REVIEW OF PARTICLE PHYSICS*

Particle Data Group

Abstract

The *Review* summarizes much of particle physics and cosmology. Using data from previous editions, plus 2,873 new measurements from 758 papers, we list, evaluate, and average measured properties of gauge bosons and the recently discovered Higgs boson, leptons, quarks, mesons, and baryons. We summarize searches for hypothetical particles such as supersymmetric particles, heavy bosons, axions, dark photons, etc. Particle properties and search limits are listed in Summary Tables. We give numerous tables, figures, formulae, and reviews of topics such as Higgs Boson Physics, Supersymmetry, Grand Unified Theories, Neutrino Mixing, Dark Energy, Dark Matter, Cosmology, Particle Detectors, Colliders, Probability and Statistics. Among the 118 reviews are many that are new or heavily revised, including a new review on Neutrinos in Cosmology.

Starting with this edition, the *Review* is divided into two volumes. Volume 1 includes the Summary Tables and all review articles. Volume 2 consists of the Particle Listings. Review articles that were previously part of the Listings are now included in volume 1.

The complete *Review* (both volumes) is published online on the website of the Particle Data Group (`http://pdg.lbl.gov`) and in a journal. Volume 1 is available in print as the *PDG Book*. A *Particle Physics Booklet* with the Summary Tables and essential tables, figures, and equations from selected review articles is also available.

DOI: 10.1103/PhysRevD.98.030001

The 2018 edition of the *Review of Particle Physics* should be cited as:
M. Tanabashi *et al.* (Particle Data Group), Phys. Rev. D **98**, 030001 (2018)

*The publication of the *Review of Particle Physics* is supported by the Director, Office of Science, Office of High Energy Physics of the U.S. Department of Energy under Contract No. DE–AC02–05CH11231; by the European Laboratory for Particle Physics (CERN); by an implementing arrangement between the governments of Japan (MEXT: Ministry of Education, Culture, Sports, Science and Technology) and the United States (DOE) on cooperative research and development; and by the Italian National Institute of Nuclear Physics (INFN). Individual collaborators receive support for their PDG activities from their respective funding agencies.

Particle Data Group

M. Tanabashi,[1,2] K. Hagiwara,[3] K. Hikasa,[4] K. Nakamura,[5,3] Y. Sumino,[4] F. Takahashi,[4] J. Tanaka,[6] K. Agashe,[7] G. Aielli,[8] C. Amsler,[9] M. Antonelli,[10] D.M. Asner,[11] H. Baer,[12] Sw. Banerjee,[13] R.M. Barnett,[14] T. Basaglia,[15] C.W. Bauer,[14] J.J. Beatty,[16] V.I. Belousov,[17] J. Beringer,[14] S. Bethke,[18] A. Bettini,[19*] H. Bichsel,[20] O. Biebel,[21] K.M. Black,[22] E. Blucher,[23] O. Buchmuller,[24] V. Burkert,[25] M.A. Bychkov,[26] R.N. Cahn,[14] M. Carena,[27,23,28] A. Ceccucci,[15] A. Cerri,[29] D. Chakraborty,[30] M.-C. Chen,[31] R.S. Chivukula,[32] G. Cowan,[33] O. Dahl,[14] G. D'Ambrosio,[34] T. Damour,[35] D. de Florian,[36] A. de Gouvêa,[37] T. DeGrand,[38] P. de Jong,[39] G. Dissertori,[40] B.A. Dobrescu,[27] M. D'Onofrio,[41] M. Doser,[15] M. Drees,[42] H.K. Dreiner,[42] D.A. Dwyer,[14] P. Eerola,[43] S. Eidelman,[44,45] J. Ellis,[46,15] J. Erler,[47] V.V. Ezhela,[17] W. Fetscher,[40] B.D. Fields,[48,49] R. Firestone,[50] B. Foster,[51,52,53] A. Freitas,[54] H. Gallagher,[55] L. Garren,[27] H.-J. Gerber,[40] G. Gerbier,[56] T. Gershon,[57] Y. Gershtein,[58] T. Gherghetta,[59] A.A. Godizov,[17] M. Goodman,[60] C. Grab,[40] A.V. Gritsan,[61] C. Grojean,[62,63] D.E. Groom,[14] M. Grünewald,[64] A. Gurtu,[65,15] T. Gutsche,[66] H.E. Haber,[67] C. Hanhart,[68] S. Hashimoto,[3] Y. Hayato,[69] K.G. Hayes,[70] A. Hebecker,[71] S. Heinemeyer,[72,73,74] B. Heltsley,[75] J. J. Hernández-Rey,[76†] J. Hisano,[2] A. Höcker,[15] J. Holder,[77,78] A. Holtkamp,[15] T. Hyodo,[79] K.D. Irwin,[80,81] K.F. Johnson,[82] M. Kado,[83,15] M. Karliner,[84] U.F. Katz,[85] S.R. Klein,[50] E. Klempt,[86] R.V. Kowalewski,[87] F. Krauss,[88] M. Kreps,[57] B. Krusche,[89] Yu.V. Kuyanov,[17‡] Y. Kwon,[90] O. Lahav,[91] J. Laiho,[92] J. Lesgourgues,[93] A. Liddle,[94] Z. Ligeti,[14] C.-J. Lin,[14] C. Lippmann,[95] T.M. Liss,[96] L. Littenberg,[11] K.S. Lugovsky,[14,17] S.B. Lugovsky,[17] A. Lusiani,[97,98] Y. Makida,[3] F. Maltoni,[99] T. Mannel,[100] A.V. Manohar,[101] W.J. Marciano,[11] A.D. Martin,[88] A. Masoni,[102] J. Matthews,[103] U.-G. Meißner,[86,68] D. Milstead,[104] R.E. Mitchell,[105] K. Mönig,[106] P. Molaro,[107] F. Moortgat,[15,108] M. Moskovic,[15] H. Murayama,[5,109,14] M. Narain,[110] P. Nason,[111] S. Navas,[112†] M. Neubert,[113] P. Nevski,[11§] Y. Nir,[114] K.A. Olive,[59] S. Pagan Griso,[14] J. Parsons,[115] C. Patrignani,[116] J.A. Peacock,[94] M. Pennington,[25] S.T. Petcov,[117,5,118] V.A. Petrov,[17] E. Pianori,[14] A. Piepke,[119] A. Pomarol,[120,121] A. Quadt,[122] J. Rademacker,[123] G. Raffelt,[124] B.N. Ratcliff,[81] P. Richardson,[88] A. Ringwald,[52] S. Roesler,[15] S. Rolli,[125] A. Romaniouk,[126] L.J. Rosenberg,[20] J.L. Rosner,[23] G. Rybka,[20] R.A. Ryutin,[17] C.T. Sachrajda,[127] Y. Sakai,[3] G.P. Salam,[15,128,129] S. Sarkar,[129,130] F. Sauli,[15§] O. Schneider,[131] K. Scholberg,[132] A.J. Schwartz,[133] D. Scott,[134] V. Sharma,[101] S.R. Sharpe,[20] T. Shutt,[81] M. Silari,[15] T. Sjöstrand,[135] P. Skands,[136] T. Skwarnicki,[92] J.G. Smith,[38] G.F. Smoot,[137,109,14] S. Spanier,[138] H. Spieler,[14§] C. Spiering,[106] A. Stahl,[139] S.L. Stone,[92] T. Sumiyoshi,[140] M.J. Syphers,[30,27] K. Terashi,[69] J. Terning,[141] U. Thoma,[86] R.S. Thorne,[91] L. Tiator,[142] M. Titov,[56] N.P. Tkachenko,[17] N.A. Törnqvist,[43‡] D.R. Tovey,[143] G. Valencia,[136] R. Van de Water,[27] N. Varelas,[144] G. Venanzoni,[98] L. Verde,[145,146] M.G. Vincter,[147] P. Vogel,[148] A. Vogt,[149] S.P. Wakely,[23,28] W. Walkowiak,[100] C.W. Walter,[132] D. Wands,[150] D.R. Ward,[151] M.O. Wascko,[24] G. Weiglein,[52] D.H. Weinberg,[152] E.J. Weinberg,[115] M. White,[109,14] L.R. Wiencke,[153] S. Willocq,[154] C.G. Wohl,[14] J. Womersley,[155] C.L. Woody,[11] R.L. Workman,[156] W.-M. Yao,[14] G.P. Zeller,[27] O.V. Zenin,[17,157] R.-Y. Zhu,[158] S.-L. Zhu,[159] F. Zimmermann,[15] P.A. Zyla[14]

Technical Associates: J. Anderson,[14] L. Fuller,[14‖] V.S. Lugovsky,[17] P. Schaffner[14]

1. *Department of Physics, Nagoya University, Nagoya, Japan*
2. *Nagoya University, Kobayashi-Maskawa Institute, Nagoya, Japan*
3. *KEK, High Energy Accelerator Research Organization, Tsukuba, Japan*
4. *Tohoku University, Department of Physics, Sendai, Japan*
5. *University of Tokyo, Kavli IPMU (WPI), The University of Tokyo Institutes for Advanced Study, Kashiwa, Japan*
6. *International Center for Elementary Particle Physics (ICEPP), University of Tokyo, Tokyo, Japan*
7. *University of Maryland, Department of Physics, College Park, MD, United States of America*
8. *Università degli Studi di Roma "Tor Vergata", Rome, Italy*
9. *Stefan Meyer Institute for Subatomic Physics, Austrian Academy of Sciences, Vienna, Austria*
10. *Lab. Nazionali di Frascati dell'INFN, Frascati, Italy*
11. *Brookhaven National Laboratory, Nuclear and Particle Physics Directorate, Upton, NY, United States of America*
12. *University of Oklahoma, Department of Physics and Astronomy, Norman, OK, United States of America*
13. *University of Louisville, Louisville, KY, United States of America*
14. *Physics Division, Lawrence Berkeley National Laboratory, Berkeley, CA, United States of America*
15. *CERN, European Organization for Nuclear Research, Genève, Switzerland*
16. *Ohio State University, Department of Physics, Columbus, OH, United States of America*
17. *Institute for High Energy Physics, COMPAS Group, Protvino, Russian Federation*
18. *Max-Planck-Institute of Physics, Munich, Germany*
19. *INFN and Dipartimento di Fisica, Università di Padova, Padova, Italy*

* Coordination activities supported directly by INFN.
† Support from Plan Estatal de Investigacion MINECO, Spain and ERDF of the European Union (FPA2015-06150-C3).
‡ Deceased.
§ Retired.
‖ Supported by the U.S. Department of Energy, Office of Science, Office of Workforce Development for Teachers and Scientists (WDTS) under the Science Undergraduate Laboratory Internship (SULI) program.

20. *University of Washington, Department of Physics, Seattle, WA, United States of America*
21. *Ludwig-Maximilians-Universität, Fakultät für Physik, München, Germany*
22. *Boston University, Department of Physics, Boston, MA, United States of America*
23. *University of Chicago, Enrico Fermi Institute and Department of Physics, Chicago, IL, United States of America*
24. *Imperial College, High Energy Physics Group, Blackett Laboratory, London, United Kingdom*
25. *Jefferson Lab, Newport News, VA, United States of America*
26. *University of Virginia, Department of Physics, Charlottesville, VA, United States of America*
27. *Fermi National Accelerator Laboratory, Batavia, IL, United States of America*
28. *University of Chicago, Kavli Institute for Cosmological Physics, Chicago, IL, United States of America*
29. *Department of Physics and Astronomy, University of Sussex, Brighton, United Kingdom*
30. *Department of Physics, Northern Illinois University, DeKalb, IL, United States of America*
31. *Department of Physics and Astronomy, University of California, Irvine, CA, United States of America*
32. *Michigan State University, Dept. of Physics and Astronomy, East Lansing, MI, United States of America*
33. *Department of Physics, Royal Holloway, University of London, London, United Kingdom*
34. *INFN Sezione di Napoli, Complesso Universitario Monte Sant'Angelo, Napoli, Italy*
35. *Institut des Hautes Etudes Scientifiques, Bures-sur-Yvette, France*
36. *UNSAM - Universidad Nacional de San Martan, International Center for Advanced Studies (ICAS), Buenos Aires, Argentina*
37. *Northwestern University, Department of Physics and Astronomy, Evanston, IL, United States of America*
38. *University of Colorado at Boulder, Department of Physics, Boulder, CO, United States of America*
39. *Nikhef and University of Amsterdam, Amsterdam, The Netherlands*
40. *ETH Zurich, Institute for Particle Physics and Astrophysics, Zurich, Switzerland*
41. *University of Liverpool, Department of Physics, Liverpool, United Kingdom*
42. *Universität Bonn, Physikalisches Institut, Bonn, Germany*
43. *University of Helsinki, Department of Physics, Helsinki, Finland*
44. *Budker Institute of Nuclear Physics SB RAS, Novosibirsk, Russian Federation*
45. *Novosibirsk State University, Novosibirsk, Russian Federation*
46. *King's College London, Department of Physics, London, United Kingdom*
47. *Universidad Nacional Autónoma de México, Departamento de Física Teórica, Instituto de Física, México, Mexico*
48. *University of Illinois, Department of Astronomy, Urbana, IL, United States of America*
49. *University of Illinois, Department of Physics, Urbana, IL, United States of America*
50. *Nuclear Science Division, Lawrence Berkeley National Laboratory, Berkeley, CA, United States of America*
51. *University of Hamburg, Hamburg, Germany*
52. *Deutsches Elektronen-Synchrotron DESY, Hamburg, Germany*
53. *University of Oxford, Denys Wilkinson Building, Department of Physics, Oxford, United Kingdom*
54. *University of Pittsburgh, Department of Physics and Astronomy, Pittsburgh, PA, United States of America*
55. *Tufts University, Department of Physics and Astronomy, Medford, MA, United States of America*
56. *CEA Saclay, DSM/IRFU/SPP, Gif-sur-Yvette, France*
57. *University of Warwick, Department of Physics, Coventry, United Kingdom*
58. *Department of Physics and Astronomy, Rutgers University, NJ, United States of America*
59. *University of Minnesota, School of Physics and Astronomy, Minneapolis, MN, United States of America*
60. *Argonne National Laboratory, Argonne, IL, United States of America*
61. *Johns Hopkins University, Baltimore, MD, United States of America*
62. *Theoriegruppe, Deutsches Elektronen-Synchrotron DESY, Hamburg, Germany*
63. *Institut für Physik, Humboldt-Universität zu Berlin, Berlin, Germany*
64. *University College Dublin, School of Physics, Dublin, Ireland*
65. *Humanitas College, Kyung Hee University, Yongin, Kymgki 17104, Republic of Korea*
66. *Universität Tübingen, Institut für Theoretische Physik, Tübingen, Germany*
67. *Santa Cruz Institute for Particle Physics, University of California, Santa Cruz, CA, United States of America*
68. *Institut für Kernphysik and Institute for Advanced Simulation, Forschungszentrum Jülich, Jülich, Germany*
69. *University of Tokyo, Department of Physics, Tokyo, Japan*
70. *Hillsdale College, Department of Physics, Hillsdale, MI, United States of America*
71. *Heidelberg University, Institute for Theoretical Physics, Heidelberg, Germany*
72. *Instituto de Física Teórica (UAM/CSIC), Universidad Autónoma de Madrid, Madrid, Spain*
73. *Campus of International Excellence UAM+CSIC, Universidad Autònoma de Madrid, Madrid, Spain*
74. *Instituto de Física de Cantabria, CSIC-UC, Santander, Spain*

75. *Cornell University, Laboratory of Elementary-Particle Physics, Ithaca, NY, United States of America*
76. *Universitat de València — C.S.I.C., IFIC — Instituto de Física Corpuscular, Valencia, Spain*
77. *University of Delaware, Department of Physics and Astronomy, Newark, DE, United States of America*
78. *University of Delaware, Bartol Research Institute, Newark, DE, United States of America*
79. *Kyoto University, Yukawa Institute for Theoretical Physics, Kyoto, Japan*
80. *Stanford University, Department of Physics, Stanford, CA, United States of America*
81. *SLAC National Accelerator Laboratory, Menlo Park, CA, United States of America*
82. *Florida State University, Department of Physics, Tallahassee, FL, United States of America*
83. *LAL, IN2P3-CNRS et Universités de Paris, Orsay CEDEX, France*
84. *Department of Particle Physics, Tel-Aviv University, Tel Aviv, Israel*
85. *Friedrich-Alexander University of Erlangen-Nürnberg, Erlangen Centre for Astroparticle Physics, Erlangen, Germany*
86. *Universität Bonn, Helmholtz-Institut für Strahlen- und Kernphysik, Bonn, Germany*
87. *University of Victoria, Victoria, BC, Canada*
88. *University of Durham, Institute for Particle Physics Phenomenology, Department of Physics, Durham, United Kingdom*
89. *University of Basel, Institute of Physics, Basel, Switzerland*
90. *Yonsei University, Department of Physics, Seoul, Republic of Korea*
91. *University College London, Department of Physics and Astronomy, London, United Kingdom*
92. *Syracuse University, Department of Physics, Syracuse, NY, United States of America*
93. *Institute of Theoretical Particle Physics and Cosmology (TTK), RWTH, Aachen, Germany*
94. *University of Edinburgh, Royal Observatory, Institute for Astronomy, Edinburgh, United Kingdom*
95. *GSI, Helmholtzzentrum für Schwerionenforschung, Darmstadt, Germany*
96. *Division of Science, City College of New York, New York, NY, United States of America*
97. *Scuola Normale Superiore, Pisa, Italy*
98. *INFN Sezione di Pisa, Pisa, Italy*
99. *Universitè catholique de Louvain, Centre for Cosmology, Particle Physics and Phenomenology (CP3), Louvain-la-Neuve, Belgium*
100. *Universität Siegen, Department für Physik, Siegen, Germany*
101. *Department of Physics, University of California at San Diego, La Jolla, CA, United States of America*
102. *INFN Sezione di Cagliari, Cittadella Universitaria di Monserrato, Monserrato, Italy*
103. *Louisana State University, Department of Physics and Astronomy, Baton Rouge, LA, United States of America*
104. *Stockholms Universitet, AlbaNova University Centre, Fysikum, Stockholm, Sweden*
105. *Indiana University, Department of Physics, Bloomington, IN, United States of America*
106. *DESY, Zeuthen, Germany*
107. *INAF-OATS, Trieste, Italy*
108. *University of Ghent, Dept. of Physics and Astronomy, Ghent, Belgium*
109. *University of California, Department of Physics, Berkeley, CA, United States of America*
110. *Brown University, Department of Physics, Providence, RI, United States of America*
111. *INFN Sezione di Milano-Bicocca, Piazza della Scienza, Milano, Italy*
112. *Universidad de Granada, Dpto. de Física Teórica y del Cosmos & C.A.F.P.E., Granada, Spain*
113. *Johannes Gutenberg University, PRISMA Cluster of Excellence and Mainz Institute for Theoretical Physics, Mainz, Germany*
114. *Department of Particle Physics and Astrophysics, Weizmann Institute of Science, Rehovot, Israel*
115. *Columbia University, Department of Physics, New York, NY, United States of America*
116. *Università di Bologna and INFN, Dip. Scienze per la Qualità della Vita, Rimini, Italy*
117. *SISSA/INFN, Trieste, Italy*
118. *INRNE, Bulgarian Academy of Sciences, Sofia, Bulgaria*
119. *University of Alabama, Department of Physics and Astronomy, Tuscaloosa, AL, United States of America*
120. *Universitat Autònoma de Barcelona, Departament de Física, Barcelona, Spain*
121. *IFAE, Universitat Autònoma de Barcelona, Barcelona, Spain*
122. *Georg-August-Universität Göttingen, II. Physikalisches Institut, Göttingen, Germany*
123. *University of Bristol, HH Wills Physics Laboratory, Bristol, United Kingdom*
124. *Max-Planck-Institut für Physik (Werner-Heisenberg-Institut), München, Germany*
125. *DOE, Washington, DC, United States of America*
126. *National Research Nuclear University "MEPhI", Moscow, Russian Federation*
127. *University of Southampton, School of Physics and Astronomy, Southampton, United Kingdom*
128. *LPTHE, UPMC Université de Paris 6, Paris, France*

129. *University of Oxford, Rudolf Peierls Centre for Theoretical Physics, Oxford, United Kingdom*
130. *Niels Bohr Institute, Copenhagen, Denmark*
131. *Institute of Physics, Ecole Polytechnique Fédérale de Lausanne (EPFL), Lausanne, Switzerland*
132. *Duke University, Physics Department, Durham, NC, United States of America*
133. *University of Cincinnati, Department of Physics, Cincinnati, OH, United States of America*
134. *University of British Columbia, Department of Physics and Astronomy, Vancouver, BC, Canada*
135. *Lund University, Department of Astronomy and Theoretical Physics, Lund, Sweden*
136. *Monash University, School of Physics, Melbourne, Australia*
137. *Paris Centre for Cosmological Physics, APC (CNRS), Université Paris Diderot, Université Sorbonne Paris Cité, Paris, France*
138. *University of Tennessee, Department of Physics and Astronomy, Knoxville, TN, United States of America*
139. *III. Physikalisches Institut, Physikzentrum, RWTH Aachen University, Aachen, Germany*
140. *High Energy Physics Laboratory, Tokyo Metropolitan University, Tokyo, Japan*
141. *Department of Physics, University of California, Davis, CA, United States of America*
142. *Institut für Kernphysik, Johannes Gutenberg University, Mainz, Germany*
143. *University of Sheffield, Department of Physics and Astronomy, Sheffield, United Kingdom*
144. *University of Illinois at Chicago, Chicago, IL, United States of America*
145. *Instituto de ciencias del Cosmos (ICC), University of Barcelona, Barcelona, Spain*
146. *Institució Catalana de Recerca i Estudis Avancats, Barcelona, Spain*
147. *Carleton University, Department of Physics, Ottawa, ON, Canada*
148. *California Institute of Technology, Kellogg Radiation Laboratory, Pasadena, CA, United States of America*
149. *The University of Liverpool, Division of Theoretical Physics, Department of Mathematical Sciences, Liverpool, United Kingdom*
150. *University of Portsmouth, Institute of Cosmology and Gravitation, Portsmouth, United Kingdom*
151. *Cavendish Laboratory, Cambridge, United Kingdom*
152. *Ohio State University, Department of Astronomy and CCAPP, Columbus, OH, United States of America*
153. *Dept. of Physics, Colorado School of Mines, Golden, CO, United States of America*
154. *University of Massachusetts, Department of Physics, Amherst, MA, United States of America*
155. *STFC Rutherford Appleton Laboratory, Didcot, United Kingdom*
156. *George Washington University Virginia Campus, Department of Physics, Ashburn, VA, United States of America*
157. *Moscow Institute of Physics and Technology, Dolgoprudny, Russian Federation*
158. *California Institute of Technology, High Energy Physics, Pasadena, CA, United States of America*
159. *School of Physics, Peking University, Beijing, China*

HIGHLIGHTS OF THE 2018 EDITION OF THE REVIEW OF PARTICLE PHYSICS

758 new papers with 2873 new measurements

- Over 367 new papers from **LHC** experiments (ATLAS, CMS, and LHCb).
- Extensive up-to-date **Higgs boson** coverage from 56 new papers with 99 measurements; provides latest results on mass, couplings, decay width, and branching ratios, plus searches for other neutral and charged Higgs bosons.
- **Supersymmetry**: 90 new papers with major exclusions.
- **Top quark**: 54 new papers.
- Latest from ***B*-meson** physics: 112 papers with 405 measurements, including some hints of possible deviations from SM predictions related to lepton flavor non-universality.
- **Improved naming scheme** for charmonium and bottomonium states (commonly referred to as X, Y or Z states).
- Many new results to and improvements in **unstable meson** Listings.
- Six **new charmed baryons** (24 in total), fitting nicely into SU(4) multiplets.
- Substantial updates to **N and Δ resonances** Summary Tables.
- New limits on neutrinoless **double-β decays**; two-neutrino mode measurements and neutrinoless mode limits now listed separately.
- **Periodic Table** with complete 7th row and newly approved names (nihonium, moscovium, tennessine, oganesson).

118 reviews (most are revised)

- New review on **Neutrinos in Cosmology**.
- **Significant update/revision** to reviews on:
  - **Status of Higgs Boson Physics** summarizes latest results and discusses non-standard models of Higgs bosons.
  - **Supersymmetry (Theory and Experiment)** interprets latest results in simplified models with various assumptions.
  - **Axions** summarizes recent searches, discusses axion as dark matter.
  - **CKM Quark-Mixing Matrix** presents latest fits to mixing matrix.
  - **Electroweak Model** provides comprehensive fit using many inputs; discusses implications of electroweak fits for constraints on new physics.
  - **Experimental Tests of Gravitational Theory** with LIGO-VIRGO observation of gravitational waves.
  - **Neutrino Masses, Mixing, and Oscillations** discusses latest results from solar, atmospheric, reactor, and accelerator-based neutrino experiments.
  - **Accelerator Physics** has latest tentative parameters of selected future colliders; **High-Energy Collider Parameters** gives parameters for running/approved colliders.
  - Discussion of Generative Adversarial Networks (GANs) added to **Monte-Carlo Techniques**.

See **pdgLive.lbl.gov** for online access to PDG data.

See **pdg.lbl.gov/AtomicNuclearProperties** for Atomic and Nuclear Properties of Materials.

VOLUME 1: SUMMARY TABLES AND REVIEWS

(Continued on next page.)

INTRODUCTION

ONLINE PARTICLE PHYSICS INFORMATION

INTRODUCTION

1. Overview

The *Review of Particle Physics* is a comprehensive review of the field of Particle Physics and of related areas in Cosmology. It consists of "Summary Tables", "Reviews, Tables, and Plots", and "Particle Listings". Starting with this edition, the *Review* is divided into two volumes. Volume 1 includes the Summary Tables and Reviews, Tables, and Plots with all review articles. Volume 2 consists of the Particle Listings. Review articles that were previously part of the Listings are now included in Reviews, Tables and Plots in volume 1.

The contents of the *Review* are updated and made available on the PDG website (`http://pdg.lbl.gov`) each year. In even-numbered years, the *Review* is published in a journal and made available in print as the *PDG Book* together with an abridged *Particle Physics Booklet* containing Summary Tables and essential tables, figures, and equations from selected review articles. This edition is an updating through January 2018.

The Summary Tables give our best values and limits for particle properties such as masses, widths or lifetimes, and branching fractions, as well as an extensive summary of searches for hypothetical particles and a summary of experimental tests of conservation laws.

The 116 review articles in Reviews, Tables and Plots cover a wide variety of theoretical and experimental topics. Together with the Summary Tables they provide a quick reference for the practicing particle physicist. Two more review articles, Online Particle Physics Information and Tests of Conservation Laws, can be found in the Introduction and Summary Tables, respectively.

The Particle Listings are a compilation/evaluation of data on particle properties. They contain all the data used to get the values given in the Summary Tables. They also give information on unconfirmed particles and particle searches. In this edition, the Particle Listings include 2,873 new measurements from 758 papers, in addition to the 38,498 measurements from 10,564 papers that first appeared in previous editions [1]. Because of the large quantity of data, the Particle Listings are not an archive of all published data on particle properties. We refer interested readers to earlier editions for data now considered to be obsolete.

We organize the particles into six categories:

Gauge and Higgs bosons
Leptons
Quarks
Mesons
Baryons
Searches not in other sections

The last category only includes searches for particles that do not belong to the previous groups. For example, it includes searches for supersymmetric particles, compositeness and extra dimensions, while searches for heavy charged leptons and massive neutrinos are with the leptons.

In Sec. 2 of this Introduction, we list the main areas of responsibility of the authors of the Particle Listings. Our many consultants, without whom we would not have been able to produce this *Review*, are acknowledged in Sec. 3. In Sec. 4, we mention briefly the naming scheme for hadrons, which has been extended in this edition. In Sec. 5, we discuss our procedures for choosing among measurements of particle properties and for obtaining best values of the properties from the measurements.

The accuracy and usefulness of this *Review* depend in large part on interaction between its users and the authors. We appreciate comments, criticisms, and suggestions for improvements of any kind. Please send them to the appropriate author, according to the list of responsibilities in Sec. 2 below, or to `pdg@lbl.gov`.

In addition to the online publication, the Review is available in different formats:

- The printed *PDG Book* includes volume 1 only, *i.e.* it contains the Summary Tables and all review articles. Since the 2016 edition the detailed tables from the Particle Listings are no longer printed.
- The *Particle Physics Booklet* includes the Summary Tables plus essential tables, figures, and equations from selected review articles. Compared to recent Booklets, we have excluded most text and explanations in order to revert back to a more pocket-sized format.
- *pdgLive* (`http://pdgLive.lbl.gov`) is a web application giving more interactive access to PDG data than the static web pages and PDF files that are also available.
- Files that can be downloaded from the PDG website include a table of masses, widths, and PDG Monte Carlo particle ID numbers; PDF files of volume 1 (PDG Book), volume 2 (Particle Listings) and Booklet; individual review articles; all figures; and an archive file containing the complete PDG website (except for pdgLive).

Copies of the *PDG Book* or the *Particle Physics Booklet* can be ordered from our website or directly at `http://pdg.lbl.gov/order`. For special requests only, please email `pdg@lbl.gov` in North and South America, Australia, and the Far East, and `pdg-products@cern.ch` in all other areas.

This *Review* is considered to be a single comprehensive review of particle physics and related areas. Therefore we prefer that it be cited as a whole, rather than citing *e.g.* an individual review article that is part of this *Review*. For the 2018 edition, the proper citation is:

M. Tanabashi *et al.* (Particle Data Group), Phys. Rev. D **98**, 030001 (2018)

If you wish to refer to a specific part of the *Review*, for example to the Higgs boson review article, the following form should be used:

Status of Higgs Boson Physics in M. Tanabashi *et al.* (Particle Data Group), Phys. Rev. D **98**, 030001 (2018)

2. Particle Listings responsibilities

* Asterisk indicates the people to contact with questions or comments about Particle Listings sections.

Gauge and Higgs bosons

γ	A. Bettini, D.E. Groom*
Gluons	R.M. Barnett,* A.V. Manohar
Graviton	A. Bettini*, D.E. Groom
W, Z	A. Gurtu,* M. Grünewald*
Higgs bosons	S. Heinemeyer,* K. Hikasa, J. Tanaka
Heavy bosons	R.M. Barnett,* M. Tanabashi
Axions	K.A. Olive, G. Raffelt,* F. Takahashi

Leptons

Neutrinos	M. Goodman, C.-J. Lin,* K. Nakamura, K.A. Olive, A. Piepke, P. Vogel
e, μ	C. Grab, A. Bettini*
τ	A. Lusiani, K. Mönig*

Quarks

Quarks	R.M. Barnett,* A.V. Manohar
Top quark	R.M. Barnett,* Y. Sumino
b', t'	R.M. Barnett,* Y. Sumino
Free quark	A. Bettini,* C.-J. Lin

Mesons

π, η	A. Bettini,* C. Grab
Unstable mesons	C. Amsler, M. Doser,* S. Eidelman,* T. Gutsche, C. Hanhart, B. Heltsley, J. J. Hernández-Rey, A. Masoni, R.E. Mitchell, S. Navas, C. Patrignani, S. Spanier, G. Venanzoni
K (stable)	G. D'Ambrosio, C.-J. Lin*
D (stable, no mix.)	J. Rademacker, C.G. Wohl*
D^0 mixing	D.M. Asner, W.-M. Yao*
B (stable)	A. Cerri,* P. Eerola, M. Kreps, Y. Kwon, W.-M. Yao*

Baryons

Stable baryons	C. Grab, C.G. Wohl*
Unstable baryons	V. Burkert, E. Klempt, U. Thoma, L. Tiator, R.L. Workman*
Charmed baryons	J. Rademacker, C.G. Wohl*
Bottom baryons	A. Cerri,* P. Eerola, M. Kreps, Y. Kwon, W.-M. Yao*

Miscellaneous searches

Monopole	A. Bettini,* D. Milstead
Supersymmetry	M. D'Onofrio, H.K. Dreiner,* A. de Gouvêa, F. Moortgat, K.A. Olive
Technicolor	K. Agashe,* M. Tanabashi
Compositeness	M. Tanabashi, J. Terning*
Extra Dimensions	D.A. Dwyer,* T. Gherghetta, K.A. Olive
WIMP, DM, Other	A. Bettini,*, H. Baer, K.A. Olive, W.-M. Yao,*

3. Consultants

The Particle Data Group benefits greatly from the assistance of hundreds of physicists who are asked to verify every piece of data entered into this *Review*. Of special value is the advice of the PDG Advisory Committee which meets biennially and thoroughly reviews all aspects of our operation. The members of the 2018 committee are:

T. Carli (CERN)
L. Hall (UC Berkeley/LBNL)
T. Nakada (EPFL)
A. Seiden (UCSC)
A. Slosar (BNL)
M. Yokoyama (Tokyo)
Q. Zhao (IHEP Beijing)

We have especially relied on the expertise of the following people for advice on particular topics:

- M. Achasov (Budker Inst., Novosibirsk)
- W. Adam (Austrian Academy of Sciences)
- E.G. Adelberger (FNAL)
- D.S. Akerib (SLAC)
- J. Alcaraz (CERN)
- A. Ali (DESY, Hamburg)
- B. Allanach (DAMPT, Cambridge U.)
- D. Amidei (Michigan U.)
- B. Ananthanarayan (IISC)
- V. Anisovich (Petersburg Nuclear Phys. Inst.)
- A. Antognini (ETH Zurich)
- F. Anulli (INFN, Rome)
- E. Aprile (Columbia U.)
- G. Arduini (CERN)
- E. Armengaud (CEA Saclay, DSM/IRFU/SPP)
- M. Artuso (Syracuse U.)
- N. Ayres (Sussex U.)
- H. Bachacou (IRFU, Saclay)
- M. Bales (Munchen Tech. U.)
- M. Bardeen (FNAL)
- J. Barranco (Guanajuato U.)
- B. Batell (Pittsburg U.)
- L. Baudis (Zürich U.)
- O. Behnke (DESY, Hamburg)
- R. Bernabei (Rome U. Tor Vergata)
- F. Bernlochner (Karlsruhe U.)
- W. Bertl (PSI)
- V. Bertone (NIKHEF)
- M. Bettler (CERN)
- S. Borghi (Manchester U.)
- D. Boscherini (INFN, Bologna)
- T. Bose (Boston U.)
- E. Braaten (Ohio State U.)
- A. Branca (INFN, Padova)
- R.A. Briere (Carnegie Mellon U.)
- T. Browder (Hawaii U.)
- B.M. Brubaker (Art Inst. of Chicago)
- P. Brun (DAPNIA, Saclay)
- R. Budnik (Weizmann Inst.)
- A. Cabrera (APC, Paris)
- W. Cairncross (Colorado U., Boulder)
- A. Canto (CERN)
- J. Cao (IHEP Beijing)
- R. Caputo (UC Santa Cruz)
- T. Carli (CERN)
- F. Cei (Pisa U.)
- F. Cerutti (LBNL)
- A. Chao (SLAC)
- K. Chetyrkin (KIT)
- G. Chiarelli (INFN, Pisa)
- J. Chou (Rutgers U.)
- X. Cid Vidal (Santiago de Compostela U.)
- D. Cinabro (Wayne State U.)
- M. Cirelli (LPTHE, Paris)
- G. Colangelo (Bern U.)
- J. Collar (Chicago U.)
- J. Conrad (Stockholm U.)
- A. Contu (INFN, Cagliary)
- A. Corsico (La Plata U.)
- K. Cranmer (NYU)
- O. Cremonesi (INFN, Milano-Bicocca)

- P.B. Cushman (Minnesota U.)
- I. Danilkin (KPH, JGU Mainz)
- C. Davies (Glasgow U.)
- A.N. Davis (Tsinghua U.)
- B. Dawson (Adelaide U.)
- J. Delahaye (CERN)
- G. de Lellis (INFN, Napoli)
- F. Della Valle (Trieste U.)
- D. Denisov (FNAL)
- D. d'Enterria (CERN)
- S. Derenzo (LBNL)
- G. DeRijk (CERN)
- U. De Sanctis (Rome U. Tor Vergata)
- S. Descotes-Genon (Paris-Sud U.)
- U. Dey (Indian Inst. Tech., Kharagpur)
- M. Diamond (Toronto U.)
- J. Donini (Clermont-Ferrand U.)
- F. Dordei (CERN)
- T. Dorigo (INFN, Padova)
- V.P. Druzhinin (Budker Inst., Novosibirsk)
- A. Dubnickova (Comenius U.)
- A. Dzyuba (Petersburg Nuclear Phys. Inst.)
- G. Edda (CERN)
- U. Egede (Imperial Coll. London)
- T. Eifert (CERN)
- G. Eigen (Bergen U.)
- S.R. Elliott (LANL)
- R.K. Ellis (FNAL)
- E. Elsen (CERN)
- C. Enss (Heidelberg U.)
- R. Essig (YITP, Stony Brook)
- G. Facini (London U.)
- A. Ferrari (CERN)
- F. Ficek (UJ, Krakow)
- L.J. Fields (FNAL)
- W. Fischer (BNL)
- V. Flambaum (New South Wales U.)
- Z. Fodor (Wuppertal U.)
- M. Fornasa (INFN, Padova)
- K. Freese (Michigan U.; Nordita, Stockholm)
- B. Fujikawa (NSD LBNL)
- P. Gambino (INFN, Torino)
- J. Gao (IHEP Beijing)
- R. Garisto (APS)
- M. Genest (CNRS)
- E. Gersabeck (Heidelberg U.)
- S. Giovannella (INFN, Frascati)
- E. Giusarma (LBNL)
- C. Glasman (U. Autònoma de Madrid)
- A. Glazov (DESY, Hamburg)
- N. Glover (Durham U.)
- S.N. Gninenko (Russian Academy of Sciences)
- C. Gobel Burlamaqui de Mello (PUC-Rio)
- T. Golan (Wrocław U.)
- T. Golling (Geneva U.)
- G. Gonzalez (Louisiana State U.)
- R. Gonzalez Suarez (Nebraska U.)
- E. Goudzovski (Birmingham U.)
- P. Grabmayr (Tübingen U.)
- B. Graner (Washington U.)
- G. Gratta (Stanford U.)
- H. Haberzettl (Georg Washington U.)
- J. Haidenbauer (Forschungszentrum Jülich)
- F. Halzen (Wisconsin U.)
- S. Hannestad (Aarhus U.)
- D.A. Harris (FNAL)
- F.A. Harris (Hawaii U.)
- A. Hasenfratz (Colorado U., Boulder)
- U. Heintz (Brown U.)
- R. Henning (North Carolina U.)
- A. Hinzmann (Hamburg U.)
- A. Hoang (HEPHY, Vienna)
- D. Holz (Chicago U., Kavli Inst.)
- J. Horandel (Radboud U.)
- Q. Huang (Beijing Inst. Theor. Phys.)
- X. Huang (Niels Bohr Inst.)
- A. Ianni (Gran Sasso)
- P. Ilten (Birmingham U.)
- T. Inada (Tokyo U.)
- K. Inoue (Tohoku U.)
- I.G. Irastorza (U. de Zaragoza)
- J. Jaeckel (Heidelberg U.)
- F. Jegerlehner (Physik, Humboldt U.)
- X. Ji (Maryland U.)
- D. Johnson (CERN)
- C. Joram (CERN)
- J. Jowett (CERN)
- K. Kaadze (CERN)
- M. Kagan (SLAC)
- F. Kahlhoefer (DESY, Hamburg)
- J. Kaminski (Bonn U.)
- K. Kampert (Wuppertal U.)
- D. Karlen (Victoria U.)
- T. Katori (Queen Mary U. of London)
- V. Kekelidze (JINR, Dubna)
- M. Kenzie (Cambridge U.)
- S. Kettell (BNL)
- J.E. Kim (Seoul National U.)
- S. Kim (Seoul National U.)
- M. Klein (Liverpool U.)
- B. Ko (IBS, Daejeon)
- R. Kogler (Hamburg U.)
- K. Kohri (KEK)
- P.S. Koppenburg (NIKHEF)
- T. Koseki (KEK)
- A. Kouchner (Paris 7)
- W. Kozanecki (U. Paris-Saclay)
- D. Kreinick (Cornell U.)
- A. Kronfeld (FNAL)
- G. Kumar (PRL, Ahmedabad)
- C.M. Kuo (NCU)
- A. Kupsc (Uppsala U.)
- G. Lambard (IFIC, Valencia)
- G. Landsberg (Brown U.)
- H. Lee (BNL)
- N. Leite (Hamburg U.)
- G.P. Lepage (Cornell U.)
- O. Leroy (CPPM Marseille)
- H. Li (IHEP Beijing)
- Z. Li (IHEP Beijing)
- J. Libby (Indian Inst. Tech., Madras)
- J. Liu (SJTU)

- D. London (U. de Montreal)
- Y. Lu (IHEP Beijing)
- P. Luo (Huazhong U. of Science and Technology)
- N. Lurkin (Birmingham U.)
- X. Lyu (UCAS, Beijing)
- Y. Maeda (Kyoto U.)
- K. Mahn (Michigan State U.)
- L. Maisenbacher (MPQ, Garching)
- B. Malaescu (CNRS)
- G. Mandaglio (Messina U.)
- B. Mansoulie (CEA Saclay, DSM/IRFU/SPP)
- M. Marsh (DAMPT, Cambridge U.)
- S.P. Martin (Northern Illinois U.)
- M. Martinelli (CERN)
- R. Maruyama (Yale U.)
- A. Melchiorri (Rome U.)
- P. Meridiani (INFN, Rome)
- P. Mermod (Geneva U.)
- M. Messier (Indiana U.)
- I. Mikulec (Austrian Academy of Sciences)
- S. Mine (UC Irvine)
- S.R. Mishra (South Carolina U.)
- M. Misiak (Warsaw U.)
- S. Moch (Hamburg U.)
- N.V. Mokhov (FNAL)
- S. Moretti (Southampton U.)
- V.M. Mostepanenko (Pulkovo Obs., St.Petersburg)
- M. Moulson (INFN, Frascati)
- B. Murray (Warwick U.)
- H. Nagahama (Tokyo U.)
- S. Nagaitsev (FNAL)
- T. Nakadaira (KEK)
- M. Nakahata (Kamioka Observ.)
- T. Nakaya (Kyoto U.)
- T. Namikawa (Stanford U.)
- S. Narison (Montpellier U.)
- S. Neubert (Ruprecht Karls U., Heidelberg)
- J.S. Nico (NIST)
- Y. Nomura (UC Berkley)
- J.A. Nowak (Lancaster U.)
- A. Nucciotti (INFN, Milano-Bicocca)
- D. Nygren (Texas U.)
- V. Obraztsov (IHEP, Protvino)
- W. Ochs (MPI Munich)
- H.B. O'Connell (Chicago U.)
- Y. Oh (IBS, Daejeon)
- J. Oller (Murcia U.)
- S.L. Olsen (Seoul National U.)
- R.A. Ong (UC Los Angeles)
- Y. Onishi (KEK)
- G. Orebi Gann (LBNL)
- A. Orso Maria Iorio (INFN, Napoli)
- P. Owen (Imperial Coll. London)
- N. Palanque-Delabrouille (Paris U.)
- S. Palestini (CERN)
- V.S. Pantuev (INR, Moscow)
- T. Papadopoulou (Athens U.)
- H. Park (IBS, Daejeon)
- S. Pastor (IFIC, Valencia)
- J.R. Pelaez (UCM, Madrid)
- S. Perazzini (CERN)
- A. Pich (IFIC, Valencia)
- M. Pieri (UC San Diego)
- A. Plante (U. de Montreal)
- R.K. Plunkett (FNAL)
- A. Pocar (Massachusetts U.)
- I. Polyakov (Syracuse U.)
- A. Poon (NSD LBNL)
- F. Porter (CALTECH)
- S. Prakhov (UC Los Angeles)
- F. Proebst (MPI Munich)
- W. Przygoda (UJ, Krakow)
- G. Pugliese (INFN, Bari)
- S. Rahatlou (UC San Diego)
- M. Redi (CERN)
- G. Ricciardi (INFN, Napoli)
- J.D. Richman (UC Santa Barbara)
- J. Rico (ICREA, Barcelona)
- T.G. Rizzo (SLAC)
- B.L. Roberts (Boston U.)
- J.M. Roney (Victoria U.)
- M. Rotondo (INFN, Frascati)
- B. Sadoulet (LBNL)
- B. Sahoo (PRL, Ahmedabad)
- A. Sakharov (NYU)
- G. Salam (LPTHE, Paris)
- R. Salerno (CNRS)
- V. Sanz (Sussex U.)
- A. Sarantsev (Bonn U.)
- X. Sarazin (LAL Orsay)
- E. Sarkisyan-Grinbaum (Texas U.)
- T. Sato (Osaka U.)
- M. Schmaltz (Boston U.)
- G. Schneider (Mainz U.)
- S. Schoenert (Munich Tech. U.)
- M. Schott (JGU, Mainz)
- D. Schulte (CERN)
- R.A. Schumacher (Carnegie Mellon U.)
- C. Schwanda (HEPHY, Vienna)
- R. Schwienhorst (Michigan State U.)
- S. Sellner (RIKEN)
- K.K. Seth (Northwestern U.)
- E. Shabalina (Georg August U. Goettingen)
- L. Shchutska (ETH Zurich)
- X. Shen (IHEP Beijing)
- Z. Shen (PMO, Nanjing)
- V. Shiltsev (FNAL)
- M. Shirasaki (NAOJ, Tokyo)
- Y. Shirman (UC Irvine)
- V. Shklyar (Giessen U.)
- P. Sikivie (Florida U.)
- P. Silva (CERN)
- A. Simone (INFN, Milano-Bicocca)
- A. Smirnov (ICTP)
- C. Smorra (RIKEN)
- D.P. Snowden-Ifft (OXY)
- J. Sobczyk (Wrocław U.)
- E.P. Solodov (Budker Inst., Novosibirsk)
- A.D. Spallicci (Orleans U.)
- P. Spradlin (Glasgow U.)
- Y. Stadnik (New South Wales U.)
- M. Strovink (UC Berkley)

- O.V. Suvorova (INR, Moscow)
- A. Svarc (Ruder Bošković I..)
- K. Tackmann (DESY, Hamburg)
- A. Tapper (Imperial Coll. London)
- X. Tata (Hawaii U.)
- R. Tenchini (INFN, Pisa)
- R. Tesarek (FNAL)
- T. Teubner (Liverpool U.)
- J. Thomas (NSD LBNL)
- P. Tiwari (Beijing Observ.)
- K. Trabelsi (KEK)
- M. Trassinelli (LPTHE, Paris)
- R.D. Tripp (LBNL)
- Y. Uchiyama (Tokyo U.)
- S. Ulmer (RIKEN)
- A. Uras (IPN, Lyon)
- P. Urquijo (School of Phys. U. of Melbourne)
- V. Vagnoni (INFN, Bologna)
- K.A. van Bibber (UC Berkley)
- C. van Eldik (Erlangen U.)
- R. Van Kooten (Indiana U.)
- Y.W. Wah (Chicago U.)
- J. Walder (Lancaster U.)
- D. Wang (IHEP Beijing)
- B. Webber (Cambridge U.)
- W. Weise (Munich Tech. U.)
- M.R. Whalley (Durham U.)
- M. Whitehead (RWTH Aachen)
- M. Wing (University Coll. London)
- E. Won (Korea U.)
- B.D. Yabsley (Sydney U.)
- A. Yamamoto (KEK)
- T. Yamanaka (Osaka U.)
- T. Yanagida (Kavli IPMU (WPI), U. Tokyo)
- L. Yang (Illinois U.)
- K. Yokoya (KEK)
- Q. Yue (Tsinghua U.)
- D. Zerwas (LAL Orsay)
- C. Zhang (IHEP Beijing)
- J. Zhang (IHEP Beijing)
- L. Zhang (Tsinghua U.)
- Y. Zhang (CNRS)
- Z. Zhang (Ningbo U.)
- K. Zhu (IHEP Beijing)
- B. Zitzer (McGill U.)
- H. Zong (Nanjing U.)
- K. Zuber (Dresden, Tech. U.)
- K. Zurek (LBNL)
- R.M. Zwaska (FNAL)

4. Naming scheme for hadrons

We introduced in the 1986 edition [2] a new naming scheme for the hadrons. Changes from older terminology affected mainly the heavier mesons made of u, d, and s quarks. Otherwise, the only important change to known hadrons was that the $F^{\pm}$ became the $D_s^{\pm}$. None of the lightest pseudoscalar or vector mesons changed names, nor did the $c\overline{c}$ or $b\overline{b}$ mesons (we do, however, now use χ_c for the $c\overline{c}$ χ states), nor did any of the established baryons. The Summary Tables give both the new and old names whenever a change has occurred.

In this edition the naming scheme is extended to address the naming of charmonium and bottomonium states that are commonly referred to as X, Y or Z states in the literature. The current scheme is described in "Naming Scheme for Hadrons" (p. 138) of this *Review*. A table details the correspondence between the names newly adopted by the PDG and those that have appeared in the literature.

We give here our conventions on type-setting style. Particle symbols are italic (or slanted) characters: e^-, p, Λ, π^0, K_L, D_s^+, b. Charge is indicated by a superscript: B^-, Δ^{++}. Charge is not normally indicated for p, n, or the quarks, and is optional for neutral isosinglets: η or η^0. Antiparticles and particles are distinguished by charge for charged leptons and mesons: τ^+, K^-. Otherwise, distinct antiparticles are indicated by a bar (overline): $\overline{\nu}_\mu$, $\overline{t}$, $\overline{p}$, $\overline{K}^0$, and $\overline{\Sigma}^+$ (the antiparticle of the Σ^-).

5. Procedures

5.1. ***Selection and treatment of data*** : The Particle Listings contain all relevant data known to us that are published in journals. With very few exceptions, we do not include results from preprints or conference reports. Nor do we include data that are of historical importance only (the Listings are not an archival record). We search every volume of 20 journals through our cutoff date for relevant data. We also include later published papers that are sent to us by the authors (or others).

In the Particle Listings, we clearly separate measurements that are used to calculate or estimate values given in the Summary Tables from measurements that are not used. We give explanatory comments in many such cases. Among the reasons a measurement might be excluded are the following:

- It is superseded by or included in later results.
- No error is given.
- It involves assumptions we question.
- It has a poor signal-to-noise ratio, low statistical significance, or is otherwise of poorer quality than other data available.
- It is clearly inconsistent with other results that appear to be more reliable. Usually we then state the criterion, which sometimes is quite subjective, for selecting "more reliable" data for averaging. See Sec. 5.4.
- It is not independent of other results.
- It is not the best limit (see below).
- It is quoted from a preprint or a conference report.

In some cases, *none* of the measurements is entirely reliable and no average is calculated. For example, the masses of many of the baryon resonances, obtained from partial-wave analyses, are quoted as estimated ranges thought to probably include the true values, rather than as averages with errors. This is discussed in the Baryon Particle Listings.

For upper limits, we normally quote in the Summary Tables the strongest limit. We do not average or combine upper limits except in a very few cases where they may be re-expressed as measured numbers with Gaussian errors.

As is customary, we assume that particle and antiparticle share the same spin, mass, and mean life. The Tests of Conservation Laws table, following the Summary Tables, lists tests of CPT as well as other conservation laws.

We use the following indicators in the Particle Listings to tell how we get values from the tabulated measurements:

- OUR AVERAGE—From a weighted average of selected data.
- OUR FIT—From a constrained or overdetermined multi-parameter fit of selected data.
- OUR EVALUATION—Not from a direct measurement, but evaluated from measurements of related quantities.
- OUR ESTIMATE—Based on the observed range of the data. Not from a formal statistical procedure.
- OUR LIMIT—For special cases where the limit is evaluated by us from measured ratios or other data. Not from a direct measurement.

An experimentalist who sees indications of a particle will of course want to know what has been seen in that region in the past. Hence we include in the Particle Listings all reported states that, in our opinion, have sufficient statistical merit and that have not been disproved by more reliable data. However, we promote to the Summary Tables only those states that we feel are well established. This judgment is, of course, somewhat subjective and no precise criteria can be given. For more detailed discussions, see the minireviews in the Particle Listings.

5.2. ***Averages and fits*** : We divide this discussion on obtaining averages and errors into three sections: (1) treatment of errors; (2) unconstrained averaging; (3) constrained fits.

5.2.1. *Treatment of errors:* In what follows, the "error" δx means that the range $x \pm \delta x$ is intended to be a 68.3% confidence interval about the central value x. We treat this error as if it were Gaussian. Thus when the error *is* Gaussian, δx is the usual one standard deviation (1σ). Many experimenters now give statistical and systematic errors separately, in which case we usually quote both errors, with the statistical error first. For averages and fits, we then add the the two errors in quadrature and use this combined error for δx.

When experimenters quote asymmetric errors $(\delta x)^+$ and $(\delta x)^-$ for a measurement x, the error that we use for that measurement in making an average or a fit with other measurements is a continuous function of these three quantities. When the resultant average or fit $\overline{x}$ is less than $x-(\delta x)^-$, we use $(\delta x)^-$; when it is greater than $x+(\delta x)^+$, we use $(\delta x)^+$. In between, the error we use is a linear function of x. Since the errors we use are functions of the result, we iterate to get the final result. Asymmetric output errors are determined from the input errors assuming a linear relation between the input and output quantities.

In fitting or averaging, we usually do not include correlations between different measurements, but we try to select data in such a way as to reduce correlations. Correlated errors are, however, treated explicitly when there are a number of results of the form $A_i \pm \sigma_i \pm \Delta$ that have identical systematic errors Δ. In this case, one can first average the $A_i \pm \sigma_i$ and then combine the resulting statistical error with Δ. One obtains, however, the same result by averaging $A_i \pm (\sigma_i^2 + \Delta_i^2)^{1/2}$, where $\Delta_i = \sigma_i \Delta [\sum (1/\sigma_j^2)]^{1/2}$. This procedure has the advantage that, with the modified systematic errors Δ_i, each measurement may be treated as independent and averaged in the usual way with other data. Therefore, when appropriate, we adopt this procedure. We tabulate Δ and invoke an automated procedure that computes Δ_i before averaging and we include a note saying that there are common systematic errors.

Another common case of correlated errors occurs when experimenters measure two quantities and then quote the two and their difference, *e.g.*, m_1, m_2, and $\Delta = m_2 - m_1$. We cannot enter all of m_1, m_2 and Δ into a constrained fit because they are not independent. In some cases, it is a good approximation to ignore the quantity with the largest error and put the other two into the fit. However, in some cases correlations are such that the errors on m_1, m_2 and Δ are comparable and none of the three values can be ignored. In this case, we put all three values into the fit and invoke an automated procedure to increase the errors prior to fitting such that the three quantities can be treated as independent measurements in the constrained fit. We include a note saying that this has been done.

5.2.2. *Unconstrained averaging:* To average data, we use a standard weighted least-squares procedure and in some cases, discussed below, increase the errors with a "scale factor." We begin by assuming that measurements of a given quantity are uncorrelated, and calculate a weighted average and error as

$$\overline{x} \pm \delta\overline{x} = \frac{\sum_i w_i\, x_i}{\sum_i w_i} \pm \left(\sum_i w_i\right)^{-1/2} , \qquad (1)$$

where

$$w_i = 1/(\delta x_i)^2 .$$

Here x_i and δx_i are the value and error reported by the ith experiment, and the sums run over the N experiments. We then calculate $\chi^2 = \sum w_i(\overline{x} - x_i)^2$ and compare it with $N-1$, which is the expectation value of χ^2 if the measurements are from a Gaussian distribution.

If $\chi^2/(N-1)$ is less than or equal to 1, and there are no known problems with the data, we accept the results.

If $\chi^2/(N-1)$ is very large, we may choose not to use the average at all. Alternatively, we may quote the calculated average, but then make an educated guess of the error, a conservative estimate designed to take into account known problems with the data.

Finally, if $\chi^2/(N-1)$ is greater than 1, but not greatly so, we still average the data, but then also do the following:

(a) We increase our quoted error, $\delta\overline{x}$ in Eq. (1), by a scale factor S defined as

$$S = \left[\chi^2/(N-1)\right]^{1/2} . \qquad (2)$$

Our reasoning is as follows. The large value of the χ^2 is likely to be due to underestimation of errors in at least one of the experiments. Not knowing which of the errors are underestimated, we assume they are all underestimated by the same factor S. If we scale up all the input errors by this factor, the χ^2 becomes $N-1$, and of course the output error $\delta\overline{x}$ scales up by the same factor. See Ref. 3.

When combining data with widely varying errors, we modify this procedure slightly. We evaluate S using only the experiments with smaller errors. Our cutoff or ceiling on δx_i is arbitrarily chosen to be

$$\delta_0 = 3N^{1/2}\, \delta\overline{x} ,$$

where $\delta\overline{x}$ is the unscaled error of the mean of all the experiments. Our reasoning is that although the low-precision experiments have little influence on the values $\overline{x}$

and $\delta\overline{x}$, they can make significant contributions to the χ^2, and the contribution of the high-precision experiments thus tends to be obscured. Note that if each experiment has the same error δx_i, then $\delta\overline{x}$ is $\delta x_i/N^{1/2}$, so each δx_i is well below the cutoff. (More often, however, we simply exclude measurements with relatively large errors from averages and fits: new, precise data chase out old, imprecise data.)

Our scaling procedure has the property that if there are two values with comparable errors separated by much more than their stated errors (with or without a number of other values of lower accuracy), the scaled-up error $\delta\,\overline{x}$ is approximately half the interval between the two discrepant values.

We emphasize that our scaling procedure for *errors* in no way affects central values. And if you wish to recover the unscaled error $\delta\overline{x}$, simply divide the quoted error by S.

(b) If the number M of experiments with an error smaller than δ_0 is at least three, and if $\chi^2/(M-1)$ is greater than 1.25, we show in the Particle Listings an ideogram of the data. Figure 1 is an example. Sometimes one or two data points lie apart from the main body; other times the data split into two or more groups. We extract no numbers from these ideograms; they are simply visual aids, which the reader may use as he or she sees fit.

Each measurement in an ideogram is represented by a Gaussian with a central value x_i, error δx_i, and area proportional to $1/\delta x_i$. The choice of $1/\delta x_i$ for the area is somewhat arbitrary. With this choice, the center of gravity of the ideogram corresponds to an average that uses weights $1/\delta x_i$ rather than the $(1/\delta x_i)^2$ actually used in the averages. This may be appropriate when some of the experiments have seriously underestimated systematic errors. However, since for this choice of area the height of the Gaussian for each measurement is proportional to $(1/\delta\, x_i)^2$, the peak position of the ideogram will often favor the high-precision measurements at least as much as does the least-squares average. See our 1986 edition [2] for a detailed discussion of the use of ideograms.

5.2.3. *Constrained fits:* In some cases, such as branching ratios or masses and mass differences, a constrained fit may be needed to obtain the best values of a set of parameters. For example, most branching ratios and rate measurements are analyzed by making a simultaneous least-squares fit to all the data and extracting the partial decay fractions P_i, the partial widths Γ_i, the full width Γ (or mean life), and the associated error matrix.

Assume, for example, that a state has m partial decay fractions P_i, where $\sum P_i = 1$. These have been measured in N_r different ratios R_r, where, e.g., $R_1 = P_1/P_2$, $R_2 = P_1/P_3$, *etc.* [We can handle any ratio R of the form $\sum \alpha_i\, P_i/\sum \beta_i\, P_i$, where α_i and β_i are constants, usually 1 or 0. The forms $R = P_iP_j$ and $R = (P_iP_j)^{1/2}$ are also allowed.] Further assume that *each* ratio R has been measured by N_k experiments (we designate each experiment with a subscript k, e.g., R_{1k}). We then find the best values of the fractions P_i by minimizing the χ^2 as a function of the $m-1$ independent parameters:

$$\chi^2 = \sum_{r=1}^{N_r}\sum_{k=1}^{N_k}\left(\frac{R_{rk}-R_r}{\delta R_{rk}}\right)^2 , \qquad (3)$$

where the R_{rk} are the measured values and R_r are the fitted values of the branching ratios.

In addition to the fitted values $\overline{P}_i$, we calculate an error matrix $\langle\delta\overline{P}_i\ \delta\overline{P}_j\rangle$. We tabulate the diagonal elements of $\delta\,\overline{P}_i = \langle\delta\,\overline{P}_i\ \delta\,\overline{P}_i\rangle^{1/2}$ (except that some errors are scaled as discussed below). In the Particle Listings, we give the complete correlation matrix; we also calculate the fitted value of each ratio, for comparison with the input data, and list it above the relevant input, along with a simple unconstrained average of the same input.

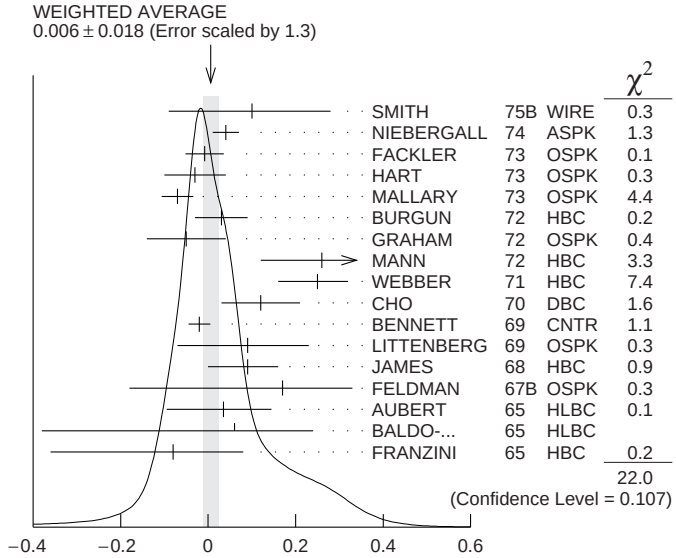

Figure 1: A typical ideogram. The arrow at the top shows the position of the weighted average, while the width of the shaded pattern shows the error in the average after scaling by the factor S. The column on the right gives the χ^2 contribution of each of the experiments. Note that the next-to-last experiment, denoted by the incomplete error flag ($\perp$), is not used in the calculation of S (see the text).

Three comments on the example above:

(1) There was no connection assumed between measurements of the full width and the branching ratios. But often we also have information on partial widths Γ_i as well as the total width Γ. In this case we must introduce Γ as a parameter in the fit, along with the P_i, and we give correlation matrices for the widths in the Particle Listings.

(2) We try to pick those ratios and widths that are as independent and as close to the original data as possible. When one experiment measures all the branching fractions and constrains their sum to be one, we leave one of them (usually the least well-determined one) out of the fit to make the set of input data more nearly independent. We now do allow for correlations between input data.

(3) We calculate scale factors for both the R_r and P_i when the measurements for any R give a larger-than-expected contribution to the χ^2. According to Eq. (3), the double sum for χ^2 is first summed over experiments $k = 1$ to N_k, leaving a single sum over ratios $\chi^2 = \sum \chi^2_r$. One is tempted to define a scale factor for the ratio r as $S_r^2 = \chi^2_r/\langle\chi^2_r\rangle$. However, since $\langle\chi^2_r\rangle$ is not a fixed quantity (it is somewhere between N_k and N_{k-1}), we do not know how to

evaluate this expression. Instead we define

$$S_r^2 = \frac{1}{N_k}\sum_{k=1}^{N_k}\frac{\left(R_{rk}-\overline{R}_r\right)^2}{\langle(R_{rk}-\overline{R}_r)^2\rangle}. \quad (4)$$

With this definition the expected value of S_r^2 is one. We can show that

$$\langle(R_{rk}-\overline{R}_r)^2\rangle = \langle(\delta R_{rk})^2\rangle - (\delta\overline{R}_r)^2\ , \quad (5)$$

where $\delta\overline{R}_r$ is the fitted error for ratio r.

The fit is redone using errors for the branching ratios that are scaled by the larger of S_r and unity, from which new and often larger errors $\delta\overline{P}_i'$ are obtained. The scale factors we finally list in such cases are defined by $S_i = \delta\overline{P}_i'/\delta\overline{P}_i$. However, in line with our policy of not letting S affect the central values, we give the values of $\overline{P}_i$ obtained from the original (unscaled) fit.

There is one special case in which the errors that are obtained by the preceding procedure may be changed. When a fitted branching ratio (or rate) $\overline{P}_i$ turns out to be less than three standard deviations ($\delta\overline{P}_i'$) from zero, a new smaller error $(\delta\overline{P}_i'')^-$ is calculated on the low side by requiring the area under the Gaussian between $\overline{P}_i - (\delta\overline{P}_i'')^-$ and $\overline{P}_i$ to be 68.3% of the area between zero and $\overline{P}_i$. A similar correction is made for branching fractions that are within three standard deviations of one. This keeps the quoted errors from overlapping the boundary of the physical region.

5.3. ***Rounding*** : While the results shown in the Particle Listings are usually exactly those published by the experiments, the numbers that appear in the Summary Tables (means, averages and limits) are subject to a set of rounding rules.

The basic rule states that if the three highest order digits of the error lie between 100 and 354, we round to two significant digits. If they lie between 355 and 949, we round to one significant digit. Finally, if they lie between 950 and 999, we round up to 1000 and keep two significant digits. In all cases, the central value is given with a precision that matches that of the error. So, for example, the result (coming from an average) 0.827 ± 0.119 would appear as 0.83 ± 0.12, while 0.827 ± 0.367 would turn into 0.8 ± 0.4.

Rounding is not performed if a result in a Summary Table comes from a single measurement, without any averaging. In that case, the number of digits published in the original paper is kept, unless we feel it inappropriate. Note that, even for a single measurement, when we combine statistical and systematic errors in quadrature, rounding rules apply to the result of the combination. It should be noted also that most of the limits in the Summary Tables come from a single source (the best limit) and, therefore, are not subject to rounding.

Finally, we should point out that in several instances, when a group of results come from a single fit to a set of data, we have chosen to keep two significant digits for all the results. This happens, for instance, for several properties of the W and Z bosons and the τ lepton.

5.4. ***Discussion*** : The problem of averaging data containing discrepant values is nicely discussed by Taylor in Ref. 4. He considers a number of algorithms that attempt to incorporate inconsistent data into a meaningful average. However, it is difficult to develop a procedure that handles simultaneously in a reasonable way two basic types of situations: (a) data that lie apart from the main body of the data are incorrect (contain unreported errors); and (b) the opposite—it is the main body of data that is incorrect. Unfortunately, as Taylor shows, case (b) is not infrequent. He concludes that the choice of procedure is less significant than the initial choice of data to include or exclude.

We place much emphasis on this choice of data. Often we solicit the help of outside experts (consultants). Sometimes, however, it is simply impossible to determine which of a set of discrepant measurements are correct. Our scale-factor technique is an attempt to address this ignorance by increasing the error. In effect, we are saying that present experiments do not allow a precise determination of this quantity because of unresolvable discrepancies, and one must await further measurements. The reader is warned of this situation by the size of the scale factor, and if he or she desires can go back to the literature (via the Particle Listings) and redo the average with a different choice of data.

Our situation is less severe than most of the cases Taylor considers, such as estimates of the fundamental constants like $\hbar$, *etc.* Most of the errors in his case are dominated by systematic effects. For our data, statistical errors are often at least as large as systematic errors, and statistical errors are usually easier to estimate. A notable exception occurs in partial-wave analyses, where different techniques applied to the same data yield different results. In this case, as stated earlier, we often do not make an average but just quote a range of values.

A brief history of early Particle Data Group averages is given in Ref. 3. Figure 2 shows some histories of our values of a few particle properties. Sometimes large changes occur. These usually reflect the introduction of significant new data or the discarding of older data. Older data are discarded in favor of newer data when it is felt that the newer data have smaller systematic errors, or have more checks on systematic errors, or have made corrections unknown at the time of the older experiments, or simply have much smaller errors. Sometimes, the scale factor becomes large near the time at which a large jump takes place, reflecting the uncertainty introduced by the new and inconsistent data. By and large, however, a full scan of our history plots shows a dull progression toward greater precision at central values quite consistent with the first data points shown.

We conclude that the reliability of the combination of experimental data and our averaging procedures is usually good, but it is important to be aware that fluctuations outside of the quoted errors can and do occur.

ACKNOWLEDGMENTS

The publication of the *Review of Particle Physics* is supported by the Director, Office of Science, Office of High Energy Physics of the U.S. Department of Energy under Contract No. DE–AC02–05CH11231; by the European Laboratory for Particle Physics (CERN); by an implementing arrangement between the governments of Japan (MEXT: Ministry of Education, Culture, Sports, Science and Technology) and the United States (DOE) on cooperative research and development; and by the Italian National Institute of

Nuclear Physics (INFN). Individual collaborators receive support for their PDG activities from their respective funding agencies.

We thank all those who have assisted in the many phases of preparing this *Review*. We particularly thank the many who have responded to our requests for verification of data entered in the Listings, and those who have made suggestions or pointed out errors.

We are grateful to the staff at CERN, IHEP Beijing, KEK, and LBNL who take care of the mailing and distribution of our products.

This work used resources of the National Energy Research Scientific Computing Center, a DOE Office of Science User Facility supported by the Office of Science of the U.S. Department of Energy under Contract No. DE-AC02-05CH11231.

REFERENCES

1. The previous edition was: C. Patrignani *et al.* (Particle Data Group), Chin. Phys. C **40**, 100001 (2016).
2. M. Aguilar-Benitez *et al.* (Particle Data Group), Phys. Lett. **170B** (1986).
3. A.H. Rosenfeld, Ann. Rev. Nucl. Sci. **25**, 555 (1975).
4. B.N. Taylor, "Numerical Comparisons of Several Algorithms for Treating Inconsistent Data in a Least-Squares Adjustment of the Fundamental Constants," U.S. National Bureau of Standards NBSIR 81-2426 (1982).

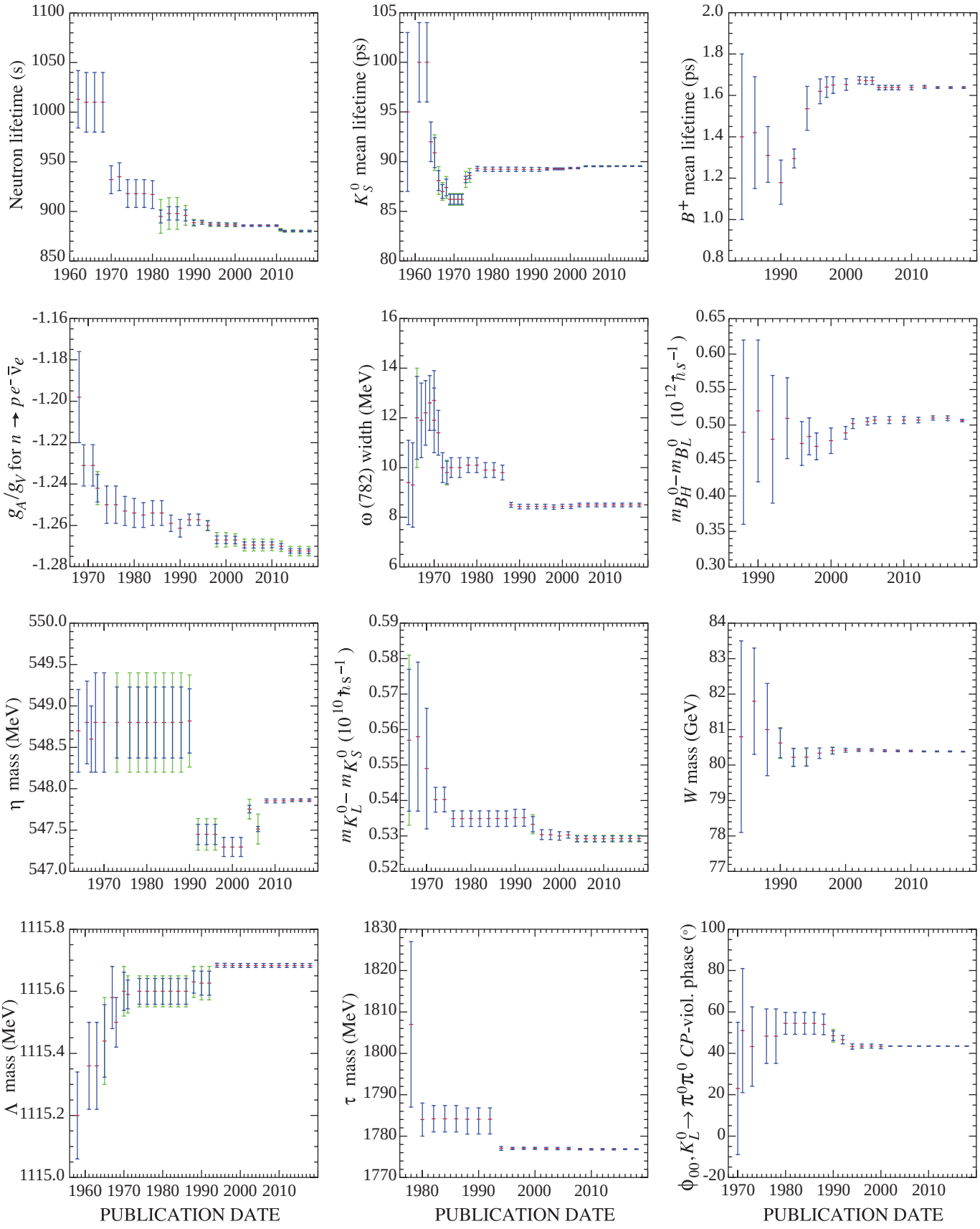

Figure 1: A historical perspective of values of a few particle properties tabulated in this *Review* as a function of date of publication of the *Review*. A full error bar indicates the quoted error; a thick-lined portion indicates the same but without the "scale factor."

Online Particle Physics Information

Updated August 2017 by A. Holtkamp and M. Moskovic (CERN)†

1. Introduction

The collection of online information resources in particle physics and related areas presented in this chapter is of necessity incomplete. An expanded and regularly updated online version can be found at:

`http://library.cern/particle_physics_information`

Suggestions for additions and updates are very welcome.†

2. Particle Data Group (PDG) resources

- **Review of Particle Physics (RPP)** A comprehensive report on the fields of particle physics and related areas of cosmology and astrophysics, including both review articles and a compilation/evaluation of data on particle properties. The review section includes articles, tables and plots on a wide variety of theoretical and experimental topics of interest to particle physicists and astrophysicists. The particle properties section provides tables of published measurements as well as the Particle Data Groups best values and limits for particle properties such as masses, widths, lifetimes, and branching fractions, and an extensive summary of searches for hypothetical particles. RPP is published as a large book every two years, with partial updates made available once each year on the web.

  All the contents of the book version of RPP are available online:

  `http://pdg.lbl.gov`

  The printed book can be ordered:

  `pdg.lbl.gov/2017/html/receive_our_products.html`

  Of historical interest is the complete RPP collection which can be found online:

  `http://pdg.lbl.gov/rpp-archive/`

  `library.cern/PDG_publications/review_particle_physics`

- **Particle Physics booklet:** An abridged version of the Review of Particle Physics available as a pocket-sized 300-page booklet. It is one of the most useful summaries of physics data. The booklet contains an abbreviated set of reviews and the summary tables from the most recent edition of the Review of Particle Physics.

  The PDF file of the booklet can be downloaded:

  `http://pdg.lbl.gov/current/booklet.pdf`

  The printed booklet can be ordered:

  `pdg.lbl.gov/2017/html/receive_our_products.html`

- **PDGLive:** A web application for browsing the contents of the PDG database that contains the information published in the Review of Particle Physics. It allows one to navigate to a particle of interest, see a summary of the information available, and then proceed to the detailed information published in the Review of Particle Physics. Data entries are directly linked to the corresponding bibliographic information in INSPIRE.

  `http://pdglive.lbl.gov`

- **Computer-readable files:** Data files that can be downloaded from PDG include tables of particle masses and widths, PDG Monte Carlo particle numbers, and cross-section data. The files are updated with each new edition of the Review of Particle Physics.

  `pdg.lbl.gov/current/html/computer_read.html`

3. Particle Physics Information Platforms

- **INSPIRE:** INSPIRE serves as a one-stop information platform for the particle physics community, comprising 8 interlinked databases on literature, conferences, institutions, journals, researchers, experiments, jobs and data. It is run in collaboration by CERN, DESY, Fermilab, IHEP and SLAC, and has been serving the scientific community for almost 50 years. Previously known as SPIRES, it was the first website outside Europe and the first database on the web. Close interaction with the user community and with arXiv, ADS, HepData, ORCID, PDG and publishers is the backbone of INSPIRE's evolution.

  `http://inspirehep.net/`

  In 2018, INSPIRE is launching a redesigned interface with more efficient searching and filtering. The INSPIRE Labs site is available at:

  `http://labs.inspirehep.net`

  `blog: http://blog.inspirehep.net/`

  `twitter:` @inspirehep

† Please send comments and corrections to `Annette.Holtkamp@cern.ch`.

4. Literature Databases

- **ADS:** The SAO/NASA Astrophysics Data System is a Digital Library portal offering access to 13 million bibliographic records in Astronomy and Physics. The ADS search engine also indexes the full-text for approximately four million publications in this collection and tracks citations, which now amount to over 80 million links. The system also provides access and links to a wealth of external resources, including electronic articles hosted by publishers and arXiv, data catalogs and a variety of data products hosted by the astronomy archives worldwide. The ADS can be accessed at

  `http://ads.harvard.edu/`

- **arXiv.org:** A repository of full text papers in physics, mathematics, computer science, statistics, nonlinear sciences, quantitative finance and quantitative biology interlinked with ADS and INSPIRE. Papers are usually submitted by their authors to arXiv in advance of submission to a journal for publication. Primarily covers 1991 to the present but authors are encouraged to post older papers retroactively. Permits searching by author, title, and words in abstract and experimentally also in the fulltext. Allows limiting by subfield archive or by date. Daily update alerts by subfield are available by email and RSS.

  `https://arXiv.org`

  `wiki: confluence.cornell.edu/display/arxivpub`

  `twitter:` @arxiv

- **CDS:** The CERN Document Server contains records of about 1,000,000 CERN and non-CERN articles, preprints, theses. It includes records for internal and technical notes, official CERN committee documents, and multimedia objects. CDS is going to focus on its role as institutional repository covering all CERN material from the early 50s and reflecting the holdings of the CERN library. Non-CERN particle and accelerator physics content is in the process of being exported to INSPIRE.

  `http://cds.cern.ch`

- **INSPIRE HEP:** The HEP collection, the flagship of the INSPIRE suite, serves more than 1.2 million bibliographic records with a growing number of fulltexts attached and metadata including author affiliations, abstracts, references, experiments, keywords as well as links to arXiv, ADS, PDG, HEPData, publisher platforms and other servers. It provides fast metadata and fulltext searches, plots extracted from fulltext, author disambiguation, author profile pages and citation analysis and is expanding its content to, e.g., experimental notes.

  `http://inspirehep.net`

- **JACoW:** The Joint Accelerator Conference Website publishes the proceedings of APAC, EPAC, PAC, IPAC, ABDW, BIW, COOL, CYCLOTRONS, DIPAC, ECRIS, FEL, HIAT, ICALEPCS, IBIC, ICAP, LINAC, North American PAC, PCaPAC, RuPAC, SRF. A custom interface allows searching on keywords, titles, authors, and in the fulltext.

  `http://www.jacow.org/`

- **KEK Library Preprints and Reports Database:** This database contains bibliographic records of preprints and technical reports held in the KEK library with links to the full text images of more than 100,000 papers scanned from their worldwide collection of preprints. Particularly useful for older scanned preprints. Links to it are included in INSPIRE HEP.

  `www.i-repository.net/il/meta_pub/engG0000128Lib`

- **MathSciNet:** This database of almost 3 million items provides reviews, abstracts and bibliographic information for much of the mathematical sciences literature. Over 100,000 new items are added each year, most of them classified according to the Mathematics Subject Classification. Authors are uniquely identified, enabling a search for publications by individual author. Over 80,000 reviews on the current published literature are added each year. Citation data allows to track the history and influence of research publications.

  `http://www.ams.org/mathscinet`

- **OSTI SciTech Connect:** A portal to free, publicly available DOE-sponsored R&D results including technical reports, bibliographic citations, journal articles, conference papers, books, multimedia and data information. SciTech Connect is a consolidation of two core DOE search engines, the Information Bridge and the Energy Citations Database. SciTech Connect incorporates all of the R&D information from these two products into one search interface. It includes over 2.9 million citations, including citations to 1.5 million journal articles. SciTech Connect also has over 440,000 full-text DOE sponsored STI reports; most of these are post-1991, but over 143,000 of the reports were published prior to 1990.

  `http://www.osti.gov/scitech/`

5. Particle Physics Journals and Conference Proceedings Series

- **CERN Journals List:** This list of journals and conference series publishing particle physics content provides information on Open Access, copyright policies and terms of use.

  `http://library.web.cern.ch/oa/where_publish`

- **INSPIRE Journals:** The database covers more than 3,550 journals publishing HEP-related articles.

  `http://inspirehep.net/collection/journals`

6. Conference Databases

- **INSPIRE Conferences:** The database of more than 22,000 past, present and future conferences, schools, and meetings of interest to high-energy physics and related fields is searchable by title, acronym, series, date, location. Included are information about published proceedings, links to conference contributions in the INSPIRE HEP database, and links to the conference Web site when available. New conferences can be submitted from the entry page.

  `http://inspirehep.net/conferences`

7. Research Institutions

- **INSPIRE Institutions:** The database of more than 11,200 institutes, laboratories, and university departments in which research on particle physics and astrophysics is performed covers six continents and over a hundred countries. Included are address and Web links where available as well as links to the papers from each institution in the HEP database, to scientists listed in HEPNames affiliated to this institution in the past or present and to experiments performed at this institution. Searches can be performed by name, acronym, location, etc. The site offers an alphabetical list by country as well as a list of the top 500 HEP and astrophysics institutions sorted by country.

  `http://inspirehep.net/institutions`

8. People

- **INSPIRE HEPNames:** Searchable worldwide database of over 119,000 active, retired and deceased people associated with particle physics and related fields. The affiliation history of these researchers, their e-mail addresses, ORCiDs, web pages, experiments they participated in, PhD advisor, information on their graduate students and links to their papers in the INSPIRE HEP, arXiv and ADS databases are provided as well as a user interface to update these informations.

  `http://inspirehep.net/hepnames`

9. Experiments

- **INSPIRE Experiments:** Contains more than 3,000 past, present, and future experiments in particle physics. Lists both accelerator and non-accelerator experiments. Includes official experiment name and number, location, and collaboration lists. Simple searches by participant, title, experiment number, institution, date approved, accelerator, or detector, return a description of the experiment, including a complete list of authors, title, overview of the experiment's goals and methods, and a link to the experiment's web page if available. Recently, it has expanded its scope to include also particle accelerators besides experiments and link them together.

  `http://inspirehep.net/Experiments`

- **Cosmic ray/Gamma ray/Neutrino and similar experiments:** This extensive collection of experimental web sites is organized by focus of study and also by location. Additional sections link to educational materials, organizations, related Web sites, etc. The site is maintained at the Max Planck Institute for Nuclear Physics, Heidelberg.

  `www.mpi-hd.mpg.de/hfm/CosmicRay/CosmicRaySites.html`

10. Jobs

- **AAS Job Register:** The American Astronomical Society publishes once a month graduate, postgraduate, faculty and other positions mainly in astronomy and astrophysics.

  `http://jobregister.aas.org/`

- **APS Careers:** A gateway for physicists, students, and physics enthusiasts to information about physics jobs and careers. Physics job listings, career advice, upcoming workshops and meetings, and career and job related resources provided by the American Physical Society.

  `http://www.aps.org/careers/employment`

- **brightrecruits.com:** A recruitment service run by IOP Publishing that connects employers from different industry sectors with jobseekers who have a background in physics and engineering.

  `http://brightrecruits.com/`

- **IOP Careers:** Careers information and resources primarily aimed at university students are provided by the UK Institute of Physics.

  `http://www.iop.org/careers/`

- **INSPIRE HEPJobs:** Lists academic and research jobs in high energy physics, nuclear physics, accelerator physics and astrophysics with the option to post a job or to receive email notices of new job listings. About 500 jobs are currently listed.

  `http://inspirehep.net/jobs`

- **Physics Today Jobs:** Online recruitment advertising website for Physics Today magazine, published by the American Institute of Physics. Physics Today Jobs is the managing partner of the AIP Career Network, an online job board network for the physical science, engineering, and computing disciplines. 8,000 resumes are currently available, and more than 2,500 jobs were posted in 2012.

  `http://www.physicstoday.org/jobs`

11. Software Packages and Repositories

Repositories

- **ASCL:** The Astrophysics Source Code Library (ASCL) is a free online registry for source codes of interest to astronomers and astrophysicists and lists codes that have been used in research that has appeared in, or been submitted to, peer-reviewed publications.

  `http://ascl.net`

- **FreeHEP:** A collection of software and information about software useful in high-energy physics and adjacent disciplines, focusing on open-source software for data analysis and visualization. Searching can be done by title, subject, date acquired, date updated, or by browsing an alphabetical list of all packages.

  `http://java.freehep.org/`

- **GenSer:** The Generator Services project collaborates with Monte Carlo (MC) generators authors and with LHC experiments in order to prepare validated LCG compliant code for both the theoretical and experimental communities at the LHC, sharing the user support duties, providing assistance for the development of the new object-oriented generators and guaranteeing the maintenance of the older packages on the LCG supported platforms. The project consists of the generators repository, validation, HepMC record and MCDB event databases.

  `ep-dep-sft.web.cern.ch/project/generator-service-project-genser`

- **Hepforge:** A development environment for high-energy physics software development projects, in particular housing many event-generator related projects, that offers a ready-made, easy-to-use set of Web based tools, including

shell account with up to date development tools, web page hosting, subversion and CVS code management systems, mailing lists, bug tracker and wiki system.

`http://www.hepforge.org/`

Particle Physics software

General purpose software packages:

- **GAMBIT:** A global fitting code for generic Beyond the Standard Model theories, designed to allow fast and easy definition of new models, observables, likelihoods, scanners and backend physics codes.

  `http://gambit.hepforge.org`

- **ROOT:** This framework for data processing in high-energy physics, born at CERN, offers applications to store, access, process, analyze and represent data or perform simulations.

  `http://root.cern.ch`

An extended list of more specialized HEP-related software can be found in the online version of this review:

`library.cern/particle_physics_information#sof`

Astrophysics Software

- **Astropy:** The Astropy Project is a community effort to develop a single core package for Astronomy in Python and foster interoperability between Python astronomy packages

  `http://www.astropy.org`

- **IRAF:** The Image Reduction and Analysis Facility is a general purpose software system for the reduction and analysis of astronomical data. IRAF is written and supported by the National Optical Astronomy Observatories (NOAO) in Tucson, Arizona.

  `http://iraf.noao.edu/`

- **Starlink:** Starlink was a UK Project supporting astronomical data processing. It was shut down in 2005 but its open-source software continued to be developed at the Joint Astronomy Centre until March 2015. It is currently maintained by the East Asian Observatory. The open-source software products are a collection of applications and libraries, usually focused on a specific aspect of data reduction or analysis.

  `http://starlink.eao.hawaii.edu/starlink`

- Links to a large number of astronomy software archives are listed at:

  `http://heasarc.nasa.gov/docs/heasarc/astro-update/`

Web Apps

- **APFEL:** This online parton density function plotter allows to compare predictions for different PDF fits.

  `https://apfel.mi.infn.it/`

- **ColliderReach:** A tool to give a simple estimate of the relation between the mass reaches of different proton-proton collider configurations.

  `http://collider-reach.web.cern.ch/`

Mobile Apps

- **arXiv mobile:** Android app for browsing and searching arXiv.org, and for reading, saving and sharing articles.

  `play.google.com/store/apps/details?id=com.commonsware.android.arXiv`

- **arXiv scanner:** Scans downloads folder for pdf files from arXiv. Adds title, authors and summary and makes all this information easily searchable from inside the application.

  `https://play.google.com/store/apps/details?id=com.agio.arxiv.scaner`

- **aNarXiv:** arXiv viewer.

  `http://github.com/nephoapp/anarxiv`

- **Collider:** This mobile app allows to see data from the ATLAS experiment at the LHC.

  `http://collider.physics.ox.ac.uk/`

- **LHSee:** This smartphone app allows to see collisions from the Large Hadron Collider.

  `http://www2.physics.ox.ac.uk/about-us/outreach/public/lhsee`

- **The Particles:** App for Apple iPad, Windows 8 and Microsoft Surface. Allows to browse a wealth of real 'event' images and videos, read popular 'biographies' of each of the particles and explore the A-Z of particle physics with its details and definitions of key concepts, laboratories and physicists. Developed by Science Photo Library in partnership with Prof. Frank Close.

  `www.sciencephoto.com/apps/particles.html`

12. Data repositories

Particle Physics

- **HEPData:** The HEPData project, funded by the STFC (UK) and based at Durham University, has been built up over the past four decades as a unique repository for scattering data from experimental particle physics papers. It currently comprises the data points from plots and tables related to several thousand publications including those from the LHC. The data from HEPData can also be accessed through INSPIRE. A new enhanced service was recently developed in collaboration with CERN.

  `https://hepdata.net`

- **CERN Open Data:** The CERN Open Data portal provides data from real collision events, as well as simulated and simplified datasets, produced by the experiments at the LHC; virtual machines to reproduce the analysis environment and software to process them. It serves over 2 PB of data in total and encourages use both for educational and research purposes.

  `http://opendata.cern.ch`

- **HepSim:** A repository with Monte Carlo simulations for particle-collision experiments. It contains predictions from parton shower models and includes Monte Carlo events after fast and full detector simulations and event reconstruction

  `http://atlaswww.hep.anl.gov/hepsim/`

- **ILDG:** The International Lattice Data Grid is an international organization which provides standards, services, methods and tools that facilitate the sharing and interchange of lattice QCD gauge configurations among scientific collaborations, by uniting their regional data grids. It offers semantic access with local tools to worldwide distributed data.

  `http://www.usqcd.org/ildg/`

- **MCDB - Monte Carlo Database:** This central database of MC events aims to facilitate communication between Monte-Carlo experts and users of event samples in LHC collaborations. Having these events stored in a public place along with the corresponding documentation allows for direct cross checks of the performances on reference samples.

  `http://mcdb.cern.ch/`

- **MCPLOTS:** mcplots is a repository of Monte Carlo plots comparing High Energy Physics event generators to a wide variety of available experimental data. The site is supported by the LHC Physics Centre at CERN.

  `http://mcplots.cern.ch/`

Astrophysics

- **CfA Dataverse:** This astronomy data repository at Harvard is open to all scientific data from astronomical institutions worldwide.

  `https://dataverse.harvard.edu/dataverse/cfa`

- **NASA's HEASARC:** The High Energy Astrophysics Science Archive Research Center (HEASARC) is the primary archive for NASA's (and other space agencies') missions dealing with electromagnetic radiation from extremely energetic phenomena ranging from black holes to the Big Bang.

  `http://heasarc.gsfc.nasa.gov/`

- **NASA archives:** The NASA archives provide access to raw and processed datasets from numerous NASA missions.

  Mikulski Archive for Space Telescopes (MAST): Hubble telescope, other missions (UV, optical):

  `http://archive.stsci.edu/`

  NASA/IPAC Infrared Science Archive: Spitzer, Herschel, Planck telescope, other missions:

  `http://irsa.ipac.caltech.edu/`

- **NASA/IPAC Extragalactic Database (NED):** An astronomical database that collates and cross-correlates information on extragalactic objects. It contains their positions, basic data, and names as well as bibliographic references to published papers, and notes from catalogs and other publications. NED supports searches for objects and references, and offers browsing capabilities for abstracts of articles of extragalactic interest.

  `http://ned.ipac.caltech.edu/`

- **SIMBAD:** The SIMBAD astronomical database provides basic data, cross-identifications, bibliography and measurements for astronomical objects outside the solar system. It can be queried by object name, coordinates and various criteria. Lists of objects and scripts can be submitted.

  `http://simbad.u-strasbg.fr/simbad/`

- **VizieR:** VizieR provides access to the most complete library of published astronomical catalogues and data tables available on line organized in a self-documented database. Query tools allow the user to select relevant data tables and to extract and format records matching given criteria. Currently, more than 16,000 catalogues are available.

  `http://vizier.u-strasbg.fr/`

General Physics

- **NIST Physical Measurement Laboratory:** The National Institute of Standards and Technology provides access to physical reference data (physical constants, atomic spectroscopy data, x-ray and gamma-ray data, radiation dosimetry data, nuclear physics data and more) and measurements and calibrations data (dimensional and electromagnetic measurements).

  `https://www.nist.gov/pml/`

- **Springer Materials - The Landolt-Börnstein Database:** Landolt-Börnstein is a data collection in all areas of physical sciences and engineering, among others particle physics, electronic structure and transport, magnetism, superconductivity. International experts scan the primary literature in more than 8,000 peer-reviewed journals and evaluate and select the most valid information to be included in the database. It includes more than 130,000 online documents, 1,2 million references, and covers 250,000 chemical substances. SPringerMaterials Interactive allows to visualise and analyse data. The search functionality is freely accessible and the search results are displayed in their context, whereas the full text is secured to subscribers.

  `http://materials.springer.com`

13. Data preservation activities

Particle Physics

- **CERN Analysis Preservation:** CERN Analysis Preservation is a platform for preserving knowledge and assets of individual physics analyses in LHC collaborations. Its aim is to capture and document all the elements needed to understand and rerun an analysis even several years later: Data, software, environment, workflow, context, and documentation. This platform is currently in a pilot stage. It is accessible by LHC experimental groups (standard collaboration access restrictions are applied).

  `https://analysispreservation.cern.ch`

- **DASPOS:** A collective effort to explore the realisation of a viable data, software and algorithm preservation architecture in High Energy Physics

  `https://daspos.crc.nd.edu`

- **DPHEP:** DPHEP coordinates the efforts to define and implement Data Preservation and Long Term Analysis in HEP. DPHEP, which was initiated as a Study Group in 2008-2009, includes all major HEP experiments and labs and since 2014 has become a Collaboration through the signature of a Collaboration Agreement by a number of large funding agencies.

Details of the organizational structure, the objectives, workshops and publications can be found on the website.

The group is endorsed by the International Committee for Future Accelerators (ICFA).

Regular workshops are organised, status reports are produced and links with similar activities in other disciplines are maintained.

`http://dphep.org`

- **REANA:** REANA (REusable ANAlyses) is a system for instantiating research data analyses on the cloud using container-based solutions. It complements CERN Analysis Preservation permitting the reuse and revalidation of preserved analyses. It is being developed in close collaboration with DASPOS and RECAST.

  `http://reanahub.io/`

- **RECAST:** Building on analysis preservation and re-use infrastructure of the LHC experiments, RECAST acts as a science gateway allowing theorists to suggest new reinterpretations of archived analyses of the LHC dataset. Experiments review suggestions and if approved, simulate the proposed models and re-run the archived analysis to determine their viability. Such reinterpretation results are then appended to the records of the original publication in the relevant digital archives. Its new website should be available soon at:

  `http://recast.cern.ch`

Astrophysics

More formal and advanced data preservation activity is ongoing in the field of Experimental Astrophysics, including:

- Fermi Data

  `http://fermi.gsfc.nasa.gov/ssc/data`

- IVOA (International Virtual Observatory Alliance)

  `www.ivoa.net/astronomers/applications.html`

- LOSC (LIGO Open Science Center)

  `https://losc.ligo.org/about/`

- PLA (Planck Legacy Archive)

  `http://pla.esac.esa.int/pla/`

- SDSS (Sloan Digital Sky Survey)

  `http://sdss.org`

14. Particle Physics Education and Outreach Sites

A useful list of resources can also be found at

`www.stfc.ac.uk/research/particle-physics-and-particle-astrophysics/particle-physics-resources`

Science Educators' Networks:

- **IPPOG:** The International Particle Physics Outreach Group is a network of particle physicists, researchers, informal science educators and science explainers aiming to raise awareness, understanding and standards of global outreach efforts in particle physics and general science by providing discussion forums and regular information exchange for science institutions, proposing and implementing strategies to share lessons learned and best practices and promoting current outreach efforts of network members.

  `http://ippog.web.cern.ch`

- **Interactions.org:** Designed to serve as a central resource for communicators of particle physics. The daily updated site provides links to current particle physics news from the world's press, high-resolution photos and graphics from the particle physics laboratories of the world; links to education and outreach programs; information about science policy and funding; a glossary; and links to many educational sites.

  `http://www.interactions.org`

- **I2U2 (Interactions in Understanding the Universe):** The I2U2 e-Labs use the Internet and distributed computing in high-school classes and provide an opportunity for students to organise and conduct authentic research; experience the environment of scientific collaborations; make real scientific contributions. It is supported by QuarkNet, NSF and DOE.

  `http://www.i2u2.org`

Master Classes

- **International Masterclasses:** Each year about 10000 high school students in 42 countries come to one of about 200 nearby universities or research centres for one day in order to unravel the mysteries of particle physics. Lectures from active scientists give insight in topics and methods of basic research at the fundaments of matter and forces, enabling the students to perform measurements on real data from particle physics experiments themselves. At the end of each day, like in an international research collaboration, the participants join in a video conference for discussion and combination of their results.

  `http://physicsmasterclasses.org/`

- **LHC physics masterclasses:** Lectures from active scientists give insight into methods of basic research, enabling the students to perform measurements on real data from LHC experiments. Like in an international research collaboration, the participants then discuss their results and compare with expectations.

  `http://cms.web.cern.ch/content/cms-physics-masterclass`

  `http://lhcb-public.web.cern.ch/lhcb-public/en/LHCb-outreach/masterclasses/en`

  `http://alice.physicsmasterclasses.org/MasterClassWebpage.html`

- **IceCube:**

  `https://masterclass.icecube.wisc.edu/`

- **MINERVA:** MINERVA (Masterclass INvolving Event recognition visualised with Atlantis) is a masterclass tool for students to learn more about the ATLAS experiment at CERN, based on a simplified setup of the ATLAS event display, Atlantis.

  `atlas-minerva.web.cern.ch/atlas-minerva/`

General Sites

- **Contemporary Physics Education Project (CPEP):** Provides charts, brochures, Web links, and classroom activities. Online interactive courses include: Fundamental

Particles and Interactions; Plasma Physics and Fusion; History and Fate of the Universe; and Nuclear Science.

`http://www.cpepweb.org/`

Particle Physics Lessons & Activities

- **Angels and Demons:** With the aim of looking at the myth versus the reality of antimatter and science at CERN this site offers teacher resources, slide shows and videos of talks given to teachers visiting CERN.

  `http://angelsanddemons.web.cern.ch/`

- **Cambridge Relativity and Cosmology:**

  `www.damtp.cam.ac.uk/research/gr/public/`

- **CERNland:** With a range of games, multimedia applications and films CERNland is a virtual theme park developed to bring the excitement of CERN's research to a young audience aged between 7 and 12. CERNland is designed to show children what is being done at CERN and inspire them with some physics at the same time.

  `http://www.cernland.net/`

- **CollidingParticles:** A series of films following a team of physicists involved in research at the LHC.

  `http://www.collidingparticles.com/`

- **Hands-On Universe:** This educational program enables students to investigate the Universe while applying tools and concepts from science, math and technology.

  `http://handsonuniverse.org/`

- **Higgs Hunters:** A web-based citizen science project to help search for unknown exotic particles in the LHC data.

  `http://HiggsHunters.org`

- **HYPATIA:** HYPATIA (Hybrid Pupil's Analysis Tool for Interactions in Atlas) is a tool for high school students to inspect the graphic visualizaton of products of particle collisions in the ATLAS detector at CERN.

  `http://hypatia.phys.uoa.gr/`

- **Imagine the Universe:** This NASA site is intended for students age 14 and up and for anyone interested in learning about the universe.

  `http://imagine.gsfc.nasa.gov/home.html`

- **In particular:** Podcast about physics and the process of discovering physics at the ATLAS experiment.

  `https://inparticular.web.cern.ch/`

- **Lancaster Particle Physics:** This site, suitable for 16+ students, offers a number of simulations and explanations of particle physics, including a section on the LHC.

  `http://www.lppp.lancs.ac.uk/`

- **LHC @ home:** Volunteer computing platform to help physicists compare theory with experiment, in the search for new fundamental particles and answers to questions about the Universe.

  `http://lhcathome.web.cern.ch`

  ATLAS @ Home is a research project that uses volunteer computing to run simulations of the ATLAS experiment at CERN.

  `http://lhcathome.web.cern.ch/projects/atlas`

  Beauty allows volunteers to participate in simulations of the LHCb experiment at CERN.

  `http://lhcathome.web.cern.ch/projects/beauty`

  CMS @ Home is currently under development.

  `http://lhcathome.web.cern.ch/projects/cms`

  The SIXTRACK project allows users with Internet-connected computers to participate in advancing Accelerator Physics.

  `lhcathome.web.cern.ch/projects/sixtrack`

  Test4Theory allows volunteers to run simulations of high-energy particle physics on their home computers. The results are submitted to a database which is used as a common resource by both experimental and theoretical scientists working on the Large Hadron Collider at CERN.

  `lhcathome.web.cern.ch/projects/test4theory`

- **Particle Adventure:** One of the most popular Web sites for learning the fundamentals of matter and force. An award-winning interactive tour of quarks, neutrinos, antimatter, extra dimensions, dark matter, accelerators and particle detectors from the Particle Data Group of Lawrence Berkeley National Laboratory. Simple elegant graphics and translations into 16 languages.

  `http://particleadventure.org/`

- **Quarked! - Adventures in the Subatomic Universe:** This project, targeted to kids aged 7-12 (and their families), brings subatomic physics to life through a multimedia project including an interactive website, a facilitated program for museums and schools, and an educational outreach program.

  `http://www.quarked.org/`

- **QuarkNet:** Brings the excitement of particle physics research to high school teachers and their students. Teachers join research groups at about 50 universities and labs across the country. These research groups are part of particle physics experiments at CERN or Fermilab. About 100,000 students from 500+ US high schools learn fundamental physics as they participate in inquiry-oriented investigations and analyze real data online. QuarkNet is supported in part by the National Science Foundation and the U.S. Department of Energy.

  `https://quarknet.i2u2.org/`

- **Rewarding Learning videos about CERN:** The three videos based on interviews with scientists and engineers at CERN introduce pupils to CERN and the type of research and work undertaken there and are accompanied by teachers' notes.

  `http://www.nicurriculum.org.uk/STEMWorks/resources/~cern/index.asp`

Lab Education Offices

- **Argonne National Laboratory (ANL) Educational Programs:**

  `http://www.anl.gov/education/`

- **Brookhaven National Laboratory (BNL) Educational Programs:** The Office of Educational Programs mission is to design, develop, implement, and facilitate workforce development and education initiatives that

support the scientific mission at Brookhaven National Laboratory and the Department of Energy.

`http://www.bnl.gov/education/`

- **CERN:** The CERN Teacher Programmes help teachers keep up-to-date with the latest developments in particle physics and related areas and enables to meet teaching colleagues from around the world.

  `http://teacher-programmes.web.cern.ch/`

In the High-School Students Internship Programme CERN invites students aged 16-19 to come to CERN for two weeks, to gain practical experience in science, technology, and innovation by shadowing, observing, and working with a member of personnel.

`http://hssip.web.cern.ch/`

- **DESY:** Offers courses for pupils and teachers as well as information for the general public, mostly in German.

  `http://www.desy.de/information__services/education/`

- **Fermilab Education Office:** Provides education resources and information about activities for educators, physicists, students and visitors to the Lab. In addition to information on 25 programs, the site provides online data-based investigations for high school students, online versions of exhibits in the Lederman Science Center, links to particle physics discovery resources, web-based instructional resources, what works for education and outreach, and links to the Lederman Science Center and the Teacher Resource Center.

  `http://ed.fnal.gov/`

- **Science Education at Jefferson Lab:**

  `http://education.jlab.org/`

- **LBL Workforce Development and Education:** This group carries out Berkeley Lab's mission to inspire and prepare the next generation of scientists, engineers, and technicians.

  `http://csee.lbl.gov/`

Educational Programs of Experiments

- **ATLAS eTours:** Give a description of the Large Hadron Collider, explain how the ATLAS detector at the LHC works and give an overview over the experiments and their physics goals.

  `http://atlasexperiment.org/etours.html`

- **Education and Outreach @ IceCube:**

  `http://icecube.wisc.edu/outreach`

- **LIGO Science Education Center:** The LIGO (Laser Interferometer Gravitational-wave Observatory) Science Education Center has over 40 interactive, hands-on exhibits that relate to the science of LIGO. The site hosts field trips for students, teacher training programs, and tours for the general public. Visitors can explore science concepts such as light, gravity, waves, and interference; learn about LIGO's search for gravitational waves; and interact with scientists and engineers.

  `https://ligo.caltech.edu/page/educational-resources`

- **Pierre Auger Observatory's Educational Pages:** The site offers information about cosmic rays and their detection, and provides material for students and teachers.

  `https://www.auger.org/index.php/edu-outreach`

News

- **Asimmetrie:** Bimonthly magazine about particle physics published by INFN, the Istituto Nazionale di Fisica Nucleare

  `http://www.asimmetrie.it/`

- **CERN Courier:**

  `http://cerncourier.com/cws/latest/cern`

- **DESY inForm:**

  `http://www.desy.de/aktuelles/desy_inform`

- **Fermilab Today:**

  `http://www.fnal.gov/pub/today/`

- **LC Newsline:** The newsletter of the Linear Collider community

  `http://newsline.linearcollider.org/`

  `twitter: @ILCnewsline`

- **IOP News:**

  `http://www.iop.org/news/`

- **JINR News:**

  `http://www1.jinr.ru/News/Jinrnews_index.html`

- **News at Interactions.org:** The InterActions site provides news and press releases on particle physics.

  `http://www.interactions.org/news-center`

  `twitter: @particlenews`

- **Symmetry:** This magazine about particle physics and its connections to other aspects of life and science, from interdisciplinary collaborations to policy to culture is published 6 times per year by Fermilab and SLAC.

  `http://www.symmetrymagazine.org/`

  `twitter: @symmetrymag`

Art in Physics

- **Arts@CERN:** Arts at CERN promotes the dialogue between artists and particle physics.

  `http://arts.cern/` The Collide@CERN residency programme aims to develop expert knowledge in the arts through the connection with fundamental science. Since 2011 the COLLIDE award calls to artists to win a fully funded residency for up to 3 months.

  `http://arts.cern/collide` Accelerate@CERN is a country specific one-month research award for artists who have never spent tine in a science lab before.

  `http://arts.cern/accelerate`

- **Art of Physics Competition:** The Canadian Association of Physicists organizes this competition, the first was launched in 1992, with the aim of stimulating interest, especially among non-scientists, in some of the captivating imagery associated with physics. The challenge is to capture photographically a beautiful or unusual physics

phenomenon and explain it in less than 200 words in terms that everyone can understand.

`https://www.cap.ca/programs/art-physics/`

medskip

- **Fermilab Art Gallery:** Arts program dedicated to the interaction between Art and Science.

  `http://events.fnal.gov/art-gallery/`

Blogs and Twitter

Lists of active blogs and tweets can be found on INSPIRE:

- **Scientist blogs:**

  `http://tinyurl.com/nmku27s`
- **Scientists with twitter accounts:**

  `http://tinyurl.com/nrg5k63`
- **Experiments with twitter accounts:**

  `http://tinyurl.com/q86kma8`
- **Institutions with twitter accounts:**

  `http://tinyurl.com/mzcm3nw`

List of physicists on Twitter at TrueSciPhi:

`http://truesciphi.org/phy.html`

Some selected particle physics related blogs:

- **ATLAS blog:**

  `https://atlas.cern/updates/blog`
- **Life and Physics:** Jon Butterworth's blog in the Guardian.

  `http://www.guardian.co.uk/science/life-and-physics`
- **Of Particular Significance:** Conversations about science, with a current focus on particle physics, with theoretical physicist Matt Strassler.

  `http://profmattstrassler.com/`
- **Particle People:** This interactions.org page highlights a new blogger involved in particle physics research each month.

  `http://www.interactions.org/particle-people`
- **Preposterous Universe:** Theoretical physicist Sean Carroll's blog.

  `http://www.preposterousuniverse.com/`
- **Quantum diaries:** Thoughts on work and life from particle physicists from around the world, from 2005 to 2016.

  `http://www.quantumdiaries.org/`
- **Quantum diaries survivor:** Experimental particle physicist Tommaso Dorigo's blog

  `http://www.quantumdiaries.org/`
- **Science blogs:** Launched in January 2006, ScienceBlogs features bloggers from a wide array of scientific disciplines, including physics.

  `http://scienceblogs.com/channel/physical-science/`
- **AstroBetter:** Blog with tips and tricks for professional astronomers

  `http://www.astrobetter.com/`

SUMMARY TABLES OF PARTICLE PHYSICS

* There are also search limits in the Summary Tables for the Gauge and Higgs Bosons, the Leptons, the Quarks, and the Mesons.

SUMMARY TABLES OF PARTICLE PROPERTIES

Extracted from the Particle Listings of the
Review of Particle Physics
M. Tanabashi *et al.* (Particle Data Group),
Phys. Rev. D **98**, 030001 (2018)
Available at `http://pdg.lbl.gov`

Particle Data Group

M. Tanabashi, K. Hagiwara, K. Hikasa, K. Nakamura, Y. Sumino, F. Takahashi, J. Tanaka, K. Agashe, G. Aielli, C. Amsler, M. Antonelli, D.M. Asner, H. Baer, Sw. Banerjee, R.M. Barnett, T. Basaglia, C.W. Bauer, J.J. Beatty, V.I. Belousov, J. Beringer, S. Bethke, A. Bettini, H. Bichsel, O. Biebel, K.M. Black, E. Blucher, O. Buchmuller, V. Burkert, M.A. Bychkov, R.N. Cahn, M. Carena, A. Ceccucci, A. Cerri, D. Chakraborty, M.-C. Chen, R.S. Chivukula, G. Cowan, O. Dahl, G. D'Ambrosio, T. Damour, D. de Florian, A. de Gouvêa, T. DeGrand, P. de Jong, G. Dissertori, B.A. Dobrescu, M. D'Onofrio, M. Doser, M. Drees, H.K. Dreiner, D.A. Dwyer, P. Eerola, S. Eidelman, J. Ellis, J. Erler, V.V. Ezhela, W. Fetscher, B.D. Fields, R. Firestone, B. Foster, A. Freitas, H. Gallagher, L. Garren, H.-J. Gerber, G. Gerbier, T. Gershon, Y. Gershtein, T. Gherghetta, A.A. Godizov, M. Goodman, C. Grab, A.V. Gritsan, C. Grojean, D.E. Groom, M. Grünewald, A. Gurtu, T. Gutsche, H.E. Haber, C. Hanhart, S. Hashimoto, Y. Hayato, K.G. Hayes, A. Hebecker, S. Heinemeyer, B. Heltsley, J. J. Hernández-Rey, J. Hisano, A. Höcker, J. Holder, A. Holtkamp, T. Hyodo, K.D. Irwin, K.F. Johnson, M. Kado, M. Karliner, U.F. Katz, S.R. Klein, E. Klempt, R.V. Kowalewski, F. Krauss, M. Kreps, B. Krusche, Yu.V. Kuyanov, Y. Kwon, O. Lahav, J. Laiho, J. Lesgourgues, A. Liddle, Z. Ligeti, C.-J. Lin, C. Lippmann, T.M. Liss, L. Littenberg, K.S. Lugovsky, S.B. Lugovsky, A. Lusiani, Y. Makida, F. Maltoni, T. Mannel, A.V. Manohar, W.J. Marciano, A.D. Martin, A. Masoni, J. Matthews, U.-G. Meißner, D. Milstead, R.E. Mitchell, K. Mönig, P. Molaro, F. Moortgat, M. Moskovic, H. Murayama, M. Narain, P. Nason, S. Navas, M. Neubert, P. Nevski, Y. Nir, K.A. Olive, S. Pagan Griso, J. Parsons, C. Patrignani, J.A. Peacock, M. Pennington, S.T. Petcov, V.A. Petrov, E. Pianori, A. Piepke, A. Pomarol, A. Quadt, J. Rademacker, G. Raffelt, B.N. Ratcliff, P. Richardson, A. Ringwald, S. Roesler, S. Rolli, A. Romaniouk, L.J. Rosenberg, J.L. Rosner, G. Rybka, R.A. Ryutin, C.T. Sachrajda, Y. Sakai, G.P. Salam, S. Sarkar, F. Sauli, O. Schneider, K. Scholberg, A.J. Schwartz, D. Scott, V. Sharma, S.R. Sharpe, T. Shutt, M. Silari, T. Sjöstrand, P. Skands, T. Skwarnicki, J.G. Smith, G.F. Smoot, S. Spanier, H. Spieler, C. Spiering, A. Stahl, S.L. Stone, T. Sumiyoshi, M.J. Syphers, K. Terashi, J. Terning, U. Thoma, R.S. Thorne, L. Tiator, M. Titov, N.P. Tkachenko, N.A. Törnqvist, D.R. Tovey, G. Valencia, R. Van de Water, N. Varelas, G. Venanzoni, L. Verde, M.G. Vincter, P. Vogel, A. Vogt, S.P. Wakely, W. Walkowiak, C.W. Walter, D. Wands, D.R. Ward, M.O. Wascko, G. Weiglein, D.H. Weinberg, E.J. Weinberg, M. White, L.R. Wiencke, S. Willocq, C.G. Wohl, J. Womersley, C.L. Woody, R.L. Workman, W.-M. Yao, G.P. Zeller, O.V. Zenin, R.-Y. Zhu, S.-L. Zhu, F. Zimmermann, P.A. Zyla

Technical Associates:

J. Anderson, L. Fuller, V.S. Lugovsky, P. Schaffner

(Approximate closing date for data: January 15, 2018)

GAUGE AND HIGGS BOSONS

γ (photon)

$I(J^{PC}) = 0,1(1^{--})$

Mass $m < 1 \times 10^{-18}$ eV
Charge $q < 1 \times 10^{-35}$ e
Mean life τ = Stable

g or gluon

$I(J^{P}) = 0(1^{-})$

Mass $m = 0$ [a]
SU(3) color octet

graviton

$J = 2$

Mass $m < 6 \times 10^{-32}$ eV

W

$J = 1$

Charge $= \pm 1$ e
Mass $m = 80.379 \pm 0.012$ GeV
W/Z mass ratio $= 0.88153 \pm 0.00017$
$m_Z - m_W = 10.803 \pm 0.015$ GeV
$m_{W^+} - m_{W^-} = -0.029 \pm 0.028$ GeV
Full width $\Gamma = 2.085 \pm 0.042$ GeV
$\langle N_{\pi^\pm} \rangle = 15.70 \pm 0.35$
$\langle N_{K^\pm} \rangle = 2.20 \pm 0.19$
$\langle N_p \rangle = 0.92 \pm 0.14$
$\langle N_{\text{charged}} \rangle = 19.39 \pm 0.08$

W^- modes are charge conjugates of the modes below.

W^+ DECAY MODES		Fraction (Γ_i/Γ)		Confidence level	p (MeV/c)
$\ell^+\nu$	[b]	(10.86± 0.09) %			–
$e^+\nu$		(10.71± 0.16) %			40189
$\mu^+\nu$		(10.63± 0.15) %			40189
$\tau^+\nu$		(11.38± 0.21) %			40170
hadrons		(67.41± 0.27) %			–
$\pi^+\gamma$		< 7	$\times 10^{-6}$	95%	40189
$D_s^+\gamma$		< 1.3	$\times 10^{-3}$	95%	40165
cX		(33.3 ± 2.6) %			–
$c\overline{s}$		(31 $^{+13}_{-11}$) %			–
invisible	[c]	(1.4 ± 2.9) %			–

Z

$J = 1$

Charge $= 0$
Mass $m = 91.1876 \pm 0.0021$ GeV [d]
Full width $\Gamma = 2.4952 \pm 0.0023$ GeV
$\Gamma(\ell^+\ell^-) = 83.984 \pm 0.086$ MeV [b]
$\Gamma(\text{invisible}) = 499.0 \pm 1.5$ MeV [e]
$\Gamma(\text{hadrons}) = 1744.4 \pm 2.0$ MeV
$\Gamma(\mu^+\mu^-)/\Gamma(e^+e^-) = 1.0009 \pm 0.0028$
$\Gamma(\tau^+\tau^-)/\Gamma(e^+e^-) = 1.0019 \pm 0.0032$ [f]

Average charged multiplicity

$\langle N_{charged} \rangle = 20.76 \pm 0.16$ (S = 2.1)

Couplings to quarks and leptons

$g_V^\ell = -0.03783 \pm 0.00041$
$g_V^u = 0.18 \pm 0.05$
$g_V^d = -0.35^{+0.05}_{-0.06}$
$g_A^\ell = -0.50123 \pm 0.00026$
$g_A^u = 0.50^{+0.04}_{-0.05}$
$g_A^d = -0.514^{+0.050}_{-0.029}$
$g^{\nu_\ell} = 0.5008 \pm 0.0008$
$g^{\nu_e} = 0.53 \pm 0.09$
$g^{\nu_\mu} = 0.502 \pm 0.017$

Gauge & Higgs Boson Summary Table

Asymmetry parameters [g]

$A_e = 0.1515 \pm 0.0019$
$A_\mu = 0.142 \pm 0.015$
$A_\tau = 0.143 \pm 0.004$
$A_s = 0.90 \pm 0.09$
$A_c = 0.670 \pm 0.027$
$A_b = 0.923 \pm 0.020$

Charge asymmetry (%) at Z pole

$A_{FB}^{(0\ell)} = 1.71 \pm 0.10$
$A_{FB}^{(0u)} = 4 \pm 7$
$A_{FB}^{(0s)} = 9.8 \pm 1.1$
$A_{FB}^{(0c)} = 7.07 \pm 0.35$
$A_{FB}^{(0b)} = 9.92 \pm 0.16$

Z DECAY MODES		Fraction (Γ_i/Γ)	Scale factor / Confidence level	p (MeV/c)
e^+e^-	[h]	(3.3632±0.0042) %		45594
$\mu^+\mu^-$	[h]	(3.3662±0.0066) %		45594
$\tau^+\tau^-$	[h]	(3.3696±0.0083) %		45559
$\ell^+\ell^-$	[b,h]	(3.3658±0.0023) %		–
$\ell^+\ell^-\ell^+\ell^-$	[i]	(4.45 ±0.32) $\times 10^{-6}$		45594
invisible	[h]	(20.000 ±0.055) %		–
hadrons	[h]	(69.911 ±0.056) %		–
$(u\overline{u}+c\overline{c})/2$		(11.6 ±0.6) %		–
$(d\overline{d}+s\overline{s}+b\overline{b})/3$		(15.6 ±0.4) %		–
$c\overline{c}$		(12.03 ±0.21) %		–
$b\overline{b}$		(15.12 ±0.05) %		–
$b\overline{b}b\overline{b}$		(3.6 ±1.3) $\times 10^{-4}$		–
ggg		< 1.1 %	CL=95%	–
$\pi^0\gamma$		< 2.01 $\times 10^{-5}$	CL=95%	45594
$\eta\gamma$		< 5.1 $\times 10^{-5}$	CL=95%	45592
$\omega\gamma$		< 6.5 $\times 10^{-4}$	CL=95%	45590
$\eta'(958)\gamma$		< 4.2 $\times 10^{-5}$	CL=95%	45589
$\phi\gamma$		< 8.3 $\times 10^{-6}$	CL=95%	45588
$\gamma\gamma$		< 1.46 $\times 10^{-5}$	CL=95%	45594
$\pi^0\pi^0$		< 1.52 $\times 10^{-5}$	CL=95%	45594
$\gamma\gamma\gamma$		< 2.2 $\times 10^{-6}$	CL=95%	45594
$\pi^\pm W^\mp$	[j]	< 7 $\times 10^{-5}$	CL=95%	10167
$\rho^\pm W^\mp$	[j]	< 8.3 $\times 10^{-5}$	CL=95%	10142
$J/\psi(1S)$X		(3.51 $^{+0.23}_{-0.25}$) $\times 10^{-3}$	S=1.1	–
$J/\psi(1S)\gamma$		< 2.6 $\times 10^{-6}$	CL=95%	45541
$\psi(2S)$X		(1.60 ±0.29) $\times 10^{-3}$		–
$\chi_{c1}(1P)$X		(2.9 ±0.7) $\times 10^{-3}$		–
$\chi_{c2}(1P)$X		< 3.2 $\times 10^{-3}$	CL=90%	–
$\Upsilon(1S)$ X + $\Upsilon(2S)$ X + $\Upsilon(3S)$ X		(1.0 ±0.5) $\times 10^{-4}$		–
$\Upsilon(1S)$X		< 3.4 $\times 10^{-6}$	CL=95%	–
$\Upsilon(2S)$X		< 6.5 $\times 10^{-6}$	CL=95%	–
$\Upsilon(3S)$X		< 5.4 $\times 10^{-6}$	CL=95%	–
$(D^0/\overline{D}^0)$ X		(20.7 ±2.0) %		–
$D^\pm$X		(12.2 ±1.7) %		–
$D^*(2010)^\pm$X	[j]	(11.4 ±1.3) %		–
$D_{s1}(2536)^\pm$X		(3.6 ±0.8) $\times 10^{-3}$		–
$D_{sJ}(2573)^\pm$X		(5.8 ±2.2) $\times 10^{-3}$		–
$D^{*\prime}(2629)^\pm$X		searched for		–
B^+X	[k]	(6.08 ±0.13) %		–
B_s^0X	[k]	(1.59 ±0.13) %		–
B_c^+X		searched for		–
Λ_c^+X		(1.54 ±0.33) %		–
Ξ_c^0X		seen		–
Ξ_bX		seen		–
b-baryon X	[k]	(1.38 ±0.22) %		–
anomalous γ+ hadrons	[l]	< 3.2 $\times 10^{-3}$	CL=95%	–
$e^+e^-\gamma$	[l]	< 5.2 $\times 10^{-4}$	CL=95%	45594
$\mu^+\mu^-\gamma$	[l]	< 5.6 $\times 10^{-4}$	CL=95%	45594
$\tau^+\tau^-\gamma$	[l]	< 7.3 $\times 10^{-4}$	CL=95%	45559
$\ell^+\ell^-\gamma\gamma$	[n]	< 6.8 $\times 10^{-6}$	CL=95%	–
$q\overline{q}\gamma\gamma$	[n]	< 5.5 $\times 10^{-6}$	CL=95%	–
$\nu\overline{\nu}\gamma\gamma$	[n]	< 3.1 $\times 10^{-6}$	CL=95%	45594
$e^\pm\mu^\mp$ LF	[j]	< 7.5 $\times 10^{-7}$	CL=95%	45594
$e^\pm\tau^\mp$ LF	[j]	< 9.8 $\times 10^{-6}$	CL=95%	45576
$\mu^\pm\tau^\mp$ LF	[j]	< 1.2 $\times 10^{-5}$	CL=95%	45576
pe L,B		< 1.8 $\times 10^{-6}$	CL=95%	45589
$p\mu$ L,B		< 1.8 $\times 10^{-6}$	CL=95%	45589

H^0

$J = 0$

Mass $m = 125.18 \pm 0.16$ GeV
Full width $\Gamma < 0.013$ GeV, CL = 95%

H^0 Signal Strengths in Different Channels

See Listings for the latest unpublished results.

Combined Final States = 1.10 ± 0.11
$WW^* = 1.08^{+0.18}_{-0.16}$
$ZZ^* = 1.14^{+0.15}_{-0.13}$
$\gamma\gamma = 1.16 \pm 0.18$
$b\overline{b} = 0.95 \pm 0.22$
$\mu^+\mu^- = 0.0 \pm 1.3$
$\tau^+\tau^- = 1.12 \pm 0.23$
$Z\gamma < 6.6$, CL = 95%
$t\overline{t}H^0$ Production = $2.3^{+0.7}_{-0.6}$

H^0 DECAY MODES	Fraction (Γ_i/Γ)	Confidence level	p (MeV/c)
e^+e^-	< 1.9 $\times 10^{-3}$	95%	62592
$J/\psi\gamma$	< 1.5 $\times 10^{-3}$	95%	62553
$\Upsilon(1S)\gamma$	< 1.3 $\times 10^{-3}$	95%	62234
$\Upsilon(2S)\gamma$	< 1.9 $\times 10^{-3}$	95%	62190
$\Upsilon(3S)\gamma$	< 1.3 $\times 10^{-3}$	95%	62163
$\phi(1020)\gamma$	< 1.4 $\times 10^{-3}$	95%	62587
$e\mu$	< 3.5 $\times 10^{-4}$	95%	62592
$e\tau$	< 6.9 $\times 10^{-3}$	95%	62579
$\mu\tau$	< 1.43 %	95%	62579
invisible	<24 %	95%	–

Neutral Higgs Bosons, Searches for

Searches for a Higgs Boson with Standard Model Couplings

Mass $m > 122$ and none 128–1000 GeV, CL = 95%

The limits for H_1^0 and A^0 in supersymmetric models refer to the m_h^{max} benchmark scenario for the supersymmetric parameters.

H_1^0 in Supersymmetric Models ($m_{H_1^0} < m_{H_2^0}$)

Mass $m > 92.8$ GeV, CL = 95%

A^0 Pseudoscalar Higgs Boson in Supersymmetric Models [o]

Mass $m > 93.4$ GeV, CL = 95% $\tan\beta > 0.4$

Charged Higgs Bosons ($H^\pm$ and $H^{\pm\pm}$), Searches for

$H^\pm$ Mass $m > 80$ GeV, CL = 95%

New Heavy Bosons (W', Z', leptoquarks, etc.), Searches for

Additional W Bosons

W' with standard couplings
Mass $m > 4.100 \times 10^3$ GeV, CL = 95% ($p\overline{p}$ direct search)
W_R (Right-handed W Boson)
Mass $m > 715$ GeV, CL = 90% (electroweak fit)

Additional Z Bosons

Z'_{SM} with standard couplings
Mass $m > 4.500 \times 10^3$ GeV, CL = 95% ($p\overline{p}$ direct search)
Z_{LR} of $SU(2)_L \times SU(2)_R \times U(1)$ (with $g_L = g_R$)
Mass $m > 630$ GeV, CL = 95% ($p\overline{p}$ direct search)
Mass $m > 1162$ GeV, CL = 95% (electroweak fit)
Z_χ of $SO(10) \rightarrow SU(5) \times U(1)_\chi$ (with $g_\chi = e/\cos\theta_W$)
Mass $m > 4.100 \times 10^3$ GeV, CL = 95% ($p\overline{p}$ direct search)
Z_ψ of $E_6 \rightarrow SO(10) \times U(1)_\psi$ (with $g_\psi = e/\cos\theta_W$)
Mass $m > 3.800 \times 10^3$ GeV, CL = 95% ($p\overline{p}$ direct search)
Z_η of $E_6 \rightarrow SU(3) \times SU(2) \times U(1) \times U(1)_\eta$ (with $g_\eta = e/\cos\theta_W$)
Mass $m > 3.900 \times 10^3$ GeV, CL = 95% ($p\overline{p}$ direct search)

Scalar Leptoquarks

Mass $m >$ 1050 GeV, CL = 95% (1st generation, pair prod.)
Mass $m >$ 1755 GeV, CL = 95% (1st generation, single prod.)
Mass $m >$ 1080 GeV, CL = 95% (2nd generation, pair prod.)
Mass $m >$ 660 GeV, CL = 95% (2nd generation, single prod.)
Mass $m >$ 850 GeV, CL = 95% (3rd generation, pair prod.)
(See the Particle Listings for assumptions on leptoquark quantum numbers and branching fractions.)

Diquarks

Mass $m >$ 6000 GeV, CL = 95% (E_6 diquark)

Axigluon

Mass $m >$ 5500 GeV, CL = 95%

Axions (A^0) and Other Very Light Bosons, Searches for

The standard Peccei-Quinn axion is ruled out. Variants with reduced couplings or much smaller masses are constrained by various data. The Particle Listings in the full *Review* contain a Note discussing axion searches.

The best limit for the half-life of neutrinoless double beta decay with Majoron emission is $> 7.2 \times 10^{24}$ years (CL = 90%).

NOTES

In this Summary Table:

When a quantity has "(S = ...)" to its right, the error on the quantity has been enlarged by the "scale factor" S, defined as $S = \sqrt{\chi^2/(N-1)}$, where N is the number of measurements used in calculating the quantity. We do this when $S > 1$, which often indicates that the measurements are inconsistent. When $S > 1.25$, we also show in the Particle Listings an ideogram of the measurements. For more about S, see the Introduction.

A decay momentum p is given for each decay mode. For a 2-body decay, p is the momentum of each decay product in the rest frame of the decaying particle. For a 3-or-more-body decay, p is the largest momentum any of the products can have in this frame.

[a] Theoretical value. A mass as large as a few MeV may not be precluded.

[b] ℓ indicates each type of lepton (e, μ, and τ), not sum over them.

[c] This represents the width for the decay of the W boson into a charged particle with momentum below detectability, p< 200 MeV.

[d] The Z-boson mass listed here corresponds to a Breit-Wigner resonance parameter. It lies approximately 34 MeV above the real part of the position of the pole (in the energy-squared plane) in the Z-boson propagator.

[e] This partial width takes into account Z decays into $\nu\overline{\nu}$ and any other possible undetected modes.

[f] This ratio has not been corrected for the τ mass.

[g] Here $A \equiv 2g_V g_A/(g_V^2+g_A^2)$.

[h] This parameter is not directly used in the overall fit but is derived using the fit results; see the note "The Z boson" and ref. LEP-SLC 06 (Physics Reports (Physics Letters C) **427** 257 (2006)).

[i] Here ℓ indicates e or μ.

[j] The value is for the sum of the charge states or particle/antiparticle states indicated.

[k] This value is updated using the product of (i) the $Z \to b\overline{b}$ fraction from this listing and (ii) the b-hadron fraction in an unbiased sample of weakly decaying b-hadrons produced in Z-decays provided by the Heavy Flavor Averaging Group (HFLAV, http://www.slac.stanford.edu/xorg/hflav/osc/PDG_2009/#FRACZ).

[l] See the Z Particle Listings for the γ energy range used in this measurement.

[n] For $m_{\gamma\gamma} = (60 \pm 5)$ GeV.

[o] The limits assume no invisible decays.

Lepton Summary Table

LEPTONS

e

$J = \frac{1}{2}$

Mass $m = (548.579909070 \pm 0.000000016) \times 10^{-6}$ u
Mass $m = 0.5109989461 \pm 0.0000000031$ MeV
$|m_{e^+} - m_{e^-}|/m < 8 \times 10^{-9}$, CL = 90%
$|q_{e^+} + q_{e^-}|/e < 4 \times 10^{-8}$
Magnetic moment anomaly
$(g-2)/2 = (1159.65218091 \pm 0.00000026) \times 10^{-6}$
$(g_{e^+} - g_{e^-}) / g_{\text{average}} = (-0.5 \pm 2.1) \times 10^{-12}$
Electric dipole moment $d < 0.87 \times 10^{-28}$ $e$cm, CL = 90%
Mean life $\tau > 6.6 \times 10^{28}$ yr, CL = 90% [a]

μ

$J = \frac{1}{2}$

Mass $m = 0.1134289257 \pm 0.0000000025$ u
Mass $m = 105.6583745 \pm 0.0000024$ MeV
Mean life $\tau = (2.1969811 \pm 0.0000022) \times 10^{-6}$ s
$\tau_{\mu^+}/\tau_{\mu^-} = 1.00002 \pm 0.00008$
$c\tau = 658.6384$ m
Magnetic moment anomaly $(g-2)/2 = (11659209 \pm 6) \times 10^{-10}$
$(g_{\mu^+} - g_{\mu^-}) / g_{\text{average}} = (-0.11 \pm 0.12) \times 10^{-8}$
Electric dipole moment $d = (-0.1 \pm 0.9) \times 10^{-19}$ $e$cm

Decay parameters [b]

$\rho = 0.74979 \pm 0.00026$
$\eta = 0.057 \pm 0.034$
$\delta = 0.75047 \pm 0.00034$
$\xi P_\mu = 1.0009^{+0.0016}_{-0.0007}$ [c]
$\xi P_\mu \delta/\rho = 1.0018^{+0.0016}_{-0.0007}$ [c]
$\xi' = 1.00 \pm 0.04$
$\xi'' = 0.98 \pm 0.04$
$\alpha/A = (0 \pm 4) \times 10^{-3}$
$\alpha'/A = (-10 \pm 20) \times 10^{-3}$
$\beta/A = (4 \pm 6) \times 10^{-3}$
$\beta'/A = (2 \pm 7) \times 10^{-3}$
$\overline{\eta} = 0.02 \pm 0.08$

μ^+ modes are charge conjugates of the modes below.

μ^- DECAY MODES		Fraction (Γ_i/Γ)	Confidence level	p (MeV/c)
$e^-\overline{\nu}_e\nu_\mu$		$\approx 100\%$		53
$e^-\overline{\nu}_e\nu_\mu\gamma$	[d]	$(6.0 \pm 0.5) \times 10^{-8}$		53
$e^-\overline{\nu}_e\nu_\mu e^+e^-$	[e]	$(3.4 \pm 0.4) \times 10^{-5}$		53
Lepton Family number (LF) violating modes				
$e^-\nu_e\overline{\nu}_\mu$	LF	[f] < 1.2 %	90%	53
$e^-\gamma$	LF	$< 4.2 \times 10^{-13}$	90%	53
$e^-e^+e^-$	LF	$< 1.0 \times 10^{-12}$	90%	53
$e^-2\gamma$	LF	$< 7.2 \times 10^{-11}$	90%	53

τ

$J = \frac{1}{2}$

Mass $m = 1776.86 \pm 0.12$ MeV
$(m_{\tau^+} - m_{\tau^-})/m_{\text{average}} < 2.8 \times 10^{-4}$, CL = 90%
Mean life $\tau = (290.3 \pm 0.5) \times 10^{-15}$ s
$c\tau = 87.03$ μm
Magnetic moment anomaly > -0.052 and < 0.013, CL = 95%
$\text{Re}(d_\tau) = -0.220$ to 0.45×10^{-16} $e$cm, CL = 95%
$\text{Im}(d_\tau) = -0.250$ to 0.0080×10^{-16} $e$cm, CL = 95%

Weak dipole moment

$\text{Re}(d_\tau^w) < 0.50 \times 10^{-17}$ $e$cm, CL = 95%
$\text{Im}(d_\tau^w) < 1.1 \times 10^{-17}$ $e$cm, CL = 95%

Weak anomalous magnetic dipole moment

$\text{Re}(\alpha_\tau^w) < 1.1 \times 10^{-3}$, CL = 95%
$\text{Im}(\alpha_\tau^w) < 2.7 \times 10^{-3}$, CL = 95%
$\tau^\pm \to \pi^\pm K_S^0 \nu_\tau$ (RATE DIFFERENCE) / (RATE SUM) = (-0.36 ± 0.25)%

Decay parameters

See the τ Particle Listings for a note concerning τ-decay parameters.

$\rho(e \text{ or } \mu) = 0.745 \pm 0.008$
$\rho(e) = 0.747 \pm 0.010$
$\rho(\mu) = 0.763 \pm 0.020$
$\xi(e \text{ or } \mu) = 0.985 \pm 0.030$
$\xi(e) = 0.994 \pm 0.040$
$\xi(\mu) = 1.030 \pm 0.059$
$\eta(e \text{ or } \mu) = 0.013 \pm 0.020$
$\eta(\mu) = 0.094 \pm 0.073$
$(\delta\xi)(e \text{ or } \mu) = 0.746 \pm 0.021$
$(\delta\xi)(e) = 0.734 \pm 0.028$
$(\delta\xi)(\mu) = 0.778 \pm 0.037$
$\xi(\pi) = 0.993 \pm 0.022$
$\xi(\rho) = 0.994 \pm 0.008$
$\xi(a_1) = 1.001 \pm 0.027$
$\xi(\text{all hadronic modes}) = 0.995 \pm 0.007$
$\overline{\eta}(\mu)$ PARAMETER $= -1.3 \pm 1.7$
$\xi_\kappa(e)$ PARAMETER $= -0.4 \pm 1.2$
$\xi_\kappa(\mu)$ PARAMETER $= 0.8 \pm 0.6$

τ^+ modes are charge conjugates of the modes below. "$h^\pm$" stands for $\pi^\pm$ or $K^\pm$. "ℓ" stands for e or μ. "Neutrals" stands for γ's and/or π^0's.

τ^- DECAY MODES		Fraction (Γ_i/Γ)	Scale factor/ Confidence level	p (MeV/c)
Modes with one charged particle				
particle$^- \geq 0$ neutrals $\geq 0K^0\nu_\tau$ ("1-prong")		(85.24 ± 0.06) %		–
particle$^- \geq 0$ neutrals $\geq 0K_L^0\nu_\tau$		(84.58 ± 0.06) %		–
$\mu^-\overline{\nu}_\mu\nu_\tau$	[g]	(17.39 ± 0.04) %		885
$\mu^-\overline{\nu}_\mu\nu_\tau\gamma$	[e]	$(3.67 \pm 0.08) \times 10^{-3}$		885
$e^-\overline{\nu}_e\nu_\tau$	[g]	(17.82 ± 0.04) %		888
$e^-\overline{\nu}_e\nu_\tau\gamma$	[e]	(1.83 ± 0.05) %		888
$h^- \geq 0K_L^0\nu_\tau$		(12.03 ± 0.05) %		883
$h^-\nu_\tau$		(11.51 ± 0.05) %		883
$\pi^-\nu_\tau$	[g]	(10.82 ± 0.05) %		883
$K^-\nu_\tau$	[g]	$(6.96 \pm 0.10) \times 10^{-3}$		820
$h^- \geq 1$ neutrals ν_τ		(37.00 ± 0.09) %		–
$h^- \geq 1\pi^0\nu_\tau$ (ex.K^0)		(36.51 ± 0.09) %		–
$h^-\pi^0\nu_\tau$		(25.93 ± 0.09) %		878
$\pi^-\pi^0\nu_\tau$	[g]	(25.49 ± 0.09) %		878
$\pi^-\pi^0$ non-$\rho(770)\,\nu_\tau$		$(3.0 \pm 3.2) \times 10^{-3}$		878
$K^-\pi^0\nu_\tau$	[g]	$(4.33 \pm 0.15) \times 10^{-3}$		814
$h^- \geq 2\pi^0\nu_\tau$		(10.81 ± 0.09) %		–
$h^-2\pi^0\nu_\tau$		(9.48 ± 0.10) %		862
$h^-2\pi^0\nu_\tau$ (ex.K^0)		(9.32 ± 0.10) %		862
$\pi^-2\pi^0\nu_\tau$ (ex.K^0)	[g]	(9.26 ± 0.10) %		862
$\pi^-2\pi^0\nu_\tau$ (ex.K^0), scalar		< 9	$\times 10^{-3}$ CL=95%	862
$\pi^-2\pi^0\nu_\tau$ (ex.K^0), vector		< 7	$\times 10^{-3}$ CL=95%	862
$K^-2\pi^0\nu_\tau$ (ex.K^0)	[g]	$(6.5 \pm 2.2) \times 10^{-4}$		796
$h^- \geq 3\pi^0\nu_\tau$		(1.34 ± 0.07) %		–
$h^- \geq 3\pi^0\nu_\tau$ (ex. K^0)		(1.25 ± 0.07) %		–
$h^-3\pi^0\nu_\tau$		(1.18 ± 0.07) %		836
$\pi^-3\pi^0\nu_\tau$ (ex.K^0)	[g]	(1.04 ± 0.07) %		836
$K^-3\pi^0\nu_\tau$ (ex.K^0, η)	[g]	$(4.8 \pm 2.1) \times 10^{-4}$		765
$h^-4\pi^0\nu_\tau$ (ex.K^0)		$(1.6 \pm 0.4) \times 10^{-3}$		800
$h^-4\pi^0\nu_\tau$ (ex.K^0,η)	[g]	$(1.1 \pm 0.4) \times 10^{-3}$		800
$a_1(1260)\nu_\tau \to \pi^-\gamma\nu_\tau$		$(3.8 \pm 1.5) \times 10^{-4}$		–
$K^- \geq 0\pi^0 \geq 0K^0 \geq 0\gamma\ \nu_\tau$		(1.552 ± 0.029) %		820
$K^- \geq 1$ (π^0 or K^0 or γ) ν_τ		$(8.59 \pm 0.28) \times 10^{-3}$		–
Modes with K^0's				
K_S^0(particles)$^-\nu_\tau$		$(9.44 \pm 0.28) \times 10^{-3}$		–
$h^-\overline{K}^0\nu_\tau$		$(9.87 \pm 0.14) \times 10^{-3}$		812
$\pi^-\overline{K}^0\nu_\tau$	[g]	$(8.40 \pm 0.14) \times 10^{-3}$		812
$\pi^-\overline{K}^0$ (non-$K^*(892)^-$)ν_τ		$(5.4 \pm 2.1) \times 10^{-4}$		812
$K^-K^0\nu_\tau$	[g]	$(1.48 \pm 0.05) \times 10^{-3}$		737
$K^-K^0 \geq 0\pi^0\nu_\tau$		$(2.98 \pm 0.08) \times 10^{-3}$		737
$h^-\overline{K}^0\pi^0\nu_\tau$		$(5.32 \pm 0.13) \times 10^{-3}$		794
$\pi^-\overline{K}^0\pi^0\nu_\tau$	[g]	$(3.82 \pm 0.13) \times 10^{-3}$		794
$\overline{K}^0\rho^-\nu_\tau$		$(2.2 \pm 0.5) \times 10^{-3}$		612

$K^- K^0 \pi^0 \nu_\tau$	[g]	$(1.50 \pm 0.07) \times 10^{-3}$			685
$\pi^- \overline{K}^0 \geq 1\pi^0 \nu_\tau$		$(4.08 \pm 0.25) \times 10^{-3}$			–
$\pi^- \overline{K}^0 \pi^0 \pi^0 \nu_\tau$ (ex. K^0)	[g]	$(2.6 \pm 2.3) \times 10^{-4}$			763
$K^- K^0 \pi^0 \pi^0 \nu_\tau$		$< 1.6 \times 10^{-4}$		CL=95%	619
$\pi^- K^0 \overline{K}^0 \nu_\tau$		$(1.55 \pm 0.24) \times 10^{-3}$			682
$\pi^- K^0_S K^0_S \nu_\tau$	[g]	$(2.33 \pm 0.07) \times 10^{-4}$			682
$\pi^- K^0_S K^0_L \nu_\tau$	[g]	$(1.08 \pm 0.24) \times 10^{-3}$			682
$\pi^- K^0_L K^0_L \nu_\tau$		$(2.33 \pm 0.07) \times 10^{-4}$			682
$\pi^- K^0 \overline{K}^0 \pi^0 \nu_\tau$		$(3.6 \pm 1.2) \times 10^{-4}$			614
$\pi^- K^0_S K^0_S \pi^0 \nu_\tau$	[g]	$(1.82 \pm 0.21) \times 10^{-5}$			614
$K^{*-} K^0 \pi^0 \nu_\tau \to \pi^- K^0_S K^0_S \pi^0 \nu_\tau$		$(1.08 \pm 0.21) \times 10^{-5}$			–
$f_1(1285) \pi^- \nu_\tau \to \pi^- K^0_S K^0_S \pi^0 \nu_\tau$		$(6.8 \pm 1.5) \times 10^{-6}$			–
$f_1(1420) \pi^- \nu_\tau \to \pi^- K^0_S K^0_S \pi^0 \nu_\tau$		$(2.4 \pm 0.8) \times 10^{-6}$			–
$\pi^- K^0_S K^0_L \pi^0 \nu_\tau$	[g]	$(3.2 \pm 1.2) \times 10^{-4}$			614
$\pi^- K^0_L K^0_L \pi^0 \nu_\tau$		$(1.82 \pm 0.21) \times 10^{-5}$			614
$K^- K^0_S K^0_S \nu_\tau$		$< 6.3 \times 10^{-7}$		CL=90%	466
$K^- K^0_S K^0_S \pi^0 \nu_\tau$		$< 4.0 \times 10^{-7}$		CL=90%	337
$K^0 h^+ h^- h^- \geq 0$ neutrals ν_τ		$< 1.7 \times 10^{-3}$		CL=95%	760
$K^0 h^+ h^- h^- \nu_\tau$	[g]	$(2.5 \pm 2.0) \times 10^{-4}$			760

Modes with three charged particles

$h^- h^- h^+ \geq 0$ neutrals $\geq 0 K^0_L \nu_\tau$		(15.21 ± 0.06) %			861
$h^- h^- h^+ \geq 0$ neutrals ν_τ (ex. $K^0_S \to \pi^+ \pi^-$) ("3-prong")		(14.55 ± 0.06) %			861
$h^- h^- h^+ \nu_\tau$		(9.80 ± 0.05) %			861
$h^- h^- h^+ \nu_\tau$ (ex. K^0)		(9.46 ± 0.05) %			861
$h^- h^- h^+ \nu_\tau$ (ex. K^0, ω)		(9.43 ± 0.05) %			861
$\pi^- \pi^+ \pi^- \nu_\tau$		(9.31 ± 0.05) %			861
$\pi^- \pi^+ \pi^- \nu_\tau$ (ex. K^0)		(9.02 ± 0.05) %			861
$\pi^- \pi^+ \pi^- \nu_\tau$ (ex. K^0), non-axial vector		< 2.4 %		CL=95%	861
$\pi^- \pi^+ \pi^- \nu_\tau$ (ex. K^0, ω)	[g]	(8.99 ± 0.05) %			861
$h^- h^- h^+ \geq 1$ neutrals ν_τ		(5.29 ± 0.05) %			–
$h^- h^- h^+ \geq 1\pi^0 \nu_\tau$ (ex. K^0)		(5.09 ± 0.05) %			–
$h^- h^- h^+ \pi^0 \nu_\tau$		(4.76 ± 0.05) %			834
$h^- h^- h^+ \pi^0 \nu_\tau$ (ex. K^0)		(4.57 ± 0.05) %			834
$h^- h^- h^+ \pi^0 \nu_\tau$ (ex. K^0, ω)		(2.79 ± 0.07) %			834
$\pi^- \pi^+ \pi^- \pi^0 \nu_\tau$		(4.62 ± 0.05) %			834
$\pi^- \pi^+ \pi^- \pi^0 \nu_\tau$ (ex. K^0)		(4.49 ± 0.05) %			834
$\pi^- \pi^+ \pi^- \pi^0 \nu_\tau$ (ex. K^0, ω)	[g]	(2.74 ± 0.07) %			834
$h^- h^- h^+ \geq 2\pi^0 \nu_\tau$ (ex. K^0)		$(5.17 \pm 0.31) \times 10^{-3}$			–
$h^- h^- h^+ 2\pi^0 \nu_\tau$		$(5.05 \pm 0.31) \times 10^{-3}$			797
$h^- h^- h^+ 2\pi^0 \nu_\tau$ (ex. K^0)		$(4.95 \pm 0.31) \times 10^{-3}$			797
$h^- h^- h^+ 2\pi^0 \nu_\tau$ (ex. K^0, ω, η)	[g]	$(10 \pm 4) \times 10^{-4}$			797
$h^- h^- h^+ 3\pi^0 \nu_\tau$		$(2.12 \pm 0.30) \times 10^{-4}$			749
$2\pi^- \pi^+ 3\pi^0 \nu_\tau$ (ex. K^0)		$(1.94 \pm 0.30) \times 10^{-4}$			749
$2\pi^- \pi^+ 3\pi^0 \nu_\tau$ (ex. K^0, η, $f_1(1285)$)		$(1.7 \pm 0.4) \times 10^{-4}$			–
$2\pi^- \pi^+ 3\pi^0 \nu_\tau$ (ex. K^0, η, ω, $f_1(1285)$)	[g]	$(1.4 \pm 2.7) \times 10^{-5}$			–
$K^- h^+ h^- \geq 0$ neutrals ν_τ		$(6.29 \pm 0.14) \times 10^{-3}$			794
$K^- h^+ \pi^- \nu_\tau$ (ex. K^0)		$(4.37 \pm 0.07) \times 10^{-3}$			794
$K^- h^+ \pi^- \pi^0 \nu_\tau$ (ex. K^0)		$(8.6 \pm 1.2) \times 10^{-4}$			763
$K^- \pi^+ \pi^- \geq 0$ neutrals ν_τ		$(4.77 \pm 0.14) \times 10^{-3}$			794
$K^- \pi^+ \pi^- \geq 0\pi^0 \nu_\tau$ (ex. K^0)		$(3.73 \pm 0.13) \times 10^{-3}$			794
$K^- \pi^+ \pi^- \nu_\tau$		$(3.45 \pm 0.07) \times 10^{-3}$			794
$K^- \pi^+ \pi^- \nu_\tau$ (ex. K^0)		$(2.93 \pm 0.07) \times 10^{-3}$			794
$K^- \pi^+ \pi^- \nu_\tau$ (ex. K^0, ω)	[g]	$(2.93 \pm 0.07) \times 10^{-3}$			794
$K^- \rho^0 \nu_\tau \to K^- \pi^+ \pi^- \nu_\tau$		$(1.4 \pm 0.5) \times 10^{-3}$			–
$K^- \pi^+ \pi^- \pi^0 \nu_\tau$		$(1.31 \pm 0.12) \times 10^{-3}$			763
$K^- \pi^+ \pi^- \pi^0 \nu_\tau$ (ex. K^0)		$(7.9 \pm 1.2) \times 10^{-4}$			763
$K^- \pi^+ \pi^- \pi^0 \nu_\tau$ (ex. K^0, η)		$(7.6 \pm 1.2) \times 10^{-4}$			763
$K^- \pi^+ \pi^- \pi^0 \nu_\tau$ (ex. K^0, ω)		$(3.7 \pm 0.9) \times 10^{-4}$			763
$K^- \pi^+ \pi^- \pi^0 \nu_\tau$ (ex. K^0, ω, η)	[g]	$(3.9 \pm 1.4) \times 10^{-4}$			763
$K^- \pi^+ K^- \geq 0$ neut. ν_τ		$< 9 \times 10^{-4}$		CL=95%	685
$K^- K^+ \pi^- \geq 0$ neut. ν_τ		$(1.496 \pm 0.033) \times 10^{-3}$			685
$K^- K^+ \pi^- \nu_\tau$	[g]	$(1.435 \pm 0.027) \times 10^{-3}$			685
$K^- K^+ \pi^- \pi^0 \nu_\tau$	[g]	$(6.1 \pm 1.8) \times 10^{-5}$			618
$K^- K^+ K^- \nu_\tau$		$(2.2 \pm 0.8) \times 10^{-5}$		S=5.4	472
$K^- K^+ K^- \nu_\tau$ (ex. ϕ)		$< 2.5 \times 10^{-6}$		CL=90%	–
$K^- K^+ K^- \pi^0 \nu_\tau$		$< 4.8 \times 10^{-6}$		CL=90%	345
$\pi^- K^+ \pi^- \geq 0$ neut. ν_τ		$< 2.5 \times 10^{-3}$		CL=95%	794
$e^- e^- e^+ \overline{\nu}_e \nu_\tau$		$(2.8 \pm 1.5) \times 10^{-5}$			888
$\mu^- e^- e^+ \overline{\nu}_\mu \nu_\tau$		$< 3.6 \times 10^{-5}$		CL=90%	885

Modes with five charged particles

$3h^- 2h^+ \geq 0$ neutrals ν_τ (ex. $K^0_S \to \pi^- \pi^+$) ("5-prong")		$(9.9 \pm 0.4) \times 10^{-4}$			794
$3h^- 2h^+ \nu_\tau$ (ex. K^0)		$(8.22 \pm 0.32) \times 10^{-4}$			794
$3\pi^- 2\pi^+ \nu_\tau$ (ex. K^0, ω)		$(8.21 \pm 0.31) \times 10^{-4}$			794
$3\pi^- 2\pi^+ \nu_\tau$ (ex. K^0, ω, $f_1(1285)$)	[g]	$(7.69 \pm 0.30) \times 10^{-4}$			–
$K^- 2\pi^- 2\pi^+ \nu_\tau$ (ex. K^0)	[g]	$(6 \pm 12) \times 10^{-7}$			716
$K^+ 3\pi^- \pi^+ \nu_\tau$		$< 5.0 \times 10^{-6}$		CL=90%	716
$K^+ K^- 2\pi^- \pi^+ \nu_\tau$		$< 4.5 \times 10^{-7}$		CL=90%	528
$3h^- 2h^+ \pi^0 \nu_\tau$ (ex. K^0)		$(1.64 \pm 0.11) \times 10^{-4}$			746
$3\pi^- 2\pi^+ \pi^0 \nu_\tau$ (ex. K^0)		$(1.62 \pm 0.11) \times 10^{-4}$			746
$3\pi^- 2\pi^+ \pi^0 \nu_\tau$ (ex. K^0, η, $f_1(1285)$)		$(1.11 \pm 0.10) \times 10^{-4}$			–
$3\pi^- 2\pi^+ \pi^0 \nu_\tau$ (ex. K^0, η, ω, $f_1(1285)$)	[g]	$(3.8 \pm 0.9) \times 10^{-5}$			–
$K^- 2\pi^- 2\pi^+ \pi^0 \nu_\tau$ (ex. K^0)	[g]	$(1.1 \pm 0.6) \times 10^{-6}$			657
$K^+ 3\pi^- \pi^+ \pi^0 \nu_\tau$		$< 8 \times 10^{-7}$		CL=90%	657
$3h^- 2h^+ 2\pi^0 \nu_\tau$		$< 3.4 \times 10^{-6}$		CL=90%	687

Miscellaneous other allowed modes

$(5\pi)^- \nu_\tau$		$(7.8 \pm 0.5) \times 10^{-3}$			800
$4h^- 3h^+ \geq 0$ neutrals ν_τ ("7-prong")		$< 3.0 \times 10^{-7}$		CL=90%	682
$4h^- 3h^+ \nu_\tau$		$< 4.3 \times 10^{-7}$		CL=90%	682
$4h^- 3h^+ \pi^0 \nu_\tau$		$< 2.5 \times 10^{-7}$		CL=90%	612
$X^-(S=-1) \nu_\tau$		(2.92 ± 0.04) %			–
$K^*(892)^- \geq 0$ neutrals $\geq 0 K^0_L \nu_\tau$		(1.42 ± 0.18) %		S=1.4	665
$K^*(892)^- \nu_\tau$		(1.20 ± 0.07) %		S=1.8	665
$K^*(892)^- \nu_\tau \to \pi^- \overline{K}^0 \nu_\tau$		$(7.83 \pm 0.26) \times 10^{-3}$			–
$K^*(892)^0 K^- \geq 0$ neutrals ν_τ		$(3.2 \pm 1.4) \times 10^{-3}$			542
$K^*(892)^0 K^- \nu_\tau$		$(2.1 \pm 0.4) \times 10^{-3}$			542
$\overline{K}^*(892)^0 \pi^- \geq 0$ neutrals ν_τ		$(3.8 \pm 1.7) \times 10^{-3}$			655
$\overline{K}^*(892)^0 \pi^- \nu_\tau$		$(2.2 \pm 0.5) \times 10^{-3}$			655
$(\overline{K}^*(892)\pi)^- \nu_\tau \to \pi^- \overline{K}^0 \pi^0 \nu_\tau$		$(1.0 \pm 0.4) \times 10^{-3}$			–
$K_1(1270)^- \nu_\tau$		$(4.7 \pm 1.1) \times 10^{-3}$			433
$K_1(1400)^- \nu_\tau$		$(1.7 \pm 2.6) \times 10^{-3}$		S=1.7	335
$K^*(1410)^- \nu_\tau$		$(1.5 \pm {}^{1.4}_{1.0}) \times 10^{-3}$			320
$K^*_0(1430)^- \nu_\tau$		$< 5 \times 10^{-4}$		CL=95%	317
$K^*_2(1430)^- \nu_\tau$		$< 3 \times 10^{-3}$		CL=95%	317
$\eta \pi^- \nu_\tau$		$< 9.9 \times 10^{-5}$		CL=95%	797
$\eta \pi^- \pi^0 \nu_\tau$	[g]	$(1.39 \pm 0.07) \times 10^{-3}$			778
$\eta \pi^- \pi^0 \pi^0 \nu_\tau$	[g]	$(1.9 \pm 0.4) \times 10^{-4}$			746
$\eta K^- \nu_\tau$	[g]	$(1.55 \pm 0.08) \times 10^{-4}$			719
$\eta K^*(892)^- \nu_\tau$		$(1.38 \pm 0.15) \times 10^{-4}$			511
$\eta K^- \pi^0 \nu_\tau$	[g]	$(4.8 \pm 1.2) \times 10^{-5}$			665
$\eta K^- \pi^0$ (non-$K^*(892)$) ν_τ		$< 3.5 \times 10^{-5}$		CL=90%	–
$\eta \overline{K}^0 \pi^- \nu_\tau$	[g]	$(9.4 \pm 1.5) \times 10^{-5}$			661
$\eta \overline{K}^0 \pi^- \pi^0 \nu_\tau$		$< 5.0 \times 10^{-5}$		CL=90%	590
$\eta K^- K^0 \nu_\tau$		$< 9.0 \times 10^{-6}$		CL=90%	430
$\eta \pi^+ \pi^- \pi^- \geq 0$ neutrals ν_τ		$< 3 \times 10^{-3}$		CL=90%	744
$\eta \pi^- \pi^+ \pi^- \nu_\tau$ (ex. K^0)	[g]	$(2.19 \pm 0.13) \times 10^{-4}$			744
$\eta \pi^- \pi^+ \pi^- \nu_\tau$ (ex. K^0, $f_1(1285)$)		$(9.9 \pm 1.6) \times 10^{-5}$			–
$\eta a_1(1260)^- \nu_\tau \to \eta \pi^- \rho^0 \nu_\tau$		$< 3.9 \times 10^{-4}$		CL=90%	–
$\eta \eta \pi^- \nu_\tau$		$< 7.4 \times 10^{-6}$		CL=90%	637
$\eta \eta \pi^- \pi^0 \nu_\tau$		$< 2.0 \times 10^{-4}$		CL=95%	559
$\eta \eta K^- \nu_\tau$		$< 3.0 \times 10^{-6}$		CL=90%	382
$\eta'(958) \pi^- \nu_\tau$		$< 4.0 \times 10^{-6}$		CL=90%	620
$\eta'(958) \pi^- \pi^0 \nu_\tau$		$< 1.2 \times 10^{-5}$		CL=90%	591
$\eta'(958) K^- \nu_\tau$		$< 2.4 \times 10^{-6}$		CL=90%	495
$\phi \pi^- \nu_\tau$		$(3.4 \pm 0.6) \times 10^{-5}$			585
$\phi K^- \nu_\tau$	[g]	$(4.4 \pm 1.6) \times 10^{-5}$			445
$f_1(1285) \pi^- \nu_\tau$		$(3.9 \pm 0.5) \times 10^{-4}$		S=1.9	408
$f_1(1285) \pi^- \nu_\tau \to \eta \pi^- \pi^+ \pi^- \nu_\tau$		$(1.18 \pm 0.07) \times 10^{-4}$		S=1.3	–
$f_1(1285) \pi^- \nu_\tau \to 3\pi^- 2\pi^+ \nu_\tau$	[g]	$(5.2 \pm 0.4) \times 10^{-5}$			–
$\pi(1300)^- \nu_\tau \to (\rho\pi)^- \nu_\tau \to (3\pi)^- \nu_\tau$		$< 1.0 \times 10^{-4}$		CL=90%	–

Lepton Summary Table

$\pi(1300)^-\nu_\tau \rightarrow$		$<$ 1.9	$\times 10^{-4}$	CL=90%	–
$((\pi\pi)_{S-\text{wave}}\,\pi)^-\nu_\tau \rightarrow$					
$(3\pi)^-\nu_\tau$					
$h^-\omega \geq 0$ neutrals ν_τ		(2.40 ± 0.08) %			708
$h^-\omega\nu_\tau$		(1.99 ± 0.06) %			708
$\pi^-\omega\nu_\tau$	[g]	(1.95 ± 0.06) %			708
$K^-\omega\nu_\tau$	[g]	(4.1 ± 0.9)	$\times 10^{-4}$		610
$h^-\omega\pi^0\nu_\tau$	[g]	(4.1 ± 0.4)	$\times 10^{-3}$		684
$h^-\omega 2\pi^0\nu_\tau$		(1.4 ± 0.5)	$\times 10^{-4}$		644
$\pi^-\omega 2\pi^0\nu_\tau$	[g]	(7.1 ± 1.6)	$\times 10^{-5}$		644
$h^-2\omega\nu_\tau$		$<$ 5.4	$\times 10^{-7}$	CL=90%	250
$2h^-h^+\omega\nu_\tau$		(1.20 ± 0.22)	$\times 10^{-4}$		641
$2\pi^-\pi^+\omega\nu_\tau$ (ex.K^0)	[g]	(8.4 ± 0.6)	$\times 10^{-5}$		641

Lepton Family number (*LF*), Lepton number (*L*), or Baryon number (*B*) violating modes

L means lepton number violation (*e.g.* $\tau^- \rightarrow e^+\pi^-\pi^-$). Following common usage, *LF* means lepton family violation *and not* lepton number violation (*e.g.* $\tau^- \rightarrow e^-\pi^+\pi^-$). *B* means baryon number violation.

$e^-\gamma$	*LF*	$<$ 3.3	$\times 10^{-8}$	CL=90%	888
$\mu^-\gamma$	*LF*	$<$ 4.4	$\times 10^{-8}$	CL=90%	885
$e^-\pi^0$	*LF*	$<$ 8.0	$\times 10^{-8}$	CL=90%	883
$\mu^-\pi^0$	*LF*	$<$ 1.1	$\times 10^{-7}$	CL=90%	880
$e^-K^0_S$	*LF*	$<$ 2.6	$\times 10^{-8}$	CL=90%	819
$\mu^-K^0_S$	*LF*	$<$ 2.3	$\times 10^{-8}$	CL=90%	815
$e^-\eta$	*LF*	$<$ 9.2	$\times 10^{-8}$	CL=90%	804
$\mu^-\eta$	*LF*	$<$ 6.5	$\times 10^{-8}$	CL=90%	800
$e^-\rho^0$	*LF*	$<$ 1.8	$\times 10^{-8}$	CL=90%	719
$\mu^-\rho^0$	*LF*	$<$ 1.2	$\times 10^{-8}$	CL=90%	715
$e^-\omega$	*LF*	$<$ 4.8	$\times 10^{-8}$	CL=90%	716
$\mu^-\omega$	*LF*	$<$ 4.7	$\times 10^{-8}$	CL=90%	711
$e^-K^*(892)^0$	*LF*	$<$ 3.2	$\times 10^{-8}$	CL=90%	665
$\mu^-K^*(892)^0$	*LF*	$<$ 5.9	$\times 10^{-8}$	CL=90%	659
$e^-\overline{K}^*(892)^0$	*LF*	$<$ 3.4	$\times 10^{-8}$	CL=90%	665
$\mu^-\overline{K}^*(892)^0$	*LF*	$<$ 7.0	$\times 10^{-8}$	CL=90%	659
$e^-\eta'(958)$	*LF*	$<$ 1.6	$\times 10^{-7}$	CL=90%	630
$\mu^-\eta'(958)$	*LF*	$<$ 1.3	$\times 10^{-7}$	CL=90%	625
$e^-f_0(980) \rightarrow e^-\pi^+\pi^-$	*LF*	$<$ 3.2	$\times 10^{-8}$	CL=90%	–
$\mu^-f_0(980) \rightarrow \mu^-\pi^+\pi^-$	*LF*	$<$ 3.4	$\times 10^{-8}$	CL=90%	–
$e^-\phi$	*LF*	$<$ 3.1	$\times 10^{-8}$	CL=90%	596
$\mu^-\phi$	*LF*	$<$ 8.4	$\times 10^{-8}$	CL=90%	590
$e^-e^+e^-$	*LF*	$<$ 2.7	$\times 10^{-8}$	CL=90%	888
$e^-\mu^+\mu^-$	*LF*	$<$ 2.7	$\times 10^{-8}$	CL=90%	882
$e^+\mu^-\mu^-$	*LF*	$<$ 1.7	$\times 10^{-8}$	CL=90%	882
$\mu^-e^+e^-$	*LF*	$<$ 1.8	$\times 10^{-8}$	CL=90%	885
$\mu^+e^-e^-$	*LF*	$<$ 1.5	$\times 10^{-8}$	CL=90%	885
$\mu^-\mu^+\mu^-$	*LF*	$<$ 2.1	$\times 10^{-8}$	CL=90%	873
$e^-\pi^+\pi^-$	*LF*	$<$ 2.3	$\times 10^{-8}$	CL=90%	877
$e^+\pi^-\pi^-$	*L*	$<$ 2.0	$\times 10^{-8}$	CL=90%	877
$\mu^-\pi^+\pi^-$	*LF*	$<$ 2.1	$\times 10^{-8}$	CL=90%	866
$\mu^+\pi^-\pi^-$	*L*	$<$ 3.9	$\times 10^{-8}$	CL=90%	866
$e^-\pi^+K^-$	*LF*	$<$ 3.7	$\times 10^{-8}$	CL=90%	813
$e^-\pi^-K^+$	*LF*	$<$ 3.1	$\times 10^{-8}$	CL=90%	813
$e^+\pi^-K^-$	*L*	$<$ 3.2	$\times 10^{-8}$	CL=90%	813
$e^-K^0_S K^0_S$	*LF*	$<$ 7.1	$\times 10^{-8}$	CL=90%	736
$e^-K^+K^-$	*LF*	$<$ 3.4	$\times 10^{-8}$	CL=90%	738
$e^+K^-K^-$	*L*	$<$ 3.3	$\times 10^{-8}$	CL=90%	738
$\mu^-\pi^+K^-$	*LF*	$<$ 8.6	$\times 10^{-8}$	CL=90%	800
$\mu^-\pi^-K^+$	*LF*	$<$ 4.5	$\times 10^{-8}$	CL=90%	800
$\mu^+\pi^-K^-$	*L*	$<$ 4.8	$\times 10^{-8}$	CL=90%	800
$\mu^-K^0_S K^0_S$	*LF*	$<$ 8.0	$\times 10^{-8}$	CL=90%	696
$\mu^-K^+K^-$	*LF*	$<$ 4.4	$\times 10^{-8}$	CL=90%	699
$\mu^+K^-K^-$	*L*	$<$ 4.7	$\times 10^{-8}$	CL=90%	699
$e^-\pi^0\pi^0$	*LF*	$<$ 6.5	$\times 10^{-6}$	CL=90%	878
$\mu^-\pi^0\pi^0$	*LF*	$<$ 1.4	$\times 10^{-5}$	CL=90%	867
$e^-\eta\eta$	*LF*	$<$ 3.5	$\times 10^{-5}$	CL=90%	699
$\mu^-\eta\eta$	*LF*	$<$ 6.0	$\times 10^{-5}$	CL=90%	653
$e^-\pi^0\eta$	*LF*	$<$ 2.4	$\times 10^{-5}$	CL=90%	798
$\mu^-\pi^0\eta$	*LF*	$<$ 2.2	$\times 10^{-5}$	CL=90%	784
$p\mu^-\mu^-$	*L*,*B*	$<$ 4.4	$\times 10^{-7}$	CL=90%	618
$\overline{p}\mu^+\mu^-$	*L*,*B*	$<$ 3.3	$\times 10^{-7}$	CL=90%	618
$\overline{p}\gamma$	*L*,*B*	$<$ 3.5	$\times 10^{-6}$	CL=90%	641
$\overline{p}\pi^0$	*L*,*B*	$<$ 1.5	$\times 10^{-5}$	CL=90%	632
$\overline{p}2\pi^0$	*L*,*B*	$<$ 3.3	$\times 10^{-5}$	CL=90%	604
$\overline{p}\eta$	*L*,*B*	$<$ 8.9	$\times 10^{-6}$	CL=90%	475
$\overline{p}\pi^0\eta$	*L*,*B*	$<$ 2.7	$\times 10^{-5}$	CL=90%	360
$\Lambda\pi^-$	*L*,*B*	$<$ 7.2	$\times 10^{-8}$	CL=90%	525
$\overline{\Lambda}\pi^-$	*L*,*B*	$<$ 1.4	$\times 10^{-7}$	CL=90%	525
e^-light boson	*LF*	$<$ 2.7	$\times 10^{-3}$	CL=95%	–
μ^-light boson	*LF*	$<$ 5	$\times 10^{-3}$	CL=95%	–

Heavy Charged Lepton Searches

$L^\pm$ – charged lepton

Mass $m >$ 100.8 GeV, CL = 95% [h] Decay to νW.

$L^\pm$ – stable charged heavy lepton

Mass $m >$ 102.6 GeV, CL = 95%

Neutrino Properties

See the note on "Neutrino properties listings" in the Particle Listings.

Mass $m <$ 2 eV (tritium decay)
Mean life/mass, $\tau/m >$ 300 s/eV, CL = 90% (reactor)
Mean life/mass, $\tau/m > 7\times10^9$ s/eV (solar)
Mean life/mass, $\tau/m >$ 15.4 s/eV, CL = 90% (accelerator)
Magnetic moment $\mu < 0.29\times10^{-10}\,\mu_B$, CL = 90% (reactor)

Number of Neutrino Types

Number $N = 2.984 \pm 0.008$ (Standard Model fits to LEP-SLC data)
Number $N = 2.92 \pm 0.05$ (S = 1.2) (Direct measurement of invisible Z width)

Neutrino Mixing

The following values are obtained through data analyses based on the 3-neutrino mixing scheme described in the review "Neutrino Mass, Mixing, and Oscillations" by K. Nakamura and S.T. Petcov in this *Review*.

$\sin^2(\theta_{12}) = 0.307 \pm 0.013$
$\Delta m^2_{21} = (7.53 \pm 0.18)\times10^{-5}$ eV^2
$\sin^2(\theta_{23}) = 0.421^{+0.033}_{-0.025}$ (S = 1.3) (Inverted order, quad. I)
$\sin^2(\theta_{23}) = 0.592^{+0.023}_{-0.030}$ (S = 1.1) (Inverted order, quad. II)
$\sin^2(\theta_{23}) = 0.417^{+0.025}_{-0.028}$ (S = 1.2) (Normal order, quad. I)
$\sin^2(\theta_{23}) = 0.597^{+0.024}_{-0.030}$ (S = 1.2) (Normal order, quad. II)
$\Delta m^2_{32} = (-2.56 \pm 0.04)\times10^{-3}$ eV^2 (Inverted order)
$\Delta m^2_{32} = (2.51 \pm 0.05)\times10^{-3}$ eV^2 (S = 1.1) (Normal order)
$\sin^2(\theta_{13}) = (2.12 \pm 0.08)\times10^{-2}$

Stable Neutral Heavy Lepton Mass Limits

Mass $m >$ 45.0 GeV, CL = 95% (Dirac)
Mass $m >$ 39.5 GeV, CL = 95% (Majorana)

Neutral Heavy Lepton Mass Limits

Mass $m >$ 90.3 GeV, CL = 95%
(Dirac ν_L coupling to e, μ, τ; conservative case(τ))
Mass $m >$ 80.5 GeV, CL = 95%
(Majorana ν_L coupling to e, μ, τ; conservative case(τ))

NOTES

In this Summary Table:

When a quantity has "(S = ...)" to its right, the error on the quantity has been enlarged by the "scale factor" S, defined as $S = \sqrt{\chi^2/(N-1)}$, where N is the number of measurements used in calculating the quantity. We do this when $S > 1$, which often indicates that the measurements are inconsistent. When $S > 1.25$, we also show in the Particle Listings an ideogram of the measurements. For more about S, see the Introduction.

A decay momentum p is given for each decay mode. For a 2-body decay, p is the momentum of each decay product in the rest frame of the decaying particle. For a 3-or-more-body decay, p is the largest momentum any of the products can have in this frame.

[a] This is the best limit for the mode $e^- \rightarrow \nu\gamma$. The best limit for "electron disappearance" is 6.4×10^{24} yr.

[b] See the "Note on Muon Decay Parameters" in the μ Particle Listings for definitions and details.

[c] P_μ is the longitudinal polarization of the muon from pion decay. In standard $V-A$ theory, $P_\mu = 1$ and $\rho = \delta = 3/4$.

[d] This only includes events with energy of $e > 45$ MeV and energy of $\gamma > 40$ MeV. Since the $e^- \overline{\nu}_e \nu_\mu$ and $e^- \overline{\nu}_e \nu_\mu \gamma$ modes cannot be clearly separated, we regard the latter mode as a subset of the former.

[e] See the relevant Particle Listings for the energy limits used in this measurement.

[f] A test of additive vs. multiplicative lepton family number conservation.

[g] Basis mode for the τ.

[h] $L^\pm$ mass limit depends on decay assumptions; see the Full Listings.

Quark Summary Table

QUARKS

The u-, d-, and s-quark masses are estimates of so-called "current-quark masses," in a mass-independent subtraction scheme such as $\overline{\text{MS}}$ at a scale $\mu \approx 2$ GeV. The c- and b-quark masses are the "running" masses in the $\overline{\text{MS}}$ scheme.

u

$I(J^P) = \frac{1}{2}(\frac{1}{2}^+)$

$m_u = 2.2^{+0.5}_{-0.4}$ MeV Charge $= \frac{2}{3}\ e$ $I_z = +\frac{1}{2}$
$m_u/m_d = 0.48^{+0.07}_{-0.08}$

d

$I(J^P) = \frac{1}{2}(\frac{1}{2}^+)$

$m_d = 4.7^{+0.5}_{-0.3}$ MeV Charge $= -\frac{1}{3}\ e$ $I_z = -\frac{1}{2}$
$m_s/m_d = 17$–22
$\overline{m} = (m_u+m_d)/2 = 3.5^{+0.5}_{-0.2}$ MeV

s

$I(J^P) = 0(\frac{1}{2}^+)$

$m_s = 95^{+9}_{-3}$ MeV Charge $= -\frac{1}{3}\ e$ Strangeness $= -1$
$m_s\ /\ ((m_u + m_d)/2) = 27.3 \pm 0.7$

c

$I(J^P) = 0(\frac{1}{2}^+)$

$m_c = 1.275^{+0.025}_{-0.035}$ GeV Charge $= \frac{2}{3}\ e$ Charm $= +1$
$m_c/m_s = 11.72 \pm 0.25$
$m_b/m_c = 4.53 \pm 0.05$
$m_b - m_c = 3.45 \pm 0.05$ GeV

b

$I(J^P) = 0(\frac{1}{2}^+)$

Mass $m = 4.18^{+0.04}_{-0.03}$ GeV Charge $= -\frac{1}{3}\ e$ Bottom $= -1$

t

$I(J^P) = 0(\frac{1}{2}^+)$

Charge $= \frac{2}{3}\ e$ Top $= +1$

Mass (direct measurements) $m = 173.0 \pm 0.4$ GeV [a,b] (S = 1.3)
Mass (from cross-section measurements) $m = 160^{+5}_{-4}$ GeV [a]
Mass (Pole from cross-section measurements) $m = 173.1 \pm 0.9$ GeV
$m_t - m_{\overline{t}} = -0.16 \pm 0.19$ GeV
Full width $\Gamma = 1.41^{+0.19}_{-0.15}$ GeV (S = 1.4)
$\Gamma(Wb)/\Gamma(Wq(q = b, s, d)) = 0.957 \pm 0.034$ (S = 1.5)

t-quark EW Couplings

$F_0 = 0.687 \pm 0.018$
$F_- = 0.320 \pm 0.013$
$F_+ = 0.002 \pm 0.011$
$F_{V+A} < 0.29$, CL = 95%

t DECAY MODES	Fraction (Γ_i/Γ)	Confidence level	p (MeV/c)
$t \to Wq(q = b, s, d)$			–
$t \to Wb$			–
$t \to e\nu_e b$	(13.3±0.6) %		–
$t \to \mu\nu_\mu b$	(13.4±0.6) %		–
$t \to \tau\nu_\tau b$	(7.1±0.6) %		–
$t \to q\overline{q}b$	(66.5±1.4) %		–
$\Delta T = 1$ weak neutral current ($T1$) modes			
$t \to Zq(q=u,c)$ $T1$	[c] < 5	$\times 10^{-4}$ 95%	–
$t \to Hu$ $T1$	< 2.4	$\times 10^{-3}$ 95%	–
$t \to Hc$ $T1$	< 2.2	$\times 10^{-3}$ 95%	–
$t \to \ell^+\overline{q}q'$ $(q=d,s,b;\ q'=u,c)$ $T1$	< 1.6	$\times 10^{-3}$ 95%	–

b′ (4th Generation) Quark, Searches for

Mass $m >$ 190 GeV, CL = 95% ($p\overline{p}$, quasi-stable b')
Mass $m >$ 755 GeV, CL = 95% (pp, neutral-current decays)
Mass $m >$ 880 GeV, CL = 95% (pp, charged-current decays)
Mass $m >$ 46.0 GeV, CL = 95% (e^+e^-, all decays)

t′ (4th Generation) Quark, Searches for

$m(t'(2/3)) >$ 1160 GeV, CL = 95% (neutral-current decays)
$m(t'(2/3)) >$ 770 GeV, CL = 95% (charged-current decays)
$m(t'(5/3)) >$ 990 GeV, CL = 95%

Free Quark Searches

All searches since 1977 have had negative results.

NOTES

[a] A discussion of the definition of the top quark mass in these measurements can be found in the review "The Top Quark."

[b] Based on published top mass measurements using data from Tevatron Run-I and Run-II and LHC at $\sqrt{s} = 7$ TeV. Including the most recent unpublished results from Tevatron Run-II, the Tevatron Electroweak Working Group reports a top mass of 173.2 ± 0.9 GeV. See the note "The Top Quark' in the Quark Particle Listings of this *Review*.

[c] This limit is for $\Gamma(t \to Zq)/\Gamma(t \to Wb)$.

LIGHT UNFLAVORED MESONS ($S = C = B = 0$)

For $I = 1$ (π, b, ρ, a): $u\overline{d}$, $(u\overline{u}-d\overline{d})/\sqrt{2}$, $d\overline{u}$;
for $I = 0$ (η, η', h, h', ω, ϕ, f, f'): $c_1(u\overline{u} + d\overline{d}) + c_2(s\overline{s})$

$\pi^\pm$

$I^G(J^P) = 1^-(0^-)$

Mass $m = 139.57061 \pm 0.00024$ MeV (S = 1.6)
Mean life $\tau = (2.6033 \pm 0.0005) \times 10^{-8}$ s (S = 1.2)
$c\tau = 7.8045$ m

$\pi^\pm \to \ell^\pm\nu\gamma$ form factors [a]

$F_V = 0.0254 \pm 0.0017$
$F_A = 0.0119 \pm 0.0001$
F_V slope parameter $a = 0.10 \pm 0.06$
$R = 0.059^{+0.009}_{-0.008}$

π^- modes are charge conjugates of the modes below.

For decay limits to particles which are not established, see the section on Searches for Axions and Other Very Light Bosons.

π^+ DECAY MODES		Fraction (Γ_i/Γ)	Confidence level	p (MeV/c)
$\mu^+\nu_\mu$		[b] (99.98770 ± 0.00004) %		30
$\mu^+\nu_\mu\gamma$		[c] (2.00 ± 0.25) × 10^{-4}		30
$e^+\nu_e$		[b] (1.230 ± 0.004) × 10^{-4}		70
$e^+\nu_e\gamma$		[c] (7.39 ± 0.05) × 10^{-7}		70
$e^+\nu_e\pi^0$		(1.036 ± 0.006) × 10^{-8}		4
$e^+\nu_e e^+e^-$		(3.2 ± 0.5) × 10^{-9}		70
$e^+\nu_e\nu\overline{\nu}$		< 5 × 10^{-6}	90%	70
Lepton Family number (LF) or Lepton number (L) violating modes				
$\mu^+\overline{\nu}_e$	L	[d] < 1.5 × 10^{-3}	90%	30
$\mu^+\nu_e$	LF	[d] < 8.0 × 10^{-3}	90%	30
$\mu^-e^+e^+\nu$	LF	< 1.6 × 10^{-6}	90%	30

π^0

$I^G(J^{PC}) = 1^-(0^{-+})$

Mass $m = 134.9770 \pm 0.0005$ MeV (S = 1.1)
$m_{\pi^\pm} - m_{\pi^0} = 4.5936 \pm 0.0005$ MeV
Mean life $\tau = (8.52 \pm 0.18) \times 10^{-17}$ s (S = 1.2)
$c\tau = 25.5$ nm

For decay limits to particles which are not established, see the appropriate Search sections (A^0 (axion) and Other Light Boson (X^0) Searches, etc.).

π^0 DECAY MODES		Fraction (Γ_i/Γ)	Scale factor/ Confidence level	p (MeV/c)
2γ		(98.823±0.034) %	S=1.5	67
$e^+e^-\gamma$		(1.174±0.035) %	S=1.5	67
γpositronium		(1.82 ±0.29) × 10^{-9}		67
$e^+e^+e^-e^-$		(3.34 ±0.16) × 10^{-5}		67
e^+e^-		(6.46 ±0.33) × 10^{-8}		67
4γ		< 2 × 10^{-8}	CL=90%	67
$\nu\overline{\nu}$		[e] < 2.7 × 10^{-7}	CL=90%	67
$\nu_e\overline{\nu}_e$		< 1.7 × 10^{-6}	CL=90%	67
$\nu_\mu\overline{\nu}_\mu$		< 1.6 × 10^{-6}	CL=90%	67
$\nu_\tau\overline{\nu}_\tau$		< 2.1 × 10^{-6}	CL=90%	67
$\gamma\nu\overline{\nu}$		< 6 × 10^{-4}	CL=90%	67
Charge conjugation (C) or Lepton Family number (LF) violating modes				
3γ	C	< 3.1 × 10^{-8}	CL=90%	67
μ^+e^-	LF	< 3.8 × 10^{-10}	CL=90%	26
μ^-e^+	LF	< 3.4 × 10^{-9}	CL=90%	26
$\mu^+e^- + \mu^-e^+$	LF	< 3.6 × 10^{-10}	CL=90%	26

η

$I^G(J^{PC}) = 0^+(0^{-+})$

Mass $m = 547.862 \pm 0.017$ MeV
Full width $\Gamma = 1.31 \pm 0.05$ keV

C-nonconserving decay parameters

$\pi^+\pi^-\pi^0$ left-right asymmetry = $(0.09^{+0.11}_{-0.12}) \times 10^{-2}$
$\pi^+\pi^-\pi^0$ sextant asymmetry = $(0.12^{+0.10}_{-0.11}) \times 10^{-2}$
$\pi^+\pi^-\pi^0$ quadrant asymmetry = $(-0.09 \pm 0.09) \times 10^{-2}$
$\pi^+\pi^-\gamma$ left-right asymmetry = $(0.9 \pm 0.4) \times 10^{-2}$
$\pi^+\pi^-\gamma$ β (D-wave) = -0.02 ± 0.07 (S = 1.3)

CP-nonconserving decay parameters

$\pi^+\pi^-e^+e^-$ decay-plane asymmetry $A_\phi = (-0.6 \pm 3.1) \times 10^{-2}$

Dalitz plot parameter

$\pi^0\pi^0\pi^0$ $\alpha = -0.0318 \pm 0.0015$
Parameter Λ in $\eta \to \ell^+\ell^-\gamma$ decay = 0.716 ± 0.011 GeV/c^2

η DECAY MODES	Fraction (Γ_i/Γ)	Scale factor/ Confidence level	p (MeV/c)
Neutral modes			
neutral modes	(72.12±0.34) %	S=1.2	–
2γ	(39.41±0.20) %	S=1.1	274
$3\pi^0$	(32.68±0.23) %	S=1.1	179
$\pi^0 2\gamma$	(2.56±0.22) × 10^{-4}		257
$2\pi^0 2\gamma$	< 1.2 × 10^{-3}	CL=90%	238
4γ	< 2.8 × 10^{-4}	CL=90%	274
invisible	< 1.0 × 10^{-4}	CL=90%	–
Charged modes			
charged modes	(28.10±0.34) %	S=1.2	–
$\pi^+\pi^-\pi^0$	(22.92±0.28) %	S=1.2	174
$\pi^+\pi^-\gamma$	(4.22±0.08) %	S=1.1	236
$e^+e^-\gamma$	(6.9 ±0.4) × 10^{-3}	S=1.3	274
$\mu^+\mu^-\gamma$	(3.1 ±0.4) × 10^{-4}		253
e^+e^-	< 2.3 × 10^{-6}	CL=90%	274
$\mu^+\mu^-$	(5.8 ±0.8) × 10^{-6}		253
$2e^+2e^-$	(2.40±0.22) × 10^{-5}		274
$\pi^+\pi^-e^+e^-(\gamma)$	(2.68±0.11) × 10^{-4}		235
$e^+e^-\mu^+\mu^-$	< 1.6 × 10^{-4}	CL=90%	253
$2\mu^+2\mu^-$	< 3.6 × 10^{-4}	CL=90%	161
$\mu^+\mu^-\pi^+\pi^-$	< 3.6 × 10^{-4}	CL=90%	113
$\pi^+e^-\overline{\nu}_e$ + c.c.	< 1.7 × 10^{-4}	CL=90%	256
$\pi^+\pi^-2\gamma$	< 2.1 × 10^{-3}		236
$\pi^+\pi^-\pi^0\gamma$	< 5 × 10^{-4}	CL=90%	174
$\pi^0\mu^+\mu^-\gamma$	< 3 × 10^{-6}	CL=90%	210
Charge conjugation (C), Parity (P), Charge conjugation × Parity (CP), or Lepton Family number (LF) violating modes			
$\pi^0\gamma$	C	< 9 × 10^{-5}	CL=90%	257
$\pi^+\pi^-$	P,CP	< 1.3 × 10^{-5}	CL=90%	236
$2\pi^0$	P,CP	< 3.5 × 10^{-4}	CL=90%	238
$2\pi^0\gamma$	C	< 5 × 10^{-4}	CL=90%	238
$3\pi^0\gamma$	C	< 6 × 10^{-5}	CL=90%	179
3γ	C	< 1.6 × 10^{-5}	CL=90%	274
$4\pi^0$	P,CP	< 6.9 × 10^{-7}	CL=90%	40
$\pi^0e^+e^-$	C	[f] < 4 × 10^{-5}	CL=90%	257
$\pi^0\mu^+\mu^-$	C	[f] < 5 × 10^{-6}	CL=90%	210
$\mu^+e^- + \mu^-e^+$	LF	< 6 × 10^{-6}	CL=90%	264

$f_0(500)$ [g]

$I^G(J^{PC}) = 0^+(0^{++})$

Mass (T-Matrix Pole $\sqrt{s}$) = (400–550)$-i$(200–350) MeV
Mass (Breit-Wigner) = (400–550) MeV
Full width (Breit-Wigner) = (400–700) MeV

$f_0(500)$ DECAY MODES	Fraction (Γ_i/Γ)	p (MeV/c)
$\pi\pi$	dominant	–
$\gamma\gamma$	seen	–

$\rho(770)$ [h]

$I^G(J^{PC}) = 1^+(1^{--})$

Mass $m = 775.26 \pm 0.25$ MeV
Full width $\Gamma = 149.1 \pm 0.8$ MeV
$\Gamma_{ee} = 7.04 \pm 0.06$ keV

Meson Summary Table

$\rho(770)$ DECAY MODES	Fraction (Γ_i/Γ)		Scale factor/ Confidence level	p (MeV/c)
$\pi\pi$	$\sim$ 100	%		363
$\rho(770)^\pm$ decays				
$\pi^\pm\gamma$	(4.5 $\pm$0.5)	$\times 10^{-4}$	S=2.2	375
$\pi^\pm\eta$	< 6	$\times 10^{-3}$	CL=84%	152
$\pi^\pm\pi^+\pi^-\pi^0$	< 2.0	$\times 10^{-3}$	CL=84%	254
$\rho(770)^0$ decays				
$\pi^+\pi^-\gamma$	(9.9 $\pm$1.6)	$\times 10^{-3}$		362
$\pi^0\gamma$	(4.7 $\pm$0.6)	$\times 10^{-4}$	S=1.4	376
$\eta\gamma$	(3.00 $\pm$0.21)	$\times 10^{-4}$		194
$\pi^0\pi^0\gamma$	(4.5 $\pm$0.8)	$\times 10^{-5}$		363
$\mu^+\mu^-$ [i]	(4.55 $\pm$0.28)	$\times 10^{-5}$		373
e^+e^- [i]	(4.72 $\pm$0.05)	$\times 10^{-5}$		388
$\pi^+\pi^-\pi^0$	($1.01^{+0.54}_{-0.36}\pm0.34$)	$\times 10^{-4}$		323
$\pi^+\pi^-\pi^+\pi^-$	(1.8 $\pm$0.9)	$\times 10^{-5}$		251
$\pi^+\pi^-\pi^0\pi^0$	(1.6 $\pm$0.8)	$\times 10^{-5}$		257
$\pi^0 e^+e^-$	< 1.2	$\times 10^{-5}$	CL=90%	376

$\omega(782)$

$I^G(J^{PC}) = 0^-(1^{--})$

Mass $m = 782.65 \pm 0.12$ MeV (S = 1.9)
Full width $\Gamma = 8.49 \pm 0.08$ MeV
$\Gamma_{ee} = 0.60 \pm 0.02$ keV

$\omega(782)$ DECAY MODES	Fraction (Γ_i/Γ)		Scale factor/ Confidence level	p (MeV/c)
$\pi^+\pi^-\pi^0$	(89.2 $\pm$0.7) %			327
$\pi^0\gamma$	(8.40 $\pm$0.22) %		S=1.8	380
$\pi^+\pi^-$	($1.53^{+0.11}_{-0.13}$) %		S=1.2	366
neutrals (excluding $\pi^0\gamma$)	($7\ ^{+7}_{-4}$)	$\times 10^{-3}$	S=1.1	–
$\eta\gamma$	(4.5 $\pm$0.4)	$\times 10^{-4}$	S=1.1	200
$\pi^0 e^+e^-$	(7.7 $\pm$0.6)	$\times 10^{-4}$		380
$\pi^0\mu^+\mu^-$	(1.34 $\pm$0.18)	$\times 10^{-4}$	S=1.5	349
e^+e^-	(7.36 $\pm$0.15)	$\times 10^{-5}$	S=1.5	391
$\pi^+\pi^-\pi^0\pi^0$	< 2	$\times 10^{-4}$	CL=90%	262
$\pi^+\pi^-\gamma$	< 3.6	$\times 10^{-3}$	CL=95%	366
$\pi^+\pi^-\pi^+\pi^-$	< 1	$\times 10^{-3}$	CL=90%	256
$\pi^0\pi^0\gamma$	(6.7 $\pm$1.1)	$\times 10^{-5}$		367
$\eta\pi^0\gamma$	< 3.3	$\times 10^{-5}$	CL=90%	162
$\mu^+\mu^-$	(7.4 $\pm$1.8)	$\times 10^{-5}$		377
3γ	< 1.9	$\times 10^{-4}$	CL=95%	391
Charge conjugation (C) violating modes				
$\eta\pi^0$ C	< 2.2	$\times 10^{-4}$	CL=90%	162
$2\pi^0$ C	< 2.2	$\times 10^{-4}$	CL=90%	367
$3\pi^0$ C	< 2.3	$\times 10^{-4}$	CL=90%	330

$\eta'(958)$

$I^G(J^{PC}) = 0^+(0^{-+})$

Mass $m = 957.78 \pm 0.06$ MeV
Full width $\Gamma = 0.196 \pm 0.009$ MeV

$\eta'(958)$ DECAY MODES	Fraction (Γ_i/Γ)	Confidence level	p (MeV/c)
$\pi^+\pi^-\eta$	(42.6 $\pm$0.7) %		232
$\rho^0\gamma$(including non-resonant $\pi^+\pi^-\gamma$)	(28.9 $\pm$0.5) %		165
$\pi^0\pi^0\eta$	(22.8 $\pm$0.8) %		239
$\omega\gamma$	(2.62 $\pm$0.13) %		159
ωe^+e^-	(2.0 $\pm$0.4) $\times 10^{-4}$		159
$\gamma\gamma$	(2.22 $\pm$0.08) %		479
$3\pi^0$	(2.54 $\pm$0.18) $\times 10^{-3}$		430
$\mu^+\mu^-\gamma$	(1.09 $\pm$0.27) $\times 10^{-4}$		467
$\pi^+\pi^-\mu^+\mu^-$	< 2.9 $\times 10^{-5}$	90%	401
$\pi^+\pi^-\pi^0$	(3.61 $\pm$0.17) $\times 10^{-3}$		428
$(\pi^+\pi^-\pi^0)$ S-wave	(3.8 $\pm$0.5) $\times 10^{-3}$		428
$\pi^\mp\rho^\pm$	(7.4 $\pm$2.3) $\times 10^{-4}$		106
$\pi^0\rho^0$	< 4 %	90%	111
$2(\pi^+\pi^-)$	(8.6 $\pm$0.9) $\times 10^{-5}$		372
$\pi^+\pi^-2\pi^0$	(1.8 $\pm$0.4) $\times 10^{-4}$		376
$2(\pi^+\pi^-)$ neutrals	< 1 %	95%	–
$2(\pi^+\pi^-)\pi^0$	< 1.8 $\times 10^{-3}$	90%	298
$2(\pi^+\pi^-)2\pi^0$	< 1 %	95%	197
$3(\pi^+\pi^-)$	< 3.1 $\times 10^{-5}$	90%	189
$K^\pm\pi^\mp$	< 4 $\times 10^{-5}$	90%	334
$\pi^+\pi^-e^+e^-$	(2.4 $^{+1.3}_{-1.0}$) $\times 10^{-3}$		458
$\pi^+e^-\nu_e$ + c.c.	< 2.1 $\times 10^{-4}$	90%	469
γe^+e^-	(4.73 $\pm$0.30) $\times 10^{-4}$		479
$\pi^0\gamma\gamma$	(3.20 $\pm$0.24) $\times 10^{-3}$		469
$\pi^0\gamma\gamma$(non resonant)	(6.2 $\pm$0.9) $\times 10^{-4}$		–
$4\pi^0$	< 3.2 $\times 10^{-4}$	90%	380
e^+e^-	< 5.6 $\times 10^{-9}$	90%	479
invisible	< 5 $\times 10^{-4}$	90%	–
Charge conjugation (C), Parity (P), Lepton family number (LF) violating modes			
$\pi^+\pi^-$ P,CP	< 1.8 $\times 10^{-5}$	90%	458
$\pi^0\pi^0$ P,CP	< 5 $\times 10^{-4}$	90%	459
$\pi^0 e^+e^-$ C [f]	< 1.4 $\times 10^{-3}$	90%	469
ηe^+e^- C [f]	< 2.4 $\times 10^{-3}$	90%	322
3γ C	< 1.1 $\times 10^{-4}$	90%	479
$\mu^+\mu^-\pi^0$ C [f]	< 6.0 $\times 10^{-5}$	90%	445
$\mu^+\mu^-\eta$ C [f]	< 1.5 $\times 10^{-5}$	90%	273
$e\mu$ LF	< 4.7 $\times 10^{-4}$	90%	473

$f_0(980)$ [j]

$I^G(J^{PC}) = 0^+(0^{++})$

Mass $m = 990 \pm 20$ MeV
Full width $\Gamma = 10$ to 100 MeV

$f_0(980)$ DECAY MODES	Fraction (Γ_i/Γ)	p (MeV/c)
$\pi\pi$	dominant	476
$K\overline{K}$	seen	36
$\gamma\gamma$	seen	495

$a_0(980)$ [j]

$I^G(J^{PC}) = 1^-(0^{++})$

Mass $m = 980 \pm 20$ MeV
Full width $\Gamma = 50$ to 100 MeV

$a_0(980)$ DECAY MODES	Fraction (Γ_i/Γ)	p (MeV/c)
$\eta\pi$	dominant	319
$K\overline{K}$	seen	†
$\gamma\gamma$	seen	490

$\phi(1020)$

$I^G(J^{PC}) = 0^-(1^{--})$

Mass $m = 1019.461 \pm 0.016$ MeV
Full width $\Gamma = 4.249 \pm 0.013$ MeV (S = 1.1)

$\phi(1020)$ DECAY MODES	Fraction (Γ_i/Γ)		Scale factor/ Confidence level	p (MeV/c)
K^+K^-	(49.2 $\pm$0.5) %		S=1.3	127
$K^0_LK^0_S$	(34.0 $\pm$0.4) %		S=1.3	110
$\rho\pi$ + $\pi^+\pi^-\pi^0$	(15.24 $\pm$0.33) %		S=1.2	–
$\eta\gamma$	(1.303 $\pm$0.025) %		S=1.2	363
$\pi^0\gamma$	(1.30 $\pm$0.05)	$\times 10^{-3}$		501
$\ell^+\ell^-$	—			510
e^+e^-	(2.973 $\pm$0.034)	$\times 10^{-4}$	S=1.3	510
$\mu^+\mu^-$	(2.86 $\pm$0.19)	$\times 10^{-4}$		499
ηe^+e^-	(1.08 $\pm$0.04)	$\times 10^{-4}$		363
$\pi^+\pi^-$	(7.3 $\pm$1.3)	$\times 10^{-5}$		490
$\omega\pi^0$	(4.7 $\pm$0.5)	$\times 10^{-5}$		171
$\omega\gamma$	< 5	%	CL=84%	209
$\rho\gamma$	< 1.2	$\times 10^{-5}$	CL=90%	215
$\pi^+\pi^-\gamma$	(4.1 $\pm$1.3)	$\times 10^{-5}$		490
$f_0(980)\gamma$	(3.22 $\pm$0.19)	$\times 10^{-4}$	S=1.1	29
$\pi^0\pi^0\gamma$	(1.12 $\pm$0.06)	$\times 10^{-4}$		492
$\pi^+\pi^-\pi^+\pi^-$	(3.9 $^{+2.8}_{-2.2}$)	$\times 10^{-6}$		410
$\pi^+\pi^+\pi^-\pi^-\pi^0$	< 4.6	$\times 10^{-6}$	CL=90%	342
$\pi^0 e^+e^-$	(1.33 $^{+0.07}_{-0.10}$)	$\times 10^{-5}$		501
$\pi^0\eta\gamma$	(7.27 $\pm$0.30)	$\times 10^{-5}$	S=1.5	346
$a_0(980)\gamma$	(7.6 $\pm$0.6)	$\times 10^{-5}$		39

$K^0\overline{K}^0\gamma$	$<$ 1.9	$\times 10^{-8}$	CL=90%	110
$\eta'(958)\gamma$	(6.22 $\pm$0.21)	$\times 10^{-5}$		60
$\eta\pi^0\pi^0\gamma$	$<$ 2	$\times 10^{-5}$	CL=90%	293
$\mu^+\mu^-\gamma$	(1.4 $\pm$0.5)	$\times 10^{-5}$		499
$\rho\gamma\gamma$	$<$ 1.2	$\times 10^{-4}$	CL=90%	215
$\eta\pi^+\pi^-$	$<$ 1.8	$\times 10^{-5}$	CL=90%	288
$\eta\mu^+\mu^-$	$<$ 9.4	$\times 10^{-6}$	CL=90%	321
$\eta U \to \eta e^+e^-$	$<$ 1	$\times 10^{-6}$	CL=90%	–

Lepton Family number (LF) violating modes

$e^\pm\mu^\mp$	*LF*	$<$ 2	$\times 10^{-6}$	CL=90%	504

$h_1(1170)$ $I^G(J^{PC}) = 0^-(1^{+-})$

Mass $m = 1170 \pm 20$ MeV
Full width $\Gamma = 360 \pm 40$ MeV

$h_1(1170)$ DECAY MODES	Fraction (Γ_i/Γ)	p (MeV/c)
$\rho\pi$	seen	308

$b_1(1235)$ $I^G(J^{PC}) = 1^+(1^{+-})$

Mass $m = 1229.5 \pm 3.2$ MeV (S = 1.6)
Full width $\Gamma = 142 \pm 9$ MeV (S = 1.2)

$b_1(1235)$ DECAY MODES	Fraction (Γ_i/Γ)	Confidence level	p (MeV/c)
$\omega\pi$	dominant		348
[D/S amplitude ratio = 0.277 $\pm$ 0.027]			
$\pi^\pm\gamma$	(1.6$\pm$0.4) $\times 10^{-3}$		607
$\eta\rho$	seen		†
$\pi^+\pi^+\pi^-\pi^0$	$<$ 50 %	84%	535
$K^*(892)^\pm K^\mp$	seen		†
$(K\overline{K})^\pm\pi^0$	$<$ 8 %	90%	248
$K^0_S K^0_L \pi^\pm$	$<$ 6 %	90%	235
$K^0_S K^0_S \pi^\pm$	$<$ 2 %	90%	235
$\phi\pi$	$<$ 1.5 %	84%	147

$a_1(1260)$ [k] $I^G(J^{PC}) = 1^-(1^{++})$

Mass $m = 1230 \pm 40$ MeV [l]
Full width $\Gamma = 250$ to 600 MeV

$a_1(1260)$ DECAY MODES	Fraction (Γ_i/Γ)	p (MeV/c)
$(\rho\pi)_{S-\text{wave}}$	seen	353
$(\rho\pi)_{D-\text{wave}}$	seen	353
$(\rho(1450)\pi)_{S-\text{wave}}$	seen	†
$(\rho(1450)\pi)_{D-\text{wave}}$	seen	†
$\sigma\pi$	seen	–
$f_0(980)\pi$	not seen	179
$f_0(1370)\pi$	seen	†
$f_2(1270)\pi$	seen	†
$K\overline{K}^*(892)+$ c.c.	seen	†
$\pi\gamma$	seen	608

$f_2(1270)$ $I^G(J^{PC}) = 0^+(2^{++})$

Mass $m = 1275.5 \pm 0.8$ MeV
Full width $\Gamma = 186.7^{+2.2}_{-2.5}$ MeV (S = 1.4)

$f_2(1270)$ DECAY MODES	Fraction (Γ_i/Γ)	Scale factor/ Confidence level	p (MeV/c)
$\pi\pi$	(84.2 $^{+2.9}_{-0.9}$) %	S=1.1	623
$\pi^+\pi^-2\pi^0$	(7.7 $^{+1.1}_{-3.2}$) %	S=1.2	563
$K\overline{K}$	(4.6 $^{+0.5}_{-0.4}$) %	S=2.7	404
$2\pi^+2\pi^-$	(2.8 $\pm$0.4) %	S=1.2	560
$\eta\eta$	(4.0 $\pm$0.8) $\times 10^{-3}$	S=2.1	326
$4\pi^0$	(3.0 $\pm$1.0) $\times 10^{-3}$		565
$\gamma\gamma$	(1.42$\pm$0.24) $\times 10^{-5}$	S=1.4	638
$\eta\pi\pi$	$<$ 8 $\times 10^{-3}$	CL=95%	478
$K^0K^-\pi^+ +$ c.c.	$<$ 3.4 $\times 10^{-3}$	CL=95%	293
e^+e^-	$<$ 6 $\times 10^{-10}$	CL=90%	638

$f_1(1285)$ $I^G(J^{PC}) = 0^+(1^{++})$

Mass $m = 1281.9 \pm 0.5$ MeV (S = 1.8)
Full width $\Gamma = 22.7 \pm 1.1$ MeV (S = 1.5)

$f_1(1285)$ DECAY MODES	Fraction (Γ_i/Γ)	Scale factor/ Confidence level	p (MeV/c)
4π	(33.5 $^{+2.0}_{-1.8}$) %	S=1.3	568
$\pi^0\pi^0\pi^+\pi^-$	(22.3 $^{+1.3}_{-1.2}$) %	S=1.3	566
$2\pi^+2\pi^-$	(11.2 $^{+0.7}_{-0.6}$) %	S=1.3	563
$\rho^0\pi^+\pi^-$	(11.2 $^{+0.7}_{-0.6}$) %	S=1.3	336
$\rho^0\rho^0$	seen		†
$4\pi^0$	$<$ 7 $\times 10^{-4}$	CL=90%	568
$\eta\pi^+\pi^-$	(35 $\pm$15) %		479
$\eta\pi\pi$	(52.0 $^{+1.8}_{-2.1}$) %	S=1.2	482
$a_0(980)\pi$ [ignoring $a_0(980) \to K\overline{K}$]	(38 $\pm$ 4) %		238
$\eta\pi\pi$ [excluding $a_0(980)\pi$]	(14 $\pm$ 4) %		482
$K\overline{K}\pi$	(9.1 $\pm$ 0.4) %	S=1.1	308
$K\overline{K}^*(892)$	not seen		†
$\pi^+\pi^-\pi^0$	(3.0 $\pm$ 0.9) $\times 10^{-3}$		603
$\rho^\pm\pi^\mp$	$<$ 3.1 $\times 10^{-3}$	CL=95%	390
$\gamma\rho^0$	(5.3 $\pm$ 1.2) %	S=2.9	406
$\phi\gamma$	(7.5 $\pm$ 2.7) $\times 10^{-4}$		236

$\eta(1295)$ $I^G(J^{PC}) = 0^+(0^{-+})$

Mass $m = 1294 \pm 4$ MeV (S = 1.6)
Full width $\Gamma = 55 \pm 5$ MeV

$\eta(1295)$ DECAY MODES	Fraction (Γ_i/Γ)	p (MeV/c)
$\eta\pi^+\pi^-$	seen	487
$a_0(980)\pi$	seen	248
$\eta\pi^0\pi^0$	seen	490
$\eta(\pi\pi)_{S\text{-wave}}$	seen	–

$\pi(1300)$ $I^G(J^{PC}) = 1^-(0^{-+})$

Mass $m = 1300 \pm 100$ MeV [l]
Full width $\Gamma = 200$ to 600 MeV

$\pi(1300)$ DECAY MODES	Fraction (Γ_i/Γ)	p (MeV/c)
$\rho\pi$	seen	404
$\pi(\pi\pi)_{S\text{-wave}}$	seen	–

$a_2(1320)$ $I^G(J^{PC}) = 1^-(2^{++})$

Mass $m = 1318.3^{+0.5}_{-0.6}$ MeV (S = 1.2)
Full width $\Gamma = 107 \pm 5$ MeV [l]

$a_2(1320)$ DECAY MODES	Fraction (Γ_i/Γ)	Scale factor/ Confidence level	p (MeV/c)
3π	(70.1 $\pm$2.7) %	S=1.2	624
$\eta\pi$	(14.5 $\pm$1.2) %		535
$\omega\pi\pi$	(10.6 $\pm$3.2) %	S=1.3	366
$K\overline{K}$	(4.9 $\pm$0.8) %		437
$\eta'(958)\pi$	(5.5 $\pm$0.9) $\times 10^{-3}$		288
$\pi^\pm\gamma$	(2.91$\pm$0.27) $\times 10^{-3}$		652
$\gamma\gamma$	(9.4 $\pm$0.7) $\times 10^{-6}$		659
e^+e^-	$<$ 5 $\times 10^{-9}$	CL=90%	659

$f_0(1370)$ [j] $I^G(J^{PC}) = 0^+(0^{++})$

Mass $m = 1200$ to 1500 MeV
Full width $\Gamma = 200$ to 500 MeV

$f_0(1370)$ DECAY MODES	Fraction (Γ_i/Γ)	p (MeV/c)
$\pi\pi$	seen	672
4π	seen	617
$4\pi^0$	seen	617
$2\pi^+2\pi^-$	seen	612

Meson Summary Table

$\pi^+\pi^-2\pi^0$	seen	615
$\rho\rho$	dominant	†
$2(\pi\pi)_S$-wave	seen	–
$\pi(1300)\pi$	seen	†
$a_1(1260)\pi$	seen	35
$\eta\eta$	seen	411
$K\overline{K}$	seen	475
$K\overline{K}n\pi$	not seen	†
6π	not seen	508
$\omega\omega$	not seen	†
$\gamma\gamma$	seen	685
e^+e^-	not seen	685

$\pi_1(1400)$ [n]

$I^G(J^{PC}) = 1^-(1^{-+})$

Mass $m = 1354 \pm 25$ MeV (S = 1.8)
Full width $\Gamma = 330 \pm 35$ MeV

$\pi_1(1400)$ DECAY MODES	Fraction (Γ_i/Γ)	p (MeV/c)
$\eta\pi^0$	seen	557
$\eta\pi^-$	seen	556

$\eta(1405)$ [o]

$I^G(J^{PC}) = 0^+(0^{-+})$

Mass $m = 1408.8 \pm 1.8$ MeV [l] (S = 2.1)
Full width $\Gamma = 51.0 \pm 2.9$ MeV [l] (S = 1.8)

$\eta(1405)$ DECAY MODES	Fraction (Γ_i/Γ)	Confidence level	p (MeV/c)
$K\overline{K}\pi$	seen		424
$\eta\pi\pi$	seen		562
$a_0(980)\pi$	seen		345
$\eta(\pi\pi)_S$-wave	seen		–
$f_0(980)\pi^0 \to \pi^+\pi^-\pi^0$	not seen		–
$f_0(980)\eta$	seen		†
4π	seen		639
$\rho\rho$	<58 %	99.85%	†
$\rho^0\gamma$	seen		491
$K^*(892)K$	seen		123

$f_1(1420)$ [p]

$I^G(J^{PC}) = 0^+(1^{++})$

Mass $m = 1426.4 \pm 0.9$ MeV (S = 1.1)
Full width $\Gamma = 54.9 \pm 2.6$ MeV

$f_1(1420)$ DECAY MODES	Fraction (Γ_i/Γ)	p (MeV/c)
$K\overline{K}\pi$	dominant	438
$K\overline{K}^*(892)+$ c.c.	dominant	163
$\eta\pi\pi$	possibly seen	573
$\phi\gamma$	seen	349

$\omega(1420)$ [q]

$I^G(J^{PC}) = 0^-(1^{--})$

Mass m (1400–1450) MeV
Full width Γ (180–250) MeV

$\omega(1420)$ DECAY MODES	Fraction (Γ_i/Γ)	p (MeV/c)
$\rho\pi$	dominant	486
$\omega\pi\pi$	seen	444
$b_1(1235)\pi$	seen	125
e^+e^-	seen	710

$a_0(1450)$ [j]

$I^G(J^{PC}) = 1^-(0^{++})$

Mass $m = 1474 \pm 19$ MeV
Full width $\Gamma = 265 \pm 13$ MeV

$a_0(1450)$ DECAY MODES	Fraction (Γ_i/Γ)	p (MeV/c)
$\pi\eta$	0.093±0.020	627
$\pi\eta'(958)$	0.033±0.017	410
$K\overline{K}$	0.082±0.028	547
$\omega\pi\pi$	**DEFINED AS 1**	484
$a_0(980)\pi\pi$	seen	342
$\gamma\gamma$	seen	737

$\rho(1450)$ [r]

$I^G(J^{PC}) = 1^+(1^{--})$

Mass $m = 1465 \pm 25$ MeV [l]
Full width $\Gamma = 400 \pm 60$ MeV [l]

$\rho(1450)$ DECAY MODES	Fraction (Γ_i/Γ)	p (MeV/c)
$\pi\pi$	seen	720
$\pi^+\pi^-$	seen	719
4π	seen	669
e^+e^-	seen	732
$\eta\rho$	seen	311
$a_2(1320)\pi$	not seen	54
$K\overline{K}$	seen	541
K^+K^-	seen	541
$K\overline{K}^*(892)+$ c.c.	possibly seen	229
$\eta\gamma$	seen	630
$f_0(500)\gamma$	not seen	–
$f_0(980)\gamma$	not seen	398
$f_0(1370)\gamma$	not seen	92
$f_2(1270)\gamma$	not seen	177

$\eta(1475)$ [o]

$I^G(J^{PC}) = 0^+(0^{-+})$

Mass $m = 1476 \pm 4$ MeV (S = 1.3)
Full width $\Gamma = 85 \pm 9$ MeV (S = 1.5)

$\eta(1475)$ DECAY MODES	Fraction (Γ_i/Γ)	p (MeV/c)
$K\overline{K}\pi$	dominant	477
$K\overline{K}^*(892)+$ c.c.	seen	245
$a_0(980)\pi$	seen	396
$\gamma\gamma$	seen	738
$K^0_SK^0_S\eta$	possibly seen	†

$f_0(1500)$ [n]

$I^G(J^{PC}) = 0^+(0^{++})$

Mass $m = 1504 \pm 6$ MeV (S = 1.3)
Full width $\Gamma = 109 \pm 7$ MeV

$f_0(1500)$ DECAY MODES	Fraction (Γ_i/Γ)	Scale factor	p (MeV/c)
$\pi\pi$	(34.9±2.3) %	1.2	740
$\pi^+\pi^-$	seen		739
$2\pi^0$	seen		740
4π	(49.5±3.3) %	1.2	691
$4\pi^0$	seen		691
$2\pi^+2\pi^-$	seen		686
$2(\pi\pi)_S$-wave	seen		–
$\rho\rho$	seen		†
$\pi(1300)\pi$	seen		143
$a_1(1260)\pi$	seen		217
$\eta\eta$	(5.1±0.9) %	1.4	515
$\eta\eta'(958)$	(1.9±0.8) %	1.7	†
$K\overline{K}$	(8.6±1.0) %	1.1	568
$\gamma\gamma$	not seen		752

$f_2'(1525)$

$I^G(J^{PC}) = 0^+(2^{++})$

Mass $m = 1525 \pm 5$ MeV [l]
Full width $\Gamma = 73^{+6}_{-5}$ MeV [l]

$f_2'(1525)$ DECAY MODES	Fraction (Γ_i/Γ)	p (MeV/c)
$K\overline{K}$	(88.7 ±2.2) %	581
$\eta\eta$	(10.4 ±2.2) %	530
$\pi\pi$	(8.2 ±1.5) $\times 10^{-3}$	750
$\gamma\gamma$	(1.10±0.14) $\times 10^{-6}$	763

$\pi_1(1600)$ [n]

$I^G(J^{PC}) = 1^-(1^{-+})$

Mass $m = 1662^{+8}_{-9}$ MeV
Full width $\Gamma = 241 \pm 40$ MeV (S = 1.4)

$\pi_1(1600)$ DECAY MODES	Fraction (Γ_i/Γ)	p (MeV/c)
$\pi\pi\pi$	seen	803
$\rho^0\pi^-$	seen	641
$f_2(1270)\pi^-$	not seen	318
$b_1(1235)\pi$	seen	357
$\eta'(958)\pi^-$	seen	543
$f_1(1285)\pi$	seen	314

$\eta_2(1645)$

$I^G(J^{PC}) = 0^+(2^{-+})$

Mass $m = 1617 \pm 5$ MeV
Full width $\Gamma = 181 \pm 11$ MeV

$\eta_2(1645)$ DECAY MODES	Fraction (Γ_i/Γ)	p (MeV/c)
$a_2(1320)\pi$	seen	242
$K\overline{K}\pi$	seen	580
$K^*\overline{K}$	seen	404
$\eta\pi^+\pi^-$	seen	685
$a_0(980)\pi$	seen	499
$f_2(1270)\eta$	not seen	†

$\omega(1650)$ [s]

$I^G(J^{PC}) = 0^-(1^{--})$

Mass $m = 1670 \pm 30$ MeV
Full width $\Gamma = 315 \pm 35$ MeV

$\omega(1650)$ DECAY MODES	Fraction (Γ_i/Γ)	p (MeV/c)
$\rho\pi$	seen	647
$\omega\pi\pi$	seen	617
$\omega\eta$	seen	500
e^+e^-	seen	835

$\omega_3(1670)$

$I^G(J^{PC}) = 0^-(3^{--})$

Mass $m = 1667 \pm 4$ MeV
Full width $\Gamma = 168 \pm 10$ MeV [l]

$\omega_3(1670)$ DECAY MODES	Fraction (Γ_i/Γ)	p (MeV/c)
$\rho\pi$	seen	645
$\omega\pi\pi$	seen	615
$b_1(1235)\pi$	possibly seen	361

$\pi_2(1670)$

$I^G(J^{PC}) = 1^-(2^{-+})$

Mass $m = 1672.2 \pm 3.0$ MeV [l] (S = 1.4)
Full width $\Gamma = 260 \pm 9$ MeV [l] (S = 1.2)

$\pi_2(1670)$ DECAY MODES	Fraction (Γ_i/Γ)	Confidence level	p (MeV/c)
3π	(95.8±1.4) %		809
$f_2(1270)\pi$	(56.3±3.2) %		328
$\rho\pi$	(31 ±4) %		648
$\sigma\pi$	(10.9±3.4) %		–
$\pi(\pi\pi)_{S\text{-wave}}$	(8.7±3.4) %		–
$K\overline{K}^*(892)+$ c.c.	(4.2±1.4) %		455
$\omega\rho$	(2.7±1.1) %		304
$\pi^\pm\gamma$	(7.0±1.1) $\times 10^{-4}$		830
$\gamma\gamma$	< 2.8 $\times 10^{-7}$	90%	836
$\rho(1450)\pi$	< 3.6 $\times 10^{-3}$	97.7%	147
$b_1(1235)\pi$	< 1.9 $\times 10^{-3}$	97.7%	365
$f_1(1285)\pi$	possibly seen		323
$a_2(1320)\pi$	not seen		292

$\phi(1680)$

$I^G(J^{PC}) = 0^-(1^{--})$

Mass $m = 1680 \pm 20$ MeV [l]
Full width $\Gamma = 150 \pm 50$ MeV [l]

$\phi(1680)$ DECAY MODES	Fraction (Γ_i/Γ)	p (MeV/c)
$K\overline{K}^*(892)+$ c.c.	dominant	462
$K^0_S K\pi$	seen	621
$K\overline{K}$	seen	680
e^+e^-	seen	840
$\omega\pi\pi$	not seen	623
$K^+K^-\pi^+\pi^-$	seen	544
$\eta\phi$	seen	290
$\eta\gamma$	seen	751

$\rho_3(1690)$

$I^G(J^{PC}) = 1^+(3^{--})$

Mass $m = 1688.8 \pm 2.1$ MeV [l]
Full width $\Gamma = 161 \pm 10$ MeV [l] (S = 1.5)

$\rho_3(1690)$ DECAY MODES	Fraction (Γ_i/Γ)	Scale factor	p (MeV/c)
4π	(71.1 ± 1.9) %		790
$\pi^\pm\pi^+\pi^-\pi^0$	(67 ±22) %		787
$\omega\pi$	(16 ± 6) %		655
$\pi\pi$	(23.6 ± 1.3) %		834
$K\overline{K}\pi$	(3.8 ± 1.2) %		629
$K\overline{K}$	(1.58± 0.26) %	1.2	685
$\eta\pi^+\pi^-$	seen		727
$\rho(770)\eta$	seen		520
$\pi\pi\rho$	seen		633
Excluding 2ρ and $a_2(1320)\pi$.			
$a_2(1320)\pi$	seen		307
$\rho\rho$	seen		335

$\rho(1700)$ [r]

$I^G(J^{PC}) = 1^+(1^{--})$

Mass $m = 1720 \pm 20$ MeV [l] ($\eta\rho^0$ and $\pi^+\pi^-$ modes)
Full width $\Gamma = 250 \pm 100$ MeV [l] ($\eta\rho^0$ and $\pi^+\pi^-$ modes)

$\rho(1700)$ DECAY MODES	Fraction (Γ_i/Γ)	p (MeV/c)
$2(\pi^+\pi^-)$	large	803
$\rho\pi\pi$	dominant	653
$\rho^0\pi^+\pi^-$	large	651
$\rho^\pm\pi^\mp\pi^0$	large	652
$a_1(1260)\pi$	seen	404
$h_1(1170)\pi$	seen	447
$\pi(1300)\pi$	seen	349
$\rho\rho$	seen	372
$\pi^+\pi^-$	seen	849
$\pi\pi$	seen	849
$K\overline{K}^*(892)+$ c.c.	seen	496
$\eta\rho$	seen	545
$a_2(1320)\pi$	not seen	334
$K\overline{K}$	seen	704
e^+e^-	seen	860
$\pi^0\omega$	seen	674

$f_0(1710)$ [t]

$I^G(J^{PC}) = 0^+(0^{++})$

Mass $m = 1723^{+6}_{-5}$ MeV (S = 1.6)
Full width $\Gamma = 139 \pm 8$ MeV (S = 1.1)

$f_0(1710)$ DECAY MODES	Fraction (Γ_i/Γ)	p (MeV/c)
$K\overline{K}$	seen	706
$\eta\eta$	seen	665
$\pi\pi$	seen	851
$\omega\omega$	seen	360

Meson Summary Table

$\pi(1800)$ $I^G(J^{PC}) = 1^-(0^{-+})$

Mass $m = 1812 \pm 12$ MeV (S = 2.3)
Full width $\Gamma = 208 \pm 12$ MeV

$\pi(1800)$ DECAY MODES	Fraction (Γ_i/Γ)	p (MeV/c)
$\pi^+\pi^-\pi^-$	seen	879
$f_0(500)\pi^-$	seen	–
$f_0(980)\pi^-$	seen	625
$f_0(1370)\pi^-$	seen	368
$f_0(1500)\pi^-$	not seen	250
$\rho\pi^-$	not seen	732
$\eta\eta\pi^-$	seen	661
$a_0(980)\eta$	seen	473
$a_2(1320)\eta$	not seen	†
$f_2(1270)\pi$	not seen	442
$f_0(1370)\pi^-$	not seen	368
$f_0(1500)\pi^-$	seen	250
$\eta\eta'(958)\pi^-$	seen	375
$K_0^*(1430)K^-$	seen	†
$K^*(892)K^-$	not seen	570

$\phi_3(1850)$ $I^G(J^{PC}) = 0^-(3^{--})$

Mass $m = 1854 \pm 7$ MeV
Full width $\Gamma = 87^{+28}_{-23}$ MeV (S = 1.2)

$\phi_3(1850)$ DECAY MODES	Fraction (Γ_i/Γ)	p (MeV/c)
$K\overline{K}$	seen	785
$K\overline{K}^*(892)+$ c.c.	seen	602

$\pi_2(1880)$ $I^G(J^{PC}) = 1^-(2^{-+})$

Mass $m = 1895 \pm 16$ MeV
Full width $\Gamma = 235 \pm 34$ MeV

$f_2(1950)$ $I^G(J^{PC}) = 0^+(2^{++})$

Mass $m = 1944 \pm 12$ MeV (S = 1.5)
Full width $\Gamma = 472 \pm 18$ MeV

$f_2(1950)$ DECAY MODES	Fraction (Γ_i/Γ)	p (MeV/c)
$K^*(892)\overline{K}^*(892)$	seen	387
$\pi^+\pi^-$	seen	962
$\pi^0\pi^0$	seen	963
4π	seen	925
$\eta\eta$	seen	803
$K\overline{K}$	seen	837
$\gamma\gamma$	seen	972
$p\overline{p}$	seen	254

$f_2(2010)$ $I^G(J^{PC}) = 0^+(2^{++})$

Mass $m = 2011^{+60}_{-80}$ MeV
Full width $\Gamma = 202 \pm 60$ MeV

$f_2(2010)$ DECAY MODES	Fraction (Γ_i/Γ)	p (MeV/c)
$\phi\phi$	seen	†
$K\overline{K}$	seen	876

$a_4(2040)$ $I^G(J^{PC}) = 1^-(4^{++})$

Mass $m = 1995^{+10}_{-8}$ MeV (S = 1.1)
Full width $\Gamma = 257^{+25}_{-23}$ MeV (S = 1.3)

$a_4(2040)$ DECAY MODES	Fraction (Γ_i/Γ)	p (MeV/c)
$K\overline{K}$	seen	867
$\pi^+\pi^-\pi^0$	seen	973
$\rho\pi$	seen	841
$f_2(1270)\pi$	seen	579
$\omega\pi^-\pi^0$	seen	818
$\omega\rho$	seen	623
$\eta\pi$	seen	917
$\eta'(958)\pi$	seen	760

$f_4(2050)$ $I^G(J^{PC}) = 0^+(4^{++})$

Mass $m = 2018 \pm 11$ MeV (S = 2.1)
Full width $\Gamma = 237 \pm 18$ MeV (S = 1.9)

$f_4(2050)$ DECAY MODES	Fraction (Γ_i/Γ)	p (MeV/c)
$\omega\omega$	seen	637
$\pi\pi$	(17.0±1.5) %	1000
$K\overline{K}$	$(6.8^{+3.4}_{-1.8}) \times 10^{-3}$	880
$\eta\eta$	$(2.1 \pm 0.8) \times 10^{-3}$	848
$4\pi^0$	< 1.2 %	964
$a_2(1320)\pi$	seen	567

$\phi(2170)$ $I^G(J^{PC}) = 0^-(1^{--})$

Mass $m = 2188 \pm 10$ MeV (S = 1.8)
Full width $\Gamma = 83 \pm 12$ MeV

$\phi(2170)$ DECAY MODES	Fraction (Γ_i/Γ)	p (MeV/c)
e^+e^-	seen	1094
$\phi f_0(980)$	seen	433
$K^+K^-f_0(980) \rightarrow K^+K^-\pi^+\pi^-$	seen	–
$K^+K^-f_0(980) \rightarrow K^+K^-\pi^0\pi^0$	seen	–
$K^{*0}K^\pm\pi^\mp$	not seen	779
$K^*(892)^0\overline{K}^*(892)^0$	not seen	634

$f_2(2300)$ $I^G(J^{PC}) = 0^+(2^{++})$

Mass $m = 2297 \pm 28$ MeV
Full width $\Gamma = 149 \pm 40$ MeV

$f_2(2300)$ DECAY MODES	Fraction (Γ_i/Γ)	p (MeV/c)
$\phi\phi$	seen	529
$K\overline{K}$	seen	1037
$\gamma\gamma$	seen	1149

$f_2(2340)$ $I^G(J^{PC}) = 0^+(2^{++})$

Mass $m = 2345^{+50}_{-40}$ MeV
Full width $\Gamma = 322^{+70}_{-60}$ MeV

$f_2(2340)$ DECAY MODES	Fraction (Γ_i/Γ)	p (MeV/c)
$\phi\phi$	seen	580
$\eta\eta$	seen	1037

STRANGE MESONS ($S = \pm 1$, $C = B = 0$)

$K^+ = u\overline{s}$, $K^0 = d\overline{s}$, $\overline{K}^0 = \overline{d}s$, $K^- = \overline{u}s$, similarly for K^*'s

$K^\pm$ $I(J^P) = \frac{1}{2}(0^-)$

Mass $m = 493.677 \pm 0.016$ MeV [u] (S = 2.8)
Mean life $\tau = (1.2380 \pm 0.0020) \times 10^{-8}$ s (S = 1.8)
$c\tau = 3.711$ m

CPT violation parameters (Δ = rate difference/sum)

$\Delta(K^\pm \rightarrow \mu^\pm\nu_\mu) = (-0.27 \pm 0.21)\%$
$\Delta(K^\pm \rightarrow \pi^\pm\pi^0) = (0.4 \pm 0.6)\%$ [v]

CP violation parameters (Δ = rate difference/sum)

$\Delta(K^\pm \rightarrow \pi^\pm e^+e^-) = (-2.2 \pm 1.6) \times 10^{-2}$
$\Delta(K^\pm \rightarrow \pi^\pm\mu^+\mu^-) = 0.010 \pm 0.023$
$\Delta(K^\pm \rightarrow \pi^\pm\pi^0\gamma) = (0.0 \pm 1.2) \times 10^{-3}$

$\Delta(K^\pm \to \pi^\pm\pi^+\pi^-) = (0.04 \pm 0.06)\%$
$\Delta(K^\pm \to \pi^\pm\pi^0\pi^0) = (-0.02 \pm 0.28)\%$

T violation parameters

$K^+ \to \pi^0\mu^+\nu_\mu \quad P_T = (-1.7 \pm 2.5) \times 10^{-3}$
$K^+ \to \mu^+\nu_\mu\gamma \quad P_T = (-0.6 \pm 1.9) \times 10^{-2}$
$K^+ \to \pi^0\mu^+\nu_\mu \quad \mathrm{Im}(\xi) = -0.006 \pm 0.008$

Slope parameter g [x]

(See Particle Listings for quadratic coefficients and alternative parametrization related to $\pi\pi$ scattering)

$K^\pm \to \pi^\pm\pi^+\pi^- \; g = -0.21134 \pm 0.00017$
$(g_+ - g_-) \,/\, (g_+ + g_-) = (-1.5 \pm 2.2) \times 10^{-4}$
$K^\pm \to \pi^\pm\pi^0\pi^0 \; g = 0.626 \pm 0.007$
$(g_+ - g_-) \,/\, (g_+ + g_-) = (1.8 \pm 1.8) \times 10^{-4}$

$K^\pm$ decay form factors [a,y]

Assuming μ-e universality
$\lambda_+(K^+_{\mu3}) = \lambda_+(K^+_{e3}) = (2.97 \pm 0.05) \times 10^{-2}$
$\lambda_0(K^+_{\mu3}) = (1.95 \pm 0.12) \times 10^{-2}$

Not assuming μ-e universality
$\lambda_+(K^+_{e3}) = (2.98 \pm 0.05) \times 10^{-2}$
$\lambda_+(K^+_{\mu3}) = (2.96 \pm 0.17) \times 10^{-2}$
$\lambda_0(K^+_{\mu3}) = (1.96 \pm 0.13) \times 10^{-2}$

K_{e3} form factor quadratic fit
$\lambda'_+\,(K^\pm_{e3})$ linear coeff. $= (2.49 \pm 0.17) \times 10^{-2}$
$\lambda''_+(K^\pm_{e3})$ quadratic coeff. $= (0.19 \pm 0.09) \times 10^{-2}$

$K^+_{e3} \quad |f_S/f_+| = (-0.3^{+0.8}_{-0.7}) \times 10^{-2}$
$K^+_{e3} \quad |f_T/f_+| = (-1.2 \pm 2.3) \times 10^{-2}$
$K^+_{\mu3} \quad |f_S/f_+| = (0.2 \pm 0.6) \times 10^{-2}$
$K^+_{\mu3} \quad |f_T/f_+| = (-0.1 \pm 0.7) \times 10^{-2}$
$K^+ \to e^+\nu_e\gamma \quad |F_A + F_V| = 0.133 \pm 0.008 \quad (S = 1.3)$
$K^+ \to \mu^+\nu_\mu\gamma \quad |F_A + F_V| = 0.165 \pm 0.013$
$K^+ \to e^+\nu_e\gamma \quad |F_A - F_V| < 0.49, \mathrm{CL} = 90\%$
$K^+ \to \mu^+\nu_\mu\gamma \quad |F_A - F_V| = -0.21 \pm 0.06$

Charge radius

$\langle r \rangle = 0.560 \pm 0.031$ fm

Forward-backward asymmetry

$A_{FB}(K^\pm_{\pi\mu\mu}) = \frac{\Gamma(\cos(\theta_{K\mu})>0) - \Gamma(\cos(\theta_{K\mu})<0)}{\Gamma(\cos(\theta_{K\mu})>0) + \Gamma(\cos(\theta_{K\mu})<0)} < 2.3 \times 10^{-2}$, CL = 90%

K^- modes are charge conjugates of the modes below.

K^+ DECAY MODES	Fraction (Γ_i/Γ)	Scale factor/ Confidence level	p (MeV/c)
Leptonic and semileptonic modes			
$e^+\nu_e$	$(1.582 \pm 0.007) \times 10^{-5}$		247
$\mu^+\nu_\mu$	(63.56 ± 0.11) %	S=1.2	236
$\pi^0 e^+\nu_e$	(5.07 ± 0.04) %	S=2.1	228
Called K^+_{e3}.			
$\pi^0\mu^+\nu_\mu$	(3.352 ± 0.033) %	S=1.9	215
Called $K^+_{\mu3}$.			
$\pi^0\pi^0 e^+\nu_e$	$(2.55 \pm 0.04) \times 10^{-5}$	S=1.1	206
$\pi^+\pi^- e^+\nu_e$	$(4.247 \pm 0.024) \times 10^{-5}$		203
$\pi^+\pi^-\mu^+\nu_\mu$	$(1.4 \pm 0.9) \times 10^{-5}$		151
$\pi^0\pi^0\pi^0 e^+\nu_e$	$< 3.5 \times 10^{-6}$	CL=90%	135
Hadronic modes			
$\pi^+\pi^0$	(20.67 ± 0.08) %	S=1.2	205
$\pi^+\pi^0\pi^0$	(1.760 ± 0.023) %	S=1.1	133
$\pi^+\pi^+\pi^-$	(5.583 ± 0.024) %		125
Leptonic and semileptonic modes with photons			
$\mu^+\nu_\mu\gamma$	[z,aa] $(6.2 \pm 0.8) \times 10^{-3}$		236
$\mu^+\nu_\mu\gamma(\mathrm{SD}^+)$	[a,bb] $(1.33 \pm 0.22) \times 10^{-5}$		–
$\mu^+\nu_\mu\gamma(\mathrm{SD}^+\mathrm{INT})$	[a,bb] $< 2.7 \times 10^{-5}$	CL=90%	–
$\mu^+\nu_\mu\gamma(\mathrm{SD}^- + \mathrm{SD}^-\mathrm{INT})$	[a,bb] $< 2.6 \times 10^{-4}$	CL=90%	–
$e^+\nu_e\gamma$	$(9.4 \pm 0.4) \times 10^{-6}$		247
$\pi^0 e^+\nu_e\gamma$	[z,aa] $(2.56 \pm 0.16) \times 10^{-4}$		228
$\pi^0 e^+\nu_e\gamma(\mathrm{SD})$	[a,bb] $< 5.3 \times 10^{-5}$	CL=90%	228
$\pi^0\mu^+\nu_\mu\gamma$	[z,aa] $(1.25 \pm 0.25) \times 10^{-5}$		215
$\pi^0\pi^0 e^+\nu_e\gamma$	$< 5 \times 10^{-6}$	CL=90%	206
Hadronic modes with photons or $\ell\overline{\ell}$ pairs			
$\pi^+\pi^0\gamma(\mathrm{INT})$	$(-4.2 \pm 0.9) \times 10^{-6}$		–
$\pi^+\pi^0\gamma(\mathrm{DE})$	[z,cc] $(6.0 \pm 0.4) \times 10^{-6}$		205
$\pi^+\pi^0\pi^0\gamma$	[z,aa] $(7.6 \pm^{6.0}_{3.0}) \times 10^{-6}$		133
$\pi^+\pi^+\pi^-\gamma$	[z,aa] $(1.04 \pm 0.31) \times 10^{-4}$		125
$\pi^+\gamma\gamma$	[z] $(1.01 \pm 0.06) \times 10^{-6}$		227
$\pi^+ 3\gamma$	[z] $< 1.0 \times 10^{-4}$	CL=90%	227
$\pi^+ e^+ e^-\gamma$	$(1.19 \pm 0.13) \times 10^{-8}$		227
Leptonic modes with $\ell\overline{\ell}$ pairs			
$e^+\nu_e\nu\overline{\nu}$	$< 6 \times 10^{-5}$	CL=90%	247
$\mu^+\nu_\mu\nu\overline{\nu}$	$< 2.4 \times 10^{-6}$	CL=90%	236
$e^+\nu_e e^+ e^-$	$(2.48 \pm 0.20) \times 10^{-8}$		247
$\mu^+\nu_\mu e^+ e^-$	$(7.06 \pm 0.31) \times 10^{-8}$		236
$e^+\nu_e\mu^+\mu^-$	$(1.7 \pm 0.5) \times 10^{-8}$		223
$\mu^+\nu_\mu\mu^+\mu^-$	$< 4.1 \times 10^{-7}$	CL=90%	185
Lepton family number (LF), Lepton number (L), $\Delta S = \Delta Q$ (SQ) violating modes, or $\Delta S = 1$ weak neutral current ($S1$) modes			
$\pi^+\pi^+ e^-\overline{\nu}_e$	SQ $< 1.3 \times 10^{-8}$	CL=90%	203
$\pi^+\pi^+\mu^-\overline{\nu}_\mu$	SQ $< 3.0 \times 10^{-6}$	CL=95%	151
$\pi^+ e^+ e^-$	$S1$ $(3.00 \pm 0.09) \times 10^{-7}$		227
$\pi^+\mu^+\mu^-$	$S1$ $(9.4 \pm 0.6) \times 10^{-8}$	S=2.6	172
$\pi^+\nu\overline{\nu}$	$S1$ $(1.7 \pm 1.1) \times 10^{-10}$		227
$\pi^+\pi^0\nu\overline{\nu}$	$S1$ $< 4.3 \times 10^{-5}$	CL=90%	205
$\mu^-\nu e^+ e^+$	LF $< 2.1 \times 10^{-8}$	CL=90%	236
$\mu^+\nu_e$	LF [d] $< 4 \times 10^{-3}$	CL=90%	236
$\pi^+\mu^+ e^-$	LF $< 1.3 \times 10^{-11}$	CL=90%	214
$\pi^+\mu^- e^+$	LF $< 5.2 \times 10^{-10}$	CL=90%	214
$\pi^-\mu^+ e^+$	L $< 5.0 \times 10^{-10}$	CL=90%	214
$\pi^- e^+ e^+$	L $< 6.4 \times 10^{-10}$	CL=90%	227
$\pi^-\mu^+\mu^+$	L [d] $< 8.6 \times 10^{-11}$	CL=90%	172
$\mu^+\overline{\nu}_e$	L [d] $< 3.3 \times 10^{-3}$	CL=90%	236
$\pi^0 e^+\overline{\nu}_e$	L $< 3 \times 10^{-3}$	CL=90%	228
$\pi^+\gamma$	[dd] $< 2.3 \times 10^{-9}$	CL=90%	227

K^0

$I(J^P) = \frac{1}{2}(0^-)$

50% K_S, 50% K_L

Mass $m = 497.611 \pm 0.013$ MeV (S = 1.2)
$m_{K^0} - m_{K^\pm} = 3.934 \pm 0.020$ MeV (S = 1.6)

Mean square charge radius

$\langle r^2 \rangle = -0.077 \pm 0.010$ fm^2

T-violation parameters in K^0-$\overline{K}^0$ mixing [y]

Asymmetry A_T in K^0-$\overline{K}^0$ mixing $= (6.6 \pm 1.6) \times 10^{-3}$

CP-violation parameters

$\mathrm{Re}(\epsilon) = (1.596 \pm 0.013) \times 10^{-3}$

CPT-violation parameters [y]

Re $\delta = (2.5 \pm 2.3) \times 10^{-4}$
Im $\delta = (-1.5 \pm 1.6) \times 10^{-5}$
Re(y), K_{e3} parameter $= (0.4 \pm 2.5) \times 10^{-3}$
Re(x$_-$), K_{e3} parameter $= (-2.9 \pm 2.0) \times 10^{-3}$
$|m_{K^0} - m_{\overline{K}^0}| \,/\, m_{\mathrm{average}} < 6 \times 10^{-19}$, CL = 90% [ee]
$(\Gamma_{K^0} - \Gamma_{\overline{K}^0})/m_{\mathrm{average}} = (8 \pm 8) \times 10^{-18}$

Tests of $\Delta S = \Delta Q$

Re(x$_+$), K_{e3} parameter $= (-0.9 \pm 3.0) \times 10^{-3}$

K^0_S

$I(J^P) = \frac{1}{2}(0^-)$

Mean life $\tau = (0.8954 \pm 0.0004) \times 10^{-10}$ s (S = 1.1) Assuming CPT
Mean life $\tau = (0.89564 \pm 0.00033) \times 10^{-10}$ s Not assuming CPT
$c\tau = 2.6844$ cm Assuming CPT

CP-violation parameters [ff]

$\mathrm{Im}(\eta_{+-0}) = -0.002 \pm 0.009$
$\mathrm{Im}(\eta_{000}) = -0.001 \pm 0.016$
$|\eta_{000}| = |A(K^0_S \to 3\pi^0)/A(K^0_L \to 3\pi^0)| < 0.0088$, CL = 90%
CP asymmetry A in $\pi^+\pi^- e^+ e^- = (-0.4 \pm 0.8)\%$

Meson Summary Table

K^0_S DECAY MODES		Fraction (Γ_i/Γ)	Scale factor/ Confidence level	p (MeV/c)
Hadronic modes				
$\pi^0\pi^0$		(30.69 ± 0.05) %		209
$\pi^+\pi^-$		(69.20 ± 0.05) %		206
$\pi^+\pi^-\pi^0$		$(3.5 \ ^{+1.1}_{-0.9}) \times 10^{-7}$		133
Modes with photons or $\ell\overline{\ell}$ pairs				
$\pi^+\pi^-\gamma$	[aa,gg]	$(1.79 \pm 0.05) \times 10^{-3}$		206
$\pi^+\pi^- e^+ e^-$		$(4.79 \pm 0.15) \times 10^{-5}$		206
$\pi^0\gamma\gamma$	[gg]	$(4.9 \pm 1.8) \times 10^{-8}$		230
$\gamma\gamma$		$(2.63 \pm 0.17) \times 10^{-6}$	S=3.0	249
Semileptonic modes				
$\pi^\pm e^\mp \nu_e$	[hh]	$(7.04 \pm 0.08) \times 10^{-4}$		229
***CP* violating (*CP*) and $\Delta S = 1$ weak neutral current (*S1*) modes**				
$3\pi^0$	*CP*	$< 2.6 \times 10^{-8}$	CL=90%	139
$\mu^+\mu^-$	*S1*	$< 8 \times 10^{-10}$	CL=90%	225
$e^+ e^-$	*S1*	$< 9 \times 10^{-9}$	CL=90%	249
$\pi^0 e^+ e^-$	*S1* [gg]	$(3.0 \ ^{+1.5}_{-1.2}) \times 10^{-9}$		230
$\pi^0\mu^+\mu^-$	*S1*	$(2.9 \ ^{+1.5}_{-1.2}) \times 10^{-9}$		177

K^0_L

$I(J^P) = \frac{1}{2}(0^-)$

$m_{K_L} - m_{K_S}$
$= (0.5293 \pm 0.0009) \times 10^{10}\ \hbar\ \mathrm{s}^{-1}$ (S = 1.3) Assuming *CPT*
$= (3.484 \pm 0.006) \times 10^{-12}$ MeV Assuming *CPT*
$= (0.5289 \pm 0.0010) \times 10^{10}\ \hbar\ \mathrm{s}^{-1}$ Not assuming *CPT*

Mean life $\tau = (5.116 \pm 0.021) \times 10^{-8}$ s (S = 1.1)
$c\tau = 15.34$ m

Slope parameters [x]

(See Particle Listings for other linear and quadratic coefficients)
$K^0_L \to \pi^+\pi^-\pi^0$: $g = 0.678 \pm 0.008$ (S = 1.5)
$K^0_L \to \pi^+\pi^-\pi^0$: $h = 0.076 \pm 0.006$
$K^0_L \to \pi^+\pi^-\pi^0$: $k = 0.0099 \pm 0.0015$
$K^0_L \to \pi^0\pi^0\pi^0$: $h = (0.6 \pm 1.2) \times 10^{-3}$

K_L decay form factors [y]

Linear parametrization assuming μ-e universality
$\lambda_+(K^0_{\mu 3}) = \lambda_+(K^0_{e3}) = (2.82 \pm 0.04) \times 10^{-2}$ (S = 1.1)
$\lambda_0(K^0_{\mu 3}) = (1.38 \pm 0.18) \times 10^{-2}$ (S = 2.2)

Quadratic parametrization assuming μ-e universality
$\lambda'_+(K^0_{\mu 3}) = \lambda'_+(K^0_{e3}) = (2.40 \pm 0.12) \times 10^{-2}$ (S = 1.2)
$\lambda''_+(K^0_{\mu 3}) = \lambda''_+(K^0_{e3}) = (0.20 \pm 0.05) \times 10^{-2}$ (S = 1.2)
$\lambda_0(K^0_{\mu 3}) = (1.16 \pm 0.09) \times 10^{-2}$ (S = 1.2)

Pole parametrization assuming μ-e universality
$M^\mu_V\ (K^0_{\mu 3}) = M^e_V\ (K^0_{e3}) = 878 \pm 6$ MeV (S = 1.1)
$M^\mu_S\ (K^0_{\mu 3}) = 1252 \pm 90$ MeV (S = 2.6)

Dispersive parametrization assuming μ-e universality
$\Lambda_+ = (0.251 \pm 0.006) \times 10^{-1}$ (S = 1.5)
$\ln(C) = (1.75 \pm 0.18) \times 10^{-1}$ (S = 2.0)

K^0_{e3} $|f_S/f_+| = (1.5^{+1.4}_{-1.6}) \times 10^{-2}$
K^0_{e3} $|f_T/f_+| = (5^{+4}_{-5}) \times 10^{-2}$
$K^0_{\mu 3}$ $|f_T/f_+| = (12 \pm 12) \times 10^{-2}$
$K_L \to \ell^+\ell^-\gamma$, $K_L \to \ell^+\ell^-\ell'^+\ell'^-$: $\alpha_{K^*} = -0.205 \pm 0.022$ (S = 1.8)
$K^0_L \to \ell^+\ell^-\gamma$, $K^0_L \to \ell^+\ell^-\ell'^+\ell'^-$: $\alpha_{DIP} = -1.69 \pm 0.08$ (S = 1.7)
$K_L \to \pi^+\pi^- e^+ e^-$: $a_1/a_2 = -0.737 \pm 0.014$ GeV^2
$K_L \to \pi^0 2\gamma$: $a_V = -0.43 \pm 0.06$ (S = 1.5)

CP-violation parameters [ff]

$A_L = (0.332 \pm 0.006)\%$
$|\eta_{00}| = (2.220 \pm 0.011) \times 10^{-3}$ (S = 1.8)
$|\eta_{+-}| = (2.232 \pm 0.011) \times 10^{-3}$ (S = 1.8)
$|\epsilon| = (2.228 \pm 0.011) \times 10^{-3}$ (S = 1.8)
$|\eta_{00}/\eta_{+-}| = 0.9950 \pm 0.0007$ [ii] (S = 1.6)
$\mathrm{Re}(\epsilon'/\epsilon) = (1.66 \pm 0.23) \times 10^{-3}$ [ii] (S = 1.6)

Assuming *CPT*
$\phi_{+-} = (43.51 \pm 0.05)^\circ$ (S = 1.2)
$\phi_{00} = (43.52 \pm 0.05)^\circ$ (S = 1.3)
$\phi_\epsilon = \phi_{SW} = (43.52 \pm 0.05)^\circ$ (S = 1.2)
$\mathrm{Im}(\epsilon'/\epsilon) = -(\phi_{00} - \phi_{+-})/3 = (-0.002 \pm 0.005)^\circ$ (S = 1.7)

Not assuming *CPT*
$\phi_{+-} = (43.4 \pm 0.5)^\circ$ (S = 1.2)
$\phi_{00} = (43.7 \pm 0.6)^\circ$ (S = 1.2)
$\phi_\epsilon = (43.5 \pm 0.5)^\circ$ (S = 1.3)

CP asymmetry A in $K^0_L \to \pi^+\pi^- e^+ e^- = (13.7 \pm 1.5)\%$
β_{CP} from $K^0_L \to e^+ e^- e^+ e^- = -0.19 \pm 0.07$
γ_{CP} from $K^0_L \to e^+ e^- e^+ e^- = 0.01 \pm 0.11$ (S = 1.6)
j for $K^0_L \to \pi^+\pi^-\pi^0 = 0.0012 \pm 0.0008$
f for $K^0_L \to \pi^+\pi^-\pi^0 = 0.004 \pm 0.006$
$|\eta_{+-\gamma}| = (2.35 \pm 0.07) \times 10^{-3}$
$\phi_{+-\gamma} = (44 \pm 4)^\circ$
$|\epsilon'_{+-\gamma}|/\epsilon < 0.3$, CL = 90%
$|g_{E1}|$ for $K^0_L \to \pi^+\pi^-\gamma < 0.21$, CL = 90%

T-violation parameters

$\mathrm{Im}(\xi)$ in $K^0_{\mu 3} = -0.007 \pm 0.026$

CPT invariance tests

$\phi_{00} - \phi_{+-} = (0.34 \pm 0.32)^\circ$
$\mathrm{Re}(\frac{2}{3}\eta_{+-} + \frac{1}{3}\eta_{00}) - \frac{A_L}{2} = (-3 \pm 35) \times 10^{-6}$

$\Delta S = -\Delta Q$ in $K^0_{\ell 3}$ decay

Re $x = -0.002 \pm 0.006$
Im $x = 0.0012 \pm 0.0021$

K^0_L DECAY MODES		Fraction (Γ_i/Γ)	Scale factor/ Confidence level	p (MeV/c)
Semileptonic modes				
$\pi^\pm e^\mp \nu_e$ Called K^0_{e3}.	[hh]	(40.55 ±0.11) %	S=1.7	229
$\pi^\pm \mu^\mp \nu_\mu$ Called $K^0_{\mu 3}$.	[hh]	(27.04 ±0.07) %	S=1.1	216
$(\pi\mu\mathrm{atom})\nu$		$(1.05 \pm 0.11) \times 10^{-7}$		188
$\pi^0\pi^\pm e^\mp \nu$	[hh]	$(5.20 \pm 0.11) \times 10^{-5}$		207
$\pi^\pm e^\mp \nu\, e^+ e^-$	[hh]	$(1.26 \pm 0.04) \times 10^{-5}$		229
Hadronic modes, including Charge conjugation×Parity Violating (*CPV*) modes				
$3\pi^0$		(19.52 ±0.12) %	S=1.6	139
$\pi^+\pi^-\pi^0$		(12.54 ±0.05) %		133
$\pi^+\pi^-$	*CPV* [jj]	$(1.967 \pm 0.010) \times 10^{-3}$	S=1.5	206
$\pi^0\pi^0$	*CPV*	$(8.64 \pm 0.06) \times 10^{-4}$	S=1.8	209
Semileptonic modes with photons				
$\pi^\pm e^\mp \nu_e \gamma$	[aa,hh,kk]	$(3.79 \pm 0.06) \times 10^{-3}$		229
$\pi^\pm \mu^\mp \nu_\mu \gamma$		$(5.65 \pm 0.23) \times 10^{-4}$		216
Hadronic modes with photons or $\ell\overline{\ell}$ pairs				
$\pi^0\pi^0\gamma$		$< 2.43 \times 10^{-7}$	CL=90%	209
$\pi^+\pi^-\gamma$	[aa,kk]	$(4.15 \pm 0.15) \times 10^{-5}$	S=2.8	206
$\pi^+\pi^-\gamma$(DE)		$(2.84 \pm 0.11) \times 10^{-5}$	S=2.0	206
$\pi^0 2\gamma$	[kk]	$(1.273 \pm 0.033) \times 10^{-6}$		230
$\pi^0\gamma\, e^+ e^-$		$(1.62 \pm 0.17) \times 10^{-8}$		230
Other modes with photons or $\ell\overline{\ell}$ pairs				
2γ		$(5.47 \pm 0.04) \times 10^{-4}$	S=1.1	249
3γ		$< 7.4 \times 10^{-8}$	CL=90%	249
$e^+ e^-\gamma$		$(9.4 \pm 0.4) \times 10^{-6}$	S=2.0	249
$\mu^+\mu^-\gamma$		$(3.59 \pm 0.11) \times 10^{-7}$	S=1.3	225
$e^+ e^-\gamma\gamma$	[kk]	$(5.95 \pm 0.33) \times 10^{-7}$		249
$\mu^+\mu^-\gamma\gamma$	[kk]	$(1.0 \ ^{+0.8}_{-0.6}) \times 10^{-8}$		225

Charge conjugation × Parity (*CP*) or Lepton Family number (*LF*) violating modes, or $\Delta S = 1$ weak neutral current (*S1*) modes

$\mu^+\mu^-$	*S1*		(6.84 ±0.11) × 10^{-9}			225
e^+e^-	*S1*		(9 $^{+6}_{-4}$) × 10^{-12}			249
$\pi^+\pi^-e^+e^-$	*S1*	[*kk*]	(3.11 ±0.19) × 10^{-7}			206
$\pi^0\pi^0e^+e^-$	*S1*		< 6.6	× 10^{-9}	CL=90%	209
$\pi^0\pi^0\mu^+\mu^-$	*S1*		< 9.2	× 10^{-11}	CL=90%	57
$\mu^+\mu^-e^+e^-$	*S1*		(2.69 ±0.27) × 10^{-9}			225
$e^+e^-e^+e^-$	*S1*		(3.56 ±0.21) × 10^{-8}			249
$\pi^0\mu^+\mu^-$	*CP,S1*	[*ll*]	< 3.8	× 10^{-10}	CL=90%	177
$\pi^0e^+e^-$	*CP,S1*	[*ll*]	< 2.8	× 10^{-10}	CL=90%	230
$\pi^0\nu\overline{\nu}$	*CP,S1*	[*nn*]	< 2.6	× 10^{-8}	CL=90%	230
$\pi^0\pi^0\nu\overline{\nu}$	*S1*		< 8.1	× 10^{-7}	CL=90%	209
$e^\pm\mu^\mp$	*LF*	[*hh*]	< 4.7	× 10^{-12}	CL=90%	238
$e^\pm e^\pm\mu^\mp\mu^\mp$	*LF*	[*hh*]	< 4.12	× 10^{-11}	CL=90%	225
$\pi^0\mu^\pm e^\mp$	*LF*	[*hh*]	< 7.6	× 10^{-11}	CL=90%	217
$\pi^0\pi^0\mu^\pm e^\mp$	*LF*		< 1.7	× 10^{-10}	CL=90%	159

$K_0^*(700)$

$I(J^P) = \frac{1}{2}(0^+)$

Mass (T-Matrix Pole $\sqrt{s}$) = (630–730) − i (260–340) MeV
Mass (Breit-Wigner) = 824 ± 30 MeV
Full width (Breit-Wigner) = 478 ± 50 MeV

$K^*(892)$

$I(J^P) = \frac{1}{2}(1^-)$

$K^*(892)^\pm$ hadroproduced mass m = 891.76 ± 0.25 MeV
$K^*(892)^\pm$ in τ decays mass m = 895.5 ± 0.8 MeV
$K^*(892)^0$ mass m = 895.55 ± 0.20 MeV (S = 1.7)
$K^*(892)^\pm$ hadroproduced full width Γ = 50.3 ± 0.8 MeV
$K^*(892)^\pm$ in τ decays full width Γ = 46.2 ± 1.3 MeV
$K^*(892)^0$ full width Γ = 47.3 ± 0.5 MeV (S = 1.9)

$K^*(892)$ DECAY MODES	Fraction (Γ_i/Γ)	Confidence level	p (MeV/c)
$K\pi$	~ 100 %		290
$K^0\gamma$	(2.46±0.21) × 10^{-3}		307
$K^\pm\gamma$	(1.00±0.09) × 10^{-3}		309
$K\pi\pi$	< 7 × 10^{-4}	95%	223

$K_1(1270)$

$I(J^P) = \frac{1}{2}(1^+)$

Mass m = 1272 ± 7 MeV [*l*]
Full width Γ = 90 ± 20 MeV [*l*]

$K_1(1270)$ DECAY MODES	Fraction (Γ_i/Γ)	p (MeV/c)
$K\rho$	(42 ±6) %	46
$K_0^*(1430)\pi$	(28 ±4) %	†
$K^*(892)\pi$	(16 ±5) %	302
$K\omega$	(11.0±2.0) %	†
$Kf_0(1370)$	(3.0±2.0) %	†
γK^0	seen	539

$K_1(1400)$

$I(J^P) = \frac{1}{2}(1^+)$

Mass m = 1403 ± 7 MeV
Full width Γ = 174 ± 13 MeV (S = 1.6)

$K_1(1400)$ DECAY MODES	Fraction (Γ_i/Γ)	p (MeV/c)
$K^*(892)\pi$	(94 ±6) %	402
$K\rho$	(3.0±3.0) %	293
$Kf_0(1370)$	(2.0±2.0) %	†
$K\omega$	(1.0±1.0) %	284
$K_0^*(1430)\pi$	not seen	†
γK^0	seen	613

$K^*(1410)$

$I(J^P) = \frac{1}{2}(1^-)$

Mass m = 1421 ± 9 MeV
Full width Γ = 236 ± 18 MeV

$K^*(1410)$ DECAY MODES	Fraction (Γ_i/Γ)	Confidence level	p (MeV/c)
$K^*(892)\pi$	> 40 %	95%	416
$K\pi$	(6.6±1.3) %		617
$K\rho$	< 7 %	95%	313
γK^0	< 2.2 × 10^{-4}	90%	623

$K_0^*(1430)$ [*oo*]

$I(J^P) = \frac{1}{2}(0^+)$

Mass m = 1425 ± 50 MeV
Full width Γ = 270 ± 80 MeV

$K_0^*(1430)$ DECAY MODES	Fraction (Γ_i/Γ)	p (MeV/c)
$K\pi$	(93 ±10) %	619
$K\eta$	(8.6$^{+\ 2.7}_{-\ 3.4}$) %	486
$K\eta'(958)$	seen	†

$K_2^*(1430)$

$I(J^P) = \frac{1}{2}(2^+)$

$K_2^*(1430)^\pm$ mass m = 1425.6 ± 1.5 MeV (S = 1.1)
$K_2^*(1430)^0$ mass m = 1432.4 ± 1.3 MeV
$K_2^*(1430)^\pm$ full width Γ = 98.5 ± 2.7 MeV (S = 1.1)
$K_2^*(1430)^0$ full width Γ = 109 ± 5 MeV (S = 1.9)

$K_2^*(1430)$ DECAY MODES	Fraction (Γ_i/Γ)	Scale factor/ Confidence level	p (MeV/c)
$K\pi$	(49.9±1.2) %		619
$K^*(892)\pi$	(24.7±1.5) %		419
$K^*(892)\pi\pi$	(13.4±2.2) %		372
$K\rho$	(8.7±0.8) %	S=1.2	318
$K\omega$	(2.9±0.8) %		311
$K^+\gamma$	(2.4±0.5) × 10^{-3}	S=1.1	627
$K\eta$	(1.5$^{+3.4}_{-1.0}$) × 10^{-3}	S=1.3	486
$K\omega\pi$	< 7.2 × 10^{-4}	CL=95%	100
$K^0\gamma$	< 9 × 10^{-4}	CL=90%	626

$K^*(1680)$

$I(J^P) = \frac{1}{2}(1^-)$

Mass m = 1718 ± 18 MeV
Full width Γ = 322 ± 110 MeV (S = 4.2)

$K^*(1680)$ DECAY MODES	Fraction (Γ_i/Γ)	p (MeV/c)
$K\pi$	(38.7±2.5) %	782
$K\rho$	(31.4$^{+5.0}_{-2.1}$) %	571
$K^*(892)\pi$	(29.9$^{+2.2}_{-5.0}$) %	618
$K\phi$	seen	387

$K_2(1770)$ [*pp*]

$I(J^P) = \frac{1}{2}(2^-)$

Mass m = 1773 ± 8 MeV
Full width Γ = 186 ± 14 MeV

$K_2(1770)$ DECAY MODES	Fraction (Γ_i/Γ)	p (MeV/c)
$K\pi\pi$		794
$K_2^*(1430)\pi$	dominant	288
$K^*(892)\pi$	seen	654
$Kf_2(1270)$	seen	53
$K\phi$	seen	441
$K\omega$	seen	607

$K_3^*(1780)$

$I(J^P) = \frac{1}{2}(3^-)$

Mass m = 1776 ± 7 MeV (S = 1.1)
Full width Γ = 159 ± 21 MeV (S = 1.3)

Meson Summary Table

$K_3^*(1780)$ DECAY MODES	Fraction (Γ_i/Γ)	Confidence level	p (MeV/c)
$K\rho$	(31 ± 9) %		613
$K^*(892)\pi$	(20 ± 5) %		656
$K\pi$	(18.8± 1.0) %		813
$K\eta$	(30 ±13) %		719
$K_2^*(1430)\pi$	< 16 %	95%	291

$K_2(1820)$ [qq]

$I(J^P) = \frac{1}{2}(2^-)$

Mass $m = 1819 \pm 12$ MeV
Full width $\Gamma = 264 \pm 34$ MeV

$K_2(1820)$ DECAY MODES	Fraction (Γ_i/Γ)	p (MeV/c)
$K_2^*(1430)\pi$	seen	329
$K^*(892)\pi$	seen	683
$Kf_2(1270)$	seen	191
$K\omega$	seen	640
$K\phi$	seen	483

$K_4^*(2045)$

$I(J^P) = \frac{1}{2}(4^+)$

Mass $m = 2045 \pm 9$ MeV (S = 1.1)
Full width $\Gamma = 198 \pm 30$ MeV

$K_4^*(2045)$ DECAY MODES	Fraction (Γ_i/Γ)	p (MeV/c)
$K\pi$	(9.9±1.2) %	958
$K^*(892)\pi\pi$	(9 ±5) %	802
$K^*(892)\pi\pi\pi$	(7 ±5) %	768
$\rho K\pi$	(5.7±3.2) %	741
$\omega K\pi$	(5.0±3.0) %	738
$\phi K\pi$	(2.8±1.4) %	594
$\phi K^*(892)$	(1.4±0.7) %	363

CHARMED MESONS ($C = \pm 1$)

$D^+ = c\overline{d}$, $D^0 = c\overline{u}$, $\overline{D}^0 = \overline{c}u$, $D^- = \overline{c}d$, similarly for D^*'s

$D^\pm$

$I(J^P) = \frac{1}{2}(0^-)$

Mass $m = 1869.65 \pm 0.05$ MeV
Mean life $\tau = (1040 \pm 7) \times 10^{-15}$ s
$c\tau = 311.8\ \mu$m

c-quark decays

$\Gamma(c \to \ell^+ \text{anything})/\Gamma(c \to \text{anything}) = 0.096 \pm 0.004$ [rr]
$\Gamma(c \to D^*(2010)^+ \text{anything})/\Gamma(c \to \text{anything}) = 0.255 \pm 0.017$

CP-violation decay-rate asymmetries

$A_{CP}(\mu^\pm\nu) = (8 \pm 8)\%$
$A_{CP}(K^0_l e^\pm\nu) = (-0.6 \pm 1.6)\%$
$A_{CP}(K^0_S\pi^\pm) = (-0.41 \pm 0.09)\%$
$A_{CP}(K^\mp 2\pi^\pm) = (-0.18 \pm 0.16)\%$
$A_{CP}(K^\mp\pi^\pm\pi^\pm\pi^0) = (-0.3 \pm 0.7)\%$
$A_{CP}(K^0_S\pi^\pm\pi^0) = (-0.1 \pm 0.7)\%$
$A_{CP}(K^0_S\pi^\pm\pi^+\pi^-) = (0.0 \pm 1.2)\%$
$A_{CP}(\pi^\pm\pi^0) = (2.4 \pm 1.2)\%$
$A_{CP}(\pi^\pm\eta) = (1.0 \pm 1.5)\%$ (S = 1.4)
$A_{CP}(\pi^\pm\eta'(958)) = (-0.6 \pm 0.7)\%$
$A_{CP}(\overline{K}^0/K^0K^\pm) = (0.11 \pm 0.17)\%$
$A_{CP}(K^0_S K^\pm) = (-0.11 \pm 0.25)\%$
$A_{CP}(K^+K^-\pi^\pm) = (0.37 \pm 0.29)\%$
$A_{CP}(K^\pm K^{*0}) = (-0.3 \pm 0.4)\%$
$A_{CP}(\phi\pi^\pm) = (0.09 \pm 0.19)\%$ (S = 1.2)
$A_{CP}(K^\pm K_0^*(1430)^0) = (8^{+7}_{-6})\%$
$A_{CP}(K^\pm K_2^*(1430)^0) = (43^{+20}_{-26})\%$
$A_{CP}(K^\pm K_0^*(700)) = (-12^{+18}_{-13})\%$
$A_{CP}(a_0(1450)^0\pi^\pm) = (-19^{+14}_{-16})\%$
$A_{CP}(\phi(1680)\pi^\pm) = (-9 \pm 26)\%$
$A_{CP}(\pi^+\pi^-\pi^\pm) = (-2 \pm 4)\%$
$A_{CP}(K^0_S K^\pm\pi^+\pi^-) = (-4 \pm 7)\%$
$A_{CP}(K^\pm\pi^0) = (-4 \pm 11)\%$

χ^2 tests of CP-violation (CPV)

Local CPV in $D^\pm \to \pi^+\pi^-\pi^\pm = 78.1\%$
Local CPV in $D^\pm \to K^+K^-\pi^\pm = 31\%$

CP violating asymmetries of P-odd (T-odd) moments

$A_T(K^0_S K^\pm\pi^+\pi^-) = (-12 \pm 11) \times 10^{-3}$ [ss]

D^+ form factors

$f_+(0)|V_{cs}|$ in $\overline{K}^0\ell^+\nu_\ell = 0.719 \pm 0.011$ (S = 1.6)
$r_1 \equiv a_1/a_0$ in $\overline{K}^0\ell^+\nu_\ell = -2.13 \pm 0.14$
$r_2 \equiv a_2/a_0$ in $\overline{K}^0\ell^+\nu_\ell = -3 \pm 12$ (S = 1.5)
$f_+(0)|V_{cd}|$ in $\pi^0\ell^+\nu_\ell = 0.1407 \pm 0.0025$
$r_1 \equiv a_1/a_0$ in $\pi^0\ell^+\nu_\ell = -2.00 \pm 0.13$
$r_2 \equiv a_2/a_0$ in $\pi^0\ell^+\nu_\ell = -4 \pm 5$
$f_+(0)|V_{cd}|$ in $D^+ \to \eta e^+\nu_e = 0.086 \pm 0.006$
$r_1 \equiv a_1/a_0$ in $D^+ \to \eta e^+\nu_e = -1.8 \pm 2.2$
$r_v \equiv V(0)/A_1(0)$ in $D^+ \to \omega e^+\nu_e = 1.24 \pm 0.11$
$r_2 \equiv A_2(0)/A_1(0)$ in $D^+ \to \omega e^+\nu_e = 1.06 \pm 0.16$
$r_v \equiv V(0)/A_1(0)$ in $D^+, D^0 \to \rho e^+\nu_e = 1.48 \pm 0.16$
$r_2 \equiv A_2(0)/A_1(0)$ in $D^+, D^0 \to \rho e^+\nu_e = 0.83 \pm 0.12$
$r_v \equiv V(0)/A_1(0)$ in $\overline{K}^*(892)^0\ell^+\nu_\ell = 1.49 \pm 0.05$ (S = 2.1)
$r_2 \equiv A_2(0)/A_1(0)$ in $\overline{K}^*(892)^0\ell^+\nu_\ell = 0.802 \pm 0.021$
$r_3 \equiv A_3(0)/A_1(0)$ in $\overline{K}^*(892)^0\ell^+\nu_\ell = 0.0 \pm 0.4$
Γ_L/Γ_T in $\overline{K}^*(892)^0\ell^+\nu_\ell = 1.13 \pm 0.08$
Γ_+/Γ_- in $\overline{K}^*(892)^0\ell^+\nu_\ell = 0.22 \pm 0.06$ (S = 1.6)

Most decay modes (other than the semileptonic modes) that involve a neutral K meson are now given as K^0_S modes, not as $\overline{K}^0$ modes. Nearly always it is a K^0_S that is measured, and interference between Cabibbo-allowed and doubly Cabibbo-suppressed modes can invalidate the assumption that $2\,\Gamma(K^0_S) = \Gamma(\overline{K}^0)$.

D^+ DECAY MODES	Fraction (Γ_i/Γ)	Scale factor/ Confidence level	p (MeV/c)
Inclusive modes			
e^+ semileptonic	(16.07±0.30) %		–
μ^+ anything	(17.6 ±3.2) %		–
K^- anything	(25.7 ±1.4) %		–
$\overline{K}^0$ anything + K^0 anything	(61 ±5) %		–
K^+ anything	(5.9 ±0.8) %		–
$\overline{K}^*(892)^-$ anything	(6 ±5) %		–
$\overline{K}^*(892)^0$ anything	(23 ±5) %		–
$K^*(892)^0$ anything	< 6.6 %	CL=90%	–
η anything	(6.3 ±0.7) %		–
η' anything	(1.04±0.18) %		–
ϕ anything	(1.03±0.12) %		–
Leptonic and semileptonic modes			
$e^+\nu_e$	< 8.8 $\times 10^{-6}$	CL=90%	935
$\gamma e^+\nu_e$	< 3.0 $\times 10^{-5}$	CL=90%	935
$\mu^+\nu_\mu$	(3.74±0.17) $\times 10^{-4}$		932
$\tau^+\nu_\tau$	< 1.2 $\times 10^{-3}$	CL=90%	90
$\overline{K}^0 e^+\nu_e$	(8.73±0.10) %		869
$\overline{K}^0\mu^+\nu_\mu$	(8.74±0.19) %		865
$K^-\pi^+e^+\nu_e$	(3.89±0.13) %	S=2.1	864
$\overline{K}^*(892)^0 e^+\nu_e$, $\overline{K}^*(892)^0 \to K^-\pi^+$	(3.66±0.12) %		722
$(K^-\pi^+)_{[0.8\text{–}1.0]\text{GeV}}\, e^+\nu_e$	(3.39±0.09) %		864
$(K^-\pi^+)_{S-wave}\, e^+\nu_e$	(2.28±0.11) $\times 10^{-3}$		–
$\overline{K}^*(1410)^0 e^+\nu_e$, $\overline{K}^*(1410)^0 \to K^-\pi^+$	< 6 $\times 10^{-3}$	CL=90%	–
$\overline{K}_2^*(1430)^0 e^+\nu_e$, $\overline{K}_2^*(1430)^0 \to K^-\pi^+$	< 5 $\times 10^{-4}$	CL=90%	–
$K^-\pi^+e^+\nu_e$ nonresonant	< 7 $\times 10^{-3}$	CL=90%	864
$K^-\pi^+\mu^+\nu_\mu$	(3.65±0.34) %		851
$\overline{K}^*(892)^0\mu^+\nu_\mu$, $\overline{K}^*(892)^0 \to K^-\pi^+$	(3.52±0.10) %		717
$K^-\pi^+\mu^+\nu_\mu$ nonresonant	(1.9 ±0.5) $\times 10^{-3}$		851
$K^-\pi^+\pi^0\mu^+\nu_\mu$	< 1.5 $\times 10^{-3}$	CL=90%	825
$\pi^0 e^+\nu_e$	(3.72±0.17) $\times 10^{-3}$	S=2.0	930
$\eta e^+\nu_e$	(1.14±0.10) $\times 10^{-3}$		855
$\rho^0 e^+\nu_e$	($2.18^{+0.17}_{-0.25}$) $\times 10^{-3}$		774
$\rho^0\mu^+\nu_\mu$	(2.4 ±0.4) $\times 10^{-3}$		770

$\omega e^+ \nu_e$		$(1.69 \pm 0.11) \times 10^{-3}$			771
$\eta'(958) e^+ \nu_e$		$(2.2 \pm 0.5) \times 10^{-4}$			690
$\phi e^+ \nu_e$		$< 1.3 \times 10^{-5}$	CL=90%		657
$D^0 e^+ \nu_e$		$< 1.0 \times 10^{-4}$	CL=90%		5
Fractions of some of the following modes with resonances have already appeared above as submodes of particular charged-particle modes.					
$\overline{K}^*(892)^0 e^+ \nu_e$		(5.40 ± 0.10) %		S=1.1	722
$\overline{K}^*(892)^0 \mu^+ \nu_\mu$		(5.25 ± 0.15) %			717
$\overline{K}_0^*(1430)^0 \mu^+ \nu_\mu$		$< 2.3 \times 10^{-4}$	CL=90%		380
$\overline{K}^*(1680)^0 \mu^+ \nu_\mu$		$< 1.5 \times 10^{-3}$	CL=90%		105
Hadronic modes with a $\overline{K}$ or $\overline{K}K\overline{K}$					
$K_S^0 \pi^+$		(1.47 ± 0.08) %		S=3.0	863
$K_L^0 \pi^+$		(1.46 ± 0.05) %			863
$K^- 2\pi^+$	$[tt]$	(8.98 ± 0.28) %		S=2.2	846
$(K^-\pi^+)_{S-\text{wave}}\pi^+$		(7.20 ± 0.25) %			846
$\overline{K}_0^*(1430)^0 \pi^+$, $\overline{K}_0^*(1430)^0 \to K^-\pi^+$	$[uu]$	(1.19 ± 0.07) %			382
$\overline{K}^*(892)^0 \pi^+$, $\overline{K}^*(892)^0 \to K^-\pi^+$		$(10.0 \pm 1.1) \times 10^{-3}$			714
$\overline{K}^*(1410)^0 \pi^+$, $\overline{K}^{*0} \to K^-\pi^+$		not seen			381
$\overline{K}_2^*(1430)^0 \pi^+$, $\overline{K}_2^*(1430)^0 \to K^-\pi^+$	$[uu]$	$(2.2 \pm 0.7) \times 10^{-4}$			371
$\overline{K}^*(1680)^0 \pi^+$, $\overline{K}^*(1680)^0 \to K^-\pi^+$	$[uu]$	$(2.1 \pm 1.0) \times 10^{-4}$			58
$K^-(2\pi^+)_{I=2}$		(1.39 ± 0.26) %			–
$K_S^0 \pi^+ \pi^0$	$[tt]$	(7.05 ± 0.27) %			845
$K_S^0 \rho^+$		(5.9 ± 0.6) %			677
$K_S^0 \rho(1450)^+$, $\rho^+ \to \pi^+\pi^0$		$(1.5 \pm 1.1) \times 10^{-3}$			–
$\overline{K}^*(892)^0 \pi^+$, $\overline{K}^*(892)^0 \to K_S^0 \pi^0$		$(2.52 \pm 0.31) \times 10^{-3}$			714
$\overline{K}_0^*(1430)^0 \pi^+$, $\overline{K}_0^{*0} \to K_S^0 \pi^0$		$(2.6 \pm 0.9) \times 10^{-3}$			–
$\overline{K}_0^*(1680)^0 \pi^+$, $\overline{K}_0^{*0} \to K_S^0 \pi^0$		$(9 \pm 9) \times 10^{-4}$			–
$\overline{\kappa}^0 \pi^+$, $\overline{\kappa}^0 \to K_S^0 \pi^0$		$(5.4 \pm 3.5) \times 10^{-3}$			–
$K_S^0 \pi^+ \pi^0$ nonresonant		$(3 \pm 4) \times 10^{-3}$			845
$K_S^0 \pi^+ \pi^0$ nonresonant and $\overline{\kappa}^0 \pi^+$		$(1.31 \pm 0.21) \%$			–
$(K_S^0 \pi^0)_{S-\text{wave}} \pi^+$		$(1.22 \pm 0.26) \%$			845
$K^- 2\pi^+ \pi^0$	$[vv]$	(5.98 ± 0.23) %			816
$K_S^0 2\pi^+ \pi^-$	$[vv]$	(2.97 ± 0.11) %			814
$K^- 3\pi^+ \pi^-$	$[tt]$	$(5.5 \pm 0.5) \times 10^{-3}$		S=1.1	772
$\overline{K}^*(892)^0 2\pi^+\pi^-$, $\overline{K}^*(892)^0 \to K^-\pi^+$		$(1.2 \pm 0.4) \times 10^{-3}$			645
$\overline{K}^*(892)^0 \rho^0 \pi^+$, $\overline{K}^*(892)^0 \to K^-\pi^+$		$(2.2 \pm 0.4) \times 10^{-3}$			239
$\overline{K}^*(892)^0 a_1(1260)^+$	$[xx]$	$(8.9 \pm 1.8) \times 10^{-3}$			†
$K^- \rho^0 2\pi^+$		$(1.65 \pm 0.27) \times 10^{-3}$			524
$K^- 3\pi^+ \pi^-$ nonresonant		$(3.9 \pm 2.8) \times 10^{-4}$			772
$K^+ 2K_S^0$		$(2.54 \pm 0.13) \times 10^{-3}$			545
$K^+ K^- K_S^0 \pi^+$		$(2.3 \pm 0.5) \times 10^{-4}$			436
Pionic modes					
$\pi^+ \pi^0$		$(1.17 \pm 0.06) \times 10^{-3}$			925
$2\pi^+ \pi^-$		$(3.13 \pm 0.19) \times 10^{-3}$			909
$\rho^0 \pi^+$		$(8.0 \pm 1.4) \times 10^{-4}$			767
$\pi^+(\pi^+\pi^-)_{S-\text{wave}}$		$(1.75 \pm 0.16) \times 10^{-3}$			909
$\sigma \pi^+$, $\sigma \to \pi^+\pi^-$		$(1.32 \pm 0.12) \times 10^{-3}$			–
$f_0(980) \pi^+$, $f_0(980) \to \pi^+\pi^-$		$(1.50 \pm 0.32) \times 10^{-4}$			669
$f_0(1370) \pi^+$, $f_0(1370) \to \pi^+\pi^-$		$(8 \pm 4) \times 10^{-5}$			–
$f_2(1270) \pi^+$, $f_2(1270) \to \pi^+\pi^-$		$(4.8 \pm 0.8) \times 10^{-4}$			485
$\rho(1450)^0 \pi^+$, $\rho(1450)^0 \to \pi^+\pi^-$		$< 8 \times 10^{-5}$	CL=95%		338
$f_0(1500) \pi^+$, $f_0(1500) \to \pi^+\pi^-$		$(1.1 \pm 0.4) \times 10^{-4}$			–
$f_0(1710) \pi^+$, $f_0(1710) \to \pi^+\pi^-$		$< 5 \times 10^{-5}$	CL=95%		–
$f_0(1790) \pi^+$, $f_0(1790) \to \pi^+\pi^-$		$< 6 \times 10^{-5}$	CL=95%		–
$(\pi^+\pi^+)_{S-\text{wave}}\pi^-$		$< 1.2 \times 10^{-4}$	CL=95%		909
$2\pi^+\pi^-$ nonresonant		$< 1.1 \times 10^{-4}$	CL=95%		909
$\pi^+ 2\pi^0$		$(4.5 \pm 0.4) \times 10^{-3}$			910
$2\pi^+\pi^-\pi^0$		(1.11 ± 0.08) %			883
$3\pi^+ 2\pi^-$		$(1.59 \pm 0.16) \times 10^{-3}$		S=1.1	845
$\eta\pi^+$		$(3.33 \pm 0.21) \times 10^{-3}$		S=1.4	848
$\eta\pi^+\pi^0$		$(1.38 \pm 0.35) \times 10^{-3}$			831
$\omega\pi^+$		$(2.8 \pm 0.6) \times 10^{-4}$			764
$\eta'(958)\pi^+$		$(4.60 \pm 0.31) \times 10^{-3}$			681
$\eta'(958)\pi^+\pi^0$		$(1.6 \pm 0.5) \times 10^{-3}$			654
Hadronic modes with a $K\overline{K}$ pair					
$K^+ K_S^0$		$(2.83 \pm 0.16) \times 10^{-3}$		S=2.8	793
$K^+ K^-\pi^+$	$[tt]$	$(9.51 \pm 0.34) \times 10^{-3}$		S=1.6	744
$\phi\pi^+$, $\phi \to K^+K^-$		$(2.64 \pm 0.11) \times 10^{-3}$			647
$K^+\overline{K}^*(892)^0$, $\overline{K}^*(892)^0 \to K^-\pi^+$		$(2.44^{+0.11}_{-0.15}) \times 10^{-3}$			613
$K^+\overline{K}_0^*(1430)^0$, $\overline{K}_0^*(1430)^0 \to K^-\pi^+$		$(1.79 \pm 0.34) \times 10^{-3}$			–
$K^+\overline{K}_2^*(1430)^0$, $\overline{K}_2^* \to K^-\pi^+$		$(1.6^{+1.2}_{-0.8}) \times 10^{-4}$			–
$K^+\overline{K}_0^*(700)$, $\overline{K}_0^* \to K^-\pi^+$		$(6.7^{+3.4}_{-2.1}) \times 10^{-4}$			–
$a_0(1450)^0\pi^+$, $a_0^0 \to K^+K^-$		$(4.4^{+7.0}_{-1.8}) \times 10^{-4}$			–
$\phi(1680)\pi^+$, $\phi \to K^+K^-$		$(4.9^{+4.0}_{-1.9}) \times 10^{-5}$			–
$K_S^0 K_S^0 \pi^+$		$(2.70 \pm 0.13) \times 10^{-3}$			741
$K^+ K_S^0 \pi^+\pi^-$		$(1.67 \pm 0.18) \times 10^{-3}$			678
$K_S^0 K^- 2\pi^+$		$(2.28 \pm 0.18) \times 10^{-3}$			678
$K^+ K^- 2\pi^+\pi^-$		$(2.2 \pm 1.2) \times 10^{-4}$			601
A few poorly measured branching fractions:					
$\phi\pi^+\pi^0$		(2.3 ± 1.0) %			619
$\phi\rho^+$		< 1.4 %		CL=90%	260
$K^+K^-\pi^+\pi^0$ non-ϕ		$(1.5^{+0.7}_{-0.6})$ %			682
$K^*(892)^+ K_S^0$		(1.6 ± 0.7) %			611
Doubly Cabibbo-suppressed modes					
$K^+\pi^0$		$(1.81 \pm 0.27) \times 10^{-4}$		S=1.4	864
$K^+\eta$		$(1.02 \pm 0.16) \times 10^{-4}$			776
$K^+\eta'(958)$		$(1.73 \pm 0.22) \times 10^{-4}$			571
$K^+\pi^+\pi^-$		$(5.19 \pm 0.26) \times 10^{-4}$			846
$K^+\rho^0$		$(2.0 \pm 0.5) \times 10^{-4}$			679
$K^*(892)^0\pi^+$, $K^*(892)^0 \to K^+\pi^-$		$(2.4 \pm 0.4) \times 10^{-4}$			714
$K^+ f_0(980)$, $f_0(980) \to \pi^+\pi^-$		$(4.6 \pm 2.8) \times 10^{-5}$			–
$K_2^*(1430)^0\pi^+$, $K_2^*(1430)^0 \to K^+\pi^-$		$(4.2 \pm 2.8) \times 10^{-5}$			–
$K^+\pi^+\pi^-$ nonresonant		not seen			846
$2K^+K^-$		$(8.5 \pm 2.0) \times 10^{-5}$			550
$\Delta C = 1$ weak neutral current ($C1$) modes, or Lepton Family number (LF) or Lepton number (L) violating modes					
$\pi^+ e^+ e^-$	$C1$	$< 1.1 \times 10^{-6}$		CL=90%	930
$\pi^+\phi$, $\phi \to e^+e^-$	$[yy]$	$(1.7^{+1.4}_{-0.9}) \times 10^{-6}$			–
$\pi^+\mu^+\mu^-$	$C1$	$< 7.3 \times 10^{-8}$		CL=90%	918
$\pi^+\phi$, $\phi \to \mu^+\mu^-$	$[yy]$	$(1.8 \pm 0.8) \times 10^{-6}$			–
$\rho^+\mu^+\mu^-$	$C1$	$< 5.6 \times 10^{-4}$		CL=90%	757
$K^+ e^+ e^-$	$[zz]$	$< 1.0 \times 10^{-6}$		CL=90%	870
$K^+\mu^+\mu^-$	$[zz]$	$< 4.3 \times 10^{-6}$		CL=90%	856
$\pi^+ e^+ \mu^-$	LF	$< 2.9 \times 10^{-6}$		CL=90%	927
$\pi^+ e^- \mu^+$	LF	$< 3.6 \times 10^{-6}$		CL=90%	927
$K^+ e^+ \mu^-$	LF	$< 1.2 \times 10^{-6}$		CL=90%	866
$K^+ e^- \mu^+$	LF	$< 2.8 \times 10^{-6}$		CL=90%	866
$\pi^- 2e^+$	L	$< 1.1 \times 10^{-6}$		CL=90%	930
$\pi^- 2\mu^+$	L	$< 2.2 \times 10^{-8}$		CL=90%	918
$\pi^- e^+ \mu^+$	L	$< 2.0 \times 10^{-6}$		CL=90%	927
$\rho^- 2\mu^+$	L	$< 5.6 \times 10^{-4}$		CL=90%	757
$K^- 2e^+$	L	$< 9 \times 10^{-7}$		CL=90%	870
$K^- 2\mu^+$	L	$< 1.0 \times 10^{-5}$		CL=90%	856
$K^- e^+ \mu^+$	L	$< 1.9 \times 10^{-6}$		CL=90%	866
$K^*(892)^- 2\mu^+$	L	$< 8.5 \times 10^{-4}$		CL=90%	703

Meson Summary Table

D^0

$I(J^P) = \frac{1}{2}(0^-)$

Mass $m = 1864.83 \pm 0.05$ MeV
$m_{D^\pm} - m_{D^0} = 4.822 \pm 0.015$ MeV
Mean life $\tau = (410.1 \pm 1.5) \times 10^{-15}$ s
$c\tau = 122.9\ \mu$m

Mixing and related parameters

$|m_{D_1^0} - m_{D_2^0}| = (0.95^{+0.41}_{-0.44}) \times 10^{10}\ \hbar\ \mathrm{s}^{-1}$
$(\Gamma_{D_1^0} - \Gamma_{D_2^0})/\Gamma = 2y = (1.29^{+0.14}_{-0.18}) \times 10^{-2}$
$|q/p| = 0.92^{+0.12}_{-0.09}$
$A_\Gamma = (-0.125 \pm 0.526) \times 10^{-3}$
$K^+\pi^-$ relative strong phase: $\cos\delta = 0.97 \pm 0.11$
$K^-\pi^+\pi^0$ coherence factor $R_{K\pi\pi^0} = 0.82 \pm 0.06$
$K^-\pi^+\pi^0$ average relative strong phase $\delta^{K\pi\pi^0} = (199 \pm 14)^\circ$
$K^-\pi^-2\pi^+$ coherence factor $R_{K3\pi} = 0.53^{+0.18}_{-0.21}$
$K^-\pi^-2\pi^+$ average relative strong phase $\delta^{K3\pi} = (125^{+22}_{-14})^\circ$
$D^0 \to K^-\pi^-2\pi^+$, $R_{K3\pi}$ (y $\cos\delta^{K3\pi}$ − x $\sin\delta^{K3\pi}$) $= (-3.0 \pm 0.7) \times 10^{-3}$ TeV^{-1}
$K^0_S K^+\pi^-$ coherence factor $R_{K^0_S K\pi} = 0.70 \pm 0.08$
$K^0_S K^+\pi^-$ average relative strong phase $\delta^{K^0_S K\pi} = (0 \pm 16)^\circ$
K^*K coherence factor $R_{K^*K} = 0.94 \pm 0.12$
K^*K average relative strong phase $\delta^{K^*K} = (-17 \pm 18)^\circ$

CP-violation decay-rate asymmetries (labeled by the D^0 decay)

$A_{CP}(K^+K^-) = (-0.07 \pm 0.11)\%$
$A_{CP}(2K^0_S) = (-0.4 \pm 1.5)\%$
$A_{CP}(\pi^+\pi^-) = (0.13 \pm 0.14)\%$
$A_{CP}(\pi^0\pi^0) = (0.0 \pm 0.6)\%$
$A_{CP}(\rho\gamma) = (6 \pm 15) \times 10^{-2}$
$A_{CP}(\phi\gamma) = (-9 \pm 7) \times 10^{-2}$
$A_{CP}(\overline{K}^*(892)^0\gamma) = (-0.3 \pm 2.0) \times 10^{-2}$
$A_{CP}(\pi^+\pi^-\pi^0) = (0.3 \pm 0.4)\%$
$A_{CP}(\rho(770)^+\pi^- \to \pi^+\pi^-\pi^0) = (1.2 \pm 0.9)\%$ [aaa]
$A_{CP}(\rho(770)^0\pi^0 \to \pi^+\pi^-\pi^0) = (-3.1 \pm 3.0)\%$ [aaa]
$A_{CP}(\rho(770)^-\pi^+ \to \pi^+\pi^-\pi^0) = (-1.0 \pm 1.7)\%$ [aaa]
$A_{CP}(\rho(1450)^+\pi^- \to \pi^+\pi^-\pi^0) = (0 \pm 70)\%$ [aaa]
$A_{CP}(\rho(1450)^0\pi^0 \to \pi^+\pi^-\pi^0) = (-20 \pm 40)\%$ [aaa]
$A_{CP}(\rho(1450)^-\pi^+ \to \pi^+\pi^-\pi^0) = (6 \pm 9)\%$ [aaa]
$A_{CP}(\rho(1700)^+\pi^- \to \pi^+\pi^-\pi^0) = (-5 \pm 14)\%$ [aaa]
$A_{CP}(\rho(1700)^0\pi^0 \to \pi^+\pi^-\pi^0) = (13 \pm 9)\%$ [aaa]
$A_{CP}(\rho(1700)^-\pi^+ \to \pi^+\pi^-\pi^0) = (8 \pm 11)\%$ [aaa]
$A_{CP}(f_0(980)\pi^0 \to \pi^+\pi^-\pi^0) = (0 \pm 35)\%$ [aaa]
$A_{CP}(f_0(1370)\pi^0 \to \pi^+\pi^-\pi^0) = (25 \pm 18)\%$ [aaa]
$A_{CP}(f_0(1500)\pi^0 \to \pi^+\pi^-\pi^0) = (0 \pm 18)\%$ [aaa]
$A_{CP}(f_0(1710)\pi^0 \to \pi^+\pi^-\pi^0) = (0 \pm 24)\%$ [aaa]
$A_{CP}(f_2(1270)\pi^0 \to \pi^+\pi^-\pi^0) = (-4 \pm 6)\%$ [aaa]
$A_{CP}(\sigma(400)\pi^0 \to \pi^+\pi^-\pi^0) = (6 \pm 8)\%$ [aaa]
$A_{CP}(\text{nonresonant}\ \pi^+\pi^-\pi^0) = (-13 \pm 23)\%$ [aaa]
$A_{CP}(a_1(1260)^+\pi^- \to 2\pi^+2\pi^-) = (5 \pm 6)\%$
$A_{CP}(a_1(1260)^-\pi^+ \to 2\pi^+2\pi^-) = (14 \pm 18)\%$
$A_{CP}(\pi(1300)^+\pi^- \to 2\pi^+2\pi^-) = (-2 \pm 15)\%$
$A_{CP}(\pi(1300)^-\pi^+ \to 2\pi^+2\pi^-) = (-6 \pm 30)\%$
$A_{CP}(a_1(1640)^+\pi^- \to 2\pi^+2\pi^-) = (9 \pm 26)\%$
$A_{CP}(\pi_2(1670)^+\pi^- \to 2\pi^+2\pi^-) = (7 \pm 18)\%$
$A_{CP}(\sigma f_0(1370) \to 2\pi^+2\pi^-) = (-15 \pm 19)\%$
$A_{CP}(\sigma\rho(770)^0 \to 2\pi^+2\pi^-) = (3 \pm 27)\%$
$A_{CP}(2\rho(770)^0 \to 2\pi^+2\pi^-) = (-6 \pm 6)\%$
$A_{CP}(2f_2(1270) \to 2\pi^+2\pi^-) = (-28 \pm 24)\%$
$A_{CP}(K^+K^-\pi^0) = (-1.0 \pm 1.7)\%$
$A_{CP}(K^*(892)^+K^- \to K^+K^-\pi^0) = (-0.9 \pm 1.3)\%$ [aaa]
$A_{CP}(K^*(1410)^+K^- \to K^+K^-\pi^0) = (-21 \pm 24)\%$ [aaa]
$A_{CP}((K^+\pi^0)_{S-wave}K^- \to K^+K^-\pi^0) = (7 \pm 15)\%$ [aaa]
$A_{CP}(\phi(1020)\pi^0 \to K^+K^-\pi^0) = (1.1 \pm 2.2)\%$ [aaa]
$A_{CP}(f_0(980)\pi^0 \to K^+K^-\pi^0) = (-3 \pm 19)\%$ [aaa]
$A_{CP}(a_0(980)^0\pi^0 \to K^+K^-\pi^0) = (-5 \pm 16)\%$ [aaa]
$A_{CP}(f_2'(1525)\pi^0 \to K^+K^-\pi^0) = (0 \pm 160)\%$ [aaa]
$A_{CP}(K^*(892)^-K^+ \to K^+K^-\pi^0) = (-5 \pm 4)\%$ [aaa]
$A_{CP}(K^*(1410)^-K^+ \to K^+K^-\pi^0) = (-17 \pm 29)\%$ [aaa]
$A_{CP}((K^-\pi^0)_{S-wave}K^+ \to K^+K^-\pi^0) = (-10 \pm 40)\%$ [aaa]
$A_{CP}(K^0_S\pi^0) = (-0.20 \pm 0.17)\%$
$A_{CP}(K^0_S\eta) = (0.5 \pm 0.5)\%$
$A_{CP}(K^0_S\eta') = (1.0 \pm 0.7)\%$
$A_{CP}(K^0_S\phi) = (-3 \pm 9)\%$
$A_{CP}(K^-\pi^+) = (0.3 \pm 0.7)\%$
$A_{CP}(K^+\pi^-) = (-0.9 \pm 1.4)\%$
$A_{CP}(D_{CP(\pm1)} \to K^\mp\pi^\pm) = (12.7 \pm 1.5)\%$
$A_{CP}(K^-\pi^+\pi^0) = (0.1 \pm 0.5)\%$
$A_{CP}(K^+\pi^-\pi^0) = (0 \pm 5)\%$
$A_{CP}(K^0_S\pi^+\pi^-) = (-0.1 \pm 0.8)\%$
$A_{CP}(K^*(892)^-\pi^+ \to K^0_S\pi^+\pi^-) = (0.4 \pm 0.5)\%$
$A_{CP}(K^*(892)^+\pi^- \to K^0_S\pi^+\pi^-) = (1 \pm 6)\%$
$A_{CP}(\overline{K}^0\rho^0 \to K^0_S\pi^+\pi^-) = (-0.1 \pm 0.5)\%$
$A_{CP}(\overline{K}^0\omega \to K^0_S\pi^+\pi^-) = (-13 \pm 7)\%$
$A_{CP}(\overline{K}^0 f_0(980) \to K^0_S\pi^+\pi^-) = (-0.4 \pm 2.7)\%$
$A_{CP}(\overline{K}^0 f_2(1270) \to K^0_S\pi^+\pi^-) = (-4 \pm 5)\%$
$A_{CP}(\overline{K}^0 f_0(1370) \to K^0_S\pi^+\pi^-) = (-1 \pm 9)\%$
$A_{CP}(\overline{K}^0\rho^0(1450) \to K^0_S\pi^+\pi^-) = (-4 \pm 10)\%$
$A_{CP}(\overline{K}^0 f_0(600) \to K^0_S\pi^+\pi^-) = (-3 \pm 5)\%$
$A_{CP}(K^*(1410)^-\pi^+ \to K^0_S\pi^+\pi^-) = (-2 \pm 9)\%$
$A_{CP}(K^*_0(1430)^-\pi^+ \to K^0_S\pi^+\pi^-) = (4 \pm 4)\%$
$A_{CP}(K^*_0(1430)^+\pi^- \to K^0_S\pi^+\pi^-) = (12 \pm 15)\%$
$A_{CP}(K^*_2(1430)^-\pi^+ \to K^0_S\pi^+\pi^-) = (3 \pm 6)\%$
$A_{CP}(K^*_2(1430)^+\pi^- \to K^0_S\pi^+\pi^-) = (-10 \pm 32)\%$
$A_{CP}(K^-\pi^+\pi^+\pi^-) = (0.2 \pm 0.5)\%$
$A_{CP}(K^+\pi^-\pi^+\pi^-) = (-2 \pm 4)\%$
$A_{CP}(K^+K^-\pi^+\pi^-) = (1.3 \pm 1.7)\%$
$A_{CP}(K^*_1(1270)^+K^- \to K^+K^-\pi^+\pi^-) = (25 \pm 16)\%$
$A_{CP}(K^*_1(1270)^+K^- \to K^{*0}\pi^+K^-) = (-1 \pm 10)\%$
$A_{CP}(K^*_1(1270)^-K^+ \to \overline{K}^{*0}\pi^-K^+) = (-10 \pm 32)\%$
$A_{CP}(K^*_1(1270)^-K^+ \to K^+K^-\pi^+\pi^-) = (-50 \pm 20)\%$
$A_{CP}(K^*_1(1270)^+K^- \to \rho^0K^+K^-) = (-7 \pm 17)\%$
$A_{CP}(K^*_1(1270)^-K^+ \to \rho^0K^-K^+) = (10 \pm 13)\%$
$A_{CP}(K^*_1(1400)^+K^- \to K^+K^-\pi^+\pi^-) = (9 \pm 25)\%$
$A_{CP}(K^*(1410)^+K^- \to K^{*0}\pi^+K^-) = (-20 \pm 17)\%$
$A_{CP}(K^*(1410)^-K^+ \to \overline{K}^{*0}\pi^-K^+) = (-1 \pm 14)\%$
$A_{CP}(K^*(1680)^+K^- \to K^+K^-\pi^+\pi^-) = (-17 \pm 29)\%$
$A_{CP}(K^{*0}\overline{K}^{*0})$ in D^0, $\overline{D}^0 \to K^{*0}\overline{K}^{*0} = (-5 \pm 14)\%$
$A_{CP}(K^{*0}\overline{K}^{*0}\ S\text{-wave}) = (10 \pm 14)\%$
$A_{CP}(\phi\rho^0)$ in D^0, $\overline{D}^0 \to \phi\rho^0 = (1 \pm 9)\%$
$A_{CP}(\phi\rho^0\ S\text{-wave}) = (-3 \pm 5)\%$
$A_{CP}(\phi\rho^0\ D\text{-wave}) = (-37 \pm 19)\%$
$A_{CP}(\phi(\pi^+\pi^-)_{S-wave}) = (0 \pm 50)\%$
$A_{CP}(K^*(892)^0(K^-\pi^+)_{S-wave}) = (-10 \pm 40)\%$
$A_{CP}(K^+K^-\pi^+\pi^-\ \text{non-resonant}) = (8 \pm 20)\%$
$A_{CP}((K^-\pi^+)_{P-wave}\ (K^+\pi^-)_{S-wave}) = (3 \pm 11)\%$

CP-even fractions (labeled by the D^0 decay)

CP-even fraction in $D^0 \to \pi^+\pi^-\pi^0$ decays $= (97.3 \pm 1.7)\%$
CP-even fraction in $D^0 \to K^+K^-\pi^0$ decays $= (73 \pm 6)\%$
CP-even fraction in $D^0 \to \pi^+\pi^-\pi^+\pi^-$ decays $= (73.7 \pm 2.8)\%$
CP-even fraction in $D^0 \to K^+K^-\pi^+\pi^-$ decays $= (75 \pm 4)\%$

CP-violation asymmetry difference

$\Delta A_{CP} = A_{CP}(K^+K^-) - A_{CP}(\pi^+\pi^-) = (-0.12 \pm 0.13)\%$ (S = 1.8)

χ^2 tests of *CP*-violation (*CPV*)

Local *CPV* in D^0, $\overline{D}^0 \to \pi^+\pi^-\pi^0 = 4.9\%$
Local *CPV* in D^0, $\overline{D}^0 \to \pi^+\pi^-\pi^+\pi^- = (0.6 \pm 0.2)\%$
Local *CPV* in D^0, $\overline{D}^0 \to K^0_S\pi^+\pi^- = 96\%$
Local *CPV* in D^0, $\overline{D}^0 \to K^+K^-\pi^0 = 16.6\%$
Local *CPV* in D^0, $\overline{D}^0 \to K^+K^-\pi^+\pi^- = 9.1\%$

T-violation decay-rate asymmetry

$A_T(K^+K^-\pi^+\pi^-) = (1.7 \pm 2.7) \times 10^{-3}$ [ss]
$A_{\text{Tviol}}(K_S\pi^+\pi^-\pi^0)$ in D^0, $\overline{D}^0 \to K_S\pi^+\pi^-\pi^0 = (-0.3^{+1.4}_{-1.6}) \times 10^{-3}$

CPT-violation decay-rate asymmetry

$A_{CPT}(K^\mp\pi^\pm) = 0.008 \pm 0.008$

Form factors

$r_V \equiv V(0)/A_1(0)$ in $D^0 \to K^*(892)^-\ell^+\nu_\ell = 1.7 \pm 0.8$
$r_2 \equiv A_2(0)/A_1(0)$ in $D^0 \to K^*(892)^-\ell^+\nu_\ell = 0.9 \pm 0.4$
$f_+(0)$ in $D^0 \to K^-\ell^+\nu_\ell = 0.736 \pm 0.004$
$f_+(0)|V_{cs}|$ in $D^0 \to K^-\ell^+\nu_\ell = 0.719 \pm 0.004$
$r_1 \equiv a_1/a_0$ in $D^0 \to K^-\ell^+\nu_\ell = -2.40 \pm 0.16$

$r_2 \equiv a_2/a_0$ in $D^0 \to K^-\ell^+\nu_\ell = 5 \pm 4$
$f_+(0)$ in $D^0 \to \pi^-\ell^+\nu_\ell = 0.637 \pm 0.009$
$f_+(0)|V_{cd}|$ in $D^0 \to \pi^-\ell^+\nu_\ell = 0.1436 \pm 0.0026$ (S = 1.5)
$r_1 \equiv a_1/a_0$ in $D^0 \to \pi^-\ell^+\nu_\ell = -1.97 \pm 0.28$ (S = 1.4)
$r_2 \equiv a_1/a_0$ in $D^0 \to \pi^-\ell^+\nu_\ell = -0.2 \pm 2.2$ (S = 1.7)

Most decay modes (other than the semileptonic modes) that involve a neutral K meson are now given as K^0_S modes, not as $\overline{K}^0$ modes. Nearly always it is a K^0_S that is measured, and interference between Cabibbo-allowed and doubly Cabibbo-suppressed modes can invalidate the assumption that $2\Gamma(K^0_S) = \Gamma(\overline{K}^0)$.

D^0 DECAY MODES	Fraction (Γ_i/Γ)	Scale factor/ Confidence level	p (MeV/c)
Topological modes			
0-prongs	[bbb] (15 ± 6) %		–
2-prongs	(70 ± 6) %		–
4-prongs	[ccc] (14.5 ± 0.5) %		–
6-prongs	[ddd] (6.4 ± 1.3) × 10^{-4}		–
Inclusive modes			
e^+ anything	[eee] (6.49 ± 0.11) %		–
μ^+ anything	(6.7 ± 0.6) %		–
K^- anything	(54.7 ± 2.8) %	S=1.3	–
$\overline{K}^0$ anything + K^0 anything	(47 ± 4) %		–
K^+ anything	(3.4 ± 0.4) %		–
$K^*(892)^-$ anything	(15 ± 9) %		–
$\overline{K}^*(892)^0$ anything	(9 ± 4) %		–
$K^*(892)^+$ anything	< 3.6 %	CL=90%	–
$K^*(892)^0$ anything	(2.8 ± 1.3) %		–
η anything	(9.5 ± 0.9) %		–
η' anything	(2.48 ± 0.27) %		–
ϕ anything	(1.05 ± 0.11) %		–
invisibles	< 9.4 × 10^{-5}	CL=90%	–
Semileptonic modes			
$K^- e^+ \nu_e$	(3.530 ± 0.028) %	S=1.1	867
$K^- \mu^+ \nu_\mu$	(3.31 ± 0.13) %		864
$K^*(892)^- e^+ \nu_e$	(2.15 ± 0.16) %		719
$K^*(892)^- \mu^+ \nu_\mu$	(1.86 ± 0.24) %		714
$K^-\pi^0 e^+ \nu_e$	(1.6 $^{+1.3}_{-0.5}$) %		861
$\overline{K}^0\pi^- e^+ \nu_e$	(2.7 $^{+0.9}_{-0.7}$) %		860
$K^-\pi^+\pi^- e^+ \nu_e$	(2.8 $^{+1.4}_{-1.1}$) × 10^{-4}		843
$K_1(1270)^- e^+ \nu_e$	(7.6 $^{+4.0}_{-3.1}$) × 10^{-4}		498
$K^-\pi^+\pi^-\mu^+\nu_\mu$	< 1.2 × 10^{-3}	CL=90%	821
$(\overline{K}^*(892)\pi)^-\mu^+\nu_\mu$	< 1.4 × 10^{-3}	CL=90%	692
$\pi^- e^+ \nu_e$	(2.91 ± 0.04) × 10^{-3}	S=1.1	927
$\pi^-\mu^+\nu_\mu$	(2.37 ± 0.24) × 10^{-3}		924
$\rho^- e^+ \nu_e$	(1.77 ± 0.16) × 10^{-3}		771
Hadronic modes with one $\overline{K}$			
$K^-\pi^+$	(3.89 ± 0.04) %	S=1.1	861
$K^0_S\pi^0$	(1.19 ± 0.04) %		860
$K^0_L\pi^0$	(10.0 ± 0.7) × 10^{-3}		860
$K^0_S\pi^+\pi^-$	[tt] (2.75 ± 0.18) %	S=1.1	842
$K^0_S\rho^0$	(6.2 $^{+0.6}_{-0.8}$) × 10^{-3}		674
$K^0_S\omega$, $\omega \to \pi^+\pi^-$	(2.0 ± 0.6) × 10^{-4}		670
$K^0_S(\pi^+\pi^-)_{S-wave}$	(3.3 ± 0.7) × 10^{-3}		842
$K^0_S f_0(980)$, $f_0 \to \pi^+\pi^-$	(1.18 $^{+0.40}_{-0.23}$) × 10^{-3}		549
$K^0_S f_0(1370)$, $f_0 \to \pi^+\pi^-$	(2.7 $^{+0.8}_{-1.3}$) × 10^{-3}		†
$K^0_S f_2(1270)$, $f_2 \to \pi^+\pi^-$	(9 $^{+10}_{-6}$) × 10^{-5}		262
$K^*(892)^-\pi^+$, $K^{*-} \to K^0_S\pi^-$	(1.62 $^{+0.14}_{-0.17}$) %		711
$K^*_0(1430)^-\pi^+$, $K^{*-}_0 \to K^0_S\pi^-$	(2.63 $^{+0.40}_{-0.32}$) × 10^{-3}		378
$K^*_2(1430)^-\pi^+$, $K^{*-}_2 \to K^0_S\pi^-$	(3.3 $^{+1.8}_{-1.0}$) × 10^{-4}		367
$K^*(1680)^-\pi^+$, $K^{*-} \to K^0_S\pi^-$	(4.3 ± 3.5) × 10^{-4}		46
$K^*(892)^+\pi^-$, $K^{*+} \to K^0_S\pi^+$	[fff] (1.11 $^{+0.60}_{-0.33}$) × 10^{-4}		711
$K^*_0(1430)^+\pi^-$, $K^{*+}_0 \to K^0_S\pi^+$	[fff] < 1.4 × 10^{-5}	CL=95%	–
$K^*_2(1430)^+\pi^-$, $K^{*+}_2 \to K^0_S\pi^+$	[fff] < 3.3 × 10^{-5}	CL=95%	–
$K^0_S\pi^+\pi^-$ nonresonant	(2.5 $^{+6.0}_{-1.6}$) × 10^{-4}		842
$K^-\pi^+\pi^0$	[tt] (14.2 ± 0.5) %	S=1.9	844
$K^-\rho^+$	(11.1 ± 0.7) %		675
$K^-\rho(1700)^+$, $\rho^+ \to \pi^+\pi^0$	(8.1 ± 1.7) × 10^{-3}		†
$K^*(892)^-\pi^+$, $K^*(892)^- \to K^-\pi^0$	(2.27 $^{+0.40}_{-0.20}$) %		711
$\overline{K}^*(892)^0\pi^0$, $\overline{K}^*(892)^0 \to K^-\pi^+$	(1.93 ± 0.24) %		711
$K^*_0(1430)^-\pi^+$, $K^{*-}_0 \to K^-\pi^0$	(4.7 ± 2.2) × 10^{-3}		378
$\overline{K}^*_0(1430)^0\pi^0$, $\overline{K}^{*0}_0 \to K^-\pi^+$	(5.8 $^{+5.0}_{-1.6}$) × 10^{-3}		379
$K^*(1680)^-\pi^+$, $K^{*-} \to K^-\pi^0$	(1.8 ± 0.7) × 10^{-3}		46
$K^-\pi^+\pi^0$ nonresonant	(1.14 $^{+0.50}_{-0.20}$) %		844
$K^0_S 2\pi^0$	(9.1 ± 1.1) × 10^{-3}	S=2.2	843
$K^0_S(2\pi^0)_{S-wave}$	(2.6 ± 0.7) × 10^{-3}		–
$\overline{K}^*(892)^0\pi^0$, $\overline{K}^{*0} \to K^0_S\pi^0$	(7.8 ± 0.7) × 10^{-3}		711
$\overline{K}^*(1430)^0\pi^0$, $\overline{K}^{*0} \to K^0_S\pi^0$	(4 ±23) × 10^{-5}		–
$\overline{K}^*(1680)^0\pi^0$, $\overline{K}^{*0} \to K^0_S\pi^0$	(1.0 ± 0.4) × 10^{-3}		–
$K^0_S f_2(1270)$, $f_2 \to 2\pi^0$	(2.3 ± 1.1) × 10^{-4}		–
$2K^0_S$, one $K^0_S \to 2\pi^0$	(3.2 ± 1.1) × 10^{-4}		–
$K^-2\pi^+\pi^-$	[tt] (8.11 ± 0.15) %	S=1.1	813
$K^-\pi^+\rho^0$ total	(6.77 ± 0.31) %		609
$K^-\pi^+\rho^0$ 3-body	(6.0 ± 1.6) × 10^{-3}		609
$\overline{K}^*(892)^0\rho^0$, $\overline{K}^{*0} \to K^-\pi^+$	(10.0 ± 0.5) × 10^{-3}		416
$(\overline{K}^*(892)^0\rho^0)_{S-wave}$, $\overline{K}^*(892)^0 \to K^-\pi^+$	(5.8 ± 0.8) × 10^{-3}		–
$(\overline{K}^*(892)^0\rho^0)_{P-wave}$, $\overline{K}^*(892)^0 \to K^-\pi^+$	(1.86 ± 0.18) × 10^{-3}		–
$(\overline{K}^*(892)^0\rho^0)_{D-wave}$, $\overline{K}^*(892)^0 \to K^-\pi^+$	(6.6 ± 0.7) × 10^{-3}		–
$\overline{K}^*(892)^0\rho^0$ transverse, $\overline{K}^{*0} \to K^-\pi^+$	(1.2 ± 0.4) %		417
$K^-a_1(1260)^+$, $a_1^+ \to \rho^0\pi^+$	(4.26 ± 0.32) %		327
$K^-a_1(1260)^+$, $a_1(1260)^+ \to (\rho^0\pi^+)_{S-wave}$	(4.3 ± 0.4) %		–
$K^-a_1(1260)^+$, $a_1(1260)^+ \to (\rho^0\pi^+)_{D-wave}$	(2.4 ± 1.1) × 10^{-4}		–
$K_1(1270)^-\pi^+$, $K_1^- \to K^-\pi^+\pi^-$ total	(5.4 ± 1.6) × 10^{-3}		–
$\overline{K}^*(892)^0\pi^+\pi^-$ 3-body, $\overline{K}^{*0} \to K^-\pi^+$	(5.9 ± 0.5) × 10^{-3}		685
$K_1(1270)^-\pi^+$, $K_1^- \to \overline{K}^*(892)^0\pi^-$, $\overline{K}^{*0} \to K^-\pi^+$	(6.5 ± 2.3) × 10^{-4}		484
$K_1(1270)^-\pi^+$, $K_1(1270)^- \to (\overline{K}^{*0}\pi^-)_{S-wave}$, $\overline{K}^*(892)^0 \to K^-\pi^+$	(8 ±11) × 10^{-5}		–
$K_1(1270)^-\pi^+$, $K_1(1270)^- \to (\overline{K}^{*0}\pi^-)_{D-wave}$, $\overline{K}^*(892)^0 \to K^-\pi^+$	(5.7 ± 2.3) × 10^{-4}		–
$K_1(1270)^-\pi^+$, $K_1(1270)^- \to (K^-\rho^0)_{S-wave}$	(2.8 ± 0.5) × 10^{-3}		–
$K^-2\pi^+\pi^-$ nonresonant	(1.78 ± 0.07) %		813
$K^0_S\pi^+\pi^-\pi^0$	[ggg] (5.1 ± 0.6) %		813
$K^0_S\eta$, $\eta \to \pi^+\pi^-\pi^0$	(1.10 ± 0.07) × 10^{-3}		772
$K^0_S\omega$, $\omega \to \pi^+\pi^-\pi^0$	(9.9 ± 0.6) × 10^{-3}		670
$K^-2\pi^+\pi^-\pi^0$	(4.2 ± 0.4) %		771
$\overline{K}^*(892)^0\pi^+\pi^-\pi^0$, $\overline{K}^{*0} \to K^-\pi^+$	(1.3 ± 0.6) %		643
$K^-\pi^+\omega$, $\omega \to \pi^+\pi^-\pi^0$	(2.7 ± 0.5) %		605

Meson Summary Table

$\overline{K}^*(892)^0\omega$, $\overline{K}^{*0} \to K^-\pi^+$, $\omega \to \pi^+\pi^-\pi^0$	(6.5 ± 3.0) × 10^{-3}			410
$K^0_S\eta\pi^0$	(5.5 ± 1.1) × 10^{-3}			721
$K^0_S a_0(980)$, $a_0 \to \eta\pi^0$	(6.5 ± 2.0) × 10^{-3}			–
$\overline{K}^*(892)^0\eta$, $\overline{K}^{*0} \to K^0_S\pi^0$	(1.6 ± 0.5) × 10^{-3}			–
$K^0_S 2\pi^+2\pi^-$	(2.61 ± 0.29) × 10^{-3}			768
$K^0_S\rho^0\pi^+\pi^-$, no $K^*(892)^-$	(1.0 ± 0.7) × 10^{-3}			–
$K^*(892)^-2\pi^+\pi^-$, $K^*(892)^- \to K^0_S\pi^-$, no ρ^0	(4 ± 7) × 10^{-4}			642
$K^*(892)^-\rho^0\pi^+$, $K^*(892)^- \to K^0_S\pi^-$	(1.6 ± 0.6) × 10^{-3}			230
$K^0_S 2\pi^+2\pi^-$ nonresonant	< 1.2 × 10^{-3}	CL=90%		768
$K^-3\pi^+2\pi^-$	(2.2 ± 0.6) × 10^{-4}			713

Fractions of some of the following modes with resonances have already appeared above as submodes of particular charged-particle modes. These nine modes below are all corrected for unseen decays of the resonances.

$K^0_S\eta$	(4.80 ± 0.30) × 10^{-3}			772
$K^0_S\omega$	(1.11 ± 0.06) %			670
$K^0_S\eta'(958)$	(9.4 ± 0.5) × 10^{-3}			565
$\overline{K}^*(892)^0\pi^+\pi^-\pi^0$	(1.9 ± 0.9) %			643
$K^-\pi^+\omega$	(3.0 ± 0.6) %			605
$\overline{K}^*(892)^0\omega$	(1.1 ± 0.5) %			410
$K^-\pi^+\eta'(958)$	(7.5 ± 1.9) × 10^{-3}			479
$\overline{K}^*(892)^0\eta'(958)$	< 1.1 × 10^{-3}	CL=90%		119

Hadronic modes with three K's

$K^0_S K^+K^-$	(4.35 ± 0.32) × 10^{-3}			544
$K^0_S a_0(980)^0$, $a_0^0 \to K^+K^-$	(2.9 ± 0.4) × 10^{-3}			–
$K^-a_0(980)^+$, $a_0^+ \to K^+K^0_S$	(5.8 ± 1.7) × 10^{-4}			–
$K^+a_0(980)^-$, $a_0^- \to K^-K^0_S$	< 1.1 × 10^{-4}	CL=95%		–
$K^0_S f_0(980)$, $f_0 \to K^+K^-$	< 9 × 10^{-5}	CL=95%		–
$K^0_S\phi$, $\phi \to K^+K^-$	(2.00 ± 0.15) × 10^{-3}			520
$K^0_S f_0(1370)$, $f_0 \to K^+K^-$	(1.7 ± 1.1) × 10^{-4}			–
$3K^0_S$	(7.5 ± 0.6) × 10^{-4}	S=1.3		539
$K^+2K^-\pi^+$	(2.22 ± 0.31) × 10^{-4}			434
$K^+K^-\overline{K}^*(892)^0$, $\overline{K}^{*0} \to K^-\pi^+$	(4.4 ± 1.7) × 10^{-5}			†
$K^-\pi^+\phi$, $\phi \to K^+K^-$	(4.0 ± 1.7) × 10^{-5}			422
$\phi\overline{K}^*(892)^0$, $\phi \to K^+K^-$, $\overline{K}^{*0} \to K^-\pi^+$	(1.06 ± 0.20) × 10^{-4}			†
$K^+2K^-\pi^+$ nonresonant	(3.3 ± 1.5) × 10^{-5}			434
$2K^0_S K^\pm\pi^\mp$	(5.8 ± 1.2) × 10^{-4}			427

Pionic modes

$\pi^+\pi^-$	(1.407 ± 0.025) × 10^{-3}		S=1.1	922
$2\pi^0$	(8.22 ± 0.25) × 10^{-4}			923
$\pi^+\pi^-\pi^0$	(1.47 ± 0.06) %		S=2.1	907
$\rho^+\pi^-$	(10.0 ± 0.4) × 10^{-3}			764
$\rho^0\pi^0$	(3.81 ± 0.23) × 10^{-3}			764
$\rho^-\pi^+$	(5.08 ± 0.25) × 10^{-3}			764
$\rho(1450)^+\pi^-$, $\rho^+ \to \pi^+\pi^0$	(1.6 ± 2.0) × 10^{-5}			–
$\rho(1450)^0\pi^0$, $\rho^0 \to \pi^+\pi^-$	(4.4 ± 1.9) × 10^{-5}			–
$\rho(1450)^-\pi^+$, $\rho^- \to \pi^-\pi^0$	(2.6 ± 0.4) × 10^{-4}			–
$\rho(1700)^+\pi^-$, $\rho^+ \to \pi^+\pi^0$	(6.0 ± 1.5) × 10^{-4}			–
$\rho(1700)^0\pi^0$, $\rho^0 \to \pi^+\pi^-$	(7.3 ± 1.7) × 10^{-4}			–
$\rho(1700)^-\pi^+$, $\rho^- \to \pi^-\pi^0$	(4.7 ± 1.1) × 10^{-4}			–
$f_0(980)\pi^0$, $f_0 \to \pi^+\pi^-$	(3.7 ± 0.8) × 10^{-5}			–
$f_0(500)\pi^0$, $f_0 \to \pi^+\pi^-$	(1.20 ± 0.21) × 10^{-4}			–
$f_0(1370)\pi^0$, $f_0 \to \pi^+\pi^-$	(5.4 ± 2.1) × 10^{-5}			–
$f_0(1500)\pi^0$, $f_0 \to \pi^+\pi^-$	(5.7 ± 1.6) × 10^{-5}			–
$f_0(1710)\pi^0$, $f_0 \to \pi^+\pi^-$	(4.5 ± 1.6) × 10^{-5}			–
$f_2(1270)\pi^0$, $f_2 \to \pi^+\pi^-$	(1.94 ± 0.21) × 10^{-4}			–
$\pi^+\pi^-\pi^0$ nonresonant	(1.2 ± 0.4) × 10^{-4}			907
$3\pi^0$	< 3.5 × 10^{-4}	CL=90%		908
$2\pi^+2\pi^-$	(7.45 ± 0.20) × 10^{-3}			880
$a_1(1260)^+\pi^-$, $a_1^+ \to 2\pi^+\pi^-$ total	(4.47 ± 0.31) × 10^{-3}			–
$a_1(1260)^+\pi^-$, $a_1^+ \to \rho^0\pi^+$ S-wave	(3.09 ± 0.21) × 10^{-3}			–
$a_1(1260)^+\pi^-$, $a_1^+ \to \rho^0\pi^+$ D-wave	(1.9 ± 0.5) × 10^{-4}			–
$a_1(1260)^+\pi^-$, $a_1^+ \to \sigma\pi^+$	(6.3 ± 0.7) × 10^{-4}			–
$a_1(1260)^-\pi^+$, $a_1^- \to \rho^0\pi^-$ S-wave	(2.3 ± 0.9) × 10^{-4}			–
$a_1(1260)^-\pi^+$, $a_1^- \to \sigma\pi^-$	(6.0 ± 3.3) × 10^{-5}			–
$\pi(1300)^+\pi^-$, $\pi(1300)^+ \to \sigma\pi^+$	(5.1 ± 2.6) × 10^{-4}			–
$\pi(1300)^-\pi^+$, $\pi(1300)^- \to \sigma\pi^-$	(2.2 ± 2.1) × 10^{-4}			–
$a_1(1640)^+\pi^-$, $a_1^+ \to \rho^0\pi^+$ D-wave	(3.1 ± 1.6) × 10^{-4}			–
$a_1(1640)^+\pi^-$, $a_1^+ \to \sigma\pi^+$	(1.8 ± 1.4) × 10^{-4}			–
$\pi_2(1670)^+\pi^-$, $\pi_2^+ \to f_2(1270)^0\pi^+$, $f_2^0 \to \pi^+\pi^-$	(2.0 ± 0.9) × 10^{-4}			–
$\pi_2(1670)^+\pi^-$, $\pi_2^+ \to \sigma\pi^+$	(2.6 ± 1.0) × 10^{-4}			–
$2\rho^0$ total	(1.83 ± 0.13) × 10^{-3}			518
$2\rho^0$, parallel helicities	(8.2 ± 3.2) × 10^{-5}			–
$2\rho^0$, perpendicular helicities	(4.8 ± 0.6) × 10^{-4}			–
$2\rho^0$, longitudinal helicities	(1.25 ± 0.10) × 10^{-3}			–
$2\rho(770)^0$, S-wave	(1.8 ± 1.2) × 10^{-4}			–
$2\rho(770)^0$, P-wave	(5.2 ± 1.3) × 10^{-4}			–
$2\rho(770)^0$, D-wave	(6.1 ± 3.0) × 10^{-4}			–
Resonant $(\pi^+\pi^-)\pi^+\pi^-$ 3-body total	(1.49 ± 0.12) × 10^{-3}			–
$\sigma\pi^+\pi^-$	(6.1 ± 0.9) × 10^{-4}			–
$\sigma\rho(770)^0$	(4.9 ± 2.5) × 10^{-4}			–
$f_0(980)\pi^+\pi^-$, $f_0 \to \pi^+\pi^-$	(1.8 ± 0.5) × 10^{-4}			–
$f_2(1270)\pi^+\pi^-$, $f_2 \to \pi^+\pi^-$	(3.7 ± 0.6) × 10^{-4}			–
$2f_2(1270)$, $f_2 \to \pi^+\pi^-$	(1.6 ± 1.8) × 10^{-4}			–
$f_0(1370)\sigma$, $f_0 \to \pi^+\pi^-$	(1.6 ± 0.5) × 10^{-3}			–
$\pi^+\pi^-2\pi^0$	(1.00 ± 0.09) %			882
$\eta\pi^0$	[hhh] (6.7 ± 0.6) × 10^{-4}			846
$\omega\pi^0$	[hhh] (1.17 ± 0.35) × 10^{-4}			761
$2\pi^+2\pi^-\pi^0$	(4.2 ± 0.5) × 10^{-3}			844
$\eta\pi^+\pi^-$	[hhh] (1.09 ± 0.16) × 10^{-3}			827
$\omega\pi^+\pi^-$	[hhh] (1.6 ± 0.5) × 10^{-3}			738
$3\pi^+3\pi^-$	(4.2 ± 1.2) × 10^{-4}			795
$\eta'(958)\pi^0$	(9.0 ± 1.4) × 10^{-4}			678
$\eta'(958)\pi^+\pi^-$	(4.5 ± 1.7) × 10^{-4}			650
2η	(1.68 ± 0.20) × 10^{-3}			754
$\eta\eta'(958)$	(1.05 ± 0.26) × 10^{-3}			537

Hadronic modes with a $K\overline{K}$ pair

K^+K^-	(3.97 ± 0.07) × 10^{-3}		S=1.4	791
$2K^0_S$	(1.70 ± 0.12) × 10^{-4}			789
$K^0_S K^-\pi^+$	(3.3 ± 0.5) × 10^{-3}		S=1.1	739
$\overline{K}^*(892)^0K^0_S$, $\overline{K}^{*0} \to K^-\pi^+$	(8.1 ± 1.6) × 10^{-5}			608
$K^*(892)^+K^-$, $K^{*+} \to K^0_S\pi^+$	(1.86 ± 0.30) × 10^{-3}			–
$\overline{K}^*(1410)^0K^0_S$, $\overline{K}^{*0} \to K^-\pi^+$	(1.2 ± 1.8) × 10^{-4}			–
$K^*(1410)^+K^-$, $K^{*+} \to K^0_S\pi^+$	(3.1 ± 1.9) × 10^{-4}			–
$(K^-\pi^+)_{S-wave}K^0_S$	(5.9 ± 2.8) × 10^{-4}			739
$(K^0_S\pi^+)_{S-wave}K^-$	(3.8 ± 1.0) × 10^{-4}			739
$a_0(980)^-\pi^+$, $a_0^- \to K^0_S K^-$	(1.3 ± 1.4) × 10^{-4}			–
$a_0(1450)^-\pi^+$, $a_0^- \to K^0_S K^-$	(2.4 ± 2.0) × 10^{-5}			–
$a_2(1320)^-\pi^+$, $a_2^- \to K^0_S K^-$	(5 ± 5) × 10^{-6}			–
$\rho(1450)^-\pi^+$, $\rho^- \to K^0_S K^-$	(4.6 ± 2.5) × 10^{-5}			–
$K^0_S K^+\pi^-$	(2.13 ± 0.34) × 10^{-3}		S=1.1	739
$K^*(892)^0K^0_S$, $K^{*0} \to K^+\pi^-$	(1.10 ± 0.21) × 10^{-4}			608
$K^*(892)^-K^+$, $K^{*-} \to K^0_S\pi^-$	(6.1 ± 1.0) × 10^{-4}			–
$K^*(1410)^0K^0_S$, $K^{*0} \to K^+\pi^-$	(5 ± 8) × 10^{-5}			–
$K^*(1410)^-K^+$, $K^{*-} \to K^0_S\pi^-$	(2.5 ± 2.0) × 10^{-4}			–
$(K^+\pi^-)_{S-wave}K^0_S$	(3.6 ± 1.9) × 10^{-4}			739

$(K^0_S\pi^-)_{S-wave}K^+$	(1.3 ± 0.6) × 10^{-4}			739
$a_0(980)^+\pi^-$, $a_0^+ \to K^0_S K^+$	(6 ± 4) × 10^{-4}			–
$a_0(1450)^+\pi^-$, $a_0^+ \to K^0_S K^+$	(3.2 ± 2.5) × 10^{-5}			–
$\rho(1700)^+\pi^-$, $\rho^+ \to K^0_S K^+$	(1.1 ± 0.6) × 10^{-5}			–
$K^+K^-\pi^0$	(3.37 ± 0.15) × 10^{-3}			743
$K^*(892)^+K^-$, $K^*(892)^+ \to K^+\pi^0$	(1.50 ± 0.07) × 10^{-3}			–
$K^*(892)^-K^+$, $K^*(892)^- \to K^-\pi^0$	(5.4 ± 0.4) × 10^{-4}			–
$(K^+\pi^0)_{S-wave}K^-$	(2.40 ± 0.17) × 10^{-3}			743
$(K^-\pi^0)_{S-wave}K^+$	(1.3 ± 0.5) × 10^{-4}			743
$f_0(980)\pi^0$, $f_0 \to K^+K^-$	(3.5 ± 0.6) × 10^{-4}			–
$\phi\pi^0$, $\phi \to K^+K^-$	(6.5 ± 0.4) × 10^{-4}			–
$2K^0_S\pi^0$	< 5.9 × 10^{-4}			740
$K^+K^-\pi^+\pi^-$	(2.44 ± 0.11) × 10^{-3}			677
$\phi(\pi^+\pi^-)_{S-wave}$, $\phi \to K^+K^-$	(10 ± 5) × 10^{-5}			614
$(\phi\rho^0)_{S-wave}$, $\phi \to K^+K^-$	(6.8 ± 0.6) × 10^{-4}			250
$(\phi\rho^0)_{P-wave}$, $\phi \to K^+K^-$	(3.9 ± 1.9) × 10^{-5}			–
$(\phi\rho^0)_{D-wave}$, $\phi \to K^+K^-$	(4.1 ± 1.4) × 10^{-5}			–
$(K^*(892)^0\overline{K}^*(892)^0)_{S-wave}$, $K^{*0} \to K^\pm\pi^\mp$	(1.1 ± 0.5) × 10^{-4}			–
$(K^*(892)^0\overline{K}^*(892)^0)_{P-wave}$, $K^* \to K^\pm\pi^\mp$	(9 ± 4) × 10^{-5}			–
$(K^*(892)^0\overline{K}^*(892)^0)_{D-wave}$, $K^* \to K^\pm\pi^\mp$	(9.7 ± 2.3) × 10^{-5}			–
$K^*(892)^0(K^-\pi^+)_{S-wave}$ 3-body, $K^{*0} \to K^+\pi^-$	(1.4 ± 0.6) × 10^{-4}			–
$K_1(1270)^+K^-$, $K_1^+ \to K^{*0}\pi^+$	(1.3 ± 0.9) × 10^{-4}			–
$K_1(1270)^+K^-$, $K_1^+ \to K^*(1430)^0\pi^+$, $K^{*0} \to K^+\pi^-$	(1.5 ± 0.5) × 10^{-4}			–
$K_1(1270)^+K^-$, $K_1^+ \to \rho^0K^+$	(2.2 ± 0.6) × 10^{-4}			–
$K_1(1270)^+K^-$, $K_1^+ \to \omega(782)K^+$, $\omega \to \pi^+\pi^-$	(1.5 ± 1.2) × 10^{-5}			–
$K_1(1270)^-K^+$, $K_1^- \to \rho^0K^-$	(1.3 ± 0.4) × 10^{-4}			–
$K_1(1400)^+K^-$, $K_1^+ \to K^*(892)^0\pi^+$, $K^{*0} \to K^+\pi^-$	(3.0 ± 1.7) × 10^{-4}			–
$K_1(1680)^+K^-$, $K_1^+ \to K^{*0}\pi^+$, $K^{*0} \to K^+\pi^-$	(8.8 ± 3.1) × 10^{-5}			–
$K^+K^-\pi^+\pi^-$ non-resonant	(2.7 ± 0.6) × 10^{-4}			–
$2K^0_S\pi^+\pi^-$	(1.20 ± 0.23) × 10^{-3}			673
$K^0_SK^-2\pi^+\pi^-$	< 1.4 × 10^{-4}	CL=90%		595
$K^+K^-\pi^+\pi^-\pi^0$	(3.1 ± 2.0) × 10^{-3}			600

Other $K\overline{K}X$ modes. They include all decay modes of the ϕ, η, and ω.

$\phi\eta$	(1.4 ± 0.5) × 10^{-4}			489
$\phi\omega$	< 2.1 × 10^{-3}	CL=90%		238

Radiative modes

$\rho^0\gamma$	(1.76 ± 0.31) × 10^{-5}			771
$\omega\gamma$	< 2.4 × 10^{-4}	CL=90%		768
$\phi\gamma$	(2.74 ± 0.19) × 10^{-5}			654
$\overline{K}^*(892)^0\gamma$	(4.1 ± 0.7) × 10^{-4}			719

Doubly Cabibbo suppressed (*DC*) modes or $\Delta C = 2$ forbidden via mixing (*C2M*) modes

$K^+\ell^-\overline{\nu}_\ell$ via $\overline{D}^0$		< 2.2 × 10^{-5}	CL=90%		–
K^+ or $K^*(892)^+e^-\overline{\nu}_e$ via $\overline{D}^0$		< 6 × 10^{-5}	CL=90%		–
$K^+\pi^-$	*DC*	(1.48 ± 0.07) × 10^{-4}	S=2.8		861
$K^+\pi^-$ via DCS		(1.366± 0.028) × 10^{-4}			–
$K^+\pi^-$ via $\overline{D}^0$		< 1.6 × 10^{-5}	CL=95%		861
$K^0_S\pi^+\pi^-$ in $D^0 \to \overline{D}^0$		< 1.7 × 10^{-4}	CL=95%		–
$K^*(892)^+\pi^-$, $K^{*+} \to K^0_S\pi^+$	*DC*	(1.11 $^{+\ 0.60}_{-\ 0.33}$) × 10^{-4}			711
$K_0^*(1430)^+\pi^-$, $K_0^{*+} \to K^0_S\pi^+$	*DC*	< 1.4 × 10^{-5}			–
$K_2^*(1430)^+\pi^-$, $K_2^{*+} \to K^0_S\pi^+$	*DC*	< 3.3 × 10^{-5}			–
$K^+\pi^-\pi^0$	*DC*	(3.01 ± 0.15) × 10^{-4}			844
$K^+\pi^-\pi^0$ via $\overline{D}^0$		(7.5 ± 0.5) × 10^{-4}			–
$K^+\pi^+2\pi^-$ via DCS		(2.45 ± 0.07) × 10^{-4}			–
$K^+\pi^+2\pi^-$	*DC*	(2.61 ± 0.06) × 10^{-4}			813
$K^+\pi^+2\pi^-$ via $\overline{D}^0$		(7.8 ± 2.9) × 10^{-6}			812
μ^- anything via $\overline{D}^0$		< 4 × 10^{-4}	CL=90%		–

$\Delta C = 1$ weak neutral current (*C1*) modes, Lepton Family number (*LF*) violating modes, Lepton (*L*) or Baryon (*B*) number violating modes

$\gamma\gamma$	*C1*	< 8.5 × 10^{-7}	CL=90%		932
e^+e^-	*C1*	< 7.9 × 10^{-8}	CL=90%		932
$\mu^+\mu^-$	*C1*	< 6.2 × 10^{-9}	CL=90%		926
$\pi^0e^+e^-$	*C1*	< 4.5 × 10^{-5}	CL=90%		928
$\pi^0\mu^+\mu^-$	*C1*	< 1.8 × 10^{-4}	CL=90%		915
ηe^+e^-	*C1*	< 1.1 × 10^{-4}	CL=90%		852
$\eta\mu^+\mu^-$	*C1*	< 5.3 × 10^{-4}	CL=90%		838
$\pi^+\pi^-e^+e^-$	*C1*	< 3.73 × 10^{-4}	CL=90%		922
$\rho^0e^+e^-$	*C1*	< 1.0 × 10^{-4}	CL=90%		771
$\pi^+\pi^-\mu^+\mu^-$	*C1*	(9.6 ± 1.2) × 10^{-7}			894
$\pi^+\pi^-\mu^+\mu^-$ (non-res)		< 5.5 × 10^{-7}	CL=90%		–
$\rho^0\mu^+\mu^-$	*C1*	< 2.2 × 10^{-5}	CL=90%		754
ωe^+e^-	*C1*	< 1.8 × 10^{-4}	CL=90%		768
$\omega\mu^+\mu^-$	*C1*	< 8.3 × 10^{-4}	CL=90%		751
$K^-K^+e^+e^-$	*C1*	< 3.15 × 10^{-4}	CL=90%		791
ϕe^+e^-	*C1*	< 5.2 × 10^{-5}	CL=90%		654
$K^-K^+\mu^+\mu^-$	*C1*	(1.54 ± 0.32) × 10^{-7}			710
$K^-K^+\mu^+\mu^-$ (non-res)		< 3.3 × 10^{-5}	CL=90%		–
$\phi\mu^+\mu^-$	*C1*	< 3.1 × 10^{-5}	CL=90%		631
$\overline{K}^0e^+e^-$	[*zz*]	< 1.1 × 10^{-4}	CL=90%		866
$\overline{K}^0\mu^+\mu^-$	[*zz*]	< 2.6 × 10^{-4}	CL=90%		852
$K^-\pi^+e^+e^-$	*C1*	< 3.85 × 10^{-4}	CL=90%		861
$\overline{K}^*(892)^0e^+e^-$	[*zz*]	< 4.7 × 10^{-5}	CL=90%		719
$K^-\pi^+\mu^+\mu^-$	*C1*	< 3.59 × 10^{-4}	CL=90%		829
$K^-\pi^+\mu^+\mu^-$, 675 < $m_{\mu\mu}$ < 875 MeV		(4.2 ± 0.4) × 10^{-6}			–
$\overline{K}^*(892)^0\mu^+\mu^-$	[*zz*]	< 2.4 × 10^{-5}	CL=90%		700
$\pi^+\pi^-\pi^0\mu^+\mu^-$	*C1*	< 8.1 × 10^{-4}	CL=90%		863
$\mu^\pm e^\mp$	*LF*	[*hh*] < 1.3 × 10^{-8}	CL=90%		929
$\pi^0e^\pm\mu^\mp$	*LF*	[*hh*] < 8.6 × 10^{-5}	CL=90%		924
$\eta e^\pm\mu^\mp$	*LF*	[*hh*] < 1.0 × 10^{-4}	CL=90%		848
$\pi^+\pi^-e^\pm\mu^\mp$	*LF*	[*hh*] < 1.5 × 10^{-5}	CL=90%		911
$\rho^0e^\pm\mu^\mp$	*LF*	[*hh*] < 4.9 × 10^{-5}	CL=90%		767
$\omega e^\pm\mu^\mp$	*LF*	[*hh*] < 1.2 × 10^{-4}	CL=90%		764
$K^-K^+e^\pm\mu^\mp$	*LF*	[*hh*] < 1.8 × 10^{-4}	CL=90%		754
$\phi e^\pm\mu^\mp$	*LF*	[*hh*] < 3.4 × 10^{-5}	CL=90%		648
$\overline{K}^0e^\pm\mu^\mp$	*LF*	[*hh*] < 1.0 × 10^{-4}	CL=90%		863
$K^-\pi^+e^\pm\mu^\mp$	*LF*	[*hh*] < 5.53 × 10^{-4}	CL=90%		848
$\overline{K}^*(892)^0e^\pm\mu^\mp$	*LF*	[*hh*] < 8.3 × 10^{-5}	CL=90%		714
$2\pi^-2e^+$ + c.c.	*L*	< 1.12 × 10^{-4}	CL=90%		922
$2\pi^-2\mu^+$ + c.c.	*L*	< 2.9 × 10^{-5}	CL=90%		894
$K^-\pi^-2e^+$ + c.c.	*L*	< 2.06 × 10^{-4}	CL=90%		861
$K^-\pi^-2\mu^+$ + c.c.	*L*	< 3.9 × 10^{-4}	CL=90%		829
$2K^-2e^+$ + c.c.	*L*	< 1.52 × 10^{-4}	CL=90%		791
$2K^-2\mu^+$ + c.c.	*L*	< 9.4 × 10^{-5}	CL=90%		710
$\pi^-\pi^-e^+\mu^+$ + c.c.	*L*	< 7.9 × 10^{-5}	CL=90%		911
$K^-\pi^-e^+\mu^+$ + c.c.	*L*	< 2.18 × 10^{-4}	CL=90%		848
$2K^-e^+\mu^+$ + c.c.	*L*	< 5.7 × 10^{-5}	CL=90%		754
pe^-	*L*,*B*	[*iii*] < 1.0 × 10^{-5}	CL=90%		696
$\overline{p}e^+$	*L*,*B*	[*jjj*] < 1.1 × 10^{-5}	CL=90%		696

$D^*(2007)^0$

$I(J^P) = \frac{1}{2}(1^-)$
I, *J*, *P* need confirmation.

Mass $m = 2006.85 \pm 0.05$ MeV (S = 1.1)
$m_{D^{*0}} - m_{D^0} = 142.016 \pm 0.030$ MeV (S = 1.5)
Full width $\Gamma < 2.1$ MeV, CL = 90%

$\overline{D}^*(2007)^0$ modes are charge conjugates of modes below.

$D^*(2007)^0$ DECAY MODES	Fraction (Γ_i/Γ)	*p* (MeV/*c*)
$D^0\pi^0$	(64.7±0.9) %	43
$D^0\gamma$	(35.3±0.9) %	137

Meson Summary Table

$D^*(2010)^\pm$

$I(J^P) = \frac{1}{2}(1^-)$
I, *J*, *P* need confirmation.

Mass $m = 2010.26 \pm 0.05$ MeV
$m_{D^*(2010)^+} - m_{D^+} = 140.603 \pm 0.015$ MeV
$m_{D^*(2010)^+} - m_{D^0} = 145.4257 \pm 0.0017$ MeV
Full width $\Gamma = 83.4 \pm 1.8$ keV

$D^*(2010)^-$ modes are charge conjugates of the modes below.

$D^*(2010)^\pm$ DECAY MODES	Fraction (Γ_i/Γ)	p (MeV/c)
$D^0\pi^+$	(67.7±0.5) %	39
$D^+\pi^0$	(30.7±0.5) %	38
$D^+\gamma$	(1.6±0.4) %	136

$D_0^*(2400)^0$

$I(J^P) = \frac{1}{2}(0^+)$

Mass $m = 2318 \pm 29$ MeV (S = 1.7)
Full width $\Gamma = 267 \pm 40$ MeV

$D_0^*(2400)^0$ DECAY MODES	Fraction (Γ_i/Γ)	p (MeV/c)
$D^+\pi^-$	seen	385

$D_1(2420)^0$

$I(J^P) = \frac{1}{2}(1^+)$
I needs confirmation.

Mass $m = 2420.8 \pm 0.5$ MeV (S = 1.3)
$m_{D_1^0} - m_{D^{*+}} = 410.6 \pm 0.5$ (S = 1.3)
Full width $\Gamma = 31.7 \pm 2.5$ MeV (S = 3.5)

$\overline{D}_1(2420)^0$ modes are charge conjugates of modes below.

$D_1(2420)^0$ DECAY MODES	Fraction (Γ_i/Γ)	p (MeV/c)
$D^*(2010)^+\pi^-$	seen	353
$D^0\pi^+\pi^-$	seen	425
$D^+\pi^-$	not seen	472
$D^{*0}\pi^+\pi^-$	not seen	279

$D_2^*(2460)^0$

$I(J^P) = \frac{1}{2}(2^+)$

$J^P = 2^+$ assignment strongly favored.

Mass $m = 2460.7 \pm 0.4$ MeV (S = 3.1)
$m_{D_2^{*0}} - m_{D^+} = 591.0 \pm 0.4$ MeV (S = 2.9)
$m_{D_2^{*0}} - m_{D^{*+}} = 450.4 \pm 0.4$ MeV (S = 2.9)
Full width $\Gamma = 47.5 \pm 1.1$ MeV (S = 1.8)

$\overline{D}_2^*(2460)^0$ modes are charge conjugates of modes below.

$D_2^*(2460)^0$ DECAY MODES	Fraction (Γ_i/Γ)	p (MeV/c)
$D^+\pi^-$	seen	505
$D^*(2010)^+\pi^-$	seen	389
$D^0\pi^+\pi^-$	not seen	462
$D^{*0}\pi^+\pi^-$	not seen	324

$D_2^*(2460)^\pm$

$I(J^P) = \frac{1}{2}(2^+)$

$J^P = 2^+$ assignment strongly favored.

Mass $m = 2465.4 \pm 1.3$ MeV (S = 3.1)
$m_{D_2^*(2460)^\pm} - m_{D_2^*(2460)^0} = 2.4 \pm 1.7$ MeV
Full width $\Gamma = 46.7 \pm 1.2$ MeV

$D_2^*(2460)^-$ modes are charge conjugates of modes below.

$D_2^*(2460)^\pm$ DECAY MODES	Fraction (Γ_i/Γ)	p (MeV/c)
$D^0\pi^+$	seen	513
$D^{*0}\pi^+$	seen	396
$D^+\pi^+\pi^-$	not seen	462
$D^{*+}\pi^+\pi^-$	not seen	326

CHARMED, STRANGE MESONS ($C = S = \pm 1$)

$D_s^+ = c\overline{s}$, $D_s^- = \overline{c}s$, similarly for D_s^*'s

$D_s^\pm$

$I(J^P) = 0(0^-)$

Mass $m = 1968.34 \pm 0.07$ MeV
$m_{D_s^\pm} - m_{D^\pm} = 98.69 \pm 0.05$ MeV
Mean life $\tau = (504 \pm 4) \times 10^{-15}$ s (S = 1.2)
$c\tau = 151.2$ μm

CP-violating decay-rate asymmetries

$A_{CP}(\mu^\pm\nu) = (5 \pm 6)\%$
$A_{CP}(K^\pm K_S^0) = (0.08 \pm 0.26)\%$
$A_{CP}(K^+K^-\pi^\pm) = (-0.5 \pm 0.9)\%$
$A_{CP}(\phi\pi^\pm) = (-0.38 \pm 0.27)\%$
$A_{CP}(K^\pm K_S^0\pi^0) = (-2 \pm 6)\%$
$A_{CP}(2K_S^0\pi^\pm) = (3 \pm 5)\%$
$A_{CP}(K^+K^-\pi^\pm\pi^0) = (0.0 \pm 3.0)\%$
$A_{CP}(K^\pm K_S^0\pi^+\pi^-) = (-6 \pm 5)\%$
$A_{CP}(K_S^0 K^\mp 2\pi^\pm) = (4.1 \pm 2.8)\%$
$A_{CP}(\pi^+\pi^-\pi^\pm) = (-0.7 \pm 3.1)\%$
$A_{CP}(\pi^\pm\eta) = (1.1 \pm 3.1)\%$
$A_{CP}(\pi^\pm\eta') = (-0.9 \pm 0.5)\%$
$A_{CP}(\eta\pi^\pm\pi^0) = (-1 \pm 4)\%$
$A_{CP}(\eta'\pi^\pm\pi^0) = (0 \pm 8)\%$
$A_{CP}(K^\pm\pi^0) = (-27 \pm 24)\%$
$A_{CP}(\overline{K}^0/K^0\pi^\pm) = (0.4 \pm 0.5)\%$
$A_{CP}(K_S^0\pi^\pm) = (3.1 \pm 2.6)\%$ (S = 1.7)
$A_{CP}(K^\pm\pi^+\pi^-) = (4 \pm 5)\%$
$A_{CP}(K^\pm\eta) = (9 \pm 15)\%$
$A_{CP}(K^\pm\eta'(958)) = (6 \pm 19)\%$

CP violating asymmetries of *P*-odd (*T*-odd) moments

$A_T(K_S^0 K^\pm\pi^+\pi^-) = (-14 \pm 8) \times 10^{-3}$ [*ss*]

$D_s^+ \to \phi\ell^+\nu_\ell$ form factors

$r_2 = 0.84 \pm 0.11$ (S = 2.4)
$r_v = 1.80 \pm 0.08$
$\Gamma_L/\Gamma_T = 0.72 \pm 0.18$

Unless otherwise noted, the branching fractions for modes with a resonance in the final state include all the decay modes of the resonance. D_s^- modes are charge conjugates of the modes below.

D_s^+ DECAY MODES		Fraction (Γ_i/Γ)	Scale factor/ Confidence level	p (MeV/c)
Inclusive modes				
e^+ semileptonic	[*kkk*]	(6.5 ±0.4) %		–
π^+ anything		(119.3 ±1.4) %		–
π^- anything		(43.2 ±0.9) %		–
π^0 anything		(123 ±7) %		–
K^- anything		(18.7 ±0.5) %		–
K^+ anything		(28.9 ±0.7) %		–
K_S^0 anything		(19.0 ±1.1) %		–
η anything	[*lll*]	(29.9 ±2.8) %		–
ω anything		(6.1 ±1.4) %		–
η' anything	[*nnn*]	(10.3 ±1.4) %	S=1.1	–
$f_0(980)$ anything, $f_0 \to \pi^+\pi^-$		< 1.3 %	CL=90%	–
ϕ anything		(15.7 ±1.0) %		–
K^+K^- anything		(15.8 ±0.7) %		–
$K_S^0 K^+$ anything		(5.8 ±0.5) %		–
$K_S^0 K^-$ anything		(1.9 ±0.4) %		–
$2K_S^0$ anything		(1.70±0.32) %		–
$2K^+$ anything		< 2.6 $\times 10^{-3}$	CL=90%	–
$2K^-$ anything		< 6 $\times 10^{-4}$	CL=90%	–
Leptonic and semileptonic modes				
$e^+\nu_e$		< 8.3 $\times 10^{-5}$	CL=90%	984
$\mu^+\nu_\mu$		(5.50±0.23) $\times 10^{-3}$		981
$\tau^+\nu_\tau$		(5.48±0.23) %		182
$K^+K^-e^+\nu_e$		—		851
$\phi e^+\nu_e$	[*ooo*]	(2.39±0.16) %	S=1.3	720
$\phi\mu^+\nu_\mu$		(1.9 ±0.5) %		715

$\eta e^+\nu_e$ + $\eta'(958) e^+\nu_e$	[ooo]	(3.03±0.24) %			–
$\eta e^+\nu_e$	[ooo]	(2.29±0.19) %			908
$\eta'(958) e^+\nu_e$	[ooo]	(7.4 ±1.4) × 10^{-3}			751
$\eta\mu^+\nu_\mu$		(2.4 ±0.5) %			905
$\eta'(958)\mu^+\nu_\mu$		(1.1 ±0.5) %			747
$\omega e^+\nu_e$	[ppp]	< 2.0 × 10^{-3}		CL=90%	829
$K^0 e^+\nu_e$		(3.9 ±0.9) × 10^{-3}			921
$K^*(892)^0 e^+\nu_e$	[ooo]	(1.8 ±0.4) × 10^{-3}			782
Hadronic modes with a $K\overline{K}$ pair					
$K^+ K^0_S$		(1.50±0.05) %			850
$K^+ \overline{K}^0$		(2.95±0.14) %			850
$K^+ K^-\pi^+$	[tt]	(5.45±0.17) %		S=1.2	805
$\phi\pi^+$	[ooo,qqq]	(4.5 ±0.4) %			712
$\phi\pi^+$, $\phi \to K^+K^-$	[qqq]	(2.27±0.08) %			712
$K^+\overline{K}^*(892)^0$, $\overline{K}^{*0} \to K^-\pi^+$		(2.61±0.09) %			416
$f_0(980)\pi^+$, $f_0 \to K^+K^-$		(1.15±0.32) %			732
$f_0(1370)\pi^+$, $f_0 \to K^+K^-$		(7 ±5) × 10^{-4}			–
$f_0(1710)\pi^+$, $f_0 \to K^+K^-$		(6.7 ±2.9) × 10^{-4}			198
$K^+\overline{K}^*_0(1430)^0$, $\overline{K}^*_0 \to K^-\pi^+$		(1.9 ±0.4) × 10^{-3}			218
$K^+ K^0_S\pi^0$		(1.52±0.22) %			805
$2K^0_S\pi^+$		(7.7 ±0.6) × 10^{-3}			802
$K^0\overline{K}^0\pi^+$		—			802
$K^*(892)^+\overline{K}^0$	[ooo]	(5.4 ±1.2) %			683
$K^+K^-\pi^+\pi^0$		(6.3 ±0.6) %			748
$\phi\rho^+$	[ooo]	(8.4 $^{+1.9}_{-2.3}$) %			401
$K^0_S K^-2\pi^+$		(1.68±0.10) %			744
$K^*(892)^+\overline{K}^*(892)^0$	[ooo]	(7.2 ±2.6) %			416
$K^+ K^0_S\pi^+\pi^-$		(1.00±0.08) %			744
$K^+K^-2\pi^+\pi^-$		(8.7 ±1.5) × 10^{-3}			673
$\phi 2\pi^+\pi^-$	[ooo]	(1.21±0.16) %			640
$K^+K^-\rho^0\pi^+$ non-ϕ		< 2.6 × 10^{-4}		CL=90%	249
$\phi\rho^0\pi^+$, $\phi \to K^+K^-$		(6.5 ±1.3) × 10^{-3}			181
$\phi a_1(1260)^+$, $\phi \to K^+K^-$, $a_1^+ \to \rho^0\pi^+$		(7.5 ±1.2) × 10^{-3}			†
$K^+K^-2\pi^+\pi^-$ nonresonant		(9 ±7) × 10^{-4}			673
$2K^0_S 2\pi^+\pi^-$		(9 ±4) × 10^{-4}			669
Hadronic modes without K's					
$\pi^+\pi^0$		< 3.5 × 10^{-4}		CL=90%	975
$2\pi^+\pi^-$		(1.09±0.05) %		S=1.1	959
$\rho^0\pi^+$		(2.0 ±1.2) × 10^{-4}			825
$\pi^+(\pi^+\pi^-)_{S-wave}$	[rrr]	(9.1 ±0.4) × 10^{-3}			959
$f_2(1270)\pi^+$, $f_2 \to \pi^+\pi^-$		(1.10±0.20) × 10^{-3}			559
$\rho(1450)^0\pi^+$, $\rho^0 \to \pi^+\pi^-$		(3.0 ±2.0) × 10^{-4}			421
$\pi^+ 2\pi^0$		(6.5 ±1.3) × 10^{-3}			961
$2\pi^+\pi^-\pi^0$		—			935
$\eta\pi^+$	[ooo]	(1.70±0.09) %		S=1.1	902
$\omega\pi^+$	[ooo]	(2.4 ±0.6) × 10^{-3}			822
$3\pi^+2\pi^-$		(8.0 ±0.8) × 10^{-3}			899
$2\pi^+\pi^-2\pi^0$		—			902
$\eta\rho^+$	[ooo]	(8.9 ±0.8) %			724
$\eta\pi^+\pi^0$		(9.2 ±1.2) %			885
$\omega\pi^+\pi^0$	[ooo]	(2.8 ±0.7) %			802
$3\pi^+2\pi^-\pi^0$		(4.9 ±3.2) %			856
$\omega 2\pi^+\pi^-$	[ooo]	(1.6 ±0.5) %			766
$\eta'(958)\pi^+$	[nnn,ooo]	(3.94±0.25) %			743
$3\pi^+2\pi^-2\pi^0$		—			803
$\omega\eta\pi^+$	[ooo]	< 2.13 %		CL=90%	654
$\eta'(958)\rho^+$	[nnn,ooo]	(5.8 ±1.5) %			465
$\eta'(958)\pi^+\pi^0$		(5.6 ±0.8) %			720
$\eta'(958)\pi^+\pi^0$ nonresonant		< 5.1 %		CL=90%	720
Modes with one or three K's					
$K^+\pi^0$		(6.3 ±2.1) × 10^{-4}			917
$K^0_S\pi^+$		(1.22±0.06) × 10^{-3}			916
$K^+\eta$	[ooo]	(1.77±0.35) × 10^{-3}			835
$K^+\omega$	[ooo]	< 2.4 × 10^{-3}		CL=90%	741
$K^+\eta'(958)$	[ooo]	(1.8 ±0.6) × 10^{-3}			646
$K^+\pi^+\pi^-$		(6.6 ±0.4) × 10^{-3}			900
$K^+\rho^0$		(2.5 ±0.4) × 10^{-3}			745
$K^+\rho(1450)^0$, $\rho^0 \to \pi^+\pi^-$		(7.0 ±2.4) × 10^{-4}			–
$K^*(892)^0\pi^+$, $K^{*0} \to K^+\pi^-$		(1.42±0.24) × 10^{-3}			775
$K^*(1410)^0\pi^+$, $K^{*0} \to K^+\pi^-$		(1.24±0.29) × 10^{-3}			–
$K^*(1430)^0\pi^+$, $K^{*0} \to K^+\pi^-$		(5.0 ±3.5) × 10^{-4}			–
$K^+\pi^+\pi^-$ nonresonant		(1.04±0.34) × 10^{-3}			900
$K^0\pi^+\pi^0$		(1.00±0.18) %			899
$K^0_S 2\pi^+\pi^-$		(3.0 ±1.1) × 10^{-3}			870
$K^+\omega\pi^0$	[ooo]	< 8.2 × 10^{-3}		CL=90%	684
$K^+\omega\pi^+\pi^-$	[ooo]	< 5.4 × 10^{-3}		CL=90%	603
$K^+\omega\eta$	[ooo]	< 7.9 × 10^{-3}		CL=90%	366
$2K^+K^-$		(2.18±0.21) × 10^{-4}			628
ϕK^+, $\phi \to K^+K^-$		(8.9 ±2.0) × 10^{-5}			–
Doubly Cabibbo-suppressed modes					
$2K^+\pi^-$		(1.27±0.13) × 10^{-4}			805
$K^+K^*(892)^0$, $K^{*0} \to K^+\pi^-$		(6.0 ±3.4) × 10^{-5}			–
Baryon-antibaryon mode					
$p\overline{n}$		(1.3 ±0.4) × 10^{-3}			295
$\Delta C = 1$ weak neutral current ($C1$) modes, Lepton family number (LF), or Lepton number (L) violating modes					
$\pi^+ e^+ e^-$	[zz]	< 1.3 × 10^{-5}		CL=90%	979
$\pi^+\phi$, $\phi \to e^+e^-$	[yy]	(6 $^{+8}_{-4}$) × 10^{-6}			–
$\pi^+\mu^+\mu^-$	[zz]	< 4.1 × 10^{-7}		CL=90%	968
$K^+ e^+ e^-$	C1	< 3.7 × 10^{-6}		CL=90%	922
$K^+\mu^+\mu^-$	C1	< 2.1 × 10^{-5}		CL=90%	909
$K^*(892)^+\mu^+\mu^-$	C1	< 1.4 × 10^{-3}		CL=90%	765
$\pi^+ e^+\mu^-$	LF	< 1.2 × 10^{-5}		CL=90%	976
$\pi^+ e^-\mu^+$	LF	< 2.0 × 10^{-5}		CL=90%	976
$K^+ e^+\mu^-$	LF	< 1.4 × 10^{-5}		CL=90%	919
$K^+ e^-\mu^+$	LF	< 9.7 × 10^{-6}		CL=90%	919
$\pi^- 2e^+$	L	< 4.1 × 10^{-6}		CL=90%	979
$\pi^- 2\mu^+$	L	< 1.2 × 10^{-7}		CL=90%	968
$\pi^- e^+\mu^+$	L	< 8.4 × 10^{-6}		CL=90%	976
$K^- 2e^+$	L	< 5.2 × 10^{-6}		CL=90%	922
$K^- 2\mu^+$	L	< 1.3 × 10^{-5}		CL=90%	909
$K^- e^+\mu^+$	L	< 6.1 × 10^{-6}		CL=90%	919
$K^*(892)^- 2\mu^+$	L	< 1.4 × 10^{-3}		CL=90%	765

$D_s^{*\pm}$

$I(J^P) = 0(?^?)$

J^P is natural, width and decay modes consistent with 1^-.

Mass $m = 2112.2 \pm 0.4$ MeV
$m_{D_s^{*\pm}} - m_{D_s^{\pm}} = 143.8 \pm 0.4$ MeV
Full width $\Gamma < 1.9$ MeV, CL = 90%

D_s^{*-} modes are charge conjugates of the modes below.

D_s^{*+} DECAY MODES	Fraction (Γ_i/Γ)	p (MeV/c)
$D_s^+\gamma$	(93.5±0.7) %	139
$D_s^+\pi^0$	(5.8±0.7) %	48
$D_s^+ e^+ e^-$	(6.7±1.6) × 10^{-3}	139

$D_{s0}^*(2317)^{\pm}$

$I(J^P) = 0(0^+)$
J, P need confirmation.

J^P is natural, low mass consistent with 0^+.

Mass $m = 2317.7 \pm 0.6$ MeV (S = 1.1)
$m_{D_{s0}^*(2317)^{\pm}} - m_{D_s^{\pm}} = 349.4 \pm 0.6$ MeV (S = 1.1)
Full width $\Gamma < 3.8$ MeV, CL = 95%

$D_{s0}^*(2317)^-$ modes are charge conjugates of modes below.

$D_{s0}^*(2317)^{\pm}$ DECAY MODES	Fraction (Γ_i/Γ)	p (MeV/c)
$D_s^+\pi^0$	seen	298
$D_s^+\pi^0\pi^0$	not seen	205

Meson Summary Table

$D_{s1}(2460)^{\pm}$

$I(J^P) = 0(1^+)$

Mass $m = 2459.5 \pm 0.6$ MeV (S = 1.1)
$m_{D_{s1}(2460)^{\pm}} - m_{D_s^{*\pm}} = 347.3 \pm 0.7$ MeV (S = 1.2)
$m_{D_{s1}(2460)^{\pm}} - m_{D_s^{\pm}} = 491.2 \pm 0.6$ MeV (S = 1.1)
Full width $\Gamma < 3.5$ MeV, CL = 95%

$D_{s1}(2460)^-$ modes are charge conjugates of the modes below.

$D_{s1}(2460)^+$ DECAY MODES	Fraction (Γ_i/Γ)	Scale factor/ Confidence level	p (MeV/c)
$D_s^{*+}\pi^0$	(48 ±11) %		297
$D_s^+\gamma$	(18 ± 4) %		442
$D_s^+\pi^+\pi^-$	(4.3± 1.3) %	S=1.1	363
$D_s^{*+}\gamma$	< 8 %	CL=90%	323
$D_{s0}^*(2317)^+\gamma$	($3.7^{+\ 5.0}_{-\ 2.4}$) %		138

$D_{s1}(2536)^{\pm}$

$I(J^P) = 0(1^+)$
J, P need confirmation.

Mass $m = 2535.10 \pm 0.06$ MeV
Full width $\Gamma = 0.92 \pm 0.05$ MeV

$D_{s1}(2536)^-$ modes are charge conjugates of the modes below.

$D_{s1}(2536)^+$ DECAY MODES	Fraction (Γ_i/Γ)	Confidence level	p (MeV/c)
$D^*(2010)^+K^0$	0.85 ±0.12		149
$(D^*(2010)^+K^0)_{S-wave}$	0.61 ±0.09		149
$D^+\pi^-K^+$	0.028±0.005		176
$D^*(2007)^0K^+$	**DEFINED AS 1**		167
D^+K^0	<0.34	90%	381
D^0K^+	<0.12	90%	391
$D_s^{*+}\gamma$	possibly seen		388
$D_s^+\pi^+\pi^-$	seen		437

$D_{s2}^*(2573)$

$I(J^P) = 0(2^+)$

J^P is natural, width and decay modes consistent with 2^+.

Mass $m = 2569.1 \pm 0.8$ MeV (S = 2.4)
Full width $\Gamma = 16.9 \pm 0.8$ MeV

$D_{s2}^*(2573)^-$ modes are charge conjugates of the modes below.

$D_{s2}^*(2573)^+$ DECAY MODES	Fraction (Γ_i/Γ)	p (MeV/c)
D^0K^+	seen	431
$D^*(2007)^0K^+$	not seen	238

$D_{s1}^*(2700)^{\pm}$

$I(J^P) = 0(1^-)$

Mass $m = 2708.3^{+4.0}_{-3.4}$ MeV
Full width $\Gamma = 120 \pm 11$ MeV

BOTTOM MESONS ($B = \pm 1$)

$B^+ = u\overline{b}$, $B^0 = d\overline{b}$, $\overline{B}^0 = \overline{d}b$, $B^- = \overline{u}b$, similarly for B^*'s

B-particle organization

Many measurements of B decays involve admixtures of B hadrons. Previously we arbitrarily included such admixtures in the $B^{\pm}$ section, but because of their importance we have created two new sections: "$B^{\pm}/B^0$ Admixture" for $\Upsilon(4S)$ results and "$B^{\pm}/B^0/B_s^0$/b-baryon Admixture" for results at higher energies. Most inclusive decay branching fractions and χ_b at high energy are found in the Admixture sections. B^0-$\overline{B}^0$ mixing data are found in the B^0 section, while B_s^0-$\overline{B}_s^0$ mixing data and B-$\overline{B}$ mixing data for a B^0/B_s^0 admixture are found in the B_s^0 section. CP-violation data are found in the $B^{\pm}$, B^0, and $B^{\pm}$ B^0 Admixture sections. b-baryons are found near the end of the Baryon section.

The organization of the B sections is now as follows, where bullets indicate particle sections and brackets indicate reviews.

- $B^{\pm}$
  mass, mean life, CP violation, branching fractions
- B^0
  mass, mean life, B^0-$\overline{B}^0$ mixing, CP violation, branching fractions
- $B^{\pm}/B^0$ Admixtures
  CP violation, branching fractions
- $B^{\pm}/B^0/B_s^0$/b-baryon Admixtures
  mean life, production fractions, branching fractions
- B^*
  mass
- $B_1(5721)^+$
  mass
- $B_1(5721)^0$
  mass
- $B_2^*(5747)^+$
  mass
- $B_2^*(5747)^0$
  mass
- $B_J^*(5970)^+$
  mass
- $B_J^*(5970)^0$
  mass
- B_s^0
  mass, mean life, B_s^0-$\overline{B}_s^0$ mixing, CP violation, branching fractions
- B_s^*
  mass
- $B_{s1}(5830)^0$
  mass
- $B_{s2}^*(5840)^0$
  mass
- $B_c^{\pm}$
  mass, mean life, branching fractions

At the end of Baryon Listings:

- Λ_b
  mass, mean life, branching fractions
- $\Lambda_b(5912)^0$
  mass, mean life
- $\Lambda_b(5920)^0$
  mass, mean life
- Σ_b
  mass
- Σ_b^*
  mass
- Ξ_b^0, Ξ_b^-
  mass, mean life, branching fractions
- $\Xi_b'(5935)^-$
  mass
- $\Xi_b(5945)^0$
  mass
- $\Xi_b^*(5955)^-$
  mass
- Ω_b^-
  mass, branching fractions

• b-baryon Admixture

mean life, branching fractions

$B^{\pm}$ $I(J^P) = \frac{1}{2}(0^-)$

I, J, P need confirmation. Quantum numbers shown are quark-model predictions.

Mass $m_{B^{\pm}} = 5279.32 \pm 0.14$ MeV (S = 1.1)
Mean life $\tau_{B^{\pm}} = (1.638 \pm 0.004) \times 10^{-12}$ s
$c\tau = 491.1\ \mu$m

CP violation

$A_{CP}(B^+ \to J/\psi(1S)K^+) = (1.8 \pm 3.0) \times 10^{-3}$ (S = 1.5)
$A_{CP}(B^+ \to J/\psi(1S)\pi^+) = (1.8 \pm 1.2) \times 10^{-2}$ (S = 1.3)
$A_{CP}(B^+ \to J/\psi\rho^+) = -0.11 \pm 0.14$
$A_{CP}(B^+ \to J/\psi K^*(892)^+) = -0.048 \pm 0.033$
$A_{CP}(B^+ \to \eta_c K^+) = 0.01 \pm 0.07$ (S = 2.2)
$A_{CP}(B^+ \to \psi(2S)\pi^+) = 0.03 \pm 0.06$
$A_{CP}(B^+ \to \psi(2S)K^+) = 0.012 \pm 0.020$ (S = 1.5)
$A_{CP}(B^+ \to \psi(2S)K^*(892)^+) = 0.08 \pm 0.21$
$A_{CP}(B^+ \to \chi_{c1}(1P)\pi^+) = 0.07 \pm 0.18$
$A_{CP}(B^+ \to \chi_{c0}K^+) = -0.20 \pm 0.18$ (S = 1.5)
$A_{CP}(B^+ \to \chi_{c1}K^+) = -0.009 \pm 0.033$
$A_{CP}(B^+ \to \chi_{c1}K^*(892)^+) = 0.5 \pm 0.5$
$A_{CP}(B^+ \to D^0\ell^+\nu_\ell) = (-0.14 \pm 0.20) \times 10^{-2}$
$A_{CP}(B^+ \to \overline{D}{}^0\pi^+) = -0.007 \pm 0.007$
$A_{CP}(B^+ \to D_{CP(+1)}\pi^+) = -0.0080 \pm 0.0026$
$A_{CP}(B^+ \to D_{CP(-1)}\pi^+) = 0.017 \pm 0.026$
$A_{CP}([K^{\mp}\pi^{\pm}\pi^+\pi^-]_D\pi^+) = 0.02 \pm 0.05$
$A_{CP}(B^+ \to [\pi^+\pi^+\pi^-\pi^-]_D K^+) = 0.10 \pm 0.04$
$A_{CP}(B^+ \to [\pi^+\pi^-\pi^+\pi^-]_D K^*(892)^+) = 0.02 \pm 0.11$
$A_{CP}(B^+ \to \overline{D}{}^0K^+) = -0.017 \pm 0.005$
$A_{CP}([K^{\mp}\pi^{\pm}\pi^+\pi^-]_D K^+) = -0.31 \pm 0.11$
$A_{CP}(B^+ \to [\pi^+\pi^+\pi^-\pi^-]_D\pi^+) = (-4 \pm 8) \times 10^{-3}$
$A_{CP}(B^+ \to [K^-\pi^+]_D K^+) = -0.58 \pm 0.21$
$A_{CP}(B^+ \to [K^-\pi^+\pi^0]_D K^+) = 0.07 \pm 0.30$ (S = 1.5)
$A_{CP}(B^+ \to [K^+K^-\pi^0]_D K^+) = 0.30 \pm 0.20$
$A_{CP}(B^+ \to [\pi^+\pi^-\pi^0]_D K^+) = 0.05 \pm 0.09$
$A_{CP}(B^+ \to \overline{D}{}^0K^*(892)^+) = -0.007 \pm 0.019$
$A_{CP}(B^+ \to [K^-\pi^+]_{\overline{D}}K^*(892)^+) = -0.75 \pm 0.16$
$A_{CP}(B^+ \to [K^-\pi^+\pi^-\pi^+]_{\overline{D}}K^*(892)^+) = -0.45 \pm 0.25$
$A_{CP}(B^+ \to [K^-\pi^+]_D\pi^+) = 0.00 \pm 0.09$
$A_{CP}(B^+ \to [K^-\pi^+\pi^0]_D\pi^+) = 0.35 \pm 0.16$
$A_{CP}(B^+ \to [K^+K^-\pi^0]_D\pi^+) = -0.03 \pm 0.04$
$A_{CP}(B^+ \to [\pi^+\pi^-\pi^0]_D\pi^+) = -0.016 \pm 0.020$
$A_{CP}(B^+ \to [K^-\pi^+]_{(D\pi)}\pi^+) = -0.09 \pm 0.27$
$A_{CP}(B^+ \to [K^-\pi^+]_{(D\gamma)}\pi^+) = -0.7 \pm 0.6$
$A_{CP}(B^+ \to [K^-\pi^+]_{(D\pi)}K^+) = 0.8 \pm 0.4$
$A_{CP}(B^+ \to [K^-\pi^+]_{(D\gamma)}K^+) = 0.4 \pm 1.0$
$A_{CP}(B^+ \to [\pi^+\pi^-\pi^0]_D K^+) = -0.02 \pm 0.15$
$A_{CP}(B^+ \to [K^0_S K^+\pi^-]_D K^+) = 0.04 \pm 0.09$
$A_{CP}(B^+ \to [K^0_S K^-\pi^+]_D K^+) = 0.23 \pm 0.13$
$A_{CP}(B^+ \to [K^0_S K^-\pi^+]_D\pi^+) = -0.052 \pm 0.034$
$A_{CP}(B^+ \to [K^0_S K^+\pi^-]_D\pi^+) = -0.025 \pm 0.026$
$A_{CP}(B^+ \to [K^*(892)^-K^+]_D K^+) = 0.03 \pm 0.11$
$A_{CP}(B^+ \to [K^*(892)^+K^-]_D K^+) = 0.34 \pm 0.21$
$A_{CP}(B^+ \to [K^*(892)^+K^-]_D\pi^+) = -0.05 \pm 0.05$
$A_{CP}(B^+ \to [K^*(892)^-K^+]_D\pi^+) = -0.012 \pm 0.030$
$A_{CP}(B^+ \to D_{CP(+1)}K^+)$ $= 0.120 \pm 0.014$ (S = 1.4)
$A_{ADS}(B^+ \to DK^+) = -0.40 \pm 0.06$
$A_{ADS}(B^+ \to D\pi^+) = 0.100 \pm 0.032$
$A_{ADS}(B^+ \to [K^-\pi^+]_D K^+\pi^-\pi^+) = -0.33 \pm 0.35$
$A_{ADS}(B^+ \to [K^-\pi^+]_D\pi^+\pi^-\pi^+) = -0.01 \pm 0.09$
$A_{CP}(B^+ \to D_{CP(-1)}K^+) = -0.10 \pm 0.07$
$A_{CP}(B^+ \to [K^+K^-]_D K^+\pi^-\pi^+) = -0.04 \pm 0.06$
$A_{CP}(B^+ \to [\pi^+\pi^-]_D K^+\pi^-\pi^+) = -0.05 \pm 0.10$
$A_{CP}(B^+ \to [K^-\pi^+]_D K^+\pi^-\pi^+) = 0.013 \pm 0.023$
$A_{CP}(B^+ \to [K^+K^-]_D\pi^+\pi^-\pi^+) = -0.019 \pm 0.015$
$A_{CP}(B^+ \to [\pi^+\pi^-]_D\pi^+\pi^-\pi^+) = -0.013 \pm 0.019$
$A_{CP}(B^+ \to [K^-\pi^+]_D\pi^+\pi^-\pi^+) = -0.002 \pm 0.011$
$A_{CP}(B^+ \to \overline{D}{}^{*0}\pi^+) = 0.0010 \pm 0.0028$
$A_{CP}(B^+ \to (D^*_{CP(+1)})^0\pi^+) = 0.016 \pm 0.010$ (S = 1.2)
$A_{CP}(B^+ \to (D^*_{CP(-1)})^0\pi^+) = -0.09 \pm 0.05$
$A_{CP}(B^+ \to D^{*0}K^+) = -0.001 \pm 0.011$ (S = 1.1)
$A_{CP}(B^+ \to D^{*0}_{CP(+1)}K^+) = -0.11 \pm 0.08$ (S = 2.7)
$A_{CP}(B^+ \to D^*_{CP(-1)}K^+) = 0.07 \pm 0.10$
$A_{CP}(B^+ \to D_{CP(+1)}K^*(892)^+) = 0.08 \pm 0.06$
$A_{CP}(B^+ \to D_{CP(-1)}K^*(892)^+) = -0.23 \pm 0.22$
$A_{CP}(B^+ \to D^+_s\phi) = 0.0 \pm 0.4$
$A_{CP}(B^+ \to D^{*+}\overline{D}{}^{*0}) = -0.15 \pm 0.11$
$A_{CP}(B^+ \to D^{*+}\overline{D}{}^0) = -0.06 \pm 0.13$
$A_{CP}(B^+ \to D^+\overline{D}{}^{*0}) = 0.13 \pm 0.18$
$A_{CP}(B^+ \to D^+\overline{D}{}^0) = -0.03 \pm 0.07$
$A_{CP}(B^+ \to K^0_S\pi^+) = -0.017 \pm 0.016$
$A_{CP}(B^+ \to K^+\pi^0) = 0.037 \pm 0.021$
$A_{CP}(B^+ \to \eta' K^+) = 0.004 \pm 0.011$
$A_{CP}(B^+ \to \eta' K^*(892)^+) = -0.26 \pm 0.27$
$A_{CP}(B^+ \to \eta' K^*_0(1430)^+) = 0.06 \pm 0.20$
$A_{CP}(B^+ \to \eta' K^*_2(1430)^+) = 0.15 \pm 0.13$
$A_{CP}(B^+ \to \eta K^+)$ $= -0.37 \pm 0.08$
$A_{CP}(B^+ \to \eta K^*(892)^+) = 0.02 \pm 0.06$
$A_{CP}(B^+ \to \eta K^*_0(1430)^+) = 0.05 \pm 0.13$
$A_{CP}(B^+ \to \eta K^*_2(1430)^+) = -0.45 \pm 0.30$
$A_{CP}(B^+ \to \omega K^+) = -0.02 \pm 0.04$
$A_{CP}(B^+ \to \omega K^{*+}) = 0.29 \pm 0.35$
$A_{CP}(B^+ \to \omega(K\pi)^{*+}_0) = -0.10 \pm 0.09$
$A_{CP}(B^+ \to \omega K^*_2(1430)^+) = 0.14 \pm 0.15$
$A_{CP}(B^+ \to K^{*0}\pi^+) = -0.04 \pm 0.09$ (S = 2.1)
$A_{CP}(B^+ \to K^*(892)^+\pi^0) = -0.39 \pm 0.21$ (S = 1.6)
$A_{CP}(B^+ \to K^+\pi^-\pi^+)$ $= 0.027 \pm 0.008$
$A_{CP}(B^+ \to K^+K^-K^+$ nonresonant$) = 0.06 \pm 0.05$
$A_{CP}(B^+ \to f(980)^0K^+) = -0.08 \pm 0.09$
$A_{CP}(B^+ \to f_2(1270)K^+)$ $= -0.68^{+0.19}_{-0.17}$
$A_{CP}(B^+ \to f_0(1500)K^+) = 0.28 \pm 0.30$
$A_{CP}(B^+ \to f'_2(1525)^0K^+) = -0.08^{+0.05}_{-0.04}$
$A_{CP}(B^+ \to \rho^0K^+)$ $= 0.37 \pm 0.10$
$A_{CP}(B^+ \to K^0\pi^+\pi^0) = 0.07 \pm 0.06$
$A_{CP}(B^+ \to K^*_0(1430)^0\pi^+) = 0.061 \pm 0.032$
$A_{CP}(B^+ \to K^*_0(1430)^+\pi^0) = 0.26^{+0.18}_{-0.14}$
$A_{CP}(B^+ \to K^*_2(1430)^0\pi^+) = 0.05^{+0.29}_{-0.24}$
$A_{CP}(B^+ \to K^+\pi^0\pi^0) = -0.06 \pm 0.07$
$A_{CP}(B^+ \to K^0\rho^+) = -0.03 \pm 0.15$
$A_{CP}(B^+ \to K^{*+}\pi^+\pi^-) = 0.07 \pm 0.08$
$A_{CP}(B^+ \to \rho^0K^*(892)^+) = 0.31 \pm 0.13$
$A_{CP}(B^+ \to K^*(892)^+f_0(980)) = -0.15 \pm 0.12$
$A_{CP}(B^+ \to a^+_1K^0) = 0.12 \pm 0.11$
$A_{CP}(B^+ \to b^+_1K^0) = -0.03 \pm 0.15$
$A_{CP}(B^+ \to K^*(892)^0\rho^+) = -0.01 \pm 0.16$
$A_{CP}(B^+ \to b^0_1K^+) = -0.46 \pm 0.20$
$A_{CP}(B^+ \to K^0K^+) = 0.04 \pm 0.14$
$A_{CP}(B^+ \to K^0_S K^+) = -0.21 \pm 0.14$
$A_{CP}(B^+ \to K^+K^0_S K^0_S) = 0.04^{+0.04}_{-0.05}$
$A_{CP}(B^+ \to K^+K^-\pi^+)$ $= -0.122 \pm 0.021$
$A_{CP}(B^+ \to K^+K^-K^+)$ $= -0.033 \pm 0.008$
$A_{CP}(B^+ \to \phi K^+) = 0.024 \pm 0.028$ (S = 2.3)
$A_{CP}(B^+ \to X_0(1550)K^+) = -0.04 \pm 0.07$
$A_{CP}(B^+ \to K^{*+}K^+K^-) = 0.11 \pm 0.09$
$A_{CP}(B^+ \to \phi K^*(892)^+) = -0.01 \pm 0.08$
$A_{CP}(B^+ \to \phi(K\pi)^{*+}_0) = 0.04 \pm 0.16$
$A_{CP}(B^+ \to \phi K_1(1270)^+) = 0.15 \pm 0.20$
$A_{CP}(B^+ \to \phi K^*_2(1430)^+) = -0.23 \pm 0.20$
$A_{CP}(B^+ \to K^+\phi\phi) = -0.10 \pm 0.08$
$A_{CP}(B^+ \to K^+[\phi\phi]_{\eta_c}) = 0.09 \pm 0.10$
$A_{CP}(B^+ \to K^*(892)^+\gamma) = 0.014 \pm 0.018$
$A_{CP}(B^+ \to \eta K^+\gamma) = -0.12 \pm 0.07$
$A_{CP}(B^+ \to \phi K^+\gamma) = -0.13 \pm 0.11$ (S = 1.1)
$A_{CP}(B^+ \to \rho^+\gamma) = -0.11 \pm 0.33$
$A_{CP}(B^+ \to \pi^+\pi^0) = 0.03 \pm 0.04$
$A_{CP}(B^+ \to \pi^+\pi^-\pi^+)$ $= 0.057 \pm 0.013$
$A_{CP}(B^+ \to \rho^0\pi^+) = 0.18^{+0.09}_{-0.17}$
$A_{CP}(B^+ \to f_2(1270)\pi^+) = 0.41 \pm 0.30$
$A_{CP}(B^+ \to \rho^0(1450)\pi^+) = -0.1^{+0.4}_{-0.5}$

Meson Summary Table

$A_{CP}(B^+ \to f_0(1370)\pi^+) = 0.72 \pm 0.22$
$A_{CP}(B^+ \to \pi^+\pi^-\pi^+ \text{ nonresonant}) = -0.14^{+0.23}_{-0.16}$
$A_{CP}(B^+ \to \rho^+\pi^0) = 0.02 \pm 0.11$
$A_{CP}(B^+ \to \rho^+\rho^0) = -0.05 \pm 0.05$
$A_{CP}(B^+ \to \omega\pi^+) = -0.04 \pm 0.06$
$A_{CP}(B^+ \to \omega\rho^+) = -0.20 \pm 0.09$
$A_{CP}(B^+ \to \eta\pi^+) = -0.14 \pm 0.07$ (S = 1.4)
$A_{CP}(B^+ \to \eta\rho^+) = 0.11 \pm 0.11$
$A_{CP}(B^+ \to \eta'\pi^+) = 0.06 \pm 0.16$
$A_{CP}(B^+ \to \eta'\rho^+) = 0.26 \pm 0.17$
$A_{CP}(B^+ \to b_1^0\pi^+) = 0.05 \pm 0.16$
$A_{CP}(B^+ \to p\overline{p}\pi^+) = 0.00 \pm 0.04$
$A_{CP}(B^+ \to p\overline{p}K^+) = 0.00 \pm 0.04$ (S = 2.2)
$A_{CP}(B^+ \to p\overline{p}K^*(892)^+) = 0.21 \pm 0.16$ (S = 1.4)
$A_{CP}(B^+ \to p\overline{\Lambda}\gamma) = 0.17 \pm 0.17$
$A_{CP}(B^+ \to p\overline{\Lambda}\pi^0) = 0.01 \pm 0.17$
$A_{CP}(B^+ \to K^+\ell^+\ell^-) = -0.02 \pm 0.08$
$A_{CP}(B^+ \to K^+e^+e^-) = 0.14 \pm 0.14$
$A_{CP}(B^+ \to K^+\mu^+\mu^-) = 0.011 \pm 0.017$
$A_{CP}(B^+ \to \pi^+\mu^+\mu^-) = -0.11 \pm 0.12$
$A_{CP}(B^+ \to K^{*+}\ell^+\ell^-) = -0.09 \pm 0.14$
$A_{CP}(B^+ \to K^*e^+e^-) = -0.14 \pm 0.23$
$A_{CP}(B^+ \to K^*\mu^+\mu^-) = -0.12 \pm 0.24$
$\gamma = (73.5^{+4.3}_{-5.0})^\circ$
$r_B(B^+ \to D^0K^+) = 0.103 \pm 0.005$
$\delta_B(B^+ \to D^0K^+) = (136.9^{+4.6}_{-5.2})^\circ$
$r_B(B^+ \to \overline{D}^0K^{*+}) = 0.075^{+0.017}_{-0.018}$
$\delta_B(B^+ \to D^0K^{*+}) = (106^{+18}_{-26})^\circ$
$r_B^*(B^+ \to D^{*0}K^+) = 0.142^{+0.019}_{-0.020}$
$\delta_B^*(B^+ \to D^{*0}K^+) = (321^{+8}_{-9})^\circ$

B^- modes are charge conjugates of the modes below. Modes which do not identify the charge state of the B are listed in the $B^\pm/B^0$ ADMIXTURE section.

The branching fractions listed below assume 50% $B^0\overline{B}^0$ and 50% B^+B^- production at the $\Upsilon(4S)$. We have attempted to bring older measurements up to date by rescaling their assumed $\Upsilon(4S)$ production ratio to 50:50 and their assumed D, D_s, D^*, and ψ branching ratios to current values whenever this would affect our averages and best limits significantly.

Indentation is used to indicate a subchannel of a previous reaction. All resonant subchannels have been corrected for resonance branching fractions to the final state so the sum of the subchannel branching fractions can exceed that of the final state.

For inclusive branching fractions, *e.g.*, $B \to D^\pm$ anything, the values usually are multiplicities, not branching fractions. They can be greater than one.

B^+ DECAY MODES		Fraction (Γ_i/Γ)	Scale factor/ Confidence level	p (MeV/c)
Semileptonic and leptonic modes				
$\ell^+\nu_\ell$ anything	[sss]	(10.99 ± 0.28) %		–
$e^+\nu_eX_c$		(10.8 ± 0.4) %		–
$D\ell^+\nu_\ell$ anything		(8.4 ± 0.5) %		–
$\overline{D}^0\ell^+\nu_\ell$	[sss]	(2.20 ± 0.10) %		2310
$\overline{D}^0\tau^+\nu_\tau$		(7.7 ± 2.5) $\times 10^{-3}$		1911
$\overline{D}^*(2007)^0\ell^+\nu_\ell$	[sss]	(4.88 ± 0.10) %		2258
$\overline{D}^*(2007)^0\tau^+\nu_\tau$		(1.88 ± 0.20) %		1839
$D^-\pi^+\ell^+\nu_\ell$		(4.1 ± 0.5) $\times 10^{-3}$		2306
$\overline{D}_0^*(2420)^0\ell^+\nu_\ell$, $\overline{D}_0^{*0} \to D^-\pi^+$		(2.5 ± 0.5) $\times 10^{-3}$		–
$\overline{D}_2^*(2460)^0\ell^+\nu_\ell$, $\overline{D}_2^{*0} \to D^-\pi^+$		(1.53 ± 0.16) $\times 10^{-3}$		2065
$D^{(*)}n\pi\ell^+\nu_\ell (n \geq 1)$		(1.60 ± 0.22) %		–
$D^{*-}\pi^+\ell^+\nu_\ell$		(6.1 ± 0.6) $\times 10^{-3}$		2254
$\overline{D}_1(2420)^0\ell^+\nu_\ell$, $\overline{D}_1^0 \to D^{*-}\pi^+$		(3.03 ± 0.20) $\times 10^{-3}$		2084
$\overline{D}_1'(2430)^0\ell^+\nu_\ell$, $\overline{D}_1'^0 \to D^{*-}\pi^+$		(2.7 ± 0.6) $\times 10^{-3}$		–
$\overline{D}_2^*(2460)^0\ell^+\nu_\ell$, $\overline{D}_2^{*0} \to D^{*-}\pi^+$		(1.01 ± 0.24) $\times 10^{-3}$	S=2.0	2065
$\overline{D}^0\pi^+\pi^-\ell^+\nu_\ell$		(1.56 ± 0.34) $\times 10^{-3}$		2301
$\overline{D}^{*0}\pi^+\pi^-\ell^+\nu_\ell$		(7 ± 4) $\times 10^{-4}$		2248
$D_s^{(*)-}K^+\ell^+\nu_\ell$		(6.1 ± 1.0) $\times 10^{-4}$		–
$D_s^-K^+\ell^+\nu_\ell$		(3.0 $^{+1.4}_{-1.2}$) $\times 10^{-4}$		2242
$D_s^{*-}K^+\ell^+\nu_\ell$		(2.9 ± 1.9) $\times 10^{-4}$		2185
$\pi^0\ell^+\nu_\ell$		(7.80 ± 0.27) $\times 10^{-5}$		2638
$\eta\ell^+\nu_\ell$		(3.9 ± 0.5) $\times 10^{-5}$		2611
$\eta'\ell^+\nu_\ell$		(2.3 ± 0.8) $\times 10^{-5}$		2553
$\omega\ell^+\nu_\ell$	[sss]	(1.19 ± 0.09) $\times 10^{-4}$		2582
$\rho^0\ell^+\nu_\ell$	[sss]	(1.58 ± 0.11) $\times 10^{-4}$		2583
$p\overline{p}\ell^+\nu_\ell$		(5.8 $^{+2.6}_{-2.3}$) $\times 10^{-6}$		2467
$p\overline{p}\mu^+\nu_\mu$		< 8.5 $\times 10^{-6}$	CL=90%	2446
$p\overline{p}e^+\nu_e$		(8.2 $^{+4.0}_{-3.3}$) $\times 10^{-6}$		2467
$e^+\nu_e$		< 9.8 $\times 10^{-7}$	CL=90%	2640
$\mu^+\nu_\mu$		< 1.0 $\times 10^{-6}$	CL=90%	2639
$\tau^+\nu_\tau$		(1.09 ± 0.24) $\times 10^{-4}$	S=1.2	2341
$\ell^+\nu_\ell\gamma$		< 3.5 $\times 10^{-6}$	CL=90%	2640
$e^+\nu_e\gamma$		< 6.1 $\times 10^{-6}$	CL=90%	2640
$\mu^+\nu_\mu\gamma$		< 3.4 $\times 10^{-6}$	CL=90%	2639
Inclusive modes				
D^0X		(8.6 ± 0.7) %		–
$\overline{D}^0X$		(79 ± 4) %		–
D^+X		(2.5 ± 0.5) %		–
D^-X		(9.9 ± 1.2) %		–
D_s^+X		(7.9 $^{+1.4}_{-1.3}$) %		–
D_s^-X		(1.10 $^{+0.40}_{-0.32}$) %		–
Λ_c^+X		(2.1 $^{+0.9}_{-0.6}$) %		–
$\overline{\Lambda}_c^-X$		(2.8 $^{+1.1}_{-0.9}$) %		–
$\overline{c}X$		(97 ± 4) %		–
cX		(23.4 $^{+2.2}_{-1.8}$) %		–
$c/\overline{c}X$		(120 ± 6) %		–
D, D^*, or D_s modes				
$\overline{D}^0\pi^+$		(4.68 ± 0.13) $\times 10^{-3}$		2308
$D_{CP(+1)}\pi^+$	[ttt]	(2.05 ± 0.18) $\times 10^{-3}$		–
$D_{CP(-1)}\pi^+$	[ttt]	(2.0 ± 0.4) $\times 10^{-3}$		–
$\overline{D}^0\rho^+$		(1.34 ± 0.18) %		2237
$\overline{D}^0K^+$		(3.63 ± 0.12) $\times 10^{-4}$		2281
$D_{CP(+1)}K^+$	[ttt]	(1.80 ± 0.07) $\times 10^{-4}$		–
$D_{CP(-1)}K^+$	[ttt]	(1.96 ± 0.18) $\times 10^{-4}$		–
$[K^-\pi^+]_DK^+$	[uuu]	< 2.8 $\times 10^{-7}$	CL=90%	–
$[K^+\pi^-]_DK^+$	[uuu]	< 1.5 $\times 10^{-5}$	CL=90%	–
$[K^-\pi^+\pi^0]_DK^+$		seen		–
$[K^+\pi^-\pi^0]_DK^+$		seen		–
$[K^-\pi^+\pi^+\pi^-]_DK^+$		seen		–
$[K^+\pi^-\pi^+\pi^-]_DK^+$		seen		–
$[K^-\pi^+]_D\pi^+$	[uuu]	(6.3 ± 1.1) $\times 10^{-7}$		–
$[K^+\pi^-]_D\pi^+$		(1.78 ± 0.32) $\times 10^{-4}$		–
$[K^-\pi^+\pi^0]_D\pi^+$		seen		–
$[K^+\pi^-\pi^0]_D\pi^+$		seen		–
$[K^-\pi^+\pi^+\pi^-]_D\pi^+$		seen		–
$[K^+\pi^-\pi^+\pi^-]_D\pi^+$		seen		–
$[\pi^+\pi^-\pi^0]_DK^-$		(4.6 ± 0.9) $\times 10^{-6}$		–
$[K^0_S K^+\pi^-]_DK^+$		seen		–
$[K^0_S K^-\pi^+]_DK^+$		seen		–
$[K^*(892)^+K^-]_DK^+$		seen		–
$[K^0_S K^-\pi^+]_D\pi^+$		seen		–
$[K^*(892)^+K^-]_D\pi^+$		seen		–
$[K^0_S K^+\pi^-]_D\pi^+$		seen		–
$[K^*(892)^-K^+]_D\pi^+$		seen		–
$\overline{D}^0K^*(892)^+$		(5.3 ± 0.4) $\times 10^{-4}$		2213
$D_{CP(-1)}K^*(892)^+$	[ttt]	(2.7 ± 0.8) $\times 10^{-4}$		–
$D_{CP(+1)}K^*(892)^+$	[ttt]	(6.2 ± 0.6) $\times 10^{-4}$		–
$\overline{D}^0K^+\pi^+\pi^-$		(5.2 ± 2.1) $\times 10^{-4}$		2237
$\overline{D}^0K^+\overline{K}^0$		(5.5 ± 1.6) $\times 10^{-4}$		2189
$\overline{D}^0K^+\overline{K}^*(892)^0$		(7.5 ± 1.7) $\times 10^{-4}$		2071
$\overline{D}^0\pi^+\pi^+\pi^-$		(5.6 ± 2.1) $\times 10^{-3}$	S=3.6	2289
$\overline{D}^0\pi^+\pi^+\pi^-$ nonresonant		(5 ± 4) $\times 10^{-3}$		2289
$\overline{D}^0\pi^+\rho^0$		(4.2 ± 3.0) $\times 10^{-3}$		2208
$\overline{D}^0a_1(1260)^+$		(4 ± 4) $\times 10^{-3}$		2123
$\overline{D}^0\omega\pi^+$		(4.1 ± 0.9) $\times 10^{-3}$		2206
$D^*(2010)^-\pi^+\pi^+$		(1.35 ± 0.22) $\times 10^{-3}$		2247
$D^*(2010)^-K^+\pi^+$		(8.2 ± 1.4) $\times 10^{-5}$		2206

$\overline{D}_1(2420)^0\pi^+,\ \overline{D}_1^0\to D^*(2010)^-\pi^+$		(5.2 ± 2.2)	$\times10^{-4}$			2081
$D^-\pi^+\pi^+$		(1.07 ± 0.05)	$\times10^{-3}$			2299
$D^-K^+\pi^+$		(7.7 ± 0.5)	$\times10^{-5}$			2260
$D_0^*(2400)^0K^+,\ D_0^{*0}\to D^-\pi^+$		(6.1 ± 2.4)	$\times10^{-6}$			–
$D_2^*(2460)^0K^+,\ D_2^{*0}\to D^-\pi^+$		(2.32 ± 0.23)	$\times10^{-5}$			–
$D_1^*(2760)^0K^+,\ D_1^{*0}\to D^-\pi^+$		(3.6 ± 1.2)	$\times10^{-6}$			–
D^+K^0		< 2.9	$\times10^{-6}$	CL=90%		2278
$D^+K^+\pi^-$		(5.6 ± 1.1)	$\times10^{-6}$			2260
$D_2^*(2460)^0K^+,\ D_2^{*0}\to D^+\pi^-$		< 6.3	$\times10^{-7}$	CL=90%		–
D^+K^{*0}		< 4.9	$\times10^{-7}$	CL=90%		2211
$D^+\overline{K}{}^{*0}$		< 1.4	$\times10^{-6}$	CL=90%		2211
$\overline{D}{}^*(2007)^0\pi^+$		(4.90 ± 0.17)	$\times10^{-3}$			2256
$\overline{D}{}^0_{CP(+1)}\pi^+$	[vvv]	(2.7 ± 0.6)	$\times10^{-3}$			–
$D^0_{CP(-1)}\pi^+$	[vvv]	(2.4 ± 0.9)	$\times10^{-3}$			–
$\overline{D}{}^*(2007)^0\omega\pi^+$		(4.5 ± 1.2)	$\times10^{-3}$			2149
$\overline{D}{}^*(2007)^0\rho^+$		(9.8 ± 1.7)	$\times10^{-3}$			2181
$\overline{D}{}^*(2007)^0K^+$		($3.97\ ^{+0.31}_{-0.28}$)	$\times10^{-4}$			2227
$\overline{D}{}^0_{CP(+1)}K^+$	[vvv]	(2.60 ± 0.33)	$\times10^{-4}$			–
$\overline{D}{}^0_{CP(-1)}K^+$	[vvv]	(2.19 ± 0.30)	$\times10^{-4}$			–
$\overline{D}{}^*(2007)^0K^*(892)^+$		(8.1 ± 1.4)	$\times10^{-4}$			2156
$\overline{D}{}^*(2007)^0K^+\overline{K}{}^0$		< 1.06	$\times10^{-3}$	CL=90%		2132
$\overline{D}{}^*(2007)^0K^+\overline{K}{}^*(892)^0$		(1.5 ± 0.4)	$\times10^{-3}$			2009
$\overline{D}{}^*(2007)^0\pi^+\pi^+\pi^-$		(1.03 ± 0.12)	%			2236
$\overline{D}{}^*(2007)^0a_1(1260)^+$		(1.9 ± 0.5)	%			2063
$\overline{D}{}^*(2007)^0\pi^-\pi^+\pi^+\pi^0$		(1.8 ± 0.4)	%			2219
$\overline{D}{}^{*0}3\pi^+2\pi^-$		(5.7 ± 1.2)	$\times10^{-3}$			2196
$D^*(2010)^+\pi^0$		< 3.6	$\times10^{-6}$			2255
$D^*(2010)^+K^0$		< 9.0	$\times10^{-6}$	CL=90%		2225
$D^*(2010)^-\pi^+\pi^+\pi^0$		(1.5 ± 0.7)	%			2235
$D^*(2010)^-\pi^+\pi^+\pi^+\pi^-$		(2.6 ± 0.4)	$\times10^{-3}$			2217
$\overline{D}{}^{**0}\pi^+$	[xxx]	(5.7 ± 1.2)	$\times10^{-3}$			–
$\overline{D}{}_1^*(2420)^0\pi^+$		(1.5 ± 0.6)	$\times10^{-3}$		S=1.3	2082
$\overline{D}_1(2420)^0\pi^+\times$ B($\overline{D}{}_1^0\to\overline{D}{}^0\pi^+\pi^-$)		($2.5\ ^{+1.6}_{-1.4}$)	$\times10^{-4}$		S=3.9	2082
$\overline{D}_1(2420)^0\pi^+\times$ B($\overline{D}{}_1^0\to\overline{D}{}^0\pi^+\pi^-$ (nonresonant))		(2.2 ± 1.0)	$\times10^{-4}$			2082
$\overline{D}{}_2^*(2462)^0\pi^+\times$ B($\overline{D}{}_2^*(2462)^0\to D^-\pi^+$)		(3.56 ± 0.24)	$\times10^{-4}$			–
$\overline{D}{}_2^*(2462)^0\pi^+\times$B($\overline{D}{}_2^{*0}\to\overline{D}{}^0\pi^-\pi^+$)		(2.2 ± 1.0)	$\times10^{-4}$			–
$\overline{D}{}_2^*(2462)^0\pi^+\times$B($\overline{D}{}_2^{*0}\to\overline{D}{}^0\pi^-\pi^+$ (nonresonant))		< 1.7	$\times10^{-4}$	CL=90%		–
$\overline{D}{}_2^*(2462)^0\pi^+\times$B($\overline{D}{}_2^{*0}\to D^*(2010)^-\pi^+$)		(2.2 ± 1.1)	$\times10^{-4}$			–
$\overline{D}{}_0^*(2400)^0\pi^+\times$ B($\overline{D}{}_0^*(2400)^0\to D^-\pi^+$)		(6.4 ± 1.4)	$\times10^{-4}$			2128
$\overline{D}_1(2421)^0\pi^+\times$ B($\overline{D}_1(2421)^0\to D^{*-}\pi^+$)		(6.8 ± 1.5)	$\times10^{-4}$			–
$\overline{D}{}_2^*(2462)^0\pi^+\times$ B($\overline{D}{}_2^*(2462)^0\to D^{*-}\pi^+$)		(1.8 ± 0.5)	$\times10^{-4}$			–
$\overline{D}{}_1'(2427)^0\pi^+\times$ B($\overline{D}{}_1'(2427)^0\to D^{*-}\pi^+$)		(5.0 ± 1.2)	$\times10^{-4}$			–
$\overline{D}_1(2420)^0\pi^+\times$B($\overline{D}{}_1^0\to\overline{D}{}^{*0}\pi^+\pi^-$)		< 6	$\times10^{-6}$	CL=90%		2082
$\overline{D}{}_1^*(2420)^0\rho^+$		< 1.4	$\times10^{-3}$	CL=90%		1996
$\overline{D}{}_2^*(2460)^0\pi^+$		< 1.3	$\times10^{-3}$	CL=90%		2063
$\overline{D}{}_2^*(2460)^0\pi^+\times$B($\overline{D}{}_2^{*0}\to\overline{D}{}^{*0}\pi^+\pi^-$)		< 2.2	$\times10^{-5}$	CL=90%		2063
$\overline{D}{}_1^*(2680)^0\pi^+,\ \overline{D}{}_1^*(2680)^0\to D^-\pi^+$		(8.4 ± 2.1)	$\times10^{-5}$			–
$\overline{D}{}_3^*(2760)^0\pi^+,\ \overline{D}{}_3^*(2760)^0\pi^+\to D^-\pi^+$		(1.00 ± 0.22)	$\times10^{-5}$			–
$\overline{D}{}_2^*(3000)^0\pi^+,\ \overline{D}{}_2^*(3000)^0\pi^+\to D^-\pi^+$		(2.0 ± 1.4)	$\times10^{-6}$			–
$\overline{D}{}_2^*(2460)^0\rho^+$		< 4.7	$\times10^{-3}$	CL=90%		1977
$\overline{D}{}^0D_s^+$		(9.0 ± 0.9)	$\times10^{-3}$			1815
$D_{s0}^*(2317)^+\overline{D}{}^0,\ D_{s0}^{*+}\to D_s^+\pi^0$		($7.9\ ^{+1.5}_{-1.3}$)	$\times10^{-4}$			1605
$D_{s0}(2317)^+\overline{D}{}^0\times$ B($D_{s0}(2317)^+\to D_s^{*+}\gamma$)		< 7.6	$\times10^{-4}$	CL=90%		1605
$D_{s0}(2317)^+\overline{D}{}^*(2007)^0\times$ B($D_{s0}(2317)^+\to D_s^+\pi^0$)		(9 ± 7)	$\times10^{-4}$			1511
$D_{sJ}(2457)^+\overline{D}{}^0$		($3.1\ ^{+1.0}_{-0.9}$)	$\times10^{-3}$			–
$D_{sJ}(2457)^+\overline{D}{}^0\times$ B($D_{sJ}(2457)^+\to D_s^+\gamma$)		($4.6\ ^{+1.3}_{-1.1}$)	$\times10^{-4}$			–
$D_{sJ}(2457)^+\overline{D}{}^0\times$ B($D_{sJ}(2457)^+\to D_s^+\pi^+\pi^-$)		< 2.2	$\times10^{-4}$	CL=90%		–
$D_{sJ}(2457)^+\overline{D}{}^0\times$ B($D_{sJ}(2457)^+\to D_s^+\pi^0$)		< 2.7	$\times10^{-4}$	CL=90%		–
$D_{sJ}(2457)^+\overline{D}{}^0\times$ B($D_{sJ}(2457)^+\to D_s^{*+}\gamma$)		< 9.8	$\times10^{-4}$	CL=90%		–
$D_{sJ}(2457)^+\overline{D}{}^*(2007)^0$		(1.20 ± 0.30)	%			–
$D_{sJ}(2457)^+\overline{D}{}^*(2007)^0\times$ B($D_{sJ}(2457)^+\to D_s^+\gamma$)		($1.4\ ^{+0.7}_{-0.6}$)	$\times10^{-3}$			–
$\overline{D}{}^0D_{s1}(2536)^+\times$ B($D_{s1}(2536)^+\to D^*(2007)^0K^+ + D^*(2010)^+K^0$)		(4.0 ± 1.0)	$\times10^{-4}$			1447
$\overline{D}{}^0D_{s1}(2536)^+\times$ B($D_{s1}(2536)^+\to D^*(2007)^0K^+$)		(2.2 ± 0.7)	$\times10^{-4}$			1447
$\overline{D}{}^*(2007)^0D_{s1}(2536)^+\times$ B($D_{s1}(2536)^+\to D^*(2007)^0K^+$)		(5.5 ± 1.6)	$\times10^{-4}$			1339
$\overline{D}{}^0D_{s1}(2536)^+\times$ B($D_{s1}(2536)^+\to D^{*+}K^0$)		(2.3 ± 1.1)	$\times10^{-4}$			1447
$\overline{D}{}^0D_{sJ}(2700)^+\times$ B($D_{sJ}(2700)^+\to D^0K^+$)		(5.6 ± 1.8)	$\times10^{-4}$		S=1.7	–
$\overline{D}{}^{*0}D_{s1}(2536)^+,\ D_{s1}^+\to D^{*+}K^0$		(3.9 ± 2.6)	$\times10^{-4}$			1339
$\overline{D}{}^0D_{sJ}(2573)^+,\ D_{sJ}^+\to D^0K^+$		(8 ±15)	$\times10^{-6}$			–
$\overline{D}{}^{*0}D_{sJ}(2573),\ D_{sJ}^+\to D^0K^+$		< 2	$\times10^{-4}$	CL=90%		1306
$\overline{D}{}^*(2007)^0D_{sJ}(2573),\ D_{sJ}^+\to D^0K^+$		< 5	$\times10^{-4}$	CL=90%		1306
$\overline{D}{}^0D_s^{*+}$		(7.6 ± 1.6)	$\times10^{-3}$			1734
$\overline{D}{}^*(2007)^0D_s^+$		(8.2 ± 1.7)	$\times10^{-3}$			1737
$\overline{D}{}^*(2007)^0D_s^{*+}$		(1.71 ± 0.24)	%			1651
$D_s^{(*)+}\overline{D}{}^{**0}$		(2.7 ± 1.2)	%			–
$\overline{D}{}^*(2007)^0D^*(2010)^+$		(8.1 ± 1.7)	$\times10^{-4}$			1713
$\overline{D}{}^0D^*(2010)^+ + \overline{D}{}^*(2007)^0D^+$		< 1.30	%		CL=90%	1792
$\overline{D}{}^0D^*(2010)^+$		(3.9 ± 0.5)	$\times10^{-4}$			1792
$\overline{D}{}^0D^+$		(3.8 ± 0.4)	$\times10^{-4}$			1866
$\overline{D}{}^0D^+K^0$		(1.55 ± 0.21)	$\times10^{-3}$			1571
$D^+\overline{D}{}^*(2007)^0$		(6.3 ± 1.7)	$\times10^{-4}$			1791
$\overline{D}{}^*(2007)^0D^+K^0$		(2.1 ± 0.5)	$\times10^{-3}$			1475
$\overline{D}{}^0D^*(2010)^+K^0$		(3.8 ± 0.4)	$\times10^{-3}$			1476
$\overline{D}{}^*(2007)^0D^*(2010)^+K^0$		(9.2 ± 1.2)	$\times10^{-3}$			1362
$\overline{D}{}^0D^0K^+$		(1.45 ± 0.33)	$\times10^{-3}$		S=2.6	1577
$\overline{D}{}^*(2007)^0D^0K^+$		(2.26 ± 0.23)	$\times10^{-3}$			1481
$\overline{D}{}^0D^*(2007)^0K^+$		(6.3 ± 0.5)	$\times10^{-3}$			1481
$\overline{D}{}^*(2007)^0D^*(2007)^0K^+$		(1.12 ± 0.13)	%			1368
$D^-D^+K^+$		(2.2 ± 0.7)	$\times10^{-4}$			1571
$D^-D^*(2010)^+K^+$		(6.3 ± 1.1)	$\times10^{-4}$			1475
$D^*(2010)^-D^+K^+$		(6.0 ± 1.3)	$\times10^{-4}$			1475
$D^*(2010)^-D^*(2010)^+K^+$		(1.32 ± 0.18)	$\times10^{-3}$			1363
$(\overline{D}+\overline{D}{}^*)(D+D^*)K$		(4.05 ± 0.30)	%			–
$D_s^+\pi^0$		(1.6 ± 0.5)	$\times10^{-5}$			2270
$D_s^{*+}\pi^0$		< 2.6	$\times10^{-4}$	CL=90%		2215
$D_s^+\eta$		< 4	$\times10^{-4}$	CL=90%		2235
$D_s^{*+}\eta$		< 6	$\times10^{-4}$	CL=90%		2178
$D_s^+\rho^0$		< 3.0	$\times10^{-4}$	CL=90%		2197
$D_s^{*+}\rho^0$		< 4	$\times10^{-4}$	CL=90%		2138
$D_s^+\omega$		< 4	$\times10^{-4}$	CL=90%		2195
$D_s^{*+}\omega$		< 6	$\times10^{-4}$	CL=90%		2136
$D_s^+a_1(1260)^0$		< 1.8	$\times10^{-3}$	CL=90%		2079

Meson Summary Table

$D_s^{*+} a_1(1260)^0$	$<$	1.3	$\times 10^{-3}$	CL=90%	2015
$D_s^+ K^+ K^-$	(	7.1 $\pm$ 1.1)	$\times 10^{-6}$		2149
$D_s^+ \phi$	$<$	4.2	$\times 10^{-7}$	CL=90%	2141
$D_s^{*+} \phi$	$<$	1.2	$\times 10^{-5}$	CL=90%	2079
$D_s^+ \overline{K}^0$	$<$	8	$\times 10^{-4}$	CL=90%	2242
$D_s^{*+} \overline{K}^0$	$<$	9	$\times 10^{-4}$	CL=90%	2185
$D_s^+ \overline{K}^*(892)^0$	$<$	4.4	$\times 10^{-6}$	CL=90%	2172
$D_s^+ K^{*0}$	$<$	3.5	$\times 10^{-6}$	CL=90%	2172
$D_s^{*+} \overline{K}^*(892)^0$	$<$	3.5	$\times 10^{-4}$	CL=90%	2112
$D_s^- \pi^+ K^+$	(	1.80 $\pm$ 0.22)	$\times 10^{-4}$		2222
$D_s^{*-} \pi^+ K^+$	(	1.45 $\pm$ 0.24)	$\times 10^{-4}$		2164
$D_s^- \pi^+ K^*(892)^+$	$<$	5	$\times 10^{-3}$	CL=90%	2138
$D_s^{*-} \pi^+ K^*(892)^+$	$<$	7	$\times 10^{-3}$	CL=90%	2076
$D_s^- K^+ K^+$	(	9.7 $\pm$ 2.1)	$\times 10^{-6}$		2149
$D_s^{*-} K^+ K^+$	$<$	1.5	$\times 10^{-5}$	CL=90%	2088

Charmonium modes

$\eta_c K^+$	(	1.09 $\pm$ 0.09)	$\times 10^{-3}$	S=1.1	1751
$\eta_c K^+,\ \eta_c \to K_S^0 K^\mp \pi^\pm$	(	2.7 $\pm$ 0.6)	$\times 10^{-5}$		–
$\eta_c K^*(892)^+$	(	1.0 $^{+\ 0.5}_{-\ 0.4}$)	$\times 10^{-3}$		1646
$\eta_c K^+ \pi^+ \pi^-$	$<$	3.9	$\times 10^{-4}$	CL=90%	1684
$\eta_c K^+ \omega(782)$	$<$	5.3	$\times 10^{-4}$	CL=90%	1475
$\eta_c K^+ \eta$	$<$	2.2	$\times 10^{-4}$	CL=90%	1588
$\eta_c K^+ \pi^0$	$<$	6.2	$\times 10^{-5}$	CL=90%	1723
$\eta_c(2S) K^+$	(	4.4 $\pm$ 1.0)	$\times 10^{-4}$		1320
$\eta_c(2S) K^+,\ \eta_c \to p\overline{p}$	(	3.5 $\pm$ 0.8)	$\times 10^{-8}$		–
$\eta_c(2S) K^+,\ \eta_c \to K_S^0 K^\mp \pi^\pm$	(	3.4 $^{+\ 2.3}_{-\ 1.6}$)	$\times 10^{-6}$		–
$h_c(1P) K^+,\ h_c \to J/\psi \pi^+ \pi^-$	$<$	3.4	$\times 10^{-6}$	CL=90%	1401
$X(3730)^0 K^+,\ X^0 \to \eta_c \eta$	$<$	4.6	$\times 10^{-5}$	CL=90%	–
$X(3730)^0 K^+,\ X^0 \to \eta_c \pi^0$	$<$	5.7	$\times 10^{-6}$	CL=90%	–
$\chi_{c1}(3872) K^+$	$<$	2.6	$\times 10^{-4}$	CL=90%	1141
$\chi_{c1}(3872) K^+,\ \chi_{c1} \to p\overline{p}$	$<$	5	$\times 10^{-9}$	CL=95%	–
$\chi_{c1}(3872) K^+,\ \chi_{c1} \to J/\psi \pi^+ \pi^-$	(	8.6 $\pm$ 0.8)	$\times 10^{-6}$		1141
$\chi_{c1}(3872) K^+,\ \chi_{c1} \to J/\psi \gamma$	(	2.1 $\pm$ 0.4)	$\times 10^{-6}$	S=1.1	1141
$\chi_{c1}(3872) K^+,\ \chi_{c1} \to \psi(2S) \gamma$	(	4 $\pm$ 4)	$\times 10^{-6}$	S=2.5	1141
$\chi_{c1}(3872) K^+,\ \chi_{c1} \to J/\psi(1S) \eta$	$<$	7.7	$\times 10^{-6}$	CL=90%	1141
$\chi_{c1}(3872) K^+,\ \chi_{c1} \to D^0 \overline{D}^0$	$<$	6.0	$\times 10^{-5}$	CL=90%	1141
$\chi_{c1}(3872) K^+,\ \chi_{c1} \to D^+ D^-$	$<$	4.0	$\times 10^{-5}$	CL=90%	1141
$\chi_{c1}(3872) K^+,\ \chi_{c1} \to D^0 \overline{D}^0 \pi^0$	(	1.0 $\pm$ 0.4)	$\times 10^{-4}$		1141
$\chi_{c1}(3872) K^+,\ \chi_{c1} \to \overline{D}^{*0} D^0$	(	8.5 $\pm$ 2.6)	$\times 10^{-5}$	S=1.4	1141
$\chi_{c1}(3872)^0 K^+,\ \chi_{c1}^0 \to \eta_c \pi^+ \pi^-$	$<$	3.0	$\times 10^{-5}$	CL=90%	–
$\chi_{c1}(3872)^0 K^+,\ \chi_{c1}^0 \to \eta_c \omega(782)$	$<$	6.9	$\times 10^{-5}$	CL=90%	–
$\chi_{c1}(3872) K^+,\ \chi_{c1} \to \chi_{c1}(1P) \pi^+ \pi^-$	$<$	1.5	$\times 10^{-6}$	CL=90%	–
$X(3915) K^+$	$<$	2.8	$\times 10^{-4}$	CL=90%	1103
$X(3915)^0 K^+,\ X^0 \to \eta_c \eta$	$<$	4.7	$\times 10^{-5}$	CL=90%	–
$X(3915)^0 K^+,\ X^0 \to \eta_c \pi^0$	$<$	1.7	$\times 10^{-5}$	CL=90%	–
$X(4014)^0 K^+,\ X^0 \to \eta_c \eta$	$<$	3.9	$\times 10^{-5}$	CL=90%	–
$X(4014)^0 K^+,\ X^0 \to \eta_c \pi^0$	$<$	1.2	$\times 10^{-5}$	CL=90%	–
$Z_c(3900)^0 K^+,\ Z_c^0 \to \eta_c \pi^+ \pi^-$	$<$	4.7	$\times 10^{-5}$	CL=90%	–
$X(4020)^0 K^+,\ X^0 \to \eta_c \pi^+ \pi^-$	$<$	1.6	$\times 10^{-5}$	CL=90%	–
$\chi_{c1}(3872) K^*(892)^+,\ \chi_{c1} \to J/\psi \gamma$	$<$	4.8	$\times 10^{-6}$	CL=90%	939
$\chi_{c1}(3872) K^*(892)^+,\ \chi_{c1} \to \psi(2S) \gamma$	$<$	2.8	$\times 10^{-5}$	CL=90%	939
$\chi_{c1}(3872)^+ K^0,\ \chi_{c1}^+ \to J/\psi(1S) \pi^+ \pi^0$ [yyy]	$<$	6.1	$\times 10^{-6}$	CL=90%	–
$\chi_{c1}(3872) K^0 \pi^+,\ \chi_{c1} \to J/\psi(1S) \pi^+ \pi^-$	(	1.06 $\pm$ 0.31)	$\times 10^{-5}$		–
$Z_c(4430)^+ K^0,\ Z_c^+ \to J/\psi \pi^+$	$<$	1.5	$\times 10^{-5}$	CL=95%	–
$Z_c(4430)^+ K^0,\ Z_c^+ \to \psi(2S) \pi^+$	$<$	4.7	$\times 10^{-5}$	CL=95%	–
$\psi(4260)^0 K^+,\ \psi^0 \to J/\psi \pi^+ \pi^-$	$<$	2.9	$\times 10^{-5}$	CL=95%	–
$X(3915) K^+,\ X \to J/\psi \gamma$	$<$	1.4	$\times 10^{-5}$	CL=90%	–
$X(3930)^0 K^+,\ X^0 \to J/\psi \gamma$	$<$	2.5	$\times 10^{-6}$	CL=90%	–
$J/\psi(1S) K^+$	(	1.010 $\pm$ 0.029)	$\times 10^{-3}$		1684
$J/\psi(1S) K^0 \pi^+$	(	1.14 $\pm$ 0.11)	$\times 10^{-3}$		1651
$J/\psi(1S) K^+ \pi^+ \pi^-$	(	8.1 $\pm$ 1.3)	$\times 10^{-4}$	S=2.5	1612
$J/\psi(1S) K^+ K^- K^+$	(	3.37 $\pm$ 0.29)	$\times 10^{-5}$		1252
$X(3915) K^+,\ X \to p\overline{p}$	$<$	7.1	$\times 10^{-8}$	CL=95%	–
$J/\psi(1S) K^*(892)^+$	(	1.43 $\pm$ 0.08)	$\times 10^{-3}$		1571
$J/\psi(1S) K(1270)^+$	(	1.8 $\pm$ 0.5)	$\times 10^{-3}$		1390
$J/\psi(1S) K(1400)^+$	$<$	5	$\times 10^{-4}$	CL=90%	1308
$J/\psi(1S) \eta K^+$	(	1.24 $\pm$ 0.14)	$\times 10^{-4}$		1510
$\chi_{c1-odd}(3872) K^+,\ \chi_{c1-odd} \to J/\psi \eta$	$<$	3.8	$\times 10^{-6}$	CL=90%	–
$\psi(4160) K^+,\ \psi \to J/\psi \eta$	$<$	7.4	$\times 10^{-6}$	CL=90%	–
$J/\psi(1S) \eta' K^+$	$<$	8.8	$\times 10^{-5}$	CL=90%	1273
$J/\psi(1S) \phi K^+$	(	5.0 $\pm$ 0.4)	$\times 10^{-5}$		1227
$J/\psi(1S) K_1(1650),\ K_1 \to \phi K^+$	(	6 $^{+10}_{-\ 6}$)	$\times 10^{-6}$		–
$J/\psi(1S) K^*(1680)^+,\ K^* \to \phi K^+$	(	3.4 $^{+\ 1.9}_{-\ 2.2}$)	$\times 10^{-6}$		–
$J/\psi(1S) K_2^*(1980),\ K_2^* \to \phi K^+$	(	1.5 $^{+\ 0.9}_{-\ 0.5}$)	$\times 10^{-6}$		–
$J/\psi(1S) K(1830)^+,\ K(1830)^+ \to \phi K^+$	(	1.3 $^{+\ 1.3}_{-\ 1.1}$)	$\times 10^{-6}$		–
$\chi_{c1}(4140) K^+,\ \chi_{c1} \to J/\psi(1S) \phi$	(	10 $\pm$ 4)	$\times 10^{-6}$		–
$\chi_{c1}(4274) K^+,\ \chi_{c1} \to J/\psi(1S) \phi$	(	3.6 $^{+\ 2.2}_{-\ 1.8}$)	$\times 10^{-6}$		–
$\chi_{c0}(4500) K^+,\ \chi_c^0 \to J/\psi(1S) \phi$	(	3.3 $^{+\ 2.1}_{-\ 1.7}$)	$\times 10^{-6}$		–
$\chi_{c0}(4700) K^+,\ \chi_{c0} \to J/\psi(1S) \phi$	(	6 $^{+\ 5}_{-\ 4}$)	$\times 10^{-6}$		–
$J/\psi(1S) \omega K^+$	(	3.20 $^{+\ 0.60}_{-\ 0.32}$)	$\times 10^{-4}$		1388
$\chi_{c1}(3872) K^+,\ \chi_{c1} \to J/\psi \omega$	(	6.0 $\pm$ 2.2)	$\times 10^{-6}$		1141
$X(3915) K^+,\ X \to J/\psi \omega$	(	3.0 $^{+\ 0.9}_{-\ 0.7}$)	$\times 10^{-5}$		1103
$J/\psi(1S) \pi^+$	(	3.88 $\pm$ 0.12)	$\times 10^{-5}$		1728
$J/\psi(1S) \pi^+ \pi^+ \pi^+ \pi^- \pi^-$	(	1.17 $\pm$ 0.13)	$\times 10^{-5}$		1635
$\psi(2S) \pi^+ \pi^+ \pi^-$	(	1.9 $\pm$ 0.4)	$\times 10^{-5}$		1304
$J/\psi(1S) \rho^+$	(	5.0 $\pm$ 0.8)	$\times 10^{-5}$		1611
$J/\psi(1S) \pi^+ \pi^0$ nonresonant	$<$	7.3	$\times 10^{-6}$	CL=90%	1717
$J/\psi(1S) a_1(1260)^+$	$<$	1.2	$\times 10^{-3}$	CL=90%	1415
$J/\psi(1S) p\overline{p} \pi^+$	$<$	5.0	$\times 10^{-7}$	CL=90%	643
$J/\psi(1S) p\overline{\Lambda}$	(	1.18 $\pm$ 0.31)	$\times 10^{-5}$		567
$J/\psi(1S) \overline{\Sigma}^0 p$	$<$	1.1	$\times 10^{-5}$	CL=90%	–
$J/\psi(1S) D^+$	$<$	1.2	$\times 10^{-4}$	CL=90%	871
$J/\psi(1S) \overline{D}^0 \pi^+$	$<$	2.5	$\times 10^{-5}$	CL=90%	665
$\psi(2S) \pi^+$	(	2.44 $\pm$ 0.30)	$\times 10^{-5}$		1347
$\psi(2S) K^+$	(	6.21 $\pm$ 0.23)	$\times 10^{-4}$		1284
$\psi(2S) K^*(892)^+$	(	6.7 $\pm$ 1.4)	$\times 10^{-4}$	S=1.3	1115
$\psi(2S) K^+ \pi^+ \pi^-$	(	4.3 $\pm$ 0.5)	$\times 10^{-4}$		1179
$\psi(2S) \phi(1020) K^+$	(	4.0 $\pm$ 0.7)	$\times 10^{-6}$		417
$\psi(3770) K^+$	(	4.9 $\pm$ 1.3)	$\times 10^{-4}$		1218
$\psi(3770) K+, \psi \to D^0 \overline{D}^0$	(	1.5 $\pm$ 0.5)	$\times 10^{-4}$	S=1.4	1218
$\psi(3770) K+, \psi \to D^+ D^-$	(	9.4 $\pm$ 3.5)	$\times 10^{-5}$		1218
$\psi(3770) K^+,\ \psi \to p\overline{p}$	$<$	2	$\times 10^{-7}$	CL=95%	–
$\psi(4040) K^+$	$<$	1.3	$\times 10^{-4}$	CL=90%	1003
$\psi(4160) K^+$	(	5.1 $\pm$ 2.7)	$\times 10^{-4}$		868
$\psi(4160) K^+,\ \psi \to \overline{D}^0 D^0$	(	8 $\pm$ 5)	$\times 10^{-5}$		–
$\chi_{c0} \pi^+,\ \chi_{c0} \to \pi^+ \pi^-$	$<$	1	$\times 10^{-7}$	CL=90%	1531
$\chi_{c0} K^+$	(	1.49 $^{+\ 0.15}_{-\ 0.14}$)	$\times 10^{-4}$		1478
$\chi_{c0} K^*(892)^+$	$<$	2.1	$\times 10^{-4}$	CL=90%	1341
$\chi_{c1}(1P) \pi^+$	(	2.2 $\pm$ 0.5)	$\times 10^{-5}$		1468
$\chi_{c1}(1P) K^+$	(	4.84 $\pm$ 0.23)	$\times 10^{-4}$		1412
$\chi_{c1}(1P) K^*(892)^+$	(	3.0 $\pm$ 0.6)	$\times 10^{-4}$	S=1.1	1265
$\chi_{c1}(1P) K^0 \pi^+$	(	5.8 $\pm$ 0.4)	$\times 10^{-4}$		1370
$\chi_{c1}(1P) K^+ \pi^0$	(	3.29 $\pm$ 0.35)	$\times 10^{-4}$		1373
$\chi_{c1}(1P) K^+ \pi^+ \pi^-$	(	3.74 $\pm$ 0.30)	$\times 10^{-4}$		1319
$\chi_{c1}(2P) K^+,\ \chi_{c1}(2P) \to \pi^+ \pi^- \chi_{c1}(1P)$	$<$	1.1	$\times 10^{-5}$	CL=90%	–
$\chi_{c2} K^+$	(	1.1 $\pm$ 0.4)	$\times 10^{-5}$		1379

$\chi_{c2}K^*(892)^+$	$<$	1.2	$\times10^{-4}$	CL=90%	1228
$\chi_{c2}K^0\pi^+$	(	1.16 ± 0.25)	$\times10^{-4}$		1336
$\chi_{c2}K^+\pi^0$	$<$	6.2	$\times10^{-5}$	CL=90%	1339
$\chi_{c2}K^+\pi^+\pi^-$	(	1.34 ± 0.19)	$\times10^{-4}$		1284
$\chi_{c2}(3930)\pi^+$, $\chi_{c2}\to\pi^+\pi^-$	$<$	1	$\times10^{-7}$	CL=90%	1437
$h_c(1P)K^+$	$<$	3.8	$\times10^{-5}$	CL=90%	1401
$h_c(1P)K^+$, $h_c\to p\overline{p}$	$<$	6.4	$\times10^{-8}$	CL=95%	–
K* or *K* **modes**					
$K^0\pi^+$	(	2.37 ± 0.08)	$\times10^{-5}$		2614
$K^+\pi^0$	(	1.29 ± 0.05)	$\times10^{-5}$		2615
$\eta' K^+$	(	7.06 ± 0.25)	$\times10^{-5}$		2528
$\eta' K^*(892)^+$	(	$4.8\ ^{+\ 1.8}_{-\ 1.6}$)	$\times10^{-6}$		2472
$\eta' K_0^*(1430)^+$	(	5.2 ± 2.1)	$\times10^{-6}$		–
$\eta' K_2^*(1430)^+$	(	2.8 ± 0.5)	$\times10^{-5}$		2346
ηK^+	(	2.4 ± 0.4)	$\times10^{-6}$	S=1.7	2588
$\eta K^*(892)^+$	(	1.93 ± 0.16)	$\times10^{-5}$		2534
$\eta K_0^*(1430)^+$	(	1.8 ± 0.4)	$\times10^{-5}$		–
$\eta K_2^*(1430)^+$	(	9.1 ± 3.0)	$\times10^{-6}$		2414
$\eta(1295)K^+\times$ B($\eta(1295)\to\eta\pi\pi$)	(	$2.9\ ^{+\ 0.8}_{-\ 0.7}$)	$\times10^{-6}$		2455
$\eta(1405)K^+\times$ B($\eta(1405)\to\eta\pi\pi$)	$<$	1.3	$\times10^{-6}$	CL=90%	2425
$\eta(1405)K^+\times$ B($\eta(1405)\to K^*K$)	$<$	1.2	$\times10^{-6}$	CL=90%	2425
$\eta(1475)K^+\times$ B($\eta(1475)\to K^*K$)	(	$1.38\ ^{+\ 0.21}_{-\ 0.18}$)	$\times10^{-5}$		2406
$f_1(1285)K^+$	$<$	2.0	$\times10^{-6}$	CL=90%	2458
$f_1(1420)K^+\times$ B($f_1(1420)\to\eta\pi\pi$)	$<$	2.9	$\times10^{-6}$	CL=90%	2420
$f_1(1420)K^+\times$ B($f_1(1420)\to K^*K$)	$<$	4.1	$\times10^{-6}$	CL=90%	2420
$\phi(1680)K^+\times$ B($\phi(1680)\to K^*K$)	$<$	3.4	$\times10^{-6}$	CL=90%	2344
$f_0(1500)K^+$	(	3.7 ± 2.2)	$\times10^{-6}$		2398
ωK^+	(	6.5 ± 0.4)	$\times10^{-6}$		2558
$\omega K^*(892)^+$	$<$	7.4	$\times10^{-6}$	CL=90%	2503
$\omega(K\pi)_0^{*+}$	(	2.8 ± 0.4)	$\times10^{-5}$		–
$\omega K_0^*(1430)^+$	(	2.4 ± 0.5)	$\times10^{-5}$		–
$\omega K_2^*(1430)^+$	(	2.1 ± 0.4)	$\times10^{-5}$		2380
$a_0(980)^+K^0\times$B($a_0(980)^+\to\eta\pi^+$)	$<$	3.9	$\times10^{-6}$	CL=90%	–
$a_0(980)^0K^+\times$B($a_0(980)^0\to\eta\pi^0$)	$<$	2.5	$\times10^{-6}$	CL=90%	–
$K^*(892)^0\pi^+$	(	1.01 ± 0.08)	$\times10^{-5}$		2562
$K^*(892)^+\pi^0$	(	6.8 ± 0.9)	$\times10^{-6}$		2563
$K^+\pi^-\pi^+$	(	5.10 ± 0.29)	$\times10^{-5}$		2609
$K^+\pi^-\pi^+$ nonresonant	(	$1.63\ ^{+\ 0.21}_{-\ 0.15}$)	$\times10^{-5}$		2609
$\omega(782)K^+$	(	6 ± 9)	$\times10^{-6}$		2558
$K^+f_0(980)\times$ B($f_0(980)\to\pi^+\pi^-$)	(	$9.4\ ^{+\ 1.0}_{-\ 1.2}$)	$\times10^{-6}$		2522
$f_2(1270)^0K^+$	(	1.07 ± 0.27)	$\times10^{-6}$		–
$f_0(1370)^0K^+\times$ B($f_0(1370)^0\to\pi^+\pi^-$)	$<$	1.07	$\times10^{-5}$	CL=90%	–
$\rho^0(1450)K^+\times$ B($\rho^0(1450)\to\pi^+\pi^-$)	$<$	1.17	$\times10^{-5}$	CL=90%	–
$f_2'(1525)K^+\times$ B($f_2'(1525)\to\pi^+\pi^-$)	$<$	3.4	$\times10^{-6}$	CL=90%	2392
$K^+\rho^0$	(	3.7 ± 0.5)	$\times10^{-6}$		2559
$K_0^*(1430)^0\pi^+$	(	$3.9\ ^{+\ 0.6}_{-\ 0.5}$)	$\times10^{-5}$	S=1.4	2445
$K_0^*(1430)^+\pi^0$	(	$1.19\ ^{+\ 0.20}_{-\ 0.23}$)	$\times10^{-5}$		–
$K_2^*(1430)^0\pi^+$	(	$5.6\ ^{+\ 2.2}_{-\ 1.5}$)	$\times10^{-6}$		2445
$K^*(1410)^0\pi^+$	$<$	4.5	$\times10^{-5}$	CL=90%	2446
$K^*(1680)^0\pi^+$	$<$	1.2	$\times10^{-5}$	CL=90%	2358
$K^+\pi^0\pi^0$	(	1.62 ± 0.19)	$\times10^{-5}$		2610
$f_0(980)K^+\times$ B($f_0\to\pi^0\pi^0$)	(	2.8 ± 0.8)	$\times10^{-6}$		2522
$K^-\pi^+\pi^+$	$<$	4.6	$\times10^{-8}$	CL=90%	2609
$K^-\pi^+\pi^+$ nonresonant	$<$	5.6	$\times10^{-5}$	CL=90%	2609
$K_1(1270)^0\pi^+$	$<$	4.0	$\times10^{-5}$	CL=90%	2484
$K_1(1400)^0\pi^+$	$<$	3.9	$\times10^{-5}$	CL=90%	2451
$K^0\pi^+\pi^0$	$<$	6.6	$\times10^{-5}$	CL=90%	2609
$K^0\rho^+$	(	$7.3\ ^{+\ 1.0}_{-\ 1.2}$)	$\times10^{-6}$		2558
$K^*(892)^+\pi^+\pi^-$	(	7.5 ± 1.0)	$\times10^{-5}$		2557
$K^*(892)^+\rho^0$	(	4.6 ± 1.1)	$\times10^{-6}$		2504
$K^*(892)^+f_0(980)$	(	4.2 ± 0.7)	$\times10^{-6}$		2466
$a_1^+K^0$	(	3.5 ± 0.7)	$\times10^{-5}$		–
$b_1^+K^0\times$ B($b_1^+\to\omega\pi^+$)	(	9.6 ± 1.9)	$\times10^{-6}$		–
$K^*(892)^0\rho^+$	(	9.2 ± 1.5)	$\times10^{-6}$		2504
$K_1(1400)^+\rho^0$	$<$	7.8	$\times10^{-4}$	CL=90%	2388
$K_2^*(1430)^+\rho^0$	$<$	1.5	$\times10^{-3}$	CL=90%	2381
$b_1^0K^+\times$ B($b_1^0\to\omega\pi^0$)	(	9.1 ± 2.0)	$\times10^{-6}$		–
$b_1^+K^{*0}\times$ B($b_1^+\to\omega\pi^+$)	$<$	5.9	$\times10^{-6}$	CL=90%	–
$b_1^0K^{*+}\times$ B($b_1^0\to\omega\pi^0$)	$<$	6.7	$\times10^{-6}$	CL=90%	–
$K^+\overline{K}^0$	(	1.31 ± 0.17)	$\times10^{-6}$	S=1.2	2593
$\overline{K}^0K^+\pi^0$	$<$	2.4	$\times10^{-5}$	CL=90%	2578
$K^+K_S^0K_S^0$	(	1.08 ± 0.06)	$\times10^{-5}$		2521
$f_0(980)K^+$, $f_0\to K_S^0K_S^0$	(	1.47 ± 0.33)	$\times10^{-5}$		–
$f_0(1710)K^+$, $f_0\to K_S^0K_S^0$	(	$4.8\ ^{+\ 4.0}_{-\ 2.6}$)	$\times10^{-7}$		–
$K^+K_S^0K_S^0$ nonresonant	(	2.0 ± 0.4)	$\times10^{-5}$		2521
$K_S^0K_S^0\pi^+$	$<$	5.1	$\times10^{-7}$	CL=90%	2577
$K^+K^-\pi^+$	(	5.2 ± 0.4)	$\times10^{-6}$		2578
$K^+K^-\pi^+$ nonresonant	$<$	7.5	$\times10^{-5}$	CL=90%	2578
$K^+\overline{K}^*(892)^0$	$<$	1.1	$\times10^{-6}$	CL=90%	2540
$K^+\overline{K}_0^*(1430)^0$	$<$	2.2	$\times10^{-6}$	CL=90%	2421
$K^+K^+\pi^-$	$<$	1.1	$\times10^{-8}$	CL=90%	2578
$K^+K^+\pi^-$ nonresonant	$<$	8.79	$\times10^{-5}$	CL=90%	2578
$f_2'(1525)K^+$	(	1.8 ± 0.5)	$\times10^{-6}$	S=1.1	2392
$K^{*+}\pi^+K^-$	$<$	1.18	$\times10^{-5}$	CL=90%	2524
$K^*(892)^+K^*(892)^0$	(	9.1 ± 2.9)	$\times10^{-7}$		2484
$K^{*+}K^+\pi^-$	$<$	6.1	$\times10^{-6}$	CL=90%	2524
$K^+K^-K^+$	(	3.40 ± 0.14)	$\times10^{-5}$	S=1.4	2523
$K^+\phi$	(	$8.8\ ^{+\ 0.7}_{-\ 0.6}$)	$\times10^{-6}$	S=1.1	2516
$f_0(980)K^+\times$ B($f_0(980)\to K^+K^-$)	(	9.4 ± 3.2)	$\times10^{-6}$		2522
$a_2(1320)K^+\times$ B($a_2(1320)\to K^+K^-$)	$<$	1.1	$\times10^{-6}$	CL=90%	2449
$X_0(1550)K^+\times$ B($X_0(1550)\to K^+K^-$)	(	4.3 ± 0.7)	$\times10^{-6}$		–
$\phi(1680)K^+\times$ B($\phi(1680)\to K^+K^-$)	$<$	8	$\times10^{-7}$	CL=90%	2344
$f_0(1710)K^+\times$ B($f_0(1710)\to K^+K^-$)	(	1.1 ± 0.6)	$\times10^{-6}$		2330
$K^+K^-K^+$ nonresonant	(	$2.38\ ^{+\ 0.28}_{-\ 0.50}$)	$\times10^{-5}$		2523
$K^*(892)^+K^+K^-$	(	3.6 ± 0.5)	$\times10^{-5}$		2466
$K^*(892)^+\phi$	(	10.0 ± 2.0)	$\times10^{-6}$	S=1.7	2460
$\phi(K\pi)_0^{*+}$	(	8.3 ± 1.6)	$\times10^{-6}$		–
$\phi K_1(1270)^+$	(	6.1 ± 1.9)	$\times10^{-6}$		2375
$\phi K_1(1400)^+$	$<$	3.2	$\times10^{-6}$	CL=90%	2339
$\phi K^*(1410)^+$	$<$	4.3	$\times10^{-6}$	CL=90%	–
$\phi K_0^*(1430)^+$	(	7.0 ± 1.6)	$\times10^{-6}$		–
$\phi K_2^*(1430)^+$	(	8.4 ± 2.1)	$\times10^{-6}$		2333
$\phi K_2^*(1770)^+$	$<$	1.50	$\times10^{-5}$	CL=90%	–
$\phi K_2^*(1820)^+$	$<$	1.63	$\times10^{-5}$	CL=90%	–
$a_1^+K^{*0}$	$<$	3.6	$\times10^{-6}$	CL=90%	–
$K^+\phi\phi$	(	5.0 ± 1.2)	$\times10^{-6}$	S=2.3	2306
$\eta'\eta'K^+$	$<$	2.5	$\times10^{-5}$	CL=90%	2338
$\omega\phi K^+$	$<$	1.9	$\times10^{-6}$	CL=90%	2374
$X(1812)K^+\times$ B($X\to\omega\phi$)	$<$	3.2	$\times10^{-7}$	CL=90%	–
$K^*(892)^+\gamma$	(	3.92 ± 0.22)	$\times10^{-5}$	S=1.7	2564
$K_1(1270)^+\gamma$	(	$4.4\ ^{+\ 0.7}_{-\ 0.6}$)	$\times10^{-5}$		2486
$\eta K^+\gamma$	(	7.9 ± 0.9)	$\times10^{-6}$		2588
$\eta' K^+\gamma$	(	$2.9\ ^{+\ 1.0}_{-\ 0.9}$)	$\times10^{-6}$		2528
$\phi K^+\gamma$	(	2.7 ± 0.4)	$\times10^{-6}$	S=1.2	2516
$K^+\pi^-\pi^+\gamma$	(	2.58 ± 0.15)	$\times10^{-5}$	S=1.3	2609
$K^*(892)^0\pi^+\gamma$	(	2.33 ± 0.12)	$\times10^{-5}$		2562
$K^+\rho^0\gamma$	(	8.2 ± 0.9)	$\times10^{-6}$		2559
$(K^+\pi^-)_{\rm NR}\pi^+\gamma$	(	$9.9\ ^{+\ 1.7}_{-\ 2.0}$)	$\times10^{-6}$		2609
$K^0\pi^+\pi^0\gamma$	(	4.6 ± 0.5)	$\times10^{-5}$		2609
$K_1(1400)^+\gamma$	(	$10\ ^{+\ 5}_{-\ 4}$)	$\times10^{-6}$		2453
$K^*(1410)^+\gamma$	(	$2.7\ ^{+\ 0.8}_{-\ 0.6}$)	$\times10^{-5}$		–
$K_0^*(1430)^0\pi^+\gamma$	(	$1.32\ ^{+\ 0.26}_{-\ 0.32}$)	$\times10^{-6}$		2445
$K_2^*(1430)^+\gamma$	(	1.4 ± 0.4)	$\times10^{-5}$		2447

Meson Summary Table

$K^*(1680)^+\gamma$		$(\ 6.7\ ^{+\ 1.7}_{-\ 1.4}\ )\times10^{-5}$			2360
$K_3^*(1780)^+\gamma$	$<$	3.9	$\times10^{-5}$	CL=90%	2341
$K_4^*(2045)^+\gamma$	$<$	9.9	$\times10^{-3}$	CL=90%	2244
Light unflavored meson modes					
$\rho^+\gamma$		$(\ 9.8\ \pm\ 2.5\ )\times10^{-7}$			2583
$\pi^+\pi^0$		$(\ 5.5\ \pm\ 0.4\ )\times10^{-6}$		S=1.2	2636
$\pi^+\pi^+\pi^-$		$(\ 1.52\ \pm\ 0.14\ )\times10^{-5}$			2630
$\rho^0\pi^+$		$(\ 8.3\ \pm\ 1.2\ )\times10^{-6}$			2581
$\pi^+ f_0(980),\ f_0\to\pi^+\pi^-$	$<$	1.5	$\times10^{-6}$	CL=90%	2545
$\pi^+ f_2(1270)$		$(\ 1.6\ ^{+\ 0.7}_{-\ 0.4}\ )\times10^{-6}$			2484
$\rho(1450)^0\pi^+,\ \rho^0\to\pi^+\pi^-$		$(\ 1.4\ ^{+\ 0.6}_{-\ 0.9}\ )\times10^{-6}$			2434
$f_0(1370)\pi^+,\ f_0\to\pi^+\pi^-$	$<$	4.0	$\times10^{-6}$	CL=90%	2460
$f_0(500)\pi^+,\ f_0\to\pi^+\pi^-$	$<$	4.1	$\times10^{-6}$	CL=90%	–
$\pi^+\pi^-\pi^+$ nonresonant		$(\ 5.3\ ^{+\ 1.5}_{-\ 1.1}\ )\times10^{-6}$			2630
$\pi^+\pi^0\pi^0$	$<$	8.9	$\times10^{-4}$	CL=90%	2631
$\rho^+\pi^0$		$(\ 1.09\ \pm\ 0.14\ )\times10^{-5}$			2581
$\pi^+\pi^-\pi^+\pi^0$	$<$	4.0	$\times10^{-3}$	CL=90%	2622
$\rho^+\rho^0$		$(\ 2.40\ \pm\ 0.19\ )\times10^{-5}$			2523
$\rho^+ f_0(980),\ f_0\to\pi^+\pi^-$	$<$	2.0	$\times10^{-6}$	CL=90%	2486
$a_1(1260)^+\pi^0$		$(\ 2.6\ \pm\ 0.7\ )\times10^{-5}$			2494
$a_1(1260)^0\pi^+$		$(\ 2.0\ \pm\ 0.6\ )\times10^{-5}$			2494
$\omega\pi^+$		$(\ 6.9\ \pm\ 0.5\ )\times10^{-6}$			2580
$\omega\rho^+$		$(\ 1.59\ \pm\ 0.21\ )\times10^{-5}$			2522
$\eta\pi^+$		$(\ 4.02\ \pm\ 0.27\ )\times10^{-6}$			2609
$\eta\rho^+$		$(\ 7.0\ \pm\ 2.9\ )\times10^{-6}$		S=2.8	2553
$\eta'\pi^+$		$(\ 2.7\ \pm\ 0.9\ )\times10^{-6}$		S=1.9	2551
$\eta'\rho^+$		$(\ 9.7\ \pm\ 2.2\ )\times10^{-6}$			2492
$\phi\pi^+$	$<$	1.5	$\times10^{-7}$	CL=90%	2539
$\phi\rho^+$	$<$	3.0	$\times10^{-6}$	CL=90%	2480
$a_0(980)^0\pi^+,\ a_0^0\to\eta\pi^0$	$<$	5.8	$\times10^{-6}$	CL=90%	–
$a_0(980)^+\pi^0,\ a_0^+\to\eta\pi^+$	$<$	1.4	$\times10^{-6}$	CL=90%	–
$\pi^+\pi^+\pi^+\pi^-\pi^-$	$<$	8.6	$\times10^{-4}$	CL=90%	2608
$\rho^0 a_1(1260)^+$	$<$	6.2	$\times10^{-4}$	CL=90%	2433
$\rho^0 a_2(1320)^+$	$<$	7.2	$\times10^{-4}$	CL=90%	2410
$b_1^0\pi^+,\ b_1^0\to\omega\pi^0$		$(\ 6.7\ \pm\ 2.0\ )\times10^{-6}$			–
$b_1^+\pi^0,\ b_1^+\to\omega\pi^+$	$<$	3.3	$\times10^{-6}$	CL=90%	–
$\pi^+\pi^+\pi^+\pi^-\pi^-\pi^0$	$<$	6.3	$\times10^{-3}$	CL=90%	2592
$b_1^+\rho^0,\ b_1^+\to\omega\pi^+$	$<$	5.2	$\times10^{-6}$	CL=90%	–
$a_1(1260)^+ a_1(1260)^0$	$<$	1.3	%	CL=90%	2336
$b_1^0\rho^+,\ b_1^0\to\omega\pi^0$	$<$	3.3	$\times10^{-6}$	CL=90%	–
Charged particle ($h^\pm$) modes					
$h^\pm = K^\pm$ or $\pi^\pm$					
$h^+\pi^0$		$(\ 1.6\ ^{+\ 0.7}_{-\ 0.6}\ )\times10^{-5}$			2636
ωh^+		$(\ 1.38\ ^{+\ 0.27}_{-\ 0.24}\ )\times10^{-5}$			2580
$h^+ X^0$ (Familon)	$<$	4.9	$\times10^{-5}$	CL=90%	–
$K^+ X^0,\ X^0\to\mu^+\mu^-$	$<$	1	$\times10^{-7}$	CL=95%	–
Baryon modes					
$p\overline{p}\pi^+$		$(\ 1.62\ \pm\ 0.20\ )\times10^{-6}$			2439
$p\overline{p}\pi^+$ nonresonant	$<$	5.3	$\times10^{-5}$	CL=90%	2439
$p\overline{p}K^+$		$(\ 5.9\ \pm\ 0.5\ )\times10^{-6}$		S=1.5	2348
$\Theta(1710)^{++}\overline{p},\ \Theta^{++}\to pK^+$	[zzz] $<$	9.1	$\times10^{-8}$	CL=90%	–
$f_J(2220)K^+,\ f_J\to p\overline{p}$	[zzz] $<$	4.1	$\times10^{-7}$	CL=90%	2135
$p\overline{\Lambda}(1520)$		$(\ 3.1\ \pm\ 0.6\ )\times10^{-7}$			2322
$p\overline{p}K^+$ nonresonant	$<$	8.9	$\times10^{-5}$	CL=90%	2348
$p\overline{p}K^*(892)^+$		$(\ 3.6\ ^{+\ 0.8}_{-\ 0.7}\ )\times10^{-6}$			2215
$f_J(2220)K^{*+},\ f_J\to p\overline{p}$	$<$	7.7	$\times10^{-7}$	CL=90%	2059
$p\overline{\Lambda}$		$(\ 2.4\ ^{+\ 1.0}_{-\ 0.9}\ )\times10^{-7}$			2430
$p\overline{\Lambda}\gamma$		$(\ 2.4\ ^{+\ 0.5}_{-\ 0.4}\ )\times10^{-6}$			2430
$p\overline{\Lambda}\pi^0$		$(\ 3.0\ ^{+\ 0.7}_{-\ 0.6}\ )\times10^{-6}$			2402
$p\overline{\Sigma}(1385)^0$	$<$	4.7	$\times10^{-7}$	CL=90%	2362
$\Delta^+\overline{\Lambda}$	$<$	8.2	$\times10^{-7}$	CL=90%	–
$p\overline{\Sigma}\gamma$	$<$	4.6	$\times10^{-6}$	CL=90%	2413
$p\overline{\Lambda}\pi^+\pi^-$		$(\ 5.9\ \pm\ 1.1\ )\times10^{-6}$			2367
$p\overline{\Lambda}\rho^0$		$(\ 4.8\ \pm\ 0.9\ )\times10^{-6}$			2214
$p\overline{\Lambda}f_2(1270)$		$(\ 2.0\ \pm\ 0.8\ )\times10^{-6}$			2026
$\Lambda\overline{\Lambda}\pi^+$	$<$	9.4	$\times10^{-7}$	CL=90%	2358
$\Lambda\overline{\Lambda}K^+$		$(\ 3.4\ \pm\ 0.6\ )\times10^{-6}$			2251
$\Lambda\overline{\Lambda}K^{*+}$		$(\ 2.2\ ^{+\ 1.2}_{-\ 0.9}\ )\times10^{-6}$			2098
$\overline{\Delta}^0 p$	$<$	1.38	$\times10^{-6}$	CL=90%	2403
$\Delta^{++}\overline{p}$	$<$	1.4	$\times10^{-7}$	CL=90%	2403
$D^+ p\overline{p}$	$<$	1.5	$\times10^{-5}$	CL=90%	1860
$D^*(2010)^+ p\overline{p}$	$<$	1.5	$\times10^{-5}$	CL=90%	1786
$\overline{D}^0 p\overline{p}\pi^+$		$(\ 3.72\ \pm\ 0.27\ )\times10^{-4}$			1789
$\overline{D}^{*0} p\overline{p}\pi^+$		$(\ 3.73\ \pm\ 0.32\ )\times10^{-4}$			1709
$D^- p\overline{p}\pi^+\pi^-$		$(\ 1.66\ \pm\ 0.30\ )\times10^{-4}$			1705
$D^{*-} p\overline{p}\pi^+\pi^-$		$(\ 1.86\ \pm\ 0.25\ )\times10^{-4}$			1621
$p\overline{\Lambda}^0\overline{D}^0$		$(\ 1.43\ \pm\ 0.32\ )\times10^{-5}$			–
$p\overline{\Lambda}^0\overline{D}^*(2007)^0$	$<$	5	$\times10^{-5}$	CL=90%	–
$\overline{\Lambda}_c^- p\pi^+$		$(\ 2.3\ \pm\ 0.4\ )\times10^{-4}$		S=2.2	1980
$\overline{\Lambda}_c^- \Delta(1232)^{++}$	$<$	1.9	$\times10^{-5}$	CL=90%	1928
$\overline{\Lambda}_c^- \Delta_X(1600)^{++}$		$(\ 4.7\ \pm\ 1.0\ )\times10^{-5}$			–
$\overline{\Lambda}_c^- \Delta_X(2420)^{++}$		$(\ 3.8\ \pm\ 0.9\ )\times10^{-5}$			–
$(\overline{\Lambda}_c^- p)_s\pi^+$	[aaaa]	$(\ 3.1\ \pm\ 0.7\ )\times10^{-5}$			–
$\overline{\Sigma}_c(2520)^0 p$	$<$	3	$\times10^{-6}$	CL=90%	1904
$\overline{\Sigma}_c(2800)^0 p$		$(\ 2.7\ \pm\ 0.9\ )\times10^{-5}$			–
$\overline{\Lambda}_c^- p\pi^+\pi^0$		$(\ 1.8\ \pm\ 0.6\ )\times10^{-3}$			1935
$\overline{\Lambda}_c^- p\pi^+\pi^+\pi^-$		$(\ 2.2\ \pm\ 0.7\ )\times10^{-3}$			1880
$\overline{\Lambda}_c^- p\pi^+\pi^+\pi^-\pi^0$	$<$	1.34	%	CL=90%	1823
$\Lambda_c^+\Lambda_c^- K^+$		$(\ 7.0\ \pm\ 2.2\ )\times10^{-4}$			–
$\overline{\Sigma}_c(2455)^0 p$		$(\ 3.0\ \pm\ 0.7\ )\times10^{-5}$			1938
$\overline{\Sigma}_c(2455)^0 p\pi^0$		$(\ 3.5\ \pm\ 1.1\ )\times10^{-4}$			1896
$\overline{\Sigma}_c(2455)^0 p\pi^-\pi^+$		$(\ 3.5\ \pm\ 1.1\ )\times10^{-4}$			1845
$\overline{\Sigma}_c(2455)^{--} p\pi^+\pi^+$		$(\ 2.39\ \pm\ 0.20\ )\times10^{-4}$			1845
$\overline{\Lambda}_c(2593)^-/\overline{\Lambda}_c(2625)^- p\pi^+$	$<$	1.9	$\times10^{-4}$	CL=90%	–
$\overline{\Xi}_c^0\Lambda_c^+,\ \overline{\Xi}_c^0\to\overline{\Xi}^+\pi^-$		$(\ 2.4\ \pm\ 0.9\ )\times10^{-5}$		S=1.4	1144
$\overline{\Xi}_c^0\Lambda_c^+,\ \overline{\Xi}_c^0\to\Lambda K^+\pi^-$		$(\ 2.1\ \pm\ 0.9\ )\times10^{-5}$		S=1.5	1144
Lepton Family number (LF) or Lepton number (L) or Baryon number (B) violating modes, or/and $\Delta B=1$ weak neutral current ($B1$) modes					
$\pi^+\ell^+\ell^-$	$B1$	$<$ 4.9	$\times10^{-8}$	CL=90%	2638
$\pi^+ e^+ e^-$	$B1$	$<$ 8.0	$\times10^{-8}$	CL=90%	2638
$\pi^+\mu^+\mu^-$	$B1$	$(\ 1.76\ \pm\ 0.23\ )\times10^{-8}$			2634
$\pi^+\nu\overline{\nu}$	$B1$	$<$ 1.4	$\times10^{-5}$	CL=90%	2638
$K^+\ell^+\ell^-$	$B1$	[sss] $(\ 4.51\ \pm\ 0.23\ )\times10^{-7}$		S=1.1	2617
$K^+ e^+ e^-$	$B1$	$(\ 5.5\ \pm\ 0.7\ )\times10^{-7}$			2617
$K^+\mu^+\mu^-$	$B1$	$(\ 4.41\ \pm\ 0.23\ )\times10^{-7}$		S=1.2	2612
$K^+\mu^+\mu^-$ nonresonant	$B1$	$(\ 4.37\ \pm\ 0.27\ )\times10^{-7}$			2612
$K^+\tau^+\tau^-$	$B1$	$<$ 2.25	$\times10^{-3}$	CL=90%	1687
$K^+\overline{\nu}\nu$	$B1$	$<$ 1.6	$\times10^{-5}$	CL=90%	2617
$\rho^+\nu\overline{\nu}$	$B1$	$<$ 3.0	$\times10^{-5}$	CL=90%	2583
$K^*(892)^+\ell^+\ell^-$	$B1$	[sss] $(\ 1.01\ \pm\ 0.11\ )\times10^{-6}$		S=1.1	2564
$K^*(892)^+ e^+ e^-$	$B1$	$(\ 1.55\ ^{+\ 0.40}_{-\ 0.31}\ )\times10^{-6}$			2564
$K^*(892)^+\mu^+\mu^-$	$B1$	$(\ 9.6\ \pm\ 1.0\ )\times10^{-7}$			2560
$K^*(892)^+\nu\overline{\nu}$	$B1$	$<$ 4.0	$\times10^{-5}$	CL=90%	2564
$K^+\pi^+\pi^-\mu^+\mu^-$	$B1$	$(\ 4.3\ \pm\ 0.4\ )\times10^{-7}$			2593
$\phi K^+\mu^+\mu^-$	$B1$	$(\ 7.9\ ^{+\ 2.1}_{-\ 1.7}\ )\times10^{-8}$			2490
$\pi^+ e^+\mu^-$	LF	$<$ 6.4	$\times10^{-3}$	CL=90%	2637
$\pi^+ e^-\mu^+$	LF	$<$ 6.4	$\times10^{-3}$	CL=90%	2637
$\pi^+ e^\pm\mu^\mp$	LF	$<$ 1.7	$\times10^{-7}$	CL=90%	2637
$\pi^+ e^+\tau^-$	LF	$<$ 7.4	$\times10^{-5}$	CL=90%	2338
$\pi^+ e^-\tau^+$	LF	$<$ 2.0	$\times10^{-5}$	CL=90%	2338
$\pi^+ e^\pm\tau^\mp$	LF	$<$ 7.5	$\times10^{-5}$	CL=90%	2338
$\pi^+\mu^+\tau^-$	LF	$<$ 6.2	$\times10^{-5}$	CL=90%	2333
$\pi^+\mu^-\tau^+$	LF	$<$ 4.5	$\times10^{-5}$	CL=90%	2333
$\pi^+\mu^\pm\tau^\mp$	LF	$<$ 7.2	$\times10^{-5}$	CL=90%	2333
$K^+ e^+\mu^-$	LF	$<$ 9.1	$\times10^{-8}$	CL=90%	2615
$K^+ e^-\mu^+$	LF	$<$ 1.3	$\times10^{-7}$	CL=90%	2615
$K^+ e^\pm\mu^\mp$	LF	$<$ 9.1	$\times10^{-8}$	CL=90%	2615
$K^+ e^+\tau^-$	LF	$<$ 4.3	$\times10^{-5}$	CL=90%	2312
$K^+ e^-\tau^+$	LF	$<$ 1.5	$\times10^{-5}$	CL=90%	2312
$K^+ e^\pm\tau^\mp$	LF	$<$ 3.0	$\times10^{-5}$	CL=90%	2312
$K^+\mu^+\tau^-$	LF	$<$ 4.5	$\times10^{-5}$	CL=90%	2298
$K^+\mu^-\tau^+$	LF	$<$ 2.8	$\times10^{-5}$	CL=90%	2298
$K^+\mu^\pm\tau^\mp$	LF	$<$ 4.8	$\times10^{-5}$	CL=90%	2298
$K^*(892)^+ e^+\mu^-$	LF	$<$ 1.3	$\times10^{-6}$	CL=90%	2563
$K^*(892)^+ e^-\mu^+$	LF	$<$ 9.9	$\times10^{-7}$	CL=90%	2563
$K^*(892)^+ e^\pm\mu^\mp$	LF	$<$ 1.4	$\times10^{-6}$	CL=90%	2563
$\pi^- e^+ e^+$	L	$<$ 2.3	$\times10^{-8}$	CL=90%	2638
$\pi^-\mu^+\mu^+$	L	$<$ 4.0	$\times10^{-9}$	CL=95%	2634
$\pi^- e^+\mu^+$	L	$<$ 1.5	$\times10^{-7}$	CL=90%	2637
$\rho^- e^+ e^+$	L	$<$ 1.7	$\times10^{-7}$	CL=90%	2583

$\rho^- \mu^+ \mu^+$	L	$<$	4.2	$\times 10^{-7}$	CL=90%	2578
$\rho^- e^+ \mu^+$	L	$<$	4.7	$\times 10^{-7}$	CL=90%	2582
$K^- e^+ e^+$	L	$<$	3.0	$\times 10^{-8}$	CL=90%	2617
$K^- \mu^+ \mu^+$	L	$<$	4.1	$\times 10^{-8}$	CL=90%	2612
$K^- e^+ \mu^+$	L	$<$	1.6	$\times 10^{-7}$	CL=90%	2615
$K^*(892)^- e^+ e^+$	L	$<$	4.0	$\times 10^{-7}$	CL=90%	2564
$K^*(892)^- \mu^+ \mu^+$	L	$<$	5.9	$\times 10^{-7}$	CL=90%	2560
$K^*(892)^- e^+ \mu^+$	L	$<$	3.0	$\times 10^{-7}$	CL=90%	2563
$D^- e^+ e^+$	L	$<$	2.6	$\times 10^{-6}$	CL=90%	2309
$D^- e^+ \mu^+$	L	$<$	1.8	$\times 10^{-6}$	CL=90%	2307
$D^- \mu^+ \mu^+$	L	$<$	6.9	$\times 10^{-7}$	CL=95%	2303
$D^{*-} \mu^+ \mu^+$	L	$<$	2.4	$\times 10^{-6}$	CL=95%	2251
$D_s^- \mu^+ \mu^+$	L	$<$	5.8	$\times 10^{-7}$	CL=95%	2267
$\overline{D}{}^0 \pi^- \mu^+ \mu^+$	L	$<$	1.5	$\times 10^{-6}$	CL=95%	2295
$\Lambda^0 \mu^+$	L,B	$<$	6	$\times 10^{-8}$	CL=90%	–
$\Lambda^0 e^+$	L,B	$<$	3.2	$\times 10^{-8}$	CL=90%	–
$\overline{\Lambda}{}^0 \mu^+$	L,B	$<$	6	$\times 10^{-8}$	CL=90%	–
$\overline{\Lambda}{}^0 e^+$	L,B	$<$	8	$\times 10^{-8}$	CL=90%	–

B^0

$I(J^P) = \frac{1}{2}(0^-)$

I, J, P need confirmation. Quantum numbers shown are quark-model predictions.

Mass $m_{B^0} = 5279.63 \pm 0.15$ MeV (S = 1.1)
$m_{B^0} - m_{B^\pm} = 0.31 \pm 0.06$ MeV
Mean life $\tau_{B^0} = (1.520 \pm 0.004) \times 10^{-12}$ s
$c\tau = 455.7\ \mu$m
$\tau_{B^+}/\tau_{B^0} = 1.076 \pm 0.004$ (direct measurements)

B^0-$\overline{B}{}^0$ mixing parameters

$\chi_d = 0.1860 \pm 0.0011$
$\Delta m_{B^0} = m_{B^0_H} - m_{B^0_L} = (0.5064 \pm 0.0019) \times 10^{12}\ \hbar\ \mathrm{s}^{-1}$
$= (3.333 \pm 0.013) \times 10^{-10}$ MeV
$x_d = \Delta m_{B^0}/\Gamma_{B^0} = 0.770 \pm 0.004$
$\mathrm{Re}(\lambda_{CP}\ /\ |\lambda_{CP}|)\ \mathrm{Re(z)} = 0.047 \pm 0.022$
$\Delta\Gamma\ \mathrm{Re(z)} = -0.007 \pm 0.004$
$\mathrm{Re(z)} = (-4 \pm 4) \times 10^{-2}$ (S = 1.4)
$\mathrm{Im(z)} = (-0.8 \pm 0.4) \times 10^{-2}$

CP violation parameters

$\mathrm{Re}(\epsilon_{B^0})/(1+|\epsilon_{B^0}|^2) = (-0.5 \pm 0.4) \times 10^{-3}$
$A_{T/CP}(B^0 \leftrightarrow \overline{B}{}^0) = 0.005 \pm 0.018$
$A_{CP}(B^0 \to D^*(2010)^+ D^-) = 0.037 \pm 0.034$
$A_{CP}(B^0 \to [K^+\pi^-]_D K^*(892)^0) = -0.03 \pm 0.04$
$R_d^+ = \Gamma(B^0 \to [\pi^+ K^-]_D K^{*0})\ /\ \Gamma(B^0 \to [\pi^- K^+]_D K^{*0}) = 0.06 \pm 0.032$
$R_d^- = \Gamma(\overline{B}{}^0 \to [\pi^- K^+]_D K^{*0})\ /\ \Gamma(\overline{B}{}^0 \to [\pi^+ K^-]_D K^{*0}) = 0.06 \pm 0.032$
$A_{CP}(B^0 \to K^+\pi^-) = -0.082 \pm 0.006$
$A_{CP}(B^0 \to \eta' K^*(892)^0) = -0.07 \pm 0.18$
$A_{CP}(B^0 \to \eta' K_0^*(1430)^0) = -0.19 \pm 0.17$
$A_{CP}(B^0 \to \eta' K_2^*(1430)^0) = 0.14 \pm 0.18$
$A_{CP}(B^0 \to \eta K^*(892)^0) = 0.19 \pm 0.05$
$A_{CP}(B^0 \to \eta K_0^*(1430)^0) = 0.06 \pm 0.13$
$A_{CP}(B^0 \to \eta K_2^*(1430)^0) = -0.07 \pm 0.19$
$A_{CP}(B^0 \to b_1 K^+) = -0.07 \pm 0.12$
$A_{CP}(B^0 \to \omega K^{*0}) = 0.45 \pm 0.25$
$A_{CP}(B^0 \to \omega (K\pi)_0^{*0}) = -0.07 \pm 0.09$
$A_{CP}(B^0 \to \omega K_2^*(1430)^0) = -0.37 \pm 0.17$
$A_{CP}(B^0 \to K^+\pi^-\pi^0) = (0 \pm 6) \times 10^{-2}$
$A_{CP}(B^0 \to \rho^- K^+) = 0.20 \pm 0.11$
$A_{CP}(B^0 \to \rho(1450)^- K^+) = -0.10 \pm 0.33$
$A_{CP}(B^0 \to \rho(1700)^- K^+) = -0.4 \pm 0.6$
$A_{CP}(B^0 \to K^+\pi^-\pi^0\ \mathrm{nonresonant}) = 0.10 \pm 0.18$
$A_{CP}(B^0 \to K^0\pi^+\pi^-) = -0.01 \pm 0.05$
$A_{CP}(B^0 \to K^*(892)^+\pi^-) = -0.22 \pm 0.06$
$A_{CP}(B^0 \to (K\pi)_0^{*+}\pi^-) = 0.09 \pm 0.07$
$A_{CP}(B^0 \to (K\pi)_0^{*0}\pi^0) = -0.15 \pm 0.11$
$A_{CP}(B^0 \to K^{*0}\pi^0) = -0.15 \pm 0.13$
$A_{CP}(B^0 \to K^*(892)^0\pi^+\pi^-) = 0.07 \pm 0.05$
$A_{CP}(B^0 \to K^*(892)^0\rho^0) = -0.06 \pm 0.09$
$A_{CP}(B^0 \to K^{*0} f_0(980)) = 0.07 \pm 0.10$
$A_{CP}(B^0 \to K^{*+}\rho^-) = 0.21 \pm 0.15$
$A_{CP}(B^0 \to K^*(892)^0 K^+ K^-) = 0.01 \pm 0.05$
$A_{CP}(B^0 \to a_1^- K^+) = -0.16 \pm 0.12$
$A_{CP}(B^0 \to K^0 K^0) = -0.6 \pm 0.7$
$A_{CP}(B^0 \to K^*(892)^0\phi) = 0.00 \pm 0.04$
$A_{CP}(B^0 \to K^*(892)^0 K^-\pi^+) = 0.2 \pm 0.4$
$A_{CP}(B^0 \to \phi(K\pi)_0^{*0}) = 0.12 \pm 0.08$
$A_{CP}(B^0 \to \phi K_2^*(1430)^0) = -0.11 \pm 0.10$
$A_{CP}(B^0 \to K^*(892)^0\gamma) = -0.006 \pm 0.011$
$A_{CP}(B^0 \to K_2^*(1430)^0\gamma) = -0.08 \pm 0.15$
$A_{CP}(B^0 \to \rho^+\pi^-) = 0.13 \pm 0.06$ (S = 1.1)
$A_{CP}(B^0 \to \rho^-\pi^+) = -0.08 \pm 0.08$
$A_{CP}(B^0 \to a_1(1260)^\pm\pi^\mp) = -0.07 \pm 0.06$
$A_{CP}(B^0 \to b_1^-\pi^+) = -0.05 \pm 0.10$
$A_{CP}(B^0 \to p\overline{p}K^*(892)^0) = 0.05 \pm 0.12$
$A_{CP}(B^0 \to p\overline{\Lambda}\pi^-) = 0.04 \pm 0.07$
$A_{CP}(B^0 \to K^{*0}\ell^+\ell^-) = -0.05 \pm 0.10$
$A_{CP}(B^0 \to K^{*0}e^+e^-) = -0.21 \pm 0.19$
$A_{CP}(B^0 \to K^{*0}\mu^+\mu^-) = -0.034 \pm 0.024$
$C_{D^{*-}D^+}\ (B^0 \to D^*(2010)^- D^+) = -0.01 \pm 0.11$
$S_{D^{*-}D^+}\ (B^0 \to D^*(2010)^- D^+) = -0.72 \pm 0.15$
$C_{D^{*+}D^-}\ (B^0 \to D^*(2010)^+ D^-) = 0.00 \pm 0.13$ (S = 1.3)
$S_{D^{*+}D^-}\ (B^0 \to D^*(2010)^+ D^-) = -0.73 \pm 0.14$
$C_{D^{*+}D^{*-}}\ (B^0 \to D^{*+} D^{*-}) = 0.01 \pm 0.09$ (S = 1.6)
$S_{D^{*+}D^{*-}}\ (B^0 \to D^{*+} D^{*-}) = -0.59 \pm 0.14$ (S = 1.8)
$C_+\ (B^0 \to D^{*+} D^{*-}) = 0.00 \pm 0.10$ (S = 1.6)
$S_+\ (B^0 \to D^{*+} D^{*-}) = -0.73 \pm 0.09$
$C_-\ (B^0 \to D^{*+} D^{*-}) = 0.19 \pm 0.31$
$S_-\ (B^0 \to D^{*+} D^{*-}) = 0.1 \pm 1.6$ (S = 3.5)
$C\ (B^0 \to D^*(2010)^+ D^*(2010)^- K_S^0) = 0.01 \pm 0.29$
$S\ (B^0 \to D^*(2010)^+ D^*(2010)^- K_S^0) = 0.1 \pm 0.4$
$C_{D^+D^-}\ (B^0 \to D^+ D^-) = -0.22 \pm 0.24$ (S = 2.5)
$S_{D^+D^-}\ (B^0 \to D^+ D^-) = -0.76^{+0.15}_{-0.13}$ (S = 1.2)
$C_{J/\psi(1S)\pi^0}\ (B^0 \to J/\psi(1S)\pi^0) = -0.13 \pm 0.13$
$S_{J/\psi(1S)\pi^0}\ (B^0 \to J/\psi(1S)\pi^0) = -0.94 \pm 0.29$ (S = 1.9)
$C(B^0 \to J/\psi(1S)\rho^0) = -0.06 \pm 0.06$
$S(B^0 \to J/\psi(1S)\rho^0) = -0.66^{+0.16}_{-0.12}$
$C_{D_{CP}^{(*)}h^0}\ (B^0 \to D_{CP}^{(*)} h^0) = -0.02 \pm 0.08$
$S_{D_{CP}^{(*)}h^0}\ (B^0 \to D_{CP}^{(*)} h^0) = -0.66 \pm 0.12$
$C_{K^0\pi^0}\ (B^0 \to K^0\pi^0) = 0.00 \pm 0.13$ (S = 1.4)
$S_{K^0\pi^0}\ (B^0 \to K^0\pi^0) = 0.58 \pm 0.17$
$C_{\eta'(958)K_S^0}\ (B^0 \to \eta'(958) K_S^0) = -0.04 \pm 0.20$ (S = 2.5)
$S_{\eta'(958)K_S^0}\ (B^0 \to \eta'(958) K_S^0) = 0.43 \pm 0.17$ (S = 1.5)
$C_{\eta' K^0}\ (B^0 \to \eta' K^0) = -0.06 \pm 0.04$
$S_{\eta' K^0}\ (B^0 \to \eta' K^0) = 0.63 \pm 0.06$
$C_{\omega K_S^0}\ (B^0 \to \omega K_S^0) = 0.0 \pm 0.4$ (S = 3.0)
$S_{\omega K_S^0}\ (B^0 \to \omega K_S^0) = 0.70 \pm 0.21$
$C\ (B^0 \to K_S^0\pi^0\pi^0) = 0.2 \pm 0.5$
$S\ (B^0 \to K_S^0\pi^0\pi^0) = 0.7 \pm 0.7$
$C_{\rho^0 K_S^0}\ (B^0 \to \rho^0 K_S^0) = -0.04 \pm 0.20$
$S_{\rho^0 K_S^0}\ (B^0 \to \rho^0 K_S^0) = 0.50^{+0.17}_{-0.21}$
$C_{f_0 K_S^0}\ (B^0 \to f_0(980) K_S^0) = 0.29 \pm 0.20$
$S_{f_0 K_S^0}\ (B^0 \to f_0(980) K_S^0) = -0.50 \pm 0.16$
$S_{f_2 K_S^0}\ (B^0 \to f_2(1270) K_S^0) = -0.5 \pm 0.5$
$C_{f_2 K_S^0}\ (B^0 \to f_2(1270) K_S^0) = 0.3 \pm 0.4$
$S_{f_x K_S^0}\ (B^0 \to f_x(1300) K_S^0) = -0.2 \pm 0.5$
$C_{f_x K_S^0}\ (B^0 \to f_x(1300) K_S^0) = 0.13 \pm 0.35$
$S_{K^0\pi^+\pi^-}\ (B^0 \to K^0\pi^+\pi^-\ \mathrm{nonresonant}) = -0.01 \pm 0.33$
$C_{K^0\pi^+\pi^-}\ (B^0 \to K^0\pi^+\pi^-\ \mathrm{nonresonant}) = 0.01 \pm 0.26$
$C_{K_S^0 K_S^0}\ (B^0 \to K_S^0 K_S^0) = 0.0 \pm 0.4$ (S = 1.4)
$S_{K_S^0 K_S^0}\ (B^0 \to K_S^0 K_S^0) = -0.8 \pm 0.5$
$C_{K^+K^-K_S^0}\ (B^0 \to K^+K^-K_S^0\ \mathrm{nonresonant}) = 0.06 \pm 0.08$
$S_{K^+K^-K_S^0}\ (B^0 \to K^+K^-K_S^0\ \mathrm{nonresonant}) = -0.66 \pm 0.11$
$C_{K^+K^-K_S^0}\ (B^0 \to K^+K^-K_S^0\ \mathrm{inclusive}) = 0.01 \pm 0.09$

Meson Summary Table

$S_{K^+K^-K^0_S}$ **($B^0 \to K^+K^-K^0_S$ inclusive)** $= -0.65 \pm 0.12$
$C_{\phi K^0_S}$ $(B^0 \to \phi K^0_S) = 0.01 \pm 0.14$
$S_{\phi K^0_S}$ $(B^0 \to \phi K^0_S)$ $= 0.59 \pm 0.14$
$C_{K_SK_SK_S}(B^0 \to K_SK_SK_S) = -0.23 \pm 0.14$
$S_{K_SK_SK_S}(B^0 \to K_SK_SK_S) = -0.5 \pm 0.6$ (S = 3.0)
$C_{K^0_S\pi^0\gamma}(B^0 \to K^0_S\pi^0\gamma) = 0.36 \pm 0.33$
$S_{K^0_S\pi^0\gamma}(B^0 \to K^0_S\pi^0\gamma) = -0.8 \pm 0.6$
$C_{K^0_S\pi^+\pi^-\gamma}(B^0 \to K^0_S\pi^+\pi^-\gamma) = -0.39 \pm 0.20$
$S_{K^0_S\pi^+\pi^-\gamma}(B^0 \to K^0_S\pi^+\pi^-\gamma) = 0.14 \pm 0.25$
$C_{K^{*0}\gamma}$ $(B^0 \to K^*(892)^0\gamma) = -0.04 \pm 0.16$ (S = 1.2)
$S_{K^{*0}\gamma}$ $(B^0 \to K^*(892)^0\gamma) = -0.15 \pm 0.22$
$C_{\eta K^0\gamma}$ $(B^0 \to \eta K^0\gamma) = -0.3 \pm 0.4$
$S_{\eta K^0\gamma}$ $(B^0 \to \eta K^0\gamma) = -0.2 \pm 0.5$
$C_{K^0\phi\gamma}$ $(B^0 \to K^0\phi\gamma) = -0.3 \pm 0.6$
$S_{K^0\phi\gamma}$ $(B^0 \to K^0\phi\gamma) = 0.7^{+0.7}_{-1.1}$
$C(B^0 \to K^0_S\rho^0\gamma) = -0.05 \pm 0.19$
$S(B^0 \to K^0_S\rho^0\gamma) = -0.04 \pm 0.23$
C $(B^0 \to \rho^0\gamma) = 0.4 \pm 0.5$
S $(B^0 \to \rho^0\gamma) = -0.8 \pm 0.7$
$C_{\pi\pi}$ $(B^0 \to \pi^+\pi^-)$ $= -0.31 \pm 0.05$
$S_{\pi\pi}$ $(B^0 \to \pi^+\pi^-)$ $= -0.67 \pm 0.06$
$C_{\pi^0\pi^0}(B^0 \to \pi^0\pi^0) = -0.33 \pm 0.22$
$C_{\rho\pi}$ $(B^0 \to \rho^+\pi^-) = -0.03 \pm 0.07$ (S = 1.2)
$S_{\rho\pi}$ $(B^0 \to \rho^+\pi^-) = 0.05 \pm 0.07$
$\Delta C_{\rho\pi}$ $(B^0 \to \rho^+\pi^-)$ $= 0.27 \pm 0.06$
$\Delta S_{\rho\pi}$ $(B^0 \to \rho^+\pi^-) = 0.01 \pm 0.08$
$C_{\rho^0\pi^0}$ $(B^0 \to \rho^0\pi^0) = 0.27 \pm 0.24$
$S_{\rho^0\pi^0}$ $(B^0 \to \rho^0\pi^0) = -0.23 \pm 0.34$
$C_{a_1\pi}$ $(B^0 \to a_1(1260)^+\pi^-) = -0.05 \pm 0.11$
$S_{a_1\pi}$ $(B^0 \to a_1(1260)^+\pi^-) = -0.2 \pm 0.4$ (S = 3.2)
$\Delta C_{a_1\pi}$ $(B^0 \to a_1(1260)^+\pi^-)$ $= 0.43 \pm 0.14$ (S = 1.3)
$\Delta S_{a_1\pi}$ $(B^0 \to a_1(1260)^+\pi^-) = -0.11 \pm 0.12$
C $(B^0 \to b_1^-K^+) = -0.22 \pm 0.24$
ΔC $(B^0 \to b_1^-\pi^+)$ $= -1.04 \pm 0.24$
$C_{\rho^0\rho^0}$ $(B^0 \to \rho^0\rho^0) = 0.2 \pm 0.9$
$S_{\rho^0\rho^0}$ $(B^0 \to \rho^0\rho^0) = 0.3 \pm 0.7$
$C_{\rho\rho}$ $(B^0 \to \rho^+\rho^-) = 0.00 \pm 0.09$
$S_{\rho\rho}$ $(B^0 \to \rho^+\rho^-) = -0.14 \pm 0.13$
$|\lambda|$ $(B^0 \to J/\psi K^*(892)^0) < 0.25$, CL = 95%
$\cos 2\beta$ $(B^0 \to J/\psi K^*(892)^0) = 1.7^{+0.7}_{-0.9}$ (S = 1.6)
$\cos 2\beta$ $(B^0 \to [K^0_S\pi^+\pi^-]_{D^{(*)}}\, h^0) = 0.84 \pm 0.31$
$(S_+ + S_-)/2$ $(B^0 \to D^{*-}\pi^+) = -0.039 \pm 0.011$
$(S_- - S_+)/2$ $(B^0 \to D^{*-}\pi^+) = -0.009 \pm 0.015$
$(S_+ + S_-)/2$ $(B^0 \to D^-\pi^+) = -0.046 \pm 0.023$
$(S_- - S_+)/2$ $(B^0 \to D^-\pi^+) = -0.022 \pm 0.021$
$(S_+ + S_-)/2$ $(B^0 \to D^-\rho^+) = -0.024 \pm 0.032$
$(S_- - S_+)/2$ $(B^0 \to D^-\rho^+) = -0.10 \pm 0.06$
$C_{\eta_c K^0_S}$ $(B^0 \to \eta_c K^0_S) = 0.08 \pm 0.13$
$S_{\eta_c K^0_S}$ $(B^0 \to \eta_c K^0_S)$ $= 0.93 \pm 0.17$
$C_{c\overline{c}K^{(*)0}}$ $(B^0 \to c\overline{c}K^{(*)0}) = (0.5 \pm 1.7) \times 10^{-2}$
$\sin(2\beta)$ $= 0.699 \pm 0.017$
$C_{J/\psi(nS)K^0}$ $(B^0 \to J/\psi(nS)K^0) = (0.5 \pm 2.0) \times 10^{-2}$
$S_{J/\psi(nS)K^0}$ $(B^0 \to J/\psi(nS)K^0)$ $= 0.701 \pm 0.017$
$C_{J/\psi K^{*0}}$ $(B^0 \to J/\psi K^{*0}) = 0.03 \pm 0.10$
$S_{J/\psi K^{*0}}$ $(B^0 \to J/\psi K^{*0}) = 0.60 \pm 0.25$
$C_{\chi_{c0}K^0_S}$ $(B^0 \to \chi_{c0}K^0_S) = -0.3^{+0.5}_{-0.4}$
$S_{\chi_{c0}K^0_S}$ $(B^0 \to \chi_{c0}K^0_S) = -0.7 \pm 0.5$
$C_{\chi_{c1}K^0_S}$ $(B^0 \to \chi_{c1}K^0_S) = 0.06 \pm 0.07$
$S_{\chi_{c1}K^0_S}$ $(B^0 \to \chi_{c1}K^0_S)$ $= 0.63 \pm 0.10$
$\sin(2\beta_{\rm eff})(B^0 \to \phi K^0) = 0.22 \pm 0.30$
$\sin(2\beta_{\rm eff})(B^0 \to \phi K^*_0(1430)^0) = 0.97^{+0.03}_{-0.52}$
$\sin(2\beta_{\rm eff})(B^0 \to K^+K^-K^0_S)$ $= 0.77^{+0.13}_{-0.12}$
$\sin(2\beta_{\rm eff})(B^0 \to [K^0_S\pi^+\pi^-]_{D^{(*)}}\, h^0) = 0.37 \pm 0.22$
$\beta_{\rm eff}(B^0 \to [K^0_S\pi^+\pi^-]_{D^{(*)}}\, h^0) = (12 \pm 8)^\circ$
$2\beta_{\rm eff}(B^0 \to J/\psi\rho^0) = (42^{+10}_{-11})^\circ$
$|\lambda|$ $(B^0 \to [K^0_S\pi^+\pi^-]_{D^{(*)}}\, h^0) = 1.01 \pm 0.08$
$|\sin(2\beta+\gamma)| > 0.40$, CL = 90%
$2\beta + \gamma = (83 \pm 60)^\circ$
$\alpha = (93 \pm 5)^\circ$
$x_+(B^0 \to DK^{*0}) = 0.04 \pm 0.17$
$x_-(B^0 \to DK^{*0}) = -0.16 \pm 0.14$
$y_+(B^0 \to DK^{*0}) = -0.68 \pm 0.22$
$y_-(B^0 \to DK^{*0}) = 0.20 \pm 0.25$ (S = 1.2)
$r_{B^0}(B^0 \to DK^{*0}) = 0.223^{+0.041}_{-0.045}$
$\delta_{B^0}(B^0 \to DK^{*0}) = (193^{+27}_{-21})^\circ$

$\overline{B}^0$ modes are charge conjugates of the modes below. Reactions indicate the weak decay vertex and do not include mixing. Modes which do not identify the charge state of the B are listed in the $B^\pm/B^0$ ADMIXTURE section.

The branching fractions listed below assume 50% $B^0\overline{B}^0$ and 50% B^+B^- production at the $\Upsilon(4S)$. We have attempted to bring older measurements up to date by rescaling their assumed $\Upsilon(4S)$ production ratio to 50:50 and their assumed D, D_s, D^*, and ψ branching ratios to current values whenever this would affect our averages and best limits significantly.

Indentation is used to indicate a subchannel of a previous reaction. All resonant subchannels have been corrected for resonance branching fractions to the final state so the sum of the subchannel branching fractions can exceed that of the final state.

For inclusive branching fractions, *e.g.*, $B \to D^\pm$ anything, the values usually are multiplicities, not branching fractions. They can be greater than one.

B^0 DECAY MODES		Fraction (Γ_i/Γ)	Scale factor/ Confidence level	p (MeV/c)
$\ell^+\nu_\ell$ anything	[sss]	(10.33± 0.28) %		–
$e^+\nu_e X_c$		(10.1 ± 0.4) %		–
$D\ell^+\nu_\ell$ anything		(9.1 ± 0.8) %		–
$D^-\ell^+\nu_\ell$	[sss]	(2.20± 0.10) %		2309
$D^-\tau^+\nu_\tau$		(1.03± 0.22) %		1909
$D^*(2010)^-\ell^+\nu_\ell$	[sss]	(4.88± 0.10) %		2257
$D^*(2010)^-\tau^+\nu_\tau$		(1.67± 0.13) %	S=1.1	1838
$\overline{D}^0\pi^-\ell^+\nu_\ell$		(4.3 ± 0.6) $\times 10^{-3}$		2308
$D_0^*(2400)^-\ell^+\nu_\ell$, $D_0^{*-} \to \overline{D}^0\pi^-$		(3.0 ± 1.2) $\times 10^{-3}$	S=1.8	–
$D_2^*(2460)^-\ell^+\nu_\ell$, $D_2^{*-} \to \overline{D}^0\pi^-$		(1.21± 0.33) $\times 10^{-3}$	S=1.8	2065
$\overline{D}^{(*)}\,n\pi\ell^+\nu_\ell$ (n $\geq$ 1)		(2.3 ± 0.4) %		–
$\overline{D}^{*0}\pi^-\ell^+\nu_\ell$		(4.9 ± 0.8) $\times 10^{-3}$		2256
$D_1(2420)^-\ell^+\nu_\ell$, $D_1^- \to \overline{D}^{*0}\pi^-$		(2.80± 0.28) $\times 10^{-3}$		–
$D_1'(2430)^-\ell^+\nu_\ell$, $D_1'^- \to \overline{D}^{*0}\pi^-$		(3.1 ± 0.9) $\times 10^{-3}$		–
$D_2^*(2460)^-\ell^+\nu_\ell$, $D_2^{*-} \to \overline{D}^{*0}\pi^-$		(6.8 ± 1.2) $\times 10^{-4}$		2065
$D^-\pi^+\pi^-\ell^+\nu_\ell$		(1.3 ± 0.5) $\times 10^{-3}$		2299
$D^{*-}\pi^+\pi^-\ell^+\nu_\ell$		(1.4 ± 0.5) $\times 10^{-3}$		2247
$\rho^-\ell^+\nu_\ell$	[sss]	(2.94± 0.21) $\times 10^{-4}$		2583
$\pi^-\ell^+\nu_\ell$	[sss]	(1.50± 0.06) $\times 10^{-4}$		2638
$\pi^-\tau^+\nu_\tau$		< 2.5 $\times 10^{-4}$	CL=90%	2338
Inclusive modes				
$K^\pm$ anything		(78 ± 8) %		–
D^0X		(8.1 ± 1.5) %		–
$\overline{D}^0X$		(47.4 ± 2.8) %		–
D^+X		< 3.9 %	CL=90%	–
D^-X		(36.9 ± 3.3) %		–
D_s^+X		(10.3 $^{+\ 2.1}_{-\ 1.8}$) %		–
D_s^-X		< 2.6 %	CL=90%	–
Λ_c^+X		< 3.1 %	CL=90%	–
$\overline{\Lambda}_c^-X$		(5.0 $^{+\ 2.1}_{-\ 1.5}$) %		–
$\overline{c}X$		(95 ± 5) %		–
cX		(24.6 ± 3.1) %		–
$\overline{c}/cX$		(119 ± 6) %		–
***D*, *D**, or D_s modes**				
$D^-\pi^+$		(2.52± 0.13) $\times 10^{-3}$	S=1.1	2306
$D^-\rho^+$		(7.9 ± 1.3) $\times 10^{-3}$		2235
$D^-K^0\pi^+$		(4.9 ± 0.9) $\times 10^{-4}$		2259
$D^-K^*(892)^+$		(4.5 ± 0.7) $\times 10^{-4}$		2211
$D^-\omega\pi^+$		(2.8 ± 0.6) $\times 10^{-3}$		2204

$D^- K^+$	(1.86± 0.20) × 10^{-4}			2279
$D^- K^+ \pi^+ \pi^-$	(3.5 ± 0.8) × 10^{-4}			2236
$D^- K^+ \overline{K}^0$	< 3.1	× 10^{-4}	CL=90%	2188
$D^- K^+ \overline{K}^*(892)^0$	(8.8 ± 1.9) × 10^{-4}			2070
$\overline{D}^0 \pi^+ \pi^-$	(8.8 ± 0.5) × 10^{-4}			2301
$D^*(2010)^- \pi^+$	(2.74± 0.13) × 10^{-3}			2255
$\overline{D}^0 K^+ K^-$	(4.9 ± 1.2) × 10^{-5}			2191
$D^- \pi^+ \pi^+ \pi^-$	(6.0 ± 0.7) × 10^{-3}		S=1.1	2287
($D^- \pi^+ \pi^+ \pi^-$) nonresonant	(3.9 ± 1.9) × 10^{-3}			2287
$D^- \pi^+ \rho^0$	(1.1 ± 1.0) × 10^{-3}			2206
$D^- a_1(1260)^+$	(6.0 ± 3.3) × 10^{-3}			2121
$D^*(2010)^- \pi^+ \pi^0$	(1.5 ± 0.5) %			2248
$D^*(2010)^- \rho^+$	(2.2 $^{+\ 1.8}_{-\ 2.7}$) × 10^{-3}		S=5.2	2180
$D^*(2010)^- K^+$	(2.12± 0.15) × 10^{-4}			2226
$D^*(2010)^- K^0 \pi^+$	(3.0 ± 0.8) × 10^{-4}			2205
$D^*(2010)^- K^*(892)^+$	(3.3 ± 0.6) × 10^{-4}			2155
$D^*(2010)^- K^+ \overline{K}^0$	< 4.7	× 10^{-4}	CL=90%	2131
$D^*(2010)^- K^+ \overline{K}^*(892)^0$	(1.29± 0.33) × 10^{-3}			2007
$D^*(2010)^- \pi^+ \pi^+ \pi^-$	(7.21± 0.29) × 10^{-3}			2235
($D^*(2010)^- \pi^+ \pi^+ \pi^-$) non-resonant	(0.0 ± 2.5) × 10^{-3}			2235
$D^*(2010)^- \pi^+ \rho^0$	(5.7 ± 3.2) × 10^{-3}			2150
$D^*(2010)^- a_1(1260)^+$	(1.30± 0.27) %			2061
$\overline{D}_1(2420)^0 \pi^- \pi^+$, $\overline{D}_1^0 \to D^{*-} \pi^+$	(1.47± 0.35) × 10^{-4}			–
$D^*(2010)^- K^+ \pi^- \pi^+$	(4.7 ± 0.4) × 10^{-4}			2181
$D^*(2010)^- \pi^+ \pi^+ \pi^- \pi^0$	(1.76± 0.27) %			2218
$D^{*-} 3\pi^+ 2\pi^-$	(4.7 ± 0.9) × 10^{-3}			2195
$\overline{D}^*(2010)^- \omega \pi^+$	(2.46± 0.18) × 10^{-3}		S=1.2	2148
$D_1(2430)^0 \omega$, $D_1^0 \to D^{*-} \pi^+$	(2.7 $^{+\ 0.8}_{-\ 0.4}$) × 10^{-4}			1992
$\overline{D}^{*-} \rho(1450)^+$	(1.07$^{+\ 0.40}_{-\ 0.34}$) × 10^{-3}			–
$\overline{D}_1(2420)^0 \omega$	(7.0 ± 2.2) × 10^{-5}			1995
$\overline{D}_2^*(2460)^0 \omega$	(4.0 ± 1.4) × 10^{-5}			1975
$\overline{D}^{*-} b_1(1235)^-$, $b_1^- \to \omega \pi^-$	< 7	× 10^{-5}	CL=90%	–
$\overline{D}^{**-} \pi^+$	[xxx] (1.9 ± 0.9) × 10^{-3}			–
$D_1(2420)^- \pi^+$, $D_1^- \to D^- \pi^+ \pi^-$	(9.9 $^{+\ 2.0}_{-\ 2.5}$) × 10^{-5}			–
$D_1(2420)^- \pi^+$, $D_1^- \to D^{*-} \pi^+ \pi^-$	< 3.3	× 10^{-5}	CL=90%	–
$\overline{D}_2^*(2460)^- \pi^+$, $(D_2^*)^- \to D^0 \pi^-$	(2.38± 0.16) × 10^{-4}			2062
$\overline{D}_0^*(2400)^- \pi^+$, $(D_0^*)^- \to D^0 \pi^-$	(7.6 ± 0.8) × 10^{-5}			2090
$D_2^*(2460)^- \pi^+$, $(D_2^*)^- \to D^{*-} \pi^+ \pi^-$	< 2.4	× 10^{-5}	CL=90%	–
$\overline{D}_2^*(2460)^- \rho^+$	< 4.9	× 10^{-3}	CL=90%	1974
$D^0 \overline{D}^0$	(1.4 ± 0.7) × 10^{-5}			1868
$D^{*0} \overline{D}^0$	< 2.9	× 10^{-4}	CL=90%	1794
$D^- D^+$	(2.11± 0.18) × 10^{-4}			1864
$D^\pm D^{*\mp}$ (CP-averaged)	(6.1 ± 0.6) × 10^{-4}			–
$D^- D_s^+$	(7.2 ± 0.8) × 10^{-3}			1812
$D^*(2010)^- D_s^+$	(8.0 ± 1.1) × 10^{-3}			1735
$D^- D_s^{*+}$	(7.4 ± 1.6) × 10^{-3}			1732
$D^*(2010)^- D_s^{*+}$	(1.77± 0.14) %			1649
$D_{s0}(2317)^- K^+$, $D_{s0}^- \to D_s^- \pi^0$	(4.2 ± 1.4) × 10^{-5}			2097
$D_{s0}(2317)^- \pi^+$, $D_{s0}^- \to D_s^- \pi^0$	< 2.5	× 10^{-5}	CL=90%	2128
$D_{sJ}(2457)^- K^+$, $D_{sJ}^- \to D_s^- \pi^0$	< 9.4	× 10^{-6}	CL=90%	–
$D_{sJ}(2457)^- \pi^+$, $D_{sJ}^- \to D_s^- \pi^0$	< 4.0	× 10^{-6}	CL=90%	–
$D_s^- D_s^+$	< 3.6	× 10^{-5}	CL=90%	1759
$D_s^{*-} D_s^+$	< 1.3	× 10^{-4}	CL=90%	1674
$D_s^{*-} D_s^{*+}$	< 2.4	× 10^{-4}	CL=90%	1583
$D_{s0}^*(2317)^+ D^-$, $D_{s0}^{*+} \to D_s^+ \pi^0$	(1.09± 0.16) × 10^{-3}			1602
$D_{s0}(2317)^+ D^-$, $D_{s0}^+ \to D_s^{*+} \gamma$	< 9.5	× 10^{-4}	CL=90%	–
$D_{s0}(2317)^+ D^*(2010)^-$, $D_{s0}^+ \to D_s^+ \pi^0$	(1.5 ± 0.6) × 10^{-3}			1509
$D_{sJ}(2457)^+ D^-$	(3.5 ± 1.1) × 10^{-3}			–
$D_{sJ}(2457)^+ D^-$, $D_{sJ}^+ \to D_s^+ \gamma$	(6.5 $^{+\ 1.7}_{-\ 1.4}$) × 10^{-4}			–
$D_{sJ}(2457)^+ D^-$, $D_{sJ}^+ \to D_s^{*+} \gamma$	< 6.0	× 10^{-4}	CL=90%	–
$D_{sJ}(2457)^+ D^-$, $D_{sJ}^+ \to D_s^+ \pi^+ \pi^-$	< 2.0	× 10^{-4}	CL=90%	–
$D_{sJ}(2457)^+ D^-$, $D_{sJ}^+ \to D_s^+ \pi^0$	< 3.6	× 10^{-4}	CL=90%	–
$D^*(2010)^- D_{sJ}(2457)^+$	(9.3 ± 2.2) × 10^{-3}			–
$D_{sJ}(2457)^+ D^*(2010)$, $D_{sJ}^+ \to D_s^+ \gamma$	(2.3 $^{+\ 0.9}_{-\ 0.7}$) × 10^{-3}			–
$D^- D_{s1}(2536)^+$, $D_{s1}^+ \to D^{*0} K^+ + D^{*+} K^0$	(2.8 ± 0.7) × 10^{-4}			1444
$D^- D_{s1}(2536)^+$, $D_{s1}^+ \to D^{*0} K^+$	(1.7 ± 0.6) × 10^{-4}			1444
$D^- D_{s1}(2536)^+$, $D_{s1}^+ \to D^{*+} K^0$	(2.6 ± 1.1) × 10^{-4}			1444
$D^*(2010)^- D_{s1}(2536)^+$, $D_{s1}^+ \to D^{*0} K^+ + D^{*+} K^0$	(5.0 ± 1.4) × 10^{-4}			1336
$D^*(2010)^- D_{s1}(2536)^+$, $D_{s1}^+ \to D^{*0} K^+$	(3.3 ± 1.1) × 10^{-4}			1336
$D^{*-} D_{s1}(2536)^+$, $D_{s1}^+ \to D^{*+} K^0$	(5.0 ± 1.7) × 10^{-4}			1336
$D^- D_{sJ}(2573)^+$, $D_{sJ}^+ \to D^0 K^+$	(3.4 ± 1.8) × 10^{-5}			1414
$D^*(2010)^- D_{sJ}(2573)^+$, $D_{sJ}^+ \to D^0 K^+$	< 2	× 10^{-4}	CL=90%	1304
$D^- D_{sJ}(2700)^+$, $D_{sJ}^+ \to D^0 K^+$	(7.1 ± 1.2) × 10^{-4}			–
$D^+ \pi^-$	(7.4 ± 1.3) × 10^{-7}			2306
$D_s^+ \pi^-$	(2.16± 0.26) × 10^{-5}			2270
$D_s^{*+} \pi^-$	(2.1 ± 0.4) × 10^{-5}		S=1.4	2215
$D_s^+ \rho^-$	< 2.4	× 10^{-5}	CL=90%	2197
$D_s^{*+} \rho^-$	(4.1 ± 1.3) × 10^{-5}			2138
$D_s^+ a_0^-$	< 1.9	× 10^{-5}	CL=90%	–
$D_s^{*+} a_0^-$	< 3.6	× 10^{-5}	CL=90%	–
$D_s^+ a_1(1260)^-$	< 2.1	× 10^{-3}	CL=90%	2080
$D_s^{*+} a_1(1260)^-$	< 1.7	× 10^{-3}	CL=90%	2015
$D_s^+ a_2^-$	< 1.9	× 10^{-4}	CL=90%	–
$D_s^{*+} a_2^-$	< 2.0	× 10^{-4}	CL=90%	–
$D_s^- K^+$	(2.7 ± 0.5) × 10^{-5}		S=2.7	2242
$D_s^{*-} K^+$	(2.19± 0.30) × 10^{-5}			2185
$D_s^- K^*(892)^+$	(3.5 ± 1.0) × 10^{-5}			2172
$D_s^{*-} K^*(892)^+$	(3.2 $^{+\ 1.5}_{-\ 1.3}$) × 10^{-5}			2112
$D_s^- \pi^+ K^0$	(9.7 ± 1.4) × 10^{-5}			2222
$D_s^{*-} \pi^+ K^0$	< 1.10	× 10^{-4}	CL=90%	2164
$D_s^- K^+ \pi^+ \pi^-$	(1.7 ± 0.5) × 10^{-4}			2198
$D_s^- \pi^+ K^*(892)^0$	< 3.0	× 10^{-3}	CL=90%	2138
$D_s^{*-} \pi^+ K^*(892)^0$	< 1.6	× 10^{-3}	CL=90%	2076
$\overline{D}^0 K^0$	(5.2 ± 0.7) × 10^{-5}			2280
$\overline{D}^0 K^+ \pi^-$	(8.8 ± 1.7) × 10^{-5}			2261
$\overline{D}^0 K^*(892)^0$	(4.5 ± 0.6) × 10^{-5}			2213
$\overline{D}^0 K^*(1410)^0$	< 6.7	× 10^{-5}	CL=90%	2059
$\overline{D}^0 K_0^*(1430)^0$	(7 ± 7) × 10^{-6}			2057
$\overline{D}^0 K_2^*(1430)^0$	(2.1 ± 0.9) × 10^{-5}			2057
$D_0^*(2400)^-$, $D_0^{*-} \to \overline{D}^0 \pi^-$	(1.9 ± 0.9) × 10^{-5}			–
$D_2^*(2460)^- K^+$, $D_2^{*-} \to \overline{D}^0 \pi^-$	(2.03± 0.35) × 10^{-5}			2029
$D_3^*(2760)^- K^+$, $D_3^{*-} \to \overline{D}^0 \pi^-$	< 1.0	× 10^{-6}	CL=90%	–
$\overline{D}^0 K^+ \pi^-$ non-resonant	< 3.7	× 10^{-5}	CL=90%	–
$\overline{D}^0 \pi^0$	(2.63± 0.14) × 10^{-4}			2308
$\overline{D}^0 \rho^0$	(3.21± 0.21) × 10^{-4}			2237
$\overline{D}^0 f_2$	(1.56± 0.21) × 10^{-4}			–
$\overline{D}^0 \eta$	(2.36± 0.32) × 10^{-4}		S=2.5	2274
$\overline{D}^0 \eta'$	(1.38± 0.16) × 10^{-4}		S=1.3	2198
$\overline{D}^0 \omega$	(2.54± 0.16) × 10^{-4}			2235
$D^0 \phi$	< 1.16	× 10^{-5}	CL=90%	2183
$D^0 K^+ \pi^-$	(5.3 ± 3.2) × 10^{-6}			2261
$D^0 K^*(892)^0$	< 1.1	× 10^{-5}	CL=90%	2213
$\overline{D}^{*0} \gamma$	< 2.5	× 10^{-5}	CL=90%	2258
$\overline{D}^*(2007)^0 \pi^0$	(2.2 ± 0.6) × 10^{-4}		S=2.6	2256

Meson Summary Table

$\overline{D}^*(2007)^0\,\rho^0$	$<$	5.1	$\times 10^{-4}$	CL=90%	2182
$\overline{D}^*(2007)^0\,\eta$	(	2.3 $\pm$ 0.6)	$\times 10^{-4}$	S=2.8	2220
$\overline{D}^*(2007)^0\,\eta'$	(	1.40 $\pm$ 0.22)	$\times 10^{-4}$		2141
$\overline{D}^*(2007)^0\,\pi^+\pi^-$	(	6.2 $\pm$ 2.2)	$\times 10^{-4}$		2249
$\overline{D}^*(2007)^0\,K^0$	(	3.6 $\pm$ 1.2)	$\times 10^{-5}$		2227
$\overline{D}^*(2007)^0\,K^*(892)^0$	$<$	6.9	$\times 10^{-5}$	CL=90%	2157
$D^*(2007)^0\,K^*(892)^0$	$<$	4.0	$\times 10^{-5}$	CL=90%	2157
$D^*(2007)^0\,\pi^+\pi^+\pi^-\pi^-$	(	2.7 $\pm$ 0.5)	$\times 10^{-3}$		2219
$D^*(2010)^+\,D^*(2010)^-$	(	8.0 $\pm$ 0.6)	$\times 10^{-4}$		1711
$\overline{D}^*(2007)^0\,\omega$	(	3.6 $\pm$ 1.1)	$\times 10^{-4}$	S=3.1	2180
$D^*(2010)^+\,D^-$	(	6.1 $\pm$ 1.5)	$\times 10^{-4}$	S=1.6	1790
$D^*(2007)^0\,\overline{D}^*(2007)^0$	$<$	9	$\times 10^{-5}$	CL=90%	1715
$D^-\,D^0\,K^+$	(	1.07 $\pm$ 0.11)	$\times 10^{-3}$		1574
$D^-\,D^*(2007)^0\,K^+$	(	3.5 $\pm$ 0.4)	$\times 10^{-3}$		1478
$D^*(2010)^-\,D^0\,K^+$	(	2.47 $\pm$ 0.21)	$\times 10^{-3}$		1479
$D^*(2010)^-\,D^*(2007)^0\,K^+$	(	1.06 $\pm$ 0.09) %			1366
$D^-\,D^+\,K^0$	(	7.5 $\pm$ 1.7)	$\times 10^{-4}$		1568
$D^*(2010)^-\,D^+\,K^0$ + $D^-\,D^*(2010)^+\,K^0$	(	6.4 $\pm$ 0.5)	$\times 10^{-3}$		1473
$D^*(2010)^-\,D^*(2010)^+\,K^0$	(	8.1 $\pm$ 0.7)	$\times 10^{-3}$		1360
$D^{*-}\,D_{s1}(2536)^+$, $D_{s1}^+ \to D^{*+}\,K^0$	(	8.0 $\pm$ 2.4)	$\times 10^{-4}$		1336
$\overline{D}^0\,D^0\,K^0$	(	2.7 $\pm$ 1.1)	$\times 10^{-4}$		1574
$\overline{D}^0\,D^*(2007)^0\,K^0$ + $\overline{D}^*(2007)^0\,D^0\,K^0$	(	1.1 $\pm$ 0.5)	$\times 10^{-3}$		1478
$\overline{D}^*(2007)^0\,D^*(2007)^0\,K^0$	(	2.4 $\pm$ 0.9)	$\times 10^{-3}$		1365
$(\overline{D}+\overline{D}^*)(D+D^*)\,K$	(	3.68 $\pm$ 0.26) %			–

Charmonium modes

$\eta_c\,K^0$	(	7.9 $\pm$ 1.2)	$\times 10^{-4}$		1751
$\eta_c\,K^*(892)^0$	(	6.9 $\pm$ 0.9)	$\times 10^{-4}$		1646
$\eta_c(2S)\,K^{*0}$	$<$	3.9	$\times 10^{-4}$	CL=90%	1159
$h_c(1P)\,K^{*0}$	$<$	4	$\times 10^{-4}$	CL=90%	1253
$J/\psi(1S)\,K^0$	(	8.73 $\pm$ 0.32)	$\times 10^{-4}$		1683
$J/\psi(1S)\,K^+\,\pi^-$	(	1.15 $\pm$ 0.05)	$\times 10^{-3}$		1652
$J/\psi(1S)\,K^*(892)^0$	(	1.27 $\pm$ 0.05)	$\times 10^{-3}$		1571
$J/\psi(1S)\,\eta\,K_S^0$	(	5.4 $\pm$ 0.9)	$\times 10^{-5}$		1508
$J/\psi(1S)\,\eta'\,K_S^0$	$<$	2.5	$\times 10^{-5}$	CL=90%	1271
$J/\psi(1S)\,\phi\,K^0$	(	4.9 $\pm$ 1.0)	$\times 10^{-5}$	S=1.3	1224
$J/\psi(1S)\,\omega\,K^0$	(	2.3 $\pm$ 0.4)	$\times 10^{-4}$		1386
$\chi_{c1}(3872)\,K^0$, $\chi_{c1} \to J/\psi\omega$	(	6.0 $\pm$ 3.2)	$\times 10^{-6}$		1140
$X(3915)$, $X \to J/\psi\omega$	(	2.1 $\pm$ 0.9)	$\times 10^{-5}$		1102
$J/\psi(1S)\,K(1270)^0$	(	1.3 $\pm$ 0.5)	$\times 10^{-3}$		1391
$J/\psi(1S)\,\pi^0$	(	1.76 $\pm$ 0.16)	$\times 10^{-5}$	S=1.1	1728
$J/\psi(1S)\,\eta$	(	1.08 $\pm$ 0.23)	$\times 10^{-5}$	S=1.5	1673
$J/\psi(1S)\,\pi^+\pi^-$	(	3.96 $\pm$ 0.17)	$\times 10^{-5}$		1716
$J/\psi(1S)\,\pi^+\pi^-$ nonresonant	$<$	1.2	$\times 10^{-5}$	CL=90%	1716
$J/\psi(1S)\,f_0(500)$, $f_0 \to \pi\pi$	(	8.0 $^{+\ 1.1}_{-\ 0.9}$)	$\times 10^{-6}$		–
$J/\psi(1S)\,f_2$	(	3.3 $\pm$ 0.5)	$\times 10^{-6}$	S=1.5	–
$J/\psi(1S)\,\rho^0$	(	2.55 $^{+\ 0.18}_{-\ 0.16}$)	$\times 10^{-5}$		1612
$J/\psi(1S)\,f_0(980)$, $f_0 \to \pi^+\pi^-$	$<$	1.1	$\times 10^{-6}$	CL=90%	–
$J/\psi(1S)\,\rho(1450)^0$, $\rho^0 \to \pi\pi$	(	2.9 $^{+\ 1.6}_{-\ 0.7}$)	$\times 10^{-6}$		–
$J/\psi\,\rho(1700)^0$, $\rho^0 \to \pi^+\pi^-$	(	2.0 $\pm$ 1.3)	$\times 10^{-6}$		–
$J/\psi(1S)\,\omega$	(	1.8 $^{+\ 0.7}_{-\ 0.5}$)	$\times 10^{-5}$		1609
$J/\psi(1S)\,K^+\,K^-$	(	2.51 $\pm$ 0.35)	$\times 10^{-6}$		1533
$J/\psi(1S)\,a_0(980)$, $a_0 \to K^+\,K^-$	(	4.7 $\pm$ 3.4)	$\times 10^{-7}$		–
$J/\psi(1S)\,\phi$	$<$	1.9	$\times 10^{-7}$	CL=90%	1520
$J/\psi(1S)\,\eta'(958)$	(	7.6 $\pm$ 2.4)	$\times 10^{-6}$		1546
$J/\psi(1S)\,K^0\,\pi^+\pi^-$	(	4.4 $\pm$ 0.4)	$\times 10^{-4}$		1611
$J/\psi(1S)\,K^0\,K^-\pi^+ +$ c.c.	$<$	2.1	$\times 10^{-5}$	CL=90%	1467
$J/\psi(1S)\,K^0\,K^+\,K^-$	(	2.5 $\pm$ 0.7)	$\times 10^{-5}$	S=1.8	1249
$J/\psi(1S)\,K^0\,\rho^0$	(	5.4 $\pm$ 3.0)	$\times 10^{-4}$		1390
$J/\psi(1S)\,K^*(892)^+\,\pi^-$	(	8 $\pm$ 4)	$\times 10^{-4}$		1514
$J/\psi(1S)\,\pi^+\pi^-\pi^+\pi^-$	(	1.43 $\pm$ 0.12)	$\times 10^{-5}$		1670
$J/\psi(1S)\,f_1(1285)$	(	8.2 $\pm$ 2.1)	$\times 10^{-6}$		1385
$J/\psi(1S)\,K^*(892)^0\,\pi^+\pi^-$	(	6.6 $\pm$ 2.2)	$\times 10^{-4}$		1447
$\chi_{c1}(3872)^-\,K^+$	$<$	5	$\times 10^{-4}$	CL=90%	–
$\chi_{c1}(3872)^-\,K^+$, $\chi_{c1}(3872)^- \to J/\psi(1S)\,\pi^-\pi^0$	[yyy] $<$	4.2	$\times 10^{-6}$	CL=90%	–
$\chi_{c1}(3872)\,K^0$, $\chi_{c1} \to J/\psi\pi^+\pi^-$	(	4.3 $\pm$ 1.3)	$\times 10^{-6}$		1140
$\chi_{c1}(3872)\,K^0$, $\chi_{c1} \to J/\psi\gamma$	$<$	2.4	$\times 10^{-6}$	CL=90%	1140
$\chi_{c1}(3872)\,K^*(892)^0$, $\chi_{c1} \to J/\psi\gamma$	$<$	2.8	$\times 10^{-6}$	CL=90%	940
$\chi_{c1}(3872)\,K^0$, $\chi_{c1} \to \psi(2S)\,\gamma$	$<$	6.62	$\times 10^{-6}$	CL=90%	1140
$\chi_{c1}(3872)\,K^*(892)^0$, $\chi_{c1} \to \psi(2S)\,\gamma$	$<$	4.4	$\times 10^{-6}$	CL=90%	940
$\chi_{c1}(3872)\,K^0$, $\chi_{c1} \to D^0\,\overline{D}^0\,\pi^0$	(	1.7 $\pm$ 0.8)	$\times 10^{-4}$		1140
$\chi_{c1}(3872)\,K^0$, $\chi_{c1} \to \overline{D}^{*0}\,D^0$	(	1.2 $\pm$ 0.4)	$\times 10^{-4}$		1140
$\chi_{c1}(3872)\,K^+\pi^-$, $\chi_{c1} \to J/\psi\pi^+\pi^-$	(	7.9 $\pm$ 1.4)	$\times 10^{-6}$		–
$\chi_{c1}(3872)\,K^*(892)^0$, $\chi_{c1} \to J/\psi\pi^+\pi^-$	(	4.0 $\pm$ 1.5)	$\times 10^{-6}$		–
$Z_c(4430)^\pm K^\mp$, $Z_c^\pm \to \psi(2S)\,\pi^\pm$	(	6.0 $^{+\ 3.0}_{-\ 2.4}$)	$\times 10^{-5}$		583
$Z_c(4430)^\pm K^\mp$, $Z_c^\pm \to J/\psi\pi^\pm$	(	5.4 $^{+\ 4.0}_{-\ 1.2}$)	$\times 10^{-6}$		583
$Z_c(3900)^\pm K^\mp$, $Z_c^\pm \to J/\psi\pi^\pm$	$<$	9	$\times 10^{-7}$		–
$Z_c(4200)^\pm K^\mp$, $X^\pm \to J/\psi\pi^\pm$	(	2.2 $^{+\ 1.3}_{-\ 0.8}$)	$\times 10^{-5}$		–
$J/\psi(1S)\,p\overline{p}$	$<$	5.2	$\times 10^{-7}$	CL=90%	862
$J/\psi(1S)\,\gamma$	$<$	1.5	$\times 10^{-6}$	CL=90%	1732
$J/\psi(1S)\,\overline{D}^0$	$<$	1.3	$\times 10^{-5}$	CL=90%	877
$\psi(2S)\,\pi^0$	(	1.17 $\pm$ 0.19)	$\times 10^{-5}$		1348
$\psi(2S)\,K^0$	(	5.8 $\pm$ 0.5)	$\times 10^{-4}$		1283
$\psi(3770)\,K^0$, $\psi \to \overline{D}^0\,D^0$	$<$	1.23	$\times 10^{-4}$	CL=90%	1217
$\psi(3770)\,K^0$, $\psi \to D^-\,D^+$	$<$	1.88	$\times 10^{-4}$	CL=90%	1217
$\psi(2S)\,\pi^+\pi^-$	(	2.22 $\pm$ 0.35)	$\times 10^{-5}$		1331
$\psi(2S)\,K^+\pi^-$	(	5.8 $\pm$ 0.4)	$\times 10^{-4}$		1239
$\psi(2S)\,K^*(892)^0$	(	5.9 $\pm$ 0.4)	$\times 10^{-4}$		1116
$\chi_{c0}\,K^0$	(	1.46 $\pm$ 0.27)	$\times 10^{-4}$		1477
$\chi_{c0}\,K^*(892)^0$	(	1.7 $\pm$ 0.4)	$\times 10^{-4}$		1342
$\chi_{c1}\,\pi^0$	(	1.12 $\pm$ 0.28)	$\times 10^{-5}$		1468
$\chi_{c1}\,K^0$	(	3.93 $\pm$ 0.27)	$\times 10^{-4}$		1411
$\chi_{c1}\,\pi^-\,K^+$	(	4.97 $\pm$ 0.30)	$\times 10^{-4}$		1371
$\chi_{c1}\,K^*(892)^0$	(	2.38 $\pm$ 0.19)	$\times 10^{-4}$	S=1.2	1265
$X(4051)^-\,K^+$, $X^- \to \chi_{c1}\,\pi^-$	(	3.0 $^{+\ 4.0}_{-\ 1.8}$)	$\times 10^{-5}$		–
$X(4248)^-\,K^+$, $X^- \to \chi_{c1}\,\pi^-$	(	4.0 $^{+20.0}_{-\ 1.0}$)	$\times 10^{-5}$		–
$\chi_{c1}\,\pi^+\pi^-\,K^0$	(	3.2 $\pm$ 0.5)	$\times 10^{-4}$		1318
$\chi_{c1}\,\pi^-\pi^0\,K^+$	(	3.5 $\pm$ 0.6)	$\times 10^{-4}$		1321
$\chi_{c2}\,K^0$	$<$	1.5	$\times 10^{-5}$	CL=90%	1379
$\chi_{c2}\,K^*(892)^0$	(	4.9 $\pm$ 1.2)	$\times 10^{-5}$	S=1.1	1228
$\chi_{c2}\,\pi^-\,K^+$	(	7.2 $\pm$ 1.0)	$\times 10^{-5}$		1338
$\chi_{c2}\,\pi^+\pi^-\,K^0$	$<$	1.70	$\times 10^{-4}$	CL=90%	1282
$\chi_{c2}\,\pi^-\pi^0\,K^+$	$<$	7.4	$\times 10^{-5}$	CL=90%	1286

K* or *K* **modes**

$K^+\pi^-$	(	1.96 $\pm$ 0.05)	$\times 10^{-5}$		2615
$K^0\pi^0$	(	9.9 $\pm$ 0.5)	$\times 10^{-6}$		2615
$\eta'\,K^0$	(	6.6 $\pm$ 0.4)	$\times 10^{-5}$	S=1.4	2528
$\eta'\,K^*(892)^0$	(	2.8 $\pm$ 0.6)	$\times 10^{-6}$		2472
$\eta'\,K_0^*(1430)^0$	(	6.3 $\pm$ 1.6)	$\times 10^{-6}$		2346
$\eta'\,K_2^*(1430)^0$	(	1.37 $\pm$ 0.32)	$\times 10^{-5}$		2346
$\eta\,K^0$	(	1.23 $^{+\ 0.27}_{-\ 0.24}$)	$\times 10^{-6}$		2587
$\eta\,K^*(892)^0$	(	1.59 $\pm$ 0.10)	$\times 10^{-5}$		2534
$\eta\,K_0^*(1430)^0$	(	1.10 $\pm$ 0.22)	$\times 10^{-5}$		2415
$\eta\,K_2^*(1430)^0$	(	9.6 $\pm$ 2.1)	$\times 10^{-6}$		2414
$\omega\,K^0$	(	4.8 $\pm$ 0.4)	$\times 10^{-6}$		2557
$a_0(980)^0\,K^0$, $a_0^0 \to \eta\pi^0$	$<$	7.8	$\times 10^{-6}$	CL=90%	–
$b_1^0\,K^0$, $b_1^0 \to \omega\pi^0$	$<$	7.8	$\times 10^{-6}$	CL=90%	–
$a_0(980)^\pm K^\mp$, $a_0^\pm \to \eta\pi^\pm$	$<$	1.9	$\times 10^{-6}$	CL=90%	–
$b_1^-\,K^+$, $b_1^- \to \omega\pi^-$	(	7.4 $\pm$ 1.4)	$\times 10^{-6}$		–
$b_1^0\,K^{*0}$, $b_1^0 \to \omega\pi^0$	$<$	8.0	$\times 10^{-6}$	CL=90%	–
$b_1^-\,K^{*+}$, $b_1^- \to \omega\pi^-$	$<$	5.0	$\times 10^{-6}$	CL=90%	–
$a_0(1450)^\pm K^\mp$, $a_0^\pm \to \eta\pi^\pm$	$<$	3.1	$\times 10^{-6}$	CL=90%	–
$K_S^0 X^0$ (Familon)	$<$	5.3	$\times 10^{-5}$	CL=90%	–
$\omega\,K^*(892)^0$	(	2.0 $\pm$ 0.5)	$\times 10^{-6}$		2503
$\omega\,(K\pi)_0^{*0}$	(	1.84 $\pm$ 0.25)	$\times 10^{-5}$		–
$\omega\,K_0^*(1430)^0$	(	1.60 $\pm$ 0.34)	$\times 10^{-5}$		2380
$\omega\,K_2^*(1430)^0$	(	1.01 $\pm$ 0.23)	$\times 10^{-5}$		2380
$\omega\,K^+\,\pi^-$ nonresonant	(	5.1 $\pm$ 1.0)	$\times 10^{-6}$		2542

$K^+\pi^-\pi^0$		$(3.78\pm0.32)\times10^{-5}$			2609
$K^+\rho^-$		$(7.0\pm0.9)\times10^{-6}$			2559
$K^+\rho(1450)^-$		$(2.4\pm1.2)\times10^{-6}$			–
$K^+\rho(1700)^-$		$(6\pm7)\times10^{-7}$			–
$(K^+\pi^-\pi^0)$ non-resonant		$(2.8\pm0.6)\times10^{-6}$			–
$(K\pi)_0^{*+}\pi^-$, $(K\pi)_0^{*+}\to K^+\pi^0$		$(3.4\pm0.5)\times10^{-5}$			–
$(K\pi)_0^{*0}\pi^0$, $(K\pi)_0^{*0}\to K^+\pi^-$		$(8.6\pm1.7)\times10^{-6}$			–
$K_2^*(1430)^0\pi^0$	$<$	4.0	$\times10^{-6}$	CL=90%	2445
$K^*(1680)^0\pi^0$	$<$	7.5	$\times10^{-6}$	CL=90%	2358
$K_x^{*0}\pi^0$	[bbaa]	$(6.1\pm1.6)\times10^{-6}$			–
$K^0\pi^+\pi^-$		$(4.94\pm0.18)\times10^{-5}$			2609
$K^0\pi^+\pi^-$ non-resonant		$(1.47^{+0.40}_{-0.26})\times10^{-5}$		S=2.1	–
$K^0\rho^0$		$(4.7\pm0.6)\times10^{-6}$			2558
$K^*(892)^+\pi^-$		$(8.4\pm0.8)\times10^{-6}$			2563
$K_0^*(1430)^+\pi^-$		$(3.3\pm0.7)\times10^{-5}$		S=2.0	–
$K_x^{*+}\pi^-$	[bbaa]	$(5.1\pm1.6)\times10^{-6}$			–
$K^*(1410)^+\pi^-$, $K^{*+}\to K^0\pi^+$	$<$	3.8	$\times10^{-6}$	CL=90%	–
$f_0(980)K^0$, $f_0\to\pi^+\pi^-$		$(7.0\pm0.9)\times10^{-6}$			2522
$f_2(1270)K^0$		$(2.7^{+1.3}_{-1.2})\times10^{-6}$			2459
$f_x(1300)K0, f_x\to\pi^+\pi^-$		$(1.8\pm0.7)\times10^{-6}$			–
$K^*(892)^0\pi^0$		$(3.3\pm0.6)\times10^{-6}$			2563
$K_2^*(1430)^+\pi^-$	$<$	6	$\times10^{-6}$	CL=90%	2445
$K^*(1680)^+\pi^-$	$<$	1.0	$\times10^{-5}$	CL=90%	2358
$K^+\pi^-\pi^+\pi^-$	[ccaa] $<$	2.3	$\times10^{-4}$	CL=90%	2600
$\rho^0K^+\pi^-$		$(2.8\pm0.7)\times10^{-6}$			2543
$f_0(980)K^+\pi^-$, $f_0\to\pi\pi$		$(1.4^{+0.5}_{-0.6})\times10^{-6}$			2506
$K^+\pi^-\pi^+\pi^-$ nonresonant	$<$	2.1	$\times10^{-6}$	CL=90%	2600
$K^*(892)^0\pi^+\pi^-$		$(5.5\pm0.5)\times10^{-5}$			2557
$K^*(892)^0\rho^0$		$(3.9\pm1.3)\times10^{-6}$		S=1.9	2504
$K^*(892)^0f_0(980)$, $f_0\to\pi\pi$		$(3.9^{+2.1}_{-1.8})\times10^{-6}$		S=3.9	2466
$K_1(1270)^+\pi^-$	$<$	3.0	$\times10^{-5}$	CL=90%	2484
$K_1(1400)^+\pi^-$	$<$	2.7	$\times10^{-5}$	CL=90%	2451
$a_1(1260)^-K^+$	[ccaa]	$(1.6\pm0.4)\times10^{-5}$			2471
$K^*(892)^+\rho^-$		$(1.03\pm0.26)\times10^{-5}$			2504
$K_0^*(1430)^+\rho^-$		$(2.8\pm1.2)\times10^{-5}$			–
$K_1(1400)^0\rho^0$	$<$	3.0	$\times10^{-3}$	CL=90%	2388
$K_0^*(1430)^0\rho^0$		$(2.7\pm0.6)\times10^{-5}$			2381
$K_0^*(1430)^0f_0(980)$, $f_0\to\pi\pi$		$(2.7\pm0.9)\times10^{-6}$			–
$K_2^*(1430)^0f_0(980)$, $f_0\to\pi\pi$		$(8.6\pm2.0)\times10^{-6}$			–
K^+K^-		$(7.8\pm1.5)\times10^{-8}$			2593
$K^0\overline{K}^0$		$(1.21\pm0.16)\times10^{-6}$			2592
$K^0K^-\pi^+$		$(6.2\pm0.7)\times10^{-6}$			2578
$K^*(892)^\pm K^\mp$	$<$	4	$\times10^{-7}$	CL=90%	2540
$\overline{K}^{*0}K^0+K^{*0}\overline{K}^0$	$<$	9.6	$\times10^{-7}$	CL=90%	–
$K^+K^-\pi^0$		$(2.2\pm0.6)\times10^{-6}$			2579
$K_S^0K_S^0\pi^0$	$<$	9	$\times10^{-7}$	CL=90%	2578
$K_S^0K_S^0\eta$	$<$	1.0	$\times10^{-6}$	CL=90%	2515
$K_S^0K_S^0\eta'$	$<$	2.0	$\times10^{-6}$	CL=90%	2453
$K^0K^+K^-$		$(2.67\pm0.11)\times10^{-5}$			2522
$K^0\phi$		$(7.3\pm0.7)\times10^{-6}$			2516
$f_0(980)K^0$, $f_0\to K^+K^-$		$(7.0^{+3.5}_{-3.0})\times10^{-6}$			–
$f_0(1500)K^0$		$(1.3^{+0.7}_{-0.5})\times10^{-5}$			2398
$f_2'(1525)^0K^0$		$(3^{+5}_{-4})\times10^{-7}$			–
$f_0(1710)K^0$, $f_0\to K^+K^-$		$(4.4\pm0.9)\times10^{-6}$			–
$K^0K^+K^-$ nonresonant		$(3.3\pm1.0)\times10^{-5}$			2522
$K_S^0K_S^0K_S^0$		$(6.0\pm0.5)\times10^{-6}$		S=1.1	2521
$f_0(980)K^0$, $f_0\to K_S^0K_S^0$		$(2.7\pm1.8)\times10^{-6}$			–
$f_0(1710)K^0$, $f_0\to K_S^0K_S^0$		$(5.0^{+5.0}_{-2.6})\times10^{-7}$			–
$f_2(2010)K^0$, $f_2\to K_S^0K_S^0$		$(5\pm6)\times10^{-7}$			–
$K_S^0K_S^0K_S^0$ nonresonant		$(1.33\pm0.31)\times10^{-5}$			2521
$K_S^0K_S^0K_L^0$	$<$	1.6	$\times10^{-5}$	CL=90%	2521
$K^*(892)^0K^+K^-$		$(2.75\pm0.26)\times10^{-5}$			2467
$K^*(892)^0\phi$		$(1.00\pm0.05)\times10^{-5}$			2460
$K^+K^-\pi^+\pi^-$ nonresonant	$<$	7.17	$\times10^{-5}$	CL=90%	2559
$K^*(892)^0K^-\pi^+$		$(4.5\pm1.3)\times10^{-6}$			2524
$K^*(892)^0\overline{K}^*(892)^0$		$(8\pm5)\times10^{-7}$		S=2.2	2485
$K^+K^+\pi^-\pi^-$ nonresonant	$<$	6.0	$\times10^{-6}$	CL=90%	2559
$K^*(892)^0K^+\pi^-$	$<$	2.2	$\times10^{-6}$	CL=90%	2524
$K^*(892)^0K^*(892)^0$	$<$	2	$\times10^{-7}$	CL=90%	2485
$K^*(892)^+K^*(892)^-$	$<$	2.0	$\times10^{-6}$	CL=90%	2485
$K_1(1400)^0\phi$	$<$	5.0	$\times10^{-3}$	CL=90%	2339
$\phi(K\pi)_0^{*0}$		$(4.3\pm0.4)\times10^{-6}$			–
$\phi(K\pi)_0^{*0}$ $(1.60<m_{K\pi}<2.15)$	ddaa] $<$	1.7	$\times10^{-6}$	CL=90%	–
$K_0^*(1430)^0K^-\pi^+$	$<$	3.18	$\times10^{-5}$	CL=90%	2403
$K_0^*(1430)^0\overline{K}^*(892)^0$	$<$	3.3	$\times10^{-6}$	CL=90%	2360
$K_0^*(1430)^0\overline{K}_0^*(1430)^0$	$<$	8.4	$\times10^{-6}$	CL=90%	2222
$K_0^*(1430)^0\phi$		$(3.9\pm0.8)\times10^{-6}$			2333
$K_0^*(1430)^0K^*(892)^0$	$<$	1.7	$\times10^{-6}$	CL=90%	2360
$K_0^*(1430)^0K_0^*(1430)^0$	$<$	4.7	$\times10^{-6}$	CL=90%	2222
$K^*(1680)^0\phi$	$<$	3.5	$\times10^{-6}$	CL=90%	2238
$K^*(1780)^0\phi$	$<$	2.7	$\times10^{-6}$	CL=90%	–
$K^*(2045)^0\phi$	$<$	1.53	$\times10^{-5}$	CL=90%	–
$K_2^*(1430)^0\rho^0$	$<$	1.1	$\times10^{-3}$	CL=90%	2381
$K_2^*(1430)^0\phi$		$(6.8\pm0.9)\times10^{-6}$		S=1.2	2333
$K^0\phi\phi$		$(4.5\pm0.9)\times10^{-6}$			2305
$\eta'\eta'K^0$	$<$	3.1	$\times10^{-5}$	CL=90%	2337
$\eta K^0\gamma$		$(7.6\pm1.8)\times10^{-6}$			2587
$\eta'K^0\gamma$	$<$	6.4	$\times10^{-6}$	CL=90%	2528
$K^0\phi\gamma$		$(2.7\pm0.7)\times10^{-6}$			2516
$K^+\pi^-\gamma$		$(4.6\pm1.4)\times10^{-6}$			2615
$K^*(892)^0\gamma$		$(4.18\pm0.25)\times10^{-5}$		S=2.1	2565
$K^*(1410)\gamma$	$<$	1.3	$\times10^{-4}$	CL=90%	2449
$K^+\pi^-\gamma$ nonresonant	$<$	2.6	$\times10^{-6}$	CL=90%	2615
$K^*(892)^0X(214)$, $X\to\mu^+\mu^-$	[eeaa] $<$	2.26	$\times10^{-8}$	CL=90%	–
$K^0\pi^+\pi^-\gamma$		$(1.99\pm0.18)\times10^{-5}$			2609
$K^+\pi^-\pi^0\gamma$		$(4.1\pm0.4)\times10^{-5}$			2609
$K_1(1270)^0\gamma$	$<$	5.8	$\times10^{-5}$	CL=90%	2486
$K_1(1400)^0\gamma$	$<$	1.2	$\times10^{-5}$	CL=90%	2454
$K_2^*(1430)^0\gamma$		$(1.24\pm0.24)\times10^{-5}$			2447
$K^*(1680)^0\gamma$	$<$	2.0	$\times10^{-3}$	CL=90%	2360
$K_3^*(1780)^0\gamma$	$<$	8.3	$\times10^{-5}$	CL=90%	2341
$K_4^*(2045)^0\gamma$	$<$	4.3	$\times10^{-3}$	CL=90%	2244

Light unflavored meson modes

$\rho^0\gamma$		$(8.6\pm1.5)\times10^{-7}$			2583
$\rho^0X(214)$, $X\to\mu^+\mu^-$	[eeaa] $<$	1.73	$\times10^{-8}$	CL=90%	–
$\omega\gamma$		$(4.4^{+1.8}_{-1.6})\times10^{-7}$			2582
$\phi\gamma$	$<$	1.0	$\times10^{-7}$	CL=90%	2541
$\pi^+\pi^-$		$(5.12\pm0.19)\times10^{-6}$			2636
$\pi^0\pi^0$		$(1.59\pm0.26)\times10^{-6}$		S=1.4	2636
$\eta\pi^0$		$(4.1\pm1.7)\times10^{-7}$			2610
$\eta\eta$	$<$	1.0	$\times10^{-6}$	CL=90%	2582
$\eta'\pi^0$		$(1.2\pm0.6)\times10^{-6}$		S=1.7	2551
$\eta'\eta'$	$<$	1.7	$\times10^{-6}$	CL=90%	2460
$\eta'\eta$	$<$	1.2	$\times10^{-6}$	CL=90%	2523
$\eta'\rho^0$	$<$	1.3	$\times10^{-6}$	CL=90%	2492
$\eta'f_0(980)$, $f_0\to\pi^+\pi^-$	$<$	9	$\times10^{-7}$	CL=90%	2454
$\eta\rho^0$	$<$	1.5	$\times10^{-6}$	CL=90%	2553
$\eta f_0(980)$, $f_0\to\pi^+\pi^-$	$<$	4	$\times10^{-7}$	CL=90%	2516
$\omega\eta$		$(9.4^{+4.0}_{-3.1})\times10^{-7}$			2552
$\omega\eta'$		$(1.0^{+0.5}_{-0.4})\times10^{-6}$			2491
$\omega\rho^0$	$<$	1.6	$\times10^{-6}$	CL=90%	2522
$\omega f_0(980)$, $f_0\to\pi^+\pi^-$	$<$	1.5	$\times10^{-6}$	CL=90%	2485
$\omega\omega$		$(1.2\pm0.4)\times10^{-6}$			2521
$\phi\pi^0$	$<$	1.5	$\times10^{-7}$	CL=90%	2540
$\phi\eta$	$<$	5	$\times10^{-7}$	CL=90%	2511
$\phi\eta'$	$<$	5	$\times10^{-7}$	CL=90%	2448
$\phi\pi^+\pi^-$		$(1.8\pm0.5)\times10^{-7}$			2533
$\phi\rho^0$	$<$	3.3	$\times10^{-7}$	CL=90%	2480
$\phi f_0(980)$, $f_0\to\pi^+\pi^-$	$<$	3.8	$\times10^{-7}$	CL=90%	2441
$\phi\omega$	$<$	7	$\times10^{-7}$	CL=90%	2479
$\phi\phi$	$<$	2.8	$\times10^{-8}$	CL=90%	2435
$a_0(980)^\pm\pi^\mp$, $a_0^\pm\to\eta\pi^\pm$	$<$	3.1	$\times10^{-6}$	CL=90%	–
$a_0(1450)^\pm\pi^\mp$, $a_0^\pm\to\eta\pi^\pm$	$<$	2.3	$\times10^{-6}$	CL=90%	–
$\pi^+\pi^-\pi^0$	$<$	7.2	$\times10^{-4}$	CL=90%	2631
$\rho^0\pi^0$		$(2.0\pm0.5)\times10^{-6}$			2581
$\rho^\mp\pi^\pm$	[hh]	$(2.30\pm0.23)\times10^{-5}$			2581
$\pi^+\pi^-\pi^+\pi^-$	$<$	1.12	$\times10^{-5}$	CL=90%	2621
$\rho^0\pi^+\pi^-$	$<$	8.8	$\times10^{-6}$	CL=90%	2575
$\rho^0\rho^0$		$(9.6\pm1.5)\times10^{-7}$			2523
$f_0(980)\pi^+\pi^-$, $f_0\to\pi^+\pi^-$	$<$	3.0	$\times10^{-6}$	CL=90%	–

Meson Summary Table

$\rho^0 f_0(980)$, $f_0 \to \pi^+\pi^-$		(7.8 ± 2.5) × 10^{-7}			2486
$f_0(980) f_0(980)$, $f_0 \to \pi^+\pi^-$, $f_0 \to \pi^+\pi^-$		< 1.9	× 10^{-7}	CL=90%	2447
$f_0(980) f_0(980)$, $f_0 \to \pi^+\pi^-$, $f_0 \to K^+K^-$		< 2.3	× 10^{-7}	CL=90%	2447
$a_1(1260)^\mp \pi^\pm$	[hh]	(2.6 ± 0.5) × 10^{-5}		S=1.9	2494
$a_2(1320)^\mp \pi^\pm$	[hh]	< 6.3	× 10^{-6}	CL=90%	2473
$\pi^+\pi^-\pi^0\pi^0$		< 3.1	× 10^{-3}	CL=90%	2622
$\rho^+\rho^-$		(2.77± 0.19) × 10^{-5}			2523
$a_1(1260)^0 \pi^0$		< 1.1	× 10^{-3}	CL=90%	2495
$\omega\pi^0$		< 5	× 10^{-7}	CL=90%	2580
$\pi^+\pi^+\pi^-\pi^-\pi^0$		< 9.0	× 10^{-3}	CL=90%	2609
$a_1(1260)^+ \rho^-$		< 6.1	× 10^{-5}	CL=90%	2433
$a_1(1260)^0 \rho^0$		< 2.4	× 10^{-3}	CL=90%	2433
$b_1^\mp \pi^\pm$, $b_1^\mp \to \omega\pi^\mp$		(1.09± 0.15) × 10^{-5}			–
$b_1^0\pi^0$, $b_1^0 \to \omega\pi^0$		< 1.9	× 10^{-6}	CL=90%	–
$b_1^- \rho^+$, $b_1^- \to \omega\pi^-$		< 1.4	× 10^{-6}	CL=90%	–
$b_1^0\rho^0$, $b_1^0 \to \omega\pi^0$		< 3.4	× 10^{-6}	CL=90%	–
$\pi^+\pi^+\pi^+\pi^-\pi^-\pi^-$		< 3.0	× 10^{-3}	CL=90%	2592
$a_1(1260)^+ a_1(1260)^-$, $a_1^+ \to 2\pi^+\pi^-$, $a_1^- \to 2\pi^-\pi^+$		(1.18± 0.31) × 10^{-5}			2336
$\pi^+\pi^+\pi^+\pi^-\pi^-\pi^-\pi^0$		< 1.1	%	CL=90%	2572

Baryon modes

$p\overline{p}$		(1.25± 0.32) × 10^{-8}			2467
$p\overline{p}\pi^+\pi^-$		(2.87± 0.19) × 10^{-6}			2406
$p\overline{p}K^+\pi^-$		(6.3 ± 0.5) × 10^{-6}			2306
$p\overline{p}K^0$		(2.66± 0.32) × 10^{-6}			2347
$\Theta(1540)^+\overline{p}$, $\Theta^+ \to p K_S^0$	[ffaa]	< 5	× 10^{-8}	CL=90%	2318
$f_J(2220) K^0$, $f_J \to p\overline{p}$		< 4.5	× 10^{-7}	CL=90%	2135
$p\overline{p}K^*(892)^0$		($1.24^{+0.28}_{-0.25}$) × 10^{-6}			2216
$f_J(2220) K_0^*$, $f_J \to p\overline{p}$		< 1.5	× 10^{-7}	CL=90%	–
$p\overline{p}K^+K^-$		(1.21± 0.32) × 10^{-7}			2179
$p\overline{\Lambda}\pi^-$		(3.14± 0.29) × 10^{-6}			2401
$p\overline{\Lambda}\pi^-\gamma$		< 6.5	× 10^{-7}	CL=90%	2401
$p\overline{\Sigma}(1385)^-$		< 2.6	× 10^{-7}	CL=90%	2363
$\Delta^0\overline{\Lambda}$		< 9.3	× 10^{-7}	CL=90%	2364
$p\overline{\Lambda}K^-$		< 8.2	× 10^{-7}	CL=90%	2308
$p\overline{\Lambda}D^-$		(2.5 ± 0.4) × 10^{-5}			1765
$p\overline{\Lambda}D^{*-}$		(3.4 ± 0.8) × 10^{-5}			1685
$p\overline{\Sigma}^0\pi^-$		< 3.8	× 10^{-6}	CL=90%	2383
$\overline{\Lambda}\Lambda$		< 3.2	× 10^{-7}	CL=90%	2392
$\overline{\Lambda}\Lambda K^0$		($4.8^{+1.0}_{-0.9}$) × 10^{-6}			2250
$\overline{\Lambda}\Lambda K^{*0}$		($2.5^{+0.9}_{-0.8}$) × 10^{-6}			2098
$\overline{\Lambda}\Lambda D^0$		($1.00^{+0.30}_{-0.26}$) × 10^{-5}			1661
$D^0\Sigma^0\overline{\Lambda}$ + c.c.		< 3.1	× 10^{-5}	CL=90%	1611
$\Delta^0\overline{\Delta}^0$		< 1.5	× 10^{-3}	CL=90%	2335
$\Delta^{++}\overline{\Delta}^{--}$		< 1.1	× 10^{-4}	CL=90%	2335
$\overline{D}^0 p\overline{p}$		(1.04± 0.07) × 10^{-4}			1863
$D_s^-\overline{\Lambda}p$		(2.8 ± 0.9) × 10^{-5}			1710
$\overline{D}^*(2007)^0 p\overline{p}$		(9.9 ± 1.1) × 10^{-5}			1788
$D^*(2010)^- p\overline{n}$		(1.4 ± 0.4) × 10^{-3}			1785
$D^- p\overline{p}\pi^+$		(3.32± 0.31) × 10^{-4}			1786
$D^*(2010)^- p\overline{p}\pi^+$		(4.7 ± 0.5) × 10^{-4}		S=1.2	1708
$\overline{D}^0 p\overline{p}\pi^+\pi^-$		(3.0 ± 0.5) × 10^{-4}			1708
$\overline{D}^{*0} p\overline{p}\pi^+\pi^-$		(1.9 ± 0.5) × 10^{-4}			1623
$\Theta_c\overline{p}\pi^+$, $\Theta_c \to D^- p$		< 9	× 10^{-6}	CL=90%	–
$\Theta_c\overline{p}\pi^+$, $\Theta_c \to D^{*-} p$		< 1.4	× 10^{-5}	CL=90%	–
$\overline{\Sigma}_c^{--}\Delta^{++}$		< 8	× 10^{-4}	CL=90%	1839
$\overline{\Lambda}_c^- p\pi^+\pi^-$		(1.03± 0.14) × 10^{-3}		S=1.3	1934
$\overline{\Lambda}_c^- p$		(1.55± 0.18) × 10^{-5}			2021
$\overline{\Lambda}_c^- p\pi^0$		(1.56± 0.19) × 10^{-4}			1982
$\Sigma_c(2455)^- p$		< 2.4	× 10^{-5}		–
$\overline{\Lambda}_c^- p\pi^+\pi^-\pi^0$		< 5.07	× 10^{-3}	CL=90%	1882
$\overline{\Lambda}_c^- p\pi^+\pi^-\pi^+\pi^-$		< 2.74	× 10^{-3}	CL=90%	1821
$\overline{\Lambda}_c^- p\pi^+\pi^-$ (nonresonant)		(5.5 ± 1.0) × 10^{-4}		S=1.3	1934
$\overline{\Sigma}_c(2520)^{--} p\pi^+$		(1.03± 0.18) × 10^{-4}			1860
$\overline{\Sigma}_c(2520)^0 p\pi^-$		< 3.1	× 10^{-5}	CL=90%	1860
$\overline{\Sigma}_c(2455)^0 p\pi^-$		(1.08± 0.16) × 10^{-4}			1895
$\overline{\Sigma}_c(2455)^0 N^0$, $N^0 \to p\pi^-$		(6.4 ± 1.7) × 10^{-5}			–
$\overline{\Sigma}_c(2455)^{--} p\pi^+$		(1.85± 0.24) × 10^{-4}			1895
$\Lambda_c^- p K^+\pi^-$		(3.5 ± 0.7) × 10^{-5}			–
$\overline{\Sigma}_c(2455)^{--} p K^+$, $\overline{\Sigma}_c^{--} \to \overline{\Lambda}_c^-\pi^-$		(8.9 ± 2.6) × 10^{-6}			1754
$\Lambda_c^- p K^*(892)^0$		< 2.42	× 10^{-5}	CL=90%	–
$\Lambda_c^- p K^+ K^-$		(2.0 ± 0.4) × 10^{-5}			–
$\Lambda_c^- p\phi$		< 1.0	× 10^{-5}	CL=90%	–
$\Lambda_c^- p\overline{p}p$		< 2.8	× 10^{-6}		–
$\overline{\Lambda}_c^- \Lambda K^+$		(4.7 ± 1.1) × 10^{-5}			1767
$\overline{\Lambda}_c^- \Lambda_c^+$		< 1.6	× 10^{-5}	CL=95%	1319
$\overline{\Lambda}_c(2593)^-$ / $\overline{\Lambda}_c(2625)^- p$		< 1.1	× 10^{-4}	CL=90%	–
$\overline{\Xi}_c^- \Lambda_c^+$, $\overline{\Xi}_c^- \to \overline{\Xi}^+\pi^-\pi^-$		(1.8 ± 1.8) × 10^{-5}		S=2.2	1147
$\Lambda_c^+\Lambda_c^- K^0$		(4.3 ± 2.3) × 10^{-4}			–

Lepton Family number (*LF*) or Lepton number (*L*) or Baryon number (*B*) violating modes, or/and $\Delta B = 1$ weak neutral current (*B1*) modes

$\gamma\gamma$	B1		< 3.2	× 10^{-7}	CL=90%	2640
e^+e^-	B1		< 8.3	× 10^{-8}	CL=90%	2640
$e^+e^-\gamma$	B1		< 1.2	× 10^{-7}	CL=90%	2640
$\mu^+\mu^-$	B1		($1.6^{+1.6}_{-1.4}$) × 10^{-10}		S=1.9	2638
$\mu^+\mu^-\gamma$	B1		< 1.6	× 10^{-7}	CL=90%	2638
$\mu^+\mu^-\mu^+\mu^-$	B1		< 6.9	× 10^{-10}	CL=95%	2629
SP, $S \to \mu^+\mu^-$, $P \to \mu^+\mu^-$	B1	[ggaa]	< 6.0	× 10^{-10}	CL=95%	–
$\tau^+\tau^-$	B1		< 2.1	× 10^{-3}	CL=95%	1952
$\pi^0\ell^+\ell^-$	B1		< 5.3	× 10^{-8}	CL=90%	2638
$\pi^0 e^+e^-$	B1		< 8.4	× 10^{-8}	CL=90%	2638
$\pi^0\mu^+\mu^-$	B1		< 6.9	× 10^{-8}	CL=90%	2634
$\eta\ell^+\ell^-$	B1		< 6.4	× 10^{-8}	CL=90%	2611
ηe^+e^-	B1		< 1.08	× 10^{-7}	CL=90%	2611
$\eta\mu^+\mu^-$	B1		< 1.12	× 10^{-7}	CL=90%	2607
$\pi^0\nu\overline{\nu}$	B1		< 9	× 10^{-6}	CL=90%	2638
$K^0\ell^+\ell^-$	B1	[sss]	($3.1^{+0.8}_{-0.7}$) × 10^{-7}			2616
$K^0 e^+e^-$	B1		($1.6^{+1.0}_{-0.8}$) × 10^{-7}			2616
$K^0\mu^+\mu^-$	B1		(3.39± 0.34) × 10^{-7}			2612
$K^0\nu\overline{\nu}$	B1		< 2.6	× 10^{-5}	CL=90%	2616
$\rho^0\nu\overline{\nu}$	B1		< 4.0	× 10^{-5}	CL=90%	2583
$K^*(892)^0\ell^+\ell^-$	B1	[sss]	($9.9^{+1.2}_{-1.1}$) × 10^{-7}			2565
$K^*(892)^0 e^+e^-$	B1		($1.03^{+0.19}_{-0.17}$) × 10^{-6}			2565
$K^*(892)^0\mu^+\mu^-$	B1		(9.4 ± 0.5) × 10^{-7}			2560
$\pi^+\pi^-\mu^+\mu^-$	B1		(2.1 ± 0.5) × 10^{-8}			2626
$K^*(892)^0\nu\overline{\nu}$	B1		< 1.8	× 10^{-5}	CL=90%	2565
invisible	B1		< 2.4	× 10^{-5}	CL=90%	–
$\nu\overline{\nu}\gamma$	B1		< 1.7	× 10^{-5}	CL=90%	2640
$\phi\nu\overline{\nu}$	B1		< 1.27	× 10^{-4}	CL=90%	2541
$e^\pm\mu^\mp$	LF	[hh]	< 2.8	× 10^{-9}	CL=90%	2639
$\pi^0 e^\pm\mu^\mp$	LF		< 1.4	× 10^{-7}	CL=90%	2637
$K^0 e^\pm\mu^\mp$	LF		< 2.7	× 10^{-7}	CL=90%	2615
$K^*(892)^0 e^+\mu^-$	LF		< 5.3	× 10^{-7}	CL=90%	2563
$K^*(892)^0 e^-\mu^+$	LF		< 3.4	× 10^{-7}	CL=90%	2563
$K^*(892)^0 e^\pm\mu^\mp$	LF		< 5.8	× 10^{-7}	CL=90%	2563
$e^\pm\tau^\mp$	LF	[hh]	< 2.8	× 10^{-5}	CL=90%	2341
$\mu^\pm\tau^\mp$	LF	[hh]	< 2.2	× 10^{-5}	CL=90%	2339
$\Lambda_c^+\mu^-$	L,B		< 1.4	× 10^{-6}	CL=90%	2143
$\Lambda_c^+ e^-$	L,B		< 4	× 10^{-6}	CL=90%	2145

$B^\pm/B^0$ ADMIXTURE

***CP* violation**

$A_{CP}(B \to K^*(892)\gamma) = -0.003 \pm 0.011$
$A_{CP}(b \to s\gamma) = 0.015 \pm 0.020$
$A_{CP}(b \to (s+d)\gamma) = 0.010 \pm 0.031$
$A_{CP}(B \to X_s\ell^+\ell^-) = 0.04 \pm 0.11$
$A_{CP}(B \to X_s\ell^+\ell^-)$ $(1.0 < q^2 < 6.0\ \mathrm{GeV}^2/c^4) = -0.06 \pm 0.22$
$A_{CP}(B \to X_s\ell^+\ell^-)$ $(10.1 < q^2 < 12.9$ or $q^2 > 14.2\ \mathrm{GeV}^2/c^4)$ $= 0.19 \pm 0.18$
$A_{CP}(B \to K^* e^+e^-) = -0.18 \pm 0.15$
$A_{CP}(B \to K^*\mu^+\mu^-) = -0.03 \pm 0.13$
$A_{CP}(B \to K^*\ell^+\ell^-) = -0.04 \pm 0.07$
$A_{CP}(B \to \eta\,\text{anything}) = -0.13^{+0.04}_{-0.05}$
$\Delta A_{CP}(X_s\gamma) = A_{CP}(B^\pm \to X_s\gamma) - A_{CP}(B^0 \to X_s\gamma) =$ 0.05 ± 0.04

$\Delta A_{CP}(B \to K^*\gamma) = A_{CP}(B^+ \to K^{*+}\gamma) - A_{CP}(B^0 \to K^{*0}\gamma) = 0.024 \pm 0.028$

$\overline{A}_{CP}(B \to K^*\gamma) = (A_{CP}(B^+ \to K^{*+}\gamma) + A_{CP}(B^0 \to K^{*0}\gamma))/2 = -0.001 \pm 0.014$

The branching fraction measurements are for an admixture of B mesons at the $\Upsilon(4S)$. The values quoted assume that $B(\Upsilon(4S) \to B\overline{B}) = 100\%$.

For inclusive branching fractions, *e.g.*, $B \to D^{\pm}$ *anything*, the treatment of multiple D's in the final state must be defined. One possibility would be to count the number of events with one-or-more D's and divide by the total number of B's. Another possibility would be to count the total number of D's and divide by the total number of B's, which is the definition of average multiplicity. The two definitions are identical if only one D is allowed in the final state. Even though the "one-or-more" definition seems sensible, for practical reasons inclusive branching fractions are almost always measured using the multiplicity definition. For heavy final state particles, authors call their results inclusive branching fractions while for light particles some authors call their results multiplicities. In the B sections, we list all results as inclusive branching fractions, adopting a multiplicity definition. This means that inclusive branching fractions can exceed 100% and that inclusive partial widths can exceed total widths, just as inclusive cross sections can exceed total cross section.

$\overline{B}$ modes are charge conjugates of the modes below. Reactions indicate the weak decay vertex and do not include mixing.

B DECAY MODES		Fraction (Γ_j/Γ)	Scale factor/ Confidence level	p (MeV/c)
Semileptonic and leptonic modes				
$\ell^+ \nu_\ell$ anything	[sss,hhaa]	(10.86 ± 0.16) %		–
$D^- \ell^+ \nu_\ell$ anything	[sss]	(2.8 ± 0.9) %		–
$\overline{D}^0 \ell^+ \nu_\ell$ anything	[sss]	(7.3 ± 1.5) %		–
$\overline{D} \ell^+ \nu_\ell$		(2.42 ± 0.12) %		2310
$D^{*-} \ell^+ \nu_\ell$ anything	[iiaa]	(6.7 ± 1.3) $\times 10^{-3}$		–
$D^* \ell^+ \nu_\ell$	[jjaa]	(4.95 ± 0.11) %		2257
$\overline{D}^{**} \ell^+ \nu_\ell$	[sss,kkaa]	(2.7 ± 0.7) %		–
$\overline{D}_1(2420) \ell^+ \nu_\ell$ anything		(3.8 ± 1.3) $\times 10^{-3}$	S=2.4	–
$D \pi \ell^+ \nu_\ell$ anything + $D^* \pi \ell^+ \nu_\ell$ anything		(2.6 ± 0.5) %	S=1.5	–
$D \pi \ell^+ \nu_\ell$ anything		(1.5 ± 0.6) %		–
$D^* \pi \ell^+ \nu_\ell$ anything		(1.9 ± 0.4) %		–
$\overline{D}_2^*(2460) \ell^+ \nu_\ell$ anything		(4.4 ± 1.6) $\times 10^{-3}$		–
$D^{*-} \pi^+ \ell^+ \nu_\ell$ anything		(1.00 ± 0.34) %		–
$\overline{D} \pi^+ \pi^- \ell^+ \nu_\ell$		(1.62 ± 0.32) $\times 10^{-3}$		2301
$\overline{D}^* \pi^+ \pi^- \ell^+ \nu_\ell$		(9.4 ± 3.2) $\times 10^{-4}$		2247
$D_s^- \ell^+ \nu_\ell$ anything	[sss]	< 7 $\times 10^{-3}$	CL=90%	–
$D_s^- \ell^+ \nu_\ell K^+$ anything	[sss]	< 5 $\times 10^{-3}$	CL=90%	–
$D_s^- \ell^+ \nu_\ell K^0$ anything	[sss]	< 7 $\times 10^{-3}$	CL=90%	–
$X_c \ell^+ \nu_\ell$		(10.65 ± 0.16) %		–
$X_u \ell^+ \nu_\ell$		(2.13 ± 0.31) $\times 10^{-3}$		–
$K^+ \ell^+ \nu_\ell$ anything	[sss]	(6.3 ± 0.6) %		–
$K^- \ell^+ \nu_\ell$ anything	[sss]	(10 ± 4) $\times 10^{-3}$		–
$K^0/\overline{K}^0 \ell^+ \nu_\ell$ anything	[sss]	(4.6 ± 0.5) %		–
$\overline{D} \tau^+ \nu_\tau$		(9.9 ± 1.2) $\times 10^{-3}$		1911
$D^* \tau^+ \nu_\tau$		(1.50 ± 0.08) %		1838
D, D^*, or D_s modes				
$D^{\pm}$ anything		(24.1 ± 1.4) %		–
$D^0/\overline{D}^0$ anything		(62.4 ± 2.9) %	S=1.3	–
$D^*(2010)^{\pm}$ anything		(22.5 ± 1.5) %		–
$D^*(2007)^0$ anything		(26.0 ± 2.7) %		–
$D_s^{\pm}$ anything	[hh]	(8.3 ± 0.8) %		–
$D_s^{*\pm}$ anything		(6.3 ± 1.0) %		–
$D_s^{*\pm} \overline{D}^{(*)}$		(3.4 ± 0.6) %		–
$\overline{D} D_{s0}(2317)$		seen		1605
$\overline{D} D_{sJ}(2457)$		seen		–
$D^{(*)} \overline{D}^{(*)} K^0$ + $D^{(*)} \overline{D}^{(*)} K^{\pm}$	[hh,llaa]	(7.1 $^{+2.7}_{-1.7}$) %		–
$b \to c\overline{c}s$		(22 ± 4) %		–
$D_s^{(*)} \overline{D}^{(*)}$	[hh,llaa]	(3.9 ± 0.4) %		–
$D^* D^*(2010)^{\pm}$	[hh]	< 5.9 $\times 10^{-3}$	CL=90%	1711
$D D^*(2010)^{\pm}$ + $D^* D^{\pm}$	[hh]	< 5.5 $\times 10^{-3}$	CL=90%	–
$D D^{\pm}$	[hh]	< 3.1 $\times 10^{-3}$	CL=90%	1866
$D_s^{(*)\pm} \overline{D}^{(*)} X(n\pi^{\pm})$	[hh,llaa]	(9 $^{+5}_{-4}$) %		–
$D^*(2010)\gamma$		< 1.1 $\times 10^{-3}$	CL=90%	2257
$D_s^+ \pi^-$, $D_s^{*+} \pi^-$, $D_s^+ \rho^-$, $D_s^{*+} \rho^-$, $D_s^+ \pi^0$, $D_s^{*+} \pi^0$, $D_s^+ \eta$, $D_s^{*+} \eta$, $D_s^+ \rho^0$, $D_s^{*+} \rho^0$, $D_s^+ \omega$, $D_s^{*+} \omega$	[hh]	< 4 $\times 10^{-4}$	CL=90%	–
$D_{s1}(2536)^+$ anything		< 9.5 $\times 10^{-3}$	CL=90%	–
Charmonium modes				
$J/\psi(1S)$ anything		(1.094 ± 0.032) %	S=1.1	–
$J/\psi(1S)$ (direct) anything		(7.8 ± 0.4) $\times 10^{-3}$	S=1.1	–
$\psi(2S)$ anything		(3.07 ± 0.21) $\times 10^{-3}$		–
$\chi_{c1}(1P)$ anything		(3.55 ± 0.27) $\times 10^{-3}$	S=1.3	–
$\chi_{c1}(1P)$ (direct) anything		(3.08 ± 0.19) $\times 10^{-3}$		–
$\chi_{c2}(1P)$ anything		(10.0 ± 1.7) $\times 10^{-4}$	S=1.6	–
$\chi_{c2}(1P)$ (direct) anything		(7.5 ± 1.1) $\times 10^{-4}$		–
$\eta_c(1S)$ anything		< 9 $\times 10^{-3}$	CL=90%	–
$K \chi_{c1}(3872)$, $\chi_{c1} \to D^0 \overline{D}^0 \pi^0$		(1.2 ± 0.4) $\times 10^{-4}$		1141
$K \chi_{c1}(3872)$, $\chi_{c1} \to D^{*0} D^0$		(8.0 ± 2.2) $\times 10^{-5}$		1141
$K X(3940)$, $X \to D^{*0} D^0$		< 6.7 $\times 10^{-5}$	CL=90%	1084
$K X(3915)$, $X \to \omega J/\psi$	[nnaa]	(7.1 ± 3.4) $\times 10^{-5}$		1103
K or K^* modes				
$K^{\pm}$ anything	[hh]	(78.9 ± 2.5) %		–
K^+ anything		(66 ± 5) %		–
K^- anything		(13 ± 4) %		–
$K^0/\overline{K}^0$ anything	[hh]	(64 ± 4) %		–
$K^*(892)^{\pm}$ anything		(18 ± 6) %		–
$K^*(892)^0/\overline{K}^*(892)^0$ anything	[hh]	(14.6 ± 2.6) %		–
$K^*(892)\gamma$		(4.2 ± 0.6) $\times 10^{-5}$		2565
$\eta K \gamma$		(8.5 $^{+1.8}_{-1.6}$) $\times 10^{-6}$		2588
$K_1(1400)\gamma$		< 1.27 $\times 10^{-4}$	CL=90%	2454
$K_2^*(1430)\gamma$		(1.7 $^{+0.6}_{-0.5}$) $\times 10^{-5}$		2447
$K_2(1770)\gamma$		< 1.2 $\times 10^{-3}$	CL=90%	2342
$K_3^*(1780)\gamma$		< 3.7 $\times 10^{-5}$	CL=90%	2341
$K_4^*(2045)\gamma$		< 1.0 $\times 10^{-3}$	CL=90%	2244
$K\eta'(958)$		(8.3 ± 1.1) $\times 10^{-5}$		2528
$K^*(892)\eta'(958)$		(4.1 ± 1.1) $\times 10^{-6}$		2472
$K\eta$		< 5.2 $\times 10^{-6}$	CL=90%	2588
$K^*(892)\eta$		(1.8 ± 0.5) $\times 10^{-5}$		2534
$K\phi\phi$		(2.3 ± 0.9) $\times 10^{-6}$		2306
$\overline{b} \to \overline{s}\gamma$		(3.49 ± 0.19) $\times 10^{-4}$		–
$\overline{b} \to \overline{d}\gamma$		(9.2 ± 3.0) $\times 10^{-6}$		–
$\overline{b} \to \overline{s}$gluon		< 6.8 %	CL=90%	–
η anything		(2.6 $^{+0.5}_{-0.8}$) $\times 10^{-4}$		–
η' anything		(4.2 ± 0.9) $\times 10^{-4}$		–
K^+gluon (charmless)		< 1.87 $\times 10^{-4}$	CL=90%	–
K^0gluon (charmless)		(1.9 ± 0.7) $\times 10^{-4}$		–
Light unflavored meson modes				
$\rho\gamma$		(1.39 ± 0.25) $\times 10^{-6}$	S=1.2	2583
$\rho/\omega\gamma$		(1.30 ± 0.23) $\times 10^{-6}$	S=1.2	–
$\pi^{\pm}$ anything	[hh,ooaa]	(358 ± 7) %		–
π^0 anything		(235 ±11) %		–
η anything		(17.6 ± 1.6) %		–
ρ^0 anything		(21 ± 5) %		–
ω anything		< 81 %	CL=90%	–
ϕ anything		(3.43 ± 0.12) %		–
$\phi K^*(892)$		< 2.2 $\times 10^{-5}$	CL=90%	2460
π^+ gluon (charmless)		(3.7 ± 0.8) $\times 10^{-4}$		–
Baryon modes				
Λ_c^+ / $\overline{\Lambda}_c^-$ anything		(3.6 ± 0.4) %		–
Λ_c^+ anything		< 1.3 %	CL=90%	–
$\overline{\Lambda}_c^-$ anything		< 7 %	CL=90%	–
$\overline{\Lambda}_c^- \ell^+$ anything		< 9 $\times 10^{-4}$	CL=90%	–
$\overline{\Lambda}_c^- e^+$ anything		< 1.8 $\times 10^{-3}$	CL=90%	–
$\overline{\Lambda}_c^- \mu^+$ anything		< − 1.4 $\times 10^{-3}$	CL=90%	–
$\overline{\Lambda}_c^- p$ anything		(2.06 ± 0.33) %		–
$\overline{\Lambda}_c^- p e^+ \nu_e$		< 8 $\times 10^{-4}$	CL=90%	2021
$\overline{\Sigma}_c^{--}$ anything		(3.4 ± 1.7) $\times 10^{-3}$		–
$\overline{\Sigma}_c^-$ anything		< 8 $\times 10^{-3}$	CL=90%	–
$\overline{\Sigma}_c^0$ anything		(3.7 ± 1.7) $\times 10^{-3}$		–
$\overline{\Sigma}_c^0 N (N = p$ or $n)$		< 1.2 $\times 10^{-3}$	CL=90%	1938
Ξ_c^0 anything, $\Xi_c^0 \to \Xi^- \pi^+$		(1.93 ± 0.30) $\times 10^{-4}$	S=1.1	–
Ξ_c^+, $\Xi_c^+ \to \Xi^- \pi^+ \pi^+$		(4.5 $^{+1.3}_{-1.2}$) $\times 10^{-4}$		–
$p/\overline{p}$ anything	[hh]	(8.0 ± 0.4) %		–
$p/\overline{p}$ (direct) anything	[hh]	(5.5 ± 0.5) %		–
$\overline{p} e^+ \nu_e$ anything		< 5.9 $\times 10^{-4}$	CL=90%	–
$\Lambda/\overline{\Lambda}$ anything	[hh]	(4.0 ± 0.5) %		–

Meson Summary Table

Λ anything			seen				–
$\overline{\Lambda}$ anything			seen				–
$\Xi^-/\overline{\Xi}^+$ anything	[hh]	(	2.7 ± 0.6)	$\times 10^{-3}$			–
baryons anything		(	6.8 ± 0.6)	%			–
$p\overline{p}$ anything		(	2.47 ± 0.23)	%			–
$\Lambda\overline{p}/\overline{\Lambda}p$ anything	[hh]	(	2.5 ± 0.4)	%			–
$\Lambda\overline{\Lambda}$ anything		<	5	$\times 10^{-3}$	CL=90%		–

Lepton Family number (LF) violating modes or $\Delta B = 1$ weak neutral current ($B1$) modes

$s\,e^+\,e^-$	$B1$	(	6.7 ± 1.7)	$\times 10^{-6}$	S=2.0		–
$s\,\mu^+\,\mu^-$	$B1$	(	4.3 ± 1.0)	$\times 10^{-6}$			–
$s\ell^+\ell^-$	$B1$	[sss] (	5.8 ± 1.3)	$\times 10^{-6}$	S=1.8		–
$\pi\ell^+\ell^-$	$B1$	<	5.9	$\times 10^{-8}$	CL=90%	2638	
$\pi\,e^+\,e^-$	$B1$	<	1.10	$\times 10^{-7}$	CL=90%	2638	
$\pi\,\mu^+\,\mu^-$	$B1$	<	5.0	$\times 10^{-8}$	CL=90%	2634	
$K\,e^+\,e^-$	$B1$	(	4.4 ± 0.6)	$\times 10^{-7}$		2617	
$K^*(892)\,e^+\,e^-$	$B1$	(	1.19 ± 0.20)	$\times 10^{-6}$	S=1.2	2565	
$K\,\mu^+\,\mu^-$	$B1$	(	4.4 ± 0.4)	$\times 10^{-7}$		2612	
$K^*(892)\mu^+\,\mu^-$	$B1$	(	1.06 ± 0.09)	$\times 10^{-6}$		2560	
$K\,\ell^+\,\ell^-$	$B1$	(	4.8 ± 0.4)	$\times 10^{-7}$		2617	
$K^*(892)\,\ell^+\,\ell^-$	$B1$	(	1.05 ± 0.10)	$\times 10^{-6}$		2565	
$K\,\nu\overline{\nu}$	$B1$	<	1.6	$\times 10^{-5}$	CL=90%	2617	
$K^*\nu\overline{\nu}$	$B1$	<	2.7	$\times 10^{-5}$	CL=90%		–
$\pi\,\nu\overline{\nu}$	$B1$	<	8	$\times 10^{-6}$	CL=90%	2638	
$\rho\nu\overline{\nu}$	$B1$	<	2.8	$\times 10^{-5}$	CL=90%	2583	
$s\,e^\pm\mu^\mp$	LF	[hh] <	2.2	$\times 10^{-5}$	CL=90%		–
$\pi\,e^\pm\mu^\mp$	LF	<	9.2	$\times 10^{-8}$	CL=90%	2637	
$\rho e^\pm\mu^\mp$	LF	<	3.2	$\times 10^{-6}$	CL=90%	2582	
$K\,e^\pm\mu^\mp$	LF	<	3.8	$\times 10^{-8}$	CL=90%	2616	
$K^*(892)\,e^\pm\mu^\mp$	LF	<	5.1	$\times 10^{-7}$	CL=90%	2563	

$B^\pm/B^0/B_s^0/b$-baryon ADMIXTURE

These measurements are for an admixture of bottom particles at high energy (LHC, LEP, Tevatron, S$p\overline{p}$S).

Mean life $\tau = (1.566 \pm 0.003) \times 10^{-12}$ s

Mean life $\tau = (1.72 \pm 0.10) \times 10^{-12}$ s Charged b-hadron admixture

Mean life $\tau = (1.58 \pm 0.14) \times 10^{-12}$ s Neutral b-hadron admixture

$\tau_{\text{charged } b\text{-hadron}}/\tau_{\text{neutral } b\text{-hadron}} = 1.09 \pm 0.13$

$|\Delta\tau_b|/\tau_{b,\overline{b}} = -0.001 \pm 0.014$

$\text{Re}(\epsilon_b)\ /\ (1 + |\epsilon_b|^2) = (-1.3 \pm 0.4) \times 10^{-3}$

The branching fraction measurements are for an admixture of B mesons and baryons at energies above the $\Upsilon(4S)$. Only the highest energy results (LHC, LEP, Tevatron, S$p\overline{p}$S) are used in the branching fraction averages. In the following, we assume that the production fractions are the same at the LHC, LEP, and at the Tevatron.

For inclusive branching fractions, *e.g.*, $B \to D^\pm$anything, the values usually are multiplicities, not branching fractions. They can be greater than one.

The modes below are listed for a $\overline{b}$ initial state. b modes are their charge conjugates. Reactions indicate the weak decay vertex and do not include mixing.

$\overline{b}$ DECAY MODES	Fraction (Γ_j/Γ)	Scale factor/ Confidence level	p (MeV/c)

PRODUCTION FRACTIONS

The production fractions for weakly decaying b-hadrons at high energy have been calculated from the best values of mean lives, mixing parameters, and branching fractions in this edition by the Heavy Flavor Averaging Group (HFLAV) as described in the note "B^0-$\overline{B}^0$ Mixing" in the B^0 Particle Listings. The production fractions in b-hadronic Z decay or $p\overline{p}$ collisions at the Tevatron are also listed at the end of the section. Values assume

$\text{B}(\overline{b} \to B^+) = \text{B}(\overline{b} \to B^0)$

$\text{B}(\overline{b} \to B^+) + \text{B}(\overline{b} \to B^0) + \text{B}(\overline{b} \to B_s^0) + \text{B}(b \to b\text{-baryon}) = 100\%.$

The correlation coefficients between production fractions are also reported:

$cor(B_s^0, b\text{-baryon}) = -0.259$

$cor(B_s^0, B^\pm{=}B^0) = -0.133$

$cor(b\text{-baryon}, B^\pm{=}B^0) = -0.923.$

The notation for production fractions varies in the literature (f_d, d_{B^0}, $f(b \to \overline{B}^0)$, $\text{Br}(b \to \overline{B}^0)$). We use our own branching fraction notation here, $\text{B}(\overline{b} \to B^0)$.

Note these production fractions are b-hadronization fractions, not the conventional branching fractions of b-quark to a B-hadron, which may have considerable dependence on the initial and final state kinematic and production environment.

B^+		(	40.5 ± 0.6)	%			–
B^0		(	40.5 ± 0.6)	%			–
B_s^0		(	10.1 ± 0.4)	%			–
b-baryon		(	8.9 ± 1.2)	%			–

DECAY MODES

Semileptonic and leptonic modes

ν anything		(	23.1 ± 1.5)	%			–
$\ell^+\nu_\ell$ anything	[sss]	(	10.69± 0.22)	%			–
$e^+\nu_e$ anything		(	10.86± 0.35)	%			–
$\mu^+\nu_\mu$ anything		(	$10.95^{+\ 0.29}_{-\ 0.25}$)	%			–
$D^-\ell^+\nu_\ell$ anything	[sss]	(	2.30± 0.34)	%		S=1.6	–
$D^-\pi^+\ell^+\nu_\ell$ anything		(	4.9 ± 1.9)	$\times 10^{-3}$			–
$D^-\pi^-\ell^+\nu_\ell$ anything		(	2.6 ± 1.6)	$\times 10^{-3}$			–
$\overline{D}^0\ell^+\nu_\ell$ anything	[sss]	(	6.83± 0.35)	%			–
$\overline{D}^0\pi^-\ell^+\nu_\ell$ anything		(	1.07± 0.27)	%			–
$\overline{D}^0\pi^+\ell^+\nu_\ell$ anything		(	2.3 ± 1.6)	$\times 10^{-3}$			–
$D^{*-}\ell^+\nu_\ell$ anything	[sss]	(	2.75± 0.19)	%			–
$D^{*-}\pi^-\ell^+\nu_\ell$ anything		(	6 ± 7)	$\times 10^{-4}$			–
$D^{*-}\pi^+\ell^+\nu_\ell$ anything		(	4.8 ± 1.0)	$\times 10^{-3}$			–
$\overline{D}_j^0\ell^+\nu_\ell$ anything $\times$ B($\overline{D}_j^0 \to D^{*+}\pi^-$)	[sss,ppaa]	(	2.6 ± 0.9)	$\times 10^{-3}$			–
$D_j^-\ell^+\nu_\ell$ anything $\times$ B($D_j^- \to D^0\pi^-$)	[sss,ppaa]	(	7.0 ± 2.3)	$\times 10^{-3}$			–
$\overline{D}_2^*(2460)^0\ell^+\nu_\ell$ anything $\times$ B($\overline{D}_2^*(2460)^0 \to D^{*-}\pi^+$)		<	1.4	$\times 10^{-3}$	CL=90%		–
$D_2^*(2460)^-\ell^+\nu_\ell$ anything $\times$ B($D_2^*(2460)^- \to D^0\pi^-$)		(	$4.2\ ^{+\ 1.5}_{-\ 1.8}$)	$\times 10^{-3}$			–
$\overline{D}_2^*(2460)^0\ell^+\nu_\ell$ anything $\times$ B($\overline{D}_2^*(2460)^0 \to D^-\pi^+$)		(	1.6 ± 0.8)	$\times 10^{-3}$			–
charmless $\ell\overline{\nu}_\ell$	[sss]	(	1.7 ± 0.5)	$\times 10^{-3}$			–
$\tau^+\nu_\tau$ anything		(	2.41± 0.23)	%			–
$D^{*-}\tau\nu_\tau$ anything		(	9 ± 4)	$\times 10^{-3}$			–
$\overline{c} \to \ell^-\overline{\nu}_\ell$ anything	[sss]	(	8.02± 0.19)	%			–
$c \to \ell^+\nu$ anything		(	$1.6\ ^{+\ 0.4}_{-\ 0.5}$)	%			–

Charmed meson and baryon modes

$\overline{D}^0$ anything		(	59.5 ± 2.9)	%			–
$D^0\,D_s^\pm$ anything	[hh]	(	$9.1\ ^{+\ 4.0}_{-\ 2.8}$)	%			–
$D^\mp D_s^\pm$ anything	[hh]	(	$4.0\ ^{+\ 2.3}_{-\ 1.8}$)	%			–
$\overline{D}^0\,D^0$ anything	[hh]	(	$5.1\ ^{+\ 2.0}_{-\ 1.8}$)	%			–
$D^0\,D^\pm$ anything	[hh]	(	$2.7\ ^{+\ 1.8}_{-\ 1.6}$)	%			–
$D^\pm\,D^\mp$ anything	[hh]	<	9	$\times 10^{-3}$	CL=90%		–
D^- anything		(	23.7 ± 1.8)	%			–
$D^*(2010)^+$ anything		(	17.3 ± 2.0)	%			–
$D_1(2420)^0$ anything		(	5.0 ± 1.5)	%			–
$D^*(2010)^\mp D_s^\pm$ anything	[hh]	(	$3.3\ ^{+\ 1.6}_{-\ 1.3}$)	%			–
$D^0\,D^*(2010)^\pm$ anything	[hh]	(	$3.0\ ^{+\ 1.1}_{-\ 0.9}$)	%			–
$D^*(2010)^\pm\,D^\mp$ anything	[hh]	(	$2.5\ ^{+\ 1.2}_{-\ 1.0}$)	%			–
$D^*(2010)^\pm\,D^*(2010)^\mp$ anything	[hh]	(	1.2 ± 0.4)	%			–
$\overline{D}\,D$ anything		(	$10\ ^{+11}_{-10}$)	%			–
$D_2^*(2460)^0$ anything		(	4.7 ± 2.7)	%			–
D_s^- anything		(	14.7 ± 2.1)	%			–
D_s^+ anything		(	10.1 ± 3.1)	%			–
Λ_c^+ anything		(	7.8 ± 1.2)	%			–
$\overline{c}/\,c$ anything	[ooaa]	(	116.2 ± 3.2)	%			–

Charmonium modes

$J/\psi(1S)$ anything		(	1.16± 0.10)	%			–
$\psi(2S)$ anything		(	2.86± 0.28)	$\times 10^{-3}$			–
$\chi_{c0}(1P)$ anything		(	1.5 ± 0.6)	%			–
$\chi_{c1}(1P)$ anything		(	1.4 ± 0.4)	%			–

$\chi_{c2}(1P)$ anything		(6.2 ± 2.9)	$\times 10^{-3}$		–
$\chi_c(2P)$ anything, $\chi_c \to \phi\phi$		< 2.8	$\times 10^{-7}$	CL=95%	–
$\eta_c(1S)$ anything		(4.5 ± 1.9)	%		–
$\eta_c(2S)$ anything, $\eta_c \to \phi\phi$		(3.2 ± 1.7)	$\times 10^{-6}$		–
$\chi_{c1}(3872)$ anything, $\chi_{c1} \to \phi\phi$		< 4.5	$\times 10^{-7}$	CL=95%	–
$X(3915)$ anything, $X \to \phi\phi$		< 3.1	$\times 10^{-7}$	CL=95%	–
K or K^* modes					
$\overline{s}\gamma$		(3.1 ± 1.1)	$\times 10^{-4}$		–
$\overline{s}\overline{\nu}\nu$	*B1*	< 6.4	$\times 10^{-4}$	CL=90%	–
$K^\pm$ anything		(74 ± 6)	%		–
K^0_S anything		(29.0 ± 2.9)	%		–
Pion modes					
$\pi^\pm$ anything		(397 ±21)	%		–
π^0 anything	[*ooaa*]	(278 ±60)	%		–
ϕ anything		(2.82± 0.23)	%		–
Baryon modes					
$p/\overline{p}$ anything		(13.1 ± 1.1)	%		–
$\Lambda/\overline{\Lambda}$ anything		(5.9 ± 0.6)	%		–
b-baryon anything		(10.2 ± 2.8)	%		–
Other modes					
charged anything	[*ooaa*]	(497 ± 7)	%		–
hadron$^+$ hadron$^-$		(1.7 $^{+\ 1.0}_{-\ 0.7}$)	$\times 10^{-5}$		–
charmless		(7 ±21)	$\times 10^{-3}$		–
$\Delta B = 1$ weak neutral current ($B1$) modes					
$\mu^+\mu^-$ anything	*B1*	< 3.2	$\times 10^{-4}$	CL=90%	–

B^*

$I(J^P) = \frac{1}{2}(1^-)$

I, *J*, *P* need confirmation. Quantum numbers shown are quark-model predictions.

Mass $m_{B^*} = 5324.65 \pm 0.25$ MeV
$m_{B^*} - m_B = 45.18 \pm 0.23$ MeV
$m_{B^{*+}} - m_{B^+} = 45.34 \pm 0.23$ MeV

B^* DECAY MODES	Fraction (Γ_i/Γ)	p (MeV/c)
$B\gamma$	dominant	45

$B_1(5721)^+$

$I(J^P) = \frac{1}{2}(1^+)$
I, *J*, *P* need confirmation.

Mass $m = 5725.9^{+2.5}_{-2.7}$ MeV
$m_{B_1^+} - m_{B^{*0}} = 401.2^{+2.4}_{-2.7}$ MeV
Full width $\Gamma = 31 \pm 6$ MeV (S = 1.1)

$B_1(5721)^+$ DECAY MODES	Fraction (Γ_i/Γ)	p (MeV/c)
$B^{*0}\pi^+$	seen	363

$B_1(5721)^0$

$I(J^P) = \frac{1}{2}(1^+)$
I, *J*, *P* need confirmation.

$B_1(5721)^0$ MASS = 5726.0 ± 1.3 MeV (S = 1.2)
$m_{B_1^0} - m_{B^+} = 446.7 \pm 1.3$ MeV (S = 1.2)
$m_{B_1^0} - m_{B^{*+}} = 401.4 \pm 1.2$ MeV (S = 1.2)
Full width $\Gamma = 27.5 \pm 3.4$ MeV (S = 1.1)

$B_1(5721)^0$ DECAY MODES	Fraction (Γ_i/Γ)	p (MeV/c)
$B^{*+}\pi^-$	dominant	363

$B_2^*(5747)^+$

$I(J^P) = \frac{1}{2}(2^+)$
I, *J*, *P* need confirmation.

Mass $m = 5737.2 \pm 0.7$ MeV
$m_{B_2^{*+}} - m_{B^0} = 457.5 \pm 0.7$ MeV
Full width $\Gamma = 20 \pm 5$ MeV (S = 2.2)

$B_2^*(5747)^+$ DECAY MODES	Fraction (Γ_i/Γ)	p (MeV/c)
$B^0\pi^+$	seen	418
$B^{*0}\pi^+$	seen	374

$B_2^*(5747)^0$

$I(J^P) = \frac{1}{2}(2^+)$
I, *J*, *P* need confirmation.

$B_2^*(5747)^0$ MASS = 5739.5 ± 0.7 MeV (S = 1.4)
$m_{B_2^{*0}} - m_{B_1^0} = 13.5 \pm 1.4$ MeV (S = 1.3)
$m_{B_2^{*0}} - m_{B^+} = 460.2 \pm 0.6$ MeV (S = 1.4)
Full width $\Gamma = 24.2 \pm 1.7$ MeV

$B_2^*(5747)^0$ DECAY MODES	Fraction (Γ_i/Γ)	p (MeV/c)
$B^+\pi^-$	dominant	421
$B^{*+}\pi^-$	dominant	377

$B_J(5970)^+$

$I(J^P) = \frac{1}{2}(?^?)$
I, *J*, *P* need confirmation.

Mass $m = 5964 \pm 5$ MeV
$m_{B_J(5970)^+} - m_{B^0} = 685 \pm 5$ MeV
Full width $\Gamma = 62 \pm 20$ MeV

$B_J(5970)^+$ DECAY MODES	Fraction (Γ_i/Γ)	p (MeV/c)
$B^0\pi^+$	possibly seen	632
$B^{*0}\pi^+$	seen	591

$B_J(5970)^0$

$I(J^P) = \frac{1}{2}(?^?)$
I, *J*, *P* need confirmation.

Mass $m = 5971 \pm 5$ MeV
$m_{B_J(5970)^0} - m_{B^+} = 691 \pm 5$ MeV
Full width $\Gamma = 81 \pm 12$ MeV

$B_J(5970)^0$ DECAY MODES	Fraction (Γ_i/Γ)	p (MeV/c)
$B^+\pi^-$	possibly seen	638
$B^{*+}\pi^-$	seen	597

BOTTOM, STRANGE MESONS ($B = \pm 1, S = \mp 1$)

$B_s^0 = s\overline{b}$, $\overline{B}_s^0 = \overline{s}b$, similarly for B_s^*'s

B_s^0

$I(J^P) = 0(0^-)$

I, *J*, *P* need confirmation. Quantum numbers shown are quark-model predictions.

Mass $m_{B_s^0} = 5366.89 \pm 0.19$ MeV
$m_{B_s^0} - m_B = 87.42 \pm 0.19$ MeV
Mean life $\tau = (1.509 \pm 0.004) \times 10^{-12}$ s
$c\tau = 452.4$ μm
$\Delta\Gamma_{B_s^0} = \Gamma_{B_{sL}^0} - \Gamma_{B_{sH}^0} = (0.088 \pm 0.006) \times 10^{12}$ s^{-1}

B_s^0-$\overline{B}_s^0$ mixing parameters

$\Delta m_{B_s^0} = m_{B_{sH}^0} - m_{B_{sL}^0} = (17.757 \pm 0.021) \times 10^{12}$ $\hbar$ s^{-1}
$= (1.1688 \pm 0.0014) \times 10^{-8}$ MeV
$x_s = \Delta m_{B_s^0}/\Gamma_{B_s^0} = 26.79 \pm 0.08$
$\chi_s = 0.499307 \pm 0.000004$

CP violation parameters in B_s^0

$\mathrm{Re}(\epsilon_{B_s^0}) / (1 + |\epsilon_{B_s^0}|^2) = (-0.15 \pm 0.70) \times 10^{-3}$
$C_{KK}(B_s^0 \to K^+K^-) = 0.14 \pm 0.11$
$S_{KK}(B_s^0 \to K^+K^-) = 0.30 \pm 0.13$
$r_B(B_s^0 \to D_s^\mp K^\pm) = 0.53 \pm 0.17$
$\delta_B(B_s^0 \to D_s^\pm K^\mp) = (3 \pm 20)^\circ$
CP Violation phase $\beta_s = (1.1 \pm 1.6) \times 10^{-2}$ rad
$|\lambda|$ $(B_s^0 \to J/\psi(1S)\phi) = 0.964 \pm 0.020$

Meson Summary Table

$|\lambda| = 1.001 \pm 0.017$
A, *CP* violation parameter $= 0.5^{+0.8}_{-0.7}$
C, *CP* violation parameter $= -0.3 \pm 0.4$
S, *CP* violation parameter $= -0.1 \pm 0.4$
$A_{CP}^{L}(B_s \to J/\psi \overline{K}^*(892)^0) = -0.05 \pm 0.06$
$A_{CP}^{\parallel}(B_s \to J/\psi \overline{K}^*(892)^0) = 0.17 \pm 0.15$
$A_{CP}^{\perp}(B_s \to J/\psi \overline{K}^*(892)^0) = -0.05 \pm 0.10$
$A_{CP}(B_s \to \pi^+ K^-) = 0.26 \pm 0.04$
$A_{CP}(B_s^0 \to [K^+ K^-]_D \overline{K}^*(892)^0) = -0.04 \pm 0.07$
$A_{CP}(B_s^0 \to [\pi^+ K^-]_D K^*(892)^0) = -0.01 \pm 0.04$
$A_{CP}(B_s^0 \to [\pi^+ \pi^-]_D K^*(892)^0) = 0.06 \pm 0.13$
$A^{\Delta}(B_s \to \phi\gamma) = -1.0 \pm 0.5$
$\Delta a_\perp < 1.2 \times 10^{-12}$ GeV, CL = 95%
$\Delta a_\parallel = (-0.9 \pm 1.5) \times 10^{-14}$ GeV
$\Delta a_X = (1.0 \pm 2.2) \times 10^{-14}$ GeV
$\Delta a_Y = (-3.8 \pm 2.2) \times 10^{-14}$ GeV
$\mathrm{Re}(\xi) = -0.022 \pm 0.033$
$\mathrm{Im}(\xi) = 0.004 \pm 0.011$

These branching fractions all scale with $B(\overline{b} \to B_s^0)$.

The branching fraction $B(B_s^0 \to D_s^- \ell^+ \nu_\ell \text{anything})$ is not a pure measurement since the measured product branching fraction $B(\overline{b} \to B_s^0) \times B(B_s^0 \to D_s^- \ell^+ \nu_\ell \text{anything})$ was used to determine $B(\overline{b} \to B_s^0)$, as described in the note on "B^0-$\overline{B}^0$ Mixing"

For inclusive branching fractions, *e.g.*, $B \to D^\pm$ anything, the values usually are multiplicities, not branching fractions. They can be greater than one.

B_s^0 DECAY MODES		Fraction (Γ_i/Γ)	Scale factor/ Confidence level	*p* (MeV/*c*)
D_s^- anything		(93 ±25) %		–
$\ell \nu_\ell X$		(9.6 ± 0.8) %		–
$e^+ \nu X^-$		(9.1 ± 0.8) %		–
$\mu^+ \nu X^-$		(10.2 ± 1.0) %		–
$D_s^- \ell^+ \nu_\ell$ anything	[qqaa]	(8.1 ± 1.3) %		–
$D_s^{*-} \ell^+ \nu_\ell$ anything		(5.4 ± 1.1) %		–
$D_{s1}(2536)^- \mu^+ \nu_\mu$, $D_{s1}^- \to D^{*-} K_S^0$		(2.6 ± 0.7) $\times 10^{-3}$		–
$D_{s1}(2536)^- X \mu^+ \nu$, $D_{s1}^- \to \overline{D}^0 K^+$		(4.4 ± 1.3) $\times 10^{-3}$		–
$D_{s2}(2573)^- X \mu^+ \nu$, $D_{s2}^- \to \overline{D}^0 K^+$		(2.7 ± 1.0) $\times 10^{-3}$		–
$D_s^- \pi^+$		(3.00± 0.23) $\times 10^{-3}$		2320
$D_s^- \rho^+$		(6.9 ± 1.4) $\times 10^{-3}$		2249
$D_s^- \pi^+ \pi^+ \pi^-$		(6.1 ± 1.0) $\times 10^{-3}$		2301
$D_{s1}(2536)^- \pi^+$, $D_{s1}^- \to D_s^- \pi^+ \pi^-$		(2.5 ± 0.8) $\times 10^{-5}$		–
$D_s^\mp K^\pm$		(2.27± 0.19) $\times 10^{-4}$		2293
$D_s^- K^+ \pi^+ \pi^-$		(3.2 ± 0.6) $\times 10^{-4}$		2249
$D_s^+ D_s^-$		(4.4 ± 0.5) $\times 10^{-3}$		1824
$D_s^- D^+$		(2.8 ± 0.5) $\times 10^{-4}$		1875
$D^+ D^-$		(2.2 ± 0.6) $\times 10^{-4}$		1925
$D^0 \overline{D}^0$		(1.9 ± 0.5) $\times 10^{-4}$		1930
$D_s^{*-} \pi^+$		(2.0 ± 0.5) $\times 10^{-3}$		2265
$D_s^{*\mp} K^\pm$		(1.33± 0.35) $\times 10^{-4}$		–
$D_s^{*-} \rho^+$		(9.6 ± 2.1) $\times 10^{-3}$		2191
$D_s^{*+} D_s^- + D_s^{*-} D_s^+$		(1.38± 0.16) %		1742
$D_s^{*+} D_s^{*-}$		(1.44± 0.20) %	S=1.1	1655
$D_s^{(*)+} D_s^{(*)-}$		(4.5 ± 1.4) %		–
$\overline{D}^{*0} \overline{K}^0$		(2.8 ± 1.1) $\times 10^{-4}$		2278
$\overline{D}^0 \overline{K}^0$		(4.3 ± 0.9) $\times 10^{-4}$		2330
$\overline{D}^0 K^- \pi^+$		(1.04± 0.13) $\times 10^{-3}$		2312
$\overline{D}^0 \overline{K}^*(892)^0$		(4.4 ± 0.6) $\times 10^{-4}$		2264
$\overline{D}^0 \overline{K}^*(1410)$		(3.9 ± 3.5) $\times 10^{-4}$		2114
$\overline{D}^0 \overline{K}_0^*(1430)$		(3.0 ± 0.7) $\times 10^{-4}$		2113
$\overline{D}^0 \overline{K}_2^*(1430)$		(1.1 ± 0.4) $\times 10^{-4}$		2113
$\overline{D}^0 \overline{K}^*(1680)$		< 7.8 $\times 10^{-5}$	CL=90%	1997
$\overline{D}^0 \overline{K}_0^*(1950)$		< 1.1 $\times 10^{-4}$	CL=90%	1890
$\overline{D}^0 \overline{K}_3^*(1780)$		< 2.6 $\times 10^{-5}$	CL=90%	1971
$\overline{D}^0 \overline{K}_4^*(2045)$		< 3.1 $\times 10^{-5}$	CL=90%	1837
$\overline{D}^0 K^- \pi^+$ (non-resonant)		(2.1 ± 0.8) $\times 10^{-4}$		2312
$D_{s2}^*(2573)^- \pi^+$, $D_{s2}^* \to \overline{D}^0 K^-$		(2.6 ± 0.4) $\times 10^{-4}$		–
$D_{s1}^*(2700)^- \pi^+$, $D_{s1}^* \to \overline{D}^0 K^-$		(1.6 ± 0.8) $\times 10^{-5}$		–
$D_{s1}^*(2860)^- \pi^+$, $D_{s1}^* \to \overline{D}^0 K^-$		(5 ± 4) $\times 10^{-5}$		–
$D_{s3}^*(2860)^- \pi^+$, $D_{s3}^* \to \overline{D}^0 K^-$		(2.2 ± 0.6) $\times 10^{-5}$		–
$\overline{D}^0 K^+ K^-$		(4.4 ± 2.0) $\times 10^{-5}$		2243
$\overline{D}^0 f_0(980)$		< 3.1 $\times 10^{-6}$	CL=90%	2242
$\overline{D}^0 \phi$		(3.0 ± 0.8) $\times 10^{-5}$		2235
$D^{*\mp} \pi^\pm$		< 6.1 $\times 10^{-6}$	CL=90%	–
$\eta_c \phi$		(5.0 ± 0.9) $\times 10^{-4}$		1663
$\eta_c \pi^+ \pi^-$		(1.8 ± 0.7) $\times 10^{-4}$		1840
$J/\psi(1S) \phi$		(1.08± 0.08) $\times 10^{-3}$		1588
$J/\psi(1S) \phi\phi$		(1.24$^{+}_{-}$ 0.17 0.19) $\times 10^{-5}$		764
$J/\psi(1S) \pi^0$		< 1.2 $\times 10^{-3}$	CL=90%	1787
$J/\psi(1S) \eta$		(4.0 ± 0.7) $\times 10^{-4}$	S=1.4	1733
$J/\psi(1S) K_S^0$		(1.88± 0.15) $\times 10^{-5}$		1743
$J/\psi(1S) \overline{K}^*(892)^0$		(4.1 ± 0.4) $\times 10^{-5}$		1637
$J/\psi(1S) \eta'$		(3.3 ± 0.4) $\times 10^{-4}$		1612
$J/\psi(1S) \pi^+ \pi^-$		(2.09± 0.23) $\times 10^{-4}$	S=1.3	1775
$J/\psi(1S) f_0(500)$, $f_0 \to \pi^+ \pi^-$		< 4 $\times 10^{-6}$	CL=90%	–
$J/\psi(1S) \rho$, $\rho \to \pi^+ \pi^-$		< 4 $\times 10^{-6}$	CL=90%	–
$J/\psi(1S) f_0(980)$, $f_0 \to \pi^+ \pi^-$		(1.28± 0.18) $\times 10^{-4}$	S=1.7	–
$J/\psi(1S) f_2(1270)$, $f_2 \to \pi^+ \pi^-$		(1.1 ± 0.4) $\times 10^{-6}$		–
$J/\psi(1S) f_2(1270)_0$, $f_2 \to \pi^+ \pi^-$		(7.5 ± 1.8) $\times 10^{-7}$		–
$J/\psi(1S) f_2(1270)_\parallel$, $f_2 \to \pi^+ \pi^-$		(1.09± 0.34) $\times 10^{-6}$		–
$J/\psi(1S) f_2(1270)_\perp$, $f_2 \to \pi^+ \pi^-$		(1.3 ± 0.8) $\times 10^{-6}$		–
$J/\psi(1S) f_0(1370)$, $f_0 \to \pi^+ \pi^-$		(4.5 $^{+}_{-}$ 0.7 4.0) $\times 10^{-5}$		–
$J/\psi(1S) f_0(1500)$, $f_0 \to \pi^+ \pi^-$		(2.11$^{+}_{-}$ 0.40 0.29) $\times 10^{-5}$		–
$J/\psi(1S) f_2'(1525)_0$, $f_2' \to \pi^+ \pi^-$		(1.07± 0.24) $\times 10^{-6}$		–
$J/\psi(1S) f_2'(1525)_\parallel$, $f_2' \to \pi^+ \pi^-$		(1.3 $^{+}_{-}$ 2.7 0.9) $\times 10^{-7}$		–
$J/\psi(1S) f_2'(1525)_\perp$, $f_2' \to \pi^+ \pi^-$		(5 ± 4) $\times 10^{-7}$		–
$J/\psi(1S) f_0(1790)$, $f_0 \to \pi^+ \pi^-$		(5.0 $^{+11.0}_{-1.1}$) $\times 10^{-6}$		–
$J/\psi(1S) \pi^+ \pi^-$ (nonresonant)		(1.8 $^{+}_{-}$ 1.1 0.4) $\times 10^{-5}$		1775
$J/\psi(1S) \overline{K}^0 \pi^+ \pi^-$		< 4.4 $\times 10^{-5}$	CL=90%	1675
$J/\psi(1S) K^+ K^-$		(7.9 ± 0.7) $\times 10^{-4}$		1601
$J/\psi(1S) K^0 K^- \pi^+ +$ c.c.		(9.3 ± 1.3) $\times 10^{-4}$		1538
$J/\psi(1S) \overline{K}^0 K^+ K^-$		< 1.2 $\times 10^{-5}$	CL=90%	1333
$J/\psi(1S) f_2'(1525)$		(2.6 ± 0.6) $\times 10^{-4}$		1304
$J/\psi(1S) p\overline{p}$		< 4.8 $\times 10^{-6}$	CL=90%	982
$J/\psi(1S) \gamma$		< 7.3 $\times 10^{-6}$	CL=90%	1790
$J/\psi(1S) \pi^+ \pi^- \pi^+ \pi^-$		(7.8 ± 1.0) $\times 10^{-5}$		1731
$J/\psi(1S) f_1(1285)$		(7.0 ± 1.4) $\times 10^{-5}$		1460
$\psi(2S) \eta$		(3.3 ± 0.9) $\times 10^{-4}$		1338
$\psi(2S) \eta'$		(1.29± 0.35) $\times 10^{-4}$		1158
$\psi(2S) \pi^+ \pi^-$		(7.1 ± 1.3) $\times 10^{-5}$		1397
$\psi(2S) \phi$		(5.4 ± 0.6) $\times 10^{-4}$		1120
$\psi(2S) K^- \pi^+$		(3.12± 0.30) $\times 10^{-5}$		1310
$\psi(2S) \overline{K}^*(892)^0$		(3.3 ± 0.5) $\times 10^{-5}$		1196
$\chi_{c1} \phi$		(2.04± 0.30) $\times 10^{-4}$		1274
$\pi^+ \pi^-$		(7.0 ± 0.8) $\times 10^{-7}$		2680
$\pi^0 \pi^0$		< 2.1 $\times 10^{-4}$	CL=90%	2680
$\eta \pi^0$		< 1.0 $\times 10^{-3}$	CL=90%	2654
$\eta\eta$		< 1.5 $\times 10^{-3}$	CL=90%	2627
$\rho^0 \rho^0$		< 3.20 $\times 10^{-4}$	CL=90%	2569
$\eta'\eta'$		(3.3 ± 0.7) $\times 10^{-5}$		2507
$\eta' \phi$		< 8.2 $\times 10^{-7}$	CL=90%	2495
$\phi f_0(980)$, $f_0(980) \to \pi^+ \pi^-$		(1.12± 0.21) $\times 10^{-6}$		–
$\phi f_2(1270)$, $f_2(1270) \to \pi^+ \pi^-$		(6.1 $^{+}_{-}$ 1.8 1.5) $\times 10^{-7}$		–
$\phi \rho^0$		(2.7 ± 0.8) $\times 10^{-7}$		2526
$\phi \pi^+ \pi^-$		(3.5 ± 0.5) $\times 10^{-6}$		2579
$\phi\phi$		(1.87± 0.15) $\times 10^{-5}$		2482
$\phi\phi\phi$		(2.2 ± 0.7) $\times 10^{-6}$		2165
$\pi^+ K^-$		(5.7 ± 0.6) $\times 10^{-6}$		2659

K^+K^-	$(2.59\pm0.17)\times10^{-5}$		2638
$K^0\overline{K}^0$	$(2.0\pm0.6)\times10^{-5}$		2637
$K^0\pi^+\pi^-$	$(9.4\pm2.1)\times10^{-6}$		2653
$K^0K^\pm\pi^\mp$	$(8.4\pm0.9)\times10^{-5}$		2622
$K^*(892)^-\pi^+$	$(3.3\pm1.2)\times10^{-6}$		2607
$K^*(892)^\pm K^\mp$	$(1.25\pm0.26)\times10^{-5}$		2585
$K_S^0\overline{K}^*(892)^0$ + c.c.	$(1.6\pm0.4)\times10^{-5}$		2585
$K^0K^+K^-$	$(1.3\pm0.6)\times10^{-6}$		2568
$\overline{K}^*(892)^0\rho^0$	$<7.67\times10^{-4}$	CL=90%	2550
$\overline{K}^*(892)^0K^*(892)^0$	$(1.11\pm0.27)\times10^{-5}$		2531
$\phi K^*(892)^0$	$(1.14\pm0.30)\times10^{-6}$		2507
$p\overline{p}$	$<1.5\times10^{-8}$	CL=90%	2514
$p\overline{p}K^+K^-$	$(4.5\pm0.5)\times10^{-6}$		2231
$p\overline{p}K^+\pi^-$	$(1.39\pm0.26)\times10^{-6}$		2355
$p\overline{p}\pi^+\pi^-$	$(4.3\pm2.0)\times10^{-7}$		2454
$p\overline{\Lambda}K^-$ + c.c.	$(5.5\pm1.0)\times10^{-6}$		2358
$\Lambda_c^-\Lambda\pi^+$	$(3.6\pm1.6)\times10^{-4}$		–
$\Lambda_c^-\Lambda_c^+$	$<8.0\times10^{-5}$	CL=95%	–

Lepton Family number (LF) violating modes or $\Delta B=1$ weak neutral current ($B1$) modes

$\gamma\gamma$	$B1$	$<3.1\times10^{-6}$	CL=90%		2683
$\phi\gamma$	$B1$	$(3.4\pm0.4)\times10^{-5}$			2587
$\mu^+\mu^-$	$B1$	$(2.7\ ^{+\ 0.6}_{-\ 0.5})\times10^{-9}$	S=1.2		2681
e^+e^-	$B1$	$<2.8\times10^{-7}$	CL=90%		2683
$\tau^+\tau^-$	$B1$	$<6.8\times10^{-3}$	CL=95%		2011
$\mu^+\mu^-\mu^+\mu^-$	$B1$	$<2.5\times10^{-9}$	CL=95%		2673
$SP,\ S\to\mu^+\mu^-,\ P\to\mu^+\mu^-$	$B1$ [ggaa]	$<2.2\times10^{-9}$	CL=95%		–
$\phi(1020)\mu^+\mu^-$	$B1$	$(8.2\pm1.2)\times10^{-7}$			2582
$\pi^+\pi^-\mu^+\mu^-$	$B1$	$(8.4\pm1.7)\times10^{-8}$			2670
$\phi\nu\overline{\nu}$	$B1$	$<5.4\times10^{-3}$	CL=90%		2587
$e^\pm\mu^\mp$	LF [hh]	$<1.1\times10^{-8}$	CL=90%		2682

B_s^*

$I(J^P)=0(1^-)$

I, J, P need confirmation. Quantum numbers shown are quark-model predictions.

Mass $m=5415.4^{+1.8}_{-1.5}$ MeV (S = 2.9)

$m_{B_s^*}-m_{B_s}=48.5^{+1.8}_{-1.5}$ MeV (S = 2.8)

B_s^* DECAY MODES	Fraction (Γ_i/Γ)	p (MeV/c)
$B_s\gamma$	dominant	48

$B_{s1}(5830)^0$

$I(J^P)=0(1^+)$
I, J, P need confirmation.

Mass $m=5828.63\pm0.27$ MeV

$m_{B_{s1}^0}-m_{B^{*+}}=503.98\pm0.18$ MeV

Full width $\Gamma=0.5\pm0.4$ MeV

$B_{s1}(5830)^0$ DECAY MODES	Fraction (Γ_i/Γ)	p (MeV/c)
$B^{*+}K^-$	dominant	97

$B_{s2}^*(5840)^0$

$I(J^P)=0(2^+)$
I, J, P need confirmation.

Mass $m=5839.85\pm0.17$ MeV (S = 1.1)

$m_{B_{s2}^{*0}}-m_{B^+}=560.53\pm0.17$ MeV (S = 1.1)

Full width $\Gamma=1.47\pm0.33$ MeV

$B_{s2}^*(5840)^0$ DECAY MODES	Fraction (Γ_i/Γ)	p (MeV/c)
B^+K^-	dominant	252

BOTTOM, CHARMED MESONS ($B=C=\pm1$)

$B_c^+=c\overline{b}$, $B_c^-=\overline{c}b$, similarly for B_c^*'s

B_c^+

$I(J^P)=0(0^-)$
I, J, P need confirmation.

Quantum numbers shown are quark-model predicitions.

Mass $m=6274.9\pm0.8$ MeV

Mean life $\tau=(0.507\pm0.009)\times10^{-12}$ s

B_c^- modes are charge conjugates of the modes below.

B_c^+ DECAY MODES × B($\overline{b}\to B_c$)	Fraction (Γ_i/Γ)	Confidence level	p (MeV/c)
The following quantities are not pure branching ratios; rather the fraction $\Gamma_i/\Gamma\times$ B($\overline{b}\to B_c$).			
$J/\psi(1S)\ell^+\nu_\ell$ anything	$(8.1\pm1.2)\times10^{-5}$		–
$J/\psi(1S)\pi^+$	seen		2371
$J/\psi(1S)K^+$	seen		2341
$J/\psi(1S)\pi^+\pi^+\pi^-$	seen		2350
$J/\psi(1S)a_1(1260)$	$<1.2\times10^{-3}$	90%	2169
$J/\psi(1S)K^+K^-\pi^+$	seen		2203
$J/\psi(1S)\pi^+\pi^+\pi^+\pi^-\pi^-$	seen		2309
$\psi(2S)\pi^+$	seen		2052
$J/\psi(1S)D^0K^+$	seen		1539
$J/\psi(1S)D^*(2007)^0K^+$	seen		1412
$J/\psi(1S)D^*(2010)^+K^{*0}$	seen		920
$J/\psi(1S)D^+K^{*0}$	seen		1122
$J/\psi(1S)D_s^+$	seen		1822
$J/\psi(1S)D_s^{*+}$	seen		1728
$J/\psi(1S)p\overline{p}\pi^+$	seen		1792
$\chi_c^0\pi^+$	$(2.4\ ^{+0.9}_{-0.8})\times10^{-5}$		2205
$p\overline{p}\pi^+$	not seen		2970
D^0K^+	$(3.8\ ^{+1.2}_{-1.0})\times10^{-7}$		2837
$D^0\pi^+$	$<1.6\times10^{-7}$	95%	2858
$D^{*0}\pi^+$	$<4\times10^{-7}$	95%	2815
$D^{*0}K^+$	$<4\times10^{-7}$	95%	2793
$D^*(2010)^+\overline{D}^0$	$<6.2\times10^{-3}$	90%	2467
D^+K^{*0}	$<0.20\times10^{-6}$	90%	2783
$D^+\overline{K}^{*0}$	$<0.16\times10^{-6}$	90%	2783
$D_s^+K^{*0}$	$<0.28\times10^{-6}$	90%	2751
$D_s^+\overline{K}^{*0}$	$<0.4\times10^{-6}$	90%	2751
$D_s^+\phi$	$<0.32\times10^{-6}$	90%	2727
K^+K^0	$<4.6\times10^{-7}$	90%	3098
$B_s^0\pi^+$ / B($\overline{b}\to B_s$)	$(2.37^{+0.37}_{-0.35})\times10^{-3}$		–

$c\overline{c}$ MESONS (including possibly non-$q\overline{q}$ states)

$\eta_c(1S)$

$I^G(J^{PC})=0^+(0^{-+})$

Mass $m=2983.9\pm0.5$ MeV (S = 1.3)

Full width $\Gamma=32.0\pm0.8$ MeV

$\eta_c(1S)$ DECAY MODES	Fraction (Γ_i/Γ)	Confidence level	p (MeV/c)
Decays involving hadronic resonances			
$\eta'(958)\pi\pi$	(4.1 ± 1.7) %		1323
$\rho\rho$	(1.8 ± 0.5) %		1275
$K^*(892)^0K^-\pi^+$ + c.c.	(2.0 ± 0.7) %		1278
$K^*(892)\overline{K}^*(892)$	$(7.1\pm1.3)\times10^{-3}$		1196
$K^*(892)^0\overline{K}^*(892)^0\pi^+\pi^-$	(1.1 ± 0.5) %		1073
ϕK^+K^-	$(2.9\pm1.4)\times10^{-3}$		1104
$\phi\phi$	$(1.79\pm0.20)\times10^{-3}$		1089
$\phi2(\pi^+\pi^-)$	$<4\times10^{-3}$	90%	1251
$a_0(980)\pi$	<2 %	90%	1327
$a_2(1320)\pi$	<2 %	90%	1196
$K^*(892)\overline{K}$ + c.c.	<1.28 %	90%	1310

Meson Summary Table

$f_2(1270)\eta$		$<$ 1.1	%	90%	1145
$\omega\omega$		$<$ 3.1	$\times 10^{-3}$	90%	1270
$\omega\phi$		$<$ 2.5	$\times 10^{-4}$	90%	1185
$f_2(1270)f_2(1270)$		(9.8 $\pm$2.5)	$\times 10^{-3}$		774
$f_2(1270)f_2'(1525)$		(9.8 $\pm$3.2)	$\times 10^{-3}$		513
$f_0(980)\eta$		seen			1264
$f_0(1500)\eta$		seen			1026
$f_0(2200)\eta$		seen			497
$a_0(980)\pi$		seen			1327
$a_0(1320)\pi$		seen			–
$a_0(1450)\pi$		seen			1123
$a_0(1950)\pi$		seen			860
$a_2(1950)\pi$		not seen			–
$K_0^*(1430)\overline{K}$		seen			–
$K_2^*(1430)\overline{K}$		seen			–
$K_0^*(1950)\overline{K}$		seen			–

Decays into stable hadrons

$K\overline{K}\pi$		(7.3 $\pm$0.5)	%		1381
$K\overline{K}\eta$		(1.36$\pm$0.16)	%		1265
$\eta\pi^+\pi^-$		(1.7 $\pm$0.5)	%		1428
$\eta 2(\pi^+\pi^-)$		(4.4 $\pm$1.3)	%		1386
$K^+K^-\pi^+\pi^-$		(6.9 $\pm$1.1)	$\times 10^{-3}$		1345
$K^+K^-\pi^+\pi^-\pi^0$		(3.5 $\pm$0.6)	%		1304
$K^0K^-\pi^+\pi^-\pi^+$+c.c.		(5.6 $\pm$1.5)	%		–
$K^+K^-2(\pi^+\pi^-)$		(7.5 $\pm$2.4)	$\times 10^{-3}$		1254
$2(K^+K^-)$		(1.47$\pm$0.31)	$\times 10^{-3}$		1055
$\pi^+\pi^-\pi^0$		$<$ 5	$\times 10^{-4}$	90%	1476
$\pi^+\pi^-\pi^0\pi^0$		(4.7 $\pm$1.0)	%		1460
$2(\pi^+\pi^-)$		(9.7 $\pm$1.2)	$\times 10^{-3}$		1459
$2(\pi^+\pi^-\pi^0)$		(17.4 $\pm$3.3)	%		1409
$3(\pi^+\pi^-)$		(1.8 $\pm$0.4)	%		1407
$p\overline{p}$		(1.52$\pm$0.16)	$\times 10^{-3}$		1160
$p\overline{p}\pi^0$		(3.6 $\pm$1.3)	$\times 10^{-3}$		1101
$\Lambda\overline{\Lambda}$		(1.09$\pm$0.24)	$\times 10^{-3}$		991
$\Sigma^+\overline{\Sigma}^-$		(2.1 $\pm$0.6)	$\times 10^{-3}$		901
$\Xi^-\overline{\Xi}^+$		(9.0 $\pm$2.6)	$\times 10^{-4}$		692
$\pi^+\pi^-p\overline{p}$		(5.3 $\pm$1.8)	$\times 10^{-3}$		1027

Radiative decays

$\gamma\gamma$		(1.57$\pm$0.12)	$\times 10^{-4}$		1492

Charge conjugation (C), Parity (P), Lepton family number (LF) violating modes

$\pi^+\pi^-$	P,CP	$<$ 1.1	$\times 10^{-4}$	90%	1485
$\pi^0\pi^0$	P,CP	$<$ 4	$\times 10^{-5}$	90%	1486
K^+K^-	P,CP	$<$ 6	$\times 10^{-4}$	90%	1408
$K_S^0K_S^0$	P,CP	$<$ 3.1	$\times 10^{-4}$	90%	1406

$J/\psi(1S)$

$I^G(J^{PC}) = 0^-(1^{--})$

Mass $m = 3096.900 \pm 0.006$ MeV
Full width $\Gamma = 92.9 \pm 2.8$ keV (S = 1.1)
$\Gamma_{ee} = 5.55 \pm 0.14 \pm 0.02$ keV

$J/\psi(1S)$ DECAY MODES		Fraction (Γ_i/Γ)	Scale factor/ Confidence level	p (MeV/c)
hadrons		(87.7 $\pm$ 0.5) %		–
virtual $\gamma \to$ hadrons		(13.50 $\pm$ 0.30) %		–
ggg		(64.1 $\pm$ 1.0) %		–
γgg		(8.8 $\pm$ 1.1) %		–
e^+e^-		(5.971$\pm$ 0.032) %		1548
$e^+e^-\gamma$	[rraa]	(8.8 $\pm$ 1.4) $\times 10^{-3}$		1548
$\mu^+\mu^-$		(5.961$\pm$ 0.033) %		1545

Decays involving hadronic resonances

$\rho\pi$	(1.69 $\pm$ 0.15) %	S=2.4		1448
$\rho^0\pi^0$	(5.6 $\pm$ 0.7) $\times 10^{-3}$			1448
$\rho(770)^\mp K^\pm K_S^0$	(1.9 $\pm$ 0.4) $\times 10^{-3}$			–
$\rho(1450)\pi \to \pi^+\pi^-\pi^0$	(2.3 $\pm$ 0.7) $\times 10^{-3}$			–
$\rho(1450)^\pm\pi^\mp \to K_S^0K^\pm\pi^\mp$	(3.5 $\pm$ 0.6) $\times 10^{-4}$			–
$\rho(1450)^0\pi^0 \to K^+K^-\pi^0$	(2.0 $\pm$ 0.5) $\times 10^{-4}$			–
$\rho(1450)\eta'(958) \to \pi^+\pi^-\eta'(958)$	(3.3 $\pm$ 0.7) $\times 10^{-6}$			–
$\rho(1700)\pi \to \pi^+\pi^-\pi^0$	(1.7 $\pm$ 1.1) $\times 10^{-4}$			–
$\rho(2150)\pi \to \pi^+\pi^-\pi^0$	(8 $\pm$40) $\times 10^{-6}$			–
$a_2(1320)\rho$	(1.09 $\pm$ 0.22) %			1123
$\omega\pi^+\pi^+\pi^-\pi^-$	(8.5 $\pm$ 3.4) $\times 10^{-3}$			1392
$\omega\pi^+\pi^-\pi^0$	(4.0 $\pm$ 0.7) $\times 10^{-3}$			1418
$\omega\pi^+\pi^-$	(8.6 $\pm$ 0.7) $\times 10^{-3}$	S=1.1		1435
$\omega f_2(1270)$	(4.3 $\pm$ 0.6) $\times 10^{-3}$			1142
$K^*(892)^0\overline{K}^*(892)^0$	(2.3 $\pm$ 0.6) $\times 10^{-4}$			1266
$K^*(892)^\pm K^*(892)^\mp$	(1.00 $^{+\ 0.22}_{-\ 0.40}$) $\times 10^{-3}$			1266
$K^*(892)^\pm K^*(700)^\mp$	(1.1 $^{+\ 1.0}_{-\ 0.6}$) $\times 10^{-3}$			–
$K_S^0\pi^- K^*(892)^+$ + c.c.	(2.0 $\pm$ 0.5) $\times 10^{-3}$			1342
$K_S^0\pi^- K^*(892)^+$ + c.c. $\to K_S^0K_S^0\pi^+\pi^-$	(6.7 $\pm$ 2.2) $\times 10^{-4}$			–
$\eta K^*(892)^0\overline{K}^*(892)^0$	(1.15 $\pm$ 0.26) $\times 10^{-3}$			1003
$K^*(1410)\overline{K}$+c.c $\to K^\pm K^\mp\pi^0$	(4.9 $\pm$ 2.8) $\times 10^{-5}$			–
$K^*(1410)\overline{K}$ + c.c. $\to K_S^0K^\pm\pi^\mp$	(8 $\pm$ 6) $\times 10^{-5}$			–
$K_2^*(1430)\overline{K}$+c.c. $\to K^\pm K^\mp\pi^0$	(7.5 $\pm$ 3.5) $\times 10^{-5}$			–
$K_2^*(1430)\overline{K}$ + c.c. $\to K_S^0K^\pm\pi^\mp$	(4.0 $\pm$ 1.0) $\times 10^{-4}$			–
$K^*(892)^0\overline{K}_2^*(1430)^0$ + c.c.	(4.66 $\pm$ 0.31) $\times 10^{-3}$			1012
$K^*(892)^+K_2^*(1430)^-$ + c.c.	(3.4 $\pm$ 2.9) $\times 10^{-3}$			1012
$K^*(892)^+K_2^*(1430)^-$ + c.c. $\to K^*(892)^+K_S^0\pi^-$ + c.c.	(4 $\pm$ 4) $\times 10^{-4}$			–
$K^*(892)^0\overline{K}_2(1770)^0$ + c.c. $\to K^*(892)^0K^-\pi^+$ + c.c.	(6.9 $\pm$ 0.9) $\times 10^{-4}$			–
$\omega K^*(892)\overline{K}$ + c.c.	(6.1 $\pm$ 0.9) $\times 10^{-3}$			1097
$\overline{K}K^*(892)$+c.c. $\to K_S^0K^\pm\pi^\mp$	(5.1 $\pm$ 0.5) $\times 10^{-3}$			–
$K^+K^*(892)^-$ + c.c.	(5.12 $\pm$ 0.30) $\times 10^{-3}$			1373
$K^+K^*(892)^-$ + c.c. $\to K^+K^-\pi^0$	(1.97 $\pm$ 0.20) $\times 10^{-3}$			–
$K^+K^*(892)^-$ + c.c. $\to K^0K^\pm\pi^\mp$ + c.c.	(3.0 $\pm$ 0.4) $\times 10^{-3}$			–
$K^0\overline{K}^*(892)^0$ + c.c.	(4.39 $\pm$ 0.31) $\times 10^{-3}$			1373
$K^0\overline{K}^*(892)^0$ + c.c. $\to K^0K^\pm\pi^\mp$ + c.c.	(3.2 $\pm$ 0.4) $\times 10^{-3}$			–
$K_1(1400)^\pm K^\mp$	(3.8 $\pm$ 1.4) $\times 10^{-3}$			1170
$\overline{K}^*(892)^0K^+\pi^-$ + c.c.	seen			1343
$K^*(892)^\pm K^\mp\pi^0$	(4.1 $\pm$ 1.3) $\times 10^{-3}$			1344
$K^*(892)^0K_S^0\pi^0$	(6 $\pm$ 4) $\times 10^{-4}$			1343
$\omega\pi^0\pi^0$	(3.4 $\pm$ 0.8) $\times 10^{-3}$			1436
$b_1(1235)^\pm\pi^\mp$	[hh] (3.0 $\pm$ 0.5) $\times 10^{-3}$			1300
$\omega K^\pm K_S^0\pi^\mp$	[hh] (3.4 $\pm$ 0.5) $\times 10^{-3}$			1210
$b_1(1235)^0\pi^0$	(2.3 $\pm$ 0.6) $\times 10^{-3}$			1300
$\eta K^\pm K_S^0\pi^\mp$	[hh] (2.2 $\pm$ 0.4) $\times 10^{-3}$			1278
$\phi K^*(892)\overline{K}$ + c.c.	(2.18 $\pm$ 0.23) $\times 10^{-3}$			969
$\omega K\overline{K}$	(1.70 $\pm$ 0.32) $\times 10^{-3}$			1268
$\omega f_0(1710) \to \omega K\overline{K}$	(4.8 $\pm$ 1.1) $\times 10^{-4}$			878
$\phi 2(\pi^+\pi^-)$	(1.66 $\pm$ 0.23) $\times 10^{-3}$			1318
$\Delta(1232)^{++}\overline{p}\pi^-$	(1.6 $\pm$ 0.5) $\times 10^{-3}$			1030
$\omega\eta$	(1.74 $\pm$ 0.20) $\times 10^{-3}$	S=1.6		1394
$\phi K\overline{K}$	(1.77 $\pm$ 0.16) $\times 10^{-3}$	S=1.3		1179
$\phi K_S^0K_S^0$	(5.9 $\pm$ 1.5) $\times 10^{-4}$			1176
$\phi f_0(1710) \to \phi K\overline{K}$	(3.6 $\pm$ 0.6) $\times 10^{-4}$			875
ϕK^+K^-	(8.3 $\pm$ 1.2) $\times 10^{-4}$			1179
$\phi f_2(1270)$	(3.2 $\pm$ 0.6) $\times 10^{-4}$			1036
$\Delta(1232)^{++}\overline{\Delta}(1232)^{--}$	(1.10 $\pm$ 0.29) $\times 10^{-3}$			938
$\Sigma(1385)^-\overline{\Sigma}(1385)^+$ (or c.c.)	[hh] (1.16 $\pm$ 0.05) $\times 10^{-3}$			697
$\Sigma(1385)^0\overline{\Sigma}(1385)^0$	(1.07 $\pm$ 0.08) $\times 10^{-3}$			697
$K^+K^-f_2'(1525)$	(1.04 $\pm$ 0.35) $\times 10^{-3}$			892
$\phi f_2'(1525)$	(8 $\pm$ 4) $\times 10^{-4}$	S=2.7		871
$\phi\pi^+\pi^-$	(8.7 $\pm$ 0.9) $\times 10^{-4}$	S=1.4		1365
$\phi\pi^0\pi^0$	(5.0 $\pm$ 1.0) $\times 10^{-4}$			1366
$\phi K^\pm K_S^0\pi^\mp$	[hh] (7.2 $\pm$ 0.8) $\times 10^{-4}$			1114
$\omega f_1(1420)$	(6.8 $\pm$ 2.4) $\times 10^{-4}$			1062
$\phi\eta$	(7.5 $\pm$ 0.8) $\times 10^{-4}$	S=1.5		1320
$\Xi^0\overline{\Xi}^0$	(1.17 $\pm$ 0.04) $\times 10^{-3}$			818
$\Xi(1530)^-\overline{\Xi}^+$	(5.9 $\pm$ 1.5) $\times 10^{-4}$			600
$pK^-\overline{\Sigma}(1385)^0$	(5.1 $\pm$ 3.2) $\times 10^{-4}$			646
$\omega\pi^0$	(4.5 $\pm$ 0.5) $\times 10^{-4}$	S=1.4		1446
$\omega\pi^0 \to \pi^+\pi^-\pi^0$	(1.7 $\pm$ 0.8) $\times 10^{-5}$			–
$\phi\eta'(958)$	(4.6 $\pm$ 0.5) $\times 10^{-4}$	S=2.2		1192
$\phi f_0(980)$	(3.2 $\pm$ 0.9) $\times 10^{-4}$	S=1.9		1178
$\phi f_0(980) \to \phi\pi^+\pi^-$	(2.59 $\pm$ 0.34) $\times 10^{-4}$			–
$\phi f_0(980) \to \phi\pi^0\pi^0$	(1.8 $\pm$ 0.5) $\times 10^{-4}$			–
$\phi\pi^0 f_0(980) \to \phi\pi^0\pi^+\pi^-$	(4.5 $\pm$ 1.0) $\times 10^{-6}$			–
$\phi\pi^0 f_0(980) \to \phi\pi^0 p^0\pi^0$	(1.7 $\pm$ 0.6) $\times 10^{-6}$			1045

$\eta\phi f_0(980) \rightarrow \eta\phi\pi^+\pi^-$		$(3.2 \pm 1.0) \times 10^{-4}$		–
$\phi a_0(980)^0 \rightarrow \phi\eta\pi^0$		$(5 \pm 4) \times 10^{-6}$		–
$\Xi(1530)^0\overline{\Xi}^0$		$(3.2 \pm 1.4) \times 10^{-4}$		608
$\Sigma(1385)^-\overline{\Sigma}^+$ (or c.c.)	[hh]	$(3.1 \pm 0.5) \times 10^{-4}$		855
$\phi f_1(1285)$		$(2.6 \pm 0.5) \times 10^{-4}$		1032
$\phi f_1(1285) \rightarrow \phi\pi^0 f_0(980) \rightarrow \phi\pi^0\pi^+\pi^-$		$(9.4 \pm 2.8) \times 10^{-7}$		952
$\phi f_1(1285) \rightarrow \phi\pi^0 f_0(980) \rightarrow \phi\pi^0\pi^0\pi^0$		$(2.1 \pm 2.2) \times 10^{-7}$		955
$\eta\pi^+\pi^-$		$(4.0 \pm 1.7) \times 10^{-4}$		1487
$\eta\rho$		$(1.93 \pm 0.23) \times 10^{-4}$		1396
$\omega\eta'(958)$		$(1.89 \pm 0.18) \times 10^{-4}$		1279
$\omega f_0(980)$		$(1.4 \pm 0.5) \times 10^{-4}$		1267
$\rho\eta'(958)$		$(8.1 \pm 0.8) \times 10^{-5}$	S=1.6	1281
$a_2(1320)^\pm\pi^\mp$	[hh]	$< 4.3 \times 10^{-3}$	CL=90%	1263
$K\overline{K}_2^*(1430)+$ c.c.		$< 4.0 \times 10^{-3}$	CL=90%	1159
$K_1(1270)^\pm K^\mp$		$< 3.0 \times 10^{-3}$	CL=90%	1231
$K_S^0\pi^- K_2^*(1430)^+ +$ c.c.		$(3.6 \pm 1.8) \times 10^{-3}$		1117
$K_S^0\pi^- K_2^*(1430)^+ +$ c.c. $\rightarrow K_S^0 K_S^0\pi^+\pi^-$		$(4.5 \pm 2.2) \times 10^{-4}$		–
$K_2^*(1430)^0\overline{K}_2^*(1430)^0$		$< 2.9 \times 10^{-3}$	CL=90%	604
$\phi\pi^0$		3×10^{-6} or 1×10^{-7}		1377
$\phi\eta(1405) \rightarrow \phi\eta\pi^+\pi^-$		$(2.0 \pm 1.0) \times 10^{-5}$		946
$\omega f_2'(1525)$		$< 2.2 \times 10^{-4}$	CL=90%	1003
$\omega X(1835) \rightarrow \omega p\overline{p}$		$< 3.9 \times 10^{-6}$	CL=95%	–
$\phi X(1835) \rightarrow \phi p\overline{p}$		$< 2.1 \times 10^{-7}$	CL=90%	–
$\phi X(1835) \rightarrow \phi\eta\pi^+\pi^-$		$< 2.8 \times 10^{-4}$	CL=90%	578
$\phi X(1870) \rightarrow \phi\eta\pi^+\pi^-$		$< 6.13 \times 10^{-5}$	CL=90%	–
$\eta\phi(2170) \rightarrow \eta\phi f_0(980) \rightarrow \eta\phi\pi^+\pi^-$		$(1.2 \pm 0.4) \times 10^{-4}$		628
$\eta\phi(2170) \rightarrow \eta K^*(892)^0\overline{K}^*(892)^0$		$< 2.52 \times 10^{-4}$	CL=90%	–
$\Sigma(1385)^0\overline{\Lambda}+$ c.c.		$< 8.2 \times 10^{-6}$	CL=90%	912
$\Delta(1232)^+\overline{p}$		$< 1 \times 10^{-4}$	CL=90%	1100
$\Lambda(1520)\overline{\Lambda}+$ c.c. $\rightarrow \gamma\Lambda\overline{\Lambda}$		$< 4.1 \times 10^{-6}$	CL=90%	–
$\Theta(1540)\overline{\Theta}(1540) \rightarrow K_S^0 p K^-\overline{n}+$ c.c.		$< 1.1 \times 10^{-5}$	CL=90%	–
$\Theta(1540)K^-\overline{n} \rightarrow K_S^0 p K^-\overline{n}$		$< 2.1 \times 10^{-5}$	CL=90%	–
$\Theta(1540)K_S^0\overline{p} \rightarrow K_S^0\overline{p}K^+ n$		$< 1.6 \times 10^{-5}$	CL=90%	–
$\overline{\Theta}(1540)K^+ n \rightarrow K_S^0\overline{p}K^+ n$		$< 5.6 \times 10^{-5}$	CL=90%	–
$\overline{\Theta}(1540)K_S^0 p \rightarrow K_S^0 p K^-\overline{n}$		$< 1.1 \times 10^{-5}$	CL=90%	–
$\Sigma^0\overline{\Lambda}$		$< 9 \times 10^{-5}$	CL=90%	1032

Decays into stable hadrons

$2(\pi^+\pi^-)\pi^0$		(4.1 ± 0.5) %	S=2.4	1496
$3(\pi^+\pi^-)\pi^0$		(2.9 ± 0.6) %		1433
$\pi^+\pi^-\pi^0$		(2.11 ± 0.07) %	S=1.5	1533
$\pi^+\pi^-\pi^0 K^+ K^-$		(1.79 ± 0.29) %	S=2.2	1368
$4(\pi^+\pi^-)\pi^0$		$(9.0 \pm 3.0) \times 10^{-3}$		1345
$\pi^+\pi^- K^+ K^-$		$(6.84 \pm 0.32) \times 10^{-3}$		1407
$\pi^+\pi^- K_S^0 K_L^0$		$(3.8 \pm 0.6) \times 10^{-3}$		1406
$\pi^+\pi^- K_S^0 K_S^0$		$(1.68 \pm 0.19) \times 10^{-3}$		1406
$\pi^\pm\pi^0 K^\mp K_S^0$		$(5.7 \pm 0.5) \times 10^{-3}$		1408
$K^+ K^- K_S^0 K_S^0$		$(4.1 \pm 0.8) \times 10^{-4}$		1127
$\pi^+\pi^- K^+ K^-\eta$		$(1.84 \pm 0.28) \times 10^{-3}$		1221
$\pi^0\pi^0 K^+ K^-$		$(2.12 \pm 0.23) \times 10^{-3}$		1410
$\pi^0\pi^0 K_S^0 K_L^0$		$(1.9 \pm 0.4) \times 10^{-3}$		1408
$K\overline{K}\pi$		$(6.1 \pm 1.0) \times 10^{-3}$		1442
$K^+ K^-\pi^0$		$(2.14 \pm 0.24) \times 10^{-3}$		1442
$K_S^0 K^\pm\pi^\mp$		$(5.6 \pm 0.5) \times 10^{-3}$		1440
$K_S^0 K_L^0\pi^0$		$(2.06 \pm 0.27) \times 10^{-3}$		1440
$K^*(892)^0\overline{K}^0+$ c.c. $\rightarrow K_S^0 K_L^0\pi^0$		$(1.21 \pm 0.18) \times 10^{-3}$		–
$K_2^*(1430)^0\overline{K}^0+$ c.c. $\rightarrow K_S^0 K_L^0\pi^0$		$(4.3 \pm 1.3) \times 10^{-4}$		–
$K_S^0 K_L^0\eta$		$(1.44 \pm 0.34) \times 10^{-3}$		1328
$2(\pi^+\pi^-)$		$(3.57 \pm 0.30) \times 10^{-3}$		1517
$3(\pi^+\pi^-)$		$(4.3 \pm 0.4) \times 10^{-3}$		1466
$2(\pi^+\pi^-\pi^0)$		(1.62 ± 0.21) %		1468
$2(\pi^+\pi^-)\eta$		$(2.29 \pm 0.24) \times 10^{-3}$		1446
$3(\pi^+\pi^-)\eta$		$(7.2 \pm 1.5) \times 10^{-4}$		1379
$p\overline{p}$		$(2.121 \pm 0.029) \times 10^{-3}$		1232
$p\overline{p}\pi^0$		$(1.19 \pm 0.08) \times 10^{-3}$	S=1.1	1176
$p\overline{p}\pi^+\pi^-$		$(6.0 \pm 0.5) \times 10^{-3}$	S=1.3	1107
$p\overline{p}\pi^+\pi^-\pi^0$	[ssaa]	$(2.3 \pm 0.9) \times 10^{-3}$	S=1.9	1033
$p\overline{p}\eta$		$(2.00 \pm 0.12) \times 10^{-3}$		948
$p\overline{p}\rho$		$< 3.1 \times 10^{-4}$	CL=90%	774
$p\overline{p}\omega$		$(9.8 \pm 1.0) \times 10^{-4}$	S=1.3	768
$p\overline{p}\eta'(958)$		$(2.1 \pm 0.4) \times 10^{-4}$		596
$p\overline{p}a_0(980) \rightarrow p\overline{p}\pi^0\eta$		$(6.8 \pm 1.8) \times 10^{-5}$		–
$p\overline{p}\phi$		$(5.19 \pm 0.33) \times 10^{-5}$		527
$n\overline{n}$		$(2.09 \pm 0.16) \times 10^{-3}$		1231
$n\overline{n}\pi^+\pi^-$		$(4 \pm 4) \times 10^{-3}$		1106
$\Sigma^+\overline{\Sigma}^-$		$(1.50 \pm 0.24) \times 10^{-3}$		992
$\Sigma^0\overline{\Sigma}^0$		$(1.172 \pm 0.031) \times 10^{-3}$	S=1.4	988
$2(\pi^+\pi^-)K^+K^-$		$(4.7 \pm 0.7) \times 10^{-3}$	S=1.3	1320
$p\overline{n}\pi^-$		$(2.12 \pm 0.09) \times 10^{-3}$		1174
$nN(1440)$		seen		978
$nN(1520)$		seen		928
$nN(1535)$		seen		917
$\Xi^-\overline{\Xi}^+$		$(9.7 \pm 0.8) \times 10^{-4}$	S=1.4	807
$\Lambda\overline{\Lambda}$		$(1.89 \pm 0.08) \times 10^{-3}$	S=2.5	1074
$\Lambda\overline{\Sigma}^-\pi^+$ (or c.c.)	[hh]	$(8.3 \pm 0.7) \times 10^{-4}$	S=1.2	950
$pK^-\overline{\Lambda}$		$(8.9 \pm 1.6) \times 10^{-4}$		876
$2(K^+K^-)$		$(7.4 \pm 0.7) \times 10^{-4}$		1131
$pK^-\overline{\Sigma}^0$		$(2.9 \pm 0.8) \times 10^{-4}$		819
K^+K^-		$(2.86 \pm 0.21) \times 10^{-4}$		1468
$K_S^0 K_L^0$		$(1.95 \pm 0.11) \times 10^{-4}$	S=2.4	1466
$\Lambda\overline{\Lambda}\pi^+\pi^-$		$(4.3 \pm 1.0) \times 10^{-3}$		903
$\Lambda\overline{\Lambda}\eta$		$(1.62 \pm 0.17) \times 10^{-4}$		672
$\Lambda\overline{\Lambda}\pi^0$		$(3.8 \pm 0.4) \times 10^{-5}$		998
$\overline{\Lambda}n K_S^0+$ c.c.		$(6.5 \pm 1.1) \times 10^{-4}$		872
$\pi^+\pi^-$		$(1.47 \pm 0.14) \times 10^{-4}$		1542
$\Lambda\overline{\Sigma}+$ c.c.		$(2.83 \pm 0.23) \times 10^{-5}$		1034
$K_S^0 K_S^0$		$< 1.4 \times 10^{-8}$	CL=95%	1466

Radiative decays

3γ		$(1.16 \pm 0.22) \times 10^{-5}$		1548
4γ		$< 9 \times 10^{-6}$	CL=90%	1548
5γ		$< 1.5 \times 10^{-5}$	CL=90%	1548
$\gamma\pi^0\pi^0$		$(1.15 \pm 0.05) \times 10^{-3}$		1543
$\gamma\eta\pi^0$		$(2.14 \pm 0.31) \times 10^{-5}$		1497
$\gamma a_0(980)^0 \rightarrow \gamma\eta\pi^0$		$< 2.5 \times 10^{-6}$	CL=95%	–
$\gamma a_2(1320)^0 \rightarrow \gamma\eta\pi^0$		$< 6.6 \times 10^{-6}$	CL=95%	–
$\gamma\eta_c(1S)$		(1.7 ± 0.4) %	S=1.5	111
$\gamma\eta_c(1S) \rightarrow 3\gamma$		$(3.8 \pm {}^{1.3}_{1.0}) \times 10^{-6}$	S=1.1	–
$\gamma\pi^+\pi^- 2\pi^0$		$(8.3 \pm 3.1) \times 10^{-3}$		1518
$\gamma\eta\pi\pi$		$(6.1 \pm 1.0) \times 10^{-3}$		1487
$\gamma\eta_2(1870) \rightarrow \gamma\eta\pi^+\pi^-$		$(6.2 \pm 2.4) \times 10^{-4}$		–
$\gamma\eta(1405/1475) \rightarrow \gamma K\overline{K}\pi$	[o]	$(2.8 \pm 0.6) \times 10^{-3}$	S=1.6	1223
$\gamma\eta(1405/1475) \rightarrow \gamma\gamma\rho^0$		$(7.8 \pm 2.0) \times 10^{-5}$	S=1.8	1223
$\gamma\eta(1405/1475) \rightarrow \gamma\eta\pi^+\pi^-$		$(3.0 \pm 0.5) \times 10^{-4}$		–
$\gamma\eta(1405/1475) \rightarrow \gamma\gamma\phi$		$< 8.2 \times 10^{-5}$	CL=95%	–
$\gamma\rho\rho$		$(4.5 \pm 0.8) \times 10^{-3}$		1340
$\gamma\rho\omega$		$< 5.4 \times 10^{-4}$	CL=90%	1338
$\gamma\rho\phi$		$< 8.8 \times 10^{-5}$	CL=90%	1258
$\gamma\eta'(958)$		$(5.13 \pm 0.17) \times 10^{-3}$	S=1.3	1400
$\gamma 2\pi^+ 2\pi^-$		$(2.8 \pm 0.5) \times 10^{-3}$	S=1.9	1517
$\gamma f_2(1270) f_2(1270)$		$(9.5 \pm 1.7) \times 10^{-4}$		878
$\gamma f_2(1270) f_2(1270)$ (non resonant)		$(8.2 \pm 1.9) \times 10^{-4}$		–
$\gamma K^+ K^-\pi^+\pi^-$		$(2.1 \pm 0.6) \times 10^{-3}$		1407
$\gamma f_4(2050)$		$(2.7 \pm 0.7) \times 10^{-3}$		891
$\gamma\omega\omega$		$(1.61 \pm 0.33) \times 10^{-3}$		1336
$\gamma\eta(1405/1475) \rightarrow \gamma\rho^0\rho^0$		$(1.7 \pm 0.4) \times 10^{-3}$	S=1.3	1223
$\gamma f_2(1270)$		$(1.64 \pm 0.12) \times 10^{-3}$	S=1.3	1286
$\gamma f_0(1370) \rightarrow \gamma K\overline{K}$		$(4.2 \pm 1.5) \times 10^{-4}$		–
$\gamma f_0(1710) \rightarrow \gamma K\overline{K}$		$(1.00 \pm {}^{0.11}_{0.09}) \times 10^{-3}$	S=1.5	1075
$\gamma f_0(1710) \rightarrow \gamma\pi\pi$		$(3.8 \pm 0.5) \times 10^{-4}$		–
$\gamma f_0(1710) \rightarrow \gamma\omega\omega$		$(3.1 \pm 1.0) \times 10^{-4}$		–
$\gamma f_0(1710) \rightarrow \gamma\eta\eta$		$(2.4 \pm {}^{1.2}_{0.7}) \times 10^{-4}$		–
$\gamma\eta$		$(1.104 \pm 0.034) \times 10^{-3}$		1500
$\gamma f_1(1420) \rightarrow \gamma K\overline{K}\pi$		$(7.9 \pm 1.3) \times 10^{-4}$		1220
$\gamma f_1(1285)$		$(6.1 \pm 0.8) \times 10^{-4}$		1283
$\gamma f_1(1510) \rightarrow \gamma\eta\pi^+\pi^-$		$(4.5 \pm 1.2) \times 10^{-4}$		–
$\gamma f_2'(1525)$		$(5.7 \pm {}^{0.8}_{0.5}) \times 10^{-4}$	S=1.5	1173
$\gamma f_2'(1525) \rightarrow \gamma\eta\eta$		$(3.4 \pm 1.4) \times 10^{-5}$		–
$\gamma f_2(1640) \rightarrow \gamma\omega\omega$		$(2.8 \pm 1.8) \times 10^{-4}$		–
$\gamma f_2(1910) \rightarrow \gamma\omega\omega$		$(2.0 \pm 1.4) \times 10^{-4}$		–

Meson Summary Table

$\gamma f_0(1800) \to \gamma\omega\phi$	$(2.5 \pm 0.6) \times 10^{-4}$		–
$\gamma f_2(1810) \to \gamma\eta\eta$	$(5.4 \,^{+\,3.5}_{-\,2.4}) \times 10^{-5}$		–
$\gamma f_2(1950) \to \gamma K^*(892)\overline{K}^*(892)$	$(7.0 \pm 2.2) \times 10^{-4}$		–
$\gamma K^*(892)\overline{K}^*(892)$	$(4.0 \pm 1.3) \times 10^{-3}$		1266
$\gamma\phi\phi$	$(4.0 \pm 1.2) \times 10^{-4}$	S=2.1	1166
$\gamma p\overline{p}$	$(3.8 \pm 1.0) \times 10^{-4}$		1232
$\gamma\eta(2225)$	$(3.14 \,^{+\,0.50}_{-\,0.19}) \times 10^{-4}$		752
$\gamma\eta(1760) \to \gamma\rho^0\rho^0$	$(1.3 \pm 0.9) \times 10^{-4}$		1048
$\gamma\eta(1760) \to \gamma\omega\omega$	$(1.98 \pm 0.33) \times 10^{-3}$		–
$\gamma X(1835) \to \gamma\pi^+\pi^-\eta'$	$(2.77 \,^{+\,0.34}_{-\,0.40}) \times 10^{-4}$	S=1.1	1006
$\gamma X(1835) \to \gamma p\overline{p}$	$(7.7 \,^{+\,1.5}_{-\,0.9}) \times 10^{-5}$		–
$\gamma X(1835) \to \gamma K_S^0 K_S^0\eta$	$(3.3 \,^{+\,2.0}_{-\,1.3}) \times 10^{-5}$		–
$\gamma X(1840) \to \gamma 3(\pi^+\pi^-)$	$(2.4 \,^{+\,0.7}_{-\,0.8}) \times 10^{-5}$		–
$\gamma(K\overline{K}\pi)$ $[J^{PC} = 0^{-+}]$	$(7 \pm 4) \times 10^{-4}$	S=2.1	1442
$\gamma\pi^0$	$(3.49 \,^{+\,0.33}_{-\,0.30}) \times 10^{-5}$		1546
$\gamma p\overline{p}\pi^+\pi^-$	$< 7.9 \times 10^{-4}$	CL=90%	1107
$\gamma\Lambda\overline{\Lambda}$	$< 1.3 \times 10^{-4}$	CL=90%	1074
$\gamma f_0(2100) \to \gamma\eta\eta$	$(1.13 \,^{+\,0.60}_{-\,0.30}) \times 10^{-4}$		–
$\gamma f_0(2100) \to \gamma\pi\pi$	$(6.2 \pm 1.0) \times 10^{-4}$		–
$\gamma f_0(2200) \to \gamma K\overline{K}$	$(5.9 \pm 1.3) \times 10^{-4}$		–
$\gamma f_J(2220) \to \gamma\pi\pi$	$< 3.9 \times 10^{-5}$	CL=90%	–
$\gamma f_J(2220) \to \gamma K\overline{K}$	$< 4.1 \times 10^{-5}$	CL=90%	–
$\gamma f_J(2220) \to \gamma p\overline{p}$	$(1.5 \pm 0.8) \times 10^{-5}$		–
$\gamma f_2(2340) \to \gamma\eta\eta$	$(5.6 \,^{+\,2.4}_{-\,2.2}) \times 10^{-5}$		–
$\gamma f_0(1500) \to \gamma\pi\pi$	$(1.09 \pm 0.24) \times 10^{-4}$		1183
$\gamma f_0(1500) \to \gamma\eta\eta$	$(1.7 \,^{+\,0.6}_{-\,1.4}) \times 10^{-5}$		–
$\gamma A \to \gamma$ invisible	[ttaa] $< 6.3 \times 10^{-6}$	CL=90%	–
$\gamma A^0 \to \gamma\mu^+\mu^-$	[uuaa] $< 5 \times 10^{-6}$	CL=90%	–

Dalitz decays

$\pi^0 e^+ e^-$	$(7.6 \pm 1.4) \times 10^{-7}$		1546
$\eta e^+ e^-$	$(1.16 \pm 0.09) \times 10^{-5}$		1500
$\eta'(958) e^+ e^-$	$(5.81 \pm 0.35) \times 10^{-5}$		1400

Weak decays

$D^- e^+\nu_e +$ c.c.	$< 1.2 \times 10^{-5}$	CL=90%	984
$\overline{D}^0 e^+ e^- +$ c.c.	$< 8.5 \times 10^{-8}$	CL=90%	987
$D_s^- e^+\nu_e +$ c.c.	$< 1.3 \times 10^{-6}$	CL=90%	923
$D_s^{*-} e^+\nu_e +$ c.c.	$< 1.8 \times 10^{-6}$	CL=90%	828
$D^-\pi^+ +$ c.c.	$< 7.5 \times 10^{-5}$	CL=90%	977
$\overline{D}^0 K^0 +$ c.c.	$< 1.7 \times 10^{-4}$	CL=90%	898
$\overline{D}^0 K^{*0} +$ c.c.	$< 2.5 \times 10^{-6}$	CL=90%	670
$D_s^-\pi^+ +$ c.c.	$< 1.3 \times 10^{-4}$	CL=90%	915
$D_s^-\rho^+ +$ c.c.	$< 1.3 \times 10^{-5}$	CL=90%	663

Charge conjugation (C), Parity (P), Lepton Family number (LF) violating modes

$\gamma\gamma$	C $< 2.7 \times 10^{-7}$	CL=90%	1548
$\gamma\phi$	C $< 1.4 \times 10^{-6}$	CL=90%	1381
$e^\pm\mu^\mp$	LF $< 1.6 \times 10^{-7}$	CL=90%	1547
$e^\pm\tau^\mp$	LF $< 8.3 \times 10^{-6}$	CL=90%	1039
$\mu^\pm\tau^\mp$	LF $< 2.0 \times 10^{-6}$	CL=90%	1035

Other decays

invisible	$< 7 \times 10^{-4}$	CL=90%	–

$\chi_{c0}(1P)$

$I^G(J^{PC}) = 0^+(0^{++})$

Mass $m = 3414.71 \pm 0.30$ MeV
Full width $\Gamma = 10.8 \pm 0.6$ MeV

$\chi_{c0}(1P)$ DECAY MODES	Fraction (Γ_i/Γ)	Scale factor/ Confidence level	p (MeV/c)

Hadronic decays

$2(\pi^+\pi^-)$	(2.34±0.18) %		1679
$\rho^0\pi^+\pi^-$	$(9.1 \pm 2.9) \times 10^{-3}$		1607
$f_0(980) f_0(980)$	$(6.6 \pm 2.1) \times 10^{-4}$		1391
$\pi^+\pi^-\pi^0\pi^0$	(3.3 ±0.4) %		1680
$\rho^+\pi^-\pi^0 +$ c.c.	(2.9 ±0.4) %		1607
$4\pi^0$	$(3.3 \pm 0.4) \times 10^{-3}$		1681
$\pi^+\pi^- K^+ K^-$	(1.81±0.14) %		1580
$K_0^*(1430)^0\overline{K}_0^*(1430)^0 \to \pi^+\pi^- K^+ K^-$	$(9.8 \,^{+\,4.0}_{-\,2.8}) \times 10^{-4}$		–
$K_0^*(1430)^0\overline{K}_2^*(1430)^0 +$ c.c. $\to \pi^+\pi^- K^+ K^-$	$(8.0 \,^{+\,2.0}_{-\,2.4}) \times 10^{-4}$		–
$K_1(1270)^+ K^- +$ c.c. $\to \pi^+\pi^- K^+ K^-$	$(6.3 \pm 1.9) \times 10^{-3}$		–
$K_1(1400)^+ K^- +$ c.c. $\to \pi^+\pi^- K^+ K^-$	$< 2.7 \times 10^{-3}$	CL=90%	–
$f_0(980) f_0(980)$	$(1.6 \,^{+\,1.0}_{-\,0.9}) \times 10^{-4}$		1391
$f_0(980) f_0(2200)$	$(7.9 \,^{+\,2.0}_{-\,2.5}) \times 10^{-4}$		584
$f_0(1370) f_0(1370)$	$< 2.7 \times 10^{-4}$	CL=90%	1019
$f_0(1370) f_0(1500)$	$< 1.7 \times 10^{-4}$	CL=90%	921
$f_0(1370) f_0(1710)$	$(6.7 \,^{+\,3.5}_{-\,2.3}) \times 10^{-4}$		720
$f_0(1500) f_0(1370)$	$< 1.3 \times 10^{-4}$	CL=90%	921
$f_0(1500) f_0(1500)$	$< 5 \times 10^{-5}$	CL=90%	807
$f_0(1500) f_0(1710)$	$< 7 \times 10^{-5}$	CL=90%	557
$K^+ K^-\pi^+\pi^-\pi^0$	$(8.6 \pm 0.9) \times 10^{-3}$		1545
$K_S^0 K^\pm\pi^\mp\pi^+\pi^-$	$(4.2 \pm 0.4) \times 10^{-3}$		1543
$K^+ K^-\pi^0\pi^0$	$(5.6 \pm 0.9) \times 10^{-3}$		1582
$K^+\pi^-\overline{K}^0\pi^0 +$ c.c.	(2.49±0.33) %		1581
$\rho^+ K^- K^0 +$ c.c.	(1.21±0.21) %		1458
$K^*(892)^- K^+\pi^0 \to K^+\pi^-\overline{K}^0\pi^0 +$ c.c.	$(4.6 \pm 1.2) \times 10^{-3}$		–
$K_S^0 K_S^0\pi^+\pi^-$	$(5.7 \pm 1.1) \times 10^{-3}$		1579
$K^+ K^-\eta\pi^0$	$(3.0 \pm 0.7) \times 10^{-3}$		1468
$3(\pi^+\pi^-)$	(1.20±0.18) %		1633
$K^+\overline{K}^*(892)^0\pi^- +$ c.c.	$(7.5 \pm 1.6) \times 10^{-3}$		1523
$K^*(892)^0\overline{K}^*(892)^0$	$(1.7 \pm 0.6) \times 10^{-3}$		1456
$\pi\pi$	$(8.51\pm0.33) \times 10^{-3}$		1702
$\pi^0\eta$	$< 1.8 \times 10^{-4}$		1661
$\pi^0\eta'$	$< 1.1 \times 10^{-3}$		1570
$\pi^0\eta_c$	$< 1.6 \times 10^{-3}$	CL=90%	383
$\eta\eta$	$(3.01\pm0.19) \times 10^{-3}$		1617
$\eta\eta'$	$(9.1 \pm 1.1) \times 10^{-5}$		1521
$\eta'\eta'$	$(2.17\pm0.12) \times 10^{-3}$		1413
$\omega\omega$	$(9.7 \pm 1.1) \times 10^{-4}$		1517
$\omega\phi$	$(1.18\pm0.22) \times 10^{-4}$		1447
$\omega K^+ K^-$	$(1.94\pm0.21) \times 10^{-3}$		1457
$K^+ K^-$	$(6.05\pm0.31) \times 10^{-3}$		1634
$K_S^0 K_S^0$	$(3.16\pm0.17) \times 10^{-3}$		1633
$\pi^+\pi^-\eta$	$< 2.0 \times 10^{-4}$	CL=90%	1651
$\pi^+\pi^-\eta'$	$< 4 \times 10^{-4}$	CL=90%	1560
$\overline{K}^0 K^+\pi^- +$ c.c.	$< 9 \times 10^{-5}$	CL=90%	1610
$K^+ K^-\pi^0$	$< 6 \times 10^{-5}$	CL=90%	1611
$K^+ K^-\eta$	$< 2.3 \times 10^{-4}$	CL=90%	1512
$K^+ K^- K_S^0 K_S^0$	$(1.4 \pm 0.5) \times 10^{-3}$		1331
$K^+ K^- K^+ K^-$	$(2.82\pm0.29) \times 10^{-3}$		1333
$K^+ K^-\phi$	$(9.7 \pm 2.5) \times 10^{-4}$		1381
$\overline{K}^0 K^+\pi^-\phi +$ c.c.	$(3.7 \pm 0.6) \times 10^{-3}$		1326
$K^+ K^-\pi^0\phi$	$(1.90\pm0.35) \times 10^{-3}$		1329
$\phi\pi^+\pi^-\pi^0$	$(1.18\pm0.15) \times 10^{-3}$		1525
$\phi\phi$	$(8.0 \pm 0.7) \times 10^{-4}$		1370
$p\overline{p}$	$(2.21\pm0.08) \times 10^{-4}$		1426
$p\overline{p}\pi^0$	$(7.0 \pm 0.7) \times 10^{-4}$	S=1.3	1379
$p\overline{p}\eta$	$(3.5 \pm 0.4) \times 10^{-4}$		1187
$p\overline{p}\omega$	$(5.2 \pm 0.6) \times 10^{-4}$		1043
$p\overline{p}\phi$	$(6.0 \pm 1.4) \times 10^{-5}$		876
$p\overline{p}\pi^+\pi^-$	$(2.1 \pm 0.7) \times 10^{-3}$	S=1.4	1320
$p\overline{p}\pi^0\pi^0$	$(1.04\pm0.28) \times 10^{-3}$		1324
$p\overline{p}K^+ K^-$ (non-resonant)	$(1.22\pm0.26) \times 10^{-4}$		890
$p\overline{p}K_S^0 K_S^0$	$< 8.8 \times 10^{-4}$	CL=90%	884
$p\overline{n}\pi^-$	$(1.27\pm0.11) \times 10^{-3}$		1376
$\overline{p}n\pi^+$	$(1.37\pm0.12) \times 10^{-3}$		1376
$p\overline{n}\pi^-\pi^0$	$(2.34\pm0.21) \times 10^{-3}$		1321
$\overline{p}n\pi^+\pi^0$	$(2.21\pm0.18) \times 10^{-3}$		1321
$\Lambda\overline{\Lambda}$	$(3.27\pm0.24) \times 10^{-4}$		1292
$\Lambda\overline{\Lambda}\pi^+\pi^-$	$(1.18\pm0.13) \times 10^{-3}$		1153
$\Lambda\overline{\Lambda}\pi^+\pi^-$ (non-resonant)	$< 5 \times 10^{-4}$	CL=90%	1153
$\Sigma(1385)^+\overline{\Lambda}\pi^- +$ c.c.	$< 5 \times 10^{-4}$	CL=90%	1083
$\Sigma(1385)^-\overline{\Lambda}\pi^+ +$ c.c.	$< 5 \times 10^{-4}$	CL=90%	1083
$K^+\overline{p}\Lambda +$ c.c.	$(1.25\pm0.12) \times 10^{-3}$	S=1.3	1132
$K^+\overline{p}\Lambda(1520) +$ c.c.	$(2.9 \pm 0.7) \times 10^{-4}$		858
$\Lambda(1520)\overline{\Lambda}(1520)$	$(3.1 \pm 1.2) \times 10^{-4}$		779
$\Sigma^0\overline{\Sigma}^0$	$(4.5 \pm 0.4) \times 10^{-4}$		1222
$\Sigma^+\overline{\Sigma}^-$	$(4.0 \pm 0.7) \times 10^{-4}$	S=1.7	1225
$\Sigma(1385)^+\overline{\Sigma}(1385)^-$	$(1.6 \pm 0.6) \times 10^{-4}$		1001

$\Sigma(1385)^-\overline{\Sigma}(1385)^+$	$(2.3 \pm 0.7) \times 10^{-4}$			1001
$K^-\Lambda\overline{\Xi}^+$ + c.c.	$(1.94 \pm 0.35) \times 10^{-4}$			873
$\Xi^0\overline{\Xi}^0$	$(3.1 \pm 0.8) \times 10^{-4}$			1089
$\Xi^-\overline{\Xi}^+$	$(4.8 \pm 0.7) \times 10^{-4}$			1081
$\eta_c\pi^+\pi^-$	$< 7 \times 10^{-4}$		CL=90%	307
Radiative decays				
$\gamma J/\psi(1S)$	(1.40 ± 0.05) %			303
$\gamma\rho^0$	$< 9 \times 10^{-6}$		CL=90%	1619
$\gamma\omega$	$< 8 \times 10^{-6}$		CL=90%	1618
$\gamma\phi$	$< 6 \times 10^{-6}$		CL=90%	1555
$\gamma\gamma$	$(2.04 \pm 0.09) \times 10^{-4}$			1707
$e^+e^-J/\psi(1S)$	$(1.54 \pm 0.33) \times 10^{-4}$			303

$\chi_{c1}(1P)$

$I^G(J^{PC}) = 0^+(1^{++})$

Mass $m = 3510.67 \pm 0.05$ MeV (S = 1.2)
Full width $\Gamma = 0.84 \pm 0.04$ MeV

$\chi_{c1}(1P)$ DECAY MODES	Fraction (Γ_i/Γ)	Scale factor/ Confidence level	p (MeV/c)
Hadronic decays			
$3(\pi^+\pi^-)$	$(5.8 \pm 1.4) \times 10^{-3}$	S=1.2	1683
$2(\pi^+\pi^-)$	$(7.6 \pm 2.6) \times 10^{-3}$		1728
$\pi^+\pi^-\pi^0\pi^0$	(1.19 ± 0.15) %		1729
$\rho^+\pi^-\pi^0$ + c.c.	(1.45 ± 0.24) %		1658
$\rho^0\pi^+\pi^-$	$(3.9 \pm 3.5) \times 10^{-3}$		1657
$4\pi^0$	$(5.4 \pm 0.8) \times 10^{-4}$		1729
$\pi^+\pi^-K^+K^-$	$(4.5 \pm 1.0) \times 10^{-3}$		1632
$K^+K^-\pi^0\pi^0$	$(1.12 \pm 0.27) \times 10^{-3}$		1634
$K^+K^-\pi^+\pi^-\pi^0$	(1.15 ± 0.13) %		1598
$K^0_S K^\pm\pi^\mp\pi^+\pi^-$	$(7.5 \pm 0.8) \times 10^{-3}$		1596
$K^+\pi^-\overline{K}^0\pi^0$ + c.c.	$(8.6 \pm 1.4) \times 10^{-3}$		1632
$\rho^-K^+\overline{K}^0$ + c.c.	$(5.0 \pm 1.2) \times 10^{-3}$		1514
$K^*(892)^0\overline{K}^0\pi^0 \to K^+\pi^-\overline{K}^0\pi^0$ + c.c.	$(2.3 \pm 0.6) \times 10^{-3}$		–
$K^+K^-\eta\pi^0$	$(1.12 \pm 0.34) \times 10^{-3}$		1523
$\pi^+\pi^-K^0_S K^0_S$	$(6.9 \pm 2.9) \times 10^{-4}$		1630
$K^+K^-\eta$	$(3.2 \pm 1.0) \times 10^{-4}$		1566
$\overline{K}^0K^+\pi^-$ + c.c.	$(7.0 \pm 0.6) \times 10^{-3}$		1661
$K^*(892)^0\overline{K}^0$ + c.c.	$(10 \pm 4) \times 10^{-3}$		1602
$K^*(892)^+K^-$ + c.c.	$(1.4 \pm 0.6) \times 10^{-3}$		1602
$K^*_J(1430)^0\overline{K}^0$ + c.c. $\to K^0_S K^+\pi^-$ + c.c.	$< 8 \times 10^{-4}$	CL=90%	–
$K^*_J(1430)^+K^-$ + c.c. $\to K^0_S K^+\pi^-$ + c.c.	$< 2.1 \times 10^{-3}$	CL=90%	–
$K^+K^-\pi^0$	$(1.81 \pm 0.24) \times 10^{-3}$		1662
$\eta\pi^+\pi^-$	$(4.62 \pm 0.23) \times 10^{-3}$		1701
$a_0(980)^+\pi^-$ + c.c. $\to \eta\pi^+\pi^-$	$(3.2 \pm 0.4) \times 10^{-3}$	S=2.2	–
$a_2(1320)^+\pi^-$ + c.c. $\to \eta\pi^+\pi^-$	$(1.76 \pm 0.24) \times 10^{-4}$		–
$a_2(1700)^+\pi^-$ + c.c. $\to \eta\pi^+\pi^-$	$(4.6 \pm 0.7) \times 10^{-5}$		–
$f_2(1270)\eta \to \eta\pi^+\pi^-$	$(3.5 \pm 0.6) \times 10^{-4}$		–
$f_4(2050)\eta \to \eta\pi^+\pi^-$	$(2.5 \pm 0.9) \times 10^{-5}$		–
$\pi_1(1400)^+\pi^-$ + c.c. $\to \eta\pi^+\pi^-$	$< 5 \times 10^{-5}$	CL=90%	–
$\pi_1(1600)^+\pi^-$ + c.c. $\to \eta\pi^+\pi^-$	$< 1.5 \times 10^{-5}$	CL=90%	–
$\pi_1(2015)^+\pi^-$ + c.c. $\to \eta\pi^+\pi^-$	$< 8 \times 10^{-6}$	CL=90%	–
$f_2(1270)\eta$	$(6.7 \pm 1.1) \times 10^{-4}$		1467
$\pi^+\pi^-\eta'$	$(2.2 \pm 0.4) \times 10^{-3}$		1612
$K^+K^-\eta'(958)$	$(8.8 \pm 0.9) \times 10^{-4}$		1461
$K^*_0(1430)^+K^-$ + c.c.	$(6.4 \, {}^{+2.2}_{-2.8}) \times 10^{-4}$		–
$f_0(980)\eta'(958)$	$(1.6 \, {}^{+1.4}_{-0.7}) \times 10^{-4}$		1460
$f_0(1710)\eta'(958)$	$(7 \, {}^{+7}_{-5}) \times 10^{-5}$		1106
$f'_2(1525)\eta'(958)$	$(9 \pm 6) \times 10^{-5}$		1225
$\pi^0 f_0(980) \to \pi^0\pi^+\pi^-$	$< 6 \times 10^{-6}$	CL=90%	–
$K^+\overline{K}^*(892)^0\pi^-$ + c.c.	$(3.2 \pm 2.1) \times 10^{-3}$		1577
$K^*(892)^0\overline{K}^*(892)^0$	$(1.4 \pm 0.4) \times 10^{-3}$		1512
$K^+K^-K^0_S K^0_S$	$< 4 \times 10^{-4}$	CL=90%	1390
$K^+K^-K^+K^-$	$(5.4 \pm 1.1) \times 10^{-4}$		1393
$K^+K^-\phi$	$(4.1 \pm 1.5) \times 10^{-4}$		1440
$\overline{K}^0K^+\pi^-\phi$ + c.c.	$(3.3 \pm 0.5) \times 10^{-3}$		1387
$K^+K^-\pi^0\phi$	$(1.62 \pm 0.30) \times 10^{-3}$		1390
$\phi\pi^+\pi^-\pi^0$	$(7.5 \pm 1.0) \times 10^{-4}$		1578
$\omega\omega$	$(5.7 \pm 0.7) \times 10^{-4}$		1571
ωK^+K^-	$(7.8 \pm 0.9) \times 10^{-4}$		1513
$\omega\phi$	$(2.1 \pm 0.6) \times 10^{-5}$		1503
$\phi\phi$	$(4.2 \pm 0.5) \times 10^{-4}$		1429
$p\overline{p}$	$(7.60 \pm 0.34) \times 10^{-5}$		1484
$p\overline{p}\pi^0$	$(1.55 \pm 0.18) \times 10^{-4}$		1438
$p\overline{p}\eta$	$(1.45 \pm 0.25) \times 10^{-4}$		1254
$p\overline{p}\omega$	$(2.12 \pm 0.31) \times 10^{-4}$		1117
$p\overline{p}\phi$	$< 1.7 \times 10^{-5}$	CL=90%	962
$p\overline{p}\pi^+\pi^-$	$(5.0 \pm 1.9) \times 10^{-4}$		1381
$p\overline{p}K^+K^-$ (non-resonant)	$(1.27 \pm 0.22) \times 10^{-4}$		974
$p\overline{p}K^0_S K^0_S$	$< 4.5 \times 10^{-4}$	CL=90%	968
$p\overline{n}\pi^-$	$(3.8 \pm 0.5) \times 10^{-4}$		1435
$\overline{p}n\pi^+$	$(3.9 \pm 0.5) \times 10^{-4}$		1435
$p\overline{n}\pi^-\pi^0$	$(1.03 \pm 0.12) \times 10^{-3}$		1383
$\overline{p}n\pi^+\pi^0$	$(1.01 \pm 0.12) \times 10^{-3}$		1383
$\Lambda\overline{\Lambda}$	$(1.14 \pm 0.11) \times 10^{-4}$		1355
$\Lambda\overline{\Lambda}\pi^+\pi^-$	$(2.9 \pm 0.5) \times 10^{-4}$		1223
$\Lambda\overline{\Lambda}\pi^+\pi^-$ (non-resonant)	$(2.5 \pm 0.6) \times 10^{-4}$		1223
$\Sigma(1385)^+\overline{\Lambda}\pi^-$ + c.c.	$< 1.3 \times 10^{-4}$	CL=90%	1157
$\Sigma(1385)^-\overline{\Lambda}\pi^+$ + c.c.	$< 1.3 \times 10^{-4}$	CL=90%	1157
$K^+\overline{p}\Lambda$	$(4.1 \pm 0.4) \times 10^{-4}$	S=1.2	1203
$K^+\overline{p}\Lambda(1520)$ + c.c.	$(1.7 \pm 0.4) \times 10^{-4}$		950
$\Lambda(1520)\overline{\Lambda}(1520)$	$< 9 \times 10^{-5}$	CL=90%	879
$\Sigma^0\overline{\Sigma}^0$	$< 4 \times 10^{-5}$	CL=90%	1288
$\Sigma^+\overline{\Sigma}^-$	$< 6 \times 10^{-5}$	CL=90%	1291
$\Sigma(1385)^+\overline{\Sigma}(1385)^-$	$< 9 \times 10^{-5}$	CL=90%	1081
$\Sigma(1385)^-\overline{\Sigma}(1385)^+$	$< 5 \times 10^{-5}$	CL=90%	1081
$K^-\Lambda\overline{\Xi}^+$ + c.c.	$(1.35 \pm 0.24) \times 10^{-4}$		963
$\Xi^0\overline{\Xi}^0$	$< 6 \times 10^{-5}$	CL=90%	1163
$\Xi^-\overline{\Xi}^+$	$(8.0 \pm 2.1) \times 10^{-5}$		1155
$\pi^+\pi^- + K^+K^-$	$< 2.1 \times 10^{-3}$		–
$K^0_S K^0_S$	$< 6 \times 10^{-5}$	CL=90%	1683
$\eta_c\pi^+\pi^-$	$< 3.2 \times 10^{-3}$	CL=90%	413
Radiative decays			
$\gamma J/\psi(1S)$	(34.3 ± 1.0) %		389
$\gamma\rho^0$	$(2.16 \pm 0.17) \times 10^{-4}$		1670
$\gamma\omega$	$(6.8 \pm 0.8) \times 10^{-5}$		1668
$\gamma\phi$	$(2.4 \pm 0.5) \times 10^{-5}$		1607
$\gamma\gamma$	$< 6.3 \times 10^{-6}$	CL=90%	1755
$e^+e^-J/\psi(1S)$	$(3.65 \pm 0.25) \times 10^{-3}$		389

$h_c(1P)$

$I^G(J^{PC}) = ?^?(1^{+-})$

Mass $m = 3525.38 \pm 0.11$ MeV
Full width $\Gamma = 0.7 \pm 0.4$ MeV

$h_c(1P)$ DECAY MODES	Fraction (Γ_i/Γ)	Confidence level	p (MeV/c)
$J/\psi(1S)\pi\pi$	not seen		312
$p\overline{p}$	$< 1.5 \times 10^{-4}$	90%	1492
$\pi^+\pi^-\pi^0$	$< 2.2 \times 10^{-3}$		1749
$2\pi^+2\pi^-\pi^0$	$(2.2^{+0.8}_{-0.7})$ %		1716
$3\pi^+3\pi^-\pi^0$	< 2.9 %		1661
Radiative decays			
$\gamma\eta$	$(4.7 \pm 2.1) \times 10^{-4}$		1720
$\gamma\eta'(958)$	$(1.5 \pm 0.4) \times 10^{-3}$		1633
$\gamma\eta_c(1S)$	(51 ± 6) %		500

$\chi_{c2}(1P)$

$I^G(J^{PC}) = 0^+(2^{++})$

Mass $m = 3556.17 \pm 0.07$ MeV
Full width $\Gamma = 1.97 \pm 0.09$ MeV

$\chi_{c2}(1P)$ DECAY MODES	Fraction (Γ_i/Γ)	Confidence level	p (MeV/c)
Hadronic decays			
$2(\pi^+\pi^-)$	(1.02 ± 0.09) %		1751
$\pi^+\pi^-\pi^0\pi^0$	(1.83 ± 0.23) %		1752
$\rho^+\pi^-\pi^0$ + c.c.	(2.19 ± 0.34) %		1682
$4\pi^0$	$(1.11 \pm 0.15) \times 10^{-3}$		1752
$K^+K^-\pi^0\pi^0$	$(2.1 \pm 0.4) \times 10^{-3}$		1658
$K^+\pi^-\overline{K}^0\pi^0$ + c.c.	(1.38 ± 0.20) %		1657
$\rho^-K^+\overline{K}^0$ + c.c.	$(4.1 \pm 1.2) \times 10^{-3}$		1540

Meson Summary Table

$K^*(892)^0 K^- \pi^+ \to K^- \pi^+ \overline{K}^0 \pi^0$ + c.c.	$(2.9 \pm 0.8) \times 10^{-3}$			–
$K^*(892)^0 \overline{K}^0 \pi^0 \to K^+ \pi^- \overline{K}^0 \pi^0$ + c.c.	$(3.8 \pm 0.9) \times 10^{-3}$			–
$K^*(892)^- K^+ \pi^0 \to K^+ \pi^- \overline{K}^0 \pi^0$ + c.c.	$(3.7 \pm 0.8) \times 10^{-3}$			–
$K^*(892)^+ \overline{K}^0 \pi^- \to K^+ \pi^- \overline{K}^0 \pi^0$ + c.c.	$(2.9 \pm 0.8) \times 10^{-3}$			–
$K^+ K^- \eta \pi^0$	$(1.3 \pm 0.4) \times 10^{-3}$			1549
$K^+ K^- \pi^+ \pi^-$	$(8.4 \pm 0.9) \times 10^{-3}$			1656
$K^+ K^- \pi^+ \pi^- \pi^0$	(1.17 ± 0.13) %			1623
$K^0_S K^\pm \pi^\mp \pi^+ \pi^-$	$(7.3 \pm 0.8) \times 10^{-3}$			1621
$K^+ \overline{K}^*(892)^0 \pi^-$ + c.c.	$(2.1 \pm 1.1) \times 10^{-3}$			1602
$K^*(892)^0 \overline{K}^*(892)^0$	$(2.3 \pm 0.4) \times 10^{-3}$			1538
$3(\pi^+ \pi^-)$	$(8.6 \pm 1.8) \times 10^{-3}$			1707
$\phi\phi$	$(1.06 \pm 0.09) \times 10^{-3}$			1457
$\omega\omega$	$(8.4 \pm 1.0) \times 10^{-4}$			1597
$\omega K^+ K^-$	$(7.3 \pm 0.9) \times 10^{-4}$			1540
$\pi\pi$	$(2.23 \pm 0.09) \times 10^{-3}$			1773
$\rho^0 \pi^+ \pi^-$	$(3.7 \pm 1.6) \times 10^{-3}$			1682
$\pi^+ \pi^- \pi^0$ (non-resonant)	$(2.0 \pm 0.4) \times 10^{-5}$			1765
$\rho(770)^\pm \pi^\mp$	$(6 \pm 4) \times 10^{-6}$			–
$\pi^+ \pi^- \eta$	$(4.8 \pm 1.3) \times 10^{-4}$			1724
$\pi^+ \pi^- \eta'$	$(5.0 \pm 1.8) \times 10^{-4}$			1636
$\eta\eta$	$(5.4 \pm 0.4) \times 10^{-4}$			1692
$K^+ K^-$	$(1.01 \pm 0.06) \times 10^{-3}$			1708
$K^0_S K^0_S$	$(5.2 \pm 0.4) \times 10^{-4}$			1707
$K^*(892)^\pm K^\mp$	$(1.44 \pm 0.21) \times 10^{-4}$			1627
$K^*(892)^0 \overline{K}^0$ + c.c.	$(1.24 \pm 0.27) \times 10^{-4}$			1627
$K_2^*(1430)^\pm K^\mp$	$(1.48 \pm 0.12) \times 10^{-3}$			–
$K_2^*(1430)^0 \overline{K}^0$ + c.c.	$(1.24 \pm 0.17) \times 10^{-3}$			1444
$K_3^*(1780)^\pm K^\mp$	$(5.2 \pm 0.8) \times 10^{-4}$			–
$K_3^*(1780)^0 \overline{K}^0$ + c.c.	$(5.6 \pm 2.1) \times 10^{-4}$			1276
$a_2(1320)^0 \pi^0$	$(1.29 \pm 0.34) \times 10^{-3}$			–
$a_2(1320)^\pm \pi^\mp$	$(1.8 \pm 0.6) \times 10^{-3}$			1530
$\overline{K}^0 K^+ \pi^-$ + c.c.	$(1.28 \pm 0.18) \times 10^{-3}$			1685
$K^+ K^- \pi^0$	$(3.0 \pm 0.8) \times 10^{-4}$			1686
$K^+ K^- \eta$	$< 3.2 \times 10^{-4}$		90%	1592
$K^+ K^- \eta'(958)$	$(1.94 \pm 0.34) \times 10^{-4}$			1488
$\eta\eta'$	$(2.2 \pm 0.5) \times 10^{-5}$			1600
$\eta'\eta'$	$(4.6 \pm 0.6) \times 10^{-5}$			1498
$\pi^+ \pi^- K^0_S K^0_S$	$(2.2 \pm 0.5) \times 10^{-3}$			1655
$K^+ K^- K^0_S K^0_S$	$< 4 \times 10^{-4}$		90%	1418
$K^+ K^- K^+ K^-$	$(1.65 \pm 0.20) \times 10^{-3}$			1421
$K^+ K^- \phi$	$(1.42 \pm 0.29) \times 10^{-3}$			1468
$\overline{K}^0 K^+ \pi^- \phi$ + c.c.	$(4.8 \pm 0.7) \times 10^{-3}$			1416
$K^+ K^- \pi^0 \phi$	$(2.7 \pm 0.5) \times 10^{-3}$			1419
$\phi \pi^+ \pi^- \pi^0$	$(9.3 \pm 1.2) \times 10^{-4}$			1603
$p\overline{p}$	$(7.33 \pm 0.33) \times 10^{-5}$			1510
$p\overline{p}\pi^0$	$(4.7 \pm 0.4) \times 10^{-4}$			1465
$p\overline{p}\eta$	$(1.74 \pm 0.25) \times 10^{-4}$			1285
$p\overline{p}\omega$	$(3.6 \pm 0.4) \times 10^{-4}$			1152
$p\overline{p}\phi$	$(2.8 \pm 0.9) \times 10^{-5}$			1002
$p\overline{p}\pi^+ \pi^-$	$(1.32 \pm 0.34) \times 10^{-3}$			1410
$p\overline{p}\pi^0 \pi^0$	$(7.8 \pm 2.3) \times 10^{-4}$			1414
$p\overline{p}K^+ K^-$ (non-resonant)	$(1.91 \pm 0.32) \times 10^{-4}$			1013
$p\overline{p}K^0_S K^0_S$	$< 7.9 \times 10^{-4}$		90%	1007
$p\overline{n}\pi^-$	$(8.5 \pm 0.9) \times 10^{-4}$			1463
$\overline{p}n\pi^+$	$(8.9 \pm 0.8) \times 10^{-4}$			1463
$p\overline{n}\pi^-\pi^0$	$(2.17 \pm 0.18) \times 10^{-3}$			1411
$\overline{p}n\pi^+\pi^0$	$(2.11 \pm 0.18) \times 10^{-3}$			1411
$\Lambda\overline{\Lambda}$	$(1.84 \pm 0.15) \times 10^{-4}$			1384
$\Lambda\overline{\Lambda}\pi^+\pi^-$	$(1.25 \pm 0.15) \times 10^{-3}$			1255
$\Lambda\overline{\Lambda}\pi^+\pi^-$ (non-resonant)	$(6.6 \pm 1.5) \times 10^{-4}$			1255
$\Sigma(1385)^+ \overline{\Lambda}\pi^-$ + c.c.	$< 4 \times 10^{-4}$		90%	1192
$\Sigma(1385)^- \overline{\Lambda}\pi^+$ + c.c.	$< 6 \times 10^{-4}$		90%	1192
$K^+ \overline{p}\Lambda$ + c.c.	$(7.8 \pm 0.5) \times 10^{-4}$			1236
$K^+ \overline{p}\Lambda(1520)$ + c.c.	$(2.8 \pm 0.7) \times 10^{-4}$			992
$\Lambda(1520)\overline{\Lambda}(1520)$	$(4.6 \pm 1.5) \times 10^{-4}$			923
$\Sigma^0 \overline{\Sigma}^0$	$< 6 \times 10^{-5}$		90%	1319
$\Sigma^+ \overline{\Sigma}^-$	$< 7 \times 10^{-5}$		90%	1322
$\Sigma(1385)^+ \overline{\Sigma}(1385)^-$	$< 1.6 \times 10^{-4}$		90%	1118
$\Sigma(1385)^- \overline{\Sigma}(1385)^+$	$< 8 \times 10^{-5}$		90%	1118
$K^- \Lambda \overline{\Xi}^+$ + c.c.	$(1.76 \pm 0.32) \times 10^{-4}$			1004
$\Xi^0 \overline{\Xi}^0$	$< 1.0 \times 10^{-4}$		90%	1197
$\Xi^- \overline{\Xi}^+$	$(1.42 \pm 0.32) \times 10^{-4}$			1189
$J/\psi(1S)\pi^+\pi^-\pi^0$	< 1.5 %		90%	185
$\pi^0 \eta_c$	$< 3.2 \times 10^{-3}$		90%	511
$\eta_c(1S)\pi^+\pi^-$	$< 5.4 \times 10^{-3}$		90%	459
Radiative decays				
$\gamma J/\psi(1S)$	(19.0 ± 0.5) %			430
$\gamma\rho^0$	$< 1.9 \times 10^{-5}$		90%	1694
$\gamma\omega$	$< 6 \times 10^{-6}$		90%	1692
$\gamma\phi$	$< 7 \times 10^{-6}$		90%	1632
$\gamma\gamma$	$(2.85 \pm 0.10) \times 10^{-4}$			1778
$e^+ e^- J/\psi(1S)$	$(2.37 \pm 0.16) \times 10^{-3}$			430

$\eta_c(2S)$

$I^G(J^{PC}) = 0^+(0^{-+})$

Quantum numbers are quark model predictions.

Mass $m = 3637.6 \pm 1.2$ MeV (S = 1.2)
Full width $\Gamma = 11.3^{+3.2}_{-2.9}$ MeV

$\eta_c(2S)$ DECAY MODES	Fraction (Γ_i/Γ)	Confidence level	p (MeV/c)
hadrons	not seen		–
$K\overline{K}\pi$	(1.9 ± 1.2) %		1729
$K\overline{K}\eta$	$(5 \pm 4) \times 10^{-3}$		1637
$2\pi^+ 2\pi^-$	not seen		1792
$\rho^0\rho^0$	not seen		1645
$3\pi^+ 3\pi^-$	not seen		1749
$K^+ K^- \pi^+ \pi^-$	not seen		1700
$K^{*0}\overline{K}^{*0}$	not seen		1585
$K^+ K^- \pi^+ \pi^- \pi^0$	(1.4 ± 1.0) %		1667
$K^+ K^- 2\pi^+ 2\pi^-$	not seen		1627
$K^0_S K^- 2\pi^+ \pi^-$ + c.c.	seen		1666
$2K^+ 2K^-$	not seen		1470
$\phi\phi$	not seen		1506
$p\overline{p}$	seen		1558
$\gamma\gamma$	$(1.9 \pm 1.3) \times 10^{-4}$		1819
$\gamma J/\psi(1S)$	< 1.4 %	90%	500
$\pi^+ \pi^- \eta$	not seen		1766
$\pi^+ \pi^- \eta'$	not seen		1680
$\pi^+ \pi^- \eta_c(1S)$	< 25 %	90%	538

$\psi(2S)$

$I^G(J^{PC}) = 0^-(1^{--})$

Mass $m = 3686.097 \pm 0.025$ MeV (S = 2.6)
Full width $\Gamma = 294 \pm 8$ keV
$\Gamma_{ee} = 2.33 \pm 0.04$ keV

$\psi(2S)$ DECAY MODES	Fraction (Γ_i/Γ)	Scale factor/ Confidence level	p (MeV/c)
hadrons	(97.85 ± 0.13) %		–
virtual $\gamma \to$ hadrons	(1.73 ± 0.14) %	S=1.5	–
ggg	(10.6 ± 1.6) %		–
γgg	(1.03 ± 0.29) %		–
light hadrons	(15.4 ± 1.5) %		–
$e^+ e^-$	$(7.93 \pm 0.17) \times 10^{-3}$		1843
$\mu^+ \mu^-$	$(8.0 \pm 0.6) \times 10^{-3}$		1840
$\tau^+ \tau^-$	$(3.1 \pm 0.4) \times 10^{-3}$		489
Decays into $J/\psi(1S)$ and anything			
$J/\psi(1S)$ anything	(61.4 ± 0.6) %		–
$J/\psi(1S)$ neutrals	(25.37 ± 0.32) %		–
$J/\psi(1S)\pi^+\pi^-$	(34.67 ± 0.30) %		477
$J/\psi(1S)\pi^0\pi^0$	(18.23 ± 0.31) %		481
$J/\psi(1S)\eta$	(3.37 ± 0.05) %		199
$J/\psi(1S)\pi^0$	$(1.268 \pm 0.032) \times 10^{-3}$		528
Hadronic decays			
$\pi^0 h_c(1P)$	$(8.6 \pm 1.3) \times 10^{-4}$		85
$3(\pi^+\pi^-)\pi^0$	$(3.5 \pm 1.6) \times 10^{-3}$		1746
$2(\pi^+\pi^-)\pi^0$	$(2.9 \pm 1.0) \times 10^{-3}$	S=4.7	1799
$\rho a_2(1320)$	$(2.6 \pm 0.9) \times 10^{-4}$		1500
$p\overline{p}$	$(2.88 \pm 0.10) \times 10^{-4}$		1586
$\Delta^{++}\overline{\Delta}^{--}$	$(1.28 \pm 0.35) \times 10^{-4}$		1371
$\Lambda\overline{\Lambda}\pi^0$	$< 2.9 \times 10^{-6}$	CL=90%	1412
$\Lambda\overline{\Lambda}\eta$	$(2.5 \pm 0.4) \times 10^{-5}$		1197
$\Lambda\overline{p}K^+$	$(1.00 \pm 0.14) \times 10^{-4}$		1327
$\Lambda\overline{p}K^+\pi^+\pi^-$	$(1.8 \pm 0.4) \times 10^{-4}$		1167
$\Lambda\overline{\Lambda}\pi^+\pi^-$	$(2.8 \pm 0.6) \times 10^{-4}$		1346

$\Lambda\overline{\Lambda}$	$(3.81 \pm 0.13) \times 10^{-4}$	S=1.4	1467
$\Lambda\overline{\Sigma}^+\pi^- +$ c.c.	$(1.40 \pm 0.13) \times 10^{-4}$		1376
$\Lambda\overline{\Sigma}^-\pi^+ +$ c.c.	$(1.54 \pm 0.14) \times 10^{-4}$		1379
$\Lambda\overline{\Sigma}^0$	$(1.23 \pm 0.24) \times 10^{-5}$		1437
$\Sigma^0\overline{p}K^+ +$ c.c.	$(1.67 \pm 0.18) \times 10^{-5}$		1291
$\Sigma^+\overline{\Sigma}^-$	$(2.32 \pm 0.12) \times 10^{-4}$		1408
$\Sigma^0\overline{\Sigma}^0$	$(2.35 \pm 0.09) \times 10^{-4}$	S=1.1	1405
$\Sigma(1385)^+\overline{\Sigma}(1385)^-$	$(8.5 \pm 0.7) \times 10^{-5}$		1218
$\Sigma(1385)^-\overline{\Sigma}(1385)^+$	$(8.5 \pm 0.8) \times 10^{-5}$		1218
$\Sigma(1385)^0\overline{\Sigma}(1385)^0$	$(6.9 \pm 0.7) \times 10^{-5}$		1218
$\Xi^-\overline{\Xi}^+$	$(2.87 \pm 0.11) \times 10^{-4}$	S=1.1	1284
$\Xi^0\overline{\Xi}^0$	$(2.3 \pm 0.4) \times 10^{-4}$	S=4.2	1291
$\Xi(1530)^0\overline{\Xi}(1530)^0$	$(5.2 \,^{+3.2}_{-1.2}) \times 10^{-5}$		1025
$K^-\Lambda\overline{\Xi}^+ +$ c.c.	$(3.9 \pm 0.4) \times 10^{-5}$		1114
$\Xi(1690)^-\overline{\Xi}^+ \to K^-\Lambda\overline{\Xi}^+ +$ c.c.	$(5.2 \pm 1.6) \times 10^{-6}$		–
$\Xi(1820)^-\overline{\Xi}^+ \to K^-\Lambda\overline{\Xi}^+ +$ c.c.	$(1.20 \pm 0.32) \times 10^{-5}$		–
$K^-\Sigma^0\overline{\Xi}^+ +$ c.c.	$(3.7 \pm 0.4) \times 10^{-5}$		1060
$\Omega^-\overline{\Omega}^+$	$(5.2 \pm 0.4) \times 10^{-5}$		774
$\pi^0 p\overline{p}$	$(1.53 \pm 0.07) \times 10^{-4}$		1543
$N(940)\overline{p}+$ c.c. $\to \pi^0 p\overline{p}$	$(6.4 \,^{+1.8}_{-1.3}) \times 10^{-5}$		–
$N(1440)\overline{p}+$ c.c. $\to \pi^0 p\overline{p}$	$(7.3 \,^{+1.7}_{-1.5}) \times 10^{-5}$	S=2.5	–
$N(1520)\overline{p}+$ c.c. $\to \pi^0 p\overline{p}$	$(6.4 \,^{+2.3}_{-1.8}) \times 10^{-6}$		–
$N(1535)\overline{p}+$ c.c. $\to \pi^0 p\overline{p}$	$(2.5 \pm 1.0) \times 10^{-5}$		–
$N(1650)\overline{p}+$ c.c. $\to \pi^0 p\overline{p}$	$(3.8 \,^{+1.4}_{-1.7}) \times 10^{-5}$		–
$N(1720)\overline{p}+$ c.c. $\to \pi^0 p\overline{p}$	$(1.79 \,^{+0.26}_{-0.70}) \times 10^{-5}$		–
$N(2300)\overline{p}+$ c.c. $\to \pi^0 p\overline{p}$	$(2.6 \,^{+1.2}_{-0.7}) \times 10^{-5}$		–
$N(2570)\overline{p}+$ c.c. $\to \pi^0 p\overline{p}$	$(2.13 \,^{+0.40}_{-0.31}) \times 10^{-5}$		–
$\pi^0 f_0(2100) \to \pi^0 p\overline{p}$	$(1.1 \pm 0.4) \times 10^{-5}$		–
$\eta p\overline{p}$	$(6.0 \pm 0.4) \times 10^{-5}$		1373
$\eta f_0(2100) \to \eta p\overline{p}$	$(1.2 \pm 0.4) \times 10^{-5}$		–
$N(1535)\overline{p} \to \eta p\overline{p}$	$(4.4 \pm 0.7) \times 10^{-5}$		–
$\omega p\overline{p}$	$(6.9 \pm 2.1) \times 10^{-5}$		1247
$\phi p\overline{p}$	$< 2.4 \times 10^{-5}$	CL=90%	1109
$\pi^+\pi^- p\overline{p}$	$(6.0 \pm 0.4) \times 10^{-4}$		1491
$p\overline{n}\pi^-$ or c.c.	$(2.48 \pm 0.17) \times 10^{-4}$		–
$p\overline{n}\pi^-\pi^0$	$(3.2 \pm 0.7) \times 10^{-4}$		1492
$2(\pi^+\pi^-\pi^0)$	$(4.8 \pm 1.5) \times 10^{-3}$		1776
$\eta\pi^+\pi^-$	$< 1.6 \times 10^{-4}$	CL=90%	1791
$\eta\pi^+\pi^-\pi^0$	$(9.5 \pm 1.7) \times 10^{-4}$		1778
$2(\pi^+\pi^-)\eta$	$(1.2 \pm 0.6) \times 10^{-3}$		1758
$\eta'\pi^+\pi^-\pi^0$	$(4.5 \pm 2.1) \times 10^{-4}$		1692
$\omega\pi^+\pi^-$	$(7.3 \pm 1.2) \times 10^{-4}$	S=2.1	1748
$b_1^\pm\pi^\mp$	$(4.0 \pm 0.6) \times 10^{-4}$	S=1.1	1635
$b_1^0\pi^0$	$(2.4 \pm 0.6) \times 10^{-4}$		–
$\omega f_2(1270)$	$(2.2 \pm 0.4) \times 10^{-4}$		1515
$\pi^0\pi^0 K^+K^-$	$(2.6 \pm 1.3) \times 10^{-4}$		1728
$\pi^+\pi^- K^+K^-$	$(7.3 \pm 0.5) \times 10^{-4}$		1726
$\pi^0\pi^0 K_S^0 K_L^0$	$(1.3 \pm 0.5) \times 10^{-3}$		1726
$\rho^0 K^+K^-$	$(2.2 \pm 0.4) \times 10^{-4}$		1616
$K^*(892)^0\overline{K}_2^*(1430)^0$	$(1.9 \pm 0.5) \times 10^{-4}$		1418
$K^+K^-\pi^+\pi^-\eta$	$(1.3 \pm 0.7) \times 10^{-3}$		1574
$K^+K^-2(\pi^+\pi^-)\pi^0$	$(1.00 \pm 0.31) \times 10^{-3}$		1611
$K^+K^-2(\pi^+\pi^-)$	$(1.9 \pm 0.9) \times 10^{-3}$		1654
$K_1(1270)^\pm K^\mp$	$(1.00 \pm 0.28) \times 10^{-3}$		1581
$K_S^0 K_S^0\pi^+\pi^-$	$(2.2 \pm 0.4) \times 10^{-4}$		1724
$\rho^0 p\overline{p}$	$(5.0 \pm 2.2) \times 10^{-5}$		1252
$K^+\overline{K}^*(892)^0\pi^- +$ c.c.	$(6.7 \pm 2.5) \times 10^{-4}$		1674
$2(\pi^+\pi^-)$	$(2.4 \pm 0.6) \times 10^{-4}$	S=2.2	1817
$\rho^0\pi^+\pi^-$	$(2.2 \pm 0.6) \times 10^{-4}$	S=1.4	1750
$K^+K^-\pi^+\pi^-\pi^0$	$(1.26 \pm 0.09) \times 10^{-3}$		1694
$\omega f_0(1710) \to \omega K^+K^-$	$(5.9 \pm 2.2) \times 10^{-5}$		–
$K^*(892)^0 K^-\pi^+\pi^0 +$ c.c.	$(8.6 \pm 2.2) \times 10^{-4}$		–
$K^*(892)^+ K^-\pi^+\pi^- +$ c.c.	$(9.6 \pm 2.8) \times 10^{-4}$		–
$K^*(892)^+ K^-\rho^0 +$ c.c.	$(7.3 \pm 2.6) \times 10^{-4}$		–
$K^*(892)^0 K^-\rho^+ +$ c.c.	$(6.1 \pm 1.8) \times 10^{-4}$		–
ηK^+K^-, no $\eta\phi$	$(3.1 \pm 0.4) \times 10^{-5}$		1664
ωK^+K^-	$(1.62 \pm 0.11) \times 10^{-4}$	S=1.1	1614
$\omega K^*(892)^+ K^-+$ c.c.	$(2.07 \pm 0.26) \times 10^{-4}$		1482
$\omega K_2^*(1430)^+ K^-+$ c.c.	$(6.1 \pm 1.2) \times 10^{-5}$		1253
$\omega\overline{K}^*(892)^0 K^0$	$(1.68 \pm 0.30) \times 10^{-4}$		1481
$\omega\overline{K}_2^*(1430)^0 K^0$	$(5.8 \pm 2.2) \times 10^{-5}$		1251
$\omega X(1440) \to \omega K_S^0 K^-\pi^+ +$ c.c.	$(1.6 \pm 0.4) \times 10^{-5}$		–
$\omega X(1440) \to \omega K^+K^-\pi^0$	$(1.09 \pm 0.26) \times 10^{-5}$		–
$\omega f_1(1285) \to \omega K_S^0 K^-\pi^+ +$ c.c.	$(3.0 \pm 1.0) \times 10^{-6}$		–
$\omega f_1(1285) \to \omega K^+K^-\pi^0$	$(1.2 \pm 0.7) \times 10^{-6}$		–
$3(\pi^+\pi^-)$	$(3.5 \pm 2.0) \times 10^{-4}$	S=2.8	1774
$p\overline{p}\pi^+\pi^-\pi^0$	$(7.3 \pm 0.7) \times 10^{-4}$		1435
K^+K^-	$(7.5 \pm 0.5) \times 10^{-5}$		1776
$K_S^0 K_L^0$	$(5.34 \pm 0.33) \times 10^{-5}$		1775
$\pi^+\pi^-\pi^0$	$(2.01 \pm 0.17) \times 10^{-4}$	S=1.7	1830
$\rho(2150)\pi \to \pi^+\pi^-\pi^0$	$(1.9 \,^{+1.2}_{-0.4}) \times 10^{-4}$		–
$\rho(770)\pi \to \pi^+\pi^-\pi^0$	$(3.2 \pm 1.2) \times 10^{-5}$	S=1.8	–
$\pi^+\pi^-$	$(7.8 \pm 2.6) \times 10^{-6}$		1838
$K_1(1400)^\pm K^\mp$	$< 3.1 \times 10^{-4}$	CL=90%	1532
$K_2^*(1430)^\pm K^\mp$	$(7.1 \,^{+1.3}_{-0.9}) \times 10^{-5}$		–
$K^+K^-\pi^0$	$(4.07 \pm 0.31) \times 10^{-5}$		1754
$K_S^0 K_L^0\pi^0$	$< 3.0 \times 10^{-4}$	CL=90%	1753
$K_S^0 K_L^0\eta$	$(1.3 \pm 0.5) \times 10^{-3}$		1661
$K^+K^*(892)^-+$ c.c.	$(2.9 \pm 0.4) \times 10^{-5}$	S=1.2	1698
$K^*(892)^0\overline{K}^0+$ c.c.	$(1.09 \pm 0.20) \times 10^{-4}$		1697
$\phi\pi^+\pi^-$	$(1.18 \pm 0.26) \times 10^{-4}$	S=1.5	1690
$\phi f_0(980) \to \pi^+\pi^-$	$(7.5 \pm 3.3) \times 10^{-5}$	S=1.6	–
$2(K^+K^-)$	$(6.3 \pm 1.3) \times 10^{-5}$		1499
ϕK^+K^-	$(7.0 \pm 1.6) \times 10^{-5}$		1546
$2(K^+K^-)\pi^0$	$(1.10 \pm 0.28) \times 10^{-4}$		1440
$\phi\eta$	$(3.10 \pm 0.31) \times 10^{-5}$		1654
$\phi\eta'$	$(3.1 \pm 1.6) \times 10^{-5}$		1555
$\omega\eta'$	$(3.2 \,^{+2.5}_{-2.1}) \times 10^{-5}$		1623
$\omega\pi^0$	$(2.1 \pm 0.6) \times 10^{-5}$		1757
$\rho\eta'$	$(1.9 \,^{+1.7}_{-1.2}) \times 10^{-5}$		1625
$\rho\eta$	$(2.2 \pm 0.6) \times 10^{-5}$	S=1.1	1717
$\omega\eta$	$< 1.1 \times 10^{-5}$	CL=90%	1715
$\phi\pi^0$	$< 4 \times 10^{-7}$	CL=90%	1699
$\eta_c\pi^+\pi^-\pi^0$	$< 1.0 \times 10^{-3}$	CL=90%	512
$p\overline{p}K^+K^-$	$(2.7 \pm 0.7) \times 10^{-5}$		1118
$\overline{\Lambda}n K_S^0+$ c.c.	$(8.1 \pm 1.8) \times 10^{-5}$		1324
$\phi f_2'(1525)$	$(4.4 \pm 1.6) \times 10^{-5}$		1321
$\Theta(1540)\overline{\Theta}(1540) \to K_S^0 p K^-\overline{n}+$ c.c.	$< 8.8 \times 10^{-6}$	CL=90%	–
$\Theta(1540)K^-\overline{n} \to K_S^0 p K^-\overline{n}$	$< 1.0 \times 10^{-5}$	CL=90%	–
$\Theta(1540)K_S^0\overline{p} \to K_S^0\overline{p}K^+ n$	$< 7.0 \times 10^{-6}$	CL=90%	–
$\overline{\Theta}(1540)K^+ n \to K_S^0\overline{p}K^+ n$	$< 2.6 \times 10^{-5}$	CL=90%	–
$\overline{\Theta}(1540)K_S^0 p \to K_S^0 p K^-\overline{n}$	$< 6.0 \times 10^{-6}$	CL=90%	–
$K_S^0 K_S^0$	$< 4.6 \times 10^{-6}$		1775

Radiative decays

$\gamma\chi_{c0}(1P)$	(9.79 ± 0.20) %		261
$\gamma\chi_{c1}(1P)$	(9.75 ± 0.24) %		171
$\gamma\chi_{c2}(1P)$	(9.52 ± 0.20) %		128
$\gamma\eta_c(1S)$	$(3.4 \pm 0.5) \times 10^{-3}$	S=1.3	635
$\gamma\eta_c(2S)$	$(7 \pm 5) \times 10^{-4}$		48
$\gamma\pi^0$	$(1.04 \pm 0.22) \times 10^{-6}$	S=1.4	1841
$\gamma\eta'(958)$	$(1.24 \pm 0.04) \times 10^{-4}$		1719
$\gamma f_2(1270)$	$(2.73 \,^{+0.29}_{-0.25}) \times 10^{-4}$	S=1.8	1622
$\gamma f_0(1370) \to \gamma K\overline{K}$	$(3.1 \pm 1.7) \times 10^{-5}$		1588
$\gamma f_0(1500)$	$(9.2 \pm 1.9) \times 10^{-5}$		1536
$\gamma f_2'(1525)$	$(3.3 \pm 0.8) \times 10^{-5}$		1528
$\gamma f_0(1710) \to \gamma\pi\pi$	$(3.5 \pm 0.6) \times 10^{-5}$		–
$\gamma f_0(1710) \to \gamma K\overline{K}$	$(6.6 \pm 0.7) \times 10^{-5}$		–
$\gamma f_0(2100) \to \gamma\pi\pi$	$(4.8 \pm 1.0) \times 10^{-6}$		1244
$\gamma f_0(2200) \to \gamma K\overline{K}$	$(3.2 \pm 1.0) \times 10^{-6}$		1193
$\gamma f_J(2220) \to \gamma\pi\pi$	$< 5.8 \times 10^{-6}$	CL=90%	1168
$\gamma f_J(2220) \to \gamma K\overline{K}$	$< 9.5 \times 10^{-6}$	CL=90%	1168
$\gamma\gamma$	$< 1.5 \times 10^{-4}$	CL=90%	1843
$\gamma\eta$	$(9.2 \pm 1.8) \times 10^{-7}$		1802
$\gamma\eta\pi^+\pi^-$	$(8.7 \pm 2.1) \times 10^{-4}$		1791
$\gamma\eta(1405) \to \gamma K\overline{K}\pi$	$< 9 \times 10^{-5}$	CL=90%	1569
$\gamma\eta(1405) \to \eta\pi^+\pi^-$	$(3.6 \pm 2.5) \times 10^{-5}$		–
$\gamma\eta(1405) \to \gamma f_0(980)\pi^0 \to \gamma\pi^+\pi^-\pi^0$	$< 5.0 \times 10^{-7}$	CL=90%	–
$\gamma\eta(1475) \to K\overline{K}\pi$	$< 1.4 \times 10^{-4}$	CL=90%	–
$\gamma\eta(1475) \to \eta\pi^+\pi^-$	$< 8.8 \times 10^{-5}$	CL=90%	–
$\gamma 2(\pi^+\pi^-)$	$(4.0 \pm 0.6) \times 10^{-4}$		1817

Meson Summary Table

$\gamma K^{*0} K^+ \pi^- +$ c.c.	$(3.7 \pm 0.9) \times 10^{-4}$			1674
$\gamma K^{*0} \overline{K}^{*0}$	$(2.4 \pm 0.7) \times 10^{-4}$			1613
$\gamma K^0_S K^+ \pi^- +$ c.c.	$(2.6 \pm 0.5) \times 10^{-4}$			1753
$\gamma K^+ K^- \pi^+ \pi^-$	$(1.9 \pm 0.5) \times 10^{-4}$			1726
$\gamma p \overline{p}$	$(3.9 \pm 0.5) \times 10^{-5}$		S=2.0	1586
$\gamma f_2(1950) \rightarrow \gamma p \overline{p}$	$(1.20 \pm 0.22) \times 10^{-5}$			–
$\gamma f_2(2150) \rightarrow \gamma p \overline{p}$	$(7.2 \pm 1.8) \times 10^{-6}$			–
$\gamma X(1835) \rightarrow \gamma p \overline{p}$	$(4.6 \, ^{+1.8}_{-4.0}) \times 10^{-6}$			–
$\gamma X \rightarrow \gamma p \overline{p}$	[vvaa] < 2	$\times 10^{-6}$	CL=90%	–
$\gamma \pi^+ \pi^- p \overline{p}$	$(2.8 \pm 1.4) \times 10^{-5}$			1491
$\gamma 2(\pi^+ \pi^-) K^+ K^-$	< 2.2	$\times 10^{-4}$	CL=90%	1654
$\gamma 3(\pi^+ \pi^-)$	< 1.7	$\times 10^{-4}$	CL=90%	1774
$\gamma K^+ K^- K^+ K^-$	< 4	$\times 10^{-5}$	CL=90%	1499
$\gamma\gamma J/\psi$	$(3.1 \, ^{+1.0}_{-1.2}) \times 10^{-4}$			542
$e^+ e^- \chi_{c0}(1P)$	$(1.06 \pm 0.24) \times 10^{-3}$			261
$e^+ e^- \chi_{c1}(1P)$	$(8.5 \pm 0.6) \times 10^{-4}$			171
$e^+ e^- \chi_{c2}(1P)$	$(7.0 \pm 0.8) \times 10^{-4}$			128
Weak decays				
$D^0 e^+ e^- +$ c.c.	< 1.4	$\times 10^{-7}$	CL=90%	1371
Other decays				
invisible	< 1.6	%	CL=90%	–

$\psi(3770)$

$I^G(J^{PC}) = 0^-(1^{--})$

Mass $m = 3773.13 \pm 0.35$ MeV (S = 1.1)
Full width $\Gamma = 27.2 \pm 1.0$ MeV
$\Gamma_{ee} = 0.262 \pm 0.018$ keV (S = 1.4)

In addition to the dominant decay mode to $D\overline{D}$, $\psi(3770)$ was found to decay into the final states containing the J/ψ (BAI 05, ADAM 06). ADAMS 06 and HUANG 06A searched for various decay modes with light hadrons and found a statistically significant signal for the decay to $\phi\eta$ only (ADAMS 06).

$\psi(3770)$ DECAY MODES	Fraction (Γ_i/Γ)	Scale factor / Confidence level	p (MeV/c)
$D\overline{D}$	$(93 \, ^{+8}_{-9}) \%$	S=2.0	286
$D^0 \overline{D}^0$	$(52 \, ^{+4}_{-5}) \%$	S=2.0	286
$D^+ D^-$	$(41 \pm 4) \%$	S=2.0	252
$J/\psi \pi^+ \pi^-$	$(1.93 \pm 0.28) \times 10^{-3}$		560
$J/\psi \pi^0 \pi^0$	$(8.0 \pm 3.0) \times 10^{-4}$		564
$J/\psi \eta$	$(9 \pm 4) \times 10^{-4}$		360
$J/\psi \pi^0$	$< 2.8 \times 10^{-4}$	CL=90%	603
$e^+ e^-$	$(9.6 \pm 0.7) \times 10^{-6}$	S=1.3	1887
Decays to light hadrons			
$b_1(1235)\pi$	$< 1.4 \times 10^{-5}$	CL=90%	1683
$\phi\eta'$	$< 7 \times 10^{-4}$	CL=90%	1607
$\omega\eta'$	$< 4 \times 10^{-4}$	CL=90%	1672
$\rho^0\eta'$	$< 6 \times 10^{-4}$	CL=90%	1674
$\phi\eta$	$(3.1 \pm 0.7) \times 10^{-4}$		1703
$\omega\eta$	$< 1.4 \times 10^{-5}$	CL=90%	1762
$\rho^0\eta$	$< 5 \times 10^{-4}$	CL=90%	1764
$\phi\pi^0$	$< 3 \times 10^{-5}$	CL=90%	1746
$\omega\pi^0$	$< 6 \times 10^{-4}$	CL=90%	1803
$\pi^+ \pi^- \pi^0$	$< 5 \times 10^{-6}$	CL=90%	1874
$\rho\pi$	$< 5 \times 10^{-6}$	CL=90%	1804
$K^*(892)^+ K^- +$ c.c.	$< 1.4 \times 10^{-5}$	CL=90%	1745
$K^*(892)^0 \overline{K}^0 +$ c.c.	$< 1.2 \times 10^{-3}$	CL=90%	1744
$K^0_S K^0_L$	$< 1.2 \times 10^{-5}$	CL=90%	1820
$2(\pi^+ \pi^-)$	$< 1.12 \times 10^{-3}$	CL=90%	1861
$2(\pi^+ \pi^-)\pi^0$	$< 1.06 \times 10^{-3}$	CL=90%	1843
$2(\pi^+ \pi^- \pi^0)$	< 5.85 %	CL=90%	1821
$\omega \pi^+ \pi^-$	$< 6.0 \times 10^{-4}$	CL=90%	1794
$3(\pi^+ \pi^-)$	$< 9.1 \times 10^{-3}$	CL=90%	1819
$3(\pi^+ \pi^-)\pi^0$	< 1.37 %	CL=90%	1792
$3(\pi^+ \pi^-) 2\pi^0$	< 11.74 %	CL=90%	1760
$\eta \pi^+ \pi^-$	$< 1.24 \times 10^{-3}$	CL=90%	1836
$\pi^+ \pi^- 2\pi^0$	$< 8.9 \times 10^{-3}$	CL=90%	1862
$\rho^0 \pi^+ \pi^-$	$< 6.9 \times 10^{-3}$	CL=90%	1796
$\eta 3\pi$	$< 1.34 \times 10^{-3}$	CL=90%	1824
$\eta 2(\pi^+ \pi^-)$	< 2.43 %	CL=90%	1804
$\eta \rho^0 \pi^+ \pi^-$	< 1.45 %	CL=90%	1708
$\eta' 3\pi$	$< 2.44 \times 10^{-3}$	CL=90%	1740
$K^+ K^- \pi^+ \pi^-$	$< 9.0 \times 10^{-4}$	CL=90%	1772
$\phi\pi^+ \pi^-$	$< 4.1 \times 10^{-4}$	CL=90%	1737
$K^+ K^- 2\pi^0$	$< 4.2 \times 10^{-3}$	CL=90%	1774
$4(\pi^+ \pi^-)$	< 1.67 %	CL=90%	1757
$4(\pi^+ \pi^-)\pi^0$	< 3.06 %	CL=90%	1720
$\phi f_0(980)$	$< 4.5 \times 10^{-4}$	CL=90%	1597
$K^+ K^- \pi^+ \pi^- \pi^0$	$< 2.36 \times 10^{-3}$	CL=90%	1741
$K^+ K^- \rho^0 \pi^0$	$< 8 \times 10^{-4}$	CL=90%	1624
$K^+ K^- \rho^+ \pi^-$	< 1.46 %	CL=90%	1622
$\omega K^+ K^-$	$< 3.4 \times 10^{-4}$	CL=90%	1664
$\phi\pi^+ \pi^- \pi^0$	$< 3.8 \times 10^{-3}$	CL=90%	1722
$K^{*0} K^- \pi^+ \pi^0 +$ c.c.	< 1.62 %	CL=90%	1693
$K^{*+} K^- \pi^+ \pi^- +$ c.c.	< 3.23 %	CL=90%	1692
$K^+ K^- \pi^+ \pi^- 2\pi^0$	< 2.67 %	CL=90%	1705
$K^+ K^- 2(\pi^+ \pi^-)$	< 1.03 %	CL=90%	1702
$K^+ K^- 2(\pi^+ \pi^-)\pi^0$	< 3.60 %	CL=90%	1660
$\eta K^+ K^-$	$< 4.1 \times 10^{-4}$	CL=90%	1712
$\eta K^+ K^- \pi^+ \pi^-$	< 1.24 %	CL=90%	1624
$\rho^0 K^+ K^-$	$< 5.0 \times 10^{-3}$	CL=90%	1665
$2(K^+ K^-)$	$< 6.0 \times 10^{-4}$	CL=90%	1552
$\phi K^+ K^-$	$< 7.5 \times 10^{-4}$	CL=90%	1598
$2(K^+ K^-)\pi^0$	$< 2.9 \times 10^{-4}$	CL=90%	1493
$2(K^+ K^-)\pi^+ \pi^-$	$< 3.2 \times 10^{-3}$	CL=90%	1425
$K^0_S K^- \pi^+$	$< 3.2 \times 10^{-3}$	CL=90%	1799
$K^0_S K^- \pi^+ \pi^0$	< 1.33 %	CL=90%	1773
$K^0_S K^- \rho^+$	$< 6.6 \times 10^{-3}$	CL=90%	1664
$K^0_S K^- 2\pi^+ \pi^-$	$< 8.7 \times 10^{-3}$	CL=90%	1739
$K^0_S K^- \pi^+ \rho^0$	< 1.6 %	CL=90%	1621
$K^0_S K^- \pi^+ \eta$	< 1.3 %	CL=90%	1669
$K^0_S K^- 2\pi^+ \pi^- \pi^0$	< 4.18 %	CL=90%	1703
$K^0_S K^- 2\pi^+ \pi^- \eta$	< 4.8 %	CL=90%	1570
$K^0_S K^- \pi^+ 2(\pi^+ \pi^-)$	< 1.22 %	CL=90%	1658
$K^0_S K^- \pi^+ 2\pi^0$	< 2.65 %	CL=90%	1742
$K^0_S K^- K^+ K^- \pi^+$	$< 4.9 \times 10^{-3}$	CL=90%	1490
$K^0_S K^- K^+ K^- \pi^+ \pi^0$	< 3.0 %	CL=90%	1427
$K^0_S K^- K^+ K^- \pi^+ \eta$	< 2.2 %	CL=90%	1214
$K^{*0} K^- \pi^+ +$ c.c.	$< 9.7 \times 10^{-3}$	CL=90%	1722
$p\overline{p}\pi^0$	$< 4 \times 10^{-5}$	CL=90%	1595
$p\overline{p}\pi^+ \pi^-$	$< 5.8 \times 10^{-4}$	CL=90%	1544
$\Lambda\overline{\Lambda}$	$< 1.2 \times 10^{-4}$	CL=90%	1521
$p\overline{p}\pi^+ \pi^- \pi^0$	$< 1.85 \times 10^{-3}$	CL=90%	1490
$\omega p\overline{p}$	$< 2.9 \times 10^{-4}$	CL=90%	1309
$\Lambda\overline{\Lambda}\pi^0$	$< 7 \times 10^{-5}$	CL=90%	1468
$p\overline{p}2(\pi^+ \pi^-)$	$< 2.6 \times 10^{-3}$	CL=90%	1425
$\eta p\overline{p}$	$< 5.4 \times 10^{-4}$	CL=90%	1430
$\eta p\overline{p}\pi^+ \pi^-$	$< 3.3 \times 10^{-3}$	CL=90%	1284
$\rho^0 p\overline{p}$	$< 1.7 \times 10^{-3}$	CL=90%	1313
$p\overline{p}K^+ K^-$	$< 3.2 \times 10^{-4}$	CL=90%	1185
$\eta p\overline{p}K^+ K^-$	$< 6.9 \times 10^{-3}$	CL=90%	736
$\pi^0 p\overline{p}K^+ K^-$	$< 1.2 \times 10^{-3}$	CL=90%	1093
$\phi p\overline{p}$	$< 1.3 \times 10^{-4}$	CL=90%	1178
$\Lambda\overline{\Lambda}\pi^+ \pi^-$	$< 2.5 \times 10^{-4}$	CL=90%	1404
$\Lambda\overline{p}K^+$	$< 2.8 \times 10^{-4}$	CL=90%	1387
$\Lambda\overline{p}K^+ \pi^+ \pi^-$	$< 6.3 \times 10^{-4}$	CL=90%	1234
$\Lambda\overline{\Lambda}\eta$	$< 1.9 \times 10^{-4}$	CL=90%	1262
$\Sigma^+ \overline{\Sigma}^-$	$< 1.0 \times 10^{-4}$	CL=90%	1464
$\Sigma^0 \overline{\Sigma}^0$	$< 4 \times 10^{-5}$	CL=90%	1462
$\Xi^+ \overline{\Xi}^-$	$< 1.5 \times 10^{-4}$	CL=90%	1346
$\Xi^0 \overline{\Xi}^0$	$< 1.4 \times 10^{-4}$	CL=90%	1353
Radiative decays			
$\gamma\chi_{c2}$	$< 6.4 \times 10^{-4}$	CL=90%	211
$\gamma\chi_{c1}$	$(2.49 \pm 0.23) \times 10^{-3}$		253
$\gamma\chi_{c0}$	$(6.9 \pm 0.6) \times 10^{-3}$		341
$\gamma\eta_c$	$< 7 \times 10^{-4}$	CL=90%	707
$\gamma\eta_c(2S)$	$< 9 \times 10^{-4}$	CL=90%	133
$\gamma\eta'$	$< 1.8 \times 10^{-4}$	CL=90%	1765
$\gamma\eta$	$< 1.5 \times 10^{-4}$	CL=90%	1847
$\gamma\pi^0$	$< 2 \times 10^{-4}$	CL=90%	1884

$\psi_2(3823)$

$I^G(J^{PC}) = 0^-(2^{--})$
I, J, P need confirmation.

Mass $m = 3822.2 \pm 1.2$ MeV
Full width $\Gamma < 16$ MeV, CL = 90%

$\psi_2(3823)$ DECAY MODES	Fraction (Γ_i/Γ)	p (MeV/c)
$\chi_{c1}\gamma$	seen	299
$\chi_{c2}\gamma$	not seen	257

$\chi_{c1}(3872)$

$I^G(J^{PC}) = 0^+(1^{++})$

Mass $m = 3871.69 \pm 0.17$ MeV
$m_{\chi_{c1}(3872)} - m_{J/\psi} = 775 \pm 4$ MeV
Full width $\Gamma < 1.2$ MeV, CL = 90%

$\chi_{c1}(3872)$ DECAY MODES	Fraction (Γ_i/Γ)	p (MeV/c)
$\pi^+\pi^- J/\psi(1S)$	> 3.2 %	650
$\omega J/\psi(1S)$	> 2.3 %	†
$D^0\overline{D}^0\pi^0$	>40 %	117
$\overline{D}^{*0}D^0$	>30 %	3
$\gamma J/\psi$	$> 7 \times 10^{-3}$	697
$\gamma\psi(2S)$	> 4 %	181
$\pi^+\pi^-\eta_c(1S)$	not seen	746
$\pi^+\pi^-\chi_{c1}$	not seen	218
$p\overline{p}$	not seen	1693

$Z_c(3900)$

$I^G(J^{PC}) = 1^+(1^{+-})$

Mass $m = 3886.6 \pm 2.4$ MeV (S = 1.6)
Full width $\Gamma = 28.2 \pm 2.6$ MeV

$Z_c(3900)$ DECAY MODES	Fraction (Γ_i/Γ)	p (MeV/c)
$J/\psi\pi$	seen	699
$h_c\pi^\pm$	not seen	318
$\eta_c\pi^+\pi^-$	not seen	758
$(D\overline{D}^*)^\pm$	seen	–
D^0D^{*-} + c.c.	seen	150
D^-D^{*0} + c.c.	seen	140
$\omega\pi^\pm$	not seen	1862
$J/\psi\eta$	not seen	509
D^+D^{*-} + c.c	seen	–
$D^0\overline{D}^{*0}$ + c.c	seen	–

$X(3915)$

$I^G(J^{PC}) = 0^+(0 \text{ or } 2^{++})$

Mass $m = 3918.4 \pm 1.9$ MeV
Full width $\Gamma = 20 \pm 5$ MeV (S = 1.1)

$X(3915)$ DECAY MODES	Fraction (Γ_i/Γ)	p (MeV/c)
$\omega J/\psi$	seen	222
$\pi^+\pi^-\eta_c(1S)$	not seen	785
$\eta_c\eta$	not seen	665
$\eta_c\pi^0$	not seen	814
$K\overline{K}$	not seen	1896
$\gamma\gamma$	seen	1959

$\chi_{c2}(3930)$

$I^G(J^{PC}) = 0^+(2^{++})$

Mass $m = 3927.2 \pm 2.6$ MeV
Full width $\Gamma = 24 \pm 6$ MeV

$\chi_{c2}(3930)$ DECAY MODES	Fraction (Γ_i/Γ)	p (MeV/c)
$\gamma\gamma$	seen	1964
$D\overline{D}$	seen	615
D^+D^-	seen	600
$D^0\overline{D}^0$	seen	615
$\pi^+\pi^-\eta_c(1S)$	not seen	792
$K\overline{K}$	not seen	1901

$X(4020)$

$I^G(J^{PC}) = 1^+(?^{?-})$

Mass $m = 4024.1 \pm 1.9$ MeV
Full width $\Gamma = 13 \pm 5$ MeV (S = 1.7)

$X(4020)$ DECAY MODES	Fraction (Γ_i/Γ)	p (MeV/c)
$h_c(1P)\pi$	seen	450
$D^*\overline{D}^*$	seen	85
$D\overline{D}^*$ + c.c.	not seen	542
$\eta_c\pi^+\pi^-$	not seen	872
$J/\psi(1S)\pi^\pm$	not seen	811

$\psi(4040)$ [xxaa]

$I^G(J^{PC}) = 0^-(1^{--})$

Mass $m = 4039 \pm 1$ MeV
Full width $\Gamma = 80 \pm 10$ MeV
$\Gamma_{ee} = 0.86 \pm 0.07$ keV
$\Gamma_{ee} < 2.9$ eV, CL = 90%
$\Gamma_{ee} < 4.6$ eV, CL = 90%

Due to the complexity of the $c\overline{c}$ threshold region, in this listing, "seen" ("not seen") means that a cross section for the mode in question has been measured at effective $\sqrt{s}$ near this particle's central mass value, more (less) than 2σ above zero, without regard to any peaking behavior in $\sqrt{s}$ or absence thereof. See mode listing(s) for details and references.

$\psi(4040)$ DECAY MODES	Fraction (Γ_i/Γ)	Confidence level	p (MeV/c)
e^+e^-	$(1.07 \pm 0.16) \times 10^{-5}$		2019
$D\overline{D}$	seen		775
$D^0\overline{D}^0$	seen		775
D^+D^-	seen		763
$D^*\overline{D}$ + c.c.	seen		569
$D^*(2007)^0\overline{D}^0$ + c.c.	seen		575
$D^*(2010)^+D^-$ + c.c.	seen		561
$D^*\overline{D}^*$	seen		193
$D^*(2007)^0\overline{D}^*(2007)^0$	seen		226
$D^*(2010)^+D^*(2010)^-$	seen		193
$D^0D^-\pi^+$ +c.c. (excl. $D^*(2007)^0\overline{D}^0$ +c.c., $D^*(2010)^+D^-$ +c.c.)	not seen		–
$D\overline{D}^*\pi$ (excl. $D^*\overline{D}^*$)	not seen		–
$D^0\overline{D}^{*-}\pi^+$ +c.c. (excl. $D^*(2010)^+D^*(2010)^-$)	seen		–
$D_s^+D_s^-$	seen		452
$J/\psi\pi^+\pi^-$	$< 4 \times 10^{-3}$	90%	794
$J/\psi\pi^0\pi^0$	$< 2 \times 10^{-3}$	90%	797
$J/\psi\eta$	$(5.2 \pm 0.7) \times 10^{-3}$		675
$J/\psi\pi^0$	$< 2.8 \times 10^{-4}$	90%	823
$J/\psi\pi^+\pi^-\pi^0$	$< 2 \times 10^{-3}$	90%	746
$\chi_{c1}\gamma$	$< 3.4 \times 10^{-3}$	90%	494
$\chi_{c2}\gamma$	$< 5 \times 10^{-3}$	90%	454
$\chi_{c1}\pi^+\pi^-\pi^0$	< 1.1 %	90%	306
$\chi_{c2}\pi^+\pi^-\pi^0$	< 3.2 %	90%	233
$h_c(1P)\pi^+\pi^-$	$< 3 \times 10^{-3}$	90%	403
$\phi\pi^+\pi^-$	$< 3 \times 10^{-3}$	90%	1880
$\Lambda\overline{\Lambda}\pi^+\pi^-$	$< 2.9 \times 10^{-4}$	90%	1578
$\Lambda\overline{\Lambda}\pi^0$	$< 9 \times 10^{-5}$	90%	1636
$\Lambda\overline{\Lambda}\eta$	$< 3.0 \times 10^{-4}$	90%	1452
$\Sigma^+\overline{\Sigma}^-$	$< 1.3 \times 10^{-4}$	90%	1632
$\Sigma^0\overline{\Sigma}^0$	$< 7 \times 10^{-5}$	90%	1630
$\Xi^+\overline{\Xi}^-$	$< 1.6 \times 10^{-4}$	90%	1527
$\Xi^0\overline{\Xi}^0$	$< 1.8 \times 10^{-4}$	90%	1533

$\chi_{c1}(4140)$

$I^G(J^{PC}) = 0^+(1^{++})$

Mass $m = 4146.8 \pm 2.4$ MeV (S = 1.1)
Full width $\Gamma = 22^{+8}_{-7}$ MeV (S = 1.3)

$\chi_{c1}(4140)$ DECAY MODES	Fraction (Γ_i/Γ)	p (MeV/c)
$J/\psi\phi$	seen	217
$\gamma\gamma$	not seen	2073

Meson Summary Table

$\psi(4160)$ [xxaa]

$I^G(J^{PC}) = 0^-(1^{--})$

Mass $m = 4191 \pm 5$ MeV
Full width $\Gamma = 70 \pm 10$ MeV
$\Gamma_{ee} = 0.48 \pm 0.22$ keV
$\Gamma_{ee} < 2.2$ eV, CL = 90%

Due to the complexity of the $c\overline{c}$ threshold region, in this listing, "seen" ("not seen") means that a cross section for the mode in question has been measured at effective $\sqrt{s}$ near this particle's central mass value, more (less) than 2σ above zero, without regard to any peaking behavior in $\sqrt{s}$ or absence thereof. See mode listing(s) for details and references.

$\psi(4160)$ DECAY MODES	Fraction (Γ_i/Γ)	Confidence level	p (MeV/c)
$e^+ e^-$	$(6.9 \pm 3.3) \times 10^{-6}$		2096
$\mu^+ \mu^-$	seen		2093
$D\overline{D}$	seen		956
$D^0 \overline{D}^0$	seen		956
$D^+ D^-$	seen		947
$D^* \overline{D}$ + c.c.	seen		798
$D^*(2007)^0 \overline{D}^0$ + c.c.	seen		802
$D^*(2010)^+ D^-$ + c.c.	seen		792
$D^* \overline{D}^*$	seen		592
$D^*(2007)^0 \overline{D}^*(2007)^0$	seen		604
$D^*(2010)^+ D^*(2010)^-$	seen		592
$D^0 D^- \pi^+$ + c.c. (excl. $D^*(2007)^0 \overline{D}^0$ + c.c., $D^*(2010)^+ D^-$ + c.c.)	not seen		–
$D\overline{D}^* \pi$ + c.c. (excl. $D^* \overline{D}^*$)	seen		–
$D^0 D^{*-} \pi^+$ + c.c. (excl. $D^*(2010)^+ D^*(2010)^-$)	not seen		–
$D_s^+ D_s^-$	not seen		719
$D_s^{*+} D_s^-$ + c.c.	seen		385
$J/\psi \pi^+ \pi^-$	$< 3 \times 10^{-3}$	90%	919
$J/\psi \pi^0 \pi^0$	$< 3 \times 10^{-3}$	90%	922
$J/\psi K^+ K^-$	$< 2 \times 10^{-3}$	90%	407
$J/\psi \eta$	$< 8 \times 10^{-3}$	90%	822
$J/\psi \pi^0$	$< 1 \times 10^{-3}$	90%	944
$J/\psi \eta'$	$< 5 \times 10^{-3}$	90%	457
$J/\psi \pi^+ \pi^- \pi^0$	$< 1 \times 10^{-3}$	90%	879
$\psi(2S) \pi^+ \pi^-$	$< 4 \times 10^{-3}$	90%	396
$\chi_{c1} \gamma$	$< 5 \times 10^{-3}$	90%	625
$\chi_{c2} \gamma$	< 1.3 %	90%	587
$\chi_{c1} \pi^+ \pi^- \pi^0$	$< 2 \times 10^{-3}$	90%	496
$\chi_{c2} \pi^+ \pi^- \pi^0$	$< 8 \times 10^{-3}$	90%	445
$h_c(1P) \pi^+ \pi^-$	$< 5 \times 10^{-3}$	90%	556
$h_c(1P) \pi^0 \pi^0$	$< 2 \times 10^{-3}$	90%	560
$h_c(1P) \eta$	$< 2 \times 10^{-3}$	90%	348
$h_c(1P) \pi^0$	$< 4 \times 10^{-4}$	90%	600
$\phi \pi^+ \pi^-$	$< 2 \times 10^{-3}$	90%	1961
$\gamma \chi_{c1}(3872) \rightarrow \gamma J/\psi \pi^+ \pi^-$	$< 6.8 \times 10^{-5}$	90%	–
$\gamma X(3915) \rightarrow \gamma J/\psi \pi^+ \pi^-$	$< 1.36 \times 10^{-4}$	90%	–
$\gamma X(3930) \rightarrow \gamma J/\psi \pi^+ \pi^-$	$< 1.18 \times 10^{-4}$	90%	–
$\gamma X(3940) \rightarrow \gamma J/\psi \pi^+ \pi^-$	$< 1.47 \times 10^{-4}$	90%	–
$\gamma \chi_{c1}(3872) \rightarrow \gamma\gamma J/\psi$	$< 1.05 \times 10^{-4}$	90%	–
$\gamma X(3915) \rightarrow \gamma\gamma J/\psi$	$< 1.26 \times 10^{-4}$	90%	–
$\gamma X(3930) \rightarrow \gamma\gamma J/\psi$	$< 8.8 \times 10^{-5}$	90%	–
$\gamma X(3940) \rightarrow \gamma\gamma J/\psi$	$< 1.79 \times 10^{-4}$	90%	–

$\psi(4260)$

$I^G(J^{PC}) = 0^-(1^{--})$

Mass $m = 4230 \pm 8$ MeV (S = 2.9)
Full width $\Gamma = 55 \pm 19$ MeV (S = 4.4)

$\psi(4260)$ DECAY MODES	Fraction (Γ_i/Γ)	p (MeV/c)
$J/\psi \pi^+ \pi^-$	seen	950
$J/\psi f_0(980)$, $f_0(980) \rightarrow \pi^+ \pi^-$	seen	–
$Z_c(3900)^\pm \pi^\mp$, $Z_c^\pm \rightarrow J/\psi \pi^\pm$	seen	–
$J/\psi \pi^0 \pi^0$	seen	952
$J/\psi K^+ K^-$	seen	477
$J/\psi K_S^0 K_S^0$	not seen	465
$J/\psi \eta$	not seen	857
$J/\psi \pi^0$	not seen	974
$J/\psi \eta'$	not seen	520
$J/\psi \pi^+ \pi^- \pi^0$	not seen	912
$J/\psi \eta \pi^0$	not seen	780
$J/\psi \eta \eta$	not seen	247
$\psi(2S) \pi^+ \pi^-$	not seen	437
$\psi(2S) \eta$	not seen	†
$\chi_{c0} \omega$	not seen	205
$\chi_{c1} \pi^+ \pi^- \pi^0$	not seen	537
$\chi_{c2} \pi^+ \pi^- \pi^0$	not seen	489
$h_c(1P) \pi^+ \pi^-$	not seen	593
$\phi \pi^+ \pi^-$	not seen	1982
$\phi f_0(980) \rightarrow \phi \pi^+ \pi^-$	not seen	–
$D\overline{D}$	not seen	998
$D^0 \overline{D}^0$	not seen	998
$D^+ D^-$	not seen	989
$D^* \overline{D}$ + c.c.	not seen	887
$D^*(2007)^0 \overline{D}^0$ + c.c.	not seen	–
$D^*(2010)^+ D^-$ + c.c.	not seen	–
$D^* \overline{D}^*$	not seen	657
$D^*(2007)^0 \overline{D}^*(2007)^0$	not seen	668
$D^*(2010)^+ D^*(2010)^-$	not seen	657
$D^0 D^- \pi^+$ + c.c. (excl. $D^*(2007)^0 \overline{D}^{*0}$ + c.c., $D^*(2010)^+ D^-$ + c.c.)	not seen	–
$D\overline{D}^* \pi$ + c.c. (excl. $D^* \overline{D}^*$)	not seen	723
$D^0 D^{*-} \pi^+$ + c.c. (excl. $D^*(2010)^+ D^*(2010)^-$)	not seen	–
$D^0 D^*(2010)^- \pi^+$ + c.c.	not seen	716
$D^* \overline{D}^* \pi$	not seen	395
$D_s^+ D_s^-$	not seen	774
$D_s^{*+} D_s^-$ + c.c.	not seen	615
$D_s^{*+} D_s^{*-}$	not seen	109
$p\overline{p}$	not seen	1896
$p\overline{p} \pi^0$	not seen	1860
$K_S^0 K^\pm \pi^\mp$	not seen	2037
$K^+ K^- \pi^0$	not seen	2038
Radiative decays		
$\eta_c(1S) \gamma$	possibly seen	1063
$\chi_{c1} \gamma$	not seen	658
$\chi_{c2} \gamma$	not seen	620
$\chi_{c1}(3872) \gamma$	seen	343

$\chi_{c1}(4274)$

$I^G(J^{PC}) = 0^+(1^{++})$

Mass $m = 4274^{+8}_{-6}$ MeV
Full width $\Gamma = 49 \pm 12$ MeV

$\chi_{c1}(4274)$ DECAY MODES	Fraction (Γ_i/Γ)	p (MeV/c)
$J/\psi \phi$	seen	503

$\psi(4360)$

$I^G(J^{PC}) = 0^-(1^{--})$
I needs confirmation.

$\psi(4360)$ MASS = 4368 ± 13 MeV (S = 3.7)
$\psi(4360)$ WIDTH = 96 ± 7 MeV
$\Gamma_{ee} < 0.57$ eV, CL = 90%
$\Gamma_{ee} < 1.9$ eV, CL = 90%

$\psi(4360)$ DECAY MODES	Fraction (Γ_i/Γ)	p (MeV/c)
$\psi(2S) \pi^+ \pi^-$	seen	573
$\psi_2(3823) \pi^+ \pi^-$	possibly seen	440

$\psi(4415)$ [xxaa]

$I^G(J^{PC}) = 0^-(1^{--})$

Mass $m = 4421 \pm 4$ MeV
Full width $\Gamma = 62 \pm 20$ MeV
$\Gamma_{ee} = 0.58 \pm 0.07$ keV
$\Gamma_{ee} < 3.6$ eV, CL = 90%
$\Gamma_{ee} < 0.47$ eV, CL = 90%
$\Gamma_{ee} < 2.3$ eV, CL = 90%

Due to the complexity of the $c\overline{c}$ threshold region, in this listing, "seen" ("not seen") means that a cross section for the mode in question has been measured at effective $\sqrt{s}$ near this particle's central mass value, more (less) than 2σ above zero, without regard to any peaking behavior in $\sqrt{s}$ or absence thereof. See mode listing(s) for details and references.

$\psi(4415)$ DECAY MODES	Fraction (Γ_i/Γ)	Confidence level	p (MeV/c)
$D\overline{D}$	seen		1187
$D^0\overline{D}^0$	seen		1187
D^+D^-	seen		1179
$D^*\overline{D}$ + c.c.	seen		1063
$D^*(2007)^0\overline{D}^0$ + c.c.	seen		1067
$D^*(2010)^+D^-$ + c.c.	seen		1059
$D^*\overline{D}^*$	seen		919
$D^*(2007)^0\overline{D}^*(2007)^0$ + c.c.	seen		927
$D^*(2010)^+D^*(2010)^-$ + c.c.	seen		919
$D^0D^-\pi^+$ (excl. $D^*(2007)^0\overline{D}^0$ +c.c., $D^*(2010)^+D^-$ +c.c.	< 2.3 %	90%	–
$D\overline{D}_2^*(2460) \to D^0D^-\pi^+$ +c.c.	(10 ±4) %		–
$D^0D^{*-}\pi^+$ +c.c.	< 11 %	90%	926
$D_s^+D_s^-$	not seen		1006
$\omega\chi_{c2}$	possibly seen		330
$D_s^{*+}D_s^-$ +c.c.	seen		–
$D_s^{*+}D_s^{*-}$	not seen		652
$\psi_2(3823)\pi^+\pi^-$	possibly seen		494
$J/\psi\eta$	$< 6 \times 10^{-3}$	90%	1022
$\chi_{c1}\gamma$	$< 8 \times 10^{-4}$	90%	817
$\chi_{c2}\gamma$	$< 4 \times 10^{-3}$	90%	780
e^+e^-	$(9.4\pm3.2)\times10^{-6}$		2210

$Z_c(4430)$

$I^G(J^{PC}) = 1^+(1^{+-})$
I, *G*, *C* need confirmation.

Quantum numbers not established.

Mass $m = 4478^{+15}_{-18}$ MeV
Full width $\Gamma = 181 \pm 31$ MeV

$Z_c(4430)$ DECAY MODES	Fraction (Γ_i/Γ)	p (MeV/c)
$\pi^+\psi(2S)$	seen	711
π^+J/ψ	seen	1162

$\psi(4660)$

$I^G(J^{PC}) = 0^-(1^{--})$
I needs confirmation.

$\psi(4660)$ MASS $= 4643 \pm 9$ MeV (S = 1.2)
$\psi(4660)$ WIDTH $= 72 \pm 11$ MeV
$\Gamma_{ee} < 0.45$ eV, CL = 90%
$\Gamma_{ee} < 2.1$ eV, CL = 90%

$\psi(4660)$ DECAY MODES	Fraction (Γ_i/Γ)	p (MeV/c)
$\psi(2S)\pi^+\pi^-$	seen	820

$b\overline{b}$ MESONS (including possibly non-$q\overline{q}$ states)

$\eta_b(1S)$

$I^G(J^{PC}) = 0^+(0^{-+})$

Mass $m = 9399.0 \pm 2.3$ MeV (S = 1.6)
Full width $\Gamma = 10^{+5}_{-4}$ MeV

$\eta_b(1S)$ DECAY MODES	Fraction (Γ_i/Γ)	Confidence level	p (MeV/c)
hadrons	seen		–
$3h^+3h^-$	not seen		4673
$2h^+2h^-$	not seen		4689
$\gamma\gamma$	not seen		4700
$\mu^+\mu^-$	$<9\times10^{-3}$	90%	4698
$\tau^+\tau^-$	<8 %	90%	4351

$\Upsilon(1S)$

$I^G(J^{PC}) = 0^-(1^{--})$

Mass $m = 9460.30 \pm 0.26$ MeV (S = 3.3)
Full width $\Gamma = 54.02 \pm 1.25$ keV
$\Gamma_{ee} = 1.340 \pm 0.018$ keV

$\Upsilon(1S)$ DECAY MODES	Fraction (Γ_i/Γ)	Scale factor/ Confidence level	p (MeV/c)
$\tau^+\tau^-$	(2.60 ±0.10) %		4384
e^+e^-	(2.38 ±0.11) %		4730
$\mu^+\mu^-$	(2.48 ±0.05) %		4729
Hadronic decays			
ggg	(81.7 ±0.7) %		–
γgg	(2.2 ±0.6) %		–
$\eta'(958)$ anything	(2.94 ±0.24) %		–
$J/\psi(1S)$ anything	(5.4 ±0.4) $\times10^{-4}$	S=1.4	4223
$J/\psi(1S)\eta_c$	< 2.2 $\times10^{-6}$	CL=90%	3623
$J/\psi(1S)\chi_{c0}$	< 3.4 $\times10^{-6}$	CL=90%	3429
$J/\psi(1S)\chi_{c1}$	(3.9 ±1.2) $\times10^{-6}$		3382
$J/\psi(1S)\chi_{c2}$	< 1.4 $\times10^{-6}$	CL=90%	3359
$J/\psi(1S)\eta_c(2S)$	< 2.2 $\times10^{-6}$	CL=90%	3317
$J/\psi(1S)X(3940)$	< 5.4 $\times10^{-6}$	CL=90%	3148
$J/\psi(1S)X(4160)$	< 5.4 $\times10^{-6}$	CL=90%	3018
$X(4350)$ anything, $X \to J/\psi(1S)\phi$	< 8.1 $\times10^{-6}$	CL=90%	–
$Z_c(3900)^\pm$ anything, $Z_c \to J/\psi(1S)\pi^\pm$	< 1.3 $\times10^{-5}$	CL=90%	–
$Z_c(4200)^\pm$ anything, $Z_c \to J/\psi(1S)\pi^\pm$	< 6.0 $\times10^{-5}$	CL=90%	–
$Z_c(4430)^\pm$ anything, $Z_c \to J/\psi(1S)\pi^\pm$	< 4.9 $\times10^{-5}$	CL=90%	–
$X_{cs}^\pm$ anything, $X \to J/\psi K^\pm$	< 5.7 $\times10^{-6}$	CL=90%	–
$\chi_{c1}(3872)$ anything, $\chi_{c1} \to J/\psi(1S)\pi^+\pi^-$	< 9.5 $\times10^{-6}$	CL=90%	–
$\psi(4260)$ anything, $\psi \to J/\psi(1S)\pi^+\pi^-$	< 3.8 $\times10^{-5}$	CL=90%	–
$\psi(4260)$ anything, $\psi \to J/\psi(1S)K^+K^-$	< 7.5 $\times10^{-6}$	CL=90%	–
$\chi_{c1}(4140)$ anything, $\chi_{c1} \to J/\psi(1S)\phi$	< 5.2 $\times10^{-6}$	CL=90%	–
χ_{c0} anything	< 4 $\times10^{-3}$	CL=90%	–
χ_{c1} anything	(1.90 ±0.35) $\times10^{-4}$		–
$\chi_{c1}(1P)X_{tetra}$	< 3.78 $\times10^{-5}$	CL=90%	–
χ_{c2} anything	(2.8 ±0.8) $\times10^{-4}$		–
$\psi(2S)$ anything	(1.23 ±0.20) $\times10^{-4}$		–
$\psi(2S)\eta_c$	< 3.6 $\times10^{-6}$	CL=90%	3345
$\psi(2S)\chi_{c0}$	< 6.5 $\times10^{-6}$	CL=90%	3124
$\psi(2S)\chi_{c1}$	< 4.5 $\times10^{-6}$	CL=90%	3070
$\psi(2S)\chi_{c2}$	< 2.1 $\times10^{-6}$	CL=90%	3043
$\psi(2S)\eta_c(2S)$	< 3.2 $\times10^{-6}$	CL=90%	2994
$\psi(2S)X(3940)$	< 2.9 $\times10^{-6}$	CL=90%	2797
$\psi(2S)X(4160)$	< 2.9 $\times10^{-6}$	CL=90%	2642
$\psi(4260)$ anything, $\psi \to \psi(2S)\pi^+\pi^-$	< 7.9 $\times10^{-5}$	CL=90%	–
$\psi(4360)$ anything, $\psi \to \psi(2S)\pi^+\pi^-$	< 5.2 $\times10^{-5}$	CL=90%	–
$\psi(4660)$ anything, $\psi \to \psi(2S)\pi^+\pi^-$	< 2.2 $\times10^{-5}$	CL=90%	–
$X(4050)^\pm$ anything, $X \to \psi(2S)\pi^\pm$	< 8.8 $\times10^{-5}$	CL=90%	–
$Z_c(4430)^\pm$ anything, $Z_c \to \psi(2S)\pi^\pm$	< 6.7 $\times10^{-5}$	CL=90%	–
$\rho\pi$	< 3.68 $\times10^{-6}$	CL=90%	4697
$\omega\pi^0$	< 3.90 $\times10^{-6}$	CL=90%	4697
$\pi^+\pi^-$	< 5 $\times10^{-4}$	CL=90%	4728
K^+K^-	< 5 $\times10^{-4}$	CL=90%	4704
$p\overline{p}$	< 5 $\times10^{-4}$	CL=90%	4636
$\pi^+\pi^-\pi^0$	(2.1 ±0.8) $\times10^{-6}$		4725
ϕK^+K^-	(2.4 ±0.5) $\times10^{-6}$		4622
$\omega\pi^+\pi^-$	(4.5 ±1.0) $\times10^{-6}$		4694
$K^*(892)^0K^-\pi^+$ + c.c.	(4.4 ±0.8) $\times10^{-6}$		4667
$\phi f_2'(1525)$	< 1.63 $\times10^{-6}$	CL=90%	4549
$\omega f_2(1270)$	< 1.79 $\times10^{-6}$	CL=90%	4611
$\rho(770)a_2(1320)$	< 2.24 $\times10^{-6}$	CL=90%	4605
$K^*(892)^0\overline{K}_2^*(1430)^0$ + c.c.	(3.0 ±0.8) $\times10^{-6}$		4579
$K_1(1270)^\pm K^\mp$	< 2.41 $\times10^{-6}$	CL=90%	4631
$K_1(1400)^\pm K^\mp$	(1.0 ±0.4) $\times10^{-6}$		4613
$b_1(1235)^\pm\pi^\mp$	< 1.25 $\times10^{-6}$	CL=90%	4649
$\pi^+\pi^-\pi^0\pi^0$	(1.28 ±0.30) $\times10^{-5}$		4720
$K_S^0K^+\pi^-$ + c.c.	(1.6 ±0.4) $\times10^{-6}$		4696
$K^*(892)^0\overline{K}^0$ + c.c.	(2.9 ±0.9) $\times10^{-6}$		4675

Meson Summary Table

$K^*(892)^- K^+ +$ c.c.		< 1.11	$\times 10^{-6}$	CL=90%	4675
$f_1(1285)$ anything		$(4.6 \pm 3.1) \times 10^{-3}$			–
$D^*(2010)^\pm$ anything		(2.52 ± 0.20) %			–
$f_1(1285) X_{tetra}$		< 6.24	$\times 10^{-5}$	CL=90%	–
^2H anything		$(2.85 \pm 0.25) \times 10^{-5}$			–
Sum of 100 exclusive modes		(1.200 ± 0.017) %			–

Radiative decays

$\gamma\pi^+\pi^-$		$(6.3 \pm 1.8) \times 10^{-5}$			4728
$\gamma\pi^0\pi^0$		$(1.7 \pm 0.7) \times 10^{-5}$			4728
$\gamma\pi^0\eta$		< 2.4	$\times 10^{-6}$	CL=90%	4713
$\gamma K^+ K^-$	[yyaa]	$(1.14 \pm 0.13) \times 10^{-5}$			4704
$\gamma p\overline{p}$	[zzaa]	< 6	$\times 10^{-6}$	CL=90%	4636
$\gamma 2h^+ 2h^-$		$(7.0 \pm 1.5) \times 10^{-4}$			4720
$\gamma 3h^+ 3h^-$		$(5.4 \pm 2.0) \times 10^{-4}$			4703
$\gamma 4h^+ 4h^-$		$(7.4 \pm 3.5) \times 10^{-4}$			4679
$\gamma\pi^+\pi^- K^+ K^-$		$(2.9 \pm 0.9) \times 10^{-4}$			4686
$\gamma 2\pi^+ 2\pi^-$		$(2.5 \pm 0.9) \times 10^{-4}$			4720
$\gamma 3\pi^+ 3\pi^-$		$(2.5 \pm 1.2) \times 10^{-4}$			4703
$\gamma 2\pi^+ 2\pi^- K^+ K^-$		$(2.4 \pm 1.2) \times 10^{-4}$			4658
$\gamma\pi^+\pi^- p\overline{p}$		$(1.5 \pm 0.6) \times 10^{-4}$			4604
$\gamma 2\pi^+ 2\pi^- p\overline{p}$		$(4 \pm 6) \times 10^{-5}$			4563
$\gamma 2K^+ 2K^-$		$(2.0 \pm 2.0) \times 10^{-5}$			4601
$\gamma\eta'(958)$		< 1.9	$\times 10^{-6}$	CL=90%	4682
$\gamma\eta$		< 1.0	$\times 10^{-6}$	CL=90%	4714
$\gamma f_0(980)$		< 3	$\times 10^{-5}$	CL=90%	4678
$\gamma f_2'(1525)$		$(3.8 \pm 0.9) \times 10^{-5}$			4607
$\gamma f_2(1270)$		$(1.01 \pm 0.09) \times 10^{-4}$			4644
$\gamma\eta(1405)$		< 8.2	$\times 10^{-5}$	CL=90%	4625
$\gamma f_0(1500)$		< 1.5	$\times 10^{-5}$	CL=90%	4611
$\gamma f_0(1710)$		< 2.6	$\times 10^{-4}$	CL=90%	4573
$\gamma f_0(1710) \to \gamma K^+ K^-$		< 7	$\times 10^{-6}$	CL=90%	–
$\gamma f_0(1710) \to \gamma\pi^0\pi^0$		< 1.4	$\times 10^{-6}$	CL=90%	–
$\gamma f_0(1710) \to \gamma\eta\eta$		< 1.8	$\times 10^{-6}$	CL=90%	–
$\gamma f_4(2050)$		< 5.3	$\times 10^{-5}$	CL=90%	4515
$\gamma f_0(2200) \to \gamma K^+ K^-$		< 2	$\times 10^{-4}$	CL=90%	4475
$\gamma f_J(2220) \to \gamma K^+ K^-$		< 8	$\times 10^{-7}$	CL=90%	4469
$\gamma f_J(2220) \to \gamma\pi^+\pi^-$		< 6	$\times 10^{-7}$	CL=90%	–
$\gamma f_J(2220) \to \gamma p\overline{p}$		< 1.1	$\times 10^{-6}$	CL=90%	–
$\gamma\eta(2225) \to \gamma\phi\phi$		< 3	$\times 10^{-3}$	CL=90%	4469
$\gamma\eta_c(1S)$		< 5.7	$\times 10^{-5}$	CL=90%	4260
$\gamma\chi_{c0}$		< 6.5	$\times 10^{-4}$	CL=90%	4114
$\gamma\chi_{c1}$		< 2.3	$\times 10^{-5}$	CL=90%	4079
$\gamma\chi_{c2}$		< 7.6	$\times 10^{-6}$	CL=90%	4062
$\gamma\chi_{c1}(3872) \to \pi^+\pi^- J/\psi$		< 1.6	$\times 10^{-6}$	CL=90%	–
$\gamma\chi_{c1}(3872) \to \pi^+\pi^-\pi^0 J/\psi$		< 2.8	$\times 10^{-6}$	CL=90%	–
$\gamma X(3915) \to \omega J/\psi$		< 3.0	$\times 10^{-6}$	CL=90%	–
$\gamma\chi_{c1}(4140) \to \phi J/\psi$		< 2.2	$\times 10^{-6}$	CL=90%	–
γX	[aabb]	< 4.5	$\times 10^{-6}$	CL=90%	–
$\gamma X\overline{X}(m_X < 3.1$ GeV)	[bbbb]	< 1	$\times 10^{-3}$	CL=90%	–
$\gamma X\overline{X}(m_X < 4.5$ GeV)	[ccbb]	< 2.4	$\times 10^{-4}$	CL=90%	–
$\gamma X \to \gamma +\geq 4$ prongs	[ddbb]	< 1.78	$\times 10^{-4}$	CL=95%	–
$\gamma a_1^0 \to \gamma\mu^+\mu^-$	[eebb]	< 9	$\times 10^{-6}$	CL=90%	–
$\gamma a_1^0 \to \gamma\tau^+\tau^-$	[yyaa]	< 1.30	$\times 10^{-4}$	CL=90%	–
$\gamma a_1^0 \to \gamma gg$	[ffbb]	< 1	%	CL=90%	–
$\gamma a_1^0 \to \gamma s\overline{s}$	[ffbb]	< 1	$\times 10^{-3}$	CL=90%	–

Lepton Family number (*LF*) violating modes

$\mu^\pm\tau^\mp$	*LF*	< 6.0	$\times 10^{-6}$	CL=95%	4563

Other decays

invisible		< 3.0	$\times 10^{-4}$	CL=90%	–

$\chi_{b0}(1P)$ [ggbb]

$I^G(J^{PC}) = 0^+(0^{++})$
J needs confirmation.

Mass $m = 9859.44 \pm 0.42 \pm 0.31$ MeV

$\chi_{b0}(1P)$ DECAY MODES	Fraction (Γ_i/Γ)	Confidence level	p (MeV/c)
$\gamma\Upsilon(1S)$	(1.94 ± 0.27) %		391
$D^0 X$	< 10.4 %	90%	–
$\pi^+\pi^- K^+ K^-\pi^0$	< 1.6 $\times 10^{-4}$	90%	4875
$2\pi^+\pi^- K^- K^0_S$	< 5 $\times 10^{-5}$	90%	4875
$2\pi^+\pi^- K^- K^0_S 2\pi^0$	< 5 $\times 10^{-4}$	90%	4846
$2\pi^+ 2\pi^- 2\pi^0$	< 2.1 $\times 10^{-4}$	90%	4905
$2\pi^+ 2\pi^- K^+ K^-$	$(1.1 \pm 0.6) \times 10^{-4}$		4861
$2\pi^+ 2\pi^- K^+ K^-\pi^0$	< 2.7 $\times 10^{-4}$	90%	4846
$2\pi^+ 2\pi^- K^+ K^- 2\pi^0$	< 5 $\times 10^{-4}$	90%	4828
$3\pi^+ 2\pi^- K^- K^0_S\pi^0$	< 1.6 $\times 10^{-4}$	90%	4827
$3\pi^+ 3\pi^-$	< 8 $\times 10^{-5}$	90%	4904
$3\pi^+ 3\pi^- 2\pi^0$	< 6 $\times 10^{-4}$	90%	4881
$3\pi^+ 3\pi^- K^+ K^-$	$(2.4 \pm 1.2) \times 10^{-4}$		4827
$3\pi^+ 3\pi^- K^+ K^-\pi^0$	< 1.0 $\times 10^{-3}$	90%	4808
$4\pi^+ 4\pi^-$	< 8 $\times 10^{-5}$	90%	4880
$4\pi^+ 4\pi^- 2\pi^0$	< 2.1 $\times 10^{-3}$	90%	4850
$J/\psi J/\psi$	< 7 $\times 10^{-5}$	90%	3836
$J/\psi\psi(2S)$	< 1.2 $\times 10^{-4}$	90%	3571
$\psi(2S)\psi(2S)$	< 3.1 $\times 10^{-5}$	90%	3273
$J/\psi(1S)$ anything	< 2.3 $\times 10^{-3}$	90%	–

$\chi_{b1}(1P)$ [ggbb]

$I^G(J^{PC}) = 0^+(1^{++})$
J needs confirmation.

Mass $m = 9892.78 \pm 0.26 \pm 0.31$ MeV

$\chi_{b1}(1P)$ DECAY MODES	Fraction (Γ_i/Γ)	Confidence level	p (MeV/c)
$\gamma\Upsilon(1S)$	(35.0 ± 2.1) %		423
$D^0 X$	(12.6 ± 2.2) %		–
$\pi^+\pi^- K^+ K^-\pi^0$	$(2.0 \pm 0.6) \times 10^{-4}$		4892
$2\pi^+\pi^- K^- K^0_S$	$(1.3 \pm 0.5) \times 10^{-4}$		4892
$2\pi^+\pi^- K^- K^0_S 2\pi^0$	< 6 $\times 10^{-4}$	90%	4863
$2\pi^+ 2\pi^- 2\pi^0$	$(8.0 \pm 2.5) \times 10^{-4}$		4921
$2\pi^+ 2\pi^- K^+ K^-$	$(1.5 \pm 0.5) \times 10^{-4}$		4878
$2\pi^+ 2\pi^- K^+ K^-\pi^0$	$(3.5 \pm 1.2) \times 10^{-4}$		4863
$2\pi^+ 2\pi^- K^+ K^- 2\pi^0$	$(8.6 \pm 3.2) \times 10^{-4}$		4845
$3\pi^+ 2\pi^- K^- K^0_S\pi^0$	$(9.3 \pm 3.3) \times 10^{-4}$		4844
$3\pi^+ 3\pi^-$	$(1.9 \pm 0.6) \times 10^{-4}$		4921
$3\pi^+ 3\pi^- 2\pi^0$	$(1.7 \pm 0.5) \times 10^{-3}$		4898
$3\pi^+ 3\pi^- K^+ K^-$	$(2.6 \pm 0.8) \times 10^{-4}$		4844
$3\pi^+ 3\pi^- K^+ K^-\pi^0$	$(7.5 \pm 2.6) \times 10^{-4}$		4825
$4\pi^+ 4\pi^-$	$(2.6 \pm 0.9) \times 10^{-4}$		4897
$4\pi^+ 4\pi^- 2\pi^0$	$(1.4 \pm 0.6) \times 10^{-3}$		4867
ω anything	(4.9 ± 1.4) %		–
ωX_{tetra}	< 4.44 $\times 10^{-4}$	90%	–
$J/\psi J/\psi$	< 2.7 $\times 10^{-5}$	90%	3857
$J/\psi\psi(2S)$	< 1.7 $\times 10^{-5}$	90%	3594
$\psi(2S)\psi(2S)$	< 6 $\times 10^{-5}$	90%	3298
$J/\psi(1S)$ anything	< 1.1 $\times 10^{-3}$	90%	–
$J/\psi(1S) X_{tetra}$	< 2.27 $\times 10^{-4}$	90%	–

$h_b(1P)$

$I^G(J^{PC}) = ?^?(1^{+-})$

Mass $m = 9899.3 \pm 0.8$ MeV

$h_b(1P)$ DECAY MODES	Fraction (Γ_i/Γ)	p (MeV/c)
$\eta_b(1S)\gamma$	(52^{+6}_{-5}) %	488

$\chi_{b2}(1P)$ [ggbb]

$I^G(J^{PC}) = 0^+(2^{++})$
J needs confirmation.

Mass $m = 9912.21 \pm 0.26 \pm 0.31$ MeV

$\chi_{b2}(1P)$ DECAY MODES	Fraction (Γ_i/Γ)	Confidence level	p (MeV/c)
$\gamma\Upsilon(1S)$	(18.8 ± 1.1) %		442
$D^0 X$	< 7.9 %	90%	–
$\pi^+\pi^- K^+ K^-\pi^0$	$(8 \pm 5) \times 10^{-5}$		4902
$2\pi^+\pi^- K^- K^0_S$	< 1.0 $\times 10^{-4}$	90%	4901
$2\pi^+\pi^- K^- K^0_S 2\pi^0$	$(5.3 \pm 2.4) \times 10^{-4}$		4873
$2\pi^+ 2\pi^- 2\pi^0$	$(3.5 \pm 1.4) \times 10^{-4}$		4931
$2\pi^+ 2\pi^- K^+ K^-$	$(1.1 \pm 0.4) \times 10^{-4}$		4888
$2\pi^+ 2\pi^- K^+ K^-\pi^0$	$(2.1 \pm 0.9) \times 10^{-4}$		4872
$2\pi^+ 2\pi^- K^+ K^- 2\pi^0$	$(3.9 \pm 1.8) \times 10^{-4}$		4855
$3\pi^+ 2\pi^- K^- K^0_S\pi^0$	< 5 $\times 10^{-4}$	90%	4854
$3\pi^+ 3\pi^-$	$(7.0 \pm 3.1) \times 10^{-5}$		4931
$3\pi^+ 3\pi^- 2\pi^0$	$(1.0 \pm 0.4) \times 10^{-3}$		4908
$3\pi^+ 3\pi^- K^+ K^-$	< 8 $\times 10^{-5}$	90%	4854
$3\pi^+ 3\pi^- K^+ K^-\pi^0$	$(3.6 \pm 1.5) \times 10^{-4}$		4835
$4\pi^+ 4\pi^-$	$(8 \pm 4) \times 10^{-5}$		4907
$4\pi^+ 4\pi^- 2\pi^0$	$(1.8 \pm 0.7) \times 10^{-3}$		4877
$J/\psi J/\psi$	< 4 $\times 10^{-5}$	90%	3869
$J/\psi\psi(2S)$	< 5 $\times 10^{-5}$	90%	3608

$\psi(2S)\psi(2S)$	$< 1.6 \times 10^{-5}$	90%	3313
$J/\psi(1S)$ anything	$(1.5 \pm 0.4) \times 10^{-3}$		–

$\Upsilon(2S)$

$I^G(J^{PC}) = 0^-(1^{--})$

Mass $m = 10023.26 \pm 0.31$ MeV
$m_{\Upsilon(3S)} - m_{\Upsilon(2S)} = 331.50 \pm 0.13$ MeV
Full width $\Gamma = 31.98 \pm 2.63$ keV
$\Gamma_{ee} = 0.612 \pm 0.011$ keV

$\Upsilon(2S)$ DECAY MODES	Fraction (Γ_i/Γ)	Scale factor/ Confidence level	p (MeV/c)
$\Upsilon(1S)\pi^+\pi^-$	(17.85 ± 0.26) %		475
$\Upsilon(1S)\pi^0\pi^0$	(8.6 ± 0.4) %		480
$\tau^+\tau^-$	(2.00 ± 0.21) %		4686
$\mu^+\mu^-$	(1.93 ± 0.17) %	S=2.2	5011
e^+e^-	(1.91 ± 0.16) %		5012
$\Upsilon(1S)\pi^0$	$< 4 \times 10^{-5}$	CL=90%	531
$\Upsilon(1S)\eta$	$(2.9 \pm 0.4) \times 10^{-4}$	S=2.0	126
$J/\psi(1S)$ anything	$< 6 \times 10^{-3}$	CL=90%	4533
$J/\psi(1S)\eta_c$	$< 5.4 \times 10^{-6}$	CL=90%	3984
$J/\psi(1S)\chi_{c0}$	$< 3.4 \times 10^{-6}$	CL=90%	3808
$J/\psi(1S)\chi_{c1}$	$< 1.2 \times 10^{-6}$	CL=90%	3765
$J/\psi(1S)\chi_{c2}$	$< 2.0 \times 10^{-6}$	CL=90%	3744
$J/\psi(1S)\eta_c(2S)$	$< 2.5 \times 10^{-6}$	CL=90%	3706
$J/\psi(1S)X(3940)$	$< 2.0 \times 10^{-6}$	CL=90%	3555
$J/\psi(1S)X(4160)$	$< 2.0 \times 10^{-6}$	CL=90%	3440
χ_{c1} anything	$(2.2 \pm 0.5) \times 10^{-4}$		–
$\chi_{c1}(1P)^0 X_{tetra}$	$< 3.67 \times 10^{-5}$	CL=90%	–
χ_{c2} anything	$(2.3 \pm 0.8) \times 10^{-4}$		–
$\psi(2S)\eta_c$	$< 5.1 \times 10^{-6}$	CL=90%	3732
$\psi(2S)\chi_{c0}$	$< 4.7 \times 10^{-6}$	CL=90%	3536
$\psi(2S)\chi_{c1}$	$< 2.5 \times 10^{-6}$	CL=90%	3488
$\psi(2S)\chi_{c2}$	$< 1.9 \times 10^{-6}$	CL=90%	3464
$\psi(2S)\eta_c(2S)$	$< 3.3 \times 10^{-6}$	CL=90%	3422
$\psi(2S)X(3940)$	$< 3.9 \times 10^{-6}$	CL=90%	3250
$\psi(2S)X(4160)$	$< 3.9 \times 10^{-6}$	CL=90%	3118
$\overline{^2H}$ anything	$(2.78^{+0.30}_{-0.26}) \times 10^{-5}$	S=1.2	–
hadrons	(94 ± 11) %		–
ggg	(58.8 ± 1.2) %		–
γgg	(1.87 ± 0.28) %		–
ϕK^+K^-	$(1.6 \pm 0.4) \times 10^{-6}$		4910
$\omega\pi^+\pi^-$	$< 2.58 \times 10^{-6}$	CL=90%	4977
$K^*(892)^0 K^-\pi^+ +$ c.c.	$(2.3 \pm 0.7) \times 10^{-6}$		4952
$\phi f_2'(1525)$	$< 1.33 \times 10^{-6}$	CL=90%	4841
$\omega f_2(1270)$	$< 5.7 \times 10^{-7}$	CL=90%	4899
$\rho(770)a_2(1320)$	$< 8.8 \times 10^{-7}$	CL=90%	4894
$K^*(892)^0\overline{K}_2^*(1430)^0 +$ c.c.	$(1.5 \pm 0.6) \times 10^{-6}$		4869
$K_1(1270)^\pm K^\mp$	$< 3.22 \times 10^{-6}$	CL=90%	4918
$K_1(1400)^\pm K^\mp$	$< 8.3 \times 10^{-7}$	CL=90%	4901
$b_1(1235)^\pm\pi^\mp$	$< 4.0 \times 10^{-7}$	CL=90%	4935
$\rho\pi$	$< 1.16 \times 10^{-6}$	CL=90%	4981
$\pi^+\pi^-\pi^0$	$< 8.0 \times 10^{-7}$	CL=90%	5007
$\omega\pi^0$	$< 1.63 \times 10^{-6}$	CL=90%	4980
$\pi^+\pi^-\pi^0\pi^0$	$(1.30 \pm 0.28) \times 10^{-5}$		5002
$K_S^0 K^+\pi^- +$ c.c.	$(1.14 \pm 0.33) \times 10^{-6}$		4979
$K^*(892)^0\overline{K}^0 +$ c.c.	$< 4.22 \times 10^{-6}$	CL=90%	4959
$K^*(892)^- K^+ +$ c.c.	$< 1.45 \times 10^{-6}$	CL=90%	4960
$f_1(1285)$ anything	$(2.2 \pm 1.6) \times 10^{-3}$		–
$f_1(1285)X_{tetra}$	$< 6.47 \times 10^{-5}$	CL=90%	–
Sum of 100 exclusive modes	$(2.90 \pm 0.30) \times 10^{-3}$		–
Radiative decays			
$\gamma\chi_{b1}(1P)$	(6.9 ± 0.4) %		130
$\gamma\chi_{b2}(1P)$	(7.15 ± 0.35) %		110
$\gamma\chi_{b0}(1P)$	(3.8 ± 0.4) %		162
$\gamma f_0(1710)$	$< 5.9 \times 10^{-4}$	CL=90%	4864
$\gamma f_2'(1525)$	$< 5.3 \times 10^{-4}$	CL=90%	4896
$\gamma f_2(1270)$	$< 2.41 \times 10^{-4}$	CL=90%	4930
$\gamma\eta_c(1S)$	$< 2.7 \times 10^{-5}$	CL=90%	4567
$\gamma\chi_{c0}$	$< 1.0 \times 10^{-4}$	CL=90%	4430
$\gamma\chi_{c1}$	$< 3.6 \times 10^{-6}$	CL=90%	4397
$\gamma\chi_{c2}$	$< 1.5 \times 10^{-5}$	CL=90%	4381
$\gamma\chi_{c1}(3872) \to \pi^+\pi^- J/\psi$	$< 8 \times 10^{-7}$	CL=90%	–
$\gamma\chi_{c1}(3872) \to \pi^+\pi^-\pi^0 J/\psi$	$< 2.4 \times 10^{-6}$	CL=90%	–
$\gamma X(3915) \to \omega J/\psi$	$< 2.8 \times 10^{-6}$	CL=90%	–
$\gamma\chi_{c1}(4140) \to \phi J/\psi$	$< 1.2 \times 10^{-6}$	CL=90%	–
$\gamma X(4350) \to \phi J/\psi$	$< 1.3 \times 10^{-6}$	CL=90%	–
$\gamma\eta_b(1S)$	$(3.9 \pm 1.5) \times 10^{-4}$		605
$\gamma\eta_b(1S) \to \gamma$Sum of 26 exclusive modes	$< 3.7 \times 10^{-6}$	CL=90%	–
$\gamma X_{b\overline{b}} \to \gamma$Sum of 26 exclusive modes	$< 4.9 \times 10^{-6}$	CL=90%	–
$\gamma X \to \gamma+ \geq 4$ prongs [hhbb]	$< 1.95 \times 10^{-4}$	CL=95%	–
$\gamma A^0 \to \gamma$hadrons	$< 8 \times 10^{-5}$	CL=90%	–
$\gamma a_1^0 \to \gamma\mu^+\mu^-$	$< 8.3 \times 10^{-6}$	CL=90%	–
Lepton Family number (LF) violating modes			
$e^\pm\tau^\mp$ LF	$< 3.2 \times 10^{-6}$	CL=90%	4854
$\mu^\pm\tau^\mp$ LF	$< 3.3 \times 10^{-6}$	CL=90%	4854

$\Upsilon_2(1D)$

$I^G(J^{PC}) = 0^-(2^{--})$

Mass $m = 10163.7 \pm 1.4$ MeV (S = 1.7)

$\Upsilon_2(1D)$ DECAY MODES	Fraction (Γ_i/Γ)	p (MeV/c)
$\gamma\gamma\,\Upsilon(1S)$	seen	679
$\gamma\chi_{bJ}(1P)$	seen	300
$\eta\,\Upsilon(1S)$	not seen	426
$\pi^+\pi^-\,\Upsilon(1S)$	$(6.6 \pm 1.6) \times 10^{-3}$	623

$\chi_{b0}(2P)$ [ggbb]

$I^G(J^{PC}) = 0^+(0^{++})$
J needs confirmation.

Mass $m = 10232.5 \pm 0.4 \pm 0.5$ MeV

$\chi_{b0}(2P)$ DECAY MODES	Fraction (Γ_i/Γ)	Confidence level	p (MeV/c)
$\gamma\,\Upsilon(2S)$	(1.38 ± 0.30) %		207
$\gamma\,\Upsilon(1S)$	$(3.8 \pm 1.7) \times 10^{-3}$		743
$D^0 X$	< 8.2 %	90%	–
$\pi^+\pi^- K^+K^-\pi^0$	$< 3.4 \times 10^{-5}$	90%	5064
$2\pi^+\pi^- K^- K_S^0$	$< 5 \times 10^{-5}$	90%	5063
$2\pi^+\pi^- K^- K_S^0 2\pi^0$	$< 2.2 \times 10^{-4}$	90%	5036
$2\pi^+ 2\pi^- 2\pi^0$	$< 2.4 \times 10^{-4}$	90%	5092
$2\pi^+ 2\pi^- K^+K^-$	$< 1.5 \times 10^{-4}$	90%	5050
$2\pi^+ 2\pi^- K^+K^-\pi^0$	$< 2.2 \times 10^{-4}$	90%	5035
$2\pi^+ 2\pi^- K^+K^- 2\pi^0$	$< 1.1 \times 10^{-3}$	90%	5019
$3\pi^+ 2\pi^- K^- K_S^0\pi^0$	$< 7 \times 10^{-4}$	90%	5018
$3\pi^+ 3\pi^-$	$< 7 \times 10^{-5}$	90%	5091
$3\pi^+ 3\pi^- 2\pi^0$	$< 1.2 \times 10^{-3}$	90%	5070
$3\pi^+ 3\pi^- K^+K^-$	$< 1.5 \times 10^{-4}$	90%	5017
$3\pi^+ 3\pi^- K^+K^-\pi^0$	$< 7 \times 10^{-4}$	90%	4999
$4\pi^+ 4\pi^-$	$< 1.7 \times 10^{-4}$	90%	5069
$4\pi^+ 4\pi^- 2\pi^0$	$< 6 \times 10^{-4}$	90%	5039

$\chi_{b1}(2P)$ [ggbb]

$I^G(J^{PC}) = 0^+(1^{++})$
J needs confirmation.

Mass $m = 10255.46 \pm 0.22 \pm 0.50$ MeV
$m_{\chi_{b1}(2P)} - m_{\chi_{b0}(2P)} = 23.5 \pm 1.0$ MeV

$\chi_{b1}(2P)$ DECAY MODES	Fraction (Γ_i/Γ)	p (MeV/c)
$\omega\,\Upsilon(1S)$	$(1.63^{+0.40}_{-0.34})$ %	135
$\gamma\,\Upsilon(2S)$	(18.1 ± 1.9) %	230
$\gamma\,\Upsilon(1S)$	(9.9 ± 1.0) %	764
$\pi\pi\chi_{b1}(1P)$	$(9.1 \pm 1.3) \times 10^{-3}$	238
$D^0 X$	(8.8 ± 1.7) %	–
$\pi^+\pi^- K^+K^-\pi^0$	$(3.1 \pm 1.0) \times 10^{-4}$	5075
$2\pi^+\pi^- K^- K_S^0$	$(1.1 \pm 0.5) \times 10^{-4}$	5075
$2\pi^+\pi^- K^- K_S^0 2\pi^0$	$(7.7 \pm 3.2) \times 10^{-4}$	5047
$2\pi^+ 2\pi^- 2\pi^0$	$(5.9 \pm 2.0) \times 10^{-4}$	5104
$2\pi^+ 2\pi^- K^+K^-$	$(10 \pm 4) \times 10^{-5}$	5062
$2\pi^+ 2\pi^- K^+K^-\pi^0$	$(5.5 \pm 1.8) \times 10^{-4}$	5047
$2\pi^+ 2\pi^- K^+K^- 2\pi^0$	$(10 \pm 4) \times 10^{-4}$	5030
$3\pi^+ 2\pi^- K^- K_S^0\pi^0$	$(6.7 \pm 2.6) \times 10^{-4}$	5029
$3\pi^+ 3\pi^-$	$(1.2 \pm 0.4) \times 10^{-4}$	5103
$3\pi^+ 3\pi^- 2\pi^0$	$(1.2 \pm 0.4) \times 10^{-3}$	5081
$3\pi^+ 3\pi^- K^+K^-$	$(2.0 \pm 0.8) \times 10^{-4}$	5029
$3\pi^+ 3\pi^- K^+K^-\pi^0$	$(6.1 \pm 2.2) \times 10^{-4}$	5011
$4\pi^+ 4\pi^-$	$(1.7 \pm 0.6) \times 10^{-4}$	5080
$4\pi^+ 4\pi^- 2\pi^0$	$(1.9 \pm 0.7) \times 10^{-3}$	5051

Meson Summary Table

$\chi_{b2}(2P)$ [ggbb]

$I^G(J^{PC}) = 0^+(2^{++})$
J needs confirmation.

Mass $m = 10268.65 \pm 0.22 \pm 0.50$ MeV
$m_{\chi_{b2}(2P)} - m_{\chi_{b1}(2P)} = 13.10 \pm 0.24$ MeV

$\chi_{b2}(2P)$ DECAY MODES	Fraction (Γ_i/Γ)	Confidence level	p (MeV/c)
$\omega\,\Upsilon(1S)$	$(1.10^{+0.34}_{-0.30})$ %		194
$\gamma\,\Upsilon(2S)$	(8.9 ±1.2) %		242
$\gamma\,\Upsilon(1S)$	(6.6 ±0.8) %		777
$\pi\pi\chi_{b2}(1P)$	(5.1 ±0.9) $\times 10^{-3}$		229
$D^0 X$	< 2.4 %	90%	–
$\pi^+\pi^- K^+ K^- \pi^0$	< 1.1 $\times 10^{-4}$	90%	5082
$2\pi^+\pi^- K^- K^0_S$	< 9 $\times 10^{-5}$	90%	5082
$2\pi^+\pi^- K^- K^0_S 2\pi^0$	< 7 $\times 10^{-4}$	90%	5054
$2\pi^+ 2\pi^- 2\pi^0$	(3.9 ±1.6) $\times 10^{-4}$		5110
$2\pi^+ 2\pi^- K^+ K^-$	(9 ±4) $\times 10^{-5}$		5068
$2\pi^+ 2\pi^- K^+ K^- \pi^0$	(2.4 ±1.1) $\times 10^{-4}$		5054
$2\pi^+ 2\pi^- K^+ K^- 2\pi^0$	(4.7 ±2.3) $\times 10^{-4}$		5037
$3\pi^+ 2\pi^- K^- K^0_S \pi^0$	< 4 $\times 10^{-4}$	90%	5036
$3\pi^+ 3\pi^-$	(9 ±4) $\times 10^{-5}$		5110
$3\pi^+ 3\pi^- 2\pi^0$	(1.2 ±0.4) $\times 10^{-3}$		5088
$3\pi^+ 3\pi^- K^+ K^-$	(1.4 ±0.7) $\times 10^{-4}$		5036
$3\pi^+ 3\pi^- K^+ K^- \pi^0$	(4.2 ±1.7) $\times 10^{-4}$		5017
$4\pi^+ 4\pi^-$	(9 ±5) $\times 10^{-5}$		5087
$4\pi^+ 4\pi^- 2\pi^0$	(1.3 ±0.5) $\times 10^{-3}$		5058

$\Upsilon(3S)$

$I^G(J^{PC}) = 0^-(1^{--})$

Mass $m = 10355.2 \pm 0.5$ MeV
$m_{\Upsilon(3S)} - m_{\Upsilon(2S)} = 331.50 \pm 0.13$ MeV
Full width $\Gamma = 20.32 \pm 1.85$ keV
$\Gamma_{ee} = 0.443 \pm 0.008$ keV

$\Upsilon(3S)$ DECAY MODES	Fraction (Γ_i/Γ)	Scale factor/ Confidence level	p (MeV/c)
$\Upsilon(2S)$ anything	(10.6 ± 0.8) %		296
$\Upsilon(2S)\pi^+\pi^-$	(2.82± 0.18) %	S=1.6	177
$\Upsilon(2S)\pi^0\pi^0$	(1.85± 0.14) %		190
$\Upsilon(2S)\gamma\gamma$	(5.0 ± 0.7) %		327
$\Upsilon(2S)\pi^0$	< 5.1 $\times 10^{-4}$	CL=90%	298
$\Upsilon(1S)\pi^+\pi^-$	(4.37± 0.08) %		813
$\Upsilon(1S)\pi^0\pi^0$	(2.20± 0.13) %		816
$\Upsilon(1S)\eta$	< 1 $\times 10^{-4}$	CL=90%	677
$\Upsilon(1S)\pi^0$	< 7 $\times 10^{-5}$	CL=90%	846
$h_b(1P)\pi^0$	< 1.2 $\times 10^{-3}$	CL=90%	426
$h_b(1P)\pi^0 \to \gamma\eta_b(1S)\pi^0$	(4.3 ± 1.4) $\times 10^{-4}$		–
$h_b(1P)\pi^+\pi^-$	< 1.2 $\times 10^{-4}$	CL=90%	353
$\tau^+\tau^-$	(2.29± 0.30) %		4863
$\mu^+\mu^-$	(2.18± 0.21) %	S=2.1	5177
e^+e^-	(2.18± 0.20) %		5178
hadrons	(93 ±12) %		–
ggg	(35.7 ± 2.6) %		–
γgg	(9.7 ± 1.8) $\times 10^{-3}$		–
^2H anything	(2.33± 0.33) $\times 10^{-5}$		–
Radiative decays			
$\gamma\chi_{b2}(2P)$	(13.1 ± 1.6) %	S=3.4	86
$\gamma\chi_{b1}(2P)$	(12.6 ± 1.2) %	S=2.4	99
$\gamma\chi_{b0}(2P)$	(5.9 ± 0.6) %	S=1.4	122
$\gamma\chi_{b2}(1P)$	(9.9 ± 1.2) $\times 10^{-3}$	S=1.9	434
$\gamma\chi_{b1}(1P)$	(9 ± 5) $\times 10^{-4}$	S=1.8	452
$\gamma\chi_{b0}(1P)$	(2.7 ± 0.4) $\times 10^{-3}$		484
$\gamma\eta_b(2S)$	< 6.2 $\times 10^{-4}$	CL=90%	350
$\gamma\eta_b(1S)$	(5.1 ± 0.7) $\times 10^{-4}$		912
$\gamma A^0 \to \gamma$ hadrons	< 8 $\times 10^{-5}$	CL=90%	–
$\gamma X \to \gamma +\geq 4$ prongs	[iibb] < 2.2 $\times 10^{-4}$	CL=95%	–
$\gamma a_1^0 \to \gamma\mu^+\mu^-$	< 5.5 $\times 10^{-6}$	CL=90%	–
$\gamma a_1^0 \to \gamma\tau^+\tau^-$	[jjbb] < 1.6 $\times 10^{-4}$	CL=90%	–
Lepton Family number (LF) violating modes			
$e^\pm\tau^\mp$	LF < 4.2 $\times 10^{-6}$	CL=90%	5025
$\mu^\pm\tau^\mp$	LF < 3.1 $\times 10^{-6}$	CL=90%	5025

$\chi_{b1}(3P)$

$I^G(J^{PC}) = 0^+(1^{++})$

Mass $m = 10512.1 \pm 2.3$ MeV

$\chi_{b1}(3P)$ DECAY MODES	Fraction (Γ_i/Γ)	p (MeV/c)
$\Upsilon(1S)\gamma$	seen	999
$\Upsilon(2S)\gamma$	seen	477
$\Upsilon(3S)\gamma$	seen	156

$\Upsilon(4S)$

$I^G(J^{PC}) = 0^-(1^{--})$

Mass $m = 10579.4 \pm 1.2$ MeV
Full width $\Gamma = 20.5 \pm 2.5$ MeV
$\Gamma_{ee} = 0.272 \pm 0.029$ keV (S = 1.5)

$\Upsilon(4S)$ DECAY MODES	Fraction (Γ_i/Γ)	Confidence level	p (MeV/c)
$B\overline{B}$	> 96 %	95%	326
B^+B^-	(51.4 ±0.6) %		331
D_s^+ anything + c.c.	(17.8 ±2.6) %		–
$B^0\overline{B}^0$	(48.6 ±0.6) %		326
$J/\psi K^0_S$ + $(J/\psi,\ \eta_c)K^0_S$	< 4 $\times 10^{-7}$	90%	–
non-$B\overline{B}$	< 4 %	95%	–
e^+e^-	(1.57±0.08) $\times 10^{-5}$		5290
$\rho^+\rho^-$	< 5.7 $\times 10^{-6}$	90%	5233
$K^*(892)^0\overline{K}^0$	< 2.0 $\times 10^{-6}$	90%	5240
$J/\psi(1S)$ anything	< 1.9 $\times 10^{-4}$	95%	–
D^{*+} anything + c.c.	< 7.4 %	90%	5099
ϕ anything	(7.1 ±0.6) %		5240
$\phi\eta$	< 1.8 $\times 10^{-6}$	90%	5226
$\phi\eta'$	< 4.3 $\times 10^{-6}$	90%	5196
$\rho\eta$	< 1.3 $\times 10^{-6}$	90%	5247
$\rho\eta'$	< 2.5 $\times 10^{-6}$	90%	5217
$\Upsilon(1S)$ anything	< 4 $\times 10^{-3}$	90%	1053
$\Upsilon(1S)\pi^+\pi^-$	(8.2 ±0.4) $\times 10^{-5}$		1026
$\Upsilon(1S)\eta$	(1.81±0.18) $\times 10^{-4}$		924
$\Upsilon(2S)\pi^+\pi^-$	(8.2 ±0.8) $\times 10^{-5}$		468
$h_b(1P)\pi^+\pi^-$	not seen		600
$h_b(1P)\eta$	(2.18±0.21) $\times 10^{-3}$		390
^2H anything	< 1.3 $\times 10^{-5}$	90%	–
Double Radiative Decays			
$\gamma\gamma\,\Upsilon(D) \to \gamma\gamma\eta\,\Upsilon(1S)$	< 2.3 $\times 10^{-5}$	90%	–

$Z_b(10610)$

$I^G(J^{PC}) = 1^+(1^{+-})$

Mass $m = 10607.2 \pm 2.0$ MeV
Full width $\Gamma = 18.4 \pm 2.4$ MeV

$Z_b(10610)$ DECAY MODES	Fraction (Γ_i/Γ)	p (MeV/c)
$\Upsilon(1S)\pi^+$	$(5.4^{+1.9}_{-1.5}) \times 10^{-3}$	1077
$\Upsilon(1S)\pi^0$	not seen	1077
$\Upsilon(2S)\pi^+$	$(3.6^{+1.1}_{-0.8})$ %	551
$\Upsilon(2S)\pi^0$	seen	552
$\Upsilon(3S)\pi^+$	$(2.1^{+0.8}_{-0.6})$ %	207
$\Upsilon(3S)\pi^0$	seen	210
$h_b(1P)\pi^+$	$(3.5^{+1.2}_{-0.9})$ %	671
$h_b(2P)\pi^+$	$(4.7^{+1.7}_{-1.3})$ %	313
$B^+\overline{B}^0$	not seen	505
$B^+\overline{B}^{*0}$ + $B^{*+}\overline{B}^0$	$(85.6^{+2.1}_{-2.9})$ %	–
$B^{*+}\overline{B}^{*0}$	not seen	†

$\Upsilon(10860)$

$I^G(J^{PC}) = 0^-(1^{--})$

Mass $m = 10889.9^{+3.2}_{-2.6}$ MeV
Full width $\Gamma = 51^{+6}_{-7}$ MeV
$\Gamma_{ee} = 0.31 \pm 0.07$ keV (S = 1.3)

$\Upsilon(10860)$ DECAY MODES	Fraction (Γ_i/Γ)	Confidence level	p (MeV/c)
$B\overline{B}X$	(76.2 $^{+2.7}_{-4.0}$) %		–
$B\overline{B}$	(5.5 ±1.0) %		1332
$B\overline{B}^* +$ c.c.	(13.7 ±1.6) %		–
$B^*\overline{B}^*$	(38.1 ±3.4) %		1138
$B\overline{B}^{(*)}\pi$	< 19.7 %	90%	1027
$B\overline{B}\pi$	(0.0 ±1.2) %		1027
$B^*\overline{B}\pi + B\overline{B}^*\pi$	(7.3 ±2.3) %		–
$B^*\overline{B}^*\pi$	(1.0 ±1.4) %		756
$B\overline{B}\pi\pi$	< 8.9 %	90%	574
$B_s^{(*)}\overline{B}_s^{(*)}$	(20.1 ±3.1) %		919
$B_s\overline{B}_s$	(5 ±5) $\times 10^{-3}$		919
$B_s\overline{B}_s^* +$ c.c.	(1.35±0.32) %		–
$B_s^*\overline{B}_s^*$	(17.6 ±2.7) %		566
no open-bottom	(3.8 $^{+5.0}_{-0.5}$) %		–
e^+e^-	(6.1 ±1.6) $\times 10^{-6}$		5445
$K^*(892)^0\overline{K}^0$	< 1.0 $\times 10^{-5}$	90%	5397
$\Upsilon(1S)\pi^+\pi^-$	(5.3 ±0.6) $\times 10^{-3}$		1310
$\Upsilon(2S)\pi^+\pi^-$	(7.8 ±1.3) $\times 10^{-3}$		788
$\Upsilon(3S)\pi^+\pi^-$	(4.8 $^{+1.9}_{-1.7}$) $\times 10^{-3}$		445
$\Upsilon(1S)K^+K^-$	(6.1 ±1.8) $\times 10^{-4}$		965
$h_b(1P)\pi^+\pi^-$	(3.5 $^{+1.0}_{-1.3}$) $\times 10^{-3}$		907
$h_b(2P)\pi^+\pi^-$	(5.7 $^{+1.7}_{-2.1}$) $\times 10^{-3}$		548
$\chi_{b0}(1P)\pi^+\pi^-\pi^0$	< 6.3 $\times 10^{-3}$	90%	899
$\chi_{b0}(1P)\omega$	< 3.9 $\times 10^{-3}$	90%	638
$\chi_{b0}(1P)(\pi^+\pi^-\pi^0)_{\text{non}-\omega}$	< 4.8 $\times 10^{-3}$	90%	–
$\chi_{b1}(1P)\pi^+\pi^-\pi^0$	(1.85±0.33) $\times 10^{-3}$		865
$\chi_{b1}(1P)\omega$	(1.57±0.30) $\times 10^{-3}$		589
$\chi_{b1}(1P)(\pi^+\pi^-\pi^0)_{\text{non}-\omega}$	(5.2 ±1.9) $\times 10^{-4}$		–
$\chi_{b2}(1P)\pi^+\pi^-\pi^0$	(1.17±0.30) $\times 10^{-3}$		846
$\chi_{b2}(1P)\omega$	(6.0 ±2.7) $\times 10^{-4}$		559
$\chi_{b2}(1P)(\pi^+\pi^-\pi^0)_{\text{non}-\omega}$	(6 ±4) $\times 10^{-4}$		–
$\gamma X_b \to \gamma\,\Upsilon(1S)\omega$	< 3.8 $\times 10^{-5}$	90%	–

Inclusive Decays.

These decay modes are submodes of one or more of the decay modes above.

ϕ anything	(13.8 $^{+2.4}_{-1.7}$) %	–
D^0 anything + c.c.	(108 ±8) %	–
D_s anything + c.c.	(46 ±6) %	–
J/ψ anything	(2.06±0.21) %	–
B^0 anything + c.c.	(77 ±8) %	–
B^+ anything + c.c.	(72 ±6) %	–

$\Upsilon(11020)$

$I^G(J^{PC}) = 0^-(1^{--})$

Mass $m = 10992.9^{+10.0}_{-3.1}$ MeV
Full width $\Gamma = 49^{+9}_{-15}$ MeV
$\Gamma_{ee} = 0.130 \pm 0.030$ keV

$\Upsilon(11020)$ DECAY MODES	Fraction (Γ_i/Γ)	p (MeV/c)
e^+e^-	$(2.7^{+1.0}_{-0.8}) \times 10^{-6}$	5496

NOTES

In this Summary Table:

When a quantity has "(S = ...)" to its right, the error on the quantity has been enlarged by the "scale factor" S, defined as $S = \sqrt{\chi^2/(N-1)}$, where N is the number of measurements used in calculating the quantity. We do this when $S > 1$, which often indicates that the measurements are inconsistent. When $S > 1.25$, we also show in the Particle Listings an ideogram of the measurements. For more about S, see the Introduction.

A decay momentum p is given for each decay mode. For a 2-body decay, p is the momentum of each decay product in the rest frame of the decaying particle. For a 3-or-more-body decay, p is the largest momentum any of the products can have in this frame.

[a] See the "Note on $\pi^\pm \to \ell^\pm\nu\gamma$ and $K^\pm \to \ell^\pm\nu\gamma$ Form Factors" in the $\pi^\pm$ Particle Listings for definitions and details.

[b] Measurements of $\Gamma(e^+\nu_e)/\Gamma(\mu^+\nu_\mu)$ always include decays with γ's, and measurements of $\Gamma(e^+\nu_e\gamma)$ and $\Gamma(\mu^+\nu_\mu\gamma)$ never include low-energy γ's. Therefore, since no clean separation is possible, we consider the modes with γ's to be subreactions of the modes without them, and let $[\Gamma(e^+\nu_e) + \Gamma(\mu^+\nu_\mu)]/\Gamma_{\text{total}} = 100\%$.

[c] See the $\pi^\pm$ Particle Listings for the energy limits used in this measurement; low-energy γ's are not included.

[d] Derived from an analysis of neutrino-oscillation experiments.

[e] Astrophysical and cosmological arguments give limits of order 10^{-13}; see the π^0 Particle Listings.

[f] C parity forbids this to occur as a single-photon process.

[g] See the "Note on scalar mesons" in the $f_0(500)$ Particle Listings . The interpretation of this entry as a particle is controversial.

[h] See the "Note on $\rho(770)$" in the $\rho(770)$ Particle Listings .

[i] The $\omega\rho$ interference is then due to $\omega\rho$ mixing only, and is expected to be small. If $e\mu$ universality holds, $\Gamma(\rho^0 \to \mu^+\mu^-) = \Gamma(\rho^0 \to e^+e^-) \times 0.99785$.

[j] See the "Note on scalar mesons" in the $f_0(500)$ Particle Listings .

[k] See the "Note on $a_1(1260)$" in the $a_1(1260)$ Particle Listings in PDG 06, Journal of Physics **G33** 1 (2006).

[l] This is only an educated guess; the error given is larger than the error on the average of the published values. See the Particle Listings for details.

[n] See the "Note on non-$q\overline{q}$ mesons" in the Particle Listings in PDG 06, Journal of Physics **G33** 1 (2006).

[o] See the "Note on the $\eta(1405)$" in the $\eta(1405)$ Particle Listings.

[p] See the "Note on the $f_1(1420)$" in the $\eta(1405)$ Particle Listings.

[q] See also the $\omega(1650)$ Particle Listings.

[r] See the "Note on the $\rho(1450)$ and the $\rho(1700)$" in the $\rho(1700)$ Particle Listings.

[s] See also the $\omega(1420)$ Particle Listings.

[t] See the "Note on $f_0(1710)$" in the $f_0(1710)$ Particle Listings in 2004 edition of *Review of Particle Physics*.

[u] See the note in the $K^\pm$ Particle Listings.

[v] Neglecting photon channels. See, *e.g.*, A. Pais and S.B. Treiman, Phys. Rev. **D12**, 2744 (1975).

[x] The definition of the slope parameters of the $K \to 3\pi$ Dalitz plot is as follows (see also "Note on Dalitz Plot Parameters for $K \to 3\pi$ Decays" in the $K^\pm$ Particle Listings):
$$|M|^2 = 1 + g(s_3 - s_0)/m^2_{\pi^+} + \cdots .$$

[y] For more details and definitions of parameters see the Particle Listings.

[z] See the $K^\pm$ Particle Listings for the energy limits used in this measurement.

[aa] Most of this radiative mode, the low-momentum γ part, is also included in the parent mode listed without γ's.

[bb] Structure-dependent part.

[cc] Direct-emission branching fraction.

[dd] Violates angular-momentum conservation.

[ee] Derived from measured values of ϕ_{+-}, ϕ_{00}, $|\eta|$, $|m_{K^0_L} - m_{K^0_S}|$, and $\tau_{K^0_S}$, as described in the introduction to "Tests of Conservation Laws."

[*ff*] The *CP*-violation parameters are defined as follows (see also "Note on *CP* Violation in $K_S \to 3\pi$" and "Note on *CP* Violation in K_L^0 Decay" in the Particle Listings):

$$\eta_{+-} = |\eta_{+-}|e^{i\phi_{+-}} = \frac{A(K_L^0 \to \pi^+\pi^-)}{A(K_S^0 \to \pi^+\pi^-)} = \epsilon + \epsilon'$$

$$\eta_{00} = |\eta_{00}|e^{i\phi_{00}} = \frac{A(K_L^0 \to \pi^0\pi^0)}{A(K_S^0 \to \pi^0\pi^0)} = \epsilon - 2\epsilon'$$

$$\delta = \frac{\Gamma(K_L^0 \to \pi^-\ell^+\nu) - \Gamma(K_L^0 \to \pi^+\ell^-\nu)}{\Gamma(K_L^0 \to \pi^-\ell^+\nu) + \Gamma(K_L^0 \to \pi^+\ell^-\nu)} ,$$

$$\mathrm{Im}(\eta_{+-0})^2 = \frac{\Gamma(K_S^0 \to \pi^+\pi^-\pi^0)^{CP \text{ viol.}}}{\Gamma(K_L^0 \to \pi^+\pi^-\pi^0)} ,$$

$$\mathrm{Im}(\eta_{000})^2 = \frac{\Gamma(K_S^0 \to \pi^0\pi^0\pi^0)}{\Gamma(K_L^0 \to \pi^0\pi^0\pi^0)} .$$

where for the last two relations *CPT* is assumed valid, *i.e.,* $\mathrm{Re}(\eta_{+-0}) \simeq 0$ and $\mathrm{Re}(\eta_{000}) \simeq 0$.

[*gg*] See the K_S^0 Particle Listings for the energy limits used in this measurement.

[*hh*] The value is for the sum of the charge states or particle/antiparticle states indicated.

[*ii*] $\mathrm{Re}(\epsilon'/\epsilon) = \epsilon'/\epsilon$ to a very good approximation provided the phases satisfy *CPT* invariance.

[*jj*] This mode includes gammas from inner bremsstrahlung but not the direct emission mode $K_L^0 \to \pi^+\pi^-\gamma$(DE).

[*kk*] See the K_L^0 Particle Listings for the energy limits used in this measurement.

[*ll*] Allowed by higher-order electroweak interactions.

[*nn*] Violates *CP* in leading order. Test of direct *CP* violation since the indirect *CP*-violating and *CP*-conserving contributions are expected to be suppressed.

[*oo*] See the "Note on $f_0(1370)$" in the $f_0(1370)$ Particle Listings and in the 1994 edition.

[*pp*] See the note in the $L(1770)$ Particle Listings in Reviews of Modern Physics **56** S1 (1984), p. S200. See also the "Note on $K_2(1770)$ and the $K_2(1820)$" in the $K_2(1770)$ Particle Listings .

[*qq*] See the "Note on $K_2(1770)$ and the $K_2(1820)$" in the $K_2(1770)$ Particle Listings .

[*rr*] This result applies to $Z^0 \to c\overline{c}$ decays only. Here ℓ^+ is an average (not a sum) of e^+ and μ^+ decays.

[*ss*] See the Particle Listings for the (complicated) definition of this quantity.

[*tt*] The branching fraction for this mode may differ from the sum of the submodes that contribute to it, due to interference effects. See the relevant papers in the Particle Listings.

[*uu*] These subfractions of the $K^-2\pi^+$ mode are uncertain: see the Particle Listings.

[*vv*] Submodes of the $D^+ \to K^-2\pi^+\pi^0$ and $K_S^0 2\pi^+\pi^-$ modes were studied by ANJOS 92C and COFFMAN 92B, but with at most 142 events for the first mode and 229 for the second – not enough for precise results. With nothing new for 18 years, we refer to our 2008 edition, Physics Letters **B667** 1 (2008), for those results.

[*xx*] The unseen decay modes of the resonances are included.

[*yy*] This is *not* a test for the ΔC=1 weak neutral current, but leads to the $\pi^+\ell^+\ell^-$ final state.

[*zz*] This mode is not a useful test for a ΔC=1 weak neutral current because both quarks must change flavor in this decay.

[*aaa*] In the 2010 *Review*, the values for these quantities were given using a measure of the asymmetry that was inconsistent with the usual definition.

[*bbb*] This value is obtained by subtracting the branching fractions for 2-, 4- and 6-prongs from unity.

[*ccc*] This is the sum of our $K^-2\pi^+\pi^-$, $K^-2\pi^+\pi^-\pi^0$, $\overline{K}^0 2\pi^+2\pi^-$, $K^+2K^-\pi^+$, $2\pi^+2\pi^-$, $2\pi^+2\pi^-\pi^0$, $K^+K^-\pi^+\pi^-$, and $K^+K^-\pi^+\pi^-\pi^0$, branching fractions.

[*ddd*] This is the sum of our $K^-3\pi^+2\pi^-$ and $3\pi^+3\pi^-$ branching fractions.

[*eee*] The branching fractions for the $K^-e^+\nu_e$, $K^*(892)^-e^+\nu_e$, $\pi^-e^+\nu_e$, and $\rho^-e^+\nu_e$ modes add up to 6.19 ± 0.17 %.

[*fff*] This is a doubly Cabibbo-suppressed mode.

[*ggg*] Submodes of the $D^0 \to K_S^0\pi^+\pi^-\pi^0$ mode with a K^* and/or ρ were studied by COFFMAN 92B, but with only 140 events. With nothing new for 18 years, we refer to our 2008 edition, Physics Letters **B667** 1 (2008), for those results.

[*hhh*] This branching fraction includes all the decay modes of the resonance in the final state.

[*iii*] This limit is for either D^0 or $\overline{D}^0$ to pe^-.

[*jjj*] This limit is for either D^0 or $\overline{D}^0$ to $\overline{p}e^+$.

[*kkk*] This is the purely e^+ semileptonic branching fraction: the e^+ fraction from τ^+ decays has been subtracted off. The sum of our (non-τ) e^+ exclusive fractions — an $e^+\nu_e$ with an η, η', ϕ, K^0, or K^{*0} — is 5.99 ± 0.31 %.

[*lll*] This fraction includes η from η' decays.

[*nnn*] The sum of our exclusive η' fractions — $\eta' e^+\nu_e$, $\eta'\mu^+\nu_\mu$, $\eta'\pi^+$, $\eta'\rho^+$, and $\eta' K^+$ — is 11.8 ± 1.6%.

[*ooo*] This branching fraction includes all the decay modes of the final-state resonance.

[*ppp*] A test for $u\overline{u}$ or $d\overline{d}$ content in the D_s^+. Neither Cabibbo-favored nor Cabibbo-suppressed decays can contribute, and $\omega - \phi$ mixing is an unlikely explanation for any fraction above about 2×10^{-4}.

[*qqq*] We decouple the $D_s^+ \to \phi\pi^+$ branching fraction obtained from mass projections (and used to get some of the other branching fractions) from the $D_s^+ \to \phi\pi^+$, $\phi \to K^+K^-$ branching fraction obtained from the Dalitz-plot analysis of $D_s^+ \to K^+K^-\pi^+$. That is, the ratio of these two branching fractions is not exactly the $\phi \to K^+K^-$ branching fraction 0.491.

[*rrr*] This is the average of a model-independent and a *K*-matrix parametrization of the $\pi^+\pi^-$ *S*-wave and is a sum over several f_0 mesons.

[*sss*] An ℓ indicates an e or a μ mode, not a sum over these modes.

[*ttt*] An $CP(\pm1)$ indicates the CP=+1 and CP=−1 eigenstates of the D^0-$\overline{D}^0$ system.

[*uuu*] D denotes D^0 or $\overline{D}^0$.

[*vvv*] D_{CP+}^{*0} decays into $D^0\pi^0$ with the D^0 reconstructed in *CP*-even eigenstates K^+K^- and $\pi^+\pi^-$.

[*xxx*] $\overline{D}^{**}$ represents an excited state with mass $2.2 < \mathrm{M} < 2.8$ GeV/c^2.

[*yyy*] $\chi_{c1}(3872)^+$ is a hypothetical charged partner of the $\chi_{c1}(3872)$.

[*zzz*] $\Theta(1710)^{++}$ is a possible narrow pentaquark state and $G(2220)$ is a possible glueball resonance.

[*aaaa*] $(\overline{\Lambda}_c^- p)_s$ denotes a low-mass enhancement near 3.35 GeV/c^2.

[*bbaa*] Stands for the possible candidates of $K^*(1410)$, $K_0^*(1430)$ and $K_2^*(1430)$.

[*ccaa*] B^0 and B_s^0 contributions not separated. Limit is on weighted average of the two decay rates.

[*ddaa*] This decay refers to the coherent sum of resonant and nonresonant $J^P = 0^+$ $K\pi$ components with $1.60 < m_{K\pi} < 2.15$ GeV/c^2.

[*eeaa*] $X(214)$ is a hypothetical particle of mass 214 MeV/c^2 reported by the HyperCP experiment, Physical Review Letters **94** 021801 (2005)

[*ffaa*] $\Theta(1540)^+$ denotes a possible narrow pentaquark state.

[*ggaa*] Here S and P are the hypothetical scalar and pseudoscalar particles with masses of 2.5 GeV/c^2 and 214.3 MeV/c^2, respectively.

[*hhaa*] These values are model dependent.

[*iiaa*] Here "anything" means at least one particle observed.

[*jjaa*] This is a $\mathrm{B}(B^0 \to D^{*-}\ell^+\nu_\ell)$ value.

[*kkaa*] D^{**} stands for the sum of the $D(1\,^1P_1)$, $D(1\,^3P_0)$, $D(1\,^3P_1)$, $D(1\,^3P_2)$, $D(2\,^1S_0)$, and $D(2\,^1S_1)$ resonances.

[*llaa*] $D^{(*)}\overline{D}^{(*)}$ stands for the sum of $D^*\overline{D}^*$, $D^*\overline{D}$, $D\overline{D}^*$, and $D\overline{D}$.

[*nnaa*] $X(3915)$ denotes a near-threshold enhancement in the $\omega J/\psi$ mass spectrum.

[*ooaa*] Inclusive branching fractions have a multiplicity definition and can be greater than 100%.

[*ppaa*] D_j represents an unresolved mixture of pseudoscalar and tensor D^{**} (P-wave) states.

[*qqaa*] Not a pure measurement. See note at head of B_s^0 Decay Modes.

[*rraa*] For $E_\gamma > 100$ MeV.

[*ssaa*] Includes $p\overline{p}\pi^+\pi^-\gamma$ and excludes $p\overline{p}\eta$, $p\overline{p}\omega$, $p\overline{p}\eta'$.

[*ttaa*] For a narrow state A with mass less than 960 MeV.

[*uuaa*] For a narrow scalar or pseudoscalar A^0 with mass 0.21–3.0 GeV.

[*vvaa*] For a narrow resonance in the range $2.2 < M(X) < 2.8$ GeV.

[*xxaa*] J^{PC} known by production in e^+e^- via single photon annihilation. I^G is not known; interpretation of this state as a single resonance is unclear because of the expectation of substantial threshold effects in this energy region.

[*yyaa*] $2m_\tau < \mathrm{M}(\tau^+\tau^-) < 9.2$ GeV

[*zzaa*] 2 GeV $< m_{K^+K^-} < 3$ GeV

[*aabb*] X = scalar with $m < 8.0$ GeV

[*bbbb*] $X\overline{X}$ = vectors with $m < 3.1$ GeV

[*ccbb*] X and $\overline{X}$ = zero spin with $m < 4.5$ GeV

[*ddbb*] 1.5 GeV $< m_X < 5.0$ GeV

[*eebb*] 201 MeV $< \mathrm{M}(\mu^+\mu^-) < 3565$ MeV

[*ffbb*] 0.5 GeV $< m_X < 9.0$ GeV, where m_X is the invariant mass of the hadronic final state.

[*ggbb*] Spectroscopic labeling for these states is theoretical, pending experimental information.

[*hhbb*] 1.5 GeV $< m_X < 5.0$ GeV

[*iibb*] 1.5 GeV $< m_X < 5.0$ GeV

[*jjbb*] For $m_{\tau^+\tau^-}$ in the ranges 4.03–9.52 and 9.61–10.10 GeV.

Meson Summary Table

See also the table of suggested $q\overline{q}$ quark-model assignments in the Quark Model section.

• Indicates particles that appear in the preceding Meson Summary Table. We do not regard the other entries as being established.

LIGHT UNFLAVORED ($S = C = B = 0$)

	$I^G(J^{PC})$
• $\pi^{\pm}$	$1^-(0^{-})$
• π^0	$1^-(0^{-+})$
• η	$0^+(0^{-+})$
• $f_0(500)$	$0^+(0^{++})$
• $\rho(770)$	$1^+(1^{--})$
• $\omega(782)$	$0^-(1^{--})$
• $\eta'(958)$	$0^+(0^{-+})$
• $f_0(980)$	$0^+(0^{++})$
• $a_0(980)$	$1^-(0^{++})$
• $\phi(1020)$	$0^-(1^{--})$
• $h_1(1170)$	$0^-(1^{+-})$
• $b_1(1235)$	$1^+(1^{+-})$
• $a_1(1260)$	$1^-(1^{++})$
• $f_2(1270)$	$0^+(2^{++})$
• $f_1(1285)$	$0^+(1^{++})$
• $\eta(1295)$	$0^+(0^{-+})$
• $\pi(1300)$	$1^-(0^{-+})$
• $a_2(1320)$	$1^-(2^{++})$
• $f_0(1370)$	$0^+(0^{++})$
$h_1(1380)$	$?^-(1^{+-})$
• $\pi_1(1400)$	$1^-(1^{-+})$
• $\eta(1405)$	$0^+(0^{-+})$
$a_1(1420)$	$1^-(1^{++})$
• $f_1(1420)$	$0^+(1^{++})$
• $\omega(1420)$	$0^-(1^{--})$
$f_2(1430)$	$0^+(2^{++})$
• $a_0(1450)$	$1^-(0^{++})$
• $\rho(1450)$	$1^+(1^{--})$
• $\eta(1475)$	$0^+(0^{-+})$
• $f_0(1500)$	$0^+(0^{++})$
$f_1(1510)$	$0^+(1^{++})$
• $f_2'(1525)$	$0^+(2^{++})$
$f_2(1565)$	$0^+(2^{++})$
$\rho(1570)$	$1^+(1^{--})$
$h_1(1595)$	$0^-(1^{+-})$
• $\pi_1(1600)$	$1^-(1^{-+})$
$a_1(1640)$	$1^-(1^{++})$
$f_2(1640)$	$0^+(2^{++})$
• $\eta_2(1645)$	$0^+(2^{-+})$
• $\omega(1650)$	$0^-(1^{--})$
• $\omega_3(1670)$	$0^-(3^{--})$
• $\pi_2(1670)$	$1^-(2^{-+})$
• $\phi(1680)$	$0^-(1^{--})$
• $\rho_3(1690)$	$1^+(3^{--})$
• $\rho(1700)$	$1^+(1^{--})$
$a_2(1700)$	$1^-(2^{++})$
• $f_0(1710)$	$0^+(0^{++})$
$\eta(1760)$	$0^+(0^{-+})$
• $\pi(1800)$	$1^-(0^{-+})$
$f_2(1810)$	$0^+(2^{++})$
$X(1835)$	$?^?(0^{-+})$
$X(1840)$	$?^?(?^{??})$
• $\phi_3(1850)$	$0^-(3^{--})$
$\eta_2(1870)$	$0^+(2^{-+})$
• $\pi_2(1880)$	$1^-(2^{-+})$
$\rho(1900)$	$1^+(1^{--})$
$f_2(1910)$	$0^+(2^{++})$
$a_0(1950)$	$1^-(0^{++})$
• $f_2(1950)$	$0^+(2^{++})$
$\rho_3(1990)$	$1^+(3^{--})$
• $f_2(2010)$	$0^+(2^{++})$
$f_0(2020)$	$0^+(0^{++})$
• $a_4(2040)$	$1^-(4^{++})$
• $f_4(2050)$	$0^+(4^{++})$
$\pi_2(2100)$	$1^-(2^{-+})$
$f_0(2100)$	$0^+(0^{++})$
$f_2(2150)$	$0^+(2^{++})$
$\rho(2150)$	$1^+(1^{--})$
• $\phi(2170)$	$0^-(1^{--})$
$f_0(2200)$	$0^+(0^{++})$
$f_J(2220)$	$0^+(2^{++}$ or $4^{++})$
$\eta(2225)$	$0^+(0^{-+})$
$\rho_3(2250)$	$1^+(3^{--})$
• $f_2(2300)$	$0^+(2^{++})$
$f_4(2300)$	$0^+(4^{++})$
$f_0(2330)$	$0^+(0^{++})$
• $f_2(2340)$	$0^+(2^{++})$
$\rho_5(2350)$	$1^+(5^{--})$
$a_6(2450)$	$1^-(6^{++})$
$f_6(2510)$	$0^+(6^{++})$

OTHER LIGHT

Further States

STRANGE ($S = \pm1$, $C = B = 0$)

	$I(J^P)$
• $K^{\pm}$	$1/2(0^-)$
• K^0	$1/2(0^-)$
• K_S^0	$1/2(0^-)$
• K_L^0	$1/2(0^-)$
• $K_0^*(700)$	$1/2(0^+)$
• $K^*(892)$	$1/2(1^-)$
• $K_1(1270)$	$1/2(1^+)$
• $K_1(1400)$	$1/2(1^+)$
• $K^*(1410)$	$1/2(1^-)$
• $K_0^*(1430)$	$1/2(0^+)$
• $K_2^*(1430)$	$1/2(2^+)$
$K(1460)$	$1/2(0^-)$
$K_2(1580)$	$1/2(2^-)$
$K(1630)$	$1/2(?^?)$
$K_1(1650)$	$1/2(1^+)$
• $K^*(1680)$	$1/2(1^-)$
• $K_2(1770)$	$1/2(2^-)$
• $K_3^*(1780)$	$1/2(3^-)$
• $K_2(1820)$	$1/2(2^-)$
$K(1830)$	$1/2(0^-)$
$K_0^*(1950)$	$1/2(0^+)$
$K_2^*(1980)$	$1/2(2^+)$
• $K_4^*(2045)$	$1/2(4^+)$
$K_2(2250)$	$1/2(2^-)$
$K_3(2320)$	$1/2(3^+)$
$K_5^*(2380)$	$1/2(5^-)$
$K_4(2500)$	$1/2(4^-)$
$K(3100)$	$?^?(?^{??})$

CHARMED ($C = \pm1$)

	$I(J^P)$
• $D^{\pm}$	$1/2(0^-)$
• D^0	$1/2(0^-)$
• $D^*(2007)^0$	$1/2(1^-)$
• $D^*(2010)^{\pm}$	$1/2(1^-)$
• $D_0^*(2400)^0$	$1/2(0^+)$
$D_0^*(2400)^{\pm}$	$1/2(0^+)$
• $D_1(2420)^0$	$1/2(1^+)$
$D_1(2420)^{\pm}$	$1/2(?^?)$
$D_1(2430)^0$	$1/2(1^+)$
• $D_2^*(2460)^0$	$1/2(2^+)$
• $D_2^*(2460)^{\pm}$	$1/2(2^+)$
$D(2550)^0$	$1/2(?^?)$
$D_J^*(2600)$	$1/2(?^?)$
$D^*(2640)^{\pm}$	$1/2(?^?)$
$D(2740)^0$	$1/2(?^?)$
$D_3^*(2750)$	$1/2(3^-)$
$D(3000)^0$	$1/2(?^?)$

CHARMED, STRANGE ($C = S = \pm1$)

	$I(J^P)$
• $D_s^{\pm}$	$0(0^-)$
• $D_s^{*\pm}$	$0(?^?)$
• $D_{s0}^*(2317)^{\pm}$	$0(0^+)$
• $D_{s1}(2460)^{\pm}$	$0(1^+)$
• $D_{s1}(2536)^{\pm}$	$0(1^+)$
• $D_{s2}^*(2573)$	$0(2^+)$
• $D_{s1}^*(2700)^{\pm}$	$0(1^-)$
$D_{s1}^*(2860)^{\pm}$	$0(1^-)$
$D_{s3}^*(2860)^{\pm}$	$0(3^-)$
$D_{sJ}(3040)^{\pm}$	$0(?^?)$

BOTTOM ($B = \pm1$)

	$I(J^P)$
• $B^{\pm}$	$1/2(0^-)$
• B^0	$1/2(0^-)$
• $B^{\pm}/B^0$ ADMIXTURE	
• $B^{\pm}/B^0/B_s^0$/b-baryon ADMIXTURE V_{cb} and V_{ub} CKM Matrix Elements	
• B^*	$1/2(1^-)$
• $B_1(5721)^+$	$1/2(1^+)$
• $B_1(5721)^0$	$1/2(1^+)$
$B_J^*(5732)$	$?(?^?)$
• $B_2^*(5747)^+$	$1/2(2^+)$
• $B_2^*(5747)^0$	$1/2(2^+)$
$B_J(5840)^+$	$1/2(?^?)$
$B_J(5840)^0$	$1/2(?^?)$
• $B_J(5970)^+$	$1/2(?^?)$
• $B_J(5970)^0$	$1/2(?^?)$

BOTTOM, STRANGE ($B = \pm1$, $S = \mp1$)

	$I(J^P)$
• B_s^0	$0(0^-)$
• B_s^*	$0(1^-)$
$X(5568)^{\pm}$	$?(?^?)$
• $B_{s1}(5830)^0$	$0(1^+)$
• $B_{s2}^*(5840)^0$	$0(2^+)$
$B_{sJ}^*(5850)$	$?(?^?)$

BOTTOM, CHARMED ($B = C = \pm1$)

	$I(J^P)$
• B_c^+	$0(0^-)$
$B_c(2S)^{\pm}$	$0(0^-)$

$c\overline{c}$

	$I^G(J^{PC})$
• $\eta_c(1S)$	$0^+(0^{-+})$
• $J/\psi(1S)$	$0^-(1^{--})$
• $\chi_{c0}(1P)$	$0^+(0^{++})$
• $\chi_{c1}(1P)$	$0^+(1^{++})$
• $h_c(1P)$	$?^?(1^{+-})$
• $\chi_{c2}(1P)$	$0^+(2^{++})$

$c\overline{c}$ (cont.)

	$I^G(J^{PC})$
• $\eta_c(2S)$	$0^+(0^{-+})$
• $\psi(2S)$	$0^-(1^{--})$
• $\psi(3770)$	$0^-(1^{--})$
• $\psi_2(3823)$	$0^-(2^{--})$
$\chi_{c0}(3860)$	$0^+(0^{++})$
• $\chi_{c1}(3872)$	$0^+(1^{++})$
• $Z_c(3900)$	$1^+(1^{+-})$
• $X(3915)$	$0^+(0/2^{++})$
• $\chi_{c2}(3930)$	$0^+(2^{++})$
$X(3940)$	$?^?(?^{??})$
• $X(4020)$	$1^+(?^{?-})$
• $\psi(4040)$	$0^-(1^{--})$
$X(4050)^{\pm}$	$1^-(?^{?+})$
$X(4055)^{\pm}$	$1^+(?^{?-})$
• $\chi_{c1}(4140)$	$0^+(1^{++})$
• $\psi(4160)$	$0^-(1^{--})$
$X(4160)$	$?^?(?^{??})$
$Z_c(4200)$	$1^+(1^{+-})$
$\psi(4230)$	$0^-(1^{--})$
$R_{c0}(4240)$	$1^+(0^{--})$
$X(4250)^{\pm}$	$1^-(?^{?+})$
• $\psi(4260)$	$0^-(1^{--})$
• $\chi_{c1}(4274)$	$0^+(1^{++})$
$X(4350)$	$0^+(?^{?+})$
• $\psi(4360)$	$0^-(1^{--})$
$\psi(4390)$	$0^-(1^{--})$
• $\psi(4415)$	$0^-(1^{--})$
• $Z_c(4430)$	$1^+(1^{+-})$
$\chi_{c0}(4500)$	$0^+(0^{++})$
• $\psi(4660)$	$0^-(1^{--})$
$\chi_{c0}(4700)$	$0^+(0^{++})$

$b\overline{b}$

	$I^G(J^{PC})$
• $\eta_b(1S)$	$0^+(0^{-+})$
• $\Upsilon(1S)$	$0^-(1^{--})$
• $\chi_{b0}(1P)$	$0^+(0^{++})$
• $\chi_{b1}(1P)$	$0^+(1^{++})$
• $h_b(1P)$	$?^?(1^{+-})$
• $\chi_{b2}(1P)$	$0^+(2^{++})$
$\eta_b(2S)$	$0^+(0^{-+})$
• $\Upsilon(2S)$	$0^-(1^{--})$
• $\Upsilon_2(1D)$	$0^-(2^{--})$
• $\chi_{b0}(2P)$	$0^+(0^{++})$
• $\chi_{b1}(2P)$	$0^+(1^{++})$
$h_b(2P)$	$?^?(1^{+-})$
• $\chi_{b2}(2P)$	$0^+(2^{++})$
• $\Upsilon(3S)$	$0^-(1^{--})$
• $\chi_{b1}(3P)$	$0^+(1^{++})$
• $\Upsilon(4S)$	$0^-(1^{--})$
• $Z_b(10610)$	$1^+(1^{+-})$
$Z_b(10650)$	$1^+(1^{+-})$
• $\Upsilon(10860)$	$0^-(1^{--})$
• $\Upsilon(11020)$	$0^-(1^{--})$

Baryon Summary Table

This short table gives the name, the quantum numbers (where known), and the status of baryons in the Review. Only the baryons with 3- or 4-star status are included in the Baryon Summary Table. Due to insufficient data or uncertain interpretation, the other entries in the table are not established baryons. The names with masses are of baryons that decay strongly. The spin-parity J^P (when known) is given with each particle. For the strongly decaying particles, the J^P values are considered to be part of the names.

p	$1/2^+$	****	$\Delta(1232)$	$3/2^+$	****	Σ^+	$1/2^+$	****	Ξ^0	$1/2^+$	****	Λ_c^+	$1/2^+$	****
n	$1/2^+$	****	$\Delta(1600)$	$3/2^+$	****	Σ^0	$1/2^+$	****	Ξ^-	$1/2^+$	****	$\Lambda_c(2595)^+$	$1/2^-$	***
$N(1440)$	$1/2^+$	****	$\Delta(1620)$	$1/2^-$	****	Σ^-	$1/2^+$	****	$\Xi(1530)$	$3/2^+$	****	$\Lambda_c(2625)^+$	$3/2^-$	***
$N(1520)$	$3/2^-$	****	$\Delta(1700)$	$3/2^-$	****	$\Sigma(1385)$	$3/2^+$	****	$\Xi(1620)$		*	$\Lambda_c(2765)^+$		*
$N(1535)$	$1/2^-$	****	$\Delta(1750)$	$1/2^+$	*	$\Sigma(1480)$		*	$\Xi(1690)$		***	$\Lambda_c(2860)^+$	$3/2^+$	***
$N(1650)$	$1/2^-$	****	$\Delta(1900)$	$1/2^-$	***	$\Sigma(1560)$		**	$\Xi(1820)$	$3/2^-$	***	$\Lambda_c(2880)^+$	$5/2^+$	***
$N(1675)$	$5/2^-$	****	$\Delta(1905)$	$5/2^+$	****	$\Sigma(1580)$	$3/2^-$	*	$\Xi(1950)$		***	$\Lambda_c(2940)^+$	$3/2^-$	***
$N(1680)$	$5/2^+$	****	$\Delta(1910)$	$1/2^+$	****	$\Sigma(1620)$	$1/2^-$	*	$\Xi(2030)$	$\geq \frac{5}{2}$?	***	$\Sigma_c(2455)$	$1/2^+$	****
$N(1700)$	$3/2^-$	***	$\Delta(1920)$	$3/2^+$	***	$\Sigma(1660)$	$1/2^+$	***	$\Xi(2120)$		*	$\Sigma_c(2520)$	$3/2^+$	***
$N(1710)$	$1/2^+$	****	$\Delta(1930)$	$5/2^-$	***	$\Sigma(1670)$	$3/2^-$	****	$\Xi(2250)$		**	$\Sigma_c(2800)$		***
$N(1720)$	$3/2^+$	****	$\Delta(1940)$	$3/2^-$	**	$\Sigma(1690)$		**	$\Xi(2370)$		**	Ξ_c^+	$1/2^+$	***
$N(1860)$	$5/2^+$	**	$\Delta(1950)$	$7/2^+$	****	$\Sigma(1730)$	$3/2^+$	*	$\Xi(2500)$		*	Ξ_c^0	$1/2^+$	***
$N(1875)$	$3/2^-$	***	$\Delta(2000)$	$5/2^+$	**	$\Sigma(1750)$	$1/2^-$	***				$\Xi_c'^+$	$1/2^+$	***
$N(1880)$	$1/2^+$	***	$\Delta(2150)$	$1/2^-$	*	$\Sigma(1770)$	$1/2^+$	*	Ω^-	$3/2^+$	****	$\Xi_c'^0$	$1/2^+$	***
$N(1895)$	$1/2^-$	****	$\Delta(2200)$	$7/2^-$	***	$\Sigma(1775)$	$5/2^-$	****	$\Omega(2250)^-$		***	$\Xi_c(2645)$	$3/2^+$	***
$N(1900)$	$3/2^+$	****	$\Delta(2300)$	$9/2^+$	**	$\Sigma(1840)$	$3/2^+$	*	$\Omega(2380)^-$		**	$\Xi_c(2790)$	$1/2^-$	***
$N(1990)$	$7/2^+$	**	$\Delta(2350)$	$5/2^-$	*	$\Sigma(1880)$	$1/2^+$	**	$\Omega(2470)^-$		**	$\Xi_c(2815)$	$3/2^-$	***
$N(2000)$	$5/2^+$	**	$\Delta(2390)$	$7/2^+$	*	$\Sigma(1900)$	$1/2^-$	*				$\Xi_c(2930)$		*
$N(2040)$	$3/2^+$	*	$\Delta(2400)$	$9/2^-$	**	$\Sigma(1915)$	$5/2^+$	****				$\Xi_c(2970)$		***
$N(2060)$	$5/2^-$	***	$\Delta(2420)$	$11/2^+$	****	$\Sigma(1940)$	$3/2^+$	*				$\Xi_c(3055)$		***
$N(2100)$	$1/2^+$	***	$\Delta(2750)$	$13/2^-$	**	$\Sigma(1940)$	$3/2^-$	***				$\Xi_c(3080)$		***
$N(2120)$	$3/2^-$	***	$\Delta(2950)$	$15/2^+$	**	$\Sigma(2000)$	$1/2^-$	*				$\Xi_c(3123)$		*
$N(2190)$	$7/2^-$	****				$\Sigma(2030)$	$7/2^+$	****				Ω_c^0	$1/2^+$	***
$N(2220)$	$9/2^+$	****	Λ	$1/2^+$	****	$\Sigma(2070)$	$5/2^+$	*				$\Omega_c(2770)^0$	$3/2^+$	***
$N(2250)$	$9/2^-$	****	$\Lambda(1405)$	$1/2^-$	****	$\Sigma(2080)$	$3/2^+$	**				$\Omega_c(3000)^0$		***
$N(2300)$	$1/2^+$	**	$\Lambda(1520)$	$3/2^-$	****	$\Sigma(2100)$	$7/2^-$	*				$\Omega_c(3050)^0$		***
$N(2570)$	$5/2^-$	**	$\Lambda(1600)$	$1/2^+$	***	$\Sigma(2250)$		***				$\Omega_c(3065)^0$		***
$N(2600)$	$11/2^-$	***	$\Lambda(1670)$	$1/2^-$	****	$\Sigma(2455)$		**				$\Omega_c(3090)^0$		***
$N(2700)$	$13/2^+$	**	$\Lambda(1690)$	$3/2^-$	****	$\Sigma(2620)$		**				$\Omega_c(3120)^0$		***
			$\Lambda(1710)$	$1/2^+$	*	$\Sigma(3000)$		*						
			$\Lambda(1800)$	$1/2^-$	***	$\Sigma(3170)$		*				Ξ_{cc}^+		*
			$\Lambda(1810)$	$1/2^+$	***							Ξ_{cc}^{++}		***
			$\Lambda(1820)$	$5/2^+$	****									
			$\Lambda(1830)$	$5/2^-$	****							Λ_b^0	$1/2^+$	***
			$\Lambda(1890)$	$3/2^+$	****							$\Lambda_b(5912)^0$	$1/2^-$	***
			$\Lambda(2000)$		*							$\Lambda_b(5920)^0$	$3/2^-$	***
			$\Lambda(2020)$	$7/2^+$	*							Σ_b	$1/2^+$	***
			$\Lambda(2050)$	$3/2^-$	*							Σ_b^*	$3/2^+$	***
			$\Lambda(2100)$	$7/2^-$	****							Ξ_b^0, Ξ_b^-	$1/2^+$	***
			$\Lambda(2110)$	$5/2^+$	***							$\Xi_b'(5935)^-$	$1/2^+$	***
			$\Lambda(2325)$	$3/2^-$	*							$\Xi_b(5945)^0$	$3/2^+$	***
			$\Lambda(2350)$	$9/2^+$	***							$\Xi_b(5955)^-$	$3/2^+$	***
			$\Lambda(2585)$		**							Ω_b^-	$1/2^+$	***
												$P_c(4380)^+$		*
												$P_c(4450)^+$		*

**** Existence is certain, and properties are at least fairly well explored.

*** Existence ranges from very likely to certain, but further confirmation is desirable and/or quantum numbers, branching fractions, etc. are not well determined.

** Evidence of existence is only fair.

* Evidence of existence is poor.

Baryon Summary Table

N BARYONS ($S = 0$, $I = 1/2$)

p, $N^+ = uud$; n, $N^0 = udd$

p

$I(J^P) = \frac{1}{2}(\frac{1}{2}^+)$

Mass $m = 1.00727646688 \pm 0.00000000009$ u
Mass $m = 938.272081 \pm 0.000006$ MeV [a]
$|m_p - m_{\overline{p}}|/m_p < 7 \times 10^{-10}$, CL = 90% [b]
$|\frac{q_{\overline{p}}}{m_{\overline{p}}}|/(\frac{q_p}{m_p}) = 1.00000000000 \pm 0.00000000007$
$|q_p + q_{\overline{p}}|/e < 7 \times 10^{-10}$, CL = 90% [b]
$|q_p + q_e|/e < 1 \times 10^{-21}$ [c]
Magnetic moment $\mu = 2.7928473446 \pm 0.0000000008\ \mu_N$
$(\mu_p + \mu_{\overline{p}})\ /\ \mu_p = (0.3 \pm 0.8) \times 10^{-6}$
Electric dipole moment $d < 0.021 \times 10^{-23}$ e cm
Electric polarizability $\alpha = (11.2 \pm 0.4) \times 10^{-4}$ fm^3
Magnetic polarizability $\beta = (2.5 \pm 0.4) \times 10^{-4}$ fm^3 (S = 1.2)
Charge radius, μp Lamb shift = 0.84087 $\pm$ 0.00039 fm [d]
Charge radius, ep CODATA value = 0.8751 $\pm$ 0.0061 fm [d]
Magnetic radius = 0.78 $\pm$ 0.04 fm [e]
Mean life $\tau > 2.1 \times 10^{29}$ years, CL = 90% [f] ($p \to$ invisible mode)
Mean life $\tau > 10^{31}$ to 10^{33} years [f] (mode dependent)

See the "Note on Nucleon Decay" in our 1994 edition (Phys. Rev. **D50**, 1173) for a short review.

The "partial mean life" limits tabulated here are the limits on τ/B_i, where τ is the total mean life and B_i is the branching fraction for the mode in question. For N decays, p and n indicate proton and neutron partial lifetimes.

p DECAY MODES	Partial mean life (10^{30} years)	Confidence level	p (MeV/c)
Antilepton + meson			
$N \to e^+\pi$	$> 2000\ (n)$, $> 8200\ (p)$	90%	459
$N \to \mu^+\pi$	$> 1000\ (n)$, $> 6600\ (p)$	90%	453
$N \to \nu\pi$	$> 1100\ (n)$, $> 390\ (p)$	90%	459
$p \to e^+\eta$	> 4200	90%	309
$p \to \mu^+\eta$	> 1300	90%	297
$n \to \nu\eta$	> 158	90%	310
$N \to e^+\rho$	$> 217\ (n)$, $> 710\ (p)$	90%	149
$N \to \mu^+\rho$	$> 228\ (n)$, $> 160\ (p)$	90%	113
$N \to \nu\rho$	$> 19\ (n)$, $> 162\ (p)$	90%	149
$p \to e^+\omega$	> 320	90%	143
$p \to \mu^+\omega$	> 780	90%	105
$n \to \nu\omega$	> 108	90%	144
$N \to e^+K$	$> 17\ (n)$, $> 1000\ (p)$	90%	339
$N \to \mu^+K$	$> 26\ (n)$, $> 1600\ (p)$	90%	329
$N \to \nu K$	$> 86\ (n)$, $> 5900\ (p)$	90%	339
$n \to \nu K^0_S$	> 260	90%	338
$p \to e^+K^*(892)^0$	> 84	90%	45
$N \to \nu K^*(892)$	$> 78\ (n)$, $> 51\ (p)$	90%	45
Antilepton + mesons			
$p \to e^+\pi^+\pi^-$	> 82	90%	448
$p \to e^+\pi^0\pi^0$	> 147	90%	449
$n \to e^+\pi^-\pi^0$	> 52	90%	449
$p \to \mu^+\pi^+\pi^-$	> 133	90%	425
$p \to \mu^+\pi^0\pi^0$	> 101	90%	427
$n \to \mu^+\pi^-\pi^0$	> 74	90%	427
$n \to e^+K^0\pi^-$	> 18	90%	319
Lepton + meson			
$n \to e^-\pi^+$	> 65	90%	459
$n \to \mu^-\pi^+$	> 49	90%	453
$n \to e^-\rho^+$	> 62	90%	150
$n \to \mu^-\rho^+$	> 7	90%	115
$n \to e^-K^+$	> 32	90%	340
$n \to \mu^-K^+$	> 57	90%	330
Lepton + mesons			
$p \to e^-\pi^+\pi^+$	> 30	90%	448
$n \to e^-\pi^+\pi^0$	> 29	90%	449
$p \to \mu^-\pi^+\pi^+$	> 17	90%	425
$n \to \mu^-\pi^+\pi^0$	> 34	90%	427
$p \to e^-\pi^+K^+$	> 75	90%	320
$p \to \mu^-\pi^+K^+$	> 245	90%	279
Antilepton + photon(s)			
$p \to e^+\gamma$	> 670	90%	469
$p \to \mu^+\gamma$	> 478	90%	463
$n \to \nu\gamma$	> 550	90%	470
$p \to e^+\gamma\gamma$	> 100	90%	469
$n \to \nu\gamma\gamma$	> 219	90%	470
Antilepton + single massless			
$p \to e^+X$	> 790	90%	–
$p \to \mu^+X$	> 410	90%	–
Three (or more) leptons			
$p \to e^+e^+e^-$	> 793	90%	469
$p \to e^+\mu^+\mu^-$	> 359	90%	457
$p \to e^+\nu\nu$	> 170	90%	469
$n \to e^+e^-\nu$	> 257	90%	470
$n \to \mu^+e^-\nu$	> 83	90%	464
$n \to \mu^+\mu^-\nu$	> 79	90%	458
$p \to \mu^+e^+e^-$	> 529	90%	463
$p \to \mu^+\mu^+\mu^-$	> 675	90%	439
$p \to \mu^+\nu\nu$	> 220	90%	463
$p \to e^-\mu^+\mu^+$	> 6	90%	457
$n \to 3\nu$	$> 5 \times 10^{-4}$	90%	470
Inclusive modes			
$N \to e^+$ anything	$> 0.6\ (n, p)$	90%	–
$N \to \mu^+$ anything	$> 12\ (n, p)$	90%	–
$N \to e^+\pi^0$ anything	$> 0.6\ (n, p)$	90%	–
$\Delta B = 2$ dinucleon modes			
The following are lifetime limits per iron nucleus.			
$pp \to \pi^+\pi^+$	> 72.2	90%	–
$pn \to \pi^+\pi^0$	> 170	90%	–
$nn \to \pi^+\pi^-$	> 0.7	90%	–
$nn \to \pi^0\pi^0$	> 404	90%	–
$pp \to K^+K^+$	> 170	90%	–
$pp \to e^+e^+$	> 5.8	90%	–
$pp \to e^+\mu^+$	> 3.6	90%	–
$pp \to \mu^+\mu^+$	> 1.7	90%	–
$pn \to e^+\overline{\nu}$	> 260	90%	–
$pn \to \mu^+\overline{\nu}$	> 200	90%	–
$pn \to \tau^+\overline{\nu}_\tau$	> 29	90%	–
$nn \to \nu_e\overline{\nu}_e$	> 1.4	90%	–
$nn \to \nu_\mu\overline{\nu}_\mu$	> 1.4	90%	–
$pn \to$ invisible	$> 2.1 \times 10^{-5}$	90%	–
$pp \to$ invisible	$> 5 \times 10^{-5}$	90%	–

$\overline{p}$ DECAY MODES

$\overline{p}$ DECAY MODES	Partial mean life (years)	Confidence level	p (MeV/c)
$\overline{p} \to e^-\gamma$	$> 7 \times 10^5$	90%	469
$\overline{p} \to \mu^-\gamma$	$> 5 \times 10^4$	90%	463
$\overline{p} \to e^-\pi^0$	$> 4 \times 10^5$	90%	459
$\overline{p} \to \mu^-\pi^0$	$> 5 \times 10^4$	90%	453
$\overline{p} \to e^-\eta$	$> 2 \times 10^4$	90%	309
$\overline{p} \to \mu^-\eta$	$> 8 \times 10^3$	90%	297
$\overline{p} \to e^-K^0_S$	> 900	90%	337
$\overline{p} \to \mu^-K^0_S$	$> 4 \times 10^3$	90%	326
$\overline{p} \to e^-K^0_L$	$> 9 \times 10^3$	90%	337
$\overline{p} \to \mu^-K^0_L$	$> 7 \times 10^3$	90%	326
$\overline{p} \to e^-\gamma\gamma$	$> 2 \times 10^4$	90%	469
$\overline{p} \to \mu^-\gamma\gamma$	$> 2 \times 10^4$	90%	463
$\overline{p} \to e^-\omega$	> 200	90%	143

n

$I(J^P) = \frac{1}{2}(\frac{1}{2}^+)$

Mass $m = 1.0086649159 \pm 0.0000000005$ u
Mass $m = 939.565413 \pm 0.000006$ MeV [a]
$(m_n - m_{\overline{n}})/\ m_n = (9 \pm 6) \times 10^{-5}$
$m_n - m_p = 1.2933321 \pm 0.0000005$ MeV
$= 0.00138844919(45)$ u
Mean life $\tau = 880.2 \pm 1.0$ s (S = 1.9)
$c\tau = 2.6387 \times 10^8$ km
Magnetic moment $\mu = -1.9130427 \pm 0.0000005\ \mu_N$
Electric dipole moment $d < 0.30 \times 10^{-25}$ $e$cm, CL = 90%
Mean-square charge radius $\langle r_n^2 \rangle = -0.1161 \pm 0.0022$ fm^2 (S = 1.3)

Magnetic radius $\sqrt{\langle r_M^2 \rangle} = 0.864 \,^{+0.009}_{-0.008}$ fm
Electric polarizability $\alpha = (11.8 \pm 1.1) \times 10^{-4}$ fm^3
Magnetic polarizability $\beta = (3.7 \pm 1.2) \times 10^{-4}$ fm^3
Charge $q = (-0.2 \pm 0.8) \times 10^{-21}$ e
Mean $n\overline{n}$-oscillation time $> 8.6 \times 10^7$ s, CL = 90% (free n)
Mean $n\overline{n}$-oscillation time $> 2.7 \times 10^8$ s, CL = 90% [g] (bound n)
Mean nn'-oscillation time > 414 s, CL = 90% [h]

$p e^- \nu_e$ decay parameters [i]

$\lambda \equiv g_A / g_V = -1.2724 \pm 0.0023$ (S = 2.2)
$A = -0.1184 \pm 0.0010$ (S = 2.4)
$B = 0.9807 \pm 0.0030$
$C = -0.2377 \pm 0.0026$
$a = -0.1059 \pm 0.0028$
$\phi_{AV} = (180.017 \pm 0.026)^\circ$ [j]
$D = (-1.2 \pm 2.0) \times 10^{-4}$ [k]
$R = 0.004 \pm 0.013$ [k]

n DECAY MODES	Fraction (Γ_i/Γ)	Confidence level	p (MeV/c)
$p e^- \overline{\nu}_e$	100 %		1
$p e^- \overline{\nu}_e \gamma$	[l] (9.2±0.7) $\times 10^{-3}$		1
Charge conservation (Q) violating mode			
$p \nu_e \overline{\nu}_e$	Q < 8 $\times 10^{-27}$	68%	1

$N(1440)$ 1/2$^+$

$I(J^P) = \frac{1}{2}(\frac{1}{2}^+)$

Re(pole position) = 1360 to 1380 (≈ 1370) MeV
−2Im(pole position) = 160 to 190 (≈ 175) MeV
Breit-Wigner mass = 1410 to 1470 (≈ 1440) MeV
Breit-Wigner full width = 250 to 450 (≈ 350) MeV

$N(1440)$ DECAY MODES	Fraction (Γ_i/Γ)	p (MeV/c)
$N\pi$	55–75 %	398
$N\eta$	<1 %	†
$N\pi\pi$	17–50 %	347
$\Delta(1232)\pi$, P-wave	6–27 %	147
$N\sigma$	11–23 %	–
$p\gamma$, helicity=1/2	0.035–0.048 %	414
$n\gamma$, helicity=1/2	0.02–0.04 %	413

$N(1520)$ 3/2$^-$

$I(J^P) = \frac{1}{2}(\frac{3}{2}^-)$

Re(pole position) = 1505 to 1515 (≈ 1510) MeV
−2Im(pole position) = 105 to 120 (≈ 110) MeV
Breit-Wigner mass = 1510 to 1520 (≈ 1515) MeV
Breit-Wigner full width = 100 to 120 (≈ 110) MeV

$N(1520)$ DECAY MODES	Fraction (Γ_i/Γ)	p (MeV/c)
$N\pi$	55–65 %	453
$N\eta$	0.07–0.09 %	142
$N\pi\pi$	25–35 %	410
$\Delta(1232)\pi$	22–34 %	225
$\Delta(1232)\pi$, S-wave	15–23 %	225
$\Delta(1232)\pi$, D-wave	7–11 %	225
$N\sigma$	< 2 %	–
$p\gamma$	0.31–0.52 %	467
$p\gamma$, helicity=1/2	0.01–0.02 %	467
$p\gamma$, helicity=3/2	0.30–0.50 %	467
$n\gamma$	0.30–0.53 %	466
$n\gamma$, helicity=1/2	0.04–0.10 %	466
$n\gamma$, helicity=3/2	0.25–0.45 %	466

$N(1535)$ 1/2$^-$

$I(J^P) = \frac{1}{2}(\frac{1}{2}^-)$

Re(pole position) = 1500 to 1520 (≈ 1510) MeV
−2Im(pole position) = 110 to 150 (≈ 130) MeV
Breit-Wigner mass = 1515 to 1545 (≈ 1530) MeV
Breit-Wigner full width = 125 to 175 (≈ 150) MeV

$N(1535)$ DECAY MODES	Fraction (Γ_i/Γ)	p (MeV/c)
$N\pi$	32–52 %	464
$N\eta$	30–55 %	176
$N\pi\pi$	3–14 %	422
$\Delta(1232)\pi$, D-wave	1–4 %	240
$N\sigma$	2–10 %	–
$N(1440)\pi$	5–12 %	†
$p\gamma$, helicity=1/2	0.15–0.30 %	477
$n\gamma$, helicity=1/2	0.01–0.25 %	477

$N(1650)$ 1/2$^-$

$I(J^P) = \frac{1}{2}(\frac{1}{2}^-)$

Re(pole position) = 1640 to 1670 (≈ 1655) MeV
−2Im(pole position) = 100 to 170 (≈ 135) MeV
Breit-Wigner mass = 1635 to 1665 (≈ 1650) MeV
Breit-Wigner full width = 100 to 150 (≈ 125) MeV

$N(1650)$ DECAY MODES	Fraction (Γ_i/Γ)	p (MeV/c)
$N\pi$	50–70 %	547
$N\eta$	15–35 %	348
ΛK	5–15 %	169
$N\pi\pi$	8–36 %	514
$\Delta(1232)\pi$, D-wave	6–18 %	345
$N\sigma$	2–18 %	–
$N(1440)\pi$	6–26 %	150
$p\gamma$, helicity=1/2	0.04–0.20 %	558
$n\gamma$, helicity=1/2	0.003–0.17 %	557

$N(1675)$ 5/2$^-$

$I(J^P) = \frac{1}{2}(\frac{5}{2}^-)$

Re(pole position) = 1655 to 1665 (≈ 1660) MeV
−2Im(pole position) = 125 to 150 (≈ 135) MeV
Breit-Wigner mass = 1665 to 1680 (≈ 1675) MeV
Breit-Wigner full width = 130 to 160 (≈ 145) MeV

$N(1675)$ DECAY MODES	Fraction (Γ_i/Γ)	p (MeV/c)
$N\pi$	38–42 %	564
$N\eta$	< 1 %	376
$N\pi\pi$	25–45 %	532
$\Delta(1232)\pi$, D-wave	23–37 %	366
$N\sigma$	3–7 %	–
$p\gamma$	0–0.02 %	575
$p\gamma$, helicity=1/2	0–0.01 %	575
$p\gamma$, helicity=3/2	0–0.01 %	575
$n\gamma$	0–0.15 %	574
$n\gamma$, helicity=1/2	0–0.05 %	574
$n\gamma$, helicity=3/2	0–0.10 %	574

$N(1680)$ 5/2$^+$

$I(J^P) = \frac{1}{2}(\frac{5}{2}^+)$

Re(pole position) = 1665 to 1680 (≈ 1675) MeV
−2Im(pole position) = 110 to 135 (≈ 120) MeV
Breit-Wigner mass = 1680 to 1690 (≈ 1685) MeV
Breit-Wigner full width = 115 to 130 (≈ 120) MeV

$N(1680)$ DECAY MODES	Fraction (Γ_i/Γ)	p (MeV/c)
$N\pi$	60–70 %	571
$N\eta$	<1 %	386
$N\pi\pi$	20–40 %	539
$\Delta(1232)\pi$	11–23 %	374
$\Delta(1232)\pi$, P-wave	4–10 %	374
$\Delta(1232)\pi$, F-wave	1–13 %	374
$N\sigma$	9–19 %	–
$p\gamma$	0.21–0.32 %	581
$p\gamma$, helicity=1/2	0.001–0.011 %	581
$p\gamma$, helicity=3/2	0.20–0.32 %	581
$n\gamma$	0.021–0.046 %	581
$n\gamma$, helicity=1/2	0.004–0.029 %	581
$n\gamma$, helicity=3/2	0.01–0.024 %	581

Baryon Summary Table

$N(1700)\ 3/2^-$

$I(J^P) = \frac{1}{2}(\frac{3}{2}^-)$

Re(pole position) = 1650 to 1750 (≈ 1700) MeV
−2Im(pole position) = 100 to 300 (≈ 200) MeV
Breit-Wigner mass = 1650 to 1800 (≈ 1720) MeV
Breit-Wigner full width = 100 to 300 (≈ 200) MeV

$N(1700)$ DECAY MODES	Fraction (Γ_i/Γ)	p (MeV/c)
$N\pi$	7–17 %	594
$N\eta$	seen	422
$N\omega$	10–34 %	†
$N\pi\pi$	60–90 %	564
$\Delta(1232)\pi$	55–85 %	402
$\Delta(1232)\pi$, S-wave	50–80 %	402
$\Delta(1232)\pi$, D-wave	4–14 %	402
$N(1440)\pi$	3–11 %	225
$N(1520)\pi$	<4 %	145
$N\rho$, S=3/2, S-wave	32–44 %	74
$N\sigma$	2–14 %	–
$p\gamma$	0.01–0.05 %	604
$p\gamma$, helicity=1/2	0.0–0.024 %	604
$p\gamma$, helicity=3/2	0.002–0.026 %	604
$n\gamma$	0.01–0.13 %	603
$n\gamma$, helicity=1/2	0.0–0.09 %	603
$n\gamma$, helicity=3/2	0.01–0.05 %	603

$N(1710)\ 1/2^+$

$I(J^P) = \frac{1}{2}(\frac{1}{2}^+)$

Re(pole position) = 1680 to 1720 (≈ 1700) MeV
−2Im(pole position) = 80 to 160 (≈ 120) MeV
Breit-Wigner mass = 1680 to 1740 (≈ 1710) MeV
Breit-Wigner full width = 80 to 200 (≈ 140) MeV

$N(1710)$ DECAY MODES	Fraction (Γ_i/Γ)	p (MeV/c)
$N\pi$	5–20 %	588
$N\eta$	10–50 %	412
$N\omega$	1–5 %	†
ΛK	5–25 %	269
ΣK	seen	138
$N\pi\pi$	seen	557
$\Delta(1232)\pi$, P-wave	3–9 %	394
$N(1535)\pi$	9–21 %	113
$N\rho$, S=1/2, P-wave	11–23 %	†
$p\gamma$, helicity=1/2	0.002–0.08 %	598
$n\gamma$, helicity=1/2	0.0–0.02%	597

$N(1720)\ 3/2^+$

$I(J^P) = \frac{1}{2}(\frac{3}{2}^+)$

Re(pole position) = 1660 to 1690 (≈ 1675) MeV
−2Im(pole position) = 150 to 400 (≈ 250) MeV
Breit-Wigner mass = 1680 to 1750 (≈ 1720) MeV
Breit-Wigner full width = 150 to 400 (≈ 250) MeV

$N(1720)$ DECAY MODES	Fraction (Γ_i/Γ)	p (MeV/c)
$N\pi$	8–14 %	594
$N\eta$	1–5 %	422
$N\omega$	12–40 %	†
ΛK	4–5 %	283
$N\pi\pi$	50–90 %	564
$\Delta(1232)\pi$	47–89 %	402
$\Delta(1232)\pi$, P-wave	47–77 %	402
$\Delta(1232)\pi$, F-wave	<12 %	402
$N\rho$, S=1/2, P-wave	1–2 %	74
$N\sigma$	2–14 %	–
$N(1440)\pi$	<2 %	225
$N(1520)\pi$, S-wave	1–5 %	145
$p\gamma$	0.05–0.25 %	604
$p\gamma$, helicity=1/2	0.05–0.15 %	604
$p\gamma$, helicity=3/2	0.002–0.16 %	604
$n\gamma$	0.0–0.016 %	603
$n\gamma$, helicity=1/2	0.0–0.01 %	603
$n\gamma$, helicity=3/2	0.0–0.015 %	603

$N(1875)\ 3/2^-$

$I(J^P) = \frac{1}{2}(\frac{3}{2}^-)$

Re(pole position) = 1850 to 1950 (≈ 1900) MeV
−2Im(pole position) = 100 to 220 (≈ 160) MeV
Breit-Wigner mass = 1850 to 1920 (≈ 1875) MeV
Breit-Wigner full width = 120 to 250 (≈ 200) MeV

$N(1875)$ DECAY MODES	Fraction (Γ_i/Γ)	p (MeV/c)
$N\pi$	3–11 %	695
$N\eta$	<1 %	559
$N\omega$	15–25 %	371
ΛK	seen	454
ΣK	seen	384
$N\pi\pi$	40–95 %	670
$\Delta(1232)\pi$	10–35 %	520
$\Delta(1232)\pi$, S-wave	7–21 %	520
$\Delta(1232)\pi$, D-wave	2–12 %	520
$N\rho$, S=3/2, S-wave	seen	379
$N\sigma$	30–60 %	–
$N(1440)\pi$	2–8 %	365
$N(1520)\pi$	<2 %	301
$p\gamma$	0.001–0.025 %	703
$p\gamma$, helicity=1/2	0.001–0.021 %	703
$p\gamma$, helicity=3/2	<0.003 %	703
$n\gamma$	<0.040 %	702
$n\gamma$, helicity=1/2	<0.007 %	702
$n\gamma$, helicity=3/2	<0.033 %	702

$N(1880)\ 1/2^+$

$I(J^P) = \frac{1}{2}(\frac{1}{2}^+)$

Re(pole position) = 1820 to 1900 (≈ 1860) MeV
−2Im(pole position) = 180 to 280 (≈ 230) MeV
Breit-Wigner mass = 1830 to 1930 (≈ 1880) MeV
Breit-Wigner full width = 200 to 400 (≈ 300) MeV

$N(1880)$ DECAY MODES	Fraction (Γ_i/Γ)	p (MeV/c)
$N\pi$	3–9 %	698
$N\eta$	5–55 %	563
$N\omega$	12–28 %	377
ΛK	12–28 %	459
ΣK	10–24 %	389
$N\pi\pi$	30–80 %	673
$\Delta(1232)\pi$	18–42 %	524
$N\sigma$	10–40 %	539
$N(1535)\pi$	4–12 %	293
$Na_0(980)$	1–5 %	†
$\Lambda K^*(892)$	0.5–1 %	†
$p\gamma$, helicity=1/2	seen	706
$n\gamma$, helicity=1/2	0.002–0.63 %	705

$N(1895)\ 1/2^-$

$I(J^P) = \frac{1}{2}(\frac{1}{2}^-)$

Re(pole position) = 1890 to 1930 (≈ 1910) MeV
−2Im(pole position) = 80 to 140 (≈ 110) MeV
Breit-Wigner mass = 1870 to 1920 (≈ 1895) MeV
Breit-Wigner full width = 80 to 200 (≈ 120) MeV

$N(1895)$ DECAY MODES	Fraction (Γ_i/Γ)	p (MeV/c)
$N\pi$	2–18 %	707
$N\eta$	15–40 %	575
$N\eta'$	10–40 %	†
$N\omega$	16–40 %	395
ΛK	13–23 %	473
ΣK	6–20 %	405
$\Delta(1232)\pi$, D-wave	3–11 %	535
$N\rho$, S=1/2, S-wave	seen	403
$N\rho$, S=3/2, D-wave	3–12 %	403
$\Lambda K^*(892)$	4–9 %	†
$N\sigma$	seen	–
$N(1440)\pi$	1–4 %	382
$p\gamma$, helicity=1/2	0.01–0.06 %	715
$n\gamma$, helicity=1/2	0.003–0.05 %	715

$N(1900)\ 3/2^+$

$I(J^P) = \frac{1}{2}(\frac{3}{2}^+)$

Re(pole position) = 1900 to 1940 (≈ 1920) MeV
−2Im(pole position) = 100 to 200 (≈ 150) MeV
Breit-Wigner mass = 1890 to 1950 (≈ 1920) MeV
Breit-Wigner full width = 100 to 320 (≈ 200) MeV

$N(1900)$ DECAY MODES	Fraction (Γ_i/Γ)	p (MeV/c)
$N\pi$	1–20 %	723
$N\eta$	2–14 %	595
$N\eta'$	4–8 %	151
$N\omega$	7–13 %	424
ΛK	2–20 %	495
ΣK	3–7 %	431
$N\pi\pi$	40–80 %	699
$\Delta(1232)\pi$	30–70 %	553
$\Delta(1232)\pi$, P-wave	9–25 %	553
$\Delta(1232)\pi$, F-wave	21–45 %	553
$\Lambda K^*(892)$	< 0.2 %	†
$N\sigma$	1–7 %	–
$N(1520)\pi$	7–23 %	341
$N(1535)\pi$	4–10 %	328
$p\gamma$	0.001–0.025 %	731
$p\gamma$, helicity=1/2	0.001–0.021 %	731
$p\gamma$, helicity=3/2	<0.003 %	731
$n\gamma$	<0.040 %	730
$n\gamma$, helicity=1/2	<0.007 %	730
$n\gamma$, helicity=3/2	<0.033 %	730

$N(2060)\ 5/2^-$

$I(J^P) = \frac{1}{2}(\frac{5}{2}^-)$

Re(pole position) = 2020 to 2130 (≈ 2070) MeV
−2Im(pole position) = 350 to 430 (≈ 400) MeV
Breit-Wigner mass = 2030 to 2200 (≈ 2100) MeV
Breit-Wigner full width = 300 to 450 (≈ 400) MeV

$N(2060)$ DECAY MODES	Fraction (Γ_i/Γ)	p (MeV/c)
$N\pi$	7–12 %	834
$N\eta$	2–6 %	729
$N\omega$	1–7 %	600
ΛK	seen	644
ΣK	1–5 %	593
$N\pi\pi$	7–19 %	814
$\Delta(1232)\pi$, D-wave	4–10 %	680
$N\rho$, S=1/2, P-wave	seen	605
$\Lambda K^*(892)$	0.3–1.3 %	307
$N\sigma$	3–9 %	–
$N(1440)\pi$	4–14 %	544
$N(1520)\pi$, P-wave	9–21 %	490
$N(1680)\pi$, S-wave	8–22 %	353
$p\gamma$	0.03–0.19 %	840
$p\gamma$, helicity=1/2	0.02–0.08 %	840
$p\gamma$, helicity=3/2	0.01–0.10 %	840
$n\gamma$	0.003–0.07 %	840
$n\gamma$, helicity=1/2	0.001–0.02 %	840
$n\gamma$, helicity=3/2	0.002–0.05 %	840

$N(2100)\ 1/2^+$

$I(J^P) = \frac{1}{2}(\frac{1}{2}^+)$

Re(pole position) = 2050 to 2150 (≈ 2100) MeV
−2Im(pole position) = 240 to 340 (≈ 300) MeV
Breit-Wigner mass = 2050 to 2150 (≈ 2100) MeV
Breit-Wigner full width = 200 to 320 (≈ 260) MeV

$N(2100)$ DECAY MODES	Fraction (Γ_i/Γ)	p (MeV/c)
$N\pi$	8–18 %	834
$N\eta$	seen	729
$N\eta'$	5–11 %	451
$N\omega$	10–25 %	600
ΛK	seen	644
$N\pi\pi$	20–40 %	814
$\Delta(1232)\pi$, P-wave	6–14 %	680
$N\rho$, S=1/2, P-wave	seen	605
$\Lambda K^*(892)$	3–11 %	307
$N\sigma$	14–26 %	–
$N(1535)\pi$	26–34 %	478
$N\gamma$, helicity=1/2	0.001–0.012 %	840

$N(2120)\ 3/2^-$

$I(J^P) = \frac{1}{2}(\frac{3}{2}^-)$

Re(pole position) = 2050 to 2150 (≈ 2100) MeV
−2Im(pole position) = 200 to 360 (≈ 280) MeV
Breit-Wigner mass = 2060 to 2160 (≈ 2120) MeV
Breit-Wigner full width = 260 to 360 (≈ 300) MeV

$N(2120)$ DECAY MODES	Fraction (Γ_i/Γ)	p (MeV/c)
$N\pi$	5–15 %	846
$N\eta'$	2–6 %	474
$N\omega$	4–20 %	617
$N\pi\pi$	50–95 %	827
$\Delta(1232)\pi$	40–90 %	693
$\Delta(1232)\pi$, S-wave	30–70 %	693
$\Delta(1232)\pi$, D-wave	8–32 %	693
$\Lambda K^*(892)$	< 0.2 %	339
$N\sigma$	7–15 %	–
$N(1535)\pi$	7–23 %	494
$p\gamma$	0.16–2.1 %	852
$p\gamma$, helicity=1/2	0.07–0.80 %	852
$p\gamma$, helicity=3/2	0.09–1.3 %	852
$n\gamma$	0.04–0.72 %	852
$n\gamma$, helicity=1/2	0.04–0.60 %	852
$n\gamma$, helicity=3/2	0.001–0.12 %	852

$N(2190)\ 7/2^-$

$I(J^P) = \frac{1}{2}(\frac{7}{2}^-)$

Re(pole position) = 2050 to 2150 (≈ 2100) MeV
−2Im(pole position) = 300 to 500 (≈ 400) MeV
Breit-Wigner mass = 2140 to 2220 (≈ 2180) MeV
Breit-Wigner full width = 300 to 500 (≈ 400) MeV

$N(2190)$ DECAY MODES	Fraction (Γ_i/Γ)	p (MeV/c)
$N\pi$	10–20 %	882
$N\eta$	1–3 %	785
$N\omega$	8–20 %	667
$\Delta(1232)\pi$, D-wave	19–31 %	734
$N\rho$, S=3/2, D-wave	seen	672
$\Lambda K^*(892)$	0.2–0.8 %	423
$N\sigma$	3–9 %	–
$p\gamma$	0.014–0.077 %	888
$n\gamma$	<0.04 %	888
$n\gamma$, helicity=3/2	<0.03 %	888

$N(2220)\ 9/2^+$

$I(J^P) = \frac{1}{2}(\frac{9}{2}^+)$

Re(pole position) = 2130 to 2200 (≈ 2170) MeV
−2Im(pole position) = 360 to 480 (≈ 400) MeV
Breit-Wigner mass = 2200 to 2300 (≈ 2250) MeV
Breit-Wigner full width = 350 to 500 (≈ 400) MeV

$N(2220)$ DECAY MODES	Fraction (Γ_i/Γ)	p (MeV/c)
$N\pi$	15–30 %	924

$N(2250)\ 9/2^-$

$I(J^P) = \frac{1}{2}(\frac{9}{2}^-)$

Re(pole position) = 2150 to 2250 (≈ 2200) MeV
−2Im(pole position) = 350 to 500 (≈ 420) MeV
Breit-Wigner mass = 2250 to 2320 (≈ 2280) MeV
Breit-Wigner full width = 300 to 600 (≈ 500) MeV

$N(2250)$ DECAY MODES	Fraction (Γ_i/Γ)	p (MeV/c)
$N\pi$	0.05 to 0.15 (≈ 0.10)	941

Baryon Summary Table

$N(2600)\ 11/2^-$

$I(J^P) = \frac{1}{2}(\frac{11}{2}^-)$

Breit-Wigner mass = 2550 to 2750 (≈ 2600) MeV
Breit-Wigner full width = 500 to 800 (≈ 650) MeV

$N(2600)$ DECAY MODES	Fraction (Γ_i/Γ)	p (MeV/c)
$N\pi$	3–8 %	1126

Δ BARYONS ($S=0, I=3/2$)

$\Delta^{++} = uuu$, $\Delta^{+} = uud$, $\Delta^{0} = udd$, $\Delta^{-} = ddd$

$\Delta(1232)\ 3/2^+$

$I(J^P) = \frac{3}{2}(\frac{3}{2}^+)$

Re(pole position) = 1209 to 1211 (≈ 1210) MeV
-2Im(pole position) = 98 to 102 (≈ 100) MeV
Breit-Wigner mass (mixed charges) = 1230 to 1234 (≈ 1232) MeV
Breit-Wigner full width (mixed charges) = 114 to 120 (≈ 117) MeV

$\Delta(1232)$ DECAY MODES	Fraction (Γ_i/Γ)	p (MeV/c)
$N\pi$	99.4 %	229
$N\gamma$	0.55–0.65 %	259
$N\gamma$, helicity=1/2	0.11–0.13 %	259
$N\gamma$, helicity=3/2	0.44–0.52 %	259
pe^+e^-	$(4.2\pm0.7)\times10^{-5}$	259

$\Delta(1600)\ 3/2^+$

$I(J^P) = \frac{3}{2}(\frac{3}{2}^+)$

Re(pole position) = 1460 to 1560 (≈ 1510) MeV
-2Im(pole position) = 200 to 340 (≈ 270) MeV
Breit-Wigner mass = 1500 to 1640 (≈ 1570) MeV
Breit-Wigner full width = 200 to 300 (≈ 250) MeV

$\Delta(1600)$ DECAY MODES	Fraction (Γ_i/Γ)	p (MeV/c)
$N\pi$	8–24 %	492
$N\pi\pi$	75–90 %	454
$\Delta(1232)\pi$	73–83 %	276
$\Delta(1232)\pi$, P-wave	72–82 %	276
$\Delta(1232)\pi$, F-wave	<2 %	276
$N(1440)\pi$, P-wave	15–25 %	†
$N\gamma$	0.001–0.035 %	505
$N\gamma$, helicity=1/2	0.0–0.02 %	505
$N\gamma$, helicity=3/2	0.001–0.015 %	505

$\Delta(1620)\ 1/2^-$

$I(J^P) = \frac{3}{2}(\frac{1}{2}^-)$

Re(pole position) = 1590 to 1610 (≈ 1600) MeV
-2Im(pole position) = 100 to 140 (≈ 120) MeV
Breit-Wigner mass = 1590 to 1630 (≈ 1610) MeV
Breit-Wigner full width = 110 to 150 (≈ 130) MeV

$\Delta(1620)$ DECAY MODES	Fraction (Γ_i/Γ)	p (MeV/c)
$N\pi$	25–35 %	520
$N\pi\pi$	55–80 %	484
$\Delta(1232)\pi$, D-wave	52–72 %	311
$N\rho$, S=1/2, S-wave	seen	†
$N\rho$, S=3/2, D-wave	seen	†
$N(1440)\pi$	3–9 %	98
$N\gamma$, helicity=1/2	0.03–0.10 %	532

$\Delta(1700)\ 3/2^-$

$I(J^P) = \frac{3}{2}(\frac{3}{2}^-)$

Re(pole position) = 1640 to 1690 (≈ 1665) MeV
-2Im(pole position) = 200 to 300 (≈ 250) MeV
Breit-Wigner mass = 1690 to 1730 (≈ 1710) MeV
Breit-Wigner full width = 220 to 380 (≈ 300) MeV

$\Delta(1700)$ DECAY MODES	Fraction (Γ_i/Γ)	p (MeV/c)
$N\pi$	10–20 %	588
$N\pi\pi$	10–55 %	557
$\Delta(1232)\pi$	10–50 %	394
$\Delta(1232)\pi$, S-wave	5–35 %	394
$\Delta(1232)\pi$, D-wave	4–16 %	394
$N\rho$, S=3/2, S-wave	seen	†
$N(1520)\pi$, P-wave	1–5 %	133
$N(1535)\pi$	0.5–1.5 %	113
$\Delta(1232)\eta$	3–7 %	†
$N\gamma$	0.22–0.60 %	598
$N\gamma$, helicity=1/2	0.12–0.30 %	598
$N\gamma$, helicity=3/2	0.10–0.30 %	598

$\Delta(1900)\ 1/2^-$

$I(J^P) = \frac{3}{2}(\frac{1}{2}^-)$

Re(pole position) = 1830 to 1900 (≈ 1865) MeV
-2Im(pole position) = 180 to 300 (≈ 240) MeV
Breit-Wigner mass = 1840 to 1920 (≈ 1860) MeV
Breit-Wigner full width = 180 to 320 (≈ 250) MeV

$\Delta(1900)$ DECAY MODES	Fraction (Γ_i/Γ)	p (MeV/c)
$N\pi$	4–12 %	685
ΣK	seen	367
$N\pi\pi$	45–85 %	660
$\Delta(1232)\pi$, D-wave	30–70 %	509
$N\rho$, S=1/2, S-wave	8–16 %	360
$N\rho$, S=3/2, D-wave	18–28 %	360
$N(1440)\pi$	8–32 %	353
$N(1520)\pi$	2–10 %	288
$\Delta(1232)\eta$	0–2 %	251
$N\gamma$, helicity=1/2	0.06–0.43 %	693

$\Delta(1905)\ 5/2^+$

$I(J^P) = \frac{3}{2}(\frac{5}{2}^+)$

Re(pole position) = 1770 to 1830 (≈ 1800) MeV
-2Im(pole position) = 260 to 340 (≈ 300) MeV
Breit-Wigner mass = 1855 to 1910 (≈ 1880) MeV
Breit-Wigner full width = 270 to 400 (≈ 330) MeV

$\Delta(1905)$ DECAY MODES	Fraction (Γ_i/Γ)	p (MeV/c)
$N\pi$	9–15 %	698
$N\pi\pi$		673
$\Delta(1232)\pi$	80–100 %	524
$\Delta(1232)\pi$, P-wave	23–43 %	524
$\Delta(1232)\pi$, F-wave	56–72 %	524
$N\rho$, S=3/2, P-wave	seen	385
$N(1535)\pi$	< 1 %	293
$N(1680)\pi$, P-wave	5–15 %	133
$\Delta(1232)\eta$	2–6 %	282
$N\gamma$	0.012–0.036 %	706
$N\gamma$, helicity=1/2	0.002–0.006 %	706
$N\gamma$, helicity=3/2	0.01–0.03 %	706

$\Delta(1910)\ 1/2^+$

$I(J^P) = \frac{3}{2}(\frac{1}{2}^+)$

Re(pole position) = 1830 to 1890 (≈ 1860) MeV
-2Im(pole position) = 200 to 400 (≈ 300) MeV
Breit-Wigner mass = 1850 to 1950 (≈ 1900) MeV
Breit-Wigner full width = 200 to 400 (≈ 300) MeV

$\Delta(1910)$ DECAY MODES	Fraction (Γ_i/Γ)	p (MeV/c)
$N\pi$	15–30 %	710
ΣK	4–14 %	410

$N\pi\pi$		686
$\Delta(1232)\pi$	34–66 %	539
$N(1440)\pi$	3–9 %	386
$\Delta(1232)\eta$	5–13 %	310
$N\gamma$, helicity=1/2	0.0–0.02 %	718

$\Delta(1920)$ 3/2$^+$

$I(J^P) = \frac{3}{2}(\frac{3}{2}^+)$

Re(pole position) = 1850 to 1950 ($\approx$ 1900) MeV
-2Im(pole position) = 200 to 400 ($\approx$ 300) MeV
Breit-Wigner mass = 1870 to 1970 ($\approx$ 1920) MeV
Breit-Wigner full width = 240 to 360 ($\approx$ 300) MeV

$\Delta(1920)$ DECAY MODES	Fraction (Γ_i/Γ)	p (MeV/c)
$N\pi$	5–20 %	723
ΣK	2–6 %	431
$N\pi\pi$		699
$\Delta(1232)\pi$	50–90 %	553
$\Delta(1232)\pi$, P-wave	8–28 %	553
$\Delta(1232)\pi$, F-wave	44–72 %	553
$N(1440)\pi$, P-wave	<4 %	403
$N(1520)\pi$, S-wave	<5 %	341
$N(1535)\pi$	<2 %	328
$Na_0(980)$	seen	41
$\Delta(1232)\eta$	5–17 %	336

$\Delta(1930)$ 5/2$^-$

$I(J^P) = \frac{3}{2}(\frac{5}{2}^-)$

Re(pole position) = 1840 to 1920 ($\approx$ 1880) MeV
-2Im(pole position) = 230 to 330 ($\approx$ 280) MeV
Breit-Wigner mass = 1900 to 2000 ($\approx$ 1950) MeV
Breit-Wigner full width = 200 to 400 ($\approx$ 300) MeV

$\Delta(1930)$ DECAY MODES	Fraction (Γ_i/Γ)	p (MeV/c)
$N\pi$	5–15 %	742
$N\gamma$	0.0–0.01 %	749
$N\gamma$, helicity=1/2	0.0–0.005 %	749
$N\gamma$, helicity=3/2	0.0–0.004 %	749

$\Delta(1950)$ 7/2$^+$

$I(J^P) = \frac{3}{2}(\frac{7}{2}^+)$

Re(pole position) = 1870 to 1890 ($\approx$ 1880) MeV
-2Im(pole position) = 220 to 260 ($\approx$ 240) MeV
Breit-Wigner mass = 1915 to 1950 ($\approx$ 1930) MeV
Breit-Wigner full width = 235 to 335 ($\approx$ 285) MeV

$\Delta(1950)$ DECAY MODES	Fraction (Γ_i/Γ)	p (MeV/c)
$N\pi$	35–45 %	729
ΣK	0.3–0.5 %	441
$N\pi\pi$		706
$\Delta(1232)\pi$, F-wave	1–9 %	560
$N(1680)\pi$, P-wave	3–9 %	191
$\Delta(1232)\eta$	< 0.6 %	349

$\Delta(2200)$ 7/2$^-$

$I(J^P) = \frac{3}{2}(\frac{7}{2}^-)$

Re(pole position) = 2050 to 2150 ($\approx$ 2100) MeV
-2Im(pole position) = 260 to 420 ($\approx$ 340) MeV
Breit-Wigner mass = 2150 to 2250 ($\approx$ 2200) MeV
Breit-Wigner full width = 200 to 500 ($\approx$ 350) MeV

$\Delta(2200)$ DECAY MODES	Fraction (Γ_i/Γ)	p (MeV/c)
$N\pi$	2–8 %	894
ΣK	1–7 %	672
$\Delta\pi$, D-wave	40–100 %	747
$\Delta\pi$, G-wave	5–25 %	747
$\Delta\eta$, D-wave	seen	614

$\Delta(2420)$ 11/2$^+$

$I(J^P) = \frac{3}{2}(\frac{11}{2}^+)$

Re(pole position) = 2300 to 2500 ($\approx$ 2400) MeV
-2Im(pole position) = 350 to 550 ($\approx$ 450) MeV
Breit-Wigner mass = 2300 to 2600 ($\approx$ 2450) MeV
Breit-Wigner full width = 300 to 700 ($\approx$ 500) MeV

$\Delta(2420)$ DECAY MODES	Fraction (Γ_i/Γ)	p (MeV/c)
$N\pi$	5–10 %	1040

Λ BARYONS
($S = -1$, $I = 0$)

$\Lambda^0 = uds$

Λ

$I(J^P) = 0(\frac{1}{2}^+)$

Mass $m = 1115.683 \pm 0.006$ MeV
$(m_\Lambda - m_{\overline{\Lambda}}) / m_\Lambda = (-0.1 \pm 1.1) \times 10^{-5}$ (S = 1.6)
Mean life $\tau = (2.632 \pm 0.020) \times 10^{-10}$ s (S = 1.6)
$(\tau_\Lambda - \tau_{\overline{\Lambda}}) / \tau_\Lambda = -0.001 \pm 0.009$
$c\tau = 7.89$ cm
Magnetic moment $\mu = -0.613 \pm 0.004\ \mu_N$
Electric dipole moment $d < 1.5 \times 10^{-16}$ e cm, CL = 95%

Decay parameters

$p\pi^-$	$\alpha_- = 0.642 \pm 0.013$
$\overline{p}\pi^+$	$\alpha_+ = -0.71 \pm 0.08$
$p\pi^-$	$\phi_- = (-6.5 \pm 3.5)^\circ$
"	$\gamma_- = 0.76$ [n]
"	$\Delta_- = (8 \pm 4)^\circ$ [n]
$n\pi^0$	$\alpha_0 = 0.65 \pm 0.04$
$pe^-\overline{\nu}_e$	$g_A/g_V = -0.718 \pm 0.015$ [i]

Λ DECAY MODES		Fraction (Γ_i/Γ)	Confidence level	p (MeV/c)
$p\pi^-$		(63.9 ±0.5) %		101
$n\pi^0$		(35.8 ±0.5) %		104
$n\gamma$		(1.75±0.15) $\times 10^{-3}$		162
$p\pi^-\gamma$	[o]	(8.4 ±1.4) $\times 10^{-4}$		101
$pe^-\overline{\nu}_e$		(8.32±0.14) $\times 10^{-4}$		163
$p\mu^-\overline{\nu}_\mu$		(1.57±0.35) $\times 10^{-4}$		131
Lepton (L) and/or Baryon (B) number violating decay modes				
π^+e^-	L,B	< 6 $\times 10^{-7}$	90%	549
$\pi^+\mu^-$	L,B	< 6 $\times 10^{-7}$	90%	544
π^-e^+	L,B	< 4 $\times 10^{-7}$	90%	549
$\pi^-\mu^+$	L,B	< 6 $\times 10^{-7}$	90%	544
K^+e^-	L,B	< 2 $\times 10^{-6}$	90%	449
$K^+\mu^-$	L,B	< 3 $\times 10^{-6}$	90%	441
K^-e^+	L,B	< 2 $\times 10^{-6}$	90%	449
$K^-\mu^+$	L,B	< 3 $\times 10^{-6}$	90%	441
$K^0_S\nu$	L,B	< 2 $\times 10^{-5}$	90%	447
$\overline{p}\pi^+$	B	< 9 $\times 10^{-7}$	90%	101

$\Lambda(1405)$ 1/2$^-$

$I(J^P) = 0(\frac{1}{2}^-)$

Mass $m = 1405.1^{+1.3}_{-1.0}$ MeV
Full width $\Gamma = 50.5 \pm 2.0$ MeV
Below $\overline{K}N$ threshold

$\Lambda(1405)$ DECAY MODES	Fraction (Γ_i/Γ)	p (MeV/c)
$\Sigma\pi$	100 %	155

$\Lambda(1520)$ 3/2$^-$

$I(J^P) = 0(\frac{3}{2}^-)$

Mass $m = 1519.5 \pm 1.0$ MeV [p]
Full width $\Gamma = 15.6 \pm 1.0$ MeV [p]

$\Lambda(1520)$ DECAY MODES	Fraction (Γ_i/Γ)	p (MeV/c)
$N\overline{K}$	(45 ±1) %	243
$\Sigma\pi$	(42 ±1) %	268

$\Lambda\pi\pi$	(10 ±1) %	259
$\Sigma\pi\pi$	(0.9 ±0.1) %	169
$\Lambda\gamma$	(0.85±0.15) %	350

$\Lambda(1600)\ 1/2^+$ $I(J^P) = 0(\frac{1}{2}^+)$

Mass m = 1560 to 1700 (≈ 1600) MeV
Full width Γ = 50 to 250 (≈ 150) MeV

Λ(1600) DECAY MODES	Fraction (Γ_i/Γ)	p (MeV/c)
$N\overline{K}$	15–30 %	343
$\Sigma\pi$	10–60 %	338

$\Lambda(1670)\ 1/2^-$ $I(J^P) = 0(\frac{1}{2}^-)$

Mass m = 1660 to 1680 (≈ 1670) MeV
Full width Γ = 25 to 50 (≈ 35) MeV

Λ(1670) DECAY MODES	Fraction (Γ_i/Γ)	p (MeV/c)
$N\overline{K}$	20–30 %	414
$\Sigma\pi$	25–55 %	394
$\Lambda\eta$	10–25 %	69
$N\overline{K}^*(892)$, S=3/2, D-wave	(5±4) %	†

$\Lambda(1690)\ 3/2^-$ $I(J^P) = 0(\frac{3}{2}^-)$

Mass m = 1685 to 1695 (≈ 1690) MeV
Full width Γ = 50 to 70 (≈ 60) MeV

Λ(1690) DECAY MODES	Fraction (Γ_i/Γ)	p (MeV/c)
$N\overline{K}$	20–30 %	433
$\Sigma\pi$	20–40 %	410
$\Lambda\pi\pi$	∼ 25 %	419
$\Sigma\pi\pi$	∼ 20 %	358

$\Lambda(1800)\ 1/2^-$ $I(J^P) = 0(\frac{1}{2}^-)$

Mass m = 1720 to 1850 (≈ 1800) MeV
Full width Γ = 200 to 400 (≈ 300) MeV

Λ(1800) DECAY MODES	Fraction (Γ_i/Γ)	p (MeV/c)
$N\overline{K}$	25–40 %	528
$\Sigma\pi$	seen	494
$\Sigma(1385)\pi$	seen	349
$\Lambda\eta$	(6±5) %	326
$N\overline{K}^*(892)$	seen	†

$\Lambda(1810)\ 1/2^+$ $I(J^P) = 0(\frac{1}{2}^+)$

Mass m = 1750 to 1850 (≈ 1810) MeV
Full width Γ = 50 to 250 (≈ 150) MeV

Λ(1810) DECAY MODES	Fraction (Γ_i/Γ)	p (MeV/c)
$N\overline{K}$	20–50 %	537
$\Sigma\pi$	10–40 %	501
$\Sigma(1385)\pi$	seen	357
$N\overline{K}^*(892)$	30–60 %	†

$\Lambda(1820)\ 5/2^+$ $I(J^P) = 0(\frac{5}{2}^+)$

Mass m = 1815 to 1825 (≈ 1820) MeV
Full width Γ = 70 to 90 (≈ 80) MeV

Λ(1820) DECAY MODES	Fraction (Γ_i/Γ)	p (MeV/c)
$N\overline{K}$	55–65 %	545
$\Sigma\pi$	8–14 %	509
$\Sigma(1385)\pi$	5–10 %	366
$N\overline{K}^*(892)$, S=3/2, P-wave	(3.0±1.0) %	†

$\Lambda(1830)\ 5/2^-$ $I(J^P) = 0(\frac{5}{2}^-)$

Mass m = 1810 to 1830 (≈ 1830) MeV
Full width Γ = 60 to 110 (≈ 95) MeV

Λ(1830) DECAY MODES	Fraction (Γ_i/Γ)	p (MeV/c)
$N\overline{K}$	3–10 %	553
$\Sigma\pi$	35–75 %	516
$\Sigma(1385)\pi$	>15 %	374
$\Sigma(1385)\pi$, D-wave	(52±6) %	374

$\Lambda(1890)\ 3/2^+$ $I(J^P) = 0(\frac{3}{2}^+)$

Mass m = 1850 to 1910 (≈ 1890) MeV
Full width Γ = 60 to 200 (≈ 100) MeV

Λ(1890) DECAY MODES	Fraction (Γ_i/Γ)	p (MeV/c)
$N\overline{K}$	20–35 %	599
$\Sigma\pi$	3–10 %	560
$\Sigma(1385)\pi$	seen	423
$N\overline{K}^*(892)$	seen	236

$\Lambda(2100)\ 7/2^-$ $I(J^P) = 0(\frac{7}{2}^-)$

Mass m = 2090 to 2110 (≈ 2100) MeV
Full width Γ = 100 to 250 (≈ 200) MeV

Λ(2100) DECAY MODES	Fraction (Γ_i/Γ)	p (MeV/c)
$N\overline{K}$	25–35 %	751
$\Sigma\pi$	∼ 5 %	705
$\Lambda\eta$	<3 %	617
ΞK	<3 %	491
$\Lambda\omega$	<8 %	443
$N\overline{K}^*(892)$	10–20 %	515

$\Lambda(2110)\ 5/2^+$ $I(J^P) = 0(\frac{5}{2}^+)$

Mass m = 2090 to 2140 (≈ 2110) MeV
Full width Γ = 150 to 250 (≈ 200) MeV

Λ(2110) DECAY MODES	Fraction (Γ_i/Γ)	p (MeV/c)
$N\overline{K}$	5–25 %	757
$\Sigma\pi$	10–40 %	711
$\Lambda\omega$	seen	455
$\Sigma(1385)\pi$	seen	591
$N\overline{K}^*(892)$	10–60 %	525

$\Lambda(2350)\ 9/2^+$ $I(J^P) = 0(\frac{9}{2}^+)$

Mass m = 2340 to 2370 (≈ 2350) MeV
Full width Γ = 100 to 250 (≈ 150) MeV

Λ(2350) DECAY MODES	Fraction (Γ_i/Γ)	p (MeV/c)
$N\overline{K}$	∼ 12 %	915
$\Sigma\pi$	∼ 10 %	867

Σ BARYONS ($S=-1, I=1$)

$\Sigma^+ = uus$, $\Sigma^0 = uds$, $\Sigma^- = dds$

Σ^+ $I(J^P) = 1(\frac{1}{2}^+)$

Mass $m = 1189.37 \pm 0.07$ MeV (S = 2.2)
Mean life $\tau = (0.8018 \pm 0.0026) \times 10^{-10}$ s
$c\tau = 2.404$ cm
$(\tau_{\Sigma^+} - \tau_{\overline{\Sigma}^-}) / \tau_{\Sigma^+} = -0.0006 \pm 0.0012$
Magnetic moment $\mu = 2.458 \pm 0.010\ \mu_N$ (S = 2.1)
$(\mu_{\Sigma^+} + \mu_{\overline{\Sigma}^-}) / \mu_{\Sigma^+} = 0.014 \pm 0.015$
$\Gamma(\Sigma^+ \to n\ell^+\nu)/\Gamma(\Sigma^- \to n\ell^-\overline{\nu}) < 0.043$

Decay parameters

$p\pi^0$	$\alpha_0 = -0.980^{+0.017}_{-0.015}$
"	$\phi_0 = (36 \pm 34)^\circ$
"	$\gamma_0 = 0.16$ [n]
"	$\Delta_0 = (187 \pm 6)^\circ$ [n]
$n\pi^+$	$\alpha_+ = 0.068 \pm 0.013$
"	$\phi_+ = (167 \pm 20)^\circ$ (S = 1.1)
"	$\gamma_+ = -0.97$ [n]
"	$\Delta_+ = (-73^{+133}_{-10})^\circ$ [n]
$p\gamma$	$\alpha_\gamma = -0.76 \pm 0.08$

Σ^+ DECAY MODES		Fraction (Γ_i/Γ)	Confidence level	p (MeV/c)
$p\pi^0$		(51.57±0.30) %		189
$n\pi^+$		(48.31±0.30) %		185
$p\gamma$		(1.23±0.05) $\times 10^{-3}$		225
$n\pi^+\gamma$	[o]	(4.5 ±0.5) $\times 10^{-4}$		185
$\Lambda e^+\nu_e$		(2.0 ±0.5) $\times 10^{-5}$		71
$\Delta S = \Delta Q$ (SQ) violating modes or $\Delta S = 1$ weak neutral current ($S1$) modes				
$ne^+\nu_e$	SQ	$< 5 \times 10^{-6}$	90%	224
$n\mu^+\nu_\mu$	SQ	$< 3.0 \times 10^{-5}$	90%	202
pe^+e^-	$S1$	$< 7 \times 10^{-6}$		225
$p\mu^+\mu^-$	$S1$	(9 $^{+9}_{-8}$) $\times 10^{-8}$		121

Σ^0 $I(J^P) = 1(\frac{1}{2}^+)$

Mass $m = 1192.642 \pm 0.024$ MeV
$m_{\Sigma^-} - m_{\Sigma^0} = 4.807 \pm 0.035$ MeV (S = 1.1)
$m_{\Sigma^0} - m_\Lambda = 76.959 \pm 0.023$ MeV
Mean life $\tau = (7.4 \pm 0.7) \times 10^{-20}$ s
$c\tau = 2.22 \times 10^{-11}$ m
Transition magnetic moment $|\mu_{\Sigma\Lambda}| = 1.61 \pm 0.08\ \mu_N$

Σ^0 DECAY MODES		Fraction (Γ_i/Γ)	Confidence level	p (MeV/c)
$\Lambda\gamma$		100 %		74
$\Lambda\gamma\gamma$		< 3 %	90%	74
Λe^+e^-	[q]	5×10^{-3}		74

Σ^- $I(J^P) = 1(\frac{1}{2}^+)$

Mass $m = 1197.449 \pm 0.030$ MeV (S = 1.2)
$m_{\Sigma^-} - m_{\Sigma^+} = 8.08 \pm 0.08$ MeV (S = 1.9)
$m_{\Sigma^-} - m_\Lambda = 81.766 \pm 0.030$ MeV (S = 1.2)
Mean life $\tau = (1.479 \pm 0.011) \times 10^{-10}$ s (S = 1.3)
$c\tau = 4.434$ cm
Magnetic moment $\mu = -1.160 \pm 0.025\ \mu_N$ (S = 1.7)
Σ^- charge radius = 0.78 ± 0.10 fm

Decay parameters

$n\pi^-$	$\alpha_- = -0.068 \pm 0.008$
"	$\phi_- = (10 \pm 15)^\circ$
"	$\gamma_- = 0.98$ [n]
"	$\Delta_- = (249^{+12}_{-120})^\circ$ [n]
$ne^-\overline{\nu}_e$	$g_A/g_V = 0.340 \pm 0.017$ [i]
"	$f_2(0)/f_1(0) = 0.97 \pm 0.14$
"	$D = 0.11 \pm 0.10$
$\Lambda e^-\overline{\nu}_e$	$g_V/g_A = 0.01 \pm 0.10$ [i] (S = 1.5)
"	$g_{WM}/g_A = 2.4 \pm 1.7$ [i]

Σ^- DECAY MODES	Fraction (Γ_i/Γ)	p (MeV/c)
$n\pi^-$	(99.848±0.005) %	193
$n\pi^-\gamma$	[o](4.6 ±0.6) $\times 10^{-4}$	193
$ne^-\overline{\nu}_e$	(1.017±0.034) $\times 10^{-3}$	230
$n\mu^-\overline{\nu}_\mu$	(4.5 ±0.4) $\times 10^{-4}$	210
$\Lambda e^-\overline{\nu}_e$	(5.73 ±0.27) $\times 10^{-5}$	79

$\Sigma(1385)$ 3/2$^+$ $I(J^P) = 1(\frac{3}{2}^+)$

$\Sigma(1385)^+$ mass $m = 1382.80 \pm 0.35$ MeV (S = 1.9)
$\Sigma(1385)^0$ mass $m = 1383.7 \pm 1.0$ MeV (S = 1.4)
$\Sigma(1385)^-$ mass $m = 1387.2 \pm 0.5$ MeV (S = 2.2)
$\Sigma(1385)^+$ full width $\Gamma = 36.0 \pm 0.7$ MeV
$\Sigma(1385)^0$ full width $\Gamma = 36 \pm 5$ MeV
$\Sigma(1385)^-$ full width $\Gamma = 39.4 \pm 2.1$ MeV (S = 1.7)
Below $\overline{K}N$ threshold

$\Sigma(1385)$ DECAY MODES	Fraction (Γ_i/Γ)	Confidence level	p (MeV/c)
$\Lambda\pi$	(87.0 ±1.5) %		208
$\Sigma\pi$	(11.7 ±1.5) %		129
$\Lambda\gamma$	(1.25$^{+0.13}_{-0.12}$) %		241
$\Sigma^+\gamma$	(7.0 ±1.7) $\times 10^{-3}$		180
$\Sigma^-\gamma$	< 2.4 $\times 10^{-4}$	90%	173

$\Sigma(1660)$ 1/2$^+$ $I(J^P) = 1(\frac{1}{2}^+)$

Mass $m = 1630$ to 1690 (≈ 1660) MeV
Full width $\Gamma = 40$ to 200 (≈ 100) MeV

$\Sigma(1660)$ DECAY MODES	Fraction (Γ_i/Γ)	p (MeV/c)
$N\overline{K}$	10–30 %	405
$\Lambda\pi$	seen	440
$\Sigma\pi$	seen	387

$\Sigma(1670)$ 3/2$^-$ $I(J^P) = 1(\frac{3}{2}^-)$

Mass $m = 1665$ to 1685 (≈ 1670) MeV
Full width $\Gamma = 40$ to 80 (≈ 60) MeV

$\Sigma(1670)$ DECAY MODES	Fraction (Γ_i/Γ)	p (MeV/c)
$N\overline{K}$	7–13 %	414
$\Lambda\pi$	5–15 %	448
$\Sigma\pi$	30–60 %	394

$\Sigma(1750)$ 1/2$^-$ $I(J^P) = 1(\frac{1}{2}^-)$

Mass $m = 1730$ to 1800 (≈ 1750) MeV
Full width $\Gamma = 60$ to 160 (≈ 90) MeV

$\Sigma(1750)$ DECAY MODES	Fraction (Γ_i/Γ)	p (MeV/c)
$N\overline{K}$	10–40 %	486
$\Lambda\pi$	seen	507
$\Sigma\pi$	<8 %	456
$\Sigma\eta$	15–55 %	98
$N\overline{K}^*(892)$, S=1/2	(8±4) %	†

$\Sigma(1775)$ 5/2$^-$ $I(J^P) = 1(\frac{5}{2}^-)$

Mass $m = 1770$ to 1780 (≈ 1775) MeV
Full width $\Gamma = 105$ to 135 (≈ 120) MeV

$\Sigma(1775)$ DECAY MODES	Fraction (Γ_i/Γ)	p (MeV/c)
$N\overline{K}$	37–43%	508
$\Lambda\pi$	14–20%	525

$\Sigma\pi$	2–5%	475
$\Sigma(1385)\pi$	8–12%	327
$\Lambda(1520)\pi$, P-wave	17–23%	201

$\Sigma(1915)\ 5/2^+$

$I(J^P) = 1(\frac{5}{2}^+)$

Mass $m = 1900$ to 1935 (≈ 1915) MeV
Full width $\Gamma = 80$ to 160 (≈ 120) MeV

$\Sigma(1915)$ DECAY MODES	Fraction (Γ_i/Γ)	p (MeV/c)
$N\overline{K}$	5–15 %	618
$\Lambda\pi$	seen	623
$\Sigma\pi$	seen	577
$\Sigma(1385)\pi$	<5 %	443

$\Sigma(1940)\ 3/2^-$

$I(J^P) = 1(\frac{3}{2}^-)$

Mass $m = 1900$ to 1950 (≈ 1940) MeV
Full width $\Gamma = 150$ to 300 (≈ 220) MeV

$\Sigma(1940)$ DECAY MODES	Fraction (Γ_i/Γ)	p (MeV/c)
$N\overline{K}$	<20 %	637
$\Lambda\pi$	seen	640
$\Sigma\pi$	seen	595
$\Sigma(1385)\pi$	seen	463
$\Lambda(1520)\pi$	seen	355
$\Delta(1232)\overline{K}$	seen	410
$N\overline{K}^*(892)$	seen	322

$\Sigma(2030)\ 7/2^+$

$I(J^P) = 1(\frac{7}{2}^+)$

Mass $m = 2025$ to 2040 (≈ 2030) MeV
Full width $\Gamma = 150$ to 200 (≈ 180) MeV

$\Sigma(2030)$ DECAY MODES	Fraction (Γ_i/Γ)	p (MeV/c)
$N\overline{K}$	17–23 %	702
$\Lambda\pi$	17–23 %	700
$\Sigma\pi$	5–10 %	657
ΞK	<2 %	422
$\Sigma(1385)\pi$	5–15 %	532
$\Lambda(1520)\pi$	10–20 %	430
$\Delta(1232)\overline{K}$	10–20 %	498
$N\overline{K}^*(892)$	<5 %	439

$\Sigma(2250)$

$I(J^P) = 1(?^?)$

Mass $m = 2210$ to 2280 (≈ 2250) MeV
Full width $\Gamma = 60$ to 150 (≈ 100) MeV

$\Sigma(2250)$ DECAY MODES	Fraction (Γ_i/Γ)	p (MeV/c)
$N\overline{K}$	<10 %	851
$\Lambda\pi$	seen	842
$\Sigma\pi$	seen	803

Ξ BARYONS ($S=-2, I=1/2$)

$\Xi^0 = uss$, $\Xi^- = dss$

Ξ^0

$I(J^P) = \frac{1}{2}(\frac{1}{2}^+)$

P is not yet measured; + is the quark model prediction.

Mass $m = 1314.86 \pm 0.20$ MeV
$m_{\Xi^-} - m_{\Xi^0} = 6.85 \pm 0.21$ MeV
Mean life $\tau = (2.90 \pm 0.09) \times 10^{-10}$ s
$c\tau = 8.71$ cm
Magnetic moment $\mu = -1.250 \pm 0.014\ \mu_N$

Decay parameters

$\Lambda\pi^0$	$\alpha = -0.406 \pm 0.013$
"	$\phi = (21 \pm 12)^\circ$
"	$\gamma = 0.85$ [n]
"	$\Delta = (218^{+12}_{-19})^\circ$ [n]
$\Lambda\gamma$	$\alpha = -0.70 \pm 0.07$
$\Lambda e^+ e^-$	$\alpha = -0.8 \pm 0.2$
$\Sigma^0\gamma$	$\alpha = -0.69 \pm 0.06$
$\Sigma^+ e^- \overline{\nu}_e$	$g_1(0)/f_1(0) = 1.22 \pm 0.05$
$\Sigma^+ e^- \overline{\nu}_e$	$f_2(0)/f_1(0) = 2.0 \pm 0.9$

Ξ^0 DECAY MODES	Fraction (Γ_i/Γ)	Confidence level	p (MeV/c)
$\Lambda\pi^0$	(99.524 ± 0.012) %		135
$\Lambda\gamma$	$(1.17 \pm 0.07) \times 10^{-3}$		184
$\Lambda e^+ e^-$	$(7.6 \pm 0.6) \times 10^{-6}$		184
$\Sigma^0\gamma$	$(3.33 \pm 0.10) \times 10^{-3}$		117
$\Sigma^+ e^- \overline{\nu}_e$	$(2.52 \pm 0.08) \times 10^{-4}$		120
$\Sigma^+ \mu^- \overline{\nu}_\mu$	$(2.33 \pm 0.35) \times 10^{-6}$		64
$\Delta S = \Delta Q$ (SQ) violating modes or $\Delta S = 2$ forbidden ($S2$) modes			
$\Sigma^- e^+ \nu_e$	SQ < 9×10^{-4}	90%	112
$\Sigma^- \mu^+ \nu_\mu$	SQ < 9×10^{-4}	90%	49
$p\pi^-$	$S2$ < 8×10^{-6}	90%	299
$p e^- \overline{\nu}_e$	$S2$ < 1.3×10^{-3}		323
$p\mu^- \overline{\nu}_\mu$	$S2$ < 1.3×10^{-3}		309

Ξ^-

$I(J^P) = \frac{1}{2}(\frac{1}{2}^+)$

P is not yet measured; + is the quark model prediction.

Mass $m = 1321.71 \pm 0.07$ MeV
$(m_{\Xi^-} - m_{\overline{\Xi}^+}) / m_{\Xi^-} = (-3 \pm 9) \times 10^{-5}$
Mean life $\tau = (1.639 \pm 0.015) \times 10^{-10}$ s
$c\tau = 4.91$ cm
$(\tau_{\Xi^-} - \tau_{\overline{\Xi}^+}) / \tau_{\Xi^-} = -0.01 \pm 0.07$
Magnetic moment $\mu = -0.6507 \pm 0.0025\ \mu_N$
$(\mu_{\Xi^-} + \mu_{\overline{\Xi}^+}) / |\mu_{\Xi^-}| = +0.01 \pm 0.05$

Decay parameters

$\Lambda\pi^-$	$\alpha = -0.458 \pm 0.012$ (S = 1.8)
	$[\alpha(\Xi^-)\alpha_-(\Lambda) - \alpha(\overline{\Xi}^+)\alpha_+(\overline{\Lambda})] / [\text{sum}] = (0 \pm 7) \times 10^{-4}$
"	$\phi = (-2.1 \pm 0.8)^\circ$
"	$\gamma = 0.89$ [n]
"	$\Delta = (175.9 \pm 1.5)^\circ$ [n]
$\Lambda e^- \overline{\nu}_e$	$g_A/g_V = -0.25 \pm 0.05$ [i]

Ξ^- DECAY MODES	Fraction (Γ_i/Γ)	Confidence level	p (MeV/c)
$\Lambda\pi^-$	(99.887 ± 0.035) %		140
$\Sigma^-\gamma$	$(1.27 \pm 0.23) \times 10^{-4}$		118
$\Lambda e^- \overline{\nu}_e$	$(5.63 \pm 0.31) \times 10^{-4}$		190
$\Lambda\mu^- \overline{\nu}_\mu$	$(3.5\ ^{+3.5}_{-2.2}) \times 10^{-4}$		163
$\Sigma^0 e^- \overline{\nu}_e$	$(8.7 \pm 1.7) \times 10^{-5}$		123
$\Sigma^0 \mu^- \overline{\nu}_\mu$	< 8×10^{-4}	90%	70
$\Xi^0 e^- \overline{\nu}_e$	< 2.3×10^{-3}	90%	7
$\Delta S = 2$ forbidden ($S2$) modes			
$n\pi^-$	$S2$ < 1.9×10^{-5}	90%	304
$n e^- \overline{\nu}_e$	$S2$ < 3.2×10^{-3}	90%	327
$n\mu^- \overline{\nu}_\mu$	$S2$ < 1.5 %	90%	314
$p\pi^-\pi^-$	$S2$ < 4×10^{-4}	90%	223
$p\pi^- e^- \overline{\nu}_e$	$S2$ < 4×10^{-4}	90%	305
$p\pi^- \mu^- \overline{\nu}_\mu$	$S2$ < 4×10^{-4}	90%	251
$p\mu^-\mu^-$	L < 4×10^{-8}	90%	272

$\Xi(1530)\ 3/2^+$

$I(J^P) = \frac{1}{2}(\frac{3}{2}^+)$

$\Xi(1530)^0$ mass $m = 1531.80 \pm 0.32$ MeV (S = 1.3)
$\Xi(1530)^-$ mass $m = 1535.0 \pm 0.6$ MeV
$\Xi(1530)^0$ full width $\Gamma = 9.1 \pm 0.5$ MeV
$\Xi(1530)^-$ full width $\Gamma = 9.9^{+1.7}_{-1.9}$ MeV

$\Xi(1530)$ DECAY MODES	Fraction (Γ_i/Γ)	Confidence level	p (MeV/c)
$\Xi\pi$	100 %		158
$\Xi\gamma$	<4 %	90%	202

$\Xi(1690)$

$I(J^P) = \frac{1}{2}(?^?)$

Mass $m = 1690 \pm 10$ MeV [p]
Full width $\Gamma < 30$ MeV

$\Xi(1690)$ DECAY MODES	Fraction (Γ_i/Γ)	p (MeV/c)
$\Lambda\overline{K}$	seen	240
$\Sigma\overline{K}$	seen	70
$\Xi\pi$	seen	311
$\Xi^-\pi^+\pi^-$	possibly seen	213

$\Xi(1820)\ 3/2^-$

$I(J^P) = \frac{1}{2}(\frac{3}{2}^-)$

Mass $m = 1823 \pm 5$ MeV [p]
Full width $\Gamma = 24^{+15}_{-10}$ MeV [p]

$\Xi(1820)$ DECAY MODES	Fraction (Γ_i/Γ)	p (MeV/c)
$\Lambda\overline{K}$	large	402
$\Sigma\overline{K}$	small	324
$\Xi\pi$	small	421
$\Xi(1530)\pi$	small	237

$\Xi(1950)$

$I(J^P) = \frac{1}{2}(?^?)$

Mass $m = 1950 \pm 15$ MeV [p]
Full width $\Gamma = 60 \pm 20$ MeV [p]

$\Xi(1950)$ DECAY MODES	Fraction (Γ_i/Γ)	p (MeV/c)
$\Lambda\overline{K}$	seen	522
$\Sigma\overline{K}$	possibly seen	460
$\Xi\pi$	seen	519

$\Xi(2030)$

$I(J^P) = \frac{1}{2}(\geq \frac{5}{2}^?)$

Mass $m = 2025 \pm 5$ MeV [p]
Full width $\Gamma = 20^{+15}_{-5}$ MeV [p]

$\Xi(2030)$ DECAY MODES	Fraction (Γ_i/Γ)	p (MeV/c)
$\Lambda\overline{K}$	~ 20 %	585
$\Sigma\overline{K}$	~ 80 %	529
$\Xi\pi$	small	574
$\Xi(1530)\pi$	small	416
$\Lambda\overline{K}\pi$	small	499
$\Sigma\overline{K}\pi$	small	428

Ω BARYONS ($S=-3, I=0$)

$\Omega^- = sss$

Ω^-

$I(J^P) = 0(\frac{3}{2}^+)$

$J^P = \frac{3}{2}^+$ is the quark-model prediction; and $J = 3/2$ is fairly well established.

Mass $m = 1672.45 \pm 0.29$ MeV
$(m_{\Omega^-} - m_{\overline{\Omega}^+}) / m_{\Omega^-} = (-1 \pm 8) \times 10^{-5}$
Mean life $\tau = (0.821 \pm 0.011) \times 10^{-10}$ s
$c\tau = 2.461$ cm
$(\tau_{\Omega^-} - \tau_{\overline{\Omega}^+}) / \tau_{\Omega^-} = 0.00 \pm 0.05$
Magnetic moment $\mu = -2.02 \pm 0.05\ \mu_N$

Decay parameters

ΛK^- $\alpha = 0.0180 \pm 0.0024$
$\Lambda K^-, \overline{\Lambda} K^+$ $(\alpha + \overline{\alpha})/(\alpha - \overline{\alpha}) = -0.02 \pm 0.13$
$\Xi^0\pi^-$ $\alpha = 0.09 \pm 0.14$
$\Xi^-\pi^0$ $\alpha = 0.05 \pm 0.21$

Ω^- DECAY MODES	Fraction (Γ_i/Γ)	Confidence level	p (MeV/c)
ΛK^-	(67.8 ± 0.7) %		211
$\Xi^0\pi^-$	(23.6 ± 0.7) %		294
$\Xi^-\pi^0$	(8.6 ± 0.4) %		289
$\Xi^-\pi^+\pi^-$	$(3.7^{+0.7}_{-0.6}) \times 10^{-4}$		189
$\Xi(1530)^0\pi^-$	$< 7 \times 10^{-5}$	90%	17
$\Xi^0 e^- \overline{\nu}_e$	$(5.6 \pm 2.8) \times 10^{-3}$		319
$\Xi^-\gamma$	$< 4.6 \times 10^{-4}$	90%	314
$\Delta S = 2$ forbidden ($S2$) modes			
$\Lambda\pi^-$	$S2$ $< 2.9 \times 10^{-6}$	90%	449

$\Omega(2250)^-$

$I(J^P) = 0(?^?)$

Mass $m = 2252 \pm 9$ MeV
Full width $\Gamma = 55 \pm 18$ MeV

$\Omega(2250)^-$ DECAY MODES	Fraction (Γ_i/Γ)	p (MeV/c)
$\Xi^-\pi^+K^-$	seen	532
$\Xi(1530)^0K^-$	seen	437

CHARMED BARYONS ($C=+1$)

$\Lambda_c^+ = udc$, $\Sigma_c^{++} = uuc$, $\Sigma_c^+ = udc$, $\Sigma_c^0 = ddc$,
$\Xi_c^+ = usc$, $\Xi_c^0 = dsc$, $\Omega_c^0 = ssc$

Λ_c^+

$I(J^P) = 0(\frac{1}{2}^+)$

Mass $m = 2286.46 \pm 0.14$ MeV
Mean life $\tau = (200 \pm 6) \times 10^{-15}$ s (S = 1.6)
$c\tau = 59.9\ \mu$m

Decay asymmetry parameters

$\Lambda\pi^+$ $\alpha = -0.91 \pm 0.15$
$\Sigma^+\pi^0$ $\alpha = -0.45 \pm 0.32$
$\Lambda\ell^+\nu_\ell$ $\alpha = -0.86 \pm 0.04$
$(\alpha + \overline{\alpha})/(\alpha - \overline{\alpha})$ in $\Lambda_c^+ \to \Lambda\pi^+, \overline{\Lambda}_c^- \to \overline{\Lambda}\pi^- = -0.07 \pm 0.31$
$(\alpha + \overline{\alpha})/(\alpha - \overline{\alpha})$ in $\Lambda_c^+ \to \Lambda e^+\nu_e, \overline{\Lambda}_c^- \to \overline{\Lambda} e^-\overline{\nu}_e = 0.00 \pm 0.04$

Branching fractions marked with a footnote, e.g. [a], have been corrected for decay modes not observed in the experiments. For example, the sub-mode fraction $\Lambda_c^+ \to p\overline{K}^*(892)^0$ seen in $\Lambda_c^+ \to pK^-\pi^+$ has been multiplied up to include $\overline{K}^*(892)^0 \to \overline{K}^0\pi^0$ decays.

Baryon Summary Table

Λ_c^+ DECAY MODES		Fraction (Γ_i/Γ)	Scale factor/ Confidence level	p (MeV/c)
Hadronic modes with a p or n: $S = -1$ final states				
pK_S^0		(1.58± 0.08) %	S=1.1	873
$pK^-\pi^+$		(6.23± 0.33) %	S=1.4	823
$p\overline{K}^*(892)^0$	[r]	(1.94± 0.27) %		685
$\Delta(1232)^{++}K^-$		(1.07± 0.25) %		710
$\Lambda(1520)\pi^+$	[r]	(2.2 ± 0.5) %		627
$pK^-\pi^+$ nonresonant		(3.4 ± 0.4) %		823
$pK_S^0\pi^0$		(1.96± 0.13) %	S=1.1	823
$nK_S^0\pi^+$		(1.82± 0.25) %		821
$p\overline{K}^0\eta$		(1.6 ± 0.4) %		568
$pK_S^0\pi^+\pi^-$		(1.59± 0.12) %	S=1.2	754
$pK^-\pi^+\pi^0$		(4.42± 0.31) %	S=1.5	759
$pK^*(892)^-\pi^+$	[r]	(1.4 ± 0.5) %		580
$p(K^-\pi^+)_{\text{nonresonant}}\pi^0$		(4.5 ± 0.8) %		759
$\Delta(1232)\overline{K}^*(892)$		seen		419
$pK^-2\pi^+\pi^-$		(1.4 ± 0.9) $\times 10^{-3}$		671
$pK^-\pi^+2\pi^0$		(10 ± 5) $\times 10^{-3}$		678
Hadronic modes with a p: $S = 0$ final states				
$p\pi^0$		< 2.7 $\times 10^{-4}$	CL=90%	945
$p\eta$		(1.24± 0.30) $\times 10^{-3}$		856
$p\pi^+\pi^-$		(4.2 ± 0.4) $\times 10^{-3}$		927
$pf_0(980)$	[r]	(3.4 ± 2.3) $\times 10^{-3}$		614
$p2\pi^+2\pi^-$		(2.2 ± 1.4) $\times 10^{-3}$		852
pK^+K^-		(10 ± 4) $\times 10^{-4}$		616
$p\phi$	[r]	(1.06± 0.14) $\times 10^{-3}$		590
pK^+K^- non-ϕ		(5.2 ± 1.2) $\times 10^{-4}$		616
$p\phi\pi^0$		(10 ± 4) $\times 10^{-5}$		460
$pK^+K^-\pi^0$ nonresonant		< 6.3 $\times 10^{-5}$	CL=90%	494
Hadronic modes with a hyperon: $S = -1$ final states				
$\Lambda\pi^+$		(1.29± 0.07) %	S=1.2	864
$\Lambda\pi^+\pi^0$		(7.0 ± 0.4) %	S=1.1	844
$\Lambda\rho^+$		< 6 %	CL=95%	636
$\Lambda\pi^-2\pi^+$		(3.61± 0.29) %	S=1.5	807
$\Sigma(1385)^+\pi^+\pi^-$, $\Sigma^{*+}\to\Lambda\pi^+$		(1.0 ± 0.5) %		688
$\Sigma(1385)^-2\pi^+$, $\Sigma^{*-}\to\Lambda\pi^-$		(7.6 ± 1.4) $\times 10^{-3}$		688
$\Lambda\pi^+\rho^0$		(1.4 ± 0.6) %		524
$\Sigma(1385)^+\rho^0$, $\Sigma^{*+}\to\Lambda\pi^+$		(5 ± 4) $\times 10^{-3}$		363
$\Lambda\pi^-2\pi^+$ nonresonant		< 1.1 %	CL=90%	807
$\Lambda\pi^-\pi^02\pi^+$ total		(2.2 ± 0.8) %		757
$\Lambda\pi^+\eta$	[r]	(2.2 ± 0.5) %		691
$\Sigma(1385)^+\eta$	[r]	(1.06± 0.32) %		570
$\Lambda\pi^+\omega$	[r]	(1.5 ± 0.5) %		517
$\Lambda\pi^-\pi^02\pi^+$, no η or ω		< 8 $\times 10^{-3}$	CL=90%	757
$\Lambda K^+\overline{K}^0$		(5.6 ± 1.1) $\times 10^{-3}$	S=1.9	443
$\Xi(1690)^0K^+$, $\Xi^{*0}\to\Lambda\overline{K}^0$		(1.6 ± 0.5) $\times 10^{-3}$		286
$\Sigma^0\pi^+$		(1.28± 0.07) %	S=1.1	825
$\Sigma^+\pi^0$		(1.24± 0.10) %		827
$\Sigma^+\eta$		(6.9 ± 2.3) $\times 10^{-3}$		713
$\Sigma^+\pi^+\pi^-$		(4.42± 0.28) %	S=1.2	804
$\Sigma^+\rho^0$		< 1.7 %	CL=95%	575
$\Sigma^-2\pi^+$		(1.86± 0.18) %		799
$\Sigma^0\pi^+\pi^0$		(2.2 ± 0.8) %		803
$\Sigma^0\pi^-2\pi^+$		(1.10± 0.30) %		763
$\Sigma^+\pi^+\pi^-\pi^0$		—		767
$\Sigma^+\omega$	[r]	(1.69± 0.21) %		569
$\Sigma^-\pi^02\pi^+$		(2.1 ± 0.4) %		762
$\Sigma^+K^+K^-$		(3.4 ± 0.4) $\times 10^{-3}$	S=1.1	349
$\Sigma^+\phi$	[r]	(3.8 ± 0.6) $\times 10^{-3}$	S=1.1	295
$\Xi(1690)^0K^+$, $\Xi^{*0}\to\Sigma^+K^-$		(10.0 ± 2.5) $\times 10^{-4}$		286
$\Sigma^+K^+K^-$ nonresonant		< 8 $\times 10^{-4}$	CL=90%	349
Ξ^0K^+		(4.9 ± 1.2) $\times 10^{-3}$		653
$\Xi^-K^+\pi^+$		(6.2 ± 0.6) $\times 10^{-3}$	S=1.1	565
$\Xi(1530)^0K^+$, $\Xi^0\to\Xi^-\pi^+$		(3.3 ± 1.2) $\times 10^{-3}$		473
Hadronic modes with a hyperon: $S = 0$ final states				
ΛK^+		(6.0 ± 1.2) $\times 10^{-4}$		781
$\Lambda K^+\pi^+\pi^-$		< 5 $\times 10^{-4}$	CL=90%	637
Σ^0K^+		(5.1 ± 0.8) $\times 10^{-4}$		735
$\Sigma^0K^+\pi^+\pi^-$		< 2.6 $\times 10^{-4}$	CL=90%	574
$\Sigma^+K^+\pi^-$		(2.1 ± 0.6) $\times 10^{-3}$		670
$\Sigma^+K^*(892)^0$	[r]	(3.4 ± 1.0) $\times 10^{-3}$		469
$\Sigma^-K^+\pi^+$		< 1.2 $\times 10^{-3}$	CL=90%	664
Doubly Cabibbo-suppressed modes				
$pK^+\pi^-$		(1.46± 0.23) $\times 10^{-4}$		823
Semileptonic modes				
$\Lambda e^+\nu_e$		(3.6 ± 0.4) %		871
$\Lambda\mu^+\nu_\mu$		(3.5 ± 0.5) %		867
Inclusive modes				
e^+ anything		(4.5 ± 1.7) %		–
pe^+ anything		(1.8 ± 0.9) %		–
p anything		(50 ±16) %		–
p anything (no Λ)		(12 ±19) %		–
n anything		(50 ±16) %		–
n anything (no Λ)		(29 ±17) %		–
Λ anything		(35 ±11) %	S=1.4	–
$\Sigma^\pm$ anything	[s]	(10 ± 5) %		–
3prongs		(24 ± 8) %		–
$\Delta C = 1$ weak neutral current ($C1$) modes, or Lepton Family number (LF), or Lepton number (L), or Baryon number (B) violating modes				
pe^+e^-	$C1$	< 5.5 $\times 10^{-6}$	CL=90%	951
$p\mu^+\mu^-$	$C1$	< 4.4 $\times 10^{-5}$	CL=90%	937
$pe^+\mu^-$	LF	< 9.9 $\times 10^{-6}$	CL=90%	947
$pe^-\mu^+$	LF	< 1.9 $\times 10^{-5}$	CL=90%	947
$\overline{p}2e^+$	L,B	< 2.7 $\times 10^{-6}$	CL=90%	951
$\overline{p}2\mu^+$	L,B	< 9.4 $\times 10^{-6}$	CL=90%	937
$\overline{p}e^+\mu^+$	L,B	< 1.6 $\times 10^{-5}$	CL=90%	947
$\Sigma^-\mu^+\mu^+$	L	< 7.0 $\times 10^{-4}$	CL=90%	812

$\Lambda_c(2595)^+$

$I(J^P) = 0(\frac{1}{2}^-)$

The spin-parity follows from the fact that $\Sigma_c(2455)\pi$ decays, with little available phase space, are dominant. This assumes that $J^P = 1/2^+$ for the $\Sigma_c(2455)$.

Mass $m = 2592.25 \pm 0.28$ MeV
$m - m_{\Lambda_c^+} = 305.79 \pm 0.24$ MeV
Full width $\Gamma = 2.6 \pm 0.6$ MeV

$\Lambda_c^+\pi\pi$ and its submode $\Sigma_c(2455)\pi$ — the latter just barely — are the only strong decays allowed to an excited Λ_c^+ having this mass; and the submode seems to dominate.

$\Lambda_c(2595)^+$ DECAY MODES		Fraction (Γ_i/Γ)	p (MeV/c)
$\Lambda_c^+\pi^+\pi^-$	[t]	—	117
$\Sigma_c(2455)^{++}\pi^-$		24 ± 7 %	†
$\Sigma_c(2455)^0\pi^+$		24 ± 7 %	†
$\Lambda_c^+\pi^+\pi^-$ 3-body		18 ± 10 %	117
$\Lambda_c^+\pi^0$	[u]	not seen	258
$\Lambda_c^+\gamma$		not seen	288

$\Lambda_c(2625)^+$

$I(J^P) = 0(\frac{3}{2}^-)$

J^P has not been measured; $\frac{3}{2}^-$ is the quark-model prediction.

Mass $m = 2628.11 \pm 0.19$ MeV (S = 1.1)
$m - m_{\Lambda_c^+} = 341.65 \pm 0.13$ MeV (S = 1.1)
Full width $\Gamma < 0.97$ MeV, CL = 90%

$\Lambda_c^+\pi\pi$ and its submode $\Sigma(2455)\pi$ are the only strong decays allowed to an excited Λ_c^+ having this mass.

$\Lambda_c(2625)^+$ DECAY MODES		Fraction (Γ_i/Γ)	Confidence level	p (MeV/c)
$\Lambda_c^+\pi^+\pi^-$		≈ 67%		184
$\Sigma_c(2455)^{++}\pi^-$		<5	90%	102
$\Sigma_c(2455)^0\pi^+$		<5	90%	102
$\Lambda_c^+\pi^+\pi^-$ 3-body		large		184
$\Lambda_c^+\pi^0$	[u]	not seen		293
$\Lambda_c^+\gamma$		not seen		319

$\Lambda_c(2860)^+$ $I(J^P) = 0(\frac{3}{2}^+)$

Mass $m = 2856.1^{+2.3}_{-6.0}$ MeV
Full width $\Gamma = 68^{+12}_{-22}$ MeV

$\Lambda_c(2860)^+$ DECAY MODES	Fraction (Γ_i/Γ)	p (MeV/c)
$D^0 p$	seen	259

$\Lambda_c(2880)^+$ $I(J^P) = 0(\frac{5}{2}^+)$

Mass $m = 2881.63 \pm 0.24$ MeV
$m - m_{\Lambda_c^+} = 595.17 \pm 0.28$ MeV
Full width $\Gamma = 5.6^{+0.8}_{-0.6}$ MeV

$\Lambda_c(2880)^+$ DECAY MODES	Fraction (Γ_i/Γ)	p (MeV/c)
$\Lambda_c^+ \pi^+ \pi^-$	seen	471
$\Sigma_c(2455)^{0,++}\pi^\pm$	seen	376
$\Sigma_c(2520)^{0,++}\pi^\pm$	seen	317
$p D^0$	seen	316

$\Lambda_c(2940)^+$ $I(J^P) = 0(\frac{3}{2}^-)$

$J^P = 3/2^-$ is favored, but is not certain

Mass $m = 2939.6^{+1.3}_{-1.5}$ MeV
Full width $\Gamma = 20^{+6}_{-5}$ MeV

$\Lambda_c(2940)^+$ DECAY MODES	Fraction (Γ_i/Γ)	p (MeV/c)
$p D^0$	seen	420
$\Sigma_c(2455)^{0,++}\pi^\pm$	seen	–

$\Sigma_c(2455)$ $I(J^P) = 1(\frac{1}{2}^+)$

$\Sigma_c(2455)^{++}$ mass $m = 2453.97 \pm 0.14$ MeV
$\Sigma_c(2455)^+$ mass $m = 2452.9 \pm 0.4$ MeV
$\Sigma_c(2455)^0$ mass $m = 2453.75 \pm 0.14$ MeV
$m_{\Sigma_c^{++}} - m_{\Lambda_c^+} = 167.510 \pm 0.017$ MeV
$m_{\Sigma_c^+} - m_{\Lambda_c^+} = 166.4 \pm 0.4$ MeV
$m_{\Sigma_c^0} - m_{\Lambda_c^+} = 167.290 \pm 0.017$ MeV
$m_{\Sigma_c^{++}} - m_{\Sigma_c^0} = 0.220 \pm 0.013$ MeV
$m_{\Sigma_c^+} - m_{\Sigma_c^0} = -0.9 \pm 0.4$ MeV
$\Sigma_c(2455)^{++}$ full width $\Gamma = 1.89^{+0.09}_{-0.18}$ MeV (S = 1.1)
$\Sigma_c(2455)^+$ full width $\Gamma < 4.6$ MeV, CL = 90%
$\Sigma_c(2455)^0$ full width $\Gamma = 1.83^{+0.11}_{-0.19}$ MeV (S = 1.2)

$\Lambda_c^+ \pi$ is the only strong decay allowed to a Σ_c having this mass.

$\Sigma_c(2455)$ DECAY MODES	Fraction (Γ_i/Γ)	p (MeV/c)
$\Lambda_c^+ \pi$	≈ 100 %	94

$\Sigma_c(2520)$ $I(J^P) = 1(\frac{3}{2}^+)$

J^P has not been measured; $\frac{3}{2}^+$ is the quark-model prediction.

$\Sigma_c(2520)^{++}$ mass $m = 2518.41^{+0.21}_{-0.19}$ MeV (S = 1.1)
$\Sigma_c(2520)^+$ mass $m = 2517.5 \pm 2.3$ MeV
$\Sigma_c(2520)^0$ mass $m = 2518.48 \pm 0.20$ MeV (S = 1.1)
$m_{\Sigma_c(2520)^{++}} - m_{\Lambda_c^+} = 231.95^{+0.17}_{-0.12}$ MeV (S = 1.3)
$m_{\Sigma_c(2520)^+} - m_{\Lambda_c^+} = 231.0 \pm 2.3$ MeV
$m_{\Sigma_c(2520)^0} - m_{\Lambda_c^+} = 232.02^{+0.15}_{-0.14}$ MeV (S = 1.3)
$m_{\Sigma_c(2520)^{++}} - m_{\Sigma_c(2520)^0} = 0.01 \pm 0.15$ MeV
$\Sigma_c(2520)^{++}$ full width $\Gamma = 14.78^{+0.30}_{-0.40}$ MeV
$\Sigma_c(2520)^+$ full width $\Gamma < 17$ MeV, CL = 90%
$\Sigma_c(2520)^0$ full width $\Gamma = 15.3^{+0.4}_{-0.5}$ MeV

$\Lambda_c^+ \pi$ is the only strong decay allowed to a Σ_c having this mass.

$\Sigma_c(2520)$ DECAY MODES	Fraction (Γ_i/Γ)	p (MeV/c)
$\Lambda_c^+ \pi$	≈ 100 %	179

$\Sigma_c(2800)$ $I(J^P) = 1(?^?)$

$\Sigma_c(2800)^{++}$ mass $m = 2801^{+4}_{-6}$ MeV
$\Sigma_c(2800)^+$ mass $m = 2792^{+14}_{-5}$ MeV
$\Sigma_c(2800)^0$ mass $m = 2806^{+5}_{-7}$ MeV (S = 1.3)
$m_{\Sigma_c(2800)^{++}} - m_{\Lambda_c^+} = 514^{+4}_{-6}$ MeV
$m_{\Sigma_c(2800)^+} - m_{\Lambda_c^+} = 505^{+14}_{-5}$ MeV
$m_{\Sigma_c(2800)^0} - m_{\Lambda_c^+} = 519^{+5}_{-7}$ MeV (S = 1.3)
$\Sigma_c(2800)^{++}$ full width $\Gamma = 75^{+22}_{-17}$ MeV
$\Sigma_c(2800)^+$ full width $\Gamma = 62^{+60}_{-40}$ MeV
$\Sigma_c(2800)^0$ full width $\Gamma = 72^{+22}_{-15}$ MeV

$\Sigma_c(2800)$ DECAY MODES	Fraction (Γ_i/Γ)	p (MeV/c)
$\Lambda_c^+ \pi$	seen	443

Ξ_c^+ $I(J^P) = \frac{1}{2}(\frac{1}{2}^+)$

J^P has not been measured; $\frac{1}{2}^+$ is the quark-model prediction.

Mass $m = 2467.87 \pm 0.30$ MeV (S = 1.1)
Mean life $\tau = (442 \pm 26) \times 10^{-15}$ s (S = 1.3)
$c\tau = 132\ \mu$m

Branching fractions marked with a footnote, e.g. [a], have been corrected for decay modes not observed in the experiments. For example, the sub-mode fraction $\Xi_c^+ \to \Sigma^+ \overline{K}^*(892)^0$ seen in $\Xi_c^+ \to \Sigma^+ K^- \pi^+$ has been multiplied up to include $\overline{K}^*(892)^0 \to \overline{K}^0 \pi^0$ decays.

Ξ_c^+ DECAY MODES	Fraction (Γ_i/Γ)	Confidence level	p (MeV/c)
No absolute branching fractions have been measured. The following are branching *ratios* relative to $\Xi^- 2\pi^+$.			
Cabibbo-favored ($S = -2$) decays — relative to $\Xi^- 2\pi^+$			
$p 2K_S^0$	0.087 ± 0.021		767
$\Lambda \overline{K}^0 \pi^+$	—		852
$\Sigma(1385)^+ \overline{K}^0$	[r] 1.0 ± 0.5		746
$\Lambda K^- 2\pi^+$	0.323 ± 0.033		787
$\Lambda \overline{K}^*(892)^0 \pi^+$	[r] <0.16	90%	608
$\Sigma(1385)^+ K^- \pi^+$	[r] <0.23	90%	678
$\Sigma^+ K^- \pi^+$	0.94 ± 0.10		811
$\Sigma^+ \overline{K}^*(892)^0$	[r] 0.81 ± 0.15		658
$\Sigma^0 K^- 2\pi^+$	0.27 ± 0.12		735
$\Xi^0 \pi^+$	0.55 ± 0.16		877
$\Xi^- 2\pi^+$	**DEFINED AS 1**		851
$\Xi(1530)^0 \pi^+$	[r] <0.10	90%	750
$\Xi^0 \pi^+ \pi^0$	2.3 ± 0.7		856
$\Xi^0 \pi^- 2\pi^+$	1.7 ± 0.5		818
$\Xi^0 e^+ \nu_e$	$2.3\ ^{+0.7}_{-0.8}$		884
$\Omega^- K^+ \pi^+$	0.07 ± 0.04		399
Cabibbo-suppressed decays — relative to $\Xi^- 2\pi^+$			
$p K^- \pi^+$	0.21 ± 0.04		944
$p \overline{K}^*(892)^0$	[r] 0.116 ± 0.030		828
$\Sigma^+ \pi^+ \pi^-$	0.48 ± 0.20		922
$\Sigma^- 2\pi^+$	0.18 ± 0.09		918
$\Sigma^+ K^+ K^-$	0.15 ± 0.06		579
$\Sigma^+ \phi$	[r] <0.11	90%	549
$\Xi(1690)^0 K^+$, $\Xi^0 \to \Sigma^+ K^-$	<0.05	90%	501

Baryon Summary Table

Ξ_c^0

$I(J^P) = \frac{1}{2}(\frac{1}{2}^+)$

J^P has not been measured; $\frac{1}{2}^+$ is the quark-model prediction.

Mass $m = 2470.87^{+0.28}_{-0.31}$ MeV
$m_{\Xi_c^0} - m_{\Xi_c^+} = 3.00 \pm 0.24$ MeV
Mean life $\tau = (112^{+13}_{-10}) \times 10^{-15}$ s
$c\tau = 33.6$ μm

Decay asymmetry parameters

$\Xi^-\pi^+$ $\quad \alpha = -0.6 \pm 0.4$

Branching fractions marked with a footnote, e.g. [a], have been corrected for decay modes not observed in the experiments. For example, the sub-mode fraction $\Xi_c^0 \to pK^-\overline{K}^*(892)^0$ seen in $\Xi_c^0 \to pK^-K^-\pi^+$ has been multiplied up to include $\overline{K}^*(892)^0 \to \overline{K}^0\pi^0$ decays.

Ξ_c^0 DECAY MODES	Fraction (Γ_i/Γ)	p (MeV/c)
No absolute branching fractions have been measured. The following are branching *ratios* relative to $\Xi^-\pi^+$.		
Cabibbo-favored ($S = -2$) decays — relative to $\Xi^-\pi^+$		
$pK^-K^-\pi^+$	0.34 $\pm$0.04	676
$pK^-\overline{K}^*(892)^0$	[r] 0.21 $\pm$0.05	413
$pK^-K^-\pi^+$ (no $\overline{K}^{*0}$)	0.21 $\pm$0.04	676
ΛK_S^0	0.210 $\pm$0.028	906
$\Lambda K^-\pi^+$	1.07 $\pm$0.14	856
$\Lambda\overline{K}^0\pi^+\pi^-$	seen	787
$\Lambda K^-\pi^+\pi^+\pi^-$	seen	703
$\Xi^-\pi^+$	**DEFINED AS 1**	875
$\Xi^-\pi^+\pi^+\pi^-$	3.3 $\pm$1.4	816
Ω^-K^+	0.297 $\pm$0.024	522
$\Xi^- e^+\nu_e$	3.1 $\pm$1.1	882
$\Xi^-\ell^+$ anything	1.0 $\pm$0.5	–
Cabibbo-suppressed decays — relative to $\Xi^-\pi^+$		
Ξ^-K^+	0.028 $\pm$0.006	790
ΛK^+K^- (no ϕ)	0.029 $\pm$0.007	648
$\Lambda\phi$	[r] 0.034 $\pm$0.007	621

$\Xi_c'^+$

$I(J^P) = \frac{1}{2}(\frac{1}{2}^+)$

J^P has not been measured; $\frac{1}{2}^+$ is the quark-model prediction.

Mass $m = 2577.4 \pm 1.2$ MeV (S = 2.9)
$m_{\Xi_c'^+} - m_{\Xi_c^+} = 109.5 \pm 1.2$ MeV (S = 3.7)
$m_{\Xi_c'^+} - m_{\Xi_c'^0} = -1.4 \pm 1.3$ MeV (S = 2.5)

The $\Xi_c'^+$–Ξ_c^+ mass difference is too small for any strong decay to occur.

$\Xi_c'^+$ DECAY MODES	Fraction (Γ_i/Γ)	p (MeV/c)
$\Xi_c^+\gamma$	seen	107

$\Xi_c'^0$

$I(J^P) = \frac{1}{2}(\frac{1}{2}^+)$

J^P has not been measured; $\frac{1}{2}^+$ is the quark-model prediction.

Mass $m = 2578.8 \pm 0.5$ MeV (S = 1.2)
$m_{\Xi_c'^0} - m_{\Xi_c^0} = 108.0 \pm 0.4$ MeV (S = 1.2)

The $\Xi_c'^0 - \Xi_c^0$ mass difference is too small for any strong decay to occur.

$\Xi_c'^0$ DECAY MODES	Fraction (Γ_i/Γ)	p (MeV/c)
$\Xi_c^0\gamma$	seen	106

$\Xi_c(2645)$

$I(J^P) = \frac{1}{2}(\frac{3}{2}^+)$

J^P has not been measured; $\frac{3}{2}^+$ is the quark-model prediction.

$\Xi_c(2645)^+$ mass $m = 2645.53 \pm 0.31$ MeV
$\Xi_c(2645)^0$ mass $m = 2646.32 \pm 0.31$ MeV (S = 1.1)
$m_{\Xi_c(2645)^+} - m_{\Xi_c^0} = 174.66 \pm 0.09$ MeV
$m_{\Xi_c(2645)^0} - m_{\Xi_c^+} = 178.44 \pm 0.11$ MeV (S = 1.1)
$m_{\Xi_c(2645)^+} - m_{\Xi_c(2645)^0} = -0.79 \pm 0.27$ MeV
$\Xi_c(2645)^+$ full width $\Gamma = 2.14 \pm 0.19$ MeV (S = 1.1)
$\Xi_c(2645)^0$ full width $\Gamma = 2.35 \pm 0.22$ MeV

$\Xi_c\pi$ is the only strong decay allowed to a Ξ_c resonance having this mass.

$\Xi_c(2645)$ DECAY MODES	Fraction (Γ_i/Γ)	p (MeV/c)
$\Xi_c^0\pi^+$	seen	102
$\Xi_c^+\pi^-$	seen	106

$\Xi_c(2790)$

$I(J^P) = \frac{1}{2}(\frac{1}{2}^-)$

J^P has not been measured; $\frac{1}{2}^-$ is the quark-model prediction.

$\Xi_c(2790)^+$ mass = 2792.0 $\pm$ 0.5 MeV (S = 1.2)
$\Xi_c(2790)^0$ mass = 2792.8 $\pm$ 1.2 MeV (S = 2.9)
$m_{\Xi_c(2790)^+} - m_{\Xi_c^0} = 321.1 \pm 0.4$ MeV (S = 1.2)
$m_{\Xi_c(2790)^0} - m_{\Xi_c^+} = 324.9 \pm 1.2$ MeV (S = 3.7)
$m_{\Xi_c(2790)^+} - m_{\Xi_c'^0} = 213.10 \pm 0.26$ MeV (S = 1.2)
$m_{\Xi_c(2790)^0} - m_{\Xi_c'^+} = 215.4 \pm 0.8$ MeV (S = 3.7)
$m_{\Xi_c(2790)^+} - m_{\Xi_c(2790)^0} = -0.9 \pm 1.3$ MeV (S = 2.5)
$\Xi_c(2790)^+$ width = 8.9 $\pm$ 1.0 MeV
$\Xi_c(2790)^0$ width = 10.0 $\pm$ 1.1 MeV

$\Xi_c(2790)$ DECAY MODES	Fraction (Γ_i/Γ)	p (MeV/c)
$\Xi_c\pi$	seen	–
$\Xi_c'\pi$	seen	160

$\Xi_c(2815)$

$I(J^P) = \frac{1}{2}(\frac{3}{2}^-)$

J^P has not been measured; $\frac{3}{2}^-$ is the quark-model prediction.

$\Xi_c(2815)^+$ mass $m = 2816.67 \pm 0.31$ MeV (S = 1.1)
$\Xi_c(2815)^0$ mass $m = 2820.22 \pm 0.32$ MeV
$m_{\Xi_c(2815)^+} - m_{\Xi_c^+} = 348.80 \pm 0.10$ MeV
$m_{\Xi_c(2815)^0} - m_{\Xi_c^0} = 349.35 \pm 0.11$ MeV
$m_{\Xi_c(2815)^+} - m_{\Xi_c(2815)^0} = -3.55 \pm 0.28$ MeV
$\Xi_c(2815)^+$ full width $\Gamma = 2.43 \pm 0.26$ MeV
$\Xi_c(2815)^0$ full width $\Gamma = 2.54 \pm 0.25$ MeV

The $\Xi_c\pi\pi$ modes are consistent with being entirely via $\Xi_c(2645)\pi$.

$\Xi_c(2815)$ DECAY MODES	Fraction (Γ_i/Γ)	p (MeV/c)
$\Xi_c\pi$	seen	–
$\Xi_c^+\pi^+\pi^-$	seen	196
$\Xi_c^0\pi^+\pi^-$	seen	191

$\Xi_c(2970)$

$I(J^P) = \frac{1}{2}(?^?)$

$\Xi_c(2970)^+$ $m = 2969.4 \pm 0.8$ MeV (S = 1.1)
$\Xi_c(2970)^0$ $m = 2967.8 \pm 0.8$ MeV (S = 1.1)
$m_{\Xi_c(2970)^+} - m_{\Xi_c^0} = 498.5 \pm 0.8$ MeV (S = 1.1)
$m_{\Xi_c(2970)^0} - m_{\Xi_c^+} = 499.9^{+0.8}_{-0.7}$ MeV (S = 1.1)
$m_{\Xi_c(2970)^+} - m_{\Xi_c(2970)^0} = 1.6 \pm 1.1$ MeV (S = 1.1)
$\Xi_c(2970)^+$ width $\Gamma = 20.9^{+2.4}_{-3.5}$ MeV (S = 1.2)
$\Xi_c(2970)^0$ width $\Gamma = 28.1^{+3.4}_{-4.0}$ MeV (S = 1.5)

$\Xi_c(2970)$ DECAY MODES	Fraction (Γ_i/Γ)	p (MeV/c)
$\Lambda_c^+\overline{K}\pi$	seen	231
$\Sigma_c(2455)\overline{K}$	seen	133
$\Lambda_c^+\overline{K}$	not seen	414
$\Xi_c 2\pi$	seen	385
$\Xi_c(2645)\pi$	seen	277

$\Xi_c(3055)$

$I(J^P) = ?(?^?)$

Mass $m = 3055.9 \pm 0.4$ MeV
Full width $\Gamma = 7.8 \pm 1.9$ MeV

$\Xi_c(3055)$ DECAY MODES	Fraction (Γ_i/Γ)	p (MeV/c)
$\Sigma^{++} K^-$	seen	–
ΛD^+	seen	316

$\Xi_c(3080)$

$I(J^P) = \frac{1}{2}(?^?)$

$\Xi_c(3080)^+$ $m = 3077.2 \pm 0.4$ MeV
$\Xi_c(3080)^0$ $m = 3079.9 \pm 1.4$ MeV (S = 1.3)
$\Xi_c(3080)^+$ width $\Gamma = 3.6 \pm 1.1$ MeV (S = 1.5)
$\Xi_c(3080)^0$ width $\Gamma = 5.6 \pm 2.2$ MeV

$\Xi_c(3080)$ DECAY MODES	Fraction (Γ_i/Γ)	p (MeV/c)
$\Lambda_c^+ \overline{K}\pi$	seen	415
$\Sigma_c(2455)\overline{K}$	seen	342
$\Sigma_c(2455)^{++} K^-$	seen	342
$\Sigma_c(2520)^{++} K^-$	seen	239
$\Sigma_c(2455)\overline{K} + \Sigma_c(2520)\overline{K}$	seen	–
$\Lambda_c^+ \overline{K}$	not seen	536
$\Lambda_c^+ \overline{K}\pi^+\pi^-$	not seen	144
ΛD^+	seen	362

Ω_c^0

$I(J^P) = 0(\frac{1}{2}^+)$

J^P has not been measured; $\frac{1}{2}^+$ is the quark-model prediction.

Mass $m = 2695.2 \pm 1.7$ MeV (S = 1.3)
Mean life $\tau = (69 \pm 12) \times 10^{-15}$ s
$c\tau = 21$ μm

Ω_c^0 DECAY MODES	Fraction (Γ_i/Γ)	Confidence level	p (MeV/c)
No absolute branching fractions have been measured. The following are branching *ratios* relative to $\Omega^-\pi^+$.			
Cabibbo-favored ($S = -3$) decays — relative to $\Omega^-\pi^+$			
$\Omega^-\pi^+$	**DEFINED AS 1**		821
$\Omega^-\pi^+\pi^0$	1.80±0.33		797
$\Omega^-\rho^+$	>1.3	90%	532
$\Omega^-\pi^-2\pi^+$	0.31±0.05		753
$\Omega^- e^+ \nu_e$	2.4 ±1.2		829
$\Xi^0\overline{K}^0$	1.64±0.29		950
$\Xi^0 K^-\pi^+$	1.20±0.18		901
$\Xi^0\overline{K}^{*0}$, $\overline{K}^{*0} \to K^-\pi^+$	0.68±0.16		764
$\Xi^-\overline{K}^0\pi^+$	2.12±0.28		895
$\Xi^- K^-2\pi^+$	0.63±0.09		830
$\Xi(1530)^0 K^-\pi^+$, $\Xi^{*0} \to \Xi^-\pi^+$	0.21±0.06		757
$\Xi^-\overline{K}^{*0}\pi^+$	0.34±0.11		653
$\Sigma^+ K^- K^-\pi^+$	<0.32	90%	689
$\Lambda\overline{K}^0 K^0$	1.72±0.35		837

$\Omega_c(2770)^0$

$I(J^P) = 0(\frac{3}{2}^+)$

J^P has not been measured; $\frac{3}{2}^+$ is the quark-model prediction.

Mass $m = 2765.9 \pm 2.0$ MeV (S = 1.2)
$m_{\Omega_c(2770)^0} - m_{\Omega_c^0} = 70.7^{+0.8}_{-0.9}$ MeV

The $\Omega_c(2770)^0$–Ω_c^0 mass difference is too small for any strong decay to occur.

$\Omega_c(2770)^0$ DECAY MODES	Fraction (Γ_i/Γ)	p (MeV/c)
$\Omega_c^0\gamma$	presumably 100%	70

$\Omega_c(3000)^0$

$I(J^P) = ?(?^?)$

Mass $m = 3000.4 \pm 0.4$ MeV
Full width $\Gamma = 4.5 \pm 0.7$ MeV

$\Omega_c(3000)^0$ DECAY MODES	Fraction (Γ_i/Γ)	p (MeV/c)
$\Xi_c^+ K^-$	seen	181

$\Omega_c(3050)^0$

$I(J^P) = ?(?^?)$

Mass $m = 3050.2 \pm 0.33$ MeV
Full width $\Gamma < 1.2$ MeV, CL = 95%

$\Omega_c(3050)^0$ DECAY MODES	Fraction (Γ_i/Γ)	p (MeV/c)
$\Xi_c^+ K^-$	seen	278

$\Omega_c(3065)^0$

$I(J^P) = ?(?^?)$

Mass $m = 3065.6 \pm 0.4$ MeV
Full width $\Gamma = 3.5 \pm 0.4$ MeV

$\Omega_c(3065)^0$ DECAY MODES	Fraction (Γ_i/Γ)	p (MeV/c)
$\Xi_c^+ K^-$	seen	303

$\Omega_c(3090)^0$

$I(J^P) = ?(?^?)$

Mass $m = 3090.2 \pm 0.7$ MeV
Full width $\Gamma = 8.7 \pm 1.3$ MeV

$\Omega_c(3090)^0$ DECAY MODES	Fraction (Γ_i/Γ)	p (MeV/c)
$\Xi_c^+ K^-$	seen	339

$\Omega_c(3120)^0$

$I(J^P) = ?(?^?)$

Mass $m = 3119.1 \pm 1.0$ MeV
Full width $\Gamma < 2.6$ MeV, CL = 95%

$\Omega_c(3120)^0$ DECAY MODES	Fraction (Γ_i/Γ)	p (MeV/c)
$\Xi_c^+ K^-$	seen	379

DOUBLY CHARMED BARYONS ($C = +2$)

$\Xi_{cc}^{++} = ucc$, $\Xi_{cc}^+ = dcc$, $\Omega_{cc}^+ = scc$

Ξ_{cc}^{++}

$I(J^P) = ?(?^?)$

Mass $m = 3621.4 \pm 0.8$ MeV

Ξ_{cc}^{++} DECAY MODES	Fraction (Γ_i/Γ)	p (MeV/c)
$\Lambda_c^+ K^-\pi^+\pi^+$	seen	880

Baryon Summary Table

BOTTOM BARYONS ($B = -1$)

$\Lambda_b^0 = udb$, $\Xi_b^0 = usb$, $\Xi_b^- = dsb$, $\Omega_b^- = ssb$

Λ_b^0

$I(J^P) = 0(\frac{1}{2}^+)$

$I(J^P)$ not yet measured; $0(\frac{1}{2}^+)$ is the quark model prediction.

Mass $m = 5619.60 \pm 0.17$ MeV
$m_{\Lambda_b^0} - m_{B^0} = 339.2 \pm 1.4$ MeV
$m_{\Lambda_b^0} - m_{B^+} = 339.72 \pm 0.28$ MeV
Mean life $\tau = (1.470 \pm 0.010) \times 10^{-12}$ s
$c\tau = 440.7\ \mu$m
$A_{CP}(\Lambda_b \to p\pi^-) = 0.06 \pm 0.08$
$A_{CP}(\Lambda_b \to pK^-) = -0.10 \pm 0.09$
$A_{CP}(\Lambda_b \to p\overline{K}^0\pi^-) = 0.22 \pm 0.13$
$\Delta A_{CP}(J/\psi p\pi^-/K^-) \equiv A_{CP}(J/\psi p\pi^-) - A_{CP}(J/\psi pK^-)$
$= (5.7 \pm 2.7) \times 10^{-2}$
$A_{CP}(\Lambda_b \to \Lambda K^+\pi^-) = -0.53 \pm 0.25$
$A_{CP}(\Lambda_b \to \Lambda K^+K^-) = -0.28 \pm 0.12$
$\Delta A_{CP}(\Lambda_b^0 \to pK^-\mu^+\mu^-) \equiv A_{CP}(pK^-\mu^+\mu^-)$
$- A_{CP}(pK^- J/\psi) = (-4 \pm 5) \times 10^{-2}$
α decay parameter for $\Lambda_b \to J/\psi\Lambda = 0.18 \pm 0.13$
$A_{FB}^{\ell}(\mu\mu)$ in $\Lambda_b \to \Lambda\mu^+\mu^- = -0.05 \pm 0.09$
$A_{FB}^{h}(p\pi)$ in $\Lambda_b \to \Lambda(p\pi)\mu^+\mu^- = -0.29 \pm 0.08$
$f_L(\mu\mu)$ longitudinal polarization fraction in $\Lambda_b \to \Lambda\mu^+\mu^- = 0.61^{+0.11}_{-0.14}$

The branching fractions B(b-baryon $\to \Lambda\ell^-\overline{\nu}_\ell$anything) and B($\Lambda_b^0 \to \Lambda_c^+\ell^-\overline{\nu}_\ell$anything) are not pure measurements because the underlying measured products of these with B($b \to b$-baryon) were used to determine B($b \to b$-baryon), as described in the note "Production and Decay of b-Flavored Hadrons."

For inclusive branching fractions, *e.g.*, $\Lambda_b \to \overline{\Lambda}_c$anything, the values usually are multiplicities, not branching fractions. They can be greater than one.

Λ_b^0 DECAY MODES		Fraction (Γ_i/Γ)	Scale factor/ Confidence level	p (MeV/c)
$J/\psi(1S)\Lambda \times$ B($b \to \Lambda_b^0$)		$(5.8 \pm 0.8) \times 10^{-5}$		1740
$pD^0\pi^-$		$(6.3 \pm 0.7) \times 10^{-4}$		2370
pD^0K^-		$(4.6 \pm 0.8) \times 10^{-5}$		2269
$pJ/\psi\pi^-$		$(2.6\ ^{+0.5}_{-0.4}) \times 10^{-5}$		1755
$p\pi^- J/\psi$, $J/\psi \to \mu^+\mu^-$		$(1.6 \pm 0.8) \times 10^{-6}$		–
$pJ/\psi K^-$		$(3.2\ ^{+0.6}_{-0.5}) \times 10^{-4}$		1589
$P_c(4380)^+K^-$, $P_c \to pJ/\psi$	[*v*]	$(2.7 \pm 1.4) \times 10^{-5}$		–
$P_c(4450)^+K^-$, $P_c \to pJ/\psi$	[*v*]	$(1.3 \pm 0.4) \times 10^{-5}$		–
$\chi_{c1}(1P)pK^-$		$(7.6\ ^{+1.5}_{-1.3}) \times 10^{-5}$		1242
$\chi_{c2}(1P)pK^-$		$(7.9\ ^{+1.6}_{-1.4}) \times 10^{-5}$		1198
$pJ/\psi(1S)\pi^+\pi^-K^-$		$(6.6\ ^{+1.3}_{-1.1}) \times 10^{-5}$		1410
$p\psi(2S)K^-$		$(6.6\ ^{+1.2}_{-1.0}) \times 10^{-5}$		1063
$p\overline{K}^0\pi^-$		$(1.3 \pm 0.4) \times 10^{-5}$		2693
pK^0K^-		$< 3.5 \times 10^{-6}$	CL=90%	2639
$\Lambda_c^+\pi^-$		$(4.9 \pm 0.4) \times 10^{-3}$	S=1.2	2342
$\Lambda_c^+K^-$		$(3.59 \pm 0.30) \times 10^{-4}$	S=1.2	2314
$\Lambda_c^+ a_1(1260)^-$		seen		2153
$\Lambda_c^+ D^-$		$(4.6 \pm 0.6) \times 10^{-4}$		1886
$\Lambda_c^+ D_s^-$		(1.10 ± 0.10) %		1833
$\Lambda_c^+\pi^+\pi^-\pi^-$		$(7.7 \pm 1.1) \times 10^{-3}$	S=1.1	2323
$\Lambda_c(2595)^+\pi^-$, $\Lambda_c(2595)^+ \to \Lambda_c^+\pi^+\pi^-$		$(3.4 \pm 1.5) \times 10^{-4}$		2210
$\Lambda_c(2625)^+\pi^-$, $\Lambda_c(2625)^+ \to \Lambda_c^+\pi^+\pi^-$		$(3.3 \pm 1.3) \times 10^{-4}$		2193
$\Sigma_c(2455)^0\pi^+\pi^-$, $\Sigma_c^0 \to \Lambda_c^+\pi^-$		$(5.7 \pm 2.2) \times 10^{-4}$		2265
$\Sigma_c(2455)^{++}\pi^-\pi^-$, $\Sigma_c^{++} \to \Lambda_c^+\pi^+$		$(3.2 \pm 1.6) \times 10^{-4}$		2265
$\Lambda_c^+\ell^-\overline{\nu}_\ell$anything	[*x*]	(10.3 ± 2.1) %		–
$\Lambda_c^+\ell^-\overline{\nu}_\ell$		$(6.2\ ^{+1.4}_{-1.3})$ %		2345
$\Lambda_c^+\pi^+\pi^-\ell^-\overline{\nu}_\ell$		(5.6 ± 3.1) %		2335
$\Lambda_c(2595)^+\ell^-\overline{\nu}_\ell$		$(7.9\ ^{+4.0}_{-3.5}) \times 10^{-3}$		2212
$\Lambda_c(2625)^+\ell^-\overline{\nu}_\ell$		$(1.3\ ^{+0.6}_{-0.5})$ %		2195
ph^-	[*y*]	$< 2.3 \times 10^{-5}$	CL=90%	2730
$p\pi^-$		$(4.2 \pm 0.8) \times 10^{-6}$		2730
pK^-		$(5.1 \pm 0.9) \times 10^{-6}$		2709
pD_s^-		$< 4.8 \times 10^{-4}$	CL=90%	2364
$p\mu^-\overline{\nu}_\mu$		$(4.1 \pm 1.0) \times 10^{-4}$		2730
$\Lambda\mu^+\mu^-$		$(1.08 \pm 0.28) \times 10^{-6}$		2695
$p\pi^-\mu^+\mu^-$		$(6.9 \pm 2.5) \times 10^{-8}$		2720
$\Lambda\gamma$		$< 1.3 \times 10^{-3}$	CL=90%	2699
$\Lambda^0\eta$		$(9\ ^{+7}_{-5}) \times 10^{-6}$		–
$\Lambda^0\eta'(958)$		$< 3.1 \times 10^{-6}$	CL=90%	–
$\Lambda\pi^+\pi^-$		$(4.6 \pm 1.9) \times 10^{-6}$		2692
$\Lambda K^+\pi^-$		$(5.7 \pm 1.2) \times 10^{-6}$		2660
ΛK^+K^-		$(1.61 \pm 0.23) \times 10^{-5}$		2605
$\Lambda^0\phi$		$(9.2 \pm 2.5) \times 10^{-6}$		–

$\Lambda_b(5912)^0$

$J^P = \frac{1}{2}^-$

Mass $m = 5912.20 \pm 0.21$ MeV
Full width $\Gamma < 0.66$ MeV, CL = 90%

$\Lambda_b(5912)^0$ DECAY MODES	Fraction (Γ_i/Γ)	p (MeV/c)
$\Lambda_b^0\pi^+\pi^-$	seen	86

$\Lambda_b(5920)^0$

$J^P = \frac{3}{2}^-$

Mass $m = 5919.92 \pm 0.19$ MeV (S = 1.1)
Full width $\Gamma < 0.63$ MeV, CL = 90%

$\Lambda_b(5920)^0$ DECAY MODES	Fraction (Γ_i/Γ)	p (MeV/c)
$\Lambda_b^0\pi^+\pi^-$	seen	108

Σ_b

$I(J^P) = 1(\frac{1}{2}^+)$
I, J, P need confirmation.

Mass $m(\Sigma_b^+) = 5811.3 \pm 1.9$ MeV
Mass $m(\Sigma_b^-) = 5815.5 \pm 1.8$ MeV
$m_{\Sigma_b^+} - m_{\Sigma_b^-} = -4.2 \pm 1.1$ MeV
$\Gamma(\Sigma_b^+) = 9.7^{+4.0}_{-3.0}$ MeV
$\Gamma(\Sigma_b^-) = 4.9^{+3.3}_{-2.4}$ MeV

Σ_b DECAY MODES	Fraction (Γ_i/Γ)	p (MeV/c)
$\Lambda_b^0\pi$	dominant	134

Σ_b^*

$I(J^P) = 1(\frac{3}{2}^+)$
I, J, P need confirmation.

Mass $m(\Sigma_b^{*+}) = 5832.1 \pm 1.9$ MeV
Mass $m(\Sigma_b^{*-}) = 5835.1 \pm 1.9$ MeV
$m_{\Sigma_b^{*+}} - m_{\Sigma_b^{*-}} = -3.0^{+1.0}_{-0.9}$ MeV
$\Gamma(\Sigma_b^{*+}) = 11.5 \pm 2.8$ MeV
$\Gamma(\Sigma_b^{*-}) = 7.5 \pm 2.3$ MeV
$m_{\Sigma_b^*} - m_{\Sigma_b} = 21.2 \pm 2.0$ MeV

Σ_b^* DECAY MODES	Fraction (Γ_i/Γ)	p (MeV/c)
$\Lambda_b^0\pi$	dominant	161

Ξ_b^0, Ξ_b^-

$I(J^P) = \frac{1}{2}(\frac{1}{2}^+)$
I, J, P need confirmation.

$m(\Xi_b^-) = 5797.0 \pm 0.9$ MeV (S = 1.8)
$m(\Xi_b^0) = 5791.9 \pm 0.5$ MeV
$m_{\Xi_b^-} - m_{\Lambda_b^0} = 177.5 \pm 0.5$ MeV (S = 1.6)
$m_{\Xi_b^0} - m_{\Lambda_b^0} = 172.5 \pm 0.4$ MeV
$m_{\Xi_b^-} - m_{\Xi_b^0} = 5.9 \pm 0.6$ MeV
Mean life $\tau_{\Xi_b^-} = (1.571 \pm 0.040) \times 10^{-12}$ s
Mean life $\tau_{\Xi_b^0} = (1.479 \pm 0.031) \times 10^{-12}$ s

Ξ_b DECAY MODES	Fraction (Γ_i/Γ)	Scale factor/ Confidence level	p (MeV/c)
$\Xi^- \ell^- \overline{\nu}_\ell X \times$ B($\overline{b} \to \Xi_b$)	$(3.9 \pm 1.2) \times 10^{-4}$	S=1.4	–
$J/\psi \Xi^- \times$ B($b \to \Xi_b^-$)	$(1.02^{+0.26}_{-0.21}) \times 10^{-5}$		1782
$J/\psi \Lambda K^- \times$ B($b \to \Xi_b^-$)	$(2.5 \pm 0.4) \times 10^{-6}$		1631
$p D^0 K^- \times$ B($\overline{b} \to \Xi_b$)	$(1.8 \pm 0.6) \times 10^{-6}$		2374
$p\overline{K}^0 \pi^- \times$ B($\overline{b} \to \Xi_b$)/B($\overline{b} \to B^0$)	$< 1.6 \times 10^{-6}$	CL=90%	2783
$p K^0 K^- \times$ B($\overline{b} \to \Xi_b$)/B($\overline{b} \to B^0$)	$< 1.1 \times 10^{-6}$	CL=90%	2730
$p K^- K^- \times$ B($\overline{b} \to \Xi_b$)	$(3.6 \pm 0.8) \times 10^{-8}$		2731
$\Lambda \pi^+ \pi^- \times$ B($b \to \Xi_b^0$)/B($b \to \Lambda_b^0$)	$< 1.7 \times 10^{-6}$	CL=90%	2781
$\Lambda K^- \pi^+ \times$ B($b \to \Xi_b^0$)/B($b \to \Lambda_b^0$)	$< 8 \times 10^{-7}$	CL=90%	2751
$\Lambda K^+ K^- \times$ B($b \to \Xi_b^0$)/B($b \to \Lambda_b^0$)	$< 3 \times 10^{-7}$	CL=90%	2698
$\Lambda_c^+ K^- \times$ B($\overline{b} \to \Xi_b$)	$(6 \pm 4) \times 10^{-7}$		2416
$\Lambda_b^0 \pi^- \times$ B($b \to \Xi_b^-$)/B($b \to \Lambda_b^0$)	$(5.7 \pm 2.0) \times 10^{-4}$		99

$\Xi_b'(5935)^-$

$J^P = \frac{1}{2}^+$

Mass $m = 5935.02 \pm 0.05$ MeV
$m_{\Xi_b'(5935)^-} - m_{\Xi_b^0} - m_{\pi^-} = 3.653 \pm 0.019$ MeV
Full width $\Gamma < 0.08$ MeV, CL = 95%

$\Xi_b'(5935)^-$ DECAY MODES	Fraction (Γ_i/Γ)	p (MeV/c)
$\Xi_b^0 \pi^- \times$ B($\overline{b} \to \Xi_b'(5935)^-$)/B($\overline{b} \to \Xi_b^0$)	(11.8±1.8) %	31

$\Xi_b(5945)^0$

$J^P = \frac{3}{2}^+$

Mass $m = 5949.8 \pm 1.4$ MeV
Full width $\Gamma = 0.90 \pm 0.18$ MeV

$\Xi_b(5945)^0$ DECAY MODES	Fraction (Γ_i/Γ)	p (MeV/c)
$\Xi_b^- \pi^+$	seen	73

$\Xi_b(5955)^-$

$J^P = \frac{3}{2}^+$

Mass $m = 5955.33 \pm 0.13$ MeV
$m_{\Xi_b(5955)^-} - m_{\Xi_b^0} - m_{\pi^-} = 23.96 \pm 0.13$ MeV
Full width $\Gamma = 1.65 \pm 0.33$ MeV

$\Xi_b(5955)^-$ DECAY MODES	Fraction (Γ_i/Γ)	p (MeV/c)
$\Xi_b^0 \pi^- \times$ B($\overline{b} \to \Xi_b^*(5955)^-$)/B($\overline{b} \to \Xi_b^0$)	(20.7±3.5) %	84

Ω_b^-

$I(J^P) = 0(\frac{1}{2}^+)$
I, J, P need confirmation.

Mass $m = 6046.1 \pm 1.7$ MeV
$m_{\Omega_b^-} - m_{\Lambda_b^0} = 426.4 \pm 2.2$ MeV
$m_{\Omega_b^-} - m_{\Xi_b^-} = 247.3 \pm 3.2$ MeV
Mean life $\tau = (1.64^{+0.18}_{-0.17}) \times 10^{-12}$ s
$\tau(\Omega_b^-)/\tau(\Xi_b^-)$ mean life ratio $= 1.11 \pm 0.16$

Ω_b^- DECAY MODES	Fraction (Γ_i/Γ)	Confidence level	p (MeV/c)
$J/\psi \Omega^- \times$B($b \to \Omega_b$)	$(2.9^{+1.1}_{-0.8}) \times 10^{-6}$		1806
$p K^- K^- \times$B($\overline{b} \to \Omega_b$)	$< 2.5 \times 10^{-9}$	90%	2866
$p \pi^- \pi^- \times$B($\overline{b} \to \Omega_b$)	$< 1.5 \times 10^{-8}$	90%	2943
$p K^- \pi^- \times$B($\overline{b} \to \Omega_b$)	$< 7 \times 10^{-9}$	90%	2915

b-baryon ADMIXTURE (Λ_b, Ξ_b, Σ_b, Ω_b)

These branching fractions are actually an average over weakly decaying b-baryons weighted by their production rates at the LHC, LEP, and Tevatron, branching ratios, and detection efficiencies. They scale with the b-baryon production fraction B($b \to b$-baryon).

The branching fractions B(b-baryon $\to \Lambda \ell^- \overline{\nu}_\ell$ anything) and B($\Lambda_b^0 \to \Lambda_c^+ \ell^- \overline{\nu}_\ell$ anything) are not pure measurements because the underlying measured products of these with B($b \to b$-baryon) were used to determine B($b \to b$-baryon), as described in the note "Production and Decay of b-Flavored Hadrons."

For inclusive branching fractions, *e.g.*, $B \to D^\pm$ anything, the values usually are multiplicities, not branching fractions. They can be greater than one.

b-baryon ADMIXTURE DECAY MODES (Λ_b,Ξ_b,Σ_b,Ω_b)	Fraction (Γ_i/Γ)	p (MeV/c)
$p\mu^-\overline{\nu}$ anything	$(5.5^{+2.2}_{-1.9})$ %	–
$p\ell\overline{\nu}_\ell$ anything	(5.3± 1.1) %	–
p anything	(66 ±21) %	–
$\Lambda\ell^-\overline{\nu}_\ell$ anything	(3.6± 0.6) %	–
$\Lambda\ell^+\nu_\ell$ anything	(3.0± 0.8) %	–
Λ anything	(37 ± 7) %	–
$\Xi^-\ell^-\overline{\nu}_\ell$ anything	$(6.2 \pm 1.6) \times 10^{-3}$	–

EXOTIC BARYONS

$P_c(4380)^+$

Mass $m = 4380 \pm 30$ MeV
Full width $\Gamma = 205 \pm 90$ MeV

$P_c(4380)^+$ DECAY MODES	Fraction (Γ_i/Γ)	p (MeV/c)
$J/\psi p$	seen	741

$P_c(4450)^+$

Mass $m = 4449.8 \pm 3.0$ MeV
Full width $\Gamma = 39 \pm 20$ MeV

$P_c(4450)^+$ DECAY MODES	Fraction (Γ_i/Γ)	p (MeV/c)
$J/\psi p$	seen	820

Baryon Summary Table

NOTES

This Summary Table only includes established baryons. The Particle Listings include evidence for other baryons. The masses, widths, and branching fractions for the resonances in this Table are Breit-Wigner parameters, but pole positions are also given for most of the N and Δ resonances.

For most of the resonances, the parameters come from various partial-wave analyses of more or less the same sets of data, and it is not appropriate to treat the results of the analyses as independent or to average them together. Furthermore, the systematic errors on the results are not well understood. Thus, we usually only give ranges for the parameters. We then also give a best guess for the mass (as part of the name of the resonance) and for the width. The *Note on N and Δ Resonances* and the *Note on Λ and Σ Resonances* in the Particle Listings review the partial-wave analyses.

When a quantity has "(S = ...)" to its right, the error on the quantity has been enlarged by the "scale factor" S, defined as $S = \sqrt{\chi^2/(N-1)}$, where N is the number of measurements used in calculating the quantity. We do this when $S > 1$, which often indicates that the measurements are inconsistent. When $S > 1.25$, we also show in the Particle Listings an ideogram of the measurements. For more about S, see the Introduction.

A decay momentum p is given for each decay mode. For a 2-body decay, p is the momentum of each decay product in the rest frame of the decaying particle. For a 3-or-more-body decay, p is the largest momentum any of the products can have in this frame. For any resonance, the *nominal* mass is used in calculating p. A dagger ("†") in this column indicates that the mode is forbidden when the nominal masses of resonances are used, but is in fact allowed due to the nonzero widths of the resonances.

[a] The masses of the p and n are most precisely known in u (unified atomic mass units). The conversion factor to MeV, 1 u = 931.494061(21) MeV, is less well known than are the masses in u.

[b] The $|m_p - m_{\overline{p}}|/m_p$ and $|q_p + q_{\overline{p}}|/e$ are not independent, and both use the more precise measurement of $|q_{\overline{p}}/m_{\overline{p}}|/(q_p/m_p)$.

[c] The limit is from neutrality-of-matter experiments; it assumes $q_n = q_p + q_e$. See also the charge of the neutron.

[d] The μp and ep values for the charge radius are much too different to average them. The disagreement is not yet understood.

[e] There is a lot of disagreement about the value of the proton magnetic charge radius. See the Listings.

[f] The first limit is for $p \to$ anything or "disappearance" modes of a bound proton. The second entry, a rough range of limits, assumes the dominant decay modes are among those investigated. For antiprotons the best limit, inferred from the observation of cosmic ray $\overline{p}$'s is $\tau_{\overline{p}} > 10^7$ yr, the cosmic-ray storage time, but this limit depends on a number of assumptions. The best direct observation of stored antiprotons gives $\tau_{\overline{p}}/\mathrm{B}(\overline{p} \to e^-\gamma) > 7 \times 10^5$ yr.

[g] There is some controversy about whether nuclear physics and model dependence complicate the analysis for bound neutrons (from which the best limit comes). The first limit here is from reactor experiments with free neutrons.

[h] Lee and Yang in 1956 proposed the existence of a mirror world in an attempt to restore global parity symmetry—thus a search for oscillations between the two worlds. Oscillations between the worlds would be maximal when the magnetic fields B and B' were equal. The limit for any B' in the range 0 to 12.5 μT is >12 s (95% CL).

[i] The parameters g_A, g_V, and g_{WM} for semileptonic modes are defined by $\overline{B}_f[\gamma_\lambda(g_V + g_A\gamma_5) + i(g_{WM}/m_{B_i})\,\sigma_{\lambda\nu}\,q^\nu]B_i$, and ϕ_{AV} is defined by $g_A/g_V = |g_A/g_V|e^{i\phi_{AV}}$. See the "Note on Baryon Decay Parameters" in the neutron Particle Listings.

[j] Time-reversal invariance requires this to be 0° or 180°.

[k] This coefficient is zero if time invariance is not violated.

[l] This limit is for γ energies between 0.4 and 782 keV.

[n] The decay parameters γ and Δ are calculated from α and ϕ using

$$\gamma = \sqrt{1-\alpha^2}\,\cos\phi\,, \qquad \tan\Delta = -\frac{1}{\alpha}\,\sqrt{1-\alpha^2}\,\sin\phi\,.$$

See the "Note on Baryon Decay Parameters" in the neutron Particle Listings.

[o] See the Listings for the pion momentum range used in this measurement.

[p] The error given here is only an educated guess. It is larger than the error on the weighted average of the published values.

[q] A theoretical value using QED.

[r] This branching fraction includes all the decay modes of the final-state resonance.

[s] The value is for the sum of the charge states or particle/antiparticle states indicated.

[t] See AALTONEN 11H, Fig. 8, for the calculated ratio of $\Lambda_c^+\pi^0\pi^0$ and $\Lambda_c^+\pi^+\pi^-$ partial widths as a function of the $\Lambda_c(2595)^+ - \Lambda_c^+$ mass difference. At our value of the mass difference, the ratio is about 4.

[u] A test that the isospin is indeed 0, so that the particle is indeed a Λ_c^+.

[v] P_c^+ is a pentaquark-charmonium state.

[x] Not a pure measurement. See note at head of Λ_b^0 Decay Modes.

[y] Here h^- means π^- or K^-.

SEARCHES not in other sections

Magnetic Monopole Searches

Isolated supermassive monopole candidate events have not been confirmed. The most sensitive experiments obtain negative results.

Best cosmic-ray supermassive monopole flux limit:

$< 1.4 \times 10^{-16}$ cm^{-2}sr^{-1}s^{-1} for $1.1 \times 10^{-4} < \beta < 1$

Supersymmetric Particle Searches

All supersymmetric mass bounds here are model dependent.

The limits assume:

1) $\widetilde{\chi}_1^0$ is the lightest supersymmetric particle; 2) R-parity is conserved;

See the Particle Listings for a Note giving details of supersymmetry.

$\widetilde{\chi}_i^0$ — neutralinos (mixtures of $\widetilde{\gamma}$, $\widetilde{Z}^0$, and $\widetilde{H}_i^0$)

Mass $m_{\widetilde{\chi}_1^0} > 0$ GeV, CL = 95%
[general MSSM, non-universal gaugino masses]

Mass $m_{\widetilde{\chi}_1^0} > 46$ GeV, CL = 95%
[all tanβ, all m_0, all $m_{\widetilde{\chi}_2^0} - m_{\widetilde{\chi}_1^0}$]

Mass $m_{\widetilde{\chi}_2^0} > 670$ GeV, CL = 95%
[$3/4\ell + \not{E}_T$, Tn2n3B, $m_{\widetilde{\chi}_1^0} < 200$GeV]

Mass $m_{\widetilde{\chi}_3^0} > 670$ GeV, CL = 95%
[$3/4\ell + \not{E}_T$, Tn2n3B, $m_{\widetilde{\chi}_1^0} < 200$GeV]

Mass $m_{\widetilde{\chi}_4^0} > 116$ GeV, CL = 95%
[1<tanβ <40, all m_0, all $m_{\widetilde{\chi}_2^0} - m_{\widetilde{\chi}_1^0}$]

$\widetilde{\chi}_i^\pm$ — charginos (mixtures of $\widetilde{W}^\pm$ and $\widetilde{H}_i^\pm$)

Mass $m_{\widetilde{\chi}_1^\pm} > 94$ GeV, CL = 95%
[tan$\beta < 40$, $m_{\widetilde{\chi}_1^\pm} - m_{\widetilde{\chi}_1^0} > 3$ GeV, all m_0]

Mass $m_{\widetilde{\chi}_1^\pm} > 500$ GeV, CL = 95%
[$2\ell^\pm + \not{E}_T$, Tchi1chi1B, $m_{\widetilde{\chi}_1^0} = 0$ GeV]

$\widetilde{\chi}^\pm$ — long-lived chargino

Mass $m_{\widetilde{\chi}^\pm} > 620$ GeV, CL = 95% [stable $\widetilde{\chi}^\pm$]

$\widetilde{\nu}$ — sneutrino

Mass $m > 41$ GeV, CL = 95% [model independent]

Mass $m > 94$ GeV, CL = 95%
[CMSSM, $1 \leq$ tan$\beta \leq 40$, $m_{\widetilde{e}_R} - m_{\widetilde{\chi}_1^0} > 10$ GeV]

Mass $m > 2300$ GeV, CL = 95%
[RPV, $\widetilde{\nu}_\tau \rightarrow e\mu$, $\lambda'_{311} = 0.11$]

$\widetilde{e}$ — scalar electron (selectron)

Mass $m(\widetilde{e}_L) > 107$ GeV, CL = 95% [all $m_{\widetilde{e}_L} - m_{\widetilde{\chi}_1^0}$]

Mass $m > 410$ GeV, CL = 95%
[RPV, $\geq 4\ell^\pm$, $\widetilde{\ell} \rightarrow l\widetilde{\chi}_1^0$, $\widetilde{\chi}_1^0 \rightarrow \ell^\pm\ell^\mp\nu$]

$\widetilde{\mu}$ — scalar muon (smuon)

Mass $m > 94$ GeV, CL = 95%
[CMSSM, $1 \leq$ tan$\beta \leq 40$, $m_{\widetilde{\mu}_R} - m_{\widetilde{\chi}_1^0} > 10$ GeV]

Mass $m > 410$ GeV, CL = 95%
[RPV, $\geq 4\ell^\pm$, $\widetilde{\ell} \rightarrow l\widetilde{\chi}_1^0$, $\widetilde{\chi}_1^0 \rightarrow \ell^\pm\ell^\mp\nu$]

$\widetilde{\tau}$ — scalar tau (stau)

Mass $m > 81.9$ GeV, CL = 95%
[$m_{\widetilde{\tau}_R} - m_{\widetilde{\chi}_1^0} > 15$ GeV, all θ_τ, B($\widetilde{\tau} \rightarrow \tau\widetilde{\chi}_1^0$) = 100%]

Mass $m > 286$ GeV, CL = 95% [long-lived $\widetilde{\tau}$]

$\widetilde{q}$ – squarks of the first two quark generations

Mass $m > 1450$ GeV, CL = 95%
[CMSSM, tan$\beta = 30$, $A_0 = -2$max$(m_0, m_{1/2})$, $\mu > 0$]

Mass $m > 1550$ GeV, CL = 95%
[mass degenerate squarks]

Mass $m > 1050$ GeV, CL = 95%
[single light squark bounds]

$\widetilde{q}$ — long-lived squark

Mass $m > 1000$, CL = 95%
[$\widetilde{t}$, charge-suppressed interaction model]

Mass $m > 845$, CL = 95% [$\widetilde{b}$, stable, Regge model]

$\widetilde{b}$ — scalar bottom (sbottom)

Mass $m > 1230$ GeV, CL = 95%
[jets+$\not{E}_T$, Tsbot1, $m_{\widetilde{\chi}_1^0} = 0$ GeV]

$\widetilde{t}$ — scalar top (stop)

Mass $m > 1120$ GeV, CL = 95%
[1ℓ+jets+$\not{E}_T$, Tstop1, $m_{\widetilde{\chi}_1^0} = 0$ GeV]

$\widetilde{g}$ — gluino

Mass $m > 1860$ GeV, CL = 95%
[≥ 1 jets + $\not{E}_T$, Tglu1A, $m_{\widetilde{\chi}_1^0} = 0$ GeV]

Technicolor

The limits for technicolor (and top-color) particles are quite varied depending on assumptions. See the Technicolor section of the full *Review* (the data listings).

Quark and Lepton Compositeness, Searches for

Scale Limits Λ for Contact Interactions
(the lowest dimensional interactions with four fermions)

If the Lagrangian has the form

$$\pm \frac{g^2}{2\Lambda^2}\, \overline{\psi}_L \gamma_\mu \psi_L\, \overline{\psi}_L \gamma^\mu \psi_L$$

(with $g^2/4\pi$ set equal to 1), then we define $\Lambda \equiv \Lambda_{LL}^\pm$. For the full definitions and for other forms, see the Note in the Listings on Searches for Quark and Lepton Compositeness in the full *Review* and the original literature.

$\Lambda_{LL}^+(eeee)$	$>$	8.3 TeV, CL = 95%
$\Lambda_{LL}^-(eeee)$	$>$	10.3 TeV, CL = 95%
$\Lambda_{LL}^+(ee\mu\mu)$	$>$	8.5 TeV, CL = 95%
$\Lambda_{LL}^-(ee\mu\mu)$	$>$	9.5 TeV, CL = 95%
$\Lambda_{LL}^+(ee\tau\tau)$	$>$	7.9 TeV, CL = 95%
$\Lambda_{LL}^-(ee\tau\tau)$	$>$	7.2 TeV, CL = 95%
$\Lambda_{LL}^+(\ell\ell\ell\ell)$	$>$	9.1 TeV, CL = 95%
$\Lambda_{LL}^-(\ell\ell\ell\ell)$	$>$	10.3 TeV, CL = 95%
$\Lambda_{LL}^+(eeqq)$	$>$	24 TeV, CL = 95%
$\Lambda_{LL}^-(eeqq)$	$>$	37 TeV, CL = 95%
$\Lambda_{LL}^+(eeuu)$	$>$	23.3 TeV, CL = 95%
$\Lambda_{LL}^-(eeuu)$	$>$	12.5 TeV, CL = 95%
$\Lambda_{LL}^+(eedd)$	$>$	11.1 TeV, CL = 95%
$\Lambda_{LL}^-(eedd)$	$>$	26.4 TeV, CL = 95%
$\Lambda_{LL}^+(eecc)$	$>$	9.4 TeV, CL = 95%
$\Lambda_{LL}^-(eecc)$	$>$	5.6 TeV, CL = 95%
$\Lambda_{LL}^+(eebb)$	$>$	9.4 TeV, CL = 95%
$\Lambda_{LL}^-(eebb)$	$>$	10.2 TeV, CL = 95%
$\Lambda_{LL}^+(\mu\mu qq)$	$>$	20 TeV, CL = 95%
$\Lambda_{LL}^-(\mu\mu qq)$	$>$	30 TeV, CL = 95%
$\Lambda(\ell\nu\ell\nu)$	$>$	3.10 TeV, CL = 90%
$\Lambda(e\nu qq)$	$>$	2.81 TeV, CL = 95%
$\Lambda_{LL}^+(qqqq)$	$>$	13.1 none 17.4–29.5 TeV, CL = 95%
$\Lambda_{LL}^-(qqqq)$	$>$	21.8 TeV, CL = 95%
$\Lambda_{LL}^+(\nu\nu qq)$	$>$	5.0 TeV, CL = 95%
$\Lambda_{LL}^-(\nu\nu qq)$	$>$	5.4 TeV, CL = 95%

Searches Summary Table

Excited Leptons

The limits from $\ell^{*+}\ell^{*-}$ do not depend on λ (where λ is the $\ell\ell^*$ transition coupling). The λ-dependent limits assume chiral coupling.

$e^{*\pm}$ — excited electron

Mass $m >$ 103.2 GeV, CL = 95% (from $e^* e^*$)
Mass $m >$ 3.000×10^3 GeV, CL = 95% (from $e e^*$)
Mass $m >$ 356 GeV, CL = 95% (if $\lambda_\gamma = 1$)

$\mu^{*\pm}$ — excited muon

Mass $m >$ 103.2 GeV, CL = 95% (from $\mu^* \mu^*$)
Mass $m >$ 3.000×10^3 GeV, CL = 95% (from $\mu \mu^*$)

$\tau^{*\pm}$ — excited tau

Mass $m >$ 103.2 GeV, CL = 95% (from $\tau^* \tau^*$)
Mass $m >$ 2.500×10^3 GeV, CL = 95% (from $\tau \tau^*$)

ν^* — excited neutrino

Mass $m >$ 1.600×10^3 GeV, CL = 95% (from $\nu^* \nu^*$)
Mass $m >$ 213 GeV, CL = 95% (from $\nu^* X$)

q^* — excited quark

Mass $m >$ 338 GeV, CL = 95% (from $q^* q^*$)
Mass $m >$ 6.000×10^3 GeV, CL = 95% (from $q^* X$)

Color Sextet and Octet Particles

Color Sextet Quarks (q_6)

Mass $m >$ 84 GeV, CL = 95% (Stable q_6)

Color Octet Charged Leptons (ℓ_8)

Mass $m >$ 86 GeV, CL = 95% (Stable ℓ_8)

Color Octet Neutrinos (ν_8)

Mass $m >$ 110 GeV, CL = 90% ($\nu_8 \rightarrow \nu g$)

Extra Dimensions

Please refer to the Extra Dimensions section of the full *Review* for a discussion of the model-dependence of these bounds, and further constraints.

Constraints on the radius of the extra dimensions, for the case of two-flat dimensions of equal radii

$R <$ 30 μm, CL = 95% (direct tests of Newton's law)
$R <$ 10.9 μm, CL = 95% ($pp \rightarrow jG$)
$R <$ 0.16–916 nm (astrophysics; limits depend on technique and assumptions)

Constraints on the fundamental gravity scale

$M_{TT} >$ 8.4 TeV, CL = 95% ($pp \rightarrow$ dijet, angular distribution)
$M_c >$ 4.16 TeV, CL = 95% ($pp \rightarrow \ell\bar{\ell}$)

Constraints on the Kaluza-Klein graviton in warped extra dimensions

$M_G >$ 4.1 TeV, CL = 95% ($pp \rightarrow \gamma\gamma$)

Constraints on the Kaluza-Klein gluon in warped extra dimensions

$M_{g_{KK}} >$ 2.5 TeV, CL = 95% ($g_{KK} \rightarrow t\bar{t}$)

TESTS OF CONSERVATION LAWS

Updated April 2018 by L. Wolfenstein (Carnegie-Mellon University), C.-J. Lin (LBNL) and E. Pianori (LBNL).

In keeping with the current interest in tests of conservation laws, we collect together a Table of experimental limits on all weak and electromagnetic decays, mass differences, and moments, and on a few reactions, whose observation would violate conservation laws. The Table is given only in the full *Review of Particle Physics*, not in the Particle Physics Booklet. For the benefit of Booklet readers, we include the best limits from the Table in the following text. Limits in this text are for CL=90% unless otherwise specified. The Table is in two parts: "Discrete Space-Time Symmetries," *i.e.*, C, P, T, CP, and CPT; and "Number Conservation Laws," *i.e.*, lepton, baryon, hadronic flavor, and charge conservation. The references for these data can be found in the the Particle Listings in the *Review*. A discussion of these tests follows.

CPT INVARIANCE

General principles of relativistic field theory require invariance under the combined transformation CPT. The simplest tests of CPT invariance are the equality of the masses and lifetimes of a particle and its antiparticle. The best test comes from the limit on the mass difference between K^0 and $\overline{K}^0$. Any such difference contributes to the CP-violating parameter ϵ. Assuming CPT invariance, ϕ_ϵ, the phase of ϵ should be very close to 44°. (See the review "CP Violation in K_L decay" in this edition.) In contrast, if the entire source of CP violation in K^0 decays were a $K^0 - \overline{K}^0$ mass difference, ϕ_ϵ would be $44° + 90°$.

Assuming that there is no other source of CPT violation than this mass difference, it is possible to deduce that [1]

$$m_{\overline{K}^0} - m_{K^0} \approx \frac{2(m_{K_L^0} - m_{K_S^0})\,|\eta|\,(\frac{2}{3}\phi_{+-} + \frac{1}{3}\phi_{00} - \phi_{\rm SW})}{\sin\phi_{\rm SW}}\ ,$$

where $\phi_{\rm SW} = (43.51 \pm 0.05)°$, the superweak angle. Using our best values of the CP-violation parameters, we get $|(m_{\overline{K}^0} - m_{K^0})/m_{K^0}| \leq 0.6 \times 10^{-18}$ at CL=90%. Limits can also be placed on specific CPT-violating decay amplitudes. Given the small value of $(1 - |\eta_{00}/\eta_{+-}|)$, the value of $\phi_{00} - \phi_{+-}$ provides a measure of CPT violation in $K_L^0 \to 2\pi$ decay. Results from CERN [1] and Fermilab [2] indicate no CPT-violating effect.

CP AND *T* INVARIANCE

Given CPT invariance, CP violation and T violation are equivalent. The original evidence for CP violation came from the measurement of $|\eta_{+-}| = |A(K_L^0 \to \pi^+\pi^-)/A(K_S^0 \to \pi^+\pi^-)| = (2.232 \pm 0.011) \times 10^{-3}$. This could be explained in terms of K^0–$\overline{K}^0$ mixing, which also leads to the asymmetry $[\Gamma(K_L^0 \to \pi^- e^+ \nu) - \Gamma(K_L^0 \to \pi^+ e^- \overline{\nu})]/[\text{sum}] = (0.334 \pm 0.007)\%$. Evidence for CP violation in the kaon decay amplitude comes from the measurement of $(1 - |\eta_{00}/\eta_{+-}|)/3 = Re(\epsilon'/\epsilon) = (1.66 \pm 0.23) \times 10^{-3}$. In the Standard Model much larger CP-violating effects are expected. The first of these, which is associated with B–$\overline{B}$ mixing, is the parameter $sin(2\beta)$ now measured quite accurately to be 0.679 ± 0.020. A number of other CP-violating observables are being measured in B decays; direct evidence for CP violation in the B decay amplitude comes from the asymmetry $[\Gamma(\overline{B}^0 \to K^-\pi^+) - \Gamma(B^0 \to K^+\pi^-)]/[\text{sum}] = -0.082 \pm 0.006$. Direct tests of T violation are much more difficult; a measurement by CPLEAR of the difference between the oscillation probabilities of K^0 to $\overline{K^0}$ and $\overline{K^0}$ to K^0 is related to T violation [3]. A nonzero value of the electric dipole moment of the neutron and electron requires both P and T violation. The current experimental results are $< 3.0 \times 10^{-26}$ e cm (neutron), and $< 8.7 \times 10^{-29}$ e cm (electron) at the 90% C.L. The BABAR experiment reported the first direct observation of T violation in the B system. The measured T-violating parameters in the time evolution of the neutral B mesons are $\Delta S_T^+ = -1.37 \pm 0.15$ and $\Delta S_T^- = 1.17 \pm 0.21$, with a significance of 14σ [4]. This observation of T violation, with exchange of initial and final states of the neutral B, was made possible in a B-factory using the Einstein-Podolsky-Rosen Entanglement of the two B's produced in the decay of the $\Upsilon(4S)$ and the two time-ordered decays of the B's as filtering measurements of the meson state [5].

CONSERVATION OF LEPTON NUMBERS

Present experimental evidence and the standard electroweak theory are consistent with the absolute conservation of three separate lepton numbers: electron number L_e, muon number L_μ, and tau number L_τ, except for the effect of neutrino mixing associated with neutrino masses. Searches for violations are of the following types:

a) $\Delta L = 2$ for one type of charged lepton. The best limit comes from the search for neutrinoless double beta decay $(Z, A) \to (Z + 2, A) + e^- + e^-$. The best laboratory limit is $t_{1/2} > 1.07 \times 10^{26}$ yr (CL=90%) for ^{136}Xe from the KamLAND-Zen experiment [6].

b) Conversion of one charged-lepton type to another. For purely leptonic processes, the best limits are on $\mu \to e\gamma$ and $\mu \to 3e$, measured as $\Gamma(\mu \to e\gamma)/\Gamma(\mu \to \text{all}) < 4.2 \times 10^{-13}$ and $\Gamma(\mu \to 3e)/\Gamma(\mu \to \text{all}) < 1.0 \times 10^{-12}$. For semileptonic processes, the best limit comes from the coherent conversion process in a muonic atom, $\mu^- + (Z, A) \to e^- + (Z, A)$, measured as $\Gamma(\mu^-\text{Ti} \to e^-\text{Ti})/\Gamma(\mu^-\text{Ti} \to \text{all}) < 4.3 \times 10^{-12}$. Of special interest is the case in which the hadronic flavor also changes, as in $K_L \to e\mu$ and $K^+ \to \pi^+ e^- \mu^+$, measured as $\Gamma(K_L \to e\mu)/\Gamma(K_L \to \text{all}) < 4.7 \times 10^{-12}$ and $\Gamma(K^+ \to \pi^+ e^- \mu^+)/\Gamma(K^+ \to \text{all}) < 1.3 \times 10^{-11}$. Limits on the conversion of τ into e or μ are found in τ decay and are much less stringent than those for $\mu \to e$ conversion, *e.g.*, $\Gamma(\tau \to \mu\gamma)/\Gamma(\tau \to \text{all}) < 4.4 \times 10^{-8}$ and $\Gamma(\tau \to e\gamma)/\Gamma(\tau \to \text{all}) < 3.3 \times 10^{-8}$.

c) Conversion of one type of charged lepton into another type of charged antilepton. The case most studied is $\mu^- + (Z, A) \to e^+ + (Z - 2, A)$, the strongest limit being $\Gamma(\mu^-\text{Ti} \to e^+\text{Ca})/\Gamma(\mu^-\text{Ti} \to \text{all}) < 3.6 \times 10^{-11}$.

d) Neutrino oscillations. It is expected even in the standard electroweak theory that the lepton numbers are not separately conserved, as a consequence of lepton mixing analogous to Cabibbo-Kobayashi-Maskawa quark mixing. However, if the only source of lepton-number violation is the mixing of low-mass neutrinos then processes such as $\mu \to e\gamma$ are expected to have extremely small unobservable probabilities. For small neutrino masses, the lepton-number violation would be observed first in neutrino oscillations, which have been the subject of extensive experimental studies. Compelling evidence for neutrino mixing has come from atmospheric, solar, accelerator, and reactor neutrinos. Recently, the reactor neutrino experiments have measured the last neutrino mixing angle θ_{13} and found it to be relatively large. For a comprehensive review on neutrino mixing, including the latest results on θ_{13}, see the review *"Neutrino Mass, Mixing, and Oscillations"* by K. Nakamura and S.T. Petcov in this edition of RPP.

CONSERVATION OF HADRONIC FLAVORS

In strong and electromagnetic interactions, hadronic flavor is conserved, *i.e.* the conversion of a quark of one flavor (d, u, s, c, b, t) into a quark of another flavor is forbidden. In the Standard Model, the weak interactions violate these conservation laws in a manner described by the Cabibbo-Kobayashi-Maskawa mixing (see the section "Cabibbo-Kobayashi-Maskawa Mixing Matrix"). The way in which these conservation laws are violated is tested as follows:

(a) $\Delta S = \Delta Q$ rule. In the strangeness-changing semileptonic decay of strange particles, the strangeness change equals the change in charge of the hadrons. Tests come from limits on decay rates such as $\Gamma(\Sigma^+ \to ne^+\nu)/\Gamma(\Sigma^+ \to \text{all}) < 5 \times 10^{-6}$, and from a detailed analysis of $K_L \to \pi e\nu$, which yields the parameter x, measured to be $(\mathrm{Re}\, x,\ \mathrm{Im}\, x) = (-0.002 \pm 0.006,\ 0.0012 \pm 0.0021)$. Corresponding rules are $\Delta C = \Delta Q$ and $\Delta B = \Delta Q$.

(b) Change of flavor by two units. In the Standard Model this occurs only in second-order weak interactions. The classic example is $\Delta S = 2$ via $K^0 - \overline{K}^0$ mixing, which is directly measured by $m(K_L) - m(K_S) = (0.5293 \pm 0.0009) \times 10^{10}\ \hbar s^{-1}$. The $\Delta B = 2$ transitions in the B^0 and B_s^0 systems via mixing are also well established. The measured mass differences between the eigenstates are $(m_{B^0_{\mathrm{H}}} - m_{B^0_{\mathrm{L}}}) = (0.5064 \pm 0.0019) \times 10^{12}\ \hbar s^{-1}$ and $(m_{B^0_{s\mathrm{H}}} - m_{B^0_{s\mathrm{L}}}) = (17.757 \pm 0.021) \times 10^{12}\ \hbar s^{-1}$. There is now strong evidence of $\Delta C = 2$ transition in the charm sector with the mass difference $m_{D^0_H} - m_{D^0_L} = (0.95^{+0.41}_{-0.44}) \times 10^{10}\ \hbar s^{-1}$. All results are consistent with the second-order calculations in the Standard Model.

(c) Flavor-changing neutral currents. In the Standard Model the neutral-current interactions do not change flavor. The low rate $\Gamma(K_L \to \mu^+\mu^-)/\Gamma(K_L \to \text{all}) = (6.84 \pm 0.11) \times 10^{-9}$ puts limits on such interactions; the nonzero value for this rate is attributed to a combination of the weak and electromagnetic interactions. The best test should come from $K^+ \to \pi^+\nu\overline{\nu}$, which occurs in the Standard Model only as a second-order weak process with a branching fraction of (0.4 to 1.2)$\times 10^{-10}$. Combining results from BNL-E787 and BNL-E949 experiments yield $\Gamma(K^+ \to \pi^+\nu\overline{\nu})/\Gamma(K^+ \to \text{all}) = (1.7 \pm 1.1) \times 10^{-10}$ [7]. Limits for charm-changing or bottom-changing neutral currents are less stringent: $\Gamma(D^0 \to \mu^+\mu^-)/\Gamma(D^0 \to \text{all}) < 6.2 \times 10^{-9}$ and $\Gamma(B^0 \to \mu^+\mu^-)/\Gamma(B^0 \to \text{all}) = (1.6^{+1.6}_{-1.4}) \times 10^{-10}$. One cannot isolate flavor-changing neutral current (FCNC) effects in non leptonic decays. For example, the FCNC transition $s \to d + (\overline{u} + u)$ is equivalent to the charged-current transition $s \to u + (\overline{u} + d)$. Tests for FCNC are therefore limited to hadron decays into lepton pairs. Such decays are expected only in second-order in the electroweak coupling in the Standard Model. The LHCb and CMS experiments have recently observed the FCNC decay of $B_s^0 \to \mu^+\mu^-$. The current world average value is $\Gamma(B_s^0 \to \mu^+\mu^-)/\Gamma(B_s^0 \to \text{all}) = (2.7^{+0.6}_{-0.5}) \times 10^{-9}$, which is consistent with the Standard Model expectation.

Unless otherwise stated, limits are given at the 90% confidence level, while errors are given as ±1 standard deviation.

References

1. R. Carosi *et al.*, Phys. Lett. **B237**, 303 (1990).
2. E. Abouzaid *et al.*, Phys. Rev. **D83**, 092001 (2011); B. Schwingenheuer *et al.*, Phys. Rev. Lett. **74**, 4376 (1995).
3. A. Angelopoulos *et al.*, Phys. Lett. **B444**, 43 (1998); L. Wolfenstein, Phys. Rev. Lett. **83**, 911 (1999).
4. J.P. Lees *et al.*, Phys. Rev. Lett. **109**, 211801 (2012).
5. M.C. Banuls, J. Bernabeu, Phys. Lett. **B464**, 117 (1999); Nucl. Phys. **B590**, 19 (2000).
6. A. Gando *et al.*, Phys. Rev. Lett. **117**, 082503 (2016).
7. A.V. Artamonov *et al.*, Phys. Rev. Lett. **101**, 191802 (2008).

TESTS OF DISCRETE SPACE-TIME SYMMETRIES

CHARGE CONJUGATION (*C*) INVARIANCE

$\Gamma(\pi^0 \to\ 3\gamma)/\Gamma_{\text{total}}$		$<3.1 \times 10^{-8}$, CL = 90%
η *C*-nonconserving decay parameters		
$\pi^+\pi^-\pi^0$ left-right asymmetry		$(0.09^{+0.11}_{-0.12}) \times 10^{-2}$
$\pi^+\pi^-\pi^0$ sextant asymmetry		$(0.12^{+0.10}_{-0.11}) \times 10^{-2}$
$\pi^+\pi^-\pi^0$ quadrant asymmetry		$(-0.09 \pm 0.09) \times 10^{-2}$
$\pi^+\pi^-\gamma$ left-right asymmetry		$(0.9 \pm 0.4) \times 10^{-2}$
$\pi^+\pi^-\gamma$ parameter β (*D*-wave)		-0.02 ± 0.07 (S = 1.3)
$\Gamma(\eta \to\ \pi^0\gamma)/\Gamma_{\text{total}}$		$<9 \times 10^{-5}$, CL = 90%
$\Gamma(\eta \to\ 2\pi^0\gamma)/\Gamma_{\text{total}}$		$<5 \times 10^{-4}$, CL = 90%
$\Gamma(\eta \to\ 3\pi^0\gamma)/\Gamma_{\text{total}}$		$<6 \times 10^{-5}$, CL = 90%
$\Gamma(\eta \to\ 3\gamma)/\Gamma_{\text{total}}$		$<1.6 \times 10^{-5}$, CL = 90%
$\Gamma(\eta \to\ \pi^0 e^+ e^-)/\Gamma_{\text{total}}$	[a]	$<4 \times 10^{-5}$, CL = 90%
$\Gamma(\eta \to\ \pi^0 \mu^+ \mu^-)/\Gamma_{\text{total}}$	[a]	$<5 \times 10^{-6}$, CL = 90%
$\Gamma(\omega(782) \to\ \eta\pi^0)/\Gamma_{\text{total}}$		$<2.2 \times 10^{-4}$, CL = 90%
$\Gamma(\omega(782) \to\ 2\pi^0)/\Gamma_{\text{total}}$		$<2.2 \times 10^{-4}$, CL = 90%
$\Gamma(\omega(782) \to\ 3\pi^0)/\Gamma_{\text{total}}$		$<2.3 \times 10^{-4}$, CL = 90%
asymmetry parameter for $\eta'(958) \to$ $\pi^+\pi^-\gamma$ decay		-0.03 ± 0.04
$\Gamma(\eta'(958) \to\ \pi^0 e^+ e^-)/\Gamma_{\text{total}}$	[a]	$<1.4 \times 10^{-3}$, CL = 90%

$\Gamma(\eta'(958) \to \eta e^+ e^-)/\Gamma_{total}$	[a]	$<2.4 \times 10^{-3}$, CL = 90%
$\Gamma(\eta'(958) \to 3\gamma)/\Gamma_{total}$		$<1.1 \times 10^{-4}$, CL = 90%
$\Gamma(\eta'(958) \to \mu^+ \mu^- \pi^0)/\Gamma_{total}$	[a]	$<6.0 \times 10^{-5}$, CL = 90%
$\Gamma(\eta'(958) \to \mu^+ \mu^- \eta)/\Gamma_{total}$	[a]	$<1.5 \times 10^{-5}$, CL = 90%
$\Gamma(J/\psi(1S) \to \gamma\gamma)/\Gamma_{total}$		$<2.7 \times 10^{-7}$, CL = 90%
$\Gamma(J/\psi(1S) \to \gamma\phi)/\Gamma_{total}$		$<1.4 \times 10^{-6}$, CL = 90%

PARITY (P) INVARIANCE

e electric dipole moment	$<0.87 \times 10^{-28}$ e cm, CL = 90%
μ electric dipole moment	$(-0.1 \pm 0.9) \times 10^{-19}$ e cm
Re(d_τ = τ electric dipole moment)	-0.220 to 0.45×10^{-16} e cm, CL = 95%
$\Gamma(\eta \to \pi^+ \pi^-)/\Gamma_{total}$	$<1.3 \times 10^{-5}$, CL = 90%
$\Gamma(\eta \to 2\pi^0)/\Gamma_{total}$	$<3.5 \times 10^{-4}$, CL = 90%
$\Gamma(\eta \to 4\pi^0)/\Gamma_{total}$	$<6.9 \times 10^{-7}$, CL = 90%
$\Gamma(\eta'(958) \to \pi^+ \pi^-)/\Gamma_{total}$	$<1.8 \times 10^{-5}$, CL = 90%
$\Gamma(\eta'(958) \to \pi^0 \pi^0)/\Gamma_{total}$	$<5 \times 10^{-4}$, CL = 90%
$\Gamma(\eta_C(1S) \to \pi^+ \pi^-)/\Gamma_{total}$	$<1.1 \times 10^{-4}$, CL = 90%
$\Gamma(\eta_C(1S) \to \pi^0 \pi^0)/\Gamma_{total}$	$<4 \times 10^{-5}$, CL = 90%
$\Gamma(\eta_C(1S) \to K^+ K^-)/\Gamma_{total}$	$<6 \times 10^{-4}$, CL = 90%
$\Gamma(\eta_C(1S) \to K^0_S K^0_S)/\Gamma_{total}$	$<3.1 \times 10^{-4}$, CL = 90%
p electric dipole moment	$<0.021 \times 10^{-23}$ e cm
n electric dipole moment	$<0.30 \times 10^{-25}$ e cm, CL = 90%
Λ electric dipole moment	$<1.5 \times 10^{-16}$ e cm, CL = 95%

TIME REVERSAL (T) INVARIANCE

e electric dipole moment		$<0.87 \times 10^{-28}$ e cm, CL = 90%
μ electric dipole moment		$(-0.1 \pm 0.9) \times 10^{-19}$ e cm
μ decay parameters		
transverse e^+ polarization normal to plane of μ spin, e^+ momentum		$(-2 \pm 8) \times 10^{-3}$
α'/A		$(-10 \pm 20) \times 10^{-3}$
β'/A		$(2 \pm 7) \times 10^{-3}$
Re(d_τ = τ electric dipole moment)		-0.220 to 0.45×10^{-16} e cm, CL = 95%
P_T in $K^+ \to \pi^0 \mu^+ \nu_\mu$		$(-1.7 \pm 2.5) \times 10^{-3}$
P_T in $K^+ \to \mu^+ \nu_\mu \gamma$		$(-0.6 \pm 1.9) \times 10^{-2}$
Im(ξ) in $K^+ \to \pi^0 \mu^+ \nu_\mu$ decay (from transverse μ pol.)		-0.006 ± 0.008
asymmetry A_T in K^0-$\overline{K}^0$ mixing		$(6.6 \pm 1.6) \times 10^{-3}$
Im(ξ) in $K^0_{\mu 3}$ decay (from transverse μ pol.)		-0.007 ± 0.026
$A_T(D^\pm \to K^0_S K^\pm \pi^+ \pi^-)$	[b]	$(-12 \pm 11) \times 10^{-3}$
$A_T(D^0 \to K^+ K^- \pi^+ \pi^-)$	[b]	$(1.7 \pm 2.7) \times 10^{-3}$
$A_T(D^\pm_s \to K^0_S K^\pm \pi^+ \pi^-)$	[b]	$(-14 \pm 8) \times 10^{-3}$
ΔS^+_T ($S^-_{\ell^-,K^0_S} - S^+_{\ell^+,K^0_S}$)		-1.37 ± 0.15
ΔS^-_T ($S^+_{\ell^-,K^0_S} - S^-_{\ell^+,K^0_S}$)		1.17 ± 0.21
ΔC^+_T ($C^-_{\ell^-,K^0_S} - C^+_{\ell^+,K^0_S}$)		0.10 ± 0.16
ΔC^-_T ($C^+_{\ell^-,K^0_S} - C^-_{\ell^+,K^0_S}$)		0.04 ± 0.16
p electric dipole moment		$<0.021 \times 10^{-23}$ e cm
n electric dipole moment		$<0.30 \times 10^{-25}$ e cm, CL = 90%
$n \to p e^- \overline{\nu}_e$ decay parameters		
ϕ_{AV}, phase of g_A relative to g_V	[c]	$(180.017 \pm 0.026)^\circ$
triple correlation coefficient D	[d]	$(-1.2 \pm 2.0) \times 10^{-4}$
triple correlation coefficient R	[d]	0.004 ± 0.013
Λ electric dipole moment		$<1.5 \times 10^{-16}$ e cm, CL = 95%
triple correlation coefficient D for $\Sigma^- \to n e^- \overline{\nu}_e$		0.11 ± 0.10

CP INVARIANCE

Re(d^W_τ)	$<0.50 \times 10^{-17}$ e cm, CL = 95%
Im(d^W_τ)	$<1.1 \times 10^{-17}$ e cm, CL = 95%
$\eta \to \pi^+ \pi^- e^+ e^-$ decay-plane asymmetry	$(-0.6 \pm 3.1) \times 10^{-2}$
$\Gamma(\eta \to \pi^+ \pi^-)/\Gamma_{total}$	$<1.3 \times 10^{-5}$, CL = 90%
$\Gamma(\eta \to 2\pi^0)/\Gamma_{total}$	$<3.5 \times 10^{-4}$, CL = 90%
$\Gamma(\eta \to 4\pi^0)/\Gamma_{total}$	$<6.9 \times 10^{-7}$, CL = 90%
$\Gamma(\eta'(958) \to \pi^+ \pi^-)/\Gamma_{total}$	$<1.8 \times 10^{-5}$, CL = 90%
$\Gamma(\eta'(958) \to \pi^0 \pi^0)/\Gamma_{total}$	$<5 \times 10^{-4}$, CL = 90%
$K^\pm \to \pi^\pm e^+ e^-$ rate difference/sum	$(-2.2 \pm 1.6) \times 10^{-2}$
$K^\pm \to \pi^\pm \mu^+ \mu^-$ rate difference/sum	0.010 ± 0.023
$K^\pm \to \pi^\pm \pi^0 \gamma$ rate difference/sum	$(0.0 \pm 1.2) \times 10^{-3}$
$K^\pm \to \pi^\pm \pi^+ \pi^-$ rate difference/sum	(0.04 ± 0.06)%
$K^\pm \to \pi^\pm \pi^0 \pi^0$ rate difference/sum	(-0.02 ± 0.28)%
$K^\pm \to \pi^\pm \pi^+ \pi^-$ $(g_+ - g_-) / (g_+ + g_-)$	$(-1.5 \pm 2.2) \times 10^{-4}$
$K^\pm \to \pi^\pm \pi^0 \pi^0$ $(g_+ - g_-) / (g_+ + g_-)$	$(1.8 \pm 1.8) \times 10^{-4}$
A_S = [$\Gamma(K^0_S \to \pi^- e^+ \nu_e)$ - $\Gamma(K^0_S \to \pi^+ e^- \overline{\nu}_e)$] / SUM	$(2 \pm 10) \times 10^{-3}$
Im(η_{+-0}) = Im(A($K^0_S \to \pi^+ \pi^- \pi^0$, CP-violating) / A($K^0_L \to \pi^+ \pi^- \pi^0$))	-0.002 ± 0.009
Im(η_{000}) = Im($A(K^0_S \to \pi^0 \pi^0 \pi^0)/A(K^0_L \to \pi^0 \pi^0 \pi^0)$)	-0.001 ± 0.016
$\lvert\eta_{000}\rvert = \lvert A(K^0_S \to 3\pi^0)/A(K^0_L \to 3\pi^0)\rvert$	<0.0088, CL = 90%
CP asymmetry A in $K^0_S \to \pi^+ \pi^- e^+ e^-$	(-0.4 ± 0.8)%
$\Gamma(K^0_S \to 3\pi^0)/\Gamma_{total}$	$<2.6 \times 10^{-8}$, CL = 90%
linear coefficient j for $K^0_L \to \pi^+ \pi^- \pi^0$	0.0012 ± 0.0008
quadratic coefficient f for $K^0_L \to \pi^+ \pi^- \pi^0$	0.004 ± 0.006
$\lvert\epsilon'_{+-\gamma}\rvert/\epsilon$ for $K^0_L \to \pi^+ \pi^- \gamma$	<0.3, CL = 90%
$\lvert g_{E1}\rvert$ for $K^0_L \to \pi^+ \pi^- \gamma$	<0.21, CL = 90%
$\Gamma(K^0_L \to \pi^0 \mu^+ \mu^-)/\Gamma_{total}$	[e] $<3.8 \times 10^{-10}$, CL = 90%
$\Gamma(K^0_L \to \pi^0 e^+ e^-)/\Gamma_{total}$	[e] $<2.8 \times 10^{-10}$, CL = 90%
$\Gamma(K^0_L \to \pi^0 \nu\overline{\nu})/\Gamma_{total}$	[f] $<2.6 \times 10^{-8}$, CL = 90%
$A_{CP}(D^\pm \to \mu^\pm \nu)$	(8 ± 8)%
$A_{CP}(D^\pm \to K^0_L e^\pm \nu)$	(-0.6 ± 1.6)%
$A_{CP}(D^\pm \to K^0_S \pi^\pm)$	(-0.41 ± 0.09)%
$A_{CP}(D^\pm \to K^\mp 2\pi^\pm)$	(-0.18 ± 0.16)%
$A_{CP}(D^\pm \to K^\mp \pi^\pm \pi^\pm \pi^0)$	(-0.3 ± 0.7)%
$A_{CP}(D^\pm \to K^0_S \pi^\pm \pi^0)$	(-0.1 ± 0.7)%
$A_{CP}(D^\pm \to K^0_S \pi^\pm \pi^+ \pi^-)$	(0.0 ± 1.2)%
$A_{CP}(D^\pm \to \pi^\pm \pi^0)$	(2.4 ± 1.2)%
$A_{CP}(D^\pm \to \pi^\pm \eta)$	(1.0 ± 1.5)% (S = 1.4)
$A_{CP}(D^\pm \to \pi^\pm \eta'(958))$	(-0.6 ± 0.7)%
$A_{CP}(D^\pm \to \overline{K}^0 / K^0 K^\pm)$	(0.11 ± 0.17)%
$A_{CP}(D^\pm \to K^0_S K^\pm)$	(-0.11 ± 0.25)%
$A_{CP}(D^\pm \to K^+ K^- \pi^\pm)$	(0.37 ± 0.29)%
$A_{CP}(D^\pm \to K^\pm K^{*0})$	(-0.3 ± 0.4)%
$A_{CP}(D^\pm \to \phi\pi^\pm)$	(0.09 ± 0.19)% (S = 1.2)
$A_{CP}(D^\pm \to K^\pm K^*_0(1430)^0)$	(8^{+7}_{-6})%
$A_{CP}(D^\pm \to K^\pm K^*_2(1430)^0)$	(43^{+20}_{-26})%
$A_{CP}(D^\pm \to K^\pm K^*_0(700))$	(-12^{+18}_{-13})%
$A_{CP}(D^\pm \to a_0(1450)^0 \pi^\pm)$	(-19^{+14}_{-16})%
$A_{CP}(D^\pm \to \phi(1680)\pi^\pm)$	(-9 ± 26)%
$A_{CP}(D^\pm \to \pi^+ \pi^- \pi^\pm)$	(-2 ± 4)%
$A_{CP}(D^\pm \to K^0_S K^\pm \pi^+ \pi^-)$	(-4 ± 7)%
$A_{CP}(D^\pm \to K^\pm \pi^0)$	(-4 ± 11)%
Local CPV in $D^\pm \to \pi^+ \pi^- \pi^\pm$	78.1%
Local CPV in $D^\pm \to K^+ K^- \pi^\pm$	31%
$\lvert q/p\rvert$ of D^0-$\overline{D}^0$ mixing	$0.92^{+0.12}_{-0.09}$
A_Γ of D^0-$\overline{D}^0$ mixing	$(-0.125 \pm 0.526) \times 10^{-3}$
Where there is ambiguity, the CP test is labelled by the D^0 decay mode.	
$A_{CP}(D^0 \to K^+ K^-)$	(-0.07 ± 0.11)%
$A_{CP}(D^0 \to K^0_S K^0_S)$	(-0.4 ± 1.5)%
$A_{CP}(D^0 \to \pi^+ \pi^-)$	(0.13 ± 0.14)%
$A_{CP}(D^0 \to \pi^0 \pi^0)$	(0.0 ± 0.6)%
$A_{CP}(D^0 \to \rho\gamma)$	$(6 \pm 15) \times 10^{-2}$
$A_{CP}(D^0 \to \phi\gamma)$	$(-9 \pm 7) \times 10^{-2}$
$A_{CP}(D^0 \to \overline{K}^*(892)^0\gamma)$	$(-0.3 \pm 2.0) \times 10^{-2}$
$A_{CP}(D^0 \to \pi^+ \pi^- \pi^0)$	(0.3 ± 0.4)%
$A_{CP}(D^0 \to \rho(770)^+ \pi^- \to \pi^+ \pi^- \pi^0)$	[g] (1.2 ± 0.9)%
$A_{CP}(D^0 \to \rho(770)^0 \pi^0 \to \pi^+ \pi^- \pi^0)$	[g] (-3.1 ± 3.0)%
$A_{CP}(D^0 \to \rho(770)^- \pi^+ \to \pi^+ \pi^- \pi^0)$	[g] (-1.0 ± 1.7)%
$A_{CP}(D^0 \to \rho(1450)^+ \pi^- \to \pi^+ \pi^- \pi^0)$	[g] (0 ± 70)%
$A_{CP}(D^0 \to \rho(1450)^0 \pi^0 \to \pi^+ \pi^- \pi^0)$	[g] (-20 ± 40)%
$A_{CP}(D^0 \to \rho(1450)^- \pi^+ \to \pi^+ \pi^- \pi^0)$	[g] (6 ± 9)%
$A_{CP}(D^0 \to \rho(1700)^+ \pi^- \to \pi^+ \pi^- \pi^0)$	[g] (-5 ± 14)%

Unless otherwise stated, limits are given at the 90% confidence level, while errors are given as ± 1 standard deviation.

Tests of Conservation Laws

$A_{CP}(D^0 \to \rho(1700)^0\pi^0 \to \pi^+\pi^-\pi^0)$	[g]	$(13 \pm 9)\%$
$A_{CP}(D^0 \to \rho(1700)^-\pi^+ \to \pi^+\pi^-\pi^0)$	[g]	$(8 \pm 11)\%$
$A_{CP}(D^0 \to f_0(980)\pi^0 \to \pi^+\pi^-\pi^0)$	[g]	$(0 \pm 35)\%$
$A_{CP}(D^0 \to f_0(1370)\pi^0 \to \pi^+\pi^-\pi^0)$	[g]	$(25 \pm 18)\%$
$A_{CP}(D^0 \to f_0(1500)\pi^0 \to \pi^+\pi^-\pi^0)$	[g]	$(0 \pm 18)\%$
$A_{CP}(D^0 \to f_0(1710)\pi^0 \to \pi^+\pi^-\pi^0)$	[g]	$(0 \pm 24)\%$
$A_{CP}(D^0 \to f_2(1270)\pi^0 \to \pi^+\pi^-\pi^0)$	[g]	$(-4 \pm 6)\%$
$A_{CP}(D^0 \to \sigma(400)\pi^0 \to \pi^+\pi^-\pi^0)$	[g]	$(6 \pm 8)\%$
$A_{CP}(\text{nonresonant } D^0 \to \pi^+\pi^-\pi^0)$	[g]	$(-13 \pm 23)\%$
$A_{CP}(D^0, \overline{D}^0 \to 2\pi^+2\pi^-)$		$(0.5 \pm 1.2)\%$
$A_{CP}(D^0 \to a_1(1260)^+\pi^- \to 2\pi^+2\pi^-)$		$(5 \pm 6)\%$
$A_{CP}(D^0 \to a_1(1260)^-\pi^+ \to 2\pi^+2\pi^-)$		$(14 \pm 18)\%$
$A_{CP}(D^0 \to \pi(1300)^+\pi^- \to 2\pi^+2\pi^-)$		$(-2 \pm 15)\%$
$A_{CP}(D^0 \to \pi(1300)^-\pi^+ \to 2\pi^+2\pi^-)$		$(-6 \pm 30)\%$
$A_{CP}(D^0 \to a_1(1640)^+\pi^- \to 2\pi^+2\pi^-)$		$(9 \pm 26)\%$
$A_{CP}(D^0 \to \pi_2(1670)^+\pi^- \to 2\pi^+2\pi^-)$		$(7 \pm 18)\%$
$A_{CP}(D^0 \to \sigma f_0(1370) \to 2\pi^+2\pi^-)$		$(-15 \pm 19)\%$
$A_{CP}(D^0 \to \sigma\rho(770)^0 \to 2\pi^+2\pi^-)$		$(3 \pm 27)\%$
$A_{CP}(D^0 \to 2\rho(770)^0 \to 2\pi^+2\pi^-)$		$(-6 \pm 6)\%$
$A_{CP}(D^0 \to 2f_2(1270) \to 2\pi^+2\pi^-)$		$(-28 \pm 24)\%$
$A_{CP}(D^0 \to K^+K^-\pi^0)$		$(-1.0 \pm 1.7)\%$
$A_{CP}(D^0 \to K^*(892)^+K^- \to K^+K^-\pi^0)$	[g]	$(-0.9 \pm 1.3)\%$
$A_{CP}(D^0 \to K^*(1410)^+K^- \to K^+K^-\pi^0)$	[g]	$(-21 \pm 24)\%$
$A_{CP}(D^0 \to (K^+\pi^0)_S K^- \to K^+K^-\pi^0)$	[g]	$(7 \pm 15)\%$
$A_{CP}(D^0 \to \phi(1020)\pi^0 \to K^+K^-\pi^0)$	[g]	$(1.1 \pm 2.2)\%$
$A_{CP}(D^0 \to f_0(980)\pi^0 \to K^+K^-\pi^0)$	[g]	$(-3 \pm 19)\%$
$A_{CP}(D^0 \to a_0(980)^0\pi^0 \to K^+K^-\pi^0)$	[g]	$(-5 \pm 16)\%$
$A_{CP}(D^0 \to f_2'(1525)\pi^0 \to K^+K^-\pi^0)$	[g]	$(0 \pm 160)\%$
$A_{CP}(D^0 \to K^*(892)^-K^+ \to K^+K^-\pi^0)$	[g]	$(-5 \pm 4)\%$
$A_{CP}(D^0 \to K^*(1410)^-K^+ \to K^+K^-\pi^0)$	[g]	$(-17 \pm 29)\%$
$A_{CP}(D^0 \to (K^-\pi^0)_{S-wave}K^+ \to K^+K^-\pi^0)$	[g]	$(-10 \pm 40)\%$
$A_{CP}(D^0 \to K^0_S\pi^0)$		$(-0.20 \pm 0.17)\%$
$A_{CP}(D^0 \to K^0_S\eta)$		$(0.5 \pm 0.5)\%$
$A_{CP}(D^0 \to K^0_S\eta')$		$(1.0 \pm 0.7)\%$
$A_{CP}(D^0 \to K^0_S\phi)$		$(-3 \pm 9)\%$
$A_{CP}(D^0 \to K^-\pi^+)$		$(0.3 \pm 0.7)\%$
$A_{CP}(D^0 \to K^+\pi^-)$		$(-0.9 \pm 1.4)\%$
$A_{CP}(D_{CP(\pm1)} \to K^\mp\pi^\pm)$		$(12.7 \pm 1.5)\%$
$A_{CP}(D^0 \to K^-\pi^+\pi^0)$		$(0.1 \pm 0.5)\%$
$A_{CP}(D^0 \to K^+\pi^-\pi^0)$		$(0 \pm 5)\%$
$A_{CP}(D^0 \to K^0_S\pi^+\pi^-)$		$(-0.1 \pm 0.8)\%$
$A_{CP}(D^0 \to K^*(892)^-\pi^+ \to K^0_S\pi^+\pi^-)$		$(0.4 \pm 0.5)\%$
$A_{CP}(D^0 \to K^*(892)^+\pi^- \to K^0_S\pi^+\pi^-)$		$(1 \pm 6)\%$
$A_{CP}(D^0 \to K^0_S\rho^0 \to K^0_S\pi^+\pi^-)$		$(-0.1 \pm 0.5)\%$
$A_{CP}(D^0 \to K^0_S\omega \to K^0_S\pi^+\pi^-)$		$(-13 \pm 7)\%$
$A_{CP}(D^0 \to K^0_S f_0(980) \to K^0_S\pi^+\pi^-)$		$(-0.4 \pm 2.7)\%$
$A_{CP}(D^0 \to K^0_S f_2(1270) \to K^0_S\pi^+\pi^-)$		$(-4 \pm 5)\%$
$A_{CP}(D^0 \to K^0_S f_0(1370) \to K^0_S\pi^+\pi^-)$		$(-1 \pm 9)\%$
$A_{CP}(D^0 \to \overline{K}^0\rho^0(1450) \to K^0_S\pi^+\pi^-)$		$(-4 \pm 10)\%$
$A_{CP}(D^0 \to \overline{K}^0 f_0(600) \to K^0_S\pi^+\pi^-)$		$(-3 \pm 5)\%$
$A_{CP}(D^0 \to K^*(1410)^-\pi^+ \to K^0_S\pi^+\pi^-)$		$(-2 \pm 9)\%$
$A_{CP}(D^0 \to K^*_0(1430)^-\pi^+ \to K^0_S\pi^+\pi^-)$		$(4 \pm 4)\%$
$A_{CP}(D^0 \to K^*_0(1430)^-\pi^+ \to K^0_S\pi^+\pi^-)$		$(12 \pm 15)\%$
$A_{CP}(D^0 \to K^*_2(1430)^-\pi^+ \to K^0_S\pi^+\pi^-)$		$(3 \pm 6)\%$
$A_{CP}(D^0 \to K^*_2(1430)^+\pi^- \to K^0_S\pi^+\pi^-)$		$(-10 \pm 32)\%$
$A_{CP}(D^0 \to K^*(1680)^-\pi^+ \to K^0_S\pi^+\pi^-)$		—
$A_{CP}(D^0 \to K^-\pi^+\pi^+\pi^-)$		$(0.2 \pm 0.5)\%$
$A_{CP}(D^0 \to K^+\pi^-\pi^+\pi^-)$		$(-2 \pm 4)\%$
$A_{CP}(D^0 \to K^+K^-\pi^+\pi^-)$		$(1.3 \pm 1.7)\%$
$A_{CP}(D^0 \to K^*_1(1270)^+K^- \to K^+K^-\pi^+\pi^-)$		$(25 \pm 16)\%$
$A_{CP}(D^0 \to K^*_1(1270)^+K^- \to K^{*0}\pi^+K^-)$		$(-1 \pm 10)\%$
$A_{CP}(D^0 \to K^*_1(1270)^-K^+ \to \overline{K}^{*0}\pi^-K^+)$		$(-10 \pm 32)\%$
$A_{CP}(D^0 \to K^*_1(1270)^-K^+ \to K^+K^-\pi^+\pi^-)$		$(-50 \pm 20)\%$
$A_{CP}(D^0 \to K^*_1(1270)^+K^- \to \rho^0K^+K^-)$		$(-7 \pm 17)\%$
$A_{CP}(D^0 \to K^*_1(1270)^-K^+ \to \rho^0K^-K^+)$		$(10 \pm 13)\%$
$A_{CP}(D^0 \to K^*_1(1400)^+K^- \to K^+K^-\pi^+\pi^-)$		$(9 \pm 25)\%$
$A_{CP}(D^0 \to K^*(1410)^+K^- \to K^{*0}\pi^+K^-)$		$(-20 \pm 17)\%$
$A_{CP}(D^0 \to K^*(1410)^-K^+ \to \overline{K}^{*0}\pi^-K^+)$		$(-1 \pm 14)\%$
$A_{CP}(D^0 \to K^*(1680)^+K^- \to K^+K^-\pi^+\pi^-)$		$(-17 \pm 29)\%$
$A_{CP}(K^{*0}\overline{K}^{*0})$ in $D^0, \overline{D}^0 \to K^{*0}\overline{K}^{*0}$		$(-5 \pm 14)\%$
$A_{CP}(D^0 \to K^{*0}\overline{K}^{*0}$ S-wave)		$(10 \pm 14)\%$
$A_{CP}(\phi\rho^0)$ in $D^0, \overline{D}^0 \to \phi\rho^0$		$(1 \pm 9)\%$
$A_{CP}(D^0 \to \phi\rho^0$ S-wave)		$(-3 \pm 5)\%$
$A_{CP}(D^0 \to \phi\rho^0$ D-wave)		$(-37 \pm 19)\%$
$A_{CP}(D^0 \to \phi(\pi^+\pi^-)_{S-wave})$		$(0 \pm 50)\%$
$A_{CP}(D^0 \to K^*(892)^0(K^-\pi^+)_{S-wave})$		$(-10 \pm 40)\%$
$A_{CP}(D^0 \to K^+K^-\pi^+\pi^-$ non-resonant)		$(8 \pm 20)\%$
$A_{CP}((K^-\pi^+)_{P-wave}(K^+\pi^-)_{S-wave})$		$(3 \pm 11)\%$
CP-even fraction in $D^0 \to \pi^+\pi^-\pi^0$ decays		$(97.3 \pm 1.7)\%$
CP-even fraction in $D^0 \to K^+K^-\pi^0$ decays		$(73 \pm 6)\%$
CP-even fraction in $D^0 \to \pi^+\pi^-\pi^+\pi^-$ decays		$(73.7 \pm 2.8)\%$
$\Delta A_{CP}^{D^0} = A_{CP}(K^+K^-) - A_{CP}(\pi^+\pi^-)$		$(-0.12 \pm 0.13)\%$ (S = 1.8)
Local CPV in $D^0, \overline{D}^0 \to \pi^+\pi^-\pi^0$		4.9%
Local CPV in $D^0, \overline{D}^0 \to \pi^+\pi^-\pi^+\pi^-$		$(0.6 \pm 0.2)\%$
Local CPV in $D^0, \overline{D}^0 \to K^0_S\pi^+\pi^-$		96%
Local CPV in $D^0, \overline{D}^0 \to K^+K^-\pi^0$		16.6%
Local CPV in $D^0, \overline{D}^0 \to K^+K^-\pi^+\pi^-$		9.1%
$A_{CP}(D_s^\pm \to \mu^\pm\nu)$		$(5 \pm 6)\%$
$A_{CP}(D_s^\pm \to K^\pm K^0_S)$		$(0.08 \pm 0.26)\%$
$A_{CP}(D_s^\pm \to K^+K^-\pi^\pm)$		$(-0.5 \pm 0.9)\%$
$A_{CP}(D_s^\pm \to \phi\pi^\pm)$		$(-0.38 \pm 0.27)\%$
$A_{CP}(D_s^\pm \to K^\pm K^0_S\pi^0)$		$(-2 \pm 6)\%$
$A_{CP}(D_s^\pm \to 2K^0_S\pi^\pm)$		$(3 \pm 5)\%$
$A_{CP}(D_s^\pm \to K^+K^-\pi^\pm\pi^0)$		$(0.0 \pm 3.0)\%$
$A_{CP}(D_s^\pm \to K^\pm K^0_S\pi^+\pi^-)$		$(-6 \pm 5)\%$
$A_{CP}(D_s^\pm \to K^0_S K^\mp 2\pi^\pm)$		$(4.1 \pm 2.8)\%$
$A_{CP}(D_s^\pm \to \pi^+\pi^-\pi^\pm)$		$(-0.7 \pm 3.1)\%$
$A_{CP}(D_s^\pm \to \pi^\pm\eta)$		$(1.1 \pm 3.1)\%$
$A_{CP}(D_s^\pm \to \pi^\pm\eta')$		$(-0.9 \pm 0.5)\%$
$A_{CP}(D_s^\pm \to \eta\pi^\pm\pi^0)$		$(-1 \pm 4)\%$
$A_{CP}(D_s^\pm \to \eta'\pi^\pm\pi^0)$		$(0 \pm 8)\%$
$A_{CP}(D_s^\pm \to K^\pm\pi^0)$		$(-27 \pm 24)\%$
$A_{CP}(D_s^\pm \to \overline{K}^0/K^0\pi^\pm)$		$(0.4 \pm 0.5)\%$
$A_{CP}(D_s^\pm \to K^0_S\pi^\pm)$		$(3.1 \pm 2.6)\%$ (S = 1.7)
$A_{CP}(D_s^\pm \to K^\pm\pi^+\pi^-)$		$(4 \pm 5)\%$
$A_{CP}(D_s^\pm \to K^\pm\eta)$		$(9 \pm 15)\%$
$A_{CP}(D_s^\pm \to K^\pm\eta'(958))$		$(6 \pm 19)\%$
$A_{CP}(B^+ \to J/\psi(1S)K^+)$		$(1.8 \pm 3.0) \times 10^{-3}$ (S = 1.5)
$A_{CP}(B^+ \to J/\psi(1S)\pi^+)$		$(1.8 \pm 1.2) \times 10^{-2}$ (S = 1.3)
$A_{CP}(B^+ \to J/\psi\rho^+)$		-0.11 ± 0.14
$A_{CP}(B^+ \to J/\psi K^*(892)^+)$		-0.048 ± 0.033
$A_{CP}(B^+ \to \eta_c K^+)$		0.01 ± 0.07 (S = 2.2)
$A_{CP}(B^+ \to \psi(2S)\pi^+)$		0.03 ± 0.06
$A_{CP}(B^+ \to \psi(2S)K^+)$		0.012 ± 0.020 (S = 1.5)
$A_{CP}(B^+ \to \psi(2S)K^*(892)^+)$		0.08 ± 0.21

Unless otherwise stated, limits are given at the 90% confidence level, while errors are given as ± 1 standard deviation.

$A_{CP}(B^+ \to \chi_{c1}(1P)\pi^+)$	0.07 ± 0.18
$A_{CP}(B^+ \to \chi_{c0} K^+)$	-0.20 ± 0.18 (S = 1.5)
$A_{CP}(B^+ \to \chi_{c1} K^+)$	-0.009 ± 0.033
$A_{CP}(B^+ \to \chi_{c1} K^*(892)^+)$	0.5 ± 0.5
$A_{CP}(B^+ \to \overline{D}^0 \pi^+)$	-0.007 ± 0.007
$A_{CP}(B^+ \to D_{CP(+1)} \pi^+)$	-0.0080 ± 0.0026
$A_{CP}(B^+ \to D_{CP(-1)} \pi^+)$	0.017 ± 0.026
$A_{CP}([K^\mp \pi^\pm \pi^+ \pi^-]_D \pi^+)$	0.02 ± 0.05
$A_{CP}(B^+ \to [\pi^+ \pi^+ \pi^- \pi^-]_D K^+)$	0.10 ± 0.04
$A_{CP}(B^+ \to [\pi^+ \pi^- \pi^+ \pi^-]_D K^*(892)^+)$	0.02 ± 0.11
$A_{CP}(B^+ \to \overline{D}^0 K^+)$	-0.017 ± 0.005
$A_{CP}([K^\mp \pi^\pm \pi^+ \pi^-]_D K^+)$	-0.31 ± 0.11
$A_{CP}(B^+ \to [\pi^+ \pi^+ \pi^- \pi^-]_D \pi^+)$	$(-4 \pm 8) \times 10^{-3}$
$A_{CP}(B^+ \to [K^- \pi^+]_D K^+)$	-0.58 ± 0.21
$A_{CP}(B^+ \to [K^- \pi^+ \pi^0]_D K^+)$	0.07 ± 0.30 (S = 1.5)
$A_{CP}(B^+ \to [K^+ K^- \pi^0]_D K^+)$	0.30 ± 0.20
$A_{CP}(B^+ \to [\pi^+ \pi^- \pi^0]_D K^+)$	0.05 ± 0.09
$A_{CP}(B^+ \to \overline{D}^0 K^*(892)^+)$	-0.007 ± 0.019
$A_{CP}(B^+ \to [K^- \pi^+]_{\overline{D}} K^*(892)^+)$	-0.75 ± 0.16
$A_{CP}(B^+ \to [K^- \pi^+ \pi^- \pi^+]_{\overline{D}} K^*(892)^+)$	-0.45 ± 0.25
$A_{CP}(B^+ \to [K^- \pi^+]_D \pi^+)$	0.00 ± 0.09
$A_{CP}(B^+ \to [K^- \pi^+ \pi^0]_D \pi^+)$	0.35 ± 0.16
$A_{CP}(B^+ \to [K^+ K^- \pi^0]_D \pi^+)$	-0.03 ± 0.04
$A_{CP}(B^+ \to [\pi^+ \pi^- \pi^0]_D \pi^+)$	-0.016 ± 0.020
$A_{CP}(B^+ \to [K^- \pi^+]_{(D\pi)} \pi^+)$	-0.09 ± 0.27
$A_{CP}(B^+ \to [K^- \pi^+]_{(D\gamma)} \pi^+)$	-0.7 ± 0.6
$A_{CP}(B^+ \to [K^- \pi^+]_{(D\pi)} K^+)$	0.8 ± 0.4
$A_{CP}(B^+ \to [K^- \pi^+]_{(D\gamma)} K^+)$	0.4 ± 1.0
$A_{CP}(B^+ \to [\pi^+ \pi^- \pi^0]_D K^+)$	-0.02 ± 0.15
$A_{CP}(B^+ \to [K^0_S K^+ \pi^-]_D K^+)$	0.04 ± 0.09
$A_{CP}(B^+ \to [K^0_S K^- \pi^+]_D K^+)$	0.23 ± 0.13
$A_{CP}(B^+ \to [K^0_S K^- \pi^+]_D \pi^+)$	-0.052 ± 0.034
$A_{CP}(B^+ \to [K^0_S K^+ \pi^-]_D \pi^+)$	-0.025 ± 0.026
$A_{CP}(B^+ \to [K^*(892)^- K^+]_D K^+)$	0.03 ± 0.11
$A_{CP}(B^+ \to [K^*(892)^+ K^-]_D K^+)$	0.34 ± 0.21
$A_{CP}(B^+ \to [K^*(892)^+ K^-]_D \pi^+)$	-0.05 ± 0.05
$A_{CP}(B^+ \to [K^*(892)^- K^+]_D \pi^+)$	-0.012 ± 0.030
$A_{CP}(B^+ \to D_{CP(+1)} K^+)$	0.120 ± 0.014 (S = 1.4)
$A_{ADS}(B^+ \to D K^+)$	-0.40 ± 0.06
$A_{ADS}(B^+ \to D \pi^+)$	0.100 ± 0.032
$A_{ADS}(B^+ \to [K^- \pi^+]_D K^+ \pi^- \pi^+)$	-0.33 ± 0.35
$A_{ADS}(B^+ \to [K^- \pi^+]_D \pi^+ \pi^- \pi^+)$	-0.01 ± 0.09
$A_{CP}(B^+ \to D_{CP(-1)} K^+)$	-0.10 ± 0.07
$A_{CP}(B^+ \to [K^+ K^-]_D K^+ \pi^- \pi^+)$	-0.04 ± 0.06
$A_{CP}(B^+ \to [\pi^+ \pi^-]_D K^+ \pi^- \pi^+)$	-0.05 ± 0.10
$A_{CP}(B^+ \to [K^- \pi^+]_D K^+ \pi^- \pi^+)$	0.013 ± 0.023
$A_{CP}(B^+ \to [K^+ K^-]_D \pi^+ \pi^- \pi^+)$	-0.019 ± 0.015
$A_{CP}(B^+ \to [\pi^+ \pi^-]_D \pi^+ \pi^- \pi^+)$	-0.013 ± 0.019
$A_{CP}(B^+ \to [K^- \pi^+]_D \pi^+ \pi^- \pi^+)$	-0.002 ± 0.011
$A_{CP}(B^+ \to \overline{D}^{*0} \pi^+)$	0.0010 ± 0.0028
$A_{CP}(B^+ \to (D^*_{CP(+1)})^0 \pi^+)$	0.016 ± 0.010 (S = 1.2)
$A_{CP}(B^+ \to (D^*_{CP(-1)})^0 \pi^+)$	-0.09 ± 0.05
$A_{CP}(B^+ \to D^{*0} K^+)$	-0.001 ± 0.011 (S = 1.1)
$A_{CP}(B^+ \to D^{*0}_{CP(+1)} K^+)$	-0.11 ± 0.08 (S = 2.7)
$A_{CP}(B^+ \to D^*_{CP(-1)} K^+)$	0.07 ± 0.10
$A_{CP}(B^+ \to D_{CP(+1)} K^*(892)^+)$	0.08 ± 0.06
$A_{CP}(B^+ \to D_{CP(-1)} K^*(892)^+)$	-0.23 ± 0.22
$A_{CP}(B^+ \to D^+_s \phi)$	0.0 ± 0.4
$A_{CP}(B^+ \to D^{*+} \overline{D}^{*0})$	-0.15 ± 0.11
$A_{CP}(B^+ \to D^{*+} \overline{D}^0)$	-0.06 ± 0.13
$A_{CP}(B^+ \to D^+ \overline{D}^{*0})$	0.13 ± 0.18
$A_{CP}(B^+ \to D^+ \overline{D}^0)$	-0.03 ± 0.07
$A_{CP}(B^+ \to K^0_S \pi^+)$	-0.017 ± 0.016
$A_{CP}(B^+ \to K^+ \pi^0)$	0.037 ± 0.021
$A_{CP}(B^+ \to \eta' K^+)$	0.004 ± 0.011
$A_{CP}(B^+ \to \eta' K^*(892)^+)$	-0.26 ± 0.27
$A_{CP}(B^+ \to \eta' K^*_0(1430)^+)$	0.06 ± 0.20
$A_{CP}(B^+ \to \eta' K^*_2(1430)^+)$	0.15 ± 0.13
$A_{CP}(B^+ \to \eta K^*(892)^+)$	0.02 ± 0.06
$A_{CP}(B^+ \to \eta K^*_0(1430)^+)$	0.05 ± 0.13
$A_{CP}(B^+ \to \eta K^*_2(1430)^+)$	-0.45 ± 0.30
$A_{CP}(B^+ \to \omega K^+)$	-0.02 ± 0.04
$A_{CP}(B^+ \to \omega K^{*+})$	0.29 ± 0.35
$A_{CP}(B^+ \to \omega (K\pi)^{*+}_0)$	-0.10 ± 0.09
$A_{CP}(B^+ \to \omega K^*_2(1430)^+)$	0.14 ± 0.15
$A_{CP}(B^+ \to K^{*0} \pi^+)$	-0.04 ± 0.09 (S = 2.1)
$A_{CP}(B^+ \to K^*(892)^+ \pi^0)$	-0.39 ± 0.21 (S = 1.6)
$A_{CP}(B^+ \to K^+ \pi^- \pi^+)$	0.027 ± 0.008
$A_{CP}(B^+ \to K^+ K^- K^+$ nonresonant)	0.06 ± 0.05
$A_{CP}(B^+ \to f(980)^0 K^+)$	-0.08 ± 0.09
$A_{CP}(B^+ \to f_0(1500) K^+)$	0.28 ± 0.30
$A_{CP}(B^+ \to f'_2(1525)^0 K^+)$	$-0.08^{+0.05}_{-0.04}$
$A_{CP}(B^+ \to K^*_0(1430)^0 \pi^+)$	0.061 ± 0.032
$A_{CP}(B^+ \to K^*_0(1430)^+ \pi^0)$	$0.26^{+0.18}_{-0.14}$
$A_{CP}(B^+ \to K^*_2(1430)^0 \pi^+)$	$0.05^{+0.29}_{-0.24}$
$A_{CP}(B^+ \to K^+ \pi^0 \pi^0)$	-0.06 ± 0.07
$A_{CP}(B^+ \to K^0 \rho^+)$	-0.03 ± 0.15
$A_{CP}(B^+ \to K^{*+} \pi^+ \pi^-)$	0.07 ± 0.08
$A_{CP}(B^+ \to \rho^0 K^*(892)^+)$	0.31 ± 0.13
$A_{CP}(B^+ \to K^*(892)^+ f_0(980))$	-0.15 ± 0.12
$A_{CP}(B^+ \to a_1^+ K^0)$	0.12 ± 0.11
$A_{CP}(B^+ \to b_1^+ K^0)$	-0.03 ± 0.15
$A_{CP}(B^+ \to K^*(892)^0 \rho^+)$	-0.01 ± 0.16
$A_{CP}(B^+ \to b_1^0 K^+)$	-0.46 ± 0.20
$A_{CP}(B^+ \to K^0 K^+)$	0.04 ± 0.14
$A_{CP}(B^+ \to K^+ K^0_S K^0_S)$	$0.04^{+0.04}_{-0.05}$
$A_{CP}(B^+ \to K^+ K^- \pi^+)$	-0.122 ± 0.021
$A_{CP}(B^+ \to K^+ K^- K^+)$	-0.033 ± 0.008
$A_{CP}(B^+ \to \phi K^+)$	0.024 ± 0.028 (S = 2.3)
$A_{CP}(B^+ \to X_0(1550) K^+)$	-0.04 ± 0.07
$A_{CP}(B^+ \to K^{*+} K^+ K^-)$	0.11 ± 0.09
$A_{CP}(B^+ \to \phi K^*(892)^+)$	-0.01 ± 0.08
$A_{CP}(B^+ \to \phi (K\pi)^{*+}_0)$	0.04 ± 0.16
$A_{CP}(B^+ \to \phi K_1(1270)^+)$	0.15 ± 0.20
$A_{CP}(B^+ \to \phi K^*_2(1430)^+)$	-0.23 ± 0.20
$A_{CP}(B^+ \to K^+ \phi\phi)$	-0.10 ± 0.08
$A_{CP}(B^+ \to K^+ [\phi\phi]_{\eta_c})$	0.09 ± 0.10
$A_{CP}(B^+ \to K^*(892)^+ \gamma)$	0.014 ± 0.018
$A_{CP}(B^+ \to \eta K^+ \gamma)$	-0.12 ± 0.07
$A_{CP}(B^+ \to \phi K^+ \gamma)$	-0.13 ± 0.11 (S = 1.1)
$A_{CP}(B^+ \to \rho^+ \gamma)$	-0.11 ± 0.33
$A_{CP}(B^+ \to \pi^+ \pi^0)$	0.03 ± 0.04
$A_{CP}(B^+ \to \pi^+ \pi^- \pi^+)$	0.057 ± 0.013
$A_{CP}(B^+ \to \rho^0 \pi^+)$	$0.18^{+0.09}_{-0.17}$
$A_{CP}(B^+ \to f_2(1270) \pi^+)$	0.41 ± 0.30
$A_{CP}(B^+ \to \rho^0(1450) \pi^+)$	$-0.1^{+0.4}_{-0.5}$
$A_{CP}(B^+ \to f_0(1370) \pi^+)$	0.72 ± 0.22
$A_{CP}(B^+ \to \pi^+ \pi^- \pi^+$ nonresonant)	$-0.14^{+0.23}_{-0.16}$
$A_{CP}(B^+ \to \rho^+ \pi^0)$	0.02 ± 0.11
$A_{CP}(B^+ \to \rho^+ \rho^0)$	-0.05 ± 0.05
$A_{CP}(B^+ \to \omega \pi^+)$	-0.04 ± 0.06
$A_{CP}(B^+ \to \omega \rho^+)$	-0.20 ± 0.09
$A_{CP}(B^+ \to \eta \pi^+)$	-0.14 ± 0.07 (S = 1.4)
$A_{CP}(B^+ \to \eta \rho^+)$	0.11 ± 0.11
$A_{CP}(B^+ \to \eta' \pi^+)$	0.06 ± 0.16
$A_{CP}(B^+ \to \eta' \rho^+)$	0.26 ± 0.17
$A_{CP}(B^+ \to b_1^0 \pi^+)$	0.05 ± 0.16
$A_{CP}(B^+ \to p\overline{p}\pi^+)$	0.00 ± 0.04
$A_{CP}(B^+ \to p\overline{p}K^+)$	0.00 ± 0.04 (S = 2.2)
$A_{CP}(B^+ \to p\overline{p}K^*(892)^+)$	0.21 ± 0.16 (S = 1.4)
$A_{CP}(B^+ \to p\overline{\Lambda}\gamma)$	0.17 ± 0.17
$A_{CP}(B^+ \to p\overline{\Lambda}\pi^0)$	0.01 ± 0.17
$A_{CP}(B^+ \to K^+ \ell^+ \ell^-)$	-0.02 ± 0.08
$A_{CP}(B^+ \to K^+ e^+ e^-)$	0.14 ± 0.14
$A_{CP}(B^+ \to K^+ \mu^+ \mu^-)$	0.011 ± 0.017
$A_{CP}(B^+ \to K^{*+} \ell^+ \ell^-)$	-0.09 ± 0.14

Unless otherwise stated, limits are given at the 90% confidence level, while errors are given as ± 1 standard deviation.

Tests of Conservation Laws

$A_{CP}(B^+ \to K^* e^+ e^-)$	-0.14 ± 0.23
$A_{CP}(B^+ \to K^* \mu^+ \mu^-)$	-0.12 ± 0.24
$r_B(B^+ \to D^0 K^+)$	0.103 ± 0.005
$\delta_B(B^+ \to D^0 K^+)$	$(136.9^{+4.6}_{-5.2})^\circ$
$r_B(B^+ \to \overline{D}^0 K^{*+})$	$0.075^{+0.017}_{-0.018}$
$\delta_B(B^+ \to D^0 K^{*+})$	$(106^{+18}_{-26})^\circ$
$r_B^*(B^+ \to D^{*0} K^+)$	$0.142^{+0.019}_{-0.020}$
$\delta_B^*(B^+ \to D^{*0} K^+)$	$(321^{+8}_{-9})^\circ$
$\mathrm{Re}(\epsilon_{B^0})/(1+\lvert\epsilon_{B^0}\rvert^2)$	$(-0.5 \pm 0.4) \times 10^{-3}$
$A_{T/CP}(B^0 \leftrightarrow \overline{B}^0)$	0.005 ± 0.018
$A_{CP}(B^0 \to D^*(2010)^+ D^-)$	0.037 ± 0.034
$A_{CP}(B^0 \to [K^+ K^-]_D K^*(892)^0)$	—
$A_{CP}(B^0 \to [K^+ \pi^-]_D K^*(892)^0)$	-0.03 ± 0.04
$A_{CP}(B^0 \to [\pi^+ \pi^-]_D K^*(892)^0)$	—
$A_{CP}(B^0 \to \eta' K^*(892)^0)$	-0.07 ± 0.18
$A_{CP}(B^0 \to \eta' K_0^*(1430)^0)$	-0.19 ± 0.17
$A_{CP}(B^0 \to \eta' K_2^*(1430)^0)$	0.14 ± 0.18
$A_{CP}(B^0 \to \eta K_0^*(1430)^0)$	0.06 ± 0.13
$A_{CP}(B^0 \to \eta K_2^*(1430)^0)$	-0.07 ± 0.19
$A_{CP}(B^0 \to b_1 K^+)$	-0.07 ± 0.12
$A_{CP}(B^0 \to \omega K^{*0})$	0.45 ± 0.25
$A_{CP}(B^0 \to \omega (K\pi)_0^{*0})$	-0.07 ± 0.09
$A_{CP}(B^0 \to \omega K_2^*(1430)^0)$	-0.37 ± 0.17
$A_{CP}(B^0 \to K^+ \pi^- \pi^0)$	$(0 \pm 6) \times 10^{-2}$
$A_{CP}(B^0 \to \rho^- K^+)$	0.20 ± 0.11
$A_{CP}(B^0 \to \rho(1450)^- K^+)$	-0.10 ± 0.33
$A_{CP}(B^0 \to \rho(1700)^- K^+)$	-0.4 ± 0.6
$A_{CP}(B^0 \to K^+ \pi^- \pi^0$ nonresonant)	0.10 ± 0.18
$A_{CP}(B^0 \to K^0 \pi^+ \pi^-)$	-0.01 ± 0.05
$A_{CP}(B^0 \to K^*(892)^+ \pi^-)$	-0.22 ± 0.06
$A_{CP}(B^0 \to (K\pi)_0^{*+} \pi^-)$	0.09 ± 0.07
$A_{CP}(B^0 \to (K\pi)_0^{*0} \pi^0)$	-0.15 ± 0.11
$A_{CP}(B^0 \to K^{*0} \pi^0)$	-0.15 ± 0.13
$A_{CP}(B^0 \to K^*(892)^0 \pi^+ \pi^-)$	0.07 ± 0.05
$A_{CP}(B^0 \to K^*(892)^0 \rho^0)$	-0.06 ± 0.09
$A_{CP}(B^0 \to K^{*0} f_0(980))$	0.07 ± 0.10
$A_{CP}(B^0 \to K^{*+} \rho^-)$	0.21 ± 0.15
$A_{CP}(B^0 \to K^*(892)^0 K^+ K^-)$	0.01 ± 0.05
$A_{CP}(B^0 \to a_1^- K^+)$	-0.16 ± 0.12
$A_{CP}(B^0 \to K^0 K^0)$	-0.6 ± 0.7
$A_{CP}(B^0 \to K^*(892)^0 \phi)$	0.00 ± 0.04
$A_{CP}(B^0 \to K^*(892)^0 K^- \pi^+)$	0.2 ± 0.4
$A_{CP}(B^0 \to \phi (K\pi)_0^{*0})$	0.12 ± 0.08
$A_{CP}(B^0 \to \phi K_2^*(1430)^0)$	-0.11 ± 0.10
$A_{CP}(B^0 \to K^*(892)^0 \gamma)$	-0.006 ± 0.011
$A_{CP}(B^0 \to K_2^*(1430)^0 \gamma)$	-0.08 ± 0.15
$A_{CP}(B^0 \to \rho^+ \pi^-)$	0.13 ± 0.06 (S = 1.1)
$A_{CP}(B^0 \to \rho^- \pi^+)$	-0.08 ± 0.08
$A_{CP}(B^0 \to a_1(1260)^\pm \pi^\mp)$	-0.07 ± 0.06
$A_{CP}(B^0 \to b_1^- \pi^+)$	-0.05 ± 0.10
$A_{CP}(B^0 \to p\overline{p} K^*(892)^0)$	0.05 ± 0.12
$A_{CP}(B^0 \to p\overline{\Lambda}\pi^-)$	0.04 ± 0.07
$A_{CP}(B^0 \to K^{*0} \ell^+ \ell^-)$	-0.05 ± 0.10
$A_{CP}(B^0 \to K^{*0} e^+ e^-)$	-0.21 ± 0.19
$A_{CP}(B^0 \to K^{*0} \mu^+ \mu^-)$	-0.034 ± 0.024
$C_{D^*(2010)^- D^+}$ ($B^0 \to D^*(2010)^- D^+$)	-0.01 ± 0.11
$C_{D^*(2010)^+ D^-}$ ($B^0 \to D^*(2010)^+ D^-$)	0.00 ± 0.13 (S = 1.3)
$C_{D^{*+} D^{*-}}$ ($B^0 \to D^{*+} D^{*-}$)	0.01 ± 0.09 (S = 1.6)
C_+ ($B^0 \to D^{*+} D^{*-}$)	0.00 ± 0.10 (S = 1.6)
C_- ($B^0 \to D^{*+} D^{*-}$)	0.19 ± 0.31
S_- ($B^0 \to D^{*+} D^{*-}$)	0.1 ± 1.6 (S = 3.5)
C ($B^0 \to D^*(2010)^+ D^*(2010)^- K_S^0$)	0.01 ± 0.29
S ($B^0 \to D^*(2010)^+ D^*(2010)^- K_S^0$)	0.1 ± 0.4
$C_{D^+ D^-}$ ($B^0 \to D^+ D^-$)	-0.22 ± 0.24 (S = 2.5)
$C_{J/\psi(1S)\pi^0}$ ($B^0 \to J/\psi(1S)\pi^0$)	-0.13 ± 0.13
$C(B^0 \to J/\psi(1S)\rho^0)$	-0.06 ± 0.06
$C_{D_{CP}^{(*)} h^0}$ ($B^0 \to D_{CP}^{(*)} h^0$)	-0.02 ± 0.08
$S_{D_{CP}^{(*)} h^0}$ ($B^0 \to D_{CP}^{(*)} h^0$)	-0.66 ± 0.12
$C_{K^0\pi^0}$ ($B^0 \to K^0 \pi^0$)	0.00 ± 0.13 (S = 1.4)
$C_{\eta'(958) K_S^0}$ ($B^0 \to \eta'(958) K_S^0$)	-0.04 ± 0.20 (S = 2.5)
$S_{\eta'(958) K_S^0}$ ($B^0 \to \eta'(958) K_S^0$)	0.43 ± 0.17 (S = 1.5)
$C_{\eta' K^0}$ ($B^0 \to \eta' K^0$)	-0.06 ± 0.04
$C_{\omega K_S^0}$ ($B^0 \to \omega K_S^0$)	0.0 ± 0.4 (S = 3.0)
$S_{\omega K_S^0}$ ($B^0 \to \omega K_S^0$)	0.70 ± 0.21
C ($B^0 \to K_S^0 \pi^0 \pi^0$)	0.2 ± 0.5
S ($B^0 \to K_S^0 \pi^0 \pi^0$)	0.7 ± 0.7
$C_{\rho^0 K_S^0}$ ($B^0 \to \rho^0 K_S^0$)	-0.04 ± 0.20
$S_{\rho^0 K_S^0}$ ($B^0 \to \rho^0 K_S^0$)	$0.50^{+0.17}_{-0.21}$
$C_{f_0(980) K_S^0}$ ($B^0 \to f_0(980) K_S^0$)	0.29 ± 0.20
$S_{f_0(980) K_S^0}$ ($B^0 \to f_0(980) K_S^0$)	-0.50 ± 0.16
$S_{f_2(1270) K_S^0}$ ($B^0 \to f_2(1270) K_S^0$)	-0.5 ± 0.5
$C_{f_2(1270) K_S^0}$ ($B^0 \to f_2(1270) K_S^0$)	0.3 ± 0.4
$S_{f_X(1300) K_S^0}$ ($B^0 \to f_X(1300) K_S^0$)	-0.2 ± 0.5
$C_{f_X(1300) K_S^0}$ ($B^0 \to f_X(1300) K_S^0$)	0.13 ± 0.35
$S_{K^0\pi^+\pi^-}$ ($B^0 \to K^0 \pi^+ \pi^-$ nonresonant)	-0.01 ± 0.33
$C_{K^0\pi^+\pi^-}$ ($B^0 \to K^0 \pi^+ \pi^-$ nonresonant)	0.01 ± 0.26
$C_{K_S^0 K_S^0}$ ($B^0 \to K_S^0 K_S^0$)	0.0 ± 0.4 (S = 1.4)
$S_{K_S^0 K_S^0}$ ($B^0 \to K_S^0 K_S^0$)	-0.8 ± 0.5
$C_{K^+K^-K_S^0}$ ($B^0 \to K^+ K^- K_S^0$ nonresonant)	0.06 ± 0.08
$C_{K^+K^-K_S^0}$ ($B^0 \to K^+ K^- K_S^0$ inclusive)	0.01 ± 0.09
$C_{\phi K_S^0}$ ($B^0 \to \phi K_S^0$)	0.01 ± 0.14
$S_{\phi K_S^0}$ ($B^0 \to \phi K_S^0$)	0.59 ± 0.14
$C_{K_S K_S K_S}(B^0 \to K_S K_S K_S)$	-0.23 ± 0.14
$S_{K_S K_S K_S}(B^0 \to K_S K_S K_S)$	-0.5 ± 0.6 (S = 3.0)
$C_{K_S^0\pi^0\gamma}(B^0 \to K_S^0 \pi^0 \gamma)$	0.36 ± 0.33
$S_{K_S^0\pi^0\gamma}(B^0 \to K_S^0 \pi^0 \gamma)$	-0.8 ± 0.6
$C_{K^*(892)^0\gamma}$ ($B^0 \to K^*(892)^0 \gamma$)	-0.04 ± 0.16 (S = 1.2)
$S_{K^*(892)^0\gamma}$ ($B^0 \to K^*(892)^0 \gamma$)	-0.15 ± 0.22
$C_{\eta K^0\gamma}$ ($B^0 \to \eta K^0 \gamma$)	-0.3 ± 0.4
$S_{\eta K^0\gamma}$ ($B^0 \to \eta K^0 \gamma$)	-0.2 ± 0.5
$C_{K^0\phi\gamma}$ ($B^0 \to K^0 \phi\gamma$)	-0.3 ± 0.6
$S_{K^0\phi\gamma}$ ($B^0 \to K^0 \phi\gamma$)	$0.7^{+0.7}_{-1.1}$
$C(B^0 \to K_S^0 \rho^0 \gamma)$	-0.05 ± 0.19
$S(B^0 \to K_S^0 \rho^0 \gamma)$	-0.04 ± 0.23
C ($B^0 \to \rho^0 \gamma$)	0.4 ± 0.5
S ($B^0 \to \rho^0 \gamma$)	-0.8 ± 0.7
$C_{\pi\pi}$ ($B^0 \to \pi^+ \pi^-$)	-0.31 ± 0.05
$C_{\pi^0\pi^0}(B^0 \to \pi^0 \pi^0)$	-0.33 ± 0.22
$C_{\rho\pi}$ ($B^0 \to \rho^+ \pi^-$)	-0.03 ± 0.07 (S = 1.2)
$S_{\rho\pi}$ ($B^0 \to \rho^+ \pi^-$)	0.05 ± 0.07
$\Delta S_{\rho\pi}$ ($B^0 \to \rho^+ \pi^-$)	0.01 ± 0.08
$C_{\rho^0\pi^0}$ ($B^0 \to \rho^0 \pi^0$)	0.27 ± 0.24
$S_{\rho^0\pi^0}$ ($B^0 \to \rho^0 \pi^0$)	-0.23 ± 0.34
$C_{a_1\pi}$ ($B^0 \to a_1(1260)^+ \pi^-$)	-0.05 ± 0.11
$S_{a_1\pi}$ ($B^0 \to a_1(1260)^+ \pi^-$)	-0.2 ± 0.4 (S = 3.2)
$\Delta C_{a_1\pi}$ ($B^0 \to a_1(1260)^+ \pi^-$)	0.43 ± 0.14 (S = 1.3)
$\Delta S_{a_1\pi}$ ($B^0 \to a_1(1260)^+ \pi^-$)	-0.11 ± 0.12
C ($B^0 \to b_1^- K^+$)	-0.22 ± 0.24
ΔC ($B^0 \to b_1^- \pi^+$)	-1.04 ± 0.24
$C_{\rho^0\rho^0}$ ($B^0 \to \rho^0 \rho^0$)	0.2 ± 0.9
$S_{\rho^0\rho^0}$ ($B^0 \to \rho^0 \rho^0$)	0.3 ± 0.7
$C_{\rho\rho}$ ($B^0 \to \rho^+ \rho^-$)	0.00 ± 0.09
$S_{\rho\rho}$ ($B^0 \to \rho^+ \rho^-$)	-0.14 ± 0.13

Unless otherwise stated, limits are given at the 90% confidence level, while errors are given as ± 1 standard deviation.

$\lvert\lambda\rvert$ ($B^0 \to J/\psi K^*(892)^0$)	<0.25, CL = 95%
cos 2β ($B^0 \to J/\psi K^*(892)^0$)	$1.7^{+0.7}_{-0.9}$ (S = 1.6)
cos 2β ($B^0 \to [K^0_S\pi^+\pi^-]_{D^{(*)}}\, h^0$)	0.84 ± 0.31
$(S_+ + S_-)/2$ ($B^0 \to D^{*-}\pi^+$)	-0.039 ± 0.011
$(S_- - S_+)/2$ ($B^0 \to D^{*-}\pi^+$)	-0.009 ± 0.015
$(S_+ + S_-)/2$ ($B^0 \to D^-\pi^+$)	-0.046 ± 0.023
$(S_- - S_+)/2$ ($B^0 \to D^-\pi^+$)	-0.022 ± 0.021
$(S_+ + S_-)/2$ ($B^0 \to D^-\rho^+$)	-0.024 ± 0.032
$(S_- - S_+)/2$ ($B^0 \to D^-\rho^+$)	-0.10 ± 0.06
$C_{\eta_c K^0_S}$ ($B^0 \to \eta_c K^0_S$)	0.08 ± 0.13
$C_{c\overline{c}K^{(*)}0}$ ($B^0 \to c\overline{c}K^{(*)}0$)	$(0.5 \pm 1.7) \times 10^{-2}$
$C_{J/\psi(\mathrm{nS})K^0}$ ($B^0 \to J/\psi(\mathrm{nS})K^0$)	$(0.5 \pm 2.0) \times 10^{-2}$
$C_{J/\psi K^{*0}}$ ($B^0 \to J/\psi K^{*0}$)	0.03 ± 0.10
$S_{J/\psi K^{*0}}$ ($B^0 \to J/\psi K^{*0}$)	0.60 ± 0.25
$C_{\chi_{c0}K^0_S}$ ($B^0 \to \chi_{c0}K^0_S$)	$-0.3^{+0.5}_{-0.4}$
$S_{\chi_{c0}K^0_S}$ ($B^0 \to \chi_{c0}K^0_S$)	-0.7 ± 0.5
$C_{\chi_{c1}K^0_S}$ ($B^0 \to \chi_{c1}K^0_S$)	0.06 ± 0.07
$\sin(2\beta_{\mathrm{eff}})(B^0 \to \phi K^0)$	0.22 ± 0.30
$\sin(2\beta_{\mathrm{eff}})(B^0 \to \phi K^*_0(1430)^0)$	$0.97^{+0.03}_{-0.52}$
$\sin(2\beta_{\mathrm{eff}})(B^0 \to [K^0_S\pi^+\pi^-]_{D^{(*)}}\, h^0)$	0.37 ± 0.22
$\lvert\lambda\rvert$ ($B^0 \to [K^0_S\pi^+\pi^-]_{D^{(*)}}\, h^0$)	1.01 ± 0.08
$\lvert\sin(2\beta+\gamma)\rvert$	>0.40, CL = 90%
$2\beta+\gamma$	$(83 \pm 60)^\circ$
$x_+(B^0 \to DK^{*0})$	0.04 ± 0.17
$x_-(B^0 \to DK^{*0})$	-0.16 ± 0.14
$y_-(B^0 \to DK^{*0})$	0.20 ± 0.25 (S = 1.2)
$A_{CP}(B \to K^*(892)\gamma)$	-0.003 ± 0.011
$A_{CP}(b \to s\gamma)$	0.015 ± 0.020
$A_{CP}(b \to (s+d)\gamma)$	0.010 ± 0.031
$A_{CP}(B \to X_s\ell^+\ell^-)$	0.04 ± 0.11
$A_{CP}(B \to K^*e^+e^-)$	-0.18 ± 0.15
$A_{CP}(B \to K^*\mu^+\mu^-)$	-0.03 ± 0.13
$A_{CP}(B \to K^*\ell^+\ell^-)$	-0.04 ± 0.07
$A_{CP}(B \to \eta\,\mathrm{anything})$	$-0.13^{+0.04}_{-0.05}$
$\mathrm{Re}(\epsilon_{B^0_s})\,/\,(1+\lvert\epsilon_{B^0_s}\rvert^2)$	$(-0.15 \pm 0.70) \times 10^{-3}$
$C_{KK}(B^0_s \to K^+K^-)$	0.14 ± 0.11
$S_{KK}(B^0_s \to K^+K^-)$	0.30 ± 0.13
$r_B(B^0_s \to D^\mp_s K^\pm)$	0.53 ± 0.17
$\delta_B(B^0_s \to D^\pm_s K^\mp)$	$(3 \pm 20)^\circ$
CP Violation phase β_s	$(1.1 \pm 1.6) \times 10^{-2}$ rad
$A^L_{CP}(B_s \to J/\psi\overline{K}^*(892)^0)$	-0.05 ± 0.06
$A^\parallel_{CP}(B_s \to J/\psi\overline{K}^*(892)^0)$	0.17 ± 0.15
$A^\perp_{CP}(B_s \to J/\psi\overline{K}^*(892)^0)$	-0.05 ± 0.10
$A_{CP}(B_s \to \pi^+K^-)$	0.26 ± 0.04
$A_{CP}(B^0_s \to [K^+K^-]_D\overline{K}^*(892)^0)$	-0.04 ± 0.07
$A_{CP}(B^0_s \to [\pi^+K^-]_D K^*(892)^0)$	-0.01 ± 0.04
$A_{CP}(B^0_s \to [\pi^+\pi^-]_D K^*(892)^0)$	0.06 ± 0.13
$\Gamma(\eta_c(1S) \to \pi^+\pi^-)/\Gamma_{\mathrm{total}}$	$<1.1 \times 10^{-4}$, CL = 90%
$\Gamma(\eta_c(1S) \to \pi^0\pi^0)/\Gamma_{\mathrm{total}}$	$<4 \times 10^{-5}$, CL = 90%
$\Gamma(\eta_c(1S) \to K^+K^-)/\Gamma_{\mathrm{total}}$	$<6 \times 10^{-4}$, CL = 90%
$\Gamma(\eta_c(1S) \to K^0_SK^0_S)/\Gamma_{\mathrm{total}}$	$<3.1 \times 10^{-4}$, CL = 90%
$(\alpha+\overline{\alpha})/(\alpha-\overline{\alpha})$ in $\Lambda \to p\pi^-$, $\overline{\Lambda} \to \overline{p}\pi^+$	0.006 ± 0.021
$\frac{[\alpha(\Xi^-)\alpha_-(\Lambda)-\alpha(\overline{\Xi}^+)\alpha_+(\overline{\Lambda})]}{[\alpha(\Xi^-)\alpha_-(\Lambda)+\alpha(\overline{\Xi}^+)\alpha_+(\overline{\Lambda})]}$	$(0 \pm 7) \times 10^{-4}$
$(\alpha+\overline{\alpha})/(\alpha-\overline{\alpha})$ in $\Omega^- \to \Lambda K^-$, $\overline{\Omega}^+ \to \overline{\Lambda}K^+$	-0.02 ± 0.13
$(\alpha+\overline{\alpha})/(\alpha-\overline{\alpha})$ in $\Lambda_c^+ \to \Lambda\pi^+$, $\overline{\Lambda}_c^- \to \overline{\Lambda}\pi^-$	-0.07 ± 0.31
$(\alpha+\overline{\alpha})/(\alpha-\overline{\alpha})$ in $\Lambda_c^+ \to \Lambda e^+\nu_e$, $\overline{\Lambda}_c^- \to \overline{\Lambda}e^-\overline{\nu}_e$	0.00 ± 0.04
$A_{CP}(\Lambda_b \to p\pi^-)$	0.06 ± 0.08
$A_{CP}(\Lambda_b \to pK^-)$	-0.10 ± 0.09

CP VIOLATION OBSERVED

$\mathrm{Re}(\epsilon)$		$(1.596 \pm 0.013) \times 10^{-3}$
charge asymmetry in $K^0_{\ell 3}$ decays		
A_L = weighted average of $A_L(\mu)$ and $A_L(e)$		$(0.332 \pm 0.006)\%$
$A_L(\mu) = [\Gamma(\pi^-\mu^+\nu_\mu) - \Gamma(\pi^+\mu^-\overline{\nu}_\mu)]$/sum		$(0.304 \pm 0.025)\%$
$A_L(e) = [\Gamma(\pi^-e^+\nu_e) - \Gamma(\pi^+e^-\overline{\nu}_e)]$/sum		$(0.334 \pm 0.007)\%$
parameters for $K^0_L \to 2\pi$ decay		
$\lvert\eta_{00}\rvert = \lvert A(K^0_L \to 2\pi^0)\,/\,A(K^0_S \to 2\pi^0)\rvert$		$(2.220 \pm 0.011) \times 10^{-3}$ (S = 1.8)
$\lvert\eta_{+-}\rvert = \lvert A(K^0_L \to \pi^+\pi^-)\,/\,A(K^0_S \to \pi^+\pi^-)\rvert$		$(2.232 \pm 0.011) \times 10^{-3}$ (S = 1.8)
$\lvert\epsilon\rvert = (2\lvert\eta_{+-}\rvert + \lvert\eta_{00}\rvert)/3$		$(2.228 \pm 0.011) \times 10^{-3}$ (S = 1.8)
$\lvert\eta_{00}/\eta_{+-}\rvert$	[*h*]	0.9950 ± 0.0007 (S = 1.6)
$\mathrm{Re}(\epsilon'/\epsilon) = (1-\lvert\eta_{00}/\eta_{+-}\rvert)/3$	[*h*]	$(1.66 \pm 0.23) \times 10^{-3}$ (S = 1.6)
Assuming CPT		
ϕ_{+-}, phase of η_{+-}		$(43.51 \pm 0.05)^\circ$ (S = 1.2)
ϕ_{00}, phase of η_{00}		$(43.52 \pm 0.05)^\circ$ (S = 1.3)
$\phi_\epsilon = (2\phi_{+-}+\phi_{00})/3$		$(43.52 \pm 0.05)^\circ$ (S = 1.2)
Not assuming CPT		
ϕ_{+-}, phase of η_{+-}		$(43.4 \pm 0.5)^\circ$ (S = 1.2)
ϕ_{00}, phase of η_{00}		$(43.7 \pm 0.6)^\circ$ (S = 1.2)
$\phi_\epsilon = (2\phi_{+-}+\phi_{00})/3$		$(43.5 \pm 0.5)^\circ$ (S = 1.3)
CP asymmetry A in $K^0_L \to \pi^+\pi^-e^+e^-$		$(13.7 \pm 1.5)\%$
β_{CP} from $K^0_L \to e^+e^-e^+e^-$		-0.19 ± 0.07
γ_{CP} from $K^0_L \to e^+e^-e^+e^-$		0.01 ± 0.11 (S = 1.6)
parameters for $K^0_L \to \pi^+\pi^-\gamma$ decay		
$\lvert\eta_{+-\gamma}\rvert = \lvert A(K^0_L \to \pi^+\pi^-\gamma,\ CP\text{ violating})/A(K^0_S \to \pi^+\pi^-\gamma)\rvert$		$(2.35 \pm 0.07) \times 10^{-3}$
$\phi_{+-\gamma}$ = phase of $\eta_{+-\gamma}$		$(44 \pm 4)^\circ$
$\Gamma(K^0_L \to \pi^+\pi^-)/\Gamma_{\mathrm{total}}$	[*i*]	$(1.967 \pm 0.010) \times 10^{-3}$ (S = 1.5)
$\Gamma(K^0_L \to \pi^0\pi^0)/\Gamma_{\mathrm{total}}$		$(8.64 \pm 0.06) \times 10^{-4}$ (S = 1.8)
$A_{CP}(B^+ \to D_{CP(+1)}K^+)$		0.120 ± 0.014 (S = 1.4)
$A_{ADS}(B^+ \to DK^+)$		-0.40 ± 0.06
$A_{CP}(B^+ \to \eta K^+)$		-0.37 ± 0.08
$A_{CP}(B^+ \to f_2(1270)K^+)$		$-0.68^{+0.19}_{-0.17}$
$A_{CP}(B^+ \to \rho^0K^+)$		0.37 ± 0.10
$A_{CP}(B^+ \to f_0(1370)\pi^+)$		0.72 ± 0.22
γ		$(73.5^{+4.3}_{-5.0})^\circ$
$r_B(B^+ \to D^0K^+)$		0.103 ± 0.005
$\delta_B(B^+ \to D^0K^+)$		$(136.9^{+4.6}_{-5.2})^\circ$
$r_B(B^+ \to \overline{D}^0K^{*+})$		$0.075^{+0.017}_{-0.018}$
$\delta_B(B^+ \to D^0K^{*+})$		$(106^{+18}_{-26})^\circ$
$r^*_B(B^+ \to D^{*0}K^+)$		$0.142^{+0.019}_{-0.020}$
$\delta^*_B(B^+ \to D^{*0}K^+)$		$(321^{+8}_{-9})^\circ$
$A_{CP}(B^0 \to K^+\pi^-)$		-0.082 ± 0.006
$A_{CP}(B^0 \to \eta K^*(892)^0)$		0.19 ± 0.05
$S_{D^*(2010)^-D^+}$ ($B^0 \to D^*(2010)^-D^+$)		-0.72 ± 0.15
$S_{D^*(2010)^+D^-}$ ($B^0 \to D^*(2010)^+D^-$)		-0.73 ± 0.14
$S_{D^{*+}D^{*-}}$ ($B^0 \to D^{*+}D^{*-}$)		-0.59 ± 0.14 (S = 1.8)
S_+ ($B^0 \to D^{*+}D^{*-}$)		-0.73 ± 0.09
$S_{D^+D^-}$ ($B^0 \to D^+D^-$)		$-0.76^{+0.15}_{-0.13}$ (S = 1.2)
$S_{J/\psi(1S)\pi^0}$ ($B^0 \to J/\psi(1S)\pi^0$)		-0.94 ± 0.29 (S = 1.9)
$S(B^0 \to J/\psi(1S)\rho^0)$		$-0.66^{+0.16}_{-0.12}$
$S_{K^0\pi^0}$ ($B^0 \to K^0\pi^0$)		0.58 ± 0.17
$S_{\eta' K^0}$ ($B^0 \to \eta' K^0$)		0.63 ± 0.06
$S_{K^+K^-K^0_S}$ ($B^0 \to K^+K^-K^0_S$ nonresonant)		-0.66 ± 0.11
$S_{K^+K^-K^0_S}$ ($B^0 \to K^+K^-K^0_S$ inclusive)		-0.65 ± 0.12
$S_{\pi\pi}$ ($B^0 \to \pi^+\pi^-$)		-0.67 ± 0.06
$\Delta C_{\rho\pi}$ ($B^0 \to \rho^+\pi^-$)		0.27 ± 0.06
$S_{\eta_c K^0_S}$ ($B^0 \to \eta_c K^0_S$)		0.93 ± 0.17
$\sin(2\beta)$ ($B^0 \to J/\psi K^0_S$)		0.699 ± 0.017

Unless otherwise stated, limits are given at the 90% confidence level, while errors are given as ± 1 standard deviation.

Tests of Conservation Laws

$S_{J/\psi(nS)K^0}$ ($B^0 \to J/\psi(nS)K^0$)	0.701 ± 0.017
$S_{\chi_{c1}K^0_S}$ ($B^0 \to \chi_{c1}K^0_S$)	0.63 ± 0.10
$\sin(2\beta_{\rm eff})$($B^0 \to K^+K^-K^0_S$)	$0.77^{+0.13}_{-0.12}$
α	$(93 \pm 5)^\circ$
r_{B^0}($B^0 \to D K^{*0}$)	$0.223^{+0.041}_{-0.045}$
δ_{B^0}($B^0 \to D K^{*0}$)	$(193^{+27}_{-21})^\circ$
$\mathrm{Re}(\epsilon_b)$ / $(1+\lvert\epsilon_b\rvert^2)$	$(-1.3 \pm 0.4) \times 10^{-3}$
$A_{CP}(B_s \to \pi^+K^-)$	0.26 ± 0.04

CPT INVARIANCE

$(m_{W^+} - m_{W^-})$ / $m_{\rm average}$		$(-3.7 \pm 3.5) \times 10^{-4}$
$(m_{e^+} - m_{e^-})$ / $m_{\rm average}$		$<8 \times 10^{-9}$, CL = 90%
$\lvert q_{e^+} + q_{e^-}\rvert/e$		$<4 \times 10^{-8}$
$(g_{e^+} - g_{e^-})$ / $g_{\rm average}$		$(-0.5 \pm 2.1) \times 10^{-12}$
$(\tau_{\mu^+} - \tau_{\mu^-})$ / $\tau_{\rm average}$		$(2 \pm 8) \times 10^{-5}$
$(g_{\mu^+} - g_{\mu^-})$ / $g_{\rm average}$		$(-0.11 \pm 0.12) \times 10^{-8}$
$(m_{\tau^+} - m_{\tau^-})/m_{\rm average}$		$<2.8 \times 10^{-4}$, CL = 90%
$m_t - m_{\overline{t}}$		-0.16 ± 0.19 GeV
$(m_{\pi^+} - m_{\pi^-})$ / $m_{\rm average}$		$(2 \pm 5) \times 10^{-4}$
$(\tau_{\pi^+} - \tau_{\pi^-})$ / $\tau_{\rm average}$		$(6 \pm 7) \times 10^{-4}$
$(m_{K^+} - m_{K^-})$ / $m_{\rm average}$		$(-0.6 \pm 1.8) \times 10^{-4}$
$(\tau_{K^+} - \tau_{K^-})$ / $\tau_{\rm average}$		$(0.10 \pm 0.09)\%$ (S = 1.2)
$K^\pm \to \mu^\pm\nu_\mu$ rate difference/sum		$(-0.27 \pm 0.21)\%$
$K^\pm \to \pi^\pm\pi^0$ rate difference/sum	[j]	$(0.4 \pm 0.6)\%$
δ in $K^0 - \overline{K}^0$ mixing		
real part of δ		$(2.5 \pm 2.3) \times 10^{-4}$
imaginary part of δ		$(-1.5 \pm 1.6) \times 10^{-5}$
Re(y), K_{e3} parameter		$(0.4 \pm 2.5) \times 10^{-3}$
Re(x$_-$), K_{e3} parameter		$(-2.9 \pm 2.0) \times 10^{-3}$
$\lvert m_{K^0} - m_{\overline{K}^0}\rvert$ / $m_{\rm average}$	[k]	$<6 \times 10^{-19}$, CL = 90%
$(\Gamma_{K^0} - \Gamma_{\overline{K}^0})/m_{\rm average}$		$(8 \pm 8) \times 10^{-18}$
phase difference $\phi_{00} - \phi_{+-}$		$(0.34 \pm 0.32)^\circ$
$\mathrm{Re}(\frac{2}{3}\eta_{+-} + \frac{1}{3}\eta_{00}) - \frac{A_L}{2}$		$(-3 \pm 35) \times 10^{-6}$
$A_{CPT}(D^0 \to K^-\pi^+)$		0.008 ± 0.008
ΔS^+_{CPT} ($S^-_{\ell^+,K^0_S} - S^+_{\ell^+,K^0_S}$)		0.16 ± 0.23
ΔS^-_{CPT} ($S^+_{\ell^+,K^0_S} - S^-_{\ell^+,K^0_S}$)		-0.03 ± 0.14
ΔC^+_{CPT} ($C^-_{\ell^+,K^0_S} - C^+_{\ell^+,K^0_S}$)		0.14 ± 0.17
ΔC^-_{CPT} ($C^+_{\ell^+,K^0_S} - C^-_{\ell^+,K^0_S}$)		0.03 ± 0.14
$\lvert m_p - m_{\overline{p}}\rvert/m_p$	[l]	$<7 \times 10^{-10}$, CL = 90%
$(\lvert\frac{q_{\overline{p}}}{m_{\overline{p}}}\rvert - \frac{q_p}{m_p})/\frac{q_p}{m_p}$		$(-9 \pm 9) \times 10^{-11}$
$\lvert q_p + q_{\overline{p}}\rvert/e$	[l]	$<7 \times 10^{-10}$, CL = 90%
$(\mu_p + \mu_{\overline{p}})$ / μ_p		$(0.3 \pm 0.8) \times 10^{-6}$
$(m_n - m_{\overline{n}})$/ m_n		$(9 \pm 6) \times 10^{-5}$
$(m_\Lambda - m_{\overline{\Lambda}})$ / m_Λ		$(-0.1 \pm 1.1) \times 10^{-5}$ (S = 1.6)
$(\tau_\Lambda - \tau_{\overline{\Lambda}})$ / τ_Λ		-0.001 ± 0.009
$(\tau_{\Sigma^+} - \tau_{\overline{\Sigma}^-})$ / τ_{Σ^+}		-0.0006 ± 0.0012
$(\mu_{\Sigma^+} + \mu_{\overline{\Sigma}^-})$ / μ_{Σ^+}		0.014 ± 0.015
$(m_{\Xi^-} - m_{\overline{\Xi}^+})$ / m_{Ξ^-}		$(-3 \pm 9) \times 10^{-5}$
$(\tau_{\Xi^-} - \tau_{\overline{\Xi}^+})$ / τ_{Ξ^-}		-0.01 ± 0.07
$(\mu_{\Xi^-} + \mu_{\overline{\Xi}^+})$ / $\lvert\mu_{\Xi^-}\rvert$		$+0.01 \pm 0.05$
$(m_{\Omega^-} - m_{\overline{\Omega}^+})$ / m_{Ω^-}		$(-1 \pm 8) \times 10^{-5}$
$(\tau_{\Omega^-} - \tau_{\overline{\Omega}^+})$ / τ_{Ω^-}		0.00 ± 0.05

TESTS OF NUMBER CONSERVATION LAWS

LEPTON FAMILY NUMBER

Lepton family number conservation means separate conservation of each of L_e, L_μ, L_τ.

$\Gamma(Z \to e^\pm\mu^\mp)/\Gamma_{\rm total}$	[n]	$<7.5 \times 10^{-7}$, CL = 95%
$\Gamma(Z \to e^\pm\tau^\mp)/\Gamma_{\rm total}$	[n]	$<9.8 \times 10^{-6}$, CL = 95%
$\Gamma(Z \to \mu^\pm\tau^\mp)/\Gamma_{\rm total}$	[n]	$<1.2 \times 10^{-5}$, CL = 95%
$\sigma(e^+e^- \to e^\pm\tau^\mp)$ / $\sigma(e^+e^- \to \mu^+\mu^-)$		$<8.9 \times 10^{-6}$, CL = 95%
$\sigma(e^+e^- \to \mu^\pm\tau^\mp)$ / $\sigma(e^+e^- \to \mu^+\mu^-)$		$<4.0 \times 10^{-6}$, CL = 95%
limit on $\mu^- \to e^-$ conversion		
$\sigma(\mu^- {}^{32}\mathrm{S} \to e^- {}^{32}\mathrm{S})$ / $\sigma(\mu^- {}^{32}\mathrm{S} \to \nu_\mu {}^{32}\mathrm{P}^*)$		$<7 \times 10^{-11}$, CL = 90%
$\sigma(\mu^-\mathrm{Ti} \to e^-\mathrm{Ti})$ / $\sigma(\mu^-\mathrm{Ti} \to \text{capture})$		$<4.3 \times 10^{-12}$, CL = 90%
$\sigma(\mu^-\mathrm{Pb} \to e^-\mathrm{Pb})$ / $\sigma(\mu^-\mathrm{Pb} \to \text{capture})$		$<4.6 \times 10^{-11}$, CL = 90%
limit on muonium $\to$ antimuonium conversion $R_g = G_C$ / G_F		<0.0030, CL = 90%
$\Gamma(\mu^- \to e^-\nu_e\overline{\nu}_\mu)/\Gamma_{\rm total}$	[o]	$<1.2 \times 10^{-2}$, CL = 90%
$\Gamma(\mu^- \to e^-\gamma)/\Gamma_{\rm total}$		$<4.2 \times 10^{-13}$, CL = 90%
$\Gamma(\mu^- \to e^-e^+e^-)/\Gamma_{\rm total}$		$<1.0 \times 10^{-12}$, CL = 90%
$\Gamma(\mu^- \to e^-2\gamma)/\Gamma_{\rm total}$		$<7.2 \times 10^{-11}$, CL = 90%
$\Gamma(\tau^- \to e^-\gamma)/\Gamma_{\rm total}$		$<3.3 \times 10^{-8}$, CL = 90%
$\Gamma(\tau^- \to \mu^-\gamma)/\Gamma_{\rm total}$		$<4.4 \times 10^{-8}$, CL = 90%
$\Gamma(\tau^- \to e^-\pi^0)/\Gamma_{\rm total}$		$<8.0 \times 10^{-8}$, CL = 90%
$\Gamma(\tau^- \to \mu^-\pi^0)/\Gamma_{\rm total}$		$<1.1 \times 10^{-7}$, CL = 90%
$\Gamma(\tau^- \to e^-K^0_S)/\Gamma_{\rm total}$		$<2.6 \times 10^{-8}$, CL = 90%
$\Gamma(\tau^- \to \mu^-K^0_S)/\Gamma_{\rm total}$		$<2.3 \times 10^{-8}$, CL = 90%
$\Gamma(\tau^- \to e^-\eta)/\Gamma_{\rm total}$		$<9.2 \times 10^{-8}$, CL = 90%
$\Gamma(\tau^- \to \mu^-\eta)/\Gamma_{\rm total}$		$<6.5 \times 10^{-8}$, CL = 90%
$\Gamma(\tau^- \to e^-\rho^0)/\Gamma_{\rm total}$		$<1.8 \times 10^{-8}$, CL = 90%
$\Gamma(\tau^- \to \mu^-\rho^0)/\Gamma_{\rm total}$		$<1.2 \times 10^{-8}$, CL = 90%
$\Gamma(\tau^- \to e^-\omega)/\Gamma_{\rm total}$		$<4.8 \times 10^{-8}$, CL = 90%
$\Gamma(\tau^- \to \mu^-\omega)/\Gamma_{\rm total}$		$<4.7 \times 10^{-8}$, CL = 90%
$\Gamma(\tau^- \to e^-K^*(892)^0)/\Gamma_{\rm total}$		$<3.2 \times 10^{-8}$, CL = 90%
$\Gamma(\tau^- \to \mu^-K^*(892)^0)/\Gamma_{\rm total}$		$<5.9 \times 10^{-8}$, CL = 90%
$\Gamma(\tau^- \to e^-\overline{K}^*(892)^0)/\Gamma_{\rm total}$		$<3.4 \times 10^{-8}$, CL = 90%
$\Gamma(\tau^- \to \mu^-\overline{K}^*(892)^0)/\Gamma_{\rm total}$		$<7.0 \times 10^{-8}$, CL = 90%
$\Gamma(\tau^- \to e^-\eta'(958))/\Gamma_{\rm total}$		$<1.6 \times 10^{-7}$, CL = 90%
$\Gamma(\tau^- \to \mu^-\eta'(958))/\Gamma_{\rm total}$		$<1.3 \times 10^{-7}$, CL = 90%
$\Gamma(\tau^- \to e^-f_0(980) \to e^-\pi^+\pi^-)/\Gamma_{\rm total}$		$<3.2 \times 10^{-8}$, CL = 90%
$\Gamma(\tau^- \to \mu^-f_0(980) \to \mu^-\pi^+\pi^-)/\Gamma_{\rm total}$		$<3.4 \times 10^{-8}$, CL = 90%
$\Gamma(\tau^- \to e^-\phi)/\Gamma_{\rm total}$		$<3.1 \times 10^{-8}$, CL = 90%
$\Gamma(\tau^- \to \mu^-\phi)/\Gamma_{\rm total}$		$<8.4 \times 10^{-8}$, CL = 90%
$\Gamma(\tau^- \to e^-e^+e^-)/\Gamma_{\rm total}$		$<2.7 \times 10^{-8}$, CL = 90%
$\Gamma(\tau^- \to e^-\mu^+\mu^-)/\Gamma_{\rm total}$		$<2.7 \times 10^{-8}$, CL = 90%
$\Gamma(\tau^- \to e^+\mu^-\mu^-)/\Gamma_{\rm total}$		$<1.7 \times 10^{-8}$, CL = 90%
$\Gamma(\tau^- \to \mu^-e^+e^-)/\Gamma_{\rm total}$		$<1.8 \times 10^{-8}$, CL = 90%
$\Gamma(\tau^- \to \mu^+e^-e^-)/\Gamma_{\rm total}$		$<1.5 \times 10^{-8}$, CL = 90%
$\Gamma(\tau^- \to \mu^-\mu^+\mu^-)/\Gamma_{\rm total}$		$<2.1 \times 10^{-8}$, CL = 90%
$\Gamma(\tau^- \to e^-\pi^+\pi^-)/\Gamma_{\rm total}$		$<2.3 \times 10^{-8}$, CL = 90%
$\Gamma(\tau^- \to \mu^-\pi^+\pi^-)/\Gamma_{\rm total}$		$<2.1 \times 10^{-8}$, CL = 90%
$\Gamma(\tau^- \to e^-\pi^+K^-)/\Gamma_{\rm total}$		$<3.7 \times 10^{-8}$, CL = 90%
$\Gamma(\tau^- \to e^-\pi^-K^+)/\Gamma_{\rm total}$		$<3.1 \times 10^{-8}$, CL = 90%
$\Gamma(\tau^- \to e^-K^0_SK^0_S)/\Gamma_{\rm total}$		$<7.1 \times 10^{-8}$, CL = 90%
$\Gamma(\tau^- \to e^-K^+K^-)/\Gamma_{\rm total}$		$<3.4 \times 10^{-8}$, CL = 90%
$\Gamma(\tau^- \to \mu^-\pi^+K^-)/\Gamma_{\rm total}$		$<8.6 \times 10^{-8}$, CL = 90%
$\Gamma(\tau^- \to \mu^-\pi^-K^+)/\Gamma_{\rm total}$		$<4.5 \times 10^{-8}$, CL = 90%
$\Gamma(\tau^- \to \mu^-K^0_SK^0_S)/\Gamma_{\rm total}$		$<8.0 \times 10^{-8}$, CL = 90%
$\Gamma(\tau^- \to \mu^-K^+K^-)/\Gamma_{\rm total}$		$<4.4 \times 10^{-8}$, CL = 90%
$\Gamma(\tau^- \to e^-\pi^0\pi^0)/\Gamma_{\rm total}$		$<6.5 \times 10^{-6}$, CL = 90%
$\Gamma(\tau^- \to \mu^-\pi^0\pi^0)/\Gamma_{\rm total}$		$<1.4 \times 10^{-5}$, CL = 90%
$\Gamma(\tau^- \to e^-\eta\eta)/\Gamma_{\rm total}$		$<3.5 \times 10^{-5}$, CL = 90%
$\Gamma(\tau^- \to \mu^-\eta\eta)/\Gamma_{\rm total}$		$<6.0 \times 10^{-5}$, CL = 90%
$\Gamma(\tau^- \to e^-\pi^0\eta)/\Gamma_{\rm total}$		$<2.4 \times 10^{-5}$, CL = 90%

Unless otherwise stated, limits are given at the 90% confidence level, while errors are given as ± 1 standard deviation.

$\Gamma(\tau^- \to \mu^- \pi^0 \eta)/\Gamma_{\text{total}}$		$<2.2 \times 10^{-5}$, CL = 90%
$\Gamma(\tau^- \to e^-$ light boson$)/\Gamma_{\text{total}}$		$<2.7 \times 10^{-3}$, CL = 95%
$\Gamma(\tau^- \to \mu^-$ light boson$)/\Gamma_{\text{total}}$		$<5 \times 10^{-3}$, CL = 95%

LEPTON FAMILY NUMBER VIOLATION IN NEUTRINOS

$\sin^2(\theta_{12})$		0.307 ± 0.013
Δm^2_{21}		$(7.53 \pm 0.18) \times 10^{-5}$ eV^2
$\sin^2(\theta_{23})$ (Inverted order, quad. I)		$0.421^{+0.033}_{-0.025}$ (S = 1.3)
$\sin^2(\theta_{23})$ (Inverted order, quad. II)		$0.592^{+0.023}_{-0.030}$ (S = 1.1)
$\sin^2(\theta_{23})$ (Normal order, quad. I)		$0.417^{+0.025}_{-0.028}$ (S = 1.2)
$\sin^2(\theta_{23})$ (Normal order, quad. II)		$0.597^{+0.024}_{-0.030}$ (S = 1.2)
Δm^2_{32} (Inverted order)		$(-2.56 \pm 0.04) \times 10^{-3}$ eV^2
Δm^2_{32} (Normal order)		$(2.51 \pm 0.05) \times 10^{-3}$ eV^2 (S = 1.1)
$\sin^2(\theta_{13})$		$(2.12 \pm 0.08) \times 10^{-2}$
$\Gamma(\pi^+ \to \mu^+ \nu_e)/\Gamma_{\text{total}}$	[p]	$<8.0 \times 10^{-3}$, CL = 90%
$\Gamma(\pi^+ \to \mu^- e^+ e^+ \nu)/\Gamma_{\text{total}}$		$<1.6 \times 10^{-6}$, CL = 90%
$\Gamma(\pi^0 \to \mu^+ e^-)/\Gamma_{\text{total}}$		$<3.8 \times 10^{-10}$, CL = 90%
$\Gamma(\pi^0 \to \mu^- e^+)/\Gamma_{\text{total}}$		$<3.4 \times 10^{-9}$, CL = 90%
$\Gamma(\pi^0 \to \mu^+ e^- + \mu^- e^+)/\Gamma_{\text{total}}$		$<3.6 \times 10^{-10}$, CL = 90%
$\Gamma(\eta \to \mu^+ e^- + \mu^- e^+)/\Gamma_{\text{total}}$		$<6 \times 10^{-6}$, CL = 90%
$\Gamma(\eta'(958) \to e\mu)/\Gamma_{\text{total}}$		$<4.7 \times 10^{-4}$, CL = 90%
$\Gamma(\phi(1020) \to e^\pm \mu^\mp)/\Gamma_{\text{total}}$		$<2 \times 10^{-6}$, CL = 90%
$\Gamma(K^+ \to \mu^- \nu e^+ e^+)/\Gamma_{\text{total}}$		$<2.1 \times 10^{-8}$, CL = 90%
$\Gamma(K^+ \to \mu^+ \nu_e)/\Gamma_{\text{total}}$	[p]	$<4 \times 10^{-3}$, CL = 90%
$\Gamma(K^+ \to \pi^+ \mu^+ e^-)/\Gamma_{\text{total}}$		$<1.3 \times 10^{-11}$, CL = 90%
$\Gamma(K^+ \to \pi^+ \mu^- e^+)/\Gamma_{\text{total}}$		$<5.2 \times 10^{-10}$, CL = 90%
$\Gamma(K^0_L \to e^\pm \mu^\mp)/\Gamma_{\text{total}}$	[n]	$<4.7 \times 10^{-12}$, CL = 90%
$\Gamma(K^0_L \to e^\pm e^\pm \mu^\mp \mu^\mp)/\Gamma_{\text{total}}$	[n]	$<4.12 \times 10^{-11}$, CL = 90%
$\Gamma(K^0_L \to \pi^0 \mu^\pm e^\mp)/\Gamma_{\text{total}}$	[n]	$<7.6 \times 10^{-11}$, CL = 90%
$\Gamma(K^0_L \to \pi^0 \pi^0 \mu^\pm e^\mp)/\Gamma_{\text{total}}$		$<1.7 \times 10^{-10}$, CL = 90%
$\Gamma(D^+ \to \pi^+ e^+ \mu^-)/\Gamma_{\text{total}}$		$<2.9 \times 10^{-6}$, CL = 90%
$\Gamma(D^+ \to \pi^+ e^- \mu^+)/\Gamma_{\text{total}}$		$<3.6 \times 10^{-6}$, CL = 90%
$\Gamma(D^+ \to K^+ e^+ \mu^-)/\Gamma_{\text{total}}$		$<1.2 \times 10^{-6}$, CL = 90%
$\Gamma(D^+ \to K^+ e^- \mu^+)/\Gamma_{\text{total}}$		$<2.8 \times 10^{-6}$, CL = 90%
$\Gamma(D^0 \to \mu^\pm e^\mp)/\Gamma_{\text{total}}$	[n]	$<1.3 \times 10^{-8}$, CL = 90%
$\Gamma(D^0 \to \pi^0 e^\pm \mu^\mp)/\Gamma_{\text{total}}$	[n]	$<8.6 \times 10^{-5}$, CL = 90%
$\Gamma(D^0 \to \eta e^\pm \mu^\mp)/\Gamma_{\text{total}}$	[n]	$<1.0 \times 10^{-4}$, CL = 90%
$\Gamma(D^0 \to \pi^+ \pi^- e^\pm \mu^\mp)/\Gamma_{\text{total}}$	[n]	$<1.5 \times 10^{-5}$, CL = 90%
$\Gamma(D^0 \to \rho^0 e^\pm \mu^\mp)/\Gamma_{\text{total}}$	[n]	$<4.9 \times 10^{-5}$, CL = 90%
$\Gamma(D^0 \to \omega e^\pm \mu^\mp)/\Gamma_{\text{total}}$	[n]	$<1.2 \times 10^{-4}$, CL = 90%
$\Gamma(D^0 \to K^- K^+ e^\pm \mu^\mp)/\Gamma_{\text{total}}$	[n]	$<1.8 \times 10^{-4}$, CL = 90%
$\Gamma(D^0 \to \phi e^\pm \mu^\mp)/\Gamma_{\text{total}}$	[n]	$<3.4 \times 10^{-5}$, CL = 90%
$\Gamma(D^0 \to \overline{K}^0 e^\pm \mu^\mp)/\Gamma_{\text{total}}$	[n]	$<1.0 \times 10^{-4}$, CL = 90%
$\Gamma(D^0 \to K^- \pi^+ e^\pm \mu^\mp)/\Gamma_{\text{total}}$	[n]	$<5.53 \times 10^{-4}$, CL = 90%
$\Gamma(D^0 \to \overline{K}^*(892)^0 e^\pm \mu^\mp)/\Gamma_{\text{total}}$	[n]	$<8.3 \times 10^{-5}$, CL = 90%
$\Gamma(D_s^+ \to \pi^+ e^+ \mu^-)/\Gamma_{\text{total}}$		$<1.2 \times 10^{-5}$, CL = 90%
$\Gamma(D_s^+ \to \pi^+ e^- \mu^+)/\Gamma_{\text{total}}$		$<2.0 \times 10^{-5}$, CL = 90%
$\Gamma(D_s^+ \to K^+ e^+ \mu^-)/\Gamma_{\text{total}}$		$<1.4 \times 10^{-5}$, CL = 90%
$\Gamma(D_s^+ \to K^+ e^- \mu^+)/\Gamma_{\text{total}}$		$<9.7 \times 10^{-6}$, CL = 90%
$\Gamma(B^+ \to \pi^+ e^+ \mu^-)/\Gamma_{\text{total}}$		$<6.4 \times 10^{-3}$, CL = 90%
$\Gamma(B^+ \to \pi^+ e^- \mu^+)/\Gamma_{\text{total}}$		$<6.4 \times 10^{-3}$, CL = 90%
$\Gamma(B^+ \to \pi^+ e^\pm \mu^\mp)/\Gamma_{\text{total}}$		$<1.7 \times 10^{-7}$, CL = 90%
$\Gamma(B^+ \to \pi^+ e^+ \tau^-)/\Gamma_{\text{total}}$		$<7.4 \times 10^{-5}$, CL = 90%
$\Gamma(B^+ \to \pi^+ e^- \tau^+)/\Gamma_{\text{total}}$		$<2.0 \times 10^{-5}$, CL = 90%
$\Gamma(B^+ \to \pi^+ e^\pm \tau^\mp)/\Gamma_{\text{total}}$		$<7.5 \times 10^{-5}$, CL = 90%
$\Gamma(B^+ \to \pi^+ \mu^+ \tau^-)/\Gamma_{\text{total}}$		$<6.2 \times 10^{-5}$, CL = 90%
$\Gamma(B^+ \to \pi^+ \mu^- \tau^+)/\Gamma_{\text{total}}$		$<4.5 \times 10^{-5}$, CL = 90%
$\Gamma(B^+ \to \pi^+ \mu^\pm \tau^\mp)/\Gamma_{\text{total}}$		$<7.2 \times 10^{-5}$, CL = 90%
$\Gamma(B^+ \to K^+ e^+ \mu^-)/\Gamma_{\text{total}}$		$<9.1 \times 10^{-8}$, CL = 90%
$\Gamma(B^+ \to K^+ e^- \mu^+)/\Gamma_{\text{total}}$		$<1.3 \times 10^{-7}$, CL = 90%
$\Gamma(B^+ \to K^+ e^\pm \mu^\mp)/\Gamma_{\text{total}}$		$<9.1 \times 10^{-8}$, CL = 90%
$\Gamma(B^+ \to K^+ e^+ \tau^-)/\Gamma_{\text{total}}$		$<4.3 \times 10^{-5}$, CL = 90%
$\Gamma(B^+ \to K^+ e^- \tau^+)/\Gamma_{\text{total}}$		$<1.5 \times 10^{-5}$, CL = 90%
$\Gamma(B^+ \to K^+ e^\pm \tau^\mp)/\Gamma_{\text{total}}$		$<3.0 \times 10^{-5}$, CL = 90%
$\Gamma(B^+ \to K^+ \mu^+ \tau^-)/\Gamma_{\text{total}}$		$<4.5 \times 10^{-5}$, CL = 90%
$\Gamma(B^+ \to K^+ \mu^- \tau^+)/\Gamma_{\text{total}}$		$<2.8 \times 10^{-5}$, CL = 90%
$\Gamma(B^+ \to K^+ \mu^\pm \tau^\mp)/\Gamma_{\text{total}}$		$<4.8 \times 10^{-5}$, CL = 90%
$\Gamma(B^+ \to K^*(892)^+ e^+ \mu^-)/\Gamma_{\text{total}}$		$<1.3 \times 10^{-6}$, CL = 90%
$\Gamma(B^+ \to K^*(892)^+ e^- \mu^+)/\Gamma_{\text{total}}$		$<9.9 \times 10^{-7}$, CL = 90%
$\Gamma(B^+ \to K^*(892)^+ e^\pm \mu^\mp)/\Gamma_{\text{total}}$		$<1.4 \times 10^{-6}$, CL = 90%
$\Gamma(B^0 \to e^\pm \mu^\mp)/\Gamma_{\text{total}}$	[n]	$<2.8 \times 10^{-9}$, CL = 90%
$\Gamma(B^0 \to \pi^0 e^\pm \mu^\mp)/\Gamma_{\text{total}}$		$<1.4 \times 10^{-7}$, CL = 90%
$\Gamma(B^0 \to K^0 e^\pm \mu^\mp)/\Gamma_{\text{total}}$		$<2.7 \times 10^{-7}$, CL = 90%
$\Gamma(B^0 \to K^*(892)^0 e^+ \mu^-)/\Gamma_{\text{total}}$		$<5.3 \times 10^{-7}$, CL = 90%
$\Gamma(B^0 \to K^*(892)^0 e^- \mu^+)/\Gamma_{\text{total}}$		$<3.4 \times 10^{-7}$, CL = 90%
$\Gamma(B^0 \to K^*(892)^0 e^\pm \mu^\mp)/\Gamma_{\text{total}}$		$<5.8 \times 10^{-7}$, CL = 90%
$\Gamma(B^0 \to e^\pm \tau^\mp)/\Gamma_{\text{total}}$	[n]	$<2.8 \times 10^{-5}$, CL = 90%
$\Gamma(B^0 \to \mu^\pm \tau^\mp)/\Gamma_{\text{total}}$	[n]	$<2.2 \times 10^{-5}$, CL = 90%
$\Gamma(B \to s e^\pm \mu^\mp)/\Gamma_{\text{total}}$	[n]	$<2.2 \times 10^{-5}$, CL = 90%
$\Gamma(B \to \pi e^\pm \mu^\mp)/\Gamma_{\text{total}}$		$<9.2 \times 10^{-8}$, CL = 90%
$\Gamma(B \to \rho e^\pm \mu^\mp)/\Gamma_{\text{total}}$		$<3.2 \times 10^{-6}$, CL = 90%
$\Gamma(B \to K e^\pm \mu^\mp)/\Gamma_{\text{total}}$		$<3.8 \times 10^{-8}$, CL = 90%
$\Gamma(B \to K^*(892) e^\pm \mu^\mp)/\Gamma_{\text{total}}$		$<5.1 \times 10^{-7}$, CL = 90%
$\Gamma(B^0_s \to e^\pm \mu^\mp)/\Gamma_{\text{total}}$	[n]	$<1.1 \times 10^{-8}$, CL = 90%
$\Gamma(J/\psi(1S) \to e^\pm \mu^\mp)/\Gamma_{\text{total}}$		$<1.6 \times 10^{-7}$, CL = 90%
$\Gamma(J/\psi(1S) \to e^\pm \tau^\mp)/\Gamma_{\text{total}}$		$<8.3 \times 10^{-6}$, CL = 90%
$\Gamma(J/\psi(1S) \to \mu^\pm \tau^\mp)/\Gamma_{\text{total}}$		$<2.0 \times 10^{-6}$, CL = 90%
$\Gamma(\Upsilon(1S) \to \mu^\pm \tau^\mp)/\Gamma_{\text{total}}$		$<6.0 \times 10^{-6}$, CL = 95%
$\Gamma(\Upsilon(2S) \to e^\pm \tau^\mp)/\Gamma_{\text{total}}$		$<3.2 \times 10^{-6}$, CL = 90%
$\Gamma(\Upsilon(2S) \to \mu^\pm \tau^\mp)/\Gamma_{\text{total}}$		$<3.3 \times 10^{-6}$, CL = 90%
$\Gamma(\Upsilon(3S) \to e^\pm \tau^\mp)/\Gamma_{\text{total}}$		$<4.2 \times 10^{-6}$, CL = 90%
$\Gamma(\Upsilon(3S) \to \mu^\pm \tau^\mp)/\Gamma_{\text{total}}$		$<3.1 \times 10^{-6}$, CL = 90%
$\Gamma(\Lambda_c^+ \to p e^+ \mu^-)/\Gamma_{\text{total}}$		$<9.9 \times 10^{-6}$, CL = 90%
$\Gamma(\Lambda_c^+ \to p e^- \mu^+)/\Gamma_{\text{total}}$		$<1.9 \times 10^{-5}$, CL = 90%

TOTAL LEPTON NUMBER

Violation of total lepton number conservation also implies violation of lepton family number conservation.

$\Gamma(Z \to pe)/\Gamma_{\text{total}}$		$<1.8 \times 10^{-6}$, CL = 95%
$\Gamma(Z \to p\mu)/\Gamma_{\text{total}}$		$<1.8 \times 10^{-6}$, CL = 95%
limit on $\mu^- \to e^+$ conversion		
$\sigma(\mu^- {}^{32}\text{S} \to e^+ {}^{32}\text{Si}^*)$ / $\sigma(\mu^- {}^{32}\text{S} \to \nu_\mu {}^{32}\text{P}^*)$		$<9 \times 10^{-10}$, CL = 90%
$\sigma(\mu^- {}^{127}\text{I} \to e^+ {}^{127}\text{Sb}^*)$ / $\sigma(\mu^- {}^{127}\text{I} \to$ anything$)$		$<3 \times 10^{-10}$, CL = 90%
$\sigma(\mu^- \text{Ti} \to e^+ \text{Ca})$ / $\sigma(\mu^- \text{Ti} \to$ capture$)$		$<3.6 \times 10^{-11}$, CL = 90%
$\Gamma(\tau^- \to e^+ \pi^- \pi^-)/\Gamma_{\text{total}}$		$<2.0 \times 10^{-8}$, CL = 90%
$\Gamma(\tau^- \to \mu^+ \pi^- \pi^-)/\Gamma_{\text{total}}$		$<3.9 \times 10^{-8}$, CL = 90%
$\Gamma(\tau^- \to e^+ \pi^- K^-)/\Gamma_{\text{total}}$		$<3.2 \times 10^{-8}$, CL = 90%
$\Gamma(\tau^- \to e^+ K^- K^-)/\Gamma_{\text{total}}$		$<3.3 \times 10^{-8}$, CL = 90%
$\Gamma(\tau^- \to \mu^+ \pi^- K^-)/\Gamma_{\text{total}}$		$<4.8 \times 10^{-8}$, CL = 90%
$\Gamma(\tau^- \to \mu^+ K^- K^-)/\Gamma_{\text{total}}$		$<4.7 \times 10^{-8}$, CL = 90%
$\Gamma(\tau^- \to p \mu^- \mu^-)/\Gamma_{\text{total}}$		$<4.4 \times 10^{-7}$, CL = 90%
$\Gamma(\tau^- \to \overline{p} \mu^+ \mu^-)/\Gamma_{\text{total}}$		$<3.3 \times 10^{-7}$, CL = 90%
$\Gamma(\tau^- \to \overline{p}\gamma)/\Gamma_{\text{total}}$		$<3.5 \times 10^{-6}$, CL = 90%
$\Gamma(\tau^- \to \overline{p}\pi^0)/\Gamma_{\text{total}}$		$<1.5 \times 10^{-5}$, CL = 90%
$\Gamma(\tau^- \to \overline{p} 2\pi^0)/\Gamma_{\text{total}}$		$<3.3 \times 10^{-5}$, CL = 90%
$\Gamma(\tau^- \to \overline{p}\eta)/\Gamma_{\text{total}}$		$<8.9 \times 10^{-6}$, CL = 90%
$\Gamma(\tau^- \to \overline{p}\pi^0 \eta)/\Gamma_{\text{total}}$		$<2.7 \times 10^{-5}$, CL = 90%
$\Gamma(\tau^- \to \Lambda \pi^-)/\Gamma_{\text{total}}$		$<7.2 \times 10^{-8}$, CL = 90%
$\Gamma(\tau^- \to \overline{\Lambda} \pi^-)/\Gamma_{\text{total}}$		$<1.4 \times 10^{-7}$, CL = 90%
$t_{1/2}(\,{}^{76}\text{Ge} \to {}^{76}\text{Se} + 2\,e^-\,)$		$>1.9 \times 10^{25}$ yr, CL = 90%
$\Gamma(\pi^+ \to \mu^+ \overline{\nu}_e)/\Gamma_{\text{total}}$	[p]	$<1.5 \times 10^{-3}$, CL = 90%
$\Gamma(K^+ \to \pi^- \mu^+ e^+)/\Gamma_{\text{total}}$		$<5.0 \times 10^{-10}$, CL = 90%
$\Gamma(K^+ \to \pi^- e^+ e^+)/\Gamma_{\text{total}}$		$<6.4 \times 10^{-10}$, CL = 90%
$\Gamma(K^+ \to \pi^- \mu^+ \mu^+)/\Gamma_{\text{total}}$	[p]	$<8.6 \times 10^{-11}$, CL = 90%
$\Gamma(K^+ \to \mu^+ \overline{\nu}_e)/\Gamma_{\text{total}}$	[p]	$<3.3 \times 10^{-3}$, CL = 90%
$\Gamma(K^+ \to \pi^0 e^+ \overline{\nu}_e)/\Gamma_{\text{total}}$		$<3 \times 10^{-3}$, CL = 90%
$\Gamma(D^+ \to \pi^- 2e^+)/\Gamma_{\text{total}}$		$<1.1 \times 10^{-6}$, CL = 90%
$\Gamma(D^+ \to \pi^- 2\mu^+)/\Gamma_{\text{total}}$		$<2.2 \times 10^{-8}$, CL = 90%
$\Gamma(D^+ \to \pi^- e^+ \mu^+)/\Gamma_{\text{total}}$		$<2.0 \times 10^{-6}$, CL = 90%
$\Gamma(D^+ \to \rho^- 2\mu^+)/\Gamma_{\text{total}}$		$<5.6 \times 10^{-4}$, CL = 90%
$\Gamma(D^+ \to K^- 2e^+)/\Gamma_{\text{total}}$		$<9 \times 10^{-7}$, CL = 90%
$\Gamma(D^+ \to K^- 2\mu^+)/\Gamma_{\text{total}}$		$<1.0 \times 10^{-5}$, CL = 90%
$\Gamma(D^+ \to K^- e^+ \mu^+)/\Gamma_{\text{total}}$		$<1.9 \times 10^{-6}$, CL = 90%
$\Gamma(D^+ \to K^*(892)^- 2\mu^+)/\Gamma_{\text{total}}$		$<8.5 \times 10^{-4}$, CL = 90%
$\Gamma(D^0 \to 2\pi^- 2e^+ + \text{c.c.})/\Gamma_{\text{total}}$		$<1.12 \times 10^{-4}$, CL = 90%
$\Gamma(D^0 \to 2\pi^- 2\mu^+ + \text{c.c.})/\Gamma_{\text{total}}$		$<2.9 \times 10^{-5}$, CL = 90%
$\Gamma(D^0 \to K^- \pi^- 2e^+ + \text{c.c.})/\Gamma_{\text{total}}$		$<2.06 \times 10^{-4}$, CL = 90%

Unless otherwise stated, limits are given at the 90% confidence level, while errors are given as ± 1 standard deviation.

Tests of Conservation Laws

$\Gamma(D^0 \to K^-\pi^-2\mu^+ + \text{c.c.})/\Gamma_{\text{total}}$		$<3.9\times10^{-4}$, CL = 90%
$\Gamma(D^0 \to 2K^-2e^+ + \text{c.c.})/\Gamma_{\text{total}}$		$<1.52\times10^{-4}$, CL = 90%
$\Gamma(D^0 \to 2K^-2\mu^+ + \text{c.c.})/\Gamma_{\text{total}}$		$<9.4\times10^{-5}$, CL = 90%
$\Gamma(D^0 \to \pi^-\pi^-e^+\mu^+ + \text{c.c.})/\Gamma_{\text{total}}$		$<7.9\times10^{-5}$, CL = 90%
$\Gamma(D^0 \to K^-\pi^-e^+\mu^+ + \text{c.c.})/\Gamma_{\text{total}}$		$<2.18\times10^{-4}$, CL = 90%
$\Gamma(D^0 \to 2K^-e^+\mu^+ + \text{c.c.})/\Gamma_{\text{total}}$		$<5.7\times10^{-5}$, CL = 90%
$\Gamma(D^0 \to pe^-)/\Gamma_{\text{total}}$	[q]	$<1.0\times10^{-5}$, CL = 90%
$\Gamma(D^0 \to \overline{p}e^+)/\Gamma_{\text{total}}$	[r]	$<1.1\times10^{-5}$, CL = 90%
$\Gamma(D_s^+ \to \pi^-2e^+)/\Gamma_{\text{total}}$		$<4.1\times10^{-6}$, CL = 90%
$\Gamma(D_s^+ \to \pi^-2\mu^+)/\Gamma_{\text{total}}$		$<1.2\times10^{-7}$, CL = 90%
$\Gamma(D_s^+ \to \pi^-e^+\mu^+)/\Gamma_{\text{total}}$		$<8.4\times10^{-6}$, CL = 90%
$\Gamma(D_s^+ \to K^-2e^+)/\Gamma_{\text{total}}$		$<5.2\times10^{-6}$, CL = 90%
$\Gamma(D_s^+ \to K^-2\mu^+)/\Gamma_{\text{total}}$		$<1.3\times10^{-5}$, CL = 90%
$\Gamma(D_s^+ \to K^-e^+\mu^+)/\Gamma_{\text{total}}$		$<6.1\times10^{-6}$, CL = 90%
$\Gamma(D_s^+ \to K^*(892)^-2\mu^+)/\Gamma_{\text{total}}$		$<1.4\times10^{-3}$, CL = 90%
$\Gamma(B^+ \to \pi^-e^+e^+)/\Gamma_{\text{total}}$		$<2.3\times10^{-8}$, CL = 90%
$\Gamma(B^+ \to \pi^-\mu^+\mu^+)/\Gamma_{\text{total}}$		$<4.0\times10^{-9}$, CL = 95%
$\Gamma(B^+ \to \pi^-e^+\mu^+)/\Gamma_{\text{total}}$		$<1.5\times10^{-7}$, CL = 90%
$\Gamma(B^+ \to \rho^-e^+e^+)/\Gamma_{\text{total}}$		$<1.7\times10^{-7}$, CL = 90%
$\Gamma(B^+ \to \rho^-\mu^+\mu^+)/\Gamma_{\text{total}}$		$<4.2\times10^{-7}$, CL = 90%
$\Gamma(B^+ \to \rho^-e^+\mu^+)/\Gamma_{\text{total}}$		$<4.7\times10^{-7}$, CL = 90%
$\Gamma(B^+ \to K^-e^+e^+)/\Gamma_{\text{total}}$		$<3.0\times10^{-8}$, CL = 90%
$\Gamma(B^+ \to K^-\mu^+\mu^+)/\Gamma_{\text{total}}$		$<4.1\times10^{-8}$, CL = 90%
$\Gamma(B^+ \to K^-e^+\mu^+)/\Gamma_{\text{total}}$		$<1.6\times10^{-7}$, CL = 90%
$\Gamma(B^+ \to K^*(892)^-e^+e^+)/\Gamma_{\text{total}}$		$<4.0\times10^{-7}$, CL = 90%
$\Gamma(B^+ \to K^*(892)^-\mu^+\mu^+)/\Gamma_{\text{total}}$		$<5.9\times10^{-7}$, CL = 90%
$\Gamma(B^+ \to K^*(892)^-e^+\mu^+)/\Gamma_{\text{total}}$		$<3.0\times10^{-7}$, CL = 90%
$\Gamma(B^+ \to D^-e^+e^+)/\Gamma_{\text{total}}$		$<2.6\times10^{-6}$, CL = 90%
$\Gamma(B^+ \to D^-e^+\mu^+)/\Gamma_{\text{total}}$		$<1.8\times10^{-6}$, CL = 90%
$\Gamma(B^+ \to D^-\mu^+\mu^+)/\Gamma_{\text{total}}$		$<6.9\times10^{-7}$, CL = 95%
$\Gamma(B^+ \to D^{*-}\mu^+\mu^+)/\Gamma_{\text{total}}$		$<2.4\times10^{-6}$, CL = 95%
$\Gamma(B^+ \to D_s^-\mu^+\mu^+)/\Gamma_{\text{total}}$		$<5.8\times10^{-7}$, CL = 95%
$\Gamma(B^+ \to \overline{D}^0\pi^-\mu^+\mu^+)/\Gamma_{\text{total}}$		$<1.5\times10^{-6}$, CL = 95%
$\Gamma(B^+ \to \Lambda^0\mu^+)/\Gamma_{\text{total}}$		$<6\times10^{-8}$, CL = 90%
$\Gamma(B^+ \to \Lambda^0e^+)/\Gamma_{\text{total}}$		$<3.2\times10^{-8}$, CL = 90%
$\Gamma(B^+ \to \overline{\Lambda}^0\mu^+)/\Gamma_{\text{total}}$		$<6\times10^{-8}$, CL = 90%
$\Gamma(B^+ \to \overline{\Lambda}^0e^+)/\Gamma_{\text{total}}$		$<8\times10^{-8}$, CL = 90%
$\Gamma(B^0 \to \Lambda_c^+\mu^-)/\Gamma_{\text{total}}$		$<1.4\times10^{-6}$, CL = 90%
$\Gamma(B^0 \to \Lambda_c^+e^-)/\Gamma_{\text{total}}$		$<4\times10^{-6}$, CL = 90%
$\Gamma(\Lambda \to \pi^+e^-)/\Gamma_{\text{total}}$		$<6\times10^{-7}$, CL = 90%
$\Gamma(\Lambda \to \pi^+\mu^-)/\Gamma_{\text{total}}$		$<6\times10^{-7}$, CL = 90%
$\Gamma(\Lambda \to \pi^-e^+)/\Gamma_{\text{total}}$		$<4\times10^{-7}$, CL = 90%
$\Gamma(\Lambda \to \pi^-\mu^+)/\Gamma_{\text{total}}$		$<6\times10^{-7}$, CL = 90%
$\Gamma(\Lambda \to K^+e^-)/\Gamma_{\text{total}}$		$<2\times10^{-6}$, CL = 90%
$\Gamma(\Lambda \to K^+\mu^-)/\Gamma_{\text{total}}$		$<3\times10^{-6}$, CL = 90%
$\Gamma(\Lambda \to K^-e^+)/\Gamma_{\text{total}}$		$<2\times10^{-6}$, CL = 90%
$\Gamma(\Lambda \to K^-\mu^+)/\Gamma_{\text{total}}$		$<3\times10^{-6}$, CL = 90%
$\Gamma(\Lambda \to K_S^0\nu)/\Gamma_{\text{total}}$		$<2\times10^{-5}$, CL = 90%
$\Gamma(\Lambda \to \overline{p}\pi^+)/\Gamma_{\text{total}}$		$<9\times10^{-7}$, CL = 90%
$\Gamma(\Lambda_c^+ \to \overline{p}2e^+)/\Gamma_{\text{total}}$		$<2.7\times10^{-6}$, CL = 90%
$\Gamma(\Lambda_c^+ \to \overline{p}2\mu^+)/\Gamma_{\text{total}}$		$<9.4\times10^{-6}$, CL = 90%
$\Gamma(\Lambda_c^+ \to \overline{p}e^+\mu^+)/\Gamma_{\text{total}}$		$<1.6\times10^{-5}$, CL = 90%

BARYON NUMBER

$\Gamma(Z \to pe)/\Gamma_{\text{total}}$		$<1.8\times10^{-6}$, CL = 95%
$\Gamma(Z \to p\mu)/\Gamma_{\text{total}}$		$<1.8\times10^{-6}$, CL = 95%
$\Gamma(\tau^- \to p\mu^-\mu^-)/\Gamma_{\text{total}}$		$<4.4\times10^{-7}$, CL = 90%
$\Gamma(\tau^- \to \overline{p}\mu^+\mu^-)/\Gamma_{\text{total}}$		$<3.3\times10^{-7}$, CL = 90%
$\Gamma(\tau^- \to \overline{p}\gamma)/\Gamma_{\text{total}}$		$<3.5\times10^{-6}$, CL = 90%
$\Gamma(\tau^- \to \overline{p}\pi^0)/\Gamma_{\text{total}}$		$<1.5\times10^{-5}$, CL = 90%
$\Gamma(\tau^- \to \overline{p}2\pi^0)/\Gamma_{\text{total}}$		$<3.3\times10^{-5}$, CL = 90%
$\Gamma(\tau^- \to \overline{p}\eta)/\Gamma_{\text{total}}$		$<8.9\times10^{-6}$, CL = 90%
$\Gamma(\tau^- \to \overline{p}\pi^0\eta)/\Gamma_{\text{total}}$		$<2.7\times10^{-5}$, CL = 90%
$\Gamma(\tau^- \to \Lambda\pi^-)/\Gamma_{\text{total}}$		$<7.2\times10^{-8}$, CL = 90%
$\Gamma(\tau^- \to \overline{\Lambda}\pi^-)/\Gamma_{\text{total}}$		$<1.4\times10^{-7}$, CL = 90%
$\Gamma(D^0 \to pe^-)/\Gamma_{\text{total}}$	[q]	$<1.0\times10^{-5}$, CL = 90%
$\Gamma(D^0 \to \overline{p}e^+)/\Gamma_{\text{total}}$	[r]	$<1.1\times10^{-5}$, CL = 90%

Unless otherwise stated, limits are given at the 90% confidence level, while errors are given as ±1 standard deviation.

$\Gamma(B^+ \to \Lambda^0\mu^+)/\Gamma_{\text{total}}$		$<6\times10^{-8}$, CL = 90%
$\Gamma(B^+ \to \Lambda^0e^+)/\Gamma_{\text{total}}$		$<3.2\times10^{-8}$, CL = 90%
$\Gamma(B^+ \to \overline{\Lambda}^0\mu^+)/\Gamma_{\text{total}}$		$<6\times10^{-8}$, CL = 90%
$\Gamma(B^+ \to \overline{\Lambda}^0e^+)/\Gamma_{\text{total}}$		$<8\times10^{-8}$, CL = 90%
$\Gamma(B^0 \to \Lambda_c^+\mu^-)/\Gamma_{\text{total}}$		$<1.4\times10^{-6}$, CL = 90%
$\Gamma(B^0 \to \Lambda_c^+e^-)/\Gamma_{\text{total}}$		$<4\times10^{-6}$, CL = 90%
p mean life	[s]	$>2.1\times10^{29}$ years, CL = 90%

A few examples of proton or bound neutron decay follow. For limits on many other nucleon decay channels, see the Baryon Summary Table.

$\tau(N \to e^+\pi)$		$>$ 2000 (n), $>$ 8200 (p) $\times10^{30}$ years, CL = 90%
$\tau(N \to \mu^+\pi)$		$>$ 1000 (n), $>$ 6600 (p) $\times10^{30}$ years, CL = 90%
$\tau(N \to e^+K)$		$>$ 17 (n), $>$ 1000 (p) $\times10^{30}$ years, CL = 90%
$\tau(N \to \mu^+K)$		$>$ 26 (n), $>$ 1600 (p) $\times10^{30}$ years, CL = 90%
limit on $n\overline{n}$ oscillations (free n)		$>0.86\times10^8$ s, CL = 90%
limit on $n\overline{n}$ oscillations (bound n)	[t]	$>1.3\times10^8$ s, CL = 90%
$\Gamma(\Lambda \to \pi^+e^-)/\Gamma_{\text{total}}$		$<6\times10^{-7}$, CL = 90%
$\Gamma(\Lambda \to \pi^+\mu^-)/\Gamma_{\text{total}}$		$<6\times10^{-7}$, CL = 90%
$\Gamma(\Lambda \to \pi^-e^+)/\Gamma_{\text{total}}$		$<4\times10^{-7}$, CL = 90%
$\Gamma(\Lambda \to \pi^-\mu^+)/\Gamma_{\text{total}}$		$<6\times10^{-7}$, CL = 90%
$\Gamma(\Lambda \to K^+e^-)/\Gamma_{\text{total}}$		$<2\times10^{-6}$, CL = 90%
$\Gamma(\Lambda \to K^+\mu^-)/\Gamma_{\text{total}}$		$<3\times10^{-6}$, CL = 90%
$\Gamma(\Lambda \to K^-e^+)/\Gamma_{\text{total}}$		$<2\times10^{-6}$, CL = 90%
$\Gamma(\Lambda \to K^-\mu^+)/\Gamma_{\text{total}}$		$<3\times10^{-6}$, CL = 90%
$\Gamma(\Lambda \to K_S^0\nu)/\Gamma_{\text{total}}$		$<2\times10^{-5}$, CL = 90%
$\Gamma(\Lambda \to \overline{p}\pi^+)/\Gamma_{\text{total}}$		$<9\times10^{-7}$, CL = 90%
$\Gamma(\Lambda_c^+ \to \overline{p}2e^+)/\Gamma_{\text{total}}$		$<2.7\times10^{-6}$, CL = 90%
$\Gamma(\Lambda_c^+ \to \overline{p}2\mu^+)/\Gamma_{\text{total}}$		$<9.4\times10^{-6}$, CL = 90%
$\Gamma(\Lambda_c^+ \to \overline{p}e^+\mu^+)/\Gamma_{\text{total}}$		$<1.6\times10^{-5}$, CL = 90%

ELECTRIC CHARGE (Q)

$e \to \nu_e\gamma$ and astrophysical limits	[u]	$>6.6\times10^{28}$ yr, CL = 90%
$\Gamma(n \to p\nu_e\overline{\nu}_e)/\Gamma_{\text{total}}$		$<8\times10^{-27}$, CL = 68%

$\Delta S = \Delta Q$ RULE

Violations allowed in second-order weak interactions.

$\Gamma(K^+ \to \pi^+\pi^+e^-\overline{\nu}_e)/\Gamma_{\text{total}}$		$<1.3\times10^{-8}$, CL = 90%
$\Gamma(K^+ \to \pi^+\pi^+\mu^-\overline{\nu}_\mu)/\Gamma_{\text{total}}$		$<3.0\times10^{-6}$, CL = 95%
Re(x_+), K_{e3} parameter		$(-0.9\pm3.0)\times10^{-3}$
$x = \text{A}(\overline{K}^0 \to \pi^-\ell^+\nu)/\text{A}(K^0 \to \pi^-\ell^+\nu) = \text{A}(\Delta S{=}-\Delta Q)/\text{A}(\Delta S{=}\Delta Q)$		
real part of x		-0.002 ± 0.006
imaginary part of x		0.0012 ± 0.0021
$\Gamma(\Sigma^+ \to n\ell^+\nu)/\Gamma(\Sigma^- \to n\ell^-\overline{\nu})$		<0.043
$\Gamma(\Sigma^+ \to ne^+\nu_e)/\Gamma_{\text{total}}$		$<5\times10^{-6}$, CL = 90%
$\Gamma(\Sigma^+ \to n\mu^+\nu_\mu)/\Gamma_{\text{total}}$		$<3.0\times10^{-5}$, CL = 90%
$\Gamma(\Xi^0 \to \Sigma^-e^+\nu_e)/\Gamma_{\text{total}}$		$<9\times10^{-4}$, CL = 90%
$\Gamma(\Xi^0 \to \Sigma^-\mu^+\nu_\mu)/\Gamma_{\text{total}}$		$<9\times10^{-4}$, CL = 90%

$\Delta S = 2$ FORBIDDEN

Allowed in second-order weak interactions.

$\Gamma(\Xi^0 \to p\pi^-)/\Gamma_{\text{total}}$		$<8\times10^{-6}$, CL = 90%
$\Gamma(\Xi^0 \to pe^-\overline{\nu}_e)/\Gamma_{\text{total}}$		$<1.3\times10^{-3}$
$\Gamma(\Xi^0 \to p\mu^-\overline{\nu}_\mu)/\Gamma_{\text{total}}$		$<1.3\times10^{-3}$
$\Gamma(\Xi^- \to n\pi^-)/\Gamma_{\text{total}}$		$<1.9\times10^{-5}$, CL = 90%
$\Gamma(\Xi^- \to ne^-\overline{\nu}_e)/\Gamma_{\text{total}}$		$<3.2\times10^{-3}$, CL = 90%
$\Gamma(\Xi^- \to n\mu^-\overline{\nu}_\mu)/\Gamma_{\text{total}}$		$<1.5\times10^{-2}$, CL = 90%
$\Gamma(\Xi^- \to p\pi^-\pi^-)/\Gamma_{\text{total}}$		$<4\times10^{-4}$, CL = 90%
$\Gamma(\Xi^- \to p\pi^-e^-\overline{\nu}_e)/\Gamma_{\text{total}}$		$<4\times10^{-4}$, CL = 90%
$\Gamma(\Xi^- \to p\pi^-\mu^-\overline{\nu}_\mu)/\Gamma_{\text{total}}$		$<4\times10^{-4}$, CL = 90%
$\Gamma(\Omega^- \to \Lambda\pi^-)/\Gamma_{\text{total}}$		$<2.9\times10^{-6}$, CL = 90%

$\Delta S = 2$ VIA MIXING

Allowed in second-order weak interactions, e.g. mixing.

$m_{K_L^0} - m_{K_S^0}$	$(0.5293 \pm 0.0009) \times 10^{10}\ \hbar\ \mathrm{s}^{-1}$ (S = 1.3)
$m_{K_L^0} - m_{K_S^0}$	$(3.484 \pm 0.006) \times 10^{-12}$ MeV

$\Delta C = 2$ VIA MIXING

Allowed in second-order weak interactions, e.g. mixing.

$\lvert m_{D_1^0} - m_{D_2^0}\rvert = x\Gamma$	$(0.95^{+0.41}_{-0.44}) \times 10^{10}\ \hbar\ \mathrm{s}^{-1}$
$(\Gamma_{D_1^0} - \Gamma_{D_2^0})/\Gamma = 2y$	$(1.29^{+0.14}_{-0.18}) \times 10^{-2}$

$\Delta B = 2$ VIA MIXING

Allowed in second-order weak interactions, e.g. mixing.

χ_d	0.1860 ± 0.0011
$\Delta m_{B^0} = m_{B_H^0} - m_{B_L^0}$	$(0.5064 \pm 0.0019) \times 10^{12}\ \hbar\ \mathrm{s}^{-1}$
$x_d = \Delta m_{B^0}/\Gamma_{B^0}$	0.770 ± 0.004
$\Delta m_{B_s^0} = m_{B_{sH}^0} - m_{B_{sL}^0}$	$(17.757 \pm 0.021) \times 10^{12}\ \hbar\ \mathrm{s}^{-1}$
$x_s = \Delta m_{B_s^0}/\Gamma_{B_s^0}$	26.72 ± 0.09
χ_s	0.499304 ± 0.000005

$\Delta S = 1$ WEAK NEUTRAL CURRENT FORBIDDEN

Allowed by higher-order electroweak interactions.

$\Gamma(K^+ \to \pi^+ e^+ e^-)/\Gamma_{\text{total}}$		$(3.00 \pm 0.09) \times 10^{-7}$
$\Gamma(K^+ \to \pi^+ \mu^+ \mu^-)/\Gamma_{\text{total}}$		$(9.4 \pm 0.6) \times 10^{-8}$ (S = 2.6)
$\Gamma(K^+ \to \pi^+ \nu\overline{\nu})/\Gamma_{\text{total}}$		$(1.7 \pm 1.1) \times 10^{-10}$
$\Gamma(K^+ \to \pi^+ \pi^0 \nu\overline{\nu})/\Gamma_{\text{total}}$		$<4.3 \times 10^{-5}$, CL = 90%
$\Gamma(K_S^0 \to \mu^+ \mu^-)/\Gamma_{\text{total}}$		$<8 \times 10^{-10}$, CL = 90%
$\Gamma(K_S^0 \to e^+ e^-)/\Gamma_{\text{total}}$		$<9 \times 10^{-9}$, CL = 90%
$\Gamma(K_S^0 \to \pi^0 e^+ e^-)/\Gamma_{\text{total}}$	[v]	$(3.0^{+1.5}_{-1.2}) \times 10^{-9}$
$\Gamma(K_S^0 \to \pi^0 \mu^+ \mu^-)/\Gamma_{\text{total}}$		$(2.9^{+1.5}_{-1.2}) \times 10^{-9}$
$\Gamma(K_L^0 \to \mu^+ \mu^-)/\Gamma_{\text{total}}$		$(6.84 \pm 0.11) \times 10^{-9}$
$\Gamma(K_L^0 \to e^+ e^-)/\Gamma_{\text{total}}$		$(9^{+6}_{-4}) \times 10^{-12}$
$\Gamma(K_L^0 \to \pi^+ \pi^- e^+ e^-)/\Gamma_{\text{total}}$	[x]	$(3.11 \pm 0.19) \times 10^{-7}$
$\Gamma(K_L^0 \to \pi^0 \pi^0 e^+ e^-)/\Gamma_{\text{total}}$		$<6.6 \times 10^{-9}$, CL = 90%
$\Gamma(K_L^0 \to \pi^0 \pi^0 \mu^+ \mu^-)/\Gamma_{\text{total}}$		$<9.2 \times 10^{-11}$, CL = 90%
$\Gamma(K_L^0 \to \mu^+ \mu^- e^+ e^-)/\Gamma_{\text{total}}$		$(2.69 \pm 0.27) \times 10^{-9}$
$\Gamma(K_L^0 \to e^+ e^- e^+ e^-)/\Gamma_{\text{total}}$		$(3.56 \pm 0.21) \times 10^{-8}$
$\Gamma(K_L^0 \to \pi^0 \mu^+ \mu^-)/\Gamma_{\text{total}}$		$<3.8 \times 10^{-10}$, CL = 90%
$\Gamma(K_L^0 \to \pi^0 e^+ e^-)/\Gamma_{\text{total}}$		$<2.8 \times 10^{-10}$, CL = 90%
$\Gamma(K_L^0 \to \pi^0 \nu\overline{\nu})/\Gamma_{\text{total}}$		$<2.6 \times 10^{-8}$, CL = 90%
$\Gamma(K_L^0 \to \pi^0 \pi^0 \nu\overline{\nu})/\Gamma_{\text{total}}$		$<8.1 \times 10^{-7}$, CL = 90%
$\Gamma(\Sigma^+ \to p e^+ e^-)/\Gamma_{\text{total}}$		$<7 \times 10^{-6}$
$\Gamma(\Sigma^+ \to p \mu^+ \mu^-)/\Gamma_{\text{total}}$		$(9^{+9}_{-8}) \times 10^{-8}$

$\Delta C = 1$ WEAK NEUTRAL CURRENT FORBIDDEN

Allowed by higher-order electroweak interactions.

$\Gamma(D^+ \to \pi^+ e^+ e^-)/\Gamma_{\text{total}}$	$<1.1 \times 10^{-6}$, CL = 90%
$\Gamma(D^+ \to \pi^+ \mu^+ \mu^-)/\Gamma_{\text{total}}$	$<7.3 \times 10^{-8}$, CL = 90%
$\Gamma(D^+ \to \rho^+ \mu^+ \mu^-)/\Gamma_{\text{total}}$	$<5.6 \times 10^{-4}$, CL = 90%
$\Gamma(D^0 \to \gamma\gamma)/\Gamma_{\text{total}}$	$<8.5 \times 10^{-7}$, CL = 90%
$\Gamma(D^0 \to e^+ e^-)/\Gamma_{\text{total}}$	$<7.9 \times 10^{-8}$, CL = 90%
$\Gamma(D^0 \to \mu^+ \mu^-)/\Gamma_{\text{total}}$	$<6.2 \times 10^{-9}$, CL = 90%
$\Gamma(D^0 \to \pi^0 e^+ e^-)/\Gamma_{\text{total}}$	$<4.5 \times 10^{-5}$, CL = 90%
$\Gamma(D^0 \to \pi^0 \mu^+ \mu^-)/\Gamma_{\text{total}}$	$<1.8 \times 10^{-4}$, CL = 90%
$\Gamma(D^0 \to \eta e^+ e^-)/\Gamma_{\text{total}}$	$<1.1 \times 10^{-4}$, CL = 90%
$\Gamma(D^0 \to \eta \mu^+ \mu^-)/\Gamma_{\text{total}}$	$<5.3 \times 10^{-4}$, CL = 90%
$\Gamma(D^0 \to \pi^+ \pi^- e^+ e^-)/\Gamma_{\text{total}}$	$<3.73 \times 10^{-4}$, CL = 90%
$\Gamma(D^0 \to \rho^0 e^+ e^-)/\Gamma_{\text{total}}$	$<1.0 \times 10^{-4}$, CL = 90%
$\Gamma(D^0 \to \pi^+ \pi^- \mu^+ \mu^-)/\Gamma_{\text{total}}$	$(9.6 \pm 1.2) \times 10^{-7}$
$\Gamma(D^0 \to \rho^0 \mu^+ \mu^-)/\Gamma_{\text{total}}$	$<2.2 \times 10^{-5}$, CL = 90%
$\Gamma(D^0 \to \omega e^+ e^-)/\Gamma_{\text{total}}$	$<1.8 \times 10^{-4}$, CL = 90%
$\Gamma(D^0 \to \omega \mu^+ \mu^-)/\Gamma_{\text{total}}$	$<8.3 \times 10^{-4}$, CL = 90%
$\Gamma(D^0 \to K^- K^+ e^+ e^-)/\Gamma_{\text{total}}$	$<3.15 \times 10^{-4}$, CL = 90%
$\Gamma(D^0 \to \phi e^+ e^-)/\Gamma_{\text{total}}$	$<5.2 \times 10^{-5}$, CL = 90%
$\Gamma(D^0 \to K^- K^+ \mu^+ \mu^-)/\Gamma_{\text{total}}$	$(1.54 \pm 0.32) \times 10^{-7}$
$\Gamma(D^0 \to \phi \mu^+ \mu^-)/\Gamma_{\text{total}}$	$<3.1 \times 10^{-5}$, CL = 90%
$\Gamma(D^0 \to K^- \pi^+ e^+ e^-)/\Gamma_{\text{total}}$	$<3.85 \times 10^{-4}$, CL = 90%
$\Gamma(D^0 \to K^- \pi^+ \mu^+ \mu^-)/\Gamma_{\text{total}}$	$<3.59 \times 10^{-4}$, CL = 90%
$\Gamma(D^0 \to \pi^+ \pi^- \pi^0 \mu^+ \mu^-)/\Gamma_{\text{total}}$	$<8.1 \times 10^{-4}$, CL = 90%
$\Gamma(D_s^+ \to K^+ e^+ e^-)/\Gamma_{\text{total}}$	$<3.7 \times 10^{-6}$, CL = 90%
$\Gamma(D_s^+ \to K^+ \mu^+ \mu^-)/\Gamma_{\text{total}}$	$<2.1 \times 10^{-5}$, CL = 90%
$\Gamma(D_s^+ \to K^*(892)^+ \mu^+ \mu^-)/\Gamma_{\text{total}}$	$<1.4 \times 10^{-3}$, CL = 90%
$\Gamma(\Lambda_c^+ \to p e^+ e^-)/\Gamma_{\text{total}}$	$<5.5 \times 10^{-6}$, CL = 90%
$\Gamma(\Lambda_c^+ \to p \mu^+ \mu^-)/\Gamma_{\text{total}}$	$<4.4 \times 10^{-5}$, CL = 90%

$\Delta B = 1$ WEAK NEUTRAL CURRENT FORBIDDEN

Allowed by higher-order electroweak interactions.

$\Gamma(B^+ \to \pi^+ \ell^+ \ell^-)/\Gamma_{\text{total}}$		$<4.9 \times 10^{-8}$, CL = 90%
$\Gamma(B^+ \to \pi^+ e^+ e^-)/\Gamma_{\text{total}}$		$<8.0 \times 10^{-8}$, CL = 90%
$\Gamma(B^+ \to \pi^+ \mu^+ \mu^-)/\Gamma_{\text{total}}$		$(1.76 \pm 0.23) \times 10^{-8}$
$\Gamma(B^+ \to \pi^+ \nu\overline{\nu})/\Gamma_{\text{total}}$		$<1.4 \times 10^{-5}$, CL = 90%
$\Gamma(B^+ \to K^+ \ell^+ \ell^-)/\Gamma_{\text{total}}$	[y]	$(4.51 \pm 0.23) \times 10^{-7}$ (S = 1.1)
$\Gamma(B^+ \to K^+ e^+ e^-)/\Gamma_{\text{total}}$		$(5.5 \pm 0.7) \times 10^{-7}$
$\Gamma(B^+ \to K^+ \mu^+ \mu^-)/\Gamma_{\text{total}}$		$(4.41 \pm 0.23) \times 10^{-7}$ (S = 1.2)
$\Gamma(B^+ \to K^+ \mu^+ \mu^-\text{nonresonant})/\Gamma_{\text{total}}$		$(4.37 \pm 0.27) \times 10^{-7}$
$\Gamma(B^+ \to K^+ \tau^+ \tau^-)/\Gamma_{\text{total}}$		$<2.25 \times 10^{-3}$, CL = 90%
$\Gamma(B^+ \to K^+ \overline{\nu}\nu)/\Gamma_{\text{total}}$		$<1.6 \times 10^{-5}$, CL = 90%
$\Gamma(B^+ \to \rho^+ \nu\overline{\nu})/\Gamma_{\text{total}}$		$<3.0 \times 10^{-5}$, CL = 90%
$\Gamma(B^+ \to K^*(892)^+ \ell^+ \ell^-)/\Gamma_{\text{total}}$	[y]	$(1.01 \pm 0.11) \times 10^{-6}$ (S = 1.1)
$\Gamma(B^+ \to K^*(892)^+ e^+ e^-)/\Gamma_{\text{total}}$		$(1.55^{+0.40}_{-0.31}) \times 10^{-6}$
$\Gamma(B^+ \to K^*(892)^+ \mu^+ \mu^-)/\Gamma_{\text{total}}$		$(9.6 \pm 1.0) \times 10^{-7}$
$\Gamma(B^+ \to K^*(892)^+ \nu\overline{\nu})/\Gamma_{\text{total}}$		$<4.0 \times 10^{-5}$, CL = 90%
$\Gamma(B^+ \to K^+ \pi^+ \pi^- \mu^+ \mu^-)/\Gamma_{\text{total}}$		$(4.3 \pm 0.4) \times 10^{-7}$
$\Gamma(B^+ \to \phi K^+ \mu^+ \mu^-)/\Gamma_{\text{total}}$		$(7.9^{+2.1}_{-1.7}) \times 10^{-8}$
$\Gamma(B^0 \to \gamma\gamma)/\Gamma_{\text{total}}$		$<3.2 \times 10^{-7}$, CL = 90%
$\Gamma(B^0 \to e^+ e^-)/\Gamma_{\text{total}}$		$<8.3 \times 10^{-8}$, CL = 90%
$\Gamma(B^0 \to e^+ e^- \gamma)/\Gamma_{\text{total}}$		$<1.2 \times 10^{-7}$, CL = 90%
$\Gamma(B^0 \to \mu^+ \mu^-)/\Gamma_{\text{total}}$		$(1.6^{+1.6}_{-1.4}) \times 10^{-10}$ (S = 1.9)
$\Gamma(B^0 \to \mu^+ \mu^- \gamma)/\Gamma_{\text{total}}$		$<1.6 \times 10^{-7}$, CL = 90%
$\Gamma(B^0 \to \mu^+ \mu^- \mu^+ \mu^-)/\Gamma_{\text{total}}$		$<6.9 \times 10^{-10}$, CL = 95%
$\Gamma(B^0 \to SP,\ S \to \mu^+ \mu^-,\ P \to \mu^+ \mu^-)/\Gamma_{\text{total}}$	[z]	$<6.0 \times 10^{-10}$, CL = 95%
$\Gamma(B^0 \to \tau^+ \tau^-)/\Gamma_{\text{total}}$		$<2.1 \times 10^{-3}$, CL = 95%
$\Gamma(B^0 \to \pi^0 \ell^+ \ell^-)/\Gamma_{\text{total}}$		$<5.3 \times 10^{-8}$, CL = 90%
$\Gamma(B^0 \to \pi^0 e^+ e^-)/\Gamma_{\text{total}}$		$<8.4 \times 10^{-8}$, CL = 90%
$\Gamma(B^0 \to \pi^0 \mu^+ \mu^-)/\Gamma_{\text{total}}$		$<6.9 \times 10^{-8}$, CL = 90%
$\Gamma(B^0 \to \eta \ell^+ \ell^-)/\Gamma_{\text{total}}$		$<6.4 \times 10^{-8}$, CL = 90%
$\Gamma(B^0 \to \eta e^+ e^-)/\Gamma_{\text{total}}$		$<1.08 \times 10^{-7}$, CL = 90%
$\Gamma(B^0 \to \eta \mu^+ \mu^-)/\Gamma_{\text{total}}$		$<1.12 \times 10^{-7}$, CL = 90%
$\Gamma(B^0 \to \pi^0 \nu\overline{\nu})/\Gamma_{\text{total}}$		$<9 \times 10^{-6}$, CL = 90%
$\Gamma(B^0 \to K^0 \ell^+ \ell^-)/\Gamma_{\text{total}}$	[y]	$(3.1^{+0.8}_{-0.7}) \times 10^{-7}$
$\Gamma(B^0 \to K^0 e^+ e^-)/\Gamma_{\text{total}}$		$(1.6^{+1.0}_{-0.8}) \times 10^{-7}$
$\Gamma(B^0 \to K^0 \mu^+ \mu^-)/\Gamma_{\text{total}}$		$(3.39 \pm 0.34) \times 10^{-7}$
$\Gamma(B^0 \to K^0 \nu\overline{\nu})/\Gamma_{\text{total}}$		$<2.6 \times 10^{-5}$, CL = 90%
$\Gamma(B^0 \to \rho^0 \nu\overline{\nu})/\Gamma_{\text{total}}$		$<4.0 \times 10^{-5}$, CL = 90%
$\Gamma(B^0 \to K^*(892)^0 \ell^+ \ell^-)/\Gamma_{\text{total}}$	[y]	$(9.9^{+1.2}_{-1.1}) \times 10^{-7}$
$\Gamma(B^0 \to K^*(892)^0 e^+ e^-)/\Gamma_{\text{total}}$		$(1.03^{+0.19}_{-0.17}) \times 10^{-6}$
$\Gamma(B^0 \to K^*(892)^0 \mu^+ \mu^-)/\Gamma_{\text{total}}$		$(9.4 \pm 0.5) \times 10^{-7}$
$\Gamma(B^0 \to K^*(892)^0 \chi,\ \chi \to \mu^+ \mu^-)/\Gamma_{\text{total}}$		—
$\Gamma(B^0 \to \pi^+ \pi^- \mu^+ \mu^-)/\Gamma_{\text{total}}$		$(2.1 \pm 0.5) \times 10^{-8}$
$\Gamma(B^0 \to K^*(892)^0 \nu\overline{\nu})/\Gamma_{\text{total}}$		$<1.8 \times 10^{-5}$, CL = 90%
$\Gamma(B^0 \to \text{invisible})/\Gamma_{\text{total}}$		$<2.4 \times 10^{-5}$, CL = 90%
$\Gamma(B^0 \to \nu\overline{\nu}\gamma)/\Gamma_{\text{total}}$		$<1.7 \times 10^{-5}$, CL = 90%

Unless otherwise stated, limits are given at the 90% confidence level, while errors are given as ± 1 standard deviation.

Tests of Conservation Laws

$\Gamma(B^0 \to \phi\nu\overline{\nu})/\Gamma_{\rm total}$		$<1.27\times10^{-4}$, CL = 90%
$\Gamma(B \to s e^+ e^-)/\Gamma_{\rm total}$		$(6.7\pm1.7)\times10^{-6}$ (S = 2.0)
$\Gamma(B \to s\mu^+\mu^-)/\Gamma_{\rm total}$		$(4.3\pm1.0)\times10^{-6}$
$\Gamma(B \to s\ell^+\ell^-)/\Gamma_{\rm total}$	[y]	$(5.8\pm1.3)\times10^{-6}$ (S = 1.8)
$\Gamma(B \to \pi\ell^+\ell^-)/\Gamma_{\rm total}$		$<5.9\times10^{-8}$, CL = 90%
$\Gamma(B \to \pi e^+ e^-)/\Gamma_{\rm total}$		$<1.10\times10^{-7}$, CL = 90%
$\Gamma(B \to \pi\mu^+\mu^-)/\Gamma_{\rm total}$		$<5.0\times10^{-8}$, CL = 90%
$\Gamma(B \to K e^+ e^-)/\Gamma_{\rm total}$		$(4.4\pm0.6)\times10^{-7}$
$\Gamma(B \to K^*(892) e^+ e^-)/\Gamma_{\rm total}$		$(1.19\pm0.20)\times10^{-6}$ (S = 1.2)
$\Gamma(B \to K\mu^+\mu^-)/\Gamma_{\rm total}$		$(4.4\pm0.4)\times10^{-7}$
$\Gamma(B \to K^*(892)\mu^+\mu^-)/\Gamma_{\rm total}$		$(1.06\pm0.09)\times10^{-6}$
$\Gamma(B \to K\ell^+\ell^-)/\Gamma_{\rm total}$		$(4.8\pm0.4)\times10^{-7}$
$\Gamma(B \to K^*(892)\ell^+\ell^-)/\Gamma_{\rm total}$		$(1.05\pm0.10)\times10^{-6}$
$\Gamma(B \to K\nu\overline{\nu})/\Gamma_{\rm total}$		$<1.6\times10^{-5}$, CL = 90%
$\Gamma(B \to K^*\nu\overline{\nu})/\Gamma_{\rm total}$		$<2.7\times10^{-5}$, CL = 90%
$\Gamma(B \to \pi\nu\overline{\nu})/\Gamma_{\rm total}$		$<8\times10^{-6}$, CL = 90%
$\Gamma(B \to \rho\nu\overline{\nu})/\Gamma_{\rm total}$		$<2.8\times10^{-5}$, CL = 90%
$\Gamma(\overline{b} \to \overline{s}\overline{\nu}\nu)/\Gamma_{\rm total}$		$<6.4\times10^{-4}$, CL = 90%
$\Gamma(\overline{b} \to e^+ e^-$ anything$)/\Gamma_{\rm total}$		—
$\Gamma(\overline{b} \to \mu^+\mu^-$ anything$)/\Gamma_{\rm total}$		$<3.2\times10^{-4}$, CL = 90%
$\Gamma(\overline{b} \to \nu\overline{\nu}$ anything$)/\Gamma_{\rm total}$		—
$\Gamma(B_s^0 \to \gamma\gamma)/\Gamma_{\rm total}$		$<3.1\times10^{-6}$, CL = 90%
$\Gamma(B_s^0 \to \phi\gamma)/\Gamma_{\rm total}$		$(3.4\pm0.4)\times10^{-5}$
$\Gamma(B_s^0 \to \mu^+\mu^-)/\Gamma_{\rm total}$		$(2.7^{+0.6}_{-0.5})\times10^{-9}$ (S = 1.2)
$\Gamma(B_s^0 \to e^+ e^-)/\Gamma_{\rm total}$		$<2.8\times10^{-7}$, CL = 90%
$\Gamma(B_s^0 \to \tau^+\tau^-)/\Gamma_{\rm total}$		$<6.8\times10^{-3}$, CL = 95%
$\Gamma(B_s^0 \to \mu^+\mu^-\mu^+\mu^-)/\Gamma_{\rm total}$		$<2.5\times10^{-9}$, CL = 95%
$\Gamma(B_s^0 \to SP,\ S \to \mu^+\mu^-,\ P \to \mu^+\mu^-)/\Gamma_{\rm total}$	[z]	$<2.2\times10^{-9}$, CL = 95%
$\Gamma(B_s^0 \to \phi(1020)\mu^+\mu^-)/\Gamma_{\rm total}$		$(8.2\pm1.2)\times10^{-7}$
$\Gamma(B_s^0 \to \pi^+\pi^-\mu^+\mu^-)/\Gamma_{\rm total}$		$(8.4\pm1.7)\times10^{-8}$
$\Gamma(B_s^0 \to \phi\nu\overline{\nu})/\Gamma_{\rm total}$		$<5.4\times10^{-3}$, CL = 90%

$\Delta T = 1$ WEAK NEUTRAL CURRENT FORBIDDEN

Allowed by higher-order electroweak interactions.

$\Gamma(t \to Zq(q{=}u,c))/\Gamma_{\rm total}$	[aa]	$<5\times10^{-4}$, CL = 95%
$\Gamma(t \to Hu)/\Gamma_{\rm total}$		$<2.4\times10^{-3}$, CL = 95%
$\Gamma(t \to Hc)/\Gamma_{\rm total}$		$<2.2\times10^{-3}$, CL = 95%
$\Gamma(t \to \ell^+\overline{q}q'(q{=}d,s,b;\ q'{=}u,c))/\Gamma_{\rm total}$		$<1.6\times10^{-3}$, CL = 95%

NOTES

In this Summary Table:

When a quantity has "(S = ...)" to its right, the error on the quantity has been enlarged by the "scale factor" S, defined as $S = \sqrt{\chi^2/(N-1)}$, where N is the number of measurements used in calculating the quantity. We do this when S > 1, which often indicates that the measurements are inconsistent. When S > 1.25, we also show in the Particle Listings an ideogram of the measurements. For more about S, see the Introduction.

[a] C parity forbids this to occur as a single-photon process.

[b] See the Particle Listings for the (complicated) definition of this quantity.

[c] Time-reversal invariance requires this to be 0° or 180°.

[d] This coefficient is zero if time invariance is not violated.

[e] Allowed by higher-order electroweak interactions.

[f] Violates CP in leading order. Test of direct CP violation since the indirect CP-violating and CP-conserving contributions are expected to be suppressed.

[g] In the 2010 *Review*, the values for these quantities were given using a measure of the asymmetry that was inconsistent with the usual definition.

[h] $\mathrm{Re}(\epsilon'/\epsilon) = \epsilon'/\epsilon$ to a very good approximation provided the phases satisfy CPT invariance.

[i] This mode includes gammas from inner bremsstrahlung but not the direct emission mode $K_L^0 \to \pi^+\pi^-\gamma$(DE).

[j] Neglecting photon channels. See, *e.g.*, A. Pais and S.B. Treiman, Phys. Rev. **D12**, 2744 (1975).

[k] Derived from measured values of ϕ_{+-}, ϕ_{00}, $|\eta|$, $|m_{K_L^0} - m_{K_S^0}|$, and $\tau_{K_S^0}$, as described in the introduction to "Tests of Conservation Laws."

[l] The $|m_p - m_{\overline{p}}|/m_p$ and $|q_p + q_{\overline{p}}|/e$ are not independent, and both use the more precise measurement of $|q_{\overline{p}}/m_{\overline{p}}|/(q_p/m_p)$.

[n] The value is for the sum of the charge states or particle/antiparticle states indicated.

[o] A test of additive vs. multiplicative lepton family number conservation.

[p] Derived from an analysis of neutrino-oscillation experiments.

[q] This limit is for either D^0 or $\overline{D}^0$ to $p e^-$.

[r] This limit is for either D^0 or $\overline{D}^0$ to $\overline{p} e^+$.

[s] The first limit is for $p \to$ anything or "disappearance" modes of a bound proton. The second entry, a rough range of limits, assumes the dominant decay modes are among those investigated. For antiprotons the best limit, inferred from the observation of cosmic ray $\overline{p}$'s is $\tau_{\overline{p}} > 10^7$ yr, the cosmic-ray storage time, but this limit depends on a number of assumptions. The best direct observation of stored antiprotons gives $\tau_{\overline{p}}/\mathrm{B}(\overline{p} \to e^-\gamma) > 7\times10^5$ yr.

[t] There is some controversy about whether nuclear physics and model dependence complicate the analysis for bound neutrons (from which the best limit comes). The first limit here is from reactor experiments with free neutrons.

[u] This is the best limit for the mode $e^- \to \nu\gamma$. The best limit for "electron disappearance" is 6.4×10^{24} yr.

[v] See the K_S^0 Particle Listings for the energy limits used in this measurement.

[x] See the K_L^0 Particle Listings for the energy limits used in this measurement.

[y] An ℓ indicates an e or a μ mode, not a sum over these modes.

[z] Here S and P are the hypothetical scalar and pseudoscalar particles with masses of 2.5 GeV/c^2 and 214.3 MeV/c^2, respectively.

[aa] This limit is for $\Gamma(t \to Zq)/\Gamma(t \to Wb)$.

REVIEWS, TABLES, AND PLOTS

(Continued on next page.)

1. Physical Constants

Table 1.1. Reviewed 2015 by P.J. Mohr and D.B. Newell (NIST). Mainly from the "CODATA Recommended Values of the Fundamental Physical Constants: 2014" by P.J. Mohr, D.B. Newell, and B.N. Taylor in Rev. Mod. Phys. **88**, 035009 (2016). The last set of constants (beginning with the Fermi coupling constant) comes from the Particle Data Group and is the only set updated for this 2018 edition. The figures in parentheses after the values give the 1-standard-deviation uncertainties in the last digits; the corresponding fractional uncertainties in parts per 10^9 (ppb) are given in the last column. This set of constants (aside from the last group) is recommended for international use by CODATA (the Committee on Data for Science and Technology). The full 2014 CODATA set of constants may be found at `http://physics.nist.gov/constants`. See also P.J. Mohr and D.B. Newell, "Resource Letter FC-1: The Physics of Fundamental Constants," Am. J. Phys. **78**, 338 (2010).

Quantity	Symbol, equation	Value	Uncertainty (ppb)
speed of light in vacuum	c	299 792 458 m s^{-1}	exact*
Planck constant	h	$6.626\ 070\ 040(81)\times10^{-34}$ J s	12
Planck constant, reduced	$\hbar \equiv h/2\pi$	$1.054\ 571\ 800(13)\times10^{-34}$ J s	12
		$= 6.582\ 119\ 514(40)\times10^{-22}$ MeV s	6.1
electron charge magnitude	e	$1.602\ 176\ 6208(98)\times10^{-19}$ C $= 4.803\ 204\ 673(30)\times10^{-10}$ esu	6.1, 6.1
conversion constant	$\hbar c$	197.326 9788(12) MeV fm	6.1
conversion constant	$(\hbar c)^2$	0.389 379 3656(48) GeV^2 mbarn	12
electron mass	m_e	$0.510\ 998\ 9461(31)$ MeV$/c^2 = 9.109\ 383\ 56(11)\times10^{-31}$ kg	6.2, 12
proton mass	m_p	$938.272\ 0813(58)$ MeV$/c^2 = 1.672\ 621\ 898(21)\times10^{-27}$ kg	6.2, 12
		$= 1.007\ 276\ 466\ 879(91)$ u $= 1836.152\ 673\ 89(17)\ m_e$	0.090, 0.095
deuteron mass	m_d	1875.612 928(12) MeV$/c^2$	6.2
unified atomic mass unit (u)	(mass ^{12}C atom)/12 = (1 g)/(N_A mol)	931.494 0954(57) MeV$/c^2 = 1.660\ 539\ 040(20)\times10^{-27}$ kg	6.2, 12
permittivity of free space	$\epsilon_0 = 1/\mu_0 c^2$	$8.854\ 187\ 817\ \ldots\ \times10^{-12}$ F m^{-1}	exact
permeability of free space	μ_0	$4\pi \times 10^{-7}$ N $A^{-2} = 12.566\ 370\ 614\ \ldots\ \times10^{-7}$ N A^{-2}	exact
fine-structure constant	$\alpha = e^2/4\pi\epsilon_0\hbar c$	$7.297\ 352\ 5664(17)\times10^{-3} = 1/137.035\ 999\ 139(31)$†	0.23, 0.23
classical electron radius	$r_e = e^2/4\pi\epsilon_0 m_e c^2$	$2.817\ 940\ 3227(19)\times10^{-15}$ m	0.68
(e^- Compton wavelength)/2π	$\lambda\!\!\!^{-}_e = \hbar/m_e c = r_e\alpha^{-1}$	$3.861\ 592\ 6764(18)\times10^{-13}$ m	0.45
Bohr radius ($m_{\rm nucleus} = \infty$)	$a_\infty = 4\pi\epsilon_0\hbar^2/m_e e^2 = r_e\alpha^{-2}$	$0.529\ 177\ 210\ 67(12)\times10^{-10}$ m	0.23
wavelength of 1 eV/c particle	hc/(1 eV)	$1.239\ 841\ 9739(76)\times10^{-6}$ m	6.1
Rydberg energy	$hcR_\infty = m_e e^4/2(4\pi\epsilon_0)^2\hbar^2 = m_e c^2\alpha^2/2$	13.605 693 009(84) eV	6.1
Thomson cross section	$\sigma_T = 8\pi r_e^2/3$	0.665 245 871 58(91) barn	1.4
Bohr magneton	$\mu_B = e\hbar/2m_e$	$5.788\ 381\ 8012(26)\times10^{-11}$ MeV T^{-1}	0.45
nuclear magneton	$\mu_N = e\hbar/2m_p$	$3.152\ 451\ 2550(15)\times10^{-14}$ MeV T^{-1}	0.46
electron cyclotron freq./field	$\omega^e_{\rm cycl}/B = e/m_e$	$1.758\ 820\ 024(11)\times10^{11}$ rad s^{-1} T^{-1}	6.2
proton cyclotron freq./field	$\omega^p_{\rm cycl}/B = e/m_p$	$9.578\ 833\ 226(59)\times10^{7}$ rad s^{-1} T^{-1}	6.2
gravitational constant‡	G_N	$6.674\ 08(31)\times10^{-11}$ m^3 kg^{-1} s^{-2}	4.7×10^4
		$= 6.708\ 61(31)\times10^{-39}\ \hbar c\ (\mathrm{GeV}/c^2)^{-2}$	4.7×10^4
standard gravitational accel.	g_N	9.806 65 m s^{-2}	exact
Avogadro constant	N_A	$6.022\ 140\ 857(74)\times10^{23}$ mol^{-1}	12
Boltzmann constant	k	$1.380\ 648\ 52(79)\times10^{-23}$ J K^{-1}	570
		$= 8.617\ 3303(50)\times10^{-5}$ eV K^{-1}	570
molar volume, ideal gas at STP	$N_A k$(273.15 K)/(101 325 Pa)	$22.413\ 962(13)\times10^{-3}$ m^3 mol^{-1}	570
Wien displacement law constant	$b = \lambda_{\rm max}T$	$2.897\ 7729(17)\times10^{-3}$ m K	570
Stefan-Boltzmann constant	$\sigma = \pi^2k^4/60\hbar^3c^2$	$5.670\ 367(13)\times10^{-8}$ W m^{-2} K^{-4}	2300
Fermi coupling constant**	$G_F/(\hbar c)^3$	$1.166\ 378\ 7(6)\times10^{-5}$ GeV^{-2}	510
weak-mixing angle	$\sin^2\widehat{\theta}(M_Z)$ ($\overline{\rm MS}$)	0.231 22(4)††	1.7×10^5
$W^\pm$ boson mass	m_W	80.379(12) GeV$/c^2$	1.5×10^5
Z^0 boson mass	m_Z	91.1876(21) GeV$/c^2$	2.3×10^4
strong coupling constant	$\alpha_s(m_Z)$	0.1181(11)	9.3×10^6

$\pi = 3.141\ 592\ 653\ 589\ 793\ 238$ e $= 2.718\ 281\ 828\ 459\ 045\ 235$ $\gamma = 0.577\ 215\ 664\ 901\ 532\ 861$

1 in $\equiv 0.0254$ m 1 G $\equiv 10^{-4}$ T 1 eV $= 1.602\ 176\ 6208(98)\times10^{-19}$ J kT at 300 K $= [38.681\ 740(22)]^{-1}$ eV

1 Å $\equiv 0.1$ nm 1 dyne $\equiv 10^{-5}$ N 1 eV$/c^2 = 1.782\ 661\ 907(11)\times10^{-36}$ kg 0 °C $\equiv 273.15$ K

1 barn $\equiv 10^{-28}$ m^2 1 erg $\equiv 10^{-7}$ J $2.997\ 924\ 58\times10^9$ esu $= 1$ C 1 atmosphere $\equiv 760$ Torr $\equiv 101\ 325$ Pa

* The meter is the length of the path traveled by light in vacuum during a time interval of 1/299 792 458 of a second.
† At $Q^2 = 0$. At $Q^2 \approx m_W^2$ the value is $\sim 1/128$.
‡ Absolute lab measurements of G_N have been made only on scales of about 1 cm to 1 m.
** See the discussion in Sec. 10, "Electroweak model and constraints on new physics."
†† The corresponding $\sin^2\theta$ for the effective angle is 0.23155(4).

2. Astrophysical Constants and Parameters

Table 2.1. Revised October 2017 by D.E. Groom (LBNL) and D. Scott (University of British Columbia). The figures in parentheses after some values give the 1-σ uncertainties in the last digit(s). Physical constants are from Ref. 1. While every effort has been made to obtain the most accurate current values of the listed quantities, the table does not represent a critical review or adjustment of the constants, and is not intended as a primary reference. The values and uncertainties for the cosmological parameters depend on the exact data sets, priors, and basis parameters used in the fit. Many of the derived parameters reported in this table have non-Gaussian likelihoods. Parameters may be highly correlated, so care must be taken in propagating errors. Unless otherwise specified, cosmological parameters are derived from a 6-parameter ΛCDM cosmology fit to *Planck* 2015 temperature (TT) + low ℓ polarization (lowP) + lensing data [2]. For more information see Ref. 3 and the original papers.

Quantity	Symbol, equation	Value	Reference, footnote
Newtonian constant of gravitation	G_N	$6.674\,08(31) \times 10^{-11}$ m^3 kg^{-1} s^{-2}	[1]
Planck mass	$\sqrt{\hbar c/G_N}$	$1.220\,910(29) \times 10^{19}$ GeV/c^2 = $2.176\,47(5) \times 10^{-8}$ kg	[1]
Planck length	$\sqrt{\hbar G_N/c^3}$	$1.616\,229(38) \times 10^{-35}$ m	[1]
tropical year (equinox to equinox) (2011)	yr	31 556 925.2 s $\approx \pi \times 10^7$ s	[4]
sidereal year (fixed star to fixed star) (2011)		31 558 149.8 s $\approx \pi \times 10^7$ s	[4]
mean sidereal day (2011) (time between vernal equinox transits)		$23^{\rm h}\,56^{\rm m}\,04^{\rm s}.090\,53$	[4]
astronomical unit	au	149 597 870 700 m	exact[5]
parsec (1 au/1 arc sec)	pc	$3.085\,677\,581\,49 \times 10^{16}$ m = 3.262 . . . ly	exact[6]
light year (deprecated unit)	ly	0.306 6 . . . pc = 0.946 053 . . . $\times 10^{16}$ m	
Solar mass	$M_\odot$	$1.988\,48(9) \times 10^{30}$ kg	[7]
Schwarzschild radius of the Sun	$2G_N M_\odot/c^2$	2.953 250 24 km	[8]
nominal Solar equatorial radius	$\mathcal{R}_\odot$	6.957×10^8 m	exact[9]
nominal Solar constant	$\mathcal{S}_\odot$	1361 W m^{-2}	exact[9,10]
nominal Solar photosphere temperature	$\mathcal{T}_\odot$	5772 K	exact[9]
nominal Solar luminosity	$\mathcal{L}_\odot$	3.828×10^{26} W	exact[9,11]
Earth mass	$M_\oplus$	$5.972\,4(3) \times 10^{24}$ kg	[7]
Schwarzschild radius of the Earth	$2G_N M_\oplus/c^2$	8.870 056 580(18) mm	[12]
nominal Earth equatorial radius	$\mathcal{R}_\oplus$	6.3781×10^6 m	exact[9]
jansky (flux density)	Jy	10^{-26} W m^{-2} Hz^{-1}	definition
luminosity conversion	L	$3.0128 \times 10^{28} \times 10^{-0.4\ M_{\rm bol}}$ W	[13]
		($M_{\rm bol}$ = absolute bolometric magnitude = bolometric magnitude at 10 pc)	
flux conversion	$\mathscr{F}$	$2.5180 \times 10^{-8} \times 10^{-0.4\ m_{\rm bol}}$ W m^{-2}	[13]
		($m_{\rm bol}$ = apparent bolometric magnitude)	
ABsolute monochromatic magnitude	AB	$-2.5 \log_{10} f_\nu - 56.10$ (for f_ν in W m^{-2} Hz^{-1})	[14]
		$= -2.5 \log_{10} f_\nu + 8.90$ (for f_ν in Jy)	
Solar angular velocity around the Galactic center	Θ_0/R_0	30.3 ± 0.9 km s^{-1} kpc^{-1}	[15]
Solar distance from Galactic center	R_0	8.00 ± 0.25 kpc	[15,16]
circular velocity at R_0	v_0 or Θ_0	254(16) km s^{-1}	[15]
escape velocity from Galaxy	$v_{\rm esc}$	498 km/s $< v_{\rm esc} <$ 608 km/s	[17]
local disk density	$\rho_{\rm disk}$	3–12 $\times 10^{-24}$ g cm^{-3} $\approx$ 2–7 GeV/c^2 cm^{-3}	[18]
local dark matter density	ρ_χ	canonical value 0.3 GeV/c^2 cm^{-3} within factor 2–3	[19]
present day CMB temperature	T_0	2.7255(6) K	[20,21]
present day CMB dipole amplitude	d	3.3645(20) mK	[20,22]
Solar velocity with respect to CMB	$v_\odot$	370.09(22) km s^{-1} towards $(\ell, b) = (263.00(3)^\circ, 48.24(2)^\circ)$	[22]
Local Group velocity with respect to CMB	$v_{\rm LG}$	627(22) km s^{-1} towards $(\ell, b) = (276(3)^\circ, 30(3)^\circ)$	[20,23]
number density of CMB photons	n_γ	410.7(3) $(T/2.7255)^3$ cm^{-3}	[24]
density of CMB photons	ρ_γ	$4.645(4)\,(T/2.7255)^4 \times 10^{-34}$ g cm^{-3} ≈ 0.260 eV cm^{-3}	[24]
entropy density/Boltzmann constant	s/k	2 891.2 $(T/2.7255)^3$ cm^{-3}	[24]
present day Hubble expansion rate	H_0	100 h km s^{-1} Mpc^{-1} = $h \times$ (9.777 752 Gyr)$^{-1}$	[25]
scale factor for Hubble expansion rate	h	0.678(9)	[2,26]
Hubble length	c/H_0	$0.925\,0629 \times 10^{26}\,h^{-1}$ m = $1.374(18) \times 10^{26}$ m	
scale factor for cosmological constant	$c^2/3H_0^2$	$2.85247 \times 10^{51}\,h^{-2}$ m^2 = $6.20(17) \times 10^{51}$ m^2	
critical density of the Universe	$\rho_{\rm crit} = 3H_0^2/8\pi G_N$	$1.878\,40(9) \times 10^{-29}\,h^2$ g cm^{-3}	
		$= 1.053\,71(5) \times 10^{-5}\,h^2$ (GeV/c^2) cm^{-3}	
		$= 2.775\,37(13) \times 10^{11}\,h^2\,M_\odot$Mpc^{-3}	
baryon-to-photon ratio (from BBN)	$\eta = n_{\rm b}/n_\gamma$	$5.8 \times 10^{-10} \le \eta \le 6.6 \times 10^{-10}$ (95% CL)	[27]
number density of baryons	$n_{\rm b}$	$2.503(26) \times 10^{-7}$ cm^{-3}	[2,3,28,29]
		$(2.4 \times 10^{-7} < n_{\rm b} < 2.7 \times 10^{-7})$ cm^{-3} (95% CL)	$\eta \times n_\gamma$
CMB radiation density of the Universe	$\Omega_\gamma = \rho_\gamma/\rho_{\rm crit}$	$2.473 \times 10^{-5}(T/2.7255)^4\,h^{-2} = 5.38(15) \times 10^{-5}$	[24]
- - - *Planck* 2015 6-parameter fit to flat ΛCDM cosmology - - -			
baryon density of the Universe	$\Omega_{\rm b} = \rho_{\rm b}/\rho_{\rm crit}$	$^\ddagger 0.02226(23)\,h^{-2}$ = $^\dagger 0.0484(10)$	[2,3,22]
cold dark matter density of the Universe	$\Omega_{\rm c} = \rho_c/\rho_{\rm crit}$	$^\ddagger 0.1186(20)\,h^{-2}$ = $^\dagger 0.258(11)$	[2,3,22]
100 × approx to $r_*/D_{\rm A}$	$100 \times \theta_{\rm MC}$	$^\ddagger 1.0410(5)$	[2,3]
reionization optical depth	τ	$^\ddagger 0.066(16)$	[2,3,30]
scalar spectral index	$n_{\rm s}$	$^\ddagger 0.968(6)$	[2,3]
ln power prim. curv. pert. (k_0=0.05 Mpc^{-1})	$\ln(10^{10}\Delta^2_{\mathcal{R}})$	$^\ddagger 3.062(29)$	[2,3]

Quantity	Symbol, equation	Value	Reference, footnote
dark energy density of the Universe	Ω_Λ	† 0.692 ± 0.012	[2,3]
pressureless matter density of the Universe	$\Omega_{\rm m} = \Omega_{\rm c} + \Omega_{\rm b}$	† 0.308 ± 0.012	[2,3]
fluctuation amplitude at $8\,h^{-1}$ Mpc scale	σ_8	† 0.815 ± 0.009	[2,3]
redshift of matter-radiation equality	$z_{\rm eq}$	† 3365 ± 44	[2]
redshift at which optical depth equals unity	z_*	† 1089.9 ± 0.4	[2]
comoving size of sound horizon at z_*	r_*	† 144.9 ± 0.4 Mpc (*Planck* CMB)	[31]
age when optical depth equals unity	t_*	373 kyr	[32]
redshift at half reionization	$z_{\rm reion}$	† $8.8^{+1.7}_{-1.4}$	[2,33]
redshift when acceleration was zero	z_q	≈ 0.65	[32]
age of the Universe	t_0	† 13.80 ± 0.04 Gyr	[2]
effective number of neutrinos	$N_{\rm eff}$	♯ 3.13 ± 0.32	[2,34,35]
sum of neutrino masses	$\sum m_\nu$	♯ < 0.68 eV (*Planck* CMB); ≥ 0.06 eV (mixing)	[2,35,36,37]
neutrino density of the Universe	$\Omega_\nu = h^{-2} \sum m_{\nu_j}/93.14\,{\rm eV}$	♯ < 0.016 (*Planck* CMB); ≥ 0.0012 (mixing)	[2,36,37]
curvature	Ω_K	♯ $-0.005^{+0.016}_{-0.017}$ (95%CL)	[2]
running spectral index slope, $k_0 = 0.002$ Mpc^{-1}	$dn_{\rm s}/d\ln k$	♯ $-0.003(15)$	[2]
tensor-to-scalar field perturbations ratio, k_0=0.002 Mpc^{-1}	$r_{0.002} = T/S$	♯ < 0.114 at 95% CL; no running	[2,3,20,38]
dark energy equation of state parameter	w	-1.01 ± 0.04	[31,39]
primordial helium fraction	$Y_{\rm p}$	0.245 ± 0.004	[20,40]

‡ Parameter in 6-parameter ΛCDM fit; † Derived parameter in 6-parameter ΛCDM fit; ♯ Extended model parameter, *Planck* data only [2].

References:

1. CODATA recommended 2014 values of the fundamental physical constants: `physics.nist.gov/constants`.
2. Planck Collab. 2015 Results XIII, Astron. & Astrophys. **594**, A13 (2016), `arXiv:1502.01589v2`.
3. O. Lahav & A.R. Liddle, "The Cosmological Parameters," Sec. 24 in this *Review*.
4. *The Astronomical Almanac Online for the year 2016*, `asa.usno.navy.mil/SecK/Constants.html`.
5. The astronomical unit of length (au) in meters is re-defined (resolution B2, IAU XXVIII General Assembly 2012) to be a conventional unit of length in agreement with the value adopted in IAU 2009 Resolution B2; it is to be used with all time scales.
6. The distance at which 1 au subtends 1 arc sec: 1 au divided by $\pi/648\,000$.
7. $G_N M$ [4] ÷ G_N [1] for either the Sun or the Earth.
8. Product of $2/c^2$ and the observationally determined Solar mass parameter $G_N M_\odot$ [4]. Truncated to 8 places so that TCB and TDB time scale values agree.
9. IAU XXIX GA, Resolution B3, "on recommended nominal conversion constants ..." Calligraphic symbol indicates recommended nominal value.
10. See also G. Kopp & J.L. Lean, Geophys. Res. Lett. **38**, L01706 (2011), who give 1360.8 ± 0.6 W m^{-2}. See paper for caveats and other measurements.
11. $4\pi\,(1\ {\rm au})^2 \times \mathcal{S}_\odot$, assuming isotropic irradiance.
12. Product of $2/c^2$ and the geocentric gravitational constant $G_N M_\oplus$ [4]. Truncated to 8 places so that TCB, TT, and TDB time scale values agree.
13. IAU XXIX GA, Resolution B2, "on recommended zero points for the absolute and apparent bolometric magnitude scales".
14. J. B. Oke and J. E. Gunn, Astrophys. J. **266**, 713 (1983). Note that in the original definition the sign of the constant is wrong.
15. M.J. Reid, *et al.*, Astrophys. J. **700**, 137 (2009). Note that Θ_0/R_0 is better determined than either Θ_0 or R_0.
16. Z.M. Malkin, `arXiv:1202.6128` and Astron. Rep. **57**, 128 (2013). 52 determinations of R_0 over 20 years are given. The weighted mean of these *unevaluated* results is 7.94 ± 0.05 kpc, with $\chi^2/N_{\rm dof} = 1.26$. If the 8 values more than 3σ from the mean are eliminated, $\langle R_0 \rangle = 8.02 \pm 0.06$ kpc and $\chi^2/N_{\rm dof} = 0.67$. The author suggests using $R_0 = 8.00 \pm 0.25$ kpc.
17. M. C. Smith *et al.*, MNRAS **379**, 755 (2007).
18. G. Gilmore, R.F.G. Wyse, & K. Kuijken, Ann. Rev. Astron. & Astrophys. **27**, 555 (1989).
19. Sampling of many references: M. Mori *et al.*, Phys. Lett. **B289**, 463 (1992); E.I. Gates *et al.*, Astrophys. J. **449**, L133 (1995); M. Kamionkowski & A. Kinkhabwala, Phys. Rev. **D57**, 325 (1998); M. Weber & W. de Boer, Astron. & Astrophys. **509**, A25 (2010); P. Salucci *et al.*, Astron. & Astrophys. **523**, A83 (2010); R. Catena & P. Ullio, JCAP **1008**, 004 (2010). The conclusion is $\rho_{\rm DM}^{\rm local} = 0.39 \pm 0.03\,{\rm GeV\,cm^{-3}}$.
20. D. Scott & G.F. Smoot, "Cosmic Microwave Background," Sec. 28 in this *Review*.
21. D. Fixsen, Astrophys. J. **707**, 916 (2009).
22. Planck Collab. 2015 Results I, Astron. & Astrophys. **594**, A1 (2016), `arXiv:1502.01581v3`.
23. D.J. Fixsen *et al.*, Astrophys. J. **473**, 576 (1996); A. Kogut *et al.*, Astrophys. J. **419**, 1 (1993).
24. $n_\gamma = \frac{2\zeta(3)}{\pi^2}\left(\frac{kT}{\hbar c}\right)^3$; $\rho_\gamma = \frac{\pi^2 kT}{15\,c^2}\left(\frac{kT}{\hbar c}\right)^3$; $s/k = \frac{2 \cdot 43 \cdot \pi^2}{11 \cdot 45}\left(\frac{kT}{\hbar c}\right)^3$; $kT/\hbar c = 11.902(3)(T/2.7255)/{\rm cm}$.
25. Conversion using length of sidereal year.
26. Measurements from traditional cosmic distance-ladder methods tend to be higher, *e.g.*, 0.732 ± 0.017 from A.G. Riess *et al.*, Astrophys. J. **826**, 56 (2016); for discussion see O. Lahav & A.R. Liddle, "The Cosmological Parameters," Sec. 24 in this *Review*.
27. B.D. Fields, P. Molarto, & S. Sarkar, "Big-Bang Nucleosynthesis," in this *Review*.
28. $n_{\rm b}$ depends only upon the measured $\Omega_{\rm b}h^2$, the average baryon mass at the present epoch [29], and G_N: $n_{\rm b} = (\Omega_{\rm b}h^2)(h^{-2}\rho_{\rm crit})/(0.93711\,{\rm GeV}/c^2$ per baryon).
29. G. Steigman, JCAP **10**, 016, (2006).
30. Planck Collab. Interm. Results XLVI, Astron. & Astrophys. **596**, A107 (2016) describes an improved study yielding the lower value 0.055 ± 0.009, although a full *Planck* polarization analysis has yet to appear.
31. D.H. Weinberg, M. White, "Dark Energy," Sec. 27 in this *Review*.
32. D. Scott, A Narimani, & D.N. Page, Phys. Canada **70**, 258 (2015), `arXiv:1309.2381v2`.
33. Planck Collab. Interm. Results XLVI, Astron. & Astrophys. **596**, A108 (2016) revise this to 7.8–8.8 (±0.9), depending on the reionization model.
34. Summary Tables in this *Review* list $N_\nu = 2.984(8)$ (Standard Model fits to LEP-SLC data). Because neutrinos are not completely decoupled at $e^\pm$ annihilation, the effective number of massless neutrino species is 3.046, rather than 3.
35. J. Lesgourgues & L. Verde, "Neutrinos in Cosmology," Sec. 25 in this *Review*.
36. The sum is over all neutrino mass eigenstates, the lower limit following from neutrino mixing results reported in this *Review* combined with the assumptions that there are three light neutrinos and that the lightest neutrino is substantially less massive than the others.
37. Astrophysical determinations of $\sum m_{\nu_j}$, reported in the Full Listings of this *Review* under "Sum of the neutrino masses," range from < 0.17 eV to < 2.3 eV in papers published since 2003.
38. Combining this with a direct upper limit on CMB B modes, cleaned using *Planck* polarization data, gives $r < 0.07$, Keck Array and BICEP2 Collabs. V, Astrophys. J. **811**, 126, (2015).
39. S. Alam *et al.*, MNRAS **470**, 2617 (2017).
40. E. Aver *et al.*, JCAP **07**, 011 (2015).

3. International System of Units (SI)

See "The International System of Units (SI)," NIST Special Publication **330**, B.N. Taylor, ed. (USGPO, Washington, DC, 1991); and "Guide for the Use of the International System of Units (SI)," NIST Special Publication **811**, 1995 edition, B.N. Taylor (USGPO, Washington, DC, 1995).

Physical quantity	Name of unit	Symbol
Base units		
length	meter	m
mass	kilogram	kg
time	second	s
electric current	ampere	A
thermodynamic temperature	kelvin	K
amount of substance	mole	mol
luminous intensity	candela	cd
Derived units with special names		
plane angle	radian	rad
solid angle	steradian	sr
frequency	hertz	Hz
energy	joule	J
force	newton	N
pressure	pascal	Pa
power	watt	W
electric charge	coulomb	C
electric potential	volt	V
electric resistance	ohm	Ω
electric conductance	siemens	S
electric capacitance	farad	F
magnetic flux	weber	Wb
inductance	henry	H
magnetic flux density	tesla	T
luminous flux	lumen	lm
illuminance	lux	lx
celsius temperature	degree celsius	°C
activity (of a radioactive source)*	becquerel	Bq
absorbed dose (of ionizing radiation)*	gray	Gy
dose equivalent*	sievert	Sv

*See our section 36, on "Radioactivity and radiation protection."

SI prefixes

10^{24}	yotta	(Y)
10^{21}	zetta	(Z)
10^{18}	exa	(E)
10^{15}	peta	(P)
10^{12}	tera	(T)
10^{9}	giga	(G)
10^{6}	mega	(M)
10^{3}	kilo	(k)
10^{2}	hecto	(h)
10	deca	(da)
10^{-1}	deci	(d)
10^{-2}	centi	(c)
10^{-3}	milli	(m)
10^{-6}	micro	(μ)
10^{-9}	nano	(n)
10^{-12}	pico	(p)
10^{-15}	femto	(f)
10^{-18}	atto	(a)
10^{-21}	zepto	(z)
10^{-24}	yocto	(y)

Table 4.1. Revised June 2017 by D.E. Groom (LBNL). The atomic number (top left) is the number of protons in the nucleus. The atomic masses (bottom) of stable elements are weighted by isotopic abundances in the Earth's surface. Atomic masses are relative to the mass of ^{12}C, defined to be exactly 12 unified atomic mass units (u) (1 u $\approx$ 1 g/mole). The exceptions are Th, Pa, and U, which have no stable isotopes but do have characteristic terrestrial compositions. Relative isotopic abundances often vary considerably, both in natural and commercial samples; this is reflected in the number of significant figures given for the mass. Masses may be found at `https://www.nist.gov/pml/atomic-weights-and-isotopic-compositions-relative-atomic-masses`. If there is no stable isotope, the atomic mass of the most stable isotope is given in parentheses.

IUPAC announced verification of the discoveries of elements 113, 115, 117, and 118 in December 2015. The names were approved November 2016. The 7th period of the periodic table is now complete.

PERIODIC TABLE OF THE ELEMENTS

1 IA																	18 VIIIA
1 H hydrogen 1.008	2 IIA											13 IIIA	14 IVA	15 VA	16 VIA	17 VIIA	2 He helium 4.002602
3 Li lithium 6.94	4 Be beryllium 9.012182											5 B boron 10.81	6 C carbon 12.0107	7 N nitrogen 14.007	8 O oxygen 15.999	9 F fluorine 18.998403163	10 Ne neon 20.1797
11 Na sodium 22.98976928	12 Mg magnesium 24.305	3 IIIB	4 IVB	5 VB	6 VIB	7 VIIB	8	9 VIII	10	11 IB	12 IIB	13 Al aluminum 26.9815385	14 Si silicon 28.085	15 P phosphorus 30.973761998	16 S sulfur 32.06	17 Cl chlorine 35.45	18 Ar argon 39.948
19 K potassium 39.0983	20 Ca calcium 40.078	21 Sc scandium 44.955908	22 Ti titanium 47.867	23 V vanadium 50.9415	24 Cr chromium 51.9961	25 Mn manganese 54.938044	26 Fe iron 55.845	27 Co cobalt 58.933195	28 Ni nickel 58.6934	29 Cu copper 63.546	30 Zn zinc 65.38	31 Ga gallium 69.723	32 Ge germanium 72.630	33 As arsenic 74.921595	34 Se selenium 78.971	35 Br bromine 79.904	36 Kr krypton 83.798
37 Rb rubidium 85.4678	38 Sr strontium 87.62	39 Y yttrium 88.90584	40 Zr zirconium 91.224	41 Nb niobium 92.90637	42 Mo molybdenum 95.95	43 Tc technetium (97.907212)	44 Ru ruthenium 101.07	45 Rh rhodium 102.90550	46 Pd palladium 106.42	47 Ag silver 107.8682	48 Cd cadmium 112.414	49 In indium 114.818	50 Sn tin 118.710	51 Sb antimony 121.760	52 Te tellurium 127.60	53 I iodine 126.90447	54 Xe xenon 131.293
55 Cs caesium 132.90545196	56 Ba barium 137.327	57–71 LANTHA- NIDES	72 Hf hafnium 178.49	73 Ta tantalum 180.94788	74 W tungsten 183.84	75 Re rhenium 186.207	76 Os osmium 190.23	77 Ir iridium 192.217	78 Pt platinum 195.084	79 Au gold 196.966569	80 Hg mercury 200.592	81 Tl thallium 204.38	82 Pb lead 207.2	83 Bi bismuth 208.98040	84 Po polonium (208.98243)	85 At astatine (209.98715)	86 Rn radon (222.01758)
87 Fr francium (223.01974)	88 Ra radium (226.02541)	89–103 ACTINIDES	104 Rf rutherford. (267.12169)	105 Db dubnium (268.12567)	106 Sg seaborgium (269.12863)	107 Bh bohrium (270.13336)	108 Hs hassium (269.13375)	109 Mt meitnerium (278.1563)	110 Ds darmstadt. (281.1645)	111 Rg roentgen. (282.16912)	112 Cn copernicium (285.17712)	113 Nh (nihonium) (286.18221)	114 Fl flerovium (289.19042)	115 Mc (moscovium) (289.19363)	116 Lv livermorium (294.2105)	117 Ts (tennessine) (294.2105)	118 Og (oganesson) (294.21392)

Lanthanide series	57 La lanthanum 138.90547	58 Ce cerium 140.116	59 Pr praseodym. 140.90766	60 Nd neodymium 144.242	61 Pm promethium (144.91276)	62 Sm samarium 150.36	63 Eu europium 151.964	64 Gd gadolinum 157.25	65 Tb terbium 158.92535	66 Dy dysprosium 162.500	67 Ho holmium 164.93033	68 Er erbium 167.259	69 Tm thulium 168.93422	70 Yb ytterbium 173.054	71 Lu lutetium 174.9668
Actinide series	89 Ac actinium (227.02775)	90 Th thorium 232.0377	91 Pa protactinium 231.03588	92 U uranium 238.02891	93 Np neptunium (237.04817)	94 Pu plutonium (244.06420)	95 Am americium (243.06138)	96 Cm curium (247.07035)	97 Bk berkelium (247.07031)	98 Cf californium (251.07959)	99 Es einsteinium (252.08298)	100 Fm fermium (257.09511)	101 Md mendelevium (258.09844)	102 No nobelium (259.10103)	103 Lr lawrencium (262.10961)

5. Electronic Structure of the Elements

Table 5.1. Reviewed 2011 by J.E. Sansonetti (NIST). The electronic configurations and the ionization energies are from the NIST database, "Ground Levels and Ionization Energies for the Neutral Atoms," W.C. Martin, A. Musgrove, S. Kotochigova, and J.E. Sansonetti, `http://www.nist.gov/pml/data/ion_energy.cfm`. The electron configuration for, say, iron indicates an argon electronic core (see argon) plus six $3d$ electrons and two $4s$ electrons.

	Element		Electron configuration ($3d^5$ = five $3d$ electrons, *etc.*)						Ground state $^{2S+1}L_J$	Ionization energy (eV)
1	H	Hydrogen	$1s$						$^2S_{1/2}$	13.5984
2	He	Helium	$1s^2$						$^1S_0$	24.5874
3	Li	Lithium	(He) $2s$						$^2S_{1/2}$	5.3917
4	Be	Beryllium	(He) $2s^2$						$^1S_0$	9.3227
5	B	Boron	(He) $2s^2$	$2p$					$^2P_{1/2}$	8.2980
6	C	Carbon	(He) $2s^2$	$2p^2$					$^3P_0$	11.2603
7	N	Nitrogen	(He) $2s^2$	$2p^3$					$^4S_{3/2}$	14.5341
8	O	Oxygen	(He) $2s^2$	$2p^4$					$^3P_2$	13.6181
9	F	Fluorine	(He) $2s^2$	$2p^5$					$^2P_{3/2}$	17.4228
10	Ne	Neon	(He) $2s^2$	$2p^6$					$^1S_0$	21.5645
11	Na	Sodium	(Ne) $3s$						$^2S_{1/2}$	5.1391
12	Mg	Magnesium	(Ne) $3s^2$						$^1S_0$	7.6462
13	Al	Aluminum	(Ne) $3s^2$	$3p$					$^2P_{1/2}$	5.9858
14	Si	Silicon	(Ne) $3s^2$	$3p^2$					$^3P_0$	8.1517
15	P	Phosphorus	(Ne) $3s^2$	$3p^3$					$^4S_{3/2}$	10.4867
16	S	Sulfur	(Ne) $3s^2$	$3p^4$					$^3P_2$	10.3600
17	Cl	Chlorine	(Ne) $3s^2$	$3p^5$					$^2P_{3/2}$	12.9676
18	Ar	Argon	(Ne) $3s^2$	$3p^6$					$^1S_0$	15.7596
19	K	Potassium	(Ar)	$4s$					$^2S_{1/2}$	4.3407
20	Ca	Calcium	(Ar)	$4s^2$					$^1S_0$	6.1132
21	Sc	Scandium	(Ar) $3d$	$4s^2$					$^2D_{3/2}$	6.5615
22	Ti	Titanium	(Ar) $3d^2$	$4s^2$					$^3F_2$	6.8281
23	V	Vanadium	(Ar) $3d^3$	$4s^2$					$^4F_{3/2}$	6.7462
24	Cr	Chromium	(Ar) $3d^5$	$4s$					$^7S_3$	6.7665
25	Mn	Manganese	(Ar) $3d^5$	$4s^2$					$^6S_{5/2}$	7.4340
26	Fe	Iron	(Ar) $3d^6$	$4s^2$					$^5D_4$	7.9024
27	Co	Cobalt	(Ar) $3d^7$	$4s^2$					$^4F_{9/2}$	7.8810
28	Ni	Nickel	(Ar) $3d^8$	$4s^2$					$^3F_4$	7.6399
29	Cu	Copper	(Ar) $3d^{10}$	$4s$					$^2S_{1/2}$	7.7264
30	Zn	Zinc	(Ar) $3d^{10}$	$4s^2$					$^1S_0$	9.3942
31	Ga	Gallium	(Ar) $3d^{10}$	$4s^2$	$4p$				$^2P_{1/2}$	5.9993
32	Ge	Germanium	(Ar) $3d^{10}$	$4s^2$	$4p^2$				$^3P_0$	7.8994
33	As	Arsenic	(Ar) $3d^{10}$	$4s^2$	$4p^3$				$^4S_{3/2}$	9.7886
34	Se	Selenium	(Ar) $3d^{10}$	$4s^2$	$4p^4$				$^3P_2$	9.7524
35	Br	Bromine	(Ar) $3d^{10}$	$4s^2$	$4p^5$				$^2P_{3/2}$	11.8138
36	Kr	Krypton	(Ar) $3d^{10}$	$4s^2$	$4p^6$				$^1S_0$	13.9996
37	Rb	Rubidium	(Kr)	$5s$					$^2S_{1/2}$	4.1771
38	Sr	Strontium	(Kr)	$5s^2$					$^1S_0$	5.6949
39	Y	Yttrium	(Kr) $4d$	$5s^2$					$^2D_{3/2}$	6.2173
40	Zr	Zirconium	(Kr) $4d^2$	$5s^2$					$^3F_2$	6.6339
41	Nb	Niobium	(Kr) $4d^4$	$5s$					$^6D_{1/2}$	6.7589
42	Mo	Molybdenum	(Kr) $4d^5$	$5s$					$^7S_3$	7.0924
43	Tc	Technetium	(Kr) $4d^5$	$5s^2$					$^6S_{5/2}$	7.28
44	Ru	Ruthenium	(Kr) $4d^7$	$5s$					$^5F_5$	7.3605
45	Rh	Rhodium	(Kr) $4d^8$	$5s$					$^4F_{9/2}$	7.4589
46	Pd	Palladium	(Kr) $4d^{10}$						$^1S_0$	8.3369
47	Ag	Silver	(Kr) $4d^{10}$	$5s$					$^2S_{1/2}$	7.5762
48	Cd	Cadmium	(Kr) $4d^{10}$	$5s^2$					$^1S_0$	8.9938

Transition elements

49	In	Indium	(Kr) $4d^{10}5s^2$	$5p$				$^2P_{1/2}$	5.7864
50	Sn	Tin	(Kr) $4d^{10}5s^2$	$5p^2$				$^3P_0$	7.3439
51	Sb	Antimony	(Kr) $4d^{10}5s^2$	$5p^3$				$^4S_{3/2}$	8.6084
52	Te	Tellurium	(Kr) $4d^{10}5s^2$	$5p^4$				$^3P_2$	9.0096
53	I	Iodine	(Kr) $4d^{10}5s^2$	$5p^5$				$^2P_{3/2}$	10.4513
54	Xe	Xenon	(Kr) $4d^{10}5s^2$	$5p^6$				$^1S_0$	12.1298
55	Cs	Cesium	(Xe)	$6s$				$^2S_{1/2}$	3.8939
56	Ba	Barium	(Xe)	$6s^2$				$^1S_0$	5.2117
57	La	Lanthanum	(Xe) $5d$	$6s^2$				$^2D_{3/2}$	5.5769
58	Ce	Cerium	(Xe) $4f$ $5d$	$6s^2$				$^1G_4$	5.5387
59	Pr	Praseodymium	(Xe) $4f^3$	$6s^2$				$^4I_{9/2}$	5.473
60	Nd	Neodymium	(Xe) $4f^4$	$6s^2$				$^5I_4$	5.5250
61	Pm	Promethium	(Xe) $4f^5$	$6s^2$				$^6H_{5/2}$	5.582
62	Sm	Samarium	(Xe) $4f^6$	$6s^2$				$^7F_0$	5.6437
63	Eu	Europium	(Xe) $4f^7$	$6s^2$				$^8S_{7/2}$	5.6704
64	Gd	Gadolinium	(Xe) $4f^7$ $5d$	$6s^2$				$^9D_2$	6.1498
65	Tb	Terbium	(Xe) $4f^9$	$6s^2$				$^6H_{15/2}$	5.8638
66	Dy	Dysprosium	(Xe) $4f^{10}$	$6s^2$				$^5I_8$	5.9389
67	Ho	Holmium	(Xe) $4f^{11}$	$6s^2$				$^4I_{15/2}$	6.0215
68	Er	Erbium	(Xe) $4f^{12}$	$6s^2$				$^3H_6$	6.1077
69	Tm	Thulium	(Xe) $4f^{13}$	$6s^2$				$^2F_{7/2}$	6.1843
70	Yb	Ytterbium	(Xe) $4f^{14}$	$6s^2$				$^1S_0$	6.2542
71	Lu	Lutetium	(Xe) $4f^{14}5d$	$6s^2$				$^2D_{3/2}$	5.4259
72	Hf	Hafnium	(Xe) $4f^{14}5d^2$	$6s^2$				$^3F_2$	6.8251
73	Ta	Tantalum	(Xe) $4f^{14}5d^3$	$6s^2$				$^4F_{3/2}$	7.5496
74	W	Tungsten	(Xe) $4f^{14}5d^4$	$6s^2$				$^5D_0$	7.8640
75	Re	Rhenium	(Xe) $4f^{14}5d^5$	$6s^2$				$^6S_{5/2}$	7.8335
76	Os	Osmium	(Xe) $4f^{14}5d^6$	$6s^2$				$^5D_4$	8.4382
77	Ir	Iridium	(Xe) $4f^{14}5d^7$	$6s^2$				$^4F_{9/2}$	8.9670
78	Pt	Platinum	(Xe) $4f^{14}5d^9$	$6s$				$^3D_3$	8.9588
79	Au	Gold	(Xe) $4f^{14}5d^{10}6s$					$^2S_{1/2}$	9.2255
80	Hg	Mercury	(Xe) $4f^{14}5d^{10}6s^2$					$^1S_0$	10.4375
81	Tl	Thallium	(Xe) $4f^{14}5d^{10}6s^2$	$6p$				$^2P_{1/2}$	6.1082
82	Pb	Lead	(Xe) $4f^{14}5d^{10}6s^2$	$6p^2$				$^3P_0$	7.4167
83	Bi	Bismuth	(Xe) $4f^{14}5d^{10}6s^2$	$6p^3$				$^4S_{3/2}$	7.2855
84	Po	Polonium	(Xe) $4f^{14}5d^{10}6s^2$	$6p^4$				$^3P_2$	8.414
85	At	Astatine	(Xe) $4f^{14}5d^{10}6s^2$	$6p^5$				$^2P_{3/2}$	
86	Rn	Radon	(Xe) $4f^{14}5d^{10}6s^2$	$6p^6$				$^1S_0$	10.7485
87	Fr	Francium	(Rn)	$7s$				$^2S_{1/2}$	4.0727
88	Ra	Radium	(Rn)	$7s^2$				$^1S_0$	5.2784
89	Ac	Actinium	(Rn) $6d$	$7s^2$				$^2D_{3/2}$	5.3807
90	Th	Thorium	(Rn) $6d^2$	$7s^2$				$^3F_2$	6.3067
91	Pa	Protactinium	(Rn)$5f^2$ $6d$	$7s^2$				$^4K_{11/2}$*	5.89
92	U	Uranium	(Rn)$5f^3$ $6d$	$7s^2$				$^5L_6$*	6.1939
93	Np	Neptunium	(Rn)$5f^4$ $6d$	$7s^2$				$^6L_{11/2}$*	6.2657
94	Pu	Plutonium	(Rn)$5f^6$	$7s^2$				$^7F_0$	6.0260
95	Am	Americium	(Rn)$5f^7$	$7s^2$				$^8S_{7/2}$	5.9738
96	Cm	Curium	(Rn)$5f^7$ $6d$	$7s^2$				$^9D_2$	5.9914
97	Bk	Berkelium	(Rn)$5f^9$	$7s^2$				$^6H_{15/2}$	6.1979
98	Cf	Californium	(Rn)$5f^{10}$	$7s^2$				$^5I_8$	6.2817
99	Es	Einsteinium	(Rn)$5f^{11}$	$7s^2$				$^4I_{15/2}$	6.3676
100	Fm	Fermium	(Rn)$5f^{12}$	$7s^2$				$^3H_6$	6.50
101	Md	Mendelevium	(Rn)$5f^{13}$	$7s^2$				$^2F_{7/2}$	6.58
102	No	Nobelium	(Rn)$5f^{14}$	$7s^2$				$^1S_0$	6.65
103	Lr	Lawrencium	(Rn)$5f^{14}$	$7s^2$	$7p$?			$^2P_{1/2}$?	4.9?
104	Rf	Rutherfordium	(Rn)$5f^{14}6d^2$	$7s^2$?				$^3F_2$?	6.0?

Lanthanides

Transition elements

Actinides

* The usual LS coupling scheme does not apply for these three elements. See the introductory note to the NIST table from which this table is taken.

6. Atomic and Nuclear Properties of Materials

Table 6.1 Abridged from `pdg.lbl.gov/AtomicNuclearProperties` by D.E. Groom (2017). See web pages for more detail about entries in this table and for several hundred others. Parentheses in the dE/dx and density columns indicate gases at 20° C and 1 atm. Boiling points are at 1 atm. Refractive indices n are evaluated at the sodium D line blend (589.2 nm); values $\gg 1$ in brackets indicate $(n-1)\times 10^6$ for gases at 0° C and 1 atm.

Material	Z	A	$\langle Z/A\rangle$	Nucl.coll. length λ_T {g cm^{-2}}	Nucl.inter. length λ_I {g cm^{-2}}	Rad.len. X_0 {g cm^{-2}}	$dE/dx\|_{\rm min}$ { MeV g^{-1}cm^2}	Density {g cm^{-3}} ({g ℓ^{-1}})	Melting point (K)	Boiling point (K)	Refract. index @ Na D
H_2	1	1.008(7)	0.99212	42.8	52.0	63.05	(4.103)	0.071(0.084)	13.81	20.28	1.11[132.]
D_2	1	2.014101764(8)	0.49650	51.3	71.8	125.97	(2.053)	0.169(0.168)	18.7	23.65	1.11[138.]
He	2	4.002602(2)	0.49967	51.8	71.0	94.32	(1.937)	0.125(0.166)		4.220	1.02[35.0]
Li	3	6.94(2)	0.43221	52.2	71.3	82.78	1.639	0.534	453.6	1615.	
Be	4	9.0121831(5)	0.44384	55.3	77.8	65.19	1.595	1.848	1560.	2744.	
C diamond	6	12.0107(8)	0.49955	59.2	85.8	42.70	1.725	3.520			2.419
C graphite	6	12.0107(8)	0.49955	59.2	85.8	42.70	1.742	2.210	Sublimes at 4098. K		
N_2	7	14.007(2)	0.49976	61.1	89.7	37.99	(1.825)	0.807(1.165)	63.15	77.29	1.20[298.]
O_2	8	15.999(3)	0.50002	61.3	90.2	34.24	(1.801)	1.141(1.332)	54.36	90.20	1.22[271.]
F_2	9	18.998403163(6)	0.47372	65.0	97.4	32.93	(1.676)	1.507(1.580)	53.53	85.03	[195.]
Ne	10	20.1797(6)	0.49555	65.7	99.0	28.93	(1.724)	1.204(0.839)	24.56	27.07	1.09[67.1]
N	13	26.9815385(7)	0.48181	69.7	107.2	24.01	1.615	2.699	933.5	2792.	
Al	13	26.9815385(7)	0.48181	69.7	107.2	24.01	1.615	2.699	933.5	2792.	
Si	14	28.0855(3)	0.49848	70.2	108.4	21.82	1.664	2.329	1687.	3538.	3.95
Cl_2	17	35.453(2)	0.47951	73.8	115.7	19.28	(1.630)	1.574(2.980)	171.6	239.1	[773.]
Ar	18	39.948(1)	0.45059	75.7	119.7	19.55	(1.519)	1.396(1.662)	83.81	87.26	1.23[281.]
Ti	22	47.867(1)	0.45961	78.8	126.2	16.16	1.477	4.540	1941.	3560.	
Fe	26	55.845(2)	0.46557	81.7	132.1	13.84	1.451	7.874	1811.	3134.	
Cu	29	63.546(3)	0.45636	84.2	137.3	12.86	1.403	8.960	1358.	2835.	
Ge	32	72.630(1)	0.44053	86.9	143.0	12.25	1.370	5.323	1211.	3106.	
Sn	50	118.710(7)	0.42119	98.2	166.7	8.82	1.263	7.310	505.1	2875.	
Xe	54	131.293(6)	0.41129	100.8	172.1	8.48	(1.255)	2.953(5.483)	161.4	165.1	1.39[701.]
W	74	183.84(1)	0.40252	110.4	191.9	6.76	1.145	19.300	3695.	5828.	
Pt	78	195.084(9)	0.39983	112.2	195.7	6.54	1.128	21.450	2042.	4098.	
Au	79	196.966569(5)	0.40108	112.5	196.3	6.46	1.134	19.320	1337.	3129.	
Pb	82	207.2(1)	0.39575	114.1	199.6	6.37	1.122	11.350	600.6	2022.	
U	92	[238.02891(3)]	0.38651	118.6	209.0	6.00	1.081	18.950	1408.	4404.	
Air (dry, 1 atm)			0.49919	61.3	90.1	36.62	(1.815)	(1.205)		78.80	[289]
Shielding concrete			0.50274	65.1	97.5	26.57	1.711	2.300			
Borosilicate glass (Pyrex)			0.49707	64.6	96.5	28.17	1.696	2.230			
Lead glass			0.42101	95.9	158.0	7.87	1.255	6.220			
Standard rock			0.50000	66.8	101.3	26.54	1.688	2.650			
Methane (CH_4)			0.62334	54.0	73.8	46.47	(2.417)	(0.667)	90.68	111.7	[444.]
Ethane (C_2H_6)			0.59861	55.0	75.9	45.66	(2.304)	(1.263)	90.36	184.5	
Propane (C_3H_8)			0.58962	55.3	76.7	45.37	(2.262)	0.493(1.868)	85.52	231.0	
Butane (C_4H_{10})			0.59497	55.5	77.1	45.23	(2.278)	(2.489)	134.9	272.6	
Octane (C_8H_{18})			0.57778	55.8	77.8	45.00	2.123	0.703	214.4	398.8	
Paraffin ($CH_3(CH_2)_{n\approx 23}CH_3$)			0.57275	56.0	78.3	44.85	2.088	0.930			
Nylon (type 6, 6/6)			0.54790	57.5	81.6	41.92	1.973	1.18			
Polycarbonate (Lexan)			0.52697	58.3	83.6	41.50	1.886	1.20			
Polyethylene ($[CH_2CH_2]_n$)			0.57034	56.1	78.5	44.77	2.079	0.89			
Polyethylene terephthalate (Mylar)			0.52037	58.9	84.9	39.95	1.848	1.40			
Polyimide film (Kapton)			0.51264	59.2	85.5	40.58	1.820	1.42			
Polymethylmethacrylate (acrylic)			0.53937	58.1	82.8	40.55	1.929	1.19			1.49
Polypropylene			0.55998	56.1	78.5	44.77	2.041	0.90			
Polystyrene ($[C_6H_5CHCH_2]_n$)			0.53768	57.5	81.7	43.79	1.936	1.06			1.59
Polytetrafluoroethylene (Teflon)			0.47992	63.5	94.4	34.84	1.671	2.20			
Polyvinyltoluene			0.54141	57.3	81.3	43.90	1.956	1.03			1.58
Aluminum oxide (sapphire)			0.49038	65.5	98.4	27.94	1.647	3.970	2327.	3273.	1.77
Barium flouride (BaF_2)			0.42207	90.8	149.0	9.91	1.303	4.893	1641.	2533.	1.47
Bismuth germanate (BGO)			0.42065	96.2	159.1	7.97	1.251	7.130	1317.		2.15
Carbon dioxide gas (CO_2)			0.49989	60.7	88.9	36.20	1.819	(1.842)			[449.]
Solid carbon dioxide (dry ice)			0.49989	60.7	88.9	36.20	1.787	1.563	Sublimes at 194.7 K		
Cesium iodide (CsI)			0.41569	100.6	171.5	8.39	1.243	4.510	894.2	1553.	1.79
Lithium fluoride (LiF)			0.46262	61.0	88.7	39.26	1.614	2.635	1121.	1946.	1.39
Lithium hydride (LiH)			0.50321	50.8	68.1	79.62	1.897	0.820	965.		
Lead tungstate ($PbWO_4$)			0.41315	100.6	168.3	7.39	1.229	8.300	1403.		2.20
Silicon dioxide (SiO_2, fused quartz)			0.49930	65.2	97.8	27.05	1.699	2.200	1986.	3223.	1.46
Sodium chloride (NaCl)			0.47910	71.2	110.1	21.91	1.847	2.170	1075.	1738.	1.54
Sodium iodide (NaI)			0.42697	93.1	154.6	9.49	1.305	3.667	933.2	1577.	1.77
Water (H_2O)			0.55509	58.5	83.3	36.08	1.992	1.000	273.1	373.1	1.33
Silica aerogel			0.50093	65.0	97.3	27.25	1.740	0.200	(0.03 H_2O, 0.97 SiO_2)		

Material	Dielectric constant ($\kappa = \epsilon/\epsilon_0$) () is ($\kappa$–1)×$10^6$ for gas	Young's modulus [10^6 psi]	Coeff. of thermal expansion [10^{-6}cm/cm-°C]	Specific heat [cal/g-°C]	Electrical resistivity [$\mu\Omega$cm(@°C)]	Thermal conductivity [cal/cm-°C-sec]
H_2	(253.9)	—	—	—	—	—
He	(64)	—	—	—	—	—
Li	—	—	56	0.86	8.55(0°)	0.17
Be	—	37	12.4	0.436	5.885(0°)	0.38
C	—	0.7	0.6–4.3	0.165	1375(0°)	0.057
N_2	(548.5)	—	—	—	—	—
O_2	(495)	—	—	—	—	—
Ne	(127)	—	—	—	—	—
Al	—	10	23.9	0.215	2.65(20°)	0.53
Si	11.9	16	2.8–7.3	0.162	—	0.20
Ar	(517)	—	—	—	—	—
Ti	—	16.8	8.5	0.126	50(0°)	—
Fe	—	28.5	11.7	0.11	9.71(20°)	0.18
Cu	—	16	16.5	0.092	1.67(20°)	0.94
Ge	16.0	—	5.75	0.073	—	0.14
Sn	—	6	20	0.052	11.5(20°)	0.16
Xe	—	—	—	—	—	—
W	—	50	4.4	0.032	5.5(20°)	0.48
Pt	—	21	8.9	0.032	9.83(0°)	0.17
Pb	—	2.6	29.3	0.038	20.65(20°)	0.083
U	—	—	36.1	0.028	29(20°)	0.064

7. Electromagnetic Relations

Revised September 2005 by H.G. Spieler (LBNL).

Quantity	Gaussian CGS	SI
Conversion factors:		
Charge:	$2.997\,924\,58 \times 10^9$ esu	$= 1$ C $= 1$ A s
Potential:	$(1/299.792\,458)$ statvolt (ergs/esu)	$= 1$ V $= 1$ J C^{-1}
Magnetic field:	10^4 gauss $= 10^4$ dyne/esu	$= 1$ T $= 1$ N A^{-1}m^{-1}
	$\mathbf{F} = q\,(\mathbf{E} + \frac{\mathbf{v}}{c} \times \mathbf{B})$	$\mathbf{F} = q\,(\mathbf{E} + \mathbf{v} \times \mathbf{B})$
	$\boldsymbol{\nabla} \cdot \mathbf{D} = 4\pi\rho$ $\boldsymbol{\nabla} \times \mathbf{H} - \frac{1}{c}\frac{\partial \mathbf{D}}{\partial t} = \frac{4\pi}{c}\mathbf{J}$ $\boldsymbol{\nabla} \cdot \mathbf{B} = 0$ $\boldsymbol{\nabla} \times \mathbf{E} + \frac{1}{c}\frac{\partial \mathbf{B}}{\partial t} = 0$	$\boldsymbol{\nabla} \cdot \mathbf{D} = \rho$ $\boldsymbol{\nabla} \times \mathbf{H} - \frac{\partial \mathbf{D}}{\partial t} = \mathbf{J}$ $\boldsymbol{\nabla} \cdot \mathbf{B} = 0$ $\boldsymbol{\nabla} \times \mathbf{E} + \frac{\partial \mathbf{B}}{\partial t} = 0$
Constitutive relations:	$\mathbf{D} = \mathbf{E} + 4\pi\mathbf{P}, \quad \mathbf{H} = \mathbf{B} - 4\pi\mathbf{M}$	$\mathbf{D} = \epsilon_0\mathbf{E} + \mathbf{P}, \quad \mathbf{H} = \mathbf{B}/\mu_0 - \mathbf{M}$
Linear media:	$\mathbf{D} = \epsilon\mathbf{E}, \quad \mathbf{H} = \mathbf{B}/\mu$ 1 1	$\mathbf{D} = \epsilon\mathbf{E}, \quad \mathbf{H} = \mathbf{B}/\mu$ $\epsilon_0 = 8.854\,187\ldots \times 10^{-12}$ F m^{-1} $\mu_0 = 4\pi \times 10^{-7}$ N A^{-2}
	$\mathbf{E} = -\boldsymbol{\nabla} V - \frac{1}{c}\frac{\partial \mathbf{A}}{\partial t}$ $\mathbf{B} = \boldsymbol{\nabla} \times \mathbf{A}$	$\mathbf{E} = -\boldsymbol{\nabla} V - \frac{\partial \mathbf{A}}{\partial t}$ $\mathbf{B} = \boldsymbol{\nabla} \times \mathbf{A}$
	$V = \sum_{\text{charges}} \frac{q_i}{r_i} = \int \frac{\rho\,(\mathbf{r}')}{\lvert\mathbf{r} - \mathbf{r}'\rvert}\, d^3x'$ $\mathbf{A} = \frac{1}{c}\oint \frac{I\,d\boldsymbol{\ell}}{\lvert\mathbf{r} - \mathbf{r}'\rvert} = \frac{1}{c}\int \frac{\mathbf{J}(\mathbf{r}')}{\lvert\mathbf{r} - \mathbf{r}'\rvert}\, d^3x'$	$V = \frac{1}{4\pi\epsilon_0}\sum_{\text{charges}} \frac{q_i}{r_i} = \frac{1}{4\pi\epsilon_0}\int \frac{\rho\,(\mathbf{r}')}{\lvert\mathbf{r} - \mathbf{r}'\rvert}\, d^3x'$ $\mathbf{A} = \frac{\mu_0}{4\pi}\oint \frac{I\,d\boldsymbol{\ell}}{\lvert\mathbf{r} - \mathbf{r}'\rvert} = \frac{\mu_0}{4\pi}\int \frac{\mathbf{J}(\mathbf{r}')}{\lvert\mathbf{r} - \mathbf{r}'\rvert}\, d^3x'$
	$\mathbf{E}'_\parallel = \mathbf{E}_\parallel$ $\mathbf{E}'_\perp = \gamma(\mathbf{E}_\perp + \frac{1}{c}\mathbf{v} \times \mathbf{B})$ $\mathbf{B}'_\parallel = \mathbf{B}_\parallel$ $\mathbf{B}'_\perp = \gamma(\mathbf{B}_\perp - \frac{1}{c}\mathbf{v} \times \mathbf{E})$	$\mathbf{E}'_\parallel = \mathbf{E}_\parallel$ $\mathbf{E}'_\perp = \gamma(\mathbf{E}_\perp + \mathbf{v} \times \mathbf{B})$ $\mathbf{B}'_\parallel = \mathbf{B}_\parallel$ $\mathbf{B}'_\perp = \gamma(\mathbf{B}_\perp - \frac{1}{c^2}\mathbf{v} \times \mathbf{E})$
$\frac{1}{4\pi\epsilon_0} = c^2 \times 10^{-7}$ N A^{-2} $= 8.987\,55\ldots \times 10^9$ m F^{-1} ; $\frac{\mu_0}{4\pi} = 10^{-7}$ N A^{-2} ; $c = \frac{1}{\sqrt{\mu_0\epsilon_0}} = 2.997\,924\;\;58 \times 10^8$ m s^{-1}		

7.1. Impedances (SI units)

ρ = resistivity at room temperature in $10^{-8}\,\Omega$ m:

~ 1.7 for Cu	~ 5.5 for W
~ 2.4 for Au	~ 73 for SS 304
~ 2.8 for Al	~ 100 for Nichrome

(Al alloys may have double the Al value.)

For alternating currents, instantaneous current I, voltage V, angular frequency ω:

$$V = V_0\, e^{j\omega t} = ZI\ . \tag{7.1}$$

Impedance of self-inductance L: $Z = j\omega L$.

Impedance of capacitance C: $Z = 1/j\omega C$.

Impedance of free space: $Z = \sqrt{\mu_0/\epsilon_0} = 376.7\ \Omega$.

High-frequency surface impedance of a good conductor:

$$Z = \frac{(1+j)\,\rho}{\delta}\ , \quad \text{where } \delta = \text{skin depth}\ ; \tag{7.2}$$

$$\delta = \sqrt{\frac{\rho}{\pi\nu\mu}} \approx \frac{6.6\text{ cm}}{\sqrt{\nu\,(\text{Hz})}} \quad \text{for Cu}\ . \tag{7.3}$$

7.2. Capacitors, inductors, and transmission Lines

The capacitance between two parallel plates of area A spaced by the distance d and enclosing a medium with the dielectric constant ε is

$$C = K\varepsilon A/d\,, \tag{7.4}$$

where the correction factor K depends on the extent of the fringing field. If the dielectric fills the capacitor volume without extending beyond the electrodes. the correction factor $K \approx 0.8$ for capacitors of typical geometry.

The inductance at high frequencies of a straight wire whose length ℓ is much greater than the wire diameter d is

$$L \approx 2.0\left[\frac{\text{nH}}{\text{cm}}\right]\cdot\ell\left(\ln\left(\frac{4\ell}{d}\right)-1\right)\ . \tag{7.5}$$

For very short wires, representative of vias in a printed circuit board, the inductance is

$$L(\text{in nH}) \approx \ell/d\,. \tag{7.6}$$

A transmission line is a pair of conductors with inductance L and capacitance C. The characteristic impedance $Z = \sqrt{L/C}$ and the phase velocity $v_p = 1/\sqrt{LC} = 1/\sqrt{\mu\varepsilon}$, which decreases with the inverse square root of the dielectric constant of the medium. Typical coaxial and ribbon cables have a propagation delay of about 5 ns/cm.

The impedance of a coaxial cable with outer diameter D and inner diameter d is

$$Z = 60\,\Omega\cdot\frac{1}{\sqrt{\varepsilon_r}}\ln\frac{D}{d}\,, \tag{7.7}$$

where the relative dielectric constant $\varepsilon_r = \varepsilon/\varepsilon_0$. A pair of parallel wires of diameter d and spacing $a > 2.5\,d$ has the impedance

$$Z = 120\,\Omega\cdot\frac{1}{\sqrt{\varepsilon_r}}\ln\frac{2a}{d}\,. \tag{7.8}$$

This yields the impedance of a wire at a spacing h above a ground plane,

$$Z = 60\,\Omega\cdot\frac{1}{\sqrt{\varepsilon_r}}\ln\frac{4h}{d}\,. \tag{7.9}$$

A common configuration utilizes a thin rectangular conductor above a ground plane with an intermediate dielectric (microstrip). Detailed calculations for this and other transmission line configurations are given by Gunston.*

* M.A.R. Gunston. Microwave Transmission Line Data, Noble Publishing Corp., Atlanta (1997) ISBN 1-884932-57-6, TK6565.T73G85.

7.3. Synchrotron radiation (CGS units)

For a particle of charge e, velocity $v = \beta c$, and energy $E = \gamma mc^2$, traveling in a circular orbit of radius R, the classical energy loss per revolution δE is

$$\delta E = \frac{4\pi}{3}\,\frac{e^2}{R}\,\beta^3\,\gamma^4\ . \tag{7.10}$$

For high-energy electrons or positrons ($\beta \approx 1$), this becomes

$$\delta E\ (\text{in MeV}) \approx 0.0885\ [E(\text{in GeV})]^4/R(\text{in m})\ . \tag{7.11}$$

For $\gamma \gg 1$, the energy radiated per revolution into the photon energy interval $d(\hbar\omega)$ is

$$dI = \frac{8\pi}{9}\alpha\,\gamma\,F(\omega/\omega_c)\,d(\hbar\omega)\ , \tag{7.12}$$

where $\alpha = e^2/\hbar c$ is the fine-structure constant and

$$\omega_c = \frac{3\gamma^3 c}{2R} \tag{7.13}$$

is the critical frequency. The normalized function $F(y)$ is

$$F(y) = \frac{9}{8\pi}\sqrt{3}\,y\int_y^\infty K_{5/3}\,(x)\ dx\ , \tag{7.14}$$

where $K_{5/3}\,(x)$ is a modified Bessel function of the third kind. For electrons or positrons,

$$\hbar\omega_c\,(\text{in keV}) \approx 2.22\ [E(\text{in GeV})]^3/R(\text{in m})\ . \tag{7.15}$$

Fig. 7.1 shows $F(y)$ over the important range of y.

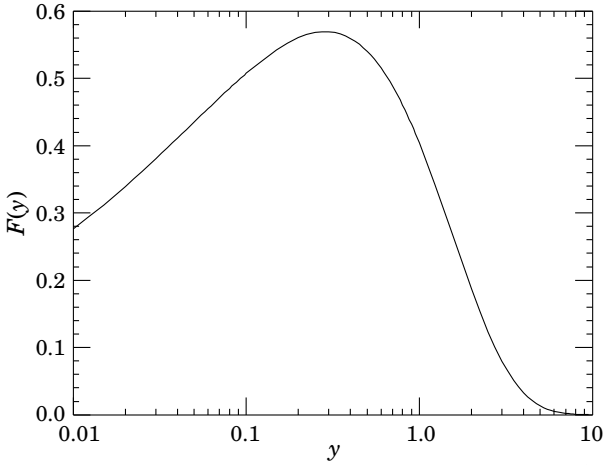

Figure 7.1: The normalized synchrotron radiation spectrum $F(y)$.

For $\gamma \gg 1$ and $\omega \ll \omega_c$,

$$\frac{dI}{d(\hbar\omega)} \approx 3.3\alpha\,(\omega R/c)^{1/3}\ , \tag{7.16}$$

whereas for

$$\gamma \gg 1 \text{ and } \omega \gtrsim 3\omega_c\ ,$$

$$\frac{dI}{d(\hbar\omega)} \approx \sqrt{\frac{3\pi}{2}}\,\alpha\,\gamma\left(\frac{\omega}{\omega_c}\right)^{1/2} e^{-\omega/\omega_c}\left[1+\frac{55}{72}\frac{\omega_c}{\omega}+\ldots\right]\ . \tag{7.17}$$

The radiation is confined to angles $\lesssim 1/\gamma$ relative to the instantaneous direction of motion. For $\gamma \gg 1$, where Eq. (7.12) applies, the mean number of photons emitted per revolution is

$$N_\gamma = \frac{5\pi}{\sqrt{3}}\alpha\gamma\ , \tag{7.18}$$

and the mean energy per photon is

$$\langle\hbar\omega\rangle = \frac{8}{15\sqrt{3}}\hbar\omega_c\ . \tag{7.19}$$

When $\langle\hbar\omega\rangle \gtrsim \mathrm{O}(E)$, quantum corrections are important.

See J.D. Jackson, *Classical Electrodynamics*, 3rd edition (John Wiley & Sons, New York, 1998) for more formulae and details. (Note that earlier editions had ω_c twice as large as Eq. (7.13).

8. Naming Scheme for Hadrons

Revised in 2017 by V. Burkert (Jefferson Lab), S. Eidelman (Budker Inst. and Novosibirsk State Univ.), C. Hanhart (Forschungszentrum Jülich), B.K. Heltsley (Cornell Univ.), E. Klempt (Bonn Univ.), R. E. Mitchell (Indiana Univ.), M.R. Pennington (Jefferson Lab), L. Tiator (Mainz Univ.), C.G. Wohl (LBNL), and R. Workman (George Washington Univ.)

In the 1986 edition [1], the Particle Data Group extended and systematized the naming scheme for mesons and baryons. The extensions were necessary in order to name the new particles containing c or b quarks that were rapidly being discovered. With the discoveries of particles that are candidates for states with more complicated structures than just $q\overline{q}$ or qqq, it is necessary to extend the naming scheme again.

8.1. "Neutral-flavor" mesons

The naming of mesons is based on their quantum numbers. Although we use names established within the naive quark model, the name does *not* necessarily designate a (predominantly) $q\overline{q}$ state. In other words, the name provides information on the quantum numbers of a given state and not about its dominant component, which might well be $q\overline{q}$ (if allowed) or tetraquark, molecule, etc. In many cases, exotic states will be difficult to distinguish from $q\overline{q}$ states and will likely mix with them, and we make no attempt to, e.g., distinguish those that are "mostly gluonium" from those that are "mostly $q\overline{q}$."

Table 8.1: Symbols for mesons with strangeness and heavy-flavor quantum numbers equal to zero. States that do not yet appear in the RPP are listed in parentheses.

$$J^{PC} = \begin{cases} 0^{-+} & 1^{+-} & 1^{--} & 0^{++} \\ 2^{-+} & 3^{+-} & 2^{--} & 1^{++} \\ \vdots & \vdots & \vdots & \vdots \end{cases}$$

Minimal quark content				
$u\overline{d}, u\overline{u}-d\overline{d}, d\overline{u}$ $(I=1)$	π	b	ρ	a
$d\overline{d}+u\overline{u}$ $(I=0)$ and/or $s\overline{s}$	η, η'	h, h'	ω, ϕ	f, f'
$c\overline{c}$	η_c	h_c	$\psi^\dagger$	χ_c
$b\overline{b}$	η_b	h_b	Υ	χ_b
$I=1$ with $c\overline{c}$	(Π_c)	Z_c	R_c	(W_c)
$I=1$ with $b\overline{b}$	(Π_b)	Z_b	(R_b)	(W_b)

†The J/ψ remains the J/ψ.

Table 8.1 shows the names for mesons having strangeness and all heavy-flavor quantum numbers equal to zero. The rows of Table 8.1 give the minimal $q\overline{q}$ content. The columns give the possible parity/charge-conjugation states,

$$PC = -+,\ +-,\ --, \text{ and } ++\ .$$

Within the naive quark model, these combinations correspond one-to-one to the angular-momentum state $^{2S+1}L_J$ of the $q\overline{q}$ system being

$$^1(L \text{ even})_J,\ ^1(L \text{ odd})_J,\ ^3(L \text{ even})_J, \text{ or } ^3(L \text{ odd})_J\ ,$$

respectively. Here S, L, and J are the spin, orbital, and total angular momenta of the $q\overline{q}$ system. Within the naive quark model, the quantum numbers are related by $P=(-1)^{L+1}$, $C=(-1)^{L+S}$, and G parity $=(-1)^{L+S+I}$, where the quantum number C is only relevant to neutral mesons with neutral-flavor quantum numbers and G extends to isovector mesons; see the review on the quark model. These expressions impose restrictions on the quantum numbers that are allowed for $q\overline{q}$ states. However, they do not apply to more complicated structures such as tetraquarks.

The spin J is added as a subscript in the name except for pseudoscalar and vector mesons, and the mass is added in parentheses for mesons that decay strongly. However, for some of the familiar mesons (e.g. η', ϕ, ω), we omit the mass.

Measurements of the mass, quark content (where relevant), and quantum numbers I, J, P, and C (or G) of a meson thus determine its symbol. Conversely, these properties may be inferred unambiguously from the symbol. The name X is used for states with still unknown quantum numbers.

The mass label used in particle names is chosen using the best information available when a name is assigned. A more accurate value of a particle mass may become available at a later time. PDG will decide on a case-by-case basis whether to revise the mass label, taking into account the updated information.

With u, d, and s quarks, there are two isospin-0 mesons. A prime is used to distinguish one from the other (e.g. η and η'). Vector mesons decoupling to $u\overline{u}+d\overline{d}$ and $s\overline{s}$ (ideal mixing) are labeled ω and ϕ, respectively. As usual, we assign the spectroscopic name (e.g. $\Upsilon(1S)$) as the primary name to most of those ψ, Υ, and χ states whose spectroscopic identity is known. We use the form $\Upsilon(9460)$ as an alternative, and as the primary name when the spectroscopic identity is not known.

Since the top quark is so heavy that it decays too rapidly to form bound states, no name is assigned to structures like $t\overline{t}$.

Mesons with quantum numbers $J^{PC}=0^{--}, 0^{+-}, 1^{-+}, 2^{+-}, 3^{-+}$, etc. cannot be $q\overline{q}$. For such a "manifestly exotic" meson, we use the same symbol as for a $q\overline{q}$ meson; the exotic nature of the meson can be inferred from the values of the P and C quantum numbers (given by the symbol), and the spin J (given by the subscript). For example, an isospin-0 1^{-+} meson containing only u, d, and s quarks and antiquarks would be denoted η_1 and an isospin-1 0^{--} meson containing only u, d, and s quarks and antiquarks would be denoted ρ_0.

The last two lines of Table 8.1 list isospin-1 states that also contain hidden heavy flavor, i.e. whose minimal quark content includes $c\overline{c}$ or $b\overline{b}$. We have assigned new names to these states, in keeping with the practice in the light-quark sector, where the $I=0$ and $I=1$ states have distinct names. The currently established $I=1$ states in the heavy-quark sector have quantum numbers $J^{PC}=1^{+-}$ and the proposed scheme keeps their original names Z.

8.2. Remarks on "neutral-flavor" mesons with hidden charm or bottom not classified as $q\overline{q}$

In the heavy-quark sector, there are several states with properties such as masses, decay patterns, and widths, which are in disagreement with predictions from the naive quark model. For example, the vector state at 4260 MeV does not decay into $D\overline{D}$, although within the naive quark model its quantum numbers would call for this decay channel to be dominant. In recent literature, these states have been called X, Y, or Z, with their masses added in parentheses. This nomenclature conflicts with the rules outlined in the previous section, since the meson names are not related to their quantum numbers. However, these states have properties in conflict with the naive quark model and therefore deserve some special labeling.

Therefore in the Review of Particle Physics we will keep two names, one that carries the quantum number information and the other the original name. However, the former name will be given priority. In particular, it will be used when the particle appears as a decay product. Thus, in the Listings as well as Summary Tables from the 2018 edition onwards (listed are only some examples of the particles that appear in the Summary Tables),

- $X(3872)$ will appear as '$\chi_{c1}(3872)$ also known as $X(3872)$';
- $X(3900)^\pm$ will appear as '$Z_c(3900)^\pm$';
- $X(4260)$ will appear as '$\psi(4260)$ also known as $Y(4260)$';

In addition, states with quantum numbers allowed by the naive quark model but showing some peculiarities, such as an unusual decay pattern, will have the following information in the header:

This state shows properties different from a conventional $q\overline{q}$ state. A candidate for an exotic structure. See the minireview on non-$q\overline{q}$ states.

The states that cannot be classified as $q\overline{q}$ states (such as charged states with strong decays to heavy quarkonia) will have in the header:

Properties incompatible with a $q\overline{q}$ structure (exotic state). See the minireview on non-$q\overline{q}$ states.

The names Z_c and Z_b used in the literature for isovector states in the $c\overline{c}$ and $b\overline{b}$ sector, respectively, will now also be the official PDG names. No heavy isovector $PC = -+, --$, or $++$ states have yet been confirmed, but provisional names for such states – Π, R, and W, respectively, – are listed in Table 8.1. Note that the heavy isovector $PC = ++$ states were predicted to exist as spin partners of the Z states in Ref. 2, where also the name W was introduced.

By analogy to the light-quark sector, states with quantum numbers that are in conflict with the naive quark model are labeled according to their I, P, C, and spin J. The exotic nature can be inferred from the quantum numbers.

8.3. Mesons with nonzero S, C and/or B

Mesons with nonzero strangeness S or heavy flavor C and/or B are not eigenstates of charge conjugation, and in each of them one of the quarks is heavier than the other (as above, states containing top quarks are not considered). The rules have been and remain:

1. The main symbol is an upper-case italic letter indicating the heavier quark as follows:

   $s \to \overline{K}$ $\quad c \to D$ $\quad b \to \overline{B}$,

   We use the convention that *the flavor quantum number and the charge of a quark have the same sign.* Thus the strangeness of the s quark is negative, the charm of the c quark is positive, and the bottomness of the b quark is negative. The effect of this convention is as follows: *any flavor carried by a charged meson has the same sign as its charge.* Thus the K^+, D^+, and B^+ have positive strangeness, charm, and bottomness, respectively, and all have positive I_3. The D_s^+ has positive charm *and* strangeness. Furthermore, the $\Delta(\text{flavor}) = \Delta Q$ rule, best known for the strange kaons, applies to every flavor.
2. If the lighter quark is not a u or a d quark, its identity is given by a subscript. The D_s^+ is an example.
3. When the spin-parity is in the natural series, $J^P = 0^+, 1^-, 2^+, \cdots$, a superscript "*" is added.
4. The spin is added as a subscript except for pseudoscalar or vector mesons.

8.4. Ordinary (3-quark) baryons

All baryons having quantum numbers consistent with a minimal quark content of three quarks are denoted by the symbols N, Δ, Λ, Σ, Ξ, and Ω introduced more than 50 years ago. These symbols are followed by J^P signifying their spin J and parity P. For those where the minimal content involves one or more heavier quarks than the light (u, d, and s) quarks, subscripts are added to their symbols, (c and b) as appropriate. The rules are:

1. Baryons with miminal content of *three* u and/or d quarks are N's (isospin 1/2) or Δ's (isospin 3/2).
2. Baryons with *two* u and/or d quarks are Λ's (isospin 0) or Σ's (isospin 1). If the third quark is a c or b quark, its identity is given by a subscript.
3. Baryons with *one* u or d quark are Ξ's (isospin 1/2). One or two subscripts are used if one or both of the remaining quarks are heavy: thus Ξ_c, Ξ_{cc}, Ξ_b, etc.*
4. Baryons with *no* u or d quarks are Ω's (isospin 0), and subscripts indicate any heavy-quark content.
5. A baryon that decays strongly has its mass in parentheses. Examples are the $\Delta(1232)$ $3/2^+$, $\Sigma(1385)$ $3/2^+$, $N(1440)$ $1/2^+$, $\Xi_c(2645)$ $3/2^+$.

In short, the minimal number of u plus d quarks together with the isospin determine the main symbol, and subscripts indicate any content of heavy quarks. A Σ always has isospin 1, an Ω always has isospin 0, etc.

8.5. Exotic baryons

In 2003, several experiments reported finding a strangeness $S = +1$, charge $Q = +1$ baryon, and one experiment reported finding an $S = -2$, $Q = -2$ baryon. Baryons with such quantum numbers cannot be made from three quarks, and thus they are exotic with respect to the naive quark model. However, these "discoveries" were then ruled out by many experiments with far larger statistics: See our 2008 *Review* [3].

The two putative pentaquark states found by LHCb [4] in the $J/\psi p$ system extracted from data on $\Lambda_b^0 \to J/\psi K^- p$ have the quantum numbers of excited nucleons, but decay into a $c\overline{c}$–state. The narrower state, for instance, is labeled as $P_c(4450)J^P$ with $J^P = 3/2^\mp$ or $5/2^\pm$, following the name given by the LHCb collaboration.**

8.6. Change of meson names

For the recently discovered particles above open-flavor threshold in the charmonium and bottomonium systems (previously the "XYZ" mesons), there are a number of differences between the names newly adopted by the PDG and those that have commonly appeared in the literature. Table 8.2 maps the names now used in the PDG to former commonly used names.

Table 8.2: A comparison of current PDG names to former names commonly used in the literature.

Mesons with complete $I^G J^{PC}$ assignment	
PDG Name	Former Common Name(s)
$\psi_2(3823)$[1]	$X(3823)$
$\chi_{c1}(3872)$	$X(3872)$
$Z_c(3900)$	$Z_c(3900)$
$\chi_{c2}(3930)$[2]	$\chi_{c2}(2P)$, $Z(3930)$
$\chi_{c1}(4140)$	$Y(4140)$
$Z_c(4200)$	$Z_c(4200)$
$\psi(4230)$	$Y(4230)$
$R_{c0}(4240)$	$Z_c(4240)$
$\psi(4260)$	$Y(4260)$
$\chi_{c1}(4274)$	$Y(4274)$
$\psi(4360)$	$Y(4360)$
$Z_c(4430)$	$Z_c(4430)$
$\chi_{c0}(4500)$	$X(4500)$
$\psi(4660)$	$X(4630)$, $Y(4660)$
$\chi_{c0}(4700)$	$X(4700)$
$Z_b(10610)$	$Z_b(10610)$
$Z_b(10650)$	$Z_b^{(\prime)}(10650)$
Mesons with incomplete $I^G J^{PC}$ assignment.	
PDG Name	Former Common Name(s)
$X(3915)$[3]	$\chi_{c0}(3915)$, $X(3915)$, $Y(3940)$
$X(3940)$	$X(3940)$
$X(4020)$	$Z_c^{(\prime)}(4020)$
$X(4050)^\pm$	$Z_1(4050)$
$X(4055)^\pm$	$Z_c(4055)$
$X(4160)$	$X(4160)$
$X(4250)^\pm$	$Z_2(4250)$
$X(4350)$	$X(4350)$

[1]The 2016 edition used $\psi(3823)$.
[2]The 2016 edition used $\chi_{c2}(2P)$. The mass is now used in the name following the current prescription.
[3]The 2016 edition used $\chi_{c0}(3915)$. The J^{PC} have since been questioned.

Footnotes and References:

* See the review on "Charmed Baryons."

** See our review on "Pentaquarks."

1. Particle Data Group: M. Aguilar-Benitez *et al.*, Phys. Lett. **170B**, 2 (1986).
2. M.B. Voloshin, Phys. Rev. **D84**, 031502 (2011).
3. Particle Data Group: C. Amsler, *et al.*, Phys. Lett. **B667**, 1 (2008).
4. R. Aaij, *et al.* [LHCb Collaboration], Phys. Rev. Lett. **115**, 072001 (2015).

9. Quantum Chromodynamics

Revised September 2017 by S. Bethke (Max-Planck-Institute of Physics, Munich), G. Dissertori (ETH Zurich), and G.P. Salam (CERN).[1]

This update retains the 2016 summary of α_s values, as few new results were available at the deadline for this Review. Those and further new results will be included in the next update.

9.1. Basics

Quantum Chromodynamics (QCD), the gauge field theory that describes the strong interactions of colored quarks and gluons, is the SU(3) component of the SU(3)×SU(2)×U(1) Standard Model of Particle Physics.

The Lagrangian of QCD is given by

$$\mathcal{L} = \sum_q \bar{\psi}_{q,a}(i\gamma^\mu \partial_\mu \delta_{ab} - g_s \gamma^\mu t^C_{ab} \mathcal{A}^C_\mu - m_q \delta_{ab})\psi_{q,b} - \frac{1}{4} F^A_{\mu\nu} F^{A\,\mu\nu} \,, \quad (9.1)$$

where repeated indices are summed over. The γ^μ are the Dirac γ-matrices. The $\psi_{q,a}$ are quark-field spinors for a quark of flavor q and mass m_q, with a color-index a that runs from $a = 1$ to $N_c = 3$, *i.e.* quarks come in three "colors." Quarks are said to be in the fundamental representation of the SU(3) color group.

The $\mathcal{A}^C_\mu$ correspond to the gluon fields, with C running from 1 to $N_c^2 - 1 = 8$, *i.e.* there are eight kinds of gluon. Gluons transform under the adjoint representation of the SU(3) color group. The t^C_{ab} correspond to eight 3×3 matrices and are the generators of the SU(3) group (*cf.* the section on "SU(3) isoscalar factors and representation matrices" in this *Review*, with $t^C_{ab} \equiv \lambda^C_{ab}/2$). They encode the fact that a gluon's interaction with a quark rotates the quark's color in SU(3) space. The quantity g_s is the QCD coupling constant. Finally, the field tensor $F^A_{\mu\nu}$ is given by

$$F^A_{\mu\nu} = \partial_\mu \mathcal{A}^A_\nu - \partial_\nu \mathcal{A}^A_\mu - g_s\, f_{ABC} \mathcal{A}^B_\mu \mathcal{A}^C_\nu \qquad [t^A, t^B] = i f_{ABC} t^C \,, \quad (9.2)$$

where the f_{ABC} are the structure constants of the SU(3) group.

Neither quarks nor gluons are observed as free particles. Hadrons are color-singlet (*i.e.* color-neutral) combinations of quarks, anti-quarks, and gluons.

Ab-initio predictive methods for QCD include lattice gauge theory and perturbative expansions in the coupling. The Feynman rules of QCD involve a quark-antiquark-gluon ($q\bar{q}g$) vertex, a 3-gluon vertex (both proportional to g_s), and a 4-gluon vertex (proportional to g_s^2). A full set of Feynman rules is to be found for example in Ref. 1.

Useful color-algebra relations include: $t^A_{ab} t^A_{bc} = C_F \delta_{ac}$, where $C_F \equiv (N_c^2 - 1)/(2N_c) = 4/3$ is the color-factor ("Casimir") associated with gluon emission from a quark; $f_{ACD} f_{BCD} = C_A \delta_{AB}$ where $C_A \equiv N_c = 3$ is the color-factor associated with gluon emission from a gluon; $t^A_{ab} t^B_{ab} = T_R \delta_{AB}$, where $T_R = 1/2$ is the color-factor for a gluon to split to a $q\bar{q}$ pair.

The fundamental parameters of QCD are the coupling g_s (or $\alpha_s = \frac{g_s^2}{4\pi}$) and the quark masses m_q.

There is freedom for an additional CP-violating term to be present in the QCD Lagrangian, $\theta \frac{\alpha_s}{8\pi} F^A_{\mu\nu} \tilde{F}^{A\,\mu\nu}$, where $\tilde{F}^{A\,\mu\nu}$ is the dual of the gluon field tensor, $\frac{1}{2}\epsilon_{\mu\nu\sigma\rho} F^{A\,\sigma\rho}$, where $\epsilon_{\mu\nu\sigma\rho}$ is the fully antisymmetric Levi-Cevita symbol. Experimental limits on the neutron electric dipole moment [2] constrain the coefficient of this contribution to satisfy $|\theta| \lesssim 10^{-10}$. Further discussion is to be found in Ref. 3 and in the Axions section in the Listings of this *Review*.

This section will concentrate mainly on perturbative aspects of QCD as they relate to collider physics. Related textbooks and reviews include Refs. 1,4–8. Aspects specific to Monte Carlo event generators are reviewed in the dedicated section 41. Lattice QCD is also reviewed in a section of its own, Sec. 17, with further discussion of perturbative and non-perturbative aspects to be found in the sections on "Quark Masses", "The CKM quark-mixing matrix", "Structure Functions", "Fragmentation Functions", and "Heavy-Quark and Soft-Collinear Effective Theory" in this *Review*. For an overview of some of the QCD issues and recent results in heavy-ion physics, see for example Refs. [9–11].

9.1.1. *Running coupling* :

In the framework of perturbative QCD (pQCD), predictions for observables are expressed in terms of the renormalized coupling $\alpha_s(\mu_R^2)$, a function of an (unphysical) renormalization scale μ_R. When one takes μ_R close to the scale of the momentum transfer Q in a given process, then $\alpha_s(\mu_R^2 \simeq Q^2)$ is indicative of the effective strength of the strong interaction in that process.

The coupling satisfies the following renormalization group equation (RGE):

$$\mu_R^2 \frac{d\alpha_s}{d\mu_R^2} = \beta(\alpha_s) = -(b_0 \alpha_s^2 + b_1 \alpha_s^3 + b_2 \alpha_s^4 + \cdots) \quad (9.3)$$

where $b_0 = (11C_A - 4n_f T_R)/(12\pi) = (33 - 2n_f)/(12\pi)$ is referred to as the 1-loop β-function coefficient, the 2-loop coefficient is $b_1 = (17C_A^2 - n_f T_R(10C_A + 6C_F))/(24\pi^2) = (153 - 19n_f)/(24\pi^2)$, and the 3-loop coefficient is $b_2 = (2857 - \frac{5033}{9} n_f + \frac{325}{27} n_f^2)/(128\pi^3)$ for the SU(3) values of C_A and C_F. The 4-loop coefficient, b_3, is to be found in Refs. 12, 13, while the 5-loop coefficient, b_4, is in Refs. 14–16. The coefficients b_2 and b_3 (and beyond) are renormalization-scheme-dependent, and given here in the modified minimal subtraction ($\overline{\rm MS}$) scheme [17], by far the most widely used scheme in QCD.

The minus sign in Eq. (9.3) is the origin of Asymptotic Freedom [18,19], *i.e.* the fact that the strong coupling becomes weak for processes involving large momentum transfers ("hard processes"). For momentum transfers in the 100 GeV – TeV range, $\alpha_s \sim 0.1$, while the theory is strongly interacting for scales around and below 1 GeV.

The β-function coefficients, the b_i, are given for the coupling of an *effective theory* in which n_f of the quark flavors are considered light ($m_q \ll \mu_R$), and in which the remaining heavier quark flavors decouple from the theory. One may relate the coupling for the theory with $n_f + 1$ light flavors to that with n_f flavors through an equation of the form

$$\alpha_s^{(n_f+1)}(\mu_R^2) = \alpha_s^{(n_f)}(\mu_R^2) \left(1 + \sum_{n=1}^{\infty} \sum_{\ell=0}^{n} c_{n\ell} \, [\alpha_s^{(n_f)}(\mu_R^2)]^n \ln^\ell \frac{\mu_R^2}{m_h^2} \right) , \quad (9.4)$$

where m_h is the mass of the $(n_f+1)^{\rm th}$ flavor, and the first few $c_{n\ell}$ coefficients are $c_{11} = \frac{1}{6\pi}$, $c_{10} = 0$, $c_{22} = c_{11}^2$, $c_{21} = \frac{19}{24\pi^2}$, and $c_{20} = -\frac{11}{72\pi^2}$ when m_h is the $\overline{\rm MS}$ mass at scale m_h ($c_{20} = \frac{7}{24\pi^2}$ when m_h is the pole mass — mass definitions are discussed below and in the review on "Quark Masses"). Terms up to $c_{4\ell}$ are to be found in Refs. 20, 21. Numerically, when one chooses $\mu_R = m_h$, the matching is a modest effect, owing to the zero value for the c_{10} coefficient. Relations between n_f and (n_f+2) flavors where the two heavy flavors are close in mass are given to three loops in Ref. 22.

Working in an energy range where the number of flavors is taken constant, a simple exact analytic solution exists for Eq. (9.3) only if one neglects all but the b_0 term, giving $\alpha_s(\mu_R^2) = (b_0 \ln(\mu_R^2/\Lambda^2))^{-1}$. Here Λ is a constant of integration, which corresponds to the scale where the perturbatively-defined coupling would diverge. Its value is indicative of the energy range where non-perturbative dynamics dominates. A convenient approximate analytic solution to the RGE that includes the terms up to b_4 is given by the iterative solution of Eq. (9.3)

$$\alpha_s(\mu_R^2) \simeq \frac{1}{b_0 t} \left(1 - \frac{b_1}{b_0^2} \frac{\ell}{t} + \frac{b_1^2(\ell^2 - \ell - 1) + b_0 b_2}{b_0^4 t^2} \right.$$
$$+ \frac{b_1^3 \left(-2\ell^3 + 5\ell^2 + 4\ell - 1\right) - 6 b_0 b_2 b_1 \ell + b_0^2 b_3}{2 b_0^6 t^3}$$
$$\left. + \frac{18 b_0 b_2 b_1^2 \left(2\ell^2 - \ell - 1\right) + b_1^4 \left(6\ell^4 - 26\ell^3 - 9\ell^2 + 24\ell + 7\right)}{6 b_0^8 t^4} \right.$$

[1] On leave from LPTHE, UMR 7589, CNRS, Paris, France

$$+\frac{-b_0^2 b_3 b_1(12\ell+1)+2b_0^2\left(5b_2^2+b_0 b_4\right)}{6b_0^8 t^4}\Bigg), \tag{9.5}$$

with $t \equiv \ln\frac{\mu_R^2}{\Lambda^2}$ and $\ell = \ln t$, again parametrized in terms of a constant Λ. Note that Eq. (9.5) is one of several possible approximate 4-loop solutions for $\alpha_s(\mu_R^2)$, and that a value for Λ only defines $\alpha_s(\mu_R^2)$ once one knows which particular approximation is being used. An alternative to the use of formulas such as Eq. (9.5) is to solve the RGE exactly, numerically (including the discontinuities, Eq. (9.4), at flavor thresholds). In such cases the quantity Λ does directly arise (though it can be defined, cf. Eqs. (1–3) of Ref.24). For these reasons, in determinations of the coupling, it has become standard practice to quote the value of α_s at a given scale (typically the mass of the Z boson, M_Z) rather than to quote a value for Λ.

The value of the coupling, as well as the exact forms of the b_2, c_{10} (and higher-order) coefficients, depend on the renormalization scheme in which the coupling is defined, *i.e.* the convention used to subtract infinities in the context of renormalization. The coefficients given above hold for a coupling defined in the $\overline{\rm MS}$ scheme.

A discussion of determinations of the coupling and a graph illustrating its scale dependence ("running") are to be found in Section 9.4. The RunDec package [25,26,27] is often used to calculate the evolution of the coupling. For a discussion of electroweak effects in the evolution of the QCD coupling, see Ref. 28 and references therein.

9.1.2. *Quark masses* :

Free quarks have never been observed, which is understood as a result of a long-distance, confining property of the strong QCD force: up, down, strange, charm, and bottom quarks all *hadronize*, *i.e.* become part of a meson or baryon, on a timescale $\sim 1/\Lambda$; the top quark instead decays before it has time to hadronize. This means that the question of what one means by the quark mass is a complex one, which requires that one adopts a specific prescription. A perturbatively defined prescription is the pole mass, m_q, which corresponds to the position of the divergence of the propagator. This is close to one's physical picture of mass. However, when relating it to observable quantities, it suffers from substantial non-perturbative ambiguities (see *e.g.* Ref. 29). An alternative is the $\overline{\rm MS}$ mass, $\overline{m}_q(\mu_R^2)$, which depends on the renormalization scale μ_R.

Results for the masses of heavier quarks are often quoted either as the pole mass or as the $\overline{\rm MS}$ mass evaluated at a scale equal to the mass, $\overline{m}_q(\overline{m}_q^2)$; light quark masses are often quoted in the $\overline{\rm MS}$ scheme at a scale $\mu_R \sim 2$ GeV. The pole and $\overline{\rm MS}$ masses are related by a slowly converging series that starts $m_q = \overline{m}_q(\overline{m}_q^2)(1+\frac{4\alpha_s(\overline{m}_q^2)}{3\pi}+\mathcal{O}(\alpha_s^2))$, while the scale-dependence of $\overline{\rm MS}$ masses is given by

$$\mu_R^2\frac{d\overline{m}_q(\mu_R^2)}{d\mu_R^2} = \left[-\frac{\alpha_s(\mu_R^2)}{\pi}+\mathcal{O}(\alpha_s^2)\right]\overline{m}_q(\mu_R^2)\,. \tag{9.6}$$

More detailed discussion is to be found in a dedicated section of the *Review*, "Quark Masses.", with detailed formulas also in Ref. 30 and references therein.

In perturbative QCD calculations of scattering processes, it is common to work in an approximation in which one neglects (*i.e.* sets to zero) the masses of all quarks whose mass is significantly smaller than the momentum transfer in the process.

9.2. Structure of QCD predictions

9.2.1. *Fully inclusive cross sections* :

The simplest observables in perturbative QCD are those that do not involve initial-state hadrons and that are fully inclusive with respect to details of the final state. One example is the total cross section for $e^+e^- \to$ hadrons at center-of-mass energy Q, for which one can write

$$\frac{\sigma(e^+e^-\to \text{hadrons}, Q)}{\sigma(e^+e^-\to\mu^+\mu^-, Q)} \equiv R(Q) = R_{\rm EW}(Q)(1+\delta_{\rm QCD}(Q))\,, \tag{9.7}$$

where $R_{\rm EW}(Q)$ is the purely electroweak prediction for the ratio and $\delta_{\rm QCD}(Q)$ is the correction due to QCD effects. To keep the discussion simple, we can restrict our attention to energies $Q \ll M_Z$, where the process is dominated by photon exchange ($R_{\rm EW} = 3\sum_q e_q^2$, neglecting finite-quark-mass corrections, where the e_q are the electric charges of the quarks),

$$\delta_{\rm QCD}(Q) = \sum_{n=1}^{\infty} c_n \cdot \left(\frac{\alpha_s(Q^2)}{\pi}\right)^n + \mathcal{O}\left(\frac{\Lambda^4}{Q^4}\right)\,. \tag{9.8}$$

The first four terms in the α_s series expansion are then to be found in Ref. 31,

$$c_1 = 1\,, \qquad c_2 = 1.9857 - 0.1152 n_f\,, \tag{9.9a}$$

$$c_3 = -6.63694 - 1.20013 n_f - 0.00518 n_f^2 - 1.240\eta\,, \tag{9.9b}$$

$$c_4 = 156.61 + 18.775 n_f - 0.7974 n_f^2 + 0.0215 n_f^3 - (17.828 - 0.575 n_f)\eta\,, \tag{9.9c}$$

with $\eta = (\sum e_q)^2/(3\sum e_q^2)$. For corresponding expressions including also Z exchange and finite-quark-mass effects, see Refs. [32–34].

A related series holds also for the QCD corrections to the hadronic decay width of the τ lepton, which essentially involves an integral of $R(Q)$ over the allowed range of invariant masses of the hadronic part of the τ decay (see *e.g.* Ref. 35). The series expansions for QCD corrections to Higgs-boson hadronic (partial) decay widths are summarized in Refs. 36, 37, 38.

One characteristic feature of Eqs. (9.8) and (9.9) is that the coefficients of α_s^n increase order by order: calculations in perturbative QCD tend to converge more slowly than would be expected based just on the size of α_s[††]. Another feature is the existence of an extra "power-correction" term $\mathcal{O}(\Lambda^4/Q^4)$ in Eq. (9.8), which accounts for contributions that are fundamentally non-perturbative. All high-energy QCD predictions involve such corrections, though the exact power of Λ/Q depends on the observable. For many processes and observables, it is possible to introduce an operator product expansion and associate power suppressed terms with specific higher-dimension (non-perturbative) operators.

Scale dependence. In Eq. (9.8) the renormalization scale for α_s has been chosen equal to Q. The result can also be expressed in terms of the coupling at an arbitrary renormalization scale μ_R,

$$\delta_{\rm QCD}(Q) = \sum_{n=1}^{\infty} \overline{c}_n\!\left(\frac{\mu_R^2}{Q^2}\right)\cdot\left(\frac{\alpha_s(\mu_R^2)}{\pi}\right)^n + \mathcal{O}\left(\frac{\Lambda^4}{Q^4}\right)\,, \tag{9.10}$$

where $\overline{c}_1(\mu_R^2/Q^2) \equiv c_1$, $\overline{c}_2(\mu_R^2/Q^2) = c_2 + \pi b_0 c_1 \ln(\mu_R^2/Q^2)$, $\overline{c}_3(\mu_R^2/Q^2) = c_3 + (2b_0c_2\pi + b_1c_1\pi^2)\ln(\mu_R^2/Q^2) + b_0^2c_1\pi^2\ln^2(\mu_R^2/Q^2)$, *etc.* Given an infinite number of terms in the α_s expansion, the μ_R dependence of the $\overline{c}_n(\mu_R^2/Q^2)$ coefficients will exactly cancel that of $\alpha_s(\mu_R^2)$, and the final result will be independent of the choice of μ_R: physical observables do not depend on unphysical scales.[**]

With just terms up to some finite $n = N$, a residual μ_R dependence will remain, which implies an uncertainty on the prediction of $R(Q)$ due to the arbitrariness of the scale choice. This uncertainty will be $\mathcal{O}(\alpha_s^{N+1})$, *i.e.* of the same order as the neglected terms. For this reason it is customary to use QCD predictions' scale dependence as an

[††] The situation is significantly worse near thresholds, *e.g.* the $t\bar{t}$ production threshold. An overview of some of the methods used in such cases is to be found for example in Ref. 39.

[**] There is an important caveat to this statement: at sufficiently high orders, perturbative series generally suffer from "renormalon" divergences $\alpha_s^n n!$ (reviewed in Ref. 29). This phenomenon is not usually visible with the limited number of perturbative terms available today. However it is closely connected with non-perturbative contributions and sets a limit on the possible precision of perturbative predictions. The cancellation of scale dependence will also ultimately be affected by this renormalon-induced breakdown of perturbation theory.

estimate of the uncertainties due to neglected terms. One usually takes a central value for $\mu_R \sim Q$, in order to avoid the poor convergence of the perturbative series that results from the large $\ln^{n-1}(\mu_R^2/Q^2)$ terms in the $\overline{c}_n$ coefficients when $\mu_R \ll Q$ or $\mu_R \gg Q$. Uncertainties are then commonly determined by varying μ_R by a factor of two up and down around the central scale choice, as discussed in more detail below in Section 9.2.4.

9.2.2. *Processes with initial-state hadrons* :

Deep Inelastic Scattering. To illustrate the key features of QCD cross sections in processes with initial-state hadrons, let us consider deep-inelastic scattering (DIS), $ep \to e + X$, where an electron e with four-momentum k emits a highly off-shell photon (momentum q) that interacts with the proton (momentum p). For photon virtualities $Q^2 \equiv -q^2$ far above the squared proton mass (but far below the Z mass), the differential cross section in terms of the kinematic variables Q^2, $x = Q^2/(2p\cdot q)$ and $y = (q\cdot p)/(k\cdot p)$ is

$$\frac{d^2\sigma}{dx dQ^2} = \frac{4\pi\alpha^2}{2xQ^4}\left[(1+(1-y)^2)F_2(x,Q^2) - y^2 F_L(x,Q^2)\right], \quad (9.11)$$

where α is the electromagnetic coupling and $F_2(x,Q^2)$ and $F_L(x,Q^2)$ are proton structure functions, which encode the interaction between the photon (in given polarization states) and the proton. In the presence of parity-violating interactions (*e.g.* νp scattering) an additional F_3 structure function is present. For an extended review, including equations for the full electroweak and polarized cases, see Sec. 18 of this *Review*.

Structure functions are not calculable in perturbative QCD, nor is any other cross section that involves initial-state hadrons. To zeroth order in α_s, the structure functions are given directly in terms of non-perturbative parton (quark or gluon) distribution functions (PDFs),

$$F_2(x,Q^2) = x\sum_q e_q^2 f_{q/p}(x), \qquad F_L(x,Q^2) = 0, \quad (9.12)$$

where $f_{q/p}(x)$ is the PDF for quarks of type q inside the proton, *i.e.* the number density of quarks of type q inside a fast-moving proton that carry a fraction x of its longitudinal momentum (the quark flavor index q, here, is not to be confused with the photon momentum q in the lines preceding Eq. (9.11)). PDFs are non-perturbative, and only just starting to be extracted in lattice QCD in a phenomenologically relevant way [40] and there is also some debate about the underlying methods [41]. Accordingly, for all practical uses, they are determined from data (*cf.* Sec. 18 of this *Review* and also Ref. 42).

The above result, with PDFs $f_{q/p}(x)$ that are independent of the scale Q, corresponds to the "quark-parton model" picture in which the photon interacts with point-like free quarks, or equivalently, one has incoherent elastic scattering between the electron and individual constituents of the proton. As a consequence, in this picture also F_2 and F_L are independent of Q [43]. When including higher orders in pQCD, Eq. (9.12) becomes

$$F_2(x,Q^2) = x\sum_{n=0}^{\infty}\frac{\alpha_s^n(\mu_R^2)}{(2\pi)^n}\sum_{i=q,g}\int_x^1\frac{dz}{z}C_{2,i}^{(n)}(z,Q^2,\mu_R^2,\mu_F^2)\, f_{i/p}\Big(\frac{x}{z},\mu_F^2\Big) + \mathcal{O}\Big(\frac{\Lambda^2}{Q^2}\Big). \quad (9.13)$$

Just as in Eq. (9.10), we have a series in powers of $\alpha_s(\mu_R^2)$, each term involving a coefficient $C_{2,i}^{(n)}$ that can be calculated using Feynman graphs. An important difference is the additional integral over z. The parton that comes from the proton can emit a gluon before it interacts with the photon. As a result, the $C_{2,i}^{(n)}$ coefficients are functions that depend on the ratio, z, of the parton's momentum before and after the gluon emission, and one must integrate over that ratio. For the electromagnetic component of DIS with light quarks and gluons, the zeroth order coefficient functions are $C_{2,q}^{(0)} = e_q^2\delta(1-z)$ and $C_{2,g}^{(0)} = 0$. Corrections are known up to $\mathcal{O}(\alpha_s^3)$ (next-to-next-next-to-leading order, N^{3}LO) for both electromagnetic [44] and weak currents [45,46]. For heavy-quark production they are known to $\mathcal{O}(\alpha_s^2)$ [47] (next-to-leading order, NLO, insofar as the series starts at $\mathcal{O}(\alpha_s)$), with ongoing work towards NNLO summarized in Ref. 48.

The majority of the emissions that modify a parton's momentum are collinear (parallel) to that parton, and don't depend on the fact that the parton is destined to interact with a photon. It is natural to view these emissions as modifying the proton's structure rather than being part of the coefficient function for the parton's interaction with the photon. Technically, one uses a procedure known as *collinear factorization* to give a well-defined meaning to this distinction, most commonly through the $\overline{\text{MS}}$ factorization scheme, defined in the context of dimensional regularization. The $\overline{\text{MS}}$ factorization scheme involves an arbitrary choice of *factorization scale*, μ_F, whose meaning can be understood roughly as follows: emissions with transverse momenta above μ_F are included in the $C_{2,q}^{(n)}(z,Q^2,\mu_R^2,\mu_F^2)$; emissions with transverse momenta below μ_F are accounted for within the PDFs, $f_{i/p}(x,\mu_F^2)$. While collinear factorization is generally believed to be valid for suitable (sufficiently inclusive) observables in processes with hard scales, Ref. 49, which reviews the factorization proofs in detail, is cautious in the statements it makes about their exhaustivity, notably for the hadron-collider processes that we shall discuss below. Further discussion is to be found in Refs. 50,51.

The PDFs' resulting dependence on μ_F is described by the Dokshitzer-Gribov-Lipatov-Altarelli-Parisi (DGLAP) equations [52], which to leading order (LO) read*

$$\mu_F^2\frac{\partial f_{i/p}(x,\mu_F^2)}{\partial\mu_F^2} = \sum_j\frac{\alpha_s(\mu_F^2)}{2\pi}\int_x^1\frac{dz}{z}P_{i\leftarrow j}^{(1)}(z)f_{j/p}\Big(\frac{x}{z},\mu_F^2\Big), \quad (9.14)$$

with, for example, $P_{q\leftarrow g}^{(1)}(z) = T_R(z^2+(1-z)^2)$. The other LO splitting functions are listed in Sec. 18 of this *Review*, while results up to NLO, α_s^2, and NNLO, α_s^3, are given in Refs. 53 and 54 respectively. A significant part ("non-singlet") of the N^{3}LO results is given in Ref. 55. Splitting functions for polarized PDFs are given in Ref. 56. Beyond LO, the coefficient functions are also μ_F dependent, for example $C_{2,i}^{(1)}(x,Q^2,\mu_R^2,\mu_F^2) = C_{2,i}^{(1)}(x,Q^2,\mu_R^2,Q^2) - \ln\big(\frac{\mu_F^2}{Q^2}\big)\sum_j\int_x^1\frac{dz}{z}C_{2,j}^{(0)}(\frac{x}{z})P_{j\leftarrow i}^{(1)}(z)$. In certain contexts, higher-order QED and mixed QED-QCD corrections to the splitting functions are also needed [57].

As with the renormalization scale, the choice of factorization scale is arbitrary, but if one has an infinite number of terms in the perturbative series, the μ_F-dependences of the coefficient functions and PDFs will compensate each other fully. Given only N terms of the series, a residual $\mathcal{O}(\alpha_s^{N+1})$ uncertainty is associated with the ambiguity in the choice of μ_F. As with μ_R, varying μ_F provides an input in estimating uncertainties on predictions. In inclusive DIS predictions, the default choice for the scales is usually $\mu_R = \mu_F = Q$.

As is the case for the running coupling, in DGLAP evolution one can introduce flavor thresholds near the heavy quark masses: below a given heavy quark's mass, that quark is not considered to be part of the proton's structure, while above it is considered to be part of the proton's structure and evolves with massless DGLAP splitting kernels. With appropriate parton distribution matching terms at threshold, such a variable flavor number scheme (VFNS), when used with massless coefficient functions, gives the full heavy-quark contributions at high Q^2 scales. For scales near the threshold, it is instead necessary to appropriately adapt the standard massive coefficient functions to

* LO is generally taken to mean the lowest order at which a quantity is non-zero. This definition is nearly always unambiguous, the one major exception being for the case of the hadronic branching ratio of virtual photons, Z, τ, *etc.*, for which two conventions exist: LO can either mean the lowest order that contributes to the hadronic branching fraction, *i.e.* the term "1" in Eq. (9.7); or it can mean the lowest order at which the hadronic branching ratio becomes sensitive to the coupling, $n = 1$ in Eq. (9.8), as is relevant when extracting the value of the coupling from a measurement of the branching ratio. Because of this ambiguity, we avoid use of the term "LO" in that context.

account for the heavy-quark contribution already included in the PDFs [58,59,60].

Hadron-hadron collisions. The extension to processes with two initial-state hadrons can be illustrated with the example of the total (inclusive) cross section for W boson production in collisions of hadrons h_1 and h_2, which can be written as

$$\begin{aligned}&\sigma(h_1h_2 \to W + X)\\ &= \sum_{n=0}^{\infty} \alpha_s^n(\mu_R^2) \sum_{i,j} \int dx_1 dx_2\, f_{i/h_1}\left(x_1, \mu_F^2\right) f_{j/h_2}\left(x_2, \mu_F^2\right)\\ &\times \hat{\sigma}^{(n)}_{ij\to W+X}\left(x_1x_2s, \mu_R^2, \mu_F^2\right) + \mathcal{O}\left(\frac{\Lambda^2}{M_W^4}\right),\end{aligned} \tag{9.15}$$

where s is the squared center-of-mass energy of the collision. At LO, $n = 0$, the hard (partonic) cross section $\hat{\sigma}^{(0)}_{ij\to W+X}(x_1x_2s, \mu_R^2, \mu_F^2)$ is simply proportional to $\delta(x_1x_2s - M_W^2)$, in the narrow W-boson width approximation (see Sec. 49 of this *Review* for detailed expressions for this and other hard scattering cross sections). It is non-zero only for choices of i, j that can directly give a W, such as $i = u$, $j = \bar{d}$. At higher orders, $n \geq 1$, new partonic channels contribute, such as gq, and there is no restriction $x_1x_2s = M_W^2$.

Equation (9.15) involves a collinear factorization between the hard cross section and the PDFs, just like Eq. (9.13). As long as the same factorization scheme is used in DIS and pp or $p\bar{p}$ (usually the $\overline{\text{MS}}$ scheme), then PDFs extracted in DIS can be directly used in pp and $p\bar{p}$ predictions [61,49] (with the anti-quark distributions in an anti-proton being the same as the quark distributions in a proton).

Fully inclusive hard cross sections are known to NNLO, *i.e.* corrections up to relative order α_s^2, for Drell-Yan (DY) lepton-pair and vector-boson production [62,63], Higgs-boson production in association with a vector boson [64], Higgs-boson production via vector-boson fusion [65] (in an approximation that factorizes the production of the two vector bosons), Higgs-pair production [66], top-antitop production [67] and vector-boson pair production [68,69]. † Recently, inclusive Higgs production through gluon fusion and vector-boson fusion were calculated at N^{3}LO [70,71]. A discussion of many other Higgs results is to be found in Ref. 72.

Photoproduction. γp (and $\gamma\gamma$) collisions are similar to pp collisions, with the subtlety that the photon can behave in two ways: there is "direct" photoproduction, in which the photon behaves as a point-like particle and takes part directly in the hard collision, with hard subprocesses such as $\gamma g \to q\bar{q}$; there is also resolved photoproduction, in which the photon behaves like a hadron, with non-perturbative partonic substructure and a corresponding PDF for its quark and gluon content, $f_{i/\gamma}(x, Q^2)$.

While useful to understand the general structure of γp collisions, the distinction between direct and resolved photoproduction is not well defined beyond leading order, as discussed for example in Ref. 73.

The high-energy (BFKL) limit. In situations in which the total center-of-mass energy $\sqrt{s}$ is much larger than all other momentum-transfer scales in the problem (*e.g.* Q in DIS, m_b for $b\bar{b}$ production in pp collisions, *etc.*), each power of α_s beyond LO can be accompanied by a power of $\ln(s/Q^2)$ (or $\ln(s/m_b^2)$, *etc.*). This is variously referred to as the high-energy, small-x or Balitsky-Fadin-Kuraev-Lipatov (BFKL) limit [74–76]. Currently it is possible to account for the dominant and first subdominant [77,78] power of $\ln s$ at each order of α_s, and also to estimate further subdominant contributions that are numerically large (see Refs. 79–82 and references therein). Progress towards NNLO is discussed in Ref. 83.

Physically, the summation of all orders in α_s can be understood as leading to a growth with s of the gluon density in the proton. At sufficiently high energies this implies non-linear effects (commonly referred to as parton saturation), whose treatment has been the subject of intense study (see for example Refs. 84, 85 and references thereto). Note that it is not straightforward to relate these results to the genuinely non-perturbative total, elastic and diffractive cross sections for hadron-hadron scattering (experimental results for which are summarized in section 51 of this *Review*).

9.2.3. ***Non fully inclusive cross sections*** :

QCD final states always consist of hadrons, while perturbative QCD calculations deal with partons. Physically, an energetic parton fragments ("showers") into many further partons, which then, on later timescales, undergo a transition to hadrons ("hadronization"). Fixed-order perturbation theory captures only a small part of these dynamics.

This does not matter for the fully inclusive cross sections discussed above: the showering and hadronization stages are approximately unitary, *i.e.* they do not substantially change the overall probability of hard scattering, because they occur long after it has taken place (they introduce at most a correction proportional to a power of the ratio of timescales involved, *i.e.* a power of Λ/Q, where Q is the hard scattering scale).

Less inclusive measurements, in contrast, may be affected by the extra dynamics. For those sensitive just to the main directions of energy flow (jet rates, event shapes, *cf.* Sec. 9.3.1) fixed order perturbation theory is often still adequate, because showering and hadronization don't substantially change the overall energy flow. This means that one can make a prediction using just a small number of partons, which should correspond well to a measurement of the same observable carried out on hadrons. For observables that instead depend on distributions of individual hadrons (which, *e.g.*, are the inputs to detector simulations), it is mandatory to account for showering and hadronization. The range of predictive techniques available for QCD final states reflects this diversity of needs of different measurements.

While illustrating the different methods, we shall for simplicity mainly use expressions that hold for e^+e^- scattering. The extension to cases with initial-state partons will be mostly straightforward (space constraints unfortunately prevent us from addressing diffraction and exclusive hadron-production processes; extensive discussion is to be found in Refs. 86, 87).

9.2.3.1. *Soft and collinear limits:*

Before examining specific predictive methods, it is useful to be aware of a general property of QCD matrix elements in the soft and collinear limits. Consider a squared tree-level matrix element $|M_n^2(p_1, \ldots, p_n)|$ for the process $e^+e^- \to n$ partons with momenta $p_1, \ldots, p_n$, and a corresponding phase-space integration measure $d\Phi_n$. If particle n is a gluon, and additionally it becomes collinear (parallel) to another particle i and its momentum tends to zero (it becomes "soft"), the matrix element simplifies as follows,

$$\begin{aligned}&\lim_{\theta_{in}\to 0,\, E_n \to 0} d\Phi_n |M_n^2(p_1, \ldots, p_n)|\\ &\qquad = d\Phi_{n-1} |M_{n-1}^2(p_1, \ldots, p_{n-1})| \frac{\alpha_s C_i}{\pi} \frac{d\theta_{in}^2}{\theta_{in}^2} \frac{dE_n}{E_n},\end{aligned} \tag{9.16}$$

where $C_i = C_F$ (C_A) if i is a quark (gluon). This formula has non-integrable divergences both for the inter-parton angle $\theta_{in} \to 0$ and for the gluon energy $E_n \to 0$, which are mirrored also in the structure of divergences in loop diagrams. These divergences are important for at least two reasons: firstly, they govern the typical structure of events (inducing many emissions either with low energy or at small angle with respect to hard partons); secondly, they will determine which observables can be calculated within perturbative QCD.

9.2.3.2. *Fixed-order predictions:*

Let us consider an observable $\mathcal{O}$ that is a function $\mathcal{O}_n(p_1, \ldots, p_n)$ of the four-momenta of the n final-state particles in an event (whether partons or hadrons). In what follows, we shall consider the cross section for events weighted with the value of the observable, $\sigma_{\mathcal{O}}$. As examples, if $\mathcal{O}_n \equiv 1$ for all n, then $\sigma_{\mathcal{O}}$ is just the total cross section; if $\mathcal{O}_n \equiv \hat{\tau}(p_1, \ldots, p_n)$ where $\hat{\tau}$ is the value of the Thrust for that event (see Sec. 9.3.1.2), then the average value of the Thrust

† Processes with jets or photons in the final state have divergent cross sections unless one places cut on the jet or photon momentum. Accordingly they are discussed below in Section 9.2.3.2.

is $\langle\tau\rangle = \sigma_{\mathcal{O}}/\sigma_{\rm tot}$; if $\mathcal{O}_n \equiv \delta(\tau - \hat{\tau}(p_1,\ldots,p_n))$ then one gets the differential cross section as a function of the Thrust, $\sigma_{\mathcal{O}} \equiv d\sigma/d\tau$.

In the expressions below, we shall omit to write the non-perturbative power correction term, which for most common observables is proportional to a single power of Λ/Q.

LO. If the observable $\mathcal{O}$ is non-zero only for events with at least n final-state particles, then the LO QCD prediction for the weighted cross section in e^+e^- annihilation is

$$\sigma_{\mathcal{O},LO} = \alpha_s^{n-2}(\mu_R^2) \int d\Phi_n |M_n^2(p_1,\ldots,p_n)|\, \mathcal{O}_n(p_1,\ldots,p_n)\,, \quad (9.17)$$

where the squared tree-level matrix element, $|M_n^2(p_1,\ldots,p_n)|$, includes relevant symmetry factors, has been summed over all subprocesses (*e.g.* $e^+e^- \to q\bar{q}q\bar{q}$, $e^+e^- \to q\bar{q}gg$) and has had all factors of α_s extracted in front. In processes other than e^+e^- collisions, the center-of-mass energy of the LO process is generally not fixed, and so the powers of the coupling are often brought inside the integrals, with the scale μ_R chosen event by event, as a function of the event kinematics.

Other than in the simplest cases (see the review on Cross Sections in this *Review*), the matrix elements in Eq. (9.17) are usually calculated automatically with programs such as CompHEP [88], MadGraph [89], Alpgen [90], Comix/Sherpa [91], and Helac/Phegas [92]. Some of these (CompHEP, MadGraph) use formulas obtained from direct evaluations of Feynman diagrams. Others (Alpgen, Helac/Phegas and Comix/Sherpa) use methods designed to be particularly efficient at high multiplicities, such as Berends-Giele recursion [93], which builds up amplitudes for complex processes from simpler ones (see also the reviews and discussion in Refs. [94–96]).

The phase-space integration is usually carried out by Monte Carlo sampling, in order to deal with the sometimes complicated cuts that are used in corresponding experimental measurements. Because of the divergences in the matrix element, Eq. (9.16), the integral converges only if the observable vanishes for kinematic configurations in which one of the n particles is arbitrarily soft or it is collinear to another particle. As an example, the cross section for producing any configuration of n partons will lead to an infinite integral, whereas a finite result will be obtained for the cross section for producing n deposits of energy (or jets, see Sec. 9.3.1.1), each above some energy threshold and well separated from each other in angle.

LO calculations can be carried out for $2 \to n$ processes with $n \lesssim 6-10$. The exact upper limit depends on the process, the method used to evaluate the matrix elements (recursive methods are more efficient), and the extent to which the phase-space integration can be optimized to work around the large variations in the values of the matrix elements.

NLO. Given an observable that is non-zero starting from n final-state particles, its prediction at NLO involves supplementing the LO result, Eq. (9.17), with the $2 \to (n+1)$-particle squared tree-level matrix element ($|M_{n+1}^2|$), and the interference of an $2 \to n$ tree-level and $2 \to n$ 1-loop amplitude ($2\mathrm{Re}(M_n M_{n,1-\mathrm{loop}}^*)$),

$$\begin{aligned}\sigma_{\mathcal{O}}^{NLO} = {}& \\ \sigma_{\mathcal{O}}^{LO} &+ \alpha_s^{n-1}(\mu_R^2) \int d\Phi_{n+1} |M_{n+1}^2(p_1,\ldots,p_{n+1})|\, \mathcal{O}_{n+1}(p_1,\ldots,p_{n+1}) \\ &+ \alpha_s^{n-1}(\mu_R^2) \int d\Phi_n\, 2\mathrm{Re}\left[\, M_n(p_1,\ldots,p_n)\, M_{n,1-\mathrm{loop}}^*(p_1,\ldots,p_n)\,\right] \\ &\times \mathcal{O}_n(p_1,\ldots,p_n)\,. \end{aligned} \quad (9.18)$$

Relative to LO calculations, two important issues appear in the NLO calculations. Firstly, the extra complexity of loop-calculations relative to tree-level calculations means that their automation has been achieved only in recent years (see below). Secondly, loop amplitudes are infinite in 4 dimensions, while tree-level amplitudes are finite, but their *integrals* are infinite, due to the divergences of Eq. (9.16). These two sources of infinities have the same soft and collinear origins and cancel after the integration only if the observable $\mathcal{O}$ satisfies the property of infrared and collinear safety,

$$\begin{aligned} \mathcal{O}_{n+1}(p_1,\ldots,p_s,\ldots,p_n) &\to \mathcal{O}_n(p_1,\ldots,p_n) \quad \text{if } p_s \to 0 \\ \mathcal{O}_{n+1}(p_1,\ldots,p_a,p_b,\ldots,p_n) &\to \mathcal{O}_n(p_1,\ldots,p_a+p_b,\ldots,p_n) \\ &\quad \text{if } p_a \,||\, p_b\,. \end{aligned} \quad (9.19)$$

Examples of infrared-safe quantities include event-shape distributions and jet cross sections (with appropriate jet algorithms, see below). Unsafe quantities include the distribution of the momentum of the hardest QCD particle (which is not conserved under collinear splitting), observables that require the complete absence of radiation in some region of phase space (*e.g.* rapidity gaps or 100% isolation cuts, which are affected by soft emissions), or the particle multiplicity (affected by both soft and collinear emissions). The non-cancellation of divergences at NLO due to infrared or collinear unsafety compromises the usefulness not only of the NLO calculation, but also that of a LO calculation, since LO is only an acceptable approximation if one can prove that higher-order terms are smaller. Infrared and collinear unsafety usually also imply large non-perturbative effects.

As with LO calculations, the phase-space integrals in Eq. (9.18) are usually carried out by Monte Carlo integration, so as to facilitate the study of arbitrary observables. Various methods exist to obtain numerically efficient cancellation among the different infinities. These include notably dipole [97], FKS [98] and antenna [99] subtraction.

NLO calculations exist for a wide range of processes. Historically, many calculations have been performed process by process and are available in dedicated packages, among them NLOJet++ [100] for e^+e^-, DIS, and hadron-hadron processes involving just light partons in the final state, MCFM [101] for hadron-hadron processes with Higgs or vector bosons and/or heavy quarks in the final state, VBFNLO for vector-boson fusion, di- and tri-boson processes [102], and the Phox family [103] for processes with photons in the final state. Many of these programs are still widely used today.

Recent years have seen very active development of automated NLO calculational tools, and a number of programs are available publicly: Madgraph5_aMC@NLO [89] and Helac-NLO [104] provide full frameworks for NLO calculations; GoSam [105], Njet [106], OpenLoops [107] and Recola [108] calculate just the 1-loop part and are typically interfaced with an external tool such as Sherpa [109] for combination with the appropriate tree-level amplitudes. Another tool, BlackHat [110] is available publicly in a pre-release form, and many of its results can be accessed in the form of ntuples [111] to which a range of cuts, and histogramming options, as well as PDF and scale-changes, can be applied *a posteriori*; an alternative approach for *a posteriori* PDF and scale change represents NLO (or NNLO) results, for a given set of cuts and binning, as an effective coefficient function on a grid in parton momentum fractions and factorization scales [112–115].

In some cases the above programs (or development versions of them) can be used to calculate also NLO electroweak or beyond-standard-model corrections [116–119]. Electroweak corrections are especially important for transverse momenta significantly above the W and Z masses, because they are enhanced by two powers of $\ln p_t/M_W$ for each power of the electroweak coupling.

The above tools rely in part on a wide array of developments reviewed in Refs. 95,120. Examples of the most complex processes for which NLO QCD corrections have been obtained so far include $e^+e^- \to 7$ jets [121], $pp \to W + 5$ jets [122] and $pp \to 5$ jets [123].

NNLO. Conceptually, NNLO and NLO calculations are similar, except that one must add a further order in α_s, consisting of: the squared $(n+2)$-parton tree-level amplitude, the interference of the $(n+1)$-parton tree-level and 1-loop amplitudes, the interference of the n-parton tree-level and 2-loop amplitudes, and the squared n-parton 1-loop amplitude.

Each of these elements involves large numbers of soft and collinear divergences, satisfying relations analogous to Eq. (9.16) that now involve multiple collinear or soft particles and higher loop orders (see *e.g.* Refs. [124–126]). Arranging for the cancellation of the divergences after numerical Monte Carlo integration has been one of the significant challenges of NNLO calculations, as has the determination of the relevant 2-loop amplitudes. For the cancellations of divergences a wide

range of methods has been developed. Some of them [127–131] retain the approach, inherent in NLO methods, of directly combining the separate loop and tree-level amplitudes. Others combine a suitably chosen, partially inclusive $2 \to n$ NNLO calculation with a fully differential $2 \to n+1$ NLO calculation [132–135].

Quite a number of processes have been calculated differentially at NNLO so far. The state of the art for e^+e^- collisions is $e^+e^- \to 3$jets [136–138]. For Deep Inelastic Scattering, dijet production is known at NNLO [139]. For hadron colliders, all $2 \to 1$ processes are known, specifically vector boson [140,141] and Higgs boson production [142,132]. For most of the above calculations there exist public codes (EERAD3 for e^+e^-, DYNNLO and FEWZ for W and Z production, fehipro and HNNLO for Higgs production), links to which are to be found among the above references. Substantial progress has been made in the past couple of years for hadron-collider $2 \to 2$ processes, with calculations having been performed for nearly all relevant processes: HH [66] (in large-top-mass approximation, see also the exact (two-loop) NLO result [143]) , WH [144] and ZH [145], ZZ [69] WW [68] and WZ [146], $\gamma\gamma$ [147,148], $Z\gamma$ [149] and $W\gamma$ [150] (many of these colour singlet processes are available also in MCFM [151]), $H+$jet [152,153,154,155], $W+$jet [133], $Z+$jet [156,157] and $\gamma+$jet [158], t-channel single-top [159,160], $t\bar{t}$ production [161], and dijet production [162]. One $2 \to 3$ process is known at NNLO, Higgs production through vector-boson fusion, using an approximation in which the two underlying DIS-like $q \to qV$ scatterings are factorised [135].

9.2.3.3. *Resummation:*

Many experimental measurements place tight constraints on emissions in the final state. For example, in e^+e^- events, that (one minus) the Thrust should be less than some value $\tau \ll 1$, or in $pp \to Z$ events that the Z-boson transverse momentum should be much smaller than its mass, $p_t^Z \ll M_Z$. A further example is the production of heavy particles or jets near threshold (so that little energy is left over for real emissions) in DIS and pp collisions.

In such cases, the constraint vetoes a significant part of the integral over the soft and collinear divergence of Eq. (9.16). As a result, there is only a partial cancellation between real emission terms (subject to the constraint) and loop (virtual) contributions (not subject to the constraint), causing each order of α_s to be accompanied by a large coefficient $\sim L^2$, where *e.g.* $L = \ln\tau$ or $L = \ln(M_Z/p_t^Z)$. One ends up with a perturbative series whose terms go as $\sim (\alpha_s L^2)^n$. It is not uncommon that $\alpha_s L^2 \gg 1$, so that the perturbative series converges very poorly if at all.** In such cases one may carry out a "resummation," which accounts for the dominant logarithmically enhanced terms to all orders in α_s, by making use of known properties of matrix elements for multiple soft and collinear emissions, and of the all-orders properties of the divergent parts of virtual corrections, following original works such as Refs. 163–172 and also through soft-collinear effective theory [173,174] (*cf.* also the section on "Heavy-Quark and Soft-Collinear Effective Theory" in this *Review*, as well as Ref. 175).

For cases with double logarithmic enhancements (two powers of logarithm per power of α_s), there are two classification schemes for resummation accuracy. Writing the cross section including the constraint as $\sigma(L)$ and the unconstrained (total) cross section as $\sigma_{\rm tot}$, the series expansion takes the form

$$\sigma(L) \simeq \sigma_{\rm tot} \sum_{n=0}^{\infty} \sum_{k=0}^{2n} R_{nk} \alpha_s^n(\mu_R^2) L^k, \qquad L \gg 1 \qquad (9.20)$$

and leading log (LL) resummation means that one accounts for all terms with $k = 2n$, next-to-leading-log (NLL) includes additionally all terms with $k = 2n-1$, *etc.* Often $\sigma(L)$ (or its Fourier or Mellin transform) *exponentiates* ‡,

$$\sigma(L) \simeq \sigma_{\rm tot} \exp\left[\sum_{n=1}^{\infty} \sum_{k=0}^{n+1} G_{nk} \alpha_s^n(\mu_R^2) L^k\right], \qquad L \gg 1\,, \qquad (9.21)$$

where one notes the different upper limit on k ($\leq n+1$) compared to Eq. (9.20). This is a more powerful form of resummation: the G_{12} term alone reproduces the full LL series in Eq. (9.20). With the form Eq. (9.21) one still uses the nomenclature LL, but this now means that all terms with $k = n+1$ are included, and NLL implies all terms with $k = n$, *etc.*

For a large number of observables, NLL resummations are available in the sense of Eq. (9.21) (see Refs. 179–181 and references therein). NNLL has been achieved for the DY and Higgs-boson p_t distributions [182–185] (also available in the CuTe [186], HRes [187] and ResBos [188] families of programs and also differentially in vector-boson decay products [189]) and related variables [190], for the p_t of vector-boson pairs [191], for the back-to-back energy-energy correlation in e^+e^- [192], the jet broadening in e^+e^- collisions [193], the jet-veto survival probability in Higgs and Z boson production in pp collisions [194], an event-shape type observable known as the beam Thrust [195], hadron-collider jet masses in specific limits [196] (see also Ref. 197), the production of top anti-top pairs near threshold [198–200] (and references therein), and high-p_t W and Z production [201]. Automation of NNLL jet-veto resummations for different processes has been achieved in Ref. 202 (*cf.* also the NLL automation in Ref. 203), while automation for a certain class of e^+e^- observables has been achieved in Ref. 204. N^{3}LL resummations are available for the Thrust variable, C-parameter and heavy-jet mass in e^+e^- annihilations [205–207] (confirmed for Thrust at NNLL in Ref. 208), for the Higgs p_t distribution [209] and for for Higgs- and vector-boson production near threshold [210]. An extensive discussion of jet masses for heavy-quark induced jets has been given in Ref. 211 (see also Ref. 212). Recently, there has also been progress in resummed calculations for jet substructure, whose observables involve more complicated definitions than is the case for standard resummations [213–217]. The inputs and methods involved in these various calculations are somewhat too diverse to discuss in detail here, so we recommend that the interested reader consult the original references for further details.

9.2.3.4. *Fragmentation functions:*

Since the parton-hadron transition is non-perturbative, it is not possible to perturbatively calculate quantities such as the energy-spectra of specific hadrons in high-energy collisions. However, one can factorize perturbative and non-perturbative contributions via the concept of fragmentation functions. These are the final-state analogue of the parton distribution functions that are used for initial-state hadrons. Like parton distribution functions, they depend on a (fragmentation) factorization scale and satisfy a DGLAP evolution equation.

It should be added that if one ignores the non-perturbative difficulties and just calculates the energy and angular spectrum of partons in perturbative QCD with some low cutoff scale $\sim \Lambda$ (using resummation to sum large logarithms of $\sqrt{s}/\Lambda$), then this reproduces many features of the corresponding hadron spectra [218]. This is often taken to suggest that hadronization is "local", in the sense it mainly involves partons that are close both in position and in momentum.

Section 19 of this *Review* provides further information (and references) on these topics, including also the question of heavy-quark fragmentation.

** To be precise one should be aware of two causes of the divergence of perturbative series. That which interests us here is associated with the presence of a new large parameter (*e.g.* ratio of scales). It is distinct from the "renormalon" induced factorial divergences of perturbation theory that were discussed above.

‡ Whether or not this happens depends on the quantity being resummed. A classic example involves jet rates in e^+e^- collisions as a function of a jet-resolution parameter $y_{\rm cut}$. The logarithms of $1/y_{\rm cut}$ exponentiate for the k_t (Durham) jet algorithm [176], but not [177] for the JADE algorithm [178] (both are discussed below in Sec. 9.3.1.1).

9.2.3.5. *Parton-shower Monte Carlo generators:*

Parton-shower Monte Carlo (MC) event generators like PYTHIA [219–221], HERWIG [222–224] and SHERPA [109] provide fully exclusive simulations of QCD events.† Because they provide access to "hadron-level" events, they are a crucial tool for all applications that involve simulating the response of detectors to QCD events. Here we give only a brief outline of how they work and refer the reader to Sec. 41 and Ref. 226 for a full overview.

The MC generation of an event involves several stages. It starts with the random generation of the kinematics and partonic channels of whatever *hard scattering process* the user has requested at some high scale Q_0 (for complex processes, this may be carried out by an external program). This is followed by a *parton shower*, usually based on the successive random generation of gluon emissions (or $g \to q\bar{q}$ splittings). Each is generated at a scale lower than the previous emission, following a (soft and collinear resummed) perturbative QCD distribution that depends on the momenta of all previous emissions. Common choices of scale for the ordering of emissions are virtuality, transverse momentum or angle. Parton showering stops at a scale of order 1 GeV, at which point a *hadronization model* is used to convert the resulting partons into hadrons. One widely-used model involves stretching a color "string" across quarks and gluons, and breaking it up into hadrons [227,228]. Another breaks each gluon into a $q\bar{q}$ pair and then groups quarks and anti-quarks into colorless "clusters", which then give the hadrons [222]. For pp and γp processes, modeling is also needed to treat the collision between the two hadron remnants, which generates an *underlying event* (UE), usually implemented via additional $2 \to 2$ scatterings ("multiple parton interactions") at a scale of a few GeV, following Ref. 229.

A deficiency of the soft and collinear approximations that underlie parton showers is that they may fail to reproduce the full pattern of hard wide-angle emissions, important, for example, in many new physics searches. It is therefore common to use LO multi-parton matrix elements to generate hard high-multiplicity partonic configurations as additional starting points for the showering, supplemented with some prescription (CKKW [230], MLM [231]) for consistently merging samples with different initial multiplicities.

MCs, as described above, generate cross sections for the requested hard process that are correct at LO. A wide variety of processes are available in MC implementations that are correct to NLO, using the MC@NLO [232] or POWHEG [233] prescriptions, notably through the Madgraph5_aMC@NLO [89], POWHEGBox [234] and Sherpa [91,235] programs. Techniques have also been developed recently to combine NLO plus shower accuracy for different multiplicities of final-state jets [236]. Building in part on some of that work, several groups have also obtained NNLO plus shower accuracy for Drell-Yan and Higgs production [237] as well as a handful of other processes.

9.2.4. ***Accuracy of predictions*** :

Estimating the accuracy of perturbative QCD predictions is not an exact science. It is often said that LO calculations are accurate to within a factor of two. This is based on experience with NLO corrections in the cases where these are available. In processes involving new partonic scattering channels at NLO and/or large ratios of scales (such as jet observables in processes with vector bosons, or the production of high-p_t jets containing B-hadrons), the ratio of the NLO to LO predictions, commonly called the "K-factor", can be substantially larger than 2.

For calculations beyond LO, a conservative approach to estimate the perturbative uncertainty is to take it to be the last known perturbative order; a more widely used method is to estimate it from the change in the prediction when varying the renormalization and factorization scales around a central value Q that is taken close to the physical scale of the process. A conventional range of variation is $Q/2 < \mu_R, \mu_F < 2Q$. This should not be assumed to always estimate the full uncertainty from missing higher orders, but it does indicate the size of one important known source of higher-order ambiguity.‡‡

There does not seem to be a broad consensus on whether μ_R and μ_F should be kept identical or varied independently. One common option is to vary them independently with the restriction $\frac{1}{2}\mu_R < \mu_F < 2\mu_R$ [245]. This limits the risk of misleadingly small uncertainties due to fortuitous cancellations between the μ_F and μ_R dependence when both are varied together, while avoiding the appearance of large logarithms of μ_R^2/μ_F^2 when both are varied completely independently.

Calculations that involve resummations usually have an additional source of uncertainty associated with the choice of argument of the logarithms being resummed, *e.g.* $\ln(2\frac{p_t^Z}{M_Z})$ as opposed to $\ln(\frac{1}{2}\frac{p_t^Z}{M_Z})$. In addition to varying renormalization and factorization scales, it is therefore also advisable to vary the argument of the logarithm by a suitable factor in either direction with respect to the "natural" argument.

The accuracy of QCD predictions is limited also by non-perturbative corrections, which typically scale as a power of Λ/Q. For measurements that are directly sensitive to the structure of the hadronic final state, the corrections are usually linear in Λ/Q. The non-perturbative corrections are further enhanced in processes with a significant underlying event (*i.e.* in pp and $p\bar{p}$ collisions) and in cases where the perturbative cross sections fall steeply as a function of p_t or some other kinematic variable, for example in inclusive jet spectra or dijet mass spectra.

Non-perturbative corrections are commonly estimated from the difference between Monte Carlo events at the parton level and after hadronization. An issue to be aware of with this procedure is that "parton level" is not a uniquely defined concept. For example, in an event generator it depends on a (somewhat arbitrary and tunable) internal cutoff scale that separates the parton showering from the hadronization. In contrast no such cutoff scale exists in a NLO or NNLO partonic calculation. For this reason there are widespread reservations as to the appropriateness of deriving hadronization corrections from a Monte Carlo program and then applying them to NLO or NNLO predictions. There exist alternative methods for estimating hadronization corrections, which attempt to analytically deduce non-perturbative effects in one observable based on measurements of other observables (see the reviews [29,246]). While they directly address the problem of different possible definitions of parton level, it should also be said that they are far less flexible than Monte Carlo programs and not always able to provide equally good descriptions of the data.

9.3. Experimental studies of QCD

Since we are not able to directly measure partons (quarks or gluons), but only hadrons and their decay products, a central issue for every experimental study of perturbative QCD is establishing a correspondence between observables obtained at the partonic and the hadronic level. The only theoretically sound correspondence is achieved by means of *infrared and collinear safe* quantities, which allow one to obtain finite predictions at any order of perturbative QCD.

As stated above, the simplest case of infrared- and collinear-safe observables are total cross sections. More generally, when measuring fully inclusive observables, the final state is not analyzed at all regarding its (topological, kinematical) structure or its composition. Basically the relevant information consists in the rate of a process ending up in a partonic or hadronic final state. In e^+e^- annihilation, widely used examples are the ratios of partial widths or branching ratios for the electroweak decay of particles into hadrons or leptons, such as Z or τ decays, (*cf.* Sec. 9.2.1). Such ratios are often favored over absolute cross sections or partial widths because of large cancellations of experimental and theoretical systematic uncertainties. The strong suppression of non-perturbative effects, $\mathcal{O}(\Lambda^4/Q^4)$, is one

† The program ARIADNE [225] has also been widely used for simulating e^+e^- and DIS collisions.

‡‡ A number of prescriptions also exist for setting the scale automatically, *e.g.* Refs. 238–241, eliminating uncertainties from scale variation, though not from the truncation of the perturbative series itself. Recently, there have also been studies of how to estimate uncertainties from missing higher orders that go beyond scale variations [242,243,244].

of the attractive features of such observables, however, at the same time the sensitivity to radiative QCD corrections is small, which for example affects the statistical uncertainty when using them for the determination of the strong coupling constant. In the case of τ decays not only the hadronic branching ratio is of interest, but also moments of the spectral functions of hadronic tau decays, which sample different parts of the decay spectrum and thus provide additional information. Other examples of fully inclusive observables are structure functions (and related sum rules) in DIS. These are extensively discussed in Sec. 18 of this *Review*.

On the other hand, often the structure or composition of the final state are analyzed and cross sections differential in one or more variables characterizing this structure are of interest. Examples are jet rates, jet substructure, event shapes or transverse momentum distributions of jets or vector bosons in hadron collisions. The case of fragmentation functions, *i.e.* the measurement of hadron production as a function of the hadron momentum relative to some hard scattering scale, is discussed in Sec. 19 of this *Review*.

It is worth mentioning that, besides the correspondence between the parton and hadron level, also a correspondence between the hadron level and the actually measured quantities in the detector has to be established. The simplest examples are corrections for finite experimental acceptance and efficiencies. Whereas acceptance corrections essentially are of theoretical nature, since they involve extrapolations from the measurable (partial) to the full phase space, other corrections such as for efficiency, resolution and response, are of experimental nature. For example, measurements of differential cross sections such as jet rates require corrections in order to relate, *e.g.* the energy deposits in a calorimeter to the jets at the hadron level. Typically detector simulations and/or data-driven methods are used in order to obtain these corrections. Care should be taken here in order to have a clear separation between the parton-to-hadron level and hadron-to-detector level corrections. Finally, for the sake of an easy comparison to the results of other experiments and/or theoretical calculations, it is suggested to provide, whenever possible, measurements corrected for detector effects and/or all necessary information related to the detector response (*e.g.* the detector response matrix).

9.3.1. *Hadronic final-state observables* :

9.3.1.1. *Jets:*

In hard interactions, final-state partons and hadrons appear predominantly in collimated bunches, which are generically called *jets*. To a first approximation, a jet can be thought of as a hard parton that has undergone soft and collinear showering and then hadronization. Jets are used both for testing our understanding and predictions of high-energy QCD processes, and also for identifying the hard partonic structure of decays of massive particles like top quarks.

In order to map observed hadrons onto a set of jets, one uses a *jet definition*. The mapping involves explicit choices: for example when a gluon is radiated from a quark, for what range of kinematics should the gluon be part of the quark jet, or instead form a separate jet? Good jet definitions are infrared and collinear safe, simple to use in theoretical and experimental contexts, applicable to any type of inputs (parton or hadron momenta, charged particle tracks, and/or energy deposits in the detectors) and lead to jets that are not too sensitive to non-perturbative effects.

An extensive treatment of the topic of jet definitions is given in Ref. 247 (for e^+e^- collisions) and Refs. [248–250]. Here we briefly review the two main classes: cone algorithms, extensively used at older hadron colliders, and sequential recombination algorithms, more widespread in e^+e^- and ep colliders and at the LHC.

Very generically, most (iterative) cone algorithms start with some seed particle i, sum the momenta of all particles j within a cone of opening-angle R, typically defined in terms of (pseudo-)rapidity and azimuthal angle. They then take the direction of this sum as a new seed and repeat until the cone is stable, and call the contents of the resulting stable cone a jet if its transverse momentum is above some threshold $p_{t,\min}$. The parameters R and $p_{t,\min}$ should be chosen according to the needs of a given analysis.

There are many variants of cone algorithm, and they differ in the set of seeds they use and the manner in which they ensure a one-to-one mapping of particles to jets, given that two stable cones may share particles ("overlap"). The use of seed particles is a problem w.r.t. infrared and collinear safety, and seeded algorithms are generally not compatible with higher-order (or sometimes even leading-order) QCD calculations, especially in multi-jet contexts, as well as potentially subject to large non-perturbative corrections and instabilities. Seeded algorithms (JetCLU, MidPoint, and various other experiment-specific iterative cone algorithms) are therefore to be deprecated. A modern alternative is to use a seedless variant, SISCone [251].

Sequential recombination algorithms at hadron colliders (and in DIS) are characterized by a distance $d_{ij} = \min(k_{t,i}^{2p}, k_{t,j}^{2p})\Delta_{ij}^2/R^2$ between all pairs of particles i, j, where Δ_{ij} is their separation in the rapidity-azimuthal plane, $k_{t,i}$ is the transverse momentum w.r.t. the incoming beams, and R is a free parameter. They also involve a "beam" distance $d_{iB} = k_{t,i}^{2p}$. One identifies the smallest of all the d_{ij} and d_{iB}, and if it is a d_{ij}, then i and j are merged into a new pseudo-particle (with some prescription, a recombination scheme, for the definition of the merged four-momentum). If the smallest distance is a d_{iB}, then i is removed from the list of particles and called a jet. As with cone algorithms, one usually considers only jets above some transverse-momentum threshold $p_{t,\min}$. The parameter p determines the kind of algorithm: $p = 1$ corresponds to the (*inclusive-*)k_t algorithm [176,252,253], $p = 0$ defines the *Cambridge-Aachen* algorithm [254,255], while for $p = -1$ we have the *anti-*k_t algorithm [256]. All these variants are infrared and collinear safe to all orders of perturbation theory. Whereas the former two lead to irregularly shaped jet boundaries, the latter results in cone-like boundaries. The *anti-*k_t algorithm has become the de-facto standard for the LHC experiments.

In e^+e^- annihilations the k_t algorithm [176] uses $y_{ij} = 2\min(E_i^2, E_j^2)(1-\cos\theta_{ij})/Q^2$ as distance measure and repeatedly merges the pair with smallest y_{ij}, until all y_{ij} distances are above some threshold $y_{\rm cut}$, the jet resolution parameter. The (pseudo)-particles that remain at this point are called the jets. Here it is $y_{\rm cut}$ (rather than R and $p_{t,\min}$) that should be chosen according to the needs of the analysis. As mentioned earlier, the k_t algorithm has the property that logarithms $\ln(1/y_{\rm cut})$ exponentiate in resummation calculations. This is one reason why it is preferred over the earlier JADE algorithm [178], which uses the distance measure $y_{ij} = 2\,E_i\,E_j\,(1-\cos\theta_{ij})/Q^2$. Note that other variants of sequential recombination algorithms for e^+e^- annhilations, using different definitions of the resolution measure y_{ij}, exhibit much larger sensitivities to fragmentation and hadronization effects than the k_t and JADE algorithms [257].

Efficient implementations of the above algorithms are available through the *FastJet* package [258].

9.3.1.2. *Event Shapes:*

Event-shape variables are functions of the four momenta of the particles in the final state and characterize the topology of an event's energy flow. They are sensitive to QCD radiation (and correspondingly to the strong coupling) insofar as gluon emission changes the shape of the energy flow.

The classic example of an event shape is the *Thrust* [259,260] in e^+e^- annihilations, defined as

$$\hat{\tau} = \max_{\vec{n}_\tau} \frac{\sum_i |\vec{p}_i \cdot \vec{n}_\tau|}{\sum_i |\vec{p}_i|} \,, \tag{9.22}$$

where $\vec{p}_i$ are the momenta of the particles or the jets in the final-state and the maximum is obtained for the Thrust axis $\vec{n}_\tau$. In the Born limit of the production of a perfect back-to-back $q\bar{q}$ pair the limit $\hat{\tau} \to 1$ is obtained, whereas a perfectly spherical many-particle configuration leads to $\hat{\tau} \to 1/2$. Further event shapes of similar nature have been extensively measured at LEP and at HERA, and for their definitions and reviews we refer to Refs. 1,4,246,261,262. The energy-energy correlation function [263], namely the energy-weighted

angular distribution of produced hadron pairs, and its associated asymmetry are further shape variables that have been studied in detail at e^+e^- colliders. For hadron colliders the appropriate modification consists in only taking the transverse momentum component [264]. More recently, the event shape *N-jettiness* has been proposed [265], that measures the degree to which the hadrons in the final state are aligned along N jet axes or the beam direction. It vanishes in the limit of exactly N infinitely narrow jets.

Phenomenological discussions of event shapes at hadron colliders can be found in Refs. [265–267]. Measurements of hadronic event-shape distributions have been published by CDF [268], ATLAS [269–273] and CMS [274–276].

Event shapes are used for many purposes. These include measuring the strong coupling, tuning the parameters of Monte Carlo programs, investigating analytical models of hadronization and distinguishing QCD events from events that might involve decays of new particles (giving event-shape values closer to the spherical limit).

9.3.1.3. *Jet substructure, quark vs. gluon jets:*

Jet substructure, which can be resolved by finding subjets or by measuring jet shapes, is sensitive to the details of QCD radiation in the shower development inside a jet and has been extensively used to study differences in the properties of quark and gluon induced jets, strongly related to their different color charges. In general there is clear experimental evidence that gluon jets have a softer particle spectrum and are "broader" than (light-) quark jets, when looking at observables such as the jet shape $\Psi(r/R)$. This is the fractional transverse momentum contained within a sub-cone of cone-size r for jets of cone-size R. It is sensitive to the relative fractions of quark and gluon jets in an inclusive jet sample and receives contributions from soft-gluon initial-state radiation and the underlying event. Therefore, it has been widely employed for validation and tuning of Monte Carlo models. Furthermore, this quantity turns out to be sensitive to the modification of the gluon radiation pattern in heavy ion collisions (see *e.g.* Ref. 277).

The most recent jet shape measurements using proton-proton collision data have been presented for inclusive jet samples [278–280] and for top-quark production [281]. Further discussions, references and recent summaries can be found in Refs. 262, 282, 283 and Sec. 4 of Ref. 284.

The use of jet substructure has also been investigated in order to distinguish QCD jets from jets that originate from hadronic decays of boosted massive particles (high-p_t electroweak bosons, top quarks and hypothesized new particles). Recently, a considerable number of experimental studies have been carried out with Tevatron and LHC data, in order to investigate on the performance of the proposed algorithms for resolving jet substructure and to apply them to searches for new physics, as well as to the reconstruction of boosted top quarks, vector bosons and the Higgs boson. For reviews of this rapidly growing field, see sec. 5.3 of Ref. 248, Ref. 250 and Refs. [284–289].

9.3.2. ***QCD measurements at colliders*** :

There exists a wealth of data on QCD-related measurements in e^+e^-, ep, pp, and $p\bar{p}$ collisions, to which a short overview like this would not be able to do any justice. Extensive reviews of the subject have been published in Refs. 261, 262 for e^+e^- colliders and in Ref. 290 for ep scattering, whereas for hadron colliders comprehensive overviews are given in, *e.g.*, Refs. 249, 283 and Refs. [291–293].

Below we concentrate our discussion on measurements that are most sensitive to hard QCD processes, with focus on jet production.

9.3.2.1. e^+e^- *colliders:* Analyses of jet production in e^+e^- collisions are mostly based on data from the JADE experiment at center-of-mass energies between 14 and 44 GeV, as well as on LEP collider data at the Z resonance and up to 209 GeV. They cover the measurements of (differential or exclusive) jet rates (with multiplicities typically up to 4, 5 or 6 jets), the study of 3-jet events and particle production between the jets as a tool for testing hadronization models, as well as 4-jet production and angular correlations in 4-jet events.

Event-shape distributions from e^+e^- data have been an important input to the tuning of parton shower MC models, typically matched to matrix elements for 3-jet production. In general these models provide good descriptions of the available, highly precise data. Especially for the large LEP data sample at the Z peak, the statistical uncertainties are mostly negligible and the experimental systematic uncertainties are at the percent level or even below. These are usually dominated by the uncertainties related to the MC model dependence of the efficiency and acceptance corrections (often referred to as "detector corrections").

Observables measured in e^+e^- collisions have been used for determinations of the strong coupling constant (*cf.* Section 9.4 below) and for putting constraints on the QCD color factors (*cf.* Sec. 9.1 for their definitions), thus probing the non-abelian nature of QCD. Typically, cross sections can be expressed as functions of these color factors, for example $\sigma = f(\alpha_s C_F, C_A/C_F, n_f T_R/C_F)$. Angular correlations in 4-jet events give sensitivity at leading order. Some sensitivity to these color factors, although only at NLO, is also obtained from event-shape distributions. Scaling violations of fragmentation functions and the different subjet structure in quark and gluon induced jets also give access to these color factors. In order to extract absolute values, *e.g.* for C_F and C_A, certain assumptions have to be made for other parameters, such as T_R, n_f or α_s, since typically only combinations (ratios, products) of all the relevant parameters appear in the perturbative predictions. A compilation of results [262] quotes world average values of $C_A = 2.89 \pm 0.03(\text{stat}) \pm 0.21(\text{syst})$ and $C_F = 1.30 \pm 0.01(\text{stat}) \pm 0.09(\text{syst})$, with a correlation coefficient of 82%. These results are in perfect agreement with the expectations from SU(3) of $C_A = 3$ and $C_F = 4/3$.

9.3.2.2. *DIS and photoproduction:* Multi-jet production in ep collisions at HERA, both in the DIS and photoproduction regime, allows for tests of QCD factorization (one initial-state proton and its associated PDF versus the hard scattering which leads to high-p_t jets) and NLO calculations which exist for 2- and 3-jet final states. Sensitivity is also obtained to the product of the coupling constant and the gluon PDF. Experimental uncertainties of the order of 5–10% have been achieved, mostly dominated by the jet energy scale, whereas statistical uncertainties are negligible to a large extent. For comparison to theoretical predictions, at large jet p_t the PDF uncertainty dominates the theoretical uncertainty (typically of order 5–10%, in some regions of phase space up to 20%), therefore jet observables become useful inputs for PDF fits.

In general, the data are well described by NLO matrix-element calculations, combined with DGLAP evolution equations, in particular at large Q^2 and central values of jet pseudo-rapidity. At low values of Q^2 and x, in particular for large jet pseudo-rapidities, certain features of the data have been interpreted as requiring BFKL-type evolution, though the predictions for such schemes are still limited. It is worth noting that there is lack of consensus throughout the community regarding this need of BFKL-evolution at currently probed x, Q^2 values, and an alternative approach [294] that implements the merging of LO matrix-element based event generation with a parton shower (using the SHERPA framework) successfully describes the data in all kinematical regions, including the low Q^2, low x domain. At moderately small x values, it should perhaps not be surprising that the BFKL approach and fixed-order matrix-element merging with parton showers may both provide adequate descriptions of the data, because some part of the multi-parton phase space that they model is common to both approaches.

In the case of photoproduction, a wealth of measurements with low p_t jets were performed in order to constrain the photon PDFs. The uncertainties related to these photon PDFs play a minor role at high jet p_t, which has allowed for precise tests of pQCD calculations.

A few examples of recent measurements can be found in Refs. 295–303 for DIS and in Refs. 304–308 for photoproduction.

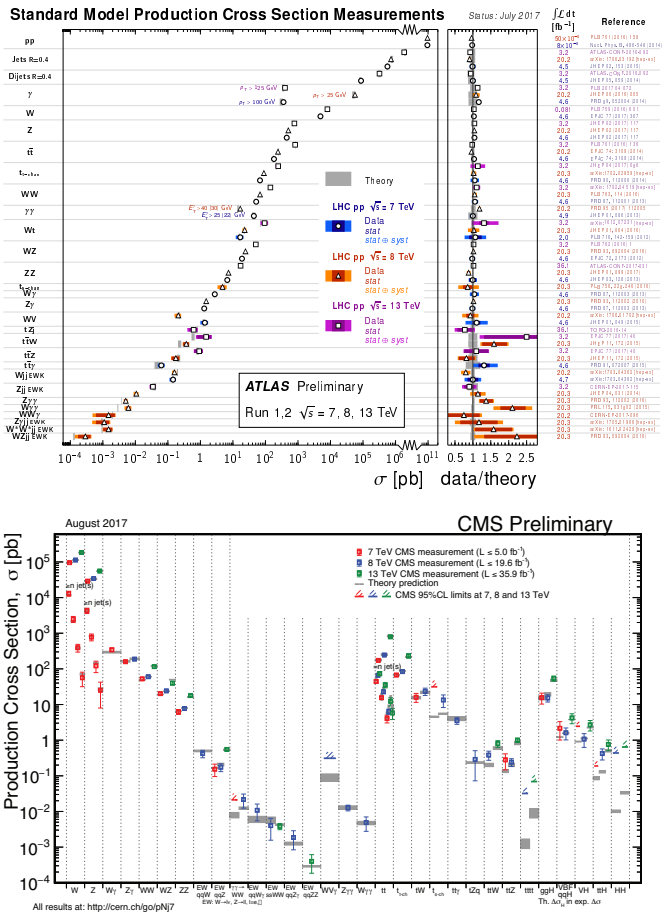

Figure 9.1: Overview of cross section measurements for a wide class of processes and observables, as obtained by the ATLAS [309] and CMS [310] experiments at the LHC, for centre-of-mass energies of 7, 8 and 13 TeV. Also shown are the theoretical predictions and their uncertainties.

9.3.2.3. *Hadron colliders:* The spectrum of observables and the number of measurements performed at hadron colliders is enormous, probing many regions of phase space and covering a huge range of cross sections, as illustrated in Fig. 9.1 for the case of the ATLAS and CMS experiments at the LHC. For the sake of brevity, in the following only certain classes of those measurements will be discussed, that allow addressing particular aspects of the various QCD studies performed. Most of our discussion will focus on recent LHC results, which are available for center-of-mass energies of 2.76, 5, 7, 8 and 13 TeV with integrated luminosities of up to 36 fb^{-1}. Generally speaking, besides representing a general test of the standard model and QCD in particular, these measurements serve several purposes, such as: (i) probing pQCD and its various approximations and implementations in MC models, in order to quantify the order of magnitude of not yet calculated contributions and to gauge their precision when used as background predictions, or (ii) extracting/constraining model parameters such as the strong coupling constant or PDFs.

Among the most important cross sections measured is the inclusive jet spectrum as a function of the jet transverse energy (E_t) or the jet transverse momentum (p_t), for several rapidity regions and for p_t up to 700 GeV at the Tevatron and ~ 2 TeV at the LHC. It is worth noting that this upper limit in p_t corresponds to a distance scale of $\sim 10^{-19}$ m: no other experiment so far is able to directly probe smaller distance scales of nature than this measurement. Whereas the Tevatron measurements (Refs. 311–313) were based on the infrared- and collinear-safe k_t algorithm in addition to the more widely used Midpoint and JetCLU algorithms of the past, the LHC experiments focus on the *anti-k_t* algorithm using various radius parameters. Measurements by ALICE, ATLAS and CMS have been published in Refs. 314–321. Reviews can be found in, *e.g.*, Refs. 283,322,323.

In general we observe a good description of the data by the NLO QCD predictions, over about 11 orders of magnitude in cross section. The experimental systematic uncertainties are dominated by the jet energy scale uncertainty, quoted to be in the range of a few percent (see for instance the review in Ref. 324), leading to uncertainties of $\sim 5-30\%$ on the cross section, increasing with p_t and rapidity. The PDF uncertainties dominate the theoretical uncertainty at large p_t and rapidity. In fact, inclusive jet data are important inputs to global PDF fits (see [325] for a recent review). Constraints on the PDFs can also be obtained from ratios of inclusive cross sections at different center-of-mass energies [315,320]. In general, ratios of jet cross sections are a means to (at least partially) cancel the jet energy scale uncertainties and thus provide jet observables with significantly improved precision.

Dijet events are analyzed in terms of their invariant mass and angular distributions, which allows for tests of NLO QCD predictions (see *e.g.* Refs. [319,326,327] for recent LHC results), and setting stringent limits on deviations from the Standard Model, such as quark compositeness or contact interactions (some examples can be found in Refs. 328–334). Furthermore, dijet azimuthal correlations between the two leading jets, normalized to the total dijet cross section, are an extremely valuable tool for studying the spectrum of gluon radiation in the event. The azimuthal separation of the two leading jets is sensitive to multi-jet production, avoiding at the same time large systematic uncertainties from the jet energy calibration. For example, results from the Tevatron [335,336] and the LHC [337–339] show that the LO (non-trivial) prediction for this observable, with at most three partons in the final state, is not able to describe the data for an azimuthal separation below $2\pi/3$, where NLO contributions (with 4 partons) restore the agreement with data. In addition, this observable can be employed to tune Monte Carlo predictions of soft gluon radiation.

Further examples of dijet observables that probe special corners of phase space are those which involve forward (large rapidity) jets and where a large rapidity separation, possibly also a rapidity gap, is required between the two jets. Reviews of such measurements can be found in Refs. [283,340], showing that no single prediction is capable of describing the data in all phase-space regions. In particular, no conclusive evidence for BFKL effects in these observables has been established so far.

Beyond dijet final states, measurements of the production of three or more jets, including cross section ratios, have been performed (see Refs. [283,341] for recent reviews), as a means of testing perturbative QCD predictions, determining the strong coupling constant (at NLO precision so far), and probing/tuning MC models, in particular those combining multi-parton matrix elements with parton showers.

In terms of precision achieved, measurements of inclusive vector boson (W, Z) production outperform the jet studies described above and provide the most precisely determined observables at hadron colliders so far. This is because the experimental signatures are based on leptons that are measured much more accurately than jets. At the LHC [342–348], the dominant uncertainty stems from the luminosity determination ($\sim$2–4%), while other uncertainties (*e.g.* statistics, lepton efficiencies) are controlled at the 1–3% level. The uncertainty from the acceptance correction of about 1–2% can be reduced by measuring so-called fiducial cross sections, ie. by applying kinematic cuts also to the particle level of the theoretical predictions. A further reduction or even complete elimination of particular uncertainties (*e.g.* luminosity) is achieved by measuring cross section ratios (W/Z or W^+/W^-) or differential distributions that are normalised to the inclusive cross section. On the theory side, as discussed earlier in this review, the production of these color-singlet states has been calculated up to NNLO accuracy. Since the dominant theoretical uncertainty is related to the choice of PDFs, these high-precision data provide useful handles for PDF determinations.

Further insights are obtained from measurements of differential vector boson production, as a function of the invariant dilepton mass, the boson's rapidity or its transverse momentum. For example, the dilepton invariant mass distribution has been measured [349–353] for masses between 15 and 2000 GeV, covering more than 8 orders of magnitude in cross section. NNLO QCD predictions, together with modern PDF sets and including higher-order electroweak and QED

final-state radiation corrections, describe the data to within 5–10% over this large range, whereas NLO predictions show larger deviations, unless matched to a parton shower.

Similar conclusions can be drawn from the observed rapidity distribution of the dilepton system (see *e.g.* [342,350]) or, in the case of W production, from the observed charged lepton rapidity distribution and its charge asymmetry. The latter is particularly sensitive to differences among PDF sets [342,354,355], also thanks to the high precision achieved by the ATLAS and CMS experiments for central rapidity ranges. These measurements are nicely extended to the very forward region, up to 4.5 in lepton rapidity, by the LHCb experiment.

An overview of this kind of measurements can be found in Ref. 283. There one can also find a discussion of and references to LHC results from studies of the vector boson's transverse momentum distribution, p_t^V (see also Refs. 356,357). This observable probes different aspects of higher-order QCD effects and is sensitive to jet production in association to the vector boson, without suffering from the large jet energy scale uncertainties since there is no explicit jet reconstruction. Whereas in the p_t^V region of several tens to hundreds of GeV the NNLO predictions (that effectively are of NLO accuracy for this variable) agree with the data to within about 10%, at transverse momentum below ∼5–10 GeV the fixed order predictions fail and soft-gluon resummation is needed to restore the agreement with data. Correspondingly, MC models implementing parton shower matching to LO or NLO matrix elements provide good predictions at low and intermediate p_t^V, but deviate up to 40% at high p_t^V.

While in principle inclusive and differential photon production represents a similar tool for studying effects as described above, the experimental results are less precise than for W and Z production, related to the greater challenges encountered in photon reconstruction and purity determination compared to lepton final states.

In terms of complexity, probably the most challenging class of processes is vector boson (photon, W, Z) production together with jets. By now the amount of results obtained both at the Tevatron and at the LHC is so extensive that a comprehensive discussion with a complete citation list would go much beyond the scope of this *Review*. We rather refer to recent summaries in Refs. 283,358 and to previous versions of this *Review*.

The measurements cover a very large phase space, *e.g.* with jet transverse momenta between 30 GeV and ∼ 800 GeV and jet rapidities up to $|y| < 4.4$. Jet multiplicities as high as seven jets accompanying the vector boson have already been probed at the LHC, together with a substantial number of other kinematical observables, such as angular correlations among the various jets or among the jets and the vector boson, or the sum of jet transverse momenta, H_T. Whereas the jet p_t and H_T distributions are dominated by jet energy scale uncertainties at levels similar to those discussed above for inclusive jet production, angular correlations and jet multiplicity ratios have been measured with a precision of ∼ 10%, see *e.g.* Refs. 359,275.

A general observation is that MC models, which implement a matching of matrix-element calculations with parton showers, provide a good description of the data within uncertainties. Also NLO calculations for up to five jets [122] in addition to the vector boson are in good agreement with the data over that phase space, where the calculations are applicable; that is, one can not expect such predictions to work for, eg., the p_t distribution of the $n+1$st jet with $V+n$ jets calculated at NLO. However, with the high statistics available to and the high precision achieved by the LHC experiments, some more detailed observations can be made. MC models that implement parton shower matching to LO matrix elements (LO+PS) tend to overpredict the data at large jet and/or boson p_t, while parton shower matching to NLO matrix elements gives better agreement. These problems of LO+PS models are less acute when looking at angular correlations.

Also, electroweak corrections are expected to become more and more relevant now that the TeV energy range starts to be explored. For example, such corrections were found [360] to be sizeable (tens of percent) when studying the ratio $(d\sigma^\gamma/dp_t)/(d\sigma^Z/dp_t)$ in $\gamma\,(Z)$+jet production, p_t being the boson's transverse momentum, and might account for (some of) the differences observed in a CMS measurement [361] of this quantity.

The challenges get even more severe in the case of vector boson plus heavy quark (b, c) production, both because of theoretical issues (an additional scale is introduced by the heavy quark mass and different schemes exist for the handling of heavy quarks and their mass effects in the initial and/or final state) and because of additional experimental uncertainties related to the heavy-flavour tagging. A review of heavy quark production at the LHC can be found in Ref. 362. There it is stated that studies of b-jet production with or without associated W and Z bosons reveal the di-b-jet p_t and mass spectra to be well modelled, within experimental and theoretical uncertainties, by most generators on the market. However, sizeable differences between data and predictions are seen in the modelling of events with single b jets, particularly at large b-jet p_t, where gluon splitting processes become dominant, as also confirmed by studies of b-hadron and b-jet angular correlations.

A number of interesting developments, in terms of probing higher-order QCD effects, have occurred in the sector of diboson production, in particular for the WW and $\gamma\gamma$ cases. Regarding the former, an early disagreement of about 10% between the LHC measurements and the NLO predictions had led to a number of speculations of possible new physics effects in this channel. However, more recent ATLAS and CMS measurements [363–365] are in agreement with the NNLO prediction [68].

In the case of diphoton production, ATLAS [366,367] and CMS [368] have provided accurate measurements, in particular for phase-space regions that are sensitive to radiative QCD corrections (multi-jet production), such as small azimuthal photon separation. While there are large deviations between data and NLO predictions in this region, a calculation [147] at NNLO accuracy manages to mostly fill this gap. This is an interesting example where scale variations can not provide a reliable estimate of missing contributions beyond NLO, since at NNLO new channels appear in the initial state (gluon fusion in this case).

In terms of heaviest particle involved, top-quark production at the LHC has become an important tool for probing higher-order QCD calculations, thanks to very impressive achievements both on the experimental and theoretical side, as extensively summarised in Ref. 369. Regarding $t\bar{t}$ production, the most precise inclusive cross section measurements are achieved using the dilepton ($e\,\mu$) final state, with a total uncertainty of 4%. This is of about the same size as the uncertainty on the most advanced theoretical prediction [67], obtained at NNLO with additional soft-gluon resummation at NNLL accuracy. There is excellent agreement between data and QCD prediction.

A large number of differential cross section measurements have been performed at 7, 8 and 13 TeV centre-of-mass energy, studying distributions such as the top-quark p_t and rapidity, the transverse momentum and invariant mass of the $t\bar{t}$ system (probing scales up to the TeV range), or the number of additional jets. These measurements have been compared to a wide range of predictions, at fixed order up to NNLO as well as using LO or NLO matrix elements matched to parton showers. While in general there is good agreement observed with data, most MC simulations predict a somewhat harder top-quark p_t distribution than seen in data.

Thanks to both the precise measurements of and predictions for the inclusive top-pair cross section, that is sensitive to the strong coupling constant and the top-quark mass, this observable has been used to measure the strong coupling constant at NNLO accuracy from hadron collider data [370,371] (*cf.* Section 9.4 below), as well as to obtain a measurement of the top-quark's pole mass without employing direct reconstruction methods [370,372,373].

Finally, it is worth mentioning that steps are being undertaken towards using the newly found Higgs boson as a new tool for QCD studies, since Higgs production, dominated by the gluon fusion process, is subject to very large QCD corrections. First studies of fiducial and differential cross sections, using the ZZ, $\gamma\gamma$ and WW decay channels, have already been performed [374–380], and the current experimental precision of ∼ 20% or more is expected to be substantially reduced with the future LHC data.

9.4. Determinations of the strong coupling constant

Beside the quark masses, the only free parameter in the QCD Lagrangian is the strong coupling constant α_s. The coupling constant in itself is not a physical observable, but rather a quantity defined in the context of perturbation theory, which enters predictions for experimentally measurable observables, such as R in Eq. (9.7).

Here, we retain the 2016 summary [381] of measurements of α_s and extraction of the world average value of $\alpha_s(M_Z^2)$, and leave an update of this section to a later version of *this Review* ♯. This is done because only very few new results satisfying the selection criteria defined below were available at the deadline for *this Review*, while further new results are expected to arrive (and actually have arrived) past-deadline.

Many experimental observables are used to determine α_s. Considerations in such determinations include:

- The observable's sensitivity to α_s as compared to the experimental precision. For example, for the e^+e^- cross section to hadrons (*cf.* R in Sec. 9.2.1), QCD effects are only a small correction, since the perturbative series starts at order α_s^0; 3-jet production or event shapes in e^+e^- annihilations are directly sensitive to α_s since they start at order α_s; the hadronic decay width of heavy quarkonia, $\Gamma(\Upsilon \to \text{hadrons})$, is very sensitive to α_s since its leading order term is $\propto \alpha_s^3$.
- The accuracy of the perturbative prediction, or equivalently of the relation between α_s and the value of the observable. The minimal requirement is generally considered to be an NLO prediction. Some observables are predicted to NNLO (many inclusive observables, 3-jet rates and event shapes in e^+e^- collisions) or even N^{3}LO (e^+e^- hadronic cross section and τ branching fraction to hadrons). In certain cases, fixed-order predictions are supplemented with resummation. The precise magnitude of theory uncertainties is usually estimated as discussed in Sec. 9.2.4.
- The size of non-perturbative effects. Sufficiently inclusive quantities, like the e^+e^- cross section to hadrons, have small non-perturbative contributions $\sim \Lambda^4/Q^4$. Others, such as event-shape distributions, have contributions $\sim \Lambda/Q$.
- The scale at which the measurement is performed. An uncertainty δ on a measurement of $\alpha_s(Q^2)$, at a scale Q, translates to an uncertainty $\delta' = (\alpha_s^2(M_Z^2)/\alpha_s^2(Q^2)) \cdot \delta$ on $\alpha_s(M_Z^2)$. For example, this enhances the already important impact of precise low-Q measurements, such as from τ decays, in combinations performed at the M_Z scale.

The selection of results from which to determine the world average value of $\alpha_s(M_Z^2)$ is restricted to those which are

- published in a peer-reviewed journal,
- based on the most complete perturbative QCD predictions, *i.e.* to those using NNLO or higher-order expansions.

This excludes *e.g.* results from jet production in DIS at HERA and at hadron colliders which are based on calculations at NLO only. These will nevertheless be discussed in this review, as they are important ingredients for the experimental evidence of the energy dependence of α_s, *i.e.* for Asymptotic Freedom, one of the key features of QCD. Note that results which do not include reliable estimates of experimental, systematic and theoretical uncertainties, which are based on not commonly accepted procedures like scale optimization, or which omit discussion or accounting of non-perturbative corrections and effects, will not be referenced at all in this review.

In order to calculate the world average value of $\alpha_s(M_Z^2)$, we apply an intermediate step of pre-averaging results within certain sub-fields like e^+e^- annihilation, DIS and hadronic τ-decays, and calculate the overall world average from those pre-averages rather than from individual measurements. This is done because in most sub-fields one observes that different determinations of the strong coupling from substantially similar datasets lead to values of α_s that are only marginally compatible with each other, or with the final world average value, which presumably is a reflection of the challenges of evaluating and including appropriate systematic uncertainties.

So for each sub-field, the *unweighted average* of all selected results is taken as the pre-average value of $\alpha_s(M_Z^2)$, and the unweighted average of the quoted uncertainties is assigned to be the respective overall error of this pre-average. However, if this error appears to be smaller than the unweighted standard deviation - i.e. the *spread* - of the results, the standard deviation is taken as the overall uncertainty instead. This is done in order to arrive at an unbiased estimator of the average value of $\alpha_s(M_Z^2)$ from this sub-field, and to avoid that singular, optimistic estimates of systematic uncertainties dominate the field if these are not backed up by a broader consensus †.

Assuming that the resulting pre-averages are largely independent of each other, we determine the final world average value using the method of 'χ^2 *averaging*', as proposed, *e.g.*, in Ref. 386, in order to treat cases of possible (unknown) correlations as well as possibly underestimated systematic uncertainties in a meaningful and well defined manner: the central value is determined as the weighted average of the different input values. An initial uncertainty of the central value is determined treating the uncertainties of all individual measurements as being uncorrelated and of Gaussian nature, and the overall χ^2 to the central value is calculated. If this initial χ^2 is larger than the number of degrees of freedom, then all individual uncertainties are enlarged by a common factor such that χ^2/d.o.f. equals unity. If the initial value of χ^2 is smaller than the number of degrees of freedom, an overall correlation coefficient is introduced and determined by requiring that the total χ^2/d.o.f. equals unity. In both cases, the resulting overall uncertainty of α_s is larger than the initial estimate of the uncertainty.

9.4.1. *Hadronic τ decays* :

Based on complete N^{3}LO predictions [35], analyses of the τ hadronic decay width and spectral functions have been performed, leading to precise determinations of α_s at the energy scale of M_τ^2 [35,387–393]. They are based on different approaches to treat perturbative and non-perturbative contributions, the impacts of which are a matter of intense discussions, see *e.g.* [391] and [394].

In particular, there is a significant difference between results obtained using fixed-order (FOPT) or contour improved perturbation theory (CIPT), such that analyses based on CIPT generally arrive at about 7% larger values of $\alpha_s(M_\tau^2)$ than those based on FOPT. When converted to $\alpha_s(M_Z^2)$, the difference is about 2%. This uncertainty is about 5 times larger than the typically achieved experimental precision. In addition, most recent results show differences of up to 10% in $\alpha_s(M_\tau^2)$ (3% at M_Z), between different groups using the same data sets and perturbative calculations, most likely due to different treatments of the non-perturbative contributions, c.f. Ref. [393] with Refs. [391,392].

We determine the pre-average value of $\alpha_s(M_Z^2)$ for this sub-field from studies which employ both, FOPT and CIPT expansions, and which include the difference among these in the quoted overall uncertainty: $\alpha_s(M_Z^2) = 0.1202 \pm 0.0019$ [35], $\alpha_s(M_Z^2) = 0.1200 \pm 0.0015$ [391], $\alpha_s(M_Z^2) = 0.1199 \pm 0.0015$ [392], and $\alpha_s(M_Z^2) = 0.1165 \pm 0.0019$ [393].

We also include the result from τ decay and lifetime measurements, obtained in Sec. *Electroweak Model and constraints on New Physics* of the 2013 edition of this *Review*, $\alpha_s(M_Z^2) = 0.1193 \pm 0.0023$. All these are summarised in Fig. 9.2. Determining the unweighted average of the central values and their overall uncertainties, we arrive at $\alpha_s(M_Z^2) = 0.1192 \pm 0.0018$ which we will use as the first input for determining the world average value of $\alpha_s(M_Z^2)$. This corresponds to $\alpha_s(M_\tau^2) = 0.325 \pm 0.015$ at the scale of the τ-mass.

♯ The time evolution of α_s combinations can be followed by consulting Refs. [383–385] as well as earlier editions of *this Review*.

† In most practical cases, this procedure arrives at similar values as obtained from the '*range averaging*' method which we used in previous *Reviews*, while it avoids potential shortcomings and biases of the latter.

9.4.2. ***Lattice QCD*** :
There are several current results on α_s from lattice QCD, see also Sec. *Lattice QCD* in this *Review*. The HPQCD collaboration [395] computes Wilson loops and similar short-distance quantities with lattice QCD and analyzes them with NNLO perturbative QCD. This yields a value for α_s, but the lattice scale must be related to a physical energy/momentum scale. This is achieved with the Υ'-Υ mass difference, however, many other quantities could be used as well [396]. HPQCD obtains $\alpha_s(M_Z^2) = 0.1184 \pm 0.0006$, where the uncertainty includes effects from truncating perturbation theory, finite lattice spacing and extrapolation of lattice data. An independent perturbative analysis of a subset of the same lattice-QCD data yields $\alpha_s(M_Z^2) = 0.1192 \pm 0.0011$ [397]. Using another, independent methodology, the current-current correlator method, HPQCD obtains $\alpha_s(M_Z^2) = 0.1182 \pm 0.0007$ [395,398]. The analysis of Ref. 399, which uses the Schroedinger functional scheme and avoids the staggered fermion treatment of Ref. 395, finds $\alpha_s(M_Z^2) = 0.1205 \pm 0.0008 \pm 0.0005\,^{+0.0000}_{-0.0017}$, where the first uncertainty is statistical and the others are from systematics. Since this approach uses a different discretization of lattice fermions and a different general methodology, it provides an independent cross check of other lattice extractions of α_s. A study of the ETM collaboration [400] used lattice data with u, d, s and c quarks in the sea and examined the ghost-gluon coupling, obtaining $\alpha_s(M_Z^2) = 0.1196 \pm 0.0012$. Finally, a determination of α_s from the QCD static potential [401] results in $\alpha_s(M_Z^2) = 0.1166^{+0.0012}_{-0.0008}$. The JLQCD collaboration, in an analysis of Adler functions, has recently corrected their initial result of $\alpha_s(M_Z^2) = 0.1181^{+0.0014}_{-0.0012}$ downwards, by more than 5 standard deviations of their assigned uncertainty, to $\alpha_s(M_Z^2) = 0.1118^{+0.0016}_{-0.0017}$ [402]. For this and other reasons discussed in [403], we do not include this result in our determination of the average lattice result.

A summary of the results discussed above is given in Fig. 9.2. They average, applying the method of taking the unweighted averages of the central values and their quoted uncertainties at face value, to $\alpha_s(M_Z^2) = 0.1188 \pm 0.0011$, which we take as our second result for the determination of the world average value of α_s. This compares well to a similar compilation and summary provided by the FLAG Working Group [403], suggesting $\alpha_s(M_Z^2) = 0.1184 \pm 0.0012$ as the overall average of lattice determinations of α_s. Both these error estimates are more conservative than the one (± 0.0005) we used in our previous *Review* where we applied the χ^2 *averaging* method.

9.4.3. ***Deep inelastic lepton-nucleon scattering (DIS)*** :
Studies of DIS final states have led to a number of precise determinations of α_s: a combination [404] of precision measurements at HERA, based on NLO fits to inclusive jet cross sections in neutral current DIS at high Q^2, provides combined values of α_s at different energy scales Q, as shown in Fig. 9.3, and quotes a combined result of $\alpha_s(M_Z^2) = 0.1198 \pm 0.0032$. A more recent study of multijet production [405], based on improved reconstruction and data calibration, confirms the general picture, albeit with a somewhat smaller value of $\alpha_s(M_Z^2) = 0.1165 \pm 0.0039$, still in NLO. An evaluation of inclusive jet production, including *approximate* NNLO contributions [406], reduces the theoretical prediction for jet production in DIS, improves the description of the final HERA data in particular at high photon virtuality Q^2 and increases the central fit value of the strong coupling constant.

Another class of studies, analyzing structure functions in NNLO QCD (and partly beyond), provide results which serve as relevant inputs for the world average of α_s. Most of these studies do *not*, however, explicitly include estimates of theoretical uncertainties when quoting fit results of α_s. In such cases we add, in quadrature, half of the difference between the results obtained in NNLO and NLO to the quoted errors: A combined analysis of non-singlet structure functions from DIS [407], based on QCD predictions up to N^{3}LO in some of its parts, results in $\alpha_s(M_Z^2) = 0.1141 \pm 0.0022$ (BBG). Studies of singlet and non-singlet structure functions, based on NNLO predictions, result in $\alpha_s(M_Z^2) = 0.1134 \pm 0.0025$ [408] (ABM) and in $\alpha_s(M_Z^2) = 0.1158 \pm 0.0036$ [409] (JR). The MSTW group [410], also including data on jet production at the Tevatron, obtains, at NNLO[♯♯], $\alpha_s(M_Z^2) = 0.1171 \pm 0.0024$. A recent update of this analysis, also including hadron collider data, determined a new set of parton density functions (MMHT2014) [411], together with $\alpha_s(M_Z^2) = 0.1172 \pm 0.0013$. The NNPDF group [412] presented a result, $\alpha_s(M_Z^2) = 0.1173 \pm 0.0011$, which is in line with the one from the MMHT group, including rather small experimental and theoretical uncertainties of only 6 and 9 per-mille, respectively.

We note that criticism has been expressed on some of the above extractions. Among the issues raised, we mention the neglect of singlet contributions at $x \geq 0.3$ in pure non-singlet fits [413], the impact and detailed treatment of particular classes of data in the fits [413,414], possible biases due to insufficiently flexible parametrizations of the PDFs [415] and the use of a fixed-flavor number scheme [416,417].

Summarizing the results from world data on structure functions, taking the *unweighted average* of the central values and errors of all selected results, leads to a pre-average value of $\alpha_s(M_Z^2) = 0.1156 \pm 0.0021$, see Fig. 9.2.

9.4.4. ***Heavy quarkonia decays*** :
The latest extraction of the strong coupling constant from an analysis of radiative Υ decays [418] resulted in $\alpha_s(M_Z^2) = 0.119^{+0.006}_{-0.005}$. This determination is based on QCD at NLO only, so it will not be considered for the final extraction of the world average value of α_s; it is, however, an important ingredient for the demonstration of Asymptotic Freedom as given in Fig. 9.3.

9.4.5. ***Hadronic final states of e^+e^- annihilations*** :
Re-analyses of event shapes in e^+e^- annihilation, measured around the Z peak and at LEP2 center-of-mass energies up to 209 GeV, using NNLO predictions matched to NLL resummation and Monte Carlo models to correct for hadronization effects, resulted in $\alpha_s(M_Z^2) = 0.1224 \pm 0.0039$ (ALEPH) [419], with a dominant theoretical uncertainty of 0.0035, and in $\alpha_s(M_Z^2) = 0.1189 \pm 0.0043$ (OPAL) [420]. Similarly, an analysis of JADE data [421] at center-of-mass energies between 14 and 46 GeV gives $\alpha_s(M_Z^2) = 0.1172 \pm 0.0051$, with contributions from hadronization model and from perturbative QCD uncertainties of 0.0035 and 0.0030, respectively. Precise determinations of α_s from 3-jet production alone, in NNLO, resulted in $\alpha_s(M_Z^2) = 0.1175 \pm 0.0025$ [422] from ALEPH data and in $\alpha_s(M_Z^2) = 0.1199 \pm 0.0059$ [423] from JADE. These results are summarized in the upper half of the e^+e^- sector of Fig. 9.2.

Another class of α_s determinations is based on analytic calculations of non-perturbative and hadronization effects, rather than on Monte Carlo models [424–427], using methods like power corrections, factorization of soft-collinear effective field theory, dispersive models and low scale QCD effective couplings. In these studies, the world data on Thrust distributions, or - most recently - C-parameter distributions, are analysed and fitted to perturbative QCD predictions in NNLO matched with resummation of leading logs up to N^{3}LL accuracy, see Sec. 9.2.3.3. The results are $\alpha_s(M_Z^2) = 0.1164^{+0.0028}_{-0.0024}$ [424], $\alpha_s(M_Z^2) = 0.1135 \pm 0.0011$ [425] and $\alpha_s(M_Z^2) = 0.1137^{+0.0034}_{-0.0027}$ [426] from Thrust, and $\alpha_s(M_Z^2) = 0.1123 \pm 0.0015$ [427] from C-parameter. They are also displayed in Fig. 9.2.

Not to be included in the computation of the world average but worth mentioning are a computation of the NLO corrections to 5-jet production and comparison to the measured 5-jet rates at LEP [428], giving $\alpha_s(M_Z^2) = 0.1156^{+0.0041}_{-0.0034}$, and a computation of non-perturbative and perturbative QCD contributions to the scale evolution of quark and gluon jet multiplicities, including resummation, resulting in $\alpha_s(M_Z^2) = 0.1199 \pm 0.0026$ [429].

We note that there is criticism on both classes of α_s extractions described above: those based on corrections of non-perturbative hadronization effects using QCD-inspired Monte Carlo generators (since the parton level of a Monte Carlo simulation is not defined in a manner equivalent to that of a fixed-order calculation), as well as studies based on non-perturbative analytic calculations, as their

[♯♯] Note that for jet production at a hadron collider, only NLO predictions are available, while for the structure functions full NNLO was utilized.

systematics have not yet been fully verified. In particular, quoting rather small overall experimental, hadronization and theoretical uncertainties of only 2, 5 and 9 per-mille, respectively [425,427], seems unrealistic and has neither been met nor supported by other authors or groups.

In view of these open questions, the determination of the *unweighted average* and uncertainties is supposed to provide the most appropriate and unbiased estimate of the average value of $\alpha_s(M_Z^2)$ for this sub-field, which results in $\alpha_s(M_Z^2) = 0.1169 \pm 0.0034$.

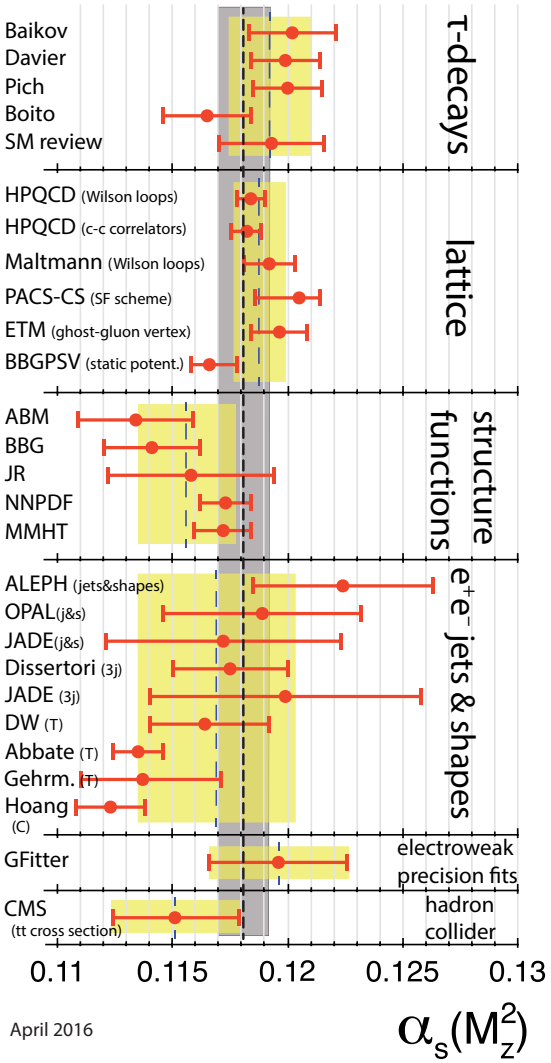

Figure 9.2: Summary of determinations of $\alpha_s(M_Z^2)$ from the six sub-fields discussed in the text. The yellow (light shaded) bands and dashed lines indicate the pre-average values of each sub-field. The dotted line and grey (dark shaded) band represent the final world average value of $\alpha_s(M_Z^2)$.

9.4.6. ***Hadron collider results*** :
Significant determinations of α_s from data at hadron colliders, *i.e.* the Tevatron and the LHC, are obtained, however mostly still limited to QCD at NLO. At $\sqrt{s} = 1.96$ TeV,

$$\alpha_s(M_Z^2) = 0.1161^{+0.0041}_{-0.0048} \text{ and}$$
$$\alpha_s(M_Z^2) = 0.1191^{+0.0048}_{-0.0071}$$

result from studies of inclusive jet cross sections [430] and from jet angular correlations [431], respectively. ATLAS data on inclusive jet production at $\sqrt{s} = 7$ TeV [432] lead to [433]

$$\alpha_s(M_Z^2) = 0.1151^{+0.0093}_{-0.0087} .$$

Here, experimental systematics, the choice of jet scale and the use of different PDFs dominate the large overall uncertainties. Determinations of α_s from CMS data on the ratio of inclusive 3-jet to 2-jet cross sections [434], from inclusive jet production [435] and from the 3-jet differential cross section [436] quoted values of

$$\alpha_s(M_Z^2) = 0.1148 \pm 0.0014(\text{exp.})^{+0.0053}_{-0.0023}(\text{theo.}) ,$$
$$\alpha_s(M_Z^2) = 0.1185 \pm 0.0019(\text{exp.})^{+0.0060}_{-0.0037}(\text{theo.}) \text{ and}$$
$$\alpha_s(M_Z^2) = 0.1171 \pm 0.0013(\text{exp.})^{+0.0073}_{-0.0047}(\text{theo.}) ,$$

respectively. Most recently, the ATLAS collaboration reported

$$\alpha_s(M_Z^2) = 0.1173 \pm 0.0010(\text{exp.})^{+0.0065}_{-0.0026}(\text{theo.}) \text{ and}$$
$$\alpha_s(M_Z^2) = 0.1195 \pm 0.0018(\text{exp.})^{+0.0062}_{-0.0022}(\text{theo.})$$

using the transverse energy-energy correlation function (TEEC) and its associated azimuthal asymmetry (ATEEC), respectively [271]. All these results are at NLO only, however they provide valuable new values of α_s at energy scales now extending up to 1.4 TeV. Although not contributing to the overall world average of α_s which we determine below, it may be worth mentioning that the collider results listed above average to a value of $\alpha_s(M_Z^2) = 0.1172 \pm 0.0059$.

So far, only one analysis is available which involves the determination of α_s from hadron collider data in NNLO of QCD: from a measurement of the $t\bar{t}$ cross section at $\sqrt{s} = 7$ TeV, CMS [370] determined

$$\alpha_s(M_Z^2) = 0.1151^{+0.0028}_{-0.0027} ,$$

whereby the dominating contributions to the overall error are experimental ($^{+0.0017}_{-0.0018}$), from parton density functions ($^{+0.0013}_{-0.0011}$) and the value of the top quark pole mass (± 0.0013).

This latter result will enter our determination of the new world average of α_s, and will thereby open a new sub-field of α_s determinations in this *Review*. We note, however, that so far there is only this one result in this sub-field. While there are more recent measurements of $t\bar{t}$ cross sections from ATLAS and from CMS, at $\sqrt{s} = 7$, 8 and at 13 TeV, none quotes further extractions of α_s. A more reliable result will thus be left to the next *Review*, however we note that the most recent measurements of $t\bar{t}$ cross sections imply larger values of $\alpha_s(M_Z^2)$ than the one which we use, at this time, as result for this sub-field.

9.4.7. ***Electroweak precision fit*** :
The N^{3}LO calculation of the hadronic Z decay width [35] was used in the latest update of the global fit to electroweak precision data [437], resulting in

$$\alpha_s(M_Z^2) = 0.1196 \pm 0.0030 ,$$

claiming a negligible theoretical uncertainty. We note that results from electroweak precision data, however, strongly depend on the strict validity of Standard Model predictions and the existence of the minimal Higgs mechanism to implement electroweak symmetry breaking. Any - even small - deviation of nature from this model could strongly influence this extraction of α_s.

9.4.8. ***Determination of the world average value of $\alpha_s(M_Z^2)$*** :
Obtaining a world average value for $\alpha_s(M_Z^2)$ is a non-trivial exercise. A certain arbitrariness and subjective component is inevitable because of the choice of measurements to be included in the average, the treatment of (non-Gaussian) systematic uncertainties of mostly theoretical nature, as well as the treatment of correlations among the various inputs, of theoretical as well as experimental origin.

We have chosen to determine pre-averages for sub-fields of measurements which are considered to exhibit a maximum of independence between each other, considering experimental as well as theoretical issues. The six pre-averages are summarized in Fig. 9.2. We recall that these are exclusively obtained from extractions which

are based on (at least) full NNLO QCD predictions, and are published in peer-reviewed journals at the time of completing this *Review*. These pre-averages are then combined to the final world average value of $\alpha_s(M_Z^2)$, using the χ^2 *averaging method* and error treatment as described above. From these, we determine the new world average value of

$$\alpha_s(M_Z^2) = 0.1181 \pm 0.0011 \ , \tag{9.23}$$

with an uncertainty of 0.9 %.*** This world average value is in reasonable agreement with that from the 2013 version of this *Review*, which was $\alpha_s(M_Z^2) = 0.1185 \pm 0.0006$, however at a somewhat decreased central value and with an overall uncertainty that has almost doubled. These changes are mainly due to the following developments:

- the uncertainty of the combined lattice result, now using the same averaging procedure as applied to the other sub-fields, is more conservative than that used in our previous *Review*, leading to a larger final uncertainty of the new world average, and to a reduced fixing power towards the central average value;
- the relatively low value of α_s from hadron collider results, which currently consists of only one measurement of the $t\bar{t}$ cross section at $\sqrt{s} = 7$ TeV [370] that is likely to be a fluctuation to the low side.

For convenience, we also provide the values for $\Lambda_{\overline{MS}}$ which correspond to the new world average:

$$\Lambda_{\overline{MS}}^{(6)} = (89 \pm 6) \ \text{MeV}, \tag{9.24a}$$
$$\Lambda_{\overline{MS}}^{(5)} = (210 \pm 14) \ \text{MeV}, \tag{9.24b}$$
$$\Lambda_{\overline{MS}}^{(4)} = (292 \pm 16) \ \text{MeV}, \tag{9.24c}$$
$$\Lambda_{\overline{MS}}^{(3)} = (332 \pm 17) \ \text{MeV}, \tag{9.24d}$$

for $n_f = 6$, 5, 4 and 3 quark flavors, which are determined using the 4-loop expression for the running of α_s according to Eq. (9.5) and 3-loop matching at the charm-, bottom- and top-quark pole masses of 1.3, 4.2 and 173 GeV/c^2, respectively. Note that for scales below a few GeV, Eq. (9.5) starts to differ significantly from the exact solution of the renormalization group equation Eq. (9.3) and the latter is then to be preferred.

In order to further test and verify the sensitivity of the new average value of $\alpha_s(M_Z^2)$ to the different pre-averages and fields of α_s determinations, we give each of the averages obtained when leaving out one of the six input values, as well as the respective, initial value of χ^2 :

$$\alpha_s(M_Z^2) = 0.1179 \pm 0.0011 \ \ (\text{w/o } \tau \text{ results};\ \chi_0^2/d.o.f. = 3.3/4), \tag{9.25a}$$
$$\alpha_s(M_Z^2) = 0.1174 \pm 0.0016 \ \ (\text{w/o lattice results};\ \chi_0^2/d.o.f. = 2.9/4), \tag{9.25b}$$
$$\alpha_s(M_Z^2) = 0.1185 \pm 0.0013 \ \ (\text{w/o DIS results};\ \chi_0^2/d.o.f. = 2.0/4), \tag{9.25c}$$
$$\alpha_s(M_Z^2) = 0.1182 \pm 0.0010 \ \ (\text{w/o } e^+e^- \text{ results};\ \chi_0^2/d.o.f. = 3.5/4), \tag{9.25d}$$
$$\alpha_s(M_Z^2) = 0.1184 \pm 0.0012 \ \ (\text{w/o hadron collider};\ \chi_0^2/d.o.f. = 2.4/4) \text{ and} \tag{9.25e}$$
$$\alpha_s(M_Z^2) = 0.1180 \pm 0.0010 \ \ (\text{w/o e.w. precision fit};\ \chi_0^2/d.o.f. = 3.4/4). \tag{9.25f}$$

They are well within the uncertainty of the overall world average quoted above. Note, however, that the average *excluding* the lattice result is no longer as close to the value obtained from lattice alone as was the case in the 2013 *Review*, but is now smaller by almost one standard deviation of its assigned uncertainty.

Notwithstanding the many open issues still present within each of the sub-fields summarised in this *Review*, the wealth of available results provides a rather precise and reasonably stable world average value of $\alpha_s(M_Z^2)$, as well as a clear signature and proof of the energy dependence of α_s, in full agreement with the QCD prediction of Asymptotic Freedom. This is demonstrated in Fig. 9.3, where results of $\alpha_s(Q^2)$ obtained at discrete energy scales Q, now also including those based just on NLO QCD, are summarized. Thanks to the results from the Tevatron and from the LHC, the energy scales at which α_s is determined now extend up to more than 1 TeV$^\diamondsuit$.

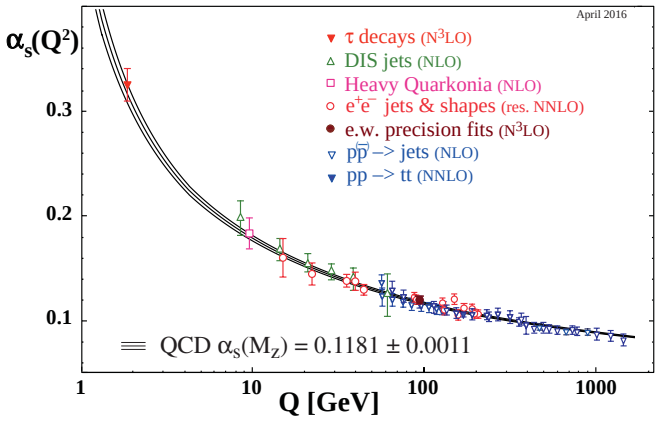

Figure 9.3: Summary of measurements of α_s as a function of the energy scale Q. The respective degree of QCD perturbation theory used in the extraction of α_s is indicated in brackets (NLO: next-to-leading order; NNLO: next-to-next-to leading order; res. NNLO: NNLO matched with resummed next-to-leading logs; N^{3}LO: next-to-NNLO).

9.5. Acknowledgments

We are grateful to J.-F. Arguin, G. Altarelli, D. Britzger, J. Butterworth, M. Cacciari, L. del Debbio, D. d'Enterria, P. Gambino, C. Glasman Kuguel, N. Glover, M. Grazzini, A. Kronfeld, K. Kousouris, M. Lüscher, Y. Ma, M. d'Onofrio, A. Ramos, S. Sharpe, R. Sommer, G. Sterman, D. Treille, N. Varelas, M. Wobisch, W.M. Yao, C.P. Yuan, and G. Zanderighi for discussions, suggestions and comments on this and earlier versions of this *Review*.

References:

1. R.K. Ellis, W.J. Stirling, and B.R. Webber, *"QCD and collider physics,"* Camb. Monogr. Part. Phys. Nucl. Phys. Cosmol. **81** (1996).
2. C.A. Baker *et al.*, Phys. Rev. Lett. **97**, 131801 (2006).
3. H.-Y. Cheng, Phys. Reports **158**, 1 (1988).
4. G. Dissertori, I.G. Knowles, and M. Schmelling, *"High energy experiments and theory,"* Oxford, UK: Clarendon (2003).
5. R. Brock *et al.*, [CTEQ Collab.], Rev. Mod. Phys. **67**, 157 (1995), see also `http://www.phys.psu.edu/~cteq/handbook/v1.1/handbook.pdf`.
6. A.S. Kronfeld and C. Quigg, Am. J. Phys. **78**, 1081 (2010).
7. T. Plehn, Lect. Notes Phys. **844**, 1 (2012).
8. J. Campbell, J. Huston, F. Krauss *"The Black Book of Quantum Chromodynamics, a Primer for the QCD Era,"* Oxford University Press, UK (2017).

*** The weighted average, treating all inputs as uncorrelated measurements with Gaussian uncertainties, results in $\alpha_s(M_Z^2) = 0.11810 \pm 0.00078$ with χ^2/d.o.f. $= 3.7/5$. Requiring χ^2/d.o.f. to reach unity calls for an overall correlation factor of 0.28, which increases the overall uncertainty to ± 0.00114.

$^\diamondsuit$ We note, however, that in many such studies, like those based on exclusive states of jet multiplicities, the relevant energy scale of the measurement is not uniquely defined. For instance, in studies of the ratio of 3- to 2-jet cross sections at the LHC, the relevant scale was taken to be the average of the transverse momenta of the two leading jets [434], but could alternatively have been chosen to be the transverse momentum of the 3^{rd} jet.

9. R. Stock (Ed.), Relativistic Heavy Ion Physics, Springer-Verlag Berlin, Heidelberg, 2010.
10. *Proceedings of the XXIV International Conference on Ultrarelativistic Nucleus–Nucleus Collisions, Quark Matter 2014*, Nucl. Phys. A, volume 931.
11. R. Hwa and X. N. Wang (Ed.), Quark Gluon Plasma 4, World Scientific Publishing Company, 2010.
12. T. van Ritbergen, J.A.M. Vermaseren, and S.A. Larin, Phys. Lett. **B400**, 379 (1997).
13. M. Czakon, Nucl. Phys. **B710**, 485 (2005).
14. P.A. Baikov, K.G. Chetyrkin, and J.H. Kühn, Phys. Rev. Lett. **118**, 082002 (2017).
15. T. Luthe *et al.*, JHEP **1607**, 127 (2016).
16. F. Herzog *et al.*, JHEP **1702**, 090 (2017).
17. W.A. Bardeen *et al.*, Phys. Rev. **D18**, 3998 (1978).
18. D.J. Gross and F. Wilczek, Phys. Rev. Lett. **30**, 1343 (1973).
19. H.D. Politzer, Phys. Rev. Lett. **30**, 1346 (1973).
20. Y. Schröder and M. Steinhauser, JHEP **0601**, 051 (2006).
21. K.G. Chetyrkin, J.H. Kühn, and C. Sturm, Nucl. Phys. **B744**, 121 (2006).
22. A.G. Grozin *et al.*, JHEP **1109**, 066 (2011).
23. K.G. Chetyrkin, B.A. Kniehl, and M. Steinhauser, Nucl. Phys. **B510**, 61 (1998).
24. M. Dalla Brida *et al.* [ALPHA Collaboration], Phys. Rev. Lett. **117**, 182001 (2016).
25. K.G. Chetyrkin, J.H. Kühn, and M. Steinhauser, Comp. Phys. Comm. **133**, 43 (2000).
26. B. Schmidt and M. Steinhauser, Comp. Phys. Comm. **183**, 1845 (2012) `http://www.ttp.kit.edu/Progdata/ttp12/ttp12-02/`.
27. F. Herren and M. Steinhauser, `arXiv:1703.03751 [hep-ph]`.
28. A.V. Bednyakov, Phys. Lett. **B741**, 262 (2015).
29. M. Beneke, Phys. Reports **317**, 1 (1999).
30. P. Marquard *et al.*, Phys. Rev. Lett. **114**, 142002 (2015).
31. P.A. Baikov *et al.*, Phys. Lett. **B714**, 62 (2012).
32. K.G. Chetyrkin, J.H. Kühn, and A. Kwiatkowski, Phys. Reports **277**, 189 (1996).
33. Y. Kiyo *et al.*, Nucl. Phys. **B823**, 269 (2009).
34. P.A. Baikov *et al.*, Phys. Rev. Lett. **108**, 222003 (2012).
35. P.A. Baikov, K.G. Chetyrkin, and J.H. Kühn, Phys. Rev. Lett. **101**, 012002 (2008).
36. P.A. Baikov, K.G. Chetyrkin, and J.H. Kühn, Phys. Rev. Lett. **96**, 012003 (2006).
37. P.A. Baikov and K.G. Chetyrkin, Phys. Rev. Lett. **97**, 061803 (2006).
38. F. Herzog *et al.*, JHEP **1708**, 113 (2017).
39. D. Asner *et al.*, `arXiv:1307.8265 [hep-ex]`.
40. H.W. Lin *et al.*, Phys. Rev. **D91**, 054510 (2015);
C. Alexandrou *et al.*, Phys. Rev. **D92**, 014502 (2015).
41. G. C. Rossi and M. Testa, Phys. Rev. **D96**, 014507 (2017).
42. J. Gao, L. Harland-Lang, and J. Rojo, `arXiv:1709.04922 [hep-ph]`.
43. J. D. Bjorken and E. A. Paschos, Phys. Rev. **185**, 1975 (1969).
44. J.A.M. Vermaseren, A. Vogt, and S. Moch, Nucl. Phys. **B724**, 3 (2005).
45. S. Moch, J.A.M. Vermaseren, and A. Vogt, Nucl. Phys. **B813**, 220 (2009).
46. J. Davies *et al.*, PoS DIS **2016** (2016) 059.
47. E. Laenen *et al.*, Nucl. Phys. **B392**, 162 (1993);
S. Riemersma, J. Smith, and W.L. van Neerven, Phys. Lett. **B347**, 143 (1995).
48. J. Blümlein, A. De Freitas, and C. Schneider, Nucl. Part. Phys. Proc. **261-262** 185 Nucl. Part. Phys. Proc. **261-262** (2015) 185.
49. J.C. Collins, D.E. Soper, and G.F. Sterman, Adv. Ser. Direct. High Energy Phys. **5**, 1 (1988).
50. J.C. Collins, *Foundations of Perturbative QCD*, Cambridge University Press, 2011.
51. G.C. Nayak, J.-W. Qiu, and G.F. Sterman, Phys. Rev. **D72**, 114012 (2005).
52. V.N. Gribov and L.N. Lipatov, Sov. J. Nucl. Phys. **15**, 438 (1972);
L.N. Lipatov, Sov. J. Nucl. Phys. **20**, 94 (1975);
G. Altarelli and G. Parisi, Nucl. Phys. **B126**, 298 (1977);
Yu.L. Dokshitzer, Sov. Phys. JETP **46**, 641 (1977).
53. G. Curci, W. Furmanski, and R. Petronzio, Nucl. Phys. **B175**, 27 (1980);
W. Furmanski and R. Petronzio, Phys. Lett. **B97**, 437 (1980).
54. A. Vogt, S. Moch, and J.A.M. Vermaseren, Nucl. Phys. **B691**, 129 (2004);
S. Moch, J.A.M. Vermaseren, and A. Vogt, Nucl. Phys. **B688**, 101 (2004).
55. S. Moch *et al.*, `arXiv:1707.08315 [hep-ph]`.
56. S. Moch, J.A.M. Vermaseren, and A. Vogt, Nucl. Phys. **B889**, 351 (2014).
57. D. de Florian, G.F.R. Sborlini, and G. Rodrigo, Eur. Phys. J. **C76**, 282 (2016);
D. de Florian, G.F.R. Sborlini, and G. Rodrigo, JHEP **1610**, 056 (2016).
58. R.S. Thorne, Phys. Rev. **D73**, 054019 (2006).
59. S. Forte *et al.*, Nucl. Phys. **B834**, 116 (2010).
60. M. Guzzi *et al.*, Phys. Rev. **D86**, 053005 (2012).
61. J.C. Collins, D.E. Soper, and G. Sterman, Nucl. Phys. **B261**, 104 (1985).
62. R. Hamberg, W.L. van Neerven, and T. Matsuura, Nucl. Phys. **B359**, 343 (1991); Erratum *ibid.*, B **644** 403, (2002).
63. R.V. Harlander and W.B. Kilgore, Phys. Rev. Lett. **88**, 201801 (2002).
64. O. Brein, A. Djouadi, and R. Harlander, Phys. Lett. **B579**, 149 (2004).
65. P. Bolzoni *et al.*, Phys. Rev. Lett. **105**, 011801 (2010).
66. D. de Florian and J. Mazzitelli, Phys. Rev. Lett. **111**, 201801 (2013).
67. M. Czakon, P. Fiedler, and A. Mitov, Phys. Rev. Lett. **110**, 252004 (2013).
68. T. Gehrmann *et al.*, Phys. Rev. Lett. **113**, 21 (2014).
69. F. Cascioli *et al.*, Phys. Lett. **B735**, 311 (2014).
70. C. Anastasiou *et al.*, Phys. Rev. Lett. **114**, 21 (2015);
C. Anastasiou *et al.*, JHEP **1605**, 058 (2016).
71. F.A. Dreyer and A. Karlberg, Phys. Rev. Lett. **117**, 072001 (2016).
72. D. de Florian *et al.* [LHC Higgs Cross Section Working Group], `arXiv:1610.07922 [hep-ph]`.
73. M. Greco and A. Vicini, Nucl. Phys. **B415**, 386 (1994).
74. L.N. Lipatov, Sov. J. Nucl. Phys. **23**, 338 (1976) [Yad. Fiz. **23**, 642 (1976)].
75. E.A. Kuraev, L.N. Lipatov, and V.S. Fadin, Sov. Phys. JETP **45**, 199 (1977) [Zh. Eksp. Teor. Fiz. **72**, 377 (1977)].
76. I.I. Balitsky and L.N. Lipatov, Sov. J. Nucl. Phys. **28**, 822 (1978) [Yad. Fiz. **28**, 1597 (1978)].
77. V.S. Fadin and L.N. Lipatov, Phys. Lett. **B429**, 127 (1998).
78. M. Ciafaloni and G. Camici, Phys. Lett. **B430**, 329 (1998).
79. G. Altarelli, R.D. Ball, and S. Forte, Nucl. Phys. **B799**, 199 (2008).
80. M. Ciafaloni *et al.*, JHEP **0708**, 046 (2007).
81. C.D. White and R.S. Thorne, Phys. Rev. **D75**, 034005 (2007).
82. E. Iancu *et al.*, Phys. Lett. **B744**, 293 (2015).
83. N. Gromov, F. Levkovich-Maslyuk, and G. Sizov, `arXiv:1507.04010 [hep-th]`;
V. N. Velizhanin, `arXiv:1508.02857 [hep-th]`;
S. Caron-Huot and M. Herranen, `arXiv:1604.07417 [hep-ph]`.
84. I. Balitsky, Nucl. Phys. **B463**, 99 (1996).
85. Y.V. Kovchegov, Phys. Rev. **D60**, 034008 (1999).
86. A. Hebecker, Phys. Reports **331**, 1 (2000).
87. A.V. Belitsky and A.V. Radyushkin, Phys. Reports **418**, 1 (2005).
88. E. Boos *et al.*, [CompHEP Collab.], Nucl. Instrum. Methods **A534**, 250 (2004) `http://comphep.sinp.msu.ru/`.
89. J. Alwall *et al.*, JHEP **1407**, 079 (2014), `https://launchpad.net/mg5amcnlo`.
90. M.L. Mangano *et al.*, JHEP **0307**, 001 (2003), `http://cern.ch/mlm/alpgen/`.

91. T. Gleisberg and S. Höche, JHEP **0812**, 039 (2008), https://sherpa.hepforge.org/trac/wiki.
92. A. Cafarella, C.G. Papadopoulos, and M. Worek, Comp. Phys. Comm. **180**, 1941 (2009), http://cern.ch/helac-phegas/.
93. F.A. Berends and W.T. Giele, Nucl. Phys. **B306**, 759 (1988).
94. L.J. Dixon, arXiv:hep-ph/9601359.
95. Z. Bern, L.J. Dixon, and D.A. Kosower, Ann. Phys. **322**, 1587 (2007).
96. S. Badger *et al.*, Phys. Rev. **D87**, 3 (2013).
97. S. Catani and M.H. Seymour, Nucl. Phys. **B485**, 291 (1997) [Erratum-ibid. B **510**,503 (1998)].
98. S. Frixione, Z. Kunszt, and A. Signer, Nucl. Phys. **B467**, 399 (1996).
99. D.A. Kosower, Phys. Rev. **D57**, 5410 (1998);
J.M. Campbell, M.A. Cullen, and E.W.N. Glover, Eur. Phys. J. **C9**, 245 (1999);
D.A. Kosower, Phys. Rev. **D71**, 045016 (2005).
100. Z. Nagy, Phys. Rev. **D68**, 094002 (2003), http://www.desy.de/znagy/Site/NLOJet++.html.
101. J.M. Campbell and R.K. Ellis, Phys. Rev. **D62**, 114012 (2000).
102. K. Arnold *et al.*, arXiv:1107.4038 [hep-ph]; http://www-itp.particle.uni-karlsruhe.de/~vbfnloweb/.
103. T. Binoth *et al.*, Eur. Phys. J. **C16**, 311 (2000), http://lapth.in2p3.fr/PHOX_FAMILY/.
104. G. Bevilacqua *et al.*, Comp. Phys. Comm. **184**, 986 (2013), http://cern.ch/helac-phegas/.
105. G. Cullen *et al.*, Eur. Phys. J. **C74**, 8 (2014), http://gosam.hepforge.org/.
106. S. Badger *et al.*, Comp. Phys. Comm. **184**, 1981 (2013), https://bitbucket.org/njet/njet/wiki/Home.
107. F. Cascioli, P. Maierhofer, and S. Pozzorini, Phys. Rev. Lett. **108**, 111601 (2012), https://openloops.hepforge.org/.
108. S. Actis *et al.*, Comp. Phys. Comm. **214**, 140 (2017).
109. T. Gleisberg *et al.*, JHEP **0902**, 007 (2009), http://projects.hepforge.org/sherpa/.
110. Z. Bern *et al.*, PoS LL **2012**,018 (2012).
111. Z. Bern *et al.*, Comp. Phys. Comm. **185**, 1443 (2014).
112. T. Kluge, K. Rabbertz, and M. Wobisch, arXiv:hep-ph/0609285, http://fastnlo.hepforge.org/.
113. T. Carli *et al.*, Eur. Phys. J. **C66**, 503 (2010), https://applgrid.hepforge.org/.
114. L. Del Debbio, N.P. Hartland, and S. Schumann, Comp. Phys. Comm. **185**, 2115 (2014), http://mcgrid.hepforge.org/.
115. V. Bertone *et al.*, JHEP **1408**, 166 (2014), https://amcfast.hepforge.org/.
116. G. Cullen, N. Greiner, and G. Heinrich, Eur. Phys. J. **C73**, 4 (2013).
117. S. Kallweit *et al.*, JHEP **1504**, 012 (2015).
118. A. Denner *et al.*, JHEP **1504**, 018 (2015).
119. S. Frixione *et al.*, JHEP **1506**, 184 (2015).
120. R.K. Ellis *et al.*, Phys. Reports **518**, 141 (2012).
121. S. Becker *et al.*, Phys. Rev. Lett. **108**, 032005 (2012).
122. Z. Bern *et al.*, Phys. Rev. **D88**, 014025 (2013).
123. S. Badger *et al.*, Phys. Rev. **D89**, 3 (2014).
124. Z. Bern *et al.*, Nucl. Phys. **B425**, 217 (1994).
125. J.M. Campbell and E.W.N. Glover, Nucl. Phys. **B527**, 264 (1998).
126. S. Catani and M. Grazzini, Phys. Lett. **B446**, 143 (1999).
127. T. Binoth and G. Heinrich, Nucl. Phys. **B585**, 741 (2000).
128. C. Anastasiou, K. Melnikov, and F. Petriello, Phys. Rev. **D69**, 076010 (2004).
129. A. Gehrmann-De Ridder, T. Gehrmann, and E.W.N. Glover, JHEP **0509**, 056 (2005).
130. G. Somogyi, Z. Trocsanyi, and V. Del Duca, JHEP **0701**, 070 (2007).
131. M. Czakon, Phys. Lett. **B693**, 259 (2010).
132. S. Catani and M. Grazzini, Phys. Rev. Lett. **98**, 222002 (2007), http://theory.fi.infn.it/grazzini/codes.html.
133. R. Boughezal *et al.*, Phys. Rev. Lett. **115**, 6 (2015).
134. J. Gaunt *et al.*, arXiv:1505.04794 [hep-ph].
135. M. Cacciari *et al.*, arXiv:1506.02660 [hep-ph].
136. A. Gehrmann-De Ridder *et al.*, Phys. Rev. Lett. **99**, 132002 (2007);
JHEP **0712**, 094 (2007);
Phys. Rev. Lett. **100**, 172001 (2008).
137. A. Gehrmann-De Ridder *et al.*, Comp. Phys. Comm. **185**, 3331 (2014), https://eerad3.hepforge.org/.
138. S. Weinzierl, Phys. Rev. Lett. **101**, 162001 (2008);
JHEP **0906**, 041 (2009).
139. J. Currie, T. Gehrmann, and J. Niehues, Phys. Rev. Lett. **117**, 042001 (2016).
140. K. Melnikov and F. Petriello, Phys. Rev. **D74**, 114017 (2006), http://gate.hep.anl.gov/fpetriello/FEWZ.html.
141. S. Catani *et al.*, Phys. Rev. Lett. **103**, 082001 (2009), http://theory.fi.infn.it/grazzini/dy.html.
142. C. Anastasiou, K. Melnikov, and F. Petriello, Nucl. Phys. **B724**, 197 (2005), http://www.phys.ethz.ch/~pheno/fehipro/.
143. S. Borowka *et al.*, Phys. Rev. Lett. **117**, 012001 (2016) Erratum:[Phys. Rev. Lett. **117**, 079901 (2016).
144. G. Ferrera, M. Grazzini, and F. Tramontano, Phys. Rev. Lett. **107**, 152003 (2011).
145. G. Ferrera, M. Grazzini, and F. Tramontano, Phys. Lett. **B740**, 51 (2015).
146. M. Grazzini *et al.*, JHEP **1705**, 139 (2017).
147. S. Catani *et al.*, Phys. Rev. Lett. **108**, 072001 (2012).
148. J.M. Campbell *et al.*, JHEP **1607**, 148 (2016).
149. M. Grazzini *et al.*, Phys. Lett. **B731**, 204 (2014).
150. M. Grazzini, S. Kallweit, and D. Rathlev, JHEP **1507**, 085 (2015).
151. R. Boughezal *et al.*, Eur. Phys. J. **C77**, 7 (2017).
152. R. Boughezal *et al.*, arXiv:1504.07922 [hep-ph].
153. R. Boughezal *et al.*, Phys. Lett. **B748**, 5 (2015).
154. F. Caola, K. Melnikov and M. Schulze, Phys. Rev. **D92**, 074032 (2015).
155. X. Chen *et al.*, JHEP **1610**, 066 (2016).
156. A. Gehrmann-De Ridder *et al.*, Phys. Rev. Lett. **117**, 022001 (2016).
157. R. Boughezal *et al.*, Phys. Rev. Lett. **116**, 152001 (2016).
158. J.M. Campbell, R.K. Ellis, and C. Williams, Phys. Rev. Lett. **118**, 222001 (2017).
159. M. Brucherseifer, F. Caola, and K. Melnikov, Phys. Lett. **B736**, 58 (2014).
160. E.L. Berger *et al.*, Phys. Rev. **D94**, 071501 (2016).
161. M. Czakon, P. Fiedler, and A. Mitov, Phys. Rev. Lett. **115**, 5 (2015).
162. J. Currie, E.W.N. Glover, and J. Pires, Phys. Rev. Lett. **118**, 072002 (2017).
163. Y.L. Dokshitzer, D.Diakonov, and S.I. Troian, Phys. Reports **58**, 269 (1980).
164. G. Parisi and R. Petronzio, Nucl. Phys. **B154**, 427 (1979).
165. G. Curci, M. Greco, and Y. Srivastava, Nucl. Phys. **B159**, 451 (1979).
166. A. Bassetto, M. Ciafaloni, and G. Marchesini, Nucl. Phys. **B163**, 477 (1980).
167. J.C. Collins and D.E. Soper, Nucl. Phys. **B193**, 381 (1981) [Erratum-*ibid.* **B213**, 545 (1983)].
168. J.C. Collins and D.E. Soper, Nucl. Phys. **B197**, 446 (1982).
169. J. Kodaira and L. Trentadue, Phys. Lett. **B112**, 66 (1982).
170. J. Kodaira and L. Trentadue, Phys. Lett. **B123**, 335 (1983).
171. J.C. Collins, D.E. Soper, and G. Sterman, Nucl. Phys. **B250**, 199 (1985).
172. S. Catani *et al.*, Nucl. Phys. **B407**, 3 (1993).
173. C. W. Bauer *et al.*, Phys. Rev. **D63**, 114020 (2001).
174. C.W. Bauer, D. Pirjol, and I.W. Stewart, Phys. Rev. **D65**, 054022 (2002).
175. T. Becher, A. Broggio, and A. Ferroglia, Lect. Notes Phys. **896** (2015) pp.1 arXiv:1410.1892 [hep-ph].
176. S. Catani *et al.*, Phys. Lett. **B269**, 432 (1991).
177. N. Brown and W.J. Stirling, Phys. Lett. **B252**, 657 (1990).

178. W. Bartel *et al.*, [JADE Collab.], Z. Phys. **C33**, 23 (1986).
179. N. Kidonakis, G. Oderda, and G. Sterman, Nucl. Phys. **B531**, 365 (1998).
180. R. Bonciani *et al.*, Phys. Lett. **B575**, 268 (2003).
181. A. Banfi, G.P. Salam, and G. Zanderighi, JHEP **0503**, 073 (2005).
182. D. de Florian and M. Grazzini, Phys. Rev. Lett. **85**, 4678 (2000).
183. G. Bozzi *et al.*, Nucl. Phys. **B737**, 73 (2006), http://theory.fi.infn.it/grazzini/codes.html.
184. G. Bozzi *et al.*, Phys. Lett. **B696**, 207 (2011).
185. T. Becher and M. Neubert, Eur. Phys. J. **C71**, 1665 (2011).
186. T. Becher, M. Neubert, and D. Wilhelm, http://cute.hepforge.org/.
187. D. de Florian *et al.*, JHEP **1206**, 132 (2012), http://theory.fi.infn.it/grazzini/codes.html.
188. C. Balazs and C.P. Yuan, Phys. Rev. **D56**, 5558 (1997).
189. S. Catani *et al.*, arXiv:1507.06937 [hep-ph].
190. A. Banfi *et al.*, Phys. Lett. **B715**, 152 (2012).
191. M. Grazzini *et al.*, arXiv:1507.02565 [hep-ph].
192. D. de Florian and M. Grazzini, Nucl. Phys. **B704**, 387 (2005).
193. T. Becher and G. Bell, JHEP **1211**, 126 (2012).
194. A. Banfi *et al.*, Phys. Rev. Lett. **109**, 202001 (2012); T. Becher, M. Neubert, and L. Rothen, JHEP **1310**, 125 (2013); I.W. Stewart *et al.*, Phys. Rev. **D89**, 5 (2014).
195. I.W. Stewart, F.J. Tackmann, and W.J. Waalewijn, Phys. Rev. Lett. **106**, 032001 (2011).
196. Y.-T. Chien *et al.*, Phys. Rev. **D87**, 014010 (2013); T.T. Jouttenus *et al.*, Phys. Rev. **D88**, 054031 (2013).
197. M. Dasgupta *et al.*, JHEP **1210**, 126 (2012).
198. V. Ahrens *et al.*, JHEP **1009**, 097 (2010).
199. M. Aliev *et al.*, Comp. Phys. Comm. **182**, 1034 (2011).
200. N. Kidonakis, Phys. Rev. **D82**, 114030 (2010).
201. T. Becher, C. Lorentzen, M. D. Schwartz, Phys. Rev. Lett. **108**, 012001 (2012).
202. T. Becher *et al.*, Eur. Phys. J. **C75**, 4 (2015).
203. E. Gerwick *et al.*, JHEP **1502**, 106 (2015).
204. A. Banfi *et al.*, JHEP **1505**, 102 (2015).
205. T. Becher and M.D. Schwartz, JHEP **0807**, 034 (2008).
206. A. H. Hoang *et al.*, Phys. Rev. **D91**, 9 (2015).
207. Y.-T. Chien and M.D. Schwartz, JHEP **1008**, 058 (2010).
208. P.F. Monni, T. Gehrmann, and G. Luisoni, JHEP **1108**, 010 (2011).
209. W. Bizon *et al.*, arXiv:1705.09127 [hep-ph].
210. S. Catani *et al.*, Nucl. Phys. **B888**, 75 (2014).
211. S. Fleming *et al.*, Phys. Rev. **D77**, 074010 (2008).
212. A.H. Hoang, P. Pietrulewicz, and D. Samitz, Phys. Rev. **D93**, 034034 (2016).
213. I. Feige *et al.*, Phys. Rev. Lett. **109**, 092001 (2012).
214. M. Dasgupta *et al.*, JHEP **1309**, 029 (2013).
215. A.J. Larkoski *et al.*, JHEP **1405**, 146 (2014).
216. M. Dasgupta, A. Powling, and A. Siodmok, arXiv:1503.01088 [hep-ph].
217. A.J. Larkoski, I. Moult, and D. Neill, arXiv:1507.03018 [hep-ph].
218. Yu.L. Dokshitzer *et al.*, *"Basics of perturbative QCD,"* Gif-sur-Yvette, France: Éditions frontières (1991), see also http://www.lpthe.jussieu.fr/~yuri/ BPQCD/cover.html.
219. T. Sjöstrand *et al.*, Comp. Phys. Comm. **135**, 238 (2001).
220. T. Sjöstrand, S. Mrenna, and P. Skands, JHEP **0605**, 026 (2006), http://projects.hepforge.org/pythia6/.
221. T. Sjöstrand *et al.*, Comp. Phys. Comm. **191**, 159 (2015), http://home.thep.lu.se/~torbjorn/Pythia.html.
222. B.R. Webber, Nucl. Phys. **B238**, 492 (1984).
223. G. Corcella *et al.*, JHEP **0101**, 010 (2001), www.hep.phy.cam.ac.uk/theory/webber/Herwig/.
224. M. Bahr *et al.*, Eur. Phys. J. **C58**, 639 (2008), projects.hepforge.org/herwig/.
225. L. Lönnblad, Comp. Phys. Comm. **71**, 15, (1992).
226. A. Buckley *et al.*, Phys. Rept. **504**, 145-233 (2011).
227. B. Andersson *et al.*, Phys. Reports **97**, 31 (1983).
228. T. Sjöstrand, Nucl. Phys. **B248**, 469 (1984).
229. T. Sjöstrand and M. van Zijl, Phys. Rev. **D36**, 2019 (1987).
230. S. Catani *et al.*, JHEP **0111**, 063 (2001).
231. J. Alwall *et al.*, Eur. Phys. J. **C53**, 473 (2008).
232. S. Frixione and B.R. Webber, JHEP **0206**, 029 (2002).
233. P. Nason, JHEP **0411**, 040 (2004).
234. S. Alioli *et al.*, JHEP **1006**, 043 (2010), http://powhegbox.mib.infn.it/.
235. S. Höche *et al.*, JHEP **1209**, 049 (2012).
236. S. Höche *et al.*, JHEP **1304**, 027 (2013); R. Frederix and S. Frixione, JHEP **1212**, 061 (2012); S. Plätzer, JHEP **1308**, 114 (2013); L. Lönnblad and S. Prestel, JHEP **1303**, 166 (2013); K. Hamilton *et al.*, JHEP **1305**, 082 (2013).
237. K. Hamilton *et al.*, JHEP **1310**, 222 (2013); A. Karlberg, E. Re, and G. Zanderighi, JHEP **1409**, 134 (2014); S. Höche, Y. Li and S. Prestel, Phys. Rev. **D91**, 074015 (2015); S. Höche, Y. Li and S. Prestel, Phys. Rev. **D90**, 054011 (2014); S. Alioli *et al.*, Phys. Rev. **D92**, 094020 (2015).
238. P.M. Stevenson, Phys. Lett. **B100**, 61 (1981).
239. P.M. Stevenson, Phys. Rev. **D23**, 2916 (1981).
240. G. Grunberg, Phys. Rev. **D29**, 2315 (1984).
241. S.J. Brodsky, G.P. Lepage, and P.B. Mackenzie, Phys. Rev. **D28**, 228 (1983).
242. M. Cacciari and N. Houdeau, JHEP **1109**, 039 (2011).
243. A. David and G. Passarino, Phys. Lett. **B726**, 266 (2013).
244. E. Bagnaschi *et al.*, JHEP **1502**, 133 (2015).
245. M. Cacciari *et al.*, JHEP **0404**, 068 (2004).
246. M. Dasgupta and G.P. Salam, J. Phys. **G30**, R143 (2004).
247. S. Moretti, L. Lönnblad, and T. Sjöstrand, JHEP **9808**, 001 (1998).
248. G.P. Salam, Eur. Phys. J. **C67**, 637 (2010).
249. S.D. Ellis *et al.*, Prog. in Part. Nucl. Phys. **60**, 484 (2008).
250. M. Cacciari, Int. J. Mod. Phys. **A30**, 1546001 (2015).
251. G.P. Salam and G. Soyez, JHEP **0705**, 086 (2007).
252. S. Catani *et al.*, Nucl. Phys. **B406**, 187 (1993).
253. S.D. Ellis and D.E. Soper, Phys. Rev. **D48**, 3160 (1993).
254. Y.L. Dokshitzer *et al.*, JHEP **9708**, 001 (1997).
255. M. Wobisch and T. Wengler, arXiv:hep-ph/9907280.
256. M. Cacciari, G.P. Salam, and G. Soyez, JHEP **0804**, 063 (2008).
257. S. Bethke *et al.*, Nucl. Phys. **B370**, 310 (1992), Nucl. Phys. **B523**, 681 (1998).
258. M. Cacciari and G.P. Salam, Phys. Lett. **B641**, 57 (2006); M. Cacciari, G.P. Salam, and G. Soyez, Eur. Phys. J. **C72**, 1896 (2012) http://fastjet.fr/.
259. S. Brandt *et al.*, Phys. Lett. **12**, 57 (1964).
260. E. Farhi, Phys. Rev. Lett. **39**, 1587 (1977).
261. O. Biebel, Phys. Reports **340**, 165 (2001).
262. S. Kluth, Rept. on Prog. in Phys. **69**, 1771 (2006).
263. C.L. Basham *et al.*, Phys. Rev. Lett. **41**, 1585 (1978).
264. A. Ali, E. Pietarinen, and W. J. Stirling, Phys. Lett. **B141**, 447 (1984).
265. I. W. Stewart, F. J. Tackmann, and W. J. Waalewijn, Phys. Rev. Lett. **105**, 092002 (2010).
266. A. Banfi, G.P. Salam, and G. Zanderighi, JHEP **0408**, 062 (2004).
267. A. Banfi, G.P. Salam, and G. Zanderighi, JHEP **1006**, 038 (2010).
268. T. Aaltonen *et al.*, [CDF Collab.], Phys. Rev. **D83**, 112007 (2011).
269. G. Aad *et al.*, [ATLAS Collab.], Eur. Phys. J. **C72**, 2211 (2012).
270. G. Aad *et al.*, [ATLAS Collab.], Phys. Rev. **D88**, 032004 (2013).
271. G. Aad *et al.*, [ATLAS Collab.], Phys. Lett. **B750**, 427 (2015).
272. G. Aad *et al.*, [ATLAS Collab.], Eur. Phys. J. **C76**, 375 (2016).
273. M. Aaboud *et al.*, [ATLAS Collab.], arXiv:1707.02562 [hep-ex].
274. V. Khachatryan *et al.*, [CMS Collab.], Phys. Lett. **B699**, 48 (2011).

275. S. Chatrchyan *et al.*, [CMS Collab.], Phys. Lett. **B722**, 238 (2013).
276. V. Khachatryan *et al.*, [CMS Collab.], JHEP **1410**, 87 (2014).
277. S. Chatrchyan *et al.*, [CMS Collab.], Phys. Lett. **B730**, 243 (2014).
278. G. Aad *et al.*, [ATLAS Collab.], Phys. Rev. **D83**, 052003 (2011).
279. S. Chatrchyan *et al.*, [CMS Collab.], JHEP **1206**, 160 (2012).
280. B. B. Abelev *et al.*, [ALICE Collab.], Phys. Rev. **D91**, 112012 (2015).
281. G. Aad *et al.*, [ATLAS Collab.], Eur. Phys. J. **C73**, 2676 (2013).
282. C. Glasman [H1 Collab. and ZEUS Collab.], Nucl. Phys. (Proc. Supp.) **191**, 121 (2009).
283. T. Carli, K. Rabbertz, and S. Schumann, `arXiv:1506.03239 [hep-ex]`.
284. A. Abdesselam *et al.*, Eur. Phys. J. **C71**, 1661 (2011).
285. A. Altheimer *et al.*, J. Phys. **G39**, 063001 (2012).
286. A. Altheimer *et al.*, Eur. Phys. J. **C74**, 2792 (2014).
287. S. Schaetzel, Eur. Phys. J. **C75**, 9 (2015).
288. A. J. Larkoski, I. Moult, and B. Nachman, `arXiv:1709.04464 [hep-ph]`.
289. D. Adams *et al.*, Eur. Phys. J. **C75**, 409 (2015).
290. T. Schörner-Sadenius, Eur. Phys. J. **C72**, 2060 (2012).
291. J.M. Campbell, J.W. Huston, and W.J. Stirling, Rept. on Prog. in Phys. **70**, 89 (2007).
292. M.L. Mangano, Phys. Usp. **53**, 109 (2010).
293. J.M. Butterworth, G. Dissertori, and G.P. Salam, Ann. Rev. Nucl. and Part. Sci. **62**, 387 (2012).
294. T. Carli, T. Gehrmann, and S. Höche, Eur. Phys. J. **C67**, 73 (2010).
295. F.D. Aaron *et al.*, [H1 Collab.], Eur. Phys. J. **C65**, 363 (2010).
296. F.D. Aaron *et al.*, [H1 Collab.], Eur. Phys. J. **C54**, 389 (2008).
297. S. Chekanov *et al.*, [ZEUS Collab.], Eur. Phys. J. **C52**, 515 (2007).
298. S. Chekanov *et al.*, [ZEUS Collab.], Phys. Rev. **D78**, 032004 (2008).
299. H. Abramowicz *et al.*, [ZEUS Collab.], Eur. Phys. J. **C70**, 965 (2010).
300. H. Abramowicz *et al.*, [ZEUS Collab.], Phys. Lett. **B691**, 127 (2010).
301. S. Chekanov *et al.*, [ZEUS Collab.], Phys. Rev. **D85**, 052008 (2012).
302. F.D. Aaron *et al.*, [H1 Collab.], Eur. Phys. J. **C67**, 1 (2010).
303. V. Andreev *et al.*, [H1 Collab.], Eur. Phys. J. **C75**, 2 (2015).
304. S. Chekanov *et al.*, [ZEUS Collab.], Nucl. Phys. **B792**, 1 (2008).
305. S. Chekanov *et al.*, [ZEUS Collab.], Phys. Rev. **D76**, 072011 (2007).
306. A. Aktas *et al.*, [H1 Collab.], Phys. Lett. **B639**, 21 (2006).
307. H. Abramowicz *et al.*, [ZEUS Collab.], Eur. Phys. J. **C71**, 1659 (2011).
308. H. Abramowicz *et al.*, [ZEUS Collab.], Nucl. Phys. **B864**, 1 (2012).
309. `http://atlas.web.cern.ch/Atlas/GROUPS/PHYSICS/CombinedSummaryPlots/SM`.
310. `twiki.cern.ch/twiki/bin/view/CMSPublic/PhysicsResultsCombined`.
311. A. Abulencia *et al.*, [CDF - Run II Collab.], Phys. Rev. **D75**, 092006 (2007) [Erratum-ibid. 119901].
312. V.M. Abazov *et al.*, [D0 Collab.], Phys. Rev. Lett. **101**, 062001 (2008).
313. V.M. Abazov *et al.*, [D0 Collab.], Phys. Rev. **D85**, 052006 (2012).
314. B. Abelev *et al.*, [ALICE Collab.], Phys. Lett. **B722**, 262 (2013).
315. G. Aad *et al.*, [ATLAS Collab.], Eur. Phys. J. **C73**, 2509 (2013).
316. G. Aad *et al.*, [ATLAS Collab.], JHEP **1502**, 153 (2015), erratum JHEP **1509**, 141 (2015).
317. M. Aaboud *et al.*, [ATLAS Collab.], JHEP **1709**, 020 (2017).
318. V. Khachatryan *et al.*, [CMS Collab.], Eur. Phys. J. **C76**, 265 (2016).
319. S. Chatrchyan *et al.*, [CMS Collab.], Phys. Rev. **D87**, 112002 (2013).
320. V. Khachatryan *et al.*, [CMS Collab.], JHEP **1703**, 156 (2017).
321. V. Khachatryan *et al.*, [CMS Collab.], Eur. Phys. J. **C76**, 451 (2016).
322. M. Wobisch *et al.*, [fastNLO Collab.], `arXiv:1109.1310 [hep-ph]`.
323. P. Francavilla, Int. J. Mod. Phys. **A30**, 1546003 (2015).
324. A. Schwartzman, Int. J. Mod. Phys. **A30**, 1546002 (2015).
325. J. Rojo, Int. J. Mod. Phys. **A30**, 1546005 (2015).
326. G. Aad *et al.*, [ATLAS Collab.], JHEP **1405**, 059 (2014).
327. A. M. Sirunyan *et al.*, [CMS Collab.], `arXiv:1705.02628 [hep-ex]`.
328. T. Aaltonen *et al.*, [CDF Collab.], Phys. Rev. **D79**, 112002 (2009).
329. V.M. Abazov *et al.*, [D0 Collab.], Phys. Rev. Lett. **103**, 191803 (2009).
330. S. Chatrchyan *et al.*, [CMS Collab.], JHEP **1205**, 055 (2012).
331. V. Khachatryan *et al.*, [CMS Collab.], Phys. Lett. **B746**, 79 (2015).
332. A.M. Sirunyan *et al.*, [CMS Collab.], JHEP **1707**, 013 (2017).
333. G. Aad *et al.*, [ATLAS Collab.], JHEP **1301**, 029 (2013).
334. M. Aaboud *et al.*, [ATLAS Collab.], `arXiv:1703.09127 [hep-ex]`.
335. V.M. Abazov *et al.*, [D0 Collab.], Phys. Rev. Lett. **94**, 221801 (2005).
336. V.M. Abazov *et al.*, [D0 Collab.], Phys. Lett. **B721**, 212 (2013).
337. G. Aad *et al.*, [ATLAS Collab.], Phys. Rev. Lett. **106**, 172002 (2011).
338. V. Khachatryan *et al.*, [CMS Collab.], Phys. Rev. Lett. **106**, 122003 (2011).
339. V. Khachatryan *et al.*, [CMS Collab.], Eur. Phys. J. **C76**, 536 (2016).
340. M. Campanelli, Int. J. Mod. Phys. **A30**, 1546006 (2015).
341. P. Kokkas, Int. J. Mod. Phys. **A30**, 1546004 (2015).
342. M. Aaboud *et al.*, [ATLAS Collab.], Eur. Phys. J. **C77**, 367 (2017).
343. G. Aad *et al. et al.*, [ATLAS Collab.], Phys. Lett. **B759**, 601 (2016).
344. S. Chatrchyan *et al.*, [CMS Collab.], JHEP **1110**, 132 (2011).
345. S. Chatrchyan *et al.*, [CMS Collab.], Phys. Rev. Lett. **112**, 191802 (2014).
346. R. Aaij *et al.*, [LHCb Collab.], JHEP **1206**, 058 (2012).
347. R. Aaij *et al.*, [LHCb Collab.], JHEP **1601**, 155 (2016).
348. R. Aaij *et al.*, [LHCb Collab.], JHEP **1609**, 136 (2016).
349. S. Chatrchyan *et al.*, [CMS Collab.], JHEP **1110**, 007 (2011).
350. V. Khachatryan *et al.*, [CMS Collab.], Eur. Phys. J. **C75**, 147 (2015).
351. G. Aad *et al.*, [ATLAS Collab.], Phys. Lett. **B725**, 223 (2013).
352. G. Aad *et al.*, [ATLAS Collab.], JHEP **1406**, 112 (2014).
353. G. Aad *et al.*, [ATLAS Collab.], JHEP **1608**, 009 (2016).
354. S. Chatrchyan *et al.*, [CMS Collab.], Phys. Rev. **D90**, 3 (2014).
355. V. Khachatryan *et al.*, [CMS Collab.], Eur. Phys. J. **C76**, 469 (2016).
356. G. Aad *et al.*, [ATLAS Collab.], Eur. Phys. J. **C76**, 291 (2016).
357. V. Khachatryan *et al.*, [CMS Collab.], JHEP **1702**, 096 (2017).
358. U. Blumenschein, Int. J. Mod. Phys. **A30**, 1546007 (2015).
359. G. Aad *et al.*, [ATLAS Collab.], JHEP **1307**, 032 (2013).
360. J. H. Kühn *et al.*, JHEP **0603**, 059 (2006).
361. V. Khachatryan *et al.*, [CMS Collab.], JHEP **1510**, 128 (2015), erratum JHEP **1604**, 010 (2016).
362. M. Voutilainen, Int. J. Mod. Phys. **A30**, 1546008 (2015).
363. G. Aad *et al.*, [ATLAS Collab.], JHEP **1609**, 029 (2016).
364. M. Aaboud *et al.*, [ATLAS Collab.], Phys. Lett. **B773**, 354 (2017).
365. V. Khachatryan *et al.*, [CMS Collab.], Eur. Phys. J. **C76**, 401 (2016).
366. G. Aad *et al.*, [ATLAS Collab.], JHEP **1301**, 086 (2013).
367. M. Aaboud *et al.*, [ATLAS Collab.], Phys. Rev. **D95**, 112005 (2017).

368. S. Chatrchyan *et al.*, [CMS Collab.], Eur. Phys. J. **C74**, 3129 (2014).
369. K. Kröninger, A. B. Meyer, and P. Uwer, `arXiv:1506.02800 [hep-ex]`.
370. S. Chatrchyan *et al.*, [CMS Collab.], Phys. Lett. **B728**, 496 (2014), Phys. Lett. **B728**, 526 (2014).
371. T. Klijnsma, S. Bethke, G. Dissertori, and G. P. Salam, `arXiv:1708.07495 [hep-ph]`.
372. G. Aad *et al.*, [ATLAS Collab.], Eur. Phys. J. **C74**, 10 (2014).
373. A.M. Sirunyan *et al.*, [CMS Collab.], JHEP **1709**, 051 (2017).
374. G. Aad *et al.*, [ATLAS Collab.], Phys. Rev. Lett. **115**, 091801 (2015).
375. G. Aad *et al.*, [ATLAS Collab.], JHEP **1608**, 104 (2016).
376. M. Aaboud *et al.*, [ATLAS Collab.], `arXiv:1708.02810 [hep-ex]`.
377. S. Chatrchyan *et al.*, [CMS Collab.], Phys. Rev. **D89**, 9 (2014).
378. V. Khachatryan *et al.*, [CMS Collab.], Eur. Phys. J. **C76**, 13 (2016).
379. V. Khachatryan *et al.*, [CMS Collab.], JHEP **1604**, 005 (2016).
380. V. Khachatryan *et al.*, [CMS Collab.], JHEP **1703**, 032 (2017).
381. S. Bethke, G. Dissertori and G.P. Salam in [382].
382. C. Patrignani *et al.*, [Particle Data Group Collaboration], Chin. Phys. **C40** (2016) 100001.
383. S. Bethke, Prog. in Part. Nucl. Phys. **58**, 351 (2007).
384. S. Bethke, Eur. Phys. J. **C64**, 689 (2009).
385. S. Bethke, J. Phys. **G26**, R27 (2000).
386. M. Schmelling, Phys. Scripta **51**, 676 (1995).
387. M. Beneke and M. Jamin, JHEP **0809**, 044 (2008).
388. K. Maltman and T. Yavin, Phys. Rev. **D78**, 094020 (2008).
389. S. Narison, Phys. Lett. **B673**, 30 (2009).
390. I. Caprini and J. Fischer, Eur. Phys. J. **C64**, 35 (2009).
391. A. Pich, Prog. in Part. Nucl. Phys. **75**, 41 (2014).
392. M. Davier *et al.*, Eur. Phys. J. **C74**, 2803 (2014).
393. D. Boito *et al.*, Phys. Rev. D 91,034003(2015).
394. G. Altarelli, PoS Corfu **2012** (2013) 002.
395. C. McNeile *et al.*, [HPQCD Collab.], Phys. Rev. **D82**, 034512 (2010).
396. C.T.H. Davies *et al.*, [HPQCD Collab., UKQCD Collab., and MILC Collab.], Phys. Rev. Lett. **92**, 022001 (2004).
397. K. Maltman *et al.*, Phys. Rev. **D78**, 114504 (2008).
398. B. Chakraborty *et al.*, [HPQCD Collab.], Phys. Rev. **D91**, 054508 (2015).
399. S. Aoki *et al.*, [PACS-CS Collab.], JHEP **0910**, 053 (2009).
400. B. Blossier *et al.*, [ETM Collab.], Phys. Rev. Lett. **108**, 262002 (2012), Phys. Rev. **D89**, 014507 (2014).
401. A. Bazavov *et al.*, [BBGPSV], Phys. Rev. **D90**, 074038 (2014).
402. E. Shintani *et al.*, [JLQCD Collab.], Phys. Rev. **D82**, 074505 (2010), erratum Phys. Rev. **D89**, 099903 (2014).
403. S. Aoki *et al.*, Eur. Phys. J. **C74**, 2890 (2014).
404. C. Glasman [H1 Collab. and ZEUS Collab.], J. Phys. Conf. Ser. **110** 022013 (2008).
405. V. Andreev *et al.*, (H1 Collab.), Eur. Phys. J. **C75**, 65 (2015).
406. T. Biekötter, M. Klasen and G. Kramer, Phys. Rev. **D92**, 074037 (2015).
407. J. Blümlein, H. Bottcher, and A. Guffanti, Nucl. Phys. **B774**, 182 (2007).
408. S. Alekhin, J. Blümlein, and S. Moch, Phys. Rev. **D86**, 054009 (2012).
409. P. Jimenez-Delgado and E. Reya, Phys. Rev. **D79**, 074023 (2009).
410. A. D. Martin *et al.*, Eur. Phys. J. **C64**, 653 (2009).
411. L. A. Harland-Lang *et al.*, Eur. Phys. J. **C75**, 435 (2015).
412. R.D. Ball *et al.*, Phys. Lett. **B707**, 66 (2012).
413. R.S. Thorne and G. Watt, JHEP **1108**, 100 (2011).
414. S. Alekhin, J. Blümlein, and S.Moch, Eur. Phys. J. **C71**, 1723 (2011).
415. R.D. Ball *et al.*, Phys. Lett. **B704**, 36 (2011).
416. R.D. Ball *et al.*, Phys. Lett. **B723**, 330 (2013).
417. R.S. Thorne *et al.*, PoS DIS **2013** (2013) 042.
418. N. Brambilla *et al.*, Phys. Rev. **D75**, 074014 (2007).
419. G. Dissertori *et al.*, JHEP **0908**, 036 (2009).
420. G. Abbiendi *et al.*, Eur. Phys. J. **C71**, 1733 (2011).
421. S. Bethke *et al.*, [JADE Collab.], Eur. Phys. J. **C64**, 351 (2009).
422. G. Dissertori *et al.*, Phys. Rev. Lett. **104**, 072002 (2010).
423. J. Schieck *et al.*, Eur. Phys. J. **C73**, 2332 (2013).
424. R.A. Davison and B.R. Webber, Eur. Phys. J. **C59**, 13 (2009).
425. R. Abbate *et al.*, Phys. Rev. **D83**, 074021 (2011).
426. T. Gehrmann *et al.*, Eur. Phys. J. **C73**, 2265 (2013).
427. A.H. Hoang *et al.*, Phys. Rev. **D91**, 094018 (2015).
428. R. Frederix *et al.*, JHEP **1011**, 050 (2010).
429. P. Bolzoni, B.A. Kniehl, and A.V. Kotikov, Nucl. Phys. **B875**, 18 (2013).
430. M. Abazov *et al.*, [D0 Collab.], Phys. Rev. **D80**, 111107 (2009).
431. M. Abazov *et al.*, [D0 Collab.], Phys. Lett. **B718**, 56 (2012).
432. G. Aad *et al.*, [ATLAS Collab.], Phys. Rev. **D86**, 014022 (2012).
433. B. Malaescu and P. Starovoitov, Eur. Phys. J. **C72**, 2041 (2012).
434. S. Chatrchyan *et al.*, [CMS Collab.], Eur. Phys. J. **C73**, 2604 (2013).
435. V. Khachatryan *et al.*, [CMS Collab.], Eur. Phys. J. **C75**, 288 (2015).
436. V. Khachatryan *et al.*, [CMS Collab.], Eur. Phys. J. **C75**, 186 (2015).
437. M. Baak *et al.*, [Gfitter group], Eur. Phys. J. **C74**, 3046 (2014).

10. Electroweak Model and Constraints on New Physics

Revised March 2018 by J. Erler (U. Mexico) and A. Freitas (Pittsburgh U.).

10.1. Introduction

The standard model of the electroweak interactions (SM) [1] is based on the gauge group SU(2) × U(1), with gauge bosons W^i_μ, $i = 1, 2, 3$, and B_μ for the SU(2) and U(1) factors, respectively, and the corresponding gauge coupling constants g and g'. The left-handed fermion fields of the $i^{\rm th}$ fermion family transform as doublets $\Psi_i = \begin{pmatrix} \nu_i \\ \ell_i^- \end{pmatrix}$ and $\begin{pmatrix} u_i \\ d'_i \end{pmatrix}$ under SU(2), where $d'_i \equiv \sum_j V_{ij}\, d_j$, and V is the Cabibbo-Kobayashi-Maskawa mixing matrix. [Constraints on V and tests of universality are discussed in Ref. 2 and in the Section on "The CKM Quark-Mixing Matrix". The extension of the formalism to allow an analogous leptonic mixing matrix is discussed in the Section on "Neutrino Mass, Mixing, and Oscillations".] The right-handed fields are SU(2) singlets. From Higgs and electroweak precision data it is known that there are precisely three sequential fermion families.

A complex scalar Higgs doublet, $\phi \equiv \begin{pmatrix} \phi^+ \\ \phi^0 \end{pmatrix}$, is added to the model for mass generation through spontaneous symmetry breaking with potential* given by,

$$V(\phi) = \mu^2 \phi^\dagger \phi + \frac{\lambda^2}{2} (\phi^\dagger \phi)^2. \tag{10.1}$$

For μ^2 negative, ϕ develops a vacuum expectation value, $v/\sqrt{2} = \mu/\lambda$, where $v \approx 246$ GeV, breaking part of the electroweak (EW) gauge symmetry, after which only one neutral Higgs scalar, H, remains in the physical particle spectrum. In non-minimal models there are additional charged and neutral scalar Higgs particles [3].

After symmetry breaking the Lagrangian for the fermion fields, ψ_i, is

$$\begin{aligned} \mathscr{L}_F = & \sum_i \overline{\psi}_i \left(i\,\partial\!\!\!/ - m_i - \frac{m_i H}{v} \right) \psi_i \\ & - \frac{g}{2\sqrt{2}} \sum_i \overline{\Psi}_i\, \gamma^\mu\, (1-\gamma^5)(T^+\, W^+_\mu + T^-\, W^-_\mu)\, \Psi_i \\ & - e \sum_i Q_i\, \overline{\psi}_i\, \gamma^\mu\, \psi_i\, A_\mu \\ & - \frac{g}{2\cos\theta_W} \sum_i \overline{\psi}_i\, \gamma^\mu (g^i_V - g^i_A \gamma^5)\, \psi_i\, Z_\mu\ . \end{aligned} \tag{10.2}$$

Here $\theta_W \equiv \tan^{-1}(g'/g)$ is the weak angle; $e = g \sin\theta_W$ is the positron electric charge; and $A \equiv B\cos\theta_W + W^3 \sin\theta_W$ is the photon field (γ). $W^\pm \equiv (W^1 \mp i W^2)/\sqrt{2}$ and $Z \equiv -B \sin\theta_W + W^3 \cos\theta_W$ are the charged and neutral weak boson fields, respectively. The Yukawa coupling of H to ψ_i in the first term in $\mathscr{L}_F$, which is flavor diagonal in the minimal model, is $g m_i/2M_W$. The boson masses in the EW sector are given (at tree level, *i.e.*, to lowest order in perturbation theory) by,

$$M_H = \lambda\, v, \tag{10.3a}$$

$$M_W = \frac{1}{2}\, g\, v = \frac{e\, v}{2 \sin\theta_W}, \tag{10.3b}$$

$$M_Z = \frac{1}{2} \sqrt{g^2 + g'^2}\, v = \frac{e\, v}{2 \sin\theta_W \cos\theta_W} = \frac{M_W}{\cos\theta_W}, \tag{10.3c}$$

$$M_\gamma = 0. \tag{10.3d}$$

* There is no generally accepted convention to write the quartic term. Our numerical coefficient simplifies Eq. (10.3*a*) below and the squared coupling preserves the relation between the number of external legs and the power counting of couplings at a given loop order. This structure also naturally emerges from physics beyond the SM, such as supersymmetry.

The second term in $\mathscr{L}_F$ represents the charged-current weak interaction [4–7], where T^+ and T^- are the weak isospin raising and lowering operators. For example, the coupling of a W to an electron and a neutrino is

$$-\frac{e}{2\sqrt{2}\sin\theta_W} \left[W^-_\mu\, \overline{e}\, \gamma^\mu (1-\gamma^5) \nu + W^+_\mu\, \overline{\nu}\, \gamma^\mu\, (1-\gamma^5) e \right]. \tag{10.4}$$

For momenta small compared to M_W, this term gives rise to the effective four-fermion interaction with the Fermi constant given by $G_F/\sqrt{2} = 1/2v^2 = g^2/8M_W^2$. CP violation is incorporated into the EW model by a single observable phase in V_{ij}.

The third term in $\mathscr{L}_F$ describes electromagnetic interactions (QED) [8,9], and the last is the weak neutral-current interaction [5–7]. The vector and axial-vector couplings are

$$g^i_V \equiv t_{3L}(i) - 2 Q_i \sin^2\theta_W, \tag{10.5a}$$

$$g^i_A \equiv t_{3L}(i), \tag{10.5b}$$

where $t_{3L}(i)$ is the weak isospin of fermion i ($+1/2$ for u_i and ν_i; $-1/2$ for d_i and e_i) and Q_i is the charge of ψ_i in units of e.

The first term in Eq. (10.2) also gives rise to fermion masses, and in the presence of right-handed neutrinos to Dirac neutrino masses. The possibility of Majorana masses is discussed in the Section on "Neutrino Mass, Mixing, and Oscillations".

10.2. Renormalization and radiative corrections

In addition to the Higgs boson mass, M_H, the fermion masses and mixings, and the strong coupling constant, α_s, the SM has three parameters. The set with the smallest experimental errors contains the Z mass**, the Fermi constant, and the fine structure constant, which will be discussed in turn (if not stated otherwise, the numerical values quoted in Sec. 10.2–10.5 correspond to the main fit result in Table 10.6):

The Z boson mass, $M_Z = 91.1876 \pm 0.0021$ GeV, has been determined from the Z lineshape scan at LEP 1 [10]. This value of M_Z corresponds to a definition based on a Breit-Wigner shape with an energy-dependent width (see the Section on "The Z Boson" in the Gauge and Higgs Boson Particle Listings of this *Review*).

The Fermi constant, $G_F = 1.1663787(6) \times 10^{-5}$ GeV^{-2}, is derived from the muon lifetime formula***,

$$\frac{\hbar}{\tau_\mu} = \frac{G_F^2 m_\mu^5}{192\pi^3}\, F(\rho) \left[1 + H_1(\rho) \frac{\widehat{\alpha}(m_\mu)}{\pi} + H_2(\rho) \frac{\widehat{\alpha}^2(m_\mu)}{\pi^2} \right], \tag{10.6}$$

where $\rho = m_e^2/m_\mu^2$, and where

$$F(\rho) = 1 - 8\rho + 8\rho^3 - \rho^4 - 12\rho^2 \ln\rho = 0.99981295, \tag{10.7a}$$

$$\begin{aligned} H_1(\rho) = & \frac{25}{8} - \frac{\pi^2}{2} - \left(9 + 4\pi^2 + 12 \ln\rho \right) \rho \\ & + 16\pi^2 \rho^{3/2} + \mathcal{O}(\rho^2) = -1.80793, \end{aligned} \tag{10.7b}$$

$$\begin{aligned} H_2(\rho) = & \frac{156815}{5184} - \frac{518}{81}\pi^2 - \frac{895}{36}\zeta(3) + \frac{67}{720}\pi^4 + \frac{53}{6}\pi^2 \ln 2 \\ & - (0.042 \pm 0.002)_{\rm had} - \frac{5}{4}\pi^2 \sqrt{\rho} + \mathcal{O}(\rho) = 6.64, \end{aligned} \tag{10.7c}$$

$$\widehat{\alpha}(m_\mu)^{-1} = \alpha^{-1} + \frac{1}{3\pi} \ln\rho + \mathcal{O}(\alpha) = 135.901 \tag{10.7d}$$

** We emphasize that in the fits described in Sec. 10.6 and Sec. 10.7 the values of the SM parameters are affected by all observables that depend on them. This is of no practical consequence for α and G_F, however, since they are very precisely known.

*** In the spirit of the Fermi theory, we incorporated the small propagator correction, $3/5\ m_\mu^2/M_W^2$, into Δr (see below). This is also the convention adopted by the MuLan collaboration [11]. While this breaks with historical consistency, the numerical difference was negligible in the past.

H_1 and H_2 capture the QED corrections within the Fermi model. The results for $\rho = 0$ have been obtained in Refs. 12 and 13, respectively, where the term in parentheses is from the hadronic vacuum polarization [13]. The mass corrections to H_1 have been known for some time [14], while those to H_2 are more recent [15]. Notice the term linear in m_e whose appearance was unforeseen and can be traced to the use of the muon pole mass in the prefactor [15]. The remaining uncertainty in G_F is experimental and has been reduced by an order of magnitude by the MuLan collaboration [11] at the PSI.

The experimental determination of the fine structure constant, $\alpha = 1/137.035999139(31)$, is currently dominated by the $e^\pm$ anomalous magnetic moment [16]. In most EW renormalization schemes, it is convenient to define a running α dependent on the energy scale of the process, with $\alpha^{-1} \sim 137$ appropriate at very low energy, *i.e.* close to the Thomson limit. (The running has also been observed [17] directly.) For scales above a few hundred MeV this introduces an uncertainty due to the low energy hadronic contribution to vacuum polarization. In the modified minimal subtraction ($\overline{\rm MS}$) scheme [18] (used for this *Review*), and with $\alpha_s(M_Z) = 0.1187 \pm 0.0016$ we have $\widehat{\alpha}^{(4)}(m_\tau)^{-1} = 133.476 \pm 0.007$ and $\widehat{\alpha}^{(5)}(M_Z)^{-1} = 127.955 \pm 0.010$. (In this Section we denote quantities defined in the modified minimal subtraction ($\overline{\rm MS}$) scheme by a caret; the exception is the strong coupling constant, α_s, which will always correspond to the $\overline{\rm MS}$ definition and where the caret will be dropped.) The latter corresponds to a quark sector contribution (without the top) to the conventional (on-shell) QED coupling, $\alpha(M_Z) = \dfrac{\alpha}{1 - \Delta\alpha(M_Z)}$, of $\Delta\alpha^{(5)}_{\rm had}(M_Z) = 0.02764 \pm 0.00007$. These values are updated from Ref. 19 with $\Delta\alpha^{(5)}_{\rm had}(M_Z)$ moved downwards and its uncertainty reduced (partly due to a more precise charm quark mass). Its correlation with the $\mu^\pm$ anomalous magnetic moment (see Sec. 10.5), as well as the non-linear α_s dependence of $\widehat{\alpha}(M_Z)$ and the resulting correlation with the input variable α_s, are fully taken into account in the fits. This is done by using as actual input (fit constraint) instead of $\Delta\alpha^{(5)}_{\rm had}(M_Z)$ the low energy contribution by the three light quarks, $\Delta\alpha^{(3)}_{\rm had}(2.0\ {\rm GeV}) = (58.71 \pm 0.50) \times 10^{-4}$ [20], and by calculating the perturbative and heavy quark contributions to $\widehat{\alpha}(M_Z)$ in each call of the fits according to Ref. 19. Part of the uncertainty ($\pm 0.37 \times 10^{-4}$) is from e^+e^- annihilation data below 1.8 GeV and τ decay data (including uncertainties from isospin breaking effects [21]) , but uncalculated higher order perturbative ($\pm 0.21 \times 10^{-4}$) and non-perturbative ($\pm 0.26 \times 10^{-4}$) [20] QCD corrections and the $\overline{\rm MS}$ quark mass values (see below) also contribute. Various evaluations of $\Delta\alpha^{(5)}_{\rm had}$ are summarized in Table 10.1, where the relation[†] between the $\overline{\rm MS}$ and on-shell definitions (obtained using Ref. 24) is given by,

$$\begin{aligned}
&\Delta\widehat{\alpha}(M_Z) - \Delta\alpha(M_Z) = \\
&\frac{\alpha}{\pi}\left[\frac{100}{27} - \frac{1}{6} - \frac{7}{4}\ln\frac{M_Z^2}{M_W^2} + \frac{\alpha_s(M_Z)}{\pi}\left(\frac{605}{108} - \frac{44}{9}\zeta(3)\right)\right. \\
&\left. + \frac{\alpha_s^2}{\pi^2}\left(\frac{976481}{23328} - \frac{253}{36}\zeta(2) - \frac{781}{18}\zeta(3) + \frac{275}{27}\zeta(5)\right)\right] = \\
&= 0.007127(2)\ , \qquad (10.8)
\end{aligned}$$

and where the first entry of the lowest order term is from fermions and the other two are from $W^\pm$ loops, which are usually excluded from the on-shell definition. Fermion mass effects and corrections of $\mathcal{O}(\alpha\alpha_s^3)$ and $\mathcal{O}(\alpha^2)$ contributing to Eq. (10.8) are small, partly cancel each other and are not included here. The most recent results on $\Delta\alpha^{(5)}_{\rm had}(M_Z)$ [20,34,35] typically assume the validity of perturbative QCD (PQCD) at scales of ~ 2 GeV or above and are in good agreement with each other. In regions where PQCD is not trusted, one can use $e^+e^- \to$ hadrons cross-section data and τ decay spectral functions [36], where the latter derive from OPAL [37], CLEO [38], ALEPH [39], and Belle [40]. Recently, new data for various $e^+e^- \to$ hadrons channels was obtained from Babar, BES3, the SND and CMD3 experiments at VEPP-2M, and the KEDR experiment at VEPP-4M (for a list of references see *e.g.* Ref. 20). While VEPP-2M and VEPP-4M scanned a range of center-of-mass energies in the ranges $\sim$ 1–2 GeV and $\sim$ 3–4 GeV, respectively, the BaBar collaboration studied multi-hadron events radiatively returned from the $\Upsilon(4S)$, reconstructing the radiated photon and normalizing to $\mu^\pm\gamma$ final states. The precision of these results generally exceed those from τ decay spectral functions. There are significant discrepancies between older and newer measurements of $e^+e^- \to K^+K^-$ at SND and CMD, which could be due to difficulties in determining the detection efficiency of low-momentum kaons. The radiative return data from BaBar is expected to be more reliable for this channel owing to an additional boost of the final-state hadrons.

Table 10.1: Evaluations of the on-shell $\Delta\alpha^{(5)}_{\rm had}(M_Z)$ by different groups (for a more complete list of evaluations see the 2012 edition of this *Review*). For better comparison we adjusted central values and errors to correspond to a common and fixed value of $\alpha_s(M_Z) = 0.120$. References quoting results without the top quark decoupled are converted to the five flavor definition. Ref. [29] uses $\Lambda_{\rm QCD} = 380 \pm 60$ MeV; for the conversion we assumed $\alpha_s(M_Z) = 0.118 \pm 0.003$.

Reference	Result	Comment
Geshkenbein, Morgunov [25]	0.02780 ± 0.00006	$\mathcal{O}(\alpha_s)$ resonance model
Swartz [26]	0.02754 ± 0.00046	use of fitting function
Krasnikov, Rodenberg [27]	0.02737 ± 0.00039	PQCD for $\sqrt{s} > 2.3$ GeV
Kühn & Steinhauser [28]	0.02778 ± 0.00016	full $\mathcal{O}(\alpha_s^2)$ for $\sqrt{s} > 1.8$ GeV
Erler [19]	0.02779 ± 0.00020	conv. from $\overline{\rm MS}$ scheme
Groote *et al.* [29]	0.02787 ± 0.00032	use of QCD sum rules
Martin *et al.* [30]	0.02741 ± 0.00019	incl. new BES data
de Troconiz, Yndurain [31]	0.02754 ± 0.00010	PQCD for $s > 2$ GeV^2
Burkhardt, Pietrzyk [32]	0.02750 ± 0.00033	PQCD for $\sqrt{s} > 12$ GeV
Hagiwara *et al.* [33]	0.02764 ± 0.00014	PQCD: $\sqrt{s} = 2.6$–3.7, >11.1 GeV
Davier *et al.* [20]	0.02761 ± 0.00008	PQCD: $\sqrt{s} = 1.8$–3.7, >5 GeV
Jegerlehner [34]	0.02755 ± 0.00011	incl. γ-ρ mixing, corrected τ data, Euclidean split technique
Keshavarzi *et al.* [35]	0.02762 ± 0.00011	PQCD for $\sqrt{s} > 11.2$ GeV

Further free parameters entering into Eq. (10.2) are the quark and lepton masses, where m_i is the mass of the $i^{\rm th}$ fermion ψ_i. For the light quarks, as described in the note on "Quark Masses" in the Quark Listings, $\widehat{m}_u = 2.2^{+0.6}_{-0.4}$ MeV, $\widehat{m}_d = 4.7^{+0.5}_{-0.4}$ MeV, and $\widehat{m}_s = 96^{+8}_{-4}$ MeV. These are running $\overline{\rm MS}$ masses evaluated at the scale $\mu = 2$ GeV. For the charm quark we use the constraint $\widehat{m}_c(\widehat{m}_c) = 1274 \pm 8 + 2616[\alpha_s(M_Z) - 0.1182]$ MeV [41], which is based on QCD sum rules [42,43] and recalculate $\widehat{m}_c$ in each call of our fits to account for its α_s dependence. For the bottom quark we use $\widehat{m}_b(\widehat{m}_b) = 4.180 \pm 0.021$ GeV. To improve the precisions in $\widehat{m}_c(\widehat{m}_c)$ and $\widehat{m}_b(\widehat{m}_b)$ in the future it would help to remeasure the threshold regions of the heavy quarks, as well as the electronic decay widths of the narrow $c\bar{c}$ and $b\bar{b}$ resonances.

The top quark "pole" mass (the quotation marks are a reminder that the experiments do not strictly measure the pole mass and that quarks do not form asymptotic states), has been kinematically reconstructed by the Tevatron Collaborations, CDF and DØ, in leptonic, hadronic, and mixed channels with the result $m_t =$

[†] In practice, $\alpha(M_Z)$ is directly evaluated in the $\overline{\rm MS}$ scheme using the FORTRAN package GAPP [22], including the QED contributions of both leptons and quarks. The leptonic three-loop contribution in the on-shell scheme has been obtained in Ref. 23.

$174.30 \pm 0.35_{\text{stat.}} \pm 0.54_{\text{syst.}}$ GeV [44]. Likewise, ATLAS (including some $t\bar{t}$ cross section information) and CMS (including results based on alternative techniques) at the LHC obtained $m_t = 172.51 \pm 0.27_{\text{stat.}} \pm 0.42_{\text{syst.}}$ GeV [45] and $m_t = 172.43 \pm 0.13_{\text{stat.}} \pm 0.46_{\text{syst.}}$ GeV [46], respectively. In addition, CMS obtained a first result with $\sqrt{s} = 13$ TeV data (Run 2) in the lepton + jets channel, $m_t = 172.25 \pm 0.08_{\text{mostly stat.}} \pm 0.62_{\text{syst.}}$ GeV [47]. Assuming a systematic error component of 0.21 GeV (the QCD, PDF and Monte Carlo type errors at ALTAS) is common to all four determinations, we arrive at the average

$$m_t = 172.74 \pm 0.33_{\text{exp.}} \pm 0.32_{\text{theory}} \text{ GeV}, \tag{10.9}$$

where the last error (taken as the uncertainty [48] in the relation [49] between the $\overline{\text{MS}}$ and pole top mass definitions) is meant to account for theoretical uncertainties associated with the precise top mass definition applied in Monte Carlo generators on the one hand, and electroweak radiative correction libraries on the other. It is conceivable that more dedicated treatments [50] of the top mass definition in the future could result in somewhat larger shifts but smaller errors in m_t. The average in Eq. (10.9) differs slightly from the value, $m_t = 173.0 \pm 0.4$ GeV, which appears in the top quark Listings in this *Review* and which is based exclusively on published results. While there seems to be generally good agreement between all these measurements, we observe a 2.8 σ discrepancy (or more in case of correlated systematics) between the two most precise determinations, 174.98 ± 0.76 GeV [51] (by the DØ Collaboration) and 172.25 ± 0.63 GeV [47] (by the CMS Collaboration), both from the lepton + jets channels. For more details, see the Section on "The Top Quark" and the Quarks Listings in this *Review*.

The observables $\sin^2\theta_W$ and M_W can be calculated from M_Z, $\widehat{\alpha}(M_Z)$, and G_F, when values for m_t and M_H are given, or conversely, M_H can be constrained by $\sin^2\theta_W$ and M_W. The value of $\sin^2\theta_W$ is extracted from neutral-current processes (see Sec. 10.3) and Z pole observables (see Sec. 10.4) and depends on the renormalization prescription. There are a number of popular schemes [52–57] leading to values which differ by small factors depending on m_t and M_H. The notation for these schemes is shown in Table 10.2.

Table 10.2: Notations used to indicate the various schemes discussed in the text. Each definition of $\sin^2\theta_W$ leads to values that differ by small factors depending on m_t and M_H. Numerical values and the uncertainties induced by the imperfectly known SM parameters are also given for illustration.

Scheme	Notation	Value	Parametric uncertainty
On-shell	s^2_W	0.22343	±0.00007
$\overline{\text{MS}}$	$\widehat{s}^2_Z$	0.23122	±0.00003
$\overline{\text{MS}}$ ND	$\widehat{s}^2_{\text{ND}}$	0.23142	±0.00003
$\overline{\text{MS}}$	$\widehat{s}^2_0$	0.23857	±0.00005
Effective angle	$\overline{s}^2_\ell$	0.23154	±0.00003

(*i*) The on-shell scheme [52] promotes the tree-level formula $\sin^2\theta_W = 1 - M^2_W/M^2_Z$ to a definition of the renormalized $\sin^2\theta_W$ to all orders in perturbation theory, *i.e.*, $\sin^2\theta_W \to s^2_W \equiv 1 - M^2_W/M^2_Z$:

$$M_W = \frac{A_0}{s_W(1-\Delta r)^{1/2}}\,, \qquad M_Z = \frac{M_W}{c_W}\,, \tag{10.10}$$

where $c_W \equiv \cos\theta_W$, $A_0 = (\pi\alpha/\sqrt{2}G_F)^{1/2} = 37.28039(1)$ GeV, and Δr includes the radiative corrections relating α, $\alpha(M_Z)$, G_F, M_W, and M_Z. One finds $\Delta r \sim \Delta r_0 - \rho_t/\tan^2\theta_W$, where $\Delta r_0 = 1 - \alpha/\widehat{\alpha}(M_Z) = 0.06627(8)$ is due to the running of α, and $\rho_t = 3G_F m_t^2/8\sqrt{2}\pi^2 = 0.00935\,(m_t/172.74\text{ GeV})^2$ represents the dominant (quadratic) m_t dependence. There are additional contributions to Δr from bosonic loops, including those which depend logarithmically on M_H and higher-order corrections[$$]. One has $\Delta r = 0.03672 \mp 0.00017 \pm 0.00008$, where the first uncertainty is from m_t and the second is from $\alpha(M_Z)$. Thus the value of s^2_W extracted from M_Z includes an uncertainty (∓ 0.00005) from the currently allowed range of m_t. This scheme is simple conceptually. However, the relatively large ($\sim 3\%$) correction from ρ_t causes large spurious contributions in higher orders.

s^2_W depends not only on the gauge couplings but also on the spontaneous-symmetry breaking, and it is awkward in the presence of any extension of the SM which perturbs the value of M_Z (or M_W). Other definitions are motivated by the tree-level coupling constant definition $\theta_W = \tan^{-1}(g'/g)$:

(*ii*) In particular, the modified minimal subtraction ($\overline{\text{MS}}$) scheme introduces the quantity $\sin^2\widehat{\theta}_W(\mu) \equiv \widehat{g}\,'^2(\mu)/\big[\widehat{g}^{\,2}(\mu) + \widehat{g}\,'^2(\mu)\big]$, where the couplings $\widehat{g}$ and $\widehat{g}'$ are defined by modified minimal subtraction and the scale μ is conveniently chosen to be M_Z for many EW processes. The value of $\widehat{s}^2_Z = \sin^2\widehat{\theta}_W(M_Z)$ extracted from M_Z is less sensitive than s^2_W to m_t (by a factor of $\tan^2\theta_W$), and is less sensitive to most types of new physics. It is also very useful for comparing with the predictions of grand unification. There are actually several variant definitions of $\sin^2\widehat{\theta}_W(M_Z)$, differing according to whether or how finite $\alpha\ln(m_t/M_Z)$ terms are decoupled (subtracted from the couplings). One cannot entirely decouple the $\alpha\ln(m_t/M_Z)$ terms from all EW quantities because $m_t \gg m_b$ breaks SU(2) symmetry. The scheme that will be adopted here decouples the $\alpha\ln(m_t/M_Z)$ terms from the γ–Z mixing [18,53], essentially eliminating any $\ln(m_t/M_Z)$ dependence in the formulae for asymmetries at the Z pole when written in terms of $\widehat{s}^2_Z$. (A similar definition is used for $\widehat{\alpha}$.) The on-shell and $\overline{\text{MS}}$ definitions are related by

$$\widehat{s}^2_Z = c\,(m_t, M_H) s^2_W = (1.0348 \pm 0.0002) s^2_W\,. \tag{10.11}$$

The quadratic m_t dependence is given by $c \sim 1 + \rho_t/\tan^2\theta_W$. The expressions for M_W and M_Z in the $\overline{\text{MS}}$ scheme are

$$M_W = \frac{A_0}{\widehat{s}_Z(1-\Delta\widehat{r}_W)^{1/2}}\,, \qquad M_Z = \frac{M_W}{\widehat{\rho}^{\,1/2}\,\widehat{c}_Z}\,, \tag{10.12}$$

and one predicts $\Delta\widehat{r}_W = 0.06916 \pm 0.00008$. $\Delta\widehat{r}_W$ has no quadratic m_t dependence, because shifts in M_W are absorbed into the observed G_F, so that the error in $\Delta\widehat{r}_W$ is almost entirely due to $\Delta r_0 = 1 - \alpha/\widehat{\alpha}(M_Z)$. The quadratic m_t dependence has been shifted into $\widehat{\rho} \sim 1 + \rho_t$, where including bosonic loops, $\widehat{\rho} = 1.01013 \pm 0.00005$.

(*iii*) A variant $\overline{\text{MS}}$ quantity $\widehat{s}^2_{\text{ND}}$ (used in the 1992 edition of this *Review*) does not decouple the $\alpha\ln(m_t/M_Z)$ terms [54]. It is related to $\widehat{s}^2_Z$ by

$$\widehat{s}^2_Z = \widehat{s}^2_{\text{ND}}/\Big(1 + \frac{\widehat{\alpha}}{\pi}d\Big), \tag{10.13a}$$

$$d = \frac{1}{3}\left(\frac{1}{\widehat{s}^2} - \frac{8}{3}\right)\left[(1 + \frac{\alpha_s}{\pi})\,\ln\frac{m_t}{M_Z} - \frac{15\alpha_s}{8\pi}\right], \tag{10.13b}$$

Thus, $\widehat{s}^2_Z - \widehat{s}^2_{\text{ND}} = -0.0002$.

(*iv*) Some of the low-energy experiments discussed in the next section are sensitive to the weak mixing angle at almost vanishing momentum transfer (for a review, see Ref. 55). Thus, Table 10.2 also includes $\widehat{s}^2_0 \equiv \sin^2\widehat{\theta}_W(0)$.

(*v*) Yet another definition, the effective angle [56,57] $\overline{s}^2_f = \sin\theta^f_{\text{eff}}$ for the Z vector coupling to fermion f, is based on Z pole observables and described in Sec. 10.4.

Experiments are at such level of precision that complete one-loop, dominant two-loop, and partial three and four-loop radiative corrections must be applied. For neutral-current and Z pole processes, these corrections are conveniently divided into two classes:

[$$] All explicit numbers quoted here and below include the two- and three-loop corrections described near the end of Sec. 10.2.

1. QED diagrams involving the emission of real photons or the exchange of virtual photons in loops, but not including vacuum polarization diagrams. These graphs often yield finite and gauge-invariant contributions to observable processes. However, they are dependent on energies, experimental cuts, *etc.*, and must be calculated individually for each experiment.
2. EW corrections, including $\gamma\gamma$, γZ, ZZ, and WW vacuum polarization diagrams, as well as vertex corrections, box graphs, *etc.*, involving virtual W and Z bosons. The one-loop corrections are included for all processes, and many two-loop corrections are also important. In particular, two-loop corrections involving the top quark modify ρ_t in $\widehat{\rho}$, Δr, and elsewhere by

$$\rho_t \to \rho_t[1 + R(M_H, m_t)\rho_t/3]. \tag{10.14}$$

$R(M_H, m_t)$ can be described as an expansion in M_Z^2/m_t^2, for which the leading m_t^4/M_Z^4 [58] and next-to-leading m_t^2/M_Z^2 [59] terms are known. The complete two-loop calculation of Δr (without further approximation) has been performed in Refs. 60 and 61 for fermionic and purely bosonic diagrams, respectively. Similarly, the EW two-loop calculation for the relation between $\overline{s}_\ell^2$ and s_W^2 is complete [62,63]. More recently, Ref. 64 obtained the $\overline{\rm MS}$ quantities $\Delta\widehat{r}_W$ and $\widehat{\rho}$ to two-loop accuracy, confirming the prediction of M_W in the on-shell scheme from Refs. 61 and 65 within about 4 MeV.

Mixed QCD-EW contributions to gauge boson self-energies of order $\alpha\alpha_s m_t^2$ [66], $\alpha\alpha_s^2 m_t^2$ [67], and $\alpha\alpha_s^3 m_t^2$ [68] increase the predicted value of m_t by 6%. This is, however, almost entirely an artifact of using the pole mass definition for m_t. The equivalent corrections when using the $\overline{\rm MS}$ definition $\widehat{m}_t(\widehat{m}_t)$ increase m_t by less than 0.5%. The subleading $\alpha\alpha_s$ corrections [69] are also included. Further three-loop corrections of order $\alpha\alpha_s^2$ [70,71], $\alpha^3 m_t^6$, and $\alpha^2\alpha_s m_t^4$ [72], are rather small. The same is true for $\alpha^3 M_H^4$ [73] corrections unless M_H approaches 1 TeV.

The theoretical uncertainty from unknown higher-order corrections is estimated to amount to 4 MeV for the prediction of M_W [65] and 4.5×10^{-5} for $\overline{s}_\ell^2$ [74].

Throughout this *Review* we utilize EW radiative corrections from the program GAPP [22], which works entirely in the $\overline{\rm MS}$ scheme, and which is independent of the package ZFITTER [57].

10.3. Low energy electroweak observables

In the following we discuss EW precision observables obtained at low momentum transfers [6], *i.e.* $Q^2 \ll M_Z^2$. It is convenient to write the four-fermion interactions relevant to ν-hadron, ν-e, as well as parity violating e-hadron and e-e neutral-current processes in a form that is valid in an arbitrary gauge theory (assuming massless left-handed neutrinos). One has★

$$-\mathscr{L}^{\nu e} = \frac{G_F}{\sqrt{2}}\,\overline{\nu}\gamma_\mu(1-\gamma^5)\nu\;\overline{e}\,\gamma^\mu(g_{LV}^{\nu e} - g_{LA}^{\nu e}\,\gamma^5)e, \tag{10.15}$$

$$-\mathscr{L}^{\nu h} = \frac{G_F}{\sqrt{2}}\,\overline{\nu}\,\gamma_\mu(1-\gamma^5)\nu\sum_q[g_{LL}^{\nu q}\,\overline{q}\,\gamma^\mu(1-\gamma^5)q + g_{LR}^{\nu q}\,\overline{q}\,\gamma^\mu(1+\gamma^5)q], \tag{10.16}$$

$$-\mathscr{L}^{ee} = -\frac{G_F}{\sqrt{2}}\,g_{AV}^{ee}\,\overline{e}\,\gamma_\mu\gamma^5 e\,\overline{e}\,\gamma^\mu e, \tag{10.17}$$

$$-\mathscr{L}^{eh} = -\frac{G_F}{\sqrt{2}}\sum_q\left[g_{AV}^{eq}\,\overline{e}\,\gamma_\mu\gamma^5 e\,\overline{q}\,\gamma^\mu q + g_{VA}^{eq}\,\overline{e}\,\gamma_\mu e\,\overline{q}\,\gamma^\mu\gamma^5 q\right], \tag{10.18}$$

★ We use here slightly different definitions (and to avoid confusion also a different notation) for the coefficients of these four-Fermi operators than we did in previous editions of this *Review*. The new couplings [75] are defined in the static limit, $Q^2 \to 0$, with specific radiative corrections included, while others (more experiment specific ones) are assumed to be removed by the experimentalist. They are convenient in that their determinations from very different types of processes can be straightforwardly combined.

where one must include the charged-current contribution for ν_e-e and $\overline{\nu}_e$-e and the parity-conserving QED contribution for electron scattering.

Table 10.3: SM tree level expressions for the neutral-current parameters for ν-hadron, ν-e, and e^--scattering processes. To obtain the SM values in the last column, the tree level expressions have to be multiplied by the low-energy neutral-current ρ parameter, $\rho_{\rm NC} = 1.00058$, and further vertex and box corrections need to be added as detailed in Ref. 75. The dominant m_t dependence is again given by $\rho_{\rm NC} \sim 1 + \rho_t$.

Quantity	SM tree level	SM value
$g_{LV}^{\nu_\mu e}$	$-\frac{1}{2} + 2\,\widehat{s}_0^2$	−0.0398
$g_{LA}^{\nu_\mu e}$	$-\frac{1}{2}$	−0.5063
$g_{LL}^{\nu_\mu u}$	$\frac{1}{2} - \frac{2}{3}\,\widehat{s}_0^2$	0.3458
$g_{LL}^{\nu_\mu d}$	$-\frac{1}{2} + \frac{1}{3}\,\widehat{s}_0^2$	−0.4288
$g_{LR}^{\nu_\mu u}$	$-\frac{2}{3}\,\widehat{s}_0^2$	−0.1552
$g_{LR}^{\nu_\mu d}$	$\frac{1}{3}\,\widehat{s}_0^2$	0.0777
g_{AV}^{ee}	$\frac{1}{2} - 2\,\widehat{s}_0^2$	0.0226
g_{AV}^{eu}	$-\frac{1}{2} + \frac{4}{3}\,\widehat{s}_0^2$	−0.1888
g_{AV}^{ed}	$\frac{1}{2} - \frac{2}{3}\,\widehat{s}_0^2$	0.3419
g_{VA}^{eu}	$-\frac{1}{2} + 2\,\widehat{s}_0^2$	−0.0352
g_{VA}^{ed}	$\frac{1}{2} - 2\,\widehat{s}_0^2$	0.0249

The SM tree level expressions for the four-Fermi couplings are given in Table 10.3. Note that they differ from the respective products of the gauge couplings in Eq. (10.5) in the radiative corrections and in the presence of possible physics beyond the SM.

10.3.1. ***Neutrino scattering*** : For a general review on ν-scattering we refer to Ref. 76 (nonstandard neutrino scattering interactions are surveyed in Ref. 77).

The cross-section in the laboratory system for $\nu_\mu e \to \nu_\mu e$ or $\overline{\nu}_\mu e \to \overline{\nu}_\mu e$ elastic scattering [78] is (in this subsection we drop the redundant index L in the effective neutrino couplings)

$$\frac{d\sigma_{\nu,\bar{\nu}}}{dy} =$$

$$\frac{G_F^2 m_e E_\nu}{2\pi}\left[(g_V^{\nu e} \pm g_A^{\nu e})^2 + (g_V^{\nu e} \mp g_A^{\nu e})^2(1-y)^2 - (g_V^{\nu e 2} - g_A^{\nu e 2})\frac{y\,m_e}{E_\nu}\right], \tag{10.19}$$

where the upper (lower) sign refers to $\nu_\mu(\overline{\nu}_\mu)$, and $y \equiv T_e/E_\nu$ (which runs from 0 to $(1 + m_e/2E_\nu)^{-1}$) is the ratio of the kinetic energy of the recoil electron to the incident ν or $\overline{\nu}$ energy. For $E_\nu \gg m_e$ this yields a total cross-section

$$\sigma = \frac{G_F^2 m_e E_\nu}{2\pi}\left[(g_V^{\nu e} \pm g_A^{\nu e})^2 + \frac{1}{3}(g_V^{\nu e} \mp g_A^{\nu e})^2\right]. \tag{10.20}$$

The most accurate measurements [78–81] of $\sin^2\theta_W$ from ν-lepton scattering (see Sec. 10.6) are from the ratio $R \equiv \sigma_{\nu_\mu e}/\sigma_{\overline{\nu}_\mu e}$, in which many of the systematic uncertainties cancel. Radiative corrections (other than m_t effects) are small compared to the precision of present experiments and have negligible effect on the extracted $\sin^2\theta_W$. The most precise experiment (CHARM II) [79] determined not only $\sin^2\theta_W$ but $g_{V,A}^{\nu e}$ as well, which are shown in Fig. 10.1. The cross-sections for ν_e-e and $\overline{\nu}_e$-e may be obtained from Eq. (10.19) by replacing $g_{V,A}^{\nu e}$ by $g_{V,A}^{\nu e} + 1$, where the 1 is due to the charged-current contribution.

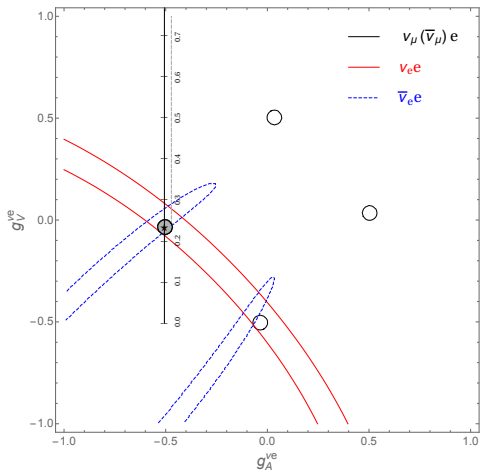

Figure 10.1: Allowed contours in $g_A^{\nu e}$ *vs.* $g_V^{\nu e}$ from neutrino-electron scattering and the SM prediction as a function of $\widehat{s}^2_Z$. (The SM best fit value $\widehat{s}^2_Z = 0.23122$ is also indicated.) The $\nu_e e$ [80] and $\bar{\nu}_e e$ [81] constraints are at 1 σ, while each of the four equivalent $\nu_\mu(\bar{\nu}_\mu)e$ [78–79] solutions ($g_{V,A} \to -g_{V,A}$ and $g_{V,A} \to g_{A,V}$) are at the 90% C.L. The global best fit region (shaded) almost exactly coincides with the corresponding $\nu_\mu(\bar{\nu}_\mu)e$ region. The solution near $g_A = 0, g_V = -0.5$ is eliminated by $e^+e^- \to \ell^+\ell^-$ data under the weak additional assumption that the neutral current is dominated by the exchange of a single Z boson.

A precise determination of the on-shell s^2_W, which depends only very weakly on m_t and M_H, is obtained from deep inelastic scattering (DIS) of neutrinos from (approximately) isoscalar targets [82]. The ratio $R_\nu \equiv \sigma^{NC}_{\nu N}/\sigma^{CC}_{\nu N}$ of neutral-to-charged-current cross-sections has been measured to 1% accuracy by CDHS [83] and CHARM [84] at CERN. CCFR [85] at Fermilab has obtained an even more precise result, so it is important to obtain theoretical expressions for R_ν and $R_{\bar{\nu}} \equiv \sigma^{NC}_{\bar{\nu}N}/\sigma^{CC}_{\bar{\nu}N}$ to comparable accuracy. Fortunately, many of the uncertainties from the strong interactions and neutrino spectra cancel in the ratio. A large theoretical uncertainty is associated with the c-threshold, which mainly affects σ^{CC}. Using the slow rescaling prescription [86] the central value of $\sin^2\theta_W$ from CCFR varies as $0.0111(m_c/\mathrm{GeV} - 1.31)$, where m_c is the effective mass which is numerically close to the $\overline{\rm MS}$ mass $\widehat{m}_c(\widehat{m}_c)$, but their exact relation is unknown at higher orders. For $m_c = 1.31 \pm 0.24$ GeV (determined from ν-induced dimuon production [87]) this contributes ± 0.003 to the total uncertainty $\Delta \sin^2\theta_W \sim \pm 0.004$. (The experimental uncertainty is also ± 0.003.) This uncertainty largely cancels, however, in the Paschos-Wolfenstein ratio [88],

$$R^- = \frac{\sigma^{NC}_{\nu N} - \sigma^{NC}_{\bar{\nu}N}}{\sigma^{CC}_{\nu N} - \sigma^{CC}_{\bar{\nu}N}} \ . \tag{10.21}$$

It was measured by Fermilab's NuTeV collaboration [89] for the first time, and required a high-intensity and high-energy anti-neutrino beam.

A simple zero$^{\rm th}$-order approximation is

$$R_\nu = g^2_L + g^2_R r \ , \ R_{\bar{\nu}} = g^2_L + \frac{g^2_R}{r} \ , \ R^- = g^2_L - g^2_R \ , \tag{10.22}$$

where

$$g^2_L \equiv (g^{\nu_\mu u}_{LL})^2 + (g^{\nu_\mu d}_{LL})^2 \approx \frac{1}{2} - \sin^2\theta_W + \frac{5}{9}\sin^4\theta_W , \tag{10.23a}$$

$$g^2_R \equiv (g^{\nu_\mu u}_{LR})^2 + (g^{\nu_\mu d}_{LR})^2 \approx \frac{5}{9}\sin^4\theta_W , \tag{10.23b}$$

and $r \equiv \sigma^{CC}_{\bar{\nu}N}/\sigma^{CC}_{\nu N}$ is the ratio of $\overline{\nu}$ to ν charged-current cross-sections, which can be measured directly. [In the simple parton model, ignoring hadron energy cuts, $r \approx (\frac{1}{3} + \epsilon)/(1 + \frac{1}{3}\epsilon)$, where $\epsilon \sim 0.125$ is the ratio of the fraction of the nucleon's momentum carried by anti-quarks to that carried by quarks.] In practice, Eq. (10.22) must be corrected for quark mixing, quark sea effects, c-quark threshold effects, non-isoscalarity, W–Z propagator differences, the finite muon mass, QED and EW radiative corrections. Details of the neutrino spectra, experimental cuts, x and Q^2 dependence of structure functions, and longitudinal structure functions enter only at the level of these corrections and therefore lead to very small uncertainties. CCFR quotes $s^2_W = 0.2236 \pm 0.0041$ for $(m_t, M_H) = (175, 150)$ GeV with very little sensitivity to (m_t, M_H).

The NuTeV collaboration found $s^2_W = 0.2277 \pm 0.0016$ (for the same reference values), which was 3.0 σ higher than the SM prediction [89]. However, since then several groups have raised concerns about interpretation of the NuTeV result, which could affect the extracted $g^2_{L,R}$ (and thus s^2_W) including their uncertainties and correlation. These include the assumption of symmetric strange and antistrange sea quark distributions, the electron neutrino contamination from K_{e3} decays, isospin symmetry violation in the parton distribution functions and from QED splitting effects, nuclear shadowing effects, and a more complete treatment of EW and QCD radiative corrections. A more detailed discussion and a list of references can be found in the 2016 edition of this *Review*. The precise impact of these effects would need to be evaluated carefully by the collaboration, but in the absence of a such an effort we do not include the νDIS constraints in our default set of fits.

10.3.2. ***Parity violation*** : For a review on weak polarized electron scattering we refer to Ref. 90. The SLAC polarized electron-deuteron DIS (eDIS) experiment [91] measured the right-left asymmetry,

$$A = \frac{\sigma_R - \sigma_L}{\sigma_R + \sigma_L} \ , \tag{10.24}$$

where $\sigma_{R,L}$ is the cross-section for the deep-inelastic scattering of a right- or left-handed electron: $e_{R,L}N \to e\mathrm{X}$. In the quark parton model,

$$\frac{A}{Q^2} = a_1 + a_2 \frac{1 - (1-y)^2}{1 + (1-y)^2} \ , \tag{10.25}$$

where $Q^2 > 0$ is the momentum transfer and y is the fractional energy transfer from the electron to the hadrons. For the deuteron or other isoscalar targets, one has, neglecting the s-quark and anti-quarks,

$$a_1 = \frac{3G_F}{5\sqrt{2}\pi\alpha}\left(g^{eu}_{AV} - \frac{1}{2}g^{ed}_{AV}\right) \approx \frac{3G_F}{5\sqrt{2}\pi\alpha}\left(-\frac{3}{4} + \frac{5}{3}\widehat{s}^2_0\right) \tag{10.26a}$$

$$a_2 = \frac{3G_F}{5\sqrt{2}\pi\alpha}\left(g^{eu}_{VA} - \frac{1}{2}g^{ed}_{VA}\right) \approx \frac{9G_F}{5\sqrt{2}\pi\alpha}\left(\widehat{s}^2_0 - \frac{1}{4}\right) . \tag{10.26b}$$

The Jefferson Lab Hall A Collaboration [92] improved on the SLAC result by determining A at $Q^2 = 1.085$ GeV and 1.901 GeV, and determined the weak mixing angle to 2% precision. In another polarized-electron scattering experiment on deuterons, but in the quasi-elastic kinematic regime, the SAMPLE experiment [93] at MIT-Bates extracted the combination $g^{eu}_{VA} - g^{ed}_{VA}$ at Q^2 values of 0.1 GeV^2 and 0.038 GeV^2. What was actually determined were nucleon form factors from which the quoted results were obtained by the removal of a multi-quark radiative correction [94]. Other linear combinations of the effective couplings have been determined in polarized-lepton scattering at CERN in μ-C DIS, at Mainz in e-Be (quasi-elastic), and at Bates in e-C (elastic). See the review articles in Refs. 95 and 96 for more details. Recent polarized electron scattering experiments, *i.e.*, SAMPLE, the PVA4 experiment at Mainz, and the HAPPEX and GØ experiments at Jefferson Lab, have focussed on the strange quark content of the nucleon. These are reviewed in Refs. 97 and 98.

The parity violating asymmetry, A_{PV}, in fixed target polarized Møller scattering, $e^-e^- \to e^-e^-$, is defined as in Eq. (10.24) and reads [99],

$$\frac{A_{PV}}{Q^2} = -2\, g^{ee}_{AV}\frac{G_F}{\sqrt{2}\pi\alpha}\frac{1-y}{1 + y^4 + (1-y)^4} \ , \tag{10.27}$$

where y is again the energy transfer. It has been measured at low $Q^2 = 0.026$ GeV^2 in the SLAC E158 experiment [100], with the result $A_{PV} = (-1.31 \pm 0.14_{\,\text{stat.}} \pm 0.10_{\,\text{syst.}}) \times 10^{-7}$. Expressed in terms of the weak mixing angle in the $\overline{\text{MS}}$ scheme, this yields $\widehat{s}^{\,2}(Q^2) = 0.2403 \pm 0.0013$, and established the scale dependence of the weak mixing angle (see $Q_W(e)$ in Fig. 10.2) at the level of 6.4 σ. One can also extract the model-independent effective coupling, $g_{AV}^{ee} = 0.0190 \pm 0.0027$ [75] (the implications are discussed in Ref. 103).

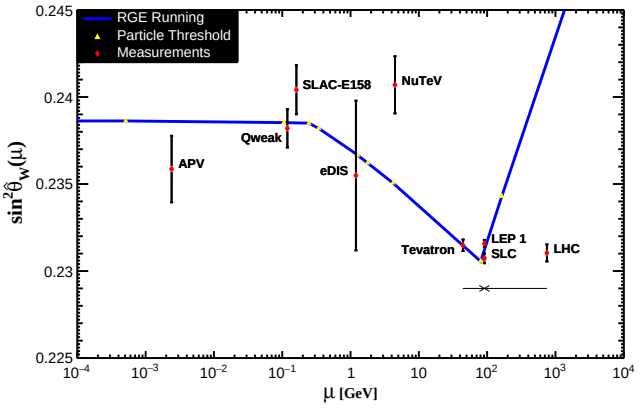

Figure 10.2: Scale dependence of the weak mixing angle defined in the $\overline{\text{MS}}$ scheme [101,102] (for the scale dependence of the weak mixing angle defined in a mass-dependent renormalization scheme, see Ref. 103). The minimum of the curve corresponds to $\mu = M_W$, below which we switch to an effective theory with the $W^\pm$ bosons integrated out, and where the β-function for the weak mixing angle changes sign. At the location of the W boson mass and each fermion mass there are also discontinuities arising from scheme dependent matching terms which are necessary to ensure that the various effective field theories within a given loop order describe the same physics. However, in the $\overline{\text{MS}}$ scheme these are very small numerically and barely visible in the figure provided one decouples quarks at $\mu = \widehat{m}_q(\widehat{m}_q)$. The width of the curve exceeds the theory uncertainty from strong interaction effects which at low energies is at the level of $\pm 2 \times 10^{-5}$ [102]. Following the estimate [104] of the typical momentum transfer for parity violation experiments in Cs, the location of the APV data point is given by $\mu = 2.4$ MeV. For NuTeV we display the updated value from Ref. 105 and chose $\mu = \sqrt{20}$ GeV which is about half-way between the averages of $\sqrt{Q^2}$ for ν and $\overline{\nu}$ interactions at NuTeV. The Tevatron and LHC measurements are strongly dominated by invariant masses of the final state dilepton pair of $\mathcal{O}(M_Z)$ and can thus be considered as additional Z pole data points. For clarity we displayed the Tevatron and LHC points horizontally to the left and to the right, respectively.

In a similar experiment and at about the same $Q^2 = 0.025$ GeV^2, Qweak at Jefferson Lab [106] measured the weak charge of the proton (which is proportional to $2g_{AV}^{eu} + g_{AV}^{ed}$) and $\sin^2\theta_W$ in polarized ep scattering with relative precisions of 6% and 0.5%, respectively. The preliminary result [107] based on the full data set corresponds to the constraint $2g_{AV}^{eu} + g_{AV}^{ed} = 0.0356 \pm 0.0023$, and to a measurement of the weak mixing angle, $\widehat{s}^{\,2}(Q^2) = 0.2382 \pm 0.0011$.

There are precise experiments measuring atomic parity violation (APV) [108,109] in cesium [110,111] (at the 0.4% level [110]), thallium [112], lead [113], and bismuth [114]. The EW physics is contained in the nuclear weak charges $Q_W^{Z,N}$, where Z and N are the numbers of protons and neutrons in the nucleus. In terms of the nucleon vector couplings,

$$g_{AV}^{ep} \equiv 2g_{AV}^{eu} + g_{AV}^{ed} \approx -\frac{1}{2} + 2\widehat{s}_0^2, \tag{10.28}$$

$$g_{AV}^{en} \equiv g_{AV}^{eu} + 2g_{AV}^{ed} \approx \frac{1}{2}, \tag{10.29}$$

one has,

$$Q_W^{Z,N} \equiv -2\left[Z(g_{AV}^{ep} + 0.00005) + N(g_{AV}^{en} + 0.00006)\right]\left(1 - \frac{\alpha}{2\pi}\right), \tag{10.30}$$

where the numerically small adjustments are discussed in Ref. 75 and include the result of the γZ-box correction from Ref. 115. *E.g.*, $Q_W(^{133}\text{Cs})$ is extracted by measuring experimentally the ratio of the parity violating amplitude, E_{PNC}, to the Stark vector transition polarizability, β, and by calculating theoretically E_{PNC} in terms of Q_W. One can then write,

$$Q_W = N\left(\frac{\text{Im}\,E_{\text{PNC}}}{\beta}\right)_{\text{exp.}}\left(\frac{|e|\,a_B}{\text{Im}\,E_{\text{PNC}}}\frac{Q_W}{N}\right)_{\text{th.}}\left(\frac{\beta}{a_B^3}\right)_{\text{exp.+th.}}\left(\frac{a_B^2}{|e|}\right),$$

where a_B is the Bohr radius. The uncertainties associated with atomic wave functions are quite small for cesium [116]. The semi-empirical value of β used in early analyses added another source of theoretical uncertainty [117]. However, the ratio of the off-diagonal hyperfine amplitude to the polarizability was subsequently measured directly by the Boulder group [118]. Combined with the precisely known hyperfine amplitude [119] one finds $\beta = (26.991 \pm 0.046)\,a_B^3$, in excellent agreement with the earlier results, reducing the overall theory uncertainty (while slightly increasing the experimental error). Utilizing the state-of-the-art many-body calculation in Ref. 120 yields $\text{Im}\,E_{\text{PNC}} = (0.8906 \pm 0.0026) \times 10^{-11}|e|\,a_B\,Q_W/N$, while the two measurements [110,111] combine to give $\text{Im}\,E_{\text{PNC}}/\beta = -1.5924 \pm 0.0055$ mV/cm, and we would obtain $Q_W(^{133}_{78}\text{Cs}) = -73.20 \pm 0.35$, or equivalently $55g_{AV}^{ep} + 78g_{AV}^{en} = 36.64 \pm 0.18$ which is in excellent agreement with the SM prediction of 36.65. However, a very recent atomic structure calculation [121] found significant corrections to two non-dominating terms, changing the result to $\text{Im}\,E_{\text{PNC}} = (0.8977 \pm 0.0040) \times 10^{-11}|e|\,a_B\,Q_W/N$, and yielding the constraint, $55g_{AV}^{ep} + 78g_{AV}^{en} = 36.35 \pm 0.21$ [$Q_W(^{133}_{78}\text{Cs}) = -72.62 \pm 0.43$], *i.e.* a 1.5 σ SM deviation. Thus, the various theoretical efforts in [120–122] together with an update of the SM calculation [123] reduced an earlier 2.3 σ discrepancy from the SM (see the year 2000 edition of this *Review*), but there still appears to remain a small deviation. The theoretical uncertainties are 3% for thallium [124] but larger for the other atoms. The Boulder experiment in cesium also observed the parity-violating weak corrections to the nuclear electromagnetic vertex (the anapole moment [125]) .

In the future it could be possible to further reduce the theoretical wave function uncertainties by taking the ratios of parity violation in different isotopes [108,126]. There would still be some residual uncertainties from differences in the neutron charge radii, however [127]. Experiments in hydrogen and deuterium are another possibility for reducing the atomic theory uncertainties [128], while measurements of single trapped radium ions are promising [129] because of the much larger parity violating effect.

10.4. Physics of the massive electroweak bosons

If the CM energy $\sqrt{s}$ is large compared to the fermion mass m_f, the unpolarized Born cross-section for $e^+e^- \to f\bar{f}$ can be written as

$$\frac{d\sigma}{d\cos\theta} = \frac{\pi\alpha^2(s)}{2s}\left[F_1(1 + \cos^2\theta) + 2F_2\cos\theta\right] + B, \tag{10.31a}$$

where

$$F_1 = Q_e^2Q_f^2 - 2\chi Q_eQ_f\overline{g}_V^e\overline{g}_V^f\cos\delta_R + \chi^2(\overline{g}_V^{e2} + \overline{g}_A^{e2})(\overline{g}_V^{f2} + \overline{g}_A^{f2}) \tag{10.31b}$$

$$F_2 = -2\chi\,Q_eQ_f\overline{g}_A^e\overline{g}_A^f\cos\delta_R + 4\chi^2\overline{g}_V^e\overline{g}_A^e\overline{g}_V^f\overline{g}_A^f \tag{10.31c}$$

$$\tan\delta_R = \frac{\overline{M}_Z\overline{\Gamma}_Z}{\overline{M}_Z^2 - s}\ ,\ \chi = \frac{G_F}{2\sqrt{2}\pi\alpha(s)}\frac{s\overline{M}_Z^2}{\left[(\overline{M}_Z^2 - s)^2 + \overline{M}_Z^2\overline{\Gamma}_Z^2\right]^{1/2}}, \tag{10.32}$$

and B accounts for box graphs involving virtual Z and W bosons, and the $\overline{g}_{V,A}^f$ are defined in Eq. (10.33) below. $\overline{M}_Z$ and $\overline{\Gamma}_Z$ correspond

to mass and width definitions based on a Breit-Wigner shape with an energy-independent width (see the Section on "The Z Boson" in the Gauge and Higgs Boson Particle Listings of this *Review*). The differential cross-section receives important corrections from QED effects in the initial and final state, and interference between the two (see *e.g.* Ref. 130). For $q\bar{q}$ production, there are additional final-state QCD corrections, which are relatively large. Note also that the equations above are written in the CM frame of the incident e^+e^- system, which may be boosted due to the initial-state QED radiation.

Some of the leading virtual EW corrections are captured by the running QED coupling $\alpha(s)$ and the Fermi constant G_F. The remaining corrections to the $Zf\bar{f}$ interaction are absorbed by replacing the tree-level couplings in Eq. (10.5) with the s-dependent *effective couplings* [131],

$$\overline{g}_V^f = \sqrt{\rho_f}\,(t_{3L}^{(f)} - 2Q_f\kappa_f \sin^2\theta_W), \qquad \overline{g}_A^f = \sqrt{\rho_f}\,t_{3L}^{(f)}. \quad (10.33)$$

In these equations, the effective couplings are to be taken at the scale $\sqrt{s}$, but for notational simplicity we do not show this explicitly. At tree-level $\rho_f = \kappa_f = 1$, but inclusion of EW radiative corrections leads to non-zero $\rho_f - 1$ and $\kappa_f - 1$, which depend on the fermion f and on the renormalization scheme. In the on-shell scheme, the quadratic m_t dependence is given by $\rho_f \sim 1 + \rho_t$, $\kappa_f \sim 1 + \rho_t/\tan^2\theta_W$, while in $\overline{\rm MS}$, $\widehat{\rho}_f \sim \widehat{\kappa}_f \sim 1$, for $f \neq b$ ($\widehat{\rho}_b \sim 1 - \frac{4}{3}\rho_t$, $\widehat{\kappa}_b \sim 1 + \frac{2}{3}\rho_t$). In the $\overline{\rm MS}$ scheme the normalization is changed according to $G_F M_Z^2/2\sqrt{2}\pi \to \widehat{\alpha}/4\widehat{s}_Z^2\widehat{c}_Z^2$ in Eq. (10.32).

For the high-precision Z-pole observables discussed below, additional bosonic and fermionic loops, vertex corrections, and higher order contributions, *etc.*, must be included [62,63,132–134]. For example, in the $\overline{\rm MS}$ scheme one has $\widehat{\rho}_\ell = 0.9977$, $\widehat{\kappa}_\ell = 1.0014$, $\widehat{\rho}_b = 0.9868$, and $\widehat{\kappa}_b = 1.0068$.

To connect to measured quantities, it is convenient to define an effective angle $\overline{s}_f^2 \equiv \sin^2\overline{\theta}_{Wf} \equiv \widehat{\kappa}_f\widehat{s}_Z^2 = \kappa_f s_W^2$, in terms of which $\overline{g}_V^f$ and $\overline{g}_A^f$ are given by $\sqrt{\rho_f}$ times their tree-level formulae. One finds that the $\widehat{\kappa}_f$ ($f \neq b$) are almost independent of (m_t, M_H), and thus one can write

$$\overline{s}_\ell^2 = \widehat{s}_Z^2 + 0.00032, \quad (10.34)$$

while the κ's for the other schemes are m_t dependent.

10.4.1. e^+e^- *scattering below the Z pole* :

Experiments at PEP, PETRA and TRISTAN have measured the unpolarized forward-backward asymmetry, A_{FB}, and the total cross-section relative to pure QED, R, for $e^+e^- \to \ell^+\ell^-$, $\ell = \mu$ or τ at CM energies $\sqrt{s} < M_Z$. They are defined as

$$A_{FB} \equiv \frac{\sigma_F - \sigma_B}{\sigma_F + \sigma_B}\,, \qquad R = \frac{\sigma}{\mathcal{R}_{\rm ini} 4\pi\alpha^2/3s}\,, \quad (10.35)$$

where σ_F (σ_B) is the cross-section for ℓ^- to travel forward (backward) with respect to the e^- direction. Neglecting box graph contribution, they are given by

$$A_{FB} = \frac{3}{4}\frac{F_2}{F_1}\,, \qquad R = F_1\,. \quad (10.36)$$

For the available data, it is sufficient to approximate the EW corrections through the leading running $\alpha(s)$ and quadratic m_t contributions [135,136] as described above. Reviews and formulae for $e^+e^- \to$ hadrons may be found in Ref. 137.

10.4.2. *Z pole physics* :

High-precision measurements of various Z pole ($\sqrt{s} \approx M_Z$) observables have been performed at LEP 1 and SLC [10,138–143], as summarized in Table 10.5. These include the Z mass and total width, Γ_Z, and partial widths $\Gamma(f\bar{f})$ for $Z \to f\bar{f}$, where $f = e$, μ, τ, light hadrons, b, or c. It is convenient to use the variables M_Z, Γ_Z, $R_\ell \equiv \Gamma({\rm had})/\Gamma(\ell^+\ell^-)$ ($\ell = e, \mu, \tau$), $\sigma_{\rm had} \equiv 12\pi\,\Gamma(e^+e^-)\,\Gamma({\rm had})/M_Z^2\,\Gamma_Z^2$ [††], $R_b \equiv \Gamma(b\bar{b})/\Gamma({\rm had})$, and $R_c \equiv \Gamma(c\bar{c})/\Gamma({\rm had})$, most of which are weakly correlated experimentally. ($\Gamma({\rm had})$ is the partial width into hadrons.) The three values for R_ℓ are consistent with lepton universality (although R_τ is somewhat low compared to R_e and R_μ), but we use the general analysis in which the three observables are treated as independent. Similar remarks apply to $A_{FB}^{0,\ell}$ defined through Eq. (10.39) with $P_e = 0$ ($A_{FB}^{0,\tau}$ is somewhat high). $\mathcal{O}(\alpha^3)$ QED corrections introduce a large anti-correlation (-30%) between Γ_Z and $\sigma_{\rm had}$. The anti-correlation between R_b and R_c is -18% [10]. The R_ℓ are insensitive to m_t except for the $Z \to b\bar{b}$ vertex and final state corrections and the implicit dependence through $\sin^2\theta_W$. Thus, they are especially useful for constraining α_s. The invisible decay width [10], $\Gamma({\rm inv}) = \Gamma_Z - 3\,\Gamma(\ell^+\ell^-) - \Gamma({\rm had}) = 499.0 \pm 1.5$ MeV, can be used to determine the number of neutrino flavors, $N_\nu = \Gamma({\rm inv})/\Gamma^{\rm theory}(\nu\overline{\nu})$, much lighter than $M_Z/2$. In practice, we determine N_ν by allowing it as an additional fit parameter and obtain,

$$N_\nu = 2.991 \pm 0.007\,. \quad (10.37)$$

Additional constraints follow from measurements of various Z-pole asymmetries. These include the forward-backward asymmetry A_{FB} and the polarization or left-right asymmetry,

$$A_{LR} \equiv \frac{\sigma_L - \sigma_R}{\sigma_L + \sigma_R}\,, \quad (10.38)$$

where $\sigma_L(\sigma_R)$ is the cross-section for a left-(right-)handed incident electron. A_{LR} was measured precisely by the SLD collaboration at the SLC [140], and has the advantages of being very sensitive to $\sin^2\theta_W$ and that systematic uncertainties largely cancel. After removing initial state QED corrections and contributions from photon exchange, γ–Z interference and EW boxes, see Eq. (10.31), one can use the effective tree-level expressions

$$A_{LR} = A_e P_e\,, \qquad A_{FB} = \frac{3}{4}A_f\,\frac{A_e + P_e}{1 + P_e A_e}\,, \quad (10.39)$$

where

$$A_f \equiv \frac{2\overline{g}_V^f\,\overline{g}_A^f}{\overline{g}_V^{f2} + \overline{g}_A^{f2}} = \frac{1 - 4|Q_f|\bar{s}_f^2}{1 - 4|Q_f|\bar{s}_f^2 + 8(|Q_f|\bar{s}_f^2)^2}\,. \quad (10.40)$$

P_e is the initial e^- polarization, so that the second equality in Eq. (10.41) is reproduced for $P_e = 1$, and the Z pole forward-backward asymmetries at LEP 1 ($P_e = 0$) are given by $A_{FB}^{(0,f)} = \frac{3}{4}A_e A_f$ where $f = e$, μ, τ, b, c, s [10], and q, and where $A_{FB}^{(0,q)}$ refers to the hadronic charge asymmetry. Corrections for t-channel exchange and s/t-channel interference cause $A_{FB}^{(0,e)}$ to be strongly anti-correlated with R_e (-37%). The correlation between $A_{FB}^{(0,b)}$ and $A_{FB}^{(0,c)}$ amounts to 15%.

In addition, SLD extracted the final-state couplings A_b, A_c [10], A_s [141], A_τ, and A_μ [142], from left-right forward-backward asymmetries, using

$$A_{LR}^{FB}(f) = \frac{\sigma_{LF}^f - \sigma_{LB}^f - \sigma_{RF}^f + \sigma_{RB}^f}{\sigma_{LF}^f + \sigma_{LB}^f + \sigma_{RF}^f + \sigma_{RB}^f} = \frac{3}{4}A_f\,, \quad (10.41)$$

where, for example, σ_{LF}^f is the cross-section for a left-handed incident electron to produce a fermion f traveling in the forward hemisphere. Similarly, A_τ and A_e were measured at LEP 1 [10] through the τ polarization, $\mathcal{P}_\tau$, as a function of the scattering angle θ, which can be written as

$$\mathcal{P}_\tau = -\frac{A_\tau(1 + \cos^2\theta) + 2A_e\cos\theta}{(1 + \cos^2\theta) + 2A_\tau A_e\cos\theta} \quad (10.42)$$

The average polarization, $\langle\mathcal{P}_\tau\rangle$, obtained by integrating over $\cos\theta$ in the numerator and denominator of Eq. (10.42), yields $\langle\mathcal{P}_\tau\rangle = -A_\tau$, while A_e can be extracted from the angular distribution of $\mathcal{P}_\tau$.

The initial state coupling, A_e, was also determined through the left-right charge asymmetry [143] and in polarized Bhabba scattering [142]

[††] Note that $\sigma_{\rm had}$ receives additional EW corrections that are not captured in the partial widths [134,144], but they only enter at two-loop order.

at SLC. Because $\overline{g}_V^\ell$ is very small, not only $A_{LR}^0 = A_e$, $A_{FB}^{(0,\ell)}$, and $\mathcal{P}_\tau$, but also $A_{FB}^{(0,b)}$, $A_{FB}^{(0,c)}$, $A_{FB}^{(0,s)}$, and the hadronic asymmetries are mainly sensitive to $\overline{s}_\ell^2$.

As mentioned in Sec. 10.2, radiative corrections to $\bar{s}_\ell^2$ have been computed with full two-loop and partial higher-order corrections. The same level of accuracy is available for $\bar{s}_b^2$ [133], while for $\bar{s}_{s,c}$ [74] the purely bosonic contributions of this order are still missing. Similarly, for the partial widths, $\Gamma(f\overline{f})$, and the hadronic peak cross-section, $\sigma_{\rm had}$, the fermionic two-loop EW corrections are known [134]. Non-factorizable $\mathcal{O}(\alpha\alpha_s)$ corrections to the $Z \to q\bar{q}$ vertex are also available [132]. They add coherently, resulting in a sizable effect and shift $\alpha_s(M_Z)$ when extracted from Z lineshape observables by $\approx +0.0007$. As an example of the precision of the Z-pole observables, the values of $\bar{g}_A^f$ and $\bar{g}_V^f$, $f = e, \mu, \tau, \ell$, extracted from the LEP and SLC lineshape and asymmetry data, are shown in Fig. 10.3, which should be compared with Fig. 10.1. (The two sets of parameters coincide in the SM at tree-level.)

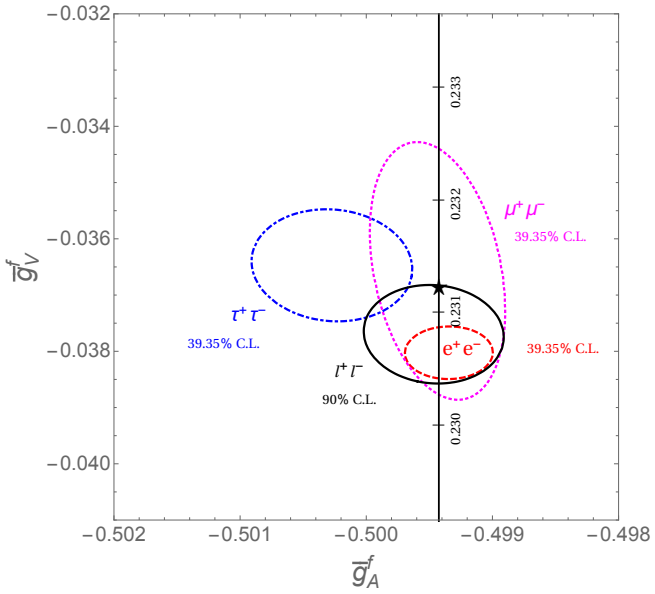

Figure 10.3: 1 σ (39.35% C.L.) contours for the Z-pole observables $\bar{g}_A^f$ and $\bar{g}_V^f$, $f = e, \mu, \tau$ obtained at LEP and SLC [10], compared to the SM expectation as a function of $\hat{s}_Z^2$. (The SM best fit value $\hat{s}_Z^2 = 0.23122$ is also indicated.) Also shown is the 90% CL allowed region in $\bar{g}_{A,V}^\ell$ obtained assuming lepton universality.

As for hadron colliders, the forward-backward asymmetry, A_{FB}, for e^+e^- and $\mu^+\mu^-$ final states (with invariant masses restricted to or dominated by values around M_Z) in $p\bar{p}$ collisions has been measured by the CDF [145] and DØ [146] collaborations, and the values $\overline{s}_\ell^2 = 0.23221 \pm 0.00046$ and $\overline{s}_\ell^2 = 0.23095 \pm 0.00040$ were extracted, respectively. The combination of these measurements yields [147]

$$\overline{s}_\ell^2 = 0.23148 \pm 0.00033 \text{ (Tevatron)}. \tag{10.43}$$

By varying the invariant mass and the scattering angle (and assuming the electron couplings), information on the effective Z couplings to light quarks, $\overline{g}_{V,A}^{u,d}$, could also be obtained [148,149], but with large uncertainties and mutual correlations and not independently of $\overline{s}_\ell^2$ above. Similar analyses have also been reported by the H1 [150] and ZEUS [151] collaborations at HERA and by the LEP collaborations [10]. This kind of measurement is harder in the pp environment due to the difficulty to assign the initial quark and antiquark in the underlying Drell-Yan process to the protons. Nevertheless, measurements of A_{FB} have been reported by the ATLAS [152], CMS [153] and LHCb [154] collaborations (the latter only for the $\mu^+\mu^-$ final state), which obtained $\overline{s}_\ell^2 = 0.2308 \pm 0.0012$, $\overline{s}_\ell^2 = 0.23101 \pm 0.00052$ and $\overline{s}_\ell^2 = 0.23142 \pm 0.00106$, respectively. Assuming that the smallest theoretical uncertainty (± 0.00034 from CMS [153]) is fully correlated among all three experiments, these measurements combine to

$$\overline{s}_\ell^2 = 0.23104 \pm 0.00049 \text{ (LHC)}, \tag{10.44}$$

in perfect agreement with DØ, but lower than the value found by CDF.

10.4.3. *LEP 2* :

LEP 2 [155,156] ran at several energies above the Z pole up to ~ 209 GeV. Measurements were made of a number of observables, including the cross-sections for $e^+e^- \to f\bar{f}$ for $f = q, \mu, \tau$; the differential cross-sections for $f = e, \mu, \tau$; R_q for $q = b, c$; $A_{FB}(f)$ for $f = \mu, \tau, b, c$; W branching ratios; and $\gamma\gamma$, WW, $WW\gamma$, ZZ, single W, and single Z cross-sections. They are in good agreement with the SM predictions, with the exceptions of R_b (2.1 σ low), $A_{FB}(b)$ (1.6 σ low), and the $W \to \tau\nu_\tau$ branching fraction (2.6 σ high).

The Z boson properties are extracted assuming the SM expressions for the γ–Z interference terms. These have also been tested experimentally by performing more general fits [155,157] to the LEP 1 and LEP 2 data. Assuming family universality this approach introduces three additional parameters relative to the standard fit [10], describing the γ–Z interference contribution to the total hadronic and leptonic cross-sections, $j_{\rm had}^{\rm tot}$ and $j_\ell^{\rm tot}$, and to the leptonic forward-backward asymmetry, $j_\ell^{\rm fb}$. *E.g.*,

$$j_{\rm had}^{\rm tot} \sim g_V^\ell g_V^{\rm had} = 0.277 \pm 0.065, \tag{10.45}$$

which is in agreement with the SM expectation [10] of 0.21 ± 0.01. These are valuable tests of the SM; but it should be cautioned that new physics is not expected to be described by this set of parameters, since (i) they do not account for extra interactions beyond the standard weak neutral current, and (ii) the photonic amplitude remains fixed to its SM value.

Strong constraints on anomalous triple and quartic gauge couplings have been obtained at LEP 2 and the Tevatron as described in the Gauge & Higgs Bosons Particle Listings.

10.4.4. *W and Z decays* :

The partial decay widths for gauge bosons to decay into massless fermions $f_1\overline{f}_2$ (the numerical values include the small EW radiative corrections and final state mass effects) are given by

$$\Gamma(W^+ \to e^+\nu_e) = \frac{G_F M_W^3}{6\sqrt{2}\pi} \approx 226.32 \pm 0.04 \text{ MeV}\ , \tag{10.46a}$$

$$\Gamma(W^+ \to u_i\overline{d}_j) = \frac{\mathcal{R}_V^q G_F M_W^3}{6\sqrt{2}\pi} |V_{ij}|^2$$
$$\approx 705.4 \pm 0.3 \text{ MeV } |V_{ij}|^2, \tag{10.46b}$$

$$\Gamma(Z \to f\bar{f}) = \frac{G_F M_Z^3}{6\sqrt{2}\pi} \left[\mathcal{R}_V^f \bar{g}_V^{f2} + \mathcal{R}_A^f \bar{g}_A^{f2}\right]$$
$$\approx \begin{cases} 167.15 \pm 0.01 \text{ MeV } (\nu\overline{\nu}), \\ 83.96 \pm 0.01 \text{ MeV } (e^+e^-), \\ 299.91 \pm 0.18 \text{ MeV } (u\overline{u}), \\ 382.78 \pm 0.13 \text{ MeV } (d\overline{d}), \\ 375.76 \mp 0.16 \text{ MeV } (b\overline{b}). \end{cases} \tag{10.46c}$$

Final-state QED and QCD corrections to the vector and axial-vector form factors are given by

$$\mathcal{R}_{V,A}^f = N_C \left[1 + \frac{3}{4}(Q_f^2 \frac{\alpha(s)}{\pi} + \frac{N_C^2 - 1}{2N_C} \frac{\alpha_s(s)}{\pi}) + \cdots\right], \tag{10.47}$$

where $N_C = 3$ (1) is the color factor for quarks (leptons) and the dots indicate finite fermion mass effects proportional to m_f^2/s which are different for $\mathcal{R}_V^f$ and $\mathcal{R}_A^f$, as well as higher-order QCD

corrections, which are known to $\mathcal{O}(\alpha_s^4)$ [158–160]. These include singlet contributions starting from two-loop order which are large, strongly top quark mass dependent, family universal, and flavor non-universal [161]. Also the $\mathcal{O}(\alpha^2)$ self-energy corrections from Ref. 162 are taken into account.

For the W decay into quarks, Eq. (10.46*b*), only the universal massless part (non-singlet and $m_q = 0$) of the final-state QCD radiator function in $\mathcal{R}_V$ from Eq. (10.47) is used, and the QED corrections are modified. Expressing the widths in terms of $G_F M_{W,Z}^3$ incorporates the largest radiative corrections from the running QED coupling [52,163]. EW corrections to the Z widths are then taken into account through the effective couplings $\overline{g}_{V,A}^{i2}$. Hence, in the on-shell scheme the Z widths are proportional to $\rho_i \sim 1 + \rho_t$. There is additional (negative) quadratic m_t dependence in the $Z \to b\overline{b}$ vertex corrections [164] which causes $\Gamma(b\overline{b})$ to decrease with m_t. The dominant effect is to multiply $\Gamma(b\overline{b})$ by the vertex correction $1 + \delta\rho_{b\overline{b}}$, where $\delta\rho_{b\overline{b}} \sim 10^{-2}(-\frac{1}{2}m_t^2/M_Z^2 + \frac{1}{5})$. In practice, the corrections are included in $\widehat{\rho}_b$ and $\widehat{\kappa}_b$, as discussed in Sec. 10.4.

For three fermion families the total widths are predicted to be

$$\Gamma_Z \approx 2.4942 \pm 0.0008 \text{ GeV}\,, \qquad \Gamma_W \approx 2.0895 \pm 0.0006 \text{ GeV}\,. \tag{10.48}$$

The uncertainties in these predictions are almost entirely induced from the fit error in $\alpha_s(M_Z) = 0.1187 \pm 0.0016$. These predictions are to be compared with the experimental results, $\Gamma_Z = 2.4952 \pm 0.0023$ GeV [10] and $\Gamma_W = 2.085 \pm 0.042$ GeV (see the Gauge & Higgs Boson Particle Listings for more details).

10.5. Precision flavor physics

In addition to cross-sections, asymmetries, parity violation, W and Z decays, there is a large number of experiments and observables testing the flavor structure of the SM. These are addressed elsewhere in this *Review*, and are generally not included in this Section. However, we identify three precision observables with sensitivity to similar types of new physics as the other processes discussed here. The branching fraction of the flavor changing transition $b \to s\gamma$ is of comparatively low precision, but since it is a loop-level process (in the SM) its sensitivity to new physics (and SM parameters, such as heavy quark masses) is enhanced. A discussion can be found in the 2010 edition of this *Review*. The τ-lepton lifetime and leptonic branching ratios are primarily sensitive to α_s and not affected significantly by many types of new physics. However, having an independent and reliable low energy measurement of α_s in a global analysis allows the comparison with the Z lineshape determination of α_s which shifts easily in the presence of new physics contributions. By far the most precise observable discussed here is the anomalous magnetic moment of the muon (the electron magnetic moment is measured to even greater precision and can be used to determine α, but its new physics sensitivity is suppressed by an additional factor of m_e^2/m_μ^2, unless there is a new light degree of freedom such as a dark Z [165] boson). Its combined experimental and theoretical uncertainty is comparable to typical new physics contributions.

The extraction of α_s from the τ lifetime [166] is standing out from other determinations because of a variety of independent reasons: (i) the τ-scale is low, so that upon extrapolation to the Z scale (where it can be compared to the theoretically clean Z lineshape determinations) the α_s error shrinks by about an order of magnitude; (ii) yet, this scale is high enough that perturbation theory and the operator product expansion (OPE) can be applied; (iii) these observables are fully inclusive and thus free of fragmentation and hadronization effects that would have to be modeled or measured; (iv) duality violation (DV) effects are most problematic near the branch cut but there they are suppressed by a double zero at $s = m_\tau^2$; (v) there are data [37,167] to constrain non-perturbative effects both within and breaking the OPE; (vi) a complete four-loop order QCD calculation is available [160]; (vii) large effects associated with the QCD β-function can be re-summed [168] in what has become known as contour improved perturbation theory (CIPT). However, while there is no doubt that CIPT shows faster convergence in the lower (calculable) orders, doubts have been cast on the method by the observation that at least in a specific model [169], which includes the exactly known coefficients and theoretical constraints on the large-order behavior, ordinary fixed order perturbation theory (FOPT) may nevertheless give a better approximation to the full result. We therefore use the expressions [43,159,160,170],

$$\tau_\tau = \hbar \frac{1 - \mathcal{B}_\tau^s}{\Gamma_\tau^e + \Gamma_\tau^\mu + \Gamma_\tau^{ud}} = 290.75 \pm 0.36 \text{ fs}, \tag{10.49}$$

$$\begin{aligned}\Gamma_\tau^{ud} =& \frac{G_F^2 m_\tau^5 |V_{ud}|^2}{64\pi^3} S(m_\tau, M_Z) \left(1 + \frac{3}{5}\frac{m_\tau^2 - m_\mu^2}{M_W^2}\right) \times \\ & [1 + \frac{\alpha_s(m_\tau)}{\pi} + 5.202\,\frac{\alpha_s^2}{\pi^2} + 26.37\,\frac{\alpha_s^3}{\pi^3} + \\ & 127.1\,\frac{\alpha_s^4}{\pi^4} + \frac{\widehat{\alpha}}{\pi}(\frac{85}{24} - \frac{\pi^2}{2}) + \delta_{\rm NP}],\end{aligned} \tag{10.50}$$

and Γ_τ^e and Γ_τ^μ can be taken from Eq. (10.6) with obvious replacements. The relative fraction of decays with $\Delta S = -1$, $\mathcal{B}_\tau^s = 0.0292 \pm 0.0004$, is based on experimental data since the value for the strange quark mass, $\widehat{m}_s(m_\tau)$, is not well known and the QCD expansion proportional to $\widehat{m}_s^2$ converges poorly and cannot be trusted. $S(m_\tau, M_Z) = 1.01907 \pm 0.0003$ is a logarithmically enhanced EW correction factor with higher orders re-summed [171]. $\delta_{\rm NP}$ collects non-perturbative and quark-mass suppressed contributions, including the dimension four, six and eight terms in the OPE, as well as DV effects. One group finds the slightly conflicting values $\delta_{\rm NP} = -0.004 \pm 0.012$ [172] and $\delta_{\rm NP} = 0.020 \pm 0.009$ [173], based on OPAL [37] and ALEPH [167] τ spectral functions, respectively. These can be combined to yield the average $\delta_{\rm NP} = 0.0114 \pm 0.0072$. Another analysis [167] obtains $\delta_{\rm NP} = -0.0064 \pm 0.0013$, based largely on the same data sets (see also Ref. 174). We take the arithmetic mean of both groups with an uncertainty that includes both central values, $\delta_{\rm NP} = 0.003 \pm 0.009$. The dominant uncertainty arises from the truncation of the FOPT series and is conservatively taken as the α_s^4 term (this is re-calculated in each call of the fits, leading to an α_s-dependent and thus asymmetric error) until a better understanding of the numerical differences between FOPT and CIPT has been gained. Our perturbative error covers almost the entire range from using CIPT to assuming that the nearly geometric series in Eq. (10.50) continues to higher orders. The experimental uncertainty in Eq. (10.49) is from the combination of the two leptonic branching ratios with the direct τ_τ. Included are also various smaller uncertainties (± 0.15 fs) from other sources. In total we obtain a $\sim 1.6\%$ determination of $\alpha_s^{(5)}(M_Z) = 0.1184^{+0.0020}_{-0.0018}$, which corresponds to $\alpha_s^{(4)}(m_\tau) = 0.323^{+0.018}_{-0.014}$, and updates the result of Refs. 43 and 175. For more details, see Refs. 172 and 173 where the τ spectral functions themselves and an estimate of the unknown α_s^5 term are used as additional inputs.

The world average of the muon anomalous magnetic moment[‡],

$$a_\mu^{\rm exp} = \frac{g_\mu - 2}{2} = (1165920.91 \pm 0.63) \times 10^{-9}, \tag{10.51}$$

is dominated by the final result of the E821 collaboration at BNL [176]. The QED contribution has been calculated to five loops [177] (fully analytic to three loops [178,179] and semi-analytic to four loops [180]) . The estimated SM EW contribution [181–183],

[‡] In what follows, we summarize the most important aspects of $g_\mu - 2$, and give some details on the evaluation in our fits. For more details see the dedicated contribution on "The Muon Anomalous Magnetic Moment" in this *Review*. There are some numerical differences, which are well understood and arise because internal consistency of the fits requires the calculation of all observables from analytical expressions and common inputs and fit parameters, so that an independent evaluation is necessary for this Section. Note, that in the spirit of a global analysis based on all available information we have chosen here to consider τ decay data, corrected for isospin breaking effects [21], as well.

$a_\mu^{\rm EW} = (1.54 \pm 0.01) \times 10^{-9}$, which includes two-loop [182] and leading three-loop [183] corrections, is at the level of twice the current uncertainty.

The limiting factor in the interpretation of the result are the uncertainties from hadronic contributions. The most recent evaluations obtained $a_\mu^{\rm had,LO} = (69.31 \pm 0.34) \times 10^{-9}$ [20], $a_\mu^{\rm had,LO} = (68.81 \pm 0.41) \times 10^{-9}$ [184], and $a_\mu^{\rm had,LO} = (69.33 \pm 0.25) \times 10^{-9}$ [35] for the leading-order hadronic effects. These are mainly based on data from $e^+e^- \to$ hadrons, including new data from BaBar and VEPP-2M (see *e.g.* Ref. 20 for a list of references). Our analysis combines the e^+e^- and τ-decay data analysis of Ref. 20 for contributions up to $\sqrt{s} = 2$ GeV, $a_\mu^{\rm had,LO}(2\ {\rm GeV}) = (64.40 \pm 0.30) \times 10^{-9}$, with analytical PQCD expressions [179] beyond 2 GeV. There are promising first results for the determination of $a_\mu^{\rm had,LO}$ from lattice QCD calculations [185], although more work will be needed to reliably control systematic uncertainties to a level comparable with e^+e^- data.

An additional uncertainty is induced by the hadronic three-loop light-by-light scattering contribution. Several recent independent model calculations yield compatible results: $a_\mu^{\rm LBLS}(\alpha^3) = (+1.36 \pm 0.25) \times 10^{-9}$ [186], $a_\mu^{\rm LBLS}(\alpha^3) = +1.37^{+0.15}_{-0.27} \times 10^{-9}$ [187], $a_\mu^{\rm LBLS}(\alpha^3) = (+1.05 \pm 0.26) \times 10^{-9}$ [188], and $a_\mu^{\rm LBLS}(\alpha^3) = (+1.03 \pm 0.29) \times 10^{-9}$ [184]. The sign of this effect is opposite [189] to the one quoted in the 2002 edition of this *Review*, and its magnitude is larger than previous evaluations [189,190]. There is also an upper bound $a_\mu^{\rm LBLS}(\alpha^3) < 1.59 \times 10^{-9}$ [187] but this requires an *ad hoc* assumption, too. Partial results (diagrams with several disconnected quark loops still need to be considered) from lattice simulations are promising, with a moderate (about 25%) statistical uncertainty [191]. Various sources of systematic uncertainties are currently being investigated. For the fits, we take the result from Ref. 184, shifted by 2×10^{-11} to account for the more accurate charm quark treatment of Ref. 187, and with increased error to cover all recent evaluations, resulting in $a_\mu^{\rm LBLS}(\alpha^3) = (+1.05 \pm 0.33) \times 10^{-9}$.

Other hadronic effects at three-loop order [192] and four-loop order [193] contribute $a_\mu^{\rm had,NLO} = (-1.01 \pm 0.01) \times 10^{-9}$ (scaled from and anti-correlated with $a_\mu^{\rm had,LO}$) and $a_\mu^{\rm had,NNLO} = (0.124 \pm 0.001) \times 10^{-9}$, respectively. Correlations with the two-loop hadronic contribution and with $\Delta\alpha(M_Z)$ (see Sec. 10.2) were considered in Ref. 179. The contributions with a hadronic LBLS subgraph have been estimated in Ref. 194, with the result $a_\mu^{\rm LBLS}(\alpha^4) = (0.03 \pm 0.02) \times 10^{-9}$.

Altogether, the SM prediction is

$$a_\mu^{\rm theory} = (1165918.36 \pm 0.44) \times 10^{-9}\ , \qquad (10.52)$$

where the error is from the hadronic uncertainties excluding parametric ones such as from α_s and the heavy quark masses. We evaluate the correlation of the total (experimental plus theoretical) uncertainty in a_μ with $\Delta\alpha(M_Z)$ to amount to 22%. The overall 3.3 σ discrepancy between the experimental and theoretical a_μ values could be due to fluctuations (the E821 result is statistics dominated) or underestimates of the theoretical uncertainties. On the other hand, the deviation could also arise from physics beyond the SM, such as supersymmetric models with large $\tan\beta$ and moderately light superparticle masses [195], or a dark Z boson [165].

10.6. Global fit results

In this section we present the results of global fits to the experimental data discussed in Sec. 10.3–Sec. 10.5. For earlier analyses see Refs. [10,96,196]

The values for m_t [44–47], M_W [155,197,198], Γ_W [155,199], ν-lepton scattering [78–81], the weak charges of the electron [100], the proton [106,107], cesium [110,111] and thallium [112], the weak mixing angle extracted from eDIS [92], the muon anomalous magnetic moment [176], and the τ lifetime are listed in Table 10.4. M_H is our average of the LHC combination from Run 1 [200], $M_H = 125.09 \pm 0.21_{\rm\,stat.} \pm 0.11_{\rm\,syst.}$ GeV, with $M_H = 124.98 \pm 0.19_{\rm\,stat.} \pm 0.21_{\rm\,syst.}$ GeV from ATLAS [201] and $M_H = 125.26 \pm 0.29_{\rm\,stat.} \pm 0.08_{\rm\,syst.}$ GeV from CMS [202] at Run 2, where we conservatively treated the smallest systematic error as common among the three determinations. Likewise, the principal Z pole observables can be found in Table 10.5, where the LEP 1 averages of the ALEPH, DELPHI, L3 and OPAL results include common systematic errors and correlations [10]. The heavy flavor results of LEP 1 and SLD are based on common inputs and correlated, as well [10]. Note that the values of $\Gamma(\ell^+\ell^-)$, Γ(had), and Γ(inv) are not independent of Γ_Z, the R_ℓ, and $\sigma_{\rm had}$ and that the SM errors in those latter are largely dominated by the uncertainty in α_s. Also shown in both tables are the SM predictions for the values of M_Z, M_H, $\alpha_s(M_Z)$, $\Delta\alpha^{(3)}_{\rm had}$ and the heavy quark masses shown in Table 10.6. The predictions result from a global least-square (χ^2) fit to all data using the minimization package MINUIT [203] and the EW library GAPP [22]. In most cases, we treat all input errors (the uncertainties of the values) as Gaussian. The reason is not that we assume that theoretical and systematic errors are intrinsically bell-shaped (which they are not) but because in most cases the input errors are either dominated by the statistical components or they are combinations of many different (including statistical) error sources, which should yield approximately Gaussian *combined* errors by the large number theorem. An exception is the theory dominated error on the τ lifetime, which we recalculate in each χ^2-function call since it depends itself on α_s. Sizes and shapes of the output errors (the uncertainties of the predictions and the SM fit parameters) are fully determined by the fit, and 1 σ errors are defined to correspond to $\Delta\chi^2 = \chi^2 - \chi^2_{\rm min} = 1$, and do not necessarily correspond to the 68.3% probability range or the 39.3% probability contour (for 2 parameters).

The agreement is generally very good. Despite the few discrepancies discussed in the following, the fit describes the data well, with a χ^2/d.o.f. = 47.0/41. The probability of a larger χ^2 is 24%. Only the final result for $g_\mu - 2$ from BNL is currently showing a larger (3.3 σ)

Table 10.4: Principal non-Z pole observables, compared with the SM best fit predictions. The first M_W and Γ_W values are from the Tevatron [197,199] and the second ones from LEP 2 [155]. The third M_W is from ATLAS [198]. The value of m_t differs from the one in the Particle Listings since it includes recent preliminary results. The world averages for $g^{\nu e}_{V,A}$ are dominated by the CHARM II [79] results, $g^{\nu e}_V = -0.035 \pm 0.017$ and $g^{\nu e}_A = -0.503 \pm 0.017$. The errors are the total (experimental plus theoretical) uncertainties. The τ_τ value is the τ lifetime world average computed by combining the direct measurements with values derived from the leptonic branching ratios [43]; in this case, the theory uncertainty is included in the SM prediction. In all other SM predictions, the uncertainty is from M_Z, M_H, m_t, m_b, m_c, $\widehat{\alpha}(M_Z)$, and α_s, and their correlations have been accounted for. The column denoted Pull gives the standard deviations.

Quantity	Value	Standard Model	Pull
m_t [GeV]	172.74 ± 0.46	172.96 ± 0.45	-0.5
M_W [GeV]	80.387 ± 0.016	80.358 ± 0.004	1.8
	80.376 ± 0.033		0.6
	80.370 ± 0.019		0.6
Γ_W [GeV]	2.046 ± 0.049	2.089 ± 0.001	-0.9
	2.195 ± 0.083		1.3
M_H [GeV]	125.14 ± 0.15	125.14 ± 0.15	0.0
$g^{\nu e}_V$	-0.040 ± 0.015	-0.0398 ± 0.0001	0.0
$g^{\nu e}_A$	-0.507 ± 0.014	-0.5063	0.0
$Q_W(e)$	-0.0403 ± 0.0053	-0.0476 ± 0.0002	1.4
$Q_W(p)$	0.0719 ± 0.0045	0.0711 ± 0.0002	0.2
Q_W(Cs)	-72.62 ± 0.43	-73.23 ± 0.01	1.4
Q_W(Tl)	-116.4 ± 3.6	-116.87 ± 0.02	0.1
$\widehat{s}^2_Z$(eDIS)	0.2299 ± 0.0043	0.23122 ± 0.00003	-0.3
τ_τ [fs]	290.75 ± 0.36	290.39 ± 2.17	0.1
$\frac{1}{2}(g_\mu - 2 - \frac{\alpha}{\pi})$	$(4511.18 \pm 0.77) \times 10^{-9}$	$(4508.63 \pm 0.03) \times 10^{-9}$	3.3

Table 10.5: Principal Z pole observables and their SM predictions (*cf.* Table 10.4). The first $\bar{s}^2_\ell$ is the effective weak mixing angle extracted from the hadronic charge asymmetry, the second is the combined value from the Tevatron [147], and the third from the LHC [152–154]. The values of A_e are (i) from A_{LR} for hadronic final states [140]; (ii) from A_{LR} for leptonic final states and from polarized Bhabba scattering [142]; and (iii) from the angular distribution of the τ polarization at LEP 1. The A_τ values are from SLD and the total τ polarization, respectively.

Quantity	Value	Standard Model	Pull
M_Z [GeV]	91.1876 ± 0.0021	91.1884 ± 0.0020	-0.4
Γ_Z [GeV]	2.4952 ± 0.0023	2.4942 ± 0.0008	0.4
Γ(had) [GeV]	1.7444 ± 0.0020	1.7411 ± 0.0008	—
Γ(inv) [MeV]	499.0 ± 1.5	501.44 ± 0.04	—
$\Gamma(\ell^+\ell^-)$ [MeV]	83.984 ± 0.086	83.959 ± 0.008	—
$\sigma_{\rm had}$[nb]	41.541 ± 0.037	41.481 ± 0.008	1.6
R_e	20.804 ± 0.050	20.737 ± 0.010	1.3
R_μ	20.785 ± 0.033	20.737 ± 0.010	1.4
R_τ	20.764 ± 0.045	20.782 ± 0.010	-0.4
R_b	0.21629 ± 0.00066	0.21582 ± 0.00002	0.7
R_c	0.1721 ± 0.0030	0.17221 ± 0.00003	0.0
$A_{FB}^{(0,e)}$	0.0145 ± 0.0025	0.01618 ± 0.00006	-0.7
$A_{FB}^{(0,\mu)}$	0.0169 ± 0.0013		0.6
$A_{FB}^{(0,\tau)}$	0.0188 ± 0.0017		1.5
$A_{FB}^{(0,b)}$	0.0992 ± 0.0016	0.1030 ± 0.0002	-2.3
$A_{FB}^{(0,c)}$	0.0707 ± 0.0035	0.0735 ± 0.0001	-0.8
$A_{FB}^{(0,s)}$	0.0976 ± 0.0114	0.1031 ± 0.0002	-0.5
$\bar{s}^2_\ell$	0.2324 ± 0.0012	0.23154 ± 0.00003	0.7
	0.23148 ± 0.00033		-0.2
	0.23104 ± 0.00049		-1.0
A_e	0.15138 ± 0.00216	0.1469 ± 0.0003	2.1
	0.1544 ± 0.0060		1.3
	0.1498 ± 0.0049		0.6
A_μ	0.142 ± 0.015		-0.3
A_τ	0.136 ± 0.015		-0.7
	0.1439 ± 0.0043		-0.7
A_b	0.923 ± 0.020	0.9347	-0.6
A_c	0.670 ± 0.027	0.6677 ± 0.0001	0.1
A_s	0.895 ± 0.091	0.9356	-0.4

conflict. In addition, $A_{FB}^{(0,b)}$ from LEP 1 and A^0_{LR} (SLD) from hadronic final states deviate at the 2 σ level. g^2_L from NuTeV is nominally in conflict with the SM, as well, but the precise status is still unresolved (see Sec. 10.3). We also recall that the values of $\bar{s}^2_\ell$ at CDF and of m_t at DØ are somewhat higher than the determinations from other experiments at hadron colliders, but this is not reflected in the overall χ^2 of the fit because Tevatron combinations are used as inputs.

A_b can be extracted from $A_{FB}^{(0,b)}$ when $A_e = 0.1501 \pm 0.0016$ is taken from a fit to leptonic asymmetries (using lepton universality). The result, $A_b = 0.881 \pm 0.017$, is 3.1 σ below the SM prediction[§] and also 1.6 σ below $A_b = 0.923 \pm 0.020$ obtained from $A_{LR}^{FB}(b)$ at SLD. Thus, it appears that at least some of the problem in A_b is due to a statistical fluctuation or other experimental effect in one of the asymmetries. Note, however, that the uncertainty in $A_{FB}^{(0,b)}$ is strongly statistics dominated. The combined value, $A_b = 0.899 \pm 0.013$ deviates by 2.8 σ.

[§] Alternatively, one can use $A_\ell = 0.1481 \pm 0.0027$, which is from LEP 1 alone and in excellent agreement with the SM, and obtain $A_b = 0.893 \pm 0.022$ which is 1.9 σ low. This illustrates that some of the discrepancy is related to the one in A_{LR}.

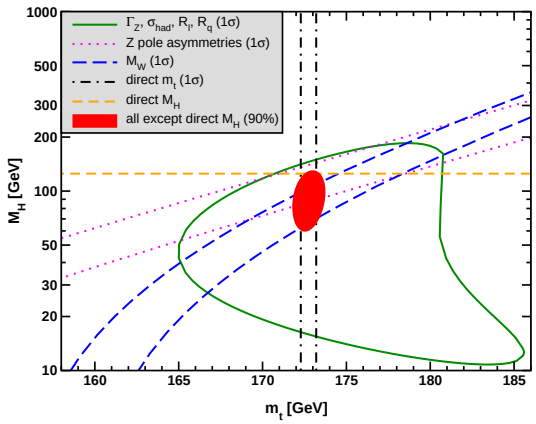

Figure 10.4: Fit result and one-standard-deviation (39.35% for the closed contours and 68% for the others) uncertainties in M_H as a function of m_t for various inputs, and the 90% CL region ($\Delta\chi^2 = 4.605$) allowed by all data. $\alpha_s(M_Z) = 0.1187$ is assumed except for the fits including the Z lineshape. The width of the horizontal dashed (yellow) band is not visible on the scale of the plot.

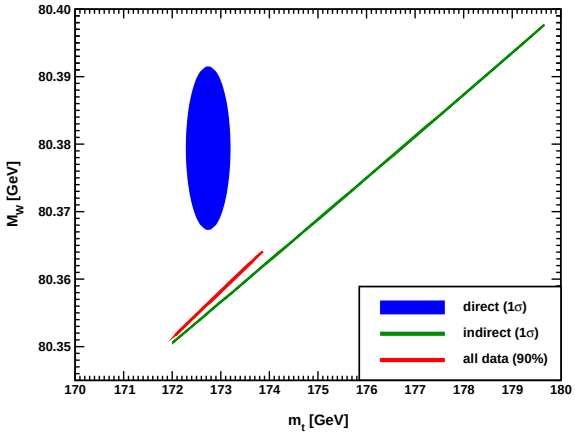

Figure 10.5: One-standard-deviation (39.35%) region in M_W as a function of m_t for the direct and indirect data, and the 90% CL region ($\Delta\chi^2 = 4.605$) allowed by all data.

The left-right asymmetry, $A^0_{LR} = 0.15138 \pm 0.00216$ [140], based on all hadronic data from 1992–1998 differs 2.1 σ from the SM expectation of 0.1469 ± 0.0003. The combined value of $A_\ell = 0.1513 \pm 0.0021$ from SLD (using lepton-family universality and including correlations) is also 2.1 σ above the SM prediction; but there is experimental agreement between this SLD value and the LEP 1 value, $A_\ell = 0.1481 \pm 0.0027$, obtained from a fit to $A_{FB}^{(0,\ell)}$, $A_e(\mathcal{P}_\tau)$, and $A_\tau(\mathcal{P}_\tau)$, again assuming universality.

The observables in Table 10.4 and Table 10.5, as well as some other less precise observables, are used in the global fits described below. In all fits, the errors include full statistical, systematic, and theoretical uncertainties. The correlations on the LEP 1 lineshape and τ polarization, the LEP/SLD heavy flavor observables, the SLD lepton asymmetries, and the ν-e scattering observables, are included. The theoretical correlations between $\Delta\alpha^{(5)}_{\rm had}$ and $g_\mu - 2$, and between the W boson mass extractions from ATLAS and the Tevatron, are also accounted for.

The electroweak data allow a simultaneous determination of M_Z, M_H, m_t, and the strong coupling $\alpha_s(M_Z)$. ($\widehat{m}_c$, $\widehat{m}_b$, and $\Delta\alpha^{(3)}_{\rm had}$ are also allowed to float in the fits, subject to the theoretical constraints [19,43] described in Sec. 10.2. These are correlated with α_s.) α_s is determined mainly from R_ℓ, Γ_Z, $\sigma_{\rm had}$, and τ_τ.

Table 10.6: Principal SM fit result including mutual correlations (all masses in GeV).

M_Z	91.1884 ± 0.0020	1.00	−0.06	0.00	0.00	0.02	0.03	0.00
$\widehat{m}_t(\widehat{m}_t)$	163.28 ± 0.44	−0.06	1.00	0.00	−0.13	−0.28	0.03	0.00
$\widehat{m}_b(\widehat{m}_b)$	4.180 ± 0.021	0.00	0.00	1.00	0.00	0.00	0.00	0.00
$\widehat{m}_c(\widehat{m}_c)$	1.275 ± 0.009	0.00	−0.13	0.00	1.00	0.45	0.00	0.00
$\alpha_s(M_Z)$	0.1187 ± 0.0016	0.02	−0.28	0.00	0.45	1.00	−0.02	0.00
$\Delta\alpha^{(3)}_{\rm had}(2\ {\rm GeV})$	0.00590 ± 0.00005	0.03	0.03	0.00	0.00	−0.02	1.00	0.00
M_H	125.14 ± 0.15	0.00	0.00	0.00	0.00	0.00	0.00	1.00

Table 10.7: Values of $\widehat{s}^2_Z$, s^2_W, α_s, m_t and M_H [both in GeV] for various data sets. In the fit to the LHC (Tevatron) data the α_s constraint is from the $t\bar{t}$ production [204] (inclusive jet [205]) cross-section.

Data	$\widehat{s}^2_Z$	s^2_W	$\alpha_s(M_Z)$	m_t	M_H
All data	0.23122(3)	0.22332(7)	0.1187(16)	173.0 ± 0.4	125
All data except M_H	0.23107(9)	0.22310(19)	0.1190(16)	172.8 ± 0.5	$90^{+\ 17}_{-\ 16}$
All data except M_Z	0.23113(6)	0.22336(8)	0.1187(16)	172.8 ± 0.5	125
All data except M_W	0.23124(3)	0.22347(7)	0.1191(16)	172.9 ± 0.5	125
All data except m_t	0.23112(6)	0.22304(21)	0.1191(16)	176.4 ± 1.8	125
M_H, M_Z, Γ_Z, m_t	0.23125(7)	0.22351(13)	0.1209(45)	172.7 ± 0.5	125
LHC	0.23110(11)	0.22332(12)	0.1143(24)	172.4 ± 0.5	125
Tevatron + M_Z	0.23102(13)	0.22295(30)	0.1160(45)	174.3 ± 0.7	$100^{+\ 31}_{-\ 26}$
LEP	0.23138(17)	0.22343(47)	0.1221(31)	182 ± 11	274^{+376}_{-152}
SLD + M_Z, Γ_Z, m_t	0.23064(28)	0.22228(54)	0.1182(47)	172.7 ± 0.5	$38^{+\ 30}_{-\ 21}$
$A^{(b,c)}_{FB}$, M_Z, Γ_Z, m_t	0.23190(29)	0.22503(69)	0.1278(50)	172.7 ± 0.5	348^{+187}_{-124}
$M_{W,Z}$, $\Gamma_{W,Z}$, m_t	0.23103(12)	0.22302(25)	0.1192(42)	172.7 ± 0.5	$84^{+\ 22}_{-\ 19}$
low energy + $M_{H,Z}$	0.23176(94)	0.2254(35)	0.1185(19)	156 ± 29	125

The global fit to all data, including the hadron collider average $m_t = 172.74 \pm 0.46$ GeV, yields the result in Table 10.6 (the $\overline{\rm MS}$ top quark mass given there corresponds to $m_t = 172.96 \pm 0.45$ GeV). The weak mixing angle, see Table 10.2, is determined to

$$\widehat{s}^2_Z = 0.23122 \pm 0.00003, \qquad s^2_W = 0.22343 \pm 0.00007,$$

while the corresponding effective angle is $\overline{s}^2_\ell = 0.23154 \pm 0.00003$.

Removing the kinematic constraint on M_H from LHC gives the loop-level determination from the precision data,

$$M_H = 90^{+17}_{-16}\ {\rm GeV}\ , \tag{10.53}$$

which is 1.9 σ below the value in Table 10.4. The latter is also slightly outside the 90% central confidence range,

$$65\ {\rm GeV} < M_H < 120\ {\rm GeV}\ . \tag{10.54}$$

This is mostly a reflection of the Tevatron determination of M_W, which is 1.8 σ higher than the SM best fit value in Table 10.4. This is illustrated in Fig. 10.4 where one sees that the precision data together with M_H from the LHC prefer that m_t is closer to the upper end of its 1σ allowed range. Conversely, one can remove the direct M_W and Γ_W constraints from the fits and use $M_H = 125.14 \pm 0.15$ GeV to obtain $M_W = 80.355 \pm 0.004$ GeV. This is 2.0 σ below the world average, $M_W = 80.379 \pm 0.012$ GeV.

Finally, one can carry out a fit without including the constraint, $m_t = 172.74 \pm 0.46$ GeV, from the hadron colliders. One obtains $m_t = 176.4 \pm 1.8$ GeV, which is 2.0 σ higher than the direct Tevatron/LHC average. (The indirect prediction is for the $\overline{\rm MS}$ mass, $\widehat{m}_t(\widehat{m}_t) = 166.5 \pm 1.7$ GeV, which is in the end converted to the pole mass.) The situation is summarized in Fig. 10.5 showing the 1 σ contours in the M_W-m_t plane from the direct and indirect determinations, as well as the combined 90% CL region.

In view of these tensions it is instructive to study the effect of doubling the uncertainty in $\Delta\alpha^{(3)}_{\rm had}(2\ {\rm GeV}) = (58.71 \pm 0.50) \times 10^{-4}$ (see Sec. 10.2) on the loop-level determination of the Higgs boson mass. The result, $M_H = 88^{+18}_{-15}$ GeV, deviates even slightly *more* (2.0 σ) than Eq. (10.53), and demonstrates that the uncertainty in $\Delta\alpha_{\rm had}$ is currently of only secondary importance. Note also that a shift of $\pm 10^{-4}$ in $\Delta\alpha^{(3)}_{\rm had}(2\ {\rm GeV})$ corresponds to a shift of ∓ 4.5 GeV in M_H. The hadronic contribution to $\alpha(M_Z)$ is correlated with $g_\mu - 2$ (see Sec. 10.5). The measurement of the latter is higher than the SM prediction, and its inclusion in the fit favors a larger $\alpha(M_Z)$ and a lower M_H from the precision data (currently by 1.7 GeV).

The weak mixing angle can be determined from Z pole observables, M_W, and from a variety of neutral-current processes spanning a very wide Q^2 range. The results (for the older low energy neutral-current data see Refs. 96 and 196, as well as earlier editions of this *Review*) shown in Table 10.7 are in reasonable agreement with each other, indicating the quantitative success of the SM. The largest discrepancy

is the value $\widehat{s}^2_Z = 0.23190 \pm 0.00029$ from the forward-backward asymmetries into bottom and charm quarks, which is 2.3 σ above the value 0.23122 ± 0.00003 from the global fit to all data (see Table 10.5). Similarly, $\widehat{s}^2_Z = 0.23064 \pm 0.00028$ from the SLD asymmetries (in both cases when combined with M_Z) is 2.1 σ low.

Table 10.8: Values of the model-independent neutral-current parameters, compared with the SM predictions. There is a second $g^{\nu e}_{LV,LA}$ solution, given approximately by $g^{\nu e}_{LV} \leftrightarrow g^{\nu e}_{LA}$, which is eliminated by e^+e^- data under the assumption that the neutral current is dominated by the exchange of a single Z boson. In the SM predictions, the parametric uncertainties from M_Z, M_H, m_t, m_b, m_c, $\widehat{\alpha}(M_Z)$, and α_s are negligible.

Quantity	Experimental Value	Standard Model	Correlation	
$g^{\nu e}_{LV}$	-0.040 ± 0.015	-0.0398		-0.05
$g^{\nu e}_{LA}$	-0.507 ± 0.014	-0.5063		
$g^{eu}_{AV} + 2\, g^{ed}_{AV}$	0.4914 ± 0.0031	0.4950	-0.88	0.19
$2\, g^{eu}_{AV} - \ g^{ed}_{AV}$	-0.7148 ± 0.0068	-0.7194		-0.22
$2\, g^{eu}_{VA} - \ g^{ed}_{VA}$	-0.13 ± 0.06	-0.0954		
g^{ee}_{VA}	0.0190 ± 0.0027	0.0226		

The extracted Z pole value of $\alpha_s(M_Z)$ is based on a formula with negligible theoretical uncertainty if one assumes the exact validity of the SM. One should keep in mind, however, that this value, $\alpha_s(M_Z) = 0.1203 \pm 0.0028$, is very sensitive to certain types of new physics such as non-universal vertex corrections. In contrast, the value derived from τ decays, $\alpha_s(M_Z) = 0.1184^{+0.0020}_{-0.0018}$, is theory dominated but less sensitive to new physics. The two values are in reasonable agreement with each other. They are also in good agreement with the averages from jet-event shapes in e^+e^- annihilation (0.1169 ± 0.0034) and lattice simulations (0.1188 ± 0.0011), whereas the DIS average (0.1156 ± 0.0021) is somewhat lower than the Z pole value. For more details, other determinations, and references, see Section 9 on "Quantum Chromodynamics" in this *Review*. In addition, there is a detailed analysis of inclusive cross section measurements for top quark pair production at hadron colliders [206], which yields $\alpha_s = 0.1170^{+0.0034}_{-0.0032}$ after adjustment of the result to correspond to the top quark mass in Eq. (10.9).

Using $\alpha(M_Z)$ and $\widehat{s}^2_Z$ as inputs, one can predict $\alpha_s(M_Z)$ assuming grand unification. One finds [207] $\alpha_s(M_Z) = 0.130 \pm 0.001 \pm 0.01$ for the simplest theories based on the minimal supersymmetric extension of the SM, where the first (second) uncertainty is from the inputs (thresholds). This is slightly larger, but consistent with $\alpha_s(M_Z) = 0.1187 \pm 0.0016$ from our fit, as well as with most other determinations. Non-supersymmetric unified theories predict the low value $\alpha_s(M_Z) = 0.073 \pm 0.001 \pm 0.001$. See also the note on "Supersymmetry" in the Searches Particle Listings.

Most of the parameters relevant to ν-hadron, ν-e, e-hadron, and $e^-e^\pm$ processes are determined uniquely and precisely from the data in "model-independent" fits (*i.e.*, fits which allow for an arbitrary EW gauge theory). The values for the parameters defined in Eqs. (10.15)–(10.18) are given in Table 10.8 along with the predictions of the SM. The agreement is very good. (The ν-hadron results including the original NuTeV data can be found in the 2006 edition of this *Review*, and fits with modified NuTeV constraints in the 2008 and 2010 editions.) The off Z pole e^+e^- results are difficult to present in a model-independent way because Z propagator effects are non-negligible at TRISTAN, PETRA, PEP, and LEP 2 energies. However, assuming e-μ-τ universality, the low energy lepton asymmetries imply [137] $4\,(g^e_A)^2 = 0.99 \pm 0.05$, in good agreement with the SM prediction $\simeq 1$.

10.7. Constraints on new physics

The masses and decay properties of the electroweak bosons and low energy data can be used to search for and set limits on deviations from the SM. We will mainly discuss the effects of exotic particles (with heavy masses $M_{\rm new} \gg M_Z$ in an expansion in $M_Z/M_{\rm new}$) on the gauge boson self-energies. (Brief remarks are made on new physics which is not of this type.) Most of the effects on precision measurements can be described by three gauge self-energy parameters S, T, and U. We will define these, as well as the related parameters ρ_0, ϵ_i, and $\widehat{\epsilon}_i$, to arise from new physics only. In other words, they are equal to zero ($\rho_0 = 1$) exactly in the SM, and do not include any (loop induced) contributions that depend on m_t or M_H, which are treated separately. Our treatment differs from most of the original papers.

The dominant effect of many extensions of the SM can be described by the ρ_0 parameter,

$$\rho_0 \equiv \frac{M_W^2}{M_Z^2\, \widehat{c}^{\,2}_Z\, \widehat{\rho}}\ , \tag{10.55}$$

which describes new sources of SU(2) breaking that cannot be accounted for by the SM Higgs doublet or m_t effects. $\widehat{\rho}$ is calculated as in Eq. (10.12) assuming the validity of the SM. In the presence of $\rho_0 \neq 1$, Eq. (10.55) generalizes the second Eq. (10.12) while the first remains unchanged. Provided that the new physics which yields $\rho_0 \neq 1$ is a small perturbation which does not significantly affect other radiative corrections, ρ_0 can be regarded as a phenomenological parameter which multiplies G_F in Eqs. (10.15)–(10.18), (10.32), and Γ_Z in Eq. (10.46*c*). There are enough data to determine ρ_0, M_H, m_t, and α_s, simultaneously. From the global fit,

$$\rho_0 = 1.00039 \pm 0.00019\ , \tag{10.56}$$

$$\alpha_s(M_Z) = 0.1189 \pm 0.0016\ , \tag{10.57}$$

where as before the uncertainty is from the experimental inputs and does not include the presumably small but difficult to quantify error from unknown higher-order electroweak corrections. The result in Eq. (10.56) is 2.0 σ above the SM expectation, $\rho_0 = 1$. It can be used to constrain higher-dimensional Higgs representations to have vacuum expectation values of less than a few percent of those of the doublets. Indeed, the relation between M_W and M_Z is modified if there are Higgs multiplets with weak isospin $> 1/2$ with significant vacuum expectation values. For a general (charge-conserving) Higgs structure,

$$\rho_0 = \frac{\sum_i [t(i)(t(i)+1) - t_3(i)^2]|v_i|^2}{2\sum_i t_3(i)^2 |v_i|^2}, \tag{10.58}$$

where v_i is the expectation value of the neutral component of a Higgs multiplet with weak isospin $t(i)$ and third component $t_3(i)$. In order to calculate to higher orders in such theories one must define a set of four fundamental renormalized parameters which one may conveniently choose to be α, G_F, M_Z, and M_W, since M_W and M_Z are directly measurable. Then $\widehat{s}^2_Z$ and ρ_0 can be considered dependent parameters.

Eq. (10.56) can also be used to constrain other types of new physics. For example, non-degenerate multiplets of heavy fermions or scalars break the vector part of weak SU(2) and lead to a decrease in the value of M_Z/M_W. Each non-degenerate SU(2) doublet $\binom{f_1}{f_2}$ yields a positive contribution to ρ_0 [208] of

$$\frac{C\, G_F}{8\sqrt{2}\pi^2} \Delta m^2, \tag{10.59}$$

where

$$\Delta m^2 \equiv m_1^2 + m_2^2 - \frac{4m_1^2 m_2^2}{m_1^2 - m_2^2} \ln \frac{m_1}{m_2} \geq (m_1 - m_2)^2, \tag{10.60}$$

and $C = 1$ (3) for color singlets (triplets). Eq. (10.56) taken together with Eq. (10.59) implies the following constraint on the mass splitting at the 90% CL,

$$(16\ \text{GeV})^2 < \sum_i \frac{C_i}{3} \Delta m_i^2 < (48\ \text{GeV})^2, \tag{10.61}$$

where the sum runs over all new-physics doublets, for example fourth-family quarks or leptons, $\binom{t'}{b'}$ or $\binom{\nu'}{\ell'-}$, vector-like fermion doublets (which contribute to the sum in Eq. (10.61) with an extra factor of 2), and scalar doublets such as $\binom{\tilde{t}}{\tilde{b}}$ in Supersymmetry (in the absence of L–R mixing).

Non-degenerate multiplets usually imply $\rho_0 > 1$. Similarly, heavy Z' bosons decrease the prediction for M_Z due to mixing and generally lead to $\rho_0 > 1$ [209]. On the other hand, additional Higgs doublets which participate in spontaneous symmetry breaking [210] or heavy lepton doublets involving Majorana neutrinos [211], both of which have more complicated expressions, as well as the vacuum expectation values of Higgs triplets or higher-dimensional representations can contribute to ρ_0 with either sign. Allowing for the presence of heavy degenerate chiral multiplets (the S parameter, to be discussed below) affects the determination of ρ_0 from the data, at present leading to a larger value.

A number of authors [212–217] have considered the general effects on neutral-current and Z and W boson observables of various types of heavy (*i.e.*, $M_{\rm new} \gg M_Z$) physics which contribute to the W and Z self-energies but which do not have any direct coupling to the ordinary fermions. In addition to non-degenerate multiplets, which break the vector part of weak SU(2), these include heavy degenerate multiplets of chiral fermions which break the axial generators.

Such effects can be described by just three parameters, S, T, and U, at the (EW) one-loop level. (Three additional parameters are needed if the new physics scale is comparable to M_Z [218]. Further generalizations, including effects relevant to LEP 2, are described in Ref. 219.) T is proportional to the difference between the W and Z self-energies at $Q^2 = 0$ (*i.e.*, vector SU(2)-breaking), while S ($S+U$) is associated with the difference between the Z (W) self-energy at $Q^2 = M^2_{Z,W}$ and $Q^2 = 0$ (axial SU(2)-breaking). Denoting the contributions of new physics to the various self-energies by $\Pi^{\rm new}_{ij}$, we have

$$\widehat{\alpha}(M_Z)T \equiv \frac{\Pi^{\rm new}_{WW}(0)}{M^2_W} - \frac{\Pi^{\rm new}_{ZZ}(0)}{M^2_Z} \ , \tag{10.62a}$$

$$\frac{\widehat{\alpha}(M_Z)}{4\,\widehat{s}^2_Z\widehat{c}^2_Z}S \equiv \frac{\Pi^{\rm new}_{ZZ}(M^2_Z) - \Pi^{\rm new}_{ZZ}(0)}{M^2_Z} - \frac{\widehat{c}^2_Z - \widehat{s}^2_Z}{\widehat{c}_Z\widehat{s}_Z}\frac{\Pi^{\rm new}_{Z\gamma}(M^2_Z)}{M^2_Z} - \frac{\Pi^{\rm new}_{\gamma\gamma}(M^2_Z)}{M^2_Z} \ , \tag{10.62b}$$

$$\frac{\widehat{\alpha}(M_Z)}{4\,\widehat{s}^2_Z}(S+U) \equiv \frac{\Pi^{\rm new}_{WW}(M^2_W) - \Pi^{\rm new}_{WW}(0)}{M^2_W} - \frac{\widehat{c}_Z}{\widehat{s}_Z}\frac{\Pi^{\rm new}_{Z\gamma}(M^2_Z)}{M^2_Z} - \frac{\Pi^{\rm new}_{\gamma\gamma}(M^2_Z)}{M^2_Z} \ . \tag{10.62c}$$

S, T, and U are defined with a factor proportional to $\widehat{\alpha}$ removed, so that they are expected to be of order unity in the presence of new physics. In the $\overline{\rm MS}$ scheme as defined in Ref. 53, the last two terms in Eqs. (10.62b) and (10.62c) can be omitted (as was done in some earlier editions of this *Review*). These three parameters are related to other parameters (S_i, h_i, $\widehat{\epsilon}_i$) defined in Refs. [53,213,214] by

$$\begin{aligned} T &= h_V = \widehat{\epsilon}_1/\widehat{\alpha}(M_Z), \\ S &= h_{AZ} = S_Z = 4\,\widehat{s}^2_Z\,\widehat{\epsilon}_3/\widehat{\alpha}(M_Z), \\ U &= h_{AW} - h_{AZ} = S_W - S_Z \\ &= -4\,\widehat{s}^2_Z\,\widehat{\epsilon}_2/\widehat{\alpha}(M_Z). \end{aligned} \tag{10.63}$$

A heavy non-degenerate multiplet of fermions or scalars contributes positively to Tas

$$\rho_0 - 1 = \frac{1}{1 - \widehat{\alpha}(M_Z)T} - 1 \simeq \widehat{\alpha}(M_Z)T, \tag{10.64}$$

where $\rho_0 - 1$ is given in Eq. (10.59). The effects of non-standard Higgs representations cannot be separated from heavy non-degenerate multiplets unless the new physics has other consequences, such as vertex corrections. Most of the original papers defined T to include the effects of loops only. However, we will redefine T to include all new sources of SU(2) breaking, including non-standard Higgs, so that T and ρ_0 are equivalent by Eq. (10.64).

A multiplet of heavy degenerate chiral fermions yields

$$S = \frac{C}{3\pi}\sum_i \Big(t_{3L}(i) - t_{3R}(i)\Big)^2, \tag{10.65}$$

where $t_{3L,R}(i)$ is the third component of weak isospin of the left-(right-)handed component of fermion i and C is the number of colors. For example, a heavy degenerate ordinary or mirror family would contribute $2/3\pi$ to S. In models with warped extra dimensions, sizeable correction to the S parameter are generated by mixing effects between the SM gauge bosons and their Kaluza-Klein (KK) excitations. One finds $S \approx 30v^2/M^2_{KK}$, where M_{KK} is the mass of the KK gauge bosons [220]. Large positive values $S > 0$ can also be generated in models with dynamical electroweak symmetry breaking, where the Higgs boson is composite. In simple composite Higgs models, the dominant contribution stems from heavy spin-1 resonances of the strong dynamics, leading to $S \approx 4\pi v^2(M_V^{-2} + M_A^{-2})$, where $M_{V,A}$ are the masses of the lightest vector and axial-vector resonances, respectively [221].

On the other hand, negative values $S < 0$ are possible, for example, for models of walking Technicolor [222] or loops involving scalars or Majorana particles [223]. The simplest origin of $S < 0$ would probably be an additional heavy Z' boson [209]. Supersymmetric extensions of the SM generally give very small effects. See Refs. 224 and 225 and the note on "Supersymmetry" in the Searches Particle Listings for a complete set of references.

Most simple types of new physics yield $U = 0$, although there are counter-examples, such as the effects of anomalous triple gauge vertices [214].

The SM expressions for observables are replaced by

$$\begin{aligned} M^2_Z &= M^2_{Z0}\,\frac{1 - \widehat{\alpha}(M_Z)T}{1 - G_F M^2_{Z0} S/2\sqrt{2}\pi} \ , \\ M^2_W &= M^2_{W0}\,\frac{1}{1 - G_F M^2_{W0}(S+U)/2\sqrt{2}\pi} \ , \end{aligned} \tag{10.66}$$

where M_{Z0} and M_{W0} are the SM expressions (as functions of m_t and M_H) in the $\overline{\rm MS}$ scheme. Furthermore,

$$\Gamma_Z = \frac{M^3_Z\beta_Z}{1 - \widehat{\alpha}(M_Z)T}, \Gamma_W = M^3_W\beta_W, A_i = \frac{A_{i0}}{1 - \widehat{\alpha}(M_Z)T} \ , \tag{10.67}$$

where β_Z and β_W are the SM expressions for the reduced widths Γ_{Z0}/M^3_{Z0} and Γ_{W0}/M^3_{W0}, M_Z and M_W are the physical masses, and A_i (A_{i0}) is a neutral-current amplitude (in the SM).

The data allow a simultaneous determination of $\widehat{s}^2_Z$ (from the Z pole asymmetries), S (from M_Z), U (from M_W), T (mainly from Γ_Z), α_s (from R_ℓ, $\sigma_{\rm had}$, and τ_τ), M_H and m_t (from the hadron colliders), with little correlation among the SM parameters:

$$\begin{aligned} S &= 0.02 \pm 0.10 \ , \\ T &= 0.07 \pm 0.12 \ , \\ U &= 0.00 \pm 0.09 \ , \end{aligned} \tag{10.68}$$

$\widehat{s}^2_Z = 0.23113 \pm 0.00014$, and $\alpha_s(M_Z) = 0.1189 \pm 0.0016$, where the uncertainties are from the inputs. The parameters in Eqs. (10.68), which by definition are due to new physics only, are in excellent agreement with the SM values of zero. Fixing $U = 0$, which is motivated by the fact that U is suppressed by an additional factor $M^2_{\rm new}/M^2_Z$ compared to S and T [226], greatly improves the precision on S and particularly T,

$$\begin{aligned} S &= 0.02 \pm 0.07 \ , \\ T &= 0.06 \pm 0.06 \ , \end{aligned} \tag{10.69}$$

see Fig. 10.6. Using Eq. (10.64), the value of ρ_0 corresponding to T in Eq. (10.68) is 1.0005 ± 0.0009, while the one corresponding to

Eq. (10.69) is 1.0005 ± 0.0005. Thus, the multi-parameter fits are consistent with $\rho_0 = 1$, in contrast to the fit with $S = U = 0$ in Eq. (10.56). There is a strong correlation (92%) between the S and T parameters. The U parameter is -66% (-86%) anti-correlated with S (T). The allowed regions in S–T are shown in Fig. 10.6. From Eqs. (10.68) one obtains $S < 0.18$ and $T < 0.26$ at 95% CL, where the former puts the constraint $M_{KK} \gtrsim 3.2$ TeV on the masses of KK gauge bosons in warped extra dimensions. In minimal composite Higgs models, the bound on S requires $M_V \gtrsim 4$ TeV [227], but this constraint can be relaxed, *e.g.*, if the fermionic sector is also allowed to be partially composite [228,229].

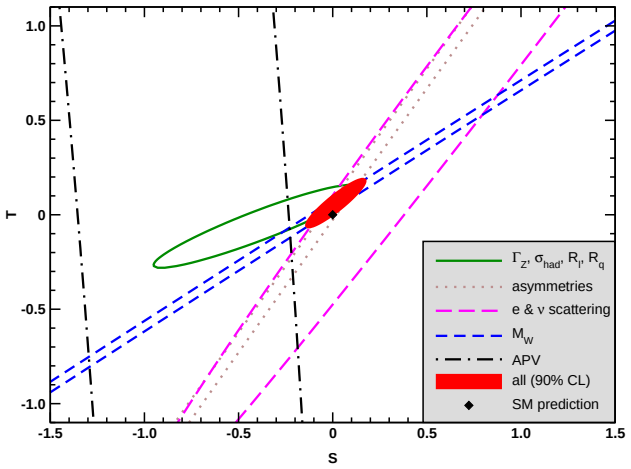

Figure 10.6: 1 σ constraints (39.35% for the closed contours and 68% for the others) on S and T (for $U = 0$) from various inputs combined with M_Z. S and T represent the contributions of new physics only. Data sets not involving M_W or Γ_W are insensitive to U. With the exception of the fit to all data, we fix $\alpha_s = 0.1187$. The black dot indicates the Standard Model values $S = T = 0$.

The S parameter can also be used to constrain the number of fermion families, *under the assumption* that there are no new contributions to T or U and therefore that any new families are degenerate; then an extra generation of SM fermions is excluded at the 9 σ level corresponding to $N_F = 2.75 \pm 0.14$. This can be compared to the fit to the number of light neutrinos given in Eq. (10.37), $N_\nu = 2.991 \pm 0.007$. However, the S parameter fits are valid even for a very heavy fourth family neutrino. Allowing T to vary as well, the constraint on a fourth family is weaker [230]. However, a heavy fourth family would increase the Higgs production cross-section through gluon fusion by a factor ~ 9, which is in considerable tension with the observed Higgs signal at LHC. Combining the limits from electroweak precision data with the measured Higgs production rate and limits from direct searches for heavy quarks [231], a fourth family of chiral fermions is now excluded by more than five standard deviations [232]. Similar remarks apply to a heavy mirror family [233] involving right-handed SU(2) doublets and left-handed singlets. In contrast, new doublets that receive most of their mass from a different source than the Higgs vacuum expectation value, such as vector-like fermion doublets or scalar doublets in Supersymmetry, give small or no contribution to S, T, U and the Higgs production cross-section and thus are still allowed. Partial or complete vector-like fermion families are predicted in many grand unified theories [234].

As discussed in Sec. 10.6, there is a 4.0% deviation in the asymmetry parameter A_b. Assuming that this is due to new physics affecting preferentially the third generation, we can perform a fit allowing additional $Z \to b\bar{b}$ vertex corrections ρ_b and κ_b as in Eq. (10.33) (here defined to be due to new physics only with the SM contributions removed), as well as S, T, U, and the SM parameters, with the result,

$$\rho_b = 0.059 \pm 0.020 \ , \qquad \kappa_b = 0.196 \pm 0.067 \ , \qquad (10.70)$$

with an almost perfect correlation of 99% (because R_b is much better determined than A_b). The central values of the oblique parameters are close to their SM values of zero, and there is little change in the SM parameters. Given that a $\sim 20\%$ correction to κ_b would be necessary, it would be difficult to account for the deviation in A_b by new physics that enters only at the level of radiative corrections. Thus, if it is due to new physics, it is most likely of tree-level type affecting preferentially the third generation. Examples include the decay of a scalar neutrino resonance [235], mixing of the b quark with heavy exotics [236], and a heavy Z' with family non-universal couplings [237,238]. It is difficult, however, to simultaneously account for R_b without tuning, which has been measured on the Z peak and off-peak [239] at LEP 1. An average of R_b measurements at LEP 2 at energies between 133 and 207 GeV is 2.1 σ below the SM prediction, while $A_{FB}^{(b)}$ (LEP 2) is 1.6 σ low [156].

There is no simple parametrization to describe the effects of every type of new physics on every possible observable. The S, T, and U formalism describes many types of heavy physics which affect only the gauge self-energies, and it can be applied to all precision observables. However, new physics which couples directly to ordinary fermions cannot be fully parametrized in the S, T, and U framework. Examples include heavy Z' bosons [209], mixing with exotic fermions [240], leptoquark exchange [155,241], supersymmetric models [225], strong EW dynamics [228], Little Higgs models [242], and TeV-scale extra spatial dimensions [243]. These types of new physics can be parametrized in a model-indepdendent way by using an effective field theory description. Here the SM is extended by a set of higher-dimensional operators, denoted $\mathcal{O}_i$,

$$\mathcal{L} = \mathcal{L}_{\rm SM} + \sum_{d>4} \sum_i \frac{C_i}{\Lambda^{d-4}} \mathcal{O}_i \ , \qquad (10.71)$$

where Λ is the characteristic scale of the new physics sector, which is assumed to satisfy $\Lambda \gg v$. For EW precision observables, the leading new operators enter at dimension $d = 6$. With current data on M_W and Z-pole observables, Λ is constrained to be larger than $\mathcal{O}$(TeV) if the Wilson coefficients C_i are of order 1 [244].

An alternate formalism [245] defines parameters, ϵ_1, ϵ_2, ϵ_3, and ϵ_b in terms of the specific observables M_W/M_Z, $\Gamma_{\ell\ell}$, $A_{FB}^{(0,\ell)}$, and R_b. The definitions coincide with those for $\widehat{\epsilon}_i$ in Eqs. (10.62) and (10.63) for physics which affects gauge self-energies only, but the ϵ's now parametrize arbitrary types of new physics. However, the ϵ's are not related to other observables unless additional model-dependent assumptions are made.

Limits on new four-Fermi operators and on leptoquarks using LEP 2 and lower energy data are given in Refs. 155 and 246. Constraints on various types of new physics are reviewed in Refs. [7,96,123,139,247,248]. For a particularly well motivated and explored type of physics beyond the SM, see the note on "The Z' Searches" in the Gauge & Higgs Boson Particle Listings.

Acknowledgments:

It is a pleasure to thank Rodolfo Ferro-Hernández for discussions, for performing some of the calculations and checks, and for producing the plot in Fig. 10.2. J.E. is supported by CONACyT (Mexico) project 252167–F and the German–Mexican research collaboration grant SP 778/4–1 (DFG) and 278017 (CONACyT). A.F. is supported in part by the National Science Foundation under grant no. PHY–1519175.

References:

1. S.L. Glashow, Nucl. Phys. **22**, 579 (1961);
S. Weinberg, Phys. Rev. Lett. **19**, 1264 (1967);
A. Salam, p. 367 of *Elementary Particle Theory*, ed. N. Svartholm (Almquist and Wiksells, Stockholm, 1969);
S.L. Glashow, J. Iliopoulos, and L. Maiani, Phys. Rev. **D2**, 1285 (1970).
2. CKMfitter Group: J. Charles *et al.*, Eur. Phys. J. **C41**, 1 (2005); updated results and plots are available at `http://ckmfitter.in2p3.fr`.
3. For reviews, see the Section on "Status of Higgs Boson Physics" in this *Review*;
J. Gunion *et al.*, *The Higgs Hunter's Guide*, (Addison-Wesley, Redwood City, 1990);

M. Carena and H.E. Haber, Prog. in Part. Nucl. Phys. **50**, 63 (2003);
A. Djouadi, Phys. Reports **457**, 1 (2008).
4. For reviews, see E.D. Commins and P.H. Bucksbaum, *Weak Interactions of Leptons and Quarks*, (Cambridge Univ. Press, 1983);
G. Barbiellini and C. Santoni, Riv. Nuovo Cimento **9(2)**, 1 (1986);
N. Severijns, M. Beck, and O. Naviliat-Cuncic, Rev. Mod. Phys. **78**, 991 (2006);
W. Fetscher and H.J. Gerber, p. 657 of Ref. 5;
J. Deutsch and P. Quin, p. 706 of Ref. 5;
P. Herczeg, p. 786 of Ref. 5;
P. Herczeg, Prog. in Part. Nucl. Phys. **46**, 413 (2001).
5. *Precision Tests of the Standard Electroweak Model*, ed. P. Langacker (World Scientific, Singapore, 1995).
6. J. Erler and M.J. Ramsey-Musolf, Prog. in Part. Nucl. Phys. **54**, 351 (2005).
7. P. Langacker, *The Standard Model and Beyond*, (CRC Press, New York, 2009).
8. T. Kinoshita, *Quantum Electrodynamics*, (World Scientific, Singapore, 1990).
9. S.G. Karshenboim, Phys. Reports **422**, 1 (2005).
10. ALEPH, DELPHI, L3, OPAL, SLD, LEP Electroweak Working Group, SLD Electroweak and Heavy Flavour Groups: S. Schael *et al.*, Phys. Reports **427**, 257 (2006); for updates see `http://lepewwg.web.cern.ch/LEPEWWG/`.
11. MuLan: D.M. Webber *et al.*, Phys. Rev. Lett. **106**, 041803 (2011).
12. T. Kinoshita and A. Sirlin, Phys. Rev. **113**, 1652 (1959).
13. T. van Ritbergen and R.G. Stuart, Nucl. Phys. **B564**, 343 (2000);
M. Steinhauser and T. Seidensticker, Phys. Lett. **B467**, 271 (1999).
14. Y. Nir, Phys. Lett. **B221**, 184 (1989).
15. A. Pak and A. Czarnecki, Phys. Rev. Lett. **100**, 241807 (2008).
16. P.J. Mohr, B.N. Taylor, and D.B. Newell, `arXiv:1507.07956 [physics.atom-ph]`.
17. For a review, see S. Mele, `arXiv:hep-ex/0610037`.
18. S. Fanchiotti, B. Kniehl, and A. Sirlin, Phys. Rev. **D48**, 307 (1993) and references thereinma.
19. J. Erler, Phys. Rev. **D59**, 054008 (1999).
20. M. Davier *et al.*, Eur. Phys. J. **C77**, 827 (2017).
21. F. Jegerlehner and R. Szafron, Eur. Phys. J. **C71**, 1632 (2011); the quoted value uses additional information thankfully provided to us by the author in a private communication.
22. J. Erler, `hep-ph/0005084`.
23. M. Steinhauser, Phys. Lett. **B429**, 158 (1998).
24. K.G. Chetyrkin, J.H. Kühn, and M. Steinhauser, Nucl. Phys. **B482**, 213 (1996).
25. B.V. Geshkenbein and V.L. Morgunov, Phys. Lett. **B352**, 456 (1995).
26. M.L. Swartz, Phys. Rev. **D53**, 5268 (1996).
27. N.V. Krasnikov and R. Rodenberg, Nuovo Cimento **111A**, 217 (1998).
28. J.H. Kühn and M. Steinhauser, Phys. Lett. **B437**, 425 (1998).
29. S. Groote *et al.*, Phys. Lett. **B440**, 375 (1998).
30. A.D. Martin, J. Outhwaite, and M.G. Ryskin, Phys. Lett. **B492**, 69 (2000).
31. J.F. de Troconiz and F.J. Yndurain, Phys. Rev. **D65**, 093002 (2002).
32. H. Burkhardt and B. Pietrzyk, Phys. Rev. **D84**, 037502 (2011).
33. K. Hagiwara *et al.*, J. Phys. **G38**, 085003 (2011).
34. F. Jegerlehner, `arXiv:1711.06089 [hep-ph]`.
35. A. Keshavarzi, D. Nomura and T. Teubner, `arXiv:1802.02995 [hep-ph]`.
36. M. Davier *et al.*, Eur. Phys. J. **C71**, 1515 (2011).
37. OPAL: K. Ackerstaff *et al.*, Eur. Phys. J. **C7**, 571 (1999).
38. CLEO: S. Anderson *et al.*, Phys. Rev. **D61**, 112002 (2000).
39. ALEPH: S. Schael *et al.*, Phys. Reports **421**, 191 (2005).
40. Belle: M. Fujikawa *et al.*: Phys. Rev. **D78**, 072006 (2008).
41. J. Erler, Eur. Phys. J. **C77**, 99 (2017).
42. V.A. Novikov *et al.*, Phys. Reports **41**, 1 (1978).
43. J. Erler and M. Luo, Phys. Lett. **B558**, 125 (2003).
44. Tevatron Electroweak Working Group for the CDF and DØ Collaborations: `arXiv:1608.01881 [hep-ex]`.
45. ATLAS: `cds.cern.ch/record/2285809/files/ATLAS-CONF-2017-071.pdf`.
46. CMS: `cds.cern.ch/record/2235162/files/TOP-15-012-pas.pdf`.
47. CMS: `cds.cern.ch/record/2284594/files/TOP-17-007-pas.pdf`.
48. M. Beneke *et al.*, Phys. Lett. **B775**, 63 (2017).
49. P. Marquard *et al.*, Phys. Rev. Lett. **114**, 142002 (2015).
50. M. Butenschoen *et al.*, Phys. Rev. Lett. **117**, 232001 (2016);
A. Andreassen, M.D. Schwartz, JHEP **1710**, 151 (2017).
51. DØ: V.M. Abazov *et al.*, Phys. Rev. Lett. **113**, 032002 (2014).
52. A. Sirlin, Phys. Rev. **D22**, 971 (1980);
D.C. Kennedy *et al.*, Nucl. Phys. **B321**, 83 (1989);
D.Yu. Bardin *et al.*, Z. Phys. **C44**, 493 (1989);
W. Hollik, Fortsch. Phys. **38**, 165 (1990);
for reviews, see W. Hollik, pp. 37 and 117, and W. Marciano, p. 170 of Ref. 5.
53. W.J. Marciano and J.L. Rosner, Phys. Rev. Lett. **65**, 2963 (1990).
54. G. Degrassi, S. Fanchiotti, and A. Sirlin, Nucl. Phys. **B351**, 49 (1991).
55. K.S. Kumar *et al.*, Ann. Rev. Nucl. and Part. Sci. **63**, 237 (2013).
56. G. Degrassi and A. Sirlin, Nucl. Phys. **B352**, 342 (1991);
P. Gambino and A. Sirlin, Phys. Rev. **D49**, 1160 (1994).
57. ZFITTER: A.B. Arbuzov *et al.*, Comput. Phys. Commun. **174**, 728 (2006) and references therein.
58. R. Barbieri *et al.*, Nucl. Phys. **B409**, 105 (1993);
J. Fleischer, O.V. Tarasov, and F. Jegerlehner, Phys. Lett. **B319**, 249 (1993).
59. G. Degrassi, P. Gambino, and A. Vicini, Phys. Lett. **B383**, 219 (1996);
G. Degrassi, P. Gambino, and A. Sirlin, Phys. Lett. **B394**, 188 (1997).
60. A. Freitas *et al.*, Phys. Lett. **B495**, 338 (2000) and *ibid.* **570**, 260(E) (2003);
M. Awramik and M. Czakon, Phys. Lett. **B568**, 48 (2003).
61. A. Freitas *et al.*, Nucl. Phys. **B632**, 189 (2002) and *ibid.* **666**, 305(E) (2003);
M. Awramik and M. Czakon, Phys. Rev. Lett. **89**, 241801 (2002);
A. Onishchenko and O. Veretin, Phys. Lett. **B551**, 111 (2003).
62. M. Awramik *et al.*, Phys. Rev. Lett. **93**, 201805 (2004);
W. Hollik, U. Meier, and S. Uccirati, Nucl. Phys. **B731**, 213 (2005).
63. M. Awramik, M. Czakon, and A. Freitas, Phys. Lett. **B642**, 563 (2006);
W. Hollik, U. Meier, and S. Uccirati, Nucl. Phys. **B765**, 154 (2007).
64. G. Degrassi, P. Gambino and P.P. Giardino, JHEP **1505**, 154 (2015).
65. M. Awramik *et al.*, Phys. Rev. **D69**, 053006 (2004).
66. A. Djouadi and C. Verzegnassi, Phys. Lett. **B195**, 265 (1987);
A. Djouadi, Nuovo Cimento **100A**, 357 (1988).
67. K.G. Chetyrkin, J.H. Kühn, and M. Steinhauser, Phys. Lett. **B351**, 331 (1995).
68. Y. Schröder and M. Steinhauser, Phys. Lett. **B622**, 124 (2005);
K.G. Chetyrkin *et al.*, Phys. Rev. Lett. **97**, 102003 (2006);
R. Boughezal and M. Czakon, Nucl. Phys. **B755**, 221 (2006);
L. Avdeev *et al.*, Phys. Lett. **B336**, 560 (1994) and *ibid.* **B349**, 597(E) (1995).
69. B.A. Kniehl, J.H. Kühn, and R.G. Stuart, Phys. Lett. **B214**, 621 (1988);
B.A. Kniehl, Nucl. Phys. **B347**, 86 (1990);
F. Halzen and B.A. Kniehl, Nucl. Phys. **B353**, 567 (1991);

A. Djouadi and P. Gambino, Phys. Rev. **D49**, 3499 (1994) and *ibid.* **53**, 4111(E) (1996).
70. A. Anselm, N. Dombey, and E. Leader, Phys. Lett. **B312**, 232 (1993).
71. K.G. Chetyrkin, J.H. Kühn, and M. Steinhauser, Phys. Rev. Lett. **75**, 3394 (1995).
72. J.J. van der Bij *et al.*, Phys. Lett. **B498**, 156 (2001); M. Faisst *et al.*, Nucl. Phys. **B665**, 649 (2003).
73. R. Boughezal, J.B. Tausk, and J.J. van der Bij, Nucl. Phys. **B725**, 3 (2005).
74. M. Awramik, M. Czakon, and A. Freitas, JHEP **0611**, 048 (2006).
75. J. Erler and S. Su, Prog. in Part. Nucl. Phys. **71**, 119 (2013).
76. J.M. Conrad, M.H. Shaevitz, and T. Bolton, Rev. Mod. Phys. **70**, 1341 (1998).
77. Z. Berezhiani and A. Rossi, Phys. Lett. **B535**, 207 (2002); S. Davidson *et al.*, JHEP **0303**, 011 (2003); A. Friedland, C. Lunardini and C. Pena-Garay, Phys. Lett. **B594**, 347 (2004).
78. J. Panman, p. 504 of Ref. 5; CHARM: J. Dorenbosch *et al.*, Z. Phys. **C41**, 567 (1989); CALO: L.A. Ahrens *et al.*, Phys. Rev. **D41**, 3297 (1990).
79. CHARM II: P. Vilain *et al.*, Phys. Lett. **B335**, 246 (1994).
80. ILM: R.C. Allen *et al.*, Phys. Rev. **D47**, 11 (1993); LSND: L.B. Auerbach *et al.*, Phys. Rev. **D63**, 112001 (2001).
81. TEXONO: M. Deniz *et al.*, Phys. Rev. **D81**, 072001 (2010).
82. For reviews, see G.L. Fogli and D. Haidt, Z. Phys. **C40**, 379 (1988); F. Perrier, p. 385 of Ref. 5.
83. CDHS: A. Blondel *et al.*, Z. Phys. **C45**, 361 (1990).
84. CHARM: J.V. Allaby *et al.*, Z. Phys. **C36**, 611 (1987).
85. CCFR: K.S. McFarland *et al.*, Eur. Phys. J. **C1**, 509 (1998).
86. R.M. Barnett, Phys. Rev. **D14**, 70 (1976); H. Georgi and H.D. Politzer, Phys. Rev. **D14**, 1829 (1976).
87. LAB-E: S.A. Rabinowitz *et al.*, Phys. Rev. Lett. **70**, 134 (1993).
88. E.A. Paschos and L. Wolfenstein, Phys. Rev. **D7**, 91 (1973).
89. NuTeV: G.P. Zeller *et al.*, Phys. Rev. Lett. **88**, 091802 (2002).
90. J. Erler *et al.*, Ann. Rev. Nucl. and Part. Sci. **64**, 269 (2014).
91. SSF: C.Y. Prescott *et al.*, Phys. Lett. **B84**, 524 (1979).
92. JLab-PVDIS: D. Wang *et al.*, Nature **506**, 67 (2014) and Phys. Rev. **C91**, 045506 (2015).
93. E.J. Beise, M.L. Pitt, and D.T. Spayde, Prog. in Part. Nucl. Phys. **54**, 289 (2005).
94. S.L. Zhu *et al.*, Phys. Rev. **D62**, 033008 (2000).
95. P. Souder, p. 599 of Ref. 5.
96. P. Langacker, p. 883 of Ref. 5.
97. R.D. Young *et al.*, Phys. Rev. Lett. **99**, 122003 (2007).
98. D.S. Armstrong and R.D. McKeown, Ann. Rev. Nucl. and Part. Sci. **62**, 337 (2012).
99. E. Derman and W.J. Marciano, Annals Phys. **121**, 147 (1979).
100. E158: P.L. Anthony *et al.*, Phys. Rev. Lett. **95**, 081601 (2005).
101. J. Erler and M.J. Ramsey-Musolf, Phys. Rev. **D72**, 073003 (2005).
102. J. Erler and R. Ferro-Hernández, JHEP **1803**, 196 (2018).
103. A. Czarnecki and W.J. Marciano, Int. J. Mod. Phys. A **15**, 2365 (2000).
104. C. Bouchiat and C.A. Piketty, Phys. Lett. **B128**, 73 (1983).
105. K.S. McFarland, in the *Proceedings of DIS* 2008.
106. Qweak: M.T. Gericke *et al.*, AIP Conf. Proc. **1149**, 237 (2009).
107. Qweak: R. Carlini *et al.*, `indico.ihep.ac.cn/event/6329/session/0/ contribution/310/material/slides/0.pdf`.
108. For reviews and references to earlier work, see M.A. Bouchiat and L. Pottier, Science **234**, 1203 (1986); B.P. Masterson and C.E. Wieman, p. 545 of Ref. 5.
109. M.S. Safronova *et al.*, `arXiv:1710.01833 [physics.atom-ph]`.
110. Cesium (Boulder): C.S. Wood *et al.*, Science **275**, 1759 (1997).
111. Cesium (Paris): J. Guéna, M. Lintz, and M.A. Bouchiat, Phys. Rev. **A71**, 042108 (2005).
112. Thallium (Oxford): N.H. Edwards *et al.*, Phys. Rev. Lett. **74**, 2654 (1995); Thallium (Seattle): P.A. Vetter *et al.*, Phys. Rev. Lett. **74**, 2658 (1995).
113. Lead (Seattle): D.M. Meekhof *et al.*, Phys. Rev. Lett. **71**, 3442 (1993).
114. Bismuth (Oxford): M.J.D. MacPherson *et al.*, Phys. Rev. Lett. **67**, 2784 (1991).
115. P.G. Blunden, W. Melnitchouk and A.W. Thomas, Phys. Rev. Lett. **109**, 262301 (2012).
116. V.A. Dzuba, V.V. Flambaum, and O.P. Sushkov, Phys. Lett. **141A**, 147 (1989); S.A. Blundell, J. Sapirstein, and W.R. Johnson, Phys. Rev. **D45**, 1602 (1992); For reviews, see S.A. Blundell, W.R. Johnson, and J. Sapirstein, p. 577 of Ref. 5; J.S.M. Ginges and V.V. Flambaum, Phys. Reports **397**, 63 (2004); J. Guéna, M. Lintz, and M.A. Bouchiat, Mod. Phys. Lett. **A20**, 375 (2005); A. Derevianko and S.G. Porsev, Eur. Phys. J. A **32**, 517 (2007).
117. V.A. Dzuba, V.V. Flambaum, and O.P. Sushkov, Phys. Rev. **A56**, R4357 (1997).
118. S.C. Bennett and C.E. Wieman, Phys. Rev. Lett. **82**, 2484 (1999).
119. M.A. Bouchiat and J. Guéna, J. Phys. (France) **49**, 2037 (1988).
120. S.G. Porsev, K. Beloy, and A. Derevianko, Phys. Rev. Lett. **102**, 181601 (2009).
121. V.A. Dzuba *et al.*, Phys. Rev. Lett. **109**, 203003 (2012); B.M. Roberts, V.A. Dzuba and V.V. Flambaum, Ann. Rev. Nucl. and Part. Sci. **65**, 63 (2015).
122. A. Derevianko, Phys. Rev. Lett. **85**, 1618 (2000); V.A. Dzuba, C. Harabati, and W.R. Johnson, Phys. Rev. **A63**, 044103 (2001); M.G. Kozlov, S.G. Porsev, and I.I. Tupitsyn, Phys. Rev. Lett. **86**, 3260 (2001); W.R. Johnson, I. Bednyakov, and G. Soff, Phys. Rev. Lett. **87**, 233001 (2001); A.I. Milstein and O.P. Sushkov, Phys. Rev. **A66**, 022108 (2002); V.A. Dzuba, V.V. Flambaum, and J.S. Ginges, Phys. Rev. **D66**, 076013 (2002); M.Y. Kuchiev and V.V. Flambaum, Phys. Rev. Lett. **89**, 283002 (2002); A.I. Milstein, O.P. Sushkov, and I.S. Terekhov, Phys. Rev. Lett. **89**, 283003 (2002); V.V. Flambaum and J.S.M. Ginges, Phys. Rev. **A72**, 052115 (2005).
123. J. Erler, A. Kurylov, and M.J. Ramsey-Musolf, Phys. Rev. **D68**, 016006 (2003).
124. V.A. Dzuba *et al.*, J. Phys. **B20**, 3297 (1987).
125. Ya.B. Zel'dovich, Sov. Phys. JETP **6**, 1184 (1958); V.V. Flambaum and D.W. Murray, Phys. Rev. **C56**, 1641 (1997); W.C. Haxton and C.E. Wieman, Ann. Rev. Nucl. Part. Sci. **51**, 261 (2001).
126. J.L. Rosner, Phys. Rev. **D53**, 2724 (1996).
127. S.J. Pollock, E.N. Fortson, and L. Wilets, Phys. Rev. **C46**, 2587 (1992); B.Q. Chen and P. Vogel, Phys. Rev. **C48**, 1392 (1993).
128. R.W. Dunford and R.J. Holt, J. Phys. **G34**, 2099 (2007).
129. O.O. Versolato *et al.*, Hyperfine Interact. **199**, 9 (2011).
130. W. Hollik and G. Duckeck, Springer Tracts Mod. Phys. **162**, 1 (2000).
131. D.Yu. Bardin *et al.*, `hep-ph/9709229`.
132. A. Czarnecki and J.H. Kühn, Phys. Rev. Lett. **77**, 3955 (1996); R. Harlander, T. Seidensticker, and M. Steinhauser, Phys. Lett. **B426**, 125 (1998); J. Fleischer *et al.*, Phys. Lett. **B459**, 625 (1999).
133. M. Awramik *et al.*, Nucl. Phys. **B813**, 174 (2009); I. Dubovyk *et al.*, Phys. Lett. **B762**, 184 (2016).
134. A. Freitas, Phys. Lett. **B730**, 50 (2014) and JHEP **1404**, 070 (2014).

135. B.W. Lynn and R.G. Stuart, Nucl. Phys. **B253**, 216 (1985).
136. *Physics at LEP*, ed. J. Ellis and R. Peccei, CERN 86–02, Vol. 1.
137. PETRA: S.L. Wu, Phys. Reports **107**, 59 (1984);
C. Kiesling, *Tests of the Standard Theory of Electroweak Interactions*, (Springer-Verlag, New York, 1988);
R. Marshall, Z. Phys. **C43**, 607 (1989);
Y. Mori *et al.*, Phys. Lett. **B218**, 499 (1989);
D. Haidt, p. 203 of Ref. 5.
138. For reviews, see D. Schaile, p. 215, and A. Blondel, p. 277 of Ref. 5; P. Langacker [7]; and S. Riemann [139].
139. S. Riemann, Rept. on Prog. in Phys. **73**, 126201 (2010).
140. SLD: K. Abe *et al.*, Phys. Rev. Lett. **84**, 5945 (2000).
141. SLD: K. Abe *et al.*, Phys. Rev. Lett. **85**, 5059 (2000).
142. SLD: K. Abe *et al.*, Phys. Rev. Lett. **86**, 1162 (2001).
143. SLD: K. Abe *et al.*, Phys. Rev. Lett. **78**, 17 (1997).
144. P.A. Grassi, B.A. Kniehl, and A. Sirlin, Phys. Rev. Lett. **86**, 389 (2001).
145. CDF: T.A. Aaltonen *et al.*, Phys. Rev. **D93**, 112016 (2016).
146. DØ: V.M. Abazov *et al.*, arXiv:1710.03951 [hep-ex].
147. CDF and DØ: T.A. Aaltonen *et al.*, arXiv:1801.06283 [hep-ex].
148. DØ: V.M. Abazov *et al.*, Phys. Rev. **D84**, 012007 (2011).
149. CDF: D. Acosta *et al.*, Phys. Rev. **D71**, 052002 (2005).
150. H1: A. Aktas *et al.*, Phys. Lett. **B632**, 35 (2006).
151. ZEUS: H. Abramowicz *et al.*, Phys. Rev. **D93**, 092002 (2016).
152. ATLAS: G. Aad *et al.*, JHEP **1509**, 049 (2015).
153. CMS: cds.cern.ch/record/2273392/files/SMP-16-007-pas.pdf.
154. LHCb: R. Aaij *et al.*, JHEP **1511**, 190 (2015).
155. ALEPH, DELPHI, L3, OPAL, and LEP Electroweak Working Group: S. Schael *et al.*, Phys. Reports **532**, 119 (2013).
156. ALEPH, DELPHI, L3, OPAL, and LEP Electroweak Working Group: J. Alcaraz *et al.*, hep-ex/0612034.
157. A. Leike, T. Riemann, and J. Rose, Phys. Lett. **B273**, 513 (1991);
T. Riemann, Phys. Lett. **B293**, 451 (1992).
158. A comprehensive report and further references can be found in K.G. Chetyrkin, J.H. Kühn, and A. Kwiatkowski, Phys. Reports **277**, 189 (1996).
159. J. Schwinger, *Particles, Sources, and Fields*, Vol. II, (Addison-Wesley, New York, 1973);
K.G. Chetyrkin, A.L. Kataev, and F.V. Tkachev, Phys. Lett. **B85**, 277 (1979);
M. Dine and J. Sapirstein, Phys. Rev. Lett. **43**, 668 (1979);
W. Celmaster and R.J. Gonsalves, Phys. Rev. Lett. **44**, 560 (1980);
S.G. Gorishnii, A.L. Kataev, and S.A. Larin, Phys. Lett. **B259**, 144 (1991);
L.R. Surguladze, M.A. Samuel, Phys. Rev. Lett. **66**, 560 (1991) and *ibid.* 2416(E).
160. P.A. Baikov, K.G. Chetyrkin, and J.H. Kühn, Phys. Rev. Lett. **101**, 012002 (2008).
161. B.A. Kniehl and J.H. Kühn, Nucl. Phys. **B329**, 547 (1990);
K.G. Chetyrkin and A. Kwiatkowski, Phys. Lett. **B319**, 307 (1993);
S.A. Larin, T. van Ritbergen, and J.A.M. Vermaseren, Phys. Lett. **B320**, 159 (1994);
K.G. Chetyrkin and O.V. Tarasov, Phys. Lett. **B327**, 114 (1994).
162. A.L. Kataev, Phys. Lett. **B287**, 209 (1992).
163. D. Albert *et al.*, Nucl. Phys. **B166**, 460 (1980);
F. Jegerlehner, Z. Phys. **C32**, 425 (1986);
A. Djouadi, J.H. Kühn, and P.M. Zerwas, Z. Phys. **C46**, 411 (1990);
A. Borrelli *et al.*, Nucl. Phys. **B333**, 357 (1990).
164. A.A. Akhundov, D.Yu. Bardin, and T. Riemann, Nucl. Phys. **B276**, 1 (1986);
W. Beenakker and W. Hollik, Z. Phys. **C40**, 141 (1988);
B.W. Lynn and R.G. Stuart, Phys. Lett. **B352**, 676 (1990);
J. Bernabeu, A. Pich, and A. Santamaria, Phys. Lett. **B200**, 569 (1988) and Nucl. Phys. **B363**, 326 (1991).
165. H. Davoudiasl, H.-S. Lee, and W.J. Marciano, Phys. Rev. **D86**, 095009 (2012).
166. E. Braaten, S. Narison, and A. Pich, Nucl. Phys. **B373**, 581 (1992).
167. M. Davier *et al.*, Eur. Phys. J. **C74**, 2803 (2014).
168. F. Le Diberder and A. Pich, Phys. Lett. **B286**, 147 (1992).
169. M. Beneke and M. Jamin, JHEP **0809**, 044 (2008).
170. E. Braaten and C.S. Li, Phys. Rev. **D42**, 3888 (1990).
171. J. Erler, Rev. Mex. Fis. **50**, 200 (2004).
172. D. Boito *et al.*, Phys. Rev. **D85**, 093015 (2012).
173. D. Boito *et al.*, Phys. Rev. **D91**, 034003 (2015).
174. A. Pich, Prog. in Part. Nucl. Phys. **75**, 41 (2014);
A. Pich and A. Rodríguez-Sánchez, Phys. Rev. **D94**, 034027 (2016).
175. J. Erler, arXiv:1102.5520 [hep-ph].
176. E821: G.W. Bennett *et al.*, Phys. Rev. Lett. **92**, 161802 (2004).
177. T. Aoyama *et al.*, Phys. Rev. Lett. **109**, 111808 (2012);
T. Aoyama *et al.*, PTEP **2012**, 01A107 (2012);
P. Baikov, A. Maier and P. Marquard, Nucl. Phys. **B877**, 647 (2013).
178. G. Li, R. Mendel, and M.A. Samuel, Phys. Rev. **D47**, 1723 (1993);
S. Laporta and E. Remiddi, Phys. Lett. **B301**, 440 (1993);
S. Laporta and E. Remiddi, Phys. Lett. **B379**, 283 (1996);
A. Czarnecki and M. Skrzypek, Phys. Lett. **B449**, 354 (1999).
179. J. Erler and M. Luo, Phys. Rev. Lett. **87**, 071804 (2001).
180. S. Laporta, Phys. Lett. **B772**, 232 (2017).
181. S.J. Brodsky and J.D. Sullivan, Phys. Rev. **D156**, 1644 (1967);
T. Burnett and M.J. Levine, Phys. Lett. **B24**, 467 (1967);
R. Jackiw and S. Weinberg, Phys. Rev. **D5**, 2473 (1972);
I. Bars and M. Yoshimura, Phys. Rev. **D6**, 374 (1972);
K. Fujikawa, B.W. Lee, and A.I. Sanda, Phys. Rev. **D6**, 2923 (1972);
G. Altarelli, N. Cabibbo, and L. Maiani, Phys. Lett. **B40**, 415 (1972);
W.A. Bardeen, R. Gastmans, and B.E. Laurup, Nucl. Phys. **B46**, 315 (1972).
182. T.V. Kukhto *et al.*, Nucl. Phys. **B371**, 567 (1992);
S. Peris, M. Perrottet, and E. de Rafael, Phys. Lett. **B355**, 523 (1995);
A. Czarnecki, B. Krause, and W.J. Marciano, Phys. Rev. **D52**, 2619 (1995);
A. Czarnecki, B. Krause, and W.J. Marciano, Phys. Rev. Lett. **76**, 3267 (1996);
C. Gnendiger, D. Stöckinger and H. Stöckinger-Kim, Phys. Rev. **D88**, 053005 (2013).
183. G. Degrassi and G. Giudice, Phys. Rev. **D58**, 053007 (1998);
A. Czarnecki, W.J. Marciano and A. Vainshtein, Phys. Rev. **D67**, 073006 (2003) and *ibid.* **D73**, 119901(E) (2006).
184. F. Jegerlehner *et al.*, EPJ Web Conf. **166**, 00022 (2018).
185. B. Chakraborty *et al.*, Phys. Rev. **D96**, 034516 (2017);
M. Della Morte *et al.*, JHEP **1710**, 020 (2017);
C. Lehner *et al.*, arXiv:1710.06874 [hep-lat];
M. Della Morte *et al.*, arXiv:1710.10072 [hep-lat];
S. Borsanyi *et al.*, arXiv:1711.04980 [hep-lat];
T. Blum *et al.*, arXiv:1801.07224 [hep-lat].
186. K. Melnikov and A. Vainshtein, Phys. Rev. **D70**, 113006 (2004).
187. J. Erler and G. Toledo Sánchez, Phys. Rev. Lett. **97**, 161801 (2006).
188. J. Prades, E. de Rafael, and A. Vainshtein, Adv. Ser. Direct. High Energy Phys. **20**, 303 (2009).
189. M. Knecht and A. Nyffeler, Phys. Rev. **D65**, 073034 (2002).
190. M. Hayakawa and T. Kinoshita, hep-ph/0112102;
J. Bijnens, E. Pallante, and J. Prades, Nucl. Phys. **B626**, 410 (2002);
A recent discussion is in J. Bijnens and J. Prades, Mod. Phys. Lett. **A22**, 767 (2007).
191. T. Blum *et al.*, Phys. Rev. Lett. **118**, 022005 (2017);
A. Gérardin *et al.*, arXiv:1712.00421 [hep-lat].
192. B. Krause, Phys. Lett. **B390**, 392 (1997).

193. A. Kurz *et al.*, Phys. Lett. **B734**, 144 (2014); A. Kurz *et al.*, EPJ Web Conf. **118**, 01033 (2016).
194. G. Colangelo *et al.*, Phys. Lett. **B735**, 90 (2014).
195. J.L. Lopez, D.V. Nanopoulos, and X. Wang, Phys. Rev. **D49**, 366 (1994).
196. U. Amaldi *et al.*, Phys. Rev. **D36**, 1385 (1987); G. Costa *et al.*, Nucl. Phys. **B297**, 244 (1988); P. Langacker and M. Luo, Phys. Rev. **D44**, 817 (1991); J. Erler and P. Langacker, Phys. Rev. **D52**, 441 (1995).
197. CDF and DØ: T. Aaltonen *et al.*, Phys. Rev. **D88**, 052018 (2013).
198. ATLAS: M. Aaboud *et al.*, Eur. Phys. J. **C78**, 110 (2018).
199. Tevatron Electroweak Working Group, CDF and DØ: arXiv:1003.2826 [hep-ex].
200. ATLAS and CMS: G. Aad *et al.*, Phys. Rev. Lett. **114**, 191803 (2015) and cds.cern.ch/record/2052552/files/ATLAS-CONF-2015-044.pdf.
201. ATLAS: cds.cern.ch/record/2273853/files/ATLAS-CONF-2017-046.pdf.
202. D. Sperka, in the *Proceedings of the 53rd Rencontres de Moriond – EW* 2018.
203. F. James and M. Roos, Comput. Phys. Commun. **10**, 343 (1975).
204. CMS: S. Chatrchyan *et al.*, Phys. Lett. **B728**, 496 (2014) and *ibid.* 526(E) (2014).
205. DØ: V.M. Abazov *et al.*, Phys. Rev. **D80**, 111107 (2009).
206. T. Klijnsma *et al.*, Eur. Phys. J. **C77**, 778 (2017).
207. P. Langacker and N. Polonsky, Phys. Rev. **D52**, 3081 (1995); J. Bagger, K.T. Matchev, and D. Pierce, Phys. Lett. **B348**, 443 (1995).
208. M. Veltman, Nucl. Phys. **B123**, 89 (1977); M. Chanowitz, M.A. Furman, and I. Hinchliffe, Phys. Lett. **B78**, 285 (1978); The two-loop correction has been obtained by J.J. van der Bij and F. Hoogeveen, Nucl. Phys. **B283**, 477 (1987).
209. P. Langacker and M. Luo, Phys. Rev. **D45**, 278 (1992) and refs. therein.
210. A. Denner, R.J. Guth, and J.H. Kühn, Phys. Lett. **B240**, 438 (1990); W. Grimus *et al.*, J. Phys. G **35**, 075001 (2008); H.E. Haber and D. O'Neil, Phys. Rev. **D83**, 055017 (2011).
211. S. Bertolini and A. Sirlin, Phys. Lett. **B257**, 179 (1991).
212. M. Peskin and T. Takeuchi, Phys. Rev. Lett. **65**, 964 (1990); M. Peskin and T. Takeuchi, Phys. Rev. **D46**, 381 (1992); M. Golden and L. Randall, Nucl. Phys. **B361**, 3 (1991).
213. D. Kennedy and P. Langacker, Phys. Rev. **D44**, 1591 (1991).
214. G. Altarelli and R. Barbieri, Phys. Lett. **B253**, 161 (1991).
215. B. Holdom and J. Terning, Phys. Lett. **B247**, 88 (1990).
216. B.W. Lynn, M.E. Peskin, and R.G. Stuart, p. 90 of Ref. 136.
217. An alternative formulation is given by K. Hagiwara *et al.*, Z. Phys. **C64**, 559 (1994), and *ibid.* **68**, 352(E) (1995); K. Hagiwara, D. Haidt, and S. Matsumoto, Eur. Phys. J. **C2**, 95 (1998).
218. I. Maksymyk, C.P. Burgess, and D. London, Phys. Rev. **D50**, 529 (1994); C.P. Burgess *et al.*, Phys. Lett. **B326**, 276 (1994); R. Barbieri, M. Frigeni, and F. Caravaglios, Phys. Lett. **B279**, 169 (1992).
219. R. Barbieri *et al.*, Nucl. Phys. **B703**, 127 (2004).
220. M.S. Carena *et al.*, Nucl. Phys. **B759**, 202 (2006).
221. R. Contino, arXiv:1005.4269 [hep-ph].
222. E. Gates and J. Terning, Phys. Rev. Lett. **67**, 1840 (1991); R. Sundrum and S.D.H. Hsu, Nucl. Phys. **B391**, 127 (1993); R. Sundrum, Nucl. Phys. **B395**, 60 (1993); M. Luty and R. Sundrum, Phys. Rev. Lett. **70**, 529 (1993); T. Appelquist and J. Terning, Phys. Lett. **B315**, 139 (1993); D.D. Dietrich, F. Sannino, and K. Tuominen, Phys. Rev. **D72**, 055001 (2005); N.D. Christensen and R. Shrock, Phys. Lett. **B632**, 92 (2006); M. Harada, M. Kurachi, and K. Yamawaki, Prog. Theor. Phys. **115**, 765 (2006).
223. H. Georgi, Nucl. Phys. **B363**, 301 (1991); M.J. Dugan and L. Randall, Phys. Lett. **B264**, 154 (1991).
224. R. Barbieri *et al.*, Nucl. Phys. **B341**, 309 (1990).
225. J. Erler and D.M. Pierce, Nucl. Phys. **B526**, 53 (1998); G.C. Cho and K. Hagiwara, Nucl. Phys. **B574**, 623 (2000); G. Altarelli *et al.*, JHEP **0106**, 018 (2001); S. Heinemeyer, W. Hollik, and G. Weiglein, Phys. Reports **425**, 265 (2006); S.P. Martin, K. Tobe, and J.D. Wells, Phys. Rev. **D71**, 073014 (2005); G. Marandella, C. Schappacher, and A. Strumia, Nucl. Phys. **B715**, 173 (2005); M.J. Ramsey-Musolf and S. Su, Phys. Reports **456**, 1 (2008); A. Djouadi, Phys. Reports **459**, 1 (2008); S. Heinemeyer *et al.*, JHEP **0804**, 039 (2008); O. Buchmueller *et al.*, Eur. Phys. J. **C72**, 2020 (2012).
226. B. Grinstein and M.B. Wise, Phys. Lett. **B265**, 326 (1991).
227. A. Pich, I. Rosell and J.J. Sanz-Cillero, JHEP **1401**, 157 (2014).
228. C.T. Hill and E.H. Simmons, Phys. Reports **381**, 235 (2003).
229. G. Panico and A. Wulzer, Lect. Notes Phys. **913**, 1 (2016).
230. J. Erler and P. Langacker, Phys. Rev. Lett. **105**, 031801 (2010).
231. CMS: S. Chatrchyan *et al.*, Phys. Rev. **D86**, 112003 (2012).
232. O. Eberhardt *et al.*, Phys. Rev. Lett. **109**, 241802 (2012); A. Djouadi and A. Lenz, Phys. Lett. **B715**, 310 (2012).
233. J. Maalampi and M. Roos, Phys. Reports **186**, 53 (1990).
234. For reviews, see "Grand Unified Theories" in this *Review*; P. Langacker, Phys. Reports **72**, 185 (1981); J.L. Hewett and T.G. Rizzo, Phys. Reports **183**, 193 (1989); J. Kang, P. Langacker and B.D. Nelson, Phys. Rev. **D77**, 035003 (2008); S.P. Martin, Phys. Rev. **D81**, 035004 (2010); P.W. Graham *et al.*, Phys. Rev. **D81**, 055016 (2010).
235. J. Erler, J.L. Feng, and N. Polonsky, Phys. Rev. Lett. **78**, 3063 (1997).
236. D. Choudhury, T.M.P. Tait, and C.E.M. Wagner, Phys. Rev. **D65**, 053002 (2002).
237. J. Erler and P. Langacker, Phys. Rev. Lett. **84**, 212 (2000).
238. P. Langacker and M. Plümacher, Phys. Rev. **D62**, 013006 (2000).
239. DELPHI: P. Abreu *et al.*, Eur. Phys. J. **C10**, 415 (1999).
240. P. Langacker and D. London, Phys. Rev. **D38**, 886 (1988); D. London, p. 951 of Ref. 5; a recent analysis is F. del Aguila, J. de Blas and M. Perez-Victoria, Phys. Rev. **D78**, 013010 (2008).
241. M. Chemtob, Prog. in Part. Nucl. Phys. **54**, 71 (2005); R. Barbier *et al.*, Phys. Reports **420**, 1 (2005).
242. T. Han, H.E. Logan, and L.T. Wang, JHEP **0601**, 099 (2006); M. Perelstein, Prog. in Part. Nucl. Phys. **58**, 247 (2007).
243. K. Agashe *et al.*, JHEP **0308**, 050 (2003); M. Carena *et al.*, Phys. Rev. **D68**, 035010 (2003); I. Gogoladze and C. Macesanu, Phys. Rev. **D74**, 093012 (2006); I. Antoniadis, hep-th/0102202; see also the note on "Extra Dimensions" in the Searches Particle Listings.
244. A. Pomarol and F. Riva, JHEP **1401**, 151 (2014); J. Ellis, V. Sanz and T. You, JHEP **1503**, 157 (2015); A. Efrati, A. Falkowski and Y. Soreq, JHEP **1507**, 018 (2015); J. de Blas *et al.*, arXiv:1710.05402 [hep-ph].
245. G. Altarelli, R. Barbieri, and S. Jadach, Nucl. Phys. **B369**, 3 (1992) and *ibid.* **B376**, 444(E) (1992).
246. G.C. Cho, K. Hagiwara, and S. Matsumoto, Eur. Phys. J. **C5**, 155 (1998); K. Cheung, Phys. Lett. **B517**, 167 (2001); Z. Han and W. Skiba, Phys. Rev. **D71**, 075009 (2005).
247. P. Langacker, M. Luo, and A.K. Mann, Rev. Mod. Phys. **64**, 87 (1992); M. Luo, p. 977 of Ref. 5.
248. F.S. Merritt *et al.*, p. 19 of *Particle Physics: Perspectives and Opportunities: Report of the DPF Committee on Long Term Planning*, ed. R. Peccei *et al.* (World Scientific, Singapore, 1995).

11. Status of Higgs Boson Physics

Revised September 2017 by M. Carena (Fermi National Accelerator Laboratory and the University of Chicago), C. Grojean (DESY, Hamburg, and Humboldt University, Berlin), M. Kado (Laboratoire de l'Accélérateur Linéaire, Orsay), and V. Sharma (University of California, San Diego).

I. Introduction

Understanding the mechanism that breaks the electroweak symmetry and generates the masses of the known elementary particles has been one of the fundamental endeavors in particle physics. The discovery in 2012 by the ATLAS [1] and the CMS [2] Collaborations of a new resonance with a mass of approximately 125 GeV and the subsequent studies of its properties with a much larger data set have provided the first portrait of this mechanism. The mass of this boson has been precisely measured and its production and decay rates are found to be consistent, within errors, with the standard model (SM) predictions. Nevertheless, several channels are yet out of reach experimentally and the couplings of the Higgs boson to light

fermions are yet to be proven. At the same time, many theoretical questions remain unanswered. New questions about what lies behind the Higgs boson have come to fore. Nonetheless, five years since its discovery, the Higgs boson has turned into a new tool to explore the manifestations of the SM and to probe the physics landscape beyond it.

In the SM [3] the electroweak interactions are described by a gauge field theory invariant under the $SU(2)_L \times U(1)_Y$ symmetry group. The mechanism of electroweak symmetry breaking (EWSB) [4] provides a general framework to keep untouched the structure of these gauge interactions at high energies and still generate the observed masses of the W and Z gauge bosons. The EWSB mechanism posits a self-interacting complex doublet scalar field, whose CP-even neutral component acquires a vacuum expectation value (VEV) $v \approx 246\,\text{GeV}$, which sets the scale of electroweak symmetry breaking. Three massless Goldstone bosons are generated and are absorbed to give masses to the W and Z gauge bosons. The remaining component of the complex doublet becomes the Higgs boson – a new fundamental scalar particle. The masses of all fermions are also a consequence of EWSB since the Higgs doublet is postulated to couple to the fermions through Yukawa interactions.

All measurements of the Higgs boson properties are so far indicating that the observations are compatible with a minimal EWSB sector. Nevertheless, within the current precision a more complex sector with additional states is not ruled out, nor has it been established whether the Higgs boson is an elementary particle or whether it has an internal structure like any other scalar particles observed before it.

Without the Higgs boson, the calculability of the SM would have been spoiled. In particular, perturbative unitarity [5, 6] would be lost at high energies since the longitudinal W/Z boson scattering amplitude would grow with the increase in centre-of-mass energy. In addition, the radiative corrections to the gauge boson self-energies would exhibit dangerous logarithmic divergences that would be difficult to reconcile with EW precision data. With the discovery of the Higgs boson, the SM is a spontaneously broken gauge theory and as such it could a priori be consistently extrapolated well above the masses of the W and Z bosons. Hence, formally there is no need for new physics at the EW scale. However, as the SM Higgs boson is a scalar particle, at the quantum level it has sensitivity to high energy thresholds. Quite generally, the Higgs mass is affected by the presence of heavy particles and receives quantum corrections proportional to highest energy scale which destabilize the weak scale barring a large fine tuning of unrelated parameters. This is known as the hierarchy or naturalness problem [7].

There are two broad classes of models addressing the naturalness problem[1]: one is based on a new fermion-boson symmetry in nature called supersymmetry (SUSY) [9–11]. This is a weakly coupled approach to EWSB, and in this case, the Higgs boson remains elementary and the corrections to its mass are screened at the scale at which SUSY is broken and remain insensitive to the details of the physics at higher scales. These theories predict at least three neutral Higgs particles and a pair of charged Higgs particles [12]. One of the neutral Higgs bosons, most often the lightest CP-even Higgs, has properties that resemble those of the SM Higgs boson. It is referred to as a SM-like Higgs boson, meaning that its couplings are close to the ones predicted in the SM.

The other approach invokes the existence of strong interactions at a scale of the order of a TeV or above and induces strong breaking of the electroweak symmetry [13]. In the original incarnation of this second approach, dubbed technicolor, the strong interactions themselves trigger EWSB without the need of a Higgs boson. Another possibility, more compatible with the ATLAS and CMS discovery, is that the strong interactions produce four light resonances identified with the Higgs doublet and EWSB proceeds through vacuum misalignment [14] (see Refs. [15, 16] for recent reviews). The Higgs boson could also correspond to the Goldstone boson associated with the spontaneous breaking of scale invariance [17, 18]. However, this dilaton/radion scenario now requires jumbled model-building to be consistent with the constraints from the coupling measurements.

Both approaches can have important effects on the phenomenology of the Higgs boson associated with EWSB. Also, in each case the Higgs role in unitarization of scattering amplitudes is shared by other particles that remain targets of experimental searches.

The naturalness problem has been the prime argument for new physics at the TeV scale, and sizable effects on the Higgs boson properties were expected. But the agreement of the Higgs couplings with the SM predictions, together with the strong bounds from precision electroweak and flavor data leaves open the possibility that the Higgs boson may well be elementary, weakly coupled and solitary up to the Planck scale, rendering the EW vacuum potentially metastable. However, absence of evidence is not evidence of absence. It is possible that new states present at the TeV scale to stabilize the Higgs mass might simply be elusive at the LHC because they do not carry a color charge. Twin Higgs [19] models were the first incarnation of this neutral naturalness idea [20]. More recent and extreme proposals [21] rely on the cosmological evolution of the Universe to drive the Higgs boson mass to a value much smaller than the cutoff of the theory and aim at alleviating the hierarchy problem without the need for TeV scale new physics.

Extensions of the SM Higgs sector without low-energy supersymmetry will also be discussed in this review. These type of models do not address the naturalness problem in a specific manner, but provide grounds to explore new Higgs boson signals in a more model-independent way, with different types of coupling structure to fermions and gauge bosons. Extended Higgs sectors are usually quite restricted by experimental constraints from precision electroweak measurements as well as constraints from flavor data.

This review is organized as follow. Section II is a theoretical review of the SM Higgs boson, its properties, production mechanisms and decay rates. In Section III, the experimental measurements are described. In Section IV, the combination of the main Higgs boson production and decay channels is presented. In Section V, measurements of the main quantum numbers and CP properties of the Higgs boson are reported and the bounds on its total width are discussed. In Section VI, a general theoretical framework to describe the deviations of the Higgs couplings from the SM predictions is introduced and the experimental measurements of these Higgs couplings is reviewed. Measurements of differential cross sections are outlined. Section VII presents, in detail, some interesting models proposed for Higgs extensions of the SM and considers their experimental signatures. Section VIII provides a short summary and a brief outlook.

II. The standard model and the mechanism of electroweak symmetry breaking

In the SM [3], electroweak symmetry breaking [4] is responsible for generating mass for the W and Z gauge bosons rendering the weak interactions short ranged. The SM scalar potential reads:

$$V(\Phi) = m^2 \Phi^\dagger \Phi + \lambda (\Phi^\dagger \Phi)^2 \tag{11.1}$$

with the Higgs field Φ being a self-interacting $SU(2)_L$ complex doublet (four real degrees of freedom) with weak hypercharge $Y{=}1$ (the hypercharge is normalized such that $Q = T_{3L} + Y/2$, Q being the electric charge and T_{3L} the diagonal generator of $SU(2)_L$):

$$\Phi = \frac{1}{\sqrt{2}} \begin{pmatrix} \sqrt{2}\phi^+ \\ \phi^0 + i a^0 \end{pmatrix}, \tag{11.2}$$

where ϕ^0 and a^0 are the CP-even and CP-odd neutral components, and ϕ^+ is the complex charged component of the Higgs doublet, respectively. $V(\Phi)$ is the most general renormalizable scalar potential and if the quadratic term is negative the neutral component of the scalar doublet acquires a non-zero vacuum expectation value (VEV)

$$\langle \Phi \rangle = \frac{1}{\sqrt{2}} \begin{pmatrix} 0 \\ v \end{pmatrix}, \tag{11.3}$$

[1] Another solution to the naturalness problem is to lower the fundamental scale of quantum gravity, like for instance in models with large extra-dimensions, see Ref. [8].

with $\phi^0 = H + \langle\phi^0\rangle$ and $\langle\phi^0\rangle \equiv v$, inducing the spontaneous breaking of the SM gauge symmetry $\mathrm{SU(3)}_C \times \mathrm{SU(2)}_L \times \mathrm{U(1)}_Y$ into $\mathrm{SU(3)}_C \times \mathrm{U(1)}_{\rm em}$. The global minimum of the theory defines the ground state, and spontaneous symmetry breaking implies that there is a symmetry of the system that is not respected by the ground state. From the four generators of the $\mathrm{SU(2)}_L \times \mathrm{U(1)}_Y$ gauge group, three are spontaneously broken, implying that they lead to non-trivial transformations of the ground state and indicate the existence of three massless Goldstone bosons identified with three of the four Higgs field degrees of freedom. The Higgs field couples to the W_μ and B_μ gauge fields associated with the $\mathrm{SU(2)}_L \times \mathrm{U(1)}_Y$ local symmetry through the covariant derivative appearing in the kinetic term of the Higgs Lagrangian,

$$\mathcal{L}_{\rm Higgs} = (D_\mu\Phi)^\dagger(D^\mu\Phi) - V(\Phi)\,, \tag{11.4}$$

where $D_\mu\Phi = (\partial_\mu + ig\sigma^a W^a_\mu/2 + ig'YB_\mu/2)\Phi$, g and g' are the SU(2) and U(1) gauge couplings, respectively, and $\sigma^a, a = 1,2,3$ are the usual Pauli matrices. As a result, the neutral and the two charged massless Goldstone degrees of freedom mix with the gauge fields corresponding to the broken generators of $\mathrm{SU(2)}_L \times \mathrm{U(1)}_Y$ and become, in the unitarity gauge, the longitudinal components of the Z and W physical gauge bosons, respectively. The Z and W gauge bosons acquire masses,

$$m_W^2 = \frac{g^2v^2}{4}\,, \quad m_Z^2 = \frac{(g'^2+g^2)v^2}{4}. \tag{11.5}$$

The fourth generator remains unbroken since it is the one associated to the conserved $\mathrm{U(1)}_{\rm em}$ gauge symmetry, and its corresponding gauge field, the photon, remains massless. Similarly the eight color gauge bosons, the gluons, corresponding to the conserved $\mathrm{SU(3)}_C$ gauge symmetry with 8 unbroken generators, also remain massless. Hence, from the initial four degrees of freedom of the Higgs field, two are absorbed by the $W^\pm$ gauge bosons, one by the Z gauge boson, and there is one remaining degree of freedom, H, that is the physical Higgs boson — a new scalar particle. The Higgs boson is neutral under the electromagnetic interactions and transforms as a singlet under $\mathrm{SU(3)}_C$ and hence does not couple at tree level to the massless photons and gluons.

The fermions of the SM acquire mass through renormalizable interactions between the Higgs field and the fermions: the Yukawa interactions,

$$\mathcal{L}_{\rm Yukawa} = -\hat{h}_{d_{ij}}\bar{q}_{L_i}\Phi\, d_{R_j} - \hat{h}_{u_{ij}}\bar{q}_{L_i}\tilde{\Phi}u_{R_j} - \hat{h}_{l_{ij}}\bar{l}_{L_i}\Phi\, e_{R_j} + h.c., \tag{11.6}$$

which respect the symmetries of the SM but generate fermion masses once EWSB occurs. In the above, $\tilde{\Phi} = i\sigma_2\Phi^*$ and q_L (l_L) and u_R, d_R (e_R) are the quark (lepton) $\mathrm{SU(2)}_L$ doublets and singlets, respectively, while each term is parametrized by a 3×3 matrix in family space. The mass term for neutrinos is omitted, but could be added in an analogous manner to the up-type quarks when right-handed neutrinos are supplementing the SM particle content (neutrinos can also acquire Majorana masses via non-renormalizable dimension-5 interactions with the Higgs field). Once the Higgs acquires a VEV, and after rotation to the fermion mass eigenstate basis that also diagonalizes the Higgs-fermion interactions, $\hat{h}_{f_{ij}} \to h_{f_i}\delta_{ij}$, all fermions acquire a mass given by $m_{f_i} = h_{f_i}v/\sqrt{2}$. The indices $i,j = 1,2,3$ refer to the three families in the up-quark, down-quark or charged lepton sectors. It should be noted that the EWSB mechanism provides no additional insight on possible underlying reasons for the large variety of masses of the fermions, often referred to as the flavor hierarchy. The fermion masses, accounting for a large number of the free parameters of the SM, are simply translated into Yukawa couplings.

II.1. The SM Higgs boson mass, couplings and quantum numbers

The SM Higgs boson is a CP-even scalar of spin 0. Its mass is given by $m_H = \sqrt{2\lambda}\,v$, where λ is the Higgs self-coupling parameter in $V(\Phi)$. The expectation value of the Higgs field, $v = (\sqrt{2}G_F)^{-1/2} \approx 246\,\mathrm{GeV}$, is fixed by the Fermi coupling G_F, which is determined with a precision of 0.6 ppm from muon decay measurements [22]. The quartic coupling λ is a free parameter in the SM, and hence, there is no a priori prediction for the Higgs mass. Moreover the sign of the mass parameter $m^2 = -\lambda v^2$ is crucial for the EW symmetry breaking to take place, but is not specified in the SM. The experimentally measured Higgs mass, $m_H \simeq 125\,\mathrm{GeV}$, implies that $\lambda \simeq 0.13$ and $|m| \simeq 88.8\,\mathrm{GeV}$.

The Higgs boson couplings to the fundamental particles are set by their masses. This is a new type of interaction; very weak for light particles, such as up and down quarks, and electrons, but strong for heavy particles such as the W and Z bosons and the top quark. More precisely, the SM Higgs couplings to fundamental fermions are linearly proportional to the fermion masses, whereas the couplings to bosons are proportional to the square of the boson masses. The SM Higgs boson couplings to gauge bosons and fermions, as well as the Higgs boson self coupling, are summarized in the following Lagrangian:

$$\mathcal{L} = -\,g_{Hff}\bar{f}fH + \frac{g_{HHH}}{6}H^3 + \frac{g_{HHHH}}{24}H^4 + \delta_V V_\mu V^\mu\left(g_{HVV}H + \frac{g_{HHVV}}{2}H^2\right) \tag{11.7}$$

with

$$g_{Hf\bar{f}} = \frac{m_f}{v},\; g_{HVV} = \frac{2m_V^2}{v},\; g_{HHVV} = \frac{2m_V^2}{v^2},\; g_{HHH} = \frac{3m_H^2}{v},\; g_{HHHH} = \frac{3m_H^2}{v^2},$$

where $V = \mathrm{W}^\pm$ or Z and $\delta_W = 1, \delta_Z = 1/2$. As a result, the dominant mechanisms for Higgs boson production and decay involve the coupling of H to W, Z and/or the third generation quarks and leptons. The Higgs boson coupling to gluons [23, 24] is induced at leading order by a one-loop process in which H couples to a virtual $t\bar{t}$ pair. Likewise, the Higgs boson coupling to photons is also generated via loops, although in this case the one-loop graph with a virtual W^+W^- pair provides the dominant contribution [12] and the one involving a virtual $t\bar{t}$ pair is subdominant.

II.2. The SM custodial symmetry

The SM Higgs Lagrangian, $\mathcal{L}_{\rm Higgs} + \mathcal{L}_{\rm Yukawa}$ of Eq. (11.4) and Eq. (11.6), is, by construction, $\mathrm{SU(2)}_L \times \mathrm{U(1)}_Y$ gauge invariant, but it also has an approximate global symmetry. In the limit $g' \to 0$ and $h_f \to 0$, the Higgs sector has a global $\mathrm{SU(2)}_R$ symmetry, and hence in such a limit it is invariant under a global $\mathrm{SU(2)}_L \times \mathrm{SU(2)}_R$ symmetry, with $\mathrm{SU(2)}_L$ just being the global variant of the SM chiral gauge symmetry. This symmetry is preserved for non-vanishing Yukawa couplings, provided $h_u = h_d$. Once the Higgs acquires a VEV, both the $\mathrm{SU(2)}_L$ and $\mathrm{SU(2)}_R$ symmetry groups are broken but the diagonal subgroup $\mathrm{SU(2)}_{L+R}$ remains unbroken and is the subgroup that defines the custodial symmetry of the SM [25].

In the limit $g' \to 0$, the W and Z gauge bosons have equal mass and form a triplet of the $\mathrm{SU(2)}_{L+R}$ unbroken global symmetry. Using the expressions for the W and Z gauge boson masses in term of the gauge couplings, one obtains

$$\frac{m_W^2}{m_Z^2} = \frac{g^2}{g'^2+g^2} = \cos^2\theta_W \quad \text{or} \quad \rho \equiv \frac{m_W^2}{m_Z^2\cos^2\theta_W} = 1 \tag{11.8}$$

at tree level. The custodial symmetry protects the above relation between the W and Z masses under radiative corrections. All corrections to the ρ parameter are therefore proportional to terms that break the custodial symmetry. For instance, radiative corrections involving the Higgs are proportional to $\sin^2\theta_W$, $\delta\rho = -11G_Fm_Z^2\sin^2\theta_W\log(m_H^2/m_Z^2)/(24\sqrt{2}\pi^2)$, and vanish in the limit $g \to 0$. Since $m_t \neq m_b$, there are also relevant radiative corrections generated by massive fermions. They are proportional to $m_t^2 + m_b^2 - 2(m_t^2m_b^2)\log(m_t^2/m_b^2)/(m_t^2 - m_b^2)$ and would indeed vanish for $m_t = m_b$ [26].

II.3. Stability of the Higgs potential

The discovery of a scalar particle with mass $m_H \approx 125\,\mathrm{GeV}$ has far reaching consequences within the SM framework. In particular, the precise value of m_H determines the value of the quartic coupling λ at the electroweak scale and makes it possible to study its behavior up to high energy scales. A larger value of m_H would have implied that

the Higgs self-coupling would become non-perturbative at some scale Λ that could be well below the Planck scale. Specifically, from the measured values of the Higgs, top, W and Z masses and of the strong gauge coupling, all within their experimental uncertainties, it follows that the Higgs quartic coupling remains perturbative all the way up to M_{Planck} [5, 6, 27], like the SM gauge and Yukawa couplings, thereby rendering the SM a consistent, calculable theory.

However, for the value of Higgs mass experimentally measured, the EW vacuum of the Higgs potential is most likely metastable. Indeed, the high energy evolution of λ shows that it becomes negative at energies $\Lambda = \mathcal{O}(10^{10} - 10^{12})$ GeV, with a broader range if the top quark mass exceeds its current measured value by 3σ. When this occurs, the SM Higgs potential develops an instability and the long term existence of the EW vacuum is challenged. This behavior may call for new physics at an intermediate scale before the instability develops, i.e., below M_{Planck} or, otherwise, the electroweak vacuum remains metastable [28]. Reference [29] studied how new physics at M_{Planck} could influence the stability of the EW vacuum and possibly modify this conclusion. The consequences of the instability of the EW vacuum on high-scale inflation have been discussed in Refs. [30].

Within the SM framework, the relevant question is the lifetime of the EW metastable vacuum that is determined by the rate of quantum tunneling from this vacuum into the true vacuum of the theory (for the most recent computation of the EW vacuum lifetime within the SM, see Refs. [31]). The running of the Higgs self coupling slows down at high energies with a cancellation of its β-function at energies just one to two orders of magnitude below the Planck scale [32, 33]. This slow evolution of the quartic coupling is responsible for saving the EW vacuum from premature collapse, allowing it to survive much longer times than those from astrophysical considerations. It might help the Higgs boson to play the role of an inflaton [34] (see, however, Ref. [35] and references therein for potential issues with this Higgs-as-an-inflaton idea).

II.4. Higgs production and decay mechanisms

Reviews of the SM Higgs boson's properties and phenomenology, with an emphasis on the impact of loop corrections to the Higgs boson decay rates and cross sections, can be found in Refs. [36–43]. The state-of-the-art of the theoretical calculations in the main different production channels is summarized in Table 11.1.

II.4.1. Production mechanisms at hadron colliders

The main production mechanisms at the Tevatron collider and the LHC are gluon fusion, weak-boson fusion, associated production with a gauge boson and associated production with a pair of $t\bar{t}$ quarks. Figure 11.1 depicts representative diagrams for these dominant Higgs production processes.

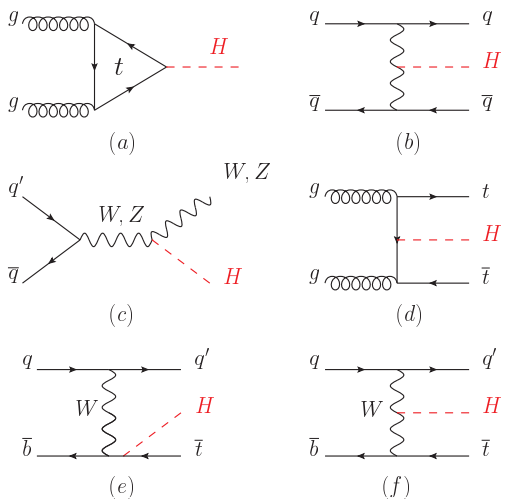

Figure 11.1: Main Leading Order Feynman diagrams contributing to the Higgs production in (a) gluon fusion, (b) Vector-boson fusion, (c) Higgs-strahlung (or associated production with a gauge boson), (d) associated production with a pair of top (or bottom) quarks, (e-f) production in association with a single top quark. with top quarks.

Table 11.2, from Refs. [40–43], summarizes the Higgs boson production cross sections and relative uncertainties for a Higgs mass of 125 GeV, for $\sqrt{s}$ = 7, 8, 13 and 14 TeV. The Higgs boson production cross sections in $p\bar{p}$ collisions at $\sqrt{s} = 1.96$ TeV for the Tevatron are obtained from Ref. [45].

Table 11.1: State-of-the-art of the theoretical calculations in the main different Higgs production channels in the SM, and main MC tools used in the simulations

ggF	VBF	VH	$t\bar{t}H$
Fixed order:	Fixed order:	Fixed order:	Fixed order:
NNLO QCD + NLO EW	NNLO QCD	NLO QCD+EW	NLO QCD
`(HIGLU, iHixs, FeHiPro, HNNLO)`	`(VBF@NNLO)`	`(V2HV and HAWK)`	`(Powheg)`
Resummed:	Fixed order:	Fixed order:	`(MG5_aMC@NLO)`
NNLO + NNLL QCD	NLO QCD + NLO EW	NNLO QCD	
`(HRes)`	`(HAWK)`	`(VH@NNLO)`	
Higgs p_T:			
NNLO+NNLL			
`(HqT, HRes)`			
Jet Veto:			
N3LO+NNLL			

The cross sections for the production of a SM Higgs boson as a function of $\sqrt{s}$, the center of mass energy, for pp collisions, including bands indicating the theoretical uncertainties, are summarized in Fig. 11.2(left) [44]. A detailed discussion, including uncertainties in the theoretical calculations due to missing higher-order effects and experimental uncertainties on the determination of SM parameters involved in the calculations can be found in Refs. [40–43]. These references also contain state-of-the-art discussions on the impact of PDF uncertainties, QCD scale uncertainties and uncertainties due to different procedures for including higher-order corrections matched to parton shower simulations as well as uncertainties due to hadronization and parton-shower events.

(i) Gluon fusion production mechanism

At high-energy hadron colliders, the Higgs boson production mechanism with the largest cross section is the gluon-fusion process, $gg \to H + X$, mediated by the exchange of a virtual, heavy top quark [46]. Contributions from lighter quarks propagating in the loop are suppressed proportional to m_q^2. QCD radiative corrections to the gluon-fusion process are very important and have been studied in detail. Including the full dependence on the (top, bottom, charm) quark and Higgs boson masses, the cross section has been calculated at the next-to-leading order (NLO) in α_s [47, 48]. To a very good approximation, the leading top-quark contribution can be evaluated

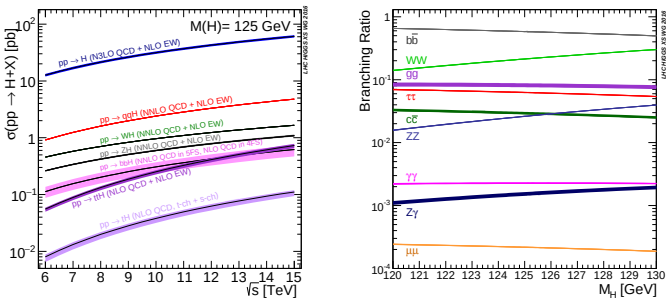

Figure 11.2: (Left) The SM Higgs boson production cross sections as a function of the center of mass energy, $\sqrt{s}$, for pp collisions [44]. The VBF process is indicated here as qqH. The theoretical uncertainties are indicated as bands. (Right) The branching ratios for the main decays of the SM Higgs boson near $m_H = 125\,\text{GeV}$ [42, 43]. The theoretical uncertainties are indicated as bands.

Table 11.2: The SM Higgs boson production cross sections for $m_H = 125\,\text{GeV}$ in pp collisions ($p\bar{p}$ collisions at $\sqrt{s} = 1.96\,\text{TeV}$ for the Tevatron), as a function of the center of mass energy, $\sqrt{s}$. The predictions for the LHC energies are taken from Refs. [40–43], the ones for the Tevatron energy are from Ref. [45]. The predictions for the ggF channel at the LHC include the latest N3LO results leading to reduced theoretical uncertainties by a factor around 2 compared to the N2LO results.

$\sqrt{s}$ (TeV)	Production cross section (in pb) for $m_H = 125\,\text{GeV}$					
	ggF	VBF	WH	ZH	$t\bar{t}H$	total
1.96	$0.95^{+17\%}_{-17\%}$	$0.065^{+8\%}_{-7\%}$	$0.13^{+8\%}_{-8\%}$	$0.079^{+8\%}_{-8\%}$	$0.004^{+10\%}_{-10\%}$	1.23
7	$16.9^{+5\%}_{-5\%}$	$1.24^{+2\%}_{-2\%}$	$0.58^{+3\%}_{-3\%}$	$0.34^{+4\%}_{-4\%}$	$0.09^{+8\%}_{-14\%}$	19.1
8	$21.4^{+5\%}_{-5\%}$	$1.60^{+2\%}_{-2\%}$	$0.70^{+3\%}_{-3\%}$	$0.42^{+5\%}_{-5\%}$	$0.13^{+8\%}_{-13\%}$	24.2
13	$48.6^{+5\%}_{-5\%}$	$3.78^{+2\%}_{-2\%}$	$1.37^{+2\%}_{-2\%}$	$0.88^{+5\%}_{-5\%}$	$0.50^{+9\%}_{-13\%}$	55.1
14	$54.7^{+5\%}_{-5\%}$	$4.28^{+2\%}_{-2\%}$	$1.51^{+2\%}_{-2\%}$	$0.99^{+5\%}_{-5\%}$	$0.60^{+9\%}_{-13\%}$	62.1

in the limit $m_t \to \infty$ by matching the SM to an effective theory. The gluon-fusion amplitude is then evaluated from an effective Lagrangian containing a local $HG^a_{\mu\nu}G^{a\,\mu\nu}$ operator [23, 24]. In this approximation the cross section is known at NLO [49], at next-to-next-to-leading order (NNLO) [50], and recently the computation at next-to-next-to-next-to-leading order (N3LO) has been completed [51]. The validity of the effective theory with infinite m_t is greatly enhanced by rescaling the result by the exact LO result: $\sigma = (\sigma^{LO}_{m_t}/\sigma^{LO}_{m_t=\infty}) \times \sigma_{m_t=\infty}$ [43]. The large top-quark mass approximation after this rescaling of the cross section yields NNLO calculations that has been established to be at the percent level accuracy by means of approximate calculations of the m_t dependence based on asymptotic expansions [52].

The LO and NLO QCD corrections amount to about 80% of the total cross section at N3LO given below. The NNLO corrections further enhance the cross section by approximately 30% of the LO plus NLO result (at $\mu_f = \mu_r = m_H/2$). Electroweak radiative corrections have been computed at NLO and increase the LO cross section by about 5% for $m_H \simeq 125\,\text{GeV}$ [53]. Mixed QCD-electroweak corrections of $O(\alpha\alpha_s)$ are presently unknown [43].

The NLO and NNLO fixed-order QCD predictions for the gluon-fusion cross section have been improved by resumming the soft, virtual and collinear gluon contributions to the cross section at next-to-next-to-leading logarithmic (NNLL) and partial NNNLL accuracy [55]. Precise predictions for the gluon-fusion cross section for different Higgs boson masses and LHC energies, and including detailed error estimates, have been obtained by combining the NNLO fixed-order QCD results with soft-gluon resummation at NNLL or NNNLL accuracy and two-loop electroweak corrections, and using the most recent sets of parton distribution functions [54, 56].

The perturbative QCD computation has been recently extended to N3LO. At this order the perturbation series is rather stable with a mere enhancement of 3% of the total cross section, with a central value quite insensitive to threshold resummation effects with the scale choice mentioned above [51, 57, 43]. At the LHC with a center-of-mass energy of 13 TeV, the most up-to-date value for the production cross section of a 125 GeV Higgs boson amounts to [43]

$$\sigma^{N3LO}_{ggF} = 48.6\,\text{pb}^{+2.2\,\text{pb}(+4.6\%)}_{-3.3\,\text{pb}(-6.7\%)}(\text{theory}) \pm 1.6\,\text{pb}(3.2\%)(\text{PDF} + \alpha_s).$$

Besides considering the inclusive Higgs boson production cross section at the LHC, it is important to study differential distributions in order to probe the properties of the Higgs boson in a detailed way. A more exclusive account of Higgs production is also required because experimental analyses often impose cuts on the final states in order to improve the signal-to-background ratio. To this end, it is useful to define benchmark cuts and compare the differential distributions obtained at various levels of theoretical accuracy (i.e., at NLO or NNLO) with Monte Carlo generators. Many search modes for the Higgs boson are carried out by separating the events according to the number of jets or the transverse momentum and rapidity of the Higgs boson. For $p_T < 30\,\text{GeV}$, predictions for the transverse-momentum distribution can only be trusted after large logarithms of the form $\alpha_s^n \ln^{2n-1}(m_H/p_T)$ have been resummed to all orders in perturbation theory [58]. This has been accomplished with NNLL accuracy [59], and the results have been matched onto the fixed-order prediction at NNLO [60]. Electroweak corrections have been studied in Ref. [61]. The effect of the non-zero quark mass on the transverse momentum spectrum has most recently been considered in Ref. [62], while the effect of the finite top mass on other differential observables has been studied in Refs. [63, 64]. There has been much activity in computing Higgs plus jet(s) production processes at NLO (see e.g. Refs. [65, 66] for associated production with one and two jets, respectively), and even at NNLO [67]. In addition, efforts to improve the calculation of the Higgs production cross section with a jet veto (the "0-jet bin") by resumming large logarithms of the form $\alpha_s^n \ln^{2n-1}(m_H/p_T^{\text{veto}})$ at NNLL order and beyond [68] have been made. Recently, reference results for the resummed cross section at NNLL have been combined with the N3LO result for the inclusive cross section to obtain accurate predictions for the jet-veto efficiency and zero-jet cross section [69]. Accurate predictions for the jet-veto cross section are required, e.g., to suppress the $t\bar{t}$ background in the $H \to WW$ channel [70].

(ii) Vector boson fusion production mechanism

The SM Higgs production mode with the second-largest cross section at the LHC is vector boson fusion (VBF). At the Tevatron collider, VBF also occurred, but for $m_H = 125\,\text{GeV}$ had a smaller cross section than Higgs production in association with a W or Z boson. Higgs production via VBF, $qq \to qqH$, proceeds by the scattering of two (anti-)quarks, mediated by t- or u-channel exchange of a W or Z boson, with the Higgs boson radiated off the weak-boson propagator. The scattered quarks give rise to two hard jets in the forward and backward regions of the detector. Because of the color-singlet nature of the weak-gauge boson exchange, gluon radiation from the central-rapidity regions is strongly suppressed. These characteristic features of VBF processes can be exploited to distinguish them from overwhelming QCD backgrounds, including gluon-fusion induced Higgs + 2 jet production, and from s-channel WH or ZH production with a hadronically decaying weak gauge boson. After the application of specific selection cuts, the VBF channel provides a clean environment, not only for Higgs searches but also for the determination of Higgs boson couplings at the LHC [71].

Computations for total cross sections and differential distributions to Higgs production via VBF including NLO QCD and EW corrections have been presented in Refs. [37, 72] and are available in the form of flexible parton-level Monte-Carlo generators. Parton-shower effects have been considered in Ref. [73]. The NNLO QCD corrections to the total rate have been presented in Refs. [74]. They reduce the residual scale uncertainties on the inclusive cross section to approximately 2%. The uncertainties due to parton distributions are estimated to be at the same level. Fully differential predictions at NNLO have been

computed recently [75], suggesting that the cross section under VBF cuts receives NNLO corrections that are larger than in the inclusive case and may reach O(5-6%).

(iii) WH and ZH associated production mechanism

The next most relevant Higgs boson production mechanisms after gluon fusion and VBF at the LHC, and the most relevant ones after gluon fusion at the Tevatron collider, are associated production with W and Z gauge bosons. The cross sections for the associated production processes, $pp \to VH + X$, with $V = W^{\pm}, Z$ receive contributions at NLO given by NLO QCD corrections to the Drell–Yan cross section [76–78] and from NLO EW corrections. The latter, unlike the QCD corrections, do not respect the factorization into Drell–Yan production since there are irreducible box contributions already at one loop [79]. At NNLO, the Drell-Yan-like corrections to WH production also give the bulk of the corrections to ZH production [80]. For ZH production there are, however, gluon-gluon induced contributions that do not involve a virtual Z gauge boson but are such that the Z gauge boson and H boson couple to gluons via top-quark loops [81]. In addition, WH and ZH production receive non Drell–Yan-like corrections in the $q\bar{q}'$ and $q\overline{q}$ initiated channels, respectively, at the NNLO level, where the Higgs is radiated off top-quark loops [82]. The full QCD corrections up to NNLO order, the NLO EW corrections and the NLO corrections to the gluon-gluon channel are available in VH@NNLO [83].

As neither the Higgs boson nor the weak gauge bosons are stable particles, their decays also have to be taken into account. Providing full kinematical information for the decay products can furthermore help in the suppression of large QCD backgrounds. Differential distributions for the processes $pp \to WH \to \nu_\ell \ell H$ and $pp \to ZH \to \ell^+\ell^- H/\nu_\ell \bar{\nu}_\ell H$, including NLO QCD and EW corrections, have been presented in Ref. [84]. The NNLO QCD corrections to differential observables for WH production at the LHC, including the leptonic decays of the W boson and the decay of the Higgs boson into a $b\bar{b}$ pair, are presented in Ref. [85]. Calculations at the same level, including also the ZH process have been performed [86, 87]. The WH production mode has also been matched to a parton shower at NNLO accuracy [88]. The WH and ZH production modes, together with Higgs production in association with a top-quark pair, provide a relatively clean environment for studying the decay of the Higgs boson into bottom quarks.

(iv) Higgs production in association with $t\bar{t}$

Higgs radiation off top quarks, $pp \to t\bar{t}H$, provides a direct probe of the top-Higgs Yukawa coupling. The LO cross section for this production process was computed in Ref. [89]. Later, the NLO QCD corrections [90] were evaluated yielding a moderate increase in the total cross section of at most 20%, but significantly reducing the scale dependence of the inclusive cross section. The total theoretical errors, estimated by combining the uncertainties from factorization and renormalization scales, strong gauge coupling, and parton distributions, amount to 10–15% of the corresponding inclusive cross section. Interfaces between NLO QCD calculations for $t\bar{t}H$ production with parton-shower Monte Carlo programs have been provided in Ref. [91]. These programs provide the most flexible tools to date for the computation of differential distributions, including experimental selection cuts and vetoes on the final-state particles and their decay products.

(v) Other single Higgs production mechanisms at the LHC

The Higgs production in association with a single top quark, though subdominant, can bring valuable information, in particular regarding the sign of the top Yukawa coupling. This is due to an almost totally destructive interference between two large contributions, one where the Higgs couples to a space-like W boson and the other where it couples to the top quark. This process has been computed at NLO in a five-flavor scheme [92] and amounts to about 90 fb at $\sqrt{s} = 14$ TeV (with the opposite sign of the top Yukawa coupling, the cross section increases by one order of magnitude).

The Higgs boson production in association with bottom quarks is known at NNLO in the case of five quark flavors [93–95]. The coupling of the Higgs boson to a b quark is suppressed in the SM by the bottom-quark mass over the Higgs VEV, m_b/v, implying that associated production of a SM Higgs boson with b quarks is small at the LHC. Yet, at high energy, large logarithms are present and need to be resummed, leading to an enhancement of the inclusive cross section. At $\sqrt{s} = 14$ TeV the $b\bar{b}H$ cross section can be as large as 550 fb, still two orders of magnitude below the ggF production cross section. In a two Higgs doublet model or a supersymmetric model, which will be discussed in Section VII, this coupling is proportional to the ratio of neutral Higgs boson vacuum expectation values, $\tan\beta$, and can be significantly enhanced for large values of this ratio. Consequently, the $b\bar{b}H$ mode can even become the dominant production process for the Higgs boson.

The Higgs production in association with charm quarks is also known at NNLO and is about 85 fb at $\sqrt{s} = 13$ TeV.

(vi) Double Higgs production at the LHC

The main interest in the double Higgs production is that it can provide invaluable information on the Higgs potential. In particular, it gives access to the Higgs cubic self-interaction. The dominant production is via gluon fusion $gg \to HH$. The NLO [96] and NNLO [97] fixed order corrections to $gg \to HH$ are known in the infinite top mass limit and, recently, the complete NLO corrections with all top quark mass effects also became available [98]. The QCD corrections are large, typically doubling the cross section from LO to NLO and further enhancing it by 20% from NLO to NNLO. At the differential level, the destructive interference between the box and the triangle contributions complicates the predictions made in the infinite top mass limit for both the HH invariant mass and the leading Higgs p_T distributions. With an inclusive cross section of about 40 fb at $\sqrt{s} = 13$ TeV and a difficult signal vs. background discrimination, the double Higgs production remains a challenging channel to probe and will greatly benefit from the high-luminosity run of the LHC.

II.4.2. Production mechanisms at e^+e^- colliders

The main Higgs boson production cross sections at an e^+e^- collider are the Higgs-strahlung process $e^+e^- \to ZH$ [6, 23, 99], and the WW fusion process [100] $e^+e^- \to \bar{\nu}_e\nu_e W^*W^* \to \bar{\nu}_e\nu_e H$. The cross-section for the Higgs-strahlung process scales as s^{-1} and is dominant at low energies, while the cross-section for the WW fusion process scales as $\ln(s/m_H^2)$ and dominates at high energies [101–103]. The ZZ fusion mechanism, $e^+e^- \to e^+e^- Z^*Z^* \to e^+e^- H$, also contributes to Higgs boson production, with a cross-section suppressed by an order of magnitude with respect to that of WW fusion. The process $e^+e^- \to t\bar{t}H$ [104, 105] becomes important for $\sqrt{s} \geq 500$ GeV. For a more detailed discussion of Higgs production properties at lepton colliders see, for example, Refs. [38, 39, 106, 107] and references therein.

II.4.3. SM Higgs branching ratios and total width

For the understanding and interpretation of the experimental results, the computation of all relevant Higgs decay widths is essential, including an estimate of their uncertainties and, when appropriate, the effects of Higgs decays into off-shell particles with successive decays into lighter SM ones. A Higgs mass of about 125 GeV allows to explore the Higgs couplings to many SM particles. In particular the dominant decay modes are $H \to b\bar{b}$ and $H \to WW^*$, followed by $H \to gg$, $H \to \tau^+\tau^-$, $H \to c\bar{c}$ and $H \to ZZ^*$. With much smaller rates follow the Higgs decays into $H \to \gamma\gamma$, $H \to \gamma Z$ and $H \to \mu^+\mu^-$. Since the decays into gluons, diphotons and $Z\gamma$ are loop induced, they provide indirect information on the Higgs couplings to WW, ZZ and $t\bar{t}$ in different combinations. The uncertainties in the branching ratios include the missing higher-order corrections in the theoretical calculations as well as the errors in the SM input parameters, in particular fermion masses and the QCD gauge coupling, involved in the decay. In the following the state-of-the-art of the theoretical calculations will be discussed and the reader is referred to Refs. [40, 41, 108] for detail.

The evaluation of the radiative corrections to the fermionic decays of the SM Higgs are implemented in HDECAY [109] at different levels of accuracy. The computations of the $H \to b\bar{b}$ and $H \to c\bar{c}$ decays include the complete massless QCD corrections up to N4LO,

with a corresponding scale dependence of about 0.1% [110]. Both the electroweak corrections to $H \to b\bar{b}$, $c\bar{c}$ as well as $H \to \tau^+\tau^-$ are known at NLO [111] providing predictions with an overall accuracy of about 1-2% for $m_H \simeq 125\,\text{GeV}$.

The loop induced decays of the SM Higgs are known at NLO and partially beyond that approximation. For $H \to gg$, the QCD corrections are known up to N3LO in the limit of heavy top quarks [112, 48] and the uncertainty from the scale dependence is about 3%. For the $H \to \gamma\gamma$, the full NLO QCD corrections are available [48, 113] and the three-loop QCD corrections have also been evaluated [114]. The NLO electroweak corrections to $H \to gg$ and $H \to \gamma\gamma$ have been computed in Ref. [115]. All these corrections are implemented in HDECAY [109]. For $m_H = 125\,\text{GeV}$, the overall impact of known QCD and EW radiative effects turns out to be well below 1%. In addition, the contribution of the $H \to \gamma e^+ e^-$ decay via virtual photon conversion has been computed in Ref. [116]. The partial decay width $H \to Z\gamma$ is only implemented at LO in HDECAY, including the virtual W, top-, bottom-, and τ-loop contributions. The QCD corrections have been calculated and are at the percent level [117], The theoretical uncertainty due to unknown electroweak corrections is estimated to be less than 5%, an accuracy that will be hard to achieve in measurements of this processes at the LHC.

The decays $H \to WW/ZZ \to 4f$ can be simulated with the Prophecy4f Monte-Carlo generator [118] that includes complete NLO QCD and EW corrections for Higgs decays into any possible four-fermion final state. All calculations are consistently performed with off-shell gauge bosons, without any on-shell approximation. For the SM Higgs boson the missing higher-order corrections are estimated to be roughly 0.5%. Such uncertainties will have to be combined with the parametric uncertainties, in particular those associated to the bottom-quark mass and the strong gauge coupling, to arrive at the full theory uncertainties. A detailed treatment of the differential distributions for a Higgs decay into four charged leptons in the final state is discussed in Refs. [42, 119].

The total width of a 125 GeV SM Higgs boson is $\Gamma_H = 4.07 \times 10^{-3}\,\text{GeV}$, with a relative uncertainty of $^{+4.0\%}_{-3.9\%}$. The branching ratios for the most relevant decay modes of the SM Higgs boson as a function of m_H, including the most recent theoretical uncertainties, are shown in Fig. 11.2(right) and listed for $m_H = 125\,\text{GeV}$ in Table 11.3. Further details of these calculations can be found in Refs. [108, 120] and in the reviews [37–43].

Table 11.3: The branching ratios and the relative uncertainty [42, 43] for a SM Higgs boson with $m_H = 125\,\text{GeV}$.

Decay channel	Branching ratio	Rel. uncertainty
$H \to \gamma\gamma$	2.27×10^{-3}	$^{+5.0\%}_{-4.9\%}$
$H \to ZZ$	2.62×10^{-2}	$^{+4.3\%}_{-4.1\%}$
$H \to W^+W^-$	2.14×10^{-1}	$^{+4.3\%}_{-4.2\%}$
$H \to \tau^+\tau^-$	6.27×10^{-2}	$^{+5.7\%}_{-5.7\%}$
$H \to b\bar{b}$	5.84×10^{-1}	$^{+3.2\%}_{-3.3\%}$
$H \to Z\gamma$	1.53×10^{-3}	$^{+9.0\%}_{-8.9\%}$
$H \to \mu^+\mu^-$	2.18×10^{-4}	$^{+6.0\%}_{-5.9\%}$

III. The experimental profile of the Higgs boson

An indirect experimental bound on the SM Higgs boson can be obtained by comparing precision electroweak data with SM predictions, that have a weak, logarithmic dependence on M_H. A global fit to electroweak data suggests $m_H = 96^{+22}_{-19}\,\text{GeV}$, or $m_H < 134\,\text{GeV}$ at 90% confidence level [121].

The announcement on July 4, 2012 of the observation [1, 2] at the LHC of a narrow resonance with a mass of about 125 GeV was an important landmark in the decades-long direct search [122, 123] for the SM Higgs boson. This was followed by a detailed exploration of properties of the Higgs boson at the different runs of the LHC at $\sqrt{s}$ = 7, 8 and 13 TeV.

The dataset delivered so far by LHC, while the Run 2 is still ongoing, corresponds to an integrated luminsoity exceeding $100\,\text{fb}^{-1}$ see Table 11.4. The datasets effectively useful for analysis need to take into account the data-taking efficiency with fully operational detecors and the data quality efficiency. The typical total inefficiency for both the ATLAS and CMS experiments are approximately 10%.

Table 11.4: The LHC running conditions and delivered data samples.

Year	$\sqrt{s}$ (TeV)	$\int$ L.dt (fb^{-1})	Run Period
2010	7	0.04	Run 1
2011	7	6.1	Run 1
2012	8	23.3	Run 1
2015	13	4.2	Run 2
2016	13	40.8	Run 2
2017	13	in progress (> 40)	Run 2

III.1. The principal decay channels to vector bosons

For a given m_H, the sensitivity of a search channel depends on the production cross section of the Higgs boson, its decay branching fraction, reconstructed mass resolution, selection efficiency and the level of background in the final state. For a low-mass Higgs boson ($110\,\text{GeV} < m_H < 150\,\text{GeV}$) where the natural width is only a few MeV, five decay channels play an important role at the LHC. In the $H \to \gamma\gamma$ and $H \to ZZ \to 4\ell$ channels, all final state particles can be very precisely measured and the reconstructed m_H resolution is excellent (typically 1-2%). While the $H \to W^+W^- \to \ell^+\nu_\ell\ell'^-\bar{\nu}_{\ell'}$ channel has relatively large branching fraction, the m_H resolution is poor (approximately 20%) due to the presence of neutrinos. The $H \to b\bar{b}$ and the $H \to \tau^+\tau^-$ channels suffer from large backgrounds and a intermediate mass resolution of about 10% and 15% respectively. For $m_H > 150\,\text{GeV}$, the sensitive search channels are $H \to WW$ and $H \to ZZ$ where the W or Z boson decays into a variety of leptonic and hadronic final states. These decay channels of the Higgs boson are searched for in the five Higgs boson production processes (ggF, VBF, WH, ZH and $t\bar{t}H$) described in Section II.4.1.

The candidate events in each Higgs boson decay channel are split into several mutually exclusive categories (or event tags) based on the specific topological, kinematic or other features present in the event. The categorization of events increases the sensitivity of the overall analysis and allows a separation of different Higgs boson production processes. Most categories are dominated by signal from one Higgs decay mode but contain an admixture of various Higgs production processes. For example, a typical VBF selection requires Higgs boson candidates to be accompanied by two energetic jets ($\geq 30\,\text{GeV}$) with a large dijet mass ($\geq 400\,\text{GeV}$) and separated by a large pseudorapidity ($\Delta\eta_{jj} \geq 3.5$). While such a category is enriched in Higgs bosons produced via VBF, the contamination from the gluon fusion production mechanism can be significant. Hence a measurement of the signal rate in the VBF category does not imply a measurement of VBF production cross-section. Simulations are used to determine the relative contributions of the various Higgs production modes in a particular category.

III.1.1. $H \to \gamma\gamma$

In the $H \to \gamma\gamma$ channel a search is performed for a narrow peak over a smoothly falling background in the invariant mass distribution of two high p_T photons. The background in this channel is conspicuous and stems from prompt $\gamma\gamma$ processes for the irreducible backgrounds, and the γ+jet and dijet processes for the reducible backgrounds where one jet fragments typically into a leading π^0. In order to optimize search sensitivity and also to separate the various Higgs production modes,

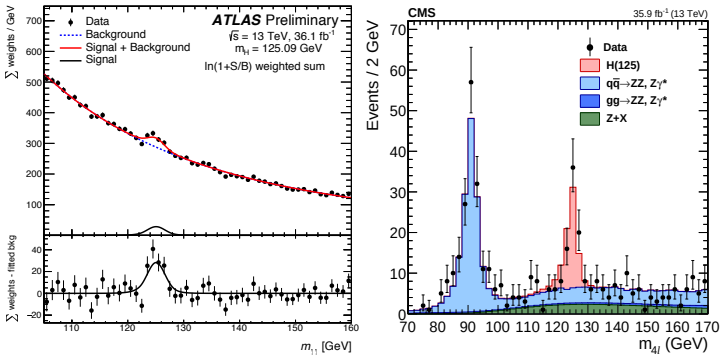

Figure 11.3: (Left) The invariant mass distribution of diphoton candidates, with each event weighted by the ratio of signal-to-background in each event category, observed by ATLAS [124] at Run 2. The residuals of the data with respect to the fitted background are displayed in the lower panel. (Right) The $m_{4\ell}$ distribution from CMS [125] Run 2 data.

ATLAS and CMS experiments split events into several mutually exclusive categories. Diphoton events containing a high p_T muon or electron, or missing energy (E_T^{miss}) consistent with the decay of a W or Z boson are tagged in the VH production category. Diphoton events containing energetic dijets with a large mass and pseudorapidity difference are assigned to the VBF production category, and the remaining events are considered either in the VH category when the two jets are compatible with the hadronic decay of a W or a Z, or in the gluon fusion production category. While the leptonic VH category is relatively pure, the VBF category has significant contamination from the gluon fusion process. Events which are not picked by any of the above selections are further categorized according to their expected $m_{\gamma\gamma}$ resolution and signal-to-background ratio. Categories with good m_H resolution and larger signal-to-background ratio contribute most to the sensitivity of the search.

Both ATLAS and CMS have studied in detail the calibration of the energy response of photons, in particular using $Z \to e^+e^-$, $Z \to \mu^+\mu^-\gamma$ and the response of muons in the calorimeter (for ATLAS) from $Z \to \mu^+\mu^-$ events. This information is used to correct the simulated signal mass lineshapes. In each category, parametric signal models are adjusted to these lineshape to provide a functional form for the signal. Simple monotonic functional forms of the backgrounds are determined by a fit to the $m_{\gamma\gamma}$ distribution in each category. All categories are fitted simultaneously to determine the signal yield at the measured combined Run 1 mass of 125.09 GeV discussed in Section III.2. The $m_{\gamma\gamma}$ distribution after combining all categories is shown for the ATLAS experiment in Fig. 11.3 using Run 2 data.

The signal strength $\mu = (\sigma \cdot \text{BR})_{\text{obs}}/(\sigma \cdot \text{BR})_{\text{SM}}$, which is the observed product of the Higgs boson production cross section (σ) and its branching ratio (BR) in units of the corresponding SM values, is 1.17 ± 0.27 for ATLAS [126] in Run 1 and 0.99 ± 0.14 in Run 2 [124]. The signal strengths [2] measured in Run 1 and Run 2 by the CMS collaboration are $0.78^{+0.26}_{-0.23}$ [127] and $1.16^{+0.15}_{-0.14}$ [128] respectively.

III.1.2. $H \to ZZ^* \to \ell^+\ell^-\ell'^+\ell'^-$

In the $H \to ZZ^* \to \ell^+\ell^-\ell'^+\ell'^-$ channel a search is performed for a narrow mass peak over a small continuous background dominated by non-resonant ZZ^* production from $q\overline{q}$ annihilation and gg fusion processes. The contribution and the shape of this irreducible background is taken from simulation. The subdominant and reducible backgrounds stem from $Z + b\bar{b}$, $t\bar{t}$ and $Z +$ jets events. Their contribution is suppressed by requirements on lepton isolation and lepton impact parameter and their yield is estimated from control samples in data.

[2] The Run 1 results for the ATLAS and CMS experiments are at fixed values of $m_H = 125.4$ GeV and 124.7 GeV.respectively.

To help distinguish the Higgs signal from the dominant non-resonant ZZ^* background, both ATLAS [129] and CMS [130] use a matrix element likelihood approach to construct a kinematic discriminant built for each 4ℓ event based on the ratio of complete leading-order matrix elements $|\mathcal{M}_{sig}{}^2/\mathcal{M}_{bkg}{}^2|$ for the signal ($gg \to H \to 4\ell$) and background($q\overline{q} \to ZZ \to 4\ell$) hypotheses. The signal matrix element $\mathcal{M}_{sig}$ is computed assuming $m_H = m_{4\ell}$. To further enhance the sensitivity to a signal, various techniques are used by the experiments based on the matrix element or a multivariate analyses.

To enhance the sensitivity to VBF and VH production processes, the ATLAS and CMS experiments divide 4ℓ events into mutually exclusive categories. Events containing dijets with a large mass and pseudorapidity difference populate the VBF category. ATLAS requires the presence of an additional lepton in the VH category. In events with less than two jets, CMS uses the $p_T^{4\ell}$ to distinguish between production via the gluon fusion and the VH/VBF processes.

Since the $m_{4\ell}$ resolutions and the reducible background levels are different in the 4μ, $4e$ and $2e2\mu$ subchannels, they are analyzed separately and the results are then combined. The distribution of the reconstructed invariant mass of the four leptons for the CMS experiment [125] is given in Fig. 11.3 (right), showing a clear excess at a mass of approximately $m_H = 125$ GeV. Both experiments also observe a clear peak at $m_{4\ell} = 91$ GeV from the production of a Z boson on-mass-shell and decaying to four leptons due typically to the emission of an off-shell photon from one of the primary leptons from the Z boson decay.

The signal strengths μ for the inclusive $H \to 4\ell$ production measured by the ATLAS and CMS experiments are $1.44^{+0.40}_{-0.33}$ at $m_H = 125.36$ GeV [129] and $0.93^{+0.29}_{-0.25}$ at $m_H = 125.6$ GeV [131] respectively, in Run 1. The signal strengths measured by the ATLAS and CMS experiments in Run 2 are $1.28^{+0.21}_{-0.19}$ [132] and $1.05^{+0.19}_{-0.25}$ [125] respectively, both measurements are made at the combined Run 1 Higgs mass of $m_H = 125.09$ GeV.

III.1.3. Measurement of the Higgs boson mass

To measure the mass of the Higgs boson, ATLAS and CMS collaborations rely on the two high mass resolution and sensitive channels, $\gamma\gamma$ and ZZ. The ATLAS & CMS approaches are very similar in these two analyses with small differences on the usage of categories, additional discriminating variables and per-event errors. In these two channels the mass resolutions range from 1.4 GeV to 2 GeV for ATLAS and from 1.0 GeV to 2.8 GeV for CMS. The best mass resolution is obtained for both experiments in the diphoton channel for central diphoton pairs (typically for events where both photons are not converted). The signal strengths in the $\gamma\gamma$ and ZZ channels are assumed to be independent and not constrained to the expected rate ($\mu = 1$) for the SM Higgs boson.

Figure 11.4 summarizes all measurements of the Higgs boson mass, including the individual and combined Run 1 measurements [133] and preliminary Run 2 measurement by ATLAS [134] for both the diphoton and the 4ℓ channels and CMS [125] for the 4ℓ channel. The CMS collaboration has also reported a preliminary best fit mass in the diphoton channel of $m_H = 125.4$ GeV with a statistical uncertainty of 150 MeV and a systematic uncertainty preliminarily evaluated as between 200 MeV and 300 MeV

In the diphoton channel, as discussed in Section V.3.2 a mass shift is expected to be induced by the deformation of the mass lineshape of the signal in presence of background, from the interference between the Higgs boson production and the continuum irreducible background. It is a small but non negligible effect of approximately 35 MeV [135] for a Higgs boson width close to that of the SM. This effect could be larger if the width of the discovered particle were to be completely different. This effect estimated by ATLAS with a full simulation is still relatively small with respect to the total uncertainty on the mass and is therefore neglected.

III.1.4. $H \to W^+W^- \to \ell^+\nu\ell^-\overline{\nu}$

In this intricate channel, experiments search for an excess of events with two leptons of opposite charge accompanied by missing energy and up to two jets. Events are divided into several categories

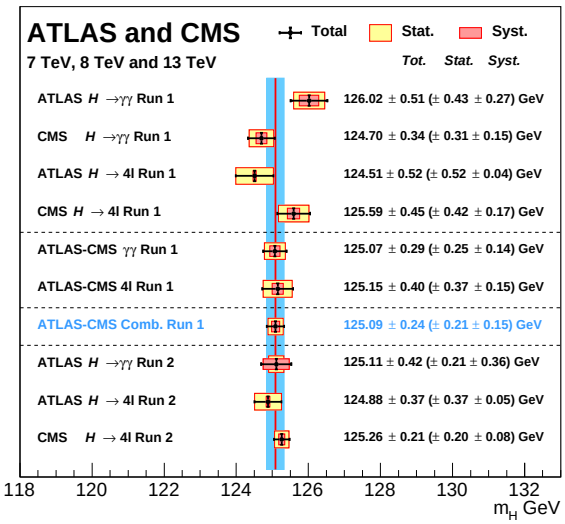

Figure 11.4: Summary of the CMS and ATLAS mass measurements in the $\gamma\gamma$ and ZZ channels in Run 1 and Run 2.

depending on the lepton flavor combination (e^+e^-, $\mu^+\mu^-$and $e^\pm\mu^\mp$) and the number of accompanying jets ($N_{\text{jet}} = 0, 1, \geq 2$). The $N_{\text{jet}} \geq 2$ category is optimized for the VBF production process by selecting two leading jets with a large pseudorapidity difference and with a large mass ($m_{jj} > 500\,\text{GeV}$).

Backgrounds contributing to this channel are numerous and depend on the category of selected events. Reducing them and accurately estimating the remainder is a major challenge in this analysis. For events with opposite-flavor lepton and no accompanying high p_T jets, the dominant background stems from non-resonant WW production. Events with same-flavor leptons suffer from large Drell–Yan contamination. The $t\bar{t}$, Wt and $W+$jets (with the jet misidentified as a lepton) events contaminate all categories. Non-resonant WZ, ZZ and $W\gamma$ processes also contribute to the background at a sub-leading level.

A requirement of large missing transverse energy (E_T^{miss}) is used to reduce the Drell–Yan and multijet backgrounds. In the e^+e^- and $\mu^+\mu^-$ categories, events with $m_{\ell\ell}$ consistent with the Z mass are vetoed. The $t\bar{t}$ background is suppressed by a veto against identified b-jets or low p_T muons (assumed to be coming from semileptonic b-hadron decays within jets) and tight isolation requirements diminish the W+jets background. The scalar nature of the Higgs boson and the $V-A$ nature of the W boson decay implies that the two charged leptons in the final state are preferentially emitted at small angles with respect to each other. Therefore the dilepton invariant mass ($m_{\ell\ell}$) and the azimuthal angle difference between the leptons ($\Delta\phi_{\ell\ell}$) are used to discriminate between the signal and non-resonant WW events. The transverse mass, constructed from the dilepton p_T ($p_T^{\ell\ell}$), E_T^{miss} and the azimuthal angle between E_T^{miss} and $p_T^{\ell\ell}$, is defined as $m_T = \sqrt{2p_T^{\ell\ell}E_T^{\text{miss}}(1-\cos\Delta\phi_{E_T^{\text{miss}}\ell\ell})}$ and serves as an effective discriminant against backgrounds. The transverse mass variable also tracks the Higgs boson mass but with a poor mass resolution. All residual background rates except for the small contributions from non-resonant WZ, ZZ and $W\gamma$ are evaluated from control samples devised from data.

ATLAS fits the m_T distributions and observes [136] an excess at $m_H = 125.36\,\text{GeV}$ with a local significance of 6.1σ similar to that expected from a 125 GeV SM Higgs boson. The measured inclusive signal strength is $\mu = 1.09^{+0.23}_{-0.21}$. In the VBF category an excess with a significance of 3.2σ corresponding to a signal strength of $\mu = 1.27^{+0.53}_{-0.45}$ is observed [136]. The CMS analysis of 0 and 1 jet categories, using all lepton flavor combinations, shows [137] an excess with an observed significance of 4.3σ, lower than the expected sensitivity of 5.8σ for a 125.6 GeV SM Higgs boson. CMS observes [137] no significant excess in the VBF production mode and sets a 95% CL limit on the signal strength of $\mu_{\text{VBF}} < 1.7$ for $m_H = 125.6\,\text{GeV}$.

The ATLAS and CMS experiments have also searched for the associated Higgs boson production (VH) in this channel. The signal consists of up to three (WH) or four (ZH) high p_T isolated leptons with missing transverse energy and low hadronic activity. The major backgrounds stem from triboson and diboson production where each boson decays leptonically. ATLAS observes [138] an excess at $m_H = 125.36\,\text{GeV}$ with a local significance of 2.5σ corresponding to a $\mu_{VH} = 3.0^{+1.6}_{-1.0}$. CMS instead sets [137] a 95% CL limit of $\mu_{VH} < 4.7$.

In this channel the full Run 2 dataset has not yet been analysed by ATLAS or CMS. The main results are still from Run 1 [136, 137]. There have been partial analyses made with Run 2 data at 13 TeV by both the ATLAS and CMS experiments. The former has analyzed the WW decay mode in the VBF and VH production mode with 2015 dataset corresponding to an integrated luminosity of $5.8\,\text{fb}^{-1}$ [139]. The latter has performed a more complete analysis with the full 2015 dataset and $15.2\,\text{fb}^{-1}$ of 2016 data, with most production channels covered in the cleaner opposite flavor electron-muon decay mode of the WW pair [140].

III.2. Decays to fermions

At hadron colliders, the most promising channel for probing the coupling of the Higgs field to the quarks and leptons are $H \to b\bar{b}$ and $H \to \tau^+\tau^-$, respectively. For a Higgs boson with $m_H \approx 125\,\text{GeV}$, the branching fraction to $b\bar{b}$ is about 57% and to $\tau^+\tau^-$ is about 6%. Nevertheless, the presence of very large backgrounds makes the isolation of a Higgs boson signal in these channels quite challenging.

III.2.1. $H \to \tau^+\tau^-$

In the $H \to \tau\tau$ search, τ leptons decaying to electrons (τ_e), muons (τ_μ) and hadrons (τ_{had}) are considered. The $\tau^+\tau^-$ invariant mass ($m_{\tau\tau}$) is reconstructed from a kinematic fit of the visible products from the two τ leptons and the missing energy observed in the event. Due to the presence of missing neutrinos, the $m_{\tau^+\tau^-}$ resolution is poor ($\approx 15\%$). As a result, a broad excess over the expected background in the $m_{\tau\tau}$ distribution is searched for. The major sources of background stem from Drell–Yan $Z \to \tau^+\tau^-$ and $Z \to e^+e^-$, W+jets, $t\bar{t}$ and multijet production. Events in all subchannels are divided into categories based on the number and kinematic properties of additional energetic jets in the event. The sensitivity of the search is generally higher for categories with one or more additional jets. The VBF category, consisting of a τ pair with two energetic jets separated by a large pseudorapidity, has the best signal-to-background ratio and search sensitivity, followed by the $\tau^+\tau^-$+1 jet category. The signal to background discrimination relies in part on the $m_{\tau\tau}$ resolution, which improves with the boost of the Higgs boson. The non-VBF categories are further subdivided according to the observed boost of the $\tau^+\tau^-$ system. CMS primarily uses the reconstructed $m_{\tau\tau}$ as the final discriminating variable [141] while the ATLAS experiment combines various kinematic properties of each event categories with multivariate techniques to build the final discriminant [142].

Searches for $H \to \tau^+\tau^-$ decays in the VH production mode are also performed in final states where the W or Z boson decays into leptons or jets. The irreducible background in this search arises from non-resonant WZ and ZZ diboson production. The reducible backgrounds originate from W, Z, and $t\bar{t}$ events that contain at least one fake lepton in the final state due to a misidentified jet. The shape and yield of the major backgrounds in each category is estimated from control samples in data. Contributions from non-resonant WZ and ZZ diboson production are estimated from simulations but corrected for reconstruction efficiency using control samples formed from observed data.

For the CMS experiment, the significance of the observed excess at $m_H = 125\,\text{GeV}$ in Run 1 is 3.2 standard deviations, close to the expected 3.7 standard deviations sensitivity, and corresponds to a signal strength of $\mu = 0.86 \pm 0.29$. The observed (expected) deviation from the background-only hypothesis in ATLAS corresponds to a local

significance of 4.5 (3.4) standard deviations and the best fit value of the signal strength is $\mu = 1.43^{+0.43}_{-0.37}$ [142].

When the ATLAS and CMS $H \to \tau\tau$ Run 1 measurements are combined [143], the significance of the observed excess corresponding to $m_H = 125.09\,\text{GeV}$ is 5.5 standard deviations and the combined signal strength is $\mu = 1.11^{+0.24}_{-0.22}$, consistent with the Standard Model expectation.

In the CMS analysis of 2016 data [144], the strategy was improved using additional categories aiming at the inclusive production of the Higgs boson and binned in transverse momentum of the $\tau^+\tau^-$ system, and for the VBF production, the analysis is binned as a function of the dijet mass. This analysis reached a sensitivity of 4.7 standard deviations with a dataset corresponding to an integrated luminosity of $35.9\,\text{fb}^{-1}$. CMS observes an excess with a significance of 4.9 standard deviations. In conjunction with the Run 1 results, this provides an unambiguous observation of the direct coupling of the Higgs boson to taus, in the vector boson fusion production mode.

III.2.2. $H \to b\overline{b}$

In the search for the decay of the Higgs boson to a pair of b-quarks the most sensitive production modes are the associated WH and ZH processes allowing use of the leptonic W and Z decays for triggering, and to purify the signal and reject QCD backgrounds. The W bosons are reconstructed via their leptonic decay $W \to \ell\bar{\nu}_\ell$ where $\ell = e, \mu$ or τ. The Z bosons are reconstructed via their decay into $e^+e^-, \mu^+\mu^-$or $\nu\bar{\nu}$. The Higgs boson candidate mass is reconstructed from two b-tagged jets in the event. Backgrounds arise from production of W and Z bosons in association with gluon, light and heavy-flavored jets (V+jets), $t\bar{t}$, diboson (ZZ and WZ with $Z \to b\overline{b}$) and QCD multijet processes. Due to the limited $m_{b\overline{b}}$ mass resolution, a SM Higgs boson signal is expected to appear as a broad enhancement in the reconstructed dijet mass distribution. The crucial elements in this search are b-jet tagging with high efficiency and low fake rate, accurate estimate of b-jet momentum and estimate of backgrounds from various signal depleted control samples constructed from data.

With varying signal/background ratios. Events with higher $p_T(V)$ have smaller backgrounds and better $m_{b\overline{b}}$ resolution. CMS uses [147] MVA classifiers based on kinematic, topological and quality of b-jet tagging and trained on different values of m_H to separate Higgs boson signal in each category from backgrounds. The MVA outputs for all categories are then fit simultaneously.

The nominal results from ATLAS are also based on a combination [148] of (i) a multivariate analysis of their 8 TeV data, incorporating various kinematic variables in addition to $m_{b\overline{b}}$ and b-tagging information and (ii) a statistical analysis of their 7 TeV data centered on $m_{b\overline{b}}$ as the main discriminant. In both cases customized control samples devised from data are used to constrain the contributions of the dominant background processes. The net observed(expected) deviation from background-only hypothesis corresponds to a significance of 1.4(2.6) standard deviations and a signal strength of $\mu = 0.5 \pm 0.4$.

In Run 2, both ATLAS and CMS have updated their results with similar analyses as those performed at Run 1. The larger dataset of approximately $36\,\text{fb}^{-1}$ of data collected in 2015 and 2016, and the increase in signal cross sections of nearly a factor of 3 at the centre-of-mass energy of 13 TeV with respect to 7 TeV, have brought the two experiment to achieve a sensitivity very close to that required to claim an evidence for this decay mode in the VH production. The expected significance for a SM Higgs boson is 3.0 standard deviations for ATLAS [149] and 2.8 standard deviations for CMS [150]. Both ATLAS and CMS observe significant excesses corresponding to 3.5 and 3.3 standard deviations respectively. When combined with results obtained in Run 1, the observed (expected) significance of the excesses are 3.6 (4.0) and 3.8 (3.8) standard deviations respectively. These results provide direct evidence for the Higgs boson decay to a $b\overline{b}$ through the VH production mode. All these results are summarized in Table 11.5.

The LHCb collaboration has also performed a search for the VH production with subsequent decay of the Higgs boson to a pair of

Table 11.5: Summary of the results of searches for a Higgs boson decaying to a pair of b-quarks by the ATLAS and CMS collaborations. The results are given in terms of measured signal strength. Where available the uncertainty the total uncertainty is reported as the statistical and systematic contributions separately and in this order.

$H \to b\overline{b}$	Tevatron	ATLAS Run 1	CMS Run 1	ATLAS Run 2	CMS Run 2
VH	1.6 ± 0.7	$0.52 \pm 0.32 \pm 0.24$	1.0 ± 0.5	$1.20 \pm 0.24 \pm 0.28$	1.2 ± 0.4
VBF	—	-0.8 ± 2.3	$2.8 \pm 1.4 \pm 0.8$	-3.9 ± 2.8	-3.7 ± 2.7
ttH	—	$1.4 \pm 0.6 \pm 0.8$	0.7 ± 1.9	$2.1 \pm 0.5 \pm 0.9$	$1.19 \pm 0.5 \pm 0.7$
Inclusive	—	—	—	—	2.3 ± 1.7
PDG Comb.	1.6 ± 0.7	0.6 ± 0.4	1.1 ± 0.5	1.2 ± 0.3	1.2 ± 0.4

At the Tevatron, the $H \to b\bar{b}$ channel contributes the majority of the Higgs boson search sensitivity below $m_H = 130\,\text{GeV}$. The CDF and D0 experiments use multivariate analysis (MVA) techniques that combine several discriminating variables into a single final discriminant used to separate signal from background. Each channel is divided into exclusive subchannels according to various lepton, jet multiplicity, and b-tagging characteristics in order to group events with similar signal-to-background ratio and thus optimize the overall search sensitivity. The combined CDF and D0 data show [145, 123] an excess of events with respect to the predicted background in the 115–140 GeV mass range in the most sensitive bins of the discriminant distributions suggesting the potential presence of a signal. At $m_H = 125\,\text{GeV}$ the observed signal strength $\mu = 1.59^{+0.69}_{-0.72}$.

In order to reduce the dominant V+jets background at the LHC, following Ref. [146], experiments select a region in the VH production phase space where the vector boson is significantly boosted and recoils from the $H \to b\overline{b}$ candidate with a large azimuthal angle $\Delta\phi_{VH}$. For each channel, events are categorized into different $p_T(V)$ regions

b-quarks [151] with $1.98\,\text{fb}^{-1}$ of data taken at a centre-of-mass energy of 8 TeV. The final state is required to have two reconstructed b quarks and one lepton in the LHCb acceptance of $2 < \eta < 5$. The sensitivity of this search is an expected 95% CL exclusion of 84 times the SM production rate. This analysis is also used to set a limit on the VH production with the subsequent decay of the Higgs boson in a pair of c quarks with a 95% CL limit at $6.4{\times}10^3$ times the SM production rate, while the expected sensitivity corresponds to an exclusion of $7.9{\times}10^3$ times the SM production rate.

ATLAS and CMS have also searched for $H \to b\overline{b}$ in the VBF production mode. The event topology consists of two "VBF-tagging" energetic light-quark jets in the forward and backward direction relative to the beam direction and two b-tagged jets in the central region of the detector. Due to the electroweak nature of the process, for the signal events, no energetic jet activity is expected in the rapidity gap between the two "VBF-tagging" jets. The dominant background in this search stems from QCD production of multijet events and the hadronic decays of vector bosons accompanied by

additional jets. A contribution of Higgs boson events produced in the ggF process but with two or more associated jets is expected in the signal sample. The signal is expected as a broad enhancement in the $m_{b\bar{b}}$ distribution over the smoothly falling contribution from the SM background processes. Both ATLAS [152] and CMS [153] have produced results in this channel with Run 1 data, but with limited sensitivity. CMS has performed a similar analysis with Run 2 data [154]. The results are summarized in Table 11.5.

Two of the main difficulties for the VBF production mode are the large QCD background and the difficulty in triggering events fully hadronic events. Both difficulties are addressed, by the proposal made in Ref. [155], where the requirement of an additional photon in the final state reduces the background through an interference effect and enhances the possibilities for triggering. This analysis has been carried out by the ATLAS experiment at Run 2 [156] (see Table 11.5).

The sensitivity in the inclusive search for the Higgs boson in the ggF production mode with $H \to b\bar{b}$ is limited by the overwhelming background from the inclusive production of $p\bar{p} \to b\bar{b} + X$ via the strong interaction. For this reason, no meaningful results exist with the Run 1 dataset for this production mode. With the increase in centre-of-mass energy to 13 TeV, and by taking advantage of the harder transverse momentum spectrum of the $gg \to H$ production mode with respect to the QCD background, a search for high p_T Higgs boson decaying to a pair of b-quarks in association with a energetic (and thus triggerable) Initial State Radiation (ISR) jet, has been performed by CMS [157]. For this novel analysis with the Run 2 data, CMS requires jets clustered with the anti-k_T algorithm [158] with a distance parameter of 0.8, with a transverse momentum in excess of 450 GeV. As in the case of VH production mode, this analysis is sensitive also to the $VZ, Z \to b\bar{b}$ production, which is an important step in the validation of the analysis chain. The $Z \to b\bar{b}$ decay is observed with a significance of 5.8 standard deviations, in good agreement with the expected sensitivity of 5.1 standard deviations. The expected sensitivity to the observation of a Higgs boson is 0.7 standard deviations while CMS observes an excess at $m_H = 125$ GeV of 1.5 standard deviations.

III.3. Higgs production in association with top quarks or in top decays

III.3.1. The associated production with top quark pairs

As discussed in Section II, the coupling of the Higgs particle to top quarks plays a special role in the electroweak symmetry breaking mechanism and in its possible extensions. Substantial indirect evidence of this coupling is provided by the compatibility of observed rates of the Higgs boson in the principal discovery channels, given that the main production process – the gluon fusion – is dominated by a top quark loop. Direct evidence of this coupling at the LHC and the future e^+e^- colliders will be mainly available through the $t\bar{t}H$ final state and will permit a clean measurement of the top quark-Higgs boson Yukawa coupling. The $t\bar{t}H$ production cross section at the LHC is small in comparison with the ggF or even VH production modes. The production cross section for a 125 GeV Higgs boson in pp collisions at $\sqrt{s} = 8$ TeV of about 130 fb makes it challenging to measure the $t\bar{t}H$ process with the LHC Run 1 dataset. However in Run 2 the increase in cross section at $\sqrt{s} = 13$ TeV is substantial, reaching approximately 510 fb. For a sensitive search, It is currently important to target as many accessible experimental signatures as possible. The analysis channels for such complex final states can be separated in four classes according to the decays of the Higgs boson. In each of these classes, most of the decay final states of the top quarks are considered. The topologies related to the decays of the top quarks are denoted 0L, 1L and 2L, for the fully hadronic, semi-leptonic and dilepton decay final states respectively of the $t\bar{t}$.

The first (i) analysis in this set is the search for $t\bar{t}H$ production in the $H \to \gamma\gamma$ channel. This analysis relies on the search for a narrow mass peak in the $m_{\gamma\gamma}$ distribution. The background is estimated from the $m_{\gamma\gamma}$ sidebands. The sensitivity in this channel is mostly limited by the available statistics. The second (ii) is the search for the Higgs boson decaying to ZZ^* and subsequently to four leptons (electrons or muons). This channel is currently limited by the low statistics due to the small branching fraction of the Z decays to leptons. The third (iii) is the search in the $H \to b\bar{b}$ channel. This search is intricate due to the large backgrounds, both physical and combinatorial in resolving the $b\bar{b}$ system from the Higgs decay, in events with six jets and four b-tagged jets. Already with the Run 1 dataset, the sensitivity of this analysis is strongly impacted by the systematic uncertainties on the background predictions. The fourth (iv) channel is a specific search for $\tau^+\tau^-$ where the two tau leptons decay to hadrons. Finally, the W^+W^- , $\tau^+\tau^-$ and ZZ^* final states can be searched for inclusively in multilepton event topologies. The corresponding $t\bar{t}H$ modes can be decomposed in terms of the decays of the Higgs boson and those of the top quarks as having two b-quarks and four W bosons (or two W and two taus, or two W and two Z) in the final state.

Table 11.6: Summary of the results of searches for a Higgs boson in association with a top quark pair by the ATLAS and CMS collaborations. The results are given in terms of measured signal strength. Where availale the uncertainty the total uncertainty is reported as the statistical and systematic contributions separately and in this order.

$t\bar{t}H$	ATLAS Run 1	CMS Run 1	ATLAS Run 2	CMS Run 2
$H \to \gamma\gamma$	$1.3\ ^{+2.6\ +2.5}_{-1.7\ -1.7}$	$1.2\ ^{+2.5\ +2.6}_{-1.7\ -1.8}$	$0.6\ ^{+0.7}_{-0.6} \pm 0.2$	$1.9^{+1.5}_{-1.2}$
$H \to 4\ell$	—	—	< 1.9 (68% CL)	0.0 ± 1.2
$b\bar{b}$	$1.4 \pm 1.0 \pm 0.6$	$1.6\ ^{+1.6}_{-1.5}$	$0.8 \pm 0.3 \pm 0.6$	-0.2 ± 0.8
$WW/\tau\tau/ZZ$	$1.4 \pm 0.6 \pm 1.0$	3.3 ± 1.4	$1.6 \pm 0.3 \pm 0.4$	1.5 ± 0.5 (0-τ)
				$0.72\ ^{+0.62}_{-0.53}$ (τ)
Comb.	$1.7 \pm 0.5 \pm 0.8$	$2.8\ ^{+1.0}_{-0.9}$	$1.2 \pm 0.2\ ^{+0.3}_{-0.2}$	—

ATLAS and CMS have provided a complete set of results in these channels and their combination with the Run 1 data [166, 167, 168]. Results for most of these channels have been updated with Run 2 data.

With the large increase in production cross section for the ttH associated production process of a factor of 3.9 from 7 TeV to 13 TeV, an outstanding goal of the Run 2 physics program is the study of these channels.

ATLAS and CMS have analyzed the Run 2 data with the full 2016 dataset and for some channels the 2015 dataset as well, to search for this production mode in most channels: the diphoton [124], $H \to 4\ell$ [132], the $H \to b\bar{b}$ [169] and multilepton [170] for ATLAS and the diphoton [128], $H \to 4\ell$ [125], and the multilepton [171, 172] for CMS. The $H \to b\bar{b}$ channel has been updated with a partial dataset corresponding to an integrated luminosity of 12.9 fb^{-1} [173] by CMS. All results are summarized in Table 11.6.

With the increase in centre-of-mass energy and recorded luminosity clean channels such as the $t\bar{t}(H \to \gamma\gamma)$ with sensitivity limited largely by the statistical uncertainty will play an increasingly important role. With the results obtained so far with the current dataset, there is substantial evidence for the production of the Higgs boson in association with a pair of top quarks.

III.3.2. The associated production with a single top quark

An additional production mode of the Higgs boson in association with a top quark is the single top associated production mode. There is an interesting similarity between this production mode and the $H \to \gamma\gamma$ decay mode. Both processes proceed through either the top Yukawa coupling or the interaction of the Higgs boson with the W-boson, with a negative interference between the two. Representative Feynman diagrams for this production process are shown in Fig. 11.1. Contrary to the diphoton decay channel, in this production mode the interference occurs at the tree level and is dominant. This process can therefore be used to further discriminate a negative relative sign between the couplings of the Higgs boson to fermions and its couplings to gauge bosons (the detailed dependence of the cross section as a function of coupling modifiers, taking into account the interference, is given in Section VI.2.1.2-ii).

The ATLAS and CMS experiments have produced specific searches for the tH production mode with the Run 1 and Run 2 data exploiting a variety of Higgs boson decay modes resulting in final states with photons, bottom quarks, and multiple charged leptons, including tau leptons. In particular the latest result with the Run 2 data obtained by CMS searches for multi-leptonic decay signatures from the $H \to WW^*$, $H \to \tau^+\tau^-$ and $H \to ZZ^*$ modes [174], this analysis restricts values of the top-Higgs coupling modifier κ_t to $[-1.25, 1.60]$ at 95% CL. CMS has also performed an analysis of the 2015 dataset to search for the $H \to b\bar{b}$ mode [175] yielding much less stringent constraints.

The diphoton channel has also been used to search specifically for this production mode by the ATLAS experiment using Run 1 data [167], yielding the restricted range of allowed values at the 95% CL to $[-1.3, 8]$.

III.3.3. Flavor changing neutral current decays of the top quark

The discovery of the Higgs boson at a mass smaller than the top quark mass opened a new decay channel for the top quark. The decays of the top quark to a Higgs boson and a charm or an up quark proceed through a Flavor Changing Neutral Current (FCNC) which are forbidden at the tree level and suppressed at higher orders through the Glashow–Iliopoulos–Maiani (GIM) mechanism [3]. The SM prediction for these branching fractions is $\mathrm{BR}(t \to Hc) = 10^{-15}$ and two orders of magnitude less for the Hu final state. These decay channels of the top quark are, therefore, very interesting to probe possible FCNC interactions in the Higgs Yukawa couplings to the quark sector, see Section VII.

ATLAS has searched for FCNC top decays specifically in channels involving a Higgs boson with subsequent decays to two photons [176] and a pair of b-quarks [178]. It has also reinterpreted a search for the ttH production in the multilepton final state (discussed in Section III.6.1) [168]. The latter channel covers Higgs boson decays to a pair of W-bosons and a pair of taus. No significant excess was observed in any of the specific channels (as discussed in Section III.6.1, a slight excess is observed in the ttH multilepton channel) and 95% CL upper limits are set on $\mathrm{BR}(t \to Hc) < 0.46\%$ with an expected sensitivity of 0.25% and $\mathrm{BR}(t \to Hu) < 0.45\%$ with an expected sensitivity of 0.29%. CMS has performed a search for these FCNC top decays in the diphoton and multilepton channels [179], placing a 95% CL upper limit on $\mathrm{BR}(t \to Hc) < 0.40\%$ with an expected sensitivity of 0.43%.

From these limits on branching fractions, constraints on non flavor-diagonal Yukawa couplings of a FCNC sector Lagrangian of the form:

$$\mathcal{L}_{FCNC} = \lambda_{tcH}\bar{t}Hc + \lambda_{tuH}\bar{t}Hu + h.c.$$

can be derived. The 95% CL observed (expected) upper limits from ATLAS on the $|\lambda_{tcH}|$ and $|\lambda_{tuH}|$ couplings are 0.13 (0.10) and 0.13 (0.10), respectively.

The results above are derived from the combination of several channels for searches performed with Run 1 data. Both ATLAS and CMS have produced updates of individual channels with Run 2 data. The ATLAS collaboration has searched for FCNC top decays with subsequent decays of the Higgs boson to a pair of photons [177], yiedling a 95% CL upper limit on $\mathrm{BR}(t \to Hc) < 0.22\%$ with an expected sensitivity of 0.16%. The CMS collaboration has searched for FCNC top decays with subsequent decays of the Higgs boson to a pair of b quarks [180], yiedling a 95% CL upper limit on $\mathrm{BR}(t \to Hc) < 0.47\%$ with an expected sensitivity of 0.44%.

III.4. Higgs boson pair production

Higgs boson pair production in the SM is rare. It is however a very interesting final state to search in two specific modes: (i) the search for non-resonant production of the Higgs boson pair and (ii) the search for resonant production of two Higgs bosons in the decay of a heavier particle.

The measurement of non-resonant Higgs pair production is important for constraining Higgs self-couplings. In the SM the main non-resonant production mode of two Higgs bosons in the final state proceeds through a loop (mainly of top quarks) (Fig. 11.5a). Another production mode is via the trilinear coupling of the Higgs boson (Fig. 11.5b), whose amplitude is not negligible compared to the former. These diagrams interfere negatively making the overall production rate smaller than what would be expected in the absence of a trilinear coupling.

Table 11.7: Summary of the final states investigated in the search for Higgs boson pair production by ATLAS and CMS. (**) denotes results obtained with the 2015 dataset corresponding to an integrated luminosity of approximately $3\,\mathrm{fb}^{-1}$, (*) denotes results obtained with a partial 2016 dataset corresponding to an integrated luminosity of approximately $12\,\mathrm{fb}^{-1}$ and the other results reported correspond to the full 2016 dataset. Results are 95% CL upper limits on the observed (expected) SM signal strengths.

Channel	ATLAS	CMS
$b\bar{b}\gamma\gamma$	117 (161)** [187]	19 (17) [188]
$b\bar{b}b\bar{b}$	29 (38)* [189]	342 (308)** [190]
$b\bar{b}\tau^+\tau^-$	—	30 (25) [191]
$b\bar{b}W^+W^-$	—	79 (89) [192]
$W^+W^-\gamma\gamma$	747 (386)* [193]	—

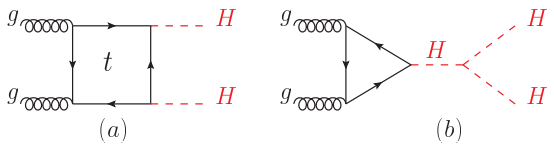

Figure 11.5: Feynman diagrams contributing to Higgs boson pair production through (a) a top- and b-quark loop and (b) through the self couplings of the Higgs boson.

III.4.1. Searches for Higgs boson pair production

The searches for Higgs boson pair production both resonant and non-resonant are very interesting probes for a variety of theories beyond the SM, and can be done in a large number of Higgs boson decay channels. At Run 1 the ATLAS and CMS collaborations have searched for both resonant and non resonant Higgs boson pair production in the following channels: (i) $HH \to b\bar{b}\gamma\gamma$ [181]; (ii) $HH \to b\bar{b}\tau^+\tau^-$ [182]; (iii) $HH \to b\bar{b}b\bar{b}$ [183]; and (iv) $HH \to WW^*\gamma\gamma$ [182]. (iv) in final states containing multiple leptons (electrons or muons) covering the WW^*WW^*, WW^*ZZ^*, ZZ^*ZZ^*, $ZZ^*\tau^+\tau^-$, $WW^*\tau^+\tau^-$, $ZZ^*b\bar{b}$, $\tau^+\tau^-\tau^+\tau^-$ channels [184]; (v) $\gamma\gamma\tau^+\tau^-$ channels [184].

At Run 2 most of these channels have been updated both by the ATLAS and CMS collaborations and the results are summarized in Table 11.7.

III.4.2. The Higgs self coupling

The Higgs boson self coupling is an extremely important direct probe of the Higgs potential with implications on our understanding of the electroweak phase transition. Constraints on the self coupling in HHH final states is an outstanding long term goal of the LHC, however with the current projected sensitivities a measurement will be extremely difficult even with the full HL-LHC dataset of 3 ab^{-1}.

In the SM the Higgs boson pair production through the trilinear Higgs has an on-shell component and a large off-shell component. The on-shell $H \to H^*H^*$ is strongly disfavored, requiring two off-shell Higgs bosons in the final state. The sensitivity region to the trilinear coupling production as in Fig. 11.5-b, is mainly in the kinematic region where the two Higgs boson in the final state are on-shell and the Higgs boson acts as a propagator (off-shell). As discussed in the introduction to this section, this process interferes negatively with the background Higgs boson pair production (Fig. 11.5a). In the SM hypothesis sensitivity to the trilinear coupling requires the

measurement of a deficit in the Higgs boson pair production, in a similar way as the off-shell couplings measurement as explained in Section V.2.

The measurements of the trilinear coupling requires separating the contributions to the overall Higgs boson pair production and in particular measure the deficit expected in the case of SM couplings. However in the regime of relatively high trilinear coupling, the observation will be an excess of events with respect to the expected background. In this case a simple limit can be set. The direct searches described in Section VII.8.i.c can be reinterpreted in terms of the ratio of the trilinear coupling to the top Yukawa coupling which controls the production rate and a limit on the trilinear coupling, assuming a top Yukawa coupling modifier of 1 can be set. Using the $b\bar{b}\gamma\gamma$ channel alone the Run 2 dataset allows to exclude trilinear couplings in excess of 15 times the SM value at 95% CL.

Preliminary studies for the sensitivity on the trilinear coupling with 3 ab^{-1} have been carried out in several channels by ATLAS and CMS. Three channels have been investigated: (i) the $HH \to b\bar{b}\gamma\gamma$; (ii) the $HH \to b\bar{b}\tau^+\tau^-$; and (iii) the $HH \to b\bar{b}W^+W^-$. The prospects in channel (i) have been studied by both the ATLAS [194] and the CMS [195] collaborations, yielding a sensitivity of 1.05σ and 1.6σ respectively to overall Higgs boson pair production. Both collaborations have studied the channel (ii) yielding a sensitivity of 0.6σ [196] and 0.9σ [195] to Higgs boson pair production respectively. CMS collaboration has studied the channel (iii) showing its low sensitivity [195]. As an example, the ATLAS prospects in the $b\bar{b}\gamma\gamma$ channel yield for the full HL-LHC luminosity, an expected significance of an excess of 1.05 standard deviations for a SM trilinear coupling [194] which will translate on an upper limit on the total HH cross section of approximately twice the SM value. This corresponds to an exclusion limit of -0.8< λ/λ_{SM} <7.7 at 95% CL. The asymmetry in the limits is due to the different acceptance of the selection when the signal is dominated by the trilinear coupling mode at high λ and by the gluon-fusion di-Higgs production dominant at low λ. It should be noted that there is a large uncertainty on these projections related both to the modeling of signal and the backgrounds, the very difficult high pile-up environment (both for reconstruction and trigger) and the design of the upgraded detectors.

Preliminary studies suggest that a direct measurement of the quartic coupling will be out of reach even at a very high energy 100 TeV hadron collider.

III.5. Searches for rare decays of the Higgs boson

III.5.1. $H \to Z\gamma$

The search for $H \to Z\gamma$ is performed in the final states where the Z boson decays into opposite sign and same flavor leptons ($\ell^+\ell^-$), ℓ here refers to e or μ. While the branching fraction for $H \to Z\gamma$ is comparable to $H \to \gamma\gamma$ (about 10^{-3}) at $m_H = 125\,\text{GeV}$, the observable signal yield is brought down by the small branching ratio of $Z \to (e^+e^- + \mu^+\mu^-) = 6.7 \times 10^{-2}$. In these channels, the $m_{\ell\ell\gamma}$ mass resolution is excellent (1-3%) so the analyses search for a narrow mass peak over a continuous background. The major backgrounds arise from the $Z + \gamma$ final state radiation in Drell–Yan decays and $Z +$ jets processes where a jet is misidentified as a photon. The ratio of signal over background in this channel is typically of the order of 0.5%. In a narrow window of a few GeV around 125 GeV, several hundreds of events are expected.

Events are divided into mutually exclusive categories on the basis of the expected $m_{Z\gamma}$ resolution and the signal-to-background ratio. A VBF category is formed for $H \to Z\gamma$ candidates which are accompanied by two energetic jets separated by a large pseudorapidity. While this category contains only about 2% of the total event count, the signal-to-noise is about an order of magnitude higher. The search for a Higgs boson is conducted independently in each category and the results from all categories are then combined.

No excess of events is observed in either ATLAS or CMS experiments in the Run 1 data. The CMS expected and observed 95% CL upper limits for $m_H = 125\,\text{GeV}$ [197] on the signal strength μ are 10 and 9.5 respectively. The ATLAS expected and observed upper limits [198] on the signal strength μ are 9 and 11 respectively for a SM $m_H = 125.5\,\text{GeV}$.

The ATLAS collaboration has performed an analysis of the full 2015 and 2016 Run 2 data to search for the $Z\gamma$ decay mode [199], no significant excess is observed and 95% CL observed (expected) upper limits on the signal strength are 6.6 (5.2).

III.5.2. $H \to \mu^+\mu^-$

The branching fraction in the $H \to \mu^+\mu^-$ channel for a 125 GeV SM Higgs boson is 2.2×10^{-4}, about ten times smaller than that for $H \to \gamma\gamma$. The dominant and irreducible background arises from the $Z/\gamma^* \to \mu^+\mu^-$ process which has a rate several orders of magnitude larger than that from the SM Higgs boson signal. Due to the precise muon momentum measurement achieved by ATLAS and CMS, the $m_{\mu^+\mu^-}$ mass resolution is excellent ($\approx 2-3\%$). A search is performed for a narrow peak over a large but smoothly falling background. For optimal search sensitivity, events are divided into several categories. Either taking advantage of the superior muon momentum measurement in the central region, events can be subdivided by the pseudorapidity of the muons, or designing selections aiming at specific production processes such in particular as the vector boson fusion.

No excess in the $m_{\mu^+\mu^-}$ spectrum is observed near 125 GeV. From an analysis of their Run 1 data, ATLAS sets [200] an observed (expected) 95% CL upper limit on the signal strength $\mu < 7.0$ (7.2). The CMS analysis [201] of their 7 and 8 TeV data sets an observed (expected) limit of $\mu < 7.4$ (6.5).

A search carried out by the ATLAS experiment using the 2015 and 2016 data [202] showed no excess at 125 GeV. A signal strength of $\mu = -0.1 \pm 1.4$ was measured, yielding an observed (expected) 95% CL upper limit on the signal strength of $\mu < 2.8$ (2.9).

III.5.3. $H \to e^+e^-$

A search similar to the $H \to \mu^+\mu^-$, is performed by CMS in the di-electron channel [201]. In this search channel there the contribution from the peaking background from Higgs boson decays to diphoton mis-identified as di-electrons (when mostly converted photons are faking electrons) needs to be assessed. The sensitivity to the SM Higgs decays is negligible given the extremely small branching fraction to e^+e^-, approximately 40,000 times smaller than the branching fraction to dimuons. It is nevertheless interesting to probe this decay channel to search for potential large anomalous couplings. Assuming a SM Higgs boson production cross section, the observed limit on the branching fraction at the 95% CL is 0.0019 [201], five orders of magnitude larger than the expected SM prediction.

III.5.4. Lepton flavor violating (LFV) Higgs boson decays

Given the Yukawa suppression of the couplings of the Higgs boson to quarks and leptons of the first two generations and the small total width of the Higgs boson, new physics contributions could easily have sizable branching fractions. One very interesting possibility is the Lepton Flavor Violating (LFV) decays of the Higgs boson, in particular in the $\tau\mu$ and τe modes. These decays are suppressed in the SM but could be enhanced in theories such as two-Higgs-doublet models (discussed in Section VII).

There are already constraints on LFV Yukawa couplings $|Y_{\tau\mu}|$ from channels such as the $\tau \to 3\mu$ or $\tau \to \mu\gamma$, or a re-interpretation of the search for Higgs decays to $\tau^+\tau^-$. A direct search at the LHC however complements these indirect limits. The search for LFV decays in the $\tau\mu$ channel have been done with the Run 1 dataset in several channels according to the subsequent decay of the τ. The results from CMS [203] and for ATLAS for the hadronic [204], the leptonic [205] decays of the tau, and their combination [205] are reported in Table 11.8. It is interesting to note that the analysis strategies for the di-lepton $\tau_{lep}\mu$ channel are very different between the ATLAS [205] and CMS [203].

As shown in Table 11.8 an excess was observed in this channel by CMS with a significance of 2.5σ, while in ATLAS the excess is smaller, about $1\ \sigma$ in Run 1. CMS has performed the search again with the full 2016 Run 2 [206] dataset and a multivariate analysis. The

Table 11.8: Summary of the results of searches for lepton flavor violating decays of the Higgs boson in the $\tau\mu$ channel from ATLAS and CMS. For the result with a *, the expected sensitivity was not reported but appears consistent with the observed.

	ATLAS (Run 1)	CMS (Run 1)	CMS (Run 2)
BR($H \to \tau\mu$)	$(0.53 \pm 0.51)\%$	$(0.84^{+0.39}_{-0.37})\%$	$(0.00 \pm 0.12)\%$
95% CL Obs.(Exp.)	1.43% (1.01%)	1.51% (0.75%)	0.25% (0.25%)
$H \to \tau e$ 95% CL Obs.(Exp.)	1.02% (1.21%)	0.69%*	0.61% (0.37%)

observed best fit branching fraction is $(0.00 \pm 0.12)\%$. These limits are reported in Table 11.8.

ATLAS and CMS have also performed a search for the LFV Higgs boson decays in the τe and μe channels [205, 207, 206], no significant excess was observed and 95% CL limits are reported in Table 11.8 for the τe channel only. For the μe channel, the constraints from the $\mu \to e\gamma$ experiments [208] are much stronger than those from the direct LFV Higgs decay search. However these indirect constraints can be relaxed by the cancellation of LFV effects from new physics.

III.5.5. Probing charm- and light-quark Yukawa couplings

Probing the Yukawa couplings to quarks of the second or even the first generation is extremely challenging given the overwhelming background and the much smaller signal rates. The possibility of probing the Yukawa coupling to the charm has been discussed in Ref. [209] where indirect bounds on the charm Yukawa coupling are estimated from a combined fit to the Higgs data. The direct impact of Higgs decays to a pair of charm quarks on the direct search for $H \to b\bar{b}$ is also investigated.

Another possibility to access the Higgs Yukawa coupling has been discussed in Ref. [210], through the decays of the Higgs boson to a final state with charmonium: $H \to J/\Psi\gamma$. Higgs decays in this final state have been searched for by the ATLAS collaboration [211]. The sensitivity of this analysis is however several orders of magnitude above the branching fraction estimated for the SM coupling BR($H \to J/\Psi\gamma$) $= (2.8 \pm 0.2) \times 10^{-6}$ [210]. The ATLAS collaboration [211] has also searched for Higgs decays to $\Upsilon(nS)\gamma$ where $(n = 1, 2, 3)$, a channel with much lower sensitivity than the $H \to b\bar{b}$ to the Yukawa coupling to b-quarks.

More recently the ATLAS collaboration has searched for another quarkonia final state where the Higgs boson decays to $\phi\gamma$ [212] at the LHC Run 2 and a center-of-mass energy of 13 TeV, with a specific trigger. This channel could probe deviations from the strange-quark Yukawa coupling of the Higgs boson. Its sensitivity is several orders of magnitude above the expectation from the SM Higgs boson. Other quarkonia final states, such as the $\rho\gamma$, which could potentially probe the Yukawa coupling to light quarks, can also be searched for.

III.5.6. Rare decays outlook

Rare decays such as those described in the above sections have a clearly limited sensitivity. They however already deliver interesting messages. For example, if the coupling of the Higgs boson to muons was as strong as it is to top quarks, this mode should have been observed. The observed Higgs boson couplings are manifestly non-universal. Further developing these rare decay modes is an important component of the high luminosity program of the LHC to directly probe the couplings of the Higgs boson, and to potentially measure the Yukawa coupling of the Higgs boson to fermions of the second generation, in particular to muons. It is also an integral part of the physics program of the discussed potential future Higgs factories.

III.6. Searches for non-standard model decay channels

The main decay and production properties of the observed Higgs boson are consistent with predictions of the SM. It may however have other decay channels beyond those anticipated in the SM. Among these and of great interest are the invisible decays into stable particles that interact very weakly with the detector, and that are undetected, such as Dark Matter particle candidates. Other non standard decay channels that have been investigated are the decays of the Higgs particle to hidden valley or dark particles.

III.6.1. Invisible decays of the Higgs boson

The discovery of the Higgs boson immediately raised the question of its couplings to dark matter and how it could be used to reveal its existence at colliders, using the Higgs boson as a portal to dark matter (see Ref. [213] and references therein). If kinematically accessible and with a sufficiently large coupling to the Higgs boson, dark matter particles, such as, e.g., neutralinos in SUSY models, graviscalars in models with extra dimensions or heavy neutrinos in the context of four-generation fermion models, would manifest themselves as invisible decays of the Higgs boson, thus strongly motivating searches for the invisible decays of the Higgs boson.

To identify an invisibly decaying Higgs boson at the LHC, it must be produced in association with other particles. Searches for invisible decays of the Higgs particle at the LHC have been carried out in three associated production modes of the Higgs boson with the highest SM cross sections and target events with large missing energy.

The ggF production mode has the largest SM cross section but it usually results in the Higgs boson being created alone and hence leaving no characteristic signature in the detector of its invisible decay. One way to search for invisible decays in ggF production mode is to look for events with the "monojet" topology arising from initial state gluon radiation and containing missing energy. The major irreducible background in such searches stems from Z + jets events where the Z boson decays into a pair of neutrinos. The analysis with the best sensitivity targets the VBF production topology but suffers from large backgrounds arising from events with two jets and large missing energy. The VH mode has much smaller cross section but the presence of a W or Z boson allows a variety of final states that can be tagged with relatively low background.

ATLAS [214–217], and CMS [218–221] have searched for such final states but have observed no significant excess over predicted backgrounds. Table 11.9 summarizes the 95% CL limits on the invisible decays of the Higgs boson assuming SM Higgs boson production cross section and corresponding detector acceptances.

Table 11.9: Summary of the channels searched for and the corresponding 95% CL limits from ATLAS and CMS on the branching fraction for the Higgs boson decay to invisible particles assuming a SM Higgs boson production cross section. The results in parentheses are the expected exclusions. [*] indicates analyses based only on 8 TeV data. When combining Run 1 results and the results from the $\approx 2\,\text{fb}^{-1}$ of 13 TeV data acquired in 2015, the CMS observed (expected) limit improves to < 32 (26) % at 95% CL.

	ATLAS (Run 1)	CMS (Run 1)	CMS (13 TeV, 2015)
ggF (monojet); $H \to$ inv.	–	67 (71) % [*]	-
VBF; $H \to$ inv.	28 (31) %	57 (40) % [*]	69 (62) %
$Z \to \ell^+\ell^-$; $H \to$ inv.	75 (62)%	75 (91) %	125 (125)%
$Z \to b\bar{b}$; $H \to$ inv.	–	182 (189) % [*]	-
$Z \to jj$; $H \to$ inv.	78 (86)%	–	-
Combination of all direct searches	25 (27)%	36 (30) %	-

The CMS experiment has updated the search for invisible decays of the Higgs boson in the gluon fusion, the vector boson fusion and the associated production with a vector boson channels (both with subsequent leptonic and hadronic decays) using Run 2 data collected in 2015 [222] and has produced a combination with Run 1 channels, yielding a limit on the invisible branching fraction of 24% with an expected sensitivity of 23%.

This constraint can then be further used to probe Higgs portal models to Dark Matter [223], where an additional weakly interacting particle χ with mass lower than $m_H/2$ is introduced as Dark Matter candidate and where the Higgs boson is considered as the only

mediator between the SM particles and Dark Matter. In this model it is interesting to express the limit on the invisible branching fraction in terms of strength of interaction of Dark Matter with standard matter, *i.e.* in terms of it interaction cross section with nucleons $\sigma_{\chi-N}$. In this model the couplings of the Higgs boson to SM particles are assumed to be those of the SM and the interaction of the Higgs boson with the nucleon is parametrized in Higgs-Nucleon form factor estimated using lattice QCD calculations [223]. The exclusion limits from the constraints on invisible Higgs decays, both direct and indirect from the measurement of the coupling properties of the Higgs boson can be compared to direct detection experiments. For comparison the limit at 90% CL on the invisible branching fraction of $\mathrm{BR}_{inv} < 24\%$ [222] is used and converted into limits on $\sigma_{\chi-N}$ under several hypotheses on the nature of Dark Matter particles depending mainly on their spin (scalar- or fermion-like). These results are shown in Fig. 11.6.

The ATLAS collaboration has performed a search for invisible decays of the Higgs boson in the associated production mode ZH with the Z boson subsequently decaying to a pair charged leptons (e^+e^- or $\mu^+\mu^-$) with the full 2015 and 2016 dataset [222].

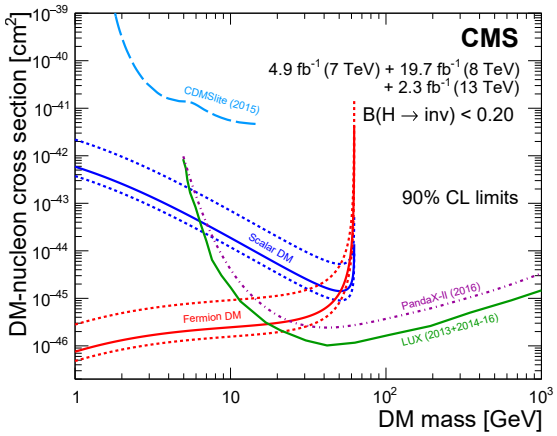

Figure 11.6: 90% CL upper limits on the WIMP-nucleon scattering cross section as a function of the Dark Matter particle mass. Spin-independent results excluded and favored regions from direct detection experiments are also shown.

III.6.2. Exotic Higgs boson decays

The 125 GeV Higgs boson not only serves as a probe for potential dark matter candidates, but also to search for other exotic particles arising from fields associated with a low-mass hidden sector. Such hidden sectors are composed of fields that are singlets under the SM gauge group $\mathrm{SU}(3) \times \mathrm{SU}(2) \times U(1)$. These models are referred to as hidden valley models [224, 225]. Since a light Higgs boson is a particle with a narrow width, even modest couplings to new states can give rise to a significant modification of Higgs phenomenology through exotic decays. Simple hidden valley models exist in which the Higgs boson decays to an invisible fundamental particle, which has a long lifetime to decay back to SM particles through a small mixing with the SM Higgs boson; Reference [225] describes an example. The Higgs boson may also decay to a pair of hidden valley "v-quarks," which subsequently hadronize in the hidden sector, forming "v-mesons." These mesons often prefer to decay to the heaviest state kinematically available, so that a possible signature is $H \to 4b$. Some of the v-mesons may be stable, implying a mixed missing energy plus heavy flavor final state. In other cases, the v-mesons may decay to leptons, implying the presence of low mass lepton resonances in high- H_T events [226]. Other scenarios have been studied [227] in which Higgs bosons decay predominantly into light hidden sector particles, either directly, or through light SUSY states, and with subsequent cascades that increase the multiplicity of hidden sector particles. In such scenarios, the high multiplicity hidden sector particles, after decaying back into the SM, appear in the detector as clusters of collimated leptons known as lepton jets.

A variety of models have been investigated searching for final states involving dark photons and hidden valley scalars. The resulting topologies searched for are prompt electron jets in the WH production process [228], displaced muonic jets [229], four muons final state, and long lived weakly interacting particles [230]. The latter occur not only in hidden valley scenarios, but also in gauge-mediated extensions of the minimal supersymmetric standard model (MSSM), the MSSM with R-parity violation, and inelastic dark matter [231]. Finally the CMS collaboration has performed a search for pair production of light bosons [232]. Such a scenario can occur in supersymmetric models with additional hidden (or dark) valleys.

IV. Combining the main channels

The analysis strategy used by the LHC and Tevatron experiments to perform the searches for the Higgs boson has been based on the Higgs decay modes. It is a natural choice given that it focusses on the decay products of the object searched for. However, for each channel, exclusive subchannels have been defined according to the Higgs production processes and in the results presented these subchannels have been combined. The natural extension of this approach in order to probe further the production and decay modes of the Higgs boson is to combine the analysis channels together. Such a combination is also used in Section VI to further measure the coupling properties of the Higgs boson.

At the LHC or the Tevatron, the total cross section cannot be measured in any of the production modes. As a consequence, neither the absolute branching fractions nor the total natural width of the Higgs boson can be directly measured. However, a combined measurement of the large variety of categories described in Section III, with different sensitivities to various production and decay modes permits a wide variety of measurements of the production, decay or in general coupling properties. These measurements require, in general, a limited but nevertheless restrictive number of assumptions.

In this section, results will be given combining not only different channels, but also the ATLAS and CMS results together [143]. These results are obtained with the Run 1 data only and are the current state-of-the-art in terms of combined measurements of the coupling properties of the Higgs boson, as no combination including the Run 2 data analyses has been performed by the experiments to date. These results were derived by the two collaborations, taking rigorously into account all correlations in the systematic uncertainties and in the large number of channels and their categories. This combination has led the two collaborations to a more precise experimental portrait of the Higgs boson. This concludes and synthesizes the analyses of the main production and decay channels of the Higgs boson at the Run 1 of the LHC.

In this section, only the results on the main Higgs boson production and decay modes will be discussed. The combination framework is briefly described herein and in more detail in the previous issue of this review [233]. This framework will also be used in Section VI, to discuss the measurements of the coupling properties of the Higgs boson.

IV.1. Principles of the combination

The combination of the Higgs boson analysis channels in each experiment and for the two experiments together is done using a fit of a signal and background model to the data. As described above the data is made of a large number of categories, aiming at reconstructing exclusive production and decay modes. In the combination of ATLAS and CMS [143] there are approximately 600 categories. The combination is a simultaneous fit to all these categories, using a reduced number of parameters of interest and a Higgs boson mass fixed at its measured value (see Section III.2). The much larger number of categories present in the ATLAS and CMS combination [143], is due to additional separation in terms of finer exclusive production regions, decay channels of the Z and the W bosons, and taus, control regions where little-to-no signal is present, and different center-of-mass energies. It should be noted that the individual combination performed by ATLAS [234] included two

additional decay channels: the $\mu^+\mu^-$ and $Z\gamma$, for the sake of simplicity these channels were omitted in the ATLAS-CMS combination. In addition, a $H \to b\overline{b}$ analysis performed by CMS [235] and included in its own combination, has been omitted from the ATLAS-CMS combination.

The key to understanding how the combination of channels works relies on the combination master formula, which expresses for each category, indexed by c, of a given channel (typically a category covers mostly one decay mode, but possibly various production modes), the measured number of signal events n_s^c as a function of a limited number of parameters as follows:

$$n_s^c = (\sum_{i,f} \mu_i \, \sigma_i^{SM} \times A_{if}^c \times \varepsilon_{if}^c \times \mu_f \, \mathrm{BR}_f^{SM}) \times \mathcal{L}^c \qquad (11.9)$$

The production index is defined as $i \in \{ggH, VBF, VH, ttH\}$ and the decay index is defined as $f \in \{\gamma\gamma, WW, ZZ, bb, \tau\tau\}$ while σ_i^{SM} and BR_f^{SM} are the corresponding production cross sections and decay branching fractions, estimated as described in Section II, assuming that the Higgs boson is that of the SM. A_{if}^c and ε_{if}^c are the signal acceptance and the reconstruction efficiency for given production and decay modes in the category c. $\mathcal{L}^c$ is the integrated luminosity used for that specific category. For the purpose of this review, these parameters can be considered as fixed[3].

The parameters of interest in the master formula are the signal strength parameters μ_i and μ_f. It is important to note that the formula relies on the factorization of the production cross section and decay branching fraction, which assumes the narrow width approximation. The width of the Higgs boson will be discussed in Section V, however for the precision needed here, the fact that the Higgs boson has been observed in decay channels with high mass resolution as a resonance is sufficient to validate this hypothesis. It is also manifest in the above equation that the ten parameters for the production modes (μ_i) and decay modes (μ_f) cannot be determined simultaneously. This illustrates that total cross sections or branching fractions cannot be measured without further assumptions in this fit.

The master formula also illustrates an important caveat to the measurement of signal strength parameters. In case these are interpreted as scale factors of the production cross sections or branching fractions, then all the other quantities such as the acceptances and efficiencies, A_{if}^c and ε_{if}^c, need to be assumed as independent and fixed to their estimated values for the SM Higgs boson. An additional important caveat to note concerning these combined results is that only the normalizations are varied, while the discriminating variables for the signal are not modified and are still used in the fit. These caveats are of particular importance in the use of the combination to measure the coupling properties of the Higgs boson as discussed in Section VI. For relatively small perturbations of the couplings of the Higgs boson from the SM values, this hypothesis is valid.

However the 25 products, $\mu_i \times \mu_f$, can be considered as free parameters and in principle measurable (if there is sufficient sensitivity from specific categories). Measuring the products of signal strengths can be viewed as the measurements of the cross sections times the branching fraction, $\sigma \cdot \mathrm{BR}$. The results are reported in Fig. 11.7 for the combination of ATLAS and CMS.

It is remarkable that of the 25 possible combinations of production and decay modes in the main channels, the fit to ATLAS and CMS data allows the measurement of 20. A coherent picture emerges with an excellent consistency between the observation in each channel and the expectation for a SM Higgs boson.

This 20 parameter fit quantifies, with very little theoretical input, the current experimental knowledge of the main production and decays modes. Other fits involving ratios of cross sections, which also are little sensitive to theory uncertainties are performed and reported in Ref. [233].

[3] In the combination performed by the ATLAS and CMS experiments the systematic uncertainties on these parameters are taken into account by allowing these parameters to vary in the fit.

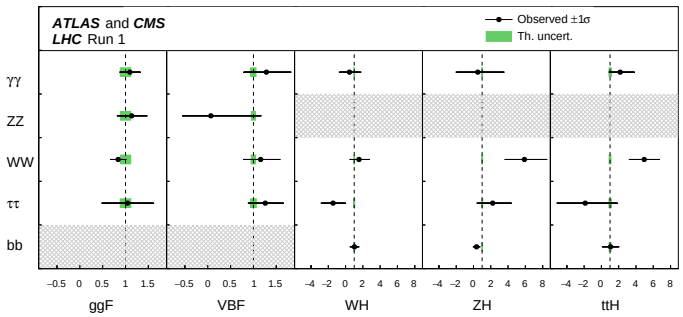

Figure 11.7: Combined measurements of the products $\sigma \cdot \mathrm{BR}$ for the five main production and five main decay modes. The hatched combinations require more data for a meaningful confidence interval to be provided.

The most constrained fit in this combination, and historically the first made, allows for only one single parameter to vary *i.e.* $\forall(i,f), \mu_i = \mu_f = \mu$. This global signal strength model provides the most precise and simple probe of the compatibility of the signal with the SM Higgs boson. This model is sensitive to any deviation from the SM Higgs boson couplings provided that these deviations do not cancel overall. The combined global signal strength is

$$\mu = 1.09 \pm 0.07\,(\mathrm{stat}) \pm 0.04\,(\mathrm{expt}) \pm 0.03\,(\mathrm{th.\,bkg}) \pm 0.07\,(\mathrm{th.\,sig})$$

This overall signal strength is fully compatible with the SM expectation of 1, with a precision of 10%. It is interesting to note that the major uncertainties in this first measurement arises from the limited precision in the theoretical predictions for the signal production processes.

IV.2. Main decay modes and observation of Higgs decays to taus

Despite the large number of decay channels, since the cross sections cannot be independently measured, from the measurements described in this section it is impossible to measure decay branching fractions without a loss of generality. The simplest assumption that can be made is that the production cross sections are those of the SM Higgs boson, which is equivalent to assuming that for all i indices $\mu_i = 1$. All branching fractions μ_f can then be measured in a simple 5 parameter fit. The result of this fit is reported in terms of significances in Table 11.10.

Table 11.10 also reports the results of a similar combination by each experiment from their data. For the main discovery modes $\gamma\gamma$, ZZ and WW, the combined significance is not computed as these decay modes have been firmly established by each experiment independently. However for the $\tau^+\tau^-$ and $b\overline{b}$ decay modes these results shed new combined light on the observation significance in these channels.

For the $\tau^+\tau^-$ channel, ATLAS and CMS are both sensitive and have observed excesses in their data. The individual results are not sufficiently significant to claim an observation, but combined they are. This conclusion can be made also in a more generic manner using the ratio of branching fractions model described above. It should be noted that in the search for $H \to \tau\tau$ decay, the most sensitive production mode is the VBF process, the experimental evidence for which is discussed in Section IV.3.

As illustrated in Table 11.10, ATLAS and CMS are both much less sensitive to the $H \to b\overline{b}$ decay mode. The available sensitivity comes mostly from the VH process, as discussed earlier in this section. The combined significance of 3.7σ at Run 1 was sufficient to suggest evidence, however ATLAS and CMS observations were both low with respect to the rate expected for the SM Higgs boson. At Run 2, this channel benefited largely from the increased production cross sections at 13 TeV and the much larger dataset expected.

Table 11.10: Summary of the significances of the excesses observed for the main decay processes. The $\gamma\gamma$, ZZ, and W^+W^- decay modes have been established at more than 5σ by both the ATLAS and CMS experiments individually, the combined observation significance therefore exceeds 5σ and is not reported here.

	Expected	Observed
$\gamma\gamma$	4.6σ (ATLAS) 5.3σ (CMS)	5.2σ (ATLAS) 4.6σ (CMS)
ZZ	6.2σ (ATLAS) 6.3σ (CMS)	8.1σ (ATLAS) 6.5σ (CMS)
WW	5.9σ (ATLAS) 5.4σ (CMS)	6.5σ (ATLAS) 4.7σ (CMS)
$\tau^+\tau^-$	3.4σ (ATLAS) 3.9σ (CMS)	4.5σ (ATLAS) 3.8σ (CMS)
$b\bar{b}$	2.6σ (ATLAS) 2.5σ (CMS)	1.4σ (ATLAS) 2.1σ (CMS)
$\tau^+\tau^-$ (Comb.)	5.0σ	5.5σ
$b\bar{b}$ (Comb.)	3.7σ	2.6σ

Table 11.11: Summary of the combined significance of observation for the main production processes. The ggF process has been established at more than 5σ by both the ATLAS and CMS experiments individually, the combined observation significance far exceeds 5σ and is not reported here.

	Expected	Observed
ggF	Ind. Obs.	Ind. Obs.
VBF	4.6σ	5.4σ
WH	2.7σ	2.4σ
ZH	2.9σ	2.3σ
VH	4.2σ	3.5σ
ttH	2.0σ	4.4σ

IV.3. Main production modes and evidence for VBF production

As discussed earlier, most analysis channels are divided into several exclusive categories allowing for an increased overall sensitivity and to measure the various Higgs production modes. The cross sections of the main production modes can be measured assuming that the branching fractions are those of the SM Higgs boson, *i.e.* for all f indices $\mu_f = 1$. These assumptions lead to a 5 parameter combination. The results are reported in terms of significances of observation of the production modes are reported in Table 11.11.

The gluon fusion production process is the dominant production mode. Although no numerical estimate of combined significance of observation for this process has been given by the experiments, it is considered as established due to the overwhelming evidence from the three main discovery channels. None of the other production modes have been firmly established by the experiments individually. These show that for the VBF mode, the combination has a large sensitivity and produced a combined observation of 5.4σ, establishing this process with a rate compatible with that expected from the SM Higgs boson. A similar conclusion can be reached but with assumptions from the fit to the ratio $\sigma_{VBF}/\sigma_{ggF}$ discussed earlier in this section.

It is interesting to note that despite the low sensitivity to the ttH production mode, the excesses observed in several ttH channels (discussed in Section III.6.1), lead to a significance of direct observation for ttH production in excess of 4σ. The compatibility of this observation with the SM production rate was at the 2.3σ level at Run 1. It improved significantly at Run 2 thanks to the higher center-of-mass energy of 13 TeV.

V. Main quantum numbers and width of the Higgs boson

V.1. Main quantum numbers J^{PC}

Probing the Higgs boson quantum numbers is essential to further unveiling its coupling properties. The measurements of the signal event yields of the observed new state in all the channels discussed in Sections III and IV and their compatibility with the SM Higgs boson predictions, give a qualitative, but nonetheless compelling indication of its nature. This qualitative picture is further complemented by the implications of the observation of the particle in the diphoton channel. According to the Landau–Yang theorem [236], the observation made in the diphoton channel excludes the spin-1 hypothesis and restricts possibilities for the spin of the observed particle to 0 or 2.

The Landau–Yang theorem does not apply if the observed state is not decaying to a pair of photons but to a pair of scalars subsequently decaying to two very collimated pairs of photons (as for example in the case of $H \to a_1 a_1 \to 4\gamma$). This possibility has not been rigorously excluded but is not experimentally favored since tight selection criteria are applied on the electromagnetic shower shapes of the reconstructed photons. A more systematic analysis of shower shapes and the fraction of conversions could be performed to further discriminate between the single prompt photon and the two overlapping photons hypotheses. There are also potential theoretical loopholes concerning the applicability of the Landau–Yang theorem, such as off-shell vector boson decays. However, for the observed particle not to be of spin 0 and +1 parity would require an improbable conspiracy of effects. It is nevertheless important to test this hypothesis independently, in particular since the measurements of coupling properties of the Higgs boson assume that the observed state is CP-even.

V.1.1. Charge conjugation

The charge conjugation quantum number is multiplicative, therefore given that the Higgs-like particle is observed in the $H \to \gamma\gamma$ channel, and given that photons are C-odd eigenstates, assuming C conservation, the observed neutral particle should be C-even.

V.1.2. Spin and parity

To probe the spin and parity quantum numbers of the discovered particle, a systematic analysis of its production and decay processes is performed in several analyses, designed to be independent of the event yields measured and relying instead on the production and the decay angles, and on the threshold distributions as long as a significant signal is observed (*i.e.* an excess over the expected background that can be used to further discriminate between signal hypotheses). These analyses are based on probing various alternative models of spin and parity. These models can be expressed in terms of an effective Lagrangian [237] or in terms of helicity amplitudes [238, 239]. The two approaches are equivalent. In the following, the effective Lagrangian formalism is chosen to describe the models considered and a restricted number of models are discussed [237]. In the analysis performed by CMS [238] a larger number of models have been investigated, however the main channels studied by both experiments are essentially the same and the main conclusions are similar and fully consistent.

(i) Spin-0 model

The interaction Lagrangian relevant for the analysis of spin-0 particle interaction with a pair of W- or Z-boson with either fixed or mixed SM and BSM CP-even couplings or CP-odd couplings, is the following:

$$\begin{aligned}\mathcal{L}_0^{W,Z} \supset \Big\{ & \cos(\alpha)\kappa_{SM}\left[\frac{1}{2} g_{HZZ} Z_\mu Z^\mu + g_{HWW} W_\mu^+ W^{-\mu}\right] \\ & - \frac{1}{4\Lambda}\left[\cos(\alpha)\kappa_{HZZ} Z_{\mu\nu} Z^{\mu\nu} + \sin(\alpha)\kappa_{AZZ} Z_{\mu\nu}\tilde{Z}^{\mu\nu}\right] \\ & - \frac{1}{2\Lambda}\left[\cos(\alpha)\kappa_{HWW} W^+_{\mu\nu} W^{-\mu\nu} + \sin(\alpha)\kappa_{AWW} W^+_{\mu\nu}\tilde{W}^{-\mu\nu}\right]\Big\} H_0,\end{aligned} \tag{11.10}$$

where $V^\mu = Z^\mu, W^{+\mu}$ are the vector boson fields, $V^{\pm\mu\nu}$ are the reduced field tensors and $\tilde{V}^{\pm\mu\nu} = 1/2\,\varepsilon^{\mu\nu\rho\sigma} V_{\rho\sigma}$ are the dual tensor fields. Ans Λ defines an effective theory energy scale. The factors $\kappa_{SM}, \kappa_{HZZ}, \kappa_{HWW}, \kappa_{AZZ}, \kappa_{AWW}$ denote the coupling constants corresponding of the coupling of the SM, BSM CP-even and CP-odd components of the Higgs field H_0 to the W and Z fields. The mixing angle α allows for the production of CP-mixed state and the CP-symmetry is broken when $\alpha \neq 0, \pi$.

This formalism can be used to probe both CP-mixing for a spin-0 state or specific alternative hypotheses such as a pure CP-odd state ($J^P = 0^-$) corresponding to $\alpha = \pi/2$, $\kappa_{SM} = \kappa_{HVV} = 0$ and $\kappa_{AVV} = 1$. A BSM CP-even state $J^P = 0^+$ corresponds to $\alpha = 0$, $\kappa_{SM} = \kappa_{AVV} = 0$ and $\kappa_{HVV} = 1$. These hypotheses are compared to the SM Higgs boson hypothesis corresponding to $\alpha = 0$ and $\kappa_{HVV} = \kappa_{AVV} = 0$ and $\kappa_{SM} = 1$.

(ii) Spin-2 model

The graviton inspired interaction Lagrangian for a spin-2 boson $X^{\mu\nu}$ for a color, weak and electromagnetic singlet spin-2 resonance uniquely interacting with the energy momentum tensor $\mathcal{T}^{V,f}$ of vector bosons V or fermions f, can be written as follows [240]:

$$\mathcal{L}_2 \supset \frac{1}{\Lambda}\left[\sum_V \xi_V \mathcal{T}^V_{\mu\nu} X^{\mu\nu} + \sum_f \xi_f \mathcal{T}^f_{\mu\nu} X^{\mu\nu}\right]$$

Where the strength of the interaction is determined by the couplings ξ_V and ξ_f. The simplest scenario, referred to as the universal couplings (UC), corresponds to $\xi_V = \xi_f$. These models predict a large branching ratio to photons (of approximately 5%) and negligible couplings to massive gauge bosons (W and Z). Such scenarios are therefore disfavored and other models are investigated where the couplings of the W, Z and γ are assumed to be independent. Universality of the couplings refers to $\xi_g = \xi_q$. Two other scenarios are considered with low light-quark fraction where $\xi_q = 0$ and the low gluon-fraction where $\xi_q = 2\xi_g$. In these scenarios a large enhancement of the tail of the transverse momentum of the spin-2 state is expected and requires a further selection requirement in order to probe the models within the range of validity of the effective field theory. Two requirements are considered, $p_T^X < 300\,\text{GeV}$ and $p_T^X < 125\,\text{GeV}$ [237].

V.1.3. Probing fixed J^P scenarios

At the LHC, the determination of the spin and *CP* properties of the Higgs boson is done independently from the total rates measurement, it uses a global angular helicity analysis and, when applicable, the study of threshold effects. The channels used for this analysis, $H \to \gamma\gamma$, $H \to W^{(*)}W^{(*)} \to \ell\nu\ell\nu$ and $H \to Z^{(*)}Z^{(*)} \to 4\ell$, are those where the observation of a signal is unambiguous.

At the Tevatron, an analysis using the threshold distribution of the production of the discovered state [241] in the associated production mode VH with subsequent decay to a pair of b-quarks was performed by the D0 collaboration.

(i) The VH production at D0

The mass of the VH system is a powerful discriminant to distinguish a $J^P = 0^+$, with a threshold behavior in $d\sigma/dM^2 \sim \beta$ from 0^- or 2^+ with threshold behaviors respectively in $\sim \beta^3$ and $\sim \beta^5$ (for a graviton like spin 2) [241]. The VH mass observable, not only discriminates signal hypotheses, but also has an increased separation between the 0^- and 2^+ hypotheses with respect to the backgrounds, thus allowing, with a small and not yet significant signal yield, to exclude that the observed state is 0^- at 98% CL [242] and 2^+ at the 99.9% CL [243].

(ii) The $\gamma\gamma$ channel at the LHC

In the $H \to \gamma\gamma$ channel, the analysis is performed inclusively using the production angle $\cos\theta^*_{CS}$ and the transverse momentum of the diphoton pair [237]. The definition chosen for the polar angle in the rest frame is the Collins–Soper frame, which is defined as the bisector axis of the momenta of the incoming protons in the diphoton rest frame. The SM Higgs signal distribution is expected to be uniform with a cutoff due to the selection requirements on the photons transverse momentum. The $H \to \gamma\gamma$ channel is mostly sensitive to the gluon-initiated spin-2 production scenarios, which yield a $\cos\theta^*_{CS}$ distribution peaking at values close to 1. The limits are derived from a fit of the signal in bins of $\cos\theta^*_{CS}$ and diphoton transverse momentum and are summarized in Fig. 11.8 (right) for ATLAS, only combined results are shown. The data shows a good compatibility with the SM 0^+ hypothesis and contributes strongly to the exclusion of several Spin-2 scenarios. The conclusions are the same from CMS results [238].

(iii) The $H \to W^{(*)}W^{(*)} \to \ell\nu\ell\nu$ channel at the LHC

In the $H \to W^{(*)}W^{(*)} \to \ell\nu\ell\nu$ channel, the production and decay angles cannot be easily reconstructed due to the presence of neutrinos in the final state, however sensitivity arises from the V-A structure of the decay of the W bosons. A scalar state thus yields a clear spin correlation pattern that implies that the charged leptons e or μ from the decays of the W bosons are produced close to one another in the transverse plane. This feature, which impacts observables such as the azimuthal angle between the two leptons $\Delta\Phi_{\ell\ell}$ or their invariant mass $M_{\ell\ell}$ in addition of the threshold behavior of the decay which is used in kinematic variables such as the transverse mass defined in Section III, can be used to discriminate between various spin and parity hypotheses. The approach adopted by ATLAS uses a multivariate discriminant, whereas CMS uses a 2D-fit of the dilepton mass and the transverse mass. The results of the $H \to W^{(*)}W^{(*)} \to \ell\nu\ell\nu$ analyses alone are summarized in Fig. 11.8 for ATLAS and in combination with other channels. Spin-1 hypotheses (1^+ and 1^-) have also been tested with this channel by ATLAS and CMS. ATLAS and CMS exclude the 1^+ and 1^- hypotheses at more than 95% CL.

(iv) The $H \to Z^{(*)}Z^{(*)} \to 4\ell$ channel at the LHC

The $H \to Z^{(*)}Z^{(*)} \to 4\ell$ coupling analysis, as described in Section III, also uses a discriminant based on the 0^+ nature of the Higgs boson to further discriminate the signal from the background. In this analysis this feature is used to discriminate between signal hypotheses. The observables sensitive to the spin and parity are [244] the masses of the two Z bosons (due to the threshold dependence of the mass of the off-shell Z boson), two production angle θ^* and Φ_1, and three decay angles, Φ, θ_1 and θ_2. The production and decay angles defined as:

– θ_1 and θ_2, the angles between the negative final state lepton and the direction of flight of Z_1 and Z_2 in the rest frame.

– Φ, the angle between the decay planes of the four final state leptons expressed in the four lepton rest frame.

– Φ_1, the angle defined between the decay plane of the leading lepton pair and a plane defined by the vector of the Z_1 in the four lepton rest frame and the positive direction of the proton axis.

– θ^*, the production angle of the Z_1 defined in the four lepton rest frame with respect to the proton axis.

These angles are illustrated in Fig. 11.8. There are two approaches to this analysis. The first, used by CMS, is a matrix element likelihood approach where a kinematic discriminant is defined based on the ratio of the signal and background probabilities. These probabilities are defined using the leading-order matrix elements. A similar approach is also performed by ATLAS as a cross check of their main result. The main approach adopted by ATLAS is the combination of sensitive observables with a Boosted Decision Tree. These analyses are sensitive to various J^P hypotheses and in particular discriminate the 0^+ hypothesis from the 0^-. In all scenarios investigated and for both the ATLAS and CMS experiments, the data are compatible with the 0^+ hypothesis. ATLAS [239] and CMS [238] exclude a pseudoscalar nature of the observed boson at CL_S levels of 98% and 99.8%.

V.1.4. Probing CP-mixing and anomalous HVV couplings

The careful study of the kinematic properties of the events observed in the $H \to Z^{(*)}Z^{(*)} \to 4\ell$ and $H \to W^{(*)}W^{(*)} \to \ell\nu\ell\nu$ channel, and in particular the angular distributions described above, allows one to further probe the HVV coupling beyond testing fixed hypotheses. Assuming that the observed particle is a spin-0 state, and using several discriminating observables in the $H \to Z^{(*)}Z^{(*)} \to 4\ell$ and $H \to W^{(*)}W^{(*)} \to \ell\nu\ell\nu$ channels, the anomalous terms in the formalism of Eq. (11.10) can be probed. In the approach of helicity amplitudes used by CMS [238], all terms are essentially equivalent, except for one additional phase which is neglected in Eq. (11.10).

Results are derived in terms of the parameters $\tilde{\kappa}_{HVV} = v/\Lambda\,\kappa_{HVV}$ and $\tilde{\kappa}_{AVV} = v/\Lambda\,\kappa_{AVV}$, and more precisely as measurements of $\tilde{\kappa}_{HVV}/\kappa_{SM}$ and $\tan\alpha\,.\,\tilde{\kappa}_{AVV}/\kappa_{SM}$ as shown in Fig. 11.9. These parameters can be interpreted as mixing parameters of a tensor anomalous CP-even coupling and a CP-odd component. The measurements are made in the $H \to Z^{(*)}Z^{(*)} \to 4\ell$ and

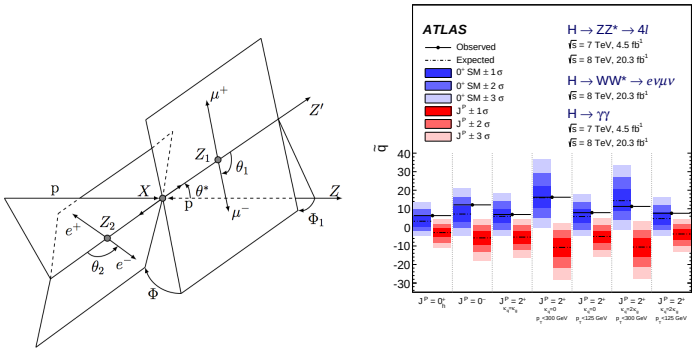

Figure 11.8: (Left) Definition of the production and decay angles defined for the $H \to Z^{(*)}Z^{(*)} \to 4\ell$ final state [238]. (Right) Expected distributions of the test statistic for the SM hypothesis (in blue) and several alternative spin and parity hypotheses (in red).

$H \to W^{(*)}W^{(*)} \to \ell\nu\ell\nu$ channels independently and then combined assuming that the $\tilde{\kappa}_{HVV}/\kappa_{SM}$ and $\tan\alpha \cdot \tilde{\kappa}_{AVV}/\kappa_{SM}$ are the same for the W and Z vector bosons. Only the combination of the WW and ZZ channels is shown in Fig. 11.9. The asymmetric shape of the likelihood as a function of $\tilde{\kappa}_{HWW,HZZ}/\kappa_{SM}$ is mainly due to the interference between the BSM and the SM contributions that give a maximal deviation from the SM predictions for negative relative values of the BSM couplings. In Fig. 11.9 the expected likelihood profiles for a SM Higgs boson are also displayed. While no significant deviation from the SM Higgs boson expectation is observed, the precision of the measurements of the mixing parameters is fairly low. The results and conclusions from the CMS measurements [238] are very similar.

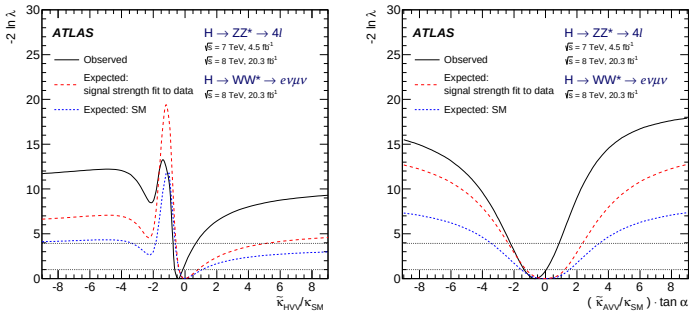

Figure 11.9: Likelihood profiles for the $\tilde{\kappa}_{HVV}$ and $\tilde{\kappa}_{AVV} \cdot \tan\alpha$ parameters, representing respectively CP-even and CP-odd anomalous couplings of the Higgs boson.

Individual ZZ^* channel measurements have been carried out at Run 2 by both ATLAS [132] and CMS [245].

V.2. Off-shell couplings of the Higgs boson

In the dominant gluon fusion production mode with a subsequent decay of the Higgs boson into a pair of Z bosons, the production cross section of a off-shell Higgs boson is known to be sizable. This follows as a consequence of the enhanced couplings of the Higgs boson to the longitudinal polarizations of the massive vector bosons at high energy.

The off-shell to on-shell cross section ratio is approximately 8% in the SM. Still the Higgs contribution to VV production at large invariant mass remains small compared to the background. It is nevertheless interesting to probe Higgs production in this regime as it is sensitive to new physics beyond the SM.

The difficulty in the off-shell VV analysis, beyond the small signal-to-background ratio, is due to a large negative interference between the signal and the $gg \to VV$ background. The resulting presence of a SM Higgs boson signal in the far off-shell domain results in a deficit of events with respect to the expectation from background only events. It is only when the off-shell couplings of the Higgs boson are larger than expected in the SM that the presence of a signal appears as an excess over the background expectation. One additional intricacy arises from the precision in the prediction of the rate for $gg \to VV$, a loop process at lowest order, and its interference with the signal. At the time of the publications of the results from the ATLAS [246] and CMS [247] a full NLO prediction had not been computed.

It is interesting to note that in this regime the Higgs boson is studied as a propagator and not as a particle. The measurement of its off-shell couplings is therefore absolute and does not rely on the knowledge of the total Higgs boson width. The off-shell couplings constraints can then be used to indirectly constrain the natural width of the Higgs boson, under specific assumptions detailed in Section V.3.3.

This measurement has been carried out in the $H \to ZZ \to 4\ell$, $H \to ZZ \to \ell\ell\nu\nu$ and $H \to WW \to \ell\nu\ell\nu$ channels. To enhance the sensitivity of the analysis the knowledge of the full kinematics of the events is important. In particular the signal and the background can be further distinguished by the invariant mass of the VV system, which is more accurately accessible in the $H \to ZZ \to 4\ell$ channel. Angular distributions also play an important role in this analysis. For these reasons the $H \to Z^{(*)}Z^{(*)} \to 4\ell$ channel is significantly more sensitive than $H \to W^{(*)}W^{(*)} \to \ell\nu\ell\nu$. The CMS results in Refs. [247] and [248] include the VBF and VH processes through the selection of two additional jets in the final state. The ATLAS results do not have a specific selection for the VBF or VH production processes, but their contributions are taken into account.

Limits on the off-shell rates have been reported for the two channels by ATLAS [246] and CMS [248]. The combined results assuming that the off-shell rates in the ZZ and WW channels scale equally, are given for two different hypotheses on the VBF production rate: fixing it to its SM value or scaling it as the gluon fusion rate. The observed (expected) limits on the off-shell rate fraction with respect to its SM expectation is 6.7 (9.1) for ATLAS [246] with the VBF rate fixed to its SM value and 2.4 (6.2) for CMS [248] where no assumption is made on the relative production rates of gluon-fusion and VBF. In both cases the custodial symmetry is assumed and the ratio of the rates in the ZZ and WW decays are fixed to those of the Standard Model. Results without this assumption have also been reported in Ref. [248].

V.3. The Higgs boson width

In the SM, the Higgs boson width is very precisely predicted once the Higgs boson mass is known. For a mass of 125.1 GeV, the Higgs boson has a very narrow width of 4.2 MeV. It is dominated by the fermionic decays partial width at approximately 75%, while the vector boson modes are suppressed and contribute 25% only.

At the LHC or the Tevatron, in all production modes, only the cross sections times branching fractions can be measured. As a consequence, the total natural width of the Higgs boson cannot be inferred from measurements of Higgs boson rates. Direct constraints on the Higgs boson width are much larger than the expected natural width of the SM Higgs boson.

V.3.1. Direct constraints

Analysis of the reconstructed mass lineshape in the two channels with a good mass resolution, the $H \to \gamma\gamma$ and $H \to Z^{(*)}Z^{(*)} \to 4\ell$, allow for a direct measurement of the width of the SM Higgs boson. The intrinsic mass resolution in these channels is about 1–2 GeV, much larger than the expected width of the SM Higgs boson. As a result only upper limits on the Higgs boson width have been measured by ATLAS [249] and CMS [125]. The two main challenges of direct constraints on the width through the measurement of the lineshape are: (i) the modeling of resolution uncertainties and (ii) the modeling of the interference between the signal and the continuum background which can be sizable for large widths, in particular in the range where direct constraints are set. Given that these interference effects are small with respect to the individual channels sensitivity, they are neglected in deriving constraints on the total width. The combined

Table 11.12: Run 1 observed (expected) direct 95% CL constraints on the natural width of the 125 GeV resonance from fits to the $\gamma\gamma$ and ZZ mass spectra and to the 4ℓ vertex lifetime. *The CMS measurement from the 4ℓ mass lineshape was performed using Run 2 data.

	$M_{\gamma\gamma}$ mass spectrum	$M_{4\ell}$ spectrum	4ℓ vertex lifetime
ATLAS	$< 5.0(6.2)$ GeV	$< 2.6(6.2)$ GeV	—
CMS	$< 2.4(3.1)$ GeV	$< 1.1(1.6)$ GeV*	$> 3.5 \times 10^{-12}$ GeV

constraints however, being more precise could be affected by the interference. ATLAS [249] has therefore not combined the constraints on the width from the two channels. The results are reported in Table 11.12. These constraints are still three orders of magnitude larger than the expected SM width and are fully compatible with the SM hypothesis.

Another direct constraint on the Higgs boson width can be obtained in the $H \to Z^{(*)}Z^{(*)} \to 4\ell$ channel, from the measurement of the average lifetime of the Higgs boson calculated from the displacement of the four-lepton vertex from the beam spot. This analysis has been carried out by CMS [247], using the measured decay length. The measured $c\tau_H$ is 2^{+25}_{-2} μm, yielding an observed (and expected) limit at the 95% CL of $c\tau_H < 57(56)\,\mu$m. From this upper limit on the lifetime of the Higgs boson. The 95% CL lower limit on its natural width is $\Gamma_H > 3.5 \times 10^{-12}$ GeV.

V.3.2. Indirect constraints from mass shift in the diphoton channel

In the diphoton channel, it was noticed in [250], that the effect of the interference between the main signal $gg \to H \to \gamma\gamma$ and the continuum irreducible background $gg \to \gamma\gamma$, taking into account detector resolution effects, is responsible for a non negligible mass shift. The size of the mass shift depends on the total width of the Higgs boson and it was suggested that measuring this mass shift could provide a constraint on the width [250]. It was further noticed that the mass shift has a dependence also on the diphoton transverse momentum. The total width of the Higgs boson could therefore be constrained using the diphoton channel alone.

Further studies were performed by the ATLAS collaboration to estimate the size of the expected mass shift [135]. The expected shift in mass in the diphoton channel is 35±9 MeV for the SM Higgs boson. Very preliminary studies of the sensitivity of this method to estimate the width of the Higgs boson in the high-luminosity regime have been made by ATLAS [251] and yield an expected 95% CL upper limit on the total width of approximately 200 MeV from 3 ab^{-1} of 14 TeV data.

V.3.3. Indirect constraints from on-shell rate in the diphoton channel

In the diphoton channel, it was noticed in Ref. [252], that the interference between the main signal $gg \to H \to \gamma\gamma$ amplitude and the continuum irreducible background $gg \to \gamma\gamma$ amplitude generates non-negligible change in the on-shell cross sections, as a result of the existence of a relative phase between these amplitudes. The size of this on-shell interference effect depends on the total width of the Higgs boson and it was suggested that measuring this on-shell cross section precisely could provide a constraint on the Higgs total width. This interference effect yields around 2% reduction for the $gg \to H \to \gamma\gamma$ cross section measurement. The current evaluation of this interference effect is performed at NLO and has $-30\% + 50\%$ uncertainty, due to the fact that the large relative phase is driven by the two-loop $gg \to \gamma\gamma$ background amplitude [250, 252]. This on-shell interference effect has dependence on the p_T of the diphoton system and the photon polar angle in the diphoton rest frame, which can be further exploited to improve the measurement to constrain the Higgs total width.

Taking the ratios of the on-shell cross section of Higgs to diphoton channel and the cross section of Higgs to four-leptons channel where the interference effect is negligible could put bound on the Higgs total width. This ratio is free from many dominant sources of systematic uncertainties for cross section measurements, *i.e.*, PDF uncertainty and luminosity uncertainty, and can be further improved by the accumulation of the LHC data. From this cross section ratio measurement alone, a preliminary estimation of the current limit from this interference effect with current 30% precision puts an upper bound of 800 MeV on the Higgs boson total width and the limit improves to 60 MeV with 3 ab^{-1} of 14 TeV data [252, 253].

V.3.4. Indirect constraints from off-shell couplings

Using simultaneously on-shell and off-shell measurements in the VV channels, it was noticed [254] that the total width of the Higgs could be constrained. This can be illustrated from the parametrization of the signal strength measurements both on-shell ($\mu_{\rm on-shell}$) and off-shell ($\mu_{\rm off-shell}$) as a function of the couplings modifiers κ_g and κ_V parameterizing the main process $gg \to H \to VV$. The on-shell signal strength can be written as:

$$\mu_{\rm on-shell} = \frac{\kappa^2_{g,\,\rm on-shell}\,\kappa^2_{V,\,\rm on-shell}}{\Gamma_H/\Gamma_{SM}}$$

while in the case of the off-shell signal strength where the Higgs boson is a propagator:

$$\mu_{\rm off-shell} = \kappa^2_{g,\,\rm off-shell}\,\kappa^2_{V,\,\rm off-shell}$$

A bound on the Higgs width can then be obtained from the measurements of the on-shell and off-shell signal strengths. This assumes that no new physics alters the Higgs boson couplings in the off-shell regime, *i.e.*, that the running of its couplings is negligible in the off-shell regime. Both ATLAS [246] and CMS [247, 248] have used their off-shell production limits to constrain the width of the Higgs boson.

Both ATLAS and CMS analyses use the kinematic event characteristics to further gain in sensitivity to discriminate between the signal and background. The ATLAS analysis assumes that there are no anomalous couplings of the Higgs boson to vector bosons, and obtains 95% CL observed (expected) upper limit on the total width of $5.7\times\Gamma_{SM}$ ($9.0\times\Gamma_{SM}$) [246]. In the CMS analysis, the observed (expected) limit on the total width is $6.2\times\Gamma_{SM}$ ($9.8\times\Gamma_{SM}$) for the ZZ channel only [247]. In addition in the CMS analysis, results are also derived allowing for anomalous couplings of the Higgs boson, therefore reducing the discriminating power of the kinematic variables used in the analysis but reducing the model dependence. The observed (expected) limit on the total width is $10.9\times\Gamma_{SM}$ ($17.4\times\Gamma_{SM}$) [247].

The CMS experiment has also combined the ZZ and W^+W^- channels while keeping the gluon-fusion and VBF production processes separate. For the gluon fusion mode the observed (expected) combined upper limit at the 95% CL on the total width of the Higgs boson is $2.4\times\Gamma_{SM}$ ($6.2\times\Gamma_{SM}$) [248], while for the VBF production mode the exclusion limits are $19.3\times\Gamma_{SM}$ ($34.4\times\Gamma_{SM}$) [248].

ATLAS has also performed a study of the prospects for measuring the Higgs width in the four lepton channel alone. Projecting to a luminosity of 3 ab^{-1}, it was concluded that, within assumptions similar to the ones mentioned above, the width of the Higgs boson could be constrained with the following precision [255]:

$$\Gamma_H = 4.2^{+1.5}_{-2.1}\,\text{MeV}.$$

VI. Probing the coupling properties of the Higgs boson

As discussed in Section II, within the SM, all the Higgs couplings are fixed unambiguously once all the particle masses are known. Any deviation in the measurement of the couplings of the Higgs boson could therefore signal physics beyond the SM.

Measuring the Higgs couplings without relying on the SM assumption requires a general framework treating deviations from the SM coherently at the quantum level in order to provide theoretical predictions for relevant observables to be confronted with experimental data. The first attempt in that direction was the development of the so-called κ-formalism [256] where the SM Higgs couplings are rescaled by factors κ, keeping the same Lorentz structure of the interactions.

This formalism allows for simple interpretation of the signal strengths μ measured in the various Higgs channels and it has been used to test various physics scenarios, like the existence of additional new particles contributing to the radiative Higgs production and decays, or to probe various symmetries of the SM itself, as for example the custodial symmetry. But the κ-formalism has obvious limitations and certainly does not capture the most general deformations of the SM, even under the assumptions of heavy and decoupling new physics. A particularly acute shortcoming at the time Higgs physics is entering a precision era is the lack of proficiency of the κ's to assert the richness of kinematical distributions beyond simple signal strength measurements. Several extensions and alternative approaches are being developed as part of the activities of the Higgs cross-section working group.

The Higgs Pseudo-Observable (HPO) approach [257] is providing a particularly elegant formalism to report the data in terms of a finite set of on-shell form factors parametrizing amplitudes of physical processes subject to constraints from Lorentz invariance and other general requirements like analyticity, unitarity, and crossing symmetry. These form factors are expanded in powers of kinematical invariants of the process around the known poles of SM particles, assuming that poles from BSM particles are absent in the relevant energy regime. A set of HPOs have been proposed to characterize both the Higgs decays and the EW Higgs production channels, thus exploring different kinematical regimes. Prospective studies concluded that these HPOs can be measured/bounded at the percent level at the HL-LHC and could therefore be used to constrain some explicit models of New Physics.

Another interesting approach to characterize the possible Higgs coupling deviations induced by physics beyond the SM is the use of Effective Field Theories (EFT). This approach assumes again that the new physics degrees of freedom are sufficiently heavy to be integrated out and they simply give rise to effective interactions among the light SM particles. By construction the effective Lagrangians cannot account for deviations in Higgs physics induced by light degrees of freedom, unless they are added themselves as extra fields in the effective Lagrangians. In Section VII, several examples of models with light degrees of freedom affecting Higgs production and decay rates will be presented. The main advantage of EFTs is their prowess to relate different observables in different sectors and at different energies to constrain a finite set of effective interactions among the SM degrees of freedom. In an EFT, the SM Lagrangian is extended by a set of higher-dimensional operators, and it reproduces the low-energy limit of a more fundamental UV description. It will be assumed that the Higgs boson is part of a CP-even EW doublet. This is motivated by the apparent relation between the Higgs couplings and the masses of the various particles which naturally follows under this assumption of a linear realization of the $\mathrm{SU}(2)_L \times \mathrm{U}(1)_Y$ symmetry of the SM. There have been some recent attempts to write the most general EFT bypassing this assumption, see for instance [258].

VI.1. Effective Lagrangian framework

The EFT has the same field content and the same linearly-realized $\mathrm{SU}(3)_C \times \mathrm{SU}(2)_L \times \mathrm{U}(1)_Y$ local symmetry as the SM. The difference is the presence of operators with canonical dimension D larger than 4. These are organized in a systematic expansion in D, where each consecutive term is suppressed by a larger power of a high mass scale. Assuming baryon and lepton number conservation, the most general Lagrangian takes the form

$$\mathcal{L}_{\text{eff}} = \mathcal{L}_{\text{SM}} + \sum_i c_i^{(6)} \mathcal{O}_i^{(6)} + \sum_j c_j^{(8)} \mathcal{O}_j^{(8)} + \cdots . \qquad (11.11)$$

The list of dimension-6 operators was first classified in a systematic way in Ref. [259] after the works of Ref. [260]. Subsequent analyses pointed out the presence of redundant operators, and a minimal and complete list of operators was finally provided in Ref. [261][4]. For a single family of fermions, there are 76 real ways to deform the SM generated by 59 independent operators (with the 3 families of fermions of the SM, flavor indices can be added to these 59 operators, and furthermore, new operator structures, that have been dismissed by means of Fierz transformations in the single family case, have to be considered, for a total of 2499 real deformations [263]). Of particular interest are the 17 CP-invariant operators, in addition to 8 dipole operators, that affect, at tree-level, the Higgs production and decay rates [264–266]. A convenient list of these operators can be found in Table 11.13, and Table 11.14. The other operators completing the basis of dimension-6 operators can be found in Ref. [266].

Table 11.13: List of 17 CP-even operators affecting, at tree-level, only Higgs production and decay rates (left) as well as EW observables (right). See text for notations.

Operators affecting Higgs physics only	Operators affecting Higgs and EW physics
$\mathcal{O}_r = \lvert\Phi\rvert^2 \lvert D_\mu\Phi\rvert^2$	$\mathcal{O}_W = \frac{ig}{2}\big(\Phi^\dagger\sigma^i \overleftrightarrow{D}^\mu\Phi\big)(D^\nu W_{\mu\nu})^i$
$\mathcal{O}_6 = \lambda\lvert\Phi\rvert^6$	$\mathcal{O}_B = \frac{ig'}{2}\big(\Phi^\dagger \overleftrightarrow{D}^\mu\Phi\big)(\partial^\nu B_{\mu\nu})$
$\mathcal{O}_{BB} = \frac{g'^2}{4}\lvert\Phi\rvert^2 B_{\mu\nu}B^{\mu\nu}$	$\mathcal{O}_T = \frac{1}{2}\big(\Phi^\dagger \overleftrightarrow{D}^\mu\Phi\big)^2$
$\mathcal{O}_{WW} = \frac{g^2}{4}\lvert\Phi\rvert^2 W^i_{\mu\nu}W^{i\,\mu\nu}$	$\mathcal{O}_{HB} = ig'\,(D^\mu\Phi)^\dagger(D^\nu\Phi)B_{\mu\nu}$
$\mathcal{O}_{GG} = \frac{g_S^2}{4}\lvert\Phi\rvert^2 G^A_{\mu\nu}G^{A\mu\nu}$	$\mathcal{O}_{Hu} = i\,(\bar{u}_R\gamma^\mu u_R)\,\big(\Phi^\dagger\overleftrightarrow{D}_\mu\Phi\big)$
$\mathcal{O}_{yu} = y_u\lvert\Phi\rvert^2\,\bar{q}_L\tilde{\Phi}u_R$	$\mathcal{O}_{Hd} = i\,\big(\bar{d}_R\gamma^\mu d_R\big)\,\big(\Phi^\dagger\overleftrightarrow{D}_\mu\Phi\big)$
$\mathcal{O}_{yd} = y_d\lvert\Phi\rvert^2\,\bar{q}_L\Phi d_R$	$\mathcal{O}_{He} = i\,\big(\bar{l}_R\gamma^\mu l_R\big)\,\big(\Phi^\dagger\overleftrightarrow{D}_\mu\Phi\big)$
$\mathcal{O}_{ye} = y_e\lvert\Phi\rvert^2\,\bar{L}_L\Phi e_R$	$\mathcal{O}_{Hq} = i\,(\bar{q}_L\gamma^\mu q_L)\,\big(\Phi^\dagger\overleftrightarrow{D}_\mu\Phi\big)$
	$\mathcal{O}^{(3)}_{Hq} = i\,\big(\bar{q}_L\gamma^\mu\sigma^i q_L\big)\,\big(\Phi^\dagger\sigma^i\overleftrightarrow{D}_\mu\Phi\big)$

Table 11.14: List of 8 dipoles operators. See text for notations.

Dipoles ops.
$\mathcal{O}_{uB} = g'\,(\bar{q}_L\tilde{\Phi}\sigma^{\mu\nu}u_R)\,B_{\mu\nu}$
$\mathcal{O}_{uW} = g\,(\bar{q}_L\sigma^i\tilde{\Phi}\sigma^{\mu\nu}u_R)\,W^i_{\mu\nu}$
$\mathcal{O}_{uG} = g_S\,(\bar{q}_L\tilde{\Phi}\sigma^{\mu\nu}t^A u_R)\,G^A_{\mu\nu}R$
$\mathcal{O}_{dB} = g'\,(\bar{q}_L\Phi\sigma^{\mu\nu}d_R)\,B_{\mu\nu}$
$\mathcal{O}_{dW} = g\,(\bar{q}_L\sigma^i\Phi\sigma^{\mu\nu}d_R)\,W^i_{\mu\nu}$
$\mathcal{O}_{dG} = g_S\,(\bar{q}_L\Phi\sigma^{\mu\nu}t^A d_R)\,G^A_{\mu\nu}$
$\mathcal{O}_{lB} = g'\,(\bar{L}_L\Phi\sigma^{\mu\nu}l_R)\,B_{\mu\nu}$
$\mathcal{O}_{lW} = g\,(\bar{L}_L\sigma^i\Phi\sigma^{\mu\nu}l_R)\,W^i_{\mu\nu}$

The SM gauge couplings are denoted by g', g, g_S while $y_{u,d,e}$ are the SM Yukawa couplings (in the mass eigenstate basis that diagonalizes the general Yukawa coupling matrices $Y_{u,d,l}$) and λ is the SM Higgs quartic coupling. We denote by $i\Phi^\dagger\overleftrightarrow{D}^\mu\Phi$ the Hermitian derivative $i\Phi^\dagger(D^\mu\Phi) - i(D^\mu\Phi)^\dagger\Phi$, $\sigma^{\mu\nu} \equiv i[\gamma^\mu,\gamma^\nu]/2$ and $\tilde{\Phi}$ is the Higgs charge-conjugate doublet: $\tilde{\Phi} = i\sigma^2\Phi^*$. Each operator $\mathcal{O}_{yu,yd,ye}$ is further assumed to be flavor-aligned with the corresponding fermion mass term, as required in order to avoid large Flavor-Changing Neutral Currents (FCNC) mediated by the tree-level exchange of the Higgs boson. This implies one coefficient for the up-type quarks (c_{yu}), one for down-type quarks (c_{yd}), and one for the charged leptons (c_{ye}), i.e. the $c_{yu,ud,ye}$ matrices should be proportional to the identity matrix in flavor space.

The choice of the basis of operators is not unique and using the equations of motion, i.e., performing field redefinitions, different dimension-6 operators can be obtained as linear combinations of the operators in the previous tables and of four-fermion operators. Some relations between common bases of operators can be found for instance in Refs. [265, 263]. Different bases have different advantages. For instance the so-called SILH basis [264] better captures the low-energy effects of universal theories in which new physics couples to SM bosons only. The Warsaw basis [261] on the other hand mostly includes vertex corrections and easily connects operators to observables [266]. The basis defined in Table 11.13, and Table 11.14 is particularly well suited for an analysis of the Higgs data. The reason is that the eight

[4] Complete classifications of D=8 operators have recently appeared in the literature, see Ref. [262]. Still, in this review, the EFT Lagrangians will be truncated at the level of dimension-6 operators.

operators of the left-hand side of Table 11.13, in the vacuum with $|\Phi|^2 = v^2/2$, merely redefine the SM input parameters and therefore were left unconstrained at tree-level before Higgs data are considered. These eight operators modify the physical Higgs vertices and can be probed via the decay processes $H \to \gamma\gamma, Z\gamma, \bar{b}b, \bar{\tau}\tau$ and the production channels $gg \to H, VV \to H, pp \to \bar{t}tH$ and $gg \to HH$. Section VI.2 illustrates how the Higgs data accumulated at the LHC can (partially) constrain these eight operators, following the initial phenomenological study of Ref. [266]. The other nine operators of Table 11.13 are tightly constrained by the LEP EW precision measurements (the measurements of the Z-boson couplings to quarks and leptons on the Z-pole) and by diboson production.[5]

The minimal flavor violation assumption imposes Yukawa dependences in the eight dipole operators. For the light generations of fermions, this dependence lowers the induced deviations in the Higgs rates below the experimental sensitivity reachable in any foreseeable future. The corresponding operators in the top sector are not suppressed but they are already constrained by the limit of the top dipole operators imposed by the bounds on the neutron electric dipole moment, on the $b \to s\gamma$ and $b \to s\ell^+\ell^-$ rates and on the $t\bar{t}$ cross section [269, 265].

Automatic tools [265, 240] are being developed to analyze the experimental data within an EFT framework.

VI.2. Probing coupling properties

As described in Section III a framework was developed by the ATLAS and CMS collaboration [143], individually and together, to combine the very large number of exclusive categories aimed at reconstructing the five main decay modes and the five main production modes of the Higgs boson. The general conclusions of this combination in terms of production cross sections and decay modes, illustrating the compatibility of the observation with the expectation from the SM Higgs boson is given in Section III. The same framework with its master formula Eq. (11.9) can be used to further measure coupling properties of the Higgs boson under specific additional assumptions.

VI.2.1. Combined measurements of the coupling properties of H

(i) From effective Lagrangians to Higgs observables

All 8 operators of the effective Lagrangian that were unconstrained before the Higgs data induce, at tree-level, deviations in the Higgs couplings that either respect the Lorentz structure of the SM interactions, or generate simple new interactions of the Higgs boson to the W and Z field strengths, or induce some contact interactions of the Higgs boson to photons (and to a photon and a Z boson) and gluons that take the form of the ones that are generated by integrating out the top quark. In other words, the Higgs couplings are described, in the unitary gauge, by the following effective Lagrangian [256, 42]

$$\begin{aligned}\mathcal{L} = {} & \kappa_3 \frac{m_H^2}{2v} H^3 + \kappa_Z \frac{m_Z^2}{v} Z_\mu Z^\mu H + \kappa_W \frac{2m_W^2}{v} W_\mu^+ W^{-\mu} H \\ & + \kappa_g \frac{\alpha_s}{12\pi v} G^a_{\mu\nu} G^{a\mu\nu} H + \kappa_\gamma \frac{\alpha}{2\pi v} A_{\mu\nu} A^{\mu\nu} H + \kappa_{Z\gamma} \frac{\alpha}{\pi v} A_{\mu\nu} Z^{\mu\nu} H \\ & + \kappa_{VV} \frac{\alpha}{2\pi v} \left(\cos^2\theta_W Z_{\mu\nu} Z^{\mu\nu} + 2\, W^+_{\mu\nu} W^{-\mu\nu} \right) H \\ & - \left(\kappa_t \sum_{f=u,c,t} \frac{m_f}{v} f\overline{f} + \kappa_b \sum_{f=d,s,b} \frac{m_f}{v} f\overline{f} + \kappa_\tau \sum_{f=e,\mu,\tau} \frac{m_f}{v} f\overline{f} \right) H. \end{aligned} \tag{11.12}$$

The correspondence between the effective coefficients of the dimension-6 operators and the κ's can be found for instance in Ref. [43]. In the SM, the Higgs boson does not couple to massless gauge bosons at tree level, hence $\kappa_g = \kappa_\gamma = \kappa_{Z\gamma} = 0$. Nonetheless, the contact operators are generated radiatively by SM particles loops. In particular, the top quark gives a contribution to the 3 coefficients $\kappa_g, \kappa_\gamma, \kappa_{Z\gamma}$ that does not decouple in the infinite top mass limit. For instance, in that limit $\kappa_\gamma = \kappa_g = 1$ [23, 24, 270].

The coefficient for the contact interactions of the Higgs boson to the W and Z field strengths is not independent but obeys the relation

$$(1 - \cos^4\theta_W)\kappa_{VV} = \sin 2\theta_W \kappa_{Z\gamma} + \sin^2\theta_W \kappa_{\gamma\gamma}. \tag{11.13}$$

This relation is a general consequence of the custodial symmetry [265], which also imposes $\kappa_Z = \kappa_W$ at leading order ($\kappa_Z/\kappa_W - 1$ is a measure of custodial symmetry breaking and as such is already constrained by electroweak precision data and the bounds on anomalous gauge couplings). When the Higgs boson is part of an $SU(2)_L$ doublet, the custodial symmetry could only be broken by the $\mathcal{O}_T = \frac{1}{2}\left(\Phi^\dagger \overleftrightarrow{D}^\mu \Phi\right)^2$ operator at the level of dimension-6 operators and it is accidentally realized among the interactions with four derivatives, like the contact interactions considered.

The coefficient κ_3 can be accessed directly only through double Higgs production processes, hence it will remain largely unconstrained at the LHC. The LHC will also have a limited sensitivity on the coefficient κ_τ since the lepton contribution to the Higgs production cross section remains subdominant and the only way to access the Higgs coupling is via the $H \to \tau^+\tau^-$ and possibly $H \to \mu^+\mu^-$ channels. Until the associated production of a Higgs with a pair of top quarks is observed, the Higgs coupling to the top quark is only probed indirectly via the one-loop gluon fusion production or the radiative decay into two photons. However, these two processes are only sensitive to the combinations of couplings $(\kappa_t + \kappa_g)$ and $(\kappa_t + \kappa_\gamma)$ and not to the individual couplings. Therefore a deviation in the Higgs coupling to the top quark can in principle always be masked by new contact interactions to photons and gluons (and this is precisely what is happening in minimal incarnations of composite Higgs models). The current limited sensitivity in the $t\bar{t}H$ channel leaves elongated ellipses in the direction $\kappa_g = \kappa_\gamma = 1 - \kappa_t$.

The operators already bounded by EW precision data and the limits on anomalous gauge couplings modify in general the Lorentz structure of the Higgs couplings and hence induce some modifications of the kinematical differential distributions [271, 272]. A promising way to have a direct access to the effective coefficients of these operators in Higgs physics is to study the VH associated production with a W or a Z at large invariant mass of the VH system [271, 273]. It has not been estimated yet whether the sensitivity on the determination of the effective coefficients in these measurements can compete with the one derived for the study of anomalous gauge couplings. In any case, these differential distributions could also be a way to directly test the hypothesis that the Higgs boson belongs to an $SU(2)_L$ doublet together with the longitudinal components of the massive electroweak gauge bosons.

(ii) Interpretations of the experimental data

The measurements of the coupling properties of the Higgs boson are entirely based on the formalism of the effective Lagrangian described in Section VI.2.1.i. Measurements of coupling properties in this framework implies assessing the parameters of the model Eq. (11.12) or combinations of these parameters with different sets of assumptions.

These measurements are carried out with the combination framework described in Section IV where the μ_i and μ_f signal strength parameters are further interpreted in terms of modifiers of the SM couplings κ_k where $k \in \{Z, W, f, g, \gamma, Z\gamma\}$ as in Eq. (11.12). These coupling modifiers κ are fully motivated as leading order coupling scale factors defined such that the cross sections σ_j and the partial decay widths Γ_j associated with the SM particle j scale with the factor κ_j^2 when compared to the corresponding SM prediction. The number of signal events per category for the various production modes are typically estimated at higher orders in the analyses but are scaled by these single LO-inspired factors, thus not taking into account possible intricacies and correlations of these parameters through the higher order corrections. This approximation is valid within the level of precision of current results and their compatibility with the SM expectation.

[5] There remains an accidental flat direction [267] in the fit of anomalous gauge boson couplings using LEP2 data on diboson production alone. This flat direction can be lifted when LHC Higgs data are considered [268].

In this formalism further assumptions are explicitly made: (i) the signals observed in the different search channels originate from a single narrow resonance with a mass of 125 GeV; (ii) similarly to the combination described in Section IV the narrow width approximation is assumed (to allow the decomposition of signal yields); (iii) the tensor structure of the couplings is assumed to be the same as that of a SM Higgs boson. This means in particular that the observed state is assumed to be a CP-even scalar as in the SM.

Loop-level couplings such as the $gg \to H$, $H \to \gamma\gamma$ and $H \to Z\gamma$ can either be treated effectively, with The κ_g, κ_γ and $\kappa_{Z\gamma}$ as free parameters in the fit or these parameters can be expressed in terms of the know SM field content and as a function of the SM coupling modifiers, in the following way:

$$\begin{aligned}\kappa_g^2(\kappa_t,\kappa_b) &= 1.06\,\kappa_t^2 - 0.07\,\kappa_t\kappa_b + 0.01\,\kappa_b^2,\\ \kappa_\gamma^2(\kappa_F,\kappa_V) &= 1.59\,\kappa_V^2 - 0.66\,\kappa_V\kappa_F + 0.07\,\kappa_F^2,\\ \kappa_{Z\gamma}^2(\kappa_F,\kappa_V) &= 1.12\,\kappa_V^2 - 0.15\,\kappa_V\kappa_F + 0.03\,\kappa_F^2.\end{aligned} \tag{11.14}$$

The $\kappa_{Z\gamma}$ parametrization is used only in the ATLAS combined measurements of the coupling properties of the Higgs boson [234]. Neither the $Z\gamma$ nor the $\mu^+\mu^-$ channels are included in the CMS [235] and the ATLAS-CMS combinations [143], which therefore do not use the $\kappa_{Z\gamma}$ or κ_μ parameters explicitly. The parametrizations are given for a Higgs boson mass hypothesis of 125.09 GeV (and in the last two expressions, all the Higgs-fermion couplings are assumed to be rescaled by an universal multiplicative factor κ_F). It can be noted from the expression of κ_γ that the coupling of the Higgs boson to photons is dominated by the loop of W bosons, and it is affected by the top quark loop mostly through its interference with the W loop. The sensitivity of the current measurements to the relative sign of the fermion and vector boson couplings to the Higgs boson is due to this large negative interference term. The κ_g parameter is expressed in terms of the scaling of production cross sections and therefore also depends on the pp collisions centre-of-mass energy. The parametrizations of κ_γ and $\kappa_{Z\gamma}$ are obtained from the scaling of partial widths and are only dependent on the Higgs boson mass hypothesis. Experiments use a more complete parametrization with the contributions from the b-quarks, τ-leptons in the loop [256, 42].

The global fit is then performed expressing the μ_i and μ_f parameters in terms of a limited number of κ_k parameters or their ratios, under various assumptions. The parametrization for the main production modes are: (i) $\mu_{ggF} = \kappa_g^2$ for the gluon fusion and an effective coupling of the Higgs boson to the gluons; (ii) $\mu_{VBF,VH} = \kappa_V^2$ for the VBF and VH processes when the W and Z couplings are assumed to scale equally, and $\mu_{VBF}^2(\kappa_W,\kappa_Z) = (\kappa_W^2\sigma_{WWH} + \kappa_Z^2\sigma_{ZZH})/(\sigma_{WWH} + \sigma_{ZZH})$, when the couplings to the W and Z bosons are varied independently (σ_{WWH} and σ_{ZZH} denote the VBF cross sections via the fusion of a W and a Z boson respectively, the small interference term is neglected); (iii) $\mu_{ttH} = \kappa_t^2$ for the $t\bar{t}$H production mode. Numerically the production modes signal strengths as a function of the coupling modifiers to the SM fields are:

$$\mu_{ggF} = 1.06\kappa_t^2 + 0.01\kappa_b^2 - 0.07\kappa_t\kappa_b, \quad \text{and} \quad \mu_{VBF} = 0.74\kappa_W^2 + 0.26\kappa_Z^2.$$

The decay mode signal strengths are parametrized as $\mu_k = \kappa_k^2/\kappa_H^2$ where $k \in \{Z, W, f, g, \gamma, Z\gamma\}$ denotes the decay mode and κ_H the overall modifier of the total width that affects all the signal yields. κ_H is a priori an independent parameter. However, when it is assumed that the Higgs boson cannot decay to new particles beyond those of the SM, κ_H can also be treated as an effective parameter and expressed in terms of the coupling modifiers to the SM field content. Its general expression is:

$$\kappa_H^2 = 0.57\kappa_b^2 + 0.06\kappa_\tau^2 + 0.03\kappa_c^2 + 0.22\kappa_W^2 + 0.03\kappa_Z^2 + 0.09\kappa_g^2 + 0.0023\kappa_\gamma^2. \tag{11.15}$$

The general expression of the total width of the Higgs boson can be written as follows:

$$\Gamma_H = \frac{\kappa_H^2\Gamma_H^{SM}}{1 - \mathrm{BR}_{\mathrm{BSM}}}$$

where Γ_H^{SM} is the total width of the SM Higgs boson and $\mathrm{BR}_{\mathrm{BSM}}$ is the branching fraction of the Higgs boson to new particles beyond the SM.

Specific parametrizations will be made in order to address the following aspects of the coupling properties of the Higgs boson under different assumptions: (i) the relative couplings of the Higgs boson to fermions and bosons; (ii) the potential impact of the presence of new particles beyond the SM either in the loops or both in the loops and the decay of the H; and (iii) also, more general models either of coupling modifiers or their ratios, under different assumptions.

(iii) Relative couplings to bosons and fermions

As will be discussed in Section VII.6.3, it is interesting to probe a model where no additional field content is considered in the decay width of the Higgs boson and where the relative couplings of the Higgs boson to W- and Z-bosons is fixed to its SM value and where all Yukawa couplings scale with one coupling modifier. In this model only SM particles are assumed to contribute to the gluon fusion and the diphoton loops, all fermion couplings modifiers are required to scale simultaneously with a unique factor κ_F and all vector boson couplings modifiers must scale simultaneously with a unique factor κ_V. This parametrization assumes that no new particles affect the direct decays or the loops. It is a two parameters fit with κ_V and κ_F as parameters of interest. The ATLAS-CMS combined results for each channel independently, the combinations of all channels for the two experiments separately and the results and the overall combination are shown in Fig. 11.10.

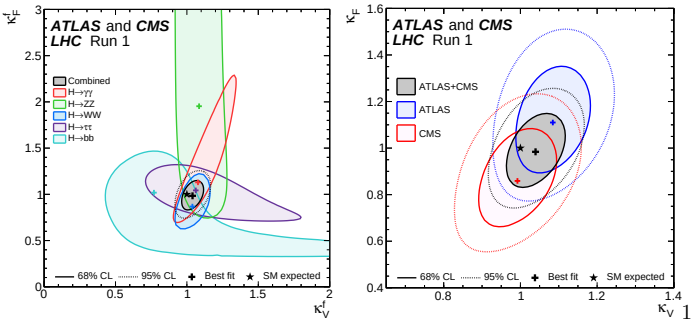

Figure 11.10: Likelihood contours in the (κ_F, κ_V) plane for the ATLAS-CMS combination for the main decay channels separately (left) and for the individual combination of all channels for ATLAS and CMS separately and the complete combined contour (right) [143].

The global fit is only sensitive to the relative sign of κ_V and κ_F. By convention negative values of κ_F can be considered. Such values are not excluded a priori, but would imply the existence of new physics at a light scale and would also raise questions about the stability of such a vacuum [274]. Among the five main Higgs decay channels, only the $\gamma\gamma$ is sensitive to the sign of κ_F through the interference of the W and t loops as shown in Eq. (11.14). The current global fit disfavors a negative value of κ_F at more than five standard deviations. A specific analysis for the Higgs boson production in association with a single top quark has been proposed [275, 276] in order to more directly probe the sign of κ_F. All available experimental data show a fair agreement of the SM prediction of the couplings of the Higgs boson to fermions and gauge bosons. The results shown in Fig. 11.10 assume that $\kappa_F \geq 0$, however in Ref. [143], a similar combination is done without this assumption. The combined sensitivity to the exclusion of a negative relative sign, is approximately 5σ in this model. It is interesting to note that although none of the channels have a significant sensitivity to resolve the sign ambiguity, the combination can, mainly through the $W-t$ interference in the $H \to \gamma\gamma$ channel and the $H \to W^+W^-$ channel. The observed exclusion is fully compatible with the expectation [143]. The combined measurements with the Run 1 dataset lead to

$$\kappa_V = 1.04 \pm 0.05 \quad \text{and} \quad \kappa_F = 0.98^{+0.11}_{-0.10},$$

already at the impressive 5% level of accuracy for the κ_V parameter.

(iv) Coupling measurements and probing new physics beyond the SM in loops and in the decay

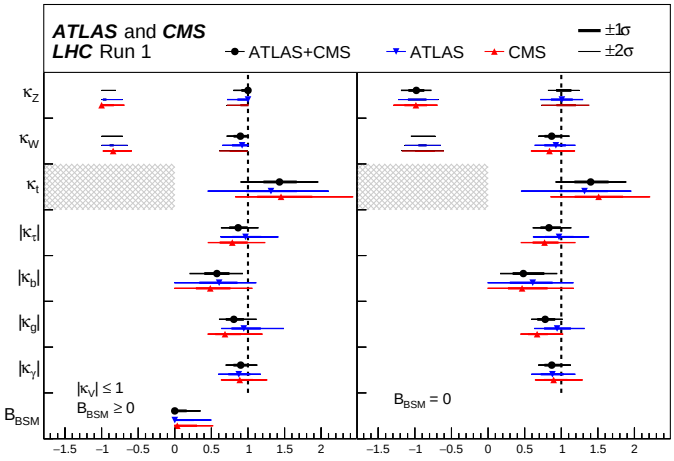

Figure 11.11: ATLAS-CMS combined measurements of coupling modifiers.

In the model described above in Section VI.2.1.iii the assumption is that no new fields distort in a perceptible way the loop contributions in the couplings of the H to gluons and photons and the total width, its couplings to known SM particles are then probed. In a first approach to simultaneously probe new physics beyond the SM in the loops and not in the decay and the couplings of the Higgs boson to SM particles, only one assumption is needed *i.e.* that $\mathrm{BR_{BSM}} = 0$. In this model the coupling of the H to photons and gluons is effective and κ_Z, κ_W, κ_t, $|\kappa_\tau|$, and $|\kappa_b|$ are measured simultaneously. The absolute value of certain coupling modifiers only indicates the complete degeneracy of combined likelihood for the two signs. It can be noted that when the coupling to gluons is not considered effective, there is some sensitivity to the sign of κ_b through the interference between the top and bottom quarks loops in the gluon fusion process. In this model it is interesting to note that the constraints on the top quark Yukawa coupling comes from the ttH direct search channels. The expected precision on κ_t is approximately 40%. As discussed in Section III the excesses observed in the ttH channel yield a large value of $\kappa_t = 1.40^{+0.24}_{-0.21}$. The complete set of results from this model is given in Fig. 11.11 (right).

This model, which assumes that no new particles enter the decay of the Higgs boson, also yields very interesting constraints on new physics in the loops through the effective coupling modifiers κ_g and κ_γ. The measured values of these parameters:

$$\kappa_g = 0.78^{+0.13}_{-0.10} \quad \text{and} \quad \kappa_\gamma = 0.87^{+0.14}_{-0.09}$$

are fully compatible with the expectation for the SM Higgs boson.

A more constrained model fully focussing on BSM scenarios with new heavy particles contributing to the loops (and not directly in the decays *i.e.* $\mathrm{BR_{BSM}} = 0$) and where all couplings to the SM particles are assumed to be the same as in the Standard Model ($\kappa_W = \kappa_Z = \kappa_t = \kappa_b = \kappa_\tau = 1$) is also used to constrain the κ_g and κ_γ parameters only. The contours of the combined likelihood in the $(\kappa_\gamma, \kappa_g)$ plane for the ATLAS and CMS experiments and their combination are shown in Fig. 11.12.

This general model requires the strong assumption that the the Higgs boson decays only to SM particles. This assumption is necessary due to the degeneracy of solutions given that κ_H is a common factor to all measured signals. The degeneracy can however be resolved using a constraint on the width of the Higgs boson as the one from the off-Shell couplings measurements. This approach was used by the ATLAS experiment [234], thus yielding a absolute measurement of the couplings of the Higgs boson.

Another well motivated constraint to resolve the aforementioned degeneracy is unitarity. Simply requiring that $\kappa_V \leq 1$ allows to free the $\mathrm{BR_{BSM}}$ parameter and further probe new physics in the decay of the Higgs boson. An intuitive understanding of how this constraint works can be given by a simple example *e.g.* VBF $H \to W^+W^-$ production where the number of signal events will be parametrized by $(1 - \mathrm{BR_{BSM}})\kappa_W^4/\kappa_H^2$, where for a number of signal events observed close to the SM expectation, large values of $\mathrm{BR_{BSM}}$ cannot be compensated by a large value of κ_W and is thus limited. Or in other terms, if $\kappa_W \sim 1$ is preferred from other channels, a low signal in the VBF $H \to W^+W^-$ channel would be a sign of the presence of new physics beyond the SM in the Higgs decays. From this general model all the above parameters can be measured in addition to $\mathrm{BR_{BSM}}$. The results of this combination are shown in Fig. 11.11 (left). The results for all parameters do not change significantly with respect to the previous model. A limit can however be set on the beyond the SM branching fraction of the Higgs boson at the 95% CL:

$$\mathrm{BR_{BSM}} < 34\%.$$

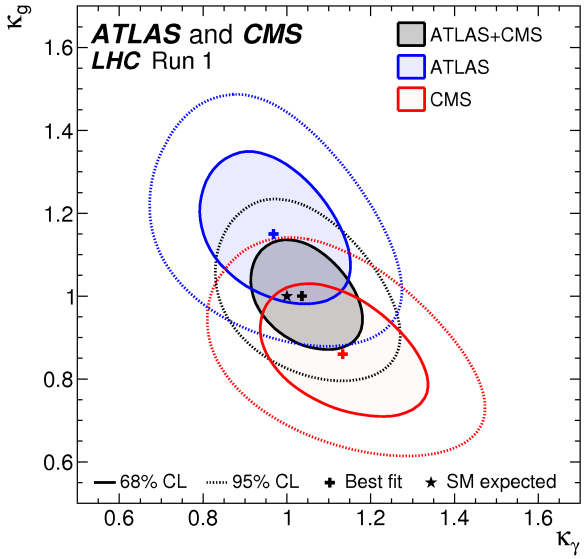

Figure 11.12: Likelihood contours of the global in the $(\kappa_g, \kappa_\gamma)$ plane for the ATLAS-CMS combination for the individual combination of all channels for ATLAS and CMS separately and the complete combined contour [143].

In the second approach, new physics is considered also in the decay thus affecting the total width of the H through decays to particles which are either "invisible" and escape detection in the experiments, or "undetected" which are not distinctive enough to be seen in the current analyses. This approach is complementary to the direct search for invisible decays of the Higgs boson described in Section III. The two approaches can be combined assuming that the undetected branching fraction is negligible. this combination was performed by the ATLAS experiment [277] and yields a limit on the invisible decays of the Higgs boson of $\mathrm{BR}_{inv} < 25\%$ at the 95% CL.

VI.2.2. Differential cross sections

To further characterize the production and decay properties of H, first measurements of fiducial and differential cross sections have been carried out by the ATLAS collaboration [278] and CMS [278] collaborations, both at Run 1 and Run 2 and in several channels: (i) the diphoton, (ii) The four leptons, and (iii) the WW channels. The selection criteria to define the fiducial volume are the following: the two highest transverse momentum (E_T), isolated final state photons, within $|\eta| < 2.37$ and with $105\,\mathrm{GeV} < M_{\gamma\gamma} < 160\,\mathrm{GeV}$ are selected (the transition region between the barrel and endcap calorimeters is not removed); after the pair is selected, the same cut on $E_T/M_{\gamma\gamma}$ as in the event selection *i.e.* in excess of 0.35 (0.25) for the two photons is applied. Several observables have been studied: the transverse

momentum rapidity of the diphoton system, the production angle in the Collins–Soper frame, the jet multiplicity, the jet veto fractions for a given jet multiplicity, and the transverse momentum distribution of the leading jet. The following additional observables: the difference in azimuthal angle between the leading and the subleading jets, and the transverse component of the vector sum of the momenta of the Higgs boson and dijet system, have also been measured in two jet events. To minimize the model dependence the differential cross sections are given within a specific fiducial region of the two photons. The observables were chosen to probe the production properties and the spin and parity of the H. The differential cross section in H transverse momentum is given in Fig. 11.13.

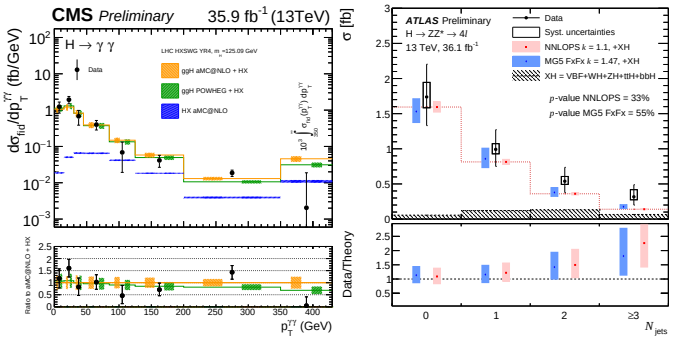

Figure 11.13: Observed differential cross sections in transverse momentum of the H in the diphoton channel, compared to the prediction of the ggF process [278].

VI.2.3. Constraints on non-SM Higgs boson interactions in an effective Lagrangian

An example of the possible use of differential cross sections in constraining non-SM Higgs boson couplings in an EFT is given by the ATLAS collaboration [279]. In this analysis, differential cross section measured in the diphoton channel are used to constrain an effective Lagrangian where the SM is supplemented by dimension six CP-even operators of the Strongly Interacting Light Higgs (SILH) formulation and corresponding CP-odd operators. The diphoton differential cross sections are mainly sensitive to the operators that affect the Higgs boson interactions with gauge bosons and the relevant terms in the effective Lagrangian can be parameterized as:

$$\begin{aligned}\mathcal{L}_{eff} =& \overline{c}_\gamma \mathcal{O}_\gamma + \overline{c}_g \mathcal{O}_g + \overline{c}_{HW} \mathcal{O}_{HW} + \overline{c}_{HB} \mathcal{O}_{HB} + \\ & \tilde{c}_\gamma \tilde{\mathcal{O}}_\gamma + \tilde{c}_g \tilde{\mathcal{O}}_g + \tilde{c}_{HW} \tilde{\mathcal{O}}_{HW} + \tilde{c}_{HB} \tilde{\mathcal{O}}_{HB} \,,\end{aligned} \tag{11.16}$$

where $\overline{c}_i$ and $\tilde{c}_i$ are the effective coefficients corresponding to the CP-even and CP-odd interactions, respectively, see Ref. [264].

The differential distributions used in this combination are: (i) the transverse momentum of the Higgs boson, (ii) the number of reconstructed jets produced in association with the diphoton pair, (iii) the invariant mass of the diphoton system and (iv) the difference in azimuthal angle of the leading and sub-leading jets in events with two or more jets.

This analysis shows how differential information significantly improves the sensitivity to operators that modify the Higgs boson interaction to photons, gluons and vector bosons both from the main gluon fusion and the vector boson fusion production modes.

VI.2.4. Simplified Template Cross Sections

An overarching subject of discussion between the Theory and Experimental communities in the field of Higgs physics has been how experimentalists could best communicate their results for them to be most efficiently used by other communities for further interpretation.

In the field of precision Standard Model measurements, the commonly used practise is that results are given at particle level within a well defined fiducial volume of phase space. The fiducial volume is usualy defined close enough to the experimental reconstruction to minimize the possible variations of the reconstruction efficiency within the particle level fiducial volume. In this way results minimize their dependence on theoretical uncertainties.

Experiments have produced fiducial and unfolded cross sections based on all objects reconstruced in the event. These measurements could be used for further interpretation. However, in order to perform a proper combination of channels taking into account all experimental systematic uncertainties is non trivial. A proposal [43] was made by the LHC Higgs Cross Section working group to produce results in each decay channel with a well defined fiducial phase space of the Higgs boson (and not its decay products) and for other associated objects pertaining to all channels, such as jets and missing transverse momentum (MET). The definition of the fiducial regions is motivated by maximizing the experimental sensitivity, the isolation of possible BSM effect, and minimizing the dependence on theoretical uncertainties. The number of regions is also minimized avoiding loss of experimental sensitivity. The observable that are measured in this approach are still the standard production cross sections (the gluon fusion, the vector boson fusion, the VH and ttH associated production modes) within the defined fiducial volumes.

In summary, this approach is hybrid. It is fiducial on specific objects to reduce the theory dependence and inclusive in the Higgs kinematics in order to allow for a more straightforward combination. This approach also allows the use of multivariate techcniques to enhance the sensitivity within given fiducial regions, at the expense of a greater extrapolation and therefore increased model dependence.

First results in this framework have been produced by experiments in several channels, including the diphoton and the 4ℓ [124, 128, 125, 132].

VII. New physics models of EWSB in the light of the Higgs boson discovery

The discovery of a light scalar with couplings to gauge bosons and fermions that are apparently consistent with SM predictions and the slow running of the Higgs self-coupling at high energies allows one to consider the SM as a valid perturbative description of nature all the way to the Planck scale. This picture is admittedly very attractive, but it posits that the Higgs boson is an elementary scalar field, which comes with an intrinsic instability of its mass under radiative corrections. This Higgs naturalness problem calls for new physics around the TeV scale. Supersymmetric models are the most elegant solution to maintain the perturbativity of the SM while alleviating the instability issue. Another possibility is that the Higgs boson itself has a finite size and is composite and thus never feels the UV degrees of freedom that would drag its mass to much higher scales. Both classes of models predict specific modifications from the SM Higgs properties.

The realization of supersymmetry at low energies has many good qualities that render it attractive as a model of new physics. First of all since for every SM degree of freedom there is superpartner of different spin but of equal mass and effective coupling to the SM-like Higgs, in the case of exact supersymmetry, an automatic cancellation of quantum corrections to the Higgs mass parameter holds. In practice, it is known that SUSY must be broken in nature since no superpartners of the SM particles have been observed so far. The mass difference between the precise value of any of the particle masses and that of its corresponding superpartner is proportional to the correlated soft supersymmetry breaking parameter, generically called M_{SUSY}. The quantum corrections to the Higgs mass parameter are proportional to M^2_{SUSY}, and provided M_{SUSY} is of order of a few TeV, the fine-tuning problem is solved, in the sense that the low energy mass parameters of the Higgs sector become insensitive to physics at the GUT or Planck scale. Another interesting feature of SUSY theories is related to the dynamical generation of EWSB [280]. In the SM a negative Higgs mass parameter, m^2, needs to be inserted by hand to induce EWSB, see Eq. (11.1). In SUSY, instead, even if the relevant Higgs mass parameter is positive in the ultraviolet, it may become negative and induce electroweak symmetry breaking radiatively through the strong effect of the top quark-Higgs boson coupling in its renormalization group evolution.

In the following, the Higgs sector will be explored in specific SUSY models. In all of them there is one neutral Higgs boson with properties that resemble those of the SM Higgs boson, whereas additional neutral and charged Higgs bosons are also predicted and are intensively being sought for at the LHC (see Section VII.8). In the simplest SUSY model the lightest Higgs boson mass, that usually plays the role of the SM-like Higgs, is predicted to be less than 135 GeV for stops in the TeV to few TeV mass range [281] whereas, larger values of the SM-like Higgs boson mass – up to about 250 GeV – can be obtained in non-minimal SUSY extensions of the SM [281]. In general, accommodating a SM-like Higgs boson with mass of 125 GeV results in constraints on the supersymmetric parameter space of specific SUSY models. While naturalness dictates relatively light stops and gluinos, the first and second generation of squarks and sleptons couple weakly to the Higgs sector and may be heavy. Moreover, small values of the μ parameter and therefore light Higgsinos, the fermionic superpartners of the Higgs bosons, would be a signature of a natural realization of electroweak symmetry breaking. Such SUSY spectra, consisting of relatively light stops and light Higgsinos, continue to be under intense scrutiny by the experimental collaborations [282] in order to understand if such natural SUSY scenarios endure [283] and can explain why the Higgs boson remains light.

In the context of weakly coupled models of EWSB one can also consider multiple Higgs $\mathrm{SU}(2)_L$ doublets as well as additional Higgs singlets, triplets or even more complicated multiplet structures, with or without low energy supersymmetry. In general for such models one needs to take into account experimental constraints from precision measurements and flavor changing neutral currents. The LHC signatures of such extended Higgs sectors are largely shaped by the role of the exotic scalar fields in EWSB.

The idea that the Higgs boson itself could be a composite bound state emerging from a new strongly-coupled sector has regained some interest. The composite Higgs idea is an interesting incarnation of EWSB via strong dynamics that smoothly interpolates between the standard Technicolor approach and the true SM limit. To avoid the usual conflict with EW data, it is sufficient if not necessary that a mass gap separates the Higgs resonance from the other resonances of the strong sector. Such a mass gap can naturally follow from dynamics if the strongly-interacting sector exhibits a global symmetry, G, broken dynamically to a subgroup H at the scale f, such that, in addition to the three Nambu–Goldstone bosons of SO(4)/SO(3) that describe the longitudinal components of the massive W and Z, the coset G/H contains a fourth Nambu–Goldstone boson that can be identified with the physical Higgs boson. Simple examples of such a coset are SU(3)/SU(2) or SO(5)/SO(4), the latter being favored since it is invariant under the custodial symmetry. It is also possible to have non-minimal custodial cosets with extra Goldstone bosons leading to additional Higgs bosons in the spectrum, see for instance Ref. [284]. Modern incarnations of composite Higgs models have been recently investigated in the framework of 5D warped models where, according to the principles of the AdS/CFT correspondence, the holographic composite Higgs boson then originates from a component of a gauge field along the 5th dimension with appropriate boundary conditions.

A last crucial ingredient in the construction of viable composite Higgs models is the concept of partial compositeness [285], i.e., the idea that there are only linear mass mixings between elementary fields and composite states. After diagonalization of the mass matrices, the SM particles, fermions and gauge bosons, are admixtures of elementary and composite states and thus they interact with the strong sector, and in particular with the Higgs boson, through their composite component. This setup has important consequences on the flavor properties, chiefly the suppression of large flavor changing neutral currents involving light fermions. It also plays an important role in dynamically generating a potential for the would-be Goldstone bosons. Partial compositeness also links the properties of the Higgs boson to the spectrum of the fermionic resonances, i.e. the partners of the top quark. As in the MSSM, these top partners are really the agents that trigger the EWSB and also generate the mass of the Higgs boson that otherwise would remain an exact Goldstone boson and hence massless. The bounds from the direct searches for the top partners in addition to the usual constraints from EW precision data force the minimal composite Higgs models into some unnatural corners of their parameter spaces [15, 286].

VII.1. Higgs bosons in the minimal supersymmetric standard model (MSSM)

The particle masses and interactions in a supersymmetric theory are uniquely defined as a function of the superpotential and the Kähler potential [287]. A fundamental theory of supersymmetry breaking, however, is unknown at this time. Nevertheless, one can parameterize the low-energy theory in terms of the most general set of soft supersymmetry-breaking operators [281]. The simplest realistic model of low-energy supersymmetry is the minimal supersymmetric extension of the SM (MSSM) [11, 287], that associates a supersymmetric partner to each gauge boson and chiral fermion of the SM, and provides a realistic model of physics at the weak scale. However, even in this minimal model with the most general set of soft supersymmetry-breaking terms more than 100 new parameters are introduced [281]. Fortunately, only a subset of these parameters impact the Higgs phenomenology either directly at tree-level or through quantum effects.

The MSSM contains the particle spectrum of a two-Higgs-doublet model (2HDM) extension of the SM and the corresponding supersymmetric partners. Two Higgs doublets, Φ_1 and Φ_2, with hypercharge $Y = -1$ and $Y = 1$, respectively, are required to ensure an anomaly-free SUSY extension of the SM and to generate mass for down-type quarks/charged leptons (Φ_1)and up-type quarks (Φ_2) [12]. The Higgs potential reads

$$\begin{aligned} V = {} & m_1^2 \Phi_1^\dagger \Phi_1 + m_2^2 \Phi_2^\dagger \Phi_2 - m_3^2 (\Phi_1^T i\sigma_2 \Phi_2 + \text{h.c.}) + \frac{1}{2}\lambda_1 (\Phi_1^\dagger \Phi_1)^2 \\ & + \frac{1}{2}\lambda_2 (\Phi_2^\dagger \Phi_2)^2 + \lambda_3 (\Phi_1^\dagger \Phi_1)(\Phi_2^\dagger \Phi_2) + \lambda_4 |\Phi_1^T i\sigma_2 \Phi_2|^2 \\ & + \frac{1}{2}\lambda_5 [(\Phi_1^T i\sigma_2 \Phi_2)^2 + \text{h.c.}] \\ & + [[\lambda_6 (\Phi_1^\dagger \Phi_1) + \lambda_7 (\Phi_2^\dagger \Phi_2)] \Phi_1^T i\sigma_2 \Phi_2 + \text{h.c.}] \end{aligned} \tag{11.17}$$

where $m_i^2 = \mu^2 + m_{H_i}^2$ $(i = 1, 2)$, with μ being the supersymmetric Higgsino mass parameter and m_{H_i} the soft supersymmetric breaking mass parameters of the two Higgs doublets; $m_3^2 \equiv B\mu$ is associated to the B-term soft SUSY breaking parameter; and λ_i, for $i = 1$ to 7, are all the Higgs quartic couplings.

After the spontaneous breaking of the electroweak symmetry (see Ref. [283] for detail), five physical Higgs particles are left in the MSSM spectrum: one charged Higgs pair, $H^\pm$, one CP-odd neutral scalar, A, and two CP-even neutral states, H and h, with h being the lightest.[6] The Higgs sector at tree level depends on the electroweak gauge coupling constants and the vacuum expectation value v – or equivalently the Z gauge boson mass – and is determined by only two free parameters: $\tan\beta$ - the ratio of the two Higgs doublets' vacuum expectation values v_2/v_1 - and one Higgs boson mass, conventionally chosen to be the CP-odd Higgs boson mass, m_A. The other tree-level Higgs boson masses are then given in terms of these parameters. The tree level value of m_h is maximized not only for $m_A \gg M_Z$ but also for $\tan\beta \gg 1$. For $m_A \gg M_Z$ it acquires a maximum value $m_h = M_Z \cos 2\beta$.

Radiative corrections have a significant impact on the values of Higgs boson masses and couplings in the MSSM. The dominant radiative effects to the SM-like Higgs mass arise from the incomplete cancellation between top and scalar-top (stop) loops and at large $\tan\beta$ also from sbottom and stau loops. The stop, sbottom and stau masses and mixing angles depend on the supersymmetric Higgsino mass parameter μ and on the soft-supersymmetry-breaking parameters [11, 287]: M_Q, M_U, M_D, M_L, M_E, and A_t, A_b A_τ. The first three of these are the left-chiral and the right-chiral top

[6] Observe that in the SM sections of this review, H denotes the SM Higgs, whereas in the sections about SUSY, or extensions of the SM with two Higgs doublets, H is used for the heaviest CP-even Higgs boson, since this is the standard notation in the literature, and the 125 GeV SM-like light Higgs boson will be denoted by h.

and bottom scalar quark mass parameters. The next two are the left-chiral stau/sneutrino and the right-chiral stau mass parameters, and the last three are the trilinear parameters that enter in the off-diagonal squark/slepton mixing elements: $X_t \equiv A_t - \mu \cot\beta$ and $X_{b,\tau} \equiv A_{b,\tau} - \mu \tan\beta$. At the two-loop level, the masses of the gluino and the electroweak gaugino also enter in the calculations. Radiative corrections to the Higgs boson masses have been computed using a number of techniques, with a variety of approximations; for a discussion see for example Refs. [38, 288, 289] and the corresponding section of the previous edition of this review.

The newly discovered SM-like Higgs boson, if interpreted as the lightest MSSM Higgs with a mass of about 125 GeV, provides information on the possible MSSM parameter space. See Fig. 11.14. and discussion in Ref. [283]

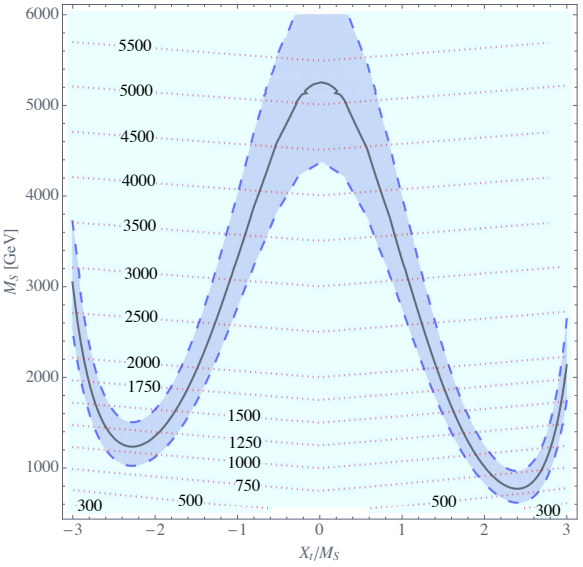

Figure 11.14: Values of the SUSY mass scale $M_{\rm SUSY} = M_S$ versus the stop mixing parameter normalized by the SUSY mass scale $X_t/M_{\rm SUSY}$, for fixed $\tan\beta = 20$, $\mu = 200\,\text{GeV}$ and $M_A = A_t = A_b = A_\tau = M_{\rm SUSY}$. The solid black line corresponds to $M_h = 125\,\text{GeV}$ while in the grey band M_h varies by $\pm 1\,\text{GeV}$. The red dotted lines are iso-values of the stop mass. This figure is based on Ref. [290].

The phenomenology of the Higgs sector depends on the couplings of the Higgs bosons to gauge bosons and fermions. At tree-level, the couplings of the two CP-even Higgs bosons to W and Z bosons are given in terms of the angles α, that diagonalizes the CP-even Higgs squared-mass matrix, and β

$$g_{hVV} = g_V m_V \sin(\beta-\alpha), \quad g_{HVV} = g_V m_V \cos(\beta-\alpha), \qquad (11.18)$$

where $g_V \equiv 2m_V/v$, for $V = \text{W}^\pm$ or Z ($g_V m_V$ is the SM hVV coupling). Observe that in the limit $\cos(\beta-\alpha) \to 0$, the lightest CP-even Higgs h behaves as the SM Higgs boson. This situation is called alignment and is achieved in specific regions of parameter space for $m_A \geq M_Z$ [291] or in the large $m_A \gg M_Z$ limit, in which alignment is achieved through decoupling [291, 292]. There are no tree-level couplings of A or $H^\pm$ to VV. The couplings of the Z boson to two neutral Higgs bosons are given by $g_{\phi AZ}(p_\phi - p_A)$, where $\phi = H$ or h, the momenta p_ϕ and p_A point into the vertex, and

$$g_{hAZ} = g_Z \cos(\beta-\alpha)/2, \quad g_{HAZ} = -g_Z \sin(\beta-\alpha)/2\,. \qquad (11.19)$$

Charged Higgs-W boson couplings to neutral Higgs bosons and four-point couplings of vector bosons and Higgs bosons can be found in Ref. [12].

The tree-level Higgs couplings to fermions obey the following property: the neutral components of one Higgs doublet, Φ_1, couple exclusively to down-type fermion pairs while the neutral components of the other doublet, Φ_2, couple exclusively to up-type fermion pairs [12]. This Higgs-fermion coupling structure defines the Type-II 2HDM [293]. In the MSSM, fermion masses are generated when both neutral Higgs components acquire vacuum expectation values, and the relations between Yukawa couplings and fermion masses are (in third-generation notation)

$$h_{b,\tau} = \sqrt{2}\, m_{b,\tau}/(v\cos\beta), \quad h_t = \sqrt{2}\, m_t/(v\sin\beta)\,. \qquad (11.20)$$

The couplings of the neutral Higgs bosons to $f\bar{f}$ relative to the SM value, $g m_f/2M_W$, are given by

$$\begin{aligned} h b\bar{b} &: -\sin\alpha/\cos\beta \qquad & h t\bar{t} &: \cos\alpha/\sin\beta\,, \\ H b\bar{b} &: \cos\alpha/\cos\beta \qquad & H t\bar{t} &: \sin\alpha/\sin\beta\,, \\ A b\bar{b} &: \gamma_5 \tan\beta \qquad & A t\bar{t} &: \gamma_5 \cot\beta\,. \end{aligned} \qquad (11.21)$$

In each relation above, the factor listed for $b\bar{b}$ also pertains to $\tau^+\tau^-$. The charged Higgs boson couplings to fermion pairs, normalized to $g/\sqrt{2}M_W$, are given by

$$g_{H^- t\bar{b}} : m_t \cot\beta \frac{1+\gamma_5}{2} + m_b \tan\beta \frac{1-\gamma_5}{2} \qquad g_{H^-\tau^+\nu} : m_\tau \tan\beta \frac{1-\gamma_5}{2}\,. \qquad (11.22)$$

The non-standard neutral Higgs bosons have significantly enhanced couplings to down-type fermions at sizeable $\tan\beta$. Radiative corrections can modify significantly the values of the Higgs boson couplings to fermion pairs and to vector boson pairs, through a "radiatively-corrected" value for $\cos(\beta-\alpha)$ [294, 295], as well as from the one-loop vertex corrections to tree-level Higgs-fermion Yukawa couplings [296–303].

VII.1.1. MSSM Higgs boson phenomenology

In the MSSM, the mass, CP properties, decay and production properties of one of the neutral Higgs bosons should agree with the LHC Higgs data. Given that present data allows only for moderate departures from the SM predictions, it implies that some degree of alignment is necessary. The SM-like branching ratios of h can be modified if decays into supersymmetric particles are kinematically allowed, and, in particular, decays into a pair of the lightest supersymmetric particles – i.e. the lightest neutralinos, $\tilde{\chi}_1^0$ – can become dominant and would be invisible if R-parity is conserved [304–306]. Moreover, if light superpartners exist that couple to photons and/or gluons, the h loop-induced coupling to gg and $\gamma\gamma$ could deviate sizably from the corresponding SM predictions [294, 307–310, 311, 312], although such deviations are also significantly constrained by present data

For the heavier Higgs states there are two possibilities to be considered: i) Alignment triggered by decoupling, hence $m_A \geq$ several hundred GeV: The HWW and HZZ couplings are very small. The dominant H, A decay branching ratios strongly depend on $\tan\beta$. The decay modes $H, A \to b\bar{b}$, $\tau^+\tau^-$ dominate when $\tan\beta$ is large (this holds even away from decoupling). For small $\tan\beta$, the $t\bar{t}$ decay mode dominates above its kinematic threshold. For the charged Higgs boson, $H^+ \to t\bar{b}$ dominates. ii) Some degree of alignment without decoupling, hence $m_A \leq$ a few hundred GeV. The main difference with the previous case is that in the low $\tan\beta$ regime ($\tan\beta \leq 5$) additional decay channels may be allowed which involve decays into the lightest SM-like Higgs boson; $A \to Zh$, $H \to hh$ as well as $H \to WW/ZZ$ decay modes are available (they are suppressed in the strict alignment limit). When kinematically open the decays $A/H \to t\bar{t}$ become relevant or even dominant for sufficiently small $\tan\beta$. For the charged Higgs boson, $H^+ \to \tau^+\nu_\tau$ dominates below the $t\bar{b}$ threshold, and also $H^\pm \to W^\pm h$ may be searched for. Both in i) and ii), the heavier Higgs states, H, A and $H^\pm$, are roughly mass degenerate (with masses $\pm$ 20 GeV or less apart). If kinematically allowed, the heavy Higgs boson decays into charginos, neutralinos and third-generation squarks and sleptons can be important [304].

At hadron colliders, the dominant neutral Higgs production mechanism at moderate values of $\tan\beta$ is gluon fusion, mediated by loops containing heavy top and bottom quarks and the corresponding supersymmetric partners [281]. The effect of light stops that may

contribute to the gluon fusion production can be partially cancelled by mixing effects. Higgs boson radiation off bottom quarks becomes important for large $\tan\beta$, where at least two of the three neutral Higgs bosons have enhanced couplings to bottom-type fermions [315–314]. Detailed discussions of the impact of radiative corrections in these search modes are presented in Refs. [316, 317]. The vector boson fusion and Higgs-strahlung production of the CP-even Higgs bosons as well as the associated production of neutral Higgs bosons with top quark pairs have lower production cross sections by at least an order of magnitude with respect to the dominant ones, depending on the precise region of MSSM parameter space [40–43]. Higgs pair production of non-standard MSSM Higgs bosons has been studied in Ref. [318]. For a discussion of charged Higgs boson production at LHC see Refs. [11, 40, 319, 281].

Summarizing, the additional Higgs bosons are sought for mainly via the channels [7]

$$\begin{aligned}
&pp \to A/H \to \tau^+\tau^- \ \text{(inclusive)},\\
&b\bar{b}A/H, A/H \to \tau^+\tau^- \ \text{(with } b\text{-tag)},\\
&b\bar{b}A/H, A/H \to b\bar{b} \ \text{(with } b\text{-tag)},\\
&pp \to t\bar{t} \to H^\pm W^\mp b\bar{b},\ H^\pm \to \tau\nu_\tau\ ,\\
&gb \to H^- t \quad \text{or} \quad g\bar{b} \to H^+\bar{t},\ H^\pm \to \tau\nu_\tau\ .
\end{aligned} \tag{11.23}$$

After the Higgs boson discovery, updated MSSM benchmarks scenarios have been defined, that highlight interesting conditions for MSSM Higgs searches [42, 321]. They include: i) a moderate mixing scenario in which the light CP-even Higgs boson can be interpreted as the newly discovered state in most of the $m_A - \tan\beta$ plane; ii) a light stop scenario with stop masses in the few to several hundred GeV range that can affect gluon fusion Higgs production; and iii) a tau-phobic scenario that exhibits variations of $\mathrm{BR}(h \to b\bar{b})$ and $\mathrm{BR}(h \to \tau^+\tau^-)$ with respect to their SM values. In the above benchmarks it is also possible to have decays of $H \to hh$ in regions of moderate m_A and moderate $\tan\beta$ as far as one is away from precise alignment. Also for the previous benchmarks, the LHC reach in the traditional $A/H \to \tau^+\tau^-$ search channel varies depending on the values of μ and M_2, that may enable the A/H decays into electroweakinos.

An alternative approach to reduce the large number of parameters relevant to the Higgs sector is to consider that, in the Higgs basis, the only important radiative corrections are those affecting the Higgs mass [322]. This approximation is called hMSSM and works well in large regions of parameter space but it breaks down for sizable values of μ and A_t, and moderate values of $\tan\beta$, for which the radiative corrections to the mixing between the two CP even eigenstates become relevant. The effect of such radiative corrections is to allow for alignment for small to intermediate values of $\tan\beta$, independent of the specific value of m_A [323]. In addition, the hMSSM assumption that the right value of the Higgs mass may be obtained for all values of m_A and $\tan\beta$ is in conflict with the MSSM predictions for the Higgs mass for small values of m_A and $\tan\beta \simeq \mathcal{O}(1)$.

Reviews of the properties and phenomenology of the Higgs bosons of the MSSM can be found for example in Refs. [38, 283, 287, 288]. Future precision measurements of the Higgs boson couplings to fermions and gauge bosons together with information on heavy Higgs searches will provide powerful information on the SUSY parameter space [323–326]. For representative references on production mechanisms for the MSSM Higgs bosons at e^+e^- see Ref. [281].

Improvements in our understanding of B-physics observables put indirect constraints on additional Higgs bosons in mass ranges that would be accessible in direct LHC searches. In particular, $\mathrm{BR}(B_s \to \mu^+\mu^-)$, $\mathrm{BR}(b \to s\gamma)$, and $\mathrm{BR}(B_u \to \tau\nu)$ play an important role within minimal flavor-violating (MFV) models [327], in which flavor effects proportional to the CKM matrix elements are induced as in the SM, see e. g. references in Ref. [281].

[7] Strong production of a heavy neutral Higgs boson followed by its decay into top pairs is a challenging channel, only most recently being searched for by ATLAS and CMS. Interference effects between the signal and the SM $t\bar{t}$ background need to be carefully taken into account [320].

VII.2. Supersymmetry with singlet extensions

The Higgs mass parameter μ is a supersymmetric parameter, and as such, it should naturally be of order M_{GUT} or M_{Planck}. The fact that phenomenologically it is required that μ be at the electroweak/TeV scale is known as the μ problem [328]. Supersymmetric models with additional singlets can provide a solution to the μ problem, by promoting the μ parameter to a dynamical singlet superfield S that only interacts with the MSSM Higgs doublets through a coupling λ_S at the level of the superpotential. An effective μ is generated when the real scalar component of S acquires a vacuum expectation value v_S, yielding $\mu_{eff} = \lambda_S v_S$. After the minimization of the Higgs potential the vacuum state relates the vacuum expectation values of the three CP-even neutral scalars, v_1, v_2 and v_S, to the scalar doublet and singlet soft supersymmetry breaking masses, hence, one expects that these VEVs should all be of order M_{SUSY} and therefore the μ problem is solved.

The addition of a singlet superfield to the MSSM may come along with additional symmetries imposed to the theory. Depending on such symmetries, different models with singlet extensions of the MSSM (xMSSM) have been proposed. Among the most studied examples are the NMSSM with an additional discrete Z_3 symmetry (first introduced in Ref. [329]), the Nearly-Minimal Supersymmetric SM (nMSSM), with additional discrete Z_5^R, and Z_7^R symmetries [330], and the $\mathrm{U}(1)'$-extended MSSM (UMSSM) [331]. A Secluded $\mathrm{U}(1)'$-extended MSSM (sMSSM) [332] contains three singlets in addition to the standard UMSSM Higgs singlet; this model is equivalent to the nMSSM in the limit that the additional singlet VEV's are large, and the trilinear singlet coupling, λ_S, is small [333].

Based on the extended models defined above, we write the most generic supersymmetric and soft supersymmetry breaking scalar potentials for the two MSSM scalar doublets: Φ_1, Φ_2 and the scalar singlet S:

$$\begin{aligned}
V_{xMSSM} = &\left|\lambda_S \Phi_2\cdot\Phi_1 + t_F + \kappa S^2\right|^2 + |\lambda_S S|^2\left(|\Phi_1|^2 + |\Phi_2|^2\right)\\
&+ \frac{g'^2+g^2}{8}\left(|\Phi_1|^2 - |\Phi_2|^2\right)^2 + \frac{g^2}{2}\left(|\Phi_1|^2|\Phi_2|^2 - |\Phi_2\cdot\Phi_1|^2\right)\\
&+ \frac{g_1'^2}{2}\left(Q_{\Phi_1}|\Phi_1|^2 + Q_{\Phi_2}|\Phi_2|^2 + Q_S|S|^2\right)^2
\end{aligned} \tag{11.24}$$

$$\begin{aligned}
V_{\mathrm{soft}} = &\, m_{H_1}^2|\Phi_1|^2 + m_{H_2}^2|\Phi_2|^2 + m_s^2|S|^2\\
&+ \left(A_s\lambda_S S H_u\cdot H_d + \frac{\kappa}{3}A_\kappa S^3 + t_S S + h.c.\right).
\end{aligned} \tag{11.25}$$

In the above, $\Phi_2\cdot\Phi_1 = \epsilon_{ij}\Phi_2^i\Phi_1^j$ and the couplings g', g, and g_1' are associated to the $\mathrm{U}(1)_Y$, $\mathrm{SU}(2)_L$, and $\mathrm{U}(1)'$ gauge symmetries, respectively. t_F and t_S are supersymmetric and SUSY breaking tadpole terms, respectively, m_s is a SUSY breaking mass term for the scalar component of the field S, and A_s and A_κ are the trilinear soft SUSY breaking mass parameters associated with the new terms $\lambda_S S\Phi_2\cdot\Phi_1$ and $\kappa S^3/3$ in the superpotential, with the B-term of the MSSM expressed as $B\mu \equiv A_s\mu_{eff}$. The UMSSM depends on the $\mathrm{U}(1)'$ charges of the Higgs fields, Q_{Φ_1}, Q_{Φ_2} and Q_S, that are free parameters with the restriction that they have to add to zero for the superpotential $\lambda_S S\Phi_2\Phi_1$ to be gauge invariant. The addition of the singlet scalar field(s) imply that additional CP-even and CP-odd Higgs bosons will appear in the spectra, whereas the charged Higgs sector remains the same as in the MSSM given that the number of Higgs doublets remains unchanged. The mixing with the extra scalar S alters the masses and properties of the physical Higgs bosons. A detailed discussion of typical mass spectra and decay properties in these models can be found for example in Refs. [334, 333]. Moreover, these models have extra neutralinos and in some cases extra neutral gauge bosons, Z'. The extra gauge boson sector is constrained by experimental data through direct Z' searches as well as the $Z - Z'$ mixing angle $\alpha_{ZZ'}$ constrained to be less that $\mathcal{O}(10^{-3})$ by precision electroweak data.

In singlet extensions of the MSSM the lightest CP-even Higgs mass at tree level, $m_{H_1}^{tree}$ receives a contribution from the singlet scalar that renders it larger than the MSSM value, in particular for small values of $\tan\beta$. The tree level upper bound reads[8]

$$m_{H_1}^{tree} \leq M_Z^2 \cos^2 2\beta + \frac{1}{2}\lambda_S^2 v^2 \sin^2 2\beta\,. \qquad (11.26)$$

At the one-loop level, the top and stop loops (as well as sbottom and stau loops for large $\tan\beta$) are the dominant contributions, that are common to the MSSM and to all the singlet extensions. Gauge couplings in the UMSSM are small compared to the top quark Yukawa coupling, hence the one-loop gauge contributions are negligible. Corrections exclusive to the NMSSM and the nMSSM enter only at the two loop level. In the decoupling limit, a value of the lightest SM Higgs mass of about 125 GeV is achievable in all these MSSM extensions, and this remains the case even after higher order corrections are implemented.

A singlet extended supersymmetric Higgs sector opens new avenues for discovery. Since the singlet pseudoscalar particle may be identified as the pseudo-Goldstone boson of a spontaneously broken Peccei–Quinn symmetry, it may become naturally light [335, 336]. Generally, there is mixing of the singlet sector with the MSSM Higgs sector, and for a sufficiently light, singlet dominated scalar or pseudoscalar, h_S or A_S, respectively, the SM-like Higgs boson h may decay to pairs of h_S or A_S. The light scalar and/or pseudoscalar may subsequently decay to $\tau\tau$ or $b\bar{b}$ pairs. Such cascade decays are more difficult to detect than standard searches due to the potentially soft decay products. There is also a rich phenomenology for the decays of the heavy CP-even and CP-odd doublets, A and H into two lighter Higgs bosons such as $H \to hh_S$, hh, h_Sh_S or $A \to A_Sh_S$, A_Sh as well as into a light Higgs boson and a gauge boson: $H \to A_SZ$; $A \to h_SZ$, hZ. If kinematically allowed the heavy Higgs bosons decay into $t\bar{t}$. If the singlet dominated scalar or pseudoscalar are somewhat heavier, the decays $h_S \to WW$ or $A_S \to h_SZ$ will be allowed.

In addition, the light singlet scenario in the NMSSM or nMSSM is typically associated with a light singlino-dominated neutralino. The recently discovered SM-like Higgs boson can then decay to pairs of this neutralino [337, 333], opening an invisible decay mode that is not excluded by present data. All of the Higgs bosons can decay into electroweakinos depending on kinematics and the singlino or higgsino composition of the electroweakinos.

In models with extended singlets, at low $\tan\beta$ it is possible to trade the requirement of a large stop mixing by a sizeable trilinear Higgs-singlet Higgs coupling λ_S, rendering more freedom on the requirements for gluon fusion production. As in the MSSM, mixing in the Higgs sector -additionally triggered by the extra new parameter λ_S - can produce variations in the Higgs–$b\bar{b}$ and Higgs–$\tau^-\tau^+$ couplings that can alter the Higgs to ZZ/WW and diphoton rates. Light charginos at low $\tan\beta$ can independently contribute to enhance the di-photon rate, without altering any other of the Higgs decay rates [310, 338].

There is much activity in exploring the NMSSM phenomenology in the light of the 125 GeV Higgs boson [339], as well as in defining benchmark scenarios with new topologies including Higgs decay chains [340]. An analytic understanding of the alignment condition in the NMSSM is presented in Ref. [341]. The NMSSM with a Higgs boson of mass 125 GeV can be compatible with stop masses of order of the electroweak/TeV scale, thereby reducing the degree of fine tuning necessary to achieve electroweak symmetry breaking (see Fig. 11.15). Interestingly, the alignment conditions point toward a more natural region of parameter space for electroweak symmetry breaking, while allowing for perturbativity of the theory up to the Planck scale and yielding a rich and interesting Higgs boson phenomenology at the LHC.

VII.3. Supersymmetry with extended gauge sectors

In the MSSM, the tree-level value of the lightest CP-even Higgs mass originates from the D-term dependence of the scalar potential

[8] Additional gauge interactions in the UMSSM contribute to this increase with a term of $\mathcal{O}(g_1'^2 v^2 (Q_{\phi_2}^2 \cos^2\beta + Q_{\phi_1}^2 \sin^2\beta))$.

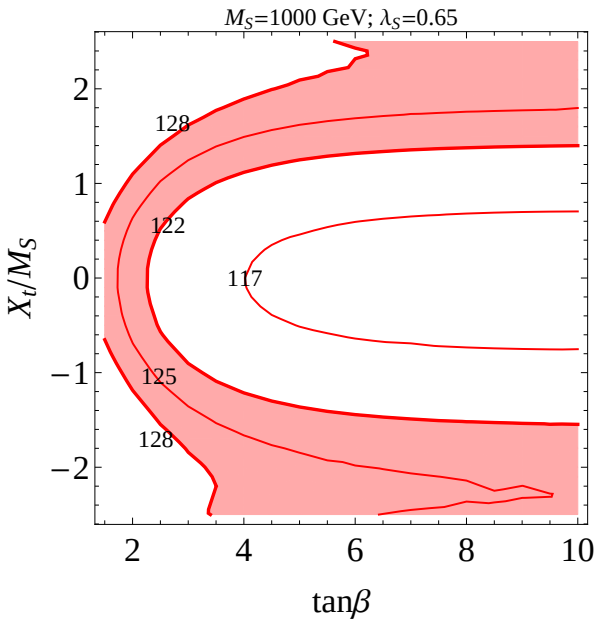

Figure 11.15: Values of the stop mixing parameter normalized to the SUSY mass scale $X_t/M_{\rm SUSY}$, as a function of $\tan\beta$, for $M_{\rm SUSY} \equiv M_S = 1000\,\text{GeV}$, $\lambda_S = 0.65$, and contours of constant values of the Higgs mass $m_h = 125 \pm 3\,\text{GeV}$ shaded in red [342].

that comes from the supersymmetric kinetic terms in the Kähler potential. The D-terms lead to tree-level quartic couplings which are governed by the squares of the gauge couplings of the weak interactions, under which the Higgs has non-trivial charges and hence the lightest Higgs mass is bounded to be smaller than M_Z. In the presence of new gauge interactions at the TeV scale, and if the Higgs fields had non-trivial charges under them, new D-term contributions would lead to an enhancement of the tree-level Higgs mass value. Since the low energy gauge interactions reduce to the known $\mathrm{SU}(3)_c \times \mathrm{SU}(2)_L \times \mathrm{U}(1)_Y$ ones, in order for this mechanism to work, the extended gauge and Higgs sectors should be integrated out in a non-supersymmetric way. This means that there must be supersymmetry breaking terms that are of the order of, or larger than, the new gauge boson masses. The tree-level quartic couplings would then be enhanced through their dependence on the square of the gauge couplings of the extended Higgs sector. This effect will be suppressed when the heavy gauge boson masses are larger than the supersymmetry breaking scale and will acquire its full potential only for large values of this scale.

One of the simplest possibilities is to extend the weak interactions to a $\mathrm{SU}(2)_1 \times \mathrm{SU}(2)_2$ sector, such that the known weak interactions are obtained after the spontaneous breaking of these groups to $\mathrm{SU}(2)_L$ [343]. This example is briefly summarized in Ref. [283]. Assuming supersymmetry breaking terms of the order of the new gauge boson masses, enhancements of order 50 percent of the MSSM D-term contribution to the Higgs mass may be obtained. Such enhancements are sufficient to obtain the measured Higgs mass value without the need for very heavy stops or large stop mixing parameters. This gauge extension leads to new, heavy gauge and Higgs bosons, as well as new neutralinos and charginos, that depending on the region of parameter space can induce novel phenomenology at the LHC. Gauge extensions including new abelian gauge groups have been considered, for instance, in Ref. [344].

Gauge extensions of the MSSM can also lead to an enhancement of the Higgs mass value by modifying the renormalization group evolution of the Higgs quartic coupling to low energies. In the MSSM, the evolution of the quartic coupling is governed by the top-quark Yukawa interactions and depends on the fourth power of the top-quark Yukawa coupling. The neutralino and chargino contributions, which depend on the fourth power of the weak gauge couplings, are small due

to the smallness of these couplings. Depending on the values of the soft supersymmetry breaking parameters in the gaugino and Higgsino sectors, the $SU(2)_1$ gauginos may become light, with masses of the order of the weak scale. Since the $SU(2)_1$ coupling may be significantly larger than the $SU(2)_L$ one, for small values of the Higgsino mass parameter μ, the associated charginos and neutralinos may modify the evolution of the quartic coupling in a significant way [345]. This may lead to a significant increase of the lightest CP-even Higgs mass, even for small values of $\tan\beta \simeq 1$ for which the D-term contributions become small.

VII.4. Effects of CP violation

SUSY scenarios with CP-violation (CPV) phases are theoretically appealing, since additional CPV beyond that observed in the K, D, and B meson systems is required to explain the observed cosmic matter-antimatter asymmetry. In the MSSM, CP-violation effects in the Higgs sector appear at the quantum level, while in singlet extensions of the MSSM CP-violation effects can already be effective at tree level. In general, CP-violation effects in the Higgs sector have significant constraints from electric dipole moments data [281].

In the MSSM, the gaugino mass parameters ($M_{1,2,3}$), the Higgsino mass parameter, μ, the bilinear Higgs squared-mass parameter, m_{12}^2, and the trilinear couplings of the squark and slepton fields to the Higgs fields, A_f, may carry non-trivial phases. The two parameter combinations $\arg[\mu A_f (m_{12}^2)^*]$ and $\arg[\mu M_i (m_{12}^2)^*]$ are invariant under phase redefinitions of the MSSM fields [346, 347]. Therefore, if one of these quantities is non-zero, there would be new sources of CP-violation affecting the Higgs sector through radiative corrections [348, 347, 349–353]. The mixing of the neutral CP-odd and CP-even Higgs boson states is no longer forbidden. Hence, m_A is no longer a physical parameter. However, the charged Higgs boson mass $m_{H^\pm}$ is still physical and can be used as an input for the computation of the neutral Higgs spectrum of the theory. For large values of $m_{H^\pm}$, corresponding to the decoupling limit, the properties of the lightest neutral Higgs boson state approach those of the SM Higgs boson. In particular, the upper bound on the lightest neutral Higgs boson mass, takes the same value as in the CP-conserving case [347]. Nevertheless, there still can be significant mixing between the two heavier neutral mass eigenstates. For a detailed study of the Higgs boson mass spectrum and parametric dependence of the associated radiative corrections, see Refs. [349, 352].

Major variations to the Higgs phenomenology occur in the presence of explicit CPV phases. In the CPV case, vector boson pairs couple to all three neutral Higgs boson mass eigenstates, H_i $(i = 1, 2, 3)$, with couplings

$$g_{H_i VV} = \cos\beta \mathcal{O}_{1i} + \sin\beta \mathcal{O}_{2i}\,, \tag{11.27}$$

$$g_{H_i H_j Z} = \mathcal{O}_{3i}\left(\cos\beta \mathcal{O}_{2j} - \sin\beta \mathcal{O}_{1j}\right) - \mathcal{O}_{3j}\left(\cos\beta \mathcal{O}_{2i} - \sin\beta \mathcal{O}_{1i}\right)\,, \tag{11.28}$$

where the $g_{H_i VV}$ couplings are normalized to the analogous SM coupling and the $g_{H_i H_j Z}$ have been normalized to $g_Z^{\rm SM}/2$. The orthogonal matrix $\mathcal{O}_{ij}$ is relating the weak eigenstates to the mass eigenstates. It has non-zero off-diagonal entries mixing the CP-even and CP-odd components of the weak eigenstates. Moreover, CPV phases imply that all neutral Higgs bosons can couple to both scalar and pseudoscalar fermion bilinear densities. The couplings of the mass eigenstates H_i to fermions depend on the loop-corrected fermion Yukawa couplings (similarly to the CPC case), on $\tan\beta$ and on the $\mathcal{O}_{ji}$ [349, 354].

The production processes of neutral MSSM Higgs bosons in the CPV scenario are similar to those in the CPC scenario. Regarding the decay properties, the lightest mass eigenstate, H_1, predominantly decays to $b\overline{b}$ if kinematically allowed, with a smaller fraction decaying to $\tau^+\tau^-$, similar to the CPC case. If kinematically allowed, a SM-like neutral Higgs boson, H_2 or H_3 can decay predominantly to $H_1 H_1$ leading to many new interesting signals both at lepton and hadron colliders; otherwise it will decay preferentially to $b\overline{b}$.

The discovery of a 125 GeV Higgs boson has put strong constraints on the realization of the CPV scenario within the MSSM. This is partly due to the fact that the observed Higgs rates are close to the SM values, and a large CP-violating component would necessarily induce a large variation in the rate of the SM-like Higgs decay into the weak gauge bosons $W^\pm$ and Z. The measured Higgs mass imposes additional constraints on the realization of this scenario. Once all effects are considered, the CP-odd Higgs A component of the lightest Higgs tends to be smaller than about 10%. This restriction can be alleviated in the NMSSM or more general two Higgs doublet models. CP-violating effects can still be significant in the heavy Higgs sector. For instance, the Higgs bosons H_2 and H_3 may be admixtures of CP-even and CP-odd scalars, and therefore both may be able to decay into pairs of weak gauge bosons. The observation of such decays would be a clear signal of CP-violation. In the MSSM the proximity of the masses of H_2 and H_3 makes the measurement of such effect quite challenging, but in generic two Higgs doublet models, the mass splitting between the two heavy mass eigenstates may become larger, facilitating the detection of CP-violating effects at collider experiments [355].

VII.5. Non-supersymmetric extensions of the Higgs sector

There are many ways to extend the minimal Higgs sector of the SM. In the preceding sections the phenomenology of SUSY Higgs sectors is considered, which at tree level implies a constrained type-II 2HDM (with restrictions on the Higgs boson masses and couplings). In the following discussion, more generic 2HDM's [12, 293, 356, 357] are presented. These models are theoretically less compelling since they do not provide an explanation for the SM Higgs naturalness problem, but can lead to different patterns of Higgs-fermion couplings, hence, to different phenomenology. It is also possible to consider models with a SM Higgs boson and one or more additional scalar SU(2) doublets that acquire no VEV and hence play no role in the EWSB mechanism. Such models are dubbed Inert Higgs Doublet Models (IHD) [358]. Without a VEV associated to it, a Higgs boson from an inert doublet has no tree-level coupling to gauge bosons and hence cannot decay into a pair of them. Moreover, imposing a Z_2 symmetry that prevents them from coupling to the fermions, it follows that, if the lightest inert Higgs boson is neutral, it becomes a good dark matter candidate with interesting associated collider signals. Recent studies of IHD models in the light of a 125 GeV Higgs have been performed in Ref. [359], showing an interesting interplay between collider and direct dark matter detection signals.

An interesting type of 2HDMs, are those in which an abelian flavor symmetry broken at the electroweak scales creates the fermion mass hierarchies and mixing angles [360]. This idea is based on the Froggatt-Nielsen model [361], where a flavon field couples differently to the SM fermions of different flavor charges. Such flavon acquires a vacuum expectation value, breaking the flavor symmetry but leaving both the flavor breaking and the new physics scales undetermined. In Refs. [362], it was proposed to relate the flavor breaking scale to the electroweak scale by identifying the flavon with the modulus square of the Higgs field. A 2HDM, however, provides a more compelling realization of the electroweak scale flavor breaking idea. In the most ambitious constructions of two Higgs doublet flavor models (2HDFM), the textures of the Yukawa couplings are a result of an abelian flavor symmetry that only allows renormalizable Yukawa couplings of the top quark to the Higgs bosons. All other Yukawa couplings are generated by higher dimensional operators that produce hierarchical entries of the Yukawa matrices, explaining the observed quark masses and mixing angles. Flavor observables, LHC Higgs signal strength measurements, electroweak precision measurements, unitarity and perturbativity bounds, as well as collider searches for new scalar resonances result in precise predictions for the parameters of these 2HDFMs. In particular, correlated departures from SM Higgs couplings, as well as additional Higgs bosons with masses < 700 GeV must be observed at the LHC. Other incarnations of 2HDFMs can aim at only partially explaining the fermion mass hierarchies and be less restrictive.

Other extensions of the Higgs sector can include multiple copies of $SU(2)_L$ doublets [334, 363], additional Higgs singlets [364], triplets or more complicated combinations of Higgs multiplets. It is also possible to enlarge the gauge symmetry beyond $SU(2)_L \times U(1)_Y$ along with the necessary Higgs structure to generate gauge boson and fermion masses.

There are two main experimental constraints on these extensions: *(i)* precision measurements which constrain $\rho = m_W^2/(m_Z^2 \cos^2\theta_W)$ to be very close to 1 and *(ii)* flavor changing neutral current (FCNC) effects. In electroweak models based on the SM gauge group, the tree-level value of ρ is determined by the Higgs multiplet structure. By suitable choices for the hypercharges, and in some cases the mass splitting between the charged and neutral Higgs sector or the vacuum expectation values of the Higgs fields, it is possible to obtain a richer combination of singlets, doublets, triplets and higher multiplets compatible with precision measurements [365]. Concerning the constraints coming from FCNC effects, the Glashow–Weinberg (GW) criterion [366] states that, in the presence of multiple Higgs doublets the tree-level FCNC's mediated by neutral Higgs bosons will be absent if all fermions of a given electric charge couple to no more than one Higgs doublet. An alternative way of suppressing FCNC in a two Higgs doublet model has been considered in Ref. [367], where it is shown that it is possible to have tree level FCNC completely fixed by the CKM matrix, as a result of an abelian symmetry.

VII.5.1. Two-Higgs-doublet models

General two Higgs doublet models [356] can have a more diverse Higgs-fermion coupling structure than in Supersymmetry, and can be viewed as a simple extension of the SM to realize the spontaneous breakdown of $\mathrm{SU(2)}_L \times \mathrm{U(1)}_Y$ to $\mathrm{U(1)}_{\rm em}$. Quite generally, if the two Higgs doublets contain opposite hypercharges, the scalar potential will contain mixing mass parameters of the kind $m_{12}^2 \Phi_1^T i\sigma_2 \Phi_2 + h.c.$. In the presence of such terms, both Higgs doublets will acquire vacuum expectation values, $v_1/\sqrt{2}$ and $v_2/\sqrt{2}$, respectively, and the gauge boson masses will keep their SM expressions with the Higgs vacuum expectation value v replaced by $v = \sqrt{v_1^2 + v_2^2}$. Apart from the mass terms, the most generic renormalizable and gauge invariant scalar potential for two Higgs doublets with opposite hypercharges contains seven quartic couplings, as presented in Eq. (11.17).

Just as in the MSSM case, after electroweak symmetry breaking and in the absence of CP-violation, the physical spectrum contains a pair of charged Higgs bosons $H^\pm$, a CP-odd Higgs boson A and two neutral CP-even Higgs bosons, h and H. The angles α and β diagonalize the CP-even, and the CP-odd and charged Higgs sectors, respectively. The complete 2HDM is defined only after considering the interactions of the Higgs fields to fermions. Yukawa couplings of the generic form

$$-h_{ij}^a \bar{\Psi}_L^i H_a \Psi_R^j + h.c. \tag{11.29}$$

may be added to the renormalizable Lagrangian of the theory. Contrary to the SM, the two Higgs doublet structure does not ensure the alignment of the fermion mass terms $m_{ij} = h_{ij}^a v_a/\sqrt{2}$ with the Yukawa couplings h_{ij}^a. This implies that quite generally, the neutral Higgs boson will mediate flavor changing interactions between the different mass eigenstates of the fermion fields. Such flavor changing interactions should be suppressed in order to describe properly the Kaon, D and B meson phenomenology. Based on the Glashow–Weinberg criterion, it is clear that the simplest way of avoiding such transitions is to assume the existence of a symmetry that ensures the couplings of the fermions of each given quantum number (up-type and down-type quarks, charged and neutral leptons) to only one of the two Higgs doublets. Different models may be defined depending on which of these fermion fields couple to a given Higgs boson, see Table 11.15. Models of type-I [357] are those in which all SM fermions couple to a single Higgs field. In type-II models [293] down-type quarks and charged leptons couple to a common Higgs field, while the up-type quarks and neutral leptons couple to the other. In models of type-III (lepton-specific) quarks couple to one of the Higgs bosons, while leptons couple to the other. Finally, in models of type-IV (flipped), up-type quarks and charged leptons couple to one of the Higgs fields while down-quarks and neutral leptons couple to the other.

The two Higgs doublet model phenomenology depends strongly on the size of the mixing angle α and therefore on the quartic couplings. For large values of m_A, $\sin\alpha \to -\cos\beta$, $\cos\alpha \to \sin\beta$, $\cos(\beta-\alpha) \to 0$, and the lightest CP-even Higgs h behaves as the SM Higgs. The same behavior is obtained if the quartic couplings are such that $\mathcal{M}_{12}^2 \sin\beta = -(\mathcal{M}_{11}^2 - m_h^2)\cos\beta$. The latter condition represents a

Table 11.15: Higgs boson couplings to up, down and charged lepton-type $SU(2)_L$ singlet fermions in the four discrete types of 2HDM models that satisfy the Glashow–Weinberg criterion, from Ref. [368].

Model	2HDM I	2HDM II	2HDM III	2HDM IV
u	Φ_2	Φ_2	Φ_2	Φ_2
d	Φ_2	Φ_1	Φ_2	Φ_1
e	Φ_2	Φ_1	Φ_1	Φ_2

situation in which the coupling of h to fermions and weak gauge bosons become the same as in the SM, without decoupling the rest of the non-standard scalars and it is of particular interest due to the fact that the recently discovered Higgs boson has SM-like properties. This situation will be referred to as alignment, as in the MSSM case.

In analogy to the effects of CP violation in the supersymmetric 2HDM, choosing m_3^2, λ_5, λ_6 and λ_7 as complex while all other parameters are real, one has a model that is explicitly CP violating. The three neutral mass eigenstates mixed with each other and the Higgs phenomenology is analogous to the one described for the SUSY case above, with the caveat that when considering the neutral Higgs couplings to the scalar and pseudoscalar fermion bilinear densities the proper weight should be considered for the respective 2HDM's.

In type-II Higgs doublet models, at large values of $\tan\beta$ and moderate values of m_A, the non-standard Higgs bosons H, A and $H^\pm$ couple strongly to bottom quarks and τ leptons. Hence the decay modes of the non-standard Higgs bosons tend to be dominated by b-quark and tau-lepton modes, including top quarks or neutrinos in the case of the charged Higgs. However, for large and negative values of λ_4, the charged Higgs boson mass may be sufficiently heavy to allow on-shell decays $H^\pm \to W^\pm + (H, A)$, via a trilinear coupling

$$g_{H^\pm W^\mp H,A} \simeq \frac{M_W}{v} \sin(\beta-\alpha)(p_{H^+} - p_{H,A}), \tag{11.30}$$

where p_{H^+} and $p_{H,A}$ are the charged and neutral scalar Higgs momenta pointing into the vertex. On the other hand, for large and positive values of λ_5, the above charged Higgs decay into a $W^\pm$ and the CP-odd Higgs boson may be allowed, but the heavy Higgs H may be sufficiently heavy to decay into a CP-odd Higgs boson and an on-shell Z, $H \to Z + A$, via

$$g_{HZA} \simeq \frac{M_Z}{v} \sin(\beta-\alpha)(p_H - p_A). \tag{11.31}$$

The decay $H^\pm \to W^\pm + H$, on the other hand may be allowed only if $\lambda_4 < -\lambda_5$. The couplings controlling all the above decay modes are proportional to $\sin(\beta-\alpha)$ and therefore they are unsuppressed in the alignment limit. Moreover, these could still be the dominant decay modes at moderate values of $\tan\beta$, offering a way to evade the current bounds obtained assuming a dominant decay into bottom quarks or τ leptons.

The quartic couplings are restricted by the condition of stability of the effective potential as well as by the restriction of obtaining the proper value of the lightest CP-even Higgs mass. Close to the alignment limit, the lightest CP-even Higgs mass becomes approximately independent of m_A and is given by

$$\begin{aligned} m_h^2 \simeq & v^2(\lambda_1 \cos^4\beta + \lambda_2 \sin^4\beta + 2\tilde{\lambda}_3 v^2 \cos^2\beta \sin^2\beta) \\ & + v^2(4\lambda_6 \cos^3\beta \sin\beta + 4\lambda_7 \sin^3\beta \cos\beta), \end{aligned} \tag{11.32}$$

where $\tilde{\lambda}_3 = \lambda_3 + \lambda_4 + \lambda_5$.

The stability conditions imply the positiveness of all masses, as well as the avoidance of run-away solutions to large negative values of the fields in the scalar potential. These conditions imply

$$\begin{aligned} & \lambda_1 \geq 0, \quad \lambda_2 \geq 0, \quad \lambda_3 + \lambda_4 - |\lambda_5| \geq -\sqrt{\lambda_1 \lambda_2}, \\ & \lambda_3 \geq -\sqrt{\lambda_1 \lambda_2}, \quad 2|\lambda_6 + \lambda_7| < \frac{\lambda_1 + \lambda_2}{2} + \tilde{\lambda}_3, \end{aligned} \tag{11.33}$$

where the first four are necessary and sufficient conditions in the case of $\lambda_6 = \lambda_7 = 0$, while the last one is a necessary condition in the case

all couplings are non-zero. Therefore, to obtain the conditions that allow the decays $H^{\pm} \to W^{\pm}H, A$ and $H \to ZA$, λ_3 should take large positive values in order to compensate for the effects of λ_4 and λ_5. For more detailed discussions about 2HDM phenomenology see for example Refs [43, 324, 363,369–372,373,320].

VII.5.2. Higgs triplets

Electroweak triplet scalars are the simplest non-doublet extension of the SM that can participate in the spontaneous breakdown of $\mathrm{SU}(2)_L \times \mathrm{U}(1)_Y$ to $\mathrm{U}(1)_{\mathrm{em}}$. Two types of model have been developed in enough detail to make a meaningful comparison to LHC data: the Higgs triplet model (HTM) [374,375] and the Georgi–Machacek model [376–379].

The Higgs triplet model extends the SM by the addition of a complex $\mathrm{SU}(2)_L$ triplet scalar field Δ with hypercharge $Y = 2$, and a general gauge-invariant renormalizable potential $V(\Phi, \Delta)$ for Δ and the SM Higgs doublet Φ. The components of the triplet field can be parameterized as

$$\Delta = \frac{1}{\sqrt{2}} \begin{pmatrix} \Delta^{+} & \sqrt{2}\Delta^{++} \\ v_{\Delta} + \delta + i\xi & -\Delta^{+} \end{pmatrix} . \tag{11.34}$$

where Δ^{+} is a singly-charged field, Δ^{++} is a doubly-charged field, δ is a neutral CP-even scalar, ξ is a neutral CP-odd scalar, and v_{Δ} is the triplet VEV. The general scalar potential mixes the doublet and triplet components. After electroweak symmetry breaking there are seven physical mass eigenstates, denoted $H^{\pm\pm}$, $H^{\pm}$, A, H, and h.

A distinguishing feature of the HTM is that it violates the custodial symmetry of the SM; thus the ρ parameter deviates from 1 even at tree level. Letting x denote the ratio of triplet and doublet VEVs, the tree level expression [380] is:

$$\rho = \frac{1 + 2x^2}{1 + 4x^2} . \tag{11.35}$$

The measured value of the ρ parameter then limits [381] the triplet VEV to be quite small, $x \lesssim 0.03$, or $v_{\Delta} < 8\,\mathrm{GeV}$. This constraint severely limits the role of the triplet scalar in the EWSB mechanism.

The small VEV of the Higgs triplet in the HTM is a virtue from the point of view of generating neutrino masses without the necessity for introducing right-handed neutrino fields. The gauge invariant dimension four interaction

$$h_{\nu_{ij}}\, \ell_i^T C^{-1} i\sigma_2\, \Delta\, \ell_j \,, \tag{11.36}$$

where ℓ_i are the lepton doublets, C is the charge conjugation matrix, and $h_{\nu_{ij}}$ is a complex symmetric coupling matrix, generates a Majorana mass matrix for the neutrinos:

$$m_{\nu_{ij}} = \sqrt{2} h_{\nu_{ij}} v_{\Delta} . \tag{11.37}$$

This can be combined with the usual neutrino seesaw to produce what is known as the type-II seesaw [382].

The HTM suggests the exciting possibility of measuring parameters of the neutrino mass matrix at the LHC. If the doubly-charged Higgs is light enough and/or its couplings to W^+W^+ are sufficiently suppressed, then its primary decay is into same-sign lepton pairs: $H^{++} \to \ell_i^+ \ell_j^+$; from Eq. (11.36) and Eq. (11.37) it is apparent that these decays are in general lepton-flavor violating with branchings proportional to elements of the neutrino mass matrix [383].

Precision electroweak data constrain the mass spectrum as well as the triplet VEV of the HTM [380,384,385]. As described in Ref. [385], these constraints favor a spectrum where H^{++} is the lightest of the exotic bosons, and where the mass difference between H^{+} and H^{++} is a few hundred GeV. The favored triplet VEV is a few GeV, which also favors H^{++} decays into W^+W^+ over same-sign dileptons.

The Georgi–Machacek model addresses the ρ parameter constraint directly by building in custodial symmetry. Writing the complex scalar doublet of the SM as a $(2,2)$ under $\mathrm{SU}(2)_L \times \mathrm{SU}(2)_R$, it is obvious that the next simplest construction respecting custodial symmetry is a scalar transforming like a $(3,3)$ [386]. These nine real degrees of freedom correspond to a complex electroweak triplet combined with a real triplet, with the scalar potential required to be invariant under $\mathrm{SU}(2)_R$. Under the custodial $\mathrm{SU}(2)_{L+R}$, they transform as $1 \oplus 3 \oplus 5$, with a CP-even neutral scalar as the custodial singlet (thus matching the SM Higgs boson), a CP-odd neutral scalar in the custodial triplet, and another CP-even neutral scalar in the custodial 5-plet.

The scalar components can be decomposed as [387]

$$\Xi = \begin{pmatrix} \chi_3^* & \xi_1 & \chi_1 \\ -\chi_2^* & \xi_2 & \chi_2 \\ \chi_1^* & -\xi_1^* & \chi_3 \end{pmatrix} , \tag{11.38}$$

where ξ_2 is a real scalar and the others are complex scalars. Linear combinations of these account for the neutral custodial singlet, a neutral and singly-charged field making up the custodial triplet, and neutral, singly-charged, and doubly-charged fields making up the custodial 5-plet.

When combined with the usual SM doublet field Φ, the electroweak scale v is now related to the doublet and triplet VEVs by

$$v^2 = v_{\Phi}^2 + 8 v_{\Xi}^2 . \tag{11.39}$$

Note that the GM triplets by themselves are sufficient to explain electroweak symmetry breaking and the existence of a 125 GeV neutral boson along with a custodial triplet of Goldstone bosons; the complex doublet field in the GM model is required to generate fermion masses via the usual dimension four Yukawa couplings. This raises the question of whether one can rule out the possibility that the 125 GeV boson is the neutral member of a custodial 5-plet rather than a custodial singlet, without invoking decays to fermions. A conclusive answer is given by observing that the ratio of the branching fractions to W versus Z bosons is completely determined by the custodial symmetry properties of the boson. For a custodial 5-plet, the ratio of the signal strength to WW over that to ZZ is predicted to be 1/4 that of a SM Higgs boson [386, 388], and thus already ruled out by the experimental results presented in Section VI.

Another interesting general feature of Higgs triplet models is that, after mixing, the SM-like neutral boson can have stronger couplings to WW and ZZ than predicted by the SM [379, 389]; this is in contrast to mixing with additional doublets and singlet, which can only reduce the WW and ZZ couplings versus the SM. This emphasizes that LHC Higgs data cannot extract model independent coupling strengths for the Higgs boson [256, 390].

Because of the built-in custodial symmetry, the triplet VEV in the GM model can be large compared to the doublet VEV. The custodial singlet neutral boson from the triplets mixes with the neutral boson from the doublet. Two interesting special cases are (i) the triplet VEV is small and the 125 GeV boson is SM-like except for small deviations, and (ii) the 125 GeV boson is mostly the custodial singlet neutral boson from the electroweak triplets. The phenomenology of the doubly-charged and singly-charged bosons is similar to that of the HTM. The constraints on the GM model from precision electroweak data, LEP data, and current LHC data are described in Refs. [387, 391–394].

VII.6. Composite Higgs models

Within the SM, EWSB is posited but has no dynamical origin. Furthermore, the Higgs boson appears to be unnaturally light. A scenario that remedies these two catches is to consider the Higgs boson as a bound state of new dynamics becoming strong around the weak scale. The Higgs boson can be made significantly lighter than the other resonances of the strong sector if it appears as a pseudo-Nambu–Goldstone boson, see Refs. [15, 16, 395] for reviews.

VII.6.1. Little Higgs models

The idea behind the Little Higgs models [396, 397] is to identify the Higgs doublet as a (pseudo) Nambu–Goldstone boson while keeping some sizable non-derivative interactions, in particular a largish Higgs quartic interaction. By analogy with QCD where the pions $\pi^{\pm,0}$ appear as Nambu–Goldstone bosons associated to the breaking of

the chiral symmetry $\mathrm{SU(2)_L \times SU(2)_R/SU(2)}$, switching on some interactions that break explicitly the global symmetry will generate masses for the would-be massless Nambu–Goldstone bosons of the order of $g\Lambda_{G/H}/(4\pi)$, where g is the coupling of the symmetry breaking interaction and $\Lambda_{G/H} = 4\pi f_{G/H}$ is the dynamical scale of the global symmetry breaking G/H. In the case of the Higgs boson, the top Yukawa interaction or the gauge interactions themselves will certainly break explicitly (part of) the global symmetry since they act non-linearly on the Higgs boson. Therefore, obtaining a Higgs mass around 100 GeV would demand a dynamical scale $\Lambda_{G/H}$ of the order of 1 TeV, which is known to lead to too large oblique corrections. Raising the strong dynamical scale by at least one order of magnitude requires an additional selection rule to ensure that a Higgs mass is generated at the 2-loop level only

$$m_H^2 = \frac{g^2}{16\pi^2}\Lambda_{G/H}^2 \to m_H^2 = \frac{g_1^2 g_2^2}{(16\pi^2)^2}\Lambda_{G/H}^2 \tag{11.40}$$

The way to enforce this selection rule is through a "collective breaking" of the global symmetry:

$$\mathcal{L} = \mathcal{L}_{G/H} + g_1\mathcal{L}_1 + g_2\mathcal{L}_2. \tag{11.41}$$

Each interaction $\mathcal{L}_1$ or $\mathcal{L}_2$ individually preserves a subset of the global symmetry such that the Higgs remains an exact Nambu–Goldstone boson whenever either g_1 or g_2 is vanishing. A mass term for the Higgs boson can be generated only by diagrams involving simultaneously both interactions. At one-loop, such diagrams are not quadratically divergent, so the Higgs mass is not UV sensitive. Explicitly, the cancellation of the SM quadratic divergences is achieved by a set of new particles around the Fermi scale: gauge bosons, vector-like quarks, and extra massive scalars, which are related, by the original global symmetry, to the SM particles with the same spin. Contrary to supersymmetry, the cancellation of the quadratic divergences is achieved by same-spin particles. These new particles, with definite couplings to SM particles as dictated by the global symmetries of the theory, are perfect goals for the LHC.

The simplest incarnation of the collective breaking idea, the so-called littlest Higgs model, is based on a non-linear σ-model describing the spontaneous breaking SU(5) down to SO(5). A subgroup $\mathrm{SU(2)_1 \times U(1)_1 \times SU(2)_2 \times U(1)_2}$ is weakly gauged. This model contains a weak doublet, that is identified with the Higgs doublet, and a complex weak triplet whose mass is not protected by collective breaking. Other popular little Higgs models are based on different coset spaces: minimal moose $(\mathrm{SU(3)^2/SU(3)})$ [398], the simplest little Higgs $(\mathrm{SU(3)^2/SU(2)^2})$ [399], the bestest little Higgs $(\mathrm{SO(6)^2/SO(6)})$ [400] *etc.*For comprehensive reviews, see Refs. [401, 402].

Generically, oblique corrections in Little Higgs models are reduced either by increasing the coupling of one of the gauge groups (in the case of product group models) or by increasing the masses of the W and Z partners, leading ultimately to a fine-tuning of the order of a few percents (see for instance Ref. [403] and references therein). The compatibility of Little Higgs models with experimental data is significantly improved when the global symmetry involves a custodial symmetry as well as a T-parity [404] under which, in analogy with R-parity in SUSY models, the SM particles are even and their partners are odd. Such Little Higgs models would therefore appear in colliders as jet(s) with missing transverse energy [405] and the ATLAS and CMS searches for squarks and gluinos [406] can be recast to obtain limits on the masses of the heavy vector-like quarks. The T-even top partner, with an expected mass below 1 TeV to cancel the top loop quadratic divergence without too much fine-tuning, would decay dominantly into a $t + Z$ pair or into a $b + W$ pair or even into $t + H$. The latest CMS and ATLAS direct searches [407] for vector-like top partners put a lower bound above one TeV on their mass, excluding the most natural region of the parameter space of these models, i.e., there is still fine-tuning at the per cent level.

The motivation for Little Higgs models is to solve the little hierarchy problem, i.e., to push the need for new physics (responsible for the stability of the weak scale) up to around 10 TeV. Per se, Little Higgs models are effective theories valid up to their cutoff scale $\Lambda_{G/H}$. Their UV completions could either be weakly or strongly coupled.

Table 11.16: Global symmetry breaking patterns and the corresponding Goldstone boson contents of the SM, the minimal composite Higgs model, the next to minimal composite Higgs model, and the minimal composite two Higgs doublet model. Note that the SU(3) model does not have a custodial invariance. a denotes a CP-odd scalar while h and H are CP-even scalars.

Model	Symmetry Pattern	Goldstones
SM	SO(4)/SO(3)	W_L, Z_L
–	SU(3)/SU(2)×U(1)	W_L, Z_L, H
MCHM	SO(5)/SO(4)	W_L, Z_L, H
NMCHM	SO(6)/SO(5)	W_L, Z_L, H, a
MC2HM	SO(6)/SO(4)×SO(2)	$W_L, Z_L, h, H, H^\pm, a$

VII.6.2. Models of partial compositeness

Even in composite models, the Higgs boson cannot appear as a regular resonance of the strong sector without endangering the viability of the setup when confronted to data. The way out is that the Higgs appears as a pseudo Nambu–Goldstone boson: the new strongly coupled sector is supposed to be invariant under a global symmetry G spontaneously broken to a subgroup H at the scale f. To avoid conflict with EW precision measurements, the strong interactions themselves should better not break the EW symmetry. Hence the SM gauge symmetry itself should be contained in H. See Table 11.16 for a few examples of coset spaces.

The SM (light) fermions and gauge bosons cannot be part of the strong sector itself since LEP data have already put stringent bounds on the compositeness scale of these particles far above the TeV scale. The gauge bosons couple to the strong sector by a weak gauging of an SU(2)×U(1) subgroup of the global symmetry G. Inspiration for the construction of such models comes from the AdS/CFT correspondence: the components of a gauge field along an extra warped space dimension can be interpreted as the Goldstone boson resulting from the breaking of global symmetry of the strong sector. The couplings of the SM fermions to the strong sector could a priori take two different forms: (i) a bilinear coupling of two SM fermions to a composite scalar operator, $\mathcal{O}$, of the form $\mathcal{L} = y\,\bar{q}_L u_R \mathcal{O} + \mathrm{hc}$ in simple analogy with the SM Yukawa interactions. This is the way fermion masses were introduced in Technicolor theories and it generically comes with severe flavor problems and calls for extended model building gymnastics [408] to circumvent them; (ii) a linear mass mixing with fermionic vector-like operators: $\mathcal{L} = \lambda_L\,\bar{q}_L \mathcal{Q}_R + \lambda_R \bar{\mathcal{U}}_L u_R$. $\mathcal{Q}$ and $\mathcal{U}$ are two fermionic composite operators of mass M_Q and M_U. Being part of the composite sector, they can have a direct coupling of generic order Y_* to the Higgs boson. In analogy with the photon-ρ mixing in QCD, once the linear mixings are diagonalized, the physical states are a linear combination of elementary and composite fields. Effective Yukawa couplings are generated and read for instance for the up-type quark

$$y = Y_* \sin\theta_L \sin\theta_R \tag{11.42}$$

where $\sin\theta_i = \lambda_i/\sqrt{M_{Q,U}^2 + \lambda_i^2}$, $i = L, R$, measure the amount of compositeness of the SM left- and right-handed up-type quark. If the strong sector is flavor-anarchic, i.e., if the couplings of the Higgs to the composite fermions does not exhibit any particular flavor structure, the relation Eq. (11.42) implies that the light fermions are mostly elementary states ($\sin\theta_i \ll 1$), while the third generation quarks need to have a sizable degree of compositeness. The partial compositeness paradigm offers an appealing dynamical explanation of the hierarchies in the fermion masses. In fact, assuming the strong sector to be almost conformal above the confinement scale, the low-energy values of the mass-mixing parameters $\lambda_{L,R}$ are determined by the (constant) anomalous dimension of the composite operator they mix with. If the UV scale at which the linear mixings are generated is large, then $\mathcal{O}(1)$ differences in the anomalous dimensions can generate naturally large hierarchies in the fermion masses via renormalization group running [409]. While the introduction of partial compositeness greatly ameliorated the flavor problem of the original composite Higgs models,

nevertheless it did not solve the issue completely, at least in the case where the strong sector is assumed to be flavor-anarchic [410]. While the partial compositeness set-up naturally emerges in models built in space-times with extra dimensions, no fully realistic microscopic realization of partial compositeness has been proposed in the literature.

Another nice aspect of the partial compositeness structure is the dynamical generation of the Higgs potential that is not arbitrary like in the SM. The Higgs being a pseudo-Nambu–Goldstone boson, its mass does not receive any contribution from the strong sector itself but it is generated at the one-loop level via the couplings of the SM particles to the strong sector since these interactions are breaking the global symmetries under which the Higgs doublet transforms non-linearly. The leading contribution to the potential arises from top loops and it takes the form

$$V(H) = m_\rho^4 \frac{\sin\theta_{tL}\sin\theta_{tR}}{16\pi^2}\left(\alpha\cos(H/f) + \beta\sin^2(H/f) + \gamma\sin^4(H/f)\right), \tag{11.43}$$

where α, β, γ are numbers of order 1 subject to selection rules following the transformation properties of the top quark under the global symmetries of the strong sector[9], and $m_\rho \approx g_\rho f$ is the typical mass scale of the strong sector resonances. The gauge contribution to the potential takes the form (g denotes the SU(2) gauge coupling)

$$m_\rho^4 \frac{g^2/g_\rho^2}{16\pi^2}\sin^2(H/f), \tag{11.44}$$

which is parametrically suppressed with respect to the top contribution by $g^2/(g_\rho y_t)$. The gauge term is always positive, and cannot trigger EWSB by itself. When $\alpha = 0$, the minimization condition of the potential simply reads

$$\sin^2\frac{\langle H\rangle}{f} = -\frac{\beta}{2\gamma}, \tag{11.45}$$

which implies that the natural expectation is that the scale f is generically of the order of the weak scale. Obtaining $v \ll f$, as required phenomenologically, requires some degree of tuning, which scales like $\xi \equiv v^2/f^2$. A mild tuning of the order of 10% ($\xi \approx 0.1$) is typically enough to comply with electroweak precision constraints. This is an important point: in partial compositeness models, the entire Higgs potential is generated at one loop, therefore the separation between v and f can only be obtained at a price of a tuning. This marks a difference with respect to the Little Higgs models, which realize a parametric hierarchy between the quartic and mass terms through the collective symmetry breaking mechanism. In fact in Little Higgs models, the quartic coupling is a tree-level effect, leading to a potential

$$V(H) \approx \frac{g_{\rm SM}^2}{16\pi^2} m_\rho^2 H^2 + g_{\rm SM}^2 H^4, \tag{11.46}$$

where $g_{\rm SM}$ generically denotes the SM couplings. The minimization condition now reads $v^2/f^2 \sim g_\rho^2/(16\pi^2)$, therefore v is formally loop suppressed with respect to f. This is the major achievement of the Little Higgs constructions, which however comes at the price of the presence of sub-TeV vectors carrying EW quantum numbers and therefore giving rise generically to large oblique corrections to the propagators of the W and the Z gauge bosons.

After minimization, the potential Eq. (11.43) leads to an estimate of the Higgs mass as

$$m_H^2 \approx g_\rho^3 y_t 2\pi^2 v^2. \tag{11.47}$$

It follows that the limit $f \to \infty$, i.e. $\xi \to 0$, is a true decoupling limit: all the resonances of the strong sector become heavy but the Higgs whose mass is protected by the symmetries of the coset G/H. When compared to the experimentally measured Higgs mass, this estimate puts an upper bound on the strength of the strong interactions: $g_\rho \lesssim 2$. In this limit of not so large coupling, the Higgs potential receives additional contributions. In particular, the fermionic resonances in the top sector which follow from the global symmetry structure of the new physics sector can help raising the Higgs mass. For instance in the minimal SO(5)/SO(4) model, using some dispersion relation techniques, one obtains [412]

$$m_H^2 \approx \frac{6}{\pi^2}\frac{m_t^2}{f^2}\frac{m_{Q_4}^2 m_{Q_1}^2}{m_{Q_1}^2 - m_{Q_4}^2}\log\left(\frac{m_{Q_1}}{m_{Q_4}}\right) \tag{11.48}$$

where Q_4 and Q_1 are fermionic color resonances transforming as a weak bi-doublet of hypercharge $Y = 1/6$ and $Y = 7/6$ and a weak singlet with hypercharge $Y = -1/3$. Therefore a 125 GeV mass can be obtained if at least one of the fermionic resonances is lighter than $\sim 1.4\, f$. As in supersymmetric scenarios, the top sector is playing a crucial role in the dynamics of EWSB and can provide the first direct signs of new physics. The direct searches for these top partners, in particular the ones with exotic electric charges 5/3, are already exploring the natural parameter spaces of these models [407], 413, 414].

The main physics properties of a pseudo Nambu–Goldstone Higgs boson can be captured in a model-independent way by a few number of higher-dimensional operators. Indeed, the strong dynamics at the origin of the composite Higgs singles out a few operators among the complete list presented earlier in Section VI: these are the operators that involve extra powers of the Higgs doublets and they are therefore generically suppressed by a factor $1/f^2$ as opposed to the operators that involve extra derivatives or gauge bosons and are suppressed by a factor $1/(g_\rho^2 f^2)$. The relevant effective Lagrangian describing a strongly interacting light Higgs is:

$$\mathcal{L}_{\rm SILH} = \frac{c_H}{2f^2}\left(\partial_\mu\left(\Phi^\dagger\Phi\right)\right)^2 + \frac{c_T}{2f^2}\left(\Phi^\dagger \overleftrightarrow{D^\mu}\Phi\right)^2 - \frac{c_6\lambda}{f^2}\left(\Phi^\dagger\Phi\right)^3 + \left(\sum_f \frac{c_f\, y_f}{f^2}\Phi^\dagger\Phi\bar{f}_L\Phi f_R + \text{h.c.}\right). \tag{11.49}$$

Typically, these new interactions induce deviations in the Higgs couplings that scale like $\mathcal{O}(v^2/f^2)$, hence the measurements of the Higgs couplings can be translated into some constraints on the compositeness scale, $4\pi f$, of the Higgs boson. The peculiarity of these composite models is that, due to the Goldstone nature of the Higgs boson, the direct couplings to photons and gluons are further suppressed and generically the coupling modifiers defined in Section VI scale like

$$\kappa_{W,Z,f} \sim 1 + \mathcal{O}\left(\frac{v^2}{f^2}\right), \quad \kappa_{Z\gamma} \sim \mathcal{O}\left(\frac{v^2}{f^2}\right), \quad \kappa_{\gamma,g} \sim \mathcal{O}\left(\frac{v^2}{f^2}\times\frac{y_t^2}{g_\rho^2}\right), \tag{11.50}$$

where g_ρ denotes the typical coupling strength among the states of the strongly coupled sector and y_t is the top Yukawa coupling, the largest interaction that breaks the Goldstone symmetry. The $\kappa_{Z\gamma,\gamma,g}$ coupling modifiers are not generated by the strong coupling operators of Eq. (11.49) but some subleading form-factor operator generated by loops of heavy resonances of the strong sector. The coupling modifiers also receive additional contributions from the other resonances of the strong sector, in particular the fermionic resonances of the top sector that are required to be light to generate a 125 GeV Higgs mass. Some indirect information on the resonance spectrum could thus be inferred by a precise measurement of the Higgs coupling deviations. However, it was realized [415] that the task is actually complicated by the fact that, in the minimal models, these top partners give a contribution to both κ_t (resulting from a modification of the top Yukawa coupling) and κ_γ and κ_g (resulting from new heavy particles running into the

[9] For instance in the SO(5)/SO(4) composite models, when the top quark is embedded into a spinorial representation of SO(5), then $\gamma = 0$ and when it is part of a **5**, **10** or **14** representation, $\alpha = 0$ as it can be inferred by looking at the structure of the H-dependent invariants built out of these representations [411]. The coefficient γ also generically comes with an extra power of the top compositeness fractions.

loops) and the structure of interactions are such that the net effect vanishes for inclusive quantities like $\sigma(gg \to H)$ or $\Gamma(H \to \gamma\gamma)$ as a consequence of the Higgs low energy theorem [23, 24, 270]. So one would need to rely on differential distribution, like the Higgs p_T distribution [416], to *see* the top partner effects in Higgs data [417]. The off-shell channel $gg \to H^* \to 4\ell$ [418] and the double Higgs production $gg \to HH$ [419] can also help to resolve the gluon loop and separate the top and top-partner contributions.

VII.6.3. Minimal composite Higgs models

The minimal composite Higgs models (MCHM) are concrete examples of the partial compositeness paradigm. The Higgs doublet is described by the coset space SO(5)/SO(4) where a subgroup $\mathrm{SU}(2)_L \times \mathrm{U}(1)_Y$ is weakly gauged under which the four Goldstone bosons transform as a doublet of hypercharge 1. There is some freedom on how the global symmetry is acting on the SM fermions: in MCHM4 [411] the quarks and leptons are embedded into spinorial representations of SO(5), while in MHCM5 [420] they are part of fundamental representations (it might also be interesting phenomenologically to consider larger representations like MCHM14 [421] with the SM fermions inside a representation of dimension 14). It is also possible to consider that fermions of different chirality and flavor are in different representations of SO(5), leading to a more varied phenomenology [422]. The non-linearly realized symmetry acting on the Goldstone bosons leads to general predictions of the coupling of the Higgs boson to the EW gauge bosons. For instance, it can be shown that the quadratic terms in the W and Z bosons read

$$m_W^2(H)\left(W_\mu W^\mu + \frac{1}{2\cos^2\theta_W} Z_\mu Z^\mu\right)$$

with $m_W(H) = \dfrac{gf}{2}\sin\dfrac{H}{f}$. Expanding around the EW vacuum, the expression of the weak scale is:

$$v = f\sin(\langle H\rangle/f), \tag{11.51}$$

and the values of the modified Higgs couplings to the W and Z:

$$g_{HVV} = \frac{2m_V^2}{v}\sqrt{1-v^2/f^2}\,, \quad g_{HHVV} = \frac{2m_V^2}{v^2}(1-2v^2/f^2)\,. \tag{11.52}$$

Note that the Higgs couplings to gauge bosons is always suppressed compared to the SM prediction. This is a general result [423] that holds as long as the coset space is compact.

The Higgs couplings to the fermions depend on the representation which the SM fermions are embedded into. For the most commonly used embedding, considering all fermion doublets and singlets embedded in the same representations, they take the following forms

$$\begin{aligned}
&\text{MCHM4}: g_{Hff} = \frac{m_f}{v}\sqrt{1-v^2/f^2}\,,\\
&\text{MCHM5}: g_{Hff} = \frac{m_f}{v}\frac{1-2v^2/f^2}{\sqrt{1-v^2/f^2}}\,,\\
&\text{MCHM14}: g_{Hff} = \frac{m_f}{v}\left(1 + A(M_{1,4,9})\frac{v^2}{f^2} + O(v^4/f^4)\right)\,,\\
&\qquad\text{with } A(M_{1,4,9}) = \frac{3M_1M_4 - 11M_1M_9 + 8M_4M_9}{2M_9(M_1-M_4)}\,.
\end{aligned} \tag{11.53}$$

While, in MHCM4 and MCHM5, the modifications of the couplings depend only on the Higgs compositeness scale, in MCHM14 the leading corrections depend also on the mass spectrum of the resonances parametrized by M_1, M_4 and M_9 [421]. This is due to the fact that more than one SO(5) invariant gives rise to SM fermion masses. The (κ_V, κ_f) experimental fit of the Higgs couplings can be used to derive a lower bound on the Higgs compositeness scale $4\pi f \gtrsim 9\,\text{TeV}$, which is less stringent than the indirect bound obtained from EW precision data, $4\pi f \gtrsim 15\,\text{TeV}$ [424] but more robust and less subject on assumptions [425].

VII.6.4. Twin Higgs models

In all composite models presented above, the particles responsible for canceling the quadratic divergences in the Higgs mass are charged under the SM gauge symmetries. In particular, the top partner carries color charge, implying a reasonably large minimal production cross section at the LHC. An alternative scenario, which is experimentally quite challenging and might explain the null result in various new physics searches, is the case nowadays referred to as "neutral naturalness" [19, 20], where the particles canceling the 1-loop quadratic divergences are neutral under the SM. The canonical example for such theories is the Twin Higgs model of Ref. [19]. This is an example of a pseudo-Goldstone boson Higgs theory, with an approximate global $SU(4)$ symmetry broken to $SU(3)$. The Twin Higgs model is obtained by gauging the $SU(2)_A \times SU(2)_B$ subgroup of $SU(4)$, where $SU(2)_A$ is identified with the SM $SU(2)_L$, while $SU(2)_B$ is the twin $SU(2)$ group. Gauging this subgroup breaks the $SU(4)$ symmetry explicitly, but quadratically divergent corrections do not involve the Higgs boson when the gauge couplings of the two SU(2) subgroups are equal, $g_A = g_B$. The $SU(4) \to SU(3)$ breaking will also result in the breaking of the twin $SU(2)_B$ group and as a result three of the seven Goldstone bosons will be eaten, leaving 4 Goldstone bosons corresponding to the SM Higgs doublet h. In fact imposing the Z_2 symmetry on the full model will ensure the cancellation of all 1-loop quadratic divergences to the Higgs mass. Logarithmically divergent terms can however arise for example from gauge loops, leading to a Higgs mass of order $g^2 f/4\pi$, which is of the order of the physical Higgs mass for $f \sim 1\,\text{TeV}$. The quadratic divergences from the top sector can be eliminated if the Z_2 protecting the Higgs mass remains unbroken by the couplings that result in the top Yukawa coupling. This can be achieved by introducing top partners charged under a twin $SU(3)_c$. In this case the quadratic divergences are cancelled by top partners that are neutral under the SM gauge symmetries.

Twin Higgs models are low-energy effective theories valid up to a cutoff scale of order $\Lambda \sim 4\pi f \sim$ 5–10 TeV, beyond which a UV completion has to be specified. The simplest such possibility is to also make the Higgs composite, and UV complete the twin-Higgs model via gauge and top partners at masses of the order of a few TeV. A concrete implementation is the holographic twin Higgs model [426], which also incorporates a custodial symmetry to protect the T-parameter from large corrections. It is based on a warped extra dimensional theory with a bulk SO(8) gauge group, which incorporates the $SU(4)$ global symmetry discussed above enlarged to contain the $\mathrm{SU}(2)_L \times \mathrm{SU}(2)_R$ custodial symmetry. In addition the bulk contains either a full $SU(7)$ group or an $SU(3) \times SU(3) \times U(1) \times U(1) \times Z_2$ subgroup of it to incorporate QCD, its twin, and hypercharge. The breaking on the UV brane is to the SM and the twin SM symmetries, while on the IR brane $SO(8) \to SO(7)$, giving rise to the 7 Goldstone bosons, three of which will be again eaten by the twin W, Z. The main difference compared to ordinary composite Higgs models is that in composite twin Higgs models the cancellation of the one-loop quadratic divergences is achieved by the twin partners of order 700 GeV– 1 TeV, which are uncharged under the SM gauge group. This allows the IR scale of the warped extra dimension to be raised to the multi-TeV range without reintroducing the hierarchy problem. The role of the composite partners is to UV complete the theory, rather than the cancellation of the one-loop quadratic divergences. For more details about the composite twin Higgs models, see Refs. [427].

VII.7. Searches for signatures of extended Higgs sectors

The measurements described in Section III have established the existence of one state of the electroweak symmetry breaking sector, compatible with a SM Higgs boson, but not that it is the only one.

Various classes of models beyond the SM discussed above require extended Higgs sectors. These models, and in particular the MSSM and the NMSSM serve as guiding principle of the experimental searches for additional scalar states beyond the SM. However these searches are made as model-independent as possible and can be summarized in the following classes: (i) the search for an additional CP-even state mostly in the high mass domain decaying to vector bosons, which would correspond to the heavy CP-even state in a generic 2HDM where the light state would be the discovered H or a generic additional singlet; (ii) the search for a state in the high mass domain decaying to pairs of fermions, which would correspond a CP-odd A and the heavy CP-even state H in a generic 2HDM; (iii)

the search for charged Higgs bosons, which also appear in generic 2HDMs; (iv) the search for a CP-odd state a in the low mass region which appears in the NMSSM; and (v) doubly charged Higgs which are motivated in extensions of the Higgs sector with triplets.

This gives a concise description of the most recent searches performed at the LHC and elsewhere. The complete of final states searched is A summary of these searches in terms of final states is given in Table 11.17 where the corresponding references are given for more details.

Table 11.17: Summary of references to searches for additional states from extended Higgs sectors, where (BBr) denotes the BaBar experiment, (TeV) the Tevatron experiments. Results using Run 2 data are marked by (*). V denotes either the W or the Z boson.

	ATLAS	CMS	Other experiments
CP-even H			
$H \to \gamma\gamma$	*[428]	*[429, 430]	—
$H \to Z\gamma$	*[431]	*[432]	—
$H \to ZZ \to 4\ell$	*[433]	*[434]	—
$H \to ZZ \to \ell\ell\nu\nu$	*[433]	*[435]	—
$H \to ZZ \to \ell\ell q\overline{q}$	*[436]	*[437]	—
$H \to ZZ \to \nu\nu q\overline{q}$	*[436]	—	—
$H \to WW \to \ell\nu\ell\nu$	[438]	*[435]	—
$H \to WW \to \ell\nu\ell\nu$ (2HDM)	[439]	[440]	—
$H \to WW \to \ell\nu q\overline{q'}$	*[441]	[442, 443]	—
$H \to VV \to q\overline{q'}q\overline{q'}(JJ)$	*[444]	—	—
$H \to hh \to b\overline{b}\tau\tau, b\overline{b}\gamma\gamma, 4b,$ $\gamma\gamma WW^*$	*[187, 189, 445]	*[188, 446]	—
CP-odd A (and/or CP-even H)			
$H, A \to \tau^+\tau^-$	*[447]	*[448]	[449, 450]-TeV [451]-LHCb
$H, A \to \mu^+\mu^-$	[452]	—	—
$H, A \to t\overline{t}$	*[453]	—	
$H, A \to b\overline{b}$	—	*[455, 456]	[457, 458]-TeV
$A \to hV \to b\overline{b}q\overline{q'}, b\overline{b}\ell\nu, b\overline{b}\ell\ell,$ $\ell\ell\tau\tau, \nu\overline{\nu}b\overline{b}$	*[459, 460]	[446]	
Charged $H^\pm$			
$H^\pm \to \tau^\pm\nu$	*[461]	*[462]	—
$H^\pm \to cs$	[463]	[464]	—
$H^\pm \to tb$	*[465]	[466]	—
$H^\pm \to W^\pm Z$	[467]	*[468]	—
$H^\pm \to cb$	—	*[469]	—
CP-odd NMSSM a			
$a \to \mu^+\mu^-$	[470]	*[471]	—
$h \to aa \to 4\mu, 4\tau, 2\mu 2\tau, 4\gamma$	[472, 473]	*[474, 475]	[476]-TeV, [477]-LEP
$\Upsilon_{1s,3s} \to a\gamma$	—	—	[478, 479]-BBr
Doubly charged $H^{\pm\pm}$	*[480, 481]	*[482]	—

(i) Searches for an additional CP-even state

(a) Exclusion limits from LEP

The LEP searches for the SM Higgs boson put a lower limit of 114 GeV on its mass, but also have relevance for non-SM Higgs bosons. These searches were also interpreted as 95% CL upper bounds on the ratio of the coupling g_{HZZ} to its SM prediction as a function of the Higgs boson mass [122]. Among the MSSM new benchmarks, the low-m_H is one example which is disfavored by these searches at low mass, and nearly ruled out by current direct constraints and charged Higgs limits from LHC. Another example is the light CP-even Higgs boson of the NMSSM which is constrained to project predominantly onto the EW singlet component. An additional motivation for these scenarios is given by the slight excess observed at LEP [122] at a Higgs boson mass hypothesis of approximately 98 GeV.

(b) Searches at the LHC

The searches for the SM Higgs boson before the discovery covered a wide range of mass hypotheses. After the discovery, the SM Higgs boson searches have been reappraised to search for a heavy CP-even state. This state could be the heavy CP-even Higgs boson of a 2HDM, or a generic additional singlet. In both cases the natural width of the additional H state can be very different from that of the SM Higgs boson. To preserve unitarity of the longitudinal vector boson scattering and the longitudinal vector boson scattering into fermion pairs, the couplings of the additional CP-even Higgs boson to gauge bosons and fermions should not be too large and should constrain the natural width to be smaller than that of a unique Higgs boson at high mass with couplings to fermions and gauge bosons as predicted by the SM (and provided that trilinear and quartic couplings are not too large and that no new state affects the heavy state total width). It is therefore reasonable to consider total widths for the high mass CP-even state smaller than the equivalent SM width. For the sake of generality these searches should be done as a function of Higgs boson mass and total width. Until recently only two cases have been investigated: (i) the SM width using the complex pole scheme (CPS), and (ii) the narrow width approximation.

Searches for the Higgs boson in the $H \to \gamma\gamma$, $H \to Z\gamma$, $H \to W^{(*)}W^{(*)}$ in the $\ell\nu\ell\nu$ and $\ell\nu q\overline{q}$ channels, and the $H \to Z^{(*)}Z^{(*)}$ searches in the 4ℓ, $\ell\ell q\overline{q}$ and $\ell\ell\nu\nu$ channels have also been done, but in most cases are simple reinterpretations of the SM Higgs search in the CPS scheme. References for these searches are summarized in Table 11.17.

(c) Searches for an additional resonance decaying to a pair of h

In addition to the rare and expected Higgs pair production mode, high mass CP-even Higgs bosons can be searched for in the resonant double Higgs mode. Searches for such processes, where the Higgs boson is used as a tool for searches for new phenomena beyond the SM, have been carried out in four distinct modes depending on the subsequent decays of each Higgs boson. The ATLAS and CMS Collaborations have searched for the $H \to hh \to b\overline{b}\tau\tau$, $b\overline{b}\gamma\gamma$ and the $H \to hh \to 4b$ final states. These channels are the most sensitive in the search for heavy Higgs bosons decaying to a hh pair. The CMS collaboration has performed a search for the $\gamma\gamma WW^*$ final states [483]. For masses hypotheses of an additional Higgs boson below 500 GeV, the two dominant search channels are the $b\overline{b}\gamma\gamma$ and the $b\overline{b}\tau\tau$. For masses above 500 GeV, the most powerful search channel is the $4b$ final state.

(d) Searches for an additional state with the presence of h

In the post-discovery era, analyses searching for additional Higgs bosons need to take into account the presence of the discovered state. For searches with sufficiently high mass resolution to disentangle the additional states which are not degenerate in mass, the strength of the observed state and limits on the signal strength of a potential additional state can be set independently, as discussed in the next section. However in some cases, such as when a channel does not have a sufficiently fine mass resolution or when the states are nearly degenerate in mass, specific analyses need to be designed. There are two examples of such analyses: (i) the search for an additional state in the $H \to W^{(*)}W^{(*)} \to \ell\nu\ell\nu$ channel in ATLAS and (ii) the search for nearly degenerate states in the $H \to \gamma\gamma$ channel with the CMS detector.

The search in the $H \to W^{(*)}W^{(*)} \to \ell\nu\ell\nu$ channel, for an additional state is done using a boosted decision tree combining several discriminating kinematic characteristics to separate the signal from the background and a high mass signal H from the lower mass

state h [439]. A simultaneous fit of the two states h and H is then made to test the presence of an additional state. In this case, the usual null hypothesis of background includes including the SM signal.

The CMS search for nearly degenerate mass states decaying to a pair of photons [484] is more generic and could for instance apply to CP-odd Higgs bosons as well. It consists of a fit to the diphoton mass spectrum using two nearly degenerate mass templates.

(e) Type I 2HDM and fermiophobia

The measurements of coupling properties of H indirectly exclude that the discovered state is fermiophobic. However, the presence of an additional fermiophobic state, as predicted by Type I 2HDMs, is not excluded. Prior to the discovery, ATLAS and CMS have performed searches for a fermiophobic Higgs boson, *i.e.* produced through couplings with vector bosons only (VBF and VH) and decaying in $h_f \to \gamma\gamma$, optimized for fermiophobic signatures in the diphoton channel [485, 486]. CMS has further combined these results with searches for $h_f \to W^+W^-$ and $h_f \to ZZ$ assuming fermiophobic production and decay [487]. CMS excludes a fermiophobic Higgs boson in the range $110\,\text{GeV} < m_H < 188\,\text{GeV}$ at the 95% C.L.

(f) Interpretation benchmarks in the light of the discovered Higgs boson

Two specific benchmark scenarios driven by unitarity relations are proposed in Ref. [42], assuming the existence of an additional state h' with coupling scale factors, i.e., deviations from the couplings predicted for the SM Higgs at the same mass, denoted κ'_V and κ'_F for the couplings of h' to vector bosons and fermions respectively. The gauge boson scattering unitarity then yields the following sum rule

$$\kappa_V^2 + \kappa_V'^2 = 1 \tag{11.54}$$

and the unitarization of the gauge boson scattering to fermions yields

$$\kappa_V \cdot \kappa_F + \kappa'_V \cdot \kappa'_F = 1 \tag{11.55}$$

The two benchmark scenarios are then defined as follows: (i) a single coupling scale factor is assumed for the gauge bosons and the fermions, with an additional parameter to take into account decays to new states; (ii) two parameters are used to describe independently the couplings to fermions and the couplings to vector bosons. A direct application of the latter can be done in the CP-even sector of the type-I 2HDM.

(ii) Searches for additional neutral states ($\phi \equiv h$, H, A) decaying to fermions

(a) Exclusion limits from LEP

In e^+e^- collisions at LEP centre-of-mass energies, the main production mechanisms of the neutral MSSM Higgs bosons were the Higgs-strahlung processes $e^+e^- \to hZ$, HZ and the pair production processes $e^+e^- \to hA$, HA, while the vector boson fusion processes played a marginal role. Higgs boson decays to $b\bar{b}$ and $\tau^+\tau^-$ were used in these searches.

The searches and limits from the four LEP experiments are described in Refs. [488, 489]. The combined LEP data did not contain any excess of events which would imply the production of a Higgs boson, and combined limits were derived [490]. For $m_A \gg M_Z$ the limit on m_h is nearly that of the SM searches, as $\sin^2(\beta-\alpha) \approx 1$. For high values of $\tan\beta$ and low m_A ($m_A \leq m_h^{max}$), the $e^+e^- \to hA$ searches become the most important, and the lightest Higgs h is non SM-like. In this region, the 95% CL mass bounds are $m_h > 92.8\,\text{GeV}$ and $m_A > 93.4\,\text{GeV}$. In the m_h^{max} scenario, values of $\tan\beta$ from 0.7 to 2.0 are excluded taking $m_t = 174.3\,\text{GeV}$, while a much larger $\tan\beta$ region is excluded for other benchmark scenarios such as the no-mixing one.

A flavor-independent limit for Higgs bosons in the Higgs-strahlung process at LEP has also been set at 112 GeV [491].

Neutral Higgs bosons may also be produced by Yukawa processes $e^+e^- \to f\bar{f}\phi$, where the Higgs particle $\phi \equiv h$, H, A, is radiated off a massive fermion ($f \equiv b$ or $\tau^\pm$). These processes can be dominant at low masses, and whenever the $e^+e^- \to hZ$ and hA processes are suppressed. The corresponding ratios of the $f\bar{f}h$ and $f\bar{f}A$ couplings to the SM coupling are $\sin\alpha/\cos\beta$ and $\tan\beta$, respectively. The LEP data have been used to search for $b\bar{b}\,b\bar{b}$, $b\bar{b}\tau^+\tau^-$, and $\tau^+\tau^-\,\tau^+\tau^-$ final states [492, 493]. Regions of low mass and high enhancement factors are excluded by these searches.

The searches for the Higgs boson at LEP also included the case where it does not predominantly decay to a pair of b quarks. All four collaborations conducted dedicated searches b for the Higgs boson with reduced model dependence, assuming it is produced via the Higgs-strahlung process, and not addressing its flavor of decay, a lower limit on the Higgs mass of 112.9 GeV is set by combining the data of all four experiments [491].

Using an effective Lagrangian approach and combining results sensitive to the $h\gamma\gamma$, $hZ\gamma$ and hZZ couplings, an interpretation of several searches for the Higgs boson was made and set a lower limit of 106.7 GeV on the mass of a Higgs boson that can couple anomalously to photons [491].

(b) Searches at the Tevatron and LHC

The best sensitivity is in the regime with low to moderate m_A and with large $\tan\beta$ which enhances the couplings of the Higgs bosons to down-type fermions. The corresponding limits on the Higgs boson production cross section times the branching ratio of the Higgs boson into down-type fermions can be interpreted in MSSM benchmark scenarios [316]. If $\phi = A, H$ for $m_A > m_h^{\max}$, and $\phi = A, h$ for $m_A < m_h^{\max}$, the most promising channels at the Tevatron are the inclusive $p\bar{p} \to \phi \to \tau^+\tau^-$ process, with contributions from both $gg \to \phi$ and $b\bar{b}\phi$ production, and $b\bar{b}\phi, \phi \to \tau^+\tau^-$ or $\phi \to b\bar{b}$, with $b\tau\tau$ or three tagged b-jets in the final state, respectively. Although Higgs boson production via gluon fusion has a higher cross section in general than via associated production, it cannot be used to study the $\phi \to b\bar{b}$ decay mode since the signal is overwhelmed by the QCD background.

The CDF and D0 collaborations have searched for neutral Higgs bosons produced in association with bottom quarks and which decay into $b\bar{b}$ [457, 458], or into $\tau^+\tau^-$ [449,450]. The most recent searches in the $b\bar{b}\phi$ channel with $\phi \to b\bar{b}$ analyze approximately $2.6\,\text{fb}^{-1}$ of data (CDF) and $5.2\,\text{fb}^{-1}$ (D0), seeking events with at least three b-tagged jets. The cross section is defined such that at least one b quark not from ϕ decay is required to have $p_T > 20\,\text{GeV}$ and $|\eta| < 5$. The invariant mass of the two leading jets as well as b-tagging variables are used to discriminate the signal from the backgrounds. The QCD background rates and shapes are inferred from data control samples, in particular, the sample with two b-tagged jets and a third, untagged jet. Separate-signal hypotheses are tested and limits are placed on $\sigma(p\bar{p} \to b\bar{b}\phi) \times \text{BR}(\phi \to b\bar{b})$. A local excess of approximately 2.5σ significance has been observed in the mass range of 130–160 GeV, but D0's search is more sensitive and sets stronger limits. The D0 result had an $\mathcal{O}(2\sigma)$ local upward fluctuation in the 110 to 125 GeV mass range. These results have been superseded by the LHC searches and the excess seen in the D0 experiment has not been confirmed elsewhere.

A substantially larger sensitivity in the search for the $\phi \to \tau^+\tau^-$ is obtained with the ATLAS and CMS analyses. The higher centre-of-mass energy reached at the Run 2 brings a substantial though not excessively large increase in sensitivity due to the intermediate masses probed. Both the ATLAS and CMS collaborations have reported the result of their searches in this important channel with the full 2016 dataset. The searches are performed in categories of the decays of the two tau leptons: $e\tau_{\text{had}}$, $\mu\tau_{\text{had}}$, $e\mu$, and $\mu\mu$, where τ_{had} denotes a tau lepton which decays to one or more hadrons plus a tau neutrino, e denotes $\tau \to e\nu\nu$, and μ denotes $\tau \to \mu\nu\nu$. The dominant background comes from $Z \to \tau^+\tau^-$ decays, although $t\bar{t}$, W+jets and Z+jets events contribute as well. Separating events into categories based on the number of b-tagged jets improves the sensitivity in the MSSM. The $b\bar{b}$ annihilation process and radiation of a Higgs boson from a b quark gives rise to events in which the Higgs boson is accompanied by a $b\bar{b}$ pair in the final state. Requiring the presence of one or more b jets reduces the background from Z+jets. Data control samples are

used to constrain background rates. The rates for jets to be identified as a hadronically decaying tau lepton are measured in dijet samples, and W+jets samples provide a measurement of the rate of events that, with a fake hadronic tau, can pass the signal selection requirements. Lepton fake rates are measured using samples of isolated lepton candidates and same-sign lepton candidates. Constraints from the CMS searches for $h \to \tau^+\tau^-$ and $h \to b\bar{b}$ are shown in Fig. 11.16 in the m_h-mod+ scenario defined in Ref. [321] and in the hMSSM approximation defined in Ref. [322]. The neutral Higgs boson searches consider the contributions of both the CP-odd and CP-even neutral Higgs bosons with enhanced couplings to bottom quarks, similarly as it was done for the Tevatron results. In Fig. 11.16, decays of the charged Higgs into $\tau\nu$ and of the heavy Higgs H decaying into a pair of SM-like Higgs bosons or gauge bosons, or of A decaying into hZ are also being constrained. In addition, decays of the neutral Higgs bosons into muon pairs are also being explored. Observe that in the $m_h$mod+ scenario the region of $\tan\beta$ lower than 5 does not allow for a Higgs mass m_h close to 125 GeV, as shown in the figure. For the hMSSM scenario, instead, the SM-like Higgs mass is fixed as an input and hence the requirement that it is close to 125 GeV is always fulfilled, although this may imply other limitations as discussed in section VII.1.1.

A search for $\phi \to \mu^+\mu^-$ has also been performed by the ATLAS collaboration [452].

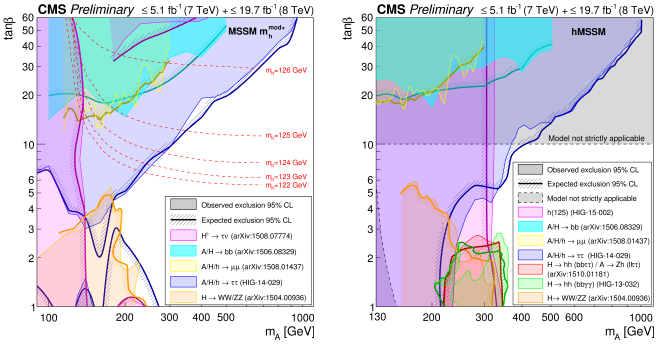

Figure 11.16: The 95% CL exclusion contours in the $(M_A, \tan\beta)$ parameter space for the hMSSM scenario (right panel) and for the m_h-mod+ scenario (left panel), for several search channels [494].

Finally searches for a resonance decaying to a top quark pair were done by ATLAS [495, 453] and CMS [496]. These searches were interpreted as searches for scalar resonances by ATLAS [495], however an important component of these searches is an accurate treatment of the interference effects between the signal and the continuum background. These can yield a dip and peak structure instead of a simple peak [373, 320]. The ATLAS Collaboration has performed a search for a high mass state decaying to a pair of top quarks taking into account the deformation in mass shape of the signal in the presence of the continuum background [454].

The LHC has the potential to explore a broad range of SUSY parameter space through the search for non-SM-like Higgs bosons. Nevertheless, Fig. 11.16 shows a broad region with intermediate $tan\beta$ and large values of m_A that is not accessed by current searches, and in which the most promising channel is the very difficult search for $t\bar{t}$ decays with its aforementioned intricacies. In this region of parameter space it is possible that only the SM-like Higgs boson can be within the LHC's reach. If no other state of the EWSB sector than H is discovered, it may be challenging to determine only from the Higgs sector whether there is a supersymmetric extension of the SM in nature.

(iii) Searches for a CP-odd state decaying to hZ

Similarly to the search for a CP-even high mass Higgs boson decaying to a pair of Higgs bosons, the search for a CP-odd states decaying hZ was carried out at the LHC by the ATLAS and CMS collaborations in various channels: (i) the $(Z \to \ell\ell)(h \to b\bar{b})$, (ii) the $(Z \to \nu\nu)(h \to b\bar{b})$, (iii) the $(Z \to \ell\ell)(h \to \tau\tau)$, (iv) and the $(Z \to \ell\ell)(h \to \tau\tau)$, final states. The searches where the A boson decays to a pair of b quarks have been performed both in the regime where both b-jets are resolved and in the boosted regime where the two b-jets are merged in a single larger radius jet. These searches have been used to constrain the parameter space of 2HDMs. In the MSSM these searches place limits on small values of $tan\beta$ for masses of A comprised between 220 GeV and 360 GeV as illustrated in Fig. 11.16.

(iv) Searches low mass states

Searches for pseudoscalar Higgs bosons at intermediate to low masses, below the Z mass (in the 25 GeV to 80 GeV mass range) have been performed by the CMS collaboration both in the $\tau^+\tau^-$ [497] and the $\mu^+\mu^-$ [498] decay channels. A light pseudoscalar in this mass range is excluded by current direct constraints in the MSSM but not in general 2HDMs [499]. These searches are done in the decay channels where the pseudoscalar Higgs boson decays to a pair of taus or muons and is produced in association with a pair of b-quarks.

Searches for low mass Higgs bosons were also performed in the diphoton channel by both the ATLAS and CMS collaborations [500, 501] and Run 1. The CMS collaboration has updated the results of this search with the full 2016 dataset [502]. A modest excess has been observed by the CMS collaboration at a mass of 95.3 GeV and a local significance of 2.8σ (the corresponding global significance is 1.3σ). An slight excess was also seen by CMS in the 8 TeV data at a slightly higher mass of 97.6 GeV with a local significance of 2.0σ (1.47σ global). No significant excess has been observed in this region with the ATLAS experiment and the Run 1 data only.

(v) Searches for charged Higgs bosons $H^\pm$

At e^+e^- colliders charged Higgs bosons can be pair produced in the s-channel via γ or Z boson exchange. This process is dominant in the LEP centre-of-mass energies range *i.e.* up to 209 GeV. At higher centre-of-mass energies, other processes can play an important role such as the production in top quark decays via $t \to b + H^+$ if $m_{H^\pm} < m_t - m_b$ or via the one-loop process $e^+e^- \to W^\pm H^\mp$ [503, 504], which allows the production of a charged Higgs boson with $m_{H^\pm} > \sqrt{s}/2$, even when H^+H^- production is kinematically forbidden. Other single charged Higgs production mechanisms include $t\bar{b}H^-/\,\bar{t}bH^+$ production [104], $\tau^+\nu H^-/\,\tau^-\bar{\nu}H^+$ production [505], and a variety of processes in which $H^\pm$ is produced in association with a one or two other gauge and/or Higgs bosons [506].

At hadron colliders, charged Higgs bosons can be produced in several different modes. If $m_{H^\pm} < m_t - m_b$, the charged Higgs boson can be produced in decays of the top quark via the decay $t \to bH^\pm$. Relevant QCD and SUSY-QCD corrections to BR$(t \to H^\pm b)$ have been computed [507–510]. For values of $m_{H^\pm}$ near m_t, width effects are important. In addition, the full $2 \to 3$ processes $pp/p\bar{p} \to H^+\bar{t}b+X$ and $pp/p\bar{p} \to H^-t\bar{b} + X$ must be considered. If $m_{H^\pm} > m_t - m_b$, then charged Higgs boson production occurs mainly through radiation from a third generation quark. Charged Higgs bosons may also be produced singly in association with a top quark via the $2 \to 3$ partonic processes gg, $q\bar{q} \to t\bar{b}H^-$. For charged Higgs boson production cross section predictions for the Tevatron and the LHC, see Refs. [11, 42, 41]. Charged Higgs bosons can also be produced via associated production with $W^\pm$ bosons through $b\bar{b}$ annihilation and gg-fusion [511] and in pairs via $q\bar{q}$ annihilation [512].

(a) Exclusion limits from LEP

Charged Higgs bosons have been searched for at LEP, where the combined data of the four experiments, ALEPH, DELPHI, L3, and OPAL, were sensitive to masses of up to about 90 GeV [490] in two decay channels, the $\tau\nu$ and $c\bar{s}$. The exclusion limit independent of the admixture of the two above mentioned branching fractions was 78.6 GeV.

(b) Exclusion limits from Tevatron

Compared to the mass domain covered by LEP searches, the Tevatron covered a complementary range of charged Higgs masses. The CDF and D0 collaborations have also searched for charged Higgs

bosons in top quark decays with subsequent decays to $\tau\nu$ or to $c\bar{s}$ [513–515]. For the $H^+ \to c\bar{s}$ channel, the limits on BR($t \to H^+b$) from CDF and D0 are $\approx 20\%$ in the mass range $90\,\text{GeV} < m_{H^+} < 160\,\text{GeV}$ and assuming a branching fraction of 100% in this specific final state. $H^+ \to \tau^+\nu_\tau$ channel, D0's limits on BR($t \to H^+b$) are also $\approx 20\%$ in the same mass range and assuming a branching fraction of 100% in this final state. These limits are valid in general 2HDMs, and they have also been interpreted in terms of the MSSM [513–515].

(c) Exclusion limits from LHC

Similarly to the Tevatron, at the LHC light charged Higgs bosons can be searched for in the decays of top quarks. The main initial production mode for light charged Higgs bosons ($m_{H^\pm} < m_t - m_b$) is top pair production. The subsequent decay modes of the charged Higgs boson for these searches are $\tau\nu$ and $c\bar{s}$. More recently ATLAS and CMS have also searched for higher mass charged Higgs bosons ($m_{H^\pm} > m_t + m_b$) in $H^+ \to t\bar{b}$. The main production modes are the associated production of a charged Higgs boson in association with a top and a bottom quark or in association with a top quark only.

The decay $H^+ \to \tau^+\nu_\tau$ is searched typically in three final state topologies: (i) lepton+jets: with $t\bar{t} \to \bar{b}WH^+ \to b\bar{b}(q\bar{q}')(\tau_{\text{lep}}\nu)$, i.e., the W boson decays hadronically and the tau decays into an electron or a muon, with two neutrinos; (ii) τ +lepton: with $t\bar{t} \to \bar{b}WH^+ \to b\bar{b}(l\nu)(\tau_{\text{had}}\nu)$ i.e., the W boson decays leptonically (with $\ell = e,\ \mu$) and the tau decays hadronically; (iii) τ+jets: $t\bar{t} \to \bar{b}WH^+ \to b\bar{b}(q\bar{q}')(\tau_{\text{had}}\nu)$, *i.e.*, both the W boson and the τ decay hadronically.

The CMS collaboration has also searched for the charged Higgs boson in the decay products of top quark pairs: $t\bar{t} \to H^\pm W^\mp b\bar{b}$ and $t\bar{t} \to H^+H^-b\bar{b}$ as well. Three types of final states with large missing transverse energy and jets originating from b-quark hadronization have been analyzed: the fully-hadronic channel with a hadronically decaying tau in association with jets, the dilepton channel with a hadronically decaying tau in association with an electron or muon and the dilepton channel with an electron-muon pair. Combining the results of these three analyses and assuming BR($H^\pm \to \tau\nu$)=1, the upper limits on BR($t \to H^+b$) are less than 2% to 3% depending on the charged Higgs boson mass in the interval $80\,\text{GeV} < m_{H^+} < 160\,\text{GeV}$.

Both the ATLAS and CMS collaborations have also searched for high mass charged Higgs bosons decaying to a top and bottom quarks. The main production mode for this search is the associated production with one top quark (5-flavor scheme) or a top quark and and bottom quark (4-flavor scheme) in the final state. The s-channel production mode where the charged Higgs boson is produced alone in the final state at tree level is also considered. This search is particularly intricate and it is sensitive to the modeling of the top pair production background produced in association with additional partons and in particular b-quarks. No excess was found and the results are expressed in terms of exclusion limits of cross section times branching fractions.

ATLAS and CMS have also searched for charged Higgs bosons in top quark decays assuming BR($H^+ \to c\bar{s}$) = 100% [463, 464], and sets limits of $\approx 20\%$ on BR($t \to H^+b$) in the $90\,\text{GeV} < m_{H^+} < 160\,\text{GeV}$ mass range.

In two Higgs doublet models the decay of the charged Higgs boson to a W- and a Z-boson is allowed only at loop level and is therefore suppressed. However the $H^\pm \to W^\pm Z$ decay channel is allowed in Higgs triplet models. The ATLAS collaboration [467] has searched for such decays, requiring that the charged Higgs boson is produced through the fusion of vector bosons. No excess with respect to the SM backgrounds has been observed in this channel, and the results are interpreted in the Georgi–Machacek model [376–379] discussed in Section VII.5.2.

At the LHC various other channels still remain to be explored, in particular searches involving additional neutral scalars in particular in WH, WA where A is the pseudo scalar MSSM Higgs boson, and Wa where a is the light CP-odd scalars of the NMSSM.

(vi) Searches for a light CP-odd Higgs boson a

A light pseudoscalar boson a is present in any two Higgs doublet mode enhanced with an additional singlet field. A prominent example is the NMSSM. The theoretical motivations for singlet extensions of the MSSM are discussed in Section VII.2. In the NMSSM, the searches now focus on the low mass pseudo-scalar boson a region for several reasons: (i) in the NMSSM, the light pseudo-scalar a boson can, as a pseudo-Goldstone boson, be a natural candidate for an axion; (ii) scenarios where $m_a > 2m_b$ and a CP-even state h decaying to a pair of a ($m_h > 2m_a$) are excluded by direct searches at LEP in the four b channel [490, 520, 476]; (iii) in the pre-discovery era, LEP limits on a CP-even Higgs boson resulted in fine tuning MSSM constraints [521] which could be evaded through non standard decays of the Higgs to aa; (iv) an NMSSM CP-odd a boson with a mass in the range 9.2–12 GeV can also account for the difference observed between the measured anomalous muon magnetic moment and its prediction [522]. A scenario that has drawn particular attention was motivated by a small excess of events 2.3σ in the SM Higgs search at LEP at Higgs boson mass of around 98 GeV. Speculative interpretations of this excess as a signal of a Higgs boson with reduced couplings to b-quarks were given [521]. Complete reviews of the NMSSM phenomenology can be found in Refs. [523, 476].

The potential benchmark scenarios have changed in the light of the Higgs boson discovery. The discovered state could be the lightest or the next-to-lightest of the three CP-even states of the NMSSM. Light pseudoscalar scenarios are still very interesting in particular for the potential axion candidate. There are three main types of direct searches for the light a boson: (i) for masses below the Υ resonance, the search is for radiative decays $\Upsilon \to a\gamma$ at B-factories; (ii) the inclusive search for in high energy pp collisions at the LHC; (iii) the search for decays of a CP-even Higgs h boson to a pair of a bosons.

Radiative decays $\Upsilon \to a\gamma$, have been searched for in various colliders, the most recent results are searches for radiative decays of the $\Upsilon(1s)$ to $a\gamma$ with a subsequent decay of the a boson to a pair of taus at CLEO [524] and the radiative decays of the $\Upsilon(1s, 2s, 3s)$ to $a\gamma$ with subsequent decays to a pair of muons or taus by the BaBar collaboration [478, 479].

Direct inclusive searches for the light pseudo scalar a boson were performed in the $a \to \mu\mu$ channel at the Tevatron by the D0 experiment [525] and by the ATLAS [470] and CMS [526] collaborations at the LHC.

Finally searches for the decays of the Higgs boson to a pair of a bosons where performed with subsequent decays to four photons, in the four muons final state, in the two muons and two taus final state, and in the four taus final state.

No significant excess in the searches for a light CP-odd a boson were found and limits on the production times branching fractions of the a boson have been set.

References for these searches are summarized in Table 11.17.

(vii) Searches for doubly charged Higgs bosons $H^{\pm\pm}$

As discussed in Section VII.5, the generation of small neutrino masses via the standard EWSB mechanism described in Section II requires unnaturally small Yukawa couplings, provided that neutrinos are Dirac-type fermions. A Majorana mass term with a see-saw mechanism for neutrinos, would allow for naturally small masses and yield a framework for the appealing scenario of leptogenesis. However within the SM Majorana mass terms correspond to (non-renomalizable) dimension-5 operators. Such effective interactions can be generated via renormalizable interactions with an electroweak triplet of complex scalar fields (corresponding to a type-II see-saw mechanism). Other models such as the Zee–Babu model, with the introduction of two $\text{SU}(2)_L$ singlets, also generate Majorana mass terms. The signature of such models would be the presence of doubly charged Higgs bosons $H^{\pm\pm}$.

The main production mechanisms of $H^{\pm\pm}$ bosons at hadron colliders are the pair production in the s-channel through the exchange of a Z boson or a photon and the associated production with a charged Higgs boson through the exchange of a W boson. Various searches for doubly charged Higgs bosons have been performed by ATLAS and CMS at Run 1 [528, 529] and Run 2 [480–482].

VII.7.1. Searches for non-standard production processes of the Higgs boson

The discovery of the Higgs boson has also allowed for searches of BSM (beyond the SM) processes involving standard decays of the Higgs boson. One example directly pertaining to the search for additional states of the EWSB sector is the search for Higgs bosons in the cascade decay of a heavy CP-even Higgs boson decaying to charged Higgs boson and a W boson, and the charged Higgs boson subsequently decaying to H and another W boson. This search has been performed by the ATLAS collaboration in $b\overline{b}$ decays of the H particle [530].

VII.7.2. Outlook of searches for additional states

The LHC program of searches for additional states covers a large variety of decay and production channels. Since the last review on the *Status of Higgs boson physics* [281] many new channels have been explored at the LHC, *e.g.* the searches for additional states decaying into hh or Zh. The search for charged Higgs bosons has been extended to include the WZ and the very difficult $t\overline{b}$ decay channel. There are however more channels to cover, *e.g.* the search for charged Higgs bosons in the HW and AW channels.

VIII. Summary and outlook

Summary– The discovery of the Higgs boson is an important milestone in the history of particle physics as well as an extraordinary achievement of the LHC machine and the ATLAS and CMS experiments. Five years after its discovery, substantial progress in the field of Higgs boson physics has been accomplished and a significant number of measurements probing its nature have been made. They are revealing an increasingly precise profile of the Higgs boson.

Since the last edition of this review [233], the LHC has delivered in Run 2 a dataset corresponding to an integrated luminosity of more than $40\,\text{fb}^{-1}$ of 13 TeV pp collisions. After data quality requirements, this leaves about $36\,\text{fb}^{-1}$ of data collected by fully operational ATLAS and CMS detectors. Due to the substantial increase in production rates at the higher center-of-mass energy, many of Run 1 results have been updated. Milestone measurements have been performed: (i) a clear observation of the Higgs boson decay to taus has been made by the CMS experiment; (ii) unambiguous evidence for the Higgs boson decay to a pair of b quarks was provided by both the ATLAS and CMS experiments; (iii) the ATLAS and CMS experiments have also provided evidence for the production of the Higgs boson through the $t\bar{t}H$ mechanism, thus yielding direct evidence for the Yukawa coupling of the Higgs boson to top quarks, with a strength compatible with that of the Standard Model. These and all other experimental measurements are consistent with the EWSB mechanism of the Standard Model.

New theoretical calculations and developments in Monte Carlo simulation pertaining to Higgs physics are still occurring at a rapid pace. For example, the theoretical prediction for the dominant gluon fusion production mode now includes the latest N3LO result, which is twice as precise as previous N2LO calculations. With these improvements in the state-of-the-art in theory predictions and the increase in luminosity and center-of-mass energy, Higgs physics has definitively entered a precision era.

Since the discovery of the Higgs boson, new ideas have emerged to probe its rare decays and production modes, as well as indirectly measure the Higgs boson width through the study of its off-shell couplings, or via on-shell interference effects. The Higgs boson has now become part of the standard toolkit in searches for new physics.

Many extensions of the SM at higher energies call for an enlargement of the EWSB sector. Hence, direct searches for additional scalar states can provide valuable insights on the dynamics of the EWSB mechanism. The ATLAS and CMS experiments have searched for additional Higgs bosons in the Run 2 data, and imposed constraints in broad ranges of mass and couplings for various extended Higgs scenarios.

The landscape of Higgs physics has been extended extraordinarily since the discovery. In addition, Run 2 is still ongoing and after its completion the amount of data collected is expected to increase three-fold. The current dataset is approximately one percent of the total dataset foreseen for the High Luminosity phase of the LHC project. This perspective brings new challenges to increase further the reach in precision and it also widens the possibilities of unveiling the nature of the electroweak symmetry breaking.

Outlook– The unitarization of the vector boson scattering (VBS) amplitudes, dominated at high energies by their longitudinal polarizations, has been the basis of the *no lose* theorem at the LHC, and was a determining consideration in the building of the accelerator and the detectors. It motivated the existence of a Higgs boson or the observability of manifestations of strong dynamics at TeV scale. Now that a Higgs boson has been found and its couplings to gauge bosons are consistent with the SM predictions, perturbative unitarity is preserved to a large amount with the sole exchange of the Higgs boson, and without the need for any additional states. VBS is, however, still an important channel to investigate further in order to better understand the nature of the Higgs sector and the possible completion of the SM at the TeV scale. In association with the double Higgs boson production channel by vector boson fusion, VBS could, for instance, confirm that the Higgs boson is part of a weak doublet and also establish whether it is an elementary object or a composite state that could emerge as a pseudo-Nambu–Goldstone boson from a new underlying broken symmetry.

The Higgs boson couplings are not dictated by any local gauge symmetry. Thus, in addition to a new particle, the LHC has also discovered a new force, different in nature from the other fundamental interactions since it is non-universal and distinguishes between the three families of quarks and leptons. The existence of the Higgs boson embodies the problem of an unnatural cancellation among the quantum corrections to its mass if new physics is present at scale significantly higher than the EW scale. The non-observation of additional states which could stabilize the Higgs boson mass is a challenge for natural scenarios like supersymmetry or models with a new strong interaction in which the Higgs boson is not a fundamental particle. This increasingly pressing paradox starts questioning the principle of naturalness.

The search for the Higgs boson has occupied the particle physics community for the last 50 years. Its discovery has shaped and sharpened the physics programs of the LHC and of prospective future accelerators. The experimental data together with the progress in theory mark the beginning of a new era of precision Higgs boson measurements.

Acknowledgements

We would like to thank many of our colleagues for proofreading this review, for useful criticism and their input in general: W. Altmannshofer, G. Branco, J. Campbell, F. Cerutti, C. Csáki, R. Contino, J. Conway, N. Craig, A. David, J.B. De Vivie, J.R. Espinosa, A. Falkowski, W. Fischer, S. Forte, M. Grazzini, H. Haber, S. Heinemeyer, J. Hubisz, A. Korytov, B. Jäger, H. Ji, T. Junk, P. Langacker, J. Lykken, F. Maltoni, B. Mansoulié R. Mishra, M. Mühlleitner, B. Murray, M. Neubert, G. Perez, G. Petrucciani, A. Pomarol, E. Pontón, D. Rebuzzi, E. Salvioni, N. Shah, G. Shaughnessy, M. Spira, O. Stål, A. Strumia, K. Tackmann, R. Tanaka, J. Terning, A. Vartak, C. Wagner, and A. Weiler. We are also most grateful to the ATLAS, CDF, CMS and D0 collaborations for their help with this review.

M.C. is supported by Fermilab, that is operated by Fermi Research Alliance, LLC under Contract No. DE–AC02–07CH11359 with the United States Department of Energy. C.G. is supported by the European Commission through the Marie Curie Career Integration Grant 631962, by the Helmholtz Association and by the Collaborative Research Center SFB676 of the Deutsche Forschungsgemeinschaft (DFG), Particles, Strings and the Early Universe. M.K. is supported by the ANR HiggsNet grant. V.S. is supported by the grant DE–SC0009919 of the United States Department of Energy.

References

1. G. Aad *et al.* [ATLAS Collab.], Phys. Lett. **B716**, 1 (2012).
2. S. Chatrchyan *et al.* [CMS Collab.], Phys. Lett. **B716**, 30 (2012).
3. S.L. Glashow, Nucl. Phys. **20**, 579 (1961);
S. Weinberg, Phys. Rev. Lett. **19**, 1264 (1967);
A. Salam, *Elementary Particle Theory*, eds.: Svartholm, Almquist and Wiksells, Stockholm, 1968;
S. Glashow, J. Iliopoulos, and L. Maiani, Phys. Rev. **D2**, 1285 (1970).
4. F. Englert and R. Brout, Phys. Rev. Lett. **13**, 321 (1964);
P.W. Higgs, Phys. Rev. Lett. **13**, 508 (1964) and Phys. Rev. **145**, 1156 (1966);
G.S. Guralnik, C.R. Hagen, and T.W. Kibble, Phys. Rev. Lett. **13**, 585 (1964).
5. J.M. Cornwall, D.N. Levin, and G. Tiktopoulos, Phys. Rev. Lett. **30**, 1286 (1973) and Phys. Rev. **D10**, 1145 (1974);
C.H. Llewellyn Smith, Phys. Lett. **B46**, 233 (1973).
6. B.W. Lee, C. Quigg, and H.B. Thacker, Phys. Rev. **D16**, 1519 (1977).
7. K. Wilson, Phys. Rev. D 3,1818(1971);
G. 't Hooft, in *Proc. of 1979 Cargèse Institute on Recent Developments in Gauge Theories,* p. 135 Press, New York 1980;
For a recent review, see G.F. Giudice, PoS EPS **-HEP2013**, 163 (2013).
8. J. Parsons, and A. Pomarol, *Extra Dimenions*, in this volume.
9. J. Wess and B. Zumino, Nucl. Phys. **B70**, 39 (1974) and Phys. Lett. **49B**, 52 (1974);
H.P. Nilles, Phys. Rev. **C110**, 1 (1984);
S.P. Martin, `arXiv:hep-ph/9709356` (1997);
P. Fayet, Phys. Lett. **B69**, 489 (1977), Phys. Lett. **B84**, 421 (1979), Phys. Lett. **B86**, 272 (1979) and Nucl. Phys. **B101**, 81 (2001).
10. E. Witten, Nucl. Phys. **B188**, 513 (1981);
R.K. Kaul, Phys. Lett. **B109**, 19 (1982) and Pramana **19**, 183 (1982);
L. Susskind, Phys. Rev. **104**, 181 (1984).
11. H.E. Haber and G.L. Kane, Phys. Rev. **C117**, 75 (1985).
12. J. F. Gunion *et al.*, *The Higgs Hunter's Guide*, Addison-Wesley (1990).
13. S. Weinberg, Phys. Rev. **D13**, 974 (1979) and Phys. Rev. **D19**, 1277 (1979);
L. Susskind, Phys. Rev. **D20**, 2619 (1979);
for a review, see C.T. Hill and E.H. Simmons, Phys. Reports **381**, 235 (2003) [E: **390**, 553 (2004)].
14. D. B. Kaplan and H. Georgi, Phys. Lett. **B136**, 183 (1984).
15. G. Panico and A. Wulzer, Lect. Notes Phys. **913**, 1 (2016).
16. C. Csaki, C. Grojean and J. Terning, Rev. Mod. Phys. **88**, 045001 (2016).
17. C. Csaki *et al.*, Phys. Rev. **D62**, 045015 (2000);
for other references, see the 2014 edition of this review.
18. W. D. Goldberger, B. Grinstein, and W. Skiba, Phys. Rev. Lett. **100**, 111802 (2008);
J. Fan *et al.*, Phys. Rev. **D79**, 035017 (2009);
B. Bellazzini *et al.*, Eur. Phys. J. **C73**, 2333 (2013);
Z. Chacko and R.K. Mishra, Phys. Rev. **D87**, 115006 (2013);
Z. Chacko, R. Franceschini, and R.K. Mishra, JHEP **1304**, 015 (2013).
19. Z. Chacko, H.S. Goh and R. Harnik, Phys. Rev. Lett. **96**, 231802 (2006) and JHEP **0601**, 108 (2006).
20. N. Craig, A. Katz, M. Strassler and R. Sundrum, JHEP **1507**, 105 (2015);
N. Craig, S. Knapen and P. Longhi, Phys. Rev. Lett. **114**, 061803 (2015).
21. P.W. Graham, D. E. Kaplan and S. Rajendran, Phys. Rev. Lett. **115**, 221801 (2015);
J.R. Espinosa *et al.*, Phys. Rev. Lett. **115**, 251803 (2015).
22. T. van Ritbergen and R.G. Stuart, Phys. Rev. Lett. **82**, 488 (1999) and Nucl. Phys. **B564**, 343 (2000);
M. Steinhauser and T. Seidensticker, Phys. Lett. **B467**, 271 (1999);
D.M. Webber *et al.* [MuLan Collab.], Phys. Rev. Lett. **106**, 041803 (2011).
23. J. Ellis, M.K. Gaillard, and D.V. Nanopoulos, Nucl. Phys. **B106**, 292 (1976).
24. M.A. Shifman *et al.*, Sov. J. Nucl. Phys. **30**, 711 (1979) [Yad. Fiz. **30**, 1368 (1979)].
25. P. Sikivie *et al.*, Nucl. Phys. **B173**, 189 (1980);
H. Georgi, Ann. Rev. Nucl. and Part. Sci. **43**, 209 (1993).
26. M.J.G. Veltman, Nucl. Phys. **B123**, 89 (1977).
27. I.V. Krive and A.D. Linde, Nucl. Phys. **B117**, 265 (1976);
for other references, see the 2014 edition of this review.
28. J.R. Espinosa and M. Quiros, Phys. Lett. **B353**, 257 (1995);
G. Isidori, G. Ridolfi, and A. Strumia, Nucl. Phys. **B609**, 387 (2001).
29. V. Branchina, E. Messina and M. Sher, Phys. Rev. **D91**, 013003 (2015).
30. A. Hook *et al.*, JHEP **1501**, 061 (2015);
J. Kearney, H. Yoo and K.M. Zurek, Phys. Rev. **D91**, 123537 (2015).
31. A. Andreassen, W. Frost and M. D. Schwartz, arXiv:1707.08124 [hep-ph].;
S. Chigusa, T. Moroi and Y. Shoji, arXiv:1707.09301 [hep-ph]..
32. J. Elias-Miro *et al.*, Phys. Lett. **B709**, 222 (2012);
G. Degrassi *et al.*, JHEP **1208**, 098 (2012);
D. Buttazzo *et al.*, JHEP **1312**, 089 (2013);
J.R. Espinosa *et al.*, JHEP **1509**, 174 (2015).
33. C.D. Froggatt and H.B. Nielsen, Phys. Lett. **B368**, 96 (1996);
M. Shaposhnikov and C. Wetterich, Phys. Lett. **B683**, 196 (2010);
M. Holthausen, K.S. Lim, and M. Lindner, JHEP **1202**, 037 (2012).
34. F.L. Bezrukov and M. Shaposhnikov, Phys. Lett. **B659**, 703 (2008);
F.L. Bezrukov, A. Magnin, and M. Shaposhnikov, Phys. Lett. **B675**, 88 (2009).
35. A. Salvio, Phys. Lett. **B727**, 234 (2013).
36. B.A. Kniehl, Phys. Reports **240**, 211 (1994).
37. M. Spira, Fortsch. Phys. **46**, 203 (1998).
38. M. Carena and H.E. Haber, Prog. in Part. Nucl. Phys. **50**, 152 (2003).
39. A. Djouadi, Phys. Reports **457**, 1 (2008).
40. S. Dittmaier *et al.*, [LHC Higgs Cross Section Working Group], CERN–2011–002, `arXiv:1101.0593 [hep-ph]` (2011).
41. S. Dittmaier *et al.*, [LHC Higgs Cross Section Working Group], CERN–2012–002, `arXiv:1201.3084 [hep-ph]` (2012).
42. S. Heinemeyer *et al.*, [LHC Higgs Cross Section Working Group], CERN–2013–004, `arXiv:1307.1347 [hep-ph]` (2013).
43. D. de Florian *et al.*, [LHC Higgs Cross Section Working Group], CERN–2017–002-M, `arXiv:1610.07922[hep-ph]` (2016).
44. LHC Higgs Cross Section Working Group, `twiki.cern.ch/twiki/bin/view/LHCPhysics/LHCHXSWG`.
45. T. Aaltonen *et al.* [CDF and D0 Collaborations], Phys. Rev. **D88**, 052014 (2013).
46. H.M. Georgi *et al.*, Phys. Rev. Lett. **40**, 692 (1978).
47. D. Graudenz, M. Spira, and P.M. Zerwas, Phys. Rev. Lett. **70**, 1372 (1993).
48. M. Spira *et al.*, Nucl. Phys. **B453**, 17 (1995).
49. S. Dawson, Nucl. Phys. **B359**, 283 (1991);
A. Djouadi, M. Spira, and P.M. Zerwas, Phys. Lett. **B264**, 440 (1991).
50. R.V. Harlander and W.B. Kilgore, Phys. Rev. Lett. **88**, 201801 (2002);
C. Anastasiou and K. Melnikov, Nucl. Phys. **B646**, 220 (2002);
V. Ravindran, J. Smith, and W.L. van Neerven, Nucl. Phys. **B665**, 325 (2003).
51. C. Anastasiou *et al.*, Phys. Rev. Lett. **114**, 212001 (2015);
C. Anastasiou *et al.*, JHEP **1605**, 058 (2016).
52. R.V. Harlander and K.J. Ozeren, JHEP **0911**, 088 (2009);
A. Pak, M. Rogal, and M. Steinhauser, JHEP **1002**, 025 (2010).

53. A. Djouadi and P. Gambino, Phys. Rev. Lett. **73**, 2528 (1994); S. Actis *et al.*, Phys. Lett. **B670**, 12 (2008); U. Aglietti *et al.*, Phys. Lett. **B595**, 432 (2004); G. Degrassi and F. Maltoni, Phys. Lett. **B600**, 255 (2004).
54. C. Anastasiou, R. Boughezal, and F. Petriello, JHEP **0904**, 003 (2009).
55. S. Catani *et al.*, JHEP **0307**, 028 (2003); S. Moch and A. Vogt, Phys. Lett. **B631**, 48 (2005); E. Laenen and L. Magnea, Phys. Lett. **B632**, 270 (2006); A. Idilbi *et al.*, Phys. Rev. **D73**, 077501 (2006); V. Ravindran, Nucl. Phys. **B752**, 173 (2006); V. Ahrens *et al.*, Eur. Phys. J. **C62**, 333 (2009).
56. V. Ahrens *et al.*, Phys. Lett. **B698**, 271 (2011); D. de Florian and M. Grazzini, Phys. Lett. **B718**, 117 (2012); C. Anastasiou *et al.*, JHEP **1204**, 004 (2012).
57. M. Bonvini *et al.*, JHEP **1608**, 105 (2016).
58. J.C. Collins, D.E. Soper and G.F. Sterman, Nucl. Phys. **B250**, 199 (1985).
59. D. de Florian *et al.*, JHEP **1111**, 064 (2011); T. Becher and M. Neubert, Eur. Phys. J. **C71**, 1665 (2011); J.Y. Chiu *et al.*, JHEP **1205**, 084 (2012); J. Wang *et al.*, Phys. Rev. **D86**, 094026 (2012); T. Becher, M. Neubert and D. Wilhelm, JHEP **1305**, 110 (2013).
60. S. Catani and M. Grazzini, Eur. Phys. J. **C72**, 2013 (2012) [E: **C72**, 2132 (2012)].
61. W.Y. Keung and F.J. Petriello, Phys. Rev. **D80**, 01007 (2009); S. Buhler *et al.*, JHEP **1207**, 115 (2012).
62. R. Frederix, S. Frixione, E. Vryonidou and M. Wiesemann, JHEP **1608**, 006 (2016);; F. Caola, S. Forte, S. Marzani, C. Muselli and G. Vita, JHEP **1608**, 50 (2016);; N. Greiner, S. Höche, G. Luisoni, M. Schönherr and J. C. Winter JHEP **1701**, 091 (2017).
63. R.V. Harlander, T. Neumann, K.J. Ozeren and M. Wiesemann, JHEP **1208**, 139 (2012); T. Neumann and M. Wiesemann, JHEP **1411**, 150 (2014).
64. R.V. Harlander, S. Liebler, and H. Mantler, Comp. Phys. Comm. **184**, 1605 (2013).
65. D. de Florian, M. Grazzini, and Z. Kunszt, Phys. Rev. Lett. **82**, 5209 (1999); C.J. Glosser and C. R. Schmidt, JHEP **0212**, 016 (2002); V. Ravindran, J. Smith and W. L. Van Neerven, Nucl. Phys. **B634**, 247 (2002); X. Liu and F. Petriello, Phys. Rev. **D87**, 014018 (2013).
66. J.M. Campbell, R.K. Ellis, and G. Zanderighi, JHEP **0610**, 028 (2006); J.M. Campbell, R.K. Ellis, and C. Williams, Phys. Rev. **D81**, 074023 (2010).
67. R. Boughezal *et al.*, JHEP **1306**, 072 (2013); R. Boughezal *et al.*, Phys. Rev. Lett. **115**, 082003 (2015).
68. C.F. Berger *et al.*, JHEP **1104**, 092 (2011); A. Banfi, G.P. Salam, and G. Zanderighi, JHEP **1206**, 159 (2012); T. Becher and M. Neubert, JHEP **1207**, 108 (2012); A. Banfi *et al.*, Phys. Rev. Lett. **109**, 202001 (2012); F.J. Tackmann, J.R. Walsh, and S. Zuberi, Phys. Rev. **D86**, 053011 (2012); T. Becher, M. Neubert, and L. Rothen, JHEP **1310**, 125 (2013).
69. A. Banfi *et al.*, JHEP **1604**, 049 (2016).
70. I. Moult and I. W. Stewart, JHEP **1409**, 129 (2014).
71. M. Duhrssen *et al.*, Phys. Rev. **D70**, 113009 (2004).
72. T. Han, G. Valencia, and S. Willenbrock, Phys. Rev. Lett. **69**, 3274 (1992); T. Figy, C. Oleari, and D. Zeppenfeld, Phys. Rev. **D68**, 073005 (2003); T. Figy and D. Zeppenfeld, Phys. Lett. **B591**, 297 (2004); E.L. Berger and J. Campbell, Phys. Rev. **D70**, 073011 (2004); M. Ciccolini, A. Denner, and S. Dittmaier, Phys. Rev. Lett. **99**, 161803 (2007); M. Ciccolini, A. Denner, and S. Dittmaier, Phys. Rev. **D77**, 103002 (2008); A. Denner, S. Dittmaier, and A. Muck, `HAWK`, `omnibus.uni-freiburg.de/~sd565/programs/hawk/hawk.html`; K. Arnold *et al.*, `VBFNLO`, Comp. Phys. Comm. **180**, 1661 (2009); M. Spira, `VV2H`, `people.web.psi.ch/spira/vv2h`; N. Adam *et al.*, `arXiv:0803.1154 [hep-ph]` (2008); T. Figy, S. Palmer, and G. Weiglein, JHEP **1202**, 105 (2012).
73. P. Nason and C. Oleari, JHEP **1002**, 037 (2010); S. Frixione, P. Torrielli, and M. Zaro, Phys. Lett. **B726**, 273 (2013); F. Maltoni, K. Mawatari, and M. Zaro, Eur. Phys. J. **C74**, 2710 (2014).
74. P. Bolzoni *et al.*, Phys. Rev. Lett. **105**, 011801 (2010); P. Bolzoni *et al.*, Phys. Rev. **D85**, 035002 (2012).
75. M. Cacciari *et al.*, Phys. Rev. Lett. **115**, 082002 (2015).
76. S.L. Glashow, D.V. Nanopoulos, and A. Yildiz, Phys. Rev. **D18**, 1724 (1978); T. Han and S. Willenbrock, Phys. Lett. **B273**, 167 (1991); T. Han, G. Valencia, and S. Willenbrock, Phys. Rev. Lett. **69**, 3274 (1992); H. Baer, B. Bailey, and J.F. Owens, Phys. Rev. **D47**, 2730 (1993); J. Ohnemus and W.J. Stirling, Phys. Rev. **D47**, 2722 (1993).
77. A. Stange, W. Marciano, and S. Willenbrock, Phys. Rev. **D49**, 1354 (1994).
78. A. Stange, W. Marciano, and S. Willenbrock, Phys. Rev. **D50**, 4491 (1994).
79. M.L. Ciccolini, S. Dittmaier, and M. Kramer, Phys. Rev. **D68**, 073003 (2003); A. Denner, S Dittmaier, and S. Kalweit, JHEP **1203**, 075 (2012).
80. R. Hamberg, W.L. van Neerven, and T. Matsuura, Nucl. Phys. **B359**, 343 (1991).
81. O. Brein, A. Djouadi, and R. Harlander, Phys. Lett. **B579**, 149 (2004); L. Altenkamp *et al.*, JHEP **1302**, 078 (2013).
82. O. Brein *et al.*, Eur. Phys. J. **C72**, 1868 (2012).
83. O. Brein, R.V. Harlander, and T.J. Zirke, Comp. Phys. Comm. **184**, 998 (2013).
84. A. Denner *et al.*, JHEP **1203**, 075 (2012).
85. G. Ferrera, M. Grazzini, and F. Tramontano, Phys. Rev. Lett. **107**, 152003 (2011).
86. G. Ferrera, M. Grazzini and F. Tramontano, Phys. Lett. **B740**, 51 (2015).
87. J.M. Campbell, R.K. Ellis and C. Williams, JHEP **1606**, 179 (2016).
88. W. Astill *et al.*, JHEP **1606**, 154 (2016).
89. R. Raitio and W.W. Wada, Phys. Rev. **D19**, 941 (1979); J.N. Ng and P. Zakarauskas, Nucl. Phys. **B247**, 339 (1984); J.F. Gunion, Phys. Lett. **B261**, 510 (1991); W.J. Marciano and F.E. Paige, Phys. Rev. Lett. **66**, 2433 (1991).
90. W. Beenakker *et al.*, Phys. Rev. Lett. **87**, 201805 (2001); L. Reina and S. Dawson, Phys. Rev. Lett. **87**, 201804 (2001); S. Dawson *et al.*, Phys. Rev. **D67**, 071503 (2003); W. Beenakker *et al.*, Nucl. Phys. **B653**, 151 (2003).
91. R. Frederix *et al.*, Phys. Lett. **B701**, 427 (2011); M. Garzelli *et al.*, Europhys. Lett. **96**, 11001 (2011).
92. F. Demartin *et al.*, Eur. Phys. J. **C75**, 267 (2015).
93. K.A. Assamagan *et al.*, [Higgs Working Group, "Physics at TeV Colliders" workshop, Les Houches, 2003], `arXiv:hep-ph/0406152` (2004).
94. R.V. Harlander and W.B. Kilgore, Phys. Rev. **D68**, 013001 (2003); J. M. Campbell *et al.*, Phys. Rev. **D67**, 095002 (2003); S. Dawson *et al.*, Phys. Rev. Lett. **94**, 031802 (2005); S. Dittmaier, M. Kramer, and M. Spira, Phys. Rev. **D70**, 074010 (2004); S. Dawson *et al.*, Phys. Rev. **D69**, 074027 (2004).

95. W.J. Stirling and D.J. Summers, Phys. Lett. **B283**, 411 (1992); F. Maltoni *et al.*, Phys. Rev. **D64**, 094023 (2001).
96. S. Dawson, S. Dittmaier and M. Spira, Phys. Rev. **D58**, 115012 (1998).
97. D. de Florian and J. Mazzitelli, Phys. Rev. Lett. **111**, 201801 (2013).
98. S. Borowka *et al.*, Phys. Rev. Lett. **117**, 012001 (2016).
99. B.L. Ioffe and V.A. Khoze, Sov. J. Nucl. Phys. **9**, 50 (1978).
100. D.R.T. Jones and S. Petcov, Phys. Lett. **B84**, 440 (1979); R.N. Cahn and S. Dawson, Phys. Lett. **B136**, 196 (1984); G.L. Kane, W.W. Repko, and W.B. Rolnick, Phys. Lett. **B148**, 367 (1984); G. Altarelli, B. Mele, and F. Pitolli, Nucl. Phys. **B287**, 205 (1987); W. Kilian, M. Kramer, and P.M. Zerwas, Phys. Lett. **B373**, 135 (1996).
101. B.A. Kniehl, Z. Phys. **C55**, 605 (1992).
102. J. Fleischer and F. Jegerlehner, Nucl. Phys. **B216**, 469 (1983); A. Denner *et al.*, Z. Phys. **C56**, 261 (1992).
103. B.A. Kniehl, Int. J. Mod. Phys. **A17**, 1457 (2002).
104. K.J. Gaemers and G.J. Gounaris, Phys. Lett. **B77**, 379 (1978); A. Djouadi, J. Kalinowski, and P. M. Zerwas, Z. Phys. **C54**, 255 (1992); B.A. Kniehl, F. Madricardo, and M. Steinhauser, Phys. Rev. **D66**, 054016 (2002).
105. S. Dittmaier *et al.*, Phys. Lett. **B441**, 383 (1998); S. Dittmaier *et al.*, Phys. Lett. **B478**, 247 (2000); S. Dawson and L. Reina, Phys. Rev. **D59**, 054012 (1999).
106. S. Dawson *et al.*, [Higgs Working Group, "Snowmass on the Mississippi" workshop] `arXiv:1310.8361 [hep-ex]` (2013).
107. D.M. Asner *et al.*, [ILC Higgs white paper, "Snowmass on the Mississippi" workshop] `arXiv:1310.0763 [hep-ph]` (2013).
108. A. Denner *et al.*, Eur. Phys. J. **C71**, 1753 (2011).
109. A. Djouadi, J. Kalinowski, and M. Spira, Comp. Phys. Comm. **108**, 56 (1998); A. Djouadi *et al.*, `arXiv:1003.1643 [hep-ph]` (2010).
110. S. Gorishnii *et al.*, Mod. Phys. Lett. **A5**, 2703 (1990); S. Gorishnii *et al.*, Phys. Rev. **D43**, 1633 (1991); A.L. Kataev and V.T. Kim, Mod. Phys. Lett. **A9**, 1309 (1994); L.R. Surguladze, Phys. Lett. **B341**, 60 (1994); S. Larin, T. van Ritbergen, and J. Vermaseren, Phys. Lett. **B362**, 134 (1995); K. Chetyrkin and A. Kwiatkowski, Nucl. Phys. **B461**, 3 (1996); K. Chetyrkin, Phys. Lett. **B390**, 309 (1997); P.A. Baikov, K.G. Chetyrkin, and J.H. Kuhn, Phys. Rev. Lett. **96**, 012003 (2006).
111. J. Fleischer and F. Jegerlehner, Phys. Rev. **D23**, 2001 (1981); D. Bardin, B. Vilensky, and P. Khristova, Sov. J. Nucl. Phys. **53**, 152 (1991); A. Dabelstein and W. Hollik, Z. Phys. **C53**, 507 (1992); B.A. Kniehl, Nucl. Phys. **B376**, 3 (1992); A. Djouadi *et al.*, *Proceedings e^+e^- collisions at 500 GeV* (1991).
112. T. Inami, T. Kubota, and Y. Okada, Z. Phys. **C18**, 69 (1983); K.G. Chetyrkin, B.A. Kniehl, and M. Steinhauser, Phys. Rev. Lett. **79**, 353 (1997); P.A. Baikov and K.G. Chetyrkin, Phys. Rev. Lett. **97**, 061803 (2006).
113. H.Q. Zheng and D.D. Wu, Phys. Rev. **D42**, 3760 (1990); A. Djouadi *et al.*, Phys. Lett. **B257**, 187 (1991); S. Dawson and R. Kauffman, Phys. Rev. **D47**, 1264 (1993); A. Djouadi, M. Spira, and P. Zerwas, Phys. Lett. **B311**, 255 (1993); K. Melnikov and O.I. Yakovlev, Phys. Lett. **B312**, 179 (1993); M. Inoue *et al.*, Mod. Phys. Lett. **A9**, 1189 (1994).
114. P. Maierhofer and P. Marquard, Phys. Lett. **B721**, 131 (2013).
115. U. Uglietti *et al.*, Phys. Lett. **B595**, 432 (2004); G. Degrassi and F. Maltoni, Phys. Lett. **B600**, 255 (2004); S. Actis *et al.*, Phys. Lett. **B670**, 12 (2008); U. Aglietti *et al.*, Phys. Lett. **B600**, 57 (2004); G. Degrassi and F. Maltoni, Nucl. Phys. **B724**, 183 (2005); U. Aglietti *et al.*, [Tevatron for LHC report: Higgs] `arXiv:hep-ph/0612172` (2006).
116. A. Abbasabadi *et al.*, Phys. Rev. **D55**, 5647 (1997); A. Abbasabadi and W.W. Repko, Phys. Rev. **D71**, 017304 (2005); A. Abbasabadi and W.W. Repko, JHEP **0608**, 048 (2006); D.A. Dicus and W.W. Repko, Phys. Rev. **D87**, 077301 (2013); L.B. Chen, C.F. Qiao, and R.L. Zhu, Phys. Lett. **B726**, 306 (2013); Y. Sun, H.R. Chang, and D.N. Gao, JHEP **1305**, 061 (2013); G. Passarino, Phys. Lett. **B727**, 424 (2013).
117. M. Spira, A. Djouadi, and P.M. Zerwas, Phys. Lett. **B276**, 350 (1992).
118. A. Bredenstein *et al.*, Phys. Rev. **D74**, 013004 (2006); A. Bredenstein *et al.*, JHEP **0702**, 080 (2007); A. Bredenstein *et al.*, `Prophecy4f`: A Monte Carlo generator for a proper description of the Higgs decay into 4 fermions, `omnibus.uni-freiburg.de/~sd565/programs/prophecy4f/prophecy4f.html`.
119. A. Ghinculov, Phys. Lett. **B337**, 137 (1994) [E: **B346**, 426 (1995)]; L. Durand, B.A. Kniehl, and K. Riesselmann, Phys. Rev. **D51**, 5007 (1995); L. Durand, K. Riesselmann, and B.A. Kniehl, Phys. Rev. Lett. **72**, 2534 (1994) [E: **74**, 1699 (1995)].
120. E. Braaten and J.P. Leveille, Phys. Rev. **D22**, 715 (1980); L. Durand, K. Riesselmann, and B.A. Kniehl, Phys. Rev. Lett. **72**, 2534 (1994); E. Gross, G. Wolf, and B.A. Kniehl, Z. Phys. **C63**, 417 (1994) [E: *ibid.*, **C66**, 32 (1995)]; A. Ghinculov, Phys. Lett. **B337**, 137 (1994) and Nucl. Phys. **B455**, 21 (1995); A. Djouadi, M. Spira, and P.M. Zerwas, Z. Phys. **C70**, 427 (1996); A. Frink *et al.*, Phys. Rev. **D54**, 4548 (1996); K.G. Chetyrkin and M. Steinhauser, Phys. Lett. **B408**, 320 (1997); R. Harlander and M. Steinhauser, Phys. Rev. **D56**, 3980 (1997); A.L. Kataev, Sov. Phys. JETP Lett. **66**, 327 (1997); S. Actis *et al.*, Nucl. Phys. **B811**, 182 (2009).
121. J. Erler and A. Freitas, *Electroweak Model and Constraints on New Physics*, in this volume.
122. R. Barate *et al.* [LEP Working Group for Higgs boson searches and ALEPH, DELPHI, L3, and OPAL Collaborations], Phys. Lett. **B565**, 61 (2003).
123. CDF and D0 Collaborations, Phys. Rev. **D88**, 052014 (2013).
124. ATLAS Collab., ATLAS-CONF-2017-045 (2017).
125. CMS Collab., CMS-PAS-HIG-16-041 (2017).
126. G. Aad *et al.* [ATLAS Collab.], Phys. Rev. **D90**, 112015 (2014).
127. S. Chatrchyan *et al.* [CMS Collab.], Eur. Phys. J. **C74**, 3076 (2014).
128. CMS Collab., CMS-PAS-HIG-16-040 (2016).
129. G. Aad *et al.* [ATLAS Collab.], Phys. Rev. **D91**, 012006 (2015).
130. S. Chatrchyan *et al.* [CMS Collab.], Phys. Rev. **D89**, 092007 (2014).
131. S. Chatrchyan *et al.* [CMS Collab.], JHEP **12**, 034 (2012).
132. ATLAS Collab., ATLAS-CONF-2017-043 (2017).
133. G. Aad *et al.* [Atlas and CMS Collaborations], Phys. Rev. Lett. **114**, 191803 (2015).
134. ATLAS Collab., ATLAS-CONF-2017-046 (2017).
135. ATLAS Collab., ATL-PHYS-PUB-2016-009 (2016).
136. G. Aad *et al.* [ATLAS Collab.], Phys. Rev. **D92**, 012006 (2015).
137. S. Chatrchyan *et al.* [CMS Collab.], JHEP **01**, 096 (2014).
138. G. Aad *et al.* [ATLAS Collab.], JHEP **08**, 137 (2015).
139. ATLAS Collab., ATLAS-CONF-2016-112 (2016).
140. CMS Collab., CMS-PAS-HIG-16-021 (2016).
141. S. Chatrchyan *et al.* [CMS Collab.], JHEP **05**, 104 (2014).
142. G. Aad *et al.* [ATLAS Collab.], JHEP **04**, 117 (2015).
143. ATLAS and CMS Collaborations, ATLAS-CONF-2015-044 and CMS-PAS-HIG-15-002 (2015).

144. CMS Collab., CERN-EP-2017-181 (2017).
145. T. Aaltonen *et al.* [CDF and D0 Collaborations], Phys. Rev. Lett. **109**, 071804 (2012).
146. J.M. Butterworth *et al.*, Phys. Rev. Lett. **100**, 242001 (2008).
147. S. Chatrchyan *et al.* [CMS Collab.], Phys. Rev. **D89**, 012003 (2014).
148. G. Aad *et al.* [ATLAS Collab.], JHEP **01**, 069 (2015).
149. ATLAS Collab., CERN-EP-2017-175 (2017).
150. CMS Collab., CERN-EP-2017-233 (2017).
151. LHCb Collab., LHCb-CONF-2016-006.
152. G. Aad *et al.* [ATLAS Collab.], JHEP **11**, 112 (2016).
153. S. Chatrchyan *et al.* [CMS Collab.], Phys. Rev. **D92**, 032008 (2015).
154. CMS Collab., CMS-PAS-HIG-16-003 (2016).
155. E. Gabrielli *et al.*, Nucl. Phys. **B781**, 64 (2007).
156. ATLAS Collab., ATLAS-CONF-2017-063 (2017).
157. CMS Collab., CERN-EP-2017-207 (2017).
158. M. Cacciari *et al.*JHEP **04**, 063 (2008).
159. ATLAS Collab., ATLAS-CONF-2015-060 (2015).
160. CMS Collab., CMS-PAS-HIG-15-005 (2016).
161. ATLAS Collab., ATLAS-CONF-2015-059 (2015).
162. CMS Collab., CMS-PAS-HIG-15-004 (2016).
163. ATLAS Collab., ATLAS-CONF-2015-069 (2015).
164. CMS Collab., CMS-PAS-HIG-15-003 (2016).
165. CMS Collab., CMS-PAS-HIG-16-003 (2016).
166. S. Chatrchyan *et al.* [CMS Collab.], JHEP **09**, 087 (2014).
167. G. Aad *et al.* [ATLAS Collab.], Phys. Lett. **B740**, 222 (2015).
168. G. Aad *et al.* [ATLAS Collab.], Phys. Lett. **B749**, 519 (2015).
169. ATLAS Collab., ATLAS-CONF-2017-076 (2017).
170. ATLAS Collab., ATLAS-CONF-2017-077 (2017).
171. CMS Collab., CMS-PAS-HIG-17-004 (2017).
172. CMS Collab., CMS-PAS-HIG-17-003 (2017).
173. CMS Collab., CMS-PAS-HIG-16-038 (2016).
174. CMS Collab., CMS-PAS-HIG-17-005 (2017).
175. CMS Collab., CMS-PAS-HIG-16-019 (2016).
176. ATLAS Collab., Phys. Lett. **B740**, 222 (2015).
177. ATLAS Collab., JHEP **129**, 010 (2017).
178. G. Aad *et al.* [ATLAS Collab.], JHEP **12**, 061 (2015).
179. CMS Collab., JHEP **02**, 079 (2017).
180. CMS Collab., CMS-PAS-TOP-2017-003 (2017).
181. G. Aad *et al.* [ATLAS Collab.], Phys. Rev. Lett. **114**, 081802 (2015).
182. G. Aad *et al.* [ATLAS Collab.], Phys. Rev. **D92**, 092004 (2015).
183. G. Aad *et al.* [ATLAS Collab.], Eur. Phys. J. **C75**, 412 (2015).
184. S. Chatrchyan *et al.* [CMS Collab.], Phys. Rev. **D90**, 112013 (2014).
185. S. Chatrchyan *et al.* [CMS Collab.], Phys. Lett. **B755**, 220 (2016).
186. S. Chatrchyan *et al.* [CMS Collab.], Phys. Lett. **B749**, 560 (2015).
187. ATLAS Collab., ATLAS-CONF-2016-004 (2016).
188. CMS Collab., CMS-PAS-HIG-2017-008 (2016).
189. ATLAS Collab., ATLAS-CONF-2016-049 (2016).
190. CMS Collab., CMS-PAS-HIG-16-026.
191. V. Khachatryan *et al.* [CMS Collab.], Phys. Lett. **B755**, 217 (2016).
192. CMS Collab., CERN-EP-2017-168.
193. ATLAS Collab., ATLAS-CONF-2016-071 (2016).
194. ATLAS Collab., ATL-PHYS-PUB-2017-001.
195. CMS Collab., CMS-PAS-FTR-15-002 (2015).
196. ATLAS Collab., ATL-PHYS-PUB-2014-019 (2014).
197. S. Chatrchyan *et al.* CMS Collab.], Phys. Lett. **B726**, 587 (2013).
198. G. Aad *et al.* [ATLAS Collab.], Phys. Lett. **B753**, 341 (2016).
199. ATLAS Collab., CERN-EP-2017-095 (2017).
200. G. Aad *et al.* [ATLAS Collab.], Phys. Lett. **B738**, 68 (2014).
201. S. Chatrchyan *et al.* [CMS Collab.], Phys. Lett. **B744**, 184 (2015).
202. G. Aad *et al.* [ATLAS Collab.], Phys. Rev. Lett. **119**, 051802 (2017).
203. S. Chatrchyan *et al.* [CMS Collab.], Phys. Lett. **B749**, 137 (2015).
204. G. Aad *et al.* [ATLAS Collab.], JHEP **1511**, 211 (2015).
205. G. Aad *et al.* [ATLAS Collab.], CERN-EP-2016-055(2016).
206. CMS Collab., CMS-PAS-HIG-17-001 (2017).
207. S. Chatrchyan *et al.* [CMS Collab.], Phys. Lett. **B763C**, 472 (2016).
208. R. Harnik *et al.*, JHEP **03**, 026 (2013).
209. C. Delaunay *et al.*, Phys. Rev. **D89**, 033014 (2014).
210. G. T. Bodwin *et al.*, Phys. Rev. **D88**, 053003 (2013).
211. G. Aad *et al.* [ATLAS Collab.], Phys. Rev. Lett. **114**, 121801 (2015).
212. ATLAS Collab., CERN-EP-2016-130 (2016).
213. A. Djouadi *et al.*, Eur. Phys. J. **C73**, 2455 (2013).
214. G. Aad *et al.* [ATLAS Collab.], Eur. Phys. J. **C75**, 337 (2015).
215. G. Aad *et al.* [ATLAS Collab.], Phys. Rev. Lett. **112**, 201802 (2014).
216. G. Aad *et al.* [ATLAS Collab.], JHEP **01**, 172 (2016).
217. G. Aad *et al.* [ATLAS Collab.], JHEP **11**, 206 (2015).
218. S. Chatrchyan *et al.* [CMS Collab.], Eur. Phys. J. **C74**, 2980 (2014).
219. S. Chatrchyan *et al.* [CMS Collab.], CMS-PAS-HIG-15-012 (2015).
220. S. Chatrchyan *et al.* [CMS Collab.], CMS-PAS-HIG-16-009 (2016).
221. S. Chatrchyan *et al.* [CMS Collab.], CMS-PAS-HIG-16-008 (2016).
222. S. Chatrchyan *et al.* [CMS Collab.], JHEP **02**, 135 (2017).
223. A. Djouadi *et al.*, Eur. Phys. J. **C73**, 2455 (2013).
224. M.J. Strassler and K.M. Zurek, Phys. Lett. **B651**, 374 (2007).
225. M.J. Strassler and K.M. Zurek, Phys. Lett. **B661**, 263 (2008).
226. T. Han *et al.*, JHEP **0807**, 008 (2008).
227. A. Falkowski *et al.*, JHEP **1005**, 077 (2010) and Phys. Rev. Lett. **105**, 241801 (2010).
228. G. Aad *et al.* [ATLAS Collab.], New J. Phys. **15**, 043009 (2013).
229. G. Aad *et al.* [ATLAS Collab.], Phys. Lett. **B721**, 32 (2013).
230. G. Aad *et al.* [ATLAS Collab.], Phys. Rev. Lett. **108**, 251801 (2012).
231. D. Tucker-Smith and N. Weiner, Phys. Rev. **D64**, 043502 (2001).
232. S. Chatrchyan *et al.* [CMS Collab.], Phys. Lett. **B726**, 564 (2013).
233. M. Carena, C. Grojean, M. Kado, and V. Sharma, *Status of Higgs boson physics*, in Review of Particle Physics, Chin. Phys. **C40** 100001 (2016).
234. G. Aad *et al.* [ATLAS Collab.], Eur. Phys. J. **C76**, 6 (2016).
235. S. Chatrchyan *et al.* [CMS Collab.], Eur. Phys. J. **C75**, 212 (2015).
236. L.D. Landau, Dokl. Akad. Nauk Ser. Fiz. **60**, 207 (1948); C.N. Yang, Phys. Rev. **D77**, 242 (1950).
237. G. Aad *et al.* [ATLAS Collab.], Eur. Phys. J. **C75**, 476 (2015).
238. V. Khachatryan *et al.* [CMS Collab.], Phys. Rev. **D92**, 012004 (2015).
239. ATLAS Collab., Phys. Lett. **B726**, 120 (2013).
240. P. Artoisenet *et al.*, JHEP **1311**, 043 (2013); A. Alloul, B. Fuks, and V. Sanz, JHEP **1404**, 110 (2014); A. Falkowski *et al.*, Eur. Phys. J. **C75**, 583 (2015).
241. J. Ellis *et al.*, JHEP **1211**, 134 (2012).
242. D0 Collab., Note 6387-CONF (2013).
243. D0 Collab., Note 6406-CONF (2013).
244. A. De Rujula *et al.*, Phys. Rev. **D82**, 013003 (2010).
245. CMS Collab., CERN-EP-2017-143 (2017).
246. ATLAS Collab., Eur. Phys. J. **C75**, 335 (2015).
247. V. Khachatryan *et al.* [CMS Collab.], Phys. Rev. **D92**, 072010 (2015).
248. V. Khachatryan *et al.* [CMS Collab.], CERN-EP-2016-054 (2016).
249. G. Aad *et al.* [ATLAS Collab.], Phys. Rev. **D90**, 052004 (2014).
250. L. Dixon and S. Siu, Phys. Rev. Lett. **90**, 252001 (2003); S. P. Martin, Phys. Rev. **D86**, 073016 (2012); L. Dixon and Y. Li, Phys. Rev. Lett. **111**, 111802 (2013).

251. ATLAS Collab., ATL-PHYS-PUB-2013-014 (2013).
252. J. Campbell, M. Carena, R. Harnik, and Z. Liu. arXiv:1704.08259 [hep-ph], Phys. Rev. Lett. to appear.
253. ATLAS Collab., ATL-PHYS-PUB-2014-016 (2014).
254. N. Kauer and G. Passarino, JHEP **08**, 116 (2012); F. Caola and K. Melnikov, Phys. Rev. **D88**, 054024 (2013); J.M. Campbell, R.K. Ellis, and C. Williams, JHEP **04**, 060 (2014); J.M. Campbell, R.K. Ellis, and C. Williams, Phys. Rev. **D89**, 053011 (2014); C. Englert and M. Spannowsky, Phys. Rev. **D90**, 053003 (2014).
255. ATLAS Collab., ATL-PHYS-PUB-2015-024 (2015).
256. A. David *et al.* [LHC Higgs Cross Section Working Group], `arXiv:1209.0040 [hep-ph]` (2012).
257. M. Gonzalez-Alonso *et al.*, Eur. Phys. J. **C75**, 128 (2015); A. Greljo *et al.*, Eur. Phys. J. **C76**, 158 (2016).
258. G. Buchalla, O. Cata and C. Krause, Nucl. Phys. **B880**, 552 (2014); I. Brivio *et al.*, JHEP **1403**, 014 (2014).
259. W. Buchmuller and D. Wyler, Nucl. Phys. **B268**, 621 (1986).
260. C.J. C. Burges and H.J. Schnitzer, Nucl. Phys. **B288**, 464 (1983); C.N. Leung, S.T. Love and S. Rao, Z. Phys. **C31**, 433 (1986).
261. B. Grzadkowski *et al.*, JHEP **1010**, 085 (2010).
262. L. Lehman and A. Martin, JHEP **1602**, 081 (2016); B. Henning *et al.*, JHEP **1708**, 016 (2017).
263. R. Alonso *et al.*, JHEP **1404**, 159 (2014).
264. G.F. Giudice *et al.*, JHEP **0706**, 045 (2007).
265. R. Contino *et al.*, JHEP **1307**, 035 (2013).
266. J. Elias-Miro *et al.*, JHEP **1311**, 066 (2013); R.S. Gupta, A. Pomarol and F. Riva, Phys. Rev. **D91**, 035001 (2015); E. Masso, JHEP **1410**, 128 (2014).
267. A. Falkowski and F. Riva, JHEP **1502**, 039 (2015).
268. A. Falkowski *et al.*, Phys. Rev. Lett. **116**, 011801 (2016).
269. C. Degrande *et al.*, JHEP **1207**, 036 (2012); J.F. Kamenik, M. Papucci, and A. Weiler, Phys. Rev. **D85**, 071501 (2012).
270. B.A. Kniehl and M. Spira, Z. Phys. **C69**, 77 (1995).
271. G. Isidori, A.V. Manohar, and M. Trott, Phys. Lett. **B728**, 131 (2014); G. Isidori and M. Trott, JHEP **1402**, 082 (2014).
272. A. Pomarol and F. Riva, JHEP **1401**, 151 (2014).
273. R. Godbole *et al.*, Phys. Lett. **B730**, 275 (2014).
274. M. Reece, New J. Phys. **15**, 043003 (2013).
275. S. Biswas, E. Gabrielli, and B. Mele, JHEP **1301**, 088 (2013); S. Biswas *et al.*, JHEP **07**, 073 (2013).
276. M. Farina *et al.*, JHEP **1305**, 022 (2013).
277. ATLAS Collab., JHEP **11**, 206 (2015).
278. ATLAS Collab., ATLAS-CONF-2013-072 (2013).
279. ATLAS Collab., Phys. Lett. **B753**, 69 (2016).
280. L.E. Ibanez and G.G. Ross, Phys. Lett. **B110**, 215 (1982); L.E. Ibanez, Phys. Lett. **B118**, 73 (1982); J. Ellis, D.V. Nanopoulos, and K. Tamvakis, Phys. Lett. **B121**, 123 (1983); L. Alvarez-Gaume, J. Polchinski, and M.B. Wise, Nucl. Phys. **B221**, 495 (1983).
281. See the list of references in the corresponding section of the 2014 edition of this review.
282. ATLAS Collab., `twiki.cern.ch/twiki/bin/view/AtlasPublic/Publications`; CMS Collab., `cms-results.web.cern.ch/cms-results/public-results/publications/SUS/STOP.html`.
283. See the list of references in the corresponding section of the 2016 edition of this review.
284. J. Mrazek *et al.*, Nucl. Phys. **B853**, 1 (2011).
285. D.B. Kaplan, Nucl. Phys. **B365**, 259 (1991).
286. G. Panico *et al.*, JHEP **1303**, 051 (2013).
287. H.E. Haber, *Supersymmetry*, in this volume.
288. A. Djouadi, Phys. Reports **459**, 1 (2008).
289. S. Heinemeyer *et al.*, Phys. Reports **425**, 265 (2006).
290. P. Draper, G. Lee and C.E.M. Wagner, Phys. Rev. **D89**, 055023 (2014).
291. J.F. Gunion and H.E. Haber, Phys. Rev. **D67**, 075019 (2003).
292. H.E. Haber and Y. Nir, Nucl. Phys. **B335**, 363 (1990); A. Dabelstein, Nucl. Phys. **B456**, 25 (1995); S. Heinemeyer, W. Hollik, and G. Weiglein, Eur. Phys. J. **C16**, 139 (2000); A. Dobado, M. J. Herrero, and S. Penaranda, Eur. Phys. J. **C17**, 487 (2000).
293. T.D. Lee, Phys. Rev. **D8**, 1226 (1973); P. Fayet, Nucl. Phys. **B78**, 14 (1974); R.D. Peccei and H.R. Quinn, Phys. Rev. Lett. **38**, 1440 (1977); P. Fayet and S. Ferrara, Phys. Reports **32**, 249 (1977); L.J. Hall and M.B. Wise, Nucl. Phys. **B187**, 397 (1981); V.D. Barger, J.L. Hewett, and R.J.N. Phillips, Phys. Rev. **D41**, 3421 (1990).
294. M. Carena *et al.*, JHEP **1203**, 014 (2012); M. Carena *et al.*, JHEP **1207**, 175 (2012).
295. M. Carena, S. Mrenna, and C.E.M. Wagner, Phys. Rev. **D60**, 075010 (1999) and Phys. Rev. **D62**, 055008 (2000).
296. A. Dabelstein, Nucl. Phys. **B456**, 25 (1995); F. Borzumati *et al.*, Nucl. Phys. **B555**, 53 (1999); H. Eberl *et al.*, Phys. Rev. **D62**, 055006 (2000).
297. J.A. Coarasa, R.A. Jimenez, and J. Sola, Phys. Lett. **B389**, 312 (1996); R.A. Jimenez and J. Sola, Phys. Lett. **B389**, 53 (1996); A. Bartl *et al.*, Phys. Lett. **B378**, 167 (1996).
298. S. Heinemeyer, W. Hollik, and G. Weiglein, Eur. Phys. J. **C16**, 139 (2000).
299. H. E. Haber *et al.*, Phys. Rev. **D63**, 055004 (2001).
300. L. Hall, R. Rattazzi, and U. Sarid, Phys. Rev. **D50**, 7048 (1994); R. Hempfling, Phys. Rev. **D49**, 6168 (1994).
301. M.S. Carena *et al.*, Nucl. Phys. **B426**, 269 (1994).
302. J. Guasch, P. Hafliger, and M. Spira, Phys. Rev. **D68**, 115001 (2003); D. Noth and M. Spira, Phys. Rev. Lett. **101**, 181801 (2008) and JHEP **1106**, 084 (2011); L. Mihaila and C. Reisser, JHEP **1008**, 021 (2010).
303. M.S. Carena *et al.*, Phys. Lett. **B499**, 141 (2001).
304. A. Djouadi, J. Kalinowski, and P.M. Zerwas, Z. Phys. **C57**, 569 (1993); H. Baer *et al.*, Phys. Rev. **D47**, 1062 (1993); A. Djouadi *et al.*, Phys. Lett. **B376**, 220 (1996); A. Djouadi *et al.*, Z. Phys. **C74**, 93 (1997); S. Heinemeyer and W. Hollik, Nucl. Phys. **B474**, 32 (1996).
305. J.F. Gunion, Phys. Rev. Lett. **72**, 199 (1994); D. Choudhury and D.P. Roy, Phys. Lett. **B322**, 368 (1994); O.J. Eboli and D. Zeppenfeld, Phys. Lett. **B495**, 147 (2000); B.P. Kersevan, M. Malawski, and E. Richter-Was, Eur. Phys. J. **C29**, 541 (2003).
306. E.L. Berger *et al.*, Phys. Rev. **D66**, 095001 (2002).
307. A. Brignole *et al.*, Nucl. Phys. **B643**, 79 (2002); R. Dermisek and I. Low, Phys. Rev. **D77**, 035012 (2008).
308. A. Djouadi, Phys. Lett. **B435**, 101 (1998).
309. M.R. Buckley and D. Hooper, Phys. Rev. **D86**, 075008 (2012); for other references, see the 2014 edition of this review.
310. J.J. Cao *et al.*, JHEP **1203**, 086 (2012); R. Benbrik *et al.*, Eur. Phys. J. **C72**, 2171 (2012); Z. Kang, J. Li, and T. Li, JHEP **1211**, 024 (2012); J.F. Gunion, Y. Jiang, and S. Kraml, Phys. Lett. **B710**, 454 (2012); U. Ellwanger, JHEP **1203**, 044 (2012).
311. T. Kitahara, JHEP **1211**, 021 (2012); M. Carena *et al.*, JHEP **1302**, 114 (2013).
312. B. Batell, S. Jung, and C.E.M. Wagner, JHEP **1312**, 075 (2013).
313. C. Balazs, H.-J. He, and C.P. Yuan, Phys. Rev. **D60**, 114001 (1999).

314. G. Lee, and C.E.M. Wagner Phys. Rev. **D92**, 075032 (2015).
315. D. Dicus *et al.*, Phys. Rev. **D59**, 094016 (1999).
316. M. Carena *et al.*, Eur. Phys. J. **C45**, 797 (2006).
317. E. Boos *et al.*, Phys. Rev. **D66**, 055004 (2002);
E. Boos, A. Djouadi, and A. Nikitenko, Phys. Lett. **B578**, 384 (2004);
E. Boos *et al.*, Phys. Lett. **B622**, 311 (2005);
M. Carena *et al.*, JHEP **1207**, 091 (2012).
318. A.A. Barrientos Bendezu and B.A. Kniehl, Phys. Rev. **D64**, 035006 (2001).
319. R.M. Barnett, H.E. Haber, and D.E. Soper, Nucl. Phys. **B306**, 697 (1988);
for other references, see the 2014 edition of this review.
320. A. Djouadi, J. Ellis and J. Quevillon, JHEP **07**, 105 (2016) `arXiv:1605.00542 [hep-ph]`(2016);
M Carena and Zhen Liu, JHEP **11**, 159 (2016).
321. M. Carena *et al.*, Eur. Phys. J. **C26**, 601 (2003);
M. Carena *et al.*, Eur. Phys. J. **C73**, 2552 (2013).
322. L. Maiani, A. D. Polosa and V. Riquer, New J. Phys. **14**, 073029 (2012) and Phys. Lett. **B718**, 465 (2012);
A. Djouadi and J. Quevillon, JHEP **1310**, 028 (2013);
A. Djouadi *et al.*, Eur. Phys. J. **C73**, 2650 (2013).
323. M. Carena *et al.*, Phys. Rev. **D91**, 035003 (2015).
324. M. Carena *et al.*, JHEP **1404**, 015 (2014).
325. K. Blum, R.T. D'Agnolo, and J. Fan, JHEP **1301**, 057 (2013);
A. Azatov *et al.*, Phys. Rev. **D86**, 075033 (2012);
J.R. Espinosa *et al.*, JHEP **1212**, 077 (2012);
R.S. Gupta, M. Montull, and F. Riva, JHEP **1304**, 132 (2013);
R.T. D'Agnolo, PhD thesis, Scuola Normale Superiore, Pisa, 2013.
326. A. Djouadi *et al.*, JHEP **1506**, 168 (2015).
327. G. D'Ambrosio *et al.*, Nucl. Phys. **B645**, 155 (2002);
R.S. Chivukula and H. Georgi, Phys. Lett. **B188**, 99 (1987);
L.J. Hall and L. Randall, Phys. Rev. Lett. **65**, 2939 (1990);
A.J. Buras *et al.*, Phys. Lett. **B500**, 161 (2001).
328. L.J. Hall, J. Lykken, and S. Weinberg, Phys. Rev. **D27**, 2359 (1983);
J.E. Kim and H.P. Nilles, Phys. Lett. **B138**, 150 (1984);
G.F. Giudice and A. Masiero, Phys. Lett. **B206**, 480 (1988);
E.J. Chun, J.E. Kim, and H.P. Nilles, Nucl. Phys. **B370**, 105 (1992);
I. Antoniadis *et al.*, Nucl. Phys. **B432**, 187 (1994).
329. P. Fayet, Phys. Lett. **B90**, 104 (1975).
330. C. Panagiotakopoulos and K. Tamvakis, Phys. Lett. **B469**, 145 (1999);
A. Dedes *et al.*, Phys. Rev. **D63**, 055009 (2001);
A. Menon, D. Morrissey, and C.E.M. Wagner, Phys. Rev. **D70**, 035005 (2004).
331. M. Cvetic *et al.*, Phys. Rev. **D56**, 2861 (1997) [E: **D58**, 119905 (1998)];
P. Langacker and J. Wang, Phys. Rev. **D58**, 115010 (1998) and references therein.
332. J. Erler, P. Langacker, and T.J. Li, Phys. Rev. **D66**, 015002 (2002);
T. Han, P. Langacker and B. McElrath, Phys. Rev. **D70**, 115006 (2004);
V. Barger *et al.*, Phys. Rev. **D73**, 115010 (2006).
333. V. Barger *et al.*, Phys. Rev. **D73**, 115010 (2006);
V. Barger, P. Langacker, and G. Shaughnessy, Phys. Rev. **D75**, 055013 (2007).
334. E. Accomando, *et al.*, `hep-ph/0608079` (2006).
335. B.A. Dobrescu, G.L. Landsberg, and K.T. Matchev, Phys. Rev. **D63**, 075003 (2001).
336. R. Dermisek and J. F. Gunion, Phys. Rev. Lett. **95**, 041801 (2005).
337. O.J.P. Eboli and D. Zeppenfeld, Phys. Lett. **B495**, 147 (2000);
H. Davoudiasl, T. Han, and H.E. Logan, Phys. Rev. **D71**, 115007 (2005).
338. L. Wang and X.F. Han, Phys. Rev. **D87**, 015015 (2013);
K. Schmidt-Hoberg and F. Staub JHEP **1210**, 195 (2012);
H. An, T. Liu, and L.T. Wang, Phys. Rev. **D86**, 075030 (2012);
D.A. Vasquez *et al.*, Phys. Rev. **D86**, 035023 (2012);
S.F. King, M. Muhlleitner, and R. Nevzorov, Nucl. Phys. **B860**, 207 (2012).
339. N.D. Christensen, T. Han, Z. Liu and S. Su, JHEP **1308**, 019 (2013);
T. Han, Z. Liu and S. Su, JHEP **1408**, 093 (2014);
S.F. King *et al.*, Phys. Rev. **D90**, 095014 (2014);
N.E. Bomark *et al.*, JHEP **1502**, 044 (2015);
P. Athron *et al.*, JHEP **1501**, 153 (2015);
N.E. Bomark, S. Moretti and L. Roszkowski, J. Phys. **G43**, 105003 (2016);
T. Li and S. Su, JHEP **1511**, 068 (2015);
G. Belanger *et al.*, JHEP **1509**, 151 (2015);
J. Baglio *et al.*, JHEP **1510**, 024 (2015);
M. Guchait and J. Kumar, Int. J. Mod. Phys. **A31**, 1650069 (2016);
D. Barducci *et al.*, JHEP **1601**, 050 (2016);
M. Carena *et al.*, Phys. Rev. **D93**, 035013 (2016);
P. Bandyopadhyay, K. Huitu and S. Niyogi, JHEP **1607**, 015 (2016);
U. Ellwanger and M. Rodriguez-Vazquez, JHEP **1602**, 096 (2016);
R. Costa *et al.*, JHEP **1606**, 034 (2016);
E. Conte *et al.*, JHEP **1605**, 100 (2016).
340. LHC Higgs Cross Section Working Group, Beyond the Standard Model Higgs – NMSSM
`twiki.cern.ch/twiki/bin/view/LHCPhysics/LHCHXSWGNMSSM`.
341. M. Carena *et al.*, Phys. Rev. **D93**, 035013 (2016).
342. Courtesy of Marcin Barziak based on the public code NMSSMTools,
`www.th.u-psud.fr/NMHDECAY/nmssmtools.html`.
343. P. Batra *et al.*, JHEP **0402**, 043 (2004).
344. P. Batra *et al.*, JHEP **0406**, 032 (2004);
A. Maloney, A. Pierce, and J.G. Wacker, JHEP **0606**, 034 (2006);
Y. Zhang *et al.*, Phys. Rev. **D78**, 011302 (2008);
C.W. Chiang *et al.*, Phys. Rev. **D81**, 015006 (2010);
A.D. Medina, N.R. Shah, and C.E.M. Wagner, Phys. Rev. **D80**, 015001 (2009);
M. Endo *et al.*, Phys. Rev. **D85**, 095006 (2012);
C. Cheung and H.L. Roberts, JHEP **1312**, 018 (2013).
345. R. Huo *et al.*, Phys. Rev. **D87**, 055011 (2013).
346. S. Dimopoulos and S. Thomas, Nucl. Phys. **B465**, 23 (1996);
S. Thomas, Int. J. Mod. Phys. **A13**, 2307 (1998).
347. A. Pilaftsis and C.E.M. Wagner, Nucl. Phys. **B553**, 3 (1999).
348. S.Y. Choi, M. Drees, and J.S. Lee, Phys. Lett. **B481**, 57 (2000);
M. Carena *et al.*, Nucl. Phys. **B625**, 345 (2002).
349. M.S. Carena *et al.*, Nucl. Phys. **B586**, 92 (2000).
350. A. Pilaftsis, Phys. Rev. **D58**, 096010 (1998) and Phys. Lett. **B435**, 88 (1998);
K.S. Babu *et al.*, Phys. Rev. **D59**, 016004 (1999).
351. G.L. Kane and L.T. Wang, Phys. Lett. **B488**, 383 (2000);
S.Y. Choi, M. Drees, and J.S. Lee, Phys. Lett. **B481**, 57 (2000);
S.Y. Choi and J.S. Lee, Phys. Rev. **D61**, 015003 (2000);
S.Y. Choi, K. Hagiwara, and J.S. Lee, Phys. Rev. **D64**, 032004 (2001) and Phys. Lett. **B529**, 212 (2002);
T. Ibrahim and P. Nath, Phys. Rev. **D63**, 035009 (2001);
T. Ibrahim, Phys. Rev. **D64**, 035009 (2001);
S. Heinemeyer, Eur. Phys. J. **C22**, 521 (2001);
S.W. Ham *et al.*, Phys. Rev. **D68**, 055003 (2003).
352. M. Frank *et al.*, JHEP **0702**, 047 (2007);
S. Heinemeyer *et al.*, Phys. Lett. **B652**, 300 (2007);
T. Hahn *et al.*, `arXiv:0710.4891` (2007).
353. D.A. Demir, Phys. Rev. **D60**, 055006 (1999);
S.Y. Choi, M. Drees, and J.S. Lee, Phys. Lett. **B481**, 57 (2000);
K. E. Williams, H. Rzehak, and G. Weiglein, Eur. Phys. J. **C71**, 1669 (2011).
354. E. Christova *et al.*, Nucl. Phys. **B639**, 263 (2002) [E: Nucl. Phys. **B647**, 359 (2002)].
355. M.D. Goodsell and F. Staub, `arXiv:1604.05335 [hep-ph]` (2016);

A. Chakraborty *et al.*, Phys. Rev. **D90**, 055005 (2014);
M. Carena *et al.*, JHEP **1602**, 123 (2016).
356. J.F. Gunion and H.E. Haber, Phys. Rev. **D67**, 075019 (2003);
G.C. Branco *et al.*, Phys. Reports **516**, 1 (2012).
357. S.L. Glashow and S. Weinberg, Phys. Rev. **D15**, 1958 (1977);
E.A. Paschos, Phys. Rev. **D15**, 1966 (1977);
H. Georgi, Hadronic J. **1,** 1227 (1978);
H. Haber, G. Kane, and T. Sterling, Nucl. Phys. **B161**, 493 (1979);
A.G. Akeroyd, Phys. Lett. **B368**, 89 (1996);
A.G. Akeroyd, Nucl. Phys. **B544**, 557 (1999);
A.G. Akeroyd, A. Arhrib, and E. Naimi, Eur. Phys. J. **C20**, 51 (2001).
358. N.G. Deshpande and E. Ma, Phys. Rev. **D18**, 2574 (1978);
R. Barbieri, L.J. Hall, and V. Rychkov, Phys. Rev. **D74**, 015007 (2006);
L. Lopez Honorez *et al.*, JCAP **0702**, 028 (2007);
E. Lundstrom, M. Gustafsson, and J. Edsjo, Phys. Rev. **D79**, 035013 (2009);
E. Dolle *et al.*, Phys. Rev. **D8**, 035003 (2010);
X. Miao, S. Su, and B. Thomas, Phys. Rev. **D82**, 035009 (2010);
L. Lopez-Honorez and C. Yaguna, JCAP **1101**, 002 (2011).
359. A. Arhrib, R. Benbrik, and N. Gaur, Phys. Rev. **D85**, 095021 (2012);
B. Swiezewska and M. Krawczyk, Phys. Rev. **D88**, 035019 (2013);
A. Goudelis, B. Herrmann, and O. Stal, JHEP **1309**, 106 (2013).
360. M. Bauer, M. Carena and K. Gemmler, JHEP **1511**, 016 (2015) and Phys. Rev. **D94**, 115030 (2016).
361. C. Froggatt and H. B. Nielsen Nucl. Phys. **B147**, 277 (1979).
362. K. Babu and S. Nandi, Phys. Rev. **D62**, 033002 (2000);
G. F. Giudice and O. Lebedev, Phys. Lett. **B665**, 79 (2008).
363. V. Barger, H.E. Logan, and G. Shaughnessy, Phys. Rev. **D79**, 115018 (2009).
364. D. O'Connell, M.J. Ramsey-Musolf, and M.B. Wise, Phys. Rev. **D75**, 037701 (2007);
V. Barger *et al.*, Phys. Rev. **D77**, 035005 (2008);
V. Barger *et al.*, Phys. Rev. **D79**, 015018 (2009);
T. Robens, and T. Stefaniak, Eur. Phys. J. **C75**, 104 (2015).
365. H.E. Haber, *Proceedings of the 1990 Theoretical Advanced Study Institute in Elementary Particle Physics,* edited by M. Cvetič and Paul Langacker (World Scientific, Singapore, 1991) pp. 340–475 and references therein.
366. S. Glashow and S. Weinberg, Phys. Rev. **D15**, 1958 (1977).
367. G.C. Branco, W. Grimus, and L. Lavoura, Phys. Lett. **B380**, 119 (1996);
F.J. Botella, G.C. Branco, M.N. Rebelo Phys. Lett. **B687**, 194 (2010).
368. N. Craig and S. Thomas, JHEP **1211**, 083 (2012).
369. G.C. Branco *et al.*, Phys. Reports **516**, 1 (2012).
370. C.Y. Chen, S. Dawson, and M. Sher, Phys. Rev. **D88**, 015018 (2013).
371. B. Swiezewska and M. Krawczyk, Phys. Rev. **D88**, 035019 (2013).
372. B. Coleppa, F. Kling and S. Su, JHEP **1409**, 161 (2014);
J. Cao *et al.*, JHEP **1412**, 026 (2014);
B. Coleppa, F. Kling and S. Su, JHEP **1412**, 148 (2014);
D. Curtin, R. Essig and Y.M. Zhong, JHEP **1506**, 025 (2015);
F. Kling, A. Pyarelal and S. Su, JHEP **1511**, 051 (2015);
J. Hajer *et al.*, JHEP **1511**, 124 (2015);
W. Bernreuther *et al.*, Phys. Rev. **D93**, 034032 (2016);
S. Gori *et al.*, Phys. Rev. **D93**, 075038 (2016);
F. Kling, J.M. No and S. Su, JHEP **1609**, 093 (2016);
N. Craig *et al.*, JHEP **1701**, 018 (2017).
373. N. Craig *et al.*,JHEP **1506**, 137 (2015);
J. Hajer *et al.*, Y. Y. Li, T. Liu and J. F. H. Shiu, JHEP **1511**, 124 (2015).
374. J. Schechter and J. W. F. Valle, Phys. Rev. **D22**, 2227 (1980).
375. T.P. Cheng and L.F. Li, Phys. Rev. **D22**, 2860 (1980).
376. H. Georgi and M. Machacek, Nucl. Phys. **B262**, 463 (1985).
377. M.S. Chanowitz and M. Golden, Phys. Lett. **B165**, 105 (1985).
378. J.F. Gunion, R. Vega, and J. Wudka, Phys. Rev. **D42**, 1673 (1990).
379. H.E. Logan and M.A. Roy, Phys. Rev. **D82**, 115011 (2010).
380. H.E. Haber and H.E. Logan, Phys. Rev. **D62**, 015011 (2000).
381. A.G. Akeroyd, M. Aoki, and H. Sugiyama, Phys. Rev. **D77**, 075010 (2008).
382. P. Nath *et al.*, Nucl. Phys. (Proc. Supp.) **B200**, 185 (2010).
383. J. Garayoa and T. Schwetz, JHEP **0803**, 009 (2008).
384. J.F. Gunion, R. Vega, and J. Wudka, Phys. Rev. **D43**, 2322 (1991).
385. S. Kanemura and K. Yagyu, Phys. Rev. **D85**, 115009 (2012).
386. I. Low and J. Lykken, JHEP **1010**, 053 (2010).
387. C. Englert, E. Re, and M. Spannowsky, Phys. Rev. **D87**, 095014 (2013).
388. I. Low, J. Lykken, and G. Shaughnessy, Phys. Rev. **D86**, 093012 (2012).
389. A. Falkowski, S. Rychkov, and A. Urbano, JHEP **1204**, 073 (2012).
390. B.A. Dobrescu and J.D. Lykken, JHEP **1302**, 073 (2013).
391. D. Carmi *et al.*, JHEP **1210**, 196 (2012).
392. C.W. Chiang and K. Yagyu, JHEP **1301**, 026 (2013).
393. G. Belanger *et al.*, Phys. Rev. **D88**, 075008 (2013).
394. C. Englert, E. Re, and M. Spannowsky, Phys. Rev. **D88**, 035024 (2013).
395. B. Bellazzini, C. Csaki and J. Serra, Eur. Phys. J. **C74**, 2766 (2014).
396. N. Arkani-Hamed *et al.*, JHEP **0207**, 034 (2002).
397. N. Arkani-Hamed, A.G. Cohen, and H. Georgi, Phys. Lett. **B513**, 232 (2001).
398. N. Arkani-Hamed *et al.*, JHEP **0208**, 021 (2002).
399. M. Schmaltz, JHEP **0408**, 056 (2004).
400. M. Schmaltz, D. Stolarski, and J. Thaler, JHEP **1009**, 018 (2010).
401. M. Perelstein, Prog. in Part. Nucl. Phys. **58**, 247 (2007).
402. M. Schmaltz and D. Tucker-Smith, Ann. Rev. Nucl. and Part. Sci. **55**, 229 (2005).
403. J.A. Casas, J.R. Espinosa, and I. Hidalgo, JHEP **0503**, 038 (2005).
404. H.C. Cheng and I. Low, JHEP **0309**, 051 (2003).
405. M.S. Carena *et al.*, Phys. Rev. **D75**, 091701 (2007).
406. ATLAS Collab., ATLAS-CONF-2012-147, ATLAS-CONF-2012-109 and ATLAS-CONF-2013-024 (2012);
CMS Collab., CMS-PAS-EXO-12-048 and CMS-SUS-12-028 (2012).
407. CMS Collab., CERN-EP/2016-279 (2016);
ATLAS Collab., JHEP **1708**, 052 (2017), CERN-EP-2017-094 (2017) and ATLAS-CONF-2017-104 (2017).
408. R.S. Chivukula, M. Narain, and J. Womersley, *Dynamical Electroweak Symmetry Breaking*, in this volume.
409. H. Georgi, A.E. Nelson, and A. Manohar, Phys. Lett. **B126**, 169 (1983);
A.E. Nelson and M.J. Strassler, JHEP **0009**, 030 (2000);
S. Davidson, G. Isidori, and S. Uhlig, Phys. Lett. **B663**, 73 (2008).
410. C. Csaki, A. Falkowski, and A. Weiler, JHEP **0809**, 008 (2008);
B. Keren-Zur *et al.*, Nucl. Phys. **B867**, 429 (2013).
411. K. Agashe, R. Contino, and A. Pomarol, Nucl. Phys. **B719**, 165 (2005).
412. O. Matsedonskyi, G. Panico, and A. Wulzer, JHEP **1301**, 164 (2013);
M. Redi and A. Tesi, JHEP **1210**, 166 (2012);
D. Marzocca, M. Serone, and J. Shu, JHEP **1208**, 013 (2012);
A. Pomarol and F. Riva, JHEP **1208**, 135 (2012).
413. R. Contino and G. Servant, JHEP **0806**, 026 (2008);
J. Mrazek and A. Wulzer, Phys. Rev. **D81**, 075006 (2010).
414. A. De Simone *et al.*, JHEP **1304**, 004 (2013);
A. Azatov *et al.*, Phys. Rev. **D89**, 075001 (2014).
415. A. Falkowski, Phys. Rev. **D77**, 055018 (2008);
I. Low and A. Vichi, Phys. Rev. **D84**, 045019 (2011);

A. Azatov and J. Galloway, Phys. Rev. **D85**, 055013 (2012); C. Delaunay, C. Grojean, and G. Perez, JHEP **1309**, 090 (2013).

416. R.K. Ellis *et al.*, Nucl. Phys. **B297**, 221 (1988); U. Baur and E.W.N. Glover, Nucl. Phys. **B339**, 38 (1990); O. Brein and W. Hollik, Phys. Rev. **D68**, 095006 (2003); U. Langenegger *et al.*, JHEP **0606**, 035 (2006).
417. A. Banfi, A. Martin, and V. Sanz, JHEP **1408**, 053 (2014); A. Azatov and A. Paul, JHEP **1401**, 014 (2014); C. Grojean *et al.*, JHEP **1405**, 022 (2014); M. Schlaffer *et al.*, Eur. Phys. J. **C74**, 3120 (2014); M. Buschmann *et al.*, Phys. Rev. **D90**, 013010 (2014); M. Buschmann *et al.*, JHEP **1502**, 038 (2015); U. Langenegger, M. Spira and I. Strebel, `arXiv:1507.01373 [hep-ph]` (2015); M. Grazzini *et al.*, JHEP **1703**, 115 (2017).
418. A. Azatov *et al.*, J. Exp. Theor. Phys. **120**, 354 (2015).
419. A. Azatov *et al.*, Phys. Rev. **D92**, 035001 (2015).
420. R. Contino, L. Da Rold, and A. Pomarol, Phys. Rev. **D75**, 055014 (2007).
421. D. Pappadopulo, A. Thamm, and R. Torre, JHEP **1307**, 058 (2013); M. Montull *et al.*, Phys. Rev. **D88**, 095006 (2013).
422. M. Carena, L. Da Rold, E Pontón JHEP **1406**, 159 (2014); D. Liu, I. Low and C. E. M. Wagner Phys. Rev. **D96**, 035013 (2017).
423. I. Low, R. Rattazzi, and A. Vichi, JHEP **1004**, 126 (2010).
424. M. Ciuchini *et al.*, JHEP **1308**, 106 (2013).
425. C. Grojean, O. Matsedonskyi, and G. Panico, JHEP **1310**, 160 (2013).
426. M. Geller and O. Telem, Phys. Rev. Lett. **114**, 191801 (2015).
427. P. Batra and Z. Chacko, Phys. Rev. D 79,095012(2009); R. Barbieri *et al.*, JHEP **1508**, 161 (2015); M. Low, A. Tesi and L. T. Wang, Phys. Rev. **D91**, 095012 (2015).
428. ATLAS Collab., CERN-EP-2017-132 (2017).
429. CMS Collab., CMS-PAS-HIG-17-13 (2017).
430. CMS Collab., Phys. Lett. **B767**, 147 (2017).
431. ATLAS Collab., CERN-EP-2017-095 (2017).
432. CMS Collab., CMS-PAS-HIG-16-014 (2016).
433. ATLAS Collab., ATLAS-CONF-2017-058 (2017).
434. CMS Collab., CMS-PAS-HIG-16-033 (2016).
435. CMS Collab., CMS-PAS-HIG-16-023 (2016).
436. ATLAS Collab., ATLAS-CONF-2016-082 (2016).
437. CMS Collab., CMS-PAS-HIG-16-034 (2016).
438. ATLAS Collab., ATLAS-CONF-2013-067 (2013).
439. ATLAS Collab., ATLAS-CONF-2013-027 (2013).
440. S. Chatrchyan *et al.* [CMS Collab.], Eur. Phys. J. **C73**, 2469 (2013).
441. ATLAS Collab., ATLAS-CONF-2012-018 (2012).
442. CMS Collab., CMS-PAS-HIG-13-008 (2013).
443. CMS Collab., CMS-PAS-HIG-12-046 (2012).
444. ATLAS Collab., CERN-EP-2017-147 (2017).
445. ATLAS Collab., ATLAS-CONF-2016-071.
446. V. Khachatryan *et al.* [CMS Collab.], Phys. Lett. **B755**, 217 (2016).
447. ATLAS Collab., ATLAS-CONF-2017-050 (2017).
448. CMS Collab., CMS-PAS-HIG-16-037 (2016).
449. V.M. Abazov *et al.* [D0 Collab.], Phys. Rev. Lett. **104**, 151801 (2010).
450. D0 Collab., D0 Note 5974-CONF (2011).
451. R. Aaij *et al.* [LHCb Collab.], JHEP **1305**, 132 (2013).
452. ATLAS Collab., ATLAS-CONF-2012-094 (2012).
453. ATLAS Collab., ATLAS-CONF-2016-104 (2016).
454. ATLAS Collab., CERN-EP-2017-134 (2017).
455. S. Chatrchyan *et al.* [CMS Collab.], Phys. Lett. **B722**, 207 (2013).
456. CMS Collab., CMS-PAS-HIG-16-025 (2016).
457. V.M. Abazov *et al.* [D0 Collab.], Phys. Lett. **B698**, 97 (2011).
458. T. Aaltonen *et al.* [CDF Collab.], Phys. Rev. **D85**, 032005 (2012).
459. ATLAS Collab., ATLAS-CONF-2017-055 (2017).
460. ATLAS Collab., Phys. Lett. **B744**, 163 (2015).
461. ATLAS Collab., Phys. Lett. **B759**, 555 (2016).
462. CMS Collab., CMS-PAS-HIG-16-031 (2016).
463. ATLAS Collab., ATLAS-CONF-2012-010 (2012).
464. V. Khachatryan *et al.* [CMS Collab.], JHEP **1512**, 178 (2015).
465. ATLAS Collab., ATLAS-CONF-2016-089 (2016).
466. V. Khachatryan *et al.* [CMS Collab.], JHEP **1511**, 018 (2015).
467. ATLAS Collab., Phys. Rev. Lett. **114**, 231801 (2015).
468. CMS Collab., CERN-EP-2017-068 (2017).
469. CMS Collab., CMS-PAS-HIG-16-030 (2016).
470. ATLAS Collab., ATLAS-CONF-2011-020 (2011).
471. CMS Collab., CMS-PAS-HIG-15-009 (2015).
472. ATLAS Collab., Phys. Rev. **D92**, 052002 (2015).
473. ATLAS Collab., ATLAS-CONF-2012-079 (2012).
474. CMS Collab., CMS-PAS-HIG-16-055 (2016).
475. CMS Collab., CERN-EP2016-292 (2016).
476. V.M. Abazov *et al.* [D0 Collab.], Phys. Rev. Lett. **103**, 061801 (2009).
477. S. Schael *et al.* [ALEPH Collab.], JHEP **1005**, 049 (2010).
478. B. Aubert *et al.* [BaBar Collab.], Phys. Rev. Lett. **103**, 081803 (2009).
479. B. Aubert *et al.* [BaBar Collab.], Phys. Rev. Lett. **103**, 181801 (2009).
480. ATLAS Collab., ATLAS-CONF-2016-051 (2016).
481. ATLAS Collab., ATLAS-CONF-2017-053 (2017).
482. CMS Collab., CMS-PAS-HIG-16-036 (2016).
483. ATLAS Collab., Phys. Rev. **D92**, 092004 (2015).
484. CMS Collab., CMS-PAS-HIG-13-016 (2013).
485. ATLAS Collab., ATLAS-CONF-2012-013 (2012).
486. CMS Collab., CMS-PAS-HIG-12-002 (2012).
487. CMS Collab., CMS-HIG-12-013 and CERN-PH-EP-2013-011 (2013).
488. ALEPH Collab., Phys. Lett. **B526**, 191 (2002).
489. L3 Collab., Phys. Lett. **B545**, 30 (2002).
490. S. Schael *et al.* [ALEPH, DELPHI, L3 and OPAL Collaborations and LEP Working Group for Higgs Boson Searches], Eur. Phys. J. **C47**, 547 (2006).
491. M.M. Kado and C.G. Tully, Ann. Rev. Nucl. and Part. Sci. **52**, 65 (2002).
492. OPAL Collab., Eur. Phys. J. **C23**, 397 (2002).
493. DELPHI Collab., Eur. Phys. J. **C38**, 1 (2004).
494. CMS Collab., CMS-PAS-HIG-16-007 (2016).
495. ATLAS Collab., JHEP **08**, 148 (2015).
496. S. Chatrchyan *et al.* [CMS Collab.], JHEP **09**, 029 (2012).
497. V. Khachatryan *et al.* [CMS Collab.], Phys. Lett. **B758**, 296 (2016).
498. CMS Collab., CERN-EP-2017-159 (2011).
499. J. Bernon *et al.*, Phys. Rev. **D91**, 075019 (2015).
500. ATLAS Collab., Phys. Rev. Lett. **113**, 171801 (2014).
501. CMS Collab., CMS-PAS-HIG-14-037 (2014).
502. CMS Collab., CMS-PAS-HIG-17-013 (2017).
503. S.H. Zhu, `hep-ph/9901221` (1999).
504. H.E. Logan and S. Su, Phys. Rev. **D66**, 035001 (2002).
505. A. Gutierrez-Rodriguez and O.A. Sampayo, Phys. Rev. **D62**, 055004 (2000).
506. S. Kanemura, S. Moretti, and K. Odagiri, JHEP **0102**, 011 (2001).
507. J.A. Coarasa Perez *et al.*, Eur. Phys. J. **C2**, 373 (1998); J.A. Coarasa Perez *et al.*, Phys. Lett. **B425**, 329 (1998).
508. C.S. Li and T.C. Yuan, Phys. Rev. **D42**, 3088 (1990) [E: **D47**, 2156 (1993)]; A. Czarnecki and S. Davidson, Phys. Rev. **D47**, 3063 (1993); C.S. Li, Y.-S. Wei, and J.-M. Yang, Phys. Lett. **B285**, 137 (1992).
509. J. Guasch, R.A. Jimenez, and J. Sola, Phys. Lett. **B360**, 47 (1995).
510. M.S. Carena *et al.*, Nucl. Phys. **B577**, 88 (2000).
511. A.A. Barrientos Bendezu and B.A. Kniehl, Phys. Rev. **D59**, 015009 (1999), Phys. Rev. **D61**, 015009 (2000) and Phys. Rev. **D63**, 015009 (2001).

512. A.A. Barrientos Bendezu and B.A. Kniehl, Nucl. Phys. **B568**, 305 (2000).
513. B. Abbott *et al.* [D0 Collab.], Phys. Rev. Lett. **82**, 4975 (1999).
514. A. Abulencia *et al.* [CDF Collab.], Phys. Rev. Lett. **96**, 042003 (2006).
515. V.M. Abazov *et al.* [D0 Collab.], Phys. Lett. **B682**, 278 (2009).
516. ATLAS Collab., JHEP **1206**, 039 (2012).
517. ATLAS Collab., JHEP **03**, 088 (2015).
518. CMS Collab., CMS-PAS-HIG-11-019 (2011).
519. G. Aad *et al.* [ATLAS Collab.], JHEP **1603**, 127 (2016).
520. J. Abdallah *et al.* [DELPHI Collab.], Eur. Phys. J. **C54**, 1 (2008) [E: **C56**, 165 (2008)].
521. R. Dermisek, Mod. Phys. Lett. **A24**, 1631 (2009).
522. J.F. Gunion, JHEP **0908**, 032 (2009).
523. U. Ellwanger, Eur. Phys. J. **C71**, 1782 (2011).
524. W. Love *et al.* [CLEO Collab.], Phys. Rev. Lett. **101**, 151802 (2008).
525. V.M. Abazov *et al.* [D0 Collab.], Phys. Rev. Lett. **103**, 061801 (2009).
526. S. Chatrchyan *et al.* [CMS Collab.], Phys. Rev. Lett. **109**, 121801 (2012).
527. CMS Collab., JHEP **01**, 079 (2016).
528. G. Aad *et al.* [ATLAS Collab.], Eur. Phys. J. **C72**, 2244 (2012).
529. S. Chatrchyan *et al.* [CMS Collab.], Eur. Phys. J. **C72**, 2189 (2012).
530. G. Aad *et al.* [ATLAS Collab.], Phys. Rev. **D89**, 032002 (2014).

12. CKM Quark-Mixing Matrix

Revised January 2018 by A. Ceccucci (CERN), Z. Ligeti (LBNL), and Y. Sakai (KEK).

12.1. Introduction

The masses and mixings of quarks have a common origin in the Standard Model (SM). They arise from the Yukawa interactions with the Higgs condensate,

$$\mathcal{L}_Y = -Y^d_{ij}\,\overline{Q^I_{Li}}\,\phi\,d^I_{Rj} - Y^u_{ij}\,\overline{Q^I_{Li}}\,\epsilon\,\phi^*\,u^I_{Rj} + \text{h.c.}, \tag{12.1}$$

where $Y^{u,d}$ are 3×3 complex matrices, ϕ is the Higgs field, i,j are generation labels, and ϵ is the 2×2 antisymmetric tensor. Q^I_L are left-handed quark doublets, and d^I_R and u^I_R are right-handed down- and up-type quark singlets, respectively, in the weak-eigenstate basis. When ϕ acquires a vacuum expectation value, $\langle\phi\rangle = (0, v/\sqrt{2})$, Eq. (12.1) yields mass terms for the quarks. The physical states are obtained by diagonalizing $Y^{u,d}$ by four unitary matrices, $V^{u,d}_{L,R}$, as $M^f_{\rm diag} = V^f_L\,Y^f\,V^{f\dagger}_R(v/\sqrt{2})$, $f = u, d$. As a result, the charged-current $W^\pm$ interactions couple to the physical u_{Lj} and d_{Lk} quarks with couplings given by

$$\frac{-g}{\sqrt{2}}(\overline{u_L},\,\overline{c_L},\,\overline{t_L})\gamma^\mu\,W^+_\mu\,V_{\rm CKM}\begin{pmatrix} d_L\\ s_L\\ b_L\end{pmatrix} + \text{h.c.},$$

$$V_{\rm CKM} \equiv V^u_L V^{d\dagger}_L = \begin{pmatrix} V_{ud} & V_{us} & V_{ub}\\ V_{cd} & V_{cs} & V_{cb}\\ V_{td} & V_{ts} & V_{tb}\end{pmatrix}. \tag{12.2}$$

This Cabibbo-Kobayashi-Maskawa (CKM) matrix [1,2] is a 3×3 unitary matrix. It can be parameterized by three mixing angles and the CP-violating KM phase [2]. Of the many possible conventions, a standard choice has become [3]

$$\begin{aligned} V_{\rm CKM} &= \begin{pmatrix} 1 & 0 & 0\\ 0 & c_{23} & s_{23}\\ 0 & -s_{23} & c_{23}\end{pmatrix}\begin{pmatrix} c_{13} & 0 & s_{13}e^{-i\delta}\\ 0 & 1 & 0\\ -s_{13}e^{i\delta} & 0 & c_{13}\end{pmatrix}\begin{pmatrix} c_{12} & s_{12} & 0\\ -s_{12} & c_{12} & 0\\ 0 & 0 & 1\end{pmatrix}\\ &= \begin{pmatrix} c_{12}c_{13} & s_{12}c_{13} & s_{13}e^{-i\delta}\\ -s_{12}c_{23}-c_{12}s_{23}s_{13}e^{i\delta} & c_{12}c_{23}-s_{12}s_{23}s_{13}e^{i\delta} & s_{23}c_{13}\\ s_{12}s_{23}-c_{12}c_{23}s_{13}e^{i\delta} & -c_{12}s_{23}-s_{12}c_{23}s_{13}e^{i\delta} & c_{23}c_{13}\end{pmatrix}, \end{aligned} \tag{12.3}$$

where $s_{ij} = \sin\theta_{ij}$, $c_{ij} = \cos\theta_{ij}$, and δ is the phase responsible for all CP-violating phenomena in flavor-changing processes in the SM. The angles θ_{ij} can be chosen to lie in the first quadrant, so $s_{ij}, c_{ij} \geq 0$.

It is known experimentally that $s_{13} \ll s_{23} \ll s_{12} \ll 1$, and it is convenient to exhibit this hierarchy using the Wolfenstein parameterization. We define [4–6]

$$\begin{aligned} s_{12} = \lambda = \frac{|V_{us}|}{\sqrt{|V_{ud}|^2+|V_{us}|^2}}, \qquad s_{23} = A\lambda^2 = \lambda\left|\frac{V_{cb}}{V_{us}}\right|,\\ s_{13}e^{i\delta} = V^*_{ub} = A\lambda^3(\rho+i\eta) = \frac{A\lambda^3(\bar\rho+i\bar\eta)\sqrt{1-A^2\lambda^4}}{\sqrt{1-\lambda^2}[1-A^2\lambda^4(\bar\rho+i\bar\eta)]}. \end{aligned} \tag{12.4}$$

These relations ensure that $\bar\rho + i\bar\eta = -(V_{ud}V^*_{ub})/(V_{cd}V^*_{cb})$ is phase convention independent, and the CKM matrix written in terms of λ, A, $\bar\rho$, and $\bar\eta$ is unitary to all orders in λ. The definitions of $\bar\rho, \bar\eta$ reproduce all approximate results in the literature. For example, $\bar\rho = \rho(1-\lambda^2/2+\ldots)$ and one can write $V_{\rm CKM}$ to $\mathcal{O}(\lambda^4)$ either in terms of $\bar\rho, \bar\eta$ or, traditionally,

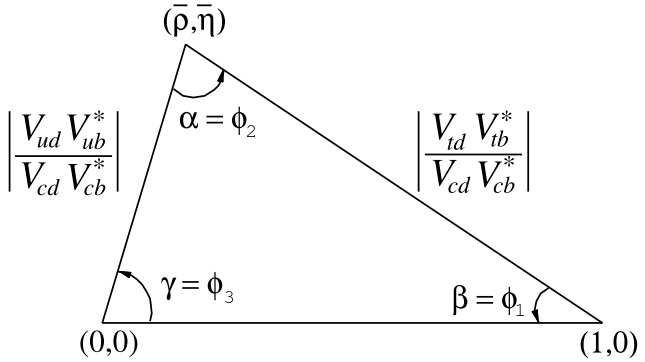

Figure 12.1: Sketch of the unitarity triangle.

$$V_{\rm CKM} = \begin{pmatrix} 1-\lambda^2/2 & \lambda & A\lambda^3(\rho-i\eta)\\ -\lambda & 1-\lambda^2/2 & A\lambda^2\\ A\lambda^3(1-\rho-i\eta) & -A\lambda^2 & 1\end{pmatrix} + \mathcal{O}(\lambda^4)\,. \tag{12.5}$$

The CKM matrix elements are fundamental parameters of the SM, so their precise determination is important. The unitarity of the CKM matrix imposes $\sum_i V_{ij}V^*_{ik} = \delta_{jk}$ and $\sum_j V_{ij}V^*_{kj} = \delta_{ik}$. The six vanishing combinations can be represented as triangles in a complex plane, of which those obtained by taking scalar products of neighboring rows or columns are nearly degenerate. The areas of all triangles are the same, half of the Jarlskog invariant, J [7], which is a phase-convention-independent measure of CP violation, defined by $\text{Im}\big[V_{ij}V_{kl}V^*_{il}V^*_{kj}\big] = J\sum_{m,n}\varepsilon_{ikm}\varepsilon_{jln}$.

The most commonly used unitarity triangle arises from

$$V_{ud}\,V^*_{ub} + V_{cd}\,V^*_{cb} + V_{td}\,V^*_{tb} = 0\,, \tag{12.6}$$

by dividing each side by the best-known one, $V_{cd}V^*_{cb}$ (see Fig. 1). Its vertices are exactly $(0,0)$, $(1,0)$, and, due to the definition in Eq. (12.4), $(\bar\rho,\bar\eta)$. An important goal of flavor physics is to overconstrain the CKM elements, and many measurements can be conveniently displayed and compared in the $\bar\rho,\bar\eta$ plane. While the Lagrangian in Eq. (12.1) is renormalized, and the CKM matrix has a well known scale dependence above the weak scale [8], below $\mu = m_W$ the CKM elements can be treated as constants, with all μ-dependence contained in the running of quark masses and higher-dimension operators.

Unless explicitly stated otherwise, we describe all measurements assuming the SM, to extract magnitudes and phases of CKM elements in Sec. 12.2 and 12.3. Processes dominated by loop-level contributions in the SM are particularly sensitive to new physics. We give the global fit results for the CKM elements in Sec. 12.4, and discuss some implications for beyond standard model physics in Sec. 12.5.

12.2. Magnitudes of CKM elements

12.2.1. $|V_{ud}|$:

The most precise determination of $|V_{ud}|$ comes from the study of superallowed $0^+ \to 0^+$ nuclear beta decays, which are pure vector transitions. Taking the average of the fourteen most precise determinations [9] yields

$$|V_{ud}| = 0.97420 \pm 0.00021. \tag{12.7}$$

The error is dominated by theoretical uncertainties stemming from nuclear Coulomb distortions and radiative corrections. A precise determination of $|V_{ud}|$ is also obtained from the measurement of the neutron lifetime. The theoretical uncertainties are very small, but the determination is limited by the knowledge of the ratio of the axial-vector and vector couplings, $g_A = G_A/G_V$ [10]. The PIBETA experiment [11] has improved the measurement of the $\pi^+ \to \pi^0 e^+\nu$ branching ratio to 0.6%, and quotes $|V_{ud}| = 0.9728 \pm 0.0030$, in agreement with the more precise result listed above. The interest in this measurement is that the determination of $|V_{ud}|$ is very clean theoretically, because it is a pure vector transition and is free from nuclear-structure uncertainties.

12.2.2. $|V_{us}|$:

The product of $|V_{us}|$ and the form factor at $q^2 = 0$, $|V_{us}|\, f_+(0)$, has been extracted traditionally from $K^0_L \to \pi e \nu$ decays in order to avoid isospin-breaking corrections ($\pi^0 - \eta$ mixing) that affect $K^\pm$ semileptonic decay, and the complications induced by a second (scalar) form factor present in the muonic decays. The last round of measurements has lead to enough experimental constraints to justify the comparison between different decay modes. Systematic errors related to the experimental quantities, *e.g.*, the lifetime of neutral or charged kaons, and the form factor determinations for electron and muonic decays, differ among decay modes, and the consistency between different determinations enhances the confidence in the final result. For this reason, we follow the prescription [12] to average $K^0_L \to \pi e \nu$, $K^0_L \to \pi \mu \nu$, $K^\pm \to \pi^0 e^\pm \nu$, $K^\pm \to \pi^0 \mu^\pm \nu$ and $K^0_S \to \pi e \nu$. The average of these five decay modes yields $|V_{us}|\, f_+(0) = 0.2165 \pm 0.0004$. Results obtained from each decay mode, and exhaustive references to the experimental data, are listed for instance in Ref. [10]. The form factor average $f_+(0) = 0.9704 \pm 0.0032$ [13] from three-flavor lattice QCD calculations gives $|V_{us}| = 0.2231 \pm 0.0008$ [10].[1] The broadly used classic calculation of $f_+(0)$ [15] is in good agreement with this value, while other calculations [16] differ by as much as 2%.

The calculation of the ratio of the kaon and pion decay constants enables one to extract $|V_{us}/V_{ud}|$ from $K \to \mu\nu(\gamma)$ and $\pi \to \mu\nu(\gamma)$, where (γ) indicates that radiative decays are included [17]. The KLOE measurement of the $K \to \mu\nu(\gamma)$ branching ratio [18], combined with the lattice QCD result, $f_K/f_\pi = 1.1933 \pm 0.0029$ [13], leads to $|V_{us}| = 0.2253 \pm 0.0007$, where the accuracy is limited by the knowledge of the ratio of the decay constants. The average of these two determinations is quoted as [10]

$$|V_{us}| = 0.2243 \pm 0.0005. \tag{12.8}$$

The latest determination from hyperon decays can be found in Ref. [19]. The authors focus on the analysis of the vector form factor, protected from first order $SU(3)$ breaking effects by the Ademollo-Gatto theorem [20], and treat the ratio between the axial and vector form factors g_1/f_1 as experimental input, thus avoiding first order $SU(3)$ breaking effects in the axial-vector contribution. They find $|V_{us}| = 0.2250 \pm 0.0027$, although this does not include an estimate of the theoretical uncertainty due to second-order $SU(3)$ breaking, contrary to Eq. (12.8). Concerning hadronic τ decays to strange particles, averaging the inclusive decay and the exclusive $\tau \to h\nu$ ($h = \pi$, K) measurements yields $|V_{us}| = 0.2216 \pm 0.0015$ [21].

12.2.3. $|V_{cd}|$:

The magnitude of V_{cd} can be extracted from semileptonic charm decays, using theoretical knowledge of the form factors. In semileptonic D decays, lattice QCD calculations have predicted the normalization of the $D \to \pi\ell\nu$ and $D \to K\ell\nu$ form factors [13]. The dependence on the invariant mass of the lepton pair, q^2, is determined from lattice QCD and theoretical constraints from analyticity [14]. Using three-flavor lattice QCD calculations for $D \to \pi\ell\nu$, $f_+^{D\pi}(0) = 0.666 \pm 0.029$ [13], and the average [21] of the measurements of BaBar [22] and BESIII [23] as well as CLEO-c [24] and Belle [25] of $D \to \pi\ell\nu$ decays, one obtains $|V_{cd}| = 0.2140 \pm 0.0029 \pm 0.0093$, where the first uncertainty is experimental, and the second is from the theoretical uncertainty of the form factor.

The determination of $|V_{cd}|$ is also possible from the leptonic decay $D^+ \to \mu^+\nu$. Its precision has been improved by a recent BESIII measurement [26]. Averaged with an earlier CLEO measurement [27] and the $N_f = 2+1+1$ lattice result, $f_D = 212.15 \pm 1.45$ MeV [13], yields $|V_{cd}| = 0.2164 \pm 0.0050 \pm 0.0014$.[2]

Earlier determinations of $|V_{cd}|$ came from neutrino scattering data. The difference of the ratio of double-muon to single-muon production by neutrino and antineutrino beams is proportional to the charm cross section off valence d quarks, and therefore to $|V_{cd}|^2$ times the average semileptonic branching ratio of charm mesons, $\mathcal{B}_\mu$. The method was used first by CDHS [28] and then by CCFR [29,30] and CHARM II [31]. Averaging these results is complicated, because it requires assumptions about the scale of the QCD corrections, and because $\mathcal{B}_\mu$ is an effective quantity, which depends on the specific neutrino beam characteristics. Given that no recent experimental input is available, we quote the average from a past review, $\mathcal{B}_\mu |V_{cd}|^2 = (0.463 \pm 0.034) \times 10^{-2}$ [32]. Analysis cuts make these experiments insensitive to neutrino energies smaller than 30 GeV. Thus, $\mathcal{B}_\mu$ should be computed using only neutrino interactions with visible energy larger than 30 GeV. An appraisal [33] based on charm-production fractions measured in neutrino interactions [34,35] gives $\mathcal{B}_\mu = 0.088 \pm 0.006$. Data from the CHORUS experiment [36] are sufficiently precise to extract $\mathcal{B}_\mu$ directly, by comparing the number of charm decays with a muon to the total number of charmed hadrons found in the nuclear emulsions. Requiring the visible energy to be larger than 30 GeV, CHORUS finds $\mathcal{B}_\mu = 0.085 \pm 0.009 \pm 0.006$. We use the average of these two determinations, $\mathcal{B}_\mu = 0.087 \pm 0.005$, and obtain $|V_{cd}| = 0.230 \pm 0.011$. Averaging the three determinations above, we find

$$|V_{cd}| = 0.218 \pm 0.004. \tag{12.9}$$

12.2.4. $|V_{cs}|$:

The direct determination of $|V_{cs}|$ is possible from semileptonic D or leptonic D_s decays, using lattice QCD calculations of the semileptonic D form factor or the D_s decay constant. For muonic decays, the average of Belle [37], CLEO-c [38], *BABAR* [39] and BESIII [40] is $\mathcal{B}(D_s^+ \to \mu^+\nu) = (5.54 \pm 0.23) \times 10^{-3}$ [21]. For decays to τ leptons, the average of CLEO-c [38,41,42], *BABAR* [39], Belle [37] and BESIII [40] gives $\mathcal{B}(D_s^+ \to \tau^+\nu) = (5.51 \pm 0.24) \times 10^{-2}$ [21]. From each of these values, determinations of $|V_{cs}|$ can be obtained using the PDG values for the mass and lifetime of the D_s, the masses of the leptons, and $f_{D_s} = (248.83 \pm 1.27)$ MeV [13]. The average of these determinations gives $|V_{cs}| = 1.006 \pm 0.019$, where the error is dominated by the experimental uncertainty. In semileptonic D decays, lattice QCD calculations of the $D \to K\ell\nu$ form factor are available [13]. Using $f_+^{DK}(0) = 0.747 \pm 0.019$ and the average of CLEO-c [24], Belle [25], *BABAR* [43] and recent BESIII [23] measurements of $D \to K\ell\nu$ decays, one obtains $|V_{cs}| = 0.967 \pm 0.025$, where the dominant uncertainty is from the theoretical calculation of the form factor. Averaging the determinations from leptonic and semileptonic decays, using the same assumptions about correlations as HFLAV [21,44], we find

$$|V_{cs}| = 0.997 \pm 0.017. \tag{12.10}$$

Measurements of on-shell $W^\pm$ decays sensitive to $|V_{cs}|$ were made by LEP-2. The W branching ratios depend on the six CKM elements involving quarks lighter than m_W. The W branching ratio to each lepton flavor is $1/\mathcal{B}(W \to \ell\bar{\nu}_\ell) = 3\big[1 + \sum_{u,c,d,s,b} |V_{ij}|^2\,(1 + \alpha_s(m_W)/\pi) + \ldots\big]$. Assuming lepton universality, the measurement $\mathcal{B}(W \to \ell\bar{\nu}_\ell) = (10.83 \pm 0.07 \pm 0.07)\,\%$ [45] implies $\sum_{u,c,d,s,b} |V_{ij}|^2 = 2.002 \pm 0.027$. This is a precise test of unitarity; however, only flavor-tagged W-decays determine $|V_{cs}|$ directly, such as DELPHI's tagged $W^+ \to c\bar{s}$ analysis, yielding $|V_{cs}| = 0.94^{+0.32}_{-0.26} \pm 0.13$ [46].

12.2.5. $|V_{cb}|$:

This matrix element can be determined from exclusive and inclusive semileptonic decays of B mesons to charm. The inclusive determinations use the semileptonic decay rate measurement, together with (certain moments of) the leptonic energy and the hadronic invariant-mass spectra. The theoretical basis is the operator product expansion [47,48], which allows calculation of the decay rate and various spectra as expansions in α_s and inverse powers of the heavy-quark mass. The dependence on m_b, m_c, and the parameters that occur at subleading order is different for different moments, and a large number of measured moments overconstrains all the parameters, and tests the consistency of the determination. The precise extraction of $|V_{cb}|$ requires using a "threshold" quark mass definition [49,50]. Inclusive measurements have been performed using B mesons from

[1] For lattice QCD inputs, we use the averages from Ref. [13], unless the minireviews [10,14] choose different values. We only use unquenched lattice QCD results.

[2] Hereafter the first error is statistical and the second is systematic, unless mentioned otherwise.

Z^0 decays at LEP, and at e^+e^- machines operated at the $\Upsilon(4S)$. At LEP, the large boost of B mesons from the Z^0 decay allows the determination of the moments throughout phase space, which is not possible otherwise, but the large statistics available at the B factories lead to more precise determinations. An average of the measurements and a compilation of the references are provided by Ref. [14]: $|V_{cb}| = (42.2 \pm 0.8) \times 10^{-3}$.

Complementary determinations are based on exclusive semileptonic B decays to D and D^*. In the $m_{b,c} \gg \Lambda_{\rm QCD}$ limit, all form factors are given by a single Isgur-Wise function [51], which depends on the product of the four-velocities of the B and $D^{(*)}$ mesons, $w = v \cdot v'$. Heavy-quark symmetry determines the rate at $w = 1$, the maximum momentum transfer to the leptons, and $|V_{cb}|$ is obtained from an extrapolation to $w = 1$. The current update of the V_{cb} and V_{ub} minireview quotes from exclusive decays $|V_{cb}| = (41.9 \pm 2.0) \times 10^{-3}$ [14], based on the only unfolded measurement of $B \to D^*$ semileptonic decay distributions [52], and using a more general fit [53] than in earlier B factory measurements. This yields the combination,

$$|V_{cb}| = (42.2 \pm 0.8) \times 10^{-3}. \tag{12.11}$$

Less precise measurements of $|V_{cb}|$, not included in this average, can be obtained from $\mathcal{B}(B \to D^{(*)}\tau\bar{\nu})$. The most precise data involving τ modes are the $|V_{cb}|$-independent ratios, $\mathcal{B}(B \to D^{(*)}\tau\bar{\nu})/\mathcal{B}(B \to D^{(*)}\ell\bar{\nu})$ [54]. If the current, approximately $4\,\sigma$, hint of lepton non-universality is confirmed, the determination of $|V_{cb}|$ becomes more complicated.

12.2.6. $|V_{ub}|$:

The determination of $|V_{ub}|$ from inclusive $B \to X_u\ell\bar{\nu}$ decay is complicated due to large $B \to X_c\ell\bar{\nu}$ backgrounds. In most regions of phase space where the charm background is kinematically forbidden, the hadronic physics enters via unknown nonperturbative functions, so-called shape functions. (In contrast, the nonperturbative physics for $|V_{cb}|$ is encoded in a few parameters.) At leading order in $\Lambda_{\rm QCD}/m_b$, there is only one shape function, which can be extracted from the photon energy spectrum in $B \to X_s\gamma$ [55,56], and applied to several spectra in $B \to X_u\ell\bar{\nu}$. The subleading shape functions are modeled in the current determinations. Phase space cuts for which the rate has only subleading dependence on the shape function are also possible [57]. The measurements of both the hadronic and the leptonic systems are important for an optimal choice of phase space. A different approach is to make the measurements more inclusive by extending them deeper into the $B \to X_c\ell\bar{\nu}$ region, and thus reduce the theoretical uncertainties. Analyses of the electron-energy endpoint from CLEO [58], *BABAR* [59], and Belle [60] quote $B \to X_u e\bar{\nu}$ partial rates for $|\vec{p}_e| \geq 2.0\,\text{GeV}$ and $1.9\,\text{GeV}$, which are well below the charm endpoint. The large and pure $B\overline{B}$ samples at the B factories permit the selection of $B \to X_u\ell\bar{\nu}$ decays in events where the other B is fully reconstructed [61]. With this full-reconstruction tag method, the four-momenta of both the leptonic and the hadronic final states can be measured. It also gives access to a wider kinematic region, because of improved signal purity. Ref. [14] quotes the inclusive average, $|V_{ub}| = (4.49 \pm 0.16\ ^{+0.16}_{-0.17} \pm 0.17) \times 10^{-3}$, where the first error is experimental, the second arises from the model dependence quoted by the individual measurements, and the third is an additional one estimated in Ref. [14].

To extract $|V_{ub}|$ from exclusive decays, the form factors have to be known. Experimentally, better signal-to-background ratios are offset by smaller yields. The $B \to \pi\ell\bar{\nu}$ branching ratio is now known to 5%. Lattice QCD calculations of the $B \to \pi\ell\bar{\nu}$ form factor are available [62,63] for the high q^2 region ($q^2 > 16$ or $18\,\text{GeV}^2$). A fit to the experimental partial rates and lattice QCD results versus q^2 yields $|V_{ub}| = (3.70 \pm 0.10 \pm 0.12) \times 10^{-3}$ [21]. Light-cone QCD sum rules are supposed to be applicable for $q^2 < 12\,\text{GeV}^2$ [64], yielding a combination, $|V_{ub}| = (3.67 \pm 0.09 \pm 0.12) \times 10^{-3}$ [21,14].

The uncertainties in extracting $|V_{ub}|$ from inclusive and exclusive decays are different to a large extent. A combination of the determinations is quoted [14] with the error scaled by $\sqrt{\chi^2} = 2.6$,

$$|V_{ub}| = (3.94 \pm 0.36) \times 10^{-3}. \tag{12.12}$$

A determination of $|V_{ub}|$ not included in this average can be obtained from $\mathcal{B}(B \to \tau\bar{\nu}) = (1.06 \pm 0.19) \times 10^{-4}$ [21]. Using $f_B = (192.0 \pm 4.3)\,\text{MeV}$ [13] and $\tau_{B^\pm} = (1.638 \pm 0.004)\,\text{ps}$ [65], we find the remarkably consistent result, $|V_{ub}| = (4.01 \pm 0.37) \times 10^{-3}$. This decay is sensitive, for example, to tree-level charged Higgs contributions, and the measured rate is consistent with the SM expectation. The recent LHCb measurement $|V_{ub}/V_{cb}| = 0.083 \pm 0.006$ [66] from the ratio of $\Lambda_b \to p^+\mu^-\bar{\nu}$ and $\Lambda_b \to \Lambda_c^+\mu^-\bar{\nu}$ in different regions of q^2, provides another complementary determination.

12.2.7. $|V_{td}|$ *and* $|V_{ts}|$:

The CKM elements $|V_{td}|$ and $|V_{ts}|$ are not likely to be precisely measurable in tree-level processes involving top quarks, so one has to rely on determinations from B–$\overline{B}$ oscillations mediated by box diagrams with top quarks, or loop-mediated rare K and B decays. Theoretical uncertainties in hadronic effects limit the accuracy of the current determinations. These can be reduced by taking ratios of processes that are equal in the flavor $SU(3)$ limit to determine $|V_{td}/V_{ts}|$.

The mixing of the two B^0 mesons was discovered by ARGUS [67], and the mass difference is precisely measured by now, $\Delta m_d = (0.5064 \pm 0.0019)\,\text{ps}^{-1}$ [68]. In the B_s^0 system, Δm_s was first measured significantly by CDF [69] and the world average, dominated by a recent LHCb measurement [70], is $\Delta m_s = (17.757 \pm 0.021)\,\text{ps}^{-1}$ [68]. Neglecting corrections suppressed by $|V_{tb}| - 1$, and using the lattice QCD results $f_{B_d}\sqrt{\widehat{B}_{B_d}} = (219 \pm 14)\,\text{MeV}$ and $f_{B_s}\sqrt{\widehat{B}_{B_s}} = (270 \pm 16)\,\text{MeV}$ [13],

$$|V_{td}| = (8.1 \pm 0.5) \times 10^{-3}, \qquad |V_{ts}| = (39.4 \pm 2.3) \times 10^{-3}. \tag{12.13}$$

The uncertainties are dominated by lattice QCD. Several uncertainties are reduced in the calculation of the ratio $\xi = \left(f_{B_s}\sqrt{\widehat{B}_{B_s}}\right)/\left(f_{B_d}\sqrt{\widehat{B}_{B_d}}\right) = 1.239 \pm 0.046$ [13] and therefore the constraint on $|V_{td}/V_{ts}|$ from $\Delta m_d/\Delta m_s$ is more reliable theoretically. These provide a theoretically clean and significantly improved constraint

$$\left|V_{td}/V_{ts}\right| = 0.210 \pm 0.001 \pm 0.008. \tag{12.14}$$

The inclusive branching ratio $\mathcal{B}(B \to X_s\gamma) = (3.32 \pm 0.15) \times 10^{-4}$ extrapolated to $E_\gamma > E_0 = 1.6\,\text{GeV}$ [21] is also sensitive to $|V_{tb}V_{ts}|$. In addition to t-quark penguins, a substantial part of the rate comes from charm contributions proportional to $V_{cb}V_{cs}^*$ via the application of 3×3 CKM unitarity (which is used here). With the NNLO calculation of $\mathcal{B}(B \to X_s\gamma)_{E_\gamma > E_0}/\mathcal{B}(B \to X_c e\bar{\nu})$ [71], we obtain $|V_{ts}/V_{cb}| = 0.98 \pm 0.04$. The $B_s \to \mu^+\mu^-$ rate is also proportional to $|V_{tb}V_{ts}|^2$ in the SM, and the world average, $\mathcal{B}(B_s \to \mu^+\mu^-) = (3.1 \pm 0.7) \times 10^{-9}$ [21], is consistent with the SM, with sizable uncertainties.

A complementary determination of $|V_{td}/V_{ts}|$ is possible from the ratio of $B \to \rho\gamma$ and $K^*\gamma$ rates. The ratio of the neutral modes is theoretically cleaner than that of the charged ones, because the poorly known spectator-interaction contribution is expected to be smaller (W-exchange vs. weak annihilation). For now, because of low statistics, we average the charged and neutral rates assuming the isospin symmetry and heavy-quark limit motivated relation, $|V_{td}/V_{ts}|^2/\xi_\gamma^2 = [\Gamma(B^+ \to \rho^+\gamma) + 2\Gamma(B^0 \to \rho^0\gamma)]/[\Gamma(B^+ \to K^{*+}\gamma) + \Gamma(B^0 \to K^{*0}\gamma)] = (3.36 \pm 0.49)\%$ [21]. Here ξ_γ contains the poorly known hadronic physics. Using $\xi_\gamma = 1.2 \pm 0.2$ [72] gives $|V_{td}/V_{ts}| = 0.220 \pm 0.016 \pm 0.037$, where the first uncertainty is experimental and the second is theoretical.

A theoretically clean determination of $|V_{td}V_{ts}^*|$ is possible from $K^+ \to \pi^+\nu\bar{\nu}$ decay [73]. Experimentally, only seven events have been observed [74] and the rate is consistent with the SM with large uncertainties. Much more data are needed for a precision measurement.

12.2.8. $|V_{tb}|$:

The determination of $|V_{tb}|$ from top decays uses the ratio of branching fractions $R = \mathcal{B}(t \to Wb)/\mathcal{B}(t \to Wq) = |V_{tb}|^2/(\sum_q |V_{tq}|^2) = |V_{tb}|^2$, where $q = b, s, d$. The CDF and DØ measurements performed on data collected during Run II of the Tevatron give $|V_{tb}| > 0.78$ [75] and $0.99 > |V_{tb}| > 0.90$ [76], respectively, at 95% CL. CMS measured the same quantity at 8 TeV and gives $|V_{tb}| > 0.975$ [77] at 95% CL.

The direct determination of $|V_{tb}|$, without assuming unitarity, is possible from the single top quark production cross section. The $(3.30^{+0.52}_{-0.40})$ pb combined cross section [78] of DØ and CDF measurements implies $|V_{tb}| = 1.02^{+0.06}_{-0.05}$. The LHC experiments, ATLAS and CMS, have measured single top quark production cross sections (and extracted $|V_{tb}|$) in t-channel, Wt-channel, and s-channel at 7 TeV, 8 TeV, and 13 TeV [79]. The average of these $|V_{tb}|$ values is calculated to be $|V_{tb}| = 1.019 \pm 0.028$, where all systematic errors and theoretical errors are treated to be fully correlated. The average of Tevatron and LHC values gives

$$|V_{tb}| = 1.019 \pm 0.025\,. \tag{12.15}$$

The experimental systematic uncertainties dominate, and a dedicated combination would be welcome.

A weak constraint on $|V_{tb}|$ can be obtained from precision electroweak data, where top quarks enter in loops. The sensitivity is best in $\Gamma(Z \to b\bar{b})$ and yields $|V_{tb}| = 0.77^{+0.18}_{-0.24}$ [80].

12.3. Phases of CKM elements

As can be seen from Fig. 12.1, the angles of the unitarity triangle are

$$\begin{aligned}
\beta &= \phi_1 = \arg\left(-\frac{V_{cd}V_{cb}^*}{V_{td}V_{tb}^*}\right),\\
\alpha &= \phi_2 = \arg\left(-\frac{V_{td}V_{tb}^*}{V_{ud}V_{ub}^*}\right),\\
\gamma &= \phi_3 = \arg\left(-\frac{V_{ud}V_{ub}^*}{V_{cd}V_{cb}^*}\right).
\end{aligned} \tag{12.16}$$

Since CP violation involves phases of CKM elements, many measurements of CP-violating observables can be used to constrain these angles and the $\bar{\rho}, \bar{\eta}$ parameters.

12.3.1. ϵ *and* ϵ' :

The measurement of CP violation in K^0–$\overline{K}^0$ mixing, $|\epsilon| = (2.228 \pm 0.011) \times 10^{-3}$ [81], provides important information about the CKM matrix. The phase of ϵ is determined by long-distance physics, $\epsilon = \frac{1}{2}\, e^{i\phi_\epsilon} \sin\phi_\epsilon \arg(-M_{12}/\Gamma_{12})$, where $\phi_\epsilon = \arctan|2\Delta m_K/\Delta\Gamma_K| \simeq 43.5^\circ$. The SM prediction can be written as

$$\begin{aligned}
\epsilon = \kappa_\epsilon\, e^{i\phi_\epsilon} \frac{G_F^2 m_W^2 m_K}{12\sqrt{2}\,\pi^2 \Delta m_K}\, f_K^2 \widehat{B}_K \Big\{ &\eta_{tt} S(x_t)\, \mathrm{Im}[(V_{ts}V_{td}^*)^2]\\
&+ 2\eta_{ct} S(x_c, x_t)\, \mathrm{Im}(V_{cs}V_{cd}^* V_{ts}V_{td}^*) + \eta_{cc}\, x_c\, \mathrm{Im}[(V_{cs}V_{cd}^*)^2] \Big\}
\end{aligned} \tag{12.17}$$

where $\kappa_\epsilon \simeq 0.94 \pm 0.02$ [82] includes the effects of $\Delta s = 1$ operators and $\phi_\epsilon \neq \pi/4$ (see also Ref. [83]). The displayed terms are the short-distance $\Delta s = 2$ contribution to $\mathrm{Im}M_{12}$ in the usual phase convention, S is an Inami-Lim function [84], $x_q = m_q^2/m_W^2$, and η_{ij} are perturbative QCD corrections. The constraint from ϵ in the $\bar{\rho}, \bar{\eta}$ plane is bounded by approximate hyperbolas. Lattice QCD determined the bag parameter $\widehat{B}_K = 0.7625 \pm 0.0097$ [13], and the main uncertainties now come from $(V_{ts}V_{td}^*)^2$, which is approximately $\sigma(|V_{cb}|^4) \sim \sigma(A^4)$, the η_{ij} coefficients, and estimates of κ_ϵ.

The measurement of $6\,\mathrm{Re}(\epsilon'/\epsilon) = 1 - |\eta_{00}/\eta_{+-}|^2$, where each $\eta_{ij} = \langle\pi^i\pi^j|\mathcal{H}|K_L\rangle\,/\,\langle\pi^i\pi^j|\mathcal{H}|K_S\rangle$ violates CP, provides a qualitative test of the CKM mechanism, and strong constraints on many new physics scenarios. Its nonzero value, $\mathrm{Re}(\epsilon'/\epsilon) = (1.67 \pm 0.23) \times 10^{-3}$ [81], demonstrated the existence of direct CP violation, a prediction of the KM ansatz. While $\mathrm{Re}(\epsilon'/\epsilon) \propto \mathrm{Im}(V_{td}V_{ts}^*)$, this quantity cannot easily be used to extract CKM parameters, because the electromagnetic penguin contributions tend to cancel the gluonic penguins for large m_t [85], thus enhancing hadronic uncertainties. Most SM estimates [86–89] agree with the observed value, indicating that $\bar{\eta}$ is positive. Progress in lattice QCD [90] may yield a precise SM prediction in the future.

12.3.2. $\boldsymbol{\beta}$ **/** $\boldsymbol{\phi_1}$:

12.3.2.1. *Charmonium modes:*

CP-violation measurements in B-meson decays provide direct information on the angles of the unitarity triangle, shown in Fig. 12.1. These overconstraining measurements serve to improve the determination of the CKM elements, or to reveal effects beyond the SM.

The time-dependent CP asymmetry of neutral B decays to a final state f common to B^0 and $\overline{B}^0$ is given by [91,92]

$$\mathcal{A}_f = \frac{\Gamma(\overline{B}^0(t) \to f) - \Gamma(B^0(t) \to f)}{\Gamma(\overline{B}^0(t) \to f) + \Gamma(B^0(t) \to f)} = S_f \sin(\Delta m_d\, t) - C_f \cos(\Delta m_d\, t), \tag{12.18}$$

where

$$S_f = \frac{2\,\mathrm{Im}\lambda_f}{1 + |\lambda_f|^2}\,, \qquad C_f = \frac{1 - |\lambda_f|^2}{1 + |\lambda_f|^2}\,, \qquad \lambda_f = \frac{q}{p}\frac{\bar{A}_f}{A_f}\,. \tag{12.19}$$

Here, q/p describes B^0–$\overline{B}^0$ mixing and, to a good approximation in the SM, $q/p = V_{tb}^* V_{td}/V_{tb}V_{td}^* = e^{-2i\beta + \mathcal{O}(\lambda^4)}$ in the usual phase convention. A_f ($\bar{A}_f$) is the amplitude of the $B^0 \to f$ ($\overline{B}^0 \to f$) decay. If f is a CP eigenstate, and amplitudes with one CKM phase dominate the decay, then $|A_f| = |\bar{A}_f|$, $C_f = 0$, and $S_f = \sin(\arg\lambda_f) = \eta_f \sin 2\phi$, where η_f is the CP eigenvalue of f and 2ϕ is the phase difference between the $B^0 \to f$ and $B^0 \to \overline{B}^0 \to f$ decay paths. A contribution of another amplitude to the decay with a different CKM phase makes the value of S_f sensitive to relative strong-interaction phases between the decay amplitudes (it also makes $C_f \neq 0$ possible).

The $b \to c\bar{c}s$ decays to CP eigenstates ($B^0 \to$ charmonium $K^0_{S,L}$) are the theoretically cleanest examples, measuring $S_f = -\eta_f \sin 2\beta$. The $b \to sq\bar{q}$ penguin amplitudes have dominantly the same weak phase as the $b \to c\bar{c}s$ tree amplitude. Since only λ^2-suppressed penguin amplitudes introduce a new CP-violating phase, amplitudes with a single weak phase dominate, and we expect $\big||\bar{A}_{\psi K}/A_{\psi K}| - 1\big| < 0.01$. The e^+e^- asymmetric-energy B-factory experiments, *BABAR* [93] and Belle [94], provide precise measurements. The world average including LHCb [95] and other measurements is [21]

$$\sin 2\beta = 0.691 \pm 0.017\,. \tag{12.20}$$

This measurement has a four-fold ambiguity in β, which can be resolved by a global fit as mentioned in Sec. 12.4. Experimentally, the two-fold ambiguity $\beta \to \pi/2 - \beta$ (but not $\beta \to \pi + \beta$) can be resolved by a time-dependent angular analysis of $B^0 \to J/\psi K^{*0}$ [96,97], or a time-dependent Dalitz plot analysis of $B^0 \to \overline{D}^0 h^0$. The time-dependent Dalitz plot analysis of $B^0 \to \overline{D}^0 h^0$ ($h^0 = \pi^0, \eta, \omega$) with $\overline{D}^0 \to K^0_S\pi^+\pi^-$, jointly performed by Belle and *BABAR*, excludes the $\pi/2 - \beta$ solution with 7.3σ condfidence level [98].

These results indicate that negative $\cos 2\beta$ solutions are very unlikely, in agreement with the global CKM fit result.

The $b \to c\bar{c}d$ mediated transitions, such as $B^0 \to J/\psi\pi^0$ and $B^0 \to D^{(*)+}D^{(*)-}$, also measure approximately $\sin 2\beta$. However, the dominant component of the $b \to d$ penguin amplitude has a different CKM phase ($V_{tb}^*V_{td}$) than the tree amplitude ($V_{cb}^*V_{cd}$), and its magnitudes are of the same order in λ. Therefore, the effect of penguins could be large, resulting in $S_f \neq -\eta_f \sin 2\beta$ and $C_f \neq 0$. Such decay modes have been measured by *BABAR*, Belle, and LHCb. The world averages [21], $S_{J/\psi\pi^0} = -0.93 \pm 0.15$, $S_{J/\psi\rho^0} = -0.66^{+0.16}_{-0.12}$, $S_{D^+D^-} = -0.84 \pm 0.12$, and $S_{D^{*+}D^{*-}} = -0.71 \pm 0.09$ (where $\eta_f = +1$ for the $J/\psi\pi^0$ and D^+D^- modes, while $J/\psi\rho^0$ and $D^{*+}D^{*-}$ are mixtures of CP even and odd states), are consistent with $\sin 2\beta$ obtained from $B^0 \to$ charmonium K^0 decays, and the C_f's are consistent with zero, although the uncertainties are sizable.

The $b \to c\bar{u}d$ decays, $B^0 \to \overline{D}{}^0 h^0$ with $\overline{D}{}^0 \to CP$ eigenstates, have no penguin contributions and provide theoretically clean $\sin 2\beta$ measurements. The joint analysis of *BABAR* and Belle data gives $S_{D^{(*)}h^0} = -0.66 \pm 0.12$ [99].

12.3.2.2. *Penguin-dominated modes:*

The $b \to s\bar{q}q$ penguin-dominated decays have the same CKM phase as the $b \to c\bar{c}s$ tree level decays, up to corrections suppressed by λ^2, since $V_{tb}^* V_{ts} = -V_{cb}^* V_{cs}[1 + \mathcal{O}(\lambda^2)]$. Therefore, decays such as $B^0 \to \phi K^0$ and $\eta' K^0$ provide $\sin 2\beta$ measurements in the SM. Any new physics contribution to the amplitude with a different weak phase would give rise to $S_f \neq -\eta_f \sin 2\beta$, and possibly $C_f \neq 0$. Therefore, the main interest in these modes is not simply to measure $\sin 2\beta$, but to search for new physics. Measurements of many other decay modes in this category, such as $B \to \pi^0 K_S^0$, $K_S^0 K_S^0 K_S^0$, *etc.*, have also been performed by *BABAR* and Belle. The results and their uncertainties are summarized in Fig. 12.3 and Table 12.1 of Ref. [92]. The comparison of CP violation measurements between tree-dominated and penguin-dominated modes in B_s^0 decays provides similar sensitivity to new physics.

12.3.3. $\boldsymbol{\alpha}$ / $\boldsymbol{\phi_2}$:

Since α is the phase between $V_{tb}^* V_{td}$ and $V_{ub}^* V_{ud}$, only time-dependent CP asymmetries in $b \to u\bar{u}d$ decay dominated modes can directly measure $\sin 2\alpha$, in contrast to $\sin 2\beta$, where several different transitions can be used. Since $b \to d$ penguin amplitudes have a different CKM phase than $b \to u\bar{u}d$ tree amplitudes, and their magnitudes are of the same order in λ, the penguin contribution can be sizable, which makes the determination of α complicated. To date, α has been measured in $B \to \pi\pi$, $\rho\pi$ and $\rho\rho$ decay modes.

12.3.3.1. $B \to \pi\pi$*:*

It is well established from the data that there is a sizable contribution of $b \to d$ penguin amplitudes in $B \to \pi\pi$ decays. Thus, $S_{\pi^+\pi^-}$ in the time-dependent $B^0 \to \pi^+\pi^-$ analysis does not measure $\sin 2\alpha$, but

$$S_{\pi^+\pi^-} = \sqrt{1 - C_{\pi^+\pi^-}^2}\, \sin(2\alpha + 2\Delta\alpha), \tag{12.21}$$

where $2\Delta\alpha$ is the phase difference between $e^{2i\gamma}\bar{A}_{\pi^+\pi^-}$ and $A_{\pi^+\pi^-}$. The value of $\Delta\alpha$, and hence α, can be extracted using the isospin relation among the amplitudes of $B^0 \to \pi^+\pi^-$, $B^0 \to \pi^0\pi^0$, and $B^+ \to \pi^+\pi^0$ decays [100],

$$\frac{1}{\sqrt{2}} A_{\pi^+\pi^-} + A_{\pi^0\pi^0} - A_{\pi^+\pi^0} = 0\,, \tag{12.22}$$

and a similar expression for the $\bar{A}_{\pi\pi}$'s. This method utilizes the fact that a pair of pions from $B \to \pi\pi$ decay must be in a zero angular momentum state, and, because of Bose statistics, they must have even isospin. Consequently, $\pi^0\pi^\pm$ is in a pure isospin-2 state, while the penguin amplitudes only contribute to the isospin-0 final state. The latter does not hold for the electroweak penguin amplitudes, but their effect is expected to be small. The isospin analysis uses the world averages of *BABAR*, Belle and LHCb measurements [21] $S_{\pi^+\pi^-} = -0.68 \pm 0.04$, $C_{\pi^+\pi^-} = -0.27 \pm 0.04$, the branching fractions of all three modes, and the direct CP asymmetry $C_{\pi^0\pi^0} = -0.33 \pm 0.22$ [21,101]. This analysis leads to 16 mirror solutions for $0 \leq \alpha < 2\pi$. Because of this, and due to the experimental uncertainties, some of these solutions are not well separated, and only the following constraint on α can be obtained at present at 68% CL: $-13.5^\circ < \alpha < 15.7^\circ$, $74.3^\circ < \alpha < 105.6^\circ$, and $118.5^\circ < \alpha < 151.5^\circ$ [21,102].

12.3.3.2. $B \to \rho\rho$*:*

The decay $B^0 \to \rho^+\rho^-$ contains two vector mesons in the final state, and so in general is a mixture of CP-even and CP-odd components. Therefore, it was thought that extracting α from this mode would be complicated.

However, the longitudinal polarization fractions in $B^+ \to \rho^+\rho^0$ and $B^0 \to \rho^+\rho^-$ decays were measured to be close to unity [103], which implies that the final states are almost purely CP-even. Furthermore, $\mathcal{B}(B^0 \to \rho^0\rho^0) = (0.95 \pm 0.16) \times 10^{-6}$ is much smaller than $\mathcal{B}(B^0 \to \rho^+\rho^-) = (24.2^{+3.1}_{-3.2}) \times 10^{-6}$ and $\mathcal{B}(B^+ \to \rho^+\rho^0) = (24.0^{+1.9}_{-2.0}) \times 10^{-6}$ [21], which implies that the effect of the penguin contributions is small. The isospin analysis using the world averages, $S_{\rho^+\rho^-} = -0.14 \pm 0.13$ and $C_{\rho^+\rho^-} = -0.00 \pm 0.09$ [21,102], together with the time-dependent CP asymmetry, $S_{\rho^0\rho^0} = -0.3 \pm 0.7$ and $C_{\rho^0\rho^0} = -0.2 \pm 0.9$ [104], and the above mentioned branching fractions and longitudinal polarisation fractions, gives $\alpha = (90.9^{+5.6}_{-5.5})^\circ$ or $\alpha = (179.1^{+5.5}_{-5.6})^\circ$ [21,102], with mirror solutions at $3\pi/2 - \alpha$. A possible small violation of Eq. (12.22) due to the finite width of the ρ [105] is neglected.

12.3.3.3. $B \to \rho\pi$*:*

The final state in $B^0 \to \rho^+\pi^-$ decay is not a CP eigenstate, but this decay proceeds via the same quark-level diagrams as $B^0 \to \pi^+\pi^-$, and both B^0 and $\overline{B}{}^0$ can decay to $\rho^+\pi^-$, while the final state in $B^0 \to \rho^0\pi^0$ is a CP eigenstate. Consequently, mixing-induced CP violation can occur in B^0 and $\overline{B}{}^0$ decays to $\rho^\pm\pi^\mp$ and $\rho^0\pi^0$. The time-dependent Dalitz plot analysis of $B^0 \to \pi^+\pi^-\pi^0$ decays permits the extraction of α with a single discrete ambiguity, $\alpha \to \alpha + \pi$, since one knows the variation of the strong phases in the interference regions of the $\rho^+\pi^-$, $\rho^-\pi^+$, and $\rho^0\pi^0$ amplitudes in the Dalitz plot [106]. The combination of Belle [107] and *BABAR* [108] measurements gives $\alpha = (54.1^{+7.7}_{-10.3})^\circ$ and $(141.8^{+4.8}_{-5.4})^\circ$ [109], $\alpha = (53.4^{+8.0}_{-11.0})^\circ$ and $(143.4^{+3.9}_{-4.8})^\circ$ [21,102], where some tension exists with the $\rho\rho$ mode and the global fit, but the constraint is still moderate.

Combining the $B \to \pi\pi$, $\rho\pi$, and $\rho\rho$ decay modes [21,102], α is constrained as

$$\alpha = (84.5^{+5.9}_{-5.2})^\circ. \tag{12.23}$$

Similar results can be found in Refs. [109,110].

12.3.4. $\boldsymbol{\gamma}$ / $\boldsymbol{\phi_3}$:

By virtue of Eq. (12.16), γ does not depend on CKM elements involving the top quark, so it can be measured in tree-level B decays. This is an important distinction from the measurements of α and β, and implies that the measurements of γ are unlikely to be affected by physics beyond the SM.

12.3.4.1. $B^\pm \to DK^\pm$*:*

The interference of $B^- \to D^0 K^-$ ($b \to c\bar{u}s$) and $B^- \to \overline{D}{}^0 K^-$ ($b \to u\bar{c}s$) transitions can be studied in final states accessible in both D^0 and $\overline{D}{}^0$ decays [91]. In principle, it is possible to extract the B and D decay amplitudes, the relative strong phases, and the weak phase γ from the data.

A practical complication is that the precision depends sensitively on the ratio of the interfering amplitudes

$$r_B = \left| A(B^- \to \overline{D}{}^0 K^-) \,/\, A(B^- \to D^0 K^-) \right|, \tag{12.24}$$

which is around 0.1. The original GLW method [111,112] considers D decays to CP eigenstates, such as $B^\pm \to D_{CP}^{(*)}(\to \pi^+\pi^-)K^{(*)\pm}$. To alleviate the smallness of r_B and make the interfering amplitudes (which are products of the B and D decay amplitudes) comparable in magnitude, the ADS method [113] considers final states where Cabibbo-allowed $\overline{D}{}^0$ and doubly-Cabibbo-suppressed D^0 decays interfere. Measurements have been made by the B factories, CDF, and LHCb, using both methods. The GLW method currently gives only a loose constraint on γ, $15.3^\circ < \gamma < 28.9^\circ$, $70.2^\circ < \gamma < 87.6^\circ$, $92.4^\circ < \gamma < 109.8^\circ$, and $151.1^\circ < \gamma < 164.7^\circ$ at 68% CL; while the ADS method provides $\gamma = (73^{+12}_{-18})^\circ$ [21,102].

It was realized that both D^0 and $\overline{D}{}^0$ have large branching fractions to certain three-body final states, such as $K_S^0\pi^+\pi^-$, and the analysis can be optimized by studying the Dalitz plot dependence of the interferences [114,115]. The best present determination of γ comes from this method. Combining the measurements by Belle [116], *BABAR* [117] and LHCb [118], $\gamma = (67.3^{+8.0}_{-7.9})^\circ$ is obtained [21,102]. The error is sensitive to the central value of the amplitude ratio r_B (and r_B^* for the D^*K mode), for which Belle found somewhat larger central values than *BABAR* and LHCb. The same values of $r_B^{(*)}$ enter

the ADS analyses, and the data can be combined to fit for $r_B^{(*)}$ and γ. The D^0–$\overline{D}^0$ mixing has been neglected in all measurements, but its effect on γ is far below the present experimental accuracy [119], unless D^0–$\overline{D}^0$ mixing is due to CP-violating new physics, in which case it can be included in the analysis [120].

Combining the GLW, ADS, and Dalitz analyses [21,102], γ is constrained as[3]

$$\gamma = (73.5^{+4.2}_{-5.1})^\circ. \tag{12.25}$$

Similar results can be found in Refs. [109,110].

12.3.4.2. $B^0 \to D^{(*)\pm}\pi^\mp$*:*

The interference of $b \to u$ and $b \to c$ transitions can be studied in $\overline{B}^0 \to D^{(*)+}\pi^-$ ($b \to c\bar{u}d$) and $\overline{B}^0 \to B^0 \to D^{(*)+}\pi^-$ ($\bar{b} \to \bar{u}c\bar{d}$) decays and their CP conjugates, since both B^0 and $\overline{B}^0$ decay to $D^{(*)\pm}\pi^\mp$ (or $D^\pm\rho^\mp$, *etc.*). Since there are only tree and no penguin contributions to these decays, in principle, it is possible to extract from the four time-dependent rates the magnitudes of the two hadronic amplitudes, their relative strong phase, and the weak phase between the two decay paths, which is $2\beta + \gamma$.

A complication is that the ratio of the interfering amplitudes is very small, $r_{D\pi} = A(B^0 \to D^+\pi^-)/A(\overline{B}^0 \to D^+\pi^-) = \mathcal{O}(0.01)$ (and similarly for $r_{D^*\pi}$ and $r_{D\rho}$), and therefore it has not been possible to measure it. To obtain $2\beta + \gamma$, $SU(3)$ flavor symmetry and dynamical assumptions have been used to relate $A(\overline{B}^0 \to D^-\pi^+)$ to $A(\overline{B}^0 \to D_s^-\pi^+)$, so this measurement is not model independent at present. Combining the $D^\pm\pi^\mp$, $D^{*\pm}\pi^\mp$ and $D^\pm\rho^\mp$ measurements [121] gives $\sin(2\beta+\gamma) > 0.68$ at 68% CL [109], consistent with the previously discussed results for β and γ. The amplitude ratio is much larger in the analogous $B_s^0 \to D_s^\pm K^\mp$ decays, which allows a model-independent extraction of $\gamma - 2\beta_s$ [122] (here $\beta_s = \arg(-V_{ts}V_{tb}^*/V_{cs}V_{cb}^*)$ is related to the phase of B_s mixing). Recent measurement by LHCb [123] gives $(127^{+17}_{-22})^\circ$ using a constraint on $2\beta_s$ (see Sec. 12.5).

12.4. Global fit in the Standard Model

Using the independently measured CKM elements mentioned in the previous sections, the unitarity of the CKM matrix can be checked. We obtain $|V_{ud}|^2+|V_{us}|^2+|V_{ub}|^2 = 0.9994\pm0.0005$ (1st row), $|V_{cd}|^2+|V_{cs}|^2+|V_{cb}|^2 = 1.043\pm0.034$ (2nd row), $|V_{ud}|^2+|V_{cd}|^2+|V_{td}|^2 = 0.9967\pm0.0018$ (1st column), and $|V_{us}|^2+|V_{cs}|^2+|V_{ts}|^2 = 1.046\pm0.034$ (2nd column), respectively. The uncertainties in the second row and column are dominated by that of $|V_{cs}|$. For the second row, a slightly better check is obtained from the measurement of $\sum_{u,c,d,s,b}|V_{ij}|^2$ in Sec. 12.2.4 minus the sum in the first row above: $|V_{cd}|^2 + |V_{cs}|^2 + |V_{cb}|^2 = 1.002 \pm 0.027$. These provide strong tests of the unitarity of the CKM matrix. With the significantly improved direct determination of $|V_{tb}|$, the unitarity checks for the third row and column have also become fairly precise, leaving decreasing room for mixing with other states. The sum of the three angles of the unitarity triangle, $\alpha + \beta + \gamma = (180 \pm 7)^\circ$, is also consistent with the SM expectation.

The CKM matrix elements can be most precisely determined using a global fit to all available measurements and imposing the SM constraints (*i.e.*, three generation unitarity). The fit must also use theory predictions for hadronic matrix elements, which sometimes have significant uncertainties. There are several approaches to combining the experimental data. CKMfitter [6,109] and Ref. [124] (which develops [125,126] further) use frequentist statistics, while UTfit [110,127] uses a Bayesian approach. These approaches provide similar results.

The constraints implied by the unitarity of the three generation CKM matrix significantly reduce the allowed range of some of the CKM elements. The fit for the Wolfenstein parameters defined in Eq. (12.4) gives

$$\begin{aligned} \lambda &= 0.22453 \pm 0.00044\,, & A &= 0.836 \pm 0.015\,, \\ \bar{\rho} &= 0.122^{+0.018}_{-0.017}\,, & \bar{\eta} &= 0.355^{+0.012}_{-0.011}\,. \end{aligned} \tag{12.26}$$

[3] The combined fit also includes other available results, such as those from $B_s \to D_s K$ and $B_s \to DK\pi$.

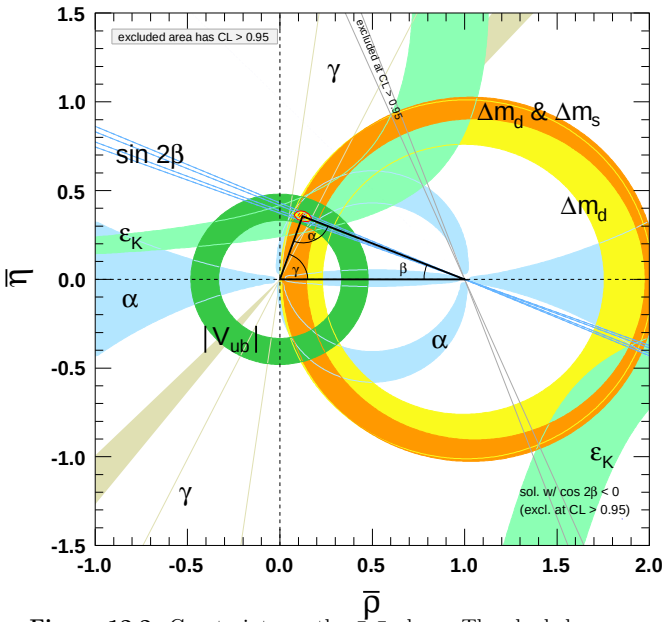

Figure 12.2: Constraints on the $\bar{\rho}, \bar{\eta}$ plane. The shaded areas have 95% CL.

These values are obtained using the method of Refs. [6,109]. Using the prescription of Refs. [110,127] gives $\lambda = 0.22465 \pm 0.00039$, $A = 0.832 \pm 0.009$, $\bar{\rho} = 0.139 \pm 0.016$, $\bar{\eta} = 0.346 \pm 0.010$ [128]. The fit results for the magnitudes of all nine CKM elements are

$$V_{\rm CKM} = \begin{pmatrix} 0.97446 \pm 0.00010 & 0.22452 \pm 0.00044 & 0.00365 \pm 0.00012 \\ 0.22438 \pm 0.00044 & 0.97359^{+0.00010}_{-0.00011} & 0.04214 \pm 0.00076 \\ 0.00896^{+0.00024}_{-0.00023} & 0.04133 \pm 0.00074 & 0.999105 \pm 0.000032 \end{pmatrix}, \tag{12.27}$$

and the Jarlskog invariant is $J = (3.18 \pm 0.15) \times 10^{-5}$.

Figure 12.2 illustrates the constraints on the $\bar{\rho}, \bar{\eta}$ plane from various measurements and the global fit result. The shaded 95% CL regions all overlap consistently around the global fit region.

12.5. Implications beyond the SM

The effects in B, B_s, K, and D decays and mixings due to high-scale physics (W, Z, t, H in the SM, and unknown heavier particles) can be parameterized by operators composed of SM fields, obeying the $SU(3) \times SU(2) \times U(1)$ gauge symmetry. Flavor-changing neutral currents, suppressed in the SM, are especially sensitive to beyond SM (BSM) contributions. Processes studied in great detail, both experimentally and theoretically, include neutral meson mixings, $B_{(s)} \to X\gamma$, $X\ell^+\ell^-$, $\ell^+\ell^-$, $K \to \pi\nu\bar{\nu}$, etc. The BSM contributions to these operators are suppressed by powers of the scale of new physics. Already at lowest order, there are many dimension-6 operators, and the observable effects of BSM interactions are encoded in their coefficients. In the SM, these coefficients are determined by just the four CKM parameters, and the W, Z, and quark masses. For example, Δm_d, $\Gamma(B \to \rho\gamma)$, $\Gamma(B \to \pi\ell^+\ell^-)$, and $\Gamma(B \to \ell^+\ell^-)$ are all proportional to $|V_{td}V_{tb}|^2$ in the SM, however, they may receive unrelated contributions from new physics. The new physics contributions may or may not obey the SM relations. (For example, the flavor sector of the MSSM contains 69 CP-conserving parameters and 41 CP-violating phases, *i.e.*, 40 new ones [129]). Thus, similar to the measurements of $\sin 2\beta$ in tree- and loop-dominated decay modes, overconstraining measurements of the magnitudes and phases of flavor-changing neutral-current amplitudes give good sensitivity to new physics.

To illustrate the level of suppression required for BSM contributions, consider a class of models in which the unitarity of the CKM matrix is maintained, and the dominant effect of new physics is to modify the neutral meson mixing amplitudes [130] by $(z_{ij}/\Lambda^2)(\overline{q}_i\gamma^\mu P_L q_j)^2$ (see [131,132]). It is only known since the measurements of γ and α that the SM gives the leading contribution to B^0–$\overline{B}^0$ mixing [6,133].

Nevertheless, new physics with a generic weak phase may still contribute to neutral meson mixings at a significant fraction of the SM [134,135,127]. The existing data imply that $\Lambda/|z_{ij}|^{1/2}$ has to exceed about 10^4 TeV for $K^0-\overline{K}^0$ mixing, 10^3 TeV for $D^0-\overline{D}^0$ mixing, 500 TeV for $B^0-\overline{B}^0$ mixing, and 100 TeV for $B_s^0-\overline{B}_s^0$ mixing [127,132]. (Some other operators are even better constrained [127].) The constraints are the strongest in the kaon sector, because the CKM suppression is the most severe. Thus, if there is new physics at the TeV scale, $|z_{ij}| \ll 1$ is required. Even if $|z_{ij}|$ are suppressed by a loop factor and $|V_{ti}^* V_{tj}|^2$ (in the down quark sector), similar to the SM, one expects percent-level effects, which may be observable in forthcoming flavor physics experiments. To constrain such extensions of the SM, many measurements irrelevant for the SM-CKM fit, such as the CP asymmetry in semileptonic $B_{d,s}^0$ decays, $A_{\rm SL}^{d,s}$, are important [136]. The current world averages [21] are consistent with the SM, with experimental uncertainties far greater than those of the theory predictions.

Many key measurements which are sensitive to BSM flavor physics are not useful to think about in terms of constraining the unitarity triangle in Fig. 12.1. For example, besides the angles in Eq. (12.16), a key quantity in the B_s system is $\beta_s = \arg(-V_{ts}V_{tb}^*/V_{cs}V_{cb}^*)$, which is the small, λ^2-suppressed, angle of a "squashed" unitarity triangle, obtained by taking the scalar product of the second and third columns. This angle can be measured via time-dependent CP violation in $B_s^0 \to J/\psi\,\phi$, similar to β in $B^0 \to J/\psi K^0$. Since the $J/\psi\,\phi$ final state is not a CP eigenstate, an angular analysis of the decay products is needed to separate the CP-even and CP-odd components, which give opposite asymmetries. In the SM, the asymmetry for the CP-even part is $2\beta_s$ (sometimes the notation $\phi_s = -2\beta_s$ plus a possible BSM contribution to the B_s mixing phase is used). Testing if the data agree with the SM prediction, $2\beta_s = 0.0370 \pm 0.0006$ [109], is another sensitive probe of the SM. The current world average, dominated by LHCb [137] including $B_s \to J/\psi\,K^+K^-$ and $J/\psi\,\pi^+\pi^-$ measurements, is $2\beta_s = 0.021 \pm 0.031$ [21]. This uncertainty is about 20 times the SM uncertainty; thus a lot will be learned from higher-precision measurements in the future. Searches for CP violation in the charm sector, in particular in $D^0-\overline{D}^0$ mixing, provide complementary sensitivity to new physics.

In the kaon sector, the two measured CP-violating observables ϵ and ϵ' are tiny, so models in which all sources of CP violation are small were viable before the B-factory measurements. Since the measurement of $\sin 2\beta$, we know that CP violation can be an $\mathcal{O}(1)$ effect, and only flavor mixing is suppressed between the three quark generations. Thus, many models with spontaneous CP violation are excluded. In the kaon sector, a very clean test of the SM will come from measurements of $K^+ \to \pi^+\nu\bar{\nu}$ and $K_L^0 \to \pi^0\nu\bar{\nu}$. These loop-induced rare decays are sensitive to new physics, and will allow a determination of β, independent of its value measured in B decays [138].

The CKM elements are fundamental parameters, so they should be measured as precisely as possible. The overconstraining measurements of CP asymmetries, mixing, semileptonic, and rare decays severely constrain the magnitudes and phases of possible new physics contributions to flavor-changing interactions. If new particles are observed at the LHC, it will be important to explore their flavor parameters as precisely as possible to understand the underlying physics.

References:

1. N. Cabibbo, Phys. Rev. Lett. **10**, 531 (1963).
2. M. Kobayashi and T. Maskawa, Prog. Theor. Phys. **49**, 652 (1973).
3. L.L. Chau and W.Y. Keung, Phys. Rev. Lett. **53**, 1802 (1984).
4. L. Wolfenstein, Phys. Rev. Lett. **51**, 1945 (1983).
5. A.J. Buras *et al.*, Phys. Rev. **D50**, 3433 (1994) [hep-ph/9403384].
6. J. Charles *et al.* [CKMfitter Group], Eur. Phys. J. **C41**, 1 (2005) [hep-ph/0406184].
7. C. Jarlskog, Phys. Rev. Lett. **55**, 1039 (1985).
8. W.J. Marciano and A. Sirlin, Nucl. Phys. **B93**, 303 (1975); K.S. Babu, Z. Phys. **C35**, 69 (1987).
9. J.C. Hardy and I. S. Towner, PoS **CKM2016**, 028 (2016).
10. E. Blucher and W.J. Marciano, "V_{ud}, V_{us}, the Cabibbo Angle and CKM Unitarity," in this *Review*.
11. D. Pocanic *et al.*, Phys. Rev. Lett. **93**, 181803 (2004) [hep-ex/0312030].
12. M. Antonelli *et al.* [The FlaviaNet Kaon Working Group], Eur. Phys. J. **C69**, 399 (2010); see also www.lnf.infn.it/wg/vus.
13. S. Aoki *et al.*, "Review of lattice results concerning low energy particle physics," Eur. Phys. J. **C77**, 112 (2017) [arXiv:1607.00299].
14. R. Kowalewski and T. Mannel, "Determination of V_{cb} and V_{ub}," in this *Review*.
15. H. Leutwyler and M. Roos, Z. Phys. **C25**, 91 (1984).
16. J. Bijnens and P. Talavera, Nucl. Phys. **B669**, 341 (2003) [hep-ph/0303103];
M. Jamin *et al.*, JHEP **402**, 047 (2004) [hep-ph/0401080];
V. Cirigliano *et al.*, JHEP **504**, 6 (2005) [hep-ph/0503108];
C. Dawson *et al.*, PoS **LAT2005**, 337 (2005) [hep-lat/0510018];
N. Tsutsui *et al.* [JLQCD Collab.], PoS **LAT2005**, 357 (2005) [hep-lat/0510068];
M. Okamoto [Fermilab Lattice Collab.], hep-lat/0412044.
17. W.J. Marciano, Phys. Rev. Lett. **93**, 231803 (2004) [hep-ph/0402299].
18. F. Ambrosino *et al.* [KLOE Collab.], Phys. Lett. **B632**, 76 (2006) [hep-ex/0509045].
19. N. Cabibbo *et al.*, Ann. Rev. Nucl. and Part. Sci. **53**, 39 (2003) [hep-ph/0307298];
Phys. Rev. Lett. **92**, 251803 (2004) [hep-ph/0307214].
20. M. Ademollo and R. Gatto, Phys. Rev. Lett. **13**, 264 (1964).
21. Y. Amhis *et al.*, Heavy Flavor Averaging Group, Eur. Phys. J. **C77**, 895 (2017) arXiv:1612.07233, and updates at http://www.slac.stanford.edu/xorg/hflav/. When we quote values updated from the above paper, we also cite the used web page.
22. J.P. Lees *et al.* [*BABAR* Collab.], Phys. Rev. **D91**, 052022 (2015) [arXiv:1412.5502].
23. M. Ablikim *et al.* [BES III Collab.] Phys. Rev. **D92**, 072012 (2015) [arXiv:1508.07560].
24. D. Besson *et al.* [CLEO Collab.], Phys. Rev. **D80**, 032005 (2009) [arXiv:0906.2983].
25. L. Widhalm *et al.* [Belle Collab.], Phys. Rev. Lett. **97**, 061804 (2006) [hep-ex/0604049].
26. M. Ablikim *et al.* [BESIII Collab.], Phys. Rev. **D89**, 051104 (2014) [arXiv:1312.0374].
27. B.I. Eisenstein *et al.* [CLEO Collab.], Phys. Rev. **D78**, 052003 (2008) [arXiv:0806.2112].
28. H. Abramowicz *et al.* [CHDS Collab.], Z. Phys. **C15**, 19 (1982).
29. S.A. Rabinowitz *et al.* [CCFR Collab.], Phys. Rev. Lett. **70**, 134 (1993).
30. A.O. Bazarko *et al.* [CCFR Collab.], Z. Phys. **C65**, 189 (1995) [hep-ex/9406007].
31. P. Vilain *et al.* [CHARM II Collab.], Eur. Phys. J. **C11**, 19 (1999).
32. F.J. Gilman *et al.*, Phys. Lett. **B592**, 793 (2004).
33. G.D. Lellis *et al.*, Phys. Rept. **399**, 227 (2004) [Erratum *ibid.* **411**, 323 (2005)].
34. N. Ushida *et al.* [Fermilab E531 Collab.], Phys. Lett. **B206**, 380 (1988).
35. T. Bolton, hep-ex/9708014.
36. A. Kayis-Topaksu *et al.* [CHORUS Collab.], Phys. Lett. **B626**, 24 (2005).
37. A. Zupanc *et al.* [Belle Collab.], JHEP **1309**, 139 (2013) [arXiv:1307.6240].
38. J.P. Alexander *et al.* [CLEO Collab.], Phys. Rev. **D79**, 052001 (2009) [arXiv:0901.1216].
39. P. del Amo Sanchez *et al.* [*BABAR* Collab.], Phys. Rev. **D82**, 091103 (2010) [arXiv:1008.4080].
40. M. Ablikim *et al.* [BESIII Collab.], Phys. Rev. **D94**, 072004 (2010) [arXiv:1608.06732].

41. P. Onyisi *et al.* [CLEO Collab.], Phys. Rev. **D79**, 052002 (2009) [arXiv:0901.1147].
42. P. Naik *et al.* [CLEO Collab.], Phys. Rev. **D80**, 112004 (2009) [arXiv:0910.3602].
43. B. Aubert *et al.* [*BABAR* Collab.], Phys. Rev. **D76**, 052005 (2007) [arXiv:0704.0020].
44. Heavy Flavor Averaging Group [21], Charm World avarage value for V_{cs}, Octover 2016 http://www.slac.stanford.edu/xorg/hflav/charm/Vcs/october16/results.html.
45. LEP W branching fraction results for this Review of Particle Physics, LEPEWWG/ XSEC/2005-01, http://lepewwg.web.cern.ch/LEPEWWG/lepww/4f/Winter05/.
46. P. Abreu *et al.* [DELPHI Collab.], Phys. Lett. **B439**, 209 (1998).
47. I. Bigi *et al.*, Phys. Rev. Lett. **71**, 496 (1993) [hep-ph/9304225].
48. A.V. Manohar and M.B. Wise, Phys. Rev. **D49**, 1310 (1994) [hep-ph/9308246].
49. I. Bigi *et al.*, Phys. Rev. **D56**, 4017 (1997) [hep-ph/9704245].
50. A.H. Hoang *et al.*, Phys. Rev. **D59**, 074017 (1999) [hep-ph/9811239]; Phys. Rev. Lett. **82**, 277 (1999) [hep-ph/9809423]; A.H. Hoang and T. Teubner, Phys. Rev. **D60**, 114027 (1999) [hep-ph/9904468].
51. N. Isgur and M.B. Wise, Phys. Lett. **B237**, 527 (1990); N. Isgur and M.B. Wise, Phys. Lett. **B232**, 113 (1989).
52. A. Abdesselam *et al.* [Belle Collab.], [arXiv:1702.01521].
53. C.G. Boyd, B. Grinstein and R.F. Lebed, Phys. Rev. **D56**, 6895 (1997) [hep-ph/9705252]; Nucl. Phys. **B461**, 493 (1996) [hep-ph/9508211].
54. J.P. Lees *et al.* [*BABAR* Collab.], Phys. Rev. Lett. **109**, 101802 (2012) [arXiv:1205.5442]; M. Huschle *et al.* [Belle Collaboration], Phys. Rev. **D92**, 072014 (2015) [arXiv:1507.03233]; R. Aaij *et al.* [LHCb Collaboration], Phys. Rev. Lett. **115**, 111803 (2015) [arXiv:1506.08614].
55. M. Neubert, Phys. Rev. **D49**, 3392 (1994) [hep-ph/9311325]; Phys. Rev. **D49**, 4623 (1994) [hep-ph/9312311].
56. I. Bigi *et al.*, Int. J. Mod. Phys. **A9**, 2467 (1994) [hep-ph/9312359].
57. C.W. Bauer *et al.*, Phys. Lett. **B479**, 395 (2000) [hep-ph/0002161]; Phys. Rev. **D64**, 113004 (2001) [hep-ph/0107074].
58. A. Bornheim *et al.* [CLEO Collab.], Phys. Rev. Lett. **88**, 231803 (2002) [hep-ex/0202019].
59. B. Aubert *et al.* [*BABAR* Collab.], Phys. Rev. **D73**, 012006 (2006) [hep-ex/0509040].
60. A. Limosani *et al.* [Belle Collab.], Phys. Lett. **B621**, 28 (2005) [hep-ex/0504046].
61. P. Urquijo *et al.* [Belle Collab.], Phys. Rev. Lett. **104**, 021801 (2010) [arXiv:0907.0379]; J.P. Lees *et al.* [*BABAR* Collab.], Phys. Rev. **D86**, 032004 (2012) [arXiv:1112.0702].
62. E. Dalgic *et al.*, Phys. Rev. **D73**, 074502 (2006) [Erratum *ibid.* **D75**, 119906 (2007)] [hep-lat/0601021].
63. J.A. Bailey *et al.* [Fermilab Lattice and MILC Collabs.], Phys. Rev. **D92**, 014024 (2015) [arXiv:1503.07839].
64. P. Ball and R. Zwicky, Phys. Rev. **D71**, 014015 (2005) [hep-ph/0406232]; A. Khodjamirian *et al.*, Phys. Rev. **D83**, 094031 (2011) [arXiv:1103.2655].
65. Particle listing, in this *Review*.
66. R. Aaij *et al.* [LHCb Collaboration], Nature Phys. **11**, 743 (2015) [arXiv:1504.01568].
67. H. Albrecht *et al.* [ARGUS Collab.], Phys. Lett. **B192**, 245 (1987).
68. O. Schneider, "B^0–$\overline{B}^0$ mixing," in this *Review*.
69. A. Abulencia *et al.* [CDF Collab.], Phys. Rev. Lett. **97**, 242003 (2006) [hep-ex/0609040].
70. R. Aaij *et al.* [LHCb Collab.], New J. Phys. 15, 053021 (2013) [arXiv:1304.4741].
71. M. Misiak *et al.*, Phys. Rev. Lett. **114**, 0221801 (2015) [arXiv:1503.01789]; M. Czakon *et al.*, JHEP **1504**, 168 (2015) [arXiv:1503.01791].
72. B. Grinstein and D. Pirjol, Phys. Rev. **D62**, 093002 (2000) [hep-ph/0002216]; A. Ali *et al.*, Phys. Lett. **B595**, 323 (2004) [hep-ph/0405075]; M. Beneke *et al.*, Nucl. Phys. **B612**, 25 (2001) [hep-ph/0106067]; S.W. Bosch and G. Buchalla, Nucl. Phys. **B621**, 459 (2002) [hep-ph/0106081]; Z. Ligeti and M. B. Wise, Phys. Rev. **D60**, 117506 (1999) [hep-ph/9905277]; D. Becirevic *et al.*, JHEP **305**, 7 (2003) [hep-lat/0301020]; P. Ball *et al.*, Phys. Rev. **D75**, 054004 (2007) [hep-ph/0612081]; W. Wang *et al.*, arXiv:0711.0432; C.D. Lu *et al.*, Phys. Rev. **D76**, 014013 (2007) [hep-ph/0701265].
73. A.J. Buras *et al.*, Phys. Rev. Lett. **95**, 261805 (2005) [hep-ph/0508165].
74. A.V. Artamonov *et al.* [E949 Collab.], Phys. Rev. Lett. **101**, 191802 (2008) [arXiv:0808.2459]; Phys. Rev. **D79**, 092004 (2009) [arXiv:0903.0030].
75. D. Acosta *et al.* [CDF Collab.], Phys. Rev. Lett. **95**, 102002 (2005) [hep-ex/0505091].
76. V.M. Abazov *et al.* [DØ Collab.], Phys. Rev. Lett. **107**, 121802 (2011) [arXiv:1106.5436].
77. V. Khachatryan *et al.* [CMS Collab.] Phys. Lett. **B736**, 33 (2014) [arXiv:1404.2292].
78. T. A. Aaltonen *et al.* [CDF and DØ Collab.], Phys. Rev. Lett. **115**, 152003 (2015) [arXiv:1503.05027].
79. LHC Top Working Group summary plots, single top quark production, Nov. 2017, https://twiki.cern.ch/twiki/bin/view/LHCPhysics/LHCTopWGSummaryPlots.
80. J. Swain and L. Taylor, Phys. Rev. **D58**, 093006 (1998) [hep-ph/9712420].
81. "K_L^0 meson" particle listing, in this *Review*.
82. A.J. Buras, D. Guadagnoli and G. Isidori, Phys. Lett. **B688**, 309 (2010) [arXiv:1002.3612]; for earlier discussions, see Ref. [83].
83. E.A. Andriyash, G.G. Ovanesyan and M.I. Vysotsky, Phys. Lett. **B599**, 253 (2004) [hep-ph/0310314]; K. Anikeev *et al.*, hep-ph/0201071; A.J. Buras and D. Guadagnoli, Phys. Rev. **D78**, 033005 (2008) [arXiv:0805.3887].
84. T. Inami and C.S. Lim, Prog. Theor. Phys. **65**, 297 (1981) [Erratum *ibid.* **65**, 1772 (1981)].
85. J.M. Flynn and L. Randall, Phys. Lett. **B224**, 221 (1989); G. Buchalla, A.J. Buras, and M.K. Harlander, Nucl. Phys. **B337**, 313 (1990).
86. M. Ciuchini *et al.*, Phys. Lett. **B301**, 263 (1993) [hep-ph/9212203]; A.J. Buras, M. Jamin, and M.E. Lautenbacher, Nucl. Phys. **B408**, 209 (1993) [hep-ph/9303284].
87. T. Hambye *et al.*, Nucl. Phys. **B564**, 391 (2000) [hep-ph/9906434].
88. S. Bertolini *et al.*, Phys. Rev. **D63**, 056009 (2001) [hep-ph/0002234].
89. A. Pich, hep-ph/0410215.
90. Z. Bai *et al.* [RBC and UKQCD Collabs.], Phys. Rev. Lett. **115**, 212001 (2015) [arXiv:1505.07863].
91. A.B. Carter and A.I. Sanda, Phys. Rev. Lett. **45**, 952 (1980); Phys. Rev. **D23**, 1567 (1981).
92. A more detailed discussion and references can be found in: T. Gershon and Y. Nir, "CP violation in meson decays," in this *Review*.
93. B. Aubert *et al.* [*BABAR* Collab.], Phys. Rev. **D79**, 072009 (2009) [arXiv:0902.1708].
94. I. Adachi *et al.* [Belle Collab.], Phys. Rev. Lett. **108**, 171802 (2012) [arXiv:1201.4643].
95. R. Aaij *et al.* [LHCb Collab.], Phys. Rev. Lett. **115**, 031601 (2015) [arXiv:1503.07089].
96. B. Aubert *et al.* [*BABAR* Collab.], Phys. Rev. **D71**, 032005 (2005) [hep-ex/0411016].

97. R. Itoh *et al.* [Belle Collab.], Phys. Rev. Lett. **95**, 091601 (2005) [hep-ex/0504030].
98. I. Adachi *et al.* [Belle and *BABAR* Collabs.], arXiv:1804.06152; arXiv:1804.06153.
99. A. Abdesselam *et al.* [*BABAR* and Belle Collab.], Phys. Rev. Lett. **115**, 121604 (2015) [arXiv:1505.04147].
100. M. Gronau and D. London, Phys. Rev. Lett. **65**, 3381 (1990).
101. Heavy Flavor Averaging Group [21] *CP* Asymmetries in Charmless B Decay, August 2017, www.slac.stanford.edu/xorg/hflav/rare/August2017/acp/index.html.
102. Heavy Flavor Averaging Group [21], Moriond 2018 updates for Unitarity Triangle Parameters: www.slac.stanford.edu/xorg/hflav/triangle/moriond2018/.
103. J. Zhang *et al.* [Belle Collab.], Phys. Rev. Lett. **91**, 221801 (2003) [hep-ex/0306007];
A. Somov *et al.* [Belle Collab.], Phys. Rev. Lett. **96**, 171801 (2006) [hep-ex/0601024];
B. Aubert *et al.* [*BABAR* Collab.], Phys. Rev. Lett. **97**, 261801 (2006) [hep-ex/0607092]; Phys. Rev. **D76**, 052007 (2007) [arXiv:0705.2157].
104. B. Aubert *et al.* [*BABAR* Collab.], Phys. Rev. **D78**, 071104 (2008) [arXiv:0807.4977].
105. A.F. Falk *et al.*, Phys. Rev. **D69**, 011502 (2004) [hep-ph/0310242].
106. H.R. Quinn and A.E. Snyder, Phys. Rev. **D48**, 2139 (1993).
107. A. Kusaka *et al.* [Belle Collab.], Phys. Rev. Lett. **98**, 221602 (2007) [hep-ex/0701015].
108. B. Aubert *et al.* [*BABAR* Collab.], Phys. Rev. **D88**, 121003 (2013) [arXiv:1304.3503].
109. A. Höcker *et al.*, Eur. Phys. J. **C21**, 225 (2001) [hep-ph/0104062]; see also Ref. [6] and updates at http://ckmfitter.in2p3.fr/.
110. M. Bona *et al.* [UTfit Collab.], JHEP **507**, 28 (2005) [hep-ph/0501199], and updates at http://www.utfit.org/.
111. M. Gronau and D. London, Phys. Lett. **B253**, 483 (1991).
112. M. Gronau and D. Wyler, Phys. Lett. **B265**, 172 (1991).
113. D. Atwood *et al.*, Phys. Rev. Lett. **78**, 3257 (1997) [hep-ph/9612433]; Phys. Rev. **D63**, 036005 (2001) [hep-ph/0008090].
114. A. Bondar, talk at the Belle analysis workshop, Novosibirsk, September 2002;
A. Poluektov *et al.* [Belle Collab.], Phys. Rev. **D70**, 072003 (2004) [hep-ex/0406067].
115. A. Giri *et al.*, Phys. Rev. **D68**, 054018 (2003) [hep-ph/0303187].
116. A. Poluektov *et al.* [Belle Collab.], Phys. Rev. **D81**, 112002 (2010) [arXiv:1003.3360].
117. B. Aubert *et al.* [*BABAR* Collab.], Phys. Rev. Lett. **105**, 121801 (2010) [arXiv:1005.1096].
118. R. Aaij *et al.*, JHEP **1410**, 097 (2014) [arXiv:1408.2748].
119. Y. Grossman *et al.*, Phys. Rev. **D72**, 031501 (2005) [hep-ph/0505270].
120. A. Amorim *et al.*, Phys. Rev. **D59**, 056001 (1999) [hep-ph/9807364].
121. B. Aubert *et al.* [*BABAR* Collab.], Phys. Rev. **D71**, 112003 (2005) [hep-ex/0504035]; Phys. Rev. **D73**, 111101 (2006) [hep-ex/0602049]; F.J. Ronga *et al.* [Belle Collab.], Phys. Rev. **D73**, 092003 (2006) [hep-ex/0604013]; S. Bahinipati *et al.* [Belle Collab.], Phys. Rev. **D84**, 021101 (2011) [arXiv:1102.0888].
122. R. Aleksan *et al.*, Z. Phys. **C54**, 653 (1992).
123. R. Aaij *et al.* [LHCb Collab.], LHCb-CONF-2016-015.
124. G.P. Dubois-Felsmann *et al.*, hep-ph/0308262; G. Eigen *et al.*, Phys. Rev. **D89**, 033004 (2014) [arXiv:1301.5867].
125. "The *BABAR* physics book: Physics at an asymmetric B factory," (P.F. Harrison and H.R. Quinn, eds.), SLAC-R-0504, 1998.
126. S. Plaszczynski and M.H. Schune, hep-ph/9911280.
127. M. Bona *et al.* [UTfit Collab.], JHEP **0803**, 049 (2008) [arXiv:0707.0636].
128. We thank the CKMfitter and UTfit groups for performing fits and preparing plots using input values from this *Review*.
129. H.E. Haber, Nucl. Phys. Proc. Supp. **62**, 469 (1998) [hep-ph/9709450];
Y. Nir, hep-ph/0109090.
130. J.M. Soares and L. Wolfenstein, Phys. Rev. **D47**, 1021 (1993); T. Goto *et al.*, Phys. Rev. **D53**, 6662 (1996) [hep-ph/9506311]; J.P. Silva and L. Wolfenstein, Phys. Rev. **D55**, 5331 (1997) [hep-ph/9610208].
131. Y. Grossman, Z. Ligeti, and Y. Nir, Prog. Theor. Phys. **122**, 125 (2009) [arXiv:0904.4262].
132. G. Isidori, Y. Nir, and G. Perez, Ann. Rev. Nucl. and Part. Sci. **60**, 355 (2010) [arXiv:1002.0900]; G. Isidori, [arXiv:1302.0661].
133. Z. Ligeti, Int. J. Mod. Phys. **A20**, 5105 (2005) [hep-ph/0408267].
134. J. Charles *et al.*, Phys. Rev. **D89**, 033016 (2014) [arXiv:1309.2293].
135. K. Agashe *et al.*, hep-ph/0509117.
136. S. Laplace *et al.*, Phys. Rev. **D65**, 094040 (2002) [hep-ph/0202010].
137. R. Aaij *et al.* [LHCb Collab.], JHEP **1708**, 037 (2017) [arXiv:1704.08217].
138. G. Buchalla and A.J. Buras, Phys. Lett. **B333**, 221 (1994) [hep-ph/9405259].

13. CP Violation in the Quark Sector

Revised August 2017 by T. Gershon (University of Warwick) and Y. Nir (Weizmann Institute).

The CP transformation combines charge conjugation C with parity P. Under C, particles and antiparticles are interchanged, by conjugating all internal quantum numbers, *e.g.*, $Q \to -Q$ for electromagnetic charge. Under P, the handedness of space is reversed, $\vec{x} \to -\vec{x}$. Thus, for example, a left-handed electron e^-_L is transformed under CP into a right-handed positron, e^+_R.

If CP were an exact symmetry, the laws of Nature would be the same for matter and for antimatter. We observe that most phenomena are C- and P-symmetric, and therefore, also CP-symmetric. In particular, these symmetries are respected by the gravitational, electromagnetic, and strong interactions. The weak interactions, on the other hand, violate C and P in the strongest possible way. For example, the charged W bosons couple to left-handed electrons, e^-_L, and to their CP-conjugate right-handed positrons, e^+_R, but to neither their C-conjugate left-handed positrons, e^+_L, nor their P-conjugate right-handed electrons, e^-_R. While weak interactions violate C and P separately, CP is still preserved in most weak interaction processes. The CP symmetry is, however, violated in certain rare processes, as discovered in neutral K decays in 1964 [1], and observed in recent years in B decays. A K_L meson decays more often to $\pi^-e^+\nu_e$ than to $\pi^+e^-\overline{\nu}_e$, thus allowing electrons and positrons to be unambiguously distinguished, but the decay-rate asymmetry is only at the 0.003 level. The CP-violating effects observed in the B system are larger: the parameter describing the CP asymmetry in the decay time distribution of $B^0/\overline{B}^0$ meson transitions to CP eigenstates like $J/\psi K_S$ is about 0.7 [2,3]. These effects are related to K^0–$\overline{K}^0$ and B^0–$\overline{B}^0$ mixing, but CP violation arising solely from decay amplitudes has also been observed, first in $K \to \pi\pi$ decays [4–6], and more recently in B^0 [7,8], B^+ [9–11], and B^0_s [12] decays. Similar effects could also occur in decays of b baryons, and evidence for CP violation in Λ^0_b decays has been found at the 3.3σ level [13]. CP violation is not yet experimentally established in the D system, where the Standard Model effects are expected to be $\mathcal{O}(10^{-3})$. Moreover, CP violation has not yet been observed in processes involving the top quark, nor in flavor-conserving processes such as electric dipole moments, nor in the lepton sector; for all of these any significant observation would be a clear indication of physics beyond the Standard Model.

In addition to parity and to continuous Lorentz transformations, there is one other spacetime operation that could be a symmetry of the interactions: time reversal T, $t \to -t$. Violations of T symmetry have been observed in neutral K decays [14]. More recently, exploiting the fact that for neutral B mesons both flavor tagging and CP tagging can be used [15], T violation has been observed between states that are not CP-conjugate [16]. Moreover, T violation is expected as a corollary of CP violation if the combined CPT transformation is a fundamental symmetry of Nature [17]. All observations indicate that CPT is indeed a symmetry of Nature. Furthermore, one cannot build a locally Lorentz-invariant quantum field theory with a Hermitian Hamiltonian that violates CPT. (At several points in our discussion, we avoid assumptions about CPT, in order to identify cases where evidence for CP violation relies on assumptions about CPT.)

Within the Standard Model, CP symmetry is broken by complex phases in the Yukawa couplings (that is, the couplings of the Higgs scalar to quarks). When all manipulations to remove unphysical phases in this model are exhausted, one finds that there is a single CP-violating parameter [18]. In the basis of mass eigenstates, this single phase appears in the 3×3 unitary matrix that gives the W-boson couplings to an up-type antiquark and a down-type quark. (If the Standard Model is supplemented with Majorana mass terms for the neutrinos, the analogous mixing matrix for leptons has three CP-violating phases.) The beautifully consistent and economical Standard-Model description of CP violation in terms of Yukawa couplings, known as the Kobayashi-Maskawa (KM) mechanism [18], agrees with all measurements to date. (Some measurements are in tension with the predictions, and are discussed in more detail below. Pending verification, the results are not considered to change the overall picture of agreement with the Standard Model.) Furthermore, one can fit the data allowing new physics contributions to loop processes to compete with, or even dominate over, the Standard Model amplitudes [19,20]. Such an analysis provides model-independent proof that the KM phase is different from zero, and that the matrix of three-generation quark mixing is the dominant source of CP violation in meson decays.

The current level of experimental accuracy and the theoretical uncertainties involved in the interpretation of the various observations leave room, however, for additional subdominant sources of CP violation from new physics. Indeed, almost all extensions of the Standard Model imply that there are such additional sources. Moreover, CP violation is a necessary condition for baryogenesis, the process of dynamically generating the matter-antimatter asymmetry of the Universe [21]. Despite the phenomenological success of the KM mechanism, it fails (by several orders of magnitude) to accommodate the observed asymmetry [22]. This discrepancy strongly suggests that Nature provides additional sources of CP violation beyond the KM mechanism. The evidence for neutrino masses implies that CP can be violated also in the lepton sector. This situation makes leptogenesis [23,24], a scenario where CP-violating phases in the Yukawa couplings of the neutrinos play a crucial role in the generation of the baryon asymmetry, a very attractive possibility. The expectation of new sources motivates the large ongoing experimental effort to find deviations from the predictions of the KM mechanism.

CP violation can be experimentally searched for in a variety of processes, such as hadron decays, electric dipole moments of neutrons, electrons and nuclei, and neutrino oscillations. Hadron decays via the weak interaction probe flavor-changing CP violation. The search for electric dipole moments may find (or constrain) sources of CP violation that, unlike the KM phase, are not related to flavor-changing couplings. Following the discovery of the Higgs boson [25,26], searches for CP violation in the Higgs sector are becoming feasible. Future searches for CP violation in neutrino oscillations might provide further input on leptogenesis.

The present measurements of CP asymmetries provide some of the strongest constraints on the weak couplings of quarks. Future measurements of CP violation in K, D, B, and B^0_s meson decays will provide additional constraints on the flavor parameters of the Standard Model, and can probe new physics. In this review, we give the formalism and basic physics that are relevant to present and near future measurements of CP violation in the quark sector.

Before going into details, we list here the observables where CP violation has been observed at a level above 5σ [27–29]:

- Indirect CP violation in $K \to \pi\pi$ and $K \to \pi\ell\nu$ decays, and in the $K_L \to \pi^+\pi^-e^+e^-$ decay, is given by

$$|\epsilon| = (2.228 \pm 0.011) \times 10^{-3}\,. \tag{13.1}$$

- Direct CP violation in $K \to \pi\pi$ decays is given by

$$\mathcal{R}e(\epsilon'/\epsilon) = (1.65 \pm 0.26) \times 10^{-3}\,. \tag{13.2}$$

- CP violation in the interference of mixing and decay in the tree-dominated $b \to c\bar{c}s$ transitions, such as $B^0 \to \psi K^0$, is given by (we use K^0 throughout to denote results that combine K_S and K_L modes, but use the sign appropriate to K_S):

$$S_{\psi K^0} = +0.691 \pm 0.017\,. \tag{13.3}$$

- CP violation in the interference of mixing and decay in modes governed by the tree-dominated $b \to c\bar{u}d$ transitions is given by

$$S_{D^{(*)}h^0} = +0.71 \pm 0.09\,, \tag{13.4}$$

- CP violation in the interference of mixing and decay in various modes related to $b \to c\bar{c}d$ transitions is given by

$$S_{\psi\pi^0} = -0.93 \pm 0.15\,, \tag{13.5}$$

$$S_{D^+D^-} = -0.84 \pm 0.12\,. \tag{13.6}$$

$$S_{D^{*+}D^{*-}} = -0.71 \pm 0.09\,. \tag{13.7}$$

- CP violation in the interference of mixing and decay in various modes related to $b \to q\bar{q}s$ (penguin) transitions is given by

$$S_{\phi K^0} = +0.74^{+0.11}_{-0.13}\,, \tag{13.8}$$

$$S_{\eta' K^0} = +0.63 \pm 0.06\,, \tag{13.9}$$

$$S_{f_0 K^0} = +0.69^{+0.10}_{-0.12}\,, \tag{13.10}$$

$$S_{K^+K^-K_S} = +0.68^{+0.09}_{-0.10}\,, \tag{13.11}$$

- CP violation in the interference of mixing and decay in the $B^0 \to \pi^+\pi^-$ mode is given by

$$S_{\pi^+\pi^-} = -0.68 \pm 0.04\,. \tag{13.12}$$

- Direct CP violation in the $B^0 \to \pi^+\pi^-$ mode is given by

$$C_{\pi^+\pi^-} = -0.27 \pm 0.04\,. \tag{13.13}$$

- Direct CP violation in the $\overline{B}^0 \to K^-\pi^+$ mode is given by

$$\mathcal{A}_{\overline{B}^0 \to K^-\pi^+} = -0.082 \pm 0.006\,. \tag{13.14}$$

- Direct CP violation in $B^+ \to D_+ K^+$ decays (D_+ is the CP-even neutral D state) is given by

$$\mathcal{A}_{B^+ \to D_+ K^+} = +0.129 \pm 0.012\,, \tag{13.15}$$

  while the corresponding quantity in the case that the neutral D meson is reconstructed in the suppressed $K^-\pi^+$ final state is

$$\mathcal{A}_{B^+ \to D_{K^-\pi^+} K^+} = -0.41 \pm 0.06\,, \tag{13.16}$$

- Direct CP violation in the $\overline{B}^0_s \to K^+\pi^-$ mode is given by

$$\mathcal{A}_{\overline{B}^0_s \to K^+\pi^-} = +0.26 \pm 0.04\,. \tag{13.17}$$

- Direct CP violation in $B^+ \to K^+K^-\pi^+$ decays is given by

$$\mathcal{A}_{B^+ \to K^+K^-\pi^+} = -0.118 \pm 0.022\,. \tag{13.18}$$

In addition, large CP violation effects have been observed in certain regions of the phase space of $B^+ \to K^+K^-K^+$, $\pi^+\pi^-K^+$, $\pi^+\pi^-\pi^+$ and $K^+K^-\pi^+$ decays.

13.1. Formalism

The phenomenology of CP violation for neutral flavored mesons is particularly interesting, since many of the observables can be cleanly interpreted. Although the phenomenology is superficially different for K^0, D^0, B^0, and B^0_s decays, this is primarily because each of these systems is governed by a different balance between decay rates, oscillations, and lifetime splitting. However, the general considerations presented in this section are identical for all flavored neutral pseudoscalar mesons. The phenomenology of CP violation for neutral mesons that do not carry flavor quantum numbers (such as the $\eta^{(\prime)}$ state) is quite different: such states are their own antiparticles and have definite CP eigenvalues, so the signature of CP violation is simply the decay to a final state with the opposite CP. Such decays are mediated by the electromagnetic or (OZI-suppressed) strong interaction, where CP violation is not expected and has not yet been observed. In the remainder of this review, we restrict ourselves to considerations of weakly decaying hadrons.

In this section, we present a general formalism for, and classification of, CP violation in the decay of a weakly decaying hadron, denoted M. We pay particular attention to the case that M is a K^0, D^0, B^0, or B^0_s meson. Subsequent sections describe the CP-violating phenomenology, approximations, and alternative formalisms that are specific to each system.

13.1.1. *Charged- and neutral-hadron decays* :

We define decay amplitudes of M (which could be charged or neutral) and its CP conjugate $\overline{M}$ to a multi-particle final state f and its CP conjugate $\overline{f}$ as

$$A_f = \langle f\,|\mathcal{H}|\,M\rangle\,, \quad \overline{A}_f = \langle f\,|\mathcal{H}|\,\overline{M}\rangle\,,$$
$$A_{\overline{f}} = \langle \overline{f}\,|\mathcal{H}|\,M\rangle\,, \quad \overline{A}_{\overline{f}} = \langle \overline{f}\,|\mathcal{H}|\,\overline{M}\rangle\,, \tag{13.19}$$

where $\mathcal{H}$ is the Hamiltonian governing weak interactions. The action of CP on these states introduces phases ξ_M and ξ_f that depend on their flavor content, according to

$$CP|M\rangle = e^{+i\xi_M}\,|\overline{M}\rangle\,, \quad CP|f\rangle = e^{+i\xi_f}\,|\overline{f}\rangle\,, \tag{13.20}$$

with

$$CP|\overline{M}\rangle = e^{-i\xi_M}\,|M\rangle\,, \quad CP|\overline{f}\rangle = e^{-i\xi_f}\,|f\rangle \tag{13.21}$$

so that $(CP)^2 = 1$. The phases ξ_M and ξ_f are arbitrary and unobservable because of the flavor symmetry of the strong interaction. If CP is conserved by the dynamics, $[CP, \mathcal{H}] = 0$, then A_f and $\overline{A}_{\overline{f}}$ have the same magnitude and an arbitrary unphysical relative phase

$$\overline{A}_{\overline{f}} = e^{i(\xi_f - \xi_M)}\,A_f\,. \tag{13.22}$$

13.1.2. *Neutral-meson mixing* :

A state that is initially a superposition of M^0 and $\overline{M}^0$, say

$$|\psi(0)\rangle = a(0)|M^0\rangle + b(0)|\overline{M}^0\rangle\,, \tag{13.23}$$

will evolve in time acquiring components that describe all possible decay final states $\{f_1, f_2, \ldots\}$, that is,

$$|\psi(t)\rangle = a(t)|M^0\rangle + b(t)|\overline{M}^0\rangle + c_1(t)|f_1\rangle + c_2(t)|f_2\rangle + \cdots\,. \tag{13.24}$$

If we are interested in computing only the values of $a(t)$ and $b(t)$ (and not the values of all $c_i(t)$), and if the times t in which we are interested are much larger than the typical strong interaction scale, then we can use a much simplified formalism [30]. The simplified time evolution is determined by a 2×2 effective Hamiltonian $\mathbf{H}$ that is not Hermitian, since otherwise the mesons would only oscillate and not decay. Any complex matrix, such as $\mathbf{H}$, can be written in terms of Hermitian matrices $\mathbf{M}$ and $\mathbf{\Gamma}$ as

$$\mathbf{H} = \mathbf{M} - \frac{i}{2}\mathbf{\Gamma}\,. \tag{13.25}$$

$\mathbf{M}$ and $\mathbf{\Gamma}$ are associated with $(M^0, \overline{M}^0) \leftrightarrow (M^0, \overline{M}^0)$ transitions via off-shell (dispersive), and on-shell (absorptive) intermediate states, respectively. Diagonal elements of $\mathbf{M}$ and $\mathbf{\Gamma}$ are associated with the flavor-conserving transitions $M^0 \to M^0$ and $\overline{M}^0 \to \overline{M}^0$, while off-diagonal elements are associated with flavor-changing transitions $M^0 \leftrightarrow \overline{M}^0$.

The eigenvectors of $\mathbf{H}$ have well-defined masses and decay widths. To specify the components of the strong interaction eigenstates, M^0 and $\overline{M}^0$, in the light (M_L) and heavy (M_H) mass eigenstates, we introduce three complex parameters: p, q, and, for the case that both CP and CPT are violated in mixing, z:

$$|M_L\rangle \propto p\sqrt{1-z}\,|M^0\rangle + q\sqrt{1+z}\,|\overline{M}^0\rangle$$
$$|M_H\rangle \propto p\sqrt{1+z}\,|M^0\rangle - q\sqrt{1-z}\,|\overline{M}^0\rangle\,, \tag{13.26}$$

with the normalization $|q|^2 + |p|^2 = 1$ when $z = 0$. (Another possible choice, which is in standard usage for K mesons, defines the mass eigenstates according to their lifetimes: K_S for the short-lived and K_L for the long-lived state. The K_L is experimentally found to be the heavier state. Yet another choice is often used for the D mesons [31]: the eigenstates are labelled according to their dominant CP content.)

The real and imaginary parts of the eigenvalues $\omega_{L,H}$ corresponding to $|M_{L,H}\rangle$ represent their masses and decay widths, respectively. The mass and width splittings are

$$\Delta m \equiv m_H - m_L = \mathcal{R}e(\omega_H - \omega_L)\,,$$
$$\Delta\Gamma \equiv \Gamma_H - \Gamma_L = -2\,\mathcal{I}m(\omega_H - \omega_L)\,. \tag{13.27}$$

Note that here Δm is positive by definition, while the sign of $\Delta\Gamma$ must be experimentally determined. The sign of $\Delta\Gamma$ has not yet been established for B^0 mesons, while $\Delta\Gamma < 0$ is established for K and B_s^0 mesons. The Standard Model predicts $\Delta\Gamma < 0$ for $B_{(s)}^0$ mesons; for this reason, $\Delta\Gamma = \Gamma_L - \Gamma_H$, which is still a signed quantity, is often used in the $B_{(s)}^0$ literature and is the convention used in the PDG experimental summaries.

Solving the eigenvalue problem for $\mathbf{H}$ yields

$$\left(\frac{q}{p}\right)^2 = \frac{\mathbf{M}_{12}^* - (i/2)\mathbf{\Gamma}_{12}^*}{\mathbf{M}_{12} - (i/2)\mathbf{\Gamma}_{12}} \tag{13.28}$$

and

$$z \equiv \frac{\delta m - (i/2)\delta\Gamma}{\Delta m - (i/2)\Delta\Gamma} \,, \tag{13.29}$$

where

$$\delta m \equiv \mathbf{M}_{11} - \mathbf{M}_{22} \,, \quad \delta\Gamma \equiv \mathbf{\Gamma}_{11} - \mathbf{\Gamma}_{22} \tag{13.30}$$

are the differences in effective mass and decay-rate expectation values for the strong interaction states M^0 and $\overline{M}^0$.

If either CP or CPT is a symmetry of $\mathbf{H}$ (independently of whether T is conserved or violated), then the values of δm and $\delta\Gamma$ are both zero, and hence $z = 0$. We also find that

$$\omega_H - \omega_L = 2\sqrt{\left(\mathbf{M}_{12} - \frac{i}{2}\mathbf{\Gamma}_{12}\right)\left(\mathbf{M}_{12}^* - \frac{i}{2}\mathbf{\Gamma}_{12}^*\right)} \,. \tag{13.31}$$

If either CP or T is a symmetry of $\mathbf{H}$ (independently of whether CPT is conserved or violated), then $\mathbf{\Gamma}_{12}/\mathbf{M}_{12}$ is real, leading to

$$\left(\frac{q}{p}\right)^2 = e^{2i\xi_M} \quad \Rightarrow \quad \left|\frac{q}{p}\right| = 1 \,, \tag{13.32}$$

where ξ_M is the arbitrary unphysical phase introduced in Eq. (13.21). If, and only if, CP is a symmetry of $\mathbf{H}$ (independently of CPT and T), then both of the above conditions hold, with the result that the mass eigenstates are orthogonal

$$\langle M_H | M_L \rangle = |p|^2 - |q|^2 = 0 \,. \tag{13.33}$$

13.1.3. *CP-violating observables* :

All CP-violating observables in M and $\overline{M}$ decays to final states f and $\overline{f}$ can be expressed in terms of phase-convention-independent combinations of A_f, $\overline{A}_f$, $A_{\overline{f}}$, and $\overline{A}_{\overline{f}}$, together with, for neutral meson decays only, q/p. CP violation in charged meson and all baryon decays depends only on the combination $|\overline{A}_{\overline{f}}/A_f|$, while CP violation in flavored neutral meson decays is complicated by $M^0 \leftrightarrow \overline{M}^0$ oscillations, and depends, additionally, on $|q/p|$ and on $\lambda_f \equiv (q/p)(\overline{A}_f/A_f)$.

The decay rates of the two neutral kaon mass eigenstates, K_S and K_L, are different enough ($\Gamma_S/\Gamma_L \sim 500$) that one can, in most cases, actually study their decays independently. For D^0, B^0, and B_s^0 mesons, however, values of $\Delta\Gamma/\Gamma$ (where $\Gamma \equiv (\Gamma_H + \Gamma_L)/2$) are relatively small, and so both mass eigenstates must be considered in their evolution. We denote the state of an initially pure $|M^0\rangle$ or $|\overline{M}^0\rangle$ after an elapsed proper time t as $|M_{\rm phys}^0(t)\rangle$ or $|\overline{M}_{\rm phys}^0(t)\rangle$, respectively. Using the effective Hamiltonian approximation, but not assuming CPT to be a good symmetry, we obtain

$$\begin{aligned} |M_{\rm phys}^0(t)\rangle &= \left(g_+(t) + z\, g_-(t)\right)|M^0\rangle - \sqrt{1-z^2}\,\frac{q}{p}\, g_-(t)|\overline{M}^0\rangle \,, \\ |\overline{M}_{\rm phys}^0(t)\rangle &= \left(g_+(t) - z\, g_-(t)\right)|\overline{M}^0\rangle - \sqrt{1-z^2}\,\frac{p}{q}\, g_-(t)|M^0\rangle \,, \end{aligned} \tag{13.34}$$

where

$$g_\pm(t) \equiv \frac{1}{2}\left(e^{-im_H t - \frac{1}{2}\Gamma_H t} \pm e^{-im_L t - \frac{1}{2}\Gamma_L t}\right) \tag{13.35}$$

and $z = 0$ if either CPT or CP is conserved.

Defining $x \equiv \Delta m/\Gamma$ and $y \equiv \Delta\Gamma/(2\Gamma)$, and assuming $z = 0$, one obtains the following time-dependent decay rates:

$$\begin{aligned} &\frac{d\Gamma\left[M_{\rm phys}^0(t) \to f\right]/dt}{e^{-\Gamma t}\mathcal{N}_f} = \\ &\quad \left(|A_f|^2 + |(q/p)\overline{A}_f|^2\right)\cosh(y\Gamma t) + \left(|A_f|^2 - |(q/p)\overline{A}_f|^2\right)\cos(x\Gamma t) \\ &\quad + 2\,\mathcal{R}e((q/p)A_f^*\overline{A}_f)\sinh(y\Gamma t) - 2\,\mathcal{I}m((q/p)A_f^*\overline{A}_f)\sin(x\Gamma t) \,, \end{aligned} \tag{13.36}$$

$$\begin{aligned} &\frac{d\Gamma\left[\overline{M}_{\rm phys}^0(t) \to f\right]/dt}{e^{-\Gamma t}\mathcal{N}_f} = \\ &\quad \left(|(p/q)A_f|^2 + |\overline{A}_f|^2\right)\cosh(y\Gamma t) - \left(|(p/q)A_f|^2 - |\overline{A}_f|^2\right)\cos(x\Gamma t) \\ &\quad + 2\,\mathcal{R}e((p/q)A_f\overline{A}_f^*)\sinh(y\Gamma t) - 2\,\mathcal{I}m((p/q)A_f\overline{A}_f^*)\sin(x\Gamma t) \,, \end{aligned} \tag{13.37}$$

where $\mathcal{N}_f$ is a common, time-independent, normalization factor that can be determined bearing in mind that the range of t is $0 < t < \infty$. Decay rates to the CP-conjugate final state $\overline{f}$ are obtained analogously, with $\mathcal{N}_f = \mathcal{N}_{\overline{f}}$ and the substitutions $A_f \to A_{\overline{f}}$ and $\overline{A}_f \to \overline{A}_{\overline{f}}$ in Eqs. (13.36, 13.37). Terms proportional to $|A_f|^2$ or $|\overline{A}_f|^2$ are associated with decays that occur without any net $M^0 \leftrightarrow \overline{M}^0$ oscillation, while terms proportional to $|(q/p)\overline{A}_f|^2$ or $|(p/q)A_f|^2$ are associated with decays following a net oscillation. The $\sinh(y\Gamma t)$ and $\sin(x\Gamma t)$ terms of Eqs. (13.36, 13.37) are associated with the interference between these two cases. Note that, in multi-body decays, amplitudes are functions of variables that describe the phase-space of the final state. Interference may be present in some regions but not others, and is strongly influenced by resonant substructure.

When neutral pseudoscalar mesons are produced coherently in pairs from the decay of a vector resonance, $V \to M^0\overline{M}^0$ (for example, $\Upsilon(4S) \to B^0\overline{B}^0$ or $\phi \to K^0\overline{K}^0$), the time-dependence of their subsequent decays to final states f_1 and f_2 has a similar form to Eqs. (13.36, 13.37):

$$\begin{aligned} &\frac{d\Gamma\left[V_{\rm phys}(t_1,t_2) \to f_1 f_2\right]/d(\Delta t)}{e^{-\Gamma|\Delta t|}\mathcal{N}_{f_1 f_2}} = \\ &\quad \left(|a_+|^2 + |a_-|^2\right)\cosh(y\Gamma\Delta t) + \left(|a_+|^2 - |a_-|^2\right)\cos(x\Gamma\Delta t) \\ &\quad - 2\,\mathcal{R}e(a_+^* a_-)\sinh(y\Gamma\Delta t) + 2\,\mathcal{I}m(a_+^* a_-)\sin(x\Gamma\Delta t) \,, \end{aligned} \tag{13.38}$$

where $\Delta t \equiv t_2 - t_1$ is the difference in the production times, t_1 and t_2, of f_1 and f_2, respectively, and the dependence on the average decay time and on decay angles has been integrated out. The normalisation factor $\mathcal{N}_{f_1 f_2}$ can be evaluated, noting that the range of Δt is $-\infty < \Delta t < \infty$. The coefficients in Eq. (13.38) are determined by the amplitudes for no net oscillation from $t_1 \to t_2$, $\overline{A}_{f_1}A_{f_2}$, and $A_{f_1}\overline{A}_{f_2}$, and for a net oscillation, $(q/p)\overline{A}_{f_1}\overline{A}_{f_2}$ and $(p/q)A_{f_1}A_{f_2}$, via

$$a_+ \equiv \overline{A}_{f_1}A_{f_2} - A_{f_1}\overline{A}_{f_2} \,, \tag{13.39}$$

$$a_- \equiv -\sqrt{1-z^2}\left(\frac{q}{p}\overline{A}_{f_1}\overline{A}_{f_2} - \frac{p}{q}A_{f_1}A_{f_2}\right) + z\left(\overline{A}_{f_1}A_{f_2} + A_{f_1}\overline{A}_{f_2}\right) \,.$$

Assuming CPT conservation, $z = 0$, and identifying $\Delta t \to t$ and $f_2 \to f$, we find that Eqs. (13.38, 13.39) reduce essentially to Eq. (13.36) with $A_{f_1} = 0$, $\overline{A}_{f_1} = 1$, or to Eq. (13.37) with $\overline{A}_{f_1} = 0$, $A_{f_1} = 1$. Indeed, such a situation plays an important role in experiments that exploit the coherence of $V \to M^0\overline{M}^0$ (for example $\psi(3770) \to D^0\overline{D}^0$ or $\Upsilon(4S) \to B^0\overline{B}^0$) production. Final states f_1 with $A_{f_1} = 0$ or $\overline{A}_{f_1} = 0$ are called tagging states, because they identify the decaying pseudoscalar meson as, respectively, $\overline{M}^0$ or M^0. Before one of M^0 or $\overline{M}^0$ decays, they evolve in phase, so that there is always one M^0 and one $\overline{M}^0$ present. A tagging decay of one meson sets the clock for the time evolution of the other: it starts at t_1 as purely M^0 or $\overline{M}^0$, with time evolution that depends only on $t_2 - t_1$.

When f_1 is a state that both M^0 and $\overline{M}^0$ can decay into, then Eq. (13.38) contains interference terms proportional to $A_{f_1}\overline{A}_{f_1} \neq 0$ that are not present in Eqs. (13.36, 13.37). Even when f_1 is dominantly produced by M^0 decays rather than $\overline{M}^0$ decays, or vice versa, $A_{f_1}\overline{A}_{f_1}$ can be non-zero owing to doubly-CKM-suppressed decays (with amplitudes suppressed by at least two powers of λ relative to the dominant amplitude, in the language of Section 13.3), and these terms should be considered for precision studies of CP violation in coherent $V \to M^0\overline{M}^0$ decays [32]. The correlations in $V \to M^0\overline{M}^0$ decays can also be exploited to determine strong phase differences between favored and suppressed decay amplitudes [33].

13.1.4. *Classification of CP-violating effects* :

We distinguish three types of CP-violating effects that can occur in the quark sector:

I. CP violation in decay is defined by

$$|\overline{A}_{\overline{f}}/A_f| \neq 1 \,. \tag{13.40}$$

In charged meson (and all baryon) decays, where mixing effects are absent, this is the only possible source of CP asymmetries:

$$\mathcal{A}_{f^\pm} \equiv \frac{\Gamma(M^- \to f^-) - \Gamma(M^+ \to f^+)}{\Gamma(M^- \to f^-) + \Gamma(M^+ \to f^+)} = \frac{|\overline{A}_{f^-}/A_{f^+}|^2 - 1}{|\overline{A}_{f^-}/A_{f^+}|^2 + 1} \,. \tag{13.41}$$

Note that the usual sign convention for CP asymmetries of hadrons is for the difference between the rate involving the particle that contains a heavy quark and that which contains an antiquark. Hence Eq. (13.41) corresponds to the definition for $B^\pm$ mesons, but the opposite sign is used for $D^\pm_{(s)}$ decays.

II. CP (and T) violation in mixing is defined by

$$|q/p| \neq 1 \,. \tag{13.42}$$

In charged-current semileptonic neutral meson decays $M, \overline{M} \to \ell^\pm X$ (taking $|A_{\ell^+X}| = |\overline{A}_{\ell^-X}|$ and $A_{\ell^-X} = \overline{A}_{\ell^+X} = 0$, as is the case in the Standard Model, to lowest order in G_F, and in most of its reasonable extensions), this is the only source of CP violation, and can be measured via the asymmetry of "wrong-sign" decays induced by oscillations:

$$\mathcal{A}_{\rm SL}(t) \equiv \frac{d\Gamma/dt\big[\overline{M}^0_{\rm phys}(t) \to \ell^+X\big] - d\Gamma/dt\big[M^0_{\rm phys}(t) \to \ell^-X\big]}{d\Gamma/dt\big[\overline{M}^0_{\rm phys}(t) \to \ell^+X\big] + d\Gamma/dt\big[M^0_{\rm phys}(t) \to \ell^-X\big]}$$
$$= \frac{1 - |q/p|^4}{1 + |q/p|^4}. \tag{13.43}$$

Note that this asymmetry of time-dependent decay rates is actually time-independent.

III. CP violation in interference between a decay without mixing, $M^0 \to f$, and a decay with mixing, $M^0 \to \overline{M}^0 \to f$ (such an effect occurs only in decays to final states that are common to M^0 and $\overline{M}^0$, including all CP eigenstates), is defined by

$$\arg(\lambda_f) + \arg(\lambda_{\overline{f}}) \neq 0 \,, \tag{13.44}$$

with

$$\lambda_f \equiv \frac{q}{p}\frac{\overline{A}_f}{A_f} \,. \tag{13.45}$$

For final CP eigenstates, f_{CP}, the condition Eq. (13.44) simplifies to

$$\mathcal{I}m(\lambda_{f_{CP}}) \neq 0 \,, \tag{13.46}$$

This form of CP violation can be observed, for example, using the asymmetry of neutral meson decays into CP eigenstates

$$\mathcal{A}_{f_{CP}}(t) \equiv \frac{d\Gamma/dt\big[\overline{M}^0_{\rm phys}(t) \to f_{CP}\big] - d\Gamma/dt\big[M^0_{\rm phys}(t) \to f_{CP}\big]}{d\Gamma/dt\big[\overline{M}^0_{\rm phys}(t) \to f_{CP}\big] + d\Gamma/dt\big[M^0_{\rm phys}(t) \to f_{CP}\big]} \,. \tag{13.47}$$

If $\Delta\Gamma = 0$, as expected to a good approximation for B^0 mesons, but not for K^0 and B^0_s mesons, and $|q/p| = 1$, then $\mathcal{A}_{f_{CP}}$ has a particularly simple form (see Eq. (13.92), below). If, in addition, the decay amplitudes fulfill $|\overline{A}_{f_{CP}}| = |A_{f_{CP}}|$, the interference between decays with and without mixing is the only source of asymmetry and $\mathcal{A}_{f_{CP}}(t) = \mathcal{I}m(\lambda_{f_{CP}})\sin(x\Gamma t)$.

Examples of these three types of CP violation will be given in Sections 13.4, 13.5, and 13.6.

13.2. Theoretical Interpretation: General Considerations

Consider the $M \to f$ decay amplitude A_f, and the CP conjugate process, $\overline{M} \to \overline{f}$, with decay amplitude $\overline{A}_{\overline{f}}$. There are two types of phases that may appear in these decay amplitudes. Complex parameters in any Lagrangian term that contributes to the amplitude will appear in complex conjugate form in the CP-conjugate amplitude. Thus, their phases appear in A_f and $\overline{A}_{\overline{f}}$ with opposite signs. In the Standard Model, these phases occur only in the couplings of the $W^\pm$ bosons, and hence, are often called "weak phases." The weak phase of any single term is convention-dependent. However, the difference between the weak phases in two different terms in A_f is convention-independent. A second type of phase can appear in scattering or decay amplitudes, even when the Lagrangian is real. This phase originates from the possible contribution from intermediate on-shell states in the decay process. Since such phases are generated by CP-invariant interactions, they are the same in A_f and $\overline{A}_{\overline{f}}$. Usually the dominant rescattering is due to strong interactions; hence the designation "strong phases" for the phase shifts so induced. Again, only the relative strong phases between different terms in the amplitude are physically meaningful.

The "weak" and "strong" phases discussed here appear in addition to the spurious CP-transformation phases of Eq. (13.22). Those spurious phases are due to an arbitrary choice of phase convention, and do not originate from any dynamics or induce any CP violation. For simplicity, we set them to zero from here on.

It is useful to write each contribution a_i to A_f in three parts: its magnitude $|a_i|$, its weak phase ϕ_i, and its strong phase δ_i. If, for example, there are two such contributions, $A_f = a_1 + a_2$, we have

$$A_f = |a_1|e^{i(\delta_1+\phi_1)} + |a_2|e^{i(\delta_2+\phi_2)},$$
$$\overline{A}_{\overline{f}} = |a_1|e^{i(\delta_1-\phi_1)} + |a_2|e^{i(\delta_2-\phi_2)}. \tag{13.48}$$

Similarly, for neutral mesons, it is useful to write

$$\mathbf{M}_{12} = |\mathbf{M}_{12}|e^{i\phi_M} \,, \quad \mathbf{\Gamma}_{12} = |\mathbf{\Gamma}_{12}|e^{i\phi_\Gamma} \,. \tag{13.49}$$

Each of the phases appearing in Eqs. (13.48, 13.49) is convention-dependent, but combinations such as $\delta_1 - \delta_2$, $\phi_1 - \phi_2$, $\phi_M - \phi_\Gamma$, and $\phi_M + \phi_1 - \overline{\phi}_1$ (where $\overline{\phi}_1$ is a weak phase contributing to $\overline{A}_f$) are physical.

It is now straightforward to evaluate the various asymmetries in terms of the theoretical parameters introduced here. We will do so with approximations that are often relevant to the most interesting measured asymmetries.

1. The CP asymmetry in charged meson and all baryon decays [Eq. (13.41)] is given by

$$\mathcal{A}_f = -\frac{2|a_1a_2|\sin(\delta_2-\delta_1)\sin(\phi_2-\phi_1)}{|a_1|^2 + |a_2|^2 + 2|a_1a_2|\cos(\delta_2-\delta_1)\cos(\phi_2-\phi_1)} \,. \tag{13.50}$$

The quantity of most interest to theory is the weak phase difference $\phi_2 - \phi_1$. Its extraction from the asymmetry requires, however, that the amplitude ratio $|a_2/a_1|$ and the strong phase difference $\delta_2 - \delta_1$ are known. Both quantities depend on non-perturbative hadronic parameters that are difficult to calculate, but in some cases can be obtained from experiment.

2. In the approximation that $|\mathbf{\Gamma}_{12}/\mathbf{M}_{12}| \ll 1$ (valid for B^0 and B^0_s mesons), the CP asymmetry in semileptonic neutral-meson decays [Eq. (13.43)] is given by

$$\mathcal{A}_{\rm SL} = -\left|\frac{\mathbf{\Gamma}_{12}}{\mathbf{M}_{12}}\right|\sin(\phi_M - \phi_\Gamma) \,. \tag{13.51}$$

The quantity of most interest to theory is the weak phase $\phi_M - \phi_\Gamma$. Its extraction from the asymmetry requires, however, that $|\mathbf{\Gamma}_{12}/\mathbf{M}_{12}|$

is known. State of the art calculations of this quantity for the B^0 and B_s^0 mesons have uncertainties of around 15–20% [34].

3. In the approximations that only a single weak phase contributes to decay, $A_f = |a_f|e^{i(\delta_f+\phi_f)}$, and that $|\mathbf{\Gamma}_{12}/\mathbf{M}_{12}| = 0$, we obtain $|\lambda_f| = 1$, and the CP asymmetries in decays to a final CP eigenstate f [Eq. (13.47)] with eigenvalue $\eta_f = \pm 1$ are given by

$$\mathcal{A}_{f_{CP}}(t) = \mathcal{I}m(\lambda_f)\ \sin(\Delta m t)\ \ \text{with}\ \ \mathcal{I}m(\lambda_f) = \eta_f \sin(\phi_M + 2\phi_f)\,. \tag{13.52}$$

Note that the phase measured is purely a weak phase, and no hadronic parameters are involved in the extraction of its value from $\mathcal{I}m(\lambda_f)$.

The discussion above allows us to introduce another classification of CP-violating effects:

1. *Indirect CP violation* is consistent with taking $\phi_M \neq 0$ and setting all other CP violating phases to zero. CP violation in mixing (type II) belongs to this class.
2. *Direct CP violation* cannot be accounted for by just $\phi_M \neq 0$. CP violation in decay (type I) belongs to this class.

The historical significance of this classification is related to theory. In superweak models [35], CP violation appears only in diagrams that contribute to $\mathbf{M}_{12}$, hence they predict that there is no direct CP violation. In most models and, in particular, in the Standard Model, CP violation is both direct and indirect. As concerns type III CP violation, a single observation of such an effect would be consistent with indirect CP violation, but observing $\eta_{f_1}\mathcal{I}m(\lambda_{f_1}) \neq \eta_{f_2}\mathcal{I}m(\lambda_{f_2})$ (for the same decaying meson and two different final CP eigenstates f_1 and f_2) would establish direct CP violation. The experimental observation of $\epsilon' \neq 0$, which was achieved by establishing that $\mathcal{I}m(\lambda_{\pi^+\pi^-}) \neq \mathcal{I}m(\lambda_{\pi^0\pi^0})$ (see Section 13.4), excluded the superweak scenario.

13.3. Theoretical Interpretation: The KM Mechanism

Of all the Standard Model quark parameters, only the Kobayashi-Maskawa (KM) phase is CP-violating. Having a single source of CP violation, the Standard Model is very predictive for CP asymmetries: some vanish, and those that do not are correlated.

To be precise, CP could be violated also by strong interactions. The experimental upper bound on the electric-dipole moment of the neutron implies, however, that $\theta_{\rm QCD}$, the non-perturbative parameter that determines the strength of this type of CP violation, is tiny, if not zero. (The smallness of $\theta_{\rm QCD}$ constitutes a theoretical puzzle, known as "the strong CP problem.") In particular, it is irrelevant to our discussion of hadron decays.

The charged current interactions (that is, the $W^\pm$ interactions) for quarks are given by

$$-\mathcal{L}_{W^\pm} = \frac{g}{\sqrt{2}}\ \overline{u_{Li}}\ \gamma^\mu\ (V_{\rm CKM})_{ij}\ d_{Lj}\ W_\mu^+ + \text{h.c.} \tag{13.53}$$

Here $i,j = 1,2,3$ are generation numbers. The Cabibbo-Kobayashi-Maskawa (CKM) mixing matrix for quarks is a 3×3 unitary matrix [36]. Ordering the quarks by their masses, *i.e.*, $(u_1,u_2,u_3) \to (u,c,t)$ and $(d_1,d_2,d_3) \to (d,s,b)$, the elements of $V_{\rm CKM}$ are written as follows:

$$V_{\rm CKM} = \begin{pmatrix} V_{ud} & V_{us} & V_{ub} \\ V_{cd} & V_{cs} & V_{cb} \\ V_{td} & V_{ts} & V_{tb} \end{pmatrix}\,. \tag{13.54}$$

While a general 3×3 unitary matrix depends on three real angles and six phases, the freedom to redefine the phases of the quark mass eigenstates can be used to remove five of the phases, leaving a single physical phase, the Kobayashi-Maskawa phase, that is responsible for all CP violation in the Standard Model.

The fact that one can parametrize $V_{\rm CKM}$ by three real and only one imaginary physical parameters can be made manifest by choosing an explicit parametrization. The Wolfenstein parametrization [37,38] is particularly useful:

$$V_{\rm CKM} = \begin{pmatrix} 1-\frac{1}{2}\lambda^2-\frac{1}{8}\lambda^4 & \lambda & A\lambda^3(\rho-i\eta) \\ -\lambda+\frac{1}{2}A^2\lambda^5[1-2(\rho+i\eta)] & 1-\frac{1}{2}\lambda^2-\frac{1}{8}\lambda^4(1+4A^2) & A\lambda^2 \\ A\lambda^3[1-(1-\frac{1}{2}\lambda^2)(\rho+i\eta)] & -A\lambda^2+\frac{1}{2}A\lambda^4[1-2(\rho+i\eta)] & 1-\frac{1}{2}A^2\lambda^4 \end{pmatrix}\,. \tag{13.55}$$

Here $\lambda \approx 0.23$ (not to be confused with λ_f), the sine of the Cabibbo angle, plays the role of an expansion parameter, and η represents the CP-violating phase. Terms of $\mathcal{O}(\lambda^6)$ have been neglected.

The unitarity of the CKM matrix, $(VV^\dagger)_{ij} = (V^\dagger V)_{ij} = \delta_{ij}$, leads to twelve distinct complex relations among the matrix elements. The six relations with $i \neq j$ can be represented geometrically as triangles in the complex plane. Two of these,

$$V_{ud}V_{ub}^* + V_{cd}V_{cb}^* + V_{td}V_{tb}^* = 0$$
$$V_{td}V_{ud}^* + V_{ts}V_{us}^* + V_{tb}V_{ub}^* = 0\,,$$

have terms of equal order, $\mathcal{O}(A\lambda^3)$, and so have corresponding triangles whose interior angles are all $\mathcal{O}(1)$ physical quantities that can be independently measured. The angles of the first triangle (see Fig. 13.1) are given by

$$\begin{aligned} \alpha \equiv \varphi_2 &\equiv \arg\left(-\frac{V_{td}V_{tb}^*}{V_{ud}V_{ub}^*}\right) \simeq \arg\left(-\frac{1-\rho-i\eta}{\rho+i\eta}\right)\,, \\ \beta \equiv \varphi_1 &\equiv \arg\left(-\frac{V_{cd}V_{cb}^*}{V_{td}V_{tb}^*}\right) \simeq \arg\left(\frac{1}{1-\rho-i\eta}\right)\,, \\ \gamma \equiv \varphi_3 &\equiv \arg\left(-\frac{V_{ud}V_{ub}^*}{V_{cd}V_{cb}^*}\right) \simeq \arg\left(\rho+i\eta\right)\,. \end{aligned} \tag{13.56}$$

The angles of the second triangle are equal to (α,β,γ) up to corrections of $\mathcal{O}(\lambda^2)$. The notations (α,β,γ) and $(\varphi_1,\varphi_2,\varphi_3)$ are both in common usage but, for convenience, we only use the first convention in the following.

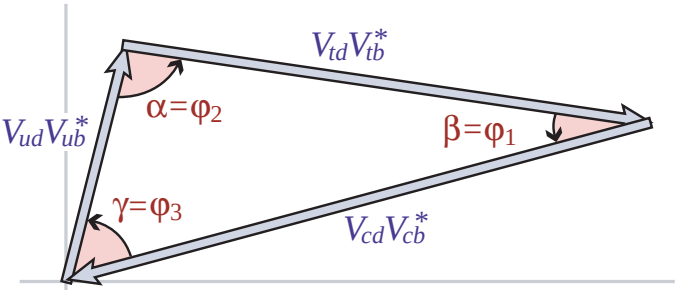

Figure 13.1: Graphical representation of the unitarity constraint $V_{ud}V_{ub}^* + V_{cd}V_{cb}^* + V_{td}V_{tb}^* = 0$ as a triangle in the complex plane.

Another relation that can be represented as a triangle,

$$V_{us}V_{ub}^* + V_{cs}V_{cb}^* + V_{ts}V_{tb}^* = 0\,, \tag{13.57}$$

and, in particular, its small angle, of $\mathcal{O}(\lambda^2)$,

$$\beta_s \equiv \arg\left(-\frac{V_{ts}V_{tb}^*}{V_{cs}V_{cb}^*}\right)\,, \tag{13.58}$$

is convenient for analyzing CP violation in the B_s^0 sector.

All unitarity triangles have the same area, commonly denoted by $J/2$ [39]. If CP is violated, J is different from zero and can be taken as the single CP-violating parameter. In the Wolfenstein parametrization of Eq. (13.55), $J \simeq \lambda^6 A^2 \eta$.

13.4. Kaons

CP violation was discovered in $K \to \pi\pi$ decays in 1964 [1]. The same mode provided the first observation of direct CP violation [4–6].

The decay amplitudes actually measured in neutral K decays refer to the mass eigenstates K_L and K_S, rather than to the K and $\overline{K}$ states referred to in Eq. (13.19). The final $\pi^+\pi^-$ and $\pi^0\pi^0$ states are CP-even. In the CP conservation limit, K_S (K_L) would be CP-even (odd), and therefore would (would not) decay to two pions. We define CP-violating amplitude ratios for two-pion final states,

$$\eta_{00} \equiv \frac{\langle \pi^0\pi^0|\mathcal{H}|K_L\rangle}{\langle \pi^0\pi^0|\mathcal{H}|K_S\rangle}\,, \quad \eta_{+-} \equiv \frac{\langle \pi^+\pi^-|\mathcal{H}|K_L\rangle}{\langle \pi^+\pi^-|\mathcal{H}|K_S\rangle}\,. \tag{13.59}$$

Another important observable is the asymmetry of time-integrated semileptonic decay rates:

$$\delta_L \equiv \frac{\Gamma(K_L \to \ell^+\nu_\ell\pi^-) - \Gamma(K_L \to \ell^-\overline{\nu}_\ell\pi^+)}{\Gamma(K_L \to \ell^+\nu_\ell\pi^-) + \Gamma(K_L \to \ell^-\overline{\nu}_\ell\pi^+)}\,. \tag{13.60}$$

CP violation has been observed as an appearance of K_L decays to two-pion final states [27],

$$|\eta_{00}| = (2.220 \pm 0.011) \times 10^{-3} \qquad |\eta_{+-}| = (2.232 \pm 0.011) \times 10^{-3} \tag{13.61}$$

$$|\eta_{00}/\eta_{+-}| = 0.9950 \pm 0.0007\,, \tag{13.62}$$

where the phase ϕ_{ij} of the amplitude ratio η_{ij} has been determined both assuming CPT invariance:

$$\phi_{00} = (43.52 \pm 0.05)^\circ\,, \qquad \phi_{+-} = (43.51 \pm 0.05)^\circ\,, \tag{13.63}$$

and without assuming CPT invariance:

$$\phi_{00} = (43.7 \pm 0.6)^\circ\,, \qquad \phi_{+-} = (43.4 \pm 0.5)^\circ\,. \tag{13.64}$$

CP violation has also been observed in semileptonic K_L decays [27]

$$\delta_L = (3.32 \pm 0.06) \times 10^{-3}\,, \tag{13.65}$$

where δ_L is a weighted average of muon and electron measurements, as well as in K_L decays to $\pi^+\pi^-\gamma$ and $\pi^+\pi^-e^+e^-$ [27]. CP violation in $K \to 3\pi$ decays has not yet been observed [27,40].

Historically, CP violation in neutral K decays has been described in terms of the complex parameters ϵ and ϵ'. The observables η_{00}, η_{+-}, and δ_L are related to these parameters, and to those of Section 13.1, by

$$\begin{aligned}
\eta_{00} &= \frac{1 - \lambda_{\pi^0\pi^0}}{1 + \lambda_{\pi^0\pi^0}} &&= \epsilon - 2\epsilon'\,, \\
\eta_{+-} &= \frac{1 - \lambda_{\pi^+\pi^-}}{1 + \lambda_{\pi^+\pi^-}} &&= \epsilon + \epsilon'\,, \\
\delta_L &= \frac{1 - |q/p|^2}{1 + |q/p|^2} &&= \frac{2\mathcal{R}e(\epsilon)}{1 + |\epsilon|^2}\,,
\end{aligned} \tag{13.66}$$

where, in the last line, we have assumed that $\left|A_{\ell^+\nu_\ell\pi^-}\right| = \left|\overline{A}_{\ell^-\overline{\nu}_\ell\pi^+}\right|$ and $\left|A_{\ell^-\overline{\nu}_\ell\pi^+}\right| = \left|\overline{A}_{\ell^+\nu_\ell\pi^-}\right| = 0$. (The convention-dependent parameter $\tilde{\epsilon} \equiv (1 - q/p)/(1 + q/p)$, sometimes used in the literature, is, in general, different from ϵ but yields a similar expression, $\delta_L = 2\mathcal{R}e(\tilde{\epsilon})/(1 + |\tilde{\epsilon}|^2)$.) A fit to the $K \to \pi\pi$ data yields [27]

$$\begin{aligned}
|\epsilon| &= (2.228 \pm 0.011) \times 10^{-3}\,, \\
\mathcal{R}e(\epsilon'/\epsilon) &= (1.66 \pm 0.23) \times 10^{-3}\,.
\end{aligned} \tag{13.67}$$

In discussing two-pion final states, it is useful to express the amplitudes $A_{\pi^0\pi^0}$ and $A_{\pi^+\pi^-}$ in terms of their isospin components via

$$\begin{aligned}
A_{\pi^0\pi^0} &= \sqrt{\frac{1}{3}}\,|A_0|\,e^{i(\delta_0+\phi_0)} - \sqrt{\frac{2}{3}}\,|A_2|\,e^{i(\delta_2+\phi_2)}, \\
A_{\pi^+\pi^-} &= \sqrt{\frac{2}{3}}\,|A_0|\,e^{i(\delta_0+\phi_0)} + \sqrt{\frac{1}{3}}\,|A_2|\,e^{i(\delta_2+\phi_2)}\,,
\end{aligned} \tag{13.68}$$

where we parameterize the amplitude $A_I(\overline{A}_I)$ for $K^0(\overline{K}^0)$ decay into two pions with total isospin $I = 0$ or 2 as

$$\begin{aligned}
A_I &\equiv \langle(\pi\pi)_I\,|\mathcal{H}|\,K^0\rangle = |A_I|\,e^{i(\delta_I+\phi_I)}\,, \\
\overline{A}_I &\equiv \langle(\pi\pi)_I\,|\mathcal{H}|\,\overline{K}^0\rangle = |A_I|\,e^{i(\delta_I-\phi_I)}\,.
\end{aligned} \tag{13.69}$$

The smallness of $|\eta_{00}|$ and $|\eta_{+-}|$ allows us to approximate

$$\epsilon \simeq \frac{1}{2}(1 - \lambda_{(\pi\pi)_{I=0}})\,, \qquad \epsilon' \simeq \frac{1}{6}\left(\lambda_{\pi^0\pi^0} - \lambda_{\pi^+\pi^-}\right)\,. \tag{13.70}$$

The parameter ϵ represents indirect CP violation, while ϵ' parameterizes direct CP violation: $\mathcal{R}e(\epsilon')$ measures CP violation in decay (type I), $\mathcal{R}e(\epsilon)$ measures CP violation in mixing (type II), and $\mathcal{I}m(\epsilon)$ and $\mathcal{I}m(\epsilon')$ measure the interference between decays with and without mixing (type III).

The following expressions for ϵ and ϵ' are useful for theoretical evaluations:

$$\epsilon \simeq \frac{e^{i\pi/4}}{\sqrt{2}}\frac{\mathcal{I}m(\mathbf{M}_{12})}{\Delta m}\,, \qquad \epsilon' = \frac{i}{\sqrt{2}}\left|\frac{A_2}{A_0}\right|e^{i(\delta_2-\delta_0)}\sin(\phi_2 - \phi_0)\,. \tag{13.71}$$

The expression for ϵ is only valid in a phase convention where $\phi_2 = 0$, corresponding to a real $V_{ud}V_{us}^*$, and in the approximation that also $\phi_0 = 0$. The phase of ϵ, $\arg(\epsilon) \approx \arctan(-2\Delta m/\Delta\Gamma)$, is independent of the electroweak model and is experimentally determined to be about $\pi/4$. The calculation of ϵ benefits from the fact that $\mathcal{I}m(\mathbf{M}_{12})$ is dominated by short distance physics. Consequently, the main sources of uncertainty in theoretical interpretations of ϵ are the values of matrix elements, such as $\langle K^0\,|(\overline{s}d)_{V-A}(\overline{s}d)_{V-A}|\,\overline{K}^0\rangle$. The expression for ϵ' is valid to first order in $|A_2/A_0| \sim 1/20$. The phase of ϵ' is experimentally determined, $\pi/2 + \delta_2 - \delta_0 \approx \pi/4$, and is independent of the electroweak model. Note that, accidentally, ϵ'/ϵ is real to a good approximation. Determination of weak phase information from the measurement of $\mathcal{R}e(\epsilon'/\epsilon)$ given in Eq. (13.67) has until now been precluded by uncertainties in the hadronic parameters, but recent advances in lattice QCD calculations [41,42] suggest that it may become possible [43].

A future measurement of much interest is that of CP violation in the rare $K \to \pi\nu\overline{\nu}$ decays. The signal for CP violation is simply observing the $K_L \to \pi^0\nu\overline{\nu}$ decay. The effect here is that of interference between decays with and without mixing (type III) [44]:

$$\frac{\Gamma(K_L \to \pi^0\nu\overline{\nu})}{\Gamma(K^+ \to \pi^+\nu\overline{\nu})} = \frac{1}{2}\left[1 + |\lambda_{\pi\nu\overline{\nu}}|^2 - 2\,\mathcal{R}e(\lambda_{\pi\nu\overline{\nu}})\right] \simeq 1 - \mathcal{R}e(\lambda_{\pi\nu\overline{\nu}}), \tag{13.72}$$

where in the last equation we neglect CP violation in decay and in mixing (expected, model-independently, to be of order 10^{-5} and 10^{-3}, respectively). Such a measurement is experimentally very challenging but would be theoretically very rewarding [45]. Similar to the CP asymmetry in $B^0 \to J/\psi K_S$, the CP violation in $K \to \pi\nu\overline{\nu}$ decay is predicted to be large (that is, the ratio in Eq. (13.72) is neither CKM- nor loop-suppressed) and can be very cleanly interpreted.

Within the Standard Model, the $K_L \to \pi^0\nu\overline{\nu}$ decay is dominated by an intermediate top quark contribution and, consequently, can be interpreted in terms of CKM parameters [46]. (For the charged mode, $K^+ \to \pi^+\nu\overline{\nu}$, the contribution from an intermediate charm quark is not negligible, and constitutes a source of hadronic uncertainty.) In particular, $\mathcal{B}(K_L \to \pi^0\nu\overline{\nu})$ provides a theoretically clean way to determine the Wolfenstein parameter η [47]:

$$\mathcal{B}(K_L \to \pi^0\nu\overline{\nu}) = \kappa_L[X(m_t^2/m_W^2)]^2A^4\eta^2\,, \tag{13.73}$$

where the hadronic parameter $\kappa_L \sim 2 \times 10^{-10}$ incorporates the value of the four-fermion matrix element which is deduced, using isospin relations, from $\mathcal{B}(K^+ \to \pi^0e^+\nu_e)$, and $X(m_t^2/m_W^2)$ is a known function of the top mass. An explicit calculation gives $\mathcal{B}(K_L \to \pi^0\nu\overline{\nu}) = (3.00 \pm 0.30) \times 10^{-11}$ [49].

The currently tightest experimental limit is $\mathcal{B}(K_L \to \pi^0\nu\overline{\nu}) < 2.6 \times 10^{-8}$ [50], which does not yet reach the bound $\mathcal{B}(K_L \to \pi^0\nu\overline{\nu}) < 4.4 \times \mathcal{B}(K^+ \to \pi^+\nu\overline{\nu})$ [44]. Significant further progress is anticipated from experiments searching for $K \to \pi\nu\overline{\nu}$ decays in the next few years [51,52].

13.5. Charm

The existence of D^0–$\overline{D}^0$ mixing has been established in recent years [53–56]. The experimental constraints read [29,57] $x \equiv \Delta m/\Gamma = (0.32 \pm 0.14) \times 10^{-2}$ and $y \equiv \Delta\Gamma/(2\Gamma) = (0.69^{+0.06}_{-0.07}) \times 10^{-2}$. Thus, the data clearly show that $y \neq 0$, but improved measurements are needed to be sure of the size of x. Long-distance contributions make it difficult to calculate Standard Model predictions for the D^0–$\overline{D}^0$ mixing parameters. Therefore, the goal of the search for D^0–$\overline{D}^0$ mixing is not to constrain the CKM parameters, but rather to probe new physics. Here CP violation plays an important role. Within the Standard Model, the CP-violating effects are predicted to be small, since the mixing and the relevant decays are described, to an excellent approximation, by the physics of the first two generations only. The expectation is that the Standard Model size of CP violation in D decays is $\mathcal{O}(10^{-3})$ or less. At present, the most sensitive searches involve the $D^0 \to K^+K^-$, $D^0 \to \pi^+\pi^-$ and $D^0 \to K^\pm\pi^\mp$ modes.

The neutral D mesons decay via a singly-Cabibbo-suppressed transition to the CP eigenstates K^+K^- and $\pi^+\pi^-$. These decays are dominated by Standard-Model tree diagrams. Thus, we can write, for $f = K^+K^-$ or $\pi^+\pi^-$,

$$\begin{aligned} A_f &= A_f^T e^{+i\phi_f^T}\left[1 + r_f e^{i(\delta_f+\phi_f)}\right] , \\ \bar{A}_f &= A_f^T e^{-i\phi_f^T}\left[1 + r_f e^{i(\delta_f-\phi_f)}\right] , \end{aligned} \tag{13.74}$$

where $A_f^T e^{\pm i\phi_f^T}$ is the Standard Model tree-level contribution, ϕ_f^T and ϕ_f are weak, CP violating phases, δ_f is a strong phase difference, and r_f is the ratio between a subleading ($r_f \ll 1$) contribution with a weak phase different from ϕ_f^T and the Standard Model tree-level contribution. Neglecting r_f, λ_f is universal, and we can define an observable phase ϕ_D via

$$\lambda_f \equiv -|q/p|e^{i\phi_D} . \tag{13.75}$$

(In the limit of CP conservation, choosing $\phi_D = 0$ is equivalent to defining the mass eigenstates by their CP eigenvalue: $|D_\mp\rangle = p|D^0\rangle \pm q|\overline{D}^0\rangle$, with D_- (D_+) being the CP-odd (CP-even) state; that is, the state that does not (does) decay into K^+K^-.)

We define the time integrated CP asymmetry for a final CP eigenstate f as follows:

$$a_f \equiv \frac{\int_0^\infty \Gamma(D^0_{\rm phys}(t) \to f)dt - \int_0^\infty \Gamma(\overline{D}^0_{\rm phys}(t) \to f)dt}{\int_0^\infty \Gamma(D^0_{\rm phys}(t) \to f)dt + \int_0^\infty \Gamma(\overline{D}^0_{\rm phys}(t) \to f)dt} . \tag{13.76}$$

(This expression corresponds to the D meson being tagged at production, hence the integration goes from 0 to $+\infty$; measurements are also possible with $\psi(3770) \to D^0\overline{D}^0$, in which case the integration goes from $-\infty$ to $+\infty$ giving slightly different results; see the discussion in Section 13.1.3.) We take $x, y, r_f \ll 1$ and expand to leading order in these parameters. We can then separate the contribution to a_f into three parts [58],

$$a_f = a_f^d + a_f^m + a_f^i , \tag{13.77}$$

with the following underlying mechanisms:

1. a_f^d signals CP violation in decay (similar to Eq. (13.41)):

$$a_f^d = 2r_f \sin\phi_f \sin\delta_f . \tag{13.78}$$

2. a_f^m signals CP violation in mixing (similar to Eq. (13.51)). With our approximations, it is universal:

$$a^m = -\frac{y}{2}\left(\left|\frac{q}{p}\right| - \left|\frac{p}{q}\right|\right)\cos\phi_D . \tag{13.79}$$

3. a_f^i signals CP violation in the interference of mixing and decay (similar to Eq. (13.52)). With our approximations, it is universal:

$$a^i = \frac{x}{2}\left(\left|\frac{q}{p}\right| + \left|\frac{p}{q}\right|\right)\sin\phi_D . \tag{13.80}$$

One can isolate the effects of direct CP violation by taking the difference between the CP asymmetries in the K^+K^- and $\pi^+\pi^-$ modes:

$$\Delta a_{CP} \equiv a_{K^+K^-} - a_{\pi^+\pi^-} = a^d_{K^+K^-} - a^d_{\pi^+\pi^-} , \tag{13.81}$$

where we neglected a residual, experiment-dependent, contribution from indirect CP violation due to the fact that there may be a decay time-dependent acceptance function that can be different for the K^+K^- and $\pi^+\pi^-$ channels. Earlier evidence for such direct CP violation [59] has become less significant when including more data, with the current average giving [29]:

$$a^d_{K^+K^-} - a^d_{\pi^+\pi^-} = (-1.3 \pm 0.7) \times 10^{-3} . \tag{13.82}$$

One can also isolate the effects of indirect CP violation in the following way. Consider the time-dependent decay rates in Eq. (13.36) and Eq. (13.37). The mixing processes modify the time dependence from a pure exponential. However, given the small values of x and y, the time dependences can be recast, to a good approximation, into purely exponential form, but with modified decay-rate parameters [60,61] (given here for the K^+K^- final state):

$$\begin{aligned} \Gamma_{D^0\to K^+K^-} &= \Gamma \times [1 + |q/p|\,(y\cos\phi_D - x\sin\phi_D)] , \\ \Gamma_{\overline{D}^0\to K^+K^-} &= \Gamma \times [1 + |p/q|\,(y\cos\phi_D + x\sin\phi_D)] . \end{aligned} \tag{13.83}$$

One can define CP-conserving and CP-violating combinations of these two observables (normalized to the true width Γ):

$$\begin{aligned} y_{CP} &\equiv \frac{\Gamma_{\overline{D}^0\to K^+K^-} + \Gamma_{D^0\to K^+K^-}}{2\Gamma} - 1 \\ &= (y/2)\,(|q/p| + |p/q|)\cos\phi_D - (x/2)\,(|q/p| - |p/q|)\sin\phi_D , \\ A_\Gamma &\equiv \frac{\Gamma_{D^0\to K^+K^-} - \Gamma_{\overline{D}^0\to K^+K^-}}{2\Gamma} \\ &= -(a^m + a^i) . \end{aligned} \tag{13.84}$$

In the limit of CP conservation (and, in particular, within the Standard Model), $y_{CP} = (\Gamma_+ - \Gamma_-)/2\Gamma = y$ (where $\Gamma_+(\Gamma_-)$ is the decay width of the CP-even (-odd) mass eigenstate) and $A_\Gamma = 0$. Indeed, present measurements imply that CP violation is small [29],

$$\begin{aligned} y_{CP} &= (+0.84 \pm 0.16) \times 10^{-2} , \\ A_\Gamma &= (-0.032 \pm 0.026) \times 10^{-2} . \end{aligned}$$

The $K^\pm\pi^\mp$ states are not CP eigenstates, but they are still common final states for D^0 and $\overline{D}^0$ decays. Since $D^0(\overline{D}^0) \to K^-\pi^+$ is a Cabibbo-favored (doubly-Cabibbo-suppressed) process, these processes are particularly sensitive to x and/or $y = \mathcal{O}(\lambda^2)$. Taking into account that $\left|\lambda_{K^-\pi^+}\right|, \left|\lambda^{-1}_{K^+\pi^-}\right| \ll 1$ and $x, y \ll 1$, assuming that there is no direct CP violation (these are Standard Model tree-level decays dominated by a single weak phase, and there is no contribution from penguin-like and chromomagnetic operators), and expanding the time-dependent rates for $xt, yt \lesssim \Gamma^{-1}$, one obtains

$$\begin{aligned} \Gamma[D^0_{\rm phys}(t) \to K^+\pi^-] = {} & e^{-\Gamma t}|\overline{A}_{K^-\pi^+}|^2 \\ \times {} & \left[r_d^2 + r_d\left|\frac{q}{p}\right|(y'\cos\phi_D - x'\sin\phi_D)\Gamma t + \left|\frac{q}{p}\right|^2\frac{y^2+x^2}{4}(\Gamma t)^2\right] , \\ \Gamma[\overline{D}^0_{\rm phys}(t) \to K^-\pi^+] = {} & e^{-\Gamma t}|\overline{A}_{K^-\pi^+}|^2 \\ \times {} & \left[r_d^2 + r_d\left|\frac{p}{q}\right|(y'\cos\phi_D + x'\sin\phi_D)\Gamma t + \left|\frac{p}{q}\right|^2\frac{y^2+x^2}{4}(\Gamma t)^2\right] , \end{aligned} \tag{13.85}$$

where

$$\begin{aligned} y' &\equiv y\cos\delta - x\sin\delta , \\ x' &\equiv x\cos\delta + y\sin\delta . \end{aligned} \tag{13.86}$$

The weak phase ϕ_D is the same as that of Eq. (13.75) (a consequence of neglecting direct CP violation) and $r_d = \mathcal{O}(\tan^2\theta_c)$ is the

amplitude ratio, $r_d = \left|\overline{A}_{K^-\pi^+}/A_{K^-\pi^+}\right| = \left|A_{K^+\pi^-}/\overline{A}_{K^+\pi^-}\right|$, that is, $\lambda_{K^-\pi^+} = r_d|q/p|e^{-i(\delta-\phi_D)}$ and $\lambda^{-1}_{K^+\pi^-} = r_d|p/q|e^{-i(\delta+\phi_D)}$. The parameter δ is a strong-phase difference for these processes, that can be obtained from measurements of quantum correlated $\psi(3770) \to D^0\overline{D}^0$ decays [62,63]. By fitting to the six coefficients of the various time-dependences, one can determine r_d, $|q/p|$, (x^2+y^2), $y'\cos\phi_D$, and $x'\sin\phi_D$. In particular, finding CP violation ($|q/p| \neq 1$ and/or $\sin\phi_D \neq 0$) at a level much higher than 10^{-3} would constitute evidence for new physics. The most stringent constraints to date on CP violation in charm mixing have been obtained with this method [64] and from the A_Γ measurement [65].

A fit to all data [29], including also results from time-dependent analyses of $D^0 \to K_S\pi^+\pi^-$ decays, from which x, y, $|q/p|$ and ϕ_D can be determined directly, yields no evidence for indirect CP violation:

$$1 - |q/p| = +0.11\,^{+0.07}_{-0.08}\,,$$
$$\phi_D = \left(-13\,^{+10}_{-9}\right)^\circ\,.$$

With the additional assumption of no direct CP violation in doubly-Cabibbo-suppressed D decays [66–68], tighter constraints are obtained:

$$1 - |q/p| = -0.001 \pm 0.014\,,$$
$$\phi_D = (0.1 \pm 0.5)^\circ\,.$$

More details on various theoretical and experimental aspects of $D^0 - \overline{D}^0$ mixing can be found in Ref. [31].

Searches for CP violation in charged $D_{(s)}$ decays have been performed in many modes. Searches in decays mediated by Cabibbo-suppressed amplitudes are particularly interesting, since in other channels effects are likely to be too small to be observable in current experiments. Examples of relevant two-body modes are $D^+ \to \pi^+\pi^0$, K_SK^+, $\phi\pi^+$ and $D_s^+ \to K^+\pi^0$, $K_S\pi^+$, ϕK^+. The most precise results are $\mathcal{A}_{D^+\to K_SK^+} = -0.0003 \pm 0.0017$ and $\mathcal{A}_{D_s^+\to K_S\pi^+} = +0.0063 \pm 0.0047$ [29]. The precision of experiments is now sufficient that the effect from CP violation in the neutral kaon system can be seen in $D^+ \to K_S\pi^+$ decays [69,70].

Three- and four-body final states provide additional possibilities to search for CP violation, since effects may vary over the phase-space [71]. A number of methods have been proposed to exploit this feature and search for CP violation in ways that do not require modelling of the decay distribution [72–74]. Such methods are useful for analysis of charm decays since they are less sensitive to biases from production asymmetries, and are well suited to address the issue of whether or not CP violation effects are present. They can also be applied to tagged neutral D meson as well as to charged $D_{(s)}$ decays (flavour tagging is typically achieved from the charge of the pion producted in $D^{*+} \to D^0\pi^+$ decays). The results of all searches to date are consistent with the absence of CP violation, with the most significant hint at the level of 2.7σ [75].

13.6. Beauty

13.6.1. *CP violation in mixing of B^0 and B_s^0 mesons* :

The upper bound on the CP asymmetry in semileptonic B decays [28] implies that CP violation in $B^0 - \overline{B}^0$ mixing is a small effect (we use $\mathcal{A}_{\rm SL}/2 \approx 1 - |q/p|$, see Eq. (13.43)):

$$\mathcal{A}^d_{\rm SL} = (-2.1 \pm 1.7) \times 10^{-3} \implies |q/p| = 1.0010 \pm 0.0008\,. \quad (13.87)$$

The Standard Model prediction is

$$\mathcal{A}^d_{\rm SL} = \mathcal{O}\left[(m_c^2/m_t^2)\sin\beta\right] \lesssim 0.001\,. \quad (13.88)$$

An explicit calculation gives $(-4.7 \pm 0.6) \times 10^{-4}$ [34].

The experimental constraint on CP violation in $B_s^0 - \overline{B}_s^0$ mixing is somewhat weaker than that in the $B^0 - \overline{B}^0$ system [28]

$$\mathcal{A}^s_{\rm SL} = (-0.6 \pm 2.8) \times 10^{-3} \implies |q/p| = 1.0003 \pm 0.0014\,. \quad (13.89)$$

The Standard Model prediction is $\mathcal{A}^s_{\rm SL} = \mathcal{O}\left[(m_c^2/m_t^2)\sin\beta_s\right] \lesssim 10^{-4}$, with an explicit calculation giving $(2.22 \pm 0.27) \times 10^{-5}$ [34].

The fit to experimental data that results in the averages quoted above has a χ^2 probability of 4.5% indicating some tension between the different measurements [29]. This originates in part from a result from the D0 collaboration for the inclusive same-sign dimuon asymmetry that deviates from the Standard Model prediction by 3.6σ [76]. As yet, this has not been confirmed by independent studies.

In models where $\mathbf{\Gamma}_{12}/\mathbf{M}_{12}$ is approximately real, such as the Standard Model, an upper bound on $\Delta\Gamma/\Delta m \approx \mathcal{R}e(\mathbf{\Gamma}_{12}/\mathbf{M}_{12})$ provides yet another upper bound on the deviation of $|q/p|$ from one. This constraint does not hold if $\mathbf{\Gamma}_{12}/\mathbf{M}_{12}$ is approximately imaginary. (An alternative parameterization uses $q/p = (1-\tilde{\epsilon}_B)/(1+\tilde{\epsilon}_B)$, leading to $\mathcal{A}_{\rm SL} \simeq 4\mathcal{R}e(\tilde{\epsilon}_B)$.)

13.6.2. *CP violation in interference of B^0 decays with and without mixing* :

The small deviation (less than one percent) of $|q/p|$ from 1 implies that, at the present level of experimental precision, CP violation in B^0 mixing is a negligible effect. Thus, for the purpose of analyzing CP asymmetries in hadronic B^0 decays, we can use

$$\lambda_f = e^{-i\phi_{M(B^0)}}(\overline{A}_f/A_f)\,, \quad (13.90)$$

where $\phi_{M(B^0)}$ refers to the phase of $\mathbf{M}_{12}$ appearing in Eq. (13.49) that is appropriate for $B^0 - \overline{B}^0$ oscillations. Within the Standard Model, the corresponding phase factor is given by

$$e^{-i\phi_{M(B^0)}} = (V_{tb}^*V_{td})/(V_{tb}V_{td}^*)\,. \quad (13.91)$$

The class of CP violation effects in interference between mixing and decay is studied with final states that are common to B^0 and $\overline{B}^0$ decays [77,78]. It is convenient to rewrite Eq. (13.47) for B^0 decays as [79–81]

$$\mathcal{A}_f(t) = S_f\sin(\Delta mt) - C_f\cos(\Delta mt)\,,$$
$$S_f \equiv \frac{2\,\mathcal{I}m(\lambda_f)}{1+|\lambda_f|^2}\,, \quad C_f \equiv \frac{1-|\lambda_f|^2}{1+|\lambda_f|^2}\,, \quad (13.92)$$

where we assume that $\Delta\Gamma = 0$ and $|q/p| = 1$. An alternative notation in use is $A_f \equiv -C_f$ – this A_f should not be confused with the A_f of Eq. (13.19), but in the limit that $|q/p| = 1$ is equivalent with the $\mathcal{A}_f$ of Eq. (13.41).

A large class of interesting processes proceed via quark transitions of the form $\overline{b} \to \overline{q}q\overline{q}'$ with $q' = s$ or d. For $q = c$ or u, there are contributions from both tree (t) and penguin (p^{q_u}, where $q_u = u, c, t$ is the quark in the loop) diagrams (see Fig. 13.2) which carry different weak phases:

$$A_f = \left(V_{qb}^*V_{qq'}\right)t_f + \sum_{q_u=u,c,t}\left(V_{q_ub}^*V_{q_uq'}\right)p_f^{q_u}\,. \quad (13.93)$$

(The distinction between tree and penguin contributions is a heuristic one; the separation by the operator that enters is more precise. A detailed discussion of the more complete operator product approach, which also includes higher order QCD corrections, can be found in Ref. [82] for example.) Using CKM unitarity, these decay amplitudes can always be written in terms of just two CKM combinations. For example, for $f = \pi\pi$, which proceeds via a $\overline{b} \to \overline{u}u\overline{d}$ transition, we can write

$$A_{\pi\pi} = (V_{ub}^*V_{ud})\,T_{\pi\pi} + (V_{tb}^*V_{td})\,P^t_{\pi\pi}\,, \quad (13.94)$$

where $T_{\pi\pi} = t_{\pi\pi} + p^u_{\pi\pi} - p^c_{\pi\pi}$ and $P^t_{\pi\pi} = p^t_{\pi\pi} - p^c_{\pi\pi}$. CP-violating phases in Eq. (13.94) appear only in the CKM elements, so that

$$\frac{\overline{A}_{\pi\pi}}{A_{\pi\pi}} = \frac{(V_{ub}V_{ud}^*)\,T_{\pi\pi} + (V_{tb}V_{td}^*)\,P^t_{\pi\pi}}{(V_{ub}^*V_{ud})\,T_{\pi\pi} + (V_{tb}^*V_{td})\,P^t_{\pi\pi}}\,. \quad (13.95)$$

For $f = J/\psi K$, which proceeds via a $\overline{b} \to \overline{c}c\overline{s}$ transition, we can write

$$A_{\psi K} = (V_{cb}^*V_{cs})\,T_{\psi K} + (V_{ub}^*V_{us})\,P^u_{\psi K}\,, \quad (13.96)$$

where $T_{\psi K} = t_{\psi K} + p^c_{\psi K} - p^t_{\psi K}$ and $P^u_{\psi K} = p^u_{\psi K} - p^t_{\psi K}$. A subtlety arises in this decay that is related to the fact that B^0 decays into a final $J/\psi K^0$ state while $\overline{B}^0$ decays into a final $J/\psi \overline{K}^0$ state. A common final state, *e.g.*, $J/\psi K_S$, is reached only via $K^0 - \overline{K}^0$ mixing. Consequently, the phase factor (defined in Eq. (13.49)) corresponding to neutral K mixing, $e^{-i\phi_{M(K)}} = (V^*_{cd}V_{cs})/(V_{cd}V^*_{cs})$, plays a role:

$$\frac{\overline{A}_{\psi K_S}}{A_{\psi K_S}} = -\frac{\left(V_{cb}V^*_{cs}\right) T_{\psi K} + \left(V_{ub}V^*_{us}\right) P^u_{\psi K}}{\left(V^*_{cb}V_{cs}\right) T_{\psi K} + \left(V^*_{ub}V_{us}\right) P^u_{\psi K}} \times \frac{V^*_{cd}V_{cs}}{V_{cd}V^*_{cs}} \,. \qquad (13.97)$$

For $q = s$ or d, there are only penguin contributions to A_f, that is, $t_f = 0$ in Eq. (13.93). (The tree $\overline{b} \to \overline{u}u\overline{q}'$ transition followed by $\overline{u}u \to \overline{q}q$ rescattering is included below in the P^u terms.) Again, CKM unitarity allows us to write A_f in terms of two CKM combinations. For example, for $f = \phi K_S$, which proceeds via a $\overline{b} \to \overline{s}s\overline{s}$ transition, we can write

$$\frac{\overline{A}_{\phi K_S}}{A_{\phi K_S}} = -\frac{\left(V_{cb}V^*_{cs}\right) P^c_{\phi K} + \left(V_{ub}V^*_{us}\right) P^u_{\phi K}}{\left(V^*_{cb}V_{cs}\right) P^c_{\phi K} + \left(V^*_{ub}V_{us}\right) P^u_{\phi K}} \times \frac{V^*_{cd}V_{cs}}{V_{cd}V^*_{cs}} \,, \qquad (13.98)$$

where $P^c_{\phi K} = p^c_{\phi K} - p^t_{\phi K}$ and $P^u_{\phi K} = p^u_{\phi K} - p^t_{\phi K}$.

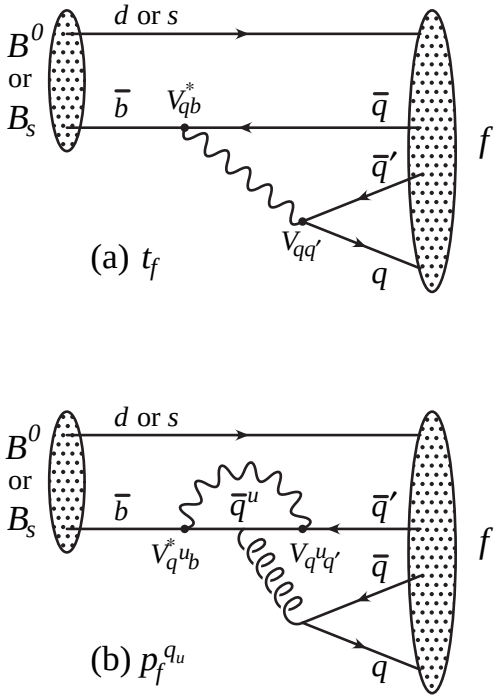

Figure 13.2: Feynman diagrams for (a) tree and (b) penguin amplitudes contributing to $B^0 \to f$ or $B^0_s \to f$ via a $\overline{b} \to \overline{q}q\overline{q}'$ quark-level process.

Since in general the amplitude A_f involves two different weak phases, the corresponding decays can exhibit both CP violation in the interference of decays with and without mixing, $S_f \neq 0$, and CP violation in decay, $C_f \neq 0$. (At the present level of experimental precision, the contribution to C_f from CP violation in mixing is negligible, see Eq. (13.87).) If the contribution from a second weak phase is suppressed, then the interpretation of S_f in terms of Lagrangian CP-violating parameters is clean, while C_f is small. If such a second contribution is not suppressed, S_f depends on hadronic parameters and, if the relevant strong phase difference is large, C_f is large.

A summary of $\overline{b} \to \overline{q}q\overline{q}'$ modes with $q' = s$ or d is given in Table 13.1. The $\overline{b} \to \overline{d}d\overline{q}$ transitions lead to final states that are similar to those from $\overline{b} \to \overline{u}u\overline{q}$ transitions and have similar phase dependence. Final states that consist of two vector mesons ($\psi\phi$ and $\phi\phi$) are not CP eigenstates, and angular analysis is needed to separate the CP-even from the CP-odd contributions.

Table 13.1: Summary of $\overline{b} \to \overline{q}q\overline{q}'$ modes with $q' = s$ or d. The second and third columns give examples of hadronic final states (usually those which are experimentally most convenient to study). The fourth column gives the CKM dependence of the amplitude A_f, using the notation of Eqs. (13.94, 13.96, 13.98), with the dominant term first and the subdominant second. The suppression factor of the second term compared to the first is given in the last column. "Loop" refers to a penguin versus tree-suppression factor (it is mode-dependent and roughly $\mathcal{O}(0.2 - 0.3)$) and $\lambda \simeq 0.23$ is the expansion parameter of Eq. (13.55).

$\overline{b} \to \overline{q}q\overline{q}'$	$B^0 \to f$	$B^0_s \to f$	CKM dependence of A_f	Suppression
$\overline{b} \to \bar{c}c\bar{s}$	ψK_S	$\psi\phi$	$(V^*_{cb}V_{cs})T + (V^*_{ub}V_{us})P^u$	loop $\times\, \lambda^2$
$\overline{b} \to \bar{s}s\bar{s}$	ϕK_S	$\phi\phi$	$(V^*_{cb}V_{cs})P^c + (V^*_{ub}V_{us})P^u$	λ^2
$\overline{b} \to \bar{u}u\bar{s}$	$\pi^0 K_S$	K^+K^-	$(V^*_{cb}V_{cs})P^c + (V^*_{ub}V_{us})T$	λ^2/loop
$\overline{b} \to \bar{c}c\bar{d}$	D^+D^-	ψK_S	$(V^*_{cb}V_{cd})T + (V^*_{tb}V_{td})P^t$	loop
$\overline{b} \to \bar{s}s\bar{d}$	K_SK_S	ϕK_S	$(V^*_{tb}V_{td})P^t + (V^*_{cb}V_{cd})P^c$	$\lesssim 1$
$\overline{b} \to \bar{u}u\bar{d}$	$\pi^+\pi^-$	$\rho^0 K_S$	$(V^*_{ub}V_{ud})T + (V^*_{tb}V_{td})P^t$	loop
$\overline{b} \to \bar{c}u\bar{d}$	$D_{CP}\pi^0$	$D_{CP}K_S$	$(V^*_{cb}V_{ud})T + (V^*_{ub}V_{cd})T'$	λ^2
$\overline{b} \to \bar{c}u\bar{s}$	$D_{CP}K_S$	$D_{CP}\phi$	$(V^*_{cb}V_{us})T + (V^*_{ub}V_{cs})T'$	$\lesssim 1$

The cleanliness of the theoretical interpretation of S_f can be assessed from the information in the last column of Table 13.1. In case of small uncertainties, the expression for S_f in terms of CKM phases can be deduced from the fourth column of Table 13.1 in combination with Eq. (13.91) (and, for $b \to q\overline{q}s$ decays, the example in Eq. (13.97)). Here we consider several interesting examples.

For $B^0 \to J/\psi K_S$ and other $\overline{b} \to \overline{c}c\overline{s}$ processes, we can neglect the P^u contribution to A_f, in the Standard Model, to an approximation that is better than one percent, giving:

$$\lambda_{\psi K_S} = -e^{-2i\beta} \;\Rightarrow\; S_{\psi K_S} = \sin 2\beta \,, \quad C_{\psi K_S} = 0 \,. \qquad (13.99)$$

It is important to verify experimentally the level of suppression of the penguin contribution. Methods based on flavor symmetries [83–86] allow limits to be obtained. All are currently consistent with the P^u term being negligible.

In the presence of new physics, A_f is still likely to be dominated by the T term, but the mixing amplitude might be modified. We learn that, model-independently, $C_f \approx 0$ while S_f cleanly determines the mixing phase ($\phi_M - 2\arg(V_{cb}V^*_{cd})$). The experimental measurement [29], $S_{\psi K} = +0.691 \pm 0.017$, gave the first precision test of the Kobayashi-Maskawa mechanism, and its consistency with the predictions for $\sin 2\beta$ makes it very likely that this mechanism is indeed the dominant source of CP violation in the quark sector.

For $B^0 \to \phi K_S$ and other $\overline{b} \to \overline{s}s\overline{s}$ processes (as well as some $\overline{b} \to \overline{u}u\overline{s}$ processes), we can neglect the subdominant contributions, in the Standard Model, to an approximation that is good to the order of a few percent:

$$\lambda_{\phi K_S} = -e^{-2i\beta} \;\Rightarrow\; S_{\phi K_S} = \sin 2\beta \,, \quad C_{\phi K_S} = 0 \,. \qquad (13.100)$$

A review of explicit calculations of the effects of subleading amplitudes can be found in Ref. [87]. In the presence of new physics, both A_f and $\mathbf{M}_{12}$ can have contributions that are comparable in size to those of the Standard Model and carry new weak phases. Such a situation gives several interesting consequences for penguin-dominated $b \to \overline{q}q\overline{s}$ decays ($q = u, d, s$) to a final state f:

1. The value of $-\eta_f S_f$ may be different from $S_{\psi K_S}$ by more than a few percent, where η_f is the CP eigenvalue of the final state.
2. The values of $\eta_f S_f$ for different final states f may be different from each other by more than a few percent (for example, $S_{\phi K_S} \neq S_{\eta' K_S}$).
3. The value of C_f may be different from zero by more than a few percent.

While a clear interpretation of such signals in terms of Lagrangian parameters will be difficult because, under these circumstances, hadronic parameters play a role, any of the above three options will clearly signal new physics. Fig. 13.3 summarizes the present experimental results: none of the possible signatures listed above is unambiguously established, but there is definitely still room for new physics.

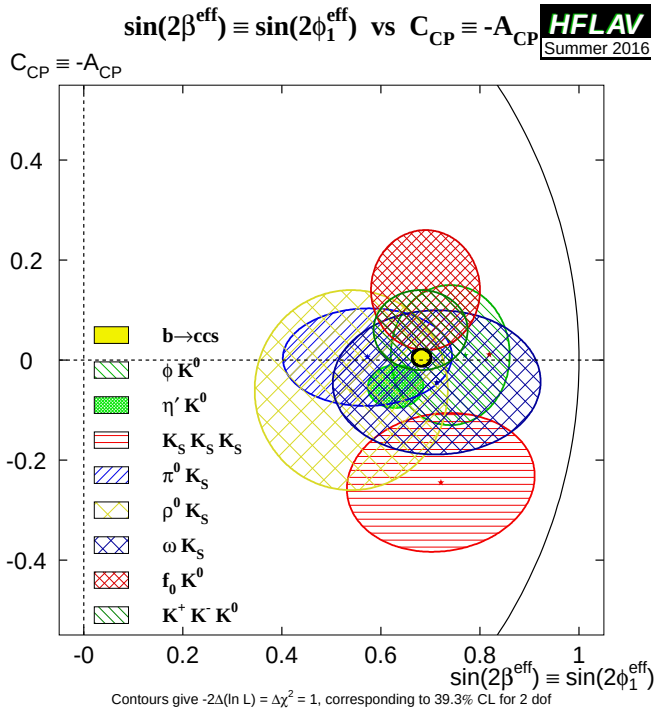

Figure 13.3: Summary of the results [29] of time-dependent analyses of $b \to q\overline{q}s$ decays, which are potentially sensitive to new physics.

For the $\overline{b} \to \overline{u}u\overline{d}$ process $B \to \pi\pi$ and other related channels, the penguin-to-tree ratio can be estimated using SU(3) relations and experimental data on related $B \to K\pi$ decays. The result (for $\pi\pi$) is that the suppression is at the level of $0.2 - 0.3$ and so cannot be neglected. The expressions for $S_{\pi\pi}$ and $C_{\pi\pi}$ to leading order in $R_{PT} \equiv (|V_{tb}V_{td}|\, P^t_{\pi\pi})/(|V_{ub}V_{ud}|\, T_{\pi\pi})$ are:

$$\lambda_{\pi\pi} = e^{2i\alpha}\left[(1 - R_{PT}e^{-i\alpha})/(1 - R_{PT}e^{+i\alpha})\right] \Rightarrow$$

$$S_{\pi\pi} \approx \sin 2\alpha + 2\,\mathcal{R}e(R_{PT})\cos 2\alpha \sin\alpha\,, \quad C_{\pi\pi} \approx 2\,\mathcal{I}m(R_{PT})\sin\alpha\,. \tag{13.101}$$

Note that R_{PT} is mode-dependent and, in particular, could be different for $\pi^+\pi^-$ and $\pi^0\pi^0$. If strong phases can be neglected, then R_{PT} is real, resulting in $C_{\pi\pi} = 0$. The size of $C_{\pi\pi}$ is an indicator of how large the strong phase is. The present experimental average is $C_{\pi^+\pi^-} = -0.27 \pm 0.04$ [29]. As concerns $S_{\pi\pi}$, it is clear from Eq. (13.101) that the relative size or strong phase of the penguin contribution must be known to extract α. This is the problem of penguin pollution.

The cleanest solution involves isospin relations among the $B \to \pi\pi$ amplitudes [88]:

$$\frac{1}{\sqrt{2}}A_{\pi^+\pi^-} + A_{\pi^0\pi^0} = A_{\pi^+\pi^0}\,. \tag{13.102}$$

The method exploits the fact that the penguin contribution to $P^t_{\pi\pi}$ is pure $\Delta I = 1/2$ (this is not true for the electroweak penguins which, however, are expected to be small), while the tree contribution to $T_{\pi\pi}$ contains pieces that are both $\Delta I = 1/2$ and $\Delta I = 3/2$. A simple geometric construction then allows one to find R_{PT} and extract α cleanly from $S_{\pi^+\pi^-}$. The key experimental difficulty is that one must measure accurately the separate rates for B^0 and $\overline{B}^0 \to \pi^0\pi^0$.

CP asymmetries in $B \to \rho\pi$ and $B \to \rho\rho$ can also be used to determine α. In particular, the $B \to \rho\rho$ measurements are presently very significant in constraining α. The extraction proceeds via isospin analysis similar to that of $B \to \pi\pi$. There are, however, several important differences. First, due to the finite width of the ρ mesons, a final $(\rho\rho)_{I=1}$ state is possible [89]. The effect is, however, of the order of $(\Gamma_\rho/m_\rho)^2 \sim 0.04$. Second, due to the presence of three helicity states for the two vector mesons, angular analysis is needed to separate the CP-even and CP-odd components. The theoretical expectation is that the CP-odd component is small, which is supported by experiments which find that the $\rho^+\rho^-$ and $\rho^\pm\rho^0$ modes are dominantly longitudinally polarized. Third, an important advantage of the $\rho\rho$ modes is that the penguin contribution is expected to be small due to different hadronic dynamics. This expectation is confirmed by the smallness of $\mathcal{B}(B^0 \to \rho^0\rho^0) = (0.95 \pm 0.16) \times 10^{-6}$ [29,90] compared to $\mathcal{B}(B^0 \to \rho^+\rho^-) = (24.2 \pm 3.1) \times 10^{-6}$ [29]. Thus, $S_{\rho^+\rho^-}$ is not far from $\sin 2\alpha$. Finally, both $S_{\rho^0\rho^0}$ and $C_{\rho^0\rho^0}$ are experimentally accessible, which may allow a precision determination of α. However, a full isospin analysis should allow that the fractions of longitudinal polarisation in B and $\overline{B}$ decays may differ, which has not yet been done by the experiments.

Detailed discussion of the determination of α with these methods, and the latest world average, can be found in Refs. [36,91]. The consistency between the range of α determined by the $B \to \pi\pi$, $\rho\pi$ and $\rho\rho$ measurements and the range allowed by CKM fits (excluding these direct determinations) provides further support to the Kobayashi-Maskawa mechanism.

All modes discussed in this Section so far have possible contributions from penguin amplitudes. As shown in Table 13.1, CP violation can also be studied with final states, typically containing charmed mesons, where no such contribution is possible. The neutral charmed meson must be reconstructed in a final state, such as a CP eigenstate, common to D^0 and $\overline{D}^0$ so that the amplitudes for the B and $\overline{B}$ meson decays interfere. Although there is a second tree amplitude with a different weak phase, the contributions of the different diagrams can in many cases be separated experimentally (for example by exploiting different decays of the $\overline{D}^0$ mesons) making these channels very clean theoretically. The first determination of $\sin(2\beta)$, with significance of CP violation over 5σ, with this method has recently been reported [92]. Moreover, the interference between the two tree diagrams gives sensitivity to γ, as will be discussed in Section 13.6.4.

13.6.3. *CP violation in interference of B^0_s decays with and without mixing*:

As discussed in Section 13.6.1, the world average for $|q/p|$ in the B^0_s system currently deviates from the Standard Model expectation due to an anomalous value of the dimuon asymmetry. Attributing the dimuon asymmetry result to a fluctuation, we again neglect the deviation of $|q/p|$ from 1, and use

$$\lambda_f = e^{-i\phi_M(B^0_s)}(\overline{A}_f/A_f)\,. \tag{13.103}$$

Within the Standard Model,

$$e^{-i\phi_{M(B^0_s)}} = (V^*_{tb}V_{ts})/(V_{tb}V^*_{ts})\,. \tag{13.104}$$

Note that $\Delta\Gamma/\Gamma = 0.122 \pm 0.009$ [29] and therefore y should not be put to zero in Eqs. (13.36, 13.37). However, $|q/p| = 1$ is expected to hold to an even better approximation than for B^0 mesons. One therefore obtains

$$\mathcal{A}_f(t) = \frac{S_f \sin(\Delta m t) - C_f \cos(\Delta m t)}{\cosh(\Delta\Gamma t/2) - A^{\Delta\Gamma}_f \sinh(\Delta\Gamma t/2)}\,,$$

$$A^{\Delta\Gamma}_f \equiv \frac{-2\,\mathcal{R}e(\lambda_f)}{1 + |\lambda_f|^2}\,. \tag{13.105}$$

The presence of the $A_f^{\Delta\Gamma}$ term implies that information on λ_f can be obtained from analyses that do not use tagging of the initial flavor, through so-called effective lifetime measurements [93].

The $B_s^0 \to J/\psi\phi$ decay proceeds via the $\overline{b} \to \overline{c}c\overline{s}$ transition. The CP asymmetry in this mode thus determines (with angular analysis to disentangle the CP-even and CP-odd components of the final state) $\sin 2\beta_s$, where β_s is defined in Eq. (13.58) [94]. The $B_s^0 \to J/\psi\pi^+\pi^-$ decay, which has a large contributions from $J/\psi f_0(980)$ and is assumed to also proceed dominantly via the $\overline{b} \to \overline{c}c\overline{s}$ transition, has also been used to determine β_s. In this case no angular analysis is necessary, since the final state has been shown to be dominated by the CP-even component [95]. The combination of measurements yields [29]

$$-2\beta_s = 0.021 \pm 0.031\,, \tag{13.106}$$

consistent with the Standard Model prediction, $\beta_s = 0.0185 \pm 0.0003$ [19].

The experimental investigation of CP violation in the B_s^0 sector is still at a relatively early stage, and far fewer modes have been studied than in the B^0 system. First results on the $\overline{b} \to \overline{q}q\overline{s}$ decays $B_s^0 \to \phi\phi$ and K^+K^- have been reported. More channels are expected to be studied in the near future.

13.6.4. *Direct CP violation in the B system* :

An interesting class of decay modes is that of the tree-level decays $B^\pm \to D^{(*)}K^\pm$. These decays provide golden methods for a clean determination of the angle γ [97–101]. The method uses the decays $B^+ \to D^0K^+$, which proceeds via the quark transition $\overline{b} \to \overline{u}c\overline{s}$, and $B^+ \to \overline{D}^0K^+$, which proceeds via the quark transition $\overline{b} \to \overline{c}u\overline{s}$, with the D^0 and $\overline{D}^0$ decaying into a common final state. The decays into common final states, such $(\pi^0K_S)_DK^+$, involve interference effects between the two amplitudes, with sensitivity to the relative phase, $\delta + \gamma$ (δ is the relevant strong phase difference). The CP-conjugate processes are sensitive to $\delta - \gamma$. Measurements of branching ratios and CP asymmetries allow the determination of γ and δ from amplitude triangle relations. The method suffers from discrete ambiguities but, since all hadronic parameters can be determined from the data, has negligible theoretical uncertainty [102].

Unfortunately, the smallness of the CKM-suppressed $b \to u$ transitions makes it difficult to use the simplest methods alone [97–99] to determine γ. These difficulties are overcome (and the discrete ambiguities are removed) by performing a Dalitz plot analysis for multi-body D decays [100,101]. Detailed discussion of the determination of γ with these methods can be found in Ref. [36].

Constraints on γ from combinations of results on various $B \to D^{(*)}K^{(*)}$ processes have been obtained by experiments [103,104]. The latest world average is [29]:

$$\gamma = \left(76.2\,^{+4.7}_{-5.0}\right)^\circ\,.$$

The consistency between the range of γ determined by the $B \to DK$ measurements and the range allowed by CKM fits (excluding these direct determinations) provides further support to the Kobayashi-Maskawa mechanism. As more data become available, determinations of γ from $B_s^0 \to D_s^\mp K^\pm$ [105,106] and $B^0 \to DK^{*0}$ [107–110] are expected to also give competitive measurements.

Decays to the final state $K^\mp\pi^\pm$ provided the first observations of direct CP violation in both B^0 and B_s^0 systems. The asymmetry arises due to interference between tree and penguin diagrams [111], similar to the effect discussed in Section 13.6.2. In principle, measurements of $\mathcal{A}_{\overline{B}^0 \to K^-\pi^+}$ and $\mathcal{A}_{\overline{B}_s^0 \to K^+\pi^-}$ could be used to determine the weak phase difference γ, but lack of knowledge of the relative magnitude and strong phase of the contributing amplitudes limits the achievable precision. The uncertainties on these hadronic parameters can be reduced by exploiting flavor symmetries, which predict a number of relations between asymmetries in different modes. One such relation is that the partial rate differences for B^0 and B_s^0 decays to $K^\mp\pi^\pm$ are expected to be approximately equal and opposite [112], which is consistent with current data. It is also expected that the partial rate asymmetries for $\overline{B}^0 \to K^-\pi^+$ and $B^- \to K^-\pi^0$ should be approximately equal; however, the experimental results currently show a significant discrepancy [29]:

$$\mathcal{A}_{\overline{B}^0 \to K^-\pi^+} = -0.082 \pm 0.006\,, \qquad \mathcal{A}_{B^- \to K^-\pi^0} = 0.040 \pm 0.021\,.$$

It is therefore of great interest to understand whether this originates from Standard Model QCD corrections, or whether it is a signature of new dynamics. Improved tests of a more precise relation between the partial rate differences of all four $K\pi$ final states [113–116], currently limited by knowledge of the CP asymmetry in $\overline{B}^0 \to K_S\pi^0$ decays, may help to resolve the situation.

It is also of interest to investigate whether similar patterns appear among the CP violating asymmetries in B meson decays to final states containing one pseudoscalar and one vector meson. Since the vector resonance decays to two particles, such channels can be studied through Dalitz plot analysis of the three-body final state. Model-independent analyses of $B^+ \to K^+K^-K^+$, $\pi^+\pi^-K^+$, $\pi^+\pi^-\pi^+$ and $K^+K^-\pi^+$ decays have revealed large CP violation effects in certain regions of phase space [117]. It remains to be seen whether these are associated to particular resonances or to interference effects, which will be necessary to understand the underlying dynamics.

13.7. Summary and Outlook

CP violation has been experimentally established in K and B meson decays. A full list of CP asymmetries that have been measured at a level higher than 5σ is given in the introduction to this review. In Section 13.1.4 we introduced three types of CP-violating effects. Examples of these three types include the following:

1. All three types of CP violation have been observed in $K \to \pi\pi$ decays:

$$\begin{aligned}
\mathcal{R}e(\epsilon') &= \frac{1}{6}\left(\left|\frac{\overline{A}_{\pi^0\pi^0}}{A_{\pi^0\pi^0}}\right| - \left|\frac{\overline{A}_{\pi^+\pi^-}}{A_{\pi^+\pi^-}}\right|\right) = (2.5 \pm 0.4) \times 10^{-6} \quad \text{(I)}\\
\mathcal{R}e(\epsilon) &= \frac{1}{2}\left(1 - \left|\frac{q}{p}\right|\right) = (1.66 \pm 0.02) \times 10^{-3} \quad \text{(II)}\\
\mathcal{I}m(\epsilon) &= -\frac{1}{2}\mathcal{I}m(\lambda_{(\pi\pi)_{I=0}}) = (1.57 \pm 0.02) \times 10^{-3}\,. \quad \text{(III)}
\end{aligned} \tag{13.107}$$

2. CP violation in decay has been observed in, for example, $B^0 \to K^+\pi^-$ transitions, while CP violation in interference of decays with and without mixing has been observed in, for example, the $B^0 \to J/\psi K_S$ channel:

$$\begin{aligned}
\mathcal{A}_{K^+\pi^-} &= \frac{|\overline{A}_{K^-\pi^+}/A_{K^+\pi^-}|^2 - 1}{|\overline{A}_{K^-\pi^+}/A_{K^+\pi^-}|^2 + 1} = -0.082 \pm 0.006 \quad \text{(I)}\\
S_{\psi K} &= \mathcal{I}m(\lambda_{\psi K}) = +0.691 \pm 0.017\,. \quad \text{(III)}
\end{aligned} \tag{13.108}$$

Based on Standard Model predictions, further observations of CP violation in B^0, B^+ and B_s^0 decays seem likely in the near future, at both LHCb and its upgrades [118–120] as well as the Belle II experiment [121]. The first observation of CP violation in b baryons is also likely to be within reach of LHCb. The same experiments have great potential to improve the sensitivity to CP violation effects in the charm sector, though uncertainty in the Standard Model predictions makes it difficult to forecast whether or not discoveries will be forthcoming. A number of upcoming experiments have potential to make significant progress on rare kaon decays. Observables that are subject to clean theoretical interpretation, such as β from $S_{\psi K_S}$, β_s from $B_s^0 \to J/\psi\phi$, $\mathcal{B}(K_L \to \pi^0\nu\overline{\nu})$ and γ from CP violation in $B \to DK$ decays, are of particular value for constraining the values of the CKM parameters and probing the flavor sector of extensions to the Standard Model. Progress in lattice QCD calculations is also needed to complement the anticipated experimental results. Other probes of CP violation now being pursued experimentally include the electric dipole moments of the neutron and electron, and the decays of tau leptons. Additional processes that are likely to play an important

role in future CP studies include top-quark production and decay, Higgs boson decays and neutrino oscillations.

All measurements of CP violation to date are consistent with the predictions of the Kobayashi-Maskawa mechanism of the Standard Model. In fact, it is now established that the KM mechanism plays a major role in the CP violation measured in the quark sector. However, a dynamically-generated matter-antimatter asymmetry of the universe requires additional sources of CP violation, and such sources are naturally generated by extensions to the Standard Model. New sources might eventually reveal themselves as small deviations from the predictions of the KM mechanism, or else might not be observable in the quark sector at all, but observable with future probes such as neutrino oscillations or electric dipole moments. The fundamental nature of CP violation demands a vigorous search.

A number of excellent reviews of CP violation are available [122–129], where the interested reader may find a detailed discussion of the various topics that are briefly reviewed here.

We thank David Kirkby for significant contributions to earlier versions of this review.

References:

1. J.H. Christenson *et al.*, Phys. Rev. Lett. **13**, 138 (1964).
2. B. Aubert *et al.* [BABAR Collab.], Phys. Rev. Lett. **87**, 091801 (2001).
3. K. Abe *et al.* [Belle Collab.], Phys. Rev. Lett. **87**, 091802 (2001).
4. H. Burkhardt *et al.* [NA31 Collab.], Phys. Lett. **B206**, 169 (1988).
5. V. Fanti *et al.* [NA48 Collab.], Phys. Lett. **B465**, 335 (1999).
6. A. Alavi-Harati *et al.* [KTeV Collab.], Phys. Rev. Lett. **83**, 22 (1999).
7. B. Aubert *et al.* [BABAR Collab.], Phys. Rev. Lett. **93**, 131801 (2004).
8. Y. Chao *et al.* [Belle Collab.], Phys. Rev. Lett. **93**, 191802 (2004).
9. A. Poluektov *et al.* [Belle Collab.], Phys. Rev. **D81**, 112002 (2010).
10. P. del Amo Sanchez *et al.* [BABAR Collab.], Phys. Rev. **D82**, 072004 (2010).
11. R. Aaij *et al.* [LHCb Collab.], Phys. Lett. **B712**, 203 (2012).
12. R. Aaij *et al.* [LHCb Collab.], Phys. Rev. Lett. **110**, 221601 (2013).
13. R. Aaij *et al.* [LHCb Collab.], Nature Phys. **13**, 391 (2017).
14. See results on the "Time reversal invariance," within the review on "Tests of Conservation Laws," in this *Review*.
15. J. Bernabeu, F. Martinez-Vidal, and P. Villanueva-Perez, JHEP **08**, 064 (2012).
16. J.P. Lees *et al.* [BABAR Collab.], Phys. Rev. Lett. **109**, 211801 (2012).
17. See, for example, R. F. Streater and A. S. Wightman, *CPT, Spin and Statistics, and All That,* reprinted by Addison-Wesley, New York (1989).
18. M. Kobayashi and T. Maskawa, Prog. Theor. Phys. **49**, 652 (1973).
19. J. Charles *et al.* [CKMfitter Group], Eur. Phys. J. **C41**, 1 (2005); updated results and plots available at: `ckmfitter.in2p3.fr`.
20. M. Bona *et al.* [UTfit Collab.], JHEP **10**, 081 (2006); updated results and plots available at: `www.utfit.org/UTfit`.
21. A.D. Sakharov, Pisma Zh. Eksp. Teor. Fiz. **5**, 32 (1967) [Sov. Phys. JETP Lett. **5**, 24 (1967)].
22. For a review, see *e.g.*, A. Riotto, "Theories of baryogenesis," `hep-ph/9807454`.
23. M. Fukugita and T. Yanagida, Phys. Lett. **B174**, 45 (1986).
24. For a review, see *e.g.*, S. Davidson, E. Nardi and Y. Nir, Phys. Reports **466**, 105 (2008).
25. G. Aad *et al.* [ATLAS Collab.], Phys. Lett. **B716**, 1 (2012).
26. S. Chatrchyan *et al.* [CMS Collab.], Phys. Lett. **B716**, 30 (2012).
27. See the K-meson Listings in this *Review*.
28. See the B-meson Listings in this *Review*.
29. Y. Amhis *et al.* [HFLAV Collab.], `arXiv:1612.07233 [hep-ex]`, and online update at `www.slac.stanford.edu/xorg/hflav`.
30. V. Weisskopf and E. P. Wigner, Z. Phys. **63**, 54 (1930); Z. Phys. **65**, 18 (1930) [See also Appendix A of P.K. Kabir, *The CP Puzzle: Strange Decays of the Neutral Kaon,* Academic Press (1968)].
31. See the review on "$D^0 - \overline{D}^0$ Mixing" in this *Review*.
32. O. Long *et al.*, Phys. Rev. **D68**, 034010 (2003).
33. M. Gronau, Y. Grossman, and J.L. Rosner, Phys. Lett. **B508**, 37 (2001).
34. M. Artuso, G. Borissov and A. Lenz, Rev. Mod. Phys. **88**, 045002 (2016).
35. L. Wolfenstein, Phys. Rev. Lett. **13**, 562 (1964).
36. See the review on "Cabibbo-Kobayashi-Maskawa Mixing Matrix," in this *Review*.
37. L. Wolfenstein, Phys. Rev. Lett. **51**, 1945 (1983).
38. A.J. Buras, M.E. Lautenbacher, and G. Ostermaier, Phys. Rev. **D50**, 3433 (1994).
39. C. Jarlskog, Phys. Rev. Lett. **55**, 1039 (1985).
40. See the review on "CP violation in $K_S \to 3\pi$," in this *Review*.
41. T. Blum *et al.*, Phys. Rev. **D91**, 074502 (2015).
42. Z. Bai *et al.*, Phys. Rev. Lett. **115**, 212001 (2015).
43. A.J. Buras *et al.*, JHEP **11**, 202 (2015).
44. Y. Grossman and Y. Nir, Phys. Lett. **B398**, 163 (1997).
45. L.S. Littenberg, Phys. Rev. **D39**, 3322 (1989).
46. A.J. Buras, Phys. Lett. **B333**, 476 (1994).
47. G. Buchalla and A.J. Buras, Nucl. Phys. **B400**, 225 (1993).
48. J. Brod, M. Gorbahn, and E. Stamou, Phys. Rev. **D83**, 034030 (2011).
49. A. J. Buras, D. Buttazzo, J. Girrbach-Noe and R. Knegjens, JHEP **11**, 033 (2015).
50. J.K. Ahn *et al.* [E391a Collab.], Phys. Rev. **D81**, 072004 (2010).
51. T. Yamanaka [KOTO Collab.], Prog. Theor. Exp. Phys. **2012**, 02B006 (2012).
52. M. Mirra [NA62 Collab.], Nuovo Cimento **C038**, 13 (2015).
53. B. Aubert *et al.* [BABAR Collab.], Phys. Rev. Lett. **98**, 211802 (2007).
54. M. Staric *et al.* [Belle Collab.], Phys. Rev. Lett. **98**, 211803 (2007).
55. T. Aaltonen *et al.* [CDF Collab.], Phys. Rev. Lett. **100**, 121802 (2008).
56. R. Aaij *et al.* [LHCb Collab.], Phys. Rev. Lett. **110**, 101802 (2013).
57. See the D-meson Listings in this *Review*.
58. Y. Grossman, A. L. Kagan, and Y. Nir, Phys. Rev. **D75**, 036008 (2007).
59. R. Aaij *et al.* [LHCb Collab.], Phys. Rev. Lett. **108**, 111602 (2012).
60. S. Bergmann *et al.*, Phys. Lett. **B486**, 418 (2000).
61. M. Gersabeck *et al.*, J. Phys. **G39**, 045005 (2012).
62. D.M. Asner *et al.* [CLEO Collab.], Phys. Rev. **D78**, 012001 (2008).
63. M. Ablikim *et al.* [BESIII Collab.], Phys. Lett. **B734**, 227 (2014).
64. R. Aaij *et al.* [LHCb Collab.], Phys. Rev. Lett. **111**, 251801 (2013).
65. R. Aaij *et al.* [LHCb Collab.], Phys. Rev. Lett. **118**, 261803 (2017).
66. M. Ciuchini *et al.*, Phys. Lett. **B655**, 162 (2007).
67. Y. Grossman, Y. Nir, and G. Perez, Phys. Rev. Lett. **103**, 071602 (2009).
68. A.L. Kagan and M.D. Sokoloff, Phys. Rev. **D80**, 076008 (2009).
69. Y. Grossman and Y. Nir, JHEP **04**, 002 (2012).
70. B.R. Ko *et al.* [Belle Collab.], Phys. Rev. Lett. **109**, 021601 (2012); Erratum-ibid. **109**, 119903 (2012).
71. See the "Review of Multibody Charm Analyses" in this *Review*.
72. B. Aubert *et al.* [BABAR Collab.], Phys. Rev. **D78**, 051102 (2008).
73. I. Bediaga *et al.*, Phys. Rev. **D80**, 096006 (2009); Phys. Rev. **D86**, 036005 (2012).
74. M. Williams, Phys. Rev. **D84**, 054015 (2011).
75. R. Aaij *et al.* [LHCb Collab.], Phys. Lett. **B769**, 345 (2017).

76. V.M. Abazov *et al.* [D0 Collab.], Phys. Rev. **D82**, 032001 (2010); Phys. Rev. **D84**, 052007 (2011); Phys. Rev. **D89**, 012002 (2014).
77. A.B. Carter and A.I. Sanda, Phys. Rev. Lett. **45**, 952 (1980); Phys. Rev. **D23**, 1567 (1981).
78. I.I. Bigi and A.I. Sanda, Nucl. Phys. **B193**, 85 (1981).
79. I. Dunietz and J.L. Rosner, Phys. Rev. **D34**, 1404 (1986).
80. Ya.I. Azimov, N.G. Uraltsev, and V.A. Khoze, Sov. J. Nucl. Phys. **45**, 878 (1987) [Yad. Fiz. **45**, 1412 (1987)].
81. I.I. Bigi and A.I. Sanda, Nucl. Phys. **B281**, 41 (1987).
82. G. Buchalla, A.J. Buras, and M.E. Lautenbacher, Rev. Mod. Phys. **68**, 1125 (1996).
83. R. Fleischer, Eur. Phys. J. **C10**, 299 (1999).
84. M. Ciuchini, M. Pierini, and L. Silvestrini, Phys. Rev. Lett. **95**, 221804 (2005).
85. S. Faller *et al.*, Phys. Rev. **D79**, 014030 (2009).
86. M. Jung, Phys. Rev. **D86**, 053008 (2012).
87. L. Silvestrini, Ann. Rev. Nucl. and Part. Sci. **57**, 405 (2007).
88. M. Gronau and D. London, Phys. Rev. Lett. **65**, 3381 (1990).
89. A.F. Falk *et al.*, Phys. Rev. **D69**, 011502 (2004).
90. R. Aaij *et al.* [LHCb Collab.], Phys. Lett. **B747**, 468 (2015).
91. J. Charles *et al.* [CKMfitter Collab.], `arXiv:1705.02981 [hep-ph]`.
92. A. Abdesselam *et al.* [BABAR and Belle Collabs.], Phys. Rev. Lett. **115**, 121604 (2015).
93. R. Fleischer and R. Knegjens, Eur. Phys. J. **C71**, 1789 (2011).
94. A.S. Dighe, I. Dunietz, and R. Fleischer, Eur. Phys. J. **C6**, 647 (1999).
95. R. Aaij *et al.* [LHCb Collab.], Phys. Rev. **D89**, 092006 (2014).
96. R. Aaij *et al.* [LHCb Collab.], Phys. Rev. Lett. **113**, 211801 (2014).
97. M. Gronau and D. London, Phys. Lett. **B253**, 483 (1991).
98. M. Gronau and D. Wyler, Phys. Lett. **B265**, 172 (1991).
99. D. Atwood, I. Dunietz, and A. Soni, Phys. Rev. Lett. **78**, 3257 (1997).
100. D. Atwood, I. Dunietz, and A. Soni, Phys. Rev. **D63**, 036005 (2001).
101. A. Giri *et al.*, Phys. Rev. **D68**, 054018 (2003).
102. J. Brod and J. Zupan, JHEP **01**, 051 (2014).
103. J. P. Lees *et al.* [BaBar Collab.], Phys. Rev. **D87**, 052015 (2013).
104. R. Aaij *et al.* [LHCb Collab.], JHEP **12**, 087 (2016), LHCb-CONF-2017-004.
105. R. Aleksan, I. Dunietz, and B. Kayser, Z. Phys. **C54**, 653 (1992).
106. R. Fleischer, Nucl. Phys. **B671**, 459 (2003).
107. I. Dunietz, Phys. Lett. **B270**, 75 (1991).
108. M. Gronau, Phys. Lett. **B557**, 198 (2003).
109. T. Gershon, Phys. Rev. **D79**, 051301 (2009).
110. T. Gershon and M. Williams, Phys. Rev. **D80**, 092002 (2009).
111. M. Bander, D. Silverman, and A. Soni, Phys. Rev. Lett. **43**, 242 (1979).
112. X.-G. He, Eur. Phys. J. **C9**, 443 (1999).
113. D. Atwood and A. Soni, Phys. Rev. **D58**, 036005 (1998).
114. M. Gronau and J. L. Rosner, Phys. Rev. **D59**, 113002 (1999).
115. H.J. Lipkin, Phys. Lett. **B445**, 403 (1999).
116. M. Gronau, Phys. Lett. **B627**, 82 (2005).
117. R. Aaij *et al.* [LHCb Collab.], Phys. Rev. Lett. **111**, 101801 (2013); Phys. Rev. Lett. **112**, 011801 (2014); Phys. Rev. **D90**, 112004 (2014).
118. A.A. Alves *et al.* [LHCb Collab.], JINST **3** S08005 (2008).
119. I. Bediaga *et al.* [LHCb Collab.], CERN-LHCC-2012-007, LHCb-TDR-12.
120. R. Aaij *et al.* [LHCb Collab.], CERN-LHCC-2017-003.
121. T. Aushev *et al.*, `arXiv:1002.5012 [hep-ex]` , KEK Report 2009-12.
122. G.C. Branco, L. Lavoura, and J.P. Silva, *CP Violation,* Oxford University Press, Oxford (1999).
123. I.I.Y. Bigi and A.I. Sanda, *CP Violation,* Cambridge Monogr., Part. Phys. Nucl. Phys. Cosmol. **9**, 1 (2000).
124. A.J. Bevan *et al.* [BABAR and Belle Collabs.], Eur. Phys. J. **C74**, 3026 (2014).
125. H.R. Quinn and Y. Nir, *"The Mystery of the Missing Antimatter,"* Princeton University Press, Princeton (2008).
126. T.E. Browder *et al.*, Rev. Mod. Phys. **81**, 1887 (2009).
127. M. Ciuchini and A. Stocchi, Ann. Rev. Nucl. and Part. Sci. **61**, 491 (2011).
128. R. Aaij *et al.* [LHCb Collab.] and A. Bharucha *et al.*, Eur. Phys. J. **C73**, 2373 (2013).
129. T. Gershon and V. V. Gligorov, Rept. on Prog. in Phys. **80**, 046201 (2017).

14. Neutrino Masses, Mixing, and Oscillations

Updated November 2017 by K. Nakamura (Kavli IPMU (WPI), U. Tokyo, KEK), and S.T. Petcov (SISSA/INFN Trieste, Kavli IPMU (WPI), U. Tokyo, Bulgarian Academy of Sciences).

The experiments with solar, atmospheric, reactor and accelerator neutrinos have provided compelling evidences for oscillations of neutrinos caused by nonzero neutrino masses and neutrino mixing. The data imply the existence of 3-neutrino mixing in vacuum. We review the theory of neutrino oscillations, the phenomenology of neutrino mixing, the problem of the nature - Dirac or Majorana, of massive neutrinos, the issue of CP violation in the lepton sector, and the current data on the neutrino masses and mixing parameters. The open questions and the main goals of future research in the field of neutrino mixing and oscillations are outlined.

14.1. Introduction: Massive neutrinos and neutrino mixing

It is a well-established experimental fact that the neutrinos and antineutrinos which take part in the standard charged current (CC) and neutral current (NC) weak interaction are of three varieties (types) or flavours: electron, ν_e and $\bar{\nu}_e$, muon, ν_μ and $\bar{\nu}_\mu$, and tauon, ν_τ and $\bar{\nu}_\tau$. The notion of neutrino type or flavour is dynamical: ν_e is the neutrino which is produced with e^+, or produces an e^-, in CC weak interaction processes; ν_μ is the neutrino which is produced with μ^+, or produces μ^-, *etc.* The flavour of a given neutrino is Lorentz invariant. Among the three different flavour neutrinos and antineutrinos, no two are identical. Correspondingly, the states which describe different flavour neutrinos must be orthogonal (within the precision of the current data): $\langle \nu_{l'}|\nu_l\rangle = \delta_{l'l}$, $\langle \bar{\nu}_{l'}|\bar{\nu}_l\rangle = \delta_{l'l}$, $\langle \bar{\nu}_{l'}|\nu_l\rangle = 0$.

It is also well-known from the existing data (all neutrino experiments were done so far with relativistic neutrinos or antineutrinos), that the flavour neutrinos ν_l (antineutrinos $\bar{\nu}_l$), are always produced in weak interaction processes in a state that is predominantly left-handed (LH) (right-handed (RH)). To account for this fact, ν_l and $\bar{\nu}_l$ are described in the Standard Model (SM) by a chiral LH flavour neutrino field $\nu_{lL}(x)$, $l = e, \mu, \tau$. For massless ν_l, the state of ν_l ($\bar{\nu}_l$) which the field $\nu_{lL}(x)$ annihilates (creates) is with helicity (-1/2) (helicity +1/2). If ν_l has a non-zero mass $m(\nu_l)$, the state of ν_l ($\bar{\nu}_l$) is a linear superposition of the helicity (-1/2) and (+1/2) states, but the helicity +1/2 state (helicity (-1/2) state) enters into the superposition with a coefficient $\propto m(\nu_l)/E$, E being the neutrino energy, and thus is strongly suppressed. Together with the LH charged lepton field $l_L(x)$, $\nu_{lL}(x)$ forms an $SU(2)_L$ doublet. In the absence of neutrino mixing and zero neutrino masses, $\nu_{lL}(x)$ and $l_L(x)$ can be assigned one unit of the additive lepton charge L_l and the three charges L_l, $l = e, \mu, \tau$, are conserved by the weak interaction.

At present there is no compelling evidence for the existence of states of relativistic neutrinos (antineutrinos), which are predominantly right-handed, ν_R (left-handed, $\bar{\nu}_L$). If RH neutrinos and LH antineutrinos exist, their interaction with matter should be much weaker than the weak interaction of the flavour LH neutrinos ν_l and RH antineutrinos $\bar{\nu}_l$, *i.e.*, ν_R ($\bar{\nu}_L$) should be "sterile" or "inert" neutrinos (antineutrinos) [1]. In the formalism of the Standard Model, the sterile ν_R and $\bar{\nu}_L$ can be described by $SU(2)_L$ singlet RH neutrino fields $\nu_R(x)$. In this case, ν_R and $\bar{\nu}_L$ will have no gauge interactions, *i.e.*, will not couple to the weak $W^\pm$ and Z^0 bosons. If present in an extension of the Standard Model, the RH neutrinos can play a crucial role i) in the generation of neutrino masses and mixing, ii) in understanding the remarkable disparity between the magnitudes of neutrino masses and the masses of the charged leptons and quarks, and iii) in the generation of the observed matter-antimatter asymmetry of the Universe (via the leptogenesis mechanism [2]) . In this scenario which is based on the see-saw theory [3], there is a link between the generation of neutrino masses and the generation of the baryon asymmetry of the Universe. The simplest hypothesis (based on symmetry considerations) is that to each LH flavour neutrino field $\nu_{lL}(x)$ there corresponds a RH neutrino field $\nu_{lR}(x)$, $l = e, \mu, \tau$, although schemes with less (more) than three RH neutrinos are also being considered.

There have been remarkable discoveries in the field of neutrino physics in the last 20 years. The experiments with solar, atmospheric, reactor and accelerator neutrinos have provided compelling evidences for the existence of neutrino oscillations [4,5], transitions in flight between the different flavour neutrinos ν_e, ν_μ, ν_τ (antineutrinos $\bar{\nu}_e$, $\bar{\nu}_\mu$, $\bar{\nu}_\tau$), caused by nonzero neutrino masses and neutrino mixing. The existence of flavour neutrino oscillations implies that if a neutrino of a given flavour, say ν_μ, with energy E is produced in some weak interaction process, at a sufficiently large distance L from the ν_μ source the probability to find a neutrino of a different flavour, say ν_τ, $P(\nu_\mu \to \nu_\tau; E, L)$, is different from zero. $P(\nu_\mu \to \nu_\tau; E, L)$ is called the $\nu_\mu \to \nu_\tau$ oscillation or transition probability. If $P(\nu_\mu \to \nu_\tau; E, L) \neq 0$, the probability that ν_μ will not change into a neutrino of a different flavour, *i.e.*, the "ν_μ survival probability" $P(\nu_\mu \to \nu_\mu; E, L)$, will be smaller than one. If only muon neutrinos ν_μ are detected in a given experiment and they take part in oscillations, one would observe a "disappearance" of muon neutrinos on the way from the ν_μ source to the detector. Disappearance of the solar ν_e, reactor $\bar{\nu}_e$ and of atmospheric ν_μ and $\bar{\nu}_\mu$ due to the oscillations have been observed respectively, in the solar neutrino [6–14], KamLAND [15,16] and Super-Kamiokande [17,18] experiments. Strong evidences for ν_μ disappearance due to oscillations were obtained also in the long-baseline accelerator neutrino experiments K2K [19]. Subsequently, the MINOS [20,21] and T2K [22,23] long baseline experiments reported compelling evidence for ν_μ disappearance due to oscillations, while

evidences for ν_τ appearance due to $\nu_\mu \to \nu_\tau$ oscillations were published by the Super-Kamiokande [24] and OPERA [25] collaborations. As a consequence of the results of the experiments quoted above the existence of oscillations or transitions of the solar ν_e, atmospheric ν_μ and $\bar{\nu}_\mu$, accelerator ν_μ (at $L \sim 250$ km, $L \sim 295$ km and $L \sim 730$ km) and reactor $\bar{\nu}_e$ (at $L \sim 180$ km), driven by nonzero neutrino masses and neutrino mixing, was firmly established. There are strong indications that the solar ν_e transitions are affected by the solar matter [26,27].

The experimental discovery of oscillations of atmospheric muon neutrinos and antineutrinos and of the flavor conversion of solar (electron) neutrinos led to the 2015 Nobel Prize for Physics awarded to Takaaki Kajita [28](from the SuperKamiokande Collaboration) and Arthur McDonald [29](from the SNO Collaboration).

Further important developments took place in the period starting from June 2011. First, the T2K Collaboration reported [30] indications for $\nu_\mu \to \nu_e$ oscillations, *i.e.*, of "appearance" of ν_e in a beam of ν_μ, which had a statistical significance of 2.5σ. The MINOS [31] Collaboration also obtained data consistent with $\nu_\mu \to \nu_e$ oscillations. Subsequently, the Double Chooz Collaboration reported [32] indications for disappearance of reactor $\bar{\nu}_e$ at $L \sim 1.1$ km. Strong evidences for reactor $\bar{\nu}_e$ disappearance at $L \sim 1.65$ km and $L \sim 1.38$ km and (with statistical significance of 5.2σ and 4.9σ) were obtained respectively in the Daya Bay [33] and RENO [34] experiments. Further evidences for reactor $\bar{\nu}_e$ disappearance (at 2.9σ) and for $\nu_\mu \to \nu_e$ oscillations (at 3.1σ) were reported by the Double Chooz [35] and T2K [36] experiments, while the Daya Bay and RENO Collaborations presented updated, more precise results on reactor $\bar{\nu}_e$ disappearance [37,38,39]. More recently the NOνA experiment reported results on $\nu_\mu \to \nu_e$ oscillations [40,42], while T2K presented data on $\bar{\nu}_\mu \to \bar{\nu}_e$ oscillation [43](for the latest results of the Daya Bay [44], RENO [45], Double Chooz [46], MINOS [47], T2K [48] and NOνA experiments, see Section 14.12).

Oscillations of neutrinos are a consequence of the presence of flavour neutrino mixing, or lepton mixing, in vacuum. In the formalism of local quantum field theory, used to construct the Standard Model, this means that the LH flavour neutrino fields $\nu_{l\mathrm{L}}(x)$, which enter into the expression for the lepton current in the CC weak interaction Lagrangian, are linear combinations of the fields of three (or more) neutrinos ν_j, having masses $m_j \neq 0$:

$$\nu_{l\mathrm{L}}(x) = \sum_j U_{lj}\, \nu_{j\mathrm{L}}(x), \quad l = e, \mu, \tau, \tag{14.1}$$

where $\nu_{j\mathrm{L}}(x)$ is the LH component of the field of ν_j possessing a mass m_j and U is a unitary matrix - the neutrino mixing matrix [1,4,5]. The matrix U is often called the Pontecorvo-Maki-Nakagawa-Sakata (PMNS) or Maki-Nakagawa-Sakata (MNS) mixing matrix. Obviously, Eq. (14.1) implies that the individual lepton charges L_l, $l = e, \mu, \tau$, are not conserved.

All compelling neutrino oscillation data can be described assuming 3-flavour neutrino mixing in vacuum. The data on the invisible decay width of the Z-boson is compatible with only 3 light flavour neutrinos coupled to Z [49]. The number of massive neutrinos ν_j, n, can, in general, be bigger than 3, $n > 3$, if, for instance, there exist sterile neutrinos and they mix with the flavour neutrinos. It is firmly established on the basis of the current data that at least 3 of the neutrinos ν_j, say ν_1, ν_2, ν_3, must be light, $m_{1,2,3} \lesssim 1$ eV (Section 14.12), and must have different masses, $m_1 \neq m_2 \neq m_3$. At present there are several experimental hints for existence of one or two light sterile neutrinos at the eV scale, which mix with the flavour neutrinos, implying the presence in the neutrino mixing of additional one or two neutrinos, ν_4 or $\nu_{4,5}$, with masses m_4 ($m_{4,5}$) ~ 1 eV. These hints will be briefly discussed in Section 14.14 of the present review.

Being electrically neutral, the neutrinos with definite mass ν_j can be Dirac fermions or Majorana particles [50,51]. The first possibility is realized when there exists a lepton charge carried by the neutrinos ν_j, which is conserved by the particle interactions. This could be, *e.g.*, the total lepton charge $L = L_e + L_\mu + L_\tau$: $L(\nu_j) = 1$, $j = 1, 2, 3$. In this case the neutrino ν_j has a distinctive antiparticle $\bar{\nu}_j$: $\bar{\nu}_j$ differs from ν_j by the value of the lepton charge L it carries, $L(\bar{\nu}_j) = -1$. The massive neutrinos ν_j can be Majorana particles if no lepton charge is conserved (see, *e.g.*, Refs. [52,53]) . A massive Majorana particle χ_j is identical with its antiparticle $\bar{\chi}_j$: $\chi_j \equiv \bar{\chi}_j$. On the basis of the existing neutrino data it is impossible to determine whether the massive neutrinos are Dirac or Majorana fermions.

In the case of n neutrino flavours and n massive neutrinos, the $n \times n$ unitary neutrino mixing matrix U can be parametrized by $n(n-1)/2$ Euler angles and $n(n+1)/2$ phases. If the massive neutrinos ν_j are Dirac particles, only $(n-1)(n-2)/2$ phases are physical and can be responsible for CP violation in the lepton sector. In this respect the neutrino (lepton) mixing with Dirac massive neutrinos is similar to the quark mixing.

For $n = 3$ there is just one CP violating phase in U, which is usually called "the Dirac CP violating phase." CP invariance holds if (in a certain standard convention) U is real, $U^* = U$.

If, however, the massive neutrinos are Majorana fermions, $\nu_j \equiv \chi_j$, the neutrino mixing matrix U contains $n(n-1)/2$ CP violation phases [54,55], *i.e.*, by $(n-1)$ phases more than in the Dirac neutrino case: in contrast to Dirac fields, the massive Majorana neutrino fields cannot "absorb" phases. In this case U can be cast in the form [54]

$$U = V\, P \tag{14.2}$$

where the matrix V contains the $(n-1)(n-2)/2$ Dirac CP violation phases, while P is a diagonal matrix with the additional $(n-1)$ Majorana CP violation phases α_{21}, α_{31},..., α_{n1},

$$P = diag\left(1, e^{i\frac{\alpha_{21}}{2}}, e^{i\frac{\alpha_{31}}{2}}, ..., e^{i\frac{\alpha_{n1}}{2}}\right). \tag{14.3}$$

The Majorana phases will conserve CP if [56] $\alpha_{j1} = \pi q_j$, $q_j = 0, 1, 2$, $j = 2, 3, ..., n$. In this case $\exp[i(\alpha_{j1} - \alpha_{k1})] = \pm 1$ has a simple physical interpretation: this is the relative CP-parity of Majorana neutrinos χ_j and χ_k. The condition of CP invariance of the leptonic CC weak interaction in the case of mixing and massive Majorana neutrinos reads [52]:

$$U^*_{lj} = U_{lj}\, \rho_j\,, \quad \rho_j = \frac{1}{i}\eta_{CP}(\chi_j) = \pm 1\,, \tag{14.4}$$

where $\eta_{CP}(\chi_j) = i\rho_j = \pm i$ is the CP parity of the Majorana neutrino χ_j [56]. Thus, if CP invariance holds, all elements of any given column of U are either real or purely imaginary.

In the case of $n = 3$ there are altogether 3 CP violation phases - one Dirac and two Majorana. Even in the mixing involving only 2 massive Majorana neutrinos there is one physical CP violation Majorana phase. In contrast, the CC weak interaction is automatically CP-invariant in the case of mixing of two massive Dirac neutrinos or of two quarks.

14.2. The three neutrino mixing

All existing compelling data on neutrino oscillations can be described assuming 3-flavour neutrino mixing in vacuum. This is the minimal neutrino mixing scheme which can account for the currently available data on the oscillations of the solar (ν_e), atmospheric (ν_μ and $\bar{\nu}_\mu$), reactor ($\bar{\nu}_e$) and accelerator (ν_μ and $\bar{\nu}_\mu$) neutrinos. The (left-handed) fields of the flavour neutrinos ν_e, ν_μ and ν_τ in the expression for the weak charged lepton current in the CC weak interaction Lagrangian, are linear combinations of the LH components of the fields of three massive neutrinos ν_j:

$$\mathcal{L}_{\mathrm{CC}} = -\,\frac{g}{\sqrt{2}} \sum_{l=e,\mu,\tau} \overline{l_L}(x)\, \gamma_\alpha\, \nu_{lL}(x)\, W^{\alpha\dagger}(x) + h.c.\,,$$

$$\nu_{l\mathrm{L}}(x) = \sum_{j=1}^{3} U_{lj}\, \nu_{j\mathrm{L}}(x), \tag{14.5}$$

where U is the 3×3 unitary neutrino mixing matrix [4,5]. As we have discussed in the preceding Section, the mixing matrix U can be parameterized by 3 angles, and, depending on whether the massive

neutrinos ν_j are Dirac or Majorana particles, by 1 or 3 CP violation phases [54,55]:

$$U = \begin{bmatrix} c_{12}c_{13} & s_{12}c_{13} & s_{13}e^{-i\delta} \\ -s_{12}c_{23} - c_{12}s_{23}s_{13}e^{i\delta} & c_{12}c_{23} - s_{12}s_{23}s_{13}e^{i\delta} & s_{23}c_{13} \\ s_{12}s_{23} - c_{12}c_{23}s_{13}e^{i\delta} & -c_{12}s_{23} - s_{12}c_{23}s_{13}e^{i\delta} & c_{23}c_{13} \end{bmatrix} \times \mathrm{diag}(1,\ e^{i\frac{\alpha_{21}}{2}},\ e^{i\frac{\alpha_{31}}{2}})\ . \quad (14.6)$$

where $c_{ij} = \cos\theta_{ij}$, $s_{ij} = \sin\theta_{ij}$, the angles $\theta_{ij} = [0, \pi/2)$, $\delta = [0, 2\pi]$ is the Dirac CP violation phase and α_{21}, α_{31} are two Majorana CP violation (CPV) phases. Thus, in the case of massive Dirac neutrinos, the neutrino mixing matrix U is similar, in what concerns the number of mixing angles and CPV phases, to the CKM quark mixing matrix. The presence of two additional physical CPV phases in U if ν_j are Majorana particles is a consequence of the special properties of the latter (see, *e.g.*, Refs. [52,54]) .

As we see, the fundamental parameters characterizing the 3-neutrino mixing are: i) the 3 angles θ_{12}, θ_{23}, θ_{13}, ii) depending on the nature of massive neutrinos ν_j - 1 Dirac (δ), or 1 Dirac + 2 Majorana ($\delta, \alpha_{21}, \alpha_{31}$), CPV phases, and iii) the 3 neutrino masses, m_1, m_2, m_3. Thus, depending on whether the massive neutrinos are Dirac or Majorana particles, this makes 7 or 9 additional parameters in the minimally extended Standard Model of particle interactions with massive neutrinos.

The angles θ_{12}, θ_{23} and θ_{13} can be defined via the elements of the neutrino mixing matrix:

$$c^2_{12} \equiv \cos^2\theta_{12} = \frac{|U_{e1}|^2}{1 - |U_{e3}|^2}\,, \quad s^2_{12} \equiv \sin^2\theta_{12} = \frac{|U_{e2}|^2}{1 - |U_{e3}|^2}\,, \quad (14.7)$$

$$s^2_{13} \equiv \sin^2\theta_{13} = |U_{e3}|^2,\ \ s^2_{23} \equiv \sin^2\theta_{23} = \frac{|U_{\mu 3}|^2}{1 - |U_{e3}|^2},$$
$$c^2_{23} \equiv \cos^2\theta_{23} = \frac{|U_{\tau 3}|^2}{1 - |U_{e3}|^2}. \quad (14.8)$$

The neutrino oscillation probabilities depend (Section 14.7), in general, on the neutrino energy, E, the source-detector distance L, on the elements of U and, for relativistic neutrinos used in all neutrino experiments performed so far, on $\Delta m^2_{ij} \equiv (m^2_i - m^2_j)$, $i \neq j$. In the case of 3-neutrino mixing there are only two independent neutrino mass squared differences, say $\Delta m^2_{21} \neq 0$ and $\Delta m^2_{31} \neq 0$. The numbering of massive neutrinos ν_j is arbitrary. It proves convenient from the point of view of relating the mixing angles θ_{12}, θ_{23} and θ_{13} to observables, to identify $|\Delta m^2_{21}|$ with the smaller of the two neutrino mass squared differences, which, as it follows from the data, is responsible for the solar ν_e and, the observed by KamLAND, reactor $\bar{\nu}_e$ oscillations. We will number (just for convenience) the massive neutrinos in such a way that $m_1 < m_2$, so that $\Delta m^2_{21} > 0$. With these choices made, there are two possibilities: either $m_1 < m_2 < m_3$, or $m_3 < m_1 < m_2$. Then the larger neutrino mass square difference $|\Delta m^2_{31}|$ or $|\Delta m^2_{32}|$, can be associated with the experimentally observed oscillations of the atmospheric and accelerator ν_μ and $\bar{\nu}_\mu$, as well as of the reactor $\bar{\nu}_e$ at $L \sim 1$ km. The effects of Δm^2_{31} or Δm^2_{32} in the oscillations of solar ν_e, and of Δm^2_{21} in the oscillations of atmospheric and accelerator ν_μ and $\bar{\nu}_\mu$ or of the reactor $\bar{\nu}_e$ at $L \sim 1$ km, are relatively small and subdominant as a consequence of the facts that i) L, E and L/E in the experiments with solar ν_e and with atmospheric and accelerator ν_μ and $\bar{\nu}_\mu$, or with reactor $\bar{\nu}_e$ and baseline $L \sim 1$ km, are very different, ii) the conditions of production and propagation (on the way to the detector) of the solar ν_e and of the atmospheric or accelerator ν_μ and $\bar{\nu}_\mu$ and of the reactor $\bar{\nu}_e$, are very different, and iii) Δm^2_{21} and $|\Delta m^2_{31}|$ ($|\Delta m^2_{32}|$) in the case of $m_1 < m_2 < m_3$ ($m_3 < m_1 < m_2$), as it follows from the data, differ by approximately a factor of 30, $\Delta m^2_{21} \ll |\Delta m^2_{31(32)}|$, $\Delta m^2_{21}/|\Delta m^2_{31(32)}| \cong 0.03$. This implies that in both cases of $m_1 < m_2 < m_3$ and $m_3 < m_1 < m_2$ we have $\Delta m^2_{32} \cong \Delta m^2_{31}$ with $|\Delta m^2_{31} - \Delta m^2_{32}| = \Delta m^2_{21} \ll |\Delta m^2_{31,32}|$. Obviously, in the case of $m_1 < m_2 < m_3$ ($m_3 < m_1 < m_2$) we have $\Delta m^2_{31(32)} > 0$ ($\Delta m^2_{31(32)} < 0$).

It followed from the results of the Chooz experiment [57] with reactor $\bar{\nu}_e$ and from the more recent data of the Daya Bay, RENO, Double Chooz and T2K experiments (which will be discussed in Section14.12), that, in the convention we use, in which $0 < \Delta m^2_{21} < |\Delta m^2_{31(32)}|$, the element $|U_{e3}|$=$\sin\theta_{13}$ of the neutrino mixing matrix U is relatively small. This makes it possible to identify the angles θ_{12} and θ_{23} as the neutrino mixing angles associated with the solar ν_e and the dominant atmospheric ν_μ (and $\bar{\nu}_\mu$) oscillations, respectively. The angles θ_{12} and θ_{23} are sometimes called "solar" and "atmospheric" neutrino mixing angles, and are sometimes denoted as $\theta_{12} = \theta_\odot$ and $\theta_{23} = \theta_{\rm A}$ (or $\theta_{\rm atm}$), while Δm^2_{21} and Δm^2_{31} are often referred to as the "solar" and "atmospheric" neutrino mass squared differences and are often denoted as $\Delta m^2_{21} \equiv \Delta m^2_\odot$, $\Delta m^2_{31} \equiv \Delta m^2_{\rm A}$ (or $\Delta m^2_{\rm atm}$).

The solar neutrino data tell us that $\Delta m^2_{21} \cos 2\theta_{12} > 0$. In the convention employed by us we have $\Delta m^2_{21} > 0$. Correspondingly, in this convention one must have $\cos 2\theta_{12} > 0$.

The enormous amount of neutrino oscillation data accumulated over many years of research allow us to determine the parameters which are responsible for the solar ν_e oscillations (flavour conversion), Δm^2_{21} and $\sin^2\theta_{12}$, for the dominant oscillations of the atmospheric ν_μ and $\bar{\nu}_\mu$, $|\Delta m^2_{31}|$ ($|\Delta m^2_{32}|$) and $\sin^2\theta_{23}$, and the angle θ_{13} responsible for the $\nu_\mu \to \nu_e$ and $\bar{\nu}_\mu \to \bar{\nu}_e$ ($\nu_\mu \to \nu_e$) oscillations observed in the T2K (NOνA) experiment as well as for the reactor $\bar{\nu}_e$ oscillations observed in the Daya Bay, RENO and Double Chooz experiments. In the two most recent global analyses of the neutrino oscillation data [58,59] the indicated 3-neutrino oscillation parameters Δm^2_{21}, θ_{12}, $|\Delta m^2_{31}|$ ($|\Delta m^2_{32}|$), θ_{23} and θ_{13} have been determined with an impressively high precision. The new data included in these analyses were, in particular, the latest T2K $\bar{\nu}_\mu \to \bar{\nu}_e$ oscillation data [43] and the latest NOνA data on ν_μ disappearance [60] and $\nu_\mu \to \nu_e$ oscillations [42], reported first at the XXVII International Conference on Neutrino Physics and Astrophysics, held in London at the beginning of July 2016, and published at the beginning of 2017. The authors of the two independent analyses [58,59] report practically the same (within 1σ) results on Δm^2_{21}, $\sin^2\theta_{12}$, $|\Delta m^2_{31}|$, $\sin^2\theta_{13}$, $\sin^2\theta_{23}$ and δ. We present in Table 14.1 the best fit values and the 99.73% confidence level (CL) allowed ranges of the neutrino oscillation parameters, as well as the 95% CL allowed range of the CP violation phases δ, found in Ref. 58.

In both analyses [58,59] the authors find, in particular, that $\sin^2\theta_{23} = 0.5$ lies outside the 2σ range allowed by the current data. This results is mainly driven by the NOνA data [60] on $\sin^2\theta_{23}$. Both groups also find that the best fit value of the Dirac CPV phases δ is close to $3\pi/2$: in [58], for example, the values found are $\delta = 1.38\pi$ (1.31π) for $\Delta m^2_{31(32)} > 0$ ($\Delta m^2_{31(32)} < 0$). The absolute χ^2 minimum takes place for $\Delta m^2_{31(32)} > 0$, the local minimum in the case of $\Delta m^2_{31(32)} < 0$ being approximately by 0.7σ higher. According to Ref. 58, the CP conserving values $\delta = 0$ or 2π are disfavored at 2.4σ (3.2σ) for $\Delta m^2_{31(32)} > 0$ ($\Delta m^2_{31(32)} < 0$); the CP conserving value $\delta = \pi$ in the case of $\Delta m^2_{31(32)} > 0$ ($\Delta m^2_{31(32)} < 0$) is statistically approximately 2.0σ (2.5σ) away from the best fit value $\delta \cong 1.38\pi$ (1.31π). In what concerns the CP violating value $\delta = \pi/2$, it is strongly disfavored at 3.4σ (3.9σ) for $\Delta m^2_{31(32)} > 0$ ($\Delta m^2_{31(32)} < 0$). The quoted confidence levels for $\delta = 0, \pi$ and $\pi/2$ are all with respect to the absolute χ^2 minimum. At 3σ, δ/π is found to lie in the case of $\Delta m^2_{31(32)} > 0$ ($\Delta m^2_{31(32)} < 0$) in the following intervals [58]: $(0.00 - 0.17(0.16)) \oplus (0.76(0.69) - 2.00))$. Similar results are obtained in [59].

It follows from the results given in Table 14.1 that the value of θ_{23} can deviate by about ± 0.1 from $\pi/4$, $\pi/4$ belonging to the 3σ allowed region, $\theta_{12} \cong \pi/5.4$ and that $\theta_{13} \cong \pi/20$. Correspondingly, the pattern of neutrino mixing is drastically different from the pattern of quark mixing.

Note also that Δm^2_{21}, $\sin^2\theta_{12}$, $|\Delta m^2_{31(32)}|$, $\sin^2\theta_{23}$ and $\sin^2\theta_{13}$ are determined from the data with a 1σ uncertainty (= 1/6 of the 3σ range) of approximately 2.3%, 5.8%, 1.6%, 9.6% and 4.0%, respectively.

Further, the existing SK atmospheric neutrino, K2K, MINOS, T2K and NOνA data do not allow to determine the sign of $\Delta m^2_{31(32)}$.

Table 14.1: The best-fit values and 3σ allowed ranges of the 3-neutrino oscillation parameters, derived from a global fit of the current neutrino oscillation data (from [58]) . For the Dirac phase δ we give the best fit value and the 2σ allowed range. The values (values in brackets) correspond to $m_1 < m_2 < m_3$ ($m_3 < m_1 < m_2$). The definition of Δm^2, which is determined in the global analysis in [58] is: $\Delta m^2 = m_3^2 - (m_2^2 + m_1^2)/2$. Thus, $\Delta m^2 = \Delta m^2_{31} - \Delta m^2_{21}/2 > 0$, if $m_1 < m_2 < m_3$, and $\Delta m^2 = \Delta m^2_{32} + \Delta m^2_{21}/2 < 0$ for $m_3 < m_1 < m_2$. We give the values of $\Delta m^2_{31} > 0$ for $m_1 < m_2 < m_3$, and of Δm^2_{23} for $m_3 < m_1 < m_2$, obtained from those for Δm^2 quoted in [58].

Parameter	best-fit	3σ
Δm^2_{21} [10^{-5} eV ^{2}]	7.37	$6.93 - 7.96$
$\Delta m^2_{31(23)}$ [10^{-3} eV ^{2}]	2.56 (2.54)	$2.45 - 2.69$ $(2.42 - 2.66)$
$\sin^2\theta_{12}$	0.297	$0.250 - 0.354$
$\sin^2\theta_{23}$, $\Delta m^2_{31(32)} > 0$	0.425	$0.381 - 0.615$
$\sin^2\theta_{23}$, $\Delta m^2_{32(31)} < 0$	0.589	$0.384 - 0.636$
$\sin^2\theta_{13}$, $\Delta m^2_{31(32)} > 0$	0.0215	$0.0190 - 0.0240$
$\sin^2\theta_{13}$, $\Delta m^2_{32(31)} < 0$	0.0216	$0.0190 - 0.0242$
δ/π	1.38 (1.31)	2σ: (1.0 - 1.9) (2σ: (0.92-1.88))

Maximal solar neutrino mixing, *i.e.*, $\theta_{12} = \pi/4$, is ruled out at more than 6σ by the data. Correspondingly, one has $\cos 2\theta_{12} \geq 0.29$ (at 99.73% CL).

Apart from the hint that the Dirac phase $\delta \cong 3\pi/2$, no other experimental information on the Dirac and Majorana CPV phases in the neutrino mixing matrix is available at present. Thus, the status of CP symmetry in the lepton sector is essentially unknown. With $\theta_{13} \cong 0.15 \neq 0$, the Dirac phase δ can generate CP violating effects in neutrino oscillations [54,61,62], *i.e.*, a difference between the probabilities of the $\nu_l \to \nu_{l'}$ and $\bar\nu_l \to \bar\nu_{l'}$ oscillations, $l \neq l' = e, \mu, \tau$. The magnitude of CP violation in $\nu_l \to \nu_{l'}$ and $\bar\nu_l \to \bar\nu_{l'}$ oscillations, $l \neq l' = e, \mu, \tau$, is determined by [63] the rephasing invariant J_{CP}, associated with the Dirac CPV phase in U:

$$J_{\rm CP} = {\rm Im}\left(U_{\mu 3}\, U^*_{e3}\, U_{e2}\, U^*_{\mu 2}\right). \tag{14.9}$$

It is analogous to the rephasing invariant associated with the Dirac CPV phase in the CKM quark mixing matrix [64]. In the "standard" parametrization of the neutrino mixing matrix (Eq. (14.6)), $J_{\rm CP}$ has the form:

$$\begin{aligned} J_{CP} &\equiv {\rm Im}\,(U_{\mu 3}\, U^*_{e3}\, U_{e2}\, U^*_{\mu 2}) \\ &= \frac{1}{8}\cos\theta_{13}\sin 2\theta_{12}\,\sin 2\theta_{23}\,\sin 2\theta_{13}\,\sin\delta\,. \end{aligned} \tag{14.10}$$

Thus, given the fact that $\sin 2\theta_{12}$, $\sin 2\theta_{23}$ and $\sin 2\theta_{13}$ have been determined experimentally with a relatively good precision, the size of CP violation effects in neutrino oscillations depends essentially only on the magnitude of the currently not well determined value of the Dirac phase δ. The current data implies $0.026(0.027)|\sin\delta| \lesssim |J_{CP}| \lesssim 0.035|\sin\delta|$, where we have used the 3σ ranges of $\sin^2\theta_{12}$, $\sin^2\theta_{23}$ and $\sin^2\theta_{13}$ given in Table 14.1. For the current best fit values of $\sin^2\theta_{12}$, $\sin^2\theta_{23}$, $\sin^2\theta_{13}$ and δ we find in the case of $\Delta m^2_{31(2)} > 0$ ($\Delta m^2_{31(2)} < 0$): $J_{CP} \cong 0.032\sin\delta \cong -0.030$ ($J_{CP} \cong 0.032\sin\delta \cong -0.027$). Thus, if the indication that δ has a value close to $3\pi/2$ is confirmed by future more precise data, i) the $J_{CP}-$ factor in the lepton sector would be approximately by 3 orders of magnitude larger in absolute value than corresponding $J_{CP}-$ factor in the quark sector, and ii) the CP violation effects in neutrino oscillations would be relatively large.

If the neutrinos with definite masses ν_i, $i = 1, 2, 3$, are Majorana particles, the 3-neutrino mixing matrix contains two additional Majorana CPV phases [54]. However, the flavour neutrino oscillation probabilities $P(\nu_l \to \nu_{l'})$ and $P(\bar\nu_l \to \bar\nu_{l'})$, $l, l' = e, \mu, \tau$, do not depend on the Majorana phases [54,65]. The Majorana phases can play important role, *e.g.*, in $|\Delta L| = 2$ processes like neutrinoless double beta ($(\beta\beta)_{0\nu}$-) decay $(A, Z) \to (A, Z+2) + e^- + e^-$, L being the total lepton charge, in which the Majorana nature of massive neutrinos ν_i manifests itself (see, *e.g.*, Refs. [52,66]) . Our interest in the CPV phases present in the neutrino mixing matrix is stimulated also by the intriguing possibility that the Dirac phase and/or the Majorana phases in $U_{\rm PMNS}$ can provide the CP violation necessary for the generation of the observed baryon asymmetry of the Universe [67,68].

As we have indicated, the existing data do not allow one to determine the sign of $\Delta m^2_{31(32)}$. In the case of 3-neutrino mixing, the two possible signs of $\Delta m^2_{31(32)}$ correspond to two types of neutrino mass spectrum. In the widely used conventions of numbering the neutrinos with definite mass in the two cases employed by us, the two spectra read:

– *i) spectrum with normal ordering (NO)*:

$$\begin{aligned} &m_1 < m_2 < m_3, \quad \Delta m^2_{31} = \Delta m^2_{\rm A} > 0, \\ &\Delta m^2_{21} \equiv \Delta m^2_{\odot} > 0, \;\; m_{2(3)} = (m_1^2 + \Delta m^2_{21(31)})^{\frac{1}{2}}. \end{aligned} \tag{14.11}$$

– *ii) spectrum with inverted ordering (IO)*:

$$\begin{aligned} &m_3 < m_1 < m_2, \quad \Delta m^2_{32} = \Delta m^2_{\rm A} < 0, \quad \Delta m^2_{21} \equiv \Delta m^2_{\odot} > 0, \\ &m_2 = (m_3^2 + \Delta m^2_{23})^{\frac{1}{2}}, \quad m_1 = (m_3^2 + \Delta m^2_{23} - \Delta m^2_{21})^{\frac{1}{2}}. \end{aligned} \tag{14.12}$$

Depending on the values of the lightest neutrino mass [69], $\min(m_j)$, the neutrino mass spectrum can be:

– *Normal Hierarchical (NH)*:

$$\begin{aligned} &m_1 \ll m_2 < m_3, \;\; m_2 \cong (\Delta m^2_{21})^{\frac{1}{2}} \cong 0.0086 \text{ eV}, \\ &m_3 \cong |\Delta m^2_{31}|^{\frac{1}{2}} \cong 0.0506 \text{ eV}; \;\; \text{or} \end{aligned} \tag{14.13}$$

– *Inverted Hierarchical (IH)*:

$$\begin{aligned} &m_3 \ll m_1 < m_2, \;\; m_1 \cong (|\Delta m^2_{32}| - \Delta m^2_{21})^{\frac{1}{2}} \cong 0.0497 \text{ eV}, \\ &m_2 \cong |\Delta m^2_{32}|^{\frac{1}{2}} \cong 0.0504 \text{ eV}; \;\; \text{or} \end{aligned} \tag{14.14}$$

– *Quasi-Degenerate (QD)*:

$$m_1 \cong m_2 \cong m_3 \cong m_0, \;\; m_j^2 \gg |\Delta m^2_{31(32)}|, \;\; m_0 \gtrsim 0.10 \text{ eV}. \tag{14.15}$$

Sometimes the determination of the neutrino mass spectrum is referred to in the literature on the subject as determination of "neutrino mass hierarchy". However, as we have seen, the neutrino mass spectrum might not be hierarchical. Therefore, determination of "neutrino mass ordering" is a more precise expression and we are going to use this expression in the present review article.

Eq. (14.11) and Eq. (14.12) suggest that, for consistency, the data on the larger neutrino mass squared difference, obtained in 3-neutrino oscillation analyses, should be presented i) either on the value of Δm^2_{32} in the case of NO spectrum and on Δm^2_{31} for IO spectrum, or ii) on the value of Δm^2_{31} for the NO spectrum and on Δm^2_{32} for IO spectrum. It would be preferable that all experimental groups which provide data on the larger neutrino mass squared difference, choose one of the indicated two possibilities to present their data - this will make straightforward the comparison of the results obtained in different experiments.

All types of neutrino mass spectrum, discussed above, are compatible with the existing constraints on the absolute scale of neutrino masses m_j. Information about the latter can be obtained, *e.g.*, by measuring the spectrum of electrons near the end point in ^{3}H β-decay experiments [70–74] and from cosmological and astrophysical data. The most stringent upper bounds on the $\bar\nu_e$ mass were obtained in the Troitzk [74,71] experiment:

$$m_{\bar\nu_e} < 2.05 \text{ eV} \quad \text{at } 95\% \text{ CL}. \tag{14.16}$$

Similar result was obtained in the Mainz experiment [72]: $m_{\bar{\nu}_e} < 2.3$ eV at 95% CL. We have $m_{\bar{\nu}_e} \cong m_{1,2,3}$ in the case of QD spectrum. The upcoming KATRIN experiment [73] is planned to reach sensitivity of $m_{\bar{\nu}_e} \sim 0.20$ eV, *i.e.*, it will probe the region of the QD spectrum.

The Cosmic Microwave Background (CMB) data of the WMAP and PLANCK experiments, combined with supernovae and other cosmological and astrophysical data can be used to obtain an upper limit on the sum of neutrinos masses (see review on "Neutrinos in Cosmology", Section 25 [75], and, *e.g.*, Ref. 76). Depending on the model complexity and the input data used one typically obtains [76]: $\sum_j m_j \lesssim (0.3 - 1.3)$ eV, 95% CL.

In March of 2013 the Planck Collaboration published their first constraints on $\sum_j m_j$ [77]. These constraints were updated in 2016 in [78]. Assuming the existence of three light massive neutrinos and the validity of the Λ CDM (Cold Dark Matter) model, and using their data on the CMB temperature power spectrum anisotropies, polarization, on gravitational lensing effects, the low l CMB polarization spectrum data (the "low P" data), etc. the Planck Collaboration reported the updated upper limit on the sum of the neutrino masses [78], which, depending on the data-set used, varies in the interval: $\sum_j m_j < (0.340 - 0.715)$ eV, 95% CL. Adding data on the Baryon Acoustic Oscillations (BAO) lowers the limit to [78]:

$$\sum_j m_j < 0.170 \ eV, \quad 95\% \ \text{CL}.$$

The quoted cosmological bound on the sum of neutrino masses might not be valid if, e.g., the neutrino masses are generated dynamically at certain relatively late epoch in the evolution of the Universe (see, e.g., Ref. [79]) .

It follows from these data that neutrino masses are much smaller than the masses of charged leptons and quarks. If we take as an indicative upper limit $m_j \lesssim 0.5$ eV, we have $m_j/m_{l,q} \lesssim 10^{-6}$, $l = e, \mu, \tau$, $q = d, s, b, u, c, t$. It is natural to suppose that the remarkable smallness of neutrino masses is related to the existence of a new fundamental mass scale in particle physics, and thus to new physics beyond that predicted by the Standard Model.

14.3. Future progress

After the spectacular experimental progress made in the studies of neutrino oscillations, further understanding of the pattern of neutrino masses and neutrino mixing, of their origins and of the status of CP symmetry in the lepton sector requires an extensive and challenging program of research. The main goals of such a research program include:

- Determining the nature - Dirac or Majorana, of massive neutrinos ν_j. This is of fundamental importance for making progress in our understanding of the origin of neutrino masses and mixing and of the symmetries governing the lepton sector of particle interactions.
- Determination of the sign of Δm^2_{31} (or Δm^2_{32}), *i.e.*, the "neutrino mass ordering", or of the type of spectrum neutrino masses obey.
- Determining, or obtaining significant constraints on, the absolute scale of neutrino masses. This, in particular, would help obtain information about the detailed structure (hierarchical, quasidegenerate, etc.) of the neutrino mass spectrum.
- Determining the status of CP symmetry in the lepton sector.
- High precision measurement of θ_{13}, Δm^2_{21}, θ_{12}, $|\Delta m^2_{31}|$ and θ_{23}.
- Understanding at a fundamental level the mechanism giving rise to neutrino masses and mixing and to L_l-non-conservation. This includes understanding the origin of the patterns of ν-mixing and ν-masses suggested by the data. Are the observed patterns of ν-mixing and of $\Delta m^2_{21,31}$ related to the existence of a new fundamental symmetry of particle interactions? Is there any relation between quark mixing and neutrino mixing? What is the physical origin of CP violation phases in the neutrino mixing matrix U? Is there any relation (correlation) between the (values of) CP violation phases and mixing angles in U? Progress in the theory of neutrino mixing might also lead to a better understanding of the mechanism of generation of baryon asymmetry of the Universe.

The high precision measurement of the value of $\sin^2 2\theta_{13}$ from the Daya Bay experiment and the subsequent results on θ_{13} obtained by the RENO, Double Chooz and T2K collaborations (see Section 1.11), have far reaching implications. The measured relatively large value of θ_{13} opened up the possibilities, in particular,

i) for searching for CP violation effects in neutrino oscillation experiments with high intensity accelerator neutrino beams, like T2K, NOνA, etc. (the sensitivities of T2K and NOνA on CP violation in neutrino oscillations are discussed in, *e.g.*, Refs. [80,81]) ; ii) for determining the sign of Δm^2_{32}, and thus the type of neutrino mass spectrum ("neutrino mass ordering") in the long baseline neutrino oscillation experiments at accelerators (NOνA, etc.), in the experiments studying the oscillations of atmospheric neutrinos (PINGU [82], ORCA [83,84], Hyper-Kamiokande [200], INO [85]), as well as in experiments with reactor antineutrinos [86–91](for reviews see, *e.g.*, Ref. 92).

There are also long term plans extending beyond 2025 for searches for CP violation and neutrino mass spectrum (ordering) determination in long baseline neutrino oscillation experiments with accelerator neutrino beams (see, *e.g.*, Refs. [93,94]) . The successful realization of this research program would be a formidable task and would require many years of extraordinary experimental efforts aided by intensive theoretical investigations and remarkable investments.

Before reviewing in detail i) the different neutrino sources and the specific characteristics of the corresponding neutrino fluxes, which have been and are being used in neutrino oscillation experiments (Section 14.6), ii) the theory and phenomenology of neutrino oscillations (Sections 14.7 and 14.8), and iii) the compelling experimental evidences of neutrino oscillations and, more generally, the results obtained in the neutrino oscillation experiments (Sections 14.9 – 14.14), we would like to discuss briefly the problem of determination of the nature - Dirac or Majorana - of massive neutrinos as well as the (type I) seesaw mechanism of neutrino mass generation.

14.4. The nature of massive neutrinos

The experiments studying flavour neutrino oscillations cannot provide information on the nature - Dirac or Majorana, of massive neutrinos [54,65]. Establishing whether the neutrinos with definite mass ν_j are Dirac fermions possessing distinct antiparticles, or Majorana fermions, *i.e.*, spin 1/2 particles that are identical with their antiparticles, is of fundamental importance for understanding the origin of ν-masses and mixing and the underlying symmetries of particle interactions (see, *e.g.*, Ref. 95). The neutrinos with definite mass ν_j will be Dirac fermions if the particle interactions conserve some additive lepton number, *e.g.*, the total lepton charge $L = L_e + L_\mu + L_\tau$. If no lepton charge is conserved, ν_j will be Majorana fermions (see, *e.g.*, Refs. [52,53]) . The massive neutrinos are predicted to be of Majorana nature by the see-saw mechanism of neutrino mass generation [3]. The observed patterns of neutrino mixing and of neutrino mass squared differences can be related to Majorana massive neutrinos and the existence of an approximate flavour symmetry in the lepton sector (see, *e.g.*, Ref. 96). Determining the nature of massive neutrinos ν_j is one of the fundamental and most challenging problems in the future studies of neutrino mixing.

The Majorana nature of massive neutrinos ν_j manifests itself in the existence of processes in which the total lepton charge L changes by two units: $K^+ \to \pi^- + \mu^+ + \mu^+$, $\mu^- + (A, Z) \to \mu^+ + (A, Z-2)$, *etc.* Extensive studies have shown that the only feasible experiments having the potential of establishing that the massive neutrinos are Majorana particles are at present the experiments searching for $(\beta\beta)_{0\nu}$-decay: $(A, Z) \to (A, Z+2) + e^- + e^-$ (see, *e.g.*, [97–99]) . The observation of $(\beta\beta)_{0\nu}$-decay and the measurement of the corresponding half-life with sufficient accuracy, would not only be a proof that the total lepton charge is not conserved, but might also provide unique information on the i) type of neutrino mass spectrum [102], ii) Majorana phases in U [66,103] and iii) the absolute scale of neutrino masses (for details see [98–104] and references quoted therein).

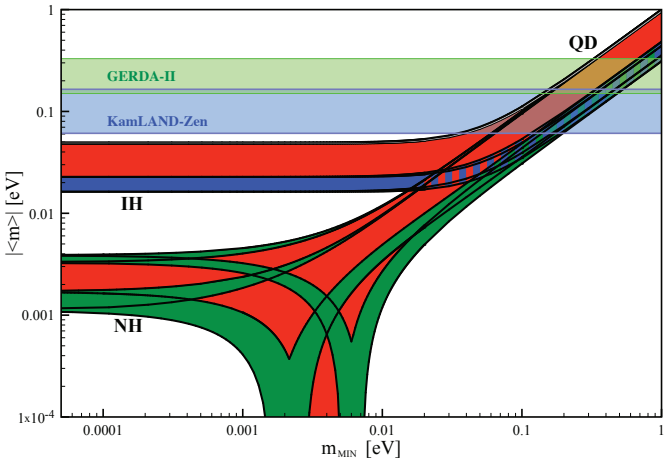

Figure 14.1: The effective Majorana mass $|<m>|$ (including a 2σ uncertainty), as a function of $\min(m_j)$. The figure is obtained using the best fit values and the 1σ ranges of allowed values of Δm^2_{21}, $\sin^2\theta_{12}$, $\sin^2\theta_{13}$ and $|\Delta m^2_{31(32)}|$ from Ref. 58 (see Table 14.1), propagated to $|<m>|$ and then taking a 2σ uncertainty. The phases α_{21} and $(\alpha_{31}-2\delta)$ are varied in the interval $[0,2\pi]$. The predictions for the NH, IH and QD spectra as well as the GERDA-II, KamLAND-Zen and the combined CUORE+CUORICINO limits, Eq. (14.20) and Eq. (14.21), are indicated. The black lines determine the ranges of values of $|<m>|$ for the different pairs of CP conserving values of α_{21} and $(\alpha_{31}-2\delta)$: $(0,0)$, $(0,\pi)$, $(\pi,0)$ and (π,π). The red regions correspond to at least one of the phases α_{21} and $(\alpha_{31}-2\delta)$ having a CP violating value, while the blue and green areas correspond to α_{21} and $(\alpha_{31}-2\delta)$ possessing CP conserving values. (Update by S. Pascoli of a figure from Ref. 112.)

Under the assumptions of 3-ν mixing, of massive neutrinos ν_j being Majorana particles, and of $(\beta\beta)_{0\nu}$-decay generated only by the (V-A) charged current weak interaction via the exchange of the three Majorana neutrinos ν_j having masses $m_j \lesssim$ few MeV, the $(\beta\beta)_{0\nu}$-decay amplitude has the form (see, *e.g.*, Refs. [52,99]): $A(\beta\beta)_{0\nu} \cong G_F^2 <m> M(A,Z)$, where G_F is the Fermi coupling constant, $M(A,Z)$ is the corresponding nuclear matrix element (NME) which does not depend on the neutrino mixing parameters, and

$$|<m>| = \left|m_1 U_{e1}^2 + m_2 U_{e2}^2 + m_3 U_{e3}^2\right| = \left|\left(m_1 c_{12}^2 + m_2 s_{12}^2 e^{i\alpha_{21}}\right) c_{13}^2 + m_3 s_{13}^2 e^{i(\alpha_{31}-2\delta)}\right|, \quad (14.17)$$

is the effective Majorana mass in $(\beta\beta)_{0\nu}$-decay. In the case of CP-invariance one has [56], $\eta_{21} \equiv e^{i\alpha_{21}} = \pm 1$, $\eta_{31} \equiv e^{i\alpha_{31}} = \pm 1$, $e^{-i2\delta} = 1$. The three neutrino masses $m_{1,2,3}$ can be expressed in terms of the two measured Δm^2_{jk} and, *e.g.*, $\min(m_j)$. Thus, given the neutrino oscillation parameters Δm^2_{21}, $\sin^2\theta_{12}$, Δm^2_{31} and $\sin^2\theta_{13}$, $|<m>|$ is a function of the lightest neutrino mass $\min(m_j)$, the type of neutrino mass spectrum, the Majorana phase α_{21}, and – in the standard parametrisation of the neutrino mixing matrix U – of the Majorana-Dirac phase difference $(\alpha_{31}-2\delta)$. In the case of NH, IH and QD spectrum we have (see, *e.g.*, Ref. 66 and Ref. 104):

$$|<m>| \cong \left|\sqrt{\Delta m^2_{21}} s^2_{12} c^2_{13} + \sqrt{\Delta m^2_{31}} s^2_{13} e^{i(\alpha_{31}-\alpha_{21}-2\delta)}\right|, \quad \text{NH}, \quad (14.18)$$

$$|<m>| \cong \tilde{m}\left(1 - \sin^2 2\theta_{12} \sin^2\frac{\alpha_{21}}{2}\right)^{\frac{1}{2}}, \quad \text{IH (IO) and QD}, \quad (14.19)$$

where $\tilde{m} \equiv \sqrt{\Delta m^2_{23}}$ ($\tilde{m} \equiv \sqrt{\Delta m^2_{23} + m_3^2}$) and $\tilde{m} \equiv m_0$ for IH (IO) and QD spectrum, respectively. In Eq. (14.19) we have exploited the fact that $\sin^2\theta_{13} \ll \cos 2\theta_{12}$. The CP conserving values of the Majorana phase α_{21} and the Majorana-Dirac phase difference $(\alpha_{31}-\alpha_{21}-2\delta)$ determine the intervals of possible values of $|<m>|$, corresponding to the different types of neutrino mass spectrum. Using the 3σ ranges of the allowed values of the neutrino oscillation parameters from Table 14.1 one finds that: i) 0.78×10^{-3} eV $\lesssim |<m>| \lesssim 4.32\times10^{-3}$ eV in the case of NH spectrum; ii) $\sqrt{\Delta m^2_{23}\cos 2\theta_{12}}\, c^2_{13} \lesssim |<m>| \lesssim \sqrt{\Delta m^2_{23}}\, c^2_{13}$, or 1.4×10^{-2} eV $\lesssim |<m>| \lesssim 5.1\times10^{-2}$ eV in the case of IH spectrum; iii) $m_0\cos 2\theta_{12} \lesssim |<m>| \lesssim m_0$, or 2.9×10^{-2} eV $\lesssim |<m>| \lesssim m_0$ eV, $m_0 \gtrsim 0.10$ eV, in the case of QD spectrum. The difference in the ranges of $|<m>|$ in the cases of NH, IH and QD spectrum opens up the possibility to get information about the type of neutrino mass spectrum from a measurement of $|<m>|$ [102]. The predicted $(\beta\beta)_{0\nu}$-decay effective Majorana mass $|<m>|$ as a function of the lightest neutrino mass $\min(m_j)$ is shown in Fig. 14.1.

The experimental searches for $(\beta\beta)_{0\nu}$-decay have a long history (see, *e.g.*, [105]) . The current best limits on $|<m>|$ have been obtained by the KamLAND-Zen [106] and GERDA phase II [107] experiments searching for $(\beta\beta)_{0\nu}$-decay of ^{136}Xe and ^{76}Ge, respectively:

$$|<m>| < (0.061-0.165)eV\,, \ ^{136}Xe$$

and

$$|<m>| < (0.15-0.33)eV\,, \ ^{76}Ge\,. \quad (14.20)$$

both at 90% CL. The intervals reflect the estimated uncertainties in the relevant NMEs used to extract the limits on $|<m>|$ from the experimentally obtained lower bounds on the ^{136}Xe and ^{76}Ge $(\beta\beta)_{0\nu}$-decay half-lives, $T^{0\nu}_{1/2}(^{136}\text{Xe}) > 1.07\times10^{26}$yr (90% CL) [106], $T^{0\nu}_{1/2}(^{76}\text{Ge}) > 8.0\times10^{25}$yr (90% CL) [107]. (For a review of the limits on $|<m>|$ obtained in other $(\beta\beta)_{0\nu}$-decay experiments and a detailed discussion of the NME calculations for $(\beta\beta)_{0\nu}$-decay and their uncertainties see, *e.g.*, Ref. 99.) In October 2017 the first results of the CUORE experiment searching for $(\beta\beta)_{0\nu}$-decay of ^{130}Te were published [108]. In this experiment the following lower limit of the half-live of ^{130}Te was obtained: $T^{0\nu}_{1/2}(^{130}\text{Te}) > 1.3\times10^{25}$yr (90% CL). Combining this limit with the limits on $T^{0\nu}_{1/2}(^{130}\text{Te})$ obtained earlier in the Cuoricino [109] and CUORE-0 [110] experiments leads to [108] $T^{0\nu}_{1/2}(^{130}\text{Te}) > 1.5\times10^{25}$yr (90% CL). Taking into account the estimated uncertainties in the relevant NMEs of the process, the following upper limit on $|<m>|$ was reported in [108]:

$$|<m>| < (0.11-0.52)eV\,, \ ^{130}\text{Te}\,. \quad (14.21)$$

The "conservative" upper limit $|<m>|^{max}_{exp} = 0.165$ eV, which is in the range of the QD spectrum, implies, as it is not difficult to show, the following upper limit on the absolute Majorana neutrino mass scale: $m_0 \cong m_{1,2,3} \lesssim |<m>|^{max}_{exp} / \cos 2\theta_{12} \lesssim 0.57$ eV.

A large number of experiments of a new generation aims at a sensitivity to $|<m>| \sim (0.01-0.05)$ eV, which will allow to probe the whole range of the predictions for $|<m>|$ in the case of IO neutrino mass spectrum [102] (see, *e.g.*, Refs. [98,99,100] for reviews of the currently running and future planned $(\beta\beta)_{0\nu}$-decay experiments and their prospective sensitivities).

Obtaining quantitative information on the neutrino mixing parameters from a measurement of $(\beta\beta)_{0\nu}$-decay half-life would be impossible without sufficiently precise knowledge of the corresponding NME of the process. At present the variation of the values of the different $(\beta\beta)_{0\nu}$-decay NMEs calculated using the various currently employed methods is typically by factors $\sim(2-3)$ (for a discussion of the current status of the calculations of the NMEs for the $(\beta\beta)_{0\nu}$-decay see [99]) . Additional source of uncertainty is the effective value of the axial-vector coupling constant g_A in $(\beta\beta)_{0\nu}$-decay. This constant is renormalized by nuclear medium effects, which tend to quench, i.e., reduce, the vacuum value of g_A. The problem of the g_A quenching arose in connection with the efforts to describe theoretically the experimental data on the two-neutrino double beta decay [101]. The physical origin of the quenching is not fully understood, and the magnitude of the quenching of g_A in $(\beta\beta)_{0\nu}$-decay is subject to debates (for further details see, e.g., [99]) . The importance of the effective value of g_A in $(\beta\beta)_{0\nu}$-decay stems from the fact that, to

a good approximation, the $(\beta\beta)_{0\nu}$-decay rate is proportional to the fourth power of the effective g_A.

The observation of $(\beta\beta)_{0\nu}$-decay of one nucleus is likely to lead to the searches and observation of the decay of other nuclei. The data on the $(\beta\beta)_{0\nu}$-decay of several nuclei might help to reduce the uncertainties in the calculations of the $(\beta\beta)_{0\nu}$-decay NMEs (see, *e.g.*, [111]) .

If the future $(\beta\beta)_{0\nu}$-decay experiments show that $|<m>| < 0.01$ eV, both the IH and the QD spectrum will be ruled out for massive Majorana neutrinos. If in addition it is established in neutrino oscillation experiments that $\Delta m^2_{31(32)} < 0$ (IO spectrum), one would be led to conclude that either the massive neutrinos ν_j are Dirac fermions, or that ν_j are Majorana particles but there are additional contributions to the $(\beta\beta)_{0\nu}$-decay amplitude which interfere destructively with that due to the exchange of ν_j. If, however, $\Delta m^2_{31(32)}$ is determined to be positive, the upper limit $|<m>| < 0.01$ eV would be perfectly compatible with massive Majorana neutrinos possessing NH mass spectrum, or NO spectrum with partial hierarchy, and the quest for $|<m>|$ would still be open (see, *e.g.*, Ref. 112).

The $(\beta\beta)_{0\nu}$-decay can be generated, in principle, by a $\Delta L = 2$ mechanism other than the light Majorana neutrino exchange considered here, or by a combination of mechanisms one of which is the light Majorana neutrino exchange (for a discussion of different mechanisms which can trigger $(\beta\beta)_{0\nu}$-decay, see, *e.g.*, Refs. [113,114] and the articles quoted therein). Actually, the predictions for $|<m>|$ in the cases of the NH, IH and QD neutrino mass spectra can be drastically modified by the existence of lepton charge non-conserving ($|\Delta L| = 2$) new physics beyond that predicted by the SM: eV or GeV to TeV scale sterile neutrinos, etc. (see, *e.g.*, Refs. [115,116]) . There is a potential synergy between the searches for $(\beta\beta)_{0\nu}$-decay and the searches for neutrino-related $|\Delta L| = 2$ beyond the SM physics at LHC: $(\beta\beta)_{0\nu}$-decay experiments with a sensitivity to half-lives of $T^{0\nu}_{1/2} = 10^{25}$ yr probe approximately values of $|<m>| \sim 0.1$ eV and "new physics" at the scale $\Lambda_{LNV} \sim 1$ TeV (see, *e.g.*, Ref. [116] and references quoted therein).

If the $(\beta\beta)_{0\nu}$-decay will be observed, it will be of fundamental importance to determine which mechanism (or mechanisms) is (are) inducing the decay. The discussion of the problem of determining the mechanisms which possibly are operative in $(\beta\beta)_{0\nu}$-decay, including the case when more than one mechanism is involved, is out of the scope of the present article. This problem has been investigated in detail in, *e.g.*, Refs. [114,117] and we refer the reader to these articles and the articles quoted therein.

14.5. The see-saw mechanism and the baryon asymmetry of the Universe

A natural explanation of the smallness of neutrino masses is provided by the (type I) see-saw mechanism of neutrino mass generation [3]. An integral part of this rather simple mechanism [118] are the RH neutrinos ν_{lR} (RH neutrino fields $\nu_{lR}(x)$). The latter are assumed to possess a Majorana mass term as well as Yukawa type coupling $\mathcal{L}_{\rm Y}(x)$ with the Standard Model lepton and Higgs doublets, $\psi_{lL}(x)$ and $\Phi(x)$, respectively, $(\psi_{lL}(x))^T = (\nu^T_{lL}(x) \quad l^T_L(x))$, $l = e, \mu, \tau$, $(\Phi(x))^T = (\Phi^{(0)}(x) \;\; \Phi^{(-)}(x))$. In the basis in which the Majorana mass matrix of RH neutrinos is diagonal, we have:

$$\mathcal{L}_{\rm Y,M}(x) = \left(\lambda_{il}\,\overline{N_{iR}}(x)\,\Phi^\dagger(x)\,\psi_{lL}(x) + \text{h.c.}\right) - \frac{1}{2}\,M_i\,\overline{N_i}(x)\,N_i(x)\,, \tag{14.22}$$

where λ_{il} is the matrix of neutrino Yukawa couplings and N_i ($N_i(x)$) is the heavy Majorana neutrino (field) possessing a mass $M_i > 0$. When the electroweak symmetry is broken spontaneously, the neutrino Yukawa coupling generates a Dirac mass term: $m^D_{il}\,\overline{N_{iR}}(x)\,\nu_{lL}(x) + \text{h.c.}$, with $m^D = v\lambda$, $v = 174$ GeV being the Higgs doublet v.e.v. In the case when the elements of m^D are much smaller than M_k, $|m^D_{il}| \ll M_k$, $i, k = 1, 2, 3$, $l = e, \mu, \tau$, the interplay between the Dirac mass term and the mass term of the heavy (RH) Majorana neutrinos N_i generates an effective Majorana mass (term) for the LH flavour neutrinos [3]:

$$m^{LL}_{l'l} \cong -(m^D)^T_{l'j} M^{-1}_j m^D_{jl} = -v^2(\lambda)^T_{l'j} M^{-1}_j \lambda_{jl}\,. \tag{14.23}$$

In grand unified theories, m^D is typically of the order of the charged fermion masses. In $SO(10)$ theories, for instance, m^D is related to the up-quark mass matrix. Taking indicatively $m^{LL} \sim 0.1$ eV, $m^D \sim 100$ GeV, one finds $M \sim 10^{14}$ GeV, which is close to the scale of unification of the electroweak and strong interactions, $M_{GUT} \cong 2 \times 10^{16}$ GeV. In GUT theories with RH neutrinos one finds that indeed the heavy Majorana neutrinos N_j naturally obtain masses which are by few to several orders of magnitude smaller than M_{GUT}. Thus, the enormous disparity between the neutrino and charged fermion masses is explained in this approach by the huge difference between effectively the electroweak symmetry breaking scale and M_{GUT}.

An additional attractive feature of the see-saw scenario is that the generation and smallness of neutrino masses is related via the leptogenesis mechanism [2] to the generation of the baryon asymmetry of the Universe. The Yukawa coupling in Eq. (14.22), in general, is not CP conserving. Due to this CP-nonconserving coupling the heavy Majorana neutrinos undergo, *e.g.*, the decays $N_j \to l^+ + \Phi^{(-)}$, $N_j \to l^- + \Phi^{(+)}$, which have different rates: $\Gamma(N_j \to l^+ + \Phi^{(-)}) \neq \Gamma(N_j \to l^- + \Phi^{(+)})$. When these decays occur in the Early Universe at temperatures somewhat below the mass of, say, N_1, so that the latter are out of equilibrium with the rest of the particles present at that epoch, CP violating asymmetries in the individual lepton charges L_l, and in the total lepton charge L, of the Universe are generated. These lepton asymmetries are converted into a baryon asymmetry by $(B - L)$ conserving, but $(B + L)$ violating, sphaleron processes, which exist in the Standard Model and are effective at temperatures $T \sim (100 - 10^{12})$ GeV. If the heavy neutrinos N_j have hierarchical spectrum, $M_1 \ll M_2 \ll M_3$, the observed baryon asymmetry can be reproduced provided the mass of the lightest one satisfies $M_1 \gtrsim 10^9$ GeV [119]. Thus, in this scenario, the neutrino masses and mixing and the baryon asymmetry have the same origin - the neutrino Yukawa couplings and the existence of (at least two) heavy Majorana neutrinos. Moreover, quantitative studies [67,68], based on advances in leptogenesis theory [120], have shown that the CP violation necessary in leptogenesis for the generation of the observed baryon asymmetry of the Universe, can be provided exclusively by the Dirac and/or Majorana phases in the neutrino mixing matrix U. This implies, in particular, that if the CP symmetry is established not to hold in the lepton sector due to U, at least some fraction (if not all) of the observed baryon asymmetry might be due to the Dirac and/or Majorana CP violation present in the neutrino mixing. More specifically, the necessary condition that the requisite CP violation for a successful leptogenesis with heirarchical in mass heavy Majorana neutrinos is due *entirely* to the Dirac CPV phase in U reads [68]: $|\sin\theta_{13}\,\sin\delta| \gtrsim 0.09$. This condition is comfortably compatible with the measured value of $\sin\theta_{13} \cong 0.15$ and the hint that $\delta \cong 3\pi/2$, found in the global analyses of the neutrino oscillation data. The scenario, in which the requisite CP violation in leptogenesis is provided exclusively by the Dirac and/or Majorana CPV phases of the neutrino mixing matrix, considered in [67,68] on purely phenomenological grounds, was shown recently to be realised in theories of lepton flavour based on non-Abelian discrete symmetries (see, *e.g.*, Ref. [121]) .

14.6. Neutrino sources

In the experimental part of this review (Sections 14.9 - 14.14), we mainly discuss neutrino oscillation experiments using neutrinos or antineutrinos produced by the Sun, cosmic-ray interactions in the air, proton accelerators, and nuclear reactors. We call neutrinos from these sources as solar neutrinos, atmospheric neutrinos, accelerator neutrinos, and reactor (anti)neutrinos. Neutrinos (and/or antineutrinos) from each of these sources have very different properties, *e.g.*, energy spectra, flavour components, and directional distributions, at production. In the literature, neutrino flavour conversion of neutrinos from gravitationally collapsed supernova explosions (supernova neutrinos) is also discussed, but this topic is out of the scope of the present review.

Solar neutrinos and atmospheric neutrinos are naturally produced neutrinos; their fluxes as well as the distance between the (point or distributed) neutrino source and the detector cannot be controlled

artificially. While the atmospheric neutrino flux involves ν_μ, $\bar{\nu}_\mu$, ν_e, and $\bar{\nu}_e$ components at production, solar neutrinos are produced as pure electron neutrinos due to thermo-nuclear fusion reactions of four protons, producing a helium nucleus. For atmospheric neutrinos with energy $\gtrsim$1 GeV, which undergo charged-current interactions in the detector, directional correlation of the charged lepton with the parent neutrino gives the way to know, within the resolution, the distance traveled by the neutrino between the production and detection.

Accelerator neutrinos and reactor (anti)neutrinos are man-made neutrinos. In principle, it is possible to choose the distance between the neutrino source and the detector arbitrarily. Accelerator neutrinos used for neutrino oscillation experiments so far have been produced by the decay of secondary mesons (pions and kaons) produced by the collision of a primary proton beam with a nuclear target. A dominant component of the accelerator neutrino flux is ν_μ or $\bar{\nu}_\mu$, depending on the secondary meson's sign selection, but a wrong-sign muon neutrino component as well as ν_e and $\bar{\nu}_e$ components are also present. The fluxes of accelerator neutrinos depend on a number of factors, *e.g.*, energy and intensity of the primary proton beam, material and geometry of the target, selection of the momentum and charge of the secondary mesons that are focused, and production angle of the secondary mesons with respect to the primary beam. In other words, it is possible to control the peak energy, energy spread, and dominant neutrino flavour, of the neutrino beam.

From the nuclear reactor, almost pure electron antineutrinos are produced by β-decays of fission products of the nuclear fuel. However, experimental groups cannot control the normalization and spectrum of the $\bar{\nu}_e$ flux from commercial nuclear reactors. They are dependent on the initial fuel composition and history of the nuclear fuel burnup. These data are provided by the power plant companies.

For neutrino oscillation experiments, knowledge of the flux of each neutrino and antineutrino flavour at production is needed for planning and designing the experiment, analyzing the data, and estimating systematic errors. Basically, for all neutrino sources, flux models are constructed and validation is made by comparing various experimentally observed quantities with the model predictions. Many of the modern accelerator long baseline and reactor neutrino oscillation experiments employ a two- or multi-detector configuration. In the accelerator long baseline experiment, a "near" detector measures non-oscillated neutrino flux. In the two- or multi-baseline reactor experiments, even a near detector measures the neutrino flux with oscillations developed to some extent. However, comparing the quantities measured with different baselines, it is possible to validate the reactor flux model and measure the oscillation parameters at the same time, or to make an analysis with minimal dependence on flux models.

14.6.1. *Standard solar model predictions of the solar neutrino fluxes* :

The Sun is an intense, well-defined neutrino source. It provides an important opportunities to investigate neutrino oscillations including matter effects, because of the wide range of matter density and the great distance from the Sun to the Earth. The solar neutrinos are produced by some of the fusion reactions in the pp chain and CNO cycle, shown in Table 14.2. In addition, electron capture on ^{13}N, ^{15}O, and ^{17}F produces line spectra of neutrinos called ecCNO neutrinos [122,123]. The combined effect of these reactions is written as

$$4p \rightarrow {}^4\mathrm{He} + 2e^+ + 2\nu_e. \qquad (14.24)$$

Positrons annihilate with electrons. Therefore, when considering the solar thermal energy generation, a relevant expression is

$$4p + 2e^- \rightarrow {}^4\mathrm{He} + 2\nu_e + 26.73\ \mathrm{MeV} - E_\nu\ , \qquad (14.25)$$

where E_ν represents the energy taken away by neutrinos, the average value being $\langle E_\nu \rangle \sim 0.6$ MeV.

The fluxes of the solar neutrinos are predicted by the calculations based on the Standard Solar Model (SSM), which describes the internal solar structure and follows its evolution from zero age to the present. A variety of input information is needed for the evolutionary

Table 14.2: Neutrino-producing reactions in the Sun (first column) and their abbreviations (second column). The neutrino fluxes predicted by the B16-GS98 standard solar model [130] are listed in the third column.

Reaction	Abbr.	Flux (cm^{-2} s^{-1})
$pp \rightarrow d\,e^+\,\nu$	*pp*	$5.98(1 \pm 0.006) \times 10^{10}$
$pe^-p \rightarrow d\,\nu$	*pep*	$1.44(1 \pm 0.01) \times 10^{8}$
$^3\mathrm{He}\ p \rightarrow {}^4\mathrm{He}\ e^+\nu$	*hep*	$7.98(1 \pm 0.30) \times 10^{3}$
$^7\mathrm{Be}\ e^- \rightarrow {}^7\mathrm{Li}\ \nu + (\gamma)$	^{7}Be	$4.93(1 \pm 0.06) \times 10^{9}$
$^8\mathrm{B} \rightarrow {}^8\mathrm{Be}^*\ e^+\nu$	^{8}B	$5.46(1 \pm 0.12) \times 10^{6}$
$^{13}\mathrm{N} \rightarrow {}^{13}\mathrm{C}\ e^+\nu$	^{13}N	$2.78(1 \pm 0.15) \times 10^{8}$
$^{15}\mathrm{O} \rightarrow {}^{15}\mathrm{N}\ e^+\nu$	^{15}O	$2.05(1 \pm 0.17) \times 10^{8}$
$^{17}\mathrm{F} \rightarrow {}^{17}\mathrm{O}\ e^+\nu$	^{17}F	$5.29(1 \pm 0.20) \times 10^{6}$

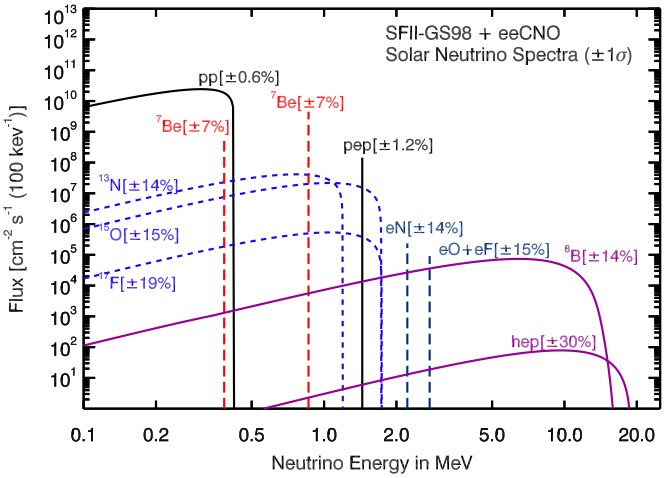

Figure 14.2: The solar neutrino spectrum predicted by the SFII-GS98 standard solar model [129]. In addition to the standard fluxes, the line spectra of the ecCNO neutrinos [123] are added. The neutrino fluxes are given in units of cm^{-2}s^{-1}MeV^{-1} for continuous spectra and cm^{-2}s^{-1} for line spectra. The numbers associated with the neutrino sources show theoretical errors of the fluxes. This figure is taken from Ref. 134.

calculations in the SSM, including the luminosity, age, radius, and mass of the Sun, its surface abundances of elements, radiative opacities, and nuclear reaction rates relevant to the pp chain and CNO cycle. Bahcall and his collaborators defined the SSM as the solar model which is constructed with the best available physics and input data [124,125,126]. Therefore, SSM calculations have been rather frequently updated in response to the changes or improvements of relevant physics and input data: there have been efforts over several decades to improve the SSM [124–130]. Observation of solar neutrinos directly addresses the theory of stellar structure and evolution, which is the basis of the SSM. There was a large discrepancy between the "observed" and predicted ^{8}B solar neutrino fluxes before the discovery of neutrino oscillations. Later, the SSM calculations of the ^{8}B solar neutrino flux turned out to be basically correct. This is one of the major successes of the SSM.

In 2011, Serenelli, Haxton, and Peña-Garay published a new SSM calculations [129] by adopting the newly analyzed solar fusion cross sections recommended in the Solar Fusion II paper by Adelberger *et al.* [131]. Hence, their SSM is referred to as the SFII SSM by Vinyoles *et al.*, who published the latest SSM calculations (referred to as the Barcelona 2016 or B16 SSM by the authors) [130]. The B16 SSM shares with the SFII SSM much of the physics but some important nuclear fusion rates are updated and the treatment of opacity uncertainties improved. Both the SFII and B16 SSM

calculations used two sets of solar abundances, GS98 [132] and AGSS09met [133]. GS98 abundances are characterized by high metal-to-hydrogen ratio $Z/X = 0.0229$ (all elements more massive than Helium are called metals and their total abundance by mass is denote by Z, while the hydrogen abundance by mass is denoted by X) and AGSS09met abundances are characterized by low Z/X (=0.0178). High-Z SSMs are referred to as SFII-GS98 and B16-GS98. These high-Z models show generally better agreement with solar data than the low-Z models with AGSS09met abundances. With regard to the solar neutrino fluxes, however, predictions of the high-Z and low-Z models are almost comparable.

The prediction of the B16-GS98 SSM [130] for the fluxes from neutrino-producing reactions is given in Table 14.2. Fig. 14.2 shows the solar-neutrino spectra calculated with the SFII-GS98 model [129], together with the line spectra of the ecCNO neutrinos [123].

14.6.2. *Atmospheric neutrino fluxes* :

Atmospheric neutrinos are produced by the decays of π and K mesons produced in the nuclear interactions of the primary component of cosmic rays in the atmosphere ((A) in Table 14.3). The primary cosmic ray components above 2 GeV/nucleon are protons ($\sim$ 95%), helium nuclei ($\sim$ 4.5%), and heavier nuclei. For neutrino producing hadronic interactions at high energies, a nucleus can be simply regarded as a sum of individual nucleons. Pions are dominantly produced in these interactions, and they predominantly decay according to (B1) in Table 14.3, followed by muon decay (E) in Table 14.3. The interactions in massive underground detectors of atmospheric neutrinos provide a means of studying neutrino oscillations because of the large range of distances traveled by these neutrinos ($\sim$10 to 1.27×10^4 km) to reach a detector on Earth and relatively well-understood atmospheric neutrino fluxes.

Table 14.3: Reactions and decays relevant to atmospheric neutrino and accelerator neutrino production. The first column shows the index of the reaction or decay, and the second column shows the reaction or decay channel. The third column shows the branching ratio [135]. (For K_L decay, the sum of the branching ratios to charge conjugate modes is shown).

	Reaction/Decay	Branching ratio (%)
(A)	$p\,(n) + A \to \pi^{\pm} X,\ K^{\pm} X,\ K_L X$	
(B1)	$\pi^{\pm} \to \mu^{\pm} + \nu_\mu\,(\bar{\nu}_\mu)$	99.9877
(B2)	$\to e^{\pm} + \nu_e\,(\bar{\nu}_e)$	0.0123
(C1)	$K^{\pm} \to \mu^{\pm} + \nu_\mu\,(\bar{\nu}_\mu)$	63.56
(C2)	$\to \pi^0 + \mu^{\pm} + \nu_\mu\,(\bar{\nu}_\mu)$	3.352
(C3)	$\to \pi^0 + e^{\pm} + \nu_e\,(\bar{\nu}_e)$	5.07
(D1)	$K_L \to \pi^{\pm} + \mu^{\mp} + \bar{\nu}_\mu\,(\nu_\mu)$	27.04
(D2)	$\to \pi^{\pm} + e^{\mp} + \bar{\nu}_e\,(\nu_e)$	40.55
(E)	$\mu^{\pm} \to e^{\pm} + \bar{\nu}_\mu(\nu_\mu) + \nu_e\,(\bar{\nu}_e)$	100

Calculation of the atmospheric neutrino fluxes requires knowledge of the primary cosmic-ray fluxes and composition, and the hadronic interactions. Atmospheric neutrinos with energy of $\sim$a few GeV are mostly produced by primary cosmic rays with energy of $\sim$100 GeV. For primary cosmic-rays in this energy range, a flux modulation due to the solar activity and the effects of Earth's geomagnetic fields should be taken into account. In particular, the atmospheric neutrino fluxes in the low-energy region depend on the location on the Earth. Detailed calculations of the atmospheric neutrino fluxes are performed by Honda et al. [136,137], Barr et al. [138], and Battistoni et al. [139], with a typical uncertainty of $10 \sim 20\%$.

From the dominant production mechanism of the atmospheric neutrinos, we can readily understand some relations that exist between the atmospheric ν_μ, $\bar{\nu}_\mu$, ν_e, and $\bar{\nu}_e$ fluxes without detailed calculations. For the ratio of the fluxes of $(\nu_\mu + \bar{\nu}_\mu)$ and $(\nu_e + \bar{\nu}_e)$ at low energies ($\lesssim$ 1 GeV), where almost all produced muons decay before reaching the ground, we have approximately $(\nu_\mu + \bar{\nu}_\mu)/(\nu_e + \bar{\nu}_e) \approx 2$. As the

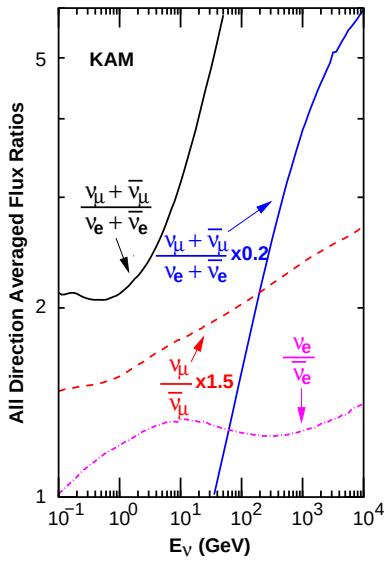

Figure 14.3: Neutrino flavour ratios calculated with the all-direction and one-year averaged atmospheric neutrino fluxes at Kamioka. This figure is provided by M. Honda, and is a part of Fig. 5 in Ref. [137], where similar plots at the INO site, the South Pole, and the Pyhäsalmi mine are also shown.

neutrino energy increases, this ratio increases because an increasing fraction of muons do not decay before reaching the ground (the Earth surface) and being absorbed. We also have $\nu_\mu/\bar{\nu}_\mu \approx 1$ at low energies. However, as the $\nu_e/\bar{\nu}_e$ ratio reflects the parent π^+/π^- ratio (see (B1) and (B2) in Table 14.3), it is expected to be slightly greater than 1 because the dominance of protons in the primary component of the cosmic rays means a π^+ excess in the secondary component. Fig. 14.3 shows these ratios at the Super-Kamiokande site, averaged over all directions and over a year, as a function of neutrino energy.

Another important feature of the atmospheric neutrino fluxes is that the zenith angle distribution for each neutrino type is up-down symmetric above $\sim$ 1 GeV, if there are no neutrino oscillations. As the neutrino energy becomes lower than $\sim$ 1 GeV, however, zenith angle distributions start to show deviations from up-down symmetric shapes due to the geomagnetic effects on primary cosmic rays.

14.6.3. *Accelerator neutrino beams* :

Conventional method to produce neutrino beams at a high-energy proton accelerator facility is to guide an intense proton beam onto a nuclear target of $1 \sim 2$ interaction lengths. For a comprehensive description of the accelerator neutrino beams, see Ref. 140. From the pA collisions, mesons are produced and their decays then produce neutrinos (see Table 14.3). In the high-energy collisions, pions are dominantly produced, with kaons produced at an order of 10% of the pion production rate. Therefore, the dominant component of the accelerator neutrinos is the muon neutrino or muon antineutrino. Mesons decay in the free space called a decay pipe or decay tunnel. This free space is evacuated or filled with helium gas. The decay tunnel is followed by a muon absorber (Earth ground or concrete), which can be several hundred meters long.

To increase the neutrino flux, it is necessary to focus the secondary pions. Modern neutrino oscillation experiments at high-energy accelerators exploit two or three magnetic horns as an approximately point-to-parallel focusing system for this purpose. A magnetic horn is a high-current pulse magnet with toroidal magnetic fields. Therefore, the use of horns also means sign selection of the secondary hadrons that are focused, which in turn means muon neutrino sign selection. Even so, a fraction of wrong sign muon neutrinos contaminate the beam. Also, there is a small ν_e and $\bar{\nu}_e$ contamination from kaon, pion, and muon decay ((C3), (B2), and (E) in Table 14.3). Precise knowledge of ν_e and $\bar{\nu}_e$ components in the neutrino flux is important for the $\nu_\mu \to \nu_e$ ($\bar{\nu}_\mu \to \bar{\nu}_e$) appearance measurement.

With a given neutrino beam line configuration, the expected

neutrino fluxes are calculated by using a simulation program tuned to that configuration. Re-interactions of the primary protons in the target and interactions of the secondary particles in the target and in the material outside the target have to be taken into account. An important input is hadron production cross sections from pA collisions for relevant target materials over wide energy and angular regions. For this purpose, some dedicated experiments such as SPY [141], HARP [142], MIPP [143], and NA61/SHINE [144] have been conducted. The data are fit to specific hadron production models to determine the model parameters.

The predicted neutrino fluxes have to be validated in some way. Modern long baseline neutrino oscillation experiments often have a two-detector configuration, with a near detector to measure an unoscillated neutrino flux immediately after the production. In the single detector experiment, the muon-neutrino flux model is calibrated by using a muon monitor which is located behind the beam dump. Since low-energy muons are absorbed in the beam dump, it is not possible to calibrate the low-energy part of the neutrino spectrum. Even in the two-detector experiments, it should be noted that the near detector does not see the same neutrino flux as the far detector sees, because the neutrino source looks like a line source for the near detector, while it looks as a point source for the far detector.

The energy E_ν of the neutrino emitted at an angle θ with respect to the parent pion direction is given by

$$E_\nu = \frac{m_\pi^2 - m_\mu^2}{2(E_\pi - p_\pi \cos\theta)}, \tag{14.26}$$

where E_π and p_π are the energy and momentum of the parent pion, m_π is the charged pion mass, m_μ is the muon mass. Suppose an ideal case that the pions are completely focused in parallel. Then, for $\theta = 0$, it can be seen from the above equation that E_ν is proportional to E_π for $E_\pi \gg m_\pi$. As the secondary pions have a wide energy spectrum, a 0 degree neutrino beam also has a wide spectrum and is called a "wide-band beam".

For a given angle θ, differentiating the above expression with respect to E_π, it can be shown that E_ν takes a maximum value $E_\nu^{\max} = (m_\pi^2 - m_\mu^2)/(2E_\pi^\circ \sin^2\theta)$ at $E_\pi^\circ = m_\pi/\sin\theta$. Numerical calculations show that a wide range of E_π, in particular that of $E_\pi \geq E_\pi^\circ$, contributes to a narrow range of $E_\nu \leq E_\nu^{\max}$ [145]. It is expected, therefore, that a narrow neutrino spectrum peaked at around $E_\nu^{\max}$ can be obtained by the off-axis beam. Fig. 14.4 shows an example of the simulated muon neutrino fluxes at $\theta = 0$ degree and 2.0° and 2.5° off-axis configurations corresponding to the T2K experiment [146]. As expected, an off-axis beam has a narrower spectrum than the 0 degree wide-band beam. Therefore, an off-axis beam is called a "narrow-band beam". This idea of an off-axis beam was proposed for BNL E889 experiment [145]. It has been employed for the T2K experiment for the first time. Currently, it is also used in the NOνA experiment [147]. For the off-axis beam, obviously the effect of a line neutrino source, namely the difference between the neutrino fluxes measured at the near and far detectors, is enhanced, and it has to be properly taken into account.

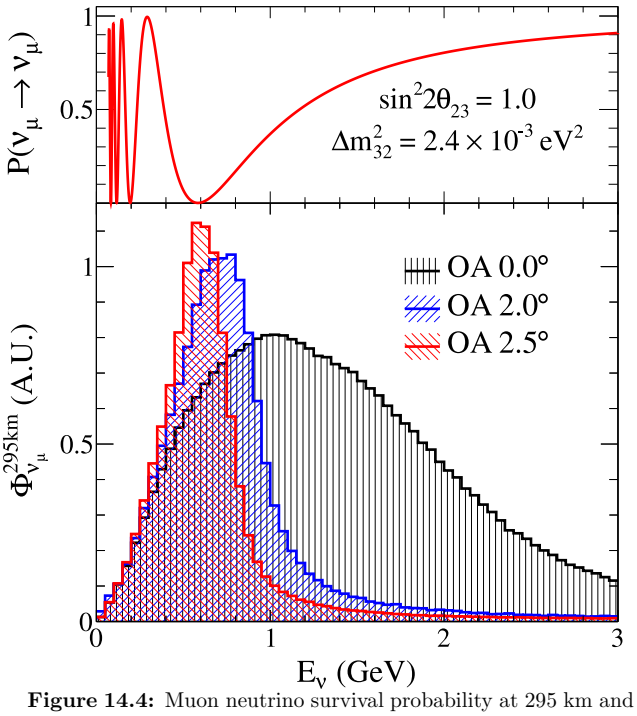

Figure 14.4: Muon neutrino survival probability at 295 km and neutrino fluxes for different off-axis angles. This figure is taken from Ref. 146.

14.6.4. *Reactor neutrino fluxes* :

In nuclear reactors, power is generated mainly by nuclear fission of four heavy isotopes, ^{235}U, ^{238}U, ^{239}Pu, and ^{241}Pu. These isotopes account for more than 99% of fissions in the reactor core. β-decays of fission products produce almost pure $\bar{\nu}_e$ flux. The rate of ν_e production is less than 10^{-5} of the rate of $\bar{\nu}_e$ production [148]. As the daughter isotopes of each fission undergo 6 β-decays on average, 6 electron antineutrinos are emitted per fission. The thermal power outputs of nuclear power reactors are usually quoted in thermal GW, GW$_{\rm th}$. The effective energy released per fission is $\sim$ 200 MeV [150]. Therefore, with 1 GW$_{\rm th}$ output, $\sim 2 \times 10^{20}$ electron antineutrinos are produced per second and emitted isotropically. Typical power plant light-water reactors have thermal power outputs of order 3 GW$_{\rm th}$. The total $\bar{\nu}_e$ flux $S(E_\nu)$ emitted from a reactor is given as a sum of contributions from the four fissioning isotopes, $S(E_\nu) = \sum_j f_j S_j(E_\nu)$, where f_j is the fission rate and $S_j(E_\nu)$ is the $\bar{\nu}_e$ flux per fission (in units of $\bar{\nu}_e/(cm^2\, fission)$) of each contributing isotope, $j = 235, 238, 239, 241$.

The fission rates, and therefore $S(E_\nu)$, are dependent on the thermal power output $W_{\rm th}$ from the reactor as a function of time. Using $W_{\rm th}$ and the total fission rate $F = \sum_j f_j$, $S(E_\nu)$ is rewritten as [149]

$$S(E_\nu) = \frac{W_{\rm th}}{\sum_j (f_j/F) E_j} \sum_j (f_j/F) S_j(E_\nu), \tag{14.27}$$

where E_j is the average energy released per fission by each isotope [150]. The thermal power output and fission fractions f_j/F are provided by the power plant companies.

Electron antineutrinos from reactors are detected via the inverse β-decay (IBD) $\bar{\nu}_e + p \rightarrow e^+ + n$. This reaction has a threshold of 1.8 MeV, so that the $\bar{\nu}_e$ flux above this threshold is detected. The event rate as a function of $\bar{\nu}_e$ energy E_ν is proportional to $\sigma(E_\nu)S(E_\nu)$, where $\sigma(E_\nu)$ is the IBD cross section. Fig. 14.5 shows $\sigma(E_\nu)$. This figure also shows the flux and event rate for a particular detector configuration (see caption to this figure) in a reactor neutrino oscillation experiment.

To estimate the flux per fission $S_j(E_\nu)$ for each fuel isotope j, two methods have been employed [151,152]. One is an *ab initio* type approach called the "summation" method. It makes use of available nuclear data information of all fission fragments and their β-decays. Then, the $\bar{\nu}_e$ spectrum of each β-decay branch is summed up with its cumulative yield in fission as a weight to give $S_j(E_\nu)$. While the conversion of the electron spectrum in β-decay to the $\bar{\nu}_e$ spectrum is trivial for a single β-decay branch, fission of the four main fuel isotopes involve $>$ 1000 daughter isotopes and $>$ 6000 individual β-decay branches. Incomplete knowledge of the nuclear data would cause rather large uncertainties in both the normalization and shape of the reactor $\bar{\nu}_e$ flux. The other method is an empirical approach called the "conversion" method. It relies on the measured cumulative electron spectrum associated with the β-decays of all fission fragments of the fuel isotope j. This spectrum is fitted by the superposition of a set of virtual allowed branches with different end points. $S_j(E_\nu)$ is then given as the sum of the $\bar{\nu}_e$ spectrum converted from each virtual β-branch.

The cumulative electron spectra were measured at the Institut Laue-Langevin (ILL) reactor in Grenoble, France in the 1980s for ^{235}U, ^{239}Pu, and ^{241}Pu, irradiated with thermal neutrons, and converted to

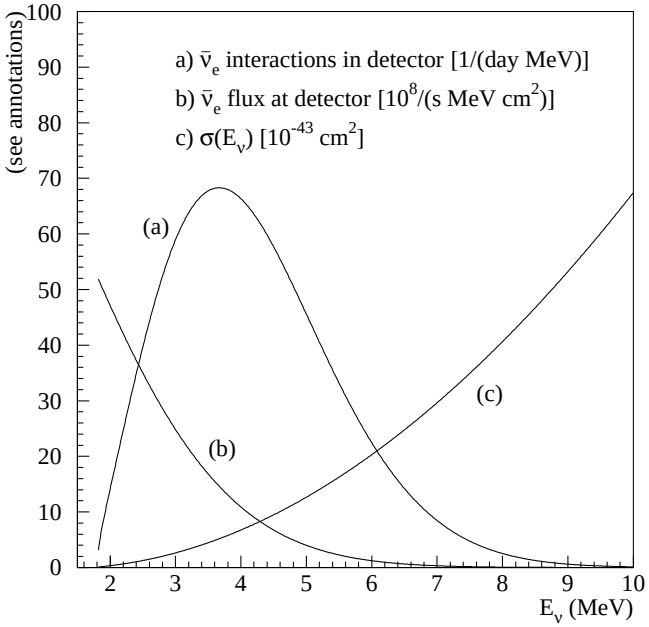

Figure 14.5: Assuming a 12-ton fiducial mass detector located 0.8 km from 12-GW$_{\rm th}$ power reactor, $\bar{\nu}_e$ interaction spectrum in the detector (curve (a)) and reactor $\bar{\nu}_e$ flux at the detector (curve (b)) are shown as a function of energy. Inverse β-decay cross section (curve (c)) is also shown. This figure is from Ref. 162.

the $\bar{\nu}_e$ spectra [153]. However, as ^{238}U undergoes fission with fast neutrons, its cumulative electron spectrum could not be measured at the ILL reactor. It was later measured at the scientific neutron source FRM II in Garching, Germany in 2014 [154].

Until 2011, a conventionally employed reactor $\bar{\nu}_e$ flux model was the predictions from the ILL conversion for ^{235}U, ^{239}Pu, and ^{241}Pu spectra [153]. For the ^{238}U $\bar{\nu}_e$ spectrum, the prediction from Vogel *et al.*'s summation [152] calculation was often used. (We refer to this reactor $\bar{\nu}_e$ flux model as the "ILL-Vogel" flux model or the "old" flux model.)

In 2011 the reactor $\bar{\nu}_e$ flux predictions were reevaluated with improved theoretical treatments [155]. The authors of [155] calculated the ^{238}U $\bar{\nu}_e$ spectrum with an improved *ab initio* approach and obtained predictions for ^{235}U, ^{239}Pu, and ^{241}Pu $\bar{\nu}_e$ spectra with a strategy to use the nuclear database information as much as possible. Their predictions for the ^{235}U, ^{239}Pu, and ^{241}Pu $\bar{\nu}_e$ spectra were found about 3% higher in normalization compared to the ILL predictions [153]. It was further pointed out in [156] that the mean ratio of the IBD event rate observed in previous short baseline reactor neutrino oscillation experiments to the rate predicted in [155] is 0.943 ± 0.023. The authors of [156] called this discrepancy (more than 2σ effect) the "reactor antineutrino anomaly."

Subsequently, the accuracy of theoretical electron spectrum in β-decay was further improved in [157]. The author of [157] took the strategy of minimizing the use of nuclear databases as much as possible, in contrast to that employed in [155], to predict the ^{235}U, ^{239}Pu, and ^{241}Pu $\bar{\nu}_e$ spectra by the conversion method. He also found that his predictions for the ^{235}U, ^{239}Pu, and ^{241}Pu $\bar{\nu}_e$ spectra were about 3% higher in normalization than the ILL predictions [153].

In view of the improved predictions of the reactor antineutrino spectra after 2011, the reactor $\bar{\nu}_e$ flux model often quoted in the literature is based on the prediction from the Huber conversion [157] for ^{235}U, ^{239}Pu, and ^{241}Pu and the prediction from Mueller *et al.*'s *ab initio* calculation for ^{238}U [155]. (We refer to this reactor $\bar{\nu}_e$ flux model as the "Saclay-Huber" flux model or the "new" flux model.) For the ^{238}U $\bar{\nu}_e$ flux, the prediction based on the measured electron spectrum [154] is also used.

If true, the results obtained with the "new" $\bar{\nu}_e$ flux model hint at possible oscillations involving sterile neutrinos (see Section 14.14). However, the reactor antineutrino flux measurement at Daya Bay [158] is consistent with the flux measurement results in the previous short-baseline reactor neutrino oscillation experiments, and shows a 7.8% lower observed IBD yield from fission of ^{235}U with respect to the prediction of the "new" flux model [159]. This result suggests that the primary source of the reactor antineutrino anomaly may be an incorrect prediction of the ^{235}U $\bar{\nu}_e$ flux by the "new" flux model. A combined analysis of the Daya Bay measurement and other reactor measurements of the $\bar{\nu}_e$ fluxes was performed also in [160], where statistically stronger results confirming the Daya Bay's observation were obtained. These results have an impact on the sterile neutrino search in reactor neutrino oscillation experiments.

In what concerns the shape of the reactor $\bar{\nu}_e$ flux, all the current reactor neutrino oscillation experiments, Daya Bay [158], RENO [45], and Double Chooz [46], observe an excess of $\bar{\nu}_e$ flux in the energy region from 4 to 6 MeV, relative to current predictions. The excess rate is found to be time independent and correlated with the reactor power. Because of this, an unknown background is unlikely for its explanation. There are certain suggestions on the possible nuclear physics origins of this excess, but this problem is not completely solved yet [161].

14.7. Neutrino oscillations in vacuum

Neutrino oscillations are a quantum mechanical consequence of the existence of nonzero neutrino masses and neutrino (lepton) mixing, Eq. (14.1), and of the relatively small splitting between the neutrino masses. The neutrino mixing and oscillation phenomena are analogous to the $K^0 - \bar{K}^0$ and $B^0 - \bar{B}^0$ mixing and oscillations.

In what follows we will present a simplified version of the derivation of the expressions for the neutrino and antineutrino oscillation probabilities. The complete derivation would require the use of the wave packet formalism for the evolution of the massive neutrino states, or, alternatively, of the field-theoretical approach, in which one takes into account the processes of production, propagation and detection of neutrinos [163].

Suppose the flavour neutrino ν_l is produced in a CC weak interaction process and after a time T it is observed by a neutrino detector, located at a distance L from the neutrino source and capable of detecting also neutrinos $\nu_{l'}$, $l' \neq l$. We will consider the evolution of the neutrino state $|\nu_l\rangle$ in the frame in which the detector is at rest (laboratory frame). The oscillation probability, as we will see, is a Lorentz invariant quantity. If lepton mixing, Eq. (14.1), takes place and the masses m_j of all neutrinos ν_j are sufficiently small, the state of the neutrino ν_l, $|\nu_l\rangle$, will be a coherent superposition of the states $|\nu_j\rangle$ of neutrinos ν_j:

$$|\nu_l\rangle = \sum_j U^*_{lj} \, |\nu_j; \tilde{p}_j\rangle, \quad l = e, \mu, \tau \,, \tag{14.28}$$

where U is the neutrino mixing matrix and $\tilde{p}_j$ is the 4-momentum of ν_j [164].

We will consider the case of relativistic neutrinos ν_j, which corresponds to the conditions in both past and currently planned future neutrino oscillation experiments [166]. In this case the state $|\nu_j; \tilde{p}_j\rangle$ practically coincides with the helicity (-1) state $|\nu_j, L; \tilde{p}_j\rangle$ of the neutrino ν_j, the admixture of the helicity (+1) state $|\nu_j, R; \tilde{p}_j\rangle$ in $|\nu_j; \tilde{p}_j\rangle$ being suppressed due to the factor $\sim m_j/E_j$, where E_j is the energy of ν_j. If ν_j are Majorana particles, $\nu_j \equiv \chi_j$, due to the presence of the helicity (+1) state $|\chi_j, R; \tilde{p}_j\rangle$ in $|\chi_j; \tilde{p}_j\rangle$, the neutrino ν_l can produce an l^+ (instead of l^-) when it interacts, *e.g.*, with nucleons. The cross section of such a $|\Delta L_l| = 2$ process is suppressed by the factor $(m_j/E_j)^2$, which renders the process unobservable at present.

If the number n of massive neutrinos ν_j is bigger than 3 due to a mixing between the active flavour and sterile neutrinos, one will have additional relations similar to that in Eq. (14.28) for the state vectors of the (predominantly LH) sterile antineutrinos. In the case of

just one RH sterile neutrino field $\nu_{sR}(x)$, for instance, we will have in addition to Eq. (14.28):

$$|\bar{\nu}_{sL}\rangle = \sum_{j=1}^{4} U^*_{sj}\,|\nu_j;\tilde{p}_j\rangle \cong \sum_{j=1}^{4} U^*_{sj}\,|\nu_j, L;\tilde{p}_j\rangle\,, \tag{14.29}$$

where the neutrino mixing matrix U is now a 4×4 unitary matrix.

For the state vector of RH flavour antineutrino $\bar{\nu}_l$, produced in a CC weak interaction process we similarly get:

$$|\bar{\nu}_l\rangle = \sum_j U_{lj}\,|\bar{\nu}_j;\tilde{p}_j\rangle \cong \sum_{j=1} U_{lj}\,|\bar{\nu}_j, R;\tilde{p}_j\rangle, \quad l = e,\mu,\tau\,, \tag{14.30}$$

where $|\bar{\nu}_j, R;\tilde{p}_j\rangle$ is the helicity (+1) state of the antineutrino $\bar{\nu}_j$ if ν_j are Dirac fermions, or the helicity (+1) state of the neutrino $\nu_j \equiv \bar{\nu}_j \equiv \chi_j$ if the massive neutrinos are Majorana particles. Thus, in the latter case we have in Eq. (14.30): $|\bar{\nu}_j;\tilde{p}_j\rangle \cong |\nu_j, R;\tilde{p}_j\rangle \equiv |\chi_j, R;\tilde{p}_j\rangle$. The presence of the matrix U in Eq. (14.30) (and not of U^*) follows directly from Eq. (14.1).

We will assume in what follows that the spectrum of masses of neutrinos is not degenerate: $m_j \neq m_k$, $j \neq k$. Then the states $|\nu_j;\tilde{p}_j\rangle$ in the linear superposition in the r.h.s. of Eq. (14.28) will have, in general, different energies and different momenta, independently of whether they are produced in a decay or interaction process: $\tilde{p}_j \neq \tilde{p}_k$, or $E_j \neq E_k$, $\mathbf{p}_j \neq \mathbf{p}_k$, $j \neq k$, where $E_j = \sqrt{p_j^2 + m_j^2}$, $p_j \equiv |\mathbf{p}_j|$. The deviations of E_j and p_j from the values for a massless neutrino E and $p = E$ are proportional to m_j^2/E_0, E_0 being a characteristic energy of the process, and are extremely small. In the case of $\pi^+ \to \mu^+ + \nu_\mu$ decay at rest, for instance, we have: $E_j = E + m_j^2/(2m_\pi)$, $p_j = E - \xi m_j^2/(2E)$, where $E = (m_\pi/2)(1 - m_\mu^2/m_\pi^2) \cong 30$ MeV, $\xi = (1 + m_\mu^2/m_\pi^2)/2 \cong 0.8$, and m_μ and m_π are the μ^+ and π^+ masses. Taking $m_j = 1$ eV we find: $E_j \cong E\,(1 + 1.2\times 10^{-16})$ and $p_j \cong E\,(1 - 4.4\times 10^{-16})$.

Given the uncorrelated uncertainties δE and δp in the knowledge of the neutrino energy E and momentum p, the quantum mechanical condition that neutrinos with definite mass ν_1, ν_2, ..., whose states are part of the linear superposition of states corresponding, for example, to $|\nu_l\rangle$ in Eq. (14.28), are emitted coherently when $|\nu_l\rangle$ is produced in some weak interaction process, has the form [167]:

$$\delta m^2 = \sqrt{(2E\delta E)^2 + (2p\delta p)^2} > \max(|m_i^2 - m_j^2|), \quad i,j = 1,2,...,n, \tag{14.31}$$

where δm^2 is the uncertainty in the square of the neutrino mass due to the uncertainties in the energy and momentum of the neutrino. Equation Eq. (14.31) follows from the well known relativistic relation $E^2 = p^2 + m^2$. In the context under discussion, δE and δp should be understood as the intrinsic quantum mechanical uncertainties in the neutrino energy and momentum for the given neutrino production and detection processes, *i.e.*, δE and δp are the minimal uncertainties with which E and p can be determined in the considered production and detection processes. Then δm^2 is the quantum mechanical uncertainty of the inferred squared neutrino mass.

Suppose that the neutrinos are observed via a CC weak interaction process and that in the detector's rest frame they are detected after time T after emission, after traveling a distance L. Then the amplitude of the probability that neutrino $\nu_{l'}$ will be observed if neutrino ν_l was produced by the neutrino source can be written as [163,165,168]:

$$A(\nu_l \to \nu_{l'}) = \sum_j U_{l'j}\,D_j\,U^\dagger_{jl}\,, \qquad l,l' = e,\mu,\tau\,, \tag{14.32}$$

where $D_j = D_j(p_j; L, T)$ describes the propagation of ν_j between the source and the detector, $U^\dagger_{jl}$ and $U_{l'j}$ are the amplitudes to find

ν_j in the initial and in the final flavour neutrino state, respectively. It follows from relativistic Quantum Mechanics considerations that [163,165]

$$D_j \equiv D_j(\tilde{p}_j; L, T) = e^{-i\tilde{p}_j\,(x_f - x_0)} = e^{-i(E_jT - p_jL)}\,, \qquad p_j \equiv |\mathbf{p}_j|\,, \tag{14.33}$$

where [169] x_0 and x_f are the space-time coordinates of the points of neutrino production and detection, $T = (t_f - t_0)$ and $L = \mathbf{k}(\mathbf{x}_f - \mathbf{x}_0)$, $\mathbf{k}$ being the unit vector in the direction of neutrino momentum, $\mathbf{p}_j = \mathbf{k}\mathrm{p_j}$. What is relevant for the calculation of the probability $P(\nu_l \to \nu_{l'}) = |A(\nu_l \to \nu_{l'})|^2$ is the interference factor $D_jD_k^*$ which depends on the phase

$$\delta\varphi_{jk} = (E_j - E_k)T - (p_j - p_k)L = (E_j - E_k)\left[T - \frac{E_j + E_k}{p_j + p_k}\,L\right] + \frac{m_j^2 - m_k^2}{p_j + p_k}\,L\,. \tag{14.34}$$

Some authors [170] have suggested that the distance traveled by the neutrinos L and the time interval T are related by $T = (E_j + E_k)\,L/(p_j + p_k) = L/\bar{v}$, $\bar{v} = (E_j/(E_j + E_k))v_j + (E_k/(E_j + E_k))v_k$ being the "average" velocity of ν_j and ν_k, where $v_{j,k} = p_{j,k}/E_{j,k}$. In this case the first term in the r.h.s. of Eq. (14.34) vanishes. The indicated relation has not emerged so far from any dynamical wave packet calculations. We arrive at the same conclusion concerning the term under discussion in Eq. (14.34) if one assumes [171] that $E_j = E_k = E_0$. Finally, it was proposed in Ref. 168 and Ref. 177 that the states of ν_j and $\bar{\nu}_j$ in Eq. (14.28) and Eq. (14.30) have the same 3-momentum, $p_j = p_k = p$. Under this condition the first term in the r.h.s. of Eq. (14.34) is negligible, being suppressed by the additional factor $(m_j^2 + m_k^2)/p^2$ since for relativistic neutrinos $L = T$ up to terms $\sim m_{j,k}^2/p^2$. We arrive at the same conclusion if $E_j \neq E_k$, $p_j \neq p_k$, $j \neq k$, and we take into account that neutrinos are relativistic and therefore, up to corrections $\sim m_{j,k}^2/E_{j,k}^2$, we have $L \cong T$ (see, *e.g.*, C. Giunti quoted in Ref. 163).

Although the cases considered above are physically quite different, they lead to the same result for the phase difference $\delta\varphi_{jk}$. Thus, we have:

$$\delta\varphi_{jk} \cong \frac{m_j^2 - m_k^2}{2p}\,L = 2\pi\,\frac{L}{L^v_{jk}}\,\mathrm{sgn}(m_j^2 - m_k^2)\,, \tag{14.35}$$

where $p = (p_j + p_k)/2$ and

$$L^v_{jk} = 4\pi\frac{p}{|\Delta m^2_{jk}|} \cong 2.48\ \mathrm{m}\ \frac{p[MeV]}{|\Delta m^2_{jk}|[eV^2]} \tag{14.36}$$

is the neutrino oscillation length associated with Δm^2_{jk}. We can safely neglect the dependence of p_j and p_k on the masses m_j and m_k and consider p to be the zero neutrino mass momentum, $p = E$. The phase difference $\delta\varphi_{jk}$, Eq. (14.35), is Lorentz-invariant.

Eq. (14.33) corresponds to a plane-wave description of the propagation of neutrinos ν_j. It accounts only for the movement of the center of the wave packet describing ν_j. In the wave packet treatment of the problem, the interference between the states of ν_j and ν_k is subject to a number of conditions [163], the localization condition and the condition of overlapping of the wave packets of ν_j and ν_k at the detection point being the most important. For relativistic neutrinos, the localisation condition in space, for instance, reads: $\sigma_{xP}, \sigma_{xD} < L^v_{jk}/(2\pi)$, $\sigma_{xP(D)}$ being the spatial width of the production (detection) wave packet. Thus, the interference will not be suppressed if the spatial width of the neutrino wave packets determined by the neutrino production and detection processes is smaller than the corresponding oscillation length in vacuum. In order for the interference to be nonzero, the wave packets describing ν_j and ν_k should also overlap in the point of neutrino detection. This requires that the spatial separation between the two wave packets at the point of neutrinos detection, caused by the two wave packets having different group velocities $v_j \neq v_k$, satisfies $|(v_j - v_k)T| \ll \max(\sigma_{xP}, \sigma_{xD})$. If the interval of time T is not measured, T in the preceding condition must be replaced by the distance L between the neutrino source and the detector (for further discussion see, *e.g.*, Refs. [163,165,168]) .

For the $\nu_l \to \nu_{l'}$ and $\bar{\nu}_l \to \bar{\nu}_{l'}$ oscillation probabilities we get from Eq. (14.32), Eq. (14.33), and Eq. (14.35):

$$P(\nu_l \to \nu_{l'}) = \sum_j |U_{l'j}|^2\,|U_{lj}|^2 + 2\sum_{j>k} |U_{l'j}\,U^*_{lj}\,U_{lk}\,U^*_{l'k}| \cos(\frac{\Delta m^2_{jk}}{2p}\,L - \phi_{l'l;jk})\,, \tag{14.37}$$

$$P(\bar{\nu}_l \to \bar{\nu}_{l'}) = \sum_j |U_{l'j}|^2 \, |U_{lj}|^2 \, + 2 \sum_{j>k} |U_{l'j} \, U^*_{lj} \, U_{lk} \, U^*_{l'k}| \cos(\frac{\Delta m^2_{jk}}{2p} \, L + \phi_{l'l;jk}) \, , \quad (14.38)$$

where $l, l' = e, \mu, \tau$ and $\phi_{l'l;jk} = \arg\left(U_{l'j} \, U^*_{lj} \, U_{lk} \, U^*_{l'k}\right)$. It follows from Eq. (14.32) - Eq. (14.34) that in order for neutrino oscillations to occur, at least two neutrinos ν_j should not be degenerate in mass and lepton mixing should take place, $U \neq \mathbf{1}$. The neutrino oscillations effects can be large if we have

$$\frac{|\Delta m^2_{jk}|}{2p} \, L = 2\pi \, \frac{L}{L^v_{jk}} \gtrsim 1 \, , \;\; j \neq k \, . \quad (14.39)$$

at least for one Δm^2_{jk}. This condition has a simple physical interpretation: the neutrino oscillation length L^v_{jk} should be of the order of, or smaller, than source-detector distance L, otherwise the oscillations will not have time to develop before neutrinos reach the detector.

We see from Eq. (14.37) and Eq. (14.38) that $P(\nu_l \to \nu_{l'}) = P(\bar{\nu}_{l'} \to \bar{\nu}_l)$, $l, l' = e, \mu, \tau$. This is a consequence of CPT invariance. The conditions of CP and T invariance read [54,61,62]: $P(\nu_l \to \nu_{l'}) = P(\bar{\nu}_l \to \bar{\nu}_{l'})$, $l, l' = e, \mu, \tau$ (CP), $P(\nu_l \to \nu_{l'}) = P(\nu_{l'} \to \nu_l)$, $P(\bar{\nu}_l \to \bar{\nu}_{l'}) = P(\bar{\nu}_{l'} \to \bar{\nu}_l)$, $l, l' = e, \mu, \tau$ (T). In the case of CPT invariance, which we will assume to hold throughout this article, we get for the survival probabilities: $P(\nu_l \to \nu_l) = P(\bar{\nu}_l \to \bar{\nu}_l)$, $l = e, \mu, \tau$. Thus, the study of the "disappearance" of ν_l and $\bar{\nu}_l$, caused by oscillations in vacuum, cannot be used to test whether CP invariance holds in the lepton sector. It follows from Eq. (14.37) and Eq. (14.38) that we can have CP violation effects in neutrino oscillations only if $\phi_{l'l;jk} \neq \pi q$, $q = 0, 1, 2$, *i.e.*, if $U_{l'j} \, U^*_{lj} \, U_{lk} \, U^*_{l'k}$, and therefore U itself, is not real. As a measure of CP and T violation in neutrino oscillations we can consider the asymmetries:

$$A^{(l'l)}_{\rm CP} \equiv P(\nu_l \to \nu_{l'}) - P(\bar{\nu}_l \to \bar{\nu}_{l'}) \, , \quad A^{(l'l)}_{\rm T} \equiv P(\nu_l \to \nu_{l'}) - P(\nu_{l'} \to \nu_l) \, . \quad (14.40)$$

CPT invariance implies: $A^{(l'l)}_{\rm CP} = -A^{(ll')}_{\rm CP}$, $A^{(l'l)}_{\rm T} = P(\bar{\nu}_{l'} \to \bar{\nu}_l) - P(\bar{\nu}_l \to \bar{\nu}_{l'}) = A^{(l'l)}_{\rm CP}$. It follows further directly from Eq. (14.37) and Eq. (14.38) that

$$A^{(l'l)}_{\rm CP} = 4 \sum_{j>k} {\rm Im}\left(U_{l'j} \, U^*_{lj} \, U_{lk} \, U^*_{l'k}\right) \, \sin\frac{\Delta m^2_{jk}}{2p} \, L \, , \;\; l, l' = e, \mu, \tau \, . \quad (14.41)$$

Eq. (14.2) and Eq. (14.37) - Eq. (14.38) imply that $P(\nu_l \to \nu_{l'})$ and $P(\bar{\nu}_l \to \bar{\nu}_{l'})$ do not depend on the Majorana CP violation phases in the neutrino mixing matrix U [54]. Thus, the experiments investigating the $\nu_l \to \nu_{l'}$ and $\bar{\nu}_l \to \bar{\nu}_{l'}$ oscillations, $l, l' = e, \mu, \tau$, cannot provide information on the nature - Dirac or Majorana, of massive neutrinos. The same conclusions hold also when the $\nu_l \to \nu_{l'}$ and $\bar{\nu}_l \to \bar{\nu}_{l'}$ oscillations take place in matter [65]. In the case of $\nu_l \leftrightarrow \nu_{l'}$ and $\bar{\nu}_l \leftrightarrow \bar{\nu}_{l'}$ oscillations in vacuum, only the Dirac phase(s) in U can cause CP violating effects leading to $P(\nu_l \to \nu_{l'}) \neq P(\bar{\nu}_l \to \bar{\nu}_{l'})$, $l \neq l'$.

In the case of 3-neutrino mixing all different ${\rm Im}(U_{l'j} U^*_{lj} U_{lk} U^*_{l'k}) \neq 0$, $l' \neq l = e, \mu, \tau$, $j \neq k = 1, 2, 3$, coincide up to a sign as a consequence of the unitarity of U. Therefore one has [63]:

$$A^{(\mu e)}_{\rm CP} = -A^{(\tau e)}_{\rm CP} = A^{(\tau\mu)}_{\rm CP} = 4 \, J_{\rm CP} \, \left(\sin\frac{\Delta m^2_{32}}{2p} \, L + \sin\frac{\Delta m^2_{21}}{2p} \, L + \sin\frac{\Delta m^2_{13}}{2p} \, L\right) \quad (14.42)$$

where

$$J_{\rm CP} = {\rm Im}\left(U_{\mu 3} \, U^*_{e3} \, U_{e2} \, U^*_{\mu 2}\right) \, , \quad (14.43)$$

is the "rephasing invariant" associated with the Dirac CP violation phase in U. It is analogous to the rephasing invariant associated with the Dirac CP violating phase in the CKM quark mixing matrix [64]. It is clear from Eq. (14.42) that $J_{\rm CP}$ controls the magnitude of CP violation effects in neutrino oscillations in the case of 3-neutrino mixing. If $\sin(\Delta m^2_{ij}/(2p)L) \cong 0$ for $(ij) = (32)$, or (21), or (13), we get $A^{(l'l)}_{\rm CP} \cong 0$. Thus, if as a consequence of the production, propagation and/or detection of neutrinos, effectively oscillations due only to one non-zero neutrino mass squared difference take place, the CP violating effects will be strongly suppressed. In particular, we get $A^{(l'l)}_{\rm CP} = 0$, unless all three $\Delta m^2_{ij} \neq 0$, $(ij) = (32), (21), (13)$.

If the number of massive neutrinos n is equal to the number of neutrino flavours, $n = 3$, one has as a consequence of the unitarity of the neutrino mixing matrix: $\sum_{l'=e,\mu,\tau} P(\nu_l \to \nu_{l'}) = 1$, $l = e, \mu, \tau$, $\sum_{l=e,\mu,\tau} P(\nu_l \to \nu_{l'}) = 1$, $l' = e, \mu, \tau$. Similar "probability conservation" equations hold for $P(\bar{\nu}_l \to \bar{\nu}_{l'})$. If, however, the number of light massive neutrinos is bigger than the number of flavour neutrinos as a consequence, *e.g.*, of a flavour neutrino - sterile neutrino mixing, we would have $\sum_{l'=e,\mu,\tau} P(\nu_l \to \nu_{l'}) = 1 - P(\nu_l \to \bar{\nu}_{sL})$, $l = e, \mu, \tau$, where we have assumed the existence of just one sterile neutrino. Obviously, in this case $\sum_{l'=e,\mu,\tau} P(\nu_l \to \nu_{l'}) < 1$ if $P(\nu_l \to \bar{\nu}_{sL}) \neq 0$. The former inequality is used in the searches for oscillations between active and sterile neutrinos.

Consider next neutrino oscillations in the case of one neutrino mass squared difference "dominance": suppose that $|\Delta m^2_{j1}| \ll |\Delta m^2_{n1}|$, $j = 2, ..., (n-1)$, $|\Delta m^2_{n1}| \, L/(2p) \gtrsim 1$ and $|\Delta m^2_{j1}| \, L/(2p) \ll 1$, so that $\exp[i(\Delta m^2_{j1} \, L/(2p)] \cong 1$, $j = 2, ..., (n-1)$. Under these conditions we obtain from Eq. (14.37) and Eq. (14.38), keeping only the oscillating terms involving Δm^2_{n1}:

$$P(\nu_{l(l')} \to \nu_{l'(l)}) \cong P(\bar{\nu}_{l(l')} \to \bar{\nu}_{l'(l)}) \cong \delta_{ll'} - 2|U_{ln}|^2 \left[\delta_{ll'} - |U_{l'n}|^2\right] (1 - \cos\frac{\Delta m^2_{n1}}{2p} \, L) \, . \quad (14.44)$$

It follows from the neutrino oscillation data discussed in Section 14.2 that in the case of 3-neutrino mixing, one of the two independent neutrino mass squared differences, $\Delta m^2_{21} > 0$, is much smaller than the absolute value of the second one, $|\Delta m^2_{31}|$: $\Delta m^2_{21} \ll |\Delta m^2_{31}|$, $\Delta m^2_{21}/|\Delta m^2_{31}| \cong 0.03$. Neglecting the effects due to Δm^2_{21} we get from Eq. (14.44) by setting $n = 3$ and choosing, *e.g.*, i) $l = l' = e$ and ii) $l = e(\mu)$, $l' = \mu(e)$ [172]:

$$P(\nu_e \to \nu_e) = P(\bar{\nu}_e \to \bar{\nu}_e) \cong 1 - 2|U_{e3}|^2 \left(1 - |U_{e3}|^2\right) \left(1 - \cos\frac{\Delta m^2_{31}}{2p} \, L\right) = 1 - \frac{1}{2} \sin^2 2\theta_{13} \left(1 - \cos\frac{\Delta m^2_{31}}{2p} \, L\right) \, , \quad (14.45)$$

$$P(\nu_{\mu(e)} \to \nu_{e(\mu)}) \cong 2 \, |U_{\mu 3}|^2 \, |U_{e3}|^2 \, \left(1 - \cos\frac{\Delta m^2_{31}}{2p} \, L\right) = \frac{|U_{\mu 3}|^2}{1 - |U_{e3}|^2} \, P^{2\nu}\left(|U_{e3}|^2, \Delta m^2_{31}\right) = \sin^2\theta_{23} P^{2\nu}\left(\sin^2\theta_{13}, \Delta m^2_{31}\right) \, , \quad (14.46)$$

and $P(\bar{\nu}_{\mu(e)} \to \bar{\nu}_{e(\mu)}) = P(\nu_{\mu(e)} \to \nu_{e(\mu)})$. Here $P^{2\nu}\left(|U_{e3}|^2, \Delta m^2_{31}\right) = 0.5 \sin^2 2\theta_{13}(1 - \cos\frac{\Delta m^2_{31}}{2p} \, L)$ is the probability of the 2-neutrino transition $\nu_e \to (s_{23}\nu_\mu + c_{23}\nu_\tau)$ due to Δm^2_{31} and a mixing with angle θ_{13}, where θ_{13} and θ_{23} are the reactor and atmospheric neutrino angles of the standard parametrization of the neutrino mixing matrix (see Eq. (14.6) and Eq. (14.8)). Eq. (14.45) describes with a relatively high precision the oscillations of reactor $\bar{\nu}_e$ on a distance $L \sim 1$ km in the case of 3-neutrino mixing. It was used in the analysis of the data of the Chooz [57], Double Chooz [32], Daya Bay [33] and RENO [34] experiments. Eq. (14.44) with $n = 3$ and $l = l' = \mu$ describes with a relatively good precision the effects of "disappearance" due to oscillations of the accelerator ν_μ, seen in the K2K [19] MINOS [20,21] and T2K [22,23] experiments. The $\nu_\mu \to \nu_\tau$ transitions due to the oscillations, which the OPERA experiment [173,174] is observing, can be described by Eq. (14.44) with $n = 3$ and $l = \mu$, $l' = \tau$.

Finally, the probability Eq. (14.46) describes with a good precision the $\nu_\mu \to \nu_e$ and $\bar\nu_\mu \to \bar\nu_e$ oscillations under the conditions of the K2K experiment [175].

It follows from the expressions for the probabilities in Eq. (14.45) and Eq. (14.46), obtained in the one Δm^2 dominance approximation, that they are not sensitive to the sign of Δm^2_{31}, i.e., to the neutrino mass ordering. However, the exact 3-neutrino mixing ν_e and $\bar\nu_e$ survival probabilities, $P(\bar\nu_e \to \bar\nu_e) = P(\nu_e \to \nu_e)$ (we assume CPT invariance), depend on the neutrino mass ordering [86,176]. Indeed, the expression of interest can be cast in the form [86,176](see also [87,89]) :

$$
\begin{aligned}
&P^{(X)}(\bar\nu_e \to \bar\nu_e) \\
&= P^{X}(\nu_e \to \nu_e) \\
&= 1 - \frac{1}{2}\,\sin^2 2\theta_{13}\,\left(1 - \cos\frac{\Delta m^2_{atm}\,L}{2\,E_\nu}\right) \\
&-\; 2\,\cos^4\theta_{13}\,X^2\,(1 - X^2)\,\left(1 - \cos\frac{\Delta m^2_{\odot}\,L}{2\,E_\nu}\right) \\
&+\; \frac{1}{2}\,\sin^2 2\theta_{13}\,X^2\,\left(\cos\left(\frac{\Delta m^2_{atm}\,L}{2\,E_\nu} - \frac{\Delta m^2_{\odot}\,L}{2\,E_\nu}\right) - \cos\frac{\Delta m^2_{atm}\,L}{2\,E_\nu}\right)\,,
\end{aligned}
\tag{14.47}
$$

where $\Delta m^2_{\odot} \equiv \Delta m^2_{21}$, $\Delta m^2_{atm} \equiv \Delta m^2_{31}$ in the NO case, $\Delta m^2_{atm} \equiv -\,\Delta m^2_{32}$ in the IO case, and we have used the fact that $\Delta m^2_{31}(NO) = -\,\Delta m^2_{32}(IO)$. Thus,

$$
\Delta m^2_{atm} \equiv \Delta m^2_{31}(NO) = -\,\Delta m^2_{32}(IO)\,. \tag{14.48}
$$

The parameter X in Eq. (14.47) is given by:

$$
\begin{aligned}
X^2 &= \sin^2\theta_{12}\,, \qquad \text{NO spectrum}\,, \\
X^2 &= \cos^2\theta_{12}\,, \qquad \text{IO spectrum}\,,
\end{aligned}
\tag{14.49}
$$

θ_{12} being the solar neutrino mixing angle of the standard parametrisation of the neutrino mixing matrix (see Eq. (14.6) and Eq. (14.7)). Thus, the probability of $\bar\nu_e$ and ν_e survival in the NO and IO cases, $P^{(NO)}(\bar\nu_e \to \bar\nu_e) = P^{(NO)}(\nu_e \to \nu_e)$ and $P^{(IO)}(\bar\nu_e \to \bar\nu_e) = P^{(IO)}(\nu_e \to \nu_e)$, differ by the coefficient X^2 in the last term in Eq. (14.47) - the interference term involving both $\Delta m^2_{\odot}$ and Δm^2_{atm}. For the current best fit value of $\sin^2\theta_{12} = 0.297$ quoted in Table 1.1 we have $\cos^2\theta_{12} \cong 0.703$, i.e., the coefficient under discussion in $P^{(IO)}(\bar\nu_e \to \bar\nu_e)$ is approximately by a factor of 2.3 larger than that in $P^{(NO)}(\bar\nu_e \to \bar\nu_e)$. It was suggested in [86] on the basis of an analysis of the distortion of $\bar\nu_e$ spectrum due to oscillations in the NO and IO cases that the indicated difference can be used for determination of the neutrino mass ordering in an experiment with reactor $\bar\nu_e$. This possibility was further studied in greater detail in [87,89] and, e.g., in [88,90]. Such an experiment is currently under preparation within the JUNO project in China [91].

In certain cases the dimensions of the neutrino source, ΔL, are not negligible in comparison with the oscillation length. Similarly, when analyzing neutrino oscillation data one has to include the energy resolution of the detector, ΔE, *etc.* in the analysis. As can be shown [52], if $2\pi\Delta L/L^v_{jk} \gg 1$, and/or $2\pi(L/L^v_{jk})(\Delta E/E) \gg 1$, the oscillating terms in the neutrino oscillation probabilities will be strongly suppressed. In this case (as well as in the case of sufficiently large separation of the ν_j and ν_k wave packets at the detection point) the interference terms in $P(\nu_l \to \nu_{l'})$ and $P(\bar\nu_{l'} \to \bar\nu_l)$ will be negligibly small and the neutrino flavour conversion will be determined by the average probabilities:

$$
\bar P(\nu_l \to \nu_{l'}) = \bar P(\bar\nu_l \to \bar\nu_{l'}) \cong \sum_j |U_{l'j}|^2\,|U_{lj}|^2\,. \tag{14.50}
$$

Suppose next that in the case of 3-neutrino mixing, $|\Delta m^2_{21}|\,L/(2p) \sim 1$, while at the same time $|\Delta m^2_{31(32)}|\,L/(2p) \gg 1$, and the oscillations due to Δm^2_{31} and Δm^2_{32} are strongly suppressed (averaged out) due to integration over the region of neutrino production, the energy resolution function, *etc.* In this case we get for the ν_e and $\bar\nu_e$ survival probabilities:

$$
\begin{aligned}
&P(\nu_e \to \nu_e) = P(\bar\nu_e \to \bar\nu_e) \cong |U_{e3}|^4 + \left(1 - |U_{e3}|^2\right)^2\,P^{2\nu}(\nu_e \to \nu_e) \\
&= \sin^4\theta_{13} + \cos^4\theta_{13} P^{2\nu}(\nu_e \to \nu_e)\,,
\end{aligned}
\tag{14.51}
$$

where

$$
\begin{aligned}
&P^{2\nu}(\nu_e \to \nu_e) = P^{2\nu}(\bar\nu_e \to \bar\nu_e) \equiv P^{2\nu}_{ee}(\theta_{12}, \Delta m^2_{21}) \\
&= 1 - \frac{1}{2}\,\sin^2 2\theta_{12}\,\left(1 - \cos\frac{\Delta m^2_{21}}{2p}\,L\right) \\
&= 1 - \sin^2 2\theta_{12}\,\sin^2\left(\frac{\Delta m^2_{21}}{4E}\,L\right)
\end{aligned}
\tag{14.52}
$$

are the ν_e and $\bar\nu_e$ survival probabilities in the case of 2-neutrino oscillations "driven" by the angle θ_{12} and Δm^2_{21}. Eq. (14.51) with $P^{2\nu}(\bar\nu_e \to \bar\nu_e)$ given by Eq. (14.52) describes the effects of neutrino oscillations of reactor $\bar\nu_e$ observed by the KamLAND experiment.

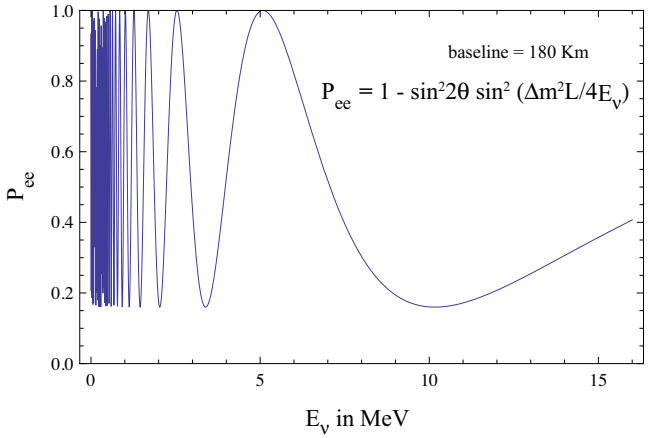

Figure 14.6: The ν_e ($\bar\nu_e$) survival probability $P(\nu_e \to \nu_e) = P(\bar\nu_e \to \bar\nu_e)$, Eq. (14.54), as a function of the neutrino energy for $L = 180$ km, $\Delta m^2 = 7.0 \times 10^{-5}$ eV^2 and $\sin^2 2\theta = 0.84$ (from Ref. 178).

The data of ν-oscillations experiments were often analyzed in the past, and in certain cases new data are still analyzed at present, assuming 2-neutrino mixing:

$$
|\nu_l\rangle \;= |\nu_1\rangle\cos\theta + |\nu_2\rangle\sin\theta\,, \quad |\nu_x\rangle \;= -|\nu_1\rangle\sin\theta + |\nu_2\rangle\cos\theta\;, \tag{14.53}
$$

where θ is the neutrino mixing angle in vacuum and ν_x is another flavour neutrino or sterile (anti-) neutrino, $x = l' \neq l$ or $\nu_x \equiv \bar\nu_{sL}$. In this case we have [177]:

$$
\begin{aligned}
P^{2\nu}(\nu_l \to \nu_l) &= 1 - \frac{1}{2}\sin^2 2\theta\,\left(1 - \cos 2\pi\frac{L}{L^v}\right) \\
&= 1 - \sin^2 2\theta\,\left(\sin^2\frac{\Delta m^2}{4E}L\right), \\
P^{2\nu}(\nu_l \to \nu_x) &= 1 - P^{2\nu}(\nu_l \to \nu_l)\,,
\end{aligned}
\tag{14.54}
$$

where $L^v = 4\pi\,E/\Delta m^2$ ($p = E$), $\Delta m^2 = m^2_2 - m^2_1 > 0$. Combining the CPT invariance constraints with the probability conservation one obtains: $P(\nu_l \to \nu_x) = P(\bar\nu_l \to \bar\nu_x) = P(\nu_x \to \nu_l) = P(\bar\nu_x \to \bar\nu_l)$. These equalities and Eq. (14.54) with $l = \mu$ and $x = \tau$ were used, for instance, in the analysis of the Super-K atmospheric neutrino data [17], in which the first compelling evidence for oscillations of neutrinos was obtained. The probability $P^{2\nu}(\nu_l \to \nu_x)$, Eq. (14.54), depends on two factors: on $(1 - \cos 2\pi L/L^v)$, which exhibits oscillatory dependence on the distance L and on the neutrino energy $p = E$ (hence the name "neutrino oscillations"), and on $\sin^2 2\theta$, which determines the amplitude of the oscillations. In order to have $P^{2\nu}(\nu_l \to \nu_x) \cong 1$,

two conditions have to be fulfilled: one should have $\sin^2 2\theta \cong 1$ and $L^v \lesssim 2\pi L$ with $\cos 2\pi L/L^v \cong -1$. If $L^v \gg 2\pi L$, the oscillations do not have enough time to develop on the way to the neutrino detector and $P(\nu_l \to \nu_x) \cong 0$, while $P(\nu_l \to \nu_l) \cong 1$. The preceding comments are illustrated in Fig. 14.6 showing the dependence of the probability $P^{2\nu}(\nu_e \to \nu_e) = P^{2\nu}(\bar{\nu}_e \to \bar{\nu}_e)$ on the neutrino energy.

Table 14.4: Sensitivity of different oscillation experiments.

Source	Type of ν	$\overline{E}$[MeV]	L[km]	min(Δm^2)[eV^2]
Reactor	$\overline{\nu}_e$	~ 1	1	$\sim 10^{-3}$
Reactor	$\overline{\nu}_e$	~ 1	100	$\sim 10^{-5}$
Accelerator	$\nu_\mu, \overline{\nu}_\mu$	$\sim 10^3$	1	~ 1
Accelerator	$\nu_\mu, \overline{\nu}_\mu$	$\sim 10^3$	1000	$\sim 10^{-3}$
Atmospheric ν's	$\nu_{\mu,e}, \overline{\nu}_{\mu,e}$	$\sim 10^3$	10^4	$\sim 10^{-4}$
Sun	ν_e	~ 1	1.5×10^8	$\sim 10^{-11}$

A given experiment searching for neutrino oscillations is specified, in particular, by the average energy of the neutrinos being studied, $\bar{E}$, and by the source-detector distance L. The requirement $L^v_{jk} \lesssim 2\pi L$ determines the minimal value of a generic neutrino mass squared difference $\Delta m^2 > 0$, to which the experiment is sensitive (figure of merit of the experiment): $\min(\Delta m^2) \sim 2\bar{E}/L$. Because of the interference nature of neutrino oscillations, experiments can probe, in general, rather small values of Δm^2 (see, *e.g.*, Ref. 168). Values of min(Δm^2), characterizing qualitatively the sensitivity of different experiments are given in Table 14.4. They correspond to the reactor experiments Chooz, Daya Bay, RENO, Double Chooz ($L \sim 1$ km) and KamLAND ($L \sim 100$ km), to accelerator experiments - past ($L \sim 1$ km), and current (K2K, MINOS, OPERA, T2K, NOνA [147]) , $L \sim (300 \div 1000)$ km), to the Super-Kamiokande, MINOS and IceCube-DeepCore experiments studying atmospheric neutrino oscillations, and to the solar neutrino experiments.

14.8. Matter effects in neutrino oscillations

The presence of matter can change drastically the pattern of neutrino oscillations: neutrinos can interact with the particles forming the matter. Accordingly, the Hamiltonian of the neutrino system in matter H_m, differs from the Hamiltonian in vacuum H_0, $H_m = H_0 + H_{int}$, where H_{int} describes the interaction of neutrinos with the particles of matter. When, for instance, ν_e and ν_μ propagate in matter, they can scatter (due to H_{int}) on the electrons (e^-), protons (p) and neutrons (n) present in matter. The incoherent elastic and the quasi-elastic scattering, in which the states of the initial particles change in the process (destroying the coherence between the neutrino states), are not of interest - they have a negligible effect on the solar neutrino propagation in the Sun and on the solar, atmospheric and reactor neutrino propagation in the Earth [179]: even in the center of the Sun, where the matter density is relatively high (~ 150 g/cm^3), a ν_e with energy of 1 MeV has a mean free path with respect to the indicated scattering processes $\sim 10^{10}$ km. We recall that the solar radius is much smaller: $R_\odot = 6.96 \times 10^5$ km. The oscillating ν_e and ν_μ can scatter also elastically in the forward direction on the e^-, p and n, with the momenta and the spin states of the particles remaining unchanged. In such a process the coherence of the neutrino states is preserved.

The ν_e and ν_μ coherent elastic scattering on the particles of matter generates nontrivial indices of refraction of the ν_e and ν_μ in matter [26]: $\kappa(\nu_e) \neq 1$, $\kappa(\nu_\mu) \neq 1$. Most importantly, we have $\kappa(\nu_e) \neq \kappa(\nu_\mu)$. The difference $\kappa(\nu_e) - \kappa(\nu_\mu)$ is determined essentially by the difference of the real parts of the forward $\nu_e - e^-$ and $\nu_\mu - e^-$ elastic scattering amplitudes [26] Re $[\mathrm{F}_{\nu_e - e^-}(0)]$ – Re $[\mathrm{F}_{\nu_\mu - e^-}(0)]$: due to the flavour symmetry of the neutrino – quark (neutrino – nucleon) neutral current interaction, the forward $\nu_e - p, n$ and $\nu_\mu - p, n$ elastic scattering amplitudes are equal and therefore do not contribute to the difference of interest [180]. The imaginary parts of the forward scattering amplitudes (responsible, in particular, for decoherence effects) are proportional to the corresponding total scattering cross-sections and in the case of interest are negligible in comparison with the real parts. The real parts of the amplitudes $\mathrm{F}_{\nu_e - e^-}(0)$ and $\mathrm{F}_{\nu_\mu - e^-}(0)$ can be calculated in the Standard Model. To leading order in the Fermi constant G_F, only the term in $\mathrm{F}_{\nu_e - e^-}(0)$ due to the diagram with exchange of a virtual $W^\pm$-boson contributes to $\mathrm{F}_{\nu_e - e^-}(0) - \mathrm{F}_{\nu_\mu - e^-}(0)$. One finds the following result for $\kappa(\nu_e) - \kappa(\nu_\mu)$ in the rest frame of the scatters [26,181,182]:

$$\kappa(\nu_e) - \kappa(\nu_\mu) = \frac{2\pi}{p^2} \left(\mathrm{Re}\ [\mathrm{F}_{\nu_e - e^-}(0)] - \mathrm{Re}\ [\mathrm{F}_{\nu_\mu - e^-}(0)] \right) = -\frac{1}{p} \sqrt{2} G_F N_e \ , \tag{14.55}$$

where N_e is the electron number density in matter. Given $\kappa(\nu_e) - \kappa(\nu_\mu)$, the system of evolution equations describing the $\nu_e \leftrightarrow \nu_\mu$ oscillations in matter reads [26]:

$$i \frac{d}{dt} \begin{pmatrix} A_e(t, t_0) \\ A_\mu(t, t_0) \end{pmatrix} = \begin{pmatrix} -\epsilon(t) & \epsilon' \\ \epsilon' & \epsilon(t) \end{pmatrix} \begin{pmatrix} A_e(t, t_0) \\ A_\mu(t, t_0) \end{pmatrix} \tag{14.56}$$

where $A_e(t, t_0)$ ($A_\mu(t, t_0)$) is the amplitude of the probability to find ν_e (ν_μ) at time t of the evolution of the system if at time $t_0 \leq t$ the neutrino ν_e or ν_μ has been produced and

$$\epsilon(t) = \frac{1}{2} \left[\frac{\Delta m^2}{2E} \cos 2\theta - \sqrt{2} G_F N_e(t) \right], \ \epsilon' = \frac{\Delta m^2}{4E} \sin 2\theta. \tag{14.57}$$

The term $\sqrt{2} G_F N_e(t)$ in $\epsilon(t)$ accounts for the effects of matter on neutrino oscillations. The system of evolution equations describing the oscillations of antineutrinos $\bar{\nu}_e \leftrightarrow \bar{\nu}_\mu$ in matter has exactly the same form except for the matter term in $\epsilon(t)$ which changes sign. The effect of matter in neutrino oscillations under discussion is usually called the Mikheyev, Smirnov, Wolfenstein (or MSW) effect.

Consider first the case of $\nu_e \leftrightarrow \nu_\mu$ oscillations in matter with constant density: $N_e(t) = N_e = const.$ Due to the interaction term H_{int} in H_m, the eigenstates of the Hamiltonian of the neutrino system in vacuum, $|\nu_{1,2}\rangle$ are not eigenstates of H_m. For the eigenstates $|\nu^m_{1,2}\rangle$ of H_m, which diagonalize the evolution matrix in the r.h.s. of the system Eq. (14.56) we have:

$$|\nu_e\rangle = |\nu^m_1\rangle \cos\theta_m + |\nu^m_2\rangle \sin\theta_m \, , \ |\nu_\mu\rangle = -|\nu^m_1\rangle \sin\theta_m \ + |\nu^m_2\rangle \cos\theta_m \ . \tag{14.58}$$

Here θ_m is the neutrino mixing angle in matter [26],

$$\sin 2\theta_m = \frac{\tan 2\theta}{\sqrt{(1 - \frac{N_e}{N^{res}_e})^2 + \tan^2 2\theta}}, \ \cos 2\theta_m = \frac{1 - N_e/N^{res}_e}{\sqrt{(1 - \frac{N_e}{N^{res}_e})^2 + \tan^2 2\theta}}, \tag{14.59}$$

where the quantity

$$N^{res}_e = \frac{\Delta m^2 \cos 2\theta}{2E\sqrt{2} G_F} \cong 6.56 \times 10^6 \ \frac{\Delta m^2[\mathrm{eV}^2]}{E[\mathrm{MeV}]} \cos 2\theta \, \mathrm{cm}^{-3} \ \mathrm{N_A} \, , \tag{14.60}$$

is called (for $\Delta m^2 \cos 2\theta > 0$) "resonance density" [27,181], $\mathrm{N_A}$ being Avogadro's number. The "adiabatic" states $|\nu^m_{1,2}\rangle$ have energies $E^m_{1,2}$ whose difference is given by

$$E^m_2 - E^m_1 = \frac{\Delta m^2}{2E} \ \left((1 - \frac{N_e}{N^{res}_e})^2 \cos^2 2\theta + \sin^2 2\theta \right)^{\frac{1}{2}} \equiv \frac{\Delta M^2}{2E} \, . \tag{14.61}$$

The probability of $\nu_{\mu(e)} \to \nu_{e(\mu)}$ transition in matter with $N_e = const.$ has the form [26,181]

$$P^{2\nu}_m(\nu_{\mu(e)} \to \nu_{e(\mu)}) = |A_{e(\mu)}(t)|^2 = \frac{1}{2} \sin^2 2\theta_m \ [1 - \cos 2\pi \frac{L}{L_m} \ ]$$
$$L_m = 2\pi/(E^m_2 - E^m_1) \, , \tag{14.62}$$

where L_m is the oscillation length in matter. As Eq. (14.59) indicates, the dependence of $\sin^2 2\theta_m$ on N_e has a resonance character [27]. Indeed, if $\Delta m^2 \cos 2\theta > 0$, for any $\sin^2 2\theta \neq 0$ there exists a value of N_e given by N^{res}_e, such that when $N_e = N^{res}_e$ we have

$\sin^2 2\theta_m = 1$ independently of the value of $\sin^2 2\theta < 1$. This implies that the presence of matter can lead to a strong enhancement of the oscillation probability $P^{2\nu}_m(\nu_{\mu(e)} \to \nu_{e(\mu)})$ even when the $\nu_{\mu(e)} \to \nu_{e(\mu)}$ oscillations in vacuum are suppressed due to a small value of $\sin^2 2\theta$. For obvious reasons

$$N_e = N_e^{res} \equiv \frac{\Delta m^2 \cos 2\theta}{2E\sqrt{2}G_F}\,, \tag{14.63}$$

is called the "resonance condition" [27,181], while the energy at which Eq. (14.63) holds for given N_e and $\Delta m^2 \cos 2\theta$, is referred to as the "resonance energy", E^{res}. The oscillation length at resonance is given by [27] $L^{res}_m = L^v/\sin 2\theta$, while the width in N_e of the resonance at half height reads $\Delta N_e^{res} = 2N_e^{res}\tan 2\theta$. Thus, if the mixing angle in vacuum is small, the resonance is narrow, $\Delta N_e^{res} \ll N_e^{res}$, and $L^{res}_m \gg L^v$. The energy difference $E^m_2 - E^m_1$ has a minimum at the resonance: $(E^m_2 - E^m_1)^{res} = \min\ (E^m_2 - E^m_1) = (\Delta m^2/(2E))\sin 2\theta$.

It is instructive to consider two limiting cases. If $N_e \ll N_e^{res}$, we have from Eq. (14.59) and Eq. (14.61), $\theta_m \cong \theta$, $\mathrm{L_m} \cong \mathrm{L^v}$ and neutrinos oscillate practically as in vacuum. In the limit $N_e \gg N_e^{res}$, $N_e^{res}\tan^2 2\theta$, one finds $\theta_m \cong \pi/2$ ($\cos 2\theta_m \cong -1$) and the presence of matter suppress the $\nu_\mu \leftrightarrow \nu_e$ oscillations. In this case $|\nu_e\rangle \cong |\nu^m_2\rangle$, $|\nu_\mu\rangle = -|\nu^m_1\rangle$, *i.e.*, ν_e practically coincides with the heavier matter-eigenstate, while ν_μ coincides with the lighter one.

Since the neutral current weak interaction of neutrinos in the Standard Model is flavour symmetric, the formulae and results we have obtained are valid for the case of $\nu_e - \nu_\tau$ mixing and $\nu_e \leftrightarrow \nu_\tau$ oscillations in matter as well. The case of $\nu_\mu - \nu_\tau$ mixing, however, is different: to a relatively good precision we have [183] $\kappa(\nu_\mu) \cong \kappa(\nu_\tau)$ and the $\nu_\mu \leftrightarrow \nu_\tau$ oscillations in the matter of the Earth and the Sun proceed practically as in vacuum [184].

The analogs of Eq. (14.59) to Eq. (14.62) for oscillations of antineutrinos, $\bar\nu_\mu \leftrightarrow \bar\nu_e$, in matter can formally be obtained by replacing N_e with $(-N_e)$ in the indicated equations. It should be clear that depending on the sign of $\Delta m^2 \cos 2\theta$, the presence of matter can lead to resonance enhancement either of the $\nu_\mu \leftrightarrow \nu_e$ or of the $\bar\nu_\mu \leftrightarrow \bar\nu_e$ oscillations, but not of both types of oscillations [181]. For $\Delta m^2 \cos 2\theta < 0$, for instance, the matter can only suppress the $\nu_{\mu(e)} \to \nu_{e(\mu)}$ oscillations, while it can enhance the $\bar\nu_{\mu(e)} \to \bar\nu_{e(\mu)}$ transitions. The dependence of the effects of matter in $\nu_\mu \to \nu_e$ and $\bar\nu_\mu \to \bar\nu_e$ oscillations on $\mathrm{sgn}(\Delta m^2 \cos 2\theta)$ is at basis of the plans to determine the sign of $\Delta m^2_{31(32)}$, and thus the type of spectrum neutrino masses obey - with normal or inverted ordering - in long baseline neutrino oscillation experiments (NOνA, DUNE,T2HKK) and in atmospheric neutrino experiments with large volume detectors (PINGU, ORCA, INO, Hyper-Kamiokande, DUNE).

The discussed disparity between the behavior of neutrinos and that of antineutrinos is a consequence of the fact that the matter in the Sun or in the Earth we are interested in is not charge-symmetric (it contains e^-, p and n, but does not contain their antiparticles) and therefore the oscillations in matter are neither CP- nor CPT-invariant [65]. Thus, even in the case of 2-neutrino mixing and oscillations we have, *e.g.*, $P^{2\nu}_m(\nu_\mu \to \nu_e) \neq P^{2\nu}_m(\bar\nu_\mu \to \bar\nu_e)$ and $P^{2\nu}_m(\nu_e \to \nu_{\mu(\tau)}) \neq P^{2\nu}_m(\bar\nu_e \to \bar\nu_{\mu(\tau)})$.

The $\nu_\mu \leftrightarrow \nu_e$ ($\bar\nu_\mu \leftrightarrow \bar\nu_e$) and $\nu_e \leftrightarrow \nu_{\mu(\tau)}$ ($\bar\nu_e \leftrightarrow \bar\nu_{\mu(\tau)}$) oscillations in matter will be invariant with respect to the operation of time reversal if the N_e distribution along the neutrino path is symmetric with respect to this operation [63,185]. The latter condition is fulfilled (to a good approximation) for the N_e distribution along a path of a neutrino crossing the Earth [186].

14.8.1. *Effects of Earth matter on oscillations of neutrinos. Analytic expressions for oscillation probabilities* :

The formalism we have developed can be applied, *e.g.*, to the study of matter effects in the $\nu_e \leftrightarrow \nu_{\mu(\tau)}$ ($\nu_{\mu(\tau)} \leftrightarrow \nu_e$) and $\bar\nu_e \leftrightarrow \bar\nu_{\mu(\tau)}$ ($\bar\nu_{\mu(\tau)} \leftrightarrow \bar\nu_e$) oscillations of neutrinos which traverse the Earth [187]. Indeed, the Earth density distribution in the existing Earth models [186] is assumed to be spherically symmetric and there are two major density structures - the core and the mantle, and a certain number of substructures (shells or layers). The Earth radius is $R_\oplus = 6371$ km; the Earth core has a radius of $R_c = 3486$ km, so the Earth mantle depth is 2885 km. For a spherically symmetric Earth density distribution, the neutrino trajectory in the Earth is specified by the value of the nadir angle θ_n of the trajectory. For $\theta_n \leq 33.17^o$, or path lengths $L \geq 10660$ km, neutrinos cross the Earth core. The path length for neutrinos which cross only the Earth mantle is given by $L = 2R_\oplus \cos\theta_n$. If neutrinos cross the Earth core, the lengths of the paths in the mantle, $2L^{\rm man}$, and in the core, $L^{\rm core}$, are determined by: $L^{\rm man} = R_\oplus\cos\theta_n - (R_c^2 - R_\oplus^2\sin^2\theta_n)^{\frac{1}{2}}$, $L^{\rm core} = 2(R_c^2 - R_\oplus^2\sin^2\theta_n)^{\frac{1}{2}}$. The mean electron number densities in the mantle and in the core according to the PREM model read [186]: $\bar N_e^{man} \cong 2.2$ cm^{-3} $\mathrm{N_A}$, $\bar N_e^c \cong 5.4$ cm^{-3} $\mathrm{N_A}$. Thus, we have $\bar N_e^c \cong 2.5\ \bar N_e^{man}$. The change of N_e from the mantle to the core can well be approximated by a step function [186]. The electron number density N_e changes relatively little around the indicated mean values along the trajectories of neutrinos which cross a substantial part of the Earth mantle, or the mantle and the core, and the two-layer constant density approximation, $N_e^{man} = const. = \bar N_e^{man}$, $N_e^c = const. = \bar N_e^c$, $\bar N_e^{man}$ *and* $\bar N_e^c$ *being the mean densities along the given neutrino path in the Earth*, was shown to be sufficiently accurate in what concerns the calculation of neutrino oscillation probabilities [63,189,190] (and references quoted in [189,190]) in a large number of specific cases. This is related to the fact that the relatively small changes of density along the path of the neutrinos in the mantle (or in the core) take place over path lengths which are typically considerably smaller than the corresponding oscillation length in matter.

In the case of 3-neutrino mixing and for neutrino energies of $E \gtrsim 2$ GeV, the effects due to Δm^2_{21} ($|\Delta m^2_{21}| \ll |\Delta m^2_{31(23)}|$, see Table 14.1) in the neutrino oscillation probabilities are sub-dominant and to leading order can be neglected: the corresponding resonance density $|N^{res}_{e21}| \lesssim 0.25\ cm^{-3}\ N_A \ll \bar N_e^{man,c}$ and the Earth matter strongly suppresses the oscillations due to Δm^2_{21}. For oscillations in vacuum this approximation is valid in the case of NO (IO) neutrino mass spectrum (see Section 2) as long as the leading order contribution due to $\Delta m^2_{31(23)}$ in the relevant probabilities is bigger than approximately 10^{-3}. In this case the 3-neutrino $\nu_e \to \nu_{\mu(\tau)}$ ($\bar\nu_e \to \bar\nu_{\mu(\tau)}$) and $\nu_{\mu(\tau)} \to \nu_e$ ($\bar\nu_{\mu(\tau)} \to \bar\nu_e$) transition probabilities for neutrinos traversing the Earth, reduce effectively to a 2-neutrino transition probability (see, *e.g.*, Refs. [190–192]) , with $\Delta m^2_{31(23)}$ and θ_{13} playing the role of the relevant 2-neutrino vacuum oscillation parameters. We note that in the approximation of negligible Δm^2_{21} we have $\Delta m^2_{31} = \Delta m^2_{32}$. Therefore in what follows in this part of the article we will use, whenever relevant, only Δm^2_{31} in the analytic expressions.

As we have discussed in Sections 14.2 and will be discussed in greater detail in Section 14.12, the value of $\sin^2 2\theta_{13}$ has been determined with a rather high precision in the Daya Bay [44] and RENO [45] experiments. The best fit values found in the two experiments read, respectively, $\sin^2 2\theta_{13} = 0.0841$ [44] and 0.086 [45]. The 3-neutrino oscillation probabilities of the atmospheric and accelerator $\nu_{e,\mu}$ having energy $E \gtrsim 2$ GeV and crossing the Earth along a trajectory characterized by a nadir angle θ_n, for instance, have the following form in the approximation of negligible Δm^2_{21}:

$$P^{3\nu}_m(\nu_e \to \nu_e) \cong 1 - P^{2\nu}_m, \tag{14.64}$$

$$P^{3\nu}_m(\nu_e \to \nu_\mu) \cong P^{3\nu}_m(\nu_\mu \to \nu_e) \cong s^2_{23}\ P^{2\nu}_m,\ \ P^{3\nu}_m(\nu_e \to \nu_\tau) \cong c^2_{23}\ P^{2\nu}_m, \tag{14.65}$$

$$P^{3\nu}_m(\nu_\mu \to \nu_\mu) \cong 1 - s^4_{23}\ P^{2\nu}_m - 2c^2_{23}s^2_{23}\ \left[1 - Re\ (e^{-i\kappa}A^{2\nu}_m(\nu' \to \nu'))\right], \tag{14.66}$$

$$P^{3\nu}_m(\nu_\mu \to \nu_\tau) = 1 - P^{3\nu}_m(\nu_\mu \to \nu_\mu) - P^{3\nu}_m(\nu_\mu \to \nu_e). \tag{14.67}$$

Here $P^{2\nu}_m \equiv P^{2\nu}_m(\Delta m^2_{31}, \theta_{13}; E, \theta_n)$ is the probability of the 2-neutrino $\nu_e \to \nu' \equiv (s_{23}\nu_\mu + c_{23}\nu_\tau)$ oscillations in the Earth, and κ and $A^{2\nu}_m(\nu' \to \nu') \equiv A^{2\nu}_m$ are known phase and 2-neutrino transition probability amplitude (see, *e.g.*, Refs. [190,191]). We note that Eq. (14.64) to Eq. (14.66) are based only on the assumptions that $|N^{res}_{e21}|$ is much smaller than the densities in the Earth mantle and core and that $|\Delta m^2_{21}| \ll |\Delta m^2_{31(23)}|$, and does not rely on the constant density approximation. Similar results are valid for the

corresponding antineutrino oscillation probabilities: one has just to replace $P^{2\nu}_m$, κ and $A^{2\nu}_m$ in the expressions given above with the corresponding quantities for antineutrinos (the latter are obtained from those for neutrinos by changing the sign in front of N_e). Obviously, we have: $P(\nu_{e(\mu)} \to \nu_{\mu(e)}), P(\bar\nu_{e(\mu)} \to \bar\nu_{\mu(e)}) \leq \sin^2\theta_{23}$, and $P(\nu_e \to \nu_\tau), P(\bar\nu_e \to \bar\nu_\tau) \leq \cos^2\theta_{23}$. The one Δm^2 dominance approximation and correspondingly Eq. (14.64) to Eq. (14.67) were used by the Super-Kamiokande Collaboration in their 2006 neutrino oscillation analysis of the multi-GeV atmospheric neutrino data [193].

In the case of neutrinos crossing only the Earth mantle and in the constant density approximation, $P^{2\nu}_m$ is given by the r.h.s. of Eq. (14.62) with θ, Δm^2 and N_e replaced respectively by θ_{13}, Δm^2_{31} and $\bar N^{man}_e$ (or $\tilde N^{man}_e$ corresponding to the given θ_n) in the relevant expressions Eq. (14.59), Eq. (14.60) and Eq. (14.61) for $\sin 2\theta_m$, N^{res}_e and $(E^m_2 - E^m_1)$, while for κ and $A^{2\nu}_m$ we have (see, *e.g.*, Ref. 190):

$$\kappa \cong \frac{1}{2}[\frac{\Delta m^2_{31}}{2E}\ L + \sqrt{2}G_F\bar N^{man}_e L - \frac{\Delta M^2_{31}L}{2E}],$$

$$A^{2\nu}_m = 1 + (e^{-i\frac{\Delta M^2_{31}L}{2E}} - 1)\cos^2\theta^m_{13}\ , \qquad (14.68)$$

where ΔM^2_{31} and θ^m_{13} can be obtained from Eq. (14.61) and Eq. (14.59) by setting $\theta = \theta_{13}$, $\Delta m^2 = \Delta m^2_{31} > 0$, $N^{res}_e = N^{res}_{e31} = \Delta m^2_{31}\cos 2\theta_{13}/(2E\sqrt{2}G_F)$ and $N_e = \bar N^{man}_e(\theta_n)$. Clearly, θ^m_{13} is the mixing angle in the mantle which coincides in vacuum with θ_{13}. In the expressions for $P^{2\nu}_m \equiv P^{2\nu}_m(\Delta m^2_{31}, \theta_{13}; E, \theta_n, \bar N^{man}_e)$, κ and $A^{2\nu}_m$ in the case of oscillations in the mantle, $L = 2R_\oplus\cos\theta_n$ is the distance the neutrino travels in the mantle. The corresponding expressions for antineutrino oscillations, as we have noticed earlier, can be obtained from those derived above by making the change $\bar N^{man}_e \to -\bar N^{man}_e$.

The analytic results for $P^{2\nu}_m(\Delta m^2_{31}, \theta_{13}; E, \theta_n, \bar N^{man}_e)$, κ and $A^{2\nu}_m$, described above and obtained in the constant mantle density approximation, as we have already remarked, provide a relatively precise description of the $\nu_{\mu(e)} \to \nu_{e(\mu)}$, $\nu_e \to \nu_{e(\tau)}$, etc. oscillation probabilities in the Earth mantle if for each given trajectory of the neutrinos in the mantle, specified by the nadir angle θ_n, in the calculations one uses for $\bar N^{man}_e$ the mean value of the electron number density along that specific trajectory: $\bar N^{man}_e = \tilde N^{man}_e(\theta_n)$, where $\tilde N^{man}_e(\theta_n)$ should be calculated using the density distribution given by the existing Earth models [186].

It follows from Eq. (14.64) and Eq. (14.65) that for $\Delta m^2_{31}\cos 2\theta_{13} > 0$, the oscillation effects of interest, *e.g.*, in the $\nu_{e(\mu)} \to \nu_{\mu(e)}$ and $\nu_e \to \nu_\tau$ transitions will be maximal if $P^{2\nu}_m \cong 1$, *i.e.*, if Eq. (14.63) leading to $\sin^2 2\theta_m \cong 1$ is fulfilled, and ii) $\cos(\Delta M^2 L/(2E)) \cong -1$. Given the value of $\bar N^{man}_e$, the first condition determines the neutrino's energy, while the second determines the path length L, for which one can have $P^{2\nu}_m \cong 1$. For $\Delta m^2_{31} \cong 2.5\times 10^{-3}$ eV^2, $\sin^2 2\theta_{13} \cong 0.090$ and $\bar{\rm N}^{\rm man}_{\rm e} \cong 2.2\ {\rm N_A cm^{-3}}$, one finds that $E_{res} \cong 7.1$ GeV and $L \cong 3522/\sin 2\theta_{13}$ km $\cong 11740$ km. Since for neutrinos crossing only the mantle $L \lesssim 10660$ km, the second condition can be satisfied only if $\sin^2 2\theta_{13} \gtrsim 0.11$, which lies outside the 3σ range of the experimentally allowed values of $\sin^2 2\theta_{13}$. We still get a significant amplification of the probability $P^{2\nu}_m$, and therefore of $P(\nu_{e(\mu)} \to \nu_{\mu(e)})$ and $P(\nu_e \to \nu_\tau)$, even when $\cos(\Delta M^2 L/(2E)) = -0.5(-0.2)$: in this case $P^{2\nu}_m \cong 0.75$ (0.60). For $\sin^2 2\theta_{13} \cong 0.090$ we have $\cos(\Delta M^2 L/(2E)) = -0.5(-0.2)$ if $L \cong 7826$ (6622) km. Thus, for $\Delta m^2_{31} > 0$, the Earth matter effects can amplify $P^{2\nu}_m$, and therefore $P(\nu_{e(\mu)} \to \nu_{\mu(e)})$ and $P(\nu_e \to \nu_\tau)$, significantly when the neutrinos cross only the mantle, for $E \sim 7$ GeV and sufficiently large path lengths L.

If $\Delta m^2_{31} < 0$ the same considerations apply for the corresponding antineutrino oscillation probabilities $\bar P^{2\nu}_m = \bar P^{2\nu}_m(\bar\nu_e \to (s_{23}\bar\nu_\mu + c_{23}\bar\nu_\tau))$ and correspondingly for $P(\bar\nu_{e(\mu)} \to \bar\nu_{\mu(e)})$ and $P(\bar\nu_e \to \bar\nu_\tau)$. For $\Delta m^2_{31} > 0$, the $\bar\nu_{e(\mu)} \to \bar\nu_{\mu(e)}$ and $\bar\nu_e \to \bar\nu_\tau$ oscillations are suppressed by the Earth matter, while if $\Delta m^2_{31} < 0$, the same conclusion holds for the $\nu_{e(\mu)} \to \nu_{\mu(e)}$ and $\nu_e \to \nu_\tau$, oscillations. The dependence on $\mathrm{sgn}(\Delta m^2_{31})$ of the effects of Earth matter - enhancement or suppression - on the $\nu_{e(\mu)} \to \nu_{\mu(e)}$ and $\bar\nu_{e(\mu)} \to \bar\nu_{\mu(e)}$ oscillations taking place when the neutrinos traverse the Earth mantle, will be exploited in the current and planned long baseline and atmospheric neutrino oscillation experiments aiming, in particular, to determine the neutrino mass ordering (NOνA, PINGU, ORCA, Hyper-Kamiokande, DUNE, INO).

The discussed features of the Earth matter effects in the $\nu_{\mu(e)} \to \nu_{e(\mu)}$ and $\bar\nu_{\mu(e)} \to \bar\nu_{e(\mu)}$ oscillation probabilities for neutrinos with a path length in the Earth mantle of 7330 km and for $\Delta m^2_{31} > 0$, $\sin^2 2\theta_{13} = 0.10$ and $\sin^2 2\theta_{23} = 1$ are illustrated in Fig. 14.7 (taken from Ref. 194). The amplification of the $\nu_{\mu(e)} \to \nu_{e(\mu)}$ oscillation probability due to the Earth matter effect in the region of the resonance value of $E/\Delta m^2_{31}$ and the suppression of the $\bar\nu_{\mu(e)} \to \bar\nu_{e(\mu)}$ oscillation probability in the same region are clearly seen in the figure.

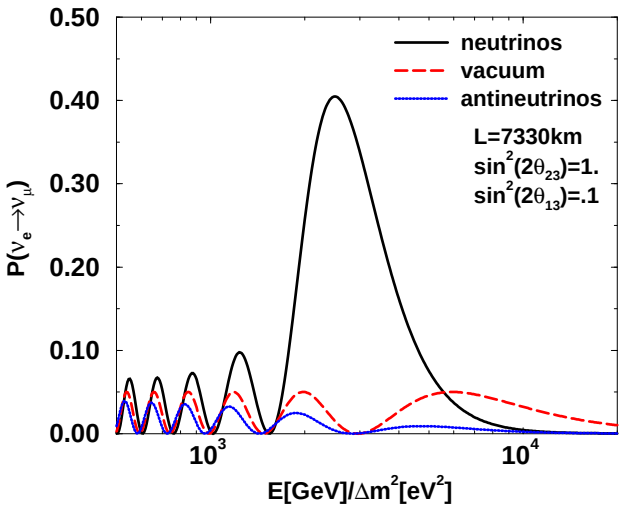

Figure 14.7: The $\nu_{e(\mu)} \to \nu_{\mu(e)}$ and $\bar\nu_{e(\mu)} \to \bar\nu_{\mu(e)}$ oscillation probabilities given in Eq. (14.65), $P(\nu_e \to \nu_\mu) = P(\nu_\mu \to \nu_e)$ (black solid line) and $P(\bar\nu_e \to \bar\nu_\mu) = P(\bar\nu_\mu \to \bar\nu_e)$ (blue solid line), as functions of $E/\Delta m^2$ for $\Delta m^2 \equiv \Delta m^2_{31} > 0$, $\sin^2 2\theta_{13} = 0.10$ and $\sin^2 2\theta_{23} = 1$. The figure is obtained for neutrinos crossing the Earth mantle along a path with length of $L = 7330$ km. The corresponding vacuum oscillation probability $P^{vac}(\nu_{e(\mu)} \to \nu_{\mu(e)}) = P^{vac}(\bar\nu_{e(\mu)} \to \bar\nu_{\mu(e)})$ is also shown (red dashed line). For $\Delta m^2 \equiv \Delta m^2_{31} < 0$, the black and blue solid lines will correspond respectively to the probabilities $P(\bar\nu_{e(\mu)} \to \bar\nu_{\mu(e)})$ and $P(\nu_{e(\mu)} \to \nu_{\mu(e)})$ (from Ref. 194).

In the case of neutrinos crossing the Earth core, new resonance-like effects become possible in the $\nu_\mu \to \nu_e$ and $\nu_e \to \nu_{\mu(\tau)}$ (or $\bar\nu_\mu \to \bar\nu_e$ and $\bar\nu_e \to \bar\nu_{\mu(\tau)}$) transitions [189–191,195–197]. For $\Delta m^2_{31} > 0$ and certain values of $\sin^2\theta_{13} \lesssim 0.05$ we can have [196] $P^{2\nu}_m(\Delta m^2_{31}, \theta_{13}) \cong 1$, and correspondingly maximal $P^{3\nu}_m(\nu_e \to \nu_\mu) = P^{3\nu}_m(\nu_\mu \to \nu_e) \cong s^2_{23}$, only due to the effect of maximal constructive interference between the amplitudes of the $\nu_e \to \nu'$ transitions in the Earth mantle and in the Earth core. The effect differs from the MSW one and the enhancement happens in the case of interest at a value of the energy between the MSW resonance energies corresponding to the density in the mantle and that of the core, or at a value of the resonance density N^{res}_e which lies between the values of N_e in the mantle and in the core [189]. In Refs. [189,190] the enhancement was called "neutrino oscillation length resonance (NOLR)", while in Refs. [191,195] the term "parametric resonance" for the same effect was used [198]. The *mantle-core enhancement effect (or NOLR)* is caused by the existence (for a given neutrino trajectory through the Earth core) of points of resonance-like maximal neutrino conversion, $P^{2\nu}_m(\Delta m^2_{31}, \theta_{13}) = 1$, in the corresponding space of neutrino oscillation parameters [196]. For $\Delta m^2_{31} < 0$ the mantle-core enhancement can take place for the antineutrino transitions, $\bar\nu_\mu \to \bar\nu_e$ and $\bar\nu_e \to \bar\nu_{\mu(\tau)}$. For neutrinos crossing the Earth core, analytic expressions for $P^{2\nu}_m(\Delta m^2_{31}, \theta_{13})$ and κ, $A^{2\nu}_m$ were derived in the two-layer constant density approximation for the Earth density distribution in [189] and [190], respectively.

A rather complete set of values of $\Delta m^2_{31}/E > 0$ and $\sin^2 2\theta_{13}$ for which $P^{2\nu}_m(\Delta m^2_{31}, \theta_{13}) = 1$ was found in Ref. 196. In the two-layer

constant density approximation, the values of $\Delta m^2_{31}/E > 0$ and $\sin^2 2\theta_{13}$ at which $P^{2\nu}_m(\Delta m^2_{31}, \theta_{13}) = 1$ can be derived as solutions of the following system of equations [196]:

$$\tan\phi^{\rm man} = \pm\sqrt{\frac{-\cos 2\theta^{core}_{13}}{\cos(2\theta^{core}_{13} - 4\theta^{man}_{13})}}\,, \tag{14.69}$$

$$\tan\phi^{\rm core} = \pm\frac{\cos 2\theta^{man}_{13}}{\sqrt{-\cos(2\theta^{core}_{13})\cos(2\theta^{core}_{13} - 4\theta^{man}_{13})}}\,, \tag{14.70}$$

where the signs in the two equations are correlated, $2\phi^{\rm man} = (E^m_3 - E^m_1)^{man} L^{man}$, $2\phi^{\rm core} = (E^m_3 - E^m_1)^{core} L^{core}$, $2L^{man}$ and L^{core} are the neutrino path lengths in the Earth mantle and the core, and θ^{man}_{13} and θ^{core}_{13} are the values of the angle θ_{13} in the mantle and in the core. The expressions for $(E^m_3 - E^m_1)^{man}$ ($(E^m_3 - E^m_1)^{core}$) and θ^{man}_{13} (θ^{core}_{13}) can be obtained respectively from Eq. (14.61) and Eq. (14.59) by setting $\theta = \theta_{13}$, $\Delta m^2 = \Delta m^2_{31}$, $N^{res}_e = N^{res}_{e31} = \Delta m^2_{31}\cos 2\theta_{13}/(2E\sqrt{2}G_F)$ and $N_e = \tilde{N}^{man}_e(\theta_n)$ ($N_e = \tilde{N}^{core}_e(\theta_n)$).

The location of the points where $P^{2\nu}_m(\Delta m^2_{31}, \theta_{13}) = 1$ in the $\Delta m^2_{31}/E - \sin^2 2\theta_{13}$ plane determines the regions in the plane where $P^{2\nu}_m(\Delta m^2_{31}, \theta_{13})$ is large, $P^{2\nu}_m(\Delta m^2_{31}, \theta_{13}) \gtrsim 0.5$. These regions vary slowly with the nadir angle, being remarkably wide in the nadir angle and rather wide in the neutrino energy [196], so that the transitions of interest can produce noticeable effects in the measured observables. For $\sin^2\theta_{13} \lesssim 0.05$, there are two sets of values of $(\Delta m^2_{31}/E, \sin^2\theta_{13})$ for which $P^{2\nu}_m(\Delta m^2_{31}, \theta_{13}) = 1$, and thus two regions in $\Delta m^2_{31}/E - \sin^2 2\theta_{13}$ plane where $P^{2\nu}_m(\Delta m^2_{31}, \theta_{13}) \gtrsim 0.5$. For $\Delta m^2_{31} = 2.5\times 10^{-3}$ eV^2 and nadir angle, *e.g.*, θ_n=0 (Earth center crossing neutrinos), we have $P^{2\nu}_m(\Delta m^2_{31}, \theta_{13}) = 1$ at $(E, \sin^2 2\theta_{13})$ =(3.4 GeV,0.034) and (5.2 GeV,0.15). At the same time for E =3.4 GeV (5.2 Gev), the probability $P^{2\nu}_m(\Delta m^2_{31}, \theta_{13}) \gtrsim 0.5$ for the values of $\sin^2 2\theta_{13}$ from the interval $0.02 \lesssim \sin^2 2\theta_{13} \lesssim 0.10$ ($0.04 \lesssim \sin^2 2\theta_{13} \lesssim 0.26$). Similar results hold for neutrinos crossing the Earth core along the trajectories with $\theta_n \neq 0$ (for further details see the last article in Ref. 196; see also the last article in Ref. 197).

The mantle-core enhancement of $P^{2\nu}_m$ (or $\bar{P}^{2\nu}_m$) is relevant, in particular, for the searches of sub-dominant $\nu_{e(\mu)} \to \nu_{\mu(e)}$ (or $\bar{\nu}_{e(\mu)} \to \bar{\nu}_{\mu(e)}$) oscillations of atmospheric neutrinos having energies $E \gtrsim 2$ GeV and crossing the Earth core on the way to the detector (see Ref. 189 to Ref. 197 and the references quoted therein).

The effects of Earth matter on the oscillations of atmospheric and accelerator neutrinos have not been observed so far. At present there are no compelling evidences for oscillations of the atmospheric ν_e and/or $\bar{\nu}_e$.

In the case of oscillations of atmospheric neutrinos in the Earth one has to take into account also the following considerations. The fluxes of atmospheric $\nu_{e,\mu}$ of energy E, which reach the detector after crossing the Earth along a given trajectory specified by the value of θ_n, $\Phi_{\nu_{e,\mu}}(E, \theta_n)$, are given by the following expressions in the case of the 3-neutrino oscillations under discussion [190,191]:

$$\Phi_{\nu_e}(E, \theta_n) \cong \Phi^0_{\nu_e}\left(1 + [s^2_{23} r - 1]\ P^{2\nu}_m\right), \tag{14.71}$$

$$\Phi_{\nu_\mu}(E, \theta_n) \cong \Phi^0_{\nu_\mu}\left(1 + s^4_{23}[(s^2_{23}\ r)^{-1} - 1]P^{2\nu}_m - 2c^2_{23}s^2_{23}\left[1 - Re\ (e^{-i\kappa}A^{2\nu}_m(\nu_\tau \to \nu_\tau))\right]\right), \tag{14.72}$$

where $\Phi^0_{\nu_{e(\mu)}} = \Phi^0_{\nu_{e(\mu)}}(E, \theta_n)$ is the $\nu_{e(\mu)}$ flux in the absence of neutrino oscillations and

$$r \equiv r(E, \theta_n) \equiv \frac{\Phi^0_{\nu_\mu}(E, \theta_n)}{\Phi^0_{\nu_e}(E, \theta_n)}\quad . \tag{14.73}$$

It follows from the global analyses of the neutrino oscillation data that the neutrino mixing parameter s^2_{23} lies (at 3σ CL) in the interval (0.38 - 0.64). For NO (IO) neutrino mass spectrum, the two groups which performed the most recent global analyses, obtained the following best values of s^2_{23}: 0.425 (0.589) [58] and 0.441 (0.587) [59]. For the predicted ratio $r(E, \theta_n)$ of the atmospheric ν_μ and ν_e fluxes for i) the Earth core crossing and ii) only mantle crossing neutrinos, having trajectories for which $0.3 \lesssim \cos\theta_n \leq 1.0$, one has [199] $r(E, \theta_n) \cong (2.6 \div 4.5)$ for neutrinos giving the main contribution to the multi-GeV samples, $E \cong (2 \div 10)$ GeV. Thus, for $s^2_{23} = 0.5$ (0.64) one finds for the multi-GeV neutrinos: $s^4_{23}[1 - (s^2_{23}\ r(E, \theta_z))^{-1}] \cong 0.06 - 0.14$ ($0.16 - 0.27$) and $(s^2_{23}\ r(E, \theta_z) - 1) \cong 0.3 - 1.3$ ($0.66 - 1.9$). Thus, the impact of the possible enhancement of $P^{2\nu}_m \cong 1$ would be largest for the flux of multi-GeV ν_e, $\Phi_{\nu_e}(E, \theta_n)$, traversing the Earth. As the preceding discussion suggests and detailed calculations show (see the first two articles quoted in Ref. 197), the sensitivity of the atmospheric neutrino experiments to the neutrino mass ordering depends strongly on the chosen value of $\sin^2\theta_{23}$ from its 3σ allowed range: it is maximal (minimal) for the maximal (minimal) allowed value of $\sin^2\theta_{23}$.

For water Cerenkov detectors, the charged current (CC) $\nu_l - N$ interaction cross section for multi-GeV neutrinos is approximately by a factor of 2 bigger than the $\bar{\nu}_l - N$ CC interaction cross section. Since these detectors do not distinguish between the neutrino and anti-neutrino induced CC events, determining that the neutrino mass spectrum is with inverted ordering would require roughly by a factor of 2 longer period of data acquisition than if the spectrum were with normal ordering.

The effects under discussion are larger, in general, for the multi-GeV neutrinos than for the sub-GeV neutrinos having energies $E \cong (0.1 - 1.0)$ GeV. Indeed, for the sub-GeV ν_e flux one finds in the limit of negligible θ_{13} [201]: $\Phi_{\nu_e}(E, \theta_n) \cong \Phi^0_{\nu_e}(1 + [c^2_{23}r - 1]\bar{P}^{2\nu}_m)$, where $\bar{P}^{2\nu}_m \equiv \bar{P}^{2\nu}_m(\Delta m^2_{21}, \theta_{12}; E, \theta_n)$ is the probability of the 2-neutrino oscillations in the Earth due to Δm^2_{21} and 2-neutrino mixing with angle θ_{12}. For the neutrinos giving contribution to the sub-GeV samples of Super-Kamiokande events one has [199] $r(E, \theta_z) \cong 2.0$. If $s^2_{23} = 0.5$ and $r(E, \theta_z) \cong 2.0$, we get $(c^2_{23}\ r(E, \theta_z) - 1) \cong 0$, and the possible effects of the $\nu_\mu \to \nu_e$ and $\nu_e \to \nu_{\mu(\tau)}$ transitions on the ν_e flux, and correspondingly in the sub-GeV $e-$like samples of events, would be rather strongly suppressed independently of the values of the corresponding transition probabilities.

The same conclusions are valid for the effects of oscillations on the fluxes of, and event rates due to, atmospheric antineutrinos $\bar{\nu}_e$ and $\bar{\nu}_\mu$. The formulae for anti-neutrino fluxes and oscillation probabilities are analogous to those for neutrinos (see, *e.g.*, Refs. [190,191,197,201]) .

The expression for the probability of the $\nu_\mu \to \nu_e$ oscillations taking place in the Earth mantle in the case of 3-neutrino mixing, in which both neutrino mass squared differences Δm^2_{21} and Δm^2_{31} contribute and the CP violation effects due to the Dirac phase in the neutrino mixing matrix are taken into account, has the following form in the constant density approximation and keeping terms up to second order in the two small parameters $|\alpha| \equiv |\Delta m^2_{21}|/|\Delta m^2_{31}| \ll 1$ and $\sin^2\theta_{13} \ll 1$ [202]:

$$P^{3\nu\ man}_m(\nu_\mu \to \nu_e) \cong P_0 + P_{\sin\delta} + P_{\cos\delta} + P_3\,. \tag{14.74}$$

Here

$$P_0 = \sin^2\theta_{23}\ \frac{\sin^2 2\theta_{13}}{(A-1)^2}\ \sin^2[(A-1)\Delta]$$

$$P_3 = \alpha^2\ \cos^2\theta_{23}\,\frac{\sin^2 2\theta_{12}}{A^2}\ \sin^2(A\Delta)\,, \tag{14.75}$$

$$P_{\sin\delta} = -\,\alpha\ \frac{8\,J_{CP}}{A(1-A)}\,(\sin\Delta)\,(\sin A\Delta)\ (\sin[(1-A)\Delta])\ , \tag{14.76}$$

$$P_{\cos\delta} = \alpha\ \frac{8\,J_{CP}\,\cot\delta}{A(1-A)}\,(\cos\Delta)\,(\sin A\Delta)\ (\sin[(1-A)\Delta])\ , \tag{14.77}$$

where

$$\alpha = \frac{\Delta m^2_{21}}{\Delta m^2_{31}}\,,\ \ \Delta = \frac{\Delta m^2_{31}\,L}{4E}\,,\ \ A = \sqrt{2}G_{\rm F}N^{man}_e\frac{2E}{\Delta m^2_{31}}\,, \tag{14.78}$$

$\cot\delta = J_{CP}^{-1}\mathrm{Re}(U_{\mu 3}U_{e3}^{*}U_{e2}U_{\mu 2}^{*}) \propto \cos\delta$, and we recall that $J_{CP} = \mathrm{Im}(U_{\mu 3}U_{e3}^{*}U_{e2}U_{\mu 2}^{*})$. The analytic expression for $P_m^{3\nu\ man}(\nu_\mu \to \nu_e)$ given above is valid for [202] neutrino path lengths in the mantle ($L \leq 10660$ km) satisfying $L \lesssim 10560\ \mathrm{km}\ E[\mathrm{GeV}]\,(7.6 \times 10^{-5}\ \mathrm{eV}^2/\Delta m^2_{21})$, and energies $E \gtrsim 0.34$ GeV $(\Delta m^2_{21}/7.6\times10^{-5}\ \mathrm{eV}^2) \times(1.4\ \mathrm{cm}^{-3}N_A/N_e^{man})$. The expression for the $\bar\nu_\mu \to \bar\nu_e$ oscillation probability can be obtained formally from that for $P_m^{3\nu\ man}(\nu_\mu \to \nu_e)$ by making the changes $A \to -A$ and $J_{CP} \to -J_{CP}$, with $J_{CP}\cot\delta \equiv \mathrm{Re}(U_{\mu 3}U_{e3}^{*}U_{e2}U_{\mu 2}^{*})$ remaining unchanged. The term $P_{\sin\delta}$ in $P_m^{3\nu\ man}(\nu_\mu \to \nu_e)$ would be equal to zero if the Dirac phase in the neutrino mixing matrix U possesses a CP-conserving value. Even in this case, however, we have $A_{CP}^{(e\mu)\ man} \equiv (P_m^{3\nu\ man}(\nu_\mu \to \nu_e) - P_m^{3\nu\ man}(\bar\nu_\mu \to \bar\nu_e)) \neq 0$ due to the effects of the Earth matter. It will be important to experimentally disentangle the effects of the Earth matter and of J_{CP} in $A_{CP}^{(e\mu)\ man}$: this will allow to get information about the Dirac CP violation phase in U. This can be done, in principle, by studying the energy dependence of $P_m^{3\nu\ man}(\nu_\mu \to \nu_e)$ and $P_m^{3\nu\ man}(\bar\nu_\mu \to \bar\nu_e)$. Since the sign of $\Delta m^2_{31(32)}$ determines for given L whether the probability $P_m^{3\nu\ man}(\nu_\mu \to \nu_e)$ or $P_m^{3\nu\ man}(\bar\nu_\mu \to \bar\nu_e)$, as a function of energy, can be resonantly enhanced or suppressed by the matter effects, the study of the energy dependence of $P_m^{3\nu\ man}(\nu_\mu \to \nu_e)$ and/or of $P_m^{3\nu\ man}(\bar\nu_\mu \to \bar\nu_e)$ can provide also information on $\mathrm{sgn}(\Delta m^2_{31(32)})$. In the vacuum limit of $N_e^{man} = 0$ ($A = 0$) we have $A_{CP}^{(e\mu)\ man} = A_{CP}^{(e\mu)}$ (see Eq. (14.42)) and only the term $P_{\sin\delta}$ contributes to the asymmetry $A_{CP}^{(e\mu)}$.

The preceding remarks apply also to the probabilities $P_m^{3\nu\ man}(\nu_e \to \nu_\mu)$ and $P_m^{3\nu\ man}(\bar\nu_e \to \bar\nu_\mu)$). The probability $P_m^{3\nu\ man}(\nu_e \to \nu_\mu)$, for example, can formally be obtained from the expression for the probability $P_m^{3\nu\ man}(\nu_\mu \to \nu_e)$ by changing the sign of the term $P_{\sin\delta}$.

The expression for the probability $P_m^{3\nu\ man}(\nu_\mu \to \nu_e)$ given in Eq. (14.74) and the corresponding expression for $P_m^{3\nu\ man}(\bar\nu_\mu \to \bar\nu_e)$ can be used for the interpretation of the data of the past, current, and future planned long baseline oscillation experiments MINOS/MINOS+, T2K, NOνA, DUNE [93] and T2HK [94].

14.8.2. *Oscillations (flavour conversion) of solar neutrinos* :

14.8.2.1. *Qualitative analysis:*

Consider next the oscillations of solar ν_e while they propagate from the central part of the Sun, where they are produced, to the surface of the Sun [27,188] (see also Ref. 26 and, *e.g.*, Ref. 203) Details concerning the production, spectrum, magnitude and particularities of the solar neutrino flux were discussed in Section 14.6, while the methods of detection of solar neutrinos, description of solar neutrino experiments and of the data they provided will be discussed in the next section (see also Ref. 204). The electron number density N_e changes considerably along the neutrino path in the Sun: it decreases monotonically from the value of $\sim 100\ \mathrm{cm}^{-3}\ N_A$ in the center of the Sun to 0 at the surface of the Sun. According to the contemporary solar models (see, *e.g.*, Ref. 204) N_e decreases approximately exponentially in the radial direction towards the surface of the Sun:

$$N_e(t) = N_e(t_0)\exp\left\{-\frac{t-t_0}{r_0}\right\}\ , \tag{14.79}$$

where $(t - t_0) \cong d$ is the distance traveled by the neutrino in the Sun, $N_e(t_0)$ is the electron number density at the point of ν_e production in the Sun, r_0 is the scale-height of the change of $N_e(t)$ and one has [204] $r_0 \sim 0.1R_\odot$

Consider the case of 2-neutrino mixing, Eq. (14.58). Obviously, if N_e changes with t (or equivalently with the distance) along the neutrino trajectory, the matter-eigenstates, their energies, the mixing angle and the oscillation length in matter, become, through their dependence on N_e, also functions of t: $|\nu^m_{1,2}\rangle = |\nu^m_{1,2}(t)\rangle$, $E^m_{1,2} = E^m_{1,2}(t)$, $\theta_m = \theta_m(t)$ and $L_m = L_m(t)$. It is not difficult to understand qualitatively the possible behavior of the neutrino system when solar neutrinos propagate from the center to the surface of the Sun if one realizes that one is dealing effectively with a two-level system whose Hamiltonian depends on time and admits "jumps" from one level to the other [205](see Eq. (14.56)). Consider the case of $\Delta m^2\cos 2\theta > 0$. Let us assume first for simplicity that the electron number density at the point of a solar ν_e production in the Sun is much bigger than the resonance density, $N_e(t_0) \gg N_e^{res}$. Actually, this is one of the cases relevant to the solar neutrinos. In this case we have $\theta_m(t_0) \cong \pi/2$ and the state of the electron neutrino in the initial moment of the evolution of the system practically coincides with the heavier of the two matter-eigenstates:

$$|\nu_e\rangle \ \cong\ |\nu^m_2(t_0)\rangle\,. \tag{14.80}$$

Thus, at t_0 the neutrino system is in a state corresponding to the "level" with energy $E^m_2(t_0)$. When neutrinos propagate to the surface of the Sun they cross a layer of matter in which $N_e = N_e^{res}$: in this layer the difference between the energies of the two "levels" $(E^m_2(t) - E^m_1(t))$ has a minimal value on the neutrino trajectory (Eq. (14.61) and Eq. (14.63)). Correspondingly, the evolution of the neutrino system can proceed basically in two ways. First, the system can stay on the "level" with energy $E^m_2(t)$, *i.e.*, can continue to be in the state $|\nu^m_2(t)\rangle$ up to the final moment t_s, when the neutrino reaches the surface of the Sun. At the surface of the Sun $N_e(t_s) = 0$ and therefore $\theta_m(t_s) = \theta$, $|\nu^m_{1,2}(t_s)\rangle \equiv |\nu_{1,2}\rangle$ and $E^m_{1,2}(t_s) = E_{1,2}$. Thus, in this case the state describing the neutrino system at t_0 will evolve continuously into the state $|\nu_2\rangle$ at the surface of the Sun. Using Eq. (14.53) with $l = e$ and $x = \mu$, it is easy to obtain the probabilities to find ν_e and ν_μ at the surface of the Sun:

$$\begin{aligned} P(\nu_e \to \nu_e; t_s, t_0) &\cong |\langle\nu_e|\nu_2\rangle|^2 = \sin^2\theta \\ P(\nu_e \to \nu_\mu; t_s, t_0) &\cong |\langle\nu_\mu|\nu_2\rangle|^2 = \cos^2\theta\,. \end{aligned} \tag{14.81}$$

It is clear that under the assumption made and if $\sin^2\theta \ll 1$, practically a total $\nu_e \to \nu_\mu$ conversion is possible. This type of evolution of the neutrino system and the $\nu_e \to \nu_\mu$ transitions taking place during the evolution, are called [27] "adiabatic." They are characterized by the fact that the probability of the "jump" from the upper "level" (having energy $E^m_2(t)$) to the lower "level" (with energy $E^m_1(t)$), P', or equivalently the probability of the $\nu^m_2(t_0) \to \nu^m_1(t_s)$ transition, $P' \equiv P'(\nu^m_2(t_0) \to \nu^m_1(t_s))$, on the whole neutrino trajectory is negligible:

$$P' \equiv P'(\nu^m_2(t_0) \to \nu^m_1(t_s)) \cong 0\ :\ \textit{adiabatic transitions}\,. \tag{14.82}$$

The second possibility is realized if in the resonance region, where the two "levels" approach each other most, the system "jumps" from the upper "level" to the lower "level" and after that continues to be in the state $|\nu^m_1(t)\rangle$ until the neutrino reaches the surface of the Sun. Evidently, now we have $P' \equiv P'(\nu^m_2(t_0) \to \nu^m_1(t_s)) \sim 1$. In this case the neutrino system ends up in the state $|\nu^m_1(t_s)\rangle \equiv |\nu_1\rangle$ at the surface of the Sun and

$$\begin{aligned} P(\nu_e \to \nu_e; t_s, t_0) &\cong |\langle\nu_e|\nu_1\rangle|^2 = \cos^2\theta \\ P(\nu_e \to \nu_\mu; t_s, t_0) &\cong |\langle\nu_\mu|\nu_1\rangle|^2 = \sin^2\theta\,. \end{aligned} \tag{14.83}$$

Obviously, if $\sin^2\theta \ll 1$, practically no transitions of the solar ν_e into ν_μ will occur. The considered regime of evolution of the neutrino system and the corresponding $\nu_e \to \nu_\mu$ transitions are usually referred to as "extremely nonadiabatic."

Clearly, the value of the "jump" probability P' plays a crucial role in the the $\nu_e \to \nu_\mu$ transitions: it fixes the type of the transition and determines to a large extent the $\nu_e \to \nu_\mu$ transition probability [188,206,207]. We have considered above two limiting cases. Obviously, there exists a whole spectrum of possibilities since P' can have any value from 0 to $\cos^2\theta$ [208,209]. In general, the transitions are called "nonadiabatic" if P' is non-negligible.

Numerical studies have shown [27] that solar neutrinos can undergo both adiabatic and nonadiabatic $\nu_e \to \nu_\mu$ transitions in the Sun and the matter effects can be substantial in the solar neutrino oscillations for $10^{-8}\ \mathrm{eV}^2 \lesssim \Delta m^2 \lesssim 10^{-4}\ \mathrm{eV}^2$, $10^{-4} \lesssim \sin^2 2\theta < 1.0$.

The condition of adiabaticity of the solar ν_e transitions in Sun can be written as [188,206]

$$\gamma(t) \equiv \sqrt{2}G_F\frac{(N_e^{res})^2}{|\dot N_e(t)|}\tan^2 2\theta\left(1+\tan^{-2}2\theta_m(t)\right)^{\frac{3}{2}} \ \gg 1$$
$$\text{adiabatic transitions}\,, \tag{14.84}$$

while if $\gamma(t) \lesssim 1$ the transitions are nonadiabatic (see also Ref. 209), where $\dot{N}_e(t) \equiv \frac{d}{dt} N_e(t)$. Condition in Eq. (14.84) implies that the $\nu_e \to \nu_{\mu(\tau)}$ transitions in the Sun will be adiabatic if $N_e(t)$ changes sufficiently slowly along the neutrino path. In order for the transitions to be adiabatic, condition in Eq. (14.84) has to be fulfilled at any point of the neutrino's path in the Sun.

14.8.2.2. *The solar ν_e survival probability:*

The system of evolution equations Eq. (14.56) can be solved exactly for N_e changing exponentially, Eq. (14.79), along the neutrino path in the Sun [208,210]. More specifically, the system in Eq. (14.56) is equivalent to one second order differential equation (with appropriate initial conditions). The latter can be shown [211] to coincide in form, in the case of N_e given by Eq. (14.79), with the Schroedinger equation for the radial part of the nonrelativistic wave function of the Hydrogen atom [212]. On the basis of the exact solution, which is expressed in terms of confluent hypergeometric functions, it was possible to derive a complete, simple and very accurate analytic description of the matter-enhanced transitions of solar neutrinos in the Sun for any values of Δm^2 and θ [26,208,209,213,214] (see also Refs. [27,188,207,215,216]) .

The probability that a ν_e, produced at time t_0 in the central part of the Sun, will not transform into $\nu_{\mu(\tau)}$ on its way to the surface of the Sun (reached at time t_s) is given by

$$P^{2\nu}_{\odot}(\nu_e \to \nu_e; t_s, t_0) = \bar{P}^{2\nu}_{\odot}(\nu_e \to \nu_e; t_s, t_0) + \ \textit{Oscillating terms}. \tag{14.85}$$

Here

$$\bar{P}^{2\nu}_{\odot}(\nu_e \to \nu_e; t_s, t_0) \equiv \bar{P}_{\odot} = \frac{1}{2} + \left(\frac{1}{2} - \mathrm{P}'\right) \cos 2\theta_m(t_0) \cos 2\theta \ , \tag{14.86}$$

is the average survival probability for ν_e having energy $\mathrm{E} \cong \mathrm{p}$ [207], where

$$P' = \frac{\exp\left[-2\pi \mathrm{r}_0 \frac{\Delta m^2}{2E} \sin^2\theta\right] - \exp\left[-2\pi \mathrm{r}_0 \frac{\Delta m^2}{2E}\right]}{1 - \exp\left[-2\pi \mathrm{r}_0 \frac{\Delta m^2}{2E}\right]}, \tag{14.87}$$

is [208] the "jump" probability for exponentially varying N_e, and $\theta_m(t_0)$ is the mixing angle in matter at the point of ν_e production [215]. The expression for $\bar{P}^{2\nu}_{\odot}(\nu_e \to \nu_e; t_s, t_0)$ with P' given by Eq. (14.87) is valid for $\Delta m^2 > 0$, but for both signs of $\cos 2\theta \neq 0$ [208](see also Ref. [216]) ; it is valid for any given value of the distance along the neutrino trajectory and does not take into account the finite dimensions of the region of ν_e production in the Sun. This can be done by integrating over the different neutrino paths, *i.e.*, over the region of ν_e production.

The oscillating terms in the probability $P^{2\nu}_{\odot}(\nu_e \to \nu_e; t_s, t_0)$ [213,211] were shown [214] to be strongly suppressed for $\Delta m^2 \gtrsim 10^{-7}$ eV^2 by the various averagings one has to perform when analyzing the solar neutrino data. The current solar neutrino and KamLAND data suggest that $\Delta m^2 \cong 7.4 \times 10^{-5} \mathrm{eV}^2$. For $\Delta m^2 \gtrsim 10^{-7}$ eV^2, the averaging over the region of neutrino production in the Sun *etc.* renders negligible all interference terms which appear in the probability of ν_e survival due to the $\nu_e \leftrightarrow \nu_{\mu(\tau)}$ oscillations in vacuum taking place on the way of the neutrinos from the surface of the Sun to the surface of the Earth. Thus, the probability that ν_e will remain ν_e while it travels from the central part of the Sun to the surface of the Earth is effectively equal to the probability of survival of the ν_e while it propagates from the central part to the surface of the Sun and is given by the average probability $\bar{P}_{\odot}(\nu_e \to \nu_e; t_s, t_0)$ (determined by Eq. (14.86) and Eq. (14.87)). For this reason the solar ν_e transition into $\nu_{\mu(\tau)}$ is sometimes referred to as "solar neutrino flavour conversion".

If the solar ν_e transitions are adiabatic ($P' \cong 0$) and $\cos 2\theta_m(t_0) \cong -1$ (*i.e.*, $N_e(t_0)/|N^{res}_e| \gg 1, |\tan 2\theta|$, the ν_e are born "above" (in N_e) the resonance region), one has [27]

$$\bar{P}^{2\nu}(\nu_e \to \nu_e; t_s, t_0) \cong \frac{1}{2} - \frac{1}{2} \cos 2\theta. \tag{14.88}$$

The regime under discussion is realized for $\sin^2 2\theta \cong 0.84$ (suggested by the data, Sections 14.2 and 14.9.1), if $E/\Delta m^2$ lies approximately in the range $(2 \times 10^4 - 3 \times 10^7)$ MeV/eV^2 (see Ref. 209). This result is relevant for the interpretation of the Super-Kamiokande and SNO solar neutrino data. We see that depending on the sign of $\cos 2\theta \neq 0$, $\bar{P}^{2\nu}(\nu_e \to \nu_e)$ is either bigger or smaller than 1/2. It follows from the solar neutrino data that in the range of validity (in $E/\Delta m^2$) of Eq. (14.88) we have $\bar{P}^{2\nu}(\nu_e \to \nu_e) \cong 0.3$. Thus, the possibility of $\cos 2\theta \leq 0$ is ruled out by the data. Given the choice $\Delta m^2 > 0$ we made, the data imply that $\Delta m^2 \cos 2\theta > 0$.

If $E/\Delta m^2$ is sufficiently small so that $N_e(t_0)/|N^{res}_e| \ll 1$, we have $P' \cong 0$, $\theta_m(t_0) \cong \theta$ and the oscillations take place in the Sun as in vacuum [27]:

$$\bar{P}^{2\nu}(\nu_e \to \nu_e; t_s, t_0) \cong 1 - \frac{1}{2} \sin^2 2\theta \,, \tag{14.89}$$

which is the average two-neutrino vacuum oscillation probability. This expression describes with good precision the transitions of the solar *pp* neutrinos (Section 14.9.1). The extremely nonadiabatic ν_e transitions in the Sun, characterized by $\gamma(t) \ll 1$, are also described by the average vacuum oscillation probability (Eq. (14.89)) (for $\Delta m^2 \cos 2\theta > 0$ in this case we have (see *e.g.*, Refs. [208,209]) $\cos 2\theta_m(t_0) \cong -1$ and $P' \cong \cos^2\theta$).

The probability of ν_e survival in the case 3-neutrino mixing takes a simple form for $|\Delta m^2_{31}| \cong 2.5 \times 10^{-3}$ $\mathrm{eV}^2 \gg |\Delta m^2_{21}|$. Indeed, for the energies of solar neutrinos $E \lesssim 10$ MeV, N^{res} corresponding to $|\Delta m^2_{31}|$ satisfies $N^{res}_{e31} \gtrsim 10^3$ cm^{-3} $\mathrm{N_A}$ and is by a factor of 10 bigger than N_e in the center of the Sun. As a consequence, the oscillations due to Δm^2_{31} proceed as in vacuum. The oscillation length associated with $|\Delta m^2_{31}|$ satisfies $L^v_{31} \lesssim 10$ km $\ll \Delta R$, ΔR being the dimension of the region of ν_e production in the Sun. We have for the different components of the solar ν_e flux [204] $\Delta R \cong (0.04 - 0.20) R_{\odot}$. Therefore the averaging over ΔR strongly suppresses the oscillations due to Δm^2_{31} and we get [192,217]:

$$P^{3\nu}_{\odot} \cong \sin^4\theta_{13} + \cos^4\theta_{13} \ P^{2\nu}_{\odot}(\Delta m^2_{21}, \theta_{12}; N_e \cos^2\theta_{13}) \,, \tag{14.90}$$

where $P^{2\nu}_{\odot}(\Delta m^2_{21}, \theta_{12}; N_e \cos^2\theta_{13})$ is given by Eq. (14.85) to Eq. (14.87) in which $\Delta m^2 = \Delta m^2_{21}$, $\theta = \theta_{12}$ and the solar e^- number density N_e is replaced by $N_e \cos^2\theta_{13}$. As can be shown [192,217], $P^{2\nu}_{\odot}(\Delta m^2_{21}, \theta_{12}; N_e \cos^2\theta_{13})$ and $(1 - P^{2\nu}_{\odot}(\Delta m^2_{21}, \theta_{12}; N_e \cos^2\theta_{13}))$ are respectively the average probabilities of solar ν_e survival and of the 2-neutrino $\nu_e \to \nu'' \equiv (c_{23}\nu_\mu - s_{23}\nu_\tau)$ transitions in the Sun. Thus, in the case of 3-neutrino mixing, the solar ν_e undergo transitions into the mixture $(c_{23}\nu_\mu - s_{23}\nu_\tau)$ of ν_μ and ν_τ.

The solar ν_e transitions observed by the Super-Kamiokande and SNO experiments are described, as it follows from Eq. (14.88) and Eq. (14.90), approximately by:

$$P^{3\nu}_{\odot} \cong \sin^4\theta_{13} + \cos^4\theta_{13} \ \ \sin^2\theta_{12} \,. \tag{14.91}$$

The data show that $P^{3\nu}_{\odot} \cong 0.3$, which is a strong evidence for matter effects in the solar ν_e transitions [218] since in the case of oscillations in vacuum $P^{3\nu}_{\odot} \cong \sin^4\theta_{13} + (1 - 0.5 \sin^2 2\theta_{12}) \cos^4\theta_{13} \gtrsim 0.52$, where we have used $\sin^2\theta_{13} \lesssim 0.0240$ and $\sin^2 2\theta_{12} \lesssim 0.915$ (see Section 14.2).

The analytic expression for the solar ν_e survival probability, Eq. (14.90), with $P^{2\nu}_{\odot}(\Delta m^2_{21}, \theta_{12}; N_e \cos^2\theta_{13})$ given by Eq. (14.85) to Eq. (14.87) and the prescriptions described above, provides a particularly precise description of the solar ν_e survival (and transitions) in the Sun - the results differ by a few percent from those obtained by solving numerically the relevant system of evolution equations using the electron number density distribution in the Sun provided by the standard solar models - if one uses as input in the calculations a "running" value of the scale-height r_0 [209], *i.e.*, if for each given values of $E/\Delta m^2_{21}$ and θ_{12} one finds the resonance density $N^{res} = N^{res}(E/\Delta m^2_{21}, \theta_{12})$, calculates the scale-height parameter $r_0 = N_e(r)/(dN_e(r)/dr)$ at the point in the Sun where $N_e \cos^2\theta_{13} = N^{res}(E/\Delta m^2_{21}, \theta_{12})$ employing the solar electron number density distribution $N_e = N_e(r)$ given by the standard solar models [204], r being the distance from the center of the Sun.

14.8.2.3. *The day-night asymmetry:*

When the solar neutrinos reaching a detector travel through the Earth at night, a partial regeneration of the flux of the solar ν_e is possible due to the inverse Earth matter-enhanced process [219,220] $\nu_{\mu(\tau)} \to \nu_e$. This can lead to a difference between the solar neutrino induced charged current day and night event rates in the detector, R_D and R_N, *i.e.*, to a non-zero day-night asymmetry $A_{D-N} = 2(R_D - R_N)/(R_D + R_N)$. An observation of $A_{D-N} \neq 0$ will be an unambiguous proof of the presence of Earth matter effects in the transitions of solar neutrinos taking place when the neutrinos traverse the Earth: in the absence of the effects of the Earth matter we have $A_{D-N} = 0$.

In the case of two-neutrino mixing, *i.e.*, neglecting the effects of the non-zero $\sin\theta_{13}$, the probability that an electron neutrino produced in the Sun will not be converted into $\nu_{\mu(\tau)}$ when it propagates in the Sun and traverses the Earth on the way to the detector is given by the following simple expression [219]:

$$P^{2\nu}_{SE}(\nu_e \to \nu_e) = \bar{P}^{2\nu}_{\odot}(\nu_e \to \nu_e) + (1 - 2\,\bar{P}^{2\nu}_{\odot}(\nu_e \to \nu_e))\,\frac{P_{e2} - \sin^2\theta_{12}}{\cos 2\theta_{12}}\,, \tag{14.92}$$

where $\bar{P}^{2\nu}_{\odot}(\nu_e \to \nu_e)$ is the average probability of solar ν_e survival in the Sun given in Eq. (14.86) and Eq. (14.87) (with $\theta = \theta_{12}$ and $\Delta m^2 = \Delta m^2_{21} > 0$) and $P_{e2} = |A(\nu_2 \to \nu_e)|^2$ is the probability of the $\nu_2 \to \nu_e$ transition after the ν_e have left the Sun, *i.e.*, of the $\nu_2 \to \nu_e$ transition in the Earth. For solar neutrinos crossing only the Earth mantle along a trajectory with nadir angle θ_n, the amplitude $A(\nu_2 \to \nu_e)$ in the constant density approximation, has the form:

$$A(\nu_2 \to \nu_e) = \sin\theta_{12} + (e^{-i\varphi^{man}} - 1)\cos(\theta_{12} - \theta^{man}_{12})\sin\theta^{man}_{12}\,, \tag{14.93}$$

where $\varphi^{man} = (E^m_2 - E^m_1)^{man} 2L^{man}$, $(E^m_2 - E^m_1)^{man}$ being the relevant difference of the energies of the two matter-eigenstate neutrinos in the Earth mantle and θ^{man}_{12} is the mixing angle in the mantle which coincides in vacuum with θ_{12}. The quantities $(E^m_2 - E^m_1)^{man}$ and θ^{man}_{12} can be obtained from Eq. (14.61) and Eq. (14.59) by setting $\theta = \theta_{12}$, $\Delta m^2 = \Delta m^2_{21}$, $N^{res}_e = N^{res}_{e21} = \Delta m^2_{21}\cos 2\theta_{12}/(2E\sqrt{2}G_F)$ and $N_e = \tilde{N}^{man}_e(\theta_n)$. The two layer constant density approximation expressions for $A(\nu_2 \to \nu_e)$ and P_{e2} for solar neutrinos crossing the Earth core at night were derived and can be found in Ref. 189.

During the day, when the neutrinos do not cross the Earth, $P_{e2} = \sin^2\theta_{12}$ and we have $P^{2\nu}_{SE}(\nu_e \to \nu_e) = \bar{P}^{2\nu}_{\odot}(\nu_e \to \nu_e)$. For Earth crossing neutrinos at night $P_{e2} \neq \sin^2\theta_{12}$ due to the Earth matter effect and $P^{2\nu}_{SE}(\nu_e \to \nu_e) \neq \bar{P}^{2\nu}_{\odot}(\nu_e \to \nu_e)$.

Detailed calculations of the day-night asymmetry $A_{D-N} \neq 0$ for the solar neutrino detectors Super-Kamiokande, SNO and BOREXINO have been performed, *e.g.*, in Refs. [221]. In Refs. [222] the effects of a $\theta_{13} \neq 0$ on the predictions for the asymmetry A_{D-N} were taken into account. The results of these calculations showed that for the experimentally determined current values of Δm^2_{21} and θ_{12}, the predicted values of the asymmetry A_{D-N} for the SNO and BOREXINO experiments are below the sensitivity of these experiments. For the Super-Kamiokande detector an asymmetry $A_{D-N} \sim -3\%$ was predicted.

14.9. Neutrino oscillation experiments

14.9.1. ***Solar neutrino experiments*** :

So far, solar neutrinos have been observed by chlorine (Homestake) [6] and gallium (SAGE [8], GALLEX [9,10], and GNO [11]) radiochemical detectors, water Cherenkov detectors using light water (Kamiokande [223,7] and Super-Kamiokande [224–228]) and heavy water (SNO [13,14,229,230]) , and liquid scintillation detectors (Borexino [231–237] and KamLAND [238,239]) .

A pioneering solar neutrino experiment by R. Davis, Jr. and collaborators at Homestake using the ^{37}Cl - ^{37}Ar method proposed by B. Pontecorvo [240] started in the late 1960s. This experiment exploited ν_e absorption on ^{37}Cl nuclei followed by the produced ^{37}Ar decay through orbital e^- capture,

$$\nu_e + {}^{37}\mathrm{Cl} \to {}^{37}\mathrm{Ar} + e^- \ \text{(threshold 814 keV)}. \tag{14.94}$$

Note that ν_e absorption reactions on nuclei are CC reactions. The detector contained 615 tons of tetrachloroethylene, C_2Cl_4. The ^{37}Ar atoms produced are radioactive, with a half life ($\tau_{1/2}$) of 34.8 days. After an exposure of the detector for two to three times $\tau_{1/2}$, the reaction products were chemically extracted and introduced into a low-background proportional counter, where they were counted for a sufficiently long period to determine the exponentially decaying signal and a constant background. Solar-model calculations [124] predict that the dominant contribution in the chlorine experiment come from ^{8}B neutrinos, the second to the dominant from ^{7}Be neutrinos, with *pep*, ^{13}N, and ^{15}O neutrinos also giving additional subdominant contributions.

Gallium experiments (GALLEX and GNO at Gran Sasso in Italy and SAGE at Baksan in Russia) utilized the reaction

$$\nu_e + {}^{71}\mathrm{Ga} \to {}^{71}\mathrm{Ge} + e^- \ \text{(threshold 233 keV)}, \tag{14.95}$$

which is sensitive to the most abundant *pp* solar neutrinos. The solar-model calculations [124] predict that more than 80% of the capture rate in gallium is due to low energy *pp* and ^{7}Be solar neutrinos with the *pp* rate being about twice the ^{7}Be rate. The ^{71}Ge atoms decay through electron capture with a half life ($\tau_{1/2}$) of 11.43 days. SAGE used approximately 50 tons of liquid gallium metal as a target. GALLEX used 101 tons of $GaCl_3$, containing 30.3 tons of gallium. Both experiments used natural gallium, containing 39.9% of ^{71}Ga isotope. SAGE started measurement from December, 1989. GALLEX experiment had been conducted between 1991 and 1997. Since April, 1998, a newly defined collaboration, GNO (Gallium Neutrino Observatory) continued the gallium experiment at Gran Sasso until April 2003.

Both GALLEX [241] and SAGE [242] tested their detectors using intense ^{51}Cr radioactive sources with known activities. Low energy neutrinos relevant to test the gallium experiments ($\sim$ 750 keV and $\sim$ 320 keV neutrinos) are emitted from decays of ^{51}Cr.

In 1987, the Kamiokande experiment at Kamioka in Japan succeeded in real-time solar neutrino observation, utilizing νe scattering,

$$\nu_x + e^- \to \nu_x + e^-\,, \tag{14.96}$$

in a 3,000-ton water-Cherenkov detector. This experiment took advantage of the directional correlation between the incoming neutrino and the recoil electron. This feature greatly helps the clear separation of the solar-neutrino signal from the background. The Kamiokande result gave the first direct evidence that neutrinos come from the direction of the Sun [223]. In 1996, the high-statistics Super-Kamiokande experiment [224–228] with a 50-kton water Cherenkov detector replaced the Kamiokande experiment. Due to the high thresholds (recoil-electron total energy of 7 MeV in Kamiokande and 4 MeV at present in Super-Kamiokande) the experiments observe pure ^{8}B solar neutrinos. It should be noted that the reaction (Eq. (14.96)) is sensitive to all active neutrinos, $x = e$, μ, and τ. However, the sensitivity to ν_μ and ν_τ is smaller than the sensitivity to ν_e since $\sigma(\nu_{\mu,\tau}e) \approx 0.16\,\sigma(\nu_e e)$.

In 1999, a new real time solar-neutrino experiment, SNO (Sudbury Neutrino Observatory), in Canada started observation. This experiment used 1000 tons of ultra-pure heavy water (D_2O) contained in a spherical acrylic vessel, surrounded by an ultra-pure H_2O shield. SNO measured ^{8}B solar neutrinos via the CC and NC reactions

$$\nu_e + d \to e^- + p + p \qquad \text{(CC)}\,, \tag{14.97}$$

and

$$\nu_x + d \to \nu_x + p + n \qquad \text{(NC)}\,, \tag{14.98}$$

as well as νe scattering, (Eq. (14.96)). The CC reaction, (Eq. (14.97)), is sensitive only to ν_e, while the NC reaction, (Eq. (14.98)), is sensitive to all active neutrinos. This is a key feature to solve the solar neutrino problem. If it is caused by flavour transitions such as neutrino oscillations, the solar neutrino fluxes measured by CC and NC reactions would show a significant difference.

The Q-value of the CC reaction is -1.4 MeV and the e^- energy is strongly correlated with the ν_e energy. Thus, the CC reaction provides

an accurate measure of the shape of the ^{8}B neutrino spectrum. The contributions from the CC reaction and νe scattering can be distinguished by using different cos θ distributions, where θ is the angle of the e^- momentum with respect to the Sun-Earth axis. While the νe scattering events have a strong forward peak, CC events have an approximate angular distribution of $(1 - 1/3 \cos\theta)$.

The neutrino energy threshold of the NC reaction is 2.2 MeV. In the pure D_2O [13,14], the signal of the NC reaction was neutron capture in deuterium, producing a 6.25-MeV γ-ray. In this case, the capture efficiency was low and the deposited energy was close to the detection threshold of 5 MeV. In order to enhance both the capture efficiency and the total γ-ray energy (8.6 MeV), 2 tons of NaCl was added to the heavy water in the second phase of the experiment [229]. Subsequently NaCl was removed and an array of ^{3}He neutron counters were installed for the third phase measurement [230]. These neutron counters provided independent NC measurement with different systematics from that of the second phase, and thus strengthened the reliability of the NC measurement. The SNO experiment completed data acquisition in 2006.

Another real time solar neutrino experiment, Borexino at Gran Sasso, started solar neutrino observation in 2007. This experiment measures solar neutrinos via νe scattering in 300 tons of ultra-pure liquid scintillator. With a detection threshold as low as 250 keV, the flux of monochromatic 0.862 MeV ^{7}Be solar neutrinos has been directly observed for the first time [231]. Further, Borexino measured the fluxes of monochromatic 1.44 MeV *pep* solar neutrinos [232] and pp solar neutrinos [233], both for the first time. Measurements of these low energy solar neutrinos are important not only to test the SSM further, but also to study the MSW effect over the energy region spanning from sub-MeV to 10 MeV. Borexino published the final results of the Phase-I (May 2007 to May 2010) low-energy solar-neutrino measurement in [235]. After Phase-I data-taking, Borexino conducted an extensive purification of its liquid scintillator, and started Phase-II data-taking in December 2011. Recently, Borexino has reported the Phase II results of the low-energy solar-neutrino measurement [236]. Borexino has also reported the ^{8}B solar-neutrino measurement between January 2008 and December 2016 [237].

The solar neutrino survival probability, relevant for the interpretation of the solar neutrino data in the terms of the MSW effect is discussed in subsection 14.8.2.2.

KamLAND is a 1-kton ultra-pure liquid scintillator detector located at the old Kamiokande's site. This experiment also measured the ^{7}Be solar neutrino flux [238]. As KamLAND is a multi-purpose experiment whose one of the primary goals was a long-baseline neutrino oscillation studies using electron antineutrinos emitted from nuclear power reactors, further description of the KamLAND experiment is given later in Section 14.9.3.

14.9.2. *Atmospheric neutrino oscillation experiments* :

Almost all large underground detectors can observe atmospheric neutrinos. In the early history of neutrino oscillation studies using atmospheric neutrinos, water Cherenkov detectors for Kamiokande [243,244] and IMB [245] (experiment in the US) and iron tracking calorimeters for the Frejus experiment [246] in France and the Soudan 2 experiment [247] at the Soudan mine in the US, measured atmospheric neutrinos, in particular, the flux ratio $\nu_\mu/\nu_e \equiv \Phi(\nu_\mu + \bar{\nu}_\mu)/\Phi(\nu_e + \bar{\nu}_e)$. The main purpose of all these experiments was search for nucleon decay, and atmospheric neutrinos were backgrounds for the main purpose. Following these initial experiments, Super-Kamiokande discovered the atmospheric neutrino oscillation [17], and a multi-purpose detector MACRO [248] at Gran Sasso obtained results consistent with neutrino oscillation. Subsequently, Soudan 2 also observed the atmospheric neutrino oscillation effects [249]. Later, the far detector of the MINOS long baseline neutrino oscillation experiment also measured atmospheric neutrinos [250], and obtained results consistent with atmospheric neutrino oscillation. This detector is a 5.4 kton iron-scintillator tracking calorimeter with toroidal magnetic field.

Atmospheric neutrino oscillations have also been observed by the neutrino telescopes for high-energy neutrino astronomy (TeV $\sim$ PeV) using Cherenkov technique, ANTARES and IceCube-DeepCore, based on the measurement of ν_μ charged-current events having an upward-going muon track to avoid contamination from atmospheric muon background. ANTARES [251] is an open water detector deployed deep under the Mediterranean Sea (depth $\sim$ 2500 m) 40 km off-shore from Toulon, France, while IceCube [252] is a detector deployed in the ice at the South Pole at the depth from 1450 m to 2450 m. Though both experiments are optimized to high-energy neutrino interactions in the TeV range, they need to measure muon neutrinos with energies as low as $\sim$ 20 GeV in order to be sensitive to atmospheric neutrino oscillations. ANTARES could reconstruct upward-going muons from ν_μ interactions down to 20 GeV [253], while IceCube used the low-energy sub-detector DeepCore, a region of denser IceCube instrumentation, to lower the muon neutrino energy threshold down to $\sim$ 6 GeV [254] (also see Ref. 255 with higher thresholds).

All these detectors, with the exception of the MINOS far detector, cannot measure the charge of the final-state leptons, and, therefore, neutrino and antineutrino induced events cannot be discriminated; the MINOS far detector can measure the charge of the muon track, and, therefore, identify ν_μ and $\bar{\nu}_\mu$ charged-current events. However, all these detectors can identify the final-state leptons to be μ-like or e-like. Taking Super-Kamiokande as an example, neutrino events having their vertex in the 22.5 kton fiducial volume are classified into fully contained (FC) events and partially contained (PC) events. The FC events are required to have no activity in the anti-counter. Single-ring events have only one charged lepton which radiates Cherenkov light in the final state, and particle identification is particularly clean for single-ring FC events. A ring produced by an e-like ($e^\pm$, γ) particle exhibits a more diffuse pattern than that produced by a μ-like ($\mu^\pm$, $\pi^\pm$) particle, since an e-like particle produces an electromagnetic shower and low-energy electrons suffer considerable multiple Coulomb scattering in water. All the PC events are assumed to be μ-like since the PC events comprise a 98% pure charged-current ν_μ sample.

In the near future, Super-Kamiokande will continue atmospheric neutrino measurements. In addition, currently several large underground detectors are proposed for construction (liquid argon detectors with a total mass of 10 - 40 kton as the far detector of the DUNE experiment [93] in the US, and a 2×0.258 Mton water Cherenkov detector, Hyper-Kamiokande (2TankHK-staged design) [200], as the far detector of the T2HK experiment [94] in Japan) or approved (a 50 kton magnetized iron tracking calorimeter, ICAL at the INO (India-based Neutrino Observatory) [85] in the southern Indian state of Tamil Nadu). Analytic expressions for the relevant atmospheric neutrino oscillation probabilities are given in subsection 14.8.1.

As high-statistics atmospheric neutrino observations in the energy region of a few to $\sim$ 10 GeV are considered to be promising for the determination of the neutrino mass ordering (see subsection 14.8.1, Fig. 14.7 and the related discussion), there are two proposed densely-instrumented neutrino telescopes PINGU (Precision IceCube Next-Generation Upgrade) [82] and ORCA (Oscillation Research with Cosmics in the Abyss) [83], both having a multi-megaton total mass. PINGU will be deployed inside the DeepCore, and will be sensitive to > 1 GeV. ORCA is proposed as part of the second phase of the KM3NeT [84], a network of neutrino telescopes deep under the Mediterranean Sea. ORCA will have sensitivity down to a few GeV, its site being Toulon, France.

14.9.3. *Accelerator neutrino oscillation experiments* :

For earlier accelerator neutrino oscillation experiments before the discovery of the atmospheric neutrino oscillation, see, *e.g.*, Ref. 257. The $\Delta m^2 \geq 2 \times 10^{-3}$ eV^2 region can be explored by accelerator-based long-baseline experiments with typically $E \sim 1$ GeV and $L \sim$ several hundred km. K2K [19], MINOS [20,21] and MINOS+ [256], OPERA [173,174], ICARUS [258], T2K [22,23], and NOνA [40,60] are completed or currently running experiments, and DUNE [93] and T2HK [94] are proposed future experiments. For analytic expressions of relevant neutrino oscillation probabilities see Eq. (14.44) and Eq. (14.74) and the discussions related to these equations. With a fixed baseline distance and a narrower, well understood neutrino energy spectrum, the value of $|\Delta m^2_{31(32)}|$ and, with higher statistics, also the relevant neutrino mixing angle,

are potentially better constrained in accelerator experiments than from atmospheric neutrino observations. With $\nu_\mu \to \nu_e$ appearance measurements, accelerator long-baseline experiments can measure θ_{13} within an uncertainty related, in particular, to the CPV phase δ. In the early phase of the accelerator long-baseline experiments, K2K used an approximate $\nu_\mu \to \nu_e$ appearance probability given by Eq. (14.46),

$$P(\nu_\mu \to \nu_e) = \sin^2 2\theta_{13} \cdot \sin^2 \theta_{23} \cdot \sin^2(1.27\Delta m^2_{31} L/E). \quad (14.99)$$

to set an upper limit to $\sin^2 2\theta_{13}$ [175]. More accurate expression for the $\nu_\mu \to \nu_e$ appearance probability relevant for the accelerator long baseline experiments, Eq. (14.74), shows that subleading terms could have rather large effects and the unknown CPV phase δ causes uncertainties if one wishes to determining the value of θ_{13} from accelerator measurements of $\nu_\mu \to \nu_e$ appearance. Now that θ_{13} has been precisely measured by reactor experiments, accelerator long-baseline experiments can potentially determine or constrain δ and the neutrino mass ordering, from the measurement of $\nu_\mu \to \nu_e$ appearance, using precise reactor results on θ_{13}, depending on the experimental conditions such as baseline distance.

The K2K (KEK-to-Kamioka) long-baseline neutrino oscillation experiment [19] is the first accelerator-based experiment with a neutrino path length extending hundreds of kilometers. A horn-focused wide-band muon neutrino beam having an average $L/E_\nu \sim 200$ ($L = 250$ km, $\langle E_\nu \rangle \sim 1.3$ GeV), was produced by 12-GeV protons from the KEK-PS and directed to the Super-Kamiokande detector. A near detector was located 300 m downstream of the production target. K2K experiment started data-taking in 1999 and was completed in 2004.

MINOS [20,21] is the second long-baseline neutrino oscillation experiment with near and far detectors. Neutrinos are produced by the NuMI (Neutrinos at the Main Injector) facility using 120 GeV protons from the Fermilab Main Injector. The far detector is a 5.4 kton (total mass) iron-scintillator tracking calorimeter with toroidal magnetic field, located underground in the Soudan mine. The baseline distance is 735 km. The near detector, located 1.04 km downstream of the production target, is also an iron-scintillator tracking calorimeter with toroidal magnetic field, with a total mass of 0.98 kton. The NuMI neutrino beam is a horn-focused wide-band beam. Its energy spectrum can be varied by moving the target position relative to the first horn and changing the horn current. MINOS started the neutrino-beam run in 2005 and was completed in 2012. Almost all the MINOS data were taken with the low-energy beam spectrum which peaked at 3 GeV. Part of the MINOS data were taken with the $\bar{\nu}_\mu$-enhanced beam by inverting the current in magnetic horns. In September, 2013, the MINOS+ experiment [256] started with the same near and far detectors as the MINOS experiment, but with the medium-energy beam spectrum which peaks at ~ 6 GeV on axis (zero degree). At zero degree, the NuMI medium-energy beam has much higher intensity than the NuMI low-energy beam. The MINOS+ experiment had run for 3 years and ended in 2016.

The T2K experiment [22,23] is the first off-axis long-baseline neutrino oscillation experiment. The baseline distance is 295 km between the J-PARC in Tokai, Japan and Super-Kamiokande. A narrow-band ν_μ beam with a peak energy of 0.6 GeV, produced by 30 GeV protons from the J-PARC Main Ring, is directed 2.5° off-axis to SK. With this configuration, the ν_μ beam is tuned to the first oscillation minimum of the ν_μ survival probability. T2K started the first physics run in 2010.

The NOνA experiment [40,41] is an off-axis long-baseline neutrino oscillation experiment using the the NuMI medium-energy beam. Its detectors are positioned 14.6 mrad off-axis. With this configuration, the neutrino beam has a narrow spectrum which peaks at around 2 GeV. The 14 kton total active mass far detector is located on the surface at Ash River, Minnesota, 810 km from the production target. The 193 ton total active mass near detector is located 100 m underground at Fermilab, approximately 1km from the target. Both detectors are fine-grained tracking calorimeters consisting of arrays of PVC cells filled with liquid scintillator. NOνA started physics run in 2014.

Although the atmospheric neutrino oscillations and accelerator long-baseline ν_μ disappearance data are fully consistent with the dominance of $\nu_\mu \to \nu_\tau$ oscillations for ν_μ at GeV energies, ν_τ appearance in the muon neutrino beam has to be demonstrated. As the τ production threshold is $E_\nu \sim 3.5$ GeV, a high-energy neutrino beam is needed for this purpose. The only experiment of this kind is OPERA [173,174] with a muon neutrino source at CERN and a detector at Gran Sasso with a baseline distance of 730 km. OPERA does not have a near detector. The CNGS (CERN Neutrinos to Gran Sasso) neutrino beam with $\langle E_\nu \rangle = 17$ GeV is produced by high-energy protons from the CERN SPS. OPERA received the CNGS neutrino beam between 2008 and 2012. The detector is a combination of the "Emulsion Cloud Chamber" and magnetized spectrometer, having a target mass of 1,290 tons. At Gran Sasso, another neutrino experiment, ICARUS [258], with a 600-ton liquid argon detector, was located and received the CNGS neutrino beam from 2010 to 2012. The ICARUS detector was transported to Fermilab in July 2017, and will be used in a short baseline experiment.

DUNE (Deep Underground Neutrino Experiment) [93] is a projected future experiment with a 1,300 km baseline. A $10 \sim 34$ kton liquid-argon far detector will be located deep underground at the Sanford Lab in South Dakota, the U.S. A fine-grained near neutrino detector will be installed at Fermilab. Based on the existing NuMI beamline and a MW class proton source, a wide-band, high-intensity ν_μ beam with a peak flux at 2.5 GeV is considered for this experiment. T2HK [94] is another future long baseline experiment from J-PARC to the 2×0.258 Mton water Cherenkov detector, Hyper-Kamiokande (2TankHK-staged design) [200], which is at the proposal stage, at Kamioka. An upgrade of the J-PARC Main Ring to achieve a MW-class beam power is also proposed.

In the context of possible hints for the existence of sterile neutrinos at the eV scale, short-baseline accelerator neutrino oscillation experiments have been drawing attention. LSND [259], Karmen 2 (and Karmen 1) [260], and MiniBooNE [261,262] are completed experiments. At Fermilab, the Short-Baseline Neutrino (SBN) Program is ongoing [263]. It consists of three new short-baseline experiments, SBND, MicroBooNE, and ICARUS in the Booster Neutrino Beamline. The detectors of all these new experiments use liquid-argon TPC technology. MicroBooNE is running, and SBND and ICARUS are in preparation.

The LSND (Liquid Scintillation Neutrino Detector) experiment [259] used the LANSE (Los Alamos Neutron Science Center, formerly known as the LAMPF) 800 MeV proton linac as a neutrino source. At this energy, kaon production is negligible. Most of the produced positive pions stop in the massive target and decay at rest, with decay muons also stop in the target and decay. Most of the produced negative pions also stop in the target and are absorbed by the target nuclei. Therefore, this neutrino source emits ν_μ, $\bar{\nu}_\mu$, and ν_e, with very small contamination of $\bar{\nu}_e$ which comes from π^- decay in flight followed by the μ^- decay at rest. Because of this small $\bar{\nu}_e$ component in the neutrino flux, LSND made a sensitive search for $\bar{\nu}_\mu \to \bar{\nu}_e$ appearance with 167 tons of diluted liquid scintillator in a tank located about 30 m from the neutrino source, using the reaction $\bar{\nu}_e + p \to e^+ + n$. Also, LSND studied $\nu_\mu \to \nu_e$ appearance above the Michel electron endpoint energy using the reaction $\nu_e + C \to e^- + N$, as the ν_e flux from μ^+ decay in flight is suppressed due to the long muon lifetime and that from π^+ decay in flight is suppressed by the small $\pi^+ \to e^+ + \nu_e$ branching ratio. The Karmen 2 experiment [260] used the 800 MeV proton synchrotron at the neutron spallation facility of the Rutherford Appleton Laboratory, also to produce low-energy $\bar{\nu}_\mu$ flux from μ^+ decay at rest. The Karmen 2 detector is a segmented liquid scintillator calorimeter located at a distance of 17.7 m from the neutrino source. MiniBooNE used a conventional horn-focused neutrino beam produced by 8 GeV protons from the Fermilab booster synchrotron. MiniBooNE investigated both ν_e [261] and $\bar{\nu}_e$ [262] appearance in ν_μ and $\bar{\nu}_\mu$ beams, respectively, with a detector containing 806 tons of mineral oil and located 541 m downstream of the production target.

14.9.4. *Reactor neutrino oscillation experiments* :

As nuclear reactors produce $\bar{\nu}_e$ flux with energy < 10 MeV, $\bar{\nu}_e$ disappearance is the only neutrino oscillation channel that can be studied using reactors and liquid scintillator detectors. To identify low-energy inverse β-decay events $\bar{\nu}_e + p \to e^+ + n$, detection of a

prompt positron signal and delayed neutron signal in coincidence is important to reject natural backgrounds. For detecting neutrons effectively, gadolinium-loaded liquid scintillator is widely used. While neutron capture on a hydrogen produces a 2.2 MeV γ, neutron capture on Gd produces multiple γ, each having average energy of ~ 2 MeV, giving a ~ 8 MeV signal in total.

For short baseline reactor neutrino oscillation experiments in the 1980s or earlier, see, *e.g.*, Refs. [264,52]. Reactor neutrino oscillation experiments with $L \sim 1$ km, $\langle E \rangle \sim 3$ MeV are sensitive down to $E/L \sim 3 \times 10^{-3}$ eV^2 $\sim \Delta m^2$. At this baseline distance, the reactor $\bar{\nu}_e$ oscillations driven by Δm^2_{21} are negligible in the three neutrino oscillation framework. The $\bar{\nu}_e$ survival probability is given in Eq. (14.45). Therefore, reactor $\bar{\nu}_e$ disappearance experiments with ~ 1 km baseline allow direct measurement of $\sin^2\theta_{13}$.

In 1990's, two experiments of this kind, Chooz [57] and Palo Verde [265], were constructed to study a possibility of rather large $\nu_\mu - \nu_e$ mixing in the Δm^2 region down to $10^{-2} \sim 10^{-3}$ eV^2 as a possible solution for the anomalous atmospheric ν_μ/ν_e ratio reported by several experiments (see, Section 14.11.1). Both Chooz and Palo Verde were single-detector experiments. The Chooz detector was located in an underground laboratory with 300 mwe (meter water equivalent) rock overburden, at about 1 km from the neutrino source. It consisted of a central 5-ton target filled with 0.09% Gd-loaded liquid scintillator, surrounded by an intermediate 17-ton and outer 90-ton regions filled with Gd-free liquid scintillator. Another experiment at the Palo Verde Nuclear Generating Station in Arizona, United States, also searched for $\bar{\nu}_e$ disappearance using 11.34 tons of Gd-loaded liquid scintillator located at a shallow (32 mwe) underground site, about 800 m from the neutrino source [265]. These two experiments found no evidence for $\bar{\nu}_e$ disappearance. The CHOOZ collaboration set a limit of $\sin^2 2\theta_{13} < 0.1$ at 90% CL. Somewhat less stringent limit was obtained by the Palo Verde collaboration.

After establishment of atmospheric and solar neutrino oscillations the importance of the reactor neutrino oscillation experiment to measure θ_{13} was widely recognized, and this led to the realization of the three new reactor experiments, Double Chooz in France, RENO in Korea, and Daya Bay in China. Given a small disappearance probability expected from the $\sin^2 2\theta_{13}$ limit reported by Chooz and Palo Verde and an uncertainty of a few% with which reactor $\bar{\nu}_e$ flux was predicted, all these experiments proposed to have near and far detectors to reduce the systematic error due to $\bar{\nu}_e$ flux uncertainty. These modern reactor neutrino oscillation experiments were approved around 2005. For their histories, see, *e.g.*, Ref. 266 for Double Chooz, Ref. 267 for Daya Bay, and Ref. 268 for RENO.

The Double Chooz experiment [32,35] measures electron antineutrinos from two 4.25 GW_{th} reactors with two identical detectors: a near detector and a far detector located at average distances of 400 m and 1050 m, respectively, from the two reactor cores. Although the far detector was completed in 2010, there was a substantial delay in the construction of the near detector, and it was completed at the end of 2014. The Daya Bay experiment [33,37] measures electron antineutrinos from the Daya Bay nuclear power complex (six 2.9 GW_{th} reactors), initially with six functionally identical detectors deployed in two near (470 m and 576 m of flux-weighted baselines) and one far (1648 m) underground halls. The first Daya Bay result [33] was obtained with this detector configuration. Later, two detectors were further installed, one in one of the near detector hall and the other in the far detector hall. The RENO experiment [34] measures electron antineutrinos from four 2.8 GW_{th} and two 2.66 GW_{th} reactors at Yonggwang Nuclear Power Plant with two identical detectors located at 294 m and 1383 m from the reactor array center (or flux-weighted baseline distance of 408.56 m and 1443.99 m, respectively). Antineutrino detectors of these experiments have similar structures. They consist of three layers and an optically independent outer veto detector. The innermost layer of the antineutrino detector is filled with Gd-loaded liquid scintillator, which is surrounded by a "γ-catcher" layer filled with Gd-free liquid scintillator, and outside the γ-catcher is a buffer layer filled with mineral oil. An outer veto detector is filled with purified water (Daya Bay and RENO) or liquid scintillator (Double Chooz). In addition, the Double Chooz near detector tank is shielded by a 1 m thick water buffer. RENO and Daya Bay started measurements with both the near and far detectors from the beginning. All these experiments published their first results on reactor $\bar{\nu}_e$ disappearance in 2012.

For longer baseline distance of $L \sim$ a few hundred km, a reactor neutrino oscillation experiment is sensitive to Δm^2 down to $\sim 10^{-5}$ eV^2. In this case the reactor $\bar{\nu}_e$ survival probability is given in Eq. (14.51). Therefore, such an experiment can test the LMA (Large Mixing Angle) solution of the solar neutrino problem, assuming CPT invariance.

However, a higher $\bar{\nu}_e$ flux and a larger target mass are needed compared to short-baseline reactor experiments to obtain statistically significant event rate. So far, KamLAND is the only experiment of this kind. It is located at the old Kamiokande's site in Japan. Its neutrino target is 1-kton ultra-pure liquid scintillator contained in a transparent balloon, which is hold inside a spherical tank with buffer oil filled between the baloon and the tank. The tank is surrounded by an outer water Cherenkov detector. Before the Great East Japan Earthquake in March 2011, many nuclear reactors were operating in Japan, and more than 79% of the $\bar{\nu}_e$ flux at KamLAND was coming from 26 reactors between 138 - 214 km away, with a flux-weighted average distance of ~ 180 km.

In future, medium baseline (~ 50 km) reactor neutrino oscillation experiments with neutrino target mass of ~ 20 kton and with a very good energy resolution of $3\%/\sqrt{E_\nu(\mathrm{MeV})}$, not reached in any previous experiment with liquid scintillator, are aiming, in particular, to determine the type of spectrum the neutrino masses obey, *i.e.*, the neutrino mass ordering (see Section 14.2). The relevant $\bar{\nu}_e$ survival probability is given in Eq. (14.47). These experiments have additional rich physics program. The Jiangmen Underground Neutrino Observatory (JUNO) [269] at Kaiping, Jiangmen in Southern China will be located at 53 km from both of the planned Yangjiang and Taishan nuclear power plants. The neutrino target of this experiment will be 20 kton liquid scintillator. JUNO is a funded project, and its construction started in January, 2015.

14.10. Results of solar neutrino experiments and KamLAND

In 1967, analyzing the possible effects of neutrino oscillations on the solar neutrino flux measurements, B. Pontecorvo predicted the solar neutrino "deficit" in experiments detecting solar neutrinos via a CC reaction [1] before the first solar neutrino data were available. The solar-neutrino problem, *i.e.*, the problem of understanding the origin of the observed deficit of solar neutrinos, remained unsolved for more than 30 years since the late 1960s, but solar neutrino experiments have achieved remarkable progress since the beginning of the new century, and the solar-neutrino problem has been understood as due to neutrino flavour conversion.

14.10.1. *Measurements of Δm^2_{21} and θ_{12}* :

From the very beginning of the solar-neutrino observation by the Homestake chlorine experiment [270] in the late 1960s, it was recognized that the observed flux was significantly smaller than the SSM prediction. The subsequent radiochemical solar neutrino experiments using ^{71}Ga, SAGE [271] and GALLEX [9] also reported smaller solar neutrino fluxes than the SSM predictions in the early 1990s. final results of these experiments [272] are compared with the SSM predictions in Table 14.5. Experiments with water Cherenkov detectors, Kamiokande and Super-Kamiokande, observed almost pure ^{8}B solar neutrinos through νe elastic scattering, and they also reported a clear deficit of ^{8}B solar neutrino flux.

In 2001, the initial SNO CC result combined with the Super-Kamiokande's high-statistics νe elastic scattering result [273] provided direct evidence for flavour conversion of solar neutrinos [13]. Later, SNO's NC measurements further strengthened this conclusion [14,229,230]. From the salt-phase measurement [229], the fluxes measured with CC, ES, and NC events were obtained as

$$\phi^{\mathrm{CC}}_{\mathrm{SNO}} = (1.68 \pm 0.06^{+0.08}_{-0.09}) \times 10^6 \mathrm{cm}^{-2}\mathrm{s}^{-1} \ , \qquad (14.100)$$

$$\phi^{\mathrm{ES}}_{\mathrm{SNO}} = (2.35 \pm 0.22 \pm 0.15) \times 10^6 \mathrm{cm}^{-2}\mathrm{s}^{-1} \ , \qquad (14.101)$$

Table 14.5: Results from radiochemical solar-neutrino experiments. The predictions of the standard solar model BPS08(GS) [128] are also shown. The first and the second errors in the experimental results are the statistical and systematic errors, respectively. SNU (Solar Neutrino Unit) is defined as 10^{-36} neutrino captures per atom per second.

	^{37}Cl→^{37}Ar (SNU)	^{71}Ga→^{71}Ge (SNU)
Homestake [6]	$2.56 \pm 0.16 \pm 0.16$	–
GALLEX [10]	–	$77.5 \pm 6.2^{+4.3}_{-4.7}$
GNO [11]	–	$62.9^{+5.5}_{-5.3} \pm 2.5$
GNO+GALLEX [11]	–	$69.3 \pm 4.1 \pm 3.6$
SAGE [8]	–	$65.4^{+3.1+2.6}_{-3.0-2.8}$
SSM [BPS08(GS)] [128]	$8.46^{+0.87}_{-0.88}$	$127.9^{+8.1}_{-8.2}$

$$\phi^{\rm NC}_{\rm SNO} = (4.94 \pm 0.21^{+0.38}_{-0.34}) \times 10^6 {\rm cm}^{-2}{\rm s}^{-1} \ , \qquad (14.102)$$

where the first errors are statistical and the second errors are systematic. In the case of $\nu_e \to \nu_{\mu,\tau}$ transitions, Eq. (14.102) is a mixing-independent result and therefore tests solar models. It shows good agreement with the ^{8}B solar-neutrino flux predicted by the solar model [125]. Fig. 14.8 shows the salt phase result on the $\nu_\mu + \nu_\tau$ flux $\phi(\nu_{\mu,\tau})$ versus the flux of electron neutrinos $\phi(\nu_e)$ with the 68%, 95%, and 99% joint probability contours. The flux of non-ν_e active neutrinos, $\phi(\nu_{\mu,\tau})$, can be deduced from these results. It is

$$\phi(\nu_{\mu,\tau}) = \left(3.26 \pm 0.25^{+0.40}_{-0.35}\right) \times 10^6 {\rm cm}^{-2}{\rm s}^{-1}. \qquad (14.103)$$

The non-zero $\phi(\nu_{\mu,\tau})$ is strong evidence for solar ν_e flavor conversion. As it follows from the discussion of the solar ν_e survival and transition probabilities in subsection 14.8.2.2 (see Eq. (14.90)), the parameters which are responsible for the solar neutrino flavour conversion are Δm^2_{21} and θ_{12}. The dependence of the survival probability on $\theta_{13} \cong 0.15$ is extremely weak, leading essentially to a rescaling of the corresponding 2-neutrino mixing ν_e survival probability by a factor of $\cos^4\theta_{13} = 0.96$ and of N_e by the factor $\cos^2\theta_{13} \cong 0.98$. The quoted experimental results are consistent with those expected from the LMA (large mixing angle) solution of solar neutrino oscillation in matter [26,27] with $\Delta m^2_{21} \sim 7.5 \times 10^{-5}$ eV^2 and $\tan^2\theta_{12} \sim 0.45$. However, with the SNO data alone, the possibility of other solutions of the solar neutrino problem cannot be excluded with sufficient statistical significance.

The KamLAND experiment solved this problem and finally identified the LMA solution as the true solution of the solar neutrino problem. With the reactor $\bar\nu_e$'s energy spectrum (< 8 MeV) and a prompt-energy analysis threshold of 2.6 MeV, this experiment has a sensitive Δm^2 range down to $\sim 10^{-5}$ eV^2. The reactor $\bar\nu_e$ survival probability relevant for the interpretation of the KamLAND data is given in Eq. (14.51) and Eq. (14.52). Assuming CPT invariance, it depends on the same parameters Δm^2_{21} and θ_{12}, which drive the solar ν_e transitions, the dependence on θ_{13} having, as in the case of the solar ν_e survival probability, a rather small rescaling effect of the corresponding 2-neutrino $\bar\nu_e$ survival probability. Therefore, if the LMA solution is the real solution of the solar neutrino problem, KamLAND should observe reactor $\bar\nu_e$ disappearance, assuming CPT invariance.

The first KamLAND results [15] with 162 ton·yr exposure were reported in December 2002. The ratio of observed to expected (assuming no $\bar\nu_e$ oscillations) number of events was

$$\frac{N_{\rm obs} - N_{\rm BG}}{N_{\rm NoOsc}} = 0.611 \pm 0.085 \pm 0.041 \qquad (14.104)$$

with obvious notation. This result showed clear evidence of an event deficit expected from neutrino oscillations. The 95% CL allowed regions are obtained from the oscillation analysis with the observed

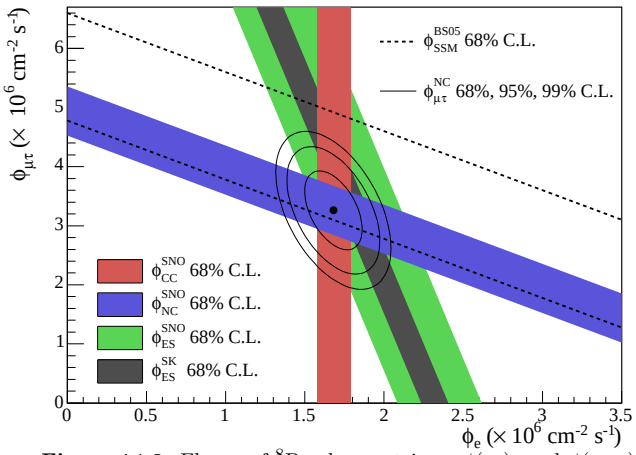

Figure 14.8: Fluxes of ^{8}B solar neutrinos, $\phi(\nu_e)$, and $\phi(\nu_{\mu,\tau})$, deduced from the SNO's CC, ES, and NC results of the salt phase measurement [229]. The Super-Kamiokande ES flux is from Ref. 274. The BS05(OP) standard solar model prediction [125] is also shown. The bands represent the 1σ error. The contours show the 68%, 95%, and 99% joint probability for $\phi(\nu_e)$ and $\phi(\nu_{\mu,\tau})$. The figure is from Ref. 229.

event rates and positron spectrum shape. A combined global solar + KamLAND analysis showed that the LMA is a unique solution to the solar neutrino problem with $> 5\sigma$ CL [275]. With increased statistics [16,276,277], KamLAND observed not only the distortion of the $\bar\nu_e$ spectrum, but also for the first time the periodic dependence on the neutrino energy of the $\bar\nu_e$ survival probability expected from neutrino oscillations (see Fig. 14.9).

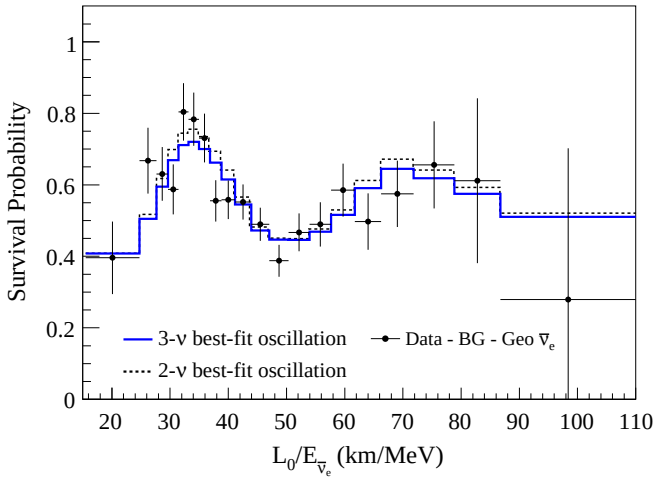

Figure 14.9: The ratio of the background and geoneutrino-subtracted $\bar\nu_e$ spectrum, observed in the KamLAND experiment, to the predicted one without oscillations (survival probability) as a function of L_0/E, where L_0=180 km. The histograms show the expected distributions based on the best-fit parameter values from the two- and three-flavor neutrino oscillation analyses. The figure is from Ref. 277.

It should be noted that with accumulation of precise solar neutrino data, analyses using only solar neutrino data [278,279,235] have attained sufficiently high statistical significance ($> 99.73\%$ or $> 3\sigma$ CL) to show the LMA solution to be the real solution to the solar neutrino problem without resorting to the KamLAND data, namely, without assuming CPT invariance, though the allowed Δm^2_{21} range is better determined by the KamLAND data.

The values of Δm^2_{21} and θ_{12} have been frequently updated by experimental groups or by phenomenological analysis groups, using the global solar neutrino data, or the KamLAND data alone, or the global solar + KamLAND data, or the global neutrino oscillation data. The latest global analysis results found in Ref. 58 are shown in Table 14.1.

Regarding the consistency between the KamLAND and solar neutrino experiments on the values of Δm^2_{21} and θ_{12}, it has been noted that there is a $\sim 2\sigma$ level tension between the best-fit value of Δm^2_{21} determined by the KamLAND collaboration and that obtained from analyses using global solar neutrino data [59]. The solar data prefer lower Δm^2_{21} value. The KamLAND and global solar best-fit values of θ_{12} are consistent.

14.10.2. *Solar neutrino flux measurements and indications of matter effects* :

So far, the pp, pep, ^{7}Be, ^{8}B solar neutrino fluxes have been measured, and upper limits have been set for the hep and CNO solar neutrino fluxes, with various techniques. Chlorine (Homestake) and gallium (SAGE, GALLEX, and GNO) radiochemical experiments measured capture rates of solar neutrinos above threshold (see Table 14.5). Light-water Cherenkov detectors, Kamiokande [7] and Super-Kamiokande [225,227,228], measured the ^{8}B neutrino flux and set an upper limit for the hep neutrino flux using νe elastic scattering [225]. A heavy-water Cherenkov detector, SNO [279], also measured the ^{8}B neutrino flux, but with three different reactions, NC, CC, and νe elastic scattering. Liquid scintillator detectors, Borexino and KamLAND, measured low-energy solar neutrinos using νe elastic scattering. In particular, Borexino successfully measured the pp [233,236], pep [232,235,236], and ^{7}Be [231,235,236] solar neutrino fluxes and set an upper limit for the CNO solar neutrino flux [232,235,236]. KamLAND also measured the ^{7}Be solar neutrino flux [238]. In addition, both Borexino [234,237] and KamLAND [239] measured the ^{8}B neutrino flux. The measured fluxes or upper limits from all these experiments are listed in the Particle Listings at the PDG website [280] except the recently reported Borexino results [236,237].

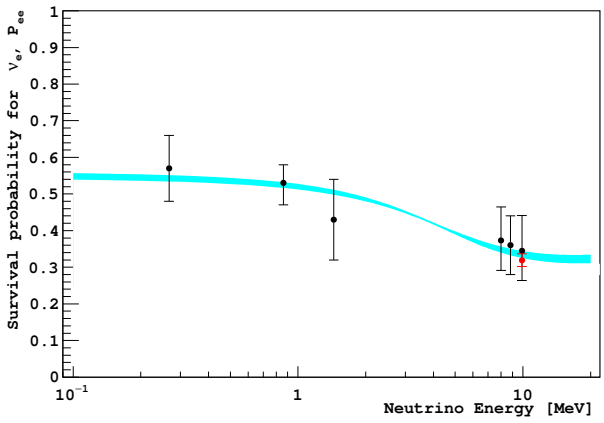

Figure 14.10: Electron neutrino survival probability as a function of neutrino energy. The points represent, from left to right, the Borexino pp, ^{7}Be, pep, and ^{8}B data (black points) and the SNO+SK ^{8}B data (red point). The three Borexino ^{8}B data points correspond, from left to right, to the low-energy (LE) range, LE+HE range, and the high-energy (HE) range. The electron neutrino survival probabilities from experimental points are determined using a high metallicity SSM from Ref. 281. The error bars represent the $\pm 1\sigma$ experimental + thoretical uncertainties. The curve corresponds to the $\pm 1\sigma$ prediction of the MSW-LMA solution using the parameter values given in Ref. 282. This figure is provided by A. Ianni.

Fig. 14.10 plots the survival probability of solar ν_e as a function of neutrino energy. The data points are from the Borexino results [236,237] except the SNO+SK ^{8}B data. The theoretical curve shows the prediction of the MSW-LMA solution. As explained in Section 14.8.2.2, matter effects on solar neutrino oscillation is expected to be given by the average two-neutrino vacuum oscillation probability, $1 - \frac{1}{2}\sin^2 2\theta_{12}$ for survival of pp neutrinos. It is ~ 0.58 for $\sin^2\theta_{12} = 0.297$. For ^{8}B neutrinos, transitions are adiabatic and the survival probability is given by $\sin^4\theta_{13} + \cos^4\theta_{13}\sin^2\theta_{12} \sim 0.28$ for $\sin^2\theta_{13} = 0.0215$ (for normal mass ordering) and $\sin^2\theta_{12} = 0.297$. All the data shown in this plot are consistent with the theoretically calculated curve. This indicates that these solar neutrino results are consistent with the MSW-LMA solution of the solar neutrino problem.

In the nighttime, solar neutrino experiments observe neutrinos propagated through the Earth. Therefore, a non-zero day-night flux (or interaction rate) asymmetry implies the Earth matter effects on flavour oscillations of solar neutrinos. In particular, if the nighttime flux is higher than the daytime flux, it implies a ν_e regeneration by the Earth matter effects (see Section 14.8.2.3). Previously, SNO [279] and Borexino [283] searched for day-night flux asymmetries of ^{8}B and ^{7}Be neutrinos, respectively, but they observed no statistically significant asymmetries. In 2014, the Super-Kamiokande experiment has reported [284] a 2.7σ indication of non-zero day-night asymmetry of ^{8}B solar neutrinos, $A_{DN} = 2(R_D - R_N)/(R_D + R_N) = -0.032 \pm 0.011 \pm 0.005$, where R_D and R_N are the average day and average night νe elastic-scattering rates of ^{8}B solar neutrinos. In 2016, Super-Kamiokande updated this day-night asymmetry as $A_{DN} = -0.033 \pm 0.010 \pm 0.005$ [228]. Statistical significance was slightly improved. This result is consistent with the Δm^2_{21} and θ_{12} values in the LMA region.

14.11. Measurements of $|\Delta m^2_{31(32)}|$ and θ_{23}, and related topics

The first compelling evidence for the neutrino oscillation was ν_μ disappearance observed by the Super-Kamiokande Collaboration in 1998 [17] in the measurement of atmospheric neutrinos produced by cosmic-ray interactions in the atmosphere. The analysis was performed using the 2-neutrino mixing ν_μ survival probability assuming $\nu_\mu \to \nu_\tau$ oscillations, Eq. (14.54) with $l = \mu$, $\theta = \theta_{23}$, $\Delta m^2 = \Delta m^2_{31}$ and $x = \tau$ (or Eq. (14.44) with $l = l' = \mu$, $n = 3$, $|U_{\mu 3}|^2 = \cos^2\theta_{13}\sin^2\theta_{23} \cong \sin^2\theta_{23}$). A striking feature of atmospheric neutrino oscillations was a surprisingly large mixing angle θ_{23}. Whether mixing is maximal, *i.e.*, $\theta_{23} = \pi/4$, or, if not, in which octant θ_{23} lies, is one of the questions drawing much interest in neutrino physics because the measurement of certain fundamental physical observables depends on the value of $\sin^2\theta_{23}$ (see, *e.g.*, Sections 14.2 and 14.8.1). The high precision measurement of $\sin^2\theta_{23}$ will provide also a test of a large class of theories of neutrino masses and mixing, based, in particular, on discrete symmetries (see, *e.g.*, the first three articles quoted in Ref. 96 and Ref. 285).

14.11.1. ν_μ *disappearance data* :

Prior to the Super-Kamiokande's discovery of atmospheric neutrino oscillations, a deficit of atmospheric $\nu_\mu + \bar{\nu}_\mu$ flux was indicated by the Kamiokande experiment [243]. Actually, Kamiokande reported the double ratio $R(\nu_\mu/\nu_e) = (\text{Measured } \nu_\mu/\nu_e)/(\text{Expected } \nu_\mu/\nu_e) < 1$ to reduce systematic effects due to rather large flux uncertainties. The IMB [245] and Soudan 2 [247] experiments also observed $R < 1$, but the Frejus experiment [246] did not see such a tendency. Kamiokande further observed zenith-dependence of $\nu_\mu + \bar{\nu}_\mu$ flux deficit [244]. However, all these results from early experiments did not have conclusive statistical significance.

In 1998, the Super-Kamiokande Collaboration reported a significant zenith-angle (Θ) dependent deficit of μ-like events compared to the no-oscillation expectation [17]. For multi-GeV (visible energy > 1.33 GeV) FC+PC muons, the asymmetry A, defined as $A = (U - D)/(U + D)$, where U is the number of upward-going events ($-1 < \cos\Theta < -0.2$) and D is the number of downward-going events ($0.2 < \cos\Theta < 1$), was observed to be $A = -0.296 \pm 0.048 \pm 0.01$ which deviates from 0 by more than 6σ. This asymmetry is expected to be ~ 0 independent of the atmospheric neutrino flux model for neutrino energy > 1 GeV. On the other hand, the zenith-angle distribution of the e-like events was consistent with the expectation

in the absence of oscillations. Fig. 14.11 shows the compilation of zenith-angle distributions of e-like and μ-like events from the Super-Kamiokande atmospheric observation. Events included in these plots are single-ring FC events subdivided into sub-GeV (visible energy < 1.33 GeV) events and multi-GeV events. The zenith-angle distribution of the multi-GeV μ-like events is shown combined with that of the PC events. The final-state leptons in these events have good directional correlation with the parent neutrinos. The dotted histograms show the Monte Carlo expectation for neutrino events. If the produced flux of atmospheric neutrinos of a given flavour remains unchanged at the detector, the data should have similar distributions to the expectation. However, the zenith-angle distribution of the μ-like events shows a strong deviation from the expectation. On the other hand, the zenith-angle distribution of the e-like events is consistent with the expectation. This characteristic feature is interpreted that muon neutrinos coming from the opposite side of the Earth's atmosphere, having travelled $\sim 10,000$ km, oscillate into other neutrinos and disappeared, while oscillations still do not take place for muon neutrinos coming from above the detector, having travelled from a few to a few tens km. These results are in good agreement with $\nu_\mu \leftrightarrow \nu_\tau$ two-flavour neutrino oscillations, because there is no indication of electron neutrino appearance. The atmospheric neutrinos corresponding to the events shown in Fig. 14.11 have $E = 1 \sim 10$ GeV. With $L = 10000$ km, neutrino oscillations suggests $\Delta m^2 \sim 10^{-3} - 10^{-4}$ eV^2. A significant deficit of μ-like events suggests a large mixing angle. Super-Kamiokande's initial results on the oscillation parameters for $\nu_\mu \leftrightarrow \nu_\tau$ were $5 \times 10^{-4} < \Delta m^2 < 6 \times 10^{-3}$ eV^2 and $\sin^2 2\theta > 0.82$ at 90% CL [17].

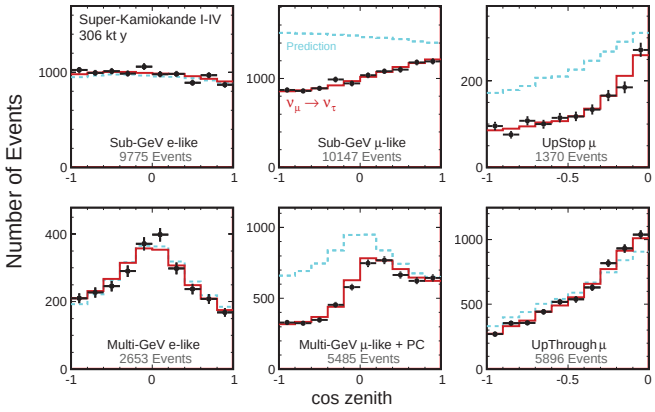

Figure 14.11: The zenith angle distributions for fully contained 1-ring e-like and μ-like events with visible energy < 1.33 GeV (sub-GeV) and > 1.33 GeV (multi-GeV). For multi-GeV μ-like events, a combined distribution with partially contained (PC) events is shown. The dotted histograms show the non-oscillated Monte Carlo events, and the solid histograms show the best-fit expectations for $\nu_\mu \leftrightarrow \nu_\tau$ oscillations. (This figure is provided by the Super-Kamiokande Collab.)

Although the Super-Kamiokande's atmospheric neutrino data are consistent with $\nu_\mu \leftrightarrow \nu_\tau$ oscillations, this interpretation will be strengthened if ν_τ appearance and characteristic sinusoidal behavior of the ν_μ survival probability as a function of L/E were observed. In fact, other exotic explanations such as neutrino decay [286] and quantum decoherence [287] cannot be completely ruled out from the zenith-angle distributions alone. By selecting events with high L/E resolution, evidence for the dip in the L/E distribution was observed at the right place expected from the interpretation of the Super-Kamiokande's data in terms of $\nu_\mu \leftrightarrow \nu_\tau$ oscillations [18], see Fig. 14.12. This dip cannot be explained by alternative hypotheses of neutrino decay and neutrino decoherence, and they are excluded at more than 3σ in comparison with the neutrino oscillation interpretation. For ν_τ appearance, see Section 14.11.4.

The muon neutrino disappearance discovered by Super-Kamiokande has been confirmed by atmospheric neutrino experiments, MACRO [248] and Soudan 2 [249], long baseline accelerator experiments, K2K [19],

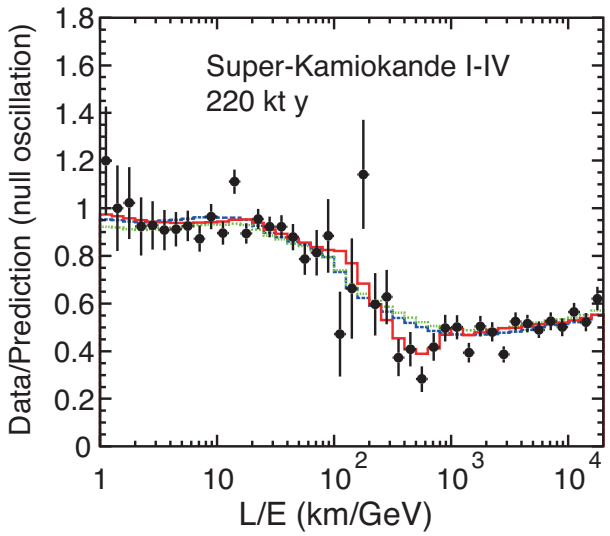

Figure 14.12: Results of the L/E analysis of SK1-SK4 atmospheric neutrino data. The points show the ratio of the data to the Monte Carlo prediction without oscillations, as a function of the reconstructed L/E. The error bars are statistical only. The solid line shows the best fit with 2-flavour $\nu_\mu \leftrightarrow \nu_\tau$ oscillations. The dashed and dotted lines show the best fit expectations for neutrino decay and neutrino decoherence hypotheses, respectively. (This figure is provided by the Super-Kamiokande Collab.)

MINOS [20,21], T2K [22,23], and NOνA [41], and neutrino telescope experiments, ANTARES [253] and IceCube-DeepCore [255]. Fig. 14.13 shows 90% CL allowed regions in the $\sin^2 2\theta_{23}$ - $\Delta m^2_{32(31)}$ plane, for the case of normal mass ordering, reported by the T2K [43], NOνA [60], MINOS [289], Super-Kamiokande [288], and IceCube-DeepCore [254] experiments. All these regions are derived from three-neutrino oscillation analyses.

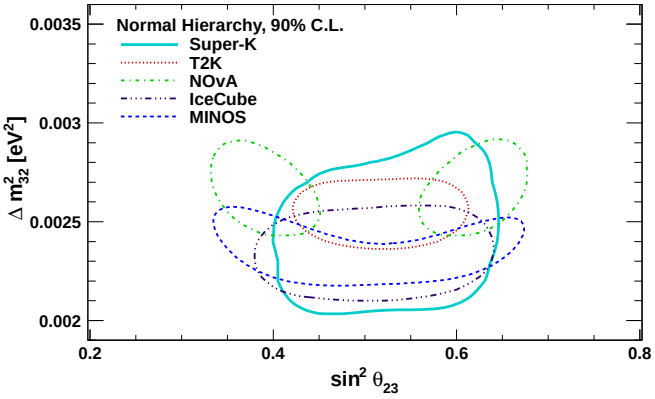

Figure 14.13: The 90% confidence regions for the $\sin^2\theta_{23}$ - Δm^2_{32} plane assuming normal mass ordering derived from the T2K [43], NOνA [60], MINOS [289], Super-Kamiokande [288], and IceCube [254] experiments. This figure is taken from [288].

14.11.2. *Octant of θ_{23}* :

The two-flavour ν_μ survival probability in vacuum $P^{2\nu}(\nu_\mu \to \nu_\mu)$ is given by Eq. (14.54) with $l = \mu$, $\theta = \theta_{23}$ and $\Delta m^2 = \Delta m^2_{31}$. It is symmetric in the mixing angle θ with respect to $\theta = \pi/4$, or degenerate with respect to the interchange $\theta \leftrightarrow \pi/2 - \theta$. In other words, in the leading order the ν_μ disappearance is not sensitive to the octant of the mixing angle θ, namely, whether θ lies in the first octant ($\theta < \pi/4$) or in the second octant ($\theta > \pi/4$). This is the reason

why $\sin^2 2\theta_{23}$ has been used in the neutrino oscillation literature until recently. However, as the mixing determined by the angle θ_{23} is known to be nearly maximal, it is important to determine whether $\theta_{23} = \pi/4$, or if not, in which octant θ_{23} lies. As we have seen in Section 14.8, the value of $\sin^2\theta_{23}$ plays a very important role in the determination of the neutrino mass ordering in the experiments with atmospheric neutrinos and in long baseline neutrino oscillation experiments. It is also one of the important parameters in the interpretation of the data on CP violation in neutrino oscillations. The value of θ_{23} might be related to the existence of a new underlying fundamental symmetry of the neutrino mixing matrix and of the lepton sector of particle physics (see, e.g., the first three articles quoted in Ref. [96]) . Precise determination of θ_{23} requires, *e.g.*, precise measurements of ν_μ disappearance and analyses in terms of full three-neutrino oscillations, or combined analysis of ν_μ disappearance and $\nu_\mu \to \nu_e$ appearance for ν_μ and $\bar{\nu}_\mu$ beams.

MINOS [289] has made a combined analysis of the ν_μ disappearance [290] and $\nu_\mu \to \nu_e$ appearance [47] data using the complete set of accelerator and atmospheric neutrino data. The results obtained are $|\Delta m^2_{32}| = (2.28 - 2.46) \times 10^{-3}$ eV^2 (68% CL) and $\sin^2\theta_{23} = 0.35 - 0.65$ (90% CL) for normal mass ordering and $|\Delta m^2_{32}| = (2.32 - 2.53) \times 10^{-3}$ eV^2 (68% CL) and $\sin^2\theta_{23} = 0.34 - 0.67$ (90% CL) for inverted mass ordering. The best-fit value in this analysis, $\sin^2\theta_{23} < 0.5$ ($\theta_{23} < \pi/4$) is obtained for inverted mass ordering.

Recently, NOνA [60] has made a precise measurement of ν_μ disappearance using the data corresponding to 6.05×10^{20} POT. Assuming the normal mass ordering, $\Delta m^2_{32} = (2.67 \pm 0.11) \times 10^{-3}$ eV^2 and two statistically degenerate values of $\sin^2\theta_{23} = 0.404^{+0.030}_{-0.022}$ and $0.624^{+0.022}_{-0.030}$ are obtained. The NOνA results disfavor the maximal mixing $\theta_{23} = \pi/2$ at 2.6σ significance.

T2K, on the other hand, has accumulated the neutrino mode data corresponding to 7.482×10^{20} POT and the antineutrino mode data corresponding to 7.471×10^{20} POT, and has made a combined analysis of ν_μ and $\bar{\nu}_\mu$ disappearance and $\nu_\mu \to \nu_e$ and $\bar{\nu}_\mu \to \bar{\nu}_e$ appearance channels [43]. In this analysis, ν_μ, $\bar{\nu}_\mu$, ν_e, and $\bar{\nu}_e$ CCQE (charged-current quasielastic event) candidates were selected from the far-detector data, and a joint maximum likelihood fit of these four event samples has been performed to estimate the oscillation parameters, $\sin^2\theta_{23}$, Δm^2_{32}, $\sin^2\theta_{13}$, and δ in the full three neutrino oscillation framework. (In the fit, the reconstructed neutrino energy $E_{\rm rec}$ is used for ν_μ and $\bar{\nu}_\mu$ samples, and $E_{\rm rec}$ and reconstructed angle between the lepton and the neutrino beam direction $\theta_{\rm rec}$ are used for ν_e and $\bar{\nu}_e$ samples.) The T2K results shown in Fig. 14.13 are obtained from this fit using the "reactor measurement" of $\sin^2 2\theta_{13} = 0.085 \pm 0.005$ [291] and assuming normal mass ordering. The obtained best-fit values are $\Delta m^2_{32} = 2.545 \times 10^{-3}$ eV^2 and $\sin^2\theta_{23} = 0.532$. The T2K result is consistent with maximal mixing. However, as the 68% CL interval for $\sin^2\theta_{23}$ is 0.464 - 0.578, T2K notes [43] that the tension between the the T2K and NOνA [60] measurements is rather mild ($1.7\ \sigma$).

14.11.3. *Comparison of ν_μ disappearance and $\bar{\nu}_\mu$ disappearance data* :

The CPT symmetry requires neutrinos and antineutrinos to have the same masses and mixing parameters. In vacuum, this means the same survival probabilities for a neutrino and an antineutrino which have the same energy and which traveled the same distance. In matter, ν_μ and $\bar{\nu}_\mu$ survival probabilities are different, but with the experimental conditions of MINOS and T2K, which reported $\bar{\nu}_\mu$ disappearance in accelerator long baseline experiments, the differences are small.

MINOS first observed muon antineutrino disappearance [292] with the NUMI beam line optimized for $\bar{\nu}_\mu$ production. Actually, MINOS produced a "ν_μ-dominated" or "$\bar{\nu}_\mu$-enhanced" beam by selectively focusing positive or negative pions and kaons. In Ref. 290, MINOS reported the results of the neutrino oscillation analysis based on the data obtained with 10.71×10^{20} POT of the ν_μ-dominated beam and 3.36×10^{20} POT of the $\bar{\nu}_\mu$-enhanced beam. In addition, they used the atmospheric neutrino data based on the MINOS far detector exposure of 37.88 kt·yr [250]. As the MINOS detector has a capability to separate neutrinos and antineutrinos on an event-by-event basis, it can use both ν_μ and $\bar{\nu}_\mu$ contained events from the ν_μ-dominated beam. From the $\bar{\nu}_\mu$-enhanced beam, $\bar{\nu}_\mu$ contained events are used. For the complete data sets used, refer to Ref. 290. Assuming the identical oscillation parameters for neutrinos and antineutrinos, the results of the fit within the two-neutrino oscillation framework using the full MINOS data sample yielded $\Delta m^2 = (2.41^{+0.09}_{-0.10}) \times 10^{-3}$ eV^2 and $\sin^2 2\theta = 0.950^{+0.035}_{-0.036}$, or $\sin^2 2\theta > 0.890$ at 90% CL. Allowing independent oscillations for neutrinos and antineutrinos, characterised respectively by Δm^2, θ and $\Delta\bar{m}^2$, $\bar{\theta}$, the results of the fit are $\Delta\bar{m}^2 = (2.50^{+0.23}_{-0.25}) \times 10^{-3}$ eV^2 and $\sin^2 2\bar{\theta} = 0.97^{+0.03}_{-0.08}$, or $\sin^2 2\bar{\theta} > 0.83$ at 90% CL, and Δm^2 - $\Delta\bar{m}^2 = (0.12^{+0.24}_{-0.26}) \times 10^{-3}$ eV^2. This result shows that the neutrino and antineutrino mass splittings are in agreement, which is compatible with CPT invariance.

T2K also observed $\bar{\nu}_\mu$ disappearance [293,294] using an off-axis quasi-monochromatic $\bar{\nu}_\mu$ beam peaked at ~ 0.6 GeV with the polarity of the horn current set to focus negative pions. Using the same ν_μ and $\bar{\nu}_\mu$ CCQE candidate events as used in Ref. 43, T2K has made a simultaneous analysis of the neutrino and antineutrino disappearance, allowing $\theta_{23} \neq \bar{\theta}_{23}$ and $\Delta m^2_{32} \neq \Delta\bar{m}^2_{32}$ [294]. This simultaneous analysis is motivated by a significant neutrino background in the antineutrino-mode running. A maximum likelihood fit has been performed to the reconstructed energy spectra of μ-like samples observed in the Super-Kamiokande in the neutrino mode and antineutrino mode. In this fit, δ is fixed to 0 since it has a negligible impact on the disappearance spectra. Other oscillation parameters, θ_{12}, θ_{13}, and Δm^2_{21} are assumed to be the same for neutrinos and antineutrinos, and are treated as nuisance parameters. Matter effects, though negligible, are included. Assuming the normal mass ordering, the best-fit values (and 68% CL intervals) obtained for the ν_μ disappearance parameters are $\Delta m^2_{32} = 2.53\ (2.40 - 2.68) \times 10^{-3}$ eV^2 and $\sin^2\theta_{23} = 0.51\ (0.44 - 0.59)$, and those for $\bar{\nu}_\mu$ disappearance parameters are $\Delta\bar{m}^2_{32} = 2.55\ (2.28 - 2.88) \times 10^{-3}$ eV^2 and $\sin^2\bar{\theta}_{23} = 0.42\ (0.35 - 0.67)$. These results show that (i) they are consistent with the MINOS $\bar{\nu}_\mu$ disappearance results [292] and (ii) no significant differences are observed between the values of ν_μ and $\bar{\nu}_\mu$ oscillation parameters.

Note also that Super-Kamiokande searched for differences in oscillation parameters for ν_μ and $\bar{\nu}_\mu$ in atmospheric neutrino observations [295]. As Super-kamiokande cannot identify ν_μ and $\bar{\nu}_\mu$ on an event by event basis, this study relied on a statistical method to fit the zenith-angle distributions of various event samples with different mixing parameters between ν_μ and $\bar{\nu}_\mu$ disappearance models. The results of this study showed no difference between neutrino and antineutrino mixing.

14.11.4. *ν_τ appearance data* :

Super-Kamiokande Collaboration searched for the appearance of τ leptons from the CC interactions of oscillation-generated ν_τ in the detector using the atmospheric neutrino data [296,24]. In the 2-neutrino mixing framework, the relevant $\nu_\mu \to \nu_\tau$ oscillation probability is given by Eq. (14.54) with $l = \mu$, $x = \tau$, $\theta = \theta_{23}$ and $\Delta m^2 = \Delta m^2_{31}$. An excess of τ-like events is expected in the upward-going direction. Though the Super-Kamiokande detector cannot identify a CC ν_τ interaction on an event by event basis, the Super-Kamiokande Collaboration excluded the no-tau-appearance hypothesis at the 3.8σ level through a neural network analysis on the zenith-angle distribution of multi-GeV contained events [24].

For the purpose of demonstrating the appearance of tau neutrinos on an event-by-event basis, a promising method is an accelerator long-baseline experiment using emulsion technique to identify short-lived τ leptons produced in the ν_τ CC interactions. OPERA adopted this strategy and searched for the appearance of ν_τ in the CNGS muon neutrino beam during 2008 and 2012, corresponding to a live exposure of 17.97×10^{19} POT in total. In 2010, OPERA reported observation of the first ν_τ candidate [173]. In 2015, OPERA has reported observation of the fifth ν_τ candidate [297]. The observed candidate events are classified into the four decay channels, $\tau \to 1h$ (hadronic 1-prong), $\tau \to 1h$ (hadronic 3-prong), $\tau \to \mu$, and $\tau \to e$, and expected signal and background events are calculated for each decay channel. The expected total signal and background events are,

respectively, 2.64 ± 0.53 and 0.25 ± 0.05. With 5 events observed, the OPERA Collaboration concludes the discovery of ν_τ appearance with a significance larger than 5σ.

14.12. Measurements of θ_{13}

The discoveries of atmospheric neutrino oscillations and solar neutrino oscillations naturally led to considerable interests in the measurements of the last neutrino mixing angle θ_{13}, because if θ_{13} is not too small, it will widen the opportunities to measure the unknown CP-violating phase δ in the PMNS matrix and the neutrino mass ordering.

In 2012, the three reactor neutrino oscillation experiments Double Chooz, Daya Bay, and RENO reported their first results on $\bar{\nu}_e$ disappearance. Under the conditions of these experiments the probability of reactor $\bar{\nu}_e$ survival is given to a very good approximation by Eq. (14.45) (the effects of Δm^2_{21} being negligible) and depends on two parameters $\sin^2 2\theta_{13}$ and Δm^2_{31}. Daya Bay obtained $\sin^2 2\theta_{13} = 0.092 \pm 0.016 \pm 0.005$ from live-time exposure in 55 days, indicating 5.2σ evidence for non-zero θ_{13} [33]. RENO obtained $\sin^2 2\theta_{13} = 0.113 \pm 0.013 \pm 0.019$ from 229 days of exposure, also indicating non-zero θ_{13} with a significance of 4.9σ [34]. Both Daya Bay and RENO results were obtained from rate-only analyses of the $\bar{\nu}_e$ disappearance measurements with near and far detectors. These results established non-zero θ_{13}, and it turned out that the measured value of θ_{13} was relatively large. It should be noted that prior to Daya Bay and RENO, Double Chooz also reported $\sin^2 2\theta_{13} = 0.086 \pm 0.041 \pm 0.030$ with measurements by a far detector, and it ruled out the no-oscillation hypothesis at the 94.6% CL [32].

The latest Daya Bay results [44] are obtained based on the combination of 217 days (December 2011 - July 2012) of measurement with six antineutrino detectors and a subsequent 1013 days (October 2012 - July 2015) of measurement with eight detectors. The Daya Bay collaboration has adopted the three-flavour oscillation scheme and analyzed the relative antineutrino rates and energy spectra between detectors using a method to predict the signal in the far hall based on measurements obtained in the near halls. With this method, they have minimized the model dependence on reactor antineutrino emission. Also, improvements in energy calibration (0.2% between detectors) and background estimation helped reduce systematic errors. Their reported new result, $\sin^2 2\theta_{13} = 0.0841 \pm 0.0027 \pm 0.0019$ is the most precise measurement of θ_{13} to date. To obtain this result, they used $\sin^2 2\theta_{12} = 0.846 \pm 0.021$ and $\Delta m^2_{21} = (7.53 \pm 0.18) \times 10^{-5}$ eV^2 [291], but the dependence on these parameters is weak. They also found for the effective mass-squared difference $|\Delta m^2_{ee}| = (2.50 \pm 0.06 \pm 0.06) \times 10^{-3}$ eV^2, where $\Delta m^2_{ee} \simeq \cos^2\theta_{12}|\Delta m^2_{31}| + \sin^2\theta_{12}|\Delta m^2_{32}|$. From the measured value of $|\Delta m^2_{ee}|$, they deduce $\Delta m^2_{32} = (2.45 \pm 0.06 \pm 0.06) \times 10^{-3}$ eV^2 for the normal mass ordering and $\Delta m^2_{32} = -(2.56 \pm 0.06 \pm 0.06) \times 10^{-3}$ eV^2 for the inverted mass ordering. These results on Δm^2_{32} are consistent with the T2K and MINOS results.

The latest RENO results are reported at TAUP2017 [45] based on 1500 live days of data. Using the observed IBD prompt rates and spectra in the near and far detectors, $\sin^2 2\theta_{13} = 0.086 \pm 0.006 \pm 0.005$ and $|\Delta m^2_{ee}| = (2.61^{+0.15}_{-0.16} \pm 0.09) \times 10^{-3}$ eV^2 have been obtained.

The latest results from Double Chooz using the data collected by the far detector in 467.90 live days have been published in Ref. 46. From a fit to the observed spectrum ("Rate + Shape analysis") in the two-flavour oscillation scheme, Double Chooz obtained $\sin^2 2\theta_{13} = 0.090^{+0.032}_{-0.029}$ for the normal mass ordering using $\Delta m^2_{31} = (2.44^{+0.09}_{-0.10}) \times 10^{-3}$ eV^2 from MINOS [289]. For the inverted mass ordering, they obtained $\sin^2 2\theta_{13} = 0.092^{+0.033}_{-0.029}$, using $|\Delta m^2_{31}| = (2.38^{+0.09}_{-0.10}) \times 10^{-3}$ eV^2 [289].

Until θ_{13} was measured by the modern reactor experiments, long-baseline accelerator $\nu_\mu \to \nu_e$ appearance experiments were considered to be another promising method to measure θ_{13}, within uncertainties mainly caused by unknown CPV phase δ. In fact, experimental indications of $\nu_\mu \to \nu_e$ oscillations and a non-zero θ_{13} was reported by the T2K experiment in 2011. T2K observed, with 1.43×10^{20} POT, six ν_e candidate events, while the expectation for $\theta_{13} = 0$ was 1.5 ± 0.3 events. This result implied a non-zero θ_{13} with statistical significance of 2.5σ [30]. However, because of the unfortunate damage of the J-PARC accelerator caused by the big Tohoku earthquake which hit Japan in March 2011, the T2K experiment stopped for more than a year, and it was in 2014 that T2K could establish non-zero θ_{13} at more than 7σ [48]. Thereafter, the focus of long baseline accelerator $\nu_\mu \to \nu_e$ appearance experiments shifted to the measurement of the CPV phase δ.

14.13. $\nu_\mu \to \nu_e$ ($\bar{\nu}_\mu \to \bar{\nu}_e$) appearance data and measurements of δ

As Eq. (14.74) shows, the probability of $\nu_\mu \to \nu_e$ oscillations in matter is given as a function of all the oscillation parameters including the sign of Δm^2_{31}, *i.e.*, mass ordering. Using the measured values of θ_{13} from the reactor experiments and Δm^2_{21} and θ_{12} from the solar neutrino experiments and KamLAND as constraints, accelerator-based long baseline experiments are able to measure the CPV phase δ and constrain mass ordering through oscillation analyses of $\nu_\mu \to \nu_e$ and $\bar{\nu}_\mu \to \bar{\nu}_e$ appearance. In these analyses, in particular in the simultaneous analyses of ν_e (and $\bar{\nu}_e$) appearance and ν_μ (and $\bar{\nu}_\mu$) disappearance, θ_{23} and $\Delta m^2_{32} \cong \Delta m^2_{31}$ are also better determined.

MINOS first used a combination of the $\nu_\mu \to \nu_e$ (and $\bar{\nu}_\mu \to \bar{\nu}_e$) appearance measurements and the reactor measurements of θ_{13} to study δ, θ_{23} octant, and mass ordering, and placed some constraints on the value of δ [47]. For this study, MINOS extracted $\nu_\mu \to \nu_e$ and $\bar{\nu}_\mu \to \bar{\nu}_e$ appearance signals statistically from the full MINOS data sample corresponding to 10.6×10^{20} POT ν-beam mode and 3.3×10^{20} POT $\bar{\nu}$-beam mode data-taking.

As noted in Section 14.12, T2K first reported observation of $\nu_\mu \to \nu_e$ appearance events in 2011 [30]. After the interruption due to the Tohoku earthquake, the resumed T2K experiment has accumulated $\nu_\mu \to \nu_e$ appearance data. In 2014, T2K reported observation of 28 ν_e events against 4.92 ± 0.55 expected background events with 1.43×10^{20} POT, and established $\nu_\mu \to \nu_e$ appearance signal with statistical significance of more than 7σ [48]. Also, T2K made an oscillation analysis using the ν_e appearance data [48], or joint analyses of ν_e appearance and ν_μ disappearance [298] with a constraint of θ_{13} value from reactor measurements. Later, T2K switched the data-taking with a ν_μ beam to that with a $\bar{\nu}_\mu$ beam. As discussed in Section 14.11.2, T2K further made a combined analysis of ν_μ and $\bar{\nu}_\mu$ disappearance and $\nu_\mu \to \nu_e$ and $\bar{\nu}_\mu \to \bar{\nu}_e$ appearance channels [43] using the neutrino-mode data corresponding to 7.482×10^{20} POT and the antineutrino-mode data corresponding to 7.471×10^{20} POT. As the appearance signal, 32 ν_e and 4 $\bar{\nu_e}$ CCQE event candidates are selected from these data. T2K further added five ν_e CC1π^+ events selected from the same data set used in Ref. 43 and made another combined analysis [299]. Fig. 14.14 shows $-2\Delta \ln \mathcal{L}$ as a function of δ, resulted from a joint maximum-likelihood fit, in which other oscillation parameters and nuisance parameters are marginalized (integrated over the prior probability density function). In this analysis, CP-conserving values $\delta = 0, \pi$ are excluded at 90% CL.

More recently, in August 2017, T2K announced the latest results with doubled POT for the neutrino-mode data taking [300]. With an improved event selection in the Super-Kamiokande in addition, T2K has observed 74 ν_e and 7 $\bar{\nu_e}$ CCQE event candidates. A combined oscillation analysis using the reactor measurement of θ_{13} has now resulted the CP conserving values of $\delta = 0$ and π falling outside of the 2σ CL intervals for both the normal and inverted mass orderings.

NOνA started physics run in February, 2014, and reported its first result of ν_e appearance measurement in 2016 [40]. Since then, NOνA has accumulated more data, and recently reported observation of 33 ν_e candidates withh 8.2 ± 0.8 background events corresponding to 6.05×10^{20} POT [42]. NOνA has made a combined analysis of ν_e appearance and ν_μ disappearance data, using the reactor measurement of θ_{13} as a constraint. Fig. 14.15 shows the significance (σ) at which each value of δ is disfavored. As the NOνA measurement of $\sin^2\theta_{23}$ has two statistically degenerate values (see Section 14.11.2), the significance is shown for four possible combinations of mass ordering (normal or inverted) and θ_{23} octant (first/lower or second/upper).

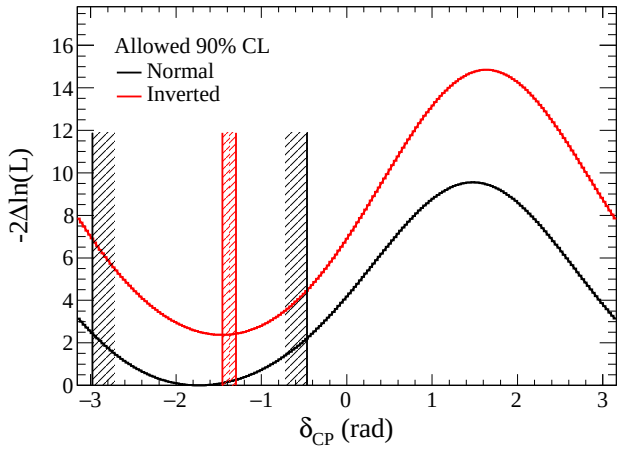

Figure 14.14: T2K's log-likelihood as a function of δ_{CP} for the normal (black) and inverted (red) mass ordering, obtained from a combined analysis of neutrino and antineutrino oscillations using both appearance and disappearance channels. The vertical lines show the corresponding allowed 90% confidence intervals, calculated using the Feldman-Cousins method. $\sin^2\theta_{13}$ is marginalized using the reactor measurement as prior probability using the value of PDG 2015 [291]. This figure is taken from [299].

As seen from this figure, there are two degenerate best-fit points for normal mass ordering, $\sin^2\theta_{23} = 0.404$ and $\delta = 1.48\pi$ and $\sin^2\theta_{23} = 0.623$ and $\delta = 0.74\pi$. The inverted mass ordering in the first octant is disfavored at $> 93\%$ for all the value of δ.

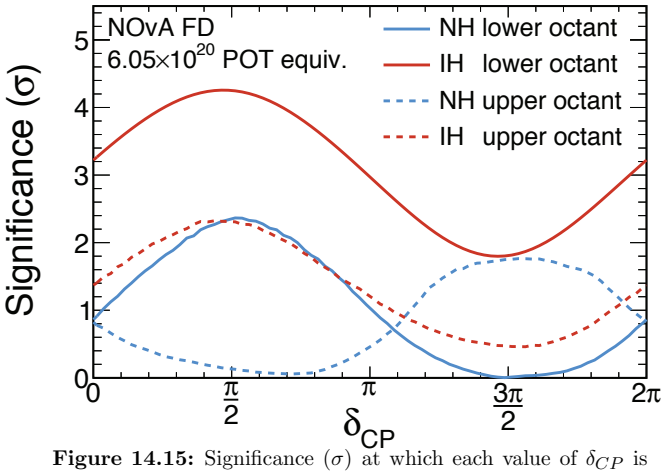

Figure 14.15: Significance (σ) at which each value of δ_{CP} is disfavored for each of the four possible combinations of mass ordering: normal (blue) or inverted (red), and θ_{23} octant: lower (solid) or upper (dashed), by the combination of ν_e appearance and NOνA's latest ν_μ disappearance measurement. This figure is taken from [42].

14.14. Search for Oscillations Involving Light Sterile Neutrinos

Although the mixing of the 3 flavour neutrino states has been experimentally well established, implying the existence of 3 light neutrinos ν_j having masses m_j not exceeding approximately 1 eV, there have been possible hints for the presence in the mixing of one or more additional neutrino states with masses at the eV scale. If these states exist, they must be related to the existence of one or more sterile neutrinos (sterile neutrino fields) which mix with the active flavour neutrinos (active flavour neutrino fields). The hints under discussion have been obtained: i) in the LSND $\bar\nu_\mu \to \bar\nu_e$ appearance experiment [259], in which a significant excess of events over the background is claimed to have been observed, ii) from the analysis of the $\bar\nu_\mu \to \bar\nu_e$ [262] and $\nu_\mu \to \nu_e$ [261] appearance data of the MiniBooNE experiment, iii) from the re-analyses of the short baseline (SBL) reactor neutrino oscillation data using newly calculated fluxes of reactor $\bar\nu_e$ [156,155], which show a possible "disappearance" of the reactor $\bar\nu_e$ ("reactor neutrino anomaly"), and iv) from the data of the radioactive neutrino source measurements of the GALLEX [241] and SAGE [242] solar neutrino experiments.

The short baseline neutrino oscillation experiment MiniBooNE at Fermilab investigated ν_e [261] and $\bar\nu_e$ [262] appearance in ν_μ and $\bar\nu_\mu$ beams, respectively, with a detector containing 800 tons of mineral oil and located 541 m downstream of the production target. With the antineutrino running mode [262], a 2.8σ excess of events over the background was observed in the energy range of $200 < E_\nu < 1250$ MeV in the charged-current quasielastic data. Excess events were observed, in particular, in the interval of energies $200 < E_\nu < 475$ MeV, which corresponds to L/E range outside of that probed in the LSND experiment. The origin of this excess is not understood. Employing a simple 2-neutrino oscillation hypothesis and using the data from the entire neutrino energy interval $200 < E_\nu < 1250$ MeV in the data analysis, this result, interpreted in terms of $\nu_\mu \to \nu_e$ oscillations, corresponds to an allowed region in the $\sin^2 2\theta - \Delta m^2$ plane, which overlaps with the allowed region obtained from the interpretation of the LSND data in terms of $\bar\nu_\mu \to \bar\nu_e$ oscillations. The overlap region at the 90% CL extends over $\Delta m^2 \sim$ a few $\times 10^{-2}$ eV^2 at $\sin^2 2\theta = 1$ to 1 eV^2 at $\sin^2 2\theta =$ a few $\times 10^{-3}$. The MiniBooNE Collaboration studied also the CP conjugate oscillation channel [261], $\nu_\mu \to \nu_e$, and observed a 3.4 σ excess of events in the same energy range. Most of the excess events lie in the interval $200 < E_\nu < 475$ MeV and are incompatible with the $\bar\nu_\mu \to \bar\nu_e$ oscillation interpretation of the LSND data. The energy spectra of the excess events observed in the ν_μ [261] and $\bar\nu_\mu$ [262] runs are only marginally compatible with each other and thus with the simple 2-neutrino oscillation hypothesis.

The reactor neutrino anomaly [156] is related to the results of a new and very detailed calculation of the reactor $\bar\nu_e$ fluxes [155] which were found to be by approximately 3.5% larger than the fluxes calculated in Ref. 153 and widely used in the past in the interpretation of the data of the SBL reactor $\bar\nu_e$ oscillation experiments. These data show indications for reactor $\bar\nu_e$ "disappearance" when analyzed using the fluxes from [155]. It should be added that there are a number of uncertainties in the calculation of the fluxes under discussion (associated, *e.g.*, with the weak magnetism term contribution to the corresponding β-decay rates [157], the contribution of a relatively large number of "forbidden" β-decays [301], etc.) which can be of the order of the difference between the "old" and "new" fluxes.

Radioactive neutrino source measurements of the GALLEX [241] and SAGE [242] experiments also showed a deficit of the measured fluxes compared to the expected fluxes ("Gallium anomaly"), and therefore might be interpreted as hints for ν_e disappearance.

Significant constraints on the parameters characterizing the oscillations involving sterile neutrinos follow from the negative results of the searches for $\nu_\mu \to \nu_e$ and/or $\bar\nu_\mu \to \bar\nu_e$ oscillations in the Karmen [260], NOMAD [302], ICARUS [258], and OPERA [303] experiments, and from the nonobservation of effects of oscillations into sterile neutrinos in the solar neutrino experiments and in the studies of ν_μ and/or $\bar\nu_\mu$ disappearance in the CDHSW [304], MINOS and SuperKamiokande experiments.

In the period May 2016 - May 2017 results of searches for active-sterile neutrino oscillations with $\Delta m^2 \sim 1$ eV^2 were presented by the IceCube [305], NEOS [306] and DANSS [307] experiments. The IceCube collaboration reported results on disappearance into sterile antineutrinos $\bar\nu_s$ of atmospheric $\bar\nu_\mu$ with energies in the interval $E_\nu \sim$(300 GeV - 10 TeV), which traverse the Earth before reaching the detector. For Earth core crossing $\bar\nu_\mu$, the $\bar\nu_\mu \to \bar\nu_s$ transitions at small mixing angles and $\Delta m^2 \sim (0.1 - 1.0)$ eV^2 can be maximally enhanced at $E_\nu \sim$3 TeV by the Earth mantle-core amplification (or NOLR) effect [190,196](see also [308]) . This allowed the IceCube collaboration to obtain stringent limits on the relevant $\bar\nu_\mu - \bar\nu_s$ mixing parameter in the region $\Delta m^2 \sim (0.1 - 0.6)$ eV^2 assuming two-neutrino mixing (for further details see [305,308]) .

The NEOS and DANSS collaborations performed searches of reactor $\bar{\nu}_e$ disappearance into $\bar{\nu}_s$. The NEOS experiment [306] used a 1 ton Gd loaded liquid scintillator detector located at a distance $L = 24$ m from the core of a reactor with thermal power of 2.8 GW, belonging to the Hanbit nuclear power complex in Yeonggwang, South Korea. In the DANSS experiment at the Kalinin nuclear power plant in Russia [307] the measurements were performed with a movable 0.9 ton segmented solid scintillator detector at 3 different distances from the core of a 3 GW reactor, spanning the (center to center) interval (10.7 - 12.7) m. The detector consists of 2500 scintillator strips, covered with gadolinium loaded reflective paint and read out by silicon PMs via wave length shifting fibers.

In the same period the Daya Bay, MINOS and Bugey-3 collaborations published results of a joint analysis of their disappearance data [309].

Two possible "minimal" phenomenological models (or schemes) with light sterile neutrinos are widely used in order to explain the data discussed in this section in terms of neutrino oscillations: the so-called "3 + 1" and "3 + 2" models. They contain respectively one and two sterile neutrinos (right-handed sterile neutrino fields). Thus, the "3 + 1" and "3 + 2" models have altogether 4 and 5 light massive neutrinos ν_j, which in the minimal versions of these models are Majorana particles. The additional neutrinos ν_4 and ν_4, ν_5 should have masses m_4 and m_4, m_5 at the eV scale (see below). It follows from the data that if ν_4 or ν_4, ν_5 exist, they couple to the electron and muon in the weak charged lepton current with couplings U_{ek} and $U_{\mu k}$, $k = 4$; $4, 5$, which are approximately $|U_{ek}| \sim 0.1$ and $|U_{\mu k}| \sim 0.1$.

In the context of the "3+1" model, the Daya Bay Collaboration searched for relative spectral distortion in their reactor antineutrino data, due to possible mixing of a light sterile neutrino in the $|\Delta m^2_{41}| < 0.3$ eV^2 region [310]. The result is consistent with no sterile neutrino mixing, leading to the most stringent limits on $\sin^2\theta_{14} = |U_{e4}|^2$ in the 10^{-3} eV$^2 < |\Delta m^2_{41}| < 0.1$ eV^2 region.

Global analysis of all the data (positive evidences and negative results) relevant for the test of the sterile neutrino hypothesis were performed most recently in [311](for earlier results of global fits see, e.g., Ref. [312] and Ref. [313]) . The authors of [311] performed the analysis within the $3 + 1$ scheme employing the so-called "pragmatic approach", i.e., excluding from the data set used the MiniBooNE data at $E_\nu < 0.475$ GeV. As we have already mentioned, these data show an excess of events over the estimated background [261,262] whose nature is presently not well understood. For the best fit values of the parameters $|U_{e4}|^2$, $|U_{\mu 4}|^2$ and $\Delta m^2_{\rm SBL} \equiv m_4^2 - m^2_{min}$, where $m_{min} = \min(m_j)$, $j = 1, 2, 3$, characterizing the active-sterile neutrino (antineutrino) oscillations in the $3 + 1$ scheme, the authors of [311] find:

$$|U_{e4}|^2 = 0.019\,, \quad |U_{\mu 4}|^2 = 0.015\,, \quad \Delta m^2_{\rm SBL} = 1.7 \text{ eV}^2\,. \qquad (14.105)$$

The existence of light sterile neutrinos has cosmological implications the discussion of which lies outside the scope of the present article (for a discussion of the cosmological constraints on light sterile neutrinos see, *e.g.*, [314,75]) .

The hypothesis of existence of light sterile neutrinos with eV scale masses and charged current couplings to the electron and muon quoted above, is already being tested, as we have discussed, in a few running experiments, and will be tested in a large number of experiments with reactor and accelerator neutrinos, and neutrinos from artificial sources, some of which are under preparation and are planned to start taking data already this (2017) year (see, *e.g.*, [315] for a detailed list and discussion of the planned experiments).

14.15. Outlook

The currently available data on neutrino oscillations are summarised in Fig. 14.16.

The program of experimental research in neutrino physics extends beyond 2030 (see, *e.g.*, Refs. [91,93,94,82,83,84,85])

In the coming years we expect a wealth of new data that, it is hoped, will shed light on the fundamental aspects of neutrino mixing: the nature - Dirac or Majorana - of massive neutrinos, the type of spectrum the neutrino masses obey, the status of CP symmetry in the lepton sector, the absolute neutrino mass scale, the origin of the observed patterns of the neutrino masses and mixing, and, eventually, on the mechanism of neutrino mass generation. We are looking forward to these exciting developments in neutrino physics.

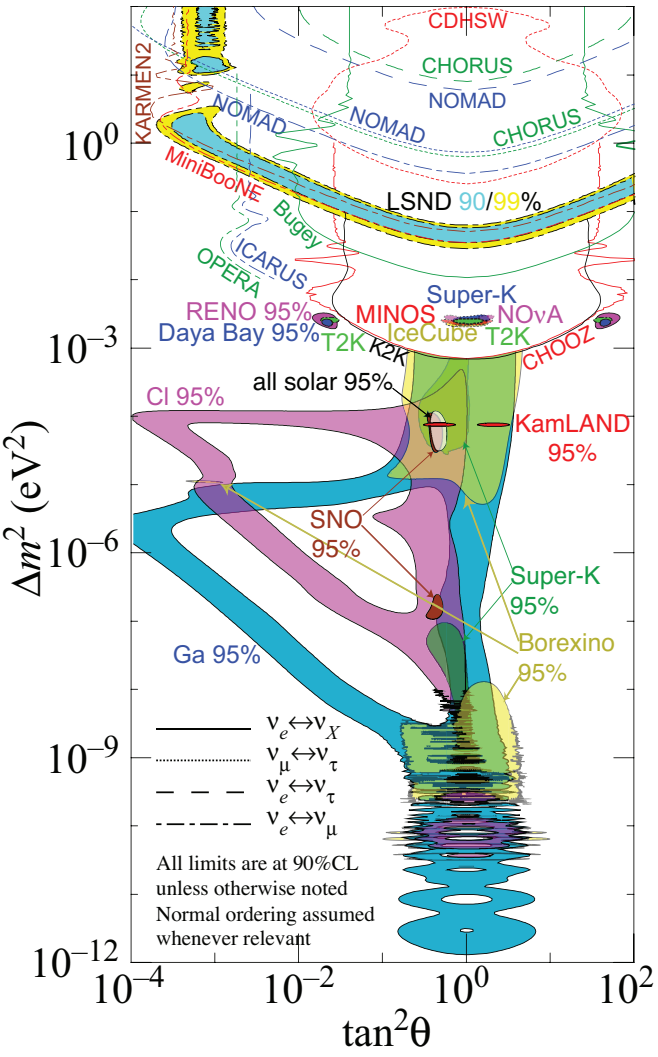

Figure 14.16: The squared-mass splittings and mixing angles favored (solid regions) or excluded (open regions) by existing neutrino oscillation measurements. Results are categorized by channels: ν_e disappearance (solid lines), $\nu_\mu \leftrightarrow \nu_\tau$ (dotted lines), $\nu_e \leftrightarrow \nu_\tau$ (dashed lines), and $\nu_e \leftrightarrow \nu_\mu$ (dashed-dotted lines). The normal mass ordering is assumed where relevant. The figure was contributed by H. Murayama (University of California, Berkeley, and Kavli IPMU, University of Tokyo, 2018).

References:

1. B. Pontecorvo, Zh. Eksp. Teor. Fiz. **53**, 1717 (1967) [Sov. Phys. JETP **26**, 984 (1968)].
2. M. Fukugita and T. Yanagida, Phys. Lett. **B174**, 45 (1986); V.A. Kuzmin, V.A. Rubakov, and M.E. Shaposhnikov, Phys. Lett. **B155**, 36 (1985).
3. P. Minkowski, Phys. Lett. **B67**, 421 (1977); see also: M. Gell-Mann, P. Ramond, and R. Slansky in *Supergravity*, p. 315, edited by F. Nieuwenhuizen and D. Friedman, North Holland, Amsterdam, 1979; T. Yanagida, *Proc. of the Workshop on Unified Theories and the Baryon Number of the Universe*, edited by O. Sawada and A. Sugamoto, KEK, Japan 1979; R.N. Mohapatra and G. Senjanović, Phys. Rev. Lett. **44**, 912 (1980).

4. B. Pontecorvo, Zh. Eksp. Teor. Fiz. **33**, 549 (1957) and **34**, 247 (1958).
5. Z. Maki, M. Nakagawa, and S. Sakata, Prog. Theor. Phys. **28**, 870 (1962).
6. B.T. Cleveland *et al.*, Astrophys. J. **496**, 505 (1988).
7. Y. Fukuda *et al.*, [Kamiokande Collab.], Phys. Rev. Lett. **77**, 1683 (1996).
8. J.N. Abdurashitov *et al.*, [SAGE Collab.], Phys. Rev. **C80**, 015807 (2009).
9. P. Anselmann *et al.*, [GALLEX Collab.], Phys. Lett. **B285**, 376 (1992).
10. W. Hampel *et al.*, [GALLEX Collab.], Phys. Lett. **B447**, 127 (1999).
11. M. Altmann *et al.*, [GNO Collab.], Phys. Lett. **B616**, 174 (2005).
12. S. Fukuda *et al.*, [Super-Kamiokande Collab.], Phys. Lett. **B539**, 179 (2002).
13. Q.R. Ahmad *et al.*, [SNO Collab.], Phys. Rev. Lett. **87**, 071301 (2001).
14. Q.R. Ahmad *et al.*, [SNO Collab.], Phys. Rev. Lett. **89**, 011301 (2002).
15. K. Eguchi *et al.*, [KamLAND Collab.], Phys. Rev. Lett. **90**, 021802 (2003).
16. T. Araki *et al.*, [KamLAND Collab.], Phys. Rev. Lett. **94**, 081801 (2005).
17. Y. Fukuda *et al.*, [Super-Kamiokande Collab.], Phys. Rev. Lett. **81**, 1562 (1998).
18. Y. Ashie *et al.*, [Super-Kamiokande Collab.], Phys. Rev. Lett. **93**, 101801 (2004).
19. M.H. Ahn *et al.*, [K2K Collab.], Phys. Rev. **D74**, 072003 (2006).
20. D.G. Michael *et al.*, [MINOS Collab.], Phys. Rev. Lett. **97**, 191801 (2006); P. Adamson *et al.*, [MINOS Collab.], Phys. Rev. Lett. **101**, 131802 (2008).
21. P. Adamson *et al.*, [MINOS Collab.], Phys. Rev. Lett. **106**, 181801 (2011).
22. K. Abe *et al.*, [T2K Collab.], Phys. Rev. **D85**, 031103 (2012).
23. K. Abe *et al.*, [T2K Collab.], Phys. Rev. Lett. **111**, 211803 (2013).
24. K. Abe *et al.*, [Super-Kamiokande Collab.], Phys. Rev. Lett. **110**, 181802 (2013).
25. A. Pastore, talk at the EPS HEP 2013 Conference, July 18-24, 2013, Stockholm.
26. L. Wolfenstein, Phys. Rev. **D17**, 2369 (1978); *Proc. of the 8th International Conference on Neutrino Physics and Astrophysics - "Neutrino'78"* (ed. E.C. Fowler, Purdue University Press, West Lafayette, 1978), p. C3.
27. S.P. Mikheev and A.Y. Smirnov, Sov. J. Nucl. Phys. **42**, 913 (1985); Nuovo Cimento **9C**, 17 (1986).
28. T. Kajita, "Nobel Diploma", www.nobelprize.org/nobel_prizes/physics/laureates/2015/kajita-diploma.html.
29. A.B. McDonald, "Nobel Diploma", www.nobelprize.org/nobel_prizes/physics/laureates/2015/mcdonald-diploma.html.
30. K. Abe *et al.*, [T2K Collab.], Phys. Rev. Lett. **107**, 041801 (2011).
31. P. Adamson *et al.*, [MINOS Collab.], Phys. Rev. Lett. **107**, 181802 (2011).
32. Y. Abe *et al.*, [Double Chooz Collab.], Phys. Rev. Lett. **108**, 131801 (2012).
33. F.P. An *et al.*, [Daya Bay Collab.], Phys. Rev. Lett. **108**, 171803 (2012).
34. J.K. Ahn *et al.*, [RENO Collab.], Phys. Rev. Lett. **108**, 191802 (2012).
35. Y. Abe *et al.*, [Double Chooz Collab.], Phys. Rev. **D86**, 052008 (2012).
36. K. Abe *et al.*, [T2K Collab.], Phys. Rev. **D88**, 032002 (2013).
37. F.P. An *et al.*, [Daya Bay Collab.], Chin. Phys. C **37**, 011001 (2013).
38. F.P. An *et al.*, [Daya Bay Collab.], Phys. Rev. Lett. **112**, 061801 (2014).
39. S.-H. Seo [for the RENO Collab.], talk at the TAUP2013 International Workshop, September 9-13, 2013, Asilomar, California, USA.
40. P. Adamson *et al.*, [NOνA Collab.] Phys. Rev. Lett. **116**, 151806 (2016).
41. P. Adamson *et al.*, [NOνA Collab.], Phys. Rev. **D93**, 051104 (2016).
42. P. Adamson *et al.*, [NOνA Collab.], Phys. Rev. Lett. **118**, 231801 (2017).
43. K. Abe *et al.*, [T2K Collab.], Phys. Rev. Lett. **118**, 151801 (2017).
44. F.P. An *et al.*, [Daya Bay Collab.], Phys. Rev. **D95**, 072006 (2017).
45. S.-H. Seo [for the RENO Collab.], talk at the TAUP2017 International Workshop, July 24-28, 2017, Sudbury, Canada; arXiv:1710.08204.
46. Y. Abe *et al.*, [Double Chooz Collab.], JHEP **1014**, 086 (2014).
47. P. Adamson *et al.*, [MINOS Collab.], Phys. Rev. Lett. **110**, 171801 (2013).
48. K. Abe *et al.*, [T2K Collab.], Phys. Rev. Lett. **112**, 061802 (2014).
49. D. Karlen in RPP2016 [Chin. Phys. **C40**, No. 10, 646 (2016)].
50. E. Majorana, Nuovo Cimento **5**, 171 (1937).
51. Majorana particles, in contrast to Dirac fermions, are their own antiparticles. An electrically charged particle (like the electron) cannot coincide with its antiparticle (the positron) which carries the opposite non-zero electric charge.
52. S.M. Bilenky and S.T. Petcov, Rev. Mod. Phys. **59**, 671 (1987).
53. S.T. Petcov, Adv. High Energy Phys. **2013**, 852987 (2013), arXiv:1303.5819.
54. S.M. Bilenky, J. Hosek, and S.T. Petcov, Phys. Lett. **B94**, 495 (1980).
55. J. Schechter and J.W.F. Valle, Phys. Rev. **D22**, 2227 (1980); M. Doi *et al.*, Phys. Lett. **B102**, 323 (1981).
56. L. Wolfenstein, Phys. Lett. **B107**, 77 (1981); J. Bernabeu and P. Pascual, Nucl. Phys. **B228**, 21 (1983); S.M. Bilenky, N.P. Nedelcheva, and S.T. Petcov, Nucl. Phys. **B247**, 61 (1984); B. Kayser, Phys. Rev. **D30**, 1023 (1984).
57. M. Apollonio *et al.*, [Chooz Collab.], Phys. Lett. **B466**, 415 (1999); Eur. Phys. J. **C27**, 331 (2003).
58. F. Capozzi *et al.*, Phys. Rev. **D95**, 096014 (2017).
59. I. Esteban *et al.*, JHEP **1701**, 087 (2017).
60. P. Adamson *et al.*, [NOνA Collab.], Phys. Rev. Lett. **118**, 151802 (2017).
61. N. Cabibbo, Phys. Lett. **B72**, 333 (1978).
62. V. Barger *et al.*, Phys. Rev. Lett. **45**, 2084 (1980).
63. P.I. Krastev and S.T. Petcov, Phys. Lett. **B205**, 84 (1988).
64. C. Jarlskog, Z. Phys. **C29**, 491 (1985).
65. P. Langacker *et al.*, Nucl. Phys. **B282**, 589 (1987).
66. S.M. Bilenky, S. Pascoli, and S.T. Petcov, Phys. Rev. **D64**, 053010 (2001), and *ibid.*, 113003.
67. S. Pascoli, S.T. Petcov, and A. Riotto, Phys. Rev. **D75**, 083511 (2007); E. Molinaro and S.T. Petcov, Phys. Lett. **B671**, 60 (2009).
68. S. Pascoli, S.T. Petcov, and A. Riotto, Nucl. Phys. **B774**, 1 (2007).
69. In the convention we use, the neutrino masses are not ordered in magnitude according to their index number: $\Delta m^2_{31} < 0$ corresponds to $m_3 < m_1 < m_2$. We can also number the massive neutrinos in such a way that one always has $m_1 < m_2 < m_3$, see, *e.g.*, Ref. 66.
70. F. Perrin, Comptes Rendus **197**, 868 (1933); E. Fermi, Nuovo Cimento **11**, 1 (1934).
71. V. Lobashev *et al.*, Nucl. Phys. **A719**, 153c, (2003).
72. Ch. Kraus *et al.*, Eur. Phys. J. **C40**, 447 (2005).
73. K. Eitel *et al.*, Nucl. Phys. (Proc. Supp.) **B143**, 197 (2005).
74. V.N. Aseev *et al.*, Phys. Rev. **D84**, 112003 (2011).
75. J. Lesgourgues and L. Verde, "Neutrinos in Cosmology" review in PDG 2017 edition at http://pdg.lbl.gov.

76. K.N. Abazajian *et al.*, Astropart. Phys. **35**, 177 (2011); K.N. Abazajian and M. Kaplinghat, Ann. Rev. Nucl. Part. Sci. **66**, 401 (2016).
77. P.A.R. Ade *et al.*, [Planck Collab.], Astron. Astrophys. **571**, A16 (2014).
78. P.A.R. Ade *et al.*, [Planck Collab.], Astron. Astrophys. **594**, A13 (2016).
79. S.M. Koksbang and S. Hannestad, JCAP **1709**, 014 (2017); see also, e.g., R. Farpon, A.E. Nelson and N. Weiner, JCAP **0410**, 005 (2004); Z. Chacko *et al.*, Phys. Rev. Lett. **94**, 111801 (2005).
80. K. Abe *et al.*, [T2K Collab.], Prog. Theor. Exp. Phys. **4**, 043C01 (2015), arXiv:1609.04111.
81. A. de Gouvea *et al.*, arXiv:1310.4340.
82. M. G. Aartsen *et al.*, [IceCube-PINGU Collab.], arXiv:1401.2046.
83. U.F. Katz (for the KM3NeT Collaboration), arXiv:1402.1022.
84. S. Adrian-Martinez *et al.*, [KM3Net Collab.], J. Phys. **G43**, 084001 (2016), arXiv:1601.07459.
85. S. Ahmed *et al.*, [INO Collab.], Pramana **88**, 79 (2017), arXiv:1505.07380.
86. S.T. Petcov and M. Piai, Phys. Lett. **B533**, 94 (2002).
87. S. Choubey, S.T. Petcov and M. Piai, Phys. Rev. **D68**, 113006 (2003).
88. J. Learned *et al.*, Phys. Rev. **D78**, 071302 (2008); L. Zhan *et al.*, Phys. Rev. **D78**, 111103 (2008) and Phys. Rev. **D79**, 073007 (2009); P. Ghoshal and S.T. Petcov, JHEP **1103**, 058 (2011); F. Capozzi, E. Lisi and A. Marrone, Phys. Rev. **D92**, 073011 (2016).
89. S.M. Bilenky, F. Capozzi and S.T. Petcov, Phys. Lett. **B772**, 179 (2017).
90. L. Stanco *et al.*, arXiv:1707.07651.
91. F. An *et al.*, J. Phys. **G43**, 030401 (2016).
92. R.N. Cahn *et al.*, arXiv:1307.5487; X. Qian and P. Vogel, Prog. Part. Nucl. Phys. **83**, 1 (2015).
93. R. Acciarri *et al.*, [DUNE Collab.] arXiv:1601.05471 and arXiv:1601.02984.
94. K. Abe *et al.*, Prog. Theor. Exp. Phys. **5**, 053C02 (2015), arXiv:1502.05199.
95. R. Mohapatra *et al.*, Rept. on Prog. in Phys. **70**, 1757 (2007); A. Bandyopadhyay *et al.*, Rept. on Prog. in Phys. **72**, 106201 (2009).
96. G. Altarelli and F. Feruglio, Rev. Mod. Phys. **82**, 2701 (2010); S.F. King *et al.*, New. J. Phys. **16**, 045018 (2014); I. Girardi *et al.*, Nucl. Phys. **B902**, 1 (2016); R. Barbieri *et al.*, JHEP **9812**, 017 (1998); S.T. Petcov, Phys. Lett. **B110**, 245 (1982).
97. A. Morales and J. Morales, Nucl. Phys. (Proc. Supp.) **B114**, 141 (2003); J. Gómez-Cadenas *et al.*, Riv. Nuovo Cimento **40**, 2 (2012).
98. S. Dell'Oro *et al.*, Adv. High Energy Phys. **2016**, 2162659 (2016).
99. J.D. Vergados, H. Ejiri and F. Simkovic, Int. J. Mod. Phys. **E25**, 1630007 (2016).
100. N. Abgrall *et al.* [LEGEND Collab.], AIP Conf. Proc. **1894**, 020027 (2017), arXiv:1709.01980 [physics.ins-det].
101. F. Iachello, J. Kotila and J. Barea, PoS NEUTEL **2015**, 047 (2015).
102. S. Pascoli and S.T. Petcov, Phys. Lett. **B544**, 239 (2002).
103. S.M. Bilenky *et al.*, Phys. Rev. **D54**, 4432 (1996).
104. S.M. Bilenky *et al.*, Phys. Lett. **B465**, 193 (1999); F. Vissani, JHEP **9906**, 022 (1999); K. Matsuda *et al.*, Phys. Rev. **D62**, 093001 (2000); K. Czakon *et al.*, hep-ph/0003161; H.V. Klapdor-Kleingrothaus, H. Päs and A.Yu. Smirnov, Phys. Rev. **D63**, 073005 (2001); S. Pascoli, S.T. Petcov and W. Rodejohann, Phys. Lett. **B549**, 177 (2002), and *ibid.* **B558**, 141 (2003); H. Murayama and Peña-Garay, Phys. Rev. **D69**, 031301 (2004); S. Pascoli, S.T. Petcov, and T. Schwetz, Nucl. Phys. **B734**, 24 (2006); M. Lindner, A. Merle, and W. Rodejohann, Phys. Rev. **D73**, 053005 (2006); A. Faessler *et al.*, Phys. Rev. **D79**, 053001 (2009); W. Rodejohann, Int. J. Mod. Phys. **E20**, 1833 (2011).
105. A. S. Barabash, Phys. Atom. Nucl. **74**, 603 (2011).
106. A.Gando *et al.* [KamLAND-Zen Collab.], Phys. Rev. Lett. **117**, 082503 (2016); Addendum: Phys. Rev. Lett. **117**, 109903 (2016).
107. M. Agostini *et al.* [GERDA Collab.], Phys. Rev. Lett. **120**, 132503 (2018).
108. C. Alduino *et al.* [CUORE Collab.], Phys. Rev. Lett. **120**, 132501 (2018).
109. E. Andreotti *et al.* [Cuoricino Collab.], Astropart. Phys. **34**, 822 (2011).
110. K. Alfonso *et al.* [CUORE Collab.], Phys. Rev. Lett. **115**, 102502 (2015).
111. S. Pascoli, S.T. Petcov, and L. Wolfenstein, Phys. Lett. **B524**, 319 (2002); S.M. Bilenky and S.T. Petcov, hep-ph/0405237.
112. S. Pascoli and S.T. Petcov, Phys. Rev. **D77**, 113003 (2008).
113. A. Halprin *et al.*, Phys. Rev. **D13**, 2567 (1976); H. Päs *et al.*, Phys. Lett. **B453**, 194 (1999), and Phys. Lett. **B498**, 35 (2001); F.F. Deppisch, M. Hirsch and H. Päs, J. Phys. **G39**, 124007 (2012); L.C. Helo *et al.*, JHEP **1505**, 092 (2015).
114. A. Halprin, S.T. Petcov and S.P. Rosen, Phys. Lett. **B125**, 335 (1983); F. Deppisch and H. Päs, Phys. Rev. Lett. **98**, 232501 (2007); V.M. Gehman and S.R. Elliott, J. Phys. **G34**, 667 (2007), Erratum J. Phys. **G35**, 029701 (2008).
115. S. M. Bilenky, S. Pascoli and S. T. Petcov, Phys. Rev. **D64**, 113003 (2001); J. Barry, W. Rodejohann and H. Zhang, JHEP **1107**, 091 (2011); I. Girardi, A. Meroni and S. T. Petcov, JHEP **1311**, 146 (2013); M. Blennow *et al.*, JHEP **1007**, 096 (2010).
116. F. Deppisch, talk given at "The XXVII International Conference on Neutrino Physics and Astrophysics" (Neutrino 2016), London (UK), 4-9 July, 2016; F. Deppisch, M. Hirsch and H. Paes, J. Phys. **G39**, 12 (2012).
117. A. Faessler *et al.*, Phys. Rev. **D83**, 113003 (2011); A. Faessler *et al.*, Phys. Rev. **D83**, 113015 (2011); F. Simkovic, J. Vergados, and A. Faessler, Phys. Rev. **D82**, 113015 (2010); A. Meroni, S.T. Petcov, and F. Simkovic, JHEP **1302**, 025 (2013).
118. For alternative mechanisms of neutrino mass generation see, *e.g.*, the first article in Ref. 95, the review article Yi Cai *et al.*, Front. Phys. **5**, 63 (2017), arXiv:1706.08524, and references quoted therein.
119. S. Davidson and A. Ibarra, Phys. Lett. **B535**, 25 (2002).
120. A. Abada *et al.*, JCAP **0604**, 004 (2006); E. Nardi *et al.*, JHEP **0601**, 164 (2006).
121. C. Hagedorn and E. Molinaro, Nucl. Phys. **B919**, 404 (2017); P. Chen, G.-J. Ding and S.F. King, JHEP **1603**, 206 (2016); C.-Ch. Li and G.-J. Ding, Phys. Rev. **D96**, 075005 (2017).
122. L.C. Stonehill, J.A. Formaggio, and R.G.H. Robertson, Phys. Rev. **C69**, 015801 (2004).
123. F.L. Villante Phys. Lett. **B742**, 279 (2015).
124. J.N. Bahcall and R.K. Ulrich, Rev. Mod. Phys. **60**, 297 (1988); J.N. Bahcall and M.H. Pinsonneault, Rev. Mod. Phys. **64**, 885 (1992); J.N. Bahcall and M.H. Pinsonneault, Rev. Mod. Phys. **67**, 781 (1995); J.N. Bahcall, M.H. Pinsonneault, and S. Basu, Astrophys. J. **555**, 990 (2001);.
125. J.N. Bahcall, A.M. Serenelli, and S. Basu, Astrophys. J. **621**, L85 (2005).
126. J.N. Bahcall, A.M. Serenelli, and S. Basu, Astrophys. J. Supp. **165**, 400 (2006).
127. S. Turck-Chieze *et al.*, Astrophys. J. **335**, 415 (1988).
128. C. Peña-Garay and A.M. Serenelli, arXiv:0811.2424.
129. A.M. Serenelli, W.C. Haxton, and C. Peña-Garay, Astrophys. J. **743**, 24 (2011).
130. N. Vinyoles *et al.*, Astrophys. J. **835**, 202 (2017).
131. E.G. Adelberger *et al.*, Rev. Mod. Phys. **83**, 195 (2011).
132. N. Grevesse and A.J. Sauval, Space Sci. Rev. **85**, 161 (1998).
133. M. Asplund *et al.*, Annu. Rev. Astron. Astrophys. **747**, 481 (2009).
134. A.M. Serenelli, Eur. Phys. J. **A52**, 78 (2016).
135. C. Patrignani *et al.*, (PDG), Chin. Phys. **C40**, No. 10 (2016).
136. M. Honda *et al.*, Phys. Rev. **D70**, 043008 (2004); Phys. Rev. **D75**, 043006 (2007); Phys. Rev. **D83**, 123001 (2011).
137. M. Honda *et al.*, Phys. Rev. **D92**, 023004 (2015).
138. G.D. Barr *et al.*, Phys. Rev. **D70**, 023006 (2004).

139. G. Battistoni *et al.*, Astopart. Phys. **19**, 269 (2003).
140. S.E. Kopp, Phys. Rep. **439**, 101 (2007).
141. A. Ambrosini *et al.*, Phys. Lett. **B420**, 225 (1998); Phys. Lett. **B425**, 208 (1998).
142. M.G. Catanesi *et al.*, Nucl. Instrum. Methods **A571**, 527 (2007).
143. R. Raja, Nucl. Instrum. Methods **A553**, 225 (2005).
144. N. Abgrall *et al.*, Phys. Rev. **C84**, 034604 (2011); Eur. Phys. J. **C76**, 84 (2016); Eur. Phys. J. **C76**, 617 (2016).
145. D. Beavis *et al.*, Physics Design Report, BNL 52459 (1995).
146. K. Abe *et al.*, [T2K Collab.], Phys. Rev. **D87**, 012001 (2013).
147. R.B. Patterson [NOνA Collab.], Nucl. Phys. (Proc. Supp.) **B235-236**, 151 (2013).
148. K. Schrenkenbach, ILL technical report 84SC26T, quoted in M. Apollonio *et al.*, Eur. Phys. J. **C27**, 331 (2003).
149. J. Cao, Nucl. Phys. (Proc. Supp.) **B229-232**, 205 (2012).
150. M.F. James, J. Nucl. Energy **23**, 517 (1969); V. Kopeikin *et al.*, Phys. Atom. Nucl. **67**, 1892 (2004).
151. B.R. Davis *et al.*. Phys. Rev. **C19**, 2259 (1979).
152. P. Vogel *et al.*. Phys. Rev. **C24**, 1543 (1981).
153. F. von Feilitzsch *et al.*, Phys. Lett. **B118**, 162 (1982); K. Schreckenbach *et al.*, Phys. Lett. **B160**, 325 (1985); A.A. Hahn *et al.*. Phys. Lett. **B218**, 365 (1989).
154. N. Haag *et al.*. Phys. Rev. Lett. **112**, 122501 (2014).
155. T.A. Mueller *et al.*, Phys. Rev. **C83**, 054615 (2011).
156. G. Mention *et al.*, Phys. Rev. **D83**, 073006 (2011).
157. P. Huber, Phys. Rev. **C84**, 024617 (2011).
158. F.P. An *et al.*, [Daya Bay Collab.], Phys. Rev. Lett. **116**, 061801 (2016).
159. F.P. An *et al.*, [Daya Bay Collab.], Phys. Rev. Lett. **118**, 251801 (2017).
160. C. Giunti, Phys. Lett. **B764**, 145 (2017); Phys. Rev. **D96**, 033005 (2017).
161. D.A. Dwyer and T.J. Langford, Phys. Rev. Lett. **114**, 012502 (2014); A.A. Sonzogni, T.D. Johnson, and E.A. McCutchan, Phys. Rev. **C91**, 011301R (2015); A.C. Hayes *et al.*, Phys. Rev. **D92**, 033015 (2015); A.A. Zakari-Issoufou *et al.*, Phys. Rev. Lett. **115**, 102503 (2015); A.A. Sonzogni *et al.*, Phys. Rev. Lett. **116**, 132502 (2016); B.C. Rasco *et al.*, Phys. Rev. Lett. **117**, 092501 (2016); C. Buck *et al.*, Phys. Lett. **B765**, 159 (2017); P. Huber, Phys. Rev. Lett. **118**, 042502 (2017).
162. C. Bemporad, G. Gratta, and P. Vogel, Rev. Mod. Phys. **74**, 292 (2002).
163. S. Nussinov, Phys. Lett. **B63**, 201 (1976); B. Kayser, Phys. Rev. **D24**, 110 (1981); J. Rich, Phys. Rev. **D48**, 4318 (1993); H. Lipkin, Phys. Lett. **B348**, 604 (1995); W. Grimus and P. Stockinger, Phys. Rev. **D54**, 3414 (1996); L. Stodolski, Phys. Rev. **D58**, 036006 (1998); W. Grimus, P. Stockinger, and S. Mohanty, Phys. Rev. **D59**, 013011 (1999); L.B. Okun, Surv. High Energy Physics **15**, 75 (2000); J.-M. Levy, `hep-ph/0004221` and `arXiv:0901.0408`; A.D. Dolgov, Phys. Reports **370**, 333 (2002); C. Giunti, Phys. Scripta **67**, 29 (2003) and Phys. Lett. **B17**, 103 (2004); M. Beuthe, Phys. Reports **375**, 105 (2003); H. Lipkin, Phys. Lett. **B642**, 366 (2006); S.M. Bilenky, F. von Feilitzsch, and W. Potzel, J. Phys. **G34**, 987 (2007); C. Giunti and C.W. Kim, *Fundamentals of Neutrino Physics and Astrophysics* (Oxford University Press, Oxford, 2007); E.Kh. Akhmedov, J. Kopp, and M. Lindner, JHEP **0805**, 005 (2008); E.Kh. Akhmedov and A.Yu. Smirnov, Phys. Atom. Nucl. **72**, 1363 (2009).
164. For the subtleties involved in the step leading from Eq. (14.1) to Eq. (14.28) see, *e.g.*, Ref. 165.
165. A.G. Cohen, S.L. Glashow, and Z. Ligeti, Phys. Lett. **B678**, 191 (2009).
166. The neutrino masses do not exceed approximately 1 eV, $m_j \lesssim 1$, while in neutrino oscillation experiments neutrinos with energy $E \gtrsim 100$ keV are detected.
167. E. K. Akhmedov, J. Kopp and M. Lindner, JHEP **0805**, 005 (2008).
168. S.M. Bilenky and B. Pontecorvo, Phys. Reports **41**, 225 (1978).
169. In Eq. (14.33) we have neglected the possible instability of neutrinos ν_j. In most theoretical models with nonzero neutrino masses and neutrino mixing, the predicted half life-time of neutrinos with mass of 1 eV exceeds the age of the Universe, see, *e.g.*, S.T. Petcov, Yad. Fiz. **25**, 641 (1977), (E) *ibid.*, **25**, 1336 (1977) [Sov. J. Nucl. Phys. **25**, 340 (1977), (E) *ibid.*, **25**, 698 (1977)], and Phys. Lett. **B115**, 401 (1982); W. Marciano and A.I. Sanda, Phys. Lett. **B67**, 303 (1977); P. Pal and L. Wolfenstein, Phys. Rev. **D25**, 766 (1982).
170. L.B. Okun (2000), J.-M. Levy (2000) and H. Lipkin (2006) quoted in Ref. 163 and Ref. 165.
171. The articles by L. Stodolsky (1998) and H. Lipkin (1995) quoted in Ref. 163.
172. A. De Rujula *et al.*, Nucl. Phys. **B168**, 54 (1980).
173. N. Agafonova *et al.*, [OPERA Collab.], Phys. Lett. **B691**, 138 (2010); New J. Phys. **14**, 033017 (2012).
174. N. Agafonova *et al.*, [OPERA Collab.], JHEP **1311**, 036 (2013).
175. M.H. Ahn *et al.*, [K2K Collab.], Phys. Rev. Lett. **93**, 051801 (2004); S. Yamamoto *et al.*, [K2K Collab.], Phys. Rev. Lett. **96**, 181801 (2006).
176. S.M. Bilenky, D. Nicolo and S.T. Petcov, Phys. Lett. **B538**, 77 (2002).
177. V. Gribov and B. Pontecorvo, Phys. Lett. **B28**, 493 (1969).
178. S. Goswami *et al.*, Nucl. Phys. (Proc. Supp.) **B143**, 121 (2005).
179. These processes are important, however, for the supernova neutrinos see, *e.g.*, G. Raffelt, *Proc. International School of Physics "Enrico Fermi", CLII Course "Neutrino Physics"*, 23 July-2 August 2002, Varenna, Italy [`hep-ph/0208024`]), and articles quoted therein.
180. We standardly assume that the weak interaction of the flavour neutrinos ν_l and antineutrinos $\bar{\nu}_l$ is described by the Standard Model (for alternatives see, *e.g.*, Ref. 26; M.M. Guzzo *et al.*, Phys. Lett. **B260**, 154 (1991); E. Roulet, Phys. Rev. **D44**, R935 (1991) and Ref. 95).
181. V. Barger *et al.*, Phys. Rev. **D22**, 2718 (1980).
182. P. Langacker, J.P. Leveille, and J. Sheiman, Phys. Rev. **D27**, 1228 (1983).
183. The difference between the ν_μ and ν_τ indices of refraction arises at one-loop level and can be relevant for the $\nu_\mu - \nu_\tau$ oscillations in very dense media, like the core of supernovae, *etc.*; see F.J. Botella, C.S. Lim, and W.J. Marciano, Phys. Rev. **D35**, 896 (1987).
184. The relevant formulae for the oscillations between the ν_e and a sterile neutrino ν_s, $\nu_e \leftrightarrow \nu_s$, can be obtained from those derived for the case of $\nu_e \leftrightarrow \nu_{\mu(\tau)}$ oscillations by Refs. [65,182] replacing N_e with $(N_e - 1/2N_n)$, N_n being the neutron number density in matter.
185. T.K. Kuo and J. Pantaleone, Phys. Lett. **B198**, 406 (1987).
186. A.D. Dziewonski and D.L. Anderson, Physics of the Earth and Planetary Interiors **25**, 297 (1981).
187. The first studies of the effects of Earth matter on the oscillations of neutrinos were performed numerically in Refs. [181,188] and in E.D. Carlson, Phys. Rev. **D34**, 1454 (1986); A. Dar *et al.*, *ibid.*, **D35**, 3607 (1988); in Ref. 63 and in G. Auriemma *et al.*, *ibid.*, **D37**, 665 (1988).
188. A.Yu. Smirnov and S.P. Mikheev, *Proc. of the VIth Moriond Workshop* (eds. O. Fackler, J. Tran Thanh Van, Frontières, Gif-sur-Yvette, 1986), p. 355.
189. S.T. Petcov, Phys. Lett. **B434**, 321 (1998), (E) *ibid.* **B444**, 584 (1998); see also Nucl. Phys. (Proc. Supp.) **B77**, 93 (1999) and `hep-ph/9811205`.
190. M.V. Chizhov, M. Maris, and S.T. Petcov, `hep-ph/9810501`.
191. E.Kh. Akhmedov *et al.*, Nucl. Phys. **B542**, 3 (1999).
192. S.T. Petcov, Phys. Lett. **B214**, 259 (1988).
193. J. Hosaka *et al.*, [Super-Kamiokande Collab.], Phys. Rev. **D74**, 032002 (2006).
194. I. Mocioiu and R. Shrock, Phys. Rev. **D62**, 053017 (2000).
195. E.Kh. Akhmedov, Nucl. Phys. **B538**, 25 (1999).
196. M.V. Chizhov and S.T. Petcov, Phys. Rev. Lett. **83**, 1096 (1999) and Phys. Rev. Lett. **85**, 3979 (2000); Phys. Rev. **D63**, 073003 (2001).

197. J. Bernabéu, S. Palomares-Ruiz, and S.T. Petcov, Nucl. Phys. **B669**, 255 (2003); S. Palomares-Ruiz and S.T. Petcov, Nucl. Phys. **B712**, 392 (2005); S.T. Petcov and T. Schwetz, Nucl. Phys. **B740**, 1 (2006); R. Gandhi *et al.*, Phys. Rev. **D76**, 073012 (2007); E.Kh. Akhmedov, M. Maltoni, and A.Yu. Smirnov, JHEP **0705**, 077 (2007).
198. The mantle-core enhancement maxima, *e.g.*, in $P_m^{2\nu}(\nu_\mu \to \nu_\mu)$, appeared in some of the early numerical calculations, but with incorrect interpretation (see, *e.g.*, the articles quoted in Ref. 187).
199. M. Honda *et al.*, Phys. Rev. **D52**, 4985 (1995); V. Agraval *et al.*, Phys. Rev. **D53**, 1314 (1996); G. Fiorentini *et al.*, Phys. Lett. **B510**, 173 (2001).
200. K. Abe *et al.*, [Hyper-Kamiokande Proto-Collab.], KEK Report 2016-21; ICRR-Report-701-2016-1.
201. O.L.G. Peres and A.Y. Smirnov, Phys. Lett. **B456**, 204 (1999), and Nucl. Phys. Proc. Suppl. **110**, 355 (2002).
202. M. Freund, Phys. Rev. **D64**, 053003 (2001).
203. M.C. Gonzalez-Garcia and Y. Nir, Rev. Mod. Phys. **75**, 345 (2003); S.M. Bilenky, W. Grimus, and C. Giunti, Prog. in Part. Nucl. Phys. **43**, 1 (1999).
204. J.N. Bahcall, *Neutrino Astrophysics*, Cambridge University Press, Cambridge, 1989; J.N. Bahcall and M. Pinsonneault, Phys. Rev. Lett. **92**, 121301 (2004); J.N. Bahcall, A.M. Serenelli and S. Basu, Astrophys. J. Supp. **165**, 400 (2006).
205. N. Cabibbo, summary talk at the International Workshop on Weak Interaction and Neutrinos (WIN), June 1985, Savonlina, Finland.
206. A. Messiah, *Proc. of the VIth Moriond Workshop* (eds. O. Fackler, J. Tran Thanh Van, Frontières, Gif-sur-Yvette, 1986), p. 373.
207. S.J. Parke, Phys. Rev. Lett. **57**, 1275 (1986).
208. S.T. Petcov, Phys. Lett. **B200**, 373 (1988).
209. P.I. Krastev and S.T. Petcov, Phys. Lett. **B207**, 64 (1988); see also M. Bruggen, W.C. Haxton, and Y.-Z. Quian, Phys. Rev. **D51**, 4028 (1995).
210. T. Kaneko, Prog. Theor. Phys. **78**, 532 (1987); S. Toshev, Phys. Lett. **B196**, 170 (1987); M. Ito, T. Kaneko, and M. Nakagawa, Prog. Theor. Phys. **79**, 13 (1988), (E) *ibid.*, **79**, 555 (1988).
211. S.T. Petcov, Phys. Lett. **B406**, 355 (1997).
212. C. Cohen-Tannoudji, B. Diu, and F. Laloe, *Quantum Mechanics*, Vol. 1 (Hermann, Paris, and John Wiley & Sons, New York, 1977).
213. S.T. Petcov, Phys. Lett. **B214**, 139 (1988); E. Lisi *et al.*, Phys. Rev. **D63**, 093002 (2000); A. Friedland, Phys. Rev. **D64**, 013008 (2001).
214. S.T. Petcov and J. Rich, Phys. Lett. **B224**, 401 (1989).
215. An expression for the "jump" probability P' for N_e varying linearly along the neutrino path was derived in W.C. Haxton, Phys. Rev. Lett. **57**, 1271 (1986) and in Ref. 207 on the basis of the old Landau-Zener result: L.D. Landau, Phys. Z. USSR **1**, 426 (1932), C. Zener, Proc. R. Soc. **A137**, 696 (1932). An analytic description of the solar ν_e transitions based on the Landau-Zener jump probability was proposed in Ref. 207 and in W.C. Haxton, Phys. Rev. **D35**, 2352 (1987). The precision limitations of this description, which is less accurate than that based on the exponential density approximation, were discussed in S.T. Petcov, Phys. Lett. **B191**, 299 (1987) and in Ref. 209.
216. A. de Gouvea, A. Friedland, and H. Murayama, JHEP **0103**, 009 (2001).
217. C.-S. Lim, Report BNL 52079, 1987; S.P. Mikheev and A.Y. Smirnov, Phys. Lett. **B200**, 560 (1988).
218. G.L. Fogli *et al.*, Phys. Lett. **B583**, 149 (2004).
219. S.P. Mikheyev and A.Yu. Smirnov, *Proc. of the VIth Moriond Workshop* (eds. O. Fackler, J. Tran Thanh Van, Frontières, Gif-sur-Yvette, 1986), p. 355.
220. M. Cribier *et al.*, Phys. Lett. **B182**, 89 (1986); J. Bouchez et al., Z. Phys. **C32**, 499 (1986).
221. E. Lisi and D. Montanino, Phys. Rev. **D56**, 1792 (1997); Q.Y. Liu, M. Maris and S.T. Petcov, Phys. Rev. **D56**, 5991 (1997); M. Maris and S.T. Petcov, Phys. Rev. **D56**, 7444 (1997); J.N. Bahcall and P.I. Krastev, Phys. Rev. **C56**, 2839 (1997); J.N. Bahcall, P.I. Krastev and A.Y. Smirnov, Phys. Rev. **D60**, 093001 (1999); M. Maris and S.T. Petcov, Phys. Rev. **D62**, 093006 (2000); J.N. Bahcall, P.I. Krastev and A.Y. Smirnov, Phys. Rev. **D62**, 093004 (2000); M.C. Gonzalez-Garcia, C. Pena-Garay and A.Y. Smirnov, Phys. Rev. **D63**, 113004 (2001); P.I. Krastev and A.Y. Smirnov, Phys. Rev. **D65**, 073022 (2002).
222. A. Bandyopadhyay *et al.*, Phys. Lett. **B583**, 134 (2004); M. Blennow, T. Ohlsson and H. Snellman, Phys. Rev. **D69**, 073006 (2004); E.K. Akhmedov, M.A. Tortola and J.W.F. Valle, JHEP **0405**, 057 (2004).
223. K.S. Hirata *et al.*, [Kamiokande Collab.], Phys. Rev. Lett. **63**, 16 (1989).
224. Y. Fukuda *et al.*, [Super-Kamiokande Collab.], Phys. Rev. Lett. **81**, 1158 (1998).
225. J. Hosaka *et al.*, [Super-Kamiokande Collab.], Phys. Rev. **D73**, 112001 (2006).
226. J.P. Cravens *et al.*, [Super-Kamiokande Collab.], Phys. Rev. **D78**, 032002 (2008).
227. K. Abe *et al.*, [Super-Kamiokande Collab.], Phys. Rev. **D83**, 052010 (2011).
228. K. Abe *et al.*, [Super-Kamiokande Collab.], Phys. Rev. **D94**, 052010 (2016).
229. B. Aharmim *et al.*, [SNO Collab.], Phys. Rev. **C72**, 055502 (2005).
230. B. Aharmim *et al.*, [SNO Collab.], Phys. Rev. Lett. **101**, 111301 (2008); Phys. Rev. **C87**, 015502 (2013).
231. G. Bellini *et al.*, [Borexino Collab.], Phys. Rev. Lett. **107**, 141302 (2011).
232. G. Bellini *et al.*, [Borexino Collab.], Phys. Rev. Lett. **108**, 051302 (2012).
233. G. Bellini *et al.*, [Borexino Collab.], Nature **512**, 383 (2014).
234. G. Bellini *et al.*, [Borexino Collab.], Phys. Rev. **D82**, 033006 (2010).
235. G. Bellini *et al.*, [Borexino Collab.], Phys. Rev. **D89**, 112007 (2014).
236. M. Agostini *et al.*, [Borexino Collab.], `arXiv:1707.09279`.
237. M. Agostini *et al.*, [Borexino Collab.], `arXiv:1709.00756`.
238. A. Gando *et al.*, [KamLAND Collab.], Phys. Rev. **C92**, 055808 (2015).
239. S. Abe *et al.*, [KamLAND Collab.], Phys. Rev. **C84**, 035804 (2011).
240. B. Pontecorvo, Chalk River Lab. report PD-205, 1946.
241. P. Anselmann *et al.*, [GALLEX Collab.], Phys. Lett. **B342**, 440 (1995); W. Hampel *et al.*, [GALLEX Collab.], Phys. Lett. **B420**, 114 (1998).
242. J.N. Abdurashitov *et al.*, [SAGE Collab], Phys. Rev. Lett. **77**, 4708 (1996); Phys. Rev. **C59**, 2246 (1999).
243. K.S. Hirata *et al.*, [Kamiokande Collab.], Phys. Lett. **B205**, 416 (1988) and Phys. Lett. **B280**, 146 (1992).
244. Y. Fukuda *et al.*, [Kamiokande Collab.], Phys. Lett. **B335**, 237 (1994).
245. D. Casper *et al.*, [IMB Collab.], Phys. Rev. Lett. **66**, 2561 (1991).
246. K. Daum *et al.*, [Frejus Collab.], Z. Phys. **C66**, 417 (1995).
247. W.W.M. Allison *et al.*, [Soudan 2 Collab.], Phys. Lett. **B391**, 491 (1997).
248. M. Ambrosio *et al.*, [MACRO Collab.], Phys. Lett. **B434**, 451 (1998); Phys. Lett. **B566**, 35 (2003).
249. M. Sanchez *et al.*, [Soudan 2 Collab.], Phys. Rev. **D68**, 113004 (2003); W.W.M. Allison *et al.*, [Soudan 2 Collab.], Phys. Rev. **D72**, 052005 (2005).
250. P. Adamson *et al.*, [MINOS Collab.], Phys. Rev. **D86**, 052007 (2012).
251. M. Ageron *et al.*, [ANTARES Collab.], Nucl. Instrum. Methods **A656**, 11 (2011).
252. M.G. *et al.*, [IceCube Collab.], Astropart. Phys. **35**, 615 (2012).
253. S. Adrián-Martínez *et al.*, [ANTARES Collab.], Phys. Lett. **B714**, 224 (2012).
254. M.G. Aartsen *et al.*, [IceCube Collab.], Phys. Rev. Lett. **120**, 071801 (2018).

255. M.G. Aartsen *et al.*, [IceCube Collab.], Phys. Rev. Lett. **111**, 081801 (2013); Phys. Rev. **D91**, 072004 (2015).
256. G. Tzanakos *et al.*, [MINOS+ Collab.], FERMILAB-PROPOSAL-1016 (2011).
257. S. Wojcicki, *Proc. of the 1997 SLAC Summer Institute.*
258. M. Antonello *et al.*, [ICARUS Collab.], Eur. Phys. J. **C73**, 2345 (2013); Eur. Phys. J. **C73**, 2599 (2013).
259. A. Aguilar *et al.*, [LSND Collab.], Phys. Rev. **D64**, 112007 (2001).
260. B. Armbruster *et al.*, [Karmen Collab.], Phys. Rev. **D65**, 112001 (2002).
261. A.A. Aguilar-Arevalo *et al.*, [MiniBooNE Collab.], Phys. Rev. Lett. **98**, 231801 (2007); Phys. Rev. Lett. **102**, 101802 (2009).
262. A.A. Aguilar-Arevalo *et al.*, [MiniBooNE Collab.], Phys. Rev. Lett. **105**, 181801 (2010); Phys. Rev. Lett. **110**, 161801 (2013).
263. For the Fermilab short-Baseline Neutrino (SBN) Program, we refer to S. Tufanli, Talk at the EPS International Conference on High Energy Physics, July 2017, Venice, Italy.
264. F. Boem and P. Vogel, *Physics of Massive Neutrinos*, Cambridge Univ. Press, 1987.
265. F. Boehm *et al.*, Phys. Rev. **D64**, 112001 (2001).
266. F. Suekane and T.J.C. Bezerra, Nucl. Phys. **B908**, 74 (2016).
267. J. Cao and K. B. Luk, Nucl. Phys. **B908**, 62 (2016).
268. S. B. Kim, Nucl. Phys. **B908**, 94 (2016).
269. Y.-F. Li Int. J. Mod. Phys.: Conf. Ser. **31**, 1460300 (2014).
270. D. Davis, Jr., D.S. Harmer, and K.C. Hoffman, Phys. Rev. Lett. **20**, 1205 (1968).
271. A.I. Abazov *et al.*, [SAGE Collab.], Phys. Rev. Lett. **67**, 3332 (1991).
272. Note that after publication of Ref. 8, the SAGE results including an extended observation period are reported by V.N. Gavrin in Phys.-Usp. **54**, 941 (2011). Also, F. Kaether *et al.*, Phys. Lett. **B685**, 47 (2010) reanalyzed a complete set of the GALLEX data with a method providing a better background reduction than that adopted in Ref. 10. The resulting GALLEX and GNO+GALLEX capture rates are slightly different from, but consistent with, those reported in Table 14.5.
273. Y. Fukuda *et al.*, [Super-Kamiokande Collab.], Phys. Rev. Lett. **86**, 5651 (2001).
274. Y. Fukuda *et al.*, [Super-Kamiokande Collab.], Phys. Lett. **B539**, 179 (2002).
275. G. L. Fogli *et al.*, Phys. Rev. **D67**, 073002 (2003); M. Maltoni, T. Schwetz, and J.W. Valle, Phys. Rev. **D67**, 093003 (2003); A. Bandyopadhyay *et al.*, Phys. Lett. **B559**, 121 (2003); J.N. Bahcall, M.C. Gonzalez-Garcia, and C. Peña-Garay, JHEP **0302**, 009 (2003); P.C. de Holanda and A.Y. Smirnov, JCAP **0302**, 001 (2003).
276. S. Abe *et al.*, [KamLAND Collab.], Phys. Rev. Lett. **100**, 221803 (2008).
277. A. Gando *et al.*, [KamLAND Collab.], Phys. Rev. **D83**, 052002 (2011).
278. B. Aharmim *et al.*, [SNO Collab.], Phys. Rev. **C81**, 055504 (2010).
279. B. Aharmim *et al.*, [SNO Collab.], Phys. Rev. **C88**, 025501 (2013).
280. http://pdg.lbl.gov/2017/listings/contents_listings.html.
281. B. Geytenbeek *et al.*, JCAP **1703**, 029 (2017).
282. J. Bergstrom *et al.*, JHEP **1603**, 132 (2016).
283. G. Bellini *et al.*, [Borexino Collab.], Phys. Lett. **B707**, 22 (2012).
284. A. Renshaw *et al.*, [Super-Kamiokande Collab.], Phys. Rev. Lett. **112**, 091805 (2014).
285. S. T. Petcov, Nucl. Phys. **B892**, 400 (2015); C. Hagedorn, A. Meroni, and E. Molinaro, Nucl. Phys. **B891**, 499 (2015); I. Girardi, S.T. Petcov, and A.V. Titov, Nucl. Phys. **B894**, 733 (2015), and Eur. Phys. J. **C75**, 345 (2015); P. Ballett, S. Pascoli, and J. Turner, Phys. Rev. **D92**, 093008 (2015); C.C. Li and G.J. Ding, JHEP **1505**, 100 (2015); J.T. Penedo, S.T. Petcov and A.V. Titov, JHEP **1712**, 022 (2017).
286. V. Barger *et al.*, Phys. Rev. Lett. **82**, 2640 (1999).
287. E. Lisi *et al.*, Phys. Rev. Lett. **85**, 1166 (2000).
288. K. Abe *et al.*, [Super-Kamiokande Collab.], Phys. Rev. **D97**, 072001 (2018).
289. P. Adamson *et al.*, [MINOS Collab.], Phys. Rev. Lett. **112**, 191801 (2014).
290. P. Adamson *et al.*, [MINOS Collab.], Phys. Rev. Lett. **110**, 251801 (2013).
291. K.A. Olive *et al.*, (PDG), Chin. Phys. **C38**, 090001 (2014) and 2015 update (http://pdg.lbl.gov/2015/).
292. P. Adamson *et al.*, [MINOS Collab.], Phys. Rev. Lett. **107**, 021801 (2011); Phys. Rev. Lett. **108**, 191801 (2012).
293. K. Abe *et al.*, [T2K Collab.], Phys. Rev. Lett. **116**, 181801 (2016).
294. K. Abe *et al.*, [T2K Collab.], Phys. Rev. **D96**, 011102 (2017).
295. K. Abe *et al.*, [Super-Kamiokande Collab.], Phys. Rev. Lett. **107**, 241801 (2011).
296. K. Abe *et al.*, [Super-Kamiokande Collab.], Phys. Rev. Lett. **97**, 171801 (2006).
297. N. Agafonova *et al.*, [OPERA Collab.], Phys. Rev. Lett. **115**, 121802 (2015).
298. K. Abe *et al.*, [T2K Collab.], Phys. Rev. **D91**, 072010 (2015).
299. K. Abe *et al.*, [T2K Collab.], Phys. Rev. **D96**, 092006 (2017).
300. M. Hartz, talk at KEK colloquium, August 2017.
301. A.C. Hayes *et al.*, Phys. Rev. Lett. **112**, 202501 (2014).
302. P. Astier *et al.*, [NOMAD Collab.], Phys. Lett. **B570**, 19 (2003).
303. N. Agafanova *et al.*, [OPERA Collab.], JHEP **1307**, 004 (2013); JHEP **1307**, 085 (2013).
304. F. Dydak *et al.*, [CDHSW Collab.], Phys. Lett. **B134**, 281 (1984).
305. M.G. Aartsen *et al.*, [IceCube Collab.], Phys. Rev. Lett. **117**, 071801 (2016).
306. Y. Ko *et al.*, [NEOS Collab.], Phys. Rev. Lett. **118**, 121802 (2017).
307. M. Danilov *et al.*, [DANSS Collab.], talk given at the Moriond Workshop on Electroweak Physics, March 2017.
308. S.T. Petcov, Int. J. Mod. Phys. **A32**, 1750018 (2017), arXiv:1611.09247.
309. P.A. Adamson *et al.*, Phys. Rev. Lett. **117**, 151801 (2016).
310. F.P. An *et al.*, [Daya Bay Collab.], Phys. Rev. Lett. **113**, 141802 (2014).
311. S. Gariazzo *et al.*, JHEP **1706**, 135 (2017).
312. J. Kopp *et al.*, JHEP **1305**, 050 (2013).
313. C. Giunti *et al.*, Phys. Rev. **D88**, 073008 (2013).
314. M. Archidiacono *et al.*, Phys. Rev. **D86**, 065028 (2012).
315. S. Gariazzo *et al.*, J. Phys. **G43**, 033001 (2016).

15. Quark Model

Revised August 2017 by C. Amsler (Stefan Meyer Institute for Subatomic Physics, Vienna), T. DeGrand (University of Colorado, Boulder), and B. Krusche (University of Basel).

15.1. Quantum numbers of the quarks

Quantum chromodynamics (QCD) is the theory of the strong interactions. QCD is a quantum field theory and its constituents are a set of fermions, the quarks, and gauge bosons, the gluons. Strongly interacting particles, the hadrons, are bound states of quark and gluon fields. As gluons carry no intrinsic quantum numbers beyond color charge, and because color is believed to be permanently confined, most of the quantum numbers of strongly interacting particles are given by the quantum numbers of their constituent quarks and antiquarks. The description of hadronic properties which strongly emphasizes the role of the minimum-quark-content part of the wave function of a hadron is generically called the quark model. It exists on many levels: from the simple, almost dynamics-free picture of strongly interacting particles as bound states of quarks and antiquarks, to more detailed descriptions of dynamics, either through models or directly from QCD itself. The different sections of this review survey the many approaches to the spectroscopy of strongly interacting particles which fall under the umbrella of the quark model.

Table 15.1: Additive quantum numbers of the quarks.

	d	u	s	c	b	t
Q – electric charge	$-\frac{1}{3}$	$+\frac{2}{3}$	$-\frac{1}{3}$	$+\frac{2}{3}$	$-\frac{1}{3}$	$+\frac{2}{3}$
I – isospin	$\frac{1}{2}$	$\frac{1}{2}$	0	0	0	0
I_z – isospin z-component	$-\frac{1}{2}$	$+\frac{1}{2}$	0	0	0	0
S – strangeness	0	0	-1	0	0	0
C – charm	0	0	0	$+1$	0	0
B – bottomness	0	0	0	0	-1	0
T – topness	0	0	0	0	0	$+1$

Quarks are strongly interacting fermions with spin 1/2 and, by convention, positive parity. Antiquarks have negative parity. Quarks have the additive baryon number 1/3, antiquarks -1/3. Table 15.1 gives the other additive quantum numbers (flavors) for the three generations of quarks. They are related to the charge Q (in units of the elementary charge e) through the generalized Gell-Mann-Nishijima formula

$$\mathsf{Q} = \mathsf{I}_z + \frac{\mathcal{B} + \mathsf{S} + \mathsf{C} + \mathsf{B} + \mathsf{T}}{2} \,, \tag{15.1}$$

where $\mathcal{B}$ is the baryon number. The convention is that the *flavor* of a quark (I_z, S, C, B, or T) has the same sign as its *charge* Q. With this convention, any flavor carried by a charged meson has the same sign as its charge, *e.g.*, the strangeness of the K^+ is $+1$, the bottomness of the B^+ is $+1$, and the charm and strangeness of the D_s^- are each -1. Antiquarks have the opposite flavor signs. The hypercharge is defined as

$$\mathsf{Y} = \mathcal{B} + \mathsf{S} - \frac{\mathsf{C} - \mathsf{B} + \mathsf{T}}{3} \,.$$

Thus Y is equal to $\frac{1}{3}$ for the u and d quarks, $-\frac{2}{3}$ for the s quark, and 0 for all other quarks.

15.2. Mesons

Mesons have baryon number $\mathcal{B} = 0$. In the quark model, they are $q\overline{q}'$ bound states of quarks q and antiquarks $\overline{q}'$ (the flavors of q and q' may be different). If the orbital angular momentum of the $q\overline{q}'$ state is ℓ, then the parity P is $(-1)^{\ell+1}$. The meson spin J is given by the usual relation $|\ell - s| \leq J \leq |\ell + s|$, where s is 0 (antiparallel quark spins) or 1 (parallel quark spins). The charge conjugation, or C-parity $C = (-1)^{\ell+s}$, is defined only for the $q\bar{q}$ states made of quarks and their own antiquarks. The C-parity can be generalized to the G-parity $G = (-1)^{I+\ell+s}$ for mesons made of quarks and their own antiquarks (isospin $\mathsf{I}_z = 0$), and for the charged $u\bar{d}$ and $d\bar{u}$ states (isospin $\mathsf{I} = 1$).

The mesons are classified in J^{PC} multiplets. The $\ell = 0$ states are the pseudoscalars (0^{-+}) and the vectors (1^{--}). The orbital excitations $\ell = 1$ are the scalars (0^{++}), the axial vectors (1^{++}) and (1^{+-}), and the tensors (2^{++}). Assignments for many of the known mesons are given in Tables 15.2 and 15.3. Radial excitations are denoted by the principal quantum number n. The very short lifetime of the t quark makes it likely that bound-state hadrons containing t quarks and/or antiquarks do not exist.

States in the natural spin-parity series $P = (-1)^J$ must, according to the above, have $s = 1$ and hence, $CP = +1$. Thus, mesons with natural spin-parity and $CP = -1$ (0^{+-}, 1^{-+}, 2^{+-}, 3^{-+}, *etc.*) are forbidden in the $q\bar{q}'$ model. The $J^{PC} = 0^{--}$ state is forbidden as well. Mesons with such *exotic* quantum numbers may exist, but would lie outside the $q\bar{q}'$ model (see section below on exotic mesons).

Following SU(3), the nine possible $q\bar{q}'$ combinations containing the light u, d, and s quarks are grouped into an octet and a singlet of light quark mesons:

$$\mathbf{3} \otimes \overline{\mathbf{3}} = \mathbf{8} \oplus \mathbf{1} \,. \tag{15.2}$$

A fourth quark such as charm c can be included by extending SU(3) to SU(4). However, SU(4) is badly broken owing to the much heavier c quark. Nevertheless, in an SU(4) classification, the sixteen mesons are grouped into a 15-plet and a singlet:

$$\mathbf{4} \otimes \overline{\mathbf{4}} = \mathbf{15} \oplus \mathbf{1} \,. \tag{15.3}$$

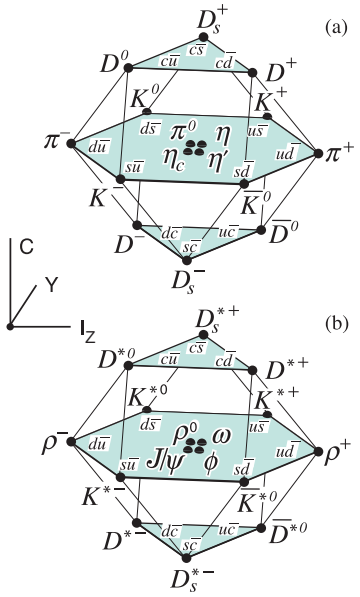

Figure 15.1: SU(4) weight diagram showing the 16-plets for the pseudoscalar (a) and vector mesons (b) made of the u, d, s, and c quarks as a function of isospin I_z, charm C, and hypercharge $\mathsf{Y} = \mathcal{B} + \mathsf{S} - \frac{\mathsf{C}}{3}$. The nonets of light mesons occupy the central planes to which the $c\bar{c}$ states have been added.

Table 15.2: Suggested $q\overline{q}$ quark-model assignments for some of the observed light mesons. Mesons in bold face are included in the Meson Summary Table. The wave functions f and f' are given in the text. The singlet-octet mixing angles from the quadratic and linear mass formulae are also given for the well established nonets. The classification of the 0^{++} mesons is tentative: the light scalars $a_0(980)$, $f_0(980)$, $f_0(500)$ and $K_0^*(800)$ are often considered to be meson-meson resonances or four-quark states, and are omitted from the table. The isoscalar 0^{++} mesons are expected to mix. In particular, the $f_0(1710)$ mixes with the $f_0(1500)$ and the $f_0(1370)$. See the "Note on Non-$q\bar{q}$ mesons" and the "Note on Scalar Mesons" in the Meson Listings for details and alternative schemes. In the 1^{++} nonet the isoscalar slot is disputed by the $f_1(1510)$. The isoscalar assignments in the 2^1S_0 (0^{-+}) nonet are also tentative. See the "Note on The Pseudoscalar and Pseudovector Mesons in the 1400 MeV Region" in the Meson Listings.

$n\,^{2s+1}\ell_J$	J^{PC}	I = 1 $u\overline{d}$, $\overline{u}d$, $\frac{1}{\sqrt{2}}(d\overline{d} - u\overline{u})$	I = $\frac{1}{2}$ $u\overline{s}$, $d\overline{s}$; $\overline{d}s$, $-\overline{u}s$	I = 0 f'	I = 0 f	$\theta_{\rm quad}$ [°]	$\theta_{\rm lin}$ [°]
$1\,^1S_0$	0^{-+}	$\boldsymbol{\pi}$	$\boldsymbol{K}$	$\boldsymbol{\eta}$	$\boldsymbol{\eta'(958)}$	−11.3	−24.5
$1\,^3S_1$	1^{--}	$\boldsymbol{\rho(770)}$	$\boldsymbol{K^*(892)}$	$\boldsymbol{\phi(1020)}$	$\boldsymbol{\omega(782)}$	39.2	36.5
$1\,^1P_1$	1^{+-}	$\boldsymbol{b_1(1235)}$	$\boldsymbol{K_{1B}}^\dagger$	$h_1(1380)$	$\boldsymbol{h_1(1170)}$		
$1\,^3P_0$	0^{++}	$\boldsymbol{a_0(1450)}$	$\boldsymbol{K_0^*(1430)}$	$\boldsymbol{f_0(1710)}$	$\boldsymbol{f_0(1370)}$		
$1\,^3P_1$	1^{++}	$\boldsymbol{a_1(1260)}$	$\boldsymbol{K_{1A}}^\dagger$	$\boldsymbol{f_1(1420)}$	$\boldsymbol{f_1(1285)}$		
$1\,^3P_2$	2^{++}	$\boldsymbol{a_2(1320)}$	$\boldsymbol{K_2^*(1430)}$	$\boldsymbol{f_2'(1525)}$	$\boldsymbol{f_2(1270)}$	29.6	28.0
$1\,^1D_2$	2^{-+}	$\boldsymbol{\pi_2(1670)}$	$\boldsymbol{K_2(1770)}^\dagger$	$\eta_2(1870)$	$\boldsymbol{\eta_2(1645)}$		
$1\,^3D_1$	1^{--}	$\boldsymbol{\rho(1700)}$	$\boldsymbol{K^*(1680)}$		$\boldsymbol{\omega(1650)}$		
$1\,^3D_2$	2^{--}		$\boldsymbol{K_2(1820)}$				
$1\,^3D_3$	3^{--}	$\boldsymbol{\rho_3(1690)}$	$\boldsymbol{K_3^*(1780)}$	$\boldsymbol{\phi_3(1850)}$	$\boldsymbol{\omega_3(1670)}$	31.8	30.8
$1\,^3F_4$	4^{++}	$\boldsymbol{a_4(2040)}$	$\boldsymbol{K_4^*(2045)}$		$\boldsymbol{f_4(2050)}$		
$1\,^3G_5$	5^{--}	$\rho_5(2350)$	$K_5^*(2380)$				
$1\,^3H_6$	6^{++}	$a_6(2450)$			$f_6(2510)$		
$2\,^1S_0$	0^{-+}	$\boldsymbol{\pi(1300)}$	$K(1460)$	$\boldsymbol{\eta(1475)}$	$\boldsymbol{\eta(1295)}$		
$2\,^3S_1$	1^{--}	$\boldsymbol{\rho(1450)}$	$\boldsymbol{K^*(1410)}$	$\boldsymbol{\phi(1680)}$	$\boldsymbol{\omega(1420)}$		
$3\,^1S_0$	0^{-+}	$\boldsymbol{\pi(1800)}$			$\eta(1760)$		

† The $1^{+\pm}$ and $2^{-\pm}$ isospin $\frac{1}{2}$ states mix. In particular, the K_{1A} and K_{1B} are nearly equal (45°) mixtures of the $K_1(1270)$ and $K_1(1400)$. The physical vector mesons listed under 1^3D_1 and 2^3S_1 may be mixtures of 1^3D_1 and 2^3S_1.

The *weight diagrams* for the ground-state pseudoscalar (0^{-+}) and vector (1^{--}) mesons are depicted in Fig. 15.1. The light quark mesons are members of nonets building the middle plane in Fig. 15.1(a) and (b).

Isoscalar states with the same J^{PC} will mix, but mixing between the two light quark isoscalar mesons, and the much heavier charmonium or bottomonium states, are generally assumed to be negligible. In the following, we shall use the generic names a for the I = 1, K for the I = 1/2, and f and f' for the I = 0 members of the light quark nonets. Thus, the physical isoscalars are mixtures of the SU(3) wave function ψ_8 and ψ_1:

$$f' = \psi_8 \cos\theta - \psi_1 \sin\theta \ , \tag{15.4}$$

$$f = \psi_8 \sin\theta + \psi_1 \cos\theta \ , \tag{15.5}$$

where θ is the nonet mixing angle and

$$\psi_8 = \frac{1}{\sqrt{6}}(u\bar{u} + d\bar{d} - 2s\bar{s}) \ , \tag{15.6}$$

$$\psi_1 = \frac{1}{\sqrt{3}}(u\bar{u} + d\bar{d} + s\bar{s}) \ . \tag{15.7}$$

These mixing relations are often rewritten to exhibit the $u\bar{u} + d\bar{d}$ and $s\bar{s}$ components which decouple for the "ideal" mixing angle θ_i, such that $\tan\theta_i = 1/\sqrt{2}$ (or $\theta_i = 35.3°$). Defining $\alpha = \theta + 54.7°$, one obtains the physical isoscalar in the flavor basis

$$f' = \frac{1}{\sqrt{2}}(u\bar{u} + d\bar{d})\cos\alpha - s\bar{s} \ \sin\alpha \ , \tag{15.8}$$

and its orthogonal partner f (replace α by α –90°). Thus for ideal mixing ($\alpha_i = 90°$), the f' becomes pure $s\bar{s}$ and the f pure $u\bar{u} + d\bar{d}$. The mixing angle θ can be derived by diagonalizing the mass matrix

$$\begin{pmatrix} m_8 & m_{81} \\ m_{18} & m_1 \end{pmatrix}$$

The mass eigenvalues are $m_{f'}$ and m_f. The mixing angle is given by

$$\tan\theta = \frac{m_8 - m_{f'}}{m_{81}} \ .$$

Calculating m_8 and m_{81} from the wave functions Eq. (15.6) and Eq. (15.7), and expressing the quark masses as a function of the I = 1/2 and I = 1 meson masses, one obtains

$$\tan\theta = \frac{4m_K - m_a - 3m_{f'}}{2\sqrt{2}(m_a - m_K)} \ , \tag{15.9}$$

Table 15.3: $q\overline{q}$ quark-model assignments for the observed heavy mesons with established J^{PC}. Mesons in bold face are included in the Meson Summary Table.

$n\,^{2s+1}\ell_J$ J^{PC}	I = 0 $c\overline{c}$	I = 0 $b\overline{b}$	I = $\frac{1}{2}$ $c\overline{u}$, $c\overline{d}$; $\overline{c}u$, $\overline{c}d$	I = 0 $c\overline{s}$; $\overline{c}s$	I = $\frac{1}{2}$ $b\overline{u}$, $b\overline{d}$; $\overline{b}u$, $\overline{b}d$	I = 0 $b\overline{s}$; $\overline{b}s$	I = 0 $b\overline{c}$; $\overline{b}c$
$1\,^1S_0$ 0^{-+}	$\boldsymbol{\eta_c(1S)}$	$\boldsymbol{\eta_b(1S)}$	$\boldsymbol{D}$	$\boldsymbol{D_s^{\pm}}$	$\boldsymbol{B}$	$\boldsymbol{B_s^0}$	$\boldsymbol{B_c^{\pm}}$
$1\,^3S_1$ 1^{--}	$\boldsymbol{J/\psi(1S)}$	$\boldsymbol{\Upsilon(1S)}$	$\boldsymbol{D^*}$	$\boldsymbol{D_s^{*\pm}}$	$\boldsymbol{B^*}$	B_s^*	
$1\,^1P_1$ 1^{+-}	$\boldsymbol{h_c(1P)}$	$\boldsymbol{h_b(1P)}$	$\boldsymbol{D_1(2420)}$	$\boldsymbol{D_{s1}(2536)^{\pm}}$	$\boldsymbol{B_1(5721)}$	$\boldsymbol{B_{s1}(5830)^0}$	
$1\,^3P_0$ 0^{++}	$\boldsymbol{\chi_{c0}(1P)}$	$\boldsymbol{\chi_{b0}(1P)}$	$\boldsymbol{D_0^*(2400)}$	$\boldsymbol{D_{s0}^*(2317)^{\pm\dagger}}$			
$1\,^3P_1$ 1^{++}	$\boldsymbol{\chi_{c1}(1P)}$	$\boldsymbol{\chi_{b1}(1P)}$	$D_1(2430)$	$\boldsymbol{D_{s1}(2460)^{\pm\dagger}}$			
$1\,^3P_2$ 2^{++}	$\boldsymbol{\chi_{c2}(1P)}$	$\boldsymbol{\chi_{b2}(1P)}$	$\boldsymbol{D_2^*(2460)}$	$\boldsymbol{D_{s2}^*(2573)^{\pm}}$	$\boldsymbol{B_2^*(5747)}$	$\boldsymbol{B_{s2}^*(5840)^0}$	
$1\,^3D_1$ 1^{--}	$\boldsymbol{\psi(3770)}$			$D_{s1}^*(2860)^{\pm\ddagger}$			
$1\,^3D_3$ 3^{--}			$D_3^*(2750)^{\pm}$	$D_{s3}^*(2860)^{\pm}$			
$2\,^1S_0$ 0^{-+}	$\boldsymbol{\eta_c(2S)}$	$\eta_b(2S)$	$D(2550)$				$B_c(2S)^{\pm}$
$2\,^3S_1$ 1^{--}	$\boldsymbol{\psi(2S)}$	$\boldsymbol{\Upsilon(2S)}$		$\boldsymbol{D_{s1}^*(2700)^{\pm\ddagger}}$			
$3\,^3S_1$ 1^{--}		$\boldsymbol{\Upsilon(3S)}$					
$4\,^3S_1$ 1^{--}		$\boldsymbol{\Upsilon(4S)}$					
$2\,^1P_1$ 1^{+-}		$h_b(2P)$					
$2\,^3P_{0,1,2}$ $0^{++}, 1^{++}, 2^{++}$	$\boldsymbol{\chi_{c2}(2P)}$	$\boldsymbol{\chi_{b0,1,2}(2P)}$					
$3\,^3P_{0,1,2}$ $0^{++}, 1^{++}, 2^{++}$		$\boldsymbol{\chi_b(3P)}$					
$1\,^3D_2$ 2^{--}		$\boldsymbol{\Upsilon(1D)}$					

† The masses of these states are considerably smaller than most theoretical predictions. They have also been considered as four-quark states.

‡ These states are mixtures of the $1\,^3D_1$ and $2\,^3S_1$ states.
The open flavor states in the 1^{+-} and 1^{++} rows are mixtures of the $1^{+\pm}$ states.

which also determines the sign of θ. Alternatively, one can express the mixing angle as a function of all nonet masses. The octet mass is given by

$$m_8 = m_{f'}\cos^2\theta + m_f \sin^2\theta$$

whence

$$\tan^2\theta = \frac{4m_K - m_a - 3m_{f'}}{-4m_K + m_a + 3m_f}\ . \qquad (15.10)$$

Eliminating θ from Eq. (15.9) and Eq. (15.10) leads to the sum rule [1]

$$(m_f + m_{f'})(4m_K - m_a) - 3m_f m_{f'} = 8m_K^2 - 8m_K m_a + 3m_a^2. \qquad (15.11)$$

This relation is verified for the ground-state vector mesons. We identify the $\phi(1020)$ with the f' and the $\omega(783)$ with the f. Thus

$$\phi(1020) = \psi_8\,\cos\theta_V - \psi_1\,\sin\theta_V\ , \qquad (15.12)$$

$$\omega(782) = \psi_8\,\sin\theta_V + \psi_1\,\cos\theta_V\ , \qquad (15.13)$$

with the vector mixing angle $\theta_V = 36.4°$ from Eq. (15.10), very close to ideal mixing. Thus $\phi(1020)$ is nearly pure $s\bar{s}$. For ideal mixing, Eq. (15.9) and Eq. (15.10) lead to the relations

$$m_K = \frac{m_f + m_{f'}}{2}\ ,\quad m_a = m_f\ , \qquad (15.14)$$

which are satisfied for the vector mesons.

The situation for the pseudoscalar and scalar mesons is not so clear cut, either theoretically or experimentally. For the pseudoscalars, the mixing angle is small. This can be understood qualitatively via gluon-line counting of the mixing process. The size of the mixing process between the nonstrange and strange mass bases scales as α_s^2, not α_s^3, because of two rather than three gluon exchange as it does for the vector mesons. It may also be that the lightest isoscalar pseudoscalars mix more strongly with excited states or with states of substantial non-$\bar{q}q$ content, as will be discussed below.

A variety of analysis methods lead to similar results: First, for these states, Eq. (15.11) is satisfied only approximately. Then Eq. (15.9) and Eq. (15.10) lead to somewhat different values for the mixing angle. Identifying the η with the f' one gets

$$\eta = \psi_8\,\cos\theta_P - \psi_1\,\sin\theta_P\ , \qquad (15.15)$$

$$\eta' = \psi_8\,\sin\theta_P + \psi_1\,\cos\theta_P\ . \qquad (15.16)$$

Following chiral perturbation theory, the meson masses in the mass formulae (Eq. (15.9) and Eq. (15.10)) might be replaced by their squares. Table 15.2 lists the mixing angle $\theta_{\rm lin}$ from Eq. (15.10) (using the neutral members of the nonets) and the corresponding $\theta_{\rm quad}$ obtained by replacing the meson masses by their squares throughout.

The pseudoscalar mixing angle θ_P can also be measured by comparing the partial widths for radiative J/ψ decay into a vector and a pseudoscalar [2], radiative $\phi(1020)$ decay into η and η' [3], radiative decays between pseudoscalar and vector mesons [4], or $\bar{p}p$ annihilation at rest into a pair of vector and pseudoscalar or into two pseudoscalars [5,6]. One obtains a mixing angle between –10° and –20°. More recently, a lattice QCD simulation, Ref. 7, has successfully

reproduced the masses of the η and η', and as a byproduct find a mixing angle $\theta_{lin} = -14.1(2.8)^\circ$. We return to this point in Sec. 15.6.

The nonet mixing angles can be measured in $\gamma\gamma$ collisions, *e.g.*, for the 0^{-+}, 0^{++}, and 2^{++} nonets. In the quark model, the amplitude for the coupling of neutral mesons to two photons is proportional to $\sum_i Q_i^2$, where Q_i is the charge of the i-th quark. The 2γ partial width of an isoscalar meson with mass m is then given in terms of the mixing angle α by

$$\Gamma_{2\gamma} = C(5\cos\alpha - \sqrt{2}\sin\alpha)^2 m^3 \ , \qquad (15.17)$$

for f' and f ($\alpha \to \alpha - 90^\circ$). The coupling C may depend on the meson mass. It is often assumed to be a constant in the nonet. For the isovector a, one then finds $\Gamma_{2\gamma} = 9\ C\ m^3$. Thus the members of an ideally mixed nonet couple to 2γ with partial widths in the ratios $f : f' : a = 25 : 2 : 9$. For tensor mesons, one finds from the ratios of the measured 2γ partial widths for the $f_2(1270)$ and $f_2'(1525)$ mesons a mixing angle α_T of $(81\pm 1)^\circ$, or $\theta_T = (27 \pm 1)^\circ$, in accord with the linear mass formula. For the pseudoscalars, one finds from the ratios of partial widths $\Gamma(\eta' \to 2\gamma)/\Gamma(\eta \to 2\gamma)$ a mixing angle $\theta_P = (-18 \pm 2)^\circ$, while the ratio $\Gamma(\eta' \to 2\gamma)/\Gamma(\pi^0 \to 2\gamma)$ leads to $\sim -24\ ^\circ$. SU(3) breaking effects for pseudoscalars are discussed in Ref. 8.

The partial width for the decay of a scalar or a tensor meson into a pair of pseudoscalar mesons is model-dependent. Following Ref. 9,

$$\Gamma = C \times \gamma^2 \times |F(q)|^2 \times q \ . \qquad (15.18)$$

C is a nonet constant, q the momentum of the decay products, $F(q)$ a form factor, and γ^2 the SU(3) coupling. The model-dependent form factor may be written as

$$|F(q)|^2 = q^{2\ell} \times \exp(-\frac{q^2}{8\beta^2}), \qquad (15.19)$$

where ℓ is the relative angular momentum between the decay products. The decay of a $q\bar{q}$ meson into a pair of mesons involves the creation of a $q\bar{q}$ pair from the vacuum, and SU(3) symmetry assumes that the matrix elements for the creation of $s\bar{s}$, $u\bar{u}$, and $d\bar{d}$ pairs are equal. The couplings γ^2 are given in Table 15.4, and their dependence upon the mixing angle α is shown in Fig. 15.2 for isoscalar decays. The generalization to unequal $s\bar{s}$, $u\bar{u}$, and $d\bar{d}$ couplings is given in Ref. 9. An excellent fit to the tensor meson decay widths is obtained assuming SU(3) symmetry, with $\beta \simeq 0.5$ GeV/c, $\theta_V \simeq 26\ ^\circ$ and $\theta_P \simeq -17\ ^\circ$ [9].

Table 15.4: SU(3) couplings γ^2 for quarkonium decays as a function of nonet mixing angle α, up to a common multiplicative factor C ($\phi \equiv 54.7^\circ + \theta_P$).

Isospin	Decay channel	γ^2
0	$\pi\pi$	$3\cos^2\alpha$
	$K\overline{K}$	$(\cos\alpha - \sqrt{2}\sin\alpha)^2$
	$\eta\eta$	$(\cos\alpha\cos^2\phi - \sqrt{2}\sin\alpha\sin^2\phi)^2$
	$\eta\eta'$	$\frac{1}{2}\sin^2 2\phi\ (\cos\alpha + \sqrt{2}\sin\alpha)^2$
1	$\eta\pi$	$2\cos^2\phi$
	$\eta'\pi$	$2\sin^2\phi$
	$K\overline{K}$	1
$\frac{1}{2}$	$K\pi$	$\frac{3}{2}$
	$K\eta$	$(\sin\phi - \frac{\cos\phi}{\sqrt{2}})^2$
	$K\eta'$	$(\cos\phi + \frac{\sin\phi}{\sqrt{2}})^2$

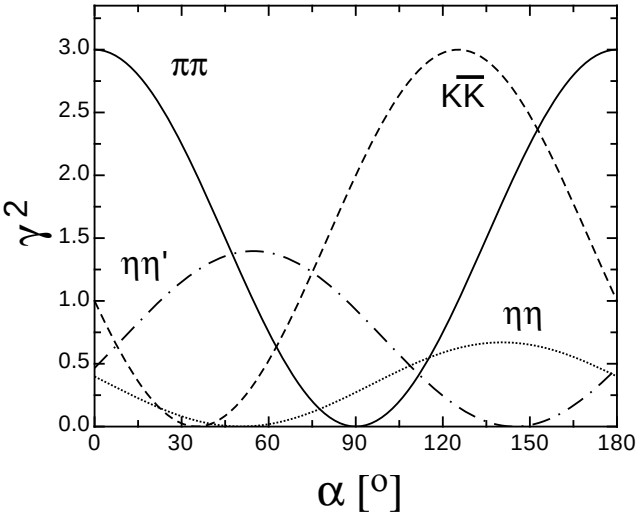

Figure 15.2: SU(3) couplings as a function of mixing angle α for isoscalar decays, up to a common multiplicative factor C and for $\theta_P = -17.3^\circ$.

15.3. Exotic mesons

The existence of a light nonet composed of four quarks (tetraquark) with masses below 1 GeV was suggested a long time ago [10]. Coupling two triplets of light quarks u, d, and s, one obtains nine states, of which the six symmetric (uu, dd, ss, $ud+du$, $us+su$, $ds+sd$) form the six dimensional representation **6**, while the three antisymmetric ($ud-du$, $us-su$, $ds-sd$) form the three dimensional representation $\overline{\mathbf{3}}$ of SU(3):

$$\mathbf{3} \otimes \mathbf{3} = \mathbf{6} \oplus \overline{\mathbf{3}} \ . \qquad (15.20)$$

Combining with spin and color and requiring antisymmetry, one finds that the most deeply bound diquark (and hence the lightest) is the one in the $\overline{\mathbf{3}}$ and spin singlet state. The combination of the diquark with an antidiquark in the **3** representation then gives a light nonet of four-quark scalar states. Letting the number of strange quarks determine the mass splitting, one obtains a mass inverted spectrum with a light isosinglet ($ud\bar{u}\bar{d}$), a medium heavy isodoublet (*e.g.*, $ud\bar{s}\bar{d}$) and a heavy isotriplet (*e.g.*, $ds\bar{u}\bar{s}$) + isosinglet (*e.g.*, $us\bar{u}\bar{s}$). It is then tempting to identify the lightest state with the $f_0(500)$, and the heaviest states with the $a_0(980)$, and $f_0(980)$. Then the meson with strangeness $K_0^*(800)$ would lie in-between.

A plethora of new states (dubbed XYZ) have been reported in the charmonium spectrum. The most prominent one, the $X(3872)$, was first observed in 2003 in B-decays in the final state $J/\psi\,\pi^+\pi^-$, and has been confirmed by high energy collider experiments which also determined its quantum numbers to be 1^{++}. The J/ψ signal points to a $cq\overline{cq}$ structure. Even more remarkable is the observation of charged mesons decaying into $c\overline{c}$ plus a charged pion, such as the $Z^{\pm}(4430)$ decaying into $\psi(2S)\pi^{\pm}$, which a priori excludes an interpretation as true $c\overline{c}$ (charmonium) state. Similar states are also observed in the bottomonium spectrum, such as the $Z_b(10610)^{\pm}$ decaying into $\Upsilon(1S, 2S, 3S)\pi^{\pm}$. Whether these mesons are tetraquark states, bound two-meson molecules or threshold effects is the subject of intense debates. Details and references can be found in a recent review Ref. 13 and in the "Note on Non-$q\bar{q}$ Mesons" in the Meson Listings.

QCD predicts the existence of extra isoscalar mesons. In the pure gauge theory they contain only gluons, and are called the glueballs. The ground state glueball is predicted by lattice gauge theories to be 0^{++}, the first excited state 2^{++}. Errors on the mass predictions are large. From Ref. 11 one obtains 1750 (50) (80) MeV for the mass of the lightest 0^{++} glueball from quenched QCD. As an example for the glueball mass spectrum, we show in Fig. 15.3 a calculation from Ref. 12. A mass of 1710 MeV is predicted for the ground state, also with an error of about 100 MeV. Earlier work by other groups produced masses at 1650 MeV [14] and 1550 MeV [15] (see also [16]). The first excited state has a mass of about 2.4 GeV, and the lightest

glueball with exotic quantum numbers (2^{+-}) has a mass of about 4 GeV.

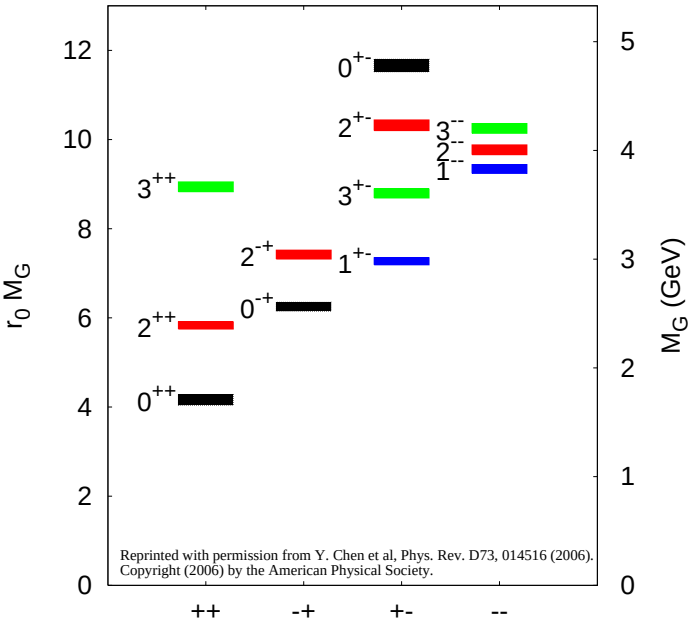

Figure 15.3: Predicted glueball mass spectrum from the lattice in quenched approximation (from Ref. 12)

These calculations are made in the so-called "quenched approximation" which neglects $q\bar{q}$ loops. However, both glue and $q\bar{q}$ states will couple to singlet scalar mesons. Therefore glueballs will mix with nearby $q\bar{q}$ states of the same quantum numbers. For example, the two isoscalar 0^{++} mesons around 1500 MeV will mix with the pure ground state glueball to generate the observed physical states $f_0(1370)$, $f_0(1500)$, and $f_0(1710)$ [9,17]. The first results from lattice calculations, which include these effects, indicate that the mass shifts are small. We return to a discussion of this point in Sec. 15.6.

The existence of three singlet scalar mesons around 1.5 GeV suggests additional degrees of freedom such as glue, since only two mesons are predicted in this mass range. The $f_0(1500)$ [9,17] or, alternatively, the $f_0(1710)$ [14], have been proposed as candidates for the scalar glueball, both states having considerable mixing also with the $f_0(1370)$. Other mixing schemes, in particular with the $f_0(500)$ and the $f_0(980)$, have also been proposed [18]. Details can be found in the "Note on Non-$q\bar{q}$ Mesons" in the Meson Listings and in Ref. 19 See also the "Note on Scalar Mesons below 2 GeV".

Mesons made of $q\bar{q}$ pairs bound by excited gluons g, the hybrid states $q\bar{q}g$, are also predicted. They should lie in the 1.9 GeV mass region, according to gluon flux tube models [20]. Lattice QCD also predicts the lightest hybrid, an exotic 1^{-+}, at a mass of 1.8 to 1.9 GeV [21]. However, the bag model predicts four nonets, among them an exotic 1^{-+} around or above 1.4 GeV [22,23]. There are so far two candidates for exotic states with quantum numbers 1^{-+}, the $\pi_1(1400)$ and $\pi_1(1600)$, which could be hybrids or four-quark states (see the "Note on Non-$q\bar{q}$ Mesons" in the Meson Listings and in Ref. 19)

15.4. Baryons: qqq states

Baryons are fermions with baryon number $\mathcal{B} = 1$, *i.e.*, in the most general case, they are composed of three quarks plus any number of quark - antiquark pairs. So far all established baryons are 3-quark (qqq) configurations (the LHCb collaboration has published the observation of two charmed 'pentaquark' states of minimal quark content $c\bar{c}uud$ at invariant masses close to 4.4 GeV [25], but their exact internal structure is not yet known). The color part of their state functions is an SU(3) singlet, a completely antisymmetric state of the three colors. Since the quarks are fermions, the state function must be antisymmetric under interchange of any two equal-mass quarks (up and down quarks in the limit of isospin symmetry). Thus it can be written as

$$|\,qqq\,\rangle_A = |\,\text{color}\,\rangle_A \times |\,\text{space, spin, flavor}\,\rangle_S\ , \tag{15.21}$$

where the subscripts S and A indicate symmetry or antisymmetry under interchange of any two equal-mass quarks. Note the contrast with the state function for the three nucleons in ^{3}H or ^{3}He:

$$|\,NNN\,\rangle_A = |\,\text{space, spin, isospin}\,\rangle_A\ . \tag{15.22}$$

This difference has major implications for internal structure, magnetic moments, *etc.* (For a nice discussion, see Ref. 26)

The "ordinary" baryons are made up of u, d, and s quarks. The three flavors imply an approximate flavor SU(3), which requires that baryons made of these quarks belong to the multiplets on the right side of

$$\mathbf{3} \otimes \mathbf{3} \otimes \mathbf{3} = \mathbf{10}_S \oplus \mathbf{8}_M \oplus \mathbf{8}_M \oplus \mathbf{1}_A \tag{15.23}$$

(see Sec. 46, on "SU(n) Multiplets and Young Diagrams"). Here the subscripts indicate symmetric, mixed-symmetry, or antisymmetric states under interchange of any two quarks. The $\mathbf{1}$ is a uds state (Λ_1), and the octet contains a similar state (Λ_8). If these have the same spin and parity, they can mix. The mechanism is the same as for the mesons (see above). In the ground state multiplet, the SU(3) flavor singlet Λ_1 is forbidden by Fermi statistics. Section 45, on "SU(3) Isoscalar Factors and Representation Matrices," shows how relative decay rates in, say, $\mathbf{10} \to \mathbf{8} \otimes \mathbf{8}$ decays may be calculated.

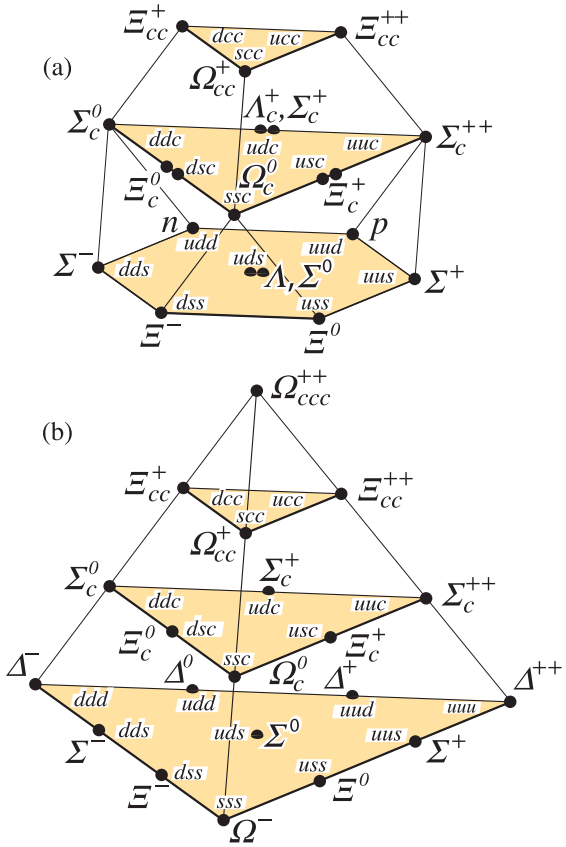

Figure 15.4: SU(4) multiplets of baryons made of u, d, s, and c quarks. (a) The 20-plet with an SU(3) octet. (b) The 20-plet with an SU(3) decuplet.

Table 15.5: N and Δ states in the N=0,1,2 harmonic oscillator bands. L^P denotes angular momentum and parity, S the three-quark spin and 'sym'=A,S,M the symmetry of the spatial wave function. Only dominant components indicated. Assignments in the N=2 band are partly tentative.

N	sym	L^P	S	$N(I=1/2)$				$\Delta(I=3/2)$			
2	A	1^+	1/2	$1/2^+$	$3/2^+$						
2	M	2^+	3/2	$1/2^+$	$3/2^+$	$5/2^+$	$7/2^+$				
2	M	2^+	1/2		$3/2^+$	$5/2^+$		$3/2^+$	$5/2^+$		
2	M	0^+	3/2		$3/2^+$						
2	M	0^+	1/2	$1/2^+$			$1/2^+$				
				$N(1710)$			$\Delta(1750)$				
2	S	2^+	3/2				$1/2^+$	$3/2^+$	$5/2^+$	$7/2^+$	
							$\Delta(1910)$	$\Delta(1920)$	$\Delta(1905)$	$\Delta(1950)$	
2	S	2^+	1/2		$3/2^+$	$5/2^+$					
					$N(1720)$	$N(1680)$					
2	S	0^+	3/2					$3/2^+$			
								$\Delta(1600)$			
2	S	0^+	1/2	$1/2^+$							
				$N(1440)$							
1	M	1^-	3/2	$1/2^-$	$3/2^-$	$5/2^-$					
				$N(1650)$	$N(1700)$	$N(1675)$					
1	M	1^-	1/2	$1/2^-$	$3/2^-$			$1/2^-$	$3/2^-$		
				$N(1535)$	$N(1520)$			$\Delta(1620)$	$\Delta(1700)$		
0	S	0^+	3/2						$3/2^+$		
									$\Delta(1232)$		
0	S	0^+	1/2	$1/2^+$							
				$N(938)$							

For the "ordinary" baryons (no c or b quark), flavor and spin may be combined in an approximate flavor-spin SU(6), in which the six basic states are $d\uparrow$, $d\downarrow$, $\cdots$, $s\downarrow$ ($\uparrow$, $\downarrow$ = spin up, down). Then the baryons belong to the multiplets on the right side of

$$\mathbf{6}\otimes\mathbf{6}\otimes\mathbf{6} = \mathbf{56}_S \oplus \mathbf{70}_M \oplus \mathbf{70}_M \oplus \mathbf{20}_A \ . \qquad (15.24)$$

These SU(6) multiplets decompose into flavor SU(3) multiplets as follows:

$$\mathbf{56} = {}^4\mathbf{10} \oplus {}^2\mathbf{8} \qquad (15.25a)$$

$$\mathbf{70} = {}^2\mathbf{10} \oplus {}^4\mathbf{8} \oplus {}^2\mathbf{8} \oplus {}^2\mathbf{1} \qquad (15.25b)$$

$$\mathbf{20} = {}^2\mathbf{8} \oplus {}^4\mathbf{1} \ , \qquad (15.25c)$$

where the superscript $(2S+1)$ gives the net spin S of the quarks for each particle in the SU(3) multiplet. The $J^P = 1/2^+$ octet containing the nucleon and the $J^P = 3/2^+$ decuplet containing the $\Delta(1232)$ together make up the "ground-state" 56-plet, in which the orbital angular momenta between the quark pairs are zero (so that the spatial part of the state function is trivially symmetric). The **70** and **20** require some excitation of the spatial part of the state function in order to make the overall state function symmetric. States with nonzero orbital angular momenta are classified in SU(6)⊗O(3) supermultiplets.

It is useful to classify the baryons into bands that have the same number N of quanta of excitation. Each band consists of a number of supermultiplets, specified by (D, L_N^P), where D is the dimensionality of the SU(6) representation, L is the total quark orbital angular momentum, and P is the total parity. Supermultiplets contained in bands up to N = 12 are given in Ref. 33. The N = 0 band, which contains the nucleon and $\Delta(1232)$, consists only of the $(56,0_0^+)$ supermultiplet. The N = 1 band consists only of the $(70,1_1^-)$ multiplet and contains the negative-parity baryons with masses below about 1.9 GeV. The N = 2 band contains five supermultiplets: $(56,0_2^+)$, $(70,0_2^+)$, $(56,2_2^+)$, $(70,2_2^+)$, and $(20,1_2^+)$.

The wave functions of the non-strange baryons in the harmonic oscillator basis are often labeled by $|X^{2S+1}L_\pi J^P\rangle$, where S, L, J, P are as above, $X = N$ or Δ, and $\pi = S, M$ or A denotes the symmetry of the spatial wave function. The possible model states for the bands with N=0,1,2 are given in Table 15.5. The assignment of experimentally observed states is only complete and well established up to the N=1 band. Some more tentative assignments for higher multiplets are suggested in Ref. 34.

In Table 15.6, quark-model assignments are given for many of the established baryons whose SU(6)⊗O(3) compositions are relatively unmixed. One must, however, keep in mind that apart from the mixing of the Λ singlet and octet states, states with same J^P but different L, S combinations can also mix. In the quark model with one-gluon exchange motivated interactions, the size of the mixing is determined by the relative strength of the tensor term with respect to the contact term (see below). The mixing is more important for the decay patterns of the states than for their positions. An example are the lowest lying $(70,1_1^-)$ states with J^P=$1/2^-$ and $3/2^-$. The physical states are:

$$|\,N(1535)1/2^-\rangle = \cos(\Theta_S)|N^2P_M1/2^-\rangle - \sin(\Theta_S)|N^4P_M1/2^-\rangle \qquad (15.26)$$

$$|\,N(1520)3/2^-\rangle = \cos(\Theta_D)|N^2P_M3/2^-\rangle - \sin(\Theta)_D|N^4P_M3/2^-\rangle \qquad (15.27)$$

and the orthogonal combinations for $N(1650)1/2^-$ and $N(1700)3/2^-$. The mixing is large for the J^P=$1/2^-$ states ($\Theta_S \approx$ -32^o), but small for the J^P=$3/2^-$ states ($\Theta_D \approx +6^o$) [35,36].

All baryons of the ground state multiplets are known. Many of their properties, in particular their masses, are in good agreement even with the most basic versions of the quark model, including harmonic (or linear) confinement and a spin-spin interaction, which is responsible for the octet - decuplet mass shifts. A consistent description of the ground-state electroweak properties, however, requires refined relativistic constituent quark models.

The situation for the excited states is much less clear. The assignment of some experimentally observed states with strange quarks to model configurations is only tentative and in many cases candidates are completely missing. Recently, Melde, Plessas and Sengl [37] have calculated baryon properties in relativistic constituent quark models, using one-gluon exchange and Goldstone-boson

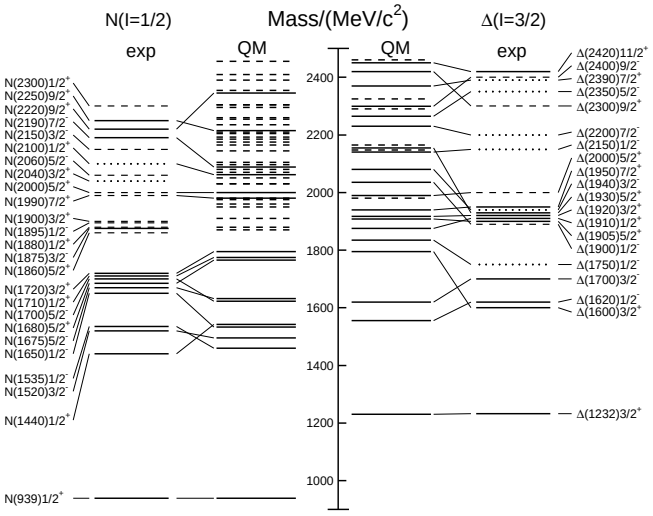

Figure 15.5: Excitation spectrum of the nucleon. Compared are the positions of the excited states identified in experiment, to those predicted by a relativized quark model calculation. Left hand side: isospin $I = 1/2$ N-states, right hand side: isospin $I = 3/2$ Δ-states. Experimental: (columns labeled 'exp'), three- and four-star states are indicated by full lines (two-star dashed lines, one-star dotted lines). At the very left and right of the figure, the spectroscopic notation of these states is given. Quark model [38]: (columns labeled 'QM'), all states for the N=1,2 bands, low-lying states for the N=3,4,5 bands. Full lines: at least tentative assignment to observed states, dashed lines: so far no observed counterparts. Many of the assignments between predicted and observed states are highly tentative.

exchange for the modeling of the hyperfine interactions (see Sec. 15.5 on Dynamics). Both types of models give qualitatively comparable results, and underestimate in general experimentally observed decay widths. Nevertheless, in particular on the basis of the observed decay patterns, the authors have assigned some additional states with strangeness to the SU(3) multiplets and suggest re-assignments for a few others. Among the new assignments are states with weak experimental evidence (two or three star ratings) and partly without firm spin/parity assignments, so that further experimental efforts are necessary before final conclusions can be drawn. We have added their suggestions in Table 15.6.

In the non-strange sector there are two main problems which are illustrated in Fig. 15.5, where the experimentally observed excitation spectrum of the nucleon (N and Δ resonances) is compared to the results of a typical quark model calculation [38]. The lowest states from the N=2 band, the $N(1440)1/2^+$, and the $\Delta(1600)3/2^+$, appear lower than the negative parity states from the N=1 band (see Table 15.5) and much lower than predicted by most models. Also negative parity Δ states from the N=3 band ($\Delta(1900)1/2^-$, $\Delta(1940)3/2^-$, and $\Delta(1930)5/2-$) are too low in energy. Part of the problem could be experimental. Among the negative parity Δ states, only the $\Delta(1930)5/2^-$ has three stars and the uncertainty in the position of the $\Delta(1600)3/2^+$ is large (1550 - 1700 MeV).

Furthermore, many more states are predicted than observed. This has been known for a long time as the 'missing resonance' problem [35]. Up to an excitation energy of 2.4 GeV, about 45 N states are predicted, but only 14 are established (four- or three-star; see Note on N and Δ Resonances for the rating of the status of resonances) and 10 are tentative (two- or one-star). Even for the N=2 band, up to now only half of the predicted states have been observed. The most recent partial wave analysis of elastic pion scattering and charge exchange data by Arndt and collaborators [39] has made the situation even worse. They found no evidence for almost half of the states listed in this review (and included in Fig. 15.5). Such analyses are of course biased against resonances which couple only weakly to the $N\pi$ channel. Quark model predictions for the couplings to other hadronic channels and to photons are given in Ref. 38. A large experimental effort is ongoing at several electron accelerators to study the baryon resonance spectrum with real and virtual photon-induced meson production reactions. This includes the search for as-yet-unobserved states, as well as detailed studies of the properties of the low lying states (decay patterns, electromagnetic couplings, magnetic moments, *etc.*) (see Ref. 40 for recent reviews). This experimental effort has currently entered its final phase with the measurement of single and double polarization observables for many different meson production channels, so that a much better understanding of the experimental spectrum can be expected. An example for the impact of the new data is given by a comparison of results from different multipole analyses of pion photoproduction [41]. It shows clearly that with the inclusion of polarization obserbvables the reaction model results start to converge. This will in the near future much improve the data basis for excited baryons in the light quark sector.

Table 15.6: Quark-model assignments for some of the known baryons in terms of a flavor-spin SU(6) basis. Only the dominant representation is listed. Assignments for several states, especially for the $\Lambda(1810)$, $\Lambda(2350)$, $\Xi(1820)$, and $\Xi(2030)$, are merely educated guesses. † recent suggestions for assignments and re-assignments from Ref. 37. For assignments of the charmed baryons, see the "Note on Charmed Baryons" in the Particle Listings.

J^P	$(D, L_N^P)\,S$	Octet members				Singlets
$1/2^+$	$(56,0_0^+)$	$1/2\,N(939)$	$\Lambda(1116)$	$\Sigma(1193)$	$\Xi(1318)$	
$1/2^+$	$(56,0_2^+)$	$1/2\,N(1440)$	$\Lambda(1600)$	$\Sigma(1660)$	$\Xi(1690)^\dagger$	
$1/2^-$	$(70,1_1^-)$	$1/2\,N(1535)$	$\Lambda(1670)$	$\Sigma(1620)$	$\Xi(?)$	$\Lambda(1405)$
				$\Sigma(1560)^\dagger$		
$3/2^-$	$(70,1_1^-)$	$1/2\,N(1520)$	$\Lambda(1690)$	$\Sigma(1670)$	$\Xi(1820)$	$\Lambda(1520)$
$1/2^-$	$(70,1_1^-)$	$3/2\,N(1650)$	$\Lambda(1800)$	$\Sigma(1750)$	$\Xi(?)$	
				$\Sigma(1620)^\dagger$		
$3/2^-$	$(70,1_1^-)$	$3/2\,N(1700)$	$\Lambda(?)$	$\Sigma(1940)^\dagger$	$\Xi(?)$	
$5/2^-$	$(70,1_1^-)$	$3/2\,N(1675)$	$\Lambda(1830)$	$\Sigma(1775)$	$\Xi(1950)^\dagger$	
$1/2^+$	$(70,0_2^+)$	$1/2\,N(1710)$	$\Lambda(1810)$	$\Sigma(1880)$	$\Xi(?)$	$\Lambda(1810)^\dagger$
$3/2^+$	$(56,2_2^+)$	$1/2\,N(1720)$	$\Lambda(1890)$	$\Sigma(?)$	$\Xi(?)$	
$5/2^+$	$(56,2_2^+)$	$1/2\,N(1680)$	$\Lambda(1820)$	$\Sigma(1915)$	$\Xi(2030)$	
$7/2^-$	$(70,3_3^-)$	$1/2\,N(2190)$	$\Lambda(?)$	$\Sigma(?)$	$\Xi(?)$	$\Lambda(2100)$
$9/2^-$	$(70,3_3^-)$	$3/2\,N(2250)$	$\Lambda(?)$	$\Sigma(?)$	$\Xi(?)$	
$9/2^+$	$(56,4_4^+)$	$1/2\,N(2220)$	$\Lambda(2350)$	$\Sigma(?)$	$\Xi(?)$	
		Decuplet members				
$3/2^+$	$(56,0_0^+)$	$3/2\,\Delta(1232)$	$\Sigma(1385)$	$\Xi(1530)$	$\Omega(1672)$	
$3/2^+$	$(56,0_2^+)$	$3/2\,\Delta(1600)$	$\Sigma(1690)^\dagger$	$\Xi(?)$	$\Omega(?)$	
$1/2^-$	$(70,1_1^-)$	$1/2\,\Delta(1620)$	$\Sigma(1750)^\dagger$	$\Xi(?)$	$\Omega(?)$	
$3/2^-$	$(70,1_1^-)$	$1/2\,\Delta(1700)$	$\Sigma(?)$	$\Xi(?)$	$\Omega(?)$	
$5/2^+$	$(56,2_2^+)$	$3/2\,\Delta(1905)$	$\Sigma(?)$	$\Xi(?)$	$\Omega(?)$	
$7/2^+$	$(56,2_2^+)$	$3/2\,\Delta(1950)$	$\Sigma(2030)$	$\Xi(?)$	$\Omega(?)$	
$11/2^+$	$(56,4_4^+)$	$3/2\,\Delta(2420)$	$\Sigma(?)$	$\Xi(?)$	$\Omega(?)$	

In quark models, the number of excited states is determined by the effective degrees of freedom, while their ordering and decay properties are related to the residual quark - quark interaction. An overview of quark models for baryons is given in Ref. 36, recent discussions of baryon spectroscopy are given in Refs. 34 and 27. The effective degrees of freedom in the standard nonrelativistic quark model are three equivalent valence quarks with one-gluon exchange-motivated, flavor-independent color-magnetic interactions. The QCD aspect of gluon-gluon interactions is emphasized by the hypercentral quark model [42], [43], which includes in a natural way three-body forces between the quarks. A different class of models uses interactions which

give rise to a quark - diquark clustering of the baryons: for a review see Ref. 44. If there is a tightly bound diquark, only two degrees of freedom are available at low energies, and thus *fewer* states are predicted. Furthermore, selection rules in the decay pattern may arise from the quantum numbers of the diquark. *More* states are predicted by collective models of the baryon like the algebraic approach in Ref. 45. In this approach, the quantum numbers of the valence quarks are distributed over a Y-shaped string-like configuration, and additional states arise *e.g.*, from vibrations of the strings. *More* states are also predicted in the framework of flux-tube models, see Ref. 46, which are motivated by lattice QCD. In addition to the quark degrees of freedom, flux-tubes responsible for the confinement of the quarks are considered as degrees of freedom. These models include hybrid baryons containing explicit excitations of the gluon fields. However, since all half integral J^P quantum numbers are possible for ordinary baryons, such 'exotics' will be very hard to identify, and probably always mix with ordinary states. So far, the experimentally observed number of states is still far lower even than predicted by the quark–diquark models.

Recently, the influence of chiral symmetry on the excitation spectrum of the nucleon has been hotly debated from a somewhat new perspective. Chiral symmetry, the fundamental symmetry of QCD, is strongly broken for the low lying states, resulting in large mass differences of parity partners like the J^P=1/2$^+$ $N(938)1/2^+$ ground state and the J^P=1/2$^-$ $N(1535)1/2^-$ excitation. However, at higher excitation energies there is some evidence for parity doublets and even some very tentative suggestions for full chiral multiplets of N^* and Δ resonances. An effective restoration of chiral symmetry at high excitation energies due to a decoupling from the quark condensate of the vacuum has been discussed (see Ref. 47 for recent reviews) as a possible cause. In this case, the mass generating mechanisms for low and high lying states would be essentially different. As a further consequence, the parity doublets would decouple from pions, so that experimental bias would be worse. However, parity doublets might also arise from the spin-orbital dynamics of the 3-quark system. Presently, the status of data does not allow final conclusions.

The most recent developments on the theory side are the first unquenched lattice calculations for the excitation spectrum discussed in Sec. 15.6. The results are basically consistent with the level counting of SU(6)⊗O(3) in the standard non-relativistic quark model and show no indication for quark-diquark structures or parity doubling. Consequently, there is as yet no indication from lattice that the mis-match between the excitation spectrum predicted by the standard quark model and experimental observations is due to inappropriate degrees of freedom in the quark model.

15.5. Dynamics

Quantum chromodynamics (QCD) is well-established as the theory for the strong interactions. As such, one of the goals of QCD is to predict the spectrum of strongly-interacting particles. To date, the only first-principles calculations of spectroscopy from QCD use lattice methods. These are the subject of Sec. 15.6. These calculations are difficult and unwieldy, and many interesting questions do not have a good lattice-based method of solution. Therefore, it is natural to build models, whose ingredients are abstracted from QCD, or from the low-energy limit of QCD (such as chiral Lagrangians) or from the data itself. The words "quark model" are a shorthand for such phenomenological models. Many specific quark models exist, but most contain a similar basic set of dynamical ingredients. These include:

i) A confining interaction, which is generally spin-independent (*e.g.*, harmonic oscillator or linear confinement);

ii) Different types of spin-dependent interactions:

a) commonly used is a color-magnetic flavor-independent interaction modeled after the effects of gluon exchange in QCD (see *e.g.*, Ref. 48). For example, in the S-wave states, there is a spin-spin hyperfine interaction of the form

$$H_{HF} = -\alpha_S M \sum_{i>j} (\overrightarrow{\sigma}\lambda_a)_i (\overrightarrow{\sigma}\lambda_a)_j \ , \qquad (15.28)$$

where M is a constant with units of energy, λ_a $(a = 1, \cdots, 8,)$ is the set of SU(3) unitary spin matrices, defined in Sec. 45, on "SU(3) Isoscalar Factors and Representation Matrices," and the sum runs over constituent quarks or antiquarks. Spin-orbit interactions, although allowed, seem to be small in general, but a tensor term is responsible for the mixing of states with the same J^P but different L, S combinations.

b) other approaches include flavor-dependent short-range quark forces from instanton effects (see *e.g.*, Ref. 49) This interaction acts only on scalar, isoscalar pairs of quarks in a relative S-wave state:

$$\langle q^2; S, L, T|W|q^2; S, L, T\rangle = -4g\delta_{S,0}\delta_{L,0}\delta_{I,0}\mathcal{W} \qquad (15.29)$$

where $\mathcal{W}$ is the radial matrix element of the contact interaction.

c) a rather different and controversially discussed approach is based on flavor-dependent spin-spin forces arising from one-boson exchange. The interaction term is of the form:

$$H_{HF} \propto \sum_{i<j} V(\overrightarrow{r}_{ij})\lambda_i^F \cdot \lambda_j^F \overrightarrow{\sigma}_i \cdot \overrightarrow{\sigma}_j \qquad (15.30)$$

where the λ_i^F are in flavor space (see *e.g.*, Ref. 50).

iii) A strange quark mass somewhat larger than the up and down quark masses, in order to split the SU(3) multiplets;

iv) In the case of spin-spin interactions (iia,c), a flavor-symmetric interaction for mixing $q\overline{q}$ configurations of different flavors (*e.g.*, $u\overline{u} \leftrightarrow d\overline{d} \leftrightarrow s\overline{s}$), in isoscalar channels, so as to reproduce *e.g.*, the η - η' and ω - ϕ mesons.

These ingredients provide the basic mechanisms that determine the hadron spectrum in the standard quark model.

15.6. Lattice Calculations of Hadronic Spectroscopy

Lattice calculations are a major source of information about QCD masses and matrix elements. The necessary theoretical background is given in Sec. 17 of this *Review*. Here we confine ourselves to some general comments and illustrations of lattice calculations for spectroscopy.

In general, the cleanest lattice results come from computations of processes in which there is only one particle in the simulation volume. These quantities include masses of hadrons, simple decay constants, like pseudoscalar meson decay constants, and semileptonic form factors (such as the ones appropriate to $B \to Dl\nu$, $Kl\nu$, $\pi l\nu$). The cleanest predictions for masses are for states which have narrow decay widths and are far below any thresholds to open channels, since the effects of final state interactions are not yet under complete control on the lattice. As a simple corollary, the lightest state in a channel is easier to study than the heavier ones. "Difficult" states for the quark model (such as exotics) are also difficult for the lattice because of the lack of simple operators which couple well to them.

Good-quality modern lattice calculations will present multi-part error budgets with their predictions. A small part of the uncertainty is statistical, from sample size. Typically, the quoted statistical uncertainty includes uncertainty from a fit: it is rare that a simulation computes one global quantity which is the desired observable. Simulations which include virtual quark-antiquark pairs (also known as "dynamical quarks" or "sea quarks") are often done at up and down quark mass values heavier than the experimental ones, and it is then necessary to extrapolate in these quark masses. Simulations can work at the physical values of the heavier quarks' masses. They are always done at nonzero lattice spacing, and so it is necessary to extrapolate to zero lattice spacing. Some theoretical input is needed to do this. Much of the uncertainty in these extrapolations is systematic, from the choice of fitting function. Other systematics include the effect of finite simulation volume, the number of flavors of dynamical quarks actually simulated, and technical issues with how these dynamical quarks are included. The particular choice of a fiducial mass (to normalize other predictions) is not standardized; there are many possible choices, each with its own set of strengths and weaknesses, and determining it usually requires a second lattice simulation from that used to calculate the quantity under consideration. A systematic error of major historical interest is the "quenched approximation," in which

dynamical quarks are simply left out of the simulation. This was done because the addition of these virtual pairs presented an expensive computational problem. No generally-accepted methodology has ever allowed one to correct for quenching effects, short of redoing all calculations with dynamical quarks. Recent advances in algorithms and computer hardware have rendered it obsolete.

With these brief remarks, we turn to examples. The field of lattice QCD simulations is vast, and so it is not possible to give a comprehensive review of them in a small space. The history of lattice QCD simulations is a story of thirty years of incremental improvements in physical understanding, algorithm development, and ever faster computers, which have combined to bring the field to a present state where it is possible to carry out very high quality calculations. We present a few representative illustrations, to show the current state of the art.

By far, the major part of all lattice spectroscopy is concerned with that of the light hadrons, and so we illustrate results in Fig. 15.6, a comprehensive summary provided by A. Kronfeld [51].

Flavor singlet mesons are at the frontier of lattice QCD calculations, because one must include the effects of "annihilation graphs," for the valence q and $\bar{q}$. Recently, several groups, Refs. 7, 58–62, have reported calculations of the η and η' mesons. The numbers of Ref. 7 are typical, finding masses of 573(6) and 947(142) MeV for the η and η'. The singlet-octet mixing angle (in the conventions of Table 15.2) is $\theta_{lin} = -14.1(2.8)°$.

The spectroscopy of mesons containing heavy quarks has become a truly high-precision endeavor. These simulations use Non-Relativistic QCD (NRQCD) or Heavy Quark Effective Theory (HQET), systematic expansions of the QCD Lagrangian in powers of the heavy quark velocity, or the heavy quark mass. Terms in the Lagrangian have obvious quark model analogs, but are derived directly from QCD. For example, the heavy quark potential is a derived quantity, extracted from simulations. Fig. 15.7 shows the mass spectrum for mesons containing at least one heavy (b or c) quark from Ref. 65. It also contains results from Refs. 67 and 68. The calculations uses a discretization of nonrelativistic QCD for bottom quarks with charm and lighter quarks being handled with an improved relativistic action.

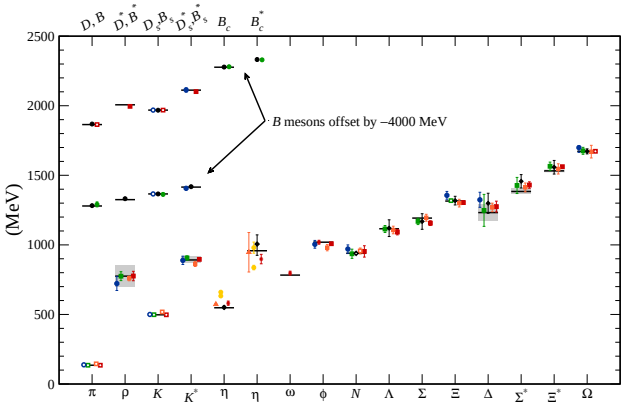

Figure 15.6: Hadron spectrum from lattice QCD. Comprehensive results for mesons and baryons are from MILC [52,53], PACS-CS [54], BMW [55], QCDSF [56], and ETM [74]. Results for η and η' are from RBC & UKQCD [7], Hadron Spectrum [59](also the only ω mass), UKQCD [58], and Michael, Ottnad, and Urbach [60]. Results for heavy-light hadrons from Fermilab-MILC [63], HPQCD [64,65], and Mohler and Woloshyn [66]. Circles, squares, diamonds, and triangles stand for staggered, Wilson, twisted-mass Wilson, and chiral sea quarks, respectively. Asterisks represent anisotropic lattices. Open symbols denote the masses used to fix parameters. Filled symbols (and asterisks) denote results. Red, orange, yellow, green, and blue stand for increasing numbers of ensembles (i.e., lattice spacing and sea quark mass). Black symbols stand for results with 2+1+1 flavors of sea quarks. Horizontal bars (gray boxes) denote experimentally measured masses (widths). b-flavored meson masses are offset by −4000 MeV.

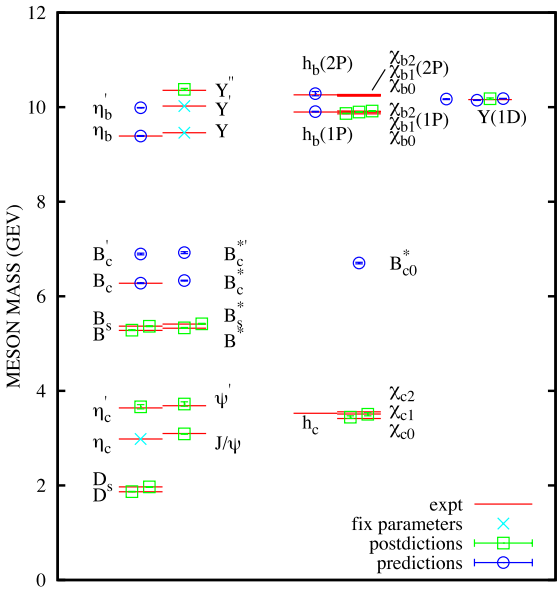

Figure 15.7: Spectroscopy for mesonic systems containing one or more heavy quarks (adapted from Ref. 65) Particles whose masses are used to fix lattice parameters are shown with crosses; the authors distinguish between "predictions" and "postdictions" of their calculation. Lines represent experiment.

Four flavors (u, d, s, c) of dynamical quarks are included.

Fig. 15.8 shows a compilation of recent lattice results for doubly and triply charmed baryons, provided by S. Meinel [69]. The state recently announced by LHCb [29] is also shown. Note that the lattice calculations for the mass of this state were predictions, not postdictions.

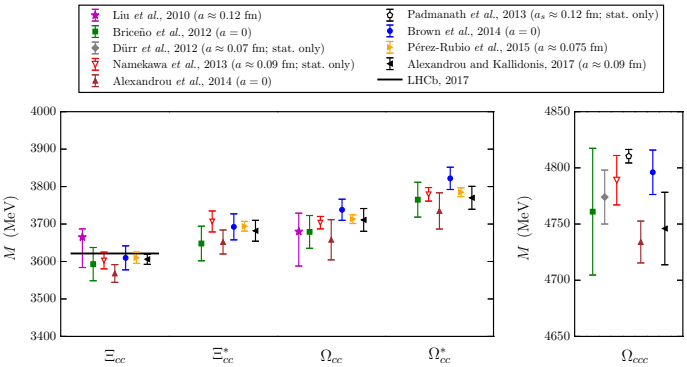

Figure 15.8: Comparison of lattice QCD results for the doubly and triply charmed baryon masses. Labels are Liu, *et al.*, [70]; Briceno, *et al.*, [71]; Namekawa, *et al.*, [72]; Padmanath, *et al.*, [73]; Alexandrou, *et al.*, [74]; Brown, *et al.*, [75]; Perez-Rubio et al., [76] Alexandrou and Kallidonis 2017, [77]. Only calculations with dynamical light quarks are included; for the doubly charmed baryons, only calculations were performed at or extrapolated to the physical pion mass are shown. Results without estimates of systematic uncertainties are labeled "stat. only". The lattice spacing values used in the calculations are also given; $a = 0$ indicates that the results have been extrapolated to the continuum limit. In the plot of the doubly charmed baryons, the recently announced experimental result for the Ξ_{cc}^{+} mass from LHCb [29] is shown with a horizontal line.

Recall that lattice calculations take operators which are interpolating fields with quantum numbers appropriate to the desired states, compute correlation functions of these operators, and fit the correlation functions to functional forms parametrized by a set of

masses and matrix elements. As we move away from hadrons which can be created by the simplest quark model operators (appropriate to the lightest meson and baryon multiplets) we encounter a host of new problems: either no good interpolating fields, or too many possible interpolating fields, and many states with the same quantum numbers. Techniques for dealing with these interrelated problems vary from collaboration to collaboration, but all share common features: typically, correlation functions from many different interpolating fields are used, and the signal is extracted in what amounts to a variational calculation using the chosen operator basis. In addition to mass spectra, wave function information can be garnered from the form of the best variational wave function. Of course, the same problems which are present in the spectroscopy of the lightest hadrons (the need to extrapolate to infinite volume, physical values of the light quark masses, and zero lattice spacing) are also present. We briefly touch on three different kinds of hadrons: excited states of mesons (including hybrids), excited states of baryons, and glueballs. The quality of the data is not as good as for the ground states, and so the results continue to evolve.

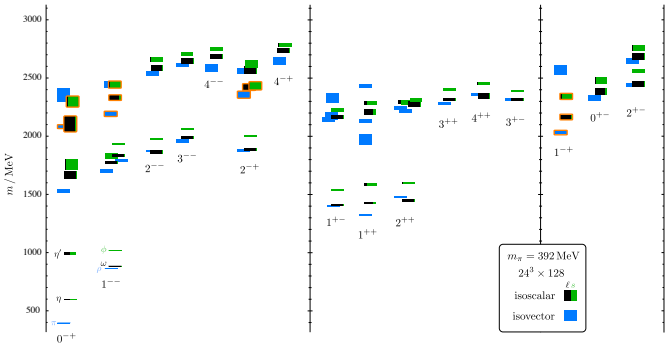

Figure 15.9: Isoscalar (green and black) and isovector (blue) spectrum from Ref. 61. States are labeled J^{PC}. The quark mass is heavier than its physical value; $m_\pi = 524$ MeV. The vertical height of each box indicates the statistical uncertainty in the mass. Black and green indicate relative nonstrange and strange composition. Orange outlines show states with a large chromomagnetic component to their wave function, which the authors of Ref. 61 argue are hybrid states. Note the exotic states in the three rightmost columns.

Modern calculations use a large bases of trial states, which allow them to probe many quantum number channels simultaneously. This is vital for studying "difficult sectors" of QCD, such as the isoscalar mesons. A recent example of meson spectroscopy where this is done, by Ref. 61, is shown in Fig. 15.9. The quark masses are still heavier than their physical values, so the pion is at 524 MeV. The authors can assign a relative composition of nonstrange and strange quark content to their states, observing, for example, a nonstrange ω and a strange ϕ. Some states also have a substantial component of gluonic excitation. Note especially the three exotic channels $J^{PC} = 1^{-+}$, 0^{+-}, and 2^{+-}, with states around 2 GeV. These calculations will continue to improve as the quark masses are carried lower.

The interesting physics questions of excited baryon spectroscopy to be addressed are precisely those enumerated in the last section. An example of a recent calculation, due to Ref. 78 is shown in Fig. 15.10. Notice that the pion is not yet at its physical value. The lightest positive parity state is the nucleon, and the Roper resonance has not yet appeared as a light state.

In Fig. 15.3 we showed a figure from Ref. 12 presenting a lattice prediction for the glueball mass spectrum in quenched approximation. A true QCD prediction of the glueball spectrum requires dynamical light quarks and (because glueball operators are intrinsically noisy) high statistics. Only recently have the first useful such calculations appeared, in Refs. 79 and 80. Fig. 15.11 shows results from Ref. 79, done with dynamical u, d and s quarks at two lattice spacings, 0.123 and 0.092 fm, along with comparisons to the quenched lattice calculation of Ref. 11 and to experimental isosinglet mesons. The

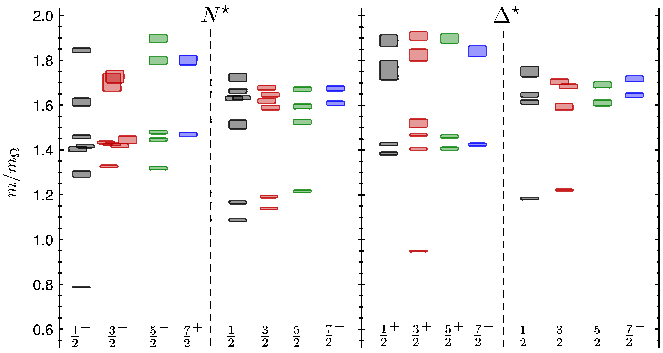

Figure 15.10: Spin-identified spectrum of nucleons and deltas, from lattices where $m_\pi = 396$ MeV, in units of the calculated Ω mass, from Ref. 78. The colors just correspond to the different J assignments: grey for $J = 1/2$, red for $J = 3/2$, green for 5/2, blue for $J = 7/2$.

dynamical simulation is, of course, not the last word on this subject, but it shows that the effects of quenching seem to be small.

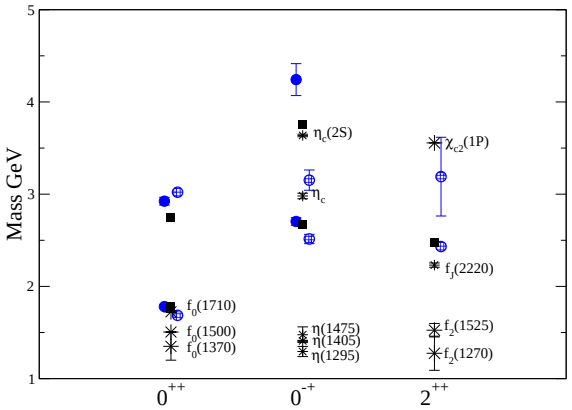

Figure 15.11: Lattice QCD predictions for glueball masses. The open and closed circles are the larger and smaller lattice spacing data of the full QCD calculation of glueball masses of Ref. 79. Squares are the quenched data for glueball masses of Ref. 11. The bursts labeled by particle names are experimental states with the appropriate quantum numbers.

Lattice calculations relevant to the extra states observed in the charmonium spectrum (section 3.1) are difficult, due to the number of nearby multiparticle states. The current status of lattice studies of these states is reviewed in Refs. 81 and 82.

Several other features of hadronic spectroscopy are also being studied on the lattice.

Electromagnetic mass splittings (such as the neutron - proton mass difference) are interesting but difficult. These calculations are important for determining the values of the quark masses (for a discussion see the review in the PDG). Knowing that the neutron is heavier than the proton tells us that these splittings have a complicated origin. One part of the shift is because the up and down quarks have slightly different masses. The second is that the quarks have (different) charges. In pre-lattice days, phenomenologists would combine Coulomb forces and spin-dependent electromagnetic hyperfine interactions to model their charge effects. These days, in order to compute hadronic mass differences on the lattice, electromagnetic interactions must be included in the simulations. This creates a host of technical issues. An important one is that electromagnetic interactions are long range, but lattice simulations are done in finite volumes. The theoretical situation is summarized in the recent review Ref. 83. A recent calculation, Ref. 84, has presented the first results for electromagnetic mass splittings in the baryon octet, with good agreement with observation.

Most hadrons are resonances, and their widths are the last target of lattice simulations we will mention. The actual calculation is of the combined mass of two (or more) hadrons in a box of finite size. The combined mass is shifted from being the sum of the individual masses because the finite box forces the hadrons to interact with each other. The volume-dependent mass shift yields the phase shift for the continuum scattering amplitude, which in turn can be used to extract the resonance mass and width, with some degree of modeling. So far only two-body resonances, the rho meson and a few others, have been well studied. This is an active research topic. A recent review, Ref. 85, summarizes the situation, and example of a calculation of the rho meson decay width is Ref. 86. The mass and decay width of the $f_0(500)$ have recently been computed in Ref. 87.

References:

1. J. Schwinger, Phys. Rev. **135**, B116 (1964).
2. A. Bramon *et al.*, Phys. Lett. **B403**, 339 (1997).
3. A. Aloisio *et al.*, Phys. Lett. **B541**, 45 (2002).
4. F. Ambrosino *et al.*, JHEP **07**, 105 (2009).
5. C. Amsler *et al.*, Phys. Lett. **B294**, 451 (1992).
6. C. Amsler, Rev. Mod. Phys. **70**, 1293 (1998).
7. N.H. Christ *et al.*, Phys. Rev. Lett. **105**, 241601 (2010).
8. T. Feldmann, Int. J. Mod. Phys. **A915**, 159 (2000).
9. C. Amsler and F.E. Close, Phys. Rev. **D53**, 295 (1996).
10. R.L. Jaffe, Phys. Rev. **D15**, 267 (1977);
    R.L. Jaffe, Phys. Rev. **D15**, 281 (1977).
11. C. Morningstar and M. Peardon, Phys. Rev. **D60**, 034509 (1999).
12. Y. Chen *et al.*, Phys. Rev. **D73**, 014516 (2006).
13. S.L. Olsen, Front. Phys. **10**, 121 (2015).
14. W.J. Lee and D. Weingarten, Phys. Rev. **D61**, 014015 (2000).
15. G.S. Bali *et al.*, Phys. Lett. **B309**, 378 (1993).
16. C. Michael, *AIP Conf. Proc.* **432**, 657 (1998).
17. F.E. Close and A. Kirk, Eur. Phys. J. **C21**, 531 (2001).
18. W. Ochs, J. Phys. **G40**, 043001 (2013).
19. C. Amsler and N.A. Törnqvist, Phys. Reports **389**, 61 (2004).
20. N. Isgur and J. Paton, Phys. Rev. **D31**, 2910 (1985).
21. P. Lacock *et al.*, Phys. Lett. **B401**, 308 (1997);
    C. Bernard *et al.*, Phys. Rev. **D56**, 7039 (1997);
    C. Bernard *et al.*, Phys. Rev. **D68**, 074505 (2003).
22. M. Chanowitz and S. Sharpe, Nucl. Phys. **B222**, 211 (1983).
23. T. Barnes *et al.*, Nucl. Phys. **B224**, 241 (1983).
24. W.-M Yao *et al.*, J. Phys. **G33**, 1 (2006).
25. R. Aaij *et al.*, Phys. Rev. Lett. **115**, 072001 (2015).
26. F.E. Close, in *Quarks and Nuclear Forces* (Springer-Verlag, 1982), p. 56.
27. V. Crede and W. Roberts, Rept. on Prog. in Phys. **76**, 076301 (2013).
28. R. Aaij *et al.*, (LHCb collaboration) Phys. Rev. Lett. **118**, 182001 (2017).
29. R. Aaij *et al.* [LHCb Collaboration], arXiv:1707.01621 [hep-ex]..
30. M. Mattson *et al.*, Phys. Rev. Lett. **89**, 112001 (2002).
31. A. Ocherashvili *et al.*, Phys. Lett. **B628**, 18 (2005).
32. M. Karliner and J.L. Rosner, Phys. Rev. **D90**, 094007 (2014).
33. R.H. Dalitz and L.J. Reinders, in "Hadron Structure as Known from Electromagnetic and Strong Interactions," *Proceedings of the Hadron '77 Conference* (Veda, 1979), p. 11.
34. E. Klempt and J.M. Richard, Rev. Mod. Phys. **82**, 1095 (2010).
35. N. Isgur and G. Karl, Phys. Rev. **D18**, 4187 (1978); *ibid.*, **D19**, 2653 (1979); *ibid.*, **D20**, 1191 (1979).
36. S. Capstick and W. Roberts, Prog. in Part. Nucl. Phys. **45**, 241 (2000).
37. T. Melde, W. Plessas, and B. Sengl, Phys. Rev. **D77**, 114002 (2008).
38. S. Capstick and W. Roberts, Phys. Rev. **D49**, 4570 (1994); *ibid.*, **D57**, 4301 (1998); *ibid.*, **D58**, 074011 (1998);
    S. Capstick, Phys. Rev. **D46**, 2864 (1992).
39. R.A. Arndt *et al.*, Phys. Rev. **C74**, 045205 (2006).
40. B. Krusche and S. Schadmand, Prog. in Part. Nucl. Phys. **51**, 399 (2003);
    V.D. Burkert, T.-S.H. Lee, Int. J. Mod. Phys. **E13**, 1035 (2004); see also A.J.G. Hey and R.L. Kelly, Phys. Reports **96**, 71 (1983).
41. A.V. Anisovich *et al.*, Eur. Phys. J. **A52**, 284 (2016).
42. M. Ferraris *et al.*, Phys. Lett. **B364**, 231 (1995).
43. M.M. Giannini and E. Santopinto, Chin. J. Phys. **53**, 020301-1 (2015).
44. M. Anselmino *et al.*, Rev. Mod. Phys. **65**, 1199 (1993).
45. R. Bijker *et al.*, Ann. Phys. **236**, 69 (1994).
46. N. Isgur and J. Paton, Phys. Rev. **D31**, 2910 (1985);
    S. Capstick and P.R. Page, Phys. Rev. **C66**, 065204 (2002).
47. R.L. Jaffe, D. Pirjol, and A. Scardicchio, Phys. Rev. **435**, 157 (2006);
    L. Ya. Glozman, Phys. Rev. **444**, 1 (2007).
48. A. De Rujula *et al.*, Phys. Rev. **D12**, 147 (1975).
49. W.H. Blask *et al.*, Z. Phys. **A337**, 327 (1990);
    U. Löring *et al.*, Eur. Phys. J. **A10**, 309 (2001);
    U. Löring *et al.*, Eur. Phys. J. **A10**, 395 (2001); *ibid.*, **A10**, 447 (2001).
50. L.Y. Glozman and D.O. Riska, Phys. Rev. **268**, 263 (1996);
    L.Y. Glozman *et al.*, Phys. Rev. **D58**, 094030 (1998);
    W. Plessas, Int. J. Mod. Phys. **A30**, 1530013 (2015).
51. A. Kronfeld, private comunication. See also Ann. Rev. Nucl. and Part. Sci. **62**, 265 (2012) for an earlier version of this figure.
52. C. Aubin *et al.*, Phys. Rev. **D70**, 094505 (2004) [hep-lat/0402030].
53. A. Bazavov *et al.*, Rev. Mod. Phys. **82**, 1349 (2010) [arXiv:0903.3598].
54. S. Aoki *et al.* [PACS-CS Collab.], Phys. Rev. **D79**, 034503 (2009) [arXiv:0807.1661].
55. S. Durr *et al.*, Science **322**, 1224 (2008) [arXiv:0906.3599].
56. W. Bietenholz *et al.*, Phys. Rev. **D84**, 054509 (2011) [arXiv:1102.5300].
57. C. Alexandrou *et al.*, Phys. Rev. **D90**, 074501 (2014) [arXiv:1406.4310].
58. E.B. Gregory *et al.* [UKQCD Collab.], Phys. Rev. **D86**, 014504 (2012) [arXiv:1112.4384].
59. J.J. Dudek *et al.*, Phys. Rev. **D83**, 111502 (2011) [arXiv:1102.4299].
60. C. Michael *et al.* [ETM Collab.], Phys. Rev. Lett. **111**, 181602 (2013) [arXiv:1310.1207].
61. J.J. Dudek *et al.* [Hadron Spectrum Collab.], Phys. Rev. **D88**, 094505 (2013) [arXiv:1309.2608].
62. K. Ottnad *et al.* [OTM Collaboration], Nucl. Phys. **B896**, 470 (2015).
63. C. Bernard *et al.* [Fermilab Lattice and MILC Collab.], Phys. Rev. **D83**, 034503 (2011) [arXiv:1003.1937].
64. E.B. Gregory *et al.*, Phys. Rev. **D83**, 014506 (2011) [arXiv:1010.3848].
65. R.J. Dowdall *et al.*, Phys. Rev. **D86**, 094510 (2012) [arXiv:1207.5149].
66. D. Mohler and R. M. Woloshyn, Phys. Rev. **D84**, 054505 (2011) [arXiv:1103.5506].
67. J.O. Daldrop *et al.* [HPQCD Collab.], Phys. Rev. Lett. **108**, 102003 (2012).
68. G.C. Donald *et al.*, Phys. Rev. **D86**, 094501 (2012).
69. S. Meinel, private comunication.
70. L. Liu *et al.*, Phys. Rev. **D81**, 094505 (2010).
71. R.A. Briceno, H.-W. Lin, and D.R. Bolton, Phys. Rev. **D86**, 094504 (2012).
72. Y. Namekawa *et al.* [PACS-CS Collab.], Phys. Rev. **D87**, 094512 (2013).
73. M. Padmanath *et al.*, Phys. Rev. **D90**, 074504 (2014).
74. C. Alexandrou *et al.*, Phys. Rev. **D90**, 074501 (2014).
75. Z.S. Brown *et al.*, Phys. Rev. **D90**, 094507 (2014).
76. P. Perez-Rubio, S. Collins and G. S. Bali, Phys. Rev. D 92,034504(2015).
77. C. Alexandrou and C. Kallidonis, arXiv:1704.02647 [hep-lat]..
78. R.G. Edwards *et al.*, Phys. Rev. **D84**, 074508 (2011) [arXiv:1104.5152].
79. C.M. Richards *et al.*, [UKQCD Collab.], Phys. Rev. **D82**, 034501 (2010).
80. E. Gregory, A. Irving, B. Lucini, C. McNeile, A. Rago, C. Richards and E. Rinaldi, JHEP **1210**, 170 (2012).

81. S. Prelovsek, PoS LATTICE **2014**, 015 (2014) [arXiv:1411.0405].
82. C. Liu, PoS LATTICE **2016**, 006 (2017) [arXiv:1612.00103 [hep-lat]]..
83. A. Patella, PoS LATTICE **2016**, 020 (2017) [arXiv:1702.03857 [hep-lat]].
84. S. Borsanyi *et al.*, Science **347**, 1452 (2015) [arXiv:1406.4088].
85. R. A. Briceno, J. J. Dudek and R. D. Young, arXiv:1706.06223 [hep-lat].
86. J. Bulava, B. Fahy, B. Hörz, K. J. Juge, C. Morningstar and C. H. Wong, Nucl. Phys. **B910**, 842 (2016).
87. R. A. Briceno, J. J. Dudek, R. G. Edwards and D. J. Wilson, Phys. Rev. Lett. **118**, 022002 (2017).

16. Heavy-Quark and Soft-Collinear Effective Theory

Updated August 2017 by C.W. Bauer (LBNL) and M. Neubert (U. Mainz).

16.1. Effective Field Theories

Quantum field theories provide the most precise computational tools for describing physics at the highest energies. One of their characteristic features is that they almost inevitably involve multiple length scales. When trying to determine the value of an observable, quantum field theory demands that all possible virtual states and hence all particles be included in the calculation. Since these particles have widely different masses, the final prediction is sensitive to many scales. This fact represents a formidable challenge from a practical point of view. No realistic quantum field theories can be solved exactly, so that one needs to resort to approximation schemes; these, however, are typically most straightforward when only a single scale is involved at a time.

Effective field theories (EFTs) provide a general theoretical framework to deal with the multi-scale problems of realistic quantum field theories. This framework aims at reducing such problems to a combination of separate and simpler single-scale problems; simultaneously, however, it provides an organization scheme whereby the other scales are not omitted but allowed to play their role in a separate step of the computation. The philosophy and basic principles of this approach are very generic, and correspondingly EFTs represent a widely used method in many different areas of high-energy physics, from the low-energy scales of atomic and nuclear physics to the high-energy scales of (partly yet unknown) elementary-particle physics, see [1–3] for some early references. EFTs can play a role both within analytic perturbative computations and in the context of non-perturbative numerical simulations; One of the simplest applications of EFTs to particle physics concerns the description of an underlying theory that is only probed at energy scales $E < \Lambda$. Any particle with mass $m > \Lambda$ cannot be produced as a real state and therefore only leads to short-distance virtual effects. Thus, one can construct an effective theory in which the quantum fluctuations of such heavy particles are "integrated out" from the generating functional for Green functions. This results in a simpler theory containing only those degrees of freedom that are relevant to the energy scales under consideration. In fact, the standard model of particle physics itself is widely viewed as an EFT of some yet unknown, more fundamental theory.

The development of any effective theory starts by identifying the degrees of freedom that are relevant to describe the physics at a given energy (or length) scale and constructing the Lagrangian describing the interactions among these fields. Short-distance quantum fluctuations associated with much smaller length scales are absorbed into the coefficients of the various operators in the effective theory. These coefficients are determined in a matching procedure, by requiring that the EFT reproduces the matrix elements of the full theory up to power corrections. In many cases the effective Lagrangian exhibits enhanced symmetries compared with the fundamental theory, allowing for simple and sometimes striking predictions relating different observables.

16.2. Heavy-Quark Effective Theory

Heavy-quark systems provide prime examples for applications of the EFT technology, because the hierarchy $m_Q \gg \Lambda_{\rm QCD}$ (with $Q = b, c$) provides a natural separation of scales. Physics at the scale m_Q is of a short-distance nature and can be treated perturbatively, while for heavy-quark systems there is always also some hadronic physics governed by the confinement scale $\Lambda_{\rm QCD}$ of the strong interaction. Being able to separate the short-distance and long-distance effects associated with these two scales is crucial for any quantitative description. For instance, if the long-distance hadronic matrix elements are obtained from lattice QCD, then it is necessary to analytically compute the effects of short-wavelength modes that do not fit on the lattice. In many other instances, the long-distance physics can be encoded in a small number of hadronic parameters.

16.2.1. ***General idea and derivation of the effective Lagrangian*** : The simplest effective theory for heavy-quark systems is the heavy-quark effective theory (HQET) [4–7] (see [8,9] for detailed discussions). It provides a simplified description of the soft interactions of a single heavy quark with light partons. This includes the interactions that bind the heavy quark with other light partons inside heavy mesons and baryons.

A softly interacting heavy quark is nearly on-shell. Its momentum may be decomposed as $p_Q = m_Q v + k$, where v is the 4-velocity of the hadron containing the heavy quark. The "residual momentum" k results from the soft interactions of the heavy quark with its environment and satisfies $v \cdot k \sim \Lambda_{\rm QCD}$ and $k^2 \sim \Lambda^2_{\rm QCD}$, which in the rest frame of the heavy hadron reduces to $k^\mu \sim \Lambda_{\rm QCD}$. In the limit $m_Q \gg \Lambda_{\rm QCD}$, the soft interactions do not change the 4-velocity of the heavy quark, which is therefore a conserved quantum number that is often used as a label on the effective heavy-quark fields. A nearly on-shell Dirac spinor has two large and two small components. We define

$$Q(x) = e^{-im_Q v\cdot x}\,[h_v(x) + H_v(x)]\,, \tag{16.1}$$

where

$$h_v(x) = e^{im_Q v\cdot x}\,\frac{1+\not{v}}{2}\,Q(x)\,, \qquad H_v(x) = e^{im_Q v\cdot x}\,\frac{1-\not{v}}{2}\,Q(x) \tag{16.2}$$

are the large ("upper") and small ("lower") components of the spinor field, respectively. The extraction of the phase factor in Eq. (16.1) implies that the fields h_v and H_v carry the residual momentum k. The field H_v is $1/m_Q$ suppressed relative to h_v and describes quantum fluctuations far off the mass shell. Integrating it out using its equations of motion yields the HQET Lagrangian

$$\mathcal{L}_{\rm HQET} = \bar h_v\, iv\cdot D_s\, h_v + \frac{1}{2m_Q}$$
$$\Big[\bar h_v (iD_s)^2 h_v + C_{\rm mag}(\mu)\,\frac{g}{2}\,\bar h_v\,\sigma_{\mu\nu}\,G_s^{\mu\nu} h_v\Big] + \ldots\,. \tag{16.3}$$

The covariant derivative $iD_s^\mu = i\partial^\mu + gA_s^\mu$ and the field strength $G_s^{\mu\nu}$ contain only the soft gluon field. Hard gluons have been integrated out, and their effects are contained in the Wilson coefficients of the operators in the effective Lagrangian. From the leading operator one derives the Feynman rules of HQET. The new operators entering at subleading order are referred to as the "kinetic energy" and "chromo-magnetic interaction". The kinetic-energy operator corresponds to the first correction term in the Taylor expansion of the relativistic energy $E = m_Q + \vec p^{\,2}/2m_Q + \ldots$. Lorentz invariance, which is encoded as a reparametrization invariance of the effective Lagrangian [10], ensures that its Wilson coefficient is not renormalized ($C_{\rm kin} \equiv 1$). The coefficient $C_{\rm mag}$ of the chromo-magnetic operator receives corrections starting at one-loop order.

16.2.2. ***Spin-flavor symmetry*** : The leading term in the HQET Lagrangian exhibits a global spin-flavor symmetry. Its physical meaning is that, in the infinite mass limit, the properties of hadronic systems containing a single heavy quark are insensitive to the spin and flavor of the heavy quark [11,12]. The spin symmetry results from the fact that there are no Dirac matrices in the leading term of the effective Lagrangian in Eq. (16.3), implying that the interactions of the heavy quark with soft gluons leave its spin unchanged. The flavor symmetry arises since the mass of the heavy quark does not appear at leading order. For n_Q heavy quarks moving at the same velocity, one can simply extend Eq. (16.3) by summing over n_Q identical terms for heavy-quark fields h_v^i. The result is invariant under rotations in flavor space. When combined with the spin symmetry, the symmetry group becomes promoted to SU($2n_Q$). These symmetries are broken by the operators at subleading power in the $1/m_Q$ expansion.

The spin-flavor symmetry leads to many interesting relations between the properties of hadrons containing a heavy quark. The most direct consequences concern the spectroscopy of such states [13]. In the heavy-quark limit, the spin of the heavy quark and the total angular momentum j of the light degrees of freedom are separately conserved by the strong interactions. Because of heavy-quark symmetry, the dynamics is independent of the spin and mass

of the heavy quark. Hadronic states can thus be classified by the quantum numbers (flavor, spin, parity, etc.) of the light degrees of freedom. The spin symmetry predicts that, for fixed $j \neq 0$, there is a doublet of degenerate states with total spin $J = j \pm 1/2$. The flavor symmetry relates the properties of states with different heavy-quark flavor.

16.2.3. ***Weak decay form factors*** : Of particular interest are the relations between the weak decay form factors of heavy mesons, which parametrize hadronic matrix elements of currents between two mesons containing a heavy quark. These relations have been derived by Isgur and Wise [12], generalizing ideas developed by Nussinov and Wetzel [14] and Voloshin and Shifman [15]. For the purpose of this discussion, it is convenient to work with a mass-independent normalization of meson states and use velocity rather than momentum variables.

Consider the elastic scattering of a pseudoscalar meson, $P(v) \to P(v')$, induced by an external vector current coupled to the heavy quark contained in P, which acts as a color source moving with the meson's velocity v. The action of the current is to replace instantaneously the color source by one moving at velocity v'. Soft gluons need to be exchanged in order to rearrange the light degrees of freedom and build up the final state meson moving at velocity v'. This rearrangement leads to a form-factor suppression. The important observation is that, in the $m_Q \to \infty$ limit, the form factor can only depend on the Lorentz boost $\gamma = v \cdot v'$ connecting the rest frames of the initial and final-state mesons (as long as $\gamma = \mathcal{O}(1)$). In the effective theory the hadronic matrix element describing the scattering process can therefore be written as

$$\langle P(v')|\,\bar h_{v'}\gamma^\mu h_v\,|P(v)\rangle = \xi(v\cdot v')(v+v')^\mu, \tag{16.4}$$

with a form factor $\xi(v \cdot v')$ that is real and independent of m_Q. By flavor symmetry, the form factor remains identical when one replaces the heavy quark Q in one of the meson states by a heavy quark Q' of a different flavor, thereby turning P into another pseudoscalar meson P'. At the same time, the current becomes a flavor-changing vector current. This universal form factor is called the Isgur-Wise function [12]. For equal velocities the vector current $J^\mu = \bar h_v \gamma^\mu h_v$ is conserved in the effective theory, irrespective of the flavor of the heavy quarks. The corresponding conserved charges are the generators of the flavor symmetry. It follows that the Isgur-Wise function is normalized at the point of equal velocities: $\xi(1) = 1$. Since the recoil energy of the daughter meson P' in the rest frame of the parent meson P is $E_{\rm recoil} = m_{P'}\,(v \cdot v' - 1)$, the point $v \cdot v' = 1$ is referred to as the zero-recoil limit. The heavy-quark spin symmetry leads to additional relations among weak decay form factors. It can be used to relate matrix elements involving vector mesons to those involving pseudoscalar mesons, which once again can be described completely in terms of the universal Isgur-Wise function.

The form factor relations imposed by heavy-quark symmetry describe the semileptonic decay processes $\bar B \to D\,\ell\,\bar\nu$ and $\bar B \to D^*\ell\,\bar\nu$ in the limit of infinite heavy-quark masses. They are model-independent consequences of QCD. The known normalization of the Isgur-Wise function at zero recoil can be used to obtain a model-independent measurement of the element $|V_{cb}|$ of the Cabibbo-Kobayashi-Maskawa (CKM) matrix. The semileptonic decay $\bar B \to D^*\ell\,\bar\nu$ is particularly well suited for this purpose [16]. Experimentally this is a very clean mode, since the reconstruction of the D^* meson mass provides a powerful rejection against background. From the theoretical point of view, it is ideal since the decay rate at zero recoil is protected by Luke's theorem against first-order power corrections in $1/m_Q$ [17]. This is described in more detail in Section 12. Corrections to the heavy-quark symmetry relations for the $\bar B \to D^{(*)}$ form factors near zero recoil can also be constrained using sum rules derived in the small-velocity limit [18,19].

16.2.4. ***Decoupling transformation*** : At leading order in $1/m_Q$, the couplings of soft gluons to heavy quarks in the effective Lagrangian Eq. (16.3) can be removed by the field redefinition $h_v(x) = Y_v(x)\,h_v^{(0)}(x)$, where $Y_v(x)$ is a soft Wilson line along the direction of v, extending from minus infinity to the point x. In terms of the new fields the leading-order HQET Lagrangian becomes $\mathcal{L}_{\rm HQET} = \bar h_v^{(0)} iv\cdot\partial\, h_v^{(0)}$. It describes a free theory as far as the strong interactions of heavy quarks are concerned. However, the theory is nevertheless non-trivial in the presence of external sources. Consider, e.g., the case of a weak-interaction heavy-quark current

$$\bar h_{v'}\gamma^\mu(1-\gamma_5)h_v = \bar h_{v'}^{(0)}\gamma^\mu(1-\gamma_5)\,Y_{v'}^\dagger Y_v\,h_v^{(0)}, \tag{16.5}$$

where v and v' are the velocities of the heavy mesons containing the heavy quarks. Unless the two velocities are equal, corresponding to the zero-recoil limit discussed above, the object $Y_{v'}^\dagger Y_v$ is non-trivial, and hence the soft gluons do not decouple from the heavy quarks inside the current operator. One may interpret $Y_{v'}^\dagger Y_v$ as a Wilson loop with a cusp at the point x, where the two paths parallel to the different velocity vectors intersect. The presence of the cusp leads to non-trivial ultra-violet behavior (for $v \neq v'$), which is described by a cusp anomalous dimension $\Gamma_c(v \cdot v')$ that was calculated at two-loop order in [20]. It coincides with the velocity-dependent anomalous dimension of heavy-quark currents, which was introduced in the context of HQET in [21]. The interpretation of heavy quarks as Wilson lines is a useful tool, which was put forward in one of the very first papers on the subject [4]. This technology will be useful in the study of the interactions of heavy quarks with collinear degrees of freedom discussed later in this review.

16.2.5. ***Heavy-quark expansion for inclusive decays*** : The theoretical description of inclusive decays of hadrons containing a heavy quark exploits two observations [22–26]: bound-state effects related to the initial state can be calculated using the heavy-quark expansion, and the fact that the final state consists of a sum over many hadronic channels eliminates the sensitivity to the properties of individual final-state hadrons. The second feature rests on the hypothesis of quark-hadron duality, i.e. the assumption that decay rates are calculable in QCD after a smearing procedure has been applied [27]. In semileptonic decays, the integration over the lepton spectrum provides a smearing over the invariant hadronic mass of the final state (global duality). For nonleptonic decays, where the total hadronic mass is fixed, the summation over many hadronic final states provides an averaging (local duality). Since global duality is a much weaker assumption, the theoretical control of inclusive semileptonic decays is on firmer footing.

Using the optical theorem, the inclusive decay width of a hadron H_b containing a b quark can be written in the form

$$\Gamma(H_b) = \frac{1}{M_{H_b}}\,{\rm Im}\,\langle H_b|\,i\int {\rm d}^4x\,T\left\{\mathcal{H}_{\rm eff}(x),\mathcal{H}_{\rm eff}(0)\right\}|H_b\rangle\,. \tag{16.6}$$

The effective weak Hamiltonian for b-quark decays consists of dimension-6 four-fermion operators and dipole operators [28]. Because of the large mass of the b quark, it follows that the separation of fields in the time-ordered product in Eq. (16.6) is small, of order $x \sim 1/m_b$. It is thus possible to construct an operator-product expansion (OPE) for the time-ordered product, in which it is represented as a series of local operators in HQET. The leading operator $\bar h_v h_v$ has a trivial matrix element. The next contributions arise at $\mathcal{O}(1/m_b^2)$ and give rise to two parameters $\mu_\pi^2(H_b)$ and $\mu_G^2(H_b)$, which are defined as the matrix elements of the heavy-quark kinetic energy and chromo-magnetic interaction inside the hadron H_b, respectively [29]. For the ground-state heavy mesons and baryons, one has $\mu_G^2(B) = 3(m_{B^*}^2 - m_B^2)/4 \simeq 0.36\,{\rm GeV}^2$ and $\mu_G^2(\Lambda_b) = 0$. Thus, the total inclusive decay rate of a hadron H_b can be written as [23,24]

$$\Gamma(H_b) = \frac{G_F^2 m_b^5 |V_{cb}|^2}{192\pi^3}\,[c_1 + c_2\,\frac{\mu_\pi^2(H_b)}{2m_b^2} + c_3\,\frac{\mu_G^2(H_b)}{2m_b^2} + \mathcal{O}(\frac{1}{m_b^3}) + \ldots], \tag{16.7}$$

where the prefactor arises from the loop integrations and is proportional to the fifth power of the b-quark mass. The coefficient functions c_i are calculable order by order in perturbation theory.

From the fully inclusive width in Eq. (16.7) one can obtain the lifetime of a heavy hadron via $\tau(H_b) = 1/\Gamma(H_b)$. Due to the

universality of the leading term in the heavy-quark expansion, lifetime ratios such as $\tau(B^-)/\tau(\bar{B}^0)$, $\tau(\bar{B}_s^0)/\tau(\bar{B}^0)$ and $\tau(\Lambda_b)/\tau(\bar{B}^0)$ are particularly sensitive to the hadronic parameters determining the power corrections in the expansion. In order to understand these ratios theoretically, it is necessary to include phase-space enhanced power corrections of order $(\Lambda_{\rm QCD}/m_b)^3$ [30,31] as well as short-distance perturbative effects [32] in the calculation.

A formula analogous to Eq. (16.7) can be derived for differential distributions in specific inclusive decay processes, assuming that these distributions are integrated over a sufficiently large region of phase space to ensure quark-hadron duality. Important examples are the distributions in the lepton energy and the lepton invariant mass, as well as moments of the invariant hadronic mass distribution in the semileptonic processes $\bar{B} \to X_u\,\ell\,\bar{\nu}$ and $\bar{B} \to X_c\,\ell\,\bar{\nu}$. A global fit of semileptonic decay distributions can be used to determine the CKM matrix elements $|V_{ub}|$ and $|V_{cb}|$ along with heavy-quark parameters such as the masses m_b, m_c and the hadronic parameters $\mu_\pi^2(B)$, $\mu_G^2(B)$. These determinations provide some of the most accurate values for these parameters [33].

16.2.6. ***Shape functions and non-local power corrections*** : In certain regions of phase space, in which the hadronic final state in an inclusive heavy-hadron decay is made up of light energetic partons, the local OPE for inclusive decays must be replaced by a more complicated expansion involving hadronic matrix elements of non-local light-ray operators [34,35]. Prominent examples are the radiative decay $\bar{B} \to X_s\gamma$ for large photon energy E_γ near $m_B/2$, and the semileptonic decay $\bar{B} \to X_u\,\ell\,\bar{\nu}$ at large lepton energy or small hadronic invariant mass. In these cases, the differential decay rates at leading order in the heavy-quark expansion can be written in the factorized form $d\Gamma = H\,J \otimes S$ [36], where the hard function H and the jet function J are calculable in perturbation theory. The characteristic scales for these functions are set by m_b and $(m_b\Lambda_{\rm QCD})^{1/2}$, respectively. The soft function

$$S(\omega) = \int \frac{dt}{4\pi}\, e^{-i\omega t}\, \langle \bar{B}(v)|\, \bar{h}_v(tn) Y_n(tn) Y_n^\dagger(0) h_v(0) |\bar{B}(v)\rangle \qquad (16.8)$$

is a genuinely non-perturbative object called the shape function [34,35]. Here Y_n are soft Wilson lines along a light-like direction n aligned with the momentum of the hadronic final-state jet. The jet function and the shape function share a common variable $\omega \sim \Lambda_{\rm QCD}$, and the symbol $\otimes$ denotes a convolution in this variable.

While the hard functions are different for the decays $\bar{B} \to X_s\gamma$ and $\bar{B} \to X_u\,\ell\bar{\nu}$, the jet and soft functions are identical at leading order in $\Lambda_{\rm QCD}/m_Q$. This is particularly important for the shape function, which introduces non-perturbative physics into the theoretical predictions for the decay rates in the regions of experimental interest. The fact that both processes depend on the same non-perturbative function makes it possible to use the measured shape of the $\bar{B} \to X_s\gamma$ photon spectrum to reduce the theoretical uncertainties in the determination of the CKM element $|V_{ub}|$ from semileptonic decays. In higher orders of the heavy-quark expansion, an increasing number of subleading jet and soft functions are required to describe the decay distributions [37]. These have been analyzed in detail at order $1/m_b$ [38–40]. In the case of $\bar{B} \to X_s\gamma$, some of these non-local effects survive in the total decay rate and give rise to irreducible hadronic uncertainties [41]. The technology for deriving the corresponding factorization theorems relies on the soft-collinear effective theory, to which we now turn.

16.3. Soft-Collinear Effective Theory

As discussed in the previous section, soft gluons that bind a heavy quark inside a heavy meson cannot change the virtuality of that heavy quark by a significant amount. The ratio $\Lambda_{\rm QCD}/m_Q$ provides the expansion parameter in HQET, which is a small parameter since $m_Q \gg \Lambda_{\rm QCD}$. This obviously does not work when considering light quarks. However, if the energy Q of the quarks is large, the ratio $\Lambda_{\rm QCD}/Q$ provides a small parameter, which can be used to construct an effective theory. One major difference to HQET is that light energetic quarks cannot only emit soft gluons, but they can also emit collinear gluons (an energetic gluon in the same direction as the original quark), without parametrically changing their virtuality. Thus, to fully reproduce the long-distance physics of energetic quarks requires that one includes their interactions with both soft and collinear particles. The resulting effective theory is therefore called soft-collinear effective theory (SCET) [42–44].

A single energetic particle can always be boosted to a frame where all momentum components have similar size, in which case there is no small expansion parameter. Thus the presence of energetic particles must refer to a reference frame defined by external kinematics. SCET has a wide range of applications; some examples are the production of energetic, light states in the decay of a heavy particle in its rest frame, the production of energetic jets in collider environments, and the scattering of energetic particles off a target at rest. In this brief review we will outline the main features of this effective theory and mention a few selected applications.

16.3.1. ***General idea of the expansion*** : Consider a quark with virtuality much less than its energy Q, moving along the direction $\vec{n}$. It is convenient to parameterize the momentum p_n of this particle in terms of its light-cone components, defined by $(p_n^-, p_n^+, p_n^\perp) = (\bar{n}\cdot p_n, n\cdot p_n, p_n^\perp)$, where $n^\mu = (1,\vec{n})$ and $\bar{n}^\mu = (1,-\vec{n})$ are light-like vectors, and $n\cdot p_n^\perp = \bar{n}\cdot p_n^\perp = 0$. The subscript n on the momentum indicates the direction of the collinear particle. In terms of these light-cone components, the virtuality satisfies $p_n^2 = p_n^+ p_n^- + p_n^{\perp 2}$. The individual components of the momentum obey

$$(p_n^-, p_n^+, p_n^\perp) \sim Q(1, \lambda^2, \lambda), \qquad (16.9)$$

where $\lambda^2 = p^2/Q^2$ is the expansion parameter of SCET. The virtuality of such an energetic particle remains parametrically unchanged if it interacts with energetic particles in the same direction n, or with soft particles with momentum scaling as

$$(p_s^-, p_s^+, p_s^\perp) \sim Q(\lambda^2, \lambda^2, \lambda^2). \qquad (16.10)$$

SCET is constructed in such a way as to reproduce the long-distance dynamics arising from the interactions of collinear and soft degrees of freedom.

In the above power counting the transverse momenta of soft degrees of freedom scale as $p_s^\perp \sim Q\lambda^2$, which is much smaller than the transverse momenta $p_c^\perp \sim Q\lambda$ of collinear fields. This theory is usually called $\rm SCET_I$. If the external kinematics require that the transverse momenta of both soft and collinear fields are of the same size, $p_c^\perp \sim p_s^\perp$, then the appropriate degrees of freedom have the scaling $p_c \sim Q(1,\lambda^2,\lambda)$ and $p_s \sim Q(\lambda,\lambda,\lambda)$. This theory is usually called $\rm SCET_{II}$ and is required, e.g., for exclusive hadronic decays such as $\bar{B} \to D\pi$, where the virtuality of both collinear and soft degrees of freedom are set by $\Lambda_{\rm QCD}$, or for the description of transverse-momentum distributions at colliders.

16.3.2. ***Leading-order Lagrangian*** : The derivation of the SCET Lagrangian follows similar steps as described for HQET in Section 16.2.1. One begins by deriving the Lagrangian for a theory containing only a single collinear sector. Similar to HQET, one separates the full QCD field into two components, $q_n(x) = \psi_n(x) + \Xi_n(x)$, where (with $n\cdot\bar{n} = 2$)

$$\psi_n(x) = \frac{\not{n}\not{\bar{n}}}{4}\, q_n(x)\,, \qquad \Xi_n(x) = \frac{\not{\bar{n}}\not{n}}{4}\, q_n(x). \qquad (16.11)$$

The degrees of freedom described by the field Ξ_n are far off shell and can therefore be eliminated using its equation of motion. This gives

$$\mathcal{L}_n = \bar{\psi}_n(x) \left[in\cdot D + i\not{D}^\perp \frac{1}{i\bar{n}\cdot D} i\not{D}^\perp \right] \frac{\not{\bar{n}}}{2}\, \psi_n(x). \qquad (16.12)$$

As a next step, one separates the large and residual momentum components by decomposing the collinear momentum into a "label" and a residual momentum, $p^\mu = P^\mu + k^\mu$ with $n\cdot P = 0$. One then performs a phase redefinition on the collinear fields, such that $\psi_n(x) = e^{iP\cdot x}\,\xi_n(x)$. Derivatives acting on the fields $\xi_n(x)$ now only pick out the residual momentum. Since unlike in HQET the label

momentum in SCET is not conserved, one defines a label operator $\mathcal{P}^\mu$ acting as $\mathcal{P}^\mu \xi_n(x) = P^\mu \xi_n(x)$ [43], as well as a corresponding covariant label operator $i\mathcal{D}_n^\mu = \mathcal{P}^\mu + gA_n^\mu(x)$. Note that at leading order in power counting $i\mathcal{D}_n^\mu$ does not contain the soft gluon field. This leads to the final SCET Lagrangian [43–46]

$$\mathcal{L}_n = \bar\xi_n(x)\left[in\cdot D_n + gn\cdot A_s + i\not{\mathcal{D}}_n^\perp \frac{1}{i\bar n\cdot \mathcal{D}_n} i\not{\mathcal{D}}_n^\perp\right]\frac{\not{\bar n}}{2}\xi_n(x) + \ldots, \tag{16.13}$$

where we have split $in\cdot D$ into a collinear piece $in\cdot D_n = in\cdot\partial + gn\cdot A_n$ and a soft piece $gn\cdot A_s$. This latter term gives rise to the only interaction between a collinear quark and soft gluons at leading power in λ. The ellipses represent higher-order interactions between soft and collinear particles.

The Lagrangian describing collinear fields in different light-like directions is simply given by the sum of the Lagrangians for each direction n, i.e. $\mathcal{L} = \sum_n \mathcal{L}_n$. The soft gluons are the same in each individual Lagrangian. An alternative way to understand the separation between large and small momentum components is to derive the Lagrangian of SCET in position space [46]. In this case no label operators are required, and the dependence on short-distance effects is contained in non-localities at short distances. An important difference between SCET and HQET is that the SCET Lagrangian is not corrected by short distance fluctuations. The physical reason is that in the construction described above no high-momentum modes have been integrated out [46]. Such hard modes arise when different collinear sectors are coupled via some external current (e.g. in jet production at e^+e^- or hadron colliders), or when collinear particles are produced in the rest frame of a decaying heavy object (such as in B decays). Short-distance effects are then incorporated in the Wilson coefficients of the external source operators.

16.3.3. ***Collinear gauge invariance and Wilson lines*** : An important aspect of SCET is the implementation of local gauge invariance. Because the effective field operators describe modes with certain momentum scalings, the effective Lagrangian respects only residual gauge symmetries. One of them satisfies the collinear scaling

$$(\bar n\cdot\partial, n\cdot\partial, \partial^\perp)\, U_n(x) \sim Q(1,\lambda^2,\lambda)\, U_n(x), \tag{16.14}$$

and one the soft scaling

$$(\bar n\cdot\partial, n\cdot\partial, \partial^\perp)\, U_s(x) \sim Q(\lambda^2,\lambda^2,\lambda^2)\, U_s(x). \tag{16.15}$$

The fact that collinear fields in different directions do not transform under the same gauge transformations implies that each collinear sector, containing particles with large momenta along a certain direction, has to be separately gauge invariant. This requires the introduction of collinear Wilson lines [43]

$$W_n(x) = P\exp\left[-ig\int_{-\infty}^0 ds\, \bar n\cdot A_n(s\bar n + x)\right], \tag{16.16}$$

which transform under collinear gauge transformations according to $W_n \to U_n W_n$. Thus, the combination $\chi_n \equiv W_n^\dagger \psi_n$ is gauge invariant. In a similar manner, one can define the gauge-invariant gluon field $B_n^\mu = g^{-1} W_n^\dagger\, iD_n^\mu W_n$ [47,48]. Collinear operators in SCET are typically constructed from such gauge-invariant building blocks.

16.3.4. ***Derivation of factorization theorems*** : One of the important applications of SCET is to understand how to factorize cross sections involving energetic particles moving in different directions into simpler pieces that can either be calculated perturbatively or determined from data. Factorization theorems have been around for much longer than SCET; see [49] for a review. However, the effective theory allows for a conceptually simpler understanding of certain classes of factorization theorems [47], since most simplifications happen already at the level of the Lagrangian. The discussion in this section is valid to leading order in the power counting of the effective theory.

As discussed in the previous section, the Lagrangian of SCET does not involve any couplings between collinear particles moving in different directions. Soft gluons couple to collinear quarks only through the term $\bar\xi_n\, g\, n\cdot A_s(\not{\bar n}/2)\,\xi_n$ in the effective Lagrangian in Eq. (16.13). This coupling is similar to the coupling of soft gluons to heavy quarks in HQET, see Section 16.2.4. It can be removed by means of the field redefinition [44]

$$\psi_n(x) = Y_n(x)\psi_n^{(0)}(x)\,, \qquad A_n^a(x) = Y_n^{ab}(x) A_n^{b(0)}(x), \tag{16.17}$$

where Y_n and Y_n^{ab} live in the fundamental and adjoint representations of SU(3), respectively. This fact greatly facilitates proofs of factorization theorems in SCET. A QCD operator $O(x)$ describing the interactions of collinear partons moving in different directions can thus be written as (omitting color indices for simplicity)

$$\langle O(x)\rangle = C_O(\mu)\,\langle \mathcal{C}_{n_a}^{(0)}(x)\mathcal{C}_{n_b}^{(0)}(x)\mathcal{C}_{n_1}^{(0)}(x)\ldots\mathcal{C}_{n_N}^{(0)}(x)$$
$$[\mathcal{Y}_{n_a}\mathcal{Y}_{n_b}\mathcal{Y}_{n_1}\ldots\mathcal{Y}_{n_N}](x)\rangle_\mu. \tag{16.18}$$

Here $\mathcal{C}_{n_i}^{(0)}(x)$ denotes a gauge-invariant combination of collinear fields (either quark or gluon fields) in the direction n_i. The hard matching coefficient C_O accounts for short-distance effects at the scale Q. The soft Wilson lines can either be in a color triplet or color octet representation, and are collectively denoted by $\mathcal{Y}_{n_i}$. Both the matrix elements and the coefficient C_O depend on the renormalization scale μ.

Having defined the operator mediating a given process, one can calculate the cross section by squaring the operator, taking the forward matrix element and integrating over the phase space of all final-state particles. The absence of interactions between collinear degrees of freedom moving along different directions or soft degrees of freedom implies that the forward matrix element can be factorized as

$$\begin{aligned}\langle \mathrm{in}|O(x)O^\dagger(0)|\mathrm{in}\rangle &= |C_0(\mu)|^2 \\ &\times \langle \mathrm{in}_a|\mathcal{C}_{n_a}(x)\mathcal{C}_{n_a}^\dagger(0)|\mathrm{in}_a\rangle_\mu \langle \mathrm{in}_b|\mathcal{C}_{n_b}(x)\mathcal{C}_{n_b}^\dagger(0)|\mathrm{in}_b\rangle_\mu \\ &\times \langle 0|\mathcal{C}_{n_1}(x)\mathcal{C}_{n_1}^\dagger(0)|0\rangle_\mu \cdots \langle 0|\mathcal{C}_{n_N}(x)\mathcal{C}_{n_N}^\dagger(0)|0\rangle_\mu \\ &\times \langle 0|[\mathcal{Y}_{n_a}\ldots\mathcal{Y}_{n_N}](x)[\mathcal{Y}_{n_a}\ldots\mathcal{Y}_{n_N}]^\dagger(0)|0\rangle_\mu.\end{aligned} \tag{16.19}$$

Thus, the matrix element can be written as a product of simpler structures, each of which can be evaluated separately.

The vacuum matrix elements of the outgoing collinear fields are determined by jet functions $J_i(\mu)$. As long as the relevant scale (for example the jet mass) is sufficiently large, these functions can be calculated perturbatively. The matrix elements of the incoming collinear fields are non-perturbative objects $B_{p/N}(\mu)$ called beam functions for parton p in nucleon N [50]. For many applications they can be related perturbatively to the well-known parton distribution functions. Finally, the vacuum matrix element of the soft Wilson lines defines a so-called soft function $S_{ab\ldots N}(\mu)$. The shared dependence on x in the above equation implies that in momentum space the various components of the factorization theorem are convoluted with one another. Deriving this convolution requires a careful treatment of the phase-space integration, in particular treating the large and residual components of each momentum appropriately.

Putting all information together, the differential cross section for a proton-proton collision with N jet-like objects can schematically be written as

$$\mathrm{d}\sigma \sim \sum_{ab} H_{ab}(\mu)[B_{a/P}(\mu)B_{b/P}(\mu)] \otimes [J_1(\mu)\ldots J_N(\mu)] \otimes S_{ab\ldots N}(\mu). \tag{16.20}$$

The hard function is equal to the square of the matching coefficient, $H_{ab}(\mu) = |C_O(\mu)|^2$. It should be mentioned that the most difficult part of traditional factorization proofs involves showing that so-called Glauber gluons do not spoil the above factorization theorem [51]. This question has not yet been fully addressed in the context of SCET.

16.3.5. ***Resummation of large logarithms*** : SCET can be used to sum the large logarithms arising in perturbative calculations to all orders in the strong coupling constant α_s. In general, perturbation theory will generate a logarithmic dependence on any ratio of scales r in a problem. For processes that involve initial or final states with energy much in excess of their mass, there are two powers of logarithms for every power of α_s. These are referred to as Sudakov logarithms. For widely separated scales these large logarithms can spoil the convergence of fixed-order perturbation theory. One thus needs to reorganize the expansion in such a way that $\alpha_s L = \mathcal{O}(1)$ is kept fixed, with $L = \ln r$. More precisely, a proper resummation requires summing logarithms of the form $\alpha_s^n L^m$ with $m \le n+1$ in the logarithm of a cross section, by writing $\ln\sigma \sim L g_0(\alpha_s L) + g_1(\alpha_s L) + \alpha_s g_2(\alpha_s L) + \ldots$, with functions $g_n(x)$ that need to be determined.

The important ingredient in achieving this resummation is the fact that SCET factorizes a given cross section into simpler pieces, each of which depends on a single physical scale. The only dependence on that scale can arise through logarithms of its ratio with the renormalization scale μ. Thus, for each of the components in the factorization theorem one can choose a renormalization scale μ for which the large logarithmic terms are absent. Of course, the factorization formula requires a common renormalization scale μ in all its components, and one therefore has to use the renormalization group (RG) to evolve the various component functions from their preferred scale to the common scale μ. A novel feature of RG equations in SCET, as opposed to other EFTs, is that the anomalous dimensions entering the evolution equations of the hard, beam, jet and soft functions in a factorization formula such as Eq. (16.20) contain a single power of the logarithm of the relevant energy scale. For example, the anomalous dimension γ_H of the hard function has the form

$$\gamma_H(\mu) = c_H\,\Gamma_{\rm cusp}(\alpha_s)\,\ln\frac{Q^2}{\mu^2} + \gamma(\alpha_s), \tag{16.21}$$

where c_H is a process-dependent coefficient and $\Gamma_{\rm cusp}$ denotes the so-called cusp anomalous dimension [20,52]. The non-cusp part γ of the anomalous dimension is process dependent. The presence of a logarithm in the anomalous dimension is characteristic of Sudakov problems and arises since the perturbative series contains double logarithms of scale ratios.

The anomalous dimension γ_H is known at two-loop order for arbitrary n-parton amplitudes containing massless or massive external partons [53–56]. Solving the RG equations one can systematically resum all large logarithms of scale ratios in the factorized cross section and express the functions $g_n(\alpha_s L)$ introduced above in terms of ratios of running coupling constants. In order to compute the first two terms $L g_0(\alpha_s L) + g_1(\alpha_s L)$ in $\ln\sigma$, corresponding to the next-to-leading logarithmic (NLL) approximation, one needs two-loop expressions for the cusp anomalous dimension and β function, one-loop expressions for the non-cusp pieces in the anomalous dimensions, and tree-level matching conditions for all component functions at their characteristic scales. To calculate the next term $\alpha_s g_2(\alpha_s L)$ in the expansion, corresponding to NNLL order, one needs to go one order higher in the loop expansion, and so on.

16.3.6. ***Factorization and resummation in*** **$\mathbf{SCET_{II}}$** : The effective theory $\mathrm{SCET_{II}}$ contains collinear and soft particles with momenta scaling as $(p_n^-, p_n^+, p_n^\perp) \sim Q(1, \lambda^2, \lambda)$ and $(p_s^-, p_s^+, p_s^\perp) \sim Q(\lambda, \lambda, \lambda)$. They have the same small virtuality ($p_n^2 \sim p_s^2 \sim Q^2\lambda^2$) but differ in their rapidities. An important class of observables, for which this scaling is relevant, contains cross sections for processes in which the transverse momenta of particles are constrained by external kinematics. The prime example are the transverse-momentum distributions of electroweak gauge bosons or Higgs bosons produced at hadron colliders. The parton transverse momenta are constrained by the fact that their vector sum must be equal and opposite to the transverse momentum q_T of the boson. Standard RG evolution in the effective theory controls the logarithms arising from the fact that the virtualities of the collinear and soft modes are much smaller than the hard scale Q in the process (the boson mass). However, additional large logarithms arise since the rapidities of collinear and soft modes are parametrically different, such that $e^{|y_c - y_s|} \sim 1/\lambda$. These logarithms need to be factorized in the cross section and resummed by other means.

Two equivalent approaches exist for how to deal with the additional rapidity logarithms. In the first approach, they are interpreted as a consequence of a "collinear anomaly" of the effective theory $\mathrm{SCET_{II}}$, resulting from the fact that a classical rescaling symmetry of the effective Lagrangian is broken by quantum effects [57]. The extra large logarithms can be resummed by means of simple differential equations, which typically state that (in an appropriate space) the logarithm of the cross section contains only a single logarithm of $\lambda \sim q_T/Q$, to all orders in perturbation theory. An alternative approach to resum the rapidity logarithms uses the "rapidity renormalization group", in which the relevant differential equations are obtained by considering a new type of scale variation in a parameter ν, which separates the phase space for collinear and soft particles along a hyperbola in the (p_-, p_+) plane [58]. In contrast to the standard RG, there is no running coupling involved in the ν evolution, since the different contributions live at the same virtuality.

$\mathrm{SCET_{II}}$ also plays an important role in the study of factorization for a variety of exclusive B meson decays, such as $\bar B \to \pi\ell\nu$, $\bar B \to K^*\gamma$ and $\bar B \to \pi\pi$, for which the virtualities of energetic (collinear) final-state particles are of order $\Lambda_{\rm QCD}$, which is also the scale for the soft light degrees of freedom contained in the initial-state B meson.

16.3.7. ***Applications*** : Most of the applications of SCET are either in flavor physics, where the decay of a heavy B meson can give rise to energetic light partons, or in collider physics, where the presence of jets naturally leads to collimated sets of energetic particles. For many of these applications alternative approaches existed before the invention of SCET, but the effective theory has opened up alternative ways to understand the physics of these processes. For several examples, however, SCET has allowed new insights. The investigation of heavy-to-light form factors has been instrumental for understanding factorization in exclusive semileptonic B decays [59]. SCET has also provided a field-theoretic basis for the QCD factorization approach to exclusive, non-leptonic decays of B mesons [60]. Using SCET methods, proofs of factorization were derived for the color-allowed decay $\bar B^0 \to D^+\pi^-$ [61], the color-suppressed decay $\bar B^0 \to D^0\pi^0$ [62], and the radiative decay $\bar B \to K^*\gamma$ [63]. Further examples are factorization theorems and the resummation of endpoint logarithms for quarkonia production [64], the resummation of large logarithmic terms for the thrust [65] and jet broadening [66] distributions in e^+e^- annihilation beyond NLL order, the development of new factorizable observables to veto extra jets [67], all-orders factorization theorems for processes containing electroweak Sudakov logarithms [68], and the resummation of threshold (soft gluon) logarithms for several important processes at hadron colliders [69–71]. Recently, there has been a lot of activity describing p_T-based resummation at hadron colliders. Examples are the transverse-momentum distributions of electroweak bosons [57] and jets [72]. We now describe three applications in more detail.

Event-shape distributions, in particular the thrust distribution, have been measured to high accuracy at LEP [73]. They can be used for a determination of the strong coupling constant α_s. SCET has increased the theoretical accuracy in the calculations of the thrust and C-parameter distributions significantly. First, it has allowed to increase the perturbative accuracy of the thrust spectrum. The resummation of logarithms of τ, which become important for $\tau \ll 1$, has been performed to N^{3}LL [65], two orders beyond what was previously available. Combining this resummation with the known two-loop spectrum [74,75] gives precise perturbative predictions both at small and large values of τ. Second, the factorization of the cross section in SCET has made it possible to include non-perturbative physics through a shape function, in analogy with the B-physics case discussed in Section 16.2.6. Comparing the theoretical predictions to the measured thrust and C-parameter distributions yields a precise value of the strong coupling constant $\alpha_s(m_Z)$, which however is lower than the average value cited in "Quantum Chromodynamics" review, Section 9, by several standard deviations [76,77]. For more discussions on this, see the mentioned "Quantum Chromodynamics" review, Section 9.

The Higgs-boson production cross section in gluon fusion at the LHC, defined with a jet veto stating that no jet in the final state has transverse momentum above a threshold $p_T^{\rm veto}$, can be factorized in the form [78,79] (see [80] for a corresponding calculation outside the SCET framework)

$$\sigma(p_T^{\rm veto}) = H(m_H,\mu)\Big(\frac{\nu_B}{\nu_S}\Big)^{-2F_{gg}(R,p_T^{\rm veto},\mu)} S_{gg}\Big(R,p_T^{\rm veto},\mu,\frac{\nu_S}{p_T^{\rm veto}}\Big) \times \int_\tau^1 \frac{dz}{z}\, B_{g/P}\Big(z,R,p_T^{\rm veto},\mu,\frac{\nu_B}{m_H}\Big)\, B_{g/P}\Big(\frac{\tau}{z},R,p_T^{\rm veto},\mu,\frac{\nu_B}{m_H}\Big), \tag{16.22}$$

where $\tau = m_H^2/s$, and $\mu \sim p_T^{\rm veto}$ is a common factorization scale. The beam functions $B_{g/P}$, the soft function S_{gg} and the exponent F_{gg} all depend on the jet radius R as well as the jet clustering algorithm. The scale dependence of the hard function H is controlled by standard RG evolution in SCET. The beam functions can be factorized further into calculable collinear kernels convoluted with parton distribution functions. In addition to the renormalization scale μ, the beam and soft functions depend on two rapidity scales $\nu_B \sim m_H$ and $\nu_S \sim p_T^{\rm veto}$, respectively. In [78] the default values $\nu_B = m_H$ and $\nu_S = p_T^{\rm veto}$ are used for these scales, and the soft function S_{gg} is absorbed into the beam functions. In [79] the exponent F_{gg} is called $-\gamma_\nu^g/2$. The second factor on the right-hand side of the factorization formula Eq. (16.22), which resums large rapidity logarithms, implies that the logarithm of the jet-veto cross section contains a single large logarithm $\ln\sigma = -2F_{gg}(R,p_T^{\rm veto},\mu)\,\ln(m_H/p_T^{\rm veto}) + \ldots$ not contained in the hard function. Its coefficient can be calculated in fixed-order perturbation theory.

Obtaining more precise fixed-order calculations has been an important goal for many years. A major difficulty in these calculations is the proper handling of the infrared singularities that arise in both virtual and real contributions. A method based on N-jettiness ($\mathcal{T}_N$) subtraction/slicing to obtain the NNLO result from a much easier NLO calculation, combined with information about the singular dependence of the cross section on the $\mathcal{T}_N$ resolution variable [81,82], has been used to compute various processes with final states containing up to one colored particle [83–85]. While the NLO calculations can be performed using well established techniques, the singular dependence on $\mathcal{T}_N$ can be calculated using SCET at NNLO. Calculations of the leading power corrections in $\mathcal{T}_0/Q$ [86,87] have helped to improved the numerical stability for several processes.

16.4. Open issues and perspectives

HQET has successfully passed many experimental tests, and there are not many open questions that still need to be addressed. One concept that has not been derived from first principles is the notion of quark-hadron duality, which underlies the application of HQET to the description of inclusive decays of B mesons. The validity of global duality (at energies even lower than those relevant in B decays) has been tested experimentally using high-precision data on semileptonic B decays and on hadronic τ decays, and good agreement between theory and data was found. However, assigning a theoretical uncertainty due to possible duality violations remains a difficult task. Another known issue is that the measured values of the CKM element $|V_{ub}|$ extracted from exclusive or inclusive decays of B mesons differ from each other by several standard deviations (see "Semileptonic Bottom Hadron Decays and the Determination of V_{cb} and V_{ub}" review, Section 89). This measurement relies on the heavy-quark limit, and the uncertainty quoted includes a theoretical estimate of the effect of power corrections arising from the finite b-quark mass. It remains an open question whether the discrepancy is due to underestimated theoretical or experimental uncertainties, or whether it may hint to the existence of new physics.

SCET, on the other hand, is still an active field of research, and new results are being obtained regularly. An important example concerns the understanding of non-global logarithms arising in hadron-collider processes with jets [88,89]. SCET-based fixed-order calculations have helped to shed some light on the nature of these logarithms [90–92]. However, for a long time a fully factorized form of jet cross sections has not been available, despite significant progress towards this goal [93,94]. A consistent factorization formula for non-global jet observables was developed in [95,96]. It requires the introduction of a new collinear-soft mode in the SCET Lagrangian. First phenomenological applications of the formalism developed in these references have been presented in [97]. Another active field concerns the study of Glauber gluons in SCET [98] and their relation to the BFKL equation familiar from small-x physics [99]. A systematic account of Glauber effects in the context of SCET has been developed in [100]. It sets the basis for a solid understanding of their impact on factorization proofs. Glauber gluons also play an important role in SCET-based analysis of jet propagation in dense QCD media [101–104], which gives rise to the jet-quenching phenomenon in heavy-ion collisions. An important open question facing some applications of SCET concerns factorized expressions containing endpoint-divergent convolution integrals. This problem arises, for example, in the description of heavy-to-light form factors such as $F_{\bar B\to\pi}(q^2)$ at large recoil [105].

We close this short review by mentioning a particularly nice application combining the methods of heavy-particle EFTs such as HQET and non-relativistic QCD with SCET in the context of describing the interactions of heavy dark matter (with mass $M \gg v$) with SM particles. In [106] it was realized that the interactions of heavy, weakly interacting massive particles (WIMPs) with nuclear targets can be described in a model-independent way using heavy-particle EFTs. The WIMPs are charged under $SU(2)_L$ and can interact with electroweak gauge bosons and the Higgs boson. The WIMP EFT was later extended by describing the produced, highly energetic electroweak gauge bosons in terms of soft or collinear fields in SCET [107–109]. This allows one to systematically separate all relevant mass scales, resum electroweak Sudakov logarithms and disentangle the so-called Sommerfeld enhancement from the short-distance hard annihilation process.

References:

1. E. Witten, Nucl. Phys. B **122**, 109 (1977).
2. S. Weinberg, Phys. Lett. B **91**, 51 (1980).
3. L.J. Hall, Nucl. Phys. B **178**, 75 (1981).
4. E. Eichten, B. Hill, Phys. Lett. B **234**, 511 (1990).
5. H. Georgi, Phys. Lett. B **240**, 447 (1990).
6. B. Grinstein, Nucl. Phys. B **339**, 253 (1990).
7. T. Mannel, W. Roberts, Z. Ryzak, Nucl. Phys. B **368**, 204 (1992).
8. M. Neubert, Phys. Rept. **245**, 259 (1994).
9. A.V. Manohar, M.B. Wise, Camb. Monogr. Part. Phys. Nucl. Phys. Cosmol. **10**, 1 (2000).
10. M.E. Luke, A.V. Manohar, Phys. Lett. B **286**, 348 (1992).
11. E.V. Shuryak, Phys. Lett. B**93**, 134 (1980).
12. N. Isgur, M.B. Wise, Phys. Lett. B **232**, 113 (1989); Phys. Lett. B **237**, 527 (1990).
13. N. Isgur, M.B. Wise, Phys. Rev. Lett. **66**, 1130 (1991).
14. S. Nussinov, W. Wetzel, Phys. Rev. D **36**, 130 (1987).
15. M.A. Shifman, M.B. Voloshin, Sov. J. Nucl. Phys. **45**, 292 (1987); Sov. J. Nucl. Phys. **47**, 511 (1988).
16. M. Neubert, Phys. Lett. B **264**, 455 (1991).
17. M.E. Luke, Phys. Lett. B **252**, 447 (1990).
18. I.I.Y. Bigi *et al.*, Phys. Rev. D **52**, 196 (1995).
19. N. Uraltsev, Phys. Lett. B **501**, 86 (2001).
20. G.P. Korchemsky, A.V. Radyushkin, Nucl. Phys. B **283**, 342 (1987).
21. A.F. Falk *et al.*, Nucl. Phys. B **343**, 1 (1990).
22. J. Chay, H. Georgi, B. Grinstein, Phys. Lett. B **247**, 399 (1990).
23. I.I.Y. Bigi, N.G. Uraltsev, A.I. Vainshtein, Phys. Lett. B **293**, 430 (1992); I.I.Y. Bigi *et al.*, Phys. Rev. Lett. **71**, 496 (1993).
24. A.V. Manohar, M.B. Wise, Phys. Rev. D **49**, 1310 (1994).
25. T. Mannel, Nucl. Phys. B **413**, 396 (1994).
26. A.F. Falk, M.E. Luke, M.J. Savage, Phys. Rev. D **49**, 3367 (1994).
27. E.C. Poggio, H.R. Quinn, S. Weinberg, Phys. Rev. D **13**, 1958 (1976).
28. G. Buchalla, A.J. Buras, M.E. Lautenbacher, Rev. Mod. Phys. **68**, 1125 (1996).
29. A.F. Falk, M. Neubert, Phys. Rev. D **47**, 2965 (1993).

30. M. Neubert, C.T. Sachrajda, Nucl. Phys. B **483**, 339 (1997).
31. M. Beneke, G. Buchalla, I. Dunietz, Phys. Rev. D **54**, 4419 (1996).
32. M. Beneke *et al.*, Phys. Lett. B **459**, 631 (1999); Nucl. Phys. B **639**, 389 (2002).
33. C.W. Bauer *et al.*, Phys. Rev. D **70**, 094017 (2004).
34. M. Neubert, Phys. Rev. D **49**, 4623 (1994).
35. I.I.Y. Bigi *et al.*, Int. J. Mod. Phys. A **9**, 2467 (1994).
36. G.P. Korchemsky, G.F. Sterman, Phys. Lett. B **340**, 96 (1994).
37. C.W. Bauer, M.E. Luke, T. Mannel, Phys. Rev. D **68**, 094001 (2003).
38. K.S.M. Lee, I.W. Stewart, Nucl. Phys. B **721**, 325 (2005).
39. S.W. Bosch, M. Neubert, G. Paz, JHEP **0411**, 073 (2004).
40. M. Beneke *et al.*, JHEP **0506**, 071 (2005).
41. M. Benzke *et al.*, JHEP **1008**, 099 (2010).
42. C.W. Bauer, S. Fleming, M.E. Luke, Phys. Rev. D **63**, 014006 (2000); C.W. Bauer *et al.*, Phys. Rev. D **63**, 114020 (2001).
43. C.W. Bauer, I.W. Stewart, Phys. Lett. B **516**, 134 (2001).
44. C.W. Bauer, D. Pirjol, I.W. Stewart, Phys. Rev. D **65**, 054022 (2002).
45. J. Chay, C. Kim, Phys. Rev. D **65**, 114016 (2002).
46. M. Beneke, A.P. Chapovsky, M. Diehl, T. Feldmann, Nucl. Phys. B **643**, 431 (2002).
47. C.W. Bauer *et al.*, Phys. Rev. D **66**, 014017 (2002).
48. R.J. Hill, M. Neubert, Nucl. Phys. B **657**, 229 (2003).
49. J.C. Collins, D.E. Soper, G.F. Sterman, Adv. Ser. Direct. High Energy Phys. **5**, 1 (1988).
50. I.W. Stewart, F.J. Tackmann, W.J. Waalewijn, Phys. Rev. D **81**, 094035 (2010).
51. J.C. Collins, D.E. Soper, G. Sterman, Nucl. Phys. B **261**, 104 (1985); Nucl. Phys. B **308**, 833 (1988).
52. I.A. Korchemskaya, G.P. Korchemsky, Phys. Lett. B **287**, 169 (1992).
53. T. Becher, M. Neubert, Phys. Rev. Lett. **102**, 162001 (2009); JHEP **0906**, 081 (2009).
54. E. Gardi, L. Magnea, JHEP **0903**, 079 (2009).
55. A. Mitov, G.F. Sterman, I. Sung, Phys. Rev. D **79**, 094015 (2009).
56. A. Ferroglia *et al.*,Phys. Rev. Lett. **103**, 201601 (2009).
57. T. Becher, M. Neubert, Eur. Phys. J. C **71**, 1665 (2011).
58. J.Y. Chiu *et al.*,JHEP **1205**, 084 (2012).
59. M. Beneke and T. Feldmann, Nucl. Phys. B **685**, 249 (2004).
60. M. Beneke *et al.*Phys. Rev. Lett. **83**, 1914 (1999); Nucl. Phys. B **591**, 313 (2000).
61. C.W. Bauer, D. Pirjol, I.W. Stewart, Phys. Rev. Lett. **87**, 201806 (2001).
62. S. Mantry, D. Pirjol, I.W. Stewart, Phys. Rev. D **68**, 114009 (2003).
63. T. Becher, R.J. Hill, M. Neubert, Phys. Rev. D **72**, 094017 (2005).
64. S. Fleming, A.K. Leibovich, T. Mehen, Phys. Rev. D **68**, 094011 (2003).
65. T. Becher, M.D. Schwartz, JHEP **0807**, 034 (2008).
66. T. Becher, G. Bell, M. Neubert, Phys. Lett. B **704**, 276 (2011).
67. I.W. Stewart, F.J. Tackmann, W.J. Waalewijn, Phys. Rev. D **81**, 094035 (2010).
68. J.-y. Chiu, R. Kelley, A.V. Manohar, Phys. Rev. D **78**, 073006 (2008).
69. T. Becher, M. Neubert, G. Xu, JHEP **0807**, 030 (2008).
70. V. Ahrens *et al.*, Eur. Phys. J. C **62**, 333 (2009); V. Ahrens, A. Ferroglia, M. Neubert, B.D. Pecjak, L.L. Yang, JHEP **1009**, 097 (2010).
71. X. Liu, S. Mantry, F. Petriello, Phys. Rev. D **86**, 074004 (2012).
72. X. Liu, F. Petriello, Phys. Rev. D **87**, no. 1, 014018 (2013).
73. For a review, see: S. Kluth, Rept. Prog. Phys. **69**, 1771 (2006).
74. A. Gehrmann-De Ridder *et al.*, Phys. Rev. Lett. **99**, 132002 (2007).
75. S. Weinzierl, Phys. Rev. Lett. **101**, 162001 (2008).
76. R. Abbate *et al.*, Phys. Rev. **D83**, 074021 (2011).
77. A.H. Hoang *et al.*, Phys. Rev. D **91**, no. 9, 094018 (2015).
78. T. Becher, M. Neubert, JHEP **1207**, 108 (2012).
79. I.W. Stewart, F.J. Tackmann, J.R. Walsh, S. Zuberi, Phys. Rev. D **89**, no. 5, 054001 (2014).
80. A. Banfi *et al.*, Phys. Rev. Lett. **109**, 202001 (2012).
81. R. Boughezal, X. Liu, F. Petriello, Phys. Rev. D **91**, no. 9, 094035 (2015).
82. J. Gaunt *et al.*, JHEP **1509**, 058 (2015).
83. R. Boughezal *et al.*, Phys. Lett. B **748**, 5 (2015).
84. R. Boughezal *et al.*, Phys. Rev. Lett. **116**, no. 15, 152001 (2016).
85. R. Boughezal, X. Liu and F. Petriello, Phys. Rev. D **94**, no. 11, 113009 (2016).
86. R. Boughezal, X. Liu and F. Petriello, JHEP **1703**, 160 (2017).
87. I. Moult, I. W. Stewart and G. Vita, JHEP **1707**, 067 (2017).
88. M. Dasgupta, G.P. Salam, Phys. Lett. B **512**, 323 (2001); JHEP **0203**, 017 (2002).
89. R.B. Appleby, M.H. Seymour, JHEP **0212**, 063 (2002).
90. R. Kelley *et al.*, Phys. Rev. D **84**, 045022 (2011); Phys. Rev. D **86**, 054017 (2012).
91. A. Hornig *et al.*, JHEP **1108**, 054 (2011).
92. A. von Manteuffel, R.M. Schabinger, H.X. Zhu, JHEP **1403**, 139 (2014).
93. S. Caron-Huot, arXiv:1501.03754 [hep-ph].
94. A.J. Larkoski, I. Moult, D. Neill, JHEP **1509**, 143 (2015).
95. T. Becher *et al.*, Phys. Rev. Lett. **116**, no. 19, 192001 (2016).
96. T. Becher *et al.*, JHEP **1611**, 019 (2016) Erratum: [JHEP **1705**, 154 (2017)].
97. T. Becher, B. D. Pecjak and D. Y. Shao, JHEP **1612**, 018 (2016).
98. C.W. Bauer, B.O. Lange, G. Ovanesyan, JHEP **1107**, 077 (2011).
99. S. Fleming, Phys. Lett. B **735**, 266 (2014).
100. I. Z. Rothstein and I. W. Stewart, JHEP **1608**, 025 (2016).
101. A. Idilbi, A. Majumder, Phys. Rev. D **80**, 054022 (2009).
102. G. Ovanesyan, I. Vitev, JHEP **1106**, 080 (2011).
103. M. Benzke *et al.*, JHEP **1302**, 129 (2013).
104. Z.B. Kang *et al.*, Phys. Rev. Lett. **114**, no. 9, 092002 (2015).
105. M. Beneke, T. Feldmann, Nucl. Phys. B **592**, 3 (2001).
106. R.J. Hill, M.P. Solon, Phys. Lett. B **707**, 539 (2012); Phys. Rev. Lett. **112**, 211602 (2014).
107. M. Bauer *et al.*, JHEP **1501**, 099 (2015); R.J. Hill, M.P. Solon, Phys. Rev. D **91**, 043505 (2015).
108. M. Baumgart, I.Z. Rothstein, V. Vaidya, Phys. Rev. Lett. **114**, 211301 (2015).
109. G. Ovanesyan, T.R. Slatyer, I.W. Stewart, Phys. Rev. Lett. **114**, no. 21, 211302 (2015).

17. Lattice Quantum Chromodynamics

Updated September 2017 by S. Hashimoto (KEK), J. Laiho (Syracuse University) and S.R. Sharpe (University of Washington).

Many physical processes considered in the Review of Particle Properties (RPP) involve hadrons. The properties of hadrons—which are composed of quarks and gluons—are governed primarily by Quantum Chromodynamics (QCD) (with small corrections from Quantum Electrodynamics [QED]). Theoretical calculations of these properties require non-perturbative methods, and Lattice Quantum Chromodynamics (LQCD) is a tool to carry out such calculations. It has been successfully applied to many properties of hadrons. Most important for the RPP are the calculation of electroweak form factors, which are needed to extract Cabbibo-Kobayashi-Maskawa (CKM) matrix elements when combined with the corresponding experimental measurements. LQCD has also been used to determine other fundamental parameters of the standard model, in particular the strong coupling constant and quark masses, as well as to predict hadronic contributions to the anomalous magnetic moment of the muon, $g_\mu - 2$.

This review describes the theoretical foundations of LQCD and sketches the methods used to calculate the quantities relevant for the RPP. It also describes the various sources of error that must be controlled in a LQCD calculation. Results for hadronic quantities are given in the corresponding dedicated reviews.

17.1. Lattice regularization of QCD

Gauge theories form the building blocks of the Standard Model. While the SU(2) and U(1) parts have weak couplings and can be studied accurately with perturbative methods, the SU(3) component—QCD—is only amenable to a perturbative treatment at high energies. The growth of the coupling constant in the infrared—the flip-side of asymptotic freedom—requires the use of non-perturbative methods to determine the low energy properties of QCD. Lattice gauge theory, proposed by K. Wilson in 1974 [1], provides such a method, for it gives a non-perturbative definition of vector-like gauge field theories like QCD. In lattice regularized QCD—commonly called lattice QCD or LQCD—Euclidean space-time is discretized, usually on a hypercubic lattice with lattice spacing a, with quark fields placed on sites and gauge fields on the links between sites. The lattice spacing plays the role of the ultraviolet regulator, rendering the quantum field theory finite. The continuum theory is recovered by taking the limit of vanishing lattice spacing, which can be reached by tuning the bare coupling constant to zero according to the renormalization group.

Unlike dimensional regularization, which is commonly used in continuum QCD calculations, the definition of LQCD does not rely on the perturbative expansion. Indeed, LQCD allows non-perturbative calculations by numerical evaluation of the path integral that defines the theory.

Practical LQCD calculations are limited by the availability of computational resources and the efficiency of algorithms. Because of this, LQCD results come with both statistical and systematic errors, the former arising from the use of Monte-Carlo integration, the latter, for example, from the use of non-zero values of a. There are also different ways in which the QCD action can be discretized, and all must give consistent results in the continuum limit, $a \to 0$. It is the purpose of this review to provide an outline of the methods of LQCD, with particular focus on applications to particle physics, and an overview of the various sources of error. This should allow the reader to better understand the LQCD results that are presented in other reviews, primarily those on "Quark Masses", "Quantum Chromodynamics", "CKM quark-mixing matrix", "V_{ud}, V_{us}, Cabibbo angle and CKM Unitarity" and "Semileptonic B-meson decays and the determination of V_{cb} and V_{ub}". For more extensive explanations the reader should consult the available textbooks or lecture notes, the most up-to-date of which are Refs. 2–4.

17.1.1. *Gauge invariance, gluon fields and the gluon action* :

A key feature of the lattice formulation of QCD is that it preserves gauge invariance. This is in contrast to perturbative calculations, where gauge fixing is an essential step. The preservation of gauge invariance leads to considerable simplifications, e.g. restricting the form of operators that can mix under renormalization.

The gauge transformations of lattice quark fields are just as in the continuum: $q(x) \longrightarrow V(x)q(x)$ and $\bar{q}(x) \longrightarrow \bar{q}(x)V^\dagger(x)$, with $V(x)$ an arbitrary element of SU(3). The only difference is that the Euclidean space-time positions x are restricted to lie on the sites of the lattice, i.e. $x = a(n_1, n_2, n_3, n_4)$ for a hypercubic lattice, with the n_j being integers. Quark bilinears involving different lattice points can be made gauge invariant by introducing the gluon field $U_\mu(x)$. For example, for adjacent points the bilinear is $\bar{q}(x)U_\mu(x)q(x+a\hat{\mu})$, with $\hat{\mu}$ the unit vector in the μ'th direction. (This form is used in the construction of the lattice covariant derivative.) This is illustrated in Fig. 17.1. The gluon field (or "gauge link") is an element of the group, SU(3), in contrast to the continuum field A_μ which takes values in the Lie algebra. The bilinear is invariant if U_μ transforms as $U_\mu(x) \to V(x)U_\mu(x)V^\dagger(x+a\hat{\mu})$. The lattice gluon field is naturally associated with the link joining x and $x+a\hat{\mu}$, and corresponds in the continuum to a Wilson line connecting these two points, $P\exp(i\int_x^{x+a\hat{\mu}} dx_\mu A_\mu^{\rm cont}(x))$ (where P indicates a path-ordered integral, and the superscript on A_μ indicates that it is a continuum field). The trace of a product of the $U_\mu(x)$ around any closed loop is easily seen to be gauge invariant and is the lattice version of a Wilson loop.

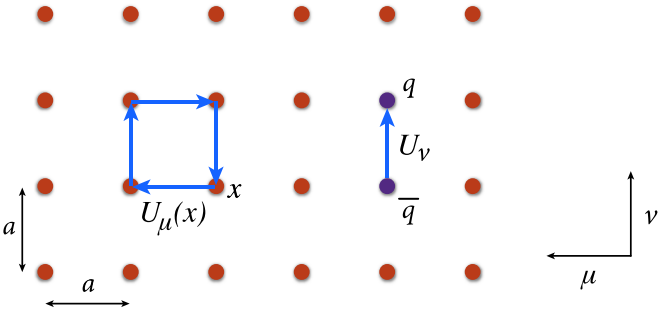

Figure 17.1: Sketch of a two-dimensional slice through the $\mu - \nu$ plane of a lattice, showing gluon fields lying on links and forming either the plaquette product appearing in the gauge action or a component of the covariant derivative connecting quark and antiquark fields.

The simplest possible gauge action, usually called the Wilson gauge action, is given by the product of gauge links around elementary plaquettes:

$$S_g = \beta \sum_{x,\mu,\nu} [1 - \frac{1}{3}{\rm ReTr}[U_\mu(x)U_\nu(x+a\hat{\mu})U_\mu^\dagger(x+a\hat{\nu})U_\nu^\dagger(x)]] \,. \quad (17.1)$$

This is illustrated in Fig. 17.1. For small a, assuming that the fields are slowly varying, one can expand the action in powers of a using $U_\mu(x) = \exp(iaA_\mu(x))$. Keeping only the leading non-vanishing term, and replacing the sum with an integral, one finds the continuum form,

$$S_g \longrightarrow \int d^4x \frac{1}{4g_{\rm lat}^2} {\rm Tr}[F_{\mu\nu}^2(x)] \,, \qquad (F_{\mu\nu} = \partial_\mu A_\nu - \partial_\nu A_\mu + i[A_\mu, A_\nu]) \quad (17.2)$$

as long as one chooses $\beta = 6/g_{\rm lat}^2$ for the lattice coupling. In this expression, $g_{\rm lat}$ is the bare coupling constant in the lattice scheme, which can be related (by combining continuum and lattice perturbation theory) to a more conventional coupling constant such as that in the $\overline{\rm MS}$ scheme (see Sec. 17.3.4 below).

In practice, the lattice spacing a is non-zero, leading to discretization errors. In particular, the lattice breaks Euclidean rotational invariance (which is the Euclidean version of Lorentz invariance) down to a discrete hypercubic subgroup. One wants to reduce discretization errors as much as possible. A very useful tool for understanding and then reducing discretization errors is the Symanzik effective action: the interactions of quarks and gluons with momenta low compared to the lattice cutoff ($|p| \ll 1/a$) are described by a continuum action consisting of the standard continuum terms (e.g. the gauge action

given in Eq. (17.2)) augmented by higher dimensional operators suppressed by powers of a [5]. For the Wilson lattice gauge action, the leading corrections come in at $\mathcal{O}(a^2)$. They take the form $\sum_j a^2 c_j O_6^{(j)}$, with the sum running over all dimension-six operators $O_6^{(j)}$ allowed by the *lattice* symmetries, and c_j unknown coefficients. Some of these operators violate Euclidean rotational invariance, and all of them lead to discretization errors of the form $a^2\Lambda^2$, where Λ is a typical momentum scale for the quantity being calculated. These errors can, however, be reduced by adding corresponding operators to the lattice action and tuning their coefficients to eliminate the dimension-six operators in the effective action to a given order in perturbation theory or even non-perturbatively. This is the idea of the Symanzik improvement program [5]. In the case of the gauge action, one adds Wilson loops involving six gauge links (as opposed to the four links needed for the original plaquette action, Eq. (17.1)) to define the $\mathcal{O}(a^2)$ improved (or "Symanzik") action [6]. In practical implementations, the improvement is either at tree-level (so that residual errors are proportional to $\alpha_s a^2$, where the coupling is evaluated at a scale $\sim 1/a$), or at one loop order (errors proportional to $\alpha_s^2 a^2$). Another popular choice is motivated by studies of renormalization group (RG) flow. It has the same terms as the $\mathcal{O}(a^2)$ improved action but with different coefficients, and is called the RG-improved or "Iwasaki" action [7].

17.1.2. ***Lattice fermions*** :

Discretizing the fermion action turns out to involve subtle issues, and the range of actions being used is more extensive than for gauge fields. Recall that the continuum fermion action is $S_f = \int d^4x \bar{q}[iD_\mu\gamma_\mu + m_q]q$, where $D_\mu = \partial_\mu + iA_\mu$ is the gauge-covariant derivative. The simplest discretization replaces the derivative with a symmetric difference:

$$D_\mu q(x) \longrightarrow \frac{1}{2a}[U_\mu(x)q(x+a\hat{\mu}) - U_\mu(x-a\hat{\mu})^\dagger q(x-a\hat{\mu})]\,. \qquad (17.3)$$

The factors of U_μ ensure that $D_\mu q(x)$ transforms under gauge transformations in the same way as $q(x)$, so that the discretized version of $\bar{q}(x)D_\mu\gamma_\mu q(x)$ is gauge invariant. The choice in Eq. (17.3) leads to the so-called naive fermion action. This, however, suffers from the fermion doubling problem—in d dimensions it describes 2^d equivalent fermion fields in the continuum limit. The appearance of the extra "doubler" fermions is related to the deeper theoretical problem of formulating chirally symmetric fermions on the lattice. This is encapsulated by the Nielsen-Ninomiya theorem [8]: one cannot define lattice fermions having exact, continuum-like chiral symmetry without producing doublers. Naive lattice fermions do have chiral symmetry but at the cost of introducing 15 unwanted doublers (for $d = 4$).

There are a number of different strategies for dealing with the doubling problem, each with their own theoretical and computational advantages and disadvantages. Wilson fermions [1] add a term proportional to $a\bar{q}\Delta q$ to the fermion action (the "Wilson term"—in which Δ is a covariant lattice Laplacian). This gives a mass of $\mathcal{O}(1/a)$ to the doublers, so that they decouple in the continuum limit. The Wilson term, however, violates chiral symmetry, and also introduces discretization errors linear in a. A commonly used variant that eliminates the $\mathcal{O}(a)$ discretization error is the $\mathcal{O}(a)$-improved Wilson (or "clover") fermion [9]. In this application of Symanzik improvement, methods have been developed to remove $\mathcal{O}(a)$ terms non-perturbatively using auxiliary simulations to tune parameters [10]. Such "non-perturbative improvement" is of great practical importance as it brings the discretization error from the fermion action down to the same level as that from the gauge action. It is used by essentially all simulations using clover fermions.

The advantages of Wilson fermions are their theoretical simplicity and relatively low computational cost. Their main disadvantage is the lack of chiral symmetry, which makes them difficult to use in cases where mixing with wrong chirality operators can occur, particularly if this involves divergences proportional to powers of $1/a$. A related problem is the presence of potential numerical instabilities due to spurious near-zero modes of the lattice Dirac operator. There are, however, recent works that successfully ameliorate these problems and increase the range of quantities for which Wilson fermions can be used (see, e.g., Refs. 11–13).

Twisted-mass fermions [14] are a variant of Wilson fermions in which two flavors are treated together with an isospin-breaking mass term (the "twisted mass" term). The main advantage of this approach is that all errors linear in a are automatically removed (without the need for tuning of parameters) by a clever choice of twisted mass and operators [15]. A disadvantage is the presence of isospin breaking effects (such as a splitting between charged and neutral pion masses even when up and down quarks are degenerate), which, however, vanish as $a^2\Lambda^2$ in the continuum limit. Strange and charm quarks can be added as a second pair, with a term added to split their masses.

Staggered fermions are a reduced version of naive fermions in which there is only a single fermion Dirac component on each lattice site, with the full Dirac structure built up from neighboring sites [16]. They have the advantages of being somewhat faster to simulate than Wilson-like fermions, of preserving some chiral symmetry, and of having discretization errors of $\mathcal{O}(a^2)$. Their disadvantage is that they retain some of the doublers (3 for $d = 4$). The action thus describes four degenerate fermions in the continuum limit. These are usually called "tastes", to distinguish them from physical flavors, and the corresponding SU(4) symmetry is referred to as the "taste symmetry". The preserved chiral symmetry in this formulation has non-singlet taste. Practical applications usually introduce one staggered fermion for each physical flavor, and remove contributions from the unwanted tastes by taking the fourth-root of the fermion determinant appearing in the path integral. The validity of this "rooting" procedure is not obvious because taste symmetry is violated for non-zero lattice spacing. Theoretical arguments, supported by numerical evidence, suggest that the procedure is valid as long as one takes the continuum limit before approaching the light quark mass region [17]. Additional issues arise for the valence quarks (those appearing in quark propagators, as described in Sec. 17.2 below), where rooting is not possible, and one must remove the extra tastes by hand [18].

Just as for Wilson fermions, the staggered action can be improved, so as to reduce discretization errors. The Asqtad (a-squared tadpole improved) action [19] was used until recently in many large scale simulations [20]. More recent calculations use the HISQ (highly improved staggered quark) action, introduced in Ref. 21. At tree-level it removes both $\mathcal{O}(a^2)$ errors and, to lowest order in the quark speed v/c, $\mathcal{O}([am]^4)$ errors. It also substantially reduces effects caused by taste-symmetry breaking. This makes it attractive not only for light quarks, but means that it is also quite accurate for heavy quarks because it suppresses $(am)^n$ errors. It is being used to directly simulate charm quarks and to approach direct simulations of bottom quarks.

There is an important class of lattice fermions, "Ginsparg-Wilsons fermions", that possess a continuum-like chiral symmetry without introducing unwanted doublers. The lattice Dirac operator D for these fermions satisfies the Ginsparg-Wilson relation $D\gamma_5 + \gamma_5 D = aD\gamma_5 D$ [22]. In the continuum, the right-hand-side vanishes, leading to chiral symmetry. On the lattice, it is non-vanishing, but with a particular form (with two factors of D) that restricts the violations of chiral symmetry in Ward-Takahashi identities to short-distance terms that do not contribute to physical matrix elements [23]. In fact, one can define a modified chiral transformation on the lattice (by including dependence on the gauge fields) such that Ginsparg-Wilson fermions have an exact chiral symmetry for on-shell quantities [24]. The net result is that such fermions essentially have the same properties under chiral transformations as do continuum fermions, including the index theorem [23]. Their leading discretization errors are of $\mathcal{O}(a^2)$.

Two types of Ginsparg-Wilson fermions are currently being used in large-scale numerical simulations. The first is Domain-wall fermions (DWF). These are defined on a five-dimensional space, in which the fifth dimension is fictitious [25]. The action is chosen so that the low-lying modes are chiral, with left- and right-handed modes localized on opposite four-dimensional surfaces. For an infinite fifth dimension, these fermions satisfy the Ginsparg-Wilson relation. In practice, the fifth dimension is kept finite, and there remains a small, controllable violation of chiral symmetry. The second type is Overlap fermions. These appeared from a completely different context and have an

explicit form that exactly satisfies the Ginsparg-Wilson relation [26]. Their numerical implementation requires an approximation of the matrix sign function of a Wilson-like fermion operator, and various approaches are being used. In fact, it is possible to rewrite these approximations in terms of a five-dimensional formulation, showing that the DWF and Overlap approaches are essentially equivalent [27]. Numerically, the five-dimensional approach appears to be more computationally efficient.

The various lattice fermion formulations are often combined with the technique of link smearing. Here one couples the fermions to a smoother gauge link, defined by averaging with adjacent links in a gauge invariant manner. Several closely related implementations are being used. All reduce the coupling of fermions to the short-distance fluctuations in the gauge field, leading to an improvement in the numerical stability and speed of algorithms. One cannot perform this smearing too agressively, however, since the smearing may distort short distance physics and enhance discretization errors.

As noted above, each fermion formulation has its own advantages and disadvantages. For instance, domain-wall and overlap fermions are theoretically preferred as they have chiral symmetry without doublers, but their computational cost is greater than for other choices. If the physics application of interest and the target precision do not require near-exact chiral symmetry, there is no strong motivation to use these expensive formulations. On the other hand, there is a class of applications (including the calculation of the $\Delta I = 1/2$ amplitude for $K \to \pi\pi$ decays and the S-parameter [28]) where chiral symmetry plays an essential role and for which the use of Ginsparg-Wilson fermions is strongly favored.

17.1.3. *Heavy quarks on the lattice* :

The fermion formulations described in the previous subsection can be used straightforwardly only for quarks whose masses are small compared to the lattice cutoff, $m_q \lesssim 1/a$. This is because there are discretization errors proportional to powers of am_q, and if $am_q \gtrsim 1$ these errors are large and uncontrolled. Present LQCD simulations typically have cutoffs in the range of $1/a = 2 - 4$ GeV (corresponding to $a \approx 0.1 - 0.05$ fm). Thus, while for the up, down and strange quarks one has $am_q \ll 1$, for bottom quarks (with $m_b \approx 4.5$ GeV) one must use alternative approaches. Charm quarks ($m_c \approx 1.5$ GeV) are an intermediate case, allowing simulations using both direct and alternative approaches.

For the charm quark, the straightforward approach is to simultaneously reduce the lattice spacing and to improve the fermion action so as to reduce the size of errors proportional to powers of am_c. This approach has, for example, been followed successfully using the HISQ and twisted-mass actions [21,29,30]. It is important to note, however, that reducing a increases the computational cost because an increased number of lattice points are needed for the same physical volume. One cannot reduce the spatial size below $2 - 3$ fm without introducing finite volume errors. Present lattices have typical sizes of $\sim 64^3 \times 128$ (with the long direction being Euclidean time), and thus allow a lattice cutoff up to $1/a \sim 4$ GeV.

Alternative approaches for discretizing heavy quarks are motivated by effective field theories. For a bottom quark in heavy-light hadrons, one can use Heavy Quark Effective Theory (HQET) to expand about the infinite quark-mass limit. In this limit, the bottom quark is a static color source, and one can straightforwardly write the corresponding lattice action [31]. Corrections, proportional to powers of $1/m_b$, can be introduced as operator insertions, with coefficients that can be determined non-perturbatively using existing techniques [32]. This method allows the continuum limit to be taken controlling all $1/m_b$ corrections.

Another way of introducing the $1/m_b$ corrections is to include the relevant terms in the effective action. This leads to a non-relativistic QCD (NRQCD) action, in which the heavy quark is described by a two-component spinor [33]. This approach has the advantage over HQET that it can also be used for heavy-heavy systems, such as the Upsilon states. A disadvantage is that some of the parameters in this effective theory are determined perturbatively (originally at tree-level, but more recently at one-loop), which limits the precision of the final results. Although discretization effects can be controlled with good numerical precision for a range of lattice spacings, these artifacts cannot be extrapolated away by taking the lattice spacing to zero. This is because NRQCD is a nonrelativistic effective field theory and so ceases to work when the cutoff π/a becomes much larger than the heavy-quark mass.

This problem can be avoided if one uses HQET power counting to analyze and reduce discretization effects for heavy quarks while using conventional fermion actions [34]. For instance, one can tune the parameters of an improved Wilson quark action so that the leading HQET corrections to the static quark limit are correctly accounted for. As the lattice spacing becomes finer, the action smoothly goes over to that of a light Wilson quark action, where the continuum limit can be taken as usual. In principle, one can improve the action in the heavy quark regime up to arbitrarily high orders using HQET, but so far large-scale simulations have typically used clover improved Wilson quarks, where tuning the parameters of the action corresponds to including all corrections through next-to-leading order in HQET. Three different methods for tuning the parameters of the clover action are being used: the Fermilab [34], Tsukuba [35] and Columbia [36] approaches. An advantage of this HQET approach is that the c and b quarks can be treated on the same footing. Parameter tuning has typically been done perturbatively, as in NRQCD, but recent work using the Columbia approach has used non-perturbative tuning of some of the parameters [37,38].

Another approach is the "ratio method" introduced in Ref. 39. Here one uses quarks with masses lying at, or slightly above, the charm mass m_c, which can be simulated with a relativistic action, and extrapolates to m_b incorporating the behavior predicted by HQET. The particular implementation relies on the use of ratios. As an example, consider the B meson decay constant f_B. According to HQET, this scales as $1/\sqrt{m_B}$ for $m_B \gg \Lambda_{\rm QCD}$, up to a logarithmic dependence that is calculable in perturbative QCD (but will be suppressed in the following). Here m_B is the B meson mass, which differs from m_b by $\sim \Lambda_{\rm QCD}$. One considers the ratio $y(\lambda, m_{b'}) \equiv f_{B''}\sqrt{m_{B''}}/f_{B'}\sqrt{m_{B'}}$ for fictitious B mesons containing b quarks with unphysical masses $m_{b'}$ and $m_{b''} = \lambda m_{b'}$. HQET implies that $y(\lambda, m_{b'})$ approaches unity for large $m_{b'}$ and any fixed $\lambda > 1$. The ratios are evaluated on the lattice for the sequence of masses $m_{b'} = m_c$, λm_c, $\lambda^2 m_c$, all well below the physical m_b, and for each the continuum limit is taken. The form of the ratio for larger values of $m_{b'}$ is obtained by fitting, incorporating the constraints implied by HQET. The result for $f_B\sqrt{m_B}$ is then obtained as a product of y's with $f_D\sqrt{m_D}$.

17.1.4. *QED on the lattice* :

Quarks in nature are electrically charged, and the resultant coupling to photons leads to shifts in the properties of hadrons that are generically of $\mathcal{O}(\alpha_{\rm EM})$. Thus, for example, the proton mass is increased by ~ 1 MeV relative to that of the neutron due to its overall charge although this effect is more than compensated for by the ~ 2.5 MeV relative decrease due to the up quark being lighter than the down quark [40]. This example shows that once pure QCD, isospin-symmetric lattice calculations reach percent level accuracy, further improvement requires the inclusion of effects due to both electromagnetism and the up-down mass difference. This level of accuracy has in fact been obtained for various quantities, e.g. light hadron masses and decay constants (see Ref. 41), and simulations including QED in addition to QCD are becoming more common.

The extension of lattice methods to include QED is straightforward, although some new subtleties arise. The essential change is that the quark must now propagate through a background field containing both gluons and photons. The gauge field U_μ that appears in the covariant derivative of Eq. (17.3) is extended from an SU(3) matrix to one living in U(3): $U_\mu \to U_\mu e^{iaqeA_\mu^{\rm EM}}$. Here $A_\mu^{\rm EM}$ is the photon field, e the electromagnetic coupling, and q the charge of the quark, *e.g.* $q = 2/3$ for up and $-1/3$ for down and strange quarks. The lattice action for the photon that is typically used is a discretized version of the continuum action Eq. (17.2), rather than the form used for the gluons, Eq. (17.1). This "non-compact" action has the advantage that it is quadratic in $A_\mu^{\rm EM}$, which simplifies the QED part of the generation of configurations.

One subtlety that arises is that Gauss' law forbids a charged particle

in a box with periodic boundary conditions. This finite volume effect can be overcome by including a uniform background charge, and this can be shown to be equivalent to removing the zero-momentum mode from the photon field. This is an example of the enhanced finite-volume effects that arise in the presence of the massless photon.

Simulations including QED have progressed over the last few years, and now a full inclusion of QED has been achieved with almost physical quark masses [40,42]. Alternative approaches have also been used: reweighting the QCD fields *a posteriori* [43,44], and keeping only the linear term in an expansion in $\alpha_{\rm EM}$ about the QCD only case [45]. In addition, some calculations have included QED effects for the valence quarks but not the sea quarks (the "electroquenched approximation")—for a recent example see Ref. 46.

17.1.5. *Basic inputs for lattice calculations* :

Since LQCD is nothing but a regularization of QCD, the renormalizability of QCD implies that the number of input parameters in LQCD is the same as for continuum QCD—the strong coupling constant $\alpha_s = g^2/(4\pi)$, the quark masses for each flavor, and the CP violating phase θ. The θ parameter is usually assumed to be zero, while the other parameters must be determined using experimental inputs.

17.1.5.1. *Lattice spacing:* In QCD, the coupling constant is a function of scale. With lattice regularization, this scale is the inverse lattice spacing $1/a$, and choosing the bare coupling constant is equivalent to fixing the lattice spacing.

In principle, a can be determined using any dimensionful quantity measured by experiments. For example, using the mass of hadron H one has $a = (am_H)^{\rm lat}/m_H^{\rm exp}$. (Of course, one must first tune the quark masses to their physical values, as discussed below.) In practice, one chooses quantities that can be calculated accurately on the lattice, and that are only weakly dependent on the light quark masses. The latter property minimizes errors from extrapolating or interpolating to the physical light quark masses or from mistuning of these masses. Commonly used choices are the spin-averaged 1S-1P or 1S-2S splittings in the Upsilon system, the mass of the Ω^- baryon, and the pion decay constant f_π. Ultimately, all choices must give consistent results for a, and that this is the case provides a highly non-trivial check of both the calculational method and of QCD.

17.1.5.2. *Light quark masses:*

In LQCD simulations, the up, down and strange quarks are usually referred to as the light quarks, in the sense that $m_q < \Lambda_{\rm QCD}$. (The standard definition of $\Lambda_{\rm QCD}$ is given in the "Quantum Chromodynamics" review; in this review we are using it only to indicate the approximate non-perturbative scale of QCD.) This condition is stronger than that used above to distinguish quarks with small discretization errors, $m_q < 1/a$. Loop effects from light quarks must be included in the simulations to accurately represent QCD. At present, most simulations are done in the isospin symmetric limit $m_u = m_d \equiv m_\ell < m_s$, and are often referred to as "$N_f = 2 + 1$" simulations. Increasingly, simulations also include loops of charm quarks (denoted $N_f = 2 + 1 + 1$ simulations), although the effect of charmed sea quarks on low-energy physics is generically expected to be at the sub-percent level [48]. Precision is now reaching the point where isospin breaking effects must be included. To do so without approximation requires simulating with nondegenerate up and down quarks (leading to $N_f = 1 + 1 + 1$ or $1 + 1 + 1 + 1$ simulations) as well as including electromagnetism (as described above). This has been done in Ref. 40. Alternatively, one can use a perturbative approach, expanding about the isospin symmetric theory and working to linear order in $\alpha_{\rm EM}$ and $m_u - m_d$ [45,47].

We now describe the tuning of m_ℓ, m_s and m_c to their physical values. (For brevity, we ignore isospin violation in the following discussion.) The most commonly used quantities for these tunings are, respectively, m_π, m_K and m_{D_s}. If the scale is being set by m_Ω, then one adjusts the lattice quark masses until the ratios m_π/m_Ω, m_K/m_Ω and m_{D_s}/m_Ω take their physical values. In the past, most calculations needed to extrapolate to the physical value of m_ℓ (typically using forms based on chiral perturbation theory [ChPT]), while simulating directly at or near to the physical values of m_s and m_c. Present calculations are increasingly done with physical or near physical values of m_ℓ, requiring at most only a short extrapolation.

17.1.5.3. *Heavy quark masses:*

The b quark is usually treated only as a valence quark, with no loop effects included. The errors introduced by this approximation can be estimated to be $\sim \alpha_s(m_b)\Lambda_{\rm QCD}^2/m_b^2$ and are likely to be very small. In the past, the same approximation has been made for the c quark, leading to errors $\sim \alpha_s(m_c)\Lambda_{\rm QCD}^2/m_c^2$. (See Ref. 48 for a quantitative estimate of the effects of including the charm quark on some low energy physical quantities, and Ref. 49 for similar estimates for B-meson matrix elements.) For high precision, however, dynamical charm quarks are necessary, and some of the most recent simulations now include them.

The b quark mass can be tuned by setting heavy-heavy (Υ) or heavy-light (B) meson masses to their experimental values. Consistency between these two determinations provides an important check that the determination of parameters in the heavy quark lattice formulations is being done correctly (see, e.g., Ref. 50).

17.1.6. *Sources of systematic error* :

Lattice results have statistical and systematic errors that must be quantified for any calculation in order for the result to be a useful input to phenomenology. The statistical error is due to the use of Monte Carlo importance sampling to evaluate the path integral (a method discussed below). There are, in addition, a number of systematic errors that are always present to some degree in lattice calculations, although the size of any given error depends on the particular quantity under consideration and the parameters of the ensembles being used. The most common lattice errors are reviewed below.

Although not strictly a systematic error, it is important to note that the presence of long autocorrelations in the sequence of lattice configurations generated by the Monte Carlo method can lead to underestimates of statistical errors [51]. It is known that the global topological charge of the gauge fields decorrelates very slowly with certain algorithms [52]. The effect of poorly sampling topological charge is expected to be most significant for the pion mass and related quantities [53,54]. This issue becomes more relevant as the precision of the final results increases.

17.1.6.1. *Continuum limit:* Physical results are obtained in the limit that the lattice spacing a goes to zero. The Symanzik effective theory determines the scaling of lattice artefacts with a. Most lattice calculations use improved actions with leading discretizations errors of $\mathcal{O}(a^2\Lambda^2)$, $\mathcal{O}(\alpha_s a^2\Lambda^2)$, or $\mathcal{O}(\alpha_s a\Lambda)$, where Λ is a typical momentum scale in the system. Knowledge of the scaling of the leading discretization errors allows controlled extrapolation to $a = 0$ when multiple lattice spacings are available, as in current state-of-the-art calculations. Residual errors arise from the exclusion of subleading a dependence from the fits.

For many quantities the typical momentum scale in the system is $\sim \Lambda_{\rm QCD} \approx 300$ MeV. Discretization errors are expected to be larger for quantities involving larger scales, for example form factors or decays involving particles with momenta larger than $\Lambda_{\rm QCD}$.

17.1.6.2. *Infinite volume limit:* LQCD calculations are necessarily carried out in finite space-time boxes, leading to departures of physical quantities (masses, decay constants, etc.) from their measured, infinite volume values. These finite-volume shifts are an important systematic that must be estimated and minimized.

Typical lattices are asymmetric, with N_s points in the three spatial directions and N_t in the (Euclidean) temporal direction. The spatial and temporal sizes in physical units are thus $L_s = aN_s$ and $L_t = aN_t$, respectively. (Anisotropic lattice spacings are also sometimes used, as discussed below in Sec. 17.2.2.) Typically, $L_t \geq 2L_s$, a longer temporal direction being used to allow excited-state contributions to correlators to decay. This means that the dominant impact of using finite volume is from the presence of a finite spatial box.

High-precision LQCD calculations are of quantities involving no more than a single particle in initial and final states (with the

exception of the $K \to \pi\pi$ decay amplitudes). For such quantities, once the volume exceeds about 2 fm (so that the particle is not "squeezed"), the dominant finite-volume effect comes from virtual pions wrapping around the lattice in the spatial directions. This effect is exponentially suppressed as the volume becomes large, roughly as $\sim \exp(-m_\pi L_s)$, and has been estimated using ChPT [55] or other methods [56]. The estimates suggest that finite volume shifts are sub-percent effects when $m_\pi L_s \gtrsim 4$, and most large-scale simulations use lattices satisfying this condition. This becomes challenging as one approaches the physical pion mass, for which $L_s \gtrsim 5$ fm is required. At present, this can only be achieved by using relatively coarse lattices, $a \gtrsim 0.07$ fm.

Finite volume errors are usually determined by repeating the simulations on two or more different volumes (with other parameters fixed). If different volumes are not available, the ChPT estimate can be used, often inflated to account for the fact that the ChPT calculation is truncated at some order.

In the future, LQCD calculations involving more than a single hadron will become increasingly precise. Examples include the calculation of resonance parameters and the above-mentioned $K \to \pi\pi$ amplitudes. Finite volume effects are much larger in these cases, with power-law terms (e.g. $1/L_s^3$) in addition to exponential dependence. Indeed, as will be discussed in Sec. 17.2.4, one can use the volume dependence to indirectly extract infinite-volume quantities such as scattering lengths. Doing so, however, requires a set of lattice volumes satisfying $m_\pi L_s \gtrsim 4$ and is thus more challenging than for single-particle quantities.

17.1.6.3. *Chiral extrapolation:*

Until recently, an important source of systematic error in LQCD calculations was the need to extrapolate in m_u and m_d (or, equivalently, in m_π). This extrapolation was usually done using functional forms based on ChPT, or with analytic functions, with the difference between different fits used as an estimate of the systematic error, which was often substantial. Increasingly, however, calculations work directly at, or very close to, the physical quark masses. This either removes entirely, or greatly reduces, the uncertainties in the extrapolation, such that this error is subdominant.

17.1.6.4. *Operator matching:*

Many of the quantities that LQCD can precisely calculate involve hadronic matrix elements of operators from the electroweak Hamiltonian. Examples include the pion and kaon decay constants, semileptonic form factors and the kaon mixing parameter B_K (the latter defined in Eq. (17.13)). The operators in the lattice matrix elements are defined in the lattice regularization scheme. To be used in tests of the Standard Model, however, they must be matched to the continuum regularization scheme in which the corresponding Wilson coefficients have been calculated. The only case in which such matching is not needed is if the operator is a conserved or partially conserved current. Similar matching is also needed for the conversion of lattice bare quark masses to those in the continuum $\overline{\rm MS}$ scheme.

Several methods are used to calculate the matching factors: perturbation theory (usually to one- or two-loop order), non-perturbative renormalization (NPR) using Landau-gauge quark and gluon external states [57], NPR using gauge-invariant methods based on the Schrödinger functional [58], and NPR using gauge-invariant hadron correlators [59]. The NPR methods replace truncation errors (which can only be approximately estimated) by statistical and systematic errors which can be determined reliably and systematically reduced.

An issue that arises in some of such calculations (e.g. for quark masses and B_K) is that, using NPR with Landau-gauge quark and gluon external states, one ends up with operators regularized in a MOM-like scheme (or a Schrödinger functional scheme), rather than the $\overline{\rm MS}$ scheme mostly used for calculating the Wilson coefficients. To make contact with this scheme requires a purely continuum perturbative matching calculation. The resultant truncation error can, however, be minimized by pushing up the momentum scale at which the matching is done using step-scaling techniques as part of the NPR calculation [60]. It should also be noted that this final step in the conversion to the $\overline{\rm MS}$ scheme could be avoided if continuum calculations used a MOM-like scheme or if one imposes a renormalization condition for quantities which are calculable both in the $\overline{\rm MS}$ scheme and in LQCD, such as the hadron correlators at short distances (see, e.g., Ref. 61).

17.2. Methods and status

Once the lattice action is chosen, it is straightforward to define the quantum theory using the path integral formulation. The Euclidean-space partition function is

$$Z = \int [dU] \prod_f [dq_f][d\bar{q}_f] e^{-S_g[U] - \sum_f \bar{q}_f (D[U]+m_f) q_f} , \qquad (17.4)$$

where link variables are integrated over the SU(3) manifold, q_f and $\bar{q}_f$ are Grassmann (anticommuting) quark and antiquark fields of flavor f, and $D[U]$ is the chosen lattice Dirac operator with m_f the quark mass in lattice units. Integrating out the quark and antiquark fields, one arrives at a form suitable for simulation:

$$Z = \int [dU] e^{-S_g[U]} \prod_f \det(D[U] + m_f) . \qquad (17.5)$$

The building blocks for calculations are expectation values of multi-local gauge-invariant operators, also known as "correlation functions",

$$\langle \mathcal{O}(U,q,\bar{q}) \rangle = (1/Z) \int [dU] \prod_f [dq_f][d\bar{q}_f] \mathcal{O}(U,q,\bar{q}) e^{-S_g[U] - \sum_f \bar{q}_f (D[U]+m_f) q_f} . \qquad (17.6)$$

If the operators depend on the (anti-)quark fields q_f and $\bar{q}_f$, then integrating these fields out leads not only to the fermion determinant but also, through Wick's theorem, to a series of quark "propagators", $(D[U]+m_f)^{-1}$, connecting the positions of the fields.

This set-up allows one to choose, by hand, the masses of the quarks in the determinant (the sea quarks) differently from those in the propagators (valence quarks). This is called "partial quenching", and is used by some calculations as a way of obtaining more data points from which to extrapolate both sea and valence quarks to their physical values.

17.2.1. ***Monte-Carlo method*** :

Since the number of integration variables U is huge ($N_s^3 \times N_t \times 4 \times 9$), direct numerical integration is impractical and one has to use Monte-Carlo techniques. In this method, one generates a Markov chain of gauge configurations (a "configuration" being the set of U's on all links) distributed according to the probability measure $[dU] e^{-S_g[U]} \prod_f \det(D[U]+m_f)$. Once the configurations are generated, expectation values $\langle \mathcal{O}(U,q,\bar{q}) \rangle$ are calculated by averaging over those configurations. In this way the configurations can be used repeatedly for many different calculations, and there are several large collections of ensembles of configurations (with a range of values of a, lattice sizes and quark masses) that are publicly available through the International Lattice Data Grid (ILDG). As the number of the configurations, N, is increased, the error decreases as $1/\sqrt{N}$.

The most challenging part of the generation of gauge configurations is the need to include the fermion determinant. Direct evaluation of the determinant is not feasible, as it requires $\mathcal{O}((N_s^3 \times N_t)^3)$ computations. Instead, one rewrites it in terms of "pseudofermion" fields ϕ (auxiliary fermion fields with bosonic statistics). For example, for two degenerate quarks one has

$$\det(D[U]+m_f)^2 = \int [d\phi] e^{-\phi^\dagger (D[U]+m_f)^{-2} \phi} . \qquad (17.7)$$

By treating the pseudofermions as additional integration variables in the path integral, one obtains a totally bosonic representation. The price one pays is that the pseudofermion effective action is highly non-local since it includes the inverse Dirac operator $(D[U]+m_f)^{-1}$. Thus, the large sparse matrix $(D[U]+m)$ has to be inverted every time one needs an evaluation of the effective action.

Present simulations generate gauge configurations using the Hybrid Monte Carlo (HMC) algorithm [62], or variants thereof. This algorithm combines molecular dynamics (MD) evolution in a fictitious time (which is also discretized) with a Metropolis "accept-reject" step. It makes a global update of the configuration, and is made exact by the Metropolis step. In its original form it can be used only for two degenerate flavors, but extensions (particularly the rational HMC [63]) are available for single flavors. Considerable speed-up of the algorithms has been achieved over the last two decades using a variety of techniques.

All these algorithms spend the bulk of their computational time on the repeated inversion of $(D[U]+m)$ acting on a source (which is required at every step of the MD evolution). Inversions are done using a variety of iterative algorithms, *e.g.* the conjugate gradient algorithm. In this class of algorithms, computational cost is proportional to the condition number of the matrix, which is the ratio of maximum and minimum eigenvalues. For $(D[U]+m)$ the smallest eigenvalue is $\approx m$, so the condition number and cost are inversely proportional to the quark mass. This is a major reason why simulations at the physical quark mass are challenging. Recent algorithmic improvements have significantly reduced this problem.

A practical concern is the inevitable presence of correlations between configurations in the Markov chain. These are characterized by an autocorrelation length in the fictitious MD time. One aims to use configurations separated in MD time by greater than this autocorrelation length. In practice, it is difficult to measure this length accurately, and this leads to some uncertainty in the resulting statistical errors, as well as the possibility of insufficient equilibration.

For most of the applications of LQCD discussed in this review, the cost of generating gauge configurations is larger than or similar to that of performing the "measurements" on those configurations. The computational cost of gauge generation grows with the lattice volume, $V_{\rm lat} = N_s^3 N_t$, as $V_{\rm lat}^{1+\delta}$. Here $\delta = 1/4$ for the HMC algorithm [64] and can be reduced slightly using modern variants. Such growth with $V_{\rm lat}$ provides a (time-dependent) limit on the largest lattice volumes that can be simulated. At present, the largest lattices being used have $N_s = 144$ and $N_t = 288$. Typically one aims to create an ensemble of $\sim 10^3$ statistically independent configurations at each choice of parameters (a, m_q and $V_{\rm lat}$). For most physical quantities of interest, this is sufficient to make the resulting statistical errors smaller than or comparable to the systematic errors.

17.2.2. *Two-point functions* :

One can extract properties of stable hadrons using two-point correlation functions, $\langle O_X(x) O_Y^\dagger(0)\rangle$. Here $O_{X,Y}(x)$ are operators that have non-zero overlaps with the hadronic state of interest $|H\rangle$, *i.e.* $\langle 0|O_{X,Y}(x)|H\rangle \neq 0$. One usually Fourier-transforms in the spatial directions and considers correlators as a function of Euclidean time:

$$C_{XY}(t;\vec{p}) = \sum_{\vec{x}} \langle O_X(t,\vec{x}) O_Y^\dagger(0)\rangle e^{-i\vec{p}\cdot\vec{x}}. \tag{17.8}$$

(Here and throughout this section all quantities are expressed in dimensionless lattice units, so that, for example, $\vec{p} = a\vec{p}_{\rm phys}$.) By inserting a complete set of states having spatial momentum $\vec{p}$, the two-point function can be written as

$$C_{XY}(t;\vec{p}) = \sum_{i=0}^{\infty} \frac{1}{2E_i(\vec{p})} \langle 0|O_X(0)|H_i(\vec{p})\rangle\langle H_i(\vec{p})|O_Y^\dagger(0)|0\rangle e^{-E_i(\vec{p})t}, \tag{17.9}$$

where the energy of the i-th state $E_i(\vec{p})$ appears as an eigenvalue of the time evolution operator e^{-Ht} in the Euclidean time direction. The factor of $1/[2E_i(\vec{p})]$ is due to the relativistic normalization used for the states. For large enough t, the dominant contribution is that of the lowest energy state $|H_0(\vec{p})\rangle$:

$$C_{XY}(t) \overset{t\to\infty}{\longrightarrow} \frac{1}{2E_0(\vec{p})} \langle 0|O_X(0)|H_0(\vec{p})\rangle\langle H_0(\vec{p})|O_Y^\dagger(0)|0\rangle e^{-E_0(\vec{p})t}\,. \tag{17.10}$$

One can thus obtain the energy $E_0(\vec{p})$, which equals the hadron mass m_H when $\vec{p} = 0$, and the product of matrix elements $\langle 0|O_X(0)|H_i(\vec{p})\rangle\langle H_i(\vec{p})|O_Y^\dagger(0)|0\rangle$.

This method can be used to determine the masses of all the stable mesons and baryons by making appropriate choices of operators. For example, if one uses the axial current, $O_X = O_Y = A_\mu = \bar{d}\gamma_\mu\gamma_5 u$, then one can determine m_{π^+} from the rate of exponential fall-off, and in addition the decay constant f_π from the coefficient of the exponential. A complication arises for states with high spins ($j \geq 4$ for bosons) because the spatial rotation group on the lattice is a discrete subgroup of the continuum group SO(3). This implies that lattice operators, even when chosen to lie in irreducible representations of the lattice rotation group, have overlap with states that have a number of values of j in the continuum limit [65]. For example $j = 0$ operators can also create mesons with $j = 4$. Methods to overcome this problem in practice are available [66,67] and have been used successfully.

The expression given above for the correlator $C_{XY}(t;\vec{p})$ shows how, in principle, one can determine the energies of the excited hadron states having the same quantum numbers as the operators $O_{X,Y}$, by fitting the correlation function to a sum of exponentials. In practice, this usually requires using a large basis of operators and adopting the variational approach such as that of Ref. 68. One can also use an anisotropic lattice in which a_t, the lattice spacing in the time direction, is smaller than its spatial counterpart a_s. This allows better separation of the different exponentials. Using a combination of these and other technical improvements extensive excited-state spectra have recently been obtained [67,69–71].

17.2.3. *Three-point functions* :

Hadronic matrix elements needed to calculate semileptonic form factors and neutral meson mixing amplitudes can be computed from three-point correlation functions. We discuss here, as a representative example, the $D \to K$ amplitude. As in the case of two-point correlation functions one constructs operators O_D and O_K having overlap, respectively, with the D and K mesons. We are interested in calculating the matrix element $\langle K|V_\mu|D\rangle$, with $V_\mu = \bar{c}\gamma_\mu s$ the vector current. To obtain this, we use the three-point correlator

$$C_{KV_\mu D}(t_x, t_y; \vec{p}) = \sum_{\vec{x},\vec{y}} \langle O_K(t_x,\vec{x}) V_\mu(0) O_D^\dagger(t_y,\vec{y})\rangle e^{-i\vec{p}\cdot\vec{x}}\,, \tag{17.11}$$

and focus on the limit $t_x \to \infty$, $t_y \to -\infty$. In this example we set the D-meson at rest while the kaon carries three-momentum $\vec{p}$. Momentum conservation then implies that the weak operator V_μ inserts three-momentum $-\vec{p}$. Inserting a pair of complete sets of states between each pair of operators, we find

$$C_{KV_\mu D}(t_x, t_y; \vec{p}) = \sum_{i,j} \frac{1}{2m_{D_i} 2E_{K_j}(\vec{p})} e^{-m_{D_i}t_x - E_{K_j}(\vec{p})|t_y|} \times$$

$$\langle 0|O_K(t_x,\vec{x})|K_i(\vec{p})\rangle\langle K_i(\vec{p})|V_\mu(0)|D_j(\vec{0})\rangle\langle D_j(\vec{0})|O_D^\dagger(0)|0\rangle. \tag{17.12}$$

The matrix element $\langle K_i(\vec{p})|V_\mu(0)|D_j(\vec{0})\rangle$ can then be extracted, since all other quantities in this expression can be obtained from two-point correlation functions. Typically one is interested in the weak matrix elements of ground states, such as the lightest pseudoscalar mesons. In the limit of large separation between the three operators in Euclidean time, the three-point correlation function yields the weak matrix element of the transition between ground states.

17.2.4. *Scattering amplitudes and resonances* :

The methods described thus far yield matrix elements involving single, stable particles (where by stable we mean here absolutely stable to strong interaction decays). Most of the particles listed in the Review of Particle Properties are, however, unstable—they are resonances decaying into final states consisting of multiple strongly interacting particles. LQCD simulations cannot directly calculate resonance properties, but methods have been developed to do so indirectly for resonances coupled to two-particle final states in the elastic regime, starting from the seminal work of Lüscher [72].

The difficulty faced by LQCD calculations is that, to obtain resonance properties, or, more generally, scattering phase-shifts, one must calculate multiparticle scattering amplitudes in momentum space and put the external particles on their mass-shells. This requires

analytically continuing from Euclidean to Minkowski momenta. Although it is straightforward in LQCD to generalize the methods described above to calculate four- and higher-point correlation functions, one necessarily obtains them at a discrete and finite set of Euclidean momenta. Analytic continuation to $p_E^2 = -m^2$ is then an ill-posed and numerically unstable problem. The same problem arises for single-particle states, but can be largely overcome by picking out the exponential fall-off of the Euclidean correlator, as described above. With a multi-particle state, however, there is no corresponding trick, except for two particles at threshold [73].

What LQCD can calculate are the energies of the eigenstates of the QCD Hamiltonian in a finite box. The energies of states containing two stable particles, e.g. two pions, clearly depend on the interactions between the particles. It is possible to invert this dependence and, with plausible assumptions, determine the scattering phase-shifts at a discrete set of momenta from a calculation of the two-particle energy levels for a variety of spatial volumes [72]. This is a challenging calculation, but it has recently been carried through in several channels with quark masses approaching physical values. Channels studied include $\pi\pi$ (for $I = 2$, 1 and 0), $\bar{K}K$, $K\pi$, KD, DD^* and $B\pi$. For a recent comprehensive review see [74]. Extensions to nucleon interactions are also being actively studied [75]. The generalization of the formalism to the case of three particles is under active consideration [76].

It is also possible to extend the methodology to calculate electroweak decay amplitudes to two particles below the inelastic threshold, e.g. $\Gamma(K \to \pi\pi)$ [77]. Results for both the $\Delta I = 3/2$ and $1/2$ amplitudes with physical quark masses have been obtained [78], the former now including a controlled continuum limit [79]. First results for the CP-violating quantity ϵ' have been obtained [80].

Partial extensions of the formalism above the elastic threshold have been worked out, in particular for the case of multiple two-particle channels [81]. Another theoretical extension is to allow the calculation of form factors between a stable particle and a resonance [82], and between two resonances [83]. The former has been used to calculate the $\gamma\pi \to \rho$ amplitude, albeit for unphysically large quark masses [84].

While a systematic extension to decays with many multiparticle channels, e.g. hadronic B decays, has, however, yet to be formulated, some interesting new ideas have been recently proposed [85].

17.2.5. ***Recent advances*** : In some physics applications, one is interested in the two-point correlation function $\langle O_X(x) O_Y^\dagger(0)\rangle$ for all values of the separation x, not just its asymptotic form for large separations (which is used to determine the hadron spectrum as sketched above). A topical example is the hadronic vacuum polarization function $\Pi_{\mu\nu}(x) = \langle V_\mu(x) V_\nu(0)\rangle$ and its Fourier transform $\Pi_{\mu\nu}(q^2)$. Since the lattice is in Euclidean space-time, only space-like momenta, $q^2 = -Q^2 < 0$, are accessible. Nevertheless, this quantity is of significant interest. It is related by a dispersion relation to the cross section for $e^+e^- \to$ hadrons, and is needed for a first-principles calculation of the "hadronic vacuum polarization" contribution to the muon anomalous magnetic moment a_μ. This is the contribution with the largest theoretical uncertainty at present. There are a number of lattice calculations of this contribution (see, e.g., Refs. 86–95 following the pioneering work Ref. 96). Since the relevant scale is set by the muon mass m_μ, this quantity is most sensitive to the low-energy region $Q^2 \simeq m_\mu^2$ of $\Pi_{\mu\nu}(-Q^2)$, where the long-range contribution of multibody states become relevant. The lattice calculation is challenging because of this and also because the necessary precision is high (below 1%). Many systematic effects must be carefully studied and controlled in order to achieve this precision, including finite volume errors and QED corrections.

Calculations of the light-by-light scattering contribution to a_μ are also underway. These involve the calculations of four-point correlation functions with various external momenta. Clever ways to sum over them to evaluate the contribution to a_μ are developed and first results have been reported [97–99]. Another approach to the light-by-light scattering is to decompose the amplitude to components using ChPT or phenomenological models, and to calculate the components in LQCD. Calculations of the $\pi \to \gamma^*\gamma^*$ amplitudes follow similar directions [100,101].

There are other processes for which lattice calculation can make significant contribution to establish quantitative understanding. One example is the long-distance contribution to the neutral kaon mass splitting, ΔM_K. This also requires the evaluation of a four-point function, constructed from the two-point functions described above by the insertion of two electroweak Hamiltonians [102]. Rare kaon decays $K \to \pi\ell^+\ell^-$ and $K \to \pi\nu\bar{\nu}$ are also important processes for which first lattice studies have recently appeared [103–105].

17.2.6. ***Status of LQCD simulations*** :

Until the 1990s, most large-scale lattice simulations were limited to the "quenched" approximation, wherein the fermion determinant is omitted from the path integral. While much of the basic methodology was developed in this era, the results obtained had uncontrolled systematic errors and were not suitable for use in placing precision constraints on the Standard Model. During the 1990s, more extensive simulations including the fermion determinant (also known as simulations with "dynamical" fermions) were begun, but with unphysically heavy quark masses ($m_\ell \sim 50 - 100$ MeV), such that the extrapolation to the physical light quark masses was a source of large systematic errors [106]. During the 2000s, advances in both algorithms and computers allowed simulations to reach much smaller quark masses ($m_\ell \sim 10 - 20$ MeV) such that LQCD calculations of selected quantities with all sources of error controlled and small became available. Their results played an important role in constraints on the CKM matrix and other phenomenological analyses. In the last few years, simulations directly at the physical isospin-symmetric light quark masses have become standard, removing the need for a chiral extrapolation and thus significantly reducing the overall error. The present frontier, as noted above, is the inclusion of isospin breaking. This will be needed to push the accuracy of calculations below the percent level.

On a more qualitative level, analytic and numerical results from LQCD have demonstrated that QCD confines color and spontaneously breaks chiral symmetry. Confinement can be seen as a linearly rising potential between heavy quark and anti-quark in the absence of quark loops. Analytically, this can be shown in the strong coupling limit $g_{\rm lat} \to \infty$ [1]. At weaker couplings there are precise numerical calculations of the potential that clearly show that this behavior persists in the continuum limit [107–109].

Chiral symmetry breaking was also demonstrated in the strong coupling limit on the lattice [16,110], and there have been a number of numerical studies showing that this holds also in the continuum limit. The accumulation of low-lying modes of the Dirac operator, which is the analog of Cooper pair condensation in superconductors, has been observed, yielding a determination of the chiral condensate [111–115]. Many relations among physical quantities that can be derived under the assumption of broken chiral symmetry have been confirmed by a number of lattice groups [41].

17.3. Physics applications

In this section we describe the main applications of LQCD that are both computationally mature and relevant for the determination of particle properties.

A general feature to keep in mind is that, since there are many different choices for lattice actions, all of which lead to the same continuum theory, a crucial test is that results for any given quantity are consistent. In many cases, different lattice calculations are completely independent and often have very different systematic errors. Thus final agreement, if found, is a highly non-trivial check, just as it is for different experimental measurements.

The number, variety and precision of the calculations has progressed to the point that an international "Flavour Lattice Averaging Group" (FLAG) has been formed. The main aims of FLAG include collecting all lattice results of relevance for a variety of phenomenologically interesting quantities and providing averages of those results which pass appropriate quality criteria. The averages attempt to account for possible correlations between results (which can arise, for example,

if they use common gauge configurations). The quantities considered are those we discuss in this section, with the exception of the hadron spectrum. The most recent FLAG review is from 2016 [41]. The interested reader can consult this review for very extensive discussions of the details of the calculations and of the sources of systematic errors.

We stress that the results we quote below are those obtained using the physical complement of light quarks (i.e. $N_f = 2+1$ or $2+1+1$ simulations).

17.3.1. ***Spectrum*** :

The most basic prediction of LQCD is of the hadron spectrum. Once the input parameters are fixed as described in Sec. 17.1.5, the masses or resonance parameters of all other states can be predicted. This includes hadrons composed of light (u, d and s) quarks, as well as heavy-light and heavy-heavy hadrons. It also includes quark-model exotics (e.g. $J^{PC} = 1^{-+}$ mesons) and glueballs. Thus, in principle, LQCD calculations should be able to reproduce many of the experimental results compiled in the Review of Particle Properties. Doing so would test both that the error budgets of LQCD calculations are accurate and that QCD indeed describes the strong interactions in the low-energy domain. The importance of the latter test can hardly be overstated.

What is the status of this fundamental test? As discussed in Sec. 1.2, LQCD calculations are most straightforward for stable, low-lying hadrons. Calculations of the properties of resonances that can decay into only two particles are more challenging, though substantial progress has been made. First theoretical work on decays to more than two particles has begun, but the methodology is not yet practical. It is also more technically challenging to calculate masses of flavor singlet states (which can annihilate into purely gluonic intermediate states) than those of flavor non-singlets, although again algorithmic and computational advances have begun to make such calculations accessible, although not yet for physical quark masses. The present status for light hadrons is that fully controlled results are available for the masses of the octet light baryons, while results with less than complete control are available for the decuplet baryon resonances, the vector meson resonances and the η and η'. In addition, it has been possible to calculate the isospin splitting in light mesons and baryons (due to the up-down mass difference and the incorporation of QED) [40]. There are also extensive results for heavy-light (D and B systems) and heavy-heavy (J/ψ and Υ systems). All present results, which are discussed in the "Quark Model" review, are consistent with experimental values, and several predictions have been made. For a recent extensive review of lattice results see Ref. 116.

17.3.2. ***Decay constants and bag parameters*** :

The pseudoscalar decay constants can be determined from two-point correlation functions involving the axial-vector current, as discussed in Sec. 17.2.2. The decay constant f_P of a meson P is extracted from the weak matrix element involving the axial-vector current using the relation $\langle 0|A_\mu(x)|P(\vec{p})\rangle = f_P p_\mu \exp(-ip\cdot x)$, where p_μ is the momentum of P and $A_\mu(x)$ is the axial-vector current. Since they are among the simplest quantities to calculate, decay constants provide good benchmarks for lattice methods, in addition to being important inputs for flavor physics phenomenology in their own right. Results from many lattice groups for the pion and kaon decay constants now have errors at the percent level or better. The decay constants in the charm and bottom sectors, f_D, f_{D_s}, f_B, and f_{B_s}, have also been calculated to high precision. Lattice results for all of these decay constants are discussed in detail in the review "Leptonic Decays of Charged Pseudoscalar Mesons."

Another important lattice quantity is the kaon bag parameter, B_K, which is needed to turn the precise measurement of CP-violation in kaon mixing into a constraint on the Standard Model. It is defined by

$$\frac{8}{3} m_K^2 f_K^2 B_K(\mu) = \langle \overline{K}^0 | Q_{\Delta S=2}(\mu) | K^0 \rangle, \qquad (17.13)$$

where m_K is the kaon mass, f_K is the kaon decay constant, $Q_{\Delta S=2} = \overline{s}\gamma_\mu(1-\gamma_5)d\,\overline{s}\gamma_\mu(1-\gamma_5)d$ is the four-quark operator of the effective electroweak Hamiltonian and μ is the renormalization scale. The short distance contribution to the electroweak Hamiltonian can be calculated perturbatively, but the hadronic matrix element parameterized by B_K must be computed using non-perturbative methods. In order to be of use to phenomenology, the renormalization factor of the four-quark operator must be matched to a continuum renormalization scheme, e.g. to $\overline{\rm MS}$, as described in Sec. 17.1.6.4. Determinations with percent-level precision using different fermion actions and $N_f = 2+1$ light sea quarks are now available using DWF [117], staggered fermions [118], DWF valence on staggered sea quarks [119], and Wilson fermions [12]. The results are all consistent, and the present FLAG average is $\hat{B}_K = 0.763(10)$ [41].

The bag parameters for B and B_s meson mixing are defined analogously to that for kaon mixing. The B and B_s mesons contain a valence b-quark so that calculations of these quantities must use one of the methods for heavy quarks described above. Calculations with $N_f = 2+1$ light fermions have been done using NRQCD [120], the Fermilab formalism [49], and static heavy quarks [121]. All results are consistent. The FLAG averages for the quantities relevant for B_s and B mixing are $f_{B_s}\sqrt{B_{B_s}} = 274(8)$ MeV and $f_B\sqrt{B_B} = 225(9)$ MeV, with their ratio (which is somewhat better determined) being $\xi = 1.206(7)$ (quoted from the 2017 web update of Ref. 41). Note that the errors for quantities involving b quarks are larger than those for quantities involving only light quarks, although the difference has decreased over the last two years.

For the K, D and B systems, one can also consider the matrix elements of four-fermion operators that arise in beyond-the-standard-model (BSM) theories, which can have a different chiral structure. Knowledge of these matrix elements allows one to constrain the parameters of the BSM theories, and is complementary to direct searches at the LHC. Reliable results are now available from lattice calculations, and are reviewed by FLAG in the case of kaon mixing [41]. Complete results for D and B mixing are presented in Ref. 122 and Ref. 49, respectively.

The results for mixing matrix elements are used in the reviews "The CKM Quark-Mixing Matrix," and "$B_0 - \bar{B}_0$ Mixing."

17.3.3. ***Form factors ($K \to \pi\ell\nu$, $D \to K\ell\nu$, $B \to \pi\ell\nu$, $B \to D^{(*)}\ell\nu$)*** :

Semileptonic decay rates can be used to extract CKM matrix elements once the semileptonic form factors are known from lattice calculations. For example, the matrix element of a pseudoscalar meson P undergoing semileptonic decay to another pseudoscalar meson D is mediated by the vector current, and can be written in terms of form factors as

$$\langle D(p_D)|V_\mu|P(p_P)\rangle = f_+(q^2)(p_D + p_P - \Delta)_\mu + f_0(q^2)\Delta_\mu\,, \qquad (17.14)$$

where $q = p_D - p_P$, $\Delta_\mu = (m_D^2 - m_P^2)q_\mu/q^2$ and V_μ is the quark vector current. The shape of the form factor is typically well determined by experiment, and the value of $f_+(q^2)$ at some reference value of q^2 is needed from the lattice in order to extract CKM matrix elements. Typically $f_+(q^2)$ dominates the decay rate, since the contribution from $f_0(q^2)$ is suppressed when the final state lepton is light.

The form factor $f_+(0)$ for $K \to \pi\ell\nu$ decays is highly constrained by the Ademollo-Gatto theorem [123] and chiral symmetry. Old estimates using chiral perturbation theory combined with quark models quote sub-percent precision [124], though they suffer from some model dependence. Utilizing the constraint from the vector current conservation that $f_+(0)$ is normalized to unity in the limit of degenerate up and strange quark masses, the lattice calculation can be made very precise and has now matched the precision of the phenomenological estimates [125–132]. The present FLAG average (from $N_f = 2+1$ simulations) is $f_+(0) = 0.968(3)$ [41].

Charm meson semileptonic decays have been calculated by different groups using methods similar to those used for charm decay constants, and results are steadily improving in precision [133,134]. For semileptonic decays involving a bottom quark, one uses HQET or NRQCD to control the discretization errors of the bottom quark. The form factors for the semileptonic decay $B \to \pi\ell\nu$ have been calculated in unquenched lattice QCD by a number of groups [135–138]. These B semileptonic form factors are difficult to calculate at low q^2,

i.e. when the mass of the B-meson must be balanced by a large pion momentum, in order to transfer a small momentum to the lepton pair. The low q^2 region has large discretization errors and very large statistical errors, while the high q^2 region is much more accessible to the lattice. For experiment, the opposite is true. To combine lattice and experimental results it has proved helpful to use the z-parameter expansion [139]. This provides a theoretically constrained parameterization of the entire q^2 range, and allows one to obtain $|V_{ub}|$ without model dependence [140,141].

The semileptonic decays $B \to D\ell\nu$ and $B \to D^*\ell\nu$ can be used to extract $|V_{cb}|$ once the corresponding form factors are known. At present only one unquenched calculation exists for the $B \to D^*\ell\nu$ form factor, where the Fermilab formulation of the heavy quark was adopted [142,143]. This calculation is done at zero-recoil because that is where the lattice systematic errors are smallest. Calculations at non-zero recoil in unquenched lattice QCD have been done for the form factors needed to extract $|V_{cb}|$ from $B \to D\ell\nu$ decays [144,145]. Semileptonic decays of the Λ_b baryon can also be used to constrain $|V_{cb}|$ and $|V_{ub}|$ using lattice calculations of the relevant form factors [146].

The rare decays $B \to K^{(*)}\ell^+\ell^-$ involve matrix elements similar to those needed for semileptonic decays, Eq. (17.14), except that the vector current V_μ is replaced by the operators $\bar{s}\gamma^\mu(1-\gamma_5)b$ or $\bar{s}\sigma^{\mu\nu}(1+\gamma_5)b$. Lattice calculations of the corresponding form factors involve similar techniques to those for the semileptonic form factors. The values of q^2 for which lattice calculations can be done are limited as for B semileptonic decays, and, in addition, the region of $c\bar{c}$ resonances has to be avoided. Recent lattice calculations [147–149] have been used to constrain the standard model and new physics contributions.

The results discussed in this section are used in the reviews "The CKM Quark-Mixing Matrix," "V_{ud}, V_{us}, the Cabibbo Angle and CKM Unitarity," and "V_{cb} and V_{ub} CKM Matrix Elements."

17.3.4. *Strong coupling constant* :

As explained in Sec. 17.1.5.1, for a given lattice action, the choice of bare lattice coupling constant, $g_{\rm lat}$, determines the lattice spacing a. If one then calculates a as described in Sec. 17.1.5.1, one knows the strong coupling constant in the bare lattice scheme at the scale $1/a$, $\alpha_{\rm lat} = g^2_{\rm lat}/(4\pi)$. This is not, however, useful for comparing to results for α_s obtained from other inputs, such as deep inelastic scattering or jet shape variables. This is because the latter results give α_s in the $\overline{\rm MS}$ scheme, which is commonly used in such analyses, and the conversion factor between these two schemes is known to converge extremely poorly in perturbation theory. Instead one must use a method which directly determines α_s on the lattice in a scheme closer to $\overline{\rm MS}$.

Several such methods have been used, all following a similar strategy. One calculates a short-distance quantity K both perturbatively ($K^{\rm PT}$) and non-perturbatively ($K^{\rm NP}$) on the lattice, and requires equality: $K^{\rm NP} = K^{\rm PT} = \sum_{i=0}^{n} c_i \alpha_s^i$. Solving this equation one obtains α_s at a scale related to the quantity being used. Often, α_s thus obtained is not defined in the conventional $\overline{\rm MS}$ scheme, and one has to convert among the different schemes using perturbation theory. Unlike for the bare lattice scheme, the required conversion factors are reasonably convergent. As a final step, one uses the renormalization group to run the resulting coupling to a canonical scale (such as M_Z).

In the work of the HPQCD collaboration [150], the short-distance quantities are Wilson loops of several sizes and their ratios. These quantities are perturbatively calculated to $\mathcal{O}(\alpha_s^3)$ using the V-scheme defined through the heavy quark potential. The coefficients of even higher orders are estimated using the data at various values of a. In addition, this work obtains a result for α_s by matching with $\alpha_{\rm lat}$ in a tadpole-improved scheme that improves convergence.

Another choice of short-distance quantities is to use current-current correlators. Appropriate moments of these correlators are ultraviolet finite, and by matching lattice results to the *continuum* perturbative predictions, one can directly extract the $\overline{\rm MS}$ coupling. The method can be applied for light meson correlators [151,152] as well as heavy meson correlators [153–157]. Yet another choice of short-distance quantity is the static-quark potential, where the lattice result for the potential is compared to perturbative calculations; this method was used to compute α_s within 2+1 flavor QCD [158–160]. There is also a determination of α_s from a comparison of lattice data for the ghost-gluon coupling with that of perturbation theory [161].

With a definition of α_s given using the Schrödinger functional, one can non-perturbatively control the evolution of α_s to high-energy scales, such as 100 GeV, where the perturbative expansion converges very well. This method developed by the ALPHA collaboration [60] has been applied to 2+1-flavor QCD in Refs. 162–164.

The various lattice methods for calculating α_s have significantly different sources of systematic error. Thus the good agreement between the approaches (which can be seen in the "Quantum Chromodynamics" review) provides a strong check on the final result.

17.3.5. *Quark masses* :

Once the quark mass parameters are tuned in the lattice action, the remaining task is to convert them to those of the conventional definition. Since the quarks do not appear as asymptotic states due to confinement, the pole mass of the quark propagator is not a physical quantity. Instead, one defines the quark mass after subtracting the ultra-violet divergences in some particular way. The conventional choice is again the $\overline{\rm MS}$ scheme at a canonical scale such as 2 or 3 GeV. Ratios such as m_c/m_s and m_b/m_c are also useful as they are free from multiplicative renormalization (in a mass-independent scheme).

As discussed in Sec. 17.1.6.4, one must convert the lattice bare quark mass to that in the $\overline{\rm MS}$ scheme. Older calculations did so directly using perturbation theory; most recent calculations use an intermediate NPR method (e.g. RI/MOM or RI/SMOM) which is then converted to the $\overline{\rm MS}$ scheme using perturbation theory.

Alternatively, one can use a definition based on the Schrödinger functional, which allows one to evolve the quark mass to a high scale non-perturbatively [165]. In practice, one can reach scales as high as ∼100 GeV, at which matching to the $\overline{\rm MS}$ scheme can be reliably calculated in perturbation theory.

Another approach available for heavy quarks is to match current-current correlators at short distances calculated on the lattice to those obtained in continuum perturbation theory in the $\overline{\rm MS}$ scheme [153–157]. This has allowed an accurate determination of m_c and is also beginning to be used for m_b [154,155].

The ratio method for heavy quarks (discussed earlier) can also be used to determine m_b [166].

Results are summarized in the review of "Quark Masses".

17.3.6. *Other applications* :

In this review we have concentrated on applications of LQCD that are relevant to the quantities discussed in the Review of Particle Properties. We have not discussed at all several other applications that are being actively pursued by simulations. Here we list the major such applications. The reader can consult the aforementioned texts [2–4] for further details, as well as the proceedings of recent lattice conferences [167].

LQCD can be used, in principle, to simulate QCD at non-zero temperature and density, and in particular to study how confinement and chiral-symmetry breaking are lost as T and μ (the chemical potential) are increased. This is of relevance to heavy-ion collisions, the early Universe and neutron-star structure. In practice, finite temperature simulations are computationally tractable and relatively mature, while simulations at finite μ suffer from a "sign problem" and are at a rudimentary stage.

Another topic under active investigation is nucleon structure and inter-nucleon interactions. The simplest nucleon matrix elements are calculable with a precision that is now starting to rival that for some mesonic quantities. Of particular interest are those of the axial current (leading to g_A) and of the scalar density (with $\langle N|\bar{s}s|N\rangle$ needed for dark matter searches).

Finally, we note that there is much recent interest in studying QCD-like theories with more fermions, possibly in other representations of the gauge group. The main interest is to find nearly conformal theories which might be candidates for "walking technicolor" models.

17.4. Outlook

While LQCD calculations have made major strides in the last decade, and are now playing an important role in constraining the Standard Model, there are many calculations that could be done in principle but are not yet mature due to limitations in computational resources. As we move to exascale resources (10^{18} floating point operations per second), the list of mature calculations will grow. Examples that we expect to mature in the next few years are results for excited hadrons, including quark-model exotics, at close to physical light-quark masses; results for moments of structure functions; results for the simplest nucleon matrix elements; $K \to \pi\pi$ amplitudes (allowing a prediction of ϵ'/ϵ from the Standard Model); hadronic vacuum polarization contributions to $g_\mu - 2$, the running of $\alpha_{\rm EM}$ and α_s; $\pi \to \gamma\gamma$ and related amplitudes; long-distance contributions to $\overline{K} \leftrightarrow K$ mixing; the light-by-light contribution to $g_\mu - 2$; and determinations of long distance contributions to rare kaon decays such as $K \to \pi\nu\bar{\nu}$. There will also be steady improvement in the precision attained for the mature quantities discussed above. As already noted, this will ultimately require simulations with $m_u \neq m_d$ and including electromagnetic effects.

References:

1. K.G. Wilson, Phys. Rev. **D10**, 2445 (1974).
2. T. Degrand & C. DeTar, "Lattice Methods for Quantum Chromodynamics," World Scientific (2006).
3. C. Gattringer & C.B. Lang, "Quantum Chromodynamics on the Lattice: An Introductory Presentation," Springer (2009).
4. "Modern Pespectives in Lattice QCD: quantum field theory and high performance computing" (Lecture notes of the Les Houches Summer School, Vol. 93) eds. L. Lellouch *et al.*, Oxford Univ. Press. (Aug. 2011).
5. W. Zimmermann, in "Lectures on Elementary Particles and Quantum Field Theory", ed. S. Deser et al., MIT Press, Cambridge, MA (1971);
   K. Symanzik, Nucl. Phys. **B226**, 187 (1983); Nucl. Phys. **B226**, 205 (1983).
6. M. Lüscher & P. Weisz, Commun. Math. Phys. **97**, 59 (1985).
7. Y. Iwasaki, UT-HEP-118.
8. H.B. Nielsen & M. Ninomiya, Phys. Lett. **B105**, 219 (1981).
9. B. Sheikholeslami & R. Wohlert, Nucl. Phys. **B259**, 572 (1985).
10. K. Jansen *et al.*, Phys. Lett. **B372**, 275 (1996).
11. M. Lüscher, JHEP **0305**, 052 (2003); Comp. Phys. Comm. **156**, 209 (2004) & Comp. Phys. Comm. **165**, 199 (2005);
    M. Hasenbusch, Phys. Lett. **B519**, 177 (2001);
    C. Urbach *et al.*, Comp. Phys. Comm. **174**, 87 (2006).
12. S. Durr *et al.*, Phys. Lett. **B705**, 477 (2011).
13. N. Ishizuka *et al.*, Phys. Rev. **D92**, 074503 (2015).
14. R. Frezzotti *et al.* [Alpha Collab.], JHEP **0108**, 058 (2001).
15. R. Frezzotti & G.C. Rossi, JHEP **0408**, 007 (2004).
16. L. Susskind, Phys. Rev. **D16**, 3031 (1977).
17. M. Golterman, PoS **CONFINEMENT8**, 014 (2008).
18. C. Bernard, Phys. Rev. **D73**, 114503 (2006);
    S.R. Sharpe, PoS LAT **2006**, 022 (2006).
19. G.P. Lepage, Phys. Rev. **D59**, 074502 (1999).
20. A. Bazavov *et al.* [MILC Collab.], Rev. Mod. Phys. **82**, 1349 (2010).
21. E. Follana *et al.* [HPQCD & UKQCD Collabs.], Phys. Rev. **D75**, 054502 (2007).
22. P.H. Ginsparg & K.G. Wilson, Phys. Rev. **D25**, 2649 (1982).
23. P. Hasenfratz *et al.*, Phys. Lett. **B427**, 125 (1998).
24. M. Lüscher, Phys. Lett. **B428**, 342 (1998).
25. D.B. Kaplan, Phys. Lett. **B288**, 342 (1992);
    Y. Shamir, Nucl. Phys. **B406**, 90 (1993);
    Y. Shamir, Nucl. Phys. **B417**, 167 (1994).
26. H. Neuberger, Phys. Lett. **B417**, 141 (1998); Phys. Lett. **B427**, 353 (1998).
27. A. Borici, `hep-lat/9912040`; A.D. Kennedy, `hep-lat/060703`.
28. E. Shintani *et al.* [JLQCD Collab.], Phys. Rev. Lett. **101**, 242001 (2008).
29. A. Bazavov *et al.* [MILC Collab.], Phys. Rev. **D87**, 054505 (2013).
30. R. Baron *et al.* [ETM Collab.], JHEP **1006**, 111 (2010).
31. E. Eichten & B. R. Hill, Phys. Lett. **B234**, 511 (1990).
32. J. Heitger & R. Sommer [ALPHA Collab.], JHEP **0402**, 022 (2004);
    B. Blossier *et al.* [ALPHA Collab.], JHEP **1012**, 039 (2010).
33. B.A. Thacker & G.P. Lepage, Phys. Rev. **D43**, 196 (1991);
    G.P. Lepage *et al.*, Phys. Rev. **D46**, 4052 (1992).
34. A.X. El-Khadra *et al.*, Phys. Rev. **D55**, 3933 (1997).
35. S. Aoki *et al.*, Prog. Theor. Phys. **109**, 383 (2003).
36. N.H. Christ *et al.*, Phys. Rev. **D76**, 074505 (2007).
37. Y. Aoki *et al.* [RBC and UKQCD Collabs.], Phys. Rev. **D86**, 116003 (2012).
38. N.H. Christ *et al.*, Phys. Rev. **D91**, 054502 (2015).
39. B. Blossier *et al.* [ETM Collab.], JHEP **1004**, 049 (2010).
40. S. Borsanyi *et al.*, Science **347**, 1452 (2015).
41. S. Aoki, *et al.*, Eur. Phys. J. **C77**, 112 (2017).
42. R. Horsley *et al.*, J. Phys. G **43**, no. 10, 10LT02 (2016)..
43. S. Aoki *et al.* [PACS-CS Collab.], PTEP **2012**, 01A102 (2012).
44. T. Ishikawa *et al.*, Phys. Rev. Lett. **109**, 072002 (2012).
45. G.M. de Divitiis *et al.* [RM123 Collab.], Phys. Rev. **D87**, 114505 (2013).
46. P. Boyle, V. Gülpers, J. Harrison, A. Jttner, C. Lehner, A. Portelli and C. T. Sachrajda, `arXiv:1706.05293 [hep-lat]`.
47. D. Giusti, V. Lubicz, C. Tarantino, G. Martinelli, S. Sanfilippo, S. Simula and N. Tantalo, Phys. Rev. **D95**, 114504 (2017).
48. M. Bruno *et al.* [ALPHA Collab.], Phys. Rev. Lett. **114**, 102001 (2015).
49. A. Bazavov *et al.* [Fermilab Lattice and MILC Collaborations], Phys. Rev. **D93**, 113016 (2016).
50. E. Follana *et al.* [HPQCD & UKQCD Collabs.], Phys. Rev. Lett. **100**, 062002 (2008);
    C.T.H. Davies *et al.* [HPQCD Collab.] Phys. Rev. **D82**, 114504 (2010).
51. S. Schaefer *et al.* [ALPHA Collab.], Nucl. Phys. **B845**, 93 (2011).
52. M. Lüscher, PoS LATTICE **2010**, 015 (2010);
    S. Schaefer *et al.* [ALPHA Collab.], Nucl. Phys. **B845**, 93 (2011).
53. R. Brower *et al.*, Phys. Lett. **B560**, 64 (2003).
54. S. Aoki *et al.*, Phys. Rev. **D76**, 054508 (2007).
55. G. Colangelo *et al.*, Nucl. Phys. **B721**, 136 (2005).
56. M. Lüscher, Commun. Math. Phys. **104**, 177 (1986).
57. G. Martinelli *et al.*, Nucl. Phys. **B445**, 81 (1995).
58. M. Lüscher *et al.*, Nucl. Phys. **B384**, 168 (1992).
59. G. Martinelli, G. C. Rossi, C. T. Sachrajda, S. R. Sharpe, M. Talevi and M. Testa, Phys. Lett. **B411**, 141 (1997).
60. M. Lüscher *et al.*, Nucl. Phys. **B413**, 481 (1994);
    M. Della Morte *et al.* [ALPHA Collab.], Nucl. Phys. **B713**, 378 (2005).
61. M. Tomii *et al.* [JLQCD Collaboration], Phys. Rev. **D94**, 054504 (2016).
62. S. Duane *et al.*, Phys. Lett. **B195**, 216 (1987).
63. M.A. Clark & A.D. Kennedy, Phys. Rev. Lett. **98**, 051601 (2007).
64. M. Creutz, Phys. Rev. **D38**, 1228 (1988);
    R. Gupta *et al.*, Phys. Rev. **D38**, 1278 (1988).
65. J.E. Mandula *et al.*, Nucl. Phys. **B228**, 91 (1983);
    J.E. Mandula & E. Shpiz, Nucl. Phys. **B232**, 180 (1984).
66. H.B. Meyer & M.J. Teper, Nucl. Phys. **B658**, 113 (2003).
67. J.J. Dudek *et al.*, Phys. Rev. **D82**, 034508 (2010);
    J.J. Dudek *et al.*, Phys. Rev. **D83**, 111502 (2011);
    R.G. Edwards *et al.*, Phys. Rev. **D84**, 074508 (2011).
68. M. Lüscher & U. Wolff, Nucl. Phys. **B339**, 222 (1990).
69. G.P. Engel *et al.* [Bern-Graz-Regensburg Collab.], Phys. Rev. **D82**, 034505 (2010).
70. M.S. Mahbub *et al.*, Ann. Phys. **342**, 270 (2014).
71. J. Bulava, B. Fahy, B. Hrz, K. J. Juge, C. Morningstar and C. H. Wong, Nucl. Phys. **B910**, 842 (2016).
72. M. Lüscher, Commun. Math. Phys. **105**, 153 (1986); Nucl. Phys. **B354**, 531 (1991), and Nucl. Phys. **B364**, 237 (1991).
73. L. Maiani & M. Testa, Phys. Lett. **B245**, 585 (1990).

74. R. A. Briceño, J. J. Dudek and R. D. Young, arXiv:1706.06223 [hep-lat].
75. M.J. Savage, Prog. in Part. Nucl. Phys. **67**, 140 (2012); T. Inoue *et al.* [HAL QCD Collaboration], Phys. Rev. **C91**, 011001 (2015).
76. K. Polejaeva & A. Rusetsky, Eur. Phys. J. **A48**, 67 (2012); R.A. Briceño & Z. Davoudi, Phys. Rev. **D87**, 094507 (2013); M.T. Hansen & S.R. Sharpe, Phys. Rev. **D90**, 116003 (2014); Phys. Rev. **D92**, 114509 (2015); R. A. Briceño, M. T. Hansen and S. R. Sharpe, Phys. Rev. **D95**, 074510 (2017); H.-W. Hammer, J.-Y. Pang and A. Rusetsky, arXiv:1707.02176 [hep-lat].
77. L. Lellouch & M. Lüscher, Commun. Math. Phys. **219**, 31 (2001).
78. T. Blum *et al.*, Phys. Rev. Lett. **108**, 141601 (2012); Phys. Rev. **D86**, 074513 (2012); Z. Bai *et al.*, Phys. Rev. Lett. **115**, 212001 (2015).
79. T. Blum *et al.*, Phys. Rev. **D91**, 074502 (2015).
80. Z. Bai *et al.* [RBC and UKQCD Collaborations], Phys. Rev. Lett. **115**, 212001 (2015).
81. B. Jager *et al.*, JHEP **1101**, 019 (2011); M. Doring *et al.*, Eur. Phys. J. **A47**, 139 (2011); M.T. Hansen & S.R. Sharpe, Phys. Rev. **D86**, 016007 (2012); R.A. Briceño & Z. Davoudi, Phys. Rev. **D88**, 094507 (2013).
82. R.A. Briceño *et al.*, Phys. Rev. **D91**, 034501 (2015).
83. R. A. Briceño and M. T. Hansen, Phys. Rev. **D94**, 013008 (2016).
84. R. A. Briceño *et al.*, Phys. Rev. **D93**, 114508 (2016).
85. D. Agadjanov *et al.*, JHEP **1606**, 043 (2016); M. T. Hansen, H. B. Meyer and D. Robaina, arXiv:1704.08993 [hep-lat]; S. Hashimoto, PTEP **2017**, 053B03 (2017).
86. X. Feng *et al.*, Phys. Rev. Lett. **107**, 081802 (2011).
87. P. Boyle *et al.*, Phys. Rev. **D85**, 074504 (2012).
88. M. Della Morte *et al.*, JHEP **1203**, 055 (2012).
89. F. Burger *et al.* [ETM Collab.], JHEP **1402**, 099 (2014).
90. B. Chakraborty *et al.* [HPQCD Collaboration], Phys. Rev. **D89**, 114501 (2014).
91. F. Burger, K. Jansen, M. Petschlies and G. Pientka, Eur. Phys. J. **C76**, 464 (2016).
92. B. Chakraborty, C. T. H. Davies, J. Koponen, G. P. Lepage, M. J. Peardon and S. M. Ryan, Phys. Rev. **D93**, 074509 (2016).
93. T. Blum *et al.* [RBC/UKQCD Collaboration], JHEP **1604**, 063 (2016).
94. S. Borsanyi *et al.*, arXiv:1612.02364 [hep-lat]..
95. M. Della Morte *et al.*, arXiv:1705.01775 [hep-lat]..
96. T. Blum, Phys. Rev. Lett. **91**, 052001 (2003).
97. T. Blum *et al.*, Phys. Rev. Lett. **114**, 012001 (2015).
98. T. Blum, N. Christ, M. Hayakawa, T. Izubuchi, L. Jin and C. Lehner, Phys. Rev. **D93**, 014503 (2016).
99. J. Green, O. Gryniuk, G. von Hippel, H. B. Meyer and V. Pascalutsa, Phys. Rev. Lett. **115**, 222003 (2015).
100. X. Feng, S. Aoki, H. Fukaya, S. Hashimoto, T. Kaneko, J. i. Noaki and E. Shintani, Phys. Rev. Lett. **109**, 182001 (2012).
101. A. Grardin, H. B. Meyer and A. Nyffeler, Phys. Rev. Lett. **94**, 074507 (2016).
102. Z. Bai *et al.*, Phys. Rev. Lett. **113**, 112003 (2014).
103. N. H. Christ *et al.* [RBC and UKQCD Collaborations], Phys. Rev. **D92**, 094512 (2015).
104. N. H. Christ, X. Feng, A. Juttner, A. Lawson, A. Portelli and C. T. Sachrajda, Phys. Rev. **D94**, 114516 (2016).
105. Z. Bai, N. H. Christ, X. Feng, A. Lawson, A. Portelli and C. T. Sachrajda, Phys. Rev. Lett. **118**, 252001 (2017).
106. C. Bernard *et al.*, Nucl. Phys. (Proc. Supp.) **119**, 170 (2003).
107. S. Perantonis & C. Michael, Nucl. Phys. **B347**, 854 (1990).
108. G.S. Bali & K. Schilling, Phys. Rev. **D46**, 2636 (1992).
109. S. Necco & R. Sommer, Nucl. Phys. **B622**, 328 (2002).
110. J.M. Blairon *et al.*, Nucl. Phys. **B180**, 439 (1981).
111. H. Fukaya *et al.* [JLQCD Collab.], Phys. Rev. Lett. **104**, 122002 (2010); H. Fukaya *et al.* [JLQCD & TWQCD Collabs.], Phys. Rev. **D83**, 074501 (2011).
112. L. Giusti & M. Lüscher, JHEP **0903**, 013 (2009).
113. K. Cichy *et al.*, JHEP **1310**, 175 (2013).
114. G.P. Engel *et al.*, Phys. Rev. Lett. **114**, 112001 (2015).
115. G.P. Engel *et al.*, Phys. Rev. **D91**, 054505 (2015).
116. Z. Fodor & C. Hoelbling, Rev. Mod. Phys. **84**, 449 (2012).
117. T. Blum *et al.* [RBC & UKQCD Collabs.], Phys. Rev. **D93**, 074505 (2016).
118. B. J. Choi *et al.* [SWME Collaboration], Phys. Rev. **D93**, 014511 (2016).
119. J. Laiho & R.S. Van de Water, PoS LATTICE **2011**, 293 (2011).
120. E. Gamiz *et al.* [HPQCD Collab.], Phys. Rev. **D80**, 014503 (2009).
121. Y. Aoki *et al.*, Phys. Rev. **D91**, 114505 (2015).
122. A. Bazavov *et al.* [Fermilab Lattice and MILC Collaborations], arXiv:1706.04622 [hep-lat].
123. M. Ademollo & R. Gatto, Phys. Rev. Lett. **13**, 264 (1964).
124. H. Leutwyler & M. Roos, Z. Phys. **C25**, 91 (1984).
125. P.A. Boyle *et al.*, Phys. Rev. Lett. **100**, 141601 (2008).
126. V. Lubicz *et al.* [ETM Collab.], Phys. Rev. **D80**, 111502 (2009); PoS LATTICE **2010**, 316 (2010).
127. P.A. Boyle *et al.*, Eur. Phys. J. **C69**, 159 (2010).
128. A. Bazavov *et al.* [FNAL/MILC Collabs.] Phys. Rev. **D87**, 073012 (2013).
129. T. Kaneko *et al.* [JLQCD Collab.], PoS LATTICE **2012**, 111 (2012).
130. P.A. Boyle *et al.*, JHEP **1308**, 132 (2013).
131. P.A. Boyle *et al.* [RBC/UKQCD Collab.], JHEP **1506**, 164 (2015).
132. N. Carrasco, P. Lami, V. Lubicz, L. Riggio, S. Simula and C. Tarantino, Phys. Rev. **D93**, 114512 (2016).
133. H. Na *et al.* [HPQCD Collab.], Phys. Rev. **D82**, 114506 (2010).
134. H. Na *et al.* [HPQCD Collab.], Phys. Rev. **D84**, 114505 (2011).
135. E. Dalgic *et al.* [HPQCD Collab.], Phys. Rev. **D73**, 074502 (2006).
136. J.M. Flynn *et al.* [RBC/UKQCD Collabs.], Phys. Rev. **D91**, 074510 (2015).
137. J. A. Bailey *et al.* [Fermilab Lattice and MILC Collaborations], Phys. Rev. **D92**, 014024 (2015).
138. B. Colquhoun, R. J. Dowdall, J. Koponen, C. T. H. Davies and G. P. Lepage, Phys. Rev. **D93**, 034502 (2016).
139. C. Bourrely *et al.*, Nucl. Phys. **B189**, 157 (1981); C.G. Boyd *et al.*, Phys. Rev. Lett. **74**, 4603 (1995); T. Becher & R.J. Hill, Phys. Lett. **B633**, 61 (2006); C. Bourrely *et al.*, Phys. Rev. **D79**, 013008 (2009).
140. M.C. Arnesen *et al.*, Phys. Rev. Lett. **95**, 071802 (2005).
141. J.A. Bailey *et al.*, Phys. Rev. **D79**, 054507 (2009).
142. C. Bernard *et al.*, Phys. Rev. **D79**, 014506 (2009);; J.A. Bailey *et al.* [Fermilab Lattice & MILC Collabs.], PoS **LATTICE2010**, 311 (2010).
143. J.A. Bailey *et al.* [Fermilab Lattice & MILC Collabs.], Phys. Rev. **D89**, 114504 (2014).
144. J. A. Bailey *et al.* [Fermilab Lattice & MILC Collaboration], Phys. Rev. **D92**, 034506 (2015).
145. H. Na, *et al.* [HPQCD Collaboration], Phys. Rev. **D92**, 054510 (2015).
146. W. Detmold, *et al.*, Phys. Rev. **D92**, 034503 (2015).
147. R. R. Horgan, Z. Liu, S. Meinel and M. Wingate, $B \to K^* \ell^+ \ell^-$ and $B_s \to \phi \ell^+ \ell^-$," Phys. Rev. **D89**, 094501 (2014).
148. J. A. Bailey *et al.*, Phys. Rev. **D93**, 025026 (2016).
149. D. Du, A. X. El-Khadra, S. Gottlieb, A. S. Kronfeld, J. Laiho, E. Lunghi, R. S. Van de Water and R. Zhou, lattice QCD," Phys. Rev. **D93**, 034005 (20156).
150. C.T. H. Davies *et al.* [HPQCD Collab.], Phys. Rev. **D78**, 114507 (2008).
151. E. Shintani *et al.*, Phys. Rev. **D82**, 074505 (2010).

152. R. J. Hudspith, R. Lewis, K. Maltman and E. Shintani, Mod. Phys. Lett. **A31**, 1630037 (2016).
153. I. Allison *et al.* [HPQCD Collab.], Phys. Rev. **D78**, 054513 (2008).
154. C. McNeile *et al.* [HPQCD Collab.], Phys. Rev. **D82**, 034512 (2010).
155. B. Chakraborty *et al.*, Phys. Rev. **D91**, 054508 (2015).
156. K. Nakayama, B. Fahy and S. Hashimoto, Phys. Rev. **D94**, 054507 (2016).
157. Y. Maezawa and P. Petreczky, Phys. Rev. **D94**, 034507 (2016).
158. Q. Mason *et al.*[HPQCD & UKQCD Collabs.], Phys. Rev. Lett. **95**, 052002 (2005).
159. A. Bazavov *et al.*, Phys. Rev. **D86**, 114031 (2012).
160. A. Bazavov, N. Brambilla, X. Garcia i Tormo, P. Petreczky, J. Soto and A. Vairo, Phys. Rev. **D90**, 074038 (2014).
161. B. Blossier *et al.*, Phys. Rev. **D85**, 034503 (2012); Phys. Rev. Lett. **108**, 262002 (2012).
162. S. Aoki *et al.* [PACS-CS Collab.], JHEP **0910**, 053 (2009).
163. P. Fritzsch *et al.*, PoS LATTICE **2014**, 291 (2014).
164. M. Bruno *et al.*, arXiv:1706.03821 [hep-lat]..
165. S. Capitani *et al.* [ALPHA Collab.], Nucl. Phys. **B544**, 669 (1999).
166. A. Bussone *et al.* [ETM Collaboration], Phys. Rev. **D93**, 114505 (2016).
167. G. Aarts *et al.* (ed.), PoS Lattice **2016** (2016).

18. Structure Functions

Updated February 2018 by B. Foster (University of Hamburg/DESY/Oxford), R.S. Thorne (University College London) and M.G. Vincter (Carleton University).

18.1. Deep inelastic scattering

High-energy lepton-nucleon scattering (deep inelastic scattering) plays a key role in determining the partonic structure of the proton. The process $\ell N \to \ell' X$ is illustrated in Fig. 18.1. The filled circle in this figure represents the internal structure of the proton which can be expressed in terms of structure functions.

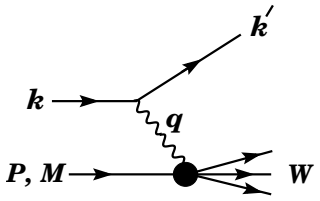

Figure 18.1: Kinematic quantities for the description of deep inelastic scattering. The quantities k and k' are the four-momenta of the incoming and outgoing leptons, P is the four-momentum of a nucleon with mass M, and W is the mass of the recoiling system X. The exchanged particle is a γ, $W^{\pm}$, or Z; it transfers four-momentum $q = k - k'$ to the nucleon.

Invariant quantities:

$\nu = \dfrac{q\cdot P}{M} = E - E'$ is the lepton's energy loss in the nucleon rest frame (in earlier literature sometimes $\nu = q\cdot P$). Here, E and E' are the initial and final lepton energies in the nucleon rest frame.

$Q^2 = -q^2 = 2(EE' - \vec{k}\cdot\vec{k}\,') - m_\ell^2 - m_{\ell'}^2$ where $m_\ell(m_{\ell'})$ is the initial (final) lepton mass. If $EE'\sin^2(\theta/2) \gg m_\ell^2,\, m_{\ell'}^2$, then

$\approx 4EE'\sin^2(\theta/2)$, where θ is the lepton's scattering angle with respect to the lepton beam direction.

$x = \dfrac{Q^2}{2M\nu}$ where, in the parton model, x is the fraction of the nucleon's momentum carried by the struck quark.

$y = \dfrac{q\cdot P}{k\cdot P} = \dfrac{\nu}{E}$ is the fraction of the lepton's energy lost in the nucleon rest frame.

$W^2 = (P+q)^2 = M^2 + 2M\nu - Q^2$ is the mass squared of the system X recoiling against the scattered lepton.

$s = (k+P)^2 = \dfrac{Q^2}{xy} + M^2 + m_\ell^2$ is the center-of-mass energy squared of the lepton-nucleon system.

The process in Fig. 18.1 is called deep ($Q^2 \gg M^2$) inelastic ($W^2 \gg M^2$) scattering (DIS). In what follows, the masses of the initial and scattered leptons, m_ℓ and $m_{\ell'}$, are neglected.

18.1.1. *DIS cross sections* :

The double-differential cross section for deep inelastic scattering can be expressed in terms of kinematic variables in several ways.

$$\frac{d^2\sigma}{dx\,dy} = x\,(s-M^2)\,\frac{d^2\sigma}{dx\,dQ^2} = \frac{2\pi\,M\nu}{E'}\frac{d^2\sigma}{d\Omega_{\rm Nrest}\,dE'}\,. \qquad (18.1)$$

In lowest-order perturbation theory, the cross section for the scattering of polarized leptons on polarized nucleons can be expressed in terms of the products of leptonic and hadronic tensors associated with the coupling of the exchanged bosons at the upper and lower vertices in Fig. 18.1 (see Refs. [1–4])

$$\frac{d^2\sigma}{dxdy} \;=\; \frac{2\pi y\alpha^2}{Q^4}\,\sum_j\,\eta_j\,L_j^{\mu\nu}\,W_{\mu\nu}^j\,. \qquad (18.2)$$

For neutral-current processes, the summation is over $j = \gamma, Z$ and γZ representing photon and Z exchange and the interference between them, whereas for charged-current interactions there is only W exchange, $j = W$. (For transverse nucleon polarization, there is a dependence on the azimuthal angle of the scattered lepton.) The lepton tensor $L_{\mu\nu}$ is associated with the coupling of the exchange boson to the leptons. For incoming leptons of charge $e = \pm 1$ and helicity $\lambda = \pm 1$,

$$\begin{aligned} L_{\mu\nu}^{\gamma} &= 2\left(k_\mu k'_\nu + k'_\mu k_\nu - (k\cdot k' - m_\ell^2)g_{\mu\nu} - i\lambda\varepsilon_{\mu\nu\alpha\beta}k^\alpha k'^\beta\right),\\ L_{\mu\nu}^{\gamma Z} &= (g_V^e + e\lambda g_A^e)\,L_{\mu\nu}^{\gamma}, \qquad L_{\mu\nu}^{Z} = (g_V^e + e\lambda g_A^e)^2\,L_{\mu\nu}^{\gamma},\\ L_{\mu\nu}^{W} &= (1+e\lambda)^2\,L_{\mu\nu}^{\gamma}, \end{aligned} \qquad (18.3)$$

where $g_V^e = -\frac{1}{2} + 2\sin^2\theta_W, \qquad g_A^e = -\frac{1}{2}$.

Although here the helicity formalism is adopted, an alternative approach is to express the tensors in Eq. (18.3) in terms of the polarization of the lepton.

The factors η_j in Eq. (18.2) denote the ratios of the corresponding propagators and couplings to the photon propagator and coupling squared

$$\begin{aligned} \eta_\gamma &= 1 \quad ; \quad \eta_{\gamma Z} = \left(\frac{G_F M_Z^2}{2\sqrt{2}\pi\alpha}\right)\left(\frac{Q^2}{Q^2+M_Z^2}\right);\\ \eta_Z &= \eta_{\gamma Z}^2 \quad ; \quad \eta_W = \tfrac{1}{2}\left(\frac{G_F M_W^2}{4\pi\alpha}\,\frac{Q^2}{Q^2+M_W^2}\right)^2. \end{aligned} \qquad (18.4)$$

The hadronic tensor, which describes the interaction of the appropriate electroweak currents with the target nucleon, is given by

$$W_{\mu\nu} \;=\; \frac{1}{4\pi}\int d^4z\; e^{iq\cdot z}\,\left\langle P,S\left|\left[J_\mu^\dagger(z), J_\nu(0)\right]\right|\,P,S\right\rangle, \qquad (18.5)$$

where S denotes the nucleon-spin 4-vector, with $S^2 = -M^2$ and $S\cdot P = 0$.

18.2. Structure functions of the proton

The structure functions are defined in terms of the hadronic tensor (see Refs. [1–3])

$$\begin{aligned} W_{\mu\nu} = &\left(-g_{\mu\nu} + \frac{q_\mu q_\nu}{q^2}\right)F_1(x,Q^2) + \frac{\hat{P}_\mu\hat{P}_\nu}{P\cdot q}\,F_2(x,Q^2)\\ &- i\varepsilon_{\mu\nu\alpha\beta}\,\frac{q^\alpha P^\beta}{2P\cdot q}\,F_3(x,Q^2)\\ &+ i\varepsilon_{\mu\nu\alpha\beta}\,\frac{q^\alpha}{P\cdot q}\left[S^\beta g_1(x,Q^2) + \left(S^\beta - \frac{S\cdot q}{P\cdot q}\,P^\beta\right)g_2(x,Q^2)\right]\\ &+ \frac{1}{P\cdot q}\left[\tfrac{1}{2}\left(\hat{P}_\mu\hat{S}_\nu + \hat{S}_\mu\hat{P}_\nu\right) - \frac{S\cdot q}{P\cdot q}\,\hat{P}_\mu\hat{P}_\nu\right]g_3(x,Q^2)\\ &+ \frac{S\cdot q}{P\cdot q}\left[\frac{\hat{P}_\mu\hat{P}_\nu}{P\cdot q}\,g_4(x,Q^2) + \left(-g_{\mu\nu} + \frac{q_\mu q_\nu}{q^2}\right)g_5(x,Q^2)\right] \end{aligned} \qquad (18.6)$$

where

$$\hat{P}_\mu \;=\; P_\mu - \frac{P\cdot q}{q^2}\,q_\mu, \qquad \hat{S}_\mu \;=\; S_\mu - \frac{S\cdot q}{q^2}\,q_\mu\,. \qquad (18.7)$$

In [2], the definition of $W_{\mu\nu}$ with $\mu \leftrightarrow \nu$ is adopted, which changes the sign of the $\varepsilon_{\mu\nu\alpha\beta}$ terms in Eq. (18.6), although the formulae given below are unchanged. Ref. [1] tabulates the relation between the structure functions defined in Eq. (18.6) and other choices available in the literature.

The cross sections for neutral- and charged-current deep inelastic scattering on unpolarized nucleons can be written in terms of the structure functions in the generic form

$$\begin{aligned} \frac{d^2\sigma^i}{dxdy} \;=\; &\frac{4\pi\alpha^2}{xyQ^2}\,\eta^i\left\{\left(1 - y - \frac{x^2y^2M^2}{Q^2}\right)F_2^i\right.\\ &\left. + y^2xF_1^i \mp \left(y - \frac{y^2}{2}\right)xF_3^i\right\}, \end{aligned} \qquad (18.8)$$

where i = NC, CC corresponds to neutral-current ($eN \to eX$) or charged-current ($eN \to \nu X$ or $\nu N \to eX$) processes, respectively. For incoming neutrinos, $L^W_{\mu\nu}$ of Eq. (18.3) is still true, but with e, λ corresponding to the outgoing charged lepton. In the last term of Eq. (18.8), the $-$ sign is taken for an incoming e^+ or $\overline{\nu}$ and the $+$ sign for an incoming e^- or ν. The factor $\eta^{\rm NC} = 1$ for unpolarized $e^\pm$ beams, whereas*

$$\eta^{\rm CC} \;=\; (1 \pm \lambda)^2 \eta_W \tag{18.9}$$

with $\pm$ for $\ell^\pm$; and where λ is the helicity of the incoming lepton and η_W is defined in Eq. (18.4); for incoming neutrinos $\eta^{\rm CC} = 4\eta_W$. The CC structure functions, which derive exclusively from W exchange, are

$$F_1^{\rm CC} = F_1^W,\; F_2^{\rm CC} = F_2^W,\; xF_3^{\rm CC} = xF_3^W. \tag{18.10}$$

The NC structure functions $F_2^\gamma, F_2^{\gamma Z}, F_2^Z$ are, for $e^\pm N \to e^\pm X$, given by [5],

$$F_2^{\rm NC} \;=\; F_2^\gamma \;-\; (g_V^e \pm \lambda g_A^e)\eta_{\gamma Z} F_2^{\gamma Z} \;+\; (g_V^{e\,2} + g_A^{e\,2} \pm 2\lambda g_V^e g_A^e)\,\eta_Z F_2^Z \tag{18.11}$$

and similarly for $F_1^{\rm NC}$, whereas

$$xF_3^{\rm NC} = \; -(g_A^e \pm \lambda g_V^e)\eta_{\gamma Z} xF_3^{\gamma Z} + [2g_V^e g_A^e \pm \lambda(g_V^{e\,2} + g_A^{e\,2})]\eta_Z xF_3^Z \;. \tag{18.12}$$

The polarized cross-section difference

$$\Delta\sigma \;=\; \sigma(\lambda_n = -1, \lambda_\ell) \;-\; \sigma(\lambda_n = 1, \lambda_\ell)\;, \tag{18.13}$$

where λ_ℓ, λ_n are the helicities (± 1) of the incoming lepton and nucleon, respectively, may be expressed in terms of the five structure functions $g_{1,\ldots 5}(x, Q^2)$ of Eq. (18.6). Thus,

$$\begin{aligned}\frac{d^2\Delta\sigma^i}{dxdy} \;=\; \frac{8\pi\alpha^2}{xyQ^2}\,\eta^i \Bigg\{ &-\lambda_\ell y\left(2 - y - 2x^2y^2\frac{M^2}{Q^2}\right)\, xg_1^i + \lambda_\ell 4x^3y^2\,\frac{M^2}{Q^2}\,g_2^i \\ &+\; 2x^2y\frac{M^2}{Q^2}\left(1 - y - x^2y^2\frac{M^2}{Q^2}\right)\, g_3^i \\ &-\; \left(1 + 2x^2y\frac{M^2}{Q^2}\right)\left[\left(1 - y - x^2y^2\frac{M^2}{Q^2}\right)\, g_4^i + xy^2 g_5^i\right]\Bigg\}\end{aligned} \tag{18.14}$$

with i = NC or CC as before. The Eq. (18.13) corresponds to the difference of antiparallel minus parallel spins of the incoming particles for e^- or ν initiated reactions, but the difference of parallel minus antiparallel for e^+ or $\overline{\nu}$ initiated processes. For longitudinal nucleon polarization, the contributions of g_2 and g_3 are suppressed by powers of M^2/Q^2. These structure functions give an unsuppressed contribution to the cross section for transverse polarization [1], but in this case the cross-section difference vanishes as $M/Q \to 0$.

Because the same tensor structure occurs in the spin-dependent and spin-independent parts of the hadronic tensor of Eq. (18.6) in the $M^2/Q^2 \to 0$ limit, the differential cross-section difference of Eq. (18.14) may be obtained from the differential cross section Eq. (18.8) by replacing

$$F_1 \;\to\; -g_5\;, \quad F_2 \;\to\; -g_4\;, \quad F_3 \;\to\; 2g_1\;, \tag{18.15}$$

and multiplying by two, since the total cross section is the average over the initial-state polarizations. In this limit, Eq. (18.8) and Eq. (18.14) may be written in the form

$$\begin{aligned}\frac{d^2\sigma^i}{dxdy} &= \frac{2\pi\alpha^2}{xyQ^2}\,\eta^i\left[Y_+ F_2^i \mp Y_- xF_3^i - y^2 F_L^i\right], \\ \frac{d^2\Delta\sigma^i}{dxdy} &= \frac{4\pi\alpha^2}{xyQ^2}\,\eta^i\left[-Y_+ g_4^i \mp Y_- 2xg_1^i + y^2 g_L^i\right],\end{aligned} \tag{18.16}$$

with i = NC or CC, where $Y_\pm = 1 \pm (1-y)^2$ and

$$F_L^i \;=\; F_2^i \;-\; 2xF_1^i\;, \qquad g_L^i \;=\; g_4^i \;-\; 2xg_5^i\;. \tag{18.17}$$

In the naive quark-parton model, the analogy with the Callan-Gross relations [6] $F_L^i = 0$, are the Dicus relations [7] $g_L^i = 0$. Therefore, there are only two independent polarized structure functions: g_1 (parity conserving) and g_5 (parity violating), in analogy with the unpolarized structure functions F_1 and F_3.

18.2.1. *Structure functions in the quark-parton model* :

In the quark-parton model [8,9], contributions to the structure functions F^i and g^i can be expressed in terms of the quark distribution functions $q(x, Q^2)$ of the proton, where $q = u, \overline{u}, d, \overline{d}$ etc. The quantity $q(x, Q^2)dx$ is the number of quarks (or antiquarks) of designated flavor that carry a momentum fraction between x and $x + dx$ of the proton's momentum in a frame in which the proton momentum is large.

For the neutral-current processes $ep \to eX$,

$$\begin{aligned}\left[F_2^\gamma,\; F_2^{\gamma Z},\; F_2^Z\right] &= x\sum_q \left[e_q^2,\; 2e_q g_V^q,\; g_V^{q\,2} + g_A^{q\,2}\right]\;(q + \overline{q})\;, \\ \left[F_3^\gamma,\; F_3^{\gamma Z},\; F_3^Z\right] &= \sum_q \left[0,\; 2e_q g_A^q,\; 2g_V^q g_A^q\right]\;(q - \overline{q})\;, \\ \left[g_1^\gamma,\; g_1^{\gamma Z},\; g_1^Z\right] &= \tfrac{1}{2}\sum_q \left[e_q^2,\; 2e_q g_V^q,\; g_V^{q\,2} + g_A^{q\,2}\right]\;(\Delta q + \Delta\overline{q})\;, \\ \left[g_5^\gamma,\; g_5^{\gamma Z},\; g_5^Z\right] &= \sum_q \left[0,\; e_q g_A^q,\; g_V^q g_A^q\right]\;(\Delta\overline{q} - \Delta q)\;,\end{aligned} \tag{18.18}$$

where $g_V^q = \pm\frac{1}{2} - 2e_q \sin^2\theta_W$ and $g_A^q = \pm\frac{1}{2}$, with $\pm$ according to whether q is a $u-$ or $d-$type quark respectively. The quantity Δq is the difference $q\uparrow - q\downarrow$ of the distributions with the quark spin parallel and antiparallel to the proton spin.

For the charged-current processes $e^-p \to \nu X$ and $\overline{\nu}p \to e^+X$, the structure functions are:

$$\begin{aligned}F_2^{W^-} &= 2x(u + \overline{d} + \overline{s} + c\ldots)\;, \\ F_3^{W^-} &= 2(u - \overline{d} - \overline{s} + c\ldots)\;, \\ g_1^{W^-} &= (\Delta u + \Delta\overline{d} + \Delta\overline{s} + \Delta c\ldots)\;, \\ g_5^{W^-} &= (-\Delta u + \Delta\overline{d} + \Delta\overline{s} - \Delta c\ldots)\;,\end{aligned} \tag{18.19}$$

where only the active flavors have been kept and where CKM mixing has been neglected. For $e^+p \to \overline{\nu}X$ and $\nu p \to e^-X$, the structure functions F^{W^+}, g^{W^+} are obtained by the flavor interchanges $d \leftrightarrow u, s \leftrightarrow c$ in the expressions for F^{W^-}, g^{W^-}. The structure functions for scattering on a neutron are obtained from those of the proton by the interchange $u \leftrightarrow d$. For both the neutral- and charged-current processes, the quark-parton model predicts $2xF_1^i = F_2^i$ and $g_4^i = 2xg_5^i$.

Neglecting masses, the structure functions g_2 and g_3 contribute only to scattering from transversely polarized nucleons (for which $S \cdot q = 0$), and have no simple interpretation in terms of the quark-parton model. They arise from off-diagonal matrix elements $\langle P, \lambda'|[J_\mu^\dagger(z), J_\nu(0)]|P, \lambda\rangle$, where the proton helicities satisfy $\lambda' \neq \lambda$. In fact, the leading-twist contributions to both g_2 and g_3 are both twist-2 and twist-3, which contribute at the same order of Q^2. The Wandzura-Wilczek relation [10] expresses the twist-2 part of g_2 in terms of g_1 as

$$g_2^i(x) \;=\; -g_1^i(x) \;+\; \int_x^1 \frac{dy}{y}\; g_1^i(y)\;. \tag{18.20}$$

However, the twist-3 component of g_2 is unknown. Similarly, there is a relation expressing the twist-2 part of g_3 in terms of g_4. A complete set of relations, including M^2/Q^2 effects, can be found in [11].

18.2.2. *Structure functions and QCD* :

One of the most striking predictions of the quark-parton model is that the structure functions F_i, g_i *scale*, i.e., $F_i(x, Q^2) \to F_i(x)$ in the Bjorken limit that Q^2 and $\nu \to \infty$ with x fixed [12]. This property is related to the assumption that the transverse momentum of the partons in the infinite-momentum frame of the proton is small. In QCD, however, the radiation of hard gluons from the quarks violates this assumption, leading to logarithmic scaling violations, which are particularly large at small x, see Fig. 18.2. The radiation of gluons produces the evolution of the structure functions. As Q^2 increases, more and more gluons are radiated, which in turn split into $q\overline{q}$ pairs. This process leads both to the softening of the initial quark momentum

distributions and to the growth of the gluon density and the $q\overline{q}$ sea as x decreases. For spin-dependent structure functions, data exists for a more restricted range of Q^2 and has lower precision, so that the scaling violations are not seen so clearly. However, spin-dependent parton distributions have been extracted by comparison to data; Fig. 18.3 shows several versions (discussed in more detail in Sec. 18.3 below) at a scale of 2.5 GeV^2 compared to the data from semi-inclusive DIS.

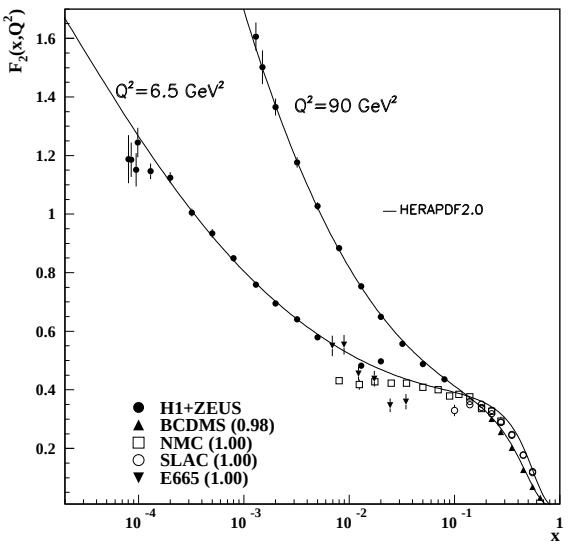

Figure 18.2: The proton structure function F_2^p given at two Q^2 values (6.5 GeV^2 and 90 GeV^2), which exhibit scaling at the 'pivot' point $x \sim 0.14$. See the captions in Fig. 18.8 and Fig. 18.10 for the references of the data. The various data sets have been renormalized by the factors shown in brackets in the key to the plot, which were globally determined in a previous HERAPDF analysis [13]. The curves were obtained using the PDFs from the HERAPDF analysis [14]. In practice, data for the reduced cross section, $F_2(x,Q^2) - (y^2/Y_+)F_L(x,Q^2)$, were fitted, rather than F_2 and F_L separately. The agreement between data and theory at low Q^2 and x can be improved by a positive higher-twist correction to $F_L(x,Q^2)$ [15,16] (see Fig. 8 of Ref. [16]).

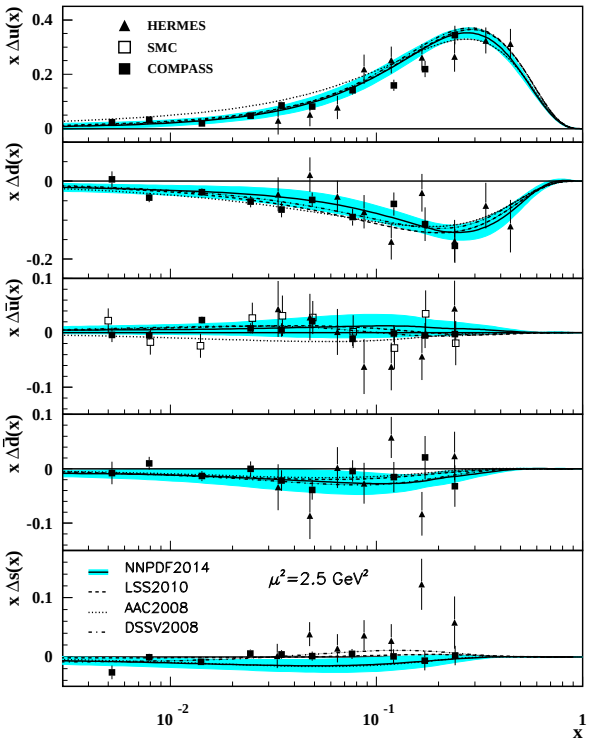

Figure 18.3: Distributions of x times the polarized parton distributions $\Delta q(x)$ (where $q = u, d, \overline{u}, \overline{d}, s$) using the NNPDF2014 [15], AAC2008 [16], DSSV2008 [17], and LSS2010 [18] parameterizations at a scale $\mu^2 = 2.5$ GeV^2, showing the blue-shaded error corridor of the NNPDF2014 set. (SMC [21] and COMPASS [22,23]) deep inelastic scattering given at $Q^2 = 2.5$ GeV^2. The SMC results were extracted under the assumption that $\Delta\overline{u}(x) = \Delta\overline{d}(x)$.

In QCD, the above processes are described in terms of scale-dependent parton distributions $f_a(x,\mu^2)$, where $a = g$ or q and, typically, μ is the scale of the probe Q. For $Q^2 \gg M^2$, the structure functions are of the form

$$F_i = \sum_a C_i^a \otimes f_a, \tag{18.21}$$

where $\otimes$ denotes the convolution integral

$$C \otimes f = \int_x^1 \frac{dy}{y}\, C(y)\, f\left(\frac{x}{y}\right) , \tag{18.22}$$

and where the coefficient functions C_i^a are given as a power series in α_s. The parton distribution f_a corresponds, at a given x, to the density of parton a in the proton integrated over transverse momentum k_t up to μ. Its evolution in μ is described in QCD by a DGLAP equation (see Refs. [24–27]) which has the schematic form

$$\frac{\partial f_a}{\partial \ln \mu^2} \sim \frac{\alpha_s(\mu^2)}{2\pi} \sum_b (P_{ab} \otimes f_b) , \tag{18.23}$$

where the P_{ab}, which describe the parton splitting $b \to a$, are also given as a power series in α_s. Although perturbative QCD can predict, via Eq. (18.23), the evolution of the parton distribution functions from a particular scale, μ_0, these DGLAP equations cannot predict them *a priori* at any particular μ_0. Thus they must be measured at a starting point μ_0 before the predictions of QCD can be compared to the data at other scales, μ. In general, all observables involving a hard hadronic interaction (such as structure functions) can be expressed as a convolution of calculable, process-dependent coefficient functions and these universal parton distributions, e.g. Eq. (18.21).

It is often convenient to write the evolution equations in terms of the gluon, non-singlet (q^{NS}) and singlet (q^S) quark distributions, such that

$$q^{NS} = q_i - \overline{q}_i \quad (\text{or } q_i - q_j), \qquad q^S = \sum_i (q_i + \overline{q}_i) . \tag{18.24}$$

The non-singlet distributions have non-zero values of flavor quantum numbers, such as isospin and baryon number. The DGLAP evolution equations then take the form

$$\frac{\partial q^{NS}}{\partial \ln \mu^2} = \frac{\alpha_s(\mu^2)}{2\pi}\, P_{qq} \otimes q^{NS} ,$$

$$\frac{\partial}{\partial \ln \mu^2} \begin{pmatrix} q^S \\ g \end{pmatrix} = \frac{\alpha_s(\mu^2)}{2\pi} \begin{pmatrix} P_{qq} & 2n_f\, P_{qg} \\ P_{gq} & P_{gg} \end{pmatrix} \otimes \begin{pmatrix} q^S \\ g \end{pmatrix} , \tag{18.25}$$

where P are splitting functions that describe the probability of a given parton splitting into two others, and n_f is the number of (active) quark flavors. The leading-order Altarelli-Parisi [26] splitting functions are

$$P_{qq} = \tfrac{4}{3}\left[\frac{1+x^2}{(1-x)}\right]_+ = \tfrac{4}{3}\left[\frac{1+x^2}{(1-x)_+}\right] + 2\delta(1-x) , \tag{18.26}$$

$$P_{qg} = \tfrac{1}{2}\left[x^2 + (1-x)^2\right] , \tag{18.27}$$

$$P_{gq} = \tfrac{4}{3}\left[\frac{1+(1-x)^2}{x}\right] , \tag{18.28}$$

$$P_{gg} = 6\left[\frac{1-x}{x} + x(1-x) + \frac{x}{(1-x)_+}\right] + \left[\frac{11}{2} - \frac{n_f}{3}\right]\delta(1-x), \quad (18.29)$$

where the notation $[F(x)]_+$ defines a distribution such that for any sufficiently regular test function, $f(x)$,

$$\int_0^1 dx f(x)[F(x)]_+ = \int_0^1 dx\ (f(x) - f(1))F(x)\ . \quad (18.30)$$

In general, the splitting functions can be expressed as a power series in α_s. The series contains both terms proportional to $\ln\mu^2$ and to $\ln(1/x)$ and $\ln(1-x)$. The leading-order DGLAP evolution sums up the $(\alpha_s \ln\mu^2)^n$ contributions, while at next-to-leading order (NLO) the sum over the $\alpha_s(\alpha_s \ln\mu^2)^{n-1}$ terms is included [28,29]. The NNLO contributions to the splitting functions and the DIS coefficient functions are also all known [30–32].

In the kinematic region of very small x, one may also sum leading terms in $\ln(1/x)$, independent of the value of $\ln\mu^2$. At leading order, LLx, this is done by the BFKL equation for the unintegrated distributions (see Refs. [33,34]). The leading-order $(\alpha_s \ln(1/x))^n$ terms result in a power-like growth, $x^{-\omega}$ with $\omega = (12\alpha_s \ln 2)/\pi$, at asymptotic values of $\ln 1/x$. The next-to-leading $\ln 1/x$ (NLLx) contributions are also available [35,36]. They are so large (and negative) that the results initially appeared to be perturbatively unstable. Methods, based on a combination of collinear and small-x resummations, have been developed which reorganize the perturbative series into a more stable hierarchy [37–40]. There are some limited indications that small-x resummations become necessary for sufficient precision for $x \lesssim 10^{-3}$ at low scales. There is not yet any very convincing indication for a 'non-linear' regime, for $Q^2 \gtrsim 2$ GeV^2, in which the gluon density would be so high that gluon-gluon recombination effects would become significant.

Table 18.1: The main processes relevant to global PDF analyses, ordered in three groups: fixed-target experiments, HERA and the $p\bar{p}$ Tevatron / pp LHC. For each process we give an indication of their dominant partonic subprocesses, the primary partons which are probed and the approximate range of x constrained by the data.

Process	Subprocess	Partons	x range
$\ell^\pm\{p,n\} \to \ell^\pm X$	$\gamma^* q \to q$	$q, \bar{q}, g$	$x \gtrsim 0.01$
$\ell^\pm n/p \to \ell^\pm X$	$\gamma^* d/u \to d/u$	d/u	$x \gtrsim 0.01$
$pp \to \mu^+\mu^- X$	$u\bar{u}, d\bar{d} \to \gamma^*$	$\bar{q}$	$0.015 \lesssim x \lesssim 0.35$
$pn/pp \to \mu^+\mu^- X$	$(u\bar{d})/(u\bar{u}) \to \gamma^*$	$\bar{d}/\bar{u}$	$0.015 \lesssim x \lesssim 0.35$
$\nu(\bar{\nu})\, N \to \mu^-(\mu^+) X$	$W^* q \to q'$	$q, \bar{q}$	$0.01 \lesssim x \lesssim 0.5$
$\nu\, N \to \mu^-\mu^+ X$	$W^* s \to c$	s	$0.01 \lesssim x \lesssim 0.2$
$\bar{\nu}\, N \to \mu^+\mu^- X$	$W^* \bar{s} \to \bar{c}$	$\bar{s}$	$0.01 \lesssim x \lesssim 0.2$
$e^\pm p \to e^\pm X$	$\gamma^* q \to q$	$g, q, \bar{q}$	$10^{-4} \lesssim x \lesssim 0.1$
$e^+ p \to \bar{\nu} X$	$W^+\{d,s\} \to \{u,c\}$	d, s	$x \gtrsim 0.01$
$e^\pm p \to e^\pm c\bar{c}X, e^\pm b\bar{b}X$	$\gamma^* c \to c$, $\gamma^* g \to c\bar{c}$	c, b, g	$10^{-4} \lesssim x \lesssim 0.01$
$e^\pm p \to$ jet$+X$	$\gamma^* g \to q\bar{q}$	g	$0.01 \lesssim x \lesssim 0.1$
$p\bar{p}, pp \to$ jet$+X$	$gg, gq, qq \to 2j$	g, q	$0.00005 \lesssim x \lesssim 0.5$
$p\bar{p} \to (W^\pm \to \ell^\pm\nu) X$	$u\bar{d} \to W^+, \bar{u}d \to W^-$	$u, d, \bar{u}, \bar{d}$	$x \gtrsim 0.05$
$pp \to (W^\pm \to \ell^\pm\nu) X$	$u\bar{d} \to W^+, d\bar{u} \to W^-$	$u, d, \bar{u}, \bar{d}, g$	$x \gtrsim 0.001$
$p\bar{p}(pp) \to (Z \to \ell^+\ell^-)X$	$uu, dd, ..(u\bar{u}, ..) \to Z$	$u, d, ..(g)$	$x \gtrsim 0.001$
$pp \to W^- c$, $W^+\bar{c}$	$gs \to W^- c$	$s, \bar{s}$	$x \sim 0.01$
$pp \to (\gamma^* \to \ell^+\ell^-)X$	$u\bar{u}, d\bar{d}, .. \to \gamma^*$	$\bar{q}, g$	$x \gtrsim 10^{-5}$
$pp \to (\gamma^* \to \ell^+\ell^-)X$	$u\gamma, d\gamma, .. \to \gamma^*$	γ	$x \gtrsim 10^{-2}$
$pp \to b\bar{b}\,X$, $t\bar{t}X$	$gg \to b\bar{b}$, $t\bar{t}$	g	$x \gtrsim 10^{-5}, 10^{-2}$
$pp \to$ exclusive J/ψ, Υ	$\gamma^*(gg) \to J/\psi$, Υ	g	$x \gtrsim 10^{-5}, 10^{-4}$
$pp \to \gamma\, X$	$gq \to \gamma q$, $g\bar{q} \to \gamma\bar{q}$	g	$x \gtrsim 0.005$

The precision of the experimental data demands that at least NLO, and preferably NNLO, DGLAP evolution be used in comparisons between QCD theory and experiment. Beyond the leading order, it is necessary to specify, and to use consistently, both a renormalization and a factorization scheme. The renormalization scheme used almost universally is the modified minimal subtraction ($\overline{\rm MS}$) scheme [41,42]. The most popular choices for the factorization scheme is also $\overline{\rm MS}$ [43]. However, sometimes the DIS [44] scheme is adopted, in which there are no higher-order corrections to the F_2 structure function. The two schemes differ in how the non-divergent pieces are assimilated in the parton distribution functions.

The discussion above relates to the Q^2 behavior of leading-twist (twist-2) contributions to the structure functions. Higher-twist terms, which involve their own non-perturbative input, exist. These die off as powers of Q; specifically twist-n terms are damped by $1/Q^{n-2}$. Provided a cut, say $W^2 > 15$ GeV^2 is imposed, the higher-twist terms appear to be numerically unimportant for Q^2 above a few GeV^2, except for x close to 1 [45–47], though it is important to note that they are likely to be larger in $xF_3(x,Q^2)$ than in $F_2(x,Q^2)$ (see e.g. [48]).

18.3. Determination of parton distributions

The parton distribution functions (PDFs) can be determined from an analysis of data for deep inelastic lepton-nucleon scattering and for related hard-scattering processes initiated by nucleons; see Refs. [49–53] for reviews. Table 18.1 highlights some of the processes, where LHC data are playing an increasing role [54], and their primary sensitivity to PDFs. Fixed-target and collider experiments have complementary kinematic reach (as is shown in Fig. 18.4), which enables the determination of PDFs over a wide range in x and Q^2. As more precise LHC data for $W^\pm$, Z, γ, jet, $b\bar{b}$, $t\bar{t}$ and J/ψ production become available, tighter constraints on the PDFs are expected in a wider kinematic range.

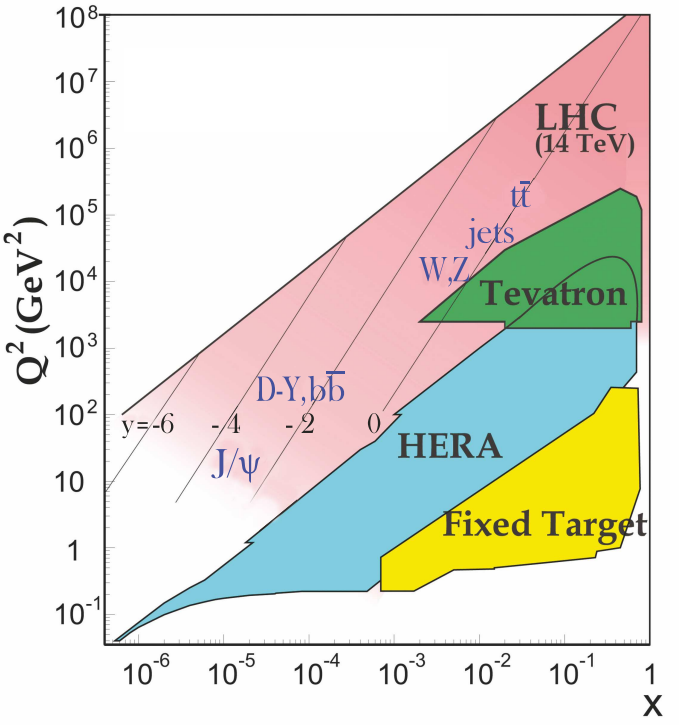

Figure 18.4: Kinematic domains in x and Q^2 probed by fixed-target and collider experiments. Some of the final states accessible at the LHC are indicated in the appropriate regions, where y is the rapidity. The incoming partons have $x_{1,2} = (M/14\ \text{TeV})e^{\pm y}$ with $Q = M$ where M is the mass of the state shown in blue in the figure. For example, exclusive J/ψ and Υ production at high $|y|$ at the LHC may probe the gluon PDF down to $x \sim 10^{-5}$.

Recent determinations and releases of the unpolarized PDFs up to NNLO have been made by six groups: MMHT [55], NNPDF [56], CT(EQ) [57], HERAPDF [14], ABMP [58] and JR [59]. JR generate 'dynamical' PDFs from a valence-like input at a very low starting scale, $Q_0^2 = 0.5$ GeV^2, whereas other groups start evolution at $Q_0^2 = 1-4$ GeV^2. Most groups use input PDFs of the form $xf = x^a(...)(1-x)^b$ with 14-28 free parameters in total. In these cases the PDF uncertainties are made available using the "Hessian" formulation. The free parameters are expanded around their best fit values, and orthogonal eigenvector sets of PDFs depending on linear combinations of the parameter variations are obtained. The uncertainty is then the quadratic sum of the uncertainties arising from each eigenvector. The NNPDF group combines a Monte Carlo representation of the probability measure in the space of PDFs with the use of neural networks. Fits are performed to a number of "replica" data sets obtained by allowing individual data points to fluctuate randomly by amounts determined by the size of the data uncertainties. This results in a set of replicas of unbiased PDF sets. In this case the best prediction is the average obtained using all PDF replicas and the uncertainty is the standard deviation over all replicas. It is now possible to convert the eigenvectors of Hessian-based PDFs to Monte Carlo replicas [60] and *vice versa* [61]. The PDFs are made available in a common format at LHAPDF [62].

In these analyses, the u, d and s quarks are taken to be massless, but the treatment of the heavy c and b quark masses, m_Q, differs, and has a long history, which may be traced from Refs. [63–74]. The MSTW, CT, NNPDF and HERAPDF analyses use different variants of the General-Mass Variable-Flavour-Number Scheme (GM-VFNS). This combines fixed-order contributions to the coefficient functions (or partonic cross sections) calculated with the full m_Q dependence, with the all-order resummation of contributions via DGLAP evolution in which the heavy quarks are treated as massless after starting evolution at some transition point. Transition matrix elements are computed, following [66], which provide the boundary conditions between n_f and $n_f + 1$ PDFs. The ABMP and JR analyses use a FFNS where only the three light (massless) quarks enter the evolution, while the heavy quarks enter the partonic cross sections with their full m_Q dependence. The GM-VFNS and FFNS approaches yield different results: in particular $\alpha_s(M_Z^2)$ and the large-x gluon PDF at large Q^2 are both significantly smaller in the FFNS. It has been argued [46,47,73] that the difference is due to the slow convergence of the $\ln^n(Q^2/m_Q^2)$ terms in certain regions in a FFNS.

The most recent determinations of the groups fitting a variety of data and using a GM-VFNS (MMHT, NNPDF and CT) have converged, so that now a good agreement has been achieved between the resulting PDFs. Indeed, the CT [57], MMHT [55], and NNPDF [56] PDF sets have been combined [75] using the Monte Carlo approach [60] mentioned above. The single combined set of PDFs is discussed in detail in Ref. [75].

For illustration, we show in Fig. 18.5 the PDFs obtained in the NNLO NNPDF analysis [56] at scales $\mu^2 = 10$ and 10^4 GeV^2. The values of α_s found by MMHT [76] may be taken as representative of those resulting from the GM-VFNS analyses

$$\text{NLO} : \alpha_s(M_Z^2) = 0.1201 \pm 0.0015,$$

$$\text{NNLO} : \alpha_s(M_Z^2) = 0.1172 \pm 0.0012,$$

where the error (at 68% C.L.) corresponds to the uncertainties resulting from the data fitted (the uncertainty that might be expected from the neglect of higher orders is at least as large), see also Ref. [77]. The ABMP analysis [58], which uses a FFNS, finds $\alpha_s(M_Z^2) = 0.1147 \pm 0.0011$ at NNLO.

A recent development has been a vastly increased understanding of the photon content of the proton. Sets of PDFs with a photon contribution were first considered in Ref. [80] and then in subsequent PDF sets [81,82]. However, due to weak data constraints, the uncertainty was extremely large. Susequently, there has been a much improved understanding of the separation into elastic and inelastic contributions [83–85]. This gives much more theoretical precision, since the elastic contribution, arising from coherent emission of a photon from the proton, can be directly related to the well-known proton electric and magnetic form factors; the model dependence of the inelastic (incoherent) contribution, related to the quark PDFs, is at the level of tens of percent. A final development directly relating the entire photon contribution to the proton structure function [86] resulted in a determination of the photon content of the proton as precise as that of the light quarks.

Spin-dependent (or polarized) PDFs have been obtained through NLO global analyses which include measurements of the g_1 structure function in inclusive polarized DIS, 'flavour-tagged' semi-inclusive DIS data, open–charm production in DIS and results from polarized pp scattering at RHIC. There are recent results on DIS from JLAB [78] (for g_1^n/F_1^n) and COMPASS [88,89]. NLO analyses are given in Refs. [16–18] and [80,91]. Improved parton-to-hadron fragmentation functions, needed to describe the semi-inclusive DIS data, can be found in Refs. [82–84]. A recent determination [85], using the NNPDF methodology, concentrates just on the inclusive polarized DIS data, and finds the errors on the polarized gluon PDF have been underestimated in the earlier analyses. An update to this [15], where jet and $W^\pm$ data from pp collisions and open–charm DIS data have been included via reweighting, reduces the uncertainty a little and suggests a positive polarized gluon PDF. The PDFs obtained in the NLO NNPDF analysis [15] at scales of $\mu^2 = 10$ and 10^4 GeV^2 are shown in Fig. 18.5.

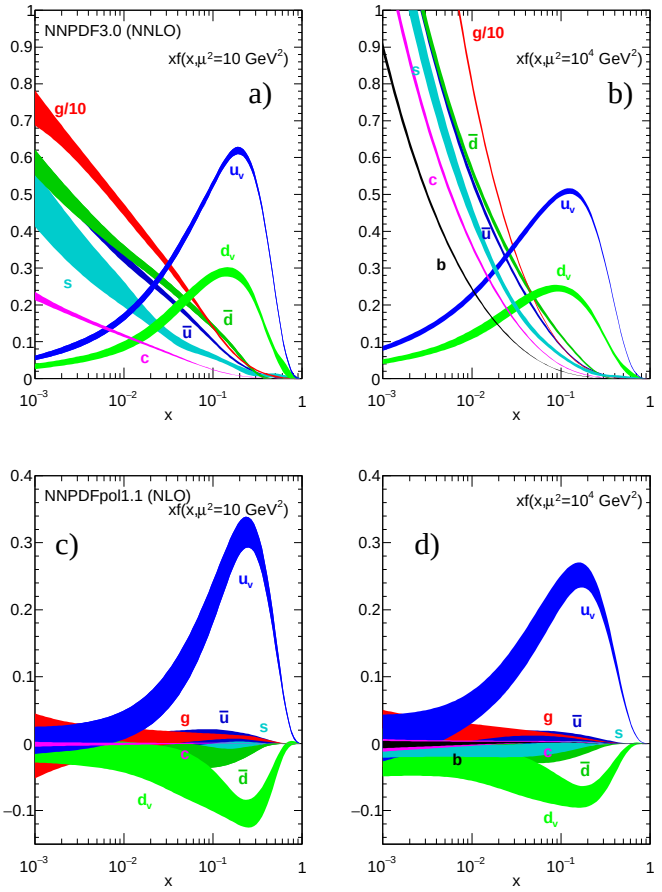

Figure 18.5: The bands are x times the unpolarized (a,b) parton distributions $f(x)$ (where $f = u_v, d_v, \overline{u}, \overline{d}, s \simeq \bar{s}, c = \bar{c}, b = \bar{b}, g$) obtained in NNLO NNPDF3.0 global analysis [56] at scales $\mu^2 = 10$ GeV^2 (left) and $\mu^2 = 10^4$ GeV^2 (right), with $\alpha_s(M_Z^2) = 0.118$. The analogous results obtained in the NNLO MMHT analysis can be found in Fig. 1 of Ref [55]. The corresponding polarized parton distributions are shown (c,d), obtained in NLO with NNPDFpol1.1 [15].

Comprehensive sets of PDFs are available as program-callable functions from the HepData website [86], which includes comparison

graphics of PDFs, and from the LHAPDF library [62], which can be linked directly into a user's programme to provide access to recent PDFs in a standard format.

18.4. The hadronic structure of the photon

Besides the *direct* interactions of the photon, it is possible for it to fluctuate into a hadronic state via the process $\gamma \to q\overline{q}$. While in this state, the partonic content of the photon may be *resolved*, for example, through the process $e^+e^- \to e^+e^-\gamma^*\gamma \to e^+e^-X$, where the virtual photon emitted by the DIS lepton probes the hadronic structure of the quasi-real photon emitted by the other lepton. The perturbative LO contributions, $\gamma \to q\overline{q}$ followed by $\gamma^* q \to q$, are subject to QCD corrections due to the coupling of quarks to gluons.

Often the equivalent-photon approximation is used to express the differential cross section for deep inelastic electron–photon scattering in terms of the structure functions of the transverse quasi-real photon times a flux factor N_γ^T (for these incoming quasi-real photons of transverse polarization)

$$\frac{d^2\sigma}{dxdQ^2} = N_\gamma^T \frac{2\pi\alpha^2}{xQ^4}\left[\left(1+(1-y)^2\right)F_2^\gamma(x,Q^2) - y^2 F_L^\gamma(x,Q^2)\right],$$

where we have used $F_2^\gamma = 2xF_T^\gamma + F_L^\gamma$, not to be confused with F_2^γ of Sec. 18.2. Complete formulae are given, for example, in the comprehensive review of [88].

The hadronic photon structure function, F_2^γ, evolves with increasing Q^2 from the 'hadron-like' behavior, calculable via the vector-meson-dominance model, to the dominating 'point-like' behaviour, calculable in perturbative QCD. Due to the point-like coupling, the logarithmic evolution of F_2^γ with Q^2 has a *positive* slope for all values of x, see Fig. 18.15. The 'loss' of quarks at large x due to gluon radiation is over-compensated by the 'creation' of quarks via the point-like $\gamma \to q\bar{q}$ coupling. The logarithmic evolution was first predicted in the quark–parton model ($\gamma^*\gamma \to q\bar{q}$) [89,90], and then in QCD in the limit of large Q^2 [91]. The evolution is now known to NLO [92–94]. The NLO data analyses to determine the parton densities of the photon can be found in Refs. [95–97].

18.5. Diffractive DIS (DDIS)

Some 10% of DIS events are diffractive, $\gamma^* p \to X + p$, in which the slightly deflected proton and the cluster X of outgoing hadrons are well-separated in rapidity. Besides x and Q^2, two extra variables are needed to describe a DDIS event: the fraction $x_{I\!P}$ of the proton's momentum transferred across the rapidity gap and t, the square of the 4-momentum transfer of the proton. The DDIS data [98,99] are usually analyzed using two levels of factorization. First, the diffractive structure function $F_2^{\rm D}$ satisfies *collinear factorization*, and can be expressed as the convolution [100]

$$F_2^{\rm D} = \sum_{a=q,g} C_2^a \otimes f_{a/p}^{\rm D}, \tag{18.31}$$

with the same coefficient functions as in DIS (see Eq. (18.21)), and where the diffractive parton distributions $f_{a/p}^{\rm D}$ $(a = q, g)$ satisfy DGLAP evolution. Second, *Regge factorization* is assumed [101],

$$f_{a/p}^{\rm D}(x_{I\!P}, t, z, \mu^2) = f_{I\!P/p}(x_{I\!P}, t)\, f_{a/I\!P}(z, \mu^2), \tag{18.32}$$

where $f_{a/I\!P}$ are the parton densities of the Pomeron, which itself is treated like a hadron, and $z \in [x/x_{I\!P}, 1]$ is the fraction of the Pomeron's momentum carried by the parton entering the hard subprocess. The Pomeron flux factor $f_{I\!P/p}(x_{I\!P}, t)$ is taken from Regge phenomenology. There are also secondary Reggeon contributions to Eq. (18.32). A sample of the t-integrated diffractive parton densities, obtained in this way, is shown in Fig. 18.6.

Although collinear factorization holds as $\mu^2 \to \infty$, there are non-negligible corrections for finite μ^2 and small $x_{I\!P}$. Besides the *resolved* interactions of the Pomeron, the perturbative QCD Pomeron may also interact *directly* with the hard subprocess, giving rise to an inhomogeneous evolution equation for the diffractive parton densities analogous to the photon case. The results of the MRW analysis [104], which includes these contributions, are also shown in Fig. 18.6. Unlike the inclusive case, the diffractive parton densities cannot be directly used to calculate diffractive hadron-hadron cross sections, since account must first be taken of "soft" rescattering effects.

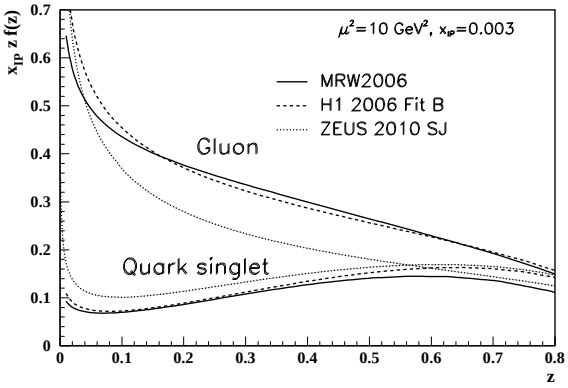

Figure 18.6: Diffractive parton distributions, $x_{I\!P}\, z f_{a/p}^{\rm D}$, obtained from fitting to the ZEUS data with $Q^2 > 5$ GeV^2 [102], H1 data with $Q^2 > 8.5$ GeV^2 assuming Regge factorization [103], and from MRW2006 [104] using a more perturbative QCD approach [104]. Only the Pomeron contributions are shown and not the secondary Reggeon contributions, which are negligible at the value of $x_{I\!P} = 0.003$ chosen here. The H1 2007 Jets distribution [105] is similar to H1 2006 Fit B.

18.6. Generalized parton distributions

The parton distributions of the proton of Sec. 18.3 are given by the diagonal matrix elements $\langle P,\lambda|\hat{O}|P,\lambda\rangle$, where P and λ are the 4-momentum and helicity of the proton, and $\hat{O}$ is a twist-2 quark or gluon operator. However, there is new information in the so-called generalised parton distributions (GPDs) defined in terms of the off-diagonal matrix elements $\langle P',\lambda'|\hat{O}|P,\lambda\rangle$; see Refs. [106–110] for reviews. Unlike the diagonal PDFs, the GPDs cannot be regarded as parton densities, but are to be interpreted as probability amplitudes.

The physical significance of GPDs is best seen using light-cone coordinates, $z^\pm = (z^0 \pm z^3)/\sqrt{2}$, and in the light-cone gauge, $A^+ = 0$. It is conventional to define the generalised quark distributions in terms of quark operators at light-like separation

$$F_q(x,\xi,t) \;=\; \frac{1}{2}\int \frac{dz^-}{2\pi}\; e^{ix\bar{P}^+z^-}\; \langle P'|\bar{\psi}(-z/2)\gamma^+\psi(z/2)|P\rangle \;\Big|_{z^+=z^1=z^2=0} \tag{18.33}$$

$$= \frac{1}{2\bar{P}^+}\left(H_q(x,\xi,t)\;\bar{u}(P')\gamma^+u(P) \;+\; E_q(x,\xi,t)\;\bar{u}(P')\frac{i\sigma^{+\alpha}\Delta_\alpha}{2m}u(P)\right) \tag{18.34}$$

with $\bar{P} = (P+P')/2$ and $\Delta = P' - P$, and where we have suppressed the helicity labels of the protons and spinors. We now have two extra kinematic variables:

$$t = \Delta^2, \qquad \xi = -\Delta^+/(P+P')^+. \tag{18.35}$$

We see that $-1 \le \xi \le 1$. Similarly, we may define GPDs $\tilde{H}_q$ and $\tilde{E}_q$ with an additional γ_5 between the quark operators in Eq. (18.33); and also an analogous set of gluon GPDs, H_g, E_g, $\tilde{H}_g$ and $\tilde{E}_g$. After a Fourier transform with respect to the transverse components of Δ, we are able to describe the spatial distribution of partons in the impact parameter plane in terms of GPDs [111,112].

For $P' = P,\ \lambda' = \lambda$ the matrix elements reduce to the ordinary PDFs of Sec. 18.2.1

$$H_q(x,0,0) = q(x), \qquad H_q(-x,0,0) = -\bar{q}(x), \qquad H_g(x,0,0) = xg(x), \tag{18.36}$$

$$\tilde{H}_q(x,0,0) = \Delta q(x), \qquad \tilde{H}_q(-x,0,0) = \Delta\bar{q}(x), \qquad \tilde{H}_g(x,0,0) = x\Delta g(x), \tag{18.37}$$

where $\Delta q = q\uparrow - q\downarrow$ as in Eq. (18.18). No corresponding relations exist for $E,\ \tilde{E}$ as they decouple in the forward limit, $\Delta = 0$.

The functions H_g, E_g are even in x, and $\tilde{H}_g, \tilde{E}_g$ are odd functions of x. We can introduce valence and 'singlet' quark distributions which are even and odd functions of x respectively. For example

$$H_q^V(x,\xi,t) \equiv H_q(x,\xi,t) + H_q(-x,\xi,t) = H_q^V(-x,\xi,t), \tag{18.38}$$

$$H_q^S(x,\xi,t) \equiv H_q(x,\xi,t) - H_q(-x,\xi,t) = -H_q^S(-x,\xi,t). \tag{18.39}$$

All the GPDs satisfy relations of the form

$$H(x,-\xi,t) = H(x,\xi,t) \qquad \text{and} \qquad H(x,-\xi,t)^* = H(x,\xi,t), \tag{18.40}$$

and so are real-valued functions. Moreover, the moments of GPDs, that is the x integrals of $x^n H_q$ etc., are *polynomials* in ξ of order $n+1$. Another important property of GPDs are Ji's sum rules [106]

$$\frac{1}{2}\int_{-1}^{1} dx\ x\left(H_q(x,\xi,t) + E_q(x,\xi,t)\right) = J_q(t), \tag{18.41}$$

where $J_q(0)$ is the total angular momentum carried by quarks and antiquarks of flavour q, with a similar relation for gluons.

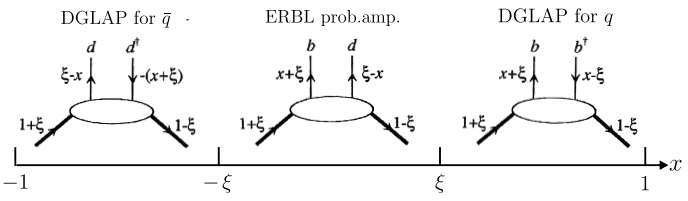

Figure 18.7: Schematic diagrams of the three distinct kinematic regions of the imaginary part of H_q. The proton and quark momentum fractions refer to $\bar{P}^+$, and x covers the interval (-1,1). In the ERBL domain the GPDs are generalisations of distribution amplitudes which occur in processes such as $p\bar{p} \to J/\psi$.

To visualize the physical content of H_q, we Fourier expand ψ and $\bar{\psi}$ in terms of quark, antiquark creation (b, d) and annihilation $(b^\dagger, d^\dagger)$ operators, and sketch the result in Fig. 18.7. There are two types of domain: (i) the time-like or 'annihilation' domain, with $|x| < |\xi|$, where the GPDs describe the wave functions of a t-channel $q\bar{q}$ (or gluon) pair and evolve according to modified ERBL equations [113,114]; (ii) the space-like or 'scattering' domain, with $|x| > |\xi|$, where the GPDs generalise the familiar $\bar{q}$, q (and gluon) PDFs and describe processes such as 'deeply virtual Compton scattering' $(\gamma^* p \to \gamma p)$, $\gamma p \to J/\psi p$, etc., and evolve according to modified DGLAP equations. The splitting functions for the evolution of GPDs are known to NLO [115].

GPDs describe new aspects of proton structure and must be determined from experiment. We can parametrise them in terms of 'double distributions' [116,117], which reduce to diagonal PDFs as $\xi \to 0$. With an additional physically reasonable 'Regge' assumption of no extra singularity at $\xi = 0$, GPDs at low ξ are uniquely given in terms of diagonal PDFs to $O(\xi)$, and have been used [118] to describe $\gamma p \to J/\psi p$ data. Alternatively, flexible $SO(3)$-based parametrisations have been used to determine GPDs from DVCS data [119]; a more recent summary may be found in Ref. [120].

* The value of $\eta^{\rm CC}$ deduced from [1] is found to be a factor of two too small; $\eta^{\rm CC}$ of Eq. (18.9) agrees with Refs. [2,3].

References:

1. J. Blümlein and N. Kochelev, Nucl. Phys. **B498**, 285 (1997).
2. S. Forte *et al.*, Nucl. Phys. **B602**, 585 (2001).
3. M. Anselmino *et al.*, Z. Phys. **C64**, 267 (1994).
4. M. Anselmino *et al.*, Phys. Rep. **261**, 1 (1995).
5. M. Klein and T. Riemann, Z. Phys. **C24**, 151 (1984).
6. C.G. Callan and D.J. Gross, Phys. Rev. Lett. **22**, 156 (1969).
7. D.A. Dicus, Phys. Rev. **D5**, 1367 (1972).
8. J.D. Bjorken and E.A. Paschos, Phys. Rev. **185**, 1975 (1969).
9. R.P. Feynman, Photon Hadron Interactions (Benjamin, New York, 1972).
10. S. Wandzura and F. Wilczek, Phys. Rev. **B72**, 195 (1977).
11. J. Blümlein and A. Tkabladze, Nucl. Phys. **B553**, 427 (1999).
12. J.D. Bjorken, Phys. Rev. **179**, 1547 (1969).
13. A.M. Cooper-Sarkar, private communication.
14. H1+ZEUS, H. Abramowicz *et al.*, Eur. Phys. J. **C75**, 580 (2015).
15. MMHT, L. Harland-Lang *et al.*, Eur. Phys. J. **C76**, 186 (2016).
16. I. Abt *et al.*, Phys. Rev. **D94**, 034032 (2016).
17. NNPDF, E.R. Nocera *et al.*, Nucl. Phys. **B887**, 276 (2014).
18. M. Hirai *et al.*, Nucl. Phys. **B813**, 106 (2009).
19. D. de Florian *et al.*, Phys. Rev. Lett. **101**, 072001 (2008); D. de Florian *et al.*, Phys. Rev. **D80**, 034030 (2009).
20. E. Leader *et al.*, Phys. Rev. **D82**, 114018 (2010).
21. HERMES, A. Airpetian *et al.*, Phys. Rev. Lett. **92**, 012005 (2004); A. Airpetian *et al.*, Phys. Rev. **D71**, 012003 (2005).
22. HERMES, A. Airpetian *et al.*, Phys. Lett. **B666**, 446 (2008).
23. SMC, B. Adeva *et al.*, Phys. Lett. **B420**, 180 (1998).
24. COMPASS, M. Alekseev *et al.*, Phys. Lett. **B680**, 217 (2009).
25. COMPASS, M. Alekseev *et al.*, Phys. Lett. **B693**, 227 (2010).
26. V.N. Gribov and L.N. Lipatov, Sov. J. Nucl. Phys. **15**, 438 (1972).
27. L.N. Lipatov, Sov. J. Nucl. Phys. **20**, 95 (1975).
28. G. Altarelli and G. Parisi, Nucl. Phys. **B126**, 298 (1977).
29. Yu.L. Dokshitzer, Sov. Phys. JETP **46**, 641 (1977).
30. G. Curci *et al.*, Nucl. Phys. **B175**, 27 (1980); W. Furmanski, and R. Petronzio, Phys. Lett. **B97**, 437 (1980).
31. R.K. Ellis *et al.*, QCD and Collider Physics (Cambridge UP, 1996).
32. E.B. Zijlstra and W.L. van Neerven, Phys. Lett. **B272**, 127 (1991); E.B. Zijlstra and W.L. van Neerven, Phys. Lett. **B273**, 476 (1991); E.B. Zijlstra and W.L. van Neerven, Phys. Lett. **B297**, 377 (1992); E.B. Zijlstra and W.L. van Neerven, Nucl. Phys. **B383**, 525 (1992).
33. S. Moch and J.A.M. Vermaseren, Nucl. Phys. **B573**, 853 (2000).
34. S. Moch *et al.*, Nucl. Phys. **B688**, 101 (2004); S. Moch *et al.*, Nucl. Phys. **B691**, 129 (2004); S. Moch *et al.*, Phys. Lett. **B606**, 123 (2005); S. Moch *et al.*, Nucl. Phys. **B724**, 3 (2005).
35. E.A. Kuraev *et al.*, Phys. Lett. **B60**, 50 (1975); E.A. Kuraev *et al.*, Sov. Phys. JETP **44**, 443 (1976); E.A. Kuraev *et al.*, Sov. Phys. JETP **45**, 199 (1977).
36. Ya.Ya. Balitsky and L.N. Lipatov, Sov. J. Nucl. Phys. **28**, 822 (1978).
37. V.S. Fadin, and L.N. Lipatov, Phys. Lett. **B429**, 127 (1998).
38. G. Camici and M. Ciafaloni, Phys. Lett. **B412**, 396 (1997), erratum-Phys. Lett. **B147**, 390 (1997); G. Camici and M. Ciafaloni, Phys. Lett. **B430**, 349 (1998).
39. M. Ciafaloni *et al.*, Phys. Rev. **D60**, 114036 (1999); M. Ciafaloni *et al.*, JHEP **0007**, 054 (2000).
40. M. Ciafaloni *et al.*, Phys. Lett. **B576**, 143 (2003); M. Ciafaloni *et al.*, Phys. Rev. **D68**, 114003 (2003).
41. G. Altarelli *et al.*, Nucl. Phys. **B742**, 1 (2006); G. Altarelli *et al.*, Nucl. Phys. **B799**, 199 (2008).
42. C.D. White and R.S. Thorne, Phys. Rev. **D75**, 034005 (2007).
43. G. 't Hooft and M. Veltman, Nucl. Phys. **B44**, 189 (1972).
44. G. 't Hooft, Nucl. Phys. **B61**, 455 (1973).

45. W.A. Bardeen *et al.*, Phys. Rev. **D18**, 3998 (1978).
46. G. Altarelli *et al.*, Nucl. Phys. **B143**, 521 (1978) and erratum: Nucl. Phys. **B146**, 544 (1978).
47. A.D. Martin *et al.*, Eur. Phys. J. **C35**, 325 (2004).
48. NNPDF, R.D. Ball *et al.*, Phys. Lett. **B723**, 330 (2013).
49. R.S. Thorne, Eur. Phys. J. **C74**, 2958 (2014).
50. M. Dasgupta and B.R. Webber, Phys. Lett. **B382**, 273 (1996).
51. A. De Roeck and R.S. Thorne, Prog. in Part. Nucl. Phys. **66**, 727 (2011).
52. S. Forte and G. Watt, Ann. Rev. Nucl. and Part. Sci. **63**, 291 (2013).
53. J. Blumlein, Prog. in Part. Nucl. Phys. **69**, 28 (2013).
54. E. Perez and E. Rizvi, Rept. on Prog. in Phys. **76**, 046201 (2013).
55. R.D. Ball *et al.*, JHEP **1304**, 125 (2013).
56. J. Rojo *et al.*, J. Phys. **G42**, 103103 (2015).
57. MMHT, L. Harland-Lang *et al.*, Eur. Phys. J. **C75**, 204 (2015).
58. NNPDF, R.D. Ball *et al.*, JHEP **1504**, 40 (2015).
59. CT14, S. Dulat *et al.*, Phys. Rev. **D93**, 033006 (2016).
60. S. Alekhin, *et al.*, Phys. Rev. **D96**, 014011 (2017).
61. P. Jimenez-Delgado and E. Reya, Phys. Rev. **D89**, 074049 (2014).
62. G. Watt and R.S. Thorne, JHEP **1208**, 052 (2012).
63. S. Carrazza *et al.*, Eur. Phys. J. **C75**, 369 (2015).
64. A. Buckley *et al.*, Eur. Phys. J. **C75**, 132 (2015).
65. J.C. Collins, F. Wilczek, and A. Zee, Phys. Rev. **D18**, 242 (1978).
66. E. Laenen *et al.*, Nucl. Phys. **B392**, 162 (1993).
67. M.A.G. Aivazis *et al.*, Phys. Rev. **D50**, 3102 (1994).
68. M. Buza *et al.*, Eur. Phys. J. **C1**, 301 (1998).
69. J.C. Collins, Phys. Rev. **D58**, 094002 (1998).
70. A. Chuvakin *et al.*, Phys. Rev. **D61**, 096004 (2000).
71. R.S. Thorne, Phys. Rev. **D73**, 054019 (2006).
72. R.S. Thorne and W.-K. Tung, Proc. 4th HERA-LHC Workshop, arXiv:0809.0714.
73. S. Alekhin and S. Moch, Phys. Lett. **B699**, 345 (2011).
74. S. Forte *et al.*, Nucl. Phys. **B834**, 116 (2010).
75. R.S. Thorne, Phys. Rev. **D86**, 074017 (2012).
76. E.G. de Oliveira *et al.*, Eur. Phys. J. **C73**, 2616 (2013).
77. J. Butterworth *et al.*, J. Phys. **G43**, 023001 (2016).
78. MMHT, L. Harland-Lang *et al.*, Eur. Phys. J. **C75**, 435 (2015).
79. NNPDF, R.D. Ball *et al.*, Phys. Lett. **B707**, 66 (2012).
80. MRST, A.D. Martin *et al.*, Eur. Phys. J. **C39**, 155 (2005).
81. NNPDF, R.D. Ball *et al.*, Nucl. Phys. **B877**, 290 (2013).
82. CT, C. Schmidt *et al.*, Phys. Rev. **D93**, 114015 (2016).
83. M. Gluck *et al.*, Phys. Lett. **B**, 540,75 (2002).
84. A.D. Martin and M.G. Ryskin, Eur. Phys. J. **C74**, 3040 (2014).
85. L.A. Harland-Lang *et al.*, Phys. Rev. **D94**, 074008 (2016).
86. A. Manohar *et al.*, Phys. Rev. Lett. **117**, 242002 (2016).
87. Jefferson Lab Hall A Collaboration, D. Flay *et al.*, Phys. Rev. **D94**, 052003 (2016).
88. COMPASS Collaboration, C. Adolph *et al.*, Phys. Lett. **B753**, 18 (2016).
89. COMPASS Collaboration, C. Adolph *et al.*, Phys. Lett. **B769**, 34 (2017).
90. J. Blümlein and H. Böttcher, Nucl. Phys. **B841**, 205 (2010).
91. N. Sato *et al.*, Phys. Rev. **D93**, 1074005 (2016).
92. D. de Florian *et al.*, Phys. Rev. **D75**, 114010 (2007); D. de Florian *et al.*, Phys. Rev. **D76**, 074033 (2007).
93. S. Albino *et al.*, Nucl. Phys. **B803**, 42 (2008).
94. M. Hirai and S. Kumano, Comp. Phys. Comm. **183**, 1002 (2012).
95. NNPDF, R.D. Ball *et al.*, Nucl. Phys. **B874**, 36 (2013).
96. http://hepdata.cedar.ac.uk/pdfs.
97. http://lhapdf.hepforge.org/.
98. R. Nisius, Phys. Reports **332**, 165 (2000).
99. T.F. Walsh and P.M. Zerwas, Phys. Lett. **B44**, 195 (1973).
100. R.L. Kingsley, Nucl. Phys. **B60**, 45 (1973).
101. E. Witten, Nucl. Phys. **B120**, 189 (1977).
102. W.A. Bardeen and A.J. Buras, Phys. Rev. **D20**, 166 (1979), erratum Phys. Rev. **D21**, 2041 (1980).
103. M. Fontannaz and E. Pilon, Phys. Rev. **D45**, 382 (1992), erratum Phys. Rev. **D46**, 484 (1992).
104. M. Glück *et al.*, Phys. Rev. **D45**, 3986 (1992).
105. F. Cornet *et al.*, Phys. Rev. **D70**, 093004 (2004).
106. P. Aurenche, *et al.*, Eur. Phys. J. **C44**, 395 (2005).
107. W. Slominski *et al.*, Eur. Phys. J. **C45**, 633 (2006).
108. H1+ZEUS, F.D. Aaron *et al.*, Eur. Phys. J. **C72**, 2175 (2012).
109. H1, F.D. Aaron *et al.*, Eur. Phys. J. **C72**, 2074 (2012).
110. J.C. Collins, Phys. Rev. **D57**, 3051 (1998); erratum Phys. Rev. **D61**, 019902 (2000).
111. G. Ingelman and P. E. Schlein, Phys. Lett. **B152**, 256 (1985).
112. ZEUS, S. Chekanov *et al.*, Nucl. Phys. **B831**, 1 (2010).
113. H1, A. Aktas *et al.*, Eur. Phys. J. **C48**, 715 (2006).
114. A.D. Martin, M.G. Ryskin, and G. Watt, Phys. Lett. **B644**, 131 (2007).
115. H1, A. Aktas *et al.*, JHEP **0710**, 042 (2007).
116. X. Ji, J. Phys. **G24**, 1181 (1998).
117. K. Goeke *et al.*, Prog. in Part. Nucl. Phys. **47**, 401 (2001).
118. M. Diehl, Phys. Rept. **388**, 41 (2003).
119. A.V. Belitsky and A.V. Radyushkin, Phys. Rept. **418**, 1 (2005).
120. S. Boffi and B. Pasquini, Riv. Nuovo Cimento **30**, 387 (2007).
121. M. Burkardt, Int. J. Mod. Phys. **A18**, 173 (2003).
122. M. Diehl, Eur. Phys. J. **C25**, 223 (2002).
123. A.V. Efremov and A.V. Radyushkin, Phys. Lett. **B94**, 245 (1980).
124. G.P. Lepage and S.J. Brodsky, Phys. Rev. **D22**, 2157 (1980).
125. A.V. Belitsky *et al.*, Phys. Lett. **B493**, 341 (2000).
126. A.V. Radyushkin, Phys. Rev. **D59**, 014030 (1999).
127. A.V. Radyushkin, Phys. Lett. **B449**, 81 (1999).
128. A.D. Martin *et al.*, Eur. Phys. J. **C63**, 57 (2009).
129. K. Kumerički and D. Müller, Nucl. Phys. **B841**, 1 (2010).
130. M. Guidal *et al.*, Rept. Prog. Phys. **76** 066202 (2013).

NOTE: THE FIGURES IN THIS SECTION ARE INTENDED TO SHOW THE REPRESENTATIVE DATA.
THEY ARE NOT MEANT TO BE COMPLETE COMPILATIONS OF ALL THE WORLD'S RELIABLE DATA.

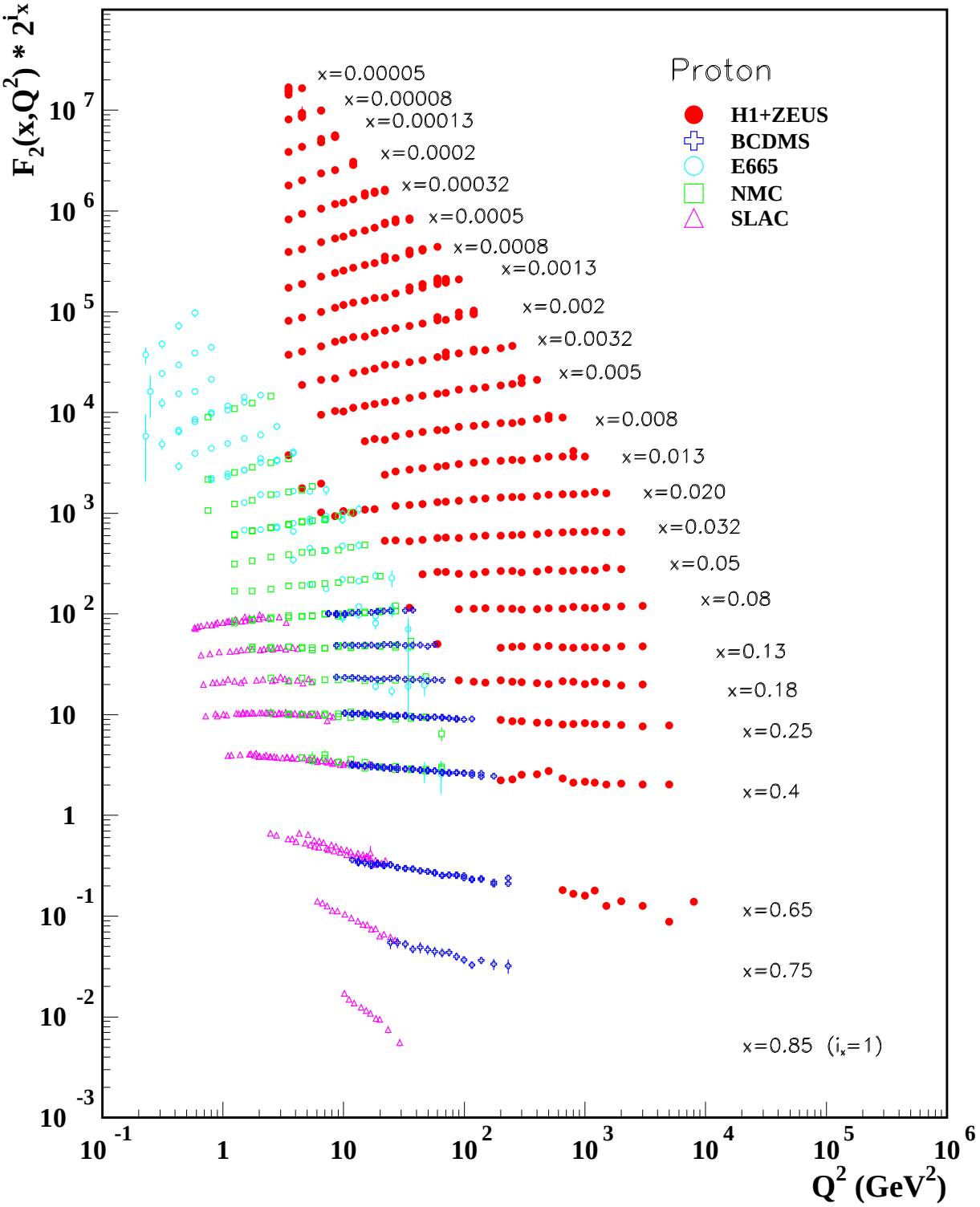

Figure 18.8: The proton structure function F_2^p measured in electromagnetic scattering of electrons and positrons on protons (collider experiments H1 and ZEUS for $Q^2 \geq 2$ GeV^2), in the kinematic domain of the HERA data (see Fig. 18.10 for data at smaller x and Q^2), and for electrons (SLAC) and muons (BCDMS, E665, NMC) on a fixed target. Statistical and systematic errors added in quadrature are shown. The H1+ZEUS combined values are obtained from the measured reduced cross section and converted to F_2^p with a HERAPDF NLO fit, for all measured points where the predicted ratio of F_2^p to reduced cross-section was within 10% of unity. The data are plotted as a function of Q^2 in bins of fixed x. Some points have been slightly offset in Q^2 for clarity. The H1+ZEUS combined binning in x is used in this plot; all other data are rebinned to the x values of these data. For the purpose of plotting, F_2^p has been multiplied by 2^{i_x}, where i_x is the number of the x bin, ranging from $i_x = 1$ ($x = 0.85$) to $i_x = 24$ ($x = 0.00005$). References: **H1 and ZEUS**—H. Abramowicz *et al.*, Eur. Phys. J. **C75**, 580 (2015) (for both data and HERAPDF parameterization); **BCDMS**—A.C. Benvenuti *et al.*, Phys. Lett. **B223**, 485 (1989) (as given in [86]); **E665**—M.R. Adams *et al.*, Phys. Rev. **D54**, 3006 (1996); **NMC**—M. Arneodo *et al.*, Nucl. Phys. **B483**, 3 (1997); **SLAC**—L.W. Whitlow *et al.*, Phys. Lett. **B282**, 475 (1992).

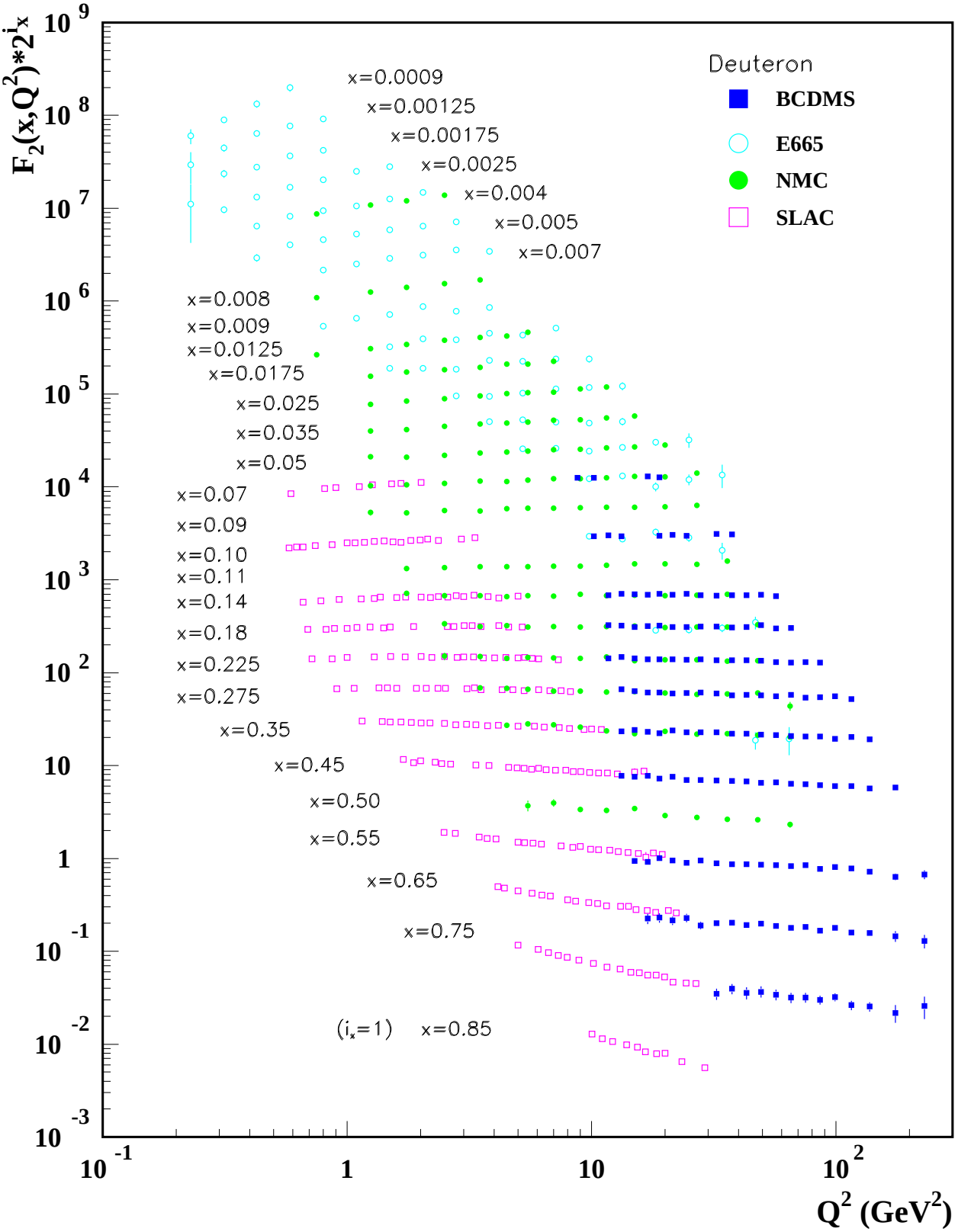

Figure 18.9: The deuteron structure function F_2^d measured in electromagnetic scattering of electrons (SLAC) and muons (BCDMS, E665, NMC) on a fixed target, shown as a function of Q^2 for bins of fixed x. Statistical and systematic errors added in quadrature are shown. For the purpose of plotting, F_2^d has been multiplied by 2^{ix}, where i_x is the number of the x bin, ranging from 1 ($x = 0.85$) to 29 ($x = 0.0009$). References: **BCDMS**—A.C. Benvenuti *et al.*, Phys. Lett. **B237**, 592 (1990). **E665, NMC, SLAC**—same references as Fig. 18.8.

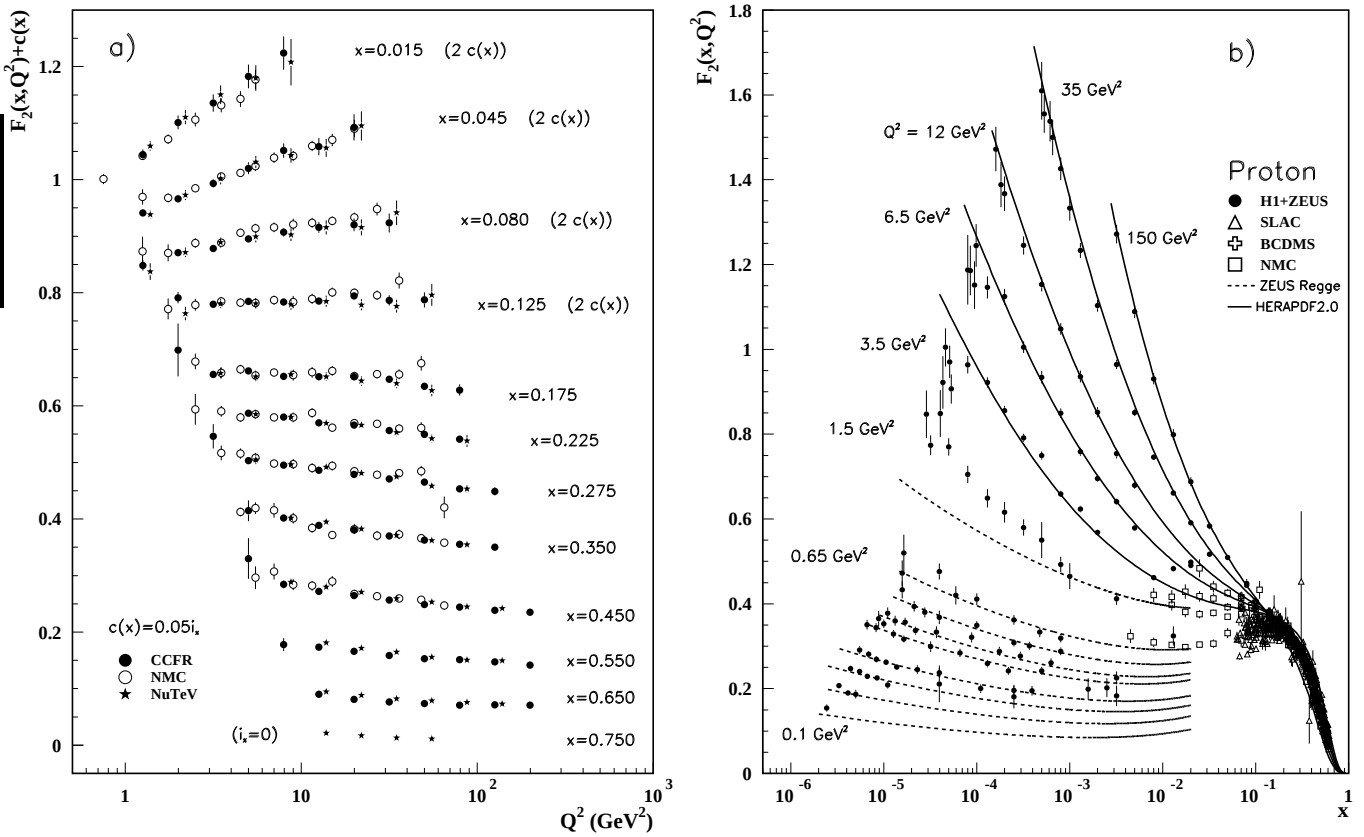

Figure 18.10: a) The deuteron structure function F_2 measured in deep inelastic scattering of muons on a fixed target (NMC) is compared to the structure function F_2 from neutrino-iron scattering (CCFR and NuTeV) using $F_2^\mu = (5/18)F_2^\nu - x(s+\overline{s})/6$, where heavy-target effects have been taken into account. The data are shown versus Q^2, for bins of fixed x. The NMC data have been rebinned to CCFR and NuTeV x values. For the purpose of plotting, a constant $c(x) = 0.05 i_x$ is added to F_2, where i_x is the number of the x bin, ranging from 0 ($x = 0.75$) to 7 ($x = 0.175$). For $i_x = 8$ ($x = 0.125$) to 11 ($x = 0.015$), $2c(x)$ has been added. References: **NMC**—M. Arneodo *et al.*, Nucl. Phys. **B483**, 3 (1997); **CCFR/NuTeV**—U.K. Yang *et al.*, Phys. Rev. Lett. **86**, 2741 (2001); **NuTeV**—M. Tzanov *et al.*, Phys. Rev. **D74**, 012008 (2006).

b) The proton structure function F_2^p mostly at small x and Q^2, measured in electromagnetic scattering of electrons and positrons (H1, ZEUS), electrons (SLAC), and muons (BCDMS, NMC) on protons. Lines are ZEUS Regge and HERAPDF parameterizations for lower and higher Q^2, respectively. The width of the bins can be up to 10% of the stated Q^2. Some points have been slightly offset in x for clarity. The H1+ZEUS combined values for $Q^2 \geq 3.5$ GeV^2 are obtained from the measured reduced cross section and converted to F_2^p with a HERAPDF NLO fit, for all measured points where the predicted ratio of F_2^p to reduced cross-section was within 10% of unity. A turn-over is visible in the low-x points at medium Q^2 (3.5 GeV^2 and 6 GeV^2) for the H1+ZEUS combined values. In order to obtain F_2^p from the measured reduced cross-section, F_L must be estimated; for the points shown, this estimate is obtained from HERAPDF2.0. No F_L value consistent with the HERA data can eliminate the turn-over. This may indicate that at low x and Q^2 there are contributions to the structure functions that cannot be described in standard DGLAP evolution.

References: **H1 and ZEUS**—F.D. Aaron *et al.*, JHEP **1001**, 109 (2010) (data for $Q^2 < 3.5$ GeV^2), H. Abramowicz *et al.*, Eur. Phys. J. **C75**, 580 (2015) (data for $Q^2 \geq 3.5$ GeV^2 and HERAPDF parameterization); **ZEUS**—J. Breitweg *et al.*, Phys. Lett. **B487**, 53 (2000) (ZEUS Regge parameterization); **BCDMS, NMC, SLAC**—same references as Fig. 18.8.

Statistical and systematic errors added in quadrature are shown for both plots.

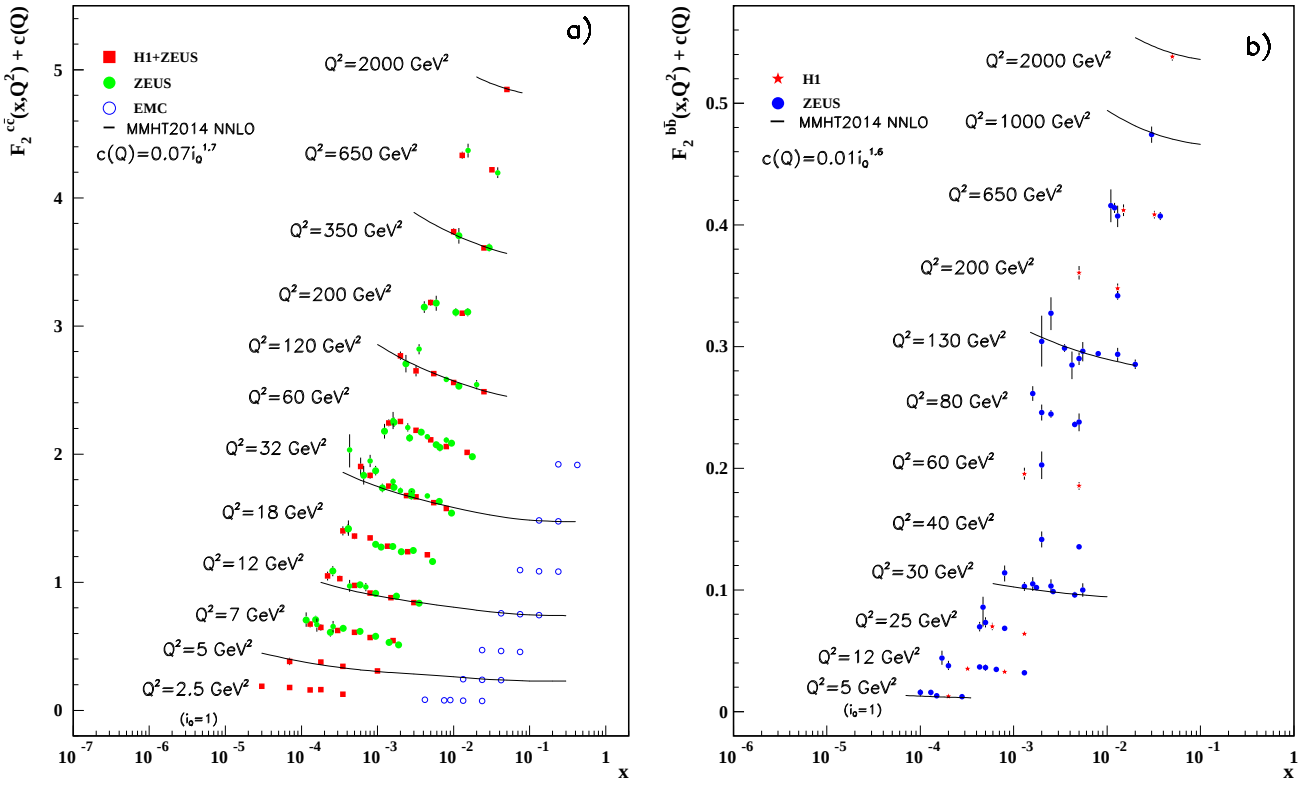

Figure 18.11: a) The charm-quark structure function $F_2^{c\bar{c}}(x)$, i.e. that part of the inclusive structure function F_2^p arising from the production of charm quarks, measured in electromagnetic scattering of positrons on protons (H1, ZEUS) and muons on iron (EMC). For the purpose of plotting, a constant $c(Q) = 0.07 i_Q{}^{1.7}$ is added to $F_2^{c\bar{c}}$ where i_Q is the number of the Q^2 bin, ranging from 1 ($Q^2 = 2.5$ GeV^2) to 12 ($Q^2 = 2000$ GeV^2). References: **H1 and ZEUS run I combination**—H. Abramowicz *et al.*, Eur. Phys. J. **C73**, 2311 (2013); **ZEUS run II**—H. Abramowicz *et al.*, JHEP **05**, 023 (2013); H. Abramowicz *et al.*, JHEP **05**, 097 (2013); H. Abramowicz *et al.*, JHEP **09**, 127 (2014); **EMC**—J.J. Aubert *et al.*, Nucl. Phys. **B213**, 31 (1983).

b) The bottom-quark structure function $F_2^{b\bar{b}}(x)$. For the purpose of plotting, a constant $c(Q) = 0.01 i_Q^{1.6}$ is added to $F_2^{b\bar{b}}$ where i_Q is the number of the Q^2 bin, ranging from 1 ($Q^2 = 5$ GeV^2) to 12 ($Q^2 = 2000$ GeV^2). References: **ZEUS**—S. Chekanov *et al.*, Eur. Phys. J. **C65**, 65 (2010); H. Abramowicz *et al.*, Eur. Phys. J. **C69**, 347 (2010); H. Abramowicz *et al.*, Eur. Phys. J. **C71**, 1573 (2011); H. Abramowicz *et al.*, JHEP **09**, 127 (2014); **H1**—F.D. Aaron *et al.*, Eur. Phys. J. **C65**, 89 (2010).

For both plots, statistical and systematic errors added in quadrature are shown. The data are given as a function of x in bins of Q^2. Points may have been slightly offset in x for clarity. Some data have been rebinned to common Q^2 values. Also shown is the MMHT2014 parameterization given at several Q^2 values (L. A. Harland-Lang *et al.*, Eur. Phys. J. **C75**, 204 (2015)).

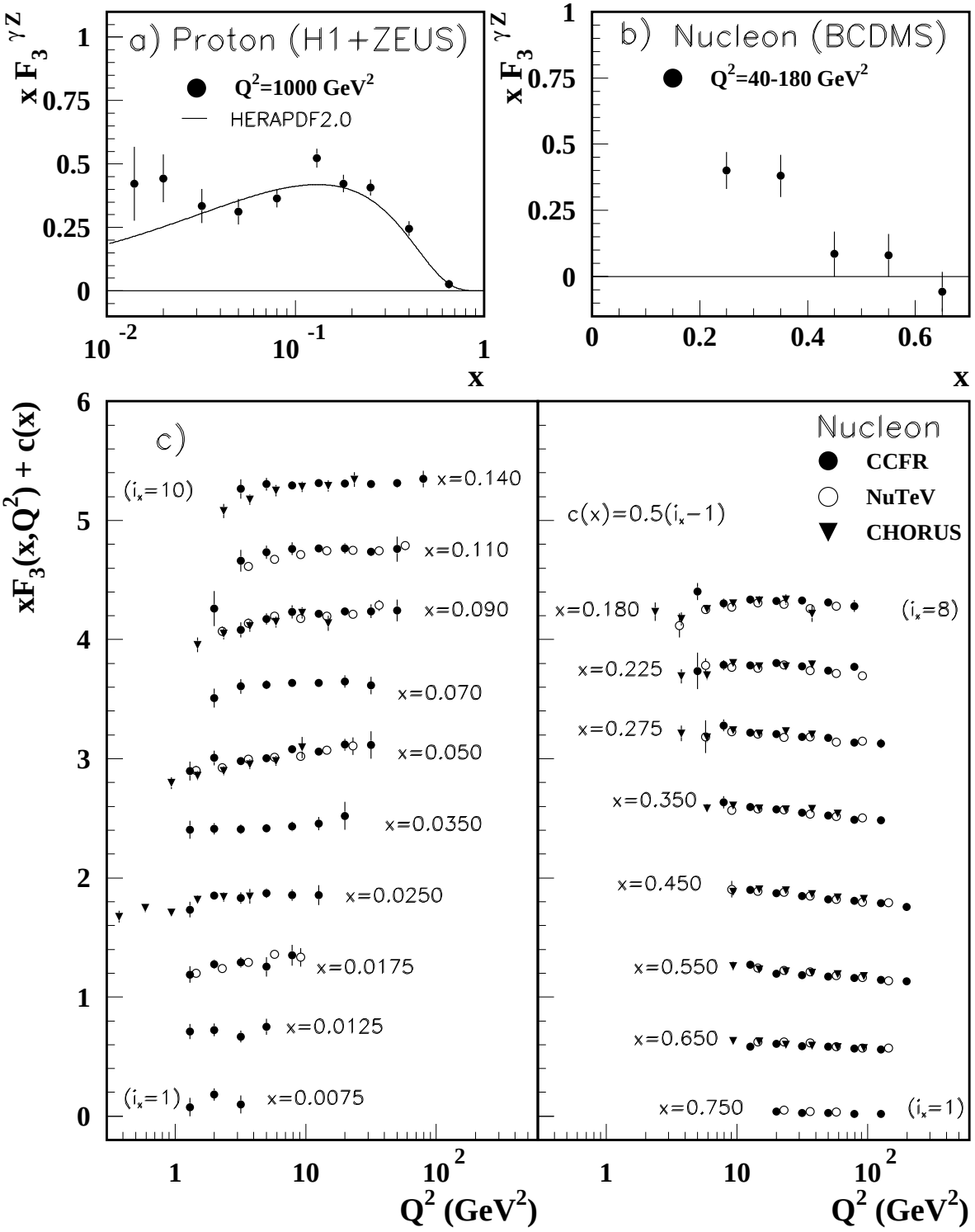

Figure 18.12: The structure function $xF_3^{\gamma Z}$ measured in electroweak scattering of **a)** electrons on protons (H1 and ZEUS) and **b)** muons on carbon (BCDMS). The line in **a)** is the HERAPDF parameterization. References: **H1 and ZEUS**—H. Abramowicz *et al.*, Eur. Phys. J. **C75**, 580 (2015) (for both data and HERAPDF parameterization); **BCDMS**—A. Argento *et al.*, Phys. Lett. **B140**, 142 (1984).
c) The structure function xF_3 of the nucleon measured in ν-Fe scattering. The data are plotted as a function of Q^2 in bins of fixed x. For the purpose of plotting, a constant $c(x) = 0.5(i_x - 1)$ is added to xF_3, where i_x is the number of the x bin as shown in the plot. The NuTeV and CHORUS points have been shifted to the nearest corresponding x bin as given in the plot and slightly offset in Q^2 for clarity. References: **CCFR**—W.G. Seligman *et al.*, Phys. Rev. Lett. **79**, 1213 (1997); **NuTeV**—M. Tzanov *et al.*, Phys. Rev. **D74**, 012008 (2006); **CHORUS**—G. Önengüt *et al.*, Phys. Lett. **B632**, 65 (2006).

Statistical and systematic errors added in quadrature are shown for all plots.

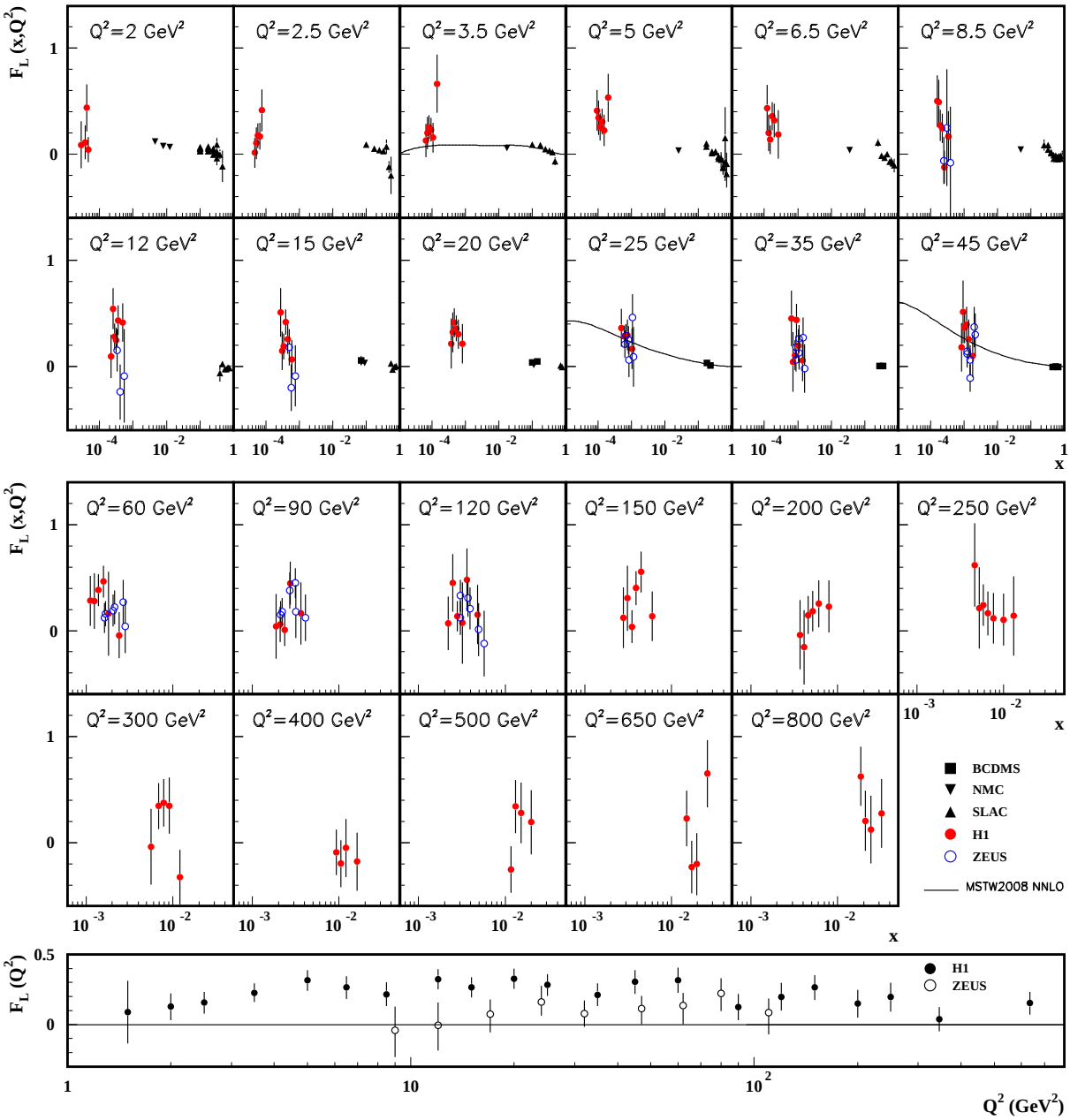

Figure 18.13: Top panels: The longitudinal structure function F_L as a function of x in bins of fixed Q^2 measured on the proton (except for the SLAC data which also contain deuterium data). BCDMS, NMC, and SLAC results are from measurements of R (the ratio of longitudinal to transverse photon absorption cross sections) which are converted to F_L by using the BDCMS parameterization of F_2 (A.C. Benvenuti *et al.*, Phys. Lett. **B223**, 485 (1989)). It is assumed that the Q^2 dependence of the fixed-target data is small within a given Q^2 bin. Some of the other data may have been rebinned to common Q^2 values. Some points have been slightly offset in x for clarity. Also shown is the MSTW2008 parameterization given at three Q^2 values (A.D. Martin *et al.*, Eur. Phys. J. **C63**, 189 (2009)). References: **H1**—V. Andreev *et al.*, Eur. Phys. J. **C74**, 2814 (2014); **ZEUS**—S. Chekanov *et al.*, Phys. Lett. **B682**, 8 (2009); H. Abramowicz et al., Phys. Rev. **D90**, 072002 (2014); **BCDMS**—A. Benvenuti *et al.*, Phys. Lett. **B223**, 485 (1989); **NMC**—M. Arneodo *et al.*, Nucl. Phys. **B483**, 3 (1997); **SLAC**—L.W. Whitlow *et al.*, Phys. Lett. **B250**, 193 (1990) and numerical values from the thesis of L.W. Whitlow (SLAC-357).

Bottom panel: The longitudinal structure function F_L as a function of Q^2. Some points have been slightly offset in Q^2 for clarity. References: **H1**—V. Andreev *et al.*, Eur. Phys. J. **C74**, 2814 (2014); **ZEUS**—H. Abramowicz et al., Phys. Rev. **D90**, 072002 (2014).

The results shown in the bottom plot require the assumption of the validity of the QCD form for the F_2 structure function in order to extract F_L. Statistical and systematic errors added in quadrature are shown for both plots.

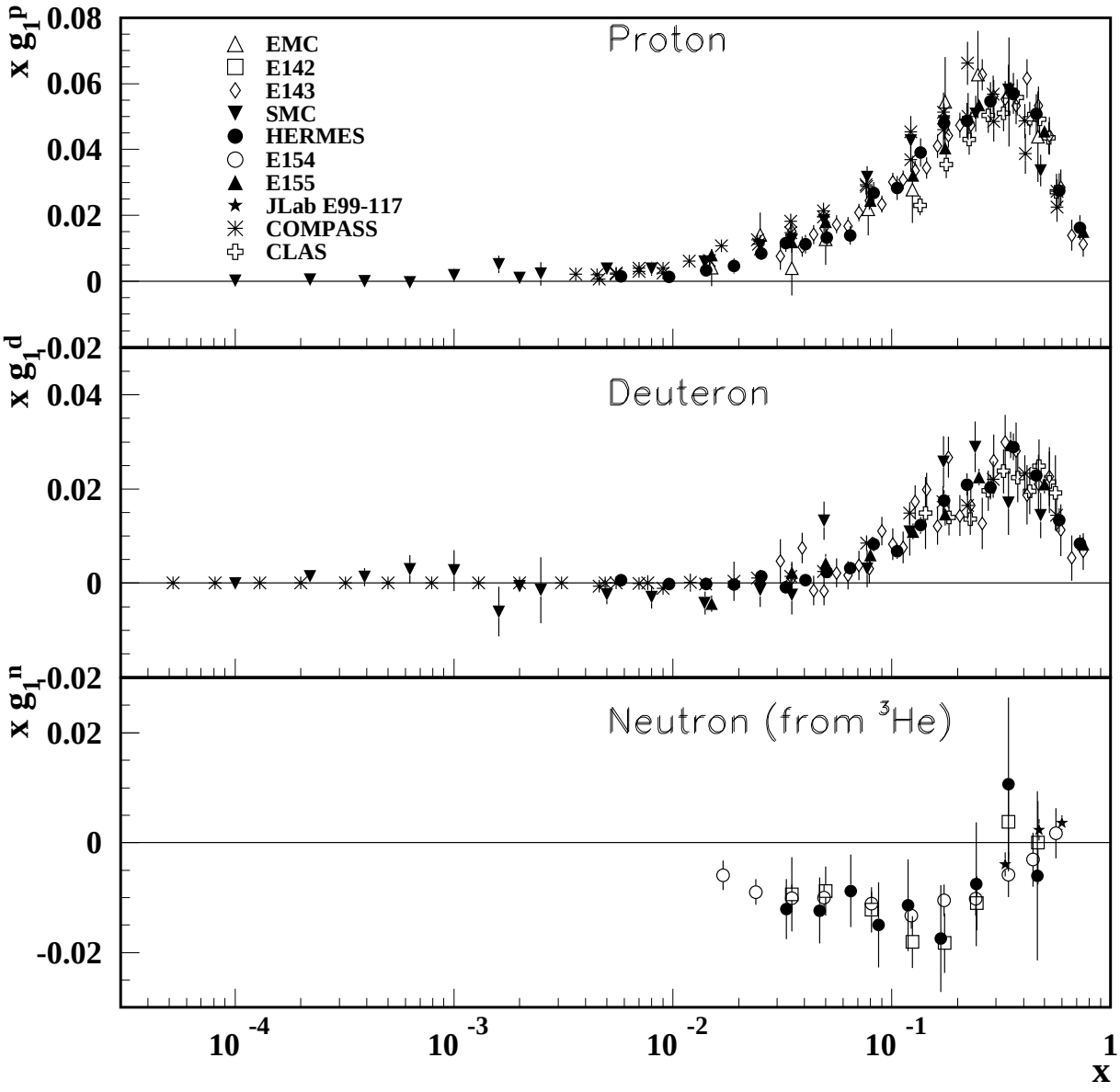

Figure 18.14: The spin-dependent structure function $xg_1(x)$ of the proton, deuteron, and neutron (from ^{3}He target) measured in deep inelastic scattering of polarized electrons/positrons: E142 ($Q^2 \sim 0.3 - 10$ GeV^2), E143 ($Q^2 \sim 0.3 - 10$ GeV^2), E154 ($Q^2 \sim 1 - 17$ GeV^2), E155 ($Q^2 \sim 1 - 40$ GeV^2), JLab E99-117 ($Q^2 \sim 2.71 - 4.83$ GeV^2), HERMES ($Q^2 \sim 0.18 - 20$ GeV^2), CLAS ($Q^2 \sim 1 - 5$ GeV^2) and muons: EMC ($Q^2 \sim 1.5 - 100$ GeV^2), SMC ($Q^2 \sim 0.01 - 100$ GeV^2), COMPASS ($Q^2 \sim 0.001 - 100$ GeV^2), shown at the measured Q^2 (except for EMC data given at $Q^2 = 10.7$ GeV^2 and E155 data given at $Q^2 = 5$ GeV^2). Note that $g_1^n(x)$ may also be extracted by taking the difference between $g_1^d(x)$ and $g_1^p(x)$, but these values have been omitted in the bottom plot for clarity. Statistical and systematic errors added in quadrature are shown. References: **EMC**—J. Ashman *et al.*, Nucl. Phys. **B328**, 1 (1989); **E142**—P.L. Anthony *et al.*, Phys. Rev. **D54**, 6620 (1996); **E143**—K. Abe *et al.*, Phys. Rev. **D58**, 112003 (1998); **SMC**—B. Adeva *et al.*, Phys. Rev. **D58**, 112001 (1998), B. Adeva *et al.*, Phys. Rev. **D60**, 072004 (1999) and Erratum-Phys. Rev. **D62**, 079902 (2000); **HERMES**—A. Airapetian *et al.*, Phys. Rev. **D75**, 012007 (2007) and K. Ackerstaff *et al.*, Phys. Lett. **B404**, 383 (1997); **E154**—K. Abe *et al.*, Phys. Rev. Lett. **79**, 26 (1997); **E155**—P.L. Anthony *et al.*, Phys. Lett. **B463**, 339 (1999) and P.L. Anthony *et al.*, Phys. Lett. **B493**, 19 (2000); **Jlab-E99-117**—X. Zheng *et al.*, Phys. Rev. **C70**, 065207 (2004); **COMPASS**—E.S. Ageev *et al.*, Phys. Lett. **B647**, 330 (2007), M.G. Alekseev *et al.*, Phys. Lett. **B690**, 466 (2010), C. Adolph, *et al.*, Phys. Lett. **B753**, 18 (2016) and C. Adolph, *et al.*, Phys. Lett. **B769**, 34 (2017); **CLAS**—K.V. Dharmawardane *et al.*, Phys. Lett. **B641**, 11 (2007) (which also includes resonance region data not shown on this plot — there is also low W^2 CLAS data in Y. Prok *et al.*, Phys. Rev. **C90**, 025212 (2014) and N. Guler *et al.*, Phys. Rev. **C92**, 055201 (2015)).

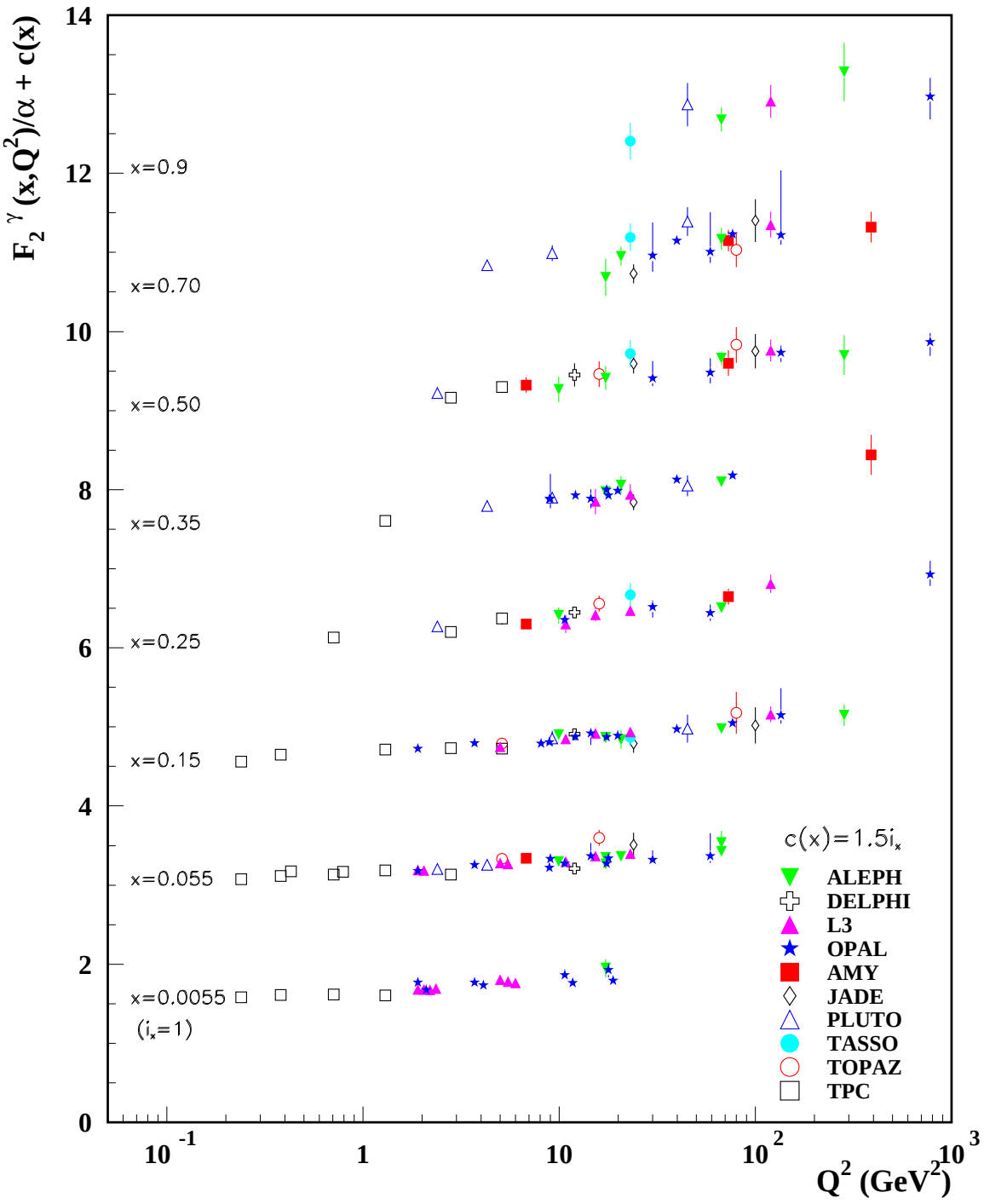

Figure 18.15: The hadronic structure function of the photon F_2^γ divided by the fine structure constant α measured in e^+e^- scattering, shown as a function of Q^2 for bins of x. Data points have been shifted to the nearest corresponding x bin as given in the plot. Some points have been offset in Q^2 for clarity. Statistical and systematic errors added in quadrature are shown. For the purpose of plotting, a constant $c(x) = 1.5i_x$ is added to F_2^γ/α where i_x is the number of the x bin, ranging from 1 ($x = 0.0055$) to 8 ($x = 0.9$). References: **ALEPH**–R. Barate *et al.*, Phys. Lett. **B458**, 152 (1999); A. Heister *et al.*, Eur. Phys. J. **C30**, 145 (2003);**DELPHI**–P. Abreu *et al.*, Z. Phys. **C69**, 223 (1995); **L3**–M. Acciarri *et al.*, Phys. Lett. **B436**, 403 (1998); M. Acciarri *et al.*, Phys. Lett. **B447**, 147 (1999); M. Acciarri *et al.*, Phys. Lett. **B483**, 373 (2000); **OPAL**–A. Ackerstaff *et al.*, Phys. Lett. **B411**, 387 (1997); A. Ackerstaff *et al.*, Z. Phys. **C74**, 33 (1997); G. Abbiendi *et al.*, Eur. Phys. J. **C18**, 15 (2000); G. Abbiendi *et al.*, Phys. Lett. **B533**, 207 (2002) (note that there is overlap of the data samples in these last two papers); **AMY**–S.K. Sahu *et al.*, Phys. Lett. **B346**, 208 (1995); T. Kojima *et al.*, Phys. Lett. **B400**, 395 (1997); **JADE**–W. Bartel *et al.*, Z. Phys. **C24**, 231 (1984); **PLUTO**–C. Berger *et al.*, Phys. Lett. **142B**, 111 (1984); C. Berger *et al.*, Nucl. Phys. **B281**, 365 (1987); **TASSO**–M. Althoff *et al.*, Z. Phys. **C31**, 527 (1986); **TOPAZ**–K. Muramatsu *et al.*, Phys. Lett. **B332**, 477 (1994); **TPC/Two Gamma**–H. Aihara *et al.*, Z. Phys. **C34**, 1 (1987).

19. Fragmentation Functions in e^+e^-, ep and pp Collisions

Revised August 2017 by O. Biebel (Ludwig-Maximilians-Universität, Munich, Germany), D. de Florian (ICAS, ECyT-UNSAM, San Martín, Argentina), D. Milstead (Fysikum, Stockholms Universitet, Sweden), and A. Vogt (Dep. of Mathematical Sciences, University of Liverpool, UK).

19.1. Introduction to fragmentation

The term 'fragmentation functions' is widely used for two conceptually different (albeit related) sets of functions describing final-state single particle energy distributions in hard scattering processes (see Refs. [1,2] for introductory reviews, and Refs. [3,4] for summaries of experimental and theoretical research in this field).

The first are cross-section observables such as the functions $F_{T,L,A}(x,s)$ in semi-inclusive e^+e^- annihilation at center-of-mass (CM) energy $\sqrt{s}$ via an intermediate photon or Z-boson, $e^+e^- \to \gamma/Z \to h + X$, given by

$$\frac{1}{\sigma_0}\frac{d^2\sigma^h}{dx\, d\cos\theta} \;=$$

$$\frac{3}{8}(1+\cos^2\theta)F_T^h(x,s) + \frac{3}{4}\sin^2\theta\, F_L^h(x,s) + \frac{3}{4}\cos\theta\, F_A^h(x,s)\,. \quad (19.1)$$

Here $x = 2E_h/\sqrt{s} \le 1$ is the scaled energy of the hadron h (in practice the approximation $x \simeq x_p = 2p_h/\sqrt{s}$ or $x \simeq p/p_{max}$ is often used), and θ is its angle relative to the electron beam in the CM frame. Eq. (19.1) is the most general form for unpolarized inclusive single-particle production via vector bosons [5]. The transverse and longitudinal fragmentation functions F_T and F_L represent the contributions from γ/Z polarizations transverse or longitudinal with respect to the direction of motion of the hadron. The parity-violating term with the asymmetric fragmentation function F_A arises from the interference between vector and axial-vector contributions. Normalization factors σ_0 used in the literature range from the total cross section $\sigma_{\rm tot}$ for $e^+e^- \to$ hadrons, including all weak and QCD contributions, to $\sigma_0 = 4\pi\alpha^2 N_c/3s$ with $N_c = 3$, the lowest-order QED cross section for $e^+e^- \to \mu^+\mu^-$ times the number of colors N_c. LEP1 measurements of all three fragmentation functions are shown in Fig. 19.1.

Integration of Eq. (19.1) over θ yields the total fragmentation function $F^h = F_T^h + F_L^h$,

$$\frac{1}{\sigma_0}\frac{d\sigma^h}{dx} \;=\; F^h(x,s) \;=$$

$$\sum_i \int_x^1 \frac{dz}{z}\, C_i(z,\alpha_{\rm s}(\mu),\frac{s}{\mu^2}) D_i^h(\frac{x}{z},\mu^2) \;+\; \mathcal{O}(\frac{1}{\sqrt{s}}) \quad (19.2)$$

with $i = u,\ \bar{u},\ d,\ \bar{d},\ \ldots,\ g$. Here the second set of functions mentioned in the first paragraph has been introduced, the parton fragmentation functions (or fragmentation densities) D_i^h. These functions are the final-state analogue of the initial-state parton distribution functions (pdf) addressed in Section 18 of this *Review*. Due to the different sign of the squared four-momentum q^2 of the intermediate gauge boson these two sets of fragmentation distributions are also referred to as the timelike (e^+e^- annihilation, $q^2 > 0$) and spacelike (deep-inelastic scattering (DIS), $q^2 < 0$) parton distribution functions. The function $D_i^h(z,\mu^2)$ describes the probability that the parton i fragments into a hadron h carrying a probability that the parton i fragments into a hadron h carrying a fraction z of the parton's momentum. Beyond the leading order (LO) of perturbative QCD these universal functions are factorization-scheme dependent, with 'reasonable' scheme choices retaining certain quark-parton-model [6] (QPM) constraints such as the momentum sum rule

$$\sum_h \int_0^1 dz\, z\, D_i^h(z,\mu^2) \;=\; 1\,. \quad (19.3)$$

The dependence of the functions D_i^h on the factorization scale μ^2 is discussed in Section 19.2. Like in Eq. (19.2) and below, this scale is often taken to be equal to the factorization or renomalization scale, but this equivalence is not required in the theory.

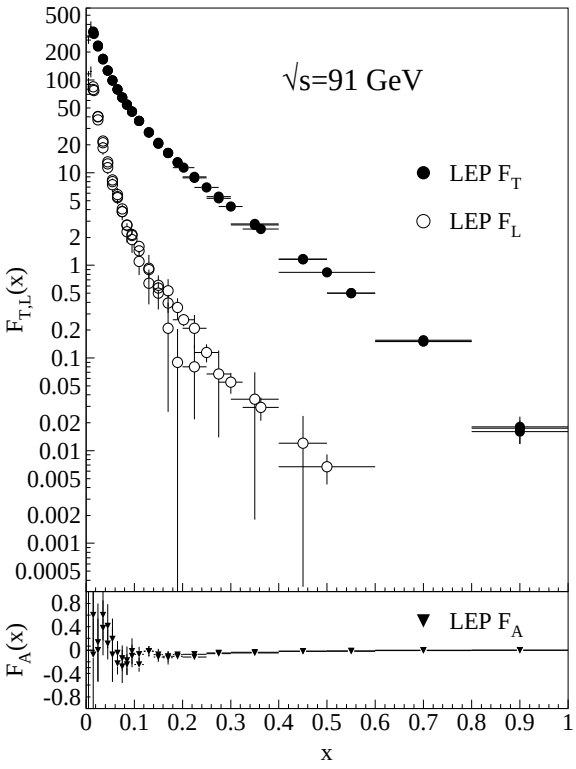

Figure 19.1: LEP1 measurements of total transverse (F_T), longitudinal (F_L), and asymmetric (F_A) fragmentation functions [7–9]. Data points with relative errors greater than 100% are omitted.

The second ingredient in Eq. (19.2), and analogous expressions for the functions $F_{T,L,A}$, are the observable-dependent coefficient functions C_i. At the zeroth order in the strong coupling $\alpha_{\rm s}$ the coefficient functions C_g for gluons are zero, while for (anti-) quarks $C_i = g_i(s)\,\delta(1-z)$ except for F_L, where $g_i(s)$ is the appropriate electroweak coupling. In particular, $g_i(s)$ is proportional to the squared charge of the quark i at $s \ll M_Z^2$, when weak effects can be neglected. The full electroweak prefactors $g_i(s)$ can be found in Ref. [5]. The power corrections in Eq. (19.2) arise from quark and hadron mass terms and from non-perturbative effects.

Measurements of fragmentation in lepton-hadron and hadron-hadron scattering are complementary to those in e^+e^- annihilation. The former are affected by contributions, in summary called the hadron remnant, arising from the partons of the initial-state hadron which are collaterally involved in the hard lepton-parton or parton-parton collision. The latter provides a clean environment (no initial-state hadron remnant) and stringent constraints on the combinations $D_{q_i}^h + D_{\bar{q}_i}^h$. However e^+e^- annihilation is far less sensitive to D_g^h and insensitive to the charge asymmetries $D_{q_i}^h - D_{\bar{q}_i}^h$. These quantities are best constrained in proton–(anti-)proton and electron-proton scattering, respectively. Especially the latter provides a more complicated environment with which it is possible to study the influence on the fragmentation process from initial-state QCD radiation, the partonic and spin structure of the hadron target, and the target remnant system (see Ref. [10] for a comprehensive review of the measurements and models of fragmentation in lepton-hadron scattering).

Moreover, unlike e^+e^- annihilation where $q^2 = s$ is fixed by the collider energy, lepton-hadron scattering has two independent scales, $Q^2 = -q^2$ and the invariant mass W^2 of the hadronic final state, which both can vary by several orders of magnitudes for a given CM energy, thus allowing the study of fragmentation in different environments by a single experiment. E.g., in photoproduction the

exchanged photon is quasi-real ($Q^2 \approx 0$) leading to processes akin to hadron-hadron scattering. In DIS ($Q^2 \gg 1$ GeV^2), using the QPM, the hadronic fragments of the struck quark can be directly compared with quark fragmentation in e^+e^- in a suitable frame. Results from lepton-hadron experiments quoted in this report primarily concern fragmentation in the DIS regime. Studies performed by lepton-hadron experiments of fragmentation with photoproduction data containing high transverse momentum jets or particles are also reported, when these are directly comparable to DIS and e^+e^- results.

Fragmentation studies in lepton-hadron collisions are usually performed in one of two frames in which the target hadron and the exchanged boson are collinear. The hadronic center-of-mass frame (HCMS) is defined as the rest system of the exchanged boson and incoming hadron, with the z^*-axis defined along the direction of the exchanged boson. The positive z^* direction defines the so-called current region. Fragmentation measurements performed in the HCMS often use the Feynman-x variable $x_F = 2p_z^*/W$, where p_z^* is the longitudinal momentum of the particle in this frame. As W is the invariant mass of the hadronic final state, x_F ranges between -1 and 1.

The Breit system [11] is connected to the HCMS by a longitudinal boost such that the time component of q vanishes, i.e, $q = (0, 0, 0, -Q)$. In the QPM, the struck parton then has the longitudinal momentum $Q/2$ which becomes $-Q/2$ after the collision. As compared with the HCMS, the current region of the Breit frame is more closely matched to the partonic scattering process, and is thus appropriate for direct comparisons of fragmentation functions in DIS with those from e^+e^- annihilation. The variable $x_p = 2p^*/Q$ is used at HERA for measurements in the Breit frame, ensuring rather directly comparable DIS and e^+e^- results, where p^* is the particle's momentum in the current region of the Breit frame.

19.2. Scaling violation

The simplest parton-model approach would predict scale-independent x-distributions ('scaling') for both the fragmentation function F^h and the parton fragmentation functions D_i^h. Perturbative QCD corrections lead, after factorization of the final-state collinear singularities for light partons, to logarithmic scaling violations via the evolution equations [12]

$$\frac{\partial}{\partial \ln \mu^2} D_i(x,\mu^2) \;=\; \sum_j \int_x^1 \frac{dz}{z} P_{ji}(z, \alpha_s(\mu^2)) D_j(\frac{x}{z}, \mu^2)\,, \qquad (19.4)$$

where the splitting functions $P_{ij}(z, \alpha_s(\mu^2))$ describe in leading order the probability to find parton i with a longitudinal momentum fraction z in parton j. Usually this system of equations is decomposed into a 2×2 flavour-singlet sector comprising gluon and the sum of all quark and antiquark fragmentation functions, and scalar ('non-singlet') equations for quark-antiquark and flavour differences. The singlet splitting-function matrix is now P_{ji}, rather than P_{ij} as for the initial-state parton distributions, since D_j represents the fragmentation of the final parton.

The splitting functions in Eq. (19.4) have perturbative expansion of the form

$$P_{ji}(z,\alpha_s) \;=\; \frac{\alpha_s}{2\pi} P_{ji}^{(0)}(z) + \Big(\frac{\alpha_s}{2\pi}\Big)^2 P_{ji}^{(1)}(z) + \Big(\frac{\alpha_s}{2\pi}\Big)^3 P_{ji}^{(2)}(z) + \ldots \quad (19.5)$$

where the leading-order (LO) functions $P^{(0)}(z)$ [12,13] are the same as those for the initial-state parton distributions. The next-to-leading order (NLO) corrections $P^{(1)}(z)$ have been calculated in Refs. [14–18] (there are well-known misprints in the journal version of Ref. [15]). Ref. [18] also includes the spin-dependent case. These functions are different from, but related to their space-like counterparts, see also Ref. [19]. These relations have facilitated recent calculations of the next-to-next-to-leading order (NNLO) quantities $P_{qq}^{(2)}(z)$ and $P_{gg}^{(2)}(z)$ in Eq. (19.5) [20,21]. The corresponding off-diagonal quantities $P_{qg}^{(2)}$ and $P_{gq}^{(2)}$ were recently obtained in Ref. [22] by using similar relations supplemented with constrains from the momentum sum rule Eq. (19.3) [21] and from the limit of $C_A = C_F = n_f$ for which QCD becomes supersymmetric. An uncertainty, which does not affect the logarithmic behaviour at small and large momentum fractions, still remains on the $P_{qg}^{(2)}$ kernel. All these results refer to the standard $\overline{\rm MS}$ scheme, with the exception of Refs. [17], with a fixed number n_f of light flavours. Fragmentation functions change when in the course of energy evolution the threshold for the production of a heavier quark flavour is crossed. The NLO treatment of these flavour thresholds in the evolution has been addressed in Ref. [23].

The QCD parts of the coefficient functions for $F_{T,L,A}(x,s)$ in Eq. (19.1) and the total fragmentation function $F_2^h \equiv F^h$ in Eq. (19.2) are given by

$$C_{a,i}(z,\alpha_s) \;=\; (1-\delta_{aL})\,\delta_{iq} + \frac{\alpha_s}{2\pi} c_{a,i}^{(1)}(z) + \Big(\frac{\alpha_s}{2\pi}\Big)^2 c_{a,i}^{(2)}(z) + \ldots\,. \quad (19.6)$$

The first-order corrections have been calculated in Refs. [24], and the second-order terms in Ref. 25. The latter results have been verified (and some typos corrected) in Refs. [20,26]. The coefficient functions are known to NNLO except for F_L where the leading contribution is of order α_s.

The effect of the evolution is similar in the timelike and spacelike cases: as the scale increases, one observes a scaling violation in which the x-distribution is shifted towards lower values. This can be seen from Fig. 19.2 where a large amount of measurements of the total fragmentation function in e^+e^- annihilation are summarized. QCD analyses of these data are discussed in Section 19.5 below.

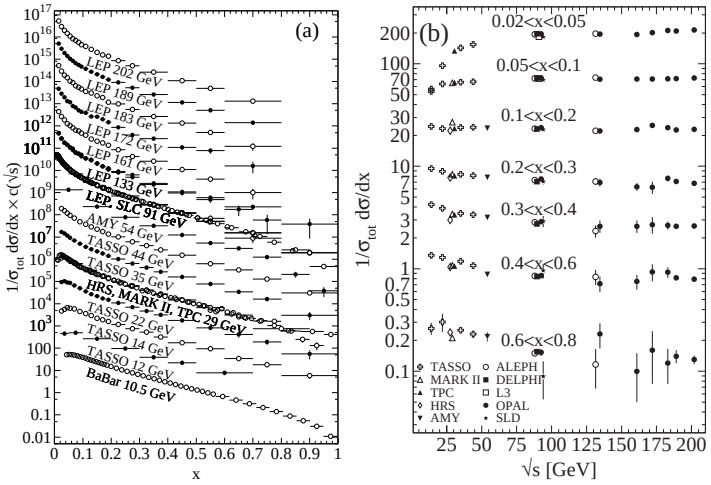

Figure 19.2: The e^+e^- fragmentation function for all charged particles is shown [9,27–44] (a) for different CM energies $\sqrt{s}$ versus x and (b) for various ranges of x versus $\sqrt{s}$. For the purpose of plotting (a), the distributions were scaled by $c(\sqrt{s}) = 10^i$ with i ranging from $i = 0$ ($\sqrt{s} = 12$ GeV) to $i = 13$ ($\sqrt{s} = 202$ GeV).

Unlike the splitting functions in Eq. (19.5), see Refs. [19–21], the coefficient functions for $F_{2,T,A}$ in Eq. (19.6) show a threshold enhancement with terms up to $\alpha_s^n (1-z)^{-1} \ln^{2n-1}(1-z)$. Such logarithms can be resummed to all orders in α_s using standard soft-gluon techniques [45–47]. Recently this resummation has been extended to the subleading (and for F_L leading) class $\alpha_s^n \ln^k(1-z)$ of large-x logarithms [48,49].

In Refs. [24] the NLO coefficient functions have been calculated also for single hadron production in lepton-proton scattering, $ep \to e + h + X$. More recently corresponding results have been obtained for the case that a non-vanishing transverse momentum is required in the HCMS frame [50].

Scaling violations in DIS are shown in Fig. 19.3 for both HCMS and Breit frame. In Fig. 1.3(a) the distribution in terms of $x_F = 2p_z^*/W$ shows a steeper slope in ep data than for the lower-energy μp data for $x_F > 0.15$, indicating the scaling violations. At smaller values of

x_F in the current jet region, the multiplicity of particles substantially increases with W owing to the increased phase space available for the fragmentation process. The EMC data access both the current region and the region of the fragmenting target remnant system. At higher values of $|x_F|$, due to the extended nature of the remnant, the multiplicity in the target region far exceeds that in the current region. For acceptance reasons the remnant hemisphere of the HCMS is only accessible by the lower-energy fixed-target experiments.

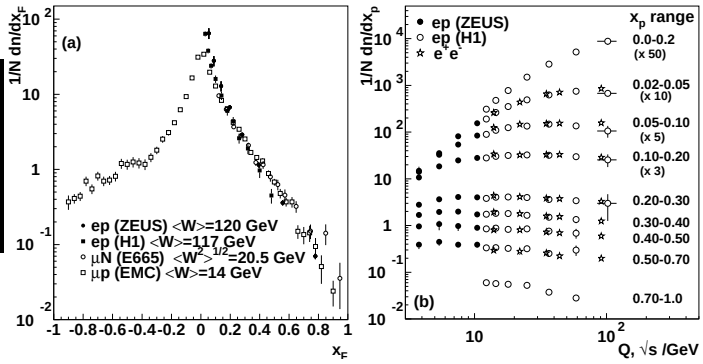

Figure 19.3: (a) The distribution $1/N \cdot dN/dx_F$ for all charged particles in DIS lepton-hadron experiments at different values of W, and measured in the HCMS [52–55]. (b) Scaling violations of the fragmentation function for all charged particles in the current region of the Breit frame of DIS [56,61] and in e^+e^- interactions [37,62]. The data are shown as a function of $\sqrt{s}$ for e^+e^- results, and as a function of Q for the DIS results, each within the same indicated intervals of the scaled momentum x_p. The data for the four lowest intervals of x_p are multiplied by factors 50, 10, 5, and 3, respectively for clarity.

Using hadrons from the current hemisphere in the Breit frame, measurements of fragmentation functions and the production properties of particles in ep scattering have been made by Refs. [56–61]. Fig. 19.3(b) compares results from ep scattering and e^+e^- experiments, the latter results are halved as they cover both event hemispheres. The agreement between the DIS and e^+e^- results is fairly good. However, processes in DIS which are not present in e^+e^- annihilation, such as boson-gluon fusion and initial-state QCD radiation, can depopulate the current region. These effects become most prominent at low values of Q and x_p. Hence, when compared with e^+e^- annihilation data at $\sqrt{s} = 5.2$, 6.5 GeV [63] not shown here, the DIS particle rates tend to lie below those from e^+e^- annihilation. A ZEUS study [64] finds that the direct comparability of the ep data to e^+e^- results at low scales is improved if twice the energy in the current hemisphere of the Breit frame, $2E_B^{\rm cr}$, is used instead of $Q/2$ as the fragmentation scale. Choosing $2 \cdot E_B^{\rm cr}$ for the fragmentation scale approximates QCD radiation effects relevant at low scales as detailed in Ref. [65].

19.3. Fragmentation functions for small particle momenta

The higher-order timelike splitting functions in Eq. (19.5) are very singular at small x. They show a double-logarithmic (LL) enhancement with leading terms of the form $\alpha_s^n \ln^{2n-2} x$ corresponding to poles $\alpha_s^n\,(N-1)^{1-2n}$ for the Mellin moments

$$P^{(n)}(N) \;=\; \int_0^1 dx\; x^{N-1}\; P^{(n)}(x)\;. \qquad (19.7)$$

Despite large cancellations between leading and non-leading logarithms at non-asymptotic value of x, the resulting small-x rise in the timelike splitting functions dwarfs that of their spacelike counterparts for the evolution of the parton distributions in Section 18 of this *Review*, see Fig. 1 of Ref. [21]. Consequently the fixed-order approximation to the evolution breaks down orders of magnitude in x earlier in fragmentation than in DIS.

The pattern of the known coefficients and other considerations suggest that the LL terms sum to all-order expressions without any pole at $N = 1$ such as [66,67]

$$P_{gg}^{\rm LL}(N) \;=\; -\frac{1}{4}(N - 1 - \sqrt{(N-1)^2 \cdot 24\,\alpha_s/\pi}\,)\;. \qquad (19.8)$$

Keeping the first three terms in the resulting expansion of Eq. (19.4) around $N = 1$ yields a Gaussian in the variable $\xi = \ln(1/x)$ for the small-x fragmentation functions,

$$xD(x,s) \;\propto\; \exp\left[-\frac{1}{2\sigma^2}(\xi - \xi_p)^2\right]\;, \qquad (19.9)$$

with the peak position and width varying with the energy as [68] (see also Ref. [2])

$$\xi_p \;\simeq\; \frac{1}{4}\ln\left(\frac{s}{\Lambda^2}\right)\;,\quad \sigma \;\propto\; \left[\ln\left(\frac{s}{\Lambda^2}\right)\right]^{3/4}\;. \qquad (19.10)$$

Next-to-leading logarithmic corrections to the above predictions have been calculated [69]. In the method of Ref. [70], see also Refs. [71,72], the corrections are included in an analytical form known as the 'modified leading logarithmic approximation' (MLLA). Alternatively they can be used to compute higher-moment corrections to the shape in Eq. (19.9) [73]. The small-x resummation of the coefficient functions for semi-inclusive e^+e^- annihilation and the timelike spitting functions in the standard $\overline{\rm MS}$ scheme was recently extended in Refs. [74,75] and has reached fully analytic next-to-next-to-leading logarithmic accuracy. First applications of these results to gluon and quark jet multiplicities have been presented in Refs. [76].

Fig. 19.4 shows the ξ distribution for charged particles produced in the current region of the Breit frame in DIS and in e^+e^- annihilation. Consistent with Eq. (19.9) (the 'hump backed plateau') and Eq. (19.10) the distributions have a Gaussian shape with the peak position and area increasing with the CM energy (e^+e^-) and Q^2 (DIS).

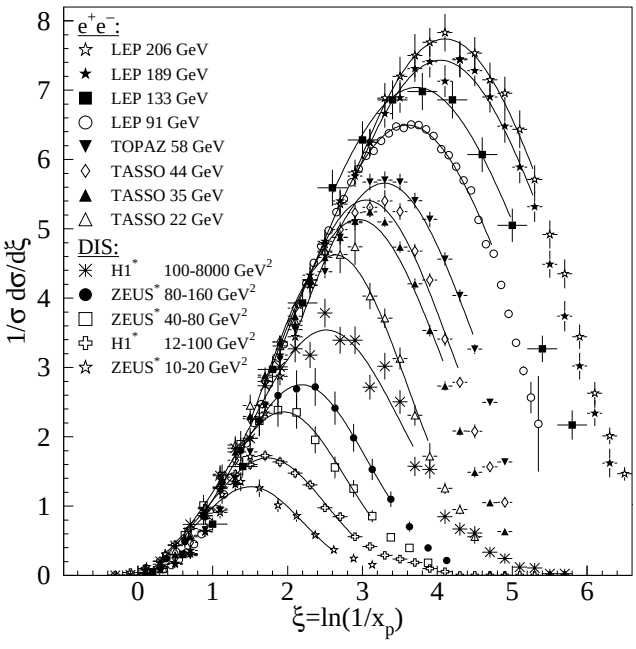

Figure 19.4: Distribution of $\xi = \ln(1/x_p)$ at several CM energies (e^+e^-) [28–29,34–37,77–80] and intervals of Q^2 (DIS) [59,60]. At each energy only one representative measurement is displayed. For clarity some measurements at intermediate CM energies (e^+e^-) or Q^2 ranges (DIS) are not shown. The DIS measurements ($*$) have been scaled by a factor of 2 for direct comparability with the e^+e^- results. Fits of simple Gaussian functions are overlaid for illustration.

The predicted energy dependence Eq. (19.10) of the peak in the ξ distribution is explained by soft gluon coherence (angular ordering), *i.e.*, the destructive interference of the color wavefunction of low energy gluon radiation, which correctly predicts the suppression of hadron production at small x. Of course, a decrease at very small x is expected on purely kinematical grounds, but this would occur at particle energies proportional to their masses, *i.e.*, at $x \propto m/\sqrt{s}$ and hence $\xi \sim \frac{1}{2}\ln s$. Thus, if the suppression were purely kinematic, the peak position ξ_p would vary twice as rapidly with the energy, which is ruled out by the data in Fig. 19.5. The e^+e^- and DIS data agree well with each other, demonstrating the universality of hadronization, and the MLLA prediction. Measurements of the higher moments of the ξ distribution in e^+e^- [37,80–82] and DIS [60] have also been performed and show consistency with each other.

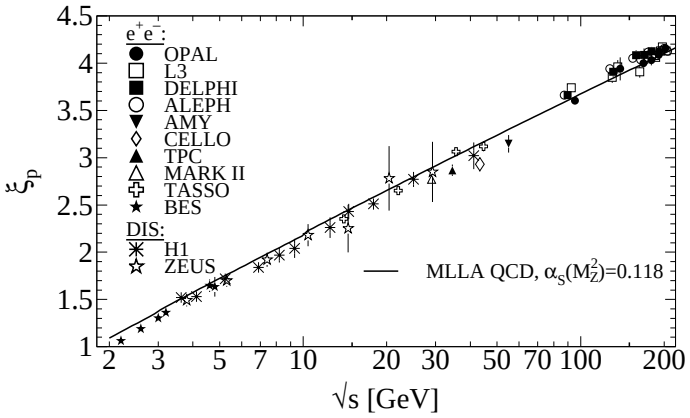

Figure 19.5: Evolution of the peak position, ξ_p, of the ξ distribution with the CM energy $\sqrt{s}$. The MLLA QCD prediction using $\alpha_S(s = M_Z^2) = 0.118$ is superimposed to the data of Refs. [28–30,33–37,58,59,78,79,82–90].

The average charged particle multiplicity is another observable sensitive to fragmentation functions for small particle momenta. Perturbative predictions using both NLO [91] and MLLA [92,94] have been obtained from solving Eq. (19.4) yielding

$$\left\langle n_G(Q^2)\right\rangle \propto \alpha_S^b(Q^2)\cdot\exp\left[\frac{c}{4\pi b_0\sqrt{\alpha_S(Q^2)}}\cdot\left(1+6a_2\frac{\alpha_S(Q^2)}{\pi}\right)\right] \tag{19.11}$$

where $b = \frac{1}{4}+\frac{10}{27}\frac{n_f}{4\pi b_0}$, $c=\sqrt{96\pi}$, with $b_0=(33-2n_f)/(12\pi)$, cp. Section 9 of this *Review*, for n_f contributing quark flavours. Higher order corrections to Eq. (19.11) are known up to next-to-next-to-next-to-leading order (3NLO), for details and references see [95]. The term proportional to $a_2 \approx -0.502 + 0.0421\,n_f - 0.00036\,n_f^2$ in Eq. (19.11) is the contribution due to NNLO corrections [96]. The quantity $\langle n_G(Q^2)\rangle$ strictly refers to the average number of gluons, while for quarks a correction factor $r = \langle n_G\rangle/\langle n_q\rangle$ weakly depending on Q^2 is required due to the different color factors in quark and gluon couplings, respectively. Higher order corrections up to 3NLO on the asymptotic value $r = C_A/C_F = 9/4$ [97] are quoted in [95].

Employing the hypothesis of 'Local Parton-Hadron Duality' (LPHD) [92], *i.e.*, that the color charge of partons is balanced locally in phase space and, hence, their hadronization occurs locally such that (Mellin transformed) parton and hadron inclusive distributions directly correspond, Eq. (19.11) can be applied to describe average charged particle multiplicities obtained in e^+e^- annihilation. The equation can also be applied to $e^\pm p$ scattering if the current fragmentation region of the Breit frame is considered for measuring the average charged particle multiplicity. Fig. 19.6 shows corresponding data and fits of Eq. (19.11) where apart from a LPHD normalization factor a constant offset has been allowed for, that is $\langle n_{\rm ch}(Q)\rangle = K_{\rm LHPD}\cdot\langle n_G(Q)\rangle/r + n_0$.

In hadron-hadron collisions beam remnants, e.g. from single-diffractive (SD) scattering where one colliding proton is negligibly deflected while hadrons are related with the other colliding proton are well-separated in rapidity from the former proton, contribute to the measurement of the hadron multiplicity from a hard parton-parton scattering, making interpretation of the data more model dependent. Experimental results are usually given for inelastic processes or for non-single diffractive processes (NSD). Due to the large beam particle momenta at Tevatron and LHC, not all final state particles can be detected within the limited detector acceptance. Therefore, experiments at Tevatron and LHC quote particle multiplicities for limited ranges of pseudo-rapidity $\eta = -\ln\tan(\vartheta/2)$ or at central rapidity, i.e. $\eta = 0$, shown in Fig. 19.6.

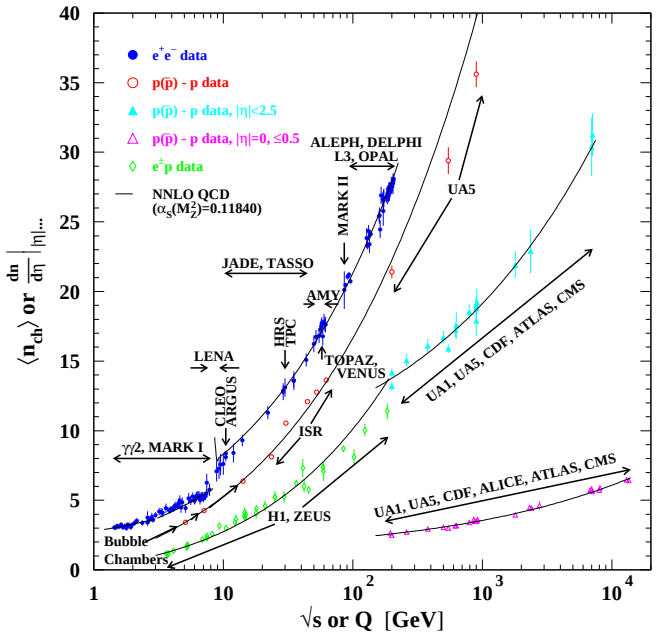

Figure 19.6: Average charged particle multiplicity $\langle n_{\rm ch}\rangle$ as a function of $\sqrt{s}$ or Q for e^+e^- and $p\overline{p}$ annihilations, and pp and ep collisions. The indicated errors are statistical and systematic uncertainties added in quadrature, except when no systematic uncertainties are given. All NNLO QCD curves are Eq. (19.11) with fitted normalization, K_{LHPD}, and offset, n_0, using a fixed $\alpha_S(M_Z^2) = 0.1184$ [93] and for e^+e^- annihilation data $n_f = 3$, 4, or 5 depending on $\sqrt{s}$, else $n_f = 3$. $\mathbf{e^+e^-}$: Contributions from K_S^0 and Λ decays included. Data compiled from Refs. [8,9,28,34,35,40,79,85,98–108]. $\mathbf{e^\pm p}$: Multiplicities have been measured in the current fragmentation region of the Breit frame. Data compiled from Refs. [59,60,64,109,110]. $\mathbf{p^{(}\overline{p}^{)}}$: Measured values above 20 GeV refer to non-single diffractive (NSD) processes. Central pseudorapidity multiplicities $(dn/d\eta)|_{|\eta|...}$ refer to either $|\eta| < 2.5$ (CMS: $|\eta| < 2.4$) or $|\eta| = 0$ (UA5, CMS, ALICE: $|\eta| < 0.5$). Data compiled from Refs. [111–126].

An universality of the average particle multiplicities in e^+e^- and $p^{(}\overline{p}^{)}$ processes has been reported in Ref. [127] when considering an effective collision energy $Q_{\rm eff} = \sqrt{s}/k$ in $p^{(}\overline{p}^{)}$ reduced by a factor of $k \approx 3$ plus a constant offset of $n_0 \approx 2$. A more detailed review is available in Ref. [128]. According to investigations presented in Ref. [129] the universality of the energy dependence of average particle multiplicities also applies to hadron-hadron and nucleus-nucleus collisions for both full and central rapidity multiplicities. Evidence for this universality is given by the good agreement for the energy dependence of Eq. (19.11) when fit to the $p^{(}\overline{p}^{)}$ data as shown in Fig. 19.6.

19.4. Fragmentation models

Although the scaling violation can be calculated perturbatively, the actual form of the parton fragmentation functions is non-perturbative. Perturbative evolution gives rise to a shower of quarks and gluons (partons). Multi-parton final states from leading and higher order matrix element calculations are linked to these parton showers using factorization prescriptions, also called matching schemes, see Ref. [130] for an overview. Phenomenological schemes are then used to model the carry-over of parton momenta and flavor to the hadrons. Implemented in Monte Carlo event generators (see Section 41 of this *Review*), these schemes have been tuned using e^+e^- data and provide good description of hadron collisions as well, thus providing evidence of the universality of the fragmentation functions.

19.5. Quark and gluon fragmentation functions

The fragmentation functions are solutions to the evolution equations Eq. (19.4), but need to be parametrized at some initial scale μ_0^2 (usually around 1 GeV^2 for light quarks and gluons and m_Q^2 for heavy quarks). A usual parametrization for light hadrons is [139–146]

$$D_i^h(x,\mu_0^2) = Nx^\alpha(1-x)^\beta\left(1+\gamma(1-x)^\delta\right) \ , \qquad (19.12)$$

where the normalization N, and the parameters α, β, γ and δ in general depend on the energy scale μ_0^2, and also on the type of the parton, i, and the hadron, h. Frequently the term involving γ and δ is left out [141–144]. Heavy flavor fragmentation into heavy mesons is discussed in Sec. 19.9. The parameters of Eq. (19.12) (see [139–144]) are obtained by performing global fits to data on various hadron types for different combinations of partons and hadrons in e^+e^-, lepton-hadron and hadron-hadron collisions.

Sets of fragmentation functions are available for pions, kaons, protons, neutrons, etas, Lambdas and charged hadrons [139–149].

Data from e^+e^- annihilation present the cleanest experimental source for the measurement of fragmentation functions, but can not contribute to disentangle quark from antiquark distributions. Since the bulk of the e^+e^- annihilation data is obtained at the mass of the Z-boson, where the electroweak couplings are roughly the same for the different partons, it provides the most precise determination of the flavor-singlet quark fragmentation. Flavor tagged results [150], distinguishing between the light quark, charm and bottom contributions are of particular value for flavor decomposition, even though those measurements can not be unambiguously interpreted in perturbative QCD. It is worth noticing that recent NNLO analysis of fragmentation functions [147,148], so far restricted to e^+e^- annihilation data, show an improvement in the theoretical description of the observable.

The most relevant source for quark-antiquark (and also flavor) separation is provided by data from semi-inclusive DIS (SIDIS). Semi-inclusive measurements are usually performed at much lower scales than for e^+e^- annihilation. The inclusion of SIDIS data in global fits allows for a wider coverage in the evolution of the fragmentation functions, resulting at the same time in a stringent test of the universality of these distributions. Charged-hadron production data in hadronic collisions also presents a sensitivity on (anti-)quark fragmentation functions.

The gluon fragmentation function $D_g(x)$ can be extracted, in principle, from the longitudinal fragmentation function F_L in Eq. (19.2), as the coefficient functions $C_{L,i}$ for quarks and gluons are comparable at order α_s. However at NLO, *i.e.*, including the $\mathcal{O}(\alpha_s^2)$ coefficient functions $C_{L,i}^{(2)}$ [25], quark fragmentation is dominant in F_L over a large part of the kinematic range, reducing the sensitivity on D_g. This distribution could be determined also analyzing the evolution of the fragmentation functions. This possibility is limited by the lack of sufficiently precise data at energy scales away from the Z-resonance and the dominance of the quark contributions and at medium and large values of x.

D_g can also be deduced from the fragmentation of three-jet events in which the gluon jet is identified, for example, by tagging the other two jets with heavy quark decays. To leading order, the measured distributions of $x = E_{\rm had}/E_{\rm jet}$ for particles in gluon jets can be identified directly with the gluon fragmentation function $D_g(x)$. At higher orders the theoretical interpretation of this observable is ambiguous.

A comparison of recent fits of NLO fragmentation functions for $\pi^+ + \pi^-$ obtained by DSS14 [146], AKK08 [140] and HKNS07 [144] is shown in Fig. 19.7. Differences between the sets are large especially for the gluon fragmentation function over the full range of x and for the quark distribution at large momentum fractions. The differences are even larger for other species of hadrons like kaons and protons [139,140,144]. Recent analyses [144,146,151] estimate the uncertainties involved in the extraction of fragmentation functions.

A direct constraint on D_g is provided by $pp, p\bar{p} \to hX$ data. At variance with e^+e^- annihilation and SIDIS, for this process gluon fragmentation starts to contribute at the lowest order in the coupling constant, introducing a strong sensitivity on D_g. At large $x \gtrsim 0.5$, where information from e^+e^- is sparse, data from hadronic colliders facilitate significantly improved extractions of D_g [139,140,146]. Recent LHC data has been included in the latest update for pion-fragmentation functions in [146], see Sec.(17.7) for more details.

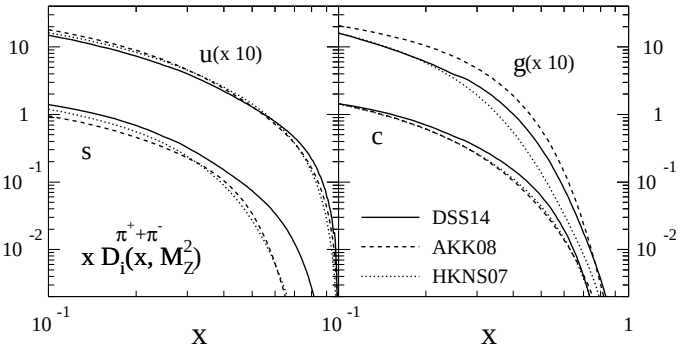

Figure 19.7: Comparison of up, strange, charm and gluon NLO fragmentation functions for $\pi^+ + \pi^-$ at the mass of the Z. The different lines correspond to the result of the most recent analyses performed in Refs. [140,144,146].

Photonic fragmentation functions play a relevant role in the theoretical understanding of inclusive photon production in (leptonic and hadronic) high energy processes. Similar to the analogy of parton fragmentation functions and parton distributions in deep inelastic scattering, also photonic fragmentation functions are analogous to the photon structure function F_2^γ (see review on structure fuctions in Section 18 of this *Review*). Since photons have a pointlike coupling to quarks [152], the corresponding fragmentation functions obey inhomogeneous evolution equations and are generally decomposed into a perturbative and a non-perturbative component [143,153,154]. The hadronic part, sometimes approximated by the Vector Meson Dominance Model, can be obtained by performing global analysis to the available prompt photon data [7,30,33,37–39,87,155,187].

19.6. Identified particles in e^+e^- and semi-inclusive DIS

A great wealth of measurements of e^+e^- fragmentation into identified particles exists. A collection of references for data on fragmentation into identified particles is given on Table 51.1 of this *Review*. Representative of this body of data is Fig. 19.8 which shows fragmentation functions as the scaled momentum spectra of charged particles at several CM energies.

Quantitative results of studies of scaling violation in e^+e^- fragmentation have been reported in [7,39,157,158]. The values of α_s obtained are consistent with the world average (see review on QCD in Section 9 of this *Review*).

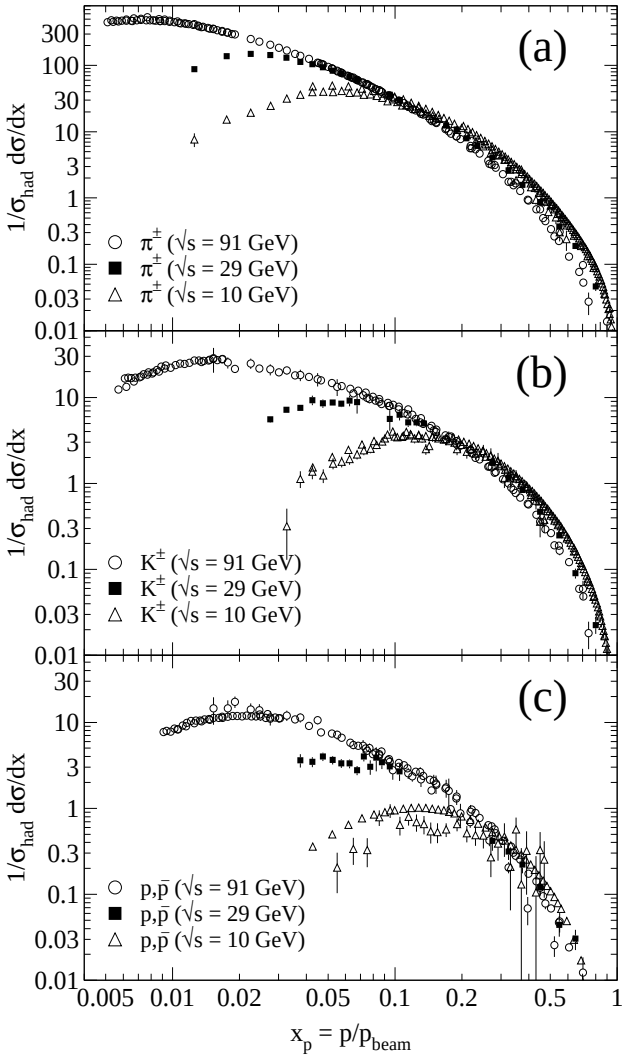

Figure 19.8: Scaled momentum spectra of (a) $\pi^\pm$, (b) $K^\pm$, and (c) $p/\overline{p}$ at $\sqrt{s} = 10$, 29, and 91 GeV [42–44,87,155,156].

Many studies have been made of identified particles produced in lepton-hadron scattering, although fewer particle species have been measured than in e^+e^- collisions. References [159–166] and [167–173] are representative of the data from fixed target and ep collider experiments, respectively.

QCD calculations performed at NLO provide an overall good description of the HERA data [55,56,60,173–175] for both SIDIS [176] and the hadron transverse momentum distribution [50] in the kinematic regions in which the calculations are predictive. A first step towards a NNLO calculation for SIDIS has been presented in [51].

Fig. 19.9(a) compares lower-energy fixed-target and HERA data on strangeness production, showing that the HERA spectra have substantially increased multiplicities, albeit with insufficient statistical precision to study scaling violations. The fixed-target data show that the Λ rate substantially exceeds the $\overline{\Lambda}$ rate in the remnant region, owing to the conserved baryon number from the baryon target. Fig. 19.9(b) shows neutral and charged pion fragmentation functions $1/N \cdot dn/dz$, where z is defined as the ratio of the pion energy to that of the exchanged boson, both measured in the laboratory frame. Results are shown from HERMES and the EMC experiments, where HERMES data have been evolved with NLO QCD to $\langle Q^2 \rangle = 25$ GeV^2 in order to be consistent with the EMC. Each of the experiments uses various kinematic cuts to ensure that the measured particles lie in the region which is expected to be associated with the struck quark. In the DIS kinematic regime accessed at these experiments, and over

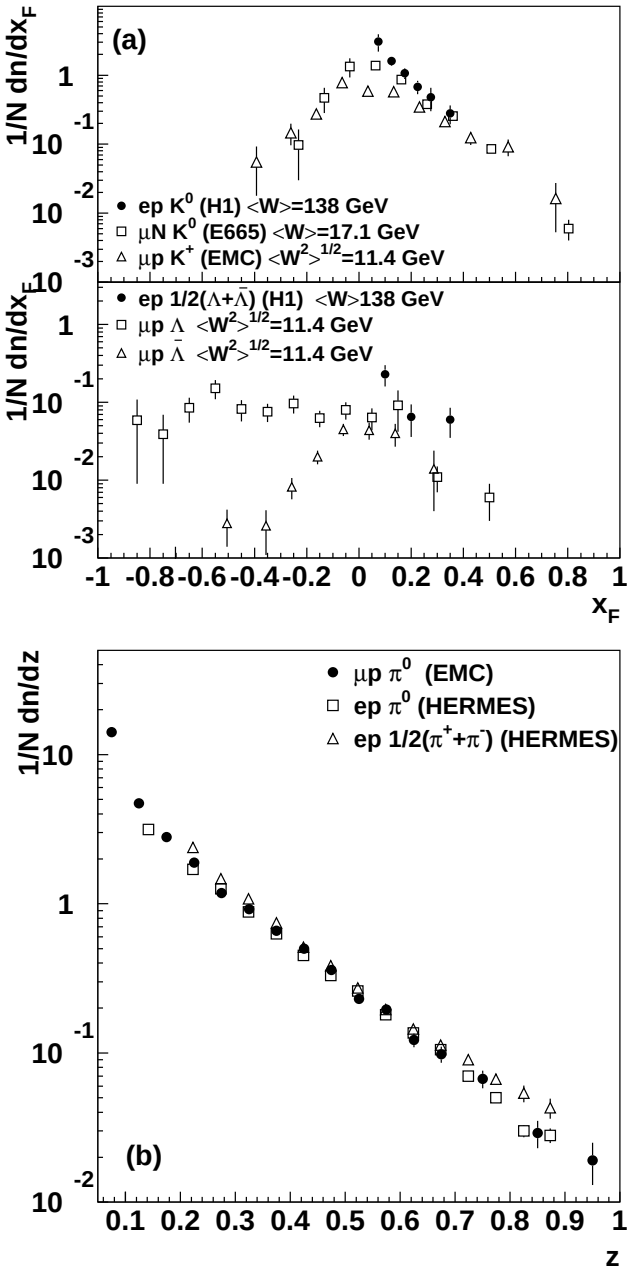

Figure 19.9: (a) $1/N \cdot dn/dx_F$ for identified strange particles in DIS at various values of W [159,162,167]. (b) $1/N \cdot dn/dz$ for measurements of pions from fixed-target DIS experiment [160,163,166].

the range in z shown in Fig. 19.9, the z and x_F variables have similar values [52]. The precision data on identified particles can be used in the study of the quark flavor content of the proton [177].

Data on identified particle production can aid the investigation of the universality of jet fragmentation in e^+e^- and DIS. The strangeness suppression factor γ_s, as derived principally from tuning the Lund string model [132] within JETSET [133], is typically found to be around 0.3 in e^+e^- experiments [77], although values closer to 0.2 [178] have also been obtained. A number of measurements of so-called V^0-particles (K^0, Λ^0) and the relative rates of V^0's and inclusively produced charged particles have been performed at HERA [167–169] and fixed target experiments [159]. These typically favour a stronger suppression ($\gamma_s \approx 0.2$) than usually obtained from e^+e^- data although values close to 0.3 have also been obtained [179,180].

However, when comparing the description of QCD-based models

for lepton-hadron interactions and e^+e^- collisions, it is important to note that the overall description by event generators of inclusively produced hadronic final states is more accurate in e^+e^- collisions than lepton-hadron interactions [181]. Predictions of particle rates in lepton-hadron scattering are affected by uncertainties in the modelling of the parton composition of the proton and photon, the extended target remnant, and initial and final-state QCD radiation. Furthermore, the tuning of event generators for e^+e^- collisions is typically based on a larger set of parameters and uses more observables [77] than are used when optimizing models for lepton-hadron data [182].

19.7. Fragmentation in hadron-hadron collisions

An extensive set on high-transverse momentum (p_T) single-inclusive hadron data has been collected in $h_1h_2 \to hX$ scattering processes, both at high energy colliders and fixed-target experiments [183–202]. Only the transverse momentum p_T is considered in hadron-hadron collisions because of lack of knowledge of the longitudinal momentum of the hard subprocess. Fig. 19.10 shows the cross section (which is proportional to the particle number) density $\frac{\mathrm{d}^3\sigma}{\mathrm{d}p^3} = \frac{\mathrm{d}^3\sigma}{\mathrm{d}p_x\mathrm{d}p_y\mathrm{d}p_z} = \frac{E}{\pi m^2}\frac{\mathrm{d}^2\sigma}{\mathrm{d}y\mathrm{d}(p_T^2)}$ for a compilation of neutral pion and charged hadron production data for energies in the range $\sqrt{s} \approx 23$ - 7000 GeV. More data for different hadron species has been recently obtained at high energy colliders [203–207].

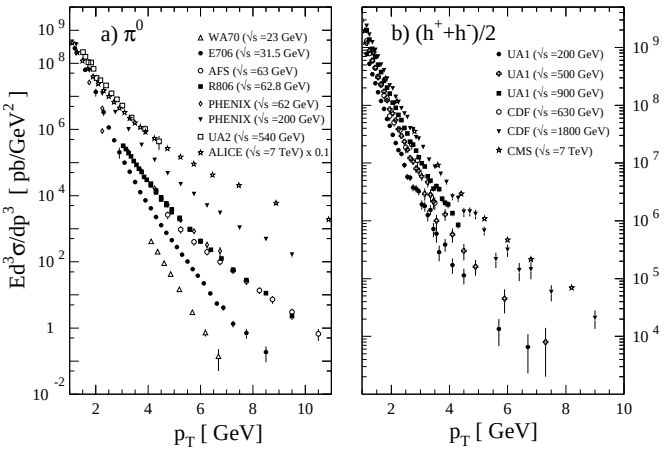

Figure 19.10: Selection of inclusive (a) π^0 and (b) charged-hadron production data from pp [121,191,195,199–202] and $p\bar{p}$ [183,186,189] collisions.

The differential cross-section for high-transverse momentum distributions has been computed to next-to-leading order accuracy in perturbative QCD [208]. The factorization, μ_f, and renomalization, μ, scales of these calculations typical range from $p_T^2/4 \leq \mu_f^2, \mu^2 \leq 4p_T^2$.

NLO calculations significantly under-predict the cross-section for several fixed-target energy data sets [209,210]. Different strategies have been developed to ameliorate the theoretical description at fixed-target energies. A possible phenomenological approach involves the introduction of a non-perturbative intrinsic partonic transverse momentum [202,211,212]. From the perturbative side, the resummation of the dominant higher order corrections at threshold produces an enhancement of the theoretical calculation that significantly improves the description of the data [213,214].

Data collected at high energy colliders are either included in global fit analyses or used as a test for the universality of fragmentation functions. Certain tension has been observed between data sets from lower-energy (RHIC) and higher-energy (LHC) collisions [215]. The tension can be largely resolved by excluding from the analysis data with transverse momentum smaller than $\approx 5 - 10$ GeV, where fixed order pQCD calculations are not expected to provide an accurate description of the process. Still, after removing the smallish p_T values where the data sets appear to be mutually exclusive in the global fit, lower-energy collisions data show a preference towards harder gluon fragmentation at large z than LHC data [146].

Measurements of hadron production in longitudinally polarized pp collisions are used mainly in the determination of the polarized gluon distribution in the proton [216,217].

Hadron production provides a critical observable for probing the high energy-density matter produced in heavy-ion collisions. Measurements at colliders show a suppression of inclusive hadron yields at high transverse momentum for AA collisions compared to pp scattering, indicating the formation of a dense medium opaque to quark and gluons, see e.g. [218].

19.8. Spin-dependent fragmentation

Measurements of charged-hadron production in unpolarized lepton-hadron scattering provide a unique tool to perform a flavor-separation determination of polarized parton densities from DIS interactions with longitudinally polarized targets [219–223].

Polarized scattering presents the possibility to measure the spin transfer from the struck quark to the final hadron, and thus develop spin-dependent fragmentation functions [224,225]. Early measurements of the longitudinal spin transfer to Lambda hyperons have been presented in [226,227]. This process is also useful in the study of the quark transversity distribution [228], which describes the probability of finding a transversely polarized quark with its spin aligned or anti-aligned with the spin of a transversely polarized nucleon. The transversity function is chiral-odd, and therefore not accessible through measurements of inclusive lepton-hadron scattering. Semi-inclusive DIS, in which another chiral-odd observable may be involved, provides a valuable tool to probe transversity. The Collins fragmentation function [229] relates the transverse polarization of the quark to that of the final hadron. It is chiral-odd and naive T-odd, leading to a characteristic single spin asymmetry in the azimuthal angular distribution of the produced hadron in the hadron scattering plane. Azimuthal angular distributions in semi-inclusive DIS can also be produced by other processes requiring non-polarized fragmentation functions, like the Sivers mechanism [230].

A number of experiments have measured these asymmetries [231–241]. Collins and Sivers asymmetries have been shown experimentally to be non zero by the HERMES measurements on transversely polarized proton targets [232–234]. Independent information on the Collins function has been provided by the BELLE Collaboration [235–236]. Measurements performed by the COMPASS collaboration on deuteron targets show results compatible with zero for both asymmetries [237–239].

19.9. Heavy quark fragmentation

It was recognized very early [242] that a heavy flavored meson should retain a large fraction of the momentum of the primordial heavy quark, and therefore its fragmentation function should be much harder than that of a light hadron. In the limit of a very heavy quark, one expects the fragmentation function for a heavy quark to go into any heavy hadron to be peaked near $x = 1$.

When the heavy quark is produced at a momentum much larger than its mass, one expects important perturbative effects, enhanced by powers of the logarithm of the transverse momentum over the heavy quark mass, to intervene and modify the shape of the fragmentation function. In leading logarithmic order (*i.e.*, including all powers of $\alpha_s \log m_Q/p_T$), the total (*i.e.*, summed over all hadron types) perturbative fragmentation function is simply obtained by solving the leading evolution equation for fragmentation functions, Eq. (19.4), with the initial condition due to the finite mass of the heavy quark given by $D_Q(z,\mu^2)\big|_{\mu^2=m_Q^2} = \delta(1-z)$ and $D_i(z,\mu^2)\big|_{\mu^2=m_Q^2} = 0$ for $i \neq$ Q (here $D_i(z,\mu^2)$, stands for the probability to produce a heavy quark Q from parton i with a fraction z of the parton momentum).

Several extensions of the leading logarithmic result have appeared in the literature. Next-to-leading-log (NLL) order results for the perturbative heavy quark fragmentation function have been obtained

in [243]. The resummation of the dominant logarithmic contributions at large z was performed in [45] to next-to-leading-log accuracy. Fixed-order calculations of the fragmentation function at order α_s^2 in e^+e^- annihilation have appeared in [244] while the initial condition for the perturbative heavy quark fragmentation function has been extended to NNLO in [245].

Inclusion of non-perturbative effects in the calculation of the heavy-quark fragmentation function is done by convoluting the perturbative result with a phenomenological non-perturbative form. This form follows from the simple kinematical consideration that the formation of a hadron by attaching light quarks/anti-quarks to the heavy quark will slightly decelerate the heavy quark. Thus its shape will show a peak which becomes increasingly centered next to $z = 1$ the higher the quark mass. Among the most popular parametrizations we have the following:

$$\text{Peterson } \textit{et al.}\ [246]: \quad D_{\rm np}(z) \propto \frac{1}{z}\left(1-\frac{1}{z}-\frac{\epsilon}{1-z}\right)^{-2} \tag{19.13}$$

$$\text{Kartvelishvili } \textit{et al.}\ [247]: \quad D_{\rm np}(z) \propto z^{\alpha}(1-z)\,, \tag{19.14}$$

$$\text{Collins\&Spiller [248]}: \quad D_{\rm np}(z) \propto \left(\frac{1-z}{z}+\frac{(2-z)\epsilon_C}{1-z}\right)\times (1+z^2)\left(1-\frac{1}{z}-\frac{\epsilon_C}{1-z}\right)^{-2} \tag{19.15}$$

$$\text{Colangelo\&Nason [249]}: \quad D_{\rm np}(z) \propto (1-z)^{\alpha} z^{\beta} \tag{19.16}$$

$$\text{Bowler [250]}: \quad D_{\rm np}(z) \propto z^{-(1+bm_{h,\perp}^2)}\,(1-z)^{a}\exp\left(-\frac{bm_{h,\perp}^2}{z}\right) \tag{19.17}$$

$$\text{Braaten } \textit{et al.}\ [251]: \quad \text{(see Eq. (31), (32) in [251])} \tag{19.18}$$

where ϵ, ϵ_C, a, $bm_{h,\perp}^2$, α, and β are non-perturbative parameters, depending upon the heavy hadron considered. The parameters entering the non-perturbative forms are fitted together with some model of hard radiation, which can be either a shower Monte Carlo, a leading-log or NLL calculation (which may or may not include Sudakov resummation), or a fixed order calculation. In [244], for example, the Peterson *et al.* [246] ϵ parameter for charm and bottom production is fitted from the measured distributions of refs. [252,265] for charm, and of [270] for bottom. If the leading-logarithmic approximation (LLA) is used for the perturbative part, one finds $\epsilon_c \approx 0.05$ and $\epsilon_b \approx 0.006$; if a second order calculation is used one finds $\epsilon_c \approx 0.035$ and $\epsilon_b \approx 0.0033$; if a NLL improved fixed order $\mathcal{O}(\alpha_S^2)$ calculation is used instead of NLO $\mathcal{O}(\alpha_S)$ one finds $\epsilon_c \approx 0.022$ and $\epsilon_b \approx 0.0023$. The larger values found in the LL approximation are consistent with what is obtained in the context of parton shower models [254], as expected. The ϵ parameter for charm and bottom scales roughly with the inverse square of the heavy flavour mass. This behaviour can be justified by several arguments [242,255,256]. It can be used to relate the non-perturbative parts of the fragmentation functions of charm and bottom quarks [244,249,257].

A more conventional approach [258] involves the introduction of a unique set of heavy quark fragmentation functions of non-perturbative nature that obey the usual massless evolution equations in Eq. (19.4). Finite mass terms of the form $(m_{\rm Q}/p_T)^n$ are kept in the corresponding short distance coefficient function for each scattering process. Within this approach, the initial condition for the perturbative fragmentation function provides the term needed to define the correct subtraction scheme to match the massless limit for the coefficient function (see e.g. [259]) . Such implementation is in line with the variable flavor number scheme introduced for parton distributions functions, as described in Section 18 of this *Review*.

High statistics data for charmed mesons production near the Υ resonance (excluding decay products of B mesons) have been published [260,261]. They include results for D and D^*, D_s (see also [262,263]) and Λ_c. Shown in Fig. 19.11(a) are the CLEO and BELLE inclusive cross-sections times branching ratio $\mathcal{B}$, $s \cdot \mathcal{B}d\sigma/dx_p$, for the production of D^0 and D^{*+}. The variable x_p approximates the light-cone momentum fraction z, but is not identical to it. The two measurements are consistent with each other.

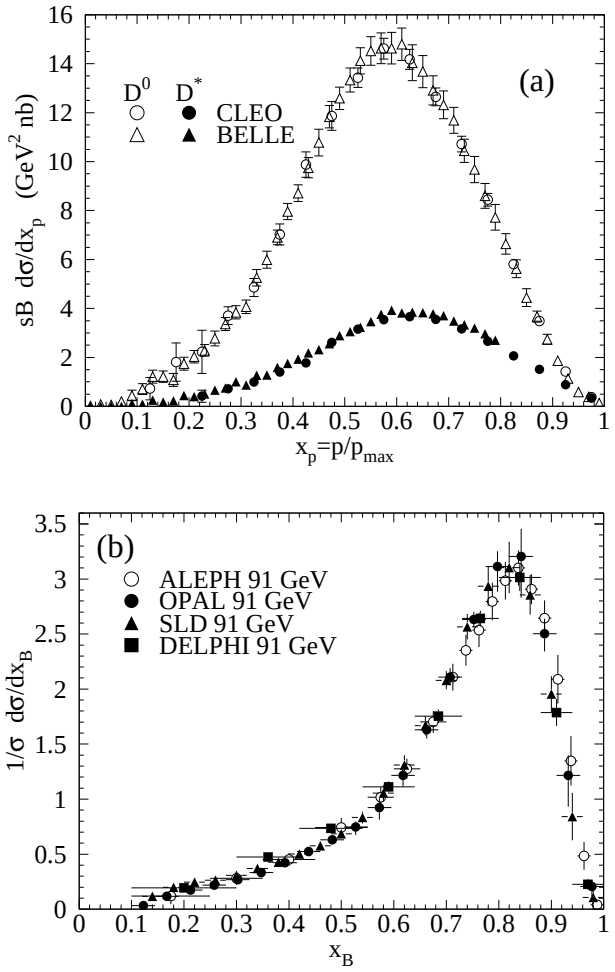

Figure 19.11: (a) Efficiency-corrected inclusive cross-section measurements for the production of D^0 and D^{*+} in e^+e^- measurements at $\sqrt{s} \approx 10.6$ GeV, excluding B decay products [260,261]. (b) Measured e^+e^- fragmentation function of b quarks into B hadrons at $\sqrt{s} \approx 91$ GeV [271].

The branching ratio $\mathcal{B}$ represents $D^0 \to K^-\pi^+$ for the D^0 results and for the D^{*+} the product branching fraction: $D^{*+} \to D^0\pi^+$, $D^0 \to K^-\pi^+$. Given the high precision of CLEO's and BELLE's data, a superposition of different parametric forms for the non-perturbative contribution is needed to obtain a good fit [23]. Older studies are reported in Refs. [264–266]. Charmed meson spectra on the Z peak have been published by OPAL and ALEPH [138,267].

Charm quark production has also been extensively studied at HERA by the H1 and ZEUS collaborations. Measurements have been made of $D^{*\pm}$, $D^{\pm}$, and $D_s^{\pm}$ mesons and the Λ_c baryon. See, for example, Refs. [268,269].

Experimental studies of the fragmentation function for b quarks, shown in Fig. 19.11(b), have been performed at LEP and SLD [270–272]. Commonly used methods identify the B meson through its semileptonic decay or based upon tracks emerging from the B secondary vertex. Heavy flavour contributions from gluon splitting are usually explicitly removed before fitting for the fragmentation functions. The studies in [271] fit the B spectrum using a Monte Carlo shower model supplemented with non-perturbative fragmentation functions yielding consistent results.

The experiments measure primarily the spectrum of B mesons. This defines a fragmentation function which includes the effect of the decay of higher mass excitations, like the B^* and B^{**}. In the literature (cf. details in Ref. [274]) , there is sometimes ambiguity in what is defined to be the bottom fragmentation function. Instead of using what is directly measured (*i.e.*, the B meson spectrum)

corrections are applied to account for B^* or B^{**} production in some cases.

Heavy-flavor production in e^+e^- collisions is the primary source of information for the role of fragmentation effects in heavy-flavor production in hadron-hadron and lepton-hadron collisions. The QCD calculations tend to underestimate the data in certain regions of phase space. Some experimental results from LHC summarized in [275] show such deviations e.g. at high transverse jet momentum and also at low di-jet separation angles, see [276] for details, and were already theoretically investigated in [277].

Both bottomed- and charmed-mesons spectra have been measured at the Tevatron with unprecedented accuracy [278]. The measured spectra are in good agreement with QCD calculations (including non-perturbative fragmentation effects inferred from e^+e^- data [279]).

The HERA collaborations have produced a number of measurements of beauty production; see, for example, Refs. [268,280–283]. As for the Tevatron data, the HERA results are described well by QCD-based calculations using fragmentation models optimised with e^+e^- data.

Besides degrading the fragmentation function by gluon radiation, QCD evolution can also generate soft heavy quarks, increasing in the small x region as $\sqrt{s}$ increases. Several theoretical studies are available on the issue of how often $b\bar{b}$ or $c\bar{c}$ pairs are produced indirectly, via a gluon splitting mechanism [284–286]. Experimental results from studies on charm and bottom production via gluon splitting, given in [267,287–291], yield weighted averages of $\overline{n}_{g\to c\bar{c}} = 3.05 \pm 0.45\%$ and $\overline{n}_{g\to b\bar{b}} = 0.277 \pm 0.072\%$, respectively.

References:

1. G. Altarelli, Phys. Reports **81**, 1 (1982).
2. R.K. Ellis *et al.*, *QCD and Collider Physics*, Cambridge University Press (1996).
3. S. Albino *et al.*, `arXiv:0804.2021` (2008).
4. F. Arleo, Eur. Phys. J. **C61**, 603 (2009).
5. P. Nason and B.R. Webber, Nucl. Phys. **B421**, 473 (1994); Erratum *ibid.* **B480**, 755 (1996).
6. J.D. Bjorken and E.A. Paschos, Phys. Rev. **185**, 1975 (1969); R.P. Feynman, *Photon Hadron Interactions*, Benjamin, New York (1972).
7. ALEPH Collab.: D. Barate *et al.*, Phys. Lett. **B357**, 487 (1995); Erratum *ibid.*, **B364**, 247 (1995).
8. OPAL Collab.: R. Akers *et al.*, Z. Phys. **C68**, 203 (1995).
9. DELPHI Collab.: P. Abreu *et al.*, Eur. Phys. J. **C6**, 19 (1999).
10. W. Kittel and E.A. De Wolf, *Soft Multihadron Dynamics*, World Scientific (2005).
11. H.F. Jones, Nuovo Cimento **40A**, 1018 (1965); K.H. Streng *et al.*, Z. Phys. **C2**, 237 (1979).
12. V.N. Gribov and L.N. Lipatov, Sov. J. Nucl. Phys. **15**, 438 (1972); V.N. Gribov and L.N. Lipatov, Sov. J. Nucl. Phys. **15**, 675 (1972); L.N. Lipatov, Sov. J. Nucl. Phys. **20**, 95 (1975); G. Altarelli and G. Parisi, Nucl. Phys. **B126**, 298 (1977); Yu.L. Dokshitzer, Sov. Phys. JETP Lett. **46**, 641 (1977).
13. H. Georgi and H.D. Politzer, Nucl. Phys. **B136**, 445 (1978); J.F. Owens, Phys. Lett. **B76**, 85 (1978); T. Uematsu, Phys. Lett. **B79**, 97 (1978).
14. G. Curci *et al.*, Nucl. Phys. **B175**, 27 (1980).
15. W. Furmanski and R. Petronzio, Phys. Lett. **97B**, 437 (1980).
16. E.G. Floratos *et al.*, Nucl. Phys. **B192**, 417 (1981); T. Munehisa *et al.*, Prog. Theor. Phys. **67**, 609 (1982).
17. J. Kalinowski *et al.*, Nucl. Phys. **B181**, 221 (1981); J. Kalinowski *et al.*, Nucl. Phys. **B181**, 253 (1981).
18. M. Stratmann and W. Vogelsang, Nucl. Phys. **B496**, 41 (1997).
19. Yu.L. Dokshitzer *et al.*, Phys. Lett. **B634**, 504 (2006).
20. A. Mitov *et al.*, Phys. Lett. **B638**, 61 (2006).
21. S. Moch and A. Vogt, Phys. Lett. **B659**, 290 (2008).
22. A.A. Almasy, A. Vogt, S. Moch, Nucl. Phys. **B854**, 133 (2013).
23. M. Cacciari *et al.*, JHEP **0604**, 006 (2006); M. Cacciari *et al.*, JHEP **0510**, 034 (2005).
24. G. Altarelli *et al.*, Nucl. Phys. **B160**, 301 (1979); R. Baier and K. Fey, Z. Phys. **C2**, 339 (1979).
25. P.J. Rijken and W.L. van Neerven, Phys. Lett. **B386**, 422 (1996); P.J. Rijken and W.L. van Neerven, Phys. Lett. **B392**, 207 (1997); P.J. Rijken and W.L. van Neerven, Nucl. Phys. **B487**, 233 (1997).
26. A. Mitov and S. Moch, Nucl. Phys. **B751**, 18 (2006).
27. ALEPH Collab.: E. Barate *et al.*, Phys. Reports **294**, 1 (1998).
28. ALEPH Collab.: D. Buskulic *et al.*, Z. Phys. **C73**, 409 (1997).
29. L3 Collab.: B. Adeva *et al.*, Phys. Lett. **B259**, 199 (1991).
30. AMY Collab.: Y.K. Li *et al.*, Phys. Rev. **D41**, 2675 (1990).
31. HRS Collab.: D.Bender *et al.*, Phys. Rev. **D31**, 1 (1984).
32. MARK II Collab.: G.S. Abrams *et al.*, Phys. Rev. Lett. **64**, 1334 (1990).
33. MARK II Collab.: A. Petersen *et al.*, Phys. Rev. **D37**, 1 (1988).
34. OPAL Collab.: R. Akers *et al.*, Z. Phys. **C72**, 191 (1996).
35. OPAL Collab.: K. Ackerstaff *et al.*, Z. Phys. **C75**, 193 (1997).
36. OPAL Collab.: G. Abbiendi *et al.*, Eur. Phys. J. **C16**, 185 (2000).
37. TASSO Collab.: W. Braunschweig *et al.*, Z. Phys. **C47**, 187 (1990).
38. OPAL Collab.: K. Ackerstaff *et al.*, Eur. Phys. J. **C7**, 369 (1998); OPAL Collab.: G. Abbiendi *et al.*, Eur. Phys. J. **C27**, 467 (2003).
39. DELPHI Collab.: P. Abreu *et al.*, Phys. Lett. **B398**, 194 (1997).
40. OPAL Collab.: G. Abbiendi *et al.*, Eur. Phys. J. **C37**, 25 (2004).
41. TASSO Collab.: R. Brandelik *et al.*, Phys. Lett. **B114**, 65 (1982).
42. SLD Collab.: K. Abe *et al.*, Phys. Rev. **D69**, 072003 (2004).
43. TPC Collab.: H. Aihara *et al.*, Phys. Rev. Lett. **61**, 1263 (1988).
44. BELLE Collab.: M. Leitgab *et al.*, Phys. Rev. Lett. **111**, 062002 (2013); BaBar Collab.: J.P. Lees *et al.*, Phys. Rev. **D88**, 032011 (2013).
45. M. Cacciari and S. Catani, Nucl. Phys. **B617**, 253 (2001).
46. J. Blümlein and V. Ravindran, Phys. Lett. **B640**, 40 (2006).
47. S. Moch and A. Vogt, Phys. Lett. **B680**, 239 (2009).
48. S. Moch and A. Vogt, JHEP **0911**, 099 (2009).
49. A. Vogt, Phys. Lett. **B691**, 77 (2010).
50. P. Aurenche *et al.*, Eur. Phys. J. **C34**, 277 (2004); A. Daleo *et al.*, Phys. Rev. **D71**, 034013 (2005); B.A. Kniehl *et al.*, Nucl. Phys. **B711**, 345 (2005); Erratum *ibid.* **B720**, 231 (2005).
51. D. de Florian *et al.*, Phys. Rev. **D95**, 0334027 (2017).
52. E665 Collab.: M.R. Adams *et al.*, Phys. Lett. **B272**, 163 (1991).
53. EMC Collab.: M. Arneodo *et al.*, Z. Phys. **C35**, 417 (1987).
54. H1 Collab.: I. Abt *et al.*, Z. Phys. **C63**, 377 (1994).
55. ZEUS Collab.: M. Derrick *et al.*, Z. Phys. **C70**, 1 (1996).
56. ZEUS Collab.: J. Breitweg *et al.*, Phys. Lett. **B414**, 428 (1997).
57. H1 Collab.: S. Aid *et al.*, Nucl. Phys. **B445**, 3 (1995).
58. ZEUS Collab.: M. Derrick *et al.*, Z. Phys. **C67**, 93 (1995).
59. H1 Collab.: C. Adloff *et al.*, Nucl. Phys. **B504**, 3 (1997).
60. ZEUS Collab.: J. Breitweg *et al.*, Eur. Phys. J. **C11**, 251 (1999).
61. H1 Collab.: F.D. Aaron *et al.*, Phys. Lett. **B654**, 148 (2007).
62. DELPHI Collab.: P. Abreu *et al.*, Phys. Lett. **B311**, 408 (1993).
63. MARK II Collab.: J.F. Patrick *et al.*, Phys. Rev. Lett. **49**, 1232, (1982).
64. ZEUS Collab.: S. Chekanov *et al.*, JHEP **0806**, 061 (2008).
65. K.H. Streng *et al.*, Z. Phys. **C2**, 237 (1979).
66. A.H. Mueller, Phys. Lett. **B104**, 161 (1981).
67. A. Bassetto *et al.*, Nucl. Phys. **B207**, 189 (1982).
68. Yu.L. Dokshitzer *et al.*, Z. Phys. **C15**, 324 (1982).
69. A.H. Mueller, Nucl. Phys. **B213**, 85 (1983); Erratum in *ibid.* **B241**, 141 (1984).
70. Yu.L. Dokshitzer *et al.*, Int. J. Mod. Phys. **A7**, 1875 (1992).

71. Yu.L. Dokshitzer *et al.*, *Basics of Perturbative QCD*, Editions Frontières (1991).
72. V.A. Khoze and W. Ochs, Int. J. Mod. Phys. **A12**, 2949 (1997).
73. C.P. Fong and B.R. Webber, Nucl. Phys. **B355**, 54 (1992).
74. S. Albino *et al.*, Nucl. Phys. **B851**, 86 (2011); S. Albino *et al.*, Nucl. Phys. **B855**, 801 (2012).
75. A. Vogt, JHEP **1110**, 025 (2011); C.-H. Kom, A. Vogt, K. Yeats, JHEP **1210**, 033 (2012).
76. P. Bolzoni, B.A. Kniehl, A.V. Kotikov, Phys. Rev. Lett. **109**, 242002 (2012); P. Bolzoni, B.A. Kniehl, A.V. Kotikov, Nucl. Phys. **B875**, 18 (2013).
77. DELPHI Collab.: P. Abreu *et al.*, Z. Phys. **C73**, 11 (1996).
78. DELPHI Collab.: P. Abreu *et al.*, Z. Phys. **C73**, 229 (1997).
79. L3 Collab.: P. Achard *et al.*, Phys. Reports **399**, 71 (2004).
80. TOPAZ Collab.: R. Itoh *et al.*, Phys. Lett. **B345**, 335 (1995).
81. TASSO Collab.: W. Braunschweig *et al.*, Z. Phys. **C22**, 307 (1990).
82. OPAL Collab.: M.Z. Akrawy *et al.*, Phys. Lett. **B247**, 617 (1990).
83. BES Collab.: J.Z. Bai *et al.*, Phys. Rev. **D69**, 072002 (2004).
84. ALEPH Collab.: D. Buskulic *et al.*, Z. Phys. **C55**, 209 (1992).
85. ALEPH Collab.: A. Heister *et al.*, Eur. Phys. J. **C35**, 457 (2004).
86. DELPHI Collab.: P. Abreu *et al.*, Phys. Lett. **B275**, 231 (1992).
87. DELPHI Collab.: P. Abreu *et al.*, Eur. Phys. J. **C5**, 585 (1998).
88. DELPHI Collab.: P. Abreu *et al.*, Phys. Lett. **B459**, 397 (1999).
89. L3 Collab.: M. Acciarri *et al.*, Phys. Lett. **B444**, 569 (1998).
90. TPC/TWO-GAMMA Collab.: H. Aihara *et al.*, LBL 23737.
91. B.R. Webber, Phys. Lett. **B143**, 501 (1984).
92. Ya.I. Azimov, Yu.L. Dokshitzer, V.A. Khoze, S.I. Troyan, Z. Phys. **C27**, 65 (1985).
93. J. Beringer *et al.* (Particle Data Group), Phys. Rev. **D86**, 010001 (2012).
94. Ya.I. Azimov, Yu.L. Dokshitzer, V.A. Khoze, S.I. Troyan, Z. Phys. **C31**, 213 (1986).
95. I.M. Dremin, J.W. Gary, Phys. Reports **349**, 301 (2001).
96. I.M. Dremin, V.A. Nechitailo, Mod. Phys. Lett. **A9**, 1471 (1994).
97. S.J. Brodsky, J.F. Gunion, Phys. Rev. Lett. **37**, 402 (1976).
98. OPAL Collab.: P.D. Acton *et al.*, Z. Phys. **C53**, 539 (1992) and references therein.
99. ALEPH Collab.: D. Buskulic *et al.*, Z. Phys. **C69**, 15 (1996).
100. DELPHI Collab.: P. Abreu *et al.*, Phys. Lett. **B372**, 172 (1996).
101. DELPHI Collab.: P. Abreu *et al.*, Phys. Lett. **B416**, 233 (1998).
102. DELPHI Collab.: P. Abreu *et al.*, Eur. Phys. J. **C18**, 203 (2000).
103. L3 Collab.: M. Acciarri *et al.*, Phys. Lett. **B371**, 137 (1996).
104. L3 Collab.: M. Acciarri *et al.*, Phys. Lett. **B404**, 390 (1997).
105. L3 Collab.: M. Acciarri *et al.*, Phys. Lett. **B444**, 569 (1998).
106. TOPAZ Collab.: K. Nakabayashi *et al.*, Phys. Lett. **B413**, 447 (1997).
107. VENUS Collab.: K. Okabe *et al.*, Phys. Lett. **B423**, 407 (1998).
108. ARGUS Collab.: H. Albrecht *et al.*, Z. Phys. **C54**, 13 (1992).
109. H1 Collab.: F.D. Aaron *et al.*, Phys. Lett. **B654**, 148 (2007).
110. ZEUS Collab.: S. Chekanov *et al.*, Phys. Lett. **B510**, 36 (2001).
111. J. Benecke *et al.*, Nucl. Phys. **B76**, 29 (1976).
112. W.M. Morse *et al.*, Phys. Rev. **D15**, 66 (1977).
113. W. Thomé *et al.*, Nucl. Phys. **B129**, 365 (1977).
114. A. Breakstone *et al.*, Phys. Rev. **D30**, 528 (1984).
115. UA5 Collab.: G.J. Alner *et al.*, Phys. Reports **154**, 247 (1987).
116. UA5 Collab.: R.E. Ansorge *et al.*, Z. Phys. **C43**, 357 (1989).
117. UA1 Collab.: C. Albajar *et al.*, Nucl. Phys. **B335**, 261 (1990).
118. CDF Collab.: F.Abe *et al.*, Phys. Rev. **D41**, 2330 (1990).
119. ALICE Collab.: K. Aamodt *et al.*, Eur. Phys. J. **C68**, 89 (2010).
120. CMS Collab.: V. Khachatryan *et al.*, JHEP **1002**, 041 (2010).
121. CMS Collab.: V. Khachatryan *et al.*, JHEP **1101**, 079 (2011).
122. CMS Collab.: V. Khachatryan *et al.*, Phys. Rev. Lett. **105**, 022002 (2010).
123. ATLAS Collab.: G. Aad *et al.*, Eur. Phys. J. **C76**, 403 (2016).
124. ATLAS Collab.: G. Aad *et al.*, Eur. Phys. J. **C76**, 502 (2016).
125. ALICE Collab.: J. Adam *et al.*, Phys. Lett. **B753**, 319 (2016).
126. ALICE Collab.: J. Adam *et al.*, Eur. Phys. J. **C77**, 33 (2017).
127. P.V. Chliapnikov, V.A. Uvarov, Phys. Lett. **B251**, 192 (1990).
128. J.F. Grosse-Oetringhaus, K. Reygers, J. Phys. **G37**, 083001 (2010).
129. E.K.G. Sarkisyan, A.S. Sakharov, hep-ph/0410324; E.K.G. Sarkisyan, A.S. Sakharov, AIP Conf. Proc. **828**, 35 (2005), [hep-ph/0510191]; E.K.G. Sarkisyan, A.S. Sakharov, Eur. Phys. J. **C70**, 533 (2010).
130. S. Höche *et al.*, hep-ph/0602031 (2006); J. Alwall *et al.*, Eur. Phys. J. **C53**, 473 (2008); S. Mrenna and P.Richardson, JHEP **0405**, 040 (2004).
131. X. Artru and G. Mennessier, Nucl. Phys. **B70**, 93 (1974).
132. B. Andersson *et al.*, Phys. Reports **97**, 31 (1983).
133. T. Sjöstrand and M. Bengtsson, Comp. Phys. Comm. **43**, 367 (1987); T. Sjöstrand, Comp. Phys. Comm. **82**, 74 (1994).
134. T. Sjöstrand, S. Mrenna, P. Skands, JHEP **0605**, 026 (2006); T. Sjöstrand, S. Mrenna, P. Skands, Comp. Phys. Comm. **178**, 852 (2008).
135. S. Chun and C. Buchanan, Phys. Reports **292**, 239 (1998).
136. G. Marchesini *et al.*, Comp. Phys. Comm. **67**, 465 (1992); G. Corcella *et al.*, JHEP **0101**, 010 (2001); M. Bähr *et al.*, Eur. Phys. J. **C58**, 639 (2008).
137. T. Gleisberg *et al.*, JHEP **0902**, 007 (2009).
138. OPAL Collab.: G. Alexander *et al.*, Z. Phys. **C69**, 543 (1996).
139. D. de Florian *et al.*, Phys. Rev. **D76**, 074033 (2007); D. de Florian *et al.*, Phys. Rev. **D75**, 114010 (2007).
140. S. Albino *et al.*, Nucl. Phys. **B803**, 42 (2008).
141. S. Kretzer *et al.*, Eur. Phys. J. **C22**, 269 (2001).
142. S. Kretzer, Phys. Rev. **D62**, 054001 (2000).
143. L. Bourhis *et al.*, Eur. Phys. J. **C19**, 89 (2001).
144. M. Hirai *et al.*, Phys. Rev. **D75**, 094009 (2007).
145. C. Aidala *et al.*, Phys. Rev. **D83**, 034002 (2011).
146. D. de Florian *et al.*, Phys. Rev. **D91**, 014035 (2015).
147. D. Anderle *et al.*, Phys. Rev. **D92**, 114017 (2015).
148. V. Bertone *et al.*[NNPDF Collab.], arXiv:1706.07049 [hep-ph].
149. D. de Florian *et al.*, Phys. Rev. **D95**, 094019 (2017).
150. ALEPH Collab.: R. Barate *et al.*, Eur. Phys. J. **C17**, 1 (2000); OPAL Collab.: R. Akers *et al.*, Z. Phys. **C68**, 179 (1995); OPAL Collab.: G. Abbiendi *et al.*, Eur. Phys. J. **C11**, 217 (1999).
151. M. Epele *et al.*, Phys. Rev. **D86**, 074028 (2012).
152. E. Witten, Nucl. Phys. **210**, 189 (1977).
153. L. Bourhis, M. Fontannaz, and J. P. Guillet, Eur. Phys. J. **C2**, 529 (1998).
154. M. Gluck, E. Reya, and A. Vogt, Phys. Rev. **D48**, 116 (1993); Erratum *ibid.* **D51**, 1427 (1995).
155. SLD Collab.: K. Abe *et al.*, Phys. Rev. **D59**, 052001 (1999).
156. ALEPH Collab.: D. Buskulic *et al.*, Z. Phys. **C66**, 355 (1995); ARGUS Collab.: H. Albrecht *et al.*, Z. Phys. **C44**, 547 (1989); OPAL Collab.: R. Akers *et al.*, Z. Phys. **C63**, 181 (1994).
157. DELPHI Collab.: P. Abreu *et al.*, Eur. Phys. J. **C13**, 573 (2000).
158. B.A. Kniehl *et al.*, Phys. Rev. Lett. **85**, 5288 (2000).
159. E665 Collab.: M.R. Adams *et al.*, Z. Phys. **C61**, 539 (1994).
160. EMC Collab.: J.J. Aubert *et al.*, Z. Phys. **C18**, 189 (1983); EMC Collab.: M. Arneodo *et al.*, Phys. Lett. **B150**, 458 (1985).
161. EMC Collab.: M. Arneodo *et al.*, Z. Phys. **C33**, 167 (1986).
162. EMC Collab.: M. Arneodo *et al.*, Z. Phys. **C34**, 283 (1987).
163. HERMES Collab.: A. Airapetian *et al.*, Eur. Phys. J. **C21**, 599 (2001).
164. HERMES Collab.: A. Airapetian *et al.*, Phys. Rev. **D87**, 074029 (2013).
165. COMPASS Collab.: N. Makke, PoS **DIS2013**, 202 (2013) [arXiv:1307.3407].
166. T.P. M$^{\rm c}$Pharlin *et al.*, Phys. Lett. **B90**, 479 (1980).
167. H1 Collab.: S. Aid *et al.*, Nucl. Phys. **B480**, 3 (1996).

168. H1 Collab.: F. D. Aaron *et al.*, Phys. Lett. **B673**, 119 (2009).
169. ZEUS Collab.: M. Derrick *et al.*, Z. Phys. **C68**, 29 (1995);
ZEUS Collab.: J. Breitweg *et al.*, Eur. Phys. J. **C2**, 77 (1998).
170. ZEUS Collab.: S. Chekanov *et al.*, Phys. Lett. **B553**, 141 (2003).
171. ZEUS Collab.: S. Chekanov *et al.*, Nucl. Phys. **B786**, 181 (2007).
172. H1 Collab.: F. D. Aaron *et al.*, Eur. Phys. J. **C61**, 185 (2009).
173. H1 Collab.: C. Adloff *et al.*, Eur. Phys. J. **C18**, 293 (2000);
H1 Collab.: A. Aktas *et al.*, Eur. Phys. J. **C36**, 413 (2004).
174. P. Dixon *et al.*, J. Phys. **G25**, 1453 (1999).
175. H1 Collab.: C. Adloff *et al.*, Phys. Lett. **B462**, 440 (1999).
176. D. Graudenz, Fortsch. Phys. **45**, 629 (1997).
177. S. Albino *et al.*, Phys. Rev. **D75**, 034018 (2007).
178. OPAL Collab.: P.D. Acton *et al.*, Phys. Lett. **B305**, 407 (1993).
179. E632 Collab.: D. DeProspo *et al.*, Phys. Rev. **D50**, 6691 (1994).
180. ZEUS Collab.: S. Chekanov *et al.*, Eur. Phys. J. **C51**, 1 (2007).
181. G. Grindhammer *et al.*, in: *Proceedings of the Workshop on Monte Carlo Generators for HERA Physics*, Hamburg, Germany, 1998/1999.
182. N. Brook *et al.*, in: *Proceedings of the Workshop for Future HERA Physics at HERA*, Hamburg, Germany, 1996.
183. CDF Collab.: F. Abe *et al.*, Phys. Rev. Lett. **61**, 1819 (1988).
184. CDF Collab.: D.E. Acosta *et al.*, Phys. Rev. **D72**, 052001 (2005).
185. UA1 Collab.: G. Arnison *et al.*, Phys. Lett. **B118**, 167 (1982).
186. UA1 Collab.: C. Albajar *et al.*, Nucl. Phys. **B335**, 261 (1990).
187. UA1 Collab.: G. Bocquet *et al.*, Phys. Lett. **B366**, 434 (1996).
188. UA2 Collab.:M. Banner *et al.*, Phys. Lett. **B122**, 322 (1983).
189. UA2 Collab.:M. Banner *et al.*, Phys. Lett. **B115**, 59 (1982).
190. UA2 Collab.:M. Banner *et al.*, Z. Phys. **C27**, 329 (1985).
191. PHENIX Collab.: S. S. Adler *et al.*, Phys. Rev. Lett. **91**, 241803 (2003).
192. PHENIX Collab.: A. Adare *et al.*, Phys. Rev. **D76**, 051106 (2007).
193. BRAHMS Collab.:, I. Arsene *et al.*, Phys. Rev. Lett. **98**, 252001 (2007).
194. STAR Collab.: J. Adams *et al.*, Phys. Lett. **B637**, 161 (2006);
STAR Collab.:, J. Adams *et al.*, Phys. Rev. Lett. **97**, 152302 (2006);
STAR Collab.: B.I. Abelev *et al.*, Phys. Rev. **C75**, 064901 (2007);
STAR Collab.:, G. Agakishiev *et al.*, Phys. Rev. Lett. **108**, 072302 (2012);
STAR Collab.: B.I. Abelev *et al.*, Phys. Rev. **C81**, 064904 (2010).
195. ALICE Collab.: B. Abelev *et al.*, Phys. Lett. **B717**, 162 (2012).
196. ALICE Collab.: B. Abelev *et al.*, Eur. Phys. J. **C73**, 2662 (2013).
197. E706 Collab.: L. Apanasevich *et al.*, Phys. Rev. Lett. **81**, 2642 (1998).
198. UA6 Collab.: G. Ballocchi *et al.*, Phys. Lett. **B436**, 222 (1998).
199. WA70 Collab.: M. Bonesini *et al.*, Z. Phys. **C38**, 371 (1988).
200. AFS Collab.: E. Anassontzis *et al.*, Sov. J. Nucl. Phys. **51**, 836 (1990).
201. R806 Collab.: C. Kourkoumelis *et al.*, Z. Phys. **C5**, 95 (1980).
202. E706 Collab.: L. Apanasevich *et al.*, Phys. Rev. **D68**, 052001 (2003).
203. ALICE Collab.: K. Aamodt *et al.*, Eur. Phys. J. **C71**, 1594 (2011);
ALICE Collab.: B. Abelev *et al.*, Phys. Lett. **B710**, 557 (2012);
ALICE Collab.: B. Abelev *et al.*, Phys. Lett. **B712**, 309 (2012);
ALICE Collab.: B. Abelev *et al.*, Eur. Phys. J. **C75**, 1 (2015);
ALICE Collab.: J. Adam *et al.*, Eur. Phys. J. **C75**, 226 (2015).
204. ATLAS Collab.: G. Aad *et al.*, Phys. Rev. **D85**, 012001 (2012);
ATLAS Collab.: G. Aad *et al.*, Eur. Phys. J. **C74**, 2895 (2014).
205. CDF Collab.: D. Acosta *et al.*, Phys. Rev. **D72**, 052001 (2005).
206. CMS Collab.: V. Khachatryan *et al.*, JHEP **1105**, 064 (2011);
CMS Collab.: S. Chatrchyan *et al.*, Eur. Phys. J. **C72**, 2164 (2012);
CMS Collab.: S. Chatrchyan *et al.*, Phys. Rev. **D88**, 052001 (2013).
207. LHCb Collab.: R. Aaij *et al.*, Phys. Lett. **B703**, 267 (2011).
208. F. Aversa *et al.*, Nucl. Phys. **B327**, 105 (1989);
D. de Florian, Phys. Rev. **D67**, 054004 (2003);
B. Jager *et al.*, Phys. Rev. **D67**, 054005 (2003).
209. U. Baur *et al.*, `hep-ph/0005226` (2000).
210. P. Aurenche, *et al.*, Eur. Phys. J. **C13**, 347 (2000).
211. L. Apanasevich *et al.*, Phys. Rev. **D59**, 074007 (1999).
212. U. D'Alesio and F. Murgia, Phys. Rev. **D70**, 074009 (2004).
213. D. de Florian and W. Vogelsang, Phys. Rev. **D71**, 114004 (2005).
214. L.G. Almeida *et al.*, Phys. Rev. **D80**, 074016 (2009).
215. D. d'Enterria *et al.*, Nucl. Phys. **B883**, 615 (2014).
216. PHENIX Collab.: A. Adare *et al.*, Phys. Rev. **D76**, 051106 (2007).
217. PHENIX Collab.: A. Adare *et al.*, Phys. Rev. **D79**, 012003 (2009).
218. PHENIX Collab.: K. Adcox *et al.*, Phys. Rev. Lett. **88**, 022301 (2002);
STAR Collab.: C. Adler *et al.*, Phys. Rev. Lett. **90**, 082302 (2003).
219. COMPASS Collab.: M. Alekseev *et al.*, Phys. Lett. **B660**, 458, (2008).
220. HERMES Collab.: A. Airapetian *et al.*, Phys. Rev. **D71**, 012003 (2005).
221. SMC Collab.: B. Adeva *et al.*, Phys. Lett. **B420**, 180 (1998).
222. HERMES Collab.: A. Airapetian *et al.*, Phys. Lett. **B666**, 446 (2008).
223. D. de Florian *et al.*, Phys. Rev. Lett. **101**, 072001 (2008).
224. P.J. Mulders and R.D. Tangerman, Nucl. Phys. **B461**, 197 (1996);
Erratum: *ibid.*, **B484**, 538 (1997).
225. R. Jacob, Nucl. Phys. **A711**, 35 (2002).
226. COMPASS Collab.: M. Alekseev *et al.*, Eur. Phys. J. **C64**, 171 (2009).
227. HERMES Collab.: A. Airapetian *et al.*, Phys. Rev. **D74**, 072004 (2006).
228. J.P. Ralston and D.E. Soper, Nucl. Phys. **B152**, 109 (1979).
229. J. Collins, Nucl. Phys. **B396**, 161 (1993).
230. D. Sivers, Phys. Rev. **D43**, 261 (1991).
231. CLAS Collab.: H. Avakian *et al.*, Phys. Rev. **D69**, 112004 (2004).
232. HERMES Collab.: A. Airapetian *et al.*, Phys. Rev. Lett. **84**, 4047 (2000).
233. HERMES Collab.: A. Airapetian *et al.*, Phys. Rev. **D64**, 097101 (2001).
234. HERMES Collab.: A. Airapetian *et al.*, Phys. Rev. Lett. **94**, 012002 (2005).
235. BELLE Collab.: K. Abe *et al.*, Phys. Rev. Lett. **96**, 232002 (2006).
236. BELLE Collab.: K. Abe *et al.*, Phys. Rev. **D78**, 032011 (2008).
237. COMPASS Collab.: V.Y Alexakhin *et al.*, Phys. Rev. Lett. **94**, 202002 (2005).
238. COMPASS Collab.: V.Y Alexakhin *et al.*, Nucl. Phys. **B765**, 31 (2007).
239. COMPASS Collab.: M. Alekseev *et al.*, Phys. Lett. **B673**, 127 (2009).
240. COMPASS Collab.: M. Alekseev *et al.*, Phys. Lett. **B692**, 240 (2010).
241. COMPASS Collab.: M. Alekseev *et al.*, Eur. Phys. J. **C70**, 39 (2010).
242. V.A. Khoze *et al.*, *Proceedings, Conference on High-Energy Physics, Tbilisi 1976*;
J.D. Bjorken, Phys. Rev. **D17**, 171 (1978).
243. B. Mele and P. Nason, Phys. Lett. **B245**, 635 (1990);
B. Mele and P. Nason, Nucl. Phys. **B361**, 626 (1991).
244. P. Nason and C. Oleari, Phys. Lett. **B418**, 199 (1998);
P. Nason and C. Oleari, Phys. Lett. **B447**, 327 (1999);
P. Nason and C. Oleari, Nucl. Phys. **B565**, 245 (2000).
245. K. Melnikov and A. Mitov, Phys. Rev. **D70**, 034027 (2004).

246. C. Peterson *et al.*, Phys. Rev. **D27**, 105 (1983).
247. V.G. Kartvelishvili *et al.*, Phys. Lett. **B78**, 615 (1978).
248. P. Collins and T. Spiller, J. Phys. **G11**, 1289 (1985).
249. G. Colangelo and P. Nason, Phys. Lett. **B285**, 167 (1992).
250. M.G. Bowler, Z. Phys. **C11**, 169 (1981).
251. E. Braaten *et al.*, Phys. Rev. **D51**, 4819 (1995).
252. OPAL Collab.: R. Akers *et al.*, Z. Phys. **C67**, 27 (1995).
253. Particle Data Group: C. Amsler *et al.*, Phys. Lett. **B667**, 1 (2008).
254. J. Chrin, Z. Phys. **C36**, 163 (1987).
255. R.L. Jaffe and L. Randall, Nucl. Phys. **B412**, 79 (1994).
256. M. Cacciari and E. Gardi, Nucl. Phys. **B664**, 299 (2003).
257. L. Randall and N. Rius, Nucl. Phys. **B441**, 167 (1995).
258. J. Collins, Phys. Rev. **D58**, 094002 (1998).
259. B.A. Kniehl *et al.*, Eur. Phys. J. **C41**, 199 (2005).
260. CLEO Collab.: M. Artuso *et al.*, Phys. Rev. **D70**, 112001 (2004).
261. BELLE Collab.: R. Seuster *et al.*, Phys. Rev. **D73**, 032002 (2006).
262. CLEO Collab.: R.A. Briere *et al.*, Phys. Rev. **D62**, 112003 (2000).
263. BABAR Collab.: B. Aubert *et al.*, Phys. Rev. **D65**, 091104 (2002).
264. CLEO Collab.: D. Bortoletto *et al.*, Phys. Rev. **D37**, 1719 (1988).
265. ARGUS Collab.: H. Albrecht *et al.*, Z. Phys. **C52**, 353 (1991).
266. ARGUS Collab.: H. Albrecht *et al.*, Z. Phys. **C54**, 1 (1992).
267. ALEPH Collab.: R. Barate *et al.*, Phys. Lett. **B561**, 213 (2003).
268. H1 Collab.: F.D. Aaron *et al.*, Eur. Phys. J. **C65**, 89 (2010).
269. ZEUS Collab.: S. Chekanov *et al.*, JHEP **0707**, 074 (2007);
ZEUS Collab: H. Abramowicz *et al.*, JHEP , 1309 (2013);
H1 Collab.: A. Aktas *et al.*, Eur. Phys. J. **C51**, 271 (2007);
H1 Collab.: F.D. Aaron *et al.*, Eur. Phys. J. **C59**, 589 (2009).
270. ALEPH Collab.: D. Buskulic *et al.*, Phys. Lett. **B357**, 699 (1995).
271. ALEPH Collab.: A. Heister *et al.*, Phys. Lett. **B512**, 30 (2001);
DELPHI Collab.: J. Abdallah *et al.*, Eur. Phys. J. **C71**, 1557 (2011);
OPAL Collab.: G. Abbiendi *et al.*, Eur. Phys. J. **C29**, 463 (2003);
SLD Collab.: K. Abe *et al.*, Phys. Rev. **D65**, 092006 (2002);
Erratum *ibid.*, **D66**, 079905 (2002).
272. L3 Collab.: B. Adeva *et al.*, Phys. Lett. **B261**, 177 (1991).
273. CDF Collab.: F. Abe *et al.*, Phys. Rev. Lett. **71**, 500 (1993);
CDF Collab.: F. Abe *et al.*, Phys. Rev. Lett. **71**, 2396 (1993);
CDF Collab.: F. Abe *et al.*, Phys. Rev. **D50**, 4252 (1994);
CDF Collab.: F. Abe *et al.*, Phys. Rev. Lett. **75**, 1451 (1995);
CDF Collab.: D. Acosta *et al.*, Phys. Rev. **D66**, 032002 (2002);
CDF Collab.: D. Acosta *et al.*, Phys. Rev. **D65**, 052005 (2002);
D0 Collab.: S. Abachi *et al.*, Phys. Rev. Lett. **74**, 3548 (1995);
UA1 Collab.: C. Albajar *et al.*, Phys. Lett. **B186**, 237 (1987);
UA1 Collab.: C. Albajar *et al.*, Phys. Lett. **B256**, 121 (1991);
Erratum *ibid.*, **B272**, 497 (1991).
274. O. Biebel, P. Nason, and B.R. Webber, Bicocca-FT-01-20, Cavendish-HEP-01/12, MPI-PhE/2001-14 [hep-ph/0109282 (2001)].
275. H. Evans, arXiv:1110.5294 (2011);
E. Aguiló, arXiv:1205.5678 (2012);
F. Simonetto, Journal of Physics: Conference Series **347**, 012014 (2012).
276. CMS Collab.: V. Khachatryan *et al.*, JHEP **1103**, 136 (2011);
ATLAS Collab.: G. Aad *et al.*, Eur. Phys. J. **C71**, 1846 (2011);
CMS Collab.: S. Chatrychyan *et al.*, JHEP **1204**, 084 (2012);
ATLAS Collab.: G. Aad *et al.*, Eur. Phys. J. **C73**, 2301 (2013).
277. H. Jung *et al.*, Phys. Rev. **D85**, 034035 (2012).
278. CDF Collab.: D. Acosta *et al.*, Phys. Rev. Lett. **91**, 241804 (2003);
CDF Collab.: D. Acosta *et al.*, Phys. Rev. **D71**, 032001 (2005).
279. M. Cacciari and P. Nason, JHEP **0309**, 006 (2003);
M. Cacciari *et al.*, JHEP **0407**, 033 (2004);
B.A. Kniehl *et al.*, Phys. Rev. Lett. **96**, 012001 (2006).
280. ZEUS Collab.: H. Abramovicz *et al.*, Eur. Phys. J. **C71**, 1573 (2011).
281. ZEUS Collab.: S. Chekanov *et al.*, Phys. Rev. **D78**, 072001 (2008).
282. ZEUS Collab.: S. Chekanov *et al.*, JHEP **0902**, 032 (2009).
283. H1 Collab.: F.D. Aaron *et al.*, Eur. Phys. J. **C72**, 2148 (2012).
284. A.H. Mueller and P. Nason, Nucl. Phys. **B266**, 265 (1986);
M.L. Mangano and P. Nason, Phys. Lett. **B285**, 160 (1992).
285. M.H. Seymour, Nucl. Phys. **B436**, 163 (1995).
286. D.J. Miller and M.H. Seymour, Phys. Lett. **B435**, 213 (1998).
287. ALEPH Collab.: R. Barate *et al.*, Phys. Lett. **B434**, 437 (1998).
288. DELPHI Collab.: P. Abreu *et al.*, Phys. Lett. **B405**, 202 (1997).
289. L3 Collab.: M. Acciarri *et al.*, Phys. Lett. **B476**, 243 (2000).
290. OPAL Collab.: G. Abbiendi *et al.*, Eur. Phys. J. **C13**, 1 (2000).
291. SLD Collab.: K. Abe *et al.*, SLAC-PUB-8157 [hep-ex/9908028 (1999)].

20. Experimental Tests of Gravitational Theory

Revised November 2017, by T. Damour (IHES, Bures-sur-Yvette, France).

Einstein's theory of General Relativity (GR), the current "standard" theory of gravitation, describes gravity as a universal deformation of the Minkowski metric:

$$g_{\mu\nu}(x^\lambda) = \eta_{\mu\nu} + h_{\mu\nu}(x^\lambda) \ , \ \text{where } \eta_{\mu\nu} = \text{diag}(-1,+1,+1,+1) \ . \quad (20.1)$$

GR is classically defined by two postulates. One postulate states that the Lagrangian density describing the propagation and self-interaction of the gravitational field is

$$\mathcal{L}_{\rm Ein}[g_{\alpha\beta}] = \frac{c^4}{16\pi G_N}\sqrt{g}g^{\mu\nu}R_{\mu\nu}(g_{\alpha\beta}) \ , \quad (20.2)$$

where G_N is Newton's constant, $g = -\det(g_{\mu\nu})$, $g^{\mu\nu}$ is the matrix inverse of $g_{\mu\nu}$, and where the Ricci tensor $R_{\mu\nu} \equiv R^\alpha_{\mu\alpha\nu}$ is the only independent trace of the curvature tensor

$$R^\alpha_{\mu\beta\nu} = \partial_\beta\Gamma^\alpha_{\mu\nu} - \partial_\nu\Gamma^\alpha_{\mu\beta} + \Gamma^\alpha_{\sigma\beta}\Gamma^\sigma_{\mu\nu} - \Gamma^\alpha_{\sigma\nu}\Gamma^\sigma_{\mu\beta} \ , \quad (20.3)$$

$$\Gamma^\lambda_{\mu\nu} = \tfrac{1}{2}g^{\lambda\sigma}(\partial_\mu g_{\nu\sigma} + \partial_\nu g_{\mu\sigma} - \partial_\sigma g_{\mu\nu}) \ , \quad (20.4)$$

A second postulate states that $g_{\mu\nu}$ couples universally, and minimally, to all the fields of the Standard Model by replacing everywhere the Minkowski metric $\eta_{\mu\nu}$. Schematically (suppressing matrix indices and labels for the various gauge fields and fermions and for the Higgs doublet),

$$\begin{aligned}\mathcal{L}_{\rm SM}[\psi, A_\mu, H, g_{\mu\nu}] = &-\tfrac{1}{4}\sum\sqrt{g}g^{\mu\alpha}g^{\nu\beta}F^a_{\mu\nu}F^a_{\alpha\beta} - \sum\sqrt{g}\,\overline{\psi}\gamma^\mu D_\mu\psi \\ &- \tfrac{1}{2}\sqrt{g}g^{\mu\nu}\overline{D_\mu H}D_\nu H - \sqrt{g}\,V(H) \\ &- \sum\lambda\sqrt{g}\,\overline{\psi}\,H\psi \ , \end{aligned} \quad (20.5)$$

where $\gamma^\mu\gamma^\nu + \gamma^\nu\gamma^\mu = 2g^{\mu\nu}$, and where the covariant derivative D_μ contains, besides the usual gauge field terms, a spin-dependent gravitational contribution. From the total action follow Einstein's field equations,

$$R_{\mu\nu} - \tfrac{1}{2}Rg_{\mu\nu} = \frac{8\pi G_N}{c^4}T_{\mu\nu} \ . \quad (20.6)$$

Here $R = g^{\mu\nu}R_{\mu\nu}$, $T_{\mu\nu} = g_{\mu\alpha}g_{\nu\beta}T^{\alpha\beta}$, and $T^{\mu\nu} = (2/\sqrt{g})\delta\mathcal{L}_{\rm SM}/\delta g_{\mu\nu}$ is the (symmetric) energy-momentum tensor of the Standard Model matter. The theory is invariant under arbitrary coordinate transformations: $x'^\mu = f^\mu(x^\nu)$. To solve the field equations Eq. (20.6), one needs to fix this coordinate gauge freedom. *E.g.*, the "harmonic gauge" (which is the analogue of the Lorenz gauge, $\partial_\mu A^\mu = 0$, in electromagnetism) corresponds to imposing the condition $\partial_\nu(\sqrt{g}g^{\mu\nu}) = 0$.

In this *Review*, we only consider the classical limit of gravitation (*i.e.* classical matter and classical gravity). Quantum gravitational effects are expected (when considered at low energy) to correct the classical action Eq. (20.3) by additional terms involving quadratic and higher powers of the curvature tensor. This suggests that the validity of classical gravity extends (at most) down to length scales of order the Planck length $L_P = \sqrt{\hbar G_N/c^3} \simeq 1.62\times10^{-33}$ cm, i.e. up to energy scales of order the Planck energy $E_P = \sqrt{\hbar c^5/G_N} \simeq 1.22\times10^{19}$ GeV. Considering quantum matter in a classical gravitational background also poses interesting challenges, notably the possibility that the zero-point fluctuations of the matter fields generate a nonvanishing vacuum energy density $\rho_{\rm vac}$, corresponding to a term $-\sqrt{g}\ \rho_{\rm vac}$ in $\mathcal{L}_{\rm SM}$ [1]. This is equivalent to adding a "cosmological constant" term $+\Lambda\, g_{\mu\nu}$ on the left-hand side of Einstein's equations Eq. (20.6), with $\Lambda = 8\pi G_N\,\rho_{\rm vac}/c^4$. Recent cosmological observations (see the following *Reviews*) suggest a positive value of Λ corresponding to $\rho_{\rm vac} \approx (2.3\times10^{-3}\text{eV})^4$. Such a small value has a negligible effect on the non cosmological tests discussed below.

20.1. Experimental tests of the matter-gravity coupling

The universality of the coupling between $g_{\mu\nu}$ and the Standard Model matter postulated in Eq. (20.5) ("Equivalence Principle") has many observable consequences. First, it predicts that the outcome of a local non-gravitational experiment, referred to local standards, does not depend on where, when, and in which locally inertial frame, the experiment is performed. This means, for instance, that local experiments should neither feel the cosmological evolution of the universe (constancy of the "constants"), nor exhibit preferred directions in spacetime (isotropy of space, local Lorentz invariance). These predictions are consistent with many experiments and observations. Stringent limits on a possible time variation of the basic coupling constants have been obtained by analyzing a natural fission reactor phenomenon which took place at Oklo, Gabon, two billion years ago [2,3]. These limits are at the 1×10^{-8} level for the fractional variation of the fine-structure constant $\alpha_{\rm em}$ [3], and at the 4×10^{-9} level for the fractional variation of the ratio m_q/Λ_{QCD} between the light quark masses and Λ_{QCD} [4]. The determination of the lifetime of Rhenium 187 from isotopic measurements of some meteorites dating back to the formation of the solar system (about 4.6 Gyr ago) yields comparably strong limits [5]. Measurements of absorption lines in astronomical spectra also give stringent limits on the variability of both $\alpha_{\rm em}$ and $\mu = m_p/m_e$ at cosmological redshifts. E.g.

$$\Delta\alpha_{\rm em}/\alpha_{\rm em} = (1.2 \pm 1.7_{\rm stat} \pm 0.9_{\rm sys})\times10^{-6} \quad (20.7)$$

at redshifts $z = 1.0$–2.4 [6], and

$$|\Delta\mu/\mu| < 4\times10^{-7}(95\%\ C.L.) \ , \quad (20.8)$$

at a redshift $z = 0.88582$ [7]. There are also strong limits on the variation of $\alpha_{\rm em}$ and $\mu = m_p/m_e$ at redshift $z \sim 10^3$ from cosmic microwave background data, e.g. $\Delta\alpha_{\rm em}/\alpha_{\rm em} = (3.6\pm3.7)\times10^{-3}$ [8]. Direct laboratory limits (based on monitoring the frequency ratio of several different atomic clocks) on the present time variation of $\alpha_{\rm em}$, $\mu = m_p/m_e$, and m_q/Λ_{QCD} have reached the levels [9]:

$$\begin{aligned} d\ln(\alpha_{\rm em})/dt &= (-2.5\pm2.6)\times10^{-17}\text{yr}^{-1}, \\ d\ln(\mu)/dt &= (-1.5\pm3.0)\times10^{-16}\text{yr}^{-1}, \\ d\ln(m_q/\Lambda_{QCD})/dt &= (7.1\pm4.4)\times10^{-15}\text{yr}^{-1}. \end{aligned} \quad (20.9)$$

There are also experimental limits on a possible dependence of coupling constants on the gravitational potential [9,10].

The highest precision tests of the isotropy of space have been performed by looking for possible quadrupolar shifts of nuclear energy levels [11]. The (null) results can be interpreted as testing the fact that the various pieces in the matter Lagrangian Eq. (20.5) are indeed coupled to one and the same external metric $g_{\mu\nu}$ to the 10^{-29} level. For astrophysical constraints on possible Planck-scale violations of Lorentz invariance, see Ref. 12.

The universal coupling to $g_{\mu\nu}$ postulated in Eq. (20.5) implies that two (electrically neutral) test bodies dropped at the same location and with the same velocity in an external gravitational field fall in the same way, independently of their masses and compositions. The universality of the acceleration of free fall has been verified, for laboratory bodies, both on the ground [13,14](at the 10^{-13} level) and, in space [15](at the 10^{-14} level):

$$\begin{aligned} (\Delta a/a)_{\rm BeTi} &= (0.3\pm1.8)\times10^{-13} \ , \\ (\Delta a/a)_{\rm BeAl} &= (-0.7\pm1.3)\times10^{-13} \ , \\ (\Delta a/a)_{\rm TiPt} &= (-1\pm9_{\rm stat}\pm9_{\rm sys})\times10^{-15} \ . \end{aligned} \quad (20.10)$$

The universality of free fall has also been verified when comparing the fall of classical and quantum objects (6×10^{-9} level [16]) , or of two quantum objects (5×10^{-7} level [17]) . The gravitational accelerations of the Earth and the Moon toward the Sun have also been verified to agree [18],

$$(\Delta a/a)_{\rm EarthMoon} = (-0.8\pm1.3)\times10^{-13} \ . \quad (20.11)$$

The latter result constrains not only how $g_{\mu\nu}$ couples to matter, but also how it couples to itself [19]("strong equivalence principle").

Finally, Eq. (20.5) also implies that two identically constructed clocks located at two different positions in a static external Newtonian potential $U(\boldsymbol{x}) = \sum G_N m/r$ exhibit, when intercompared by means of electromagnetic signals, the (apparent) difference in clock rate, $\tau_1/\tau_2 = \nu_2/\nu_1 = 1 + [U(\boldsymbol{x}_1) - U(\boldsymbol{x}_2)]/c^2 + O(1/c^4)$, independently of their nature and constitution. This universal gravitational redshift of clock rates has been verified at the 10^{-4} level by comparing a hydrogen-maser clock flying on a rocket up to an altitude $\sim 10,000$ km to a similar clock on the ground [20]. The redshift due to a height change of only 33 cm has been detected by comparing two optical clocks based on $^{27}Al^+$ ions [21].

20.2. Tests of the dynamics of the gravitational field in the weak field regime

The effect on matter of one-graviton exchange, *i.e.*, the interaction Lagrangian obtained when solving Einstein's field equations Eq. (20.6) written in, say, the harmonic gauge at first order in $h_{\mu\nu}$,

$$\Box h_{\mu\nu} = -\frac{16\pi G_N}{c^4}(T_{\mu\nu} - \tfrac{1}{2}T\eta_{\mu\nu}) + O(h^2) + O(hT) \ , \qquad (20.12)$$

reads $-(8\pi G_N/c^4)T^{\mu\nu}\Box^{-1}(T_{\mu\nu} - \frac{1}{2}T\eta_{\mu\nu})$. For a system of N moving point masses, with free Lagrangian $L^{(1)} = \sum_{A=1}^{N} - m_A c^2\sqrt{1 - \boldsymbol{v}_A^2/c^2}$, this interaction, expanded to order v^2/c^2, reads (with $r_{AB} \equiv |\boldsymbol{x}_A - \boldsymbol{x}_B|$, $\boldsymbol{n}_{AB} \equiv (\boldsymbol{x}_A - \boldsymbol{x}_B)/r_{AB}$)

$$L^{(2)} = \tfrac{1}{2}\sum_{A\neq B} \frac{G_N\, m_A\, m_B}{r_{AB}}\Big[1 + \frac{3}{2c^2}(\boldsymbol{v}_A^2 + \boldsymbol{v}_B^2) - \frac{7}{2c^2}(\boldsymbol{v}_A\cdot\boldsymbol{v}_B) - \frac{1}{2c^2}(\boldsymbol{n}_{AB}\cdot\boldsymbol{v}_A)(\boldsymbol{n}_{AB}\cdot\boldsymbol{v}_B) + O\left(\frac{1}{c^4}\right)\Big] \ . \qquad (20.13)$$

The two-body interactions, Eq. (20.13), exhibit v^2/c^2 corrections to Newton's $1/r$ potential induced by spin-2 exchange ("gravito-magnetism"). Consistency at the "post-Newtonian" level $v^2/c^2 \sim G_N\, m/rc^2$ requires that one also considers the three-body interactions induced by some of the three-graviton vertices and other nonlinearities (terms $O(h^2)$ and $O(hT)$ in Eq. (20.12)),

$$L^{(3)} = -\frac{1}{2}\sum_{B\neq A\neq C} \frac{G_N^2\, m_A\, m_B\, m_C}{r_{AB}\, r_{AC}\, c^2} + O\left(\frac{1}{c^4}\right) \ . \qquad (20.14)$$

All currently performed gravitational experiments in the solar system, including perihelion advances of planetary orbits, the bending and delay of electromagnetic signals passing near the Sun, and very accurate ranging data to the Moon obtained by laser echoes, are compatible with the post-Newtonian results Eqs. (20.12)–(20.14). The "gravito-magnetic" interactions $\propto v_A v_B$ contained in Eq. (20.13) are involved in many of these experimental tests. They have been particularly tested in lunar laser ranging data [18], in the combined LAGEOS-LARES satellite data [22,23], and in the dedicated Gravity Probe B mission [24].

Similar to what is done in discussions of precision electroweak experiments, it is useful to quantify the significance of precision gravitational experiments by parametrizing plausible deviations from GR. Here, we shall focus on the simplest, and most conservative deviations from Einstein's pure spin-2 theory defined by adding new, bosonic light or massless, macroscopically coupled fields. The possibility of new gravitational-strength couplings leading (on small, and possibly large, scales) to deviations from Einsteinian (and Newtonian) gravity is suggested by String Theory [25], and by Brane World ideas [26]. Experiments have set limits on non-Newtonian forces down to the micrometer range [27].

Here, we shall focus on the parametrization of long-range deviations from relativistic gravity obtained by adding a strictly massless (*i.e.* without self-interaction $V(\varphi) = 0$) scalar field φ coupled to the trace of the energy-momentum tensor $T = g_{\mu\nu}T^{\mu\nu}$ [28,29]. The most general such theory contains an arbitrary function $a(\varphi)$ of the scalar field, and can be defined by the Lagrangian

$$\mathcal{L}_{\rm tot}[g_{\mu\nu},\varphi,\psi,A_\mu,H] = \frac{c^4}{16\pi G}\sqrt{g}(R(g_{\mu\nu}) - 2g^{\mu\nu}\partial_\mu\varphi\partial_\nu\varphi) + \mathcal{L}_{\rm SM}[\psi, A_\mu, H, \widetilde{g}_{\mu\nu}] \ , \qquad (20.15)$$

where G is a "bare" Newton constant, and where the Standard Model matter is coupled not to the "Einstein" (pure spin-2) metric $g_{\mu\nu}$, but to the conformally related ("Jordan-Fierz") metric $\widetilde{g}_{\mu\nu} = \exp(2a(\varphi))g_{\mu\nu}$. The scalar field equation $\Box_g\varphi = -(4\pi G/c^4)\alpha(\varphi)T$ displays $\alpha(\varphi) \equiv \partial a(\varphi)/\partial\varphi$ as the basic (field-dependent) coupling between φ and matter [29,30]. The one-parameter (ω) Jordan-Fierz-Brans-Dicke theory [28] is the special case $a(\varphi) = \alpha_0\varphi$ leading to a field-independent coupling $\alpha(\varphi) = \alpha_0$ (with ${\alpha_0}^2 = 1/(2\omega + 3)$). The addition of a self-interaction term $V(\varphi)$ in Eq. (20.15) introduces new phenomenological possibilities; notably the "chameleon mechanism" [31].

In the weak-field slow-motion limit appropriate to describing gravitational experiments in the solar system, the addition of φ modifies Einstein's predictions only through the appearance of two "post-Einstein" dimensionless parameters: $\overline{\gamma} = -2\alpha_0^2/(1+\alpha_0^2)$ and $\overline{\beta} = +\frac{1}{2}\beta_0\alpha_0^2/(1+\alpha_0^2)^2$, where $\alpha_0 \equiv \alpha(\varphi_0)$, $\beta_0 \equiv \partial\alpha(\varphi_0)/\partial\varphi_0$, φ_0 denoting the vacuum expectation value of φ. These parameters show up also naturally (in the form $\gamma_{\rm PPN} = 1 + \overline{\gamma}$, $\beta_{\rm PPN} = 1 + \overline{\beta}$) in phenomenological discussions of possible deviations from GR [32]. The parameter $\overline{\gamma}$ measures the admixture of spin 0 to Einstein's graviton, and contributes an extra term $+\overline{\gamma}(\boldsymbol{v}_A - \boldsymbol{v}_B)^2/c^2$ in the square brackets of the two-body Lagrangian Eq. (20.13). The parameter $\overline{\beta}$ modifies the three-body interaction Eq. (20.14) by an overall multiplicative factor $1 + 2\overline{\beta}$. Moreover, the combination $\eta \equiv 4\overline{\beta} - \overline{\gamma}$ parametrizes the lowest order effect of the self-gravity of orbiting masses by modifying the Newtonian interaction energy terms in Eq. (20.13) into $G_{AB}m_Am_B/r_{AB}$, with a body-dependent gravitational "constant" $G_{AB} = G_N[1 + \eta(E_A^{\rm grav}/m_Ac^2 + E_B^{\rm grav}/m_Bc^2) + O(1/c^4)]$, where $G_N = G\exp[2a(\varphi_0)](1+\alpha_0^2)$ and where $E_A^{\rm grav}$ denotes the gravitational binding energy of body A.

The best current limits on the post-Einstein parameters $\overline{\gamma}$ and $\overline{\beta}$ are (at the 68% confidence level):

$$\overline{\gamma} = (2.1 \pm 2.3)\times 10^{-5} \ , \qquad (20.16)$$

deduced from the additional Doppler shift experienced by radio-wave beams connecting the Earth to the Cassini spacecraft when they passed near the Sun [33], and

$$|\overline{\beta}| < 7\times 10^{-5} \ , \qquad (20.17)$$

from a study of the global sensitivity of planetary ephemerides to post-Einstein parameters [34]. More stringent limits on $\overline{\gamma}$ are obtained in models (*e.g.*, string-inspired ones [25]) where scalar couplings violate the Equivalence Principle.

20.3. Tests of the dynamics of the gravitational field in the radiative and/or strong field regimes: pulsars

The discovery of pulsars (*i.e.*, rotating neutron stars emitting a beam of radio noise) in gravitationally bound orbits [35,36] has given us our first experimental handle on the regime of radiative and/or strong gravitational fields. In these systems, the finite velocity of propagation of the gravitational interaction between the pulsar and its companion generates damping-like terms at order $(v/c)^5$ in the equations of motion [37]. These damping forces are the local counterparts of the gravitational radiation emitted at infinity by the system ("gravitational radiation reaction"). They cause the binary orbit to shrink and its orbital period P_b to decrease. The remarkable stability of pulsar clocks has allowed one to measure the corresponding very small orbital period decay $\dot{P}_b \equiv dP_b/dt \sim -(v/c)^5 \sim -10^{-12}$

in several binary systems, thereby giving us a direct experimental confirmation of the propagation properties of the gravitational field, and, in particular, an experimental confirmation that the speed of propagation of gravity c_g is equal to the velocity of light c to better than a part in a thousand. In addition, the surface gravitational potential of a neutron star $h_{00}(R_{\rm NS}) \simeq 2Gm/c^2R_{\rm NS} \simeq 0.4$ being a factor $\sim 10^8$ higher than the surface potential of the Earth, and a mere factor 2.5 below the black hole limit ($h_{00}(R_{\rm BH}) = 1$), pulsar data have allowed one to obtain several accurate tests of the strong-gravitational-field regime, as we discuss next.

Binary pulsar timing data record the times of arrival of successive electromagnetic pulses emitted by a pulsar orbiting around the center of mass of a binary system. After correcting for the Earth motion around the Sun and for the dispersion due to propagation in the interstellar plasma, the time of arrival of the Nth pulse t_N can be described by a generic, parametrized "timing formula" [38] whose functional form is common to the whole class of tensor-scalar gravitation theories:

$$t_N - t_0 = F[T_N(\nu_p, \dot\nu_p, \ddot\nu_p)\,;\,\{p^K\}\,;\,\{p^{PK}\}] \ . \tag{20.18}$$

Here, T_N is the pulsar proper time corresponding to the Nth turn given by $N/2\pi = \nu_p T_N + \frac{1}{2}\dot\nu_p T_N^2 + \frac{1}{6}\ddot\nu_p T_N^3$ (with $\nu_p \equiv 1/P_p$ the spin frequency of the pulsar, *etc.*), $\{p^K\} = \{P_b, T_0, e, \omega_0, x\}$ is the set of "Keplerian" parameters (notably, orbital period P_b, eccentricity e, periastron longitude ω_0 and projected semi-major axis $x = a\sin i/c$), and $\{p^{PK}\} = \{k, \gamma_{\rm timing}, \dot P_b, r, s, \delta_\theta, \dot e, \dot x\}$ denotes the set of (separately measurable) "post-Keplerian" parameters. Most important among these are: the fractional periastron advance per orbit $k \equiv \dot\omega P_b/2\pi$, a dimensionful time-dilation parameter $\gamma_{\rm timing}$, the orbital period derivative $\dot P_b$, and the "range" and "shape" parameters of the gravitational time delay caused by the companion, r and s.

Without assuming any specific theory of gravity, one can phenomenologically analyze the data from any binary pulsar by least-squares fitting the observed sequence of pulse arrival times to the timing formula Eq. (20.18). This fit yields the "measured" values of the parameters $\{\nu_p, \dot\nu_p, \ddot\nu_p\}$, $\{p^K\}$, $\{p^{PK}\}$. Now, each specific relativistic theory of gravity predicts that, for instance, k, $\gamma_{\rm timing}$, $\dot P_b$, r and s (to quote parameters that have been successfully measured from some binary pulsar data) are some theory-dependent functions of the Keplerian parameters and of the (unknown) masses m_1, m_2 of the pulsar and its companion. For instance, in GR, one finds (with $M \equiv m_1 + m_2$, $n \equiv 2\pi/P_b$)

$$\begin{aligned}
k^{\rm GR}(m_1,m_2) =& 3(1-e^2)^{-1}(G_N Mn/c^3)^{2/3} \ , \\
\gamma^{\rm GR}_{\rm timing}(m_1,m_2) =& e n^{-1}(G_N Mn/c^3)^{2/3} m_2(m_1+2m_2)/M^2 \ , \\
\dot P_b^{\rm GR}(m_1,m_2) =& -(192\pi/5)(1-e^2)^{-7/2}\left(1+\tfrac{73}{24}e^2+\tfrac{37}{96}e^4\right) \\
& \times (G_N Mn/c^3)^{5/3} m_1 m_2/M^2 \ , \\
r(m_1,m_2) =& G_N m_2/c^3 \ , \\
s(m_1,m_2) =& nx(G_N Mn/c^3)^{-1/3} M/m_2 \ .
\end{aligned} \tag{20.19}$$

In tensor-scalar theories, each of the functions $k^{\rm theory}(m_1,m_2)$, $\gamma^{\rm theory}_{\rm timing}(m_1,m_2)$, $\dot P_b^{\rm theory}(m_1,m_2)$, *etc.*, is modified by quasi-static strong field effects (associated with the self-gravities of the pulsar and its companion), while the particular function $\dot P_b^{\rm theory}(m_1,m_2)$ is further modified by radiative effects (associated with the spin 0 propagator) [30,39,40].

Let us give some highlights of the current experimental situation. In the first discovered binary pulsar PSR 1913+16 [35,36], it has been (recently [41]) possible to measure *five* post-Keplerian parameters: k, $\gamma_{\rm timing}$, $\dot P_b$, and (with less accuracy) r and s. [Even more post-Keplerian parameters have been recently measured [41], but they cannot be currently used to test gravity theories.] The five equations $k^{\rm measured} = k^{\rm theory}(m_1,m_2)$, $\gamma^{\rm measured}_{\rm timing} = \gamma^{\rm theory}_{\rm timing}(m_1,m_2)$, $\dot P_b^{\rm measured} = \dot P_b^{\rm theory}(m_1,m_2)$, $r^{\rm measured} = r^{\rm theory}(m_1,m_2)$, $s^{\rm measured} = s^{\rm theory}(m_1,m_2)$, determine, for each given theory, five curves in the two-dimensional mass plane. [The less accurate measurements of r and s determine strips rather than thin curves.] This yields *three* tests of the specified theory, according to whether the five curves (or strips) have one point in common, as they should. After subtracting a small ($\sim 10^{-14}$ level in $\dot P_b^{\rm obs} = (-2.423 \pm 0.001)\times 10^{-12}$), but significant, "galactic" perturbing effect (linked to galactic accelerations and to the pulsar proper motion) [42], one finds that GR passes these three (combined radiative/strong-field) tests with flying colors. The most accurate of these three tests involves the three quantities $(k - \gamma_{\rm timing} - \dot P_b)_{1913+16}$, and is passed with complete success at the 10^{-3} level [36,43,41]

$$\left[\frac{\dot P_b^{\rm obs} - \dot P_b^{\rm gal}}{\dot P_b^{\rm GR}[k^{\rm obs}, \gamma^{\rm obs}_{\rm timing}]}\right]_{1913+16} = 0.9983 \pm 0.0016 \ . \tag{20.20}$$

Here $\dot P_b^{\rm GR}[k^{\rm obs}, \gamma^{\rm obs}_{\rm timing}]$ is the result of inserting in $\dot P_b^{\rm GR}(m_1,m_2)$ the values of the masses predicted by the two equations $k^{\rm obs} = k^{\rm GR}(m_1,m_2)$, $\gamma^{\rm obs}_{\rm timing} = \gamma^{\rm GR}_{\rm timing}(m_1,m_2)$. This yields experimental evidence for the reality of gravitational radiation damping forces at the $(-1.7 \pm 1.6)\times 10^{-3}$ level.

In the binary pulsar PSR 1534+12 [44] one has measured *five* post-Keplerian parameters: k, $\gamma_{\rm timing}$, r, s, and (with less accuracy)$\dot P_b$ [45,46]. This yields *three* more tests of relativistic gravity. Two among these tests accurately probe strong field gravity, without mixing of radiative effects [45]. General Relativity passes all these tests within the measurement accuracy. The most precise of the pure strong-field tests is the one obtained by combining the measurements of k, $\gamma_{\rm timing}$, and s. Using the most recent data [46], one finds agreement at the $(2 \pm 2)\times 10^{-3}$ level:

$$\left[\frac{s^{\rm obs}}{s^{\rm GR}[k^{\rm obs}, \gamma^{\rm obs}_{\rm timing}]}\right]_{1534+12} = 1.002 \pm 0.002 \ . \tag{20.21}$$

In the binary pulsar PSR J1141−6545 [47](whose companion is probably a white dwarf) one has measured *four* observable parameters: $k, \gamma_{\rm timing}, \dot P_b$ [48,49], and the parameter s [50,49]. The latter parameter (which is equal to the sine of the inclination angle, $s = \sin i$) was consistently measured in two ways: from a scintillation analysis [50], and from timing measurements [49]. GR passes all the corresponding tests within measurement accuracy. See Fig. 20.1 which uses the (more precise) scintillation measurement of $s = \sin i$.

The discovery of the remarkable *double* binary pulsar PSR J0737−3039 A and B [51,52] has led to the measurement of *seven* independent parameters [53,54,55]: five of them are the post-Keplerian parameters k, $\gamma_{\rm timing}$, r, s and $\dot P_b$ entering the relativistic timing formula of the fast-spinning pulsar PSR J0737−3039 A, a sixth is the ratio $R = x_B/x_A$ between the projected semi-major axis of the more slowly spinning companion pulsar PSR J0737−3039 B, and that of PSR J0737−3039 A. [The theoretical prediction for the ratio $R = x_B/x_A$, considered as a function of the (inertial) masses $m_1 = m_A$ and $m_2 = m_B$, is $R^{\rm theory} = m_1/m_2 + O((v/c)^4)$ [38], independently of the gravitational theory considered.] Finally, the seventh parameter $\Omega_{\rm SO,B}$ is the angular rate of (spin-orbit) precession of PSR J0737−3039 B around the total angular momentum [54,55]. These seven measurements give us *five* tests of relativistic gravity [53,56,57]. GR passes all those tests with flying colors (see Fig. 20.1). Let us highlight here two of them (from [57]) .

One test is a new confirmation of the reality of gravitational radiation at the 10^{-3} level

$$\left[\frac{\dot P_b^{\rm obs}}{\dot P_b^{\rm GR}[k^{\rm obs}, R^{\rm obs}]}\right]_{0737-3039} = 1.000 \pm 0.001 \ . \tag{20.22}$$

Another one is a new, 5×10^{-4} level, strong-field confirmation of GR:

$$\left[\frac{s^{\rm obs}}{s^{\rm GR}[k^{\rm obs}, R^{\rm obs}]}\right]_{0737-3039} = 1.0000 \pm 0.0005 \ . \tag{20.23}$$

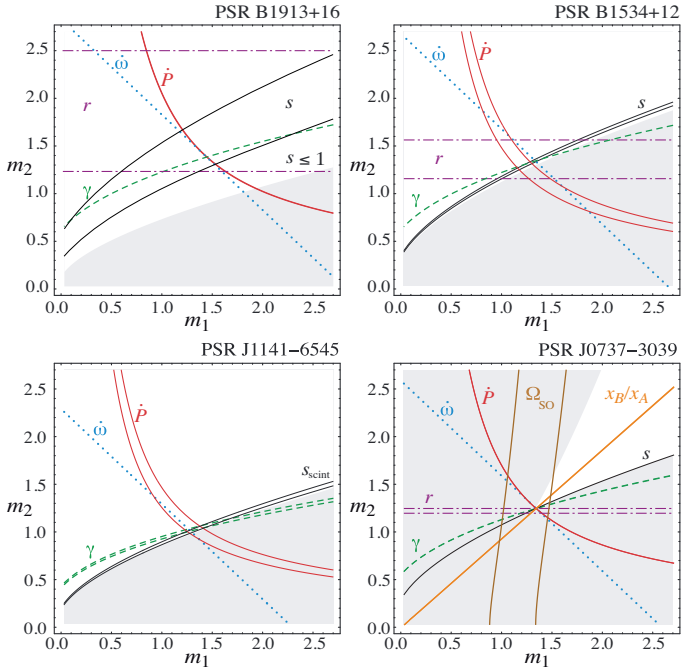

Figure 20.1: Illustration of the *thirteen* tests of relativistic gravity obtained in the four different binary pulsar systems PSR1913+16 (3 tests), PSR1534+12 (3 tests), PSR J1141−6545 (2 tests), and PSR J0737−3039 A,B (5 tests). Each curve (or strip) in the mass plane corresponds to the interpretation, within GR, of some observable parameter among: $\dot{P}_b$, $k \equiv \dot{\omega} P_b/2\pi$, $\gamma_{\rm timing}$, r, $s = \sin i$, $\Omega_{\rm SO,B}$ and R. The shaded regions are excluded because they would correspond (in GR) to $s = |\sin i| > 1$. (Figure updated from [71]; courtesy of G. Esposito-Farèse.)

Fig. 20.1 illustrates the thirteen tests of strong-field and radiative gravity derived from the above-mentioned binary pulsars: $(5-2=)$ 3 tests from PSR1913+16, $(5-2=)$ 3 tests from PSR1534+12, $(4-2=)$ 2 tests from PSR J1141−6545, and $(7-2=)$ 5 tests from PSR J0737−3039. [See, also, [58] for additional, less accurate, and partially discrepant, tests of relativistic gravity.]

Data from several nearly circular binary systems (made of a neutron star and a white dwarf) have also led to strong-field confirmations (at the 4.6×10^{-3} level) of the 'strong equivalence principle,' *i.e.*, the fact that neutron stars and white dwarfs fall with the same acceleration in the gravitational field of the Galaxy [59,60,61]. The measurements of $\dot{P}_b$ in some pulsar-white dwarf systems lead to strong constraints on the variation of Newton's G_N, and on the existence of gravitational dipole radiation [62,63,64,66,67]. In addition, arrays of millisecond pulsars are sensitive detectors of ultra low frequency gravitational waves ($f \sim 10^{-9} - 10^{-8}$ Hz) [68,69]. Such waves might be generated by supermassive black-hole binary systems, by cosmic strings and/or during the inflationary era. Pulsar timing arrays have recently put strong constraints on current models of supermassive black-hole binaries by finding no evidence for a background of gravitational waves with periods between ~ 1 and ~ 10 years [70].

The constraints on tensor-scalar theories provided by the various binary-pulsar "experiments" have been analyzed in [45,40,64,65,71,72] and shown to exclude a large portion of the parameter space allowed by solar-system tests. Some of the most stringent tests follow from the measurement of the orbital period decay $\dot{P}_b$ of low-eccentricity pulsar-white dwarf systems (notably PSR J1738+0333 [64]) . Indeed, asymmetric binary systems are strong emitters of dipolar gravitational radiation in tensor-scalar theories, with $\dot{P}_b$ scaling (modulo matter-scalar couplings) like $m_1 m_2/(m_1+m_2)^2 (v/c)^3$, instead of the parametrically smaller quadrupolar radiation $\dot{P}_b \sim (v/c)^5$ [32,30]. As a result the basic matter-scalar coupling α_0^2 is more strongly constrained, over most of the parameter space, than the best current solar-system limits Eq. (20.16), Eq. (20.17) (namely below the 10^{-5} level) [64,65].

Measurements over several years of the pulse profiles of various pulsars have detected secular profile changes compatible with the prediction [73] that the general relativistic spin-orbit coupling should cause a secular change in the orientation of the pulsar beam with respect to the line of sight ("geodetic precession"). Such confirmations of general-relativistic spin-orbit effects were obtained in PSR 1913+16 [74], PSR B1534+12 [46], PSR J1141−6545 [75], PSR J0737−3039 [54,55] and PSR J1906+0746 [76]. In some cases (notably PSR 1913+16 and PSR J1906+0746) the secular change in the orientation of the pulsar beam is expected to lead to the disappearance of the beam (as seen on the Earth) on a human time scale (the second pulsar in the double system PSR J0737−3039 has already disappeared in March 2008 and is expected to reappear around 2035 [55]) .

20.4. Tests of the dynamics of the gravitational field in the radiative and strong field regimes: gravitational waves

The observation, by the US-based Laser Interferometer Gravitational -wave Observatory (LIGO), later joined by the Europe-based Virgo detector, of gravitational-wave (GW) signals [77,78,79,80,81], has opened up a novel testing ground for relativistic gravity. The four transient signals GW150914, GW151226, GW170104 and GW170814, are most readily interpreted as the GW signals emitted ($\gtrsim 400$ Mpc away) by the last inspiralling orbits and the merger of binary black holes. The longer (~ 100 s) and louder (signal-to-noise ratio [SNR] ~ 32) signal GW170817 is most readily interpreted as coming from a binary neutron star inspiral (~ 40 Mpc away), and was associated with a subsequent γ-ray burst, followed by transient counterparts across the electromagnetic spectrum [82]. Thanks to the rather high SNRs, respectively, ~ 24, ~ 13, ~ 13, ~ 18, ~ 32, of the LIGO-Virgo observations, one could test consistency with GR in several ways.

For the binary black hole events, a first level of consistency check follows from the good global agreement between the full observed signal and the signal predicted by both analytical [83] and numerical [84] calculations of the gravitational waveform emitted by coalescing black holes. In particular, the noise-weighted correlation between the observed strain signal GW150914 and the best-fit GR-predicted waveform was found to be $\geq 96\%$ [85]. In other words, GR-violation effects that cannot be reabsorbed in a redefinition of physical parameters are limited (in a noise-weighted sense) to less than 4%. A perturbed black hole has characteristic ringing GW modes [86], whose frequencies and decay times are functions of the mass and spin of the black hole. The final black hole (with mass M_f and dimensionless spin parameter $a_f = J_f/(G_N M_f^2)$) formed by the coalescence of the two initial black holes emits, just after merger, a superposition of such (rapidly decaying) ringing GW modes. Currently, only GW150914 has allowed one to test the consistency between the observed signal and the (separately considered) GR predictions for the inspiral signal (up to the GW frequency $f^{\rm end\,inspiral} = 132$ Hz), the post-inspiral one ($f_{\rm GW} \geq f^{\rm end\,inspiral}$), and also, to some extent, the post-merger signal (merger being defined as the moment where the GW amplitude $h_{\mu\nu}$ reaches a maximum). First, the joint posterior distribution for M_f and a_f, obtained by separately best fitting to the corresponding GR predictions either the inspiral signal or the post-inspiral one, have been found to be consistent (see Fig. 4 in [85]) . A second, less accurate, check has found consistency between the measurement of the frequency and decay time of the first (least-damped) ringing mode from the latish post-merger signal, and the values inferred (using GR predictions) from fitting the entire signal (see Fig. 5 in [85]) .

Quantitatively more precise tests have been obtained from GW151226, which features a much longer signal (~ 55 GW cycles). The most accurate test has consisted in phenomenologically allowing the numerical coefficient φ_3 (parametrizing the contribution proportional to $f_{\rm GW}^{-2/3}$ in the frequency evolution of the Fourier-domain phase of the GW signal during the early inspiral) to vary [87,88]. [This contribution is physically related to "tail" effects in the curved spacetime propagation of the GW signal.] The 90 % credible limit

on the fractional variation of φ_3 obtained from GW151226 data is $\Delta\varphi_3/\varphi_3 \leq 0.1$ [88]. The three-detector observation of GW170814 has allowed one to probe the polarization content of the GW signal: the data were found to strongly favor the GR-predicted pure tensor polarization of GWs [80].

GR predicts that GWs are non dispersive, and propagate at the same velocity as light. One can phenomenologically modify the GR-predicted GW phase evolution by adding the putative effect of an anomalous dispersion relation of the form $E^2 = p^2c^2 + Ap^\alpha c^\alpha$. GW data have been used to set bounds on the anomalous coefficient A for various values of the exponent α (see Fig. 5 in [79]) . The case $\alpha = 0$ is equivalent to assuming that gravitons disperse as a massive particle [89]. Combined GW data lead to the following phenomenological limit on the graviton mass: $m_g \leq 7.7 \times 10^{-23} eV/c^2$ [79]. [See [90] for other graviton mass bounds.] Finally, the observed time delay of ~ 1.7 s between GW170817 and the associated γ-ray burst constrains the fractional difference between the speed of GWs and the speed of light to be between -3×10^{-15} and $+7 \times 10^{-16}$ [91].

Contrary to the solar-system, and binary-pulsar, tests, the phenomenological GW emission tests deduced from black hole merger signals do not directly constrain the most conservative class of theoretical deviations from GR obtained by adding a light scalar field φ, as in Eq. (20.15). Indeed, the no-hair properties of (4-dimensional) black holes mean that φ does not couple to black holes, so that, when neglecting large-scale external gradients (or fine-tuned initial data), light scalar fields have no effect on either the dynamics or the GW emission of black hole binaries.

20.5. Conclusions

All present experimental tests are compatible with the predictions of the current "standard" theory of gravitation: Einstein's General Relativity. The universality of the coupling between matter and gravity (Equivalence Principle) has been verified around the 10^{-14} level. Solar system experiments have tested the weak-field predictions of Einstein's theory at the few 10^{-5} level. The propagation properties (in the near zone) of relativistic gravity, as well as several of its static strong-field aspects, have been verified at the 10^{-3} level (or better) in several binary pulsar experiments. Interferometric detectors of gravitational radiation have given direct observational proofs of the existence, and properties, of gravitational waves (in the wave zone), and of the existence of coalescing black holes, and they have started to explore several dynamic aspects of strong-field gravity. Recent laboratory experiments have set strong constraints on sub-millimeter modifications of Newtonian gravity. Quantitative confirmations of GR have also been obtained on astrophysical scales. The GR action on light and matter of an external gravitational field has been verified in many gravitational lensing systems [92]. Some tests on cosmological scales are also available [93]. Beyond the quantitative limits on various parametrized theoretical models discussed in the latter reference, one should remember the striking (strong-field-type) qualitative verification of GR embodied in the fact that relativistic cosmological models give an accurate picture of the Universe over a period during which the spatial metric has been blown up by a gigantic factor, say $(1+z)^2 \sim 10^{19}$ between Big Bang nucleosynthesis and now (though a skeptic might wish to keep in mind the two "dark clouds" of current cosmology, namely the need to assume dark matter and a cosmological constant).

References:

1. S. Weinberg, Rev. Mod. Phys. **61**, 1 (1989).
2. A.I. Shlyakhter, Nature **264**, 340 (1976).
3. T. Damour and F. Dyson, Nucl. Phys. **B480**, 37 (1996);
   C.R. Gould, E.I. Sharapov, and S.K. Lamoreaux, Phys. Rev. **C74**, 024607 (2006);
   E. D. Davis and L. Hamdan,, Phys. Rev. **C92**, 014319 (2015);
   Yu.V. Petrov *et al.*, Phys. Rev. **C74**, 064610 (2006).
4. V.V. Flambaum and R.B. Wiringa, Phys. Rev. **C79**, 034302 (2009).
5. K.A. Olive *et al.*, Phys. Rev. **D69**, 027701 (2004).
6. M. T. Murphy, A. L. Malec and J. X. Prochaska, Mon. Not. Roy. Astron. Soc. **461**, no. 3, 2461 (2016).
7. N. Kanekar *et al.*, Mon. Not. Roy. Astron. Soc. **448**, no. 1, L104 (2015).
8. P. A. R. Ade *et al.* [Planck Collaboration], Astron. Astrophys. **580**, A22 (2015).
9. T. Rosenband *et al.*, Science **319**, 1808 (2008);
   J. Guéna *et al.*, Phys. Rev. Lett. **109**, 080801 (2012);
   R. M. Godun *et al.*, Phys. Rev. Lett. **113**, 210801 (2014).
10. T.M. Fortier *et al.*, Phys. Rev. Lett. **98**, 070801 (2007);
    S. Blatt *et al.*, Phys. Rev. Lett. **100**, 140801 (2008);
    T. Dent, Phys. Rev. Lett. **101**, 041102 (2008).
11. M. Smiciklas *et al.*, Phys. Rev. Lett. **107**, 171604 (2011).
12. S. Liberati, J. Phys. Conf. Ser. **631**, no. 1, 012011 (2015).
13. S. Schlamminger *et al.*, Phys. Rev. Lett. **100**, 041101 (2008).
14. T.A. Wagner *et al.*, Class. Quantum Grav. **29**, 184002 (2012).
15. P. Touboul *et al.*, Phys. Rev. Lett. , in press.
16. S. Merlet *et al.*, Metrologia, **47**, L9-L11 (2010).
17. D. Schlippert *et al.*, Phys. Rev. Lett. **112**, 203002 (2014).
18. J.G. Williams, S.G. Turyshev, and D.H. Boggs, Class. Quantum Grav. **29**, 184004 (2012);
    J. Müller, F. Hofmann, and L. Biskupek, Class. Quantum Grav. **29**, 184006 (2012).
19. K. Nordtvedt, Phys. Rev. **170**, 1186 (1968).
20. R.F.C. Vessot and M.W. Levine, Gen. Rel. Grav. **10**, 181 (1978);
    R.F.C. Vessot *et al.*, Phys. Rev. Lett. **45**, 2081 (1980).
21. C.W. Chou *et al.*, Science **329**, 1630 (2010).
22. I. Ciufolini and E.C. Pavlis, Nature **431**, 958 (2004).
23. I. Ciufolini *et al.*, Eur. Phys. J. C **76**, no. 3, 120 (2016).
24. C.W.F. Everitt *et al.*, Phys. Rev. Lett. **106**, 221101 (2011).
25. T.R. Taylor and G. Veneziano, Phys. Lett. **B213**, 450 (1988);
    T. Damour and A.M. Polyakov, Nucl. Phys. **B423**, 532 (1994);
    S. Dimopoulos and G. Giudice, Phys. Lett. **B379**, 105 (1996);
    I. Antoniadis, S. Dimopoulos, and G. Dvali, Nucl. Phys. **B516**, 70 (1998).
26. V.A. Rubakov, Phys. Usp **44**, 871 (2001);
    R. Maartens and K. Koyama, Living Rev. Rel. **13**, 5 (2010).
27. D. J. Kapner *et al.*, Phys. Rev. Lett. **98**, 021101 (2007);
    A. O. Sushkov *et al.*, Phys. Rev. Lett. **107**, 171101 (2011).
28. P. Jordan, *Schwerkraft und Weltall* (Vieweg, Braunschweig, 1955);
    M. Fierz, Helv. Phys. Acta **29**, 128 (1956);
    C. Brans and R.H. Dicke, Phys. Rev. **124**, 925 (1961).
29. R. V. Wagoner, Phys. Rev. D **1**, 3209 (1970).
30. T. Damour and G. Esposito-Farèse, Class. Quantum Grav. **9**, 2093 (1992).
31. J. Khoury and A. Weltman, Phys. Rev. Lett. **93**, 171104 (2004).
32. C.M. Will, *Theory and Experiment in Gravitational Physics* (Cambridge University Press, Cambridge, 1993); and Living Rev. Rel. **17**, 4 (2014).
33. B. Bertotti, L. Iess, and P. Tortora, Nature **425**, 374 (2003).
34. A. Fienga *et al.*, Cel. Mech. Dyn. Astr. **123**, Issue 2, 1 (2015).
35. R.A. Hulse, Rev. Mod. Phys. **66**, 699 (1994).
36. J.H. Taylor, Rev. Mod. Phys. **66**, 711 (1994).
37. T. Damour and N. Deruelle, Phys. Lett. **A87**, 81 (1981);
    T. Damour, C.R. Acad. Sci. Paris **294**, 1335 (1982).
38. T. Damour and N. Deruelle, Ann. Inst. H. Poincaré A, **44**, 263 (1986);
    T. Damour and J.H. Taylor, Phys. Rev. **D45**, 1840 (1992).
39. C.M. Will and H.W. Zaglauer, Astrophys. J. **346**, 366 (1989).
40. T. Damour and G. Esposito-Farèse, Phys. Rev. **D54**, 1474 (1996);
    idem, Phys. Rev. **D58**, 042001 (1998).
41. J. M. Weisberg and Y. Huang, Astrophys. J. **829**, no. 1, 55 (2016).
42. T. Damour and J.H. Taylor, Astrophys. J. **366**, 501 (1991).
43. J.M. Weisberg, D.J. Nice, and J.H. Taylor, Astrophys. J. **722**, 1030 (2010).
44. A. Wolszczan, Nature **350**, 688 (1991).
45. J.H. Taylor *et al.*, Nature **355**, 132 (1992).

46. E. Fonseca, I.H. Stairs and S.E. Thorsett, Astrophys. J. **787**, 82 (2014).
47. V.M. Kaspi *et al.*, Astrophys. J. **528**, 445 (2000).
48. M. Bailes *et al.*, Astrophys. J. **595**, L49 (2003).
49. N.D.R. Bhat, M. Bailes, and J.P.W. Verbiest, Phys. Rev. **D77**, 124017 (2008).
50. S.M. Ord *et al.*, Astrophys. J. **574**, L75 (2002).
51. M. Burgay *et al.*, Nature **426**, 531 (2003).
52. A.G. Lyne *et al.*, Science **303**, 1153 (2004).
53. M. Kramer *et al.*, Science **314**, 97 (2006).
54. R.P. Breton *et al.*, Science **321**, 104 (2008).
55. B. Perera *et al.*, AIP Conf. Proc. **1357**, 105 (2011) [Astrophys. J. **721**, 1193 (2010)].
56. M. Kramer and N. Wex, Class. Quantum Grav. **26**, 073001 (2009).
57. M. Kramer, in *Neutron Stars and Pulsars: Challenges and Opportunities after 80 Years; Proceedings of the International Astronomical Union Symposium S291, 2012*, J. van Leeuwen, ed. (Cambridge University Press, 2013), pp 19-26, [arXiv:1211.2457 [astro-ph.HE]].
58. R.D. Ferdman *et al.*, Mon. Not. Roy. Astron. Soc. **443**, no. 3, 2183 (2014).
59. T. Damour and G. Schäfer, Phys. Rev. Lett. **66**, 2549 (1991).
60. M.E. Gonzalez *et al.*, Astrophys. J. 743,102 (2011).
61. P.C.C. Freire, M. Kramer, and N. Wex , Class. Quantum Grav. **29**, 184007 (2012).
62. J.P.W. Verbiest *et al.*, Astrophys. J. **679**, 675 (2008).
63. K. Lazaridis *et al.*, Mon. Not. Roy. Astron. Soc. **400**, 805 (2009).
64. P.C.C. Freire *et al.*, Mon. Not. Roy. Astron. Soc. **423**, 3328 (2012).
65. L. Shao *et al.*, Phys. Rev. X, in press; arXiv:1704.07561 [gr-qc].
66. J. Antoniadis *et al.*, Science **340**, 6131 (2013).
67. W.W. Zhu *et al.*, Astrophys. J. **809**, 41 (2015).
68. R.S. Foster and D.C. Backer Astrophys. J. **361**, 300 (1990).
69. J. P. W. Verbiest *et al.*, Mon. Not. Roy. Astron. Soc. **458**, no. 2, 1267 (2016).
70. R. M. Shannon *et al.*, Science **349**, no. 6255, 1522 (2015).
71. G. Esposito-Farèse, in *Proceedings of the 10th Marcel Grossmann Meeting on Recent Developments in Theoretical and Experimental General Relativity*, edited by M. Novello *et al.*, (World Scientific, 2006), part A, pp 647-666.
72. G. Esposito-Farèse, in *Mass and Motion in General Relativity*, eds L. Blanchet *et al.*, series Fundam. Theor. Phys. **162** (Springer, Dordrecht, 2011) 461-489.
73. T. Damour and R. Ruffini, C. R. Acad. Sc. Paris **279**, série A, 971 (1974);
B.M. Barker and R.F. O'Connell, Phys. Rev. **D12**, 329 (1975).
74. M. Kramer, Astrophys. J. **509**, 856 (1998);
J.M. Weisberg and J.H. Taylor, Astrophys. J. **576**, 942 (2002).
75. R.N. Manchester *et al.*, Astrophys. J. **710**, 1694 (2010).
76. J. van Leeuwen *et al.*, Astrophys. J. **798**, 118 (2015).
77. B. P. Abbott *et al.*, Phys. Rev. Lett. **116**, 061102 (2016).
78. B. P. Abbott *et al.*, Phys. Rev. Lett. **116**, 241103 (2016).
79. B. P. Abbott *et al.*, Phys. Rev. Lett. **118**, 221101 (2017).
80. B. P. Abbott *et al.*, Phys. Rev. Lett. **119**, 141101 (2017).
81. B. P. Abbott *et al.*, Phys. Rev. Lett. **119**, 161101 (2017).
82. B. P. Abbott *et al.* , Astrophys. J. **848**, L12 (2017).
83. A. Buonanno and T. Damour, Phys. Rev. **D62**, 064015 (2000).
84. F. Pretorius, Phys. Rev. Lett. **95**, 121101 (2005);
M. Campanelli *et al.*, Phys. Rev. Lett. **96**, 111101 (2006);
J.G. Baker *et al.*, Phys. Rev. Lett. **96**, 111102 (2006).
85. B. P. Abbott *et al.*, Phys. Rev. Lett. **116**, 221101 (2016).
86. C.V. Vishveshwara, Nature **227**, 936 (1970).
87. L. Blanchet and B. S. Sathyaprakash, Phys. Rev. Lett. **74**, 1067 (1995).
88. B. P. Abbott *et al.*, Phys. Rev. X **6**, 041015 (2016).
89. C. M. Will, Phys. Rev. D 57, 2061 (1998).
90. C. de Rham *et al.*, Rev. Mod. Phys. **89**, no. 2, 025004 (2017).
91. B. P. Abbott *et al.*, Astrophys. J. **848**, L13 (2017).
92. J. Schwab, A.S. Bolton, and S.A. Rappaport, Astrophys. J. **708**, 750 (2010);
S. Cao *et al.*, Astrophys. J. **835**, no. 1, 92 (2017).
93. B. Jain and J. Khoury, Ann. Phys. **325**, 1479 (2010);
K. Koyama, Rept. Prog. Phys. **79**, no. 4, 046902 (2016).

21. Big-Bang Cosmology

Revised September 2017 by K.A. Olive (University of Minnesota) and J.A. Peacock (University of Edinburgh).

21.1. Introduction to Standard Big-Bang Model

The observed expansion of the Universe [1–3] is a natural (almost inevitable) result of any homogeneous and isotropic cosmological model based on general relativity. However, by itself, the Hubble expansion does not provide sufficient evidence for what we generally refer to as the Big-Bang model of cosmology. While general relativity is in principle capable of describing the cosmology of any given distribution of matter, it is extremely fortunate that our Universe appears to be homogeneous and isotropic on large scales. Together, homogeneity and isotropy allow us to extend the Copernican Principle to the Cosmological Principle, stating that all spatial positions in the Universe are essentially equivalent.

The formulation of the Big-Bang model began in the 1940s with the work of George Gamow and his collaborators, Alpher and Herman. In order to account for the possibility that the abundances of the elements had a cosmological origin, they proposed that the early Universe which was once very hot and dense (enough so as to allow for the nucleosynthetic processing of hydrogen), and has expanded and cooled to its present state [4,5]. In 1948, Alpher and Herman predicted that a direct consequence of this model is the presence of a relic background radiation with a temperature of order a few K [6,7]. Of course this radiation was observed 16 years later as the microwave background radiation [8]. Indeed, it was the observation of the 3 K background radiation that singled out the Big-Bang model as the prime candidate to describe our Universe. Subsequent work on Big-Bang nucleosynthesis further confirmed the necessity of our hot and dense past. (See Sec. 21.3.7 for a brief discussion of BBN and the review on BBN—Sec. 23 of this *Review* for a detailed discussion of BBN.) These relativistic cosmological models face severe problems with their initial conditions, to which the best modern solution is inflationary cosmology, discussed in Sec. 21.3.5 and in —Sec. 22 of this *Review*. If correct, these ideas would strictly render the term 'Big Bang' redundant, since it was first coined by Hoyle to represent a criticism of the lack of understanding of the initial conditions.

21.1.1. *The Robertson-Walker Universe* :

The observed homogeneity and isotropy enable us to describe the overall geometry and evolution of the Universe in terms of two cosmological parameters accounting for the spatial curvature and the overall expansion (or contraction) of the Universe. These two quantities appear in the most general expression for a space-time metric which has a (3D) maximally symmetric subspace of a 4D space-time, known as the Robertson-Walker metric:

$$ds^2 = dt^2 - R^2(t)\left[\frac{dr^2}{1-kr^2} + r^2\left(d\theta^2 + \sin^2\theta\, d\phi^2\right)\right] \ . \qquad (21.1)$$

Note that we adopt $c = 1$ throughout. By rescaling the radial coordinate, we can choose the curvature constant k to take only the discrete values $+1$, -1, or 0 corresponding to closed, open, or spatially flat geometries. In this case, it is often more convenient to re-express the metric as

$$ds^2 = dt^2 - R^2(t)\left[d\chi^2 + S_k^2(\chi)\left(d\theta^2 + \sin^2\theta\, d\phi^2\right)\right] \ , \qquad (21.2)$$

where the function $S_k(\chi)$ is $(\sin\chi, \chi, \sinh\chi)$ for $k = (+1, 0, -1)$. The coordinate r [in Eq. (21.1)] and the 'angle' χ (in Eq. (21.2)) are both dimensionless; the dimensions are carried by $R(t)$, which is the cosmological scale factor which determines proper distances in terms of the comoving coordinates. A common alternative is to define a dimensionless scale factor, $a(t) = R(t)/R_0$, where $R_0 \equiv R(t_0)$ is R at the present epoch. It is also sometimes convenient to define a dimensionless or conformal time coordinate, η, by $d\eta = dt/R(t)$. Along constant spatial sections, the proper time is defined by the time coordinate, t. Similarly, for $dt = d\theta = d\phi = 0$, the proper distance is given by $R(t)\chi$. For standard texts on cosmological models see *e.g.*, Refs. [9–16].

21.1.2. *The redshift* :

The cosmological redshift is a direct consequence of the Hubble expansion, determined by $R(t)$. A local observer detecting light from a distant emitter sees a redshift in frequency. We can define the redshift as

$$z \equiv \frac{\nu_1 - \nu_2}{\nu_2} \simeq v_{12} \ , \qquad (21.3)$$

where ν_1 is the frequency of the emitted light, ν_2 is the observed frequency and v_{12} is the relative velocity between the emitter and the observer. While the definition, $z = (\nu_1 - \nu_2)/\nu_2$ is valid on all distance scales, relating the redshift to the relative velocity in this simple way is only true on small scales (*i.e.*, less than cosmological scales) such that the expansion velocity is non-relativistic. For light signals, we can use the metric given by Eq. (21.1) and $ds^2 = 0$ to write

$$v_{12} = \dot{R}\,\delta r = \frac{\dot{R}}{R}\,\delta t = \frac{\delta R}{R} = \frac{R_2 - R_1}{R_1} \ , \qquad (21.4)$$

where $\delta r(\delta t)$ is the radial coordinate (temporal) separation between the emitter and observer. Noting that physical distance, D, is $R\delta r$ or δt, Eq. (21.4) gives us Hubble's law, $v = HD$. In addition, we obtain the simple relation between the redshift and the scale factor

$$1 + z = \frac{\nu_1}{\nu_2} = \frac{R_2}{R_1} \ . \qquad (21.5)$$

This result does not depend on the non-relativistic approximation.

21.1.3. *The Friedmann equations of motion* :

The cosmological equations of motion are derived from Einstein's equations

$$\mathcal{R}_{\mu\nu} - \tfrac{1}{2} g_{\mu\nu}\mathcal{R} = 8\pi G_{\rm N} T_{\mu\nu} + \Lambda g_{\mu\nu} \ . \qquad (21.6)$$

Gliner [17] and Zeldovich [18] have pioneered the modern view, in which the Λ term is set on the rhs and interpreted as an effective energy–momentum tensor $T_{\mu\nu}$ for the vacuum of $\Lambda g_{\mu\nu}/8\pi G_{\rm N}$. It is common to assume that the matter content of the Universe is a perfect fluid, for which

$$T_{\mu\nu} = -p g_{\mu\nu} + (p + \rho)\, u_\mu u_\nu \ , \qquad (21.7)$$

where $g_{\mu\nu}$ is the space-time metric described by Eq. (21.1), p is the isotropic pressure, ρ is the energy density and $u = (1, 0, 0, 0)$ is the velocity vector for the isotropic fluid in co-moving coordinates. With the perfect fluid source, Einstein's equations lead to the Friedmann equations

$$H^2 \equiv \left(\frac{\dot{R}}{R}\right)^2 = \frac{8\pi\, G_{\rm N}\, \rho}{3} - \frac{k}{R^2} + \frac{\Lambda}{3} \ , \qquad (21.8)$$

and

$$\frac{\ddot{R}}{R} = \frac{\Lambda}{3} - \frac{4\pi G_{\rm N}}{3}\ (\rho + 3p) \ , \qquad (21.9)$$

where $H(t)$ is the Hubble parameter and Λ is the cosmological constant. The first of these is sometimes called the Friedmann equation. Energy conservation via $T^{\mu\nu}_{\ \ ;\mu} = 0$, leads to a third useful equation [which can also be derived from Eq. (21.8) and Eq. (21.9)]

$$\dot{\rho} = -3H\,(\rho + p) \ . \qquad (21.10)$$

Eq. (21.10) can also be simply derived as a consequence of the first law of thermodynamics.

Eq. (21.8) has a simple classical mechanical analog if we neglect (for the moment) the cosmological term Λ. By interpreting $-k/R^2$ Newtonianly as a 'total energy', then we see that the evolution of the Universe is governed by a competition between the potential energy, $8\pi G_{\rm N}\rho/3$, and the kinetic term $(\dot{R}/R)^2$. For $\Lambda = 0$, it is clear that the Universe must be expanding or contracting (except at the turning point prior to collapse in a closed Universe). The ultimate fate of the Universe is determined by the curvature constant k. For $k = +1$, the Universe will recollapse in a finite time, whereas for $k = 0, -1$, the Universe will expand indefinitely. These simple conclusions can be altered when $\Lambda \neq 0$ or more generally with some component with $(\rho + 3p) < 0$.

21.1.4. ***Definition of cosmological parameters*** :

In addition to the Hubble parameter, it is useful to define several other measurable cosmological parameters. The Friedmann equation can be used to define a critical density such that $k = 0$ when $\Lambda = 0$,

$$\rho_{\rm c} \equiv \frac{3H^2}{8\pi G_{\rm N}} = 1.88 \times 10^{-26}\, h^2 \text{ kg m}^{-3} = 1.05 \times 10^{-5}\, h^2 \text{ GeV cm}^{-3} \,, \tag{21.11}$$

where the scaled Hubble parameter, h, is defined by

$$H \equiv 100\, h \text{ km s}^{-1} \text{ Mpc}^{-1} \Rightarrow H^{-1} = 9.78\, h^{-1} \text{ Gyr} = 2998\, h^{-1} \text{ Mpc} \,. \tag{21.12}$$

The cosmological density parameter $\Omega_{\rm tot}$ is defined as the energy density relative to the critical density,

$$\Omega_{\rm tot} = \rho/\rho_{\rm c} \,. \tag{21.13}$$

Note that one can now rewrite the Friedmann equation as

$$k/R^2 = H^2(\Omega_{\rm tot} - 1) \,. \tag{21.14}$$

From Eq. (21.14), one can see that when $\Omega_{\rm tot} > 1$, $k = +1$ and the Universe is closed, when $\Omega_{\rm tot} < 1$, $k = -1$ and the Universe is open, and when $\Omega_{\rm tot} = 1$, $k = 0$, and the Universe is spatially flat.

It is often necessary to distinguish different contributions to the density. It is therefore convenient to define present-day density parameters for pressureless matter ($\Omega_{\rm m}$) and relativistic particles ($\Omega_{\rm r}$), plus the quantity $\Omega_\Lambda = \Lambda/3H^2$. In more general models, we may wish to drop the assumption that the vacuum energy density is constant, and we therefore denote the present-day density parameter of the vacuum by $\Omega_{\rm v}$. The Friedmann equation then becomes

$$k/R_0^2 = H_0^2(\Omega_{\rm m} + \Omega_{\rm r} + \Omega_{\rm v} - 1) \,, \tag{21.15}$$

where the subscript 0 indicates present-day values. Thus, it is the sum of the densities in matter, relativistic particles, and vacuum that determines the overall sign of the curvature. Note that the quantity $-k/R_0^2H_0^2$ is sometimes referred to as Ω_k. This usage is unfortunate: it encourages one to think of curvature as a contribution to the energy density of the Universe, which is not correct.

21.1.5. ***Standard Model solutions*** :

Much of the history of the Universe in the standard Big-Bang model can be easily described by assuming that either matter or radiation dominates the total energy density. During inflation and again today the expansion rate for the Universe is accelerating, and domination by a cosmological constant or some other form of dark energy should be considered. In the following, we shall delineate the solutions to the Friedmann equation when a single component dominates the energy density. Each component is distinguished by an equation of state parameter $w = p/\rho$. We concentrate on solutions that expand at early times, the Friedmann equation also permits a time-reversed contracting solution.

21.1.5.1. *Solutions for a general equation of state:*

Let us first assume a general equation of state parameter for a single component, w which is constant. In this case, Eq. (21.10) can be written as $\dot\rho = -3(1+w)\rho\dot R/R$ and is easily integrated to yield

$$\rho \propto R^{-3(1+w)} \,. \tag{21.16}$$

Note that at early times when R is small, the less singular curvature term k/R^2 in the Friedmann equation can be neglected so long as $w > -1/3$. Curvature domination occurs at rather late times (if a cosmological constant term does not dominate sooner). For $w \neq -1$, one can insert this result into the Friedmann equation Eq. (21.8), and if one neglects the curvature and cosmological constant terms, it is easy to integrate the equation to obtain,

$$R(t) \propto t^{2/[3(1+w)]} \,. \tag{21.17}$$

21.1.5.2. *A Radiation-dominated Universe:*

In the early hot and dense Universe, it is appropriate to assume an equation of state corresponding to a gas of radiation (or relativistic particles) for which $w = 1/3$. In this case, Eq. (21.16) becomes $\rho \propto R^{-4}$. The 'extra' factor of $1/R$ is due to the cosmological redshift; not only is the number density of particles in the radiation background decreasing as R^{-3} since volume scales as R^3, but in addition, each particle's energy is decreasing as $E \propto \nu \propto R^{-1}$. Similarly, one can substitute $w = 1/3$ into Eq. (21.17) to obtain

$$R(t) \propto t^{1/2} \,; \qquad H = 1/2t \,. \tag{21.18}$$

21.1.5.3. *A Matter-dominated Universe:*

At relatively late times, non-relativistic matter eventually dominates the energy density over radiation (see Sec. 21.3.8). A pressureless gas ($w = 0$) leads to the expected dependence $\rho \propto R^{-3}$ from Eq. (21.16) and, if $k = 0$, we get

$$R(t) \propto t^{2/3} \,; \qquad H = 2/3t \,. \tag{21.19}$$

21.1.5.4. *A Universe dominated by vacuum energy:*

If there is a dominant source of vacuum energy, V_0, it would act as a cosmological constant with $\Lambda = 8\pi G_{\rm N} V_0$ and equation of state $w = -1$. In this case, the solution to the Friedmann equation when curvature is neglected is particularly simple and leads to an exponential expansion of the Universe:

$$R(t) \propto e^{\sqrt{\Lambda/3}\,t} \,. \tag{21.20}$$

More generally we could write

$$a(t) = \sinh^{2/3}(\sqrt{3\Lambda}t/2), \tag{21.21}$$

which describes a flat universe containing both matter and vacuum energy, with $a(t)$ being the scale factor normalized to unity when both components are equal.

A key parameter is the equation of state of the vacuum, $w \equiv p/\rho$: this need not be the $w = -1$ of Λ, and may not even be constant [19–21]. There is now much interest in the more general possibility of a dynamically evolving vacuum energy, for which the name 'dark energy' has become commonly used. A variety of techniques exist whereby the vacuum density as a function of time may be measured, usually expressed as the value of w as a function of epoch [22,23]. The best current measurement for the equation of state (assumed constant, but without assuming zero curvature) is $w = -1.01 \pm 0.04$ [24]. Unless stated otherwise, we will assume that the vacuum energy is a cosmological constant with $w = -1$ exactly.

The presence of vacuum energy can dramatically alter the fate of the Universe. For example, if $\Lambda < 0$, the Universe will eventually recollapse independent of the sign of k. For large values of $\Lambda > 0$ (larger than the Einstein static value needed to halt any cosmological expansion or contraction), even a closed Universe will expand forever. One way to quantify this is the deceleration parameter, q_0, defined as

$$q_0 = -\left.\frac{R\ddot R}{\dot R^2}\right|_0 = \frac{1}{2}\Omega_{\rm m} + \Omega_{\rm r} + \frac{(1+3w)}{2}\Omega_{\rm v} \,. \tag{21.22}$$

This equation shows us that $w < -1/3$ for the vacuum may lead to an accelerating expansion. To the continuing astonishment of cosmologists, such an effect has been observed; one piece of direct evidence is the Supernova Hubble diagram [25–30] (see Fig. 21.1 below); current data indicate that vacuum energy is indeed the largest contributor to the cosmological density budget, with $\Omega_{\rm v} = 0.692 \pm 0.012$ and $\Omega_{\rm m} = 0.308 \pm 0.012$ if $k = 0$ is assumed (Planck) [31].

The existence of this constituent is without doubt the greatest puzzle raised by the current cosmological model; the final section of this review discusses some of the ways in which the vacuum-energy problem is being addressed. For more details, see the review on Dark Energy—Sec. 27.

21.2. Introduction to Observational Cosmology

21.2.1. *Fluxes, luminosities, and distances* :

The key quantities for observational cosmology can be deduced quite directly from the metric.

(1) The *proper* transverse size of an object seen by us to subtend an angle $d\psi$ is its comoving size $d\psi\, S_k(\chi)$ times the scale factor at the time of emission:

$$d\ell = d\psi\; R_0 S_k(\chi)/(1+z)\;. \tag{21.23}$$

(2) The apparent flux density of an object is deduced by allowing its photons to flow through a sphere of current radius $R_0 S_k(\chi)$; but photon energies and arrival rates are redshifted, and the bandwidth $d\nu$ is reduced. The observed photons at frequency ν_0 were emitted at frequency $\nu_0(1+z)$, so the flux density is the luminosity at this frequency, divided by the total area, divided by $1+z$:

$$S_\nu(\nu_0) = \frac{L_\nu([1+z]\nu_0)}{4\pi R_0^2 S_k^2(\chi)(1+z)}\;. \tag{21.24}$$

These relations lead to the following common definitions:

$$\begin{aligned} \text{angular-diameter distance:}\quad & D_\mathrm{A} = (1+z)^{-1} R_0 S_k(\chi) \\ \text{luminosity distance:}\quad & D_\mathrm{L} = (1+z)\; R_0 S_k(\chi)\;. \end{aligned} \tag{21.25}$$

These distance-redshift relations are expressed in terms of observables by using the equation of a null radial geodesic ($R(t)d\chi = dt$) plus the Friedmann equation:

$$\begin{aligned} R_0 d\chi =& \frac{1}{H(z)}\,dz = \frac{1}{H_0}\,\Big[(1-\Omega_\mathrm{m}-\Omega_\mathrm{v}-\Omega_\mathrm{r})(1+z)^2 \\ &+\;\Omega_\mathrm{v}(1+z)^{3+3w} + \Omega_\mathrm{m}(1+z)^3 + \Omega_\mathrm{r}(1+z)^4\Big]^{-1/2}\,dz\;. \end{aligned} \tag{21.26}$$

The main scale for the distance here is the Hubble length, $1/H_0$.

The flux density is the product of the specific intensity I_ν and the solid angle $d\Omega$ subtended by the source: $S_\nu = I_\nu\, d\Omega$. Combining the angular size and flux-density relations thus gives the relativistic version of surface-brightness conservation:

$$I_\nu(\nu_0) = \frac{B_\nu([1+z]\nu_0)}{(1+z)^3}\;, \tag{21.27}$$

where B_ν is surface brightness (luminosity emitted into unit solid angle per unit area of source). We can integrate over ν_0 to obtain the corresponding total or bolometric formula:

$$I_\mathrm{tot} = \frac{B_\mathrm{tot}}{(1+z)^4}\;. \tag{21.28}$$

This cosmology-independent form expresses Liouville's Theorem: photon phase-space density is conserved along rays.

21.2.2. *Distance data and geometrical tests of cosmology* :

In order to confront these theoretical predictions with data, we have to bridge the divide between two extremes. Nearby objects may have their distances measured quite easily, but their radial velocities are dominated by deviations from the ideal Hubble flow, which typically have a magnitude of several hundred $\mathrm{km\,s^{-1}}$. On the other hand, objects at redshifts $z \gtrsim 0.01$ will have observed recessional velocities that differ from their ideal values by $\lesssim 10\%$, but absolute distances are much harder to supply in this case. The traditional solution to this problem is the construction of the distance ladder: an interlocking set of methods for obtaining relative distances between various classes of object, which begins with absolute distances at the 10 to 100 pc level, and terminates with galaxies at significant redshifts. This is reviewed in the review on Cosmological Parameters—Sec. 24 of this *Review*.

By far the most exciting development in this area has been the use of type Ia Supernovae (SNe), which now allow measurement of relative distances with 5% precision. In combination with improved Cepheid data from the HST and a direct geometrical distance to the maser galaxy NGC4258, an improved measurement of the distance to the LMC, SNe results extend the distance ladder to the point where deviations from uniform expansion are negligible, leading to the best existing direct value for H_0: $73.24 \pm 1.74\,\mathrm{km\,s^{-1}Mpc^{-1}}$ [32]. Better still, the analysis of high-z SNe has allowed a simple and direct test of cosmological geometry to be carried out: as shown in Fig. 21.1 and Fig. 21.2, supernova data and measurements of microwave-background anisotropies strongly favor a $k = 0$ model dominated by vacuum energy. It is worth noting that there is some tension ($2.8\ \sigma$) between the local and CMB determinations of H_0 (the latter is 67.8 ± 0.9 [31]. It is nevertheless remarkable that the two very different methods give such similar results. (See the review on Cosmological Parameters—Sec. 24 of this *Review* for a more comprehensive review of Hubble parameter determinations.)

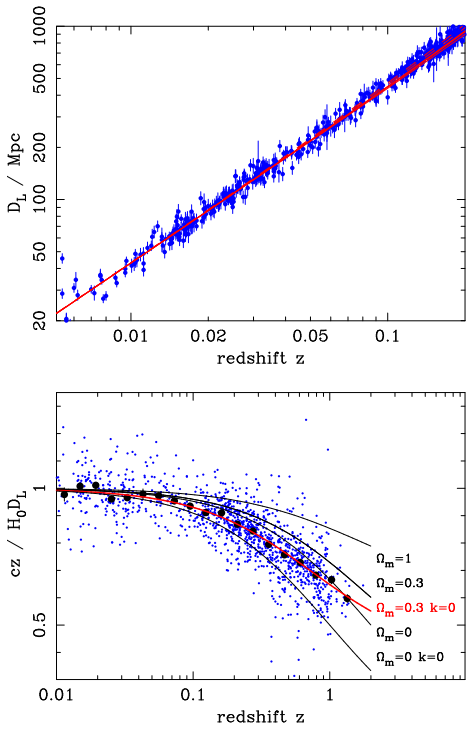

Figure 21.1: The type Ia supernova Hubble diagram, based on over 1200 publicly available supernova distance estimates [28–30]. The first panel shows that for $z \ll 1$ the large-scale Hubble flow is indeed linear and uniform; the second panel shows an expanded scale, with the linear trend divided out, and with the redshift range extended to show how the Hubble law becomes nonlinear. ($\Omega_\mathrm{r} = 0$ is assumed.) Larger points with errors show median values in redshift bins. Comparison with the prediction of Friedmann models appears to favor a vacuum-dominated Universe.

21.2.3. *Age of the Universe* :

The most striking conclusion of relativistic cosmology is that the Universe has not existed forever. The dynamical result for the age of the Universe may be written as

$$\begin{aligned} H_0 t_0 &= \int_0^\infty \frac{dz}{(1+z)H(z)} \\ &= \int_0^\infty \frac{dz}{(1+z)\,\left[(1+z)^2(1+\Omega_\mathrm{m}z) - z(2+z)\Omega_\mathrm{v}\right]^{1/2}}\;, \end{aligned} \tag{21.29}$$

where we have neglected Ω_r and chosen $w = -1$. Over the range of interest ($0.1 \lesssim \Omega_\mathrm{m} \lesssim 1$, $|\Omega_\mathrm{v}| \lesssim 1$), this exact answer may be approximated to a few % accuracy by

$$H_0 t_0 \simeq \tfrac{2}{3}\,(0.7\Omega_\mathrm{m} + 0.3 - 0.3\Omega_\mathrm{v})^{-0.3}\;. \tag{21.30}$$

For the special case that $\Omega_{\rm m} + \Omega_{\rm v} = 1$, the integral in Eq. (21.29) can be expressed analytically as

$$H_0 t_0 = \frac{2}{3\sqrt{\Omega_{\rm v}}} \ln \frac{1+\sqrt{\Omega_{\rm v}}}{\sqrt{1-\Omega_{\rm v}}} \quad (\Omega_{\rm m} < 1) \ . \tag{21.31}$$

The most accurate means of obtaining ages for astronomical objects is based on the natural clocks provided by radioactive decay. The use of these clocks is complicated by a lack of knowledge of the initial conditions of the decay. In the Solar System, chemical fractionation of different elements helps pin down a precise age for the pre-Solar nebula of 4.6 Gyr, but for stars it is necessary to attempt an a priori calculation of the relative abundances of nuclei that result from supernova explosions. In this way, a lower limit for the age of stars in the local part of the Milky Way of about 11 Gyr is obtained [34,35].

The other major means of obtaining cosmological age estimates is based on the theory of stellar evolution. In principle, the main-sequence turnoff point in the color-magnitude diagram of a globular cluster should yield a reliable age. However, these have been controversial owing to theoretical uncertainties in the evolution model, as well as observational uncertainties in the distance, dust extinction, and metallicity of clusters. The present consensus favors ages for the oldest clusters of about 13 Gyr [36].

These methods are all consistent with the age deduced from studies of structure formation, using the microwave background and large-scale structure: $t_0 = 13.80 \pm 0.04$ Gyr [31], where the extra accuracy comes at the price of assuming the Cold Dark Matter model to be true.

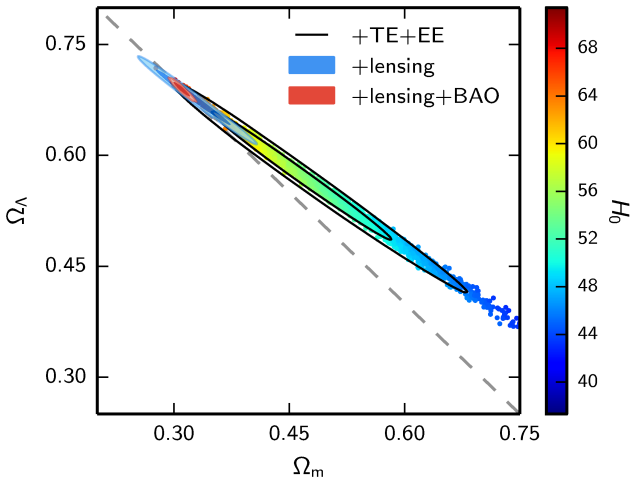

Figure 21.2: Likelihood-based probability densities on the plane Ω_Λ (*i.e.*, $\Omega_{\rm v}$ assuming $w = -1$) vs $\Omega_{\rm m}$. The colored locus derives from Planck [31] and shows that the CMB alone requires a flat universe $\Omega_{\rm v} + \Omega_{\rm m} \simeq 1$ if the Hubble constant is not too high. The SNe Ia results [33] very nearly constrain the orthogonal combination $\Omega_{\rm v} - \Omega_{\rm m}$, and the intersection of these constraints directly favors a flat model with $\Omega_{\rm m} \simeq 0.3$, as does the measurement of the Baryon Acoustic Oscillation lengthscale (for which a joint constraint is shown on this plot). The CMB alone is capable of breaking the degeneracy with H_0 by using the measurements of gravitational lensing that can be made with modern high-resolution CMB data.

21.2.4. *Horizon, isotropy, flatness problems* :

For photons, the radial equation of motion is just $c\,dt = R\,d\chi$. How far can a photon get in a given time? The answer is clearly

$$\Delta\chi = \int_{t_1}^{t_2} \frac{dt}{R(t)} \equiv \Delta\eta \ , \tag{21.32}$$

i.e., just the interval of conformal time. We can replace dt by $dR/\dot{R}$, which the Friedmann equation says is $\propto dR/\sqrt{\rho R^2}$ at early times. Thus, this integral converges if $\rho R^2 \to \infty$ as $t_1 \to 0$, otherwise it diverges. Provided the equation of state is such that ρ changes faster than R^{-2}, light signals can only propagate a finite distance between the Big Bang and the present; there is then said to be a particle horizon. Such a horizon therefore exists in conventional Big-Bang models, which are dominated by radiation ($\rho \propto R^{-4}$) at early times.

At late times, the integral for the horizon is largely determined by the matter-dominated phase, for which

$$D_{\rm H} = R_0\,\chi_{\rm H} \equiv R_0 \int_0^{t(z)} \frac{dt}{R(t)} \simeq \frac{6000}{\sqrt{\Omega_{\rm m} z}}\ h^{-1}\,{\rm Mpc} \quad (z \gg 1) \ . \tag{21.33}$$

The horizon at the time of formation of the microwave background ('last scattering': $z \simeq 1100$) was thus of order 100 Mpc in size, subtending an angle of about 1°. Why then are the large number of causally disconnected regions we see on the microwave sky all at the same temperature? The Universe is very nearly isotropic and homogeneous, even though the initial conditions appear not to permit such a state to be constructed.

A related problem is that the $\Omega = 1$ Universe is unstable:

$$\Omega(a) - 1 = \frac{\Omega - 1}{1 - \Omega + \Omega_{\rm v} a^2 + \Omega_{\rm m} a^{-1} + \Omega_{\rm r} a^{-2}} \ , \tag{21.34}$$

where Ω with no subscript is the total density parameter, and $a(t) = R(t)/R_0$. This requires $\Omega(t)$ to be unity to arbitrary precision as the initial time tends to zero; a universe of non-zero curvature today requires very finely tuned initial conditions.

21.3. The Hot Thermal Universe

21.3.1. *Thermodynamics of the early Universe* :

As alluded to above, we expect that much of the early Universe can be described by a radiation-dominated equation of state. In addition, through much of the radiation-dominated period, thermal equilibrium is established by the rapid rate of particle interactions relative to the expansion rate of the Universe (see Sec. 21.3.3 below). In equilibrium, it is straightforward to compute the thermodynamic quantities, ρ, p, and the entropy density, s. In general, the energy density for a given particle type i can be written as

$$\rho_i = \int E_i\, dn_{q_i} \ , \tag{21.35}$$

with the density of states given by

$$dn_{q_i} = \frac{g_i}{2\pi^2} \left(\exp[(E_{q_i} - \mu_i)/T_i] \pm 1\right)^{-1}\ q_i^2\, dq_i \ , \tag{21.36}$$

where g_i counts the number of degrees of freedom for particle type i, $E_{q_i}^2 = m_i^2 + q_i^2$, μ_i is the chemical potential, and the $\pm$ corresponds to either Fermi or Bose statistics. Similarly, we can define the pressure of a perfect gas as

$$p_i = \frac{1}{3} \int \frac{q_i^2}{E_i}\, dn_{q_i} \ . \tag{21.37}$$

The number density of species i is simply

$$n_i = \int dn_{q_i} \ , \tag{21.38}$$

and the entropy density is

$$s_i = \frac{\rho_i + p_i - \mu_i n_i}{T_i} \ . \tag{21.39}$$

In the Standard Model, a chemical potential is often associated with baryon number, and since the net baryon density relative to the photon density is known to be very small (of order 10^{-10}), we can neglect any such chemical potential when computing total thermodynamic quantities.

For photons, we can compute all of the thermodynamic quantities rather easily. Taking $g_i = 2$ for the 2 photon polarization states, we have (in units where $\hbar = k_{\rm B} = 1$)

$$\rho_\gamma = \frac{\pi^2}{15} T^4 \ ; \quad p_\gamma = \frac{1}{3}\rho_\gamma \ ; \quad s_\gamma = \frac{4\rho_\gamma}{3T} \ ; \quad n_\gamma = \frac{2\zeta(3)}{\pi^2} T^3 \ , \tag{21.40}$$

with $2\zeta(3)/\pi^2 \simeq 0.2436$. Note that Eq. (21.10) can be converted into an equation for entropy conservation. Recognizing that $\dot{p} = s\dot{T}$, Eq. (21.10) becomes

$$d(sR^3)/dt = 0 \ . \tag{21.41}$$

For radiation, this corresponds to the relationship between expansion and cooling, $T \propto R^{-1}$ in an adiabatically expanding universe. Note also that both s and n_γ scale as T^3.

21.3.2. ***Radiation content of the Early Universe*** :

At the very high temperatures associated with the early Universe, massive particles are pair produced, and are part of the thermal bath. If for a given particle species i we have $T \gg m_i$, then we can neglect the mass in Eq. (21.35) to Eq. (21.39), and the thermodynamic quantities are easily computed as in Eq. (21.40). In general, we can approximate the energy density (at high temperatures) by including only those particles with $m_i \ll T$. In this case, we have

$$\rho = \left(\sum_{\rm B} g_{\rm B} + \frac{7}{8} \sum_{\rm F} g_{\rm F} \right) \frac{\pi^2}{30} T^4 \equiv \frac{\pi^2}{30} N(T)\, T^4 \ , \tag{21.42}$$

where $g_{\rm B(F)}$ is the number of degrees of freedom of each boson (fermion) and the sum runs over all boson and fermion states with $m \ll T$. The factor of 7/8 is due to the difference between the Fermi and Bose integrals. Eq. (21.42) defines the effective number of degrees of freedom, $N(T)$, by taking into account new particle degrees of freedom as the temperature is raised. This quantity calculated from high temperature lattice QCD is plotted in Fig. 21.3 [37]. Near the QCD transition, there is a slight difference between the coefficient of T^4 for ρ and the coefficient of T^3 for the entropy density $s = (2\pi^2/45) N_s(T) T^3$ as seen in the figure [38].

The value of $N(T)$ at any given temperature depends on the particle physics model. In the standard SU(3) × SU(2) × U(1) model, we can specify $N(T)$ up to temperatures of $O(100)$ GeV. The change in N (ignoring mass effects) can be seen in the table below.

Temperature	New Particles	$4N(T)$
$T < m_e$	γ's + ν's	29
$m_e < T < m_\mu$	$e^\pm$	43
$m_\mu < T < m_\pi$	$\mu^\pm$	57
$m_\pi < T < T_c$ †	π's	69
$T_c < T < m_{\rm strange}$	π's + $u, \bar{u}, d, \bar{d}$ + gluons	205
$m_s < T < m_{\rm charm}$	$s, \bar{s}$	247
$m_c < T < m_\tau$	$c, \bar{c}$	289
$m_\tau < T < m_{\rm bottom}$	$\tau^\pm$	303
$m_b < T < m_{\rm W,Z}$	$b, \bar{b}$	345
$m_{W,Z} < T < m_{\rm Higgs}$	$W^\pm, Z$	381
$m_H < T < m_{\rm top}$	H^0	385
$m_t < T$	$t, \bar{t}$	427

†T_c corresponds to the confinement-deconfinement transition between quarks and hadrons.

At higher temperatures, $N(T)$ will be model-dependent. For example, in the minimal SU(5) model, one needs to add 24 states to $N(T)$ for the charged and colored X and Y gauge bosons, another 24 from the adjoint Higgs, and another 6 scalar degrees of freedom (in addition to the 4 associated with the complex Higgs doublet already counted in the longitudinal components of $W^\pm$ and Z, and in H) from the $\overline{5}$ of Higgs. Hence for $T > m_{\rm X}$ in minimal SU(5), $N(T) = 160.75$. In a supersymmetric model this would at least double, with some changes possibly necessary in the table if the lightest supersymmetric particle has a mass below m_t.

In the radiation-dominated epoch, Eq. (21.10) can be integrated (neglecting the T-dependence of N) giving us a relationship between the age of the Universe and its temperature

$$t = \left(\frac{90}{32\pi^3 G_{\rm N} N(T)} \right)^{1/2} T^{-2} \ . \tag{21.43}$$

Put into a more convenient form

$$t\, T_{\rm MeV}^2 = 2.4 [N(T)]^{-1/2} \ , \tag{21.44}$$

where t is measured in seconds and $T_{\rm MeV}$ in units of MeV.

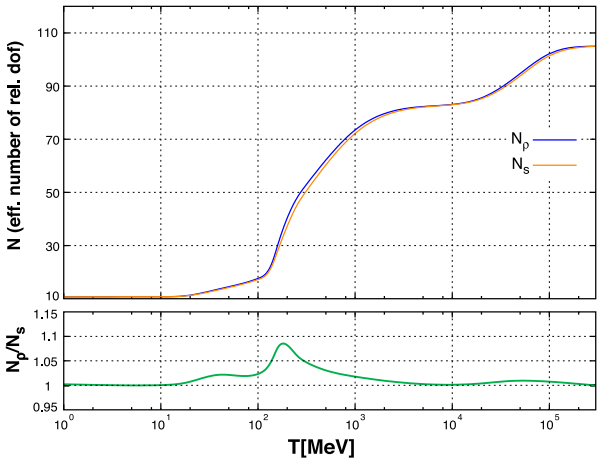

Figure 21.3: The effective numbers of relativistic degrees of freedom as a function of temperature. The sharp drop corresponds to the quark-hadron transition. The solid curve assume a QCD scale of 150 MeV, while the dashed curve assumes 450 MeV.

21.3.3. ***Neutrinos and equilibrium*** : Due to the expansion of the Universe, certain rates may be too slow to either establish or maintain equilibrium. Quantitatively, for each particle i, as a minimal condition for equilibrium, we will require that some rate Γ_i involving that type be larger than the expansion rate of the Universe or

$$\Gamma_i > H \ . \tag{21.45}$$

Recalling that the age of the Universe is determined by H^{-1}, this condition is equivalent to requiring that on average, at least one interaction has occurred over the lifetime of the Universe.

A good example for a process which goes in and out of equilibrium is the weak interactions of neutrinos. On dimensional grounds, one can estimate the thermally averaged scattering cross section:

$$\langle \sigma v \rangle \sim O(10^{-2}) T^2 / m_{\rm W}^4 \tag{21.46}$$

for $T \lesssim m_{\rm W}$. Recalling that the number density of leptons is $n \propto T^3$, we can compare the weak interaction rate, $\Gamma_{\rm wk} \sim n \langle \sigma v \rangle$, with the expansion rate,

$$\begin{aligned} H = \left(\frac{8\pi G_{\rm N} \rho}{3} \right)^{1/2} &= \left(\frac{8\pi^3}{90} N(T) \right)^{1/2} T^2 / M_{\rm P} \\ &\sim 1.66 N(T)^{1/2} T^2 / M_{\rm P}, \end{aligned} \tag{21.47}$$

where the Planck mass $M_{\rm P} = G_{\rm N}^{-1/2} = 1.22 \times 10^{19}$ GeV.

Neutrinos will be in equilibrium when $\Gamma_{\rm wk} > H$ or

$$T > (500\, m_{\rm W}^4 / M_{\rm P})^{1/3} \sim 1 \ \text{MeV} \ . \tag{21.48}$$

However, this condition assumes $T \ll m_{\rm W}$; for higher temperatures, we should write $\langle \sigma v \rangle \sim O(10^{-2})/T^2$, so that $\Gamma \sim 10^{-2} T$. Thus, in the very early stages of expansion, at temperatures $T \gtrsim 10^{-2} M_{\rm P}/\sqrt{N}$, equilibrium will not have been established.

Having attained a quasi-equilibrium stage, the Universe then cools further to the point where the interaction and expansion timescales match once again. The temperature at which these rates are equal is commonly referred to as the neutrino decoupling or freeze-out temperature and is defined by $\Gamma_{\rm wk}(T_d) = H(T_d)$. For $T < T_d$, neutrinos drop out of equilibrium. The Universe becomes transparent to neutrinos and their momenta simply redshift with the cosmic expansion. The effective neutrino temperature will simply fall with $T \sim 1/R$.

Soon after decoupling, $e^\pm$ pairs in the thermal background begin to annihilate (when $T \lesssim m_e$). Because the neutrinos are decoupled, the

energy released due to annihilation heats up the photon background relative to the neutrinos. The change in the photon temperature can be easily computed from entropy conservation. The neutrino entropy must be conserved separately from the entropy of interacting particles. A straightforward computation yields

$$T_\nu = (4/11)^{1/3}\, T_\gamma \simeq 1.9\ \mathrm{K}\ . \tag{21.49}$$

The total entropy density is therefore given by the contribution from photons and 3 flavors of neutrinos

$$s = \frac{4}{3}\frac{\pi^2}{30}\left(2 + \frac{21}{4}(T_\nu/T_\gamma)^3\right) T_\gamma^3 = \frac{4}{3}\frac{\pi^2}{30}\left(2 + \frac{21}{11}\right) T_\gamma^3 = 7.04\, n_\gamma\ . \tag{21.50}$$

Similarly, the total relativistic energy density is given by

$$\rho_r = \frac{\pi^2}{30}\left[2 + \frac{21}{4}(T_\nu/T_\gamma)^4\right] T_\gamma^4 \simeq 1.68\rho_\gamma\ . \tag{21.51}$$

In practice, a small correction is needed to this, since neutrinos are not totally decoupled at $e^\pm$ annihilation: the effective number of massless neutrino species is 3.046, rather than 3 [39].

This expression ignores neutrino rest masses, but current oscillation data require at least one neutrino eigenstate to have a mass exceeding 0.05 eV. In this minimal case, $\Omega_\nu h^2 = 5 \times 10^{-4}$, so the neutrino contribution to the matter budget would be negligibly small (which is our normal assumption). However, a nearly degenerate pattern of mass eigenstates could allow larger densities, since oscillation experiments only measure differences in m^2 values. Note that a 0.05-eV neutrino has $kT_\nu = m_\nu$ at $z \simeq 297$, so the above expression for the total present relativistic density is really only an extrapolation. However, neutrinos are almost certainly relativistic at all epochs where the radiation content of the Universe is dynamically significant.

21.3.4. *Field Theory and Phase transitions* :

It is very likely that the Universe has undergone one or more phase transitions during the course of its evolution [40–43]. Our current vacuum state is described by $\mathrm{SU}(3)_c \times \mathrm{U}(1)_{\mathrm{em}}$, which in the Standard Model is a remnant of an unbroken $\mathrm{SU}(3)_c \times \mathrm{SU}(2)_L \times \mathrm{U}(1)_Y$ gauge symmetry. Symmetry breaking occurs when a non-singlet gauge field (the Higgs field in the Standard Model) picks up a non-vanishing vacuum expectation value, determined by a scalar potential. For example, a simple (non-gauged) potential describing symmetry breaking is $V(\phi) = \frac{1}{4}\lambda\phi^4 - \frac{1}{2}\mu^2\phi^2 + V(0)$. The resulting expectation value is simply $\langle\phi\rangle = \mu/\sqrt{\lambda}$.

In the early Universe, finite temperature radiative corrections typically add terms to the potential of the form $\phi^2 T^2$. Thus, at very high temperatures, the symmetry is restored and $\langle\phi\rangle = 0$. As the Universe cools, depending on the details of the potential, symmetry breaking will occur via a first order phase transition in which the field tunnels through a potential barrier, or via a second order transition in which the field evolves smoothly from one state to another (as would be the case for the above example potential).

The evolution of scalar fields can have a profound impact on the early Universe. The equation of motion for a scalar field ϕ can be derived from the energy-momentum tensor

$$T_{\mu\nu} = \partial_\mu\phi\partial_\nu\phi - \frac{1}{2}g_{\mu\nu}\partial_\rho\phi\partial^\rho\phi - g_{\mu\nu}V(\phi)\ . \tag{21.52}$$

By associating $\rho = T_{00}$ and $p = R^{-2}(t)T_{ii}$ we have

$$\begin{aligned} \rho &= \frac{1}{2}\dot\phi^2 + \frac{1}{2}R^{-2}(t)(\nabla\phi)^2 + V(\phi) \\ p &= \frac{1}{2}\dot\phi^2 - \frac{1}{6}R^{-2}(t)(\nabla\phi)^2 - V(\phi)\ , \end{aligned} \tag{21.53}$$

and from Eq. (21.10) we can write the equation of motion (by considering a homogeneous region, we can ignore the gradient terms)

$$\ddot\phi + 3H\dot\phi = -\partial V/\partial\phi\ . \tag{21.54}$$

21.3.5. *Inflation* :

In Sec. 21.2.4, we discussed some of the problems associated with the standard Big-Bang model. However, during a phase transition, our assumptions of an adiabatically expanding universe are generally not valid. If, for example, a phase transition occurred in the early Universe such that the field evolved slowly from the symmetric state to the global minimum, the Universe may have been dominated by the vacuum energy density associated with the potential near $\phi \approx 0$. During this period of slow evolution, the energy density due to radiation will fall below the vacuum energy density, $\rho \ll V(0)$. When this happens, the expansion rate will be dominated by the constant V(0), and we obtain the exponentially expanding solution given in Eq. (21.20). When the field evolves towards the global minimum it will begin to oscillate about the minimum, energy will be released during its decay, and a hot thermal universe will be restored. If released fast enough, it will produce radiation at a temperature $NT_R{}^4 \lesssim V(0)$. In this reheating process, entropy has been created and the final value of RT is greater than the initial value of RT. Thus, we see that, during a phase transition, the relation $RT \sim$ constant need not hold true. This is the basis of the inflationary Universe scenario [44–46].

If, during the phase transition, the value of RT changed by a factor of $O(10^{29})$, the cosmological problems discussed above would be solved. The observed isotropy would be generated by the immense expansion; one small causal region could get blown up, and thus our entire visible Universe would have been in thermal contact some time in the past. In addition, the density parameter Ω would have been driven to 1 (with exponential precision). Density perturbations will be stretched by the expansion, $\lambda \sim R(t)$. Thus it will appear that $\lambda \gg H^{-1}$ or that the perturbations have left the horizon, where in fact the size of the causally connected region is now no longer simply H^{-1}. However, not only does inflation offer an explanation for large scale perturbations, it also offers a source for the perturbations themselves through quantum fluctuations.

Problems with early models of inflation based on a either first order [47] or second order [48,49] phase transition of a Grand Unified Theory led to models invoking a completely new scalar field: the inflaton, ϕ. The potential of this field, $V(\phi)$, needs to have a very low gradient and curvature in order to match observed metric fluctuations. For a more thorough discussion of the problems of early models and a host of current models being studying see the review on inflation—Sec. 22 of this *Review*. In most current inflation models, reheated bubbles typically do not percolate, so inflation is 'eternal' and continues with exponential expansion in the region outside bubbles. These causally disconnected bubble universes constitute a 'multiverse', where low-energy physics can vary between different bubbles. This has led to a controversial 'anthropic' approach to cosmology [50–52], where observer selection within the multiverse can be introduced as a means of understanding e.g. why the observed level of vacuum energy is so low (because larger values suppress growth of structure).

21.3.6. *Baryogenesis* :

The Universe appears to be populated exclusively with matter rather than antimatter. Indeed antimatter is only detected in accelerators or in cosmic rays. However, the presence of antimatter in the latter is understood to be the result of collisions of primary particles in the interstellar medium. There is in fact strong evidence against primary forms of antimatter in the Universe. Furthermore, the density of baryons compared to the density of photons is extremely small, $\eta \sim 10^{-10}$.

The production of a net baryon asymmetry requires baryon number violating interactions, C and CP violation and a departure from thermal equilibrium [53]. The first two of these ingredients are expected to be contained in grand unified theories as well as in the non-perturbative sector of the Standard Model, the third can be realized in an expanding universe where as we have seen interactions come in and out of equilibrium.

There are several interesting and viable mechanisms for the production of the baryon asymmetry. While we can not review any of them here in any detail, we mention some of the important scenarios. In all cases, all three ingredients listed above are incorporated. One of the first mechanisms was based on the out of equilibrium

decay of a massive particle such as a superheavy GUT gauge of Higgs boson [54,55]. A novel mechanism involving the decay of flat directions in supersymmetric models is known as the Affleck-Dine scenario [56]. There is also the possibility of generating the baryon asymmetry at the electro-weak scale using the non-perturbative interactions of sphalerons [57]. Because these interactions conserve the sum of baryon and lepton number, $B + L$, it is possible to first generate a lepton asymmetry (*e.g.*, by the out-of-equilibrium decay of a superheavy right-handed neutrino), which is converted to a baryon asymmetry at the electro-weak scale [58]. This mechanism is known as lepto-baryogenesis.

21.3.7. *Nucleosynthesis* :

An essential element of the standard cosmological model is Big-Bang nucleosynthesis (BBN), the theory which predicts the abundances of the light element isotopes D, ^{3}He, ^{4}He, and ^{7}Li. Nucleosynthesis takes place at a temperature scale of order 1 MeV. The nuclear processes lead primarily to ^{4}He, with a primordial mass fraction of about 25%. Lesser amounts of the other light elements are produced: about 10^{-5} of D and ^{3}He and about 10^{-10} of ^{7}Li by number relative to H. The abundances of the light elements depend almost solely on one key parameter, the baryon-to-photon ratio, η. The nucleosynthesis predictions can be compared with observational determinations of the abundances of the light elements. Consistency between theory and observations driven primarily by recent D/H measurements [59] leads to a range of

$$5.8 \times 10^{-10} < \eta < 6.6 \times 10^{-10} \ . \tag{21.55}$$

η is related to the fraction of Ω contained in baryons, $\Omega_{\rm b}$

$$\Omega_{\rm b} = 3.66 \times 10^7 \eta \, h^{-2} \ , \tag{21.56}$$

or $10^{10}\eta = 274\Omega_{\rm b}h^2$. The Planck result [31] for $\Omega_{\rm b}h^2$ of 0.0223 ± 0.0002 translates into a value of $\eta = 6.09 \pm 0.06$. This result can be used to 'predict' the light element abundance which can in turn be compared with observation [60]. The resulting D/H abundance is in excellent agreement with that found in quasar absorption systems. It is in reasonable agreement with the helium abundance observed in extra-galactic HII regions (once systematic uncertainties are accounted for), but is in poor agreement with the Li abundance observed in the atmospheres of halo dwarf stars [61]. (See the review on BBN—Sec. 23 of this *Review* for a detailed discussion of BBN or references [62,63,64].)

21.3.8. *The transition to a matter-dominated Universe* :

In the Standard Model, the temperature (or redshift) at which the Universe undergoes a transition from a radiation dominated to a matter dominated Universe is determined by the amount of dark matter. Assuming three nearly massless neutrinos, the energy density in radiation at temperatures $T \ll 1$ MeV, is given by

$$\rho_{\rm r} = \frac{\pi^2}{30}\left[2 + \frac{21}{4}\left(\frac{4}{11}\right)^{4/3}\right] T^4 \ . \tag{21.57}$$

In the absence of non-baryonic dark matter, the matter density can be written as

$$\rho_{\rm m} = m_{\rm N} \eta \, n_\gamma \ , \tag{21.58}$$

where $m_{\rm N}$ is the nucleon mass. Recalling that $n_\gamma \propto T^3$ [cf. Eq. (21.40)], we can solve for the temperature or redshift at the matter-radiation equality when $\rho_{\rm r} = \rho_{\rm m}$,

$$T_{\rm eq} = 0.22 \, m_{\rm N} \, \eta \qquad \text{or} \qquad (1 + z_{\rm eq}) = 0.22 \, \eta \frac{m_{\rm N}}{T_0} \ , \tag{21.59}$$

where T_0 is the present temperature of the microwave background. For $\eta = 6.1 \times 10^{-10}$, this corresponds to a temperature $T_{\rm eq} \simeq 0.13$ eV or $(1 + z_{\rm eq}) \simeq 550$. A transition this late is very problematic for structure formation (see Sec. 21.4.5).

The redshift of matter domination can be pushed back significantly if non-baryonic dark matter is present. If instead of Eq. (21.58), we write

$$\rho_{\rm m} = \Omega_{\rm m} \rho_{\rm c} \left(\frac{T}{T_0}\right)^3 \ , \tag{21.60}$$

we find that

$$T_{\rm eq} = 0.9 \frac{\Omega_{\rm m}\rho_{\rm c}}{T_0^3} \qquad \text{or} \qquad (1 + z_{\rm eq}) = 2.4 \times 10^4 \Omega_{\rm m} h^2 \ . \tag{21.61}$$

21.4. The Universe at late times

21.4.1. *The CMB* :

One form of the infamous Olbers' paradox says that, in Euclidean space, surface brightness is independent of distance. Every line of sight will terminate on matter that is hot enough to be ionized and so scatter photons: $T \gtrsim 10^3$ K; the sky should therefore shine as brightly as the surface of the Sun. The reason the night sky is dark is entirely due to the expansion, which cools the radiation temperature to 2.73 K. This gives a Planck function peaking at around 1 mm to produce the microwave background (CMB).

The CMB spectrum is a very accurate match to a Planck function [65]. (See the review on CBR–Sec. 28 of this *Review*.) The COBE estimate of the temperature is [66]

$$T = 2.7255 \pm 0.0006 \, {\rm K} \ . \tag{21.62}$$

The lack of any distortion of the Planck spectrum is a strong physical constraint. It is very difficult to account for in any expanding universe other than one that passes through a hot stage. Alternative schemes for generating the radiation, such as thermalization of starlight by dust grains, inevitably generate a superposition of temperatures. What is required in addition to thermal equilibrium is that $T \propto 1/R$, so that radiation from different parts of space appears identical.

Although it is common to speak of the CMB as originating at 'recombination', a more accurate terminology is the era of 'last scattering'. In practice, this takes place at $z \simeq 1100$, almost independently of the main cosmological parameters, at which time the fractional ionization is very small. This occurred when the age of the Universe was about 370,000 years. But the CMB photons themselves were not generated at this point, and were the result of thermalization at $z \sim 10^7$. (See the review on CBR–Sec. 28 of this *Review* for a full discussion of the CMB.)

21.4.2. *Matter in the Universe* :

One of the main tasks of cosmology is to measure the density of the Universe, and how this is divided between dark matter and baryons. The baryons consist partly of stars, with $0.002 \lesssim \Omega_* \lesssim 0.003$ [67] but mainly inhabit the intergalactic medium (IGM). One powerful way in which this can be studied is via the absorption of light from distant luminous objects such as quasars. Even very small amounts of neutral hydrogen can absorb rest-frame UV photons (the Gunn-Peterson effect), and should suppress the continuum by a factor $\exp(-\tau)$, where

$$\tau \simeq 10^{4.62} h^{-1} \left[\frac{n_{\rm HI}(z)/{\rm m}^{-3}}{(1+z)\sqrt{1+\Omega_{\rm m} z}}\right] \ , \tag{21.63}$$

and this expression applies while the Universe is matter dominated ($z \gtrsim 1$ in the $\Omega_{\rm m} = 0.3$ $\Omega_{\rm v} = 0.7$ model). At $z < 6$, the dominant effect on quasar spectra is a 'forest' of narrow absorption lines, which produce a mean $\tau = 1$ in the Lyα forest at about $z = 3$, and so we have $\Omega_{\rm HI} \simeq 10^{-6.7} h^{-1}$. This is such a small number that the IGM must be very highly ionized at these redshifts apart from a few high-density clumps. But at $z > 6$ there is good evidence for a 'reionization' era at which the general IGM is not so strongly ionized [68]. As discussed below, this ionized IGM at low z is also detectable via the secondary Compton scattering of CMB photons.

The Lyα forest is of great importance in pinning down the abundance of deuterium. Because electrons in deuterium differ in reduced mass by about 1 part in 4000 compared to hydrogen, each absorption system in the Lyα forest is accompanied by an offset deuterium line. By careful selection of systems with an optimal HI column density, a measurement of the D/H ratio can be made. This has now been done with high accuracy in 10 quasars, with consistent results [59]. Combining these determinations with the

theory of primordial nucleosynthesis yields a baryon density of $\Omega_{\rm b}h^2 = 0.021 - 0.023$ (95% confidence) in excellent agreement with the Planck result. (See also the review on BBN—Sec. 23 of this *Review*.)

Ionized IGM can also be detected in emission when it is densely clumped, via bremsstrahlung radiation. This generates the spectacular X-ray emission from rich clusters of galaxies. Studies of this phenomenon allow us to achieve an accounting of the total baryonic material in clusters. Within the central $\simeq 1$ Mpc, the masses in stars, X-ray emitting gas and total dark matter can be determined with reasonable accuracy (perhaps 20% rms), and this allows a minimum baryon fraction to be determined [69,70]:

$$\frac{M_{\rm baryons}}{M_{\rm total}} \gtrsim 0.009 + (0.066 \pm 0.003)\, h^{-3/2} \ . \tag{21.64}$$

Because clusters are the largest collapsed structures, it is reasonable to take this as applying to the Universe as a whole. This equation implies a minimum baryon fraction of perhaps 12% (for reasonable h), which is too high for $\Omega_{\rm m} = 1$ if we take $\Omega_{\rm b}h^2 \simeq 0.02$ from nucleosynthesis. This is therefore one of the more robust arguments in favor of $\Omega_{\rm m} \simeq 0.3$. (See the review on Cosmological Parameters—Sec. 24 of this *Review*.) This argument is also consistent with the inference on $\Omega_{\rm m}$ that can be made from Fig. 21.2.

This method is much more robust than the older classical technique for weighing the Universe: '$L \times M/L$'. The overall light density of the Universe is reasonably well determined from redshift surveys of galaxies, so that a good determination of mass M and luminosity L for a single object suffices to determine $\Omega_{\rm m}$ – but only *if* the mass-to-light ratio were universal.

21.4.3. *Gravitational lensing* :

A robust method for determining masses in cosmology is to use gravitational light deflection. Most systems can be treated as a geometrically thin gravitational lens, where the light bending is assumed to take place only at a single distance. Simple geometry then determines a mapping between the coordinates in the intrinsic source plane (S) and the observed image plane (I):

$$\alpha(D_{\rm L}\theta_{\rm I}) = \frac{D_{\rm S}}{D_{\rm LS}}(\theta_{\rm I} - \theta_{\rm S}) \ , \tag{21.65}$$

where the angles $\theta_{\rm I}, \theta_{\rm S}$ and α are in general two-dimensional vectors on the sky. The distances $D_{\rm LS}$ etc. are given by an extension of the usual distance-redshift formula:

$$D_{\rm LS} = \frac{R_0 S_k(\chi_{\rm S} - \chi_{\rm L})}{1 + z_{\rm S}} \ . \tag{21.66}$$

This is the angular-diameter distance for objects on the source plane as perceived by an observer on the lens.

Solutions of this equation divide into weak lensing, where the mapping between source plane and image plane is one-to-one, and strong lensing, in which multiple imaging is possible. For circularly-symmetric lenses, an on-axis source is multiply imaged into a 'caustic' ring, whose radius is the Einstein radius:

$$\begin{aligned} \theta_{\rm E} &= \left(4GM\,\frac{D_{\rm LS}}{D_{\rm L}D_{\rm S}}\right)^{1/2} \\ &= \left(\frac{M}{10^{11.09}M_\odot}\right)^{1/2} \left(\frac{D_{\rm L}D_{\rm S}/D_{\rm LS}}{\rm Gpc}\right)^{-1/2} \quad \text{arcsec} \ . \end{aligned} \tag{21.67}$$

The observation of 'arcs' (segments of near-perfect Einstein rings) in rich clusters of galaxies has thus given very accurate masses for the central parts of clusters—generally in good agreement with other indicators, such as analysis of X-ray emission from the cluster IGM [71,72].

Gravitational lensing has also developed into a particularly promising probe of cosmological structure on 10 to 100 Mpc scales. Weak image distortions manifest themselves as an additional ellipticity of galaxy images ('shear'), which can be observed by averaging many images together (the corresponding flux amplification is less readily detected). The result is a 'cosmic shear' field of order 1% ellipticity, coherent over scales of around 30 arcmin, which is directly related to the cosmic mass field, without any astrophysical uncertainties. For this reason, weak lensing is seen as potentially the cleanest probe of matter fluctuations, next to the CMB. Already, impressive results have been obtained in measuring cosmological parameters, based on survey data from only ~ 450 deg^2 [73]. A particular strength of lensing is its ability to measure the amplitude of mass fluctuations; this can be deduced from the amplitude of CMB fluctuations, but only with low precision on account of the poorly-known optical depth due to Compton scattering after reionization. However, the effect of weak lensing on the CMB map itself can be detected via the induced non-Gaussian signal, and this gives the CMB greater internal power [74].

21.4.4. *Density Fluctuations* :

The overall properties of the Universe are very close to being homogeneous; and yet telescopes reveal a wealth of detail on scales varying from single galaxies to large-scale structures of size exceeding 100 Mpc. The existence of these structures must be telling us something important about the initial conditions of the Big Bang, and about the physical processes that have operated subsequently. This motivates the study of the density perturbation field, defined as

$$\delta(\mathbf{x}) \equiv \frac{\rho(\mathbf{x}) - \langle\rho\rangle}{\langle\rho\rangle} \ . \tag{21.68}$$

A critical feature of the δ field is that it inhabits a universe that is isotropic and homogeneous in its large-scale properties. This suggests that the statistical properties of δ should also be statistically homogeneous—*i.e.*, it is a stationary random process.

It is often convenient to describe δ as a Fourier superposition:

$$\delta(\mathbf{x}) = \sum \delta_{\mathbf{k}} e^{-i\mathbf{k}\cdot\mathbf{x}} \ . \tag{21.69}$$

We avoid difficulties with an infinite universe by applying periodic boundary conditions in a cube of some large volume V. The cross-terms vanish when we compute the variance in the field, which is just a sum over modes of the power spectrum

$$\langle\delta^2\rangle = \sum |\delta_{\mathbf{k}}|^2 \equiv \sum P(k) \ . \tag{21.70}$$

Note that the statistical nature of the fluctuations must be isotropic, so we write $P(k)$ rather than $P(\mathbf{k})$. The $\langle\ldots\rangle$ average here is a volume average. Cosmological density fields are an example of an ergodic process, in which the average over a large volume tends to the same answer as the average over a statistical ensemble.

The statistical properties of discrete objects sampled from the density field are often described in terms of N-point correlation functions, which represent the excess probability over random for finding one particle in each of N boxes in a given configuration. For the 2-point case, the correlation function is readily shown to be identical to the autocorrelation function of the δ field: $\xi(r) = \langle\delta(x)\delta(x+r)\rangle$.

The power spectrum and correlation function are Fourier conjugates, and thus are equivalent descriptions of the density field (similarly, k-space equivalents exist for the higher-order correlations). It is convenient to take the limit $V \to \infty$ and use k-space integrals, defining a dimensionless power spectrum, which measures the contribution to the fractional variance in density per unit logarithmic range of scale, as $\Delta^2(k) = d\langle\delta^2\rangle/d\ln k = Vk^3P(k)/2\pi^2$:

$$\xi(r) = \int \Delta^2(k)\,\frac{\sin kr}{kr}\,d\ln k; \quad \Delta^2(k) = \frac{2}{\pi}k^3\int_0^\infty \xi(r)\,\frac{\sin kr}{kr}\,r^2\,dr \ . \tag{21.71}$$

For many years, an adequate approximation to observational data on galaxies was $\xi = (r/r_0)^{-\gamma}$, with $\gamma \simeq 1.8$ and $r_0 \simeq 5\,h^{-1}\,$Mpc. Modern surveys are now able to probe into the large-scale linear regime where unaltered traces of the curved post-recombination spectrum can be detected [75–77].

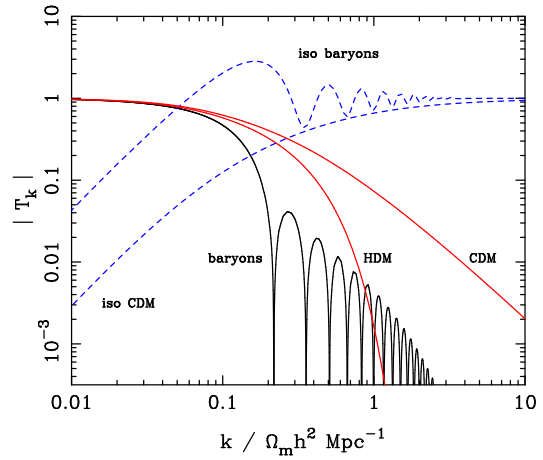

Figure 21.4: A plot of transfer functions for various models. For adiabatic models, $T_k \to 1$ at small k, whereas the opposite is true for isocurvature models. For dark-matter models, the characteristic wavenumber scales proportional to $\Omega_{\rm m}h^2$. The scaling for baryonic models does not obey this exactly; the plotted cases correspond to $\Omega_{\rm m} = 1$, $h = 0.5$.

21.4.5. *Formation of cosmological structure* :

The simplest model for the generation of cosmological structure is gravitational instability acting on some small initial fluctuations (for the origin of which a theory such as inflation is required). If the perturbations are adiabatic (*i.e.*, fractionally perturb number densities of photons and matter equally), the linear growth law for matter perturbations is simple:

$$\delta \propto \begin{cases} a^2(t) & \text{(radiation domination; } \Omega_{\rm r} = 1\text{)} \\ a(t) & \text{(matter domination; } \Omega_{\rm m} = 1\text{)} \, . \end{cases} \tag{21.72}$$

For low-density universes, the growth is slower:

$$d\ln\delta/d\ln a \simeq \Omega_{\rm m}^{\gamma}(a), \tag{21.73}$$

where the parameter γ is close to 0.55 independent of the vacuum density [78,79].

The alternative perturbation mode is isocurvature: only the equation of state changes, and the total density is initially unperturbed. These modes perturb the total entropy density, and thus induce additional large-scale CMB anisotropies [80]. Although the character of perturbations in the simplest inflationary theories are purely adiabatic, correlated adiabatic and isocurvature modes are predicted in many models; the simplest example is the curvaton, which is a scalar field that decays to yield a perturbed radiation density. If the matter content already exists at this time, the overall perturbation field will have a significant isocurvature component. Such a prediction is inconsistent with current CMB data [81], and most analyses of CMB and large scale structure (LSS) data assume the adiabatic case to hold exactly.

Linear evolution preserves the shape of the power spectrum. However, a variety of processes mean that growth actually depends on the matter content:

(1) Pressure opposes gravity effectively for wavelengths below the horizon length while the Universe is radiation dominated. The *comoving* horizon size at $z_{\rm eq}$ is therefore an important scale:

$$D_{\rm H}(z_{\rm eq}) = \frac{2(\sqrt{2}-1)}{(\Omega_{\rm m}z_{\rm eq})^{1/2}H_0} = \frac{16.0}{\Omega_{\rm m}h^2}\,{\rm Mpc} \, . \tag{21.74}$$

(2) At early times, dark matter particles will undergo free streaming at the speed of light, and so erase all scales up to the horizon—a process that only ceases when the particles go nonrelativistic. For light massive neutrinos, this happens at $z_{\rm eq}$; all structure up to the horizon-scale power-spectrum break is in fact erased. Hot(cold) dark matter models are thus sometimes dubbed large(small)-scale damping models.

(3) A further important scale arises where photon diffusion can erase perturbations in the matter–radiation fluid; this process is named Silk damping.

The overall effect is encapsulated in the transfer function, which gives the ratio of the late-time amplitude of a mode to its initial value (see Fig. 21.4). The overall power spectrum is thus the primordial scalar-mode power law, times the square of the transfer function:

$$P(k) \propto k^{n_{\rm s}}\, T_k^2 \, . \tag{21.75}$$

The most generic power-law index is $n_{\rm s} = 1$: the 'Zeldovich' or 'scale-invariant' spectrum. Inflationary models tend to predict a small 'tilt:' $|n_{\rm s} - 1| \lesssim 0.03$ [12,13]. On the assumption that the dark matter is cold, the power spectrum then depends on 5 parameters: $n_{\rm s}$, h, $\Omega_{\rm b}$, $\Omega_{\rm c}$ ($\equiv \Omega_{\rm m} - \Omega_{\rm b}$) and an overall amplitude. The latter is often specified as σ_8, the linear-theory fractional rms in density when a spherical filter of radius $8\,h^{-1}\,$Mpc is applied in linear theory. This scale can be probed directly via weak gravitational lensing, and also via its effect on the abundance of rich galaxy clusters. The favored value from the latter is approximately [82]

$$\sigma_8 \simeq [0.746 \pm 0.012\,({\rm stat}) \pm 0.022\,({\rm sys})]\,(\Omega_{\rm m}/0.3)^{-0.47}, \tag{21.76}$$

which is rather similar to the normalization inferred from weak lensing: $\sigma_8 \simeq [0.745 \pm 0.039](\Omega_{\rm m}/0.3)^{-0.5}$ [73]. These figures are in $> 2\sigma$ tension with the Planck values of $(\sigma_8, \Omega_{\rm m}) = (0.815 \pm 0.009, 0.308 \pm 0.012)$. If real, such a discrepancy could indicate interesting new physics; but the current evidence is not strong enough to make such a claim.

A direct measure of mass inhomogeneity is valuable, since the galaxies inevitably are biased with respect to the mass. This means that the fractional fluctuations in galaxy number, $\delta n/n$, may differ from the mass fluctuations, $\delta\rho/\rho$. It is commonly assumed that the two fields obey some proportionality on large scales where the fluctuations are small, $\delta n/n = b\delta\rho/\rho$, but even this is not guaranteed [83].

The main shape of the transfer function is a break around the horizon scale at $z_{\rm eq}$, which depends just on $\Omega_{\rm m}h$ when wavenumbers are measured in observable units ($h\,{\rm Mpc}^{-1}$). For reasonable baryon content, weak oscillations in the transfer function are also expected, and these BAOs (Baryon Acoustic Oscillations) have been clearly detected [84,85]. As well as directly measuring the baryon fraction, the scale of the oscillations directly measures the acoustic horizon at decoupling; this can be used as an additional standard ruler for cosmological tests, and the BAO signature has become one of the most important applications of large galaxy surveys. Overall, current power-spectrum data [75–77] favor $\Omega_{\rm m}h \simeq 0.20$ and a baryon fraction of about 0.15 for $n_{\rm s} = 1$ (see Fig. 21.5).

In principle, accurate data over a wide range of k could determine both $\Omega_{\rm m}h$ and n, but in practice there is a strong degeneracy between these. In order to constrain $n_{\rm s}$ itself, it is necessary to examine data on anisotropies in the CMB.

21.4.6. *CMB anisotropies* :

The CMB has a clear dipole anisotropy, of magnitude 1.23×10^{-3}. This is interpreted as being due to the Earth's motion, which is equivalent to a peculiar velocity for the Milky Way of

$$v_{\rm MW} \simeq 600\,{\rm km\,s^{-1}} \quad \text{towards} \quad (\ell, b) \simeq (270^\circ, 30^\circ) \, . \tag{21.77}$$

All higher-order multipole moments of the CMB are however much smaller (of order 10^{-5}), and interpreted as signatures of density fluctuations at last scattering ($\simeq 1100$). To analyze these, the sky is expanded in spherical harmonics as explained in the review on CBR–Sec. 28 of this *Review*. The dimensionless power per ln k or 'bandpower' for the CMB is defined as

$$\mathcal{T}^2(\ell) = \frac{\ell(\ell+1)}{2\pi} C_\ell \, . \tag{21.78}$$

This function encodes information from the three distinct mechanisms that cause CMB anisotropies:

(1) Gravitational (Sachs–Wolfe) perturbations. Photons from high-density regions at last scattering have to climb out of potential wells, and are thus redshifted.

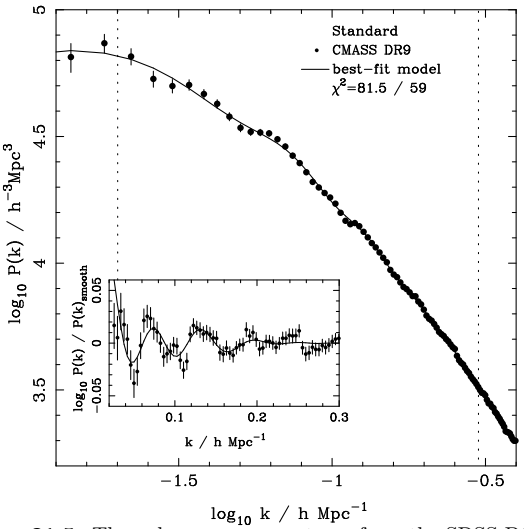

Figure 21.5: The galaxy power spectrum from the SDSS BOSS survey [77]. The solid points with error bars show the power estimate. The solid line shows a standard ΛCDM model with $\Omega_{\rm b}h^2 \simeq 0.02$ and $\Omega_{\rm m}h \simeq 0.2$. The inset amplifies the region where BAO features are visible. The fact that these perturb the power by $\sim 20\%$ rather than order unity is direct evidence that the matter content of the universe is dominated by collisionless dark matter.

(2) Intrinsic (adiabatic) perturbations. In high-density regions, the coupling of matter and radiation can compress the radiation also, giving a higher temperature.

(3) Velocity (Doppler) perturbations. The plasma has a non-zero velocity at recombination, which leads to Doppler shifts in frequency and hence shifts in brightness temperature.

Because the potential fluctuations obey Poisson's equation, $\nabla^2\Phi = 4\pi G\rho\delta$, and the velocity field satisfies the continuity equation $\nabla\cdot\mathbf{u} = -\dot{\delta}$, the resulting different powers of k ensure that the Sachs-Wolfe effect dominates on large scales and adiabatic effects on small scales.

The relation between angle and comoving distance on the last-scattering sphere requires the comoving angular-diameter distance to the last-scattering sphere; because of its high redshift, this is effectively identical to the horizon size at the present epoch, $D_{\rm H}$:

$$\begin{aligned} D_{\rm H} &= \frac{2}{\Omega_{\rm m}H_0} \quad (\Omega_{\rm v}=0) \\ D_{\rm H} &\simeq \frac{2}{\Omega_{\rm m}^{0.4}H_0} \quad (\text{flat}: \Omega_{\rm m}+\Omega_{\rm v}=1)\ . \end{aligned} \tag{21.79}$$

These relations show how the CMB is strongly sensitive to curvature: the horizon length at last scattering is $\propto 1/\sqrt{\Omega_{\rm m}}$, so that this subtends an angle that is virtually independent of $\Omega_{\rm m}$ for a flat model. Observations of a peak in the CMB power spectrum at relatively large scales ($\ell \simeq 225$) are thus strongly inconsistent with zero-Λ models with low density: current CMB + BAO + lensing data require $\Omega_{\rm m}+\Omega_{\rm v} = 1.000\pm0.005$ (95%) [31]. (See *e.g.*, Fig. 21.2). This result is unchanged when SN data and the prior on H_0 are included.

In addition to curvature, the CMB encodes information about several other key cosmological parameters. Within the compass of simple adiabatic CDM models, there are 9 of these:

$$\omega_{\rm c},\ \omega_{\rm b},\ \Omega_{\rm tot},\ h,\ \tau,\ n_{\rm s},\ n_{\rm t},\ r,\ Q\ . \tag{21.80}$$

The symbol ω denotes the physical density, Ωh^2: the transfer function depends only on the densities of CDM ($\omega_{\rm c}$) and baryons ($\omega_{\rm b}$). Transcribing the power spectrum at last scattering into an angular power spectrum brings in the total density parameter ($\Omega_{\rm tot} \equiv \Omega_{\rm m}+\Omega_{\rm v} = \Omega_{\rm c}+\Omega_{\rm b}+\Omega_{\rm v}$) and h: there is an exact geometrical degeneracy [86] between these that keeps the angular-diameter distance to last scattering invariant, so that models with substantial spatial curvature and large vacuum energy cannot be ruled out without prior knowledge of the Hubble parameter. Alternatively, the CMB alone cannot measure the Hubble parameter without taking into account foreground effects.

A further possible degeneracy involves the tensor contribution to the CMB anisotropies. These are important at large scales (up to the horizon scales); for smaller scales, only scalar fluctuations (density perturbations) are important. Each of these components is characterized by a spectral index, n, and a ratio between the power spectra of tensors and scalars (r). See the review on Cosmological Parameters—Sec. 24 of this *Review* for a technical definition of the r parameter. Finally, the overall amplitude of the spectrum must be specified (Q), together with the optical depth to Compton scattering owing to recent reionization (τ). Adding a large tensor contribution reduces the contrast between low ℓ and the peak at $\ell \simeq 225$ (because the tensor spectrum has no acoustic component). The previous relative height of the peak can be recovered by increasing $n_{\rm s}$ to increase the small-scale power in the scalar component; this in turn over-predicts the power at $\ell \sim 1000$, but this effect can be counteracted by raising the baryon density [87]. This approximate 3-way degeneracy is broken as we increase the range of multipoles sampled.

The reason the tensor component is introduced, and why it is so important, is that it is the only non-generic prediction of inflation. Slow-roll models of inflation involve two dimensionless parameters:

$$\epsilon \equiv \frac{M_{\rm P}^2}{16\pi}\left(\frac{V'}{V}\right)^2 \qquad \eta \equiv \frac{M_{\rm P}^2}{8\pi}\left(\frac{V''}{V}\right)\ , \tag{21.81}$$

where V is the inflaton potential, and dashes denote derivatives with respect to the inflation field. In terms of these, the tensor-to-scalar ratio is $r \simeq 16\epsilon$, and the spectral indices are $n_{\rm s} = 1-6\epsilon+2\eta$ and $n_{\rm t} = -2\epsilon$. The natural expectation of inflation is that the quasi-exponential phase ends once the slow-roll parameters become significantly non-zero, so that both $n_{\rm s} \neq 1$ and a significant tensor component are expected. These predictions can be avoided in some models, but it is undeniable that observation of such features would be a great triumph for inflation. Cosmology therefore stands at a fascinating point given that the most recent CMB data reject the zero-tensor $n_{\rm s} = 1$ model at almost 6σ: $n_{\rm s} = 0.968\pm0.006$ [31]. This rejection is strong enough that it is also able to break the tensor degeneracy, so that no model with $n_{\rm s} = 1$ is acceptable, whatever the value of r.

The current limit on r is < 0.07 at 95% confidence [88]. In conjunction with the measured value of $n_{\rm s}$, this upper limit sits close to the prediction of a linear potential (i.e. $|\eta| \ll |\epsilon|$). Any further reduction in the limit on r will force η to be negative – i.e. a convex potential at the point where LSS scales were generated (sometimes called a 'hilltop'), in contrast to simple early models such as $V(\phi) = m^2\phi^2$ or $\lambda\phi^4$, which are now excluded. Examples of models which are currently in excellent agreement with the Planck results are the Starobinsky model of $\mathcal{R}+\mathcal{R}^2$ gravity [89], or the Higgs-inflation model where the Higgs field is non-minimally coupled [90]. Assuming 55 e-foldings of inflation, these models predict $n_{\rm s} = 0.965$ and $r = 0.0035$. Assuming that no systematic error in the CMB data can be identified, cosmology has passed a critical hurdle in rejecting scale-invariant fluctuations. The years ahead will be devoted to the task of searching for the tensor fluctuations – for which the main tool will be the polarization of the CMB [14].

21.4.6.1. *CMB foregrounds:*

As the quality of CMB data improves, there is a growing interest in effects that arise along the line of sight. The CMB temperature is perturbed by dark-matter structures and by Compton scattering from ionized gas. In the former case, we have the Integrated Sachs-Wolfe effect, which is sensitive to the time derivative of the gravitational potential. In the linear regime, this is damped when the universe becomes Λ-dominated, and this is an independent way of detecting Λ [91]. The potential also causes gravitational lensing of the CMB: structures at $z \sim 1-2$ displace features on the CMB sky by about 2 arcmin over coherent degree-scale patches. Detection of these distortions allows a map to be made of overdensity projected from

$z = 0$ to 1100 [74]. This is a very powerful calibration for direct studies of gravitational lensing using galaxies. Finally, Comptonization affects the CMB in two ways: the thermal Sunyaev-Zeldovich effect measures the blurring of photon energies by hot gas; the kinetic Sunyaev-Zeldovich effect is sensitive to the bulk velocity of the gas. Both these effects start to dominate over the intrinsic CMB fluctuations at multipoles $\ell \gtrsim 2000$ [92].

21.4.7. ***Probing dark energy and the nature of gravity*** :

The most radical element of our current cosmological model is the dark energy that accelerates the expansion. The energy density of this component is approximately $(2.2\,\mathrm{meV})^4$ (for $w = -1$, $\Omega_v = 0.68$, $h = 0.67$), or roughly $10^{-123} M_{\rm P}^4$, and such an un-naturally small number is hard to understand. Various quantum effects (most simply zero-point energy) should make contributions to the vacuum energy density: these may be truncated by new physics at high energy, but this presumably occurs at $> 1\,\mathrm{TeV}$ scales, not meV; thus the apparent energy scale of the vacuum is at least 10^{15} times smaller than its natural value. A classic review of this situation is given in [50], which lists extreme escape routes – especially the multiverse viewpoint, according to which low values of Λ are rare, but high values suppress the formation of structure and observers. It is certainly impressive that Weinberg used such reasoning to predict the value of Λ before any data strongly indicated a non-zero value.

But it may be that the phenomenon of dark energy is entirely illusory. The necessity for this constituent arises from using the Friedmann equation to describe the evolution of the cosmic expansion; if this equation is incorrect, it would require the replacement of Einstein's relativistic theory of gravity with some new alternative. A frontier of current cosmological research is to distinguish these possibilities [93,94]. We also note that it has been suggested that dark energy might be an illusion even within general relativity, owing to an incorrect treatment of averaging in an inhomogeneous Universe [95,96]. Most would argue that a standard Newtonian treatment of such issues should be adequate inside the cosmological horizon, but debate on this issue continues.

Dark Energy can differ from a classical cosmological constant in being a dynamical phenomenon [97,98], *e.g.*, a rolling scalar field (sometimes dubbed 'quintessence'). Empirically, this means that it is endowed with two thermodynamic properties that astronomers can try to measure: the bulk equation of state and the sound speed. If the sound speed is close to the speed of light, the effect of this property is confined to very large scales, and mainly manifests itself in the large-angle multipoles of the CMB anisotropies [99]. The equation of state parameter governs the rate of change of the vacuum density: $d\ln\rho_v/d\ln a = -3(1+w)$, so it can be accessed via the evolving expansion rate, $H(a)$. This can be measured most cleanly by using the inbuilt natural ruler of large-scale structure: the Baryon Acoustic Oscillation horizon scale [100]:

$$D_{\rm BAO} \simeq 147\,(\Omega_{\rm m}h^2/0.13)^{-0.25}(\Omega_{\rm b}h^2/0.023)^{-0.08}\ \mathrm{Mpc}\ . \qquad (21.82)$$

$H(a)$ is measured by radial clustering, since $dr/dz = c/H$; clustering in the plane of the sky measures the integral of this. The expansion rate is also measured by the growth of density fluctuations, where the pressure-free growth equation for the density perturbation is $\ddot{\delta} + 2H(a)\dot{\delta} = 4\pi G\rho_0\,\delta$. Thus, both the scale and amplitude of density fluctuations are sensitive to $w(a)$ – but only weakly. These observables change by only typically 0.2% for a 1% change in w. Current constraints [31] place a constant w to within 5-10% of -1, depending on the data combination chosen. A substantial improvement in this precision will require us to limit systematics in data to a few parts in 1000.

Testing whether theories of gravity require revision can also be done using data on cosmological inhomogeneities. Two separate issues arise, concerning the metric perturbation potentials Ψ and Φ, which affect respectively the time and space parts of the metric. In Einstein gravity, these potentials are both equal to the Newtonian gravitational potential, which satisfies Poisson's equation: $\nabla^2\Phi/a^2 = 4\pi G\bar{\rho}\delta$. Empirically, modifications of gravity require us to explore a change with scale and with time of the 'slip' (Ψ/Φ) and the effective G on the rhs of the Poisson equation. The former aspect can only be probed via gravitational lensing, whereas the latter can be addressed on 10-100 Mpc scales via the growth of clustering. Various schemes for parameterising modified gravity exist, but a practical approach is to assume that the growth rate can be tied to the density parameter: $d\ln\delta/d\ln a = \Omega_{\rm m}^{\gamma}(a)$ [78,79]. The parameter γ is close to 0.55 for standard relativistic gravity, but can differ by around 0.1 from this value in many non-standard models. Clearly this parameterization is incomplete, since it explicitly rejects the possibility of early dark energy ($\Omega_{\rm m}(a) \to 1$ as $a \to 0$), but it is a convenient way of capturing the power of various experiments. Current data are consistent with standard ΛCDM [101], and exclude variations in slip or effective G of larger than a few times 10%.

Current planning envisages a set of satellite probes that, a decade hence, will pursue these fundamental tests via gravitational lensing measurements over thousands of square degrees, $> 10^8$ redshifts, and photometry of > 1000 supernovae (WFIRST in the USA, Euclid in Europe) [22,23]. These experiments will measure both w and the perturbation growth rate to an accuracy of around 1%. The outcome will be either a validation of the standard relativistic vacuum-dominated big bang cosmology at a level of precision far beyond anything attempted to date, or the opening of entirely new directions in cosmological models. For a more complete discussion of dark energy and future probes see the review on Dark Energy—Sec. 27

References:

1. V.M. Slipher, Pop. Astr. **23**, 21 (1915).
2. K. Lundmark, Mon. Not. R. Astron. Soc **84**, 747 (1924).
3. E. Hubble and M.L. Humason, Astrophys. J. **74**, 43 (1931).
4. G. Gamow, Phys. Rev. **70**, 572 (1946).
5. R.A. Alpher *et al.*, Phys. Rev. **73**, 803 (1948).
6. R.A. Alpher and R.C. Herman, Phys. Rev. **74**, 1737 (1948).
7. R.A. Alpher and R.C. Herman, Phys. Rev. **75**, 1089 (1949).
8. A.A. Penzias and R.W. Wilson, Astrophys. J. **142**, 419 (1965).
9. P.J.E. Peebles, *Principles of Physical Cosmology*, Princeton University Press (1993).
10. G. Börner, *The Early Universe: Facts and Fiction*, Springer-Verlag (1988).
11. E.W. Kolb and M.S. Turner, *The Early Universe*, Addison-Wesley (1990).
12. J.A. Peacock, *Cosmological Physics*, Cambridge Univ. Press (1999).
13. A.R. Liddle and D. Lyth, *Cosmological Inflation and Large-Scale Structure*, Cambridge University Press (2000).
14. S. Dodelson, *Modern Cosmology*, Academic Press (2003).
15. V. Mukhanov, *Physical Foundations of Cosmology*, Cambridge University Press (2005).
16. S. Weinberg, *Cosmology*, Oxford Press (2008).
17. E.B. Gliner, Sov. Phys. JETP **22**, 378 (1966).
18. Y.B. Zeldovich, (1967), Sov. Phys. Usp. **11**, 381 (1968).
19. P.M. Garnavich *et al.*, Astrophys. J. **507**, 74 (1998).
20. S. Perlmutter *et al.*, Phys. Rev. Lett. **83**, 670 (1999).
21. I. Maor *et al.*, Phys. Rev. **D65**, 123003 (2002).
22. A. Albrecht *et al.*, `astro-ph/0609591`.
23. J. Peacock *et al.*, `astro-ph/0610906`.
24. S. Alam *et al.*, Mon. Not. R. Astron. Soc **470**, 2617 (2017).
25. A.G. Riess *et al.*, Astrophys. J. **116**, 1009 (1998).
26. S. Perlmutter *et al.*, Astrophys. J. **517**, 565 (1999).
27. A.G. Riess, Pub. Astron. Soc. Pac. **112**, 1284 (2000).
28. J.L. Tonry *et al.*, Astrophys. J. **594**, 1 (2003).
29. R. Amanullah *et al.*, Astrophys. J. **716**, 712 (2010).
30. M. Betoul *et al.*, Astron. & Astrophys. **568**, A22 (2014).
31. Planck Collab. 2015 Results XIII, Astron. & Astrophys. **594**, A13 (2016).
32. A.G. Riess *et al.*, Astrophys. J. **826**, 56 (2016).
33. P. Astier *et al.*, Astron. & Astrophys. **447**, 31 (2006).
34. J.A. Johnson and M. Bolte, Astrophys. J. **554**, 888 (2001).
35. R. Cayrel *et al.*, Nature **409**, 691 (2001).
36. D. VandenBerg *et al.*, Astrophys. J. 775,134(2013).
37. S. Borsanyi *et al.*, Nature **539**, 69 (2016).
38. M. Srednicki *et al.*, Nucl. Phys. **B310**, 693 (1988).

39. G. Mangano *et al.*, Phys. Lett. **B534**, 8 (2002).
40. A. Linde, Phys. Rev. **D14**, 3345 (1976).
41. A. Linde, Rept. on Prog. in Phys. **42**, 389 (1979).
42. C.E. Vayonakis, Surv. High Energy Physics **5**, 87 (1986).
43. S.A. Bonometto and A. Masiero, Nuovo Cimento **9N5**, 1 (1986).
44. A. Linde, *Particle Physics And Inflationary Cosmology*, Harwood (1990).
45. K.A. Olive, Phys. Reports **190**, 307 (1990).
46. D. Lyth and A. Riotto, Phys. Reports **314**, 1 (1999).
47. A.H. Guth, Phys. Rev. **D23**, 347 (1981).
48. A.D. Linde, Phys. Lett. **108B**, 389 (1982).
49. A. Albrecht, P.J. Steinhardt, Phys. Rev. Lett. **48**, 1220 (1982).
50. S. Weinberg, Rev. Mod. Phys. **60**, 1 (1989).
51. L. Susskind, `hep-th/0302219` (2003).
52. B. Carr, *Universe or multiverse?* C.U.P. (2007).
53. A.D. Sakharov, Sov. Phys. JETP Lett. **5**, 24 (1967).
54. S. Weinberg, Phys. Rev. Lett. **42**, 850 (1979).
55. D. Toussaint *et al.*, Phys. Rev. **D19**, 1036 (1979).
56. I. Affleck and M. Dine, Nucl. Phys. **B249**, 361 (1985).
57. V. Kuzmin *et al.*, Phys. Lett. **B155**, 36 (1985).
58. M. Fukugita and T. Yanagida, Phys. Lett. **B174**, 45 (1986).
59. S. Riemer-Sorensen and S. Jenssen, Universe **3**, 44 (2017).
60. R.H. Cyburt *et al.*, Phys. Lett. **B567**, 227 (2003).
61. R.H. Cyburt *et al.*, JCAP **0811**, 012 (2008).
62. K.A. Olive *et al.*, Phys. Reports **333**, 389 (2000).
63. F. Iocco *et al.*, Phys. Reports **472**, 1 (2009).
64. R.H. Cyburt *et al.*, Rev. Mod. Phys. **88**, 015004 (2016).
65. D.J. Fixsen *et al.*, Astrophys. J. **473**, 576 (1996).
66. J.C. Mather *et al.*, Astrophys. J. **512**, 511 (1999).
67. S.M. Cole *et al.*, Mon. Not. R. Astron. Soc **326**, 255 (2001).
68. J. Schroeder, A. Mesinger and Z. Haiman, Mon. Not. R. Astron. Soc **428**, 3058 (2012).
69. S.D.M. White *et al.*, Nature **366**, 429 (1993).
70. S.W. Allen *et al.*, Mon. Not. R. Astron. Soc **334**, L11 (2002).
71. S.W. Allen, Mon. Not. R. Astron. Soc **296**, 392 (1998).
72. G.P. Smith *et al.*, Mon. Not. R. Astron. Soc **456**, L74 (2016).
73. H. Hildebrandt *et al.*, Mon. Not. R. Astron. Soc **465**, 1454 (2017).
74. Planck Collab. 2015 Results XV, Astron. & Astrophys. **594**, A15 (2016).
75. S.M. Cole *et al.*, Mon. Not. R. Astron. Soc **362**, 505 (2005).
76. W.J. Percival *et al.*, Astrophys. J. **657**, 645 (2007).
77. L. Anderson *et al.*, Mon. Not. R. Astron. Soc **427**, 3435 (2012).
78. E. Linder, Phys. Rev. **D72**, 43529 (2005).
79. D. Polarski and R. Gannouji, Phys. Lett. **B660**, 439 (2008).
80. G. Efstathiou and J.R. Bond, Mon. Not. R. Astron. Soc **218**, 103 (1986).
81. C. Gordon and A. Lewis, Phys. Rev. **D67**, 123513 (2003).
82. A. Vikhlinin *et al.*, Astrophys. J. **692**, 1060 (2009).
83. A. Dekel and O. Lahav, Astrophys. J. **520**, 24 (1999).
84. W.J. Percival *et al.*, Mon. Not. R. Astron. Soc **381**, 1053 (2007).
85. W.J. Percival *et al.*, Mon. Not. R. Astron. Soc **401**, 2148 (2010).
86. G. Efstathiou and J.R. Bond, Mon. Not. R. Astron. Soc **304**, 75 (1999).
87. G.P. Efstathiou *et al.*, Mon. Not. R. Astron. Soc **330**, L29 (2002).
88. P.A.R. Ade *et al.*, Phys. Rev. Lett. **116**, 031302 (2016).
89. A. A. Starobinsky, Phys. Lett. **B91**, 99 (1980).
90. F. Bezrukov and M. Shaposhnikov, JHEP **0907**, 089 (2009).
91. Planck Collab. 2015 Results XXI, Astron. & Astrophys. **594**, A21 (2016).
92. Planck Collab. 2015 Results XXII, Astron. & Astrophys. **594**, A22 (2016).
93. W. Hu and I. Sawicki, Phys. Rev. **D76**, 4043 (2007).
94. B. Jain and P. Zhang, Phys. Rev. **D78**, 3503 (2008).
95. D.L. Wiltshire, Phys. Rev. Lett. **99**, 251101 (2007).
96. T. Buchert, Gen. Rel. Grav. **40**, 467 (2008).
97. I. Zlatev *et al.*, Phys. Rev. Lett. **82**, 896 (1999).
98. C. Armendariz-Picon, V. Mukhanov, and P.J. Steinhardt, Phys. Rev. **D63**, 3510 (2001).
99. S. DeDeo, R.R. Caldwell, and P.J. Steinhardt, Phys. Rev. **D67**, 3509 (2003).
100. W. Hu, `arXiv:astro-ph/0407158` (2004).
101. S.F. Daniel *et al.*, Phys. Rev. **D81**, 123508 (2010).

22. Inflation

Written August 2017 by J. Ellis (King's College London; CERN) and D. Wands (U. of Portsmouth).

22.1. Motivation and Introduction

The standard Big-Bang model of cosmology provides a successful framework in which to understand the thermal history of our Universe and the growth of cosmic structure, but it is essentially incomplete. As described in Sec. 21.2.4 in "Big Bang Cosmology" review, Big-Bang cosmology requires very specific initial conditions. It postulates a uniform cosmological background, described by a spatially-flat, homogeneous and isotropic Robertson-Walker (RW) metric (Eq. (21.1) in "Big Bang Cosmology" review), with scale factor $R(t)$. Within this setting, it also requires an initial almost scale-invariant distribution of primordial density perturbations as seen, for example, in the cosmic microwave background (CMB) radiation (described in Chap. 28, "Cosmic Microwave Background" review), on scales far larger than the causal horizon at the time the CMB photons last scattered.

The Hubble expansion rate, $H \equiv \dot{R}/R$, in a Robertson-Walker cosmology is given by the Friedmann constraint equation (Eq. (21.8) in "Big Bang Cosmology" review)

$$H^2 = \frac{8\pi\rho}{3M_P^2} + \frac{\Lambda}{3} - \frac{k}{R^2}\,, \tag{22.1}$$

where k/R^2 is the intrinsic spatial curvature. We use natural units such that the speed of light $c = 1$ and hence we have the Planck mass $M_P = G_N^{-1/2} \simeq 10^{19}$ GeV (see "Astrophysical Constants and Parameters"). A cosmological constant, Λ, of the magnitude required to accelerate the Universe today (see Chap. 27, "Dark Energy" review) would have been completely negligible in the early Universe where the energy density $\rho \gg M_P^2\Lambda \sim 10^{-12}(\mathrm{eV})^4$. The standard early Universe cosmology, described in Sec. 21.1.5 in "Big Bang Cosmology" review, is thus dominated by non-relativistic matter ($p_m = 0$) or radiation ($p_r = \rho_r/3$ for an isotropic distribution). This leads to a decelerating expansion with $\ddot{R} < 0$.

The hypothesis of inflation [1,2] postulates a period of accelerated expansion, $\ddot{R} > 0$, in the very early Universe, preceding the standard radiation-dominated era, which offers a physical model for the origin of these initial conditions, as reviewed in [3,4,5,6,7]. Such a period of accelerated expansion (i) drives a curved RW spacetime (with spherical or hyperbolic spatial geometry) towards spatial flatness, and (ii) it also expands the causal horizon beyond the present Hubble length, so as to encompass all the scales relevant to describe the large-scale structure observed in our Universe today, via the following two mechanisms.

(i) A spatially-flat universe with vanishing spatial curvature, $k = 0$, has the dimensionless density parameter $\Omega_{\rm tot} = 1$, where we define (Eq. (21.13) in "Big Bang Cosmology" review; see Chap. 24, "Cosmological Parameters" review for more complete definitions)

$$\Omega_{\rm tot} \equiv \frac{8\pi\rho_{\rm tot}}{3M_P^2H^2}\,, \tag{22.2}$$

with $\rho_{\rm tot} \equiv \rho + \Lambda M_P^2/8\pi$. If we re-write the Friedmann constraint (Eq. (22.1)) in terms of $\Omega_{\rm tot}$ we have

$$1 - \Omega_{\rm tot} = -\frac{k}{\dot{R}^2}\,. \tag{22.3}$$

Observations require $|1 - \Omega_{\rm tot,0}| < 0.005$ today [8], where the subscript 0 denotes the present-day value. Taking the time derivative of Eq. (22.3) we obtain

$$\frac{d}{dt}\left(1 - \Omega_{\rm tot}\right) = -2\frac{\ddot{R}}{\dot{R}}\left(1 - \Omega_{\rm tot}\right)\,. \tag{22.4}$$

Thus in a decelerating expansion, $\dot{R} > 0$ and $\ddot{R} < 0$, any small initial deviation from spatial flatness grows, $(d/dt)|1 - \Omega_{\rm tot}| > 0$. A small value such as $|1 - \Omega_{\rm tot,0}| < 0.005$ today requires an even smaller value at earlier times, e.g., $|1 - \Omega_{\rm tot}| < 10^{-5}$ at the last scattering of the CMB, which appears unlikely, unless for some reason space is exactly flat. However, an extended period of accelerated expansion in the very early Universe, with $\dot{R} > 0$ and $\ddot{R} > 0$ and hence $(d/dt)|1 - \Omega_{\rm tot}| < 0$, can drive $\Omega_{\rm tot}$ sufficiently close to unity, so that $|1 - \Omega_{\rm tot,0}|$ remains unobservably small today, even after the radiation- and matter-dominated eras, for a wide range of initial values of $\Omega_{\rm tot}$.

(ii) The comoving distance (the present-day proper distance) traversed by light between cosmic time t_1 and t_2 in an expanding universe can be written, (see Eq. (21.32) in "Big Bang Cosmology" review), as

$$D_0(t_1, t_2) = R_0\int_{t_1}^{t_2}\frac{dt}{R(t)} = R_0\int_{\ln R_1}^{\ln R_2}\frac{d(\ln R)}{\dot{R}}\,. \tag{22.5}$$

In standard decelerated (radiation- or matter-dominated) cosmology the integrand, $1/\dot{R}$, decreases towards the past, and there is a finite comoving distance traversed by light (a particle horizon) since the Big Bang ($R_1 \to 0$). For example, the comoving size of the particle horizon at the CMB last-scattering surface ($R_2 = R_{\rm lss}$) corresponds to $D_0 \sim 100\,$Mpc, or approximately 1° on the CMB sky today (see Sec. 21.2.4 in "Big Bang Cosmology" review). However, during a period of inflation, $1/\dot{R}$ increases towards the past, and hence the integral (Eq. (22.5)) diverges as $R_1 \to 0$, allowing an arbitrarily large causal horizon, dependent only upon the duration of the accelerated expansion. Assuming that the Universe inflates with a finite Hubble rate H_* at $t_1 = t_*$, ending with $H_{\rm end} < H_*$ at $t_2 = t_{\rm end}$, we have

$$D_0(t_*, t_{\rm end}) > \left(\frac{R_0}{R_{\rm end}}\right)H_*^{-1}\left(e^{N_*} - 1\right)\,, \tag{22.6}$$

where $N_* \equiv \ln(R_{\rm end}/R_*)$ describes the duration of inflation, measured in terms of the logarithmic expansion (or "e-folds") from $t_1 = t_*$ up to the end of inflation at $t_2 = t_{\rm end}$, and $R_0/R_{\rm end}$ is the subsequent expansion from the end of inflation to the present day. If inflation occurs above the TeV scale, the comoving Hubble scale at the end of inflation, $(R_0/R_{\rm end})H_{\rm end}^{-1}$, is less than one astronomical unit ($\sim 10^{11}$ m), and a causally-connected patch can encompass our entire observable Universe today, which has a size $D_0 > 30$ Gpc, if there were more than 40 e-folds of inflation ($N_* > 40$). If inflation occurs at the GUT scale (10^{15} GeV) then we require more than 60 e-folds.

Producing an accelerated expansion in general relativity requires an energy-momentum tensor with negative pressure, $p < -\rho/3$ (see Eq. (21.9) in "Big Bang Cosmology" review and Chap. 27, "Dark Energy" review), quite different from the hot dense plasma of relativistic particles in the hot Big Bang. However a positive vacuum energy $V > 0$ does exert a negative pressure, $p_V = -\rho_V$. The work done by the cosmological expansion must be negative in this case so that the local vacuum energy density remains constant in an expanding universe, $\dot{\rho}_V = -3H(\rho_V + p_V) = 0$. Therefore, a false vacuum state can drive an exponential expansion, corresponding to a de Sitter spacetime with a constant Hubble rate $H^2 = 8\pi\rho_V/3M_P^2$ on spatially-flat hypersurfaces.

A constant vacuum energy V, equivalent to a cosmological constant Λ in the Friedmann equation Eq. (22.1), cannot provide a complete description of inflation in the early Universe, since inflation must necessarily have come to an end in order for the standard Big-Bang cosmology to follow. A phase transition to the present true vacuum is required to release the false vacuum energy into the energetic plasma of the hot Big Bang and produce the large total entropy of our observed Universe today. Thus we must necessarily study dynamical models of inflation, where the time-invariance of the false vacuum state is broken by a time-dependent field. A first-order phase transition would produce a very inhomogeneous Universe [9] unless a time-dependent scalar field leads to a rapidly changing percolation rate [10,11,12]. However, a second-order phase transition [13,14], controlled by a slowly-rolling scalar field, can lead to a smooth classical exit from the vacuum-dominated phase.

As a spectacular bonus, quantum fluctuations in that scalar field could provide a source of almost scale-invariant density

fluctuations [15,16], as detected in the CMB (see Chap. 28), which are thought to be the origin of the structures seen in the Universe today.

Accelerated expansion and primordial perturbations can also be produced in some modified gravity theories (e.g., [1,17]) , which introduce additional non-minimally coupled degrees of freedom. Such inflation models can often be conveniently studied by transforming variables to an 'Einstein frame' in which Einstein's equations apply with minimally coupled scalar fields [18,19,20].

In the following we will review scalar field cosmology in general relativity and the spectra of primordial fluctuations produced during inflation, before studying selected inflation models.

22.2. Scalar Field Cosmology

The energy-momentum tensor for a canonical scalar field ϕ with self-interaction potential $V(\phi)$ is given in Eq. (21.52) in "Big Bang Cosmology" review. In a homogeneous background this corresponds to a perfect fluid with density

$$\rho = \frac{1}{2}\dot{\phi}^2 + V(\phi)\,, \tag{22.7}$$

and isotropic pressure

$$p = \frac{1}{2}\dot{\phi}^2 - V(\phi)\,, \tag{22.8}$$

while the 4-velocity is proportional to the gradient of the field, $u^\mu \propto \nabla^\mu\phi$.

A field with vanishing potential energy acts like a stiff fluid with $p = \rho = \dot{\phi}^2/2$, whereas if the time-dependence vanishes we have $p = -\rho = -V$ and the scalar field is uniform in time and space. Thus a classical, potential-dominated scalar-field cosmology, with $p \simeq -\rho$, can naturally drive a quasi-de Sitter expansion; the slow time-evolution of the energy density weakly breaks the exact $O(1,3)$ symmetry of four-dimensional de Sitter spacetime down to a Robertson-Walker (RW) spacetime, where the scalar field plays the role of the cosmic time coordinate.

In a scalar-field RW cosmology the Friedmann constraint equation (Eq. (22.1)) reduces to

$$H^2 = \frac{8\pi}{3M_P^2}\left(\frac{1}{2}\dot{\phi}^2 + V\right) - \frac{k}{R^2}\,, \tag{22.9}$$

while energy conservation (Eq. (21.10) in "Big Bang Cosmology" review) for a homogeneous scalar field reduces to the Klein-Gordon equation of motion (Eq. (21.54) in "Big Bang Cosmology" review)

$$\ddot{\phi} = -3H\dot{\phi} - V'(\phi)\,. \tag{22.10}$$

The evolution of the scalar field is thus driven by the potential gradient $V' = dV/d\phi$, subject to damping by the Hubble expansion $3H\dot{\phi}$.

If we define the Hubble slow-roll parameter

$$\epsilon_H \equiv -\frac{\dot{H}}{H^2}\,, \tag{22.11}$$

then we see that inflation ($\ddot{R} > 0$ and hence $\dot{H} > -H^2$) requires $\epsilon_H < 1$. In this case the spatial curvature decreases relative to the scalar field energy density as the Universe expands. Hence in the following we drop the spatial curvature and consider a spatially-flat RW cosmology, assuming that inflation has lasted sufficiently long that our observable universe is very close to spatially flatness. However, we note that bubble nucleation, leading to a first-order phase transition during inflation, can lead to homogeneous hypersurfaces with a hyperbolic ('open') geometry, effectively resetting the spatial curvature inside the bubble [21]. This is the basis of so-called open inflation models [22,23,24], where inflation inside the bubble has a finite duration, leaving a finite negative spatial curvature.

In a scalar field-dominated cosmology (Eq. (22.11)) gives

$$\epsilon_H = \frac{3\dot{\phi}^2}{2V + \dot{\phi}^2}\,, \tag{22.12}$$

in which case we see that inflation requires a potential-dominated expansion, $\dot{\phi}^2 < V$.

22.2.1. *Slow-Roll Inflation* :

It is commonly assumed that the field acceleration term, $\ddot{\phi}$, in (Eq. (22.10)) can be neglected, in which case one can give an approximate solution for the inflationary attractor [25]. This slow-roll approximation reduces the second-order Klein-Gordon equation (Eq. (22.10)) to a first-order system, which is over-damped, with the potential gradient being approximately balanced against to the Hubble damping:

$$3H\dot{\phi} \simeq -V'\,, \tag{22.13}$$

and at the same time that the Hubble expansion (Eq. (22.9)) is dominated by the potential energy

$$H^2 \simeq \frac{8\pi}{3M_P^2}V(\phi)\,, \tag{22.14}$$

corresponding to $\epsilon_H \ll 1$.

A necessary condition for the validity of the slow-roll approximation is that the potential slow-roll parameters

$$\epsilon \equiv \frac{M_P^2}{16\pi}\left(\frac{V'}{V}\right)^2\,, \quad \eta \equiv \frac{M_P^2}{8\pi}\left(\frac{V''}{V}\right)\,, \tag{22.15}$$

are small, i.e., $\epsilon \ll 1$ and $|\eta| \ll 1$, requiring the potential to be correspondingly flat. If we identify V'' with the effective mass of the field, we see that the slow-roll approximation requires that the mass of the scalar field must be small compared with the Hubble scale. We note that the Hubble slow-roll parameter coincides with the potential slow-roll parameter, $\epsilon_H \simeq \epsilon$, to leading order in the slow-roll approximation.

The slow-roll approximation allows one to determine the Hubble expansion rate as a function of the scalar field value, and vice versa. In particular, we can express, in terms of the scalar field value during inflation, the total logarithmic expansion, or number of "e-folds":

$$N_* \equiv \ln\left(\frac{R_{\rm end}}{R_*}\right) = \int_{t_*}^{t_{\rm end}} H dt \simeq -\int_{\phi_*}^{\phi_{\rm end}} \sqrt{\frac{4\pi}{\epsilon}}\frac{d\phi}{M_P} \text{ for } V' > 0\,. \tag{22.16}$$

Given that the slow-roll parameters are approximately constant during slow-roll inflation, $d\epsilon/dN \simeq 2\epsilon(\eta - 2\epsilon) = \mathcal{O}(\epsilon^2)$, we have

$$N_* \simeq \frac{4}{\sqrt{\epsilon}}\frac{\Delta\phi}{M_P}\,. \tag{22.17}$$

Since we require $N > 40$ to solve the flatness, horizon and entropy problems of the standard Big Bang cosmology, we require either very slow roll, $\epsilon < 0.01$, or a large change in the value of the scalar field relative to the Planck scale, $\Delta\phi > M_P$.

22.2.2. *Reheating* :

Slow-roll inflation can lead to an exponentially large universe, close to spatial flatness and homogeneity, but the energy density is locked in the potential energy of the scalar field, and needs to be converted to particles and thermalised to recover a hot Big Bang cosmology at the end of inflation [26,27]. This process is usually referred to as reheating, although there was not necessarily any preceding thermal era. Reheating can occur when the scalar field evolves towards the minimum of its potential, converting the potential energy first to kinetic energy. This can occur either through the breakdown of the slow-roll condition in single-field models, or due to an instability triggered by the inflaton reaching a critical value, in multi-field models known as hybrid inflation models [28].

Close to a simple minimum, the scalar field potential can be described by a quadratic function, $V = m^2\phi^2/2$, where m is the mass of the field. We can obtain slow-roll inflation in such a potential at large field values, $\phi \gg M_P$. However, for $\phi \ll M_P$ the field approaches an oscillatory solution:

$$\phi(t) \simeq \frac{M_P}{\sqrt{3\pi}}\frac{\sin(mt)}{mt}\,. \tag{22.18}$$

For $|\phi| < M_P$ the Hubble rate drops below the inflaton mass, $H < m$, and the field oscillates many times over a Hubble time. Averaging

over several oscillations, $\Delta t \gg m^{-1}$, we find $\langle \dot\phi^2/2\rangle_{\Delta t} \simeq \langle m^2\phi^2/2\rangle_{\Delta t}$ and hence

$$\langle\rho\rangle_{\Delta t} \simeq \frac{M_P^2}{6\pi t^2}\,, \quad \langle p\rangle_{\Delta t} \simeq 0\,. \tag{22.19}$$

This coherent oscillating field corresponds to a condensate of non-relativistic massive inflaton particles, driving a matter-dominated era at the end of inflation, with scale factor $R \propto t^{2/3}$.

The inflaton condensate can lose energy through perturbative decays due to terms in the interaction Lagrangian, such as

$$\mathcal{L}_{\rm int} \subset -\lambda_i\sigma\phi\chi_i^2 - \lambda_j\phi\bar\psi_j\psi_j \tag{22.20}$$

that couple the inflation to scalar fields χ_i or fermions ψ_j, where σ has dimensions of mass and the λ_i are dimensionless couplings. When the mass of the inflaton is much larger than the decay products, the decay rate is given by [29]

$$\Gamma_i = \frac{\lambda_i^2\sigma^2}{8\pi m}\,, \quad \Gamma_j = \frac{\lambda_j^2 m}{8\pi}\,. \tag{22.21}$$

These decay products must in turn thermalise with Standard Model particles before we recover conventional hot Big Bang cosmology. An upper limit on the reheating temperature after inflation is given by [27]

$$T_{rh} = 0.2\left(\frac{100}{g_*}\right)^{1/4}\sqrt{M_P\Gamma_{\rm tot}}\,, \tag{22.22}$$

where g_* is the effective number of degrees of freedom and $\Gamma_{\rm tot}$ is the total decay rate for the inflaton, which is required to be less than m for perturbative decay.

The baryon asymmetry of the Universe must be generated after the main release of entropy during inflation, which is an important constraint on possible models. Also, the fact that the inflaton mass is much larger than the mass scale of the Standard Model opens up the possibility that it may decay into massive stable or metastable particles that could be connected with dark matter, constraining possible models. For example, in the context of supergravity models the reheat temperature is constrained by the requirement that gravitinos are not overproduced, potentially destroying the successes of Big Bang nucleosynthesis. For a range of gravitino masses one must require $T_{rh} < 10^9$ GeV [30,31].

The process of inflaton decay and reheating can be significantly altered by interactions leading to space-time dependences in the effective masses of the fields. In particular, parametric resonance can lead to explosive, non-perturbative decay of the inflaton in some cases, a process often referred to as preheating [32,26]. For example, an interaction term of the form

$$\mathcal{L}_{\rm int} \subset -\lambda^2\phi^2\chi^2\,, \tag{22.23}$$

leads to a time-dependent effective mass for the χ field as the inflaton ϕ oscillates. This can lead to non-adiabatic particle production if the bare mass of the χ field is small for large couplings or for rapid changes of the inflaton field. The process of preheating is highly model-dependent, but it highlights the possible role of non-thermal particle production after and even during inflation.

22.3. Primordial Perturbations from Inflation

Although inflation was originally discussed as a solution to the problem of initial conditions required for homogeneous and isotropic hot Big Bang cosmology, it was soon realised that inflation also offered a mechanism to generate the inhomogeneous initial conditions required for the formation of large-scale structure [15,16,17,33].

22.3.1. *Metric Perturbations* :

In a homogeneous classical inflationary cosmology driven by a scalar field, the inflaton field is uniform on constant-time hypersurfaces, $\phi = \phi_0(t)$. However, quantum fluctuations inevitably break the spatial symmetry leading to an inhomogeneous field:

$$\phi(t, x^i) = \phi_0(t) + \delta\phi(t, x^i)\,. \tag{22.24}$$

At the same time, one should consider inhomogeneous perturbations of the RW spacetime metric (see, e.g., [34,35,36]) :

$$ds^2 = (1{+}2A)dt^2 - 2RB_i dt dx^i - R^2\left[(1+2C)\delta_{ij} + \partial_i\partial_j E + h_{ij}\right]dx^i dx^j, \tag{22.25}$$

where A, B, E and C are scalar perturbations while h_{ij} represents transverse and tracefree, tensor metric perturbations. Vector metric perturbations can be eliminated using Einstein constraint equations in a scalar field cosmology.

The tensor perturbations remain invariant under a temporal gauge transformation $t \to t + \delta t(t, x^i)$, but both the scalar field and the scalar metric perturbations transform. For example, we have

$$\delta\phi \to \delta\phi - \dot\phi_0\delta t\,, \quad C \to C - H\delta t\,. \tag{22.26}$$

However, there are gauge invariant combinations, such as [37]

$$Q = \delta\phi - \frac{\dot\phi_0}{H}C\,, \tag{22.27}$$

which describes the scalar field perturbations on spatially-flat ($C = 0$) hypersurfaces. This is simply related to the curvature perturbation on uniform-field ($\delta\phi = 0$) hypersurfaces:

$$\mathcal{R} = C - \frac{H}{\dot\phi_0}\delta\phi = -\frac{H}{\dot\phi_0}Q\,, \tag{22.28}$$

which coincides in slow-roll inflation, $\rho \simeq \rho(\phi)$, with the curvature perturbation on uniform-density hypersurfaces [16]

$$\zeta = C - \frac{H}{\dot\rho_0}\delta\rho\,. \tag{22.29}$$

Thus scalar field and scalar metric perturbations are coupled by the evolution of the inflaton field.

22.3.2. *Gravitational waves from inflation* :

The tensor metric perturbation, h_{ij} in Eq. (22.25), is gauge-invariant and decoupled from the scalar perturbations at first order. This represents the free excitations of the spacetime, i.e., gravitational waves, which are the simplest metric perturbations to study at linear order.

Each tensor mode, with wavevector $\vec k$, has two linearly-independent transverse and trace-free polarisation states:

$$h_{ij}(\vec k) = h_{\vec k}q_{ij} + \bar h_{\vec k}\bar q_{ij}\,. \tag{22.30}$$

The linearised Einstein equations then yield the same evolution equation for the amplitude as that for a massless field in RW spacetime:

$$\ddot h_{\vec k} + 3H\dot h_{\vec k} + \frac{k^2}{R^2}h_{\vec k} = 0\,, \tag{22.31}$$

(and similarly for $\bar h_{\vec k}$). This can be re-written in terms of the conformal time, $\eta = \int dt/R$, and the conformally rescaled field:

$$u_{\vec k} = \frac{M_P R h_{\vec k}}{\sqrt{32\pi}}\,. \tag{22.32}$$

This conformal field then obeys the wave equation for a canonical scalar field in Minkowski spacetime with a time-dependent mass:

$$u_{\vec k}'' + \left(k^2 - \frac{R''}{R}\right)u_{\vec k} = 0\,. \tag{22.33}$$

During slow-roll

$$\frac{R''}{R} \simeq (2-\epsilon)R^2H^2\,. \tag{22.34}$$

This makes it possible to quantise the linearised metric fluctuations, $u_{\vec k} \to \hat u_{\vec k}$, on sub-Hubble scales, $k^2/R^2 \gg H^2$, where the background expansion can be neglected.

Crucially, in an inflationary expansion, where $\ddot R > 0$, the comoving Hubble length $H^{-1}/R = 1/\dot R$ decreases with time. Thus all modes

start inside the Hubble horizon and it is possible to take the initial field fluctuations to be in a vacuum state at early times or on small scales:

$$\langle u_{\vec{k}_1}\, u_{\vec{k}_2}\rangle = \frac{i}{2}(2\pi)^3\delta^{(3)}\left(\vec{k}_1+\vec{k}_2\right) . \tag{22.35}$$

In terms of the amplitude of the tensor metric perturbations, this corresponds to

$$\langle h_{\vec{k}_1}\, h_{\vec{k}_2}\rangle = \frac{1}{2}\frac{\mathcal{P}_t(k_1)}{4\pi k_1^3}(2\pi)^3\delta^{(3)}\left(\vec{k}_1+\vec{k}_2\right) , \tag{22.36}$$

where the factor $1/2$ appears due to the two polarisation states that contribute to the total tensor power spectrum:

$$\mathcal{P}_t(k) = \frac{64\pi}{M_P^2}\left(\frac{k}{2\pi R}\right)^2 . \tag{22.37}$$

On super-Hubble scales, $k^2/R^2 \ll H^2$, we have the growing mode solution to Eq. (22.33), $u_{\vec{k}} \propto R$, corresponding to $h_{\vec{k}} \to$ constant, i.e., tensor modes are frozen-in on super-Hubble scales, both during and after inflation. Thus, connecting the initial vacuum fluctuations on sub-Hubble scales to the late-time power spectrum for tensor modes at Hubble exit during inflation, $k = R_*H_*$, we obtain

$$\mathcal{P}_t(k) \simeq \frac{64\pi}{M_P^2}\left(\frac{H_*}{2\pi}\right)^2 . \tag{22.38}$$

In the de Sitter limit, $\epsilon \to 0$, the Hubble rate becomes time-independent and the tensor spectrum on super-Hubble scales becomes scale-invariant [38]. However slow-roll evolution leads to weak time dependence of H_* and thus a scale-dependent spectrum on large scales, with a spectral tilt

$$n_t \equiv \frac{d\ln\mathcal{P}_T}{d\ln k} \simeq -2\epsilon_* . \tag{22.39}$$

22.3.3. *Density Perturbations from single-field inflation* :

The inflaton field fluctuations on spatially-flat hypersurfaces are coupled to scalar metric perturbations at first order, but these can be eliminated using the Einstein constraint equations to yield an evolution equation

$$\ddot{Q}_{\vec{k}} + 3H\dot{Q}_{\vec{k}} + \left[\frac{k^2}{R^2} + V'' - \frac{8\pi}{3M_P^2}\frac{d}{dt}\left(\frac{R^3\dot{\phi}^2}{H}\right)\right]Q_{\vec{k}} = 0 . \tag{22.40}$$

Terms proportional to M_P^{-2} represent the effect on the field fluctuations of gravity at first order. As can be seen, this vanishes in the limit of a constant background field, and hence is suppressed in the slow-roll limit, but it is of the same order as the effective mass, $V'' = 3\eta H^2$, so must be included if we wish to model deviations from exact de Sitter symmetry.

This wave equation can also be written in the canonical form for a free field in Minkowski spacetime if we define [37]

$$v_{\vec{k}} \equiv RQ_{\vec{k}} , \tag{22.41}$$

to yield

$$v_{\vec{k}}'' + \left(k^2 - \frac{z''}{z}\right)v_{\vec{k}} = 0 , \tag{22.42}$$

where we define

$$z \equiv \frac{R\dot{\phi}}{H} , \qquad \frac{z''}{z} \simeq (2+5\epsilon-3\eta)R^2H^2 , \tag{22.43}$$

where the last approximate equality holds to leading order in the slow-roll approximation.

As previously done for gravitational waves, we quantise the linearised field fluctuations $v_{\vec{k}} \to \hat{v}_{\vec{k}}$ on sub-Hubble scales, $k^2/R^2 \gg H^2$, where the background expansion can be neglected. Thus we impose

$$\langle v_{\vec{k}_1}\, v'_{\vec{k}_2}\rangle = \frac{i}{2}\delta^{(3)}\left(\vec{k}_1+\vec{k}_2\right) . \tag{22.44}$$

In terms of the field perturbations, this corresponds to

$$\langle Q_{\vec{k}_1}\, Q_{\vec{k}_2}\rangle = \frac{\mathcal{P}_Q(k_1)}{4\pi k_1^3}(2\pi)^3\delta^{(3)}\left(\vec{k}_1+\vec{k}_2\right) , \tag{22.45}$$

where the power spectrum for vacuum field fluctuations on sub-Hubble scales, $k^2/R^2 \gg H^2$, is simply

$$\mathcal{P}_Q(k) = \left(\frac{k}{2\pi R}\right)^2 , \tag{22.46}$$

yielding the classic result for the vacuum fluctuations for a massless field in de Sitter at Hubble exit, $k = R_*H_*$:

$$\mathcal{P}_Q(k) \simeq \left(\frac{H}{2\pi}\right)_*^2 . \tag{22.47}$$

In practice there are slow-roll corrections due to the small but finite mass (η) and field evolution (ϵ) [39].

Slow-roll corrections to the field fluctuations are small on sub-Hubble scales, but can become significant as the field and its perturbations evolve over time on super-Hubble scales. Thus it is helpful to work instead with the curvature perturbation, ζ defined in equation (Eq. (22.29)), which remains constant on super-Hubble scales for adiabatic density perturbations both during and after inflation [16,40]. Thus we have an expression for the primordial curvature perturbation on super-Hubble scales produced by single-field inflation:

$$\mathcal{P}_\zeta(k) = \left[\left(\frac{H}{\dot{\phi}}\right)^2\mathcal{P}_Q(k)\right]_* \simeq \frac{4\pi}{M_P^2}\left[\frac{1}{\epsilon}\left(\frac{H}{2\pi}\right)^2\right]_* . \tag{22.48}$$

Comparing this with the primordial gravitational wave power spectrum (Eq. (22.38)) we obtain the tensor-to-scalar ratio for single-field slow-roll inflation

$$r \equiv \frac{\mathcal{P}_t}{\mathcal{P}_\zeta} \simeq 16\epsilon_* . \tag{22.49}$$

Note that the scalar amplitude is boosted by a factor $1/\epsilon_*$ during slow-roll inflation, because small scalar field fluctuations can lead to relatively large curvature perturbations on hypersurfaces defined with respect to the density if the potential energy is only weakly dependent on the scalar field, as in slow-roll. Indeed, the de Sitter limit is singular, since the potential energy becomes independent of the scalar field at first order, $\epsilon \to 0$, and the curvature perturbation on uniform-density hypersurfaces becomes ill-defined.

We note that in single-field inflation the tensor-to-scalar ratio and the tensor tilt (Eq. (22.39)) at the same scale are both determined by the first slow-roll parameter at Hubble exit, ϵ_*, giving rise to an important consistency test for single-field inflation:

$$n_t = -\frac{r}{8} . \tag{22.50}$$

This may be hard to verify if r is small, making any tensor tilt n_t difficult to measure. On the other hand, it does offer a way to rule out single-field slow-roll inflation if either r or n_t is large.

Given the relatively large scalar power spectrum, it has proved easier to measure the scalar tilt, conventionally defined as $n_s - 1$. Slow-roll corrections lead to slow time-dependence of both H_* and ϵ_*, giving a weak scale-dependence of the scalar power spectrum:

$$n_s - 1 \equiv \frac{d\ln\mathcal{P}_\zeta}{d\ln k} \simeq -6\epsilon_* + 2\eta_* , \tag{22.51}$$

and a running of this tilt at second-order in slow-roll:

$$\frac{dn_s}{d\ln k} \simeq -8\epsilon_*(3\epsilon_* - 2\eta_*) - 2\xi_*^2 , \tag{22.52}$$

where the running introduces a new slow-roll parameter at second-order:

$$\xi^2 = \frac{M_P^4}{64\pi^2}\frac{V'V'''}{V^2} . \tag{22.53}$$

22.3.4. *Observational Bounds* :

The observed scale-dependence of the power spectrum makes it necessary to specify the comoving scale, k, at which quantities are constrained and hence the Hubble-exit time, $k = a_* H_*$, when the corresponding theoretical quantities are calculated during inflation. This is usually expressed in terms of the number of e-folds from the end of inflation [41]:

$$N_*(k) \simeq 67 - \ln\left(\frac{k}{a_0 H_0}\right) + \frac{1}{4}\ln\left(\frac{V_*^2}{M_P^4 \rho_{\rm end}}\right) + \frac{1}{12}\ln\left(\frac{\rho_{rh}}{\rho_{\rm end}}\right) - \frac{1}{12}\ln(g_*), \tag{22.54}$$

where H_0^{-1}/a_0 is the present comoving Hubble length. Different models of reheating and and thus different reheat temperatures and densities, ρ_{rh} in Eq. (22.54), lead to a range of possible values for N_* corresponding to a fixed physical scale, and hence we have a range of observational predictions for a given inflation model, as seen in Fig. 22.1.

The Planck 2015 temperature and polarisation data (see Chap. 28, "Cosmic Microwave Background" review) are consistent with a smooth featureless power spectrum over a range of comoving wavenumbers, $0.008\ h^{-1}\ {\rm Mpc}^{-1} \leq k \leq 0.1\ h\ {\rm Mpc}^{-1}$. In the absence of running, the data measure the the spectral index

$$n_s = 0.968 \pm 0.006\,, \tag{22.55}$$

corresponding to a deviation from scale-invariance exceeding the 5σ level. If running of the spectral tilt is included in the model, this is constrained to be

$$\frac{dn_s}{d\ln k} = -0.003 \pm 0.007\,. \tag{22.56}$$

A recent analysis of the BICEP2/Keck Array, Planck and other data places an upper bound on the tensor-to-scalar ratio at $k = 0.05\ {\rm Mpc}^{-1}$ [42]

$$r < 0.07 \tag{22.57}$$

at the 95% CL.

These observational bounds can be converted into bounds on the slow-roll parameters and hence the potential during slow-roll inflation. Setting higher-order slow-roll parameters (beyond second-order in horizon-flow parameters [43]) to zero the Planck collaboration obtain the following bounds [44]

$$\epsilon < 0.012\,, \tag{22.58}$$

$$\eta = -0.0080^{+0.0088}_{-0.0146}\,, \tag{22.59}$$

$$\xi^2 = 0.0070^{+0.0045}_{-0.0069}\,, \tag{22.60}$$

which can be used to constrain models, as discussed in the next Section.

Fig. 22.1, which is taken from [44], compares observational CMB constraints on the tilt, n_s, in the spectrum of scalar perturbations and the ratio, r, between the magnitudes of tensor and scalar perturbations. Important rôles are played by data from the Planck satellite, the BICEP2/Keck Array (BKP) and measurements of baryon acoustic oscillations (BAO). The reader is referred to [44] for technical details. These experimental constraints are compared with the predictions of some of the inflationary models discussed in this review. Generally speaking, models with a concave potential are favoured over those with a convex potential, and models with power-law inflation, as opposed to de Sitter-like (quasi-)exponential expansion, are now excluded.

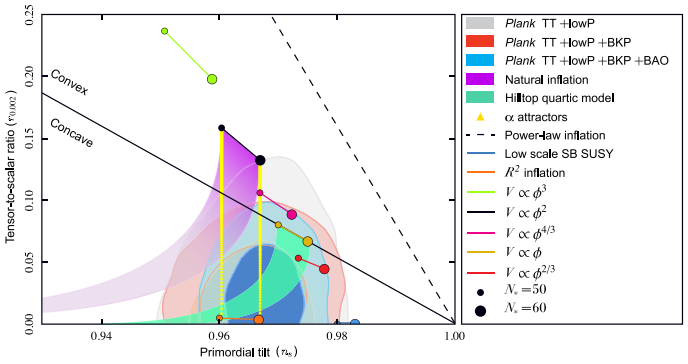

Figure 22.1: The marginalized joint 68 and 95% CL regions for the tilt in the scalar perturbation spectrum, n_s, and the relative magnitude of the tensor perturbations, r, obtained from the Planck 2015 data and their combinations with BICEP2/Keck Array and/or BAO data, confronted with the predictions of some of the inflationary models discussed in this review. This figure is taken from [44].

22.4. Models

22.4.1. *Pioneering Models* :

The paradigm of the inflationary Universe was proposed in [2], where it was pointed out that an early period of (near-)exponential expansion, in addition to resolving the horizon and flatness problems of conventional Big-Bang cosmology as discussed above (the possibility of a de Sitter phase in the early history of the Universe was also proposed in the non-minimal gravity model of [1], with the motivation of avoiding an initial singularity), would also dilute the prior abundance of any unseen heavy, (meta-)stable particles, as exemplified by monopoles in grand unified theories (GUTs; see Chap. 114, "Grand Unified Theories" review). The original proposal was that this inflationary expansion took place while the Universe was in a metastable state (a similar suggestion was made in [45,46], where in [45] it was also pointed out that such a mechanism could address the horizon problem) and was terminated by a first-order transition due to tunnelling though a potential barrier. However, it was recognized already in [2] that this 'old inflation' scenario would need modification if the transition to the post-inflationary universe were to be completed smoothly without generating unacceptable inhomogeneities.

This 'graceful exit' problem was addressed in the 'new inflation' model of [13](see also [14] and footnote [39] of [2]) , which studied models based on an SU(5) GUT with an effective potential of the Coleman-Weinberg type (i.e., dominated by radiative corrections), in which inflation could occur during the roll-down from the local maximum of the potential towards a global minimum. However, it was realized that the Universe would evolve to a different minimum from the Standard Model [47], and it was also recognized that density fluctuations would necessarily be too large [15], since they were related to the GUT coupling strength.

These early models of inflation assumed initial conditions enforced by thermal equilibrium in the early Universe. However, this assumption was questionable: indeed, it was not made in the model of [1], in which a higher-order gravitational curvature term was assumed to arise from quantum corrections, and the assumption of initial thermal equilibrium was jettisoned in the 'chaotic' inflationary model of [48]. These are the inspirations for much recent inflationary model building, so we now discuss them in more detail, before reviewing contemporary models.

In this section we will work in natural units where we set the reduced Planck mass to unity, i.e., $8\pi/M_P^2 = 1$. All masses are thus relative to the reduced Planck scale.

22.4.2. R^2 *Inflation* :

The first-order Einstein-Hilbert action, $(1/2)\int d^4x\sqrt{-g}R$, where R is the Ricci scalar curvature, is the minimal possible theory consistent with general coordinate invariance. However, it is possible that there might be non-minimal corrections to this action, and the unique second-order possibility is

$$S = \frac{1}{2}\int d^4x\sqrt{-g}\left(R + \frac{R^2}{6M^2}\right)\,. \tag{22.61}$$

It was pointed out in [1] that an R^2 term could be generated by quantum effects, and that (Eq. (22.61)) could lead to de Sitter-like expansion of the Universe. Scalar density perturbations in this model were calculated in [17]. Because the initial phase was (almost) de Sitter, these perturbations were (approximately) scale-invariant, with

magnitude $\propto M$. It was pointed out in [17] that requiring the scalar density perturbations to lie in the range 10^{-3} to 10^{-5}, consistent with upper limits at that time, would require $M \sim 10^{-3}$ to 10^{-5} in Planck units, and it was further suggested in that these perturbations could lead to the observed large-scale structure of the Universe, including the formation of galaxies.

Although the action (Eq. (22.61)) does not contain an explicit scalar field, [17] reduced the calculation of density perturbations to that of fluctuations in the scalar curvature R, which could be identified (up to a factor) with a scalar field of mass M. The formal equivalence of R^2 gravity (Eq. (22.61)) to a theory of gravity with a massive scalar ϕ had been shown in [18], see also [19]. The effective scalar potential for what we would nowadays call the 'inflaton' [49] takes the form

$$S = \frac{1}{2}\int d^4x\sqrt{-g}\left[R + (\partial_\mu\phi)^2 - \frac{3}{2}M^2(1-e^{-\sqrt{2/3}\phi})^2\right] \qquad (22.62)$$

when the action is written in the Einstein frame, and the potential is shown as the solid black line in Fig. 22.2. Using (Eq. (22.48)), one finds that the amplitude of the scalar density perturbations in this model is given by

$$\Delta_{\mathcal{R}} = \frac{3M^2}{8\pi^2}\sinh^4\left(\frac{\phi}{\sqrt{6}}\right), \qquad (22.63)$$

The measured magnitude of the density fluctuations in the CMB requires $M \simeq 1.3\times10^{-5}$ in Planck units (assuming $N_* \simeq 55$), so one of the open questions in this model is why M is so small. Obtaining $N_* \simeq 55$ also requires an initial value of $\phi \simeq 5.5$, i.e., a super-Planckian initial condition, and another issue for this and many other models is how the form of the effective potential is protected and remains valid at such large field values. Using Eq. (22.51) one finds that $n_s \simeq 0.965$ for $N_* \simeq 55$ and using (Eq. (22.49)) one finds that $r \simeq 0.0035$. These predictions are consistent with the present data from Planck and other experiments, as seen in Fig. 22.1.

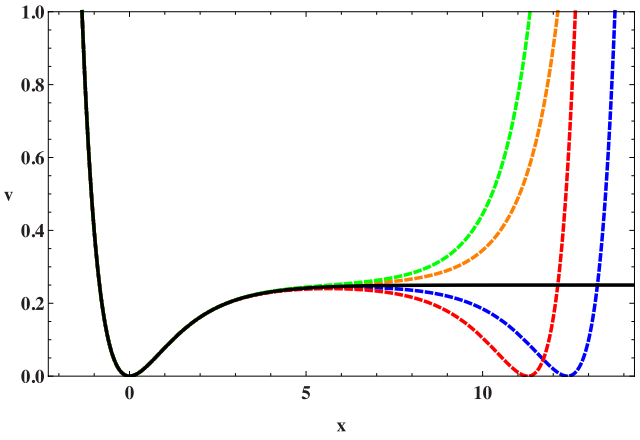

Figure 22.2: The inflationary potential V in the R^2 model (solid black line) compared with its form in various no-scale models discussed in detail in [50](dashed coloured lines).

22.4.3. *Chaotic Models with Power-Law Potentials* :

As has already been mentioned, a key innovation in inflationary model-building was the suggestion to abandon the questionable assumption of a thermal initial state, and consider 'chaotic' initial conditions with very general forms of potential [48]. (Indeed, the R^2 model discussed above can be regarded as a prototype of this approach.) The chaotic approach was first proposed in the context of a simple power-law potential of the form $\mu^{4-\alpha}\phi^\alpha$, and the specific example of $\lambda\phi^4$ was studied in [48]. Such models make the following predictions for the slow-roll parameters ϵ and η:

$$\epsilon = \frac{1}{2}\left(\frac{\alpha}{\phi}\right)^2, \quad \eta = \frac{\alpha(\alpha-1)}{\phi^2}, \qquad (22.64)$$

leading to the predictions

$$r \approx \frac{4\alpha}{N_*}, \qquad n_s - 1 \approx -\frac{\alpha+2}{2N_*}, \qquad (22.65)$$

which are shown in Fig. 22.1 for some illustrative values of α. We note that the prediction of the original ϕ^4 model lies out of the frame, with values of r that are too large and values of n_s that are too small. The ϕ^3 model has similar problems, and would in any case require modification in order to have a well-defined minimum. The simplest possibility is ϕ^2, but this is now also disfavoured by the data, at the 95% CL if only the Planck data are considered, and more strongly if other data are included, as seen in Fig. 22.1. (For non-minimal models of quadratic inflation that avoid this problem, see, e.g., [51].)

Indeed, as can be seen in Fig. 22.1, all single-field models with a convex potential (i.e., one curving upwards) are disfavoured compared to models with a concave potential. Thus, a model with a $\phi^{2/3}$ potential may just be compatible with the data at the 68% CL, whereas linear and $\phi^{4/3}$ potentials are allowed only at about the 95% CL.

22.4.4. *Hilltop Models* :

This preference for a concave potential motivates interest in 'hilltop' models [52], whose starting-point is a potential of the form

$$V(\phi) = \Lambda^4\left[1 - \left(\frac{\phi}{\mu}\right)^p + \ldots\right], \qquad (22.66)$$

where the ... represent extra terms that yield a positive semi-definite potential. To first order in the slow-roll parameters, when $x \equiv \phi/\mu$ is small, one has

$$n_s \simeq 1 - p(p-1)\mu^{-2}\frac{x^{p-2}}{(1-x^p)} - \frac{3}{8}r, \qquad r \simeq 8p^2\mu^{-2}\frac{x^{2p-2}}{(1-x^p)^2}. \qquad (22.67)$$

As seen in Fig. 22.1, a hilltop model with $p = 4$ can be compatible with the Planck and other measurements, if $\mu \gg M_P$.

22.4.5. *D-Brane Inflation* :

Many scenarios for inflation involving extra dimensions have been proposed, e.g., the possibility that observable physics resides on a three-dimensional brane, and that there is an inflationary potential that depends on the distance between our brane and an antibrane, with a potential of the form [53]

$$V(\phi) = \Lambda^4\left[1 - \left(\frac{\mu}{\phi}\right)^p + \ldots\right]. \qquad (22.68)$$

In this scenario the effective potential vanishes in the limit $\phi \to \infty$, corresponding to complete separation between our brane and the antibrane. The predictions for n_s and r in this model can be obtained from (Eq. (22.67)) by exchanging $p \leftrightarrow -p$, and are also consistent with the Planck and other data.

22.4.6. *Natural Inflation* :

Also seen in Fig. 22.1 are the predictions of 'natural inflation' [54], in which one postulates a non-perturbative shift symmetry that suppresses quantum corrections, so that a hierarchically small scale of inflation, $H \ll M_P$, is technically natural. In the simplest models, there is a periodic potential of the form

$$V(\phi) = \Lambda^4\left[1 + \cos\left(\frac{\phi}{f}\right)\right], \qquad (22.69)$$

where f is a dimensional parameter reminiscent of an axion decay constant (see the next subsection) [55], which must have a value $> M_P$. Natural inflation can yield predictions similar to quadratic inflation (which are no longer favoured, as already discussed), but can also yield an effective convex potential. Thus, it may lead to values of r that are acceptably small, but for values of n_s that are in tension with the data, as seen in Fig. 22.1.

22.4.7. ***Axion Monodromy Models*** :

The effective potentials in stringy models [56,57] motivated by axion monodromy may be of the form

$$V(\phi) \;=\; \mu^{4-\alpha}\phi^{\alpha} + \Lambda^4 e^{-C\left(\frac{\phi}{\phi_0}\right)^{p_\Lambda}} \cos\left[\gamma + \frac{\phi}{f}\left(\frac{\phi}{\phi_0}\right)^{p_f+1}\right] , \quad (22.70)$$

where μ, Λ, f and ϕ_0 are parameters with the dimension of mass, and C, p, p_Λ, p_f and γ are dimensionless constants, generalizing the potential ([54]) in the simplest models of natural inflation. The oscillations in (Eq. (22.70)) are associated with the axion field, and powers $p_\Lambda, p_f \neq 0$ may arise from ϕ-dependent evolutions of string moduli. Since the exponential prefactor in (Eq. (22.70)) is due to non-perturbative effects that may be strongly suppressed, the oscillations may be unobservably small. Specific string models having ϕ^α with $\alpha = 4/3, 1$ or $2/3$ have been constructed in [56,57], providing some motivation for the low-power models mentioned above.

As seen in Fig. 22.1, the simplest axion monodromy models with these values of the power α are compatible with all the available data at the 95% CL, though not at the 68% CL. The Planck Collaboration has also searched for characteristic effects associated with the second term in (Eq. (22.70)), such as a possible drift in the modulation amplitude (setting $p_\Lambda = C = 0$), and a possible drifting frequency generated by $p_f \neq 0$, without finding any compelling evidence [44].

22.4.8. ***Higgs Inflation*** :

Since the energy scale during inflation is commonly expected to lie between the Planck and TeV scales, it may serve as a useful bridge with contacts both to string theory or some other quantum theory of gravity, on the one side, and particle physics on the other side. However, as the above discussion shows, much of the activity in building models of inflation has been largely independent of specific connections with these subjects, though some examples of string-motivated models of inflation were mentioned above.

The most economical scenario for inflation might be to use as inflaton the only established scalar field, namely the Higgs field (see Chap. 11, "Status of Higgs boson physics" review). A specific model assuming a non-minimal coupling of the Higgs field h to gravity was constructed in [58]. Its starting-point is the action

$$S \;=\; \int d^4x\sqrt{-g}\left[\frac{M^2+\xi h^2}{2}R + \frac{1}{2}\partial_\mu h \partial^\mu h - \frac{\lambda}{4}(h^2-v^2)^2\right] , \quad (22.71)$$

where v is the Higgs vacuum expectation value. The model requires $\xi \gg 1$, in which case it can be rewritten in the Einstein frame as

$$S \;=\; \int d^4x\sqrt{-g}\left[\frac{1}{2}R + \frac{1}{2}\partial_\mu\chi\partial^\mu\chi - U(\chi)\right] , \quad (22.72)$$

where the effective potential for the canonically-normalized inflaton field χ has the form

$$U(\chi) \;=\; \frac{\lambda}{4\xi^2}\left[1+\exp\left(-\frac{2\chi}{\sqrt{6}M_P}\right)\right]^{-2} , \quad (22.73)$$

which is similar to the effective potential of the R^2 model at large field values. As such, the model inflates successfully if $\xi \simeq 5\times 10^4\ m_h/(\sqrt{2}v)$, with predictions for n_s and r that are indistinguishable from the predictions of the R^2 model shown in Fig. 22.1.

This model is very appealing, but must confront several issues. One is to understand the value of ξ, and another is the possibility of unitarity violation. However, a more fundamental issue is whether the effective quartic Higgs coupling is positive at the scale of the Higgs field during inflation. Extrapolations of the effective potential in the Standard Model using the measured values of the masses of the Higgs boson and the top quark indicate that probably $\lambda < 0$ at this scale [59], though there are still significant uncertainties associated with the appropriate input value of the top mass and the extrapolation to high renormalization scales.

22.4.9. ***Supersymmetric Models of Inflation*** :

Supersymmetry [60] is widely considered to be a well-motivated possible extension of the Standard Model that might become apparent at the TeV scale. It is therefore natural to consider supersymmetric models of inflation. These were originally proposed because of the problems of the the new inflationary theory [13,14] based on the one-loop (Coleman-Weinberg) potential for breaking SU(5). Several of these problems are related to the magnitude of the effective potential parameters: in any model of inflation based on an elementary scalar field, some parameter in the effective potential must be small in natural units, e.g., the quartic coupling λ in a chaotic model with a quartic potential, or the mass parameter μ in a model of chaotic quadratic inflation. These parameters are renormalized multiplicatively in a supersymmetric theory, so that the quantum corrections to small values would be under control. Hence it was suggested that inflation cries out for supersymmetry [61], though non-supersymmetric resolutions of the problems of Coleman-Weinberg inflation are also possible: see, e.g., Ref. [62].

In the Standard Model there is only one scalar field that could be a candidate for the inflaton, namely the Higgs field discussed above, but even the minimal supersymmetric extension of the Standard Model (MSSM) contains many scalar fields. However, none of these is a promising candidate for the inflaton. The minimal extension of the MSSM that may contain a suitable candidate is the supersymmetric version of the minimal seesaw model of neutrino masses, which contains the three supersymmetric partners of the heavy singlet (right-handed) neutrinos. One of these singlet sneutrinos $\tilde{\nu}$ could be the inflaton [63]: it would have a quadratic potential, the mass coefficient required would be $\sim 10^{13}$ GeV, very much in the expected ball-park for singlet (right-handed) neutrino masses, and sneutrino inflaton decays also could give rise to the cosmological baryon asymmetry via leptogenesis. However, as seen in Fig. 22.1 and already discussed, a purely quadratic inflationary potential is no longer favoured by the data. This difficulty could in principle be resolved in models with multiple sneutrinos [64], or by postulating a trilinear sneutrino coupling and hence a superpotential of Wess-Zumino type [65], which can yield successful inflation with predictions intermediate between those of natural inflation and hilltop inflation in Fig. 22.1.

Finally, we note that it is also possible to obtain inflation via supersymmetry breaking, as in the model [66] whose predictions are illustrated in Fig. 22.1.

22.4.10. ***Supergravity Models*** :

Any model of early-Universe cosmology, and specifically inflation, must necessarily incorporate gravity. In the context of supersymmetry this requires an embedding in some supergravity theory [67,68]. An $\mathcal{N} = 1$ supergravity theory is specified by three functions: a Hermitian function of the matter scalar fields ϕ^i, called the Kähler potential K, that describes its geometry, a holomorphic function of the superfields, called the superpotential W, which describes their interactions, and another holomorphic function $f_{\alpha\beta}$, which describes their couplings to gauge fields V_α [69].

The simplest possibility is that the Kähler metric is flat:

$$K = \phi^i\phi_i^* , \quad (22.74)$$

where the sum is over all scalar fields in the theory, and the simplest inflationary model in minimal supergravity had the superpotential [70]

$$W = m^2(1-\phi)^2 , \quad (22.75)$$

Where ϕ is the inflaton. However, this model predicts a tilted scalar perturbation spectrum, $n_s = 0.933$, which is now in serious disagreement with the data from Planck and other experiments shown in Fig. 22.1.

Moreover, there is a general problem that arises in any supergravity theory coupled to matter, namely that, since its effective scalar potential contains a factor of e^K, scalars typically receive squared masses $\propto H^2 \sim V$, where H is the Hubble parameter [71], an issue called the 'η problem'. The theory given by (Eq. (22.75)) avoids this η problem, but a generic supergravity inflationary model encounters

this problem of a large inflaton mass. Moreover, there are additional challenges for supergravity inflation associated with the spontaneous breaking of local supersymmetry [72,73,74].

Various approaches to the η problem in supergravity have been proposed, including the possibility of a shift symmetry [75], and one possibility that has attracted renewed attention recently is no-scale supergravity [76,77]. This is a form of supergravity with a Kähler potential that can be written in the form [78]

$$K \;=\; -3\ln\left(T+T^*-\frac{\sum_i|\phi^i|^2}{3}\right)\,, \tag{22.76}$$

which has the special property that it naturally has a flat potential, at the classical level and before specifying a non-trivial superpotential. As such, no-scale supergravity is well-suited for constructing models of inflation. Adding to its attraction is the feature that compactifications of string theory to supersymmetric four-dimensional models yield effective supergravity theories of the no-scale type [79]. There are many examples of superpotentials that yield effective inflationary potentials for either the T field (which is akin to a modulus field in some string compactification) or a ϕ field (generically representing matter) that are of the same form as the effective potential of the R^2 model (Eq. (22.62)) when the magnitude of the inflaton field $\gg 1$ in Planck units, as required to obtain sufficiently many e-folds of inflation, N_* [80,81]. This framework also offers the possibility of using a suitable superpotential to construct models with effective potentials that are similar, but not identical, to the R^2 model, as shown by the dashed coloured lines in Fig. 22.2.

22.4.11. ***Other Exponential Potential Models*** :

This framework also offers the possibility [80] of constructing models in which the asymptotic constant value of the potential at large inflaton field values is approached via a different exponentially-suppressed term:

$$V(\phi) \;=\; A\left[1-\delta e^{-B\phi}+\mathcal{O}(e^{-2B\phi})\right]\,, \tag{22.77}$$

where the magnitude of the scalar density perturbations fixes A, but δ and B are regarded as free parameters. In the case of R^2 inflation $\delta = 2$ and $B = \sqrt{2/3}$. In a model such as (Eq. (22.77)), one finds at leading order in the small quantity $e^{-B\phi}$ that

$$\begin{aligned} n_s &= 1-2B^2\delta e^{-B\phi}\,,\\ r &= 8B^2\delta^2 e^{-2B\phi}\,,\\ N_* &= \frac{1}{B^2\delta}e^{+B\phi}\,. \end{aligned} \tag{22.78}$$

yielding the relations

$$n_s \;=\; 1-\frac{2}{N_*}\,, r \;=\; \frac{8}{B^2N_*^2}\,. \tag{22.79}$$

This model leads to the class of predictions labelled by 'α attractors' [82] in Fig. 22.1. There are generalizations of the simplest no-scale model (Eq. (22.76)) with prefactors before the $\ln(\ldots)$ that are 1 or 2, leading to larger values of $B = \sqrt{2}$ or 1, respectively, and hence smaller values of r than in the R^2 model.

22.5. Model Comparison

Given a particular inflationary model, one can obtain constraints on the model parameters, informed by the likelihood, corresponding to the probability of the data given a particular choice of parameters (see Chap. 39, "Statistics" review). In the light of the detailed constraints on the statistical distribution of primordial perturbations now inferred from high-precision observations of the cosmic microwave background, it is also possible to make quantitative comparison of the statistical evidence for or against different inflationary models. This can be done either by comparing the logarithm of the maximum likelihood that can be obtained for the data using each model, i.e., the minimum χ^2 (with some correction for the number of free parameters in each model), or by a Bayesian model comparison [83](see also Sec. 39.3.3 in "Statistics" review).

In such a Bayesian model comparison one computes [7] the evidence, $\mathcal{E}(\mathcal{D}|\mathcal{M}_A)$ for a model, $\mathcal{M}_A$, given the data $\mathcal{D}$. This corresponds to the likelihood, $\mathcal{L}(\theta_{Aj}) = p(\mathcal{D}|\theta_{Aj},\mathcal{M}_A)$, integrated over the assumed prior distribution, $\pi(\theta_{Aj}|\mathcal{M}_A)$, for all the model parameters θ_{Aj}:

$$\mathcal{E}(\mathcal{D}|\mathcal{M}_A) = \int \mathcal{L}(\theta_{Aj})\pi(\theta_{Aj}|\mathcal{M}_A)d\theta_{Aj}\,. \tag{22.80}$$

The posterior probability of the model given the data follows from Bayes' theorem

$$p(\mathcal{M}_A|\mathcal{D}) = \frac{\mathcal{E}(\mathcal{D}|\mathcal{M}_A)\pi(\mathcal{M}_A)}{p(\mathcal{D})}\,, \tag{22.81}$$

where the prior probability of the model is given by $\pi(\mathcal{M}_A)$. Assuming that all models are equally likely a priori, $\pi(\mathcal{M}_A) = \pi(\mathcal{M}_B)$, the relative probability of model A relative to a reference model, in the light of the data, is thus given by the Bayes factor

$$B_{A,\mathrm{ref}} = \frac{\mathcal{E}(\mathcal{D}|\mathcal{M}_A)}{\mathcal{E}(\mathcal{D}|\mathcal{M}_{\mathrm{ref}})}\,. \tag{22.82}$$

Computation of the multi-dimensional integral (Eq. (22.80)) is a challenging numerical task. Even using an efficient sampling algorithm requires hundreds of thousands of likelihood computations for each model, though slow-roll approximations can be used to calculate rapidly the primordial power spectrum using the APSIC numerical library [7] for a large number of single-field, slow-roll inflation models.

The change in χ^2 for selected slow-roll models relative to a baseline ΛCDM model is given in Table 22.1 (taken from [44]) . All the inflation models require some amplitude of tensors and so have an increased χ^2 with respect to the baseline ΛCDM model with a scalar tilt but no tensors. Table 22.1 also shows the Bayesian evidence for ($\ln B_{A,\mathrm{ref}} > 0$) or against ($\ln B_{A,\mathrm{ref}} < 0$) a selection of inflation models using the Planck analysis priors [44]. The Starobinsky R^2 inflationary model may be chosen as a reference [44] that provides a good fit to current data. Higgs inflation [58] is indistinguishable using current data, making the model comparison "inconclusive" on the Jeffrey's scale ($|\ln B_{A,\mathrm{ref}}| < 1$). (Recall, though, that this model is disfavoured by the measured values of the Higgs and top quark masses [59].) On the other hand, there is now moderate evidence ($|\ln B_{A,\mathrm{ref}}| > 2.5$) against large-field models such as chaotic inflation with a quadratic potential and strong evidence ($|\ln B_{A,\mathrm{ref}}| > 5$) against chaotic inflation with a quartic potential. Indeed, over 30% of the slow-roll inflation models considered in Ref. [7] are strongly disfavoured by the Planck data.

Table 22.1: Observational evidence for and against selected inflation models: $\Delta\chi^2$ is determined relative to a baseline ΛCDM model, and the Bayes factors are calculated relative to Starobinsky R^2 inflation. Results from Planck 2015 analysis [44].

Model	$\Delta\chi^2$	$\ln B_{A,\mathrm{ref}}$
R^2 inflation	+0.8	0
Power-law potential $\phi^{2/3}$	+6.5	−2.4
Power-law potential ϕ^2	+8.6	−4.7
Power-law potential ϕ^4	+43.3	−23.3
Natural inflation	+7.2	−2.4
SUSY α-attractor	+0.7	−1.8

The Bayes factors for a wide selection of slow-roll inflationary models are displayed in Fig. 22.3, which is adapted from Fig. 3 in [84], where more complete descriptions of the models and the calculations of the Bayes factors are given. Models discussed in this review are highlighted in yellow, and numbered as follows: (1) R^2 inflation

(Sec. 22.4) and models with similar predictions, such as Higgs inflation (Sec. 22.4) and no-scale supergravity inflation (Sec. 22.4); chaotic inflation models (2) with a ϕ^2 potential; (3) with a ϕ^4 potential; (4) with a $\phi^{2/3}$ potential, and (5) with a ϕ^p potential marginalising over $p \in [0.2, 6]$ (Sec. 22.4); hilltop inflation models (6) with $p = 2$; (7) with $p = 4$ and (8) marginalising over p (Sec. 22.4); (9) brane inflation (Sec. 22.4); (10) natural inflation (Sec. 22.4); (11) exponential potential models such as α-attractors (Sec. 22.4). As seen in Fig. 22.3 and discussed in the next Section, constraints on reheating are starting to provide additional information about models of inflation.

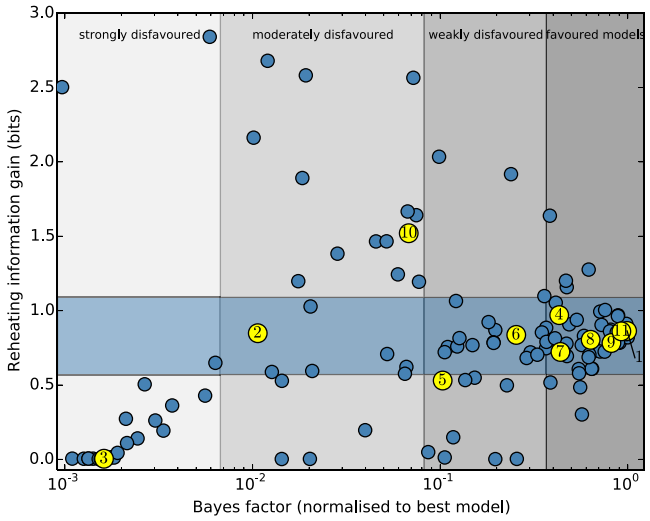

Figure 22.3: The Bayes factors calculated in [84] for a large sample of inflationary models. Those highlighted in yellow are featured in the this review, according tothe numbers listed in the text.

22.6. Constraints on Reheating

One connection between inflation and particle physics is provided by inflaton decay, whose products are expected to have thermalized subsequently. As seen in (Eq. (22.54)), the number of e-folds required during inflation depends on details of this reheating process, including the matter density upon reheating, denoted by $\rho_{\rm th}$, which depends in turn on the inflaton decay rate Γ_ϕ. We see in Fig. 22.1 that, within any specific inflationary model, both n_s and particularly r are sensitive to the value of N_*. In particular, the one-σ uncertainty in the experimental measurement of n_s is comparable to the variation in many model predictions for $N_* \in [50, 60]$. This implies that the data start to constrain scenarios for inflaton decay in many models. For example, it is clear from Fig. 22.1 that $N_* = 60$ would be preferred over $N_* = 50$ in a chaotic inflationary model with a quadratic potential.

As a specific example, let us consider R^2 models and related models such as Higgs and no-scale inflation models that predict small values of r [85]. As seen in Fig. 22.1, within these models the combination of Planck, BICEP2/Keck Array and BAO data would require a limited range of n_s, corresponding to a limited range of N_*, as seen by comparing the left and right vertical axes in Fig. 22.4:

$$N_* \gtrsim 52 \quad (68\%\ \text{CL}), \quad N_* \gtrsim 44 \quad (95\%\ \text{CL}). \tag{22.83}$$

Within any specific model for inflaton decay, these bounds can be translated into constraints on the effective decay coupling. For example, if one postulates a two-body inflaton decay coupling y, the bounds (Eq. (22.83)) can be translated into bounds on y. This is illustrated in Fig. 22.4, where any value of N_* (on the left vertical axis), projected onto the diagonal line representing the correlation predicted in R^2-like models, corresponds to a specific value of the inflaton decay rate Γ_ϕ/m (lower horizontal axis) and hence y (upper horizontal axis):

$$y \gtrsim 10^{-5} \quad (68\%\ \text{CL}), \quad y \gtrsim 10^{-15} \quad (95\%\ \text{CL}). \tag{22.84}$$

These bounds are not very constraining – although the 68% CL lower bound on y is already comparable with the electron Yukawa coupling – but can be expected to improve significantly in the coming years and thereby provide significant information on the connections between inflation and particle physics.

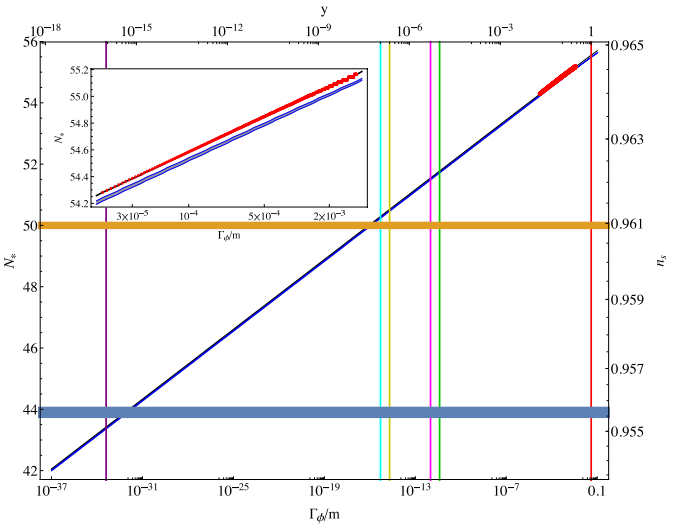

Figure 22.4: The values of N_* (left axis) and n_s (right axis) in R^2 inflation and related models for a wide range of decay rates, Γ_ϕ/m, (bottom axis) and corresponding two-body couplings, y (top axis). The diagonal red line segment shows full numerical results over a restricted range of Γ_ϕ/m (which are shown in more detail in the insert), while the diagonal blue strip represents an analytical approximation described in [85]. The difference between these results is indistinguishable in the main plot, but is visible in the insert. The horizontal yellow and blue lines show the 68 and 95% CL lower limits from the Planck 2015 data [44], and the vertical coloured lines correspond to specific models of inflaton decay. Figure taken from [85].

22.7. Beyond Single-Field Slow-Roll Inflation

There are numerous possible scenarios beyond the simplest single-field models of slow-roll inflation. These include theories in which non-canonical fields are considered, such as k-inflation [86] or DBI inflation [87], and multiple-field models, such as the curvaton scenario [88]. As well as altering the single-field predictions for the primordial curvature power spectrum (Eq. (22.48)) and the tensor-scalar ratio (Eq. (22.49)), they may introduce new quantities that vanish in single-field slow-roll models, such as isocurvature matter perturbations, corresponding to entropy fluctuations in the photon-to-matter ratio, at first order:

$$S_m = \frac{\delta n_m}{n_m} - \frac{\delta n_\gamma}{n_\gamma} = \frac{\delta \rho_m}{\rho_m} - \frac{3}{4}\frac{\delta \rho_\gamma}{\rho_\gamma}. \tag{22.85}$$

Another possibility is non-Gaussianity in the distribution of the primordial curvature perturbation (see Chap. 28, "Cosmic Microwave Background" review), encoded in higher-order correlators such as the primordial bispectrum [89]

$$\langle \zeta(\mathbf{k})\zeta(\mathbf{k}')\zeta(\mathbf{k}'')\rangle \equiv (2\pi)^3 \delta(\mathbf{k}+\mathbf{k}'+\mathbf{k}'') B_\zeta(k,k',k''), \tag{22.86}$$

which is often expressed in terms of a dimensionless non-linearity parameter $f_{\rm NL} \propto B_\zeta(k,k',k'')/P_\zeta(k)P_\zeta(k')$. The three-point function (Eq. (22.86)) can be thought of as defined on a triangle whose sides are

$\mathbf{k}, \mathbf{k}', \mathbf{k}''$, of which only two are independent, since they sum to zero. Further assuming statistical isotropy ensures that the bispectrum depends only on the magnitudes of the three vectors, k, k' and k''. The search for $f_{\rm NL}$ and other non-Gaussian effects was a prime objective of the Planck data analysis [90].

22.7.1. ***Effective Field Theory of Inflation*** :

Since slow-roll inflation is a phase of accelerated expansion with an almost constant Hubble parameter, one may think of inflation in terms of an effective theory where the de Sitter spacetime symmetry is spontaneously broken down to RW symmetry by the time-evolution of the Hubble rate, $\dot{H} \neq 0$. There is then a Goldstone boson, π, associated with the spontaneous breaking of time-translation invariance, which can be used to study model-independent properties of inflation. The Goldstone boson describes a spacetime-dependent shift of the time coordinate, corresponding to an adiabatic perturbation of the matter fields:

$$\delta\phi_i(t,\vec{x}) = \phi_i(t+\pi(t,\vec{x})) - \phi_i(t)\,. \tag{22.87}$$

Thus adiabatic field fluctuations can be absorbed into the spatial metric perturbation, $\mathcal{R}$ in Eq. (22.28) at first order, in the comoving gauge:

$$\mathcal{R} = -H\pi\,, \tag{22.88}$$

where we define π on spatially-flat hypersurfaces. In terms of inflaton field fluctuations, we can identify $\pi \equiv \delta\phi/\dot{\phi}$, but in principle this analysis is not restricted to inflation driven by scalar fields.

The low-energy effective action for π can be obtained by writing down the most general Lorentz-invariant action and expanding in terms of π. The second-order effective action for the free-field wave modes, π_k, to leading order in slow roll is then

$$S_\pi^{(2)} = -\int d^4x\sqrt{-g}\frac{M_P^2\dot{H}}{c_s^2}\left[\dot{\pi}_k^2 - \frac{c_s^2}{R^2}(\nabla\pi)^2\right], \tag{22.89}$$

where ϵ_H is the Hubble slow-roll parameter (Eq. (22.11)). We identify c_s^2 with an effective sound speed, generalising canonical slow-roll inflation, which is recovered in the limit $c_s^2 \to 1$.

The scalar power spectrum on super-Hubble scales (Eq. (22.48)) is enhanced for a reduced sound speed, leading to a reduced tensor-scalar ratio (Eq. (22.49))

$$\mathcal{P}_\zeta(k) \simeq \frac{4\pi}{M_P^2}\frac{1}{c_s^2\epsilon}\left(\frac{H}{2\pi}\right)^2_*, \qquad r \simeq 16(c_s^2\epsilon)_*\,. \tag{22.90}$$

At third perturbative order and to lowest order in derivatives, one obtains [91]

$$S_\pi^{(3)} = \int d^4x\sqrt{-g}\frac{M_P^2(1-c_s^2)\dot{H}}{c_s^2}\left[\frac{\dot{\pi}(\nabla\pi)^2}{R^2} - \left(1+\frac{2}{3}\frac{\tilde{c}_3}{c_s^2}\right)\dot{\pi}^3\right]. \tag{22.91}$$

Note that this expression vanishes for canonical fields with $c_s^2 = 1$. For $c_s^2 \neq 1$ the cubic action is determined by the sound speed and an additional parameter $\tilde{c}_3$. Both terms in the cubic action give rise to primordial bispectra that are well approximated by equilateral bispectra. However, the shapes are not identical, so one can find a linear combination for which the equilateral bispectra of each term cancel, giving rise to a distinctive orthogonal-type bispectrum [91].

Analysis based on Planck 2015 temperature and polarisation data has placed bounds on several bispectrum shapes including equilateral and orthogonal shapes [90]:

$$f_{\rm NL}^{\rm equil} = -4 \pm 43\,, \qquad f_{\rm NL}^{\rm orthog} = -26 \pm 21 \quad (68\%\ {\rm CL})\,. \tag{22.92}$$

For the simplest case of a constant sound speed, and marginalising over $\tilde{c}_3$, this provides a bound on the inflaton sound speed [90]

$$c_s \geq 0.024 \quad (95\%\ {\rm CL})\,. \tag{22.93}$$

For a specific model such as DBI inflation [87], corresponding to $\tilde{c}_3 = 3(1-c_s^2)/2$, one obtains a tighter bound [90]:

$$c_s^{DBI} \geq 0.087 \quad (95\%\ {\rm CL})\,. \tag{22.94}$$

The Planck team have analysed a wide range of non-Gaussian templates from different inflation models, including tests for deviations from an initial Bunch-Davies vacuum state, direction-dependent non-Gaussianity, and feature models with oscillatory bispectra [90]. No individual feature or resonance is above the three-σ significance level after accounting for the look-elsewhere effect. These results are consistent with the simplest canonical, slow-roll inflation models, but do not rule out most alternative models; rather, bounds on primordial non-Gaussianity place important constraints on the parameter space for non-canonical models.

22.7.2. ***Multi-Field Fluctuations*** :

There is a very large literature on two- and multi-field models of inflation, most of which lies beyond the scope of this review [92]. However, two important general topics merit being mentioned here, namely residual isocurvature perturbations and the possibility of non-Gaussian effects in the primordial perturbations.

One might expect that other scalar fields besides the inflaton might have non-negligible values that evolve and fluctuate in parallel with the inflaton, without necessarily making the dominant contribution to the energy density during the inflationary epoch. However, the energy density in such a field might persist beyond the end of inflation before decaying, at which point it might come to dominate (or at least make a non-negligible contribution to) the total energy density. In such a case, its perturbations could end up generating the density perturbations detected in the CMB. This could occur due to a late-decaying scalar field [88] or a field fluctuation that modulates the end of inflation [93] or the inflaton decay [94].

22.7.2.1. *Isocurvature Perturbations:*

Primordial perturbations arising in single-field slow-roll inflation are necessarily adiabatic, i.e., they affect the overall density without changing the ratios of different contributions, such as the photon-matter ratio, $\delta(n_\gamma/n_m)/(n_\gamma/n_m)$. This is because inflaton perturbations represent a local shift of the time, as described in section Sec. 22.7:

$$\pi = \frac{\delta n_\gamma}{\dot{n}_\gamma} = \frac{\delta n_m}{\dot{n}_m}\,. \tag{22.95}$$

However, any light scalar field (i.e., one with effective mass less than the Hubble scale) acquires a spectrum of nearly scale-invariant perturbations during inflation. Fluctuations orthogonal to the inflaton in field space are decoupled from the inflaton at Hubble-exit, but can affect the subsequent evolution of the density perturbation. In particular, they can give rise to local variations in the equation of state (non-adabatic pressure perturbations) that can alter the primordial curvature perturbation ζ on super-Hubble scales. Since these fluctuations are statistically independent of the inflaton perturbations at leading order in slow-roll [95], non-adiabatic field fluctuations can only increase the scalar power spectrum with respect to adiabatic perturbations at Hubble exit, while leaving the tensor modes unaffected at first perturbative order. Thus the single-field result for the tensor-scalar ratio (Eq. (22.49)) becomes an inequality [96]

$$r \leq 16\epsilon_*\,. \tag{22.96}$$

Hence an observational upper bound on the tensor-scalar ratio does not bound the slow-roll parameter ϵ in multi-field models.

If all the scalar fields present during inflation eventually decay completely into fully thermalized radiation, these field fluctuations are converted fully into adiabatic perturbations in the primordial plasma [97]. On the other hand, non-adiabatic field fluctuations can also leave behind primordial isocurvature perturbations (Eq. (22.85)) after inflation. In multi-field inflation models it is thus possible for non-adiabatic field fluctuations to generate both curvature and isocurvature perturbations leading to correlated primordial perturbations [98].

The amplitudes of any primordial isocurvature perturbations (Eq. (22.85)) are strongly constrained by the current CMB data, especially on large angular scales. Using temperature and low-ℓ polarisation data yields the following bound on the amplitude of cold dark matter isocurvature perturbations at scale $k = 0.002h^{-1}{\rm Mpc}^{-1}$

(marginalising over the correlation angle and in the absence of primordial tensor perturbations) [44]:

$$\frac{\mathcal{P}_{S_m}}{\mathcal{P}_\zeta + \mathcal{P}_{S_m}} < 0.020 \text{ at } 95\% \text{ CL}\,. \tag{22.97}$$

For fully (anti-)correlated isocurvature perturbations, corresponding to a single isocurvature field providing a source for both the curvature and residual isocurvature perturbations, the bounds become significantly tighter [44]:

$$\frac{\mathcal{P}_{S_m}}{\mathcal{P}_\zeta + \mathcal{P}_{S_m}} < 0.0013 \text{ at } 95\% \text{ CL}, \text{correlated}\,, \tag{22.98}$$

$$\frac{\mathcal{P}_{S_m}}{\mathcal{P}_\zeta + \mathcal{P}_{S_m}} < 0.0008 \text{ at } 95\% \text{ CL}, \text{anti}-\text{correlated}\,. \tag{22.99}$$

22.7.2.2. *Local-Type Non-Gaussianity:*

Since non-adiabatic field fluctuations in multi-field inflation may lead the to evolution of the primordial curvature perturbation at all orders, it becomes possible to generate significant non-Gaussianity in the primordial curvature perturbation. Non-linear evolution on super-Hubble scales leads to local-type non-Gaussianity, where the local integrated expansion is a non-linear function of the local field values during inflation, $N(\phi_i)$. While the field fluctuations at Hubble exit, $\delta\phi_{i*}$, are Gaussian in the slow-roll limit, the curvature perturbation, $\zeta = \delta N$, becomes a non-Gaussian distribution [99]:

$$\zeta = \sum_i \frac{\partial N}{\partial \phi_i}\delta\phi_i + \frac{1}{2}\sum_{i,j}\frac{\partial^2 N}{\partial\phi_i\partial\phi_j}\delta\phi_i\delta\phi_j + \ldots \tag{22.100}$$

with non-vanishing bispectrum in the squeezed limit ($k_1 \approx k_2 \gg k_3$):

$$B_\zeta(k_1,k_2,k_3) \approx \frac{12}{5} f_{\rm NL}^{\rm local} \frac{\mathcal{P}_\zeta(k_1)}{4\pi k_1^3}\frac{\mathcal{P}_\zeta(k_3)}{4\pi k_3^3}\,, \tag{22.101}$$

where

$$\frac{6}{5} f_{\rm NL}^{\rm local} = \frac{\sum_{i,j}\frac{\partial^2 N}{\partial\phi_i\partial\phi_j}}{\left(\sum_i \frac{\partial N}{\partial\phi_i}\right)^2}\,. \tag{22.102}$$

Both equilateral and orthogonal bispectra, discussed above in the context of generalised single field inflation, vanish in the squeezed limit, enabling the three types of non-Gaussianity to be distinguished by observations, in principle.

Non-Gaussianity during multi-field inflation is highly model dependent, though $f_{\rm NL}^{\rm local}$ can often be smaller than unity in multi-field slow-roll inflation [100]. Scenarios where a second light field plays a role during or after inflation can make distinctive predictions for $f_{\rm NL}^{\rm local}$, such as $f_{\rm NL}^{\rm local} = -5/4$ in some curvaton scenarios [99,101] or $f_{\rm NL}^{\rm local} = 5$ in simple modulated reheating scenarios [94,102]. By contrast the constancy of ζ on super-Hubble scales in single-field slow-roll inflation leads to a very small non-Gaussianity [103,104], and in the squeezed limit we have the simple result $f_{\rm NL}^{\rm local} = 5(1-n_S)/12$ [105,106].

A combined analysis of the Planck temperature and polarization data yields the following range for $f_{\rm NL}^{\rm local}$ defined in (Eq. (22.102)):

$$f_{\rm NL}^{\rm local} \;=\; 0.8 \pm 5.0 \quad (95\%\ \text{CL})\,. \tag{22.103}$$

This sensitivity is sufficient to rule out parameter regimes giving rise to relatively large non-Gaussianity, but insufficient to probe $f_{\rm NL}^{\rm local} = \mathcal{O}(\epsilon)$, as expected in single-field models, or the range $f_{\rm NL}^{\rm local} = \mathcal{O}(1)$ found in the simplest two-field models.

Local-type primordial non-Gaussianity can also give rise to a striking scale-dependent bias in the distribution of collapsed dark matter halos and thus the galaxy distribution [107,108]. However, bounds from high-redshift galaxy surveys are not yet competitive with the best CMB constraints.

22.8. Pre-Inflation and Anomalies in the CMB

Most work on inflation is done in the context of RW cosmology, which already assumes a high degree of symmetry, or small inhomogeneous perturbations (usually first order) about an RW cosmology. The isotropic RW spacetime is an attractor for many homogeneous, but anisotropic cosmologies in the presence of a false vacuum energy density [109] or a scalar field with suitable self-interaction potential energy [110,111]. However it is much harder to establish the range of highly inhomogeneous initial conditions that yield a successful RW Universe, with only limited studies to date (see, e.g., [112,113,114]) .

One of the open questions in inflation is the nature of the pre-inflationary state that should have provided suitable initial conditions for inflation. This would need to have satisfied non-trivial homogeneity and isotropy conditions, and one may ask how these could have arisen and whether there may be some observable signature of the pre-inflationary state. In general, one would expect any such effects to appear at large angular scales, i.e., low multipoles ℓ.

Indeed, various anomalies have been noted in the large-scale CMB anisotropies, also discussed in Chap. 28, "Cosmic Microwave Background" review, including a possible suppression of the quadrupole and other very large-scale anisotropies, an apparent feature in the range $\ell \approx 20$ to 30, and a possible hemispheric asymmetry. None of these are highly statistically significant in view of the limitations due to cosmic variance [44], and they cannot yet be regarded as signatures of some pre-inflationary dynamics such as string theory or the multiverse. However, is a hot topic for present and future analysis.

22.9. Prospects for Future Probes of Inflation

When inflation was first proposed [1,2] there was no evidence for the existence of scalar fields or the accelerated expansion of the universe. The situation has changed dramatically in recent years with the observational evidence that the cosmic expansion is currently accelerating and with the discovery of a scalar particle, namely the Higgs boson (see Chap. 11, "Status of Higgs boson physics" review). These discoveries encourage interest in the idea of primordial accelerated expansion driven by a scalar field, i.e., cosmological inflation. In parallel, successive CMB experiments have been consistent with generic predictions of inflationary models, although without yet providing irrefutable evidence.

Prospective future CMB experiments, both ground- and space-based are reviewed in the separate PDG "Cosmic Microwave Background" review, Chap. 28. The main emphasis in CMB experiments in the coming years will be on ground-based experiments providing improved measurements of B-mode polarization and greater sensitivity to the tensor-to-scalar ratio r, and more precise measurements at higher ℓ that will constrain n_s better. As is apparent from Fig. 22.1 and the discussion of models such as R^2 inflation, there is a strong incentive to reach a 5-σ sensitivity to $r \sim 3$ to 4×10^{-3}. This could be achieved with a moderately-sized space mission with large sky coverage [115], improvements in de-lensing and foreground measurements. The discussion in Sec. 22.3 (see also Fig. 22.4), also brought out the importance of reducing the uncertainty in n_s, as a way to constrain post-inflationary reheating and the connection to particle physics. CMB temperature anisotropies probe primordial density perturbations down to comoving scales of order 50 Mpc, beyond which scale secondary sources of anisotropy dominate. CMB spectral distortions could potentially constrain the amplitude and shape of primordial density perturbations on comoving scales from Mpc to kpc due to distortions caused by the Silk damping of pressure waves in the radiation dominated era, before the last scattering of the CMB photons but after the plasma can be fully thermalised [116].

Improved sensitivity to non-Gaussianities is also a priority. In addition to CMB measurements, future large-scale structure surveys will also have roles to play as probes into models of inflation, for which there are excellent prospects. High-redshift galaxy surveys are sensitive to local-type non-Gaussianity due to the scale-dependent bias induced on large scales. Current surveys such as eBOSS, probing out to redshift $z \sim 2$, can reach a precision $\Delta f_{NL} \sim 15$, from measurements of the galaxy power spectrum, or possibly $\Delta f_{NL} \sim 10$,

if the galaxy bias can be determined independently [117]. Upcoming surveys such as DESI may reach $\Delta f_{NL} \sim 4$ [118] comparable with the Planck sensitivity. In the future, radio surveys such as SKA will measure large-scale structure out to redshift $z \sim 3$ [119], initially through mapping the intensity of the neutral hydrogen 21-cm line, and eventually through radio galaxy surveys which will probe local-type non-Gaussianity to $f_{NL} \sim 1$.

Galaxy clustering using DESI and Euclid satellite data could also constrain the running of the scalar tilt to a precision of $\Delta\alpha_s \approx 0.0028$, a factor of 2 improvement on Planck constraints, or a precision of 0.0016 using LSST data [118].

The proposed SPHEREx satellite mission [120] will use measurements of the galaxy power spectrum to target a measurement of the running of the scalar spectral index with a sensitivity $\Delta\alpha_s \sim 10^{-3}$ and local-type primordial non-Gaussianity, $\Delta f_{NL} \sim 1$. Including information from the galaxy bispectrum one might reduce the measurement error on non-Gaussianity to $\Delta f_{NL} \sim 0.2$, making it possible to distinguish between single-field slow-roll models and alternatives such as the curvaton scenario for the origin of structure, which generate $f_{NL} \sim 1$.

Acknowledgements

The authors are grateful to Vincent Vennin for his careful reading of this manuscript and preparing Fig. 22.3 for this review. The work of J.E. was supported in part by the London Centre for Terauniverse Studies (LCTS), using funding from the European Research Council via the Advanced Investigator Grant 267352 and from the UK STFC via the research grant ST/L000326/1. The work of D.W. was supported in part by the UK STFC research grant ST/K00090X/1 and ST/N000668/1.

References:

1. A.A. Starobinsky, Phys. Lett. **B91**, 99 (1980).
2. A.H. Guth, Phys. Rev. **D23**, 347 (1981).
3. K.A. Olive, Phys. Rept. **190**, 307 (1990).
4. D.H. Lyth and A. Riotto, Phys. Rep. **314**, 1 (1999).
5. A.R. Liddle and D.H. Lyth, *Cosmological inflation and large-scale structure* (Cambridge University Press, 2000).
6. D. Baumann, arXiv:0907.5424 [hep-th].
7. J. Martin, C. Ringeval and V. Vennin, Phys. Dark Univ. **5-6**, 75-235 (2014) [arXiv:1303.3787 [astro-ph.CO]]; J. Martin *et al.*, JCAP **1403** (2014) 039 [arXiv:1312.3529 [astro-ph.CO]]; J. Martin, arXiv:1502.05733 [astro-ph.CO].
8. P.A.R. Ade *et al.* [Planck Collab.], arXiv:1502.01589 [astro-ph.CO].
9. A.H. Guth and E.J. Weinberg, Nucl. Phys. B **212**, 321 (1983).
10. D. La and P.J. Steinhardt, Phys. Rev. Lett. **62**, 376 (1989) [Phys. Rev. Lett. **62**, 1066 (1989)].
11. A.D. Linde, Phys. Lett. **B249**, 18 (1990).
12. F.C. Adams and K. Freese, Phys. Rev. **D43**, 353 (1991) [hep-ph/0504135].
13. A.D. Linde, Phys. Lett. **B108**, 389 (1982).
14. A. Albrecht and P.J. Steinhardt, Phys. Rev. Lett. **48**, 1220 (1982).
15. W.H. Press, Phys. Scr. **21** (1980) 702; S.W. Hawking, Phys. Lett. **115B** (1982) 295; A.A. Starobinsky, Phys. Lett. **117B** (1982) 175; A.H. Guth and S.Y. Pi, Phys. Rev. Lett. **49** (1982) 1110.
16. J.M. Bardeen, P.J. Steinhardt and M.S. Turner, Phys. Rev. **D28**, 679 (1983).
17. V.F. Mukhanov and G.V. Chibisov, JETP Lett. **33** (1981) 532.
18. K.S. Stelle, Gen. Rel. Grav. **9** (1978) 353.
19. B. Whitt, Phys. Lett. **B145**, 176 (1984).
20. D. Wands, Class. Quant. Grav. **11**, 269 (1994) [gr-qc/9307034].
21. S.R. Coleman and F. De Luccia, Phys. Rev. **D21**, 3305 (1980).
22. M. Sasaki *et al.*, Phys. Lett. **B317**, 510 (1993).
23. M. Bucher, A.S. Goldhaber and N. Turok, Phys. Rev. **D52**, 3314 (1995) [hep-ph/9411206].
24. A.D. Linde and A. Mezhlumian, Phys. Rev. **D52**, 6789 (1995) [astro-ph/9506017].
25. A.R. Liddle, P. Parsons and J.D. Barrow, Phys. Rev. **D50**, 7222 (1994) [astro-ph/9408015].
26. L. Kofman, A.D. Linde and A.A. Starobinsky, Phys. Rev. **D56**, 3258 (1997) [hep-ph/9704452].
27. B.A. Bassett, S. Tsujikawa and D. Wands, Rev. Mod. Phys. **78**, 537 (2006) [astro-ph/0507632].
28. A.D. Linde, Phys. Rev. **D49**, 748 (1994) [astro-ph/9307002].
29. A.D. Dolgov and A.D. Linde, Phys. Lett. **B116**, 329 (1982).
30. J.R. Ellis *et al.*, Nucl. Phys. B **238**, 453 (1984).
31. M. Kawasaki and T. Moroi, Prog. Theor. Phys. **93**, 879 (1995) [hep-ph/9403364, hep-ph/9403061].
32. J.H. Traschen and R.H. Brandenberger, Phys. Rev. **D42**, 2491 (1990).
33. G.V. Chibisov and V.F. Mukhanov, Mon. Not. Roy. Astron. Soc. **200**, 535 (1982).
34. H. Kodama and M. Sasaki, Prog. Theor. Phys. Suppl. **78**, 1 (1984).
35. V.F. Mukhanov, H.A. Feldman and R.H. Brandenberger, Phys. Rept. **215**, 203 (1992).
36. K.A. Malik and D. Wands, Phys. Rept. **475**, 1 (2009) [arXiv:0809.4944 [astro-ph]].
37. M. Sasaki, Prog. Theor. Phys. **76**, 1036 (1986) V.F. Mukhanov, Sov. Phys. JETP **67**, 1297 (1988) [Zh. Eksp. Teor. Fiz. **94N7**, 1 (1988)].
38. A.A. Starobinsky, JETP Lett. **30**, 682 (1979) [Pisma Zh. Eksp. Teor. Fiz. **30**, 719 (1979)].
39. E.D. Stewart and D.H. Lyth, Phys. Lett. **B302**, 171 (1993) [gr-qc/9302019].
40. D. Wands *et al.*, Phys. Rev. **D62**, 043527 (2000) [astro-ph/0003278].
41. A.R. Liddle and S.M. Leach, Phys. Rev. **D68**, 103503 (2003) [astro-ph/0305263].
42. P.A.R. Ade *et al.* [BICEP2/Keck and Planck Collabs.], Phys. Rev. Lett. **114**, 101301 (2015) [arXiv:1502.00612 [astro-ph.CO]]; P.A.R. Ade *et al.* [BICEP2 and Keck Array Collabs.], Phys. Rev. Lett. **116**, 031302 (2016) [arXiv:1510.09217 [astro-ph.CO]].
43. S.M. Leach, A.R. Liddle, J. Martin, and D.J. Schwarz, Phys. Rev. **D66**, 23515 (2002).
44. P.A.R. Ade *et al.* [Planck Collab.], arXiv:1502.02114 [astro-ph.CO].
45. D. Kazanas, Astrophys. J. **241** (1980) L59.
46. K. Sato, Mon. Not. Roy. Astron. Soc. **195**, 467 (1981).
47. A. Billoire and K. Tamvakis, Nucl. Phys. B **200** (1982) 329; J.D. Breit, S. Gupta and A. Zaks, Phys. Rev. Lett. **51**, 1007 (1983).
48. A.D. Linde, Phys. Lett. **B129**, 177 (1983).
49. D.V. Nanopoulos, K.A. Olive and M. Srednicki, Phys. Lett. **B127**, 30 (1983).
50. J. Ellis, D.V. Nanopoulos and K.A. Olive, Phys. Rev. Lett. **111**, 111301 (2013) [Phys. Rev. Lett. **111**, 129902 (2013)] [arXiv:1305.1247 [hep-th]].
51. C. Pallis and Q. Shafi, JCAP **1503** (2015) 03, 023 [arXiv:1412.3757 [hep-ph]].
52. L. Boubekeur and D.H. Lyth, JCAP **0507** (2005) 010 [hep-ph/0502047].
53. G.R. Dvali, Q. Shafi and S. Solganik, hep-th/0105203; J. Garcia-Bellido, R. Rabadan and F. Zamora, JHEP **0201** (2002) 036 [hep-th/0112147]; S. Kachru *et al.*, JCAP **0310** (2003) 013 [hep-th/0308055].
54. K. Freese, J.A. Frieman and A.V. Olinto, Phys. Rev. Lett. **65**, 3233 (1990) F.C. Adams *et al.*, Phys. Rev. **D47**, 426 (1993) [hep-ph/9207245].
55. For a recent review of axion inflation, see E. Pajer and M. Peloso, Class. Quant. Grav. **30** (2013) 214002 [arXiv:1305.3557 [hep-th]].
56. E. Silverstein and A. Westphal, Phys. Rev. **D78**, 106003 (2008) [arXiv:0803.3085 [hep-th]].
57. L. McAllister, E. Silverstein and A. Westphal, Phys. Rev. **D82**, 046003 (2010) [arXiv:0808.0706 [hep-th]].
58. F.L. Bezrukov and M. Shaposhnikov, Phys. Lett. **B659**, 703 (2008) [arXiv:0710.3755 [hep-th]].

59. D. Buttazzo *et al.*, JHEP **1312** (2013) 089 [arXiv:1307.3536 [hep-ph]].
60. H.P. Nilles, Phys. Rept. **110** (1984) 1; H.E. Haber and G.L. Kane, Phys. Rept. **117** (1985) 75.
61. J.R. Ellis *et al.*, Phys. Lett. **B118**, 336 (1982).
62. N. Okada and Q. Shafi, arXiv:1311.0921 [hep-ph].
63. H. Murayama *et al.*, Phys. Rev. Lett. **70**, 1912 (1993).
64. J. Ellis, M. Fairbairn and M. Sueiro, JCAP **1402** (2014) 044 [arXiv:1312.1353 [astro-ph.CO]].
65. D. Croon, J. Ellis and N.E. Mavromatos, Phys. Lett. **B724**, 165 (2013) [arXiv:1303.6253 [astro-ph.CO]].
66. G.R. Dvali, Q. Shafi and R.K. Schaefer, Phys. Rev. Lett. **73**, 1886 (1994) [hep-ph/9406319].
67. D.V. Nanopoulos *et al.*, Phys. Lett. **B123**, 41 (1983).
68. A.B. Goncharov and A.D. Linde, Phys. Lett. **B139**, 27 (1984).
69. E. Cremmer *et al.*, Nucl. Phys. B **212** (1983) 413.
70. R. Holman, P. Ramond and G.G. Ross, Phys. Lett. **B137**, 343 (1984).
71. E.J. Copeland *et al.*, Phys. Rev. **D49**, 6410 (1994) [astro-ph/9401011]; E.D. Stewart, Phys. Rev. **D51**, 6847 (1995) [hep-ph/9405389].
72. G.D. Coughlan *et al.*, Phys. Lett. B **131**, 59 (1983); A.S. Goncharov, A.D. Linde and M.I. Vysotsky, Phys. Lett. **B147**, 279 (1984); T. Banks, D.B. Kaplan and A.E. Nelson, Phys. Rev. **D49**, 779 (1994) [hep-ph/9308292]; B. De Carlos *et al.*, Phys. Lett. **B318**, 447 (1993) [hep-ph/9308325]; M. Kawasaki, T. Moroi and T. Yanagida Phys. Lett. **B370**, 52 (1996) [hep-ph/9509399].
73. J. Ellis, D.V. Nanopoulos, and M. Quiros, Phys. Lett. **B174**, 176 (1986).
74. T. Moroi, M. Yamaguchi and T. Yanagida Phys. Lett. **B342**, 105 (1995) [hep-ph/9409367].
75. M. Kawasaki, M. Yamaguchi and T. Yanagida, Phys. Rev. Lett. **85**, 3572 (2000) [hep-ph/0004243]; K. Nakayama, F. Takahashi and T.T. Yanagida, JCAP **1308** (2013) 038 [arXiv:1305.5099 [hep-ph]].
76. E. Cremmer *et al.*, Phys. Lett. **B133**, 61 (1983).
77. For some older examples of no-scale inflationary models see, e.g., A.S. Goncharov and A.D. Linde, Class. Quant. Grav. **1**, L75 (1984); C. Kounnas and M. Quiros, Phys. Lett. **B151**, 189 (1985); J.R. Ellis *et al.*, Phys. Lett. **B152**, 175 (1985) [Erratum-ibid. **156B** (1985) 452].
78. J.R. Ellis, C. Kounnas and D.V. Nanopoulos, Nucl. Phys. B **247** (1984) 373.
79. E. Witten, Phys. Lett. **B155**, 151 (1985).
80. J. Ellis, D.V. Nanopoulos and K.A. Olive, JCAP **1310** (2013) 009 [arXiv:1307.3537].
81. For a recent review and more references, see J. Ellis *et al.*, arXiv:1507.02308 [hep-ph].
82. R. Kallosh, A. Linde and D. Roest, JHEP **1311** (2013) 198 [arXiv:1311.0472].
83. A.R. Liddle, Mon. Not. Roy. Astron. Soc. **377**, L74 (2007) [astro-ph/0701113].
84. J. Martin, C. Ringeval and V. Vennin, arXiv:1603.02606 [astro-ph.CO] We thank Vincent Vennin for providing the adapted version of Fig. 3 from this reference.
85. J. Ellis *et al.*, JCAP **1507** (2015) 07, 050 [arXiv:1505.06986 [hep-ph]].
86. C. Armendariz-Picon, T. Damour and V.F. Mukhanov, Phys. Lett. **B458**, 209 (1999) [hep-th/9904075].
87. M. Alishahiha, E. Silverstein and D. Tong, Phys. Rev. **D70**, 123505 (2004) [hep-th/0404084].
88. K. Enqvist and M.S. Sloth, Nucl. Phys. B **626** (2002) 395 [hep-ph/0109214]; D.H. Lyth and D. Wands, Phys. Lett. **B524**, 5 (2002) [hep-ph/0110002]; T. Moroi and T. Takahashi, Phys. Lett. **B522**, 215 (2001) [Phys. Lett. **B539**, 303 (2002)] [hep-ph/0110096].
89. N. Bartolo *et al.*, Phys. Rept. **402**, 103 (2004) [astro-ph/0406398].
90. P.A.R. Ade *et al.* [Planck Collab.], arXiv:1502.01592 [astro-ph.CO].
91. L. Senatore, K.M. Smith and M. Zaldarriaga, JCAP **1001**, 028 (2010) [arXiv:0905.3746 [astro-ph.CO]].
92. See, for example, C. Gordon *et al.*, Phys. Rev. **D63**, 023506 (2001) [astro-ph/0009131]; C.T. Byrnes and D. Wands, Phys. Rev. **D74**, 043529 (2006) [astro-ph/0605679]; R. Easther *et al.*, Phys. Rev. Lett. **112**, 161302 (2014) [arXiv:1312.4035 [astro-ph.CO]]; J. Ellis *et al.*, JCAP **1501** (2015) 01, 010 [arXiv:1409.8197 [hep-ph]]; S. Renaux-Petel and K. Turzynski, JCAP **1506** (2015) 06, 010 [arXiv:1405.6195 [astro-ph.CO]].
93. D.H. Lyth, JCAP **0511**, 006 (2005) [astro-ph/0510443].
94. G. Dvali, A. Gruzinov and M. Zaldarriaga, Phys. Rev. **D69**, 023505 (2004) [astro-ph/0303591].
95. C.T. Byrnes and D. Wands, Phys. Rev. **D74**, 043529 (2006) [astro-ph/0605679].
96. D. Wands *et al.*, Phys. Rev. **D66**, 043520 (2002) [astro-ph/0205253].
97. S. Weinberg, Phys. Rev. **D67**, 123504 (2003) [astro-ph/0302326].
98. D. Langlois, Phys. Rev. **D59**, 123512 (1999) [astro-ph/9906080].
99. D.H. Lyth and Y. Rodriguez, Phys. Rev. Lett. **95**, 121302 (2005) [astro-ph/0504045].
100. F. Vernizzi and D. Wands, JCAP **0605**, 019 (2006) [astro-ph/0603799].
101. M. Sasaki, J. Valiviita and D. Wands, Phys. Rev. **D74**, 103003 (2006) [astro-ph/0607627].
102. G. Dvali, A. Gruzinov and M. Zaldarriaga, Phys. Rev. **D69**, 083505 (2004) [astro-ph/0305548].
103. D.S. Salopek and J.R. Bond, Phys. Rev. **D43**, 1005 (1991).
104. A. Gangui *et al.*, Astrophys. J. **430**, 447 (1994) [astro-ph/9312033].
105. J.M. Maldacena, JHEP **0305**, 013 (2003) [astro-ph/0210603].
106. V. Acquaviva *et al.*, Nucl. Phys. B **667**, 119 (2003) [astro-ph/0209156].
107. N. Dalal *et al.*, Phys. Rev. **D77**, 123514 (2008) [arXiv:0710.4560 [astro-ph]].
108. S. Matarrese and L. Verde, Astrophys. J. **677**, L77 (2008) [arXiv:0801.4826 [astro-ph]].
109. R.M. Wald, Phys. Rev. **D28**, 2118 (1983).
110. M. Heusler, Phys. Lett. **B253**, 33 (1991).
111. Y. Kitada and K.-i. Maeda, Phys. Rev. **D45**, 1416 (1992).
112. D.S. Goldwirth and T. Piran, Phys. Rept. **214**, 223 (1992).
113. T. Vachaspati and M. Trodden, Phys. Rev. **D61**, 023502 (1999) [gr-qc/9811037].
114. W.E. East *et al.*, arXiv:1511.05143 [hep-th].
115. Proposed space missions include PIXIE: A. Kogut *et al.*, JCAP **1107** (2011) 025 [arXiv:1105.2044 [astro-ph.CO]]; LiteBird: `http://litebird.jp/eng/` and Cosmic Origins Explorer (COrE): `http://www.core-mission.org`.
116. J. Chluba, J. Hamann and S.P. Patil, Int. J. Mod. Phys. D **24**, no. 10, 1530023 (2015) [arXiv:1505.01834 [astro-ph.CO]].
117. G.B. Zhao *et al.*, Mon. Not. Roy. Astron. Soc. **457**, 2377 (2016) [arXiv:1510.08216 [astro-ph.CO]].
118. A. Font-Ribera *et al.*, JCAP **1405**, 023 (2014) [arXiv:1308.4164 [astro-ph.CO]].
119. R. Maartens *et al.* [SKA Cosmology SWG Collab.], PoS AASKA **14**, 016 (2015) [arXiv:1501.04076 [astro-ph.CO]].
120. O. Dor *et al.*, arXiv:1412.4872 [astro-ph.CO].

23. Big-Bang Nucleosynthesis

Revised September 2017 by B.D. Fields, (Univ. of Illinois) P. Molaro (Trieste Observatory) and S. Sarkar (Univ. of Oxford & Niels Bohr Institute, Copenhagen).

Big-Bang nucleosynthesis (BBN) offers the deepest reliable probe of the early Universe, being based on well-understood Standard Model physics [1]. Predictions of the abundances of the light elements, D, ^{3}He, ^{4}He, and ^{7}Li, synthesized at the end of the 'first three minutes,' are in good overall agreement with the primordial abundances inferred from observational data, thus validating the standard hot Big-Bang cosmology (see [2–5] for reviews). This is particularly impressive given that these abundances span nine orders of magnitude – from ^{4}He/H ~ 0.08 down to ^{7}Li/H $\sim 10^{-10}$ (ratios by number). Thus BBN provides powerful constraints on possible deviations from the standard cosmology, and on new physics beyond the Standard Model [6–9].

23.1. Theory

The synthesis of the light elements is sensitive to physical conditions in the early radiation-dominated era at a temperature $T \sim 1$ MeV, corresponding to an age $t \sim 1$ s. At higher temperatures, weak interactions were in thermal equilibrium, thus fixing the ratio of the neutron and proton number densities to be $n/p = \mathrm{e}^{-Q/T}$, where $Q = 1.293$ MeV is the neutron-proton mass difference. As the temperature dropped, the neutron-proton inter-conversion rate per nucleon, $\Gamma_{n\leftrightarrow p} \sim G_{\rm F}^2 T^5$, fell faster than the Hubble expansion rate, $H \sim \sqrt{g_* G_{\rm N}}\, T^2$, where g_* counts the number of relativistic particle species determining the energy density in radiation (see 'Big Bang Cosmology' Chapter 21 of this *Review*). This resulted in departure from chemical equilibrium ('freeze-out') at $T_{\rm fr} \sim (g_* G_{\rm N}/G_{\rm F}^4)^{1/6} \simeq 1$ MeV. The neutron fraction at this time, $n/p = \mathrm{e}^{-Q/T_{\rm fr}} \simeq 1/6$, is thus sensitive to every known physical interaction, since Q is determined by both strong and electromagnetic interactions while $T_{\rm fr}$ depends on the weak as well as gravitational interactions. Moreover, the sensitivity to the Hubble expansion rate affords a probe of, *e.g.,* the number of relativistic neutrino species [10]. After freeze-out, the neutrons were free to β-decay, so the neutron fraction dropped to $n/p \simeq 1/7$ by the time nuclear reactions began. A simplified analytic model of freeze-out yields the n/p ratio to an accuracy of $\sim 1\%$ [11,12].

The rates of these reactions depend on the density of baryons (strictly speaking, nucleons), which is usually expressed normalized to the relic blackbody photon density as $\eta \equiv n_{\rm b}/n_\gamma$. As we shall see, all the light-element abundances can be explained with $\eta_{10} \equiv \eta \times 10^{10}$ in the range 5.8–6.6 (95% CL). With n_γ fixed by the present CMB temperature 2.7255 K (see 'Cosmic Microwave Background' Chapter 28 of this *Review*), this can be stated as the allowed range for the baryon mass density today, $\rho_{\rm b} = (3.9\text{–}4.6) \times 10^{-31}$ g cm^{-3}, or as the baryonic fraction of the critical density, $\Omega_{\rm b} = \rho_{\rm b}/\rho_{\rm crit} \simeq \eta_{10} h^{-2}/274 = (0.021\text{–}0.024) h^{-2}$, where $h \equiv H_0/100$ km s^{-1} Mpc^{-1} is the present Hubble parameter (see Cosmological Parameters review Chapter 24).

The nucleosynthesis chain begins with the formation of deuterium in the process $p(n,\gamma)$D. However, photo-dissociation by the high number density of photons delays production of deuterium (and other complex nuclei) until well after T drops below the binding energy of deuterium, $\Delta_{\rm D} = 2.23$ MeV. The quantity $\eta^{-1}\mathrm{e}^{-\Delta_{\rm D}/T}$, *i.e.,* the number of photons per baryon above the deuterium photo-dissociation threshold, falls below unity at $T \simeq 0.1$ MeV; nuclei can then begin to form without being immediately photo-dissociated again. Only 2-body reactions, such as D$(p,\gamma)^3$He and ^{3}He$(\mathrm{D},p)^4$He are important because the density by this time has become rather low – comparable to that of air!

Nearly all neutrons end up bound in the most stable light element ^{4}He. Heavier nuclei do not form in any significant quantity both because of the absence of stable nuclei with mass number 5 or 8 (which impedes nucleosynthesis via n^4He, p^4He or ^{4}He^{4}He reactions), and the large Coulomb barriers for reactions such as ^{3}He$(^4\mathrm{He},\gamma)^7$Li and ^{3}He$(^4\mathrm{He},\gamma)^7$Be. Hence the primordial mass fraction of ^{4}He, $Y_{\rm p} \equiv \rho(^4\mathrm{He})/\rho_{\rm b}$, can be estimated by the simple counting argument

$$Y_{\rm p} = \frac{2(n/p)}{1 + n/p} \simeq 0.25 \ . \qquad (23.1)$$

There is little sensitivity here to the actual nuclear reaction rates, which are, however, important in determining the other 'left-over' abundances: D and ^{3}He at the level of a few times 10^{-5} by number relative to H, and ^{7}Li/H at the level of about 10^{-10} (when η_{10} is in the range 1–10). These values can be understood in terms of approximate analytic arguments [12,13]. The experimental parameter most important in determining $Y_{\rm p}$ is the neutron lifetime, τ_n, which normalizes (the inverse of) $\Gamma_{n\leftrightarrow p}$. Its value has recently been significantly revised downwards to $\tau_n = 880.2 \pm 1.0$ s (see *N* Baryons Listing).

The elemental abundances shown in Fig. 23.1 as a function of η_{10} were calculated [14] using an updated version [15] of the Wagoner code [1]; other versions [16–18] too are publicly available. The ^{4}He curve includes small corrections due to radiative processes at zero and finite temperatures [19], non-equilibrium neutrino heating during $e^\pm$ annihilation [20], and finite nucleon mass effects [21]; the range primarily reflects the 2σ uncertainty in the neutron lifetime. The spread in the curves for D, ^{3}He, and ^{7}Li corresponds to the 2σ uncertainties in nuclear cross sections, as estimated by Monte Carlo methods [15, 22–24]. The input nuclear data have been carefully reassessed [14, 24–28], leading to improved precision for the abundance predictions. In particular, the uncertainty in ^{7}Li/H at interesting values of η has been reduced recently by a factor ~ 2, a consequence of a similar reduction in the error budget [29] for the dominant mass-7 production channel ^{3}He$(^4\mathrm{He},\gamma)^7$Be. Polynomial fits to the predicted abundances and the error correlation matrix have been given in refs. [23,30]. The boxes in Fig. 23.1 show the observationally inferred primordial abundances with their associated uncertainties, as discussed below.

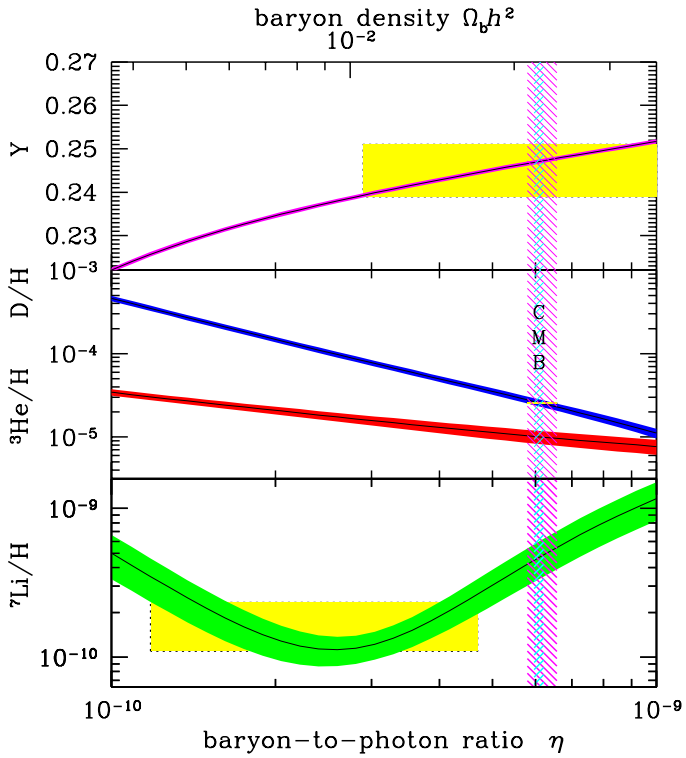

Figure 23.1: The primordial abundances of ^{4}He, D, ^{3}He, and ^{7}Li as predicted by the standard model of Big-Bang nucleosynthesis — the bands show the 95% CL range [5]. Boxes indicate the observed light element abundances. The narrow vertical band indicates the CMB measure of the cosmic baryon density, while the wider band indicates the BBN D+^{4}He concordance range (both at 95% CL).

The nuclear reaction cross sections important for BBN have all been measured at the relevant energies. Recently however there have been substantial advances in the precision of light element observations (e.g., D/H) and in the determination of cosmological parameters (e.g.,

from *Planck*). This motivates corresponding improvement in BBN predictions and thus in the key reaction cross sections. For example, it has been suggested [31,32] that $d(p,\gamma)^3$He measurements may suffer from systematic errors and be inferior to *ab initio* theory; if so, this could alter D/H abundances at a level that is now significant. Ongoing low-background cross section measurements should resolve this issue [33].

23.2. Light Element Abundances

BBN theory predicts the universal abundances of D, ^{3}He, ^{4}He, and ^{7}Li, which are essentially fixed by $t \sim 180$ s. Abundances are, however, observed at much later epochs, after stellar nucleosynthesis has commenced. This produces heavy elements such as C, N, O, and Fe ("metals"), while the ejected remains of this stellar processing alters the light element abundances from their primordial values. Thus, one seeks astrophysical sites with low metal abundances in order to measure light element abundances that are closer to primordial. For all light elements, systematic errors are the dominant limitation to the precision with which primordial abundances can be inferred.

BBN is the only significant source of deuterium, which is entirely destroyed when it is cycled into stars [34]. Thus, any detection provides a lower limit to primordial D/H, and an upper limit on η_{10}; for example, the local interstellar value of $\mathrm{D/H} = (1.56 \pm 0.40) \times 10^{-5}$ [35] requires $\eta_{10} \leq 9$. The best proxy to the primordial value of D is its measure in distant and chemically unprocessed matter, where stellar processing (astration) is minimal [34]. This has become possible with the advent of large telescopes, but after two decades of observational efforts we have only around a dozen determinations [36–49]. The available D measurements are for systems with metallicities of $(0.001 - 0.03)\times$ Solar where no significant astration is expected [37].

High-resolution spectra reveal the presence of D in high-redshift, low-metallicity quasar absorption systems via its isotope-shifted Lyman-α absorption features, though, unfortunately, these are usually obscured or contaminated by the Lyman-α forest of hydrogen features.

Damped Lyman-α systems (DLAs: $N(\mathrm{H}) > 5 \times 10^{20}$ cm^{-2}) correspond to sightlines through dense regions in high-z galaxies. These systems make possible a precise measure of the hydrogen column density by means of the Lorentzian damping wings of Lyman-α and Lyman-β (if relatively uncontaminated by Lyman-α clouds)[36, 38]. Systems with a simple kinematic structure are desirable to avoid uncertainties with complex, only partially resolved components. A few DLA systems show D lines resolved up to the higher members of the Lyman series. Recent determinations [40, 42], and reanalyses [41, 49], provide strikingly improved precision over earlier work. There are now 10 good measurements which provide a weighted mean of $\log(\mathrm{D/H}) = -4.590 \pm 0.004$, i.e.:

$$\mathrm{D/H}|_\mathrm{p} = (2.569 \pm 0.027) \times 10^{-5}. \tag{23.2}$$

D/H shows no correlation with metallicity, redshift, or the hydrogen column density $N(\mathrm{H})$ $(= \int_\mathrm{los} n_\mathrm{H}\, ds)$ integrated over the line-of-sight through the absorber. This is consistent with the measured D/H being representative of the primordial value. By contrast, D/H measurements in the Galaxy are scattered by a factor of ~ 2 [50], with a bimodal distribution as well as being anti-correlated with metal abundances. This suggests that interstellar D not only suffers stellar astration but also partly resides in dust particles that evade gas-phase observations. However, in the DLA used for deuterium the dust content is apparently quite small as implied by Solar proportions of the abundances of refractory and non refractory elements.

The primordial ^{4}He abundance is best determined through recombination emission lines of He and H in the most metal-poor extragalactic H II (ionized) regions, *viz.* blue compact galaxies, generally found at low redshift. There is now a large body of data on ^{4}He and CNO in these galaxies, with over 1000 such systems in the Sloan Digital Sky Survey alone [51, 59]. These data confirm that the small stellar contribution to the helium abundance is positively correlated with metal production, so extrapolation to zero metallicity gives the primordial ^{4}He abundance Y_p. However, H II regions are complex systems and several physical parameters enter in the He/H determination, notably the electron density and temperature, as well as reddening. Thus systematic effects dominate the uncertainties in the abundance determination [51, 52]. A major step forward has been the inclusion of the He λ10830 infrared emission line which shows a strong dependence on the electron density and is thus useful to break the degeneracy with the temperature, allowing for a more robust helium abundance determination. In recent work that has accounted for the underlying ^{4}He stellar absorption, and/or the newly derived values of the HeI-recombination and H-excitation-collisional coefficients, the ^{4}He abundances have increased significantly. Recent results are $Y_\mathrm{p} = 0.2446 \pm 0.0029$ [54], $Y_\mathrm{p} = 0.2449 \pm 0.0040$ [57] and $Y_\mathrm{p} = 0.2551 \pm 0.0022$ [58]- – see Ref. [59] and references therein for previous determinations. Our recommended ^{4}He abundance is

$$Y_\mathrm{p} = 0.245 \pm 0.003, \tag{23.3}$$

but the matter is far from settled given that the measurements are only marginally consistent.

As we will see in more detail below, the primordial abundance of ^{7}Li now plays a central role in BBN, and possibly points to new physics. The systems best suited for Li observations are metal-poor ("Pop II") stars in the spheroid of the Galaxy, which have metallicities going down to perhaps 10^{-5} of the solar value [62]. Observations have long shown [63–66] that Li does not vary significantly in Pop II stars with metallicities $\lesssim 1/30$ of Solar — the "Spite plateau" [63]. However, there are systematic uncertainties due to different techniques used to determine the physical parameters (*e.g.*, the temperature) of the stellar atmosphere in which the Li absorption line is formed. Different analyses and in some cases different stars and stellar systems (globular clusters), yield $\mathrm{Li/H}|_\mathrm{p} = (1.7 \pm 0.3) \times 10^{-10}$ [66], $\mathrm{Li/H}|_\mathrm{p} = (2.19 \pm 0.28) \times 10^{-10}$ [67], and $\mathrm{Li/H}|_\mathrm{p} = (1.86 \pm 0.23) \times 10^{-10}$ [68].

Recent observations find a puzzling drop in Li/H in metal-poor stars with $[\mathrm{Fe/H}] \equiv \log_{10}[(\mathrm{Fe/H})/(\mathrm{Fe/H})_\odot] < -3.0$ [69, 71] particularly at the very low metallicity end. Li is not detected at all, or is well below the Spite Plateau, in *all* the 5 extremely metal poor dwarfs with metallicities $[\mathrm{Fe/H}] \lesssim -4.5$, where it ought to be present. The reason is not known and the same effect(s) may also produce the 'melting' of the Li plateau at metallicities $[\mathrm{Fe/H} \approx -3.0$ [70, 71], thus making quite uncertain any primordial Li value extracted by extrapolating to zero metallicity. To estimate the primordial value it is therefore safer to consider stars with $-2.8 < [\mathrm{Fe/H}] < -1.5$ [71], which yields

$$\mathrm{Li/H}|_\mathrm{p} = (1.6 \pm 0.3) \times 10^{-10}. \tag{23.4}$$

However, the evidence that something is depleting Li at the low metallicity end suggests that its abundance may also be modified in halo stars with moderate metallicity. The observed abundance should thus be considered a *lower bound* rather than a measure of primordial Li. In fact, Li in Pop II stars may have been partially destroyed due to mixing of the outer layers with the hotter interior [75]. Such processes can be constrained by the absence of significant scatter in Li versus Fe [65], but Li depletion by a factor as large as ~ 1.8 may have occured [76]. A recent model [74] predicts that Li is significantly destroyed in the pre-main-sequence phase by overshoot mixing and then partially restored by late accretion of fresh non-Li depleted material; the Spite plateau is recovered starting from an initial $\mathrm{Li/H}|_\mathrm{p} = 5.3 \times 10^{-10}$ which corresponds to the baryon density indicated by both the CMB and the D abundance [73, 74].

Stellar determination of Li abundances typically sum over both stable isotopes ^{6}Li and ^{7}Li. Recent high-precision measurements are sensitive to the tiny isotopic shift in Li absorption (which manifests itself in the shape of the blended, thermally broadened line) and indicate $^6\mathrm{Li}/^7\mathrm{Li} \leq 0.05$ [77, 78], thus confirming that ^{7}Li is dominant. A ^{6}Li plateau (analogous to the ^{7}Li plateau) has also been claimed [77]. This has, however, been challenged by new observations and analyses [78, 79, 80], which show that stellar convective motions can generate asymmetries in the line shape that mimic the presence of ^{6}Li. Hence the deduced ratio in the best studied stars should be interpreted as an *upper limit* on the ^{6}Li abundance [78].

Turning to ^{3}He, the only data available are from the Solar system and (high-metallicity) H II regions in our Galaxy [81]. This makes

inferring the primordial abundance difficult, a problem compounded by the fact that stellar nucleosynthesis models for ^{3}He are in conflict with observations [82]. Consequently, it is inappropriate to use ^{3}He or D+^{3}He as cosmological probes; instead, one might hope to turn the problem around and constrain stellar astrophysics using the predicted primordial ^{3}He abundance [83].

23.3. Concordance, Dark Matter, and the CMB

We now use the observed light element abundances to test the theory. We first consider standard BBN, which is based on Standard Model physics alone, so $N_\nu = 3$ and the only free parameter is the baryon-to-photon ratio η. (The implications of BBN for physics beyond the Standard Model will be considered below, Section 23.5). Thus, any abundance measurement determines η, and additional measurements overconstrain the theory and thereby provide a consistency check.

While the η ranges spanned by the boxes in Fig. 23.1 do not all overlap, they are all within a factor ~ 2 of each other. In particular, the lithium abundance corresponds to η values that are inconsistent with that of the (now very precise) D/H abundance as well as the less-constraining ^{4}He abundance. This discrepancy marks the 'lithium problem.' The problem could simply reflect difficulty in determining the primordial lithium abundance, or could hint at a more fundamental omission in the theory. The possibility that lithium reveals new physics is addressed in detail in the next section. If however we exclude the lithium constraint because its inferred abundance may suffer from systematic uncertainties, then D/H and ^{4}He are in agreement. The concordant η range is essentially that implied by D/H, namely

$$5.8 \leq \eta_{10} \leq 6.6 \text{ (95\% CL)}. \tag{23.5}$$

Despite the lithium problem, the overall concordance remains remarkable: using only well-established microphysics we can extrapolate back to $t \sim 1$ s to predict light element abundances spanning nine orders of magnitude, in approximate agreement with observation. This is a major success for the standard cosmology, and inspires confidence in extrapolation back to still earlier times.

This concordance provides a measure of the baryon content:

$$0.021 \leq \Omega_{\rm b} h^2 \leq 0.024 \text{ (95\% CL)}, \tag{23.6}$$

a result that plays a key role in our understanding of the matter budget of the Universe. First we note that $\Omega_{\rm b} \ll 1$, *i.e.*, baryons cannot close the Universe [85]. Furthermore, the cosmic density of (optically) luminous matter is $\Omega_{\rm lum} \simeq 0.0024 h^{-1}$ [86], so that $\Omega_{\rm b} \gg \Omega_{\rm lum}$: most baryons are optically dark, probably in the form of a diffuse intergalactic medium [87]. Finally, given that $\Omega_{\rm m} \sim 0.3$ (see Dark Matter and Cosmological Parameters reviews, Chapter 26 Chapter 24), we infer that most matter in the Universe is not only dark, but also takes some non-baryonic (more precisely, non-nucleonic) form.

The BBN prediction for the cosmic baryon density can be tested through precision measurements of CMB temperature fluctuations (see Cosmic Microwave Background review, Chapter 28). One can determine η from the amplitudes of the acoustic peaks in the CMB angular power spectrum [88], making it possible to compare two measures of η using very different physics, at two widely separated epochs. In the standard cosmology, there is no change in η between BBN and CMB decoupling, thus, a comparison of $\eta_{\rm BBN}$ and $\eta_{\rm CMB}$ is a key test. Agreement would endorse the standard picture, while disagreement could point to new physics during/between the BBN and CMB epochs.

The analysis described in the Cosmic Microwave Background review, based on *Planck* 2015 data, yields $\Omega_{\rm b} h^2 = 0.0223 \pm 0.0002$ which corresponds to $\eta_{10} = 6.09 \pm 0.06$ [61]. This result depends weakly on the primordial helium abundance, and the fiducial *Planck* analysis uses BBN theory to fix $Y_{\rm p}(\eta)$. As shown in Fig. 23.1, this CMB estimate of the baryon density (narrow vertical band) is consistent with the BBN range, *i.e.*, in good agreement with the value inferred from high-redshift D/H measurements [39] and local ^{4}He determinations; together these observations span diverse environments from redshifts $z \sim 1000$ to the present [89].

The CMB damping tail is sensitive to the primordial ^{4}He abundance and this is independent of both BBN and local ^{4}He measurements [60]. The *Planck* 2015 analysis using TT+lowP but not lensing yields $Y_{\rm p} = 0.253^{+0.041}_{-0.042}$ [61], *i.e.*, consistent with the H II region helium abundance determination. Moreover, this value is consistent with the Standard ($N_\nu = 3$) BBN prediction for $Y_{\rm p}$ with the *Planck*-determined baryon density. This concordance represents a successful CMB-only test of BBN.

The precision determination of the baryon density using the CMB motivates using this as an input to BBN calculations. Within the context of the Standard Model, BBN then becomes a zero-parameter theory, and the light element abundances are completely determined to within the uncertainties in $\eta_{\rm CMB}$ and the BBN theoretical errors. Comparison with the observed abundances then can be used to test the astrophysics of post-BBN light element evolution [90]. Alternatively, one can consider possible physics beyond the Standard Model (*e.g.*, which might change the expansion rate during BBN) and then use all of the abundances to test such models; this is discussed in Section 23.5.

23.4. The Lithium Problem

As Fig. 23.1 shows, stellar Li/H measurements are inconsistent with the CMB (and D/H), given the error budgets we have quoted. Recent updates in nuclear cross sections and stellar abundance systematics *increase* the discrepancy to over 5σ, depending on the stellar abundance analysis adopted [14].

The question then becomes pressing as to whether this mismatch comes from systematic errors in the observed abundances, and/or uncertainties in stellar astrophysics or nuclear inputs, or whether there might be new physics at work [9]. Nuclear inputs (cross sections) for BBN reactions are constrained by extensive laboratory measurements; to increase ^{7}Be destruction requires enhancement of otherwise subdominant processes that can be attained by missed resonances in a few reactions such as ^{7}Be$(d,p)2\alpha$ if the compound nuclear state properties are particularly favorable [91]. However, experimental searches have now closed off these possibilities [92], making a "nuclear fix" increasingly unlikely.

Another conventional means to solve the lithium problem is by *in situ* destruction over the long lifetimes of the host halo stars. Stellar depletion mechanisms include diffusion, rotationally induced mixing, or pre-main-sequence depletion. These effects certainly occur, but to reduce lithium to the required levels generally requires some *ad hoc* mechanism and fine tuning of the initial stellar parameters [73, 74, 93]. A putative signature of diffusion has been reported for the globular clusters NGC 6397 and NGC 6752, where the "turnoff" stars exhibit slightly lower (by a factor ~ 1.3) abundances of Fe II, Ti II, Sc II, Ca I and Mg I, than in more evolved stars [76,94]. General features of diffusive models are a dispersion in the Li abundances and a pronounced downturn in the Li abundances at the hot end of the Li plateau. Some extra turbulence needs to be invoked to limit diffusion in the hotter stars and to restore uniform Li abundance along the Spite plateau [93]. In the framework of these models (and also assuming identical initial stellar rotation) depletion by at most a factor ~ 1.8 is conceivable [76, 94].

As nuclear and astrophysical solutions to the lithium problem become increasingly constrained (even if difficult to rule out definitively), the possibility of new physics arises. Nucleosynthesis models in which the baryon-to-photon ratio is inhomogeneous can alter abundances for a given $\eta_{\rm BBN}$, but will overproduce ^{7}Li [95]. Entropy generation by some non-standard process could have decreased η between the BBN era and CMB decoupling, however the lack of spectral distortions in the CMB rules out any significant energy injection upto a redshift $z \sim 10^7$ [96]. The most intriguing resolution of the lithium problem thus involves new physics during BBN [7–9].

We summarize the general features of such solutions here, and later consider examples in the context of specific particle physics models. Many proposed solutions introduce perturbations to light-element formation during BBN; while all element abundances may suffer

perturbations, the interplay of ^{7}Li and D is often the most important *i.e.* observations of D often provide the strongest constraints on the allowed perturbations to ^{7}Li. In this connection it is important to note that the new, very precise determination of D/H [39] will significantly constrain the ability of such models to ameliorate or solve the lithium problem.

A well studied class of models invokes the injection of suprathermal hadronic or electromagnetic particles due to decays of dark matter particles. The effects are complex and depend on the nature of the decaying particles and their branchings and spectra. However, the models that most successfully solve the lithium problem generally feature non-thermal nucleons, which dissociate all light elements. Dissociation of even a small fraction of ^{4}He introduces a large abundance of free neutrons, which quickly thermalize. The thermal neutrons drive the ^{7}Be$(n,p)^7$Li conversion of ^{7}Be. The resulting ^{7}Li has a lower Coulomb barrier relative to ^{7}Be and is readily destroyed via ^{7}Li$(p,\alpha)^4$He [84, 97]. But ^{4}He dissociation also produces D directly as well as via nonthermal neutron $n(p,\gamma)d$ reactions. This introduces a tension between Li/H reduction and D/H enhancement that becomes increasingly restrictive with the increasing precision of deuterium observations. Indeed, this now forces particle injection scenarios to make very small ^{7}Li perturbations — far short of the level needed. An exception is a recent model wherein MeV-scale decays by construction avoid ^{4}He dissociation and associated D/H overproduction, instead "borrowing" neutrons by dissociating only deuterons [98].

Another important class of models retains the standard cosmic particle content, but changes their interactions via time variations in the fundamental constants [99]. Here too, the details are model-dependent, but scenarios that solve or alleviate the lithium problem often feature perturbations to the deuteron binding energy. A weaker D binding leads to the D bottleneck being overcome later, so that element formation commences at a lower temperature and lower density. This leads in turn to slower nuclear rates that freeze out earlier. The net result is a *higher* final D/H, due to less efficient processing into ^{4}He, but also *lower* Li, due to suppressed production via ^{3}He$(\alpha,\gamma)^7$Be.

The lithium problem remains an unresolved issue in BBN. Nevertheless, the remarkable concordance between the CMB and the D (as well as ^{4}He) abundance, is a non-trivial success, and provides important constraints on the early Universe.

23.5. Beyond the Standard Model

Given the simple physics underlying BBN, it is remarkable that it still provides the most effective test for the cosmological viability of ideas concerning physics beyond the Standard Model. Although baryogenesis and inflation must have occurred at higher temperatures in the early Universe, we do not as yet have 'standard models' for these, so BBN still marks the boundary between the established and the speculative in Big Bang cosmology. It might appear possible to push the boundary back to the quark-hadron transition at $T \sim \Lambda_{\rm QCD}$, or electroweak symmetry breaking at $T \sim 1/\sqrt{G_{\rm F}}$; however, so far no observable relics of these epochs have been identified, either theoretically or observationally. Thus, although the Standard Model provides a precise description of physics up to the Fermi scale, cosmology cannot be traced in detail before the BBN era.

Limits on new physics come mainly from the observational bounds on the ^{4}He abundance. This is proportional to the n/p ratio when the weak-interaction rate falls behind the Hubble expansion rate at $T_{\rm fr} \sim 1$ MeV. The presence of additional neutrino flavors (or of any other relativistic species) at this time increases g_*, hence the expansion rate, leading to a larger value of $T_{\rm fr}$, n/p, and therefore $Y_{\rm p}$ [10,100]. In the Standard Model at $T = 1$ MeV, $g_* = 5.5 + \frac{7}{4}N_\nu$, where N_ν is the *effective* number of (nearly) massless neutrino flavors (see Big Bang Cosmology review Chapter 21). The helium curves in Fig. 23.1 were computed taking $N_\nu = 3$; small corrections for non-equilibrium neutrino heating [20] are included in the thermal evolution and lead to an effective $N_\nu = 3.04$ compared to assuming instantaneous neutrino freezeout (Chapter 21). The computed ^{4}He abundance scales as $\Delta Y_{\rm p} \simeq 0.013\Delta N_\nu$ [11]. Clearly the central value for N_ν from BBN will depend on η, which is independently determined (with weaker sensitivity to N_ν) by the adopted D or ^{7}Li abundance. For example, if the best value for the observed primordial ^{4}He abundance is 0.249, then, for $\eta_{10} \sim 6$, the central value for N_ν is very close to 3. A maximum likelihood analysis on η and N_ν based on the above ^{4}He and D abundances finds the (correlated) 95% CL ranges to be $5.6 < \eta_{10} < 6.6$ and $2.3 < N_\nu < 3.4$ [5]. Identical results are obtained using a simpler method to extract such bounds based on χ^2 statistics, given a set of input abundances [101].

The CMB power spectrum in the damping tail is independently sensitive to N_ν (*e.g.* [102]) . The CMB value $N_\nu^{\rm CMB}$ probes the cosmic radiation content at (re)combination, so a discrepancy would imply new physics or astrophysics. Indeed, observations by the South Pole Telescope implied $N_\nu^{\rm CMB} = 3.85 \pm 0.62$ [103], prompting discussion of "dark radiation" such as sterile neutrinos [104]. However, *Planck* 2015 results give $N_\nu^{\rm CMB} = 3.13 \pm 0.31$ when using the BBN $Y_{\rm p}(\eta)$, a result quite consistent with the Standard Model neutrinos [61]. If we *assume* that η did not change between BBN and (re)combination, the constraint can be improved by including the recent D/H and astrophysical $Y_{\rm p}$ measurements, which yields $N_\nu = 2.88 \pm 0.16$ [5].

Just as one can use the measured helium abundance to place limits on g_* [100], any changes in the strong, weak, electromagnetic, or gravitational coupling constants, arising *e.g.*, from the dynamics of new dimensions, can be similarly constrained [105], as can any speed-up of the expansion rate in, *e.g.*, scalar-tensor theories of gravity [106].

The limits on N_ν can be translated into limits on other types of particles or particle masses that would affect the expansion rate of the Universe during nucleosynthesis. For example, consider 'sterile' neutrinos with only right-handed interactions of strength $G_{\rm R} < G_{\rm F}$. Such particles would decouple at higher temperature than (left-handed) neutrinos, so their number density ($\propto T^3$) relative to neutrinos would be reduced by any subsequent entropy release, *e.g.*, due to annihilations of massive particles that become non-relativistic between the two decoupling temperatures. Thus (relativistic) particles with less than full strength weak interactions contribute less to the energy density than particles that remain in equilibrium up to the time of nucleosynthesis [107]. If we impose $N_\nu < 4$ as an illustrative constraint, then the three right-handed neutrinos must have a temperature $3(T_{\nu_{\rm R}}/T_{\nu_{\rm L}})^4 < 1$. Since the temperature of the decoupled $\nu_{\rm R}$ is determined by entropy conservation (see Big Bang Cosmology review, Chapter 21), $T_{\nu_{\rm R}}/T_{\nu_{\rm L}} = [(43/4)/g_*(T_{\rm d})]^{1/3} < 0.76$, where $T_{\rm d}$ is the decoupling temperature of the $\nu_{\rm R}$. This requires $g_*(T_{\rm d}) > 24$, so decoupling must have occurred at $T_{\rm d} > 140$ MeV. The decoupling temperature is related to $G_{\rm R}$ through $(G_{\rm R}/G_{\rm F})^2 \sim (T_{\rm d}/3\,{\rm MeV})^{-3}$, where 3 MeV is the decoupling temperature for $\nu_{\rm L}$s. This yields a limit $G_{\rm R} \lesssim 10^{-2} G_{\rm F}$. The above argument sets lower limits on the masses of new Z' gauge bosons to which right-handed neutrinos would be coupled in models of superstrings [108], or extended technicolour [109]. Similarly a Dirac magnetic moment for neutrinos, which would allow the right-handed states to be produced through scattering and thus increase g_*, can be significantly constrained [110], as can any new interactions for neutrinos that have a similar effect [111]. Right-handed states can be populated directly by helicity-flip scattering if the neutrino mass is large enough, and this property has been used to infer a bound of $m_{\nu_\tau} \lesssim 1$ MeV (taking $N_\nu < 4$) [112]. If there is mixing between active and sterile neutrinos then the effect on BBN is more complicated [113].

BBN limits on the cosmic expansion rate constrain supersymmetric scenarios in which the neutralino or gravitino are very light, so that they contribute to g_* [114]. A gravitino in the mass range $\sim 10^{-4} - 10$ eV will affect the expansion rate of the Universe similarly to a light neutralino (which is however now probably ruled out by collider data, especially the decays of the Higgs-like boson). The net contribution to N_ν then ranges between 0.74 and 1.69, depending on the gravitino and slepton masses [115].

The limit on the expansion rate during BBN can also be translated into bounds on the mass/lifetime of non-relativistic particles that decay during BBN. This results in an even faster speed-up rate, and typically also changes the entropy [116]. If the decays include

Standard Model particles, the resulting electromagnetic [117–118] and/or hadronic [119] cascades can strongly perturb the light elements, which leads to even stronger constraints. Such arguments have been applied to rule out an MeV mass for ν_τ, which decays during nucleosynthesis [120].

Decaying-particle arguments have proved very effective in probing supersymmetry. Light-element abundances generally are complementary to accelerator data in constraining SUSY parameter space, with BBN reaching to values kinematically inaccessible to the LHC. Much recent interest has focused on the case in which the next-to-lightest supersymmetric particle is metastable and decays during or after BBN. The constraints on unstable particles discussed above imply stringent bounds on the allowed abundance of such particles [119]; if the metastable particle is charged (*e.g.*, the stau), then it is possible for it to form atom-like electromagnetic bound states with nuclei, and the resulting impact on light elements can be quite complex [121]. Moreover, SUSY decays can destroy ^{7}Li and/or produce ^{6}Li, leading to a possible supersymmetric solution to the lithium problems noted above [122](see [7] for a review).

These arguments impose powerful constraints on supersymmetric inflationary cosmology [118–119], particularly thermal leptogenesis [123]. These limits can be evaded only if the gravitino is massive enough to decay before BBN, *i.e.*, $m_{3/2} \gtrsim 50$ TeV [124](which would be unnatural), or if it is in fact the lightest supersymmetric particle and thus stable [118,125]. Similar constraints apply to moduli – very weakly coupled fields in string theory that obtain an electroweak-scale mass from supersymmetry breaking [126].

Finally, we mention that BBN places powerful constraints on the possibility that there are new large dimensions in nature, perhaps enabling the scale of quantum gravity to be as low as the electroweak scale [127]. Thus, Standard Model fields may be localized on a 'brane,' while gravity alone propagates in the 'bulk.' It has been further noted that the new dimensions may be non-compact, even infinite [128], and the cosmology of such models has attracted considerable attention. The expansion rate in the early Universe can be significantly modified, so BBN is able to set interesting constraints on such possibilities [129].

References:

1. R.V. Wagoner *et al.*, Astrophys. J. **148**, 3 (1967).
2. D.N. Schramm and M.S. Turner, Rev. Mod. Phys. **70**, 303 (1998).
3. G. Steigman, Ann. Rev. Nucl. and Part. Sci. **57**, 463 (2007).
4. F. Iocco *et al.*, Phys. Reports **472**, 1 (2009).
5. R.H. Cyburt *et al.*, Rev. Mod. Phys. **88**, 015004 (2016).
6. S. Sarkar, Rept. on Prog. in Phys. **59**, 1493 (1996).
7. K. Jedamzik and M. Pospelov, New J. Phys. **11**, 105028 (2009).
8. M. Pospelov and J. Pradler, Ann. Rev. Nucl. and Part. Sci. **60**, 539 (2010).
9. B.D. Fields, Ann. Rev. Nucl. and Part. Sci. **61**, 47 (2011).
10. P.J.E. Peebles, Phys. Rev. Lett. **16**, 411 (1966).
11. J. Bernstein *et al.*, Rev. Mod. Phys. **61**, 25 (1989).
12. S. Mukhanov, Int. J. Theor. Phys. **143**, 669 (2004).
13. R. Esmailzadeh *et al.*, Astrophys. J. **378**, 504 (1991).
14. R.H. Cyburt *et al.*, JCAP **0811**, 012 (2008).
15. R.H. Cyburt *et al.*, New Astron. **6**, 215 (2001).
16. L. Kawano, FERMILAB-PUB-92/04-A.
17. O. Pisanti *et al.*, Comput. Phys. Commun. **178**, 956 (2008).
18. A. Arbey, Comput. Phys. Commun. **183**, 1822 (2012).
19. S. Esposito *et al.*, Nucl. Phys. **B568**, 421 (2000).
20. S. Dodelson and M.S. Turner, Phys. Rev. **D46**, 3372 (1992).
21. D. Seckel, `hep-ph/9305311`; R. Lopez and M.S. Turner, Phys. Rev. **D59**, 103502 (1999).
22. M.S. Smith *et al.*, Astrophys. J. Supp. **85**, 219 (1993).
23. G. Fiorentini *et al.*, Phys. Rev. **D58**, 063506 (1998).
24. A. Coc *et al.*, Astrophys. J. **744**, 158 (2012).
25. K.M. Nollett and S. Burles, Phys. Rev. **D61**, 123505 (2000).
26. R.H. Cyburt, Phys. Rev. **D70**, 023505 (2004).
27. P.D. Serpico *et al.*, JCAP **12**, 010 (2004).
28. R.N. Boyd *et al.*, Phys. Rev. **D82**, 105005 (2010).
29. R.H. Cyburt and B. Davids, Phys. Rev. **C78**, 012 (2008).
30. K.M. Nollett *et al.*, Astrophys. J. Lett. **552**, L1 (2001).
31. K.M. Nollett and G.P. Holder, `arXiv:1112.2683`.
32. L.E. Marcucci *et al.*, Phys. Rev. Lett. **116**, 102501 (2016).
33. C. Gustavino, Euro. Phys. J. Web of Conferences, 136, 01009 (2017).
34. R.I. Epstein *et al.*, Nature **263**, 198 (1976).
35. B.E. Wood *et al.*, Astrophys. J. **609**, 838 (2004).
36. S. D'Odorico *et al.*, Astron. & Astrophys. **368**, L21 (2001).
37. D. Romano *et al.*, Mon. Not. R. Astron. Soc **369**, 295 (2006).
38. M. Pettini and D. Bowen, Astrophys. J. **560**, 41 (2001).
39. R. Cooke *et al.*, Astrophys. J. **781**, 31 (2014).
40. R. Cooke *et al.*, Astrophys. J. **830**, 148 (2016).
41. E.O. Zavarygin *et al.*, `arXiv:1706.09512`(2017).
42. S.A. Balashev *et al.*, Mon. Not. R. Astron. Soc **458**, 2188 (2016).
43. S.A. Levshakov *et al.*, Astrophys. J. **565**, 696 (2002).
44. M. Fumagalli *et al.*, Science **334**, 1245 (2011).
45. R. Srianand *et al.*, Mon. Not. R. Astron. Soc **405**, 1888 (2010).
46. P. Noterdaeme *et al.*, Astron. & Astrophys. **542**, L33 (2012).
47. M. Pettini and R. Cooke, Mon. Not. R. Astron. Soc **425**, 2477 (2012).
48. S. Riemer-Sørensen *et al.*, Mon. Not. R. Astron. Soc **447**, 2925 (2015).
49. S. Riemer-Sørensen *et al.*, Mon. Not. R. Astron. Soc **468**, 3239 (2017).
50. J.L. Linsky *et al.*, Astrophys. J. **647**, 1106 (2006).
51. Y.I. Izotov *et al.*, Astrophys. J. **527**, 757 (1999).
52. K.A. Olive and E. Skillman, Astrophys. J. **617**, 29 (2004).
53. M. Peimbert *et al.*, Astrophys. J. **667**, 636 (2007).
54. A. Peimbert *et al.*, RMxAA **52**,419(2016).
55. Y.I. Izotov *et al.*, Astrophys. J. **662**, 15 (2007).
56. E. Aver *et al.*, JCAP **04**, 004 (2012).
57. E. Aver *et al.*, JCAP **07**, 011 (2015).
58. Y.I. Izotov *et al.*, Mon. Not. R. Astron. Soc **445**, 778 (2014).
59. Y.I. Izotov *et al.*, Astron. & Astrophys. **558**, A57 (2013).
60. R. Trotta and S.H. Hansen, Phys. Rev. **D69**, 023509 (2004).
61. P.A.R. Ade *et al.*, Astron. & Astrophys. **594**, A13 (2016).
62. N. Christlieb *et al.*, Nature **419**, 904 (2002).
63. M. Spite and F. Spite, Nature **297**, 483 (1982).
64. E. Vangioni-Flam *et al.*, New Astron. **4**, 245 (1999).
65. S.G. Ryan *et al.*, Astrophys. J. Lett. **530**, L57 (2000).
66. P. Bonifacio and P. Molaro, Mon. Not. R. Astron. Soc **285**, 847 (1997).
67. P. Bonifacio *et al.*, Astron. & Astrophys. **390**, 91 (2002).
68. J. Melendez *et al.*, Astron. & Astrophys. **515**, L3 (2010).
69. P. Bonifacio *et al.*, Astron. & Astrophys. **462**, 851 (2007).
70. W. Aoki, Astrophys. J. **698**, 1803 (2009); A. Hosford *et al.*, Astron. & Astrophys. **493**, 601 (2009).
71. L. Sbordone *et al.*, Astron. & Astrophys. **522**, A26 (2010).
72. E. Caffau *et al.*, Nature **477**, 67 (2011).
73. P. Molaro *et al.*, Memorie della Soc. Astronomica Italiana Supp. **22**, 233 (2012).
74. X. Fu *et al.*, Mon. Not. R. Astron. Soc **452**, 325 (2015).
75. M.H. Pinsonneault *et al.*, Astrophys. J. **574**, 389 (2002).
76. A.J. Korn *et al.*, Nature **442**, 657 (2006).
77. M. Asplund *et al.*, Astrophys. J. **644**, 229 (2006).
78. K. Lind *et al.*, Astron. & Astrophys. **554**, 96 (2013).
79. R. Cayrel *et al.*, Astron. & Astrophys. **473**, L37 (2007).
80. M. Steffen *et al.*, Memorie della Soc. Astronomica Italiana Supp. **22**, 152 (2012).
81. T.M. Bania *et al.*, Nature **415**, 54 (2002).
82. K.A. Olive *et al.*, Astrophys. J. **479**, 752 (1997).
83. E. Vangioni-Flam *et al.*, Astrophys. J. **585**, 611 (2003).
84. M. Kawasaki *et al.*, Phys. Rev. **D71**, 083502 (2005).
85. H. Reeves *et al.*, Astrophys. J. **179**, 909 (1973).
86. M. Fukugita and P.J.E. Peebles, Astrophys. J. **616**, 643 (2004).
87. R. Cen and J.P. Ostriker, Astrophys. J. **514**, 1 (1999).
88. G. Jungman *et al.*, Phys. Rev. **D54**, 1332 (1996).
89. A. Coc *et al.*, `arXiv:1307:6955`.
90. R.H. Cyburt *et al.*, Phys. Lett. **B567**, 227 (2003).

91. R.H. Cyburt and M. Pospelov, Int. J. Mod. Phys. E **21**, 1250004 (2012);
R.N. Boyd *et al.*, Phys. Rev. **D82**, 105005 (2010);
N. Chakraborty *et al.*, Phys. Rev. **D83**, 063006 (2011);
C. Broggini *et al.*, JCAP **06**, 030 (2012).
92. P.D. O'Malley *et al.*, Phys. Rev. **C84**, 042801 (2011);
Hammache, F., *et al.*, Phys. Rev. C 88, 062802 (2013);
Paris, M. *et al.*, Nuclear Data Sheets, 120, 184 (2014).
93. O. Richard *et al.*, Astrophys. J. **619**, 538 (2005).
94. P. Gruyters *et al.*, Astron. Astrophys. **555**, 31 (2013).
95. K. Jedamzik and J.B. Rehm, Phys. Rev. **D64**, 023510 (2001).
96. D.J. Fixsen *et al.*, Astrophys. J. **473**, 576 (1996).
97. K. Jedamzik, Phys. Rev. **D70**, 063524 (2004).
98. A. Goudelis, M. Pospelov, and J. Pradler, Phys. Rev. Lett. **116**, 211303 (2016).
99. J.D. Barrow, Phys. Rev. **D35**, 1805 (1987);
B.A. Campbell and K.A. Olive, Phys. Lett. **B345**, 429 (1995);
L. Bergström, Phys. Rev. **D60**, 045005 (1999);
V.V. Flambaum and E.V. Shuryak, Phys. Rev. **D65**, 103503 (2002);
A. Coc *et al.*, Phys. Rev. **D76**, 023511 (2007);
J.C. Berengut *et al.*, Phys. Rev. **D87**, 085018 (2013).
100. G. Steigman *et al.*, Phys. Lett. **B66**, 202 (1977).
101. E. Lisi *et al.*, Phys. Rev. **D59**, 123520 (1999).
102. Z. Hou *et al.*, Phys. Rev. **D87**, 083008 (2013).
103. R. Keisler *et al.*, Astrophys. J. **743**, 28 (2011).
104. J. Hamann *et al.*, Phys. Rev. Lett. **105**, 181301 (2010).
105. E.W. Kolb *et al.*, Phys. Rev. **D33**, 869 (1986);
F.S. Accetta *et al.*, Phys. Lett. **B248**, 146 (1990);
B.A. Campbell and K.A. Olive, Phys. Lett. **B345**, 429 (1995);
K.M. Nollett and R. Lopez, Phys. Rev. **D66**, 063507 (2002);
C. Bambi *et al.*, Phys. Rev. **D71**, 123524 (2005).
106. A. Coc *et al.*, Phys. Rev. **D73**, 083525 (2006).
107. K.A. Olive *et al.*, Nucl. Phys. **B180**, 497 (1981).
108. J. Ellis *et al.*, Phys. Lett. **B167**, 457 (1986).
109. L.M. Krauss *et al.*, Phys. Rev. Lett. **71**, 823 (1993).
110. J.A. Morgan, Phys. Lett. **B102**, 247 (1981).
111. E.W. Kolb *et al.*, Phys. Rev. **D34**, 2197 (1986);
J.A. Grifols and E. Massó, Mod. Phys. Lett. **A2**, 205 (1987);
K.S. Babu *et al.*, Phys. Rev. Lett. **67**, 545 (1991).
112. A.D. Dolgov *et al.*, Nucl. Phys. **B524**, 621 (1998).
113. K. Enqvist *et al.*, Nucl. Phys. **B373**, 498 (1992);
A.D. Dolgov, Phys. Reports **370**, 333 (2002).
114. J.A. Grifols *et al.*, Phys. Lett. **B400**, 124 (1997).
115. H. Dreiner *et al.*, Phys. Rev. **D85**, 065027 (2012).
116. K. Sato and M. Kobayashi, Prog. Theor. Phys. **58**, 1775 (1977);
D.A. Dicus *et al.*, Phys. Rev. **D17**, 1529 (1978);
R.J. Scherrer and M.S. Turner, Astrophys. J. **331**, 19 (1988).
117. D. Lindley, Mon. Not. R. Astron. Soc **188**, 15 (1979); Astrophys. J. **294**, 1 (1985).
118. J. Ellis *et al.*, Nucl. Phys. **B259**, 175 (1985);
J. Ellis *et al.*, Nucl. Phys. **B373**, 399 (1992);
R.H. Cyburt *et al.*, Phys. Rev. **D67**, 103521 (2003).
119. M.H. Reno and D. Seckel, Phys. Rev. **D37**, 3441 (1988);
S. Dimopoulos *et al.*, Nucl. Phys. **B311**, 699 (1989);
K. Kohri *et al.*, Phys. Rev. **D71**, 083502 (2005).
120. S. Sarkar and A.M. Cooper, Phys. Lett. **B148**, 347 (1984).
121. M. Pospelov *et al.*, Phys. Rev. Lett. **98**, 231301 (2007);
M. Kawasaki *et al.*, Phys. Lett. **B649**, 436 (2007);
R.H. Cyburt *et al.*, JCAP **05**, 014 (2013).
122. K. Jedamzik *et al.*, JCAP **07**, 007 (2006).
123. S. Davidson *et al.*, Phys. Rev. **466**, 105 (2008).
124. S. Weinberg, Phys. Rev. Lett. **48**, 1303 (1979).
125. M. Bolz *et al.*, Nucl. Phys. **B606**, 518 (2001).
126. G. Coughlan *et al.*, Phys. Lett. **B131**, 59 (1983).
127. N. Arkani-Hamed *et al.*, Phys. Rev. **D59**, 086004 (1999).
128. L. Randall and R. Sundrum, Phys. Rev. Lett. **83**, 3370 (1999).
129. J.M. Cline *et al.*, Phys. Rev. Lett. **83**, 4245 (1999);
P. Binetruy *et al.*, Phys. Lett. **B477**, 285 (2000).

24. Cosmological Parameters

Updated October 2017, by O. Lahav (University College London) and A.R. Liddle (University of Edinburgh).

24.1. Parametrizing the Universe

Rapid advances in observational cosmology have led to the establishment of a precision cosmological model, with many of the key cosmological parameters determined to one or two significant figure accuracy. Particularly prominent are measurements of cosmic microwave background (CMB) anisotropies, with the highest precision observations being those of the *Planck* Satellite [1,2] which supersede the iconic *WMAP* results [3,4]. However the most accurate model of the Universe requires consideration of a range of observations, with complementary probes providing consistency checks, lifting parameter degeneracies, and enabling the strongest constraints to be placed.

The term 'cosmological parameters' is forever increasing in its scope, and nowadays often includes the parameterization of some functions, as well as simple numbers describing properties of the Universe. The original usage referred to the parameters describing the global dynamics of the Universe, such as its expansion rate and curvature. Also now of great interest is how the matter budget of the Universe is built up from its constituents: baryons, photons, neutrinos, dark matter, and dark energy. We need to describe the nature of perturbations in the Universe, through global statistical descriptors such as the matter and radiation power spectra. There may also be parameters describing the physical state of the Universe, such as the ionization fraction as a function of time during the era since recombination. Typical comparisons of cosmological models with observational data now feature between five and ten parameters.

24.1.1. *The global description of the Universe* :

Ordinarily, the Universe is taken to be a perturbed Robertson–Walker space-time with dynamics governed by Einstein's equations. This is described in detail in the Big-Bang Cosmology chapter in this volume. Using the density parameters Ω_i for the various matter species and Ω_Λ for the cosmological constant, the Friedmann equation can be written

$$\sum_i \Omega_i + \Omega_\Lambda - 1 = \frac{k}{R^2 H^2}\,, \tag{24.1}$$

where the sum is over all the different species of material in the Universe. This equation applies at any epoch, but later in this article we will use the symbols Ω_i and Ω_Λ to refer to the present-epoch values.

The complete present-epoch state of the homogeneous Universe can be described by giving the current-epoch values of all the density parameters and the Hubble constant h (the present-day Hubble parameter being written $H_0 = 100h\,\mathrm{km\,s^{-1}\,Mpc^{-1}}$). A typical collection would be baryons Ω_b, photons Ω_γ, neutrinos Ω_ν, and cold dark matter Ω_c (given charge neutrality, the electron density is guaranteed to be too small to be worth considering separately and is effectively included with the baryons). The spatial curvature can then be determined from the other parameters using Eq. (24.1). The total present matter density $\Omega_\mathrm{m} = \Omega_\mathrm{c} + \Omega_\mathrm{b}$ may be used in place of the cold dark matter density Ω_c.

These parameters also allow us to track the history of the Universe, at least back until an epoch where interactions allow interchanges between the densities of the different species; this is believed to have last happened at neutrino decoupling, shortly before Big Bang Nucleosynthesis (BBN). To probe further back into the Universe's history requires assumptions about particle interactions, and perhaps about the nature of physical laws themselves.

The standard neutrino sector has three flavors. For neutrinos of mass in the range $5\times10^{-4}\,\mathrm{eV}$ to $1\,\mathrm{MeV}$, the density parameter in neutrinos is predicted to be

$$\Omega_\nu h^2 = \frac{\sum m_\nu}{93.14\,\mathrm{eV}}\,, \tag{24.2}$$

where the sum is over all families with mass in that range (higher masses need a more sophisticated calculation). We use units with $c = 1$ throughout. Results on atmospheric and Solar neutrino oscillations [5] imply non-zero mass-squared differences between the three neutrino flavors. These oscillation experiments cannot tell us the absolute neutrino masses, but within the simple assumption of a mass hierarchy suggest a lower limit of approximately $0.06\,\mathrm{eV}$ for the sum of the neutrino masses (see the Neutrino chapter).

Even a mass this small has a potentially observable effect on the formation of structure, as neutrino free-streaming damps the growth of perturbations. Analyses commonly now either assume a neutrino mass sum fixed at this lower limit, or allow the neutrino mass sum as a variable parameter. To date there is no decisive evidence of any effects from either neutrino masses or an otherwise non-standard neutrino sector, and observations impose quite stringent limits; see the Neutrinos in Cosmology section. However, we note that the inclusion of the neutrino mass sum as a free parameter can affect the derived values of other cosmological parameters.

24.1.2. *Inflation and perturbations* :

A complete model of the Universe should include a description of deviations from homogeneity, at least in a statistical way. Indeed, some of the most powerful probes of the parameters described above come from the evolution of perturbations, so their study is naturally intertwined with the determination of cosmological parameters.

There are many different notations used to describe the perturbations, both in terms of the quantity used to describe the perturbations and the definition of the statistical measure. We use the dimensionless power spectrum Δ^2 as defined in the Big Bang Cosmology section (also denoted $\mathcal{P}$ in some of the literature). If the perturbations obey Gaussian statistics, the power spectrum provides a complete description of their properties.

From a theoretical perspective, a useful quantity to describe the perturbations is the curvature perturbation $\mathcal{R}$, which measures the spatial curvature of a comoving slicing of the space-time. A simple case is the Harrison–Zeldovich spectrum, which corresponds to a constant $\Delta^2_\mathcal{R}$. More generally, one can approximate the spectrum by a power-law, writing

$$\Delta^2_\mathcal{R}(k) = \Delta^2_\mathcal{R}(k_*)\left[\frac{k}{k_*}\right]^{n_\mathrm{s}-1}\,, \tag{24.3}$$

where n_s is known as the spectral index, always defined so that $n_\mathrm{s} = 1$ for the Harrison–Zeldovich spectrum, and k_* is an arbitrarily chosen scale. The initial spectrum, defined at some early epoch of the Universe's history, is usually taken to have a simple form such as this power law, and we will see that observations require n_s close to one. Subsequent evolution will modify the spectrum from its initial form.

The simplest mechanism for generating the observed perturbations is the inflationary cosmology, which posits a period of accelerated expansion in the Universe's early stages [6,7]. It is a useful working hypothesis that this is the sole mechanism for generating perturbations, and it may further be assumed to be the simplest class of inflationary model, where the dynamics are equivalent to that of a single scalar field ϕ with canonical kinetic energy slowly rolling on a potential $V(\phi)$. One may seek to verify that this simple picture can match observations and to determine the properties of $V(\phi)$ from the observational data. Alternatively, more complicated models, perhaps motivated by contemporary fundamental physics ideas, may be tested on a model-by-model basis (see more in the Inflation chapter in this volume).

Inflation generates perturbations through the amplification of quantum fluctuations, which are stretched to astrophysical scales by the rapid expansion. The simplest models generate two types, density perturbations that come from fluctuations in the scalar field and its corresponding scalar metric perturbation, and gravitational waves that are tensor metric fluctuations. The former experience gravitational instability and lead to structure formation, while the latter can influence the CMB anisotropies. Defining slow-roll parameters, with primes indicating derivatives with respect to the scalar field, as

$$\epsilon = \frac{m_\mathrm{Pl}^2}{16\pi}\left(\frac{V'}{V}\right)^2 \quad,\quad \eta = \frac{m_\mathrm{Pl}^2}{8\pi}\frac{V''}{V}\,, \tag{24.4}$$

which should satisfy $\epsilon, |\eta| \ll 1$, the spectra can be computed using the slow-roll approximation as

$$\Delta^2_\mathcal{R}(k) \simeq \left.\frac{8}{3m_\mathrm{Pl}^4}\frac{V}{\epsilon}\right|_{k=aH} \quad,\quad \Delta^2_\mathrm{t}(k) \simeq \left.\frac{128}{3m_\mathrm{Pl}^4}V\right|_{k=aH}\,. \tag{24.5}$$

In each case, the expressions on the right-hand side are to be evaluated when the scale k is equal to the Hubble radius during inflation. The symbol '$\simeq$' here indicates use of the slow-roll approximation, which is expected to be accurate to a few percent or better.

From these expressions, we can compute the spectral indices [8]:

$$n_{\rm s} \simeq 1 - 6\epsilon + 2\eta \quad ; \quad n_{\rm t} \simeq -2\epsilon\,. \tag{24.6}$$

Another useful quantity is the ratio of the two spectra, defined by

$$r \equiv \frac{\Delta^2_{\rm t}(k_*)}{\Delta^2_{\mathcal{R}}(k_*)}\,. \tag{24.7}$$

We have

$$r \simeq 16\epsilon \simeq -8 n_{\rm t}\,, \tag{24.8}$$

which is known as the consistency equation.

One could consider corrections to the power-law approximation, which we discuss later. However, for now we make the working assumption that the spectra can be approximated by such power laws. The consistency equation shows that r and $n_{\rm t}$ are not independent parameters, and so the simplest inflation models give initial conditions described by three parameters, usually taken as $\Delta^2_{\mathcal{R}}$, $n_{\rm s}$, and r, all to be evaluated at some scale k_*, usually the 'statistical center' of the range explored by the data. Alternatively, one could use the parametrization V, ϵ, and η, all evaluated at a point on the putative inflationary potential.

After the perturbations are created in the early Universe, they undergo a complex evolution up until the time they are observed in the present Universe. When the perturbations are small, this can be accurately followed using a linear theory numerical code such as CAMB or CLASS [9]. This works right up to the present for the CMB, but for density perturbations on small scales non-linear evolution is important and can be addressed by a variety of semi-analytical and numerical techniques. However the analysis is made, the outcome of the evolution is in principle determined by the cosmological model and by the parameters describing the initial perturbations, and hence can be used to determine them.

Of particular interest are CMB anisotropies. Both the total intensity and two independent polarization modes are predicted to have anisotropies. These can be described by the radiation angular power spectra C_ℓ as defined in the CMB article in this volume, and again provide a complete description if the density perturbations are Gaussian.

24.1.3. *The standard cosmological model* :

We now have most of the ingredients in place to describe the cosmological model. Beyond those of the previous subsections, we need a measure of the ionization state of the Universe. The Universe is known to be highly ionized at low redshifts (otherwise radiation from distant quasars would be heavily absorbed in the ultra-violet), and the ionized electrons can scatter microwave photons, altering the pattern of observed anisotropies. The most convenient parameter to describe this is the optical depth to scattering τ (*i.e.*, the probability that a given photon scatters once); in the approximation of instantaneous and complete reionization, this could equivalently be described by the redshift of reionization $z_{\rm ion}$.

As described in Sec. 24.4, models based on these parameters are able to give a good fit to the complete set of high-quality data available at present, and indeed some simplification is possible. Observations are consistent with spatial flatness, and the inflation models so far described automatically generate negligible spatial curvature, so we can set $k = 0$; the density parameters then must sum to unity, and so one of them can be eliminated. The neutrino energy density is often not taken as an independent parameter. Provided that the neutrino sector has the standard interactions, the neutrino energy density, while relativistic, can be related to the photon density using thermal physics arguments, and a minimal assumption takes the neutrino mass sum to be that of the lowest mass solution to the neutrino oscillation constraints, namely 0.06 eV. In addition, there is no observational evidence for the existence of tensor perturbations (though the upper limits are fairly weak), and so r could be set to zero. This leaves seven parameters, which is the smallest set that can usefully be compared to the present cosmological dataset. This model is referred to by various names, including ΛCDM, the concordance cosmology, and the standard cosmological model.

Of these parameters, only Ω_γ is accurately measured directly. The radiation density is dominated by the energy in the CMB, and the COBE satellite FIRAS experiment determined its temperature to be $T = 2.7255 \pm 0.0006\,{\rm K}$ [10], ‡ corresponding to $\Omega_\gamma = 2.47 \times 10^{-5} h^{-2}$. It typically need not be varied in fitting other data. Hence the minimum number of cosmological parameters varied in fits to data is six, though as described below there may additionally be many 'nuisance' parameters necessary to describe astrophysical processes influencing the data.

In addition to this minimal set, there is a range of other parameters that might prove important in future as the data-sets further improve, but for which there is so far no direct evidence, allowing them to be set to a specific value for now. We discuss various speculative options in the next section. For completeness at this point, we mention one other interesting parameter, the helium fraction, which is a non-zero parameter that can affect the CMB anisotropies at a subtle level. It is usually fixed in microwave anisotropy studies, but the data are approaching a level where allowing its variation may become mandatory.

Most attention to date has been on parameter estimation, where a set of parameters is chosen by hand and the aim is to constrain them. Interest has been growing towards the higher-level inference problem of model selection, which compares different choices of parameter sets. Bayesian inference offers an attractive framework for cosmological model selection, setting a tension between model predictiveness and ability to fit the data [11].

24.1.4. *Derived parameters* :

The parameter list of the previous subsection is sufficient to give a complete description of cosmological models that agree with observational data. However, it is not a unique parameterization, and one could instead use parameters derived from that basic set. Parameters that can be obtained from the set given above include the age of the Universe, the present horizon distance, the present neutrino background temperature, the epoch of matter–radiation equality, the epochs of recombination and decoupling, the epoch of transition to an accelerating Universe, the baryon-to-photon ratio, and the baryon to dark matter density ratio. In addition, the physical densities of the matter components, $\Omega_i h^2$, are often more useful than the density parameters. The density perturbation amplitude can be specified in many different ways other than the large-scale primordial amplitude, for instance, in terms of its effect on the CMB, or by specifying a short-scale quantity, a common choice being the present linear-theory mass dispersion on a scale of $8\,h^{-1}$Mpc, known as σ_8.

Different types of observation are sensitive to different subsets of the full cosmological parameter set, and some are more naturally interpreted in terms of some of the derived parameters of this subsection than on the original base parameter set. In particular, most types of observation feature degeneracies whereby they are unable to separate the effects of simultaneously varying specific combinations of several of the base parameters.

24.2. Extensions to the standard model

At present, there is no positive evidence in favor of extensions of the standard model. These are becoming increasingly constrained by the data, though there always remains the possibility of trace effects at a level below present observational capability.

‡ Unless stated otherwise, all quoted uncertainties in this article are one-sigma/68% confidence and all upper limits are 95% confidence. Cosmological parameters sometimes have significantly non-Gaussian uncertainties. Throughout we have rounded central values, and especially uncertainties, from original sources, in cases where they appear to be given to excessive precision.

24.2.1. ***More general perturbations*** :

The standard cosmology assumes adiabatic, Gaussian perturbations. Adiabaticity means that all types of material in the Universe share a common perturbation, so that if the space-time is foliated by constant-density hypersurfaces, then all fluids and fields are homogeneous on those slices, with the perturbations completely described by the variation of the spatial curvature of the slices. Gaussianity means that the initial perturbations obey Gaussian statistics, with the amplitudes of waves of different wavenumbers being randomly drawn from a Gaussian distribution of width given by the power spectrum. Note that gravitational instability generates non-Gaussianity; in this context, Gaussianity refers to a property of the initial perturbations, before they evolve.

The simplest inflation models, based on one dynamical field, predict adiabatic perturbations and a level of non-Gaussianity that is too small to be detected by any experiment so far conceived. For present data, the primordial spectra are usually assumed to be power laws.

24.2.1.1. *Non-power-law spectra:*

For typical inflation models, it is an approximation to take the spectra as power laws, albeit usually a good one. As data quality improves, one might expect this approximation to come under pressure, requiring a more accurate description of the initial spectra, particularly for the density perturbations. In general, one can expand $\ln \Delta^2_{\mathcal{R}}$ as

$$\ln \Delta^2_{\mathcal{R}}(k) = \ln \Delta^2_{\mathcal{R}}(k_*) + (n_{\rm s,*} - 1) \ln \frac{k}{k_*} + \frac{1}{2} \left. \frac{dn_{\rm s}}{d \ln k} \right|_* \ln^2 \frac{k}{k_*} + \cdots \,, \quad (24.9)$$

where the coefficients are all evaluated at some scale k_*. The term $dn_{\rm s}/d\ln k|_*$ is often called the running of the spectral index [12]. Once non-power-law spectra are allowed, it is necessary to specify the scale k_* at which the spectral index is defined.

24.2.1.2. *Isocurvature perturbations:*

An isocurvature perturbation is one that leaves the total density unperturbed, while perturbing the relative amounts of different materials. If the Universe contains N fluids, there is one growing adiabatic mode and $N-1$ growing isocurvature modes (for reviews see Ref. 7 and Ref. 13). These can be excited, for example, in inflationary models where there are two or more fields that acquire dynamically-important perturbations. If one field decays to form normal matter, while the second survives to become the dark matter, this will generate a cold dark matter isocurvature perturbation.

In general, there are also correlations between the different modes, and so the full set of perturbations is described by a matrix giving the spectra and their correlations. Constraining such a general construct is challenging, though constraints on individual modes are beginning to become meaningful, with no evidence that any other than the adiabatic mode must be non-zero.

24.2.1.3. *Seeded perturbations:*

An alternative to laying down perturbations at very early epochs is that they are seeded throughout cosmic history, for instance by topological defects such as cosmic strings. It has long been excluded that these are the sole original of structure, but they could contribute part of the perturbation signal, current limits being just a few percent [14]. In particular, cosmic defects formed in a phase transition ending inflation is a plausible scenario for such a contribution.

24.2.1.4. *Non-Gaussianity:*

Multi-field inflation models can also generate primordial non-Gaussianity (reviewed, *e.g.*, in Ref. 7). The extra fields can either be in the same sector of the underlying theory as the inflaton, or completely separate, an interesting example of the latter being the curvaton model [15]. Current upper limits on non-Gaussianity are becoming stringent, but there remains strong motivation to push down those limits and perhaps reveal trace non-Gaussianity in the data. If non-Gaussianity is observed, its nature may favor an inflationary origin, or a different one such as topological defects.

24.2.2. ***Dark matter properties*** :

Dark matter properties are discussed in the Dark Matter chapter in this volume. The simplest assumption concerning the dark matter is that it has no significant interactions with other matter, and that its particles have a negligible velocity as far as structure formation is concerned. Such dark matter is described as 'cold,' and candidates include the lightest supersymmetric particle, the axion, and primordial black holes. As far as astrophysicists are concerned, a complete specification of the relevant cold dark matter properties is given by the density parameter $\Omega_{\rm c}$, though those seeking to detect it directly are as interested in its interaction properties.

Cold dark matter is the standard assumption and gives an excellent fit to observations, except possibly on the shortest scales where there remains some controversy concerning the structure of dwarf galaxies and possible substructure in galaxy halos. It has long been excluded for all the dark matter to have a large velocity dispersion, so-called 'hot' dark matter, as it does not permit galaxies to form; for thermal relics the mass must be above about 1 keV to satisfy this constraint, though relics produced non-thermally, such as the axion, need not obey this limit. However, in future further parameters might need to be introduced to describe dark matter properties relevant to astrophysical observations. Suggestions that have been made include a modest velocity dispersion (warm dark matter) and dark matter self-interactions. There remains the possibility that the dark matter is comprized of two separate components, *e.g.*, a cold one and a hot one, an example being if massive neutrinos have a non-negligible effect.

24.2.3. ***Relativistic species*** :

The number of relativistic species in the young Universe (omitting photons) is denoted $N_{\rm eff}$. In the standard cosmological model only the three neutrino species contribute, and its baseline value is assumed fixed at 3.045 (the small shift from 3 is because of a slight predicted deviation from a thermal distribution [16]) . However other species could contribute, for example an extra neutrino, possibly of sterile type, or massless Goldstone bosons or other scalars. It is hence interesting to study the effect of allowing this parameter to vary, and indeed although 3.045 is consistent with the data, most analyses currently suggest a somewhat higher value (*e.g.*, Ref. 17).

24.2.4. ***Dark energy*** :

While the standard cosmological model given above features a cosmological constant, in order to explain observations indicating that the Universe is presently accelerating, further possibilities exist under the general headings of 'dark energy' and 'modified gravity'. These topics are described in detail in the Dark Energy chapter in this volume. This article focuses on the case of the cosmological constant, as this simple model is a good match to existing data. We note that more general treatments of dark energy/modified gravity will lead to weaker constraints on other parameters.

24.2.5. ***Complex ionization history*** :

The full ionization history of the Universe is given by the ionization fraction as a function of redshift z. The simplest scenario takes the ionization to have the small residual value left after recombination up to some redshift $z_{\rm ion}$, at which point the Universe instantaneously reionizes completely. Then there is a one-to-one correspondence between τ and $z_{\rm ion}$ (that relation, however, also depending on other cosmological parameters). An accurate treatment of this process will track separate histories for hydrogen and helium. While currently rapid ionization appears to be a good approximation, as data improve a more complex ionization history may need to be considered.

24.2.6. ***Varying 'constants'*** :

Variation of the fundamental constants of Nature over cosmological times is another possible enhancement of the standard cosmology. There is a long history of study of variation of the gravitational constant $G_{\rm N}$, and more recently attention has been drawn to the possibility of small fractional variations in the fine-structure constant. There is presently no observational evidence for the former, which is tightly constrained by a variety of measurements. Evidence for the latter has been claimed from studies of spectral line shifts in quasar spectra at redshift $z \approx 2$ [18], but this is presently controversial and

in need of further observational study. See constraints from the CMB in the *Planck* 2015 papers.

24.2.7. *Cosmic topology* :

The usual hypothesis is that the Universe has the simplest topology consistent with its geometry, for example that a flat Universe extends forever. Observations cannot tell us whether that is true, but they can test the possibility of a non-trivial topology on scales up to roughly the present Hubble scale. Extra parameters would be needed to specify both the type and scale of the topology, for example, a cuboidal topology would need specification of the three principal axis lengths. At present, there is no evidence for non-trivial cosmic topology [19].

24.3. Cosmological Probes

The goal of the observational cosmologist is to utilize astronomical information to derive cosmological parameters. The transformation from the observables to the parameters usually involves many assumptions about the nature of the objects, as well as of the dark sector. Below we outline the physical processes involved in each of the major probes, and the main recent results. The first two subsections concern probes of the homogeneous Universe, while the remainder consider constraints from perturbations.

In addition to statistical uncertainties we note three sources of systematic uncertainties that will apply to the cosmological parameters of interest: (i) due to the assumptions on the cosmological model and its priors (*i.e.*, the number of assumed cosmological parameters and their allowed range); (ii) due to the uncertainty in the astrophysics of the objects (*e.g.*, light curve fitting for supernovae or the mass–temperature relation of galaxy clusters); and (iii) due to instrumental and observational limitations (*e.g.*, the effect of 'seeing' on weak gravitational lensing measurements, or beam shape on CMB anisotropy measurements).

These systematics, the last two of which appear as 'nuisance parameters', pose a challenging problem to the statistical analysis. We attempt to fit the whole Universe with 6 to 12 parameters, but we might need to include hundreds of nuisance parameters, some of them highly correlated with the cosmological parameters of interest (for example time-dependent galaxy biasing could mimic the growth of mass fluctuations). Fortunately, there is some astrophysical prior knowledge on these effects, and a small number of physically-motivated free parameters would ideally be preferred in the cosmological parameter analysis.

24.3.1. *Direct measures of the Hubble constant* :

In 1929, Edwin Hubble discovered the law of expansion of the Universe by measuring distances to nearby galaxies. The slope of the relation between the distance and recession velocity is defined to be the Hubble constant, H_0. Astronomers argued for decades about the systematic uncertainties in various methods and derived values over the wide range $40\,\mathrm{km\,s^{-1}\,Mpc^{-1}} \lesssim H_0 \lesssim 100\,\mathrm{km\,s^{-1}\,Mpc^{-1}}$.

One of the most reliable results on the Hubble constant came from the Hubble Space Telescope Key Project [20]. This study used the empirical period–luminosity relation for Cepheid variable stars, and calibrated a number of secondary distance indicators—Type Ia Supernovae (SNe Ia), the Tully–Fisher relation, surface-brightness fluctuations, and Type II Supernovae. A recent derivation based on this approach utilizes the maser-based distance to NGC4258 to re-calibrate its Cepheid distance scale to obtain $H_0 = 73.2 \pm 1.7\,\mathrm{km\,s^{-1}\,Mpc^{-1}}$ [21]. The major sources of uncertainty in this result are due to the heavy element abundance of the Cepheids and the distance to the fiducial nearby galaxy, the Large Magellanic Cloud, relative to which all Cepheid distances are measured.

The indirect determination of H_0 by the *Planck* Collaboration [2] found a lower value, $H_0 = 67.8 \pm 0.9\,\mathrm{km\,s^{-1}\,Mpc^{-1}}$. As discussed in that paper, there is strong degeneracy of H_0 with other parameters, *e.g.*, Ω_m and the neutrino mass. The tension between the H_0 from *Planck* and the traditional cosmic distance-ladder methods is under investigation.

24.3.2. *Supernovae as cosmological probes* :

Empirically, the peak luminosity of SNe Ia can be used as an efficient distance indicator (*e.g.*, Ref. 22), thus allowing cosmology to be constrained via the distance–redshift relation. The favorite theoretical explanation for SNe Ia is the thermonuclear disruption of carbon–oxygen white dwarfs. Although not perfect 'standard candles', it has been demonstrated that by correcting for a relation between the light-curve shape, color, and luminosity at maximum brightness, the dispersion of the measured luminosities can be greatly reduced. There are several possible systematic effects that may affect the accuracy of the use of SNe Ia as distance indicators, *e.g.*, evolution with redshift and interstellar extinction in the host galaxy and in the Milky Way.

Two major studies, the Supernova Cosmology Project and the High-z Supernova Search Team, found evidence for an accelerating Universe [23], interpreted as due to a cosmological constant or a dark energy component. When combined with the CMB data (which indicate flatness, *i.e.*, $\Omega_\mathrm{m} + \Omega_\Lambda = 1$), the best-fit values were $\Omega_\mathrm{m} \approx 0.3$ and $\Omega_\Lambda \approx 0.7$. Most results in the literature are consistent with the $w = -1$ cosmological constant case. A recent study [24] deduced, from a sample of 740 spectroscopically-confirmed SNe Ia, that $\Omega_\mathrm{m} = 0.295 \pm 0.034$ (stat+sym) for an assumed flat ΛCDM model. This is consistent with the latest CMB measurements. Future experiments will aim to set constraints on the cosmic equation of state $w(z)$.

24.3.3. *Cosmic microwave background* :

The physics of the CMB is described in detail in the CMB chapter in this volume. Before recombination, the baryons and photons are tightly coupled, and the perturbations oscillate in the potential wells generated primarily by the dark matter perturbations. After decoupling, the baryons are free to collapse into those potential wells. The CMB carries a record of conditions at the time of last scattering, often called primary anisotropies. In addition, it is affected by various processes as it propagates towards us, including the effect of a time-varying gravitational potential (the integrated Sachs–Wolfe effect), gravitational lensing, and scattering from ionized gas at low redshift.

The primary anisotropies, the integrated Sachs–Wolfe effect, and the scattering from a homogeneous distribution of ionized gas, can all be calculated using linear perturbation theory. Available codes include CAMB and CLASS [9], the former widely used embedded within the analysis package CosmoMC [25] and in higher-level analysis packages such as CosmoSIS [26] and CosmoLike [27]. Gravitational lensing is also calculated in these codes. Secondary effects such as inhomogeneities in the reionization process, and scattering from gravitationally-collapsed gas (the Sunyaev–Zeldovich (SZ) effect), require more complicated, and more uncertain, calculations.

The upshot is that the detailed pattern of anisotropies depends on all of the cosmological parameters. In a typical cosmology, the anisotropy power spectrum [usually plotted as $\ell(\ell+1)C_\ell$] features a flat plateau at large angular scales (small ℓ), followed by a series of oscillatory features at higher angular scales, the first and most prominent being at around one degree ($\ell \simeq 200$). These features, known as acoustic peaks, represent the oscillations of the photon–baryon fluid around the time of decoupling. Some features can be closely related to specific parameters—for instance, the location in multipole space of the set of peaks probes the spatial geometry, while the relative heights of the peaks probe the baryon density—but many other parameters combine to determine the overall shape.

The 2015 data release from the *Planck* satellite [1] gives the most powerful results to date on the spectrum of CMB temperature anisotropies, with a precision determination of the temperature power spectrum to beyond $\ell = 2000$. The Atacama Cosmology Telescope (ACT) and South Pole Telescope (SPT) experiments extend these results to higher angular resolution, though without full-sky coverage. *Planck* and the *WMAP* satellite final (9-year) data release [3] give the state of the art in measuring the spectrum of E-polarization anisotropies and the correlation spectrum between temperature and polarization (those spectra having first been detected by DASI [28]) . These are consistent with models based on the parameters we have described, and provide accurate determinations of many of those parameters [2]. Primordial B-mode polarization has not been

detected (although the gravitational lensing effect on B-mode has been measured).

The data provide an exquisite measurement of the location of the set of acoustic peaks, determining the angular-diameter distance of the last-scattering surface. In combination with other data this strongly constrains the spatial geometry, in a manner consistent with spatial flatness and excluding significantly-curved Universes. CMB data give a precision measurement of the age of the Universe. The CMB also gives a baryon density consistent with, and at higher precision than, that coming from BBN. It affirms the need for both dark matter and dark energy. It shows no evidence for dynamics of the dark energy, being consistent with a pure cosmological constant ($w = -1$). The density perturbations are consistent with a power-law primordial spectrum, and there is no indication yet of tensor perturbations. The current best-fit for the reionization optical depth from CMB data, $\tau = 0.066$, is in line with models of how early structure formation induces reionization.

Planck has also made the first all-sky map of the CMB lensing field, which probes the entire matter distribution in the Universe and adds some additional constraining power to the CMB-only data-sets. ACT previously announced the first detection of gravitational lensing of the CMB from the four-point correlation of temperature variations [29]. These measurements agree with the expected effect in the standard cosmology.

24.3.4. *Galaxy clustering* :

The power spectrum of density perturbations depends on the nature of the dark matter. Within the ΛCDM model, the power spectrum shape depends primarily on the primordial power spectrum and on the combination $\Omega_{\rm m}h$, which determines the horizon scale at matter–radiation equality, with a subdominant dependence on the baryon density. The matter distribution is most easily probed by observing the galaxy distribution, but this must be done with care since the galaxies do not perfectly trace the dark matter distribution. Rather, they are a 'biased' tracer of the dark matter [30]. The need to allow for such bias is emphasized by the observation that different types of galaxies show bias with respect to each other. In particular, scale-dependent and stochastic biasing may introduce a systematic effect on the determination of cosmological parameters from redshift surveys [31]. Prior knowledge from simulations of galaxy formation or from gravitational lensing data could help to quantify biasing. Furthermore, the observed 3D galaxy distribution is in redshift space, *i.e.*, the observed redshift is the sum of the Hubble expansion and the line-of-sight peculiar velocity, leading to linear and non-linear dynamical effects that also depend on the cosmological parameters. On the largest length scales, the galaxies are expected to trace the location of the dark matter, except for a constant multiplier b to the power spectrum, known as the linear bias parameter. On scales smaller than 20 h^{-1} Mpc or so, the clustering pattern is 'squashed' in the radial direction due to coherent infall, which depends approximately on the parameter $\beta \equiv \Omega_{\rm m}^{0.6}/b$ (on these shorter scales, more complicated forms of biasing are not excluded by the data). On scales of a few h^{-1} Mpc, there is an effect of elongation along the line of sight (colloquially known as the 'finger of God' effect) that depends on the galaxy velocity dispersion.

24.3.4.1. *Baryonic acoustic oscillations:*

The power spectra of the 2-degree Field (2dF) Galaxy Redshift Survey and the Sloan Digital Sky Survey (SDSS) are well fit by a ΛCDM model and both surveys showed evidence for baryon acoustic oscillations (BAOs) [32,33]. The Baryon Oscillation Spectroscopic Survey (BOSS) of Luminous Red Galaxies (LRGs) in the SDSS found consistency with the dark energy equation of state $w = -1$ [34]. Similar results for w were obtained by the WiggleZ survey [35].

24.3.4.2. *Redshift distortion:*

There is renewed interest in the 'redshift distortion' effect. This distortion depends on cosmological parameters [36] via the perturbation growth rate in linear theory $f(z) = d\ln\delta/d\ln a \approx \Omega^{\gamma}(z)$, where $\gamma \simeq 0.55$ for the ΛCDM model and may be different for modified gravity models. By measuring $f(z)$ it is feasible to constrain γ and rule out certain modified gravity models [37,38]. We note the degeneracy of the redshift-distortion pattern and the geometric distortion (the so-called Alcock–Paczynski effect [39]), *e.g.*, as illustrated by the WiggleZ survey [40] and the BOSS Survey [41].

24.3.4.3. *Limits on neutrino mass from galaxy surveys and other probes:*

Large-scale structure data place constraints on Ω_ν due to the neutrino free-streaming effect [42]. Presently there is no clear detection, and upper limits on neutrino mass are commonly estimated by comparing the observed galaxy power spectrum with a four-component model of baryons, cold dark matter, a cosmological constant, and massive neutrinos. Such analyses also assume that the primordial power spectrum is adiabatic, scale-invariant, and Gaussian. Potential systematic effects include biasing of the galaxy distribution and non-linearities of the power spectrum. An upper limit can also be derived from CMB anisotropies alone, while combination with additional cosmological data-sets can improve the results.

The most recent results on neutrino mass upper limits and other neutrino properties are summarised in the Neutrinos in Cosmology chapter in this volume. While the latest cosmological data do not yet constrain the sum of neutrino masses to below 0.2 eV, since the lower limit on this sum from oscillation experiments is 0.06 eV it is expected that future cosmological surveys will soon detect effects from the neutrino mass. Also, current cosmological datasets are in good agreement with the standard value for the effective number of neutrino species $N_{\rm eff} = 3.045$.

24.3.5. *Clustering in the inter-galactic medium* :

It is commonly assumed, based on hydrodynamic simulations, that the neutral hydrogen in the inter-galactic medium (IGM) can be related to the underlying mass distribution. It is then possible to estimate the matter power spectrum on scales of a few megaparsecs from the absorption observed in quasar spectra, the so-called Lyman-α forest. The usual procedure is to measure the power spectrum of the transmitted flux, and then to infer the mass power spectrum. Photo-ionization heating by the ultraviolet background radiation and adiabatic cooling by the expansion of the Universe combine to give a simple power-law relation between the gas temperature and the baryon density. It also follows that there is a power-law relation between the optical depth τ and $\rho_{\rm b}$. Therefore, the observed flux $F = \exp(-\tau)$ is strongly correlated with $\rho_{\rm b}$, which itself traces the mass density. The matter and flux power spectra can be related by a biasing function that is calibrated from simulations. The BOSS survey has been used to detect and measure the BAO feature in the Lyman-α forest fluctuation at redshift $z = 2.4$, with a result impressively consistent with the standard ΛCDM model [43,44]. The Lyman-α flux power spectrum has also been used to constrain the nature of dark matter, for example constraining the amount of warm dark matter [45].

24.3.6. *Gravitational lensing* :

Images of background galaxies are distorted by the gravitational effect of mass variations along the line of sight. Deep gravitational potential wells such as galaxy clusters generate 'strong lensing', leading to arcs, arclets and multiple images, while more moderate perturbations give rise to 'weak lensing'. Weak lensing is now widely used to measure the mass power spectrum in selected regions of the sky (see Ref. 46 for reviews). As the signal is weak, the image of deformed galaxy shapes (the 'shear map') must be analyzed statistically to measure the power spectrum, higher moments, and cosmological parameters. There are various systematic effects in the interpretation of weak lensing, *e.g.*, due to atmospheric distortions during observations, the redshift distribution of the background galaxies, the intrinsic correlation of galaxy shapes, and non-linear modeling uncertainties.

24.3.7. *Other probes* :

Other probes that have been used to constrain cosmological parameters, but that are not presently competitive in terms of accuracy, are the integrated Sachs–Wolfe effect [47,48], the number density or composition of galaxy clusters [49], and galaxy peculiar velocities which probe the mass fluctuations in the local universe [50].

24.4. Bringing probes together

Although it contains two ingredients—dark matter and dark energy—which have not yet been verified by laboratory experiments, the ΛCDM model is almost universally accepted by cosmologists as the best description of the present data. The approximate values of some of the key parameters are $\Omega_b \approx 0.05$, $\Omega_c \approx 0.25$, $\Omega_\Lambda \approx 0.70$, and a Hubble constant $h \approx 0.70$. The spatial geometry is very close to flat (and usually assumed to be precisely flat), and the initial perturbations Gaussian, adiabatic, and nearly scale-invariant.

The most powerful data source is the CMB, which on its own supports all these main tenets. Values for some parameters, as given in Ref. 2, are reproduced in Table 24.1. These particular results presume a flat Universe. The constraints are somewhat strengthened by adding additional data-sets such as BAO and supernovae, as shown in the Table, though most of the constraining power resides in the CMB data. Similar constraints were previously obtained by the *WMAP* collaboration; the additional precision of *Planck* data versus *WMAP* is only really apparent when considering larger parameter sets.

Table 24.1: Parameter constraints reproduced from Ref. 2 (Table 4), with some additional rounding. Both columns assume the ΛCDM cosmology with a power-law initial spectrum, no tensors, spatial flatness, a cosmological constant as dark energy, and the sum of neutrino masses fixed to 0.06 eV. Above the line are the six parameter combinations actually fit to the data (θ_{MC} is a measure of the sound horizon at last scattering); those below the line are derived from these. The first column uses *Planck* primary CMB data, restricting polarization data to low multipoles as currently recommended by the *Planck* collaboration, plus the *Planck* measurement of CMB lensing. This column gives our present recommended values. The second column adds additional data and is included to show that the effect of its inclusion is modest; the extra data are the Hubble parameter, BAO measurements from the SDSS, BOSS, and 6dF surveys, and supernova constraints from the JLA analysis. The perturbation amplitude $\Delta^2_{\mathcal{R}}$ (denoted A_s in the original paper) is specified at the scale $0.05\,\mathrm{Mpc}^{-1}$. Uncertainties are shown at 68% confidence.

	Planck TT+lowP+lensing	*Planck* TT+lowP+lensing+ext
$\Omega_b h^2$	0.02226 ± 0.00023	0.02227 ± 0.00020
$\Omega_c h^2$	0.1186 ± 0.0020	0.1184 ± 0.0012
$100\,\theta_{MC}$	1.0410 ± 0.0005	1.0411 ± 0.0004
n_s	0.968 ± 0.006	0.968 ± 0.004
τ	0.066 ± 0.016	0.067 ± 0.013
$\ln(10^{10}\Delta^2_{\mathcal{R}})$	3.062 ± 0.029	3.064 ± 0.024
h	0.678 ± 0.009	0.679 ± 0.006
σ_8	0.815 ± 0.009	0.815 ± 0.009
Ω_m	0.308 ± 0.012	0.306 ± 0.007
Ω_Λ	0.692 ± 0.012	0.694 ± 0.007

If the assumption of spatial flatness is lifted, it turns out that the CMB on its own only weakly constrains the spatial curvature, due to a parameter degeneracy in the angular-diameter distance. However, inclusion of other data readily removes this. For example, adding the usual non-CMB data-sets, plus the assumption that the dark energy is a cosmological constant, yields a 68% confidence constraint on $\Omega_{tot} \equiv \sum \Omega_i + \Omega_\Lambda = 1.0002 \pm 0.0026$ [2]. Results of this type are normally taken as justifying the restriction to flat cosmologies.

One derived parameter that is very robust is the age of the Universe, since there is a useful coincidence that for a flat Universe the position of the first peak is strongly correlated with the age. The CMB data give 13.80 ± 0.04 Gyr (assuming flatness). This is in good agreement with the ages of the oldest globular clusters and with radioactive dating.

The baryon density Ω_b is now measured with high accuracy from CMB data alone, and is consistent with and much more precise than the determination from BBN. The value quoted in the Big Bang Nucleosynthesis chapter in this volume is $0.021 \leq \Omega_b h^2 \leq 0.024$ (95% confidence).

A somewhat smaller value of the optical depth, $\tau = 0.055 \pm 0.009$, has been found in more recent *Planck* collaboration analyses, as described in the CMB chapter in this volume. However these have not yet been propogated into simultaneous measurements of all the cosmological parameters.

While Ω_Λ is measured to be non-zero with very high confidence, there is no evidence of evolution of the dark energy density. As described in the Dark Energy chapter in this volume, from a compilation of CMB, SN and BAO measurements, assuming a flat universe, Ref. 52 found $w = -1.01 \pm 0.04$, consistent with the cosmological constant case $w = -1$. Allowing more complicated forms of dark energy weakens the limits.

The data provide strong support for the main predictions of the simplest inflation models: spatial flatness and adiabatic, Gaussian, nearly scale-invariant density perturbations. But it is disappointing that there is no sign of primordial gravitational waves, with an upper limit $r < 0.07$ at 95% confidence [53] (weakening if running is allowed). The spectral index is clearly required to be less than one by current data, though the strength of that conclusion can weaken if additional parameters are included in the model fits.

Tests have been made for various types of non-Gaussianity, a particular example being a parameter f_{NL} that measures a quadratic contribution to the perturbations. Various non-Gaussian shapes are possible (see Ref. 51 for details), and current constraints on the popular 'local', 'equilateral', and 'orthogonal' types combining temperature and polarization data are $f_{NL}^{local} = 1 \pm 5$, $f_{NL}^{equil} = -4 \pm 43$, and $f_{NL}^{ortho} = -26 \pm 21$ respectively (these look weak, but prominent non-Gaussianity requires the product $f_{NL}\Delta_{\mathcal{R}}$ to be large, and $\Delta_{\mathcal{R}}$ is of order 10^{-5}). Clearly none of these give any indication of primordial non-gaussianity.

While the above results come from the CMB alone, other probes are becoming competitive (especially when considering more complex cosmological models), and so combination of probes is of growing importance. We note that it has become fashionable to combine probes at the level of power-spectrum data vectors, taking into account nuisance parameters in each probe. Recent examples include KiDS+GAMA [54] and Dark Energy Survey (DES) Year 1 [55]. For example, the DES analysis includes galaxy position–position clustering, galaxy–galaxy lensing, and weak lensing shear. Discussions on 'tension' in resulting cosmological parameters depend on the statistical approaches used. Commonly the cosmology community works within the Bayesian framework, and assesses agreement amongst data sets with respect to a model via Bayesian Evidence, essentially the denominator in Bayes's theorem. As an example of results, combining DES Y1 with *Planck*, Baryonic Acoustic Oscillation measurements from SDSS, 6dF, and BOSS, and type Ia supernovae from the Joint Lightcurve Analysis (JLA) dataset has shown the datasets to be mutually compatible and yields very tight constraints on cosmological parameters: $S_8 \equiv \sigma_8(\Omega_m/0.3)^{0.5} = 0.799^{+0.014}_{-0.009}$, and $\Omega_m = 0.301^{+0.006}_{-0.008}$ in ΛCDM, and $w = -1.00^{+0.04}_{-0.05}$ in wCDM [55]. The combined measurement of the Hubble constant h within ΛCDM gives $h = 0.682 \pm 0.006$, still leaving some level of tension with the local measurements described earlier. Future analyses and the next generation of surveys will test for deviations from ΛCDM, for example epoch-dependent $w(z)$ and modifications to General Relativity.

24.5. Outlook for the future

The concordance model is now well established, and there seems little room left for any dramatic revision of this paradigm. A measure of the strength of that statement is how difficult it has proven to formulate convincing alternatives.

Should there indeed be no major revision of the current paradigm, we can expect future developments to take one of two directions.

Either the existing parameter set will continue to prove sufficient to explain the data, with the parameters subject to ever-tightening constraints, or it will become necessary to deploy new parameters. The latter outcome would be very much the more interesting, offering a route towards understanding new physical processes relevant to the cosmological evolution. There are many possibilities on offer for striking discoveries, for example:

- the cosmological effects of a neutrino mass may be unambiguously detected, shedding light on fundamental neutrino properties;
- detection of primordial non-Gaussianities would indicate that non-linear processes influence the perturbation generation mechanism;
- detection of variation in the dark-energy density (*i.e.*, $w \neq -1$) would provide much-needed experimental input into its nature.

These provide more than enough motivation for continued efforts to test the cosmological model and improve its accuracy. Over the coming years, there are a wide range of new observations that will bring further precision to cosmological studies. Indeed, there are far too many for us to be able to mention them all here, and so we will just highlight a few areas.

The CMB observations will improve in several directions. A current frontier is the study of polarization, for which power spectrum measurements have now been made by several experiments. Detection of primordial B-mode anisotropies is the next major goal and a variety of projects are targeting this, though theory gives little guidance as to the likely signal level.

An impressive array of comology surveys are already operational, under construction, or proposed, including the ground-based Dark Energy Survey (DES), Hyper Suprime Camera (HSC) and Large Synoptic Survey Telescope (LSST), imaging surveys, spectroscopic surveys such as the Dark Energy Spectroscopic Instrument (DESI), and space missions Euclid and the Wide-Field Infrared Survey (WFIRST).

An exciting area for the future is radio surveys of the redshifted 21-cm line of hydrogen. Because of the intrinsic narrowness of this line, by tuning the bandpass the emission from narrow redshift slices of the Universe will be measured to extremely high redshift, probing the details of the reionization process at redshifts up to perhaps 20, as well as measuring large scale features such as the BAOs. LOFAR is the first instrument able to do this and has begun its operations. In the longer term, the Square Kilometre Array (SKA) will take these studies to a precision level.

The development of the first precision cosmological model is a major achievement. However, it is important not to lose sight of the motivation for developing such a model, which is to understand the underlying physical processes at work governing the Universe's evolution. On that angle, progress has been much less dramatic. For instance, there are many proposals for the nature of the dark matter, but no consensus as to which is correct. The nature of the dark energy remains a mystery. Even the baryon density, now measured to an accuracy of a percent, lacks an underlying theory able to predict it within orders of magnitude. Precision cosmology may have arrived, but at present many key questions remain to motivate and challenge the cosmology community.

References:

1. Planck Collab. 2015 Results I, Astron. & Astrophys. **594**, A1 (2016).
2. Planck Collab. 2015 Results XIII, Astron. & Astrophys. **594**, A13 (2016).
3. C. Bennett *et al.*, Astrophys. J. Supp., **208**, 20 (2013).
4. G. Hinshaw *et al.*, Astrophys. J. Supp., **208**, 19 (2013).
5. S. Fukuda *et al.*, Phys. Rev. Lett. **85**, 3999 (2000); Q.R. Ahmad *et al.*, Phys. Rev. Lett. **87**, 071301 (2001).
6. E.W. Kolb and M.S. Turner, *The Early Universe*, Addison–Wesley (Redwood City, 1990).
7. D.H. Lyth and A.R. Liddle, *The Primordial Density Perturbation*, Cambridge University Press (2009).
8. A.R. Liddle and D.H. Lyth, Phys. Lett. **B291**, 391 (1992).
9. A. Lewis, A Challinor, and A. Lasenby, Astrophys. J. **538**, 473 (2000); D. Blas, J. Lesgourgues, and T. Tram, JCAP **1107**, 034 (2011).
10. D. Fixsen, Astrophys. J. **707**, 916 (2009).
11. M. Hobson et al. (eds). *Bayesian Methods in Cosmology*, Cambridge University Press (2009).
12. A. Kosowsky and M.S. Turner, Phys. Rev. **D52**, 1739 (1995).
13. K.A. Malik and D. Wands, Phys. Reports **475**, 1 (2009).
14. Planck Collab. 2013 Results XXV, Astron. & Astrophys. **571**, A25 (2014).
15. D.H. Lyth and D. Wands, Phys. Lett. **B524**, 5 (2002); K. Enqvist and M.S. Sloth, Nucl. Phys. **B626**, 395 (2002); T. Moroi and T. Takahashi, Phys. Lett. **B522**, 215 (2001).
16. P. F. de Salas and S. Pastor, JCAP **1607**, 051 (2016).
17. S. Riemer-Sørensen, D. Parkinson, and T.M. Davis, Publications of Astronmilcal Society of the Pacific **30**, e029 (2013).
18. J.K. Webb *et al.*, Phys. Rev. Lett. **107**, 191101 (2011); J.A. King *et al.*, MNRAS **422**, 3370 (2012); P. Molaro *et al.*, Astron. & Astrophys. **555**, 68 (2013).
19. Planck Collab. 2015 Results XVIII, Astron. & Astrophys. **594**, A18 (2016).
20. W.L. Freedman *et al.*, Astrophys. J. **553**, 47 (2001).
21. A.G. Riess *et al.*, Astrophys. J. **826**, 56 (2016).
22. B. Leibundgut, Ann. Rev. Astron. Astrophys. **39**, 67 (2001).
23. A.G. Riess *et al.*, Astron. J. **116**, 1009 (1998); P. Garnavich *et al.*, Astrophys. J. **509**, 74 (1998); S. Perlmutter *et al.*, Astrophys. J. **517**, 565 (1999).
24. M. Betoule *et al.*, Astron. & Astrophys., 568, 22 (2014).
25. A. Lewis and S. Bridle, Phys. Rev. **D66**, 103511 (2002).
26. J. Zuntz *et al.*, arXiv:1409.3409 (2014).
27. E. Krause and T. Eifler, MNRAS **470**, 2100 (2017).
28. J. Kovac *et al.*, Nature **420**, 772 (2002).
29. S. Das *et al.*, Phys. Rev. Lett. **107**, 021301 (2011).
30. N. Kaiser, Astrophys. J. **284**, L9 (1984).
31. A. Dekel and O. Lahav, Astrophys. J. **520**, 24 (1999).
32. D. Eisenstein *et al.*, Astrophys. J. **633**, 560 (2005).
33. S. Cole *et al.*, MNRAS **362**, 505 (2005).
34. L. Anderson *et al.*, MNRAS **441**, 24 (2014).
35. D. Parkinson *et al.*, Phys. Rev. **D86**, 103518 (2012).
36. N. Kaiser, MNRAS **227**, 1 (1987).
37. L. Guzzo *et al.*, Nature **451**, 541 (2008).
38. A. Nusser and M. Davis, Astrophys. J. **736**, 93 (2011).
39. C. Alcock and B. Paczynski, Nature **281**, 358 (1979).
40. C. Blake *et al.*, MNRAS **425**, 405 (2012).
41. H. Gil-Marín *et al.*, MNRAS **465**, 1757 (2017).
42. J. Lesgourgues and S. Pastor, Phys. Reports **429**, 307 (2006).
43. A. Slosar *et al.*, JCAP **1404**, 026 (2014).
44. T. Delubac *et al.*, Astron. & Astrophys. **574**, A59 (2015).
45. M. Viel *et al.*, Phys. Rev. **D88**, 043502 (2013).
46. A. Refregier, Ann. Rev. Astron. Astrophys. **41**, 645 (2003); R. Massey *et al.*, Nature **445**, 286 (2007); H. Hoekstra and B. Jain, Ann. Rev. Nucl. and Part. Sci. **58**, 99 (2008).
47. R.G. Crittenden and N. Turok, Phys. Rev. Lett. **75**, 2642 (1995).
48. Planck Collab. 2015 Results XIX, Astron. & Astrophys. **594**, A21 (2016).
49. Planck Collab. 2015 Results XX, Astron. & Astrophys. **594**, A24 (2016).
50. A. Dekel, Ann. Rev. Astron. Astrophys. **32**, 371 (1994).
51. Planck Collab. 2015 Results XVII, Astron. & Astrophys. **594**, A17 (2016).
52. S. Alam *et al.*, MNRAS **470**, 2617 (2017).
53. P. A. R. Ade *et al.*, Phys. Rev. Lett. **116**, 031302 (2016).
54. E. van Uitert *et al.*, arXiv:1706.05004 (2017).
55. DES Collab., arXiv:1708.01530 (2017).

25. Neutrinos in Cosmology

Written August 2017 by J. Lesgourgues (RWTH Aachen U.) and L. Verde (U. of Barcelona & ICREA).

25.1. Standard neutrino cosmology

Neutrino properties leave detectable imprints on cosmological observations that can then be used to constrain neutrino properties. This is a great example of the remarkable interconnection and interplay between nuclear physics, particle physics, astrophysics and cosmology (for general reviews see *e.g.*, [1,2,3,4]) . Present cosmological data are already providing constraints on neutrino properties not only complementary but also competitive with terrestrial experiments; for instance, upper bounds on the total neutrino mass have shrinked by a factor of about 10 in the past 15 years. Forthcoming cosmological data may soon provide key information, not obtainable in other ways like *e.g.*, a measurement of the absolute neutrino mass scale. This new section is motivated by this exciting prospect.

A relic neutrino background pervading the Universe (the Cosmic Neutrino background, CνB) is a generic prediction of the standard hot Big Bang model (see Big Bang Nucleosynthesis – Chap. 23 of this *Review*). While it has not yet been detected directly, it has been indirectly confirmed by the accurate agreement of predictions and observations of: *a)* the primordial abundance of light elements (see Big Bang Nucleosynthesis – Chap. 23) of this *Review*; *b)* the power spectrum of Cosmic Microwave Background (CMB) anisotropies (see Cosmic Microwave Background – Chap. 28 of this *Review*); and *c)* the large scale clustering of cosmological structures. Within the hot Big Bang model such good agreement would fail dramatically without a CνB with properties matching closely those predicted by the standard neutrino decoupling process (*i.e.*, involving only weak interactions).

We will illustrate below that cosmology is sensitive to the following neutrino properties: their density, related to the number of active (*i.e.*, left-handed, see Neutrino Mass, Mixing, and Oscillations - Chap. 14 of this *Review*) neutrino species, and their masses. At first order, cosmology is sensitive to the total neutrino mass, but is blind to the mixing angles and CP violation phase as discussed in Neutrino Mass, Mixing, and Oscillations (Chap. 14 of this *Review*). This makes cosmological constraints nicely complementary to measurements from terrestrial neutrino experiments.

The minimal cosmological model, ΛCDM, currently providing a good fit to most cosmological data sets (up to moderate tensions discussed in The Cosmological Parameters Chap. 24 of this *Review*), assumes that the only massless or light (sub-keV) relic particles since the Big Bang Nucleosynthesis (BBN) epoch are photons and active neutrinos. Extended models with light sterile neutrinos, light thermal axions or other light relics –sometimes referred to as "dark radiation"– would produce effects similar to, and potentially degenerate with, those of active neutrinos. Thus neutrino bounds are often discussed together with limits on such scenarios. In case of anomalies in cosmological data, it might not be obvious to discriminate between interpretation in terms of active neutrinos with non-standard decoupling, additional production mechanisms, non-standard interactions, etc., or in terms of some additional light particles. At the moment, such extensions are, however, not required by the cosmological data at any significant level.

Hence neutrino density and mass bounds can be derived under the assumption of no additional massless or light relic particles, and the neutrino density measured in that way provides a test of standard (*i.e.*, involving only weak interactions) neutrino decoupling.

In that model, the three active neutrino types thermalize in the early Universe, with a negligible leptonic asymmetry. Then they can be viewed as three propagating mass eigenstates sharing the same temperature and identical Fermi-Dirac distributions, thus with no visible effects of flavour oscillations. Neutrinos decouple gradually from the thermal plasma at temperatures $T \sim 2\,\mathrm{MeV}$. In the instantaneous neutrino decoupling limit, *i.e.*, assuming that neutrinos were fully decoupled at the time when electron-positrons annihilate and release entropy in the thermal bath, the neutrino-to-photon density ratio between the time of electron-positron annihilation and the non-relativistic transition of neutrinos would be given by

$$\frac{\rho_\nu}{\rho_\gamma} = \frac{7}{8} N_{\rm eff} \left(\frac{4}{11}\right)^{4/3} , \qquad (25.1)$$

with $N_{\rm eff} = 3$, and the last factor comes from the fourth power of the temperature ratio $T_\nu/T_\gamma = (4/11)^{1/3}$ (see Big Bang Cosmology – Chap. 21 in this *Review*). In the above formula, $N_{\rm eff}$ is called the effective number of neutrino species because it can be viewed as a convenient parametrisation of the relativistic energy density of the Universe beyond that of photons, in units of one neutrino in the instantaneous decoupling limit. Precise simulations of neutrino decoupling and electron-positron annihilation, taking into account flavor oscillations, provide precise predictions for the actual phase-space distribution of relic neutrinos [5,6,7,8]. These distributions differ from the instantaneous decoupling approximation through a combination of a small shift in the photon temperature and small non-thermal distortions, all at the percent level. The final result for the density ratio ρ_ν/ρ_γ in the relativistic regime can always be expressed as in Eq. (25.1), but with a different value of $N_{\rm eff}$. The most recent analysis, that includes the effect of neutrino oscillations with the present values of the mixing parameters and an improved calculation of the collision terms, gives $N_{\rm eff} = 3.045$ [8]. The precise number density ratio n_ν/n_γ can also be derived from such studies, and is important for computing the ratio $\Omega_\nu h^2/\sum_i m_i$ (ratio of the physical density of neutrinos in units of the critical density to the sum of neutrino masses) in the non-relativistic regime.

The neutrino temperature today, $T_\nu^0 \simeq 1.7 \times 10^{-4}$ eV $\simeq 1.9$ K, is smaller than at least two of the neutrino masses, since the two squared-mass differences are $|\Delta m^2_{31}|^{1/2} > |\Delta m^2_{21}|^{1/2} > T_\nu^0$ (see Neutrino mass, Mixing, and oscillations – Chap. 14 of this *Review*). Thus at least two neutrino mass eigenstates are non-relativistic today and behave as a small "hot" fraction of the total dark matter (they cannot be all the dark matter, as explained in Chap. 26 in this *Review*). This fraction of hot dark matter can be probed by cosmological experiments, for two related reasons, as we now describe.

First, neutrinos are the only known particles behaving as radiation at early times (during the CMB acoustic oscillations) and dark matter at late times (during structure formation), which has consequences on the background evolution. Neutrinos become non-relativistic when their mass is equal to their average momentum, given for any Fermi-Dirac-distributed particle by $\langle p \rangle = 3.15\,T$. Thus the redshift of the non-relativistic transition is given by $z_i^{\rm nr} = m_i/(3.15\,T_\nu^0) - 1 = m_i/[0.53\,\mathrm{meV}] - 1$ for each eigenstate of mass m_i, giving for instance $z_i^{\rm nr} = 110$ for $m_i = 60\,\mathrm{meV}$, corresponding to a time deep inside the matter-dominated regime. Second, until the non-relativistic transition, neutrinos travel at the speed of light, and later on they move at a typical velocity $\langle v_i/c \rangle = 3.15\,T_\nu(z)/m_i = 0.53(1+z)\,\mathrm{meV}/m_i$, which is several orders of magnitude larger than that of the dominant cold (or even of possibly warm) dark matter component(s). This brings their characteristic diffusion scale, called the "free-streaming length", to cosmological relevant values, with consequences on gravitational clustering and the growth of structure.

Once neutrinos are non-relativistic, their energy density is given by $\rho_\nu \simeq \sum m_i n_i$. Since the number densities n_i are equal to each other (up to negligible corrections coming from flavour effects in the decoupling phase), the total mass $(\sum m_\nu) = m_1 + m_2 + m_3$ can be factorized out. It is possible that the lightest neutrino is still relativistic today, in which case this relation is slightly incorrect, but given that the total density is always strongly dominated by that of non-relativistic neutrinos, the error made is completely negligible. Using the expression for n_i/n_γ obtained from precise neutrino decoupling studies, and knowing n_γ from the measurement of the CMB temperature, one can compute ρ_ν^0, the total neutrino density today, in units of the critical density $\rho_{\rm crit}^0$ [7]:

$$\Omega_\nu = \frac{\rho_\nu^0}{\rho_{\rm crit}^0} = \frac{\sum m_\nu}{93.14 h^2\,\mathrm{eV}} , \qquad (25.2)$$

and the total neutrino average number density today: $n_\nu^0 = 339.5\ \mathrm{cm}^{-3}$. Here h is the Hubble constant in units of 100 km s^{-1} Mpc^{-1}.

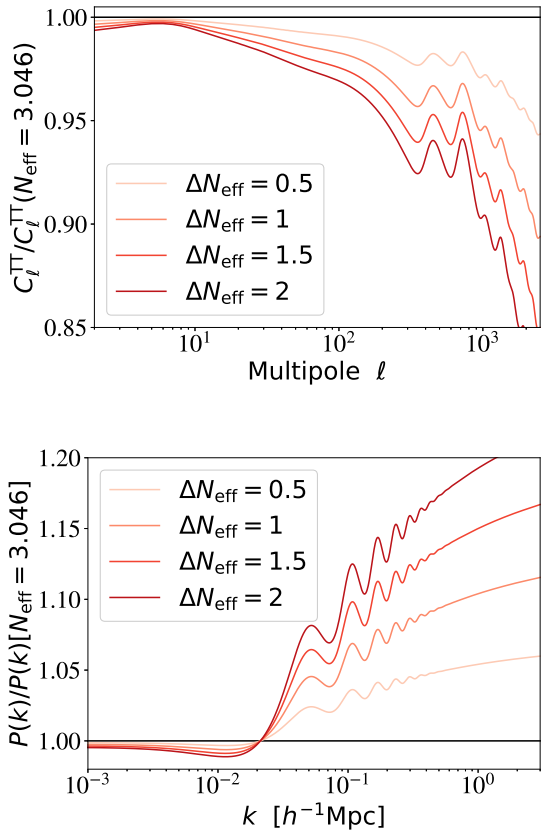

Figure 25.1: Ratio of the CMB C_ℓ^{TT} (left, including lensing effects) and matter power spectrum $P(k)$ (right, computed for each model in units of $(h^{-1}\mathrm{Mpc})^3$) for different values of $\Delta N_{\rm eff} \equiv N_{\rm eff} - 3.045$ over those of a reference model with $\Delta N_{\rm eff} = 0$. In order to minimize and better characterise the effect of $N_{\rm eff}$ on the CMB, the parameters that are kept fixed are $\{z_{\rm eq},\, z_\Lambda,\, \omega_{\rm b},\, \tau\}$ and the primordial spectrum parameters. Fixing $\{z_{\rm eq},\, z_\Lambda\}$ is equivalent to fixing the fractional density of total radiation, of total matter and of cosmological constant $\{\Omega_{\rm r}, \Omega_{\rm m}, \Omega_\Lambda\}$ while increasing the Hubble parameter as a function of $N_{\rm eff}$. The statistical errors on the C_ℓ are $\sim 1\%$ for a band power of $\Delta\ell = 30$ at $\ell \sim 1000$. The error on $P(k)$ is estimated to be of the order of 5%.

25.2. Effects of neutrino properties on cosmological observables

As long as they are relativistic, *i.e.*, until some time deep inside the matter-dominated regime for neutrinos with a mass $m_i \ll 3.15\, T_\nu^{\rm eq} \sim 1.5$ eV (see Big Bang Cosmology, Chap. 21 in this *Review*), neutrinos enhance the density of radiation: this effect is parameterised by $N_{\rm eff}$ and can be discussed separately from the effect of the mass that will be described later in this section. Increasing $N_{\rm eff}$ impacts the observable spectra of CMB anisotropies and matter fluctuations through background and perturbation effects.

25.2.1. ***Effect of $N_{\rm eff}$ on the CMB*** : The background effects depend on what is kept fixed when increasing $N_{\rm eff}$. If the densities of other species are kept fixed, a higher $N_{\rm eff}$ implies a smaller redshift of radiation-to-matter equality, with very strong effects on the CMB spectrum: when the amount of expansion between radiation-to-matter equality and photon decoupling is larger, the CMB peaks are suppressed. This effect is not truly characteristic of the neutrino density, since it can be produced by varying several other parameters. Hence, to characterise the effect of $N_{\rm eff}$, it is more useful and illuminating to enhance the density of total radiation, of total matter and of Λ by exactly the same amount, in order to keep the redshift of radiation-to-matter equality $z_{\rm eq}$ and matter-to-Λ equality z_Λ fixed [9,10,4]. The primordial spectrum parameters, the baryon density $\omega_{\rm b} \equiv \Omega_{\rm b} h^2$ and the optical depth to reionization τ can be kept fixed at the same time, since we can simply vary $N_{\rm eff}$ together with the Hubble parameter h with fixed $\{\omega_{\rm b},\, \Omega_{\rm c},\, \Omega_\Lambda\}$. The impact of such a transformation is shown in Fig. 25.1 for the CMB temperature spectrum C_ℓ^{TT} (defined in Chap. 28 in this *Review*) and for the matter power spectrum $P(k)$ (defined in Chap. 21 in this *Review*) for several representative values of $N_{\rm eff}$. These effects are within the reach of cosmological observations given current error bars, as discussed in Section 25.3 (for instance, with the *Planck* satellite data, the statistical error on the C_ℓ's is of the order of one per cent for a band power of $\Delta\ell = 30$ at $\ell \sim 1000$).

With this transformation, the main background effect of $N_{\rm eff}$ is an increase in the diffusion scale (or Silk damping scale, see Cosmic Microwave Background – Chap. 28 in this *Review*) at the time of decoupling, responsible for the decrease in C_ℓ^{TT} at high ℓ, plus smaller effects coming from a slight increase in the redshift of photon decoupling [4,9,10]. At the level of perturbations, a higher $N_{\rm eff}$ implies that photons feel gravitational forces from a denser neutrino component; this tends to decrease the acoustic peaks (because neutrinos are distributed in a smoother way than photons) and to shift them to larger scales / smaller multipoles (because photon perturbations traveling at the speed of sound in the photon-baryon fluid feel some dragging effect from neutrino perturbations travelling at the speed of light) [9,4,11]. The combination of these effects is truly characteristic of the radiation density parameter $N_{\rm eff}$ and cannot be mimicked by other parameters; thus $N_{\rm eff}$ can be accurately measured from the CMB alone. However, there are correlations between $N_{\rm eff}$ and other parameters. In particular, we have seen (Fig. 25.1) that in order to minimise the effect of $N_{\rm eff}$ on the CMB spectrum, one should vary h at the same time, hence there is a correlation between $N_{\rm eff}$ and h, which implies that independent measurements reducing the error bar on h also reduce that on $N_{\rm eff}$. Note that this correlation is not equivalent to a perfect degeneracy, so both parameters can anyway be constrained with CMB data alone.

25.2.2. ***Effect of $N_{\rm eff}$ on the matter spectrum*** : We have discussed the effect of increasing $N_{\rm eff}$ while keeping $z_{\rm eq}$ and $\omega_{\rm b}$ fixed, because the latter two quantities are very accurately constrained by CMB data. This implies that $\omega_{\rm c}$ increases with $N_{\rm eff}$, and that the ratio $\omega_{\rm b}/\omega_{\rm c} = \Omega_{\rm b}/\Omega_{\rm c}$ decreases. However, the ratio of baryonic-to-dark matter has a strong impact on the shape of the matter power spectrum, because until the time of decoupling of the baryons from the photons, CDM experiences gravitational collapse, while baryons are kept smoothly distributed by photon pressure and affected by acoustic oscillations. The decrease of $\Omega_{\rm b}/\Omega_{\rm c}$ following from the increase of $N_{\rm eff}$ gives more weight to the most clustered of the two components, namely the dark matter one, and produces an enhancement of the small-scale matter power spectrum and a damping of the amplitude of baryon acoustic oscillations (BAOs), clearly visible in Fig. 25.1 (right plot). The scale of BAOs is also slightly shifted.

The increase in the small-scale matter power spectrum is also responsible for a last effect on the CMB spectra : the CMB last scattering surface is slightly more affected by weak lensing from large-scale structures. This tends to smooth the maxima, the minima, and the damping scale of the CMB spectra [12].

25.2.3. ***Effect of neutrino masses on the CMB*** : Neutrino eigenstates with a mass $m_i \ll 0.57$ eV become non-relativistic after photon decoupling. They contribute to the non-relativistic matter budget today, but not at the time of equality or recombination. If we increase the neutrino mass while keeping fixed the density of baryons and dark matter ($\omega_{\rm b}$ and $\omega_{\rm c}$), the early cosmological evolution remains fixed and independent of the neutrino mass, until the time of the non-relativistic transition. Thus one might expect that the CMB temperature and polarisation power spectra are left invariant. This is not true for four reasons.

First, the neutrino density enhances the total non-relativistic density at late times, $\omega_{\rm m} = \omega_{\rm b} + \omega_{\rm c} + \omega_\nu$, where $\omega_\nu \equiv \Omega_\nu h^2$ is given as a function of the total mass $\sum m_\nu$ by Eq. (25.2). The late background evolution impacts the CMB spectrum through the relation between

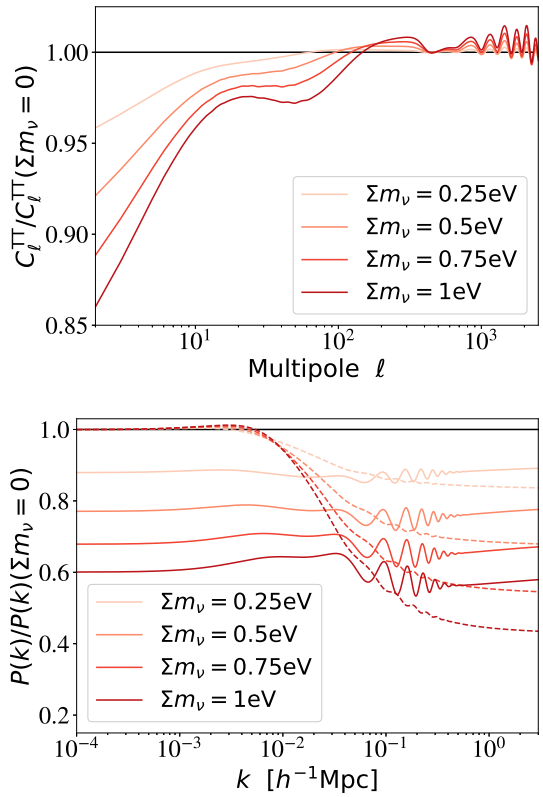

Figure 25.2: Ratio of the CMB C_ℓ^{TT} and matter power spectrum $P(k)$ (computed for each model in units of $(h^{-1}\mathrm{Mpc})^3$) for different values of $\sum m_\nu$ over those of a reference model with massless neutrinos. In order to minimize and better characterise the effect of $\sum m_\nu$ on the CMB, the parameters that are kept fixed are ω_b, ω_c, τ, the angular scale of the sound horizon θ_s and the primordial spectrum parameters (solid lines). This implies that we are increasing the Hubble parameter h as a function of $\sum m_\nu$. For the matter power spectrum, in order to single out the effect of neutrino free-streaming on $P(k)$, the dashed lines show the spectrum ratio when $\{\omega_\mathrm{m}, \omega_\mathrm{b}, \Omega_\Lambda\}$ are kept fixed. For comparison, the error on $P(k)$ is of the order of 5% with current observations, and the fractional C_ℓ errors are of the order of $1/\sqrt{\ell}$ at low ℓ.

scales on the last scattering surface and angles on the sky, and through the late ISW effect (see Cosmic Microwave Background – Chap. 28 of this *Review*). These two effects depend respectively on the angular diameter distance to recombination, $d_A(z_\mathrm{rec})$, and on the redshift of matter-to-Λ equality. Increasing $\sum m_\nu$ tends to modify these two quantities. By playing with h and Ω_Λ, it is possible to keep one of them fixed, but not both at the same time. Since the CMB measures the angular scale of acoustic oscillations with exquisite precision, and is only loosely sensitive to the late ISW effect due to cosmic variance, we choose in Fig. 25.2 to play with the Hubble parameter in order to maintain a fixed scale $d_A(z_\mathrm{rec})$. With such a choice, an increase in neutrino mass comes together with a decrease in the late ISW effect explaining the depletion of the CMB spectrum for $l \leq 20$. The fact that both $\sum m_\nu$ and h enter the expression of $d_A(z_\mathrm{rec})$ implies that measurements of the neutrino mass from CMB data are strongly correlated with h. Second, the non-relativistic transition of neutrinos affects the total pressure-to-density ratio of the universe, and causes a small variation of the metric fluctuations. If this transition takes place not too long after photon decoupling, this variation is observable through the early ISW effect [4,13,14]. It is responsible for the dip seen in Fig. 25.2 for $20 \leq \ell \leq 200$. Third, when the neutrino mass is higher, the CMB spectrum is less affected by the weak lensing effect induced by the large-scale structure at small redshift. This is due to a decrease in the matter power spectrum described in the next paragraphs. This reduced lensing effect is responsible for most of the oscillatory patterns visible in Fig. 25.2 (left plot) for $\ell \geq 200$. Fourth, the neutrinos with the smallest momenta start to be non-relativistic earlier than the average ones. The photon perturbations feel this through their gravitational coupling with neutrinos. This leads to a small enhancement of C_l^{TT} for $\ell \geq 500$, hardly visible on Fig. 25.2 because it is balanced by the lensing effect.

25.2.4. ***Effect of neutrino masses on the matter spectrum*** : The physical effect of neutrinos on the matter power spectrum is related to their velocity dispersion. Neutrinos free-stream over large distances without falling into small potential wells. The free-streaming scale is roughly defined as the distance travel by neutrinos over a Hubble time scale $t_\mathrm{H} = (a/\dot{a})$, and approximates the scale below which neutrinos remain very smooth. On larger scales, they cluster in the same way as cold dark matter. The power spectrum of total matter fluctuations, related to the squared fluctuation δ_m^2 with $\delta_\mathrm{m} \equiv \delta_\mathrm{b} + \delta_\mathrm{c} + \delta_\nu$, gets a negligible contribution from the neutrino component on small scales, and is reduced by a factor $(1 - 2f_\nu)$, where $f_\nu = \omega_\nu/\omega_\mathrm{m}$. Additionally, on scales below the free-streaming scale, the growth of ordinary cold dark matter and baryon fluctuations is modified by the fact that neutrinos contribute to the background density, but not to the density fluctuations. This changes the balance between the gravitational forces responsible for clustering, and the Hubble friction term slowing it down. Thus the growth rate of CDM and baryon fluctuations is reduced [15]. This results today in an additional suppression of the small-scale linear matter power spectrum by approximately $(1 - 6f_\nu)$. These two effects sum up to a factor $(1 - 8f_\nu)$ [16] (more precise approximations can be found in [2,4]). The non-linear spectrum is even more suppressed on mildly non-linear scales [17,18,19,20,21,3].

This effect is often illustrated by plots of the matter power spectrum ratio with fixed parameters $\{\omega_\mathrm{m}, \omega_\mathrm{b}, \Omega_\Lambda\}$ and varying f_ν, *i.e.*, with the CDM density adjusted to get a fixed total dark matter density [2,4,16](see Fig. 25.2, right plot, dashed lines). This transformation does not leave the redshift of equality z_eq invariant, and has very large effects on the CMB spectra. If one follows the logic of minimizing CMB variations and fixing z_eq like in the previous paragraphs, the increase in $\sum m_\nu$ must take place together with an increase of h, which tends to suppress the large-scale power spectrum, by approximately the same amount as the neutrino free-streaming effect [22]. In that case, the impact of neutrino masses on the matter power spectrum appears as an overall amplitude suppression, which can be seen in Fig. 25.2 (right plot, solid lines). The oscillations on intermediate wavenumbers come from a small shift in the BAO scale [22]. This global effect is not degenerate with a variation of the primordial spectrum amplitude A_s, because it only affects the matter power spectrum, and not the CMB spectra. However, the amplitude of the CMB temperature and polarization spectrum is given by the combination $A_\mathrm{s}e^{-2\tau}$. Hence a measurement of τ is necessary in order to fix A_s from CMB data, and avoid a parameter degeneracy between $\sum m_\nu$ and A_s [22,23,24].

A few of the neutrino mass effects described above–free-streaming scale, early ISW– depend on individual masses m_i, but most of them depend only on the total mass through f_ν –suppression of the matter power spectrum, CMB lensing, shift in angular diameter distance–. Because the latter effects are easier to measure, cosmology is primarily sensitive to the total mass $\sum m_\nu$ [25,26]. The possibility that future data sets might be able to measure individual masses or the mass hierarchy, despite systematic errors and parameter degeneracies, has recently become a subject of investigation [27,28].

25.3. Cosmological Constraints on neutrino properties

In this review we focus on cosmological constraints on the abundance and mass of ordinary active neutrinos. Several stringent but model-dependent constraints on non-standard neutrinos (*e.g.*, sterile neutrinos, active neutrinos with interactions beyond the weak force, unstable neutrinos with invisible decay, etc.) can also be found in the literature.

25.3.1. ***Neutrino abundance*** :

Table 25.1 shows a list of constraints on $N_{\rm eff}$ obtained with several combination of data sets. 'Pl15' denotes the *Planck* 2015 data, composed of a high-ℓ temperature likelihood (TT), low-ℓ temperature+polarization likelihood (lowP) and CMB lensing spectrum likelihood (lensing) based on lensing extraction from quadratic estimators [29]. 'BAO' refers to measurements of the BAO scale (and hence of the angular diameter distance) from various recent data sets, described in detail in the references given in the table. 'JLA' refers to the supernovae luminosity distance measurements [30]. 'HST' refers to the direct measurement of the Hubble scale from cepheids and supernovae [31].

Within the framework of a 7-parameter cosmological model (ΛCDM+$N_{\rm eff}$), the most conservative constraint on $N_{\rm eff}$ comes from the *Planck* 2015 data release with robust temperature and large-angle polarization information: $N_{\rm eff} = 3.13 \pm 0.32$ (68%CL). This number is perfectly compatible with the prediction of the standard neutrino decoupling model, $N_{\rm eff} = 3.045$, and can be viewed as a proof of self-consistency of the cosmological model.

The bounds can be tightened by adding more CMB polarization data, but the *Planck* Collaboration warns that there might be some unremoved systematics in the full TT,TE,EE likelihood; or, more conservatively, by adding information on the low-redshift background expansion from BAOs, supernovae or direct H_0 measurements. Finally, one can also add information on large scale structure (LSS), *i.e.*, on the growth rate and clustering amplitude of matter as a function of scale. However, LSS data are not very constraining for the $N_{\rm eff}$ parameter, and the only LSS data included in Table 25.1 is the measurement of the CMB lensing spectrum.

Combinations of *Planck* 2015 data with BAO, supernovae or CMB lensing constraints, all return measurements consistent with the standard expectation.

The situation is different with the inclusion of the direct measurement of H_0 heavily relying on the *Hubble Space Telescope* (HST) data, [31], known to be in tension with *Planck* in the ΛCDM framework. As explained in Section 25.2, the positive correlation between $N_{\rm eff}$ and h means that inclusion of the H_0 measurement pushes $N_{\rm eff}$ to higher values, $N_{\rm eff} = 3.41 \pm 0.22$ (68%CL, Pl15[TT+lowP+lensing] + BAO + JLA + HST), but still compatible with the standard expectation at the 1.7σ level. It remains to be seen whether the 3.2σ tension between CMB data and direct measurements of H_0 results from systematics, or from a departure from the ΛCDM model [33].

The error bars on $N_{\rm eff}$ degrade when the data are analysed in the context of more extended cosmological scenarios. Adding the neutrino mass as an 8th free parameter, the Pl15[TT+lowP+lensing]+BAO data set of Ref. [29] returns $N_{\rm eff} = 3.2 \pm 0.5$ instead of 3.07 ± 0.23 (68%CL). The authors of Ref. [34] take an extreme point of view and fit a 12-parameter model to Pl15[TT,TE,EE+lowP+lensing] data; they obtain $N_{\rm eff} = 2.93^{+0.51}_{-0.48}$ (95%CL), showing that it is very difficult with current cosmological data to accommodate shifts of more than 0.5 from the standard $N_{\rm eff}$ value, and to obtain good fits with, for instance, a fourth (sterile) thermalized neutrino. This is interesting since the anomalies in some oscillation data could be interpreted as evidence for at least one sterile neutrino with a large mixing angle, which would need to be thermalised unless non-standard interactions come into play [36]. In other words cosmology disfavours the explanation of the oscillations anomalies in terms of 1 or more extra neutrinos if they are thermalized.

25.3.2. ***Are they really neutrinos, as expected?*** : While a value of $N_{\rm eff}$ significantly different from zero (at more than 10σ) and consistent with the expected number 3.045 yields a powerful indirect confirmation of the CνB, departures from standard $N_{\rm eff}$ could be caused by any ingredient affecting the early-time expansion rate of the Universe. Extra relativistic particles (either decoupled, self-interacting, or interacting with a dark sector), a background of gravitational waves, an oscillating scalar field with quartic potential, departures from Einstein gravity, or large extra dimensions are some of the possibilities for such ingredients. In principle one could even assume that the cosmic neutrino background never existed or has decayed (like in the "neutrinoless universe" model of [37]) while another dark radiation component is responsible for $N_{\rm eff}$. At least, cosmological data allow to narrow the range of possible interpretations of $N_{\rm eff} \simeq 3$ to the presence of decoupled relativistic relics like standard neutrinos. Indeed, free-streaming particles leave specific signatures, especially in the CMB, because their density and pressure perturbations, bulk velocities and anisotropic stress also source the metric perturbations. These signatures can be tested in several ways.

Table 25.1: Summary of $N_{\rm eff}$ constraints.

	Model	68%CL	Ref.
CMB alone			
Pl15[TT+lowP]	ΛCDM+$N_{\rm eff}$	3.13 ± 0.32	[29]
Pl15[TT+lowP]	ΛCDM+$N_{\rm eff}$+$\sum m_\nu$	3.08 ± 0.31	[35]
CMB + probes of background evolution			
Pl15[TT+lowP] + BAO	ΛCDM+$N_{\rm eff}$	3.15 ± 0.23	[29]
Pl15[TT+lowP] + BAO	ΛCDM+$N_{\rm eff}$+$\sum m_\nu$	$3.18^{+0.24}_{-0.27}$	[35]
CMB + probes of background evolution + LSS			
Pl15[TT+lowP+lensing] + BAO	ΛCDM+$N_{\rm eff}$	$3.08^{+0.22}_{-0.24}$	[35]
" + BAO + JLA + HST	ΛCDM+$N_{\rm eff}$	3.41 ± 0.22	[31]
" + BAO	ΛCDM+$N_{\rm eff}$+$\sum m_\nu$	3.2 ± 0.5	[29]
Pl15[TT,TE,EE+lowP+lensing]	ΛCDM+$N_{\rm eff}$+5-params.	$2.93^{+0.51}_{-0.48}$	[34]

A first approach consists of introducing a self-interaction term in the neutrino equations. Refs [38,39] find that the Pl15+BAO data are compatible with no self-interactions. The upper limits to the effective coupling constant $G_{\rm eff}$ for a Fermi-like four-fermions interaction at 95% confidence is $\log_{10}(G_{\rm eff}{\rm MeV}^2) < -3.5(-2.7)$ for Planck CMB temperature data only [38](+BAO [39]) .

A second approach consists of introducing two phenomenological parameters, $c_{\rm eff}$ and $c_{\rm vis}$ (see *e.g.*, [40,41,42]): $c^2_{\rm eff}$ generalizes the linear relation between isotropic pressure perturbations and density perturbations, while $c^2_{\rm vis}$ modifies the neutrino anisotropic stress equation. While relativistic free-streaming species have $(c^2_{\rm eff}, c^2_{\rm vis}) = (1/3, 1/3)$, a perfect relativistic fluid would have $(c^2_{\rm eff}, c^2_{\rm vis}) = (1/3, 0)$. Other values do not necessarily refer to a concrete model, but make it possible to interpolate between these limits. The latest *Planck* data strongly suggests $(c^2_{\rm eff}, c^2_{\rm vis}) = (1/3, 1/3)$ [43,29]. Finally, Ref. [11] shows that *Planck* data are precise enough to detect the "neutrino drag" effect mentioned in Sec. 25.2, caused by gravitational interactions between neutrino and photon perturbations, and shifting the CMB peaks towards larger angular scales. These findings show that current cosmological data are able to detect not just the average density of some relativistic relics, but also their anisotropies.

25.3.3. ***Neutrino masses*** :

Table 25.2 shows a list of constraints on $\sum m_\nu$ obtained with several combinations of data sets. The acronyms "Pl15", "BAO", "JLA", and "HST" have been described in the previous subsection. "Pl16" refers to Planck intermediate results from 2016 in which the high-ℓ and lensing likelihood are identical to the 2015 version, but the low-ℓ temperature+polarization likelihood based on the Low Frequency Instrument (lowP) data is replaced by a newer version based on the High Frequency Instrument (SimLow) [32]. There "P(k)" refers to the several measurements of the matter power spectrum shape (and hence of the growth rate and of the clustering amplitude as function of scale) for "WZ", by the WiggleZ survey [44], for "DR7", from the Data Release 7 of the Sloan Digital Sky Survey [45], and for "DR12", from the Data Release 12 of the Baryon Oscillation Spectroscopic Survey (BOSS) [46,47]. "Lyα" refers to the BOSS measurement of the Lyman-α flux power spectrum in quasar spectra [48].

Given that most determinations of $N_{\rm eff}$ are compatible with the standard prediction, $N_{\rm eff} = 3.045$, it is reasonable to adopt this value as a theoretical prior and to investigate neutrino mass constraints in

Table 25.2: Summary of $\sum m_\nu$ constraints.

	Model	95% CL (eV)	Ref.
CMB alone			
Pl15[TT+lowP]	ΛCDM+$\sum m_\nu$	< 0.72	[29]
Pl15[TT+lowP]	ΛCDM+$\sum m_\nu$+$N_{\rm eff}$	< 0.73	[35]
Pl16[TT+SimLow]	ΛCDM+$\sum m_\nu$	< 0.59	[32]
CMB + probes of background evolution			
Pl15[TT+lowP] + BAO	ΛCDM+$\sum m_\nu$	< 0.21	[29]
Pl15[TT+lowP] + JLA	ΛCDM+$\sum m_\nu$	< 0.33	[35]
Pl15[TT+lowP] + BAO	ΛCDM+$\sum m_\nu$+$N_{\rm eff}$	< 0.27	[35]
CMB + probes of background evolution + LSS			
Pl15[TT+lowP+lensing]	ΛCDM+$\sum m_\nu$	< 0.68	[29]
Pl15[TT+lowP+lensing] + BAO	ΛCDM+$\sum m_\nu$	< 0.25	[35]
Pl15[TT+lowP] + P(k)$_{\rm DR12}$	ΛCDM+$\sum m_\nu$	< 0.30	[50]
Pl15[TT,TE,EE+lowP] + BAO+ P(k)$_{\rm WZ}$	ΛCDM+$\sum m_\nu$	< 0.14	[52]
Pl15[TT,TE,EE+lowP] + BAO+ P(k)$_{\rm DR7}$	ΛCDM+$\sum m_\nu$	< 0.13	[52]
Pl15[TT+lowP+lensing] + Lyα	ΛCDM+$\sum m_\nu$	< 0.12	[48]
Pl16[TT+SimLow+lensing] + BAO	ΛCDM+$\sum m_\nu$	< 0.17	[48]
Pl15[TT+lowP+lensing] + BAO	ΛCDM+$\sum m_\nu$+Ω_k	< 0.37	[35]
Pl15[TT+lowP+lensing] + BAO	ΛCDM+$\sum m_\nu$+w	< 0.37	[35]
Pl15[TT+lowP+lensing] + BAO	ΛCDM+$\sum m_\nu$+$N_{\rm eff}$	< 0.32	[29]
Pl15[TT,TE,EE+lowP+lensing]	ΛCDM+$\sum m_\nu$+5-params.	< 0.66	[34]

the context of a minimal 7-parameter model, ΛCDM+$\sum m_\nu$. Under this assumption, the most robust constraints come from *Planck* temperature data and large-angle polarization information: $\sum m_\nu < 0.72\,$eV (95%CL) using the 2015 low-ℓ polarization likelihood [29], or $\sum m_\nu < 0.59\,$eV (95%CL) using the one from 2016 [32] (see also Ref. [49]). The high-ℓ polarization likelihood from *Planck* 2015, which should be used with caution, pushes the bound to $\sum m_\nu < 0.34\,$eV (95%CL). Among the four effects of neutrino masses on the CMB spectra described before, current bounds are dominated by the first and the third effects (modified late background evolution, and distorsions of the temperature and polarisation spectra through weak lensing).

Adding data on BAO scales is crucial, since the measurement of the angular diameter distance at small redshift allows us to break parameter degeneracies, for instance between $\sum m_\nu$ and h. Combined with conservative Planck 2015 data, BAO experiments give $\sum m_\nu < 0.21\,$eV (95%CL). Supernovae data are less constraining than BAO data for the neutrino mass determination. Because the parameter correlation between $\sum m_\nu$ and H_0 is negative, the inclusion of HST data provides stronger bounds on neutrinos masses, down to $\sum m_\nu < 0.11$ eV (95% CL) when including LSS [52], but such bounds are subject to caution, since they come from a combination of slightly discrepant data sets (at the 3.2σ level).

It is interesting to add LSS data sets, sensitive to the small-scale suppression of the matter power spectrum due to neutrino free-streaming. The inclusion of the *Planck* 2015 CMB lensing likelihood is not very constraining. Overall, adding CMB lensing to conservative *Planck* 2015 data gives stronger bounds, but only marginally (from $\sum m_\nu < 0.72\,$eV to $\sum m_\nu < 0.68\,$eV at 95%CL). The inclusion of several matter power spectrum determinations, listed in Table 25.2, also provides rather marginal improvements: the constraint $\sum m_\nu < 0.17\,$eV (95%CL) from Pl15[TT,TE,EE+lowP]+BAO is only pushed down to 0.14 eV (0.13 eV, 0.16 eV) when adding matter power spectrum data from WiggleZ (blue galaxies) [50](SDSS-DR7 [52], BOSS-DR12 [52], red galaxies). The Lyman-α power spectrum data from BOSS are more constraining, since this leads to $\sum m_\nu < 0.12\,$eV (95% CL) in the absence of BAO or high-ℓ polarization data, but only with Pl15[TT+lowP+lensing] [48]. However, it is often stressed that the bounds coming from Lyman-α data involve more modelling of non-linear effects that the other techniques presented in this summary.

Upper bounds on neutrino masses become weaker when the data are analysed in the context of extended cosmological models, but not considerably weaker. For instance, one can see in Table 25.2 that bounds from Pl15[TT+lowP+lensing] + BAO tend to degrade from 0.25 eV to 0.37 eV (95% CL) when introducing an 8th free parameter accounting for spatial curvature or dynamical dark energy. In the extreme case considered by Ref. [34], with 12 free cosmological parameters, the bound from Pl15[TT,TE,EE+lowP+lensing] increases from 0.59 eV to 0.66 eV (95% CL). This shows that current cosmological data are precise enough to disentangle the effect of several extended cosmological parameters, and that neutrino mass bounds are becoming increasingly robust.

25.4. Future prospects and outlook

The cosmic neutrino background has been detected indirectly at very high statistical significance. Direct detection experiments are now being planned, *e.g.*, at the Princeton Tritium Observatory for Light, Early-universe, Massive-neutrino Yield (PTOLEMY) [53]. The detection prospects crucially depend on the exact value of neutrino masses and on the enhancement of their density at the location of the Earth through gravitational clustering in the Milky Way and its sub-halos – an effect however expected to be small [54,55,56].

Over the past few years the upper limit on the sum of neutrino masses has become increasingly stringent, first indicating that the mass ordering is hierarchical and recently putting the inverted hierarchy under pressure and favouring the normal hierarchy (although quantitative estimates of how disfavoured the inverted hierarchy is vary depending on assumptions, see *e.g.* [57,58]) which has consequences for planning future double beta decay experiments.

Neutrino mass and density bounds are expected to keep improving significantly over the next years, thanks to new LSS experiments like DES [59], Euclid [60], LSST [61], and SKA [62], or possible new CMB experiments like CMB-S4 [63], Pixie [65], CMBPol or CORE [64]. If the ΛCDM model is confirmed, and if neutrinos have standard properties, the total neutrino mass should be detected at the level of at least 3–4σ even at the minimum level allowed by oscillations. This is the conclusion reached by several independent studies, using different dataset combinations (see *e.g.*, [66,67,68,69,70,71]). One should note that at the minimum level allowed by oscillations $\sum m_\nu \sim 0.06$, neutrinos constitute $\sim 0.5\%$ of the Universe matter density, and

their effects on the matter power spectrum is only at the 5% level, implying that exquisite control of systematic errors will be crucial to achieve the required accuracy. At this level, the information coming from the power spectrum shape is more powerful than that coming from geometrical measurements (e.g., BAO). But exploiting the shape information requires improved understanding of the non-linear regime, and of galaxy bias for galaxy surveys. The fact that different surveys and different data set combinations have enough statistical power to reach this level, offers a much needed redundancy and the possibility to perform consistency checks which in turns helps immensely with the control of systematic errors and in making the measurement robust. Using the entire Universe as a particle detector, the on-going and future observational efforts hold the exciting prospect to provide a measurement of the sum of neutrino masses and possibly indication of their mass hierarchy.

References:

1. A. D. Dolgov, Phys. Reports **370**, 333 (2002).
2. J. Lesgourgues and S. Pastor, Phys. Reports **429**, 307 (2006).
3. S. Hannestad, Prog. in Part. Nucl. Phys. **65**, 185 (2010).
4. J. Lesgourgues *et al.*, *Neutrino cosmology* (Cambridge University Press, 2013).
5. J. Birrell, C.-T. Yang, and J. Rafelski, Nucl. Phys. **B890**, 481 (2014).
6. G. Mangano *et al.*, Nucl. Phys. **B729**, 221 (2005).
7. E. Grohs *et al.*, Phys. Rev. **D93**, 083522 (2016).
8. P. F. de Salas and S. Pastor, JCAP **1607**, 051 (2016).
9. S. Bashinsky and U. Seljak, Phys. Rev. **D69**, 083002 (2004).
10. Z. Hou *et al.*, Phys. Rev. **D87**, 083008 (2013).
11. B. Follin *et al.*, Phys. Rev. Lett. **115**, 091301 (2015).
12. A. Lewis and A. Challinor, Phys. Reports **429**, 1 (2006).
13. J. Lesgourgues and S. Pastor, Adv. High Energy Phys. **2012**, 608515 (2012).
14. Z. Hou *et al.*, Astrophys. J. **782**, 74 (2014).
15. J. R. Bond, G. Efstathiou and J. Silk, Phys. Rev. Lett. **45**, 1980 (1980).
16. W. Hu, D. J. Eisenstein and M. Tegmark, Phys. Rev. Lett. **80**, 5255 (1998).
17. S. Bird, M. Viel and M. G. Haehnelt, Mon. Not. R. Astron. Soc **420**, 2551 (2012).
18. C. Wagner, L. Verde and R. Jimenez, Astrophys. J. **752**, L31 (2012).
19. E. Castorina *et al.*, JCAP **1507**, 042 (2015).
20. J. Brandbyge and S. Hannestad, JCAP **1710**, 015 (2017).
21. J. Adamek, R. Durrer and M. Kunz, JCAP **1711**, 004 (2017).
22. M. Archidiacono *et al.*, JCAP **1702**, 052 (2017).
23. A. Liu *et al.*, Phys. Rev. **D93**, 043013 (2016).
24. R. Allison *et al.*, Phys. Rev. **D92**, 123535 (2015).
25. J. Lesgourgues, S. Pastor and L. Perotto, Phys. Rev. **D70**, 045016 (2004).
26. A. Slosar, Phys. Rev. **D73**, 123501 (2006).
27. R. Jimenez *et al.*, JCAP **1005**, 035 (2010).
28. R. Jimenez, C. Pena-Garay and L. Verde, Phys. Dark Univ. **15**, 31 (2017).
29. P. A. R. Ade *et al.*, [Planck Collaboration], Astron. & Astrophys. **594**, A13 (2016).
30. M. Betoule *et al.*, [SDSS Collaboration], Astron. & Astrophys. **568**, A22 (2014).
31. A. G. Riess *et al.*, Astrophys. J. **826**, 56 (2016).
32. N. Aghanim *et al.*, [Planck Collaboration], Astron. & Astrophys. **596**, A107 (2016).
33. J. L. Bernal, L. Verde and A. G. Riess, JCAP **1610**, 019 (2016).
34. E. Di Valentino, A. Melchiorri and J. Silk, Phys. Rev. **D92**, 12,1302 (2015).
35. Planck 2015 explanatory supplement, `wiki.cosmos.esa.int/planckpla2015/`, "Mission Products: Cosmological parameters: Parameter Tables".
36. M. Archidiacono *et al.*, JCAP **1608**, 067 (2016).
37. J. F. Beacom, N. F. Bell and S. Dodelson, Phys. Rev. Lett. **93**, 121302 (2004).
38. L. Lancaster *et al.*, JCAP **1707**, 033 (2017).
39. I. M. Oldengott *et al.*, JCAP **1711**, 027 (2017).
40. W. Hu, Astrophys. J. **506**, 485 (1998).
41. W. Hu *et al.*, Phys. Rev. **D59**, 023512 (1999).
42. M. Gerbino, E. Di Valentino and N. Said, Phys. Rev. **D88**, 063538 (2013).
43. B. Audren *et al.*, JCAP **1503**, 036 (2015).
44. S. Riemer-Sorensen, D. Parkinson and T. M. Davis, Phys. Rev. D 89,103505(2014).
45. B. A. Reid *et al.*, Mon. Not. R. Astron. Soc **404**, 60 (2010).
46. S. Alam *et al.*, [BOSS Collaboration], Mon. Not. R. Astron. Soc **470**, 2617 (2017).
47. H. Gil-Marín *et al.*, Mon. Not. R. Astron. Soc **460**, 4188 (2016).
48. N. Palanque-Delabrouille *et al.*, JCAP **1511**, 011 (2015).
49. F. Capozzi *et al.*, Phys. Rev. D 95,096014(2017).
50. S. Vagnozzi *et al.*, Phys. Rev. **D96**, 123503 (2017).
51. C. Yeche *et al.*, JCAP **1706**, 047 (2017).
52. A. J. Cuesta, V. Niro and L. Verde, Phys. Dark Univ. **13**, 77 (2016).
53. S. Betts *et al.*, `arXiv:1307.4738 [astro-ph.IM]`..
54. A. Ringwald and Y. Y. Y. Wong, JCAP **0412**, 005 (2004).
55. F. Villaescusa-Navarro *et al.*, JCAP **03**, 019 (2013).
56. P. F. de Salas *et al.*, JCAP **1709**, 034 (2017).
57. F. Simpson *et al.*, JCAP **06**, 029 (2017).
58. S. Hannestadt, T. Schwetz, JCAP **1611**, 035 (2016).
59. Dark Energy Survey Collaboration *et al.*, Mon. Not. R. Astron. Soc **460**, 1270 (2016).
60. R. Laureijs *et al.*, (2011) `arXiv:1110.3193`.
61. Paul A. Abell *et al.*; LSST Science and LSST Project Collaborations, `lss.fnal.gov/archive/test-tm/2000/fermilab-tm-2495-a.pdf`, (2009) `arXiv:0912.0201`.
62. `http://www.skatelescope.org`.
63. K. Abajiazan *et al.*, 2016, `arXiv:1610.02743`.
64. J. Delabrouille *et al.*, JCAP **1804**, 014 (2018).
65. A. Kogut, JCAP **1107**, 025 (2011).
66. C. Carbone *et al.*, JCAP **1103**, 030 (2011).
67. J. Hamann, S. Hannestad, Y. Wong, JCAP **1211**, 052 (2012).
68. B. Audren *et al.*, JCAP **1301**, 026 (2013).
69. R. Pearson, O. Zhan, Phys. Rev. **D89**, 043516 (2014).
70. R. Alison *et al.*, Phys. Rev. **D92**, 123535 (2015).
71. F. Villaescusa-Navarro, P. Bull, M. Viel, Astrophys. J. **814**, 146 (2015).

26. Dark Matter

Revised September 2017 by M. Drees (Bonn University) and G. Gerbier (Queen's University, Canada).

26.1. Theory

26.1.1. *Evidence for Dark Matter* :

The existence of Dark (*i.e.*, non-luminous and non-absorbing) Matter (DM) is by now well established [1,2]. The earliest, and perhaps still most convincing, evidence for DM came from the observation that various luminous objects (stars, gas clouds, globular clusters, or entire galaxies) move faster than one would expect if they only felt the gravitational attraction of other visible objects. An important example is the measurement of galactic rotation curves. The rotational velocity v of an object on a stable Keplerian orbit with radius r around a galaxy scales like $v(r) \propto \sqrt{M(r)/r}$, where $M(r)$ is the mass inside the orbit. If r lies outside the visible part of the galaxy and mass tracks light, one would expect $v(r) \propto 1/\sqrt{r}$. Instead, in most galaxies one finds that v becomes approximately constant out to the largest values of r where the rotation curve can be measured; in our own galaxy, $v \simeq 240$ km/s at the location of our solar system, with little change out to the largest observable radius. This implies the existence of a *dark halo*, with mass density $\rho(r) \propto 1/r^2$, *i.e.*, $M(r) \propto r$; at some point ρ will have to fall off faster (in order to keep the total mass of the galaxy finite), but we do not know at what radius this will happen. This leads to a lower bound on the DM mass density, $\Omega_{\rm DM} \gtrsim 0.1$, where $\Omega_X \equiv \rho_X/\rho_{\rm crit}$, $\rho_{\rm crit}$ being the critical mass density (*i.e.*, $\Omega_{\rm tot} = 1$ corresponds to a flat Universe).

The observation of clusters of galaxies tends to give somewhat larger values, $\Omega_{\rm DM} \simeq 0.2$. These observations include measurements of the peculiar velocities of galaxies in the cluster, which are a measure of their potential energy if the cluster is virialized; measurements of the *X-ray* temperature of hot gas in the cluster, which again correlates with the gravitational potential felt by the gas; and—most directly—studies of (weak) gravitational lensing of background galaxies on the cluster.

A particularly compelling example involves the bullet cluster (1E0657-558) which recently (on cosmological time scales) passed through another cluster. As a result, the hot gas forming most of the clusters' baryonic mass was shocked and decelerated, whereas the galaxies in the clusters proceeded on ballistic trajectories. Gravitational lensing shows that most of the total mass also moved ballistically, indicating that DM self-interactions are indeed weak [1].

Many cosmologists consider the existence of old galaxies (detected at redshift $z \sim 10$) to be the strongest argument for the existence of DM. Observations of the cosmic microwave background (CMB) show that density perturbations at $z \simeq 1,300$ were very small, $\delta\rho/\rho < 10^{-4}$. Since (sub–horizon sized) density perturbations grow only in the matter–dominated epoch, and matter domination starts earlier in the presence of DM, density perturbations start to grow earlier when DM is present, therefore allowing an earlier formation of the first galaxies [3].

All these arguments rely on Einsteinian, or Newtonian, gravity. One might thus ask whether the necessity to postulate the existence of DM, sometimes perceived to be ad hoc, could be avoided by modifying the theory of gravity. Indeed, the so–called Modified Newtonian Dynamics (MOND) allows to reproduce many observations on galactic scales, in particular galactic rotation curves, without introducing DM [4]. However, MOND is a purely non–relativistic theory. Attempts to embed it into a relativistic field theory require the existence of additional fields (e.g. a vector field or a second metric), and introduce considerably arbitrariness [4]. Moreover, the correct description of large–scale structure formation seems to require some sort of DM even in these theories [5]. In contrast, successful models of particle DM (see below) can be described in the well established language of quantum field theory, and do not need any modification of General Relativity, which has passed a large number of tests with flying colors [6].

The currently most accurate, if somewhat indirect, determination of $\Omega_{\rm DM}$ comes from global fits of cosmological parameters to a variety of observations; see the Section on Cosmological Parameters for details. For example, using measurements of the anisotropy of the cosmic microwave background (CMB) and of the spatial distribution of galaxies, Ref. 7 finds a density of cold, non-baryonic matter

$$\Omega_{\rm nbm} h^2 = 0.1186 \pm 0.0020 \ , \tag{26.1}$$

where h is the Hubble constant in units of 100 km/(s·Mpc). Some part of the baryonic matter density [7],

$$\Omega_{\rm b} h^2 = 0.02226 \pm 0.00023 \ , \tag{26.2}$$

may well contribute to (baryonic) DM, *e.g.*, MACHOs [8] or cold molecular gas clouds [9].

The DM density in the "neighborhood" of our solar system is also of considerable interest. This was first estimated as early as 1922 by J.H. Jeans, who analyzed the motion of nearby stars transverse to the galactic plane [2]. He concluded that in our galactic neighborhood, the average density of DM must be roughly equal to that of luminous matter (stars, gas, dust). Remarkably enough, a recent estimate finds a quite similar result for the smooth component of the local Dark Matter density [10]:

$$\rho_{\rm DM}^{\rm local} = (0.39 \pm 0.03) \cdot (1.2 \pm 0.2) \cdot (1 \pm \delta_{\rm triax}) \, \frac{\rm GeV}{\rm cm^3} \ . \tag{26.3}$$

The first term on the right-hand side of Eq. (26.3) gives the average Dark Matter density at a point one solar distance from the center of our galaxy. The second factor accounts for the fact that the baryons in the galactic disk, in which the solar system is located, also increase the local DM density [11]. The third factor in Eq. (26.3) corrects for possible deviations from a purely spherical halo; according to [12], $\delta_{\rm triax} \leq 0.2$. Small substructures (minihaloes, streams) are not likely to change the local DM density significantly [1]. Note that the first factor in Eq. (26.3) has been derived by fitting a complete model of our galaxy to a host of data, including the galactic rotation curve. A "purely local" analysis, only using the motion of nearby stars, gives a consistent result, with an error three times as large [13].

26.1.2. *Candidates for Dark Matter* :

Analyses of structure formation in the Universe indicate that most DM should be "cold" or "cool", *i.e.*, should have been non-relativistic at the onset of galaxy formation (when there was a galactic mass inside the causal horizon) [1]. This agrees well with the upper bound [7] on the contribution of light neutrinos to Eq. (26.1),

$$\Omega_\nu h^2 \leq 0.0062 \quad 95\% \ {\rm CL} \ . \tag{26.4}$$

Candidates for non-baryonic DM in Eq. (26.1) must satisfy several conditions: they must be stable on cosmological time scales (otherwise they would have decayed by now), they must interact very weakly with electromagnetic radiation (otherwise they wouldn't qualify as *dark* matter), and they must have the right relic density. Candidates include primordial black holes, axions, sterile neutrinos, and weakly interacting massive particles (WIMPs).

Primordial black holes (PBHs) must have formed before the era of Big-Bang nucleosynthesis, since otherwise they would have been counted in Eq. (26.2) rather than Eq. (26.1). Such an early creation of a large number of black holes is possible only in certain somewhat contrived cosmological models [14]. Moreover, a large number of astrophysical observations constrain PBH DM, leaving at best a narrow range of masses [15].

The existence of axions [16] was first postulated to solve the strong *CP* problem of QCD; they also occur naturally in superstring theories. They are pseudo Nambu-Goldstone bosons associated with the (mostly) spontaneous breaking of a new global "Peccei-Quinn" (PQ) U(1) symmetry at scale f_a; see the Section on Axions in this *Review* for further details. Although very light, axions would constitute cold DM, since they were produced non-thermally. At temperatures well above the QCD phase transition, the axion is massless, and the axion field can take any value, parameterized by the "misalignment angle" θ_i. At $T \lesssim 1$ GeV, the axion develops a mass $m_a \sim f_\pi m_\pi / f_a$ due to instanton effects. Unless the axion field happens to find itself at

the minimum of its potential ($\theta_i = 0$), it will begin to oscillate once m_a becomes comparable to the Hubble parameter H. These coherent oscillations transform the energy originally stored in the axion field into physical axion quanta. The contribution of this mechanism to the present axion relic density is [1]

$$\Omega_a h^2 = \kappa_a \left(f_a / 10^{12}\ \text{GeV} \right)^{1.175} \theta_i^2 \ , \tag{26.5}$$

where the numerical factor κ_a lies roughly between 0.5 and a few. If $\theta_i \sim \mathcal{O}(1)$, Eq. (26.5) will saturate Eq. (26.1) for $f_a \sim 10^{11}$ GeV, comfortably above laboratory and astrophysical constraints [16]; this would correspond to an axion mass around 0.1 meV. However, if the post-inflationary reheat temperature $T_R > f_a$, cosmic strings will form during the PQ phase transition at $T \simeq f_a$. Their decay will give an additional contribution to Ω_a, which is often bigger than that in Eq. (26.5) [1], leading to a smaller preferred value of f_a, *i.e.*, larger m_a. On the other hand, values of f_a near the Planck scale become possible if θ_i is for some reason very small.

"Sterile" $SU(2) \times U(1)_Y$ singlet neutrinos with keV masses [17] could alleviate the "cusp/core problem" [1] of cold DM models. If they were produced non-thermally through mixing with standard neutrinos, they would eventually decay into a standard neutrino and a photon or into three neutrinos.

Weakly interacting massive particles (WIMPs) χ are particles with mass roughly between 10 GeV and a few TeV, and with cross sections of approximately weak strength. Within standard cosmology, their present relic density can be calculated reliably if the WIMPs were in thermal and chemical equilibrium with the hot "soup" of Standard Model (SM) particles after inflation. In this case, their density would become exponentially (Boltzmann) suppressed at $T < m_\chi$. The WIMPs therefore drop out of thermal equilibrium ("freeze out") once the rate of reactions that change SM particles into WIMPs or vice versa, which is proportional to the product of the WIMP number density and the WIMP pair annihilation cross section into SM particles σ_A times velocity, becomes smaller than the Hubble expansion rate of the Universe. After freeze out, the co-moving WIMP density remains essentially constant; if the Universe evolved adiabatically after WIMP decoupling, this implies a constant WIMP number to entropy density ratio. Their present relic density is then approximately given by (ignoring logarithmic corrections) [3]

$$\Omega_\chi h^2 \simeq const. \cdot \frac{T_0^3}{M_{\rm Pl}^3 \langle \sigma_A v \rangle} \simeq \frac{0.1\ \text{pb} \cdot c}{\langle \sigma_A v \rangle} \ . \tag{26.6}$$

Here T_0 is the current CMB temperature, $M_{\rm Pl}$ is the Planck mass, c is the speed of light, σ_A is the total annihilation cross section of a pair of WIMPs into SM particles, v is the relative velocity between the two WIMPs in their cms system, and $\langle \ldots \rangle$ denotes thermal averaging. Freeze out happens at temperature $T_F \simeq m_\chi/20$ almost independently of the properties of the WIMP. This means that WIMPs are already non-relativistic when they decouple from the thermal plasma; it also implies that Eq. (26.6) is applicable if $T_R > T_F$. Notice that the 0.1 pb in Eq. (26.6) contains factors of T_0 and $M_{\rm Pl}$; it is, therefore, quite intriguing that it "happens" to come out near the typical size of weak interaction cross sections.

The seemingly most obvious WIMP candidate is a heavy neutrino. However, an SU(2) doublet neutrino will have too small a relic density if its mass exceeds $M_Z/2$, as required by LEP data. One can suppress the annihilation cross section, and hence increase the relic density, by postulating mixing between a heavy SU(2) doublet and some sterile neutrino. However, one also has to require the neutrino to be stable; it is not obvious why a massive neutrino should not be allowed to decay.

The currently best motivated WIMP candidate is, therefore, the lightest superparticle (LSP) in supersymmetric models [18] with exact R-parity (which guarantees the stability of the LSP). Searches for exotic isotopes [19] imply that a stable LSP has to be neutral. This leaves basically two candidates among the superpartners of ordinary particles, a sneutrino, and a neutralino. The negative outcome of various WIMP searches (see below) rules out "ordinary" sneutrinos as primary component of the DM halo of our galaxy. The most widely studied WIMP is therefore the lightest neutralino. Detailed calculations [1] show that the lightest neutralino will have the desired thermal relic density Eq. (26.1) in at least four distinct regions of parameter space. χ could be (mostly) a bino or photino (the superpartner of the $U(1)_Y$ gauge boson and photon, respectively), if both χ and some sleptons have mass below ~ 150 GeV, or if m_χ is close to the mass of some sfermion (so that its relic density is reduced through co-annihilation with this sfermion), or if $2m_\chi$ is close to the mass of the *CP*-odd Higgs boson present in supersymmetric models. Finally, Eq. (26.1) can also be satisfied if χ has a large higgsino or wino component.

Many non-supersymmetric extensions of the Standard Model also contain viable WIMP candidates [1]. Examples are the lightest $T-$odd particle in "Little Higgs" models with conserved $T-$parity, or "techni-baryons" in scenarios with an additional, strongly interacting ("technicolor" or similar) gauge group.

Although thermally produced WIMPs are attractive DM candidates because their relic density naturally has at least the right order of magnitude, non-thermal production mechanisms have also been suggested, *e.g.*, LSP production from the decay of some moduli fields [20], from the decay of the inflaton [21], or from the decay of "$Q-$balls" (non-topological solitons) formed in the wake of Affleck-Dine baryogenesis [22]. Although LSPs from these sources are typically highly relativistic when produced, they quickly achieve kinetic (but not chemical) equilibrium if T_R exceeds a few MeV [23] (but stays below $m_\chi/20$). They therefore also contribute to cold DM. Finally, if the WIMPs aren't their own antiparticles, an asymmetry between WIMPs and antiWIMPs might have been created in the early Universe, possibly by the same (unknown) mechanism that created the baryon antibaryon asymmetry. In such "asymmetric DM" models [24] the WIMP antiWIMP annihilation cross section $\langle \sigma_A v \rangle$ should be significantly larger than $0.1\,\text{pb} \cdot c$, cf Eq. (26.6).

The absence of signals at the LHC for physics beyond the Standard Model, as well as the discovery of an SM-like Higgs boson with mass near 125 GeV, constrains many well-motivated WIMP models. For example, in constrained versions of the minimal supersymmetrized Standard Model (MSSM) both the absence of supersymmetric signals and the relatively large mass of the Higgs boson favor larger WIMP masses and lower scattering cross sections on nucleons. However, constraints from "new physics" searches apply most directly to strongly interacting particles. Many WIMP models therefore can still accommodate a viable WIMP for a wide range of masses. For example, in supersymmetric models where the bino mass is not related to the other gaugino masses a bino with mass as small as 15 GeV can still have the correct thermal relic density [25]. Even lighter supersymmetric WIMPs can be realized in models with extended Higgs sector [26].

The lack of signals at the LHC may have weakened the argument for WIMPs being embedded in a larger theory that addresses the hierarchy problem. This, and the increasingly stronger limits from direct and indirect WIMP searches (see below), has spawned a plethora of new models of particle DM. For example, particles with masses in the MeV to GeV range still naturally form cold DM, but are difficult to detect with current methods. These models typically require rather light "mediator" particles in order to achieve the correct thermal relic density. Light bosons coupling to (possibly quite heavy) DM particles have also been invoked in order to greatly increase the annihilation cross section of the latter at small velocities, through the so-called Sommerfeld enhancement [27]. Several collider and fixed target experiments have searched for such light mediators, but no signal has been found [28].

Another mechanism to achieve the correct thermal relic density is based on $2 \leftrightarrow 3$ reactions purely within the dark sector. This requires quite large self interactions between the DM particles, which have therefore been dubbed SIMPs (strongly interacting massive particles) [29]. The SIMP-SIMP elastic scattering cross section σ might even be large enough to affect cosmological structure formation, which roughly requires $\sigma/m_\chi > 0.1$ b/GeV, where m_χ is the mass of the SIMP; this is considerably larger than the elastic scattering cross section of protons. Scalar SIMPs could interact with ordinary matter via Higgs exchange.

Primary black holes (as MACHOs), axions, sterile neutrinos, and WIMPs are all (in principle) detectable with present or near-future technology (see below). There are also particle physics DM candidates which currently seem almost impossible to detect, unless they decay; the present lower limit on their lifetime is of order 10^{25} to 10^{26} s for 100 GeV particles. These include the gravitino (the spin-3/2 superpartner of the graviton), states from the "hidden sector" thought responsible for supersymmetry breaking, and the axino (the spin-1/2 superpartner of the axion) [1].

26.2. Experimental detection of Dark Matter

26.2.1. *The case of baryonic matter in our galaxy* :

The search for hidden galactic baryonic matter in the form of MAssive Compact Halo Objects (MACHOs) has been initiated following the suggestion that they may represent a large part of the galactic DM and could be detected through the microlensing effect [8]. The MACHO, EROS, and OGLE collaborations have performed a program of observation of such objects by monitoring the luminosity of millions of stars in the Large and Small Magellanic Clouds for several years. EROS concluded that MACHOs cannot contribute more than 8% to the mass of the galactic halo [30], while MACHO observed a signal at 0.4 solar mass and put an upper limit of 40%. Overall, this strengthens the need for non-baryonic DM, also supported by the arguments developed above.

26.2.2. *Axion searches* :

Axions can be detected by looking for $a \to \gamma$ conversion in a strong magnetic field [1]. Such a conversion proceeds through the loop-induced $a\gamma\gamma$ coupling, whose strength $g_{a\gamma\gamma}$ is an important parameter of axion models. There is currently only one experiment searching for axionic DM: the ADMX experiment [31], originally situated at the LLNL in California but now running at the University of Washington, started taking data in the first half of 1996. It employs a high quality cavity, whose "Q factor" enhances the conversion rate on resonance, *i.e.*, for $m_a(c^2 + v_a^2/2) = \hbar\omega_{\rm res}$. One then needs to scan the resonance frequency in order to cover a significant range in m_a or, equivalently, f_a. ADMX now uses SQUIDs as first-stage amplifiers; their extremely low noise temperature (1.2 K) enhances the conversion signal. Published results [32], combining data taken with conventional amplifiers and SQUIDs, exclude axions with mass between 1.9 and 3.53 μeV, corresponding to $f_a \simeq 4 \cdot 10^{13}$ GeV, for an assumed local DM density of 0.45 GeV/cm^3, if $g_{a\gamma\gamma}$ is near the upper end of the theoretically expected range. About five times better limits on $g_{a\gamma\gamma}$ were achieved [33] for 1.98 μeV $\leq m_a \leq$ 2.18 μeV as well as for 3.3 μeV $\leq m_a \leq$ 3.65 μeV, if a large fraction of the local DM density is due to a single flow of axions with very low velocity dispersion. The ADMX experiment is being upgraded by reducing the cavity and SQUID temperature from the current 1.2 K to about 0.1 K. This should increase the frequency scanning speed for given sensitivity by more than two orders of magnitude, or increase the sensitivity for fixed observation time.

Recently several new DM axion search experiments have been proposed and are in various stages of development; see ref. [34] for brief descriptions and further references. However, none of them has produced any limits yet.

26.2.3. *Searches for keV Neutrinos* :

Relic keV neutrinos ν_s can only be detected if they mix with the ordinary neutrinos. This mixing leads to radiative $\nu_s \to \nu\gamma$ decays, with lifetime $\tau_{\nu_s} \simeq 1.8 \cdot 10^{21}$ s $\cdot (\sin\theta)^{-2} \cdot (1\ {\rm keV}/m_{\nu_s})^5$, where θ is the mixing angle [17]. This gives rise to a flux of mono-energetic photons with $E_\gamma = m_{\nu_s}/2$, which might be observable by *X-ray* satellites. In the simplest case the relic ν_s are produced only by oscillations of standard neutrinos. Assuming that all lepton-antilepton asymmetries are well below 10^{-3}, the ν_s relic density can then be computed uniquely in terms of the mixing angle θ and the mass m_{ν_s}. The combination of lower bounds on m_{ν_s} from analyses of structure formation (in particular, the Lyα "forest") and upper bounds on *X-ray* fluxes from various (clusters of) galaxies exclude this scenario if ν_s forms all of DM. This conclusion can be evaded if ν_s forms only part of DM, and/or if there is a lepton asymmetry $\geq 10^{-3}$ (i.e. some 7 orders of magnitude above the observed baryon-antibaryon asymmetry), and/or if there is an additional source of ν_s production in the early Universe, e.g. from the decay of heavier particles [17].

Recently some evidence for a weak *X-ray* line at ~ 3.5 keV has been found in data released by the XMM-Newton satellite [35]. However, the existence of this line was not confirmed by data from the Suzaku and (very short-lived) Hitomi missions [36]. Although this line has been interpreted in terms of decaying keV DM particles, e.g. sterile neutrinos with mass $m_{\nu_s} \simeq 7$ keV, it might also be due to certain inner-shell transitions of highly ionized K atoms [37].

26.2.4. *Basics of direct WIMP search* :

As stated above, WIMPs should be gravitationally trapped inside galaxies and should have the adequate density profile to account for the observed rotational curves. These two constraints determine the main features of experimental detection of WIMPs, which have been detailed in the reviews in [1].

Their mean velocity inside our galaxy relative to its center is expected to be similar to that of stars, *i.e.*, a few hundred kilometers per second at the location of our solar system. For these velocities, WIMPs interact with ordinary matter through elastic scattering on nuclei. With expected WIMP masses in the range 10 GeV to 10 TeV, typical nuclear recoil energies are of order of 1 to 100 keV.

The shape of the nuclear recoil spectrum results from a convolution of the WIMP velocity distribution, usually taken as a Maxwellian distribution in the galactic rest frame, shifted into the Earth rest frame, with the angular scattering distribution, which is isotropic to first approximation but forward-peaked for high nuclear mass (typically higher than Ge mass) due to the nuclear form factor. Overall, this results in a roughly exponential spectrum. The higher the WIMP mass, the higher the mean value of the exponential. This points to the need for low nuclear recoil energy threshold detectors.

On the other hand, expected interaction rates depend on the product of the local WIMP flux and the interaction cross section. The first term is fixed by the local density of dark matter, taken as 0.39 GeV/cm^3 [see Eq. (26.3)], the mean WIMP velocity, typically 220 km/s, the galactic escape velocity, typically 544 km/s [38] and the mass of the WIMP. The expected interaction rate then mainly depends on two unknowns, the mass and cross section of the WIMP (with some uncertainty [10] due to the halo model). This is why the experimental observable, which is basically the scattering rate as a function of energy, is usually expressed as a contour in the WIMP mass–cross section plane.

The cross section depends on the nature of the couplings. For non-relativistic WIMPs, one in general has to distinguish spin-independent and spin-dependent couplings. The former can involve scalar and vector WIMP and nucleon currents (vector currents are absent for Majorana WIMPs, *e.g.*, the neutralino), while the latter involve axial vector currents (and obviously only exist if χ carries spin). Due to coherence effects, the spin-independent cross section scales approximately as the square of the mass of the nucleus, so higher mass nuclei, from Ge to Xe, are preferred for this search. For spin-dependent coupling, the cross section depends on the nuclear spin factor; used target nuclei include ^{19}F, ^{23}Na, ^{73}Ge, ^{127}I, ^{129}Xe, ^{131}Xe, and ^{133}Cs.

Cross sections calculated in MSSM models [39] induce rates of at most 1 evt day^{-1} kg^{-1} of detector, much lower than the usual radioactive backgrounds. This indicates the need for underground laboratories to protect against cosmic ray induced backgrounds, and for the selection of extremely radio-pure materials.

The typical shape of exclusion contours can be anticipated from this discussion: at low WIMP mass, the sensitivity drops because of the detector energy threshold, whereas at high masses, the sensitivity also decreases because, for a fixed mass density, the WIMP flux decreases $\propto 1/m_\chi$. The sensitivity is best for WIMP masses near the mass of the recoiling nucleus.

Two important points are to be kept in mind when comparing exclusion curves from various experiments between them or with positive indications of a signal.

For an experiment with a fixed nuclear recoil energy threshold, the lower is the considered WIMP mass, the lower is the fraction of the spectrum to which the experiment is sensitive. This fraction may be extremely small in some cases. For illustration, some figures from some early experiments are used in the following. CoGeNT [40], using a Germanium detector with an energy threshold of around 2 keV, is sensitive to about 10 % of the total recoil spectrum of a 7 GeV WIMP, while for XENON100 [41], using a liquid Xenon detector with a threshold of 8.4 keV, this fraction is only 0.05 % (that is the extreme tail of the distribution), for the same WIMP mass. The two experiments are then sensitive to very different parts of the WIMP velocity distribution.

A second important point to consider is the energy resolution of the detector. Again at low WIMP mass, the expected roughly exponential spectrum is very steep and when the characteristic energy of the exponential becomes of the same order as the energy resolution, the energy smearing becomes important. In particular, a significant fraction of the expected spectrum below effective threshold is smeared above threshold, increasing artificially the sensitivity. For instance, a Xenon detector with a threshold of 8 keV and infinitely good resolution is actually insensitive to a 7 GeV mass WIMP, because the expected energy distribution has a cut-off at roughly 5 keV. When folding in the experimental resolution of XENON100 (corresponding to a photostatistics of 0.5 photoelectron per keV), then around 1 % of the signal is smeared above 5 keV and 0.05 % above 8 keV. Setting reliable cross section limits in this mass range thus requires a complete understanding of the response of the detector at energies well below the nominal threshold.

Two experimental signatures are predicted for WIMP signals. One is a strong daily forward/backward asymmetry of the nuclear recoil direction, due to the alternate sweeping of the WIMP cloud by the rotating Earth. Detection of this effect requires gaseous detectors, anisotropic response scintillators (stilbene) or extremely fine grain solid state detector (emulsion). The second is a few percent annual modulation of the recoil rate due to the Earth speed adding to or subtracting from the speed of the Sun. This tiny effect can only be detected with large masses; nuclear recoil identification should also be performed, as the otherwise much larger background may also be subject to seasonal modulation.

26.2.5. *Status and prospects of direct WIMP searches* :

Given the intense activity of the field, readers interested in more details than the ones given below may refer to [1], to presentations at recent conferences [31] and to the previous versions of this review.

The first searches have been performed with ultra-pure semiconductors installed in pure lead and copper shields in underground environments. Combining a priori excellent energy resolutions and very pure detector material, they produced the first limits on WIMP searches (Heidelberg-Moscow, IGEX, COSME-II, HDMS) [1]. Planned experiments using several tens of kg to a ton of Germanium run at liquid nitrogen temperature (designed for double-beta decay search) – GERDA, MAJORANA – are based in addition on passive reduction of the external and internal electromagnetic and neutron background by using Point Contact detectors (discussed below), minimal detector housing, close electronics, pulse shape discrimination and large liquid nitrogen or argon shields. Their sensitivity to WIMP interactions will depend on their ability to lower the energy threshold sufficiently, while keeping the background rate small.

Development of so called Point Contact Germanium detectors, with a very small capacitance allowed one to reach sub-keV thresholds, though performance seems to stall now at around 400 eV. The CoGeNT collaboration was first operating a single 440 g Germanium detector with an effective threshold of 400 eV in the Soudan Underground Laboratory for 56 days [40]. No new result has been published these last two years. A possible excess that had originally been observed has been understood, while a possible annual modulation in the data fell short of being significant as well.

The CDEX collaboration has also operated a single Point Contact detector in the Jinping underground laboratory, with a 475 eV threshold and a background rate too high to lead to a competitive limit [42]. The next step is CDEX-10, an array with a total mass of 10 kg, planned to be immersed in a ton-scale liquid argon chamber as active shield.

In order to make progress in the reliability of any claimed signal, active background rejection and signal identification questions have to be addressed. Active background rejection in detectors relies on the relatively small ionization in nuclear recoils due to their low velocity. This induces a reduction ("quenching") of the ionization/scintillation signal for nuclear recoil signal events relative to e or γ induced backgrounds of the same energy. Energies calibrated with gamma sources are then called "electron equivalent energies" (keVee unit used below). This effect has been both calculated and measured [1]. It is exploited in cryogenic detectors described later. In scintillation detectors, it induces in addition a difference in decay times of pulses induced by e/γ events vs nuclear recoils. In most cases, due to the limited resolution and discrimination power of this technique at low energies, this effect allows only a statistical background rejection. It has been used in NaI(Tl) (DAMA, LIBRA, NAIAD, Saclay NaI), in CsI(Tl) (KIMS), and Xe (ZEPLIN-I) [1,31]. In liquid argon, pulse shape discrimination applied to the pulse of primary scintillation light is particularly efficient and allows an event by event discrimination, however, at some high energy, roughly above 20 keVee (see later in this review).

The DAMA collaboration is the only group in the community claiming a signal at more than 5 σ level, observed now for 14 years. The claim results from a total of 7 years exposure with the LIBRA phase involving 250 kg of detectors, plus the earlier 6 years exposure of the original DAMA/NaI experiment with 100 kg of detectors [43], for a total exposure of 1.33 t·y. They observe an annual modulation of the signal in the 2 to 6 keVee bin, with the expected period (1 year) and phase (maximum around June 2), at 9.3 σ level. If interpreted within the standard halo model described above, two possible solutions have been proposed: a WIMP with $m \simeq 50$ GeV and $\sigma_{\chi p} \simeq 7 \cdot 10^{-6}$ pb (central values) or at low mass, in the 6 to 16 GeV range with $\sigma_{\chi p} \simeq 2 \cdot 10^{-4}$ pb; the cross section could be somewhat lower if there is a significant channeling effect [1]. No new result has been reported by DAMA over the two last years.

Interpreting these observations as positive WIMP signal raises several issues of internal consistency. First, the proposed WIMP solutions would induce a sizable fraction of nuclear recoils in the total measured rate in the 2 to 6 keVee bin. No pulse shape analysis has been reported by the authors to check whether the unmodulated signal was detectable this way. Secondly, the residual e/γ-induced background, inferred by subtracting the signal predicted by the WIMP interpretation from the data, has an unexpected shape [44], starting near zero at threshold and quickly rising to reach its maximum near 3 to 3.5 keVee; from general arguments one would expect the background (e.g. due to electronic noise) to increase towards the threshold. Finally, the amplitude of the annual modulation shows a tendency to decrease with time [45].

Under standard assumptions, many experiments – see below – exclude both the high and low mass DAMA/LIBRA solutions by increasingly many orders of magnitude. In particular, the large WIMP mass (60 GeV) interpretation of the DAMA/LIBRA signal induced by scattering on Iodine nuclei is excluded directly by the Korean collaboration KIMS. It has conducted an experiment in the underground Yangyang laboratory in South Korea using CsI(Tl), *i.e.* the identical nucleus of Iodine, and set an upper limit on the cross section roughly two orders of magnitude below that required to explain the DAMA signal [46]. On the other hand, no convincing non-WIMP explanation of the annual modulation of the DAMA/LIBRA signal has yet been put forward.

The last few years have seen a growing number of projects using NaI(Tl) scintillators (SABRE, COSINE; and DM-ICE, KIMS and ANAIS now taking data). Some of them have now reached the needed maturity to test the DAMA result. Thanks to the progress in powder selection and reduction of key contaminants, the background rate at low energy obtained by COSINE is only about a factor 2 higher than DAMA's. Moreover, they obtained a light yield two times higher than the ones previously achieved. This opens the possibility of a significant nuclear recoil-electron recoil discrimination at energies down to 2 keV [47]. The COSINE team is now operating 100 kg of detectors and

prepares a second phase of 200 kg.

DM-ICE has published results [48] of a 3.6 y run with 18 kg operated within the Ice Cube neutrino Telescope, at a threshold of 4 keV. Not surprisingly, no modulation was observed.

SABRE plans to run NaI(Tl) detectors immersed in liquid scintillatior in two similar set-ups at LNGS and in the Southern hemisphere, in the new underground laboratory site STAWELL in Australia (in a gold mine 240 km west of Melbourne) in order to test for a possible shift of the phase of the annual modulation. Such a shift would be expected if the modulation is somehow related to the seasons on Earth, whereas a WIMP induced annual modulation should have the same phase in both hemispheres. SABRE has conducted an R&D program to improve the radiopurity of their crystals and light detectors and will soon start first proof of principle measurements at LNGS.

Liquid noble gas (Xe, Ar) detectors have achieved tremendous progress. Due to their relatively easy scalability they currently have the highest sensitivity for "high mass" WIMPs (masses above ~ 10 GeV). Dual (liquid and gas) phase detectors allow one to measure both the primary scintillation S1 and the ionization electrons drifted through the liquid, amplified in the gas and giving rise to a second scintillation pulse S2. S1 and S2 are used to discriminate between nuclear and electron recoils as well as 3D position reconstruction within the detector. In the single phase mode (DEAP, XMASS), only S1 is measured; discrimination is then ensured by the pulse shape analysis in the case of Argon and by the self shielding in the case of Xenon.

The suite of XENON-n detectors [31] are operated at the Gran Sasso laboratory. After XENON10, XENON 100 in 2012 was the first to clearly show the supremacy of liquid noble gas detectors for high mass WIMP searches. Recently the last avatar, Xenon1t, has delivered its first results [49]. With a fiducial mass of 1042 kg and 32 days of operating time, they set the best limit on the cross section for spin-independent interactions at 7.7×10^{-11} pb for a WIMP mass of 35 GeV.

This result surpasses the most recent limit set by LUX, a 370 kg double phase Xenon detector installed in a large water shield, operated in the SURF (previously Homestake) laboratory in the US. Thanks to a total exposure of 33500 kg·d, a limit is set at 1.1×10^{-10} pb for a WIMP mass of 50 GeV [50]. This data set provides the best published limit for spin dependent WIMPs with pure neutron couplings at all masses [51]. LUX is now preparing the next phase, LZ, which will operate several tons of Xenon.

PandaX, another double phase liquid Xenon based project, has been quickly evolving in the Chinese Jinping lab. From a first phase of 54 kg, the detector has been upgraded within about one year to a mass of 500 kg. The latest result was obtained by PandaX-II with a fiducial mass of 364 kg and a running time of 77 days [52]. Combined with previous data, the total exposure of 54 000 kg·d allows one to set a limit of 8.6×10^{-11} pb for a WIMP mass of 40 GeV [53]. There is now a strong competition between these three experiments.

XMASS [31], a single-phase 800 kg Xenon detector (100 kg fiducial mass, allowing a strong self shielding) operated in Japan at the SuperKamiokande site, has seen its detector repaired. The observed spectrum is consistent with the expected background and allows to set limits about 2 orders of magnitude higher than the other, double phase, detectors. The next phase of XMASS is XMASS-1.5 with a 1.5 ton fiducial mass.

The ArDM-1t detector [31], an Argon detector with a total mass of 1.1 t installed at the Canfranc laboratory, is still in the commissioning phase.

DarkSide50, installed in LNGS, is a two phase liquid argon TPC with fiducial mass of 46 kg. The detector is immersed in a spherical vessel containing 30 t of liquid scintillator, which in turn is immersed in a tank containing one kiloton of pure water. Results from the first use of Argon from underground sources, which is depleted in the radioactive isotope ^{39}Ar, have been published recently [54]. Combined with previous results obtained with natural Argon, the obtained limit is 2.0×10^{-8} pb for a WIMP mass of 100 GeV.

DEAP-3600 [31], designed to operate in single phase mode in spherical geometry, started operating at SNOLAB 3600 kg of Argon, the so far largest mass of liquid noble gas for dark matter search. A short data taking run of 4.2 days in August 2016 resulted in a sizable exposure of 9 870 kg·d in which no candidate event was observed in the region of interest, allowing to set a limit of 1.2×10^{-8} pb for a WIMP mass of 100 GeV [55]. This is currently the best limit for an Argon based detector. However, in the background free regime, even with a fiducial mass a factor 2 higher than Xenon1t, the rate of increase in sensitivity per unit time of DEAP is around a factor 6 lower than Xenon1t. This is due to the high threshold of DEAP and the lower enhancement factor for spin independent interactions on Argon compared to Xenon. The final "winner" will then be the one with the lowest ultimate background, which DEAP projects to be.

Candidates for the next generation of multiton Ar and Xe detectors are XENONnT, DARWIN, DEAP-50T, and DarkSide-20k.

At mK temperature, the simultaneous measurement of the phonon and ionization signals in semiconductor detectors permits event by event discrimination between nuclear and electronic recoils down to few keV recoil energy. This feature is being used by the CDMS [31] and EDELWEISS [31] collaborations. Surface interactions, exhibiting incomplete charge collection, are an important residual background. Both experiments now use an interleaved ionization read-out electrodes scheme in order to control this background. On the other hand, the cryogenic experiment CRESST [31] in the Gran Sasso laboratory uses scintillating crystals as detectors and thus employs the scintillation signal as second variable for background discrimination.

Somewhat paradoxically, all three cryogenic experiments now tend to turn their efforts towards a mode of operating their detectors which gives up their discrimination power. Indeed, given the overwhelming progress of liquid noble gas detectors for WIMP masses above 10 GeV, cryogenic detectors are now tuned towards access to low mass WIMPs, by decreasing their thresholds. Given that the current limits on cross sections below a WIMP mass of 10 GeV are rather high, the detector mass required to get significant improvements does not need to be large, and discrimination against electron recoils is less crucial. Typically, in the present situation, the current limits on scattering cross sections of 3 GeV WIMPs are 5 orders of magnitude higher than at 30 GeV, which means that a detector mass of about 100 g is enough to gain in sensitivity at a WIMP mass of 3 GeV. In order to reach the "neutrino floor" due to the irreducible background rate from the elastic scattering of (mostly solar) neutrinos off the target nuclei [56] in the 7 GeV region, that is 10^{-8} pb for the WIMP–proton cross section, a detector mass of 50 to 200 kg would be needed.

The SuperCDMS collaboration has now stopped operations at Soudan and is preparing to install its large cryostat, able to house up to 200 kg of detectors, at SNOLAB. They reported recently the results from the majority of the Soudan data set, involving 15 Germanium IZIP detectors and an exposure of 1690 kg·d. A new spin-independent WIMP nucleon cross sections limit is set at 1.4×10^{-8} pb, at 90% CL for a 46 GeV WIMP [57]. This is a 20% improvement relative to the 2015 result involving 612 kg·d . Combining both results provides a limit of 1.0×10^{-8} pb at 90% CL for a 46 GeV WIMP. For comparison, the best limit at the same WIMP mass set by Xenon detectors is around 0.8×10^{-11} pb, *i.e.* two orders of magnitude lower.

Some detectors at Soudan have been operated with "high" voltage (*i.e.* 70 V instead of 6 to 8 V) across the electrodes measuring the ionization. The phonons generated by the ionization electrons traveling inside the crystal – the so-called Neganov Luke effect – then give a stronger phonon signal than the normal phonon pulse induced by the initial interaction. This is equivalent to an amplification of the ionization pulse, but at the expense of losing the discrimination between electron and nuclear recoils. This running mode allowed to lower the energy threshold to 50 to 70 eVee [58]. The sensitivity is then determined by the counting rate at the threshold. A significant improvement of the cross section limit, to 2.0×10^{-5} pb, has been obtained at around 3 GeV of WIMP mass. A projection paper [59] details expected performances for the SNOLAB set-up. A typical figure for the sensitivity goal is 4.0×10^{-8} pb for a 3 GeV WIMP. Calculated sensitivities down to a WIMP mass of 1 GeV rely on the extrapolation of knowledge of the radioactive background down to 10

eVee and of the quenching factor down to 50 eVNR.

The EDELWEISS collaboration [31] also operates cryogenic Germanium detectors (so-called FID800 detectors, featuring a complete coverage of the crystal with annular electrodes, and better rejection of non-nuclear recoil events) in the Laboratoire Souterrain de Modane. Two new results based on the same data set have been published. From an exposure of 496 kg·d obtained with 8 detectors selected out of 24 detectors for their very low threshold [60], a profile likelihood analysis has been applied and provided limits ranging from 1.6×10^{-3} pb at around 4 GeV to 7.0×10^{-8} pb at 30 GeV, all limits being higher than the ones obtained by SuperCDMS in similar mass ranges. A strategy paper [61] details expected performances under various hypothesis of R&D outcomes and running conditions. An improvement of a factor 3 over the current SuperCDMS result is anticipated at a WIMP mass of 3 GeV in 2018. The route towards the detection of solar ^{8}B neutrinos, involving several hundred kg of discrimination detectors in the SNOLAB SuperCDMS set-up, assumes an improvement in ionization channel energy rms resolution of 50 eVee, which is considered to be at hand. The solar neutrinos would be detected by elastic (coherent) scattering off the Germanium nuclei; coherent neutrino–nucleus scattering has very recently been detected experimentally for the first time [62].

The cryogenic experiment CRESST [31] in the Gran Sasso laboratory uses the scintillation of $CaWO_4$ crystals as second variable for background discrimination. CRESST puts focus on lowering the energy threshold in order to access low mass WIMPs, by implementing a new generation of detectors with improved vetoing of low energy surface events induced by external alpha particles. Results [63] from a single detector show a quite low threshold of 0.31 keVNR, allowing one to set a limit on WIMP–proton cross section for spin independent couplings of 3×10^{-4} pb for a WIMP mass around 3 GeV and 10^{-2} pb at 1 GeV, assuming interactions on the Oxygen nuclei in the target. Interestingly, the obtained limit excludes the signals reported by the same collaboration two years before, which are now believed to have been caused by an inadequate description of the background from external alpha particles. Low mass 20 g detectors with thresholds of around 100 eV are now being operated. As illustration of the shift towards extremely low threshold, 1 g detectors with 20 eV threshold have been operated at the surface in order to set limits on MeV mass particles [64].

The two following experiments also aim to search for very low mass WIMPs, that is down to 0.1 GeV. DAMIC [31], using CCDs at SNOLAB, obtained a threshold of around 100 eV. Thanks to a series of exposures of 2.9 g CCDS in different conditions adding to 0.6 kg·d, an exclusion limit [65] has been produced, ranging from 1 pb at 1.5 GeV to 1×10^{-3} pb at 3 GeV, above the limits set by CRESST. The DAMIC100 project will use 16 CCDs of 5.8 g each. The renamed NEWS-G collaboration [31] exploits an unconventional gas detector, based on a spherical geometry, able to achieve a very low energy threshold, down to a single ionization electron. A 60 cm diameter prototype, SEDINE, has being operated in the Fréjus laboratory with Neon gas at a pressure of 3.1 bars for 42 days. With a 150 eV analysis threshold, a quite competitive limit [66] of 4.4×10^{-1} pb is set at a WIMP mass of 0.5 GeV. The NEWS-SNO project involving a 1.4 m diameter spherical detector has been accepted at SNOLAB, and will allow to reach sensitivity to WIMP masses down to 0.1 GeV thanks to the use of Helium and Hydrogen targets.

Detectors based on metastable liquids or gels have the advantage of being insensitive to electromagnetic interactions, and the drawback of being threshold yes/no detectors. PICO, the merging of the Picasso and COUPP collaborations, has operated at SNOLAB a series of bubble chamber type detectors with compounds rich in Fluorine, therefore orienting their search towards spin dependent interactions. Spectacular progress has been achieved in the last two years thanks to the removal of particulates responsible for anomalous nuclear recoil like events. Using PICO60, filled with 54 kg of C_3F_8, no single scatter compatible with a nuclear recoil has been observed in an exposure of 1167 kg·d, allowing to set a limit on the spin dependent proton cross section of 3.4×10^{-5} pb for a 30 GeV WIMP, a gain of almost a factor 20 relative to the previous limit. This experiment has the best sensitivity worldwide for spin dependent couplings at all WIMP masses, similar to the ones derived from the bound on WIMP-induced muon neutrinos from the Sun (see below). The collaboration has submitted the PICO-500 project, a ton scale detector, which has been funded and will be operated at SNOLAB.

If a hint for a signal is observed in calorimetric detectors, the only convincing way to prove the galactic origin of a possible signal would be to show that the direction of nuclear recoils is indeed compatible with that of the expected WIMP wind on Earth. Until recently the low pressure Time Projection Chamber technique seemed the only feasible way to measure tracks [1]. The DRIFT collaboration [31] has operated a 1 m^3 volume detector filled with CS2 in the UK Boulby mine. Results from a 55 days run with a partial pressure of 10 torr of CF4 did not show any candidate event but the extracted limit of 0.28 pb at 100 GeV WIMP mass is 5 orders of magnitude higher than the limit set by PICO. The MIMAC collaboration [31], who operates an unshielded 2.5 l 1000 channel prototype in the Laboratoire Souterrain de Modane, did not conduct any WIMP search. Other groups developing similar techniques, though with lower sensitivity, are DMTPC in the US and NewAge in Japan. A newcomer in the WIMP directional measurement hunt, NEWSdm, an Italo-Japanese collaboration building on know-how acquired with the emulsion technique in the OPERA experiment, proposes to measure the expected 0.1 micron long nuclear tracks in an extremely finely grained emulsion. R&D is ongoing and proponents aim at operating a target mass of 1 kg, with a final sensitivity expected to be at around the DAMA signal, *i.e.* well above current limits set by most calorimetric experiments.

To complete this review about direct detection of dark matter, it is certainly worth mentioning a growing wave of ideas for new avenues towards detection of dark matter particles with ever lower masses, ranging from MeV down to the meV mass scale. Suggested methods include scattering on nuclei, scattering on electrons, absorption of bosonic particles by electrons, and chemical bond breaking. Since these proposals have the potential to explore new territories, small scale experiments can quickly cover orders of magnitude in mass and sensitivity of new parameter space.

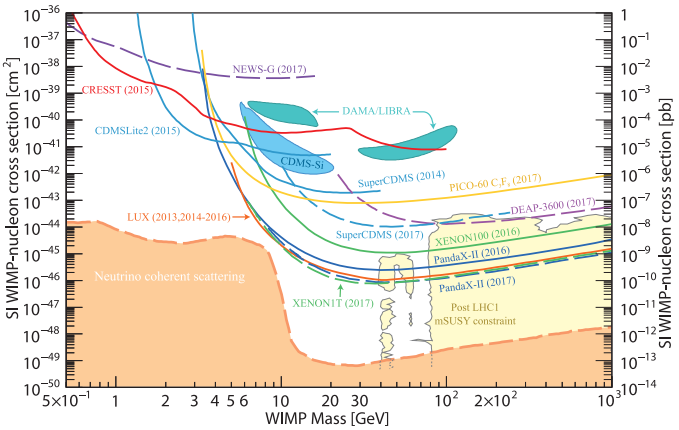

Figure 26.1: WIMP cross sections (normalized to a single nucleon) for spin-independent coupling versus mass. The DAMA/LIBRA [72], and CDMS-Si enclosed areas are regions of interest from possible signal events. References to the experimental results are given in the text. For context, the black contour shows a scan of the parameter space of 4 typical SUSY models, CMSSM, NUHM1, NUHM2, pMSSM10 [73], which integrates constraints set by ATLAS Run 1.

Figures 26.1 and 26.2 illustrate the limits and positive claims for WIMP scattering cross sections, normalized to scattering on a single nucleon, for spin independent and spin dependent couplings, respectively, as functions of WIMP mass. Only the two or three currently best limits are presented. Also shown are constraints from indirect observations (see the next section) and a typical region of a SUSY model after the LHC run-1 results.

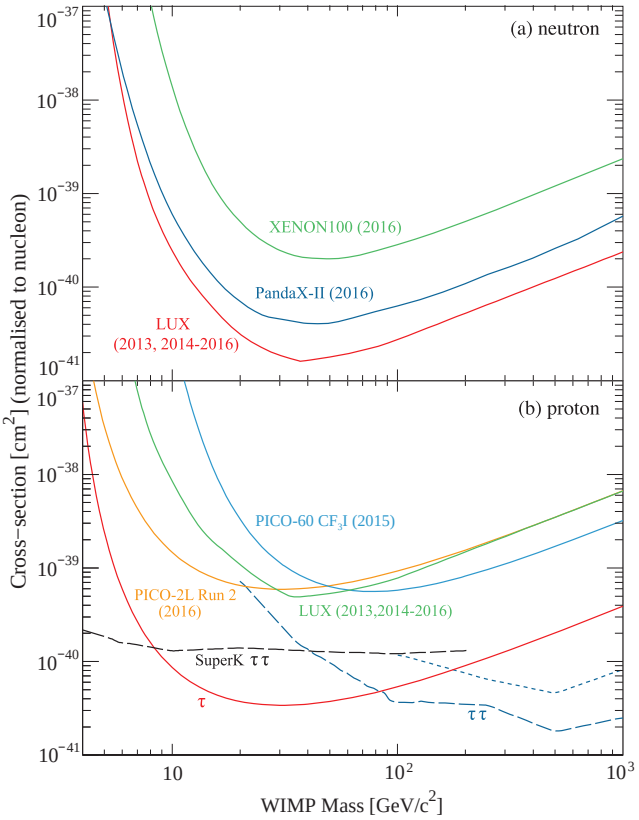

Figure 26.2: WIMP cross sections for spin dependent coupling versus mass. (a) interactions with the neutron; (b) interactions with the proton. References to the experimental results are given in the text. Indirect detection results are from SuperKamiokande (annihilation into $b\bar{b}$ and $\tau^+\tau^-$ channels) together with IceCube (annihilation into W^+W^-); for details see the indirect WIMP searches section below.

Table 25.1 summarizes the best experimental performances in terms of the upper limit on cross sections for spin independent and spin dependent couplings, at the optimized WIMP mass of each experiment. Also included are some new significant results (using Argon for example).

In summary, the confused situation at low WIMP mass has largely been cleared up (with the notable exception of the DAMA claim). Liquid noble gas detectors have achieved large progress in sensitivity to spin independent coupling WIMPs without seeing any hint of a signal. A lot of progress has also been achieved by the PICO experiment for spin dependent couplings. Many new projects focus on the very low mass range of 0.1-10 GeV. Sensitivities down to $\sigma_{\chi p}$ of 10^{-13} pb, as needed to probe nearly all of the MSSM parameter space [39] at WIMP masses above 10 GeV and to saturate the limit of the irreducible neutrino-induced background [56], will be reached with Ar and/or Xe detectors of multi-ton masses, assuming nearly perfect background discrimination capabilities. For WIMP masses below 10 GeV, this cross section limit is set by the solar neutrinos, inducing an irreducible background at an equivalent cross section around 10^{-9} pb, which is accessible with less massive low threshold detectors [31].

26.2.6. *Status and prospects of indirect WIMP searches* :

WIMPs can annihilate and their annihilation products can be detected; these include neutrinos, gamma rays, positrons, antiprotons, and antinuclei [1]. These methods are complementary to direct detection and might be able to explore higher masses and different coupling scenarios. "Smoking gun" signals for indirect detection are GeV neutrinos coming from the center of the Sun or Earth, and monoenergetic photons from WIMP annihilation in space.

WIMPs can be slowed down, captured, and trapped in celestial objects like the Earth or the Sun, thus enhancing their density and their probability of annihilation. This is a source of muon neutrinos which can interact in the Earth. Upward going muons can then be detected in large neutrino telescopes such as MACRO, BAKSAN, SuperKamiokande, Baikal, AMANDA, ANTARES, NESTOR, and the large sensitive area IceCube [1]. For standard halo velocity profiles, only the limits from the Sun, which mostly probe spin-dependent couplings, are competitive with direct WIMP search limits.

The best upper limit for low WIMP masses comes from SuperKamiokande [31]. By including events where the muon is produced inside the detector, in addition to the upgoing events used in earlier analyses, they have been able to extend the sensitivity to the few GeV regime. For example, for WIMPs annihilating into $b\bar{b}$ pairs, the resulting upper limit on the spin-dependent scattering cross section on protons is about 1.5 (2.3) fb for $m_\chi = 10$ (50) GeV; for WIMPs annihilating exclusively into $\tau^+\tau^-$ pairs the bounds are about one order of magnitude stronger [74]. These upper bounds are more than two orders of magnitude below the cross sections required to explain the DAMA signal through spin-dependent scattering on protons.

For heavier WIMPs, giving rise to more energetic muons, the best bounds have been derived from IceCube/DeepCore data. These supersede the SuperKamiokande limits for $m_\chi > 40$ (100) GeV if WIMPs annihilate into $\tau^+\tau^-$ ($b\bar{b}$) pairs. For example, the upper bound on the spin-dependent scattering cross section on protons for a 1 TeV WIMP annihilating into W^+W^- is about 0.02 fb; for WIMPs exclusively annihilating into $b\bar{b}$ the bound is about 30 to 100 times weaker [75]. The corresponding upper bounds on spin-independent scattering cross section on protons are about three orders of magnitude stronger; however, they are still at least one order of magnitude weaker than those derived from direct WIMP searches.

WIMP annihilation in the halo can give a continuous spectrum of gamma rays and (at one-loop level) also monoenergetic photon contributions from the $\gamma\gamma$ and γZ channels. These channels also allow to search for WIMPs for which direct detection experiments have little sensitivity, *e.g.*, almost pure higgsinos. The size of this

Table 26.1: Summary of performances of the best direct detection experiments, for spin independent and spin dependent couplings. For the "low mass" section, in most cases, there is no minimum in the exclusion curve and a best "typical" WIMP mass cross section point has been chosen.

	Target	Fiducial Mass [kg]	Cross section [pb]	WIMP mass [GeV]	Ref.
Spin independent high mass (>10 GeV)					
Xenon1t	Xe	1042	7.7×10^{-11}	35	[49]
PANDAX II	Xe	364	8.6×10^{-11}	40	[53]
LUX	Xe	118	1.1×10^{-10}	50	[50]
SuperCDMS	Ge	12	1.0×10^{-8}	46	[57]
DEAP	Ar	2000	1.2×10^{-8}	100	[55]
Spin independent low mass (<10 GeV)					
LUX	Xe	118	2×10^{-9}	10	[50]
Xenon1t	Xe	1042	2×10^{-9}	10	[49]
PANDAX II	Xe	364	2×10^{-9}	10	[53]
PICO60	C_3F_8 - F	46	2×10^{-7}	10	[67]
SuperCDMS	Ge HV	0.6	3×10^{-5}	3	[58]
CRESST	$CaWO_4$ - O	0.25	1×10^{-2}	1	[63]
NEWS-G	Ne	0.3	6×10^{-2}	1	[66]
Spin dependent p					
PICO60	C_3F_8 - F	54	3.4×10^{-5}	30	[67]
Spin dependent n					
LUX	Xe	118	1.6×10^{-5}	35	[51]

signal depends strongly on the halo model, but is expected to be most prominent near the galactic center. The central region of our galaxy hosts a strong TeV point source discovered [76] by the H.E.S.S. Cherenkov telescope [31]. Moreover, Fermi-LAT [31] data revealed a new extended source of GeV photons near the galactic center above and below the galactic plane, the so-called Fermi bubbles [77], as well as several dozen point sources of GeV photons in the inner kpc of our galaxy [77]. These sources are very likely of (mostly) astrophysical origin. The presence of these unexpected backgrounds makes it more difficult to discover WIMPs in this channel.

Nevertheless analyses of publicly available Fermi-LAT data claimed an excess of events in the few GeV range from an extended region around the center of our galaxy, consistent with several WIMP interpretations [78]. A recent analysis by the Fermi-LAT collaboration [77] indeed found evidence for emission of GeV photons from this region not accounted for by their modeling of astrophysical sources. However, the size, spectrum and morphology of the fitted "excess" depend strongly on the details of the fits. For example, assumptions about the selected region of interest; the template used to model the inverse Compton background; the existence of cosmic ray sources in the inner galaxy; the extension of the "Fermi bubbles" into the galactic center; and about the template for point sources, each can modify the overall flux of the "excess" by a factor $\gtrsim 2$. The latter two sources of background might each describe the entire "excess" for $E_\gamma \geq 10$ GeV. Note also that most photons detected from directions around the galactic center actually originate from astrophysical foregrounds, not from the central region, and this foreground is not well understood. As a result, a possible signal from WIMP annihilation can contribute at most about 5% of the total photon flux from the direction of the galactic center. Moreover, fitting "WIMP annihilation" templates at different locations around the galactic disk can give even larger "signal-to-background" ratios than that for the galactic center [77]; these "signals" cannot be due to WIMP annihilation, but are due to imperfections of the model used. Fermi-LAT therefore does not claim a signal, but uses these data to constrain a possible contribution from WIMP annihilation. The derived upper bound on the annihilation cross section depends sensitively on the assumed distribution of WIMPs near the galactic center, but is not far worse than the best current bound.

Due to the large astrophysical background near the galactic center, the best bound on WIMPs annihilating into photons in today's universe comes from a combination of Fermi-LAT observations of dwarf galaxies [79]. It excludes WIMPs annihilating either hadronically or into $\tau^+\tau^-$ pairs with the standard cross section needed for thermal relics, if the WIMP mass is below ~ 100 GeV; the main assumption is annihilation from an $S-$wave initial state. Only slightly weaker limits can be derived from detailed analyses of the CMB by the Planck satellite [80]. The CMB bound assumes otherwise standard cosmology, but also holds if WIMPs dominantly annihilate into light charged leptons.

Antiparticles arise as additional WIMP annihilation products in the halo. To date the best measurements of the antiproton flux come from the PAMELA satellite and the AMS-02 experiment [31] on the International Space Station, and cover kinetic energies between 60 MeV and 350 GeV [81]. The result is in fair to good agreement with secondary production and propagation models. These data exclude WIMP models that attempt to explain the "$e^\pm$ excesses" (see below) via annihilation into $W^\pm$ or Z^0 boson pairs; however, largely due to systematic uncertainties they do not significantly constrain conventional WIMP models. The AMS-02 data are sufficiently precise to look for subdominant contributions from WIMP annihilation. Two analyses [82] found statistically quite significant features that could be explained by WIMP annihilation. However, these fits are "suspiciously good". For example, Cuoco *et al.*quote an overall χ^2 of 46 for 163 degrees of freedom. The probability for obtaining this small a χ^2 is below 10^{-20}. The same analysis quotes a χ^2 of 71 for 165 degrees of freedom without a WIMP component. One possible explanation for these anomalously small values of χ^2 are correlations between the experimental errors that have not been accounted for.

The best measurements of the positron (and electron) flux at energies of tens to hundreds GeV also come from AMS02 [83] and PAMELA [84], showing a rather marked rise of the positron fraction between 10 and 200 GeV; the AMS02 data are compatible with a flattening of the positron fraction at the highest energies. While the observed positron spectrum falls within the one order of magnitude span (largely due to differences in the propagation model used) of fluxes predicted by secondary production models [85], the increase of the positron fraction is difficult to reconcile with the rather hard electron spectrum measured by PAMELA [86], if all positrons were due to secondary interactions of cosmic ray particles. Measurements of the total electron+positron energy spectrum by ATIC [87], Fermi-LAT [88] and H.E.S.S. [89] between 100 and 2000 GeV also exceed the predicted purely secondary spectrum, but with very large dispersion of the magnitude of these excesses. These observations can in principle be explained through WIMP annihilation. However, this requires cross sections well above that indicated by Eq. (26.6) for a thermal WIMP. This tension can be resolved only in somewhat baroque WIMP models. Most of these models have by now been excluded by the stringent bounds from Fermi-LAT and from analyses of the CMB on the flux of high energy photons due to WIMP annihilation. This is true also for models trying to explain the leptonic excesses through the decay of WIMPs with lifetime of the order of 10^{26} s. In contrast, viable astrophysical explanations of these excesses introducing new primary sources of electrons and positrons, e.g. pulsars [90] or a nearby supernova that exploded about two million years ago [91], have been suggested. On the other hand, the high quality of the AMS02 data on the positron fraction, which does not show any marked features, allows one to impose stringent bounds on WIMPs with mass below 300 GeV annihilating directly into leptons [92]. However, for energies between 100 GeV and 1 TeV the latest Fermi-LAT result for the summed electron+positron flux is significantly above that from AMS-02.

Last but not least, an antideuteron signal [1], as potentially observable by AMS02 or PAMELA, could constitute a signal for WIMP annihilation in the halo.

An interesting comparison of respective sensitivities to MSSM parameter space of future direct and various indirect searches has been performed with the DARKSUSY tool [93]. A web-based up-to-date collection of results from direct WIMP searches, theoretical predictions, and sensitivities of future experiments can be found in [71]. Also, the web page [94] allows to make predictions for WIMP signals in various experiments, within a variety of SUSY models and to extract limits from simply parameterized data. Integrated analysis of all data from direct and indirect WIMP detection, and also from LHC experiments should converge to a comprehensive approach, required to fully unravel the mysteries of dark matter.

References:

1. For details, recent reviews and many more references about particle dark matter, see G. Bertone, *Particle Dark Matter* (Cambridge University Press, 2010).
2. For a brief but delightful history of DM, see V. Trimble, in *Proceedings of the First International Symposium on Sources of Dark Matter in the Universe*, Bel Air, California, 1994, published by World Scientific, Singapore (ed. D.B. Cline). See also the recent review G. Bertone, D. Hooper, and J. Silk, Phys. Reports **405**, 279 (2005).
3. E.W. Kolb and M.E. Turner, *The Early Universe*, Addison-Wesley (1990).
4. M. Milgrom, Can. J. Phys. **93**, 107 (2015), and references therein.
5. See e.g. L. Bernard and L. Blanchet, Phys. Rev. D 91, 103536(2015).
6. See the section on *Experimental Tests of Gravitational Theory* in this *Review*.
7. See *Cosmological Parameters* in this *Review*.
8. B. Paczynski, Astrophys. J. **304**, 1 (1986); K. Griest, Astrophys. J. **366**, 412 (1991).
9. F. De Paolis *et al.*, Phys. Rev. Lett. **74**, 14 (1995).
10. R. Catena and P. Ullio, JCAP **1008**, 004 (2010).
11. M. Pato *et al.*, Phys. Rev. **D82**, 023531 (2010).
12. N. Bernal *et al.*, JCAP **1409**, 004 (2014).

13. J. Bovy and S. Tremaine, Astrophys. J. **756**, 89 (2012).
14. K. Kohri, D.H. Lyth, and A. Melchiorri, JCAP **0804**, 038 (2008).
15. B. Carr *et al.*, Phys. Rev. **D96**, 023514 (2017).
16. See *Axions and Other Very Light Bosons* in this *Review*.
17. A. Kusenko, Phys. Reports **481**, 1 (2009).
18. For a general introduction to SUSY, see the section devoted in this *Review of Particle Physics*. For a review of SUSY Dark Matter, see G. Jungman, M. Kamionkowski, and K. Griest, Phys. Reports **267**, 195 (1996).
19. See *Searches for WIMPs and Other Particles* in this *Review*.
20. T. Moroi and L. Randall, Nucl. Phys. **B570**, 455 (2000).
21. R. Allahverdi and M. Drees, Phys. Rev. Lett. **89**, 091302 (2002).
22. M. Fujii and T. Yanagida, Phys. Lett. **B542**, 80 (2002).
23. J. Hisano, K. Kohri, and M.M. Nojiri, Phys. Lett. **B505**, 169 (2001).
24. D.E. Kaplan, M.A. Luty, and K.M. Zurek, Phys. Rev. **D79**, 115016 (2009).
25. G. Belanger *et al.*, Phys. Lett. **B726**, 773 (2013).
26. J. Kozaczuk and S. Profumo, Phys. Rev. **D89**, 095012 (2014).
27. N. Arkani-Hamed *et al.*, Phys. Rev. **D79**, 015014 (2009).
28. A. Soffner, `arXiv:1507.02330`, and references therein; BaBar Collab., J.P. Lees *et al.*, `arXiv:1702.03327`.
29. Y. Hochberg *et al.*, Phys. Rev. Lett. **113**, 171301 (2014).
30. MACHO Collab., C. Alcock *et al.*, Astrophys. J. **542**, 257 (2000);
    EROS-2 Collab., P. Tisserand *et al.*, Astron. & Astrophys. **469**, 387 (2007);
    OGLE Collab., L. Wyrzykowski *et al.*, Mon. Not. R. Astron. Soc **416**, 2949 (2011).
31. A very useful collection of web links to the homepages of Dark Matter related conferences, and of experiments searching for WIMP Dark Matter, is the "Dark Matter Portal" at `lpsc.in2p3.fr/mayet/dm.php`. See also the TAUP and IDM conference series sites : `www.taup-conference.to.infn.it` and `kicp-workshops.uchicago.edu/IDM2012/overview.php`.
32. S.J. Asztalos *et al.*, Phys. Rev. **D69**, 011101 (2004);
    S.J. Asztalos *et al.*, Phys. Rev. Lett. **104**, 041301 (2010).
33. L.D. Duffy *et al.*, Phys. Rev. **D74**, 012006 (2006);
    J. Hoskins *et al.*, Phys. Rev. **D84**, 121302 (2011).
34. A. Ringwald, t arXiv:1612.08933.
35. E. Bulbul *et al.*, Astrophys. J. **789**, 13 (2014);
    O. Ruchayskiy *et al.*, Mon. Not. R. Astron. Soc **460**, 1390 (2016);
    J. Franse *et al.*, Astrophys. J. **829**, 124 (2016).
36. O. Urban *et al.*, Mon. Not. R. Astron. Soc **451**, 2447 (2015);
    F.A. Aharonian *et al.*, Astrophys. J. **837**, L15 (2017).
37. T.E. Jeltema and S. Profumo, Mon. Not. R. Astron. Soc **450**, 2143 (2015) and references therein.
38. M.C. Smith *et al.*, Mon. Not. R. Astron. Soc **379**, 755 (2007).
39. J. Ellis *et al.*, Phys. Rev. **D77**, 065026 (2008).
40. C.E. Aalseth *et al.*, Phys. Rev. Lett. **106**, 131301 (2011).
41. XENON100 Collab., E. Aprile *et al.*, Phys. Rev. Lett. **109**, 181301 (2012).
42. CDEX Collab., W. Zhao *et al.*, Phys. Rev. **D93**, 092003 (2016).
43. DAMA Collab., R. Bernabei *et al.*, Phys. of Part. and Nucl. **46**, 2 (2015), Phys. of Part. and Nucl. **46**, 138 (2015).
44. M. Fairbairn and T. Schwetz, JCAP **0901**, 037 (2009).
45. C. Kelso, AIP Conf. Proc. **1743**, 050007 (2016).
46. S.C. Kim *et al.*, Phys. Rev. Lett. **108**, 181301 (2012).
47. K. Kim *et al.*, IEEE Trans. **NS63**, 534 (2016).
48. DM Ice Collab., E. Barbosa de Souza *et al.*, Phys. Rev. **D95**, 032006 (2017).
49. XENON Collab., E. Aprile *et al.*, `arXiv:1705.06655`, Phys. Rev. **D94**, 122001 (2016).
50. LUX Collab., D.S. Akerib *et al.*, Phys. Rev. Lett. **118**, 021303 (2017).
51. LUX Collab., D.S. Akerib *et al.*, Phys. Rev. Lett. **118**, 251302 (2017).
52. PandaX Collab., A. Tan *et al.*, Phys. Rev. Lett. **117**, 121303 (2016).
53. PandaX-II Collab., X. Cui *et al.*, `arXiv:1708.06917`.
54. DarkSide Collab., P. Agnes *et al.*, Phys. Rev. **D93**, 081101 (2016).
55. DEAP Collab., P.-A. Amaudruz *et al.*, `arXiv:1707.08042`.
56. J. Billard, L. Strigari, E. Figueroa-Feliciano, Phys. Rev. **D89**, 023524 (2014).
57. SuperCDMS Collab., R. Agnese *et al.*, `arXiv:1708.08869`, Phys. Rev. Lett. **112**, 241302 (2014), Phys. Rev. **D92**, 072003 (2015).
58. SuperCDMS Collab., R. Agnese *et al.*, Phys. Rev. Lett. **116**, 071301 (2016).
59. SuperCDMS Collab., R. Agnese *et al.*, Phys. Rev. **D95**, 082002 (2017).
60. Edelweiss Collab., L. Hehn *et al.*, Eur. Phys. J. **C76**, 548 (2016).
61. Edelweiss Collab., Q. Arnaud *et al.*, `arXiv:1707.04308`.
62. COHERENT Collab., D. Akimov *et al.*., `arXiv:1708.04255`, published in Science (Aug. 2017).
63. CRESST Collab., G. Angloher *et al.*, Eur. Phys. J. **C76**, 25 (2016).
64. CRESST Collab., G. Angloher *et al.*, `arXiv:1707.06749`.
65. DAMIC Collab., A. Aguilar-Arevalo *et al.*, Phys. Rev. **D94**, 082006 (2016).
66. NEWS-G Collab., Q. Arnaud *et al.*, `arXiv:1706.04934`.
67. PICO Collab., C. Amole *et al.*, Phys. Rev. Lett. **118**, 251301 (2017).
68. DRIFT Collab., J.B.R. Battat *et al.*, Astropart. Phys. **91**, 65 (2017).
69. NEWSdm Collab., N. di Marco *et al.*, J. Phys. Conf. Ser. **718**, 042018 (2016).
70. Community paper `arXiv:1707.04591`, proceedings of U.S. Cosmic Visions: New Ideas in Dark Matter, `endico.fnal.gov/event/13702/`.
71. DMTOOLS site : `dmtools.brown.edu:8080/`.
72. C. Savage *et al.*., JCAP **0904**, 010 (2009).
73. E.A. Bagnaschi *et al.*, Eur. Phys. J. **C75**, 500 (2015).
74. SuperKamiokande Collab., K. Choi *et al.*, Phys. Rev. Lett. **114**, 141301 (2015).
75. IceCube Collab., M.G. Aartsen *et al.*, Eur. Phys. J. **C77**, 146 (2017).
76. H.E.S.S. Collab., F. Aharonian *et al.*, Astron. & Astrophys. **503**, 817 (2009);
    H.E.S.S. Collab., F. Acero *et al.*, Mon. Not. R. Astron. Soc **402**, 1877 (2010).
77. Fermi-LAT Collab., M. Ackermann *et al.*, Astrophys. J. **840**, 43 (2017).
78. D. Hooper and L. Goodenough, Phys. Lett. **B697**, 412 (2011);
    T. Daylan *et al.*, Phys. Dark Univ. **12**, 1 (2016).
79. Fermi-LAT Collab., M. Ackermann *et al.*, Phys. Rev. Lett. **115**, 231301 (2015).
80. G. Steigman, Phys. Rev. **D91**, 083538 (2015).
81. PAMELA Collab., O. Adriani *et al.*, Phys. Rev. Lett. **105**, 121101 (2010);
    AMS-02 Collab., M. Aguilar *et al.*, Phys. Rev. Lett. **117**, 091103 (2016).
82. M.Y. Cui, Q. Yuan, Y.L. Sming Tsai and Y.Z. Fan, Phys. Rev. Lett. **118**, 191101 (2017);
    A. Cuoco, M. Krämer and M. Korsmeier, Phys. Rev. Lett. **118**, 191102 (2017).
83. AMS02 Collab., M. Aguilar *et al.*, Phys. Rev. Lett. **113**, 121101 (2014) and Phys. Rev. Lett. **113**, 121102 (2014).
84. PAMELA Collab., O. Adriani *et al.*, Phys. Rev. Lett. **111**, 081102 (2013).
85. T. Delahaye *et al.*, Astron. & Astrophys. **501**, 821 (2009).
86. PAMELA Collab., O. Adriani *et al.*, Phys. Rev. Lett. **106**, 201101 (2011).
87. ATIC Collab., J. Chang *et al.*, Nature **456**, 362 (2008).
88. Fermi-LAT Collab., S. Abdollahi *et al.*, Phys. Rev. **D95**, 082007 (2017).
89. H.E.S.S. Collab., F. Aharonian *et al.*, Astron. & Astrophys. **508**, 561 (2009).
90. M. Cirelli, Pramana **79**, 1021 (2012);
    S. Profumo, Central Eur. J. Phys. **10**, 1 (2011).

91. M. Kachelriess, A. Neronov, D.V. Semikoz, Phys. Rev. Lett. **115**, 181103 (2015).
92. L. Bergstrom *et al.*, Phys. Rev. Lett. **111**, 171101 (2013).
93. DARKSUSY site: `www.physto.se/~edsjo/darksusy/`.
94. ILIAS web page: `pisrv0.pit.physik.uni-tuebingen.de/darkmatter/`.

27. Dark Energy

Revised September 2017 by D. H. Weinberg (OSU) and M. White (UCB, LBL)

27.1. Repulsive Gravity and Cosmic Acceleration

In the first modern cosmological model, Einstein [1] modified his field equation of General Relativity (GR), introducing a "cosmological term" that enabled a solution with time-independent, spatially homogeneous matter density $\rho_{\rm m}$ and constant positive space curvature. Although Einstein did not frame it this way, one can view the "cosmological constant" Λ as representing a constant energy density of the vacuum [2], whose repulsive gravitational effect balances the attractive gravity of matter and thereby allows a static solution. After the development of dynamic cosmological models [3,4] and the discovery of cosmic expansion [5], the cosmological term appeared unnecessary, and Einstein and de Sitter [6] advocated adopting an expanding, homogeneous and isotropic, spatially flat, matter-dominated universe as the default cosmology until observations dictated otherwise. Such a model has matter density equal to the critical density, $\Omega_{\rm m} \equiv \rho_{\rm m}/\rho_{\rm c} = 1$, and negligible contribution from other energy components [7].

By the mid-1990s, the Einstein-de Sitter model was showing numerous cracks, under the combined onslaught of data from the cosmic microwave background (CMB), large-scale galaxy clustering, and direct estimates of the matter density, the expansion rate (H_0), and the age of the Universe. As noted in a number of papers from this time, introducing a cosmological constant offered a potential resolution of many of these tensions, yielding the most empirically successful version of the inflationary cold dark matter scenario. In the late 1990s, supernova surveys by two independent teams provided direct evidence for accelerating cosmic expansion [8,9], establishing the cosmological constant model (with $\Omega_{\rm m} \simeq 0.3$, $\Omega_\Lambda \simeq 0.7$) as the preferred alternative to the $\Omega_{\rm m} = 1$ scenario. Shortly thereafter, CMB evidence for a spatially flat universe [10,11], and thus for $\Omega_{\rm tot} \simeq 1$, cemented the case for cosmic acceleration by firmly eliminating the free-expansion alternative with $\Omega_{\rm m} \ll 1$ and $\Omega_\Lambda = 0$. Today, the accelerating universe is well established by multiple lines of independent evidence from a tight web of precise cosmological measurements.

As discussed in the Big Bang Cosmology article of this *Review* (Sec. 21), the scale factor $R(t)$ of a homogeneous and isotropic universe governed by GR grows at an accelerating rate if the pressure $p < -\frac{1}{3}\rho$ (in $c = 1$ units). A cosmological constant has $\rho_\Lambda =$ constant and pressure $p_\Lambda = -\rho_\Lambda$ (see Eq. 21.10), so it will drive acceleration if it dominates the total energy density. However, acceleration could arise from a more general form of "dark energy" that has negative pressure, typically specified in terms of the equation-of-state-parameter $w = p/\rho$ ($= -1$ for a cosmological constant). Furthermore, the conclusion that acceleration requires a new energy component beyond matter and radiation relies on the assumption that GR is the correct description of gravity on cosmological scales. The title of this article follows the common but inexact usage of "dark energy" as a catch-all term for the origin of cosmic acceleration, regardless of whether it arises from a new form of energy or a modification of GR. Our account here draws on the much longer review of cosmic acceleration by Ref. [12], which provides background explanation and extensive literature references for most of the points in this article, but is less up to date in its description of current empirical constraints.

Below we will use the abbreviation ΛCDM to refer to a model with cold dark matter, a cosmological constant, inflationary initial conditions, standard radiation and neutrino content, and a flat universe with $\Omega_{\rm tot} = 1$ (though we will sometimes describe this model as "flat ΛCDM" to emphasize this last restriction). We will use wCDM to denote a model with the same assumptions but a free, constant value of w. Models with the prefix "o" (*e.g.*, owCDM) allow non-zero space curvature.

27.2. Theories of Cosmic Acceleration

27.2.1. *Dark Energy or Modified Gravity?* :

A cosmological constant is the mathematically simplest, and perhaps the physically simplest, theoretical explanation for the accelerating universe. The problem is explaining its unnaturally small magnitude, as discussed in Sec. 21.4.7 of this *Review*. An alternative (which still requires finding a way to make the cosmological constant zero or at least negligibly small) is that the accelerating cosmic expansion is driven by a new form of energy such as a scalar field [13] with potential $V(\phi)$. The energy density and pressure of the field $\phi(\mathbf{x})$ take the same forms as for inflationary scalar fields, given in Eq. (21.52) of the Big Bang Cosmology article. In the limit that $\frac{1}{2}\dot\phi^2 \ll |V(\phi)|$, the scalar field acts like a cosmological constant, with $p_\phi \simeq -\rho_\phi$. In this scenario, today's cosmic acceleration is closely akin to the epoch of inflation, but with radically different energy and timescale.

More generally, the value of $w = p_\phi/\rho_\phi$ in scalar field models evolves with time in a way that depends on $V(\phi)$ and on the initial conditions $(\phi_i, \dot\phi_i)$; some forms of $V(\phi)$ have attractor solutions in which the late-time behavior is insensitive to initial values. Many forms of time evolution are possible, including ones where w is approximately constant and broad classes where w "freezes" towards or "thaws" away from $w = -1$, with the transition occurring when the field comes to dominate the total energy budget. If ρ_ϕ is even approximately constant, then it becomes dynamically insignificant at high redshift, because the matter density scales as $\rho_{\rm m} \propto (1+z)^3$. "Early dark energy" models are ones in which ρ_ϕ is a small but not negligible fraction (*e.g.*, a few percent) of the total energy throughout the matter- and radiation-dominated eras, tracking the dominant component before itself coming to dominate at low redshift.

Instead of introducing a new energy component, one can attempt to modify gravity in a way that leads to accelerated expansion [14]. One option is to replace the Ricci scalar $\mathcal{R}$ with a function $\mathcal{R} + f(\mathcal{R})$ in the gravitational action [15]. Other changes can be more radical, such as introducing extra dimensions and allowing gravitons to "leak" off the brane that represents the observable universe (the "DGP" model [16]) . The DGP example has inspired a more general class of "galileon" and massive gravity models. Constructing viable modified gravity models is challenging, in part because it is easy to introduce theoretical inconsistencies (such as "ghost" fields with negative kinetic energy), but above all because GR is a theory with many high-precision empirical successes on solar system scales [17]. Modified gravity models typically invoke screening mechanisms that force model predictions to approach those of GR in regions of high density or strong gravitational potential. Screening offers potentially distinctive signatures, as the strength of gravity (*i.e.*, the effective value of $G_{\rm N}$) can vary by order unity in environments with different gravitational potentials.

More generally, one can search for signatures of modified gravity by comparing the history of cosmic structure growth to the history of cosmic expansion. Within GR, these two are linked by a consistency relation, as described below (Eq. (27.2)). Modifying gravity can change the predicted rate of structure growth, and it can make the growth rate dependent on scale or environment. In some circumstances, modifying gravity alters the combinations of potentials responsible for gravitational lensing and the dynamics of non-relativistic tracers (such as galaxies or stars) in different ways (see Sec. 21.4.7 in this *Review*), leading to order unity mismatches between the masses of objects inferred from lensing and those inferred from dynamics in unscreened environments.

At present there are no fully realized and empirically viable modified gravity theories that explain the observed level of cosmic acceleration. The constraints on $f(\mathcal{R})$ models now force them so close to GR that they cannot produce acceleration without introducing a separate dark energy component [18]. The DGP model is empirically ruled out by several tests, including the expansion history, the integrated Sachs-Wolfe effect, and redshift-space distortion measurements of the structure growth rate [19]. The elimination of these models should be considered an important success of the program to empirically test theories of cosmic acceleration. However, it is worth recalling that there was no fully realized gravitational explanation for the precession of Mercury's orbit prior to the completion of GR in 1915, and the fact that no complete and viable modified gravity theory exists today does not mean that one will not arise in the future. In the meantime, we can continue empirical investigations that can tighten restrictions on

such theories or perhaps point towards the gravitational sector as the origin of accelerating expansion.

27.2.2. ***Expansion History and Growth of Structure*** :

The main line of empirical attack on dark energy is to measure the history of cosmic expansion and the history of matter clustering with the greatest achievable precision over a wide range of redshift. Within GR, the expansion rate $H(z)$ is governed by the Friedmann equation (see the articles on Big Bang Cosmology and Cosmological Parameters—Secs. 21 and 24 in this *Review*). For dark energy with an equation of state $w(z)$, the cosmological constant contribution to the expansion, Ω_Λ, is replaced by a redshift-dependent contribution. The evolution of the dark energy density follows from Eq. (21.10),

$$\Omega_{\rm de}\frac{\rho_{\rm de}(z)}{\rho_{\rm de}(z=0)} = \Omega_{\rm de}\exp\left[3\int_0^z [1+w(z')]\frac{dz'}{1+z'}\right] = \Omega_{\rm de}(1+z)^{3(1+w)}, \tag{27.1}$$

where the second equality holds for constant w. If $\Omega_{\rm m}$, $\Omega_{\rm r}$, and the present value of $\Omega_{\rm tot}$ are known, then measuring $H(z)$ pins down $w(z)$. (Note that $\Omega_{\rm de}$ is the same quantity denoted $\Omega_{\rm v}$ in Sec. 21, but we have adopted the de subscript to avoid implying that dark energy is necessarily a vacuum effect.)

While some observations can probe $H(z)$ directly, others measure the distance-redshift relation. The basic relations between angular diameter distance or luminosity distance and $H(z)$ are given in Ch. 21 —and these are generally unaltered in time-dependent dark energy or modified gravity models. For convenience, in later sections, we will sometimes refer to the comoving angular distance, $D_{\rm A,c}(z) = (1+z)D_{\rm A}(z)$.

In GR-based linear perturbation theory, the density contrast $\delta(\mathbf{x},t) \equiv \rho(\mathbf{x},t)/\bar\rho(t) - 1$ of pressureless matter grows in proportion to the linear growth function $G(t)$ (not to be confused with the gravitational constant $G_{\rm N}$), which follows the differential equation

$$\ddot G + 2H(z)\dot G - \frac{3}{2}\Omega_{\rm m}H_0^2(1+z)^3 G = 0\ . \tag{27.2}$$

To a good approximation, the logarithmic derivative of $G(z)$ is

$$f(z) \equiv -\frac{d\ln G}{d\ln(1+z)} \simeq \left[\Omega_{\rm m}(1+z)^3\frac{H_0^2}{H^2(z)}\right]^\gamma\ , \tag{27.3}$$

where $\gamma \simeq 0.55$ for relevant values of cosmological parameters [20]. In an $\Omega_{\rm m} = 1$ universe, $G(z) \propto (1+z)^{-1}$, but growth slows when $\Omega_{\rm m}$ drops significantly below unity. One can integrate Eq. (27.3) to get an approximate integral relation between $G(z)$ and $H(z)$, but the full (numerical) solution to Eq. (27.2) should be used for precision calculations. Even in the non-linear regime, the amplitude of clustering is determined mainly by $G(z)$, so observations of non-linear structure can be used to infer the linear $G(z)$, provided one has good theoretical modeling to relate the two.

In modified gravity models the growth rate of gravitational clustering may differ from the GR prediction. A general strategy to test modified gravity, therefore, is to measure both the expansion history and the growth history to see whether they yield consistent results for $H(z)$ or $w(z)$.

27.2.3. ***Parameters*** :

Constraining a general history of $w(z)$ is nearly impossible, because the dark energy density, which affects $H(z)$, is given by an integral over $w(z)$, and distances and the growth factor involve a further integration over functions of $H(z)$. Oscillations in $w(z)$ over a range $\Delta z/(1+z) \ll 1$ are therefore extremely difficult to constrain. It has become conventional to phrase constraints or projected constraints on $w(z)$ in terms of a linear evolution model,

$$w(a) = w_0 + w_{\rm a}(1-a) = w_{\rm p} + w_{\rm a}(a_{\rm p} - a), \tag{27.4}$$

where $a \equiv (1+z)^{-1}$, w_0 is the value of w at $z = 0$, and $w_{\rm p}$ is the value of w at a "pivot" redshift $z_{\rm p} \equiv a_{\rm p}^{-1} - 1$, where it is best constrained by a given set of experiments. For typical data combinations, $z_{\rm p} \simeq 0.5$. This simple parameterization can provide a good approximation to the predictions of many physically motivated models for observables measured with percent-level precision. A widely used "Figure of Merit" (FoM) for dark energy experiments [21] is the projected combination of errors $[\sigma(w_{\rm p})\sigma(w_{\rm a})]^{-1}$. Ambitious future experiments with 0.1–0.3% precision on observables can constrain richer descriptions of $w(z)$, which can be characterized by principal components.

There has been less convergence on a standard parameterization for describing modified gravity theories. Deviations from the GR-predicted growth rate can be described by a deviation $\Delta\gamma$ in the index of Eq. (27.3), together with an overall multiplicative offset relative to the $G(z)$ expected from extrapolating the CMB-measured fluctuation amplitude to low redshift. However, these two parameters may not accurately capture the growth predictions of all physically interesting models. Another important parameter to constrain is the ratio of the gravitational potentials governing space curvature and the acceleration of non-relativistic test particles. The possible phenomenology of modified gravity models is rich, which enables many consistency tests but complicates the task of constructing parameterized descriptions.

The more general set of cosmological parameters is discussed elsewhere in this *Review* (Sec. 24), but here we highlight a few that are particularly important to the dark energy discussion:

- The dimensionless Hubble parameter $h \equiv H_0/100\ {\rm km\,s^{-1}\,Mpc^{-1}}$ determines the present day value of the critical density and the overall scaling of distances inferred from redshifts.
- $\Omega_{\rm m}$ and $\Omega_{\rm tot}$ affect the expansion history and the distance-redshift relation.
- The sound horizon $r_{\rm s} = \int_0^{t_{\rm rec}} c_{\rm s}(t)dt/a(t)$, the comoving distance that pressure waves can propagate between $t = 0$ and recombination, determines the physical scale of the acoustic peaks in the CMB and the baryon acoustic oscillation (BAO) feature in low redshift matter clustering [22].
- The amplitude of matter fluctuations, conventionally represented by the quantity $\sigma_8(z)$, scales the overall amplitude of growth measures such as weak lensing or redshift-space distortions (discussed in the next section).

Specifically, $\sigma_8(z)$ refers to the rms fluctuation of the matter overdensity $\rho/\bar\rho$ in spheres of radius $8\,h^{-1}$Mpc, computed from the linear theory matter power spectrum at redshift z, and σ_8 on its own refers to the value at $z = 0$ (just like our convention for $\Omega_{\rm m}$).

While discussions of dark energy are frequently phrased in terms of values and errors on quantities like $w_{\rm p}$, $w_{\rm a}$, $\Delta\gamma$, and $\Omega_{\rm tot}$, parameter precision is the means to an end, not an end in itself. The underlying goal of empirical studies of cosmic acceleration is to address two physically profound questions:

1. Does acceleration arise from a breakdown of GR on cosmological scales or from a new energy component that exerts repulsive gravity within GR?
2. If acceleration is caused by a new energy component, is its energy density constant in space and time, as expected for a fundamental vacuum energy, or does it show variations that indicate a dynamical field?

Substantial progress towards answering these questions, in particular any definitive rejection of the cosmological constant "null hypothesis," would be a major breakthrough in cosmology and fundamental physics.

27.3. Observational Probes

We briefly summarize the observational probes that play the greatest role in current constraints on dark energy. Further discussion can be found in other articles of this *Review*, in particular Secs. 24 (Cosmological Parameters) and 28 (The Cosmic Microwave Background), and in Ref. [12], which provides extensive references to background literature. Recent observational results from these methods are discussed in 27.4.

27.3.1. ***Methods, Sensitivity, Systematics*** :

Cosmic Microwave Background Anisotropies: Although CMB anisotropies provide limited information about dark energy on their own, CMB constraints on the geometry, matter content, and radiation content of the Universe play a critical role in dark energy studies when combined with low redshift probes. In particular, CMB data supply measurements of $\theta_s = r_s/D_{A,c}(z_{rec})$, the angular size of the sound horizon at recombination, from the angular location of the acoustic peaks, measurements of $\Omega_m h^2$ and $\Omega_b h^2$ from the heights of the peaks, and normalization of the amplitude of matter fluctuations at z_{rec} from the amplitude of the CMB fluctuations themselves. *Planck* data yield a 0.3% determination of r_s, which scales as $(\Omega_m h^2)^{-0.25}$ for cosmologies with standard matter and radiation content. The uncertainty in the matter fluctuation amplitude is $1-2\%$. Improvements in the measurement of the electron scattering optical depth τ, with future analyses of *Planck* polarization maps, would reduce this uncertainty further. Secondary anisotropies, including the Integrated Sachs-Wolfe effect, the Sunyaev-Zeldovich (SZ, [23]) effect, and gravitational lensing of primary anisotropies provide additional information about dark energy by constraining low-redshift structure growth.

Type Ia Supernovae (SN): Type Ia supernovae, produced by the thermonuclear explosions of white dwarfs, exhibit $10-15\%$ scatter in peak luminosity after correction for light curve duration (the time to rise and fall) and color (which is a diagnostic of dust extinction). Since the peak luminosity is not known *a priori*, supernova surveys constrain ratios of luminosity distances at different redshifts. If one is comparing a high redshift sample to a local calibrator sample measured with much higher precision (and distances inferred from Hubble's law), then one essentially measures the luminosity distance in h^{-1}Mpc, constraining the combination $hD_L(z)$. With distance uncertainties of 5–8% per well observed supernova, a sample of around 100 SNe is sufficient to achieve sub-percent statistical precision. The 1–2% systematic uncertainties in current samples are dominated by uncertainties associated with photometric calibration and dust extinction corrections plus the observed dependence of luminosity on host galaxy properties. Another potential systematic is redshift evolution of the supernova population itself, which can be tested by analyzing subsamples grouped by spectral properties or host galaxy properties to confirm that they yield consistent results.

Baryon Acoustic Oscillations (BAO): Pressure waves that propagate in the pre-recombination photon-baryon fluid imprint a characteristic scale in the clustering of matter and galaxies, which appears in the galaxy correlation function as a localized peak at the sound horizon scale r_s, or in the power spectrum as a series of oscillations. Since observed galaxy coordinates consist of angles and redshifts, measuring this "standard ruler" scale in a galaxy redshift survey determines the angular diameter distance $D_A(z)$ and the expansion rate $H(z)$, which convert coordinate separations to comoving distances. Errors on the two quantities are correlated, and in existing galaxy surveys the best determined combination is approximately $D_V(z) = [czD^2_{A,c}(z)/H(z)]^{1/3}$. As an approximate rule of thumb, a survey that fully samples structures at redshift z over a comoving volume V, and is therefore limited by cosmic variance rather than shot noise, measures $D_{A,c}(z)$ with a fractional error of $0.005(V/10\,\mathrm{Gpc}^3)^{-1/2}$ and $H(z)$ with a fractional error $1.6-1.8$ times higher. The most precise BAO measurements to date come from large galaxy redshift surveys probing $z < 0.8$, and these will be extended to higher redshifts by future projects. At redshifts $z > 2$, BAO can also be measured in the Lyman-α forest of intergalactic hydrogen absorption towards background quasars, where the fluctuating absorption pattern provides tens or hundreds of samples of the density field along each quasar sightline. For Lyman-α forest BAO, the best measured parameter combination is more heavily weighted towards $H(z)$ because of strong redshift-space distortions that enhance clustering in the line-of-sight direction. Radio intensity mapping, which maps large-scale structure in redshifted 21cm hydrogen emission without resolving individual galaxies, offers a potentially promising route to measuring BAO over large volumes at relatively low cost, but the technique is still under development. Photometric redshifts in optical imaging surveys can be used to measure BAO in the angular direction, though the typical distance precision is a factor of $3-4$ lower compared to a well sampled spectroscopic survey of the same area, and angular BAO measurements do not directly constrain $H(z)$. BAO distance measurements complement SN distance measurements by providing absolute rather than relative distances (with precise calibration of r_s from the CMB) and by having greater achievable precision at high redshift thanks to the increasing comoving volume available. Theoretical modeling suggests that BAO measurements from even the largest feasible redshift surveys will be limited by statistical rather than systematic uncertainties.

Weak Gravitational Lensing: Gravitational light bending by a clustered distribution of matter shears the shapes of higher redshift background galaxies in a spatially coherent manner, producing a correlated pattern of apparent ellipticities. By studying the weak lensing signal for source galaxies binned by photometric redshift (estimated from broad-band colors), one can probe the history of structure growth. For a specified expansion history, the predicted signal scales approximately as $\sigma_8\Omega_m^\alpha$, with $\alpha \simeq 0.3$–0.5. The predicted signal also depends on the distance-redshift relation, so weak lensing becomes more powerful in concert with SN or BAO measurements that can pin this relation down independently. The most challenging systematics are shape measurement biases, biases in the distribution of photometric redshifts, and intrinsic alignments of galaxy orientations that could contaminate the lensing-induced signal. Predicting the large-scale weak lensing signal is straightforward in principle, but the number of independent modes on large scales is small, and the inferences are therefore dominated by sample variance. Exploiting small-scale measurements, for tighter constraints, requires modeling the effects of complex physical processes such as star formation and feedback on the matter power spectrum. Strong gravitational lensing can also provide constraints on dark energy, either through time delay measurements that probe the absolute distance scale, or through measurements of multiple-redshift lenses that constrain distance ratios. The primary uncertainty for strong lensing constraints is modeling the mass distribution of the lens systems.

Clusters of Galaxies: Like weak lensing, the abundance of massive dark matter halos probes structure growth by constraining $\sigma_8\Omega_m^\alpha$, where $\alpha \simeq 0.3$–0.5. These halos can be identified as dense concentrations of galaxies or through the signatures of hot (10^7–10^8 K) gas in X-ray emission or SZ distortion of the CMB. The critical challenge in cluster cosmology is calibrating the relation $P(M_{halo}|O)$ between the halo mass as predicted from theory and the observable O used for cluster identification. Measuring the stacked weak lensing signal from clusters has emerged as a promising approach to achieve percent-level accuracy in calibration of the mean relation, which is required for clusters to remain competitive with other growth probes. This method requires accurate modeling of completeness and contamination of cluster catalogs, projection effects on cluster selection and weak lensing measurements, and possible baryonic physics effects on the mass distribution within clusters.

Redshift-Space Distortions (RSD) and the Alcock-Paczynksi (AP) Effect: Redshift-space distortions of galaxy clustering, induced by peculiar motions, probe structure growth by constraining the parameter combination $f(z)\sigma_8(z)$, where $f(z)$ is the growth rate defined by Eq. (27.3). Uncertainties in theoretical modeling of non-linear gravitational evolution and the non-linear bias between the galaxy and matter distributions currently limit application of the method to large scales (comoving separations $r \gtrsim 10\,h^{-1}$Mpc or wavenumbers $k \lesssim 0.2h\,\mathrm{Mpc}^{-1}$). A second source of anisotropy arises if one adopts the wrong cosmological metric to convert angles and redshifts into comoving separations, a phenomenon known as the Alcock-Paczynksi effect [24]. Demanding isotropy of clustering at redshift z constrains the parameter combination $H(z)D_A(z)$. The main challenge for the AP method is correcting for the anisotropy induced by peculiar velocity RSD.

Direct Determination of H_0: The value of H_0 sets the current value of the critical density $\rho_c = 3H_0^2/8\pi G_N$, and combination with CMB measurements provides a long lever arm for constraining the evolution of dark energy. The challenge in direct H_0 measurements is establishing distances to galaxies that are "in the Hubble flow," *i.e.*, far enough away that their peculiar velocities are small compared

Table 27.1: A selection of major dark energy experiments, based on Ref. [25]. Abbreviations in the "Data" column refer to optical (Opt) or near-infrared (NIR) imaging (I) or spectroscopy (S). For spectroscopic experiments, the "Spec-z" column lists the primary redshift range for galaxies (gals), quasars (QSOs), or the Lyman-α forest (LyαF). Abbreviations in the "Methods" column are weak lensing (WL), clusters (CL), supernovae (SN), baryon acoustic oscillations (BAO), and redshift-space distortions (RSD).

Project	Dates	Area/deg^2	Data	Spec-z Range	Methods
BOSS	2008-2014	10,000	Opt-S	$0.3-0.7$ (gals)	BAO/RSD
				$2-3.5$ (LyαF)	
DES	2013-2018	5000	Opt-I	——	WL/CL
					SN/BAO
eBOSS	2014-2020	7500	Opt-S	$0.6-2.0$ (gal/QSO)	BAO/RSD
				$2-3.5$ (LyαF)	
SuMIRE	2014-2024	1500	Opt-I		WL/CL
			Opt/NIR-S	$0.8-2.4$ (gals)	BAO/RSD
HETDEX	2014-2019	300	Opt-S	$1.9 < z < 3.5$ (gals)	BAO/RSD
DESI	2019-2024	14,000	Opt-S	$0-1.7$ (gals)	BAO/RSD
				$2-3.5$ (LyαF)	
LSST	2020-2030	20,000	Opt-I	——	WL/CL
					SN/BAO
Euclid	2020-2026	15,000	Opt-I		WL/CL
			NIR-S	$0.7-2.2$ (gals)	BAO/RSD
WFIRST	2024-2030	2200	NIR-I		WL/CL/SN
			NIR-S	$1.0-3.0$ (gals)	BAO/RSD

to the expansion velocity $v = H_0 d$. This can be done by building a ladder of distance indicators tied to stellar parallax on its lowest rung, or by using gravitational lens time delays or geometrical measurements of maser data to circumvent this ladder.

27.3.2. *Dark Energy Experiments* :

Most observational applications of these methods now take place in the context of large cosmological surveys, for which constraining dark energy and modified gravity theories is a central objective. Table 27.1 lists a selection of current and planned dark energy experiments, taken from the Snowmass 2013 Dark Energy Facilities review [25], which focused on projects in which the U.S. has either a leading role or significant participation. References and links to further information about these projects can be found in Ref. [25].

Beginning our discussion with imaging surveys, the Dark Energy Survey (DES) is covering 1/8 of the sky to an eventual depth roughly 2 magnitudes deeper than the Sloan Digital Sky Survey (SDSS), enabling weak lensing measurements with unprecedented statistical precision, cluster measurements calibrated by weak lensing, and angular BAO measurements based on photometric redshifts. With repeat imaging over a smaller area, DES will identify thousands of Type Ia SNe, which together with spectroscopic follow-up data will enable significant improvements on the current state-of-the-art for supernova (SN) cosmology. Cosmological results from weak lensing and galaxy clustering analyses of the first year DES data have recently been announced [26] and are discussed further below. The Hyper-Suprime Camera (HSC) on the Subaru 8.2-meter telescope is carrying out a similar type of optical imaging survey, probing a smaller area than DES but to greater depth. A number of results based on early HSC data have appeared recently, but cosmological weak lensing analyses are still underway. The HSC survey is one component of the Subaru Measurement of Images and Redshifts (SuMIRE) project. Beginning in the early 2020s, the dedicated Large Synoptic Survey Telescope (LSST) will scan the southern sky to SDSS-like depth every four nights. LSST imaging co-added over its decade-long primary survey will reach extraordinary depth, enabling weak lensing, cluster, and photometric BAO studies from billions of galaxies. LSST time-domain monitoring will identify and measure light curves for thousands of Type Ia SNe per year.

Turning to spectroscopic surveys, the Baryon Oscillation Spectroscopic Survey (BOSS) and its successor eBOSS use fiber-fed optical spectrographs to map the redshift-space distributions of millions of galaxies and quasars. These 3-dimensional maps enable BAO and RSD measurements, and Lyman-α forest spectra of high-redshift quasars extend these measurements to redshifts $z > 2$. As discussed below, the BOSS Collaboration has now published BAO and RSD analyses of its final data sets, and eBOSS has released the first BAO measurements from quasar clustering at $z = 1-2$. The Hobby-Eberly Telescope Dark Energy Experiment (HETDEX) uses integral field spectrographs to detect Lyman-α emission-line galaxies at $z \simeq 1.9-3.5$, probing a small sky area but a substantial comoving volume. The Dark Energy Spectroscopic Instument (DESI) follows a strategy similar to BOSS/eBOSS but on a much grander scale, using a larger telescope (4-meter vs. 2.5-meter) and a much higher fiber multiplex (5000 vs. 1000) to survey an order-of-magnitude more galaxies. A new Prime Focus Spectrograph (PFS) for the Subaru telescope will enable the spectroscopic component of SuMIRE, with the large telescope aperture and wavelength sensitivity that extends to the near-infrared (NIR) allowing it to probe a higher redshift galaxy population than DESI, over a smaller area of sky.

Compared to ground-based observations, space observations afford higher angular resolution and a far lower NIR sky background. The *Euclid* and *WFIRST* (*Wide Field Infrared Survey Telescope*) missions will exploit these advantages, conducting large area imaging surveys for weak lensing and cluster studies and slitless spectroscopic surveys of emission-line galaxies for BAO and RSD studies. *WFIRST* also incorporates an imaging and spectrophotometric supernova (SN) survey, extending to redshift $z \simeq 1.7$. Survey details are likely to evolve prior to launch, but in the current designs one can roughly characterize the difference between the *Euclid* and *WFIRST* dark energy experiments as "wide vs. deep," with planned survey areas of 15,000 deg^2 and 2200 deg^2, respectively. For weak lensing shape measurements, *Euclid* uses a single wide optical filter, while *WFIRST* uses three NIR filters. The *Euclid* galaxy redshift survey covers a large volume at relatively low space density, while the *WFIRST* survey provides denser sampling of structure in a smaller volume. There are numerous synergies among the LSST, *Euclid*, and *WFIRST* dark energy programs, as discussed in Ref. [27].

27.4. Current Constraints on Expansion, Growth, and Dark Energy

The last decade has seen dramatic progress in measurements of the cosmic expansion history and structure growth, leading to much tighter constraints on the parameters of dark energy models. CMB data from the *WMAP* and *Planck* satellites and from higher resolution ground-based experiments have provided an exquisitely detailed picture of structure at the recombination epoch and the first CMB-based measures of low redshift structure through lensing and SZ cluster counts. Cosmological supernova samples have increased in size from tens to many hundreds, with continuous coverage from $z = 0$ to $z \simeq 1.4$, alongside major improvements in data quality, analysis methods, and detailed understanding of local populations. BAO measurements have advanced from the first detections to $1-2\%$ precision at multiple redshifts, with increasingly sophisticated methods for testing systematics, fitting models, and evaluating statistical errors. Advances in X-ray, SZ, and weak lensing observations of large samples of galaxy clusters allow a multi-faceted approach to mass calibration, improving statistical precision but also revealing sources of astrophysical uncertainty. Cluster constraints have been joined by the first precise matter clustering constraints from cosmic shear weak lensing and galaxy-galaxy lensing, and by redshift-space distortion measurements that probe different aspects of structure growth at somewhat lower precision. The precision of direct H_0 measurements has sharpened from the roughly 10% error of the *HST* Key Project [28] to 2–4% in some recent analyses.

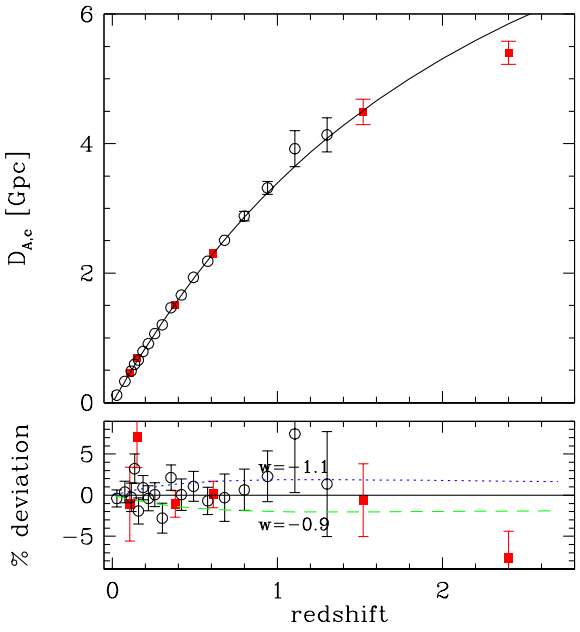

Figure 27.1: Distance-redshift relation measured from Type Ia SNe and BAO compared to the predictions (black curve) of a flat ΛCDM model with $\Omega_{\rm m} = 0.308$ and $h = 0.678$, the best-fit parameters inferred from *Planck* CMB data [29]. Circles show binned luminosity distances from the JLA SN sample [30], multiplied by $(1+z)^{-1}$ to convert to comoving angular diameter distance. Red squares show BAO distance measurements from the 6dFGS, SDSS-II, BOSS, and eBOSS surveys (see text for details and references). The lower panel plots residuals from the ΛCDM prediction, with dashed and dotted curves that show the effect of changing w by ± 0.1 while all other parameters are held fixed. Note that the SN data points can be shifted up or down by a constant factor to account for freedom in the peak luminosity, while the BAO points are calibrated to 0.3% precision by the sound horizon scale computed from *Planck* data. The errors on the BAO data points are approximately independent. In the upper panel, error bars are plotted only at $z > 0.7$ to avoid visual confusion.

As an illustration of current measurements of the cosmic expansion history, Fig. 27.1 compares distance-redshift measurements from SN and BAO data to the predictions for a flat universe with a cosmological constant. SN cosmology relies on compilation analyses that try to bring data from different surveys probing distinct redshift ranges to a common scale. Here we use the "joint light curve analysis" (JLA) sample of Ref. [30], who carried out a careful intercalibration of the 3-year Supernova Legacy Survey (SNLS3, [31]) and the full SDSS-II Supernova Survey [32] data in combination with several local supernova samples and high-redshift supernovae from *HST*. Results from the Union2.1 sample [33], which partly overlaps JLA but has different analysis procedures, would be similar. For illustration purposes, we have binned the JLA data in redshift and plotted the diagonal elements of the covariance matrix as error bars, and we have converted the SN luminosity distances to an equivalent comoving angular diameter distance. Because the peak luminosity of a fiducial SN Ia is an unknown free parameter, the SN distance measurements could all be shifted up and down by a constant multiplicative factor; cosmological information resides in the relative distances as a function of redshift. The normalization used here corresponds to a Hubble parameter $h = 0.678$.

The $z < 2$ BAO data points come from the 6-degree-Field Galaxy Survey 6dFGS survey [34], the SDSS-II Main Galaxy Sample [35], the final galaxy clustering data set from BOSS [36], and the first BAO measurement from quasar clustering in eBOSS [37]. For the 6dFGS, SDSS-II, and eBOSS data points, values of $D_{\rm V}$ have been converted to $D_{\rm A,c}$. The BOSS analysis measures $D_{\rm A,c}$ directly; we have taken values from the "BAO only" column of table 7 of Ref. [36]. At $z = 2.4$ we plot $D_{\rm A,c}$ measured from the BAO analysis of the BOSS Lyman-α forest auto-correlation and cross-correlation with quasars [38]. The BAO measurements are converted to absolute distances using the sound horizon scale $r_{\rm s} = 147.60$ Mpc from *Planck* 2015 CMB data, whose 0.29% uncertainty is small compared to the current BAO measurement errors. The BOSS galaxy and Lyman-α forest analyses also measure $H(z)$ at the same redshifts, providing further leverage on expansion history that is not captured in Fig. 27.1.

The plotted cosmological model has $\Omega_{\rm m} = 0.308$ and $h = 0.678$, the best-fit values from *Planck* (TT+lowP+lensing) assuming $w = -1$ and $\Omega_{\rm tot} = 1$ [29]. The SN, BAO, and CMB data sets, probing a wide range of redshifts with radically different techniques, are for the most part mutually consistent with the predictions of a flat ΛCDM cosmology. Other curves in the lower panel of Fig. 27.1 show the effect of changing w by ± 0.1 with all other parameters held fixed. However, such a single-parameter comparison does not capture the impact of parameter degeneracies or the ability of complementary data sets to break them, and if one instead forced a match to CMB data by changing h and $\Omega_{\rm m}$ when changing w then the predicted BAO distances would diverge at $z = 0$ rather than converging there.

As discussed by [38], the Lyman-α forest BAO measurements of $D_{\rm A,c}(z)$ and $H(z)$ at $z = 2.4$ deviate from the *Planck* ΛCDM model predictions by about 2.3σ, but the ensemble of BAO measurements (including the Lyman-α forest points)) yields a statistically acceptable χ^2 of 14.8 for 12 data points. The analyses in [38] examine a wide range of possible systematic errors but find none that are comparable in magnitude to the statistical errors. Simple extensions of the ΛCDM model (including $w \neq -1$, non-zero curvature, decaying dark matter, early dark energy, massive neutrinos, and additional relativistic species) do not remove the tension with the Lyman-α forest data points [39]. The lack of a plausible alternative model, and the acceptable total χ^2 when all data points are considered equally, suggests that the discrepancy with Lyman-α forest BAO is either a statistical fluke or a still unrecognized systematic bias in the measurement. This remains an interesting area for future investigation, as a tightening of error bars without a change in central value would imply a breakdown of this entire class of dark energy models at $z \simeq 2-3$, or an unanticipated astrophysical effect on the imprint of BAO in the Lyman-α forest.

Figure 27.2, taken from [36], presents constraints on models that allow a free but constant value of w with non-zero space curvature (`owCDM`, left panel) or the evolving equation of state of Eq. (27.4) in a flat universe (`w0waCDM`, right panel). Green contours show constraints from the combination of *Planck* 2015 CMB data and the JLA supernova sample. Gray contours show the combination of *Planck*

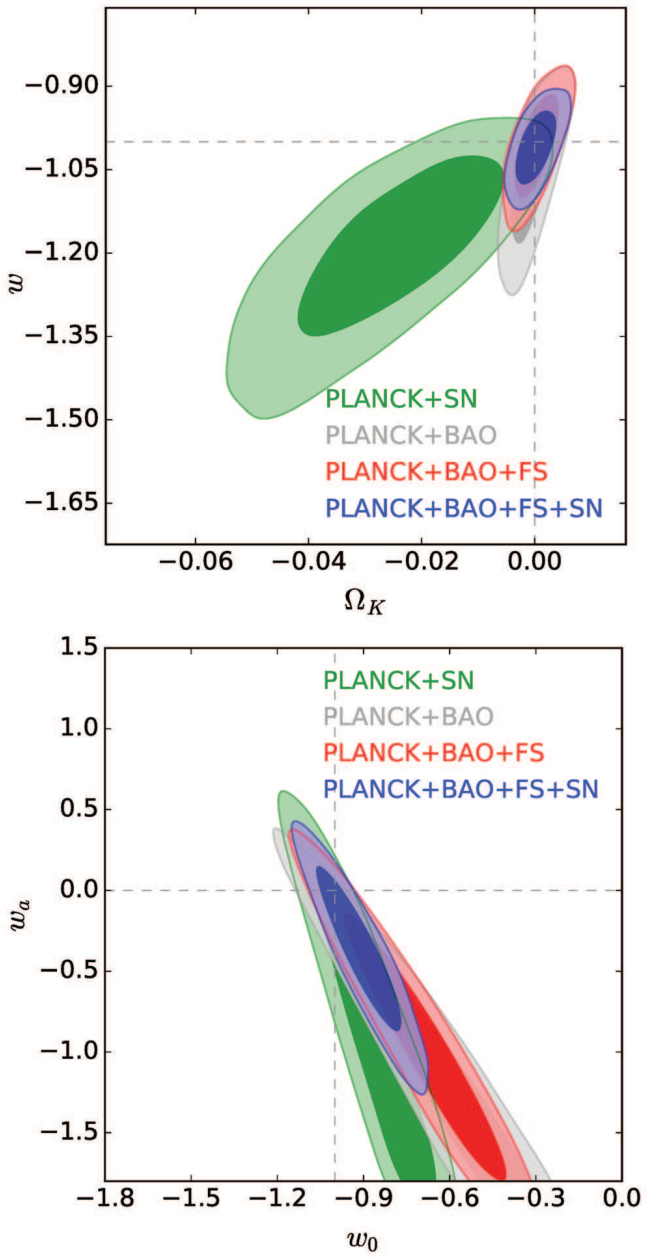

Figure 27.2: Constraints on dark energy model parameters from combinations of CMB, BAO, galaxy clustering, and supernova (SN) data, taken from Ref. [36]. The top panel shows 68% and 95% confidence contours in the `owCDM` model, with constant equation-of-state parameter w and non-zero space curvature $\Omega_K \equiv 1 - \Omega_{tot}$. Green and gray contours show the combination of *Planck* CMB data with SN or BAO data, respectively. Red contours combine CMB, BAO, and the full shape (FS) of redshift-space galaxy clustering. Blue contours add SN data to this combination. The bottom panel shows confidence contours for the same data combinations in the w_0w_a`CDM` model, which assumes a flat universe and an evolving equation of state with $w(a) = w_0 + w_a(1 - a)$.

with BAO measurements from BOSS, 6dFGS, and SDSS-II. Red contours adopt a more aggressive analysis of the BOSS galaxy data that uses the full shape (FS) of the redshift-space power spectrum and correlation function, modeled via perturbation theory, in addition to the measurement of the BAO scale itself. The full shape analysis improves the constraining power of the data, primarily because measurement of the Alcock-Paczynski effect on sub-BAO scales helps to break degeneracy between $D_{A,c}(z)$ and $H(z)$. Blue contours show constraints from the full combination of CMB, BAO+FS, and SN data. Supernovae provide fine-grained relative distance measurements with good bin-by-bin precision at $z < 0.7$ (see Fig. 27.1), which is complementary to BAO for constraining redshift evolution of w. In both classes of models, the flat ΛCDM parameters ($w = w_0 = -1$, $\Omega_K = w_a = 0$) lie within the 68% confidence contour.

The precision on dark energy parameters depends, of course, on both the data being considered and the flexibility of the model being assumed. For the `owCDM` model and the Planck+BAO+FS+SN data combination, Ref. [36] finds

$$w = -1.01 \pm 0.04 \ , \tag{27.5}$$

which we consider a reasonable characterization of current knowledge about the dark energy equation of state. The use of full shape clustering information at this level of precision is relatively new, and with the more conservative Planck+BAO combination [36] find $w = -1.05 \pm 0.08$ for `owCDM`. Similar values and uncertainties are found for similar data and model combinations by Ref. [29]. In the w_0w_a`CDM` model there is strong degeneracy between w_0 and w_a, as one can see in Fig. 27.2. However, the value of w at the pivot redshift $z_p = 0.29$ is well constrained by the Planck+BAO+FS+SN data combination, with $w_p = -1.05 \pm 0.06$ [36]. The constraint on the evolution parameter, by contrast, remains poor even with this data combination, $w_a = -0.39 \pm 0.34$. For examinations of a wide range of dark energy, dark matter, neutrino content, and modified gravity models, see Refs. [36,29,40].

A flat ΛCDM model fit to *Planck* CMB data alone predicts $H_0 = 67.8 \pm 0.9$ km s^{-1} Mpc^{-1} (see Chapter 28 of this *Review*). This is lower than most recent determinations of H_0 that use *HST* observations of Cepheid variables in external galaxies to calibrate secondary distance indicators, particularly Type Ia SNe, which can in turn measure distances to galaxies in the Hubble flow. With analyses of the same underlying data sets but different choices about data selection, calibration, and treatments of outliers and systematics, Refs. [41], [42], and [43] all found central values of H_0 above 70 km s^{-1} Mpc^{-1}, but with different error estimates implying varying levels of disagreement with *Planck*-normalized ΛCDM. Recently Ref. [44] analyzed a larger Cepheid and supernova data set and addressed several of the issues raised in earlier papers, finding $H_0 = 73.24 \pm 1.74$ km s^{-1} Mpc^{-1}, a $\sim 2.5\sigma$ discrepancy. Gravitational lensing time delays provide an alternative route to H_0 that is independent of the Cepheid distance ladder, and a recent combination of results from three systems analyzed with a consistent underlying approach yields $H_0 = 71.9^{+2.4}_{-3.1}$ km s^{-1} Mpc^{-1} [45]. With the current uncertainties, this result is consistent with both the Cepheid distance ladder and *Planck* ΛCDM values, but analysis of additional systems should shrink the error bars in the near future.

The precise inference of H_0 from *Planck* CMB data relies on the assumption of a flat ΛCDM model, and the uncertainties in H_0 become much larger once curvature or $w \neq -1$ are allowed. However, this is no longer the case once BAO and SN data are included. Ref. [39] presents an "inverse distance ladder" measurement of H_0 that uses *Planck* data *only* to constrain the sound horizon scale r_s. BOSS BAO measurements then provide $\sim 1\%$ determinations of the absolute distance scale at $z = 0.3 - 0.6$, and JLA supernovae provide precise relative distances that transfer these measurements to $z = 0$, using empirical data instead of an adopted dark energy model. Even allowing very flexible dark energy parameterizations and non-zero space curvature, Ref. [39] obtains 1.7% precision on H_0, with a value $H_0 = 67.3 \pm 1.1$ km s^{-1} Mpc^{-1} in excellent agreement with the *Planck*+ΛCDM prediction. These measurements could be reconciled with $H_0 \geq 70$ km s^{-1} Mpc^{-1} by altering the *pre-recombination* physics of the standard model in a way that shrinks the BAO standard ruler, for instance by adding extra relativistic degrees of freedom, or perhaps by rapidly accelerating expansion at very low redshift. The former solution is increasingly disfavored by the CMB measurements themselves, which constrain the energy density at recombination through its impact on the damping tail of the anisotropy spectrum. The latter solution would require dark energy dynamics more extreme than allowed by the parameterizations considered to date. Alternatively, the "H_0 tension" may reflect a

systematic bias, or at least an underestimated level of observational uncertainty, in one or more of the data sets that leads to it.

The amplitude of CMB anisotropies is proportional to the amplitude of density fluctuations present at recombination, and by assuming GR and a specified dark energy model one can extrapolate the growth of structure forward to the present day to predict σ_8. Probes of low redshift structure yield constraints in the (σ_8, Ω_m) plane, which can be summarized in terms of the parameter combination $S_8 \equiv \sigma_8(\Omega_m/0.3)^{0.5}$. As discussed in the 2014 and 2016 editions of this *Review*, and in more detail by [39], most but not all weak lensing and cluster studies to date yield S_8 values lower than those predicted for *Planck*-normalized ΛCDM. The most recent developments in this active field come from weak lensing measurements based on the first 450 deg^2 of the Kilo Degree Survey (KiDS-450) or the Year 1 data of the Dark Energy Survey (DES Y1).

Planck TT+lowP+lensing data predict $S_8 = 0.825 \pm 0.016$ after marginalizing over ΛCDM parameter uncertainties, tightening to $S_8 = 0.824 \pm 0.012$ when BAO and SN data are added [46]. Cosmic shear analysis of KiDS-450 yields $S_8 = 0.745 \pm 0.039$ [47], and combination with galaxy-galaxy lensing and galaxy clustering in overlapping 2dFLens and BOSS data gives the slightly tighter constraint $S_8 = 0.742 \pm 0.035$ [48]. However, a similar analysis combining KiDS-450 with the GAMA redshift survey yields $S_8 = 0.801 \pm 0.032$ [49], which is statistically compatible with the other KiDS-450 analyses but in much better agreement with the *Planck* ΛCDM prediction. The DES Y1 analysis combines cosmic shear, galaxy-galaxy lensing, and galaxy clustering in the DES data set to obtain $S_8 = 0.797 \pm 0.022$ [46], intermediate between the KiDS-450 cosmic shear result and the *Planck* ΛCDM prediction, and compatible with either. On smaller scales [50] find that mock catalogs of the BOSS CMASS galaxy sample with *Planck* ΛCDM cosmological parameters overpredict measurements of CMASS galaxy-galaxy lensing, by about 20% over the projected separation range $0.4 - 4\,h^{-1}$Mpc and a larger factor at smaller separations. This discrepancy is large compared to the statistical errors and to any recognized systematics in the measurement, but interpreting its significance requires more comprehensive theoretical investigation of non-linear galaxy-galaxy lensing and of astrophysical effects on the small-scale mass distribution.

In sum, current data do not provide strong evidence for a discrepancy between measured matter clustering and predictions of the CMB-normalized ΛCDM cosmology, but the mild tension between them has not disappeared. The situation should evolve rapidly over the next two years with multiple weak lensing data sets reaching the few-percent level of statistical precision, improvements in non-linear modeling of galaxy-galaxy lensing, and sharpened predictions from the final *Planck* analysis and new CMB data from the SPT and ACT experiments (see Chapter 28 of this review). CMB lensing and Lyman-α forest measurements imply that deviation from GR-predicted structure growth, if it occurs, must set in mainly at $z < 2$. A low redshift onset would not necessarily be surprising, however, as it would coincide with the era of cosmic acceleration.

27.5. Summary and Outlook

Figure 27.2 focuses on model parameter constraints, but as a description of the observational situation it is most useful to characterize the precision, redshift range, and systematic uncertainties of the basic expansion and growth measurements. At present, supernova surveys constrain distance ratios at the 1–2% level in redshift bins of width $\Delta z = 0.1$ over the range $0 < z < 0.6$, with larger but still interesting error bars out to $z \simeq 1.3$. These measurements are currently limited by systematics tied to photometric calibration, dust reddening, host galaxy correlations, and possible evolution of the SN population. BAO surveys have measured the absolute distance scale (calibrated to the sound horizon r_s) to 4% at $z = 0.15$, 1% at $z = 0.38$ and $z = 0.61$, and 2% at $z = 2.4$. Multiple studies have used clusters of galaxies or weak lensing cosmic shear or galaxy-galaxy lensing to measure a parameter combination $\sigma_8\Omega_m^\alpha$ with $\alpha \simeq 0.3$–0.5. The estimated errors of the most recent studies, including both statistical contributions and identified systematic uncertainties, are 3–5%. RSD measurements constrain the combination $f(z)\sigma_8(z)$, with recent determinations spanning the redshift range $0 < z < 0.9$ with typical estimated errors of about 10%. These errors are dominated by statistics, but shrinking them further will require improvements in modeling non-linear effects on small scales. Direct distance-ladder estimates of H_0 now span a small range (using overlapping data but distinct treatments of key steps), with individual studies quoting uncertainties of 2–5%, with similar statistical and systematic contributions. *Planck* data and higher resolution ground-based experiments now measure CMB anisotropy with exquisite precision; for example, CMB measurements now constrain the physical size of the BAO sound horizon to 0.3% and the angular scale of the sound horizon to 0.01%.

A flat ΛCDM model with standard radiation and neutrino content can fit the CMB data and the BAO and SN distance measurements to within their estimated uncertainties, excepting a moderately significant discrepancy for Lyman-α forest BAO at $z = 2.4$. However the CMB+BAO parameters for this model are in approximately 2σ tension with some of the direct H_0 measurements and many but not all of the cluster and weak lensing analyses, disagreeing by 5–10% in each case. Agreement of the "inverse distance ladder" value of H_0 with the *Planck*+ΛCDM value suggests that the current direct measurements are systematically high. Alternatively, a change to pre-recombination physics (such as extra relativistic energy density) could shrink the BAO standard ruler and raise the inferred H_0, but changes large enough to allow $H_0 \geq 70$ km s^{-1} Mpc^{-1} might run afoul of the observed CMB power spectrum. CMB lensing and Lyman-α forest measurements show good agreement with ΛCDM-predicted structure growth at $z \simeq 2 - 4$, so if the discrepancies with lower redshift measurements are real then the deviations in growth must set in at late times. At present, none of the tensions in the data provide compelling evidence for new physics. Moving forward, the community will have to balance the requirement of strong evidence for interesting claims (such as $w \neq -1$ or deviations from GR) against the danger of confirmation bias, *i.e.*, discounting observations or error estimates when they do not overlap simple theoretical expectations.

There are many ongoing projects that should lead to improvement in observational constraints in the near-term and over the next 15 years, as summarized above in Table 27.1. Final analyses of *Planck* temperature, polarization, and CMB lensing maps will improve estimates of the electron scattering optical depth and tighten other parameter constraints, thus sharpening tests based on structure growth. Preliminary results suggest a small reduction in the inferred σ_8, which goes in the direction of reducing tensions. eBOSS is measuring BAO in the previously unexplored redshift range $1 < z < 2$, and it will improve the precision of BOSS BAO measurements at lower and higher redshifts. The HETDEX project will measure BAO with Lyman-α emission line galaxies at $z = 2$–3, providing an independent check on Lyman-α forest results with completely different structure tracers. The same galaxy surveys carried out for BAO also provide data for RSD measurements of structure growth and AP measurements of cosmic geometry. With improved theoretical modeling there is potential for significant precision gains over current constraints from these methods. Analyses of Year 1 DES data already provide the tightest constraints on low redshift matter clustering, and analyses of the 3-year data (in hand) and the final 5-year data sets should yield substantial further improvements. DES is also obtaining a sample of several thousand Type Ia SNe, enabling smaller statistical errors and division of the sample into subsets for cross-checking evolutionary effects and other systematics. Weak lensing surveys from HSC on the Subaru telescope will be smaller in area than DES but deeper, with a comparable number of lensed galaxies. These new weak lensing data sets hold the promise of providing structure growth constraints at the same (roughly 1%) level of precision as the best current expansion history constraints, allowing a much more comprehensive test of cosmic acceleration models. Controlling measurement and modeling systematics at the level demanded by these surveys' statistical power will be a major challenge, but the payoff in improved precision is large. Uncertainties in direct determinations of H_0 should be reduced by further observations with *HST* and, in the longer run, by Cepheid parallaxes from the *Gaia* mission, by the ability of the *James Webb Space Telescope* to discover Cepheids in more distant SN Ia calibrator galaxies, and by independent estimates

from larger samples of maser galaxies and gravitational lensing time delays.

A still more ambitious period begins late in this decade and continues through the 2020s, with experiments that include DESI, Subaru PFS, LSST, and the space missions *Euclid* and *WFIRST*. DESI and PFS both aim for major improvements in the precision of BAO, RSD, and other measurements of galaxy clustering in the redshift range $0.8 < z < 2$, where large comoving volume allows much smaller cosmic variance errors than low redshift surveys like BOSS. LSST will be the ultimate ground-based optical weak lensing experiment, measuring several billion galaxy shapes over 20,000 deg^2 of the southern hemisphere sky, and it will detect and monitor many thousands of SNe per year. *Euclid* and *WFIRST* also have weak lensing as a primary science goal, taking advantage of the high angular resolution and extremely stable image quality achievable from space. Both missions plan large spectroscopic galaxy surveys, which will provide better sampling at high redshifts than DESI or PFS because of the lower infrared sky background above the atmosphere. *WFIRST* is also designed to carry out what should be the ultimate supernova cosmology experiment, with deep, high resolution, near-IR observations and the stable calibration achievable with a space platform.

Performance forecasts necessarily become more uncertain the further ahead we look, but collectively these experiments are likely to achieve 1–2 order of magnitude improvements over the precision of current expansion and growth measurements, while simultaneously extending their redshift range, improving control of systematics, and enabling much tighter cross-checks of results from entirely independent methods. The critical clue to the origin of cosmic acceleration could also come from a surprising direction, such as laboratory or solar system tests that challenge GR, time variation of fundamental "constants," or anomalous behavior of gravity in some astronomical environments. Experimental advances along these multiple axes could confirm today's relatively simple, but frustratingly incomplete, "standard model" of cosmology, or they could force yet another radical revision in our understanding of energy, or gravity, or the spacetime structure of the Universe.

References:

1. A. Einstein, Sitzungsber. Preuss. Akad. Wiss. Berlin (Math. Phys.), 142 (1917).
2. Y.B. Zeldovich, Soviet Physics Uspekhi **11**, 381 (1968).
3. A. Friedmann, On the curvature of space. Z. Phys. **10**, 377 (1922).
4. G. Lemaître, Annales de la Societe Scietifique de Bruxelles **47**, 49 (1927).
5. E. Hubble, Proc. Nat. Acad. Sci. **15**, 168 (1929).
6. A. Einstein and W. de Sitter, Proc. Nat. Acad. Sci. **18**, 213 (1932).
7. For background and definitions, see Big-Bang Cosmology – Sec. 21 of this *Review*.
8. A.G. Riess *et al.* [Supernova Search Team Collab.], Astron. J. **116**, 1009 (1998).
9. S. Perlmutter *et al.* [Supernova Cosmology Project Collab.], Astrophys. J. **517**, 565 (1999).
10. P. de Bernardis *et al.* [Boomerang Collab.], Nature **404**, 955 (2000).
11. S. Hanany *et al.*, Astrophys. J. **545**, L5 (2000).
12. D.H. Weinberg *et al.*, Phys. Reports **530**, 87 (2013).
13. B. Ratra and P.J.E. Peebles, Phys. Rev. **D37**, 3406 (1988) C. Wetterich, Nucl. Phys. **B302**, 668 (1988).
14. Excellent overviews of the theory and phenomenology of modified gravity models can be found in the review articles of B. Jain and J. Khoury, Ann. Phys. **325**, 1479 (2010) and A. Joyce *et al.*, Phys. Reports **568**, 1 (2015).
15. S.M. Carroll *et al.*, Phys. Rev. **D70**, 043528 (2004).
16. G.R. Dvali, G. Gabadadze, and M. Porrati, Phys. Lett. **B485**, 208 (2000).
17. C.M. Will, Living Reviews in Relativity, **9**, 3 (2006). See also the chapter on Experimental Tests of Gravitational Theory — in this *Review*.
18. B. Jain, V. Vikram, and J. Sakstein, Astrophys. J. **779**, 39 (2013) J. Wang, L. Hui, and J. Khoury, Phys. Rev. Lett. **109**, 241301 (2012).
19. Multiple investigations including M. Fairbairn and A. Goobar, Phys. Lett. **B642**, 432 (2006); Y.-S. Song, I. Sawicki, and W. Hu, Phys. Rev. **D75**, 064003 (2007); C. Blake *et al.*, Mon. Not. Roy. Astron. Soc. **415**, 2876 (2011).
20. E.V. Linder, Phys. Rev. **D72**, 043529 (2005).
21. This is essentially the FoM proposed in the Dark Energy Task Force (DETF) report, A. Albrecht *et al.*, `astro-ph/0609591`,though they based their FoM on the area of the 95% confidence ellipse in the $w_0 - w_a$ plane.
22. For high accuracy, the impact of acoustic oscillations must be computed with a full Boltzmann code, but the simple integral for r_s captures the essential physics and the scaling with cosmological parameters.
23. R.A. Sunyaev and Y.B. Zeldovich, Astrophys. Space Sci. **7**, 3 (1970).
24. C. Alcock and B. Paczynski, Nature **281**, 358 (1979).
25. D. Weinberg *et al.*, Snowmass 2013 report on Facilities for Dark Energy Investigations, `arXiv:1309.5380`.
26. DES Collaboration, T. Abbott *et al.*, `arXiv:1708.01530`.
27. B. Jain *et al.*, The Whole is Greater than the Sum of the Parts: Optimizing the Joint Science Return from LSST, Euclid and WFIRST, `arXiv:1501.07897`.
28. W.L. Freedman et al., Astrophys. J. **553**, 47 (2001).
29. Planck Collab. 2015 Results XIII, Astron. & Astrophys. **594**, A13 (2016).
30. M. Betoule *et al.*, Astron. & Astrophys. **568**, 22 (2014).
31. M. Sullivan *et al.*, Astrophys. J. **737**, 102 (2011).
32. A. Friedmann, On the curvature of space. Z. Phys. **10**, 377 (1922).
33. N. Suzuki *et al.*, Astrophys. J. **746**, 85 (2012).
34. F. Beutler *et al.*, Mon. Not. Roy. Astron. Soc. **416**, 3017 (2011).
35. A.J. Ross *et al.*, Mon. Not. Roy. Astron. Soc. **449**, 835 (2015).
36. S. Alam *et al.*, Mon. Not. Roy. Astron. Soc. **470**, 2617 (2017).
37. M. Ata *et al.*, `arXiv:1705.06373`.
38. J. Bautista *et al.*, Astron. Astrophys. **603**, A12 (2017) ; H. du Mas des Bourboux *et al.*, `arXiv:1708.02225`.
39. E. Aubourg *et al.*, Phys. Rev. D **92**, 123516 (2015).
40. Planck Collab. 2015 Results XIV, Astron. & Astrophys. **594**, A14 (2016).
41. A.G. Riess *et al.*, Astrophys. J. **730**, 119 (2011).
42. G. Efstathiou, Mon. Not. Roy. Astron. Soc. **440**, 1138 (2014).
43. B. Zhang *et al.*, Mon. Not. Roy. Astron. Soc. **471**, 2254 (2017).
44. A. Riess *et al.*, Astrophys. J. **826**, 56 (2016).
45. V. Bonvin *et al.*, Mon. Not. Roy. Astron. Soc. **465**, 4914 (2017).
46. For *Planck* we quote values from Table 4 of Ref. [29]. For DES Y1 we quote the value from equation VII.7 of Ref. [26], which assumes a neutrino mass sum of 0.06 eV as in the other analyses quoted..
47. H. Hildebrandt *et al.*, Mon. Not. Roy. Astron. Soc. **465**, 1454 (2017).
48. S. Joudaki *et al.*, `arXiv:1707.06627`.
49. E. van Uitert *et al.*, `arXiv:1706.05004`.
50. A. Leauthaud *et al.*, Mon. Not. Roy. Astron. Soc. **467**, 3024 (2017).

28. Cosmic Microwave Background

Revised August 2017 by D. Scott (University of British Columbia) and G.F. Smoot (UCB/LBNL).

28.1. Introduction

The energy content in radiation from beyond our Galaxy is dominated by the cosmic microwave background (CMB), discovered in 1965 [1]. The spectrum of the CMB is well described by a blackbody function with $T = 2.7255\,\mathrm{K}$. This spectral form is a main supporting pillar of the hot Big Bang model for the Universe. The lack of any observed deviations from a blackbody spectrum constrains physical processes over cosmic history at redshifts $z \lesssim 10^7$ (see earlier versions of this review).

Currently the key CMB observable is the angular variation in temperature (or intensity) correlations, and now to some extent polarization [2]. Since the first detection of these anisotropies by the Cosmic Background Explorer (*COBE*) satellite [3], there has been intense activity to map the sky at increasing levels of sensitivity and angular resolution by ground-based and balloon-borne measurements. These were joined in 2003 by the first results from NASA's Wilkinson Microwave Anisotropy Probe (*WMAP*) [4], which were improved upon by analyses of the 3-year, 5-year, 7-year, and 9-year *WMAP* data [5,6,7,8]. In 2013 we had the first results [9] from the third generation CMB satellite, ESA's *Planck* mission [10,11], which were enhanced by results from the the 2015 *Planck* data release [12,13]. Additionally, CMB anisotropies have been extended to smaller angular scales by ground-based experiments, particularly the Atacama Cosmology Telescope (ACT) [14] and the South Pole Telescope (SPT) [15]. Together these observations have led to a stunning confirmation of the 'Standard Model of Cosmology.' In combination with other astrophysical data, the CMB anisotropy measurements place quite precise constraints on a number of cosmological parameters, and have launched us into an era of precision cosmology. With the study of the CMB passing the half-century mark, the program to map temperature anisotropies is effectively wrapping up, and attention is increasingly focussing on polarization measurements as the future arena in which to test fundamental physics.

28.2. CMB Spectrum

It is well known that the spectrum of the microwave background is very precisely that of blackbody radiation, whose temperature evolves with redshift as $T(z) = T_0(1+z)$ in an expanding universe. As a direct test of its cosmological origin, this relationship has been tested by measuring the strengths of emission and absorption lines in high-redshift systems [16].

Measurements of the spectrum are consistent with a blackbody distribution over more than three decades in frequency (there is a claim by ARCADE [17] of a possible unexpected extragalactic emission signal at low frequency, but the interpretation is debated [18]). All viable cosmological models predict a very nearly Planckian spectrum to within the current observational limits. Because of this, measurements of deviations from a blackbody spectrum have received little attention in recent years, with only a few exceptions. However, that situation will eventually change, since proposed experiments (such as PIXIE [19]) have the potential to dramatically improve the constraints on energy release in the early Universe. It now seems feasible to probe spectral distortion mechanisms that are *required* in the standard picture, such as those arising from the damping and dissipation of relatively small primordial perturbations, or the average effect of inverse Compton scattering. A more ambitious goal would be to reach the precision needed to detect the residual lines from the cosmological recombination of hydrogen and helium and hence test whether conditions at $z \gtrsim 1000$ accurately follow those in the standard picture [20].

28.3. Description of CMB Anisotropies

Observations show that the CMB contains temperature anisotropies at the 10^{-5} level and polarization anisotropies at the 10^{-6} (and lower) level, over a wide range of angular scales. These anisotropies are usually expressed by using a spherical harmonic expansion of the CMB sky:

$$T(\theta,\phi) = \sum_{\ell m} a_{\ell m} Y_{\ell m}(\theta,\phi)$$

(with the linear polarization pattern written in a similar way using the so-called spin-2 spherical harmonics). Increasing angular resolution requires that the expansion goes to higher and higher multipoles. Because there are only very weak phase correlations seen in the CMB sky and since we notice no preferred direction, the vast majority of the cosmological information is contained in the temperature 2-point function, *i.e.*, the variance as a function only of angular separation. Equivalently, the power per unit $\ln \ell$ is $\ell \sum_m |a_{\ell m}|^2 / 4\pi$.

28.3.1. *The Monopole* :

The CMB has a mean temperature of $T_\gamma = 2.7255 \pm 0.0006\,\mathrm{K}$ (1σ) [21], which can be considered as the monopole component of CMB maps, a_{00}. Since all mapping experiments involve difference measurements, they are insensitive to this average level; monopole measurements can only be made with absolute temperature devices, such as the FIRAS instrument on the *COBE* satellite [22]. The measured kT_γ is equivalent to $0.234\,\mathrm{meV}$ or $4.60 \times 10^{-10}\, m_e c^2$. A blackbody of the measured temperature has a number density $n_\gamma = (2\zeta(3)/\pi^2)\, T_\gamma^3 \simeq 411\,\mathrm{cm}^{-3}$, energy density $\rho_\gamma = (\pi^2/15)\, T_\gamma^4 \simeq 4.64 \times 10^{-34}\,\mathrm{g\,cm}^{-3} \simeq 0.260\,\mathrm{eV\,cm}^{-3}$, and a fraction of the critical density $\Omega_\gamma \simeq 5.38 \times 10^{-5}$.

28.3.2. *The Dipole* :

The largest anisotropy is in the $\ell = 1$ (dipole) first spherical harmonic, with amplitude $3.3645 \pm 0.0020\,\mathrm{mK}$ [12]. The dipole is interpreted to be the result of the Doppler boosting of the monopole caused by the solar system motion relative to the nearly isotropic blackbody field, as broadly confirmed by measurements of the radial velocities of local galaxies (*e.g.*, Ref. [23]); the intrinsic part of the signal is expected to be 2 orders of magnitude smaller (and fundamentally difficult to distinguish). The motion of an observer with velocity $\beta \equiv v/c$ relative to an isotropic Planckian radiation field of temperature T_0 produces a Lorentz-boosted temperature pattern

$$\begin{aligned} T(\theta) &= T_0(1-\beta^2)^{1/2}/(1-\beta\cos\theta) \\ &\simeq T_0\left[1 + \beta\cos\theta + \left(\beta^2/2\right)\cos 2\theta + \mathrm{O}\left(\beta^3\right)\right]. \end{aligned}$$

At every point in the sky, one observes a blackbody spectrum, with temperature $T(\theta)$. The spectrum of the dipole has been confirmed to be the differential of a blackbody spectrum [24]. At higher order there are additional effects arising from aberration and from modulation of the anisotropy pattern, which have also been observed [25].

The implied velocity for the solar system barycenter is $v = 370.09 \pm 0.22\,\mathrm{km\,s}^{-1}$, assuming a value $T_0 = T_\gamma$, towards $(l,b) = (264.00^\circ \pm 0.03^\circ, 48.24^\circ \pm 0.02^\circ)$ [12]. Such a solar system motion implies a velocity for the Galaxy and the Local Group of galaxies relative to the CMB. The derived value is $v_{\mathrm{LG}} = 627 \pm 22\,\mathrm{km\,s}^{-1}$ towards $(l,b) = (276^\circ \pm 3^\circ, 30^\circ \pm 3^\circ)$ [26], where most of the error comes from uncertainty in the velocity of the solar system relative to the Local Group.

The dipole is a frame-dependent quantity, and one can thus determine the 'absolute rest frame' as that in which the CMB dipole would be zero. Our velocity relative to the Local Group, as well as the velocity of the Earth around the Sun, and any velocity of the receiver relative to the Earth, is normally removed for the purposes of CMB anisotropy study. The dipole is now routinely used as a primary calibrator for mapping experiments, either via the time-varying orbital motion of the Earth, or through the cosmological dipole measured by satellite experiments.

28.3.3. *Higher-Order Multipoles* :

The variations in the CMB temperature maps at higher multipoles ($\ell \geq 2$) are interpreted as being mostly the result of perturbations in the density of the early Universe, manifesting themselves at the epoch of the last scattering of the CMB photons. In the hot Big Bang picture, the expansion of the Universe cools the plasma so that by a redshift $z \simeq 1100$ (with little dependence on the details of the model), the hydrogen and helium nuclei can bind electrons into neutral atoms, a process usually referred to as recombination [27]. Before this epoch, the CMB photons were tightly coupled to the baryons, while afterwards they could freely stream towards us. By measuring the $a_{\ell m}$s we are thus learning directly about physical conditions in the early Universe.

A statistically isotropic sky means that all ms are equivalent, *i.e.*, there is no preferred axis, so that the temperature correlation function between two positions on the sky depends only on angular separation and not orientation. Together with the assumption of Gaussian statistics (*i.e.*, no correlations between the modes), the variance of the temperature field (or equivalently the power spectrum in ℓ) then fully characterizes the anisotropies. The power summed over all ms at each ℓ is $(2\ell+1)C_\ell/(4\pi)$, where $C_\ell \equiv \langle |a_{\ell m}|^2 \rangle$. Thus averages of $a_{\ell m}$s over m can be used as estimators of the C_ℓs to constrain their expectation values, which are the quantities predicted by a theoretical model. For an idealized full-sky observation, the variance of each measured C_ℓ (*i.e.*, the variance of the variance) is $[2/(2\ell+1)]C_\ell^2$. This sampling uncertainty (known as 'cosmic variance') comes about because each C_ℓ is χ^2 distributed with $(2\ell+1)$ degrees of freedom for our observable volume of the Universe. For fractional sky coverage, $f_{\rm sky}$, this variance is increased by $1/f_{\rm sky}$ and the modes become partially correlated.

It is important to understand that theories predict the expectation value of the power spectrum, whereas our sky is a single realization. Hence the cosmic variance is an unavoidable source of uncertainty when constraining models; it dominates the scatter at lower ℓs, while the effects of instrumental noise and resolution dominate at higher ℓs [28].

Theoretical models generally predict that the $a_{\ell m}$ modes are Gaussian random fields to high precision, matching the empirical tests, *e.g.*, standard slow-roll inflation's non-Gaussian contribution is expected to be at least an order of magnitude below current observational limits [29]. Although non-Gaussianity of various forms is possible in early Universe models, tests show that Gaussianity is an extremely good simplifying approximation [30]. The only current indications of any non-Gaussianity or statistical anisotropy are some relatively weak signatures at large scales, seen in both *WMAP* [31] and *Planck* data [32], but not of high enough significance to reject the simplifying assumption. Nevertheless, models that deviate from the inflationary slow-roll conditions can have measurable non-Gaussian signatures. So while the current observational limits make the power spectrum the dominant probe of cosmology, it is worth noting that higher-order correlations are beginning to be a tool for constraining otherwise viable theories.

28.3.4. *Angular Resolution and Binning* :

There is no one-to-one conversion between multipole ℓ and the angle subtended by a particular spatial scale projected onto the sky. However, a single spherical harmonic $Y_{\ell m}$ corresponds to angular variations of $\theta \sim \pi/\ell$. CMB maps contain anisotropy information from the size of the map (or in practice some fraction of that size) down to the beam-size of the instrument, σ (the standard deviation of the beam, in radians). One can think of the effect of a Gaussian beam as rolling off the power spectrum with the function $\mathrm{e}^{-\ell(\ell+1)\sigma^2}$.

For less than full sky coverage, the ℓ modes become correlated. Hence, experimental results are usually quoted as a series of 'band powers,' defined as estimators of $\ell(\ell+1)C_\ell/2\pi$ over different ranges of ℓ. Because of the strong foreground signals in the Galactic Plane, even 'all-sky' surveys, such as *WMAP* and *Planck* involve a cut sky. The amount of binning required to obtain uncorrelated estimates of power also depends on the map size.

28.4. Cosmological Parameters

The current 'Standard Model' of cosmology contains around 10 free parameters (see The Cosmological Parameters—Sec. 24 of this *Review*). The basic framework is the Friedmann-Robertson-Walker (FRW) metric (*i.e.*, a universe that is approximately homogeneous and isotropic on large scales), with density perturbations laid down at early times and evolving into today's structures (see Big-Bang cosmology—Sec. 21 of this *Review*). The most general possible set of density variations is a linear combination of an adiabatic density perturbation and some isocurvature perturbations. Adiabatic means that there is no change to the entropy per particle for each species, *i.e.*, $\delta\rho/\rho$ for matter is $(3/4)\delta\rho/\rho$ for radiation. Isocurvature means that the set of individual density perturbations adds to zero, for example, matter perturbations compensate radiation perturbations so that the total energy density remains unperturbed, *i.e.*, $\delta\rho$ for matter is $-\delta\rho$ for radiation. These different modes give rise to distinct (temporal) phases during growth, with those of the adiabatic scenario looking exactly like the data. Models that generate mainly isocurvature type perturbations (such as most topological defect scenarios) are no longer considered to be viable. However, an admixture of the adiabatic mode with up to about 4% isocurvature contribution (depending on details of the mode) is still allowed [33,34].

28.4.1. *Initial Condition Parameters* :

Within the adiabatic family of models, there is, in principle, a free function describing the variation of comoving curvature perturbations, $\mathcal{R}(\mathbf{x}, t)$. The great virtue of $\mathcal{R}$ is that it is constant in time for a purely adiabatic perturbation. There are physical reasons to anticipate that the variance of these perturbations will be described well by a power law in scale, *i.e.*, in Fourier space $\left\langle |\mathcal{R}|_k^2 \right\rangle \propto k^{n_{\rm s}-4}$, where k is wavenumber and $n_{\rm s}$ is the usual definition of spectral index. So-called 'scale-invariant' initial conditions (meaning gravitational potential fluctuations that are independent of k) correspond to $n_{\rm s} = 1$. In inflationary models [35] (see Inflation—Sec. 22 of this *Review*), perturbations are generated by quantum fluctuations, which are set by the energy scale of inflation, together with the slope and higher derivatives of the inflationary potential. One generally expects that the Taylor series expansion of $\ln \mathcal{R}_k(\ln k)$ has terms of steadily decreasing size. For the simplest models, there are thus two parameters describing the initial conditions for density perturbations, namely the amplitude and slope of the power spectrum. These can be explicitly defined, for example, through:

$$\Delta^2_{\mathcal{R}} \equiv (k^3/2\pi^2)\left\langle |\mathcal{R}|_k^2 \right\rangle \simeq A_{\rm s}\,(k/k_0)^{n_{\rm s}-1}\,,$$

with $A_{\rm s} \equiv \Delta^2_{\mathcal{R}}(k_0)$ and $k_0 = 0.05\,\mathrm{Mpc}^{-1}$, say. There are many other equally valid definitions of the amplitude parameter (see also Secs. 21, 24, and 22 of this *Review*), and we caution that the relationships between some of them can be cosmology-dependent. In 'slow roll' inflationary models, this normalization is proportional to the combination $V^3/(V')^2$, for the inflationary potential $V(\phi)$. The slope $n_{\rm s}$ also involves V'', and so the combination of $A_{\rm s}$ and $n_{\rm s}$ can constrain potentials.

Inflation generates tensor (gravitational wave) modes, as well as scalar (density perturbation) modes. This fact introduces another parameter, measuring the amplitude of a possible tensor component, or equivalently the ratio of the tensor to scalar contributions. The tensor amplitude is $A_{\rm t} \propto V$, and thus one expects a larger gravitational wave contribution in models where inflation happens at higher energies. The tensor power spectrum also has a slope, often denoted $n_{\rm t}$, but since this seems unlikely to be measured in the near future, it is sufficient for now to focus only on the amplitude of the gravitational wave component. It is most common to define the tensor contribution through r, the ratio of tensor to scalar perturbation spectra at some small value of k (*e.g.*, $k = 0.002\,\mathrm{Mpc}^{-1}$, although sometimes it is defined in terms of the ratio of contributions at $\ell = 2$). Different inflationary potentials will lead to different predictions, *e.g.*, for 50 e-folds $\lambda\phi^4$ inflation gives $r = 0.32$ and $m^2\phi^2$ inflation gives $r = 0.16$ (both now disfavored by the data), while other models can have arbitrarily small values of r. In any case, whatever the specific definition, and whether they come from inflation or something else, the 'initial conditions' give rise to a minimum of three parameters, $A_{\rm s}$, $n_{\rm s}$, and r.

28.4.2. *Background Cosmology Parameters* :

The FRW cosmology requires an expansion parameter (the Hubble Constant, H_0, often represented through $H_0 = 100\,h\,\mathrm{km\,s^{-1}Mpc^{-1}}$) and several parameters to describe the matter and energy content of the Universe. These are usually given in terms of the critical density, *i.e.*, for species 'x,' $\Omega_{\rm x} \equiv \rho_{\rm x}/\rho_{\rm crit}$, where $\rho_{\rm crit} \equiv 3H_0^2/8\pi G$. Since physical densities $\rho_{\rm x} \propto \Omega_{\rm x}h^2 \equiv \omega_{\rm x}$ are what govern the physics of the CMB anisotropies, it is these ωs that are best constrained by CMB data. In particular CMB, observations constrain $\Omega_{\rm b}h^2$ for baryons and $\Omega_{\rm c}h^2$ for cold dark matter (with $\rho_{\rm m} = \rho_{\rm c} + \rho_{\rm b}$ for the sum).

The contribution of a cosmological constant Λ (or other form of dark energy, see Dark Energy—Sec. 27) is usually included via a parameter that quantifies the curvature, $\Omega_K \equiv 1 - \Omega_{\rm tot}$, where $\Omega_{\rm tot} = \Omega_{\rm m} + \Omega_\Lambda$. The radiation content, while in principle a free parameter, is precisely enough determined by the measurement of T_γ that it can be considered fixed, and makes a $< 10^{-4}$ contribution to $\Omega_{\rm tot}$ today.

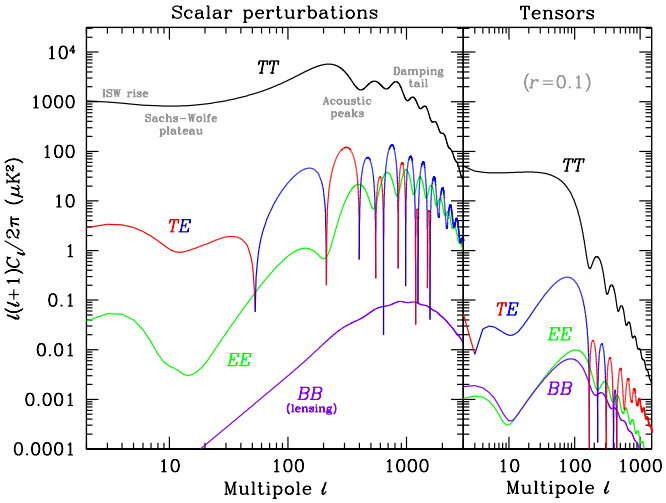

Figure 28.1: Theoretical CMB anisotropy power spectra, using the best-fitting ΛCDM model from *Planck*, calculated using `CAMB`. The panel on the left shows the theoretical expectation for scalar perturbations, while the panel on the right is for tensor perturbations, with an amplitude set to $r = 0.1$ for illustration. Note that the x-axis is logarithmic here. For the well-measured scalar TT spectrum, the regions, each covering roughly a decade in ℓ, are labeled as in the text: the ISW rise; Sachs-Wolfe plateau; acoustic peaks; and damping tail. The TE cross-correlation power spectra change sign, and that has been indicated by plotting the absolute value, but switching color for the negative parts.

Astrophysical processes at relatively low redshift can also affect the C_ℓs, with a particularly significant effect coming through reionization. The Universe became reionized at some redshift $z_{\rm i}$, long after recombination, affecting the CMB through the integrated Thomson scattering optical depth:

$$\tau = \int_0^{z_{\rm i}} \sigma_{\rm T} n_{\rm e}(z) \frac{dt}{dz} dz,$$

where $\sigma_{\rm T}$ is the Thomson cross-section, $n_{\rm e}(z)$ is the number density of free electrons (which depends on astrophysics), and dt/dz is fixed by the background cosmology. In principle, τ can be determined from the small-scale matter power spectrum, together with the physics of structure formation and radiative feedback processes; however, this is a sufficiently intricate calculation that in practice τ needs to be considered as a free parameter.

Thus, we have eight basic cosmological parameters: $A_{\rm s}$, $n_{\rm s}$, r, h, $\Omega_{\rm b}h^2$, $\Omega_{\rm c}h^2$, $\Omega_{\rm tot}$, and τ. One can add additional parameters to this list, particularly when using the CMB in combination with other data sets. The next most relevant ones might be: $\Omega_\nu h^2$, the massive neutrino contribution; w ($\equiv p/\rho$), the equation of state parameter for the dark energy; and $dn_{\rm s}/d\ln k$, measuring deviations from a constant spectral index. To these 11 one could of course add further parameters describing additional physics, such as details of the reionization process, features in the initial power spectrum, a sub-dominant contribution of isocurvature modes, *etc.*

As well as these underlying parameters, there are other (dependent) quantities that can be obtained from them. Such derived parameters include the actual Ωs of the various components (*e.g.*, $\Omega_{\rm m}$), the variance of density perturbations at particular scales (*e.g.*, σ_8), the angular scale of the sound horizon (θ_*), the age of the Universe today (t_0), the age of the Universe at recombination, reionization, *etc.* (see The Cosmological Parameters—Sec. 24).

28.5. Physics of Anisotropies

The cosmological parameters affect the anisotropies through the well understood physics of the evolution of linear perturbations within a background FRW cosmology. There are very effective, fast, and publicly available software codes for computing the CMB anisotropy, polarization, and matter power spectra, *e.g.*, `CMBFAST` [36], `CAMB` [37], and `CLASS` [38]. These have been tested over a wide range of cosmological parameters and are considered to be accurate to much better than the 1% level [39], so that numerical errors are less than 10% of the parameter uncertainties for *Planck* [9].

For pedagogical purposes, it is easiest to focus on the temperature anisotropies, before moving to the polarization power spectra. A description of the physics underlying the C_ℓ^{TT}s can be separated into four main regions (the first two combined below), as shown in the top left part of Fig. 28.1.

28.5.1. *The ISW Rise, $\ell \lesssim 10$, and Sachs-Wolfe Plateau, $10 \lesssim \ell \lesssim 100$* :

The horizon scale (or more precisely, the angle subtended by the Hubble radius) at last scattering corresponds to $\ell \simeq 100$. Anisotropies at larger scales have not evolved significantly, and hence directly reflect the 'initial conditions.' Temperature variations are $\delta T/T = -(1/5)\mathcal{R}(\mathbf{x}_{\rm LSS}) \simeq (1/3)\delta\phi/c^2$, where $\delta\phi$ is the perturbation to the gravitational potential, evaluated on the last scattering surface (LSS). This is a result of the combination of gravitational redshift and intrinsic temperature fluctuations, and is usually referred to as the Sachs-Wolfe effect [40].

Assuming that a nearly scale-invariant spectrum of curvature and corresponding density perturbations was laid down at early times (*i.e.*, $n_{\rm s} \simeq 1$, meaning equal power per decade in k), then $\ell(\ell+1)C_\ell \simeq$ constant at low ℓs. This effect is hard to see unless the multipole axis is plotted logarithmically (as in Fig. 28.1, and part of Fig. 28.2).

Time variation of the potentials (*i.e.*, time-dependent metric perturbations) leads to an upturn in the C_ℓs in the lowest several multipoles; any deviation from a total equation of state $w = 0$ has such an effect. So the dominance of the dark energy at low redshift (see Dark Energy—Sec. 27) makes the lowest ℓs rise above the plateau. This is sometimes called the integrated Sachs-Wolfe effect (or ISW rise), since it comes from the line integral of $\dot\phi$; it has been confirmed through correlations between the large-angle anisotropies and large-scale structure [41]. Specific models can also give additional contributions at low ℓ (*e.g.*, perturbations in the dark energy component itself [42]), but typically these are buried in the cosmic variance.

In principle, the mechanism that produces primordial perturbations could generate scalar, vector, and tensor modes. However, the vector (vorticity) modes decay with the expansion of the Universe. The tensors (transverse trace-free perturbations to the metric) generate temperature anisotropies through the integrated effect of the locally anisotropic expansion of space. Since the tensor modes also redshift away after they enter the horizon, they contribute only to angular scales above about 1° (see Fig. 28.1). Hence some fraction of the low-ℓ signal could be due to a gravitational wave contribution, although small amounts of tensors are essentially impossible to discriminate from other effects that might raise the level of the plateau. Nevertheless, the tensors *can* be distinguished using polarization information (see Sec. 28.7).

28.5.2. *The Acoustic Peaks, $100 \lesssim \ell \lesssim 1000$* :

On sub-degree scales, the rich structure in the anisotropy spectrum is the consequence of gravity-driven acoustic oscillations occurring before the atoms in the Universe became neutral [43]. Perturbations inside the horizon at last scattering have been able to evolve causally and produce anisotropy at the last scattering epoch, which reflects this evolution. The frozen-in phases of these sound waves imprint a dependence on the cosmological parameters, which gives CMB anisotropies their great constraining power.

The underlying physics can be understood as follows. Before the Universe became neutral, the proton-electron plasma was tightly coupled to the photons, and these components behaved as a single 'photon-baryon fluid.' Perturbations in the gravitational potential, dominated by the dark matter component, were steadily evolving.

They drove oscillations in the photon-baryon fluid, with photon pressure providing most of the restoring force and baryons giving some additional inertia. The perturbations were quite small in amplitude, $O(10^{-5})$, and so evolved linearly. That means each Fourier mode developed independently, and hence can be described by a driven harmonic oscillator, with frequency determined by the sound speed in the fluid. Thus the fluid density underwent oscillations, giving time variations in temperature. These combine with a velocity effect, which is $\pi/2$ out of phase and has its amplitude reduced by the sound speed.

After the Universe recombined, the radiation decoupled from the baryons and could travel freely towards us. At that point, the (temporal) phases of the oscillations were frozen-in, and became projected on the sky as a harmonic series of peaks. The main peak is the mode that went through 1/4 of a period, reaching maximal compression. The even peaks are maximal *under*-densities, which are generally of smaller amplitude because the rebound has to fight against the baryon inertia. The troughs, which do not extend to zero power, are partially filled by the Doppler effect because they are at the velocity maxima.

The physical length scale associated with the peaks is the sound horizon at last scattering, which can be straightforwardly calculated. This length is projected onto the sky, leading to an angular scale that depends on the geometry of space, as well as the distance to last scattering. Hence the angular position of the peaks is a sensitive probe of a particular combination of cosmological parameters. In fact, the angular scale, θ_*, is the most precisely measured observable, and hence is usually treated as an element of the cosmological parameter set.

One additional effect arises from reionization at redshift $z_{\rm i}$. A fraction of photons (τ) will be isotropically scattered at $z < z_{\rm i}$, partially erasing the anisotropies at angular scales smaller than those subtended by the Hubble radius at $z_{\rm i}$. This corresponds typically to ℓs above about 10, depending on the specific reionization model. The acoustic peaks are therefore reduced by a factor $e^{-2\tau}$ relative to the plateau.

These peaks were a clear theoretical prediction going back to about 1970 [44]. One can think of them as a snapshot of stochastic standing waves. Since the physics governing them is simple and their structure rich, one can see how they encode extractable information about the cosmological parameters. Their empirical existence started to become clear around 1994 [45], and the emergence, over the following decade, of a coherent series of acoustic peaks and troughs is a triumph of modern cosmology. This picture has received further confirmation with the detection in the power spectrum of galaxies (at redshifts close to zero) of the imprint of these same acoustic oscillations in the baryon component [46], as well as through detection of the expected oscillations in CMB polarization power spectra (see Sec. 28.7).

28.5.3. *The Damping Tail, $\ell \gtrsim 1000$* :

The recombination process is not instantaneous, which imparts a thickness to the last scattering surface. This leads to a damping of the anisotropies at the highest ℓs, corresponding to scales smaller than that subtended by this thickness. One can also think of the photon-baryon fluid as having imperfect coupling, so that there is diffusion between the two components, and hence the amplitudes of the oscillations decrease with time. These effects lead to a damping of the C_ℓs, sometimes called Silk damping [47], which cuts off the anisotropies at multipoles above about 2000. So, although in principle it is possible to measure to ever smaller scales, this becomes increasingly difficult in practice.

28.5.4. *Gravitational Lensing Effects* :

An extra effect at high ℓs comes from gravitational lensing, caused mainly by non-linear structures at low redshift. The C_ℓs are convolved with a smoothing function in a calculable way, partially flattening the peaks and troughs, generating a power-law tail at the highest multipoles, and complicating the polarization signal [48]. The expected effects of lensing on the CMB have been definitively detected through the 4-point function, which correlates temperature gradients and small-scale anisotropies (enabling a map of the lensing potential to be constructed [49,50]), as well as through the smoothing effect on the shape of the C_ℓs. Lensing is important because it gives an independent estimate of $A_{\rm s}$, breaking the parameter combination $A_{\rm s}e^{-2\tau}$ that is largely degenerate in the anisotropy power spectra.

Lensing is an example of a 'secondary effect,' *i.e.*, the processing of anisotropies due to relatively nearby structures (see Sec. 28.8.2). Galaxies and clusters of galaxies give several such effects; all are expected to be of low amplitude, but are increasingly important at the highest ℓs. Such effects carry additional cosmological information (about evolving gravitational potentials in the low-redshift Universe) and are increasing in importance as experiments push to higher sensitivity and angular resolution. The lensing power spectrum provides independent constraints on the amplitude of perturbations, as well as potentially constraining dark energy evolution, while future measurements at high ℓ are a particularly sensitive probe of the sum of the neutrino masses [51].

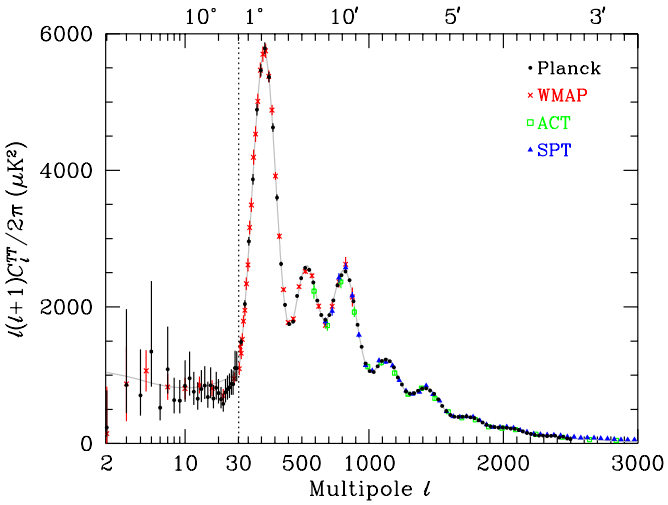

Figure 28.2: CMB temperature anisotropy band-power estimates from the *Planck*, *WMAP*, ACT, and SPT experiments. Note that the widths of the ℓ-bands vary between experiments and have not been plotted. This figure represents only a selection of the most recent available experimental results, and some points with large error bars have been omitted. At the higher multipoles these band-powers involve subtraction of particular foreground models, and so proper analysis requires simultaneous fitting of CMB and foregrounds over multiple frequencies. The x-axis here is logarithmic for the lowest multipoles, to show the Sachs-Wolfe plateau, and linear for the other multipoles. The acoustic peaks and damping region are very clearly observed, with no need for a theoretical curve to guide the eye; however, the curve plotted is the best-fit *Planck* ΛCDM model.

28.6. Current Temperature Anisotropy Data

There has been a steady improvement in the quality of CMB data that has led to the development of the present-day cosmological model. The most robust constraints currently available come from *Planck* satellite [52,53] data (together with constraints from non-CMB cosmological data-sets), although smaller scale results from the ACT [54] and SPT [55] experiments are becoming competetive. We plot power spectrum estimates from these experiments in Fig. 28.2, along with *WMAP* data [8] to show the consistency (see previous versions of this review for data from earlier experiments). Comparisons among data-sets show very good agreement, both in maps and in derived power spectra (up to systematic uncertainties in the overall calibration for some experiments). This makes it clear that systematic effects are largely under control.

The band-powers shown in Fig. 28.2 are in very good agreement with a 'ΛCDM' model. As described earlier, several (at least eight) of the peaks and troughs are quite apparent. For details of how these estimates were arrived at, the strength of correlations between band-powers and other information required to properly interpret them, the original papers should be consulted.

28.7. CMB Polarization

Since Thomson scattering of an anisotropic radiation field also generates linear polarization, the CMB is predicted to be polarized at the level of roughly 5% of the temperature anisotropies [56]. Polarization is a spin-2 field on the sky, and the algebra of the modes in ℓ-space is strongly analogous to spin-orbit coupling in quantum mechanics [57]. The linear polarization pattern can be decomposed in a number of ways, with two quantities required for each pixel in a map, often given as the Q and U Stokes parameters. However, the most intuitive and physical decomposition is a geometrical one, splitting the polarization pattern into a part that comes from a divergence (often referred to as the 'E-mode') and a part with a curl (called the 'B-mode') [58]. More explicitly, the modes are defined in terms of second derivatives of the polarization amplitude, with the Hessian for the E-modes having principle axes in the same sense as the polarization, while the B-mode pattern can be thought of as a 45° rotation of the E-mode pattern. Globally one sees that the E-modes have $(-1)^\ell$ parity (like the spherical harmonics), while the B-modes have $(-1)^{\ell+1}$ parity.

The existence of this linear polarization allows for six different cross-power spectra to be determined from data that measure the full temperature and polarization anisotropy information. Parity considerations make two of these zero, and we are left with four potential observables, C_ℓ^{TT}, C_ℓ^{TE}, C_ℓ^{EE}, and C_ℓ^{BB} (see Fig. 28.1). Because scalar perturbations have no handedness, the B-mode power spectrum can only be sourced by vectors or tensors. Moreover, since inflationary scalar perturbations give only E-modes, while tensors generate roughly equal amounts of E- and B-modes, then the determination of a non-zero B-mode signal is a way to measure the gravitational wave contribution (and thus potentially derive the energy scale of inflation). However, since the signal is expected to be rather weak, one must first eliminate the foreground contributions and other systematic effects down to very low levels.

Like with temperature, the polarization C_ℓs exhibit a series of acoustic peaks generated by the oscillating photon-baryon fluid. The main 'EE' power spectrum has peaks that are out of phase with those in the 'TT' spectrum because the polarization anisotropies are sourced by the fluid velocity. The 'TE' part of the polarization and temperature patterns comes from correlations between density and velocity perturbations on the last scattering surface, which can be both positive and negative, and is of larger amplitude than the EE signal. There is no polarization Sachs-Wolfe effect, and hence no large-angle plateau. However, scattering during a recent period of reionization can create a polarization 'bump' at large angular scales.

Because the polarization anisotropies have only a fraction of the amplitude of the temperature anisotropies, they took longer to detect. The first measurement of a polarization signal came in 2002 from the DASI experiment [59], which provided a convincing detection, confirming the general paradigm, but of low enough significance that it lent no real constraint to models. Despite dramatic progress since then, it is still the case that polarization data mainly support the basic paradigm, without dramatically reducing error bars on parameters. However, there are exceptions to this, specifically in the reionization optical depth, and the potential to constrain primordial gravitational waves.

28.7.1. *T–E Power Spectrum*:

Since the T and E skies are correlated, one has to measure the TE power spectrum, as well as TT and EE, in order to extract all the cosmological information. This TE signal has now been mapped out extremely accurately by *Planck* [53], and these band-powers are shown in Fig. 28.3, along with those from *WMAP* [60] and BICEP2/Keck [61], with ACTPol [62,63] and SPTPol [64] extending to smaller angular scales. The anti-correlation at $\ell \simeq 150$ and the peak at $\ell \simeq 300$ were the first features to become distinct, but now a whole series of oscillations is clearly seen in this power spectrum. The measured shape of the cross-correlation power spectrum provides supporting evidence for the general cosmological picture, as well as directly constraining the thickness of the last scattering surface. Since the polarization anisotropies are generated in this scattering surface, the existence of correlations at angles above about a degree demonstrates that there were super-Hubble fluctuations at the recombination epoch. The sign of this correlation also confirms the adiabatic paradigm.

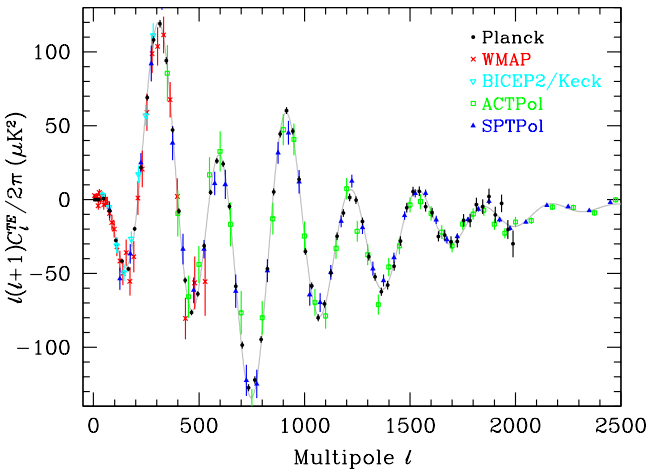

Figure 28.3: Cross-power spectrum band-powers of the temperature anisotropies and E-mode polarization signal from *Planck* (the low multipole data have been binned here), as well as *WMAP*, BICEP2/Keck, ACTPol, and SPTPol. The curve is the prediction from the best fit to the *Planck* temperature band-powers (as well as the $\ell < 30$ polarization and CMB lensing results) and is not a fit to these data; however, these TE measurements follow the curve very closely, showing the expected oscillatory structure. Note that each band-power is an average over a range of multipoles, and hence to compare in detail with a model one has to integrate the theoretical curve through the band.

The overall picture of the source of CMB polarization and its oscillations has also been confirmed through tests that average the maps around both temperature hot spots and cold spots [65,11]. One sees precisely the expected patterns of radial and tangential polarization configurations, as well as the phase shift between polarization and temperature. This leaves no doubt that the oscillation picture is the correct one and that the polarization is coming from Thomson scattering at $z \simeq 1100$.

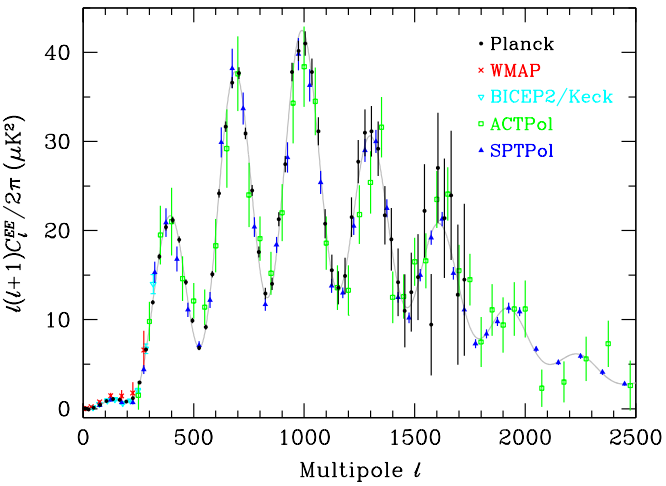

Figure 28.4: Power spectrum of E-mode polarization from *Planck*, together with *WMAP*, BICEP2/Keck, ACTPol, and SPTPol. Note that some band-powers with larger uncertainties have been omitted and that the unbinned *Planck* low-ℓ data have been binned here. Also plotted is the best-fit theoretical model from *Planck* TT data (plus polarization at $\ell < 30$ and CMB lensing).

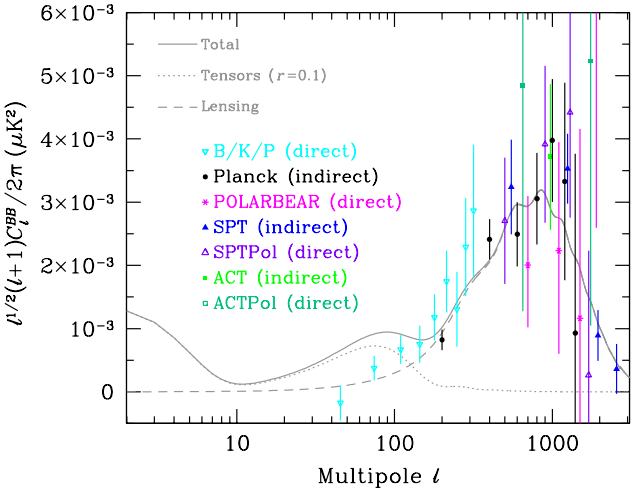

Figure 28.5: Power spectrum of B-mode polarization, including results from the BICEP2/Keck Array/*Planck* combined analysis (B/K/P), *Planck*, POLARBEAR, SPT, and ACT. Note that some of the measurements are direct estimates of B-modes on the sky, while others are only sensitive to the lensing signal and come from combining E-mode and lensing potential measurements. Several earlier experiments reported upper limits, which are all off the top of this plot. A logarithmic x-axis is adopted here and the y-axis has been divided by a factor of $\sqrt{\ell}$ in order to show all three theoretically expected contributions: the low-ℓ reionization bump; the $\ell \sim 100$ recombination peak; and the high-ℓ lensing signature. The dotted line is for a tensor (primordial gravitational wave) fraction $r = 0.1$, simply as an example, with all other cosmological parameters set at the best *Planck*-derived values, for which model the expected lensing B-modes have also been shown with a dashed line.

28.7.2. *E–E Power Spectrum* :

Experimental band-powers for C_ℓ^{EE} from *Planck*, *WMAP*, BICEP2/Keck Array [61], ACTPol [63], and SPTPol [64] are shown in Fig. 28.4. Without the benefit of correlating with the temperature anisotropies (*i.e.*, measuring C_ℓ^{TE}), the polarization anisotropies are very weak and challenging to measure. Nevertheless, the oscillatory pattern is becoming well established and the data closely match the TT-derived theoretical prediction. In Fig. 28.4 one can clearly see the 'shoulder' expected at $\ell \simeq 140$, the first main peak at $\ell \simeq 400$ (corresponding to the first trough in C_ℓ^{TT}), and the series of oscillations that is out of phase with those of the temperature anisotropy power spectrum.

Perhaps the most notable result from the polarization measurements is at the largest angular scales ($\ell < 10$) in C_ℓ^{TE} and C_ℓ^{EE}, where there is evidence for an excess signal (not visible in Fig. 28.4) compared to that expected from the temperature power spectrum alone. This is precisely the signal anticipated from an early period of reionization, arising from Doppler shifts during the partial scattering at $z < z_{\rm i}$. The amplitude of the signal indicates that the first stars, presumably the source of the ionizing radiation, formed around $z \simeq 8$ (although the uncertainty is still quite large). Since this corresponds to scattering optical depth $\tau \simeq 0.06$, then roughly 6% of CMB photons were re-scattered at the reionization epoch, with the other 94% last scattering at $z \simeq 1100$. However, estimates of the amplitude of this reionization excess have come down since the first measurements by *WMAP* (indicating that this is an extremely difficult measurement to make) and the latest *Planck* results have reduced the value further [66].

28.7.3. *B–B Power Spectrum* :

The expected amplitude of C_ℓ^{BB} is very small, and so measurements of this polarization curl-mode are extremely challenging. The first indication of the existence of the BB signal has come from the detection of the expected conversion of E-modes to B-modes by gravitational lensing, through a correlation technique using the lensing potential and polarization measurements from SPT [67]. However, the real promise of B-modes lies in the detection of primordial gravitational waves at larger scales. This tensor signature could be seen either in the 'recombination bump' at around $\ell = 100$ (caused by an ISW effect as gravitational waves redshift away at the last-scattering epoch) or the 'reionization bump' (from additional scattering at low redshifts).

Results from the BICEP-2 experiment [68] in 2014 suggested a detection of the primordial B-mode signature around the recombination peak. BICEP-2 mapped a small part of the CMB sky with the the lowest sensitivity level reached at that time (below 100 nK), but at a single frequency. Higher frequency data from *Planck* indicated that much of the BICEP2 signal was due to dust within out Galaxy, and a combined analysis by the BICEP-2, Keck Array, and *Planck* teams [69] indicated that the data are consistent with no primordial B-modes, with an upper limit of $r < 0.12$ (95%, from BB alone). This limit was reduced to $r < 0.09$ with the inclusion of Keck Array data at 95 GHz [70].

Several experiments are continuing to push down the sensitivity of B-mode measurements, motivated by the enormous importance of a future detection of this telltale signature of inflation (or other physics at the highest energies). A compilation of experimental results for C_ℓ^{BB} is shown in Fig. 28.5, coming from a combination of direct estimates of the B-modes (BICEP2/Keck Array [61], POLARBEAR [71], SPTPol [72], and ACTPol [63]) and indirect determinations of the lensing B-modes based on estimating the effect of measured lensing on measured E-modes (*Planck* [50], SPT [67], and ACT [73]) . Additional band-power estimates are expected from these and other experiments in the near future, with the so-called 'Stage 4' CMB project holding great promise for pushing down to the $r \sim 0.001$ level [74].

28.8. Complications

There are a number of issues that complicate the interpretation of CMB anisotropy data (and are considered to be *signal* by many astrophysicists), some of which we sketch out below.

28.8.1. *Foregrounds* :

The microwave sky contains significant emission from our Galaxy and from extra-galactic sources [75] . Fortunately, the frequency dependence of these various sources is in general substantially different from that of the CMB anisotropy signals. The combination of Galactic synchrotron, bremsstrahlung, and dust emission reaches a minimum at a frequency of roughly 100 GHz (or wavelength of about 3 mm). As one moves to greater angular resolution, the minimum moves to slightly higher frequencies, but becomes more sensitive to unresolved (point-like) sources.

At frequencies around 100 GHz, and for portions of the sky away from the Galactic Plane, the foregrounds are typically 1 to 10% of the CMB anisotropies. By making observations at multiple frequencies, it is relatively straightforward to separate the various components and determine the CMB signal to the few per cent level. For greater sensitivity, it is necessary to use the spatial information and statistical properties of the foregrounds to separate them from the CMB. Furthermore, at higher ℓs it is essential to carefully model extragalactic foregrounds, particularly the clustering of infrared-emitting galaxies, which dominate the measured power spectrum as we move into the damping tail.

The foregrounds for CMB polarization follow a similar pattern to those for temperature, but are intrinsically brighter relative to CMB anisotropies. *WMAP* showed that the polarized foregrounds dominate at large angular scales, and that they must be well characterized in order to be discriminated [76]. *Planck* has shown that it is possible to characterize the foreground polarization signals, with synchrotron dominating at low frequencies and dust at high frequencies [77]. On smaller scales there are no strongly polarized foregrounds, and hence it is in principle easier to measure foreground-free modes at high multipoles in polarization than in temperature. Although foreground contamination will no doubt become more complicated as we push down in sensitivity, and they will make analysis more difficult, for the time being, foreground contamination is not a fundamental limit for CMB experiments.

28.8.2. ***Secondary Anisotropies*** :

With increasingly precise measurements of the primary anisotropies, there is growing theoretical and experimental interest in 'secondary anisotropies,' pushing experiments to higher angular resolution and sensitivity. These secondary effects arise from the processing of the CMB due to ionization history and the evolution of structure, including gravitational lensing (which was already discussed) and patchy reionization effects [78] . Additional information can thus be extracted about the Universe at $z \ll 1000$. This tends to be most effectively done through correlating CMB maps with other cosmological probes of structure. Secondary signals are also typically non-Gaussian, unlike the primary CMB anisotropies.

A secondary signal of great current interest is the Sunyaev-Zeldovich (SZ) effect [79] , which is Compton scattering ($\gamma e \to \gamma' e'$) of the CMB photons by hot electron gas. This creates spectral distortions by transferring energy from the electrons to the photons. It is particularly important for clusters of galaxies, through which one observes a partially Comptonized spectrum, resulting in a decrement at radio wavelengths and an increment in the submillimeter.

The imprint on the CMB sky is of the form $\Delta T/T = y\, f(x)$, with the y-parameter being the integral of Thomson optical depth times $kT_{\rm e}/m_{\rm e}c^2$ through the cluster, and $f(x)$ describing the frequency dependence. This is simply $x\coth(x/2) - 4$ for a non-relativistic gas (the electron temperature in a cluster is typically a few keV), where the dimensionless frequency $x \equiv h\nu/kT_\gamma$. As well as this 'thermal' SZ effect, there is also a smaller 'kinetic' effect due to the bulk motion of the cluster gas, giving $\Delta T/T \sim \tau(v/c)$, with either sign, but having the same spectrum as the primary CMB anisotropies.

A significant advantage in finding galaxy clusters this way is that the SZ effect is largely independent of redshift, so in principle clusters can be found to arbitrarily large distances. The SZ effect can be used to find and study individual clusters, and to obtain estimates of the Hubble constant. There is also the potential to constrain cosmological parameters, such as the clustering amplitude σ_8 and the equation of state of the dark energy, through counts of detected clusters as a function of redshift. The promise of the method has been realized through detections of clusters purely through the SZ effect by SPT [80] , ACT [81], and *Planck* [82]. Results from *Planck* clusters [83] suggest a somewhat lower value of σ_8 than inferred from CMB anisotropies, but there are still systematic uncertainties that might encompass the difference, and a more recent analysis of SPT-detected clusters shows more agreement [84]. Further analysis of scaling relations among cluster properties should enable more robust cosmological constraints to be placed in future, so that we can understand whether this 'tension' might be a sign of new physics.

28.8.3. ***Higher-order Statistics*** :

Although most of the CMB anisotropy information is contained in the power spectra, there will also be weak signals present in higher-order statistics. These can measure any primordial non-Gaussianity in the perturbations, as well as non-linear growth of the fluctuations on small scales and other secondary effects (plus residual foreground contamination of course). Although there are an infinite variety of ways in which the CMB could be non-Gaussian [29] , there is a generic form to consider for the initial conditions, where a quadratic contribution to the curvature perturbations is parameterized through a dimensionless number $f_{\rm NL}$. This weakly non-linear component can be constrained in several ways, the most popular being through measurements of the bispectrum.

The constraints depend on the shape of the triangles in harmonic space, and it has become common to distinguish the 'local' or 'squeezed' configuration (in which one side is much smaller than the other two) from the 'equilateral' configuration. Other configurations are also relevant for specific theories, such as 'orthogonal' non-Gaussianity, which has positive correlations for $k_1 \simeq 2k_2 \simeq 2k_3$, and negative correlations for the equilateral configuration. The results from the *Planck* team [85](including polarization here) are $f_{\rm NL}^{\rm local} = 1 \pm 5$, $f_{\rm NL}^{\rm equil} = 0 \pm 40$, and $f_{\rm NL}^{\rm ortho} = -26 \pm 21$.

These results are consistent with zero, but are at a level that is now interesting for model predictions. The amplitude of $f_{\rm NL}$ expected is small, so that a detection of $f_{\rm NL} \gg 1$ would rule out all single-field, slow-roll inflationary models. It is still possible to improve upon these *Planck* results, and it certainly seems feasible that a measurement of primordial non-Gaussianity may yet be within reach. *Non*-primordial detections of non-Gaussianity from expected signatures have already been made. For example, the bispectrum and trispectrum contain evidence of gravitational lensing, the ISW effect, and Doppler boosting. For now the primordial signal is elusive, but should it be detected, then detailed measurements of non-Gaussianity will become a unique probe of inflationary-era physics. Because of that, much effort continues to be devoted to honing predictions and measurement techniques, with the expectation that we will need to go beyond the CMB to dramatically improve the constraints.

28.8.4. ***Anomalies*** :

Several features seen in the *Planck* data [32] confirm those found earlier with *WMAP* [31] , showing mild deviations from a simple description of the data; these are often referred to as 'anomalies.' One such feature is the apparent lack of power in the multipole range $\ell \simeq 20$–30 [9,53]. The other examples involve the breaking of statistical anisotropy, caused by alignment of the lowest multipoles, or a somewhat excessive cold spot, or a power asymmetry between hemispheres. No such feature is significant at more than the roughly 3σ level, and the importance of 'a posteriori' statistics here has been emphasized by many authors. Since these effects are at large angular scales, where cosmic variance dominates, the results will not increase in significance with more data, although there is the potential for polarization to provide independent tests.

28.9. Constraints on Cosmological Parameters

The most striking outcome of the newer experimental results is that the standard cosmological paradigm is in very good shape. A large amount of high precision data on the power spectrum is adequately fit with fewer than 10 free parameters (and only six need non-trivial values). The framework is that of FRW models, which have nearly flat geometry, containing dark matter and dark energy, and with adiabatic perturbations having close to scale-invariant initial conditions.

Within this basic picture, the values of the cosmological parameters can be constrained. Of course, much more stringent bounds can be placed on models that cover a restricted parameter space, *e.g.*, assuming that $\Omega_{\rm tot} = 1$ or $r = 0$. More generally, the constraints depend upon the adopted prior probability distributions, even if they are implicit, for example by restricting the parameter freedom or their ranges (particularly where likelihoods peak near the boundaries), or by using different choices of other data in combination with the CMB. As the data become even more precise, these considerations will be less important, but for now we caution that restrictions on model space and choice of non-CMB data-sets and priors need to be kept in mind when adopting specific parameter values and uncertainties.

There are some combinations of parameters that fit the CMB anisotropies almost equivalently. For example, there is a nearly exact geometric degeneracy, where any combination of $\Omega_{\rm m}$ and Ω_Λ that provides the same angular diameter distance to last scattering will give nearly identical C_ℓs. There are also other less exact degeneracies among the parameters. Such degeneracies can be broken when using the CMB results in combination with other cosmological data-sets. Particularly useful are complementary constraints from baryon acoustic oscillations, galaxy clustering, the abundance of galaxy clusters, weak gravitational lensing measurements, and Type Ia supernova distances. For an overview of some of these other cosmological constraints, see The Cosmological Parameters—Sec. 24 of this *Review*.

Within the context of a six parameter family of models (which fixes $\Omega_{\rm tot} = 1$, $dn_{\rm s}/d\ln k = 0$, $r = 0$, and $w = -1$) the *Planck* results for TT, together with low-ℓ polarization and CMB lensing, yields [13]: $\ln(10^{10}A_{\rm s}) = 3.062 \pm 0.029$; $n_{\rm s} = 0.968 \pm 0.006$; $\Omega_{\rm b}h^2 = 0.02226 \pm 0.00023$; $\Omega_{\rm c}h^2 = 0.1186 \pm 0.0020$; $100\theta_* = 1.0410 \pm 0.0005$; and $\tau = 0.066 \pm 0.016$ (more recently reduced to 0.055 ± 0.009 [66]) . Other parameters can be derived from this basic set, including $h = 0.678 \pm 0.009$, $\Omega_\Lambda = 0.692 \pm 0.012$ ($= 1 - \Omega_{\rm m}$) and $\sigma_8 = 0.815 \pm 0.009$. Somewhat different (although consistent) values are obtained using other data combinations, such as including BAO, supernova, H_0, or weak lensing constraints (see Sec. 24 of this *Review*). However, the results quoted above are currently the best available from CMB anisotropies alone. The uncertainties decrease by around 25% when

adding *Planck* polarization data, although the recommendation for now is not to include these 2015 polarization data in fits, since there are still some unmodeled systematic effects present [53].

The standard cosmological model continues to fit the data well, with the error bars on the parameters continuing to shrink. Improved measurement of higher acoustic peaks has dramatically reduced the uncertainty in the θ_* parameter, which is now detected at $> 2000\sigma$. The evidence for $n_s < 1$ remains above the 5σ level. The value of the reionization optical depth has decreased compared with earlier estimates; it is convincingly detected, but still not of very high significance.

Constraints can also be placed on parameters beyond the basic six, particularly when including other astrophysical data-sets. Relaxing the flatness assumption, the constraint on $\Omega_{\rm tot}$ is 1.005 ± 0.008. Note that for h, the CMB data alone provide only a very weak constraint if spatial flatness is not assumed. However, with the addition of other data (particularly powerful in this context being a compilation of BAO measurements [86]), the constraints on the Hubble constant and curvature improve considerably, leading to $\Omega_{\rm tot} = 1.0002 \pm 0.0026$ [13].

For $\Omega_{\rm b}h^2$ the CMB-derived value is generally consistent with completely independent constraints from Big Bang nucleosynthesis (see Sec. 23 of this *Review*). Related are constraints on additional neutrino-like relativistic degrees of freedom, which lead to $N_{\rm eff} = 3.15 \pm 0.23$ (including BAO), *i.e.*, no evidence for extra neutrino species.

The 95% confidence upper limit on r (measured at $k = 0.002\,{\rm Mpc}^{-1}$) from the effect of tensors solely on C_ℓ^{TT} (see Fig. 28.1) is 0.11. This limit depends on how the slope n is restricted and whether $dn_{\rm s}/d\ln k \neq 0$ is allowed. The joint constraints on $n_{\rm s}$ and r allow specific inflationary models to be tested [33,34]. The limit on r is even tighter when combined with the BICEP/Keck/*Planck* results for C_ℓ^{BB}, yielding $r < 0.07$ at 95% confidence [34,70]. Looking at the $(n_{\rm s}, r)$ plane, this means that $m^2\phi^2$ (mass-term quadratic) inflation is now disfavored by the data, as well as $\lambda\phi^4$ (self-coupled) inflation.

The addition of the dark energy equation of state w adds the partial degeneracy of being able to fit a ridge in (w, h) space, extending to low values of both parameters. This degeneracy is broken when the CMB is used in combination with other data-sets, *e.g.*, adding a compilation of BAO data gives $w = -1.01 \pm 0.05$. Constraints can also be placed on more general dark energy and modified gravity models [87]. However, when extending the search space, one needs to be careful not to over-interpret some tensions between data-sets as evidence for new physics.

For the reionization optical depth, a reanalysis of *Planck* data in 2016 resulted in a reduction in the value of τ, with the tightest result (from low-ℓ HFI EE data) giving $\tau = 0.055 \pm 0.009$. This corresponds to $z_{\rm i} = 7.8$–8.8 (depending on the functional form of the reionization history), with an uncertainty of ± 0.9 [66]. This redshift is only slightly higher that that suggested from studies of absorption lines in high-z quasar spectra [88] and Ly α-emitting galaxies [89], perhaps hinting that the process of reionization was not as complex as previously suspected. The important constraint provided by CMB polarization, in combination with astrophysical measurements, thus allows us to investigate how the first stars formed and brought about the end of the cosmic dark ages.

28.10. Particle Physics Constraints

CMB data place limits on parameters that are directly relevant for particle physics models. For example, there is a limit on the sum of the masses of the neutrinos, $\sum m_\nu < 0.21\,{\rm eV}$ (95%) [9] coming from *Planck* together with BAO measurements (although limits are weaker when considering both $N_{\rm eff}$ and $\sum m_\nu$ as free parameters). This assumes the usual number density of fermions, which decoupled when they were relativistic. The limit is tantalizingly only a factor of a few higher than the minimum value coming from neutrino mixing experiments (see Neutrino Mixings—Secs. 14 and 25). As well as being an indirect probe of the neutrino background, *Planck* data also require that the neutrino background has perturbations, *i.e.*, that it possesses a sound speed $c_{\rm s}^2 \simeq 1/3$, as expected [13].

The current suite of data suggests that $n_{\rm s} < 1$, with a best-fitting value about 0.03 below unity. This is already quite constraining for inflationary models, particularly along with r limits. There is no current evidence for running of the spectral index, with $dn_{\rm s}/d\ln k = -0.003 \pm 0.008$ from *Planck* alone [13], although this is less of a constraint on models. Similarly, primordial non-Gaussianity is being probed to interesting levels, although tests of simple inflationary models will only come with significant reductions in uncertainty.

The large-angle anomalies, such as the hemispheric modulation of power and the dip in power at $\ell \simeq 20$–30, have the potential to be hints of new physics. Such effects might be expected in a universe that has a large-scale power cut-off, or anisotropy in the initial power spectrum, or is topologically non-trivial. However, cosmic variance and *a posteriori* statistics limit the significance of these anomalies, absent the existence of a model that naturally yields some of these features (and ideally also predicting other phenomena that can be tested).

Constraints on 'cosmic birefringence' (*i.e.*, rotation of the plane of CMB polarization that generates non-zero TB and EB power) can be used to place limits on theories involving parity violation, Lorentz violation, or axion-photon mixing [90].

It is possible to place limits on additional areas of physics [91], for example annihilating dark matter [13], primordial magnetic fields [92], and time variation of the fine-structure constant [93], as well as parity violation, the neutrino chemical potential, a contribution of warm dark matter, topological defects, or physics beyond general relativity. Further particle physics constraints will follow as the smaller scale and polarization measurements continue to improve.

The CMB anisotropy measurements precisely pin down physics at the time of last-scattering, and so any change of physics can be constrained if it affects the relevant energies or timescales. Future, higher sensitivity measurements of the CMB frequency spectrum will push the constraints back to cover energy injection at much earlier times ($\sim 1\,{\rm year}$). Comparison of CMB and BBN observables extend these constraints to timescales of order seconds, and energies in the MeV range. And to the extent that inflation provides an effective description of the generation of perturbations, the inflationary observables will constrain physics at GUT-type energy scales.

More generally, careful measurement of the CMB power spectra and non-Gaussianity can in principle put constraints on physics at the highest energies, including ideas of string theory, extra dimensions, colliding branes, *etc.* At the moment any calculation of predictions appears to be far from definitive. However, there is a great deal of activity on implications of string theory for the early Universe, and hence a very real chance that there might be observational implications for specific scenarios.

28.11. Fundamental Lessons

More important than the precise values of parameters is what we have learned about the general features that describe our observable Universe. Beyond the basic hot Big Bang picture, the CMB has taught us that:

- The Universe recombined at $z \sim 1000$ and started to become ionized again at $z \sim 10$.
- The geometry of the Universe is close to flat.
- Both dark matter and dark energy are required.
- Gravitational instability is sufficient to grow all of the observed large structures in the Universe.
- Topological defects were not important for structure formation.
- There are 'synchronized' super-Hubble modes generated in the early Universe.
- The initial perturbations were predominantly adiabatic in nature.
- The perturbation spectrum has a slightly red tilt.
- The perturbations had close to Gaussian (*i.e.*, maximally random) initial conditions.

These features form the basis of the cosmological standard model, ΛCDM, for which it is tempting to make an analogy with the Standard Model of particle physics (see earlier Sections of this *Review*). The cosmological model is much further from any underlying 'fundamental theory,' which may ultimately provide the values of the parameters from first principles. Nevertheless, any genuinely complete 'theory of everything' must include an explanation for the values of these

cosmological parameters as well as the parameters of the Standard Model of particle physics.

28.12. Future Directions

Given the significant progress in measuring the CMB sky, which has been instrumental in tying down the cosmological model, what can we anticipate for the future? There will be a steady improvement in the precision and confidence with which we can determine the appropriate cosmological parameters. Ground-based experiments operating at smaller angular scales will continue to place tighter constraints on the damping tail. New polarization experiments at small scales will probe further into the damping tail, without the limitation of extragalactic foregrounds. And polarization experiments at large angular scales will push down the limits on primordial B-modes.

Planck, the third generation CMB satellite mission, was launched in May 2009, and has produced a large number of papers, including a set of cosmological studies based on the first two full surveys of the sky (accompanied by a public release of data products) in 2013 and a further series based on analysis of the full mission data release in 2015 (eight surveys for the Low Frequency Instrument and five surveys for the High Frequency Instrument). In late 2017 results are expected from a final analysis, including full constraints from polarization data.

A set of cosmological parameters is now known to percent level accuracy, and that may seem sufficient for many people. However, we should certainly demand more of measurements that describe *the entire observable Universe!* Hence a lot of activity in the coming years will continue to focus on determining those parameters with increasing precision. This necessarily includes testing for consistency among different predictions of the cosmological Standard Model, and searching for signals that might require additional physics.

A second area of focus will be the smaller scale anisotropies and 'secondary effects.' There is a great deal of information about structure formation at $z \ll 1000$ encoded in the CMB sky. This may involve higher-order statistics and cross-correlations with other large-scale structure tracers, as well as spectral signatures, with many experiments targeting the galaxy cluster SZ effect. The current status of CMB lensing is similar (in terms of total signal-to-noise) to the quality of the first CMB anisotropy measurements by *COBE*, and thus we can expect that experimental probes of lensing will improve dramatically in the coming years. All of these investigations can provide constraints on the dark energy equation of state, for example, which is a major area of focus for several future cosmological surveys at optical wavelengths. CMB lensing also promises to yield a measurement of the sum of the neutrino masses.

A third direction is increasingly sensitive searches for specific signatures of physics at the highest energies. The most promising of these may be the primordial gravitational wave signals in C_ℓ^{BB}, which could be a probe of the $\sim 10^{16}$ GeV energy range. There are several ground- and balloon-based experiments underway that are designed to search for the polarization B-modes. Additionally, non-Gaussianity holds the promise of constraining models beyond single-field slow-roll inflation.

Anisotropies in the CMB have proven to be the premier probe of cosmology and the early Universe. Theoretically the CMB involves well understood physics in the linear regime, and is under very good calculational control. A substantial and improving set of observational data now exists. Systematics appear to be under control and not a limiting factor. And so for the next few years we can expect an increasing amount of cosmological information to be gleaned from CMB anisotropies, with the prospect also of some genuine surprises.

References:

1. A.A. Penzias and R. Wilson, Astrophys. J. **142**, 419 (1965); R.H. Dicke *et al.*, Astrophys. J. **142**, 414 (1965).
2. M. White, D. Scott, and J. Silk, Ann. Rev. Astron. Astrophys. **32**, 329 (1994); W. Hu and S. Dodelson, Ann. Rev. Astron. Astrophys. **40**, 171 (2002); A. Challinor and H. Peiris, Proc. Astro. Soc. Pacific Conf. Ser. Vol. 1132, 86 (2009).
3. G.F. Smoot *et al.*, Astrophys. J. **396**, L1 (1992).
4. C.L. Bennett *et al.*, Astrophys. J. Supp. **148**, 1 (2003).
5. N. Jarosik *et al.*, Astrophys. J. Supp. **170**, 263 (2007).
6. G. Hinshaw *et al.*, Astrophys. J. Supp. **180**, 225 (2009).
7. N. Jarosik *et al.*, Astrophys. J. Supp. **192**, 14 (2011).
8. G. Hinshaw *et al.*, Astrophys. J. Supp. **208**, 19 (2013).
9. Planck Collab. 2013 Results XVI, Astron. & Astrophys. **571**, A16 (2014).
10. J.A. Tauber *et al.*, Astron. & Astrophys. **520**, 1 (2010); Planck Collab. Early Results I, Astron. & Astrophys. **536**, 1 (2011).
11. Planck Collab. 2013 Results I, Astron. & Astrophys. **571**, A1 (2014).
12. Planck Collab. 2015 Results I, Astron. & Astrophys. **594**, A1 (2016).
13. Planck Collab. 2015 Results XIII, Astron. & Astrophys. **594**, A13 (2016).
14. D.S. Swetz *et al.*,Astrophys. J. Supp. **194**, 41 (2011).
15. J.E. Carlstron *et al.*, Publ. Astron. Soc. Pacific **123**, 568 (2011).
16. P. Noterdaeme *et al.*, Astron. & Astrophys. **526**, L7 (2011); S. Muller *et al.*, Astron. & Astrophys. **551**, A109 (2013).
17. D.J. Fixsen *et al.*, Astrophys. J. **734**, 5 (2011).
18. R. Subrahmanyan and R. Cowsik, Astrophys. J. **776**, 42 (2013).
19. A. Kogut *et al.*, Proc. SPIE, vol. 9143, 1E (2014).
20. V. Desjacques *et al.*, Mon. Not. R. Astron. Soc **451**, 4460 (2015).
21. D.J. Fixsen, Astrophys. J. **707**, 916 (2009).
22. J.C. Mather *et al.*, Astrophys. J. **512**, 511 (1999).
23. Y. Hoffman, H.M. Courtois, and R.B. Tully, Mon. Not. R. Astron. Soc **449**, 4494 (2015).
24. D.J. Fixsen *et al.*, Astrophys. J. **420**, 445 (1994).
25. Planck Collab. 2013 Results XXVII, Astron. & Astrophys. **571**, A27 (2014).
26. A. Kogut *et al.*, Astrophys. J. **419**, 1 (1993).
27. S. Seager, D.D. Sasselov, and D. Scott, Astrophys. J. Supp. **128**, 407 (2000).
28. L. Knox, Phys. Rev. **D52**, 4307 (1995).
29. N. Bartolo *et al.*, Phys. Reports **402**, 103 (2004); E. Komatsu, Class. Quantum Grav. **27**, 124010 (2010); A.P.S. Yadav and B.D. Wandelt, Adv. Astron. **2010**, 565248 (2010).
30. Planck Collab. 2013 Results XXIV, Astron. & Astrophys. **571**, A24 (2014).
31. C.L. Bennett *et al.*, Astrophys. J. Supp. **192**, 17 (2011).
32. Planck Collab. 2013 Results XXIII, Astron. & Astrophys. **571**, A23 (2014); Planck Collab. 2015 Results XVI, Astron. & Astrophys. **594**, A16 (2016).
33. Planck Collab. 2013 Results XXII, Astron. & Astrophys. **571**, A22 (2014).
34. Planck Collab. 2015 Results XX, Astron. & Astrophys. **594**, A20 (2016).
35. A.R. Liddle and D.H. Lyth, Cosmological Inflation and Large-Scale Structure, Cambridge University Press (2000).
36. U. Seljak and M. Zaldarriaga, Astrophys. J. **469**, 437 (1996).
37. A. Lewis, A. Challinor, and A. Lasenby, Astrophys. J. **538**, 473 (2000).
38. D., Blas, J. Lesgourgues, and T. Tram, JCAP **07**, 034 (2011).
39. U. Seljak *et al.*, Phys. Rev. **D68**, 083507 (2003); C. Howlett *et al.*, JCAP **04**, 027 (2012).
40. R.K. Sachs and A.M. Wolfe, Astrophys. J. **147**, 73 (1967).
41. R. Crittenden and N. Turok, Phys. Rev. Lett. **76**, 575 (1996); Planck Collab. 2015 Results XXI, Astron. & Astrophys. **594**, A21 (2016).
42. W. Hu *et al.*, Phys. Rev. **D59**, 023512 (1999).
43. W. Hu *et al.*, Nature **386**, 37 (1997).
44. P.J.E. Peebles and J.T. Yu, Astrophys. J. **162**, 815 (1970); R.A. Sunyaev and Ya.B. Zeldovich, Astrophys. & Space Sci. **7**, 3 (1970).
45. D. Scott, J. Silk, and M. White, Science **268**, 829 (1995).
46. D.J. Eisenstein, New Astron. Rev. **49**, 360 (2005); W.J. Percival *et al.*, Mon. Not. R. Astron. Soc **381**, 1053 (2007).
47. J. Silk, Astrophys. J. **151**, 459 (1968).

48. M. Zaldarriaga and U. Seljak, Phys. Rev. **D58**, 023003 (1998); A. Lewis and A. Challinor, Phys. Reports **429**, 1 (2006).
49. Planck Collab. 2013 Result XVII, Astron. & Astrophys. **571**, A17 (2014).
50. Planck Collab. 2015 Results XV, Astron. & Astrophys. **594**, A15 (2016).
51. M. Kaplighat, L. Knox, and Y.-S. Song, Phys. Rev. Lett. **91**, 241301 (2003).
52. Planck Collab. 2013 Results XV, Astron. & Astrophys. **571**, A15 (2014).
53. Planck Collab. 2015 Results XI, Astron. & Astrophys. **594**, A11 (2016).
54. S. Das *et al.*, JCAP **04**, 014 (2014).
55. K.T. Story *et al.*, Astrophys. J. **779**, 86 (2013).
56. W. Hu and M. White, New Astron. **2**, 323 (1997).
57. W. Hu and M. White, Phys. Rev. **D56**, 596 (1997).
58. M. Zaldarriaga and U. Seljak, Phys. Rev. **D55**, 1830 (1997); M. Kamionkowski, A. Kosowsky, and A. Stebbins, Phys. Rev. **D55**, 7368 (1997).
59. J. Kovac *et al.*, Nature **420**, 772 (2002).
60. D. Larson *et al.*, Astrophys. J. Supp. **192**, 16 (2011).
61. Keck Array and BICEP2 Collabs. V, Astrophys. J. **811**, 126, (2015).
62. S. Naess *et al.*, J. Cosm. & Astropart. Phys. **10**, 007 (2014).
63. T. Louis *et al.*, Astrophys. J. in press, `arXiv:1610.02360`.
64. A.T. Crites *et al.*, Astrophys. J. **805**, 36 (2015); J.W. Henning *et al.*, Astrophys. J. in press, `arXiv:1707.09353`.
65. E. Komatsu *et al.*, Astrophys. J. Supp. **192**, 18 (2011).
66. Planck Collab. Interm. Results XLVI, Astron. & Astrophys. **596**, A107 (2016); Planck Collab. Interm. Results XLVII, Astron. & Astrophys. **596**, A108 (2016).
67. D. Hanson *et al.*, Phys. Rev. Lett. **111**, 141301 (2013).
68. BICEP2 Collab., Phys. Rev. Lett. **112**, 1101 (2014).
69. BICEP/Keck and Planck Collabs., Phys. Rev. Lett. **114**, 1301 (2015).
70. BICEP2 and Keck Array Collab. Phys. Rev. Lett. **116**, 1302 (2016).
71. POLARBEAR Collab., Astrophys. J. in press, `arXiv:1705.02907`.
72. R. Keisler *et al.*, Astrophys. J. **807**, 151 (2015).
73. A. van Engelen *et al.*, Astrophys. J. **808**, 7 (2015).
74. K.N. Abazajian *et al.*, CMB-S4 Science Book, `arXiv:1610.02743`.
75. Planck Collab. 2013 Results XII, Astron. & Astrophys. **571**, A12 (2014); Planck Collab. 2015 Results IX, Astron. & Astrophys. **594**, A9 (2016); Planck Collab. 2015 Results X, Astron. & Astrophys. **594**, A10 (2016).
76. B. Gold *et al.*, Astrophys. J. Supp. **192**, 15 (2011).
77. Planck Collab. Interm. Results XXX, Astron. & Astrophys. **586**, A133 (2016); Planck Collab. 2015 Results XXV, Astron. & Astrophys. **594**, A25 (2016).
78. M. Millea *et al.*, Astrophys. J. **746**, 4 (2012); E. Calabrese *et al.*, JCAP **8**, 010 (2014).
79. R.A. Sunyaev and Ya.B. Zeldovich, Ann. Rev. Astron. Astrophys. **18**, 537 (1980); M. Birkinshaw, Phys. Reports **310**, 98 (1999); J.E. Carlstrom, G.P. Holder, and E.D. Reese, Ann. Rev. Astron. Astrophys. **40**, 643 (2002).
80. R. Williamson *et al.*, Astrophys. J. **738**, 139 (2011); L.E. Bleem *et al.*, Astrophys. J. Supp. **216**, 27 (2015).
81. T.A. Marriage *et al.*, Astrophys. J. **737**, 61 (2011); M. Hasselfield *et al.*, JCAP **07**, 008 (2013).
82. Planck Collab. Early Results VIII, Astron. & Astrophys. **536**, 8 (2011); Planck Collab. 2013 Results XXIX, Astron. & Astrophys. **571**, A29 (2014); Planck Collab. 2015 Results XXVII, Astron. & Astrophys. **594**, A27 (2016).
83. Planck Collab. 2013 Results XX, Astron. & Astrophys. **571**, A20 (2014); Planck Collab. 2015 Results XXIV, Astron. & Astrophys. **594**, A24 (2016).
84. T. de Haan *et al.*, Astrophys. J. **832**, 95 (2016).
85. Planck Collab. 2013 Results XXIV, Astron. & Astrophys. **571**, A24 (2014); Planck Collab. 2015 Results XVII, Astron. & Astrophys. **594**, A17 (2016).
86. F. Beutler *et al.*, Mon. Not. R. Astron. Soc **416**, 3017 (2011); L. Anderson *et al.*, Mon. Not. R. Astron. Soc **441**, 24 (2014); E.A. Kazin *et al.*, Mon. Not. R. Astron. Soc **441**, 3524 (2014); A.J. Ross *et al.*, Mon. Not. R. Astron. Soc **449**, 835 (2014).
87. Planck Collab. 2015 Results XIV, Astron. & Astrophys. **594**, A14 (2016).
88. X. Fan, C.L. Carilli, and B. Keating, Ann. Rev. Astron. Astrophys. **44**, 415 (2006).
89. T.R. Choudhury *et al.*, Mon. Not. R. Astron. Soc **452**, 261 (2015).
90. B. Feng *et al.*, Phys. Rev. Lett. **96**, 1302 (2006); Planck Collab. Interm. Results XLIX, Astron. & Astrophys. **596**, A110 (2016).
91. M. Kamionkowski and A. Kosowsky, Ann. Rev. Nucl. and Part. Sci. **49**, 77 (1999); A. Lasenby, Space Sci. Rev. **148**, 329 (2009).
92. Planck Collab. 2015 Results XIX, Astron. & Astrophys. **594**, A19 (2016).
93. Planck Collab. Interm. Results XXIV, Astron. & Astrophys. **580**, A22 (2015).
94. R. Maartens, Living Rev. Rel. **7**, 7 (2004).

29. Cosmic Rays

Revised October 2017 by J.J. Beatty (Ohio State Univ.), J. Matthews (Louisiana State Univ.), and S.P. Wakely (Univ. of Chicago).

29.1. Primary spectra

The cosmic radiation incident at the top of the terrestrial atmosphere includes all stable charged particles and nuclei with lifetimes of order 10^6 years or longer. When discussing the astrophysical origin of cosmic rays, "primary" cosmic rays are those particles accelerated at astrophysical sources and "secondaries" are those particles produced in interaction of the primaries with interstellar gas†. Thus electrons, protons and helium, as well as carbon, oxygen, iron, and other nuclei synthesized in stars, are primaries. Nuclei such as lithium, beryllium, and boron (which are not abundant end-products of stellar nucleosynthesis) are secondaries. Antiprotons and positrons are also in large part secondary. Whether a small fraction of these particles may be primary is a question of current interest.

Apart from particles associated with solar flares, the cosmic radiation comes from outside the solar system. The incoming charged particles are "modulated" by the solar wind, the expanding magnetized plasma generated by the Sun, which decelerates and partially excludes the lower energy galactic cosmic rays from the inner solar system. There is a significant anticorrelation between solar activity (which has an alternating eleven-year cycle) and the intensity of the cosmic rays with rigidities below about 10 GV. In addition, the lower-energy cosmic rays are affected by the geomagnetic field, which they must penetrate to reach the top of the atmosphere. Thus the intensity of any component of the cosmic radiation in the GeV range depends both on the location and time.

There are four different ways to describe the spectra of the components of the cosmic radiation: (1) By particles per unit rigidity. Propagation (and probably also acceleration) through cosmic magnetic fields depends on gyroradius or *magnetic rigidity,* R, which is gyroradius multiplied by the magnetic field strength:

$$R = \frac{p\,c}{Z\,e} = r_L B \ . \qquad (29.1)$$

(2) By particles per energy-per-nucleon. Fragmentation of nuclei propagating through the interstellar gas depends on energy per nucleon, since that quantity is approximately conserved when a nucleus breaks up on interaction with the gas. (3) By nucleons per energy-per-nucleon. Production of secondary cosmic rays in the atmosphere depends on the intensity of nucleons per energy-per-nucleon, approximately independently of whether the incident nucleons are free protons or bound in nuclei. (4) By particles per energy-per-nucleus. Air shower experiments that use the atmosphere as a calorimeter generally measure a quantity that is related to total energy per particle.

The units of differential intensity I are $[\mathrm{m}^{-2}\,\mathrm{s}^{-1}\mathrm{sr}^{-1}\mathcal{E}^{-1}]$, where $\mathcal{E}$ represents the units of one of the four variables listed above.

The intensity of primary nucleons in the energy range from several GeV to somewhat beyond 100 TeV is given approximately by

$$I_N(E) \ \approx \ 1.8 \times 10^4 \ (E/1\ \mathrm{GeV})^{-\alpha} \ \frac{\mathrm{nucleons}}{\mathrm{m}^2\ \mathrm{s}\ \mathrm{sr}\ \mathrm{GeV}} \ , \qquad (29.2)$$

where E is the energy-per-nucleon (including rest mass energy) and $\alpha\ (\equiv \gamma + 1) = 2.7$ is the differential spectral index of the cosmic-ray flux and γ is the integral spectral index. About 74% of the primary nucleons are free protons and about 70% of the rest are nucleons bound in helium nuclei. The fractions of the primary nuclei are nearly constant over this energy range (with a few interesting variations, e.g. [2]) . Fractions of both primary and secondary incident nuclei are listed in Table 29.1. Figure 29.1 shows the major components for kinetic energies greater than 0.22 GeV/nucleus. A useful compendium of experimental data for cosmic-ray nuclei and electrons is described in [1].

† 'Primary' and 'secondary' are used in a different but analogous sense when discussing cosmic ray interactions in the atmosphere.

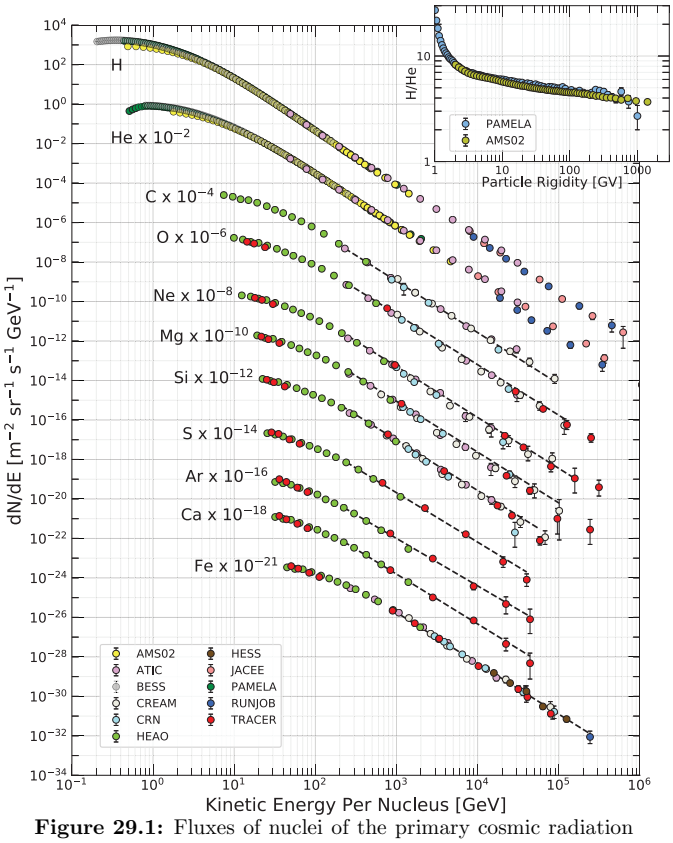

Figure 29.1: Fluxes of nuclei of the primary cosmic radiation in particles per energy-per-nucleus are plotted vs energy-per-nucleus using data from Refs. [2–13]. The inset shows the H/He ratio at constant rigidity [2,4].

The composition and energy spectra of nuclei are typically interpreted in the context of propagation models, in which the sources of the primary cosmic radiation are located within the Galaxy [14]. The ratio of secondary to primary nuclei is observed to decrease with increasing energy, a fact often interpreted to mean that the lifetime of cosmic rays in the Galaxy decreases with energy. Measurements of radioactive "clock" isotopes in the low energy cosmic radiation are consistent with a lifetime in the Galaxy of about 15 Myr [15].

Table 29.1: Relative abundances F of cosmic-ray nuclei at 10.6 GeV/nucleon normalized to oxygen ($\equiv 1$) [10]. The oxygen flux at kinetic energy of 10.6 GeV/nucleon is 3.29×10^{-2} $(\mathrm{m}^2\ \mathrm{s\ sr\ GeV/nucleon})^{-1}$. Abundances of hydrogen and helium are from Refs. [3–5]. Note that one can not use these values to extend the cosmic-ray flux to high energy because the power law indices for each element may differ slightly.

Z	Element	F	Z	Element	F
1	H	550	13–14	Al-Si	0.19
2	He	34	15–16	P-S	0.03
3–5	Li-B	0.40	17–18	Cl-Ar	0.01
6–8	C-O	2.20	19–20	K-Ca	0.02
9–10	F-Ne	0.30	21–25	Sc-Mn	0.05
11–12	Na-Mg	0.22	26–28	Fe-Ni	0.12

Cosmic rays are nearly isotropic at most energies due to diffusive propagation in the galactic magnetic field. Milagro [16], IceCube [17], and the Tibet-III air shower array [18] have observed anisotropy at the level of about 10^{-3} for cosmic rays with energy of a few TeV, possibly due to the distribution of sources and the direction of local Galactic magnetic fields.

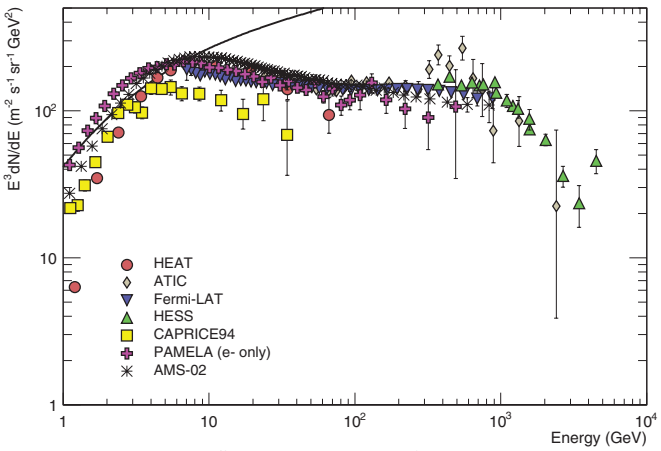

Figure 29.2: Differential spectrum of electrons plus positrons (except PAMELA data, which are electrons only) multiplied by E^3 [19–23,33,34]. The line shows the proton spectrum [25] multiplied by 0.01.

The spectrum of electrons and positrons incident at the top of the atmosphere is generally expected to steepen by one power of E at an energy of ∼5 GeV because of strong radiative energy loss effects in the Galaxy. The ATIC experiment [19] measured a sharp excess of electrons over propagation model expectations, at energies of ∼300-800 GeV. The *Fermi*/LAT γ-ray observatory measured a not-entirely flat spectrum [20] without confirming the peak of the ATIC excess at ∼600 GeV. Measurements in the same energy range by AMS-02 also show no sharp features and are compatible with a single power law above 30.2 GeV [21]. The HESS imaging atmospheric Cherenkov array also measured the electron flux above ∼400 GeV, finding indications of a cutoff above ∼1 TeV [22], but no evidence for a pronounced peak below this.

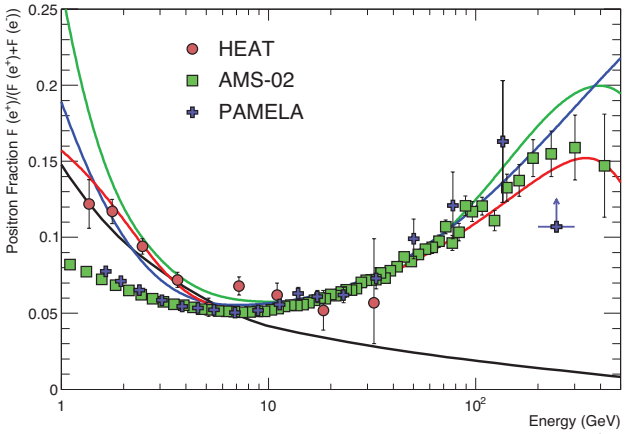

Figure 29.3: The positron fraction (ratio of the flux of e^+ to the total flux of e^+ and e^-) [26,24,30]. The heavy black line is a model of pure secondary production [28] and the three thin lines show three representative attempts to model the positron excess with different phenomena: green: dark matter decay [29]; blue: propagation physics [32]; red: production in pulsars [40]. The ratio below 10 GeV is dependent on the polarity of the solar magnetic field.

The PAMELA [26] and AMS-02 [27,24] satellite experiments measured the positron to electron ratio to increase above 10 GeV instead of the expected decrease [28] at higher energy, confirming earlier hints seen by the HEAT balloon-borne experiment [30]. The structure in the electron spectrum, as well as the increase in the positron fraction, may be related to contributions from individual nearby sources (supernova remnants or pulsars) emerging above a background suppressed at high energy by synchrotron losses [31]. Other explanations have invoked propagation effects [32] or dark matter decay/annihilation processes (see, e.g., [29]) . The significant disagreement in the ratio below ∼10 GeV is attributable to differences in charge-sign dependent solar modulation effects present near Earth at the times of measurement.

The ratio of antiprotons to protons is $\sim 2\times10^{-4}$ [35] at around 10–20 GeV, and there is clear evidence [36] for the kinematic suppression at lower energy that is the signature of secondary antiprotons. The $\overline{p}/p$ ratio also shows a strong dependence on the phase and polarity of the solar cycle [37] in the opposite sense to that of the positron fraction. There is at this time no evidence for a significant primary component of antiprotons. No antihelium or antideuteron has been found in the cosmic radiation. The best measured upper limit on the ratio antihelium/helium is currently approximately 1×10^{-7} [38] The upper limit on the flux of antideuterons around 1 GeV/nucleon is approximately $2\times10^{-4}\,(\mathrm{m^2\ s\ sr\ GeV/nucleon})^{-1}$ [39].

29.2. Cosmic rays in the atmosphere

Figure 29.4 shows the vertical fluxes of the major cosmic-ray components in the atmosphere in the energy region where the particles are most numerous (except for electrons, which are most numerous near their critical energy, which is about 81 MeV in air). Except for protons and electrons near the top of the atmosphere, all particles are produced in interactions of the primary‡ cosmic rays in the air. Muons and neutrinos are products of the decay chain of charged mesons, while electrons and photons originate in decays of neutral mesons.

Most measurements are made at ground level or near the top of the atmosphere, but there are also measurements of muons and electrons from airplanes and balloons. Fig. 29.4 includes recent measurements of negative muons [41–45]. Since $\mu^+(\mu^-)$ are produced in association with $\nu_\mu(\overline{\nu}_\mu)$, the measurement of muons near the maximum of the intensity curve for the parent pions serves to calibrate the atmospheric ν_μ beam [46]. Because muons typically lose almost 2 GeV in passing through the atmosphere, the comparison near the production altitude is important for the sub-GeV range of $\nu_\mu(\overline{\nu}_\mu)$ energies.

The flux of cosmic rays through the atmosphere is described by a set of coupled cascade equations with boundary conditions at the top of the atmosphere to match the primary spectrum. Numerical or Monte Carlo calculations are needed to account accurately for decay and energy-loss processes, and for the energy-dependences of the cross sections and of the primary spectral index γ. Approximate analytic solutions are, however, useful in limited regions of energy [47,48]. For example, the vertical intensity of charged pions with energy $E_\pi \ll \epsilon_\pi = 115$ GeV is

$$I_\pi(E_\pi, X) \;\approx\; \frac{Z_{N\pi}}{\lambda_N}\, I_N(E_\pi, 0)\, e^{-X/\Lambda}\, \frac{X\, E_\pi}{\epsilon_\pi}\ , \qquad (29.3)$$

where Λ is the characteristic length for exponential attenuation of the parent nucleon flux in the atmosphere. This expression has a maximum at $X = \Lambda \approx 121\pm4$ g cm^{-2} [49], which corresponds to an altitude of 15 kilometers. The quantity $Z_{N\pi}$ is the spectrum-weighted moment of the inclusive distribution of charged pions in interactions of nucleons with nuclei of the atmosphere. The intensity of low-energy pions is much less than that of nucleons because $Z_{N\pi} \approx 0.079$ is small and because most pions with energy much less than the critical energy ϵ_π decay rather than interact.

‡ When discussing cosmic rays in the atmosphere, 'primary' is used to denote the original particle and 'secondary' to denote the particles produced in interactions.

29.3. Cosmic rays at the surface

29.3.1. ***Muons*** : Muons are the most numerous charged particles at sea level (see Fig. 29.4). Most muons are produced high in the atmosphere (typically 15 km) and lose about 2 GeV to ionization before reaching the ground. Their energy and angular distribution reflect a convolution of the production spectrum, energy loss in the atmosphere, and decay. For example, 2.4 GeV muons have a decay length of 15 km, which is reduced to 8.7 km by energy loss. The mean energy of muons at the ground is ≈ 4 GeV. The energy spectrum is almost flat below 1 GeV, steepens gradually to reflect the primary spectrum in the 10–100 GeV range, and steepens further at higher energies because pions with $E_\pi > \epsilon_\pi$ tend to interact in the atmosphere before they decay. Asymptotically ($E_\mu \gg 1$ TeV), the energy spectrum of atmospheric muons is one power steeper than the primary spectrum. The integral intensity of vertical muons above 1 GeV/c at sea level is ≈ 70 m^{-2}s^{-1}sr^{-1} [50,51], with recent measurements [52–54] favoring a lower normalization by 10-15%. Experimentalists are familiar with this number in the form $I \approx 1$ cm^{-2} min^{-1} for horizontal detectors. The overall angular distribution of muons at the ground as a funxtion of zenith angle θ is $\propto \cos^2\theta$, which is characteristic of muons with $E_\mu \sim 3$ GeV. At lower energy the angular distribution becomes increasingly steep, while at higher energy it flattens, approaching a $\sec\theta$ distribution for $E_\mu \gg \epsilon_\pi$ and $\theta < 70°$.

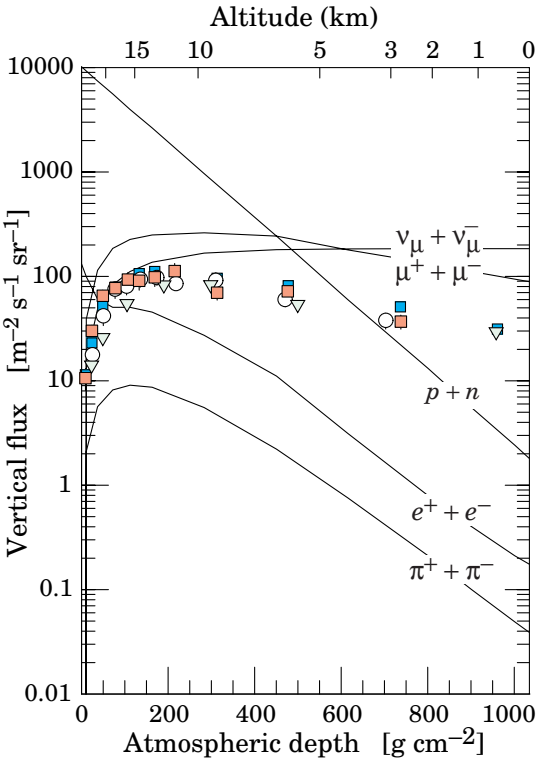

Figure 29.4: Vertical fluxes of cosmic rays in the atmosphere with $E > 1$ GeV estimated from the nucleon flux of Eq. (29.2). The points show measurements of negative muons with $E_\mu > 1$ GeV [41–45].

Figure 29.5 shows the muon energy spectrum at sea level for two angles. At large angles low energy muons decay before reaching the surface and high energy pions decay before they interact, thus the average muon energy increases. An approximate extrapolation formula valid when muon decay is negligible ($E_\mu > 100/\cos\theta$ GeV) and the curvature of the Earth can be neglected ($\theta < 70°$) is

$$\frac{dN_\mu}{dE_\mu d\Omega} \approx \frac{0.14\, E_\mu^{-2.7}}{\text{cm}^2 \text{ s sr GeV}} \times \left\{ \frac{1}{1 + \frac{1.1 E_\mu \cos\theta}{115\,\text{GeV}}} + \frac{0.054}{1 + \frac{1.1 E_\mu \cos\theta}{850\,\text{GeV}}} \right\}, \qquad (29.4)$$

where the two terms give the contribution of pions and charged kaons. Eq. (29.4) neglects a small contribution from charm and heavier flavors which is negligible except at very high energy [55].

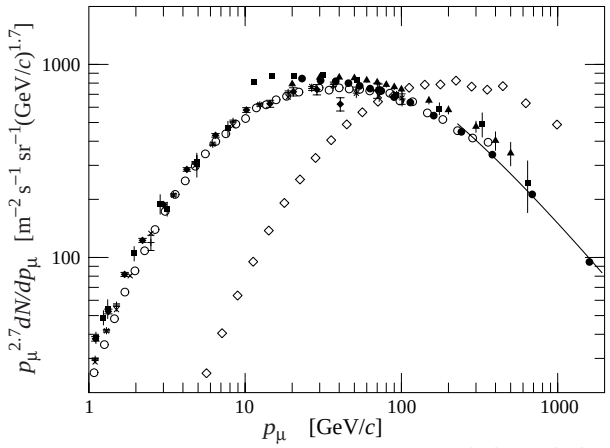

Figure 29.5: Spectrum of muons at $\theta = 0°$ (♦ [50], ■ [56], ▼ [57], ▲ [58], ×, + [52], ○ [53], and • [54] and $\theta = 75°$ ◇ [59]). The line plots the result from Eq. (29.4) for vertical showers.

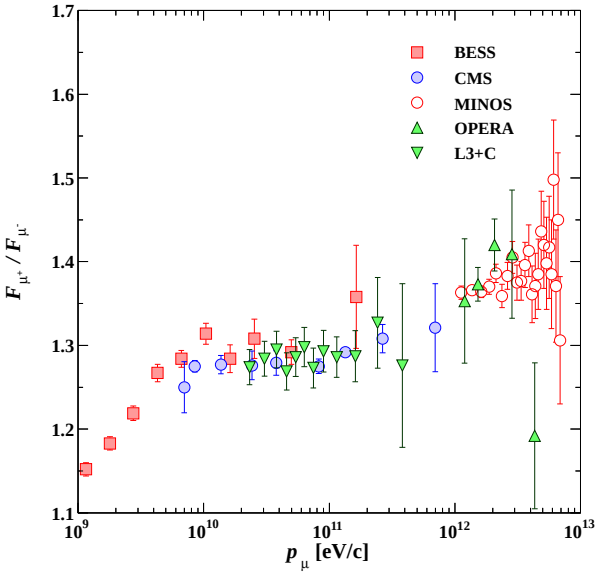

Figure 29.6: Muon charge ratio as a function of the muon momentum from Refs. [53,54,60,65,66].

The muon charge ratio reflects the excess of π^+ over π^- and K^+ over K^- in the forward fragmentation region of proton initiated interactions together with the fact that there are more free and bound protons than free and bound neutrons in the primary spectrum. The increase with energy of μ^+/μ^- shown in Fig. 29.6 reflects the increasing importance of kaons in the TeV range [60] and indicates a significant contribution of associated production by cosmic-ray protons ($p \to \Lambda + K^+$). The same process is even more important for atmospheric neutrinos at high energy.

29.3.2. ***Electromagnetic component*** : At the ground, this component consists of electrons, positrons, and photons primarily from cascades initiated by decay of neutral and charged mesons. Muon decay is the dominant source of low-energy electrons at sea level. Decay of neutral pions is more important at high altitude or when the energy threshold is high. Knock-on electrons also make a small contribution at low energy [61]. The integral vertical intensity of electrons plus positrons is very approximately 30, 6, and 0.2 $\mathrm{m^{-2}s^{-1}sr^{-1}}$ above 10, 100, and 1000 MeV respectively [51,62], but the exact numbers depend sensitively on altitude, and the angular dependence is complex because of the different altitude dependence of the different sources of electrons [61–63]. The ratio of photons to electrons plus positrons is approximately 1.3 above 1 GeV and 1.7 below the critical energy [63].

29.3.3. ***Protons*** : Nucleons above 1 GeV/c at ground level are degraded remnants of the primary cosmic radiation. The intensity is approximately $I_N(E,0) \times \exp(-X/\cos\theta\Lambda)$ for $\theta < 70°$. At sea level, about 1/3 of the nucleons in the vertical direction are neutrons (up from $\approx 10\%$ at the top of the atmosphere as the n/p ratio approaches equilibrium). The integral intensity of vertical protons above 1 GeV/c at sea level is ≈ 0.9 $\mathrm{m^{-2}s^{-1}sr^{-1}}$ [51,64].

29.4. Cosmic rays underground

Only muons and neutrinos penetrate to significant depths underground. The muons produce tertiary fluxes of photons, electrons, and hadrons.

29.4.1. ***Muons*** : As discussed in Section 33.6 of this *Review*, muons lose energy by ionization and by radiative processes: bremsstrahlung, direct production of e^+e^- pairs, and photonuclear interactions. The total muon energy loss may be expressed as a function of the amount of matter traversed as

$$-\frac{dE_\mu}{dX} = a + b\,E_\mu \ , \tag{29.5}$$

where a is the ionization loss and b is the fractional energy loss by the three radiation processes. Both are slowly varying functions of energy. The quantity $\epsilon \equiv a/b$ (≈ 500 GeV in standard rock) defines a critical energy below which continuous ionization loss is more important than radiative losses. Table 29.2 shows a and b values for standard rock, and b for ice, as a function of muon energy. The second column of Table 29.2 shows the muon range in standard rock ($A = 22$, $Z = 11$, $\rho = 2.65$ g $\mathrm{cm^{-3}}$). These parameters are quite sensitive to the chemical composition of the rock, which must be evaluated for each location.

Table 29.2: Average muon range R and energy loss parameters a and b calculated for standard rock [67] and the total energy loss parameter b for ice. Range is given in km-water-equivalent, or 10^5 g $\mathrm{cm^{-2}}$.

E_μ	R	a	$b_{\rm brems}$	$b_{\rm pair}$	$b_{\rm nucl}$	$\sum b_i$	$\sum b$(ice)
GeV	km.w.e.	$\mathrm{MeV\,g^{-1}\,cm^2}$	—	10^{-6} $\mathrm{g^{-1}\,cm^2}$		—	
10	0.05	2.17	0.70	0.70	0.50	1.90	1.66
100	0.41	2.44	1.10	1.53	0.41	3.04	2.51
1000	2.45	2.68	1.44	2.07	0.41	3.92	3.17
10000	6.09	2.93	1.62	2.27	0.46	4.35	3.78

The intensity of muons underground can be estimated from the muon intensity in the atmosphere and their rate of energy loss. To the extent that the mild energy dependence of a and b can be neglected, Eq. (29.5) can be integrated to provide the following relation between the energy $E_{\mu,0}$ of a muon at production in the atmosphere and its average energy E_μ after traversing a thickness X of rock (or ice or water):

$$E_{\mu,0} = (E_\mu + \epsilon)\, e^{bX} - \epsilon \ . \tag{29.6}$$

Especially at high energy, however, fluctuations are important and an accurate calculation requires a simulation that accounts for stochastic energy-loss processes [68].

There are two depth regimes for which Eq. (29.6) can be simplified. For $X \ll b^{-1} \approx 2.5$ km water equivalent, $E_{\mu,0} \approx E_\mu(X) + aX$, while for $X \gg b^{-1}$ $E_{\mu,0} \approx (\epsilon + E_\mu(X))\exp(bX)$. Thus at shallow depths the differential muon energy spectrum is approximately constant for $E_\mu < aX$ and steepens to reflect the surface muon spectrum for $E_\mu > aX$, whereas for $X > 2.5$ km.w.e. the differential spectrum underground is again constant for small muon energies but steepens to reflect the surface muon spectrum for $E_\mu > \epsilon \approx 0.5$ TeV. In the deep regime the shape is independent of depth although the intensity decreases exponentially with depth. In general the muon spectrum at slant depth X is

$$\frac{dN_\mu(X)}{dE_\mu} = \frac{dN_\mu}{dE_{\mu,0}}\,\frac{dE_{\mu,0}}{dE_\mu} = \frac{dN_\mu}{dE_{\mu,0}}\,e^{bX} \ , \tag{29.7}$$

where $E_{\mu,0}$ is the solution of Eq. (29.6) in the approximation neglecting fluctuations.

Fig. 29.7 shows the vertical muon intensity versus depth. In constructing this "depth-intensity curve," each group has taken account of the angular distribution of the muons in the atmosphere, the map of the overburden at each detector, and the properties of the local medium in connecting measurements at various slant depths and zenith angles to the vertical intensity. Use of data from a range of angles allows a fixed detector to cover a wide range of depths. The flat portion of the curve is due to muons produced locally by charged-current interactions of ν_μ. The inset shows the vertical intensity curve for water and ice published in Refs. [70–73]. It is not as steep as the one for rock because of the lower muon energy loss in water.

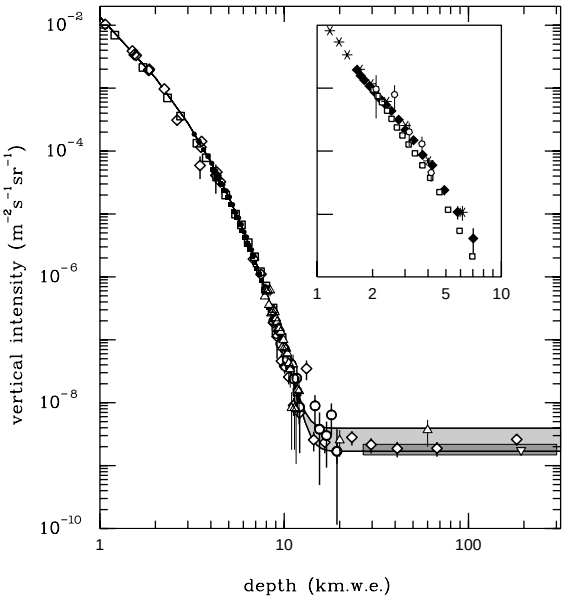

Figure 29.7: Vertical muon intensity vs depth (1 km.w.e. = 10^5 g $\mathrm{cm^{-2}}$ of standard rock). The experimental data are from: ◊: the compilations of Crouch [69], □: Baksan [75], ○: LVD [76], •: MACRO [77], ■: Frejus [78], and △: SNO [79]. The shaded area at large depths represents neutrino-induced muons of energy above 2 GeV. The upper line is for horizontal neutrino-induced muons, the lower one for vertically upward muons. Darker shading shows the muon flux measured by the SuperKamiokande experiment. The inset shows the vertical intensity curve for water and ice published in Refs. [70–73]. Additional data extending to slant depths of 13 km are available in [74].

Table 29.3: Measured fluxes (10^{-9} m^{-2} s^{-1} sr^{-1}) of neutrino-induced muons as a function of the effective minimum muon energy E_μ.

$E_\mu >$	1 GeV	1 GeV	1 GeV	2 GeV	3 GeV	3 GeV
Ref.	CWI [83]	Baksan [84]	MACRO [85]	IMB [86]	Kam [87]	SuperK [88]
F_μ	2.17±0.21	2.77±0.17	2.29 ± 0.15	2.26±0.11	1.94±0.12	1.74±0.07

29.4.2. ***Neutrinos*** : Because neutrinos have small interaction cross sections, measurements of atmospheric neutrinos require a deep detector to avoid backgrounds. There are two types of measurements: contained (or semi-contained) events, in which the vertex is determined to originate inside the detector, and neutrino-induced muons. The latter are muons that enter the detector from zenith angles so large (*e.g.*, nearly horizontal or upward) that they cannot be muons produced in the atmosphere. In neither case is the neutrino flux measured directly. What is measured is a convolution of the neutrino flux and cross section with the properties of the detector (which includes the surrounding medium in the case of entering muons).

Contained and semi-contained events reflect neutrinos in the sub-GeV to multi-GeV region where the product of increasing cross section and decreasing flux is maximum. In the GeV region the neutrino flux and its angular distribution depend on the geomagnetic location of the detector and, to a lesser extent, on the phase of the solar cycle. Naively, we expect $\nu_\mu/\nu_e = 2$ from counting neutrinos of the two flavors coming from the chain of pion and muon decays. Contrary to expectation, however, the numbers of the two classes of events are similar rather than different by a factor of two. This is now understood to be a consequence of neutrino flavor oscillations [82]. (See the article on neutrino properties in this *Review*.)

Two well-understood properties of atmospheric cosmic rays provide a standard for comparison of the measurements of atmospheric neutrinos to expectation. These are the "$\sec\theta$ effect" and the "east-west effect" [81]. The former refers originally to the enhancement of the flux of > 10 GeV muons (and neutrinos) at large zenith angles because the parent pions propagate more in the low density upper atmosphere where decay is enhanced relative to interaction. For neutrinos from muon decay, the enhancement near the horizontal becomes important for $E_\nu > 1$ GeV and arises mainly from the increased pathlength through the atmosphere for muon decay in flight.

Fig. 14.11 from Ref. 80 shows a comparison between measurement and expectation for the zenith angle dependence of multi-GeV electron-like (mostly ν_e) and muon-like (mostly ν_μ) events separately. The ν_e show an enhancement near the horizontal and approximate equality for nearly upward ($\cos\theta \approx -1$) and nearly downward ($\cos\theta \approx 1$) events. There is, however, a very significant deficit of upward ($\cos\theta < 0$) ν_μ events, which have long pathlengths comparable to the radius of the Earth. This feature is the principal signature for atmospheric neutrino oscillations [82].

Muons that enter the detector from outside after production in charged-current interactions of neutrinos naturally reflect a higher energy portion of the neutrino spectrum than contained events because the muon range increases with energy as well as the cross section. The relevant energy range is $\sim 10 < E_\nu < 1000$ GeV, depending somewhat on angle. Neutrinos in this energy range show a $\sec\theta$ effect similar to muons (see Eq. (29.4)). This causes the flux of horizontal neutrino-induced muons to be approximately a factor two higher than the vertically upward flux. The upper and lower edges of the horizontal shaded region in Fig. 29.7 correspond to horizontal and vertical intensities of neutrino-induced muons. Table 29.3 gives the measured fluxes of upward-moving neutrino-induced muons averaged over the lower hemisphere. Generally the definition of minimum muon energy depends on where it passes through the detector. The tabulated effective minimum energy estimates the average over various accepted trajectories.

29.5. Air showers

So far we have discussed inclusive or uncorrelated fluxes of various components of the cosmic radiation. An air shower is caused by a single cosmic ray with energy high enough for its cascade to be detectable at the ground. The shower has a hadronic core, which acts as a collimated source of electromagnetic subshowers, generated mostly from $\pi^0 \to \gamma\,\gamma$ decays. The resulting electrons and positrons are the most numerous charged particles in the shower. The number of muons, produced by decays of charged mesons, is an order of magnitude lower. Air showers spread over a large area on the ground, and arrays of detectors operated for long times are useful for studying cosmic rays with primary energy $E_0 > 100$ TeV, where the low flux makes measurements with small detectors in balloons and satellites difficult.

Greisen [89] gives the following approximate expressions for the numbers and lateral distributions of particles in showers at ground level. The total number of muons N_μ with energies above 1 GeV is

$$N_\mu(> 1 \text{ GeV}) \;\approx\; 0.95 \times 10^5 \left(N_e/10^6\right)^{3/4} \;, \tag{29.8}$$

where N_e is the total number of charged particles in the shower (not just $e^\pm$). The number of muons per square meter, ρ_μ, as a function of the lateral distance r (in meters) from the center of the shower is

$$\rho_\mu = \frac{1.25\,N_\mu}{2\pi\,\Gamma(1.25)} \left(\frac{1}{320}\right)^{1.25} r^{-0.75} \left(1 + \frac{r}{320}\right)^{-2.5} \;, \tag{29.9}$$

where Γ is the gamma function. The number density of charged particles is

$$\rho_e = C_1(s, d, C_2)\, x^{(s-2)} (1 + x)^{(s-4.5)} (1 + C_2 x^d) \;. \tag{29.10}$$

Here s, d, and C_2 are parameters in terms of which the overall normalization constant $C_1(s, d, C_2)$ is given by

$$C_1(s, d, C_2) = \frac{N_e}{2\pi r_1^2} \left[\, B(s, 4.5 - 2s) + C_2\, B(s + d,\, 4.5 - d - 2s)\right]^{-1} \;, \tag{29.11}$$

where $B(m, n)$ is the beta function. The values of the parameters depend on shower size (N_e), depth in the atmosphere, identity of the primary nucleus, etc. For showers with $N_e \approx 10^6$ at sea level, Greisen uses $s = 1.25$, $d = 1$, and $C_2 = 0.088$. Finally, x is r/r_1, where r_1 is the Molière radius, which depends on the density of the atmosphere and hence on the altitude at which showers are detected. At sea level $r_1 \approx 78$ m. It increases with altitude as the air density decreases. (See the section on electromagnetic cascades in the article on the passage of particles through matter in this *Review*).

The lateral spread of a shower is determined largely by Coulomb scattering of the many low-energy electrons and is characterized by the Moliere radius. The lateral spread of the muons (ρ_μ) is larger and depends on the transverse momenta of the muons at production as well as multiple scattering.

There are large fluctuations in development from shower to shower, even for showers of the same energy and primary mass—especially for small showers, which are usually well past maximum development

when observed at the ground. Thus the shower size N_e and primary energy E_0 are only related in an average sense, and even this relation depends on depth in the atmosphere. One estimate of the relation is [96]

$$E_0 \sim 3.9 \times 10^6 \text{ GeV } (N_e/10^6)^{0.9} \quad (29.12)$$

for vertical showers with $10^{14} < E < 10^{17}$ eV at 920 g cm^{-2} (965 m above sea level). As E_0 increases the shower maximum (on average) moves down into the atmosphere and the relation between N_e and E_0 changes. Moreover, because of fluctuations, N_e as a function of E_0 is not correctly obtained by inverting Eq. (29.12). At the maximum of shower development, there are approximately 2/3 particles per GeV of primary energy.

There are three common types of air shower detectors: shower arrays that measure a ground parameter related to shower size N_e and muon number N_μ as well as the lateral distribution on the ground, Cherenkov detectors that detect the Cherenkov radiation emitted by the charged particles of the shower, and fluorescence detectors that study the nitrogen fluorescence excited by the charged particles in the shower. The fluorescence light is emitted isotropically so the showers can be observed from the side. Detection of radiofrequency emission from showers via geosynchrotron and Askaryan mechanisms has also been successfully employed in recent experiments. Detailed simulations and cross-calibrations between different types of detectors are necessary to establish the primary energy spectrum from air-shower experiments.

Figure 29.8 shows the "all-particle" spectrum. The differential energy spectrum has been multiplied by $E^{2.6}$ in order to display the features of the steep spectrum that are otherwise difficult to discern. The steepening that occurs between 10^{15} and 10^{16} eV is known as the *knee* of the spectrum. The feature around $10^{18.5}$ eV is called the *ankle* of the spectrum.

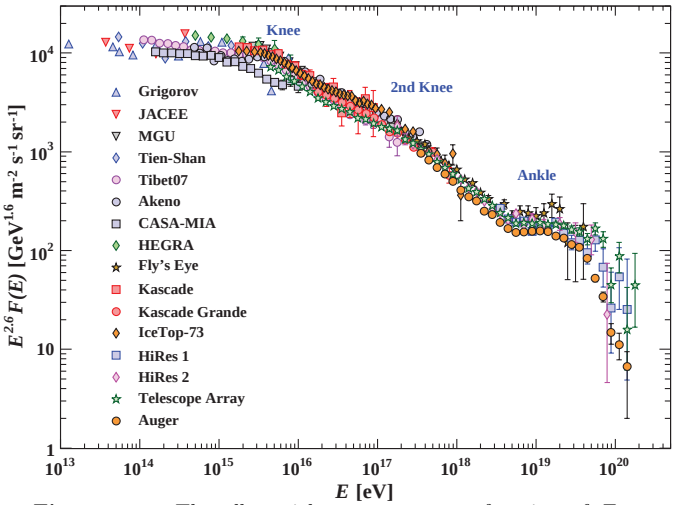

Figure 29.8: The all-particle spectrum as a function of E (energy-per-nucleus) from air shower measurements [91–106].

Measurements of flux with air shower experiments in the knee region differ by as much as a factor of two, indicative of systematic uncertainties in interpretation of the data. (For a review see Ref. 90.) In establishing the spectrum shown in Fig. 29.8, efforts have been made to minimize the dependence of the analysis on the primary composition. Ref. 99 uses an unfolding procedure to obtain the spectra of the individual components, giving a result for the all-particle spectrum between 10^{15} and 10^{17} eV that lies toward the upper range of the data shown in Fig. 29.8. In the energy range above 10^{17} eV, the fluorescence technique [107] is particularly useful because it can establish the primary energy in a model-independent way by observing most of the longitudinal development of each shower, from which E_0 is obtained by integrating the energy deposition in the atmosphere. The result, however, depends strongly on the light absorption in the atmosphere and the calculation of the detector's aperture.

Assuming the cosmic-ray spectrum below 10^{18} eV is of galactic origin, the *knee* could reflect the fact that most cosmic accelerators in the Galaxy have reached their maximum energy. Some types of expanding supernova remnants, for example, are estimated not to be able to accelerate protons above energies in the range of 10^{15} eV. Effects of propagation and confinement in the Galaxy [111] also need to be considered. A discussion of models of the knee may be found in Ref. 112. The Kascade-Grande experiment [101] has reported observation of a second steepening of the spectrum near 8×10^{16} eV, with evidence that this structure is accompanied a transition to heavy primaries.

Concerning the ankle, one possibility is that it is the result of a higher energy population of particles overtaking a lower energy population, for example an extragalactic flux beginning to dominate over the galactic flux (e.g. Ref. 107). Another possibility is that the dip structure in the region of the ankle is due to $p\gamma \to e^+ + e^-$ energy losses of extragalactic protons on the 2.7 K cosmic microwave radiation (CMB) [114]. This dip structure has been cited as a robust signature of both the protonic and extragalactic nature of the highest energy cosmic rays [113]. If this interpretation is correct, then the galactic cosmic rays do not contribute significantly to the flux above 10^{18} eV.

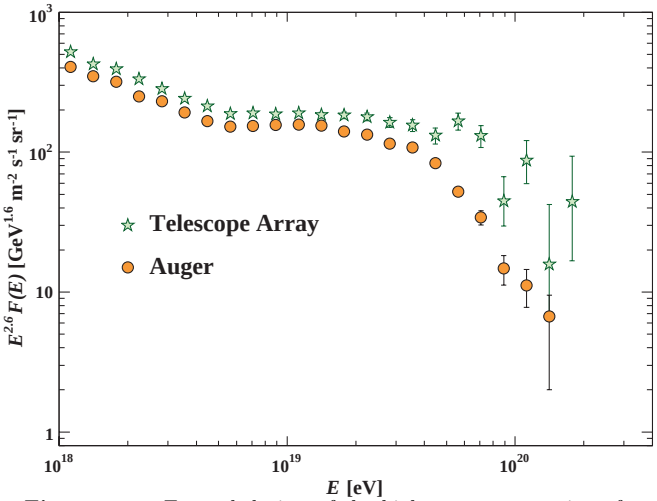

Figure 29.9: Expanded view of the highest energy portion of the cosmic-ray spectrum from data of the Telescope Array [105], and the Pierre Auger Observatory [106].

The energy-dependence of the composition from the knee through the ankle is useful in discriminating between these two viewpoints, since a heavy composition above 10^{18} eV is inconsistent with the formation of the ankle by pair production losses on the CMB. The TA and Auger experiments, however, have shown somewhat different interpretations of data on the depth of shower maximum X_{max}, a quantity that correlates strongly with $ln(E/A)$ and with the interaction cross section of the primary particle. The Telescope Array (TA) collaboration [115] has interpreted their data as implying a light primary composition (mainly p and He) of ultrahigh-energy cosmic-rays (UHECR) from 1.3×10^{18} to 4×10^{19} eV. The Pierre Auger collaboration [116], using post-LHC hadronic interaction models, reports a composition becoming light up to 2×10^{18} eV but then becoming heavier above that energy, with the mean mass intermediate between protons and iron at 3×10^{19} eV. Auger and TA have also conducted a thorough joint analysis [117] and state that, at the current level of statistics and understanding of systematics, both data sets are compatible with being drawn from the same parent distribution, and that the TA data is compatible both with a protonic compsition below 10^{19} eV and with the mixed compostion above 10^{19} eV as reported by Auger.

If the cosmic-ray flux at the highest energies is cosmological in origin, there should be a rapid steepening of the spectrum (called the GZK feature) around 5×10^{19} eV, resulting from the onset of

inelastic interactions of UHE cosmic rays with the cosmic microwave background [118,119]. Photo-dissociation of heavy nuclei in the mixed composition model [120] would have a similar effect. UHECR experiments have detected events of energy above 10^{20} eV [107–108]. The HiRes fluorescence experiment [103,131] detected evidence of the GZK suppression, and the Auger observatory [104–106] has also presented spectra showing this suppression based on surface detector measurements calibrated against fluorescence detectors using events detected in hybrid mode, i.e. with both the surface and the fluorescence detectors. The Telescope Array (TA) [105] has also presented a spectrum showing this suppression. The differential energy spectra measured by the TA and by Auger agree within systematic errors below 10^{19} eV (Fig. 29.9). At higher energies, TA observes more cosmic rays than would be expected if the spectral shape were the same as that seen by Auger. TA has also reported a 'hot spot' in the Northern Hemisphere at energies above 5.5×10^{19} eV of radius $\sim 20°$ with a post-trials statistical significance of this excess with respect to an isotropic distribution of 3.4σ [109]. Auger has reported the observation of a dipole of amplitude $6.5^{+1.3}_{-0.9}\%$ with a significance of 5.2σ for cosmic rays with energies above 8×10^{18} eV. The direction of the dipole indicates an extragalactic origin for these particles [110].

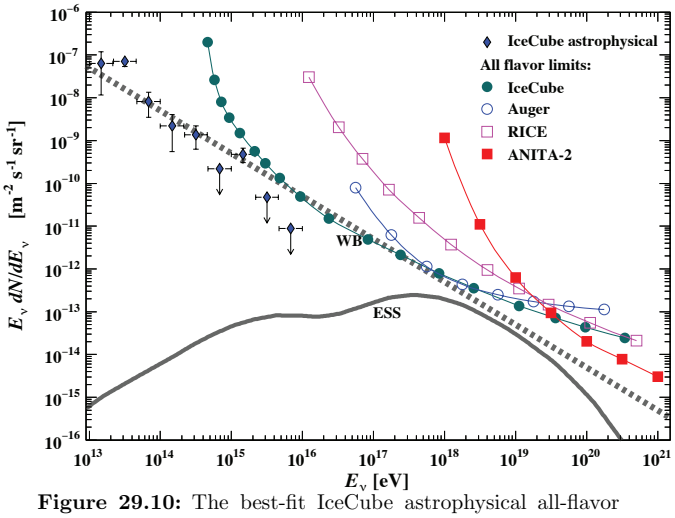

Figure 29.10: The best-fit IceCube astrophysical all-flavor neutrino flux [123]. Also shown are differential limits on the flux of cosmogenic neutrinos set by four experiments [125–128]. The curves show the Waxman-Bahcall benchmark flux (WB, [130]) and a representative midrange model for the expected flux of cosmogenic neutrinos (ESS, [129]) . The expected flux is uncertain by over an order of magnitude in either direction.

Neutrinos are expected to be produced in hadronic interactions in a variety of astrophysical objects. IceCube has reported a population of astrophysical neutrino events extending from tens of TeV up to several PeV [121–123].

There is also expected to be a neutrino flux produced in cosmic ray GZK interactions. One half of the energy that UHECR protons lose in photoproduction interactions that cause the GZK effects ends up in neutrinos [124]. Measuring this *cosmogenic* neutrino flux above 10^{18} eV would help resolve the UHECR uncertainties mentioned above. The magnitude of this flux depends strongly on the cosmic-ray spectrum at acceleration, the cosmic-ray composition, and the cosmological evolution of the cosmic-ray sources. In the case that UHECR have mixed composition only the proton fraction would produce cosmogenic neutrinos. Heavy nuclei propagation produces mostly $\bar{\nu}_e$ at lower energy from neutron decay.

The expected rate of cosmogenic neutrinos is lower than current limits obtained by IceCube [125], the Auger observatory [126], RICE [127], and ANITA-2 [128], which are shown in Fig. 29.10 together with a model for cosmogenic neutrino production [129] and the Waxman-Bahcall benchmark flux of neutrinos produced in cosmic ray sources [130]. At production, the dominant component of neutrinos comes from $\pi^\pm$ decays and has flavor content $\nu_e : \nu_\mu : \nu_\tau = 1 : 2 : 0$. After oscillations, the arriving cosmogenic neutrinos are expected to be an equal mixture of all three flavors. The sensitivity of each experiment depends on neutrino flavor. IceCube, RICE, and ANITA are sensitive to all three flavors, and the sensitivity to different flavors is energy dependent. The limit of Auger is only for ν_τ and $\bar{\nu}_\tau$ which should be about 1/3 of the total neutrino flux after oscillations, so this limit is plotted multiplied by a factor of three for comparison with the other limits and with the theoretical estimates.

References:

1. D. Maurin *et al.*, Astron. & Astrophys. **569**, A32 (2014).
2. O. Adriani *et al.* (PAMELA Collab.), Science **332**, 69 (2011).
3. M. Aguilar *et al.* (AMS02 Collab.), Phys. Rev. Lett. **114**, 171103 (2015).
4. M. Aguilar *et al.* (AMS02 Collab.), Phys. Rev. Lett. **115**, 211101 (2015).
5. K. Abe *et al.* (BESS Collab.), Astrophys. J. **822**, 65 (2016).
6. K. Asakimori *et al.* (JACEE Collab.), Astrophys. J. **502**, 278 (1998).
7. A.D. Panov *et al.*(ATIC Collab.), Bull. Russian Acad. of Science, Physics, **73**, 564 (2009).
8. V.A. Derbina *et al.*(RUNJOB Collab.), Astrophys. J. **628**, L41 (2005).
9. H.S. Ahn, *et al.* (CREAM Collab.), Astrophys. J. **707**, 593 (2009).
10. J.J. Engelmann *et al.*(HEAO3-C2 Collab.), Astron. & Astrophys. **233**, 96 (1990).
11. D. Müller *et al.*(CRN Collab.), Astrophys. J. **374**, 356 (1991).
12. M. Ave *et al.* (TRACER Collab.), Astrophys. J. **678**, 262 (2008).
13. F. Aharonian *et al.* (HESS Collab.), Phys. Rev. **D75**, 042004 (2007).
14. A.W. Strong *et al.*, Ann. Rev. Nucl. and Part. Sci. **57**, 285 (2007).
15. R.A. Mewaldt *et al.*, Space Science Reviews 99,27(2001).
16. A.A. Abdo *et al.*, Astrophys. J. **698**, 2121 (2009).
17. R. Abbasi *et al.*, Astrophys. J. **718**, L194 (2010).
18. M. Amenomori *et al.*, Astrophys. J. **711**, 119 (2010).
19. J. Chang *et al.* (ATIC Collab.), Nature **456**, 362 (2008).
20. A.A. Abdo *et al.* (Fermi/LAT Collab.), Phys. Rev. Lett. **102**, 181101 (2009); M. Ackermann *et al.*, Phys. Rev. **D82**, 092004 (2010).
21. M. Aguilar *et al.* (AMS-02 Collab.), Phys. Rev. Lett. **113**, 221102 (2014).
22. F. Aharonian *et al.* (HESS Collab.), Phys. Rev. Lett. **101**, 261104 (2008) and Astron. & Astrophys. **508**, 561 (2009).
23. O Adriani *et al.*, Phys. Rev. Lett. **106**, 201101 (2011).
24. L. Accardo *et al.* (AMS-02 Collab.), Phys. Rev. Lett. **113**, 121101 (2014).
25. Y. Shizake *et al.*, Astropart. Phys. **28**, 154 (2007).
26. O. Adriani *et al.* (Pamela Collab.), Nature **458**, 607 (2009); Phys. Rev. Lett. **102**, 051101 (2009).
27. M. Aguilar *et al.*, Phys. Rev. Lett. **110**, 141102 (2013).
28. I.V. Moskalenko and A.W. Strong, Astrophys. J. **493**, 694 (1998).
29. A. Ibarra *et al.*, Int. J. Mod. Phys. **A28**, 1330040 (2013).
30. J.J. Beatty *et al.*, Phys. Rev. Lett. **93**, 24112 (2004).
31. J. Nishimura *et al.*, Adv. Space Research **19**, 767 (1997).
32. D. Gaggero *et al.*, Phys. Rev. Lett. **111**, 021102 (2013).
33. M.A. DuVernois *et al.*, Astrophys. J. **559**, 296 (2001).
34. M. Boezio *et al.*, Astrophys. J. **532**, 653 (2000).
35. A.S. Beach *et al.*, Phys. Rev. Lett. **87**, 271101 (2001).
36. A. Yamamoto *et al.*, Adv. Space Research**42**, 443(2008).
37. Y. Asaoka *et al.*, Phys. Rev. Lett. **88**, 51101 (2002).
38. K. Abe *et al.*, Phys. Rev. Lett. **108**, 081102 (2012).
39. H. Fuke *et al.*, Phys. Rev. Lett. **95**, 081101 (2005).
40. P. Yin *et al.*, Phys. Rev. **D88**, 023001 (2013).
41. R. Bellotti *et al.*, Phys. Rev. **D53**, 35 (1996).
42. R. Bellotti *et al.*, Phys. Rev. **D60**, 052002 (1999).

43. M. Boezio *et al.*, Phys. Rev. **D62**, 032007 (2000); M. Boezio *et al.*, Phys. Rev. **D67**, 072003 (2003).
44. S. Coutu *et al.*, Phys. Rev. **D62**, 032001 (2000).
45. S. Haino *et al.*, Phys. Lett. **B594**, 35 (2004).
46. T. Sanuki *et al.*, Phys. Rev. **D75**, 043005 (2007).
47. T.K. Gaisser, R. Engel, and E. Resconi, *Cosmic Rays and Particle Physics (second edition)*, Cambridge University Press (2016).
48. P. Lipari, Astropart. Phys. **1**, 195 (1993).
49. E. Mocchiutto *et al.*, in *Proc. 28th Int. Cosmic Ray Conf.*, Tsukuba, 1627 (2003). [adsabs.harvard.edu/abs/2003ICRC....3.1627M].
50. M.P. De Pascale *et al.*, J. Geophys. Res. **98**, 3501 (1993).
51. P.K.F. Grieder, *Cosmic Rays at Earth*, Elsevier Science (2001).
52. J. Kremer *et al.*, Phys. Rev. Lett. **83**, 4241 (1999).
53. S. Haino *et al.* (BESS Collab.), Phys. Lett. **B594**, 35 (2004).
54. P. Archard *et al.* (L3+C Collab.), Phys. Lett. **B598**, 15 (2004).
55. C.G.S. Costa, Astropart. Phys. **16**, 193 (2001).
56. O.C. Allkofer, K. Carstensen, and W.D. Dau, Phys. Lett. **B36**, 425 (1971).
57. B.C. Rastin, J. Phys. **G10**, 1609 (1984).
58. C.A. Ayre *et al.*, J. Phys. **G1**, 584 (1975).
59. H. Jokisch *et al.*, Phys. Rev. **D19**, 1368 (1979).
60. P. Adamson *et al.* (MINOS Collab.), Phys. Rev. **D76**, 052003 (2007).
61. S. Hayakawa, *Cosmic Ray Physics*, Wiley, Interscience, New York (1969).
62. R.R. Daniel and S.A. Stephens, Revs. Geophysics & Space Sci. **12**, 233 (1974).
63. K.P. Beuermann and G. Wibberenz, Can. J. Phys. **46**, S1034 (1968).
64. I.S. Diggory *et al.*, J. Phys. **A7**, 741 (1974).
65. V. Khachatryan *et al.* (CMS Collab.) Phys. Lett. **B692**, 83 (2010).
66. N. Agafonova *et al.* (OPERA Collab.) Eur. Phys. J. **C67**, 25 (2010).
67. D.E. Groom, N.V. Mokhov, and S.I. Striganov, *"Muon stopping-power and range tables,"*Atomic Data and Nuclear Data Tables, **78**, 183 (2001).
68. P. Lipari and T. Stanev, Phys. Rev. **D44**, 3543 (1991).
69. M. Crouch, in *Proc. 20th Int. Cosmic Ray Conf.*, Moscow, **6**, 165 (1987) [http://adsabs.harvard.edu/abs/1987ICRC....6..165C].
70. I.A. Belolaptikov *et al.*, Astropart. Phys. **7**, 263 (1997).
71. J. Babson *et al.*, Phys. Rev. **D42**, 3613 (1990).
72. P. Desiati *et al.*, in *Proc. 28th Int. Cosmic Ray Conf.*, Tsukuba, 1373 (2003) [adsabs.harvard.edu/abs/2003ICRC....3.1373D].
73. T. Pradier *et al.* (ANTARES Collab.), arXiv:0805.2545 and 31st ICRC, 7-15 July 2009, Łódź, Poland (paper #0340).
74. S. Aiello *et al.* (NEMO Collab), Astropart. Phys. **66**, 1 (2015).
75. Yu.M. Andreev, V.I. Gurentzov, and I.M. Kogai, in *Proc. 20th Int. Cosmic Ray Conf.*, Moscow, **6**, 200 (1987), [adsabs.harvard.edu/abs/1987ICRC....6..200A].
76. M. Aglietta *et al.* (LVD Collab.), Astropart. Phys. **3**, 311 (1995).
77. M. Ambrosio *et al.* (MACRO Collab.), Phys. Rev. **D52**, 3793 (1995).
78. Ch. Berger *et al.* (Frejus Collab.), Phys. Rev. **D40**, 2163 (1989).
79. C. Waltham *et al.*, in *Proc. 27th Int. Cosmic Ray Conf.*, Hamburg, 991 (2001), [adsabs.harvard.edu/abs/2001ICRC....3..991W].
80. Y. Ashie *et al.* (SuperKamiokande Collab.), Phys. Rev. **D71**, 112005 (2005).
81. T. Futagami *et al.*, Phys. Rev. Lett. **82**, 5194 (1999).
82. Y. Fukuda *et al.*, Phys. Rev. Lett. **81**, 1562 (1998).
83. F. Reines *et al.*, Phys. Rev. Lett. **15**, 429 (1965).
84. M.M. Boliev *et al.*, in *Proc. 3rd Int. Workshop on Neutrino Telescopes* (ed. Milla Baldo Ceolin), 235 (1991).
85. M. Ambrosio *et al.*, (MACRO) Phys. Lett. **B434**, 451 (1998). The number quoted for MACRO is the average over 90% of the lower hemisphere, $\cos\theta < -0.1$; see F. Ronga *et al.*, hep-ex/9905025.
86. R. Becker-Szendy *et al.*, Phys. Rev. Lett. **69**, 1010 (1992); *Proc. 25th Int. Conf. High-Energy Physics*, Singapore (eds. K.K. Phua and Y. Yamaguchi, World Scientific), 662 1991.
87. S. Hatakeyama *et al.*, Phys. Rev. Lett. **81**, 2016 (1998).
88. Y. Fukuda *et al.*, Phys. Rev. Lett. **82**, 2644 (1999).
89. K. Greisen, Ann. Rev. Nucl. Sci. **10**, 63 (1960).
90. S.P. Swordy *et al.*, Astropart. Phys. **18**, 129 (2002).
91. N.L. Grigorov *et al.*, *Sov. J. Nucl. Phys.* 11, 588. *Proc. 12th Int. Cosmic Ray Conf.*, Hobart, **1**, 1746 and 1752 (1971).
92. K. Asakimori *et al.*, *Proc. 23rd Int. Cosmic Ray Conf.*, Calgary, **2**, 25 (1993); *Proc. 22nd Int. Cosmic Ray Conf.*, Dublin, **2**, 57 and 97 (1991) [adsabs.harvard.edu/abs/1991ICRC....2...57A] [adsabs.harvard.edu/abs/1991ICRC....2...97A].
93. T.V. Danilova *et al.*, *Proc. 15th Int. Cosmic Ray Conf.*, Plovdiv, **8**, 129 (1977) [adsabs.harvard.edu/abs/1977ICRC....8..129D].
94. Yu. A. Fomin *et al.*, *Proc. 22nd Int. Cosmic Ray Conf.*, Dublin, **2**, 85 (1991) [adsabs.harvard.edu/abs/1991ICRC....2...85F].
95. M. Amenomori *et al.*, Astrophys. J. **461**, 408 (1996).
96. M. Nagano *et al.*, J. Phys. **G10**, 1295 (1984).
97. F. Arqueros *et al.*, Astron. & Astrophys. **359**, 682 (2000).
98. M.A.K. Glasmacher *et al.*, Astropart. Phys. **10**, 291 (1999).
99. T. Antoni *et al.* (Kascade Collab.), Astropart. Phys. **24**, 1 (2005).
100. M. Amenomori *et al.*, Astrophys. J. **268**, 1165 (2008).
101. W.D. Apel *et al.*, Phys. Rev. Lett. **107**, 171104 (2011).
102. M.G. Aartson *et al.*, (IceCube Collab.) arXiv:1307.3795v1(2013).
103. R. Abbasi *et al.*, (HiRes Collab.), Phys. Rev. Lett. **100**, 101101 (2008).
104. J. Abraham *et al.*, (Auger Collab.), Phys. Rev. Lett. **101**, 061101 (2008).
105. D. Ivanov *et al.*, (Telescope Array Collab.), *Proceedings of Science* (ICRC2015), 349 (2015).
106. F. Fenu *et al.*, (Auger Collab.), *Proceedings of Science* (ICRC2017), 486 (2017).
107. D.J. Bird *et al.*, (Fly's Eye Collab.), Astrophys. J. **424**, 491 (1994).
108. M. Takeda *et al.*, (AGASA Collab.), Astropart. Phys. **19**, 447 (2003).
109. P. Tinyakov *et al.*, (Telescope Array Collab.), *Proceedings of Science* (ICRC2015), 326 (2015).
110. A. Aab *et al.*, (Auger Collab.), *Science* 57, 1266 (2017).
111. V.S. Ptuskin *et al.*, Astron. & Astrophys. **268**, 726 (1993).
112. J.R. Hörandel, Astropart. Phys. **21**, 241 (2004).
113. V.S. Berezinsky and S.I. Grigor'eva, Astron. & Astrophys. **199**, 1 (1988).
114. V. Berezinsky, A. Gazizov, and S. Grigorieva, Phys. Rev. **D74**, 043005 (2006).
115. D. Ikeda *et al.*(TA Collab.), Proceedings of Science(ICRC2017), 515 (2017).
116. J. Bellido *et al.*(Auger Collab.), Proceedings of Science(ICRC2017), 506 (2017).
117. V. de Souza *et al.*(TA and Auger Collabs.), Proceedings of Science(ICRC2017), 522 (2017).
118. K. Greisen, Phys. Rev. Lett. **16**, 748 (1966).
119. G.T. Zatsepin and V.A. Kuz'min, Sov. Phys. JETP Lett. **4**, 78 (1966).
120. D. Allard *et al.*, Astron. & Astrophys. **443**, L29 (2005).
121. M. Aartsen *et al.*, (IceCube Collab.) Science **342**, 1242856 (2013).
122. M. Aartsen *et al.*, (IceCube Collab.) Phys. Rev. Lett. **113**, 101101 (2013).
123. M.G. Aartsen *et al.*(IceCube Collab.), Astrophys. J. **809**, 98 (2015).
124. V.S. Berezinsky and G.T. Zatsepin, Phys. Lett. **B28**, 423 (1969).

125. M.G. Aartsen *et al.*, (IceCube Collab.), Phys. Rev. **D88**, 112008 (2013).
126. A. Aab *et al.*, (Auger Collab.), Phys. Rev. **D91**, 092008 (2015).
127. I. Kravchenko *et al.*(RICE Collab.), Phys. Rev. **D73**, 082002 (2006);
I. Kravchenko *et al.*(RICE collab.), Phys. Rev. **D85**, 062004 (2012).
128. P. Gorham *et al.*, (ANITA Collab.), Phys. Rev. **D82**, 022004 (2010);
P. Gorham *et al.*, (ANITA Collab.), Phys. Rev. **D85**, 049901 (2012).
129. R. Engel, D. Seckel, and T. Stanev, Phys. Rev. **D64**, 09310 (2001).
130. E. Waxman and J. Bahcall, Phys. Rev. **D59**, 023002 (1999).
131. R.U. Abbasi *et al.*, (HiRes Collab.), Astropart. Phys. **32**, 53 (2009).

30. Accelerator Physics of Colliders

Revised March 2018 by M.J. Syphers (NIU/FNAL) and F. Zimmermann (CERN).

30.1. Luminosity

This article provides background for the High-Energy Collider Parameter Tables that follow. The number of events, N_{exp}, is the product of the cross section of interest, σ_{exp}, and the time integral over the instantaneous *luminosity*, $\mathscr{L}$:

$$N_{exp} = \sigma_{exp} \times \int \mathscr{L}(t)dt. \tag{30.1}$$

Today's colliders all employ bunched beams. If two bunches containing n_1 and n_2 particles collide head-on with frequency $f_{\rm coll}$, a basic expression for the luminosity is

$$\mathscr{L} = f_{\rm coll}\frac{n_1 n_2}{4\pi\sigma_x^*\sigma_y^*} \tag{30.2}$$

where σ_x^* and σ_y^* characterize the rms transverse beam sizes in the horizontal (bend) and vertical directions at the interaction point. In this form it is assumed that the bunches are identical in transverse profile, that the profiles are Gaussian and independent of position along the bunch, and the particle distributions are not altered during bunch crossing. Nonzero beam crossing angles θ_c in the horizontal plane and long bunches (rms bunch length σ_z) will reduce the luminosity from the above value, e.g. by a factor $1/(1+\phi^2)^{1/2}$, where the parameter $\phi \equiv \theta_c\sigma_z/(2\sigma_x^*)$ is known as the Piwinski angle.

Whatever the distribution at the source, by the time the beam reaches high energy, the normal form is a useful approximation as suggested by the σ-notation. In the case of an electron storage ring, synchrotron radiation leads to a Gaussian distribution in equilibrium, but even in the absence of radiation the central limit theorem of probability and the diminished importance of space charge effects produce a similar result.

The luminosity may be obtained directly by measurement of the beam properties in Eq. (30.2). For continuous measurements, an expression similar to Eq. (30.1) with N_{ref} from a known reference cross section, σ_{ref}, may be used to determine σ_{exp} according to $\sigma_{exp} = (N_{exp}/N_{ref})\sigma_{ref}$.

In the Tables, luminosity is stated in units of $\rm cm^{-2}s^{-1}$. Integrated luminosity, on the other hand is usually quoted as the inverse of the standard measures of cross section such as femtobarns and, recently, attobarns. Subsequent sections in this report briefly expand on the dynamics behind collider design, comment on the realization of collider performance in a selection of today's facilities, and end with some remarks on future possibilities.

30.2. Beam Dynamics

The first concern of beam dynamics is stability. While a reference particle proceeds along the design, or reference, trajectory other particles in the bunch are to remain close by. Assume that the reference particle carries a right-handed Cartesian coordinate system, with the z-coordinate pointed in the direction of motion along the reference trajectory. The independent variable is the distance s of the reference particle along this trajectory rather than time, and for simplicity this path is taken to be planar. The transverse coordinates are x and y, where $\{x, z\}$ defines the plane of the reference trajectory.

Several time scales are involved, and the approximations used in writing the equations of motion reflect that circumstance. All of today's high energy colliders are alternating-gradient synchrotrons or, respectively, storage rings [1,2], and the shortest time scale is that associated with transverse motion, that is described in terms of betatron oscillations, so called because of their analysis for the betatron accelerator species years ago. The linearized equations of motion of a particle displaced from the reference particle are

$$\begin{aligned} x'' + K_x x = 0, \qquad & K_x \equiv \frac{q}{p}\frac{\partial B}{\partial x} + \frac{1}{\rho^2} \\ y'' + K_y y = 0, \qquad & K_y \equiv -\frac{q}{p}\frac{\partial B}{\partial x} \\ z' = -x/\rho & \end{aligned} \tag{30.3}$$

where the magnetic field $B(s)$ along the design trajectory is only in the y direction, contains only dipole and quadrupole terms, and is treated as static here. The radius of curvature due to the field on the reference orbit is ρ; z represents the longitudinal distance from the reference particle; p and q are the particle's momentum and charge, respectively. The prime denotes d/ds. The pair $(x,\ x')$ describes approximately-canonical variables. For more general cases (e.g. acceleration) one should use $(x,\ p_x)$ instead, where p_x denotes the transverse momentum in the x-direction.

The equations for x and y are those of harmonic oscillators but with a restoring force periodic in s; that is, they are instances of Hill's equation. The solution may be written in the form

$$\begin{aligned} x(s) &= A_x\sqrt{\beta_x}\ \cos\psi_x \\ x'(s) &= -\frac{A_x}{\sqrt{\beta_x}}\left[\alpha_x\cos\psi_x + \sin\psi_x\right] \end{aligned} \tag{30.4}$$

where A_x is a constant of integration, $\alpha_x \equiv -(1/2)d\beta_x(s)/ds$, and the envelope of the motion is modulated by the *amplitude function*, β_x. A solution of the same form describes the motion in y. The subscripts will be suppressed in the following discussion.

The amplitude function satisfies

$$2\beta\beta'' - \beta'^2 + 4\beta^2 K = 4, \tag{30.5}$$

and in a region free of magnetic field it should be noted that the solution of Eq. (30.5) is a parabola. Expressing A in terms of $x,\ x'$ yields

$$\begin{aligned} A^2 &= \gamma x^2 + 2\alpha x x' + \beta x'^2 \\ &= \frac{1}{\beta}\left[x^2 + (\alpha x + \beta x')^2\right] \end{aligned} \tag{30.6}$$

with $\gamma \equiv (1+\alpha^2)/\beta$. In a single pass system such as a linac, the *Courant-Snyder parameters* α, β, γ may be selected to match the $x,\ x'$ distribution of the input beam; in a recursive system, the parameters are usually defined by the structure rather than by the beam.

The relationships between the parameters and the structure may be seen by treatment of a simple *lattice* consisting of equally-spaced thin-lens quadrupoles whose magnetic-field gradients are equal in magnitude but alternating in sign. For this discussion, the weak focusing effects of the bending magnets may be neglected. The propagation of $X \equiv \{x, x'\}$ through a repetition period may be written $X_2 = MX_1$, with the matrix $M = FODO$ composed of the matrices

$$F = \begin{pmatrix} 1 & 0 \\ -1/f & 1 \end{pmatrix},\ D = \begin{pmatrix} 1 & 0 \\ 1/f & 1 \end{pmatrix},\ O = \begin{pmatrix} 1 & L \\ 0 & 1 \end{pmatrix},$$

where f is the magnitude of the focal length and L the lens spacing. Then

$$M = \begin{pmatrix} 1+\dfrac{L}{f} & 2L+\dfrac{L^2}{f} \\ -\dfrac{L}{f^2} & 1-\dfrac{L}{f}-\dfrac{L^2}{f^2} \end{pmatrix}. \tag{30.7}$$

The matrix for y is identical in form differing only by a change in sign of the terms linear in $1/f$. An eigenvector-eigenvalue analysis of the matrix M shows that the motion is stable provided $f > L/2$. While that criterion is easily met, in practice instability may be caused by many other factors, including the beam-beam interaction itself.

Standard focus-drift-defocus-drift, or *FODO*, cells such as characterized in simple form by Eq. (30.7) occupy most of the layout of a large collider ring and may be used to set the scale of the amplitude function and related phase advance. Conversion of Eq. (30.4) to a matrix form equivalent to Eq. (30.7) (but more generally valid, i.e. for any stable periodic linear motion) gives

$$M = \begin{pmatrix} C+\alpha S & \beta S \\ -\gamma S & C-\alpha S \end{pmatrix} \tag{30.8}$$

where $C \equiv \cos\Delta\psi$, $S \equiv \sin\Delta\psi$, and the relation between structure and amplitude function is specified by setting the values of the

latter to be the same at both ends of the cell. By comparison of Eq. (30.7) and Eq. (30.8) one finds $C = 1 - L^2/(2f^2)$, so that the choice $f = L/\sqrt{2}$ would give a phase advance $\Delta\psi$ of 90 degrees for the standard cell. The amplitude function would have a maximum at the focusing quadrupole of magnitude $\hat{\beta} = 2.7L$, illustrating the relationship of alternating gradient focusing amplitudes to relatively local aspects of the design. Other functionalities such as injection, extraction, and HEP experiments are included by lattice sections matched to the standard cell parameters (β, α) at the insertion points.

The phase advances according to $d\psi/ds = 1/\beta$; that is, β also plays the role of a local $\lambda/2\pi$, and the *tune*, ν, is the number of such oscillations per turn about the closed path. In the neighborhood of an interaction point (IP), the beam optics of the ring is configured so as to produce a narrow focus; the value of the amplitude function at this point is designated β^*.

The motion as it develops with s describes an ellipse in $\{x, x' \equiv dx/ds\}$ phase space, the area of which is πA^2, where A is the constant in Eq. (30.4). If the interior of that ellipse is populated by an ensemble of non-interacting particles, that area, given the name *emittance* and denoted by ε, would change only with energy. More precisely, for a beam with a Gaussian distribution in x, x', the area containing one standard deviation σ_x, divided by π, is used as the definition of emittance in the Tables:

$$\varepsilon_x \equiv \frac{\sigma_x^2}{\beta_x}\,, \tag{30.9}$$

with a corresponding expression in the other transverse direction, y. This definition includes 39% of the beam. For most of the entries in the Tables the standard deviation is used as the beam radius.

To complete the coordinates used to describe the motion, we take as the variable conjugate to z the fractional momentum deviation $\delta p/p$ from that of the reference particle. Radiofrequency electric fields in the s direction provide a means for longitudinal oscillations, and the frequency determines the bunch length. The frequency of this system appears in the Tables as does the rms value of $\delta p/p$ characterized as "energy spread" of the beam.

For HEP bunch length is a significant quantity for a variety of reasons, but in the present context if the bunch length, or (with nonzero crossing angle) the effective interaction length, becomes larger than β^* the luminosity is adversely affected. This is because β grows parabolically as one proceeds away from the interaction point and so the beam size increases thus lowering the contribution to the luminosity from such locations. This is often called the "hourglass" effect.

The other major external electromagnetic field interaction in the single particle context is the production of synchrotron radiation due to centripetal acceleration, given by the Larmor formula multiplied by a relativistic magnification factor of γ^4 [3]. In the case of electron rings this process determines the equilibrium emittance through a balance between radiation damping and excitation of oscillations, and further serves as a barrier to future higher energy versions in this variety of collider. A more comprehensive discussion of betatron oscillations, longitudinal motion, and synchrotron radiation is available in the 2008 version of the PDG review [5].

Synchrotron radiation emitted during the collision in the field of the opposing beam is called beamstrahlung. Beamstrahlung is relevant for both linear colliders (where it degrades the luminosity spectrum) and future highest-energy circular colliders (where it limits the beam lifetime). For both types of colliders the beamstrahlung is mitigated by making the colliding beams as flat as possible at the interaction point ($\sigma_x^* \gg \sigma_y^*$). The photon energy spectrum of the beamstrahlung is characterized by the parameter Upsilon $\Upsilon = (2/3)\hbar\omega_c/E_b$ [4], with $\hbar\omega_c$ denoting the critical photon energy and E_b the beam energy. The spectrum strongly deviates from the classical synchrotron radiation spectrum for Υ approaching 1.

30.3. Road to High Luminosity

Eq. (30.2) can be recast in terms of emittances and amplitude functions as

$$\mathscr{L} = f\frac{n_1 n_2}{4\pi\sqrt{\epsilon_x\,\beta_x^*\,\epsilon_y\,\beta_y^*}}\;\mathcal{F}. \tag{30.10}$$

Here, $\mathcal{F} \leq 1$ is a factor that takes into account effects such as crossing angles, hour glass factors, pinch effects, and so on. So to achieve high luminosity, all one has to do is make high population bunches of low emittance collide at high frequency at locations where the beam optics provides as low values of the amplitude functions as possible.

Expressions for the reductions due to crossing angle and other effects can be found elsewhere [6]. While there are no fundamental limits to producing luminosity, there are certainly challenges. Here we have space to mention only a few of these. The beam-beam tune shift appears in the Tables. A bunch in beam 1 presents a (nonlinear) lens to a particle in beam 2 resulting in changes to the particle's transverse tune with a range characterized by the beam-beam parameter [6]

$$\xi_{y,2} = \left(\frac{\mu_0}{8\pi^2}\right)\frac{q_1 q_2 n_1 \beta_{y,2}^*}{m_{A,2}\gamma_2\sigma_{y,1}^*(\sigma_{x,1}^* + \sigma_{y,1}^*)} \tag{30.11}$$

where q_1 (q_2) denotes the particle charge of beam 1 (2) in units of the elementary charge, $m_{A,2}$ the mass of beam-2 particles, and μ_0 the vacuum permeability. The transverse oscillations are susceptible to resonant perturbations from a variety of sources such as imperfections in the magnetic guide field, so that certain values of the tune must be avoided. Accordingly, the tune spread arising from ξ is limited, but limited to a value difficult to predict. But a glance at the Tables shows that electrons are more forgiving than protons thanks to the damping effects of synchrotron radiation; the ξ-values for the former are about an order of magnitude larger than those for protons. In linear colliders, the strength of the collision is measured by the ratio of the rms bunch length σ_z to the approximate (linear, thin-lens) beam-beam focal length. This ratio, called disruption parameter D_y [4], is related to ξ_y via $D_y = 4\pi\sigma_z\xi_y/\beta_y^*$.

A subject of present intense interest is the *electron-cloud effect* [7,8]; actually a variety of related processes come under this heading. They typically involve a buildup of electron density in the vacuum chamber due to emission from the chamber walls stimulated by electrons or photons originating from the beam itself. For instance, there is a process closely resembling the multipacting effects familiar from radiofrequency system commissioning. Low energy electrons are ejected from the walls by photons from positron or proton beam-produced synchrotron radiation. These electrons are accelerated toward a beam bunch, but by the time they reach the center of the vacuum chamber the bunch has gone and so the now-energetic electrons strike the opposite wall to produce more secondaries. These secondaries are now accelerated by a subsequent bunch, and so on. Among the disturbances that this electron accumulation can produce is an enhancement of the tune spread within the bunch; the near-cancellation of bunch-induced electric and magnetic fields is no longer in effect.

If the luminosity of Eq. (30.10) is rewritten in terms of the beam-beam parameter, Eq. (30.11), the emittance itself disappears. However, the emittance must be sufficiently small to realize a desired magnitude of beam-beam parameter, but once ξ_y reaches this limit, further lowering the emittance does not lead to higher luminosity.

For electron synchrotrons and storage rings, radiation damping provides an automatic route to achieve a small emittance. In fact, synchrotron radiation is of key importance in the design and optimization of e^+e^- colliders. While vacuum stability and electron clouds can be of concern in the positron rings, synchrotron radiation along with the restoration of longitudinal momentum by the RF system has the positive effect of generating very small transverse beam sizes and small momentum spread. Further reduction of beam size at the interaction points using standard beam optics techniques and successfully contending with high beam currents has led to record luminosities in these rings. To maximize integrated luminosity the beam can be "topped off" by injecting new particles without removing existing ones – a feature difficult to imitate in hadron colliders.

For hadrons, particularly antiprotons, two inventions have played a prominent role. Stochastic cooling [9] was employed first to prepare beams for the $S\bar{p}pS$ and subsequently in the Tevatron, and to cool the beams at full energy in RHIC [10,11,12]. Electron cooling [13] was also used in the Tevatron complex to great advantage. Further

innovations are underway driven by the needs of potential future projects; these are noted in the final section.

30.4. Recent High Energy Colliders

Collider accelerator physics of course goes far beyond the elements of the preceding sections. In this and the following section elaboration is made on various issues associated with some of the recently operating colliders, particularly factors which impact integrated luminosity. The various colliders utilizing hadrons each have unique characteristics and are, therefore, discussed separately. As space is limited, general references are provided where much further information can be obtained. A more complete list of recent colliders and their parameters can be found in the High-Energy Collider Parameters tables.

30.4.1. ***Tevatron*** : [15] The first synchrotron in history using superconducting magnets, the Tevatron, was the highest energy collider for 25 years. Operation was terminated in September 2011, after delivering more than 10 fb^{-1} to the p-$\bar{\text{p}}$ collider experiments CDF and D0. The route to high integrated luminosity in the Tevatron was governed by the antiproton production rate, the turn-around time to produce another store, and the resulting optimization of store time. The proton and antiproton beams in the Tevatron circulated in a single vacuum pipe and thus were placed on separated orbits which wrapped around each other in a helical pattern outside of the interaction regions. Hence, long-range encounters played an important role here as well, with the 70 long-range encounters distributed about the synchrotron, and mitigation was limited by the available aperture. The Tevatron ultimately achieved luminosities a factor of 400 over its original design specification.

30.4.2. ***HERA*** : [16] HERA, operated between 1992 and 2007, delivered nearly 1 fb^{-1} of integrated luminosity to the electron-proton collider experiments H1 and ZEUS. HERA was the first high-energy lepton-hadron collider, and also the first facility to employ both applications of superconductivity: magnets and accelerating structures. The proton beams of HERA had a maximum energy of 920 GeV. The lepton beams (positrons or electrons) were provided by the existing DESY complex, and were accelerated to 27.5 GeV using conventional magnets. At collision a 4-times higher frequency RF system, compared with the injection RF, was used to generate shorter bunches, thus helping alleviate the hourglass effect at the collision points. The lepton beam naturally would become transversely polarized (within about 40 minutes) and "spin rotators" were implemented on either side of an IP to produce longitudinal polarization at the experiment.

30.4.3. ***LEP*** : [17] Installed in a tunnel of 27 km circumference, LEP was the largest circular e^+e^- collider built so far. It was operated from 1989 to 2000 with beam energies ranging from 45.6 to 104.5 GeV and a maximum luminosity of 10^{32} $\text{cm}^{-2}\text{s}^{-1}$, at 98 GeV, surpassing all relevant design parameters.

30.4.4. ***SLC*** : [18] Based on an existing 3-km long S-band linac, the SLC was the first and only linear collider. It was operated from 1987 to 1998 with a constant beam energy of 45.6 GeV, up to about 80% electron-beam polarization, quasi-flat beams, and, in its last year, a typical peak luminosity of 2×10^{30} $\text{cm}^{-2}\text{s}^{-1}$, a third of the design value.

30.5. Present Collider Facilities

30.5.1. ***LHC*** : [19] The superconducting Large Hadron Collider is the world's highest energy collider. Early operations for HEP were at 4 TeV per proton [20], with the beam energy increased to 6.5 TeV in 2015. The current status is best checked at the Web site [21]. In 2017 peak luminosities above 2×10^{34} $\text{cm}^{-2}\text{s}^{-1}$ (more than twice the design value) have been achieved. To meet its luminosity goals the LHC operates with a high beam current of approximately 0.5 A, leading to stored energies of several hundred MJ per beam. Component protection, beam collimation, and controlled energy deposition were given very high priorities. Additionally, at energies of 5-7 TeV per particle, synchrotron radiation moves from being a curiosity to a challenge in a hadron accelerator for the first time. At design beam current the cryogenic system must remove roughly 7 kW due to synchrotron radiation, intercepted at a temperature of 4.5-20 K. As the photons are emitted their interactions with the vacuum chamber wall can generate free electrons, with consequent "electron cloud" development. Much care was taken to design a special beam screen for the chamber to mitigate this issue.

The two proton beams are contained in separate pipes throughout most of the circumference, and are brought together into a single pipe at the interaction points. The large number of bunches, and subsequent short bunch spacing, would lead to approximately 30 head-on collisions through 120 m of common beam pipe at each IP. Thus, a small crossing angle is employed, which reduces the luminosity by about 15%. Still, the bunches moving in one direction will have long-range encounters with the counter-rotating bunches and the resulting perturbations of the particle motion constitute a continued course of study. The luminosity scale is absolutely calibrated by the "van der Meer method" as was invented for the ISR [22], and followed by multiple, redundant luminosity monitors (see for example [23] and references therein). The Tables also show the 2015 LHC luminosity performance in Pb-Pb collisions, which for the ATLAS and CMS experiments well exceeded the design value, while for the ALICE [24] experiment, the luminosity was "levelled" at the Pb-Pb design value of 10^{27} $\text{cm}^{-2}\text{s}^{-1}$. The LHC can also provide Pb-p collisions as it did in 2013 and 2016, and other ion-ion or ion-proton collisions, at different energies.

In the coming years, an ambitious upgrade program, HL-LHC [25,26], has as its target an order-of-magnitude increase in integrated luminosity through the utilization of Nb_3Sn superconducting magnets, superconducting compact "crab" cavities and luminosity leveling also for ATLAS and CMS as its key ingredients.

30.5.2. ***e^+e^- Rings*** : Asymmetric energies of the two beams have allowed for the enhancement of B-physics research and for interesting interaction region designs. As the bunch spacing can be quite short, the lepton beams sometimes pass through each other at an angle and hence have reduced luminosity. Recently, however, the use of high frequency "crab crossing" schemes has produced full restoration of the luminous region. KEK-B attained over 1 fb^{-1} of integrated luminosity in a single day, and its upgrade, SuperKEKB, is aiming for luminosities of 8×10^{35} $\text{cm}^{-2}\text{s}^{-1}$ [27]. A different collision approach, called "crab waist", which relies on special sextupoles together with a large crossing angle, has been successfully implemented at DAΦNE [28] and has become a key ingredient for proposed future e^+e^- circular colliders. Other e^+e^- ring colliders in operation are BEPC-II, VEPP-2000 and VEPP-4M [27].

30.5.3. ***RHIC*** : [29] The Relativistic Heavy Ion Collider employs superconducting magnets, and collides combinations of fully-stripped ions such as H-H (p-p), p-Al, p-Au, d-Au, h-Au, Cu-Cu, Cu-Au, Au-Au, and U-U over a wide energy range [30]. The high charge per particle (+79 for gold, for instance) makes intra-beam scattering of particles within the bunch a special concern, even for seemingly moderate bunch intensities. In 2012, 3-D stochastic cooling was successfully implemented in RHIC [12] and is now routinely used. With stochastic cooling, steady increases in the bunch intensity, and numerous other upgrades, RHIC now operates at 44 times the Au-Au design average luminosity. Another special feature of accelerating heavy ions in RHIC is that the beams cross the "transition energy" during acceleration – a point where the derivative with respect to momentum of the revolution period is zero. This is more typical of low-energy accelerators, where the necessary phase jump required of the RF system is implemented rapidly and little time is spent near this condition. In the case of RHIC with heavy ions, the superconducting magnets do not ramp very quickly and the period of time spent crossing transition is long and must be dealt with carefully. For p-p operation the beams are always above their transition energy and so this condition is completely avoided.

RHIC is also unique in its ability to accelerate and collide polarized proton beams. As proton beam polarization must be maintained from its low-energy source, successful acceleration through the myriad of

depolarizing resonance conditions in high energy circular accelerators has taken years to accomplish. An energy of 255 GeV per proton with 55% final polarization per beam has been realized. As part of a scheme to compensate the head-on beam-beam effect, electron lenses operated routinely during the polarized proton operation at 100 GeV in 2015 [31].

30.6. Future High Energy Colliders and Prospects

Recent accomplishments of particle physics have been obtained through high-energy and high-intensity experiments using hadron-hadron, lepton-lepton, and lepton-proton colliders. Following the discovery of the Higgs particle at the LHC and in view of ongoing searches for "new physics" and rare phenomena, various options are under discussions and development to pursue future particle-physics research at higher energy and with appropriate luminosity. This is the basis for several new projects, ideas, and R&D activities, which can only briefly be summarized here. Specifically, the following projects are noted: an energy upgrade of the LHC based on 16 T dipole magnets (HE-LHC), two approaches to an electron-positron linear collider, larger 100-km circular tunnels supporting e^+e^- collisions up to either 240 or 365 GeV in the centre of mass along with a 100-TeV proton-proton collider or 70–140 TeV muon ring collider, and potential use of plasma acceleration and other advanced schemes. Complementary studies are ongoing of a high-energy lepton-hadron collider bringing into collision a 60-GeV electron beam from an energy-recovery linac with the 7 TeV protons circulating in the LHC (LHeC) [32,33], with the 13.5 TeV protons in the HE-LHC (HE-LHeC), or with the 50(35) TeV protons of the 100(70) TeV collider (FCC-he,SPPC), and of $\gamma\gamma$ collider Higgs factories based on recirculating electron linacs (e.g. SAPPHiRE [34]) . Tentative parameters of some of the colliders discussed, or mentioned, in this section are summarized in Table 30.1 and Table 30.2.

30.6.1. ***Electron-Positron Linear Colliders*** : For three decades efforts have been devoted to develop high-gradient technology e^+e^- colliders in order to overcome the synchrotron radiation limitations of circular e^+e^- machines in the TeV energy range.

The primary challenge confronting a high energy, high luminosity single pass collider design is the power requirement, so that measures must be taken to keep the demand within bounds as illustrated in a transformed Eq. (30.2) [35]:

Table 30.1: Tentative parameters of selected future e^+e^- high-energy colliders. Parameters associated with different beam energy scenarios are comma-separated.

	FCC-ee	CEPC	ILC	CLIC
Species	e^+e^-	e^+e^-	e^+e^-	e^+e^-
Beam energy (GeV)	46, 120, 183	46, 120	125, 250	190, 1500
Circumference / Length (km)	97.75	100	20.5, 31	11, 50
Interaction regions	2	2	1	1
Estimated integrated luminosity per exp. (ab^{-1}/year)	26, 0.9, 0.17	4, 0.4	0.2, 0.2	0.2, 0.6
Peak luminosity (10^{34} cm^{-2} s^{-1})	200, 7, 1.5	32, 3	1.4, 1.8	1.5, 6
Time between collisions (μs)	0.015, 0.75, 8.5	0.025, 0.68	0.55	0.0005
Energy spread (rms, 10^{-3})	1.3, 1.65, 2.0	0.4, 1.0	e^-: 1.9, 1.2 e^+: 1.5, 0.7	3.5
Bunch length (rms, mm)	12.1, 5.3, 3.8	8.5, 3.3	0.3	0.09, 0.044
IP beam size (μm)	H: 6.3, 14, 38 V: 0.03, 0.04, 0.07	H: 5.9, 21 V: 0.04, 0.07	H: 0.52, 0.47 V: 0.008, 0.006	H: 0.15, 0.04 V: 0.003, 0.001
Injection energy (GeV)	on energy (topping off)	on energy (topping off)	5.0 (linac)	9.0 (linac)
Transv. geom. emittance (rms, pm)	H: 270, 630, 1340 V: 1, 1, 3	H: 170, 1210 V: 2, 3	H: 20, 10 V: 0.14, 0.07	H: 2.4, 0.22 V: 0.08, 0.01
β^* at interaction point (cm)	H: 15, 30, 100 V: 0.08, 0.1, 0.16	H: 20, 36 V: 0.1, 0.15	H: 1.3, 2.2 V: 0.041, 0.048	H: 0.8, 0.69 V: 0.01, 6.8×10^{-3}
Full crossing angle (mrad)	30	33	14	20
Crossing scheme	crab waist	crab waist	crab crossing	crab crossing
Piwinski angle $\phi=\sigma_z\theta_c/(2\sigma_x^*)$	28.5, 5.8, 1.5	23.8, 2.6	0	0
Beam-beam parameter ξ_y (10^{-3})	133, 118, 144	72, 109	n/a	n/a
Disruption parameter D_y	0.9, 1.1, 1.9	0.3, 1.0	34, 25	8, 12
Average Upsilon Υ	0.0002, 0.0004, 0.0006	0.0001, 0.0005	0.03, 0.06	0.26, 3.4
RF frequency (MHz)	400, 400, 800	650	1300	11994
Particles per bunch (10^{10})	17, 15, 27	8, 15	2	0.52, 0.37
Bunches per beam	16640, 328, 33	12000, 242	1312 (pulse)	352, 312 (trains at 50 Hz)
Average beam current (mA)	1390, 29, 5.4	19.2	6 (in train)	1660, 1200 (in train)
RF gradient (MV/m)	1.3, 9.8, 19.8	3.6, 19.7	31.5	72, 100
Polarization (%)	$\geq$10, 0, 0	5–10, 0	e^-: 80% e^+: 30%	e^-: 70% at IP
SR power loss (MW)	100	64	n/a	n/a
Beam power/beam (MW)	n/a	n/a	5.3, 10.5	3, 14
Novel technology	—	—	high grad. SC RF	two-beam accel.

Table 30.2: Tentative parameters of selected future high-energy hadronic colliders. Parameters associated with different beam energy scenarios for a μ collider are comma-separated. Parameters of HL-LHC can be found in the High-Energy Collider Parameters review tables.

	LHeC	HE-LHeC	HE-LHC	FCC-hh	SPPC	μ collider
Species	ep	ep	pp	pp	pp	$\mu^+\mu^-$
Beam Energy (TeV)	0.06(e), 7 (p)	0.06(e), 13.5 (p)	13.5	50	37.5	0.063, 3
Circumference (km)	9(e), 26.7 (p)	9(e), 26.7 (p)	26.7	97.75	100	0.3, 6
Interaction regions	1	1	2 (4)	4	2	1, 2
Estimated integrated luminosity per exp. (ab^{-1}/year)	0.1	0.1	1.0	0.2–1.0	0.4	0.001, 1.0
Peak luminosity (10^{34} cm^{-2} s^{-1})	0.8	1.2	28	5–30	10	2.2, 71
Time between collisions (μs)	0.025	0.025	0.025	0.025	0.025	1, 20
Energy spread (rms, 10^{-3})	0.03 (e), 0.1(p)	0.03 (e), 0.1(p)	0.1	0.1	0.2	0.04, 1
Bunch length (rms, mm)	0.06 (e), 75.5(p)	0.06 (e), 80 (p)	80	80	75.5	63, 2
IP beam size (μm)	4.3 (round)	3.5 (round)	6.6	6.8 (inj.)	6.8 (inj.)	75, 1.5
Injection energy (GeV)	1(e), 450(p)	1(e), 450(p)	450	3300	2100	on energy
Transverse emittance (rms, nm)	0.45(e), 0.27(p)	0.45(e), 0.17(p)	0.17	0.04 (inj.)	0.06 (inj.)	335, 0.9
β^*, amplitude function at interaction point (cm)	5.0(e), 7.0(p)	4.0(e), 10.0(p)	25	110–30	75	1.7, 0.25
Beam-beam parameter/IP (10^{-3})	−(e), 0.4(p)	−(e), 0.3(p)	12	5–15	7.5	20, 90
RF frequency (MHz)	800(e), 400(p)	800(e), 400(p)	400	400	400/200	805
Particles per bunch (10^{10})	0.23(e), 22(p)	0.30(e), 22(p)	10	10	15	400, 200
Bunches per beam	−(e), 2808(p)	−(e), 2808(p)	2808	10600	10080	1
Average beam current (mA)	15(e), 883(p)	20(e), 1120(p)	1120	500	730	640, 16 (peak)
Length of standard cell (m)	52.4(e arc), 107(p)	52.4(e arc), 107(p)	137	213	148	N/A
Phase advance per cell (deg)	310/90(eH/V) 90(p)	310/90(eH/V) 90(p)	90	90	90	N/A
Peak magnetic field (T)	0.264(e), 8.33(p)	0.264(e), 16(p)	16	16	12	10
Polarization (%)	90(e), 0(p)	90(e), 0(p)	0	0	0	0
SR power loss/beam (MW)	30(e), 0.01(p)	30(e), 0.1(p)	0.1	2.4	1.1	3×10^{-5}, 0.068
Novel technology	high-energy ERL	h.-e. ERL 16 T magnets	16 T Nb_3Sn magnets	16 T Nb_3Sn magnets	HTS magnets	muon prod.

$$\mathscr{L} \approx \frac{137}{8\pi r_e}\,\frac{P_{\rm wall}}{E_{cm}}\,\frac{\eta}{\sigma_y^*}\,N_\gamma\,H_D\,. \qquad (30.12)$$

Here, $P_{\rm wall}$ is the total wall-plug power of the collider, $\eta \equiv P_b/P_{\rm wall}$ the efficiency of converting wall-plug power into beam power $P_b = f_{\rm coll} n E_{cm}$, E_{cm} the cms energy, n $(= n_1 = n_2)$ the bunch population, and σ_y^* the vertical rms beam size at the collision point. In formulating Eq. (30.12) the number of beamstrahlung photons emitted per $e^\pm$, was approximated as $N_\gamma \approx 2\alpha r_e n/\sigma_x^*$, where α denotes the fine-structure constant. The management of $P_{\rm wall}$ leads to an upward push on the bunch population n with an attendant rise in the energy radiated due to the electromagnetic field of one bunch acting on the particles of the other. Keeping a significant fraction of the luminosity close to the nominal energy represents a design goal, which is met if N_γ does not exceed a value of about 1. A consequence is the use of flat beams, where N_γ is managed by the beam width, and luminosity adjusted by the beam height, thus the explicit appearance of the vertical beam size σ_y^*. The final factor in Eq. (30.12), H_D, represents the enhancement of luminosity due to the pinch effect during bunch crossing (the effect of which has been neglected in the expression for N_γ).

The approach designated by the International Linear Collider (ILC) is presented in the Tables, and the contrast with the collision-point parameters of the circular colliders is striking, though reminiscent in direction of those of the SLAC Linear Collider. The ILC *Technical Design Report* [36,37] has a baseline cms energy of 500 GeV with upgrade provision for 1 TeV, and luminosity comparable to the LHC; recent tendancies have been toward a baseline of 250 GeV. The ILC is based on superconducting accelerating structures of the 1.3 GHz TESLA variety. Progress toward higher field gradients and Q values continues to be made, with nitrogen-doping techniques being a recent example [38].

At CERN, a design effort is underway on the Compact Linear Collider (CLIC), each linac of which is itself a two-beam accelerator, in that a high energy, low current beam is fed by a low energy, high current driver [39]. The CLIC design employs normal conducting 12 GHz accelerating structures at a gradient of 100 MeV/m, some three times the current capability of the superconducting ILC cavities. The design cms energy is 3 TeV, though recent staging options – 0.38, 1.5, and 3 TeV – have been developed [40].

30.6.2. ***Future Circular Colliders*** : The discovery, in 2012, of the Higgs boson at the LHC has stimulated interest in constructing a large circular tunnel which could host a variety of energy-frontier machines, including high-energy electron-positron, proton-proton, and lepton-hadron colliders. Such projects are under study by a global collaboration hosted at CERN (FCC) [41] and another one centered in China (CEPC/SPPC) [42], following earlier proposals for a Very Large Hadron Collider (VLHC) [43] and a Very Large Lepton Collider (VLLC) in the US, which would have been housed in the same 230-km long tunnel.

The maximum beam energy of a hadron collider is directly proportional to the magnetic field and to the ring circumference. The LHC magnets,

based on Nb-Ti superconductor, achieve a maximum operational field of 8.33 T. The HL-LHC project develops the technology of higher field Nb_3Sn magnets as well as cables made from high-temperature superconductor (HTS). Nb_3Sn dipoles could ultimately reach an operational field around 16 T, and HTS inserts, requiring new engineering materials and substantial dedicated R&D, could boost this further. More cost-effective hybrid magnet designs incorporating Nb-Ti, two types of Nb_3Sn, and an inner layer of HTS providing fields of about 20 T have been examined [44]. However present project efforts are not utilizing this hybrid approach as of yet.

Aside from the magnets, the cryogenic beam vacuum system is another key component of any future hadron collider. A beam screen inside the cold bore of the magnets can intercept the synchrotron radiation at an elevated temperature, allowing a more efficient extraction of the synchrotron-radiation heat load. While the LHC beam screen has a temperature of 5–20 K, future, higher-energy machines are likely to raise this temperature to 50 K or 100 K.

Further substantial increases in collision energy are possible only with a larger tunnel. The FCC hadron collider (FCC-hh) [45], formerly called VHE-LHC [46,46], is based on a new tunnel of about 100 km circumference, which would allow exploring energies up to 100 TeV in the centre of mass with proton-proton collisions, using 16 T magnets. This new tunnel could also accommodate a high-luminosity circular e^+e^- Higgs factory (FCC-ee) as well as a lepton-hadron collider (FCC-he). The SPPC is a 100 km hadron collider based on 12 T (later 24 T) iron-based high-temperature superconducting magnets, which could be installed in the same tunnel as the e^+e^- collider CEPC.

In order to serve as a Higgs factory a new circular e^+e^- collider needs to achieve a cms energy of at least 240 GeV. FCC-ee (formerly TLEP [48]) , installed in the ∼100 km tunnel of the FCC-hh, could reach even higher energies, e.g. 365 GeV cms for $t\bar{t}$ production. At these energies, the luminosity, limited by the synchrotron radiation power, would still be above 10^{34} $cm^{-2}s^{-1}$ at each of two or four collision points. At lower energies (Z pole and WW threshold) FCC-ee could deliver up to three orders of magnitude higher luminosities, and also profit from radiative self polarization for precise energy calibration. The short beam lifetime at the high target luminosity, due to radiative Bhabha scattering, requires FCC-ee to be constructed as a double ring, where the collider ring operating at constant energy is complemented by a second injector ring installed in the same tunnel to "top off" the collider current. Beamstrahlung, i.e. synchrotron radiation emitted during the collision in the field of the opposing beam, introduces an additional beam lifetime limitation depending on momentum acceptance (so that achieving sufficient off-momentum dynamic aperture becomes one of the design challenges), as well as some bunch lengthening.

30.6.3. ***Muon Collider*** : The muon to electron mass ratio of 210 implies less concern about synchrotron radiation by a factor of about 2×10^9 and its 2.2 μs lifetime means that it will last for some $150B$ turns in a ring about half of which is occupied by bend magnets with average field B (Tesla). Design effort became serious in the mid 1990s and a collider outline emerged quickly.

Removal of the synchrotron radiation barrier reduces the scale of a muon collider facility to a level compatible with on-site placement at existing accelerator laboratories. The Higgs production cross section in the s-channel is enhanced by a factor of $(m_\mu/m_e)^2$ compared to that in e^+e^- collisions. And a neutrino factory could potentially be realized in the course of construction [49].

The challenges to luminosity achievement are clear and amenable to immediate study: targeting, collection, and emittance reduction are paramount, as well as the bunch manipulation required to produce $> 10^{12}$ muons per bunch without emittance degradation. The proton source needs to deliver a beam power of several MW, collection would be aided by magnetic fields common on neutron stars (though scaled back for application on earth), and the emittance requirements have inspired fascinating investigations into phase space manipulations that are finding applications in other facilities. The status was summarized in a White Paper submitted to "Snowmass 2013" [50]. More recently, direct production of a low-emittance muon beam by positron annihilation [51](or alternatively laser-hadron collisions [52,53]) has been proposed as a possible path towards a simpler and cheaper muon collider.

30.6.4. ***Plasma Acceleration and Other Advanced Concepts*** : At the 1956 CERN Symposium, a paper by Veksler, in which he suggested acceleration of protons to the TeV scale using a bunch of electrons, anticipated current interest in plasma acceleration [54]. A half-century later this became more than a suggestion, with the demonstration, as a striking example, of electron energy doubling from 42 to 84 GeV over 85 cm at SLAC [55] and the creation of a 1 GeV electron bunch with relatively small energy spread accelerated through a cm-scale plasma [56].

Whether plasma acceleration will find application in an HEP facility is not yet clear, given the necessity of staging and phase-locking acceleration in multiple plasma chambers. However, strides continue to be made, as multi-stage coupling of independent laser plasma accelerators have been demonstrated recently [57].

Maintaining beam quality and beam position as well as the acceleration of high-repetition bunch trains are also primary feasibility issues, addressed by active R&D. For recent discussions of parameters for a laser-plasma based electron positron collider, see, for example, relevant papers from the proceedings of the 2016 Advanced Accelerator Concepts Workshop [58] and the ICFA-ICUIL White Paper from 2011 [59].

Additional approaches aiming at accelerating gradients higher, or much higher, than those achievable with conventional metal cavities include the use of dielectric materials and, for the long-term future, crystals. Combining several innovative ideas, even a linear crystal muon collider driven by X-ray lasers has been proposed [60], as well as "accelerators on a chip" [61,62]. Not only the achievable accelerating gradient, but also the overall power efficiency, e.g. the attainable luminosity as a function of electrical input power, will determine the suitability of any novel technology for use in future high-energy accelerators.

References:

1. E. D. Courant and H. S. Snyder, Ann. Phys. **3**, 1 (1958). This is the classic article on the alternating gradient synchrotron.
2. A.W. Chao *et al.*, *eds.*, *Handbook of Accelerator Physics and Engineering*, World Science Publishing Co. (Singapore, 2nd edition, 2013.), Sec. 2.1, 2.2.
3. H. Wiedemann, *Handbook of Accelerator Physics and Engineering*, *ibid*, Sec. 3.1.
4. K. Yokoya and P. Chen, "Beam-Beam Phenomena in Linear Colliders," KEK Preprint 91-2 (1991).
5. C. Amsler *et al.* (Particle Data Group), Phys. Lett. **B667**, 1 (2008) [http://pdg.lbl.gov/2008/reviews/contents_sports.html].
6. M.A. Furman and M.S. Zisman, *Handbook of Accelerator Physics and Engineering*, *ibid*, Sec. 4.1.
7. M.A. Furman, *Handbook of Accelerator Physics and Engineering*, *ibid*, Sec. 2.4.14.
8. http://ab-abp-rlc.web.cern.ch/ab-abp-rlc-ecloud/. This site contains many references as well as videos of electron cloud simulations.
9. D. Möhl *et al.*, Phys. Reports **58**, 73 (1980).
10. M. Blaskiewicz and J.M. Brennan, Phys. Rev. ST Accel. Beams **10**, 061001 (2007).
11. M. Blaskiewicz, J.M. Brennan and F. Severino, Phys. Rev. Lett. **100**, 174802 (2008).
12. M. Blaskiewicz, J.M. Brennan and K. Mernick, Phys. Rev. Lett. **105**, 094801 (2010).
13. G.I. Budker, *Proc. Int. Symp. Electron & Positron Storage Rings*, (1966).
14. S. Nagaitsev *et al.*, Phys. Rev. Lett. **96**, 044801 (2006).
15. H.T. Edwards, "The Tevatron Energy Doubler: A Superconducting Accelerator," Ann. Rev. Nucl. and Part. Sci. **35**, 605 (1985).
16. Brief history at en.wikipedia.org/wiki/Hadron_Elektron_Ring_Anlage.
17. R. Assmann *et al.*, Nucl. Phys. (Proc. Supp.) **B9**, 17 (2002).
18. N. Phinney, arXiv:physics/0010008 (2000).

19. L. Evans, "The Large Hadron Collider," Ann. Rev. Nucl. and Part. Sci. **61**, 435 (2011).
20. M. Draper (ed.), *Proc. Chamonix 2014: LHC Performance Workshop*, CERN-2015-002, http://cds.cern.ch/record/2020930 (2015).
21. Detailed information from the multi-volume design report to present status may be found at http://lhc.web.cern.ch/lhc/.
22. S. van der Meer, "Calibration of the Effective Beam Height at the ISR," CERN-ISR-PO/68-31 (1968).
23. ATLAS Collaboration, "Improved Luminosity Determination in pp Collisions at $\sqrt{s} = 7$ TeV using the ATLAS Detector at the LHC," Eur. Phys. J. **C73**, 2518 (2013).
24. http://aliceinfo.cern.ch/Public/Welcome.html.
25. http://hilumilhc.web.cern.ch.
26. G. Apollinari *et al.*, CERN Yellow Report CERN-2015-005 (2015).
27. An overview of electron-positron colliders past and present may be found in ICFA Beam Dynamics Newsletter No. 46, April 2009, http://icfa-bd.kek.jp/. A day-by-day account of the luminosity progress at KEK-B may be found at http://belle.kek.jp/bdocs/lumi_belle.png.
28. M. Zobov *et al.*, "Test of 'Crab-Waist' Collisions at the DAΦNE Φ Factory," Phys. Rev. Lett. **104**, 174801 (2010).
29. M. Harrison, T. Ludlam, and S. Ozaki, *eds.*, "Special Issue: The Relativisitic Heavy Ion Collider Project: RHIC and its Detectors," Nucl. Instrum. Methods **A499**, 1 (2003).
30. http://www.rhichome.bnl.gov/RHIC/Runs/.
31. W. Fischer *et al.*, Phys. Rev. Lett. **115**, 264801 (2015).
32. J.L. Abelleira *et al.*, J. Phys. **G39**, 075001 (2012).
33. J.L. Abelleira *et al.*, arXiv:1211.5102 (2012).
34. S.A. Bogacz *et al.*, arXiv:1208.2827 (2012).
35. F. Zimmermann, "Tutorial on Linear Colliders," AIP Conf. Proc. **592**, 494 (2001).
36. http://www.linearcollider.org/ILC/Publications/Technical-Design-Report.
37. The International Linear Collider Machine Staging Report 2017, arXiv:1108:00568.
38. A. Grassellino *et al.*, "Nitrogen and argon doping of niobium for superconducting radio frequency cavities: a pathway to highly efficient accelerating structures", Superconductor Sci. and Tech. **26**, 10 (2013).
39. http://lcd.web.cern.ch/lcd/CDR/CDR.html.
40. https://cds.cern.ch/record/2210892.
41. http://www.cern.ch/fcc.
42. J. Gao, "CEPC-SPPC Accelerator Status Towards CDR," to be published in Int. J. Mod. Phys. A (2017).
43. http://vlhc.org.
44. L. Rossi, E. Todesco, arXiv:1108:1619, in *Proc. HE-LHC10*, Malta, 14–16 October 2010, *CERN Yellow Report CERN-2011-003*.
45. F. Zimmermann *et al.*, "Challenges for Highest Energy Circular Colliders," *Proc. IPAC'14 Dresden*.
46. M. Benedikt, D. Schulte, F. Zimmermann, "Optimizing integrated luminosity of future hadron colliders", Phys. Rev. ST Accel. Beams **18**, 101002 (12015).
47. M. Benedikt and F. Zimmermann "Towards Future Circular Colliders", J. Korean Phys. Soc., Vol. 69, **6**, 893-902 (2016).
48. http://tlep.web.cern.ch/.
49. http://en.wikipedia.org/wiki/Neutrino_Factory.
50. J.P. Delahaye *et al.*, arXiv:1308.0494 (2013); M. Palmer, Discussion of the Scientific Potential of Muon Beams, FNAL, 18 November 2015 (2015)..
51. M. Antonelli, M. Boscolo, R. Di Nardo, P. Raimondi, "Novel proposal for a low emittance muon beam using positron beam on target," Nucl. Instrum. Meth. A **807** 101-107 (2016).
52. C. Curatolo, F. Broggi, L. Serafini, "Phase space analysis of secondary beams generated in hadron-photon collisions," Nucl. Instrum. Meth. A **865** 128-132 (2017).
53. M.W. Krasny, "The Gamma Factory proposal for CERN," arXiv:1511.07794 [hep-ex] (2015).
54. V.I. Veksler, CERN Symposium on High Energy Accelerators and Pion Physics, 11–23 June 1956, p. 80. This paper may be downloaded from http://cdsweb.cern.ch/record/1241563?ln=en.
55. I. Blumenfeld *et al.*, Nature **445**, 741 (2007).
56. W.P. Leemans *et al.*, "GeV electron beams from a cm-scale accelerator," Nature Physics **2**, 696-699 (2006).
57. S. Steinke *et al.*, "Multistage coupling of independent laser plasma accelerators," Nature **530**, 190193 (2016).
58. Advanced Accelerator Concepts (AAC 2016), edited by S.H. Gold, G.S. Nusinovich, K.P. Wootton and D.F. Gordon, *AIP Conference Proceedings 1812*, National Harbor MD 31 July – 5 August 2016.
59. White Paper of ICFA-ICUIL Joint Task Force — High Power Laser Technology for Accelerators, published in ICFA Beam Dynamics Newsletter No. 56, December 2011, http://icfa-bd.kek.jp/.
60. V. Shiltsev, Sov. Phys. Usp. **55**, 965 (2012).
61. J. Breuer and P. Hommelhoff, Laser-Based Acceleration of Nonrelativistic Electrons at a Dielectric Structure, Phys. Rev. Lett. **111**, 134803 (2013).
62. Demonstration of electron acceleration in a laser-driven dielectric microstructure E.A. Peralta *et al.*, Nature, **503** (2013).

High-Energy Collider Parameters: e^+e^- Colliders (I)

Updated in March 2018 with numbers received from representatives of the colliders (contact E. Pianori, LBNL). The table shows the parameter values achieved. Quantities are, where appropriate, r.m.s.; unless noted otherwise, energies refer to beam energy; H and V indicate horizontal and vertical directions; s.c. stands for superconducting. Parameters for the defunct SPEAR, DORIS, PETRA, PEP, TRISTAN, and VEPP-2M colliders may be found in our 1996 edition (Phys. Rev. **D54**, 1 July 1996, Part I).

	VEPP-2000 (Novosibirsk)	VEPP-4M (Novosibirsk)	BEPC (China)	BEPC-II (China)	DAΦNE (Frascati)
Physics start date	2010	1994	1989	2008	1999
Physics end date	—	—	2005	—	—
Maximum beam energy (GeV)	1.0	6	2.5	1.89 (2.3 max)	0.510
Delivered integrated luminosity per exp. (fb^{-1})	0.125	0.027	0.11	17.5	$\approx$ 4.7 in 2001-2007 $\approx$ 2.7 w/crab-waist $\approx$ 1.8 since Nov 2014
Luminosity (10^{30} $cm^{-2}s^{-1}$)	40	20	12.6 at 1.843 GeV 5 at 1.55 GeV	1000	453
Time between collisions (μs)	0.04	0.6	0.8	0.008	0.0027
Full crossing angle (μ rad)	0	0	0	2.2×10^4	5×10^4
Energy spread (units 10^{-3})	0.71	1	0.58 at 2.2 GeV	0.52	0.40
Bunch length (cm)	4	5	$\approx$ 5	$\approx$ 1.2	low current: 1 at 15mA: 2
Beam radius (10^{-6} m)	125 (round)	H: 1000 V: 30	H: 890 V: 37	H: 347 V: 4.5	H: 260 V: 4.8
Free space at interaction point (m)	$\pm$0.5	$\pm$2	$\pm$2.15	$\pm$0.63	$\pm$0.295
Luminosity lifetime (hr)	continuous	2	7–12	1.5	0.2
Turn-around time (min)	continuous	18	32	15	2 (topping up)
Injection energy (GeV)	0.2–1.0	1.8	1.55	1.89	on energy
Transverse emittance (10^{-9} m)	H: 150 V: 150	H: 200 V: 20	H: 660 V: 28	H: 121 V: 1.56	H: 260 V: 2.6
β^*, amplitude function at interaction point (m)	H: 0.05 – 0.11 V: 0.05 – 0.11	H: 0.75 V: 0.05	H: 1.2 V: 0.05	H: 1.0 V: 0.0129	H: 0.26 V: 0.009
Beam-beam tune shift per crossing (units 10^{-4})	H: 850 V: 850	500	350	383	440 (crab-waist test)
RF frequency (MHz)	172	180	199.53	499.8	356
Particles per bunch (units 10^{10})	8	15	20 at 2 GeV 11 at 1.55 GeV	3.8	e^-: 3.2 e^+: 2.1
Bunches per ring per species	1	2	1	119	100 to 105 (120 buckets)
Average beam current per species (mA)	160	80	40 at 2 GeV 22 at 1.55 GeV	851	e^-: 1250 e^+: 800
Circumference or length (km)	0.024	0.366	0.2404	0.23753	0.098
Interaction regions	2	1	2	1	1
Magnetic length of dipole (m)	1.1	2	1.6	outer ring: 1.6 inner ring: 1.41	outer ring: 1.2 inner ring: 1
Length of standard cell (m)	12	7.2	6.6	outer ring: 6.6 inner ring: 6.2	n/a
Phase advance per cell (deg)	H: 745 V: 385	65	$\approx$ 60	60–90 non-standard cells	—
Dipoles in ring	8	78	40 + 4 weak	84 + 8 weak	8
Quadrupoles in ring	24 + 4 s.c.	150	68	134+2 s.c.	48
Peak magnetic field (T)	2.4	0.6	0.903 at 2.8 GeV	outer ring: 0.677 inner ring: 0.766	1.2

High-Energy Collider Parameters: e^+e^- Colliders (II)

Updated in March 2018 with numbers received from representatives of the colliders (contact E. Pianori, LBNL). The table shows the parameter values achieved. Quantities are, where appropriate, r.m.s.; unless noted otherwise, energies refer to beam energy; H and V indicate horizontal and vertical directions; s.c. stands for superconducting. ILC and CLIC parameters are documented in the Accelerator physics of colliders review.

	CESR (Cornell)	CESR-C (Cornell)	LEP (CERN)	SLC (SLAC)
Physics start date	1979	2002	1989	1989
Physics end date	2002	2008	2000	1998
Maximum beam energy (GeV)	6	6	100 - 104.6	50
Delivered integrated luminosity per experiment (fb^{-1})	41.5	2.0	0.221 at Z peak 0.501 at $65-100$ GeV 0.275 at >100 GeV	0.022
Luminosity (10^{30} $cm^{-2}s^{-1}$)	1280 at 5.3 GeV	76 at 2.08 GeV	24 at Z peak 100 at > 90 GeV	2.5
Time between collisions (μs)	0.014 to 0.22	0.014 to 0.22	22	8300
Full crossing angle (μ rad)	±2000	±3300	0	0
Energy spread (units 10^{-3})	0.6 at 5.3 GeV	0.82 at 2.08 GeV	0.7→1.5	1.2
Bunch length (cm)	1.8	1.2	1.0	0.1
Beam radius (μm)	H: 460 V: 4	H: 340 V: 6.5	H: 200 → 300 V: 2.5 → 8	H: 1.5 V: 0.5
Free space at interaction point (m)	±2.2 (±0.6 to REC quads)	±2.2 (±0.3 to PM quads)	±3.5	±2.8
Luminosity lifetime (hr)	2–3	2–3	20 at Z peak 10 at > 90 GeV	—
Turn-around time (min)	5 (topping up)	1.5 (topping up)	50	120 Hz (pulsed)
Injection energy (GeV)	1.8–6	1.5–6	22	45.64
Transverse emittance (10^{-9} m)	H: 210 V: 1	H: 120 V: 3.5	H: 20–45 V: 0.25 → 1	H: 0.5 V: 0.05
β^*, amplitude function at interaction point (m)	H: 1.0 V: 0.018	H: 0.94 V: 0.012	H: 1.5 V: 0.05	H: 0.0025 V: 0.0015
Beam-beam tune shift per crossing (10^{-4}) or disruption	H: 250 V: 620	e^-: 420 (H), 280 (V) e^+: 410 (H), 270 (V)	830	0.75 (H) 2.0 (V)
RF frequency (MHz)	500	500	352.2	2856
Particles per bunch (units 10^{10})	1.15	4.7	45 in collision 60 in single beam	4.0
Bunches per ring per species	9 trains of 5 bunches	8 trains of 3 bunches	4 trains of 1 or 2	1
Average beam current per species (mA)	340	72	4 at Z peak 4→6 at > 90 GeV	0.0008
Beam polarization (%)	—	—	55 at 45 GeV 5 at 61 GeV	e^-: 80
Circumference or length (km)	0.768	0.768	26.66	1.45 +1.47
Interaction regions	1	1	4	1
Magnetic length of dipole (m)	1.6–6.6	1.6–6.6	11.66/pair	2.5
Length of standard cell (m)	16	16	79	5.2
Phase advance per cell (deg)	45–90 (no standard cell)	45–90 (no standard cell)	102/90	108
Dipoles in ring	86	84	3280 + 24 inj. + 64 weak	460+440
Quadrupoles in ring	101 + 4 s.c.	101 + 4 s.c.	520 + 288 + 8 s.c.	—
Peak magnetic field (T)	0.3 / 0.8 at 8 GeV	0.3 / 0.8 at 8 GeV, 2.1 wigglers at 1.9 GeV	0.135	0.597

High-Energy Collider Parameters: e^+e^- Colliders (III)

Updated in March 2018 with numbers received from representatives of the colliders (contact E. Pianori, LBNL). The table shows the parameter values achieved. For future colliders, design values are quoted. Quantities are, where appropriate, r.m.s.; unless noted otherwise, energies refer to beam energy; H and V indicate horizontal and vertical directions; s.c. stands for superconducting.

	KEKB (KEK)	PEP-II (SLAC)	SuperKEKB (KEK)
Physics start date	1999	1999	2018
Physics end date	2010	2008	—
Maximum beam energy (GeV)	e^-: 8.33 (8.0 nominal) e^+: 3.64 (3.5 nominal)	e^-: 7–12 (9.0 nominal) e^+: 2.5–4 (3.1 nominal)	e^-: 7 e^+: 4
Delivered integrated luminosity per exp. (fb^{-1})	1040	557	—
Luminosity (10^{30} $cm^{-2}s^{-1}$)	21083	12069 (design: 3000)	8×10^5
Time between collisions (μs)	0.00590 or 0.00786	0.0042	0.004
Full crossing angle (μ rad)	±11000*	0	±41500
Energy spread (units 10^{-3})	0.7	e^-/e^+: 0.61/0.77	e^-/e^+: 0.64/0.81
Bunch length (cm)	0.65	e^-/e^+: 1.1/1.0	e^-/e^+: 0.5/0.6
Beam radius (μm)	H: 124 (e^-), 117 (e^+) V: 1.9	H: 157 V: 4.7	e^-: 11 (H), 0.062 (V) e^+: 10 (H), 0.048 (V)
Free space at interaction point (m)	+0.75/−0.58 (+300/−500) mrad cone	±0.2, ±300 mrad cone	e^- : +1.20/ − 1.28, e^+ : +0.78/ − 0.73 (+300/−500) mrad cone
Luminosity lifetime (hr)	continuous	continuous	continuous
Turn-around time (min)	continuous	continuous	continuous
Injection energy (GeV)	e^-/e^+ : 8.0/3.5 (nominal)	e^-/e^+ : 9.0/3.1 (nominal)	e^-/e^+ : 7/4
Transverse emittance (10^{-9} m)	e^-: 24 (57†) (H), 0.61 (V) e^+: 18 (55†) (H), 0.56 (V)	e^-: 48 (H), 1.8 (V) e^+: 24 (H), 1.8 (V)	e^-: 4.6 (H), 0.013 (V) e^+: 3.2 (H), 0.0086 (V)
β^*, amplitude function at interaction point (m)	e^-: 1.2 (0.27†) (H), 0.0059 (V) e^+: 1.2 (0.23†) (H), 0.0059 (V)	e^-: 0.50 (H), 0.012 (V) e^+: 0.50 (H), 0.012 (V)	e^-: 0.025 (H), 3×10^{-4} (V) e^+: 0.032 (H), 2.7×10^{-4} (V)
Beam-beam tune shift per crossing (units 10^{-4})	e^-: 1020 (H), 900 (V) e^+: 1270 (H), 1290 (V)	e^-: 703 (H), 498 (V) e^+: 510 (H), 727 (V)	e^-: 12 (H), 807 (V) e^+: 28 (H), 881 (V)
RF frequency (MHz)	508.887	476	508.887
Particles per bunch (units 10^{10})	e^-/e^+: 4.7/6.4	e^-/e^+: 5.2/8.0	e^-/e^+: 6.53/9.04
Bunches per ring per species	1585	1732	2500
Average beam current per species (mA)	e^-/e^+: 1188/1637	e^-/e^+: 1960/3026	e^-/e^+: 2600/3600
Beam polarization (%)	—	—	—
Circumference or length (km)	3.016	2.2	3.016
Interaction regions	1	1	1
Magnetic length of dipole (m)	e^-/e^+ : 5.86/0.915	e^-/e^+: 5.4/0.45	e^-/e^+ : 5.9/4.0
Length of standard cell (m)	e^-/e^+ : 75.7/76.1	15.2	e^-/e^+ : 75.7/76.1
Phase advance per cell (deg)	450	e^-/e^+: 60/90	450
Dipoles in ring	e^-/e^+ : 116/112	e^-/e^+: 192/192	e^-/e^+ : 116/112
Quadrupoles in ring	e^-/e^+ : 452/452	e^-/e^+: 290/326	e^-/e^+ : 466/460
Peak magnetic field (T)	e^-/e^+ : 0.25/0.72	e^-/e^+: 0.18/0.75	e^-/e^+ : 0.22/0.19

*KEKB was operated with crab crossing from 2007 to 2010.

†With dynamic beam-beam effect.

High-Energy Collider Parameters: ep, $\overline{\text{p}}$p, pp Colliders

Updated in March 2018 with numbers received from representatives of the colliders (contact E. Pianori, LBNL). The table shows the parameter values achieved. Parameters for the defunct S$p\overline{p}$S collider may be found in our 2002 edition (Phys. Rev. **D66**, 010001 (2002)). Quantities are, where appropriate, r.m.s.; unless noted otherwise, energies refer to beam energy; H and V indicate horizontal and vertical directions; s.c. stands for superconducting.

	HERA (DESY)	TEVATRON* (Fermilab)	RHIC (Brookhaven)	LHC (CERN)		
Physics start date	1992	1987	2001	2009	2015	2026 (HL-LHC)
Physics end date	2007	2011	—	—		
Particles collided	ep	$p\overline{p}$	pp (polarized)	pp		
Maximum beam energy (TeV)	e: 0.030 p: 0.92	0.980	0.255 55% polarization	4.0	6.5	7.0
Maximum delivered integrated luminosity per exp. (fb^{-1})	0.8	12	0.38 at 100 GeV 1.3 at 250/255 GeV	23.3 at 4.0 TeV 6.1 at 3.5 TeV	94.5	250/y
Luminosity (10^{30} $\text{cm}^{-2}\text{s}^{-1}$)	75	431	245 (pk) 160 (avg)	7.7×10^3	2×10^4	5.0×10^4 (leveled)
Time between collisions (ns)	96	396	107	49.90	24.95	24.95
Full crossing angle (μ rad)	0	0	0	290	$300 \rightarrow 240^\dagger$	500
Energy spread (units 10^{-3})	e: 0.91 p: 0.2	0.14	0.15	0.1445	0.105	0.129
Bunch length (cm)	e: 0.83 p: 8.5	p: 50 $\bar{\text{p}}$: 45	60	9.4	8	9
Beam radius (10^{-6} m)	e: $110(H), 30(V)$ p: $111(H), 30(V)$	p: 28 $\bar{\text{p}}$: 16	85	18.8	10	7
Free space at interaction point (m)	± 2	± 6.5	16	38	38	38
Initial luminosity decay time, $-L/(dL/dt)$ (hr)	10	6 (avg)	7.5	≈ 6	≈ 15	≈ 15 (leveled)
Turn-around time (min)	e: 75, p: 135	90	25	180	150	145
Injection energy (TeV)	e: 0.012 p: 0.040	0.15	0.023	0.450	0.450	0.450
Transverse emittance (10^{-9} m)	e: $20(H), 3.5(V)$ p: $5(H), 5(V)$	p: 3 $\bar{\text{p}}$: 1	11	0.59	0.3	0.33
β^*, ampl. function at interaction point (m)	e: $0.6(H), 0.26(V)$ p: $2.45(H), 0.18(V)$	0.28	0.65	0.6	0.3	0.15
Beam-beam tune shift per crossing (units 10^{-4})	e: $190(H), 450(V)$ p: $12(H), 9(V)$	p: 120 $\bar{\text{p}}$: 120	73	72	45	86
RF frequency (MHz)	e: 499.7 p: 208.2/52.05	53	accel: 9 store: 28	400.8	400.8	400.8
Particles per bunch (units 10^{10})	e: 3 p: 7	p: 26 $\bar{\text{p}}$: 9	18.5	16	12.5	22
Bunches per ring per species	e: 189 p: 180	36	111	1380	1868 1868 (i.r. $1/5^\ddagger$)	2760 2748 (i.r. $1/5^\ddagger$)
Average beam current per species (mA)	e: 40 p: 90	p: 70 $\bar{\text{p}}$: 24	257	400	420	1100
Circumference (km)	6.336	6.28	3.834	26.659		
Interaction regions	2 colliding beams 1 fixed target (e beam)	2 high $\mathscr{L}$	6 total, 2 high $\mathscr{L}$	4 total, 2 high $\mathscr{L}$		
Magnetic length of dipole (m)	e: 9.185 p: 8.82	6.12	9.45	14.3		
Length of standard cell (m)	e: 23.5 p: 47	59.5	29.7	106.90		
Phase advance per cell (deg)	e: 60 p: 90	67.8	84	90		
Dipoles in ring	e: 396 p: 416	774	192 per ring + 12 common	1232 main dipoles		
Quadrupoles in ring	e: 580 p: 280	216	246 per ring	482 2-in-1 24 1-in-1		
Magnet types	e: C-shaped p: s.c., collared, warm iron	s.c., $\cos\theta$ warm iron	s.c., $\cos\theta$ cold iron	s.c., 2 in 1 cold iron		
Peak magnetic field (T)	e: 0.274, p: 5	4.4	3.5	$8.3^\S$		

*Other TEVATRON parameters: $\overline{p}$ source accum. rate: $25{\times}10^{10}$ hr^{-1}; max. no. of $\overline{p}$ stored: $3.4{\times}10^{12}$ (Accumulator), $6.1{\times}10^{12}$ (Recycler).

†Variable crossing angle decreasing during the fill with the reduction in bunch population

‡Number of bunches colliding at the interaction regions (i.r.) 1 (ATLAS) and 5 (CMS).

§Value for design beam energy of 7 TeV.

High-Energy Collider Parameters: Heavy Ion Colliders

Updated in March 2018 with numbers received from representatives of the colliders (contact E. Pianori, LBNL). The table shows the parameter values achieved. For the LHC, only maximum values for the ATLAS and CMS experiments are provided (ALICE and LHCb have different requirements for energy and luminosity). Design values for a high-luminosity upgrade are also given. Quantities are, where appropriate, r.m.s.; unless noted otherwise, energies refer to beam energy; s.c. stands for superconducting. pk and avg denote peak and average values.

	RHIC (Brookhaven)		LHC (CERN)			
Physics start date	2000	2012 / 2012 / 2004 / 2014 2002 / 2015 / 2015	2010	2012	2017	$\geq$ 2021 (high lum.)[§]
Physics end date		—		—		
Particles collided	Au Au	U U / Cu Au / Cu Cu / h Au d Au / p Au / p Al	Pb Pb	p Pb	Xe Xe	Pb Pb
Maximum beam energy (TeV/n)	0.1	0.1	2.51	p: 6.5 Pb: 2.56	2.72	2.76
$\sqrt{s_{NN}}$ (TeV)	0.2	0.2	5.02	8.16	5.44	5.5
Max. delivered int. nucleon-pair lumin. per exp. (pb^{-1})	2639 (at 100 GeV/n)	21 / 167 / 60 / 43 169 / 124 / 63 (all at 100 GeV/n)	30.3	194	0.05	$\approx 150/y$
Luminosity (10^{27} $\text{cm}^{-2}\text{s}^{-1}$)	pk: 15.5 avg: 8.7	pk: 0.4 / 12 / 21 / 170 850 / 880 / 7600 avg: 0.6 / 10 / 8 / 100 500 / 450 / 3800	3.6	900	0.4	6 (leveled)
Time between collisions (ns)	107	107 / 107 / 321 / 107 107 / 107 / 107	99.8 / 149.7	99.8 / 149.7	≈ 5500	49.9
Full crossing angle (μ rad)	0	0	290	280	300	> 200
Energy spread (units 10^{-3})	0.75	0.75	0.11	0.11	0.11	0.11
Bunch length (cm)	30	30	8.0	p / Pb: 9 / 11.5	11	7.9
Beam radius (10^{-6} m)	114*	123*/ 163*/ 145*/ 136* 124*/ 147*/ 128*	55	19	12	16
Free space at interaction point (m)	16	16	38	38	38	38
Initial luminosity decay time, $-L/(dL/dt)$ (hr)	1	-0.35‡/ ∞‡/ 1.8 / 0.6 ∞‡/ 0.5 / 0.25	2.6	≈ 2	≈ 6	∞
Turn-around time (min)	30	60 / 160 / 90 / 45 90 / 60 / 50	≈ 180	150	180	≈ 180
Injection energy (TeV/n)	0.011	0.011	0.177	p / Pb: 0.45 / 0.177	0.188	0.177
Transverse emittance (10^{-9} m)	19*	22*/ 38*/ 23*/ 19* 22*/ 26*/ 21*	1.5	0.29	0.3	0.5
β^*, ampl. function at interaction point (m)	0.7	0.7 / 0.7 / 0.9 / 1.0 0.7 / 0.8 / 0.8	0.8	0.5	0.4	0.5
Beam-beam tune shift per crossing (units 10^{-4})	39†	6†/ 14†(Cu), 14†(Au) / 30† 42†(h), 22†(Au) / 40†(d), 27†(Au) 53†(p), 41†(Au) / 80†(p) 59†(Au)	9	15	≈ 10	10
RF frequency (MHz)	accel: 28, store: 197	accel: 28, store: 197	400.8	400.8	400.8	400.8
Particles per bunch (units 10^{10})	0.20	0.03 / 0.4 (Cu), 0.13 (Au) / 0.45 4.5 (h), 0.13 (Au) / 13 (d), 0.20 (Au) 22.5 (p), 0.16 (Au) / 24 (p), 1.1 (Al)	0.019 (r.m.s.)	p: 2.6 Pb: 0.022	0.027	0.017
Bunches per ring per species	111	111 / 111 / 37 / 111 111 / 111 / 111	518	p: 540 Pb: 684	16	≈ 1100
Average beam current per species (mA)	224	38 / 160 (Cu), 138 (Au) / 60 125 (h), 143 (Au) / 181 (d), 213 (Au) 313 (p), 176 (Au) / 334 (p), 199 (Al)	14.9	p: 16 Pb: 15	0.54	28
Circumference (km)	3.834		26.659			
Interaction regions	6 total, 2 high $\mathscr{L}$		3 high $\mathscr{L}$ + 1			
Magnetic length of dipole (m)	9.45		14.3			
Length of standard cell (m)	29.7		106.90			
Phase advance per cell (deg)	93	84 / 84 / 84 / 93 84 (d), 93 (Au) / 84 (p), 93 (Au) 84 (p), 93 (Al)	90			
Dipoles in ring	192 per ring, + 12 common		1232, main dipoles			
Quadrupoles in ring	246 per ring		482 2-in-1, 24 1-in-1			
Magnet Type	s.c. $\cos\theta$, cold iron		s.c., 2 in 1, cold iron			
Peak magnetic field (T)	3.5		8.3			

*Initial value, smaller after cooling

†Initial value, possibly larger after cooling

‡Negative or infinite decay time is effect of cooling.

§High luminosity upgrade expected >= 2021; will extend throughout HL-LHC running. Very preliminary, conservative estimates.

32. Neutrino Beam Lines at High-Energy Proton Synchrotrons

Revised October 2017 with numbers verified by representatives of the synchrotrons (contact C.-J. Lin, LBNL). For existing (future) neutrino beam lines the latest achieved (design) values are given.

The main source of neutrinos at proton synchrotrons is from the decay of pions and kaons produced by protons striking a nuclear target. There are different schemes to focus the secondary particles to enhance neutrino flux and/or tune the neutrino energy profile. In wide-band beams (WBB), the neutrino parent mesons are focused over a wide momentum range to obtain maximum neutrino intensity. In narrow-band beams (NBB), the secondary particles are first momentum-selected to produce a monochromatic parent beam. Another approach to generate a narrow-band neutrino spectrum is to select neutrinos that are emitted off-axis relative to the momentum of the parent mesons. For a comprehensive review of the topic, including other historical neutrino beam lines, see the article by S. E. Kopp, "Accelerator-based neutrino beams," Phys. Rept. **439**, 101 (2007).

	PS (CERN)				SPS (CERN)				PS (KEK)	Main Ring (JPARC)
Date	1963	1969	1972	1983	1977	1977	1995	2006	1999	2017
Proton Kinetic Energy (GeV)	20.6	20.6	26	19	350	350	450	400	12	30 (50)
Protons per Cycle (10^{12})	0.7	0.6	5	5	10	10	36	48	6	240 (330)
Cycle Time (s)	3	2.3	-	-	-	-	14.4	6	2.2	2.48 (3.5)
Beam Power (kW)	0.8	0.9	-	-	-	-	180	510	5	500 (750)
Target	-	-	-	-	-	-	Be	Graphite	Al	Graphite
Target Length (cm)	-	-	-	-	-	-	290	1000	66	91
Secondary Focussing	1-horn WBB	3-horn WBB	2-horn WBB	bare target	dichromatic NBB	2-horn WBB	2-horn WBB	2-horn WBB	2-horn WBB	3-horn off-axis
Decay Pipe Length (m)	-	-	-	-	-	-	110	130	200	96
$\langle E_\nu \rangle$ (GeV)	1.5	1.5	1.5	1	50,150[†]	20	24.3	17	1.3	0.6
Experiments	HLBC, Spark Ch.	HLBC, Spark Ch.	GGM, Aachen-Padova	CDHS, CHARM	CDHS, CHARM, BEBC	GGM,CDHS, CHARM, BEBC	NOMAD, CHORUS	OPERA, ICARUS	K2K	T2K

	Main Ring (Fermilab)							Booster (Fermilab)	Main Injector (Fermilab)	
Date	1975	1975	1974	1979	1976	1991	1998	2002	2005	2017
Proton Kinetic Energy (GeV)	300,400	300,400	300	400	350	800	800	8	120	120
Protons per Cycle (10^{12})	10	10	10	10	13	10	12	4.5	37	54
Cycle Time (s)	-	-	-	-	-	60	60	0.2	2	1.333
Beam Power (kW)	-	-	-	-	-	20	25	29	350	720
Target	-	-	-	-	-	-	BeO	Be	Graphite	Graphite
Target Length (cm)	-	-	-	-	-	-	31	71	95	120
Secondary Focussing	bare target	quad trip., SSBT	dichromatic NBB	2-horn WBB	1-horn WBB	quad trip.	SSQT WBB	1-horn WBB	2-horn WBB	2-horn off-axis
Decay Pipe Length (m)	350	350	400	400	400	400	400	50	675	675
$\langle E_\nu \rangle$ (GeV)	40	50,180[†]	50,180[†]	25	100	90,260	70,180	1	3-20[‡]	2
Experiments	HPWF	CITF, HPWF	CITF, HPWF, 15' BC	15' BC	HPWF 15' BC	15' BC, CCFRR	NuTeV	MiniBooNE, SciBooNE, MicroBooNE	MINOS, MINERνA	NOνA, MINERνA, MINOS+

[†]Pion and kaon peaks in the momentum-selected channel.

[‡]Tunable WBB energy spectrum.

33. Passage of Particles Through Matter

Revised August 2015 by H. Bichsel (University of Washington), D.E. Groom (LBNL), and S.R. Klein (LBNL).

This review covers the interactions of photons and electrically charged particles in matter, concentrating on energies of interest for high-energy physics and astrophysics and processes of interest for particle detectors (ionization, Cherenkov radiation, transition radiation). Much of the focus is on particles heavier than electrons ($\pi^{\pm}$, p, etc.). Although the charge number z of the projectile is included in the equations, only $z = 1$ is discussed in detail. Muon radiative losses are discussed, as are photon/electron interactions at high to ultrahigh energies. Neutrons are not discussed.

33.1. Notation

The notation and important numerical values are shown in Table 33.1.

Table 33.1: Summary of variables used in this section. The kinematic variables β and γ have their usual relativistic meanings.

Symbol	Definition	Value or (usual) units
$m_e c^2$	electron mass $\times\, c^2$	0.510 998 9461(31) MeV
r_e	classical electron radius $e^2/4\pi\epsilon_0 m_e c^2$	2.817 940 3227(19) fm
α	fine structure constant $e^2/4\pi\epsilon_0\hbar c$	1/137.035 999 139(31)
N_A	Avogadro's number	$6.022\,140\,857(74) \times 10^{23}$ mol^{-1}
ρ	density	g cm^{-3}
x	mass per unit area	g cm^{-2}
M	incident particle mass	MeV/c^2
E	incident part. energy γMc^2	MeV
T	kinetic energy, $(\gamma - 1)Mc^2$	MeV
W	energy transfer to an electron in a single collision	MeV
k	bremsstrahlung photon energy	MeV
z	charge number of incident particle	
Z	atomic number of absorber	
A	atomic mass of absorber	g mol^{-1}
K	$4\pi N_A r_e^2 m_e c^2$ (Coefficient for dE/dx)	0.307 075 MeV mol^{-1} cm^2
I	mean excitation energy	eV (*Nota bene!*)
$\delta(\beta\gamma)$	density effect correction to ionization energy loss	
$\hbar\omega_p$	plasma energy $\sqrt{4\pi N_e r_e^3}\, m_e c^2/\alpha$	$\sqrt{\rho\,\langle Z/A\rangle} \times 28.816$ eV, ρ in g cm^{-3}
N_e	electron density	(units of r_e)$^{-3}$
w_j	weight fraction of the jth element in a compound or mixture	
n_j	$\propto$ number of jth kind of atoms in a compound or mixture	
X_0	radiation length	g cm^{-2}
E_c	critical energy for electrons	MeV
$E_{\mu c}$	critical energy for muons	GeV
E_s	scale energy $\sqrt{4\pi/\alpha}\, m_e c^2$	21.2052 MeV
R_M	Molière radius	g cm^{-2}

33.2. Electronic energy loss by heavy particles [1–33]

33.2.1. *Moments and cross sections* :

The electronic interactions of fast charged particles with speed $v = \beta c$ occur in *single collisions with energy losses* W [1], leading to ionization, atomic, or collective excitation. Most frequently the energy losses are small (for 90% of all collisions the energy losses are less than 100 eV). In thin absorbers few collisions will take place and the total energy loss will show a large variance [1]; also see Sec. 33.2.9 below. For particles with charge ze more massive than electrons ("heavy"

particles), scattering from free electrons is adequately described by the Rutherford differential cross section [2],

$$\frac{d\sigma_R(W;\beta)}{dW} = \frac{2\pi r_e^2 m_e c^2 z^2}{\beta^2}\frac{(1-\beta^2 W/W_{\rm max})}{W^2}\ , \qquad (33.1)$$

where $W_{\rm max}$ is the maximum energy transfer possible in a single collision. But in matter electrons are not free. W must be finite and depends on atomic and bulk structure. For electrons bound in atoms Bethe [3] used "Born Theorie" to obtain the differential cross section

$$\frac{d\sigma_B(W;\beta)}{dW} = \frac{d\sigma_R(W,\beta)}{dW}B(W)\ . \qquad (33.2)$$

Electronic binding is accounted for by the correction factor $B(W)$. Examples of $B(W)$ and $d\sigma_B/dW$ can be seen in Figs. 5 and 6 of Ref. 1.

Bethe's theory extends only to some energy above which atomic effects are not important. The free-electron cross section (Eq. (33.1)) can be used to extend the cross section to $W_{\rm max}$. At high energies σ_B is further modified by polarization of the medium, and this "density effect," discussed in Sec. 33.2.5, must also be included. Less important corrections are discussed below.

The mean number of collisions with energy loss between W and $W + dW$ occurring in a distance δx is $N_e\delta x\,(d\sigma/dW)dW$, where $d\sigma(W;\beta)/dW$ contains all contributions. It is convenient to define the moments

$$M_j(\beta) = N_e\,\delta x \int W^j \frac{d\sigma(W;\beta)}{dW}dW\ , \qquad (33.3)$$

so that M_0 is the mean number of collisions in δx, M_1 is the mean energy loss in δx, $(M_2 - M_1)^2$ is the variance, *etc.* The number of collisions is Poisson-distributed with mean M_0. N_e is either measured in electrons/g ($N_e = N_A Z/A$) or electrons/cm^3 ($N_e = N_A\,\rho Z/A$). The former is used throughout this chapter, since quantities of interest (dE/dx, X_0, *etc.*) vary smoothly with composition when there is no density dependence.

copper, the error thus introduced into dE/dx is greater than 6% at 100 GeV. For $2\gamma m_e \gg M$, $W_{\rm max} = Mc^2\,\beta^2\gamma$.

At energies of order 100 GeV, the maximum 4-momentum transfer to the electron can exceed 1 GeV/c, where hadronic structure effects significantly modify the cross sections. This problem has been investigated by J.D. Jackson [9], who concluded that for hadrons (but not for large nuclei) corrections to dE/dx are negligible below energies where radiative effects dominate. While the cross section for rare hard collisions is modified, the average stopping power, dominated by many softer collisions, is almost unchanged.

33.2.3. *Stopping power at intermediate energies* :

The mean rate of energy loss by moderately relativistic charged heavy particles is well-described by the "Bethe equation,"

$$\left\langle -\frac{dE}{dx}\right\rangle = Kz^2\frac{Z}{A}\frac{1}{\beta^2}\left[\frac{1}{2}\ln\frac{2m_e c^2\beta^2\gamma^2 W_{\rm max}}{I^2} - \beta^2 - \frac{\delta(\beta\gamma)}{2}\right]\ . \qquad (33.5)$$

It describes the mean rate of energy loss in the region $0.1 \lesssim \beta\gamma \lesssim 1000$ for intermediate-Z materials with an accuracy of a few percent.

This is the *mass stopping power*; with the symbol definitions and values given in Table 33.1, the units are MeV g^{-1}cm^2. As can be seen from Fig. 33.2, $\langle -dE/dx\rangle$ defined in this way is about the same for most materials, decreasing slowly with Z. The *linear stopping power*, in MeV/cm, is $\langle -dE/dx\rangle\,\rho$, where ρ is the density in g/cm^3.

$W_{\rm max}$ is defined in Sec. 33.2.2. At the lower limit the projectile velocity becomes comparable to atomic electron "velocities" (Sec. 33.2.6), and at the upper limit radiative effects begin to be important (Sec. 33.6). Both limits are Z dependent. A minor dependence on M at the highest energies is introduced through $W_{\rm max}$, but for all practical purposes $\langle dE/dx\rangle$ in a given material is a function of β alone.

Few concepts in high-energy physics are as misused as $\langle dE/dx\rangle$. The main problem is that the mean is weighted by very rare events

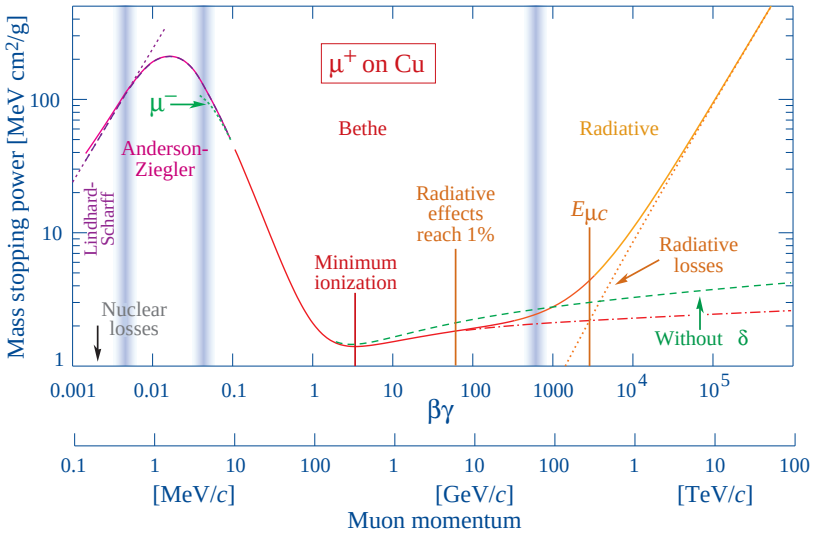

Fig. 33.1: Mass stopping power (= $\langle -dE/dx\rangle$) for positive muons in copper as a function of $\beta\gamma = p/Mc$ over nine orders of magnitude in momentum (12 orders of magnitude in kinetic energy). Solid curves indicate the total stopping power. Data below the break at $\beta\gamma \approx 0.1$ are taken from ICRU 49 [4], and data at higher energies are from Ref. 5. Vertical bands indicate boundaries between different approximations discussed in the text. The short dotted lines labeled "μ^-" illustrate the "Barkas effect," the dependence of stopping power on projectile charge at very low energies [6]. dE/dx in the radiative region is not simply a function of β.

33.2.2. *Maximum energy transfer in a single collision* :

For a particle with mass M,

$$W_{\rm max} = \frac{2m_e c^2\,\beta^2\gamma^2}{1 + 2\gamma m_e/M + (m_e/M)^2}\ . \qquad (33.4)$$

In older references [2,8] the "low-energy" approximation $W_{\rm max} = 2m_e c^2\,\beta^2\gamma^2$, valid for $2\gamma m_e \ll M$, is often implicit. For a pion in

with large single-collision energy deposits. Even with samples of hundreds of events a dependable value for the mean energy loss cannot be obtained. Far better and more easily measured is the most probable energy loss, discussed in Sec. 33.2.9. The most probable energy loss in a detector is considerably below the mean given by the Bethe equation.

In a TPC (Sec. 34.6.5), the mean of 50%–70% of the samples

with the smallest signals is often used as an estimator. Although it must be used with cautions and caveats, $\langle dE/dx \rangle$ as described in Eq. (33.5) still forms the basis of much of our understanding of energy loss by charged particles. Extensive tables are available [4,5, `pdg.lbl.gov/AtomicNuclearProperties/`].

For heavy projectiles, like ions, additional terms are required to account for higher-order photon coupling to the target, and to account for the finite target radius. These can change dE/dx by a factor of two or more for the heaviest nuclei in certain kinematic regimes [7].

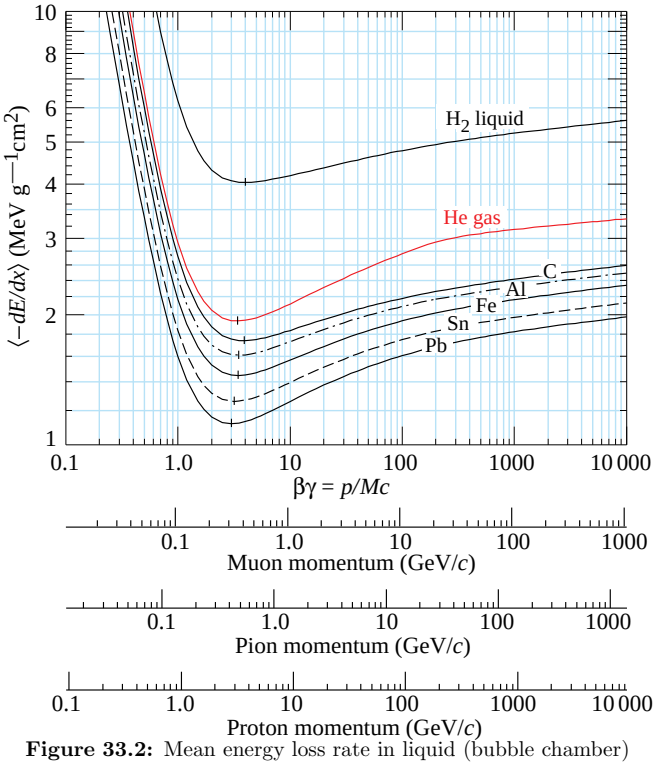

Figure 33.2: Mean energy loss rate in liquid (bubble chamber) hydrogen, gaseous helium, carbon, aluminum, iron, tin, and lead. Radiative effects, relevant for muons and pions, are not included. These become significant for muons in iron for $\beta\gamma \gtrsim 1000$, and at lower momenta for muons in higher-Z absorbers. See Fig. 33.23.

The function as computed for muons on copper is shown as the "Bethe" region of Fig. 33.1. Mean energy loss behavior below this region is discussed in Sec. 33.2.6, and the radiative effects at high energy are discussed in Sec. 33.6. Only in the Bethe region is it a function of β alone; the mass dependence is more complicated elsewhere. The stopping power in several other materials is shown in Fig. 33.2. Except in hydrogen, particles with the same velocity have similar rates of energy loss in different materials, although there is a slow decrease in the rate of energy loss with increasing Z. The qualitative behavior difference at high energies between a gas (He in the figure) and the other materials shown in the figure is due to the density-effect correction, $\delta(\beta\gamma)$, discussed in Sec. 33.2.5. The stopping power functions are characterized by broad minima whose position drops from $\beta\gamma = 3.5$ to 3.0 as Z goes from 7 to 100. The values of minimum ionization as a function of atomic number are shown in Fig. 33.3.

In practical cases, most relativistic particles (*e.g.*, cosmic-ray muons) have mean energy loss rates close to the minimum; they are "minimum-ionizing particles," or mip's.

Eq. (33.5) may be integrated to find the total (or partial) "continuous slowing-down approximation" (CSDA) range R for a particle which loses energy only through ionization and atomic excitation. Since dE/dx depends only on β, R/M is a function of E/M or pc/M. In practice, range is a useful concept only for low-energy hadrons ($R \lesssim \lambda_I$, where λ_I is the nuclear interaction length), and for muons below a few hundred GeV (above which

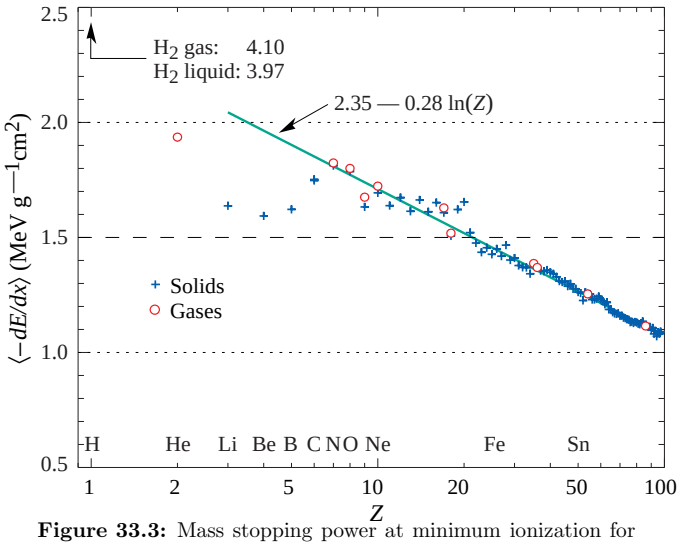

Figure 33.3: Mass stopping power at minimum ionization for the chemical elements. The straight line is fitted for $Z > 6$. A simple functional dependence on Z is not to be expected, since $\langle -dE/dx \rangle$ also depends on other variables.

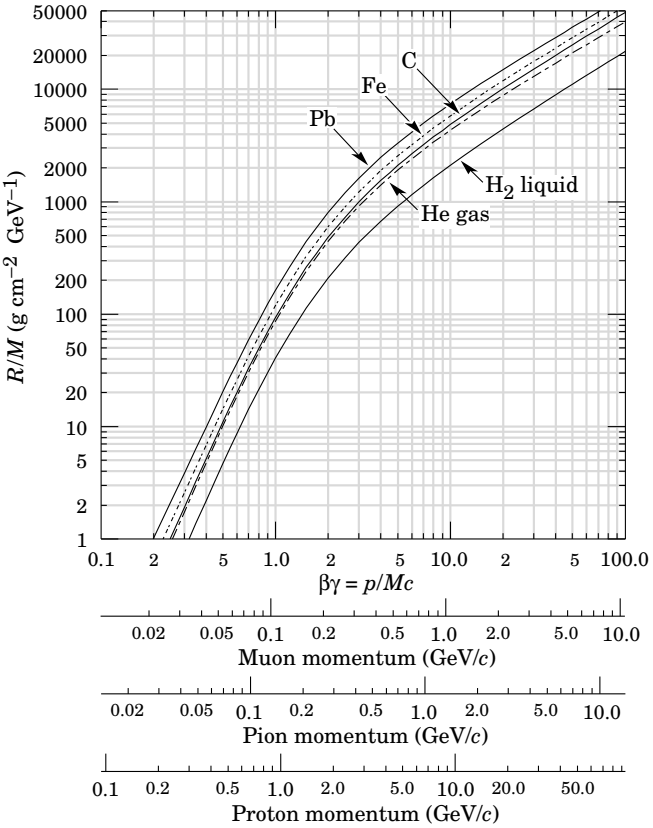

Figure 33.4: Range of heavy charged particles in liquid (bubble chamber) hydrogen, helium gas, carbon, iron, and lead. For example: For a K^+ whose momentum is 700 MeV/c, $\beta\gamma = 1.42$. For lead we read $R/M \approx 396$, and so the range is 195 g cm^{-2} (17 cm).

radiative effects dominate). R/M as a function of $\beta\gamma = p/Mc$ is shown for a variety of materials in Fig. 33.4.

The mass scaling of dE/dx and range is valid for the electronic losses described by the Bethe equation, but not for radiative losses, relevant only for muons and pions.

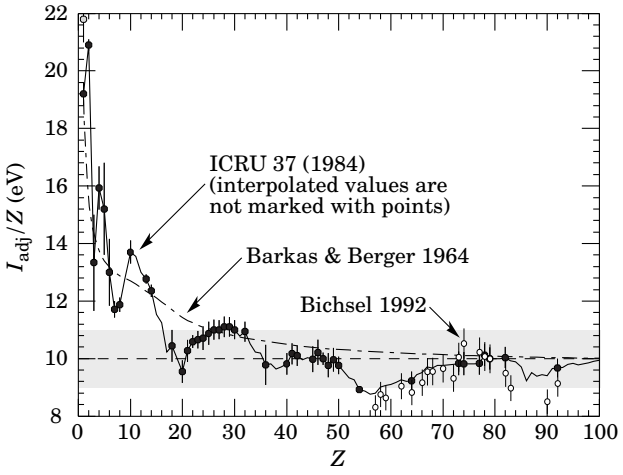

Figure 33.5: Mean excitation energies (divided by Z) as adopted by the ICRU [11]. Those based on experimental measurements are shown by symbols with error flags; the interpolated values are simply joined. The grey point is for liquid H_2; the black point at 19.2 eV is for H_2 gas. The open circles show more recent determinations by Bichsel [13]. The dash-dotted curve is from the approximate formula of Barkas [14] used in early editions of this *Review*.

33.2.4. ***Mean excitation energy*** :

"The determination of the mean excitation energy is the principal non-trivial task in the evaluation of the Bethe stopping-power formula" [10]. Recommended values have varied substantially with time. Estimates based on experimental stopping-power measurements for protons, deuterons, and alpha particles and on oscillator-strength distributions and dielectric-response functions were given in ICRU 49 [4]. See also ICRU 37 [11]. These values, shown in Fig. 33.5, have since been widely used. Machine-readable versions can also be found [12].

33.2.5. ***Density effect*** :

As the particle energy increases, its electric field flattens and extends, so that the distant-collision contribution to Eq. (33.5) increases as $\ln\beta\gamma$. However, real media become polarized, limiting the field extension and effectively truncating this part of the logarithmic rise [2–8,15–16]. At very high energies,

$$\delta/2 \to \ln(\hbar\omega_p/I) + \ln\beta\gamma - 1/2 \ , \tag{33.6}$$

where $\delta(\beta\gamma)/2$ is the density effect correction introduced in Eq. (33.5) and $\hbar\omega_p$ is the plasma energy defined in Table 33.1. A comparison with Eq. (33.5) shows that $|dE/dx|$ then grows as $\ln\beta\gamma$ rather than $\ln\beta^2\gamma^2$, and that the mean excitation energy I is replaced by the plasma energy $\hbar\omega_p$. The ionization stopping power as calculated with and without the density effect correction is shown in Fig. 33.1. Since the plasma frequency scales as the square root of the electron density, the correction is much larger for a liquid or solid than for a gas, as is illustrated by the examples in Fig. 33.2.

The density effect correction is usually computed using Sternheimer's parameterization [15]:

$$\delta(\beta\gamma) = \begin{cases} 2(\ln 10)x - \overline{C} & \text{if } x \geq x_1; \\ 2(\ln 10)x - \overline{C} + a(x_1 - x)^k & \text{if } x_0 \leq x < x_1; \\ 0 & \text{if } x < x_0 \text{ (nonconductors);} \\ \delta_0 10^{2(x-x_0)} & \text{if } x < x_0 \text{ (conductors)} \end{cases} \tag{33.7}$$

Here $x = \log_{10}\eta = \log_{10}(p/Mc)$. $\overline{C}$ (the negative of the C used in Ref. 15) is obtained by equating the high-energy case of Eq. (33.7) with the limit given in Eq. (33.6). The other parameters are adjusted to give a best fit to the results of detailed calculations for momenta below $Mc\exp(x_1)$. Parameters for elements and nearly 200 compounds and mixtures of interest are published in a variety of places, notably in Ref. 16. A recipe for finding the coefficients for nontabulated materials is given by Sternheimer and Peierls [17], and is summarized in Ref. 5.

The remaining relativistic rise comes from the $\beta^2\gamma$ growth of $W_{\max}$, which in turn is due to (rare) large energy transfers to a few electrons. When these events are excluded, the energy deposit in an absorbing layer approaches a constant value, the Fermi plateau (see Sec. 33.2.8 below). At even higher energies (*e.g.*, > 332 GeV for muons in iron, and at a considerably higher energy for protons in iron), radiative effects are more important than ionization losses. These are especially relevant for high-energy muons, as discussed in Sec. 33.6.

33.2.6. ***Energy loss at low energies*** :

Shell corrections C/Z must be included in the square brackets of of Eq. (33.5) [4,11,13,14] to correct for atomic binding having been neglected in calculating some of the contributions to Eq. (33.5). The Barkas form [14] was used in generating Fig. 33.1. For copper it contributes about 1% at $\beta\gamma = 0.3$ (kinetic energy 6 MeV for a pion), and the correction decreases very rapidly with increasing energy.

Equation 33.2, and therefore Eq. (33.5), are based on a first-order Born approximation. Higher-order corrections, again important only at lower energies, are normally included by adding the "Bloch correction" $z^2L_2(\beta)$ inside the square brackets (Eq.(2.5) in [4]) .

An additional "Barkas correction" $zL_1(\beta)$ reduces the stopping power for a negative particle below that for a positive particle with the same mass and velocity. In a 1956 paper, Barkas *et al.* noted that negative pions had a longer range than positive pions [6]. The effect has been measured for a number of negative/positive particle pairs, including a detailed study with antiprotons [18].

A detailed discussion of low-energy corrections to the Bethe formula is given in ICRU 49 [4]. When the corrections are properly included, the Bethe treatment is accurate to about 1% down to $\beta \approx 0.05$, or about 1 MeV for protons.

For $0.01 < \beta < 0.05$, there is no satisfactory theory. For protons, one usually relies on the phenomenological fitting formulae developed by Andersen and Ziegler [4,19]. As tabulated in ICRU 49 [4], the nuclear plus electronic proton stopping power in copper is 113 MeV cm^2 g^{-1} at $T = 10$ keV ($\beta\gamma = 0.005$), rises to a maximum of 210 MeV cm^2 g^{-1} at $T \approx 120$ keV ($\beta\gamma = 0.016$), then falls to 118 MeV cm^2 g^{-1} at $T = 1$ MeV ($\beta\gamma = 0.046$). Above 0.5–1.0 MeV the corrected Bethe theory is adequate.

For particles moving more slowly than $\approx 0.01c$ (more or less the velocity of the outer atomic electrons), Lindhard has been quite successful in describing electronic stopping power, which is proportional to β [20]. Finally, we note that at even lower energies, *e.g.*, for protons of less than several hundred eV, non-ionizing nuclear recoil energy loss dominates the total energy loss [4,20,21].

33.2.7. ***Energetic knock-on electrons (δ rays)*** :

The distribution of secondary electrons with kinetic energies $T \gg I$ is [2]

$$\frac{d^2N}{dTdx} = \frac{1}{2}\,Kz^2\frac{Z}{A}\,\frac{1}{\beta^2}\,\frac{F(T)}{T^2} \tag{33.8}$$

for $I \ll T \leq W_{\max}$, where $W_{\max}$ is given by Eq. (33.4). Here β is the velocity of the primary particle. The factor F is spin-dependent, but is about unity for $T \ll W_{\max}$. For spin-0 particles $F(T) = (1 - \beta^2 T/W_{\max})$; forms for spins 1/2 and 1 are also given by Rossi [2](Sec. 2.3, Eqns. 7 and 8). Additional formulae are given in Ref. 22. Equation (33.8) is inaccurate for T close to I [23].

δ rays of even modest energy are rare. For a $\beta \approx 1$ particle, for example, on average only one collision with $T_e > 10$ keV will occur along a path length of 90 cm of Ar gas [1].

A δ ray with kinetic energy T_e and corresponding momentum p_e is produced at an angle θ given by

$$\cos\theta = (T_e/p_e)(p_{\max}/W_{\max}) \ , \tag{33.9}$$

where $p_{\max}$ is the momentum of an electron with the maximum possible energy transfer $W_{\max}$.

33.2.8. ***Restricted energy loss rates for relativistic ionizing particles*** : Further insight can be obtained by examining the mean energy deposit by an ionizing particle when energy transfers are restricted to $T \leq W_{\rm cut} \leq W_{\rm max}$. The restricted energy loss rate is

$$-\frac{dE}{dx}\Big|_{T<W_{\rm cut}} = Kz^2\frac{Z}{A}\frac{1}{\beta^2}\left[\frac{1}{2}\ln\frac{2m_ec^2\beta^2\gamma^2W_{\rm cut}}{I^2} - \frac{\beta^2}{2}\left(1+\frac{W_{\rm cut}}{W_{\rm max}}\right) - \frac{\delta}{2}\right] . \quad (33.10)$$

This form approaches the normal Bethe function (Eq. (33.5)) as $W_{\rm cut} \to W_{\rm max}$. It can be verified that the difference between Eq. (33.5) and Eq. (33.10) is equal to $\int_{W_{\rm cut}}^{W_{\rm max}} T(d^2N/dTdx)dT$, where $d^2N/dTdx$ is given by Eq. (33.8).

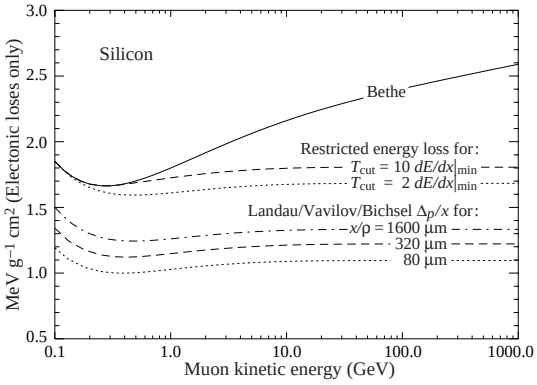

Figure 33.6: Bethe dE/dx, two examples of restricted energy loss, and the Landau most probable energy per unit thickness in silicon. The change of Δ_p/x with thickness x illustrates its $a\ln x + b$ dependence. Minimum ionization ($dE/dx|_{\rm min}$) is 1.664 MeV g^{-1} cm^2. Radiative losses are excluded. The incident particles are muons.

Since $W_{\rm cut}$ replaces $W_{\rm max}$ in the argument of the logarithmic term of Eq. (33.5), the $\beta\gamma$ term producing the relativistic rise in the close-collision part of dE/dx is replaced by a constant, and $|dE/dx|_{T<W_{\rm cut}}$ approaches the constant "Fermi plateau." (The density effect correction δ eliminates the explicit $\beta\gamma$ dependence produced by the distant-collision contribution.) This behavior is illustrated in Fig. 33.6, where restricted loss rates for two examples of $W_{\rm cut}$ are shown in comparison with the full Bethe dE/dx and the Landau-Vavilov most probable energy loss (to be discussed in Sec. 33.2.9 below).

"Restricted energy loss" is cut at the total mean energy, not the single-collision energy above $W_{\rm cut}$ It is of limited use. The most probable energy loss, discussed in the next Section, is far more useful in situations where single-particle energy loss is observed.

33.2.9. ***Fluctuations in energy loss*** :

For detectors of moderate thickness x (*e.g.* scintillators or LAr cells),* the energy loss probability distribution $f(\Delta;\beta\gamma,x)$ is adequately described by the highly-skewed Landau (or Landau-Vavilov) distribution [24,25]. The most probable energy loss is [26] †

$$\Delta_p = \xi\left[\ln\frac{2mc^2\beta^2\gamma^2}{I} + \ln\frac{\xi}{I} + j - \beta^2 - \delta(\beta\gamma)\right] , \quad (33.11)$$

where $\xi = (K/2)\langle Z/A\rangle z^2(x/\beta^2)$ MeV for a detector with a thickness x in g cm^{-2}, and $j = 0.200$ [26]. ‡ While dE/dx is independent of thickness, Δ_p/x scales as $a\ln x + b$. The density correction $\delta(\beta\gamma)$ was not included in Landau's or Vavilov's work, but it was later included by Bichsel [26]. The high-energy behavior of $\delta(\beta\gamma)$ (Eq. (33.6)) is such that

$$\Delta_p \underset{\beta\gamma\gtrsim 100}{\longrightarrow} \xi\left[\ln\frac{2mc^2\xi}{(\hbar\omega_p)^2} + j\right] . \quad (33.12)$$

Thus the Landau-Vavilov most probable energy loss, like the restricted energy loss, reaches a Fermi plateau. The Bethe dE/dx and Landau-Vavilov-Bichsel Δ_p/x in silicon are shown as a function of muon energy in Fig. 33.6. The energy deposit in the 1600 μm case is roughly the same as in a 3 mm thick plastic scintillator.

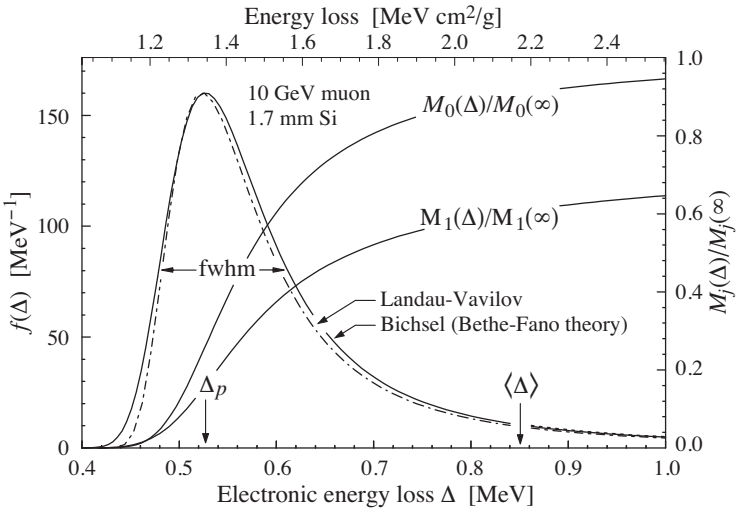

Figure 33.7: Electronic energy deposit distribution for a 10 GeV muon traversing 1.7 mm of silicon, the stopping power equivalent of about 0.3 cm of PVT-based scintillator [1,13,28]. The Landau-Vavilov function (dot-dashed) uses a Rutherford cross section without atomic binding corrections but with a kinetic energy transfer limit of $W_{\rm max}$. The solid curve was calculated using Bethe-Fano theory. $M_0(\Delta)$ and $M_1(\Delta)$ are the cumulative 0th moment (mean number of collisions) and 1st moment (mean energy loss) in crossing the silicon. (See Sec. 33.2.1. The fwhm of the Landau-Vavilov function is about 4ξ for detectors of moderate thickness. Δ_p is the most probable energy loss, and $\langle\Delta\rangle$ divided by the thickness is the Bethe $\langle dE/dx\rangle$.

The distribution function for the energy deposit by a 10 GeV muon going through a detector of about this thickness is shown in Fig. 33.7. In this case the most probable energy loss is 62% of the mean ($M_1(\langle\Delta\rangle)/M_1(\infty)$). Folding in experimental resolution displaces the peak of the distribution, usually toward a higher value. 90% of the collisions ($M_1(\langle\Delta\rangle)/M_1(\infty)$) contribute to energy deposits below the mean. It is the very rare high-energy-transfer collisions, extending to $W_{\rm max}$ at several GeV, that drives the mean into the tail of the distribution. The large weight of these rare events makes the mean of an experimental distribution consisting of a few hundred events subject to large fluctuations and sensitive to cuts. *The mean of the energy loss given by the Bethe equation, Eq. (*33.5*), is thus ill-defined experimentally and is not useful for describing energy loss by single particles.*♮ It rises as $\ln\gamma$ because $W_{\rm max}$ increases as γ at high energies. *The most probable energy loss should be used.*

A practical example: For muons traversing 0.25 inches (0.64 cm) of PVT (polyvinyltolulene) based plastic scintillator, the ratio of the

* "Moderate thickness" means $G \lesssim 0.05$–0.1, where G is given by Rossi [Ref. 2, Eq. 2.7(10)]. It is Vavilov's κ [25]. G is proportional to the absorber's thickness, and as such parameterizes the constants describing the Landau distribution. These are fairly insensitive to thickness for $G \lesssim 0.1$, the case for most detectors.

† Practical calculations can be expedited by using the tables of δ and β from the text versions of the muon energy loss tables to be found at `pdg.lbl.gov/AtomicNuclearProperties`.

‡ Rossi [2], Talman [27], and others give somewhat different values for j. The most probable loss is not sensitive to its value.

♮ It does find application in dosimetry, where only bulk deposit is relevant.

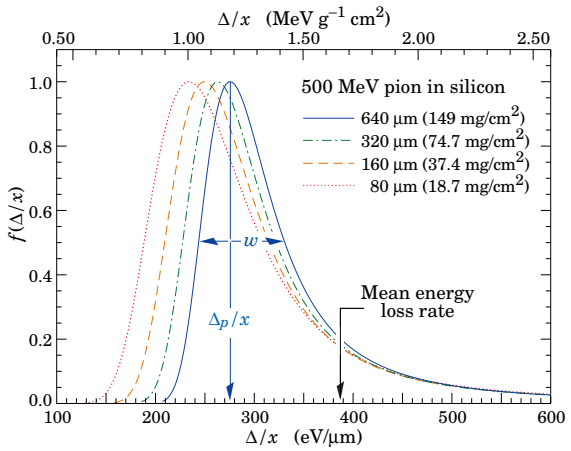

Figure 33.8: Straggling functions in silicon for 500 MeV pions, normalized to unity at the most probable value Δ_p/x. The width w is the full width at half maximum.

most probable E loss rate to the mean loss rate via the Bethe equation is $[0.69, 0.57, 0.49, 0.42, 0.38]$ for $T_\mu = [0.01, 0.1, 1, 10, 100]$ GeV. Radiative losses add less than 0.5% to the total mean energy deposit at 10 GeV, but add 7% at 100 GeV. The most probable E loss rate rises slightly beyond the minimum ionization energy, then is essentially constant.

The Landau distribution fails to describe energy loss in thin absorbers such as gas TPC cells [1] and Si detectors [26], as shown clearly in Fig. 1 of Ref. 1 for an argon-filled TPC cell. Also see Talman [27]. While Δ_p/x may be calculated adequately with Eq. (33.11), the distributions are significantly wider than the Landau width $w = 4\xi$ [Ref. 26, Fig. 15]. Examples for 500 MeV pions incident on thin silicon detectors are shown in Fig. 33.8. For very thick absorbers the distribution is less skewed but never approaches a Gaussian.

The most probable energy loss, scaled to the mean loss at minimum ionization, is shown in Fig. 33.9 for several silicon detector thicknesses.

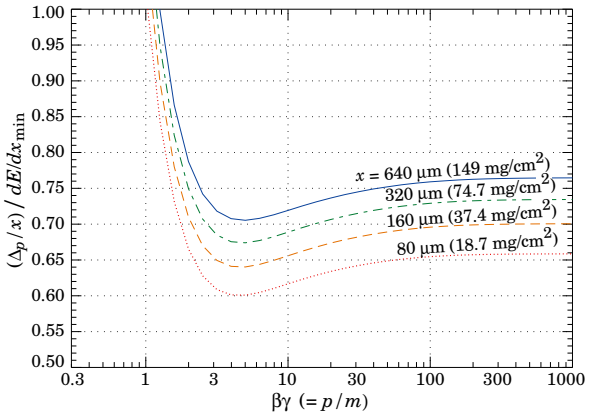

Figure 33.9: Most probable energy loss in silicon, scaled to the mean loss of a minimum ionizing particle, 388 eV/μm (1.66 MeV g^{-1}cm^2).

33.2.10. *Energy loss in mixtures and compounds* :

A mixture or compound can be thought of as made up of thin layers of pure elements in the right proportion (Bragg additivity). In this case,

$$\left\langle \frac{dE}{dx} \right\rangle = \sum w_j \left\langle \frac{dE}{dx} \right\rangle_j , \tag{33.13}$$

where $dE/dx|_j$ is the mean rate of energy loss (in MeV g cm^{-2}) in the jth element. Eq. (33.5) can be inserted into Eq. (33.13) to find expressions for $\langle Z/A \rangle$, $\langle I \rangle$, and $\langle \delta \rangle$; for example, $\langle Z/A \rangle = \sum w_j Z_j/A_j = \sum n_j Z_j / \sum n_j A_j$. However, $\langle I \rangle$ as defined this way is an underestimate, because in a compound electrons are more tightly bound than in the free elements, and $\langle \delta \rangle$ as calculated this way has little relevance, because it is the electron density that matters. If possible, one uses the tables given in Refs. 16 and 29, that include effective excitation energies and interpolation coefficients for calculating the density effect correction for the chemical elements and nearly 200 mixtures and compounds. Otherwise, use the recipe for δ given in Ref. 5 and 17, and calculate $\langle I \rangle$ following the discussion in Ref. 10. (Note the "13%" rule!)

33.2.11. *Ionization yields* :

Physicists frequently relate total energy loss to the number of ion pairs produced near the particle's track. This relation becomes complicated for relativistic particles due to the wandering of energetic knock-on electrons whose ranges exceed the dimensions of the fiducial volume. For a qualitative appraisal of the nonlocality of energy deposition in various media by such modestly energetic knock-on electrons, see Ref. 30. The mean local energy dissipation per local ion pair produced, W, while essentially constant for relativistic particles, increases at slow particle speeds [31]. For gases, W can be surprisingly sensitive to trace amounts of various contaminants [31]. Furthermore, ionization yields in practical cases may be greatly influenced by such factors as subsequent recombination [32].

33.3. Multiple scattering through small angles

A charged particle traversing a medium is deflected by many small-angle scatters. Most of this deflection is due to Coulomb scattering from nuclei as described by the Rutherford cross section. (However, for hadronic projectiles, the strong interactions also contribute to multiple scattering.) For many small-angle scatters the net scattering and displacement distributions are Gaussian via the central limit theorem. Less frequent "hard" scatters produce non-Gaussian tails. These Coulomb scattering distributions are well-represented by the theory of Molière [34]. Accessible discussions are given by Rossi [2] and Jackson [33], and exhaustive reviews have been published by Scott [35] and Motz *et al.* [36]. Experimental measurements have been published by Bichsel [37](low energy protons) and by Shen *et al.* [38](relativistic pions, kaons, and protons).*

If we define

$$\theta_0 = \theta_{\text{plane}}^{\text{rms}} = \frac{1}{\sqrt{2}} \theta_{\text{space}}^{\text{rms}} , \tag{33.14}$$

then it is sufficient for many applications to use a Gaussian approximation for the central 98% of the projected angular distribution, with an rms width given by Lynch & Dahl [39]:

$$\begin{aligned} \theta_0 &= \frac{13.6 \text{ MeV}}{\beta c p} \, z \sqrt{\frac{x}{X_0}} \left[1 + 0.088 \log_{10}\left(\frac{x\, z^2}{X_0 \beta^2}\right) \right] \\ &= \frac{13.6 \text{ MeV}}{\beta c p} \, z \sqrt{\frac{x}{X_0}} \left[1 + 0.038 \ln\left(\frac{x\, z^2}{X_0 \beta^2}\right) \right] \end{aligned} \tag{33.15}$$

Here p, βc, and z are the momentum, velocity, and charge number of the incident particle, and x/X_0 is the thickness of the scattering medium in radiation lengths (defined below). This takes into account the p and z dependence quite well at small Z, but for large Z and small x the β-dependence is not well represented. Further improvements are discussed in Ref. 39.

Eq. (33.15) describes scattering from a single material, while the usual problem involves the multiple scattering of a particle traversing many different layers and mixtures. Since it is from a fit to a Molière distribution, it is incorrect to add the individual θ_0 contributions in quadrature; the result is systematically too small. It is much more accurate to apply Eq. (33.15) once, after finding x and X_0 for the combined scatterer.

The nonprojected (space) and projected (plane) angular distributions are given approximately by [34]

$$\frac{1}{2\pi\, \theta_0^2} \exp\left(-\frac{\theta_{\text{space}}^2}{2\theta_0^2} \right) d\Omega , \tag{33.16}$$

$$\frac{1}{\sqrt{2\pi}\, \theta_0} \exp\left(-\frac{\theta_{\text{plane}}^2}{2\theta_0^2} \right) d\theta_{\text{plane}} , \tag{33.17}$$

* Shen *et al.*'s measurements show that Bethe's simpler methods of including atomic electron effects agrees better with experiment than does Scott's treatment.

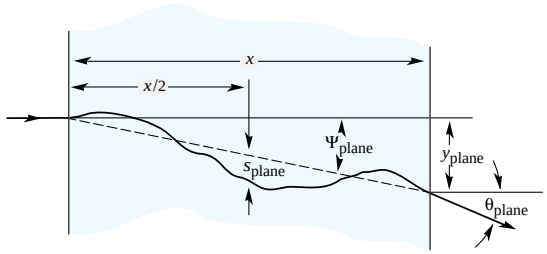

Figure 33.10: Quantities used to describe multiple Coulomb scattering. The particle is incident in the plane of the figure.

where θ is the deflection angle. In this approximation, $\theta^2_{\rm space} \approx (\theta^2_{{\rm plane},x} + \theta^2_{{\rm plane},y})$, where the x and y axes are orthogonal to the direction of motion, and $d\Omega \approx d\theta_{{\rm plane},x}\, d\theta_{{\rm plane},y}$. Deflections into $\theta_{{\rm plane},x}$ and $\theta_{{\rm plane},y}$ are independent and identically distributed.

Fig. 33.10 shows these and other quantities sometimes used to describe multiple Coulomb scattering. They are

$$\psi^{\rm rms}_{\rm plane} = \frac{1}{\sqrt{3}}\,\theta^{\rm rms}_{\rm plane} = \frac{1}{\sqrt{3}}\,\theta_0\ , \tag{33.18}$$

$$y^{\rm rms}_{\rm plane} = \frac{1}{\sqrt{3}}\,x\,\theta^{\rm rms}_{\rm plane} = \frac{1}{\sqrt{3}}\,x\,\theta_0\ , \tag{33.19}$$

$$s^{\rm rms}_{\rm plane} = \frac{1}{4\sqrt{3}}\,x\,\theta^{\rm rms}_{\rm plane} = \frac{1}{4\sqrt{3}}\,x\,\theta_0\ . \tag{33.20}$$

All the quantitative estimates in this section apply only in the limit of small $\theta^{\rm rms}_{\rm plane}$ and in the absence of large-angle scatters. The random variables s, ψ, y, and θ in a given plane are correlated. Obviously, $y \approx x\psi$. In addition, y and θ have the correlation coefficient $\rho_{y\theta} = \sqrt{3}/2 \approx 0.87$. For Monte Carlo generation of a joint $(y_{\rm\,plane}, \theta_{\rm plane})$ distribution, or for other calculations, it may be most convenient to work with independent Gaussian random variables (z_1, z_2) with mean zero and variance one, and then set

$$y_{\rm plane} = z_1\, x\,\theta_0(1-\rho^2_{y\theta})^{1/2}/\sqrt{3} + z_2\,\rho_{y\theta} x\,\theta_0/\sqrt{3} \tag{33.21}$$

$$= z_1\, x\,\theta_0/\sqrt{12} + z_2\, x\,\theta_0/2\ ; \tag{33.22}$$

$$\theta_{\rm plane} = z_2\,\theta_0\ . \tag{33.23}$$

Note that the second term for $y_{\rm\,plane}$ equals $x\,\theta_{\rm plane}/2$ and represents the displacement that would have occurred had the deflection $\theta_{\rm plane}$ all occurred at the single point $x/2$.

For heavy ions the multiple Coulomb scattering has been measured and compared with various theoretical distributions [40].

33.4. Photon and electron interactions in matter

At low energies electrons and positrons primarily lose energy by ionization, although other processes (Møller scattering, Bhabha scattering, e^+ annihilation) contribute, as shown in Fig. 33.11. While ionization loss rates rise logarithmically with energy, bremsstrahlung losses rise nearly linearly (fractional loss is nearly independent of energy), and dominates above the critical energy (Sec. 33.4.4 below), a few tens of MeV in most materials

33.4.1. *Collision energy losses by $e^\pm$* :

Stopping power differs somewhat for electrons and positrons, and both differ from stopping power for heavy particles because of the kinematics, spin, charge, and the identity of the incident electron with the electrons that it ionizes. Complete discussions and tables can be found in Refs. 10, 11, and 29.

For electrons, large energy transfers to atomic electrons (taken as free) are described by the Møller cross section. From Eq. (33.4), the maximum energy transfer in a single collision should be the entire kinetic energy, $W_{\rm max} = m_e c^2(\gamma-1)$, but because the particles are identical, the maximum is half this, $W_{\rm max}/2$. (The results are the same if the transferred energy is ϵ or if the transferred energy is $W_{\rm max} - \epsilon$. The stopping power is by convention calculated for the faster of the two emerging electrons.) The first moment of the Møller cross section [22](divided by dx) is the stopping power:

$$\left\langle -\frac{dE}{dx}\right\rangle = \frac{1}{2}K\frac{Z}{A}\frac{1}{\beta^2}\left[\ln\frac{m_e c^2\beta^2\gamma^2\{m_e c^2(\gamma-1)/2\}}{I^2}\right.$$
$$\left. +(1-\beta^2) - \frac{2\gamma-1}{\gamma^2}\ln 2 + \frac{1}{8}\left(\frac{\gamma-1}{\gamma}\right)^2 - \delta\right] \tag{33.24}$$

The logarithmic term can be compared with the logarithmic term in the Bethe equation (Eq. (33.2)) by substituting $W_{\rm max} = m_e c^2(\gamma-1)/2$. The two forms differ by $\ln 2$.

Electron-positron scattering is described by the fairly complicated Bhabha cross section [22]. There is no identical particle problem, so $W_{\rm max} = m_e c^2(\gamma-1)$. The first moment of the Bhabha equation yields

$$\left\langle -\frac{dE}{dx}\right\rangle = \frac{1}{2}K\frac{Z}{A}\frac{1}{\beta^2}\left[\ln\frac{m_e c^2\beta^2\gamma^2\{m_e c^2(\gamma-1)\}}{2I^2}\right.$$
$$\left. +2\ln 2 - \frac{\beta^2}{12}\left(23 + \frac{14}{\gamma+1} + \frac{10}{(\gamma+1)^2} + \frac{4}{(\gamma+1)^3}\right)\right] \tag{33.25}$$

Following ICRU 37 [11], the density effect correction δ has been added to Uehling's equations [22] in both cases.

For heavy particles, shell corrections were developed assuming that the projectile is equivalent to a perturbing potential whose center moves with constant velocity. This assumption has no sound theoretical basis for electrons. The authors of ICRU 37 [11] estimated the possible error in omitting it by assuming the correction was twice as great as for a proton of the same velocity. At $T = 10$ keV, the error was estimated to be ≈2% for water, ≈9% for Cu, and ≈21% for Au.

As shown in Fig. 33.11, stopping powers for e^-, e^+, and heavy particles are not dramatically different. In silicon, the minimum value for electrons is 1.50 MeV cm^2/g (at $\gamma = 3.3$); for positrons, 1.46 MeV cm^2/g (at $\gamma = 3.7$), and for muons, 1.66 MeV cm^2/g (at $\gamma = 3.58$).

33.4.2. *Radiation length* :

High-energy electrons predominantly lose energy in matter by bremsstrahlung, and high-energy photons by e^+e^- pair production. The characteristic amount of matter traversed for these related interactions is called the radiation length X_0, usually measured in g cm^{-2}. It is both (a) the mean distance over which a high-energy electron loses all but $1/e$ of its energy by bremsstrahlung, and (b) $\frac{7}{9}$ of the mean free path for pair production by a high-energy photon [41]. It is also the appropriate scale length for describing high-energy electromagnetic cascades. X_0 has been calculated and tabulated by Y.S. Tsai [42]:

$$\frac{1}{X_0} = 4\alpha r_e^2\frac{N_A}{A}\left\{Z^2\left[L_{\rm rad} - f(Z)\right] + Z\,L'_{\rm rad}\right\}\ . \tag{33.26}$$

For $A = 1$ g mol^{-1}, $4\alpha r_e^2 N_A/A = (716.408\ {\rm g\ cm^{-2}})^{-1}$. $L_{\rm rad}$ and $L'_{\rm rad}$ are given in Table 33.2. The function $f(Z)$ is an infinite sum, but for elements up to uranium can be represented to 4-place accuracy by

$$f(Z) = a^2\left[(1+a^2)^{-1} + 0.20206 - 0.0369\,a^2 + 0.0083\,a^4 - 0.002\,a^6\right]\ , \tag{33.27}$$

where $a = \alpha Z$ [43].

Table 33.2: Tsai's $L_{\rm rad}$ and $L'_{\rm rad}$, for use in calculating the radiation length in an element using Eq. (33.26).

Element	Z	$L_{\rm rad}$	$L'_{\rm rad}$
H	1	5.31	6.144
He	2	4.79	5.621
Li	3	4.74	5.805
Be	4	4.71	5.924
Others	> 4	$\ln(184.15\,Z^{-1/3})$	$\ln(1194\,Z^{-2/3})$

The radiation length in a mixture or compound may be approximated by

$$1/X_0 = \sum w_j/X_j\ , \tag{33.28}$$

where w_j and X_j are the fraction by weight and the radiation length for the jth element.

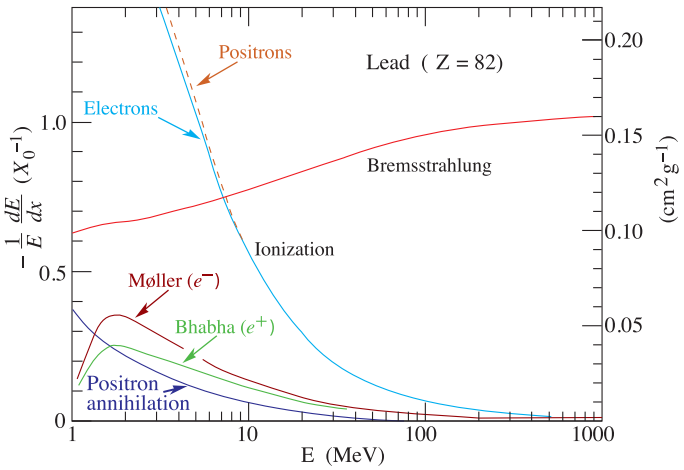

Figure 33.11: Fractional energy loss per radiation length in lead as a function of electron or positron energy. Electron (positron) scattering is considered as ionization when the energy loss per collision is below 0.255 MeV, and as Møller (Bhabha) scattering when it is above. Adapted from Fig. 3.2 from Messel and Crawford, *Electron-Photon Shower Distribution Function Tables for Lead, Copper, and Air Absorbers*, Pergamon Press, 1970. Messel and Crawford use $X_0(\mathrm{Pb}) = 5.82$ g/cm^2, but we have modified the figures to reflect the value given in the Table of Atomic and Nuclear Properties of Materials ($X_0(\mathrm{Pb}) = 6.37$ g/cm^2).

33.4.3. *Bremsstrahlung energy loss by $e^{\pm}$* :

At very high energies and except at the high-energy tip of the bremsstrahlung spectrum, the cross section can be approximated in the "complete screening case" as [42]

$$d\sigma/dk = (1/k)4\alpha r_e^2\{(\tfrac{4}{3} - \tfrac{4}{3}y + y^2)[Z^2(L_{\mathrm{rad}} - f(Z)) + Z\,L'_{\mathrm{rad}}] + \tfrac{1}{9}(1-y)(Z^2+Z)\}\ , \tag{33.29}$$

where $y = k/E$ is the fraction of the electron's energy transferred to the radiated photon. At small y (the "infrared limit") the term on the second line ranges from 1.7% (low Z) to 2.5% (high Z) of the total. If it is ignored and the first line simplified with the definition of X_0 given in Eq. (33.26), we have

$$\frac{d\sigma}{dk} = \frac{A}{X_0 N_A k}\left(\tfrac{4}{3} - \tfrac{4}{3}y + y^2\right)\ . \tag{33.30}$$

This cross section (times k) is shown by the top curve in Fig. 33.12.

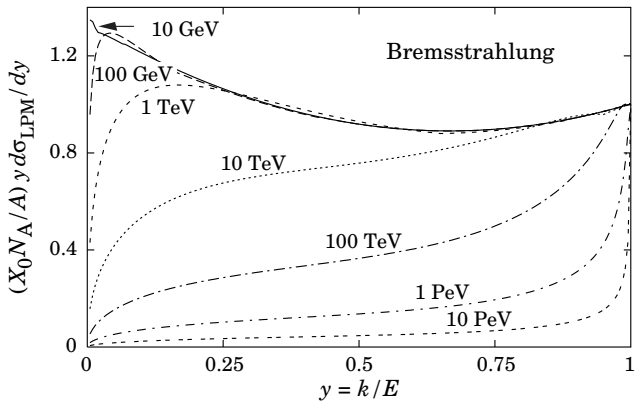

Figure 33.12: The normalized bremsstrahlung cross section $k\,d\sigma_{LPM}/dk$ in lead versus the fractional photon energy $y = k/E$. The vertical axis has units of photons per radiation length.

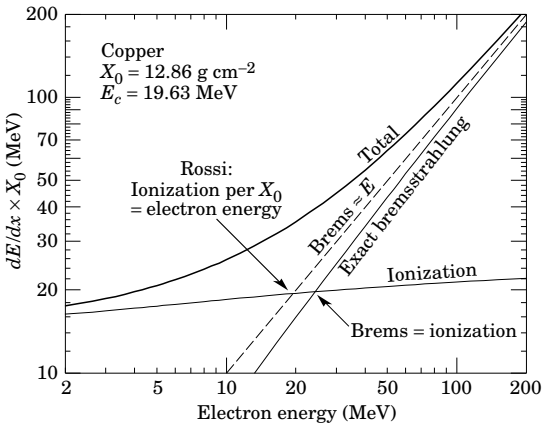

Figure 33.13: Two definitions of the critical energy E_c.

This formula is accurate except in near $y = 1$, where screening may become incomplete, and near $y = 0$, where the infrared divergence is removed by the interference of bremsstrahlung amplitudes from nearby scattering centers (the LPM effect) [44,45] and dielectric suppression [46,47]. These and other suppression effects in bulk media are discussed in Sec. 33.4.6.

With decreasing energy ($E \lesssim 10$ GeV) the high-y cross section drops and the curves become rounded as $y \to 1$. Curves of this familar shape can be seen in Rossi [2] (Figs. 2.11.2,3); see also the review by Koch & Motz [48].

Except at these extremes, and still in the complete-screening approximation, the number of photons with energies between $k_{\min}$ and $k_{\max}$ emitted by an electron travelling a distance $d \ll X_0$ is

$$N_\gamma = \frac{d}{X_0}\left[\frac{4}{3}\ln\left(\frac{k_{\max}}{k_{\min}}\right) - \frac{4(k_{\max} - k_{\min})}{3E} + \frac{k_{\max}^2 - k_{\min}^2}{2E^2}\right]\ . \tag{33.31}$$

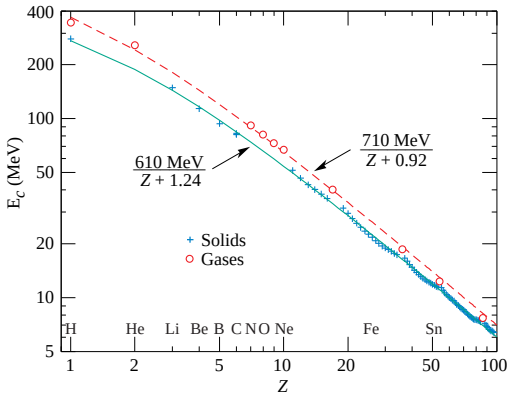

Figure 33.14: Electron critical energy for the chemical elements, using Rossi's definition [2]. The fits shown are for solids and liquids (solid line) and gases (dashed line). The rms deviation is 2.2% for the solids and 4.0% for the gases. (Computed with code supplied by A. Fassó.)

33.4.4. *Critical energy* :

An electron loses energy by bremsstrahlung at a rate nearly proportional to its energy, while the ionization loss rate varies only logarithmically with the electron energy. The *critical energy* E_c is sometimes defined as the energy at which the two loss rates are equal [49]. Among alternate definitions is that of Rossi [2], who defines the critical energy as the energy at which the ionization loss per radiation length is equal to the electron energy. Equivalently, it is the same as the first definition with the approximation $|dE/dx|_{\mathrm{brems}} \approx E/X_0$. This form has been found to describe transverse electromagnetic shower development more accurately (see below). These definitions are illustrated in the case of copper in Fig. 33.13.

The accuracy of approximate forms for E_c has been limited by the failure to distinguish between gases and solid or liquids, where there is a substantial difference in ionization at the relevant energy because of the density effect. We distinguish these two cases in Fig. 33.14. Fits were also made with functions of the form $a/(Z+b)^{\alpha}$, but α was found to be essentially unity. Since E_c also depends on A, I, and other factors, such forms are at best approximate.

Values of E_c for both electrons and positrons in more than 300 materials can be found at `pdg.lbl.gov/AtomicNuclearProperties`.

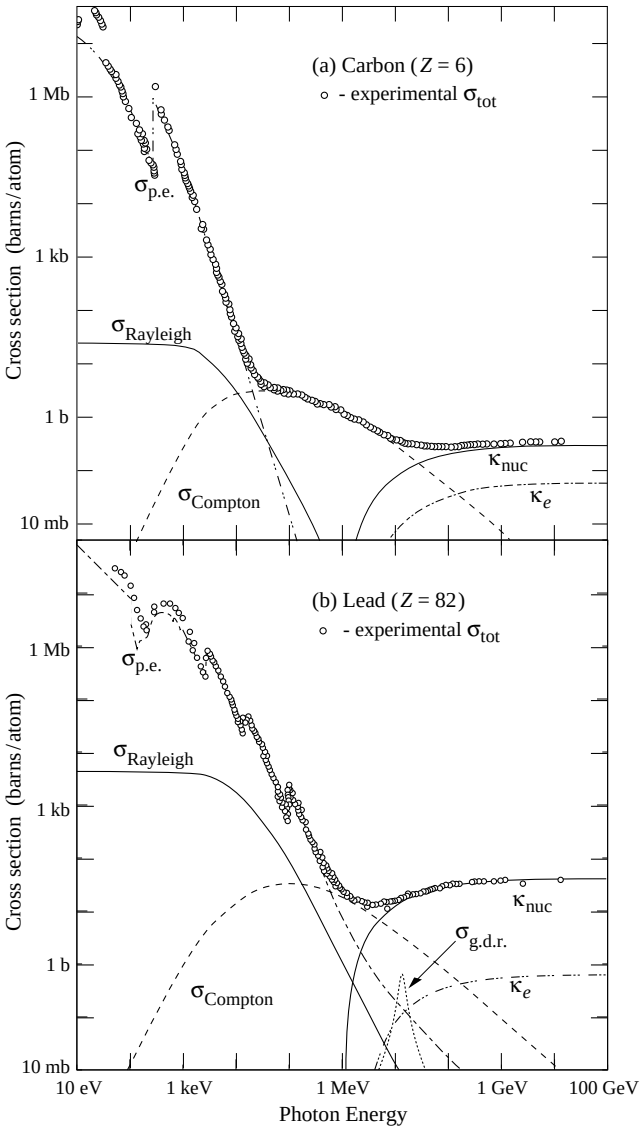

Figure 33.15: Photon total cross sections as a function of energy in carbon and lead, showing the contributions of different processes [50]:

$\sigma_{\rm p.e.}$ = Atomic photoelectric effect (electron ejection, photon absorption)
$\sigma_{\rm Rayleigh}$ = Rayleigh (coherent) scattering–atom neither ionized nor excited
$\sigma_{\rm Compton}$ = Incoherent scattering (Compton scattering off an electron)
$\kappa_{\rm nuc}$ = Pair production, nuclear field
κ_e = Pair production, electron field
$\sigma_{\rm g.d.r.}$ = Photonuclear interactions, most notably the Giant Dipole Resonance [51]. In these interactions, the target nucleus is broken up.

Original figures through the courtesy of John H. Hubbell (NIST).

33.4.5. ***Energy loss by photons*** :

Contributions to the photon cross section in a light element (carbon) and a heavy element (lead) are shown in Fig. 33.15. At low energies it is seen that the photoelectric effect dominates, although Compton scattering, Rayleigh scattering, and photonuclear absorption also contribute. The photoelectric cross section is characterized by discontinuities (absorption edges) as thresholds for photoionization of various atomic levels are reached. Photon attenuation lengths for a variety of elements are shown in Fig. 33.19, and data for 30 eV< k <100 GeV for all elements are available from the web pages given in the caption. Here k is the photon energy.

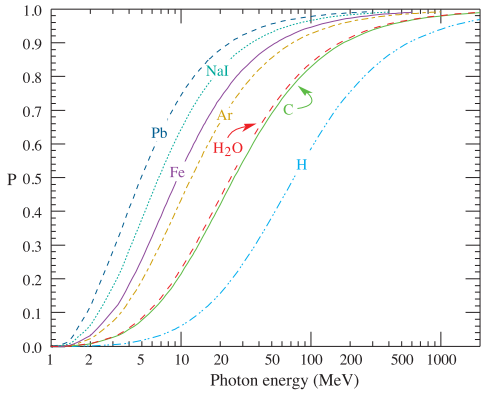

Figure 33.16: Probability P that a photon interaction will result in conversion to an e^+e^- pair. Except for a few-percent contribution from photonuclear absorption around 10 or 20 MeV, essentially all other interactions in this energy range result in Compton scattering off an atomic electron. For a photon attenuation length λ (Fig. 33.19), the probability that a given photon will produce an electron pair (without first Compton scattering) in thickness t of absorber is $P[1-\exp(-t/\lambda)]$.

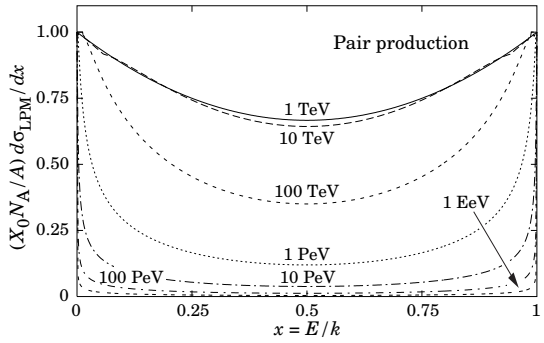

Figure 33.17: The normalized pair production cross section $d\sigma_{LPM}/dy$, versus fractional electron energy $x = E/k$.

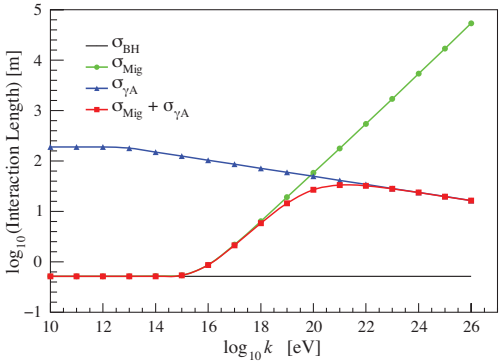

Figure 33.18: Interaction length for a photon in ice as a function of photon energy for the Bethe-Heitler (BH), LPM (Mig) and photonuclear (γA) cross sections [55]. The Bethe-Heitler interaction length is $9X_0/7$, and X_0 is 0.393 m in ice.

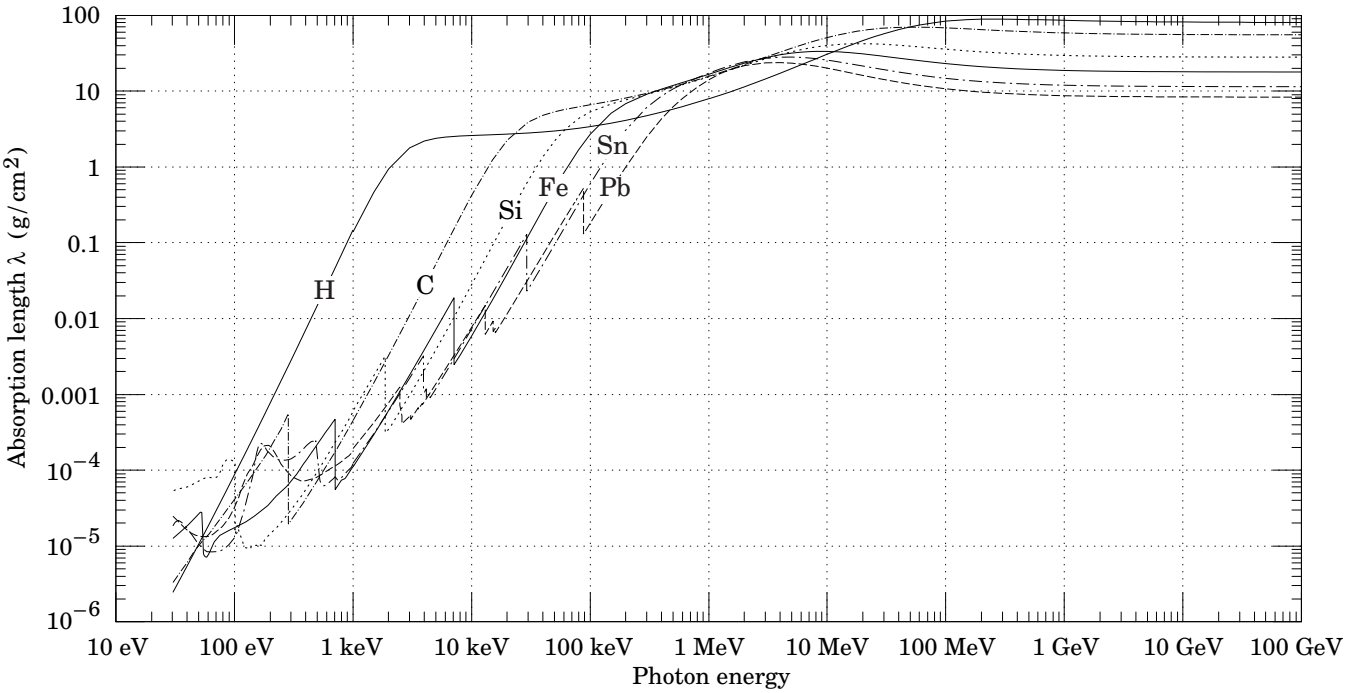

Figure 33.19: The photon mass attenuation length (or mean free path) $\lambda = 1/(\mu/\rho)$ for various elemental absorbers as a function of photon energy. The mass attenuation coefficient is μ/ρ, where ρ is the density. The intensity I remaining after traversal of thickness t (in mass/unit area) is given by $I = I_0\ \exp(-t/\lambda)$. The accuracy is a few percent. For a chemical compound or mixture, $1/\lambda_{\rm eff} \approx \sum_{\rm elements} w_Z/\lambda_Z$, where w_Z is the proportion by weight of the element with atomic number Z. The processes responsible for attenuation are given in Fig. 33.11. Since coherent processes are included, not all these processes result in energy deposition. The data for 30 eV $< E <$ 1 keV are obtained from `http://www-cxro.lbl.gov/optical_constants` (courtesy of Eric M. Gullikson, LBNL). The data for 1 keV $< E <$ 100 GeV are from `http://physics.nist.gov/PhysRefData`, through the courtesy of John H. Hubbell (NIST).

The increasing domination of pair production as the energy increases is shown in Fig. 33.16. Using approximations similar to those used to obtain Eq. (33.30), Tsai's formula for the differential cross section [42] reduces to

$$\frac{d\sigma}{dx} = \frac{A}{X_0 N_A}\left[1 - \tfrac{4}{3}x(1-x)\right] \tag{33.32}$$

in the complete-screening limit valid at high energies. Here $x = E/k$ is the fractional energy transfer to the pair-produced electron (or positron), and k is the incident photon energy. The cross section is very closely related to that for bremsstrahlung, since the Feynman diagrams are variants of one another. The cross section is of necessity symmetric between x and $1-x$, as can be seen by the solid curve in Fig. 33.17. See the review by Motz, Olsen, & Koch for a more detailed treatment [52].

Eq. (33.32) may be integrated to find the high-energy limit for the total e^+e^- pair-production cross section:

$$\sigma = \tfrac{7}{9}(A/X_0 N_A)\ . \tag{33.33}$$

Equation Eq. (33.33) is accurate to within a few percent down to energies as low as 1 GeV, particularly for high-Z materials.

33.4.6. *Bremsstrahlung and pair production at very high energies* :

At ultrahigh energies, Eqns. 33.29–33.33 will fail because of quantum mechanical interference between amplitudes from different scattering centers. Since the longitudinal momentum transfer to a given center is small ($\propto k/E(E-k)$, in the case of bremsstrahlung), the interaction is spread over a comparatively long distance called the formation length ($\propto E(E-k)/k$) via the uncertainty principle. In alternate language, the formation length is the distance over which the highly relativistic electron and the photon "split apart." The interference is usually destructive. Calculations of the "Landau-Pomeranchuk-Migdal" (LPM) effect may be made semi-classically based on the average multiple scattering, or more rigorously using a quantum transport approach [44,45].

In amorphous media, bremsstrahlung is suppressed if the photon energy k is less than $E^2/(E + E_{LPM})$ [45], where*

$$E_{LPM} = \frac{(m_e c^2)^2 \alpha X_0}{4\pi\hbar c\rho} = (7.7\ \text{TeV/cm}) \times \frac{X_0}{\rho}\ . \tag{33.34}$$

Since physical distances are involved, X_0/ρ, in cm, appears. The energy-weighted bremsstrahlung spectrum for lead, $k\,d\sigma_{LPM}/dk$, is shown in Fig. 33.12. With appropriate scaling by X_0/ρ, other materials behave similarly.

For photons, pair production is reduced for $E(k-E) > k\,E_{LPM}$. The pair-production cross sections for different photon energies are shown in Fig. 33.17.

If $k \ll E$, several additional mechanisms can also produce suppression. When the formation length is long, even weak factors can perturb the interaction. For example, the emitted photon can coherently forward scatter off of the electrons in the media. Because of this, for $k < \omega_p E/m_e \sim 10^{-4}$, bremsstrahlung is suppressed by a factor $(km_e/\omega_p E)^2$ [47]. Magnetic fields can also suppress bremsstrahlung.

In crystalline media, the situation is more complicated, with coherent enhancement or suppression possible. The cross section depends on the electron and photon energies and the angles between the particle direction and the crystalline axes [54].

33.4.7. *Photonuclear and electronuclear interactions at still higher energies* :

At still higher photon and electron energies, where the bremsstrahlung and pair production cross-sections are heavily suppressed by the LPM effect, photonuclear and electronuclear interactions predominate over electromagnetic interactions.

At photon energies above about 10^{20} eV, for example, photons usually interact hadronically. The exact cross-over energy depends on the model used for the photonuclear interactions. These processes are illustrated in Fig. 33.18. At still higher energies ($\gtrsim 10^{23}$ eV),

* This definition differs from that of Ref. 53 by a factor of two. E_{LPM} scales as the 4th power of the mass of the incident particle, so that $E_{LPM} = (1.4 \times 10^{10}\ \text{TeV/cm}) \times X_0/\rho$ for a muon.

photonuclear interactions can become coherent, with the photon interaction spread over multiple nuclei. Essentially, the photon coherently converts to a ρ^0, in a process that is somewhat similar to kaon regeneration [55].

Similar processes occur for electrons. As electron energies increase and the LPM effect suppresses bremsstrahlung, electronuclear interactions become more important. At energies above 10^{21}eV, these electronuclear interactions dominate electron energy loss [55].

33.5. Electromagnetic cascades

When a high-energy electron or photon is incident on a thick absorber, it initiates an electromagnetic cascade as pair production and bremsstrahlung generate more electrons and photons with lower energy. The longitudinal development is governed by the high-energy part of the cascade, and therefore scales as the radiation length in the material. Electron energies eventually fall below the critical energy, and then dissipate their energy by ionization and excitation rather than by the generation of more shower particles. In describing shower behavior, it is therefore convenient to introduce the scale variables

$$t = x/X_0 \ , \qquad y = E/E_c \ , \tag{33.35}$$

so that distance is measured in units of radiation length and energy in units of critical energy.

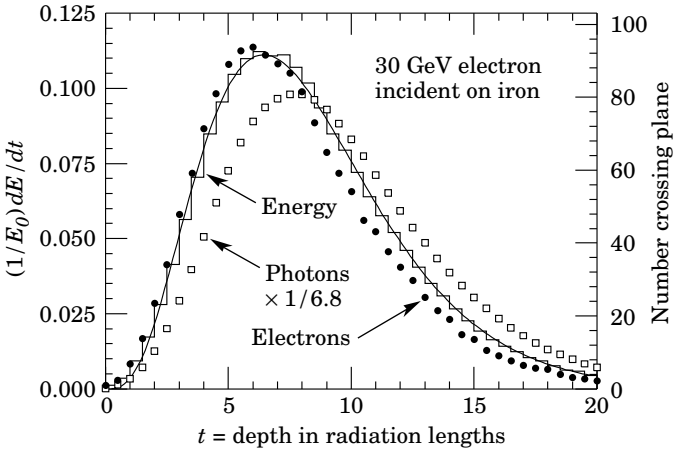

Figure 33.20: An EGS4 simulation of a 30 GeV electron-induced cascade in iron. The histogram shows fractional energy deposition per radiation length, and the curve is a gamma-function fit to the distribution. Circles indicate the number of electrons with total energy greater than 1.5 MeV crossing planes at $X_0/2$ intervals (scale on right) and the squares the number of photons with $E \geq 1.5$ MeV crossing the planes (scaled down to have same area as the electron distribution).

Longitudinal profiles from an EGS4 [56] simulation of a 30 GeV electron-induced cascade in iron are shown in Fig. 33.20. The number of particles crossing a plane (very close to Rossi's Π function [2]) is sensitive to the cutoff energy, here chosen as a total energy of 1.5 MeV for both electrons and photons. The electron number falls off more quickly than energy deposition. This is because, with increasing depth, a larger fraction of the cascade energy is carried by photons. Exactly what a calorimeter measures depends on the device, but it is not likely to be exactly any of the profiles shown. In gas counters it may be very close to the electron number, but in glass Cherenkov detectors and other devices with "thick" sensitive regions it is closer to the energy deposition (total track length). In such detectors the signal is proportional to the "detectable" track length T_d, which is in general less than the total track length T. Practical devices are sensitive to electrons with energy above some detection threshold E_d, and $T_d = T\,F(E_d/E_c)$. An analytic form for $F(E_d/E_c)$ obtained by Rossi [2] is given by Fabjan in Ref. 57; see also Amaldi [58].

The mean longitudinal profile of the energy deposition in an electromagnetic cascade is reasonably well described by a gamma distribution [59]:

$$\frac{dE}{dt} = E_0\, b\, \frac{(bt)^{a-1} e^{-bt}}{\Gamma(a)} \tag{33.36}$$

The maximum $t_{\rm max}$ occurs at $(a-1)/b$. We have made fits to shower profiles in elements ranging from carbon to uranium, at energies from 1 GeV to 100 GeV. The energy deposition profiles are well described by Eq. (33.36) with

$$t_{\rm max} = (a-1)/b = 1.0 \times (\ln y + C_j) \ , \qquad j = e, \gamma \ , \tag{33.37}$$

where $C_e = -0.5$ for electron-induced cascades and $C_\gamma = +0.5$ for photon-induced cascades. To use Eq. (33.36), one finds $(a-1)/b$ from Eq. (33.37) and Eq. (33.35), then finds a either by assuming $b \approx 0.5$ or by finding a more accurate value from Fig. 33.21. The results are very similar for the electron number profiles, but there is some dependence on the atomic number of the medium. A similar form for the electron number maximum was obtained by Rossi in the context of his "Approximation B," [2] (see Fabjan's review in Ref. 57), but with $C_e = -1.0$ and $C_\gamma = -0.5$; we regard this as superseded by the EGS4 result.

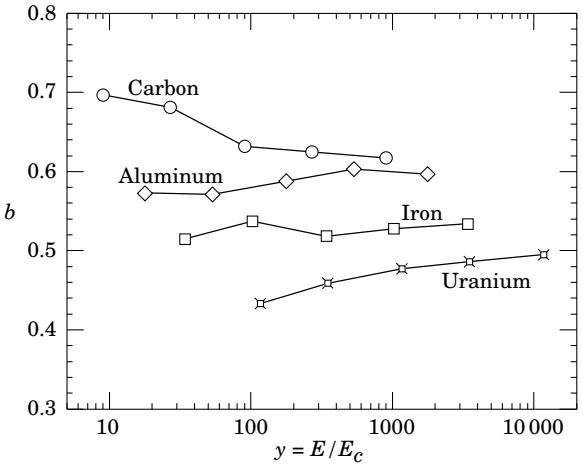

Figure 33.21: Fitted values of the scale factor b for energy deposition profiles obtained with EGS4 for a variety of elements for incident electrons with $1 \leq E_0 \leq 100$ GeV. Values obtained for incident photons are essentially the same.

The "shower length" $X_s = X_0/b$ is less conveniently parameterized, since b depends upon both Z and incident energy, as shown in Fig. 33.21. As a corollary of this Z dependence, the number of electrons crossing a plane near shower maximum is underestimated using Rossi's approximation for carbon and seriously overestimated for uranium. Essentially the same b values are obtained for incident electrons and photons. For many purposes it is sufficient to take $b \approx 0.5$.

The length of showers initiated by ultra-high energy photons and electrons is somewhat greater than at lower energies since the first or first few interaction lengths are increased via the mechanisms discussed above.

The gamma function distribution is very flat near the origin, while the EGS4 cascade (or a real cascade) increases more rapidly. As a result Eq. (33.36) fails badly for about the first two radiation lengths; it was necessary to exclude this region in making fits.

Because fluctuations are important, Eq. (33.36) should be used only in applications where average behavior is adequate. Grindhammer *et al.* have developed fast simulation algorithms in which the variance and correlation of a and b are obtained by fitting Eq. (33.36) to individually simulated cascades, then generating profiles for cascades using a and b chosen from the correlated distributions [60].

The transverse development of electromagnetic showers in different materials scales fairly accurately with the *Molière radius* R_M, given by [61,62]

$$R_M = X_0\, E_s/E_c \ , \tag{33.38}$$

where $E_s \approx 21$ MeV (Table 33.1), and the Rossi definition of E_c is used.

In a material containing a weight fraction w_j of the element with critical energy E_{cj} and radiation length X_j, the Molière radius is given by

$$\frac{1}{R_M} = \frac{1}{E_s} \sum \frac{w_j\, E_{cj}}{X_j} \ . \tag{33.39}$$

Measurements of the lateral distribution in electromagnetic cascades are shown in Refs. 61 and 62. On the average, only 10% of the energy lies outside the cylinder with radius R_M. About 99% is contained inside of $3.5R_M$, but at this radius and beyond composition effects become important and the scaling with R_M fails. The distributions are characterized by a narrow core, and broaden as the shower develops. They are often represented as the sum of two Gaussians, and Grindhammer [60] describes them with the function

$$f(r) = \frac{2r\, R^2}{(r^2 + R^2)^2} \ , \tag{33.40}$$

where R is a phenomenological function of x/X_0 and $\ln E$.

At high enough energies, the LPM effect (Sec. 33.4.6) reduces the cross sections for bremsstrahlung and pair production, and hence can cause significant elongation of electromagnetic cascades [45].

33.6. Muon energy loss at high energy

At sufficiently high energies, radiative processes become more important than ionization for all charged particles. For muons and pions in materials such as iron, this "critical energy" occurs at several hundred GeV. (There is no simple scaling with particle mass, but for protons the "critical energy" is much, much higher.) Radiative effects dominate the energy loss of energetic muons found in cosmic rays or produced at the newest accelerators. These processes are characterized by small cross sections, hard spectra, large energy fluctuations, and the associated generation of electromagnetic and (in the case of photonuclear interactions) hadronic showers [63–71]. As a consequence, at these energies the treatment of energy loss as a uniform and continuous process is for many purposes inadequate.

It is convenient to write the average rate of muon energy loss as [72]

$$-dE/dx = a(E) + b(E)\, E \ . \tag{33.41}$$

Here $a(E)$ is the ionization energy loss given by Eq. (33.5), and $b(E)$ is the sum of e^+e^- pair production, bremsstrahlung, and photonuclear contributions. To the approximation that these slowly-varying functions are constant, the mean range x_0 of a muon with initial energy E_0 is given by

$$x_0 \approx (1/b) \ln(1 + E_0/E_{\mu c}) \ , \tag{33.42}$$

where $E_{\mu c} = a/b$. Fig. 33.22 shows contributions to $b(E)$ for iron. Since $a(E) \approx 0.002$ GeV g^{-1} cm^2, $b(E)E$ dominates the energy loss above several hundred GeV, where $b(E)$ is nearly constant. The rates of energy loss for muons in hydrogen, uranium, and iron are shown in Fig. 33.23 [5].

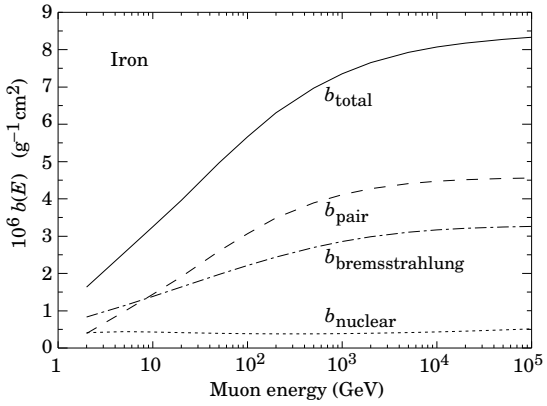

Figure 33.22: Contributions to the fractional energy loss by muons in iron due to e^+e^- pair production, bremsstrahlung, and photonuclear interactions, as obtained from Groom *et al.* [5] except for post-Born corrections to the cross section for direct pair production from atomic electrons.

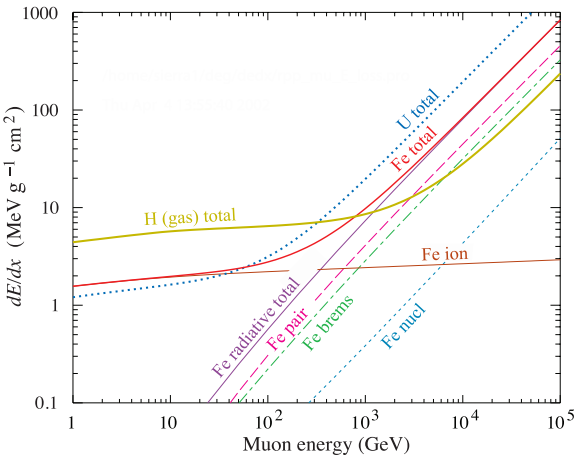

Figure 33.23: The average energy loss of a muon in hydrogen, iron, and uranium as a function of muon energy. Contributions to dE/dx in iron from ionization and the processes shown in Fig. 33.22 are also shown.

The "muon critical energy" $E_{\mu c}$ can be defined more exactly as the energy at which radiative and ionization losses are equal, and can be found by solving $E_{\mu c} = a(E_{\mu c})/b(E_{\mu c})$. This definition corresponds to the solid-line intersection in Fig. 33.13, and is different from the Rossi definition we used for electrons. It serves the same function: below $E_{\mu c}$ ionization losses dominate, and above $E_{\mu c}$ radiative effects dominate. The dependence of $E_{\mu c}$ on atomic number Z is shown in Fig. 33.24.

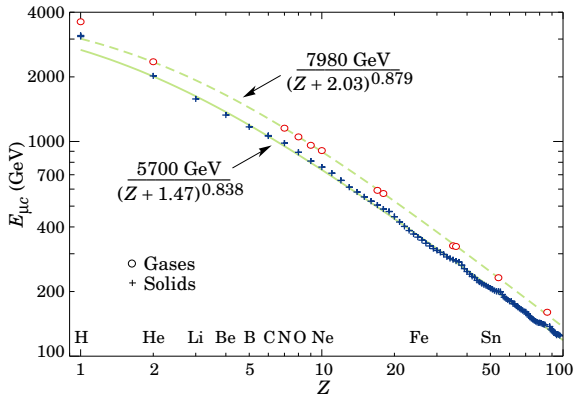

Figure 33.24: Muon critical energy for the chemical elements, defined as the energy at which radiative and ionization energy loss rates are equal [5]. The equality comes at a higher energy for gases than for solids or liquids with the same atomic number because of a smaller density effect reduction of the ionization losses. The fits shown in the figure exclude hydrogen. Alkali metals fall 3–4% above the fitted function, while most other solids are within 2% of the function. Among the gases the worst fit is for radon (2.7% high).

The radiative cross sections are expressed as functions of the fractional energy loss ν. The bremsstrahlung cross section goes roughly as $1/\nu$ over most of the range, while for the pair production case the distribution goes as ν^{-3} to ν^{-2} [73]. "Hard" losses are therefore more probable in bremsstrahlung, and in fact energy losses due to pair production may very nearly be treated as continuous. The simulated [71] momentum distribution of an incident 1 TeV/c muon beam after it crosses 3 m of iron is shown in Fig. 33.25. The most probable loss is 8 GeV, or 3.4 MeV g^{-1}cm^2. The full width at half maximum is 9 GeV/c, or 0.9%. The radiative tail is almost entirely due to bremsstrahlung, although most of the events in which more than 10% of the incident energy lost experienced relatively hard photonuclear interactions. The latter can exceed detector resolution [74], necessitating the reconstruction of lost energy. Tables

in Ref. 5 list the stopping power as 9.82 MeV $g^{-1}cm^2$ for a 1 TeV muon, so that the mean loss should be 23 GeV ($\approx$ 23 GeV/c), for a final momentum of 977 GeV/c, far below the peak. This agrees with the indicated mean calculated from the simulation. Electromagnetic and hadronic cascades in detector materials can obscure muon tracks in detector planes and reduce tracking efficiency [75].

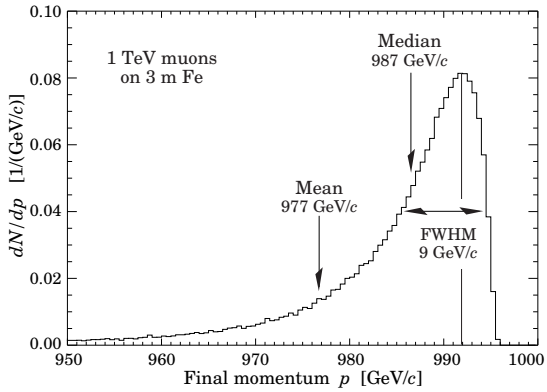

Figure 33.25: The momentum distribution of 1 TeV/c muons after traversing 3 m of iron as calculated with the MARS15 Monte Carlo code [71] by S.I. Striganov [5].

33.7. Cherenkov and transition radiation [33,76,77]

A charged particle radiates if its velocity is greater than the local phase velocity of light (Cherenkov radiation) or if it crosses suddenly from one medium to another with different optical properties (transition radiation). Neither process is important for energy loss, but both are used in high-energy and cosmic-ray physics detectors.

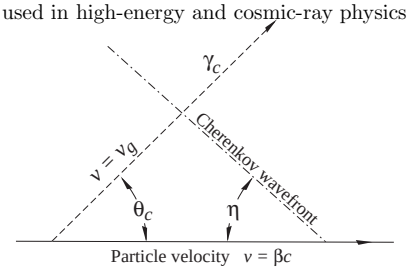

Figure 33.26: Cherenkov light emission and wavefront angles. In a dispersive medium, $\theta_c + \eta \neq 90^0$.

33.7.1. *Optical Cherenkov radiation* :

The angle θ_c of Cherenkov radiation, relative to the particle's direction, for a particle with velocity βc in a medium with index of refraction n is

$$\cos\theta_c = (1/n\beta)$$
$$\text{or} \quad \tan\theta_c = \sqrt{\beta^2 n^2 - 1} \approx \sqrt{2(1-1/n\beta)} \quad \text{for small } \theta_c, \textit{e.g.} \text{ in gases.} \tag{33.43}$$

The threshold velocity β_t is $1/n$, and $\gamma_t = 1/(1-\beta_t^2)^{1/2}$. Therefore, $\beta_t\gamma_t = 1/(2\delta+\delta^2)^{1/2}$, where $\delta = n-1$. Values of δ for various commonly used gases are given as a function of pressure and wavelength in Ref. 78. For values at atmospheric pressure, see Table 6.1. Data for other commonly used materials are given in Ref. 79.

Practical Cherenkov radiator materials are dispersive. Let ω be the photon's frequency, and let $k = 2\pi/\lambda$ be its wavenumber. The photons propage at the group velocity $v_g = d\omega/dk = c/[n(\omega) + \omega(dn/d\omega)]$. In a non-dispersive medium, this simplies to $v_g = c/n$.

In his classical paper, Tamm [80] showed that for dispersive media the radiation is concentrated in a thin conical shell whose vertex is at the moving charge, and whose opening half-angle η is given by

$$\cot\eta = \left[\frac{d}{d\omega}(\omega\tan\theta_c)\right]_{\omega_0} = \left[\tan\theta_c + \beta^2\omega\, n(\omega)\,\frac{dn}{d\omega}\cot\theta_c\right]_{\omega_0} , \tag{33.44}$$

where ω_0 is the central value of the small frequency range under consideration. (See Fig. 33.26.) This cone has a opening half-angle η, and, unless the medium is non-dispersive ($dn/d\omega = 0$), $\theta_c + \eta \neq 90^0$. The Cherenkov wavefront 'sideslips' along with the particle [81]. This effect has timing implications for ring imaging Cherenkov counters [82], but it is probably unimportant for most applications.

The number of photons produced per unit path length of a particle with charge ze and per unit energy interval of the photons is

$$\frac{d^2N}{dEdx} = \frac{\alpha z^2}{\hbar c}\sin^2\theta_c = \frac{\alpha^2 z^2}{r_e\, m_e c^2}\left(1 - \frac{1}{\beta^2 n^2(E)}\right) \approx 370\,\sin^2\theta_c(E)\ \text{eV}^{-1}\text{cm}^{-1} \qquad (z=1)\ , \tag{33.45}$$

or, equivalently,

$$\frac{d^2N}{dxd\lambda} = \frac{2\pi\alpha z^2}{\lambda^2}\ \left(1 - \frac{1}{\beta^2 n^2(\lambda)}\right)\ . \tag{33.46}$$

The index of refraction n is a function of photon energy $E = \hbar\omega$, as is the sensitivity of the transducer used to detect the light. For practical use, Eq. (33.45) must be multiplied by the the transducer response function and integrated over the region for which $\beta\, n(\omega) > 1$. Further details are given in the discussion of Cherenkov detectors in the Particle Detectors section (Sec. 34 of this *Review*).

When two particles are close together (lateral separation $\lesssim 1$ wavelength), the electromagnetic fields from the particles may add coherently, affecting the Cherenkov radiation. Because of their opposite charges, the radiation from an e^+e^- pair at close separation is suppressed compared to two independent leptons [83].

33.7.2. *Coherent radio Cherenkov radiation* :

Coherent Cherenkov radiation is produced by many charged particles with a non-zero net charge moving through matter on an approximately common "wavefront"—for example, the electrons and positrons in a high-energy electromagnetic cascade. The signals can be visible above backgrounds for shower energies as low as 10^{17} eV; see Sec. 35.3.3 for more details. The phenomenon is called the Askaryan effect [84]. Near the end of a shower, when typical particle energies are below E_c (but still relativistic), a charge imbalance develops. Photons can Compton-scatter atomic electrons, and positrons can annihilate with atomic electrons to contribute even more photons which can in turn Compton scatter. These processes result in a roughly 20% excess of electrons over positrons in a shower. The net negative charge leads to coherent radio Cherenkov emission. The radiation includes a component from the decelerating charges (as in bremsstrahlung). Because the emission is coherent, the electric field strength is proportional to the shower energy, and the signal power increases as its square. The electric field strength also increases linearly with frequency, up to a maximum frequency determined by the lateral spread of the shower. This cutoff occurs at about 1 GHz in ice, and scales inversely with the Moliere radius. At low frequencies, the radiation is roughly isotropic, but, as the frequency rises toward the cutoff frequency, the radiation becomes increasingly peaked around the Cherenkov angle. The radiation is linearly polarized in the plane containing the shower axis and the photon direction. A measurement of the signal polarization can be used to help determine the shower direction. The characteristics of this radiation have been nicely demonstrated in a series of experiments at SLAC [85]. A detailed discussion of the radiation can be found in Ref. 86.

33.7.3. *Transition radiation* :

The energy radiated when a particle with charge ze crosses the boundary between vacuum and a medium with plasma frequency ω_p is

$$I = \alpha z^2 \gamma \hbar\omega_p/3\ , \tag{33.47}$$

where

$$\hbar\omega_p = \sqrt{4\pi N_e r_e^3}\ m_e c^2/\alpha = \sqrt{\rho\ (\text{in g/cm}^3)\ \langle Z/A\rangle} \times 28.81\ \text{eV}\ . \tag{33.48}$$

For styrene and similar materials, $\hbar\omega_p \approx 20$ eV; for air it is 0.7 eV.

The number spectrum $dN_\gamma/d(\hbar\omega$ diverges logarithmically at low energies and decreases rapidly for $\hbar\omega/\gamma\hbar\omega_p > 1$. About half the energy is emitted in the range $0.1 \leq \hbar\omega/\gamma\hbar\omega_p \leq 1$. Inevitable absorption in a

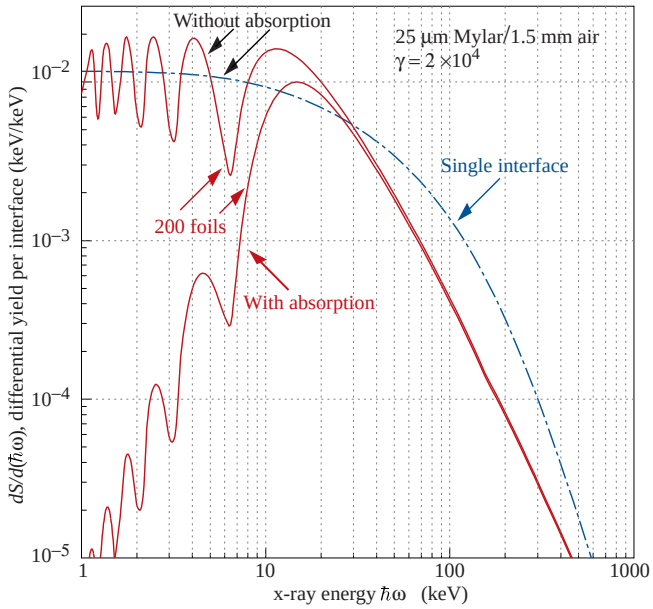

Figure 33.27: X-ray photon energy spectra for a radiator consisting of 200 25 μm thick foils of Mylar with 1.5 mm spacing in air (solid lines) and for a single surface (dashed line). Curves are shown with and without absorption. Adapted from Ref. 87.

practical detector removes the divergence. For a particle with $\gamma = 10^3$, the radiated photons are in the soft x-ray range 2 to 40 keV. The γ dependence of the emitted energy thus comes from the hardening of the spectrum rather than from an increased quantum yield.

The number of photons with energy $\hbar\omega > \hbar\omega_0$ is given by the answer to problem 13.15 in Ref. 33,

$$N_\gamma(\hbar\omega > \hbar\omega_0) = \frac{\alpha z^2}{\pi}\left[\left(\ln\frac{\gamma\hbar\omega_p}{\hbar\omega_0} - 1\right)^2 + \frac{\pi^2}{12}\right] , \qquad (33.49)$$

within corrections of order $(\hbar\omega_0/\gamma\hbar\omega_p)^2$. The number of photons above a fixed energy $\hbar\omega_0 \ll \gamma\hbar\omega_p$ thus grows as $(\ln\gamma)^2$, but the number above a fixed fraction of $\gamma\hbar\omega_p$ (as in the example above) is constant. For example, for $\hbar\omega > \gamma\hbar\omega_p/10$, $N_\gamma = 2.519\,\alpha z^2/\pi = 0.59\% \times z^2$.

The particle stays "in phase" with the x ray over a distance called the formation length, $d(\omega) = (2c/\omega)(1/\gamma^2 + \theta^2 + \omega_p^2/\omega^2)^{-1}$. Most of the radiation is produced in this distance. Here θ is the x-ray emission angle, characteristically $1/\gamma$. For $\theta = 1/\gamma$ the formation length has a maximum at $d(\gamma\omega_p/\sqrt{2}) = \gamma c/\sqrt{2}\,\omega_p$. In practical situations it is tens of μm.

Since the useful x-ray yield from a single interface is low, in practical detectors it is enhanced by using a stack of N foil radiators—foils L thick, where L is typically several formation lengths—separated by gas-filled gaps. The amplitudes at successive interfaces interfere to cause oscillations about the single-interface spectrum. At increasing frequencies above the position of the last interference maximum ($L/d(w) = \pi/2$), the formation zones, which have opposite phase, overlap more and more and the spectrum saturates, $dI/d\omega$ approaching zero as $L/d(\omega) \to 0$. This is illustrated in Fig. 33.27 for a realistic detector configuration.

For regular spacing of the layers fairly complicated analytic solutions for the intensity have been obtained [87,88]. Although one might expect the intensity of coherent radiation from the stack of foils to be proportional to N^2, the angular dependence of the formation length conspires to make the intensity $\propto N$.

References:

1. H. Bichsel, Nucl. Instrum. Methods **A562**, 154 (2006).
2. B. Rossi, *High Energy Particles*, Prentice-Hall, Inc., Englewood Cliffs, NJ, 1952.
3. H.A. Bethe, *Zur Theorie des Durchgangs schneller Korpuskularstrahlen durch Materie,* H. Bethe, Ann. Phys. **5**, 325 (1930).
4. "Stopping Powers and Ranges for Protons and Alpha Particles," ICRU Report No. 49 (1993); tables and graphs of these data are available at `physics.nist.gov/PhysRefData/`.
5. D.E. Groom, N.V. Mokhov, and S.I. Striganov, "Muon stopping-power and range tables: 10 MeV–100 TeV," Atomic Data and Nuclear Data Tables **78**, 183–356 (2001). Since submission of this paper it has become likely that post-Born corrections to the direct pair production cross section should be made. Code used to make Figs. 33.22–33.24 included these corrections [D.Yu. Ivanov *et al.*, Phys. Lett. **B442**, 453 (1998)]. The effect is negligible except at high Z. (It is less than 1% for iron.); More extensive printable and machine-readable tables are given at `pdg.lbl.gov/AtomicNuclearProperties/`.
6. W.H. Barkas, W. Birnbaum, and F.M. Smith, Phys. Rev. **101**, 778 (1956).
7. J. Lindhard and A. H. Sørensen, Phys. Rev. **A53**, 2443 (1996).
8. U. Fano, Ann. Rev. Nucl. Sci. **13**, 1 (1963).
9. J.D. Jackson, Phys. Rev. **D59**, 017301 (1999).
10. S.M. Seltzer and M.J. Berger, Int. J. of Applied Rad. **33**, 1189 (1982).
11. "Stopping Powers for Electrons and Positrons," ICRU Report No. 37 (1984).
12. `physics.nist.gov/PhysRefData/XrayMassCoef/tab1.html`.
13. H. Bichsel, Phys. Rev. **A46**, 5761 (1992).
14. W.H. Barkas and M.J. Berger, *Tables of Energy Losses and Ranges of Heavy Charged Particles*, NASA-SP-3013 (1964).
15. R.M. Sternheimer, Phys. Rev. **88**, 851 (1952).
16. R.M. Sternheimer, S.M. Seltzer, and M.J. Berger, "The Density Effect for the Ionization Loss of Charged Particles in Various Substances," Atomic Data and Nuclear Data Tables **30**, 261 (1984). Minor errors are corrected in Ref. 5. Chemical composition for the tabulated materials is given in Ref. 10.
17. R.M. Sternheimer and R.F. Peierls, Phys. Rev. **B3**, 3681 (1971).
18. S.P. Møller *et al.*, Phys. Rev. **A56**, 2930 (1997).
19. H.H. Andersen and J.F. Ziegler, *Hydrogen: Stopping Powers and Ranges in All Elements.* Vol. 3 of *The Stopping and Ranges of Ions in Matter* (Pergamon Press 1977).
20. J. Lindhard, Kgl. Danske Videnskab. Selskab, Mat.-Fys. Medd. **28**, No. 8 (1954); J. Lindhard, M. Scharff, and H.E. Schiøtt, Kgl. Danske Videnskab. Selskab, Mat.-Fys. Medd. **33**, No. 14 (1963).
21. J.F. Ziegler, J.F. Biersac, and U. Littmark, *The Stopping and Range of Ions in Solids*, Pergamon Press 1985.
22. E.A. Uehling, Ann. Rev. Nucl. Sci. **4**, 315 (1954) (For heavy particles with unit charge, but $e^\pm$ cross sections and stopping powers are also given).
23. N.F. Mott and H.S.W. Massey, *The Theory of Atomic Collisions*, Oxford Press, London, 1965.
24. L.D. Landau, J. Exp. Phys. (USSR) **8**, 201 (1944).
25. P.V. Vavilov, Sov. Phys. JETP **5**, 749 (1957).
26. H. Bichsel, Rev. Mod. Phys. **60**, 663 (1988).
27. R. Talman, Nucl. Instrum. Methods **159**, 189 (1979).
28. H. Bichsel, Ch. 87 in the Atomic, Molecular and Optical Physics Handbook, G.W.F. Drake, editor (Am. Inst. Phys. Press, Woodbury NY, 1996).
29. S.M. Seltzer and M.J. Berger, Int. J. of Applied Rad. **35**, 665 (1984). This paper corrects and extends the results of Ref. 10.
30. L.V. Spencer "Energy Dissipation by Fast Electrons," Nat'l Bureau of Standards Monograph No. 1 (1959).
31. "Average Energy Required to Produce an Ion Pair," ICRU Report No. 31 (1979).
32. N. Hadley *et al.*, "List of Poisoning Times for Materials," Lawrence Berkeley Lab Report TPC-LBL-79-8 (1981).
33. J.D. Jackson, *Classical Electrodynamics*, 3rd edition, (John Wiley and Sons, New York, 1998).
34. H.A. Bethe, Phys. Rev. **89**, 1256 (1953).
35. W.T. Scott, Rev. Mod. Phys. **35**, 231 (1963).
36. J.W. Motz, H. Olsen, and H.W. Koch, Rev. Mod. Phys. **36**, 881 (1964).
37. H. Bichsel, Phys. Rev. **112**, 182 (1958).
38. G. Shen *et al.*, Phys. Rev. **D20**, 1584 (1979).
39. G.R. Lynch and O.I Dahl, Nucl. Instrum. Methods **B58**, 6 (1991). Eq. (33.15) is Eq. 12 from this paper.
40. M. Wong *et al.*, Med. Phys. **17**, 163 (1990).

41. E. Segrè, *Nuclei and Particles*, New York, Benjamin (1964) p. 65 ff.
42. Y.S. Tsai, Rev. Mod. Phys. **46**, 815 (1974).
43. H. Davies, H.A. Bethe, and L.C. Maximon, Phys. Rev. **93**, 788 (1954).
44. L.D. Landau and I.J. Pomeranchuk, Dokl. Akad. Nauk. SSSR **92**, 535 (1953); **92**, 735 (1953). These papers are available in English in L. Landau, *The Collected Papers of L.D. Landau*, Pergamon Press, 1965; A.B. Migdal, Phys. Rev. **103**, 1811 (1956).
45. S. Klein, Rev. Mod. Phys. **71**, 1501 (1999).
46. M.L. Ter-Mikaelian, SSSR **94**, 1033 (1954);
M.L. Ter-Mikaelian, *High Energy Electromagnetic Processes in Condensed Media* (John Wiley and Sons, New York, 1972).
47. P. Anthony *et al.*, Phys. Rev. Lett. **76**, 3550 (1996).
48. H.W. Koch and J.W. Motz, Rev. Mod. Phys. **31**, 920 (1959).
49. M.J. Berger and S.M. Seltzer, "Tables of Energy Losses and Ranges of Electrons and Positrons," National Aeronautics and Space Administration Report NASA-SP-3012 (Washington DC 1964).
50. Data from J.H. Hubbell, H. Gimm, and I. Øverbø, J. Phys. Chem. Ref. Data **9**, 1023 (1980); parameters for $\sigma_{\text{g.d.r.}}$ from A. Veyssiere *et al.*, Nucl. Phys. **A159**, 561 (1970). Curves for these and other elements, compounds, and mixtures may be obtained from `physics.nist.gov/PhysRefData`. The photon total cross section is approximately flat for at least two decades beyond the energy range shown.
51. B.L. Berman and S.C. Fultz, Rev. Mod. Phys. **47**, 713 (1975).
52. J.W. Motz, H.A. Olsen, and H.W. Koch, Rev. Mod. Phys. **41**, 581 (1969).
53. P. Anthony *et al.*, Phys. Rev. Lett. **75**, 1949 (1995).
54. U.I. Uggerhoj, Rev. Mod. Phys. **77**, 1131 (2005).
55. L. Gerhardt and S.R. Klein, Phys. Rev. **D82**, 074017 (2010).
56. W.R. Nelson, H. Hirayama, and D.W.O. Rogers, "The EGS4 Code System," SLAC-265, Stanford Linear Accelerator Center (Dec. 1985).
57. *Experimental Techniques in High Energy Physics*, ed. T. Ferbel (Addison-Wesley, Menlo Park CA 1987).
58. U. Amaldi, Phys. Scripta **23**, 409 (1981).
59. E. Longo and I. Sestili, Nucl. Instrum. Methods **128**, 283 (1975).
60. G. Grindhammer *et al.*, in *Proceedings of the Workshop on Calorimetry for the Supercollider*, Tuscaloosa, AL, March 13–17, 1989, edited by R. Donaldson and M.G.D. Gilchriese (World Scientific, Teaneck, NJ, 1989), p. 151.
61. W.R. Nelson *et al.*, Phys. Rev. **149**, 201 (1966).
62. G. Bathow *et al.*, Nucl. Phys. **B20**, 592 (1970).
63. H.A. Bethe and W. Heitler, Proc. Royal Soc. London **A146**, 83 (1934);
H.A. Bethe, *Proc. Cambridge Phil. Soc.* **30**, 542 (1934).
64. A.A. Petrukhin and V.V. Shestakov, Can. J. Phys. **46**, S377 (1968).
65. V.M. Galitskii and S.R. Kel'ner, Sov. Phys. JETP **25**, 948 (1967).
66. S.R. Kel'ner and Yu.D. Kotov, Sov. J. Nucl. Phys. **7**, 237 (1968).
67. R.P. Kokoulin and A.A. Petrukhin, in *Proceedings of the International Conference on Cosmic Rays*, Hobart, Australia, August 16–25, 1971, Vol. **4**, p. 2436.
68. A.I. Nikishov, Sov. J. Nucl. Phys. **27**, 677 (1978).
69. Y.M. Andreev *et al.*, Phys. Atom. Nucl. **57**, 2066 (1994).
70. L.B. Bezrukov and E.V. Bugaev, Sov. J. Nucl. Phys. **33**, 635 (1981).
71. N.V. Mokhov, "The MARS Code System User's Guide," Fermilab-FN-628 (1995);
N.V. Mokhov *et al.*, Radiation Protection and Dosimetry, vol. 116, part 2, pp. 99 (2005);
Fermilab-Conf-04/053 (2004);
N.V. Mokhov *et al.*, in *Proc. of Intl. Conf. on Nuclear Data for Science and Tech*, (Santa Fe, NM, 2004), AIP C onf. Proc. 769, part 2, p. 1618;
Fermilab-Conf-04/269-AD (2004);
`www-ap.fnal.gov/MARS/`.
72. P.H. Barrett *et al.*, Rev. Mod. Phys. **24**, 133 (1952).
73. A. Van Ginneken, Nucl. Instrum. Methods **A251**, 21 (1986).
74. U. Becker *et al.*, Nucl. Instrum. Methods **A253**, 15 (1986).
75. J.J. Eastman and S.C. Loken, in *Proceedings of the Workshop on Experiments, Detectors, and Experimental Areas for the Supercollider*, Berkeley, CA, July 7–17, 1987, edited by R. Donaldson and M.G.D. Gilchriese (World Scientific, Singapore, 1988), p. 542.
76. *Methods of Experimental Physics*, L.C.L. Yuan and C.-S. Wu, editors, Academic Press, 1961, Vol. 5A, p. 163.
77. W.W.M. Allison and P.R.S. Wright, "The Physics of Charged Particle Identification: dE/dx, Cherenkov Radiation, and Transition Radiation," p. 371 in *Experimental Techniques in High Energy Physics*, T. Ferbel, editor, (Addison-Wesley 1987).
78. E.R. Hayes, R.A. Schluter, and A. Tamosaitis, "Index and Dispersion of Some Cherenkov Counter Gases," ANL-6916 (1964).
79. T. Ypsilantis, "Particle Identification at Hadron Colliders," CERN-EP/89-150 (1989), or ECFA 89-124, **2** 661 (1989).
80. I. Tamm, J. Phys. U.S.S.R., **1**, 439 (1939).
81. H. Motz and L.I. Schiff, Am. J. Phys. **21**, 258 (1953).
82. B.N. Ratcliff, Nucl. Instrum. Methods **A502**, 211 (2003).
83. S.K. Mandal, S.R. Klein, and J. D. Jackson, Phys. Rev. **D72**, 093003 (2005).
84. G.A. Askaryan, Sov. Phys. JETP **14**, 441 (1962).
85. P.W. Gorham *et al.*, Phys. Rev. **D72**, 023002 (2005).
86. E. Zas, F. Halzen, and T. Stanev, Phys. Rev. D 45,362(1992).
87. M.L. Cherry, Phys. Rev. **D10**, 3594 (1974);
M.L. Cherry, Phys. Rev. **D17**, 2245 (1978).
88. B. Dolgoshein, Nucl. Instrum. Methods **A326**, 434 (1993).

34. Particle Detectors at Accelerators

Revised 2017. See the various sections for authors.

34.1. Introduction

This review summarizes the detector technologies employed at accelerator particle physics experiments. Several of these detectors are also used in a non-accelerator context and examples of such applications will be provided. The detector techniques which are specific to non-accelerator particle physics experiments are the subject of Chap. 35. More detailed discussions of detectors and their underlying physics can be found in books by Ferbel [1], Kleinknecht [2], Knoll [3], Green [4], Leroy & Rancoita [5], and Grupen [6].

In Table 34.1 are given typical resolutions and deadtimes of common charged particle detectors. The quoted numbers are usually based on typical devices, and should be regarded only as rough approximations for new designs. The spatial resolution refers to the intrinsic detector resolution, i.e. without multiple scattering. We note that analog detector readout can provide better spatial resolution than digital readout by measuring the deposited charge in neighboring channels. Quoted ranges attempt to be representative of both possibilities. The time resolution is defined by how accurately the time at which a particle crossed the detector can be determined. The deadtime is the minimum separation in time between two resolved hits on the same channel. Typical performance of calorimetry and particle identification are provided in the relevant sections below.

Table 34.1: Typical resolutions and deadtimes of common charged particle detectors. Revised November 2011.

Detector Type	Intrinsinc Spatial Resolution (rms)	Time Resolution	Dead Time
Resistive plate chamber	$\lesssim$10 mm	1 ns (50 ps[a])	—
Streamer chamber	300 μm[b]	2 μs	100 ms
Liquid argon drift [7]	∼175–450 μm	∼ 200 ns	∼ 2 μs
Scintillation tracker	∼100 μm	100 ps/n[c]	10 ns
Bubble chamber	10–150 μm	1 ms	50 ms[d]
Proportional chamber	50–100 μm[e]	2 ns	20-200 ns
Drift chamber	50–100 μm	2 ns[f]	20-100 ns
Micro-pattern gas detectors	30–40 μm	< 10 ns	10-100 ns
Silicon strip	pitch/(3 to 7)[g]	few ns[h]	$\lesssim$50 ns[h]
Silicon pixel	$\lesssim$10 μm	few ns[h]	$\lesssim$50 ns[h]
Emulsion	1 μm	—	—

[a] For multiple-gap RPCs.
[b] 300 μm is for 1 mm pitch (wirespacing/$\sqrt{12}$).
[c] n = index of refraction.
[d] Multiple pulsing time.
[e] Delay line cathode readout can give ±150 μm parallel to anode wire.
[f] For two chambers.
[g] The highest resolution ("7") is obtained for small-pitch detectors ($\lesssim$25 μm) with pulse-height-weighted center finding.
[h] Limited by the readout electronics [8].

34.2. Photon detectors

Updated August 2011 by D. Chakraborty (Northern Illinois U) and T. Sumiyoshi (Tokyo Metro U).

Most detectors in high-energy, nuclear, and astrophysics rely on the detection of photons in or near the visible range, 100 nm $\lesssim\lambda\lesssim$ 1000 nm, or $E\approx$ a few eV. This range covers scintillation and Cherenkov radiation as well as the light detected in many astronomical observations.

Generally, photodetection involves generating a detectable electrical signal proportional to the (usually very small) number of incident photons. The process involves three distinct steps:

1. generation of a primary photoelectron or electron-hole (e-h) pair by an incident photon by the photoelectric or photoconductive effect,
2. amplification of the p.e. signal to detectable levels by one or more multiplicative bombardment steps and/or an avalanche process (usually), and,
3. collection of the secondary electrons to form the electrical signal.

The important characteristics of a photodetector include the following in statistical averages:

1. quantum efficiency (QE or ϵ_Q): the number of primary photoelectrons generated per incident photon ($0 \leq \epsilon_Q \leq 1$; in silicon more than one e-h pair per incident photon can be generated for $\lambda \lesssim 165$ nm),
2. collection efficiency (CE or ϵ_C): the overall acceptance factor other than the generation of photoelectrons ($0 \leq \epsilon_C \leq 1$),
3. gain (G): the number of electrons collected for each photoelectron generated,
4. dark current or dark noise: the electrical signal when there is no photon,
5. energy resolution: electronic noise (ENC or N_e) and statistical fluctuations in the amplification process compound the Poisson distribution of n_γ photons from a given source:

$$\frac{\sigma(E)}{\langle E \rangle} = \sqrt{\frac{f_N}{n_\gamma \epsilon_Q \epsilon_C} + \left(\frac{N_e}{G n_\gamma \epsilon_Q \epsilon_C}\right)^2}, \qquad (34.1)$$

where f_N, or the excess noise factor (ENF), is the contribution to the energy distribution variance due to amplification statistics [9],

6. dynamic range: the maximum signal available from the detector (this is usually expressed in units of the response to noise-equivalent power, or NEP, which is the optical input power that produces a signal-to-noise ratio of 1),
7. time dependence of the response: this includes the transit time, which is the time between the arrival of the photon and the electrical pulse, and the transit time spread, which contributes to the pulse rise time and width, and
8. rate capability: inversely proportional to the time needed, after the arrival of one photon, to get ready to receive the next.

area to be covered and the efficiency required, the volume available to accommodate the detectors, characteristics of the environment such as chemical composition, temperature, magnetic field, ambient background, as well as ambient radiation of different types and, mode of operation (continuous or triggered), bias (high-voltage) requirements, power consumption, calibration needs, aging, cost, and so on. Several technologies employing different phenomena for the three steps described above, and many variants within each, offer a wide range of solutions to choose from. The salient features of the main technologies and the common variants are described below. Some key characteristics are summarized in Table 34.2.

34.2.1. ***Vacuum photodetectors*** : Vacuum photodetectors can be broadly subdivided into three types: photomultiplier tubes, microchannel plates, and hybrid photodetectors.

34.2.1.1. *Photomultiplier tubes:* A versatile class of photon detectors, vacuum photomultiplier tubes (PMT) has been employed by a vast majority of all particle physics experiments to date [9]. Both "transmission-" and "reflection-type" PMT's are widely used. In the former, the photocathode material is deposited on the inside of a transparent window through which the photons enter, while in the latter, the photocathode material rests on a separate surface that the incident photons strike. The cathode material has a low work function, chosen for the wavelength band of interest. When a photon hits the cathode and liberates an electron (the photoelectric effect), the latter is accelerated and guided by electric fields to impinge on a secondary-emission electrode, or dynode, which then emits a few (~ 5) secondary electrons. The multiplication process is repeated typically 10 times in series to generate a sufficient number of electrons, which are collected at the anode for delivery to the external circuit. The total gain of a PMT depends on the applied high voltage V as $G = AV^{kn}$, where $k \approx 0.7$–0.8 (depending on the dynode material), n is the number of dynodes in the chain, and A a constant (which also depends on n). Typically, G is in the range of 10^5–10^6. Pulse risetimes are usually in the few nanosecond range. With *e.g.* two-level discrimination the effective time resolution can be much better.

A large variety of PMT's, including many just recently developed, covers a wide span of wavelength ranges from infrared (IR) to extreme

Table 34.2: Representative characteristics of some photodetectors commonly used in particle physics. The time resolution of the devices listed here vary in the 10–2000 ps range.

Type	λ (nm)	$\epsilon_Q\,\epsilon_C$	Gain	Risetime (ns)	Area (mm^2)	1-p.e noise (Hz)	HV (V)	Price (USD)
PMT*	115–1700	0.15–0.25	10^3–10^7	0.7–10	10^2–10^5	10–10^4	500–3000	100–5000
MCP*	100–650	0.01–0.10	10^3–10^7	0.15–0.3	10^2–10^4	0.1–200	500–3500	10–6000
HPD*	115–850	0.1–0.3	10^3–10^4	7	10^2–10^5	10–10^3	$\sim 2 \times 10^4$	$\sim$600
GPM*	115–500	0.15–0.3	10^3–10^6	$O(0.1)$	$O(10)$	10–10^3	300–2000	$O(10)$
APD	300–1700	$\sim$0.7	10–10^8	$O(1)$	10–10^3	1–10^3	400–1400	$O(100)$
PPD	320–900	0.15–0.3	10^5–10^6	~ 1	1–10	$O(10^6)$	30–60	$O(100)$
VLPC	500–600	$\sim$0.9	$\sim 5 \times 10^4$	~ 10	1	$O(10^4)$	$\sim$7	$\sim$1

∗These devices often come in multi-anode configurations. In such cases, area, noise, and price are to be considered on a "per readout-channel" basis.

The QE is a strong function of the photon wavelength (λ), and is usually quoted at maximum, together with a range of λ where the QE is comparable to its maximum. Spatial uniformity and linearity with respect to the number of photons are highly desirable in a photodetector's response.

Optimization of these factors involves many trade-offs and vary widely between applications. For example, while a large gain is desirable, attempts to increase the gain for a given device also increases the ENF and after-pulsing ("echos" of the main pulse). In solid-state devices, a higher QE often requires a compromise in the timing properties. In other types, coverage of large areas by focusing increases the transit time spread.

Other important considerations also are highly application-specific. These include the photon flux and wavelength range, the total

ultraviolet (XUV) [10]. They are categorized by the window materials, photocathode materials, dynode structures, anode configurations, *etc.* Common window materials are borosilicate glass for IR to near-UV, fused quartz and sapphire (Al_2O_3) for UV, and MgF_2 or LiF for XUV. The choice of photocathode materials include a variety of mostly Cs- and/or Sb-based compounds such as CsI, CsTe, bi-alkali (SbRbCs, SbKCs), multi-alkali ($SbNa_2KCs$), GaAs(Cs), GaAsP, *etc.* Sensitive wavelengths and peak quantum efficiencies for these materials are summarized in Table 34.3. Typical dynode structures used in PMT's are circular cage, line focusing, box and grid, venetian blind, and fine mesh. In some cases, limited spatial resolution can be obtained by using a mosaic of multiple anodes. Fast PMT's with very large windows—measuring up to 508 mm across—have been developed in recent years for detection of Cherenkov radiation in neutrino

experiments such as Super-Kamiokande and KamLAND among many others. Specially prepared low-radioactivity glass is used to make these PMT's, and they are also able to withstand the high pressure of the surrounding liquid.

PMT's are vulnerable to magnetic fields—sometimes even the geomagnetic field causes large orientation-dependent gain changes. A high-permeability metal shield is often necessary. However, proximity-focused PMT's, *e.g.* the fine-mesh types, can be used even in a high magnetic field (≥ 1 T) if the electron drift direction is parallel to the field. CMS uses custom-made vacuum phototriodes (VPT) mounted on the back face of projective lead tungstate crystals to detect scintillation light in the endcap sections of its electromagnetic calorimeters, which are inside a 3.8 T superconducting solenoid. A VPT employs a single dynode (thus, $G \approx 10$) placed close to the photocathode, and a mesh anode plane between the two, to help it cope with the strong magnetic field, which is not too unfavorably oriented with respect to the photodetector axis in the endcaps (within 25°), but where the radiation level is too high for Avalanche Photodiodes (APD's) like those used in the barrel section.

34.2.1.2. *Microchannel plates:* A typical Microchannel plate (MCP) photodetector consists of one or more ∼2 mm thick glass plates with densely packed $O(10\ \mu\text{m})$-diameter cylindrical holes, or "channels", sitting between the transmission-type photocathode and anode planes, separated by $O(1$ mm) gaps. Instead of discrete dynodes, the inner surface of each cylindrical tube serves as a continuous dynode for the entire cascade of multiplicative bombardments initiated by a photoelectron. Gain fluctuations can be minimized by operating in a saturation mode, whence each channel is only capable of a binary output, but the sum of all channel outputs remains proportional to the number of photons received so long as the photon flux is low enough to ensure that the probability of a single channel receiving more than one photon during a single time gate is negligible. MCP's are thin, offer good spatial resolution, have excellent time resolution (∼20 ps), and can tolerate random magnetic fields up to 0.1 T and axial fields up to ∼ 1 T. However, they suffer from relatively long recovery time per channel and short lifetime. MCP's are widely employed as image-intensifiers, although not so much in HEP or astrophysics.

34.2.1.3. *Hybrid photon detectors:* Hybrid photon detectors (HPD) combine the sensitivity of a vacuum PMT with the excellent spatial and energy resolutions of a Si sensor [11]. A single photoelectron ejected from the photocathode is accelerated through a potential difference of ∼20 kV before it impinges on the silicon sensor/anode. The gain nearly equals the maximum number of e-h pairs that could be created from the entire kinetic energy of the accelerated electron: $G \approx \text{eV}/w$, where e is the electronic charge, V is the applied potential difference, and $w \approx 3.7$ eV is the mean energy required to create an e-h pair in Si at room temperature. Since the gain is achieved in a single step, one might expect to have the excellent resolution of a simple Poisson statistic with large mean, but in fact it is even better, thanks to the Fano effect discussed in Sec. 34.7.

Low-noise electronics must be used to read out HPD's if one intends to take advantage of the low fluctuations in gain, *e.g.* when counting small numbers of photons. HPD's can have the same $\epsilon_Q\,\epsilon_C$ and window geometries as PMT's and can be segmented down to ∼50 μm. However, they require rather high biases and will not function in a magnetic field. The exception is proximity-focused devices (⇒ no (de)magnification) in an axial field. With time resolutions of ∼10 ps and superior rate capability, proximity-focused HPD's can be an alternative to MCP's. Current applications of HPD's include the CMS hadronic calorimeter and the RICH detector in LHCb. Large-size HPD's with sophisticated focusing may be suitable for future water Cherenkov experiments.

Hybrid APD's (HAPD's) add an avalanche multiplication step following the electron bombardment to boost the gain by a factor of ∼50. This affords a higher gain and/or lower electrical bias, but also degrades the signal definition.

34.2.2. ***Gaseous photon detectors*** : In gaseous photomultipliers (GPM) a photoelectron in a suitable gas mixture initiates an avalanche in a high-field region, producing a large number of secondary impact-ionization electrons. In principle the charge multiplication and collection processes are identical to those employed in gaseous tracking detectors such as multiwire proportional chambers, micromesh gaseous detectors (Micromegas), or gas electron multipliers (GEM). These are discussed in Sec. 34.6.4.

Table 34.3: Properties of photocathode and window materials commonly used in vacuum photodetectors [10].

Photocathode material	λ (nm)	Window material	Peak ϵ_Q (λ/nm)
CsI	115–200	MgF_2	0.11 (140)
CsTe	115–320	MgF_2	0.14 (240)
Bi-alkali	300–650	Borosilicate	0.27 (390)
	160-650	Synthetic Silica	0.27 (390)
"Ultra Bi-alkali"	300–650	Borosilicate	0.43 (350)
	160-650	Synthetic Silica	0.43 (350)
Multi-alkali	300–850	Borosilicate	0.20 (360)
	160-850	Synthetic Silica	0.20 (360)
GaAs(Cs)*	160–930	Synthetic Silica	0.23 (280)
GaAsP(Cs)	300-750	Borosilicate	0.50 (500)
InP/InGaAsP†	350-1700	Borosilicate	0.01 (1100)

*Reflection type photocathode is used. †Requires cooling to ~ -80°C.

The devices can be divided into two types depending on the photocathode material. One type uses solid photocathode materials much in the same way as PMT's. Since it is resistant to gas mixtures typically used in tracking chambers, CsI is a common choice. In the other type, photoionization occurs on suitable molecules vaporized and mixed in the drift volume. Most gases have photoionization work functions in excess of 10 eV, which would limit their sensitivity to wavelengths far too short. However, vapors of TMAE (tetrakis dimethyl-amine ethylene) or TEA (tri-ethyl-amine), which have smaller work functions (5.3 eV for TMAE and 7.5 eV for TEA), are suited for XUV photon detection [12]. Since devices like GEM's offer sub-mm spatial resolution, GPM's are often used as position-sensitive photon detectors. They can be made into flat panels to cover large areas ($O(1\ \text{m}^2)$), can operate in high magnetic fields, and are relatively inexpensive. Many of the ring imaging Cherenkov (RICH) detectors to date have used GPM's for the detection of Cherenkov light [13]. Special care must be taken to suppress the photon-feedback process in GPM's. It is also important to maintain high purity of the gas as minute traces of O_2 can significantly degrade the detection efficiency.

34.2.3. ***Solid-state photon detectors*** : In a phase of rapid development, solid-state photodetectors are competing with vacuum- or gas-based devices for many existing applications and making way for a multitude of new ones. Compared to traditional vacuum- and gaseous photodetectors, solid-state devices are more compact, lightweight, rugged, tolerant to magnetic fields, and often cheaper. They also allow fine pixelization, are easy to integrate into large systems, and can operate at low electric potentials, while matching or exceeding most performance criteria. They are particularly well suited for detection of γ- and X-rays. Except for applications where coverage of very large areas or dynamic range is required, solid-state detectors are proving to be the better choice. Some hybrid devices attempt to combine the best features of different technologies while applications of nanotechnology are opening up exciting new possibilities.

Silicon photodiodes (PD) are widely used in high-energy physics as particle detectors and in a great number of applications (including solar cells!) as light detectors. The structure is discussed in some detail in Sec. 34.7. In its simplest form, the PD is a reverse-biased p-n junction. Photons with energies above the indirect bandgap energy (wavelengths shorter than about 1050 nm, depending on the temperature) can create e-h pairs (the photoconductive effect), which are collected on the p and n sides, respectively. Often, as in the PD's used for crystal scintillator readout in CLEO, L3, Belle, BaBar, and GLAST, intrinsic silicon is doped to create a p-i-n structure. The reverse bias increases the thickness of the depleted region; in the case

of these particular detectors, to full depletion at a depth of about 100 μm. Increasing the depletion depth decreases the capacitance (and hence electronic noise) and extends the red response. Quantum efficiency can exceed 90%, but falls toward the red because of the increasing absorption length of light in silicon. The absorption length reaches 100 μm at 985 nm. However, since $G = 1$, amplification is necessary. Optimal low-noise amplifiers are slow, but, even so, noise limits the minimum detectable signal in room-temperature devices to several hundred photons.

Very large arrays containing $O(10^7)$ of $O(10\ \mu\text{m}^2)$-sized photodiodes pixelizing a plane are widely used to photograph all sorts of things from everyday subjects at visible wavelengths to crystal structures with X-rays and astronomical objects from infrared to UV. To limit the number of readout channels, these are made into charge-coupled devices (CCD), where pixel-to-pixel signal transfer takes place over thousands of synchronous cycles with sequential output through shift registers [14]. Thus, high spatial resolution is achieved at the expense of speed and timing precision. Custom-made CCD's have virtually replaced photographic plates and other imagers for astronomy and in spacecraft. Typical QE's exceed 90% over much of the visible spectrum, and "thick" CCD's have useful QE up to $\lambda = 1\ \mu$m. Active Pixel Sensor (APS) arrays with a preamplifier on each pixel and CMOS processing afford higher speeds, but are challenged at longer wavelengths. Much R&D is underway to overcome the limitations of both CCD and CMOS imagers.

In APD's, an exponential cascade of impact ionizations initiated by the original photogenerated e-h pair under a large reverse-bias voltage leads to an avalanche breakdown [15]. As a result, detectable electrical response can be obtained from low-intensity optical signals down to single photons. Excellent junction uniformity is critical, and a guard ring is generally used as a protection against edge breakdown. Well-designed APD's, such as those used in CMS' crystal-based electromagnetic calorimeter, have achieved $\epsilon_Q\,\epsilon_C \approx 0.7$ with sub-ns response time. The sensitive wavelength window and gain depend on the semiconductor used. The gain is typically 10–200 in linear and up to 10^8 in Geiger mode of operation. Stability and close monitoring of the operating temperature are important for linear-mode operation, and substantial cooling is often necessary. Position-sensitive APD's use time information at multiple anodes to calculate the hit position.

One of the most promising recent developments in the field is that of devices consisting of large arrays ($O(10^3)$) of tiny APD's packed over a small area ($O(1\ \text{mm}^2)$) and operated in a limited Geiger mode [16]. Among different names used for this class of photodetectors, "PPD" (for "Pixelized Photon Detector") is most widely accepted (formerly "SiPM"). Although each cell only offers a binary output, linearity with respect to the number of photons is achieved by summing the cell outputs in the same way as with a MCP in saturation mode (see above). PPD's are being adopted as the preferred solution for various purposes including medical imaging, *e.g.* positron emission tomography (PET). These compact, rugged, and economical devices allow auto-calibration through decent separation of photoelectron peaks and offer gains of $O(10^6)$ at a moderate bias voltage (∼50 V). However, the single-photoelectron noise of a PPD, being the logical "or" of $O(10^3)$ Geiger APD's, is rather large: $O(1\ \text{MHz/mm}^2)$ at room temperature. PPD's are particularly well-suited for applications where triggered pulses of several photons are expected over a small area, *e.g.* fiber-guided scintillation light. Intense R&D is expected to lower the noise level and improve radiation hardness, resulting in coverage of larger areas and wider applications. Attempts are being made to combine the fabrication of the sensors and the front-end electronics (ASIC) in the same process with the goal of making PPD's and other finely pixelized solid-state photodetectors extremely easy to use.

Of late, much R&D has been directed to p-i-n diode arrays based on thin polycrystalline diamond films formed by chemical vapor deposition (CVD) on a hot substrate (∼1000 K) from a hydrocarbon-containing gas mixture under low pressure (∼100 mbar). These devices have maximum sensitivity in the extreme- to moderate-UV region [17]. Many desirable characteristics, including high tolerance to radiation and temperature fluctuations, low dark noise, blindness to most of the solar radiation spectrum, and relatively low cost make them ideal for space-based UV/XUV astronomy, measurement of synchrotron radiation, and luminosity monitoring at (future) lepton collider(s).

Visible-light photon counters (VLPC) utilize the formation of an impurity band only 50 meV below the conduction band in As-doped Si to generate strong ($G \approx 5 \times 10^4$) yet sharp response to single photons with $\epsilon_Q \approx 0.9$ [18]. The smallness of the band gap considerably reduces the gain dispersion. Only a very small bias (∼7 V) is needed, but high sensitivity to infrared photons requires cooling below 10 K. The dark noise increases sharply and exponentially with both temperature and bias. The Run 2 DØ detector used 86000 VLPC's to read the optical signal from its scintillating-fiber tracker and scintillator-strip preshower detectors.

34.3. Organic scintillators

Revised August 2017 by Kurtis F. Johnson (FSU).

Organic scintillators are broadly classed into three types, crystalline, liquid, and plastic, all of which utilize the ionization produced by charged particles (see Sec. 33.2 of this *Review*) to generate optical photons, usually in the blue to green wavelength regions [19]. Plastic scintillators are by far the most widely used, liquid organic scintillator is finding increased use, and crystal organic scintillators are practically unused in high-energy physics. Plastic scintillator densities range from 1.03 to 1.20 g cm^{-3}. Typical photon yields are about 1 photon per 100 eV of energy deposit [20]. A one-cm-thick scintillator traversed by a minimum-ionizing particle will therefore yield $\approx 2 \times 10^4$ photons. The resulting photoelectron signal will depend on the collection and transport efficiency of the optical package and the quantum efficiency of the photodetector.

Organic scintillator does not respond linearly to the ionization density. Very dense ionization columns emit less light than expected on the basis of dE/dx for minimum-ionizing particles. A widely used semi-empirical model by Birks posits that recombination and quenching effects between the excited molecules reduce the light yield [21]. These effects are more pronounced the greater the density of the excited molecules. Birks' formula is

$$\frac{d\mathscr{L}}{dx} = \mathscr{L}_0 \frac{dE/dx}{1 + k_B\, dE/dx}\ , \tag{34.2}$$

where $\mathscr{L}$ is the luminescence, $\mathscr{L}_0$ is the luminescence at low specific ionization density, and k_B is Birks' constant, which must be determined for each scintillator by measurement. Decay times are in the ns range; rise times are much faster. The high light yield and fast response time allow the possibility of sub-ns timing resolution [22]. The fraction of light emitted during the decay "tail" can depend on the exciting particle. This allows pulse shape discrimination as a technique to carry out particle identification. Because of the hydrogen content (carbon to hydrogen ratio ≈ 1) plastic scintillator is sensitive to proton recoils from neutrons. Ease of fabrication into desired shapes and low cost has made plastic scintillator a common detector element. In the form of scintillating fiber it has found widespread use in tracking and calorimetry [23].

Demand for large volume detectors has lead to increased use of liquid organic scintillator, which has the same scintillation mechanism as plastic scintillator, due to its cost advantage. The containment vessel defines the detector shape; photodetectors or waveshifters may be immersed in the liquid.

34.3.1. *Scintillation mechanism* :

A charged particle traversing matter leaves behind it a wake of excited molecules. Certain types of molecules, however,

will release a small fraction (≈ 3%) of this energy as optical photons. This process, scintillation, is especially marked in those organic substances which contain aromatic rings, such as polystyrene (PS) and polyvinyltoluene (PVT). Liquids which scintillate include toluene, xylene and pseudocumene.

In fluorescence, the initial excitation takes place via the absorption of a photon, and de-excitation by emission of a longer wavelength photon. Fluors are used as "waveshifters" to shift scintillation light to a more convenient wavelength. Occurring in complex molecules, the absorption and emission are spread out over a wide band of photon

energies, and have some overlap, that is, there is some fraction of the emitted light which can be re-absorbed [24]. This "self-absorption" is undesirable for detector applications because it causes a shortened attenuation length. The wavelength difference between the major absorption and emission peaks is called the Stokes' shift. It is usually the case that the greater the Stokes' shift, the smaller the self absorption thus, a large Stokes' shift is a desirable property for a fluor.

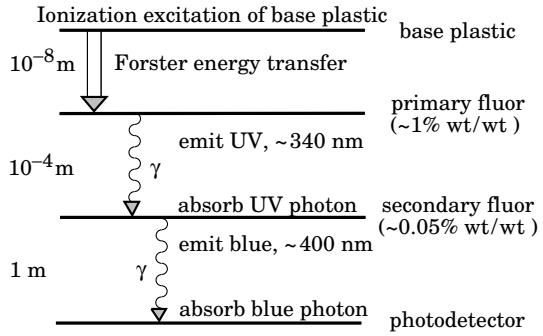

Figure 34.1: Cartoon of scintillation "ladder" depicting the operating mechanism of organic scintillator. Approximate fluor concentrations and energy transfer distances for the separate sub-processes are shown.

The plastic scintillators used in high-energy physics are binary or ternary solutions of selected fluors in a plastic base containing aromatic rings. (See appendix in Ref. 25 for a comprehensive list of components.) Virtually all plastic scintillators contain as a base either PVT or PS. PVT-based scintillator can be up to 50% brighter.

Ionization in the plastic base produces UV photons with short attenuation length (several mm). Longer attenuation lengths are obtained by dissolving a "primary" fluor in high concentration (1% by weight) into the base, which is selected to efficiently re-radiate absorbed energy at wavelengths where the base is more transparent (see Fig. 34.1).

The primary fluor has a second important function. The decay time of the scintillator base material can be quite long – in pure polystyrene it is 16 ns, for example. The addition of the primary fluor in high concentration can shorten the decay time by an order of magnitude and increase the total light yield. At the concentrations used (1% and greater), the average distance between a fluor molecule and an excited base unit is around 100 Å, much less than a wavelength of light. At these distances the predominant mode of energy transfer from base to fluor is not the radiation of a photon, but a resonant dipole-dipole interaction, first described by Foerster, which strongly couples the base and fluor [26]. The strong coupling sharply increases the speed and the light yield of the plastic scintillators.

Normally a fluor which fulfills other requirements is not adequate with respect to emission wavelength or attenuation length, so it is necessary to add yet another waveshifter (the "secondary" fluor), at fractional percent levels, and occasionally a third (not shown in Fig. 34.1).

External wavelength shifters are widely used to aid light collection in complex geometries. Scintillation light is captured by a lightpipe comprising a wave-shifting fluor dissolved in a nonscintillating base. The wavelength shifter must be insensitive to ionizing radiation and Cherenkov light. A typical wavelength shifter uses an acrylic base because of its good optical qualities, a single fluor to shift the light emerging from the plastic scintillator to the blue-green, and contains ultra-violet absorbing additives to deaden response to Cherenkov light.

By drastically increasing fluor concentrations beyond those discussed above, scintillators of increased radiation resistance or with special properties such as neutron/gamma discrimination may be made [35].

34.3.2. ***Caveats and cautions*** :

Plastic scintillators are reliable, robust, and convenient. However, exposure to solvent vapors, high temperatures, mechanical flexing, irradiation, or rough handling will cause degradation. A The surface is particularly fragile region and can "craze" – develop microcracks which degrade transmission of light by total internal reflection. Crazing is particularly likely where oils, solvents, or *fingerprints* have contacted the surface.

They have a long-lived luminescence which does not follow a simple exponential decay. Intensities at the 10^{-4} level of the initial fluorescence can persist for hundreds of ns [19,27].

They can decrease their light yield with increasing partial pressure of oxygen. This can be a 10% effect in an artificial atmosphere [28].

Their light yield may be changed by a magnetic field. Increases of $\approx 3\%$ at 0.45 T have been reported [29].

Irradiation of plastic scintillator creates color centers which absorb light more strongly in the UV and blue than at longer wavelengths. This poorly understood effect appears as a reduction both of light yield and attenuation length. Radiation damage depends not only on the integrated dose, but on the dose rate, atmosphere, and temperature, before, during and after irradiation, as well as the materials properties of the base such as glass transition temperature, polymer chain length, *etc.* Annealing also occurs, accelerated by the diffusion of atmospheric oxygen and elevated temperatures. The phenomena are complex, unpredictable, and not well understood [30]. Since color centers are most disruptive at shorter wavelengths, the most reliable method of mitigating radiation damage is to shift emissions at every step to the longest practical wavelengths, *e.g.*, utilize fluors with large Stokes' shifts (aka the "Better red than dead" strategy).

34.3.3. ***Scintillating and wavelength-shifting fibers*** :

The clad optical fiber comprising scintillator and wavelength shifter (WLS) is particularly useful [31]. Since the initial demonstration of the scintillating fiber (SCIFI) calorimeter [32], SCIFI techniques have become mainstream [33]. SCIFI calorimeters are fast, dense, radiation hard, and can have leadglass-like resolution. SCIFI trackers can handle high rates and are radiation tolerant, but the low photon yield at the end of a long fiber (see below) requires use of sensitive photodetectors. WLS-only fiber readout of a calorimeter allows a very high level of hermeticity since the solid angle blocked by the fiber on its way to the photodetector is very small. The sensitive region of scintillating fibers can be controlled by splicing them onto clear (non-scintillating/non-WLS) fibers.

A typical configuration would be fibers with a core of polystyrene-based scintillator or WLS (index of refraction $n = 1.59$), surrounded by a cladding of PMMA ($n = 1.49$) a few microns thick, or, for added light capture, with another cladding of fluorinated PMMA with $n = 1.42$, for an overall diameter of 0.5 to 1 mm. The fraction of generated light which is transported down the optical fiber is denoted the capture fraction and is about 6% for the single-clad fiber and 10% for the double-clad fiber. A minimum-ionizing particle traversing a high-quality 1 mm diameter fiber perpendicular to its axis will produce fewer than 2000 photons, of which about 200 are captured. Attenuation may eliminate 95% of these photons in a large collider tracker.

A scintillating or WLS fiber is often characterized by its attenuation length, over which the signal is attenuated to $1/e$ of its original value. Factors determining attenuation length include re-absorption of emitted photons by the polymer base or dissolved fluors, the level of crystallinity of the base polymer, variation of photodetector sensitivity to emitted wavelengths, and the quality of the internal surface [34]. Attenuation lengths of several meters are obtained by high quality fibers.

34.4. Inorganic scintillators:

Revised November 2017 by R.-Y. Zhu (California Institute of Technology) and C.L. Woody (BNL).

Inorganic crystals form a class of scintillating materials with much higher densities than organic plastic scintillators (typically $\sim$ 4–8 g/cm^3) with a variety of different properties for use as scintillation detectors. Due to their high density and high effective atomic number, they can be used in applications where high stopping power or a high conversion efficiency for electrons or photons is required. These include total absorption electromagnetic calorimeters (see Sec. 34.9.1), which consist of a totally active absorber (as opposed to a sampling calorimeter), as well as serving as gamma ray detectors over a wide range of energies. Many of these crystals also have very high light output, and can therefore provide excellent energy resolution down to very low energies ($\sim$ few hundred keV).

Some crystals are intrinsic scintillators in which the luminescence is produced by a part of the crystal lattice itself. However, other crystals require the addition of a dopant, typically fluorescent ions such as thallium (Tl) or cerium (Ce) which is responsible for producing the scintillation light. However, in both cases, the scintillation mechanism is the same. Energy is deposited in the crystal by ionization, either directly by charged particles, or by the conversion of photons into electrons or positrons which subsequently produce ionization. This energy is transferred to the luminescent centers which then radiate scintillation photons. The light yield L in terms of the number of scintillation photons produced per MeV of energy deposit in the crystal can be expressed as [36]

$$L = 10^6 \;\; S \cdot Q/(\beta \cdot E_g), \tag{34.3}$$

where $\beta \cdot E_g$ is is the energy required to create an e-h pair expressed as a multiple of the band gap energy Eg (eV), S is the efficiency of energy transfer to the luminescent center and Q is the quantum efficiency of the luminescent center. The values of β, S and Q are crystal dependent and are the main factors in determining the intrinsic light yield of the scintillator. The decay time of the scintillator is mainly dominated by the decay time of the luminescent center.

Table 34.4 lists the basic properties of some commonly used inorganic crystals. NaI(Tl) is one of the most common and widely used scintillators, with an emission that is well matched to a bialkali photomultiplier tube, but it is highly hygroscopic and difficult to work with, and has a rather low density. CsI(Tl) and CsI(Na) have high light yield, low cost, and are mechanically robust (high plasticity and resistance to cracking). However, they need careful surface treatment and are slightly and highly hygroscopic respectively. Pure CsI has identical mechanical properties as CsI(Tl), but faster emission at shorter wavelength and a much lower light output. BaF_2 has a fast component with a sub-nanosecond decay time, and is the fastest known scintillator. However, it also has a slow component with a much longer decay time ($\sim$ 630 ns). Bismuth gemanate ($Bi_4Ge_3O_{12}$ or BGO) has a high density, and consequently a short radiation length X_0 and Molière radius R_M. Similar to CsI(Tl), BGO's emission is well-matched to the spectral sensitivity of photodiodes, and it is easy to handle and not hygroscopic. Lead tungstate ($PbWO_4$ or PWO) has a very high density, with a very short X_0 and R_M, but its intrinsic light yield is rather low.

Cerium doped lutetium oxyorthosilicate (Lu_2SiO_5:Ce, or LSO:Ce) [37] and cerium doped lutetium-yttrium oxyorthosilicate ($Lu_{2(1-x)}Y_{2x}SiO_5$, LYSO:Ce) [38] are dense crystal scintillators which have a high light yield and a fast decay time. Only the properties of LSO:Ce are listed in Table 34.4 since the properties of LYSO:Ce are similar to that of LSO:Ce except a slightly lower density than LSO:Ce depending on the yttrium fraction in LYSO:Ce. This material is also featured with excellent radiation hardness [39], so is expected to be used where extraordinary radiation hardness is required.

Also listed in Table 34.4 are other fluoride crystals such as PbF_2 as a Cherenkov material and CeF_3, which have been shown to provide excellent energy resolution in calorimeter applications. Table 34.4 also includes cerium doped lanthanum tri-halides, such as $LaBr_3$ [40] and $CeBr_3$ [41], which are brighter and faster than LSO:Ce, but they are highly hygroscopic and have a lower density. The FWHM energy resolution measured for these materials coupled to a PMT with bi-alkali photocathode for 0.662 MeV γ-rays from a ^{137}Cs source is about 3%, and has recently been improved to 2% by co-doping with cerium and strontium [42], which is the best among all inorganic crystal scintillators. For this reason, $LaBr_3$ and $CeBr_3$ are expected to be used in applications where a good energy resolution for low energy photons are required, such as homeland security.

Beside the crystals listed in Table 34.4, a number of new crystals are being developed that may have potential applications in high energy or nuclear physics. Of particular interest is the family of yttrium and lutetium perovskites and garnet, which include YAP ($YAlO_3$:Ce), LuAP ($LuAlO_3$:Ce), YAG ($Y_3Al_5O_{12}$:Ce) and LuAG ($Lu_3Al_5O_{12}$:Ce) and their mixed compositions. These have been shown to be linear over a large energy range [43], and have the potential for providing good intrinsic energy resolution.

Aiming at the best jet-mass resolution inorganic scintillators are being investigated for HEP calorimeters with dual readout for both Cherenkov and scintillation light to be used at future linear colliders. These materials may be used for an electromagnetic calorimeter [44] or a homogeneous hadronic calorimetry (HHCAL) detector concept, including both electromagnetic and hadronic parts [45]. Because of the unprecedented volume (70 to 100 m^3) foreseen for the HHCAL detector concept the materials must be (1) dense (to minimize the leakage) and (2) cost-effective. It should also be UV transparent (for effective collection of the Cherenkov light) and allow for a clear discrimination between the Cherenkov and scintillation light. The preferred scintillation light is thus at a longer wavelength, and not necessarily bright or fast. Dense crystals, scintillating glasses and ceramics offer a very attractive implementation for this detector concept [46].

The fast scintillation light provides timing information about electromagnetic interactions and showers, which may be used to mitigate pile-up effects and/or for particle identification since the time development of electromagnetic and hadronic showers, as well as minimum ionizing particles, are different. The timing information is primarily determined by the scintillator rise time and decay time, and the number of photons produced. For fast timing, it is important to have a large number of photons emitted in the initial part of the scintillation pulse, e.g. in the first ns, since one is often measuring the arrival time of the particle in the crystal using the leading edge of the light pulse. A good example of this is BaF_2, which has $\sim$ 10% of its light in its fast component with a decay time of < 1 ns. The light propagation can spread out the arrival time of the scintillation photons at the photodetector due to time dispersion [47]. The time response of the photodetector also plays a major role in achieving good time resolution with fast scintillating crystals.

Table 34.4 gives the light output of other crystals relative to NaI(Tl) and their dependence to the temperature variations measured for 1.5 X_0 cube crystal samples with a Tyvek paper wrapping and a full end face coupled to a photodetector [48]. The quantum efficiencies of the photodetector is taken out to facilitate a direct comparison of crystal's light output. However, the useful signal produced by a scintillator is usually quoted in terms of the number of photoelectrons per MeV produced by a given photodetector. The relationship between the number of photons/MeV produced (L) and photoelectrons/MeV detected ($N_{\rm p.e.}$/MeV) involves the factors for the light collection efficiency (LC) and the quantum efficiency (QE) of the photodetector:

$$N_{\rm p.e.}/{\rm MeV} = L \cdot LC \cdot QE. \tag{34.4}$$

LC depends on the size and shape of the crystal, and includes effects such as the transmission of scintillation light within the crystal (i.e., the bulk attenuation length of the material), scattering from within the crystal, reflections and scattering from the crystal surfaces, and re-bouncing back into the crystal by wrapping materials. These factors can vary considerably depending on the sample, but can be in the range of $\sim$10–60%. The internal light transmission depends on the intrinsic properties of the material, e.g. the density and type of the scattering centers and defects that can produce internal absorption within the crystal, and can be highly affected by factors such as radiation damage, as discussed below.

The quantum efficiency depends on the type of photodetector used to detect the scintillation light, which is typically $\sim$15–30% for

photomultiplier tubes and ∼70% for silicon photodiodes for visible wavelengths. The quantum efficiency of the detector is usually highly wavelength dependent and should be matched to the particular crystal of interest to give the highest quantum yield at the wavelength corresponding to the peak of the scintillation emission. Fig. 34.2 shows the quantum efficiencies of two photodetectors, a Hamamatsu R2059 PMT with bi-alkali cathode and quartz window and a Hamamatsu S8664 avalanche photodiode (APD) as a function of wavelength. Also shown in the figure are emission spectra of three crystal scintillators, BGO, LSO:Ce/LYSO:Ce and CsI(Tl), and the numerical values of the emission weighted quantum efficiency. The area under each emission spectrum is proportional to crystal's light yield, as shown in Table 34.4, where the quantum efficiencies of the photodetector has been taken out. Results with different photodetectors can be significantly different. For example, the response of CsI(Tl) relative to NaI(Tl) with a standard photomultiplier tube with a bi-alkali photo-cathode, e.g. Hamamatsu R2059, would be 45 rather than 165 because of the photomultiplier's low quantum efficiency at longer wavelengths. For scintillators which emit in the UV, a detector with a quartz window should be used.

For very low energy applications (typically below 1 MeV), non-proportionality of the scintillation light yield may be important. It has been known for a long time that the conversion factor between the energy deposited in a crystal scintillator and the number of photons produced is not constant. It is also known that the energy resolution measured by all crystal scintillators for low energy γ-rays is significantly worse than the contribution from photo-electron statistics alone, indicating an intrinsic contribution from the scintillator itself. Precision measurement using low energy electron beam shows that this non-proportionality is crystal dependent [49]. Recent study on this issue also shows that this effect is also sample dependent even for the same crystal [50]. Further work is therefore needed to fully understand this subject.

One important issue related to the application of a crystal scintillator is its radiation hardness. Stability of its light output, or the ability to track and monitor the variation of its light output in a radiation environment, is required for high resolution and precision calibration [51]. All known crystal scintillators suffer from ionization dose induced radiation damage [52], where a common damage phenomenon is the appearance of radiation induced absorption caused by the formation of color centers originated from the impurities or point defects in the crystal. This radiation induced absorption reduces the light attenuation length in the crystal, and hence its light output. For crystals with high defect density, a severe reduction of light attenuation length may cause a distortion of the light response uniformity, leading to a degradation of the energy resolution. Additional radiation damage effects may include a reduced intrinsic scintillation light yield (damage to the luminescent centers) and an increased phosphorescence (afterglow). For crystals to be used in a high precision calorimeter in a radiation environment, its scintillation mechanism must not be damaged and its light attenuation length in the expected radiation environment must be long enough so that its light response uniformity, and thus its energy resolution, does not change.

While radiation damage induced by ionization dose is well understood [53], investigation is on-going to understand radiation damage caused by hadrons, including both charged hadrons and neutrons [54]. Two additional fundamental processes may cause defects by hadrons: displacement damage and nuclear breakup. While charged hadrons can produce all three types of damage (and it's often difficult to separate them), neutrons can produce only the last two, and electrons and photons only produce ionization damage. Studies on hadron induced radiation damage to lead tungstate [56] show a proton-specific damage component caused by fragments from fission induced in lead and tungsten by particles in the hadronic shower. The fragments cause a severe, local damage to the crystalline lattice due to

Table 34.4: Properties of several inorganic crystals. Most of the notation is defined in Sec. 6 of this *Review*.

Parameter:	ρ	MP	X_0^*	R_M^*	dE^*/dx	λ_I^*	$\tau_{\rm decay}$	$\lambda_{\rm max}$	$n^\natural$	Relative	Hygro-	d(LY)/dT
Units:	g/cm^3	°C	cm	cm	MeV/cm	cm	ns	nm		output†	scopic?	%/°C‡
NaI(Tl)	3.67	651	2.59	4.13	4.8	42.9	245	410	1.85	100	yes	−0.2
BGO	7.13	1050	1.12	2.23	9.0	22.8	300	480	2.15	21	no	−0.9
BaF_2	4.89	1280	2.03	3.10	6.5	30.7	650^s	300^s	1.50	36^s	no	-1.9^s
							0.9^f	220^f		4.1^f		0.1^f
CsI(Tl)	4.51	621	1.86	3.57	5.6	39.3	1220	550	1.79	165	slight	0.4
CsI(Na)	4.51	621	1.86	3.57	5.6	39.3	690	420	1.84	88	yes	0.4
CsI(pure)	4.51	621	1.86	3.57	5.6	39.3	30^s	310	1.95	3.6^s	slight	−1.4
							6^f			1.1^f		
$PbWO_4$	8.30	1123	0.89	2.00	10.1	20.7	30^s	425^s	2.20	0.3^s	no	−2.5
							10^f	420^f		0.077^f		
LSO(Ce)	7.40	2050	1.14	2.07	9.6	20.9	40	402	1.82	85	no	−0.2
PbF_2	7.77	824	0.93	2.21	9.4	21.0	-	-	-	Cherenkov	no	-
CeF_3	6.16	1460	1.70	2.41	8.42	23.2	30	340	1.62	7.3	no	0
$LaBr_3$(Ce)	5.29	783	1.88	2.85	6.90	30.4	20	356	1.9	180	yes	0.2
$CeBr_3$	5.23	722	1.96	2.97	6.65	31.5	17	371	1.9	165	yes	−0.1

* Numerical values calculated using formulae in this review.
$^\natural$ Refractive index at the wavelength of the emission maximum.
† Relative light output measured for samples of 1.5 X_0 cube with a Tyvek paper wrapping and a full end face coupled to a photodetector. The quantum efficiencies of the photodetector are taken out.
‡ Variation of light yield with temperature evaluated at the room temperature.
f = fast component, s = slow component

their extremely high energy loss over a short distance [56]. Investigation on neutron-specific damage in lead tungstate [57] up to 4×10^{19} n/cm^2 show no neutron-specific damage in PWO [58].

Most of the crystals listed in Table 34.4 have been used in high energy or nuclear physics experiments when the ultimate energy resolution for electrons and photons is desired. Examples are the Crystal Ball NaI(Tl) calorimeter at SPEAR, the L3 BGO calorimeter at LEP, the CLEO CsI(Tl) calorimeter at CESR, the KTeV CsI calorimeter at the Tevatron, the BaBar, BELLE and BES II CsI(Tl) calorimeters at PEP-II, KEK and BEPC III. Because of their high density and relative low cost, PWO calorimeters are used by CMS and ALICE at LHC, by CLAS and PrimEx at CEBAF and by PANDA at GSI, and PbF_2 calorimeters are used by the A4 experiment at MAINZ and by the g-2 experiment at Fermilab. A LYSO:Ce calorimeter is being built for the COMET experiment at J-PARC and a CsI calorimeter is being built for the Mu2e experiment at Fermilab.

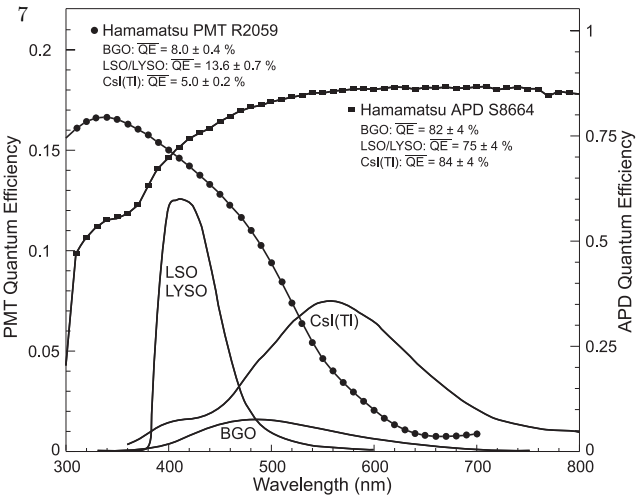

Figure 34.2: The quantum efficiencies of two photodetectors, a Hamamatsu R2059 PMT with bi-alkali cathode and a Hamamatsu S8664 avalanche photodiode (APD), are shown as a function of wavelength. Also shown in the figure are emission spectra of three crystal scintillators, BGO, LSO and CsI(Tl), and the numerical values of the emission weighted quantum efficiencies. The area under each emission spectrum is proportional to crystal's light yield.

34.5. Cherenkov detectors

Revised August 2015 by B.N. Ratcliff (SLAC).

Although devices using Cherenkov radiation are often thought of as only particle identification (PID) detectors, in practice they are used over a much broader range of applications including; (1) fast particle counters; (2) hadronic PID; and (3) tracking detectors performing complete event reconstruction. Examples of applications from each category include; (1) the Quartic fast timing counter designed to measure small angle scatters at the LHC [59]; (2) the hadronic PID detectors at the B factory detectors—DIRC in BaBar [60] and the aerogel threshold Cherenkov in Belle [61]; and (3) large water Cherenkov counters such as Super-Kamiokande [62]. Cherenkov counters contain two main elements; (1) a radiator through which the charged particle passes, and (2) a photodetector. As Cherenkov radiation is a weak source of photons, light collection and detection must be as efficient as possible. The refractive index n and the particle's path length through the radiator L appear in the Cherenkov relations allowing the tuning of these quantities for particular applications.

Cherenkov detectors utilize one or more of the properties of Cherenkov radiation discussed in the Passages of Particles through Matter section (Sec. 33 of this *Review*): the prompt emission of a light pulse; the existence of a velocity threshold for radiation; and the dependence of the Cherenkov cone half-angle θ_c and the number of emitted photons on the velocity of the particle and the refractive index of the medium.

The number of photoelectrons ($N_{\rm p.e.}$) detected in a given device is

$$N_{\rm p.e.} = L\frac{\alpha^2 z^2}{r_e\, m_e c^2}\int \epsilon(E)\, \sin^2\theta_c(E) dE\ , \qquad (34.5)$$

where ϵ(E) is the efficiency for collecting the Cherenkov light and transducing it into photoelectrons, and $\alpha^2/(r_e\, m_e c^2) = 370\ {\rm cm}^{-1}{\rm eV}^{-1}$.

The quantities ϵ and θ_c are functions of the photon energy E. As the typical energy dependent variation of the index of refraction is modest, a quantity called the *Cherenkov detector quality factor* N_0 can be defined as

$$N_0 = \frac{\alpha^2 z^2}{r_e\, m_e c^2}\ \int \epsilon\, dE\ , \qquad (34.6)$$

so that, taking $z = 1$ (the usual case in high-energy physics),

$$N_{\rm p.e.} \approx L N_0 \langle \sin^2\theta_c\rangle\ . \qquad (34.7)$$

This definition of the quality factor N_0 is not universal, nor, indeed, very useful for those common situations where ϵ factorizes as $\epsilon = \epsilon_{\rm coll}\epsilon_{\rm det}$ with the geometrical photon collection efficiency ($\epsilon_{\rm coll}$) varying substantially for different tracks while the photon detector efficiency ($\epsilon_{\rm det}$) remains nearly track independent. In this case, it can be useful to explicitly remove ($\epsilon_{\rm coll}$) from the definition of N_0. A typical value of N_0 for a photomultiplier (PMT) detection system working in the visible and near UV, and collecting most of the Cherenkov light, is about 100 cm^{-1}. Practical counters, utilizing a variety of different photodetectors, have values ranging between about 30 and 180 cm^{-1}. Radiators can be chosen from a variety of transparent materials (Sec. 33 of this *Review* and Table 6.1). In addition to refractive index, the choice requires consideration of factors such as material density, radiation length and radiation hardness, transmission bandwidth, absorption length, chromatic dispersion, optical workability (for solids), availability, and cost. When the momenta of particles to be identified is high, the refractive index must be set close to one, so that the photon yield per unit length is low and a long particle path in the radiator is required. Recently, the gap in refractive index that has traditionally existed between gases and liquid or solid materials has been partially closed with transparent *silica aerogels* with indices that range between about 1.007 and 1.13.

Cherenkov counters may be classified as either *imaging* or *threshold* types, depending on whether they do or do not make use of Cherenkov angle (θ_c) information. Imaging counters may be used to track particles as well as identify them. The recent development of very fast photodetectors such as micro-channel plate PMTs (MCP PMT) (see Sec. 34.2 of this *Review*) also potentially allows very fast Cherenkov based time of flight (TOF) detectors of either class [63]. The track timing resolution of imaging detectors can be extremely good as it scales approximately as $\frac{1}{\sqrt{N_{\rm p.e.}}}$.

Threshold Cherenkov detectors [64], in their simplest form, make a yes/no decision based on whether the particle is above or below the Cherenkov threshold velocity $\beta_t = 1/n$. A straightforward enhancement of such detectors uses the number of observed photoelectrons (or a calibrated pulse height) to discriminate between species or to set probabilities for each particle species [65]. This strategy can increase the momentum range of particle separation by a modest amount (to a momentum some 20% above the threshold momentum of the heavier particle in a typical case).

Careful designs give $\langle\epsilon_{\rm coll}\rangle \gtrsim 90\%$. For a photomultiplier with a typical bialkali cathode, $\int \epsilon_{\rm det} dE \approx 0.27$ eV, so that

$$N_{\rm p.e.}/L \approx 90\ {\rm cm}^{-1}\,\langle\sin^2\theta_c\rangle \quad (i.e.,\ N_0 = 90\ {\rm cm}^{-1})\ . \qquad (34.8)$$

Suppose, for example, that n is chosen so that the threshold for species a is p_t; that is, at this momentum species a has velocity $\beta_a = 1/n$. A second, lighter, species b with the same momentum has velocity β_b, so $\cos\theta_c = \beta_a/\beta_b$, and

$$N_{\rm p.e.}/L \approx 90\ {\rm cm}^{-1}\,\frac{m_a^2 - m_b^2}{p_t^2 + m_a^2}\ . \qquad (34.9)$$

For K/π separation at $p = p_t = 1(5)$ GeV/c, $N_{\rm p.e.}/L \approx 16(0.8)$ cm^{-1} for π's and (by design) 0 for K's.

For limited path lengths $N_{\rm p.e.}$ will usually be small. The overall efficiency of the device is controlled by Poisson fluctuations, which can be especially critical for separation of species where one particle type is dominant. Moreover, the effective number of photoelectrons is often less than the average number calculated above due to additional equivalent noise from the photodetector (see the discussion of the excess noise factor in Sec. 34.2 of this *Review*). It is common to design for at least 10 photoelectrons for the high velocity particle in order to obtain a robust counter. As rejection of the particle that is below threshold depends on *not* seeing a signal, electronic and other background noise, especially overlapping tracks, can be important. Physics sources of light production for the below threshold particle, such as decay to an above threshold particle, scintillation light, or the production of delta rays in the radiator, often limit the separation attainable, and need to be carefully considered. Well designed, modern multi-channel counters, such as the ACC at Belle [61], can attain adequate particle separation performance over a substantial momentum range.

Imaging counters make the most powerful use of the information available by measuring the ring-correlated angles of emission of the individual Cherenkov photons. They typically provide positive ID information both for the "wanted" and the "unwanted" particles, thus reducing mis-identification substantially. Since low-energy photon detectors can measure only the position (and, perhaps, a precise detection time) of the individual Cherenkov photons (not the angles directly), the photons must be "imaged" onto a detector so that their angles can be derived [66]. Typically the optics map the Cherenkov cone onto (a portion of) a distorted "circle" at the photodetector. Though the imaging process is directly analogous to familiar imaging techniques used in telescopes and other optical instruments, there is a somewhat bewildering variety of methods used in a wide variety of counter types with different names. Some of the imaging methods used include (1) focusing by a lens or mirror; (2) proximity focusing (i.e., focusing by limiting the emission region of the radiation); and (3) focusing through an aperture (a pinhole). In addition, the prompt Cherenkov emission coupled with the speed of some modern photon detectors allows the use of (4) time imaging, a method which is little used in conventional imaging technology, and may allow some separation with particle TOF. Finally, (5) correlated tracking (and event reconstruction) can be performed in large water counters by combining the individual space position and time of each photon together with the constraint that Cherenkov photons are emitted from each track at the same polar angle (Sec. 35.3.1 of this *Review*).

In a simple model of an imaging PID counter, the fractional error on the particle velocity (δ_β) is given by

$$\delta_\beta = \frac{\sigma_\beta}{\beta} = \tan\theta_c \sigma(\theta_c) \quad , \tag{34.10}$$

where

$$\sigma(\theta_c) = \frac{\langle\sigma(\theta_i)\rangle}{\sqrt{N_{\rm p.e.}}} \oplus C \ , \tag{34.11}$$

and $\langle\sigma(\theta_i)\rangle$ is the average single photoelectron resolution, as defined by the optics, detector resolution and the intrinsic chromaticity spread of the radiator index of refraction averaged over the photon detection bandwidth. C combines a number of other contributions to resolution including, (1) correlated terms such as tracking, alignment, and multiple scattering, (2) hit ambiguities, (3) background hits from random sources, and (4) hits coming from other tracks. The actual separation performance is also limited by physics effects such as decays in flight and particle interactions in the material of the detector. In many practical cases, the performance is limited by these effects.

For a $\beta \approx 1$ particle of momentum (p) well above threshold entering a radiator with index of refraction (n), the number of σ separation (N_σ) between particles of mass m_1 and m_2 is approximately

$$N_\sigma \approx \frac{|m_1^2 - m_2^2|}{2p^2\sigma(\theta_c)\sqrt{n^2-1}} \ . \tag{34.12}$$

In practical counters, the angular resolution term $\sigma(\theta_c)$ varies between about 0.1 and 5 mrad depending on the size, radiator, and photodetector type of the particular counter. The range of momenta over which a particular counter can separate particle species extends from the point at which the number of photons emitted becomes sufficient for the counter to operate efficiently as a threshold device ($\sim$20% above the threshold for the lighter species) to the value in the imaging region given by the equation above. For example, for $\sigma(\theta_c) = 2$mrad, a fused silica radiator($n = 1.474$), or a fluorocarbon gas radiator (C_5F_{12}, $n = 1.0017$), would separate π/K's from the threshold region starting around 0.15(3) GeV/c through the imaging region up to about 4.2(18) GeV/c at better than 3σ.

Many different imaging counters have been built during the last several decades [63]. Among the earliest examples of this class of counters are the very limited acceptance Differential Cherenkov detectors, designed for particle selection in high momentum beam lines. These devices use optical focusing and/or geometrical masking to select particles having velocities in a specified region. With careful design, a velocity resolution of $\sigma_\beta/\beta \approx 10^{-4}$–$10^{-5}$ can be obtained [64].

Practical multi-track Ring-Imaging Cherenkov detectors (generically called RICH counters) are a more recent development. RICH counters are sometimes further classified by 'generations' that differ based on historical timing, performance, design, and photodetection techniques.

Prototypical examples of first generation RICH counters are those used in the DELPHI and SLD detectors at the LEP and SLC Z factory e^+e^- colliders [63]. They have both liquid (C_6F_{14}, $n = 1.276$) and gas (C_5F_{12}, $n = 1.0017$) radiators, the former being proximity imaged with the latter using mirrors. The phototransducers are a TPC/wire-chamber combination. They are made sensitive to photons by doping the TPC gas (usually, ethane/methane) with $\sim 0.05\%$ TMAE (tetrakis(dimethylamino)ethylene). Great attention to detail is required, (1) to avoid absorbing the UV photons to which TMAE is sensitive, (2) to avoid absorbing the single photoelectrons as they drift in the long TPC, and (3) to keep the chemically active TMAE vapor from interacting with materials in the system. In spite of their unforgiving operational characteristics, these counters attained good $e/\pi/K/p$ separation over wide momentum ranges (from about 0.25 to 20 GeV/c) during several years of operation at LEP and SLC. Related but smaller acceptance devices include the OMEGA RICH at the CERN SPS, and the RICH in the balloon-borne CAPRICE detector [63].

Later generation counters [63] generally operate at much higher rates, with more detection channels, than the first generation detectors just described. They also utilize faster, more forgiving photon detectors, covering different photon detection bandwidths. Radiator choices have broadened to include materials such as lithium fluoride, fused silica, and aerogel. Vacuum based photodetection systems (*e.g.*, single or multi anode PMTs, MCP PMTs, or hybrid photodiodes (HPD)) have become increasingly common (see Sec. 34.2 of this *Review*). They handle high rates, and can be used with a wide choice of radiators. Examples include (1) the SELEX RICH at Fermilab, which mirror focuses the Cherenkov photons from a neon radiator onto a camera array made of $\sim$ 2000 PMTs to separate hadrons over a wide momentum range (to well above 200 GeV/c for heavy hadrons); (2) the HERMES RICH at HERA, which mirror focuses photons from C_4F_{10}($n = 1.00137$) and aerogel($n = 1.0304$) radiators within the same volume onto a PMT camera array to separate hadrons in the momentum range from 2 to 15 GeV/c; and (3) the LHCb detector now running at the LHC. It uses two separate counters readout by hybrid PMTs. One volume, like HERMES, contains two radiators (aerogel and C_4F_{10}) while the second volume contains CF_4. Photons are mirror focused onto detector arrays of HPDs to cover a π/K separation momentum range between 1 and 150 GeV/c. This device will be upgraded to deal with the higher luminosities provided by LHC after 2018 by modifying the optics and removing the aerogel radiator of the upstream RICH and replacing the Hybrid PMTs with multi-anode PMTs (MaPMTs).

Other fast detection systems that use solid cesium iodide (CsI) photocathodes or triethylamine (TEA) doping in proportional chambers are useful with certain radiator types and geometries. Examples include (1) the CLEO-III RICH at CESR that uses a LiF radiator with TEA doped proportional chambers; (2) the ALICE

detector at the LHC that uses proximity focused liquid (C_6F_{14} radiators and solid CSI photocathodes (similar photodectors have been used for several years by the HADES and COMPASS detectors), and the hadron blind detector (HBD) in the PHENIX detector at RHIC that couples a low index CF_4 radiator to a photodetector based on electron multiplier (GEM) chambers with reflective CSI photocathodes [63].

A DIRC (Detection [of] Internally Reflected Cherenkov [light]) is a distinctive, compact RICH subtype first used in the BaBar detector [60,63]. A DIRC "inverts" the usual RICH principle for use of light from the radiator by collecting and imaging the total internally reflected light rather than the transmitted light. It utilizes the optical material of the radiator in two ways, simultaneously; first as a Cherenkov radiator, and second, as a light pipe. The magnitudes of the photon angles are preserved during transport by the flat, rectangular cross section radiators, allowing the photons to be efficiently transported to a detector outside the path of the particle where they may be imaged in up to three independent dimensions (the usual two in space and, due to the long photon paths lengths, one in time). Because the index of refraction in the radiator is large (~ 1.48 for fused silica), light collection efficiency is good, but the momentum range with good π/K separation is rather low. The BaBar DIRC range extends up to ~ 4 GeV/c. It is plausible, but challenging, to extend it up to about 10 GeV/c with an improved design. New DIRC detectors are being developed that take advantage of the new, very fast, pixelated photodetectors becoming available, such as flat panel MaPMTs and MCP PMTs. They typically utilize either time imaging or mirror focused optics, or both, leading not only to a precision measurement of the Cherenkov angle, but in some cases, to a precise measurement of the particle TOF, and/or to correction of the chromatic dispersion in the radiator. Examples [63] include (1) the time of propagation (TOP) counter being fabricated for the BELLE-II upgrade at KEKB emphasizing precision timing for both Cherenkov imaging and TOF, which is scheduled for installation in 2016; (2) the full scale 3-dimensional imaging FDIRC prototype using the BaBar DIRC radiators which was designed for the SuperB detector at the Italian SuperB collider and uses precision timing not only for improving the angle reconstruction and TOF precision, but also to correct the chromatic dispersion; (3) the DIRCs being developed for the PANDA detector at FAIR that use elegant focusing optics and fast timing; and (4) the TORCH proposal being developed for an LHCb upgrade after 2019 which uses DIRC imaging with fast photo detectors to provide particle separation via particle TOF over a path length of 9.5m.

34.6. Gaseous detectors

34.6.1. ***Energy loss and charge transport in gases*** : Revised March 2010 by F. Sauli (CERN) and M. Titov (CEA Saclay).

Gas-filled detectors localize the ionization produced by charged particles, generally after charge multiplication. The statistics of ionization processes having asymmetries in the ionization trails, affe the coordinate determination deduced from the measurement of dri time, or of the center of gravity of the collected charge. For thin ga layers, the width of the energy loss distribution can be larger than its average, requiring multiple sample or truncated mean analysis t achieve good particle identification. In the truncated mean metho for calculating $\langle dE/dx \rangle$, the ionization measurements along the trac length are broken into many samples and then a fixed fraction of high-side (and sometimes also low-side) values are rejected [67].

The energy loss of charged particles and photons in matter is discussed in Sec. 33. Table 34.5 provides values of relevant parameters in some commonly used gases at NTP (normal temperature, 20° C, and pressure, 1 atm) for unit-charge minimum-ionizing particles (MIPs) [68–74]. Values often differ, depending on the source, so those in the table should be taken only as approximate. For different conditions and for mixtures, and neglecting internal energy transfer processes (*e.g.*, Penning effect), one can scale the density, N_P, and N_T with temperature and pressure assuming a perfect gas law.

When an ionizing particle passes through the gas it creates electron-ion pairs, but often the ejected electrons have sufficient energy to further ionize the medium. As shown in Table 34.5, the total number of electron-ion pairs (N_T) is usually a few times larger than the number of primaries (N_P).

Table 34.5: Properties of noble and molecular gases at normal temperature and pressure (NTP: 20° C, one atm). E_X, E_I: first excitation, ionization energy; W_I: average energy per ion pair; $dE/dx|_{\rm min}$, N_P, N_T: differential energy loss, primary and total number of electron-ion pairs per cm, for unit charge minimum ionizing particles.

Gas	Density, mg cm^{-3}	E_x eV	E_I eV	W_I eV	$dE/dx\|_{\rm min}$ keV cm^{-1}	N_P cm^{-1}	N_T cm^{-1}
He	0.179	19.8	24.6	41.3	0.32	3.5	8
Ne	0.839	16.7	21.6	37	1.45	13	40
Ar	1.66	11.6	15.7	26	2.53	25	97
Xe	5.495	8.4	12.1	22	6.87	41	312
CH_4	0.667	8.8	12.6	30	1.61	28	54
C_2H_6	1.26	8.2	11.5	26	2.91	48	112
iC_4H_{10}	2.49	6.5	10.6	26	5.67	90	220
CO_2	1.84	7.0	13.8	34	3.35	35	100
CF_4	3.78	10.0	16.0	54	6.38	63	120

The probability for a released electron to have an energy E or larger follows an approximate $1/E^2$ dependence (Rutherford law), shown in Fig. 34.3 for Ar/CH_4 at NTP (dotted line, left scale). More detailed estimates taking into account the electronic structure of the medium are shown in the figure, for three values of the particle velocity factor $\beta\gamma$ [69]. The dot-dashed line provides, on the right scale, the practical range of electrons (including scattering) of energy E. As an example, about 0.6% of released electrons have 1 keV or more energy, substantially increasing the ionization loss rate. The practical range of 1 keV electrons in argon (dot-dashed line, right scale) is 70 μm and this can contribute to the error in the coordinate determination.

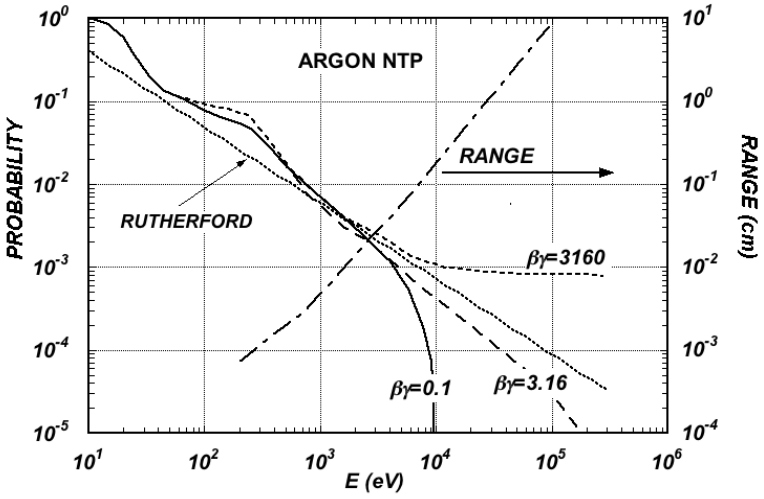

Figure 34.3: Probability of single collisions in which released electrons have an energy E or larger (left scale) and practical range of electrons in Ar/CH_4 (P10) at NTP (dot-dashed curve, right scale) [69].

The number of electron-ion pairs per primary ionization, or cluster size, has an exponentially decreasing probability; for argon, there is about 1% probability for primary clusters to contain ten or more electron-ion pairs [70].

Once released in the gas, and under the influence of an applied electric field, electrons and ions drift in opposite directions and diffuse towards the electrodes. The scattering cross section is determined by the details of atomic and molecular structure. Therefore, the drift velocity and diffusion of electrons depend very strongly on the

nature of the gas, specifically on the inelastic cross-section involving the rotational and vibrational levels of molecules. In noble gases, the inelastic cross section is zero below excitation and ionization thresholds. Large drift velocities are achieved by adding polyatomic gases (usually CH_4, CO_2, or CF_4) having large inelastic cross sections at moderate energies, which results in "cooling" electrons into the energy range of the Ramsauer-Townsend minimum (at $\sim$0.5 eV) of the elastic cross-section of argon. The reduction in both the total electron scattering cross-section and the electron energy results in a large increase of electron drift velocity (for a compilation of electron-molecule cross sections see Ref. 71). Another principal role of the polyatomic gas is to absorb the ultraviolet photons emitted by the excited noble gas atoms. Extensive collections of experimental data [72] and theoretical calculations based on transport theory [73] permit estimates of drift and diffusion properties in pure gases and their mixtures. In a simple approximation, gas kinetic theory provides the drift velocity v as a function of the mean collision time τ and the electric field E: $v = eE\tau/m_e$ (Townsend's expression). Values of drift velocity and diffusion for some commonly used gases at NTP are given in Fig. 34.4 and Fig. 34.5. These have been computed with the MAGBOLTZ program [74]. For different conditions, the horizontal axis must be scaled inversely with the gas density. Standard deviations for longitudinal (σ_L) and transverse diffusion (σ_T) are given for one cm of drift, and scale with the the square root of the drift distance. Since the collection time is inversely proportional to the drift velocity, diffusion is less in gases such as CF_4 that have high drift velocities. In the presence of an external magnetic field, the Lorentz force acting on electrons between collisions deflects the drifting electrons and modifies the drift properties. The electron trajectories, velocities and diffusion parameters can be computed with MAGBOLTZ. A simple theory, the friction force model, provides an expression for the vector drift velocity $\boldsymbol{v}$ as a function of electric and magnetic field vectors $\boldsymbol{E}$ and $\boldsymbol{B}$, of the Larmor frequency $\omega = eB/m_e$, and of the mean collision time τ:

$$\boldsymbol{v} = \frac{e}{m_e}\frac{\tau}{1+\omega^2\tau^2}\left(\boldsymbol{E} + \frac{\omega\tau}{B}(\boldsymbol{E}\times\boldsymbol{B}) + \frac{\omega^2\tau^2}{B^2}(\boldsymbol{E}\cdot\boldsymbol{B})\boldsymbol{B}\right) \qquad (34.13)$$

To a good approximation, and for moderate fields, one can assume that the energy of the electrons is not affected by B, and use for τ the values deduced from the drift velocity at $B = 0$ (the Townsend expression). For $\boldsymbol{E}$ perpendicular to $\boldsymbol{B}$, the drift angle to the relative to the electric field vector is $\tan\theta_B = \omega\tau$ and $v = (E/B)(\omega\tau/\sqrt{1+\omega^2\tau^2})$. For parallel electric and magnetic fields, drift velocity and longitudinal diffusion are not affected, while the transverse diffusion can be strongly reduced: $\sigma_T(B) = \sigma_T(B=0)/\sqrt{1+\omega^2\tau^2}$. The dotted line in Fig. 34.5 represents σ_T for the classic Ar/CH_4 (90:10) mixture at 4 T. Large values of $\omega\tau \sim 20$ at 5 T are consistent with the measurement of diffusion coefficient in $Ar/CF_4/iC_4H_{10}$ (95:3:2). This reduction is exploited in time projection chambers (Sec. 34.6.5) to improve spatial resolution.

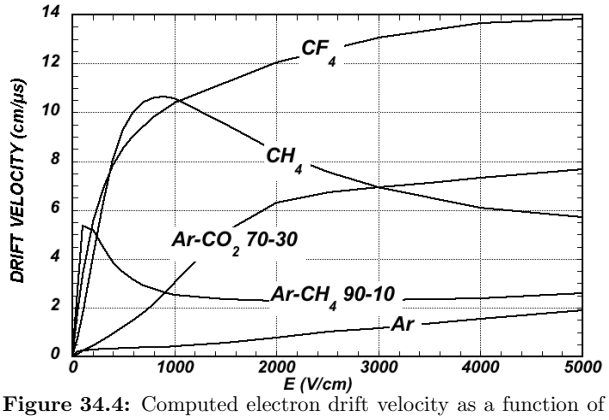

Figure 34.4: Computed electron drift velocity as a function of electric field in several gases at NTP and $B = 0$ [74].

In mixtures containing electronegative molecules, such as O_2 or H_2O, electrons can be captured to form negative ions. Capture cross-sections are strongly energy-dependent, and therefore the capture probability is a function of applied field. For example, the electron is attached to the oxygen molecule at energies below 1 eV. The three-body electron attachment coefficients may differ greatly for the same additive in different mixtures. As an example, at moderate fields (up to 1 kV/cm) the addition of 0.1% of oxygen to an Ar/CO_2 mixture results in an electron capture probability about twenty times larger than the same addition to Ar/CH_4.

Carbon tetrafluoride is not electronegative at low and moderate fields, making its use attractive as drift gas due to its very low diffusion. However, CF_4 has a large electron capture cross section at fields above $\sim$8 kV/cm, before reaching avalanche field strengths. Depending on detector geometry, some signal reduction and resolution loss can be expected using this gas.

If the electric field is increased sufficiently, electrons gain enough energy between collisions to ionize molecules. Above a gas-dependent threshold, the mean free path for ionization, λ_i, decreases exponentially with the field; its inverse, $\alpha = 1/\lambda_i$, is the first Townsend coefficient. In wire chambers, most of the increase of avalanche particle density occurs very close to the anode wires, and a simple electrostatic consideration shows that the largest fraction of the detected signal is due to the motion of positive ions receding from the wires. The electron component, although very fast, contributes very little to the signal. This determines the characteristic shape of the detected signals in the proportional mode: a fast rise followed by a gradual increase. The slow component, the so-called "ion tail" that limits the time resolution of the detector, is usually removed by differentiation of the signal. In uniform fields, N_0 initial electrons multiply over a length x forming an electron avalanche of size $N = N_0\, e^{\alpha x}$; N/N_0 is the gain of the detector. Fig. 34.6 shows examples of Townsend coefficients for several gas mixtures, computed with MAGBOLTZ [74].

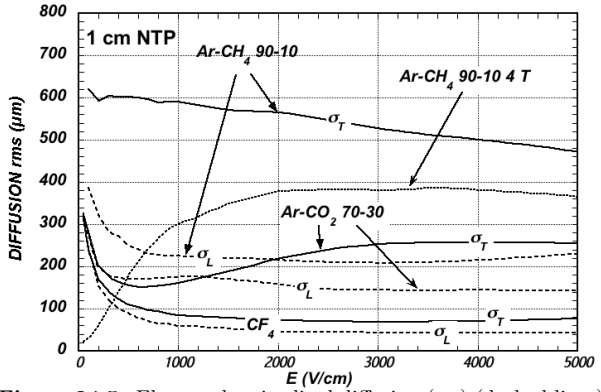

Figure 34.5: Electron longitudinal diffusion (σ_L) (dashed lines) and transverse diffusion (σ_T) (full lines) for 1 cm of drift at NTP and $B = 0$. The dotted line shows σ_T for the P10 mixture at 4 T [74].

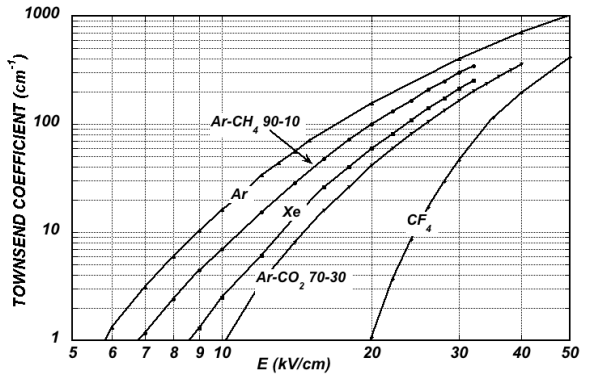

Figure 34.6: Computed first Townsend coefficient α as a function of electric field in several gases at NTP [74].

Positive ions released by the primary ionization or produced in the avalanches drift and diffuse under the influence of the electric field. Negative ions may also be produced by electron attachment to gas molecules. The drift velocity of ions in the fields encountered in gaseous detectors (up to few kV/cm) is typically about three orders of magnitude less than for electrons. The ion mobility μ, the ratio of drift velocity to electric field, is constant for a given ion type up to very high fields. Values of mobility at NTP for ions in their own and other gases are given in Table 34.6 [75]. For different temperatures and pressures, the mobility can be scaled inversely with the density assuming an ideal gas law. For mixtures, due to a very effective charge transfer mechanism, only ions with the lowest ionization potential survive after a short path in the gas. Both the lateral and transverse diffusion of ions are proportional to the square root of the drift time, with a coefficient that depends on temperature but not on the ion mass. Accumulation of ions in the gas drift volume may induce field distortions (see Sec. 34.6.5).

Table 34.6: Mobility of ions in gases at NTP [75].

Gas	Ion	Mobility μ ($cm^2\ V^{-1}\ s^{-1}$)
He	He^+	10.4
Ne	Ne^+	4.7
Ar	Ar^+	1.54
Ar/CH_4	CH_4^+	1.87
Ar/CO_2	CO_2^+	1.72
CH_4	CH_4^+	2.26
CO_2	CO_2^+	1.09

34.6.2. ***Multi-Wire Proportional and Drift Chambers*** : Revised March 2010 by Fabio Sauli (CERN) and Maxim Titov (CEA Saclay).

Single-wire counters that detect the ionization produced in a gas by a charged particle, followed by charge multiplication and collection around a thin wire have been used for decades. Good energy resolution is obtained in the proportional amplification mode, while very large saturated pulses can be detected in the streamer and Geiger modes [3].

Multiwire proportional chambers (MWPCs) [76,77], introduced in the late '60's, detect, localize and measure energy deposit by charged particles over large areas. A mesh of parallel anode wires at a suitable potential, inserted between two cathodes, acts almost as a set of independent proportional counters (see Fig. 34.7a). Electrons released in the gas volume drift towards the anodes and produce avalanches in the increasing field. Analytic expressions for the electric field can be found in many textbooks. The fields close to the wires $E(r)$, in the drift region E_D, and the capacitance C per unit length of anode wire are approximately given by

$$E(r) = \frac{CV_0}{2\pi\epsilon_0}\frac{1}{r} \qquad E_D = \frac{CV_0}{2\epsilon_0 s} \qquad C = \frac{2\pi\epsilon_0}{\pi(\ell/s) - \ln(2\pi a/s)}\ , \quad (34.14)$$

where r is the distance from the center of the anode, s the wire spacing, ℓ and V_0 the distance and potential difference between anode and cathode, and a the anode wire radius.

Because of electrostatic forces, anode wires are in equilibrium only for a perfect geometry. Small deviations result in forces displacing the wires alternatively below and above the symmetry plane, sometimes with catastrophic results. These displacement forces are countered by the mechanical tension of the wire, up to a maximum unsupported stable length, L_M [67], above which the wire deforms:

$$L_M = \frac{s}{CV_0}\sqrt{4\pi\epsilon_0 T_M} \quad (34.15)$$

The maximum tension T_M depends on the wire diameter and modulus of elasticity. Table 34.7 gives approximate values for tungsten and the corresponding maximum stable wire length under reasonable assumptions for the operating voltage ($V_0 = 5\,kV$) [78]. Internal supports and spacers can be used in the construction of longer detectors to overcome limits on the wire length imposed by Eq. (34.15).

Table 34.7: Maximum tension T_M and stable unsupported length L_M for tungsten wires with spacing s, operated at $V_0 = 5$ kV. No safety factor is included.

Wire diameter (μm)	T_M (newton)	s (mm)	L_M (cm)
10	0.16	1	25
20	0.65	2	85

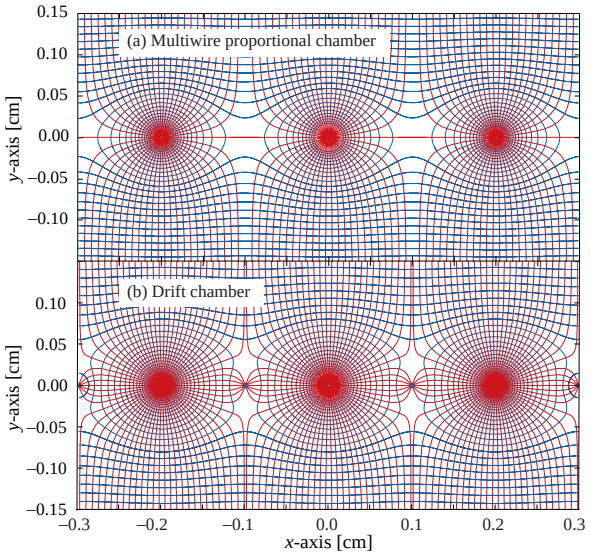

Figure 34.7: Electric field lines and equipotentials in (a) a multiwire proportional chamber and (b) a drift chamber.

Detection of charge on the wires over a predefined threshold provides the transverse coordinate to the wire with an accuracy comparable to that of the wire spacing. The coordinate along each wire can be obtained by measuring the ratio of collected charge at the two ends of resistive wires. Making use of the charge profile induced on segmented cathodes, the so-called center-of gravity (COG) method, permits localization of tracks to sub-mm accuracy. Due to the statistics of energy loss and asymmetric ionization clusters, the position accuracy is $\sim$ 50 μm rms for tracks perpendicular to the wire plane, but degrades to $\sim$250 μmat 30° to the normal [79]. The intrinsic bi-dimensional characteristic of the COG readout has found numerous applications in medical imaging.

Drift chambers, developed in the early '70's, can be used to estimate the longitudinal position of a track by exploiting the arrival time of electrons at the anodes if the time of interaction is known [80]. The distance between anode wires is usually several cm, allowing coverage of large areas at reduced cost. In the original design, a thicker wire (the field wire) at the proper voltage, placed between the anode wires, reduces the field at the mid-point between anodes and improves charge collection (Fig. 34.7b). In some drift chamber designs, and with the help of suitable voltages applied to field-shaping electrodes, the electric field structure is adjusted to improve the linearity of space-to-drift-time relation, resulting in better spatial resolution [81].

Drift chambers can reach a longitudinal spatial resolution from timing measurement of order 100 μm (rms) or better for minimum ionizing particles, depending on the geometry and operating conditions. However, a degradation of resolution is observed [82] due to primary ionization statistics for tracks close to the anode wires, caused by the spread in arrival time of the nearest ionization clusters. The effect can be reduced by operating the detector at higher pressures. Sampling

the drift time on rows of anodes led to the concept of multiple arrays such as the multi-drift module [83] and the JET chamber [84]. A measurement of drift time, together with the recording of charge sharing from the two ends of the anode wires provides the coordinates of segments of tracks. The total charge gives information on the differential energy loss and is exploited for particle identification. The time projection chamber (TPC) [85] combines a measurement of drift time and charge induction on cathodes, to obtain excellent tracking for high multiplicity topologies occurring at moderate rates (see Sec. 34.6.5). In all cases, a good knowledge of electron drift velocity and diffusion properties is required. This has to be combined with the knowledge of the electric fields in the structures, computed with commercial or custom-developed software [74,86]. For an overview of detectors exploiting the drift time for coordinate measurement see Refs. 6 and 67.

Multiwire and drift chambers have been operated with a variety of gas fillings and operating modes, depending on experimental requirements. The so-called "Magic Gas," a mixture of argon, isobutane and Freon [77], permits very high and saturated gains ($\sim 10^6$). This gas mixture was used in early wire chambers, but was found to be susceptible to severe aging processes. With present-day electronics, proportional gains around 10^4 are sufficient for detection of minimum ionizing particles, and noble gases with moderate amounts of polyatomic gases, such as methane or carbon dioxide, are used.

Although very powerful in terms of performance, multi-wire structures have reliability problems when used in harsh or hard-to-access environments, since a single broken wire can disable the entire detector. Introduced in the '80's, straw and drift tube systems make use of large arrays of wire counters encased in individual enclosures, each acting as an independent wire counter [87]. Techniques for low-cost mass production of these detectors have been developed for large experiments, such as the Transition Radiation Tracker and the Drift Tubes arrays for CERN's LHC experiments [88].

34.6.3. ***High Rate Effects*** : Revised March 2010 by Fabio Sauli (CERN) and Maxim Titov (CEA Saclay).

The production of positive ions in the avalanches and their slow drift before neutralization result in a rate-dependent accumulation of positive charge in the detector. This may result in significant field distortion, gain reduction and degradation of spatial resolution. As shown in Fig. 34.8 [89], the proportional gain drops above a charge production rate around 10^9 electrons per second and mm of wire, independently of the avalanche size. For a proportional gain of 10^4 and 100 electrons per track, this corresponds to a particle flux of $10^3\,\mathrm{s}^{-1}\mathrm{mm}^{-1}$ (1 kHz/mm^2 for 1 mm wire spacing).

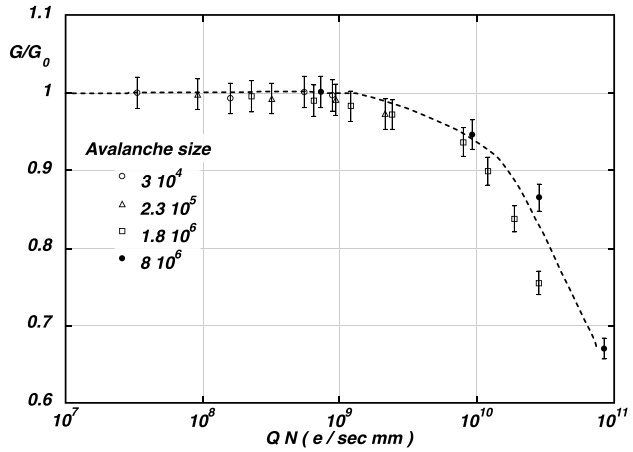

Figure 34.8: Charge rate dependence of normalized gas gain G/G_0 (relative to zero counting rate) in proportional thin-wire detectors [89]. Q is the total charge in single avalanche; N is the particle rate per wire length.

At high radiation fluxes, a fast degradation of detectors due to the formation of polymers deposits (aging) is often observed. The process has been extensively investigated, often with conflicting results. Several causes have been identified, including organic pollutants and silicone oils. Addition of small amounts of water in many (but not all) cases has been shown to extend the lifetime of the detectors. Addition of fluorinated gases (*e.g.*, CF_4) or oxygen may result in an etching action that can overcome polymer formation, or even eliminate already existing deposits. However, the issue of long-term survival of gas detectors with these gases is controversial [90]. Under optimum operating conditions, a total collected charge of a few coulombs per cm of wire can usually be reached before noticeable degradation occurs. This corresponds, for one mm spacing and at a gain of 10^4, to a total particle flux of $\sim 10^{14}$ MIPs/cm^2.

34.6.4. ***Micro-Pattern Gas Detectors*** : Revised March 2010 by Fabio Sauli (CERN) and Maxim Titov (CEA Saclay)

Despite various improvements, position-sensitive detectors based on wire structures are limited by basic diffusion processes and space charge effects to localization accuracies of 50–100 μm [91]. Modern photolithographic technology led to the development of novel Micro-Pattern Gas Detector (MPGD) concepts [92], revolutionizing cell size limitations for many gas detector applications. By using pitch size of a few hundred μm, an order of magnitude improvement in granularity over wire chambers, these detectors offer intrinsic high rate capability ($> 10^6$ Hz/mm^2), excellent spatial resolution ($\sim$ 30 μm), multi-particle resolution ($\sim$ 500 μm), and single photo-electron time resolution in the ns range.

The Micro-Strip Gas Chamber (MSGC), invented in 1988, was the first of the micro-structure gas chambers [93]. It consists of a set of tiny parallel metal strips laid on a thin resistive support, alternatively connected as anodes and cathodes. Owing to the small anode-to-cathode distance ($\sim$ 100 μm), the fast collection of positive ions reduces space charge build-up, and provides a greatly increased rate capability. Unfortunately, the fragile electrode structure of the MSGC turned out to be easily destroyed by discharges induced by heavily ionizing particles [94]. Nevertheless, detailed studies of their properties, and in particular, on the radiation-induced processes leading to discharge breakdown, led to the development of the more powerful devices: GEM and Micromegas. These have improved reliability and radiation hardness. The absence of space-charge effects in GEM detectors at the highest rates reached so far and the fine granularity of MPGDs improve the maximum rate capability by more than two orders of magnitude (Fig. 34.9) [81,95]. Even larger rate capability has been reported for Micromegas [96].

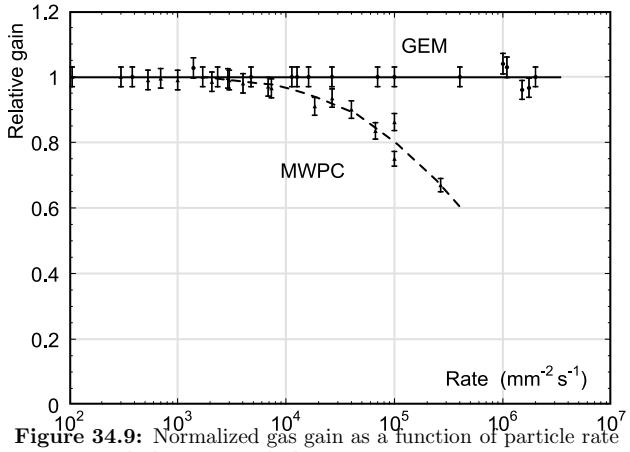

Figure 34.9: Normalized gas gain as a function of particle rate for MWPC [81] and GEM [95].

The Gas Electron Multiplier (GEM) detector consists of a thin-foil copper-insulator-copper sandwich chemically perforated to obtain a high density of holes in which avalanches occur [97]. The hole diameter is typically between 25 μm and 150 μm, while the corresponding distance between holes varies between 50 μm and 200 μm. The central insulator is usually (in the original design) the polymer Kapton, with a thickness of 50 μm. Application of a potential difference between the two sides of the GEM generates the electric fields indicated in Fig. 34.10. Each hole acts as an independent

proportional counter. Electrons released by the primary ionization particle in the upper conversion region (above the GEM foil) drift into the holes, where charge multiplication occurs in the high electric field (50–70 kV/cm). Most of avalanche electrons are transferred into the gap below the GEM. Several GEM foils can be cascaded, allowing the multi-layer GEM detectors to operate at overall gas gain above 10^4 in the presence of highly ionizing particles, while strongly reducing the risk of discharges. This is a major advantage of the GEM technology [98]. Localization can then be performed by collecting the charge on a patterned one- or two-dimensional readout board of arbitrary pattern, placed below the last GEM.

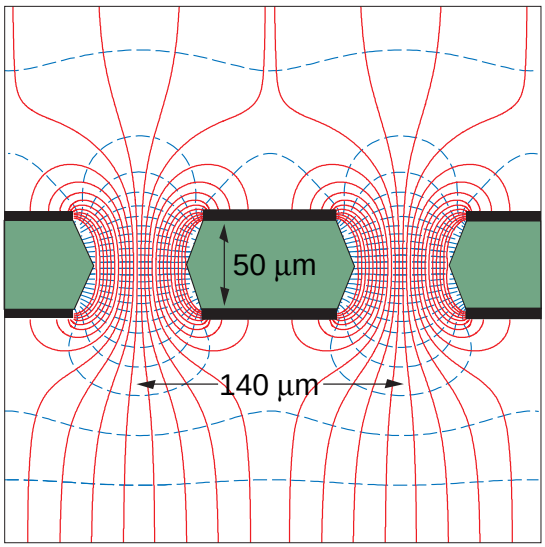

Figure 34.10: Schematic view and typical dimensions of the hole structure in the GEM amplification cell. Electric field lines (solid) and equipotentials (dashed) are shown.

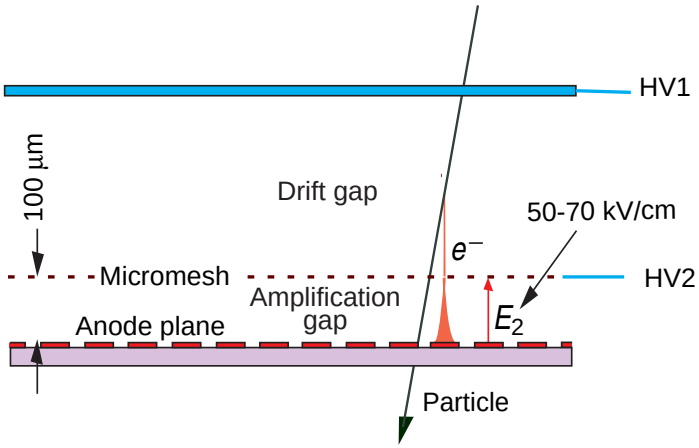

Figure 34.11: Schematic drawing of the Micromegas detector.

The micro-mesh gaseous structure (Micromegas) is a thin parallel-plate avalanche counter, as shown in Fig. 34.11 [99]. It consists of a drift region and a narrow multiplication gap (25–150 μm) between a thin metal grid (micromesh) and the readout electrode (strips or pads of conductor printed on an insulator board). Electrons from the primary ionization drift through the holes of the mesh into the narrow multiplication gap, where they are amplified. The electric field is homogeneous both in the drift (electric field $\sim$1 kV/cm) and amplification (50–70 kV/cm) gaps. In the narrow multiplication region, gain variations due to small variations of the amplification gap are approximately compensated by an inverse variation of the amplification coefficient, resulting in a more uniform gain. The small amplification gap produces a narrow avalanche, giving rise to excellent spatial resolution: 12 μm accuracy, limited by the micro-mesh pitch, has been achieved for MIPs, as well as very good time resolution and energy resolution ($\sim$12% FWHM with 6 keV x rays) [100].

The performance and robustness of GEM and Micromegas have encouraged their use in high-energy and nuclear physics, UV and visible photon detection, astroparticle and neutrino physics, neutron detection and medical physics. Most structures were originally optimized for high-rate particle tracking in nuclear and high-energy physics experiments. COMPASS, a high-luminosity experiment at CERN, pioneered the use of large-area ($\sim 40 \times 40$ cm^2) GEM and Micromegas detectors close to the beam line with particle rates of 25 kHz/mm^2. Both technologies achieved a tracking efficiency of close to 100% at gas gains of about 10^4, a spatial resolution of 70–100 μm and a time resolution of $\sim$10 ns. GEM detectors are also used for triggering in the LHCb Muon System and for tracking in the TOTEM Telescopes. Both GEM and Micromegas devices are foreseen for the upgrade of the LHC experiments and for one of the readout options for the Time Projection Chamber (TPC) at the International Linear Collider (ILC). The development of new fabrication techniques—"bulk" Micromegas technology [101] and single-mask GEMs [102] —is a big step toward industrial production of large-size MPGDs. In some applications requiring very large-area coverage with moderate spatial resolution, coarse macro-patterned detectors, such as Thick GEMs (THGEM) [103] or patterned resistive-plate devices [104] might offer economically interesting solutions.

Sensitive and low-noise electronics enlarge the range of the MPGD applications. Recently, the GEM and Micromegas detectors were read out by high-granularity ($\sim$50 μm pitch) CMOS chips assembled directly below the GEM or Micromegas amplification structures [105]. These detectors use the bump-bonding pads of a pixel chip as an integrated charge collecting anode. With this arrangement signals are induced at the input gate of a charge-sensitive preamplifier (top metal layer of the CMOS chip). Every pixel is then directly connected to the amplification and digitization circuits, integrated in the underlying active layers of the CMOS technology, yielding timing and charge measurements as well as precise spatial information in 3D.

The operation of a MPGD with a Timepix CMOS chip has demonstrated the possibility of reconstructing 3D-space points of individual primary electron clusters with $\sim$30 μm spatial resolution and event-time resolution with nanosecond precision. This has become indispensable for tracking and triggering and also for discriminating between ionizing tracks and photon conversions. The GEM, in conjunction with a CMOS ASIC,* can directly view the absorption process of a few keV x-ray quanta and simultaneously reconstruct the direction of emission, which is sensitive to the x-ray polarization. Thanks to these developments, a micro-pattern device with finely segmented CMOS readout can serve as a high-precision "electronic bubble chamber." This may open new opportunities for x-ray polarimeters, detection of weakly interacting massive particles (WIMPs) and axions, Compton telescopes, and 3D imaging of nuclear recoils.

An elegant solution for the construction of the Micromegas with pixel readout is the integration of the amplification grid and CMOS chip by means of an advanced "wafer post-processing" technology [106]. This novel concept is called "Ingrid" (see Fig. 34.12). With this technique, the structure of a thin (1 μm) aluminum grid is fabricated on top of an array of insulating pillars. which stands $\sim$50 μm above the CMOS chip. The sub-μm precision of the grid dimensions and avalanche gap size results in a uniform gas gain. The grid hole size, pitch and pattern can be easily adapted to match the geometry of any pixel readout chip.

Recent developments in radiation hardness research with state-of-the-art MPGDs are reviewed in Ref. 107. Earlier aging studies of GEM and Micromegas concepts revealed that they might be even less vulnerable to radiation-induced performance degradation than standard silicon microstrip detectors.

The RD51 collaboration was established in 2008 to further advance technological developments of micro-pattern detectors and associated electronic-readout systems for applications in basic and applied research [108].

* Application Specific Integrated Circuit

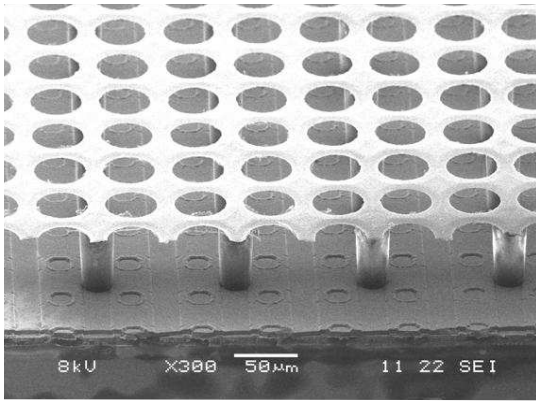

Figure 34.12: Photo of the Micromegas "Ingrid" detector. The grid holes can be accurately aligned with readout pixels of CMOS chip. The insulating pillars are centered between the grid holes, thus avoiding dead regions.

34.6.5. ***Time-projection chambers*** : Written August 2015 by C. Lippmann (GSI Helmholtzzentrum für Schwerionenforschung, Darmstadt, Germany)

The Time Projection Chamber (TPC) concept was invented by David Nygren in the late 1970's [85]. It consists of a cylindrical or square field cage filled with a detection medium that is usually a gas or a liquid. Charged particles produce tracks of ionization electrons that drift in a uniform electric field towards a position-sensitive amplification stage which provides a 2D projection of the particle trajectories. The third coordinate can be calculated from the arrival times of the drifted electrons. The start for this drift time measurement is usually derived from an external detector, e.g. a fast interaction trigger detector.

This section focuses on the gas-filled TPCs that are typically used in particle or nuclear physics experiments at accelerators due to their low material budget. For neutrino physics (Sec. 34.10) or for detecting rare events (Sec. 35.4), on the contrary, usually high density and large active mass are required, and a liquid detection medium is favored.

The TPC enables full 3D measurements of charged particle tracks, which gives it a distinct advantage over other tracking detector designs which record information only in two-dimensional detector planes and have less overall segmentation. This advantage is often exploited for pattern recognition in events with large numbers of particles, e.g. heavy-ion collisions. Two examples of modern large-volume gaseous TPCs are shown in Fig. 34.13 and Fig. 34.14.

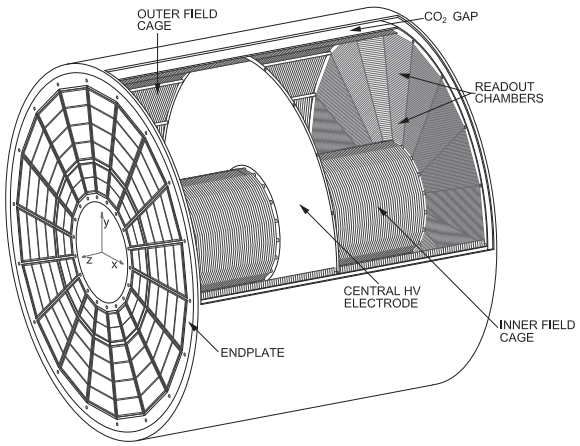

Figure 34.13: Schematic view of the ALICE TPC [109]. The drift volume with 5 m diameter is divided into two halves, each providing 2.5 m drift length.

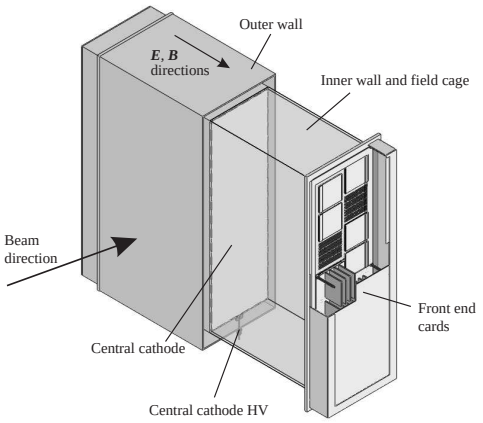

Figure 34.14: One of the 3 TPC modules for the near detector of the T2K experiment [110]. The size is $2 \times 2 \times 0.8\,\mathrm{m}^3$. Micromegas devices are used for gas amplification and readout.

Identification of the charged particles crossing the TPC is possible by simultaneously measuring their momentum and specific energy deposit through ionisation ($\mathrm{d}E/\mathrm{d}x$). The momentum, as well as the charge sign, are calculated from a helix fit to the particle trajectory in the presence of a magnetic field (typically parallel to the drift field). For this application, precise spatial measurements in the plane transverse to the magnetic field are most important. The specific energy deposit is estimated from many charge measurements along the particle trajectory (e.g. one measurement per anode wire or per row of readout pads). As the charge collected per readout segment depends on the track angle and on the ambient conditions, the measured values are corrected for the effective length of the track segments and for variations of the gas temperature and pressure. The most probable value of the corrected signal amplitudes provides the best estimator for the specific energy deposit (see Sec. 33.2.3); it is usually approximated by the truncated mean, i.e. the average of the 50%-70% smallest values. The resulting particle identification performance is illustrated in Fig. 34.15, for the ALICE TPC.

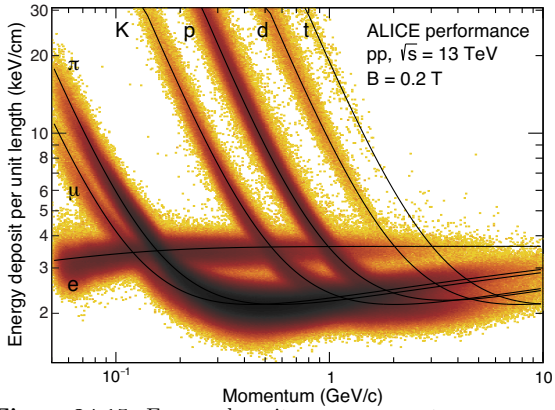

Figure 34.15: Energy deposit versus momentum measured in the ALICE TPC [111].

The dependence of the achievable energy resolution on the number of measurements N, on the thickness of the sampling layers t, and on the gas pressure P can be estimated using an empirical formula [112]:

$$\sigma_{dE/dx} = 0.41\ N^{-0.43}(t\,P)^{-0.32}. \qquad (34.16)$$

Typical values at nominal pressure are $\sigma_{dE/dx} = 4.5$ to 7.5%, with $t = 0.4$ to 1.5 cm and $N = 40$ up to more than 300. Due to the high gas pressure of 8.5 bar, the resolution achieved with the PEP-4/9 TPC was an unprecedented 3% [113].

The greatest challenges for a large TPC are due to the length of the drift of up to several meters. In particular, it can make the device sensitive to small distortions in the electric field. Such distortions can arise from a number of sources, e.g. imperfections in the field cage construction or the presence of ions in the drift volume. The electron drift in a TPC in the presence of a magnetic field is defined by Eq. (34.13). The $\boldsymbol{E} \times \boldsymbol{B}$ term of Eq. (34.13) vanishes for perfectly aligned electric and magnetic fields, which can however be difficult to achieve in practice. Furthermore, the electron drift depends on the $\omega\tau$ factor, which is defined by the chosen gas mixture and magnetic field strength. The electrons will tend to follow the magnetic field lines for $\omega\tau > 1$ or the electric field lines for $\omega\tau < 1$. The former mode of operation makes the TPC less sensitive to non-uniformities of the electric field, which is usually desirable.

The drift of the ionization electrons is superposed with a random diffusion motion which degrades their position information. The ultimate resolution of a single position measurement is limited to around

$$\sigma_x = \frac{\sigma_D \sqrt{L}}{\sqrt{n}}\,, \tag{34.17}$$

where σ_D is the transverse diffusion coefficient for 1 cm drift, L is the drift length in cm and n is the effective number of electrons collected. Without a magnetic field, $\sigma_{D,B=0}\sqrt{L}$ is typically a few mm after a drift of $L = 100\,\text{cm}$. However, in a strong magnetic field parallel to the drift field, a large value of $\omega\tau$ can significantly reduce diffusion:

$$\frac{\sigma_{D,B>0}}{\sigma_{D,B=0}} = \frac{1}{\sqrt{1+\omega^2\tau^2}}\,. \tag{34.18}$$

This factor can reach values of up to 10. In practice, the final resolution limit due to diffusion will typically be around $\sigma_x = 100\,\mu\text{m}$.

The drift and diffusion of electrons depend strongly on the nature of the gas that is used. The optimal gas mixture varies according to the environment in which the TPC will operate. In all cases, the oxygen concentration must be kept very low (few ten parts per million in a large TPC) in order to avoid electron loss through attachment. Ideally, the drift velocity should depend only weakly on the electric field at the nominal operating condition. The classic Ar/CH_4 (90:10) mixture, known as P10, has a drift velocity maximum of $5\,\text{cm}/\mu\text{s}$ at an electric field of only $125\,\text{V/cm}$ (Fig. 34.4). In this regime, the electron arrival time is not affected by small variations in the ambient conditions. Moreover, low electric fields simplify the design and operation of the field cage. The mixture has a large transverse diffusion at $B = 0$, but this can be reduced significantly in a strong magnetic field due to the relatively large value of $\omega\tau$.

For certain applications, organic gases like CH_4 are not desirable, since they may cause aging. An alternative is to replace CH_4 with CO_2. An Ar/CO_2 (90:10) mixture features a low transverse diffusion at all magnetic field strengths, but does not provide a saturated drift velocity for the typical electric fields used in TPCs (up to a few $100\,\text{V/cm}$), so it is quite sensitive to the ambient conditions. Freon admixtures like CF_4 can be an attractive option for a TPC as well, since the resulting gas mixtures provide high drift velocities at low electric fields. However, the use of CF_4 always needs to be thoroughly validated for compatibility with all materials of the detector and the gas system.

Historically, the amplification stages used in gaseous TPCs have been planes of anode wires operated in proportional mode. The performance is limited by effects related to the feature size of a few mm (wire spacing). Since near the wires the electric and magnetic fields are not parallel, the incoming ionisation electrons are displaced in the direction of the wires ("wire $E \times B$ effect"), which degrades the resolution. The smaller feature sizes of Micro-Pattern Gas Detectors (MPGDs) like GEMs and Micromegas lead to many advantages as compared to wire planes (see Sec. 34.6.4). In particular, $E \times B$ effects in the amplification stage are much smaller. Moreover, the signal induction process in MPGDs leads to a very narrow pad response, allowing for a much finer segmentation and improving the separation of two nearby tracks. Combinations of MPGDs with silicon sensors have resulted in the highest granularity readout systems so far (see Sec. 34.6.4). These devices make it possible to count the number of ionization clusters along the length of a track, which can, in principle, improve the particle identification capability. However, the big challenge for such a system is the huge number of read-out channels for a TPC of a typical size.

The accumulation of the positive ions created by the ionization from the particle tracks can lead to time-dependent distortions of the drift field. Due to their small drift velocity, ions from many events may coexist in the drift volume. To reduce the effect of such a build-up of space charge, Argon can be replaced by Neon as the main component of the gas mixture. Neon features a lower number of ionisation electrons per unit of track length (see Table 34.5) and a higher ion mobility (see Table 34.6).

Of much greater concern are the ions produced in the gas amplification stage. In order to prevent them from entering the drift volume, large TPCs built until now usually have a gating grid. The gating grid can be switched to transparent mode (usually in the presence of an interaction trigger) to allow the ionization electrons to pass into the amplification region. After all electrons have reached the amplification region, it is usually closed such that it is rendered opaque to electrons and ions.

Alternatively, new readout schemes are being developed using MPGDs. These can be optimized in a way that they release many fewer positive ions than wire planes operating at the same effective gain. This is an exciting possibility for future TPCs.

34.6.6. ***Transition radiation detectors (TRD's)*** : Revised August 2017 by P. Nevski (BNL) and A. Romaniouk (Moscow Eng. & Phys. Inst.)

Transition radiation (TR) x-rays are produced when a highly relativistic particle ($\gamma \gtrsim 10^3$) crosses a refractive index interface, as discussed in Sec. 33.7. Since the TR yield is about 1% per boundary crossing, radiation from multiple surface crossings is used in practical detectors. The x-rays, ranging from a few keV to a few dozen keV or more, are emitted in a forward direction at small angles ($\sim$ few mrad) to the particle trajectory. The TR intensity for a single boundary crossing always increases with γ, but, for multiple boundary crossings, interference leads to saturation above a Lorentz factor $\gamma_{\text{sat}} = 0.6\ \omega_1\sqrt{\ell_1\ell_2}/c$ [114], where ω_1 is the radiator material plasma frequency, ℓ_1 is its thickness, and ℓ_2 the spacing. The probability density function of TR is a fairly complex function of γ, radiator parameters, angle (θ) and photon energy (ω). Integration over the angle yields the TR spectrum, which typically features many maxima (see Sec. 33.7). Most of the radiation is emitted near the last maximum of the spectra determined by radiator material parameters at $\omega_{max} = \ell_1\omega_1^2/2\pi c$. The effective TR photon emission starts at about $\gamma_{thr} = \ell_1\omega_1/c$. By varying radiator parameters one may optimize the particle separation for a given range of the γ-factor. The angular distribution of TR photons has a few maxima and extends up to $\theta_{max} = (1/\gamma^2 + \omega_1^2/\omega^2)^{1/2}$ (see Ref. 87 in Sec. 33.7). The largest part of the TR energy is emitted around the most probable angle $\theta = (1/\gamma^2 + \omega_2^2/\omega^2)^{1/2}$, where ω_2 is the plasma frequency of the gas surrounding the radiator material elements.

In the simplest concept, a detector module might consist of low-Z TR radiator followed by a high-Z active layer made of proportional counters filled with a Xe-rich gas mixture. The atomic number considerations follow from the dominant photoelectric absorption cross section per atom going roughly as Z^n/E_x^3, where n varies between 4 and 5 over the region of interest, and the x-ray energy is E_x.* To minimize self-absorption, materials such as polypropylene, Mylar, carbon, and (rarely) lithium in the form of foils, fibers or foams are used as radiators. The TR signal in the active regions is in most cases superimposed upon the particle ionization losses, which are proportional to Z. In most of the detectors used in particle physics the radiator parameters are chosen to provide $\gamma_{\text{sat}} \approx 2000$. Those detectors normally work as threshold devices, ensuring the best electron/pion separation in the momentum range $1\ \text{GeV}/c \lesssim p \lesssim 150\ \text{GeV}/c$.

One can distinguish two design concepts—"thick" and "thin" detectors:

* Photon absorption coefficients for the elements (via a NIST link), and $dE/dx|_{\text{min}}$ and plasma energies for many materials are given in `pdg.lbl.gov/AtomicNuclearProperties`.

In "thick" detectors the radiator, optimized for a minimum total radiation length at maximum TR yield and total TR absorption in the detector, consists of few hundred foils (for instance 300 20 μm thick polypropylene foils). Most of the TR photons are absorbed in the radiator itself. To maximise the number of TR photons reaching the detector, part of the radiator far from the active layers is often made of thicker foils, which shifts the x-ray spectrum to higher energies. The detector thickness, about 2-4 cm for Xe-filled gas chambers, is optimized to absorb the incoming x-ray spectrum. A classical detector is composed of several similar modules which respond nearly independently. Such detectors were used in the UA2, NA34 and other experiments [115], and are being used in the ALICE experiment [116], [117].

In another TRD concept a fine granular radiator/detector structure exploits the soft part of the TR spectrum more efficiently and thereby may act also as an integral part of the tracking detector providing many points of measurements on the particle track . This can be achieved, for instance, by distributing small-diameter straw-tube detectors uniformly or in thin layers throughout the radiator material. Even with a relatively thin radiator stack, radiation below 5 keV is mostly lost in the radiators themselves. However for photon energies above this value, the absorption is reduced and the radiation can be registered by several consecutive detector layers, thus creating a strong TR build-up effect. This approach allows to realise a TRD as an integral part of a tracking detector. Descriptions of detectors using this approach in both accelerator and space experiments can be found in [116,117]. For example, in the ATLAS TR tracker (TRT), charged particles cross about 35 effective straw tube layers embedded in the radiator material [116]. The effective thickness of the Xe gas per straw is about 2.2 mm and the average number of foils per straw is about 40 with an effective foil thickness of about 18 μm.

Although the values mentioned above are typical for most of the plastic radiators used with Xe-based detectors, they vary significantly depending on the detector parameters: radiator material, thickness and spacing, the geometry and position of the sensitive chambers, *etc.* Thus careful simulations are usually needed to build a detector optimized for a particular application. For TRD simulations the codes are based on well understood TR emission formulas (see for instance Ref. 87 in Sec. 33.7). They give a reasonably good agreement of the TR energy spectra with data (see in [117] and [120]) , both for the stand-alone simulation programs (see ATLAS TRT in [116]) and for GEANT4 based ones [118], [119]. However non of them include correct angular distribution of the TR photons.

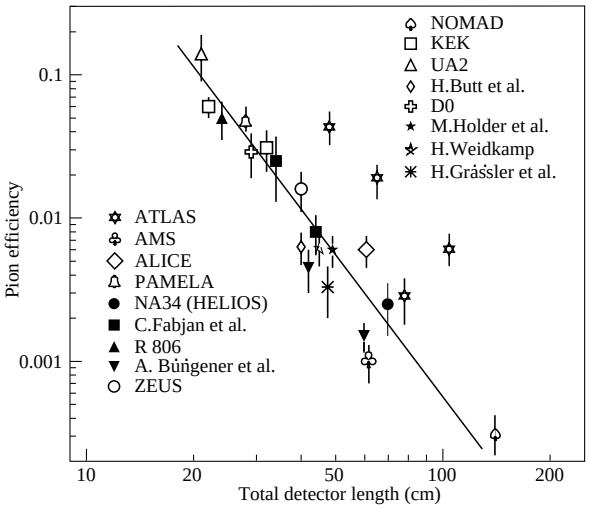

Figure 34.16: Pion efficiency measured (or predicted) for different TRDs as a function of the detector length for a fixed electron efficiency of 90%. The plot is taken from [115]. Results from more recent detectors are added from [116] and [117].

The discrimination between electrons and pions can be based on the charge deposition measured in each detection module, on the number of clusters – energy depositions observed above an optimal threshold (usually it is 5–7 keV), or on more sophisticated methods such as analyzing the pulse shape as a function of time. The total energy measurement technique is more suitable for thick gas volumes, which absorb most of the TR radiation and where the ionization loss fluctuations are relatively small. The cluster-counting method works better for detectors with thin gas layers, where the fluctuations of the ionization losses are bigger. Cluster-counting replaces the Landau-Vavilov distribution of background ionization energy losses with the Poisson statistics of δ-electrons, responsible for the distribution tails. The latter distribution is narrower than the Landau-Vavilov distribution. In practice, most of the experiments use a likelihood method, which exploits detailed knowledge of the detector response for different particles and gives the best separation. The more parameters that are considered, the better separation power may be achieved. For example, for the TRD in the AMS experiment the rejection power achieved in the real experiment is better by almost one order of magnitude than that obtained in the beam test if stringent criteria for track selection are applied, see in [117]. Another example is the neural network method used by the ALICE TRD (ALICE point in Fig. 34.16) which gives another factor of 2–3 in rejection power with respect to the likelihood method [121].

The major factor in the performance of any TRD is its overall length. This is illustrated in Fig. 34.16, which shows, for a variety of detectors, the pion efficiency at a fixed electron efficiency of 90% as a function of the overall detector length. As TRD performance depends on particle energy, the experimental data in this figure covering a range of particle energies from 1 GeV to 40 GeV, are rescaled to an energy of 10 GeV when possible. Phenomenologically, the rejection power against pions increases as $5 \cdot 10^{L/38}$, where the range of validity is $L \approx 20$–100 cm. Apart from the beam energy variations, the observed scattering of the points in the plot reflects how effectively the detector space is used and how well the exact response to different particles is taken into account in the analysis. For instance, the ATLAS TRT was built as a compromise between TR and tracking requirements; that is why the test-beam prototype result (lower point) is better than the real TRT performance at the LHC shown in Fig. 34.16 for different regions in the detector (in agreement with MC).

In most cases, recent TRDs combine particle identification with charged-track measurement in the same detector [116,117,122]. This is particularly important for collider experiments, where the available space for the inner detector is very limited. For a modest increase of the radiation length due to the radiator (∼4% X0), a significant enhancement of the electron identification was obtained in the case of the ATLAS TRT. Here, the combination of the two detector functions provides a powerful tool for electron identification even at very high particle densities.

In addition to the enhancement of the electron identification during offline data analysis, TRD signatures are often used in the trigger algorithms at collider experiments. The ALICE experiment [117] is a good example for the use of the TRD in a First Level Trigger. In the ATLAS experiment, the TRT information is used in the High Level Trigger (HLT) algorithms. At increasing luminosities, the electron trigger output rate becomes so high, that a significant increase of the calorimeter energy threshold is required to keep it at an acceptable level. This may affect the trigger efficiency of very important physics channels (e.g. $W \to e\nu$ inclusive decay). Even a very soft TR cut at the HLT level, which preserves high electron efficiency (98%), allows to suppress a significant part of fake triggers and enhance the purity for physics events with electrons in a final state. The TRT also plays a crucial role in the studies where an electron suppression is required (e.g. hadronic mode of τ–decays). TR information is a completely independent tool for electron identification and allows to study systematic uncertainties of other electron reconstruction methods.

Electron identification is not the only TRD application. Recent TRDs for particle astrophysics are designed to directly measure the Lorentz factor of high-energy nuclei by using the quadratic dependence of the TR yield on nuclear charge; see, for instance, in [116]. The radiator configuration (ℓ_1, ℓ_2) is tuned to extend the TR yield rise up to $\gamma \approx 10^5$ using the more energetic part of the TR spectrum (up to

100 keV). High density radiator materials (such as Al) are the best for this purpose. Direct absorption of the TR-photons of these energies with thin detectors becomes problematic and TR detection methods based on Compton scattering have been proposed, see in [116], [117].

The high granularity of the Si-pixel or the Si-microstrip detectors provides spatial separation of the TR photons and dE/dx losses at relatively modest distances between radiator and detector. These detectors may be the basis for novel devices which combine precise tracking and PID properties. TR measurements using a pixel detector with 20 μm pitch size are described in [117]. The presence of a magnetic field could enhance the separation between TR photons and dE/dx losses. Simulations made on the basis of the beam-test results has shown that in a magnetic field of 2 T and for the geometry of the ATLAS Si-tracker proposed for sLHC, a rejection factor of > 30 can be obtained for an electron efficiency above 90% in the particle momentum range from 2 to 30 GeV/c, see in [116] and [117]. New detector techniques for TRDs are also under development. In particular, GasPixel detectors allow to obtain a space point accuracy of < 30 μm and exploit all details of the particle tracks to highlight individual TR clusters in the gas, see in [117]. Thin films of heavy scintillators might be a very attractive option for non-gas based TRD [117].

34.6.7. ***Resistive-plate chambers*** : Revised August 2017 by G. Aielli (U. Roma Tor Vergata).

The resistive-plate chamber (RPC) is a gaseous detector developed by R. Santonico and R. Cardarelli in the early 1980's [123] *. Although its original purpose was to provide a competitive alternative to large scintillator counters, the RPC's potential for timing tracker systems was quickly recognized given its excellent temporal and spatial resolutions and the ease of constructing large-format single detectors. The RPC, as sketched in Fig. 34.17, is a large planar capacitor with two parallel high bulk resistivity electrode plates (10^9–10^{13} Ω·cm) separated by a set of insulating spacers. The spacers define a gap in the range from a few millimeters down to 0.1 mm with a precision of a few $\sim$ μm. The gap is filled with a suitable atmospheric-pressure gas mixture which serves as a target for ionizing radiation. Primary ionization for sub-millimeter gas gaps can be insufficient, thus multiple gaps can be combined to ensure an acceptable detection efficiency [125].

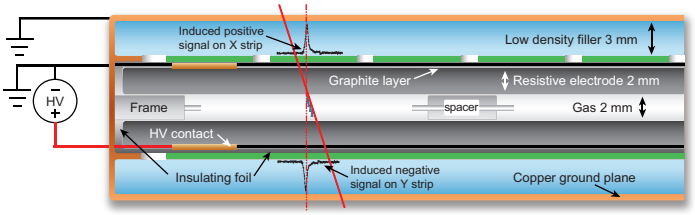

Figure 34.17: Schematic cross section of a generic single gap RPC.

The electrodes are most commonly made of high pressure phenolic-melaminic laminate (HPL), improperly referred to as "bakelite", or glass. A moderate electrode resistivity ($\sim 10^5$ $\Omega/\Box$) establishes a uniform electric field of several kV/mm across the gap, which initiates an electron avalanche following primary ionization. The above resistivity is low enough to ensure uniformity of the electric field, yet still transparent to fast signal transients from avalanches. This field configuration allows an excellent space-time localization of the signal. Due to the high electrode resistivity in RPCs, the electrode time constant is much longer than discharge processes. Therefore only the locally-stored electrostatic energy contributes to the discharge, which prevents the formation of sparks and leaves the rest of the detector field unaffected. The gas-facing surface of HPL electrodes are commonly coated with a few μm-thick layer of polymerized linseed oil. This layer has a similar resistivity as the electrode, and is smooth to aid the uniformity of the electric field. It also protects the electrode from the free radicals generated in the discharge e.g. in presence of hydrocarbons or fluorocarbons. As with other gaseous detectors, the gas mixture is optimized for each specific application. In general it needs to contain a component to quench UV photons, thus avoiding discharge propagation. An electronegative component controls the avalanche growth in case of very high electric fields [126,127]. To first order, each primary ionization in an RPC is exponentially amplified according to its distance from the anode. Therefore RPC signals span a large dynamic range, unlike gaseous detectors where ionization and amplification occur in separate regions (e.g. wire chambers or MPGDs). For increasingly stronger fields, the avalanche exponential growth progressively saturates to linear [128], and finally reaches a strongly-saturated "streamer" transition which exhausts all the locally-available energy [129]. A set of metallic readout electrodes (e.g. pads or strips) placed behind the resistive electrodes detect the charge pulse induced by the fast movement of the avalanche electrons. The signal is isotropically distributed with respect to the field direction and present with equal but opposite amplitude on the two electrodes. This feature allows for 2D localization of the signal with uniform spatial resolution. The induced charge density projected in 1D can be calculated for a simplified RPC model [130] as: $\sigma(x) = A/\cosh[(x-\overline{x})/\delta]$ where $\overline{x}$ is the center of the avalanche and $\delta = (g+2d)/\pi$ depends on the gap and electrode width (g and d, respectively). The spatial extent of actual signals are generally larger than those given by this model [131,132]. Conductivity of the graphite layer results in the most prominent broadening. Cross-talk from parasitic coupling of neighboring electrodes can also spread the signal spatially. Although the broadened charge distribution preserves most of the original spatial resolution, it can adversely impact signal clustering, so the detector layout must be calculated according to the expected application. Sensitivity to high-frequency electron avalanche signals over large RPC areas requires a correspondingly adequate Faraday cage and readout structure design. In particular, the front end electronics must be time-sensitive with a fast response and low noise, although these requirements are usually in competition [133].

34.6.7.1. *RPC types and applications:* RPCs are generally classified in two categories depending on the gas gap structure: single gap RPCs (described above) and multiple gap RPCs (typically referred as mRPCs or timing RPCs). While they are both based on the same principle they have different construction techniques, performance and limitations, making them suitable for different applications. Due to its simplicity and robustness, the single gap RPC is ideal for covering very large surfaces. Typical detector systems can have sensitive surface areas up to $\sim 10^4$ m^2, with single module areas of a few m^2, and a space-time resolution down to $\sim$0.4 ns $\times$ 100 μm [134,135]. Typical applications are in muon systems (e.g. the muon trigger systems of the LHC experiments) or ground and underground based cosmic rays and neutrino arrays [136]. Moreover, single gap RPCs have recently found an application in tracking calorimetry [137]. The mRPC allows for smaller gas gap thicknesses while still maintaining a sufficient gaseous target. The most common version [138] consists of a stack of floating glass electrodes separated by monofilament (i.e. fishing line), sandwiched between two external electrodes which provide the high-voltage bias. The floating glass electrodes assume a potential determined by the avalanche processes occurring between them. mRPCs have been largely used in TOF systems and in applications such as timing PET.

34.6.7.2. *Time and space resolution:* The RPC field configuration generates an avalanche which is strongly correlated in space and time to the original ionizing event. Space-time uncertainties generally arise from the statistical fluctuations of the ionization and multiplication processes, and from the characteristics of the readout and front-end electronics. The intrinsic signal latency is commonly in the ns range, making the RPC suitable for applications where a low latency is essential. A higher time resolution and shorter signal duration is correlated with a thinner gas gap, although a higher electric field is required for sufficient avalanche development [138,139]. Typical timing performances are from around 1 ns with a 2 mm gas gap, down to 20 ps for a stack of several 0.1 mm gaps [140]. The mechanical delicacy of sub-mm-gap structures makes this technique less suitable for large detector areas. Digital strip readouts are commonly used, with spatial resolution determined by the strip pitch and the cluster

* The RPC was based on earlier work on a spark counter with one metallic and one high-resistivity plate [124].

size (∼0.5 cm). Recent developments toward higher spatial resolutions are mostly based on charge centroid techniques, benefiting from the availability of low-cost high-performance readout electronics. The present state of the art detectors have a combined space-time resolution of ∼50 ps × 40 μm [141].

34.6.7.3. *Rate capability and ageing:* RPC rate capability is limited by the voltage drop on resistive electrodes, $\Delta V = V_{\rm a} - V_{\rm gas} = I \cdot R$ [142]. Here $V_{\rm a}$ is the applied voltage, $V_{\rm gas}$ is the effective voltage on the gas, $R = \rho \cdot d/S$ is the total electrode resistance and I is the working current. Expressing I as the particle flux Φ times an average charge per avalanche $\langle Q \rangle$ gives $\Delta V/\Phi = \rho \cdot d \cdot \langle Q \rangle$. A large I not only limits the rate capability but also affects the long term performance of the detector. Discharges deplete the conductive properties of HPL electrodes [143]. In the presence of fluorocarbons and water, discharges generate hydrofluoric acid (HF) which damages internal detector surfaces, particularly glass electrodes [144]. HF damage can be mitigated by preventing water vapor contamination (for glass electrodes) or by sufficient flushing of the gas gap (for HPL electrodes). Operating in the streamer regime puts low requirements on the front end electronics sensitivity, but generally limits the counting rate capability to ∼100 Hz/cm^2 and requires stability over a large gain range. Higher-rate operation can be achieved by reducing gas gain in favor of electronic amplification, operating the detector in avalanche mode. Increasing concentrations of electronegative gases, such as $C_2H_2F_4$ and SF_6 [127], shifts the streamer transition to higher gains. The avalanche signal has a higher dynamic range, a drawback which can be compensated with appropriate electronics. With these techniques, stable performance at high rates (e.g. 10 kHz/cm^2) has been achieved for large area single gap RPCs [133]. Additional techniques rely on the natural redundancy and small gain of multiple gap structures [145] and electrodes made with lower resistivity materials [146].

34.7. Semiconductor detectors

Updated November 2013 by H. Spieler.

Semiconductor detectors provide a unique combination of energy and position resolution. In collider detectors they are most widely used as position sensing devices and photodetectors (Sec. 34.2). Integrated circuit technology allows the formation of high-density micron-scale electrodes on large (15–20 cm diameter) wafers, providing excellent position resolution. Furthermore, the density of silicon and its small ionization energy yield adequate signals with active layers only 100–300 μm thick, so the signals are also fast (typically tens of ns). The high energy resolution is a key parameter in x-ray, gamma, and charged particle spectroscopy, *e.g.*, in neutrinoless double beta decay searches. Silicon and germanium are the most commonly used materials, but gallium-arsenide, CdTe, CdZnTe, and other materials are also useful. CdZnTe provides a higher stopping power and the ratio of Cd to Zn concentrations changes the bandgap. Ge detectors are commonly operated at liquid nitrogen temperature to reduce the bias current, which depends exponentially on temperature. Semiconductor detectors depend crucially on low-noise electronics (see Sec. 34.8), so the detection sensitivity is determined by signal charge and capacitance. For a comprehensive discussion of semiconductor detectors and electronics see Ref. 147 or the tutorial website `http://www-physics.lbl.gov/ spieler`.

34.7.1. ***Materials Requirements*** :

Semiconductor detectors are essentially solid state ionization chambers. Absorbed energy forms electron-hole pairs, *i.e.*, negative and positive charge carriers, which under an applied electric field move towards their respective collection electrodes, where they induce a signal current. The energy required to form an electron-hole pair is proportional to the bandgap. In tracking detectors the energy loss in the detector should be minimal, whereas for energy spectroscopy the stopping power should be maximized, so for gamma rays high-Z materials are desirable.

Measurements on silicon photodiodes [148] show that for photon energies below 4 eV one electron-hole (e-h) pair is formed per incident photon. The mean energy E_i required to produce an e-h pair peaks at 4.4 eV for a photon energy around 6 eV. Above ∼1.5 keV it assumes a constant value, 3.67 eV at room temperature. It is larger than the bandgap energy because momentum conservation requires excitation of lattice vibrations (phonons). For minimum-ionizing particles, the most probable charge deposition in a 300 μm thick silicon detector is about 3.5 fC (22000 electrons). Other typical ionization energies are 2.96 eV in Ge, 4.2 eV in GaAs, and 4.43 eV in CdTe.

Since both electronic and lattice excitations are involved, the variance in the number of charge carriers $N = E/E_i$ produced by an absorbed energy E is reduced by the Fano factor F (about 0.1 in Si and Ge). Thus, $\sigma_N = \sqrt{FN}$ and the energy resolution $\sigma_E/E = \sqrt{FE_i/E}$. However, the measured signal fluctuations are usually dominated by electronic noise or energy loss fluctuations in the detector. The electronic noise contributions depend on the pulse shaping in the signal processing electronics, so the choice of the shaping time is critical (see Sec. 34.8).

A smaller bandgap would produce a larger signal and improve energy resolution, but the intrinsic resistance of the material is critical. Thermal excitation, given by the Fermi-Dirac distribution, promotes electrons into the conduction band, so the thermally excited carrier concentration increases exponentially with decreasing bandgaps. In pure Si the carrier concentration is $\sim 10^{10}$cm^{-3} at 300 K, corresponding to a resistivity $\rho \approx 400\,$k$\Omega\,$cm. In reality, crystal imperfections and minute impurity concentrations limit Si carrier concentrations to $\sim 10^{11}$ cm^{-3} at 300 K, corresponding to a resistivity $\rho \approx 40\,$k$\Omega\,$cm. In practice, resistivities up to 20 k$\Omega\,$cm are available, with mass production ranging from 5 to 10 k$\Omega\,$cm. Signal currents at keV scale energies are of order μA. However, for a resistivity of 10^4 Ωcm a 300 μm thick sensor with 1 cm^2 area would have a resistance of 300 Ω , so 30 V would lead to a current flow of 100 mA and a power dissipation of 3 W. On the other hand, high-quality single crystals of Si and Ge can be grown economically with suitably large volumes, so to mitigate the effect of resistivity one resorts to reverse-biased diode structures. Although this reduces the bias current relative to a resistive material, the thermally excited leakage current can still be excessive at room temperature, so Ge diodes are typically operated at liquid nitrogen temperature (77 K).

A major effort is to find high-Z materials with a bandgap that is sufficiently high to allow room-temperature operation while still providing good energy resolution. Compound semiconductors, *e.g.*, CdZnTe, can allow this, but typically suffer from charge collection problems, characterized by the product $\mu\tau$ of mobility and carrier lifetime. In Si and Ge $\mu\tau > 1\,$cm$^2\,$V^{-1} for both electrons and holes, whereas in compound semiconductors it is in the range 10^{-3}–10^{-8}. Since for holes $\mu\tau$ is typically an order of magnitude smaller than for electrons, detector configurations where the electron contribution to the charge signal dominates—*e.g.*, strip or pixel structures—can provide better performance.

34.7.2. ***Detector Configurations*** :

A p-n junction operated at reverse bias forms a sensitive region depleted of mobile charge and sets up an electric field that sweeps charge liberated by radiation to the electrodes. Detectors typically use an asymmetric structure, *e.g.*, a highly doped p electrode and a lightly doped n region, so that the depletion region extends predominantly into the lightly doped volume.
In a planar device the thickness of the depleted region is

$$W = \sqrt{2\epsilon\,(V + V_{bi})/Ne} = \sqrt{2\rho\mu\epsilon(V + V_{bi})}\ , \qquad (34.19)$$

where $V =$ external bias voltage
$V_{bi} =$ "built-in" voltage (≈ 0.5 V for resistivities typically used in Si detectors)
$N =$ doping concentration
$e =$ electronic charge
$\epsilon =$ dielectric constant = 11.9 $\epsilon_0 \approx 1$ pF/cm in Si
$\rho =$ resistivity (typically 1–10 kΩ cm in Si)
$\mu =$ charge carrier mobility
= 1350 cm^2 V^{-1} s^{-1} for electrons in Si
= 450 cm^2 V^{-1} s^{-1} for holes in Si

In Si

$W = 0.5\ [\mu\text{m}/\sqrt{\Omega\text{-cm} \cdot \text{V}}] \times \sqrt{\rho(V + V_{bi})}$ for n-type Si, and

$W = 0.3\ [\mu\text{m}/\sqrt{\Omega\text{-cm} \cdot \text{V}}] \times \sqrt{\rho(V + V_{bi})}$ for p-type Si.

The conductive p and n regions together with the depleted volume form a capacitor with the capacitance per unit area

$$C = \epsilon/W \approx 1\,[\mathrm{pF/cm}]\,/W \text{ in Si.} \tag{34.20}$$

In strip and pixel detectors the capacitance is dominated by the fringing capacitance to neighboring electrodes. For example, the strip-to-strip Si fringing capacitance is $\sim$ 1–1.5 pF cm^{-1} of strip length at a strip pitch of 25–50 μm.

Large volume ($\sim 10^2$–10^3 cm^3) Ge detectors are commonly configured as coaxial detectors, *e.g.*, a cylindrical n-type crystal with 5–10 cm diameter and 10 cm length with an inner 5–10 mm diameter n^+ electrode and an outer p^+ layer forming the diode junction. Ge can be grown with very low impurity levels, 10^9–10^{10} cm^{-3} (HPGe), so these large volumes can be depleted with several kV.

34.7.3. ***Signal Formation*** :

The signal pulse shape depends on the instantaneous carrier velocity $v(x) = \mu E(x)$ and the electrode geometry, which determines the distribution of induced charge (*e.g.*, see Ref. 147, pp. 71–83). Charge collection time decreases with increasing bias voltage, and can be reduced further by operating the detector with "overbias," *i.e.*, a bias voltage exceeding the value required to fully deplete the device. Note that in partial depletion the electric field goes to zero, whereas going beyond full depletion adds a constantly distributed field. The collection time is limited by velocity saturation at high fields (in Si approaching 10^7 cm/s at $E > 10^4$ V/cm); at an average field of 10^4 V/cm the collection time is about 15 ps/μm for electrons and 30 ps/μm for holes. In typical fully-depleted detectors 300 μm thick, electrons are collected within about 10 ns, and holes within about 25 ns.

Position resolution is limited by transverse diffusion during charge collection (typically 5 μm for 300 μm thickness) and by knock-on electrons. Resolutions of 2–4 μm (rms) have been obtained in beam tests. In magnetic fields, the Lorentz drift deflects the electron and hole trajectories and the detector must be tilted to reduce spatial spreading (see "Hall effect" in semiconductor textbooks).

Electrodes can be in the form of cm-scale pads, strips, or μm-scale pixels. Various readout structures have been developed for pixels, *e.g.*, CCDs, DEPFETs, monolithic pixel devices that integrate sensor and electronics (MAPS), and hybrid pixel devices that utilize separate sensors and readout ICs connected by two-dimensional arrays of solder bumps. For an overview and further discussion see Ref. 147.

In gamma ray spectroscopy ($E_\gamma > 10^2$ keV) Compton scattering dominates, so for a significant fraction of events the incident gamma energy is not completely absorbed, *i.e.*, the Compton scattered photon escapes from the detector and the energy deposited by the Compton electron is only a fraction of the total. Distinguishing multi-interaction events, *e.g.*, multiple Compton scatters with a final photoelectric absorption, from single Compton scatters allows background suppression. Since the individual interactions take place in different parts of the detector volume, these events can be distinguished by segmenting the outer electrode of a coaxial detector and analyzing the current pulse shapes. The different collection times can be made more distinguishable by using "point" electrodes, where most of the signal is induced when charges are close to the electrode, similarly to strip or pixel detectors. Charge clusters arriving from different positions in the detector will arrive at different times and produce current pulses whose major components are separated in time. Point electrodes also reduce the electrode capacitance, which reduces electronic noise, but careful design is necessary to avoid low-field regions in the detector volume.

34.7.4. ***Radiation Damage*** : Radiation damage occurs through two basic mechanisms:

1. Bulk damage due to displacement of atoms from their lattice sites. This leads to increased leakage current, carrier trapping, and build-up of space charge that changes the required operating voltage. Displacement damage depends on the nonionizing energy loss and the energy imparted to the recoil atoms, which can initiate a chain of subsequent displacements, *i.e.*, damage clusters. Hence, it is critical to consider both particle type and energy.
2. Surface damage due to charge build-up in surface layers, which leads to increased surface leakage currents. In strip detectors the inter-strip isolation is affected. The effects of charge build-up are strongly dependent on the device structure and on fabrication details. Since the damage is proportional to the absorbed energy (when ionization dominates), the dose can be specified in rad (or Gray) independent of particle type.

The increase in reverse bias current due to bulk damage is $\Delta I_r = \alpha\Phi$ per unit volume, where Φ is the particle fluence and α the damage coefficient ($\alpha \approx 3 \times 10^{-17}$ A/cm for minimum ionizing protons and pions after long-term annealing; $\alpha \approx 2 \times 10^{-17}$ A/cm for 1 MeV neutrons). The reverse bias current depends strongly on temperature

$$\frac{I_R(T_2)}{I_R(T_1)} = \left(\frac{T_2}{T_1}\right)^2 \exp\left[-\frac{E}{2k}\left(\frac{T_1 - T_2}{T_1 T_2}\right)\right] , \tag{34.21}$$

where $E = 1.2$ eV, so rather modest cooling can reduce the current substantially ($\sim$ 6-fold current reduction in cooling from room temperature to 0°C).

Displacement damage forms acceptor-like states. These trap electrons, building up a negative space charge, which in turn requires an increase in the applied voltage to sweep signal charge through the detector thickness. This has the same effect as a change in resistivity, *i.e.*, the required voltage drops initially with fluence, until the positive and negative space charge balance and very little voltage is required to collect all signal charge. At larger fluences the negative space charge dominates, and the required operating voltage increases ($V \propto N$). The safe limit on operating voltage ultimately limits the detector lifetime. Strip detectors specifically designed for high voltages have been extensively operated at bias voltages >500 V. Since the effect of radiation damage depends on the electronic activity of defects, various techniques have been applied to neutralize the damage sites. For example, additional doping with oxygen can increase the allowable charged hadron fluence roughly three-fold [149]. Detectors with columnar electrodes normal to the surface can also extend operational lifetime [150]. The increase in leakage current with fluence, on the other hand, appears to be unaffected by resistivity and whether the material is n or p-type. At fluences beyond 10^{15} cm^{-2} decreased carrier lifetime becomes critical [151,152].

Strip and pixel detectors have remained functional at fluences beyond 10^{15} cm^{-2} for minimum ionizing protons. At this damage level, charge loss due to recombination and trapping becomes significant and the high signal-to-noise ratio obtainable with low-capacitance pixel structures extends detector lifetime. The higher mobility of electrons makes them less sensitive to carrier lifetime than holes, so detector configurations that emphasize the electron contribution to the charge signal are advantageous, *e.g.*, n^+ strips or pixels on a p- or n-substrate. The occupancy of the defect charge states is strongly temperature dependent; competing processes can increase or decrease the required operating voltage. It is critical to choose the operating temperature judiciously (−10 to 0°C in typical collider detectors) and limit warm-up periods during maintenance. For a more detailed summary see Ref. 153 and and the web-sites of the ROSE and RD50 collaborations at `http://RD48.web.cern.ch/rd48` and `http://RD50.web.cern.ch/rd50`. Materials engineering, *e.g.*, introducing oxygen interstitials, can improve certain aspects and is under investigation. At high fluences diamond is an alternative, but operates as an insulator rather than a reverse-biased diode.

Currently, the lifetime of detector systems is still limited by the detectors; in the electronics use of standard "deep submicron" CMOS fabrication processes with appropriately designed circuitry has increased the radiation resistance to fluences $> 10^{15}$ cm^{-2} of minimum

ionizing protons or pions. For a comprehensive discussion of radiation effects see Ref. 154.

34.8. Low-noise electronics

Revised November 2013 by H. Spieler.

Many detectors rely critically on low-noise electronics, either to improve energy resolution or to allow a low detection threshold. A typical detector front-end is shown in Fig. 34.18.

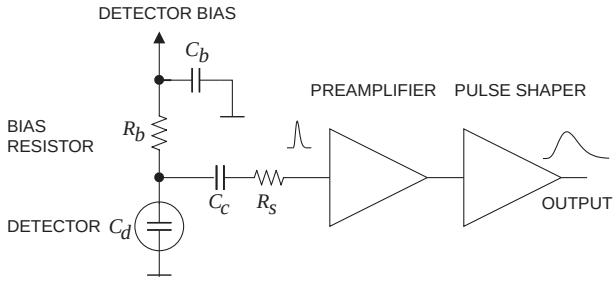

Figure 34.18: Typical detector front-end circuit.

The detector is represented by a capacitance C_d, a relevant model for most detectors. Bias voltage is applied through resistor R_b and the signal is coupled to the preamplifier through a blocking capacitor C_c. The series resistance R_s represents the sum of all resistances present in the input signal path, *e.g.* the electrode resistance, any input protection networks, and parasitic resistances in the input transistor. The preamplifier provides gain and feeds a pulse shaper, which tailors the overall frequency response to optimize signal-to-noise ratio while limiting the duration of the signal pulse to accommodate the signal pulse rate. Even if not explicitly stated, all amplifiers provide some form of pulse shaping due to their limited frequency response.

The equivalent circuit for the noise analysis (Fig. 34.19) includes both current and voltage noise sources. The leakage current of a semiconductor detector, for example, fluctuates due to continuous electron emission statistics. The statistical fluctuations in the charge measurement will scale with the square root of the total number of recorded charges, so this noise contribution increases with the width of the shaped output pulse. This "shot noise" i_{nd} is represented by a current noise generator in parallel with the detector. Resistors exhibit noise due to thermal velocity fluctuations of the charge carriers. This yields a constant noise power density vs. frequency, so increasing the bandwidth of the shaped output pulse, *i.e.* reducing the shaping time, will increase the noise. This noise source can be modeled either as a voltage or current generator. Generally, resistors shunting the input act as noise current sources and resistors in series with the input act as noise voltage sources (which is why some in the detector community refer to current and voltage noise as "parallel" and "series" noise). Since the bias resistor effectively shunts the input, as the capacitor C_b passes current fluctuations to ground, it acts as a current generator i_{nb} and its noise current has the same effect as the shot noise current from the detector. Any other shunt resistances can be incorporated in the same way. Conversely, the series resistor R_s acts as a voltage generator. The electronic noise of the amplifier is described fully by a combination of voltage and current sources at its input, shown as e_{na} and i_{na}.

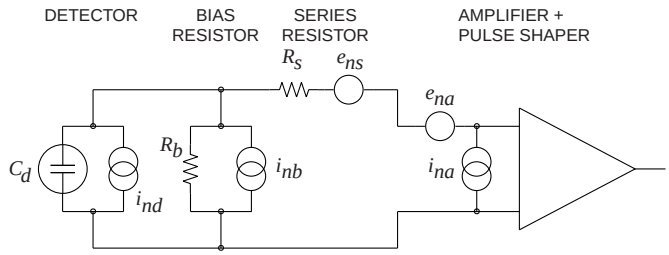

Figure 34.19: Equivalent circuit for noise analysis.

Shot noise and thermal noise have a "white" frequency distribution, *i.e.* the spectral power densities $dP_n/df \propto di_n^2/df \propto de_n^2/df$ are constant with the magnitudes

$$\begin{aligned} i_{nd}^2 &= 2eI_d \ , \\ i_{nb}^2 &= \frac{4kT}{R_b} \ , \\ e_{ns}^2 &= 4kTR_s \ , \end{aligned} \tag{34.22}$$

where e is the electronic charge, I_d the detector bias current, k the Boltzmann constant and T the temperature. Typical amplifier noise parameters e_{na} and i_{na} are of order $\mathrm{nV}/\sqrt{\mathrm{Hz}}$ and $\mathrm{pA}/\sqrt{\mathrm{Hz}}$. Trapping and detrapping processes in resistors, dielectrics and semiconductors can introduce additional fluctuations whose noise power frequently exhibits a $1/f$ spectrum. The spectral density of the $1/f$ noise voltage is

$$e_{nf}^2 = \frac{A_f}{f} \ , \tag{34.23}$$

where the noise coefficient A_f is device specific and of order 10^{-10}–$10^{-12}\,\mathrm{V}^2$.

A fraction of the noise current flows through the detector capacitance, resulting in a frequency-dependent noise voltage $i_n/(\omega C_d)$, which is added to the noise voltage in the input circuit. Thus, the current noise contribution increases with lowering frequency, so its contribution increases with shaping pulse width. Since the individual noise contributions are random and uncorrelated, they add in quadrature. The total noise at the output of the pulse shaper is obtained by integrating over the full bandwidth of the system. Superimposed on repetitive detector signal pulses of constant magnitude, purely random noise produces a Gaussian signal distribution.

Since radiation detectors typically convert the deposited energy into charge, the system's noise level is conveniently expressed as an equivalent noise charge Q_n, which is equal to the detector signal that yields a signal-to-noise ratio of one. The equivalent noise charge is commonly expressed in Coulombs, the corresponding number of electrons, or the equivalent deposited energy (eV). For a capacitive sensor

$$Q_n^2 = i_n^2 F_i T_S + e_n^2 F_v \frac{C^2}{T_S} + F_{vf} A_f C^2 \ , \tag{34.24}$$

where C is the sum of all capacitances shunting the input, F_i, F_v, and F_{vf} depend on the shape of the pulse determined by the shaper and T_s is a characteristic time, for example, the peaking time of a semi-gaussian pulse or the sampling interval in a correlated double sampler. The form factors F_i, F_v are easily calculated

$$F_i = \frac{1}{2T_S}\int_{-\infty}^{\infty} [W(t)]^2\,dt \ , \qquad F_v = \frac{T_S}{2}\int_{-\infty}^{\infty}\left[\frac{dW(t)}{dt}\right]^2 dt \ , \tag{34.25}$$

where for time-invariant pulse-shaping $W(t)$ is simply the system's impulse response (the output signal seen on an oscilloscope) for a short input pulse with the peak output signal normalized to unity. For more details see Refs. 155 and 156.

A pulse shaper formed by a single differentiator and integrator with equal time constants has $F_i = F_v = 0.9$ and $F_{vf} = 4$, independent of the shaping time constant. The overall noise bandwidth, however, depends on the time constant, *i.e.* the characteristic time T_s. The contribution from noise currents increases with shaping time, *i.e.*, pulse duration, whereas the voltage noise decreases with increasing shaping time, *i.e.* reduced bandwidth. Noise with a $1/f$ spectrum depends only on the ratio of upper to lower cutoff frequencies (integrator to differentiator time constants), so for a given shaper topology the $1/f$ contribution to Q_n is independent of T_s. Furthermore, the contribution of noise voltage sources to Q_n increases with detector capacitance. Pulse shapers can be designed to reduce the effect of current noise, *e.g.*, mitigate radiation damage. Increasing pulse symmetry tends to decrease F_i and increase F_v (*e.g.*, to 0.45 and 1.0 for a shaper with one CR differentiator and four cascaded integrators). For the circuit shown in Fig. 34.19,

$$\begin{aligned} Q_n^2 = &\left(2eI_d + 4kT/R_b + i_{na}^2\right)F_i T_S \\ &+ \left(4kTR_s + e_{na}^2\right)F_v C_d^2/T_S + F_{vf}A_f C_d^2 \ . \end{aligned} \tag{34.26}$$

As the characteristic time T_S is changed, the total noise goes through a minimum, where the current and voltage contributions are equal. Fig. 34.20 shows a typical example. At short shaping times the voltage noise dominates, whereas at long shaping times the current noise takes over. The noise minimum is flattened by the presence of $1/f$ noise. Increasing the detector capacitance will increase the voltage noise and shift the noise minimum to longer shaping times.

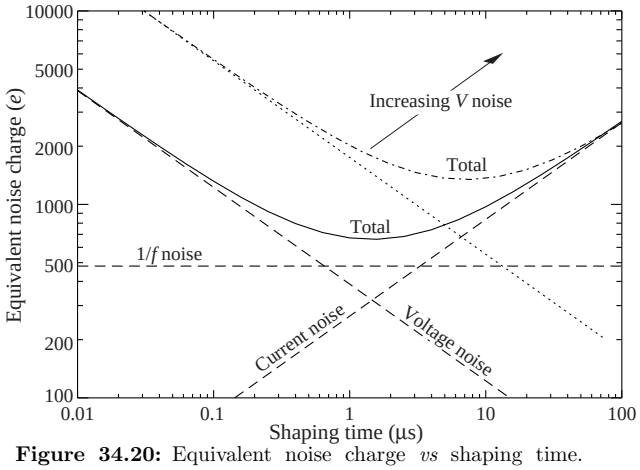

Figure 34.20: Equivalent noise charge *vs* shaping time. Changing the voltage or current noise contribution shifts the noise minimum. Increased voltage noise is shown as an example.

For quick estimates, one can use the following equation, which assumes an FET amplifier (negligible i_{na}) and a simple CR–RC shaper with time constants τ (equal to the peaking time):

$$(Q_n/e)^2 = 12\left[\frac{1}{\mathrm{nA\cdot ns}}\right] I_d\tau + 6\times 10^5\left[\frac{\mathrm{k\Omega}}{\mathrm{ns}}\right]\frac{\tau}{R_b} + 3.6\times 10^4\left[\frac{\mathrm{ns}}{(\mathrm{pF})^2(\mathrm{nV})^2/\mathrm{Hz}}\right] e_n^2\frac{C^2}{\tau}\ . \quad (34.27)$$

Noise is improved by reducing the detector capacitance and leakage current, judiciously selecting all resistances in the input circuit, and choosing the optimum shaping time constant. Another noise contribution to consider is that noise cross-couples from the neighboring front-ends in strip and pixel detectors through the inter-electrode capacitance.

The noise parameters of the amplifier depend primarily on the input device. In field effect transistors, the noise current contribution is very small, so reducing the detector leakage current and increasing the bias resistance will allow long shaping times with correspondingly lower noise. In bipolar transistors, the base current sets a lower bound on the noise current, so these devices are best at short shaping times. In special cases where the noise of a transistor scales with geometry, *i.e.*, decreasing noise voltage with increasing input capacitance, the lowest noise is obtained when the input capacitance of the transistor is equal to the detector capacitance, albeit at the expense of power dissipation. Capacitive matching is useful with field-effect transistors, but not bipolar transistors. In bipolar transistors, the minimum obtainable noise is independent of shaping time, but only at the optimum collector current I_C, which does depend on shaping time.

$$Q^2_{n,\min} = 4kT\frac{C}{\sqrt{\beta_{DC}}}\sqrt{F_iF_v} \ \text{ at } \ I_c = \frac{kT}{e}C\sqrt{\beta_{DC}}\sqrt{\frac{F_v}{F_i}}\frac{1}{T_S}\ , \quad (34.28)$$

where β_{DC} is the DC current gain. For a CR–RC shaper and $\beta_{DC} = 100$,

$$Q_{n,\min}/e \approx 250\sqrt{C/\mathrm{pF}}\ . \quad (34.29)$$

Practical noise levels range from $\sim 1e$ for CCD's at long shaping times to $\sim 10^4$ e in high-capacitance liquid argon calorimeters. Silicon strip detectors typically operate at $\sim 10^3$ electrons, whereas pixel detectors with fast readout provide noise of several hundred electrons.

In timing measurements, the slope-to-noise ratio must be optimized, rather than the signal-to-noise ratio alone, so the rise time t_r of the pulse is important. The "jitter" σ_t of the timing distribution is

$$\sigma_t = \frac{\sigma_n}{(dS/dt)_{S_T}} \approx \frac{t_r}{S/N}\ , \quad (34.30)$$

where σ_n is the rms noise and the derivative of the signal dS/dt is evaluated at the trigger level S_T. To increase dS/dt without incurring excessive noise, the amplifier bandwidth should match the rise-time of the detector signal. The 10 to 90% rise time of an amplifier with bandwidth f_U is $0.35/f_U$. For example, an oscilloscope with 350 MHz bandwidth has a 1 ns rise time. When amplifiers are cascaded, which is invariably necessary, the individual rise times add in quadrature.

$$t_r \approx \sqrt{t_{r1}^2 + t_{r2}^2 + ... + t_{rn}^2}\ . \quad (34.31)$$

Increasing signal-to-noise ratio also improves time resolution, so minimizing the total capacitance at the input is also important. At high signal-to-noise ratios, the time jitter can be much smaller than the rise time. The timing distribution may shift with signal level ("walk"), but this can be corrected by various means, either in hardware or software [8].

The basic principles discussed above apply to both analog and digital signal processing. In digital signal processing the pulse shaper shown in Fig. 34.18 is replaced by an analog to digital converter (ADC) followed by a digital processor that determines the pulse shape. Digital signal processing allows great flexibility in implementing filtering functions. The software can be changed readily to adapt to a wide variety of operating conditions and it is possible to implement filters that are impractical or even impossible using analog circuitry. However, this comes at the expense of increased circuit complexity and increased demands on the ADC compared to analog shaping.

If the sampling rate of the ADC is too low, high frequency components will be transferred to lower frequencies ("aliasing"). The sampling rate of the ADC must be high enough to capture the maximum frequency component of the input signal. Apart from missing information on the fast components of the pulse, undersampling introduces spurious artifacts. If the frequency range of the input signal is much greater, the noise at the higher frequencies will be transferred to lower frequencies and increase the noise level in the frequency range of pulses formed in the subsequent digital shaper. The Nyquist criterion states that the sampling frequency must be at least twice the maximum relevant input frequency. This requires that the bandwith of the circuitry preceding the ADC must be limited. The most reliable technique is to insert a low-pass filter.

The digitization process also introduces inherent noise, since the voltage range ΔV corresponding to a minimum bit introduces quasi-random fluctuations relative to the exact amplitude

$$\sigma_n = \frac{\Delta V}{\sqrt{12}}\ . \quad (34.32)$$

When the Nyquist condition is fulfilled the noise bandwidth Δf_n is spread nearly uniformly and extends to 1/2 the sampling frequency f_S, so the spectral noise density

$$e_n = \frac{\sigma_n}{\sqrt{\Delta f_n}} = \frac{\Delta V}{\sqrt{12}}\cdot\frac{1}{\sqrt{f_S/2}} = \frac{\Delta V}{\sqrt{6f_S}}\ . \quad (34.33)$$

Sampling at a higher frequency spreads the total noise over a larger frequency range, so oversampling can be used to increase the effective resolution. In practice, this quantization noise is increased by differential nonlinearity. Furthermore, the equivalent input noise of ADCs is often rather high, so the overall gain of the stages preceding the ADC must be sufficiently large for the preamplifier input noise to override.

When implemented properly, digital signal processing provides significant advantages in systems where the shape of detector signal pulses changes greatly, for example in large semiconductor detectors for gamma rays or in gaseous detectors (*e.g.* TPCs) where the duration of the current pulse varies with drift time, which can range

over orders of magnitude. Where is analog signal processing best (most efficient)? In systems that require fast time response the high power requirements of high-speed ADCs are prohibitive. Systems that are not sensitive to pulse shape can use fixed shaper constants and rather simple filters, which can be either continuous or sampled. In high density systems that require small circuit area and low power (*e.g.* strip and pixel detectors), analog filtering often yields the required response and tends to be most efficient.

It is important to consider that additional noise is often introduced by external electronics, *e.g.* power supplies and digital systems. External noise can couple to the input. Often the "common grounding" allows additional noise current to couple to the current loop connecting the detector to the preamp. Recognizing additional noise sources and minimizing cross-coupling to the detector current loop is often important. Understanding basic physics and its practical effects is important in forming a broad view of the detector system and recognizing potential problems (*e.g.* modified data), rather than merely following standard recipes.

For a more detailed introduction to detector signal processing and electronics see Ref. 147 or the tutorial website `http://www-physics.lbl.gov/spieler`.

34.9. Calorimeters

A calorimeter is designed to measure a particle's (or jet's) energy and direction for an (ideally) contained electromagnetic (EM) or hadronic shower. The characteristic interaction distance for an electromagnetic interaction is the radiation length X_0, which ranges from 13.8 g cm^{-2} in iron to 6.0 g cm^{-2} in uranium.* Similarly, the characteristic nuclear interaction length λ_I varies from 132.1 g cm^{-2} (Fe) to 209 g cm^{-2} (U).† In either case, a calorimeter must be many interaction lengths deep, where "many" is determined by physical size, cost, and other factors. EM calorimeters tend to be 15–30 X_0 deep, while hadronic calorimeters are usually compromised at 5–8 λ_I. In real experiments there is likely to be an EM calorimeter in front of the hadronic section, which in turn has less sampling density in the back, so the hadronic cascade occurs in a succession of different structures.

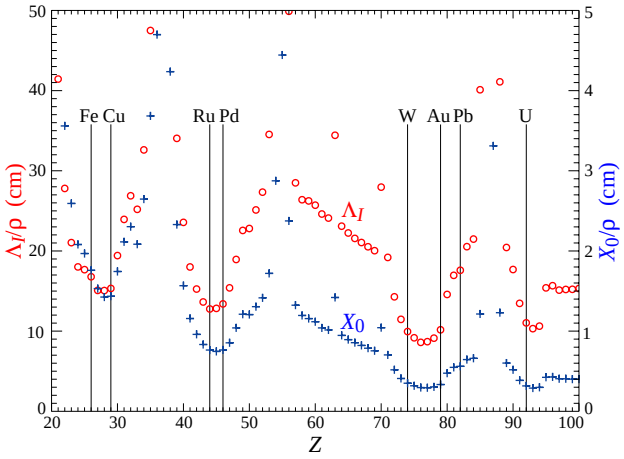

Figure 34.21: Nuclear interaction length λ_I/ρ (circles) and radiation length X_0/ρ (+'s) in cm for the chemical elements with $Z > 20$ and $\lambda_I < 50$ cm.

In all cases there is a premium on small λ_I/ρ and X_0/ρ (both with units of length). These quantities are shown for $Z > 20$ for the chemical elements in Fig. 34.21. For the hadronic case, metallic absorbers in the W–Au region are best, followed by U. The Ru–Pd region elements are rare and expensive. Lead is a bad choice. Given cost considerations, Fe and Cu might be appropriate choices. For EM calorimeters high Z is preferred, and lead is not a bad choice.

These considerations are for *sampling calorimeters* consisting of metallic absorber sandwiched or (threaded) with an active material which generates signal. The active medium may be a scintillator, an ionizing noble liquid, a gas chamber, a semiconductor, or a Cherenkov radiator. The average interaction length is thus greater than that of the absorber alone, sometimes substantially so.

There are also *homogeneous calorimeters,* in which the entire volume is sensitive, *i.e.*, contributes signal. Homogeneous calorimeters (so far usually electromagnetic) may be built with inorganic heavy (high density, high $\langle Z \rangle$) scintillating crystals, or non-scintillating Cherenkov radiators such as lead glass and lead fluoride. Scintillation light and/or ionization in noble liquids can be detected. Nuclear interaction lengths in inorganic crystals range from 17.8 cm ($LuAlO_3$) to 42.2 cm (NaI). Popular choices have been BGO with $\lambda_I = 22.3$ cm and $X_0 = 1.12$ cm, and $PbWO_4$ (20.3 cm and 0.89 cm). Properties of these and other commonly used inorganic crystal scintillators can be found in Table 34.4.

34.9.1. *Electromagnetic calorimeters* :

Revised September 2015 by R.-Y. Zhu (California Institute of Technology).

The development of electromagnetic showers is discussed in the section on "Passage of Particles Through Matter" (Sec. 33 of this *Review*). Formulae are given which approximately describe average showers, but since the physics of electromagnetic showers is well understood, detailed and reliable Monte Carlo simulation is possible. EGS4 [157] and GEANT [158] have emerged as the standards.

There are homogeneous and sampling electromagnetic calorimeters. In a homogeneous calorimeter the entire volume is sensitive, *i.e.*, contributes signal. Homogeneous electromagnetic calorimeters may be built with inorganic heavy (high-Z) scintillating crystals such as BaF_2, BGO, CsI, LYSO, NaI and PWO, non-scintillating Cherenkov radiators such as lead glass and lead fluoride (PbF_2), or ionizing noble liquids. Properties of commonly used inorganic crystal scintillators can be found in Table 34.4. A sampling calorimeter consists of an active medium which generates signal and a passive medium which functions as an absorber. The active medium may be a scintillator, an ionizing noble liquid, a semiconductor, or a gas chamber. The passive medium is usually a material of high density, such as lead, tungsten, iron, copper, or depleted uranium.

The energy resolution σ_E/E of a calorimeter can be parameterized as $a/\sqrt{E} \oplus b \oplus c/E$, where $\oplus$ represents addition in quadrature and E is in GeV. The stochastic term a represents statistics-related fluctuations such as intrinsic shower fluctuations, photoelectron statistics, dead material at the front of the calorimeter, and sampling fluctuations. For a fixed number of radiation lengths, the stochastic term a for a sampling calorimeter is expected to be proportional to $\sqrt{t/f}$, where t is plate thickness and f is sampling fraction [159,160]. While a is at a few percent level for a homogeneous calorimeter, it is typically 10% for sampling calorimeters.

The main contributions to the systematic, or constant, term b are detector non-uniformity and calibration uncertainty. In the case of the hadronic cascades discussed below, non-compensation also contributes to the constant term. One additional contribution to the constant term for calorimeters built for modern high-energy physics experiments, operated in a high-beam intensity environment, is radiation damage of the active medium. This can be mitigated by developing radiation-hard active media [52], by reducing the signal path length [55] and by frequent *in situ* calibration and monitoring [51,160]. With effort, the constant term b can be reduced to below one percent. The term c is due to electronic noise summed over readout channels within a few Molière radii. The best energy resolution for electromagnetic shower measurement is obtained in total absorption homogeneous calorimeters, *e.g.* calorimeters built with heavy crystal scintillators. These are used when ultimate performance is pursued.

The position resolution depends on the effective Molière radius and the transverse granularity of the calorimeter. Like the energy resolution, it can be factored as $a/\sqrt{E} \oplus b$, where a is a few to 20 mm and b can be as small as a fraction of mm for a dense calorimeter with fine granularity. Electromagnetic calorimeters may also provide direction measurement for electrons and photons. This is important for photon-related physics when there are uncertainties in event origin, since photons do not leave information in the particle tracking system.

* $X_0 = 120\ \mathrm{g\,cm^{-2}}\ Z^{-2/3}$ to better than 5% for $Z > 23$.

† $\lambda_I = 37.8\ \mathrm{g\,cm^{-2}}\ A^{0.312}$ to within 0.8% for $Z > 15$.

See `pdg.lbl.gov/AtomicNuclearProperties` for actual values.

Typical photon angular resolution is about 45 mrad/$\sqrt{E}$, which can be provided by implementing longitudinal segmentation [161] for a sampling calorimeter or by adding a preshower detector [162] for a homogeneous calorimeter without longitudinal segmentation.

Novel technologies have been developed for electromagnetic calorimetry. New heavy crystal scintillators, such as PWO and LYSO:Ce (see Sec. 34.4), have attracted much attention. In some cases, such as PWO, it has received broad applications in high-energy and nuclear physics experiments. The "spaghetti" structure has been developed for sampling calorimetry with scintillating fibers as the sensitive medium. The "shashlik" structure has been developed for sampling calorimetry with wavelength shifting fibers functioning as both the converter and transporter for light generated in the sensitive medium. The "accordion" structure has been developed for sampling calorimetry with ionizing noble liquid as the sensitive medium.

Table 34.8 provides a brief description of typical electromagnetic calorimeters built recently for high-energy physics experiments. Also listed in this table are calorimeter depths in radiation lengths (X_0) and the achieved energy resolution. Whenever possible, the performance of calorimeters *in situ* is quoted, which is usually in good agreement with prototype test beam results as well as EGS or GEANT simulations, provided that all systematic effects are properly included. Detailed references on detector design and performance can be found in Appendix C of reference [160] and Proceedings of the International Conference series on Calorimetry in High Energy Physics.

Table 34.8: Resolution of typical electromagnetic calorimeters. E is in GeV.

Technology (Experiment)	Depth	Energy resolution	Date
NaI(Tl) (Crystal Ball)	$20X_0$	$2.7\%/\mathrm{E}^{1/4}$	1983
$Bi_4Ge_3O_{12}$ (BGO) (L3)	$22X_0$	$2\%/\sqrt{E}\oplus 0.7\%$	1993
CsI (KTeV)	$27X_0$	$2\%/\sqrt{E}\oplus 0.45\%$	1996
CsI(Tl) (BaBar)	16–$18X_0$	$2.3\%/E^{1/4}\oplus 1.4\%$	1999
CsI(Tl) (BELLE)	$16X_0$	1.7% for $E_\gamma > 3.5$ GeV	1998
$PbWO_4$ (PWO) (CMS)	$25X_0$	$3\%/\sqrt{E}\oplus 0.5\%\oplus 0.2/E$	1997
Lead glass (OPAL)	$20.5X_0$	$5\%/\sqrt{E}$	1990
Liquid Kr (NA48)	$27X_0$	$3.2\%/\sqrt{E}\oplus 0.42\%\oplus 0.09/E$	1998
Scintillator/depleted U (ZEUS)	20–$30X_0$	$18\%/\sqrt{E}$	1988
Scintillator/Pb (CDF)	$18X_0$	$13.5\%/\sqrt{E}$	1988
Scintillator fiber/Pb spaghetti (KLOE)	$15X_0$	$5.7\%/\sqrt{E}\oplus 0.6\%$	1995
Liquid Ar/Pb (NA31)	$27X_0$	$7.5\%/\sqrt{E}\oplus 0.5\%\oplus 0.1/E$	1988
Liquid Ar/Pb (SLD)	$21X_0$	$8\%/\sqrt{E}$	1993
Liquid Ar/Pb (H1)	20–$30X_0$	$12\%/\sqrt{E}\oplus 1\%$	1998
Liquid Ar/depl. U (DØ)	$20.5X_0$	$16\%/\sqrt{E}\oplus 0.3\%\oplus 0.3/E$	1993
Liquid Ar/Pb accordion (ATLAS)	$25X_0$	$10\%/\sqrt{E}\oplus 0.4\%\oplus 0.3/E$	1996

34.9.2. ***Hadronic calorimeters*** : [1–5,160]
Revised September 2013 by D. E. Groom (LBNL).

Hadronic calorimetry is considerably more difficult than EM calorimetry. For the same cascade containment fraction discussed in the previous section, the calorimeter would need to be ∼30 times deeper. Electromagnetic energy deposit from the decay of a small number of π^0's are usually detected with greater efficiency than are the hadronic parts of the cascade, themselves subject to large fluctuations in neutron production, undetectable energy loss to nuclear disassociation, and other effects.

Most large hadron calorimeters are parts of large 4π detectors at colliding beam facilities. At present these are sampling calorimeters: plates of absorber (Fe, Pb, Cu, or occasionally U or W) alternating with plastic scintillators (plates, tiles, bars), liquid argon (LAr), or gaseous detectors. The ionization is measured directly, as in LAr calorimeters, or via scintillation light observed by photodetectors (usually PMT's or silicon photodiodes). Wavelength-shifting fibers are often used to solve difficult problems of geometry and light collection uniformity. Silicon sensors are being studied for ILC detectors; in this case e-h pairs are collected. There are as many variants of these schemes as there are calorimeters, including variations in geometry of the absorber and sensors, *e.g.*, scintillating fibers threading an absorber [163], and the "accordion" LAr detector [164]. The latter has zig-zag absorber plates to minimize channeling effects; the calorimeter is hermitic (no cracks), and plates are oriented so that cascades cross the same plate repeatedly. Another departure from the traditional sandwich structure is the LAr-tube design shown in Fig. 34.22(a) [165].

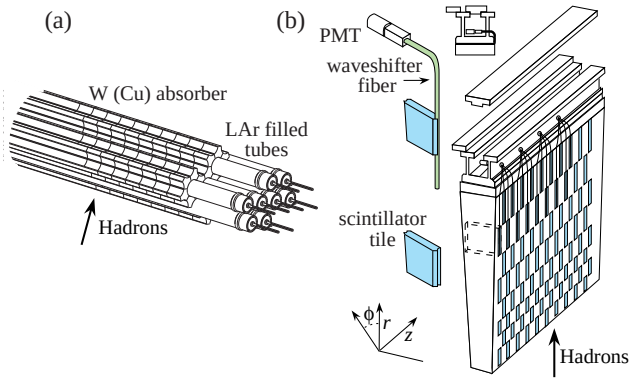

Figure 34.22: (a) ATLAS forward hadronic calorimeter structure (FCal2, 3) [165]. Tubes containing LAr are embedded in a mainly tungsten matrix. (b) ATLAS central calorimeter wedge; iron with plastic scintillator tile with wavelength-shifting fiber readout [166].

A relatively new variant in hadron calorimetry is the detection of Cerenkov light. Such a calorimeter is sensitive to relativistic $e^{\pm}$'s in the EM showers plus a few relativistic pions. An example is the radiation-hard forward calorimeter in CMS, with iron absorber and quartz fiber readout by PMT's [167].

Ideally the calorimeter is segmented in ϕ and θ (or $\eta = -\ln\tan(\theta/2)$). Fine segmentation, while desirable, is limited by cost, readout complexity, practical geometry, and the transverse size of the cascades—but see Ref. 168. An example, a wedge of the ATLAS central barrel calorimeter, is shown in Fig. 34.22(b) [166].

Much of the following discussion assumes an idealized calorimeter, with the same structure throughout and without leakage. "Real" calorimeters usually have an EM detector in front and a coarse "catcher" in the back. Complete containment is generally impractical.

In an inelastic hadronic collision a significant fraction f_{em} of the energy is removed from further hadronic interaction by the production of secondary π^0's and η's, whose decay photons generate high-energy electromagnetic (EM) showers. Charged secondaries ($\pi^{\pm}$, p, ...) deposit energy via ionization and excitation, but also interact with nuclei, producing spallation protons and neutrons, evaporation neutrons, and spallation products. The charged collision products

produce detectable ionization, as do the showering γ-rays from the prompt de-excitation of highly excited nuclei. The recoiling nuclei generate little or no detectable signal. The neutrons lose kinetic energy in elastic collisions, thermalize on a time scale of several μs, and are captured, with the production of more γ-rays—usually outside the acceptance gate of the electronics. Between endothermic spallation losses, nuclear recoils, and late neutron capture, a significant fraction of the hadronic energy (20%–40%, depending on the absorber and energy of the incident particle) is used to overcome nuclear binding energies and is therefore lost or "invisible."

In contrast to EM showers, hadronic cascade processes are characterized by the production of relatively few high-energy particles. The lost energy and f_{em} are highly variable from event to event. Until there is event-by-event knowledge of both the EM fraction and the invisible energy loss, the energy resolution of a hadron calorimeter will remain significantly worse than that of its EM counterpart.

The efficiency e with which EM deposit is detected varies from event to event, but because of the large multiplicity in EM showers the variation is small. In contrast, because a variable fraction of the hadronic energy deposit is detectable, the efficiency h with which hadronic energy is detected is subject to considerably larger fluctuations. It thus makes sense to consider the ratio h/e as a stochastic variable.

Most energy deposit is by very low-energy electrons and charged hadrons. Because so many generations are involved in a high-energy cascade, the hadron spectra in a given material are essentially independent of energy except for overall normalization [170]. For this reason $\langle h/e\rangle$ is a robust concept, independently of hadron energy and species.

If the detection efficiency for the EM sector is e and that for the hadronic sector is h, then the ratio of the mean response to a pion relative to that for an electron is

$$\langle \pi/e\rangle = \langle f_{em}\rangle + \langle f_h\rangle\langle h/e\rangle^* = 1 - (1 - \langle h/e\rangle)\langle f_h\rangle \qquad (34.34)$$

It has been shown by a simple induction argument and verified by experiment, that the decrease in the average value of the hadronic energy fraction $\langle f_h\rangle = 1 - \langle f_{em}\rangle$ as the projectile energy E increases is fairly well described by the power law [169,170]

$$\langle f_h\rangle \approx (E/E_0)^{m-1} \qquad (\text{for } E > E_0)\ , \qquad (34.35)$$

at least up to a few hundred GeV. The exponent m depends logarithmically on the mean multiplicity and the mean fractional loss to π^0 production in a single interaction. It is in the range 0.80–0.87. E_0, roughly the energy for the onset of inelastic collisions, is 1 GeV or a little less for incident pions [169]. Both m and E_0 must be obtained experimentally for a given calorimeter configuration.

Only the product $(1 - \langle h/e\rangle)E_0^{1-m}$ can be obtained by measuring $\langle \pi/e\rangle$ as a function of energy. Since $1 - m$ is small and $E_0 \approx 1$ GeV for pion-induced cascades, this fact is usually ignored and $\langle h/e\rangle$ is reported.

In a hadron-nucleus collision a large fraction of the incident energy is carried by a "leading particle" with the same quark content as the incident hadron. If the projectile is a charged pion, the leading particle is usually a pion, which can be neutral and hence contributes to the EM sector. This is not true for incident protons. The result is an increased mean hadronic fraction for incident protons: $E_0 \approx 2.6$ GeV [169–172].

By definition, $0 \le f_{em} \le 1$. Its variance $\sigma^2_{f_{em}}$ changes only slowly with energy, but perforce $\langle f_{em}\rangle \to 1$ as the projectile energy increases. An empirical power law (unrelated to Eq. (34.34)) of the form $\sigma_{f_{em}} = (E/E_1)^{1-\ell}$ (where $\ell < 1$) describes the energy dependence of the variance adequately and has the right asymptotic properties [160]. For $\langle h/e\rangle \neq 1$ (*noncompensation*), fluctuations in f_{em} significantly contribute to or even dominate the resolution. Since the f_{em} distribution has a high-energy tail, the calorimeter response is non-Gaussian with a high-energy tail if $\langle h/e\rangle < 1$. Noncompensation thus seriously degrades resolution and produces a nonlinear response.

It is clearly desirable to *compensate* the response, *i.e.*, to design the calorimeter such that $\langle h/e\rangle = 1$. This is possible only with a sampling calorimeter, where several variables can be chosen or tuned:

1. Decrease the EM sensitivity. EM cross sections increase with Z,[†] and most of the energy in an EM shower is deposited by low-energy electrons. A disproportionate fraction of the EM energy is thus deposited in the higher-Z absorber. Lower-Z cladding, such as the steel cladding on ZEUS U plates, preferentially absorbs low-energy γ's in EM showers and thus also lowers the electronic response. G10 signal boards in the DØ calorimeters and G10 next to slicon readout detectors has the same effect. The degree of EM signal suppression can be somewhat controlled by tuning the sensor/absorber thickness ratio.
2. Increase the hadronic sensitivity. The abundant neutrons produced in the cascade have large n-p elastic scattering cross sections, so that low-energy scattered protons are produced in hydrogenous sampling materials such as butane-filled proportional counters or plastic scintillator. (The maximal fractional energy loss when a neutron scatters from a nucleus with mass number A is $4A/(1 + A)^2$.) The down side in the scintillator case is that the signal from a highly-ionizing stopping proton can be reduced by as much as 90% by recombination and quenching parameterized by Birks' Law (Eq. (34.2)).
3. Fabjan and Willis proposed that the additional signal generated in the aftermath of fission in ^{238}U absorber plates should compensate nuclear fluctuations [173]. The production of fission fragments due to fast n capture was later observed [174]. However, while a very large amount of energy is released, it is mostly carried by low-velocity, very highly ionizing fission fragments which produce very little observable signal because of recombination and quenching. But in fact much of the compensation observed with the ZEUS ^{238}U/scintillator calorimeter was mainly the result of methods 1 and 2 above.

Motivated very much by the work of Brau, Gabriel, Brückmann, and Wigmans [175], several groups built calorimeters which were very nearly compensating. The degree of compensation was sensitive to the acceptance gate width, and so could be somewhat further tuned. These included

a) HELIOS with 2.5 mm thick scintillator plates sandwiched between 2 mm thick ^{238}U plates (one of several structures); $\sigma/E = 0.34/\sqrt{E}$ was obtained,
b) ZEUS, 2.6 cm thick scintillator plates between 3.3 mm ^{238}U plates; $\sigma/E = 0.35/\sqrt{E}$,
c) a ZEUS prototype with 10 mm Pb plates and 2.5 mm scintillator sheets; $\sigma/E = 0.44/\sqrt{E}$, and
d) DØ, where the sandwich cell consists of a 4–6 mm thick ^{238}U plate, 2.3 mm LAr, a G-10 signal board, and another 2.3 mm LAr gap; $\sigma/E \approx 0.45/\sqrt{E}$.

Given geometrical and cost constraints, the calorimeters used in modern collider detectors are not compensating: $\langle h/e\rangle \approx 0.7$, for the ATLAS central barrel calorimeter, is typical.

A more versatile approach to compensation is provided by a *dual-readout calorimeter*, in which the signal is sensed by two readout systems with highly contrasting $\langle h/e\rangle$. Although the concept is more than two decades old [176], it was only recently been implemented by the DREAM collaboration [177]. The test beam calorimeter consisted of copper tubes, each filled with scintillator and quartz fibers. If the two signals C and S (quartz and scintillator) are both normalized to electron response, then for each event Eq. (34.34) takes the form

$$\begin{aligned} C &= E[f_{em} + \langle h/e\rangle|_C(1 - f_{em})] \\ S &= E[f_{em} + \langle h/e\rangle|_S(1 - f_{em})] \end{aligned} \qquad (34.36)$$

for the Cherenkov and scintillator responses. On a dotplot of C/E vs S/E, events scatter about a line-segment locus described in Fig. 34.23. With increasing energy the distribution moves upward along the locus and becomes tighter. Equations 34.36 are linear in $1/E$ and f_{em}, and are easily solved to obtain estimators of the *corrected* energy and f_{em} for each event. Both are subject to resolution effects, but

* Technically, we should write $\langle f_h(h/e)\rangle$, but we approximate it as $\langle f_h\rangle\langle h/e\rangle$ to facilitate the rest of the discussion.

† The asymptotic pair-production cross section scales roughly as $Z^{0.75}$, and $|dE/dx|$ slowly decreases with increasing Z.

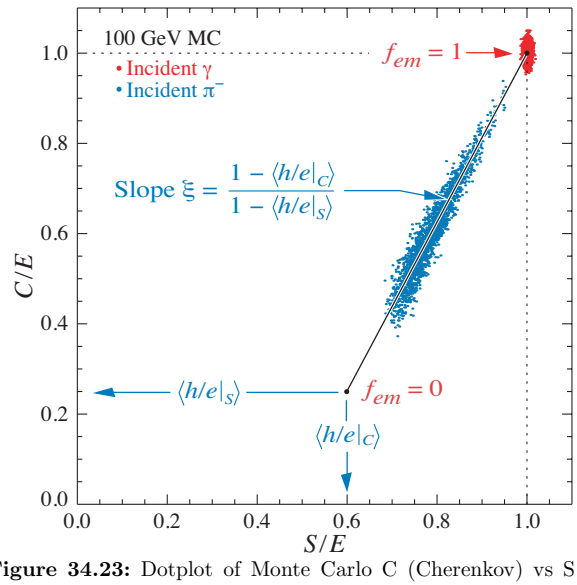

Figure 34.23: Dotplot of Monte Carlo C (Cherenkov) vs S (scintillator) signals for individual events in a dual readout calorimeter. Hadronic (π^-) induced events are shown in blue, and scatter about the indicated event locus. Electromagnetic events cluster about (C,S) = (0,0). In this case worse resolution (fewer p.e.'s) was assumed for the Cherenkov events, leading to the "elliptical" distribution.

contributions due to fluctuations in f_{em} are eliminated. The solution for the corrected energy is given by [170]:

$$E = \frac{\xi S - C}{\xi - 1} \text{ , where } \xi = \frac{1 - \langle h/e \rangle|_C}{1 - \langle h/e \rangle|_S} \tag{34.37}$$

ξ is the energy-independent slope of the event locus on a plot of C vs S. It can be found either from the fitted slope or by measuring π/e as a function of E. Because we have no knowledge of h/e on an event-by-event basis, it has been replaced by $\langle h/e \rangle$ in Eq. (34.37). ξ must be as far from unity as possible to optimize resolution, which means in practical terms that the scintillator readout of the calorimeter must be as compensating as possible.

Although the usually-dominant contribution of the f_{em} distribution to the resolution can be minimized by compensation or the use of dual calorimetry, there remain significant contributions to the resolution:

1. Incomplete corrections for leakage, differences in light collection efficiency, and electronics calibration.
2. Readout transducer shot noise (usually photoelectron statistics), plus electronic noise.
3. Sampling fluctuations. Only a small part of the energy deposit takes place in the scintillator or other sensor, and that fraction is subject to large fluctuations. This can be as high as $40\%/\sqrt{E}$ (lead/scintillator). It is even greater in the Fe/scint case because of the very small sampling fraction (if the calorimeter is to be compensating), and substantially lower in a U/scint calorimeter. It is obviously zero for a homogeneous calorimeter.
4. Intrinisic fluctuations. The many ways ionization can be produced in a hadronic shower have different detection efficiencies and are subject to stochastic fluctuations. In particular, a very large fraction of the hadronic energy (~20% for Fe/scint, ~40% for U/scint) is "invisible," going into nuclear dissociation, thermalized neutrons, etc. The lost fraction depends on readout—it will be greater for a Cherenkov readout, less for an organic scintillator readout.

Except in a sampling calorimeter especially designed for the purpose, sampling and intrinsic resolution contributions cannot be separated. This may have been best studied by Drews *et al.* [178], who used a calorimeter in which even- and odd-numbered scintillators were separately read out. Sums and differences of the variances were used to separate sampling and intrinsic contributions.

The fractional energy resolution can be represented by

$$\frac{\sigma}{E} = \frac{a_1(E)}{\sqrt{E}} \oplus \left| 1 - \left\langle \frac{h}{e} \right\rangle \right| \left(\frac{E}{E_1} \right)^{1-\ell} \tag{34.38}$$

The coefficient a_1 is expected to have mild energy dependence for a number of reasons. For example, the sampling variance is $(\pi/e)E$ rather than E. The term $(E/E_1)^{1-\ell}$ is the parametrization of $\sigma_{f_{em}}$ discussed above. Usually a plot of $(\sigma/E)^2$ vs $1/E$ ia well-described by a straight line (constant a_1) with a finite intercept—the square of the right term in Eq. (34.38), is called "the constant term." Precise data show the slight downturn [163].

After the first interaction of the incident hadron, the average longitudinal distribution rises to a smooth peak. The peak position increases slowly with energy. The distribution becomes nearly exponential after several interaction lengths. Examples from the CDHS magnetized iron-scintillator sandwich calorimeter test beam calibration runs [179] are shown in Fig. 34.24. Proton-induced cascades are somewhat shorter and broader than pion-induced cascades [172]. A gamma distribution fairly well describes the longitudinal development of an EM shower, as discussed in Sec. 33.5. Following this logic, Bock *et al.* suggested that the profile of a hadronic cascade could be fitted by the sum of two Γ distributions, one with a characteristic length X_0 and the other with length λ_I [180]. Fits to this 4-parameter function are commonly used, *e.g.*, by the ATLAS Tilecal collaboration [172]. If the interaction point is not known (the usual case), the distribution must be convoluted with an exponential in the interaction length of the incident particle. Adragna *et al.* give an analytic form for the convoluted function [172].

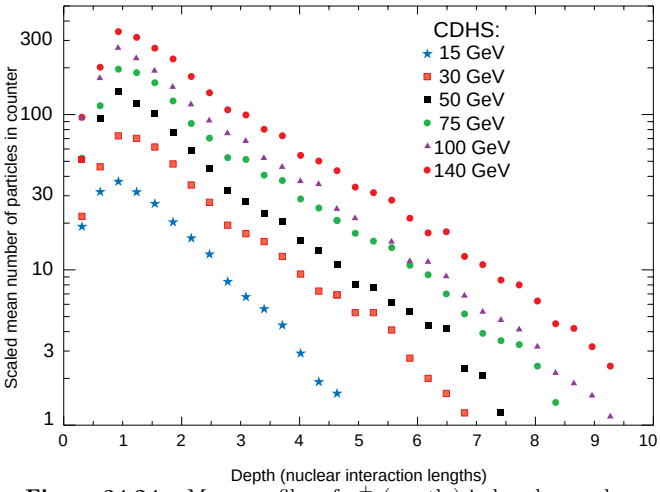

Figure 34.24: Mean profiles of π^+ (mostly) induced cascades in the CDHS neutrino detector [179]. Corresponding results for the ATLAS tile calorimeter can be found in Ref. 172.

The transverse energy deposit is characterized by a central core dominated by EM cascades, together with a wide "skirt" produced by wide-angle hadronic interactions [181].

The CALICE collaboration has tested a "tracking" calorimeter (AHCAL) with highly granular scintillator readout [168]. Since the position of the first interaction is observed, the average longitudinal and radial shower distributions are obtained.

While the average distributions might be useful in designing a calorimeter, they have little meaning for individual events, whose distributions are extremely variable because of the small number of particles involved early in the cascade.

Particle identification, primarily e-π discrimination, is accomplished in most calorimeters by depth development. An EM shower is mostly contained in $15X_0$ while a hadronic shower takes about $4\lambda_I$. In high-A absorbers such as Pb, $X_0/\lambda_I \sim 0.03$. In a fiber calorimeter, such as the RD52 dual-readout calorimeter [182], e-π discrimination is achieved by differences in the Cerenkov and scintillation signals, lateral spread, and timing differences, ultimately achieving about 500:1 discrimination.

34.9.3. ***Free electron drift velocities in liquid ionization chambers*** :
Written August 2009 by W. Walkowiak (U. Siegen)

Drift velocities of free electrons in LAr [183] are given as a function of electric field strength for different temperatures of the medium in Fig. 34.25. The drift velocites in LAr have been measured using a double-gridded drift chamber with electrons produced by a laser pulse on a gold-plated cathode. The average temperature gradient of the drift velocity of the free electrons in LAr is described [183] by

$$\frac{\Delta v_d}{\Delta T\, v_d} = (-1.72 \pm 0.08)\ \%/\mathrm{K}.$$

Earlier measurements [184–187] used different techniques and show systematic deviations of the drift velocities for free electrons which cannot be explained by the temperature dependence mentioned above.

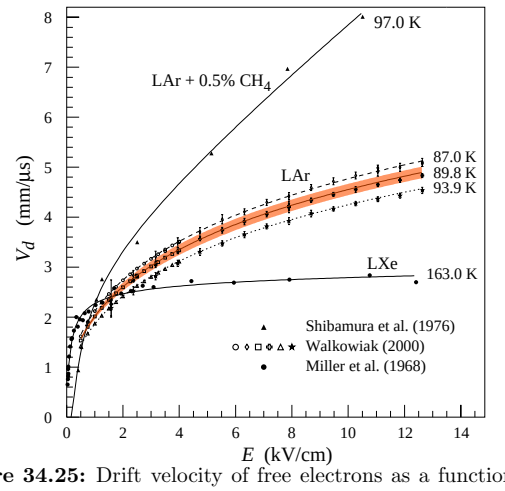

Figure 34.25: Drift velocity of free electrons as a function of electric field strength for LAr [183], LAr + 0.5% CH_4 [185] and LXe [184]. The average temperatures of the liquids are indicated. Results of a fit to an empirical function [189] are superimposed. In case of LAr at 91 K the error band for the global fit [183] including statistical and systematic errors as well as correlations of the data points is given. Only statistical errors are shown for the individual LAr data points.

Drift velocities of free electrons in LXe [185] as a function of electric field strength are also displayed in Fig. 34.25. The drift velocity saturates for $|\boldsymbol{E}| > 3$ kV/cm, and decreases with increasing temperature for LXe as well as measured e.g. by [188].

The addition of small concentrations of other molecules like N_2, H_2 and CH_4 in solution to the liquid typically increases the drift velocities of free electrons above the saturation value [185,186], see example for CH_4 admixture to LAr in Fig. 34.25. Therefore, actual drift velocities are critically dependent on even small additions or contaminations.

34.10. Accelerator-based Neutrino Detectors

Revised August 2017 by M.O. Wascko (Imperial College London).

34.10.1. ***Introduction*** :

Accelerator-based neutrino experiments span many orders of magnitude in neutrino energy, from a few MeV to hundreds of GeV. This wide range of neutrino energy is driven by the many physics applications of accelerator-based neutrino beams. Foremost among them is neutrino oscillation, which varies as the ratio L/E_ν, where L is the neutrino baseline (distance traveled), and E_ν is the neutrino energy. But accelerator-based neutrino beams have also been used to study the nature of the weak interaction, to probe nucleon form factors and structure functions, and to study nuclear structure.

The first accelerator-based neutrino experiment used neutrinos from the decays of high energy pions in flight to show that the neutrinos emitted from pion decay are different from the neutrinos emitted by beta decay [190]. The field of accelerator-based neutrino experiments would likely not have expanded beyond this without Simon van der Meer's invention of the magnetic focusing horn [191], which significantly increased the flux of neutrinos aimed toward the detector. In this mini-review, we focus on experiments employing decay-in-flight beams—pions, kaons, charmed mesons, and taus—producing fluxes of neutrinos and antineutrinos from ~ 10 MeV to ~ 100 GeV.

Neutrino interactions with matter proceed only through the weak interaction, making the cross section extremely small and requiring high fluxes of neutrinos and large detector masses in order to achieve satisfactory event rates. Therefore, neutrino detector design is a balancing act taking into account sufficient numbers of nuclear targets (often achieved with inactive detector materials), adequate sampling/segmentation to ensure accurate reconstruction of the tracks and showers produced by neutrino-interaction secondary particles, and practical readout systems to allow timely analysis of data.

34.10.2. ***Signals and Backgrounds*** :

The neutrino interaction processes available increase with increasing neutrino energy as interaction thresholds are crossed; in general neutrino-interaction cross sections grow with energy; for a detailed discussion of neutrino interactions see [192]. The multiplicity of secondary particles from each interaction process grows in complexity with neutrino energy, while the forward-boost due to increasing E_ν compresses the occupied phase space in the lab frame, impacting detector designs. Because decay-in-fight beams produce neutrinos at well-defined times, leading to very small duty factors, the predominant backgrounds usually stem from unwanted beam-induced neutrino interactions, i.e. neutrinos interacting via other processes than the one being studied. A noteworthy exception is time projection chambers, wherein the long drift times can admit substantially more cosmic backgrounds than most other detection methods. Cosmic backgrounds are more rare at higher energies because the secondary particles produced by neutrino interactions yield detector signals that resemble cosmic backgrounds less and less.

Below, we describe a few of the dominant neutrino interaction processes, with a focus on the final state particle content and topologies.

34.10.2.1. *Charged-Current Quasi-Elastic Scattering and Pion Production:*

Below ~ 2 GeV neutrino energy, the dominant neutrino-nucleus interaction process is quasi-elastic (QE) scattering. In the charged current (CC) mode, the CCQE base neutrino reaction is $\nu_\ell\, n \to \ell^-\, p$, where $\ell = e, \mu, \tau$, and similarly for antineutrinos, $\overline{\nu}_\ell\, p \to \ell^+\, n$. The final state particles are a charged lepton, and perhaps a recoiling nucleon if it is given enough energy to escape the nucleus. Detectors designed to observe this process should have good single-particle track resolution for muon neutrino interactions, but should have good μ/e separation for electron neutrino interactions. Because the interaction cross section falls sharply with Q^2, the lepton typically carries away more of the neutrino's kinetic energy than the recoiling nucleon. The fraction of backward-scattered leptons is large, however, so detectors with 4π coverage are desirable. The dominant backgrounds in this channel tend to come from single pion production events in which the pion is not detected.

Near 1 GeV, the quasi-elastic cross section is eclipsed by pion production processes. A typical single pion production (CC1π) reaction is $\nu_\ell\, n \to \ell^-\, \pi^+\, n$, but many more final state particle combinations are possible. Single pion production proceeds through the coherent channel and many incoherent processes, dominated by resonance production. With increasing neutrino energy, higher-order resonances can be excited, leading to multiple pions in the final state. Separating these processes from quasi-elastic scattering, and indeed from each other, requires tagging, and ideally reconstructing, the pions. Since these processes can produce neutral pions, electromagnetic (EM) shower reconstruction is more important here than it is for the quasi-elastic channel. The predominant backgrounds for pion production change with increasing neutrino energy. Detection of pion processes is also complicated because near threshold the quasi-elastic channel creates pion backgrounds through final state interactions of the recoiling nucleon, and at higher energies backgrounds come from migration of multiple pion events in which one or more pions is not detected.

34.10.2.2. *Deep Inelastic Scattering:*

Beyond a few GeV, the neutrino has enough energy to probe the nucleon at the parton scale, leading to deep inelastic scattering (DIS). In the charged-current channel, the DIS neutrino reaction is $\nu_\ell N \to \ell^- X$, where N is a nucleon and X encompasses the entire recoiling hadronic system. The final state particle reconstruction revolves around accurate reconstruction of the lepton momentum and containment and reconstruction of the hadronic shower energy. Because of the high neutrino energies involved, DIS events are very forward boosted, and can have extremely long particle tracks. For this reason, detectors measuring DIS interactions must be large to contain the hadronic showers in the detector volume.

34.10.2.3. *Neutral Currents:*

Neutrino interactions proceeding through the neutral current (NC) channel are identified by the lack of a charged lepton in the final state. For example, the NC elastic reaction is $\nu_l N \to \nu_l N$, and the NC DIS reaction is $\nu_l N \to \nu_l X$. NC interactions are suppressed relative to CC interactions by a factor involving the weak mixing angle; the primary backgrounds for NC interactions come from CC interactions in which the charged lepton is misidentified.

34.10.3. ***Instances of Neutrino Detector Technology*** :

Below we describe many of the actual detectors that have been built and operated for use in accelerator-based neutrino beams.

34.10.3.1. *Spark Chambers:*

In the first accelerator-based neutrino beam experiment, Lederman, Schwartz, and Steinberger [190] used an internally-triggered spark chamber detector, filled with 10 tons of Al planes and surrounded by external scintillator veto planes, to distinguish muon tracks from electron showers, and hence muon neutrinos from electron neutrinos. The inactive Al planes served as the neutrino interaction target and as radiators for EM shower development. The detector successfully showed the presence of muon tracks from neutrino interactions. It was also sensitive to the hadronic showers induced by NC interactions, which were unknown at the time. In 1963, CERN also built and ran a large (20 ton) Al plane spark chamber in a wideband beam based on the PS accelerator. [193]. More than a decade later, the Aachen-Padova [195] experiment at CERN employed a 30 ton Al spark chamber in the PS-WBB.

34.10.3.2. *Bubble Chambers:*

Several large bubble chamber detectors were employed as accelerator neutrino detectors in the 1970s and 80s, performing many of the first studies of the properties of the weak interaction. Bubble chambers provide exquisite granularity in the reconstruction of secondary particles, allowing very accurate separation of interaction processes. However, the extremely slow and labor-intensive acquisition and analysis of the data from photographic film led to them being phased out in favor of electronically read out detectors.

Table 34.9: Properties of detectors for accelerator-based neutrino beams.

Name	Type	Target	Mass* (t)	Location	$\langle E_\nu \rangle$(GeV)	Dates
Lederman et al.	Spark	Al	10	BNL	0.2–2	1962
CERN-spark	Spark	Al	20	CERN	1.5	1964
Serpukhov	Spark	Al	20	IHEP	4	1977
Aachen-Padova	Spark	Al	30	CERN	1.5	1976–77
Gargamelle	Bubble	Freon	6	CERN	1.5,20	1972,1977
BEBC	Bubble	H,D,Ne-H	2–42	CERN	50,150 & 20	1977–84
SKAT	Bubble	Freon	8	IHEP	4	1977-1987
ANL-12ft	Bubble	H,D	1–2	ANL	0.5	1970
BNL-7ft	Bubble	H,D	0.4–0.9	BNL	1.3,3	1976–82
Fermilab-15ft	Bubble	D,Ne	1–20	FNAL	50,180&25,100	1974–92
CITF	Iron	Fe	92	FNAL	50,180	1977–83
CDHS	Iron	Fe	750	CERN	50,150	1977–83
MINOS	Iron	Fe	980,5.4k	FNAL	4–15	2005–2016
INGRID	Iron	Fe	99	J-PARC	0.7–3	2009–
Super-Kamiokande	Cherenkov	H_2O	22,500	Kamioka	0.6	1996–
K2K-1kt	Cherenkov	H_2O	25	KEK	0.8	1998–2004
MiniBooNE	Cherenkov	CH_2	440	FNAL	0.6	2002–12
HWPF	Scintillation	CH_2	2	FNAL	2	2014–
LSND	Scintillation	CH_2	130	LANL	0.06	1993–98
NOvA	Scintillation	CH_2	300,14k	FNAL/Ash River	2	2013–
SciBar	Scintillation	CH	12	KEK/FNAL	0.8,0.6	2004,2007–8
ICARUS	LArTPC	Ar	760	LNGS	20	2006–12
Argoneut	LArTPC	Ar	0.025	FNAL	3	2009–10
MicroBooNE	LArTPC	Ar	170	FNAL	0.8	2014–
FNAL-E-531	Emulsion	Ag, Br	0.009	FNAL	25	1984
CHORUS	Emulsion	Ag, Br	1.6	CERN	20	1995
DONuT	Emulsion	Fe	0.26	FNAL	100	1997
OPERA	Emulsion	Pb	1.3k	LNGS	20	2006–12
NINJA	Emulsion	Fe	0.001	J-PARC	0.6	2016–
CHARM	Hybrid	$CaCO_3O$	150	CERN	20	1977
CHARM-II	Hybrid	Si	692	CERN	20	1983
BNL-E-734	Hybrid	CH_2	172	BNL	1.3	1987
BNL-E-776	Hybrid	concrete	240	BNL	3	1990
NOMAD	Hybrid	CH	3	CERN	20	1995–98
CCFR	Hybrid	Fe	690	FNAL	90,260	1991
NuTeV	Hybrid	Fe	690	FNAL	70,180	1996–97
MINERvA	Hybrid	CH,H_2O,Fe,Pb,C,He	8	FNAL	3,8	2009–
T2K-ND280	Hybrid	CH,H_2O,Pb,Cu	4	J-PARC	0.6	2009–

* Fiducial.

The Gargamelle [196] detector at CERN used Freon and propane gas targets to make the first observation of neutrino-induced NC interactions and more. The BEBC [197] detector at CERN was a bubble chamber that was alternately filled with liquid hydrogen, deuterium, and a neon-hydrogen mixture; BEBC was also outfitted with a track-sensitive detector to improve event tagging, and sometimes used with a small emulsion chamber. The SKAT [194] Freon bubble chamber was exposed to wideband neutrino and antineutrino beams at the Serpukhov laboratory in the former Soviet Union. A series of American bubble chambers in the 1970's and 1980's made measurements on free nucleons that are still crucial inputs for neutrino-nucleus scattering predictions. The 12-foot bubble chamber at ANL [210] in the USA used both deuterium and hydrogen targets, as did the 7-foot bubble chamber at BNL [199]. Fermilab's 15 foot bubble chamber [200] used deuterium and neon targets.

34.10.3.3. *Iron Tracking Calorimeters:*

Because of the forward boost of high energy interactions, long detectors made of magnetized iron interspersed with active detector layers have been very successfully employed. The long magnetized detectors allow measurements of the momentum of penetrating muons. The iron planes also act as shower-inducing layers, allowing separation of EM and hadronic showers; the large number of iron planes provide enough mass for high statistics and/or shower containment. Magnetized iron spectrometers have been used for studies of the weak interaction, measurements of structure functions, and searches for neutrino oscillation. Non-magnetized iron detectors have also been successfully employed as neutrino monitors for oscillation experiments and also for neutrino-nucleus interaction studies.

The Caltech-Fermilab counter (CITF) [210] combined a 92 ton iron-scintillator target-calorimeter detector with a downstream toroidal magnet to perform early studies of weak interactions—including observations of neutral currents. The CDHS [211] detector used layers of magnetized iron modules interspersed with wire drift chambers, with a fiducial mass of 750 t, to detector neutrinos in the range 30–300 GeV. Within each iron module, 5 cm (or 15 cm) iron plates were interspersed with scintillation counters. The MINOS [214] detectors, a near detector of 980 t at FNAL and a far detector of 5400 t in the Soudan mine, were functionally identical magnetized iron calorimeters, comprised of iron plates interleaved with layers of 4 cm wide plastic scintillator strips in alternating orientations. The T2K [234] on-axis detector, INGRID, consists of 16 non-magnetized iron scintillator sandwich detectors, each with nine 6.5 cm iron plane (7.1 t total) interspersed between layers of 5 cm wide plastic scintillator strips readout out by multi-pixel photon counters (MPPCs) coupled to WLS fibers. Fourteen of the INGRID modules are arranged in a cross-hair configuration centered on the neutrino beam axis.

34.10.3.4. *Cherenkov Detectors:*

Open volume water Cherenkov detectors were originally built to search for proton decay. Large volumes of ultra-pure water were lined with photomultipliers to collect Cherenkov light emitted by the passage of relativistic charged particles. See Sec. 35.3.1 for a detailed discussion of deep liquid detectors for rare processes. The Cherenkov light, which has significant production in the visible range, appears on the walls of the detectors in distinctive ring patterns, and topological characteristics of the rings are employed to separate muon-induced rings from electron-induced with very high accuracy. As neutrino detectors, Cherenkov detectors optimize the design balance since the entire neutrino target is also active detector medium.

When used to detect $\sim$ GeV neutrinos, the detector medium acts as a natural filter for final state particles below the Cherenkov threshold; this feature has been exploited successfully by the K2K, MiniBooNE (using mineral oil instead of water), and T2K neutrino oscillation experiments. This makes event reconstruction simple and robust since electrons and muons have very different signatures, but does require making assumptions when inferring neutrino energy since not all final state particles are observed. At higher energies Cherenkov detectors become less accurate because the overlapping rings from many final state particles become increasingly difficult to resolve.

The second-generation Cherenkov detector in Japan, Super-Kamiokande [202](Super-K), comprises 22.5 kt of water viewed by 50 cm photomultiplier tubes with 40% photocathode coverage; it is surrounded by an outer detector region viewed by 20 cm photomultipliers. Super-K is the far detector for K2K and T2K, and is described in greater detail elsewhere in this review. The K2K experiment also employed a 1 kt water Cherenkov detector in the suite of near detectors [203], with 40% photocathode coverage. The MiniBooNE detector at FNAL was a 0.8 kt [204] mineral oil Cherenkov detector, with 20 cm photomultipliers giving 10% photocathode coverage, surrounded by a veto detector also with 20 cm photomultipliers.

34.10.3.5. *Scintillation Detectors:*

Liquid and solid scintillator detectors also employ fully (or nearly fully) active detector media. Typically organic scintillators, which emit into the ultraviolet range, are dissolved in mineral oil or plastic and read out by photomultipliers coupled to wavelength shifters (WLS). Open volume scintillation detectors lined with photomultipliers are conceptually similar to Cherenkov detectors, although energy reconstruction is calorimetric in nature as opposed to kinematic (see also Sec. 35.3.1). For higher energies and higher particle multiplicities, it becomes beneficial to use segmented detectors to help distinguish particle tracks and showers from each other.

The HWPF collaboration [206] employed a 2 t liquid scintillator total-absorption hadron calorimeter followed by a magnetic spectrometer to observe neutral current events in the early days of Fermilab. The LSND [207] detector at LANL was a 130 t open volume liquid scintillator detector employed to detect relatively low energy ($<$300 MeV) neutrinos. The NOvA [209] detectors use segmented volumes of liquid scintillator in which the scintillation light is collected by WLS fibers in the segments that are coupled to avalanche photodiodes (APDs) at the ends of the volumes. The NOvA far detector, located in Ash River, MN, is comprised of 896 layers of 15.6 m long extruded PVC scintillator cells for a total mass of 14 kt; the NOνA near detector is comprised of 214 layers of 4.1 m scintillator volumes for a total mass of of 300 t. Both are placed in the NuMI beamline at 0.8° off-axis. The SciBar (Scintillation Bar) detector was originally built for K2K at KEK in Japan and then re-used for SciBooNE [208] at FNAL. SciBar used plastic scintillator strips with 1.5 cm$\times$2.5 cm rectangular cross section, read out by multianode photomultipliers (MAPMTs) coupled to WLS fibers, arranged in alternating horizontal and vertical layers. Both SciBooNE and K2K employed an EM calorimeter downstream of SciBar and a muon range detector (MRD) downstream of that.

34.10.3.6. *Liquid Argon Time Projection Chambers:*

Liquid argon time projection chambers (LAr-TPCs) were conceived in the 1970s as a way to achieve a fully active detector with sub-centimeter track reconstruction [215]. A massive volume of purified liquid argon is put under a strong electric field (hundreds of V/cm), so that the liberated electrons from the paths of ionizing particles can be drifted to the edge of the volume and read out, directly by collecting charge from wire planes or non-destructively through charge induction in the wire planes. A dual-phase readout method is also being developed, in which the charge is drifted vertically and then passed through an amplification region inside a gas volume above the liquid volume; the bottom of the liquid volume is equipped with a PMT array for detecting scintillation photons form the liquid argon. The first large scale LAr-TPC was the ICARUS T-600 module [216], comprising 760 t of liquid argon with a charge drift length of 1.5 m read out by wires with 3 mm pitch, which operated in LNGS, both standalone and also exposed to the CNGS high energy neutrino beam. The ICARUS detector has been transported to Fermilab and is being installed in an on-axis position in the Booster Neutrino Beamline, where it will also be exposed to off-axis neutrinos from the NuMI beamline. The ArgoNeuT [217] detector at FNAL, with fiducial mass 25 kg of argon read out with 4 mm pitch wires, was exposed to the NuMI neutrino and antineutrino beams. The MicroBooNE [218] detector at FNAL comprises 170 t of liquid Ar, read out with 3 mm wire pitch, which began collecting data in the Booster Neutrino Beam Oct 2015. A LAr-TPC has also been chosen as the detector design for the future DUNE neutrino oscillation experiment, from FNAL to Sanford Underground Research Facility; both single and dual phase modules are planned.

34.10.3.7. *Emulsion Detectors:*

Photographic film emulsions have been employed in particle physics experiments since the 1940s [219]. Thanks to advances in scanning technology and automation [223], they have been successfully employed as neutrino detectors. Emulsions are used for experiments observing CC tau neutrino interactions, where the short lifetime of the tau, $\tau_\tau = 2.90 \times 10^{-13}$s, leading to the short mean path length, $c \times \tau = 87\mu$m, requires extremely precise track resolution. They are employed in hybrid detectors in which the emulsion bricks are embedded inside fine-grained tracker detectors. In the data analysis, the tracker data are used to select events with characteristics typical of a tau decay in the final state, such as missing energy and unbalanced transverse momentum. The reconstructed tracks are projected back into an emulsion brick and used as the search seed for a neutrino interaction vertex.

E531 [220] at Fermilab tested many of the emulsion-tracker hybrid techniques employed by later neutrino experiments, in a detector with approximately 9 kg of emulsion target. The CHORUS [221] experiment at CERN used 1,600 kg of emulsion, in a hybrid detector with a fiber tracker, high resolution calorimeter, and muon spectrometer, to search for $\nu_\mu \to \nu_\tau$ oscillation. The DONuT [222] experiment at FNAL used a hybrid detector, with 260 kg of emulsion bricks interspersed with fiber trackers, followed by a magnetic spectrometer, and calorimeter, to make the first direct observation of tau neutrino CC interactions. The OPERA [224,225,226] experiment used an automated hybrid emulsion detector, with 1,300 t of emulsion, to make the first direct observation of the appearance of ν_τ in a ν_μ beam. Recently, the NINJA collaboration has developed an emulsion cloud chamber detector to observe neutrinos in the J-PARC neutrino beam [227].

34.10.3.8. *Hybrid Detectors:*

In the previous neutrino detector examples, one can point to a specific detection technology or configuration that defines a category of detectors. In this section we look at detectors that combine multiple elements or techniques, without one facet being specifically dominant or crucial; we call these detectors hybrids.

The CHARM detector [228] at CERN was built to study neutral-current interactions and search for muon neutrino oscillation. It was a fine-grained ionization calorimeter tracker with approximately 150 t of marble as neutrino target, surrounded by a magnetized iron muon system for tagging high angle muons, and followed downstream by a muon spectrometer. The CHARM II detector [229] at CERN comprised a target calorimeter followed by a downstream muon spectrometer. Each target calorimeter module consists of a 4.8 cm thick glass plate followed by a layer of plastic streamer tubes, with spacing 1 cm, instrumented with 2 cm wide pickup strips. Every fifth module is followed by a 3 cm thick scintillator layer. The total mass of the target calorimeter was 692 t.

The Brookhaven E-734 [230] detector was a tracking calorimeter made up of 172 t liquid scintillator modules interspersed with proportional drift tubes, followed by a dense EM calorimeter and a muon spectrometer downstream of that. The detector was exposed to a wideband horn-focused beam with peak neutrino energy near 1 GeV. The Brookhaven E-776 [231] experiment comprised a finely segmented EM calorimeter, with 2.54 cm concrete absorbers interspersed with planes of drift tubes and acrylic scintillation counters, with total mass 240 t, followed by a muon spectrometer.

The FNAL Lab-E neutrino detector was used by the CCFR [212] and NuTeV [213] collaborations to perform a series of experiments in the Fermilab high energy neutrino beam (50 GeV$< E_\nu <$ 300 GeV). The detector was comprised of six iron target calorimeter modules, with 690 t total target mass, followed by three muon spectrometer modules, followed by two drift chambers. Each iron target calorimeter module comprised 5.2 cm thick steel plates interspersed with liquid scintillation counters and drift chambers.

The NOMAD [232] detector at CERN consisted of central tracker detector inside a 0.4 T dipole magnet (the magnet was originally used by the UA1 experiment at CERN) followed by a hadronic calorimeter and muon detectors downstream of the magnet. The main neutrino target is 3 t of drift chambers followed downstream by transition radiation detectors which are followed by an EM calorimeter. NOMAD was exposed to the same wideband neutrino beam as was CHORUS.

MINERvA [233] is a hybrid detector based around a central plastic scintillator tracker: 8.3 t of plastic scintillator strips with triangular cross section read out by MAPMTs coupled to WLS fibers. The scintillator tracker is surrounded by electromagnetic and hadronic calorimetry, which is achieved by interleaving thin lead (steel) layers between the scintillator layers for the ECAL (HCAL). MINERvA is situated upstream of the MINOS near detector which acts as a muon spectrometer. Upstream of the scintillator tracker is a nuclear target region containing inactive layers of C (graphite), Pb, Fe (steel), and O (water). MINERvA's physics goals span a wide range of neutrino-nucleus interaction studies, from form factors to nuclear effects.

T2K [234] in Japan employs two near detectors at 280 m from the neutrino beam target, one centered on the axis of the horn-focused J-PARC neutrino beam and one placed 2.5° off-axis. The on-axis detector, INGRID, is described above. The 2.5° off-axis detector, ND280, employs the UA1 magnet (at 0.2 T) previously used by NOMAD. Inside the magnet volume are three separate detector systems: the trackers, the Pi0 Detector (P0D), and several ECal modules. The tracker detectors comprise two fine-grained scintillator detectors (FGDs), read out by MPPCs coupled to WLS fibers, interleaved between three gas TPCs read out by micromegas planes. The downstream FGD contains inactive water layers in addition to the scintillators. Upstream of the tracker is the P0D, a sampling tracker calorimeter with active detector materials comprising plastic scintillator read out by MPPCs and WLS fibers, and inactive sheets of brass radiators and refillable water modules. Surrounding the tracker and P0D, but still inside the magnet, are lead-scintillator EM sampling calorimeters.

34.10.4. ***Outlook*** :

Detectors for accelerator-based neutrino beams have been in use, and constantly evolving, for six decades now. The rich program of neutrino oscillation physics and attendant need for newer and better neutrino-nucleus scattering measurements means that more neutrino detectors with broader capabilities will be needed in the coming decades.

One of the most intriguing prospects is a large volume, high pressure gas time projection chamber (HPTPC). With the prospect of megawatt power accelerator-based neutrino beams, it is entirely feasible to collect high statistics data sets with a gas target. The low momentum thresholds for particle detection, and excellent momentum resolution and particle identification capabilities, of an HPTPC would open a new window into the physics of neutrino-nucleus scattering. Moreover, the ability to change the gas mixtures in the HPTPC would allow measurements in the same detector on multiple nuclear targets, which would, in turn, allow unprecedentedly accurate constraints and tuning of neutrino-nucleus interaction models.

34.11. Superconducting magnets for collider detectors

Revised August 2017 by Y. Makida (KEK)

34.11.1. ***Solenoid Magnets*** : In all cases SI unit are assumed, so that the magnetic field, B, is in Tesla, the stored energy, E, is in joules, the dimensions are in meters, and vacuum permeability of $\mu_0 = 4\pi \times 10^{-7}$.

The magnetic field (B) in an simple solenoid with a flux return iron yoke, in which the magnetic field is lower than magnetic saturation of < 2 T, is given by

$$B = \frac{\mu_0 \, n \, I}{L} \tag{34.39}$$

where n is the number of turns, I is the current and L is the coil length.

In an air-core solenoid case, the central field is given by

$$B(0,0) = \mu_0 \, n \, I \frac{1}{\sqrt{L^2 + 4R^2}} \, , \tag{34.40}$$

where R is the coil radius.

In most cases, momentum analysis is made by measuring the circular trajectory of the passing particles according to $p = mv = qrB$,

where p is the momentum, m the mass, q the charge, r the bending radius. The sagitta, s, of the trajectory is given by

$$s = q\,B\,\ell^2/8p\ , \tag{34.41}$$

where ℓ is the path length in the magnetic field. In a practical momentum measurement in colliding beam detectors, it is more effective to increase the magnetic volume than the field strength, since

$$dp/p \propto p/B\,\ell^2\ , \tag{34.42}$$

where ℓ corresponds to the solenoid coil radius R. The energy stored in the magnetic field of any magnet is calculated by integrating B^2 over all space:

$$E = \frac{1}{2\mu_0}\int B^2 dV \tag{34.43}$$

If the coil thin and inside an iron return yoke , (which is the case if it is to superconducting coil), then

$$E \approx (B^2/2\mu_0)\pi R^2 L\ . \tag{34.44}$$

For a detector in which the calorimetry is outside the aperture of the solenoid, the coil must be transparent in terms of radiation and absorption lengths. This usually means that the superconducting solenoid and its cryostat is of minimum real thickness and is made of a material with long radiation length. There are two major contributors to the thickness of a thin solenoid:

1) The conductor consisting of the current-carrying superconducting material (usually Nb-Ti/Cu) and the quench protecting stabilizer (usually aluminum) are wound on the inside of a structural support cylinder (usually aluminum also). The coil thickness scales as B^2R, so the thickness in radiation lengths (X_0) is

$$t_{\rm coil}/X_0 = (R/\sigma_h X_0)(B^2/2\mu_0)\ , \tag{34.45}$$

where $t_{\rm coil}$ is the physical thickness of the coil, X_0 the average radiation length of the coil/stabilizer material, and σ_h is the hoop stress in the coil [237]. $B^2/2\mu_0$ is the magnetic pressure. In large detector solenoids, the aluminum stabilizer and support cylinders dominate the thickness; the superconductor (Nb-TI/Cu) contributes a smaller fraction. The main coil and support cylinder components typically contribute about 2/3 of the total thickness in radiation lengths.

2) Another contribution to the material comes from the outer cylindrical shell of the vacuum vessel. Since this shell is susceptible to buckling collapse, its thickness is determined by the diameter, length and the modulus of the material of which it is fabricated. The outer vacuum shell represents about 1/3 of the total thickness in radiation length.

34.11.2. *Properties of collider detector magnets* :

The physical dimensions, central field stored energy and thickness in radiation lengths normal to the beam line of the superconducting solenoids associated with the major collider are given in Table 34.10 [236]. Fig. 34.26 shows thickness in radiation lengths as a function of B^2R in various collider detector solenoids.

Table 34.10: Progress of superconducting magnets for particle physics detectors.

Experiment	Laboratory	B [T]	Radius [m]	Length [m]	Energy [MJ]	X/X_0	E/M [kJ/kg]
TOPAZ*	KEK	1.2	1.45	5.4	20	0.70	4.3
CDF*	Tsukuba/Fermi	1.5	1.5	5.07	30	0.84	5.4
VENUS*	KEK	0.75	1.75	5.64	12	0.52	2.8
AMY*	KEK	3	1.29	3	40	†	
CLEO-II*	Cornell	1.5	1.55	3.8	25	2.5	3.7
ALEPH*	Saclay/CERN	1.5	2.75	7.0	130	2.0	5.5
DELPHI*	RAL/CERN	1.2	2.8	7.4	109	1.7	4.2
ZEUS*	INFN/DESY	1.8	1.5	2.85	11	0.9	5.5
H1*	RAL/DESY	1.2	2.8	5.75	120	1.8	4.8
BaBar*	INFN/SLAC	1.5	1.5	3.46	27	†	3.6
D0*	Fermi	2.0	0.6	2.73	5.6	0.9	3.7
BELLE*	KEK	1.5	1.8	4	42	†	5.3
BES-III	IHEP	1.0	1.475	3.5	9.5	†	2.6
ATLAS-CS	ATLAS/CERN	2.0	1.25	5.3	38	0.66	7.0
ATLAS-BT	ATLAS/CERN	1	4.7–9.75	26	1080	(Toroid)†	
ATLAS-ET	ATLAS/CERN	1	0.825–5.35	5	2×250	(Toroid)†	
CMS	CMS/CERN	4	6	12.5	2600	†	12
SiD**	ILC	5	2.9	5.6	1560	†	12
ILD**	ILC	4	3.8	7.5	2300	†	13
SiD**	CLIC	5	2.8	6.2	2300	†	14
ILD**	CLIC	4	3.8	7.9	2300	†	
FCC**		6	6	23	54000	†	12

* No longer in service
**Conceptual design in future
† EM calorimeter is inside solenoid, so small X/X_0 is not a goal

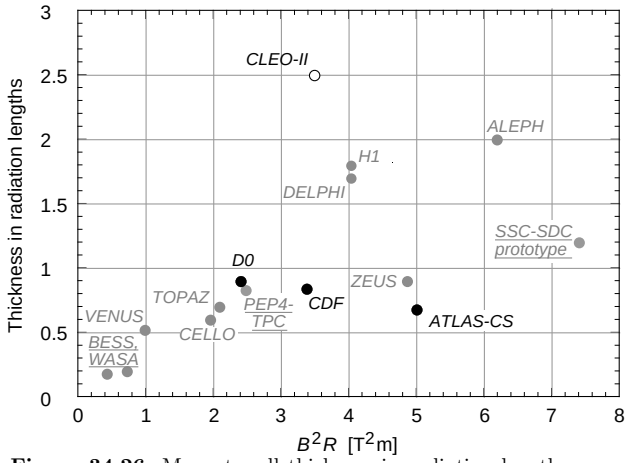

Figure 34.26: Magnet wall thickness in radiation length as a function of B^2R for various detector solenoids. Gray entries are for magnets no longer in use, and entries underlined are not listed in Table 34.10. Open circles are for magnets not designed to be "thin." The SSC-SDC prototype provided important R&D for LHC magnets.

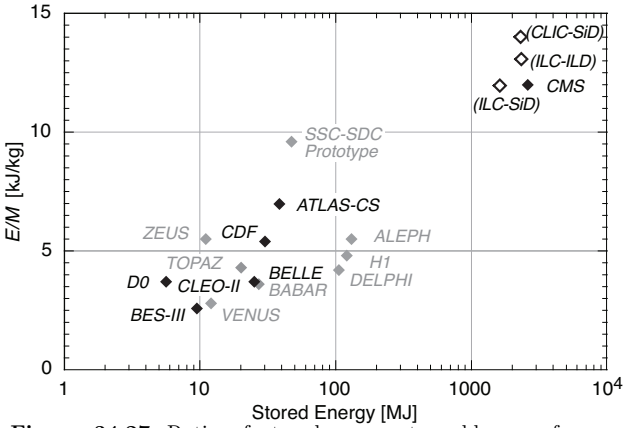

Figure 34.27: Ratio of stored energy to cold mass for major detector solenoids. Gray indicates magnets no longer in operation.

The ratio of stored energy to cold mass (E/M) is a useful performance measure. It can also be expressed as the ratio of the stress, σ_h, to twice the equivalent density, ρ, in the coil [237]:

$$\frac{E}{M} = \frac{E}{\rho\, 2\pi t_{\rm coil} RL} \approx \frac{\sigma_h}{2\rho} \qquad (34.46)$$

The E/M ratio in the coil is approximately equivalent to H,* the enthalpy of the coil, and it determines the average coil temperature rise after energy absorption in a quench:

$$E/M = H(T_2) - H(T_1) \approx H(T_2) \qquad (34.47)$$

where T_2 is the average coil temperature after the full energy absorption in a quench, and T_1 is the initial temperature. E/M ratios of 5, 10, and 20 kJ/kg correspond to ∼65, ∼80, and ∼100 K, respectively. The E/M ratios of various detector magnets are shown in Fig. 34.27 as a function of total stored energy. One would like the cold mass to be as small as possible to minimize the thickness, but temperature rise during a quench must also be minimized. An E/M ratio as large as 12 kJ/kg is designed into the CMS solenoid, with the possibility that about half of the stored energy can go to an external dump resistor. Thus the coil temperature can be kept below 80 K if the energy extraction system works well. The limit is set by the maximum temperature that the coil design can tolerate during a quench. This maximum local temperature should be <130 K (50 K + 80 K), so that thermal expansion effects, which are remarkable beyond 80 K, in the coil are manageable less than 50 K.

* The enthalpy, or heat content, is called H in the thermodynamics literature. It is not to be confused with the magnetic field intensity B/μ.

34.11.3. *Toroidal magnets* :

Toroidal coils uniquely provide a closed magnetic field without the necessity of an iron flux-return yoke. Because no field exists at the collision point and along the beam line, there is, in principle, no effect on the beam. On the other hand, the field profile generally has $1/r$ dependence. The particle momentum may be determined by measurements of the deflection angle combined with the sagitta. The deflection (bending) power BL is

$$BL \approx \int_{R_i}^{R_0} \frac{B_i R_i\, dR}{R\, \sin\theta} = \frac{B_i\, R_i}{\sin\theta} \ln(R_0/R_i)\ , \qquad (34.48)$$

where R_i is the inner coil radius, R_0 is the outer coil radius, and θ is the angle between the particle trajectory and the beam line axis . The momentum resolution given by the deflection may be expressed as

$$\frac{\Delta p}{p} \propto \frac{p}{BL} \approx \frac{p\, \sin\theta}{B_i R_i\, \ln(R_0/R_i)}\ . \qquad (34.49)$$

The momentum resolution is better in the forward/backward (smaller θ) direction. The geometry has been found to be optimal when $R_0/R_i \approx$ 3–4. In practical designs, the coil is divided into 6–12 lumped coils in order to have reasonable acceptance and accessibility. This causes the coil design to be much more complex. The mechanical structure needs to sustain the decentering force between adjacent coils, and the peak field in the coil is 3–5 times higher than the useful magnetic field for the momentum analysis [235].

34.12. Measurement of particle momenta in a uniform magnetic field [238,239]

The trajectory of a particle with momentum p (in GeV/c) and charge ze in a constant magnetic field $\overrightarrow{B}$ is a helix, with radius of curvature R and pitch angle λ. The radius of curvature and momentum component perpendicular to $\overrightarrow{B}$ are related by

$$p\cos\lambda = 0.3\, z\, B\, R\ , \qquad (34.50)$$

where B is in tesla and R is in meters.

The distribution of measurements of the curvature $k \equiv 1/R$ is approximately Gaussian. The curvature error for a large number of uniformly spaced measurements on the trajectory of a charged particle in a uniform magnetic field can be approximated by

$$(\delta k)^2 = (\delta k_{\rm res})^2 + (\delta k_{\rm ms})^2\ , \qquad (34.51)$$

where $\delta k =$ curvature error
$\delta k_{\rm res} =$ curvature error due to finite measurement resolution
$\delta k_{\rm ms} =$ curvature error due to multiple scattering.

If many (≥ 10) uniformly spaced position measurements are made along a trajectory in a uniform medium,

$$\delta k_{\rm res} = \frac{\epsilon}{L'^2}\sqrt{\frac{720}{N+4}}\ , \qquad (34.52)$$

where $N =$ number of points measured along track
$L' =$ the projected length of the track onto the bending plane
$\epsilon =$ measurement error for each point, perpendicular to the trajectory.

If a vertex constraint is applied at the origin of the track, the coefficient under the radical becomes 320.

For arbitrary spacing of coordinates s_i measured along the projected trajectory and with variable measurement errors ϵ_i the curvature error $\delta k_{\rm res}$ is calculated from:

$$(\delta k_{\rm res})^2 = \frac{4}{w}\ \frac{V_{ss}}{V_{ss}V_{s^2s^2} - (V_{ss^2})^2}\ , \qquad (34.53)$$

where V are covariances defined as $V_{s^m s^n} = \langle s^m s^n \rangle - \langle s^m \rangle \langle s^n \rangle$ with $\langle s^m \rangle = w^{-1} \sum ({s_i}^m / {\epsilon_i}^2)$ and $w = \sum {\epsilon_i}^{-2}$.

The contribution due to multiple Coulomb scattering is approximately

$$\delta k_{\rm ms} \approx \frac{(0.016)({\rm GeV}/c)z}{Lp\beta\cos^2\lambda}\sqrt{\frac{L}{X_0}}\,, \qquad (34.54)$$

where $p =$ momentum (GeV/c)
$z =$ charge of incident particle in units of e
$L =$ the total track length
$X_0 =$ radiation length of the scattering medium (in units of length; the X_0 defined elsewhere must be multiplied by density)
$\beta =$ the kinematic variable v/c.

More accurate approximations for multiple scattering may be found in the section on Passage of Particles Through Matter (Sec. 33 of this *Review*). The contribution to the curvature error is given approximately by $\delta k_{\rm ms} \approx 8 s^{\rm rms}_{\rm plane}/L^2$, where $s^{\rm rms}_{\rm plane}$ is defined there.

References:

1. T. Ferbel (ed.), *Experimental Techniques in High Energy Physics*, Addison-Wesley, Menlo Park, CA (1987).
2. K. Kleinknecht, *Detectors for Particle Radiation*, Cambridge University Press, Cambridge (1998).
3. G.F. Knoll, *Radiation Detection and Measurement*, 3nd edition, John Wiley & Sons, New York (1999).
4. D.R. Green, *The Physics of Particle Detectors*, Cambridge Monographs on Particle Physics, Nuclear Physics and Cosmology, Cambridge University Press, Cambridge (2000).
5. C. Leroy and P.-G. Rancoita, *Principles of Radiation Interaction in Matter and Detection*, World Scientific, Singapore (2004).
6. C. Grupen, *Particle Detectors*, Cambridge Monographs on Particle Physics, Nuclear Physics and Cosmology, Cambridge University Press (2008).
7. ICARUS Collab., ICARUS-TM/2001-09 [LGNS-EXP 13/89 add.2/01] (2001).
8. H. Spieler, IEEE Trans. **NS29**, 1142 (1982).
9. K. Arisaka, Nucl. Instrum. Methods **A442**, 80 (2000).
10. T. Hakamata (ed.), *Photomultiplier Tubes: Basics and Applications*, 3rd edition, Hamamatsu Photonics K.K., Hamamatsu (2006).
11. A. Braem *et al.*, Nucl. Instrum. Methods **A518**, 574 (2004).
12. R. Arnold *et al.*, Nucl. Instrum. Methods **A314**, 465 (1992).
13. P. Mangeot *et al.*, Nucl. Instrum. Methods **A216**, 79 (1983);
R. Apsimon *et al.*, IEEE Trans. **NS33**, 112 (1986);
R. Arnold *et al.*, Nucl. Instrum. Methods **A270**, 255 (1988);
D. Aston *et al.*, Nucl. Instrum. Methods **A283**, 582 (1989).
14. J. Janesick, *Scientific charge-coupled devices*, SPIE Press, Bellingham, WA (2001).
15. R. Haitz *et al.*, J. Appl. Phys. **36**, 3123 (1965);
R. McIntyre, IEEE Trans. Electron Devices **13**, 164 (1966);
H. Dautet *et al.*, Applied Optics, **32**, 3894 (1993);
Perkin-Elmer Optoelectronics, *Avalanche Photodiodes: A User's Guide*, (2003).
16. P. Buzhan *et al.*, Nucl. Instrum. Methods **A504**, 48 (2003);
Z. Sadygov *et al.*, Nucl. Instrum. Methods **A504**, 301 (2003);
V. Golovin and V. Saveliev, Nucl. Instrum. Methods **A518**, 560 (2004).
17. M. Landstrass *et al.*, Diam. & Rel. Matter, **2**, 1033 (1993);
R. McKeag and R. Jackman, Diam. & Rel. Matter, **7**, 513 (1998);
R. Brascia *et al.*, Phys. Stat. Sol. **199**, 113 (2003).
18. M. Petrov, M. Stapelbroek, and W. Kleinhans, Appl. Phys. Lett. **51**, 406 (1987);
M. Atac and M. Petrov, IEEE Trans. **NS36**, 163 (1989);
M. Atac *et al.*, Nucl. Instrum. Methods **A314**, 56 (1994).
19. J.B. Birks, *The Theory and Practice of Scintillation Counting*, Pergamon, London (1964).
20. D. Clark, Nucl. Instrum. Methods **117**, 295 (1974).
21. J.B. Birks, Proc. Phys. Soc. **A64**, 874 (1951).
22. B. Bengston and M. Moszynski, Nucl. Instrum. Methods **117**, 227 (1974);
J. Bialkowski *et al.*, Nucl. Instrum. Methods **117**, 221 (1974).
23. C. P. Achenbach, `arXiv:nucl-ex/0404008` (2004).
24. I.B. Berlman, *Handbook of Fluorescence Spectra of Aromatic Molecules*, 2nd edition, Academic Press, New York (1971).
25. F. Sauli (ed.), *Instrumentation in High Energy Physics*, World Scientific, Singapore (1992), see pp. 218–279 by C. Zorn.
26. T. Foerster, Ann. Phys. **2**, 55 (1948).
27. J.M. Fluornoy, Rad. Phys. and Chem. **41**, 389 (1993).
28. D. Horstman and U. Holm, Rad. Phys. and Chem. **41**, 395 (1993).
29. D. Blomker *et al.*, Nucl. Instrum. Methods **A311**, 505 (1992);
J. Mainusch *et al.*, Nucl. Instrum. Methods **A312**, 451 (1992).
30. K.F. Johnson and R.L. Clough (eds.), *Proceedings of the International Conference on Radiation-Tolerant Plastic Scintillators and Detectors*, Rad. Phys. and Chem. **41** (1993).
31. S.R. Borenstein and R.C. Strand, IEEE Trans. **NS31**, 396 (1984).
32. P. Sonderegger, Nucl. Instrum. Methods **A257**, 523 (1987).
33. P. Achenbach *et al.*, Nucl. Instrum. Methods **A593**, 353 (2008).
34. C.M. Hawkes *et al.*, Nucl. Instrum. Methods **A292**, 329 (1990).
35. N. Zaitseva *et al.*, Nucl. Instrum. Methods **A668**, 88 (2012).
36. S.E. Derenzo, W.-S. Choong and W.W. Moses, Phys. Med. Biol. **59**, 3261 (2014).
37. C. Melcher and J. Schweitzer, Nucl. Instrum. Methods **A314**, 212 (1992).
38. D.W. Cooke *et al.*, J. Appl. Phys. **88**, 7360 (2000).
39. J.M. Chen *et al.*, IEEE Trans. **NS54**, 718 (2007);
J.M. Chen *et al.*, IEEE Trans. **NS54**, 1319 (2007).
40. E.V.D. van Loef *et al.*, Nucl. Instrum. Methods **A486**, 254 (2002).
41. W. Drozdowski *et al.*, IEEE Trans. **NS55**, 1391 (2008).
42. M.S. Alekhin *et al.*, Appl. Phys. Lett. **102**, 161915 (2013).
43. C. Kuntner *et al.*, Nucl. Instrum. Methods **A493**, 131 (2002).
44. N. Akchurin *et al.*, Nucl. Instrum. Methods **A595**, 359 (2008).
45. A. Para, FERMILAB-CONF-11-519-CD (2011);
H. Wenzel *et al.*, FERMILAB-PUB-11-531-CD-E (2011).
46. R.H. Mao, L.Y. Zhang and R.Y. Zhu, IEEE Trans. **NS59**, 2229 (2012).
47. W.W. Moses, W.-S. Choong and S.E. Derenzo, Acta Physica Polonica **B7**, 725 (2014).
48. R.H. Mao, L.Y. Zhang and R.Y. Zhu, IEEE Trans. **NS55**, 2425 (2008).
49. B.D. Rooney and J.D. Valentine, IEEE Trans. **NS44**, 509 (1997).
50. W.W. Moses *et al.*, IEEE Trans. **NS55**, 1049 (2008).
51. G. Gratta, H. Newman, and R.Y. Zhu, Ann. Rev. Nucl. and Part. Sci. **44**, 453 (1994).
52. R.Y. Zhu, Nucl. Instrum. Methods **A413**, 297 (1998).
53. F. Yang *et al.*, IEEE Trans. **NS63**, 612 (2016).
54. F. Yang *et al.*, IEEE Trans. **NS64**, 665 (2017).
55. R.Y. Zhu, Journal of Physics: Conference Series **587**, 012055 (2015).
56. G. Dissertori *et al.*, Nucl. Instrum. Methods **745**, 1 (2014), and references therein.
57. R. Chipaux *et al.*, *Proc. of the 8th Int. Conf. on Inorganic Scintillators (SCINT2005)*, 369 (2005).
58. The CMS Electromagnetic Calorimeter Group, JINST **5** P03010 (2010).
59. M.G. Albrow *et al.*, JINST **7**, P10027 (2012).
60. B. Aubert *et al.* [BaBar Collab.], Nucl. Instrum. Methods **A479**, 1 (2002).
61. A. Abashian *et al.*, Nucl. Instrum. Methods **A479**, 117 (2002).
62. M. Shiozawa *et al.* [Super-Kamiokande Collab.], Nucl. Instrum. Methods **A433**, 240 (1999).
63. *Proceedings of the International Workshops on Ring Imaging Cherenkov Detectors*, Nucl. Instrum. Methods **A343**, 1 (1993); Nucl. Instrum. Methods **A371**, 1 (1996);
Nucl. Instrum. Methods **A433**, 1 (1999); Nucl. Instrum. Methods **A502**, 1 (2003);

Nucl. Instrum. Methods **A553**, 1 (2005); Nucl. Instrum. Methods **A595**, 1 (2008);
Nucl. Instrum. Methods **A639**, 1 (2011); Nucl. Instrum. Methods **A766**, 1 (2014).
64. J. Litt and R. Meunier, Ann. Rev. Nucl. Sci. **23**, 1 (1973).
65. D. Bartlett *et al.*, Nucl. Instrum. Methods **A260**, 55 (1987).
66. B. Ratcliff, Nucl. Instrum. Methods **A502**, 211 (2003).
67. W. Blum, W. Riegler, and L. Rolandi, *Particle Detection with Drift Chambers*, Springer-Verlag, Berlin (2008).
68. L.G. Christophorou, *Atomic and Molecular Radiation Physics*, John Wiley & Sons, Hoboken (1971);
I.B. Smirnov, Nucl. Instrum. Methods **A554**, 474 (2005);
J. Berkowitz, *Atomic and Molecular Photoabsorption*, Academic Press, Cambridge (2002);
http://pdg.lbl.gov/2007/AtomicNuclearProperties.
69. H. Bichsel, Nucl. Instrum. Methods **A562**, 154 (2006).
70. H. Fischle *et al.*, Nucl. Instrum. Methods **A301**, 202 (1991).
71. http://rjd.web.cern.ch/rjd/cgi-bin/cross.
72. A. Peisert and F. Sauli, CERN 84-08 (1984).
73. S. Biagi, Nucl. Instrum. Methods **A421**, 234 (1999).
74. http://consult.cern.ch/writeup/magboltz/.
75. E. McDaniel and E. Mason, *The Mobility and Diffusion of Ions in Gases*, John Wiley & Sons, Hoboken (1973);
G. Shultz *et al.*, Rev. Phys. Appl. **12**, 67 (1977).
76. G. Charpak *et al.*, Nucl. Instrum. Methods **A62**, 262 (1968).
77. G. Charpak and F. Sauli, Ann. Rev. Nucl. Sci. **34**, 285 (1984).
78. T. Ferbel (ed.), *Experimental Techniques in High Energy Physics*, Addison-Wesley, Menlo Park, CA (1987), see "Principles of Operation of Multiwire Proportional and Drift Chambers".
79. G. Charpak *et al.*, Nucl. Instrum. Methods **A167**, 455 (1979).
80. A.H. Walenta *et al.*, Nucl. Instrum. Methods **A92**, 373 (1971).
81. A. Breskin *et al.*, Nucl. Instrum. Methods **A124**, 189 (1975).
82. A. Breskin *et al.*, Nucl. Instrum. Methods **A156**, 147 (1978).
83. R. Bouclier *et al.*, Nucl. Instrum. Methods **A265**, 78 (1988).
84. H. Drumm *et al.*, Nucl. Instrum. Methods **A176**, 333 (1980).
85. D.R. Nygren and J.N. Marx, Phys. Today **31N10**, 46 (1978).
86. http://www.ansoft.com.
87. P. Beringer *et al.*, Nucl. Instrum. Methods **A254**, 542 (1987).
88. J. Virdee, Phys. Reports **403**, 401 (2004).
89. H. Walenta, Phys. Scripta **23**, 354 (1981).
90. J. Va'vra, Nucl. Instrum. Methods **A515**, 1 (2003);
M. Titov, arXiv:physics/0403055 (2004).
91. M. Aleksa *et al.*, Nucl. Instrum. Methods **A446**, 435 (2000).
92. F. Sauli and A. Sharma, Ann. Rev. Nucl. Part. Sci. **49**, 341 (1999).
93. A. Oed, Nucl. Instrum. Methods **A263**, 351 (1988);
A. Barr *et al.*, Nucl. Phys. (Proc. Supp.) **B61**, 264 (1988).
94. Y. Bagaturia *et al.*, Nucl. Instrum. Methods **A490**, 223 (2002).
95. J. Benlloch *et al.*, IEEE Trans. **NS45**, 234 (1998).
96. Y. Giomataris, Nucl. Instrum. Methods **A419**, 239 (1998).
97. F. Sauli, Nucl. Instrum. Methods **A386**, 531 (1997);
A. Bressan *et al.*, Nucl. Instrum. Methods **A425**, 262 (1999).
98. S. Bachmann *et al.*, Nucl. Instrum. Methods **A479**, 294 (2002);
A. Bressan *et al.*, Nucl. Instrum. Methods **A424**, 321 (1999).
99. Y. Giomataris *et al.*, Nucl. Instrum. Methods **A376**, 29 (1996).
100. J. Derre *et al.*, Nucl. Instrum. Methods **A459**, 523 (2001);
G. Charpak *et al.*, Nucl. Instrum. Methods **A478**, 26 (2002).
101. I. Giomataris *et al.*, Nucl. Instrum. Methods **A560**, 405 (2006).
102. S. Duarte Pinto *et al.*, IEEE NSS Conf. Record **N08-4**, 1426 (2008).
103. L. Periale *et al.*, Nucl. Instrum. Methods **A478**, 377 (2002);
R. Chechik *et al.*, Nucl. Instrum. Methods **A535**, 303 (2004);
A. Breskin *et al.*, Nucl. Instrum. Methods **A598**, 107 (2009).
104. A. Di Mauro *et al.*, Nucl. Instrum. Methods **A581**, 225 (2007).
105. R. Bellazzini *et al.*, Nucl. Instrum. Methods **A535**, 477 (2004);
M. Campbell *et al.*, Nucl. Instrum. Methods **A540**, 295 (2005);
A. Bamberger *et al.*, Nucl. Instrum. Methods **A573**, 361 (2007);
T.Kim *et al.*, Nucl. Instrum. Methods **A599**, 173 (2008).
106. M. Chefdeville *et al.*, Nucl. Instrum. Methods **A556**, 490 (2006).
107. M. Titov, arXiv:physics/0403055 (2004).
108. http://rd51-public.web.cern.ch/RD51-Public.
109. J. Alme *et al.*, Nucl. Instrum. Methods **A622**, 316 (2010).
110. N. Abgrall *et al.*, Nucl. Instrum. Methods **A637**, 25 (2011).
111. ALICE Collab., ALICE-PUBLIC-2015-004 (2015).
112. A.H. Walenta *et al.*, Nucl. Instrum. Methods **161**, 45 (1979).
113. H. Aihara *et al.*, IEEE Trans. **NS30**, 63 (1983).
114. X. Artru *et al.*, Phys. Rev. **D12**, 1289 (1975);
G.M. Garibian *et al.*, Nucl. Instrum. Methods **125**, 133 (1975).
115. B. Dolgoshein, Nucl. Instrum. Methods **A326**, 434 (1993).
116. *TRDs for the Third Millenium: Proc. 2nd Workshop on Advanced Transition Radiation Detectors for Accelerator and Space Applications*, Nucl. Instrum. Methods **A522**, 1 (2004).
117. *TRDs for the Third Millenium: Proc. 4th Workshop on Advanced Transition Radiation Detectors for Accelerator and Space Applications*, Nucl. Instrum. Methods **A706**, 1 (2013).
118. V.M. Grichine and S.S. Sadilov Nucl. Instrum. Methods **A522**, 122 (2004).
119. J. Apostolakis *et al.*, Rad. Phys. and Chem. **78**, 859 (2009).
120. B. Beischer *et al.*, Nucl. Instrum. Methods **A583**, 485 (2007).
121. A. Adronic and J.P Wessels, Nucl. Instrum. Methods **A666**, 130 (2012).
122. M. Petris *et al.*, Nucl. Instrum. Methods **A714**, 17 (2007).
123. R. Santonico and R. Cardarelli, Nucl. Instrum. Methods **A187**, 377 (1981).
124. V.V. Parkhomchuck, Yu.N. Pestov, and N.V. Petrovykh, Nucl. Instrum. Methods **93**, 269 (1971).
125. E. Cerron Zeballos *et al.*, Nucl. Instrum. Methods **A374**, 132 (1996).
126. R. Cardarelli *et al.*, Nucl. Instrum. Methods **A333**, 399 (1993).
127. P. Camarri *et al.*, Nucl. Instrum. Methods **A414**, 317 (1998).
128. G. Aielli *et al.*, Nucl. Instrum. Methods **A508**, 6 (2003).
129. R. Cardarelli *et al.*, Nucl. Instrum. Methods **A382**, 470 (1996).
130. I. Crotty *et al.*, Nucl. Instrum. Methods **A505**, 203 (2006).
131. V. Ammosov *et al.*, Nucl. Instrum. Methods **A456**, 1-2 (2000).
132. W. Riegler and D. Burgarth, Nucl. Instrum. Methods **A481**, 130-13 (2001).
133. R. Cardarelli *et al.*, JINST **8**, P01003 (2013).
134. G. Aielli *et al.*, JINST **9**, C09030 (2014).
135. R. Santonico, JINST **9**, C11007 (2014).
136. R. Santonico *et al.*, Nucl. Instrum. Methods **A661**, S2 (2012).
137. M. Bedjidian *et al.*, JINST **6** P02001 (2011).
138. P. Fonte *et al.*, Nucl. Instrum. Methods **A443**, 201 (2000).
139. L. Paolozzi *et al.*, PoS(RPC2012)065 (2012).
140. S. An *et al.*, Nucl. Instrum. Methods **A594**, 39 (2008).
141. C. Iacobaeus *et al.*, Nucl. Instrum. Methods **A513**, 244 (2003).
142. G. Aielli *et al.*, Nucl. Instrum. Methods **A456**, 82 (2000).
143. G. Aielli *et al.*, IEEE Trans. **NS53**, 567 (2006).
144. H. Sakai *et al.*, Nucl. Instrum. Methods **A484**, 153 (2002).
145. R. Santonico, JINST **8**, P04023 (2013).
146. L. Lopes *et al.*, Nucl. Instrum. Methods **A533**, 69 (2003).
147. H. Spieler, *Semiconductor Detector Systems*, Oxford Univ. Press, Oxford (2005).
148. F. Scholze *et al.*, Nucl. Instrum. Methods **A439**, 208 (2000).
149. G. Lindström *et al.*, Nucl. Instrum. Methods **A465**, 60 (2001).
150. C. Da Via *et al.*, Nucl. Instrum. Methods **A509**, 86 (2003).
151. G. Kramberger *et al.*, Nucl. Instrum. Methods **A481**, 297 (2002).
152. O. Krasel *et al.*, IEEE Trans. **NS51**, 3055 (2004).
153. G. Lindström *et al.*, Nucl. Instrum. Methods **A426**, 1 (1999).
154. A. Holmes-Siedle and L. Adams, *Handbook of Radiation Effects*, 2nd edition, Oxford Univ. Press, Oxford (2002).
155. V. Radeka, IEEE Trans. **NS15**, 455 (1968);
V. Radeka, IEEE Trans. **NS21**, 51 (1974).
156. F.S. Goulding, Nucl. Instrum. Methods **100**, 493 (1972);
F.S. Goulding and D.A. Landis, IEEE Trans. **NS29**, 1125 (1982).
157. W.R. Nelson, H. Hirayama, and D.W.O. Rogers, SLAC-265 (1985).
158. R. Brun *et al.*, CERN DD/EE/84-1 (1987).

159. D. Hitlin *et al.*, Nucl. Instrum. Methods **137**, 225 (1976); See also W. J. Willis and V. Radeka, Nucl. Instrum. Methods **120**, 221 (1974), for a more detailed discussion.
160. R. Wigmans, *Calorimetry: Energy Measurement in Particle Physics*, Inter. Series of Monographs on Phys. **107**, Clarendon Press, Oxford (2000).
161. ATLAS Collab., CERN/LHCC 96-41 (1996).
162. CMS Collab., CERN/LHCC 97-33 (1997).
163. N. Akchurin *et al.*, Nucl. Instrum. Methods **A399**, 202 (1997).
164. B. Aubert *et al.*, Nucl. Instrum. Methods **A321**, 467 (1992).
165. A. Artamonov *et al.*, JINST **3**, P02010 (2008).
166. F. Ariztizabal *et al.*, Nucl. Instrum. Methods **A349**, 384 (1994).
167. S. Abdullin *et al.*, Eur. Phys. J. **C53**, 139 (2008).
168. M. Romalli, J. Phys. Conf. Series **404** 012050 (2012); C. Adloff *et al.*, `arXiv:1306.3037` (2013).
169. T.A. Gabriel *et al.*, Nucl. Instrum. Methods **A338**, 336 (1994).
170. D.E. Groom, Nucl. Instrum. Methods **A572**, 633 (2007); Erratum: D.E. Groom, Nucl. Instrum. Methods **A593**, 638 (2008).
171. N. Akchurin *et al.*, Nucl. Instrum. Methods **A408**, 380 (1998); An energy-independent analysis of these data is given in Ref. 170.
172. P. Adragna *et al.*, Nucl. Instrum. Methods **A615**, 158 (2010).
173. C.W. Fabjan *et al.*, Phys. Lett. **B60**, 105 (1975).
174. C. Leroy, J. Sirois, and R. Wigmans, Nucl. Instrum. Methods **A252**, 4 (1986).
175. J.E. Brau and T.A. Gabriel, Nucl. Instrum. Methods **A238**, 489 (1985); H. Brückmann and H. Kowalski, ZEUS Int. Note 86/026 DESY, Hamburg (1986); R. Wigmans, Nucl. Instrum. Methods **A259**, 389 (1987); R. Wigmans, Nucl. Instrum. Methods **A265**, 273 (1988).
176. P. Mockett, SLAC-267, 335 (1987).
177. R. Wigmans, *Proc. 7th Inter. Conf. on Calorimetry in High Energy Physics*, 182 World Scientific, River Edge, NJ, (1998); N. Akchurin *et al.*, Nucl. Instrum. Methods **A537**, 537 (2005).
178. G. Drews *et al.*, Nucl. Instrum. Methods **A335**, 335 (1990).
179. M. Holder *et al.*, Nucl. Instrum. Methods **151**, 69 (1978).
180. R.K. Bock, T. Hansl-Kozanecka, and T.P. Shah, Nucl. Instrum. Methods **186**, 533 (1981); Y.A. Kulchitsky and V.B. Vinogradov, Nucl. Instrum. Methods **A455**, 499 (2000).
181. D. Acosta *et al.*, Nucl. Instrum. Methods **A316**, 184 (1997).
182. N. Akchurin, *et al.*, Nucl. Instrum. Methods **A735**, 120 (2013).
183. W. Walkowiak, Nucl. Instrum. Methods **A449**, 288 (2000).
184. L.S. Miller *et al.*, Phys. Rev. **166**, 871 (1968).
185. E. Shibamura *et al.*, Nucl. Instrum. Methods **A316**, 184 (1975).
186. K. Yoshino *et al.*, Phys. Rev. **A14**, 438 (1976).
187. A.O. Allen *et al.*, NSRDS-NBS-58 (1976).
188. P. Benetti *et al.*, Nucl. Instrum. Methods **A32**, 361 (1993).
189. A.M. Kalinin *et al.*, ATLAS-LARG-NO-058 (1996).
190. G. Danby *et al.*, Phys. Rev. Lett. **9**, 36 (1962).
191. S. van der Meer, CERN 61-07 (1961).
192. J.A. Formaggio and G.P. Zeller, Rev. Mod. Phys. **84**, 1307 (2013).
193. H. Faissner, "CERN Spark Chamber Neutrino Experiment", INSPIRE-1377455.
194. A.E. Asratien *et al.*, Phys. Lett. **79**, 497 (1978).
195. H. Faissner *et al.*, Phys. Lett. **B68**, 377 (1977).
196. F.J. Hasert *et al.*, Nucl. Phys. **B73**, 1 (1974).
197. N. Armenise *et al.*, Phys. Lett. **B81**, 385 (1979).
198. S.J. Barish *et al.*, Phys. Rev. **D16**, 3103 (1977).
199. N.J. Baker *et al.*, Phys. Rev. **D23**, 2499 (1981).
200. J.W. Chapman *et al.*, Phys. Rev. **D14**, 5 (1976).
201. E.P. Kuznetsov*et al.*, Preprint IHEP 71-75, Serpukhov, (1971).
202. Y. Fukuda *et al.*, Nucl. Instrum. Methods **A501**, 418 (2003).
203. Y. Fukuda *et al.*, Phys. Rev. **D74**, 072003 (2006).
204. A.A. Aguilar-Arevalo *et al.*, Nucl. Instrum. Methods **A599**, 28 (2009).
205. A.A. Aguilar-Arevalo *et al.*, Phys. Rev. **D79**, 072002 (2009).
206. A. Benvenuti *et al.*, Nucl. Instrum. Methods **125**, 447 (1975).
207. C. Athanassopoulos *et al.*, Nucl. Instrum. Methods **A388**, 149 (1997).
208. K. Hiraide *et al.*, Phys. Rev. **D78**, 112004 (2008).
209. D.S. Ayres *et al.*, FERMILAB-DESIGN-2007-01 (2007).
210. B. C. Barish, Phys. Rept. **39**, 279 (1978).
211. M. Holder *et al.*, Nucl. Instrum. Methods **148**, 203 (1978).
212. W.K. Sakumoto *et al.*, Nucl. Instrum. Methods **A294**, 179 (1990).
213. D.A. Harris *et al.*, Nucl. Instrum. Methods **A447**, 377 (2000).
214. I. Ambats *et al.*, FERMILAB-DESIGN-1998-02 (1998).
215. C. Rubbia, CERN-EP-INT-77-08 (1977).
216. S. Amerio *et al.*, Nucl. Instrum. Methods **A527**, 329 (2004).
217. C. Anderson *et al.*, JINST **7**, 10020 (2012).
218. H. Chen *et al.*, FERMILAB-PROPOSAL-0974 (2007).
219. D.H. Perkins, Nature **159**, 126 (1947).
220. N. Uhida *et al.*, Nucl. Instrum. Methods **224**, 50 (1984).
221. S. Aoki *et al.*, Nucl. Instrum. Methods **A447**, 361 (2000).
222. K. Kodama *et al.*, Nucl. Instrum. Methods **B93**, 340 (1994).
223. S. Aoki, Nucl. Instrum. Methods **A473**, 192 (2001).
224. T. Adam *et al.*, Nucl. Instrum. Methods **A577**, 523 (2007).
225. D. Di Ferdinando *et al.*, Radiat. Meas. **44**, 840 (2009).
226. R. Acquafredda *et al.*, New J. Phys. **8**, 303 (2006).
227. T. Fukuda *et al.*, PTEP **2017**, no. 6, 063C02 (2017).
228. A.N. Diddens *et al.*, Nucl. Instrum. Methods **178**, 27 (1980).
229. D. Geiregat *et al.*, Nucl. Instrum. Methods **A325**, 92 (1993).
230. L.A. Ahrens *et al.*, Nucl. Instrum. Methods **A254**, 515 (1987).
231. G. Gidal, LBL-91 Suppl., Rev. (1985).
232. J. Altegoer *et al.*, Nucl. Instrum. Methods **A404**, 96 (1998).
233. L. Aliaga *et al.*, Nucl. Instrum. Methods **A743**, 130 (2014).
234. K. Abe *et al.*, Nucl. Instrum. Methods **A659**, 106 (2011).
235. T. Taylor, Phys. Scripta **23**, 459 (1980).
236. A. Yamamoto, Nucl. Instrum. Methods **A494**, 255 (2003).
237. A. Yamamoto, Nucl. Instrum. Methods **A453**, 445 (2000).
238. R.L. Gluckstern, Nucl. Instrum. Methods **24**, 381 (1963).
239. V. Karimäki, Nucl. Instrum. Methods **A410**, 284 (1998).

35. Particle Detectors for Non-Accelerator Physics

Revised 2017. See the various sections for authors.

35.1. Introduction

Non-accelerator experiments have become increasingly important in particle physics. These include classical cosmic ray experiments, neutrino oscillation measurements, and searches for double-beta decay, dark matter candidates, and magnetic monopoles. The experimental methods are sometimes those familiar at accelerators (plastic scintillators, drift chambers, TRD's, *etc.*) but there is also instrumentation either not found at accelerators or applied in a radically different way. Examples are atmospheric scintillation detectors (Fly's Eye), massive Cherenkov detectors (Super-Kamiokande, IceCube), ultracold solid state detectors (CDMS). And, except for the cosmic ray detectors, radiologically ultra-pure materials are required.

In this section, some more important detectors special to terrestrial non-accelerator experiments are discussed. Techniques used in both accelerator and non-accelerator experiments are described in Sec. 28, Particle Detectors at Accelerators, some of which have been modified to accommodate the non-accelerator nuances.

Space-based detectors also use some unique instrumentation, but these are beyond the present scope of RPP.

35.2. High-energy cosmic-ray hadron and gamma-ray detectors

35.2.1. *Atmospheric fluorescence detectors* :

Revised August 2017 by L.R. Wiencke (Colorado School of Mines).

Cosmic-ray fluorescence detectors (FDs) use the atmosphere as a giant calorimeter to measure isotropic scintillation light that traces the development profiles of extensive air showers. An extensive air shower (EAS) is produced by the interactions of ultra high-energy ($E > 10^{17}$ eV) subatomic particles in the stratosphere and upper troposphere. The amount of scintillation light generated by an EAS is proportional to the energy deposited in the atmosphere and nearly independent of the primary species. With energies extending beyond 10^{20} eV these are the highest energy subatomic particles known to exist. In addition to particle arrival directions, energy spectra and primary composition, the astroparticle science investigated with FDs also includes multi-messenger studies, searches for high energy photons, neutrinos, monopoles and deeply penetrating forms of dark matter.

Previous experiments with FDs included the pioneering Fly's Eye [1,2], and the High Resolution Fly's Eye (HiRes and HiRes prototype) [3]. The current generation of experiments include the Telescope Array (TA) [4] in the northern hemisphere, and the much larger Pierre Auger Observatory (Auger) [5] in the southern hemisphere. Both are hybrid observatories. Their FD telescopes overlook sparse arrays of particle detectors on the ground. Select parameters are listed in Table 35.1. TA and Auger have each one FD site populated with additional telescopes that view up to 60° in elevation to measure lower EASs using a combination of scintillation and direct Cherenkov light. The Auger FD also measures UV scintillation that traces the development of atmospheric transient luminous events called "Elves" that are initiated by lightning [6]. At TA a prototype FD telescope, dubbed FAST [7], has observed EASs using wide field of view PMTs and fast timing.

The fluorescence light is emitted primarily between 290 and 430 nm (Fig. 35.1) with major lines at 337, 357, and 391 nm, when relativistic charged particles, primarily electrons and positrons, excite nitrogen molecules in air, resulting in transitions of the 1P and 2P systems. Reviews and references for the pioneering and recent laboratory measurements of fluorescence yield, $Y(\lambda, P, T, u)$, including dependence on wavelength (λ), temperature (T), pressure (p), and humidity (u) may be found in Refs. 8–10. The results of various laboratory experiments have been combined (Fig. 35.2) to obtain an absolute average and uncertainty for Y(337 nm, 800 hPa, 293 K, dry air) of 7.04 ± 0.24 ph/MeV after corrections for different electron beam energies and other factors. The units of ph/MeV correspond to the number of fluorescence photons produced per MeV of energy deposited in the atmosphere by the electromagnetic component of an EAS.

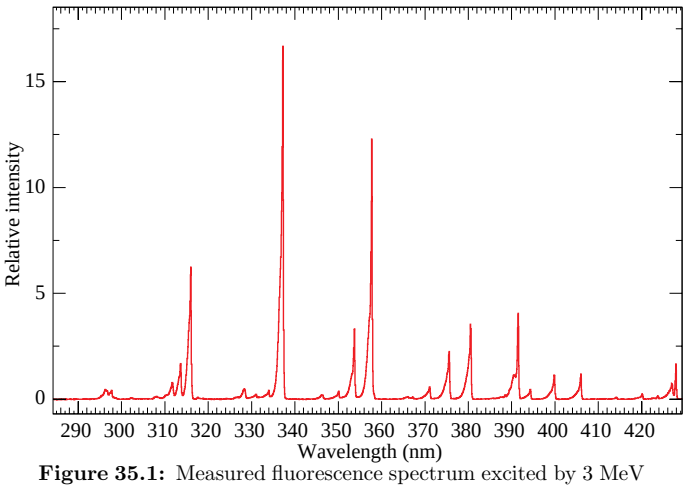

Figure 35.1: Measured fluorescence spectrum excited by 3 MeV electrons in dry air at 800 hPa and 293 K [12].

Table 35.1: Parameters of major fluorescence detectors. Note 1: Year when all FD sites were operational. Note 2: At TA 1 of the 3 FD sites features 24 telescopes from the HiRes experiment. Note 3: A-C for one telescope where A is the full area and C the area obscured by the camera and support structures. Thus A-C is the effective light collecting area. For the modified Schmidt design at Auger, the area of the entrance pupil, A, is listed because the pupil is smaller than the mirror and thus defines the entrance aperture. For the other experiments, the area of the mirror, A, is listed.

Observatory	Fly's Eye	HiRes	Telescope Array	Pierre Auger
Location	Dugway UT US	Dugway UT US	Delta UT US	Malargüe AR
Start-End	1981-1992	1996-2006	2008-present	2005-present
Sites (note 1)	2 (1986)	2 (1999)	3 (2008)	4 (2008)
Separation	3.3 km	12.6 km	31-40 km	39-62 km
Telescopes/site	67,18	21,42	12,12,14+10	6, 6, 6, 6+3
Pixel FOV	5.5°	1°	1°	1.5°
Telescope FOV Azi×Elv	≈18°×≈18°	16°×13.5°	18°×15° (note 2)	30°×28.1°
Light collection area (note 3)	1.95 m^2 - 0.25 m^2	3.72 m^2 - 0.5 m^2	6.8 m^2 - 0.85 m^2 (for 2 sites)	3.80 m^2 - 0.80 m^2 (modified schmidt)
Energy Scale Uncertainty	≤40%	≈20%	≈20%	14%

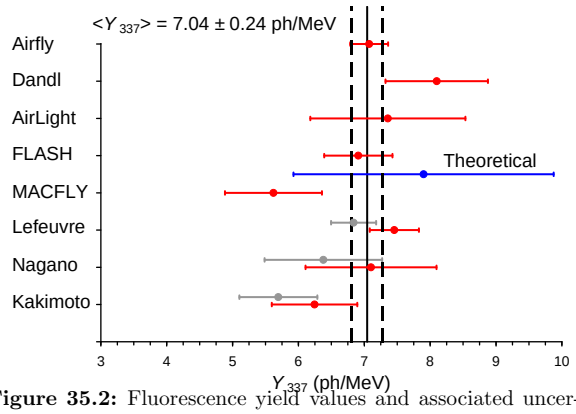

Figure 35.2: Fluorescence yield values and associated uncertainties at 337 nm (Y_{337}) in dry air at 800 hPa and 293 K The methodology and corrections that were applied to obtain the average and the uncertainty are discussed extensively in this reference. The vertical axis denotes different laboratory experiments that measured FY. The gray bars show three of the original measurements to illustrate the scale of the corrections applied. Figure from Ref [13].

An FD element (telescope) consists of a non-tracking spherical mirror of less than astronomical quality, a close-packed "camera" of photomultiplier tubes (PMTs) near the focal plane, and a flash ADC readout system with a pulse and track-finding trigger scheme [11]. The major experiments listed in Table 35.1 all use conventional PMTs (for example, Hamamatsu R9508 or Photonis XP3062) with grounded cathodes and AC coupled readout. Segmented mirrors have been fabricated from slumped or slumped/polished glass with an anodized aluminum coating or fabricated using shaped aluminum that was then chemically anodized with $AlMgSiO_5$. A broadband UV filter (custom fabricated or Schott MUG-6) reduces background light such as starlight, airglow, man-made light pollution, and airplane strobe-lights.

At 10^{20} eV, where the flux drops below 1 EAS/km^2century, the aperture for an eye of adjacent FD telescopes that span the horizon can reach 10^4 km^2 sr. FD operation requires (nearly) moonless nights and clear atmospheric conditions, which imposes a duty cycle of about 10%. Arrangements of LEDs, calibrated diffuse sources [14], pulsed UV lasers [15], LIDARs* and IR detectors that are sensitive to clouds are used for photometric calibration, atmospheric calibration [16], and determination of exposure [17]. For purposes of optical transmission, the atmosphere is treated as a dominant molecular component and a secondary aerosol component. The latter is well described [18] by molecular scattering theory and models derived from radiosonde measurements. The aerosol component can include dust, haze and pollution and the aerosol optical depth profile must be measured on site in the UV during FD data taking.

The EAS generates a track consistent with a light source moving at $v = c$ across the FOV. The number of photons (N_γ) as a function of atmospheric depth (X) can be expressed as [9]

$$\frac{\mathrm{d}N_\gamma}{\mathrm{d}X} = \frac{dE^{\mathrm{tot}}_{\mathrm{dep}}}{dX} \int Y(\lambda, P, T, u) \cdot \tau_{\mathrm{atm}}(\lambda, X) \cdot \varepsilon_{\mathrm{FD}}(\lambda)\mathrm{d}\lambda, \qquad (35.1)$$

where $\tau_{atm}(\lambda, X)$ is the atmospheric transmission, including wavelength (λ) dependence, and $\varepsilon_{\mathrm{FD}}(\lambda)$ is the FD efficiency. $\varepsilon_{\mathrm{FD}}(\lambda)$ includes geometric factors and collection efficiency of the optics, quantum efficiency of the PMTs, and other throughput factors. The typical systematic uncertainties, τ_{atm} (10%) and $\varepsilon_{\mathrm{FD}}$ (photometric calibration 10%), currently dominate the systematic uncertainty the absolute EAS energy scale. FD energy resolution, defined as event-to-event statistical uncertainty, is typically less than 10% for final data samples used for science analysis.

Analysis methods to reconstruct the EAS profile and deconvolve the contributions of re-scattered scintillation light, and direct and scattered Cherenkov light are described in [1] and more recently in [19]. The EAS energy is typically obtained by integrating over the Gaisser-Hillas function [20]

$$E_{\mathrm{cal}} = \int_0^\infty [w_{\max} \left(\frac{X - X_0}{X_{\max} - X_0} \right)^{(X_{\max} - X_0)/\lambda} e^{(X\max - X)/\lambda}] \mathrm{d}X, \qquad (35.2)$$

where E_{cal} is the energy of electromagnetic energy component of the EAS and $X_{\max}$ is the atmospheric slant depth at which the shower reaches its maximum energy deposit rate. This maximum dE/dX is denoted as $w_{\max}$. X_0 and λ are two shape parameters. The energy of the primary cosmic ray is obtained by correcting E_{cal} upward by about

* "LIDAR stands for "Light Detection and Ranging" and refers here to systems that measure atmospheric properties from the light scattered backwards from laser pulses directed into the sky.

10% to account for the invisible energy carried by particles that do not interact in the atmosphere. Energy resolution, $\Delta E/E$, of 15-20% is achievable, provided the geometric fit of the EAS axis is constrained, typically by multi-eye stereo projection or hybrid observations, and the profile fit of EAS development along the track is constrained by the observed rise and fall about $X_{\max}$. An example of a recorded EAS light profile and its corresponding dE/dX development profile are shown in Fig. 35.3.

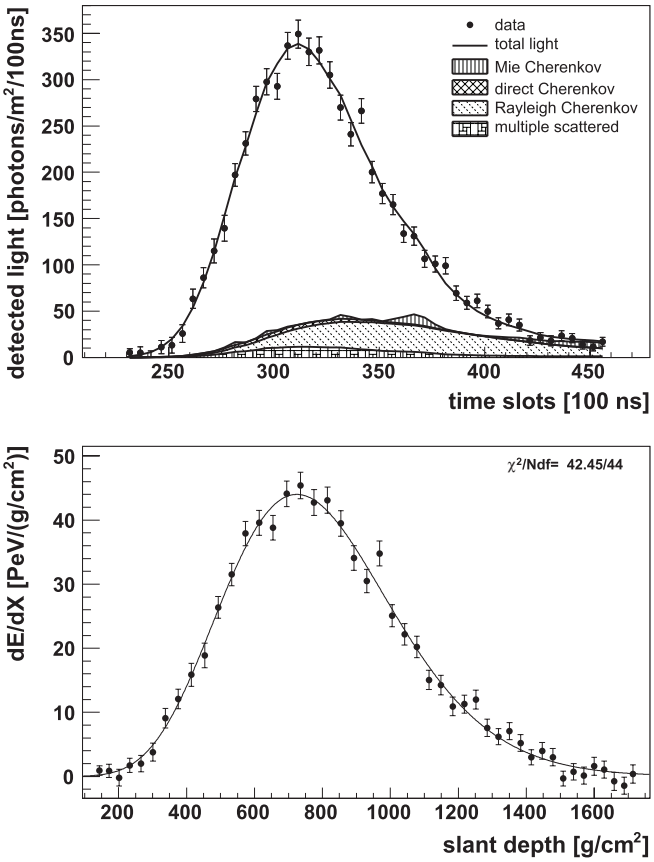

Figure 35.3: Example light profile (top) of one EAS recorded by the Pierre Auger FD and the corresponding profile (bottom) of energy deposited in the atmosphere vs atmospheric slant depth. The light profiles include the estimated components of Cherenkov light that have been scattered out of the forward beam by the molecular and aerosol (Mie) components of the atmosphere. The reconstructed energy of this EAS was $3.0 \pm 0.2 \times 10^{19}$ eV. Figure from Ref [21].

R&D toward an FD in space is at the design and prototype phase. A proposed space based FD instrument [22] by the JEM-EUSO collaboration would look down on the earth's atmosphere from space to view a much larger area than ground based instruments. Prototypes that have been built and flown include the TUS instrument [23] launched in 2016 onboard the Lomonosov satellite and two FD telescopes flown on stratospheric balloons in 2014 [24] and 2017 [25]. The proposed POEMMA space mission [26] would record scintillation and Cherenkov light from EASs the atmosphere to measure UHECRs and PeV scale cosmogenic tau neutrinos.

35.2.2. *Atmospheric Cherenkov telescopes for high-energy γ-ray astronomy* :

Revised July 2017 by J. Holder (Dept. of Physics and Astronomy & Bartol Research Inst., Univ. of Delaware).

A wide variety of astrophysical objects are now known to produce high-energy γ-ray photons. Leptonic or hadronic particles, accelerated to relativistic energies in the source, produce γ-rays typically through inverse Compton boosting of ambient photons or through the decay of neutral pions produced in hadronic interactions. At energies below ∼30 GeV, γ-ray emission can be efficiently detected using satellite or balloon-borne instrumentation, with an effective area approximately equal to the size of the detector (typically < 1 m^2). At higher energies, a technique with much larger effective collection area is desirable to measure astrophysical γ-ray fluxes, which decrease rapidly with increasing energy. Atmospheric Cherenkov detectors achieve effective collection areas of $>10^5$ m^2 by employing the Earth's atmosphere as an intrinsic part of the detection technique.

As described in Chapter 29, a hadronic cosmic ray or high energy γ-ray incident on the Earth's atmosphere triggers a particle cascade, or air shower. Relativistic charged particles in the cascade generate Cherenkov radiation, which is emitted along the shower direction, resulting in a light pool on the ground with a radius of ∼130 m. Cherenkov light is produced throughout the cascade development, with the maximum emission occurring when the number of particles in the cascade is largest, at an altitude of ∼10 km for primary energies of 100 GeV–1 TeV. Following absorption and scattering in the atmosphere, the Cherenkov light at ground level peaks at a wavelength, $\lambda \approx 300$–350 nm. The photon density is typically ∼100 photons/m^2 for a 1 TeV primary, arriving in a brief flash of a few nanoseconds duration. This Cherenkov pulse can be detected from any point within the light pool radius by using large reflecting surfaces to focus the Cherenkov light on to fast photon detectors (Fig. 35.4).

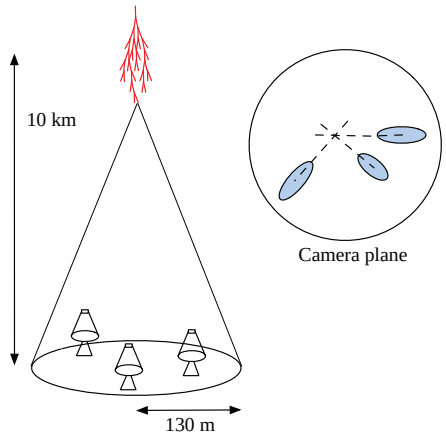

Figure 35.4: A schematic illustration of an imaging atmospheric Cherenkov telescope array. The primary particle initiates an air shower, resulting in a cone of Cherenkov radiation. Telescopes within the Cherenkov light pool record elliptical images; the intersection of the long axes of these images indicates the arrival direction of the primary, and hence the location of a γ-ray source in the sky.

Modern atmospheric Cherenkov telescopes, such as those built and operated by the VERITAS [27], H.E.S.S. [28] and MAGIC [29] collaborations, consist of large ($> 100\,\mathrm{m}^2$) segmented mirrors on steerable altitude-azimuth mounts. A camera made from an array of photosensors is placed at the focus of each mirror and used to record a Cherenkov image of each air shower. In these imaging atmospheric Cherenkov telescopes, single-anode photomultipliers tubes (PMTs) have traditionally been used (2048, in the case of H.E.S.S. II), but multi-anode PMTs and silicon devices now feature in more modern designs. The telescope cameras typically cover a field-of-view of $3-10^\circ$ in diameter. Images are recorded at kHz rates, the vast majority of which are due to showers with hadronic cosmic-ray primaries. The shape and orientation of the Cherenkov images are used to discriminate γ-ray photon events from this cosmic-ray background, and to reconstruct the photon energy and arrival direction. γ-ray images result from purely electromagnetic cascades and appear as narrow, elongated ellipses in the camera plane. The long axis of the ellipse corresponds to the vertical extension of the air shower, and points back towards the source position in the field-of-view. If multiple telescopes are used to view the same shower ("stereoscopy"), the

source position is simply the intersection point of the various image axes. Cosmic-ray primaries produce secondaries with large transverse momenta, which initiate sub-showers. Their images are consequently wider and less regular than those with γ-ray primaries and, since the original charged particle has been deflected by Galactic magnetic fields before reaching the Earth, the images have no preferred orientation.

The measurable differences in Cherenkov image orientation and morphology provide the background discrimination which makes ground-based γ-ray astronomy possible. For point-like sources, such as distant active galactic nuclei, modern instruments can reject over 99.999% of the triggered cosmic-ray events, while retaining up to 50% of the γ-ray population. In the case of spatially extended sources, such as Galactic supernova remnants, the background rejection is less efficient, but the technique can be used to produce γ-ray maps of the emission from the source. The angular resolution depends upon the number of telescopes which view the image and the energy of the primary γ-ray, but is typically less than 0.1° per event (68% containment radius) at energies above a few hundred GeV.

The total Cherenkov yield from the air shower is proportional to the energy of the primary particle. The image intensity, combined with the reconstructed distance of the shower core from each telescope, can therefore be used to estimate the primary energy. The energy resolution of this technique, also energy-dependent, is typically 15–20% at energies above a few hundred GeV. Energy spectra of γ-ray sources can be measured over a wide range, depending upon the instrument characteristics, source properties (flux, spectral slope, elevation angle, *etc.*), and exposure time. The effective energy range is typically from 30 GeV to 100 TeV and peak sensitivity lies in the range from 100 GeV to a few TeV.

The first astrophysical source to be convincingly detected using the imaging atmospheric Cherenkov technique was the Crab Nebula [30], with an integral flux of 2.1×10^{-11} photons cm^{-2} s^{-1} above 1 TeV [31]. Modern imaging atmospheric Cherenkov telescopes have sensitivity sufficient to detect sources with less than 1% of the Crab Nebula flux in a few tens of hours. The TeV source catalog now consists of approximately 200 sources (see e.g. Ref. 32). A large fraction of these were detected by scanning the Galactic plane from the southern hemisphere with the H.E.S.S. telescope array [33]. Recent reviews of the field include [34] and [35], and a historical overview can be found in [36].

Major upgrades of the existing telescope arrays have recently been completed, including the addition of a 28 m diameter central telescope to H.E.S.S. (H.E.S.S. II). Development is also underway for the next generation instrument, the Cherenkov Telescope Array (CTA), which will consist of a northern and a southern hemisphere observatory, with a combined total of more than 100 telescopes [37]. Telescopes of three different sizes are planned, spread over an area of > 1 km^2, providing wider energy coverage, improved angular and energy resolutions, and an order of magnitude improvement in sensitivity relative to existing imaging atmospheric Cherenkov telescopes. Baseline telescope designs are similar to existing devices, but exploit technological developments such as dual mirror optics and silicon photo-detectors.

35.3. Large neutrino detectors

35.3.1. *Deep liquid detectors for rare processes* :

Revised August 2017 by K. Scholberg & C.W. Walter (Duke University)

Deep, large detectors for rare processes tend to be multi-purpose with physics reach that includes not only solar, reactor, supernova and atmospheric neutrinos, but also searches for baryon number violation, searches for exotic particles such as magnetic monopoles, and neutrino and cosmic-ray astrophysics in different energy regimes. The detectors may also serve as targets for long-baseline neutrino beams for neutrino oscillation physics studies. In general, detector design considerations can be divided into high-and low-energy regimes, for which background and event reconstruction issues differ. The high-energy regime, from about 100 MeV to a few hundred GeV, is relevant for proton decay searches, atmospheric neutrinos and high-energy astrophysical neutrinos. The low-energy regime (a few tens of MeV or less) is relevant for supernova, solar, reactor and geological neutrinos.

Large water Cherenkov and scintillator detectors (see Table 34.9) usually consist of a volume of transparent liquid viewed by photomultiplier tubes (PMTs) (see Sec. 34.2); the liquid serves as active target. PMT hit charges and times are recorded and digitized, and triggering is usually based on coincidence of PMT hits within a time window comparable to the detector's light-crossing time. Because photosensors lining an inner surface represent a driving cost that scales as surface area, very large volumes can be used for comparatively reasonable cost. Some detectors are segmented into subvolumes individually viewed by PMTs, and may include other detector elements (*e.g.*, tracking detectors). Devices to increase light collection, *e.g.*, reflectors or waveshifter plates, may be employed. A common configuration is to have at least one concentric outer layer of liquid material separated from the inner part of the detector to serve as shielding against ambient background. If optically separated and instrumented with PMTs, an outer layer may also serve as an active veto against entering cosmic rays and other background events. The PMTs for large detectors typically range in size from 20 cm to 51 cm diameter, and typical quantum efficiencies are in the 20–25% range for scintillation and water-Cherenkov photons. PMTs with higher quantum efficiencies, 35% or higher, have recently become available. The active liquid volume requires purification and there may be continuous recirculation of liquid. For large homogeneous detectors, the event interaction vertex is determined using relative timing of PMT hits, and energy deposition is determined from the number of recorded photoelectrons. A "fiducial volume" is usually defined within the full detector volume, some distance away from the PMT array. Inside the fiducial volume, enough PMTs are illuminated per event that reconstruction is considered reliable, and furthermore, entering background from the enclosing walls is suppressed by a buffer of self-shielding. PMT and detector optical parameters are calibrated using laser, LED, or other light sources. Quality of event reconstruction typically depends on photoelectron yield, pixelization and timing.

Because in most cases one is searching for rare events, large detectors are usually sited underground to reduce cosmic-ray-related background (see Chapter 29). The minimum depth required varies according to the physics goals [38].

35.3.1.1. *Liquid scintillator detectors:*

Past and current large underground detectors based on hydrocarbon scintillators include LVD, MACRO, Baksan, Borexino, KamLAND and SNO+; JUNO is a future detector. Experiments at nuclear reactors include CHOOZ, Double CHOOZ, Daya Bay, and RENO. Organic liquid scintillators (see Sec. 34.3.0) for large detectors are chosen for high light yield and attenuation length, good stability, compatibility with other detector materials, high flash point, low toxicity, appropriate density for mechanical stability, and low cost. They may be doped with waveshifters and stabilizing agents. Popular choices are pseudocumene (1,2,4-trimethylbenzene) with a few g/L of the PPO (2,5-diphenyloxazole) fluor, and linear alkylbenzene (LAB). In a typical detector configuration there will be active or passive regions of undoped scintillator, non-scintillating mineral oil or water surrounding the inner neutrino target volume. A thin vessel or balloon made of nylon, acrylic or other material transparent to scintillation light may contain the inner target; if the scintillator is buoyant with respect to its buffer, ropes may hold the balloon in place. For phototube surface coverages in the 20–40% range, yields in the few hundreds of photoelectrons per MeV of energy deposition can be obtained. Typical energy resolution is about $7\%/\sqrt{E(\mathrm{MeV})}$, and typical position reconstruction resolution is a few tens of cm at $\sim$ 1 MeV, scaling as $\sim N^{-1/2}$, where N is the number of photoelectrons detected.

Shallow detectors for reactor neutrino oscillation experiments require excellent muon veto capabilities. For $\bar{\nu}_e$ detection via inverse beta decay on free protons, $\bar{\nu}_e + p \to n + e^+$, the neutron is captured by a proton on a $\sim$180 μs timescale, resulting in a 2.2 MeV γ ray, observable by Compton scattering and which can be used as a tag in coincidence with the positron signal. The positron annihilation γ rays may also contribute. Inverse beta decay tagging may be improved by addition of Gd at $\sim$0.1% by mass, which for natural isotope abundance has a $\sim$49,000 barn cross-section for neutron capture (in contrast to

Table 34.9: Properties of large detectors for rare processes. If total target mass is divided into large submodules, the number of subdetectors is indicated in parentheses. Projects with first data expected in 2020 or later are indicated in italics.

Detector	Mass, kton (modules)	PMTs (diameter, cm)	ξ	p.e./MeV	Dates
Baksan	0.33, scint (3150)	1/module (15)	segmented	40	1980–
MACRO	0.56, scint (476)	2-4/module (20)	segmented	18	1989–2000
LVD	1, scint. (840)	3/module (15)	segmented	15	1992–
KamLAND	0.41^f, scint	1325(43)+554(51)*	34%	460	2002–
Borexino	0.1^f, scint	2212 (20)	30%	500	2007–
SNO+	0.78, scint	9438 (20)	54%	400–900	2017 (exp.)
CHOOZ	0.005, scint (Gd)	192 (20)	15%	130	1997–1998
Double Chooz	0.017, scint (Gd)(2)	534/module (20)	13%	180	2011–
Daya Bay	0.160, scint (Gd)(8)	192/module (20)	5.6%†	100	2011–
RENO	0.032, scint (Gd)(2)	342/module (25)	12.6%	100	2011–
JUNO	20.0^f, scint	17000 (51)/25000 (8)	75%	1200	2020 (exp.)
IMB-1	3.3^f, H_2O	2048 (12.5)	1%	0.25	1982–1985
IMB-2	3.3^f, H_2O	2048 (20)	4.5%	1.1	1987–1990
Kam I	$0.88/0.78^f$, H_2O	1000/948 (51)	20%	3.4	1983–1985
Kam II	1.04^f, H_2O	948 (51)	20%	3.4	1986–1990
Kam III	1.04^f, H_2O	948 (51)	20%‡	4.3	1990–1995
SK I	22.5^f, H_2O	11146 (51)	40%	6	1996–2001
SK II	22.5^f, H_2O	5182 (51)	19%	3	2002–2005
SK III-IV	22.5^f, H_2O	11129 (51)	40%	6	2006–
SK-Gd	22.5^f, H_2O (Gd)	11129 (51)	40%	6	2019 (exp.)
Hyper-K	187^f, H_2O**	40000 (51)	40%	12	2026 (exp.)
SNO	1, $D_2O/1.7$, H_2O	9438 (20)	31% §	9	1999–2006

f indicates typical fiducial mass used for data analysis; this may vary by physics topic.
* Measurements made before 2003 only considered data from the 43 cm PMTs.
† The effective Daya Bay coverage is 12% with top and bottom reflectors.
‡ The effective Kamiokande III coverage was 25% with light collectors.
** A second staged module is planned.
§ The effective SNO coverage was 54% with light collectors.

the 0.3 barn cross-section for capture on free protons). Gd capture takes ∼30 μs, and is followed by a cascade of γ rays adding up to about 8 MeV. Gadolinium doping of scintillator requires specialized formulation to ensure adequate attenuation length and stability.

Scintillation detectors have an advantage over water Cherenkov detectors in the lack of Cherenkov threshold and the high light yield. However, scintillation light emission is nearly isotropic, and therefore directional capabilities are relatively weak. Liquid scintillator is especially suitable for detection of low-energy events. Radioactive backgrounds are a serious issue, and include long-lived cosmogenics. To go below a few MeV, very careful selection of materials and purification of the scintillator is required (see Sec. 35.6). Fiducialization and tagging can reduce background. One can also dissolve neutrinoless double beta decay ($0\nu\beta\beta$) isotopes in scintillator. This has been realized by KamLAND-Zen, which deployed a 1.5 m-radius balloon containing enriched Xe dissolved in scintillator inside KamLAND, and ^{130}Te is planned for SNO+. Although for this approach, energy resolution is poor compared to other $0\nu\beta\beta$ search experiments, the quantity of isotope can be so large that the kinematic signature of $0\nu\beta\beta$ would be visible as a clear feature in the spectrum.

35.3.1.2. *Water Cherenkov detectors:*

Very large imaging water detectors reconstruct ten-meter-scale Cherenkov rings produced by charged particles (see Sec. 34.5.0). The first such large detectors were IMB and Kamiokande. The only currently existing instance of this class of detector, with fiducial mass of 22.5 kton and total mass of 50 kton, is Super-Kamiokande (Super-K, SK). Hyper-Kamiokande (Hyper-K) plans at least one, and possibly two, detectors with 187-kton fiducial mass. For volumes of this scale, absorption and scattering of Cherenkov light are non-negligible, and a wavelength-dependent factor $\exp(-d/L(\lambda))$ (where d is the distance from emission to the sensor and $L(\lambda)$ is the attenuation length of the medium) must be included in the integral of Eq. (34.5) for the photoelectron yield. Attenuation lengths on the order of 100 meters have been achieved.

Cherenkov detectors are excellent electromagnetic calorimeters, and the number of Cherenkov photons produced by an e/γ is nearly proportional to its kinetic energy. For massive particles, the number of photons produced is also related to the energy, but not linearly. For any type of particle, the *visible energy* $E_{\rm vis}$ is defined as the energy of an electron which would produce the same number of Cherenkov photons. The number of collected photoelectrons depends on the scattering and attenuation in the water along with the photocathode coverage, quantum efficiency and the optical parameters of any external light collection systems or protective material surrounding them. Event-by-event corrections are made for geometry and attenuation. For a typical case, in water $N_{\rm p.e.} \sim 15\,\xi\,E_{\rm vis}({\rm MeV})$, where ξ is the effective fractional photosensor coverage. Cherenkov photoelectron yield per MeV of energy is relatively small compared to that for scintillator, *e.g.*, ∼ 6 pe/MeV for Super-K with a PMT surface coverage of ∼ 40%. In spite of light yield and Cherenkov threshold issues, the intrinsic directionality of Cherenkov light allows individual particle tracks to be reconstructed. Vertex and direction fits are performed using PMT hit charges and times, requiring that the hit pattern be consistent with a Cherenkov ring.

High-energy (∼100 MeV or more) neutrinos from the atmosphere or beams interact with nucleons; for the nucleons bound inside the

^{16}O nucleus, nuclear effects must be considered both at the interaction and as the particles leave the nucleus. Various event topologies can be distinguished by their timing and fit patterns, and by presence or absence of light in a veto. "Fully-contained" events are those for which the neutrino interaction final state particles do not leave the inner part of the detector; these have their energies relatively well measured. Neutrino interactions for which the lepton is not contained in the inner detector sample have higher-energy parent neutrino energy distributions. For example, in "partially-contained" events, the neutrino interacts inside the inner part of the detector but the lepton (almost always a muon, since only muons are penetrating) exits. "Upward-going muons" can arise from neutrinos which interact in the rock below the detector and create muons which enter the detector and either stop, or go all the way through (entering downward-going muons cannot be distinguished from cosmic rays). At high energies, multi-photoelectron hits are likely and the charge collected by each PMT (rather than the number of PMTs firing) must be used; this degrades the energy resolution to approximately $2\%/\sqrt{\xi\, E_{\rm vis}({\rm GeV})}$. The absolute energy scale in this regime can be known to ∼2–3% using cosmic-ray muon energy deposition, Michel electrons and π^0 from atmospheric neutrino interactions. Typical vertex resolutions for GeV energies are a few tens of cm [39]. Angular resolution for determination of the direction of a charged particle track is a few degrees. For a neutrino interaction, because some final-state particles are usually below Cherenkov threshold, knowledge of direction of the incoming neutrino direction itself is generally worse than that of the lepton direction, and dependent on neutrino energy.

Multiple particles in an interaction (so long as they are above Cherenkov threshold) may be reconstructed, allowing for the exclusive reconstruction of final states. In searches for proton decay, multiple particles can be kinematically reconstructed to form a decaying nucleon. High-quality particle identification is also possible: γ rays and electrons shower, and electrons scatter, which results in fuzzy rings, whereas muons, pions and protons make sharp rings. These patterns can be quantitatively separated with high reliability using maximum likelihood methods [40]. A e/μ misidentification probability of $\sim 0.4\%/\xi$ in the sub-GeV range is consistent with the performance of several experiments for $4\% < \xi < 40\%$. Sources of background for high energy interactions include misidentified cosmic muons and anomalous light patterns when the PMTs sometimes "flash" and emit photons themselves. The latter class of events can be removed using its distinctive PMT signal patterns, which may be repeated. More information about high energy event selection and reconstruction may be found in reference [41].

In spite of the fairly low light yield, large water Cherenkov detectors may be employed for reconstructing low-energy events, down to *e.g.* ∼ 4-5 MeV for Super-K [42]. Low-energy neutrino interactions of solar neutrinos in water are predominantly elastic scattering off atomic electrons; single electron events are then reconstructed. At solar neutrino energies, the visible energy resolution ($\sim 30\%/\sqrt{\xi\, E_{\rm vis}({\rm MeV})}$) is about 20% worse than photoelectron counting statistics would imply. Using an electron LINAC and/or nuclear sources, approximately 0.5% determination of the absolute energy scale has been achieved at solar neutrino energies. Angular resolution is limited by multiple scattering in this energy regime (25–30°). At these energies, radioactive backgrounds become a dominant issue. These backgrounds include radon in the water itself or emanated from detector materials, and γ rays from the rock and detector materials. In the few to few tens of MeV range, radioactive products of cosmic-ray-muon-induced spallation are troublesome, and are removed by proximity in time and space to preceding muons, at some cost in dead time. Gadolinium doping using 0.2% $Gd_2(SO_4)_3$ is planned for Super-K to improve selection of low-energy $\bar{\nu}_e$ and other events with accompanying neutrons [43].

The Sudbury Neutrino Observatory (SNO) detector [44] is the only instance of a large heavy water detector and deserves mention here. In addition to an outer 1.7 kton of light water, SNO contained 1 kton of D_2O, giving it unique sensitivity to neutrino neutral current ($\nu_x + d \to \nu_x + p + n$), and charged current ($\nu_e + d \to p + p + e^-$) deuteron breakup reactions. The neutrons were detected in three ways: In the first phase, via the reaction $n + d \to t + \gamma + 6.25$ MeV; Cherenkov radiation from electrons Compton-scattered by the γ rays was observed. In the second phase, NaCl was dissolved in the water. ^{35}Cl captures neutrons, $n + {}^{35}{\rm Cl} \to {}^{36}{\rm Cl} + \gamma + 8.6$ MeV. The γ rays were observed via Compton scattering. In a final phase, specialized low-background ^{3}He counters ("neutral current detectors" or NCDs) were deployed in the detector. These counters detected neutrons via $n + {}^3{\rm He} \to p + t + 0.76$ MeV; ionization charge from energy loss of the products was recorded in proportional counters.

35.3.2. *Neutrino telescopes* :

Revised Aug. 2017 by Ch. Spiering (DESY/Zeuthen) and U.F. Katz (Univ. Erlangen)

The primary goal of neutrino telescopes (NTs) is the detection of astrophysical neutrinos, in particularly those which are expected to accompany the production of high-energy cosmic rays in astrophysical accelerators. NTs in addition address a variety of other fundamental physics issues like indirect search for dark matter, study of neutrino oscillations, search for exotic particles like magnetic monopoles or study of cosmic rays and their interactions [45,46,47].

NTs are large-volume arrays of "optical modules" (OMs) installed in open transparent media like water or ice, at depths that completely block the daylight. The OMs record the Cherenkov light induced by charged secondary particles produced in reactions of high-energy neutrinos in or around the instrumented volume. The neutrino energy, E_ν, and direction can be reconstructed from the hit pattern recorded. NTs typically target an energy range $E_\nu \gtrsim 100\,{\rm GeV}$; sensitivity to lower energies is achieved in dedicated setups with denser instrumentation.

In detecting cosmic neutrinos, three sources of backgrounds have to be considered: (i) *atmospheric neutrinos* from cosmic-ray interactions in the atmosphere, which can be separated from cosmic neutrinos on a statistical basis, or, for down-going neutrinos, by vetoing accompanying muons; (ii) down-going punch-through *atmospheric muons* from cosmic-ray interactions, which are suppressed by several orders of magnitude with respect to the ground level due to the large detector depths. They can be further reduced by selecting upward-going or high-energy neutrinos or by self-veto methods; (iii) random backgrounds due to photomultiplier (PMT) dark counts, ^{40}K decays (mainly in sea water) or bioluminescence (only water), which impact adversely on event recognition and reconstruction. Note that atmospheric neutrinos and muons allow for investigating neutrino oscillations and cosmic ray anisotropies, respectively. Recently, it has become obvious that a precise measurement of the energy-zenith-distribution of atmospheric neutrinos may allow for determining the neutrino mass hierarchy by exploiting matter-induced oscillation effects in the Earth [48,49].

Neutrinos can interact with target nucleons N through charged current ($\overset{(-)}{\nu}_\ell N \to \ell^\mp X$, CC) or neutral current ($\overset{(-)}{\nu}_\ell N \to \overset{(-)}{\nu}_\ell X$, NC) processes. A CC reaction of a $\overset{(-)}{\nu}_\mu$ produces a muon track and a hadronic particle cascade, whereas all NC reactions and CC reactions of $\overset{(-)}{\nu}_e$ produce particle cascades only. CC interactions of $\overset{(-)}{\nu}_\tau$ can have either signature, depending on the τ decay mode. In most astrophysical models, neutrinos are expected to be produced through the $\pi/K \to \mu \to e$ decay chain, *i.e.*, with a flavour ratio $\nu_e : \nu_\mu : \nu_\tau \approx 1 : 2 : 0$. For sources outside the solar system, neutrino oscillations turn this ratio to $\nu_e : \nu_\mu : \nu_\tau \approx 1 : 1 : 1$ upon arrival on Earth.

The total neutrino-nucleon cross section is about $10^{-35}\,{\rm cm}^2$ at $E_\nu = 1\,{\rm TeV}$ and rises roughly linearly with E_ν below this energy and as $E_\nu^{0.3-0.5}$ above, flattening out towards high energies. The CC:NC cross-section ratio is about 2:1. At energies above some TeV, neutrino absorption in the Earth becomes noticeable; for vertically upward-moving neutrinos (zenith angle $\theta = 180°$), the survival probability is $74\,(27, < 2)\%$ for $10\,(100, 1000)\,{\rm TeV}$. On average, between 50% (65%) and 75% of E_ν is transfered to the final-state lepton in neutrino (antineutrino) reactions between 100 GeV and 10 PeV.

The final-state lepton follows the initial neutrino direction with a RMS mismatch angle $\langle\phi_{\nu\ell}\rangle \approx 1.5°/\sqrt{E_\nu\,[{\rm TeV}]}$, indicating the intrinsic kinematic limit to the angular resolution of NTs. For CC $\overset{(-)}{\nu}_\mu$ reactions at energies above about 10 TeV, the angular resolution is dominated by the muon reconstruction accuracy of a few times 0.1° at most. For muon energies $E_\mu \gtrsim 1\,{\rm TeV}$, the increasing light emission due to

radiative processes allows for reconstructing E_μ from the measured dE_μ/dx with an accuracy of $\sigma(\log E_\mu) \approx 0.3$; at lower energies, E_μ can be estimated from the length of the muon track if it is contained in the detector. These properties make CC $\overset{(-)}{\nu}_\mu$ reactions the prime channel for the identification of individual astrophysical neutrino sources.

Hadronic and electromagnetic particle cascades at the relevant energies are 5–20 m long, *i.e.*, short compared to typical OM distances. The total amount of Cherenkov light provides a direct measurement of the cascade energy with an accuracy of about 20% at energies above 10 TeV and 10% beyond 100 TeV for events contained in the instrumented volume. Neutrino flavour and reaction mechanism can, however, hardly be determined and neutrinos from NC reactions or τ decays may carry away significant "invisible" energy. Above 100 TeV, the average directional reconstruction accuracy of cascades is 10–15 degrees in polar ice and better than 2 degrees in water, the difference being due to the inhomogeneity of the ice and stronger light scattering in ice. These features, together with the small background of atmospheric $\overset{(-)}{\nu}_e$ and $\overset{(-)}{\nu}_\tau$ events, makes the cascade channel particularly interesting for searches for a diffuse, high-energy excess of extraterrestrial over atmospheric neutrinos. In water, cascade events can also be used for the search for point sources of cosmic neutrinos, albeit the inferior angular accuracy compared to muon tracks leads to a higher background from atmospheric neutrinos.

The detection efficiency of a NT is quantified by its effective area, *e.g.*, the fictitious area for which the full incoming neutrino flux would be recorded (see Fig. 35.5). The increase with E_ν is due to the rise of neutrino cross section and muon range, while neutrino absorption in the Earth causes the decrease at large θ. Identification of downward-going neutrinos requires strong cuts against atmospheric muons, hence the cut-off towards low E_ν. Due to the small cross section, the effective area is many orders of magnitude smaller than the geometrical dimension of the detector; a $\overset{(-)}{\nu}_\mu$ with 1 TeV can, *e.g.*, be detected with a probability of the order 10^{-6} if the telescope is on its path.

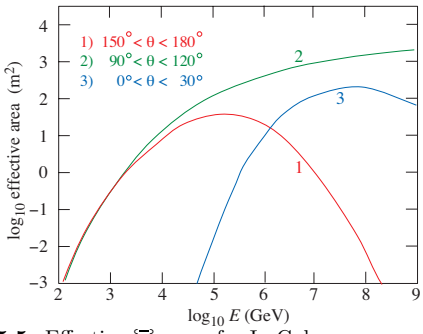

Figure 35.5: Effective $\overset{(-)}{\nu}_\mu$ area for IceCube as an example of a cubic-kilometre NT, as a function of neutrino energy for three intervals of the zenith angle θ. The values shown here correspond to a specific event selection for point source searches.

Detection of upward-going muons allows for identifying neutrino interactions far outside the instrumented volume. This method, however, is only sensitive to CC $\overset{(-)}{\nu}_\mu$ interactions and cannot be extended to more than 5–10 degrees above the geometric horizon, where the background of atmospheric muons becomes prohibitive. Alternatively, one can select events that start inside the instrumented volume and thus remove incoming muons that generate early hits in the outer layers of the detector. Such a veto-based event selection is sensitive to neutrinos of all flavours from all directions, albeit with a reduced efficiency since a part of the instrumented volume is sacrificed for the veto. Such a muon veto, or vetoing events with a coincident signal in the surface array, also rejects down-going atmospheric neutrinos that are accompanied by muons from the same air shower and thus reduces the atmospheric-neutrino background. Actually, the breakthrough in detecting high-energy cosmic neutrinos has been achieved with this technique.

Note that the fields of view of NTs at the South Pole and in the Northern hemisphere are complementary for each reaction channel and neutrino energy.

35.3.2.1. *The Projects:*

Table 35.2: Past, present and future neutrino telescope projects and their main parameters. The milestone years give the times of project start, of first data taking with partial configurations, of detector completion, and of project termination. Projects with first data expected past 2020 are indicated in italics. The size refers to the largest instrumented volume reached during the project development. See [47] for references to the different projects where unspecified.

Experiment	Milestones	Medium/ Location	Size (km^3)	Remarks
DUMAND	1978/–/–/1995	Pacific/Hawaii		Terminated due to technical/funding problems
NT-200	1980/1993/1998/2015	Lake Baikal	10^{-4}	First proof of principle
GVD [50]	2012/2015/–/–	Lake Baikal	0.5–1.5	High-energy ν astronomy, first 2 clusters installed
NESTOR	1991/–/–/–	Med. Sea		2004 data taking with prototype
NEMO	1998/–/–/–	Med. Sea		R&D project, prototype tests
AMANDA	1990/1996/2000/2009	Ice/South Pole	0.015	First deep-ice neutrino telescope
ANTARES	1997/2006/2008/–	Med. Sea	0.010	First deep-sea neutrino telescope
IceCube	2001/2005/2010/–	Ice/South Pole	1.0	First km^3-sized detector
IceCube-Gen2 [51]	2014/–/–/–	Ice/South Pole	5–10	Planned extension of IceCube covering low and high energies, a surface array and radio detection
KM3NeT/ARCA [49]	2013/(2015)/–/–	Med. Sea	1–2	First construction phase started
KM3NeT/ORCA [49]	2014/(2017)/–/–	Med. Sea	0.003	Low-energy configuration for neutrino mass hierarchy
KM3NeT Phase 3	2013/–/–/–	Med. Sea	3–6	6 building blocks + ORCA

35.3.2.2. *Properties of media:*

The efficiency and quality of event reconstruction depend strongly on the optical properties (absorption and scattering length, intrinsic optical activity) of the medium in the spectral range of bialkali photocathodes (300–550 nm). Large absorption lengths result in a better light collection, large scattering lengths in superior angular resolution. Deep-sea sites typically have effective scattering lengths of > 100 m and, at their peak transparency around 450 nm, absorption lengths of 50–65 m. The absorption length for Lake Baikal is 22–24 m. The properties of South Polar ice vary strongly with depth; at the peak transparency wave length (400 nm), the scattering length is between 5 and 75 m and the absorption length between 15 and 250 m, with the best values in the depth region 220 ones in the layer 1950–2100 m.

Noise rates measured by 25 cm PMTs in deep polar ice are about 0.5 kHz per PMT and almost entirely due to radioactivity in the OM components. The corresponding rates in sea water are typically 60 kHz, mostly due to ^{40}K decays. Bioluminescence activity can locally cause rates on the MHz scale for seconds; the frequency and intensity of such "bursts" depends strongly on the sea current, the season, the geographic location, and the detector geometry. Experience from ANTARES shows that these backgrounds are manageable without a major loss of efficiency or experimental resolution.

35.3.2.3. *Technical realisation:*

Optical modules (OMs) and PMTs: An OM is a pressure-tight glass sphere housing one or several PMTs with a time resolution in the nanosecond range, and in most cases also electronics for control, HV generation, operation of calibration LEDs, time synchronisation and signal digitisation.

Hybrid PMTs with 37 cm diameter have been used for NT-200, conventional hemispheric PMTs for AMANDA (20 cm) and for ANTARES, IceCube and Baikal-GVD (25 cm). A novel concept has been chosen for KM3NeT. The OMs (43 cm) are equipped with 31 PMTs (7.5 cm), plus control, calibration and digitisation electronics. The main advantages are that (i) the overall photocathode area exceeds that of a 25 cm PMT by more than a factor of 3; (ii) the individual readout of the PMTs results in a very good separation between one- and two-photoelectron signals which is essential for online data filtering and random background suppression; (iii) the hit pattern on an OM provides directional information; (iv) no mu-metal shielding against the Earth magnetic field is required. Figure 35.6 shows the OM designs of IceCube and KM3NeT.

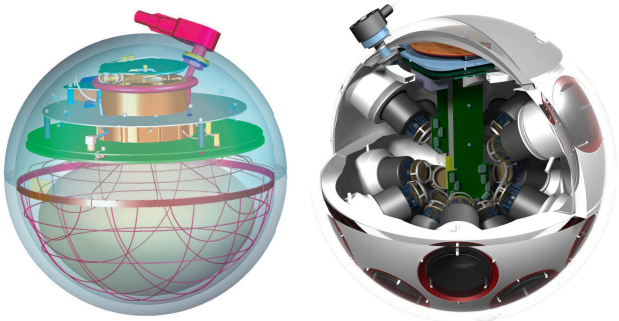

Figure 35.6: Schematic views of the digital OMs of IceCube (left) and KM3NeT (right).

Readout and data filtering: In current NTs the PMT data are digitised in situ, for ANTARES and Baikal-GVD in special electronics containers close to the OMs, for IceCube and KM3NeT inside the OMs. For IceCube, data are transmitted via electrical cables of up to 3.3 km length, depending on the location of the strings and the depth of the OMs; for ANTARES, KM3NeT and Baikal-GVD optical fibre connections have been chosen (several 10 km for the first two and 4 km for GVD).

The full digitised waveforms of the IceCube OMs are transmitted to the surface for pulses appearing in local coincidences on a string; for other pulses, only time and charge information is provided. For ANTARES (time and charge) and KM3NeT (time over threshold), all PMT signals above an adjustable noise threshold are sent to shore.

The raw data are subsequently processed on online computer farms, where multiplicity and topology-driven filter algorithms are applied to select event candidates. The filter output data rate is about 10 GByte/day for ANTARES and of the order 1 TByte/day for IceCube (100 GByte/day transfered via satellite) and KM3NeT.

Calibration: For efficient event recognition and reconstruction, the OM timing must be synchronised at the few-nanosecond level and the OM positions and orientations must be known to a few 10 cm and a few degrees, respectively. Time calibration is achieved by sending synchronisation signals to the OM electronics and also by light calibration signals emitted at known times by LED or laser flashers emitted in situ (ANTARES, KM3NeT). Precise position calibration is achieved by measuring the travel time of light calibration signals sent from OM to OM (IceCube) or acoustic signals sent from transducer at the sea floor to receivers on the detector strings (ANTARES, KM3NeT, Baikal-GVD). Absolute pointing and angular resolution can be determined by measuring the "shadow of the moon" (*i.e.*, the directional depletion of muons generated in cosmic-ray interactions). IceCube has shown that both are below 1°, confirming MC calculations which indicate a precision of $\approx 0.5°$ for energies above 10 TeV. For KM3NeT, simulations indicate that sub-degree precision in the absolute pointing can be reached within a few weeks of operation.

Detector configurations: IceCube (see Fig. 35.7) consists of 5160 Digital OMs (DOMs) installed on 86 strings at depths of 1450 to 2450 m in the Antarctic ice; except for the DeepCore region, string distances are 125 m and vertical distances between OMs 17 m. 324 further DOMs are installed in IceTop, an array of detector stations on the ice surface above the strings. DeepCore is a high-density sub-array at large depths (*i.e.*, in the best ice layer) at the centre of IceCube.

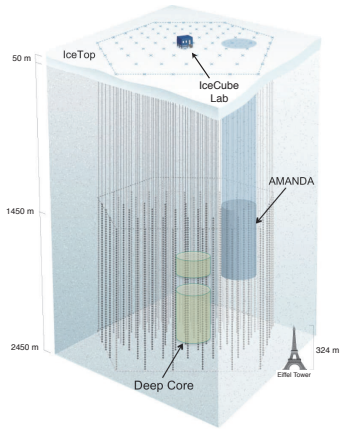

Figure 35.7: Schematic view of the IceCube neutrino observatory comprising the deep-ice detector including its nested dense part DeepCore, and the surface air shower array IceTop. The IceCube Lab houses data acquisition electronics and the computer farm for online processing. Operation of AMANDA was terminated in 2009.

The NT200 detector in Lake Baikal at a depth of 1100 m consisted of 8 strings attached to an umbrella-like frame, with 12 pairs of OMs per string. The diameter of the instrumented volume was 42m, its height 70 m. Meanwhile (2017), the Baikal collaboration has installed the first two clusters of a future cubic-kilometre array. A first phase, covering a volume of about 0.4 km^3, will consist of 8 clusters, each with 288 OMs at 8 strings; its completion is scheduled for 2020. A next stage could comprise about 20 clusters and cover up to 1.5 km^3.

ANTARES comprises 12 strings with lateral distances of 60–70 m, each carrying 25 triplets of OMs at vertical distances of 14.5 m. The OMs are located at depths 2.1–2.4 km, starting 100 m above the sea floor. A further string carries devices for calibration and environmental monitoring. A system to investigate the feasibility of acoustic neutrino detection is also implemented.

KM3NeT will consist of building blocks of 115 strings each, with 18 OMs per string. Prototype operations have successfully verified

the KM3NeT technology [52]. In the upcoming phase 2.0 of its staged implementation, KM3NeT aims at two building blocks for neutrino astronomy, with vertical distances between OMs of 36 m and a lateral distance between adjacent strings of 90 m (ARCA, for *Astroparticle Research with Cosmics in the Abyss*) and at one block for the measurement of the neutrino mass hierarchy, with vertical distances between OMs of 9 m and a lateral distance between adjacent strings of about 20 m (ORCA, for *Oscillation Research with Cosmics in the Abyss*) [49]. A first installation phase of ARCA near Capo Passero, East of Sicily and of ORCA near Toulon has started in 2015 and comprises 24 (7) ARCA (ORCA) strings to be deployed by end of 2018. Completion of the full three blocks is expected for 2021.

35.3.2.4. *Results:*

Atmospheric neutrino fluxes have been precisely measured with AMANDA and ANTARES ($\overset{(-)}{\nu}_\mu$) and with IceCube ($\overset{(-)}{\nu}_\mu, \overset{(-)}{\nu}_e$); the results are in agreement with predicted spectra. No astrophysical point sources have been identified yet, and no indications of neutrino fluxes from dark matter annihilations or of exotic phenomena have been found (see [47] and references therein). IceCube has furthermore reported an energy-dependent anisotropy of cosmic-ray induced muons.

In 2013, an excess of track and cascade events between 30 TeV and 1 PeV above background expectations was reported by IceCube; this analysis used the data taken in 2010 and 2011 and for the first time employed containment conditions and an atmospheric muon veto for suppression of down-going atmospheric neutrinos (High-Energy Starting Event analysis, HESE). A display of one of the selected events is shown in Fig. 35.8. The observed excess reached a significance of 5.7σ in a subsequent analysis of 3 years of data [53] and cannot be explained by atmospheric neutrinos and misidentified atmospheric muons alone. Some clustering of the HESE events close to the Galactic Centre was observed. The hypothesis that this low-significance excess could be due to a point source with a spectral index of ≥ 2 was constrained by an analysis of ANTARES data looking at lower energies and with superior pointing to the same sky region [54]. In a six-year HESE sample, combined with a sample of high-energy through-going muons, the mentioned excess close to the Galactic Centre has essentially disappeared (see Fig. 35.9). Meanwhile the energy range of the IceCube HESE analysis has been extended down to 1 TeV and the high-energy excess confirmed; also, events with through-going muons showed a corresponding excess of cosmic origin. In [55], the various analyses have been combined. Assuming the cosmic neutrino flux to be isotropic, flavour-symmetric and ν-$\overline{\nu}$-symmetric at Earth, the all-flavour spectrum is well described by a power law with normalisation $6.7^{+1.1}_{-1.2} \times 10^{-18}\,\mathrm{GeV^{-1}s^{-1}sr^{-1}cm^{-2}}$ at 100 TeV and a spectral index -2.50 ± 0.09 for energies between 25 TeV and 2.8 PeV. A spectral index of -2, an often quoted benchmark value, is disfavoured with a significance of 3.8σ.

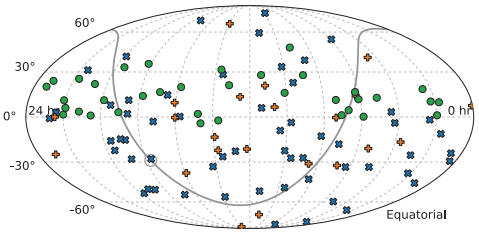

Figure 35.9: Arrival directions of IceCube candidate events for cosmic neutrinos in equatorial coordinates. The plot contains 82 HESE events, with shower-like events marked as blue × and muon tracks as orange +, and in addition 36 through-going muons tracks with an energy deposit exceeding 200 TeV (green circles). Approximately 40% of the events are expected to originate from atmospheric backgrounds. The grey curve denotes the Galactic Plane and the grey circle the Galactic Centre (from [58]) .

At lower energies, down to 10 GeV, IceCube/DeepCore and ANTARES have identified clear signals of oscillations of atmospheric neutrinos. The closely spaced OMs of DeepCore allow for selecting a very pure sample of low-energy $\overset{(-)}{\nu}_\mu$ (6–56 GeV) that produce upward moving muons inside the detector. The neutrino energy is determined from the energy of the hadronic shower at the vertex and the muon range. Fits to the energy/zenith-dependent deficit of muon neutrinos provide constraints on the oscillation parameters $\sin^2\theta_{23}$ and Δm^2_{23} (see Fig. 14.13 in "Neutrino masses, mixing, and oscillations" review).

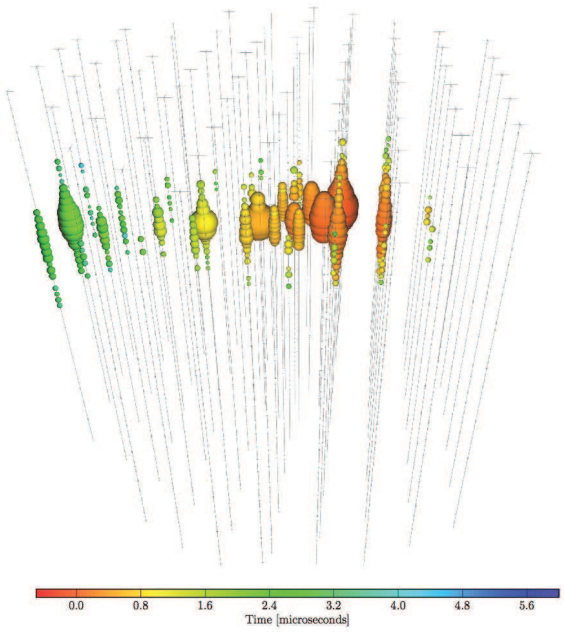

Figure 35.8: Event display of one of the starting-track events from [53]. The deposited energy is 70 TeV, the colour code indicates the signal timing (red: early; green: late).

See [56] and [57] for summaries of recent results of IceCube and ANTARES, respectively.

35.3.2.5. *Plans beyond 2020:*

Within the future IceCube-Gen2 project, it is planned to extend the sensitivity of IceCube towards both lower and higher energies. A substantially denser instrumentation of a sub-volume of DeepCore would lead to an energy threshold for neutrino detection of a few GeV (PINGU project, aiming primarily at measuring the neutrino mass hierarchy). For higher energies, a large-volume extension, combined with a powerful surface veto, is envisaged [7]. A very first phase with 7 closely spaced strings is discussed, aiming to cover part of the PINGU program, to better calibrate the existing IceCube and to test new technologies. More information on the future extensions of GVD and KM3NeT are given above, in Table 35.2 and in [49].

35.3.3. ***Coherent radio Cherenkov radiation detectors*** :
Revised August 2017 by S.R. Klein (LBNL/UC Berkeley)

Radio-frequency (RF) pulses are an attractive signature for coherent Cherenkov radiation from showers produced from interactions of ultra-high energy cosmic neutrinos. RF detectors can be used to search for energetic neutrinos from three types of sources: astrophysical objects (*i.e.* extending measurements the neutrino energy spectrum observed at TeV to PeV energies upward in energy, searching for 'GZK' neutrinos associated with cosmic-ray-cosmic microwave background radiation interactions, and searching for neutrinos from beyond-standard-model physics. These types are roughly associated with energies below 10^{18} eV, the energy range 10^{18} to 10^{20} eV, and above 10^{20} eV. GZK neutrinos are produced when protons with energy $E > 4 \times 10^{19}$ eV interact with cosmic microwave background radiation (CMB) and are excited to a Δ^+ resonance. The subsequent $\Delta^+ \to n\pi^+$ decay leads to the production of neutrinos with energies above 10^{18} eV [59]. Neutrinos are the only long-range probe of the ultra-high energy cosmos, because protons, heavier nuclei and photons with energies above 5×10^{19} eV are limited to ranges of less than 100 Mpc by interactions with the CMB and early starlight.

To detect a GZK neutrino signal of at least a few events per year (assuming that ultra-high energy cosmic-rays are protons) requires

a detector with an active volume of about 100 km^3, made out of a non-conducting solid (or potentially liquid) medium, with a long absorption length for radio waves. The huge volumes require that this be a common material. A dense medium would be ideal to reduce the detector volume, but, unfortunately, the available natural media have only moderate density. Optical Cherenkov and acoustical detectors are limited by short ($<$ 300 m) attenuation lengths [60] so would require a prohibitive number of sensors. Radio-detection is the only current approach that can scale to this volume. Table 35.3 compares the characteristics of commonly used media - the lunar regolith and several locations on the polar ice pack [61].

Electromagnetic and hadronic showers produce radio pulses via the Askaryan effect [62], as discussed in Sec. 33. The shower contains more electrons than positrons, leading to coherent emission.

High-frequency radiation is concentrated around the Cherenkov angle. On the cone, the electric field strength, $E_{\rm ch}$ at a frequency f from an electromagnetic shower from a ν_e may be roughly parameterized as [63]

$$E_{\rm Ch}(V/{\rm MHz}) = 2.53\times10^{-7}\frac{E_\nu}{1{\rm TeV}}\frac{f}{f_c}\left[\frac{1}{1+(f/f_c)^{1.44}}\right]. \qquad (35.3)$$

The electric field strength increases linearly with frequency, up to a cut-off f_c, which is set by the transverse size of the shower [64]. The maximum wavelength is roughly the Moliere radius divided by $\cos(\theta_C)$ where θ_C is the Cherenkov angle. Some examples are given in Table 35.3.

Near f_c, radiation is narrowly concentrated around the Cherenov angle [64]. At lower frequencies, the limited length of the emitting region leads to a broadening in emission angle around the Cherenkov cone. Away from θ_C, the electric field from Eq. (35.3) is reduced by [63],

$$\frac{E}{E_{\rm Ch}} = \exp\left(-\frac{1}{2}\frac{(\theta-\theta_C)^2}{(2.2^0\times[1{\rm GHz}/f])^2}\right), \qquad (35.4)$$

At very low frequencies, the distribution is nearly isotropic.

Table 35.3: Characteristics of different detection media for radio-Cherenkov signals. The attenuation length is at a frequency of 300 MHz; the Greenland figure is extrapolated upward from the 75 MHz measurements. The lunar regolith and ice have similar Cherenkov angles because they have similar indices of refraction.

Medium	Density	Cherenkov Ang.	Cutoff Freq.	Atten. Length
Lunar Regolith	2.5 g/cm^3	56^0	3.0 GHz	9m/f(GHz) [61]
Antarctic Ice (South Pole)	0.92 g/cm^3	56^0	1.15 GHz	900 m [65]
Ross Ice Shelf	0.92 g/cm^3	56^0	1.15 GHz	406 m [66]
Greenland	0.92 g/cm^3	56^0	1.15 GHz	1022 m [67]

Along the Cherenkov cone, the initial pulse width is $\approx$ 1 nsec, but it may be broadened by dispersion as it propagates, particularly for signals from the Moon traversing the ionosphere. As long as the dispersion can be compensated for, a large bandwidth detector is the most sensitive. Spectral information can be used to reject background, and to help reconstruct the neutrino direction, because the cutoff frequency depends on the observation angle (with respect to the Cherenkov cone).

The electric field is linearly proportional to the neutrino energy, so the power (field strength squared) is proportional to the square of the neutrino energy. Since the signal is a radio wave, the field amplitude decreases as $1/R$, plus absorption in the intervening medium. The detection threshold is determined by the distance to the antenna and the noise characteristics of the detector. For an antenna located in the detection medium, the typical threshold is around 10^{17} eV; for stand-off (remote sensing) detectors, the threshold rises roughly linearly with the distance. These thresholds can be reduced significantly by using directional antennas and/or combining the signals from multiple antennas using beam-forming techniques. Experiments have used both approaches to reduce trigger-level noise, or to reject background at the analysis level. For multi-element arrays, the threshold drops as the square root of number of antennas, since the signal adds in-phase while the backgrounds add with random phases [68].

The main background sources are anthropogenic noise, antenna/preamp noise, cosmic-ray air showers, charge generated by blowing snow, and lightning. The need to limit anthropogenic noise has led most experimental groups to select remote locations for their detectors.

The signal is linearly polarized in the plane perpendicular to the neutrino direction. This polarization is an important check that any observed signal is indeed coherent Cherenkov radiation. Polarization measurements can be used to help reconstruct the neutrino direction.

At energies above 10^{20} eV, the Landau-Pomeranchuk-Migdal effect significantly spreads out electromagnetic showers, producing what are effectively subshowers with significant separation. The radio emission becomes even more concentrated around the Cherenkov cone, and then, at higher energies the emission begins to vary event-by-event. Because of this, many of the experiments that study higher energy neutrinos focus on the hadronic shower from the struck nucleus. This contains on average only about 20% of the energy, but with large fluctuations. The hadronic shower is useful for very high energy searches ($\gg 10^{20}$ eV) because it is much less subject to the LPM effects.

Radio detectors have observed cosmic-ray air showers in the atmosphere. The physics of radio-wave generation in air showers is more complex because of the large contribution due to charge separation as electrons and positrons bend in different directions as they propagate, leading to a growing charge dipole (transverse current) [69]. This time-varying transverse current emits radiation, spread over the transverse size of the shower. Since the radiating particles are moving relativistically downward, a ground-based observer sees a Lorentz contracted pulse which can have frequency components reaching the GHz range, limited by the thickness of the particle shower. There is also a contribution from geosynchrotron radiation, as $e^\pm$ are bent in the same field [69]. Coherent Cherenkov radiation is less important than these other sources. Experiments for ν detection may also detect air showers [70], which is also a potential background. Magnetic monopoles would also emit radio waves, and neutrino experiments have also set monpole flux limits [71].

35.3.4. *The Moon as a target* :

Because of its large size and non-conducting regolith, and the availability of large radio-telescopes, the Moon is an attractive target [72]. TableMoonList lists some lunar experiments. Conventional radio-telescopes are quite well suited to lunar neutrino searches, with natural beam widths not too dissimilar from the size of the Moon. Still, there are experimental challenges. The composition of the lunar regolith is not well known, and the attenuation length for radio waves must be estimated. The big limitation of lunar experiments is that the 240,000 km target-antenna separation leads to neutrino energy thresholds above 10^{20} eV.

Table 35.4: Experiments that have set limits on neutrino interactions in the Moon; current limits are shown in Fig. 1 of [61], with Lunaska (2015) from [73].

Experiment	Year	Dish Size	Frequency	Bandwidth	Obs. Time
Parkes	1995	64 m	1425 MHz	500 MHz	10 hrs
Glue	1999+	70 m, 34 m	2200 MHz	40-150 MHz	120 hrs
NuMoon	2008	11×25 m	115–180 MHz	—	50 hrs
Lunaska	2008	3× 22 m	1200–1800 MHz	—	6 nights
Lunaska	2015	64	1200-1500 MHz	300 MHz	127 hours
Resun	2008	4× 25 m	1450 MHz	50 MHz	45 hours

The effective volume probed by experiments depends on the geometry, which itself depends on the frequency range used. At high frequencies f, the electric field strength is high, leading to a lower energy threshold, but the sensitive volume is limited because the

Cherenkov cone only points toward the Earth for a narrow range of geometries. Lower frequency radiation is more isotropic, so the effective volume is larger, but, because the electric field is weaker, the energy threshold is higher. The $1/f$ dependence of the attenuation length in the lunar regolith further increases the effective volume at low frequencies.

With modern technology, it is increasingly viable to search over very broad frequency ranges [74]. One technical challenge is due to dispersion (frequency dependent time delays) in the ionosphere. Dispersion can be largely removed with a de-dispersion filter, using either analog circuitry or post-collection digital processing.

Lunar experiments use different techniques to reduce the anthropogenic background. Some experiments use multiple antennas, separated by at least hundreds of meters; by requiring a coincidence within a small time window, anthropogenic noise can be rejected. With good enough timing, beam-forming techniques can be used to further reduce the background. An alternative approach is to use beam forming with multiple feed antennas viewing a single reflector, to ensure that the signal points back to the moon.

In the near future, several large radio detector arrays should reach significantly lower limits. The LOFAR array is beginning to take data with 36 detector clusters spread over Northwest Europe. In the longer term, the Square Kilometer Array (SKA) with 1 km^2 effective area will push thresholds down to near 10^{20} eV [74].

35.3.5. ***Ice-based detectors*** :

Lower energy thresholds require a smaller antenna-target separation. Natural ice is an attractive medium for this, with attenuation lengths over 300 m. The attenuation length varies with the frequency and ice temperature, with higher attenuation in warmer ice. Table 35.3 lists some radio attenuation measurements.

Although ice is mostly uniform, the top $\approx$ 100 m of Antarctic ice, the 'firn,' exhibits a gradual transition from packed snow at the surface (typical density 0.35 g/cm^3) to solid ice (density 0.92 g/cm^3) below [75]. The index of refraction depends linearly on the density, so radio waves curve downward in the firn. This bending reduces the effectiveness of surface or aerial antennas. The thickness of the firn varies with location; it is thicker in central Antarctica than in the coastal ice sheets. For aerial observations, the surface roughness of the ice can affect signals as they transition from the ice to the atmosphere. There are also indications that the increase in firn density is non-monotonic. This can lead to a non-monotonic change in index of refraction which may create waveguides which trap and propagate waves horizontally [76].

There are two types of Antarctic neutrino experiments. In one class, antennas mounted on scientific balloons observe the ice from above. The ANITA experiment is one example. It has made four flights around Antarctica, floating at an altitude around 35 km [77]. Its 32/40/48 (depending on the flight) dual-polarization horn antennas scanned the surrounding ice, out to the horizon (650 km away). Because of the small angle of incidence, ANITA could make use of polarization information; ν signals should be vertically polarized, while most background from cosmic-ray air showers is expected to be horizontally polarized.

Because of the significant source-detector separation, ANITA is most sensitive at energies above 10^{19} eV, above the peak of the GZK neutrino spectrum. As with the lunar experiments, ANITA had to contend with anthropogenic backgrounds. The ANITA collaboration uses their multiple antennas as a phased array to achieve good pointing accuracy, and used that to remove all apparent signals that pointed toward known or suspected areas of human habitation. By using the several-meter separation between antennas, they achieved a pointing accuracy of 0.2-0.4^0 in elevation, and 0.5-1.1^0 in azimuth. ANITA has set the most stringent limits on GZK neutrinos to date.

The proposed EVA experiment will use a portion of a fixed-shape balloon as a large parabolic radio antenna. Because of the large antenna surface, they hope to achieve threshold around 10^{17} eV.

Other ice based experiments use antennas located within the active volume, allowing them to reach thresholds around 10^{17} eV. This approach was pioneered by the RICE experiment [78], which buried 18 half-wave dipole antennas in holes drilled for AMANDA at the South Pole, at depths from 100 to 300 m. The hardware was sensitive from 200 MHz to 1 GHz. Each antenna fed an in-situ preamplifier which transmitted the signals to surface digitizing electronics.

Two groups are have deployed prototype arrays, with the goal of a building a detector with a $\sim$100 km^3 active volume. In both concepts, the hardware is modular, so the detector volume scales roughly linearly with the available funding. The Askaryan Radio Array (ARA) is located at the South Pole [79], while the Antarctic Ross Iceshelf Antenna Neutrino Array (ARIANNA) is on the Ross Ice Shelf [80], about 110 km north of McMurdo station. Both experiments use multiple antennas, with varying degrees of connection. They use the timing between multiple antennas in a single station to determine the arrival direction, and have angular resolutions of a few degrees. At larger distance scales, such as between ARA and ARIANNA stations, the relative timing uncertainty is larger, and the stations are effectively independent, with independent triggers, and the data is only combined offline.

The two approaches have many differences. ARA [79] is located at the South Pole, where the ice is very cold and more than 2800 m thick, leading to long attenuation lengths and allowing a large active volume, while ARIANNA [80] is on the Ross Ice Shelf, about 110 km north of McMurdo station, where the ice is 575 m thick. The ice is warmer there, but it sits atop the Ross Sea. At the site, the ice-water interface is smooth, so it acts as a reflector for radio waves. These reflections give ARIANNA sensitivity to downward going neutrinos, and to more of the Cherenkov cone for horizontal neutrinos.

The two experiments have different antenna deployment schemes. ARA buries their antennas up to 200 m deep in the ice, to avoid radio wave refraction in the firn and give their antennas a clear field of view. However, drilling holes has costs, and the limited hole diameter (15 cm in ARA) requires compromises between antenna design (particularly for horizontally polarized waves), mechanical support, power and communications. In contrast, the ARIANNA antennas are placed in shallow holes. This greatly simplifies deployment and avoids limitations on antenna design, but at a cost of reduced sensitivity to neutrino interactions near the surface.

The current ARA proposal, ARA-37 [79], calls for an array of 37 stations, each consisting of 16 embedded antennas deployed in narrow boreholes 50-200 m deep. The antennas will detect signals from 150 to 850 MHz for vertical polarization, and 250 MHz to 850 MHz for horizontal polarization. ARA plans to use bicone antennas for vertical polarization, and quad-slotted cylinders for horizontal polarization. The collaboration uses notch filters and surface veto antennas to eliminate most anthropogenic noise, and vetos events when aircraft are in the area, or weather balloons are being launched. Each ARIANNA station (1296 have been proposed) [80] will include multiple log-periodic dipole antennas sensitive to the frequency range from about 80 MHz to 1 GHz. The multiple antennas allow for single-station directional and polarization measurements. A few of the antennas will point upward to help veto cosmic-ray air showers and other external backgrounds.

35.4. Large time-projection chambers for rare event detection

Revised Aug. 2017 by T. Shutt (SLAC).

Rare event searches require detectors that combine large target masses and low levels of radioactivity, and that are located deep underground to eliminate cosmic-ray related backgrounds. Past and present efforts include searches for the scattering of particle dark matter, neutrinoless double beta decay, and the measurement of solar neutrinos, while next generation experiments will also probe coherent scattering of solar, atmospheric and diffuse supernova background neutrinos. Large time project chambers (TPCs), adapted from particle collider experiments, have emerged as a leading technology for these efforts. Events are measured in a central region confined by a field cage and usually filled with a liquid noble element target. Ionized electrons are drifted (in the z direction) to an anode region by use of electrode grids and field shaping rings, where their magnitude and $x-y$ location is measured. In low background TPCs, scintillation generated at the initial event site is also measured, and the time difference between this prompt signal and the later-arriving charge signal gives the event location in z for a known electron drift speed.

Thus, 3D imaging is a achieved in a monolithic central volume. Noble elements have relatively high light yields (comparable to or exceeding the best inorganic scintillators), and the charge signal can be amplified by multiplication or electroluminescence. Radioactive backgrounds are distinguished by event imaging, the separate measurements of charge and light, and scintillation pulse shape. For recent reviews of noble element detectors, see [81,82].

Methods for achieving very low radioactive backgrounds are discussed in general in section 34.6. The basic architecture of large TPCs is very favorable for this application because gas or liquid targets can be relatively easily purified, while the generally more radioactive readout and support materials are confined to the periphery. The 3D imaging of the TPC then allows self shielding in the target material, which is quite powerful when the target is large compared to mean scattering lengths of $\sim$ MeV neutrons and gammas from radioactivity ($\sim$ 10 cm in LXe, for example). The use of higher density targets (i.e., liquid instead of gas and/or higher mass elements) maximizes the ratio of target to surrounding material mass. The TPC geometry allows highly hermetic external shielding, with recent experiments using large water shields, in some cases enhanced with an active liquid scintillator layer.

In noble element targets, all non-noble impurities are readily removed (e.g., by chemical reaction in a commercial getter) so that only radioactive noble isotopes are a significant background concern. Xe, Ne and He have have no long lived radioactive isotopes (apart from the ^{136}Xe, discussed below). Kr has $\sim$ 1 MBq/kg of the beta emitter ^{85}Kr created by nuclear fuel reprocessing, making it unusable as a target, while the 1 Bq/kg level of the beta emitter ^{39}Ar is a nuisance for Ar-based experiments. Both of these can be backgrounds in other target materials, as can Rn emanating from detector components. Relatively low background materials are available for most of the structures surrounding the central target, with the exception of radioactive glasses and ceramics usually present in PMTs, feedthroughs and electrical components. Very low background PMTs with synthetic quartz windows, developed over the last decade, have been a key enabling technology for dark matter searches. These are not yet low enough in background for some double beta decay searches, which use radio-clean Si-based photon detectors.

An important technical challenge in liquid detectors is achieving the high voltages needed for electron drift and measurement. Quench gases which stabilize charge gain and speed electron transport in wire chambers cannot be used, since these absorb scintillation light (and also suppress charge extraction in dual-phase detectors, discussed below). At low energies (e.g., in a dark matter search) it is also important to suppress low-level emission of electrons and associated photons. Drift of electrons over meter scales with minimal loss from attachment on trace levels of dissolved impurities (e.g., O_2) has so far required continuous circulating purification. The relatively slow readout due to $\sim$ msec/m drift speeds is not a major pile-up concern in low background experiments.

35.4.1. *Dark matter and other low energy signals* :

A major goal of low background experiments is detection of WIMP (Weakly Interacting Massive Particle) dark matter through scattering on nuclei in a terrestrial detector (for a recent review, see [83]) . Energy transfers are generally small, a few tens of keV at most. Liquid noble TPCs distinguish nuclear recoils (NR) from dark matter from the usually dominant background of electron recoils (ER) from gamma rays and beta decays by requiring single scatters and based on their charge to light ratio or scintillation pulse shape, as described below. Neutrons are a NR background, but can be recognized in a large imaging TPC if they multiply scatter. To detect small charge signals, a dual phase technique is used wherein electrons from interactions in the liquid target are drifted to the liquid surface and extracted with high field ($\sim$ 5 kV/cm) into the gas phase leading to an amplified electroluminescence signal measured by an array of PMTs located just above. (Both charge multiplication and electroluminescence are possible in liquid, but have seen little use because the signals have very broad dispersion). This technique readily measures single electrons with $\sim$ cm $x-y$ resolution. The sides of the chamber are lined with highly (diffusively) reflective PTFE, and a second PMT array is located below the active volume to maximize the sensitivity to the initial scintillation signal.

The microscopic processes leading to signals in liquid nobles are complex. Energy deposited by an event generates pairs of free electron and ions, and also atoms in their lowest excited state. These rapidly form excimers which de-excite by emitting light. Excimers arise in both triplet and singlet states which have the same energy but different decay times. In an event track, some fraction of electrons recombine with ions, while the rest escape and are measured. Recombination leads to further excimer formation and hence more scintillation photons. Finally, some part of the energy is lost as heat - a small fraction for ER but a dominant and energy dependent fraction for NR. This complexity distinguishes ER and NR: for the same visible energy, the slower nuclear recoils form a denser track with less charge and more light than recoiling electrons, and they generate fewer long-lived triplet state scintillation photons than singlet-state photons. Charge and light yields depend on drift field, energy, and the initial particle (ER or NR), requiring extensive calibrations. The existing data has been incorporated into the NEST Monte Carlo framework. Typical yields are several tens of electrons and photons per keV of deposited energy (with up to 10-15 % efficiency for these photons being detected).

The scattering rates of WIMPs are model dependent, but are usually highest for spin-independent scattering which has an A^2 dependence, so that experiments to date have used LXe and LAr targets. LXe experiments have had the best WIMP sensitivity for all but the lowest most WIMP masses for the last decade, with the ton-scale XENON1T [84] and PANDAX-II [85] experiments now eclipsing LUX with world-leading results. Previous significant experiments also include XENON10/100, and ZEPLIN II/III. Next generation experiments under construction include LZ and XENONnT with roughly 7 tons active mass. If a dark matter signal is seen, its spin dependence could be probed with Xe targets isotopically separated into spin-rich and spin-poor targets.

The reach of LXe TPCs depends critically on the level of ER background rejection provided by the ratio of charge to light. Most reported values (at 50% NR acceptance) are near the 99.6% result obtained by LUX, while ZEPLIN III had 99.99%, possibly because of its very high drift field (4 kV/cm). While there is a basic framework [86] for how this improves with light collection and varies with electric field, a fully predictive understanding is not yet in hand. Pulse shape discrimination is present, but weak at low energy. The $\sim$ 178 nm scintillation light of Xe is just long enough to be transmitted through high purity synthetic quartz PMTs windows. Kr suppression to the $\sim$ ppt or better level is needed, and has been accomplished via distillation or chromatography.

Two experiments to date have produced dark matter limits using dual phase Ar TPCs: WARP and DarkSide-50, while ArDM is under development. A primary attraction of Ar compared to Xe is much lower raw material costs. However beta decays from ^{39}Ar, produced by cosmic-ray interactions in the atmosphere, give a low energy ER background roughly 10^8 times higher than the fundamental ER background from p-p solar neutrinos. Remarkably, however, pulse shape discrimination (PSD) of ER backgrounds is very powerful in LAr for sufficiently high energy, based on the favorably different ratio of populations of the singlet (6 ns lifetime) and triplet ($\sim$ 1.5 μ s lifetime) states. DarkSide has shown roughly 10^8 discrimination with $\geq$ 50% WIMP acceptance above 47 keV. They have also extracted "aged" Ar with the 32.9 yr half-life ^{39} Ar reduced by a factor of 1400, via processing of underground (cosmic ray shielded) gas deposits. This lowers the energy threshold and allows ton-scale experiments without significant pile-up. Charge and light discrimination has also been demonstrated at high energy, but it is less well characterized than in LXe and appears weak at low energy. While the strong PSD in LAr allows relaxed requirements for ER backgrounds, U and Th contamination must still be kept very low because their decay chains create neutrons via (α, n) reactions, particularly in low Z elements such as PMT glass and PTFE. Waveshifter is used (typically TPB) because PMTs are blind to the 128 nm scintillation light.

LZ and XENONnT project sensitivity to WIMPs about a decade above the "floor" of coherent electron scattering of astrophysical

neutrinos, which, absent a directional measurement (see below), are essentially indistinguishable from WIMPs. A 30-50 ton LXe TPC would approach the practical limit set by this floor for WIMP masses above $\sim$ 5 GeV if a $\sim$ 99.98% rejection (at 30% NR acceptance) of p-p solar ν ER backgrounds [87] is achieved, while a $\sim$ 200 ton LAr detector would achieve similar sensitivity for WIMPs above $\sim$ 50 GeV. Sensitivity to lower WIMP mass could be obtained by adding Ne to a LXe TPC, or, more speculatively,with a superfluid He TPC [88] read out with superconducting sensors (similar to the proposed HERON solar neutrino experiment). With sufficient control of dissolved Kr and especially Rn, the ER background in the next LXe experiments could be dominated by the poorly measured low energy spectrum of solar neutrinos from the main p-p burning reaction.

Measurement of NR recoil track direction would provide proof of the galactic origin of a dark matter signal since the prevailing WIMP direction varies on a daily basis as the earth spins. This cannot be achieved for the sub-micron tracks in any existing solid or liquid technology, but the mm-scale tracks in a low pressure gas (typically, P $\sim$ 50 Torr) could be imaged with sufficiently dense instrumentation. Directionality can be established with $O(10^2)$ events by measuring just the track direction, while, with finer resolution that distinguishes the diffuse (dense) tail and dense (diffuse) head of NR (ER) tracks, only $O(10)$ events are required. Such imaging requires a high energy threshold, decreasing WIMP sensitivity, but also powerfully rejecting less dense ER background tracks.

A variety of TPC configurations are being pursued to accomplish this, most with a CF_4 target. The longest established effort, DRIFT, avoids diffusion washing out tracks for electron drift distances greater than $\sim$ 20 cm by attaching electrons to CS_2, which drifts with vastly reduced diffusion. Other efforts drift electrons directly and use a variety of techniques for their measurement: DMTPC (electroluminescence + CCDs), MIMAC (MicroMegas), NEWAGE (GEMs), and D^3 (Si pixels). WIMP limits have been obtained by DRIFT, NEWAGE, and DMTPC. A related suggestion is that the amount of recombination in a high pressure Xe gas with an electron-cooling additive could be sensitive to the angle between the track and electric field [89], eliminating the need for track imaging. Directional measurements appear to be the only possibility to push beyond the floor of coherent neutrino scatters [90], though this would require extraodinarily large target mass.

35.4.2. $0\nu\beta\beta$ *Decay* :

Another major class of rare event search is neutrinoless double beta decay ($0\nu\beta\beta$). A limited set of nuclei are unstable against simultaneous beta decay of two neutrons. Observation of the lepton-number violating neutrinoless version of this decay would establish that neutrinos are Majorana particles and provide a direct measure of neutrino mass. For a recent review, see [91]. The signal in $0\nu\beta\beta$ decay is distinctive: the full Q-value energy of the nuclear decay appears as equal energy back-to-back recoil electrons. A large TPC is advantageous for observing this low rate decay for all the reasons described above. The first detector to observe the standard model process 2 neutrino double beta decay was a gaseous TPC which imaged the two electrons tracks from ^{82}Se embedded in a foil. Modern detectors use Xe as the detector medium because it includes the $\beta\beta$ isotope ^{136}Xe (Q-value 2458 keV), which, as an inert gas, can also be more readily enriched from its natural 8.9% abundance than any other $\beta\beta$ isotope. EXO-200, which currently has one of the best search limits [93], is a large single-phase LXe TPC with roughly 110 active kg of Xe enriched to 80.7 % ^{136}Xe, and a multi-ton successor nEXO has been proposed which would fully cover the inverted neutrino mass hierarchy. These detectors are similar to dark matter TPCs, but, not needing charge gain, use single phase with charge measured directly on crossed wire grids. Light readout is done with LAAPDs (EXO-200) and SiPMTs (nEXO).

The dominant background is gamma rays originating outside the active volume. Most of these undergo multiple Compton-scatters which are efficiently recognized and rejected through sub-cm position resolution, though the few percent of gammas at this energy that photoabsorb are not. Self shielding of gamma rays is less powerful than in dark matter, since in the former case there is some small probability of penetrating to some depth followed by the modestly small probability of photo-absorption. The latter case consists of three small probability processes: penetration to some depth, a very low-energy scatter, and the gamma exiting without a second interaction. Because of this and the fact that background and the signal are both electron recoils, the requirements on radioactivity in all the materials of a $\beta\beta$ TPC are much more stringent than an otherwise similar dark matter detector, unless other background rejection tools are available. Percent-level energy resolution is crucial to avoid background from $2\nu\beta\beta$ decays and gammas including the prominent 2615 MeV line from ^{208}Tl in the Th chain. Here the combined charge and light measurement eliminates the otherwise dominant fluctuations in recombination which lead to anti-correlated fluctuations in charge and light. EXO-200 has achieved $\sigma \approx 1.5\%$ (at 2458 keV), and values below 1% appear possible.

A related approach being pursued by the NEXT and PandaX-III collaborations is to use high pressure gaseous Xe TPC. With mm-scale charge readout, the two-electron topology of $0\nu\beta\beta$ events can be distinguished from single electrons from photoabsorption of background gammas. In addition, the low recombination fraction in the gas phase suppresses recombination fluctuations, in principle allowing σ below 0.2% via the charge channel alone. Finally, a definitive identification of a $0\nu\beta\beta$ signal would be provided by extraction and tagging of the ionized Ba daughter via atomic physics techniques [94], either in gas or liquid and gas phases.

35.5. Sub-Kelvin detectors

Written September 2015 by K. Irwin (Stanford and SLAC).

Many particle physics experiments utilize detectors operated at temperatures below 1 K. These include WIMP searches, beta-decay experiments to measure the absolute mass of the electron neutrino, and searches for neutrinoless-double-beta decay ($0\nu\beta\beta$) to probe the properties of Majorana neutrinos. Sub-Kelvin detectors also provide important cosmological constraints on particle physics through sensitive measurement of the cosmic microwave background (CMB). CMB measurements probe the physics of inflation at $\sim 10^{16}$ GeV, and the absolute mass, hierarchy, and number of neutrino species.

Detectors that operate below 1 K benefit from reduced thermal noise and lower material specific heat and thermal conductivity. At these temperatures, superconducting materials, sensors with high responsivity, and cryogenic preamplifiers and multiplexers are available. We provide a simple overview of the techniques and the experiments using sub-K detectors. A useful review of the broad application of low-temperature detectors is provided in [95], and the proceedings of the International Workshop on Low Temperature Detectors [96] provide an overview of the field.

Sub-Kelvin detectors can be categorized as equilibrium thermal detectors or non-equilibrium detectors. Equilibrium detectors measure a temperature rise in a material when energy is deposited. Non-equilibrium detectors are based on the measurement of prompt, non-equilibrated signals and on the excitation of materials with an energy gap.

35.5.1. *Equilibrium thermal detectors* :

An equilibrium thermal detector consists of a thermometer and absorber with combined heat capacity C coupled to a heat bath through a weak thermal conductance G. The rise time of a thermal detector is limited by the internal equilibration time of the thermometer-absorber system and the electrical time constant of the thermometer. The thermal relaxation time over which heat escapes to the heat bath is $\tau = C/G$. Thermal detectors are often designed so that an energy input to the absorber is thermalized and equilibrated through the absorber and thermometer on timescales shorter than τ, making the operation particularly simple. An equilibrium thermal detector can be operated as either a calorimeter, which measures an incident energy deposition E, or as a bolometer, which measures an incident power P.

In a calorimeter, an energy E deposited by a particle interaction causes a transient change in the temperature $\Delta T = E/C$, where the heat capacity C can be dominated by the phonons in a lattice, the quasiparticle excitations in a superconductor, or the electronic heat capacity of a metal. The thermodynamic energy fluctuations in the

absorber and thermometer have variance

$$\Delta E_{\rm rms}^2 = k_{\rm B} T^2 C \tag{35.5}$$

when operated near equilibrium, where $\Delta E_{\rm rms}$ is the root-mean-square energy fluctuation, $k_{\rm B}$ is the Boltzmann constant and T is the equilibrium temperature. When a sufficiently sensitive thermometer is used, and the energy is thermalized at frequencies large compared to the thermal response frequency ($f_{\rm th} = 1/2\pi\tau$), the signal-to-noise ratio is nonzero at frequencies higher than $f_{\rm th}$. In this case, detector energy resolution can be somewhat better than $\Delta E_{\rm rms}$ [97]. Deviations from the ideal calorimeter model can cause excess noise and position and energy dependence in the signal shape, leading to degradation in achieved energy resolution.

also have superior thermalization properties, making them attractive for some applications in which extreme precision and high energy resolution are required (e.g. beta endpoint experiments to measure neutrino mass using ^{163}Ho). At low temperature, the heat capacity of normal metals is dominated by electrons, and is linear in temperature, with convenient form

$$C = \frac{\rho}{A}\gamma V T, \tag{35.8}$$

where V is the sample volume, γ is the molar specific heat of the material, ρ is the mass density, and A is the atomic weight. Superconducting absorbers are also used. Superconductors combine some of the thermalization advantages of normal metals with the lower specific heats associated with insulators when operated well below $T_{\rm c}$,

Table 35.5: Some selected experiments using sub-Kelvin equilibrium bolometers to measure the CMB. These experiments constrain the physics of inflation and the absolute mass, hierarchy, and number of neutrino species. The experiment location determines the part of the sky that is observed. The size of the aperture determines the angular resolution. The table also indicates the type of sensor used, the number of sensors, the frequency range, and the number of frequency bands. The number of sensors and frequency range and bands for ongoing upgrades are provided for some experiments in parentheses.

Sub-K CMB Experiment	Location	Aperture	Sensor type	# Sensors (planned)	Frequency (planned)	Bands (planned)
Ground-based						
Atacama Cosmology Telescope (2007–)	Chile	6 m	TES	1,800 (5,334)	90–150 GHz (28–220 GHz)	2 (5)
BICEP/Keck (2006–)	South Pole	26/68 cm	TES	3,200	95–220 GHz	3
CLASS (2015–)	Chile	60 cm	TES	36 (5,108)	40 GHz (40–220 GHz)	1 (4)
POLARBEAR / Simons (2012–)	Chile	3.5 m	TES	1,274 (22,764)	150 GHz (90–220 GHz)	1 (3)
South Pole Telescope (2007–)	South Pole	10 m	TES	1,536 (16,260)	95–150 GHz (95–220 GHz)	2 (3)
Balloon						
EBEX (2013–)	McMurdo	1.5 m	TES	∼1,000	150–410 GHz	3
PIPER (2016–)	New Mexico	2 m	TES	5,120	200–600 GHz	4
SPIDER (2014–)	McMurdo	30 cm	TES	1,959	90–280 GHz	3
Satellite						
Planck HFI (2003–)	L2	1.5 m	NTD	52	100-857 GHz	9

In a bolometer, a power P deposited by a stream of particles causes a change in the equilibrium temperature $\Delta T = P/G$. The weak thermal conductance G to the heat bath is usually limited by the flow of heat through a phonon or electron system. The thermodynamic power fluctuations in the absorber and thermometer have power spectral density

$$S_{\rm P} = NEP^2 = 4k_{\rm B}T^2 G \tag{35.6}$$

when operated near equilibrium, where the units of NEP (noise equivalent power) are $\mathrm{W}/\sqrt{\mathrm{Hz}}$.

The minimization of thermodynamic energy and power fluctuations is a primary motivation for the use of sub-Kelvin thermal detectors. These low temperatures also enable the use of materials and structures with extremely low C and G, and the use of superconducting materials and amplifiers.

When very large absorbers are required (e.g. WIMP dark matter searches), dielectric crystals with extremely low specific heat are often used. These materials are operated well below the Debye temperature $T_{\rm D}$ of a crystal, where the specific heat scales as T^3. In this low-temperature limit, the dimensionless phononic heat capacity at fixed volume reduces to

$$\frac{C_{\rm V}}{N\,k_{\rm B}} = \frac{12\,\pi^4}{5}\left(\frac{T}{T_{\rm D}}\right)^3, \tag{35.7}$$

where N is the number of atoms in the crystal. Normal metals have higher low-temperature specific heat than dielectric crystals, but they where the electronic heat capacity freezes out, and the material is dominated by phononic heat capacity. At higher temperatures, superconducting materials have more complicated heat capacities, but at their transition temperature $T_{\rm c}$, BCS theory predicts that the electronic heat capacity of a superconductor is ∼2.43 times the normal metal value.

When very low thermal conductances are required for power measurement (e.g. the measurement of the cosmic microwave background), the weak thermal link is sometimes provided by thin membranes of non-stoichiometric silicon nitride. The thermal conductance of these membranes is:

$$G = 4\sigma A T^3 \xi, \tag{35.9}$$

where σ has a value of 15.7 $\mathrm{mW/cm^2K^4}$, A is the cross-sectional area perpendicular to the heat flow, and ξ is a numerical factor with a value of one in the case of specular surface scattering but less than one for diffuse surface scattering. The thermal impedance between the electron and phonon systems can also limit the thermal conductance.

The most commonly used sub-Kelvin thermometer is the superconducting transition-edge sensor (TES) [98]. The TES consists of a superconductor biased at the transition temperature $T_{\rm c}$, in the region between the superconducting and normal state, where its resistance is a strong function of temperature. The TES is voltage biased. The Joule power provides strong negative electrothermal feedback, which improves linearity, speeds up response to faster than $\tau = C/G$,

and provides tolerance for T_c variation between multiple TESs in a large array. The current flowing through a TES is read out by a superconducting quantum interference device (SQUID) amplifier. These amplifiers can be cryogenically multiplexed, allowing a large number of TES devices to be read out with a small number of wires to room temperature.

Neutron-transmutation-doped (NTD) germanium and implanted silicon semiconductors read out by cryogenic FET amplifiers are also used as thermometers [97]. Their electrical resistance is exponentially dependent on $1/T$, and is determined by phonon-assisted hopping conduction between impurity sites. Finally, the temperature dependence of the permeability of a paramagnetic material is used as a thermometer. Detectors using these thermometers are referred to as metallic magnetic calorimeters (MMC) [99]. These detectors operate without dissipation and are inductively readout by SQUIDs.

In WIMP and neutrino experiments using sub-Kelvin dielectric semiconductors, the recoil energy is typically $\gtrsim 0.1$ keV. The majority of the energy is deposited in phonons and a minority in ionization and, in some cases, scintillation. The semiconductor bandgap is typically $\sim$ eV, and $k_B T < 10$ μeV at $T < 1$ K. Thus, high-energy charge pairs and athermal phonons are initially produced. The charge pairs cascade quickly to the gap edge. The high-energy phonons experience isotopic scattering and anharmonic decay, which downshifts the phonon spectrum until the phonon mean free path approaches the characteristic dimension of the absorber. If the crystal is sufficiently pure, these phonons propagate ballistically, preserving information about the interaction location. They are not thermalized, and thus not affected by an increase in the crystal heat capacity, allowing the use of larger absorbers. Sensors similar to those used in sub-K equilibrium thermal detectors measure the athermal phonons at the crystal surface.

Table 35.6: Selected experiments using sub-Kelvin calorimeters. The table shows only currently operated experiments, and is not exhaustive. WIMP experiments search for dark matter, and beta-decay and neutrinoless double beta decay ($0\nu\beta\beta$) experiments constrain neutrino mass, hierarchy, and Majorana nature. The experiment location determines the characteristics of the radioactive background. The dates of current program phase, detection mode (equilibrium or nonequilibrium phonon measurements, and measurement of ionization or scintillation signals), the absorber and total mass, the sensor type, and the number of sensors and crystals (if different) are given. Many sub-K calorimeter experiments are also in planning and construction phases, including EURECA (dark matter), HOLMES and NuMECs (beta decay), and CUPID-0 ($0\nu\beta\beta$ decay). Many of the existing experiments are being upgraded to larger mass absorbers, different absorber materials, or lower energy threshhold.

Sub-K Calorimeter	Location	Detection mode	Absorber Total mass	Sensor type	# Sensor # Crystal
WIMP					
CRESST II (2003–)	Gran Sasso Italy	Noneq. phon. and scint.	$CaWO_4$ 5.4 kg	TES	18
EDELWEISS III (2015–)	LSM Modane France	Eq. thermal and ion.	Ge 22 kg	NTD Ge +HEMT	36
SuperCDMS (2012–)	Soudan, USA SNOLAB, Canada	Noneq. phon. and ion.	Ge 9 kg	TES +JFET	120 15
Beta decay					
ECHo (2012–)	Heidelberg Germany	Eq. thermal	Au:^{163}Ho 0.2μg	MMC	16
$0\nu\beta\beta$ decay					
CUORE (2015–)	Gran Sasso Italy	Eq. thermal	TeO_2 741 kg	NTD Ge	988
AMoRe Pilot (2015–)	Yang Yang S. Korea	Noneq. phon. and scint.	$CaMoO_4$ 1.5 kg	MMC	5
LUCIFER (2010–)	Gran Sasso Italy	Eq. thermal and scint.	ZnSe 431 g	NTD Ge	1

Equilibrium thermal detectors are simple, and they have important advantages in precision measurements because of their insensitivity to statistical variations in energy down-conversion pathways, as long as the incident energy equilibrates into an equilibrium thermal distribution that can be measured by a thermometer.

35.5.2. *Nonequilibrium Detectors* :

Nonequilibrium detectors use many of the same principles and techniques as equilibrium detectors, but are also sensitive to details of the energy down-conversion before thermalization. Sub-Kelvin nonequilibrium detectors measure athermal phonon signals in a dielectric crystal, electron-hole pairs in a semiconductor crystal, athermal quasiparticle excitations in a superconductor, photon emission from a scintillator, or a combination of two of the above to better discriminate recoils from nuclei or electrons. Because the phonons are athermal, sub-Kelvin nonequilibrium detectors can use absorbers with larger heat capacity, and they use information about the details of energy down-conversion pathways in order to better discriminate signal from background.

Superconductors can also be used as absorbers in sub-Kelvin detectors when $T \ll T_c$. The superconducting gap is typically $\sim$ meV. Energy absorption breaks Cooper pairs and produces quasiparticles. These particles cascade to the superconducting gap edge, and then recombine after a material-dependent lifetime. During the quasiparticle lifetime, they diffuse through the material. In superconductors with large mean free path, the diffusion length can be more than 1 mm, allowing diffusion to a detector.

In some experiments (e.g. SuperCDMS and CRESST), athermal phonons and quasiparticle diffusion are combined to increase achievable absorber mass. Athermal phonons in a three-dimensional dielectric crystal break Cooper pairs in a two-dimensional superconducting film on the detector surface. The resulting quasiparticles diffuse to thermal sensors (typically a TES) where they are absorbed and detected. While thin superconducting films have diffusion lengths shorter than the diffusion lengths in single crystal superconductors, segmenting the films into small sections and coupling them to multiple TES sensors allows the instrumentation of large absorber volume. The TES sensors

can be wired in parallel to combine their output signal.

The combined measurement of the phonon signal and a secondary signal (ionization or scintillation) can provide a powerful discrimination of signal from background events. Nuclear-recoil events in WIMP searches produce proportionally smaller ionization or scintillation signal than electron-scattering events. Since many of the background events are electron recoils, this discrimination provides a powerful veto. Similarly, beta-decay events produce proportionally smaller scintillation signal than alpha-particle events, allowing rejection of alpha backgrounds in neutrino experiments.

Combined phonon and ionization measurement has been implemented in experiments including CDMS I/II, SuperCDMS, and EDELWEISS I/II/III. These experiments use semiconductor crystal absorbers, in which dark-matter scattering events would produce recoiling particles and generate electron-hole pairs and phonons. The electron-hole pairs are separated and drifted to the surface of the crystal by applying an electric field, where they are measured by a JFET or HEMT using similar techniques to those used in 77 K Ge x-ray spectrometers. However, the field strength must be much lower in sub-K detectors to limit the generation of phonon signals by the Neganov-Luke effect, which can confuse the background discrimination. For detectors with very low threshhold, the Neganov-Luke effect can also be used to detect generated charge through the induced phonon signal.

Combined phonon and scintillation measurement has been implemented in CRESST II, ROSEBUD, AMoRE and LUCIFER. For example, the CRESST-II experiment uses $CaWO_4$ crystal absorbers, and measures both the phonon signal and the scintillation signal with TES calorimeters. A wide variety of scintillating crystals are under consideration, including different tungstates and molybdates, BaF_2, ZnSe, and bismuth germanate (BGO).

35.6. Low-radioactivity background techniques

Revised August 2015 by A. Piepke (University of Alabama).

The physics reach of low-energy rare-event searches *e.g.* for dark matter, neutrino oscillations, or double beta decay is often limited by background caused by radioactivity. Depending on the chosen detector design, the separation of the physics signal from this unwanted interference can be achieved on an event-by-event basis by active event tagging, utilizing some unique event features, or by reducing the flux of the background radiation by appropriate shielding and material selection. In both cases, the background rate is proportional to the flux of the interfering radiation. Its reduction is thus essential for realizing the full physics potential of the experiment. In this context, "low energy" may be defined as the regime of natural, anthropogenic, or cosmogenic radioactivity, all at energies up to about 10 MeV. See [100,101] for in-depth reviews of this subject. Following the classification of [100], sources of background may be categorized into the following classes:

1. environmental radioactivity,
2. radio-impurities in detector or shielding components,
3. radon and its progeny,
4. cosmic rays,
5. neutrons from natural fission, (α, n) reactions and from cosmic-ray muon spallation and capture.

35.6.1. ***Defining the problem*** : The application defines the requirements. Background goals can be as demanding as a few low-energy events per year in a ton-size detector. The strength of the physics signal of interest can often be estimated theoretically or from limits derived by earlier experiments. The experiments are then designed for the desired signal-to-background ratio. This requires finding the right balance between "clarity of measurement", ease of construction, and budget. In a practical sense, it is important to formulate background goals that are sufficient for the task at hand but achievable, in a finite time. It is standard practice to use detector simulations to translate the background requirements into limits for the radioactivity content of various detector components, requirements for radiation shielding, and allowable cosmic-ray fluxes. This strategy allows the identification of the most critical components early and facilitates the allocation of analysis and development resources in a rational way. The CERN code GEANT4 [102] is a widely used tool for this purpose. It has incorporated sufficient nuclear physics to allow accurate background estimations. Custom-written event generators, modeling *e.g.*, particle correlations in complex decay schemes, deviations from allowed beta spectra or $\gamma - \gamma$-angular correlations, are used as well.

35.6.2. ***Environmental radioactivity*** : The long-lived natural radio-nuclides ^{40}K, ^{232}Th, and ^{238}U have average abundances of 1.6, 11.1 and 2.7 ppm (corresponding to 412, 45 and 33 Bq/kg, respectively) in the earth's crust, with large local variations. In most applications, γ radiation emitted due to the decay of natural radioactivity and its unstable daughters constitutes the dominant contribution to the local radiation field. Typical low-background applications require levels of natural radioactivity on the order of ppb or ppt in the detector components. Passive or active shielding is used to suppress external γ radiation down to an equivalent level. Fig. 35.10 shows the energy-dependent attenuation length $\lambda(E_\gamma)$ as a function of γ-ray energy E_γ for three common shielding materials (water, copper, lead). The thickness ℓ required to reduce the external flux by a factor $f > 1$ is estimated, assuming exponential damping:

$$\ell \;=\; \lambda(E_\gamma) \cdot \ln f \;. \qquad (35.10)$$

At 100 keV, a typical energy scale for dark matter searches (or 2.615 MeV, for a typical double-beta decay experiment), attenuation by a factor $f = 10^5$ requires 67(269) cm of H_2O, 2.8(34) cm of Cu, or 0.18(23) cm of Pb. Such estimates allow for an order-of-magnitude determination of the experiment dimensions.

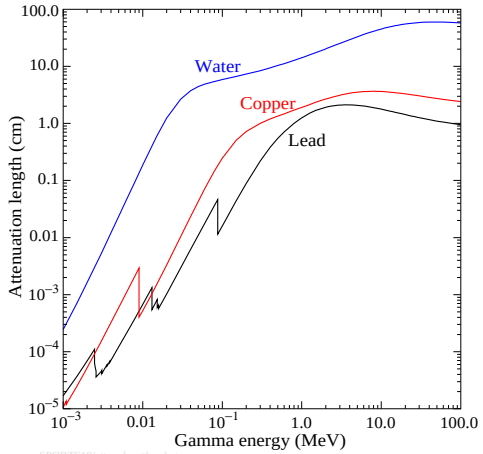

Figure 35.10: γ-ray attenuation lengths in some common shielding materials. The mass attenuation data has been taken from the NIST data base XCOM; see "Atomic Nuclear Properties" at `pdg.lbl.gov`.

A precise estimation of the the magnitude of the external gamma-ray background, including scattering and the effect of analysis-energy cuts, requires Monte Carlo simulations based on the the knowledge of the radioactivity present in the laboratory. Detailed modeling of the γ-ray flux in a large laboratory, or inside the hermetic shielding, needs to cope with a very small probability of generating any signal in the detector. It is often advantageous to calculate solid angle of the detector to the background sources and mass attenuation of the radiation shield separately, or to employ importance sampling. The former method can lead to loss of energy-direction correlations while in the latter has to balance CPU-time consumption against the loss of statistical independence. These approaches reduce the computation time required for a statistically meaningful number of detector hits to manageable levels.

Water is commonly used as shielding medium for large detectors, as it can be obtained cheaply and purified effectively in large quantity. Water purification technology is commercially available. Ultra-pure water, instrumented with photomultiplier tubes, can serve as active cosmic-ray veto counter. Water is also an effective neutron moderator and shield. In more recent underground experiments that involve

detectors operating at cryogenic temperature, liquefied gases (e.g. argon) are being used for shielding as well.

35.6.3. ***Radioactive impurities in detector and shielding components*** : After suppressing the effect of external radioactivity, radioactive impurities, contained in the detector components or attached to their surfaces, become important. Every material contains radioactivity at some level. The activity can be natural, cosmogenic, man-made, or a combination of them. The determination of the activity content of a specific material or component requires case-by-case analyses, and is rarely obtainable from the manufacturer. However, there are some general rules that can be used to guide the pre-selection. For detectors designed to look for electrons (for example in double-beta decay searches or neutrino detection via inverse beta decay or elastic scattering), intrinsic radioactivity is often the principal source of background. For devices detecting nuclear recoils (for example in dark matter searches), this is often of secondary importance as ionization signals can be actively discriminated on an event-by-event basis. Decay induced nuclear reactions become a concern.

For natural radioactivity, a rule of thumb is that synthetic substances are cleaner than natural materials. Typically, more highly processed materials have lower activity content than raw substances. Substances with high electro-negativity tend to be cleaner as the refining process preferentially removes K, Th, and U. For example, Al is often found to contain considerable amounts of Th and U, while electrolytic Cu is very low in primordial activities. Plastics or liquid hydrocarbons, having been refined by distillation, are often quite radiopure. Tabulated radioassay results for a wide range of materials can be found in Refs. [103] and [104]. Radioassay results from previous underground physics experiments are being archived at an online database [105].

The long-lived ^{238}U daughter ^{210}Pb ($T_{1/2}$=22.3 y) is found in all shielding lead, and is a background concern at low energies. This is due to the relatively high endpoint energy (Q_β=1.162 MeV) of its beta-unstable daughter ^{210}Bi. Lead refined from selected low-U ores have specific activities of about 5–30 Bq/kg. For applications that require lower specific activity, ancient lead (for example from Roman ships) is sometimes used. Because the ore processing and lead refining removed most of the ^{238}U, the ^{210}Pb decayed during the long waiting time to the level supported by the U-content of the refined lead. Lining the lead with copper to range out the low-energy radiation is another remedy. However, intermediate-Z materials carry additional cosmogenic-activation risks when handled above ground, as will be discussed below. ^{210}Pb is also found in solders.

Man-made radioactivity, released during above-ground nuclear testing and nuclear power production, is a source of background. The fission product ^{137}Cs can often be found attached to the surface of materials. The radioactive noble gas ^{85}Kr, released into the atmosphere by nuclear reactors and nuclear fuel re-processing, is sometimes a background concern, especially due to its high solubility in organic materials. Post-World War II steel typically contains a few tens of mBq/kg of ^{60}Co.

Surface activity is not a material property per se but is added during manufacturing and handling. Surface contamination can often be effectively removed by clean machining, etching, or a combination of both. The assembly of low-background detectors is often performed in controlled enclosures (e.g. clean rooms or glove boxes) to avoid contaminating surfaces with environmental substances, such as dust, containing radioactivity at much higher concentrations than the detector components. Surfaces are cleaned with high purity chemicals and de-ionized water. When not being processed components are best stored in sealed bags to limit dust deposition on the surface, even inside clean rooms. Surface contamination can be quantified by means of wipe-testing with acid or alcohol wetted Whatman 41 filters. Pre-soaking of the filters in clean acid reduces the amount of Th and U contained in the paper and boosts analysis sensitivity. The paper filters are ashed after wiping and the residue is digested in acid. Subsequent analysis by means of mass spectroscopy or neutron activation analysis is capable of detecting less than 1 pg/cm^2 of Th and U.

The most demanding low-rate experiments require screening of *all* components, which can be a time consuming task. The requirements for activity characterization depend on the experiment and the location and amount of a particular component. Monte Carlo simulations are used to quantify these requirements. Sensitivities of the order μBq/kg or less are sometimes required for the most critical detector components. At such a level of sensitivity, the characterization becomes a challenging problem in itself. Low-background α, β, and γ-ray counting, mass spectroscopy, and neutron activation analysis are the commonly used diagnostic techniques.

35.6.4. ***Radon and its progeny*** : The noble gas ^{222}Rn, a pure α-emitter, is a ^{238}U decay product. Due to its relatively long half-life of 3.8 d it is released by surface soil and is found in the atmosphere everywhere. ^{220}Rn (^{232}Th decay product) is mostly unimportant for most low-background experiments because of its short half-life. The ^{222}Rn activity in air ranges from 10 to 100 mBq/L outdoors and 100 to thousands of mBq/L indoors. The natural radon concentration depends on the weather and shows daily and seasonal variations. Radon levels are lowest above the oceans. For electron detectors, it is not the Rn itself that creates background, but its progeny ^{214}Pb, ^{214}Bi, ^{210}Bi, which emit energetic beta and γ radiation. Thus, not only the detector itself has to be separated from contact with air, but also internal voids in the shield which contain air can be a background concern. Radon is quite soluble in water and even more so in organic solvents. For large liquid scintillation detectors, radon mobility due to convection and diffusion is a concern. To define a scale: typical double-beta-decay searches are are restricted to $< \mu\text{Bq/kg}_{\text{detector}}$ (or 1 decay per $\text{kg}_{\text{detector}}$ and per 11.6 days) activities of ^{222}Rn in the active medium. This corresponds to a steady-state population of 0.5 atoms/$\text{kg}_{\text{detector}}$ or 50 $\mu\text{L/kg}_{\text{detector}}$ of air (assuming 20 mBq/L of radon in the air). The demand on leak tightness can thus be quite demanding. The decay of Rn itself is a concern for some recoil type detectors, as nuclear recoil energies in α decays are substantial (76 keV in the case of ^{222}Rn).

Low-background detectors are often kept sealed from the air and continuously flushed with boil-off nitrogen, which contains only small amounts of Rn. For the most demanding applications, the nitrogen is purified by multiple distillations, or by using pressure swing adsorption chromatography. Then only the Rn outgassing of the piping (due to its intrinsic U content) determines the radon concentration. Radon diffuses readily through thin plastic barriers. If the detector is to be isolated from its environment by means of a membrane, the choice of material is important [106].

Prolonged exposure of detector components or raw materials to air leads to the accumulation of the long-lived radon daughter ^{210}Pb on surfaces. Due to its low Q-value of 63.5 keV, ^{210}Pb itself is only a problem when extreme low energy response is important. However, because of its higher Q-value, the lead daughter ^{210}Bi, is a concern up to the MeV scale. The alpha unstable Bi-daughter ^{210}Po (E_α = 5304 keV) contributes not only to the alpha background but can also induce the emission of energetic neutrons via (α,n) reactions on low-Z materials (such as F, C, Si...etc). The neutrons, in turn, may capture on other detector components, creating energetic background. The (α,n) reaction yield induced by the α decay of ^{210}Po is typically small ($6 \cdot 10^{-6}$ n/α in Teflon, for example). Some data is available on the deposition of radon daughters from air onto materials, see e.g. [108]. This data indicates effective radon daughter collection distances of a a few *cm* in air. These considerations limit the allowable air exposure time. In case raw materials (e.g. in the form of granules) were exposed to air at the production site, the bulk of the finished detector components may be loaded with ^{210}Pb and its daughters. These are difficult to detect as no energetic gamma radiation is emitted in their decays. Careful air-exposure management is the only way to reduce this source of background. This can be achieved by storing the parts under a protective low-radon cover gas or keeping them sealed from radon.

State-of-the-art detectors can detect radon even at the level of few atoms. Solid state, scintillation, or gas detectors utilize alpha spectroscopy or are exploiting the fast $\beta - \alpha$ decay sequences of ^{214}Bi and ^{214}Po. The efficiency of these devices is sometimes boosted by electrostatic collection of charged radon from a large gas volume into a small detector.

35.6.5. ***Cosmic rays*** : Cosmic radiation, discussed in detail in Chapter 29, is a source of background for just about any non-accelerator experiment. Primary cosmic rays are about 90% protons, 9% alpha particles, and the rest heavier nuclei (Fig. 29.1). They are totally attenuated within the first the first few hg/cm^2 of atmospheric thickness. At sea level secondary particles ($\pi^{\pm} : p : e^{\pm} : n : \mu^{\pm}$) are observed with relative intensities 1 : 13 : 340 : 480 : 1420 (Ref. 109; also see Fig. 29.4).

All but the muon and the neutron components are readily absorbed by overburden such as building ceilings and passive shielding. Only if there is very little overburden ($\lesssim$10 g/cm^2 or so [100]) do pions and protons need to be considered when estimating the production rate of cosmogenic radioactivity.

Sensitive experiments are thus operated deep underground where essentially only muons can penetrate. As shown in Fig. 29.7, the muon intensity falls off rapidly with depth. Active detection systems, capable of tagging events correlated in time with cosmic-ray activity, are needed, depending on the overburden.

The muonic background is related to low-radioactivity techniques insofar as photo-nuclear interactions with atomic nuclei can produce long-lived radioactivity directly or indirectly via the creation of neutrons. This happens at any overburden, however, at strongly depth dependent rates. Muon bremsstrahlung, created in high-Z shielding materials, contributes to the low energy background too. Active muon detection systems are effective in reducing this background, but only for activities with sufficiently short half-lives, allowing vetoing with reasonable detector dead time.

Cosmogenic activation of detector components at the surface can be an issue for low-background experiments. Proper management of parts and materials above ground during manufacturing and detector assembly minimizes the accumulation of long-lived activity. Cosmogenic activation is most important for intermediate-Z materials such as Cu and Fe. For the most demanding applications, metals are stored and transported under sufficient shielding to stop the hadronic component of the cosmic rays. Parts can be stored underground for long periods before being used. Underground machine shops are sometimes used to limit the duration of exposure at the surface. Some experiments are even electro-forming copper underground.

35.6.6. ***Neutrons*** : Neutrons contribute to the background of low-energy experiments in different ways: directly through nuclear recoil in the detector medium, and indirectly, through the production of radio-nuclides, capture γs and inelastic scattering inside the detector and its components. The indirect mechanisms allow even remote materials to contribute to the background by means of penetrating γ radiation. Neutrons are thus an important source of low-energy background. They are produced in different ways:

1. At the earth's surface the flux of cosmic-ray secondary neutrons is exceeded only by that of muons;
2. Energetic tertiary neutrons are produced by cosmic-ray muons by nuclear spallation in the detector and laboratory walls;
3. In high-Z materials, often used in radiation shields, nuclear capture of negative muons results in the emission of neutrons;
4. Natural radioactivity has a neutron component through spontaneous fission and (α, n)-reactions.

A calculation with the hadronic simulation code FLUKA [107], using the known energy distribution of secondary neutrons at the earth's surface [110], yields a mass attenuation of 1.5 hg/cm^2 in concrete for secondary neutrons. In case energy-dependent neutron-capture cross sections are known, such calculations can be used to obtain the production rate of particular radio-nuclides.

At an overburden of only few meters water equivalent, neutron production by muons becomes the dominant mechanism. Neutron production rates are high in high-Z shielding materials. A high-Z radiation shield, discussed earlier as being effective in reducing background due to external radioactivity, thus acts as a source for cosmogenic tertiary high-energy neutrons. Depending on the overburden and the radioactivity content of the laboratory, there is an optimal shielding thickness. Water shields, although bulky, are an attractive alternative due to their low neutron production yield and self-shielding.

Shields made from plastic or water are commonly used to reduce the neutron flux. The shield is sometimes doped with a substance having a high thermal neutron capture cross section (such as boron) to absorb thermal neutrons more quickly. The hydrogen, contained in these shields, serves as a target for elastic scattering, and is effective in reducing the neutron energy. Neutrons from natural radioactivity have relatively low energies and can be effectively suppressed by a neutron shield. Ideally, such a neutron shield should be inside the lead to be effective for tertiary neutrons. However, this is rarely done as it increases the neutron production target (in form of the passive shield), and the costs increase as the cube of the linear dimensions. An active cosmic-ray veto is an effective solution, correlating a neutron with its parent muon. This solution works best if the veto system is as far away from the detector as feasible (outside the radiation shield) in order to correlate as many background-producing muons with neutrons as possible. The vetoed time after a muon hit needs to be sufficiently long to assure muon bremsstrahlung and neutron-induced backgrounds are sufficiently suppressed. An upper limit to the allowable veto period is given by the veto-induced deadtime, which is related to the muon hit rate on the veto detector. This consideration also constitutes the limiting factor for the physical size of the veto system (besides the cost). The background caused by neutron-induced radioactivity with live-times exceeding the veto time cannot be addressed in this way. Moving the detector deep underground, and thus reducing the muon flux, is the only technique that addresses all sources of cosmogenic the neutron background.

References:

1. R.M. Baltrusaitis *et al.*, Nucl. Instrum. Methods **A20**, 410 (1985).
2. D.J. Bird *et al.*, The Atrophysics Journal 424,491(1994).
3. T. Abu-Zayyad *et al.*, Nucl. Instrum. Methods **A450**, 253 (2000).
4. H. Tokuno *et al.*, Nucl. Instrum. Methods **A676**, 54 (2012).
5. J. Abraham *et al.* [Pierre Auger Collab.], Nucl. Instrum. Methods **A620**, 227 (2010).
6. J. Abraham *et al.* [Pierre Auger Collab.], Eur. Phys. J. Plus **127**, 94 (2012).
7. T. Fujii et al., Astropart. Phys. **74**, 64 (2016).
8. F. Arqueros, J. Hrandel, and B. Keilhauer, Nucl. Instrum. Methods **A597**, 23 (2008).
9. F. Arqueros, J. Hrandel, and B. Keilhauer, Nucl. Instrum. Methods **A597**, 1 (2008).
10. J. Rosado, F. Blanco, and F. Arqueros, Astropart. Phys. **34**, 164 (2010).
11. J. Boyer *et al.*, Nucl. Instrum. Methods **A482**, 457 (2002); J.Abraham *et al.* [Pierre Auger Collab.], Nucl. Instrum. Methods **A620**, 227 (2010).
12. M. Ave *et al.* [AIRFLY Collab.], Astropart. Phys. **28**, 41 (2007).
13. J. Rosado, F. Blanci, and F. Arqueros, Astropart. Phys. **55**, 51 (2014).
14. J.T. Brack *et al.*, Astropart. Phys. **20**, 653, (2004).
15. B. Fick *et al.*, JINST **1**, 11003 (2006).
16. J. Abraham *et al.* [Pierre Auger Collab.], Astropart. Phys. **33**, 108 (2010).
17. J. Abraham *et al.* [Pierre Auger Collab.], Astropart. Phys. **34**, 368 (2011).
18. R. Thalman *et al.* Journal of Quantitative Spectroscopy and Radiative Transfer , **147**, 171 (2014), Erratum-ibid. **189**, 281 (2017).
19. M. Unger *et al.*, Nucl. Instrum. Methods **A588**, 433 (2008).
20. T.K. Gaisser and A.M. Hillas, *Proc. 15th Int. Cosmic Ray Conf.* Bulgarska Akademiia na Naukite, Conf. Papers **8**, 353 (1978), (archived at http://adsabs.harvard.edu/abs/1977ICRC....8..353G).
21. J.Abraham *et al.* [Pierre Auger Collab.], Nucl. Instrum. Methods **A789**, 172 (2015).
22. A. Huangs, G. Medina-Tanco and A. Santangelo, Experimental Astronomy **40**, 1 (2015).
23. P.A. Klimov *et al.* Space Science Reviews, Aug. 21 (2017).
24. G. Abedellaoui *et al.* [JEM-EUSO Collab.], Nucl. Instrum. Methods **A866**, 150, (2017).
25. L. Wiencke and A. Olinto for the JEM-EUSO Collaboration, PoS(ICRC2017) 1097 (2017).

26. A. Olinto et al.,PoS(ICRC2017) 542 (2017).
27. J. Holder *et al.*, AIP Conf. Proc. **1085**, 657 (2008).
28. F. Aharonian *et al.*, Astron. & Astrophys. **457**, 899 (2006).
29. J. Albert *et al.*, Astrophys. J. **674**, 1037 (2008).
30. T.C. Weekes *et al.*, Astrophys. J. **342**, 379 (1989).
31. A.M. Hillas *et al.*, Astrophys. J. **503**, 744 (1998).
32. `http://tevcat.uchicago.edu/`.
33. F.A. Aharonian *et al.*, Astrophys. J. **636**, 777 (2006).
34. M. de Naurois and D. Mazin, Comptes Rendus Physique 16,610(2015).
35. M. Lemoine-Goumard, Proc. 34th ICRC (2015).
36. A.M. Hillas, Astropart. Phys. **43**, 19 (2013).
37. B.S. Acharya *et al.*, Astropart. Phys. **43**, 3 (2013).
38. L.A. Bernstein *et al.*, `arXiv:0907.4183` (2009).
39. Y. Ashie *et al.*, Phys. Rev. **D71**, 112005 (2005).
40. S. Kasuga *et al.*, Phys. Lett. **B374**, 238 (1996).
41. M. Shiozawa, Nucl. Instrum. Methods **A433**, 240 (1999).
42. K. Abe *et al.*, Phys. Rev. **D83**, 052010 (2011).
43. J. Beacom and M. Vagins, Phys. Rev. Lett. **93**, 171101 (2004).
44. J. Boger *et al.*, Nucl. Instrum. Methods **A449**, 172 (2000).
45. T.K. Gaisser, F. Halzen, and T. Stanev, Phys. Reports **258**, 173 (1995) and Phys. Reports **271**, 355 (1995).
46. J.G. Learned and K. Mannheim, Ann. Rev. Nucl. and Part. Sci. **50**, 679 (2000).
47. U.F. Katz and C. Spiering, Prog. in Part. Nucl. Phys. **67**, 651 (2012).
48. M.G. Aartsen et al. (IceCube Collab.), J. Phys. G44, 054006 (2017);.
49. S. Adrián-Martínez et al. (KM3NeT Collab.), J. Phys. G43, 084001 (2016);.
50. A. Avronin et al. (Baikal Collab.), Phys. Part. Nucl. **46**, 211 (2015).
51. M.G. Aartsen et al. (IceCube-Gen2 Collab.), *IceCube-Gen2: A vision for the Future of Neutrino Astronomy in Antarctica*, `arXiv:1412.5106v2[astro-ph.HE]`.
52. S. Adrián-Martínez et al. (KM3NeT Collab.), Eur. Phys. J. C74, 3056 (2014);
S. Adrián-Martínez et al. (KM3NeT Collab.), Eur. Phys. J. C76, 54 (2016).
53. M.G. Aartsen *et al.* (IceCube Collab.), Phys. Rev. Lett. 113, 101101 (2014).
54. S. Adrián-Martínez *et al.* (ANTARES Collab.), Astrophys. Journ. 786, L5 (2014).
55. M.G. Aartsen *et al.* (IceCube Collab.), Phys. Rev. D 91, 072004, (2015).
56. J. van Santen (for the IceCube Collab.), contribution to ICRC2017.
57. A. Heijboer (for the ANTARES and KM3NeT Collabs.), contribution to ICRC2017.
58. C. Kopper (for the IceCube Collab.), contribution to ICRC2017.
59. K. Griesen, Phys. Rev. Lett. **16**, 748 (1966);
G.T. Zatsepin and V.A. Kuzmin, JETP Lett. **4**, 78 (1966).
60. R. Abbasi *et al.* [IceCube Collab.], Astropart. Phys. **34**, 382 (2011).
61. S.R. Klein, `arXiv:1012.1407` (2010).
62. G.A. Askaryan, Sov. Phys. JETP **14**, 441 (1962);
G.A. Askaryan, Sov. Phys. JETP **21**, 658 (1965).
63. J. Alvarez-Muniz *et al.*, Phys. Rev. **D62**, 063001 (2000).
64. D. Saltzberg *et al.*, Phys. Rev. Lett. **86**, 2802 (2001);
O. Scholten *et al.*, J. Phys. Conf. Ser. **81**, 012004 (2007).
65. P. Allison *et al.* [ARA Collab.], Astropart. Phys. **70**, 62 (2015).
66. J.C. Hanson *et al.* [ARIANNA Collab.], J. Glaciology **61**, 438 (2015).
67. J. Avva *et al.*, J. Glaciology **61**, 1005 (2015)..
68. A. G. Vieregg, K. Bechtol and A. Romero-Wolf, JCAP **1602**, no. 02, 005 (2016).
69. T. Huege, Braz. J. Phys. **44**, 520 (2014).
70. S. Hoover *et al.*, Phys. Rev. Lett. **105**, 151101 (2010).
71. M. Detrixhe *et al.* [ANITA-II Collab.], Phys. Rev. **D83**, 023513 (2011).
72. R.D. Dagkesamanskii and I.M. Zheleznykh, Sov. Phys. JETP Lett. **50**, 233 (1989).
73. J.D. Bray *et al.*, Phys. Rev. **D91**, 063002 (2015).
74. C. W. James *et al.*, EPJ Web Conf. **135**, 04001 (2017).
75. J.A. Dowdeswell and S. Evans, Rept. on Prog. in Phys. **67**, 1821 (2004).
76. S. Barwick, presented at the 35th Intl. Cosmic Ray Conf. (2017).
77. P. Gorham *et al.* [ANITA Collab.], Phys. Rev. Lett. **103**, 051103 (2009). The published limit is corrected in an erratum, P. Gorham *et al.*, `arXiv:1011.5004` (2010).
78. I. Kravchenko *et al.* [RICE Collab.], Phys. Rev. **D73**, 082002 (2006);
I. Kravchenko *et al.* [RICE Collab.] Astropart. Phys. **19**, 15 (2003).
79. P. Allison *et al.* [ARA Collab.], Phys. Rev. **D93**, 082003 (2016).
80. S.W. Barwick *et al.* [ARIANNA Collab.], IEEE Trans. Nucl. Sci. **62**, 2202 (2015);
S.W. Barwick *et al.* [ARIANNA Collab.], Astropart. Phys. **70**, 12 (2015).
81. E. Aprile and T. Doke, Rev. Mod. Phys. **82**, 2053 (2010).
82. V. Chepel and H. Araújo, J. Instrum. **8**, R04001 (2013).
83. T.M. Undagoitia and L. Rauch, `arXiv:1509.08767` (2015).
84. E. Aprile *et al.*, `arXiv:1705.06655` (2017).
85. X. Cui *et al.*, `arXiv:1708.06917` (2017).
86. C.E. Dahl, PhD thesis, Princeton U. (2009).
87. M. Schumann *et al.*, JCAP **10**, 16 (2015).
88. W. Guo and D.N. McKinsey, Phys. Rev. **D87**, 115001 (2013).
89. D.R. Nygren, J. Phys. Conf. Ser. **460**, 012006 (2013).
90. C.A.J. O'Hare *et al.*, Phys. Rev. **D92**, 063518 (2015).
91. S.M. Bilenky and Carlo Giunti, Mod. Phys. Lett. **A27**, 1230015 (2012).
92. J.B. Albert *et al.*, Nature **510**, 229 (2014).
93. J.B. Albert *et al.*, `arXiv:1707.08707` (2017).
94. M.L. Moe, Phys. Rev. **C44**, 931 (1991).
95. C. Enss (ed.), *Cryogenic Particle Detection*, Springer-Verlag, Berlin (2005).
96. E. Shirokoff (ed.), *Proc. 15th Int. Workshop on Low Temperature Detectors (LTD-15)*, J. Low Temp. Phys. **176**, 131–1108 (2014); see also previous *Proceedings* of this workshop.
97. S.H. Moseley, J.C. Mather, and D. McCammon, J. Appl. Phys. **56**, 1257 (1984).
98. K.D. Irwin, Appl. Phys. Lett. **66**, 1998 (1995).
99. S.R. Bandler *et al.*, J. Low. Temp. Phys. **93**, 709 (1993).
100. G. Heusser, Ann. Rev. Nucl. and Part. Sci. **45**, 543 (1995).
101. J.A. Formaggio and C.J. Martoff, Ann. Rev. Nucl. and Part. Sci. **54**, 361 (2004).
102. S. Agostinelli *et al.*, Nucl. Instrum. Methods **A506**, 250 (2003).
103. P. Jagam and J.J. Simpson, Nucl. Instrum. Methods **A324**, 389 (1993).
104. D.S. Leonard *et al.*, Nucl. Instrum. Methods **A591**, 490 (2008).
105. `http://www.radiopurity.org`.
106. M. Wojcik *et al.*, Nucl. Instrum. Methods **A449**, 158 (2000).
107. `http://www.fluka.org/fluka.php?id=faq&sub=13`.
108. V.E. Guiseppe *et al.*, `arXiv:1101.0126` (2011).
109. National Council on Radiation Protection and Measurement, Report 94, Bethesda, MD (1987).
110. M.S. Gordon *et al.*, IEEE Trans. **NS51**, 3427 (2004).

36. Radioactivity and Radiation Protection

Revised October 2017 by S. Roesler and M. Silari (CERN).

36.1. Definitions [1,2,3]

It would be desirable if legal protection limits could be expressed in directly measurable *physical quantities*. However, this does not allow to quantify biological effects of the exposure of the human body to ionizing radiation.

For this reason, protection limits are expressed in terms of so-called *protection quantities* which, although calculable, are not measurable. Protection quantities quantify the extent of exposure of the human body to ionizing radiation from both whole and partial body external irradiation and from intakes of radionuclides.

In order to demonstrate compliance with dose limits, so-called *operational quantities* are typically used which aim at providing conservative estimates of protection quantities. Often radiation protection detectors used for individual and area monitoring are calibrated in terms of operational quantities and, thus, these quantities become "measurable".

36.1.1. *Physical quantities* :

• **Fluence,** Φ (unit: $1/m^2$): The fluence is the quotient of the sum of the particle trajectory lengths dl in the volume dV

$$\Phi = dl/dV \ . \tag{36.1}$$

It can also be expressed in terms of number of particles dN incident upon a small sphere of cross-sectional area da

$$\Phi = dN/da \ .$$

• **Absorbed dose,** D (unit: gray, 1 Gy=1 J/kg=100 rad): The absorbed dose is the energy imparted by ionizing radiation in a volume element of a specified material divided by the mass of this volume element.

• **Kerma,** K (unit: gray): Kerma is the sum of the initial kinetic energies of all charged particles liberated by indirectly ionizing radiation in a volume element of the specified material divided by the mass of this volume element.

• **Linear energy transfer,** L **or** LET (unit: J/m, often given in keV/μm, 1 keV/μm$\approx 1.602 \times 10^{-10}$ J/m): The linear energy transfer is the mean energy, dE, lost by a charged particle owing to collisions with electrons in traversing a distance dl in matter. *Low-LET radiation:* X rays and gamma rays (accompanied by charged particles due to interactions with the surrounding medium) or light charged particles such as electrons that produce sparse ionizing events far apart at a molecular scale ($L < 10$ keV/μm). *High-LET radiation:* neutrons and heavy charged particles that produce ionizing events densely spaced at a molecular scale ($L > 10$ keV/μm). While the above LET definition refers to electronic stopping power only, at low energy nuclear stopping power could be a significant fraction of the total stopping power.

• **Activity,** A (unit: becquerel, 1 Bq=1/s=27 pCi): Activity is the expectation value of the number of nuclear decays occurring in a given quantity of material per unit time.

36.1.2. *Protection quantities* :

• **Organ absorbed dose,** D_T (unit: gray): The mean absorbed dose in an organ or tissue T of mass m_T is defined as

$$D_T = \frac{1}{m_T} \int_{m_T} D dm \ .$$

• **Equivalent dose,** H_T (unit: sievert, 1 Sv=100 rem): The equivalent dose H_T in an organ or tissue T is equal to the sum of the absorbed doses $D_{T,R}$ in the organ or tissue caused by different radiation types R weighted with so-called radiation weighting factors w_R:

$$H_T = \sum_R w_R \times D_{T,R} \ . \tag{36.2}$$

Table 36.1: Radiation weighting factors, w_R.

Radiation type	w_R
Photons, electrons and muons	1
Neutrons, $E_n < 1$ MeV	$2.5 + 18.2 \times \exp[-(\ln E_n)^2/6]$
1 MeV $\leq E_n \leq$ 50 MeV	$5.0 + 17.0 \times \exp[-(\ln(2E_n))^2/6]$
$E_n >$ 50 MeV	$2.5 + 3.25 \times \exp[-(\ln(0.04E_n))^2/6]$
Protons and charged pions	2
Alpha particles, fission fragments, heavy ions	20

It expresses long-term risks (primarily cancer and leukemia) from low-level chronic exposure. The values for w_R recommended by ICRP [2] are given in Table 36.1.

• **Effective dose,** E (unit: sievert): The sum of the equivalent doses, weighted by the tissue weighting factors w_T ($\sum_T w_T = 1$) of several organs and tissues T of the body that are considered to be most sensitive [2], is called "effective dose":

$$E = \sum_T w_T \times H_T \ . \tag{36.3}$$

36.1.3. *Operational quantities* :

• **Dose equivalent,** H (unit: sievert): The dose equivalent at a point in tissue is given by:

$$H = D \times Q \tag{36.4}$$

where D is the absorbed dose and Q is the quality factor at that point. The quality factor at a point in tissue, is given by:

$$Q = \frac{1}{D} \int_{L=0}^{\infty} Q(L) D_L dL$$

where D_L is the distribution of D in unrestricted linear energy transfer L at the point of interest, and $Q(L)$ is the quality factor as a function of L. The integration is to be performed over D_L, due to all charged particles, excluding their secondary electrons.

• **Ambient dose equivalent,** $H^*(10)$ (unit: sievert): The dose equivalent at a point in a radiation field that would be produced by the corresponding expanded and aligned field in a 30 cm diameter sphere of unit density tissue (ICRU sphere) at a depth of 10 mm on the radius vector opposing the direction of the aligned field. Ambient dose equivalent is the operational quantity for *area monitoring*.

• **Personal dose equivalent,** $H_p(d)$ (unit: sievert): The dose equivalent in ICRU tissue at an appropriate depth, d, below a specified point on the human body. The specified point is normally taken to be where the individual dosimeter is worn. For the assessment of effective dose, $H_p(10)$ with a depth $d = 10$ mm is chosen, and for the assessment of the dose to the skin and to the hands and feet the personal dose equivalent, $H_p(0.07)$, with a depth $d = 0.07$ mm, is used. Personal dose equivalent is the operational quantity for *individual monitoring*.

36.1.4. *Dose conversion coefficients* :

Dose conversion coefficients allow direct calculation of protection or operational quantities from particle fluence and are functions of particle type, energy and irradiation configuration. The most common coefficients are those for effective dose and ambient dose equivalent. The former are based on simulations in which the dose to organs of anthropomorphic phantoms is calculated for approximate actual conditions of exposure, such as irradiation of the front of the body (antero-posterior irradiation) or isotropic irradiation.

Conversion coefficients from fluence to effective dose are given for anterior-posterior irradiation and various particles in Fig. 36.1 [4]. For example, the effective dose from an anterior-posterior irradiation in a field of 1-MeV neutrons with a fluence of 1 neutron per cm^2 is about 290 pSv. In Monte Carlo simulations such coefficients allow multiplication with fluence at scoring time such that effective dose to a human body at the considered location is directly obtained.

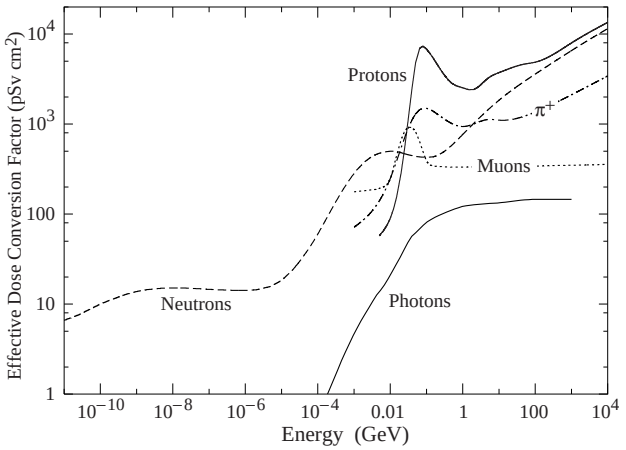

Figure 36.1: Fluence to effective dose conversion coefficients for anterior-posterior irradiation and various particles [4].

36.2. Radiation levels [5]

• **Natural background radiation**: On a worldwide average, the annual whole-body dose equivalent due to all sources of natural background radiation ranges from 1.0 to 13 mSv (0.1–1.3 rem) with an annual average of 2.4 mSv [6]. In certain areas values up to 50 mSv (5 rem) have been measured. A large fraction (typically more than 50%) originates from inhaled natural radioactivity, mostly radon and radon daughters. The latter can vary by more than one order of magnitude: it is 0.1–0.2 mSv in open areas, 2 mSv on average in a house and more than 20 mSv in poorly ventilated mines.

• **Cosmic ray background radiation**: At sea level, the whole-body dose equivalent due to cosmic ray background radiation is dominated by muons; at higher altitudes also nucleons contribute. Dose equivalent rates range from less than 0.1 μSv/h at sea level to a few μSv/h at aircraft altitudes. Details on cosmic ray fluence levels are given in the Cosmic Rays section (Sec. 29 of this *Review*).

36.3. Health effects of ionizing radiation

Radiation can cause two types of health effects, deterministic and stochastic:

• **Deterministic effects** are tissue reactions which cause injury to a population of cells if a given threshold of absorbed dose is exceeded. The severity of the reaction increases with dose. The quantity in use for tissue reactions is the absorbed dose, D. When particles other than photons and electrons (low-LET radiation) are involved, a Relative Biological Effectiveness (RBE)-weighted dose may be used. The RBE of a given radiation is the reciprocal of the ratio of the absorbed dose of that radiation to the absorbed dose of a reference radiation (usually X rays) required to produce the same degree of biological effect. It is a complex quantity that depends on many factors such as cell type, dose rate, fractionation, etc.

• **Stochastic effects** are malignant diseases and heritable effects for which the probability of an effect occurring, but not its severity, is a function of dose without threshold.

• **Lethal dose**: The whole-body dose from penetrating ionizing radiation resulting in 50% mortality in 30 days (assuming no medical treatment) is 2.5–4.5 Gy (250–450 rad)†, as measured internally on the body longitudinal center line. The surface dose varies due to variable body attenuation and may be a strong function of energy.

• **Cancer induction**: The cancer induction probability is about 5% per Sv on average for the entire population [3].

• **Recommended effective dose limits**: The International Commission on Radiological Protection (ICRP) recommends a limit for radiation workers of 20 mSv effective dose per year averaged over 5 years, with the provision that the dose should not exceed 50 mSv in any single year [3]. The limit in the EU-countries and Switzerland is 20 mSv per year, in the U.S. it is 50 mSv per year (5 rem per year). Many physics laboratories in the U.S. and elsewhere set lower limits. The effective dose limit for general public is typically 1 mSv per year.

† RBE-weighted when necessary

36.4. Prompt neutrons at accelerators

Neutrons dominate the particle environment outside thick shielding (*e.g.*, > 1 m of concrete) for high energy (> a few hundred MeV) electron and hadron accelerators. In addition, for accelerators with energies above about 10 GeV, muons contribute significantly at small angles with regard to the beam, even behind several meters of shielding. Another special case are synchrotron light sources where particular care has to be taken to shield the very intense low-energy photons extracted from the electron synchrotron into the experimental areas. Due to its importance at high energy accelerators this section focuses on prompt neutrons.

36.4.1. *Electron accelerators* :

At electron accelerators, neutrons are generated via photonuclear reactions from bremsstrahlung photons. Neutron production takes place above a threshold value which varies from 10 to 19 MeV for light nuclei (with important exceptions, such as 2.23 MeV for deuterium and 1.67 MeV for beryllium) and from 4 to 6 MeV for heavy nuclei. It is commonly described by different mechanisms depending on the photon energy: the giant dipole resonance interactions (from threshold up to about 30 MeV, often the dominant process), the quasi-deuteron effect (between 30 MeV and a few hundred MeV), the delta resonance mechanism (between 200 MeV and a few GeV) and the vector meson dominance model at higher energies.

The giant dipole resonance reaction consists in a collective excitation of the nucleus, in which neutrons and protons oscillate in the direction of the photon electric field. The oscillation is damped by friction in a few cycles, with the photon energy being transferred to the nucleus in a process similar to evaporation. Nucleons emitted in the dipolar interaction have an anisotropic angular distribution, with a maximum at 90°, while those leaving the nucleus as a result of evaporation are emitted isotropically with a Maxwellian energy distribution described as [7]:

$$\frac{dN}{dE_n} = \frac{E_n}{T^2} e^{-E_n/T} \ , \tag{36.5}$$

where T is a nuclear 'temperature' (in units of MeV) characteristic of the particular target nucleus and its excitation energy. For heavy nuclei the 'temperature' generally lies in the range of T = 0.5–1.0 MeV. Neutron yields from semi-infinite targets per kW of electron beam power are plotted in Fig. 36.2 as a function of the electron beam energy [7].

While for thick targets neutron production is mainly due to photonuclear interactions, for thin targets (thickness of fractions of the radiation length) electronuclear interactions are the dominating process.

Typical neutron energy spectra outside of concrete (80 cm thick, 2.35 g/cm^3) and iron (40 cm thick) shields are shown in Fig. 36.3. In order to compare these spectra to those caused by proton beams (see below) the spectra are scaled by a factor of 100, which roughly corresponds to the difference in the high energy hadronic cross sections for photons and hadrons (*e.g.*, the fine structure constant). The shape of these spectra are generally characterized by a low-energy peak at around 1 MeV (evaporation neutrons) and a high-energy shoulder at around 70–80 MeV. In case of concrete shielding, the spectrum also shows a pronounced peak at thermal neutron energies.

36.4.2. *Proton accelerators* :

At proton accelerators, neutron yields emitted per incident proton by different target materials are roughly independent of proton energy between 20 MeV and 1 GeV, and are given by the ratio C : Al : Cu-Fe : Sn : Ta-Pb = 0.3 : 0.6 : 1.0 : 1.5 : 1.7 [10]. Above about 1 GeV, the neutron yield is proportional to E^m, where $0.80 \leq m \leq 0.85$ [11].

Typical neutron energy spectra outside of concrete and iron shielding are shown in Fig. 36.3. Here, the radiation fields are caused

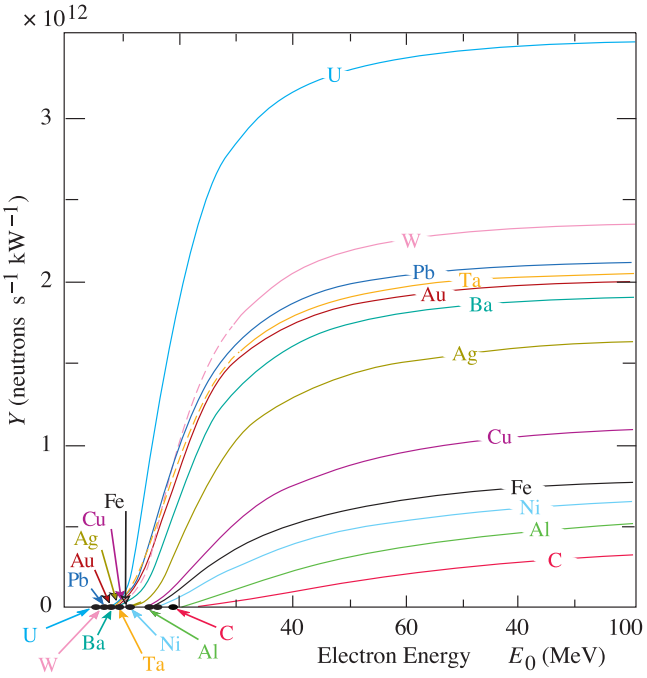

Figure 36.2: Neutron yields from semi-infinite targets per kW of electron beam power, as a function of the electron beam energy, disregarding target self-shielding [7].

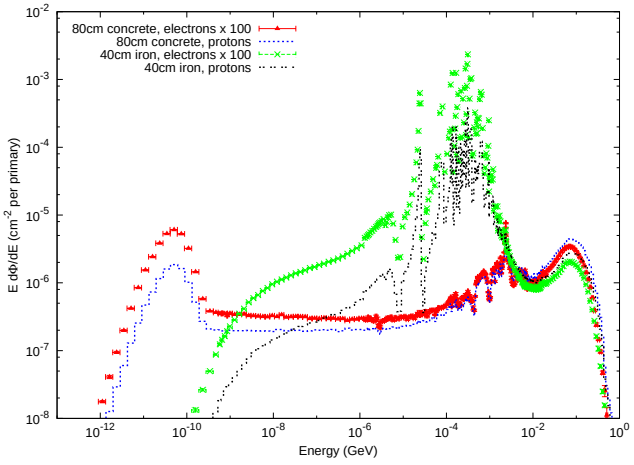

Figure 36.3: Neutron energy spectra calculated with the FLUKA code [8,9] from 25 GeV proton and electron beams on a thick copper target. Spectra are evaluated at 90° to the beam direction behind 80 cm of concrete or 40 cm of iron. All spectra are normalized per beam particle. In addition, spectra for electron beam are multiplied by a factor of 100.

by a 25 GeV proton beam interacting with a thick copper target. The comparison of these spectra with those for an electron beam of the same energy reflects the difference in the hadronic cross sections between photons and hadrons above a few 100 MeV. Differences are increasing towards lower energies because of different interaction mechanisms. Furthermore, the slight shift in energy above about 100 MeV follows from the fact that the energies of the interacting photons are lower than 25 GeV. Apart from this the shapes of the two spectra are similar.

The neutron-attenuation length is shown in Fig. 36.4 for concrete and mono-energetic broad-beam conditions. As can be seen in the figure it reaches a value of about 117 g/cm^2 above 200 MeV. As the cascade through thick shielding is carried by particles with energies between about 100 MeV and 300 MeV (in this energy range non-elastic cross sections are at minimum and are dominated by quasi-elastic processes leading to low attenuation) this value is equal to the equilibrium attenuation length for particles emitted at 90 degrees in concrete.

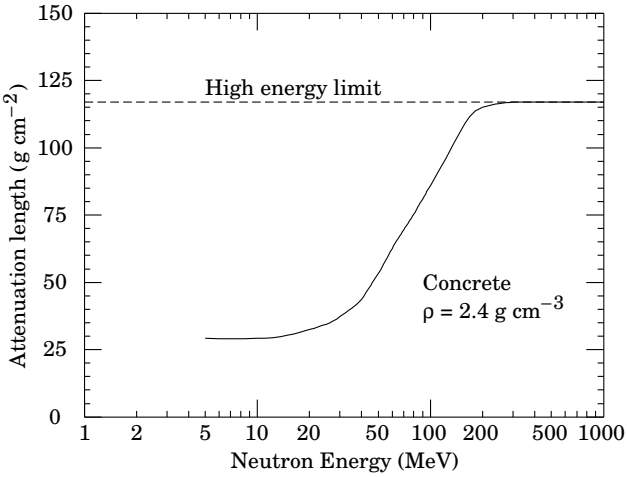

Figure 36.4: The variation of the attenuation length for mono-energetic neutrons in concrete as a function of neutron energy [10].

36.5. Photon sources

The dose equivalent rate in tissue (in mSv/h) from a gamma point source emitting one photon of energy E (in MeV) per second at a distance of 1 m is $4.6 \times 10^{-9}\,\mu_{en}/\rho\,E$, where μ_{en}/ρ is the mass energy absorption coefficient. The latter has a value of 0.029 ± 0.004 cm^2/g for photons in tissue over an energy range between 60 keV and 2 MeV (see Ref. 12 for tabulated values).

Similarly, the dose equivalent rate in tissue (in mSv/h) at the surface of a semi-infinite slab of uniformly activated material containing 1 Bq/g of a gamma emitter of energy E (in MeV) is $2.9 \times 10^{-4}\,R_\mu\,E$, where R_μ is the ratio of the mass energy absorption coefficients of the photons in tissue and in the material.

36.6. Accelerator-induced radioactivity

Typical medium- and long-lived activation products in metallic components of accelerators are ^{22}Na, ^{46}Sc, ^{48}V, ^{51}Cr, ^{54}Mn, ^{55}Fe, ^{59}Fe, ^{56}Co, ^{57}Co, ^{58}Co, ^{60}Co, ^{63}Ni and ^{65}Zn. Gamma-emitting nuclides dominate doses by external irradiation at longer decay times (more than one day) while at short decay times β^+ emitters are also important (through photons produced by β^+ annihilation). Due to their short range, β^- emitters are relevant, for example, only for dose to the skin and eyes or for doses due to inhalation or ingestion. Fig. 36.5 and Fig. 36.6 show the contributions of gamma and β^+ emitters to the total dose rate at 12.4 cm distance to a copper sample [13]. The sample was activated by the stray radiation field created by a 120 GeV mixed hadron beam dumped in a copper target during about 8 hours at intensities between $10^7 - 10^8$ hadrons per second. Typically, dose rates at a certain decay time are mainly determined by radionuclides having a half-life of the order of the decay time. Extended irradiation periods might be an exception to this general rule as in this case the activity of long-lived nuclides can build up sufficiently so that it dominates that one of short-lived even at short cooling times.

Activation in concrete is dominated by ^{24}Na (short decay times) and ^{22}Na (long decay times). Both nuclides can be produced either by low-energy neutron reactions on the sodium-component in the concrete or by spallation reactions on silicon, calcium and other constituents such as aluminum. At long decay times nuclides of radiological interest in activated concrete can also be ^{60}Co, ^{152}Eu, ^{154}Eu and ^{134}Cs, all of which produced by (n,γ)-reactions with traces of natural cobalt, europium and cesium, Thus, such trace elements might be important

even if their content in concrete is only a few parts per million or less by weight.

The explicit simulation of radionuclide production with general-purpose Monte Carlo codes has become the most commonly applied method to calculate induced radioactivity and its radiological consequences [13](see also Sec. 36.8). They are complemented by analytical codes based on folding particle fluence spectra with nuclide production cross sections. ActiWiz [14,15] is an example of such a code targeting the domain of radiological characterization and material optimization. It allows for calculating nuclide inventories by convolution of fluence spectra with nuclide production data for 85 chemical elements and arbitrary compounds from threshold to an energy of 100 TeV.

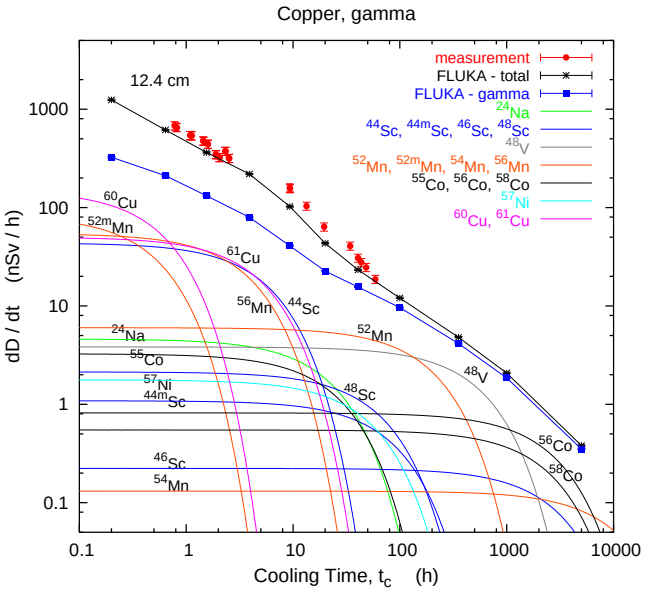

Figure 36.5: Contribution of individual gamma-emitting nuclides to the total dose rate at 12.4 cm distance to an activated copper sample [13].

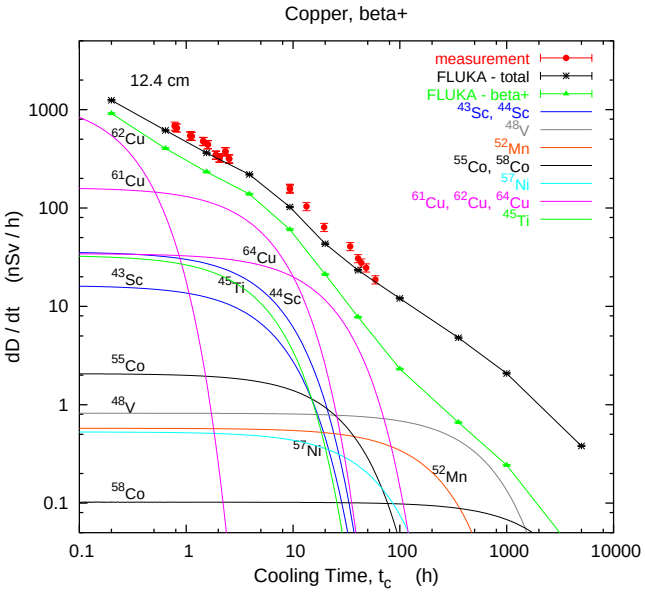

Figure 36.6: Contribution of individual positron-emitting nuclides to the total dose rate at 12.4 cm distance to an activated copper sample [13].

36.7. Radiation protection instrumentation

The capacity to distinguish and measure the high-LET (mostly neutrons) and the low-LET components (photons, electrons, muons) of the radiation field at workplaces is of primary importance to evaluate the exposure of personnel. At proton machines the prompt dose equivalent outside a shield is mainly due to neutrons, with some contribution from photons and, to a minor extent, charged particles. At high-energy electron accelerators the dominant stray radiation during operation consists of high-energy neutrons, because the shielding is normally thick enough to absorb most of the bremsstrahlung photons. Most of the personnel exposure at accelerator facilities is often received during maintenance interventions, and is due to gamma/beta radiation coming from residual radioactivity in accelerator components.

Radiation detectors used both for radiation surveys and area monitoring are normally calibrated in ambient dose equivalent $H^*(10)$.

36.7.1. *Neutron detectors* :

• **Rem counters:** A rem counter [16] is a portable detector consisting of a thermal neutron counter embedded in a polyethylene moderator, with a response function that approximately follows the curve of the conversion coefficients from neutron fluence to $H^*(10)$ over a wide energy range. Conventional rem counters provide a response to neutrons up to approximately 10-15 MeV, extended-range units are heavier as they include a high-A converter but correctly measure $H^*(10)$ up to several hundred MeV [17].

• **Bonner Sphere Spectrometer (BSS):** A BSS [18] is made up of a thermal neutron detector at the centre of moderating spheres of different diameters made of polyethylene (PE) or a combination of PE and a high-A material to enhance its response to high energy neutrons (similar to rem counters). Each sphere has a different response function versus neutron energy, and the neutron energy, at which the sensitivity peaks, increases with sphere diameter. The energy resolution of the system is rather low but satisfactory for radiation protection purposes. The neutron spectrum is obtained by unfolding the experimental counts of the BSS with its response matrix by a computer code that is often based on an iterative algorithm. BSS exist in active (using ^{3}He or BF_3 proportional counters or ^{6}LiI scintillators) and passive versions (using CR-39 track detectors or LiF), for use *e.g.* in strongly pulsed fields. With ^{3}He counters the discrimination with respect to gamma rays and noise is excellent.

• **Bubble detectors:** A bubble detector [19] is a dosimeter based on a super-heated emulsion (super-heated droplets suspended in a gel) contained in a vial and acting as a continuously sensitive, miniature bubble chamber. The total number of bubbles evolved from the radiation-induced nucleation of drops gives an integrated measure of the total neutron exposure. Various techniques exist to record and count the bubbles, *e.g.*, visual inspection, automated reading with video cameras or acoustic counting. Bubble detectors are insensitive to low-LET radiation. Super-heated emulsions are used as personal, area and environmental dosimeters, as well as neutron spectrometers.

• **Track etched detectors:** Track etched detectors (TEDs) [20] are based on the preferential dissolution of suitable, mostly insulator, materials along the damage trails of charged particles of sufficiently high-energy deposition density. The detectors are effectively not sensitive to radiation which deposits the energy through the interactions of particles with low LET. These dosimeters are generally able to determine neutron ambient dose equivalent down to around 100 μSv. They are used both as personal dosimeters and for area monitoring, *e.g.*, in BSS.

36.7.2. *Photon detectors* [21] :

• **GM counters:** Geiger Müller (GM) counters are low cost devices and simple to operate. They work in pulse mode and since they only count radiation-induced events, any spectrometric information is lost. In general they are calibrated in terms of air kerma, for instance in a ^{60}Co field. The response of GM counters to photons is constant within 15% for energies up to 2 MeV and shows considerable energy dependence above.

• **Ionization chambers:** Ionization chambers are gas-filled detectors used both as hand-held instruments (*e.g.*, for radiation surveys)

and environmental monitors. They are normally operated in current mode although pulse-mode operation is also possible. They possess a relatively flat response to a wide range of X- and gamma ray energies (typically from 10 keV to several MeV), can measure radiation over a wide intensity range and are capable of discriminating between the beta and gamma components of a radiation field (by use of, *e.g.*, a beta window). Pressurized ion chambers (filled, *e.g.*, with Ar or H gas to several tens of bars) are used for environmental monitoring applications. They have good sensitivity to neutrons and charged hadrons in addition to low LET radiation (gammas and muons), with the response function to the former being strongly non-linear with energy.

• **Scintillators:** Scintillation-based detectors are used in radiation protection as hand-held probes and in fixed installations, *e.g.*, portal monitors. A scintillation detector or counter is obtained coupling a scintillator to an electronic light sensor such as a photomultiplier tube (PMT), a photodiode or a silicon photomultiplier (SiPM). There is a wide range of scintillating materials, inorganic (such as CsI and BGO), organic or plastic; they find application in both photon dosimetry and spectrometry.

36.7.3. *Operation in pulsed radiation fields* :

There are many practical situations with particle accelerators used for scientific, industrial and medical applications where the time structure of the stray radiation limits the use of active monitors. Pulsed neutron and gamma fields may be present because of beam losses at, *e.g.*, targets, collimators and beam dumps. The time duration of a single burst can range from a few ns to about 1 ms with a typical repetition rate in the range 0.1–100Hz. Conventional detectors generally suffer from dead time effects and have strong limitations in the measurements of pulsed fields. Severe under response has been observed, *e.g.*, in commercial rem counters, with tremendous underestimation of the ambient dose equivalent, $H^*(10)$, up to three orders of magnitude. The common techniques used to correct the response of radiation detectors which include dead-time corrections operate properly in a steady-state radiation field, whereas it is much more difficult to cope with dead time losses in a pulsed radiation field of unknown time structure and burst dose. Generally speaking the monitoring instrumentation must be chosen on the basis of the knowledge of the radiation field. Detectors with specifically designed electronics must be employed in pulsed field conditions, such as the recently developed LUPIN [22] in place of conventional rem counters for neutrons. If real-time monitoring is not required, passive detectors or dosimeters such as TEDs mentioned in Sec. 36.7.1 or LiF mentioned in Sec. 36.7.4 can be employed, as they are insensitive to the time structure of the radiation.

36.7.4. *Personal dosimeters* :

Personal dosimeters, calibrated in $H_p(10)$, are worn by persons exposed to ionizing radiation for professional reasons to record the dose received. They are typically passive detectors, either film, track etched detectors, ^{6}Li/^{7}Li-based dosimeters (*e.g.* LiF), optically stimulated luminescence (OSL) or radiophotoluminescence detectors (RPL) but semi-active dosimeters using miniaturized ion-chambers also exist.

Electronic personal dosimeters are small active units for on-line monitoring of individual exposure, designed to be worn on the body. They can give an alarm on both the integral dose received or dose rate once a pre-set threshold is exceeded.

36.8. Monte Carlo codes for radiation protection studies

The use of general-purpose particle interaction and transport Monte Carlo codes is often the most accurate and efficient choice for assessing radiation protection quantities at accelerators. Due to the vast spread of such codes to all areas of particle physics and the associated extensive benchmarking with experimental data, the modeling has reached an unprecedented accuracy. Furthermore, most codes allow the user to simulate all aspects of a high energy particle cascade in one and the same run: from the first interaction of a TeV nucleus over the transport and re-interactions (hadronic and electromagnetic) of the produced secondaries, to detailed nuclear fragmentation, the calculation of radioactive decays and even of the electromagnetic shower caused by the radiation from such decays. A brief account of the codes most widely used for radiation protection studies at high energy accelerators is given in the following.

• **FLUKA [8,9]:** FLUKA is a general-purpose particle interaction and transport code. It comprises all features needed for radiation protection, such as detailed hadronic and nuclear interaction models up to 10 PeV, full coupling between hadronic and electromagnetic processes and numerous variance reduction options. The latter include weight windows, region importance biasing, and leading particle, interaction, and decay length biasing (among others). The capabilities of FLUKA are unique for studies of induced radioactivity, especially with regard to nuclide production, decay, and transport of residual radiation. In particular, particle cascades by prompt and residual radiation are simulated in parallel based on the microscopic models for nuclide production and a solution of the Bateman equations for activity build-up and decay.

• **GEANT4 [23,24,25]:** GEANT4 is an object-oriented toolkit consisting of a kernel that provides the framework for particle transport, including tracking, geometry description, material specifications, management of events and interfaces to external graphics systems. The kernel also provides interfaces to physics processes. It allows the user to freely select the physics models that best serve the particular application needs. Implementations of interaction models exist over an extended range of energies, from optical photons and thermal neutrons to high-energy interactions required for the simulation of accelerator and cosmic ray experiments. To facilitate the use of variance reduction techniques, general-purpose biasing methods such as importance biasing, weight windows, and a weight cut-off method have been introduced directly into the toolkit. Other variance reduction methods, such as leading particle biasing for hadronic processes, come with the respective physics packages.

• **MARS15 [26,27,28]:** The MARS15 code system is a set of Monte Carlo programs for the simulation of hadronic and electromagnetic cascades. It covers a wide energy range: 1 keV to 100 TeV for muons, charged hadrons, heavy ions and electromagnetic showers; and 0.00215 eV to 100 TeV for neutrons. Hadron-nucleus interactions as well as practically all other strong, weak and electromagnetic interactions in the entire energy range can be simulated either inclusively or exclusively. MARS15 uses ENDFB-VII nuclear data to handle interactions of neutrons with energies below 14 MeV. Several variance reduction techniques, such as weight windows, particle splitting, and Russian roulette, are available in MARS15. A tagging module allows one to tag the origin of a given signal for source term or sensitivity analyses. The geometry module allows either a basic solid body representation option or a ROOT-based powerful engine. Further features of MARS15 include a MAD-MARS merge for a convenient creation of accelerator models and multi-turn tracking and cascade simulation in accelerator and beamline lattices.

• **MCNP6 [29,30]:** MCNP6 is the latest version of the Monte Carlo N-Particle transport (MCNP) family of neutron interaction and transport codes and, therefore, features one of the most comprehensive and detailed descriptions of the related physical processes. It transports 37 different particle types, including ions and electromagnetic particles. The neutron interaction and transport modules use standard evaluated data libraries mixed with physics models where such libraries are not available. The transport is continuous in energy. MCNP6 contains one of the most powerful implementations of variance reduction techniques. Spherical mesh weight windows can be created by a generator in order to focus the simulation time on certain spatial regions of interest. In addition, a more generalized phase space biasing is also possible through energy- and time-dependent weight windows. Other biasing options include pulse-height tallies with variance reduction and criticality source convergence acceleration.

• **PHITS [31,32]:** The Particle and Heavy-Ion Transport code System PHITS was among the first general-purpose codes to simulate the transport and interactions of heavy ions in a wide energy range, from 10 MeV/nucleon to 100 GeV/nucleon. It is based on the high-energy hadron transport code NMTC/JAM that was extended to heavy ions.

The transport of low-energy neutrons employs cross sections from evaluated nuclear data libraries such as ENDF and JENDL below 20 MeV. Electromagnetic interactions are simulated based on the ITS code in the energy range between 1 keV and 100 MeV for electrons and positrons and between 1 keV and 100 GeV for photons. Several variance reduction techniques, including weight windows and region importance biasing, are available in PHITS.

References:

1. International Commission on Radiation Units and Measurements, *Fundamental Quantities and Units for Ionizing Radiation*, ICRU Report 60 (1998).
2. ICRP, 2010. *Conversion Coefficients for Radiological Protection Quantities for External Radiation Exposures*, ICRP Publication 116, Annals of the ICRP 40(2-5).
3. ICRP Publication 103, *The 2007 Recommendations of the International Commission on Radiological Protection*, Annals of the ICRP, Elsevier (2007).
4. M. Pelliccioni, Radiation Protection Dosimetry **88**, 279 (2000).
5. E. Pochin, *Nuclear Radiation: Risks and Benefits*, Clarendon Press, Oxford, 1983.
6. United Nations, *Report of the United Nations Scientific Committee on the Effect of Atomic Radiation*, General Assembly, Official Records A/63/46 (2008).
7. W.P. Swanson, *Radiological Safety Aspects of the Operation of Electron Linear Accelerators*, IAEA Technical Reports Series No. 188 (1979).
8. A. Ferrari, *et al.*, FLUKA, A Multi-particle Transport Code (Program Version 2005), CERN-2005-010 (2005), `www.fluka.org`.
9. T.T. Böhlen, *et al.*, The FLUKA code: Developments and Challenges for High Energy and Medical Applications, Nuclear Data Sheets **120**, 211 (2014).
10. R.H. Thomas and G.R. Stevenson, *Radiological Safety Aspects of the Operation of Proton Accelerators,* IAEA Technical Report Series No. 283 (1988).
11. T.A. Gabriel, *et al.*, Nucl. Instrum. Methods **A338**, 336 (1994).
12. `physics.nist.gov/PhysRefData/XrayMassCoef/cover.html`.
13. S. Roesler, *et al.*, "Simulation of Remanent Dose Rates and Benchmark Measurements at the CERN-EU High Energy Reference Field Facility," in *Proceedings of the Sixth International Meeting on Nuclear Applications of Accelerator Technology,* San Diego, CA, 1-5 June 2003, 655–662 (2003).
14. C. Theis and H. Vincke, "The use of ActiWiz in operational radiation protection," in *Proceedings of the Twelfth Meeting of Task-Force on Shielding Aspects of Accelerators, Targets and Irradiation Facilities of Accelerator Technology, SATIF12* FNAL, 28-30 April 2014, Nuclear Science Report NEA/NSC/R 3, (2015).
15. C. Theis and H. Vincke, "ActiWiz3 an overview of the concepts, architecture and new features," CERN Technical Note CERN-RP-2016-117-REPORTS-TN (2016), `actiwiz.web.cern.ch`.
16. I.O. Andersson and J. Braun, A neutron rem counter with uniform sensitivity from 0.025 eV to 10 MeV in *Proceedings of the IAEA Symposium on Neutron dosimetry,* IAEA, Vienna, Vol. II, 87–95, (1963).
17. C. Birattari, *et al.*, Radiation Protection Dosimetry **76**, 135 (1998).
18. R.L. Bramblett, R.I. Ewing and T.W. Bonner, Nuclear Instruments and Methods **9**, 1 (1960).
19. F. d'Errico, Nucl. Instrum. Methods **B184**, 229 (2001).
20. K. Becker, Dosimetric applications of track etching, in *Topics in Radiation Dosimetry* Ed. F.H. Attix, Academic Press, London, 79–143, (1972).
21. G.F. Knoll, *Radiation detection and measurements,* Wiley (2010).
22. M. Caresana, *et al.*, A new version of the LUPIN detector: Improvements and latest experimental verification, Review of Scientific Instruments **85**, 065102 (2014).
23. S. Agostinelli, *et al.*, Nucl. Instrum. Methods **A506**, 250 (2003).
24. J. Allison, *et al.*, IEEE Transactions on Nuclear Science **53**, 270 (2006).
25. J. Allison, *et al.*, Nucl. Instrum. Methods **A835**, 186 (2016), `geant4.cern.ch`.
26. N.V. Mokhov, S.I. Striganov, MARS15 Overview *Proceedings of the Hadronic Shower Simulation Workshop 2006,* Fermilab 6–8 September 2006, M. Albrow, R. Raja, eds., *AIP Conference Proceeding 896*, 50–60, (2007).
27. N.V. Mokhov, MARS Code System, Version 15 (2016), `mars.fnal.gov`.
28. N.V. Mokhov, *et al.*, Prog. Nucl. Sci. Technol. **4**, 496 (2014).
29. D. Pelowitz, *et al.*, Los Alamos National Laboratory report, LA-CP-14-00745 (2014), `mcnp.lanl.gov`.
30. J.T. Goorley, *et al.*, Nuclear Technology **180**, 298 (2012).
31. T. Sato, *et al.*, Journal of Nuclear Science and Technology **50**, 913 (2013).
32. T. Sato, *et al.*, PHITS Particle and Heavy Ion Transport code System, Version 2.88 (2017), `phits.jaea.go.jp`.

37. Commonly Used Radioactive Sources

Table 37.1. Revised August 2017 by D.E. Groom (LBNL) and R.B. Firestone (LBNL).

			Particle		Photon	
Nuclide	Half-life	Type of decay	Energy (MeV)	Emission prob.	Energy (MeV)	Emission prob.
$^{22}_{11}$Na	2.603 y	β^+, EC	0.546	90%	0.511	Annih.
					1.275	100%
$^{51}_{24}$Cr	27.70 d	EC			0.340	10%
					V K x rays	100%
Neutrino calibration source						
$^{54}_{25}$Mn	0.855 y	EC			0.835	100%
					Cr K x rays	26%
$^{55}_{26}$Fe	2.747 y	EC			Mn K x rays:	
					0.00590	24.4%
					0.00649	2.86%
$^{57}_{27}$Co	271.8 d	EC			0.014	9%
					0.122	86%
					0.136	11%
					Fe K x rays	58%
$^{60}_{27}$Co	5.271 y	β^-	0.317	99.9%	1.173	99.9%
					1.333	99.9%
$^{68}_{32}$Ge	271.0 d	EC			Ga K x rays	42%
→ $^{68}_{31}$Ga	67.8 m	β^+, EC	1.899	90%	0.511	Annih.
					1.077	3%
$^{90}_{38}$Sr	28.8 y	β^-	0.546	100%		
→ $^{90}_{39}$Y	2.67 d	β^-	2.279	100%		
$^{106}_{44}$Ru	371.5 d	β^-	0.039	100%		
→ $^{106}_{45}$Rh	30.1 s	β^-	3.546	79%	0.512	21%
					0.622	10%
$^{109}_{48}$Cd	1.265 y	EC	0.063 e^-	42%	0.088	3.7%
			0.084 e^-	44%	Ag K x rays	100%
$^{113}_{50}$Sn	115.1 d	EC	0.364 e^-	28%	0.392	65%
			0.388 e^-	6%	In K x rays	97%
$^{137}_{55}$Cs	30.0 y	β^-	0.514	94%	0.662	85%
			1.176	6%		
$^{133}_{56}$Ba	10.55 y	EC	0.045 e^-	50%	0.081	33%
			0.075 e^-	6%	0.356	62%
					Cs K x rays	121%
$^{152}_{63}$Eu	13.537 y	EC		72.1%	Many γ's	
		β^-		27.9%	0.1218–1.408 MeV	
$^{207}_{83}$Bi	32.9 y	EC	0.481 e^-	2%	0.569	98%
			0.975 e^-	7%	1.063	75%
			1.047 e^-	2%	1.770	7%
					Pb K x rays	78%
$^{228}_{90}$Th	1.912 y	6α:	5.341 to 8.785		0.239	44%
		3β^-:	0.334 to 2.246		0.583	31%
					2.614	36%
(→$^{224}_{88}$Ra	→ $^{220}_{86}$Rn	→ $^{216}_{84}$Po	→ $^{212}_{82}$Pb	→ $^{212}_{83}$Bi	→ $^{212}_{84}$Po)	
(361 d	55.8 s	0.148 s	10.64 h	60.54 m	300 ns)	
$^{241}_{95}$Am	432.6 y	α	5.443	13%	0.060	36%
			5.486	84%	Np L x rays	38%
$^{241}_{95}$Am/Be	432.6 y	6×10^{-5} neutrons ($\langle E \rangle = 4$ MeV) and $4 \times 10^{-5}\gamma$'s (4.43 MeV from $^{9}_{4}$ Be(α, n))				
$^{244}_{96}$Cm	18.11 y	α	5.763	24%	Pu L x rays	$\sim 9\%$
			5.805	76%		
$^{252}_{98}$Cf	2.645 y	α (97%)	6.076	15%		
			6.118	82%		
Fission (3.1%): Average 7.8 γ's/fission; $\langle E_\gamma \rangle = 0.88$ MeV ≈ 4 neutrons/fission; $\langle E_n \rangle = 2.14$ MeV						

"Emission probability" is the probability per decay of a given emission; because of cascades these may total more than 100%. Only principal emissions are listed. EC means electron capture, and e^- means monoenergetic internal conversion (Auger) electron. The intensity of 0.511 MeV e^+e^- annihilation photons depends upon the number of stopped positrons. Endpoint $\beta^\pm$ energies are listed. In some cases when energies are closely spaced, the γ-ray values are approximate weighted averages. Radiation from short-lived daughter isotopes is included where relevant.

Half-lives, energies, and intensities may be found in `www-pub.iaea.org/books/IAEABooks/7551/Update-of-X-Ray-and-Gamma-Ray-Decay-Data-Standards-for-Detector-Calibration-and-Other-Applications` IAEA (2007)
or Nuclear Data Sheets (`www.journals.elsevier.com/nuclear-data-sheets`) (2007).

Neutron sources: See *e.g.* "Neutron Calibration Sources in the Daya Bay Experiment," J. Liu *et al.*, Nuclear Instrum. Methods **A797,** 260 (2005) (arXiv.1504.07911).

$^{51}_{24}$Cr calibration of neutrino detectors is discussed in *e.g.* J.N. Abdurashitov *et al.* [SAGE Collaboration], Phys. Rev. **C59**, 2246 (1999). The use of $^{75}_{34}$Se and other isotopes has also been proposed.

38. Probability

Revised September 2015 by G. Cowan (RHUL).

38.1. General [1–8]

An abstract definition of probability can be given by considering a set S, called the sample space, and possible subsets $A, B, \ldots$, the interpretation of which is left open. The probability P is a real-valued function defined by the following axioms due to Kolmogorov [9]:

1. For every subset A in S, $P(A) \geq 0$;
2. For disjoint subsets (*i.e.*, $A \cap B = \emptyset$), $P(A \cup B) = P(A) + P(B)$;
3. $P(S) = 1$.

In addition, one defines the conditional probability $P(A|B)$ (read as P of A given B) as

$$P(A|B) = \frac{P(A \cap B)}{P(B)} \, . \tag{38.1}$$

From this definition and using the fact that $A \cap B$ and $B \cap A$ are the same, one obtains *Bayes' theorem*,

$$P(A|B) = \frac{P(B|A)P(A)}{P(B)} \, . \tag{38.2}$$

From the three axioms of probability and the definition of conditional probability, one obtains the *law of total probability*,

$$P(B) = \sum_i P(B|A_i)P(A_i) \, , \tag{38.3}$$

for any subset B and for disjoint A_i with $\cup_i A_i = S$. This can be combined with Bayes' theorem (Eq. (38.2)) to give

$$P(A|B) = \frac{P(B|A)P(A)}{\sum_i P(B|A_i)P(A_i)} \, , \tag{38.4}$$

where the subset A could, for example, be one of the A_i.

The most commonly used interpretation of the elements of the sample space are outcomes of a repeatable experiment. The probability $P(A)$ is assigned a value equal to the limiting frequency of occurrence of A. This interpretation forms the basis of *frequentist statistics*.

The elements of the sample space might also be interpreted as *hypotheses*, *i.e.*, statements that are either true or false, such as 'The mass of the W boson lies between 80.3 and 80.5 GeV.' Upon repetition of a measurement, however, such statements are either always true or always false, *i.e.*, the corresponding probabilities in the frequentist interpretation are either 0 or 1. Using *subjective probability*, however, $P(A)$ is interpreted as the degree of belief that the hypothesis A is true. Subjective probability is used in *Bayesian* (as opposed to frequentist) statistics. Bayes' theorem can be written

$$P(\text{theory}|\text{data}) \propto P(\text{data}|\text{theory})P(\text{theory}) \, , \tag{38.5}$$

where 'theory' represents some hypothesis and 'data' is the outcome of the experiment. Here $P(\text{theory})$ is the *prior* probability for the theory, which reflects the experimenter's degree of belief before carrying out the measurement, and $P(\text{data}|\text{theory})$ is the probability to have gotten the data actually obtained, given the theory, which is also called the *likelihood*.

Bayesian statistics provides no fundamental rule for obtaining the prior probability, which may depend on previous measurements, theoretical prejudices, *etc.* Once this has been specified, however, Eq. (38.5) tells how the probability for the theory must be modified in the light of the new data to give the *posterior* probability, $P(\text{theory}|\text{data})$. As Eq. (38.5) is stated as a proportionality, the probability must be normalized by summing (or integrating) over all possible hypotheses.

38.2. Random variables

A *random variable* is a numerical characteristic assigned to an element of the sample space. In the frequency interpretation of probability, it corresponds to an outcome of a repeatable experiment. Let x be a possible outcome of an observation. If x can take on any value from a continuous range, we write $f(x;\theta)dx$ as the probability that the measurement's outcome lies between x and $x + dx$. The function $f(x;\theta)$ is called the *probability density function* (p.d.f.), which may depend on one or more parameters θ. If x can take on only discrete values (*e.g.*, the non-negative integers), then we use $f(x;\theta)$ to denote the probability to find the value x. In the following the term p.d.f. is often taken to cover both the continuous and discrete cases, although technically the term density should only be used in the continuous case.

The p.d.f. is always normalized to unity. Both x and θ may have multiple components and are then often written as vectors. If θ is unknown, we may wish to estimate its value from a given set of measurements of x; this is a central topic of *statistics* (see Sec. 39).

The *cumulative distribution function* $F(a)$ is the probability that $x \leq a$:

$$F(a) = \int_{-\infty}^{a} f(x)\, dx \, . \tag{38.6}$$

Here and below, if x is discrete-valued, the integral is replaced by a sum. The endpoint a is expressly included in the integral or sum. Then $0 \leq F(x) \leq 1$, $F(x)$ is nondecreasing, and $P(a < x \leq b) = F(b) - F(a)$. If x is discrete, $F(x)$ is flat except at allowed values of x, where it has discontinuous jumps equal to $f(x)$.

Any function of random variables is itself a random variable, with (in general) a different p.d.f. The *expectation value* of any function $u(x)$ is

$$E[u(x)] = \int_{-\infty}^{\infty} u(x)\, f(x)\, dx \, , \tag{38.7}$$

assuming the integral is finite. The expectation value is linear, *i.e.*, for any two functions u and v of x and constants c_1 and c_2, $E[c_1 u + c_2 v] = c_1 E[u] + c_2 E[v]$.

The n^{th} moment of a random variable x is

$$\alpha_n \equiv E[x^n] = \int_{-\infty}^{\infty} x^n f(x)\, dx \, , \tag{38.8a}$$

and the n^{th} central moment of x (or moment about the mean, α_1) is

$$m_n \equiv E[(x - \alpha_1)^n] = \int_{-\infty}^{\infty} (x - \alpha_1)^n f(x)\, dx \, . \tag{38.8b}$$

The most commonly used moments are the mean μ and variance σ^2:

$$\mu \equiv \alpha_1 \, , \tag{38.9a}$$

$$\sigma^2 \equiv V[x] \equiv m_2 = \alpha_2 - \mu^2 \, . \tag{38.9b}$$

The mean is the location of the "center of mass" of the p.d.f., and the variance is a measure of the square of its width. Note that $V[cx + k] = c^2 V[x]$. It is often convenient to use the *standard deviation* of x, σ, defined as the square root of the variance.

Any odd moment about the mean is a measure of the skewness of the p.d.f. The simplest of these is the dimensionless coefficient of skewness $\gamma_1 = m_3/\sigma^3$.

The fourth central moment m_4 provides a convenient measure of the tails of a distribution. For the Gaussian distribution (see Sec. 38.4), one has $m_4 = 3\sigma^4$. The *kurtosis* is defined as $\gamma_2 = m_4/\sigma^4 - 3$, *i.e.*, it is zero for a Gaussian, positive for a *leptokurtic* distribution with longer tails, and negative for a *platykurtic* distribution with tails that die off more quickly than those of a Gaussian.

The *quantile* x_α is the value of the random variable x at which the cumulative distribution is equal to α. That is, the quantile is the inverse of the cumulative distribution function, *i.e.*, $x_\alpha = F^{-1}(\alpha)$. An important special case is the *median*, x_{med}, defined by $F(x_{\text{med}}) = 1/2$, *i.e.*, half the probability lies above and half lies below x_{med}. (More rigorously, x_{med} is a median if $P(x \geq x_{\text{med}}) \geq 1/2$ and $P(x \leq x_{\text{med}}) \geq 1/2$. If only one value exists, it is called '*the* median.')

Under a monotonic change of variable $x \to y(x)$, the quantiles of a distribution (and hence also the median) obey $y_\alpha = y(x_\alpha)$. In

general the expectation value and *mode* (most probable value) of a distribution do not, however, transform in this way.

Let x and y be two random variables with a *joint* p.d.f. $f(x,y)$. The *marginal* p.d.f. of x (the distribution of x with y unobserved) is

$$f_1(x) = \int_{-\infty}^{\infty} f(x,y)\,dy\ , \tag{38.10}$$

and similarly for the marginal p.d.f. $f_2(y)$. The *conditional* p.d.f. of y given fixed x (with $f_1(x) \neq 0$) is defined by $f_3(y|x) = f(x,y)/f_1(x)$, and similarly $f_4(x|y) = f(x,y)/f_2(y)$. From these, we immediately obtain Bayes' theorem (see Eqs. (38.2) and (38.4)),

$$f_4(x|y) = \frac{f_3(y|x)f_1(x)}{f_2(y)} = \frac{f_3(y|x)f_1(x)}{\int f_3(y|x')f_1(x')\,dx'}\ . \tag{38.11}$$

The mean of x is

$$\mu_x = \int_{-\infty}^{\infty}\int_{-\infty}^{\infty} x\,f(x,y)\,dx\,dy = \int_{-\infty}^{\infty} x\,f_1(x)\,dx\ , \tag{38.12}$$

and similarly for y. The *covariance* of x and y is

$$\mathrm{cov}[x,y] = E[(x-\mu_x)(y-\mu_y)] = E[xy] - \mu_x\mu_y\ . \tag{38.13}$$

A dimensionless measure of the covariance of x and y is given by the *correlation coefficient*,

$$\rho_{xy} = \mathrm{cov}[x,y]/\sigma_x\sigma_y\ , \tag{38.14}$$

where σ_x and σ_y are the standard deviations of x and y. It can be shown that $-1 \leq \rho_{xy} \leq 1$.

Two random variables x and y are *independent* if and only if

$$f(x,y) = f_1(x)f_2(y)\ . \tag{38.15}$$

If x and y are independent, then $\rho_{xy} = 0$; the converse is not necessarily true. If x and y are independent, $E[u(x)v(y)] = E[u(x)]E[v(y)]$, and $V[x+y] = V[x] + V[y]$; otherwise, $V[x+y] = V[x] + V[y] + 2\mathrm{cov}[x,y]$, and $E[uv]$ does not necessarily factorize.

Consider a set of n continuous random variables $\boldsymbol{x} = (x_1,\ldots,x_n)$ with joint p.d.f. $f(\boldsymbol{x})$, and a set of n new variables $\boldsymbol{y} = (y_1,\ldots,y_n)$, related to $\boldsymbol{x}$ by means of a function $\boldsymbol{y}(\boldsymbol{x})$ that is one-to-one, *i.e.*, the inverse $\boldsymbol{x}(\boldsymbol{y})$ exists. The joint p.d.f. for $\boldsymbol{y}$ is given by

$$g(\boldsymbol{y}) = f(\boldsymbol{x}(\boldsymbol{y}))|J|\ \ , \tag{38.16}$$

where $|J|$ is the absolute value of the determinant of the square matrix $J_{ij} = \partial x_i/\partial y_j$ (the Jacobian determinant). If the transformation from $\boldsymbol{x}$ to $\boldsymbol{y}$ is not one-to-one, the $\boldsymbol{x}$-space must be broken into regions where the function $\boldsymbol{y}(\boldsymbol{x})$ can be inverted, and the contributions to $g(\boldsymbol{y})$ from each region summed.

Given a set of functions $\boldsymbol{y} = (y_1,\ldots,y_m)$ with $m < n$, one can construct $n-m$ additional independent functions, apply the procedure above, then integrate the resulting $g(\boldsymbol{y})$ over the unwanted y_i to find the marginal distribution of those of interest.

For a one-to-one transformation of discrete random variables, the probability is obtained by simple substitution; no Jacobian is necessary because in this case f is a probability rather than a probability density. If the transformation is not one-to-one, then one must sum the probabilities for all values of the original variable that contribute to a given value of the transformed variable. If f depends on a set of parameters $\boldsymbol{\theta}$, a change to a different parameter set $\boldsymbol{\eta}(\boldsymbol{\theta})$ is made by simple substitution; no Jacobian is used.

38.3. Characteristic functions

The characteristic function $\phi(u)$ associated with the p.d.f. $f(x)$ is essentially its Fourier transform, or the expectation value of e^{iux}:

$$\phi(u) = E\left[e^{iux}\right] = \int_{-\infty}^{\infty} e^{iux} f(x)\,dx\ . \tag{38.17}$$

Once $\phi(u)$ is specified, the p.d.f. $f(x)$ is uniquely determined and vice versa; knowing one is equivalent to the other. Characteristic functions are useful in deriving a number of important results about moments and sums of random variables.

It follows from Eqs. (38.8a) and (38.17) that the n^{th} moment of a random variable x that follows $f(x)$ is given by

$$i^{-n}\ \frac{d^n\phi}{du^n}\bigg|_{u=0} = \int_{-\infty}^{\infty} x^n f(x)\,dx = \alpha_n\ . \tag{38.18}$$

Thus it is often easy to calculate all the moments of a distribution defined by $\phi(u)$, even when $f(x)$ cannot be written down explicitly.

If the p.d.f.s $f_1(x)$ and $f_2(y)$ for independent random variables x and y have characteristic functions $\phi_1(u)$ and $\phi_2(u)$, then the characteristic function of the weighted sum $ax+by$ is $\phi_1(au)\phi_2(bu)$. The rules of addition for several important distributions (*e.g.*, that the sum of two Gaussian distributed variables also follows a Gaussian distribution) easily follow from this observation.

Let the (partial) characteristic function corresponding to the conditional p.d.f. $f_2(x|z)$ be $\phi_2(u|z)$, and the p.d.f. of z be $f_1(z)$. The characteristic function after integration over the conditional value is

$$\phi(u) = \int \phi_2(u|z)f_1(z)\,dz\ . \tag{38.19}$$

Suppose we can write ϕ_2 in the form

$$\phi_2(u|z) = A(u)e^{ig(u)z}\ . \tag{38.20}$$

Then

$$\phi(u) = A(u)\phi_1(g(u))\ . \tag{38.21}$$

The cumulants (semi-invariants) κ_n of a distribution with characteristic function $\phi(u)$ are defined by the relation

$$\phi(u) = \exp\left[\sum_{n=1}^{\infty}\frac{\kappa_n}{n!}(iu)^n\right] = \exp\left(i\kappa_1 u - \tfrac{1}{2}\kappa_2 u^2 + \ldots\right)\ . \tag{38.22}$$

The values κ_n are related to the moments α_n and m_n. The first few relations are

$$\begin{aligned}
&\kappa_1 = \alpha_1\ (= \mu, \text{ the mean})\\
&\kappa_2 = m_2\ = \alpha_2 - \alpha_1^2\ (= \sigma^2,\ \text{ the variance})\\
&\kappa_3 = m_3 = \alpha_3 - 3\alpha_1\alpha_2 + 2\alpha_1^3\ .
\end{aligned} \tag{38.23}$$

38.4. Commonly used probability distributions

Table 38.1 gives a number of common probability density functions and corresponding characteristic functions, means, and variances. Further information may be found in Refs. [1– 8], [10], and [11], which has particularly detailed tables. Monte Carlo techniques for generating each of them may be found in our Sec. 40.4 and in Ref. [10]. We comment below on all except the trivial uniform distribution.

38.4.1. *Binomial and multinomial distributions* :

A random process with exactly two possible outcomes which occur with fixed probabilities is called a *Bernoulli* process. If the probability of obtaining a certain outcome (a "success") in an individual trial is p, then the probability of obtaining exactly r successes ($r = 0, 1, 2, \ldots, N$) in N independent trials, without regard to the order of the successes and failures, is given by the binomial distribution $f(r;N,p)$ in Table 38.1. If r and s are binomially distributed with parameters (N_r,p) and (N_s,p), then $t = r+s$ follows a binomial distribution with parameters (N_r+N_s,p).

If there are are m possible outcomes for each trial having probabilities $p_1, p_2, \ldots, p_m$, then the joint probability to find $r_1, r_2, \ldots, r_m$ of each outcome after a total of N independent trials is given by the multinomial distribution as shown in Table 38.1. We can regard outcome i as "success" and all the rest as "failure", so individually, any of the r_i follow a binomial distribution for N trials and a success probability p_i.

38.4.2. ***Poisson distribution*** :

The Poisson distribution $f(n;\nu)$ gives the probability of finding exactly n events in a given interval of x (*e.g.*, space or time) when the events occur independently of one another and of x at an average rate of ν per the given interval. The variance σ^2 equals ν. It is the limiting case $p \to 0$, $N \to \infty$, $Np = \nu$ of the binomial distribution. The Poisson distribution approaches the Gaussian distribution for large ν.

For example, a large number of radioactive nuclei of a given type will result in a certain number of decays in a fixed time interval. If this interval is small compared to the mean lifetime, then the probability for a given nucleus to decay is small, and thus the number of decays in the time interval is well modeled as a Poisson variable.

38.4.3. ***Normal or Gaussian distribution*** :

The normal (or Gaussian) probability density function $f(x;\mu,\sigma^2)$ given in Table 38.1 has mean $E[x] = \mu$ and variance $V[x] = \sigma^2$. Comparison of the characteristic function $\phi(u)$ given in Table 38.1 with Eq. (38.22) shows that all cumulants κ_n beyond κ_2 vanish; this is a unique property of the Gaussian distribution. Some other properties are:

$P(x \text{ in range } \mu \pm \sigma) = 0.6827,$

$P(x \text{ in range } \mu \pm 0.6745\sigma) = 0.5,$

$E[|x-\mu|] = \sqrt{2/\pi}\sigma = 0.7979\sigma,$

half-width at half maximum $= \sqrt{2\ln 2}\,\sigma = 1.177\sigma.$

Table 38.1. Some common probability density functions, with corresponding characteristic functions and means and variances. In the Table, $\Gamma(k)$ is the gamma function, equal to $(k-1)!$ when k is an integer; ${}_1F_1$ is the confluent hypergeometric function of the 1st kind [11].

Distribution	Probability density function f (variable; parameters)	Characteristic function $\phi(u)$	Mean	Variance
Uniform	$f(x;a,b) = \begin{cases} 1/(b-a) & a \le x \le b \\ 0 & \text{otherwise} \end{cases}$	$\dfrac{e^{ibu} - e^{iau}}{(b-a)iu}$	$\dfrac{a+b}{2}$	$\dfrac{(b-a)^2}{12}$
Binomial	$f(r;N,p) = \dfrac{N!}{r!(N-r)!}\, p^r q^{N-r}$ $r = 0,1,2,\ldots,N\ ;\quad 0 \le p \le 1\ ;\quad q = 1-p$	$(q + pe^{iu})^N$	Np	Npq
Multinomial	$f(r_1,\ldots,r_m;N,p_1,\ldots,p_m) = \dfrac{N!}{r_1!\cdots r_m!} p_1^{r_1}\cdots p_m^{r_m}$ $r_k = 0,1,2,\ldots,N\ ;\quad 0 \le p_k \le 1\ ;\quad \sum_{k=1}^m r_k = N$	$\left(\sum_{k=1}^m p_k e^{iu_k}\right)^N$	$E[r_i] = Np_i$	$\text{cov}[r_i,r_j] = Np_i(\delta_{ij} - p_j)$
Poisson	$f(n;\nu) = \dfrac{\nu^n e^{-\nu}}{n!}\ ;\quad n = 0,1,2,\ldots\ ;\quad \nu > 0$	$\exp[\nu(e^{iu}-1)]$	ν	ν
Normal (Gaussian)	$f(x;\mu,\sigma^2) = \dfrac{1}{\sigma\sqrt{2\pi}}\ \exp(-(x-\mu)^2/2\sigma^2)$ $-\infty < x < \infty\ ;\quad -\infty < \mu < \infty\ ;\quad \sigma > 0$	$\exp(i\mu u - \frac{1}{2}\sigma^2 u^2)$	μ	σ^2
Multivariate Gaussian	$f(\boldsymbol{x};\boldsymbol{\mu},V) = \dfrac{1}{(2\pi)^{n/2}\sqrt{\lvert V\rvert}}$ $\times \exp\left[-\frac{1}{2}(\boldsymbol{x}-\boldsymbol{\mu})^T V^{-1}(\boldsymbol{x}-\boldsymbol{\mu})\right]$ $-\infty < x_j < \infty;\quad -\infty < \mu_j < \infty;\quad \lvert V\rvert > 0$	$\exp\left[i\boldsymbol{\mu}\cdot\boldsymbol{u} - \frac{1}{2}\boldsymbol{u}^T V \boldsymbol{u}\right]$	$\boldsymbol{\mu}$	V_{jk}
Log-normal	$f(x;\mu,\sigma^2) = \dfrac{1}{\sigma\sqrt{2\pi}}\dfrac{1}{x}\ \exp(-(\ln x-\mu)^2/2\sigma^2)$ $0 < x < \infty\ ;\quad -\infty < \mu < \infty\ ;\quad \sigma > 0$	—	$\exp(\mu + \sigma^2/2)$	$\exp(2\mu+\sigma^2)$ $\times[\exp(\sigma^2)-1]$
χ^2	$f(z;n) = \dfrac{z^{n/2-1}e^{-z/2}}{2^{n/2}\Gamma(n/2)}\ ;\quad z \ge 0$	$(1-2iu)^{-n/2}$	n	$2n$
Student's t	$f(t;n) = \dfrac{1}{\sqrt{n\pi}}\ \dfrac{\Gamma[(n+1)/2]}{\Gamma(n/2)}\left(1+\dfrac{t^2}{n}\right)^{-(n+1)/2}$ $-\infty < t < \infty\ ;\quad n$ not required to be integer	—	0 for $n > 1$	$n/(n-2)$ for $n > 2$
Gamma	$f(x;\lambda,k) = \dfrac{x^{k-1}\lambda^k e^{-\lambda x}}{\Gamma(k)}\ ;\quad 0 \le x < \infty\ ;$ k not required to be integer	$(1-iu/\lambda)^{-k}$	k/λ	k/λ^2
Beta	$f(x;\alpha,\beta) = \dfrac{\Gamma(\alpha+\beta)}{\Gamma(\alpha)\Gamma(\beta)} x^{\alpha-1}(1-x)^{\beta-1}$ $0 \le x \le 1$	${}_1F_1(\alpha;\alpha+\beta;iu)$	$\dfrac{\alpha}{\alpha+\beta}$	$\dfrac{\alpha\beta}{(\alpha+\beta)^2(\alpha+\beta+1)}$

For a Gaussian with $\mu = 0$ and $\sigma^2 = 1$ (the *standard normal*) the cumulative distribution, often written $\Phi(x)$, is related to the error function erf by

$$F(x; 0, 1) \equiv \Phi(x) = \tfrac{1}{2}\left[1 + \mathrm{erf}(x/\sqrt{2})\right] . \quad (38.24)$$

The error function and standard Gaussian are tabulated in many references (*e.g.*, Ref. [11,12]) and are available in software packages such as ROOT [13]. For a mean μ and variance σ^2, replace x by $(x - \mu)/\sigma$. The probability of x in a given range can be calculated with Eq. (39.70).

For x and y independent and normally distributed, $z = ax + by$ follows a normal p.d.f. $f(z; a\mu_x + b\mu_y, a^2\sigma_x^2 + b^2\sigma_y^2)$; that is, the weighted means and variances add.

The Gaussian derives its importance in large part from the *central limit theorem*:

If independent random variables $x_1, \ldots, x_n$ are distributed according to *any* p.d.f. with finite mean and variance, then the sum $y = \sum_{i=1}^{n} x_i$ will have a p.d.f. that approaches a Gaussian for large n. If the p.d.f.s of the x_i are not identical, the theorem still holds under somewhat more restrictive conditions. The mean and variance are given by the sums of corresponding terms from the individual x_i. Therefore, the sum of a large number of fluctuations x_i will be distributed as a Gaussian, even if the x_i themselves are not.

For a set of n Gaussian random variables $\boldsymbol{x}$ with means $\boldsymbol{\mu}$ and covariances $V_{ij} = \mathrm{cov}[x_i, x_j]$, the p.d.f. for the one-dimensional Gaussian is generalized to

$$f(\boldsymbol{x}; \boldsymbol{\mu}, V) = \frac{1}{(2\pi)^{n/2}\sqrt{|V|}} \exp\left[-\tfrac{1}{2}(\boldsymbol{x} - \boldsymbol{\mu})^T V^{-1} (\boldsymbol{x} - \boldsymbol{\mu})\right] , \quad (38.25)$$

where the determinant $|V|$ must be greater than 0. For diagonal V (independent variables), $f(\boldsymbol{x}; \boldsymbol{\mu}, V)$ is the product of the p.d.f.s of n Gaussian distributions.

For $n = 2$, $f(\boldsymbol{x}; \boldsymbol{\mu}, V)$ is

$$f(x_1, x_2;\ \mu_1, \mu_2, \sigma_1, \sigma_2, \rho) = \frac{1}{2\pi\sigma_1\sigma_2\sqrt{1-\rho^2}}$$

$$\times \exp\left\{\frac{-1}{2(1-\rho^2)}\left[\frac{(x_1-\mu_1)^2}{\sigma_1^2} \ \frac{2\rho(x_1-\mu_1)(x_2-\mu_2)}{\sigma_1\sigma_2} \ + \frac{(x_2-\mu_2)^2}{\sigma_2^2}\right]\right\} . \quad (38.26)$$

The characteristic function for the multivariate Gaussian is

$$\phi(\boldsymbol{u}; \boldsymbol{\mu}, V) = \exp\left[i\boldsymbol{\mu}\cdot\boldsymbol{u} - \tfrac{1}{2}\boldsymbol{u}^T V \boldsymbol{u}\right] . \quad (38.27)$$

If the components of $\boldsymbol{x}$ are independent, then Eq. (38.27) is the product of the characteristic functions of n Gaussians.

For an n-dimensional Gaussian distribution for $\boldsymbol{x}$ with mean $\boldsymbol{\mu}$ and covariance matrix V, the marginal distribution for any single x_i is is a one-dimensional Gaussian with mean μ_i and variance V_{ii}. The equation $(\boldsymbol{x} - \boldsymbol{a})^T V^{-1} (\boldsymbol{x} - \boldsymbol{a}) = C$, where C is any positive number, defines an n-dimensional ellipse centered about $\boldsymbol{a}$. If $\boldsymbol{a}$ is equal to the mean $\boldsymbol{\mu}$, then C is a random variable obeying the χ^2 distribution for n degrees of freedom, which is discussed in the following section. The probability that $\boldsymbol{x}$ lies outside the ellipsoid for a given value of C is given by $1 - F_{\chi^2}(C; n)$, where F_{χ^2} is the cumulative χ^2 distribution. This may be read from Fig. 39.1. For example, the "s-standard-deviation ellipsoid" occurs at $C = s^2$. For the two-variable case ($n = 2$), the point $\boldsymbol{x}$ lies outside the one-standard-deviation ellipsoid with 61% probability. The use of these ellipsoids as indicators of probable error is described in Sec. 39.4.2.2; the validity of those indicators assumes that $\boldsymbol{\mu}$ and V are correct.

38.4.4. *Log-normal distribution* :

If a random variable y follows a Gaussian distribution with mean μ and variance σ^2, then $x = e^y$ follows a log-normal distribution, as given in Table 38.1. As a consequence of the central limit theorem described in Sec. 38.4.3, the distribution of the product of a large number of positive random variables approaches a log-normal. It is bounded below by zero and is thus well suited for modeling quantities that are intrinsically non-negative such as an efficiency. One can implement a log-normal model for a random variable x by defining $y = \ln x$ so that y follows a Gaussian distribution.

38.4.5. χ^2 *distribution* :

If $x_1, \ldots, x_n$ are independent Gaussian random variables, the sum $z = \sum_{i=1}^{n} (x_i - \mu_i)^2/\sigma_i^2$ follows the χ^2 p.d.f. with n *degrees of freedom*, which we denote by $\chi^2(n)$. More generally, for n correlated Gaussian variables as components of a vector $\boldsymbol{X}$ with covariance matrix V, $z = \boldsymbol{X}^T V^{-1} \boldsymbol{X}$ follows $\chi^2(n)$ as in the previous section. For a set of z_i, each of which follows $\chi^2(n_i)$, $\sum z_i$ follows $\chi^2(\sum n_i)$. For large n, the χ^2 p.d.f. approaches a Gaussian with a mean and variance given by $\mu = n$ and $\sigma^2 = 2n$, respectively (here the formulae for μ and σ^2 are valid for all n).

The χ^2 p.d.f. is often used in evaluating the level of compatibility between observed data and a hypothesis for the p.d.f. that the data might follow. This is discussed further in Sec. 39.3.2 on significance tests.

38.4.6. *Student's t distribution* :

Suppose that y and $x_1, \ldots, x_n$ are independent and Gaussian distributed with mean 0 and variance 1. We then define

$$z = \sum_{i=1}^{n} x_i^2 \quad \text{and} \quad t = \frac{y}{\sqrt{z/n}} . \quad (38.28)$$

The variable z thus follows a $\chi^2(n)$ distribution. Then t is distributed according to Student's t distribution with n degrees of freedom, $f(t; n)$, given in Table 38.1.

If defined through gamma functions as in Table 38.1, the parameter n is not required to be an integer. As $n \to \infty$, the distribution approaches a Gaussian, and for $n = 1$ it is a *Cauchy* or *Breit–Wigner* distribution.

As an example, consider the *sample mean* $\overline{x} = \sum x_i/n$ and the *sample variance* $s^2 = \sum (x_i - \overline{x})^2/(n-1)$ for normally distributed x_i with unknown mean μ and variance σ^2. The sample mean has a Gaussian distribution with a variance σ^2/n, so the variable $(\overline{x} - \mu)/\sqrt{\sigma^2/n}$ is normal with mean 0 and variance 1. The quantity $(n-1)s^2/\sigma^2$ is independent of this and follows $\chi^2(n-1)$. The ratio

$$t = \frac{(\overline{x} - \mu)/\sqrt{\sigma^2/n}}{\sqrt{(n-1)s^2/\sigma^2(n-1)}} = \frac{\overline{x} - \mu}{\sqrt{s^2/n}} \quad (38.29)$$

is distributed as $f(t; n-1)$. The unknown variance σ^2 cancels, and t can be used to test the hypothesis that the true mean is some particular value μ.

38.4.7. *Gamma distribution* :

For a process that generates events as a function of x (*e.g.*, space or time) according to a Poisson distribution, the distance in x from an arbitrary starting point (which may be some particular event) to the k^{th} event follows a *gamma* distribution, $f(x; \lambda, k)$. The Poisson parameter μ is λ per unit x. The special case $k = 1$ (*i.e.*, $f(x; \lambda, 1) = \lambda e^{-\lambda x}$) is called the *exponential* distribution. A sum of k' exponential random variables x_i is distributed as $f(\sum x_i; \lambda, k')$.

The parameter k is not required to be an integer. For $\lambda = 1/2$ and $k = n/2$, the gamma distribution reduces to the $\chi^2(n)$ distribution.

38.4.8. *Beta distribution* :

The beta distribution describes a continuous random variable x in the interval $[0, 1]$. By scaling and translation one can easily generalize it to have arbitrary endpoints. In Bayesian inference about the parameter p of a binomial process, if the prior p.d.f. is a beta distribution $f(p; \alpha, \beta)$ then the observation of r successes out of N trials gives a posterior beta distribution $f(p; r+\alpha, N-r+\beta)$ (Bayesian methods are discussed further in Sec. 39). The uniform distribution is a beta distribution with $\alpha = \beta = 1$.

References:

1. H. Cramér, *Mathematical Methods of Statistics,* (Princeton Univ. Press, New Jersey, 1958).
2. A. Stuart and J.K. Ord, *Kendall's Advanced Theory of Statistics*, Vol. 1 *Distribution Theory* 6th Ed., (Halsted Press, New York, 1994), and earlier editions by Kendall and Stuart.

3. F.E. James, *Statistical Methods in Experimental Physics*, 2nd Ed., (World Scientific, Singapore, 2006).
4. L. Lyons, *Statistics for Nuclear and Particle Physicists*, (Cambridge University Press, New York, 1986).
5. B.R. Roe, *Probability and Statistics in Experimental Physics,* 2nd Ed., (Springer, New York, 2001).
6. R.J. Barlow, *Statistics: A Guide to the Use of Statistical Methods in the Physical Sciences*, (John Wiley, New York, 1989).
7. S. Brandt, *Data Analysis*, 3rd Ed., (Springer, New York, 1999).
8. G. Cowan, *Statistical Data Analysis*, (Oxford University Press, Oxford, 1998).
9. A.N. Kolmogorov, *Grundbegriffe der Wahrscheinlichkeitsrechnung*, (Springer, Berlin, 1933); *Foundations of the Theory of Probability*, 2nd Ed., (Chelsea, New York 1956).
10. Ch. Walck, *Hand-book on Statistical Distributions for Experimentalists*, University of Stockholm Internal Report SUF-PFY/96-01, available from `www.physto.se/~walck`.
11. M. Abramowitz and I. Stegun, eds., *Handbook of Mathematical Functions*, (Dover, New York, 1972).
12. F.W.J. Olver *et al.*, eds., NIST Handbook of Mathematical Functions, (Cambridge University Press, 2010); a companion Digital Library of Mathematical Functions is available at `dlmf.nist.gov`.
13. Rene Brun and Fons Rademakers, Nucl. Instrum. Methods **A389**, 81 (1997); see also `root.cern.ch`.

39. Statistics

Revised September 2017 by G. Cowan (RHUL).

This chapter gives an overview of statistical methods used in high-energy physics. In statistics, we are interested in using a given sample of data to make inferences about a probabilistic model, *e.g.*, to assess the model's validity or to determine the values of its parameters. There are two main approaches to statistical inference, which we may call frequentist and Bayesian.

In frequentist statistics, probability is interpreted as the frequency of the outcome of a repeatable experiment. The most important tools in this framework are parameter estimation, covered in Section 39.2, statistical tests, discussed in Section 39.3, and confidence intervals, which are constructed so as to cover the true value of a parameter with a specified probability, as described in Section 39.4.2. Note that in frequentist statistics one does not define a probability for a hypothesis or for the value of a parameter.

In Bayesian statistics, the interpretation of probability is more general and includes *degree of belief* (called subjective probability). One can then speak of a probability density function (p.d.f.) for a parameter, which expresses one's state of knowledge about where its true value lies. Bayesian methods provide a natural means to include additional information, which in general may be subjective; in fact they *require* prior probabilities for the hypotheses (or parameters) in question, *i.e.*, the degree of belief about the parameters' values, before carrying out the measurement. Using Bayes' theorem (Eq. (38.4)), the prior degree of belief is updated by the data from the experiment. Bayesian methods for interval estimation are discussed in Sections 39.4.1 and 39.4.2.4.

For many inference problems, the frequentist and Bayesian approaches give similar numerical values, even though they answer different questions and are based on fundamentally different interpretations of probability. In some important cases, however, the two approaches may yield very different results. For a discussion of Bayesian vs. non-Bayesian methods, see references written by a statistician [1], by a physicist [2], or the detailed comparison in Ref. [3].

39.1. Fundamental concepts

Consider an experiment whose outcome is characterized by one or more data values, which we can write as a vector $\boldsymbol{x}$. A *hypothesis* H is a statement about the probability for the data, often written $P(\boldsymbol{x}|H)$. (We will usually use a capital letter for a probability and lower case for a probability density. Often the term p.d.f. is used loosely to refer to either a probability or a probability density.) This could, for example, define completely the p.d.f. for the data (a *simple* hypothesis), or it could specify only the functional form of the p.d.f., with the values of one or more parameters not determined (a *composite* hypothesis).

If the probability $P(\boldsymbol{x}|H)$ for data $\boldsymbol{x}$ is regarded as a function of the hypothesis H, then it is called the *likelihood* of H, usually written $L(H)$. Often the hypothesis is characterized by one or more parameters $\boldsymbol{\theta}$, in which case $L(\boldsymbol{\theta}) = P(\boldsymbol{x}|\boldsymbol{\theta})$ is called the likelihood function.

In some cases one can obtain at least approximate frequentist results using the likelihood evaluated only with the data obtained. In general, however, the frequentist approach requires a full specification of the probability model $P(\boldsymbol{x}|H)$ both as a function of the data $\boldsymbol{x}$ and hypothesis H.

In the Bayesian approach, inference is based on the posterior probability for H given the data $\boldsymbol{x}$, which represents one's degree of belief that H is true given the data. This is obtained from Bayes' theorem (38.4), which can be written

$$P(H|\boldsymbol{x}) = \frac{P(\boldsymbol{x}|H)\pi(H)}{\int P(\boldsymbol{x}|H')\pi(H')\,dH'}\,. \tag{39.1}$$

Here $P(\boldsymbol{x}|H)$ is the likelihood for H, which depends only on the data actually obtained. The quantity $\pi(H)$ is the prior probability for H, which represents one's degree of belief for H before carrying out the measurement. The integral in the denominator (or sum, for discrete hypotheses) serves as a normalization factor. If H is characterized by a continuous parameter θ then the posterior probability is a p.d.f. $p(\theta|\boldsymbol{x})$. Note that the likelihood function itself is not a p.d.f. for θ.

39.2. Parameter estimation

Here we review *point estimation* of parameters, first with an overview of the frequentist approach and its two most important methods, maximum likelihood and least squares, treated in Sections 39.2.2 and 39.2.3. The Bayesian approach is outlined in Sec. 39.2.5.

An *estimator* $\widehat{\theta}$ (written with a hat) is a function of the data used to estimate the value of the parameter θ. Sometimes the word 'estimate' is used to denote the value of the estimator when evaluated with given data. There is no fundamental rule dictating how an estimator must be constructed. One tries, therefore, to choose that estimator which has the best properties. The most important of these are (a) *consistency*, (b) *bias*, (c) *efficiency*, and (d) *robustness*.

(a) An estimator is said to be *consistent* if the estimate $\widehat{\theta}$ converges in probability (see Ref. [3]) to the true value θ as the amount of data increases. This property is so important that it is possessed by all commonly used estimators.

(b) The *bias*, $b = E[\widehat{\theta}] - \theta$, is the difference between the expectation value of the estimator and the true value of the parameter. The expectation value is taken over a hypothetical set of similar experiments in which $\widehat{\theta}$ is constructed in the same way. When $b = 0$, the estimator is said to be unbiased. The bias depends on the chosen metric, *i.e.*, if $\widehat{\theta}$ is an unbiased estimator of θ, then $\widehat{\theta}^{\,2}$ is not in general an unbiased estimator for θ^2.

(c) *Efficiency* is the ratio of the minimum possible variance for any estimator of θ to the variance $V[\widehat{\theta}]$ of the estimator $\widehat{\theta}$. For the case of a single parameter, under rather general conditions the minimum variance is given by the Rao-Cramér-Fréchet bound,

$$\sigma^2_{\rm min} = \left(1 + \frac{\partial b}{\partial \theta}\right)^2 / I(\theta)\,, \tag{39.2}$$

where

$$I(\theta) = E\left[\left(\frac{\partial \ln L}{\partial \theta}\right)^2\right] = -E\left[\frac{\partial^2 \ln L}{\partial \theta^2}\right] \tag{39.3}$$

is the *Fisher information*, L is the likelihood, and the operator $E[]$ in (39.3) is the expectation value with respect to the data. For the final equality to hold, the range of allowed data values must not depend on θ.

The *mean-squared error*,

$$\text{MSE} = E[(\widehat{\theta} - \theta)^2] = V[\widehat{\theta}] + b^2\,, \tag{39.4}$$

is a measure of an estimator's quality which combines bias and variance.

(d) *Robustness* is the property of being insensitive to departures from assumptions in the p.d.f., *e.g.*, owing to uncertainties in the distribution's tails.

It is not in general possible to optimize simultaneously for all the measures of estimator quality described above. For example, there is in general a trade-off between bias and variance. For some common estimators, the properties above are known exactly. More generally, it is possible to evaluate them by Monte Carlo simulation. Note that they will in general depend on the unknown θ.

39.2.1. *Estimators for mean, variance, and median* :

Suppose we have a set of n independent measurements, $x_1, \ldots, x_n$, each assumed to follow a p.d.f. with unknown mean μ and unknown variance σ^2 (the measurements do not necessarily have to follow a Gaussian distribution). Then

$$\widehat{\mu} = \frac{1}{n}\sum_{i=1}^{n} x_i \tag{39.5}$$

$$\widehat{\sigma^2} = \frac{1}{n-1}\sum_{i=1}^{n}(x_i - \widehat{\mu})^2 \tag{39.6}$$

are unbiased estimators of μ and σ^2. The variance of $\widehat{\mu}$ is σ^2/n and the variance of $\widehat{\sigma^2}$ is

$$V\left[\widehat{\sigma^2}\right] = \frac{1}{n}\left(m_4 - \frac{n-3}{n-1}\sigma^4\right) , \tag{39.7}$$

where m_4 is the 4^{th} central moment of x (see Eq. (38.8b)). For Gaussian distributed x_i, this becomes $2\sigma^4/(n-1)$ for any $n \geq 2$, and for large n the standard deviation of $\widehat{\sigma}$ is $\sigma/\sqrt{2n}$. For any n and Gaussian x_i, $\widehat{\mu}$ is an efficient estimator for μ, and the estimators $\widehat{\mu}$ and $\widehat{\sigma^2}$ are uncorrelated. Otherwise the arithmetic mean (39.5) is not necessarily the most efficient estimator; this is discussed further in Sec. 8.7 of Ref. [4].

If σ^2 is known, it does not improve the estimate $\widehat{\mu}$, as can be seen from Eq. (39.5); however, if μ is known, one can substitute it for $\widehat{\mu}$ in Eq. (39.6) and replace $n-1$ by n to obtain an estimator of σ^2 still with zero bias but smaller variance. If the x_i have different, known variances σ_i^2, then the weighted average

$$\widehat{\mu} = \frac{1}{w}\sum_{i=1}^{n} w_i x_i , \tag{39.8}$$

where $w_i = 1/\sigma_i^2$ and $w = \sum_i w_i$, is an unbiased estimator for μ with a smaller variance than an unweighted average. The standard deviation of $\widehat{\mu}$ is $1/\sqrt{w}$.

As an estimator for the median x_{med}, one can use the value $\widehat{x}_{\text{med}}$ such that half the x_i are below and half above (the sample median). If there are an even number of observations and the sample median lies between two observed values, the estimator is set by convention to their arithmetic average. If the p.d.f. of x has the form $f(x-\mu)$ and μ is both mean and median, then for large n the variance of the sample median approaches $1/[4nf^2(0)]$, provided $f(0) > 0$. Although estimating the median can often be more difficult computationally than the mean, the resulting estimator is generally more robust, as it is insensitive to the exact shape of the tails of a distribution.

39.2.2. *The method of maximum likelihood* :

Suppose we have a set of measured quantities $\boldsymbol{x}$ and the likelihood $L(\boldsymbol{\theta}) = P(\boldsymbol{x}|\boldsymbol{\theta})$ for a set of parameters $\boldsymbol{\theta} = (\theta_1, \ldots, \theta_N)$. The *maximum likelihood* (ML) estimators for $\boldsymbol{\theta}$ are defined as the values that give the maximum of L. Because of the properties of the logarithm, it is usually easier to work with $\ln L$, and since both are maximized for the same parameter values $\boldsymbol{\theta}$, the ML estimators can be found by solving the *likelihood equations*,

$$\frac{\partial \ln L}{\partial \theta_i} = 0 , \qquad i = 1, \ldots, N . \tag{39.9}$$

Often the solution must be found numerically. Maximum likelihood estimators are important because they are unbiased and efficient asymptotically (*i.e.*, for large data samples), under quite general conditions, and the method has a wide range of applicability.

In general the likelihood function is obtained from the probability of the data under assumption of the parameters. An important special case is when the data consist of *i.i.d.* (independent and identically distributed) values. Here one has a set of n statistically independent quantities $\boldsymbol{x} = (x_1, \ldots, x_n)$, where each component follows the same p.d.f. $f(x;\boldsymbol{\theta})$. In this case the joint p.d.f. of the data sample factorizes and the likelihood function is

$$L(\boldsymbol{\theta}) = \prod_{i=1}^{n} f(x_i;\boldsymbol{\theta}) . \tag{39.10}$$

In this case the number of events n is regarded as fixed. If however the probability to observe n events itself depends on the parameters $\boldsymbol{\theta}$, then this dependence should be included in the likelihood. For example, if n follows a Poisson distribution with mean μ and the independent x values all follow $f(x;\boldsymbol{\theta})$, then the likelihood becomes

$$L(\boldsymbol{\theta}) = \frac{\mu^n}{n!}e^{-\mu}\prod_{i=1}^{n} f(x_i;\boldsymbol{\theta}) . \tag{39.11}$$

Equation (39.11) is often called the *extended likelihood* (see, *e.g.*, Refs. [6–8]). If μ is given as a function of $\boldsymbol{\theta}$, then including the probability for n given $\boldsymbol{\theta}$ in the likelihood provides additional information about the parameters. This therefore leads to a reduction in their statistical uncertainties and in general changes their estimated values.

In evaluating the likelihood function, it is important that any normalization factors in the p.d.f. that involve $\boldsymbol{\theta}$ be included. However, we will only be interested in the maximum of L and in ratios of L at different values of the parameters; hence any multiplicative factors that do not involve the parameters that we want to estimate may be dropped, including factors that depend on the data but not on $\boldsymbol{\theta}$.

Under a one-to-one change of parameters from $\boldsymbol{\theta}$ to $\boldsymbol{\eta}$, the ML estimators $\widehat{\boldsymbol{\theta}}$ transform to $\boldsymbol{\eta}(\widehat{\boldsymbol{\theta}})$. That is, the ML solution is invariant under change of parameter. However, other properties of ML estimators, in particular the bias, are not invariant under change of parameter.

The inverse V^{-1} of the covariance matrix $V_{ij} = \text{cov}[\widehat{\theta}_i, \widehat{\theta}_j]$ for a set of ML estimators can be estimated by using

$$(\widehat{V}^{-1})_{ij} = -\left.\frac{\partial^2 \ln L}{\partial\theta_i \partial\theta_j}\right|_{\widehat{\theta}} . \tag{39.12}$$

For finite samples, however, Eq. (39.12) can result in a misestimation of the variances. In the large sample limit (or in a linear model with Gaussian data), L has a Gaussian form and $\ln L$ is (hyper)parabolic. In this case, s times the standard deviations σ_i of the estimators for the parameters can be obtained from the hypersurface defined by the $\boldsymbol{\theta}$ such that

$$\ln L(\boldsymbol{\theta}) = \ln L_{\max} - s^2/2 , \tag{39.13}$$

where $\ln L_{\max}$ is the value of $\ln L$ at the solution point (compare with Eq. (39.73)). The minimum and maximum values of θ_i on the hypersurface then give an approximate s-standard deviation confidence interval for θ_i (see Section 39.4.2.2).

39.2.2.1. *ML with binned data:*

If the total number of data values x_i, $(i = 1, \ldots, n_{\text{tot}})$, is small, the unbinned maximum likelihood method, *i.e.*, use of Equation (39.10) (or (39.11) for extended ML), is preferred since binning can only result in a loss of information, and hence larger statistical errors for the parameter estimates. If the sample is large, it can be convenient to bin the values in a histogram with N bins, so that one obtains a vector of data $\boldsymbol{n} = (n_1, \ldots, n_N)$ with expectation values $\boldsymbol{\mu} = E[\boldsymbol{n}]$ and probabilities $f(\boldsymbol{n};\boldsymbol{\mu})$. Suppose the mean values $\boldsymbol{\mu}$ can be determined as a function of a set of parameters $\boldsymbol{\theta}$. Then one may maximize the likelihood function based on the contents of the bins.

As mentioned in Sec. 39.2.2, the total number of events $n_{\text{tot}} = \sum_i n_i$ can be regarded either as fixed or as a random variable. If it is fixed, the histogram follows a multinomial distribution,

$$f_{\text{M}}(\boldsymbol{n};\boldsymbol{\theta}) = \frac{n_{\text{tot}}!}{n_1! \cdots n_N!} p_1^{n_1} \cdots p_N^{n_N} , \tag{39.14}$$

where we assume the probabilities p_i are given functions of the parameters $\boldsymbol{\theta}$. The distribution can be written equivalently in terms of the expected number of events in each bin, $\mu_i = n_{\text{tot}} p_i$. If the n_i are regarded as independent and Poisson distributed, then the data are instead described by a product of Poisson probabilities,

$$f_{\text{P}}(\boldsymbol{n};\boldsymbol{\theta}) = \prod_{i=1}^{N} \frac{\mu_i^{n_i}}{n_i!} e^{-\mu_i} , \tag{39.15}$$

where the mean values μ_i are given functions of $\boldsymbol{\theta}$. The total number of events n_{tot} thus follows a Poisson distribution with mean $\mu_{\text{tot}} = \sum_i \mu_i$.

When using maximum likelihood with binned data, one can find the ML estimators and at the same time obtain a statistic usable for a test of goodness-of-fit (see Sec. 39.3.2). Maximizing the likelihood $L(\boldsymbol{\theta}) = f_{\text{M/P}}(\boldsymbol{n};\boldsymbol{\theta})$ is equivalent to maximizing the likelihood ratio $\lambda(\boldsymbol{\theta}) = f_{\text{M/P}}(\boldsymbol{n};\boldsymbol{\theta})/f(\boldsymbol{n};\hat{\boldsymbol{\mu}})$, where in the denominator $f(\boldsymbol{n};\boldsymbol{\mu})$ is a

model with an adjustable parameter for each bin, $\boldsymbol{\mu} = (\mu_1, \ldots, \mu_N)$, and the corresponding estimators are $\hat{\boldsymbol{\mu}} = (n_1, \ldots, n_N)$. Equivalently one often minimizes the quantity $-2\ln\lambda(\boldsymbol{\theta})$. For independent Poisson distributed n_i this is [9]

$$-2\ln\lambda(\boldsymbol{\theta}) = 2\sum_{i=1}^{N}\left[\mu_i(\boldsymbol{\theta}) - n_i + n_i\ln\frac{n_i}{\mu_i(\boldsymbol{\theta})}\right] , \tag{39.16}$$

where for bins with $n_i = 0$, the last term in (39.16) is zero. The expression (39.16) without the terms $\mu_i - n_i$ also gives $-2\ln\lambda(\boldsymbol{\theta})$ for multinomially distributed n_i, *i.e.*, when the total number of entries is regarded as fixed. In the limit of zero bin width, minimizing (39.16) is equivalent to maximizing the unbinned extended likelihood function (39.11); in the corresponding multinomial case without the $\mu_i - n_i$ terms one obtains Eq. (39.10).

A smaller value of $-2\ln\lambda(\widehat{\boldsymbol{\theta}})$ corresponds to better agreement between the data and the hypothesized form of $\boldsymbol{\mu}(\boldsymbol{\theta})$. The value of $-2\ln\lambda(\widehat{\boldsymbol{\theta}})$ can thus be translated into a p-value as a measure of goodness-of-fit, as described in Sec. 39.3.2. Assuming the model is correct, then according to Wilks' theorem [10], for sufficiently large μ_i and provided certain regularity conditions are met, the minimum of $-2\ln\lambda$ as defined by Eq. (39.16) follows a χ^2 distribution (see, *e.g.*, Ref. [9]) . If there are N bins and m fitted parameters, then the number of degrees of freedom for the χ^2 distribution is $N - m$ if the data are treated as Poisson-distributed, and $N - m - 1$ if the n_i are multinomially distributed.

Suppose the n_i are Poisson-distributed and the overall normalization $\mu_{\rm tot} = \sum_i \mu_i$ is taken as an adjustable parameter, so that $\mu_i = \mu_{\rm tot} p_i(\boldsymbol{\theta})$, where the probability to be in the ith bin, $p_i(\boldsymbol{\theta})$, does not depend on $\mu_{\rm tot}$. Then by minimizing Eq. (39.16), one obtains that the area under the fitted function is equal to the sum of the histogram contents, *i.e.*, $\sum_i \hat{\mu}_i = \sum_i n_i$. This is a property not possessed by the estimators from the method of least squares (see, *e.g.*, Sec. 39.2.3 and Ref. [8]) .

39.2.2.2. *Frequentist treatment of nuisance parameters:*

Suppose we want to determine the values of parameters $\boldsymbol{\theta}$ using a set of measurements $\boldsymbol{x}$ described by a probability model $P_x(\boldsymbol{x}|\boldsymbol{\theta})$. In general the model is not perfect, which is to say it can not provide an accurate description of the data even at the most optimal point of its parameter space. As a result, the estimated parameters can have a systematic bias.

One can improve the model by including in it additional parameters. That is, $P_x(\boldsymbol{x}|\boldsymbol{\theta})$ is replaced by a more general model $P_x(\boldsymbol{x}|\boldsymbol{\theta},\boldsymbol{\nu})$, which depends on parameters of interest $\boldsymbol{\theta}$ and *nuisance parameters* $\boldsymbol{\nu}$. The additional parameters are not of intrinsic interest but must be included for the model to be accurate for some point in the enlarged parameter space.

Although including additional parameters may eliminate or at least reduce the effect of systematic uncertainties, their presence will result in increased statistical uncertainties for the parameters of interest. This occurs because the estimators for the nuisance parameters and those of interest will in general be correlated, which results in an enlargement of the contour defined by Eq. (39.13).

To reduce the impact of the nuisance parameters one often tries to constrain their values by means of control or calibration measurements, say, having data $\boldsymbol{y}$. For example, some components of $\boldsymbol{y}$ could represent estimates of the nuisance parameters, often from separate experiments. Suppose the measurements $\boldsymbol{y}$ are statistically independent from $\boldsymbol{x}$ and are described by a model $P_y(\boldsymbol{y}|\boldsymbol{\nu})$. The joint model for both $\boldsymbol{x}$ and $\boldsymbol{y}$ is in this case therefore the product of the probabilities for $\boldsymbol{x}$ and $\boldsymbol{y}$, and thus the likelihood function for the full set of parameters is

$$L(\boldsymbol{\theta},\boldsymbol{\nu}) = P_x(\boldsymbol{x}|\boldsymbol{\theta},\boldsymbol{\nu})P_y(\boldsymbol{y}|\boldsymbol{\nu}) . \tag{39.17}$$

Note that in this case if one wants to simulate the experiment by means of Monte Carlo, both the primary and control measurements, $\boldsymbol{x}$ and $\boldsymbol{y}$, must be generated for each repetition under assumption of fixed values for the parameters $\boldsymbol{\theta}$ and $\boldsymbol{\nu}$.

Using all of the parameters $(\boldsymbol{\theta},\boldsymbol{\nu})$ in Eq. (39.13) to find the statistical errors in the parameters of interest $\boldsymbol{\theta}$ is equivalent to using the *profile likelihood*, which depends only on $\boldsymbol{\theta}$. It is defined as

$$L_{\rm p}(\boldsymbol{\theta}) = L(\boldsymbol{\theta},\widehat{\widehat{\boldsymbol{\nu}}}(\boldsymbol{\theta})), \tag{39.18}$$

where the double-hat notation indicates the profiled values of the parameters $\boldsymbol{\nu}$, defined as the values that maximize L for the specified $\boldsymbol{\theta}$. The profile likelihood is discussed further in Section 39.3.2.1 in connection with hypothesis tests.

39.2.3. ***The method of least squares*** :

The *method of least squares* (LS) coincides with the method of maximum likelihood in the following special case. Consider a set of N independent measurements y_i at known points x_i. The measurement y_i is assumed to be Gaussian distributed with mean $\mu(x_i;\boldsymbol{\theta})$ and known variance σ_i^2. The goal is to construct estimators for the unknown parameters $\boldsymbol{\theta}$. The log-likelihood function contains the sum of squares

$$\chi^2(\boldsymbol{\theta}) = -2\ln L(\boldsymbol{\theta}) + \text{ constant } = \sum_{i=1}^{N}\frac{(y_i - \mu(x_i;\boldsymbol{\theta}))^2}{\sigma_i^2} . \tag{39.19}$$

The parameter values that maximize L are the same as those which minimize χ^2.

The minimum of the chi-square function in Equation (39.19) defines the least-squares estimators $\widehat{\boldsymbol{\theta}}$ for the more general case where the y_i are not Gaussian distributed as long as they are independent. If they are not independent but rather have a covariance matrix $V_{ij} = \text{cov}[y_i, y_j]$, then the LS estimators are determined by the minimum of

$$\chi^2(\boldsymbol{\theta}) = (\boldsymbol{y} - \boldsymbol{\mu}(\boldsymbol{\theta}))^T V^{-1}(\boldsymbol{y} - \boldsymbol{\mu}(\boldsymbol{\theta})) , \tag{39.20}$$

where $\boldsymbol{y} = (y_1, \ldots, y_N)$ is the (column) vector of measurements, $\boldsymbol{\mu}(\boldsymbol{\theta})$ is the corresponding vector of predicted values, and the superscript T denotes the transpose. If the y_i are not Gaussian distributed, then the LS and ML estimators will not in general coincide.

Often one further restricts the problem to the case where $\mu(x_i;\boldsymbol{\theta})$ is a linear function of the parameters, *i.e.*,

$$\mu(x_i;\boldsymbol{\theta}) = \sum_{j=1}^{m}\theta_j h_j(x_i) . \tag{39.21}$$

Here the $h_j(x)$ are m linearly independent functions, *e.g.*, $1, x, x^2, \ldots, x^{m-1}$ or Legendre polynomials. We require $m < N$ and at least m of the x_i must be distinct.

Minimizing χ^2 in this case with m parameters reduces to solving a system of m linear equations. Defining $H_{ij} = h_j(x_i)$ and minimizing χ^2 by setting its derivatives with respect to the θ_i equal to zero gives the LS estimators,

$$\widehat{\boldsymbol{\theta}} = (H^T V^{-1} H)^{-1} H^T V^{-1}\boldsymbol{y} \equiv D\boldsymbol{y} . \tag{39.22}$$

The covariance matrix for the estimators $U_{ij} = \text{cov}[\widehat{\theta}_i, \widehat{\theta}_j]$ is given by

$$U = DVD^T = (H^T V^{-1} H)^{-1} , \tag{39.23}$$

or equivalently, its inverse U^{-1} can be found from

$$(U^{-1})_{ij} = \frac{1}{2}\frac{\partial^2\chi^2}{\partial\theta_i\partial\theta_j}\bigg|_{\theta=\widehat{\theta}} = \sum_{k,l=1}^{N} h_i(x_k)(V^{-1})_{kl}h_j(x_l) . \tag{39.24}$$

The LS estimators can also be found from the expression

$$\widehat{\boldsymbol{\theta}} = U\boldsymbol{g} , \tag{39.25}$$

where the vector $\boldsymbol{g}$ is defined by

$$g_i = \sum_{j,k=1}^{N} y_j h_i(x_k)(V^{-1})_{jk} . \tag{39.26}$$

For the case of uncorrelated y_i, for example, one can use (39.25) with

$$(U^{-1})_{ij} = \sum_{k=1}^{N} \frac{h_i(x_k)h_j(x_k)}{\sigma_k^2} \,, \tag{39.27}$$

$$g_i = \sum_{k=1}^{N} \frac{y_k h_i(x_k)}{\sigma_k^2} \,. \tag{39.28}$$

Expanding $\chi^2(\boldsymbol{\theta})$ about $\widehat{\boldsymbol{\theta}}$, one finds that the contour in parameter space defined by

$$\chi^2(\boldsymbol{\theta}) = \chi^2(\widehat{\boldsymbol{\theta}}) + 1 = \chi^2_{\rm min} + 1 \tag{39.29}$$

has tangent planes located at approximately plus-or-minus-one standard deviation $\sigma_{\widehat{\theta}}$ from the LS estimates $\widehat{\boldsymbol{\theta}}$.

In constructing the quantity $\chi^2(\boldsymbol{\theta})$ one requires the variances or, in the case of correlated measurements, the covariance matrix. Often these quantities are not known *a priori* and must be estimated from the data. An important example is where the measured value y_i represents the event count in a histogram bin. If, for example, y_i represents a Poisson variable, for which the variance is equal to the mean, then one can either estimate the variance from the predicted value, $\mu(x_i;\boldsymbol{\theta})$, or from the observed number itself, y_i. In the first option, the variances become functions of the parameters, and as a result the estimators may need to be found numerically. The second option can be undefined if y_i is zero, and for small y_i, the variance will be poorly estimated. In either case, one should constrain the normalization of the fitted curve to the correct value, *i.e.*, one should determine the area under the fitted curve directly from the number of entries in the histogram (see Ref. [8], Section 7.4). As noted in Sec. 39.2.2.1, this issue is avoided when using the method of extended maximum likelihood with binned data by minimizing Eq. (39.16). In that case if the expected number of events $\mu_{\rm tot}$ does not depend on the other fitted parameters $\boldsymbol{\theta}$, then its extended ML estimator is equal to the observed total number of events.

As the minimum value of the χ^2 represents the level of agreement between the measurements and the fitted function, it can be used for assessing the goodness-of-fit; this is discussed further in Section 39.3.2.

39.2.4. *Parameter estimation with constraints* :

In some applications one is interested in using a set of measured quantities $\boldsymbol{y} = (y_1, \ldots, y_N)$ to estimate a set of parameters $\boldsymbol{\theta} = (\theta_1, \ldots, \theta_M)$ subject to a number of constraints. For example, one may have measured coordinates from two tracks, and one wishes to estimate their momentum vectors subject to the constraint that the tracks have a common vertex. The parameters can also include momenta of undetected particles such as neutrinos, as long as the constraints from conservation of energy and momentum and from known masses of particles involved in the reaction chain provide enough information for these quantities to be inferred.

A set of K constraints can be given in the form of equations

$$c_k(\boldsymbol{\theta}) = 0 \,, \quad k = 1, \ldots, K \,. \tag{39.30}$$

In some problems it may be possible to define a new set of parameters $\boldsymbol{\eta} = (\eta_1, \ldots, \eta_L)$ with $L = M - K$ such that every point in $\boldsymbol{\eta}$-space automatically satisfies the constraints. If this is possible then the problem reduces to one of estimating $\boldsymbol{\eta}$ with, *e.g.*, maximum likelihood or least squares and then transforming the estimators back into $\boldsymbol{\theta}$-space.

In many cases it may be difficult or impossible to find an appropriate transformation $\boldsymbol{\eta}(\boldsymbol{\theta})$. Suppose that the parameters are determined through minimizing an objective function such as $\chi^2(\boldsymbol{\theta})$ in the method of least squares. Here one may enforce the constraints by finding the stationary points of the *Lagrange function*

$$\mathcal{L}(\boldsymbol{\theta}, \boldsymbol{\lambda}, \boldsymbol{y}) = \chi^2(\boldsymbol{\theta}, \boldsymbol{y}) + \sum_{k=1}^{K} \lambda_k c_k(\boldsymbol{\theta}) \tag{39.31}$$

with respect to both the parameters $\boldsymbol{\theta}$ and a set of *Lagrange multipliers* $\boldsymbol{\lambda} = (\lambda_1, \ldots, \lambda_K)$. Combining the parameters and Lagrange multipliers into an $(M + K)$-component vector $\boldsymbol{\gamma} = (\theta_1, \ldots, \theta_M, \lambda_1, \ldots, \lambda_K)$, the solutions for $\boldsymbol{\gamma}$, *i.e.*, the estimators $\hat{\boldsymbol{\gamma}}$, are found (*e.g.*, numerically) from the system of equations

$$F_i(\boldsymbol{\gamma}, \boldsymbol{y}) \equiv \frac{\partial \mathcal{L}}{\partial \gamma_i} = 0 \,, \quad i = 1, \ldots, M + K \,. \tag{39.32}$$

To obtain the covariance matrix of the estimated parameters one can find solutions $\tilde{\boldsymbol{\gamma}}$ corresponding to the expectation values of the data $\langle \boldsymbol{y} \rangle$ and expand $F_i(\hat{\boldsymbol{\gamma}}, \boldsymbol{y})$ to first order about these values. This gives (see, e.g., Sec. 11.6 of Ref. [8]) linearized approximations for the estimators, $\hat{\boldsymbol{\gamma}}(\boldsymbol{y}) \approx \tilde{\boldsymbol{\gamma}} + C(\boldsymbol{y} - \langle \boldsymbol{y} \rangle)$, where the matrix $C = -A^{-1}B$, and A and B are given by

$$A_{ij} = \left[\frac{\partial F_i}{\partial \gamma_j}\right]_{\tilde{\gamma}, \langle y \rangle} \quad \text{and} \quad B_{ij} = \left[\frac{\partial F_i}{\partial y_j}\right]_{\tilde{\gamma}, \langle y \rangle} \,. \tag{39.33}$$

In practice the values $\langle \boldsymbol{y} \rangle$ and corresponding solutions $\tilde{\boldsymbol{\gamma}}$ are estimated using the data from the actual measurement. Using this approximation for $\hat{\boldsymbol{\gamma}}(\boldsymbol{y})$, one can find the covariance matrix $U_{ij} = \mathrm{cov}[\hat{\gamma}_i, \hat{\gamma}_j]$ of the the estimators for the γ_i in terms of that of the data $V_{ij} = \mathrm{cov}[y_i, y_j]$ using error propagation (cf. Eqs. (39.42) and (39.43)),

$$U = CVC^T \,. \tag{39.34}$$

The upper-left $M \times M$ block of the matrix U gives the covariance matrix for the estimated parameters $\mathrm{cov}[\hat{\theta}_i, \hat{\theta}_j]$. If the parameters are estimated using the method of least squares, then the number of degrees of freedom for the distribution of the minimized χ^2 is increased by the number of constraints, *i.e.*, it becomes $N - M + K$. Further details can be found in, *e.g.*, Ch. 7 of Ref. [31].

39.2.5. *The Bayesian approach* :

In the frequentist methods discussed above, probability is associated only with data, not with the value of a parameter. This is no longer the case in Bayesian statistics, however, which we introduce in this section. For general introductions to Bayesian statistics see, *e.g.*, Refs. [26–29].

Suppose the outcome of an experiment is characterized by a vector of data $\boldsymbol{x}$, whose probability distribution depends on an unknown parameter (or parameters) $\boldsymbol{\theta}$ that we wish to determine. In Bayesian statistics, all knowledge about $\boldsymbol{\theta}$ is summarized by the posterior p.d.f. $p(\boldsymbol{\theta}|\boldsymbol{x})$, whose integral over any given region gives the degree of belief for $\boldsymbol{\theta}$ to take on values in that region, given the data $\boldsymbol{x}$. It is obtained by using Bayes' theorem,

$$p(\boldsymbol{\theta}|\boldsymbol{x}) = \frac{P(\boldsymbol{x}|\boldsymbol{\theta})\pi(\boldsymbol{\theta})}{\int P(\boldsymbol{x}|\boldsymbol{\theta}')\pi(\boldsymbol{\theta}')\, d\boldsymbol{\theta}'} \,, \tag{39.35}$$

where $P(\boldsymbol{x}|\boldsymbol{\theta})$ is the likelihood function, *i.e.*, the joint p.d.f. for the data viewed as a function of $\boldsymbol{\theta}$, evaluated with the data actually obtained in the experiment, and $\pi(\boldsymbol{\theta})$ is the prior p.d.f. for $\boldsymbol{\theta}$. Note that the denominator in Eq. (39.35) serves to normalize the posterior p.d.f. to unity.

As it can be difficult to report the full posterior p.d.f. $p(\boldsymbol{\theta}|\boldsymbol{x})$, one would usually summarize it with statistics such as the mean (or median) value, and covariance matrix. In addition one may construct intervals with a given probability content, as is discussed in Sec. 39.4.1 on Bayesian interval estimation.

39.2.5.1. *Priors:*

Bayesian statistics supplies no unique rule for determining the prior $\pi(\boldsymbol{\theta})$; this reflects the analyst's subjective degree of belief (or state of knowledge) about $\boldsymbol{\theta}$ before the measurement was carried out. For the result to be of value to the broader community, whose members may not share these beliefs, it is important to carry out a *sensitivity analysis*, that is, to show how the result changes under a reasonable variation of the prior probabilities.

One might like to construct $\pi(\boldsymbol{\theta})$ to represent complete ignorance about the parameters by setting it equal to a constant. A problem here is that if the prior p.d.f. is flat in $\boldsymbol{\theta}$, then it is not flat for a

nonlinear function of $\boldsymbol{\theta}$, and so a different parametrization of the problem would lead in general to a non-equivalent posterior p.d.f.

For the special case of a constant prior, one can see from Bayes' theorem (39.35) that the posterior is proportional to the likelihood, and therefore the mode (peak position) of the posterior is equal to the ML estimator. The posterior mode, however, will change in general upon a transformation of parameter. One may use as the Bayesian estimator a summary statistic other than the mode, such as the median, which is invariant under parameter transformation. But this will not in general coincide with the ML estimator.

The difficult and subjective nature of encoding personal knowledge into priors has led to what is called *objective Bayesian statistics*, where prior probabilities are based not on an actual degree of belief but rather derived from formal rules. These give, for example, priors which are invariant under a transformation of parameters, or ones which result in a maximum gain in information for a given set of measurements. For an extensive review see, *e.g.*, [30].

Objective priors do not in general reflect degree of belief, but they could in some cases be taken as possible, although perhaps extreme, subjective priors. The posterior probabilities as well therefore do not necessarily reflect a degree of belief. However one may regard investigating a variety of objective priors to be an important part of the sensitivity analysis. Furthermore, use of objective priors with Bayes' theorem can be viewed as a recipe for producing estimators or intervals which have desirable frequentist properties.

An important procedure for deriving objective priors is due to Jeffreys. According to *Jeffreys' rule* one takes the prior as

$$\pi(\boldsymbol{\theta}) \propto \sqrt{\det(I(\boldsymbol{\theta}))}\,, \tag{39.36}$$

where

$$I_{ij}(\boldsymbol{\theta}) = -E\left[\frac{\partial^2 \ln P(\boldsymbol{x}|\boldsymbol{\theta})}{\partial\theta_i \partial\theta_j}\right] \tag{39.37}$$

is the *Fisher information matrix*. One can show that the Jeffreys prior leads to inference that is invariant under a transformation of parameters. One should note that the Jeffreys prior does not in general correspond to one's degree of belief about the value of a parameter. As examples, the Jeffreys prior for the mean μ of a Gaussian distribution is a constant, and for the mean of a Poisson distribution one finds $\pi(\mu) \propto 1/\sqrt{\mu}$.

Neither the constant nor $1/\sqrt{\mu}$ priors can be normalized to unit area and are therefore said to be *improper*. This can be allowed because the prior always appears multiplied by the likelihood function, and if the likelihood falls to zero sufficiently quickly then one may have a normalizable posterior density.

An important type of objective prior is the reference prior due to Bernardo and Berger [32]. To find the reference prior for a given problem one considers the Kullback-Leibler divergence $D_n[\pi, p]$ of the posterior $p(\boldsymbol{\theta}|\boldsymbol{x})$ relative to a prior $\pi(\boldsymbol{\theta})$, obtained from a set of i.i.d. data $\boldsymbol{x} = (x_1, \ldots, x_n)$:

$$D_n[\pi, p] = \int p(\boldsymbol{\theta}|\boldsymbol{x}) \ln \frac{p(\boldsymbol{\theta}|\boldsymbol{x})}{\pi(\boldsymbol{\theta})}\, d\boldsymbol{\theta}\,. \tag{39.38}$$

This is effectively a measure of the gain in information provided by the data. The reference prior is chosen so that the expectation value of this information gain is maximized for the limiting case of $n \to \infty$, where the expectation is computed with respect to the marginal distribution of the data,

$$p(\boldsymbol{x}) = \int p(\boldsymbol{x}|\boldsymbol{\theta})\pi(\boldsymbol{\theta})\, d\boldsymbol{\theta}\,. \tag{39.39}$$

For a single, continuous parameter the reference prior is usually identical to the Jeffreys prior. In the multiparameter case an iterative algorithm exists, which requires sorting the parameters by order of inferential importance. Often the result does not depend on this order, but when it does, this can be part of a sensitivity analysis. Further discussion and applications to particle physics problems can be found in Ref. [33].

39.2.5.2. *Bayesian treatment of nuisance parameters:*

As discussed in Sec. 39.2.2, a model may depend on parameters of interest $\boldsymbol{\theta}$ as well as on nuisance parameters $\boldsymbol{\nu}$, which must be included for an accurate description of the data. Knowledge about the values of $\boldsymbol{\nu}$ may be supplied by control measurements, theoretical insights, physical constraints, etc. Suppose, for example, one has data $\boldsymbol{y}$ from a control measurement which is characterized by a probability $P_y(\boldsymbol{y}|\boldsymbol{\nu})$. Suppose further that before carrying out the control measurement one's state of knowledge about $\boldsymbol{\nu}$ is described by an initial prior $\pi_0(\boldsymbol{\nu})$, which in practice is often taken to be a constant or in any case very broad. By using Bayes' theorem (39.1) one obtains the updated prior $\pi(\boldsymbol{\nu})$ (*i.e.*, now $\pi(\boldsymbol{\nu}) = \pi(\boldsymbol{\nu}|\boldsymbol{y})$, the probability for $\boldsymbol{\nu}$ given $\boldsymbol{y}$),

$$\pi(\boldsymbol{\nu}|\boldsymbol{y}) \propto P(\boldsymbol{y}|\boldsymbol{\nu})\pi_0(\boldsymbol{\nu})\,. \tag{39.40}$$

In the absence of a model for $P(\boldsymbol{y}|\boldsymbol{\nu})$ one may make some reasonable but *ad hoc* choices. For a single nuisance parameter ν, for example, one might characterize the uncertainty by a p.d.f. $\pi(\nu)$ centered about its nominal value with a certain standard deviation σ_ν. Often a Gaussian p.d.f. provides a reasonable model for one's degree of belief about a nuisance parameter; in other cases, more complicated shapes may be appropriate. If, for example, the parameter represents a non-negative quantity then a log-normal or gamma p.d.f. can be a more natural choice than a Gaussian truncated at zero. Note also that truncation of the prior of a nuisance parameter ν at zero will in general make $\pi(\nu)$ nonzero at $\nu = 0$, which can lead to an unnormalizable posterior for a parameter of interest that appears multiplied by ν.

The likelihood function, prior, and posterior p.d.f.s all depend on both $\boldsymbol{\theta}$ and $\boldsymbol{\nu}$, and are related by Bayes' theorem, as usual. Note that the likelihood here only refers to the primary measurement $\boldsymbol{x}$. Once any control measurements $\boldsymbol{y}$ are used to find the updated prior $\pi(\boldsymbol{\nu})$ for the nuisance parameters, this information is fully encapsulated in $\pi(\boldsymbol{\nu})$ and the control measurements do not appear further.

One can obtain the posterior p.d.f. for $\boldsymbol{\theta}$ alone by integrating over the nuisance parameters, *i.e.*,

$$p(\boldsymbol{\theta}|\boldsymbol{x}) = \int p(\boldsymbol{\theta}, \boldsymbol{\nu}|\boldsymbol{x})\, d\boldsymbol{\nu}\,. \tag{39.41}$$

Such integrals can often not be carried out in closed form, and if the number of nuisance parameters is large, then they can be difficult to compute with standard Monte Carlo methods. *Markov Chain Monte Carlo* (MCMC) techniques are often used for computing integrals of this type (see Sec. 40.5).

39.2.6. ***Propagation of errors*** :

Consider a set of n quantities $\boldsymbol{\theta} = (\theta_1, \ldots, \theta_n)$ and a set of m functions $\boldsymbol{\eta}(\boldsymbol{\theta}) = (\eta_1(\boldsymbol{\theta}), \ldots, \eta_m(\boldsymbol{\theta}))$. Suppose we have estimated $\widehat{\boldsymbol{\theta}} = (\widehat{\theta}_1, \ldots, \widehat{\theta}_n)$, using, say, maximum-likelihood or least-squares, and we also know or have estimated the covariance matrix $V_{ij} = \mathrm{cov}[\widehat{\theta}_i, \widehat{\theta}_j]$. The goal of *error propagation* is to determine the covariance matrix for the functions, $U_{ij} = \mathrm{cov}[\widehat{\eta}_i, \widehat{\eta}_j]$, where $\widehat{\boldsymbol{\eta}} = \boldsymbol{\eta}(\widehat{\boldsymbol{\theta}})$. In particular, the diagonal elements $U_{ii} = V[\widehat{\eta}_i]$ give the variances. The new covariance matrix can be found by expanding the functions $\boldsymbol{\eta}(\boldsymbol{\theta})$ about the estimates $\widehat{\boldsymbol{\theta}}$ to first order in a Taylor series. Using this one finds

$$U_{ij} \approx \sum_{k,l} \left.\frac{\partial\eta_i}{\partial\theta_k}\frac{\partial\eta_j}{\partial\theta_l}\right|_{\widehat{\theta}} V_{kl}\,. \tag{39.42}$$

This can be written in matrix notation as $U \approx AVA^T$ where the matrix of derivatives A is

$$A_{ij} = \left.\frac{\partial\eta_i}{\partial\theta_j}\right|_{\widehat{\theta}}\,, \tag{39.43}$$

and A^T is its transpose. The approximation is exact if $\boldsymbol{\eta}(\boldsymbol{\theta})$ is linear (it holds, for example, in Equation (39.23)). If this is not the case, the approximation can break down if, for example, $\boldsymbol{\eta}(\boldsymbol{\theta})$ is significantly nonlinear close to $\widehat{\boldsymbol{\theta}}$ in a region of a size comparable to the standard deviations of $\widehat{\boldsymbol{\theta}}$.

39.3. Statistical tests

In addition to estimating parameters, one often wants to assess the validity of certain statements concerning the data's underlying distribution. Frequentist *hypothesis tests*, described in Sec. 39.3.1, provide a rule for accepting or rejecting hypotheses depending on the outcome of a measurement. In *significance tests*, covered in Sec. 39.3.2, one gives the probability to obtain a level of incompatibility with a certain hypothesis that is greater than or equal to the level observed with the actual data. In the Bayesian approach, the corresponding procedure is based fundamentally on the posterior probabilities of the competing hypotheses. In Sec. 39.3.3 we describe a related construct called the Bayes factor, which can be used to quantify the degree to which the data prefer one or another hypothesis.

39.3.1. *Hypothesis tests* :

A frequentist *test* of a hypothesis (often called the null hypothesis, H_0) is a rule that states for which data values $\boldsymbol{x}$ the hypothesis is rejected. A region of $\boldsymbol{x}$-space called the critical region, w, is specified such that there is no more than a given probability under H_0, α, called the *size* or *significance level* of the test, to find $\boldsymbol{x} \in w$. If the data are discrete, it may not be possible to find a critical region with exact probability content α, and thus we require $P(\boldsymbol{x} \in w|H_0) \leq \alpha$. If the data are observed in the critical region, H_0 is rejected.

The data $\boldsymbol{x}$ used to construct a test could be, for example, a set of values that characterizes an individual event. In this case the test corresponds to classification as, *e.g.*, signal or background. Alternatively the data could represent a set of values from a collection of events. Often one is interested in knowing whether all of the events are of a certain type (background), or whether the sample contains at least some events of a new type (signal). Here the background-only hypothesis plays the role of H_0, and in the alternative H_1 both signal and background are present. Rejecting H_0 is, from the standpoint of frequentist statistics, the required step to establish discovery of the signal process.

The critical region is not unique. Its choice should take into account the probabilities for the data predicted by some alternative hypothesis (or set of alternatives) H_1. Rejecting H_0 if it is true is called a *type-I error*, and occurs by construction with probability no greater than α. Not rejecting H_0 if an alternative H_1 is true is called a *type-II error*, and for a given test this will have a certain probability $\beta = P(\boldsymbol{x} \notin w|H_1)$. The quantity $1 - \beta$ is called the *power* of the test of H_0 with respect to the alternative H_1. A strategy for defining the critical region can therefore be to maximize the power with respect to some alternative (or alternatives) given a fixed size α.

To maximize the power of a test of H_0 with respect to the alternative H_1, the *Neyman–Pearson lemma* states that the critical region w should be chosen such that for all data values $\boldsymbol{x}$ inside w, the likelihood ratio

$$\lambda(\boldsymbol{x}) = \frac{f(\boldsymbol{x}|H_1)}{f(\boldsymbol{x}|H_0)} \tag{39.44}$$

is greater than or equal to a given constant c_α, and everywhere outside the critical region one has $\lambda(\boldsymbol{x}) < c_\alpha$, where the value of c_α is determined by the size of the test α. Here H_0 and H_1 must be simple hypotheses, *i.e.*, they should not contain undetermined parameters.

It is convenient to define the test using a scalar function of the data $\boldsymbol{x}$ called a *test statistic*, $t(\boldsymbol{x})$, such that the boundary of the critical region is given by a surface of constant $t(\boldsymbol{x})$. The Neyman–Pearson lemma is equivalent to the statement that the likelihood ratio (39.44) represents the optimal test statistic. It can be difficult in practice, however, to determine $\lambda(\boldsymbol{x})$, since this requires knowledge of the joint p.d.f.s $f(\boldsymbol{x}|H_0)$ and $f(\boldsymbol{x}|H_1)$. Often one does not have explicit formulae for these, but rather Monte Carlo models that allow one to generate instances of $\boldsymbol{x}$ that follow the p.d.f.s.

In the case where the likelihood ratio (39.44) cannot be used explicitly, there exist a variety of other multivariate methods for constructing a test statistic that may approach its performance. These are based on machine-learning algorithms that use samples of *training data* corresponding to the hypotheses in question, often generated from Monte Carlo models. Methods often used in HEP include *Fisher Discriminants*, *Neural Networks*, *Boosted Decision Trees* and *Support Vector Machines*. Descriptions of these and other methods can be found in Refs. [11–14] and *Proceedings of the PHYSTAT* conference series [15]. Software for HEP includes the `TMVA` [16] and `scikit-learn` [18] packages.

An important issue in constructing a test is the choice of variables that enter into the data vector $\boldsymbol{x}$. For purposes of classification one may choose, for example, to form certain functions of particle momenta such as, *e.g.*, invariant masses that are felt to be physically meaningful in the context of a particular event type. It may be difficult to know, however, whether there may exist further features that would help distinguish between signal and background. Recently, so-called *Deep* Neural Networks containing several or more hidden layers have been applied in HEP [19]; these allow one to use directly as inputs the elements of the data vector $\boldsymbol{x}$ (features) that represent lower-level quantities such as individual particle momenta, rather than needing to first construct "by hand" higher level features. Each hidden layer then allows the network to construct significant high-level features in an automatic way.

The multivariate algorithms designed to classify events into signal and background types also form the basis of tests of the hypothesis that a sample of events consists of background only. Such a test can be constructed using the distributions of the test statistic $t(\boldsymbol{x})$ for event classification obtained from a multivariate algorithm such as a Neural Network output. The distributions $p(t|s)$ and $p(t|b)$ for signal and background events, respectively, are used to construct the likelihood ratio of the signal-plus-background hypothesis relative to that of background only. To the extent that the test statistic $t(\boldsymbol{x})$ approximates the likelihood ratio (or a monotonic function thereof) for individual events given by (39.44), the resulting test of the background-only hypothesis for the event sample will have maximum power with respect to the signal-plus-background alternative (see Ref. [20]) .

39.3.2. *Tests of significance (goodness-of-fit)* :

Often one wants to quantify the level of agreement between the data and a hypothesis without explicit reference to alternative hypotheses. This can be done by defining a statistic t whose value reflects in some way the level of agreement between the data and the hypothesis. The analyst must decide what values of the statistic correspond to better or worse levels of agreement with the hypothesis in question; the choice will in general depend on the relevant alternative hypotheses.

The hypothesis in question, H_0, will determine the p.d.f. $f(t|H_0)$ for the statistic. The significance of a discrepancy between the data and what one expects under the assumption of H_0 is quantified by giving the p-value, defined as the probability to find t in the region of equal or lesser compatibility with H_0 than the level of compatibility observed with the actual data. For example, if t is defined such that large values correspond to poor agreement with the hypothesis, then the p-value would be

$$p = \int_{t_{\rm obs}}^{\infty} f(t|H_0)\, dt\ , \tag{39.45}$$

where $t_{\rm obs}$ is the value of the statistic obtained in the actual experiment.

The p-value should not be confused with the size (significance level) of a test, or the confidence level of a confidence interval (Section 39.4), both of which are pre-specified constants. We may formulate a hypothesis test, however, by defining the critical region to correspond to the data outcomes that give the lowest p-values, so that finding $p \leq \alpha$ implies that the data outcome was in the critical region. When constructing a p-value, one generally chooses the region of data space deemed to have lower compatibility with the model being tested as one having higher compatibility with a given alternative, such that the corresponding test will have a high power with respect to this alternative.

The p-value is a function of the data, and is therefore itself a random variable. If the hypothesis used to compute the p-value is true, then for continuous data p will be uniformly distributed between zero and one. Note that the p-value is not the probability for the hypothesis; in frequentist statistics, this is not defined.

When searching for a new phenomenon, one tries to reject the hypothesis H_0 that the data are consistent with known (*e.g.*, Standard Model) processes. If the p-value of H_0 is sufficiently low, then one is willing to accept that some alternative hypothesis is true. Often one converts the p-value into an equivalent significance Z, defined so that a Z standard deviation upward fluctuation of a Gaussian random variable would have an upper tail area equal to p, *i.e.*,

$$Z = \Phi^{-1}(1-p) \; . \tag{39.46}$$

Here Φ is the cumulative distribution of the standard Gaussian, and Φ^{-1} is its inverse (quantile) function. Often in HEP the level of significance where an effect is said to qualify as a discovery is $Z = 5$, *i.e.*, a 5σ effect, corresponding to a p-value of 2.87×10^{-7}. One's actual degree of belief that a new process is present, however, will depend in general on other factors as well, such as the plausibility of the new signal hypothesis and the degree to which it can describe the data, one's confidence in the model that led to the observed p-value, and possible corrections for multiple observations out of which one focuses on the smallest p-value obtained (the "look-elsewhere effect", discussed in Section 39.3.2.2).

39.3.2.1. *Treatment of nuisance parameters for frequentist tests:*

Suppose one wants to test hypothetical values of parameters $\boldsymbol{\theta}$, but the model also contains nuisance parameters $\boldsymbol{\nu}$. To find a p-value for $\boldsymbol{\theta}$ we can construct a test statistic q_θ such that larger values constitute increasing incompatibility between the data and the hypothesis. Then for an observed value of the statistic $q_{\theta,\mathrm{obs}}$, the p-value of $\boldsymbol{\theta}$ is

$$p_\theta(\boldsymbol{\nu}) = \int_{q_{\theta,\mathrm{obs}}}^{\infty} f(q_\theta|\boldsymbol{\theta},\boldsymbol{\nu})\, dq_\theta \; , \tag{39.47}$$

which depends in general on the nuisance parameters $\boldsymbol{\nu}$. In the strict frequentist approach, $\boldsymbol{\theta}$ is rejected only if the p-value is less than α for all possible values of the nuisance parameters.

The difficulty described above is effectively solved if we can define the test statistic q_θ in such a way that its distribution $f(q_\theta|\boldsymbol{\theta})$ is independent of the nuisance parameters. Although exact independence is only found in special cases, it can be achieved approximately by use of the *profile likelihood ratio*. This is given by the profile likelihood from Eq.(39.18) divided by the value of the likelihood at its maximum, *i.e.*, when evaluated with the ML estimators $\widehat{\boldsymbol{\theta}}$ and $\widehat{\boldsymbol{\nu}}$:

$$\lambda_p(\boldsymbol{\theta}) = \frac{L(\boldsymbol{\theta}, \widehat{\widehat{\boldsymbol{\nu}}}(\boldsymbol{\theta}))}{L(\widehat{\boldsymbol{\theta}}, \widehat{\boldsymbol{\nu}})} \; . \tag{39.48}$$

Wilks' theorem [10] states that, providing certain general conditions are satisfied, the distribution of $-2\ln\lambda_{\mathrm{p}}(\boldsymbol{\theta})$, under assumption of $\boldsymbol{\theta}$, approaches a χ^2 distribution in the limit where the data sample is very large, independent of the values of the nuisance parameters $\boldsymbol{\nu}$. Here the number of degrees of freedom is equal to the number of components of $\boldsymbol{\theta}$. More details on use of the profile likelihood are given in Refs. [41–42] and in contributions to the PHYSTAT conferences [15]; explicit formulae for special cases can be found in Ref. [43]. Further discussion on how to incorporate systematic uncertainties into p-values can be found in Ref. [21].

Even with use of the profile likelihood ratio, for a finite data sample the p-value of hypothesized parameters $\boldsymbol{\theta}$ will retain in general some dependence on the nuisance parameters $\boldsymbol{\nu}$. Ideally one would find the the maximum of $p_\theta(\boldsymbol{\nu})$ from Eq. (39.47) explicitly, but that is often impractical. An approximate and computationally feasible technique is to use $p_\theta(\widehat{\widehat{\boldsymbol{\nu}}}(\theta))$, where $\widehat{\widehat{\boldsymbol{\nu}}}(\theta)$ are the profiled values of the nuisance parameters as defined in Section 39.2.2.2. The resulting p-value is correct if the true values of the nuisance parameters are equal to the profiled values used; otherwise it could be either too high or too low. This is discussed further in Section 39.4.2 on confidence intervals.

One may also treat model uncertainties in a Bayesian manner but then use the resulting model in a frequentist test. Suppose the uncertainty in a set of nuisance parameters $\boldsymbol{\nu}$ is characterized by a Bayesian prior p.d.f. $\pi(\boldsymbol{\nu})$. This can be used to construct the marginal (also called the prior predictive) model for the data $\boldsymbol{x}$ and parameters of interest $\boldsymbol{\theta}$,

$$P_{\mathrm{m}}(\boldsymbol{x}|\boldsymbol{\theta}) = \int P(\boldsymbol{x}|\boldsymbol{\theta},\boldsymbol{\nu})\pi(\boldsymbol{\nu})\, d\boldsymbol{\nu} \; . \tag{39.49}$$

The marginal model does not represent the probability of data that would be generated if one were really to repeat the experiment, as in that case one would assume that the nuisance parameters do not vary. Rather, the marginal model represents a situation in which every repetition of the experiment is carried out with new values of $\boldsymbol{\nu}$, randomly sampled from $\pi(\boldsymbol{\nu})$. It is in effect an average of models each with a given $\boldsymbol{\nu}$, where the average is carried out with respect to the prior p.d.f. $\pi(\boldsymbol{\nu})$.

The marginal model for the data $\boldsymbol{x}$ can be used to determine the distribution of a test statistic Q, which can be written

$$P_{\mathrm{m}}(Q|\boldsymbol{\theta}) = \int P(Q|\boldsymbol{\theta},\boldsymbol{\nu})\pi(\boldsymbol{\nu})\, d\boldsymbol{\nu} \; . \tag{39.50}$$

In a search for a new signal process, the test statistic can be based on the ratio of likelihoods corresponding to the experiments where signal and background events are both present, L_{s+b}, to that of background only, L_b. Often the likelihoods are evaluated with the profiled values of the nuisance parameters, which may give improved performance. It is important to note, however, that it is through use of the marginal model for the distribution of Q that the uncertainties related to the nuisance parameters are incorporated into the result of the test. Different choices for the test statistic itself only result in variations of the power of the test with respect to different alternatives.

39.3.2.2. *The look-elsewhere effect:*

The "look-elsewhere effect" relates to multiple measurements used to test a single hypothesis. The classic example is when one searches in a distribution for a peak whose position is not predicted in advance. Here the no-peak hypothesis is tested using data in a given range of the distribution. In the frequentist approach the correct p-value of the no-peak hypothesis is the probability, assuming background only, to find a signal as significant as the one found or more so anywhere in the search region. This can be substantially higher than the probability to find a peak of equal or greater significance in the particular place where it appeared. There is in general some ambiguity as to what constitutes the relevant search region or even the broader set of relevant measurements. Although the desired p-value is well defined once the search region has been fixed, an exact treatment can require extensive computation.

The "brute-force" solution to this problem by Monte Carlo involves generating data under the background-only hypothesis and for each data set, fitting a peak of unknown position and recording a measure of its significance. To establish a discovery one often requires a p-value smaller than 2.87×10^{-7}, corresponding to a 5σ or larger effect. Determining this with Monte Carlo thus requires generating and fitting a very large number of experiments, perhaps several times 10^7. In contrast, if the position of the peak is fixed, then the fit to the distribution is much easier, and furthermore one can in many cases use formulae valid for sufficiently large samples that bypass completely the need for Monte Carlo (see, *e.g.*, [43]) . However, this fixed-position or "local" p-value would not be correct in general, as it assumes the position of the peak was known in advance.

A method that allows one to modify the local p-value computed under assumption of a fixed position to obtain an approximation to the correct "global" value using a relatively simple calculation is described in Ref. [22]. Suppose a test statistic q_0, defined so that larger values indicate increasing disagreement with the data, is observed to have a value u. Furthermore suppose the model contains a nuisance parameter θ (such as the peak position) which is only defined under the signal model (there is no peak in the background-only model). An approximation for the global p-value is found to be

$$p_{\mathrm{global}} \approx p_{\mathrm{local}} + \langle N_u \rangle \; , \tag{39.51}$$

where $\langle N_u \rangle$, which is much smaller than one in cases of interest, is the mean number of "upcrossings" of the statistic q_0 above the level u in the range of the nuisance parameter considered (*e.g.*, the mass range).

The value of $\langle N_u \rangle$ can be estimated from the number of upcrossings $\langle N_{u_0} \rangle$ above some much lower value, u_0, by using a relation due to Davis [23],

$$\langle N_u \rangle \approx \langle N_{u_0} \rangle e^{-(u-u_0)/2} \; . \tag{39.52}$$

By choosing u_0 sufficiently low, the value of $\langle N_u \rangle$ can be estimated by simulating only a very small number of experiments, or even from the observed data, rather than the 10^7 needed if one is dealing with a 5σ effect.

39.3.2.3. *Goodness-of-fit with the method of least squares:*

When estimating parameters using the method of least squares, one obtains the minimum value of the quantity χ^2 (39.19). This statistic can be used to test the *goodness-of-fit*, *i.e.*, the test provides a measure of the significance of a discrepancy between the data and the hypothesized functional form used in the fit. It may also happen that no parameters are estimated from the data, but that one simply wants to compare a histogram, *e.g.*, a vector of Poisson distributed numbers $\boldsymbol{n} = (n_1, \ldots, n_N)$, with a hypothesis for their expectation values $\mu_i = E[n_i]$. As the distribution is Poisson with variances $\sigma_i^2 = \mu_i$, the χ^2 (39.19) becomes *Pearson's* χ^2 *statistic*,

$$\chi^2 = \sum_{i=1}^{N} \frac{(n_i - \mu_i)^2}{\mu_i} \; . \tag{39.53}$$

If the hypothesis $\boldsymbol{\mu} = (\mu_1, \ldots, \mu_N)$ is correct, and if the expected values μ_i in (39.53) are sufficiently large (or equivalently, if the measurements n_i can be treated as following a Gaussian distribution), then the χ^2 statistic will follow the χ^2 p.d.f. with the number of degrees of freedom equal to the number of measurements N minus the number of fitted parameters.

Alternatively, one may fit parameters and evaluate goodness-of-fit by minimizing $-2 \ln \lambda$ from Eq. (39.16). One finds that the distribution of this statistic approaches the asymptotic limit faster than does Pearson's χ^2. Therefore if one uses the asymptotic χ^2 p.d.f. as the statistic's approximate sampling distribution to compute a p-value, one obtains in general a more accurate result from $-2 \ln \lambda$ than from Pearson's χ^2 (see Ref. [9] and references therein).

Assuming the goodness-of-fit statistic follows a χ^2 p.d.f., the p-value for the hypothesis is then

$$p = \int_{\chi^2}^{\infty} f(z; n_\mathrm{d}) \, dz \; , \tag{39.54}$$

where $f(z; n_\mathrm{d})$ is the χ^2 p.d.f. and n_d is the appropriate number of degrees of freedom. Values are shown in Fig. 39.1 or obtained from the ROOT function `TMath::Prob`. If the conditions for using the χ^2 p.d.f. do not hold, the statistic can still be defined as before, but its p.d.f. must be determined by other means in order to obtain the p-value, *e.g.*, using a Monte Carlo calculation.

Since the mean of the χ^2 distribution is equal to n_d, one expects in a "reasonable" experiment to obtain $\chi^2 \approx n_\mathrm{d}$. Hence the quantity χ^2/n_d is sometimes reported. Since the p.d.f. of χ^2/n_d depends on n_d, however, one must report n_d as well if one wishes to determine the p-value. The p-values obtained for different values of χ^2/n_d are shown in Fig. 39.2.

If the minimized χ^2 value indicates a low level of agreement between data and hypothesis, one may be tempted to expect a high degree of uncertainty for any fitted parameters. Poor goodness-of-fit, however, does not mean that one will have large statistical errors for parameter estimates. If, for example, the error bars (or covariance matrix) used in constructing the χ^2 are underestimated, then this will lead to underestimated statistical errors for the fitted parameters. The standard deviations of estimators that one finds from, say, Eq. (39.13) reflect how widely the estimates would be distributed if one were to repeat the measurement many times, assuming that the hypothesis and measurement errors used in the χ^2 are also correct. They do not include the systematic error which may result from an incorrect hypothesis or incorrectly estimated measurement errors in the χ^2.

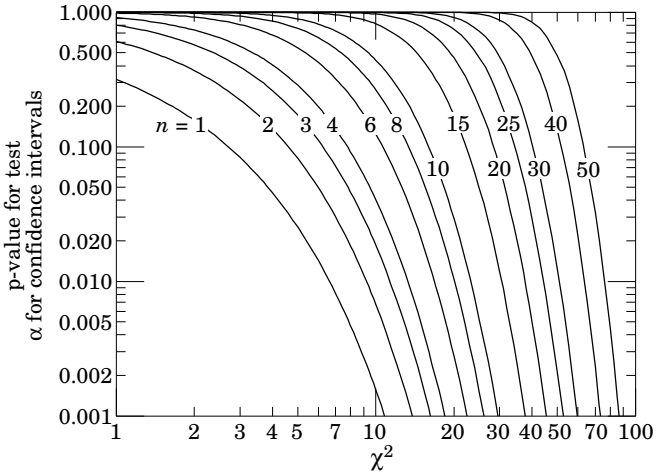

Figure 39.1: One minus the χ^2 cumulative distribution, $1 - F(\chi^2; n)$, for n degrees of freedom. This gives the p-value for the χ^2 goodness-of-fit test as well as one minus the coverage probability for confidence regions (see Sec. 39.4.2.2).

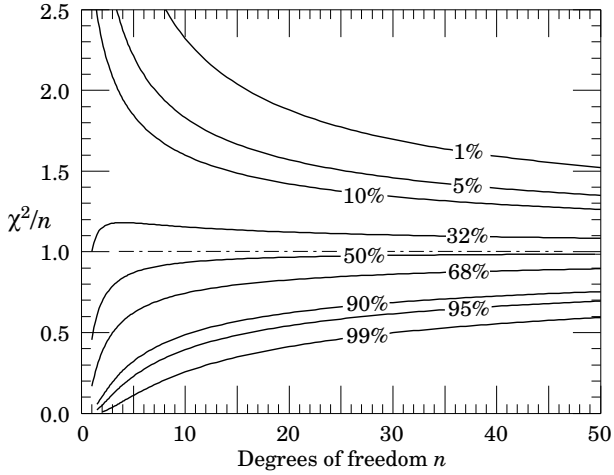

Figure 39.2: The 'reduced' χ^2, equal to χ^2/n, for n degrees of freedom. The curves show as a function of n the χ^2/n that corresponds to a given p-value.

39.3.3. ***Bayes factors*** :

In Bayesian statistics, all of one's knowledge about a model is contained in its posterior probability, which one obtains using Bayes' theorem (Eq. (39.35)). Thus one could reject a hypothesis H if its posterior probability $P(H|\boldsymbol{x})$ is sufficiently small. The difficulty here is that $P(H|\boldsymbol{x})$ is proportional to the prior probability $P(H)$, and there will not be a consensus about the prior probabilities for the existence of new phenomena. Nevertheless one can construct a quantity called the Bayes factor (described below), which can be used to quantify the degree to which the data prefer one hypothesis over another, and is independent of their prior probabilities.

Consider two models (hypotheses), H_i and H_j, described by vectors of parameters $\boldsymbol{\theta}_i$ and $\boldsymbol{\theta}_j$, respectively. Some of the components will be common to both models and others may be distinct. The full prior probability for each model can be written in the form

$$\pi(H_i, \boldsymbol{\theta}_i) = P(H_i) \pi(\boldsymbol{\theta}_i | H_i) \; . \tag{39.55}$$

Here $P(H_i)$ is the overall prior probability for H_i, and $\pi(\boldsymbol{\theta}_i|H_i)$ is the normalized p.d.f. of its parameters. For each model, the posterior probability is found using Bayes' theorem,

$$P(H_i|\boldsymbol{x}) = \frac{\int P(\boldsymbol{x}|\boldsymbol{\theta}_i, H_i) P(H_i) \pi(\boldsymbol{\theta}_i|H_i) \, d\boldsymbol{\theta}_i}{P(\boldsymbol{x})} \; , \tag{39.56}$$

where the integration is carried out over the internal parameters $\boldsymbol{\theta}_i$ of the model. The ratio of posterior probabilities for the models is therefore

$$\frac{P(H_i|\boldsymbol{x})}{P(H_j|\boldsymbol{x})} = \frac{\int P(\boldsymbol{x}|\boldsymbol{\theta}_i, H_i)\pi(\boldsymbol{\theta}_i|H_i)\, d\boldsymbol{\theta}_i}{\int P(\boldsymbol{x}|\boldsymbol{\theta}_j, H_j)\pi(\boldsymbol{\theta}_j|H_j)\, d\boldsymbol{\theta}_j} \frac{P(H_i)}{P(H_j)} \,. \tag{39.57}$$

The *Bayes factor* is defined as

$$B_{ij} = \frac{\int P(\boldsymbol{x}|\boldsymbol{\theta}_i, H_i)\pi(\boldsymbol{\theta}_i|H_i)\, d\boldsymbol{\theta}_i}{\int P(\boldsymbol{x}|\boldsymbol{\theta}_j, H_j)\pi(\boldsymbol{\theta}_j|H_j)\, d\boldsymbol{\theta}_j} \,. \tag{39.58}$$

This gives what the ratio of posterior probabilities for models i and j would be if the overall prior probabilities for the two models were equal. If the models have no nuisance parameters, *i.e.*, no internal parameters described by priors, then the Bayes factor is simply the likelihood ratio. The Bayes factor therefore shows by how much the probability ratio of model i to model j changes in the light of the data, and thus can be viewed as a numerical measure of evidence supplied by the data in favour of one hypothesis over the other.

Although the Bayes factor is by construction independent of the overall prior probabilities $P(H_i)$ and $P(H_j)$, it does require priors for all internal parameters of a model, *i.e.*, one needs the functions $\pi(\boldsymbol{\theta}_i|H_i)$ and $\pi(\boldsymbol{\theta}_j|H_j)$. In a Bayesian analysis where one is only interested in the posterior p.d.f. of a parameter, it may be acceptable to take an unnormalizable function for the prior (an improper prior) as long as the product of likelihood and prior can be normalized. But improper priors are only defined up to an arbitrary multiplicative constant, and so the Bayes factor would depend on this constant. Furthermore, although the range of a constant normalized prior is unimportant for parameter determination (provided it is wider than the likelihood), this is not so for the Bayes factor when such a prior is used for only one of the hypotheses. So to compute a Bayes factor, all internal parameters must be described by normalized priors that represent meaningful probabilities over the entire range where they are defined.

An exception to this rule may be considered when the identical parameter appears in the models for both numerator and denominator of the Bayes factor. In this case one can argue that the arbitrary constants would cancel. One must exercise some caution, however, as parameters with the same name and physical meaning may still play different roles in the two models.

Both integrals in Equation (39.58) are of the form

$$m = \int P(\boldsymbol{x}|\boldsymbol{\theta})\pi(\boldsymbol{\theta})\, d\boldsymbol{\theta} \,, \tag{39.59}$$

which is the marginal likelihood seen previously in Eq. (39.49) (in some fields this quantity is called the *evidence*). Computing marginal likelihoods can be difficult; in many cases it can be done with the nested sampling algorithm [35] as implemented, *e.g.*, in the program `MultiNest` [36]. A review of Bayes factors can be found in Ref. [37].

39.4. Intervals and limits

When the goal of an experiment is to determine a parameter θ, the result is usually expressed by quoting, in addition to the point estimate, some sort of interval which reflects the statistical precision of the measurement. In the simplest case, this can be given by the parameter's estimated value $\widehat{\theta}$ plus or minus an estimate of the standard deviation of $\widehat{\theta}$, $\widehat{\sigma}_{\widehat{\theta}}$. If, however, the p.d.f. of the estimator is not Gaussian or if there are physical boundaries on the possible values of the parameter, then one usually quotes instead an interval according to one of the procedures described below.

In reporting an interval or limit, the experimenter may wish to

- communicate as objectively as possible the result of the experiment;
- provide an interval that is constructed to cover on average the true value of the parameter with a specified probability;
- provide the information needed by the consumer of the result to draw conclusions about the parameter or to make a particular decision;
- draw conclusions about the parameter that incorporate stated prior beliefs.

With a sufficiently large data sample, the point estimate and standard deviation (or for the multiparameter case, the parameter estimates and covariance matrix) satisfy essentially all of these goals. For finite data samples, no single method for quoting an interval will achieve all of them.

In addition to the goals listed above, the choice of method may be influenced by practical considerations such as ease of producing an interval from the results of several measurements. Of course the experimenter is not restricted to quoting a single interval or limit; one may choose, for example, first to communicate the result with a confidence interval having certain frequentist properties, and then in addition to draw conclusions about a parameter using a judiciously chosen subjective Bayesian prior. It is recommended, however, that there be a clear separation between these two aspects of reporting a result. In the remainder of this section, we assess the extent to which various types of intervals achieve the goals stated here.

39.4.1. *Bayesian intervals* :

As described in Sec. 39.2.5, a Bayesian posterior probability may be used to determine regions that will have a given probability of containing the true value of a parameter. In the single parameter case, for example, an interval (called a Bayesian or credible interval) $[\theta_{\rm lo}, \theta_{\rm up}]$ can be determined which contains a given fraction $1-\alpha$ of the posterior probability, *i.e.*,

$$1-\alpha = \int_{\theta_{\rm lo}}^{\theta_{\rm up}} p(\theta|\boldsymbol{x})\, d\theta \,. \tag{39.60}$$

Sometimes an upper or lower limit is desired, *i.e.*, $\theta_{\rm lo}$ or $\theta_{\rm up}$ can be set to a physical boundary or to plus or minus infinity. In other cases, one might be interested in the set of θ values for which $p(\theta|\boldsymbol{x})$ is higher than for any θ not belonging to the set, which may constitute a single interval or a set of disjoint regions; these are called highest posterior density (HPD) intervals. Note that HPD intervals are not invariant under a nonlinear transformation of the parameter.

If a parameter is constrained to be non-negative, then the prior p.d.f. can simply be set to zero for negative values. An important example is the case of a Poisson variable n, which counts signal events with unknown mean s, as well as background with mean b, assumed known. For the signal mean s, one often uses the prior

$$\pi(s) = \begin{cases} 0 & s < 0 \\ 1 & s \geq 0 \end{cases} \,. \tag{39.61}$$

This prior is regarded as providing an interval whose frequentist properties can be studied, rather than as representing a degree of belief. For example, to obtain an upper limit on s, one may proceed as follows. The likelihood for s is given by the Poisson distribution for n with mean $s+b$,

$$P(n|s) = \frac{(s+b)^n}{n!} e^{-(s+b)} \,, \tag{39.62}$$

along with the prior (39.61) in (39.35) gives the posterior density for s. An upper limit $s_{\rm up}$ at confidence level (or here, rather, *credibility* level) $1-\alpha$ can be obtained by requiring

$$1-\alpha = \int_{-\infty}^{s_{\rm up}} p(s|n) ds = \frac{\int_{-\infty}^{s_{\rm up}} P(n|s)\, \pi(s)\, ds}{\int_{-\infty}^{\infty} P(n|s)\, \pi(s)\, ds} \,, \tag{39.63}$$

where the lower limit of integration is effectively zero because of the cut-off in $\pi(s)$. By relating the integrals in Eq. (39.63) to incomplete gamma functions, the solution for the upper limit is found to be

$$s_{\rm up} = \tfrac{1}{2} F_{\chi^2}^{-1} [p, 2(n+1)] - b \,, \tag{39.64}$$

where $F_{\chi^2}^{-1}$ is the quantile of the χ^2 distribution (inverse of the cumulative distribution). Here the quantity p is

$$p = 1 - \alpha \left(1 - F_{\chi^2} [2b, 2(n+1)]\right) \,, \tag{39.65}$$

where F_{χ^2} is the cumulative χ^2 distribution. For both F_{χ^2} and $F^{-1}_{\chi^2}$ above, the argument $2(n+1)$ gives the number of degrees of freedom. For the special case of $b = 0$, the limit reduces to

$$s_{\rm up} = \tfrac{1}{2} F^{-1}_{\chi^2}(1-\alpha; 2(n+1)) \,. \tag{39.66}$$

It happens that for the case of $b = 0$, the upper limit from Eq. (39.66) coincides numerically with the frequentist upper limit discussed in Section 39.4.2.3. Values for $1-\alpha = 0.9$ and 0.95 are given by the values $\mu_{\rm up}$ in Table 39.3. The frequentist properties of confidence intervals for the Poisson mean found in this way are discussed in Refs. [2] and [25].

As in any Bayesian analysis, it is important to show how the result changes under assumption of different prior probabilities. For example, one could consider the Jeffreys prior as described in Sec. 39.2.5. For this problem one finds the Jeffreys prior $\pi(s) \propto 1/\sqrt{s+b}$ for $s \geq 0$ and zero otherwise. As with the constant prior, one would not regard this as representing one's prior beliefs about s, both because it is improper and also as it depends on b. Rather it is used with Bayes' theorem to produce an interval whose frequentist properties can be studied.

If the model contains nuisance parameters then these are eliminated by marginalizing, as in Eq. (39.41), to obtain the p.d.f. for the parameters of interest. For example, if the parameter b in the Poisson counting problem above were to be characterized by a prior p.d.f. $\pi(b)$, then one would first use Bayes' theorem to find $p(s, b|n)$. This is then marginalized to find $p(s|n) = \int p(s, b|n)\pi(b)\, db$, from which one may determine an interval for s. One may not be certain whether to extend a model by including more nuisance parameters. In this case, a Bayes factor may be used to determine to what extent the data prefer a model with additional parameters, as described in Section 39.3.3.

39.4.2. *Frequentist confidence intervals* :

The unqualified phrase "confidence intervals" refers to frequentist intervals obtained with a procedure due to Neyman [34], described below. The boundary of the interval (or in the multiparameter case, region) is given by a specific function of the data, which would fluctuate if one were to repeat the experiment many times. The *coverage probability* refers to the fraction of intervals in such an ensemble that contain the true parameter value. Confidence intervals are constructed so as to have a coverage probability greater than or equal to a given *confidence level*, regardless of the true parameter's value. It is important to note that in the frequentist approach, such a probability is not meaningful for a fixed interval. In this section we discuss several techniques for producing intervals that have, at least approximately, this property of coverage.

39.4.2.1. *The Neyman construction for confidence intervals:*

Consider a p.d.f. $f(x;\theta)$ where x represents the outcome of the experiment and θ is the unknown parameter for which we want to construct a confidence interval. The variable x could (and often does) represent an estimator for θ. Using $f(x;\theta)$, we can find using a pre-defined rule and probability $1-\alpha$ for every value of θ, a set of values $x_1(\theta,\alpha)$ and $x_2(\theta,\alpha)$ such that

$$P(x_1 < x < x_2; \theta) = \int_{x_1}^{x_2} f(x;\theta)\, dx \geq 1-\alpha \,. \tag{39.67}$$

If x is discrete, the integral is replaced by the corresponding sum. In that case there may not exist a range of x values whose summed probability is exactly equal to a given value of $1-\alpha$, and one requires by convention $P(x_1 < x < x_2; \theta) \geq 1-\alpha$.

This is illustrated for continuous x in Fig. 39.3: a horizontal line segment $[x_1(\theta,\alpha), x_2(\theta,\alpha)]$ is drawn for representative values of θ. The union of such intervals for all values of θ, designated in the figure as $D(\alpha)$, is known as a *confidence belt*. Typically the curves $x_1(\theta,\alpha)$ and $x_2(\theta,\alpha)$ are monotonic functions of θ, which we assume for this discussion.

Upon performing an experiment to measure x and obtaining a value x_0, one draws a vertical line through x_0. The confidence interval for θ is the set of all values of θ for which the corresponding line segment

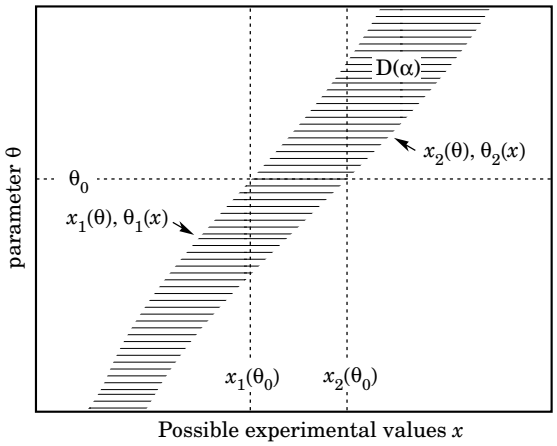

Figure 39.3: Construction of the confidence belt (see text).

$[x_1(\theta,\alpha), x_2(\theta,\alpha)]$ is intercepted by this vertical line. Such confidence intervals are said to have a *confidence level* (CL) equal to $1-\alpha$.

Now suppose that the true value of θ is θ_0, indicated in the figure. We see from the figure that θ_0 lies between $\theta_1(x)$ and $\theta_2(x)$ if and only if x lies between $x_1(\theta_0)$ and $x_2(\theta_0)$. The two events thus have the same probability, and since this is true for any value θ_0, we can drop the subscript 0 and obtain

$$1-\alpha = P(x_1(\theta) < x < x_2(\theta)) = P(\theta_2(x) < \theta < \theta_1(x)) \,. \tag{39.68}$$

In this probability statement, $\theta_1(x)$ and $\theta_2(x)$, *i.e.*, the endpoints of the interval, are the random variables and θ is an unknown constant. If the experiment were to be repeated a large number of times, the interval $[\theta_1, \theta_2]$ would vary, covering the fixed value θ in a fraction $1-\alpha$ of the experiments.

The condition of coverage in Eq. (39.67) does not determine x_1 and x_2 uniquely, and additional criteria are needed. One possibility is to choose *central intervals* such that the probabilities to find x below x_1 and above x_2 are each $\alpha/2$. In other cases, one may want to report only an upper or lower limit, in which case one of $P(x \leq x_1)$ or $P(x \geq x_2)$ can be set to α and the other to zero. Another principle based on *likelihood ratio ordering* for determining which values of x should be included in the confidence belt is discussed below.

When the observed random variable x is continuous, the coverage probability obtained with the Neyman construction is $1-\alpha$, regardless of the true value of the parameter. Because of the requirement $P(x_1 < x < x_2) \geq 1-\alpha$ when x is discrete, one obtains in that case confidence intervals that include the true parameter with a probability greater than or equal to $1-\alpha$.

An equivalent method of constructing confidence intervals is to consider a test (see Sec. 39.3) of the hypothesis that the parameter's true value is θ (assume one constructs a test for all physical values of θ). One then excludes all values of θ where the hypothesis would be rejected in a test of size α or less. The remaining values constitute the confidence interval at confidence level $1-\alpha$. If the critical region of the test is characterized by having a p-value $p_\theta \leq \alpha$, then the endpoints of the confidence interval are found in practice by solving $p_\theta = \alpha$ for θ.

In the procedure outlined above, one is still free to choose the test to be used; this corresponds to the freedom in the Neyman construction as to which values of the data are included in the confidence belt. One possibility is to use a test statistic based on the *likelihood ratio*,

$$\lambda(\theta) = \frac{f(x;\theta)}{f(x;\widehat{\theta}\,)} \,, \tag{39.69}$$

where $\widehat{\theta}$ is the value of the parameter which, out of all allowed values, maximizes $f(x;\theta)$. This results in the intervals described in Ref. [38] by Feldman and Cousins. The same intervals can be obtained from the Neyman construction described above by including in the confidence belt those values of x which give the greatest values of $\lambda(\theta)$.

If the model contains nuisance parameters $\boldsymbol{\nu}$, then these can be incorporated into the test (or the p-values) used to determine the limit by profiling as discussed in Section 39.3.2.1. As mentioned there, the strict frequentist approach is to regard the parameter of interest θ as excluded only if it is rejected for all possible values of $\boldsymbol{\nu}$. The resulting interval for θ will then cover the true value with a probability greater than or equal to the nominal confidence level for all points in $\boldsymbol{\nu}$-space.

If the p-value is based on the profiled values of the nuisance parameters, *i.e.*, with $\boldsymbol{\nu} = \widehat{\widehat{\boldsymbol{\nu}}}(\theta)$ used in Eq. (39.47), then the resulting interval for the parameter of interest will have the correct coverage if the true values of $\boldsymbol{\nu}$ are equal to the profiled values. Otherwise the coverage probability may be too high or too low. This procedure has been called *profile construction* in HEP [24] (see also [21]) .

39.4.2.2. *Gaussian distributed measurements:*

An important example of constructing a confidence interval is when the data consists of a single random variable x that follows a Gaussian distribution; this is often the case when x represents an estimator for a parameter and one has a sufficiently large data sample. If there is more than one parameter being estimated, the multivariate Gaussian is used. For the univariate case with known σ, the probability that the measured value x will fall within $\pm\delta$ of the true value μ is

$$1 - \alpha = \frac{1}{\sqrt{2\pi}\sigma} \int_{\mu-\delta}^{\mu+\delta} e^{-(x-\mu)^2/2\sigma^2}\, dx = \mathrm{erf}\left(\frac{\delta}{\sqrt{2}\,\sigma}\right) = 2\Phi\left(\frac{\delta}{\sigma}\right) - 1 \,, \tag{39.70}$$

where erf is the Gaussian error function, which is rewritten in the final equality using Φ, the Gaussian cumulative distribution. Fig. 39.4 shows a $\delta = 1.64\sigma$ confidence interval unshaded. The choice $\delta = \sigma$ gives an interval called the *standard error* which has $1 - \alpha = 68.27\%$ if σ is known. Values of α for other frequently used choices of δ are given in Table 39.1.

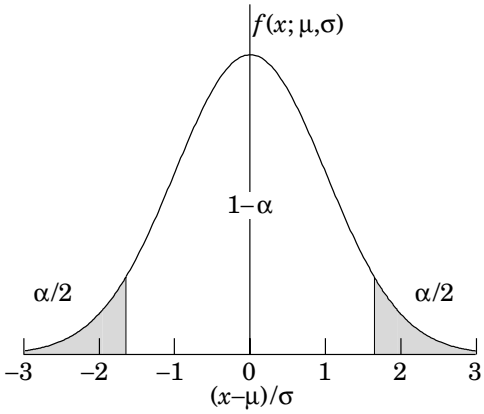

Figure 39.4: Illustration of a symmetric 90% confidence interval (unshaded) for a Gaussian-distributed measurement of a single quantity. Integrated probabilities, defined by $\alpha = 0.1$, are as shown.

Table 39.1: Area of the tails α outside $\pm\delta$ from the mean of a Gaussian distribution.

α	δ	α	δ
0.3173	1σ	0.2	1.28σ
4.55×10^{-2}	2σ	0.1	1.64σ
2.7×10^{-3}	3σ	0.05	1.96σ
6.3×10^{-5}	4σ	0.01	2.58σ
5.7×10^{-7}	5σ	0.001	3.29σ
2.0×10^{-9}	6σ	10^{-4}	3.89σ

We can set a one-sided (upper or lower) limit by excluding above $x + \delta$ (or below $x - \delta$). The values of α for such limits are half the values in Table 39.1.

The relation (39.70) can be re-expressed using the cumulative distribution function for the χ^2 distribution as

$$\alpha = 1 - F(\chi^2; n) \,, \tag{39.71}$$

for $\chi^2 = (\delta/\sigma)^2$ and $n = 1$ degree of freedom. This can be seen as the $n = 1$ curve in Fig. 39.1 or obtained by using the ROOT function `TMath::Prob`.

For multivariate measurements of, say, n parameter estimates $\widehat{\boldsymbol{\theta}} = (\widehat{\theta}_1, \ldots, \widehat{\theta}_n)$, one requires the full covariance matrix $V_{ij} = \mathrm{cov}[\widehat{\theta}_i, \widehat{\theta}_j]$, which can be estimated as described in Sections 39.2.2 and 39.2.3. Under fairly general conditions with the methods of maximum-likelihood or least-squares in the large sample limit, the estimators will be distributed according to a multivariate Gaussian centered about the true (unknown) values $\boldsymbol{\theta}$, and furthermore, the likelihood function itself will take on a Gaussian shape.

The standard error ellipse for the pair $(\widehat{\theta}_i, \widehat{\theta}_j)$ is shown in Fig. 39.5, corresponding to a contour $\chi^2 = \chi^2_{\mathrm{min}} + 1$ or $\ln L = \ln L_{\mathrm{max}} - 1/2$. The ellipse is centered about the estimated values $\widehat{\boldsymbol{\theta}}$, and the tangents to the ellipse give the standard deviations of the estimators, σ_i and σ_j. The angle of the major axis of the ellipse is given by

$$\tan 2\phi = \frac{2\rho_{ij}\sigma_i\sigma_j}{\sigma_j^2 - \sigma_i^2} \,, \tag{39.72}$$

where $\rho_{ij} = \mathrm{cov}[\widehat{\theta}_i, \widehat{\theta}_j]/\sigma_i\sigma_j$ is the correlation coefficient.

The correlation coefficient can be visualized as the fraction of the distance σ_i from the ellipse's horizontal center-line at which the ellipse becomes tangent to vertical, *i.e.*, at the distance $\rho_{ij}\sigma_i$ below the center-line as shown. As ρ_{ij} goes to $+1$ or -1, the ellipse thins to a diagonal line.

It could happen that one of the parameters, say, θ_j, is known from previous measurements to a precision much better than σ_j, so that the current measurement contributes almost nothing to the knowledge of θ_j. However, the current measurement of θ_i and its dependence on θ_j may still be important. In this case, instead of quoting both parameter estimates and their correlation, one sometimes reports the value of θ_i, which minimizes χ^2 at a fixed value of θ_j, such as the PDG best value. This θ_i value lies along the dotted line between the points where the ellipse becomes tangent to vertical, and has statistical error σ_{inner} as shown on the figure, where $\sigma_{\mathrm{inner}} = (1 - \rho_{ij}^2)^{1/2}\sigma_i$. Instead of the correlation ρ_{ij}, one reports the dependency $d\widehat{\theta}_i/d\theta_j$, which is the slope of the dotted line. This slope is related to the correlation coefficient by $d\widehat{\theta}_i/d\theta_j = \rho_{ij} \times \frac{\sigma_i}{\sigma_j}$.

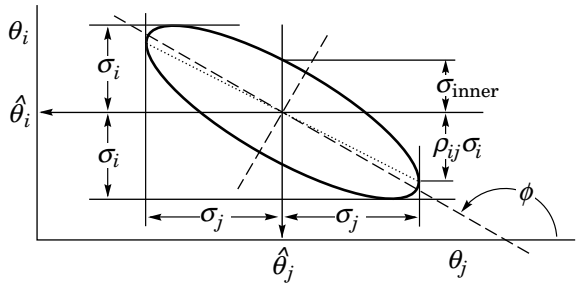

Figure 39.5: Standard error ellipse for the estimators $\widehat{\theta}_i$ and $\widehat{\theta}_j$. In the case shown the correlation is negative.

As in the single-variable case, because of the symmetry of the Gaussian function between $\boldsymbol{\theta}$ and $\widehat{\boldsymbol{\theta}}$, one finds that contours of constant $\ln L$ or χ^2 cover the true values with a certain, fixed probability. That is, the confidence region is determined by

$$\ln L(\boldsymbol{\theta}) \geq \ln L_{\mathrm{max}} - \Delta \ln L \,, \tag{39.73}$$

or where a χ^2 has been defined for use with the method of least-squares,

$$\chi^2(\boldsymbol{\theta}) \leq \chi^2_{\mathrm{min}} + \Delta\chi^2 \,. \tag{39.74}$$

Table 39.2: Values of $\Delta\chi^2$ or $2\Delta\ln L$ corresponding to a coverage probability $1-\alpha$ in the large data sample limit, for joint estimation of m parameters.

$(1-\alpha)$ (%)	$m=1$	$m=2$	$m=3$
68.27	1.00	2.30	3.53
90.	2.71	4.61	6.25
95.	3.84	5.99	7.82
95.45	4.00	6.18	8.03
99.	6.63	9.21	11.34
99.73	9.00	11.83	14.16

Values of $\Delta\chi^2$ or $2\Delta\ln L$ are given in Table 39.2 for several values of the coverage probability $1-\alpha$ and number of fitted parameters m. For Gaussian distributed data, these are related by $\Delta\chi^2 = 2\Delta\ln L = F^{-1}_{\chi^2_m}(1-\alpha)$, where $F^{-1}_{\chi^2_m}$ is the chi-square quantile (inverse of the cumulative distribution) for m degrees of freedom.

For non-Gaussian data samples, the probability for the regions determined by Equations (39.73) or (39.74) to cover the true value of $\boldsymbol{\theta}$ becomes independent of $\boldsymbol{\theta}$ only in the large-sample limit. So for a finite data sample these are not exact confidence regions according to our previous definition. Nevertheless, they can still have a coverage probability only weakly dependent on the true parameter, and approximately as given in Table 39.2. In any case, the coverage probability of the intervals or regions obtained according to this procedure can in principle be determined as a function of the true parameter(s), for example, using a Monte Carlo calculation.

One of the practical advantages of intervals that can be constructed from the log-likelihood function or χ^2 is that it is relatively simple to produce the interval for the combination of several experiments. If N independent measurements result in log-likelihood functions $\ln L_i(\boldsymbol{\theta})$, then the combined log-likelihood function is simply the sum,

$$\ln L(\boldsymbol{\theta}) = \sum_{i=1}^{N} \ln L_i(\boldsymbol{\theta}) \; . \tag{39.75}$$

This can then be used to determine an approximate confidence interval or region with Eq. (39.73), just as with a single experiment.

39.4.2.3. *Poisson or binomial data:*

Another important class of measurements consists of counting a certain number of events, n. In this section, we will assume these are all events of the desired type, *i.e.*, there is no background. If n represents the number of events produced in a reaction with cross section σ, say, in a fixed integrated luminosity $\mathcal{L}$, then it follows a Poisson distribution with mean $\mu = \sigma\mathcal{L}$. If, on the other hand, one has selected a larger sample of N events and found n of them to have a particular property, then n follows a binomial distribution where the parameter p gives the probability for the event to possess the property in question. This is appropriate, *e.g.*, for estimates of branching ratios or selection efficiencies based on a given total number of events.

For the case of Poisson distributed n, limits on the mean value μ can be found from the Neyman procedure as discussed in Section 39.4.2.1 with n used directly as the statistic x . The upper and lower limits are found to be

$$\mu_{\rm lo} = \tfrac{1}{2} F^{-1}_{\chi^2}(\alpha_{\rm lo}; 2n) \; , \tag{39.76a}$$

$$\mu_{\rm up} = \tfrac{1}{2} F^{-1}_{\chi^2}(1-\alpha_{\rm up}; 2(n+1)) \; , \tag{39.76b}$$

where confidence levels of $1-\alpha_{\rm lo}$ and $1-\alpha_{\rm up}$ refer separately to the corresponding intervals $\mu \geq \mu_{\rm lo}$ and $\mu \leq \mu_{\rm up}$, and $F^{-1}_{\chi^2}$ is the quantile of the χ^2 distribution (inverse of the cumulative distribution). The quantiles $F^{-1}_{\chi^2}$ can be obtained from standard tables or from the ROOT routine `TMath::ChisquareQuantile`. For central confidence intervals at confidence level $1-\alpha$, set $\alpha_{\rm lo} = \alpha_{\rm up} = \alpha/2$.

Table 39.3: Lower and upper (one-sided) limits for the mean μ of a Poisson variable given n observed events in the absence of background, for confidence levels of 90% and 95%.

	$1-\alpha$ =90%		$1-\alpha$ =95%	
n	$\mu_{\rm lo}$	$\mu_{\rm up}$	$\mu_{\rm lo}$	$\mu_{\rm up}$
0	–	2.30	–	3.00
1	0.105	3.89	0.051	4.74
2	0.532	5.32	0.355	6.30
3	1.10	6.68	0.818	7.75
4	1.74	7.99	1.37	9.15
5	2.43	9.27	1.97	10.51
6	3.15	10.53	2.61	11.84
7	3.89	11.77	3.29	13.15
8	4.66	12.99	3.98	14.43
9	5.43	14.21	4.70	15.71
10	6.22	15.41	5.43	16.96

It happens that the upper limit from Eq. (39.76*b*) coincides numerically with the Bayesian upper limit for a Poisson parameter, using a uniform prior p.d.f. for μ. Values for confidence levels of 90% and 95% are shown in Table 39.3. For the case of binomially distributed n successes out of N trials with probability of success p, the upper and lower limits on p are found to be

$$p_{\rm lo} = \frac{nF^{-1}_F[\alpha_{\rm lo}; 2n, 2(N-n+1)]}{N-n+1 \, + \, nF^{-1}_F[\alpha_{\rm lo}; 2n, 2(N-n+1)]} \; , \tag{39.77a}$$

$$p_{\rm up} = \frac{(n+1)F^{-1}_F[1-\alpha_{\rm up}; 2(n+1), 2(N-n)]}{(N-n) \, + \, (n+1)F^{-1}_F[1-\alpha_{\rm up}; 2(n+1), 2(N-n)]} \; . \tag{39.77b}$$

Here F^{-1}_F is the quantile of the F distribution (also called the Fisher–Snedecor distribution; see Ref. [4]) .

39.4.2.4. *Parameter exclusion in cases of low sensitivity:*

An important example of a statistical test arises in the search for a new signal process. Suppose the parameter μ is defined such that it is proportional to the signal cross section. A statistical test may be carried out for hypothesized values of μ, which may be done by computing a p-value, p_μ, for all μ. Those values not rejected in a test of size α, *i.e.*, for which one does not find $p_\mu \leq \alpha$, constitute a confidence interval with confidence level $1-\alpha$.

In general one will find that for some regions in the parameter space of the signal model, the predictions for data are almost indistinguishable from those of the background-only model. This corresponds to the case where μ is very small, as would occur, *e.g.*, in a search for a new particle with a mass so high that its production rate in a given experiment is negligible. That is, one has essentially no experimental sensitivity to such a model.

One would prefer that if the sensitivity to a model (or a point in a model's parameter space) is very low, then it should not be excluded. Even if the outcomes predicted with or without signal are identical, however, the probability to reject the signal model will equal α, the type-I error rate. As one often takes α to be 5%, this would mean that in a large number of searches covering a broad range of a signal model's parameter space, there would inevitably be excluded regions in which the experimental sensitivity is very small, and thus one may question whether it is justified to regard such parameter values as disfavored.

Exclusion of models to which one has little or no sensitivity occurs, for example, if the data fluctuate very low relative to the expectation of the background-only hypothesis. In this case the resulting upper limit on μ may be anomalously low. As a means of controlling this effect one often determines the mean or median limit under assumption of the background-only hypothesis, as discussed in Sec. 39.5.

One way to mitigate the problem of excluding models to which one is not sensitive is the CL_s method, where the measure used to test a parameter is increased for decreasing sensitivity [39,40]. The procedure is based on a statistic called CL_s, which is defined as

$$CL_s = \frac{p_\mu}{1 - p_b} , \tag{39.78}$$

where p_b is the p-value of the background-only hypothesis. In the usual formulation of the method, both p_μ and p_b are defined using a single test statistic, and the definition of CL_s above assumes this statistic is continuous; more details can be found in Refs. [39–40].

A point in a model's parameter space is regarded as excluded if one finds $CL_s \leq \alpha$. As the denominator in Eq. (39.78) is always less than or equal to unity, the exclusion criterion based on CL_s is more stringent than the usual requirement $p_\mu \leq \alpha$. In this sense the CL_s procedure is conservative, and the coverage probability of the corresponding intervals will exceed the nominal confidence level $1 - \alpha$. If the experimental sensitivity to a given value of μ is very low, then one finds that as p_μ decreases, so does the denominator $1 - p_b$, and thus the condition $CL_s \leq \alpha$ is effectively prevented from being satisfied. In this way the exclusion of parameters in the case of low sensitivity is suppressed.

The CL_s procedure has the attractive feature that the resulting intervals coincide with those obtained from the Bayesian method in two important cases: the mean value of a Poisson or Gaussian distributed measurement with a constant prior. The CL_s intervals overcover for all values of the parameter μ, however, by an amount that depends on μ.

The problem of excluding parameter values to which one has little sensitivity is particularly acute when one wants to set a one-sided limit, *e.g.*, an upper limit on a cross section. Here one tests a value of a rate parameter μ against the alternative of a lower rate, and therefore the critical region of the test is taken to correspond to data outcomes with a low event yield. If the number of events found in the search region fluctuates low enough, however, it can happen that all physically meaningful signal parameter values, including those to which one has very little sensitivity, are rejected by the test.

Another solution to this problem, therefore, is to replace the one-sided test by one based on the likelihood ratio, where the critical region is not restricted to low rates. This is the approach followed in the Feldman-Cousins procedure described in Section 39.4.2.1. The critical region for the test of a given value of μ contains data values characteristic of both higher and lower rates. As a result, for a given observed rate one can in general obtain a two-sided interval. If, however, the parameter estimate $\hat{\mu}$ is sufficiently close to the lower limit of zero, then only high values of μ are rejected, and the lower edge of the confidence interval is at zero. Note, however, that the coverage property of $1 - \alpha$ pertains to the entire interval, not to the probability for the upper edge μ_{up} to be greater than the true value μ. For parameter estimates increasingly far away from the boundary, *i.e.*, for increasing signal significance, the point $\mu = 0$ is excluded and the interval has nonzero upper and lower edges.

An additional difficulty arises when a parameter estimate is not significantly far away from the boundary, in which case it is natural to report a one-sided confidence interval (often an upper limit). It is straightforward to force the Neyman prescription to produce only an upper limit by setting $x_2 = \infty$ in Eq. (39.67). Then x_1 is uniquely determined and the upper limit can be obtained. If, however, the data come out such that the parameter estimate is not so close to the boundary, one might wish to report a central confidence interval (*i.e.*, an interval based on a two-sided test with equal upper and lower tail areas). As pointed out by Feldman and Cousins [38], if the decision to report an upper limit or two-sided interval is made by looking at the data ("flip-flopping"), then in general there will be parameter values for which the resulting intervals have a coverage probability less than $1 - \alpha$. With the confidence intervals suggested in [38], the prescription determines whether the interval is one- or two-sided in a way which preserves the coverage probability (and are thus said to be *unified*).

The intervals according to this method for the mean of Poisson variable in the absence of background are given in Table 39.4. (Note that α in Ref. [38] is defined following Neyman [34] as the coverage probability; this is opposite the modern convention used here in which the coverage probability is $1 - \alpha$.) The values of $1 - \alpha$ given here refer to the coverage of the true parameter by the whole interval $[\mu_1, \mu_2]$. In Table 39.3 for the one-sided upper limit, however, $1 - \alpha$ refers to the probability to have $\mu_{up} \geq \mu$ (or $\mu_{lo} \leq \mu$ for lower limits).

Table 39.4: Unified confidence intervals $[\mu_1, \mu_2]$ for a the mean of a Poisson variable given n observed events in the absence of background, for confidence levels of 90% and 95%.

	$1 - \alpha$ =90%		$1 - \alpha$ =95%	
n	μ_1	μ_2	μ_1	μ_2
0	0.00	2.44	0.00	3.09
1	0.11	4.36	0.05	5.14
2	0.53	5.91	0.36	6.72
3	1.10	7.42	0.82	8.25
4	1.47	8.60	1.37	9.76
5	1.84	9.99	1.84	11.26
6	2.21	11.47	2.21	12.75
7	3.56	12.53	2.58	13.81
8	3.96	13.99	2.94	15.29
9	4.36	15.30	4.36	16.77
10	5.50	16.50	4.75	17.82

A potential difficulty with unified intervals arises if, for example, one constructs such an interval for a Poisson parameter s of some yet to be discovered signal process with, say, $1 - \alpha = 0.9$. If the true signal parameter is zero, or in any case much less than the expected background, one will usually obtain a one-sided upper limit on s. In a certain fraction of the experiments, however, a two-sided interval for s will result. Since, however, one typically chooses $1 - \alpha$ to be only 0.9 or 0.95 when setting limits, the value $s = 0$ may be found below the lower edge of the interval before the existence of the effect is well established. It must then be communicated carefully that in excluding $s = 0$ at, say, 90% or 95% confidence level from the interval, one is not necessarily claiming to have discovered the effect, for which one would usually require a higher level of significance (*e.g.*, 5 σ).

Another possibility is to construct a Bayesian interval as described in Section 39.4.1. The presence of the boundary can be incorporated simply by setting the prior density to zero in the unphysical region. More specifically, the prior may be chosen using formal rules such as the reference prior or Jeffreys prior mentioned in Sec. 39.2.5.

In HEP a widely used prior for the mean μ of a Poisson distributed measurement has been the uniform distribution for $\mu \geq 0$. This prior does not follow from any fundamental rule nor can it be regarded as reflecting a reasonable degree of belief, since the prior probability for μ to lie between any two finite values is zero. The procedure above can be more appropriately regarded as a way for obtaining intervals with frequentist properties that can be investigated. The resulting upper limits have a coverage probability that depends on the true value of the Poisson parameter, and is nowhere smaller than the stated probability content. Lower limits and two-sided intervals for the Poisson mean based on flat priors undercover, however, for some values of the parameter, although to an extent that in practical cases may not be too severe [2,25]. Intervals constructed in this way have the advantage of being easy to derive; if several independent measurements are to be combined then one simply multiplies the likelihood functions (cf. Eq. (39.75)).

In any case, it is important to always report sufficient information so that the result can be combined with other measurements. Often this means giving an unbiased estimator and its standard deviation, even if the estimated value is in the unphysical region.

It can also be useful with a frequentist interval to calculate its subjective probability content using the posterior p.d.f. based on one or several reasonable guesses for the prior p.d.f. If it turns out to be significantly less than the stated confidence level, this warns that

it would be particularly misleading to draw conclusions about the parameter's value from the interval alone.

39.5. Experimental sensitivity

In this section we describe methods for characterizing the sensitivity of a search for a new physics signal. As discussed in Sec. 39.3,an experimental analysis can often be formulated as a test of hypothetical model parameters. Therefore we may quantify the sensitivity by giving the results that we expect from such a test under specific assumptions about the signal process.

Here to be concrete we will consider a parameter μ proportional to the rate of a signal process, although the concepts described in this section may be easily generalized to other parameters. One may wish to establish discovery of the signal process by testing and rejecting the hypothesis that $\mu = 0$, and in addition one often wants to test nonzero values of μ to construct a confidence interval (*e.g.*, limits) as described in Sec. 39.4. In the frequentist framework, the result of each tested value of μ is the p-value p_μ or equivalently the significance $Z_\mu = \Phi^{-1}(1 - p_\mu)$, where as usual Φ is the standard Gaussian cumulative distribution and its inverse Φ^{-1} is the standard Gaussian quantile.

Prior to carrying out the experiment, one generally wants to quantify what significance Z_μ is expected under given assumptions for the presence or absence of the signal process. Specifically, for the significance of a test of $\mu = 0$ (the discovery significance) one usually quotes the Z_0 one would expect if the signal is present at a given nominal rate, which we can define in general to correspond to $\mu = 1$. For limits, one often gives the expected limit under assumption of the background-only ($\mu = 0$) model. These quantities are used to optimize the analysis and to quantify the experimental sensitivity, that is, to characterize how likely it is to make a discovery if the signal is present, and to say what values of μ one may be able to exclude if the signal is in fact absent.

First we clarify the notion of *expected significance*. Because the significance Z_μ is a function of the data, it is itself a random quantity characterized by a certain sampling distribution. This distribution depends on the assumed value of μ, which is not necessarily the same as the hypothesized value of μ being tested. We may therefore consider the distribution $f(Z_\mu|\mu')$, *i.e.*, the distribution of Z_μ that would be obtained by considering data samples generated under assumption of μ'. In a similar way one can talk about the sampling distribution of an upper limit for μ, $f(\mu_{\rm up}|\mu')$.

One can identify the expected significance or limit with either the mean or median of these distributions, but the median may be preferred since it is invariant under monotonic transformations. For example, the monotonic relation between p-value and significance, $p = 1 - \Phi(Z)$, then gives $\mathrm{med}[p_\mu|\mu'] = 1 - \Phi(\mathrm{med}[Z_\mu|\mu'])$, whereas the corresponding relation does not hold in general for the mean.

In some cases one may be able to write down approximate formulae for the distributions of Z_μ and for limits, but more generally they must be determined from Monte Carlo calculations. In many cases of interest, the significance Z_μ and the limits on μ will have approximate Gaussian distributions.

As an example, consider a Poisson counting experiment, where the result consists of an observed number n of events, modeled as a Poisson distributed variable with a mean of $\mu s + b$. Here s and b, the expected numbers of events from signal and background processes, are taken to be known. If we are interested in discovering the signal process we test and try to reject the hypothesis $\mu = 0$. To characterize the experimental sensitivity, we want to give the discovery significance expected under the assumption of $\mu = 1$.

In the limit where its mean value is large, the Poisson variable n can be approximated as an almost continuous Gaussian variable with mean $\mu s + b$ and standard deviation $\sigma = \sqrt{\mu s + b}$. In the usual case where a physical signal model corresponds to $\mu > 0$, the p-value of $\mu = 0$ is the probability to find n greater than or equal to the value observed,

$$p_0 = \Phi\left(\frac{n-b}{\sqrt{b}}\right) , \tag{39.79}$$

and the corresponding significance is $Z_0 = \Phi^{-1}(1 - p_0) = (n - b)/\sqrt{b}$. The median (here equal to the mean) of n assuming $\mu = 1$ is $s + b$, and therefore the median discovery significance is

$$\mathrm{med}[Z_0|\mu = 1] = \frac{s}{\sqrt{b}} . \tag{39.80}$$

The figure of merit "$s/\sqrt{b}$" has been widely used in HEP as a measure of expected discovery significance. A better approximation for the Poisson counting experiment, however, may be obtained by testing $\mu = 0$ using the likelihood ratio (39.48) $\lambda(0) = L(0)/L(\hat{\mu})$, where

$$L(\mu) = \frac{(\mu s + b)^n}{n!} e^{-(\mu s + b)} \tag{39.81}$$

is the likelihood function, $\hat{\mu} = (n - b)/s$ is the ML estimator. In this example there are no nuisance parameters, as s and b are taken to be known. For the case where the relevant signal models correspond to positive μ, one may test the $\mu = 0$ hypothesis with the statistic $q_0 = -2 \ln \lambda(0)$ when $\hat{\mu} > 0$, *i.e.*, an excess is observed, and $q_0 = 0$ otherwise. One can show (see, *e.g.*, [43]) that in the large-sample limit, the discovery significance is then $Z_0 = \sqrt{q_0}$, for which one finds

$$Z_0 = \sqrt{2\left(n \ln \frac{n}{b} + b - n\right)} \tag{39.82}$$

for $n > b$ and $Z_0 = 0$ otherwise. To approximate the expected discovery significance assuming $\mu = 1$, one may simply replace n with the expected value $E[n|\mu = 1] = s + b$ (the so-called "Asimov data set"), giving

$$\mathrm{med}[Z_0|\mu = 1] = \sqrt{2\left((s + b) \ln\left(1 + \frac{s}{b}\right) - s\right)} . \tag{39.83}$$

This has been shown in Ref. [43] to provide a good approximation to the median discovery significance for values of s of several and for b well below unity. The right-hand side of Eq. (39.83) reduces to $s/\sqrt{b}$ in the limit $s \ll b$.

Beyond the simple Poisson counting experiment, in general one may test values of a parameter μ with more complicated functions of the measured data to obtain a p-value p_μ, and from this one can quote the equivalent significance Z_μ or find, *e.g.*, an upper limit $\mu_{\rm up}$. In this case as well one may quantify the experimental sensitivity by giving the significance Z_μ expected if the data are generated with a different value of the parameter μ'. In some problems, finding the sampling distribution of the significance or limits may be possible using large-sample formulae as described, *e.g.*, in Ref. [43]. In other cases a Monte Carlo study may be needed. Using whatever method of calculation is most appropriate, one usually quotes the expected (mean or, preferably, median) significance or limit as the primary measures of experimental sensitivity.

Even if the true signal is present at its nominal rate, the actual discovery significance Z_0 obtained from the real data is subject to statistical fluctuations and will not in general be equal to its expected value. In an analogous way, the observed limit will differ from the expected limit even if the signal is absent. Upon observing such a difference one would like to know how large this is compared to expected statistical fluctuations. Therefore, in addition to the observed significance and limits it is useful to communicate not only their expected values but also a measure of the width of their distributions.

As the distributions of significance and limits are often well approximated by a Gaussian, one may indicate the intervals corresponding to plus-or-minus one and/or two standard deviations. If the distributions are significantly non-Gaussian, one may use instead the quantiles that give the same probability content, *i.e.*, $[0.1587, 0.8413]$ for $\pm 1\sigma$, $[0.02275, 0.97725]$ for $\pm 2\sigma$. An upper limit found significantly below the background-only expectation may indicate a strong downward fluctuation of the data, or perhaps as well an incorrect estimate of the background rate.

The procedures described above pertain to frequentist hypothesis tests and limits. Bayesian limits, just like those found from a

frequentist procedure, are functions of the data and one may therefore find, usually with approximations or Monte Carlo studies, their sampling distribution and corresponding mean (or, preferably, median) and standard deviation.

When trying to establish discovery of a signal process, the Bayesian approach may employ a Bayes factor as described in Sec. 39.3.3. In the case of the Poisson counting experiment with the likelihood from Eq. (39.81), the log of the Bayes factor that compares $\mu = 1$ to $\mu = 0$ is $\ln B_{10} = \ln(L(1)/L(0)) = n \ln(1 + s/b) - s$. That is, the expectation value, assuming $\mu = 1$, of $\ln B_{10}$ for this problem is

$$E[\ln B_{10}|\mu = 1] = (s + b) \ln \left(1 + \frac{s}{b}\right) - s \, . \tag{39.84}$$

Comparing this to Eq. (39.83), one finds $\mathrm{med}[Z_0|1] = \sqrt{2E[\ln B_{10}|1]}$. Thus for this particular problem the frequentist median discovery significance can be related to the corresponding Bayes factor in a simple way.

In some analyses, the goal may not be to establish discovery of a signal process but rather to measure, as accurately as possible, the signal rate. If we consider again the Poisson counting experiment described by the likelihood function of Eq. (39.81), the ML estimator $\hat{\mu} = (n - b)/s$ has a variance, assuming $\mu = 1$, of

$$V[\hat{\mu}] = V\left[\frac{n - b}{s}\right] = \frac{1}{s^2} V[n] = \frac{s + b}{s^2} \, , \tag{39.85}$$

so that the standard deviation of $\hat{\mu}$ is $\sigma_{\hat{\mu}} = \sqrt{s + b}/s$. One may therefore use $s/\sqrt{s + b}$ as a figure of merit to be maximized in order to obtain the best measurement accuracy of a rate parameter. The quantity $s/\sqrt{s + b}$ is also the expected significance with which one rejects s assuming the signal is absent, and thus can be used to optimize the expected upper limit on s.

References:

1. B. Efron, Am. Stat. **40**, 11 (1986).
2. R.D. Cousins, Am. J. Phys. **63**, 398 (1995).
3. A. Stuart, J.K. Ord, and S. Arnold, *Kendall's Advanced Theory of Statistics*, Vol. 2A: *Classical Inference and the Linear Model*, 6th ed., Oxford Univ. Press (1999), and earlier editions by Kendall and Stuart. The likelihood-ratio ordering principle is described at the beginning of Ch. 23. Chapter 26 compares different schools of statistical inference.
4. F. James, *Statistical Methods in Experimental Physics*, 2nd ed., (World Scientific, Singapore, 2007).
5. H. Cramér, *Mathematical Methods of Statistics,* Princeton Univ. Press, New Jersey (1958).
6. L. Lyons, *Statistics for Nuclear and Particle Physicists*, (Cambridge University Press, New York, 1986).
7. R. Barlow, Nucl. Instrum. Methods **A297**, 496 (1990).
8. G. Cowan, *Statistical Data Analysis*, (Oxford University Press, Oxford, 1998).
9. For a review, see S. Baker and R. Cousins, Nucl. Instrum. Methods **221**, 437 (1984).
10. S.S. Wilks, Ann. Math. Statist. **9**, 60 (1938).
11. Christopher M. Bishop, *Pattern Recognition and Machine Learning*, (Springer, New York, 2006).
12. T. Hastie, R. Tibshirani, and J. Friedman, *The Elements of Statistical Learning*, (2nd edition, Springer, New York, 2009).
13. A. Webb, *Statistical Pattern Recognition*, 2nd ed., (Wiley, New York, 2002).
14. L.I. Kuncheva, *Combining Pattern Classifiers*, (Wiley, New York, 2004).
15. Links to the *Proceedings of the PHYSTAT* conference series (Durham 2002, Stanford 2003, Oxford 2005, and Geneva 2007, 2011) can be found at `phystat.org`.
16. A. Höcker *et al.*, *TMVA Users Guide*, `physics/0703039`(2007); software available from `tmva.sourceforge.net`.
17. I. Narsky, *StatPatternRecognition: A C++ Package for Statistical Analysis of High Energy Physics Data*, `physics/0507143`(2005); software avail. from `sourceforge.net/projects/statpatrec`.
18. F. Pedregosa et al., *Scikit-learn: Machine Learning in Python*, Journal of Machine Learning Research **12** 2825–2830 (2011).
19. P. Baldi, P. Sadowski and D. Whiteson, Nature Commun. 5, 4308 (2014); e-print `arXiv:1402.4735` [hep-ph].
20. K. Cranmer, J. Pavez and G. Louppe, `arXiv:1506.02169` [stat.AP] (2015).
21. L. Demortier, *P-Values and Nuisance Parameters*, *Proceedings of PHYSTAT 2007*, CERN-2008-001, p. 23.
22. E. Gross and O. Vitells, Eur. Phys. J. **C70**, 525 (2010); `arXiv:1005.1891`.
23. R.B. Davis, Biometrica **74**, 33 (1987).
24. K. Cranmer, *Statistical Challenges for Searches for New Physics at the LHC*, in Proceedings of PHYSTSAT 2005, L. Lyons and M. Karagoz Unel (eds.), Oxford (2005); `arXiv:physics/0511028`.
25. B.P. Roe and M.B. Woodroofe, Phys. Rev. **D63**, 13009 (2000).
26. A. O'Hagan and J.J. Forster, *Bayesian Inference*, (2nd edition, volume 2B of *Kendall's Advanced Theory of Statistics*, Arnold, London, 2004).
27. D. Sivia and J. Skilling, *Data Analysis: A Bayesian Tutorial*, (Oxford University Press, 2006).
28. P.C. Gregory, *Bayesian Logical Data Analysis for the Physical Sciences*, (Cambridge University Press, 2005).
29. J.M. Bernardo and A.F.M. Smith, *Bayesian Theory*, (Wiley, 2000).
30. Robert E. Kass and Larry Wasserman, J. Am. Stat. Assoc. **91**, 1343 (1996).
31. Olaf Behnke et al., *Data Analysis in High Energy Physics: A Practical Guide to Statistical Methods*, (Wiley, 2013).
32. J.M. Bernardo, J. R. Statist. Soc. **B41**, 113 (1979); J.M. Bernardo and J.O. Berger, J. Am. Stat. Assoc. **84**, 200 (1989). See also J.M. Bernardo, *Reference Analysis*, in *Handbook of Statistics*, 25 (D.K. Dey and C.R. Rao, eds.), 17-90, Elsevier (2005) and references therein.
33. L. Demortier, S. Jain, and H. Prosper, Phys. Rev. **D82**, 034002 (2010) [`arXiv:1002.1111`].
34. J. Neyman, Phil. Trans. Royal Soc. London, Series A, **236**, 333 (1937), reprinted in *A Selection of Early Statistical Papers on J. Neyman*, (University of California Press, Berkeley, 1967).
35. J. Skilling, *Nested Sampling*, *AIP Conference Proceedings*, **735**, 395–405 (2004).
36. F. Feroz, M.P. Hobson, and M. Bridges, Mon. Not. Roy. Astron. Soc. **398**, 1601-1614 (2009); `arXiv:0809.3437`.
37. R. E. Kass and A. E. Raftery, J. Am. Stat. Assoc. **90**, 773 (1995).
38. G.J. Feldman and R.D. Cousins, Phys. Rev. **D57**, 3873 (1998). This paper does not specify what to do if the ordering principle gives equal rank to some values of x. Eq. 21.6 of Ref. [3] gives the rule: all such points are included in the acceptance region (the domain $D(\alpha)$). Some authors have assumed the contrary, and shown that one can then obtain null intervals.
39. A.L. Read, *Modified frequentist analysis of search results (the CL_s method)*, in F. James, L. Lyons, and Y. Perrin (eds.), *Workshop on Confidence Limits*, CERN Yellow Report 2000-005, available through `cdsweb.cern.ch`.
40. T. Junk, Nucl. Instrum. Methods **A434**, 435 (1999).
41. N. Reid, *Likelihood Inference in the Presence of Nuisance Parameters*, *Proceedings of PHYSTAT2003*, L. Lyons, R. Mount, and R. Reitmeyer, eds., eConf C030908, Stanford, 2003.
42. W.A. Rolke, A.M. Lopez, and J. Conrad, Nucl. Instrum. Methods **A551**, 493 (2005).
43. G. Cowan *et al.*, Eur. Phys. J. **C71**, 1554 (2011).

40. Monte Carlo Techniques

Revised September 2017 by G. Cowan (RHUL).

Monte Carlo techniques are often the only practical way to evaluate difficult integrals or to sample random variables governed by complicated probability density functions. Here we describe an assortment of methods for sampling some commonly occurring probability density functions.

40.1. Sampling the uniform distribution

Most Monte Carlo sampling or integration techniques assume a "random number generator," which generates uniform statistically independent values on the half open interval $[0, 1)$; for reviews see, *e.g.*, Refs. [1,2].

Uniform random number generators are available in software libraries such as CLHEP [3], and ROOT [4]. For example, in addition to a basic congruential generator `TRandom` (see below), ROOT provides three more sophisticated routines: `TRandom1` implements the RANLUX generator [5] based on the method by Lüscher, and allows the user to select different quality levels, trading off quality with speed; `TRandom2` is based on the maximally equidistributed combined Tausworthe generator by L'Ecuyer [6]; the `TRandom3` generator implements the Mersenne twister algorithm of Matsumoto and Nishimura [7]. All of the algorithms produce a periodic sequence of numbers, and to obtain effectively random values, one must not use more than a small subset of a single period. The Mersenne twister algorithm has an extremely long period of $2^{19937} - 1$.

The performance of the generators can be investigated with tests such as DIEHARD [8] or TestU01 [9]. Many commonly available congruential generators fail these tests and often have sequences (typically with periods less than 2^{32}), which can be easily exhausted on modern computers. A short period is a problem for the `TRandom` generator in ROOT, which, however, has the advantage that its state is stored in a single 32-bit word. The generators `TRandom1`, `TRandom2`, or `TRandom3` have much longer periods, with `TRandom3` being recommended by the ROOT authors as providing the best combination of speed and good random properties. For further information see, *e.g.*, Ref. [10].

40.2. Inverse transform method

If the desired probability density function is $f(x)$ on the range $-\infty < x < \infty$, its cumulative distribution function (expressing the probability that $x \leq a$) is given by Eq. (38.6). If a is chosen with probability density $f(a)$, then the integrated probability up to point a, $F(a)$, is itself a random variable which will occur with uniform probability density on $[0, 1]$. Suppose u is generated according to a uniformly distributed in $(0, 1)$. If x can take on any value, and ignoring the endpoints, we can then find a unique x chosen from the p.d.f. $f(x)$ for a given u if we set

$$u = F(x) \ , \tag{40.1}$$

provided we can find an inverse of F, defined by

$$x = F^{-1}(u) \ . \tag{40.2}$$

This method is shown in Fig. 40.1a. It is most convenient when one can calculate by hand the inverse function of the indefinite integral of f. This is the case for some common functions $f(x)$ such as $\exp(x)$, $(1 - x)^n$, and $1/(1 + x^2)$ (Cauchy or Breit-Wigner), although it does not necessarily produce the fastest generator. Standard libraries contain software to implement this method numerically, working from functions or histograms in one or more dimensions, *e.g.*, the UNU.RAN package [11], available in ROOT.

For a discrete distribution, $F(x)$ will have a discontinuous jump of size $f(x_k)$ at each allowed $x_k, k = 1, 2, \cdots$. Choose u from a uniform distribution on (0,1) as before. Find x_k such that

$$F(x_{k-1}) < u \leq F(x_k) \equiv \text{Prob}\,(x \leq x_k) = \sum_{i=1}^{k} f(x_i) \ ; \tag{40.3}$$

then x_k is the value we seek (note: $F(x_0) \equiv 0$). This algorithm is illustrated in Fig. 40.1b.

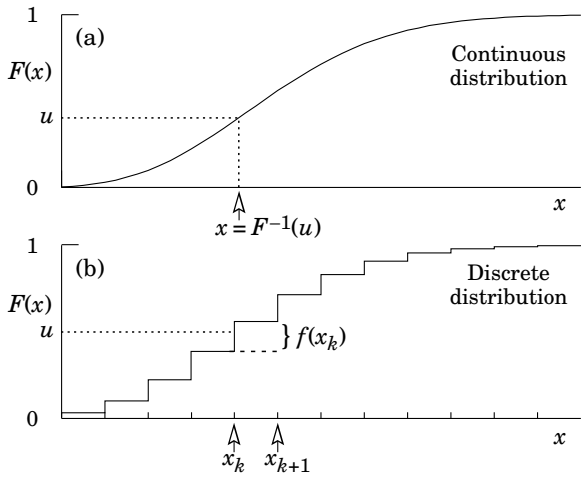

Figure 40.1: Use of a random number u chosen from a uniform distribution (0,1) to find a random number x from a distribution with cumulative distribution function $F(x)$.

40.3. Acceptance-rejection method (Von Neumann)

Very commonly an analytic form for $F(x)$ is unknown or too complex to work with, so that obtaining an inverse as in Eq. (40.2) is impractical. We suppose that for any given value of x, the probability density function $f(x)$ can be computed, and further that enough is known about $f(x)$ that we can enclose it entirely inside a shape which is C times an easily generated distribution $h(x)$, as illustrated in Fig. 40.2. That is, $Ch(x) \geq f(x)$ must hold for all x.

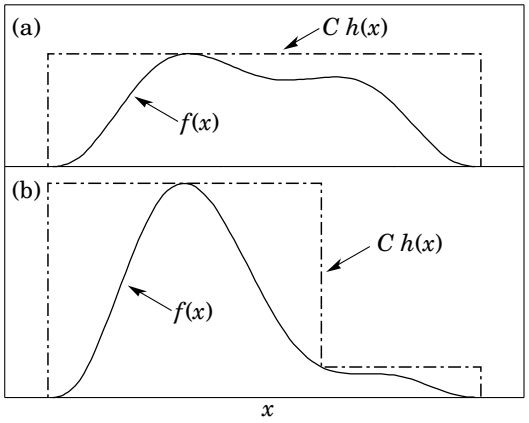

Figure 40.2: Illustration of the acceptance-rejection method. Random points are chosen inside the upper bounding figure, and rejected if the ordinate exceeds $f(x)$. The lower figure illustrates a method to increase the efficiency (see text).

Frequently $h(x)$ is uniform or is a normalized sum of uniform distributions. Note that both $f(x)$ and $h(x)$ must be normalized to unit area, and therefore, the proportionality constant $C > 1$. To generate $f(x)$, first generate a candidate x according to $h(x)$. Calculate $f(x)$ and the height of the envelope $C\,h(x)$; generate u and test if $uC\,h(x) \leq f(x)$. If so, accept x; if not reject x and try again. If we regard x and $uC\,h(x)$ as the abscissa and ordinate of a point in a two-dimensional plot, these points will populate the entire area $C\,h(x)$ in a smooth manner; then we accept those which fall under $f(x)$. The efficiency is the ratio of areas, which must equal $1/C$; therefore we must keep C as close as possible to 1.0. Therefore, we try to choose $C\,h(x)$ to be as close to $f(x)$ as convenience dictates, as in the lower part of Fig. 40.2.

40.4. Algorithms

Algorithms for generating random numbers belonging to many different distributions are given for example by Press [12], Ahrens and Dieter [13], Rubinstein [14], Devroye [15], Walck [16] and Gentle [17]. For many distributions, alternative algorithms exist, varying in complexity, speed, and accuracy. For time-critical applications, these algorithms may be coded in-line to remove the significant overhead often encountered in making function calls.

In the examples given below, we use the notation for the variables and parameters given in Table 38.1. Variables named "u" are assumed to be independent and uniform on [0,1). Denominators must be verified to be non-zero where relevant.

40.4.1. ***Exponential decay*** :

This is a common application of the inverse transform method, and uses the fact that if u is uniformly distributed in $[0,1]$, then $(1-u)$ is as well. Consider an exponential p.d.f. $f(t) = (1/\tau)\exp(-t/\tau)$ that is truncated so as to lie between two values, a and b, and renormalized to unit area. To generate decay times t according to this p.d.f., first let $\alpha = \exp(-a/\tau)$ and $\beta = \exp(-b/\tau)$; then generate u and let

$$t = -\tau \ln(\beta + u(\alpha - \beta)). \tag{40.4}$$

For $(a,b) = (0,\infty)$, we have simply $t = -\tau \ln u$. (See also Sec. 40.4.6.)

40.4.2. ***Isotropic direction in 3D*** :

Isotropy means the density is proportional to solid angle, the differential element of which is $d\Omega = d(\cos\theta)d\phi$. Hence $\cos\theta$ is uniform $(2u_1 - 1)$ and ϕ is uniform $(2\pi u_2)$. For alternative generation of $\sin\phi$ and $\cos\phi$, see the next subsection.

40.4.3. ***Sine and cosine of random angle in 2D*** :

Generate u_1 and u_2. Then $v_1 = 2u_1 - 1$ is uniform on (−1,1), and $v_2 = u_2$ is uniform on (0,1). Calculate $r^2 = v_1^2 + v_2^2$. If $r^2 > 1$, start over. Otherwise, the sine (S) and cosine (C) of a random angle (*i.e.*, uniformly distributed between zero and 2π) are given by

$$S = 2v_1v_2/r^2 \quad \text{and} \quad C = (v_1^2 - v_2^2)/r^2\ . \tag{40.5}$$

40.4.4. ***Gaussian distribution*** :

If u_1 and u_2 are uniform on (0,1), then

$$z_1 = \sin(2\pi u_1)\sqrt{-2\ln u_2} \quad \text{and} \quad z_2 = \cos(2\pi u_1)\sqrt{-2\ln u_2} \tag{40.6}$$

are independent and Gaussian distributed with mean 0 and $\sigma = 1$.

There are many variants of this basic algorithm, which may be faster. For example, construct $v_1 = 2u_1 - 1$ and $v_2 = 2u_2 - 1$, which are uniform on (−1,1). Calculate $r^2 = v_1^2 + v_2^2$, and if $r^2 > 1$ start over. If $r^2 < 1$, it is uniform on (0,1). Then

$$z_1 = v_1\sqrt{\frac{-2\ln r^2}{r^2}} \quad \text{and} \quad z_2 = v_2\sqrt{\frac{-2\ln r^2}{r^2}} \tag{40.7}$$

are independent numbers chosen from a normal distribution with mean 0 and variance 1. $z_i' = \mu + \sigma z_i$ distributes with mean μ and variance σ^2.

For a multivariate Gaussian with an $n \times n$ covariance matrix V, one can start by generating n independent Gaussian variables, $\{\eta_j\}$, with mean 0 and variance 1 as above. Then the new set $\{x_i\}$ is obtained as $x_i = \mu_i + \sum_j L_{ij}\eta_j$, where μ_i is the mean of x_i, and L_{ij} are the components of L, the unique lower triangular matrix that fulfils $V = LL^T$. The matrix L can be easily computed by the following recursive relation (Cholesky's method):

$$L_{jj} = \left(V_{jj} - \sum_{k=1}^{j-1} L_{jk}^2\right)^{1/2}\ , \tag{40.8a}$$

$$L_{ij} = \frac{V_{ij} - \sum_{k=1}^{j-1} L_{ik}L_{jk}}{L_{jj}}\ ,\ j = 1,...,n\ ;\ i = j+1,...,n, \tag{40.8b}$$

where $V_{ij} = \rho_{ij}\sigma_i\sigma_j$ are the components of V. For $n = 2$ one has

$$L = \begin{pmatrix} \sigma_1 & 0 \\ \rho\sigma_2 & \sqrt{1-\rho^2}\,\sigma_2 \end{pmatrix}\ , \tag{40.9}$$

and therefore the correlated Gaussian variables are generated as $x_1 = \mu_1 + \sigma_1\eta_1$, $x_2 = \mu_2 + \rho\sigma_2\eta_1 + \sqrt{1-\rho^2}\,\sigma_2\eta_2$.

40.4.5. **$\chi^2(n)$ distribution** :

To generate a variable following the χ^2 distribution for n degrees of freedom, use the Gamma distribution with $k = n/2$ and $\lambda = 1/2$ using the method of Sec. 40.4.6.

40.4.6. ***Gamma distribution*** :

All of the following algorithms are given for $\lambda = 1$. For $\lambda \neq 1$, divide the resulting random number x by λ.

- If $k = 1$ (the *exponential* distribution), accept $x = -\ln u$. (See also Sec. 40.4.1.)

- If $0 < k < 1$, initialize with $v_1 = (e + k)/e$ (with $e = 2.71828...$ being the natural log base). Generate u_1, u_2. Define $v_2 = v_1u_1$.

  Case 1: $v_2 \leq 1$. Define $x = v_2^{1/k}$. If $u_2 \leq e^{-x}$, accept x and stop, else restart by generating new u_1, u_2.
  Case 2: $v_2 > 1$. Define $x = -\ln([v_1 - v_2]/k)$. If $u_2 \leq x^{k-1}$, accept x and stop, else restart by generating new u_1, u_2. Note that, for $k < 1$, the probability density has a pole at $x = 0$, so that return values of zero due to underflow must be accepted or otherwise dealt with.

- Otherwise, if $k > 1$, initialize with $c = 3k - 0.75$. Generate u_1 and compute $v_1 = u_1(1 - u_1)$ and $v_2 = (u_1 - 0.5)\sqrt{c/v_1}$. If $x = k + v_2 - 1 \leq 0$, go back and generate new u_1; otherwise generate u_2 and compute $v_3 = 64v_1^3u_2^2$. If $v_3 \leq 1 - 2v_2^2/x$ **or** if $\ln v_3 \leq 2\{[k-1]\ln[x/(k-1)] - v_2\}$, accept x and stop; otherwise go back and generate new u_1.

40.4.7. ***Binomial distribution*** :

Begin with $k = 0$ and generate u uniform in $[0,1)$. Compute $P_k = (1-p)^n$ and store P_k into B. If $u \leq B$ accept $r_k = k$ and stop. Otherwise, increment k by one; compute the next P_k as $P_k \cdot (p/(1-p)) \cdot (n-k)/(k+1)$; add this to B. Again, if $u \leq B$, accept $r_k = k$ and stop, otherwise iterate until a value is accepted. If $p > 1/2$, it will be more efficient to generate r from $f(r; n, q)$, *i.e.*, with p and q interchanged, and then set $r_k = n - r$.

40.4.8. ***Poisson distribution*** :

Iterate until a successful choice is made: Begin with $k = 1$ and set $A = 1$ to start. Generate u. Replace A with uA; if now $A < \exp(-\mu)$, where μ is the Poisson parameter, accept $n_k = k - 1$ and stop. Otherwise increment k by 1, generate a new u and repeat, always starting with the value of A left from the previous try.

Note that the Poisson generator used in ROOT's `TRandom` classes before version 5.12 (including the derived classes `TRandom1, TRandom2, TRandom3`) uses a Gaussian approximation when μ exceeds a given threshold. This may be satisfactory (and much faster) for some applications. To do this, generate z from a Gaussian with zero mean and unit standard deviation; then use $x = \max(0, [\mu + z\sqrt{\mu} + 0.5])$ where $[\,]$ signifies the greatest integer $\leq$ the expression. The routines from Numerical Recipes [12] and CLHEP's routine `RandPoisson` do not make this approximation (see, *e.g.*, Ref. 10).

40.4.9. ***Student's t distribution*** :

Generate u_1 and u_2 uniform in $(0,1)$; then $t = \sin(2\pi u_1)[n(u_2^{-2/n} - 1)]^{1/2}$ follows the Student's t distribution for $n > 0$ degrees of freedom (n not necessarily an integer).

Alternatively, generate x from a Gaussian with mean 0 and $\sigma^2 = 1$ according to the method of 40.4.4. Next generate y, an independent gamma random variate, according to 40.4.6 with $\lambda = 1/2$ and $k = n/2$. Then $z = x/\sqrt{y/n}$ is distributed as a t with n degrees of freedom.

For the special case $n = 1$, the Breit-Wigner distribution, generate u_1 and u_2; set $v_1 = 2u_1 - 1$ and $v_2 = 2u_2 - 1$. If $v_1^2 + v_2^2 \leq 1$ accept $z = v_1/v_2$ as a Breit-Wigner distribution with unit area, center at 0.0, and FWHM 2.0. Otherwise start over. For center M_0 and FWHM Γ, use $W = z\Gamma/2 + M_0$.

40.4.10. ***Beta distribution*** :

The choice of an appropriate algorithm for generation of beta distributed random numbers depends on the values of the parameters α and β. For, *e.g.*, $\alpha = 1$, one can use the transformation method to find $x = 1 - u^{1/\beta}$, and similarly if $\beta = 1$ one has $x = u^{1/\alpha}$. For more general cases see, *e.g.*, Refs. [16,17] and references therein.

40.5. Markov Chain Monte Carlo

In applications involving generation of random numbers following a multivariate distribution with a high number of dimensions, the transformation method may not be possible and the acceptance-rejection technique may have too low of an efficiency to be practical. If it is not required to have independent random values, but only that they follow a certain distribution, then Markov Chain Monte Carlo (MCMC) methods can be used. In depth treatments of MCMC can be found, *e.g.*, in the texts by Robert and Casella [18], Liu [19], and the review by Neal [20]. HEP-oriented software for MCMC is available from the Bayesian Analysis Toolkit (BAT) [21].

MCMC is particularly useful in connection with Bayesian statistics, where a p.d.f. $p(\boldsymbol{\theta})$ for an n-dimensional vector of parameters $\boldsymbol{\theta} = (\theta_1, \ldots, \theta_n)$ is obtained, and one needs the marginal distribution of a subset of the components. Here one samples $\boldsymbol{\theta}$ from $p(\boldsymbol{\theta})$ and simply records the marginal distribution for the components of interest.

A simple and broadly applicable MCMC method is the Metropolis-Hastings algorithm, which allows one to generate multidimensional points $\boldsymbol{\theta}$ distributed according to a target p.d.f. that is proportional to a given function $p(\boldsymbol{\theta})$. It is not necessary to have $p(\boldsymbol{\theta})$ normalized to unit area, which is useful in Bayesian statistics, as posterior probability densities are often determined only up to an unknown normalization constant.

To generate points that follow $p(\boldsymbol{\theta})$, one first needs a proposal p.d.f. $q(\boldsymbol{\theta}; \boldsymbol{\theta}_0)$, which can be (almost) any p.d.f. from which independent random values $\boldsymbol{\theta}$ can be generated, and which contains as a parameter another point in the same space $\boldsymbol{\theta}_0$. For example, a multivariate Gaussian centered about $\boldsymbol{\theta}_0$ can be used. Beginning at an arbitrary starting point $\boldsymbol{\theta}_0$, the Hastings algorithm iterates the following steps:

1. Generate a value $\boldsymbol{\theta}$ using the proposal density $q(\boldsymbol{\theta}; \boldsymbol{\theta}_0)$;
2. Form the Hastings test ratio, $\alpha = \min\left[1, \dfrac{p(\boldsymbol{\theta})q(\boldsymbol{\theta}_0; \boldsymbol{\theta})}{p(\boldsymbol{\theta}_0)q(\boldsymbol{\theta}; \boldsymbol{\theta}_0)}\right]$;
3. Generate a value u uniformly distributed in $[0, 1]$;
4. If $u \leq \alpha$, take $\boldsymbol{\theta}_1 = \boldsymbol{\theta}$. Otherwise, repeat the old point, *i.e.*, $\boldsymbol{\theta}_1 = \boldsymbol{\theta}_0$.
5. Set $\boldsymbol{\theta}_0 = \boldsymbol{\theta}_1$ and return to step 1.

If one takes the proposal density to be symmetric in $\boldsymbol{\theta}$ and $\boldsymbol{\theta}_0$, then this is the *Metropolis*-Hastings algorithm, and the test ratio becomes $\alpha = \min[1, p(\boldsymbol{\theta})/p(\boldsymbol{\theta}_0)]$. That is, if the proposed $\boldsymbol{\theta}$ is at a value of probability higher than $\boldsymbol{\theta}_0$, the step is taken. If the proposed step is rejected, the old point is repeated.

Methods for assessing and optimizing the performance of the algorithm are discussed in, *e.g.*, Refs. [18–20]. One can, for example, examine the autocorrelation as a function of the lag k, *i.e.*, the correlation of a sampled point with that k steps removed. This should decrease as quickly as possible for increasing k.

Generally one chooses the proposal density so as to optimize some quality measure such as the autocorrelation. For certain problems it has been shown that one achieves optimal performance when the acceptance fraction, that is, the fraction of points with $u \leq \alpha$, is around 40%. This can be adjusted by varying the width of the proposal density. For example, one can use for the proposal p.d.f. a multivariate Gaussian with the same covariance matrix as that of the target p.d.f., but scaled by a constant.

40.6. Generative Adversarial Networks

Recent developments in Machine Learning have led to new types of Monte Carlo methods based on generative models. The goal is to generate events each consisting of a vector of quantities $\boldsymbol{x}$, which could represent the set of pixels in an image or energy deposits in the cells of a calorimeter. Suppose, however, that we do not have direct access to the underlying probability density $f(\boldsymbol{x})$, but rather we only have an implicit model (*e.g.*, a computer program able to simulate the complexities of the physical system), which can provide a set of events usable as training data. In the case of a calorimeter, for example, this could represent real events from a control measurement or simply the output from a detailed simulation.

Generative models such as such as Variational Autoencoders (VAEs) [22,23] and Generative Adversarial Networks (GANs) [24] are algorithms for generating events that mimic the training data. Recently GANs have been investigated in HEP for simulation of energy deposits in calorimeters, so far in a simplified setting. They are able to generate events that capture detailed properties of those from a detailed Monte Carlo simulation but require far less computing time (for a recent example see, *e.g.*, Ref. [25]).

Here we sketch the main ideas behind GANs used to simulate a random vector $\boldsymbol{x}$. This follows some distribution $f(\boldsymbol{x})$ which itself is not known, but we have a set of instances (events) $\boldsymbol{x}_1, \ldots, \boldsymbol{x}_N$ as training data, here regarded as representative of the true distribution. We seek a function (the generator) $G(\boldsymbol{z})$ which takes as input a vector of random numbers $\boldsymbol{z}$ and produces directly as output an event vector, *i.e.*, $\boldsymbol{x} = G(\boldsymbol{z})$. The method is in this sense similar to the transformation method described in 40.2, but here both the function G and the input of random values $\boldsymbol{z}$ are multidimensional. As a prototypical example we can take the components of $\boldsymbol{z}$ as independent and Gaussian distributed about zero with unit variance.

The GAN makes use of two functions, the generator $G(\boldsymbol{z})$ and a discriminator $D(\boldsymbol{x})$. The generator tries to produce events $\boldsymbol{x}$ that mimic the (real) training data and thus look as if they were sampled from the unknown distribution $f(\boldsymbol{x})$. Simultaneously, the discriminator is trained to do its best to distinguish the generated events from the real ones.

To find the function $G(\boldsymbol{z})$ that generates events that are as similar as possible to the training data, one may use a Deep Neural Network (DNN), *i.e.*, a neural network with a sufficiently large number of hidden layers, and thus having a large set of parameters $\boldsymbol{\theta}_g$. This is needed so that network is capable of modelling accurately the potentially complex density $f(\boldsymbol{x})$. The input layer corresponds to the components of the random vector $\boldsymbol{z}$ and the multidimensional output layer to $\boldsymbol{x}$. The goal is thus reduced to finding optimal values of the parameters $\boldsymbol{\theta}_g$ using the training data.

The discriminator function $D(\boldsymbol{x}; \boldsymbol{\theta}_d)$ can also be a DNN containing parameters $\boldsymbol{\theta}_d$. It takes as input an event (an instance in $\boldsymbol{x}$-space) and provides a single scalar output in $[0, 1]$, which should be as close as possible to zero for generated and one for real events.

The parameters of the generator and discriminator are chosen such that the function

$$V(\boldsymbol{\theta}_g, \boldsymbol{\theta}_d) = E_x[\log(D(\boldsymbol{x}; \boldsymbol{\theta}_d))] + E_z[\log(1 - D(G(\boldsymbol{z}; \boldsymbol{\theta}_g); \boldsymbol{\theta}_d))] \quad (40.10)$$

is minimized with respect to $\boldsymbol{\theta}_g$ and simultaneously maximized with respect to $\boldsymbol{\theta}_d$. For the expectation value in the first term, $\boldsymbol{x}$ is sampled from the (real) training data; for the second term $\boldsymbol{z}$ follows its given distribution, *e.g.*, a multivariate standard Gaussian. That is, the discriminator is adjusted to maximize the probability that it will correctly identify an event as real or generated, and simultaneously the generator is tuned such that it produces events which appear as real as possible when evaluated by the discriminator.

Challenges with GANs such as difficulty training the networks are an active area of research in Machine Learning. Once an optimal set of parameters is found, the transformation $\boldsymbol{x} = G(\boldsymbol{z}; \boldsymbol{\theta}_g)$ can be used to generate events in $\boldsymbol{x}$-space that capture detailed properties of the training data. Further information on applications, network architecture and training procedures can be found in, *e.g.*, Ref. [25] and references therein.

References:

1. F. James, Comp. Phys. Comm. **60**, 329 (1990).
2. P. L'Ecuyer, *Proc. 1997 Winter Simulation Conference*, IEEE Press, Dec. 1997, 127–134.
3. Leif Lönnblad, Comp. Phys. Comm. **84**, 307 (1994).
4. Rene Brun and Fons Rademakers, Nucl. Inst. Meth. **A389**, 81 (1997); see also `root.cern.ch`.
5. F. James, Comp. Phys. Comm. **79**, 111 (1994), based on M. Lüscher, Comp. Phys. Comm. **79**, 100 (1994).
6. P. L'Ecuyer, Mathematics of Computation, **65**, 213 (1996) and **65**, 225 (1999).
7. M. Matsumoto and T. Nishimura, *ACM Transactions on Modeling and Computer Simulation*, Vol. 8, No. 1, January 1998, 3–30.
8. Much of DIEHARD is described in: G. Marsaglia, *A Current View of Random Number Generators*, keynote address, *Computer Science and Statistics: 16th Symposium on the Interface*, Elsevier (1985).
9. P. L'Ecuyer and R. Simard, *ACM Transactions on Mathematical Software* 33, 4, Article 1, December 2007.
10. J. Heinrich, CDF Note CDF/MEMO/STATISTICS/PUBLIC /8032, 2006.
11. UNU.RAN is described at `statmath.wu.ac.at/software/unuran`; see also W. Hörmann, J. Leydold, and G. Derflinger, *Automatic Nonuniform Random Variate Generation*, (Springer, New York, 2004).
12. W.H. Press *et al.*, *Numerical Recipes*, 3rd edition, (Cambridge University Press, New York, 2007).
13. J.H. Ahrens and U. Dieter, Computing **12**, 223 (1974).
14. R.Y. Rubinstein, *Simulation and the Monte Carlo Method*, (John Wiley and Sons, Inc., New York, 1981).
15. L. Devroye, *Non-Uniform Random Variate Generation*, (Springer-Verlag, New York, 1986); available online at `luc.devroye.org/rnbookindex.html`.
16. C. Walck, *Handbook on Statistical Distributions for Experimentalists*, University of Stockholm Report SUF-PFY/96-01, available from `www.fysik.su.se/~walck`.
17. J.E. Gentle, *Random Number Generation and Monte Carlo Methods*, 2nd ed., (Springer, New York, 2003).
18. C.P. Robert and G. Casella, *Monte Carlo Statistical Methods*, 2nd ed., (Springer, New York, 2004).
19. J.S. Liu, *Monte Carlo Strategies in Scientific Computing*, (Springer, New York, 2001).
20. R.M. Neal, *Probabilistic Inference Using Markov Chain Monte Carlo Methods*, Technical Report CRG-TR-93-1, Dept. of Computer Science, University of Toronto, available from `www.cs.toronto.edu/~radford/res-mcmc.html`.
21. A. Caldwell, D. Kollar, K. Krninger, Comput. Phys. Commun. 180 (2009) pages 2197-2209; e-print: arXiv:0808.2552.
22. D.P. Kingma and M. Welling, *Auto-Encoding Variational Bayes*, Int. Conf. on Learning Representations, ICLR, 2014; e-print: arXiv:1312.6114 [stat.ML].
23. D.J. Rezende, S. Mohamed and D. Wierstra, *Stochastic Backpropagation and Approximate Inference in Deep Generative Models*, Proc. 31st Int. Conf. on Machine Learning, Beijing, 2014. JMLR: W&CP vol. 32; e-print: arXiv:1401.4082 [stat.ML].
24. I.J. Goodfellow et al., *Generative Adversarial Nets*, Proceedings of Advances in Neural Information Processing Systems 27 (Z. Ghahramani et al., eds., NIPS 2014) pages 26722680; e-print: arXiv:1406.2661 [stat.ML].
25. M. Paganini, L. de Oliveira and B. Nachman, *CaloGAN: Simulating 3D High Energy Particle Showers in Multi-Layer Electromagnetic Calorimeters with Generative Adversarial Networks* e-print: arXiv:1705.02355 [hep-ex].

41. Monte Carlo Event Generators

Revised September 2017 by P. Nason (INFN, Milan) and P.Z. Skands (Monash University).

General-purpose Monte Carlo (GPMC) generators like HERWIG [1,2,3], PYTHIA [4,5], and SHERPA [6], provide detailed simulations of high-energy collisions. They play an essential role in QCD modeling (in particular for aspects beyond fixed-order perturbative QCD) and in data analysis and the planning of new experiments, where they are used together with detector simulation to estimate signals and backgrounds in high-energy processes. They are built from several components, that describe the physics starting from very short distance scales, up to the typical scale of hadron formation and decay. Since QCD is weakly interacting at short distances (below a femtometer), the components of the GPMC dealing with short-distance physics are based upon perturbation theory. At larger distances, all soft hadronic phenomena, like hadronization and the formation of the underlying event in hadron collisions, cannot be computed from first principles at present, and one must rely upon QCD-inspired models.

The purpose of this review is to illustrate the main components of these generators. It is divided into four sections. The first one deals with short-distance, perturbative phenomena. The basic concepts leading to the simulations of the dominant QCD processes are illustrated here. In the second section, the nonperturbative transition from partons to hadrons ("hadronization") is treated. The two most popular hadronization models, the string and cluster models, are illustrated. The basics of the implementation of decay chains of unstable "primary" hadrons into stable "secondaries" is also illustrated here. In the third section, models for soft hadron physics are discussed. These include models for the underlying event and for minimum-bias interactions. Issues of Bose-Einstein and color-reconnection effects are also discussed here. The fourth section briefly introduces the challenges of MC uncertainty estimates and tuning.

We use natural units throughout, such that $c = 1$ and $\hbar = 1$, with energy, momenta and masses measured in GeV, and time and distances measured in GeV^{-1}.

41.1. Short-distance physics in GPMC generators

The short-distance components of a GPMC generator deal with the computation of the primary process at hand, with decays of short-lived particles, and with the generation of QCD and QED radiation. QCD radiation is computable in perturbation theory as long as the time scales involved are well below $1/\Lambda$, where Λ is a typical hadronic scale of few hundred MeV. Because of the presence of logarithmic enhancements due to both collinear and soft emissions, this description involves an indefinite number of final-state particles that are emitted at time scales below $1/\Lambda$. In e^+e^- annihilation into hadrons, for example, the time scale of the primary process is of the order of the inverse of the annihilation energy Q. Collinear and soft emissions take place at all time scales between $1/Q$ and $1/\Lambda$, Technically, the computation of the dominant collinear and soft radiation is carried out by the so called shower algorithms. Historically, such algorithms were first developed for resummation of collinear singularities, leading to the so called "Parton Shower" algorithms. We will briefly describe this approach in this section. We stress, however, that many modern generators adopt approaches that focus initially upon soft singularities, leading to the so called "Dipole Showers" discussed in Sec. 41.1.3.

Collinear singularities arise when the angle between two emitted light partons becomes small. For example, in a process in which a quark and a gluon are emitted, if the angle θ among them is very small (and is smaller than the angles among all other pairs of light partons in the process) the squared amplitude factorizes as follows

$$|M_{qg}|^2 \mathrm{d}\Phi_{qg} \approx |M_q|^2 \,\mathrm{d}\Phi_q \frac{\alpha_s}{2\pi} P_{q,qg}(z) \mathrm{d}z \frac{\mathrm{d}\phi}{2\pi} \frac{\mathrm{d}\theta^2}{\theta^2} \qquad (41.1)$$

where M_{qg}, $\mathrm{d}\Phi_{qg}$ are the amplitude and phase space when both the gluon and the quark are emitted; M_q, $\mathrm{d}\Phi_q$ are the amplitude and phase space when only the quark is emitted; $z = E_q/(E_q + E_g)$ is the fraction of energy carried by the quark; ϕ is the azimuth of the splitting plane, and $P_{q,qg}(z) = C_F(1+z^2)/(1-z)$ is the Altarelli-Parisi splitting kernel for gluon emission from a quark line, with color factor $C_F = 4/3$. The factorized form of Eq. (41.1) is due to the fact that for small angle the process is dominated by a single amplitude in which the splitting quark is almost on shell and hence propagates for long distances. We define the energy scale corresponding to the inverse of this distance as the *hardness* of the splitting process, so that larger hardness corresponds to shorter distance. We can define the hardness t as the product $E^2\theta^2$, or as the virtuality of the splitting parton p^2, or as a measure of the relative transverse momentum in the splitting such as the k_t of an emitted parton relative to its parent, defined by

$$p^2 = 2E^2 z(1-z)(1-\cos\theta) \approx z(1-z)E^2\theta^2\,, \quad k_T^2 = z^2(1-z)^2E^2\theta^2\,. \qquad (41.2)$$

If the region of small values of z and $1-z$ was not important, these definitions would be equivalent. In QCD we also have soft divergences, arising when soft gluons are emitted. In Eq. (41.1) they appear as $z \to 1$, because of the $1/(1-z)$ singularity of $P_{q,qg}(z)$. Thus, we expect that the choice of the appropriate ordering variable will be relevant when dealing with soft divergences (see Sec. 41.3). The $\mathrm{d}\theta^2/\theta^2$ factor in Eq. (41.1) can be equivalently written in terms of the hardness $\mathrm{d}t/t$. After integration it gives rise to a logarithmic factor $\log(Q^2/\Lambda^2)$. We can have many subsequent splittings, that we can describe by applying Eq. (41.1) recursively, as long as the splittings are strongly ordered in decreasing hardness. This means that, from a typical final-state configuration, by clustering together final-state parton pairs with the smallest hardness recursively, we can reconstruct a branching tree, that may be viewed as the splitting history of the event. We stress that all hardness values between the hardness of the primary process and the cutoff scale Λ are equally involved here. The collinear approximation is applied recursively to splitting processes that have much smaller hardness with respect to all previous ones.

By integrating over the phase space, a process with n collinear splittings will be of order $(\alpha_S(Q^2)\log(Q^2/\Lambda^2))^n$ with respect to the primary process. Since $\alpha_S(Q^2) \propto 1/\log(Q^2/\Lambda^2)$ [7], these corrections are not small. The so-called KLN theorem [8,9] guarantees that large logarithmic enhancements arising from final-state collinear splitting cancel against the virtual corrections in inclusive cross sections, order by order in perturbation theory. Furthermore, the factorization theorem guarantees that initial-state collinear singularities can be factorized into the parton density functions (PDFs) [7]. Therefore, the cross section for the basic process remains accurate up to corrections of higher orders in $\alpha_S(Q)$, provided it is interpreted as an inclusive cross section, rather than as a bare partonic cross section. For example, the leading order (LO) cross section for $e^+e^- \to q\bar{q}$ is a good LO estimate of the e^+e^- cross section for the production of a pair of quarks accompanied by an arbitrary number of collinear and soft gluons, but is not a good estimate of the cross section for the production of a $q\bar{q}$ pair with no extra radiation. In summary, perturbation theory at fixed order can yield increasingly accurate predictions for inclusive observables, but cannot be used to describe the indefinite sequence of collinear and soft radiations that accompany the hard partons.

Parton-Shower algorithms are used to compute the cross section for generic hard processes including all dominant collinear radiation. These algorithms begin with the generation of the kinematics of the basic process, performed with a probability proportional to its LO partonic cross section. This is interpreted physically as the inclusive cross section for the basic process, followed by an arbitrary sequence of shower splittings. The algorithm then assigns a probability to each splitting sequence, so that the initial LO cross section is partitioned into the cross sections for a multitude of final states of arbitrary multiplicity, with their sum equal to the cross section of the primary process. This property of the GPMCs reflects the KLN cancellation mentioned earlier, and it is often called "unitarity of the shower process", a name that reminds us that the KLN cancellation itself is a consequence of unitarity. The fact that a quantum mechanical process can be described in terms of composition of probabilities, rather than amplitudes, follows from the collinear approximation. In fact, because of strong ordering, a radiated parton cannot be collinear to more than one parton in the amplitude, and this suppresses interference effects.

We now illustrate the basic parton-shower algorithm, as first introduced in Ref. 11. (For more pedagogical introductions see Ref. 18

and references therein.) For simplicity, we consider the example of e^+e^- annihilation into $q\bar{q}$ pairs, where we only have to deal with final state radiation (FSR). We consider all final states that can be built by dressing the q and $\bar{q}$ partons with an indefinite number of splitting processes. By recursively clustering together final state parton pairs with the smallest relative hardness, from each final state configuration we can construct two trees rooted at the q and $\bar{q}$ partons. The momenta of all intermediate lines of the tree diagrams are then uniquely determined from the final-state momenta. Hardnesses in the trees are ordered. One assigns to each splitting vertex the hardness t, the energy fractions z and $1-z$ of the two generated partons, and the azimuth ϕ of the splitting process with respect to the momentum of the incoming parton. For definiteness, we assume that z and ϕ are defined in the center-of-mass (CM) frame of the e^+e^- collision. The differential cross section for a given final state is given by the product of the differential cross section for the initial $e^+e^- \to q\bar{q}$ process, multiplied by a factor

$$\Delta_i(t_m,t_n)\frac{\alpha_S(t)}{2\pi}P_{i,jk}(z)\frac{dt_m}{t_m}dz\frac{d\phi}{2\pi} \tag{41.3}$$

for each intermediate line arising from the $n^{\rm th}$ and ending in the $m^{\rm th}$ splitting vertex. $\Delta(t_m,t_n)$ is the so-called Sudakov form factor

$$\Delta_i(t_m,t_n) = \exp\left[-\int_{t_m}^{t_n}\frac{dq^2}{q^2}\,\frac{\alpha_S(q^2)}{2\pi}\sum_{jk}P_{i,jk}(z)dz\frac{d\phi}{2\pi}\right]. \tag{41.4}$$

The suffixes i and jk represent the parton species of the incoming and final partons, respectively, and $P_{i,jk}(z)$ are the Altarelli-Parisi [12] splitting kernels. Notice that the endpoints on the z integration depend upon the definition of hardness. For example, in case of virtuality or transverse momentum ordering, the z integration is automatically cut-off near the extremes, see eq. (1.2). When this is not the case (as, for example, for angular ordering) an explicit cut-off on z must be introduced, corresponding to the requirement that an emission must have some mininum energy to be distinguishable from no emission. For lines originating at the primary vertex, the scale t_n is replaced by the typical scale of the primary process and for lines ending without any further splitting the scale t_m is replaced by t_0, an infrared cutoff defined by the shower hadronization scale (at which the charges are screened by hadronization) or, for an unstable particle, its width (a source cannot emit radiation with a period exceeding its lifetime).

Eq. (41.3) can be obtained by iterating formula Eq. (41.1) recursively, with two important corrections: a) the strong coupling is evaluated at a scale corresponding to the hardness of the splitting process; b) the presence of the Sudakov form factor. Both these modifications arise from the inclusion of all collinear-dominant virtual corrections.

Notice that the Sudakov form factor for a small hardness interval $\Delta_i(t,t+\delta t)$ is equal to one minus the integrated emission probability of Eq. (41.3), i.e. it can be interpreted as the probability of no emission in the interval $t,t+\delta t$. From this, it immediately follows that $\Delta_i(t_m,t_n)$ can be interpreted as the no-emission probability in the full t_m,t_n interval. This interpretation allows to formulate the shower process as a probabilistic algorithm. We first notice that $0<\Delta_i(t_m,t_n)\le 1$, where the upper extreme is reached for $t_m=t_n$, and the lower extreme is approached for $t_m=t_0$. Starting from each of the partons in the primary process (e.g., $e^+e^-\to q\bar{q}$), event generation then proceeds recursively as follows. Given a parton exiting a vertex with hardness t_n, (taken to be of order the annihilation scale Q^2 for the first branching) one seeks a solution of the equation $r=\Delta_i(t_m,t_n)$, with $r\in[0,1]$ a uniform random number, and solves it for the hardness of the next branching t_m. If $t_m\le t_0$, no splitting is generated and the line is interpreted as a final parton. If $t_m>t_0$, a branching is generated at the scale t_m. Its z value and the final parton species jk are generated with a probability proportional to $P_{i,jk}(z)$. The azimuth is generated uniformly, neglecting angular correlations (see Sec. 41.1.1). This procedure is started with each of the primary process partons, and is applied recursively to all generated partons. It may generate an arbitrary number of partons, and it stops when no final-state partons undergo further splitting.

The four-momenta of the final-state partons are reconstructed from the momenta of the initial ones, and from the whole sequence of splitting variables, subject to overall momentum conservation. Different algorithms employ different strategies to treat recoil effects due to momentum conservation, which may be applied either locally for each splitting, or globally for the entire set of partons (a procedure called *momentum reshuffling*.) This has a subleading effect with respect to the collinear approximation.

We emphasize that the shower cross sections described above can be derived from perturbative QCD by keeping only the collinear-dominant real and virtual contributions to the cross section. As such it is unpredictive for large-angle radiation. It is thus unsafe to rely upon Parton Shower Monte Carlo alone to compute backgrounds to new physics signals that are characterized by several widely separated jets.

A Shower Monte Carlo builds its final state as if it developed from an iterative process, often with each intermediate stage made available to the user. It should be remarked that the meaning of these intermediate stages is only relevant within the approximation adopted by the generator, and could also differ in different implementations.

41.1.1. ***Angular correlations*** :
In gluon-splitting processes ($g\to q\bar{q}$, $g\to gg$) in the collinear approximation, the distribution of the split pair is not uniform in azimuth, and the Altarelli-Parisi splitting functions are recovered only after azimuthal averaging. This dependence is due to the interference of positive and negative helicity states for the gluon that undergoes splitting. Spin correlations propagate through the splitting process, and determine acausal correlations of the EPR kind [13]. A method to partially account for these effects was introduced in Ref. 14, in which the azimuthal correlation between two successive splittings is computed by averaging over polarizations. This can then be applied at each branching step. Acausal correlations are argued to be small, and are discarded with this method, that is still used in `PYTHIA` [4]. A method that fully includes spin correlation effects was later proposed [15], and has been implemented in `HERWIG` [16,3].

41.1.2. ***Initial-state radiation*** :
Initial-state radiation (ISR) arises because incoming particles may undergo collinear radiation before entering the hard-scattering process. In doing so, they acquire a non-vanishing transverse momentum, and their virtuality becomes negative (spacelike). It turns out to be convenient to develop the ISR shower starting with the highest hardness (i.e. with the hard process) and ending with the smallest (i.e. with the incoming parton in the hadron). Unlike the case of FSR, however, hardness ordering is opposite to time ordering in the ISR case. A corresponding backwards-evolution algorithm was formulated by Sjöstrand [17], and was basically adopted in all shower models. It can be illustrated by considering a primary interaction initiated by a quark where no collinear emission of hardness $\ge t$ have taken place, and the same process where the quark also emits a collinear gluon of hardness t. The respective cross sections are proportional to

$$|M_q(x)|^2 {\rm d}x f_q(x,t), {\rm and} |M_q(x)|^2\,{\rm d}x\frac{\alpha_s(t)}{2\pi}f_q(x/z,t)P_{q,qg}(z){\rm d}z\frac{{\rm d}\phi}{2\pi}\frac{{\rm d}t}{t}\,. \tag{41.5}$$

Here f_q is the quark PDF in the incoming hadron, x is the fraction of momentum of the incoming quark that enters the basic process, while x/z is the fraction of momentum of the incoming quark *before* it emits the collinear gluon. The elementary *emission probability* is the ratio of the second over the first expression in Eq. (41.5). In analogy with the final state radiation case, this ratio will appear in the exponent of the Sudakov form factor, that (after the inclusion of all splitting subprocesses) is given by

$$\Delta_i^{\rm ISR}(t,t') = \exp\left[-\int_{t'}^{t}\frac{dt''}{t''}\frac{\alpha_S(t'')}{2\pi}\int_x^1\frac{dz}{z}\sum_{jk}P_{j,ik}(z)\frac{f_j(t'',x/z)}{f_i(t'',x)}\right]. \tag{41.6}$$

Notice that there are two uses of the PDFs: they are used to compute the cross section for the basic hard process, and they control

ISR via backward evolution. Since the evolution is generated with leading-logarithmic accuracy, it is acceptable to use two different PDF sets for these two tasks, provided they agree at the LO level.

In the context of GPMC evolution, each ISR emission generates a finite amount of transverse momentum. Details on how the recoils generated by these transverse "kicks" are distributed among other partons in the event, in particular the ones involved in the hard process, constitute one of the main areas of difference between existing algorithms, see Ref. 18. An additional $\mathcal{O}(1\,\mathrm{GeV})$ of "primordial k_T" is typically added, to represent the sum of unresolved and/or non-perturbative motion below the shower cutoff scale.

41.1.3. ***Soft emissions and QCD coherence*** :
Soft singularities arise in QCD due to the real or virtual emission of soft gluons. For example, the cross section for the emission of a soft gluon in e^+e^- annihilation into hadrons is given by

$$\mathrm{d}\sigma_{q\bar{q}g} \approx \mathrm{d}\sigma_{q\bar{q}} \frac{4}{3}(4\pi\alpha_s)\left[\frac{2\; p_q \cdot p_{\bar{q}}}{p_q \cdot l\; p_{\bar{q}} \cdot l}\right] \frac{\mathrm{d}^3 l}{2l^0(2\pi)^3}$$

$$= \mathrm{d}\sigma_{q\bar{q}} \frac{\alpha_s}{2\pi}\frac{4}{3}\frac{\mathrm{d}l^0}{l^0}\frac{\mathrm{d}\phi}{2\pi}\frac{\mathrm{d}\cos\theta}{1-\cos^2\theta}, \qquad (41.7)$$

where p_q, $p_{\bar{q}}$ and l are the quark, antiquark and gluon momentum, and θ and ϕ are the polar and azimuthal angle of the gluon momentum with respect to the quark direction. Since the gluon is soft, we may assume that p_q and $p_{\bar{q}}$ are unaffected by the gluon emission. The soft singularity is manifest in the $\mathrm{d}l^0/l^0$ factor. Notice that also collinear singularities are present at the same time when $\theta \to 0$ and $\theta \to \pi$, corresponding to the gluon becoming collinear to either the quark or the antiquark. It is easy to check that in the collinear limits Eq. (41.7) becomes equivalent to Eq. (41.1) with $P_{q,qg}(z) = (4/3)2/(1-z)$, i.e. the limiting form of $P_{q,qg}(z)$ when z approaches 1. Thus, soft singularities coexist with collinear ones, so that two potentially large logarithms can arise simultaneously due to gluon emission.

Unlike the case of collinear emission, soft emission is not tied to a single emitting particle. The amplitude for the emission of a soft gluon from an external (incoming or outgoing) line with momentum p is proportional to $p \cdot \epsilon / p \cdot l$. When squaring the amplitude, products like the one appearing in the square bracket of Eq. (41.1) arise for all pairs of external particles, with the product of a single emission amplitude with itself appearing only if $p^2 > 0$, i.e. for massive coloured particles. Thus interference plays here a crucial role. This is unlike the case of collinear singularities, where because of strong ordering a radiated parton cannot be collinear to more than one other parton.

It was shown in a set of publications (see Ref. 19) that, within the conventional parton-shower formalism based on collinear factorization, the region of collinear and soft emissions can be correctly described by using the angle of the emissions as the ordering variable, rather than the virtuality, and by setting the argument of α_S at the splitting vertex equal to the relative parton transverse momentum after the splitting. Physically, the ordering in angle approximates the coherent interference arising from large-angle soft emission from a bunch of collinear partons. Without this effect, the particle multiplicity would grow too rapidly with energy, in conflict with e^+e^- data. For this reason, angular ordering is used as the default evolution variable in all versions of `HERWIG` (see Ref. 20). To partially account for soft interference effects, an angular veto is imposed on the virtuality-ordered evolution in `PYTHIA` 6 [21].

A radical alternative formulation of QCD cascades first proposed in Ref. 22 focuses upon soft emission, rather than collinear emission, as the basic splitting mechanism. It then becomes natural to consider a branching process where it is a parton pair (i.e. a dipole) rather than a single parton, that emits a soft parton. Adding a suitable correction for non-soft, collinear partons, one can simultaneously achieve the correct logarithmic structure for both the collinear and soft emissions in the so called leading color approximation, i.e. when terms suppressed by a power of the number of colors are neglected. The `ARIADNE` [23] and `VINCIA` [25] programs are based on this approach. Dipole-type showers [26] are also used by default in `SHERPA` [27] and exist as an option in `HERWIG` [28]. An alternative dipole-based model is available in `PYTHIA` and `SHERPA` via the `DIRE` [29] plugin. The $p_\perp$-ordered showers in `PYTHIA` 6 and 8 represent a hybrid, combining collinear splitting kernels with dipole kinematics [30].

41.1.4. ***Resummation*** :
It is notoriously difficult to assess the accuracy of shower Monte Carlos in comparison with QCD resummation calculations [7]. The latter start from the definition of a specific infrared-safe observable, which develops towers of large logarithms in certain regions of phase space. A dedicated resummation calculation must in general be performed for each new observable. The predictions of shower MCs, on the other hand, are cast in terms of complete sets of final-state momenta, on which one can evaluate any observable; i.e., the shower algorithm itself is normally independent of the specific observable(s) under study.

Generally, shower MCs perform much better than strict LL resummations; this is related to their inclusion of several universal but formally subleading aspects. But there are no guarantees. A shower MC may do well for some specific observables, and not for others. At present, it is difficult to make more precise and general statements than that. Instead, it is common to specify what kind of corrections are included. Typically, collinear emissions are accounted for, although not always including angular correlations. Soft emissions are dealt with to some extent via angular ordering or dipole approaches. The most important and ubiquitous aspects beyond the strict LL approximation are momentum conservation and optimised scale choices. The former is obviously physical, hence including it should yield better results than not doing so (indeed, momentum conservation does become an aspect of QCD resummation calculations beyond LL), although the precise way of how the resulting recoil effects are handled in the shower is ambiguous. The latter can be tied, e.g., to reaching NLL accuracy for soft emissions for observables such as the transverse momentum of Drell-Yan pairs [101].

41.1.5. ***Massive quarks*** :
Quark masses act as a cut-off on collinear singularities. If the mass of a quark is below, or of the order of Λ, its effect in the shower is small. For larger quark masses, like in c, b, or t production, it is the mass, rather than the typical hadronic scale, that cuts off collinear radiation. For a quark with energy E and mass m_Q, the divergent behavior $d\theta/\theta$ of the collinear splitting process is regulated for $\theta \leq \theta_0 = m_Q/E$. We thus expect less collinear activity for heavy quarks than for light ones, which in turn is the reason why heavy quarks carry a larger fraction of the momentum acquired in the hard production process.

This feature can be implemented with different levels of sophistication. Using the fact that soft emission exhibits a zero at zero emission angle, older parton shower algorithms simply limited the shower emission to be not smaller than the angle θ_0. More modern approaches are used in both `PYTHIA`, where mass effects are included using a kind of matrix-element correction method [31], and in `HERWIG++` and `SHERPA`, where a generalization of the Altarelli-Parisi splitting kernel is used for massive quarks [32].

41.1.6. ***Color information*** :
In event generators, quarks and antiquarks are represented by color lines, with arrows indicating the direction of color flow. In the limit of infinitely many colors (called the leading color approximation), each such line can be associated with a unique label; the probability for two quarks (or antiquarks) to have the same color (anticolor) vanishes. Moreover, in the same limit gluons can be represented by a pair of color lines with opposite arrows, as can be realised e.g. from the SU(3) group relation $8 = 3 \otimes \bar{3} \ominus 1$. The rules for color propagation are:

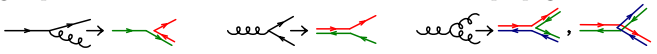

During the shower development, partons are connected by color lines. We can have a quark directly connected by a color line to an antiquark, or via an arbitrary number of intermediate gluons, as shown in Fig. 41.1. It is also possible for a set of gluons to be connected cyclically in color, as e.g. in the decay $\Upsilon \to ggg$.

The color information is used in angular-ordered showers, where the angle of color-connected partons (i.e. partons connected by the same color line) determines the initial angle for the shower development, and in dipole showers, where dipoles are always color-connected partons. It is also used in hadronization models, where the initial strings or

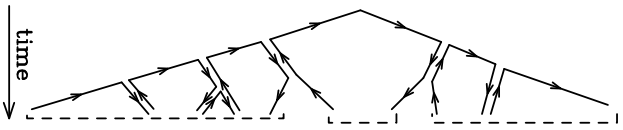

Figure 41.1: Color development of a shower in e^+e^- annihilation. Color-neutral clusters of partons are indicated by the dashed under-brackets.

clusters used for hadronization are formed by color-neutral clusters of partons.

41.1.7. ***Electromagnetic corrections*** :
The physics of photon emission from light charged particles can also be treated with a shower MC algorithm. High-energy electrons and quarks, for example, are accompanied by bremsstrahlung photons. Also here, similarly to the QCD case, electromagnetic corrections are of order $\alpha_{\rm em}\ln(Q/m)$, where m is the mass of the radiating particle, or even of order $\alpha_{\rm em}\ln(Q/m)\ln(E_\gamma/E)$ in the region where soft photon emission is important, so that, especially for the case of electrons, their inclusion in the simulation process is mandatory. This is done in most of the GPMC's (for a recent comparative study see [33]) . The specialized generator PHOTOS [34] is sometimes used as an afterburner for an improved treatment of QED radiation in non-hadronic resonance decays.

For photon emissions off leptons, the shower can be continued down to virtualities arbitrarily close to the lepton mass shell (unlike the case in QCD). In practice, an infrared cutoff is still required for the shower algorithm to terminate. Therefore, there is always an energy cut-off for emitted photons that depends upon the implementations [33]. In the case of electrons, this energy is typically of the order of its mass. Electromagnetic radiation below this scale is not enhanced by collinear singularities, and is thus bound to be soft, so that the electron momentum is not affected by it.

For photons emitted from quarks, we have instead the obvious limitation that the photon wavelength cannot exceed the typical hadronic size. Longer-wavelength photons are in fact emitted by hadrons, rather than quarks. This last effect is in practice never modeled by existing shower MC implementations. Thus, electromagnetic radiation from quarks is cut off at a typical hadronic scale. Finally, hadron (and τ) decays involving charged particles can produce additional soft bremsstrahlung. This is implemented in a general way in `HERWIG++`/`HERWIG 7` [35] and `SHERPA` [36].

41.1.8. ***Beyond-the-Standard-Model Physics*** :
The inclusion of processes for physics beyond the Standard Model (BSM) in event generators is to some extent only a matter of implementing the relevant hard processes and (chains of) decays, with the level of difficulty depending on the complexity of the model and the degree of automation [37,38]. Notable exceptions are long-lived colored particles [39], particles in exotic color representations, and particles showering under new gauge symmetries, with a growing set of implementations documented in the individual GPMC manuals. Further complications that may be relevant are finite-width effects (discussed in Sec. 41.1.9) and the assumed threshold behavior.

In addition to code-specific implementations [18], there are a few commonly adopted standards that are useful for transferring information and events between codes. Currently, the most important of these is the Les Houches Event File (LHEF) standard [40], normally used to transfer parton-level events from a hard-process generator to a shower generator. Another important standard is the Supersymmetry Les Houches Accord (SLHA) format [41], originally used to transfer information on supersymmetric particle spectra and couplings, but by now extended to apply also to more general BSM frameworks and incorporated within the LHEF standard [42].

41.1.9. ***Decay Chains and Particle Widths*** :
In most BSM processes and some SM ones, an important aspect of the event simulation is how decays of short-lived particles, such as top quarks, EW and Higgs bosons, and new BSM resonances, are handled. We here briefly summarize the spectrum of possibilities, but emphasize that there is no universal standard. Users are advised to check whether the treatment of a given code is adequate for the physics study at hand.

The appearance of an unstable resonance as a physical particle at an intermediate stage of the event generation implies that its production and decay processes are treated as being factorized. This is valid up to corrections of order Γ/m_0, with Γ the width and m_0 the pole mass. States whose widths are a substantial fraction of their mass should instead be treated as intrinsically off-shell internal propagator lines.

For states treated as physical particles, two aspects are relevant: the mass distribution of the decaying particle itself and the distributions of its decay products. For the former, matrix-element generators often use a simple δ function at m_0. The next level up, typically used in GPMCs, is to use a Breit-Wigner distribution (relativistic or non-relativistic), which formally resums higher-order virtual corrections to the mass distribution. Note, however, that this still only generates an improved picture for *moderate* fluctuations away from m_0. Similarly to above, particles that are significantly off-shell (in units of Γ) should not be treated as resonant, but rather as internal off-shell propagator lines. In most GPMCs, further refinements are included, for instance by letting Γ be a function of m ("running widths") and by limiting the magnitude of the allowed fluctuations away from m_0. We finally point out that recently NLO+PS generators have appeared that can deal with resonances including off-shell effects, non-resonance contributions and interference of radiation generated in resonance decay and production, see [24] and references therein.

For the distributions of the decay products, the simplest treatment is again to assign them their respective m_0 values, with a uniform phase-space distribution. A more sophisticated treatment distributes the decay products according to the differential decay matrix elements, capturing at least the internal dynamics and helicity structure of the decay process, including EPR-like correlations. Further refinements include polarizations of the external states [43] and assigning the decay products their own Breit-Wigner distributions, the latter of which opens the possibility to include also intrinsically off-shell decay channels, like $H \to WW^*$.

GPMC manuals often give instructions on how to include new decay modes, at varying levels of sophistications ranging from simple uniform phase-space sampling (which the user can reweight a posteriori) and step-function thresholds, to fully matrix-element weighted decay implementations including potential off-shell / threshold effects.

During subsequent showering of the decay products, most parton-shower models will preserve the total invariant mass of the decayed resonance, so as not to skew the original resonance shape. In the context of passing externally generated LHEF files [40] to a GPMC for showering, note that this is only possible if the intermediate resonances are present (with status code 2) in the LHEF event record [44].

41.1.10. ***Matching with Matrix Elements*** :
Shower algorithms are based upon a combination of the collinear (small-angle) and soft (small-energy) approximations and are thus normally inaccurate for hard, wide-angle emissions (i.e., additional well-resolved jets). They also contain only the leading singular pieces of next-to-leading order (NLO) and higher corrections to the basic process.

Traditional GPMCs, like `HERWIG` and `PYTHIA`, have included for a long time the so called Matrix Element Corrections (MEC), first formulated in Ref. 45 with later developments summarized in Ref. 18. They are typically available for $2 \to 1$ or $1 \to 2$ processes, like DIS, vector boson and Higgs production and decays, and top decays. The MEC corrects the emission of the hardest jet at large angles, so that it becomes exact at LO. A generalization of the method to multiple emissions was formulated recently [46].

Aside from MECs implemented directly in the GPMCs, the improvements on the parton-shower description of hard collisions have been made in two main directions: the so called Matrix Elements and Parton Shower matching (ME+PS from now on), and the matching of NLO calculations and Parton Showers (NLO+PS). We now discuss

each of these, and then briefly summarise techniques becoming available for combining them.

The ME+PS method allows one to use tree-level matrix elements for hard, large-angle emissions. It was first formulated in the so-called CKKW paper [47], and several variants have appeared, including the CKKW-L, MLM, and pseudoshower methods, see Refs. 48, 18 for summaries. So called "Truncated Showers" are required [49] to maintain color coherence when interfacing to angular-ordered parton showers, and care must be taken to use consistent α_S choices for the real (ME-driven) and virtual (PS-driven) corrections [50].

In the ME+PS method one typically starts by generating LO matrix elements for the production of the basic process plus a certain number $\leq n$ of other partons. A minimum separation is imposed on the produced partons, requiring, for example, that the relative transverse momentum in any pair of partons is above a given cut $Q_{\rm cut}$. One then reweights these amplitudes in such a way that, in the strongly ordered region, the virtual effects that are included in the shower algorithm (i.e. running couplings and Sudakov form factors) are also accounted for. At this stage, before parton showers are added, the generated configurations are tree-level accurate at large angle, and at small angle they match the results of the shower algorithm, except that there are no emissions below the scale $Q_{\rm cut}$, and no final states with more than n partons. These kinematic configurations are thus fed into a GPMC, that must generate all splittings with relative transverse momentum below the scale $Q_{\rm cut}$, for initial events with less than n partons, or below the scale of the smallest pair transverse momentum, for events with n partons. The matching parameter $Q_{\rm cut}$ must be chosen to be large enough for fixed-order perturbation theory to hold, but small enough so that the shower is accurate for emissions below it. Notice that the accuracy achieved with MEC is equivalent to that of ME+PS with $n = 1$, where MEC has the advantage of not having a matching parameter $Q_{\rm cut}$.

The popularity of the ME+PS method is due to the fact that processes with many jets appear often as backgrounds to new-physics searches. These jets are typically required to be well separated, and to have large transverse momenta. These kinematical configurations are exactly those for which pure shower algorithms are unreliable, hence it is mandatory to describe them using at least LO matrix elements.

Several ME+PS implementations use existing LO generators, like `ALPGEN` [51], `MADGRAPH` [52], and others summarized in Ref. 48, for the calculation of the matrix elements, and feed the partonic events to a GPMC like `PYTHIA` or `HERWIG` using the Les Houches Interface for User Processes (LHI/LHEF) [44,40]. `SHERPA` and `HERWIG 7` also include their own matrix-element generators.

The NLO+PS methods promote the accuracy of the generation of the basic process from LO to NLO in QCD. They must thus include the radiation of one extra parton with tree-level accuracy, since this radiation constitutes a NLO correction to the basic process. They must also include NLO virtual corrections. They can be viewed as an extension of the MEC methods with the inclusion of NLO virtual corrections. They are however more general, since they are applicable to processes of arbitrary complexity. Two of these methods are now widely used: `MC@NLO` [53] and `POWHEG` [49,54], with several alternative methods now also being pursued, see Ref. 18 and references therein.

NLO+PS generators produce NLO accurate distributions for inclusive quantities, and generate the hardest jet with tree-level accuracy. It should be recalled, though, that in $2 \to 1$ processes like Z/W production, GPMCs including MEC and weighted by a constant K factor may perform nearly as well, and, if suitably tuned, may even yield a better description of data. In this context, note also that the optimal tuning of an NLO+PS generator may well be different from that of the pure PS.

Several NLO+PS processes are implemented in the `MC@NLO` program [53], together with the new `AMC@NLO` development [55], and in the `POWHEG BOX` framework [54]. `HERWIG 7` supports now its own variants of `POWHEG` and `MC@NLO` for several processes. `SHERPA` instead implements a variant of the `MC@NLO` method.

For applications that require an accurate description of more than one hard, large-angle jet associated with the primary process, ME+PS schemes are still superior to NLO+PS ones. Ideally, one would like to improve NLO generators in such a way that also the production of associated jets achieves NLO accuracy. The FXFX [57], UNLOPS [58], MiNLO [59] and `MEPS@NLO` [60] methods address this problem. In turn, its solution is a prerequisite for the construction of NNLO+PS generators, that in fact have already appeared for the $gg \to H$ and Drell-Yan processes (see ref. [61] and references therein).

41.2. Hadronization Models

In the context of GPMCs, *hadronization* denotes the process by which a set of colored partons (*after* showering) is transformed into a set of "primary hadrons", which may then subsequently decay further (to "secondary hadrons"). This non-perturbative transition takes place at the *hadronization scale* $Q_{\rm had}$, which by construction is equal to the infrared cutoff of the parton shower. In the absence of a first-principles solution to the relevant dynamics, GPMCs use QCD-inspired phenomenological models to describe this transition.

An important result in "quenched" lattice QCD (see Chap. 17 of PDG book) is that the potential energy between two partons with opposite color charges grows linearly with their separation, at distances greater than about a femtometer. This is known as "linear confinement", and it forms the starting point for the *string model of hadronization*, discussed below in Sec. 41.2.1. Alternatively, a property of perturbative QCD called "preconfinement" is the basis of the *cluster model of hadronization*, discussed in Sec. 41.2.2.

A key difference between MC hadronization models and the fragmentation-function (FF) formalism used to describe inclusive hadron spectra in perturbative QCD (see Chap. 9 and Chap. 19 of PDG book) is that FFs can be defined at an arbitrary perturbative scale Q while MC hadronization models are intrinsically defined at the scale $Q_{\rm had}$. Direct comparisons are therefore only meaningful if the perturbative evolution between Q and $Q_{\rm had}$ is taken into account. FFs are calculable in pQCD, given a non-perturbative initial condition obtained by fits to hadron spectra. In the MC context, one can prove that the correct QCD evolution of the FFs arises from the shower formalism, with the hadronization model providing an explicit parameterization of the non-perturbative component. However, the MC modeling of shower and hadronization includes much more information on the final state since it is fully exclusive (i.e., it addresses all particles in the final state explicitly), while FFs only describe inclusive spectra. This exclusivity also enables MC models to make use of the color-flow information coming from the perturbative shower evolution (see Sec. 41.1.6) to determine between which partons confining potentials should arise. E.g., in the string picture, the nonperturbative limit of a QCD dipole is a string piece [62].

Given an exact hadronization model, its dependence on the scale $Q_{\rm had}$ should in principle be compensated by the corresponding scale dependence of the shower algorithm, which stops generating branchings at the scale $Q_{\rm had}$. However, due to their complicated and fully exclusive nature, it is generally not possible to enforce this compensation automatically in MC models. One must therefore be aware that the nonperturbative model parameters must be "retuned" by hand if the infrared cutoff is modified. Any other changes to the perturbative part of the calculation, such as matching to further (fixed-order or resummed) coefficients, may also necessitate a retuning. Tuning is discussed briefly in Sec. 41.4.

Finally, it should be emphasized that the so-called "parton level" that can be obtained by switching off hadronization in a GPMC, is not a universal concept, since each model defines $Q_{\rm had}$ differently (e.g. via a cutoff in $p_\perp$, invariant mass, etc., with different tunes using different values for the cutoff). Comparisons to distributions at this level may therefore be used to provide an idea of the overall impact of hadronization corrections within a given model, but should be avoided in the context of physical observables.

41.2.1. *The String Model* :

Starting from early concepts [63], several hadronization models based on strings have been proposed [18]. Of these, the most widely used today is the so-called Lund model [64,65], implemented in `PYTHIA` [4,5]. We concentrate on that particular model here, though many of the overall concepts would be shared by any string-inspired method.

Consider a color-connected quark-antiquark pair emerging from the parton shower (like the $\bar{q}q$ pair in the center of Fig. 41.1). As the charges move apart, linear confinement implies that a potential $V(r) = \kappa r$ is reached for large distances r. (At short distances, there is a Coulomb term $\propto 1/r$ as well, but this is neglected in the Lund string.) This potential describes a string with tension $\kappa \sim 1\,\text{GeV/fm} \sim 0.2\,\text{GeV}^2$. The physical picture is that of a color flux tube being stretched between the q and the $\bar{q}$.

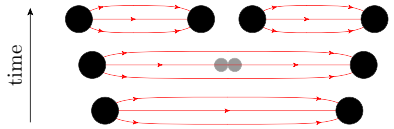

Figure 41.2: Illustration of string breaking by quark pair-creation in the string field.

As the string grows, the nonperturbative creation of quark-antiquark pairs can break the string, via the process illustrated in Fig. 41.2. The model is Lorentz invariant, so considerations involving boosted string systems are straightforward, involving the usual Lorentz effects. More complicated configurations involving intermediate gluons are treated by representing gluons as transverse "kinks", illustrated in Fig. 41.3, and considerations involving boosted string systems are subject to the usual Lorentz effects. In the leading-color approximation, the order of these kinks follows directly from the color ordering produced by the parton shower, cf. the $\bar{q}gggq$ and $\bar{q}gq$ systems on the left and right part of Fig. 41.1. (Modifications to this order, by possible color reconnection/rearrangement effects, are discussed in Sec. 41.3.3.)

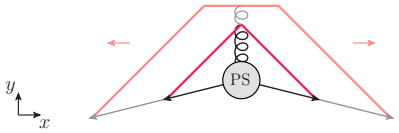

Figure 41.3: Schematic illustration of an $e^+e^- \to qg\bar{q}$ configuration emerging from the parton shower (PS). Snapshots of string positions are shown at two different times (full and shaded lines respectively). The gluon forms a transverse kink which grows in the y direction until all the gluon's kinetic energy has been used up.

Thus gluons effectively build up a transverse structure in the originally one-dimensional object, with infinitely soft ones smoothly absorbed into the string. Note: cyclic topologies made entirely of gluons (closed strings) are also possible, e.g. in decays such as $H \to gg$ or $\Upsilon \to ggg$. The space-time evolution is more involved when kinks are taken into account [65], but no additional free parameters need to be introduced. The main difference between quark and gluon hadronization stems from the fact that gluons are connected to two string pieces (one on either side), while quarks are only connected to a single string piece. Hence, the relative rate of energy loss per unit invariant time — and consequently also the rate of hadron production — is larger by a factor of 2 for gluons (similar to the ratio of color Casimirs $C_A/C_F = 2.25$).

To convert a set of partons to hadrons, the first step is thus to map color-connected pairs of partons to string pieces, with quarks as endpoints and gluons as kinks. Next, the strings evolve, with a constant probability density for string breaks to occur per unit string space-time area. In this context, it is important to note that the individual string breaks are causally disconnected [65], hence they do not have to be generated in any particular time-ordered sequence. This is exploited in the Lund model to allow to consider the formation of a single on-shell hadron at a time, in an order that corresponds to decreasing average absolute rapidity (along the string). Selecting randomly between the left and right sides of the string, the first hadron to be generated is thus the "outermost" one, formed by combining the original hadronizing endpoint quark (or antiquark) q_0 with an antiquark (or quark) $\bar{q}_1$ produced by a breakup. The new leftover quark (or antiquark) q_1 becomes the string endpoint for the next iteration, in a Markov chain which continues, alternating randomly between the left and right ends of the string, until finally a small last bit of string is decayed directly to two hadrons, with no energy left over.

For each breakup vertex, quantum mechanical tunneling is assumed to control the masses and $p_\perp$ kicks (transverse to the string axis, in a frame in which the string itself has no transverse motion) that can be produced, leading to a Gaussian suppression

$$\text{Prob}(m_q^2, p_{\perp q}^2) \;\propto\; \exp\left(\frac{-\pi m_q^2}{\kappa}\right) \exp\left(\frac{-\pi p_{\perp q}^2}{\kappa}\right) \;, \qquad (41.8)$$

where m_q is the mass of the produced quark flavor and $p_\perp$ is the nonperturbative transverse momentum imparted to it by the breakup process, with a universal average value of $\left\langle p_{\perp q}^2 \right\rangle = \kappa/\pi \sim (250\,\text{MeV})^2$. The antiquark has the same mass and opposite $p_\perp$.

In an MC model with a fixed shower cutoff t_0, the effective amount of $p_\perp$ in string breaks may be larger than the purely nonperturbative κ/π above, to account for effects of additional (unresolved) radiation below t_0.

From the mass term in Eq. (41.8), one concludes that charm and bottom quarks are too heavy to be produced in string breaks, while strange quarks will be suppressed relative to up and down ones. Lacking unambiguous and precise mass definitions for light quarks, however, the effective amount of strangeness suppression is normally extracted from experimental data, using observables such as K/π and K^*/ρ ratios.

Baryon production can also be incorporated, by allowing string breaks to produce pairs of *diquarks*, loosely bound states of two quarks in an overall $\bar{3}$ representation. Again, since diquark masses are difficult to define, the relative rate of diquark to quark production is extracted, e.g. from the p/π ratio. Since the perturbative shower splittings do not produce diquarks, the optimal value for this parameter is mildly correlated with the amount of $g \to q\bar{q}$ splittings produced by the shower. More advanced scenarios for baryon production have also been proposed, see Ref. 65. Within the PYTHIA framework, a hadronization model including baryon string junctions [66] is also available.

The next step of the algorithm is the assignment of the produced quarks within hadron multiplets. Using a nonrelativistic classification of spin states, the hadronizing q may combine with the $\bar{q}'$ from a newly created breakup to produce a meson — or baryon, if diquarks are involved — of a given spin S and angular momentum L. The lowest-lying pseudoscalar and vector meson multiplets, and spin-1/2 and -3/2 baryons, are assumed to dominate in a string framework[1], but individual rates are not predicted by the model. This is therefore the sector that contains the largest amount of free parameters. The ratio V/P of vectors to pseudoscalars is expected to be 3, but in practice it is only in the B meson sector that this is approximately true. For lighter flavors, the difference in phase space caused by the V–P mass splittings implies a suppression of vector production. When extracting the corresponding parameters from data, it is advisable to begin with the heaviest states, since so-called feed-down from the decays of higher-lying hadron states complicates the extraction for lighter particles, see Sec. 41.2.3. For baryons, additional parameters control the relative rates of spin-1 diquarks vs. spin-0 ones.

With $p_\perp^2$ and m^2 now fixed, the final step is to select the longitudinal momentum component of the created hadron along the string axis. This is parameterized by a nonperturbative *fragmentation function*, $f(z)$, which governs the probability for a hadron to take a fraction $z \in [0, 1]$ of the total available momentum. In a string framework, the requirement that the hadronization be independent of

[1] PYTHIA includes the lightest pseudoscalar and vector mesons, with the four $L = 1$ multiplets (scalar, tensor, and 2 pseudovectors) available but disabled by default, largely because several states are poorly known and thus may result in a worse overall description when included. For baryons, the lightest spin-1/2 and -3/2 multiplets are included.

the sequence in which breakups are considered (causality) imposes a "left-right symmetry" which strongly constrains the functional form of $f(z)$, with the solution

$$f(z) \propto \frac{1}{z}(1-z)^a \exp\left(-\frac{b\,(m_h^2 + p_{\perp h}^2)}{z}\right) \quad . \tag{41.9}$$

This is known as the Lund symmetric fragmentation function (normalized to unit integral). The dimensionless parameter a dampens the hard tail of the fragmentation function, towards $z \to 1$, and may in principle be flavor-dependent, while b, with dimension GeV^{-2}, is a universal constant related to the string tension [65] which determines the behavior in the soft limit, $z \to 0$. Note that the dependence on the hadron mass, m_h, in $f(z)$ implies that heavier hadrons have higher $\langle z \rangle$.

As a by-product, the probability distribution in invariant time τ of $q'\bar{q}$ breakup vertices, or equivalently $\Gamma = (\kappa\tau)^2$, is also obtained, with $dP/d\Gamma \propto \Gamma^a \exp(-b\Gamma)$ implying an area law for the color flux, and the average breakup time lying along a hyperbola of constant invariant time $\tau_0 \sim 10^{-23}$s [65].

For massive endpoints (e.g. c and b quarks), which do not move along straight lightcone sections, the exponential suppression with string area leads to modifications of the form $f(z) \to f(z)/z^{b m_Q^2}$, with m_Q the mass of the heavy quark [67]. Although different forms, such as the Peterson formula [68], can also be used to describe inclusive heavy-meson spectra (see Sec 19.9 of PDG book), such choices are not strictly consistent with causality in the string framework.

41.2.2. *The Cluster Model* :

The cluster hadronization model is based on *preconfinement*, i.e., on the observation [69,70] that the color structure of a perturbative QCD shower evolution at any scale Q_0 is such that color-singlet subsystems of partons (labeled "clusters") occur with a universal invariant mass distribution which is power suppressed at large masses. For any starting scale $Q \gg Q_0 \gg \Lambda_{\mathrm{QCD}}$, only the number of such clusters depends on Q, while the shape of their mass distribution only depends on Q_0 and on Λ_{QCD}.

Following early models based on this universality [11,71], the cluster model developed by Webber [72] has for many years been a hallmark of the `HERWIG` generators, with an alternative implementation [73] now available in the `SHERPA` generator. The key idea, in addition to preconfinement, is to force "by hand" all gluons to split into quark-antiquark pairs at the end of the parton shower. Compared with the string description, this effectively amounts to viewing gluons as "seeds" for string breaks, rather than as kinks in a continuous object. After the splittings, a new set of low-mass color-singlet clusters is obtained, formed only by quark-antiquark pairs. These can be decayed to on-shell hadrons in a simple manner, with the relative yields of different hadron species mainly governed by their masses and the size of the phase space.

The algorithm starts by generating the forced $g \to q\bar{q}$ breakups, and by assigning flavors and momenta to the produced quark pairs. For a typical shower cutoff corresponding to a gluon virtuality of $Q_{\mathrm{had}} \sim 1\,\mathrm{GeV}$, the $p_\perp$ generated by the splittings can be neglected. The constituent light-quark masses, $m_{u,d} \sim 300\,\mathrm{MeV}$ and $m_s \sim 450\,\mathrm{MeV}$, imply a suppression (typically even an absence) of strangeness production. In principle, the model also allows for diquarks to be produced at this stage, but due to the larger constituent masses this would only become relevant for shower cutoffs larger than 1 GeV.

If a cluster formed in this way has an invariant mass above some cutoff value, typically 3–4 GeV, it is forced to undergo sequential $1 \to 2$ cluster breakups, along an axis defined by the constituent partons of the original cluster, until all sub-cluster masses fall below the cutoff value. Due to the preservation of the original axis in these breakups, this treatment has some resemblance to the string-like picture, though the nonperturbative $p_\perp$ kicks generated in this way are generally larger, up to half the allowed cluster mass.

Next, on the low-mass side of the spectrum, some clusters are allowed to decay directly to a single hadron, with nearby clusters absorbing any excess momentum. This improves the description of the high-z part of the spectrum — where the hadron carries almost all the momentum of its parent jet — at the cost of introducing one additional parameter, controlling the probability for single-hadron cluster decay.

Having obtained a final distribution of small-mass clusters, now with a strict cutoff at 3–4 GeV and with the component destined to decay to single hadrons already removed, the remaining clusters are interpreted as a smoothed-out spectrum of excited mesons, each of which decays isotropically to two hadrons, with relative probabilities proportional to the available phase space for each possible two-hadron combination that is consistent with the cluster's internal flavors, including spin degeneracy. It is important that all the light members (containing only uds) of each hadron multiplet be included, as the absence of members can lead to unphysical isospin or SU(3) flavor violation. Typically, the lightest pseudoscalar, vector, scalar, even and odd charge conjugation pseudovector, and tensor multiplets of light mesons are included. In addition, some excited vector multiplets of light mesons may be available. For baryons, usually only the lightest flavor-octet, -decuplet and -singlet baryons are present, although both the `HERWIG++` and `SHERPA` implementations now include some heavier baryon multiplets as well.

Differently from the string model, the mechanism of phase-space suppression employed here leads to a natural enhancement of the lighter pseudoscalars, and no parameters beyond the spectrum of hadron masses need to be introduced at this point. The phase space also limits the transverse momenta of the produced hadrons relative to the jet axis.

Note that, since the masses and decays of excited heavy-flavor hadrons in particular are not well known, there is some freedom in the model to adjust these, which in turn will affect their relative phase-space populations.

41.2.3. *Hadron and τ Decays* :

Of the so-called primary hadrons, originating directly from string breaks and/or cluster decays (see above), many are unstable and so decay further, until a set of particles is obtained that can be considered stable on time scales relevant to the given measurement. (A typical hadron-collider definition of a "stable particle" $c\tau \geq 10\,\mathrm{mm}$ includes weakly-decaying strange hadrons K, Λ, $\Sigma^\pm$, $\bar{\Sigma}^\pm$, Ξ, Ω.) The decay modeling can therefore have a significant impact on final particle yields and spectra, especially for the lowest-lying hadronic states, which receive the largest relative contributions from decays (feed-down). This interplay also implies that hadronization parameters may need to be retuned if significant changes to the decay treatment are made.

Particle summary tables, such as those given elsewhere in this *Review*, represent a condensed summary of the available experimental measurements and hence may be incomplete and/or exhibit inconsistencies within the experimental precision. In an MC decay package, on the other hand, all information must be quantified and consistent, with all branching ratios summing to unity. When adapting particle summary information for use in a decay package, a number of choices must therefore be made. The amount of ambiguity increases as more excited hadron multiplets are added to the simulation, about which less and less is known from experiment, with each GPMC making its own choices.

A related choice is how to distribute the decay products differentially in phase space, in particular which matrix elements to use. Historically, MC generators contained matrix elements only for selected (generator-specific) classes of hadron and τ decays, coupled with a Breit-Wigner smearing of the masses, truncated at the edges of the physical decay phase space (the treatment of decay thresholds can be important for certain modes [18]) . A more sophisticated treatment can then be obtained by reweighting the generated events using the obtained particle four-momenta and/or by using specialized external packages such as `EVTGEN` [74] for hadron decays and `TAUOLA` [75] for τ decays.

More recently, `HERWIG++` and `SHERPA` include helicity-dependence in τ decays [76,6], with a more limited treatment available in `PYTHIA 8` [5]. The `HERWIG++` and `SHERPA` generators have also included significantly improved internal simulations of hadronic

decays, which include spin correlations between those decays for which matrix elements are used. Photon-bremsstrahlung effects are discussed in Sec. 41.1.7.

HERWIG++ and PYTHIA include the probability for B mesons to oscillate into $\bar{B}$ ones before decay. SHERPA and EVTGEN also include CP-violating effects and, for common decay modes of the neutral meson and its antiparticle, the interference between the direct decay and oscillation followed by decay.

We end on a note of warning on double counting. This may occur if a particle can decay via an intermediate on-shell resonance. An example is $a_1 \to \pi\pi\pi$ which may proceed via $a_1 \to \rho\pi$, $\rho \to \pi\pi$. If these decay channels of the a_1 are both included, each with their full partial width, a double counting of the on-shell $a_1 \to \rho\pi$ contribution would result. Such cases are normally dealt with consistently in the default MC generator packages, so this warning is mostly for users that wish to edit decay tables on their own.

41.3. Models for Soft Hadron-Hadron Physics

41.3.1. ***Minimum-Bias and Diffraction*** :
The term "minimum bias" (MB) originates from the experimental requirement of a minimal number of tracks (or hits) in a given instrumented region. In order to make MC predictions for such observables, all possible contributions to the relevant phase-space region must be accounted for. There are essentially four types of physics processes, which together make up the total hadron-hadron (hh) cross section: 1) elastic scattering[2]: $hh \to hh$, 2) single diffractive dissociation: $hh \to h + \text{gap} + X$, with X denoting anything that is not the original beam particle, and "gap" denoting a rapidity region devoid of observed activity; 3) double diffractive dissociation: $hh \to X + \text{gap} + X$, and 4) inelastic non-diffractive scattering: everything else. A fifth class may also be defined, called central diffraction ($hh \to h + \text{gap} + X + \text{gap} + h$). Note that different terminologies exist [77]: in experimental settings, diffraction is typically defined by an observable gap, of some minimal size in rapidity, while in the MC context, each diffractive physics process produces a whole spectrum of gaps, with small ones suppressed but not excluded.

The inelastic non-diffractive part of the cross section is typically modeled either by smoothly regulating and extending the perturbative QCD scattering cross sections all the way to zero $p_\perp$ [78] (PYTHIA and SHERPA), or by regulating the QCD cross sections with a sharp cutoff [79] and adding a separate class of nonperturbative scatterings below that scale [80](HERWIG). See also Sec. 41.3.2. In all cases, the most important ingredients are: 1) the IR regularization of the perturbative scattering cross sections, including their PDF dependence, 2) the assumed matter distribution of the colliding hadrons, possibly including multi-parton correlations [66] and/or x dependence [81], and 3) additional soft-QCD effects such as color reconnections, discussed in Sec. 41.3.3.

Currently, there are essentially three methods for simulating diffraction in the main MC models: 1) in PYTHIA 6, one picks a diffractive mass according to parameterized cross sections $\propto \mathrm{d}M^2/M^2$ [82]. This mass is represented as a string, which is hadronized as described in Sec. 41.2.1, though differences in the effective scale of the hadronization may necessitate a (re)tuning of the hadronization parameters for diffraction; 2) in PYTHIA 8, the high-mass tail beyond $M \sim 10\,\text{GeV}$ is augmented by a partonic description in terms of pomeron PDFs [83], allowing diffractive jet production including showers and underlying event [84]; 3) the PHOJET and DPMJET programs also include central diffraction and rely directly on a formulation in terms of pomerons (color-singlet multi-gluon states) [85–87]. Cut pomerons correspond to exchanges of soft gluons while uncut ones give elastic and diffractive topologies as well as virtual corrections that help preserve unitarity. So-called "hard pomerons" provide a transition to the perturbative regime. Hadronization is still handled using the Lund string model, so there is some overlap with the above models at the hadronization stage.

[2] The QED elastic cross section diverges and is normally a non-default option.

In addition, a pomeron-based package exists for HERWIG [88], and an effort is underway to construct an MC implementation of the "KMR" model [89] within the SHERPA generator. Color reconnections (Sec. 41.3.3) may also play a role in creating rapidity gaps and the underlying event (Sec. 41.3.2) in filling them.

41.3.2. ***Underlying Event and Jet Pedestals*** :
In the GPMC context, "underlying event" (UE) denotes any additional activity *beyond* the basic process and its associated ISR and FSR activity. The UE is thus only defined in the context of events selected with a "hard" (i.e., high-$\mathrm{p}_\perp$) trigger which defines the basic process at hand. (This is distinct from the MB selection which does not require any hard perturbative activity.) The dominant contribution to the UE is believed to come from additional color exchanges between the colliding hadronic states. These multiple exchanges can be modeled either as additional perturbative (mainly t-channel gluon) exchanges, called multiple parton-parton interactions (MPI), or nonperturbatively using so-called cut pomerons (roughly equivalent to exchange of gluons with $p_\perp \to 0$). The experimental observation that events with a hard trigger are accompanied by a higher-than-average level of associated activity (UE particle densities and related quantities are greater than those of MB events at the same CM energy) is called the "jet pedestal" effect.

The most clearly identifiable consequence of MPI is arguably the possibility of observing several hard parton-parton interactions in one and the same hadron-hadron event. Typically, these are QCD $2 \to 2$ interactions, which produce additional back-to-back jet pairs, with each pair having a small value of $\text{sum}(\vec{p}_\perp)$. The fraction of MPI that give rise to additional reconstructible jets is, however, small. Soft interactions, that exchange color and a small amount of momentum without giving rise to observable jets, are much more plentiful, and can give significant corrections to the color flow and total scattered energy of the event. This affects the final-state activity in a more global way, increasing hadron-multiplicity and summed E_T distributions, and contributing to the break-up of the beam remnants in the forward direction.

The first detailed Monte Carlo model for perturbative MPI was proposed in Ref. 78, and with some variation this still forms the basis for most modern implementations. Some useful additional references can be found in Ref. 18. The first crucial observation is that the t-channel propagators appearing in perturbative QCD $2 \to 2$ scattering almost go on shell at low $p_\perp$, causing the differential cross sections to behave roughly as

$$d\sigma_{2\to 2} \propto \frac{dt}{t^2} \sim \frac{dp_\perp^2}{p_\perp^4} \ . \tag{41.10}$$

This cross section represents the inclusive scattering of partons against partons in perturbative QCD, summed over all partons. Thus, if a single hadron-hadron scattering contains *two* parton-parton interactions, that event will contribute twice to the parton-parton cross section $\sigma_{2\to 2}$ but only once to the hadron-hadron one σ_{tot}, and so on. In the limit that all the parton-parton interactions are independent and equivalent, one has

$$\sigma_{2\to 2} = \langle n \rangle \ \sigma_{\text{tot}} \ , \tag{41.11}$$

with $\langle n \rangle$ the average number of parton-parton interactions, typically defined with some minimal $p_\perp > p_{\perp\text{min}}$ to render the parton-parton cross section finite. The probability for n parton-parton scatterings then follows a Poisson distribution,

$$\mathcal{P}_n = \langle n \rangle^n \frac{\exp\left(-\langle n \rangle\right)}{n!} \ . \tag{41.12}$$

This simple argument expresses unitarity; instead of the total hadron-hadron interaction cross section diverging as the parton-parton $p_\perp \to 0$ (which would violate unitarity), we have restated the problem so that it is now the *number of parton-parton interactions per hadron-hadron collision* that diverges, with the total hadron-hadron cross section remaining finite. At LHC energies, the parton-parton scattering cross sections computed using the LO QCD cross section folded with modern PDFs become larger than the total pp one for $p_{\perp\text{min}}$ values of

order 4–5 GeV (see e.g. [90,91]) . One therefore expects the average number of perturbative MPI to exceed unity at around that scale.

Two ingredients remain to fully regulate the remaining divergence. Firstly, the interactions cannot use up more momentum than is available in the parent hadron. This suppresses the large-n tail of the estimate above. In PYTHIA-based models, the MPI are ordered in $p_\perp$, and the parton densities for each successive interaction are explicitly constructed so that the sum of x fractions can never be greater than unity. In the HERWIG models, the Poisson estimate of $\langle n \rangle$ above is used as an initial guess, but the generation of actual MPI is stopped once the energy-momentum conservation limit is reached. Both of these approaches generate momentum (conservation) correlations among the MPI.

The second ingredient invoked to suppress the number of interactions, at low $p_\perp$ and x, is color screening; if the wavelength $\sim 1/p_\perp$ of an exchanged colored parton becomes larger than a typical color-anticolor separation distance, it will only see an *average* color charge that vanishes in the limit $p_\perp \to 0$. This provides an infrared cutoff for MPI similar to that provided by the hadronization scale for parton showers. A first estimate of the color-screening cutoff would be the proton size, $p_{\perp\min} \approx \hbar/r_p \approx 0.3\,\text{GeV} \approx \Lambda_{\rm QCD}$, but empirically this appears to be far too low. In current models, one replaces the proton radius r_p in the above formula by a "typical color screening distance," i.e., an average size of a region within which the net compensation of a given color charge occurs. This number is not known from first principles [89] and is perceived of simply as an effective cutoff parameter. The simplest choice is to introduce a step function $\Theta(p_\perp - p_{\perp\min})$. Alternatively, one may note that the jet cross section is divergent like $\alpha_{\rm S}^2(p_\perp^2)/p_\perp^4$, cf. Eq. (41.10), and that therefore a factor

$$\frac{\alpha_{\rm S}^2(p_{\perp 0}^2 + p_\perp^2)}{\alpha_{\rm S}^2(p_\perp^2)} \, \frac{p_\perp^4}{(p_{\perp 0}^2 + p_\perp^2)^2} \tag{41.13}$$

would smoothly regulate the divergences, now with $p_{\perp 0}$ as the free parameter. Regardless of whether it is imposed as a smooth (PYTHIA and SHERPA) or steep (HERWIG++) function, this is effectively the main "tuning" parameter in such models.

Note that the numerical value obtained for the cross section depends upon the PDF set used, and therefore the optimal value to use for the cutoff will also depend on this choice. Note also that the cutoff does not have to be energy-independent. Higher energies imply that parton densities can be probed at smaller x values, where the number of partons rapidly increases. Partons then become closer packed and the color screening distance d decreases. The uncertainty on the energy and/or x scaling of the cutoff is a major concern when extrapolating between different collider energies [92].

We now turn to the origin of the observational fact that hard jets appear to sit on top of a higher "pedestal" of underlying activity than events with no hard jets. This is interpreted as a consequence of impact-parameter-dependence: in peripheral collisions, only a small fraction of events contain any high-$p_\perp$ activity, whereas central collisions are more likely to contain at least one hard scattering; a high-$p_\perp$ triggered sample will therefore be biased towards small impact parameters, b. The ability of a model to describe the shape of the pedestal (e.g. to describe both MB and UE distributions simultaneously) therefore depends upon its modeling of the b-dependence, and correspondingly the impact-parameter shape constitutes another main tuning parameter.

For each impact parameter b, the number of interactions $\tilde{n}(b)$ can still be assumed to be distributed according to Eq. (41.12), again modulo momentum conservation, but now with the mean value of the Poisson distribution depending on impact parameter, $\langle \tilde{n}(b) \rangle$. This causes the final n-distribution (integrated over b) to be wider than a Poissonian.

Finally, there are two perturbative modeling aspects which go beyond the introduction of MPI themselves: 1) parton showers off the MPI, and 2) perturbative parton-rescattering effects. Without showers, MPI models would generate very sharp peaks for back-to-back MPI jets, caused by unshowered partons passed directly to the hadronization model. However, with the exception of the oldest PYTHIA6 model, all GPMC models do include such showers [18], and hence should exhibit more realistic (i.e., broader and more decorrelated) MPI jets. On the initial-state side, the main questions are whether and how correlated multi-parton densities are taken into account and, as discussed previously, how the showers are regulated at low $p_\perp$ and/or low x. Although none of the MC models currently impose a rigorous correlated multi-parton evolution, all of them include some elementary aspects. The most significant for parton-level results is arguably momentum conservation, which is enforced explicitly in all the models. The so-called "interleaved" models [30] attempt to go a step further, generating an explicitly correlated multi-parton evolution in which flavor sum rules are imposed to conserve, e.g. the total numbers of valence and sea quarks [66].

Perturbative rescattering in the final state can occur if partons are allowed to undergo several distinct interactions, with showering activity possibly taking place in-between. This has so far not been studied extensively, but a first exploratory model is available [93]. In the initial state, parton rescattering/recombination effects have so far not been included in any of the GPMC models.

41.3.3. ***Bose-Einstein and Color-Reconnection Effects*** :
In the context of e^+e^- collisions, Bose-Einstein (BE) correlations have mostly been discussed as a source of uncertainty on high-precision W mass determinations at LEP [94]. In hadron-hadron (and nucleus-nucleus) collisions, however, BE correlations are used extensively to study the space-time structure of hadronizing matter ("femtoscopy").

In MC models of hadronization, each string break or particle/cluster decay is normally factorized from all other ones. This reduces the number of variables that must be considered in each step, but also makes it intrinsically difficult to introduce correlations among particles from different breaks/decays. In GPMCs, a few semi-classical models are available within the PYTHIA 6 and 8 generators [95], in which the BE effect is mimicked by an attractive interaction between pairs of identical particles in the final state, with no higher correlations included. Variants of this model differ mainly by the assumed shape of the correlation function and how overall momentum conservation is handled.

As discussed in Sec. 41.2, leading-color ("planar") color flows are used to set up the hadronizing systems (clusters or strings) at the hadronization stage. If the systems do not overlap significantly in space and time, subleading-color ambiguities and/or nonperturbative reconnections are expected to be small. However, if the density of displaced color charges is sufficiently high that several systems can overlap significantly, full-color and/or reconnection effects should become progressively larger.

In the specific context of MPI, a crucial question is how color is neutralized *between* different MPI systems, including the remnants. The large rapidity differences involved imply large invariant masses (though normally low $p_\perp$), and hence large amounts of (soft) particle production. Indeed, in the context of soft-inclusive physics, it is these "inter-system" strings/clusters that furnish the dominant particle-production mechanism, and hence their modeling is an essential part of the soft-physics description, affecting topics such as MB/UE multiplicity and $p_\perp$ distributions, rapidity gaps, and precision mass measurements. Reviews of color-reconnection effects can be found in Refs. 18,96.

41.4. Uncertainties and Tuning

The accuracy that can be achieved by a GPMC model depends on the sophistication of the theory models it incorporates, on the available constraints on its free parameters, and on the nature of the observable(s) under study. Using existing data (or more accurate theory calculations) to constrain the model parameters is referred to as generator tuning. Although tuned models do tend to yield improved results also for observables that they have not been tuned to, the question of evaluating the remaining uncertainties reliably is still far from solved. It is worth noting, however, that all of the GPMCs now provide options for automatic evaluation of perturbative shower uncertainties (e.g., via renormalization-scale variations), in the form

of vectors of alternative event weights [97,98,99] although significant weight fluctuations can be a problem for processes with many or large shower phase spaces. One must be aware that these variations are not necessarily exhaustive and care must be taken in their interpretation. Nonperturbative uncertainties must normally still be evaluated by varying salient model parameters by hand. A general method called eigentunes [100] is also available, based on global fits to data.

Typically, the overall event properties are determined by only a few, very important parameters, such as the value of α_S, for perturbative corrections, and the shape of the fragmentation functions, for nonperturbative ones. More parameters may then be introduced to describe successively more detailed aspects (e.g., the rates and decays of individual hadron species), but these should have progressively less impact on the overall modeling. One may therefore take a factorized approach, first constraining the perturbative parameters and thereafter the nonperturbative ones, in order of decreasing significance to the overall modeling. Furthermore, by identifying which measurements are most sensitive to each parameter, this ordering can be reflected in the way that data is selected and applied to constrain the models. Thus, measurements sensitive to global event properties would typically be applied first, to constrain the most inclusive parameters, and so on for progressively more exclusive aspects.

At LO×LL, perturbation theory is doing well if it agrees with an IR safe measurement within $\sim 10\%$. It would therefore not make much sense to tune a GPMC beyond roughly 5% (it might even be dangerous, due to overfitting). The advent of NLO Monte Carlos may reduce this number slightly, but only for quantities for which one expects NLO precision. For quantities governed by nonperturbative physics, uncertainties are larger. For some quantities, e.g. ones for which the underlying modeling is known to be poor, an order-of-magnitude agreement or worse may have to be accepted. Note further that the unitarity of shower and hadronization models implies that the Born-level cross-section normalization is not tunable, hence in tuning contexts one tends to focus on the shapes of distributions rather than their normalizations.

In the context of LO×LL GPMC tuning, subleading aspects of coupling-constant and PDF choices are relevant. In particular, one should be aware that the choice of QCD Λ parameter $\Lambda_{\rm MC} = 1.569\Lambda_{\overline{\rm MS}}$ (for 5 active flavors) improves the predictions of coherent shower algorithms at the NLL level for a class of relevant observables [101], and hence this scheme is often considered the baseline for shower tuning. The question of LO vs. NLO PDFs is more involved [18], but it should be emphasized that the gluon PDF at (very) low x is important for determining the level of the underlying event in MPI models (Sec. 41.3.2), and hence the MB/UE tuning (and energy scaling [92]) is linked to the choice of PDF in such models. Further issues and an example of a specific recipe that could be followed in a realistic set-up can be found in Ref. 90. A useful online resource can be found at the mcplots.cern.ch web site [102], based on the RIVET tool [103].

Recent years have seen the emergence of automated tools to reduce the amount of both computer and manpower required for tuning [100]. Automating the human expert input is more difficult. In the tools currently on the market, this is addressed by a combination of input solicited from the GPMC authors (e.g., which parameters and ranges to consider, which observables constitute a complete set, etc) and a set of weights determining the relative priority given to each bin in each distribution. The final result is therefore still subjective but at least reproducible. When backed by careful demonstrations of sensitivities, correlations, and uncertainties, the quality of the resulting tunes is by now competitive. The field is still burgeoning, with future sophistications to be expected.

References:

1. G. Corcella *et al.*, JHEP **0101**, 010 (2001), hep-ph/0011363.
2. M.Bähr *et al.*, Eur. Phys. J. **C58**, 639 (2008), arXiv:0803.0883.
3. J. Bellm *et al.*, Eur. Phys. J. **C76**, 196 (2016), arXiv:1512.01178.
4. T. Sjöstrand, S. Mrenna, and P. Z. Skands, JHEP **05**, 026 (2006), hep-ph/0603175.
5. T. Sjöstrand *et al.*, Comp. Phys. Comm. **191**, 159 (2015), arXiv:1410.3012.
6. T. Gleisberg *et al.*, JHEP **0902**, 007 (2009), arXiv:0811.4622.
7. QCD summary, PDG..
8. T. Kinoshita, J. Math. Phys. **3**, 650 (1962).
9. T. Lee and M. Nauenberg, Phys. Rev. **133**, 1549 (1964).
10. A. Buckley *et al.*, arXiv:1101.2599, and references therein..
11. G.C. Fox and S. Wolfram, Nucl. Phys. **B168**, 285 (1980).
12. G. Altarelli and G. Parisi, Nucl. Phys. **B126**, 298 (1977).
13. A. Einstein, B. Podolsky, and N. Rosen, Phys. Rev. **47**, 777 (1935).
14. B.R. Webber, Phys. Lett. **B193**, 91 (1987).
15. J.C. Collins, Nucl. Phys. **B304**, 794 (1988).
16. I.G. Knowles, Comp. Phys. Comm. **58**, 271 (1990).
17. T. Sjöstrand, Phys. Lett. **B157**, 321 (1985).
18. A. Buckley *et al.*, Phys. Reports **504**, 145 (2011), arXiv:1101.2599.
19. G. Marchesini and B.R. Webber, Nucl. Phys. **B310**, 461 (1988).
20. S. Gieseke, P. Stephens, and B. Webber, JHEP **0312**, 045 (2003), hep-ph/0310083.
21. M. Bengtsson and T. Sjöstrand, Nucl. Phys. **B289**, 810 (1987).
22. G. Gustafson and U. Pettersson, Nucl. Phys. **B306**, 746 (1988).
23. L. Lönnblad, Comp. Phys. Comm. **71**, 15 (1992).
24. T. Ježo *et al.*, Eur. Phys. J. **C76**, 691 (2016), arXiv:1607.04538.
25. W.T. Giele, D.A. Kosower, and P.Z. Skands, Phys. Rev. **D78**, 014026 (2008), arXiv:0707.3652.
26. Z. Nagy and D.E. Soper, JHEP **0510**, 024 (2005), hep-ph/0503053.
27. S. Schumann and F. Krauss, JHEP **0803**, 038 (2008), arXiv:0709.1027.
28. S. Plätzer and S. Gieseke, Eur. Phys. J. **C72**, 2187 (2012), arXiv:1109.6256.
29. S. Höche and S. Prestel, Eur. Phys. J. **C75**, 461 (2015), arXiv:1506.05057.
30. T. Sjöstrand and P.Z. Skands, Eur. Phys. J. **C39**, 129 (2005), hep-ph/0408302.
31. E. Norrbin and T. Sjöstrand, Nucl. Phys. **B603**, 297 (2001), hep-ph/0010012.
32. S. Catani *et al.*, Nucl. Phys. **B627**, 189 (2002), hep-ph/0201036.
33. J. Cembranos *et al.*, (2013), arXiv:1305.2124.
34. N. Davidson, T. Przedzinski, and Z. Was, (2010), arXiv:1011.0937.
35. K. Hamilton and P. Richardson, JHEP **0607**, 010 (2006), hep-ph/0603034.
36. M. Schönherr and F. Krauss, JHEP **0812**, 018 (2008), arXiv:0810.5071.
37. A. Semenov, Comp. Phys. Comm. **180**, 431 (2009), arXiv:0805.0555.
38. N.D. Christensen and C. Duhr, Comp. Phys. Comm. **180**, 1614 (2009), arXiv:0806.4194.
39. M. Fairbairn *et al.*, Phys. Reports **438**, 1 (2007), hep-ph/0611040.
40. J. Alwall *et al.*, Comp. Phys. Comm. **176**, 300 (2007), hep-ph/0609017.
41. P.Z. Skands *et al.*, JHEP **0407**, 036 (2004), hep-ph/0311123.
42. J. Alwall *et al.*, (2007), arXiv:0712.3311.
43. P. Richardson, JHEP **0111**, 029 (2001), hep-ph/0110108.
44. E. Boos *et al.*, (2007), hep-ph/0109068.
45. M. Bengtsson and T. Sjöstrand, Phys. Lett. **B185**, 435 (1987).
46. W. T. Giele, D. A. Kosower and P. Z. Skands, Phys. Rev. **D84**, 054003 (2011), arXiv:1102.2126.
47. S. Catani *et al.*, JHEP **11**, 063 (2001), hep-ph/0109231.
48. J. Alwall *et al.*, Eur. Phys. J. **C53**, 473 (2008), arXiv:0706.2569.
49. P. Nason, JHEP **11**, 040 (2004), hep-ph/0409146.
50. B. Cooper *et al.*, Eur. Phys. J. **C72**, 2078 (2012), arXiv:1109.5295.
51. M.L. Mangano *et al.*, JHEP **0307**, 001 (2003), hep-ph/0206293.
52. J. Alwall *et al.*, JHEP **1106**, 128 (2011), arXiv:1106.0522.

53. S. Frixione and B.R. Webber, JHEP **06**, 029 (2002), hep-ph/0204244.
54. S. Alioli *et al.*, JHEP **1006**, 043 (2010), arXiv:1002.2581.
55. J. Alwall *et al.*, JHEP **07**, 079 (2014), arXiv:1405.0301.
56. S. Alioli, K. Hamilton, and E. Re, JHEP **09**, 104 (2011), arXiv:1108.0909.
57. R. Frederix and S. Frixione, JHEP **12**, 061 (2012), arXiv:1209.6215.
58. L. Lönnblad and S. Prestel, JHEP **03**, 166 (2013), arXiv:1211.7278.
59. K. Hamilton, P. Nason and G. Zanderighi, JHEP **10**, 155 (2012), arXiv:1206.3572.
60. S. Höche *et al.*, JHEP **04**, 027 (2013), arXiv:1207.5030.
61. K. Hamilton, P. Nason and G. Zanderighi, JHEP **05**, 140 (2015), arXiv:1501.04637.
62. G. Gustafson, Phys. Lett. **B175**, 453 (1986).
63. X. Artru and G. Mennessier, Nucl. Phys. **B70**, 93 (1974).
64. B. Andersson *et al.*, Phys. Reports **97**, 31 (1983).
65. B. Andersson, Camb. Monogr. Part. Phys. Nucl. Phys. Cosmol. **7** (1997).
66. T. Sjöstrand and P.Z. Skands, JHEP **0403**, 053 (2004), hep-ph/0402078.
67. M. Bowler, Z. Phys. **C11**, 169 (1981).
68. C. Peterson *et al.*, Phys. Rev. **D27**, 105 (1983).
69. D. Amati and G. Veneziano, Phys. Lett. **B83**, 87 (1979).
70. A. Bassetto, M. Ciafaloni, and G. Marchesini, Phys. Lett. **B83**, 207 (1979).
71. R.D. Field and S. Wolfram, Nucl. Phys. **B213**, 65 (1983).
72. B.R. Webber, Nucl. Phys. **B238**, 492 (1984).
73. J.-C. Winter, F. Krauss, and G. Soff, Eur. Phys. J. **C36**, 381 (2004), hep-ph/0311085.
74. D. Lange, Nucl. Instrum. Methods **A462**, 152 (2001).
75. S. Jadach *et al.*, Comp. Phys. Comm. **76**, 361 (1993).
76. D. Grellscheid and P. Richardson, (2007), arXiv:0710.1951.
77. V. Khoze *et al.*, Eur. Phys. J. **C69**, 85 (2010), arXiv:1005.4839.
78. T. Sjöstrand and M. van Zijl, Phys. Rev. **D36**, 2019 (1987).
79. J.M. Butterworth, J.R. Forshaw, and M.H. Seymour, Z. Phys. **C72**, 637 (1996), hep-ph/9601371.
80. M. Bähr *et al.*, (2009), arXiv:0905.4671.
81. R. Corke and T. Sjöstrand, JHEP **1105**, 009 (2011), 1101.5953.
82. G.A. Schuler and T. Sjöstrand, Phys. Rev. **D49**, 2257 (1994).
83. G. Ingelman and P. Schlein, Phys. Lett. **B152**, 256 (1985).
84. S. Navin, (2010), arXiv:1005.3894.
85. P. Aurenche *et al.*, Comp. Phys. Comm. **83**, 107 (1994), hep-ph/9402351.
86. F.W. Bopp, R. Engel, and J. Ranft, (1998), hep-ph/9803437.
87. S. Roesler, R. Engel, and J. Ranft, p. 1033 (2000), hep-ph/0012252.
88. B.E. Cox and J.R. Forshaw, Comp. Phys. Comm. **144**, 104 (2002), hep-ph/0010303.
89. M. Ryskin, A. Martin, and V. Khoze, Eur. Phys. J. **C71**, 1617 (2011), arXiv:1102.2844.
90. P. Skands, S. Carrazza and J. Rojo, Eur. Phys. J. **C74**, 3024 (2014), arXiv:1404.5630.
91. M. Bähr, J.M. Butterworth, and M.H. Seymour, JHEP **01**, 065 (2009), arXiv:0806.2949.
92. H. Schulz and P.Z. Skands, Eur. Phys. J. **C71**, 1644 (2011), arXiv:1103.3649.
93. R. Corke and T. Sjöstrand, JHEP **01**, 035 (2009), arXiv:0911.1901.
94. LEP Electroweak Working Group, (2005), hep-ex/0511027.
95. L. Lönnblad and T. Sjöstrand, Eur. Phys. J. **C2**, 165 (1998), hep-ph/9711460.
96. J. R. Christiansen and P. Z. Skands, JHEP **08**, 003 (2015), arXiv:1505.01681.
97. J. Bellm *et al.*, Phys. Rev. **D94**, 034028 (2016), arXiv:1605.08256.
98. S. Mrenna and P. Skands, Phys. Rev. **D94**, 074005 (2016), arXiv:1605.08352.
99. E. Bothmann, M. Schnherr and S. Schumann, Eur. Phys. J. **C76**, 590 (2016), arXiv:1606.08753.
100. A. Buckley *et al.*, Eur. Phys. J. **C65**, 331 (2010), arXiv:0907.2973.
101. S. Catani, B. R. Webber, and G. Marchesini, Nucl. Phys. **B349**, 635 (1991).
102. A. Karneyeu *et al.*, Eur. Phys. J. **C74**, 2714 (2013), arXiv:1306.3436.
103. A. Buckley *et al.*, Comp. Phys. Comm. **184**, 2803 (2010), arXiv:1003.0694.

42. Monte Carlo Neutrino Generators

Updated September 2017 by H. Gallagher (Tufts U.) and Y. Hayato (Tokyo U.)

Monte Carlo neutrino generators are programs or libraries which simulate neutrino interactions with electrons, nucleons and nuclei. In this capacity their usual task is to take an input neutrino and nucleus and produce a set of 4-vectors for particles emerging from the interaction, which are then input to full detector simulations. Since these generators have to simulate not only the initial interaction of neutrinos with target particles, but re-interactions of the generated particles in the nucleus, they contain a wide range of elementary particle and nuclear physics. Viewed more broadly, they are the access point for neutrino experimentalists to the theory inputs needed for analysis. Examples include cross section libraries for event rate calculations and parameter uncertainties and reweighting tools for systematic error evaluation.

Neutrino experiments typically operate in neutrino beams that are neither completely pure nor mono-energetic. Generators are a crucial component in the convolution of beam flux, neutrino interaction physics, and detector response that is necessary to make predictions about observable quantities. Similarly they are used to relate reconstructed quantities back to true quantities. In these various capacities they are used from the detector design stage through the extraction of physics measurements from reconstructed observables. Monte Carlo neutrino generators play unique and important roles in the experimental study of neutrino interactions and oscillations.

There are several neutrino event generators available, such as ANIS [1], GENIE [2], GiBUU [3,4], MARLEY [5], NEGN [6], NEUT [7], NUANCE [8], the FLUKA routines NUNDIS/NUNRES [9,10], and NuWro [11], as well as tools to facilitate cross-generator comparisons [12]. Historically, experiments would develop their own generators. This was often because they were focused on a particular measurement, energy range, or target, and wanted to ensure that the best physics was included for it. These 'home-grown' generators were often tuned primarily or exclusively to the neutrino data most similar to the data that the experiment would be collecting. A major advance in the field was the introduction of conference series devoted to the topic of neutrino interaction physics, NuINT (https://nuint2017.physics.utoronto.ca) and NuFACT (https://indico.uu.se/event/324/) in particular. Event generator comparisons have been a regular staple of the NuINT conference series from its inception, and a great deal of information on this topic can be found in the Proceedings of these meetings. These meetings have facilitated experiment-theory discussions leading to the first generator developed by a theory group (NuWro) [11], the extension of established nuclear interaction codes (FLUKA and GiBUU) to include neutrino-nuclear processes [3,4,9,10], and inclusion of theorists in existing generator development teams.

These activites have led to more careful scrutiny of the crucial nuclear theory inputs to these generators, which is evaluated in particular through comparisons to electron-scattering data. At this point in time all simulation codes face challenges in describing the full extent of the lepton scattering data, and the tension between incorporating the best available theory versus obtaining the best agreement with the data plays out in a variety of ways within the field. For the field to make progress, inclusion of state of the art theory needs to be coupled to global analyses that correctly incorporate correlations between measurements. Given the rapid pace of new data and the complexity of analyses, this is a significant challenge for the field in the coming years.

There are many neutrino experiments which use various sources of neutrinos, from reactors, accelerators, the atmosphere, and astrophysical sources, thereby covering a range of energies from MeV to TeV. Much of the emphasis has been on the few-GeV region in the generators, as this is the relevant energy range for short- and long-baseline neutrino oscillation experiments. These generators use the impulse approximation, which treats the nucleus as a collection of independent nucleons and the primary interaction occurs between the probe and a single nucleon, for most of the initial interaction, and subsequently simulates the interactions of secondary particles in the nucleus in semi-classical ways. Semi-classical hadron transport approaches are commonly used as they are able simulate a variety of nuclei in a single model, and for practical considerations as these approaches are fast. However, there are several challenges facing these simulations coming mainly from the complexity of the nuclear physics, and avoiding double counting in combining perturbative and non-perturbative models for the neutrino-nucleon scattering processes. The overall validity of this impulse approximation-based scheme, and in particular the importance of scattering channels that involve more than one nucleon, is a crucial question that is the topic of much current work. While generators share many common ingredients, differences in implementation, parameter values, and approaches to avoid double counting can yield dramatically different predictions [13]. In the following sections, interaction models and their implementations including the interactions of generated particles in the nuclei are described.

In order to assure its validity, neutrino event generators are tuned and validated against a wide variety of data, including data from photon, charged lepton, neutrino, and hadron probes. The results from these external data tuning exercises are important for experiments as they quantify the uncertainty on model paramaters, needed by experiments in the evaluation of generator-related systematic errors. Electron scattering data plays an important role in determining the vector contribution to the form-factors and structure functions, as well as in evaluating specific aspects of the nuclear model [14]. Hadron scattering data is used in validating the nuclear model, in particular of interactions between hadrons produced in the primary interaction and the residual target nucleus (final state interactions). Tuning of neutrino-nucleon scattering and hadronization models relies heavily on the previous generation of high energy neutrino scattering and hydrogen and deuterium bubble chamber experiments, and more recent data from the K2K, MiniBooNE, NOMAD, SciBooNE, MINOS, T2K, ArgoNEUT, MINERvA, NOvA, MicroBooNE, and SBND experiments either has been, or will be, used for this purpose.

42.1. Neutrino-Nucleon Scattering

Event generators typically begin with free-nucleon cross sections which are then embedded into a nuclear physics model. The most important processes are quasi-elastic (elastic for neutral current (NC)) scattering, resonance production, and non-resonant inelastic scattering, which make comparable contributions for few-GeV interactions. The neutrino cross sections in this energy range can be seen in Figures 50.1 through 50.3 of this *Review*.

42.1.1. ***Quasi-Elastic Scattering*** : The cross section for the neutrino nucleon charged current quasi-elastic scattering is described in terms of the leptonic and hadronic weak currents, where dominant contributions to the hadronic current come from the vector (V) and axial-vector (A) form factors. Contributions from the pseudo-scalar form factor (P) are typically small for muon and electron and neutrinos are are related to the axial form factor (A) assuming partially conserved axial currents (PCAC). The vector form factors are related via the conserved vector current (CVC) hypothesis to those measured by precise electron scattering experiments, which are known to have some deviation from the simple dipole form [15]. Therefore, most of the generators use parametrizations of this form factor taken directly from the data. For the axial form factor there is no such precise experiment, and most of the generators use a dipole form [16]. Generally, the value of axial form factor at $q^2 = 0$ (q is the four-momentum transfer) is extracted from the polarized nucleon beta decay experiment. However, the selection of the axial vector mass parameter depends on each generator, with values typically around 1.00 GeV/c^2. Recently, there are several attempts to use the other fucntions for the axial form factors [17,18] and some generators have already implemented these form factors [19].

42.1.2. ***Resonance Production*** : Most generators use the prescriptions of Rein-Sehgal [20] to simulate neutrino-induced single pion production. To obtain the cross section for a particular channel, they calculate the amplitude for the production of each resonance multiplied by the probability for the decay of that resonance into that particular channel. Implementation differences include the number of resonances included, whether the amplitudes are added coherently or

incoherently, the invariant mass range over which the model is used, how non-resonant backgrounds are included, inclusion of lepton mass terms, and the model parameter values (in particular the axial mass). In this model it is also possible to calculate the cross-sections of single photon, kaon and η productions by changing the decay probability of the resonances, which are included in some of the programs. However, it is known that discrepancies exist between the recent pion electro/photoproduction data and the results from the simulation data with the same framework, i.e. vector part of this model. There are several attempts to overcome this issue [21] and some of the generators started using more appropriate form factors. The GiBUU and NuWro generators do not use the Rein-Sehgal model, and instead rely directly on electro-production data for the vector contribution and fit bubble chamber data to determine the remaining parameters for the axial contribution [22,23,24].

42.1.3. ***Deep and Shallow Inelastic Scattering*** : For this process the fundamental target shifts from the nucleon to its quark constituents. Therefore, the generators use the standard expression for the constructions for the nucleon structure functions F_2 and xF_3 from parton distributions for high Q^2 (the DIS regime: W$>$ 2 GeV/c^2 and $Q^2 > 1$ GeV^2) to calculate direction and momentum of lepton. The first challenge is in extending this picture to the lower values of Q^2 and W that dominate the available phase space for few-GeV interactions (the so-called 'shallow inelastic scattering', or SIS regime). GRV98LO parton distribution functions [25] with the corrections proposed in [26] are widely used, while others [9] implement their own modifictions to the parton distributions at low Q^2. Both DIS and SIS generates hadrons but their production depends on each generator's implementation of a hadronization model as described in the next section. There are various difficulties not only in the actual hadronization but the relation with the single meson production. It is necessary to avoid double counting between the resonance and SIS/DIS models, and all generators are different in this regard. The scheme chosen can have a significant impact on the results of simulations at a few-GeV neutrino energies.

42.2. Hadronization Models

For hadrons produced via baryonic resonances, the underlying model amplitudes and resonance branching fractions can be used to fully characterize the hadronic system. For non-resonant production, a hadronization model is required. Most generators use PYTHIA [27] for this purpose, although some with modified parameters. In addition some implement their own models to handle invariant masses that are too low for PYTHIA, typically somewhere around 2.0 GeV/c^2. Such models rely heavily on measurements of neutrino hadro-production in high-resolution devices, such as bubble chambers and the CHORUS [28] and NOMAD experiments [29], to construct empirical parametrizations that reproduce the key features of the data [30,31]. The basic ingredients are the emperical observations that average charged particle multiplicites increase logarithmically with the invariant mass of the hadronic system, and that the distribution of charged particle multiplicities about this average are described by a single function (an observation known as KNO scaling [32]) . Neutral particles are assumed to be produced with an average multiplicity that is 50% of the charged particle multiplicity. Simple parametrizations to more accurately reproduce differences observed in the forward/backward hemispheres of hadronic systems are included in GENIE, NEUT, and NuWro.

42.3. Nuclear Physics

The nuclear physics relevant to neutrino-nucleus scattering at few-GeV energies is complicated, involving Fermi motion, nuclear binding, Pauli blocking, in-medium modifications of form factors and hadronization, intranuclear rescattering of hadrons, and many-body scattering mechanisms including long- and short-range nucleon-nucleon correlations.

42.3.1. ***Scattering Mechanisms*** :

Most of the models used for neutrino-nuclear scattering kinematics were developed in the context of few-GeV inclusive electron scattering, by experiments going back nearly 50 years. A topic of considerable discussion within this community has been to what extent the impulse approximation, whereby the nucleus is envisioned as collection of bound, moving, single nucleons, is appropriate. The question arose initially in the context of measurements of the quasi-elastic axial mass, with a number of recent experiments using nuclear targets measuring values that were significantly higher than those obtained by an earlier generation of bubble chamber experiments using hydrogen or deuterium [16]. These differences arise for several reasons; a suppression of forward going muons (low Q^2), a high Q^2 enhancement in the event rate, and an overall larger than expected number of observed events. The mismodeling of the Q^2 distribution suggests that the simple nuclear model is not appropriate in describing the data, and the larger interaction rate indicates that there may be the other interactions included in the signal sample which have not been taken into account. These led to a revisitation of the role played by scattering from multi-particle/hole states in the nucleus, and the experimental search for evidence of these scattering channels is an area of intense experimental interest [33]. The contribution of these scattering processes is an extremely active area of theoretical research as well, with significant implications for generators and analyses [34]. Several approaches, ranging from strictly phenomenological descriptions to full theoretical calculations, have recently been incorporated into generators [35,36,37]. One example of a phenomenological approach utilizes an Effective Spectral Function [38] and a Transerse Enhancement Model [39], which together encapsulate information derived from electron scattering experiments at relevant kinematics. The microscopic model of Nieves and collaborators is now available in GENIE and NEUT [40,41]. One of the challenges in incoporating full theoretical models of these processes is that they are typically slow, so generators have developed new approaches whereby much of the computation is done offline, and the generators simply read in the hadronic tensor components. This allows for a full prediction of the lepton kinematics, however the ability to simulate the hadronic component of these multinucleon states then relies on separate models.

In order to obtain the cross-section off nucleons in the nucleus, it is necessary to take into account the in-medium effects. The basic models imployed in event generators rely on impulse approximation schemes, the most simple of which is the Relativistic Fermi Gas Model. The most common implementations are the Smith-Moniz [42] and Bodek-Ritchie [43] models. However, these simple Fermi-Gas model can not reproduce the strong suppression of the forward going muons, which has been observed in K2K, MiniBooNE and the other experiments. This kind of small q^2 suppression could be reproduced by taking into account more realistic nuclear binding effects. For example, medium correction for rather simple local Fermi-Gas model, which is calculated with random phase approximation, is known to give large suppression in small q^2. Some of the generators started implementing this kind of nuclear medium corrections. Recent hadronic energy measurements by MINERvA have shown that the simple global Fermi-gas model is not appropriate to reproduce the small energy deposit. Therefore, several generators implemented local Fermi-gas model or more sophisticated models. Within the electron scattering community, the analogous calculations have for decades relied on spectral functions, which incorporate information about nucleon momenta and binding energies in the impulse approximation scheme. The NuWro and GiBUU generators currently use spectral functions, they are incorporated into NEUT as an option, and several of the other generators are incorporating spectral function models at this time. It is known from photo and electro-nuclear scattering that the Delta width is affected by Pauli blocking and collisional broadening. These effects are included in some, but not all, generators.

When scattering from a nucleus, coherent scattering of various kinds is possible. Most simulations incorporate, at least, neutral and charged coherent single pion production. While the interaction rate for these interactions is typically around a percent of the total yield, the unique kinematic features of these events can make them potential

backgrounds for oscillation searches. Implemented in Monte Carlo are several PCAC-based methods [44,45], and microscopic models [46,47], valid at lower neutrino energies, have also been implemented in several generators. One of the commonly used model by Rein and Sehgal [44] predicts much larger charged current cross-section compared to the recent measurements of MINERνA and T2K gives a few times smaller cross-section for the charged current coherent pion production. However, the cross-section is sensitive to the pion cross-section used in the model as parameters and improved models with lepton mass correction [45] give better agreement with the recent data. This improved model is implemented in most of the generators.

42.3.2. *Hadron Production in Nuclei* :

Neutrino pion production is one of the dominant interactions in a few-GeV region and the interaction cross sections of pions in nucleus from those interactions are quite large. Therefore, the interactions of pions in nucleus changes the kinematics of the pions and can have large effects on the results of simulations at these energies. Most generators implement this physics through an intranuclear cascade simulation. In generators which utilize cascade models, a hadron, which has been formed in the nucleus, is moved step by step until it interacts with the other nucleon or escapes from the nucleus. The probabilities of each interaction in nucleus are usually given as the mean free paths and used to determine whether the hadron is interacted or not. If the hadron is found to be interacted, appropriate interactions are selected and simulated. Usually, absorption, elastic, charge exchange, and inelastic scatterings including particle productions are simulated as intranuclear interactions. The determination method of the kinematics for the final state particles heavily depends on the generators but most of them use experimentally validated models to simulate hadron interactions in nucleus. No two interanuclear cascade simulations implemented in neutrino event generators are the same. In all cases hadrons propagate from an interaction vertex chosen based on the density distribution of the target nucleus. In determining the generated position of the hadrons in nucleus, the concept of the formation length is sometimes employed. Based on this idea, the hadronization process is not instantaneous and it takes some time before generating the hadrons [11]. The basis for formation times are measurements at relatively high energy and Q^2, and most generators that employ the concept do not apply them to resonance interactions.

GiBUU does not employ an intranuclear cascade simulation, instead, it utilizes a semiclassical transport model in coupled channels that describes the space-time evolution of a manybody system in the presence of potentials and a collision term [3]. This approach assures consistency between nuclear effects in the initial state, such as Fermi motion, Pauli blocking, hadron self-energies, and modified cross sections, and the final state, such as particle reinteractions, since the two are derived from the same model. This model has been previously used to describe a wide variety of nuclear interaction data. Similarly, the hadronic simulation of the NUNDIS/NUNRES programs are handled by the well-established FLUKA hadronic simulation package [9].

References:

1. A. Gazizov and M. P. Kowalski, Comp. Phys. Comm. **172**, 203 (2005) [astro-ph/0406439].
2. C. Andreopoulos *et al.*, Nucl. Instrum. Methods **A614**, 87 (2010) [arXiv:0905.2517].
3. O. Buss *et al.*, Phys. Reports **512**, 1 (2012) [arXiv:1106.1344].
4. K. Gallmeister *et al.*, Phys. Rev. **C94**, 035502 (2016) [arXiv:1615.09391].
5. S. Gardiner, C. Grant, E. Pantic, and R. Svoboda, www.marleygen.org.
6. D. Autiero, Nucl. Phys. (Proc. Supp.) **139**, 253 (2005).
7. Y. Hayato, Nucl. Phys. (Proc. Supp.) **112**, 171 (2002).
8. D. Casper, Nucl. Phys. (Proc. Supp.) **112**, 161 (2002) [hep-ph/0208030].
9. G. Battiston *et al.*, Acta Phys. Polon. **B40**, 2491 (2009).
10. T.T. Böhlen *et al.*, Nuclear Data Sheets **120**, 211 (2014).
11. T. Golan, C. Juszczak, and J. Sobczyk, Phys. Rev. **C86**, 015505 (2012) [arXiv:1202.4197].
12. P. Stowell *et al.*, JINST 12, P01016 (2017).
13. S. Boyd *et al.*, AIP Conf. Proc. **1189**, 60 (2009).
14. O. Benhar, D. Day, and I. Sick, Rev. Mod. Phys. **80**, 189 (2008).
15. A. Bodek *et al.*, Eur. Phys. J. **C53**, 349 (2008) [arXiv:0708.1946].
16. H. Gallagher, G. Garvey, G. Zeller, Ann. Rev. Nucl. and Part. Sci. **61**, 355 (2011).
17. E. Tomasi-Gustafsson *et al.*, Phys. Rev. **C73**, 045204 (2006).
18. B. Bhattacharya, R. Hill, and G. Paz, Phys. Rev. D 84,073006(2011).
19. A.S. Meyer *et al.*, Phys. Rev. **D93**, 113015 (2016).
20. D. Rein, and L.M. Sehgal, Ann. Phys. **133**, 79 (1981).
21. K.M. Graczyk and J.T. Sobczyk, Phys. Rev. **D77**, 053001 (2008); Erratum-ibid. **D79**, 079903 (2009) [arXiv:0707.3561].
22. O. Lalakulich and E.A. Paschos, Phys. Rev. **D71**, 074003 (2005) [hep-ph/0501109].
23. J. Nowak, Phys. Scripta **T127**, 70 (2006).
24. L. Alvarez-Ruso, S.K. Singh, and M.J. Vicente-Vacas, Phys. Rev. **C57**, 2693 (1998) [nucl-th/9712058].
25. M. Glueck, E. Reya, and A. Vogt, Eur. Phys. J. **C5**, 461 (1998).
26. A. Bodek and U.K. Yang, J. Phys. **G29**, 1899 (2003) [hep-ex/0210024].
27. T. Sjostrand, S. Mrenna, and P. Skands, JHEP **0605**, 026 (2006) [hep-ph/0603175].
28. A. Kayis-Topaksu *et al.*, Eur. Phys. J. **C51**, 775 (2007) [arXiv:0707.1586].
29. J. Altegoer *et al.*, Phys. Lett. **B445**, 439 (1999).
30. T. Yang *et al.*, Eur. Phys. J. **C63**, 1 (2009) [hep-ph/0904.4043].
31. J. Nowak and J. Sobczyk, Acta Phys. Polon. **B37**, 2371 (2006) [hep-ph/0608108].
32. Z. Koba, H. Nielsen, and P. Olesen Nucl. Phys. **B40**, 317 (1972).
33. P. Rodrigues *et al.*, Phys. Rev. Lett. **116**, 071802 (2016).
34. L. Alvarez-Ruso *et al.*, arXiv:1706.03621 (2017).
35. T. Katori, AIP Conf. Proc. **1663**, 030001 (2015) [arXiv:1304.6014].
36. M. Alam *et al.*, arXiv:1512.06882 (2015).
37. C. Wilkinson *et al.*, Phys. Rev. **D93**, 072010 (2016).
38. A. Bodek, M. Christy, and B. Coopersmith, Eur. Phys. J. **C74**, 3091 (2014).
39. A. Bodek, H. Budd, and M. Christy, Eur. Phys. J. **C71**, 1726 (2011).
40. J. Nieves, I. Ruiz Simo, and M. Vicente Vacas, Phys. Rev. **C83**, 045501 (2011).
41. R. Gran *et al.*, Phys. Rev. **D88**, 113007 (2013).
42. R. Smith and E. Moniz, Nucl. Phys. **B43**, 605 (1972).
43. A. Bodek and J. Ritchie, Phys. Rev. **D24**, 1400 (1981).
44. D. Rein and L. Sehgal, Nucl. Phys. **B223**, 29 (1983).
45. C. Berger and L. Sehgal, Phys. Rev. **D79**, 053003 (2009).
46. L. Alvarez-Ruso *et al.*, Phys. Rev. **C75**, 055501 (2007).
47. L. Alvarez-Ruso *et al.*, Phys. Rev. **C76**, 068501 (2007).

43. Monte Carlo Particle Numbering Scheme

Revised October 2017 by L. Garren (Fermilab), F. Krauss (Durham U.), C.-J. Lin (LBNL), S. Navas (U. Granada), P. Richardson (Durham U.), and T. Sjöstrand (Lund U.).

The Monte Carlo particle numbering scheme presented here is intended to facilitate interfacing between event generators, detector simulators, and analysis packages used in particle physics. The numbering scheme was introduced in 1988 [1] and a revised version [2,3] was adopted in 1998 in order to allow systematic inclusion of quark model states which are as yet undiscovered and hypothetical particles such as SUSY particles. The numbering scheme is used in several event generators, *e.g.* HERWIG, PYTHIA, and SHERPA, and interfaces, *e.g.* `/HEPEVT/` and HepMC.

The general form is a 7–digit number:

$$\pm n\, n_r\, n_L\, n_{q_1}\, n_{q_2}\, n_{q_3}\, n_J\ .$$

This encodes information about the particle's spin, flavor content, and internal quantum numbers. The details are as follows:

1. Particles are given positive numbers, antiparticles negative numbers. The PDG convention for mesons is used, so that K^+ and B^+ are particles.
2. Quarks and leptons are numbered consecutively starting from 1 and 11 respectively; to do this they are first ordered by family and within families by weak isospin.
3. In composite quark systems (diquarks, mesons, and baryons) n_{q1-3} are quark numbers used to specify the quark content, while the rightmost digit $n_J = 2J + 1$ gives the system's spin (except for the K^0_S and K^0_L). The scheme does not cover particles of spin $J > 4$.
4. Diquarks have 4-digit numbers with $n_{q_1} \geq n_{q_2}$ and $n_{q_3} = 0$.
5. The numbering of mesons is guided by the nonrelativistic (L–S decoupled) quark model, as listed in Tables 15.2 and 15.3.
   a. The numbers specifying the meson's quark content conform to the convention $n_{q_1} = 0$ and $n_{q_2} \geq n_{q_3}$. The special case K^0_L is the sole exception to this rule.
   b. The quark numbers of flavorless, light (u, d, s) mesons are: 11 for the member of the isotriplet $(\pi^0, \rho^0, \ldots)$, 22 for the lighter isosinglet $(\eta, \omega, \ldots)$, and 33 for the heavier isosinglet $(\eta', \phi, \ldots)$. Since isosinglet mesons are often large mixtures of $u\overline{u} + d\overline{d}$ and $s\overline{s}$ states, 22 and 33 are assigned by mass and do not necessarily specify the dominant quark composition.
   c. The special numbers 310 and 130 are given to the K^0_S and K^0_L respectively.
   d. The fifth digit n_L is reserved to distinguish mesons of the same total (J) but different spin (S) and orbital (L) angular momentum quantum numbers. For $J > 0$ the numbers are: $(L, S) = (J - 1, 1)$ $n_L = 0$, $(J, 0)$ $n_L = 1$, $(J, 1)$ $n_L = 2$ and $(J + 1, 1)$ $n_L = 3$. For the exceptional case $J = 0$ the numbers are $(0, 0)$ $n_L = 0$ and $(1, 1)$ $n_L = 1$ (*i.e.* $n_L = L$). See Table 43.1.

   Table 43.1: Meson numbering logic. Here qq stands for $n_{q2}\, n_{q3}$.

	$L = J-1$, $S = 1$			$L = J$, $S = 0$			$L = J$, $S = 1$			$L = J+1$, $S = 1$		
J	code	J^{PC}	L	code	J^{PC}	L	code	J^{PC}	L	code	J^{PC}	L
0	—	—	—	00qq1	0^{-+}	0	—	—	—	10qq1	0^{++}	1
1	00qq3	1^{--}	0	10qq3	1^{+-}	1	20qq3	1^{++}	1	30qq3	1^{--}	2
2	00qq5	2^{++}	1	10qq5	2^{-+}	2	20qq5	2^{--}	2	30qq5	2^{++}	3
3	00qq7	3^{--}	2	10qq7	3^{+-}	3	20qq7	3^{++}	3	30qq7	3^{--}	4
4	00qq9	4^{++}	3	10qq9	4^{-+}	4	20qq9	4^{--}	4	30qq9	4^{++}	5

   e. If a set of physical mesons correspond to a (non-negligible) mixture of basis states, differing in their internal quantum numbers, then the lightest physical state gets the smallest basis state number. For example the $K_1(1270)$ is numbered 10313 (1^1P_1 K_{1B}) and the $K_1(1400)$ is numbered 20313 (1^3P_1 K_{1A}).
   f. The sixth digit n_r is used to label mesons radially excited above the ground state.
   g. Numbers have been assigned for complete $n_r = 0$ S- and P-wave multiplets, even where states remain to be identified.
   h. In some instances assignments within the $q\bar{q}$ meson model are only tentative; here best guess assignments are made.
   i. Many states appearing in the Meson Listings are not yet assigned within the $q\bar{q}$ model. Here $n_{q_{2-3}}$ and n_J are assigned according to the state's likely flavors and spin; all such unassigned light isoscalar states are given the flavor code 22. Within these groups $n_L = 0, 1, 2, \ldots$ is used to distinguish states of increasing mass. These states are flagged using $n = 9$. It is to be expected that these numbers will evolve as the nature of the states are elucidated. Codes are assigned to all mesons which are listed in the one-page table at the end of the Meson Summary Table as long as they have a prefered or established spin. Additional heavy meson states expected from heavy quark spectroscopy are also assigned codes.
6. The numbering of baryons is again guided by the nonrelativistic quark model, see Table 15.6. This numbering scheme is illustrated through a few examples in Table 43.2.
   a. The numbers specifying a baryon's quark content are such that in general $n_{q_1} \geq n_{q_2} \geq n_{q_3}$.
   b. Two states exist for $J = 1/2$ baryons containing 3 different types of quarks. In the lighter baryon $(\Lambda, \Xi, \Omega, \ldots)$ the light quarks are in an antisymmetric $(J = 0)$ state while for the heavier baryon $(\Sigma^0, \Xi', \Omega', \ldots)$ they are in a symmetric $(J = 1)$ state. In this situation n_{q_2} and n_{q_3} are reversed for the lighter state, so that the smaller number corresponds to the lighter baryon.
   c. For excited baryons a scheme is adopted, where the n_r label is used to denote the excitation bands in the harmonic oscillator model, see Sec. 15.4. Using the notation employed there, n_r is given by the N-index of the D_N band identifier.
   d. Further degeneracies of excited hadron multiplets with the same excitation number n_r and spin J are lifted by labelling such multiplets with the n_L index according to their mass, as given by its N or Δ-equivalent.
   e. In such excited multiplets extra singlets may occur, the $\Lambda(1520)$ being a prominent example. In such cases the ordering is reversed such that the heaviest quark label is pushed to the last position: $n_{q_3} > n_{q_1} > n_{q_2}$.
   f. For pentaquark states $n = 9$, $n_r n_L n_{q_1} n_{q_2}$ gives the four quark numbers in order $n_r \geq n_L \geq n_{q_1} \geq n_{q_2}$, n_{q_3} gives the antiquark number, and $n_J = 2J + 1$, with the assumption that $J = 1/2$ for the states currently reported.
7. The gluon, when considered as a gauge boson, has official number 21. In codes for glueballs, however, 9 is used to allow a notation in close analogy with that of hadrons.
8. The pomeron and odderon trajectories and a generic reggeon trajectory of states in QCD are assigned codes 990, 9990, and 110 respectively, where the final 0 indicates the indeterminate nature of the spin, and the other digits reflect the expected "valence" flavor content. We do not attempt a complete classification of all reggeon trajectories, since there is currently no need to distinguish a specific such trajectory from its lowest-lying member.
9. Two-digit numbers in the range 21–30 are provided for the Standard Model gauge bosons and Higgs.
10. Codes 81–100 are reserved for generator-specific pseudoparticles and concepts. Codes 901–930, 1901–1930, 2901–2930, and 3901–3930 are for additional components of Standard Model parton distribution functions, where the latter three ranges are intended to distinguish left/right/longitudinal components.
11. The search for physics beyond the Standard Model is an active area, so these codes are also standardized as far as possible.
    a. A standard fourth generation of fermions is included by analogy with the first three.
    b. The graviton and the boson content of a two-Higgs-doublet scenario and of additional SU(2)×U(1) groups are found in the range 31–40.
    c. "One-of-a-kind" exotic particles are assigned numbers in the range 41–80.
    d. Fundamental supersymmetric particles are identified by adding a nonzero n to the particle number. The superpartner of a boson or a left-handed fermion has $n = 1$ while the superpartner of a right-handed fermion has $n = 2$. When mixing occurs, such as between the winos and charged Higgsinos to give charginos, or between left and right

Table 43.2: Some examples of octet (top) and decuplet (bottom) members for the numbering scheme for excited baryons. Here qqq stands for $n_{q_1}n_{q_2}n_{q_3}$. See the text for the definition of the notation. The numbers in parenthesis correspond to the mass of the baryons. The states marked as (?) are not experimentally confirmed.

J^P	(D, L_N^P)	$n_r n_L n_{q_1} n_{q_2} n_{q_3} n_J$	N	Λ_8	Σ	Ξ	Λ_1
Octet			211,221	312	311,321,322	331,332	213
$1/2^+$	$(\mathbf{56}, \mathbf{0_0^+})$	$00qqq2$	(939)	(1116)	(1193)	(1318)	—
$1/2^+$	$(\mathbf{56}, \mathbf{0_2^+})$	$20qqq2$	(1440)	(1600)	(1660)	(1690)	—
$1/2^+$	$(\mathbf{70}, \mathbf{0_2^+})$	$21qqq2$	(1710)	(1810)	(1880)	(?)	(?)
$1/2^-$	$(\mathbf{70}, \mathbf{1_1^-})$	$10qqq2$	(1535)	(1670)	(1620)	(1750)	(1405)
J^P	(D, L_N^P)	$n_r n_L n_{q_1} n_{q_2} n_{q_3} n_J$	Δ		Σ	Ξ	Ω
Decuplet			111,211,221,222		311,321,322	331,332	333
$3/2^+$	$(\mathbf{56}, \mathbf{0_0^+})$	$00qqq4$	(1232)		(1385)	(1530)	(1672)
$3/2^+$	$(\mathbf{56}, \mathbf{0_2^+})$	$20qqq4$	(1600)		(1690)	(?)	(?)
$1/2^-$	$(\mathbf{70}, \mathbf{1_1^-})$	$11qqq2$	(1620)		(1750)	(?)	(?)
$3/2^-$	$(\mathbf{70}, \mathbf{1_1^-})$	$12qqq4$	(1700)		(?)	(?)	(?)

sfermions, the lighter physical state is given the smaller basis state number.

e. Technicolor states have $n = 3$, with technifermions treated like ordinary fermions. States which are ordinary color singlets have $n_r = 0$. Color octets have $n_r = 1$. If a state has non-trivial quantum numbers under the topcolor groups $\mathrm{SU}(3)_1 \times \mathrm{SU}(3)_2$, the quantum numbers are specified by tech,ij, where i and j are 1 or 2. n_L is then $2i + j$. The coloron, V_8, is a heavy gluon color octet and thus is 3100021.

f. Excited (composite) quarks and leptons are identified by setting $n = 4$ and $n_r = 0$.

g. Within several scenarios of new physics, it is possible to have colored particles sufficiently long-lived for color-singlet hadronic states to form around them. In the context of supersymmetric scenarios, these states are called R-hadrons, since they carry odd R-parity. R-hadron codes, defined here, should be viewed as templates for corresponding codes also in other scenarios, for any long-lived particle that is either an unflavored color octet or a flavored color triplet. The R-hadron code is obtained by combining the SUSY particle code with a code for the light degrees of freedom, with as many intermediate zeros removed from the former as required to make place for the latter at the end. (To exemplify, a sparticle $n00000n_{\tilde{q}}$ combined with quarks q_1 and q_2 obtains code $n00n_{\tilde{q}}n_{q_1}n_{q_2}n_J$.) Specifically, the new-particle spin decouples in the limit of large masses, so that the final n_J digit is defined by the spin state of the light-quark system alone. An appropriate number of n_q digits is used to define the ordinary-quark content. As usual, 9 rather than 21 is used to denote a gluon/gluino in composite states. The sign of the hadron agrees with that of the constituent new particle (a color triplet) where there is a distinct new antiparticle, and else is defined as for normal hadrons. Particle names are R with the flavor content as lower index.

h. A black hole in models with extra dimensions has code 5000040. Kaluza-Klein excitations in models with extra dimensions have $n = 5$ or $n = 6$, to distinquish excitations of left- or right-handed fermions or, in case of mixing, the lighter or heavier state (cf. 11d). The nonzero n_r digit gives the radial excitation number, in scenarios where the level spacing allow these to be distinguished. Should the model also contain supersymmetry, excited SUSY states would be denoted by an $n_r > 0$, with $n = 1$ or 2 as usual. Should some colored states be long-lived enough that hadrons would form around them, the coding strategy of 11g applies, with the initial two nn_r digits preserved in the combined code.

i. Magnetic monopoles and dyons are assumed to have one unit of Dirac monopole charge and a variable integer number $n_{q1}n_{q2}n_{q3}$ units of electric charge. Codes $411n_{q1}n_{q2}n_{q3}0$ are then used when the magnetic and electrical charge sign agree and $412n_{q1}n_{q2}n_{q3}0$ when they disagree, with the overall sign of the particle set by the magnetic charge. For now no spin information is provided.

j. The nature of Dark Matter (DM) is not known, and therefore a definitive classification is too early. Candidates within specific scenarios are classified therein, such as 1000022 for the lightest neutralino. Generic fundamental states can be given temporary codes in the range 51 - 60, with 51, 52 and 53 reserved for spin 0, 1/2 and 1 ones. Generic mediators of s-channel DM pair creation of annihilation can be given codes 54 and 55 for spin 0 or 1 ones. Separate antiparticles, with negative codes, may or may not exist. More elaborate new scenarios should be constructed with $n = 5$ and $n_r = 9$.

k. Hidden Valley particles have $n = 4$ and $n_r = 9$, and trailing numbers in agreement with their nearest-analog standard particles, as far as possible. Thus 4900021 is the gauge boson g_v of a confining gauge field, $490000n_{q_v}$ and $490001n_{\ell_v}$ fundamental constituents charged or not under this, 4900022 is the γ_v of a non-confining field, and $4900n_{q_{v1}}n_{q_{v2}}n_J$ a Hidden Valley meson.

12. Occasionally program authors add their own states. To avoid confusion, these should be flagged by setting $nn_r = 99$.

13. Concerning the non-99 numbers, it may be noted that only quarks, excited quarks, squarks, and diquarks have $n_{q_3} = 0$; only diquarks, baryons (including pentaquarks), and the odderon have $n_{q_1} \neq 0$; and only mesons, the reggeon, and the pomeron have $n_{q_1} = 0$ and $n_{q_2} \neq 0$. Concerning mesons (not antimesons), if n_{q_1} is odd then it labels a quark and an antiquark if even.

14. Nuclear codes are given as 10-digit numbers $\pm 10LZZZAAAI$. For a (hyper)nucleus consisting of n_p protons, n_n neutrons and n_Λ Λ's, $A = n_p + n_n + n_\Lambda$ gives the total baryon number, $Z = n_p$ the total charge and $L = n_\Lambda$ the total number of strange quarks. I gives the isomer level, with $I = 0$ corresponding to the ground state and $I > 0$ to excitations, see [4], where states denoted m, n, p, q translate to $I = 1 - 4$. As examples, the deuteron is 1000010020 and ^{235}U is 1000922350. To avoid ambiguities, nuclear codes should not be applied to a single hadron, like p, n or Λ^0, where quark-contents-based codes already exist.

This text and full lists of particle numbers can be found online [5].

References:

1. G.P. Yost *et al.*, Particle Data Group, Phys. Lett. **B204**, 1 (1988).
2. I.G. Knowles *et al.*, CERN 96-01, v. 2, p. 103.
3. C. Caso *et al.*, Particle Data Group, Eur. Phys. J. **C3**, 1 (1998).
4. G. Audi *et al.*, Nucl. Phys. **A729**, 3 (2003).
5. `http://pdg.lbl.gov/current/mc-particle-id/`.

QUARKS

d	1
u	2
s	3
c	4
b	5
t	6
b'	7
t'	8

LEPTONS

e^-	11
ν_e	12
μ^-	13
ν_μ	14
τ^-	15
ν_τ	16
τ'^-	17
$\nu_{\tau'}$	18

GAUGE AND HIGGS BOSONS

g	(9) 21
γ	22
Z^0	23
W^+	24
h^0/H_1^0	25
Z'/Z_2^0	32
Z''/Z_3^0	33
W'/W_2^+	34
H^0/H_2^0	35
A^0/H_3^0	36
H^+	37

SPECIAL PARTICLES

G (graviton)	39
R^0	41
LQ^c	42
$DM(S=0)$	51
$DM(S=1/2)$	52
$DM(S=1)$	53
reggeon	110
pomeron	990
odderon	9990

for MC internal use 81–100, 901–**930***, **1901**–**1930***, **2901**–**2930*** and **3901**–**3930***

DIQUARKS

$(dd)_1$	1103
$(ud)_0$	2101
$(ud)_1$	2103
$(uu)_1$	2203
$(sd)_0$	3101
$(sd)_1$	3103
$(su)_0$	3201
$(su)_1$	3203
$(ss)_1$	3303
$(cd)_0$	4101
$(cd)_1$	4103
$(cu)_0$	4201
$(cu)_1$	4203
$(cs)_0$	4301
$(cs)_1$	4303
$(cc)_1$	4403
$(bd)_0$	5101
$(bd)_1$	5103
$(bu)_0$	5201
$(bu)_1$	5203
$(bs)_0$	5301
$(bs)_1$	5303
$(bc)_0$	5401
$(bc)_1$	5403
$(bb)_1$	5503

SUSY PARTICLES

$\widetilde{d}_L$	1000001
$\widetilde{u}_L$	1000002
$\widetilde{s}_L$	1000003
$\widetilde{c}_L$	1000004
$\widetilde{b}_1$	1000005[a]
$\widetilde{t}_1$	1000006[a]
$\widetilde{e}_L^-$	1000011
$\widetilde{\nu}_{eL}$	1000012
$\widetilde{\mu}_L^-$	1000013
$\widetilde{\nu}_{\mu L}$	1000014
$\widetilde{\tau}_1^-$	1000015[a]
$\widetilde{\nu}_{\tau L}$	1000016
$\widetilde{d}_R$	2000001
$\widetilde{u}_R$	2000002
$\widetilde{s}_R$	2000003
$\widetilde{c}_R$	2000004
$\widetilde{b}_2$	2000005[a]
$\widetilde{t}_2$	2000006[a]
$\widetilde{e}_R^-$	2000011
$\widetilde{\mu}_R^-$	2000013
$\widetilde{\tau}_2^-$	2000015[a]
$\widetilde{g}$	1000021
$\widetilde{\chi}_1^0$	1000022[b]
$\widetilde{\chi}_2^0$	1000023[b]
$\widetilde{\chi}_1^+$	1000024[b]
$\widetilde{\chi}_3^0$	1000025[b]
$\widetilde{\chi}_4^0$	1000035[b]
$\widetilde{\chi}_2^+$	1000037[b]
$\widetilde{G}$	1000039

LIGHT $I = 1$ MESONS

π^0	111
π^+	211
$a_0(980)^0$	9000111
$a_0(980)^+$	9000211
$\pi(1300)^0$	100111
$\pi(1300)^+$	100211
$a_0(1450)^0$	10111
$a_0(1450)^+$	10211
$\pi(1800)^0$	9010111
$\pi(1800)^+$	9010211
$\rho(770)^0$	113
$\rho(770)^+$	213
$b_1(1235)^0$	10113
$b_1(1235)^+$	10213
$a_1(1260)^0$	20113
$a_1(1260)^+$	20213
$\pi_1(1400)^0$	9000113
$\pi_1(1400)^+$	9000213
$\rho(1450)^0$	100113
$\rho(1450)^+$	100213
$\pi_1(1600)^0$	9010113
$\pi_1(1600)^+$	9010213
$a_1(1640)^0$	9020113
$a_1(1640)^+$	9020213
$\rho(1700)^0$	30113
$\rho(1700)^+$	30213
$\rho(1900)^0$	9030113
$\rho(1900)^+$	9030213
$\rho(2150)^0$	9040113
$\rho(2150)^+$	9040213
$a_2(1320)^0$	115
$a_2(1320)^+$	215
$\pi_2(1670)^0$	10115
$\pi_2(1670)^+$	10215
$a_2(1700)^0$	9000115
$a_2(1700)^+$	9000215
$\pi_2(2100)^0$	9010115
$\pi_2(2100)^+$	9010215
$\rho_3(1690)^0$	117
$\rho_3(1690)^+$	217
$\rho_3(1990)^0$	9000117
$\rho_3(1990)^+$	9000217
$\rho_3(2250)^0$	9010117
$\rho_3(2250)^+$	9010217
$a_4(2040)^0$	119
$a_4(2040)^+$	219

LIGHT $I = 0$ MESONS

($u\overline{u}$, $d\overline{d}$, and $s\overline{s}$ Admixtures)

η	221
$\eta'(958)$	331
$f_0(500)$	9000221
$f_0(980)$	9010221
$\eta(1295)$	100221
$f_0(1370)$	10221
$\eta(1405)$	9020221
$\eta(1475)$	100331
$f_0(1500)$	9030221
$f_0(1710)$	10331
$\eta(1760)$	9040221
$f_0(2020)$	9050221
$f_0(2100)$	9060221
$f_0(2200)$	9070221
$\eta(2225)$	9080221
$\omega(782)$	223
$\phi(1020)$	333
$h_1(1170)$	10223
$f_1(1285)$	20223
$h_1(1380)$	10333
$f_1(1420)$	20333
$\omega(1420)$	1000223
$f_1(1510)$	9000223
$h_1(1595)$	9010223
$\omega(1650)$	30223
$\phi(1680)$	100333
$f_2(1270)$	225
$f_2(1430)$	9000225
$f_2'(1525)$	335
$f_2(1565)$	9010225
$f_2(1640)$	9020225
$\eta_2(1645)$	10225
$f_2(1810)$	9030225
$\eta_2(1870)$	10335
$f_2(1910)$	9040225
$f_2(1950)$	9050225
$f_2(2010)$	9060225
$f_2(2150)$	9070225
$f_2(2300)$	9080225
$f_2(2340)$	9090225
$\omega_3(1670)$	227
$\phi_3(1850)$	337
$f_4(2050)$	229
$f_J(2220)$	9000229
$f_4(2300)$	9010229

STRANGE MESONS

K_L^0	130
K_S^0	310
K^0	311
K^+	321
$K_0^*(700)^0$	9000311
$K_0^*(700)^+$	9000321
$K_0^*(1430)^0$	10311
$K_0^*(1430)^+$	10321
$K(1460)^0$	100311
$K(1460)^+$	100321
$K(1830)^0$	9010311
$K(1830)^+$	9010321
$K_0^*(1950)^0$	9020311
$K_0^*(1950)^+$	9020321
$K^*(892)^0$	313
$K^*(892)^+$	323
$K_1(1270)^0$	10313
$K_1(1270)^+$	10323
$K_1(1400)^0$	20313
$K_1(1400)^+$	20323
$K^*(1410)^0$	100313
$K^*(1410)^+$	100323
$K_1(1650)^0$	9000313
$K_1(1650)^+$	9000323
$K^*(1680)^0$	30313
$K^*(1680)^+$	30323
$K_2^*(1430)^0$	315
$K_2^*(1430)^+$	325
$K_2(1580)^0$	9000315
$K_2(1580)^+$	9000325
$K_2(1770)^0$	10315
$K_2(1770)^+$	10325
$K_2(1820)^0$	20315
$K_2(1820)^+$	20325
$K_2^*(1980)^0$	9010315
$K_2^*(1980)^+$	9010325
$K_2(2250)^0$	9020315
$K_2(2250)^+$	9020325
$K_3^*(1780)^0$	317
$K_3^*(1780)^+$	327
$K_3(2320)^0$	9010317
$K_3(2320)^+$	9010327
$K_4^*(2045)^0$	319
$K_4^*(2045)^+$	329
$K_4(2500)^0$	9000319
$K_4(2500)^+$	9000329

CHARMED MESONS

D^+	411
D^0	421
$D_0^*(2400)^+$	10411
$D_0^*(2400)^0$	10421
$D^*(2010)^+$	413
$D^*(2007)^0$	423
$D_1(2420)^+$	10413
$D_1(2420)^0$	10423
$D_1(H)^+$	20413
$D_1(2430)^0$	20423
$D_2^*(2460)^+$	415
$D_2^*(2460)^0$	425
D_s^+	431
$D_{s0}^*(2317)^+$	10431
D_s^{*+}	433
$D_{s1}(2536)^+$	10433
$D_{s1}(2460)^+$	20433
$D_{s2}^*(2573)^+$	435

BOTTOM MESONS

B^0	511
B^+	521
B_0^{*0}	10511
B_0^{*+}	10521
B^{*0}	513
B^{*+}	523
$B_1(L)^0$	10513
$B_1(L)^+$	10523
$B_1(H)^0$	20513
$B_1(H)^+$	20523
B_2^{*0}	515
B_2^{*+}	525
B_s^0	531
B_{s0}^{*0}	10531
B_s^{*0}	533
$B_{s1}(L)^0$	10533
$B_{s1}(H)^0$	20533
B_{s2}^{*0}	535
B_c^+	541
B_{c0}^{*+}	10541
B_c^{*+}	543
$B_{c1}(L)^+$	10543
$B_{c1}(H)^+$	20543
B_{c2}^{*+}	545

***c*$\overline{c}$ MESONS**

$\eta_c(1S)$	441
$\chi_{c0}(1P)$	10441
$\eta_c(2S)$	100441
$J/\psi(1S)$	443
$h_c(1P)$	10443
$\chi_{c1}(1P)$	20443
$\psi(2S)$	100443
$\psi(3770)$	30443
$\psi(4040)$	9000443
$\psi(4160)$	9010443
$\psi(4415)$	9020443
$\chi_{c2}(1P)$	445
$\chi_{c2}(3930)$	100445

***b*$\overline{b}$ MESONS**

$\eta_b(1S)$	551
$\chi_{b0}(1P)$	10551
$\eta_b(2S)$	100551
$\chi_{b0}(2P)$	110551
$\eta_b(3S)$	200551
$\chi_{b0}(3P)$	210551
$\Upsilon(1S)$	553
$h_b(1P)$	10553
$\chi_{b1}(1P)$	20553
$\Upsilon_2(1D)$	30553
$\Upsilon(2S)$	100553
$h_b(2P)$	110553
$\chi_{b1}(2P)$	120553
$\Upsilon_1(2D)$	130553
$\Upsilon(3S)$	200553
$h_b(3P)$	210553
$\chi_{b1}(3P)$	220553
$\Upsilon(4S)$	300553
$\Upsilon(10860)$	9000553
$\Upsilon(11020)$	9010553
$\chi_{b2}(1P)$	555
$\eta_{b2}(1D)$	10555
$\Upsilon_2(1D)$	20555
$\chi_{b2}(2P)$	100555
$\eta_{b2}(2D)$	110555
$\Upsilon_2(2D)$	120555
$\chi_{b2}(3P)$	200555
$\Upsilon_3(1D)$	557
$\Upsilon_3(2D)$	100557

LIGHT BARYONS

p	2212
n	2112
Δ^{++}	2224
Δ^+	2214
Δ^0	2114
Δ^-	1114

STRANGE BARYONS

Λ	3122
Σ^+	3222
Σ^0	3212
Σ^-	3112
Σ^{*+}	3224[c]
Σ^{*0}	3214[c]
Σ^{*-}	3114[c]
Ξ^0	3322
Ξ^-	3312
Ξ^{*0}	3324[c]
Ξ^{*-}	3314[c]
Ω^-	3334

CHARMED BARYONS

Λ_c^+	4122
Σ_c^{++}	4222
Σ_c^+	4212
Σ_c^0	4112
Σ_c^{*++}	4224
Σ_c^{*+}	4214
Σ_c^{*0}	4114
Ξ_c^+	4232
Ξ_c^0	4132
$\Xi_c^{\prime+}$	4322
$\Xi_c^{\prime0}$	4312
Ξ_c^{*+}	4324
Ξ_c^{*0}	4314
Ω_c^0	4332
Ω_c^{*0}	4334
Ξ_{cc}^+	4412
Ξ_{cc}^{++}	4422
Ξ_{cc}^{*+}	4414
Ξ_{cc}^{*++}	4424
Ω_{cc}^+	4432
Ω_{cc}^{*+}	4434
Ω_{ccc}^{++}	4444

BOTTOM BARYONS

Λ_b^0	5122
Σ_b^-	5112
Σ_b^0	5212
Σ_b^+	5222
Σ_b^{*-}	5114
Σ_b^{*0}	5214
Σ_b^{*+}	5224
Ξ_b^-	5132
Ξ_b^0	5232
$\Xi_b^{\prime-}$	5312
$\Xi_b^{\prime0}$	5322
Ξ_b^{*-}	5314
Ξ_b^{*0}	5324
Ω_b^-	5332
Ω_b^{*-}	5334
Ξ_{bc}^0	5142
Ξ_{bc}^+	5242
$\Xi_{bc}^{\prime0}$	5412
$\Xi_{bc}^{\prime+}$	5422
Ξ_{bc}^{*0}	5414
Ξ_{bc}^{*+}	5424
Ω_{bc}^0	5342
$\Omega_{bc}^{\prime0}$	5432
Ω_{bc}^{*0}	5434
Ω_{bcc}^+	5442
Ω_{bcc}^{*+}	5444
Ξ_{bb}^-	5512
Ξ_{bb}^0	5522
Ξ_{bb}^{*-}	5514
Ξ_{bb}^{*0}	5524
Ω_{bb}^-	5532
Ω_{bb}^{*-}	5534
Ω_{bbc}^0	5542
Ω_{bbc}^{*0}	5544
Ω_{bbb}^-	5554

Footnotes to the Tables:

∗) Numbers or names in bold face are new or have changed since the 2016 *Review*.

a) Particulary in the third generation, the left and right sfermion states may mix, as shown. The lighter mixed state is given the smaller number.

b) The physical $\widetilde{\chi}$ states are admixtures of the pure $\widetilde{\gamma}$, $\widetilde{Z}^0$, $\widetilde{W}^+$, $\widetilde{H}_1^0$, $\widetilde{H}_2^0$, and $\widetilde{H}^+$ states.

c) Σ^* and Ξ^* are alternate names for $\Sigma(1385)$ and $\Xi(1530)$.

44. Clebsch-Gordan Coefficients, Spherical Harmonics, and d Functions

Note: A square-root sign is to be understood over *every* coefficient, *e.g.*, for $-8/15$ read $-\sqrt{8/15}$.

Notation:

J	J	...
M	M	...

m_1	m_2	
m_1	m_2	Coefficients
.	.	
.	.	
.	.	

1/2×1/2

	+1/2	−1/2
+1/2	1	0
−1/2	0	1

	+1/2	−1/2
+1/2	1/2	1/2
−1/2	1/2	−1/2

1×1/2

	+1	0	−1
+1/2	1	0	0
−1/2	0	1	0

	+1/2	−1/2
+1	2/3	1/3
0	1/3	−2/3
−1	0	1

	+1/2	−1/2
+1	1/3	2/3
0	2/3	−1/3
−1	1/2	1/2

2×1/2

	+2	+1	0	−1
+1/2	1	0	0	0
−1/2	0	1/5	4/5	0
−3/2	0	4/5	−1/5	0
−5/2	0	0	0	1

	+2	+1	0	−1
+1/2	1/5	4/5	0	0
−1/2	4/5	−1/5	0	0
−3/2	0	0	1/2	1/2
−5/2	0	0	1/2	−1/2

	+2	+1	0	−1
+1/2	4/5	−1/5	0	0
−1/2	1/5	4/5	0	0
−3/2	0	0	3/5	2/5
−5/2	0	0	2/5	−3/5

	+2	+1	0	−1
+1/2	2/5	3/5	0	0
−1/2	3/5	−2/5	0	0
−3/2	0	0	3/5	2/5
−5/2	0	0	2/5	−3/5

3/2×1/2

	+3/2	+1/2	−1/2	−3/2
+1/2	1/4	3/4	0	0
−1/2	3/4	−1/4	0	0
+3/2	0	0	1/2	1/2
−3/2	0	0	1/2	−1/2

	+3/2	+1/2	−1/2	−3/2
+1/2	1/4	3/4	0	0
−1/2	3/4	−1/4	0	0
+3/2	0	0	3/4	1/4
−3/2	0	0	1/4	−3/4

	+3/2	+1/2	−1/2	−3/2
+1/2	3/4	1/4	0	0
−1/2	1/4	−3/4	0	0
+3/2	0	0	3/4	1/4
−3/2	0	0	1/4	−3/4

2×1

	+2	+1	0	−1
+1	1/3	2/3	0	0
0	2/3	−1/3	0	0
−1	0	0	2/3	1/3
−2	0	0	1/3	−2/3

	+2	+1	0	−1
+1	1/15	1/3	3/5	0
0	8/15	1/6	−3/10	0
−1	2/5	−1/2	1/10	0
−2	0	0	0	1

	+2	+1	0	−1
+1	1/5	1/2	3/10	0
0	3/5	0	−2/5	0
−1	1/5	−1/2	3/10	0
−2	0	0	0	0

	+2	+1	0	−1
+1	2/5	1/2	1/10	0
0	8/15	−1/6	−3/10	0
−1	1/15	−1/3	3/5	0
−2	0	0	0	0

3/2×1

	+3/2	+1/2	−1/2	−3/2
+1/2	2/5	3/5	0	0
−1/2	3/5	−2/5	0	0
+3/2	0	0	2/5	3/5
−3/2	0	0	3/5	−2/5

	+3/2	+1/2	−1/2	−3/2
+1/2	1/10	2/5	1/2	0
−1/2	3/5	1/15	−1/3	0
+3/2	3/10	−8/15	1/6	0
−3/2	0	0	0	1

	+3/2	+1/2	−1/2	−3/2
+1/2	3/10	8/15	1/6	0
−1/2	0	3/5	−1/15	−1/3
−3/2	0	1/10	−2/5	1/2
−5/2	0	0	2/5	−3/5

1×1

	+1	0	−1
+1	1/2	1/2	0
0	1/2	−1/2	0
−1	0	0	1

	+1	0	−1
+1	1/6	1/2	1/3
0	2/3	0	−1/3
−1	1/6	−1/2	1/3

	+1	0	−1
+1	1/2	1/2	0
0	1/2	−1/2	0
−1	0	0	1

$$Y_1^0 = \sqrt{\frac{3}{4\pi}}\cos\theta$$

$$Y_1^1 = -\sqrt{\frac{3}{8\pi}}\sin\theta\, e^{i\phi}$$

$$Y_2^0 = \sqrt{\frac{5}{4\pi}}\left(\frac{3}{2}\cos^2\theta - \frac{1}{2}\right)$$

$$Y_2^1 = -\sqrt{\frac{15}{8\pi}}\sin\theta\cos\theta\, e^{i\phi}$$

$$Y_2^2 = \frac{1}{4}\sqrt{\frac{15}{2\pi}}\sin^2\theta\, e^{2i\phi}$$

$$Y_\ell^{-m} = (-1)^m Y_\ell^{m*}$$

$$d^\ell_{m,0} = \sqrt{\frac{4\pi}{2\ell+1}}\, Y_\ell^m\, e^{-im\phi}$$

$$\langle j_1 j_2 m_1 m_2 | j_1 j_2 J M\rangle = (-1)^{J-j_1-j_2}\langle j_2 j_1 m_2 m_1 | j_2 j_1 J M\rangle$$

$$d^j_{m',m} = (-1)^{m-m'} d^j_{m,m'} = d^j_{-m,-m'}$$

2×3/2

	+3/2	+1/2	−1/2	−3/2
+2	3/7	4/7	0	0
+1	4/7	−3/7	0	0
0	0	0	2/5	3/5
−1	0	0	3/5	−2/5

	+3/2	+1/2	−1/2	−3/2
+2	1/7	16/35	2/5	0
+1	4/7	1/35	−2/5	0
0	2/7	−18/35	1/5	0
−1	0	0	0	1

	+3/2	+1/2	−1/2	−3/2
+2	1/35	6/35	2/5	2/5
+1	12/35	5/14	0	−3/10
0	18/35	−3/35	−1/5	1/5
−1	4/35	−27/70	2/5	−1/10

	+3/2	+1/2	−1/2	−3/2
+2	4/35	27/70	2/5	1/10
+1	18/35	3/35	−1/5	−1/5
0	12/35	−5/14	0	3/10
−1	1/35	−6/35	2/5	−2/5

	+3/2	+1/2	−1/2	−3/2
+2	1/20	1/4	9/20	1/4
+1	9/20	1/4	−1/20	−1/4
0	9/20	−1/4	−1/20	1/4
−1	1/20	−1/4	9/20	−1/4

3/2×3/2

	+3/2	+1/2	−1/2	−3/2
+3/2	1/2	1/2	0	0
+1/2	1/2	−1/2	0	0
−1/2	0	0	1/2	1/2
−3/2	0	0	1/2	−1/2

	+3/2	+1/2	−1/2	−3/2
+3/2	1/5	1/2	3/10	0
+1/2	3/5	0	−2/5	0
−1/2	1/5	−1/2	3/10	0
−3/2	0	0	0	0

	+3/2	+1/2	−1/2	−3/2
+3/2	3/5	2/5	0	0
+1/2	2/5	−3/5	0	0
−1/2	0	0	3/5	2/5
−3/2	0	0	2/5	−3/5

	+3/2	+1/2	−1/2	−3/2
+3/2	1/20	1/4	9/20	1/4
+1/2	9/20	1/4	−1/20	−1/4
−1/2	9/20	−1/4	−1/20	1/4
−3/2	1/20	−1/4	9/20	−1/4

2×2

	+2	+1	0
+2	3/14	1/2	2/7
+1	4/7	0	−3/7
0	3/14	−1/2	2/7

	+2	+1	0	−1
+2	1/14	3/10	3/7	1/5
+1	3/7	1/5	−1/14	−3/10
0	3/7	−1/5	−1/14	3/10
−1	1/14	−3/10	3/7	−1/5

	+2	+1	0	−1
+2	1/70	1/10	2/7	2/5
+1	8/35	2/5	1/14	−1/10
0	18/35	0	−2/7	0
−1	8/35	−2/5	1/14	1/10
−2	1/70	−1/10	2/7	−2/5

	+2	+1	0	−1
+1	1/14	3/10	3/7	1/5
0	3/7	1/5	−1/14	−3/10
−1	3/7	−1/5	−1/14	3/10
−2	1/14	−3/10	3/7	−1/5

	+2	+1	0	−1
+1	1/14	3/10	3/7	1/5
0	3/7	1/5	−1/14	−3/10
−1	3/7	−1/5	−1/14	3/10
−2	1/14	−3/10	3/7	−1/5

	+2	+1	0	−1
+1	1/14	3/10	3/7	1/5
0	3/7	1/5	−1/14	−3/10
−1	3/7	−1/5	−1/14	3/10
−2	1/14	−3/10	3/7	−1/5

$$d^1_{0,0} = \cos\theta \qquad d^{1/2}_{1/2,1/2} = \cos\frac{\theta}{2} \qquad d^1_{1,1} = \frac{1+\cos\theta}{2}$$

$$d^{1/2}_{1/2,-1/2} = -\sin\frac{\theta}{2} \qquad d^1_{1,0} = -\frac{\sin\theta}{\sqrt{2}}$$

$$d^1_{1,-1} = \frac{1-\cos\theta}{2}$$

$$d^{3/2}_{3/2,3/2} = \frac{1+\cos\theta}{2}\cos\frac{\theta}{2}$$

$$d^{3/2}_{3/2,1/2} = -\sqrt{3}\frac{1+\cos\theta}{2}\sin\frac{\theta}{2} \qquad d^2_{2,2} = \left(\frac{1+\cos\theta}{2}\right)^2$$

$$d^{3/2}_{3/2,-1/2} = \sqrt{3}\frac{1-\cos\theta}{2}\cos\frac{\theta}{2} \qquad d^2_{2,1} = -\frac{1+\cos\theta}{2}\sin\theta$$

$$d^{3/2}_{3/2,-3/2} = -\frac{1-\cos\theta}{2}\sin\frac{\theta}{2} \qquad d^2_{2,0} = \frac{\sqrt{6}}{4}\sin^2\theta \qquad d^2_{1,1} = \frac{1+\cos\theta}{2}(2\cos\theta - 1)$$

$$d^{3/2}_{1/2,1/2} = \frac{3\cos\theta - 1}{2}\cos\frac{\theta}{2} \qquad d^2_{2,-1} = -\frac{1-\cos\theta}{2}\sin\theta \qquad d^2_{1,0} = -\sqrt{\frac{3}{2}}\sin\theta\cos\theta$$

$$d^{3/2}_{1/2,-1/2} = -\frac{3\cos\theta + 1}{2}\sin\frac{\theta}{2} \qquad d^2_{2,-2} = \left(\frac{1-\cos\theta}{2}\right)^2 \qquad d^2_{1,-1} = \frac{1-\cos\theta}{2}(2\cos\theta + 1) \qquad d^2_{0,0} = \left(\frac{3}{2}\cos^2\theta - \frac{1}{2}\right)$$

Figure 44.1: The sign convention is that of Wigner (*Group Theory*, Academic Press, New York, 1959), also used by Condon and Shortley (*The Theory of Atomic Spectra*, Cambridge Univ. Press, New York, 1953), Rose (*Elementary Theory of Angular Momentum*, Wiley, New York, 1957), and Cohen (*Tables of the Clebsch-Gordan Coefficients*, North American Rockwell Science Center, Thousand Oaks, Calif., 1974).

45. SU(3) isoscalar factors and representation matrices

Written by R.L. Kelly (LBNL).

The most commonly used SU(3) isoscalar factors, corresponding to the singlet, octet, and decuplet content of $8 \otimes 8$ and $10 \otimes 8$, are shown at the right. The notation uses particle names to identify the coefficients, so that the pattern of relative couplings may be seen at a glance. We illustrate the use of the coefficients below. See J.J de Swart, Rev. Mod. Phys. **35**, 916 (1963) for detailed explanations and phase conventions.

A $\sqrt{\ }$ is to be understood over every integer in the matrices; the exponent 1/2 on each matrix is a reminder of this. For example, the $\Xi \to \Omega K$ element of the $10 \to 10 \otimes 8$ matrix is $-\sqrt{6}/\sqrt{24} = -1/2$.

Intramultiplet relative decay strengths may be read directly from the matrices. For example, in decuplet → octet + octet decays, the ratio of $\Omega^* \to \Xi\overline{K}$ and $\Delta \to N\pi$ partial widths is, from the $10 \to 8 \times 8$ matrix,

$$\frac{\Gamma\,(\Omega^* \to \Xi\overline{K})}{\Gamma\,(\Delta \to N\pi)} = \frac{12}{6} \times \text{ (phase space factors)} \,. \tag{45.1}$$

Including isospin Clebsch-Gordan coefficients, we obtain, *e.g.*,

$$\frac{\Gamma(\Omega^{*-} \to \Xi^0 K^-)}{\Gamma(\Delta^+ \to p\,\pi^0)} = \frac{1/2}{2/3} \times \frac{12}{6} \times p.s.f. = \frac{3}{2} \times p.s.f. \tag{45.2}$$

Partial widths for $8 \to 8 \otimes 8$ involve a linear superposition of 8_1 (symmetric) and 8_2 (antisymmetric) couplings. For example,

$$\Gamma(\Xi^* \to \Xi\pi) \sim \left(-\sqrt{\frac{9}{20}}\, g_1 + \sqrt{\frac{3}{12}}\, g_2\right)^2 \,. \tag{45.3}$$

The relations between g_1 and g_2 (with de Swart's normalization) and the standard D and F couplings that appear in the interaction Lagrangian,

$$\mathscr{L} = -\sqrt{2}\; D\; Tr\,(\{\overline{B}, B\}M) + \sqrt{2}\; F\; Tr\,([\overline{B}, B]\,M) \;\;, \tag{45.4}$$

where $[\overline{B}, B] \equiv \overline{B}B - B\overline{B}$ and $\{\overline{B}, B\} \equiv \overline{B}B + B\overline{B}$, are

$$D = \frac{\sqrt{30}}{40}\, g_1 \;, \qquad F = \frac{\sqrt{6}}{24}\, g_2 \;. \tag{45.5}$$

Thus, for example,

$$\Gamma(\Xi^* \to \Xi\pi) \sim (F - D)^2 \sim (1 - 2\alpha)^2 \;, \tag{45.6}$$

where $\alpha \equiv F/(D + F)$. (This definition of α is de Swart's. The alternative $D/(D + F)$, due to Gell-Mann, is also used.)

The generators of SU(3) transformations, λ_a $(a = 1, 8)$, are 3×3 matrices that obey the following commutation and anticommutation relationships:

$$[\lambda_a,\ \lambda_b] \equiv \lambda_a\lambda_b - \lambda_b\lambda_a = 2i f_{abc}\lambda_c \tag{45.7}$$

$$\{\lambda_a,\ \lambda_b\} \equiv \lambda_a\lambda_b + \lambda_b\lambda_a = \frac{4}{3}\delta_{ab} I + 2 d_{abc}\lambda_c \;, \tag{45.8}$$

where I is the 3×3 identity matrix, and δ_{ab} is the Kronecker delta symbol. The f_{abc} are odd under the permutation of any pair of indices, while the d_{abc} are even. The nonzero values are

$1 \to 8 \otimes 8$

$$\begin{pmatrix}\Lambda\end{pmatrix} \to \begin{pmatrix} N\overline{K} & \Sigma\pi & \Lambda\eta & \Xi K \end{pmatrix} = \frac{1}{\sqrt{8}} \begin{pmatrix} 2 & 3 & -1 & -2 \end{pmatrix}^{1/2}$$

$8_1 \to 8 \otimes 8$

$$\begin{pmatrix} N \\ \Sigma \\ \Lambda \\ \Xi \end{pmatrix} \to \begin{pmatrix} N\pi & N\eta & \Sigma K & \Lambda K \\ N\overline{K} & \Sigma\pi & \Lambda\pi & \Sigma\eta & \Xi K \\ & N\overline{K} & \Sigma\pi & \Lambda\eta & \Xi K \\ & & \Sigma\overline{K} & \Lambda\overline{K} & \Xi\pi & \Xi\eta \end{pmatrix} = \frac{1}{\sqrt{20}} \begin{pmatrix} 9 & -1 & -9 & -1 \\ -6 & 0 & 4 & 4 & -6 \\ 2 & -12 & -4 & -2 \\ 9 & -1 & -9 & -1 \end{pmatrix}^{1/2}$$

$8_2 \to 8 \otimes 8$

$$\begin{pmatrix} N \\ \Sigma \\ \Lambda \\ \Xi \end{pmatrix} \to \begin{pmatrix} N\pi & N\eta & \Sigma K & \Lambda K \\ N\overline{K} & \Sigma\pi & \Lambda\pi & \Sigma\eta & \Xi K \\ & N\overline{K} & \Sigma\pi & \Lambda\eta & \Xi K \\ & & \Sigma\overline{K} & \Lambda\overline{K} & \Xi\pi & \Xi\eta \end{pmatrix} = \frac{1}{\sqrt{12}} \begin{pmatrix} 3 & 3 & 3 & -3 \\ 2 & 8 & 0 & 0 & -2 \\ 6 & 0 & 0 & 6 \\ 3 & 3 & 3 & -3 \end{pmatrix}^{1/2}$$

$10 \to 8 \otimes 8$

$$\begin{pmatrix} \Delta \\ \Sigma \\ \Xi \\ \Omega \end{pmatrix} \to \begin{pmatrix} N\pi & \Sigma K \\ N\overline{K} & \Sigma\pi & \Lambda\pi & \Sigma\eta & \Xi K \\ & \Sigma\overline{K} & \Lambda\overline{K} & \Xi\pi & \Xi\eta \\ & & \Xi\overline{K} \end{pmatrix} = \frac{1}{\sqrt{12}} \begin{pmatrix} -6 & 6 \\ -2 & 2 & -3 & 3 & 2 \\ 3 & -3 & 3 & 3 \\ 12 \end{pmatrix}^{1/2}$$

$8 \to 10 \otimes 8$

$$\begin{pmatrix} N \\ \Sigma \\ \Lambda \\ \Xi \end{pmatrix} \to \begin{pmatrix} \Delta\pi & \Sigma K \\ \Delta\overline{K} & \Sigma\pi & \Sigma\eta & \Xi K \\ & \Sigma\pi & \Xi K \\ \Sigma\overline{K} & \Xi\pi & \Xi\eta & \Omega K \end{pmatrix} = \frac{1}{\sqrt{15}} \begin{pmatrix} -12 & 3 \\ 8 & -2 & -3 & 2 \\ & -9 & 6 \\ 3 & -3 & -3 & 6 \end{pmatrix}^{1/2}$$

$10 \to 10 \otimes 8$

$$\begin{pmatrix} \Delta \\ \Sigma \\ \Xi \\ \Omega \end{pmatrix} \to \begin{pmatrix} \Delta\pi & \Delta\eta & \Sigma K \\ \Delta\overline{K} & \Sigma\pi & \Sigma\eta & \Xi K \\ \Sigma\overline{K} & \Xi\pi & \Xi\eta & \Omega K \\ & \Xi\overline{K} & \Omega\eta \end{pmatrix} = \frac{1}{\sqrt{24}} \begin{pmatrix} 15 & 3 & -6 \\ 8 & 8 & 0 & -8 \\ 12 & 3 & -3 & -6 \\ & 12 & -12 \end{pmatrix}^{1/2}$$

abc	f_{abc}
123	1
147	1/2
156	−1/2
246	1/2
257	1/2
345	1/2
367	−1/2
458	$\sqrt{3}/2$
678	$\sqrt{3}/2$

abc	d_{abc}
118	$1/\sqrt{3}$
146	1/2
157	1/2
228	$1/\sqrt{3}$
247	−1/2
256	1/2
338	$1/\sqrt{3}$
344	1/2

abc	d_{abc}
355	1/2
366	−1/2
377	−1/2
448	$-1/(2\sqrt{3})$
558	$-1/(2\sqrt{3})$
668	$-1/(2\sqrt{3})$
778	$-1/(2\sqrt{3})$
888	$-1/\sqrt{3}$

The λ_a's are

$$\lambda_1 = \begin{pmatrix} 0 & 1 & 0 \\ 1 & 0 & 0 \\ 0 & 0 & 0 \end{pmatrix} \quad \lambda_2 = \begin{pmatrix} 0 & -i & 0 \\ i & 0 & 0 \\ 0 & 0 & 0 \end{pmatrix} \quad \lambda_3 = \begin{pmatrix} 1 & 0 & 0 \\ 0 & -1 & 0 \\ 0 & 0 & 0 \end{pmatrix}$$

$$\lambda_4 = \begin{pmatrix} 0 & 0 & 1 \\ 0 & 0 & 0 \\ 1 & 0 & 0 \end{pmatrix} \quad \lambda_5 = \begin{pmatrix} 0 & 0 & -i \\ 0 & 0 & 0 \\ i & 0 & 0 \end{pmatrix} \quad \lambda_6 = \begin{pmatrix} 0 & 0 & 0 \\ 0 & 0 & 1 \\ 0 & 1 & 0 \end{pmatrix}$$

$$\lambda_7 = \begin{pmatrix} 0 & 0 & 0 \\ 0 & 0 & -i \\ 0 & i & 0 \end{pmatrix} \quad \lambda_8 = \frac{1}{\sqrt{3}} \begin{pmatrix} 1 & 0 & 0 \\ 0 & 1 & 0 \\ 0 & 0 & -2 \end{pmatrix}$$

Equation (45.7) defines the Lie algebra of SU(3). A general d-dimensional representation is given by a set of $d \times d$ matrices satisfying Eq. (45.7) with the f_{abc} given above. Equation (45.8) is specific to the defining 3-dimensional representation.

46. SU(n) Multiplets and Young Diagrams

Written by C.G. Wohl (LBNL).

This note tells (1) how SU(n) particle multiplets are identified or labeled, (2) how to find the number of particles in a multiplet from its label, (3) how to draw the Young diagram for a multiplet, and (4) how to use Young diagrams to determine the overall multiplet structure of a composite system, such as a 3-quark or a meson-baryon system.

In much of the literature, the word "representation" is used where we use "multiplet," and "tableau" is used where we use "diagram."

46.1. Multiplet labels

An SU(n) multiplet is uniquely identified by a string of ($n-1$) nonnegative integers: $(\alpha, \beta, \gamma, \ldots)$. Any such set of integers specifies a multiplet. For an SU(2) multiplet such as an isospin multiplet, the single integer α is the number of *steps* from one end of the multiplet to the other (*i.e.*, it is one fewer than the number of particles in the multiplet). In SU(3), the two integers α and β are the numbers of steps across the top and bottom levels of the multiplet diagram. Thus the labels for the SU(3) octet and decuplet

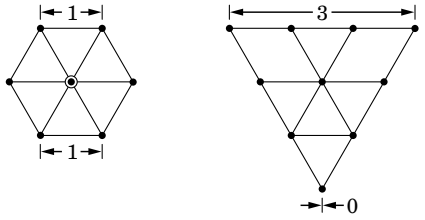

are (1,1) and (3,0). For larger n, the interpretation of the integers in terms of the geometry of the multiplets, which exist in an ($n-1$)-dimensional space, is not so readily apparent.

The label for the SU(n) singlet is $(0, 0, \ldots, 0)$. In a flavor SU(n), the n quarks together form a $(1, 0, \ldots, 0)$ multiplet, and the n antiquarks belong to a $(0, \ldots, 0, 1)$ multiplet. These two multiplets are *conjugate* to one another, which means their labels are related by $(\alpha, \beta, \ldots) \leftrightarrow (\ldots, \beta, \alpha)$.

46.2. Number of particles

The number of particles in a multiplet, $N = N(\alpha, \beta, \ldots)$, is given as follows (note the pattern of the equations).

In SU(2), $N = N(\alpha)$ is

$$N = \frac{(\alpha + 1)}{1} \, . \tag{46.1}$$

In SU(3), $N = N(\alpha, \beta)$ is

$$N = \frac{(\alpha + 1)}{1} \cdot \frac{(\beta + 1)}{1} \cdot \frac{(\alpha + \beta + 2)}{2} \, . \tag{46.2}$$

In SU(4), $N = N(\alpha, \beta, \gamma)$ is

$$N = \frac{(\alpha+1)}{1} \cdot \frac{(\beta+1)}{1} \cdot \frac{(\gamma+1)}{1} \cdot \frac{(\alpha+\beta+2)}{2} \cdot \frac{(\beta+\gamma+2)}{2} \cdot \frac{(\alpha+\beta+\gamma+3)}{3} \, . \tag{46.3}$$

Note that in Eq. (46.3) there is no factor with $(\alpha + \gamma + 2)$: only a *consecutive* sequence of the label integers appears in any factor. One more example should make the pattern clear for any SU(n). In SU(5), $N = N(\alpha, \beta, \gamma, \delta)$ is

$$N = \frac{(\alpha+1)}{1} \cdot \frac{(\beta+1)}{1} \cdot \frac{(\gamma+1)}{1} \cdot \frac{(\delta+1)}{1} \cdot \frac{(\alpha+\beta+2)}{2} \cdot \frac{(\beta+\gamma+2)}{2} \times \frac{(\gamma+\delta+2)}{2} \cdot \frac{(\alpha+\beta+\gamma+3)}{3} \cdot \frac{(\beta+\gamma+\delta+3)}{3} \cdot \frac{(\alpha+\beta+\gamma+\delta+4)}{4} \tag{46.4}$$

From the symmetry of these equations, it is clear that multiplets that are conjugate to one another have the same number of particles, but so can other multiplets. For example, the SU(4) multiplets (3,0,0) and (1,1,0) each have 20 particles. Try the equations and see.

46.3. Young diagrams

A Young diagram consists of an array of boxes (or some other symbol) arranged in one or more *left-justified* rows, with each row being *at least as long* as the row beneath. The correspondence between a diagram and a multiplet label is: The top row juts out α boxes to the right past the end of the second row, the second row juts out β boxes to the right past the end of the third row, *etc.* A diagram in SU(n) has at most n rows. There can be any number of "completed" columns of n boxes buttressing the left of a diagram; these don't affect the label. Thus in SU(3) the diagrams

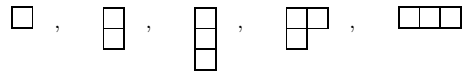

represent the multiplets (1,0), (0,1), (0,0), (1,1), and (3,0). In any SU(n), the quark multiplet is represented by a single box, the antiquark multiplet by a column of ($n-1$) boxes, and a singlet by a completed column of n boxes.

46.4. Coupling multiplets together

The following recipe tells how to find the multiplets that occur in coupling two multiplets together. To couple together more than two multiplets, first couple two, then couple a third with each of the multiplets obtained from the first two, *etc.*

First a definition: A sequence of the letters $a, b, c, \ldots$ is *admissible* if at any point in the sequence at least as many a's have occurred as b's, at least as many b's have occurred as c's, *etc.* Thus *abcd* and *aabcb* are admissible sequences and *abb* and *acb* are not. Now the recipe:

(a) Draw the Young diagrams for the two multiplets, but in one of the diagrams replace the boxes in the first row with a's, the boxes in the second row with b's, *etc.* Thus, to couple two SU(3) octets (such as the π-meson octet and the baryon octet), we start with  and  . The *unlettered* diagram forms the *upper left-hand corner* of all the enlarged diagrams constructed below.

(b) Add the a's from the lettered diagram to the right-hand ends of the rows of the unlettered diagram to form all possible legitimate Young diagrams that have no more than one a per column. In general, there will be several distinct diagrams, and all the a's appear in each diagram. At this stage, for the coupling of the two SU(3) octets, we have:

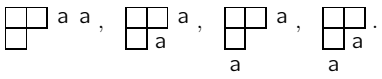

(c) Use the b's to further enlarge the diagrams already obtained, subject to the same rules. Then throw away any diagram in which the full sequence of letters formed by reading *right to left* in the first row, then the second row, *etc.*, is not admissible.

(d) Proceed as in (c) with the c's (if any), *etc.*

The final result of the coupling of the two SU(3) octets is:

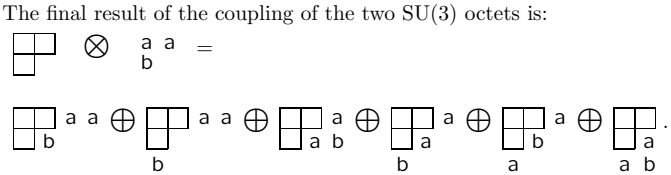

Here only the diagrams with admissible sequences of a's and b's and with fewer than four rows (since $n = 3$) have been kept. In terms of multiplet labels, the above may be written

$$(1,1) \otimes (1,1) = (2,2) \oplus (3,0) \oplus (0,3) \oplus (1,1) \oplus (1,1) \oplus (0,0) \, .$$

In terms of numbers of particles, it may be written

$$\mathbf{8} \otimes \mathbf{8} = \mathbf{27} \oplus \mathbf{10} \oplus \overline{\mathbf{10}} \oplus \mathbf{8} \oplus \mathbf{8} \oplus \mathbf{1} \, .$$

The product of the numbers on the left here is equal to the sum on the right, a useful check. (See also Sec. 15 on the Quark Model.)

47. Kinematics

Revised August 2017 by D.R. Tovey (Sheffield) and January 2000 by J.D. Jackson (LBNL).

Throughout this section units are used in which $\hbar = c = 1$. The following conversions are useful: $\hbar c = 197.3$ MeV fm, $(\hbar c)^2 = 0.3894$ $(\mathrm{GeV})^2$ mb.

47.1. Lorentz transformations

The energy E and 3-momentum $\boldsymbol{p}$ of a particle of mass m form a 4-vector $p = (E, \boldsymbol{p})$ whose square $p^2 \equiv E^2 - |\boldsymbol{p}|^2 = m^2$. The velocity of the particle is $\boldsymbol{\beta} = \boldsymbol{p}/E$. The energy and momentum $(E^*, \boldsymbol{p}^*)$ viewed from a frame moving with velocity $\boldsymbol{\beta}_f$ are given by

$$\begin{pmatrix} E^* \\ p_\parallel^* \end{pmatrix} = \begin{pmatrix} \gamma_f & -\gamma_f\beta_f \\ -\gamma_f\beta_f & \gamma_f \end{pmatrix} \begin{pmatrix} E \\ p_\parallel \end{pmatrix} , \quad p_T^* = p_T , \tag{47.1}$$

where $\gamma_f = (1-\beta_f^2)^{-1/2}$ and p_T ($p_\parallel$) are the components of $\boldsymbol{p}$ perpendicular (parallel) to $\boldsymbol{\beta}_f$. Other 4-vectors, such as the space-time coordinates of events, of course transform in the same way. The scalar product of two 4-momenta $p_1 \cdot p_2 = E_1E_2 - \boldsymbol{p}_1 \cdot \boldsymbol{p}_2$ is invariant (frame independent).

47.2. Center-of-mass energy and momentum

In the collision of two particles of masses m_1 and m_2 the total center-of-mass energy can be expressed in the Lorentz-invariant form

$$\begin{aligned} E_{\mathrm{cm}} &= \left[(E_1+E_2)^2 - (\boldsymbol{p}_1+\boldsymbol{p}_2)^2\right]^{1/2} , \\ &= \left[m_1^2 + m_2^2 + 2E_1E_2(1-\beta_1\beta_2\cos\theta)\right]^{1/2} , \end{aligned} \tag{47.2}$$

where θ is the angle between the particles. In the frame where one particle (of mass m_2) is at rest (lab frame),

$$E_{\mathrm{cm}} = (m_1^2 + m_2^2 + 2E_{1\,\mathrm{lab}}\, m_2)^{1/2} . \tag{47.3}$$

The velocity of the center-of-mass in the lab frame is

$$\boldsymbol{\beta}_{\mathrm{cm}} = \boldsymbol{p}_{\mathrm{lab}}/(E_{1\,\mathrm{lab}} + m_2) , \tag{47.4}$$

where $\boldsymbol{p}_{\mathrm{lab}} \equiv \boldsymbol{p}_{1\,\mathrm{lab}}$ and

$$\gamma_{\mathrm{cm}} = (E_{1\,\mathrm{lab}} + m_2)/E_{\mathrm{cm}} . \tag{47.5}$$

The c.m. momenta of particles 1 and 2 are of magnitude

$$p_{\mathrm{cm}} = p_{\mathrm{lab}}\frac{m_2}{E_{\mathrm{cm}}} . \tag{47.6}$$

For example, if a 0.80 GeV/c kaon beam is incident on a proton target, the center of mass energy is 1.699 GeV and the center of mass momentum of either particle is 0.442 GeV/c. It is also useful to note that

$$E_{\mathrm{cm}}\, dE_{\mathrm{cm}} = m_2\, dE_{1\,\mathrm{lab}} = m_2\, \beta_{1\,\mathrm{lab}}\, dp_{\mathrm{lab}} . \tag{47.7}$$

47.3. Lorentz-invariant amplitudes

The matrix elements for a scattering or decay process are written in terms of an invariant amplitude $-i\mathscr{M}$. As an example, the S-matrix for $2 \to 2$ scattering is related to $\mathscr{M}$ by

$$\begin{aligned} \langle p_1'p_2' \,|S|\, p_1p_2\rangle &= I - i(2\pi)^4\, \delta^4(p_1+p_2-p_1'-p_2') \\ &\quad \times \frac{\mathscr{M}(p_1,\, p_2;\, p_1',\, p_2')}{(2E_1)^{1/2}\,(2E_2)^{1/2}\,(2E_1')^{1/2}\,(2E_2')^{1/2}} . \end{aligned} \tag{47.8}$$

The state normalization is such that

$$\langle p'|p\rangle = (2\pi)^3\delta^3(\boldsymbol{p}-\boldsymbol{p}') . \tag{47.9}$$

For a $2 \to 2$ scattering process producing unstable particles $1'$ and $2'$ decaying via $1' \to 3'4'$ and $2' \to 5'6'$ the matrix element for the complete process can be written in the narrow width approximation as:

$$\begin{aligned} &\mathscr{M}(12 \to 3'4'5'6') = \\ &\sum_{h_{1'},h_{2'}} \frac{\mathscr{M}(12 \to 1'2')\mathscr{M}(1' \to 3'4')\mathscr{M}(2' \to 5'6')}{(m_{3'4'}^2 - m_{1'}^2 + im_{1'}\Gamma_{1'})(m_{5'6'}^2 - m_{2'}^2 + im_{2'}\Gamma_{2'})} . \end{aligned} \tag{47.10}$$

Here, m_{ij} is the invariant mass of particles i and j, m_k and Γ_k are the mass and total width of particle k, and the sum runs over the helicities of the intermediate particles. This enables the cross section for such a process to be written as the product of the cross section for the initial $2 \to 2$ scattering process with the branching ratios (relative partial decay rates) of the subsequent decays.

47.4. Particle decays

The partial decay rate of a particle of mass M into n bodies in its rest frame is given in terms of the Lorentz-invariant matrix element $\mathscr{M}$ by

$$d\Gamma = \frac{(2\pi)^4}{2M}\, |\mathscr{M}|^2\, d\Phi_n\, (P;\, p_1,\, \ldots,\, p_n), \tag{47.11}$$

where $d\Phi_n$ is an element of n-body phase space given by

$$d\Phi_n(P;\, p_1,\, \ldots,\, p_n) = \delta^4\,(P - \sum_{i=1}^{n} p_i)\, \prod_{i=1}^{n} \frac{d^3p_i}{(2\pi)^3 2E_i} . \tag{47.12}$$

This phase space can be generated recursively, viz.

$$\begin{aligned} &d\Phi_n(P;\, p_1,\, \ldots,\, p_n) = d\Phi_j(q;\, p_1,\, \ldots,\, p_j) \\ &\times\ d\Phi_{n-j+1}\,(P;\, q,\, p_{j+1},\, \ldots,\, p_n)(2\pi)^3 dq^2 , \end{aligned} \tag{47.13}$$

where $q^2 = (\sum_{i=1}^{j} E_i)^2 - \left|\sum_{i=1}^{j} \boldsymbol{p}_i\right|^2$. This form is particularly useful in the case where a particle decays into another particle that subsequently decays.

47.4.1. ***Survival probability*** : If a particle of mass M has mean proper lifetime τ $(= 1/\Gamma)$ and has momentum $(E, \boldsymbol{p})$, then the probability that it lives for a time t_0 or greater before decaying is given by

$$P(t_0) = e^{-t_0\,\Gamma/\gamma} = e^{-Mt_0\,\Gamma/E} , \tag{47.14}$$

and the probability that it travels a distance x_0 or greater is

$$P(x_0) = e^{-Mx_0\,\Gamma/|\boldsymbol{p}|} . \tag{47.15}$$

47.4.2. ***Two-body decays*** :

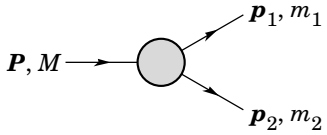

Figure 47.1: Definitions of variables for two-body decays.

In the rest frame of a particle of mass M, decaying into 2 particles labeled 1 and 2,

$$E_1 = \frac{M^2 - m_2^2 + m_1^2}{2M} , \tag{47.16}$$

$$\begin{aligned} |\boldsymbol{p}_1| &= |\boldsymbol{p}_2| \\ &= \frac{\left[\left(M^2 - (m_1+m_2)^2\right)\left(M^2 - (m_1-m_2)^2\right)\right]^{1/2}}{2M} , \end{aligned} \tag{47.17}$$

and

$$d\Gamma = \frac{1}{32\pi^2}\, |\mathscr{M}|^2\, \frac{|\boldsymbol{p}_1|}{M^2}\, d\Omega , \tag{47.18}$$

where $d\Omega = d\phi_1 d(\cos\theta_1)$ is the solid angle of particle 1. The invariant mass M can be determined from the energies and momenta using Eq. (47.2) with $M = E_{\mathrm{cm}}$.

47.4.3. ***Three-body decays*** :

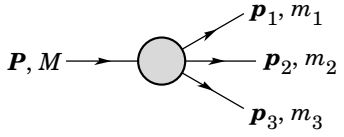

Figure 47.2: Definitions of variables for three-body decays.

Defining $p_{ij} = p_i + p_j$ and $m_{ij}^2 = p_{ij}^2$, then $m_{12}^2 + m_{23}^2 + m_{13}^2 = M^2 + m_1^2 + m_2^2 + m_3^2$ and $m_{12}^2 = (P - p_3)^2 = M^2 + m_3^2 - 2ME_3$, where E_3 is the energy of particle 3 in the rest frame of M. In that frame, the momenta of the three decay particles lie in a plane. The relative orientation of these three momenta is fixed if their energies are known. The momenta can therefore be specified in space by giving three Euler angles (α, β, γ) that specify the orientation of the final system relative to the initial particle. The direction of any one of the particles relative to the frame in which the initial particle is described can be specified in space by two angles (α, β) while a third angle, γ, can be set as the azimuthal angle of a second particle around the first [1]. Then

$$d\Gamma = \frac{1}{(2\pi)^5} \frac{1}{16M} |\mathscr{M}|^2 \, dE_1 \, dE_3 \, d\alpha \, d(\cos\beta) \, d\gamma \; . \tag{47.19}$$

Alternatively

$$d\Gamma = \frac{1}{(2\pi)^5} \frac{1}{16M^2} |\mathscr{M}|^2 \, |\boldsymbol{p}_1^*| \, |\boldsymbol{p}_3| \, dm_{12} \, d\Omega_1^* \, d\Omega_3 \; , \tag{47.20}$$

where $(|\boldsymbol{p}_1^*|, \, \Omega_1^*)$ is the momentum of particle 1 in the rest frame of 1 and 2, and Ω_3 is the angle of particle 3 in the rest frame of the decaying particle. $|\boldsymbol{p}_1^*|$ and $|\boldsymbol{p}_3|$ are given by

$$|\boldsymbol{p}_1^*| = \frac{\left[(m_{12}^2 - (m_1 + m_2)^2)\,(m_{12}^2 - (m_1 - m_2)^2)\right]^{1/2}}{2m_{12}} \; , \tag{47.21a}$$

and

$$|\boldsymbol{p}_3| = \frac{\left[(M^2 - (m_{12} + m_3)^2)\,(M^2 - (m_{12} - m_3)^2)\right]^{1/2}}{2M} \; . \tag{47.21b}$$

[Compare with Eq. (47.17).]

If the decaying particle is a scalar or we average over its spin states, then integration over the angles in Eq. (47.19) gives

$$d\Gamma = \frac{1}{(2\pi)^3} \frac{1}{8M} \overline{|\mathscr{M}|^2} \, dE_1 \, dE_3$$

$$= \frac{1}{(2\pi)^3} \frac{1}{32M^3} \overline{|\mathscr{M}|^2} \, dm_{12}^2 \, dm_{23}^2 \; . \tag{47.22}$$

This is the standard form for the Dalitz plot.

47.4.3.1. *Dalitz plot:* For a given value of m_{12}^2, the range of m_{23}^2 is determined by its values when $\boldsymbol{p}_2$ is parallel or antiparallel to $\boldsymbol{p}_3$:

$$(m_{23}^2)_{\rm max} =$$

$$(E_2^* + E_3^*)^2 - \left(\sqrt{E_2^{*2} - m_2^2} - \sqrt{E_3^{*2} - m_3^2}\right)^2 \; , \tag{47.23a}$$

$$(m_{23}^2)_{\rm min} =$$

$$(E_2^* + E_3^*)^2 - \left(\sqrt{E_2^{*2} - m_2^2} + \sqrt{E_3^{*2} - m_3^2}\right)^2 \; . \tag{47.23b}$$

Here $E_2^* = (m_{12}^2 - m_1^2 + m_2^2)/2m_{12}$ and $E_3^* = (M^2 - m_{12}^2 - m_3^2)/2m_{12}$ are the energies of particles 2 and 3 in the m_{12} rest frame. The scatter plot in m_{12}^2 and m_{23}^2 is called a Dalitz plot. If $\overline{|\mathscr{M}|^2}$ is constant, the allowed region of the plot will be uniformly populated with events [see Eq. (47.22)]. A nonuniformity in the plot gives immediate information on $|\mathscr{M}|^2$. For example, in the case of $D \to K\pi\pi$, bands appear when $m_{(K\pi)} = m_{K^*(892)}$, reflecting the appearance of the decay chain $D \to K^*(892)\pi \to K\pi\pi$.

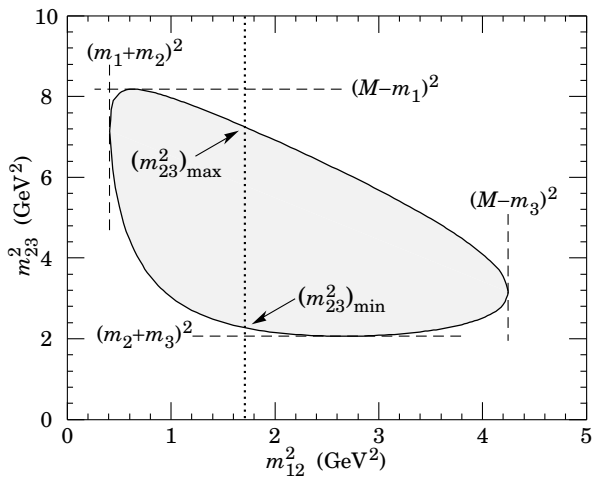

Figure 47.3: Dalitz plot for a three-body final state. In this example, the state is $\pi^+\overline{K}^0 p$ at 3 GeV. Four-momentum conservation restricts events to the shaded region.

47.4.4. ***Kinematic limits*** :

47.4.4.1. *Three-body decays:* In a three-body decay (Fig. 47.2) the maximum of $|\boldsymbol{p}_3|$, [given by Eq. (47.21)], is achieved when $m_{12} = m_1 + m_2$, *i.e.*, particles 1 and 2 have the same vector velocity in the rest frame of the decaying particle. If, in addition, $m_3 > m_1, m_2$, then $|\boldsymbol{p}_3|_{\rm max} > |\boldsymbol{p}_1|_{\rm max}$, $|\boldsymbol{p}_2|_{\rm max}$. The distribution of m_{12} values possesses an end-point or maximum value at $m_{12} = M - m_3$. This can be used to constrain the mass difference of a parent particle and one invisible decay product.

47.4.4.2. *Sequential two-body decays:*

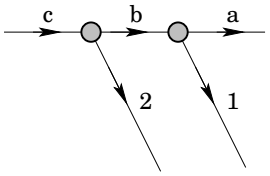

Figure 47.4: Particles participating in sequential two-body decay chain. Particles labeled 1 and 2 are visible while the particle terminating the chain (a) is invisible.

When a heavy particle initiates a sequential chain of two-body decays terminating in an invisible particle, constraints on the masses of the states participating in the chain can be obtained from end-points and thresholds in invariant mass distributions of the aggregated decay products. For the two-step decay chain depicted in Fig. 47.4 the invariant mass distribution of the two visible particles possesses an end-point given by:

$$(m_{12}^{\rm max})^2 = \frac{(m_{\rm c}^2 - m_{\rm b}^2)(m_{\rm b}^2 - m_{\rm a}^2)}{m_{\rm b}^2} \; , \tag{47.24}$$

provided particles 1 and 2 are massless. If visible particle 1 has non-zero mass m_1 then Eq. (47.24) is replaced by

$$(m_{12}^{\rm max})^2 = m_1^2 + \frac{(m_{\rm c}^2 - m_{\rm b}^2)}{2m_{\rm b}^2} \times$$

$$\left(m_1^2 + m_{\rm b}^2 - m_{\rm a}^2 + \sqrt{(-m_1^2 + m_{\rm b}^2 - m_{\rm a}^2)^2 - 4m_1^2 m_{\rm a}^2}\right) . \tag{47.25}$$

See Refs. 2 and 3 for other cases.

47.4.5. ***Multibody decays*** : The above results may be generalized to final states containing any number of particles by combining some of the particles into "effective particles" and treating the final states as 2 or 3 "effective particle" states. Thus, if $p_{ijk\ldots} = p_i + p_j + p_k + \ldots$, then

$$m_{ijk\ldots} = \sqrt{p^2_{ijk\ldots}} \ , \tag{47.26}$$

and $m_{ijk\ldots}$ may be used in place of *e.g.*, m_{12} in the relations in Sec. 47.4.3 or Sec. 47.4.4 above.

47.5. Cross sections

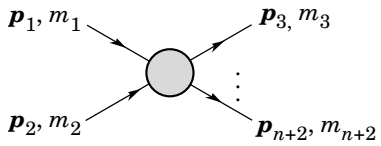

Figure 47.5: Definitions of variables for production of an n-body final state.

The differential cross section is given by

$$d\sigma = \frac{(2\pi)^4 |\mathscr{M}|^2}{4\sqrt{(p_1 \cdot p_2)^2 - m_1^2 m_2^2}} \times \ d\Phi_n(p_1 + p_2;\ p_3,\ \ldots,\ p_{n+2}) \ . \tag{47.27}$$

[See Eq. (47.12).] In the rest frame of m_2(lab),

$$\sqrt{(p_1 \cdot p_2)^2 - m_1^2 m_2^2} = m_2 p_{1\,\mathrm{lab}} \ ; \tag{47.28a}$$

while in the center-of-mass frame

$$\sqrt{(p_1 \cdot p_2)^2 - m_1^2 m_2^2} = p_{1\mathrm{cm}} \sqrt{s} \ . \tag{47.28b}$$

47.5.1. ***Two-body reactions*** :

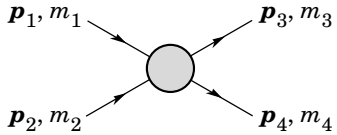

Figure 47.6: Definitions of variables for a two-body final state.

Two particles of momenta p_1 and p_2 and masses m_1 and m_2 scatter to particles of momenta p_3 and p_4 and masses m_3 and m_4; the Lorentz-invariant Mandelstam variables are defined by

$$\begin{aligned} s &= (p_1 + p_2)^2 = (p_3 + p_4)^2 \\ &= m_1^2 + 2E_1E_2 - 2\boldsymbol{p}_1 \cdot \boldsymbol{p}_2 + m_2^2 \ , \qquad (47.29) \\ t &= (p_1 - p_3)^2 = (p_2 - p_4)^2 \\ &= m_1^2 - 2E_1E_3 + 2\boldsymbol{p}_1 \cdot \boldsymbol{p}_3 + m_3^2 \ , \qquad (47.30) \\ u &= (p_1 - p_4)^2 = (p_2 - p_3)^2 \\ &= m_1^2 - 2E_1E_4 + 2\boldsymbol{p}_1 \cdot \boldsymbol{p}_4 + m_4^2 \ , \qquad (47.31) \end{aligned}$$

and they satisfy

$$s + t + u = m_1^2 + m_2^2 + m_3^2 + m_4^2 \ . \tag{47.32}$$

The two-body cross section may be written as

$$\frac{d\sigma}{dt} = \frac{1}{64\pi s} \ \frac{1}{|\boldsymbol{p}_{1\mathrm{cm}}|^2} \ |\mathscr{M}|^2 \ . \tag{47.33}$$

In the center-of-mass frame

$$\begin{aligned} t = (E_{1\mathrm{cm}} - E_{3\mathrm{cm}})^2 - (p_{1\mathrm{cm}} - p_{3\mathrm{cm}})^2 \qquad & \\ - 4p_{1\mathrm{cm}}\, p_{3\mathrm{cm}}\, \sin^2(\theta_{\mathrm{cm}}/2) & \\ = t_0 - 4p_{1\mathrm{cm}}\, p_{3\mathrm{cm}}\, \sin^2(\theta_{\mathrm{cm}}/2) \ , & \qquad (47.34) \end{aligned}$$

where θ_{cm} is the angle between particle 1 and 3. The limiting values t_0 ($\theta_{\mathrm{cm}} = 0$) and t_1 ($\theta_{\mathrm{cm}} = \pi$) for $2 \to 2$ scattering are

$$t_0(t_1) = \left[\frac{m_1^2 - m_3^2 - m_2^2 + m_4^2}{2\sqrt{s}}\right]^2 - (p_{1\,\mathrm{cm}} \mp p_{3\,\mathrm{cm}})^2 \ . \tag{47.35}$$

In the literature the notation $t_{\min}$ ($t_{\max}$) for t_0 (t_1) is sometimes used, which should be discouraged since $t_0 > t_1$. The center-of-mass energies and momenta of the incoming particles are

$$E_{1\mathrm{cm}} = \frac{s + m_1^2 - m_2^2}{2\sqrt{s}} \ , \qquad E_{2\mathrm{cm}} = \frac{s + m_2^2 - m_1^2}{2\sqrt{s}} \ , \tag{47.36}$$

For $E_{3\mathrm{cm}}$ and $E_{4\mathrm{cm}}$, change m_1 to m_3 and m_2 to m_4. Then

$$p_{i\,\mathrm{cm}} = \sqrt{E_{i\,\mathrm{cm}}^2 - m_i^2} \text{ and } p_{1\mathrm{cm}} = \frac{p_{1\,\mathrm{lab}}\, m_2}{\sqrt{s}} \ . \tag{47.37}$$

Here the subscript lab refers to the frame where particle 2 is at rest. [For other relations see Eqs. (47.2)–(47.4).]

47.5.2. ***Inclusive reactions*** : Choose some direction (usually the beam direction) for the z-axis; then the energy and momentum of a particle can be written as

$$E = m_{_T} \cosh y \ , \ p_x \ , \ p_y \ , \ p_z = m_{_T} \sinh y \ , \tag{47.38}$$

where $m_{_T}$, conventionally called the 'transverse mass', is given by

$$m_{_T}^2 = m^2 + p_x^2 + p_y^2 \ . \tag{47.39}$$

and the rapidity y is defined by

$$\begin{aligned} y &= \frac{1}{2} \ln \left(\frac{E + p_z}{E - p_z}\right) \\ &= \ln \left(\frac{E + p_z}{m_{_T}}\right) = \tanh^{-1}\left(\frac{p_z}{E}\right) \ . \qquad (47.40) \end{aligned}$$

Note that the definition of the transverse mass in Eq. (47.39) differs from that used by experimentalists at hadron colliders (see Sec. 47.6.1 below). Under a boost in the z-direction to a frame with velocity β, $y \to y - \tanh^{-1}\beta$. Hence the shape of the rapidity distribution dN/dy is invariant, as are differences in rapidity. The invariant cross section may also be rewritten

$$E\frac{d^3\sigma}{d^3p} = \frac{d^3\sigma}{d\phi\, dy\, p_{_T} dp_{_T}} \Longrightarrow \frac{d^2\sigma}{\pi\, dy\, d(p_{_T}^2)} \ . \tag{47.41}$$

The second form is obtained using the identity $dy/dp_z = 1/E$, and the third form represents the average over ϕ.

Feynman's x variable is given by

$$x = \frac{p_z}{p_{z\,\max}} \approx \frac{E + p_z}{(E + p_z)_{\max}} \quad (p_{_T} \ll |p_z|) \ . \tag{47.42}$$

In the c.m. frame,

$$x \approx \frac{2p_{z\,\mathrm{cm}}}{\sqrt{s}} = \frac{2m_{_T} \sinh y_{\mathrm{cm}}}{\sqrt{s}} \tag{47.43}$$

and

$$= (y_{\mathrm{cm}})_{\max} = \ln(\sqrt{s}/m) \ . \tag{47.44}$$

The invariant mass M of the two-particle system described in Sec. 47.4.2 can be written in terms of these variables as

$$M^2 = m_1^2 + m_2^2 + 2[E_{_T}(1)E_{_T}(2)\cosh\Delta y - \boldsymbol{p}_{_T}(1) \cdot \boldsymbol{p}_{_T}(2)] \ , \tag{47.45}$$

where

$$E_{_T}(i) = \sqrt{|\boldsymbol{p}_{_T}(i)|^2 + m_i^2} \ , \tag{47.46}$$

and $\boldsymbol{p}_{_T}(i)$ denotes the transverse momentum vector of particle i.

For $p \gg m$, the rapidity [Eq. (47.40)] may be expanded to obtain

$$\begin{aligned} y &= \frac{1}{2} \ln \frac{\cos^2(\theta/2) + m^2/4p^2 + \ldots}{\sin^2(\theta/2) + m^2/4p^2 + \ldots} \\ &\approx -\ln \tan(\theta/2) \equiv \eta \qquad (47.47) \end{aligned}$$

where $\cos\theta = p_z/p$. The pseudorapidity η defined by the second line is approximately equal to the rapidity y for $p \gg m$ and $\theta \gg 1/\gamma$, and in any case can be measured when the mass and momentum of the particle are unknown. From the definition one can obtain the identities

$$\sinh\eta = \cot\theta \ , \quad \cosh\eta = 1/\sin\theta \ , \quad \tanh\eta = \cos\theta \ . \tag{47.48}$$

47.6. Transverse variables

At hadron colliders, a significant and unknown proportion of the energy of the incoming hadrons in each event escapes down the beam-pipe. Consequently if invisible particles are created in the final state, their net momentum can only be constrained in the plane transverse to the beam direction. Defining the z-axis as the beam direction, this net momentum is equal to the missing transverse energy vector

$$\boldsymbol{E}_T^{\rm miss} = -\sum_i \boldsymbol{p}_T(i) \ , \tag{47.49}$$

where the sum runs over the transverse momenta of all visible final state particles.

47.6.1. *Single production with semi-invisible final state* :

Consider a single heavy particle of mass M produced in association with visible particles which decays as in Fig. 47.1 to two particles, of which one (labeled particle 1) is invisible. The mass of the parent particle can be constrained with the quantity M_T defined by

$$\begin{aligned} M_T^2 &\equiv [E_T(1) + E_T(2)]^2 - [\boldsymbol{p}_T(1) + \boldsymbol{p}_T(2)]^2 \\ &= m_1^2 + m_2^2 + 2[E_T(1)E_T(2) - \boldsymbol{p}_T(1) \cdot \boldsymbol{p}_T(2)] \ , \end{aligned} \tag{47.50}$$

where

$$\boldsymbol{p}_T(1) = \boldsymbol{E}_T^{\rm miss} \ . \tag{47.51}$$

This quantity is called the 'transverse mass' by hadron collider experimentalists but it should be noted that it is quite different from that used in the description of inclusive reactions [Eq. (47.39)]. The distribution of event M_T values possesses an end-point at $M_T^{\rm max} = M$. If $m_1 = m_2 = 0$ then

$$M_T^2 = 2|\boldsymbol{p}_T(1)||\boldsymbol{p}_T(2)|(1 - \cos\phi_{12}) \ , \tag{47.52}$$

where ϕ_{ij} is defined as the angle between particles i and j in the transverse plane.

47.6.2. *Pair production with semi-invisible final states* :

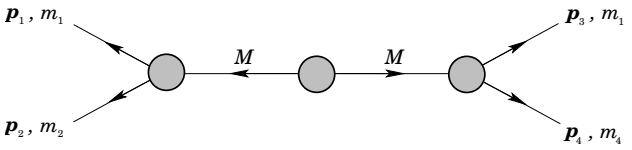

Figure 47.7: Definitions of variables for pair production of semi-invisible final states. Particles 1 and 3 are invisible while particles 2 and 4 are visible.

Consider two identical heavy particles of mass M produced such that their combined center-of-mass is at rest in the transverse plane (Fig. 47.7). Each particle decays to a final state consisting of an invisible particle of fixed mass m_1 together with an additional visible particle. M and m_1 can be constrained with the variables M_{T2} and M_{CT} which are defined in Refs. 4 and 5.

References:

1. See, for example, J.D. Jackson in *High Energy Physics, Les Houches 1965 Summer School*, GORDON AND BREACH Science Publishers (1965), p. 348.
2. I. Hinchliffe *et al.*, Phys. Rev. **D55**, 5520 (1997).
3. B.C. Allanach *et al.*, JHEP **0009**, 004 (2000).
4. C.G. Lester and D.J. Summers, Phys. Lett. **B463**, 99 (1999).
5. D.R. Tovey, JHEP **0804**, 034 (2008).

48. Resonances

Updated 2017 by D.M. Asner (Brookhaven National Laboratory), C. Hanhart (Forschungszentrum Jülich) and E. Klempt (Bonn).

48.1. General Considerations

Perturbative methods can be applied to systems of quarks and gluons only for large momentum transfers (see review on 'Quantum chromodynamics') and, under certain conditions, to some properties of systems that contain heavy quarks (see review on 'Heavy-Quark and Soft-Collinear Effective Theory'). In general, however, dealing with QCD in the low momentum transfer region is a very complicated non–perturbative problem where quarks and gluons are confined within color neutral hadrons. Physical states show up as poles of the S–matrix either on the physical sheet (bound states) or on the unphysical sheets (resonances) and manifest themselves as structures in experimental observables.

Resonances can show up either in so–called formation experiments, typically of the kind

$$A + B \to R \to C_1 + ... + C_n \ ,$$

where they become visible in an energy scan (a perfect example of this being the R–function measured in e^+e^- annihilations — *cf.* the corresponding plots in the review on 'Plots of Cross sections and related quantities'), or together with a spectator particle S in production experiments of the kind

$$A \to R + S \to [C_1 + ... + C_n] + S \ .$$

In the latter case the resonances properties are commonly extracted from a Dalitz plot analysis (see review on 'Kinematics') or projections thereof. Multi–particle final states are often parametrized in terms of successive decays of two–body resonances.

Resonance phenomena are very rich: while typical hadronic widths are of the order of 100 MeV (e.g., for the meson resonances $\rho(770)$ or $\psi(4040)$ or the baryon resonance $\Delta(1232)$) corresponding to a life time of 10^{-23} s, the widths can also be as small as sub MeV (e.g. of $X(3872)$) or as large as several hundred MeV (e.g. of the meson resonances $f_0(500)$ or $D_1(2430)$ or the baryon resonance $N(2190)$).

Ideally a resonance appears as a peak in the total cross section. If the structure is narrow and if there are no relevant thresholds or other resonances nearby, the resonance properties may be extracted employing a standard Breit-Wigner parametrization if necessary improved by using an energy dependent width term (*cf.* Sec. 2.1 of this review). However, in general, unitarity and analyticity call for the use of more refined tools. When there are overlapping resonances with the same quantum numbers, the resonance terms should not simply be added but combined in a non–trivial way either in a K–matrix approximation (*cf.* Sec. 2.3 of this review) or using more refined methods (*cf.* Sec. 1.4 of this review). Only then the proper pole parameters can be extracted that are universal resonance properties — on the contrary, Breit–Wigner parameters are typically reaction dependent. In addition, for broad resonances there is no direct relation anymore between pole location and the total width/life time — then the pole residues need to be used in order to quantify the decay properties of a given state (*cf.* Sec. 3 of this review).

For simplicity, throughout this review the formulas are given for distinguishable, scalar particles. The additional complications that appear in the presence of spins can be controlled in the helicity framework developed by Jacob and Wick [1], or in a non-relativistic [2] or relativistic [3] tensor operator formalism. Within these frames, sequential (cascade) decays are commonly treated as a coherent sum of two-body interactions. Therefore below most explicit expressions are given for two–body kinematics.

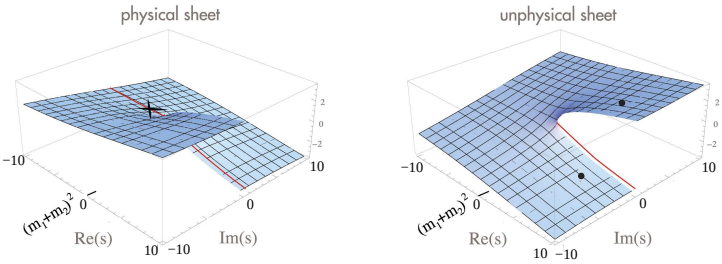

Figure 48.1: Sketch of the imaginary part of a typical single–channel amplitude in the complex s-plane. The solid dots indicate allowed positions for resonance poles, the cross for a bound state. The solid line is the physical axis (shifted by $i\epsilon$ into the physical sheet). The two sheets are connected smoothly along their discontinuities.

48.1.1. *Properties of the S-matrix* :

The unitary operator that connects asymptotic *in* and *out* states is called the S–matrix. It is an analytic function in the Mandelstam plane up to its branch points and poles. Branch points appear whenever there is a channel opening — at each threshold for massive particles the number of Riemann sheets doubles. Poles refer either to bound states or to resonances. The former poles are located on the physical sheet, the latter are located on the unphysical sheet closest to the physical one, often called the second sheet; each can be accompanied by mirror poles. If there are resonances in subsystems of multi–particle states, branch points appear in the complex plane of the unphysical sheet(s). Any of these singularities leads to some structure in the observables (see also Ref. [4]). In a partial wave decomposed amplitude additional singularities not related to resonance physics may emerge as a result of the partial-wave projection. For a discussion see, e.g., Ref. [5].

For simplicity we now restrict ourselves to reactions involving four particles. Then the kinematics of the reaction is fully described by the Mandelstam variables s, t and u, only two of them being independent (cf. Eqs. (28)-(31) of the kinematics review). Bound state poles are allowed only on the real s–axis below the lowest threshold. There is no restriction for the location of poles on the unphysical sheets. Analyticity requires, however, that, if there is a pole at some complex value of s, there must be another pole at its complex conjugate value, s^*. The pole with a negative imaginary part is closer to the physical axis and thus influences the observables in the vicinity of the resonance region more strongly, however, at the threshold both poles are always equally important. This is illustrated in Fig. 48.1.

The S-matrix is related to the scattering matrix $\mathscr{M}$ (c.f. Eq. (8) of the kinematics review). For two–body scattering it can be cast into the form

$$S_{ab} = I_{ab} - 2i\sqrt{\rho_a}\mathscr{M}_{ab}\sqrt{\rho_b}\,. \tag{48.1}$$

$\mathscr{M}$ is a matrix in channel space and depends, for two–body scattering, on both s and t. The channel indices a and b are multi–indices specifying all properties of the channel including the conserved quantum numbers. The two-body phase-space ρ is given (cf. Eq. 12 of the kinematics review) by

$$\rho_a(s) = \frac{1}{16\pi}\frac{2|\vec{q}_a|}{\sqrt{s}}\,. \tag{48.2}$$

with q_a denoting the relative momentum of the decay particles of channel a, with masses m_1 and m_2, cf. Eq. (20a) of the kinematics review.

As discussed below, unitarity puts strong constraints on the scattering matrix. Further constraints come, e.g., from crossing symmetry and duality [6].

48.1.2. ***Consequences from unitarity*** :

In what follows, scattering amplitudes $\mathscr{M}$ and decay amplitudes $\mathcal{A}$ will be distinguished, since unitarity puts different constraints on these. The discontinuity of the scattering amplitude from channel a to channel b [7] is constrained by unitarity to

$$i\,[\mathscr{M}_{ba} - \mathscr{M}^*_{ab}] = (2\pi)^4 \sum_c \int d\Phi_c \mathscr{M}^*_{cb} \mathscr{M}_{ca} \ . \tag{48.3}$$

Using $\mathrm{Disc}(\mathscr{M}(s)) = 2i\,\mathrm{Im}(\mathscr{M}(s+i\epsilon))$ the optical theorem follows

$$\mathrm{Im}\,(\mathscr{M}_{aa}|_{\mathrm{forward}}) = 2q_a\sqrt{s}\,\sigma_{\mathrm{tot}}(a \to \mathrm{anything}) \ . \tag{48.4}$$

The unitarity relation for a decay amplitude of a heavy state H into a channel a is given by

$$i\left[\mathcal{A}^H_a - \mathcal{A}^{H\,*}_a\right] = (2\pi)^4 \sum_c \int d\Phi_c \mathscr{M}^*_{ca} \mathcal{A}^H_c \ . \tag{48.5}$$

From Eq. (48.5) Watson's theorem follows straightforwardly: the phase of $\mathcal{A}$ agrees with that of $\mathscr{M}$ as long as only a single channel contributes. For systems where the phase shifts are known like $\pi\pi$ in S– and P–waves for low energies, $\mathcal{A}^H$ can be calculated in a model-independent way using dispersion theory [8]. Those methods can also be generalized to three–body final states [9] and were applied to $\eta \to \pi\pi\pi$ in Refs. [10,11,12] and to ϕ and ω to 3π in Ref. [13].

48.1.3. ***Partial-wave decomposition*** :

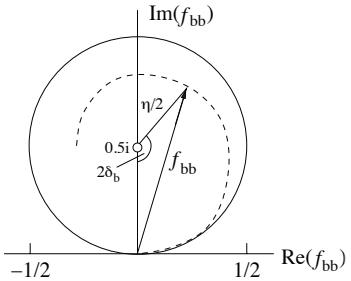

Figure 48.2: Argand plot showing a diagonal element of a partial-wave amplitude, a_{bb}, as a function of energy. The amplitude leaves the unitary circle (solid line) as soon as inelasticity sets in, $\eta < 1$ (dashed line).

In general, a physical amplitude $\mathscr{M}$ (c.f. Eq. (8) of the kinematics review) is a matrix in channel space. It depends, for two–body scattering, on both s and t. It is often convenient to expand the amplitudes in partial waves. For this purpose one defines for the transition matrix from channel a to channel b

$$\mathscr{M}_{ba}(s,t) = \sum_{L=0}^{\infty} (2L+1) \mathscr{M}^L_{ba}(s) P_L(\cos(\theta)) \ , \tag{48.6}$$

where L denotes the angular momentum—in the presence of spins the initial and final value of L does not need to be equal. To simplify notations below we will drop the label L. The function $\mathscr{M}_{ba}(s)$ is expressed in terms of the partial-wave amplitudes $f_{ba}(s)$ via

$$\mathscr{M}_{ba}(s) = -f_{ba}(s)/\sqrt{\rho_a \rho_b} \ . \tag{48.7}$$

The partial-wave amplitudes f_{ba} depend on s only. Using $S_{ba} = \delta_{ba} + 2i f_{ba}$ one gets from the unitarity of the S-matrix

$$f_{bb} = (\eta \exp(2i\delta_b) - 1)/2i \ , \tag{48.8}$$

where δ_b (η) denotes the phase shift (elasticity parameter — also called inelasticity) for the scattering from channel b to channel b. One has $0 \le \eta \le 1$, where $\eta = 1$ refers to purely elastic scattering. The evolution with energy of a partial-wave amplitude f_{bb} can be displayed as a trajectory in an Argand plot, as shown in Fig. 48.2. In case of a two–channel problem the off–diagonal element is typically parametrized as $f_{ba} = \sqrt{1-\eta^2}/2\,\exp(i(\delta_b + \delta_a))$.

48.1.4. ***Explicit parametrizations for scattering and production amplitudes*** :

It is often convenient to decompose the physical amplitude $\mathscr{M}$ into a pole part and a non–pole part, often called background

$$\mathscr{M} = \mathscr{M}^{\mathrm{b.g.}} + \mathscr{M}^{\mathrm{pole}} \ . \tag{48.9}$$

The splitting given in Eq. (48.9) is reaction dependent and not unique (see, e.g., the discussion in Ref. [14]) , such that some resonances show up differently in different reactions. Independent of the reaction are, however, the location of the pole of a given resonance R in the complex s-plane, s_{R}, and its residues, or, more accurately, the pole couplings introduced in the last section of this review. Those parameters capture all the properties of a given resonance. The decomposition of Eq. (48.9) is employed, e.g., in Ref. [15] to study the lineshape of $\psi(3770)$ and in Refs. [16,17] to investigate πN scattering. Traditionally one introduces the notation

$$\sqrt{s_{\mathrm{R}}} = M_{\mathrm{R}} - i\Gamma_{\mathrm{R}}/2 \ , \tag{48.10}$$

where M_{R} and Γ_{R} are referred to as mass and total width of the resonance R, respectively. Note, the standard Breit-Wigner parameters M_{BW} and Γ_{BW}, also introduced below, in general deviate from the pole parameters, e.g., due to finite width effects and the influence of thresholds.

If there are N resonances in a particular channel,

$$\mathscr{M}^{\mathrm{pole}}_{ba}(s) = \gamma_b(s)[1 - V^{\mathrm{R}}(s)\Sigma(s)]^{-1}_{bc} V^{\mathrm{R}}_{ca}(s)\gamma_a(s) \ . \tag{48.11}$$

where all ingredients are matrices in channel space. Especially

$$V^{\mathrm{R}}_{ab}(s) = -\sum_{n=1}^{N} \frac{g_{n\,b}\ g_{n\,a}}{s - M_n^2} \ , \tag{48.12}$$

γ_a and Σ_a denote the normalized vertex function and the self-energy, respectively, while $g_{n\,a}$ denotes the coupling of the resonance R_n to channel a and M_n its mass parameter (not to be confused with the pole position). The sign in Eq. (48.12) is necessary to render the g–parameters real. A relation analogous to Eq. (48.5) holds for any kind of production amplitude — especially for the normalized vertex functions, however, with the final state interaction provided by $\mathscr{M}^{\mathrm{b.g.}}$

$$i\,[\gamma_a - \gamma^*_a] = (2\pi)^4 \sum_c d\Phi_c \left(\mathscr{M}^{\mathrm{b.g.}}\right)^*_{ca} \gamma_c \ . \tag{48.13}$$

The discontinuity of the self-energy $\Sigma_a(s)$ is

$$i\,[\Sigma_a - \Sigma^*_a] = (2\pi)^4 \int d\Phi_a |\gamma_a|^2 \ . \tag{48.14}$$

The real part of Σ_a can be calculated from Eq. (48.14) via a properly subtracted dispersion integral. If $\mathscr{M}^{\mathrm{b.g.}}$ is unitary, the use of Eq. (48.11) leads to a unitary full amplitude, cf. Eq. (48.9).

For a single resonance ($N = 1$) Eq. (48.11) reads

$$\mathscr{M}_{\mathrm{pole}}(s)_{ba}\big|_{N=1} = -\gamma_b(s) \frac{g_b\ g_a}{s - \hat{M}_{\mathrm{R}}(s)^2 + i\sqrt{s}\Gamma^{\mathrm{R}}(s)_{\mathrm{tot}}} \gamma_a(s) \ , \tag{48.15}$$

where the mass function $\hat{M}_{\mathrm{R}}(s)^2 = M^2 + \sum_c g_c^2 \mathrm{Re}(\Sigma_c)$. The imaginary part of the self-energy gives the width of the resonance via

$$\Gamma^{\mathrm{R}}_c(s) = \frac{(2\pi)^4}{2\sqrt{s}} g_c^2 \int d\Phi_c |\gamma_c|^2; \ \Gamma^{\mathrm{R}}(s)_{\mathrm{tot}} = \sum_c \Gamma^{\mathrm{R}}_c(s) \ . \tag{48.16}$$

Here the sum runs over all channels. Eq. (48.16) agrees with Eq. (10) of the kinematics review.

In the absence of left–hand cuts in the production mechanism, the decay amplitude of some heavy state H can be written as

$$\mathcal{A}^H_a(s) = \gamma_a(s) \left[1 - V^{\mathrm{R}}(s)\Sigma(s)\right]^{-1}_{ab} \mathcal{P}^H_b(s) \ , \tag{48.17}$$

where $\mathcal{P}^H$ is a vector in channel space that may be parametrized as

$$\mathcal{P}^H_b(s) = p_b(s) - \sum_{n=1}^{N} \frac{g_{n\,b}\ \alpha^H_n}{s - M^2_n} \tag{48.18}$$

and the masses M_n need to agree with those in $V_{\rm R}$. The function $p_a(s)$ is a background term and the α^H_n denote the coupling of the heavy state H to the particular resonance R_n. If there are additional particles in the final state of the studied decay of the heavy state H, not included in the non-perturbative treatment of Eq. (48.17), then they also contain the corresponding kinematic factors related to their coupling. If these additional particles are interacting strongly, a complete few–body treatment of the final state becomes necessary, especially since rescattering effects can introduce additional complex phases [18]. However, in practice those effects as well as those from missing channels are often parametrized by choosing the parameters α^H_n complex valued. With some additional assumptions, Eq. (48.9) and Eq. (48.17) were employed in Ref. [19] to study the pion vector form factor. An alternative parametrization for the production amplitude that is convenient, if the full matrix $\mathscr{M}$ — including the resonances — is known, cf. Ref. [20]

$$\mathcal{A}^H_a(s) = \mathscr{M}_{ab}(s)\tilde{\mathcal{P}}^H_b(s)\ . \tag{48.19}$$

The function $\tilde{\mathcal{P}}_H(s)_b$ needs to cancel the left–hand cuts of $\mathscr{M}$ and therefore could be strongly energy dependent. In actual applications a low-order polynomial turned out to be sufficient — c.f. Ref. [21,22] for a study of $\gamma\gamma \to \pi\pi$. As above, to preserve unitarity the coefficients of $\tilde{\mathcal{P}}_H(s)_b$ need to be real, however, in practice rescattering effects or missing channels are parametrized by complex valued parameters.

Three-body decays are often represented by Dalitz plots. It is often of interest to quantify the contribution of a single amplitude $\mathcal{A}^H_a$ to the decay of a heavy resonance H, where now $\mathcal{A}^H_a$ needs to be generalized to three body kinematics either completely by considering the full three–body final state interactions or effectively by choosing complex vertex parameters. Then fractional contributions are introduced (since different intermediate states leading to the same final state interfere, the assignment of branching ratios is to be taken with some caution) via

$$\mathrm{F}^H_a = \frac{\int d\Phi |\mathcal{A}^H_a|^2}{\int d\Phi |\sum_a \mathcal{A}^H_a|^2} \tag{48.20}$$

where the phase space integral $d\Phi$ extends over the Dalitz plot region and the angular dependence of the subsystems needs to be kept (cf. Eq. (48.6)). Typically the effect of interference terms in the denominator is small.

The formulas given so far are completely general. However, they require as input, e.g., information on all relevant channels. It is therefore often necessary and appropriate to find approximations/parameterizations.

48.2. Common parameterizations for resonances

In most common parameterizations the non–pole interaction, $\mathscr{M}^{\rm b.g.}$, is omitted. While this is a bad approximation for, e.g., scalar–isoscalar $\pi\pi$ interactions at very low energies [23], under more favorable conditions this can be justified. Thus in what follows we will assume $\mathscr{M}^{\rm b.g.} = 0$, which leads to real vertex functions. For two–body channels one writes

$$\gamma(s)_a = q_a^{L_a} F_{L_a}(q_a, q_{\rm o})\ ,$$

where L_a denotes the angular momentum of the decay products, giving rise to the centrifugal barrier $q_a^{L_a}$, where q_a denotes the relative momentum of the outgoing particle pair defined in the rest frame of the decaying particle, cf. Eq. (20a) of the kinematics review. Often one introduces a phenomenological form factor, here denoted by $F_{L_a}(q_a, q_{\rm o})$. It depends on the channel momentum as well as some intrinsic scale $q_{\rm o}$. Often the Blatt-Weisskopf form is chosen [24,25], where, e.g., $F^2_0 = 1$, $F^2_1 = 2/(q_a + q_{\rm o})$ and $F^2_2 = 13/((q_a - 3q_{\rm o})^2 + 9q_a q_{\rm o})$. In addition, for isolated, narrow resonances the couplings g_a can be related to the partial widths, $\Gamma_{\mathrm{R}\to a}$, via

$$g_a = \frac{1}{\gamma_a(s_{\rm R})} \sqrt{\frac{M_{\rm R}\Gamma_{\mathrm{R}\to a}}{\rho_a}}\ , \tag{48.21}$$

where $M_{\rm R}$ was defined in Eq. (48.10).

48.2.1. *The Breit–Wigner and Flatté Parametrizations* :

If there is only a single resonance present and all relevant thresholds are far away, then one may replace $\Gamma_{\rm R}(s)_{\rm tot}$ with a constant, $\Gamma_{\rm BW}$. Under these conditions also the real part of Σ is a constant that can be absorbed into the mass parameter and Eq. (48.15) simplifies to

$$\mathscr{M}^{\rm pole}_{ba}\Big|_{N=1} = -\frac{g_b\ g_a}{s - M^2_{\rm BW} + i\sqrt{s}\Gamma_{\rm BW}}\ , \tag{48.22}$$

which is the standard Breit–Wigner parametrization. For a narrow resonance it is common to replace $\sqrt{s}$ by $M_{\rm BW}$. If there are nearby relevant thresholds, $\Gamma_{\rm BW}$ needs to be replaced by $\Gamma(s)$. For two–body decays one writes

$$\Gamma(s) = \sum_c \Gamma_{\mathrm{R}\to c} \left(\frac{q_c}{q_{\mathrm{R}\,c}}\right)^{2L_c+1} \left(\frac{M_R}{\sqrt{s}}\right) \left(\frac{F_{L_c}(q_c, q_{\rm o})}{F_{L_c}(q_{\mathrm{R}\,c}, q_{\rm o})}\right)^2\ , \tag{48.23}$$

where $q_{\mathrm{R}\,c} = q(M_{\rm BW})_c$ denotes the decay momentum of resonance R into channel c. The Breit-Wigner parameters $M_{\rm BW}$ and $\Gamma_{\rm BW}$ agree with the pole parameters only if $M_{\rm R}\Gamma(M_{\rm R}) \ll M^2_{\rm thr.} - M^2_{\rm R}$, with $M_{\rm thr.}$ for the closest relevant threshold. Otherwise the Breit-Wigner parameters deviate from the pole parameters and are reaction dependent.

If there is more than one resonance in one partial wave that significantly couples to the same channels, it is in general incorrect to use a sum of Breit-Wigner functions, for it may violate unitarity constraints. Then more refined methods should be used, like the K–matrix approximation described in the next section.

Below the corresponding threshold, q_c in Eq. (48.23) must be continued analytically: if, e.g., the particles in channel c have equal mass m_c, then

$$q_c = \frac{i}{2}\sqrt{4m_c^2 - s} \quad \text{for} \quad \sqrt{s} < 2m_c\ . \tag{48.24}$$

The resulting line shape above and below the threshold of channel c is called Flatté parametrization [26]. If the coupling of a resonance to the channel opening nearby is very strong, the Flatté parametrization shows a scaling invariance and does not allow for an extraction of individual partial decay widths, but only of ratios [27].

48.2.2. *The K–matrix approximation* :

As soon as there is more than one resonance in one channel, the use of the K–matrix approximation should be preferred compared to the Breit–Wigner parametrization discussed above. From the considerations formulated in Eq. (48.11), the K–matrix approximation follows straightforwardly by replacing the self-energy Σ_c by its imaginary part in the absence of $\mathscr{M}^{\rm b.g.}$, but keeping the full matrix structure of $V^{\rm R}$. Thus, for two–body intermediate states one writes within this scheme for the self-energy

$$\Sigma(s)_c \to i\rho_c\gamma(s)^2_c\ . \tag{48.25}$$

However, in distinction to the Breit-Wigner approach, $V^{\rm R}$, then called K–matrix, is kept in the form of Eq. (48.12). The decay amplitude given in Eq. (48.17) then takes the form of the standard P–vector formalism introduced in Ref. [28]. For $N = 1$ the amplitude derived from the K–matrix is identical to that of Eq. (48.22).

Some authors use the analytic continuation of ρ_c below the threshold via the analytic continuation of the particle momentum as described above [29,30].

48.2.3. *Further improvements* :

The K–matrix described above usually allows one to get a proper fit of physical amplitudes and it is easy to deal with, however, it also has an important deficit: it violates constraints from analyticity — e.g., ρ_a, defined in Eq. (48.2), is ill-defined at $s = 0$ and for unequal masses develops an unphysical cut. In addition, the analytic continuation of the amplitudes into the complex plane is not controlled and typically the parameters of broad resonances come out wrong (see, e.g., minireview on scalar mesons). A method to improve the analytic properties was suggested in Refs. [31–34]. It basically

amounts to replacing the phase-space factor $i\rho_a$ in Eq. (48.25) by an analytic function that produces the identical imaginary part on the right-hand cut. In the simplest case of a channel with equal masses the expressions that can be used for real values of s read

$$-\frac{\hat{\rho}_a}{\pi}\log\left|\frac{1+\hat{\rho}_a}{1-\hat{\rho}_a}\right|,\ -\frac{2\hat{\rho}_a}{\pi}\arctan\left(\frac{1}{\hat{\rho}_a}\right),\ -\frac{\hat{\rho}_a}{\pi}\log\left|\frac{1+\hat{\rho}_a}{1-\hat{\rho}_a}\right|+i\hat{\rho}_a$$

for $s<0$, $0<s<4m_a^2$, and $4m_a^2<s$, respectively, with $\hat{\rho}_a=\sqrt{|1-4m_a^2/s|}$ for all values of s, extending the expression of Eq. (48.2) into the regime below threshold. The more complicated expression for the case of different masses can be found, e.g., in Ref. [32].

If there is only a single resonance in a given channel, it is possible to feed the imaginary part of the Breit-Wigner function, Eq. (48.22) with an energy-dependent width, directly into a dispersion integral to get a resonance propagator with the correct analytic structure [35,36].

48.3. Properties of resonances

A resonance is characterized not only by its complex pole position but also by its residues that quantify its couplings to the various channels and allow one to define a branching ratio also for broader resonances. In the Meson Particle Listings the two-photon width of $f_0(500)$ is defined in terms of the corresponding residue. The Baryon Particle Listings give the elastic pole residues and normalized transition residues. However, different conventions are used in the two sectors, which are shortly outlined here.

In the close vicinity of a pole the scattering matrix $\mathscr{M}$ can be written as

$$\lim_{s\to s_R}\mathscr{M}_{ba}=-\frac{\mathscr{R}_{ba}}{s-s_{\rm R}}\ , \tag{48.26}$$

where $s_{\rm R}$ denotes the pole position of the resonance R. The sign convention in Eq. (48.26) is consistent with that of Eq. (48.12). The residues may be calculated via an integration along a closed contour around the pole using

$$\mathscr{R}_{ba}=\frac{i}{2\pi}\oint ds.\mathscr{M}_{ba}\ .$$

The factorization of the residue $(\mathscr{R}_{ba})^2=\mathscr{R}_{aa}\times\mathscr{R}_{bb}$ allows one to introduce pole couplings according to

$$\tilde{g}_a=\mathscr{R}_{ba}/\sqrt{\mathscr{R}_{bb}}\ . \tag{48.27}$$

The pole couplings are the only quantities that allow one quantify the transition strength of a given resonance to some channel a independent of how the particular resonance got produced. For a single, narrow state with an energy-independent background in the resonance region, far away from all relevant thresholds one finds $\tilde{g}_a=\gamma_a(s_{\rm R})g_a$ with the real valued resonance couplings g_a defined in Eq. (48.12) accompanied by the complex valued vertex functions γ_a introduced in Eq. (48.11). Based on this observation one may use the straightforward generalization of Eq. (48.21) to define a partial width and a branching fraction even for a broad resonance via

$$\Gamma_{{\rm R}\to a}=\frac{|\tilde{g}_a|^2}{M_{\rm R}}\rho_a(M_{\rm R}^2)\quad\text{and}\quad Br_a=\Gamma_{{\rm R}\to a}/\Gamma_{\rm R}\ , \tag{48.28}$$

where $M_{\rm R}$ and $\Gamma_{\rm R}$ were introduced in Eq. (48.10). This expression was used to define a two–photon width for the broad $f_0(500)$ (also called σ) [21,22]. Eq. (48.28) defines a partial decay width independent of the reaction used to extract the parameters. It maps smoothly onto the standard definitions for narrow resonances — cf. Eq. (48.16). There are cases where a resonance couples to a channel that opens only above $M_{\rm R}$. A prominent example for this being $f_0(980)$ to $\bar{K}K$. If one wants to define a branching fraction that also captures this situation one may define

$$Br'_a=\int\limits_{\rm threshold}^{\infty}\frac{ds}{\pi}\frac{|\tilde{g}_a|^2\rho(s)}{|D(s)|^2}\ . \tag{48.29}$$

Here one needs to assume a line shape for the resonance R. A possible choice is a Flatté form

$$|D(s)|^2=(M_{\rm R}^2-s)^2+(\sum_a|\tilde{g}_a|^2\rho_a(s))^2\ . \tag{48.30}$$

If the s–dependence of the phase space factors is large (as is the case, e.g., for multi–particle final states) the spectral shape that emerges from the choice in Eq. (48.30) may deviate significantly from what one would expect from the corresponding pole in the complex plane. In those situations it might be appropriate to refine the parameters of Eq. (48.29) somewhat as was suggested, e.g., in Ref. [38]. In any case the only model-independent quantities are the pole couplings/residues — both forms, Eq. (48.28) and Eq. (48.29), are in general not directly related to observables but only meant to quantify the effect of the pole couplings by employing better known quantities.

In the baryon sector it is common to define the residue with respect to the partial-wave amplitudes $f_{ba}(s)$ defined in Eq. (48.7) and with respect to $\sqrt{s}$ instead of s. Accordingly in the baryon listings the elastic pole residue, which refers to $\pi N\to\pi N$ scattering, is related to the residues introduced above via

$$r=\frac{\rho_{\pi N}(s_{\rm R})}{\sqrt{4s_{\rm R}}}\mathscr{R}_{\pi N,\pi N}\ , \tag{48.31}$$

where the phase space factor is to be evaluated at the pole.

References:

1. M. Jacob and G.C. Wick, Annals Phys. **7**, 404 (1959) [Annals Phys. **281**, 774 (2000)].
2. C. Zemach, Phys. Rev. **140B**, 97, 109 (1965).
3. A.V. Anisovich *et al.*, J. Phys. G **28**, 15 (2002), Eur. Phys. J. A **24**, 111 (2005).
4. A rapid change in an amplitude is not an unambiguous signal of a singularity of the S–matrix [37], however, for realistic interactions this connection holds.
5. G. Höhler, *Pion-Nucleon Scattering – Methods and Results of Phenomenological Analyses*, Springer-Verlag Berlin, Heidelberg, New York, 1983.
6. M. Fukugita and K. Igi, Phys. Rept. **31** (1977) 237.
7. M.P. Peskin and D.V. Schroeder, *An Introduction to Quantum Field Theory*, Westview Press, 1995.
8. R. Omnes, Nuovo Cim. **8**, 316 (1958).
9. N.N. Khuri and S.B. Treiman, Phys. Rev. **119**, 1115 (1960).
10. J. Kambor, C. Wiesendanger and D. Wyler, Nucl. Phys. B **465**, 215 (1996).
11. A.V. Anisovich and H. Leutwyler, Phys. Lett. B **375**, 335 (1996).
12. S.P. Schneider, B. Kubis and C. Ditsche, JHEP **1102**, 028 (2011).
13. F. Niecknig, B. Kubis and S.P. Schneider, Eur. Phys. J. C **72**, 2014 (2012).
14. D. Djukanovic, J. Gegelia and S. Scherer, Phys. Rev. D **76** (2007) 037501.
15. N.N. Achasov and G.N. Shestakov, Phys. Rev. D **86**, 114013 (2012).
16. A. Matsuyama, T. Sato and T.-S.H. Lee, Phys. Rept. **439**, 193 (2007).
17. M. Döring et al., Phys. Lett. B **681**, 26 (2009).
18. I. Caprini, Phys. Lett. B **638**, 468 (2006).
19. C. Hanhart, Phys. Lett. B **715**, 170 (2012).
20. K.L. Au, D. Morgan and M.R. Pennington, Phys. Rev. D **35**, 1633 (1987).
21. D. Morgan and M.R. Pennington, Z. Phys. C **37** (1988) 431 [Erratum-ibid. C **39** (1988) 590].
22. D. Morgan and M.R. Pennington, Z. Phys. **C48**, 623 (1990).
23. J. Gasser and U.G. Meißner, Nucl. Phys. B **357**, 90 (1991).
24. J. Blatt and V. Weisskopf, *Theoretical Nuclear Physics*, New York: John Wiley & Sons (1952).
25. S.U. Chung *et al.*, Annalen Phys. **4**, 404 (1995).
26. S.M. Flatté, Phys. Lett. B **63**, 224 (1976).
27. V. Baru *et al.*, Eur. Phys. J. A **23**, 523 (2005).
28. I.J.R. Aitchison, Nucl. Phys. **A189**, 417 (1972).
29. J.H. Reid and N.N. Trofimenkoff, J. Math. Phys. **25**, 3540 (1984)..

30. V.V. Anisovich and A.V. Sarantsev, Eur. Phys. J. A **16**, 229 (2003).
31. M.R. Pennington *et al.*, Eur. Phys. J. **C56**, 1 (2008).
32. J.A. Oller and E. Oset, Phys. Rev. D **60**, 074023 (1999).
33. N.N. Achasov and A.V. Kiselev, Phys. Rev. D **83**, 054008 (2011).
34. A.V. Anisovich *et al.*, Phys. Rev. D **84**, 076001 (2011).
35. E.L. Lomon and S. Pacetti, Phys. Rev. D **85**, 113004 (2012) [Erratum-ibid. D **86**, 039901 (2012)].
36. B. Moussallam, Eur. Phys. J. C **73** (2013) 2539.
37. G. Calucci, L. Fonda and G.C. Ghirardi, Phys. Rev. **166**, 1719 (1968).
38. A.V. Anisovich *et al.*, Phys. Lett. B **772** (2017) 247.

49. Cross-section formulae for specific processes

Revised October 2009 by H. Baer (University of Oklahoma) and R.N. Cahn (LBNL).

PART I: STANDARD MODEL PROCESSES

Setting aside leptoproduction (for which, see Sec. 16 of this *Review*), the cross sections of primary interest are those with light incident particles, e^+e^-, $\gamma\gamma$, $q\overline{q}$, gq , gg, *etc.*, where g and q represent gluons and light quarks. The produced particles include both light particles and heavy ones - t, W, Z, and the Higgs boson H. We provide the production cross sections calculated within the Standard Model for several such processes.

49.1. Resonance Formation

Resonant cross sections are generally described by the Breit-Wigner formula (Sec. 18 of this *Review*).

$$\sigma(E) = \frac{2J+1}{(2S_1+1)(2S_2+1)}\frac{4\pi}{k^2}\left[\frac{\Gamma^2/4}{(E-E_0)^2+\Gamma^2/4}\right]B_{in}B_{out}, \quad (49.1)$$

where E is the c.m. energy, J is the spin of the resonance, and the number of polarization states of the two incident particles are $2S_1+1$ and $2S_2+1$. The c.m. momentum in the initial state is k, E_0 is the c.m. energy at the resonance, and Γ is the full width at half maximum height of the resonance. The branching fraction for the resonance into the initial-state channel is B_{in} and into the final-state channel is B_{out}. For a narrow resonance, the factor in square brackets may be replaced by $\pi\Gamma\delta(E-E_0)/2$.

49.2. Production of light particles

The production of point-like, spin-1/2 fermions in e^+e^- annihilation through a virtual photon, $e^+e^- \to \gamma^* \to f\overline{f}$, at c.m. energy squared s is given by

$$\frac{d\sigma}{d\Omega} = N_c\frac{\alpha^2}{4s}\beta\left[1+\cos^2\theta+(1-\beta^2)\sin^2\theta\right]Q_f^2 \ , \quad (49.2)$$

where β is v/c for the produced fermions in the c.m., θ is the c.m. scattering angle, and Q_f is the charge of the fermion. The factor N_c is 1 for charged leptons and 3 for quarks. In the ultrarelativistic limit, $\beta \to 1$,

$$\sigma = N_cQ_f^2\frac{4\pi\alpha^2}{3s} = N_cQ_f^2\frac{86.8\text{ nb}}{s\,(\text{GeV}^2)} \ . \quad (49.3)$$

The cross section for the annihilation of a $q\overline{q}$ pair into a distinct pair $q'\overline{q}'$ through a gluon is completely analogous up to color factors, with the replacement $\alpha \to \alpha_s$. Treating all quarks as massless, averaging over the colors of the initial quarks and defining $t = -s\sin^2(\theta/2)$, $u = -s\cos^2(\theta/2)$, one finds [1]

$$\frac{d\sigma}{d\Omega}(q\overline{q} \to q'\overline{q}') = \frac{\alpha_s^2}{9s}\frac{t^2+u^2}{s^2} \ . \quad (49.4)$$

Crossing symmetry gives

$$\frac{d\sigma}{d\Omega}(qq' \to qq') = \frac{\alpha_s^2}{9s}\frac{s^2+u^2}{t^2} \ . \quad (49.5)$$

If the quarks q and q' are identical, we have

$$\frac{d\sigma}{d\Omega}(q\overline{q} \to q\overline{q}) = \frac{\alpha_s^2}{9s}\left[\frac{t^2+u^2}{s^2}+\frac{s^2+u^2}{t^2}-\frac{2u^2}{3st}\right] \ , \quad (49.6)$$

and by crossing

$$\frac{d\sigma}{d\Omega}(qq \to qq) = \frac{\alpha_s^2}{9s}\left[\frac{t^2+s^2}{u^2}+\frac{s^2+u^2}{t^2}-\frac{2s^2}{3ut}\right] . \quad (49.7)$$

Annihilation of e^+e^- into $\gamma\gamma$ has the cross section

$$\frac{d\sigma}{d\Omega}(e^+e^- \to \gamma\gamma) = \frac{\alpha^2}{2s}\frac{u^2+t^2}{tu} \ . \quad (49.8)$$

The related QCD process also has a triple-gluon coupling. The cross section is

$$\frac{d\sigma}{d\Omega}(q\overline{q} \to gg) = \frac{8\alpha_s^2}{27s}(t^2+u^2)\left(\frac{1}{tu}-\frac{9}{4s^2}\right) \ . \quad (49.9)$$

The crossed reactions are

$$\frac{d\sigma}{d\Omega}(qg \to qg) = \frac{\alpha_s^2}{9s}(s^2+u^2)(-\frac{1}{su}+\frac{9}{4t^2}) \quad (49.10)$$

and

$$\frac{d\sigma}{d\Omega}(gg \to q\overline{q}) = \frac{\alpha_s^2}{24s}(t^2+u^2)(\frac{1}{tu}-\frac{9}{4s^2}) \ . \quad (49.11)$$

Finally,

$$\frac{d\sigma}{d\Omega}(gg \to gg) = \frac{9\alpha_s^2}{8s}(3-\frac{ut}{s^2}-\frac{su}{t^2}-\frac{st}{u^2}) \ . \quad (49.12)$$

Lepton-quark scattering is analogous (neglecting Z exchange)

$$\frac{d\sigma}{d\Omega}(eq \to eq) = \frac{\alpha^2}{2s}e_q^2\frac{s^2+u^2}{t^2} \ . \quad (49.13)$$

where e_q is the charge of the quark. For neutrino scattering with the four-Fermi interaction

$$\frac{d\sigma}{d\Omega}(\nu d \to \ell^- u) = \frac{G_F^2 s}{4\pi^2} \ , \quad (49.14)$$

where the Cabibbo angle suppression is ignored. Similarly

$$\frac{d\sigma}{d\Omega}(\nu\overline{u} \to \ell^-\overline{d}) = \frac{G_F^2 s}{4\pi^2}\frac{(1+\cos\theta)^2}{4} \ . \quad (49.15)$$

To obtain the formulae for deep inelastic scattering (presented in more detail in Section 16) we consider quarks of type i carrying a fraction $x = Q^2/(2M\nu)$ of the nucleon's energy, where $\nu = E-E'$ is the energy lost by the lepton in the nucleon rest frame. With $y = \nu/E$ we have the correspondences

$$1+\cos\theta \to 2(1-y) \ ,$$
$$d\Omega_{cm} \to 4\pi f_i(x)dx\,dy \ , \quad (49.16)$$

where the latter incorporates the quark distribution, $f_i(x)$. In this way we find

$$\frac{d\sigma}{dx\,dy}(eN \to eX) = \frac{4\pi\alpha^2 xs}{Q^4}\frac{1}{2}\left[1+(1-y)^2\right] \times \left[\frac{4}{9}(u(x)+\overline{u}(x)+\ldots)+\frac{1}{9}(d(x)+\overline{d}(x)+\ldots)\right] \quad (49.17)$$

where now $s = 2ME$ is the cm energy squared for the electron-nucleon collision and we have suppressed contributions from higher mass quarks.

Similarly,

$$\frac{d\sigma}{dx\,dy}(\nu N \to \ell^- X) = \frac{G_F^2 xs}{\pi}[(d(x)+\ldots)+(1-y)^2(\overline{u}(x)+\ldots)] \quad (49.18)$$

and

$$\frac{d\sigma}{dx\,dy}(\overline{\nu}N \to \ell^+ X) = \frac{G_F^2 xs}{\pi}[(\overline{d}(x)+\ldots)+(1-y)^2(u(x)+\ldots)] \ . \quad (49.19)$$

Quasi-elastic neutrino scattering ($\nu_\mu n \to \mu^- p$, $\overline{\nu}_\mu p \to \mu^+ n$) is directly related to the crossed reaction, neutron decay. The formula for the differential cross section is presented, for example, in N.J. Baker *et al.*, Phys. Rev. **D23**, 2499 (1981).

49.3. Hadroproduction of heavy quarks

For hadroproduction of heavy quarks $Q = c,\ b,\ t$, it is important to include mass effects in the formulae. For $q\bar{q} \to Q\bar{Q}$, one has

$$\frac{d\sigma}{d\Omega}(q\bar{q} \to Q\bar{Q}) = \frac{\alpha_s^2}{9s^3}\sqrt{1-\frac{4m_Q^2}{s}}\left[(m_Q^2-t)^2+(m_Q^2-u)^2+2m_Q^2 s\right], \tag{49.20}$$

while for $gg \to Q\bar{Q}$ one has

$$\begin{aligned}\frac{d\sigma}{d\Omega}(gg \to Q\bar{Q}) = \frac{\alpha_s^2}{32s}\sqrt{1-\frac{4m_Q^2}{s}}\Bigg[&\frac{6}{s^2}(m_Q^2-t)(m_Q^2-u)\\ &-\frac{m_Q^2(s-4m_Q^2)}{3(m_Q^2-t)(m_Q^2-u)}\\ &+\frac{4}{3}\frac{(m_Q^2-t)(m_Q^2-u)-2m_Q^2(m_Q^2+t)}{(m_Q^2-t)^2}\\ &+\frac{4}{3}\frac{(m_Q^2-t)(m_Q^2-u)-2m_Q^2(m_Q^2+u)}{(m_Q^2-u)^2}\\ &-3\,\frac{(m_Q^2-t)(m_Q^2-u)+m_Q^2(u-t)}{s(m_Q^2-t)}\\ &-3\,\frac{(m_Q^2-t)(m_Q^2-u)+m_Q^2(t-u)}{s(m_Q^2-u)}\Bigg].\end{aligned} \tag{49.21}$$

49.4. Production of Weak Gauge Bosons

49.4.1. ***W and Z resonant production*** :

Resonant production of a single W or Z is governed by the partial widths

$$\Gamma(W \to \ell_i \overline{\nu}_i) = \frac{\sqrt{2}G_F m_W^3}{12\pi} \tag{49.22}$$

$$\Gamma(W \to q_i \overline{q}_j) = 3\frac{\sqrt{2}G_F|V_{ij}|^2 m_W^3}{12\pi} \tag{49.23}$$

$$\Gamma(Z \to f\overline{f}) = N_c\frac{\sqrt{2}G_F m_Z^3}{6\pi} \times\left[(T_3 - Q_f\sin^2\theta_W)^2+(Q_f\sin^2\theta_W)^2\right] \tag{49.24}$$

The weak mixing angle is θ_W. The CKM matrix elements are indicated by V_{ij} and N_c is 3 for $q\overline{q}$ final states and 1 for leptonic final states.

The full differential cross section for $f_i\overline{f}_j \to (W,Z) \to f_{i'}\overline{f}_{j'}$ is given by

$$\begin{aligned}\frac{d\sigma}{d\Omega} = \frac{N_c^f}{N_c^i}\cdot\frac{1}{256\pi^2 s}\cdot\frac{s^2}{(s-M^2)^2+s\Gamma^2}\\ \times\Big[(L^2+R^2)(L'^2+R'^2)(1+\cos^2\theta)\\ +(L^2-R^2)(L'^2-R'^2)2\,cos\theta\Big]\end{aligned} \tag{49.25}$$

where M is the mass of the W or Z. The couplings for the W are $L = (8G_F m_W^2/\sqrt{2})^{1/2}V_{ij}/\sqrt{2}; R = 0$ where V_{ij} is the corresponding CKM matrix element, with an analogous expression for L' and R'. For Z, the couplings are $L = (8G_F m_Z^2/\sqrt{2})^{1/2}(T_3 - \sin^2\theta_W Q); R = -(8G_F m_Z^2/\sqrt{2})^{1/2}\sin^2\theta_W Q$, where T_3 is the weak isospin of the initial left-handed fermion and Q is the initial fermion's electric charge. The expressions for L' and R' are analogous. The color factors $N_c^{i,f}$ are 3 for initial or final quarks and 1 for initial or final leptons.

49.4.2. ***Production of pairs of weak gauge bosons*** :

The cross section for $f\overline{f} \to W^+W^-$ is given in term of the couplings of the left-handed and right-handed fermion f, $\ell = 2(T_3 - Qx_W)$, $r = -2Qx_W$, where T_3 is the third component of weak isospin for the left-handed f, Q is its electric charge (in units of the proton charge), and $x_W = \sin^2\theta_W$:

$$\begin{aligned}\frac{d\sigma}{dt} = \frac{2\pi\alpha^2}{N_c s^2}\Bigg\{&\left[\left(Q+\frac{\ell+r}{4x_W}\frac{s}{s-m_Z^2}\right)^2+\left(\frac{\ell-r}{4x_W}\frac{s}{s-m_Z^2}\right)^2\right]A(s,t,u)\\ &+\frac{1}{2x_W}\left(Q+\frac{\ell}{2x_W}\frac{s}{s-m_Z^2}\right)(\Theta(-Q)I(s,t,u)-\Theta(Q)I(s,u,t))\\ &+\frac{1}{8x_W^2}(\Theta(-Q)E(s,t,u)+\Theta(Q)E(s,u,t))\Bigg\},\end{aligned} \tag{49.26}$$

where $\Theta(x)$ is 1 for $x > 0$ and 0 for $x < 0$, and where

$$\begin{aligned}A(s,t,u) &= \left(\frac{tu}{m_W^4}-1\right)\left(\frac{1}{4}-\frac{m_W^2}{s}+3\frac{m_W^4}{s^2}\right)+\frac{s}{m_W^2}-4,\\ I(s,t,u) &= \left(\frac{tu}{m_W^4}-1\right)\left(\frac{1}{4}-\frac{m_W^2}{2s}-\frac{m_W^4}{st}\right)+\frac{s}{m_W^2}-2+2\frac{m_W^2}{t},\\ E(s,t,u) &= \left(\frac{tu}{m_W^4}-1\right)\left(\frac{1}{4}+\frac{m_W^4}{t^2}\right)+\frac{s}{m_W^2},\end{aligned} \tag{49.27}$$

and s,t,u are the usual Mandelstam variables with $s = (p_f + p_{\overline{f}})^2, t = (p_f - p_{W^-})^2, u = (p_f - p_{W^+})^2$. The factor N_c is 3 for quarks and 1 for leptons.

The analogous cross-section for $q_i\overline{q}_j \to W^\pm Z^0$ is

$$\begin{aligned}\frac{d\sigma}{dt} = \frac{\pi\alpha^2|V_{ij}|^2}{6s^2x_W^2}\Bigg\{&\left(\frac{1}{s-m_W^2}\right)^2\left[\left(\frac{9-8x_W}{4}\right)\left(ut-m_W^2m_Z^2\right)\right.\\ &\left.+(8x_W-6)\,s\left(m_W^2+m_Z^2\right)\right]\\ &+\left[\frac{ut-m_W^2m_Z^2-s(m_W^2+m_Z^2)}{s-m_W^2}\right]\left[\frac{\ell_j}{t}-\frac{\ell_i}{u}\right]\\ &+\frac{ut-m_W^2m_Z^2}{4(1-x_W)}\left[\frac{\ell_j^2}{t^2}+\frac{\ell_i^2}{u^2}\right]+\frac{s(m_W^2+m_Z^2)}{2(1-x_W)}\frac{\ell_i\ell_j}{tu}\Bigg\},\end{aligned} \tag{49.28}$$

where ℓ_i and ℓ_j are the couplings of the left-handed q_i and q_j as defined above. The CKM matrix element between q_i and q_j is V_{ij}.

The cross section for $q_i\overline{q}_i \to Z^0Z^0$ is

$$\frac{d\sigma}{dt} = \frac{\pi\alpha^2}{96}\frac{\ell_i^4+r_i^4}{x_W^2(1-x_W^2)^2s^2}\left[\frac{t}{u}+\frac{u}{t}+\frac{4m_Z^2s}{tu}-m_Z^4\left(\frac{1}{t^2}+\frac{1}{u^2}\right)\right]. \tag{49.29}$$

49.5. Production of Higgs Bosons

49.5.1. ***Resonant Production*** : The Higgs boson of the Standard Model can be produced resonantly in the collisions of quarks, leptons, W or Z bosons, gluons, or photons. The production cross section is thus controlled by the partial width of the Higgs boson into the entrance channel and its total width. The branching fractions for the Standard Model Higgs boson are shown in Fig. 1 of the "Searches for Higgs bosons" review in the Particle Listings section, as a function of the Higgs boson mass. The partial widths are given by the relations

$$\Gamma(H \to f\overline{f}) = \frac{G_F m_f^2 m_H N_c}{4\pi\sqrt{2}}\left(1-4m_f^2/m_H^2\right)^{3/2}, \tag{49.30}$$

$$\Gamma(H \to W^+W^-) = \frac{G_F m_H^3\beta_W}{32\pi\sqrt{2}}\left(4-4a_W+3a_W^2\right), \tag{49.31}$$

$$\Gamma(H \to ZZ) = \frac{G_F m_H^3\beta_Z}{64\pi\sqrt{2}}\left(4-4a_Z+3a_Z^2\right), \tag{49.32}$$

where N_c is 3 for quarks and 1 for leptons and where $a_W = 1 - \beta_W^2 = 4m_W^2/m_H^2$ and $a_Z = 1 - \beta_Z^2 = 4m_Z^2/m_H^2$. The decay to two gluons proceeds through quark loops, with the t quark dominating [2]. Explicitly,

$$\Gamma(H \to gg) = \frac{\alpha_s^2 G_F m_H^3}{36\pi^3\sqrt{2}} \left| \sum_q I(m_q^2/m_H^2) \right|^2 , \tag{49.33}$$

where $I(z)$ is complex for $z < 1/4$. For $z < 2 \times 10^{-3}$, $|I(z)|$ is small so the light quarks contribute negligibly. For $m_H < 2m_t$, $z > 1/4$ and

$$I(z) = 3\left[2z + 2z(1-4z)\left(\sin^{-1}\frac{1}{2\sqrt{z}}\right)^2\right], \tag{49.34}$$

which has the limit $I(z) \to 1$ as $z \to \infty$.

49.5.2. *Higgs Boson Production in W^* and Z^* decay* :

The Standard Model Higgs boson can be produced in the decay of a virtual W or Z ("Higgstrahlung") [3,4]: In particular, if k is the c.m. momentum of the Higgs boson,

$$\sigma(q_i\overline{q}_j \to WH) = \frac{\pi\alpha^2|V_{ij}|^2}{36\sin^4\theta_W}\frac{2k}{\sqrt{s}}\frac{k^2+3m_W^2}{(s-m_W^2)^2} \tag{49.35}$$

$$\sigma(f\overline{f} \to ZH) = \frac{2\pi\alpha^2(\ell_f^2+r_f^2)}{48N_c\sin^4\theta_W\cos^4\theta_W}\frac{2k}{\sqrt{s}}\frac{k^2+3m_Z^2}{(s-m_Z^2)^2}, \tag{49.36}$$

where ℓ and r are defined as above.

49.5.3. *W and Z Fusion* :

Just as high-energy electrons can be regarded as sources of virtual photon beams, at very high energies they are sources of virtual W and Z beams. For Higgs boson production, it is the longitudinal components of the Ws and Zs that are important [5]. The distribution of longitudinal Ws carrying a fraction y of the electron's energy is [6]

$$f(y) = \frac{g^2}{16\pi^2}\frac{1-y}{y}, \tag{49.37}$$

where $g = e/\sin\theta_W$. In the limit $s \gg m_H \gg m_W$, the partial decay rate is $\Gamma(H \to W_L W_L) = (g^2/64\pi)(m_H^3/m_W^2)$ and in the equivalent W approximation [7]

$$\sigma(e^+e^- \to \overline{\nu}_e\nu_e H) = \frac{1}{16m_W^2}\left(\frac{\alpha}{\sin^2\theta_W}\right)^3 \times \left[\left(1+\frac{m_H^2}{s}\right)\log\frac{s}{m_H^2} - 2 + 2\frac{m_H^2}{s}\right]. \tag{49.38}$$

There are significant corrections to this relation when m_H is not large compared to m_W [8]. For $m_H = 150$ GeV, the estimate is too high by 51% for $\sqrt{s} = 1000$ GeV, 32% too high at $\sqrt{s} = 2000$ GeV, and 22% too high at $\sqrt{s} = 4000$ GeV. Fusion of ZZ to make a Higgs boson can be treated similarly. Identical formulae apply for Higgs production in the collisions of quarks whose charges permit the emission of a W^+ and a W^-, except that QCD corrections and CKM matrix elements are required. Even in the absence of QCD corrections, the fine-structure constant ought to be evaluated at the scale of the collision, say m_W. All quarks contribute to the ZZ fusion process.

49.6. Inclusive hadronic reactions

One-particle inclusive cross sections $Ed^3\sigma/d^3p$ for the production of a particle of momentum p are conveniently expressed in terms of rapidity y (see above) and the momentum p_T transverse to the beam direction (in the c.m.):

$$E\frac{d^3\sigma}{d^3p} = \frac{d^3\sigma}{d\phi\, dy\, p_T dp_T^2} . \tag{49.39}$$

In appropriate circumstances, the cross section may be decomposed as a partonic cross section multiplied by the probabilities of finding partons of the prescribed momenta:

$$\sigma_{\rm hadronic} = \sum_{ij}\int dx_1\, dx_2\, f_i(x_1)\, f_j(x_2)\, d\hat{\sigma}_{\rm partonic} , \tag{49.40}$$

The probability that a parton of type i carries a fraction of the incident particle's that lies between x_1 and $x_1 + dx_1$ is $f_i(x_1)dx_1$ and similarly for partons in the other incident particle. The partonic collision is specified by its c.m. energy squared $\hat{s} = x_1x_2s$ and the momentum transfer squared $\hat{t}$. The final hadronic state is more conveniently specified by the rapidities y_1, y_2 of the two jets resulting from the collision and the transverse momentum p_T. The connection between the differentials is

$$dx_1dx_2d\hat{t} = dy_1dy_2\frac{\hat{s}}{s}dp_T^2, \tag{49.41}$$

so that

$$\frac{d^3\sigma}{dy_1dy_2dp_T^2} = \frac{\hat{s}}{s}\left[f_i(x_1)f_j(x_2)\frac{d\hat{\sigma}}{d\hat{t}}(\hat{s},\hat{t},\hat{u}) + f_i(x_2)f_j(x_1)\frac{d\hat{\sigma}}{d\hat{t}}(\hat{s},\hat{u},\hat{t})\right], \tag{49.42}$$

where we have taken into account the possibility that the incident parton types might arise from either incident particle. The second term should be dropped if the types are identical: $i = j$.

49.7. Two-photon processes

In the Weizsäcker-Williams picture, a high-energy electron beam is accompanied by a spectrum of virtual photons of energies ω and invariant-mass squared $q^2 = -Q^2$, for which the photon number density is

$$dn = \frac{\alpha}{\pi}\left[1 - \frac{\omega}{E} + \frac{\omega^2}{E^2} - \frac{m_e^2\,\omega^2}{Q^2E^2}\right]\frac{d\omega}{\omega}\frac{dQ^2}{Q^2}, \tag{49.43}$$

where E is the energy of the electron beam. The cross section for $e^+e^- \to e^+e^-X$ is then [9]

$$d\sigma_{e^+e^-\to e^+e^-X}(s) = dn_1dn_2d\sigma_{\gamma\gamma\to X}(W^2), \tag{49.44}$$

where $W^2 = m_X^2$. Integrating from the lower limit $Q^2 = m_e^2\frac{\omega_i^2}{E_i(E_i-\omega_i)}$ to a maximum Q^2 gives

$$\sigma_{e^+e^-\to e^+e^-X}(s) = \frac{\alpha^2}{\pi^2}\int_{z_{th}}^1\frac{dz}{z} \times \left[\left(\ln\frac{Q^2_{max}}{zm_e^2} - 1\right)^2 f(z) + \frac{1}{3}(\ln z)^3\right]\sigma_{\gamma\gamma\to X}(zs), \tag{49.45}$$

where

$$f(z) = \left(1+\tfrac{1}{2}z\right)^2\ln(1/z) - \tfrac{1}{2}(1-z)(3+z). \tag{49.46}$$

The appropriate value of Q^2_{max} depends on the properties of the produced system X. For production of hadronic systems, $Q^2_{max} \approx m_\rho^2$,

while for lepton-pair production, $Q^2 \approx W^2$. For production of a resonance with spin $J \neq 1$, we have

$$\sigma_{e^+e^-\to e^+e^-R}(s) = (2J+1)\frac{8\alpha^2\Gamma_{R\to\gamma\gamma}}{m_R^3} \times \left[f(m_R^2/s)\left(\ln\frac{m_V^2 s}{m_e^2 m_R^2} - 1\right)^2 - \frac{1}{3}\left(\ln\frac{s}{M_R^2}\right)^3\right], \quad (49.47)$$

where m_V is the mass that enters into the form factor for the $\gamma\gamma \to R$ transition, typically m_ρ.

PART II: PROCESSES BEYOND THE STANDARD MODEL

49.8. Production of supersymmetric particles

In supersymmetric (SUSY) theories (see Supersymmetric Particle Searches in this *Review*), every boson has a fermionic superpartner, and every fermion has a bosonic superpartner. The minimal supersymmetric Standard Model (MSSM) is a direct supersymmetrization of the Standard Model (SM), although a second Higgs doublet is needed to avoid triangle anomalies [10]. Under *soft* SUSY breaking, superpartner masses are lifted above the SM particle masses. In weak scale SUSY, the superpartners are invoked to stabilize the weak scale under radiative corrections, so the superpartners are expected to have masses of order the TeV scale.

49.8.1. *Gluino and squark production* :

The superpartners of gluons are the color octet, spin$-\frac{1}{2}$ gluinos ($\tilde{g}$), while each helicity component of quark flavor has a spin-0 *squark* partner, *e.g.* $\tilde{q}_L$ and $\tilde{q}_R$. Third generation left- and right- squarks are expected to have large mixing, resulting in mass eigenstates $\tilde{q}_1$ and $\tilde{q}_2$, with $m_{\tilde{q}_1} < m_{\tilde{q}_2}$ (here, q denotes any of the SM flavors of quarks and $\tilde{q}_i$ the corresponding flavor and type ($i = L, R$ or $1, 2$) of squark). Gluino pair production ($\tilde{g}\tilde{g}$) takes place via either glue-glue or quark-antiquark annihilation [11].

The subprocess cross sections are usually presented as differential distributions in the Mandelstam variables s, t and u. Note that for a $2 \to 2$ scattering subprocess $ab \to cd$, the Mandelstam variable $s = (p_a + p_b)^2 = (p_c + p_d)^2$, where p_a is the 4-momentum of particle a, and so forth. The variable $t = (p_c - p_a)^2$, where c and a are taken conventionally to be the most similar particles in the subprocess. The variable u would then be equal to $(p_d - p_a)^2$. Note that since s, t and u are squares of 4-vectors, they are invariants in any inertial reference frame.

Gluino pair production at hadron colliders is described by:

$$\frac{d\sigma}{dt}(gg \to \tilde{g}\tilde{g}) = \frac{9\pi\alpha_s^2}{4s^2}\left\{\frac{2(m_{\tilde{g}}^2 - t)(m_{\tilde{g}}^2 - u)}{s^2} + \frac{(m_{\tilde{g}}^2 - t)(m_{\tilde{g}}^2 - u) - 2m_{\tilde{g}}^2(m_{\tilde{g}}^2 + t)}{(m_{\tilde{g}}^2 - t)^2} + \frac{(m_{\tilde{g}}^2 - t)(m_{\tilde{g}}^2 - u) - 2m_{\tilde{g}}^2(m_{\tilde{g}}^2 + u)}{(m_{\tilde{g}}^2 - u)^2} + \frac{m_{\tilde{g}}^2(s - 4m_{\tilde{g}}^2)}{(m_{\tilde{g}}^2 - t)(m_{\tilde{g}}^2 - u)} - \frac{(m_{\tilde{g}}^2 - t)(m_{\tilde{g}}^2 - u) + m_{\tilde{g}}^2(u - t)}{s(m_{\tilde{g}}^2 - t)} - \frac{(m_{\tilde{g}}^2 - t)(m_{\tilde{g}}^2 - u) + m_{\tilde{g}}^2(t - u)}{s(m_{\tilde{g}}^2 - u)}\right\}, \quad (49.48)$$

where α_s is the strong fine structure constant. Also,

$$\frac{d\sigma}{dt}(q\bar{q} \to \tilde{g}\tilde{g}) = \frac{8\pi\alpha_s^2}{9s^2}\left\{\frac{4}{3}\left(\frac{m_{\tilde{g}}^2 - t}{m_{\tilde{q}}^2 - t}\right)^2 + \frac{4}{3}\left(\frac{m_{\tilde{g}}^2 - u}{m_{\tilde{q}}^2 - u}\right)^2 + \frac{3}{s^2}\left[(m_{\tilde{g}}^2 - t)^2 + (m_{\tilde{g}}^2 - u)^2 + 2m_{\tilde{g}}^2 s\right] - 3\frac{\left[(m_{\tilde{g}}^2 - t)^2 + m_{\tilde{g}}^2 s\right]}{s(m_{\tilde{q}}^2 - t)} - 3\frac{\left[(m_{\tilde{g}}^2 - u)^2 + m_{\tilde{g}}^2 s\right]}{s(m_{\tilde{q}}^2 - u)} + \frac{1}{3}\frac{m_{\tilde{g}}^2 s}{(m_{\tilde{q}}^2 - t)(m_{\tilde{q}}^2 - u)}\right\}. \quad (49.49)$$

Gluinos can also be produced in association with squarks: $\tilde{g}\tilde{q}_i$ production, where $\tilde{q}_i$ represents any of the various types (left-, right- or mixed) and flavors of squarks. The subprocess cross section is independent of whether the squark is the right-, left- or mixed type:

$$\frac{d\sigma}{dt}(gq \to \tilde{g}\tilde{q}_i) = \frac{\pi\alpha_s^2}{24s^2}\frac{\left[\frac{16}{3}(s^2 + (m_{\tilde{q}_i}^2 - u)^2) + \frac{4}{3}s(m_{\tilde{q}_i}^2 - u)\right]}{s(m_{\tilde{g}}^2 - t)(m_{\tilde{q}_i}^2 - u)^2} \times \left((m_{\tilde{g}}^2 - u)^2 + (m_{\tilde{q}_i}^2 - m_{\tilde{g}}^2)^2 + \frac{2sm_{\tilde{g}}^2(m_{\tilde{q}_i}^2 - m_{\tilde{g}}^2)}{(m_{\tilde{g}}^2 - t)}\right). \quad (49.50)$$

There are many different subprocesses for production of squark pairs. Since left- and right- squarks generally have different masses and different decay patterns, we present the differential cross section for each subprocess of $\tilde{q}_i$ ($i = L,\ R$ or $1,\ 2$) separately. (In early literature, the following formulae were often combined into a single equation which didn't differentiate the various squark types.) The result for $gg \to \tilde{q}_i\bar{\tilde{q}}_i$ is:

$$\frac{d\sigma}{dt}(gg \to \tilde{q}_i\bar{\tilde{q}}_i) = \frac{\pi\alpha_s^2}{4s^2}\left\{\frac{1}{3}\left(\frac{m_{\tilde{q}}^2 + t}{m_{\tilde{q}}^2 - t}\right)^2 + \frac{1}{3}\left(\frac{m_{\tilde{q}}^2 + u}{m_{\tilde{q}}^2 - u}\right)^2 + \frac{3}{32s^2}\left(8s(4m_{\tilde{q}}^2 - s) + 4(u - t)^2\right) + \frac{7}{12} - \frac{1}{48}\frac{(4m_{\tilde{q}}^2 - s)^2}{(m_{\tilde{q}}^2 - t)(m_{\tilde{q}}^2 - u)} + \frac{3}{32}\frac{\left[(t - u)(4m_{\tilde{q}}^2 + 4t - s) - 2(m_{\tilde{q}}^2 - u)(6m_{\tilde{q}}^2 + 2t - s)\right]}{s(m_{\tilde{q}}^2 - t)} + \frac{3}{32}\frac{\left[(u - t)(4m_{\tilde{q}}^2 + 4u - s) - 2(m_{\tilde{q}}^2 - t)(6m_{\tilde{q}}^2 + 2u - s)\right]}{s(m_{\tilde{q}}^2 - u)} + \frac{7}{96}\frac{\left[4m_{\tilde{q}}^2 + 4t - s\right]}{m_{\tilde{q}}^2 - t} + \frac{7}{96}\frac{\left[4m_{\tilde{q}}^2 + 4u - s\right]}{m_{\tilde{q}}^2 - u}\right\}, \quad (49.51)$$

which has an obvious $u \leftrightarrow t$ symmetry.

For $q\bar{q} \to \tilde{q}_i\bar{\tilde{q}}_i$ with the same initial and final state flavors, we have

$$\frac{d\sigma}{dt}(q\bar{q} \to \tilde{q}_i\bar{\tilde{q}}_i) = \frac{2\pi\alpha_s^2}{9s^2}\left\{\frac{1}{(t - m_{\tilde{g}}^2)^2} + \frac{2}{s^2} - \frac{2/3}{s(t - m_{\tilde{g}}^2)}\right\} \times \left[-st - (t - m_{\tilde{q}_i}^2)^2\right], \quad (49.52)$$

while if initial and final state flavors are different ($q\bar{q} \to \tilde{q}_i'\bar{\tilde{q}}_i'$) we instead have

$$\frac{d\sigma}{dt}(q\bar{q} \to \tilde{q}_i'\bar{\tilde{q}}_i') = \frac{4\pi\alpha_s^2}{9s^4}\left[-st - (t - m_{\tilde{q}_i'}^2)^2\right]. \quad (49.53)$$

If the two initial state quarks are of different flavors, then we have

$$\frac{d\sigma}{dt}(q\bar{q}' \to \tilde{q}_i\bar{\tilde{q}}_i') = \frac{2\pi\alpha_s^2}{9s^2}\frac{-st - (t - m_{\tilde{q}_i}^2)^2}{(t - m_{\tilde{g}}^2)^2}. \quad (49.54)$$

If the initial quarks are of different flavor and final state squarks are of different type ($i \neq j$) then

$$\frac{d\sigma}{dt}(q\bar{q}' \to \tilde{q}_i\bar{\tilde{q}}_j') = \frac{2\pi\alpha_s^2}{9s^2}\frac{m_{\tilde{g}}^2 s}{(t - m_{\tilde{g}}^2)^2}. \quad (49.55)$$

For same-flavor initial state quarks, but final state unlike-type squarks, we also have

$$\frac{d\sigma}{dt}(q\bar{q} \to \tilde{q}_i\bar{\tilde{q}}_j) = \frac{2\pi\alpha_s^2}{9s^2}\frac{m_{\tilde{g}}^2 s}{(t - m_{\tilde{g}}^2)^2}. \quad (49.56)$$

There also exist cross sections for quark-quark annihilation to squark pairs. For same flavor quark-quark annihilation to same flavor/same type final state squarks,

$$\frac{d\sigma}{dt}(qq \to \tilde{q}_i\tilde{q}_i) =$$

$$= \frac{\pi\alpha_s^2}{9s^2} m_{\tilde{g}}^2 s \left\{ \frac{1}{(t-m_{\tilde{g}}^2)^2} + \frac{1}{(u-m_{\tilde{g}}^2)^2} - \frac{2/3}{(t-m_{\tilde{g}}^2)(u-m_{\tilde{g}}^2)} \right\}, \quad (49.57)$$

while if the final type squarks are different ($i \neq j$), we have

$$\frac{d\sigma}{dt}(qq \to \tilde{q}_i\tilde{q}_j) =$$

$$\frac{2\pi\alpha_s^2}{9s^2} \left\{ \frac{[-st-(t-m_{\tilde{q}_i}^2)(t-m_{\tilde{q}_j}^2)]}{(t-m_{\tilde{g}}^2)} + \frac{[-su-(u-m_{\tilde{q}_i}^2)(u-m_{\tilde{q}_j}^2)]}{(u-m_{\tilde{g}}^2)} \right\}. \quad (49.58)$$

If initial/final state flavors are different, but final state squark types are the same, then

$$\frac{d\sigma}{dt}(qq' \to \tilde{q}_i\tilde{q}_i') = \frac{2\pi\alpha_s^2}{9s^2} \frac{m_{\tilde{g}}^2 s}{(t-m_{\tilde{g}}^2)^2}. \quad (49.59)$$

If initial quark flavors are different and final squark types are different, then

$$\frac{d\sigma}{dt}(qq' \to \tilde{q}_i\tilde{q}_j') = \frac{2\pi\alpha_s^2}{9s^2} \frac{-st-(t-m_{\tilde{q}_i}^2)(t-m_{\tilde{q}_j}^2)}{(t-m_{\tilde{g}}^2)^2}. \quad (49.60)$$

49.8.2. *Gluino and squark associated production* :

In the MSSM, the charged spin-$\frac{1}{2}$ winos and higgsinos mix to make chargino states $\chi_1^\pm$ and $\chi_2^\pm$, with $m_{\chi_1^\pm} < m_{\chi_2^\pm}$. The spin$-\frac{1}{2}$ neutral bino, wino and higgsino fields mix to give four neutralino mass eigenstates $\chi_{1,2,3,4}^0$ ordered according to mass. We sometimes denote the charginos and neutralinos collectively as -inos for notational simplicity

For gluino and squark production in association with charginos and neutralinos [12], the quark-squark-neutralino couplings* are defined by the interaction Lagrangian terms $\mathcal{L}_{\bar{f}f\chi_i^0} = \left[iA^f_{\tilde{\chi}_i^0} \tilde{f}_L^\dagger \bar{\tilde{\chi}}_i^0 P_L f + iB^f_{\tilde{\chi}_i^0} \tilde{f}_R^\dagger \bar{\tilde{\chi}}_i^0 P_R f + \text{h.c.} \right]$, where $A^f_{\tilde{\chi}_i^0}$ and $B^f_{\tilde{\chi}_i^0}$ are coupling constants involving gauge couplings, neutralino mixing elements and in the case of third generation fermions, Yukawa couplings. Their form depends on the conventions used for setting up the MSSM Lagrangian, and can be found in various reviews [13] and textbooks [14,15]. P_L and P_R are the usual left- and right-spinor projection operators and f denotes any of the SM fermions u, d, e, $\nu_e, \cdots$. The fermion-sfermion- chargino couplings have the form $\mathcal{L} = \left[iA^d_{\tilde{\chi}_i^-} \tilde{u}_L^\dagger \overline{\tilde{\chi}_i^-} P_L d + iA^u_{\tilde{\chi}_i^-} \tilde{d}_L^\dagger \overline{\tilde{\chi}_i^c} P_L u + \text{h.c.} \right]$ for u and d quarks, where the $A^d_{\tilde{\chi}_i^-}$ and $A^u_{\tilde{\chi}_i^-}$ couplings are again convention-dependent, and can be found in textbooks. The superscript c denotes "charge conjugate spinor", defined by $\psi^c \equiv C\bar{\psi}^T$.

The subprocess cross sections for chargino-squark associated production occur via squark exchange and are given by

$$\frac{d\sigma}{dt}(\bar{u}g \to \tilde{\chi}_i^- \bar{\tilde{d}}_L) = \frac{\alpha_s}{24s^2} |A^u_{\tilde{\chi}_i^-}|^2 \psi(m_{\tilde{d}_L}, m_{\tilde{\chi}_i^-}, t), \quad (49.61)$$

$$\frac{d\sigma}{dt}(dg \to \tilde{\chi}_i^- \tilde{u}_L) = \frac{\alpha_s}{24s^2} |A^d_{\tilde{\chi}_i^-}|^2 \psi(m_{\tilde{u}_L}, m_{\tilde{\chi}_i^-}, t), \quad (49.62)$$

while neutralino-squark production is given by

$$\frac{d\sigma}{dt}(qg \to \tilde{\chi}_i^0 \tilde{q}) = \frac{\alpha_s}{24s^2} \left(|A^q_{\tilde{\chi}_i^0}|^2 + |B^q_{\tilde{\chi}_i^0}|^2 \right) \psi(m_{\tilde{q}}, m_{\tilde{\chi}_i^0}, t), \quad (49.63)$$

where

$$\psi(m_1, m_2, t) = \frac{s+t-m_1^2}{2s} - \frac{m_1^2(m_2^2-t)}{(m_1^2-t)^2} + \frac{t(m_2^2-m_1^2)+m_2^2(s-m_2^2+m_1^2)}{s(m_1^2-t)}. \quad (49.64)$$

Here, the variable t is given by the square of "squark-minus-quark" four-momentum. The neutralino-gluino associated production cross section also occurs via squark exchange and is given by

$$\frac{d\sigma}{dt}(q\bar{q} \to \tilde{\chi}_i^0 \tilde{g}) = \frac{\alpha_s}{18s^2} \left(|A^q_{\tilde{\chi}_i^0}|^2 + |B^q_{\tilde{\chi}_i^0}|^2 \right) \left[\frac{(m^2_{\tilde{\chi}_i^0}-t)(m_{\tilde{g}}^2-t)}{(m_{\tilde{q}}^2-t)^2} + \frac{(m^2_{\tilde{\chi}_i^0}-u)(m_{\tilde{g}}^2-u)}{(m_{\tilde{q}}^2-u)^2} - \frac{2\eta_i\eta_{\tilde{g}} m_{\tilde{g}} m_{\tilde{\chi}_i^0} s}{(m_{\tilde{q}}^2-t)(m_{\tilde{q}}^2-u)} \right], \quad (49.65)$$

where η_i is the sign of the neutralino mass eigenvalue and $\eta_{\tilde{g}}$ is the sign of the gluino mass eigenvalue. We also have chargino-gluino associated production:

$$\frac{d\sigma}{dt}(\bar{u}d \to \tilde{\chi}_i^- \tilde{g}) = \frac{\alpha_s}{18s^2} \left[|A^u_{\tilde{\chi}_i^-}|^2 \frac{(m^2_{\tilde{\chi}_i^-}-t)(m_{\tilde{g}}^2-t)}{(m^2_{\tilde{d}_L}-t)^2} + |A^d_{\tilde{\chi}_i^-}|^2 \frac{(m^2_{\tilde{\chi}_i^-}-u)(m_{\tilde{g}}^2-u)}{(m^2_{\tilde{u}_L}-u)^2} + \frac{2\eta_{\tilde{g}} Re(A^u_{\tilde{\chi}_i^-} A^d_{\tilde{\chi}_i^-}) m_{\tilde{g}} m_{\tilde{\chi}_i} s}{(m^2_{\tilde{d}_L}-t)(m^2_{\tilde{u}_L}-u)} \right], \quad (49.66)$$

where $\hat{t} = (\tilde{g}-d)^2$ and in the third term one must take the real part of the in general complex coupling constant product.

49.8.3. *Slepton and sneutrino production* :

The subprocess cross section for $\tilde{\ell}_L\bar{\tilde{\nu}}_{\ell_L}$ production ($\ell = e$ or μ) occurs via s-channel W exchange and is given by

$$\frac{d\sigma}{dt}(d\bar{u} \to \tilde{\ell}_L\bar{\tilde{\nu}}_{\ell_L}) = \frac{g^4 |D_W(s)|^2}{192\pi s^2} \left(tu - m^2_{\tilde{\ell}_L} m^2_{\tilde{\nu}_{\ell_L}} \right), \quad (49.67)$$

where $D_W(s) = 1/(s - M_W^2 + iM_W\Gamma_W)$ is the W-boson propagator denominator. The production of $\tilde{\tau}_1\bar{\tilde{\nu}}_\tau$ is given as above, but replacing $m_{\tilde{\ell}_L} \to m_{\tilde{\tau}_1}$, $m_{\tilde{\nu}_{\ell_L}} \to m_{\tilde{\nu}_\tau}$ and multiplying by an overall factor of $\cos^2\theta_\tau$ (where θ_τ is the tau-slepton mixing angle). Similar substitutions hold for $\tilde{\tau}_2\bar{\tilde{\nu}}_\tau$ production, except the overall factor is $\sin^2\theta_\tau$.

Table 49.1: The constants α_f and β_f that appear in in the SM neutral current Lagrangian. Here $t \equiv \tan\theta_W$ and $c \equiv \cot\theta_W$.

f	q_f	α_f	β_f
ℓ	-1	$\frac{1}{4}(3t-c)$	$\frac{1}{4}(t+c)$
ν_ℓ	0	$\frac{1}{4}(t+c)$	$-\frac{1}{4}(t+c)$
u	$\frac{2}{3}$	$-\frac{5}{12}t+\frac{1}{4}c$	$-\frac{1}{4}(t+c)$
d	$-\frac{1}{3}$	$\frac{1}{12}t-\frac{1}{4}c$	$\frac{1}{4}(t+c)$

* The couplings $A^f_{\tilde{\chi}_i^0}$ and $B^f_{\tilde{\chi}_i^0}$ are given explicitly in Ref. 15 in Eq. (8.87). Also, the couplings $A^d_{\tilde{\chi}_i^-}$ and $A^u_{\tilde{\chi}_i^-}$ are given in Eq. (8.93). The couplings X_i^j and Y_i^j are given by Eq. (8.103), while the x_i and y_i couplings are given in Eq. (8.100). Finally, the couplings W_{ij} are given in Eq. (8.101).

The subprocess cross section for $\tilde{\ell}_L\bar{\tilde{\ell}}_L$ production occurs via s-channel γ and Z exchange, and depends on the neutral current interaction, with fermion couplings to γ and Z^0 given by $\mathcal{L}_{\rm neutral} = -eq_f\bar{f}\gamma^\mu f A_\mu + e\bar{f}\gamma^\mu(\alpha_f+\beta_f\gamma_5)fZ_\mu$ (with values of q_f, α_f, and β_f given in Table 49.1.

The subprocess cross section is given by

$$\frac{d\sigma}{dt}(q\bar{q}\to\tilde{\ell}_L\bar{\tilde{\ell}}_L) = \frac{e^4}{24\pi s^2}\left(tu-m_{\tilde{\ell}_L}^4\right)\times$$

$$\left\{\frac{q_\ell^2 q_q^2}{s^2}+(\alpha_\ell-\beta_\ell)^2(\alpha_q^2+\beta_q^2)|D_Z(s)|^2\right.$$

$$\left.+\frac{2q_\ell q_q\alpha_q(\alpha_\ell-\beta_\ell)(s-M_Z^2)}{s}|D_Z(s)|^2\right\}, \qquad (49.68)$$

where $D_Z(s) = 1/(s-M_Z^2+iM_Z\Gamma_Z)$. The cross section for sneutrino production is given by the same formula, but with α_ℓ, β_ℓ, q_ℓ and $m_{\tilde{\ell}_L}$ replaced by α_ν, β_ν, 0 and $m_{\tilde{\nu}_{L_\ell}}$, respectively. The cross section for $\tilde{\tau}_1\bar{\tilde{\tau}}_1$ production is obtained by replacing $m_{\tilde{\ell}_L}\to m_{\tilde{\tau}_1}$ and $\beta_\ell\to\beta_\ell\cos 2\theta_\tau$. The cross section for $\tilde{\ell}_R\bar{\tilde{\ell}}_R$ production is given by substituting $\alpha_\ell-\beta_\ell\to\alpha_\ell+\beta_\ell$ and $m_{\tilde{\ell}_L}\to m_{\tilde{\ell}_R}$ in the equation above. The cross section for $\tilde{\tau}_2\bar{\tilde{\tau}}_2$ production is obtained from the formula for $\tilde{\ell}_R\bar{\tilde{\ell}}_R$ production by replacing $m_{\tilde{\ell}_R}\to m_{\tilde{\tau}_2}$ and $\beta_\ell\to\beta_\ell\cos 2\theta_\tau$.

Finally, the cross section for $\tilde{\tau}_1\bar{\tilde{\tau}}_2$ production occurs only via Z exchange, and is given by

$$\frac{d\sigma}{dt}(q\bar{q}\to\tilde{\tau}_1\bar{\tilde{\tau}}_2) = \frac{d\sigma}{dt}(q\bar{q}\to\bar{\tilde{\tau}}_1\tilde{\tau}_2) =$$

$$\frac{e^4}{24\pi s^2}(\alpha_q^2+\beta_q^2)\beta_\ell^2\sin^2 2\theta_\tau|D_Z(s)|^2(ut-m_{\tilde{\tau}_1}^2 m_{\tilde{\tau}_2}^2). \qquad (49.69)$$

49.8.4. *Chargino and neutralino pair production* :

49.8.4.1. $\tilde{\chi}_i^-\tilde{\chi}_j^0$ *production:*

The subprocess cross section for $d\bar{u}\to\tilde{\chi}_i^-\tilde{\chi}_j^0$ depends on Lagrangian couplings $\mathcal{L}_{W\bar{u}d} = -\frac{g}{\sqrt{2}}\bar{u}\gamma_\mu P_L d W^{+\mu}$ + h.c., $\mathcal{L}_{W\tilde{\chi}_i^-\tilde{\chi}_j^0} = -g(-i)^{\theta_j}\overline{\tilde{\chi}^-}_i[X_i^j+Y_i^j\gamma_5]\gamma_\mu\tilde{\chi}_j^0 W^{-\mu}$ + h.c., $\mathcal{L}_{q\tilde{q}\tilde{\chi}_i^-} = iA^d_{\tilde{\chi}_i^-}\tilde{u}_L^\dagger\overline{\tilde{\chi}_i^-}P_L d + iA^u_{\tilde{\chi}_i^-}\tilde{d}_L^\dagger\overline{\tilde{\chi}_i^c}P_L u$ +h.c. and $\mathcal{L}_{q\tilde{q}\tilde{\chi}_j^0} = iA^q_{\tilde{\chi}_j^0}\tilde{q}_L^\dagger\overline{\tilde{\chi}^0}_j P_L q$ +h.c.. Contributing diagrams include W exchange and also $\tilde{d}_L$ and $\tilde{u}_L$ squark exchange. The X_i^j and Y_i^j couplings are new, and again convention-dependent: the cross section formulae works if the interaction Lagrangian is written in the above form, so that the couplings can be suitably extracted. The term $\theta_j = 0$ (1) if $m_{\tilde{\chi}_j^0} > 0$ (< 0); it comes about because the neutralino field must be re-defined by a $-i\gamma_5$ transformation if its mass eigenvalue is negative [15]. The subprocess cross section is given in terms of dot products of four momenta, where particle labels are used to denote their four-momenta; note that all mass terms in the cross section formulae are positive definite, so that the signs of mass eigenstates have been absorbed into the Lagrangian couplings, as for instance in Ref. [15]. We then have

$$\frac{d\sigma}{dt}(d\overline{u}\to\tilde{\chi}_i^-\tilde{\chi}_j^0) = \frac{1}{192\pi s^2}$$

$$\left[T_W + T_{\tilde{d}_L} + T_{\tilde{u}_L} + T_{W\tilde{d}_L} + T_{W\tilde{u}_L} + T_{\tilde{d}_L\tilde{u}_L}\right] \qquad (49.70)$$

where

$$T_W = 8g^4|D_W(s)|^2\left\{[X_i^{j2}+Y_i^{j2}](\tilde{\chi}_j^0\cdot d\tilde{\chi}_i^-\cdot\overline{u}+\tilde{\chi}_j^0\cdot\overline{u}\tilde{\chi}_i^-\cdot d)\right.$$
$$\left.+2(X_i^jY_i^j)(\tilde{\chi}_j^0\cdot d\tilde{\chi}_i^-\cdot\overline{u}-\tilde{\chi}_j^0\cdot\overline{u}\tilde{\chi}_i^-\cdot d)+[X_i^{j2}-Y_i^{j2}]m_{\tilde{\chi}_i^-}m_{\tilde{\chi}_j^0}d\cdot\overline{u}\right\}, \qquad (49.71)$$

$$T_{\tilde{d}_L} = \frac{4|A^u_{\tilde{\chi}_i^-}|^2|A^d_{\tilde{\chi}_j^0}|^2}{[(\tilde{\chi}_i^- - \overline{u})^2 - m^2_{\tilde{d}_L}]^2}\; d\cdot\tilde{\chi}_j^0\tilde{\chi}_i^-\cdot\overline{u}, \qquad (49.72)$$

$$T_{\tilde{u}_L} = \frac{4|A^d_{\tilde{\chi}_i^-}|^2|A^u_{\tilde{\chi}_j^0}|^2}{[(\tilde{\chi}_j^0 - \overline{u})^2 - m^2_{\tilde{u}_L}]^2}\; \overline{u}\cdot\tilde{\chi}_j^0\tilde{\chi}_i^-\cdot d \qquad (49.73)$$

$$T_{W\tilde{d}_L} = \frac{-\sqrt{2}g^2 Re[A^{d*}_{\tilde{\chi}_j^0}A^u_{\tilde{\chi}_i^-}(-i)^{\theta_j}](s-M_W^2)|D_W(s)|^2}{(\tilde{\chi}_i^- - \overline{u})^2 - m^2_{\tilde{d}_L}}$$
$$\times\left\{8(X_i^j+Y_i^j)\tilde{\chi}_j^0\cdot d\overline{u}\cdot\tilde{\chi}_i^- + 4(X_i^j-Y_i^j)m_{\tilde{\chi}_i^-}m_{\tilde{\chi}_j^0}d\cdot\overline{u}\right\} \qquad (49.74)$$

$$T_{W\tilde{u}_L} = \frac{\sqrt{2}g^2 Re[A^{d*}_{\tilde{\chi}_i^-}A^u_{\tilde{\chi}_j^0}(-i)^{\theta_j}](s-M_W^2)|D_W(s)|^2}{(\tilde{\chi}_j^0 - \overline{u})^2 - m^2_{\tilde{u}_L}}$$
$$\times\left\{8(X_i^j-Y_i^j)\tilde{\chi}_j^0\cdot\overline{u}d\cdot\tilde{\chi}_i^- + 4(X_i^j+Y_i^j)m_{\tilde{\chi}_i^-}m_{\tilde{\chi}_j^0}d\cdot\overline{u}\right\} \qquad (49.75)$$

and

$$T_{\tilde{d}_L\tilde{u}_L} = -\frac{4Re[A^d_{\tilde{\chi}_j^0}A^{u*}_{\tilde{\chi}_i^-}A^{d*}_{\tilde{\chi}_i^-}A^u_{\tilde{\chi}_j^0}]m_{\tilde{\chi}_i^-}m_{\tilde{\chi}_j^0}d\cdot\overline{u}}{[(\tilde{\chi}_i^- - \overline{u})^2 - m^2_{\tilde{d}_L}][(\tilde{\chi}_j^0 - \overline{u})^2 - m^2_{\tilde{u}_L}]}. \qquad (49.76)$$

49.8.4.2. *Chargino pair production:*

The subprocess cross section for $d\bar{d}\to\tilde{\chi}_i^-\tilde{\chi}_i^+$ $(i=1,2)$ depends on Lagrangian couplings $\mathcal{L} = e\overline{\tilde{\chi}_i^-}\gamma_\mu\tilde{\chi}_i^- A^\mu - e\cot\theta_W\overline{\tilde{\chi}_i^-}\gamma_\mu(x_i-y_i\gamma_5)\tilde{\chi}_i^- Z^\mu$ and also $\mathcal{L}\ni iA^d_{\tilde{\chi}_i^-}\tilde{u}_L^\dagger\overline{\tilde{\chi}_i^-}P_L d + iA^u_{\tilde{\chi}_i^-}\tilde{d}_L^\dagger\overline{\tilde{\chi}_i^{-c}}P_L u$ + h.c.. Contributing diagrams include s-channel γ, Z^0 exchange and t-channel $\tilde{u}_L$ exchange [16,17]. The couplings x_i and y_i are again new and as usual convention-dependent.

The subprocess cross section is given by

$$\frac{d\sigma}{dt}(d\overline{d}\to\tilde{\chi}_i^-\tilde{\chi}_i^+) = \frac{1}{192\pi s^2}\left[T_\gamma + T_Z + T_{\tilde{u}_L} + T_{\gamma Z} + T_{\gamma\tilde{u}_L} + T_{Z\tilde{u}_L}\right] \qquad (49.77)$$

where

$$T_\gamma = \frac{32e^4q_d^2}{s^2}\left[d\cdot\tilde{\chi}_i^+\overline{d}\cdot\tilde{\chi}_i^- + d\cdot\tilde{\chi}_i^-\overline{d}\cdot\tilde{\chi}_i^+ + m^2_{\tilde{\chi}_i^-}d\cdot\overline{d}\right] \qquad (49.78)$$

$$T_Z = 32e^4\cot^2\theta_W|D_Z(s)|^2$$
$$\left\{(\alpha_d^2+\beta_d^2)(x_i^2+y_i^2)\left[d\cdot\tilde{\chi}_i^+\overline{d}\cdot\tilde{\chi}_i^- + d\cdot\tilde{\chi}_i^-\overline{d}\cdot\tilde{\chi}_i^+ + m^2_{\tilde{\chi}_i^-}d\cdot\overline{d}\right]\right.$$
$$\left.\mp 4\alpha_d\beta_d x_i y_i\left[d\cdot\tilde{\chi}_i^+\overline{d}\cdot\tilde{\chi}_i^- - d\cdot\tilde{\chi}_i^-\overline{d}\cdot\tilde{\chi}_i^+\right] - 2y_i^2(\alpha_d^2+\beta_d^2)m^2_{\tilde{\chi}_i^-}d\cdot\overline{d}\right\}, \qquad (49.79)$$

$$T_{\tilde{u}_L} = \frac{4|A^d_{\tilde{\chi}_i^-}|^4}{[(d-\tilde{\chi}_i^-)^2 - m^2_{\tilde{u}_L}]^2}\; d\cdot\tilde{\chi}_i^-\overline{d}\cdot\tilde{\chi}_i^+ \qquad (49.80)$$

$$T_{\gamma Z} = \frac{64e^4\cot\theta_W q_d(s-M_Z^2)|D_Z(s)|^2}{s}\times$$
$$\left\{\alpha_d x_i\left(d\cdot\tilde{\chi}_i^+\overline{d}\cdot\tilde{\chi}_i^- + d\cdot\tilde{\chi}_i^-\overline{d}\cdot\tilde{\chi}_i^+ + m^2_{\tilde{\chi}_i^-}d\cdot\overline{d}\right)\right.$$
$$\left.\pm\beta_d y_i\left(d\cdot\tilde{\chi}_i^-\overline{d}\cdot\tilde{\chi}_i^+ - d\cdot\tilde{\chi}_i^+\overline{d}\cdot\tilde{\chi}_i^-\right)\right\} \qquad (49.81)$$

$$T_{\gamma\tilde{u}_L} = \mp\frac{8e^2q_d}{s}\frac{|A^d_{\tilde{\chi}_i^-}|^2}{[(d-\tilde{\chi}_i^-)^2 - m^2_{\tilde{u}_L}]}\left\{2\overline{d}\cdot\tilde{\chi}_i^+ d\cdot\tilde{\chi}_i^- + m^2_{\tilde{\chi}_i^-}d\cdot\overline{d}\right\} \qquad (49.82)$$

and

$$T_{Z\tilde{u}_L} = \mp 8e^2 \cot\theta_W |D_Z(s)|^2 \frac{|A^d_{\tilde{\chi}_i^-}|^2 (s-M_Z^2)}{[(d-\tilde{\chi}_i^-)^2 - m^2_{\tilde{u}_L}]} (\alpha_d - \beta_d) \times \left\{ 2(x_i \mp y_i) d\cdot\tilde{\chi}_i^- \overline{d}\cdot\tilde{\chi}_i^+ + m^2_{\tilde{\chi}_i^-}(x_i \pm y_i) d\cdot\overline{d} \right\} \quad (49.83)$$

using the upper of the sign choices.

The cross section for $u\overline{u} \to \tilde{\chi}_i^+ \tilde{\chi}_i^-$ can be obtained from the above by replacing $\alpha_d \to \alpha_u$, $\beta_d \to \beta_u$, $q_d \to q_u$, $\tilde{u}_L \to \tilde{d}_L$, $A^d_{\tilde{\chi}_i^-} \to A^u_{\tilde{\chi}_i^-}$, $d \to \overline{u}$, $\overline{d} \to u$ and adopting the lower of the sign choices everywhere.

The cross section for $q\bar{q} \to \tilde{\chi}_1^- \tilde{\chi}_2^+$, $\tilde{\chi}_1^+ \tilde{\chi}_2^-$ can occur via Z and $\tilde{q}_L$ exchange. It is usually much smaller than $\tilde{\chi}^-_{1,2}\tilde{\chi}^+_{1,2}$ production, so the cross section will not be presented here. It can be found in Appendix A of Ref. 15.

49.8.4.3. *Neutralino pair production:*

Neutralino pair production via $q\bar{q}$ fusion takes place via s-channel Z exchange plus t- and u-channel left- and right- squark exchange (5 diagrams) [17,18]. The Lagrangian couplings (see previous footnote*) needed include terms given above plus terms of the form $\mathcal{L} = W_{ij}\overline{\tilde{\chi}^0}_i \gamma_\mu (\gamma_5)^{\theta_i+\theta_j+1} \tilde{\chi}^0_j Z^\mu$. The couplings W_{ij} depend only on the *higgsino* components of the neutralinos i and j. The subprocess cross section is given by:

$$\frac{d\sigma}{dt}(q\bar{q} \to \tilde{\chi}_i^0 \tilde{\chi}_j^0) = \frac{1}{192\pi s^2} \left[T_Z + T_{\tilde{q}_L} + T_{\tilde{q}_R} + T_{Z\tilde{q}_L} + T_{Z\tilde{q}_R} \right] \quad (49.84)$$

where

$$T_Z = 128e^2 |W_{ij}|^2 (\alpha_q^2 + \beta_q^2) |D_Z(s)|^2 \left[q\cdot\tilde{\chi}_i^0 \bar{q}\cdot\tilde{\chi}_j^0 + q\cdot\tilde{\chi}_j^0 \bar{q}\cdot\tilde{\chi}_i^0 - \eta_i\eta_j m_{\tilde{\chi}_i^0} m_{\tilde{\chi}_j^0} q\cdot\bar{q} \right], \quad (49.85)$$

$$T_{\tilde{q}_L} = 4|A^q_{\tilde{\chi}_i^0}|^2 |A^q_{\tilde{\chi}_j^0}|^2 \left\{ \frac{q\cdot\tilde{\chi}_i^0 \bar{q}\cdot\tilde{\chi}_j^0}{[(\tilde{\chi}_i^0 - q)^2 - m^2_{\tilde{q}_L}]^2} + \frac{q\cdot\tilde{\chi}_j^0 \bar{q}\cdot\tilde{\chi}_i^0}{[(\tilde{\chi}_j^0 - q)^2 - m^2_{\tilde{q}_L}]^2} - \eta_i\eta_j \frac{m_{\tilde{\chi}_i^0} m_{\tilde{\chi}_j^0} q\cdot\bar{q}}{[(\tilde{\chi}_i^0 - q)^2 - m^2_{\tilde{q}_L}][(\tilde{\chi}_j^0 - q)^2 - m^2_{\tilde{q}_L}]} \right\} \quad (49.86)$$

$$T_{\tilde{q}_R} = 4|B^q_{\tilde{\chi}_i^0}|^2 |B^q_{\tilde{\chi}_j^0}|^2 \left\{ \frac{q\cdot\tilde{\chi}_i^0 \bar{q}\cdot\tilde{\chi}_j^0}{[(\tilde{\chi}_i^0 - q)^2 - m^2_{\tilde{q}_R}]^2} + \frac{q\cdot\tilde{\chi}_j^0 \bar{q}\cdot\tilde{\chi}_i^0}{[(\tilde{\chi}_j^0 - q)^2 - m^2_{\tilde{q}_R}]^2} - \eta_i\eta_j \frac{m_{\tilde{\chi}_i^0} m_{\tilde{\chi}_j^0} q\cdot\bar{q}}{[(\tilde{\chi}_i^0 - q)^2 - m^2_{\tilde{q}_R}][(\tilde{\chi}_j^0 - q)^2 - m^2_{\tilde{q}_R}]} \right\} \quad (49.87)$$

$$T_{Z\tilde{q}_L} = 16e(\alpha_q - \beta_q)(s - M_Z^2) |D_Z(s)|^2 \left\{ \frac{Re(W_{ij} A^{q*}_{\tilde{\chi}_i^0} A^q_{\tilde{\chi}_j^0})}{[(\tilde{\chi}_i^0 - q)^2 - m^2_{\tilde{q}_L}]} \left[2q\cdot\tilde{\chi}_i^0 \bar{q}\cdot\tilde{\chi}_j^0 - \eta_i\eta_j m_{\tilde{\chi}_i^0} m_{\tilde{\chi}_j^0} q\cdot\bar{q} \right] + \eta_i\eta_j \frac{Re(W_{ij} A^q_{\tilde{\chi}_i^0} A^{q*}_{\tilde{\chi}_j^0})}{[(\tilde{\chi}_j^0 - q)^2 - m^2_{\tilde{q}_L}]} \left[2q\cdot\tilde{\chi}_j^0 \bar{q}\cdot\tilde{\chi}_i^0 - \eta_i\eta_j m_{\tilde{\chi}_i^0} m_{\tilde{\chi}_j^0} q\cdot\bar{q} \right] \right\} \quad (49.88)$$

$$T_{Z\tilde{q}_R} = 16e(\alpha_q + \beta_q)(s - M_Z^2) |D_Z(s)|^2 \left\{ \frac{Re(W_{ij} B^{q*}_{\tilde{\chi}_i^0} B^q_{\tilde{\chi}_j^0})}{[(\tilde{\chi}_i^0 - q)^2 - m^2_{\tilde{q}_R}]} \left[2q\cdot\tilde{\chi}_i^0 \bar{q}\cdot\tilde{\chi}_j^0 - \eta_i\eta_j m_{\tilde{\chi}_i^0} m_{\tilde{\chi}_j^0} q\cdot\bar{q} \right] - \frac{Re(W_{ij} B^q_{\tilde{\chi}_i^0} B^{q*}_{\tilde{\chi}_j^0})}{[(\tilde{\chi}_j^0 - q)^2 - m^2_{\tilde{q}_R}]} \left[2q\cdot\tilde{\chi}_j^0 \bar{q}\cdot\tilde{\chi}_i^0 - \eta_i\eta_j m_{\tilde{\chi}_i^0} m_{\tilde{\chi}_j^0} q\cdot\bar{q} \right] \right\}. \quad (49.89)$$

As before, $\eta_i = \pm 1$ corresponding to whether the neutralino mass eigenvalue is positive or negative. When $i = j$ in the above formula, one must remember to integrate over just 2π steradians of solid angle to avoid double counting in the total cross section.

49.9. Universal extra dimensions

In the Universal Extra Dimension (UED) model of Ref. [19] (see Ref. [20] for a review of models with extra spacetime dimensions), the Standard Model is embedded in a five dimensional theory, where the fifth dimension is compactified on an S_1/Z_2 orbifold. Each SM chirality state is then the zero mode of an infinite tower of Kaluza-Klein excitations labelled by $n = 0 - \infty$. A KK parity is usually assumed to hold, where each state is assigned KK-parity $P = (-1)^n$. If the compactification scale is around a TeV, then the $n = 1$ (or even higher) KK modes may be accessible to collider searches.

Of interest for hadron colliders are the production of massive $n \geq 1$ quark or gluon pairs. These production cross sections have been calculated in Ref. [21,22]. We list here results for the $n = 1$ case only with $M_1 = 1/R$ (R is the compactification radius) and s, t and u are the usual Mandelstam variables; more general formulae can be found in Ref. [22]. The superscript $*$ stands for any KK excited state, while $\bullet$ stands for left chirality states and $\circ$ stands for right chirality states.

$$\frac{d\sigma}{dt} = \frac{1}{16\pi s^2} T \quad (49.90)$$

where

$$T(q\bar{q} \to g^* g^*) = \frac{2g_s^4}{27} \left[M_1^2 \left(-\frac{4s^3}{t'^2 u'^2} + \frac{57s}{t'u'} - \frac{108}{s} \right) + \frac{20s^2}{t'u'} - 93 + \frac{108 t'u'}{s^2} \right] \quad (49.91)$$

and

$$T(gg \to g^* g^*) = \frac{9g_s^4}{27} \left[3M_1^4 \frac{s^2 + t'^2 + u'^2}{t'^2 u'^2} - 3M_1^2 \frac{s^2 + t'^2 + u'^2}{st'u'} + 1 + \frac{(s^2 + t'^2 + u'^2)^3}{4s^2 t'^2 u'^2} - \frac{t'u'}{s^2} \right] \quad (49.92)$$

where $t' = t - M_1^2$ and $u' = u - M_1^2$.

Also,

$$T(q\bar{q} \to q_1^{*\prime} \bar{q}_1^{*\prime}) = \frac{4g_s^4}{9} \left[\frac{2M_1^2}{s} + \frac{t'^2 + u'^2}{s^2} \right],$$

$$T(q\bar{q} \to q_1^* \bar{q}_1^*) = \frac{g_2^4}{9} \left[2M_1^2 \left(\frac{4}{s} + \frac{s}{t'^2} - \frac{1}{t'} \right) + \frac{23}{6} + \frac{2s^2}{t'^2} + \frac{8s}{3t'} + \frac{6t'}{s} + \frac{8t'^2}{s^2} \right],$$

$$T(qq \to q_1^* q_1^*) = \frac{g_s^4}{27} \left[M_1^2 \left(6\frac{t'}{u'^2} + 6\frac{u'}{t'^2} - \frac{s}{t'u'} \right) + 2 \left(3\frac{t'^2}{u'^2} + 3\frac{u'^2}{t'^2} + 4\frac{s^2}{t'u'} - 5 \right) \right],$$

$$T(gg \to q_1^* \bar{q}_1^*) = g_s^4 \left[M_1^4 \frac{-4}{t'u'} \left(\frac{s^2}{6t'u'} - \frac{3}{8} \right) + M_1^2 \frac{4}{s} \left(\frac{s^2}{6t'u'} - \frac{3}{8} \right) + \frac{s^2}{6t'u'} - \frac{17}{24} + \frac{3t'u'}{4s^2} \right],$$

$$T(gq \to g^* q_1^*) = \frac{-g_s^4}{3} \left[\frac{5s^2}{12t'^2} + \frac{s^3}{t'^2 u'} + \frac{11su'}{6t'^2} + \frac{5u'^2}{12t'^2} + \frac{u'^3}{st'^2} \right],$$

$$T(q\bar{q}' \to q_1^* \bar{q}_1^{*\prime}) = \frac{g_s^4}{18} \left[4M_1^4 \frac{s}{t'^2} + 5 + 4\frac{s^2}{t'^2} + 8\frac{s}{t'} \right],$$

$$T(qq' \to q_1^* q_1^{*\prime}) = \frac{2g_s^4}{9} \left[-M_1^2 \frac{s}{t'^2} + \frac{1}{4} + \frac{s^2}{t'^2} \right],$$

$$T(qq \to q_1^\bullet q_1^\circ) = \frac{g_s^4}{9}\left[M_1^2\left(\frac{2s^3}{t'^2u'^2} - \frac{4s}{t'u'}\right) + 2\frac{s^4}{t'^2u'^2} - 8\frac{s^2}{t'u'} + 5\right],$$

$$T(q\bar{q}' \to q_1^\bullet \bar{q}_1'^\circ) = \frac{g_s^4}{9}\left[2M_1^2\left(\frac{1}{t'} + \frac{u'}{t'^2}\right) + \frac{5}{2} + \frac{4u'}{t'} + \frac{2u'^2}{t'^2}\right],$$

and

$$T(qq' \to q_1^\bullet q_1'^\circ) = \frac{g_s^4}{9}\left[-2M_1^2\left(\frac{1}{t'} + \frac{u'}{t'^2}\right) + \frac{1}{2} + \frac{2u'^2}{t'^2}\right].$$

49.10. Large extra dimensions

In the ADD theory [23] with large extra dimensions (LED), the SM particles are confined to a 3-brane, while gravity propagates in the bulk. It is assumed that the n extra dimensions are compactified on an n-dimensional torus of volume $(2\pi r)^n$, so that the fundamental $4+n$ dimensional Planck scale M_* is related to the usual 4-dimensional Planck scale M_{Pl} by $M_{Pl}^2 = M_*^{n+2}(2\pi r)^n$. If $M_* \sim 1$ TeV, then the $M_W - M_{Pl}$ hierarchy problem is just due to gravity propagating in the large extra dimensions.

In these theories, the KK-excited graviton states $G_{\mu\nu}^n$ for $n = 1-\infty$ can be produced at collider experiments. The graviton couplings to matter are suppressed by $1/M_{Pl}$, so that graviton emission cross sections $d\sigma/dt \sim 1/M_{Pl}^2$. However, the mass splittings between the excited graviton states can be tiny, so the graviton eigenstates are usually approximated by a continuum distribution. A summation (integration) over all allowed graviton emissions ends up cancelling the $1/M_{Pl}^2$ factor, so that observable cross section rates can be attained. Some of the fundamental production formulae for a KK graviton (denoted G) of mass m at hadron colliders include the subprocesses

$$\frac{d\sigma_m}{dt}(f\bar{f} \to \gamma G) = \frac{\alpha Q_f^2}{16N_f}\frac{1}{sM_{Pl}^2}F_1(\frac{t}{s}, \frac{m^2}{s}), \tag{49.93}$$

where Q_f is the charge of fermion f and N_f is the number of QCD colors of f. Also,

$$\frac{d\sigma_m}{dt}(q\bar{q} \to gG) = \frac{\alpha_s}{36}\frac{1}{sM_{Pl}^2}F_1(\frac{t}{s}, \frac{m^2}{s}), \tag{49.94}$$

$$\frac{d\sigma_m}{dt}(qg \to qG) = \frac{\alpha_s}{96}\frac{1}{sM_{Pl}^2}F_2(\frac{t}{s}, \frac{m^2}{s}), \tag{49.95}$$

$$\frac{d\sigma_m}{dt}(gg \to gG) = \frac{3\alpha_s}{16}\frac{1}{sM_{Pl}^2}F_3(\frac{t}{s}, \frac{m^2}{s}), \tag{49.96}$$

where

$$F_1(x,y) = \frac{1}{x(y-1-x)}\Big[-4x(1+x)(1+2x+2x^2) + y(1+6x+18x^2+16x^3) - 6y^2x(1+2x) + y^3(1+4x)\Big] \tag{49.97}$$

$$F_2(x,y) = -(y-1-x)F_1\left(\frac{x}{y-1-x}, \frac{y}{y-1-x}\right) \tag{49.98}$$

and

$$F_3(x,y) = \frac{1}{x(y-1-x)}\Big[1+2x+3x^2+2x^3+x^4 - 2y(1+x^3) + 3y^2(1+x^2) - 2y^3(1+x) + y^4\Big]. \tag{49.99}$$

These formulae must then be multiplied by the graviton density of states formula $dN = S_{n-1}\frac{M_{Pl}^2}{M_*^{n+2}}m^{n-1}dm$ to gain the cross section

$$\frac{d^2\sigma}{dtdm} = S_{n-1}\frac{M_{Pl}^2}{M_*^{n+2}}m^{n-1}\frac{d\sigma_m}{dt} \tag{49.100}$$

where $S_n = \frac{(2\pi)^{n/2}}{\Gamma(n/2)}$ is the surface area of an n-dimensional sphere of unit radius.

Virtual graviton processes can also be searched for at colliders. For instance, in Ref. [24] the cross section for Drell-Yan production of lepton pairs via gluon fusion was calculated, where it is found that, in the center-of-mass system

$$\frac{d\sigma}{dz}(gg \to \ell^+\ell^-) = \frac{\lambda^2 s^3}{64\pi M_*^8}(1-z^2)(1+z^2) \tag{49.101}$$

where $z = \cos\theta$ and λ is a model-dependent coupling constant ~ 1. Formulae for Drell-Yan production via $q\bar{q}$ fusion can also be found in Refs. [24,25].

49.11. Warped extra dimensions

In the Randall-Sundrum model [26] of warped extra dimensions, the arena for physics is a 5-d anti-deSitter (AdS_5) spacetime, for which a non-factorizable metric exists with a metric warp factor $e^{-2\sigma(\phi)}$. It is assumed that two opposite tension 3-branes exist within AdS_5 at the two ends of an S_1/Z_2 orbifold parametrized by co-ordinate ϕ which runs from $0-\pi$. The 4-D solution of the Einstein equations yields $\sigma(\phi) = kr_c|\phi|$, where r_c is the compactification radius of the extra dimension and $k \sim M_{Pl}$. The 4-D effective action allows one to identify $\overline{M}_{Pl}^2 = \frac{M^3}{k}(1 - e^{-2kr_c\pi})$, where M is the 5-D Planck scale. Physical particles on the TeV scale (SM) brane have mass $m = e^{-kr_c\pi}m_0$, where m_0 is a fundamental mass of order the Planck scale. Thus, the weak scale-Planck scale hierarchy occurs due to the existence of the exponential warp factor if $kr_c \sim 12$.

In the simplest versions of the RS model, the TeV-scale brane contains only SM particles plus a tower of KK gravitons. The RS gravitons have mass $m_n = kx_ne^{-kr_c\pi}$, where the x_i are roots of Bessel functions $J_1(x_n) = 0$, with $x_1 \simeq 3.83$, $x_2 \simeq 7.02$ etc. While the RS zero-mode graviton couplings suppressed by $1/\overline{M}_{Pl}$ and are thus inconsequential for collider searches, the $n=1$ and higher modes have couplings suppressed instead by $\Lambda_\pi = e^{-kr_c\pi}\overline{M}_{Pl} \sim TeV$. The $n=1$ RS graviton should have width $\Gamma_1 = \rho m_1 x_1^2(k/\overline{M}_{Pl})^2$, where ρ is a constant depending on how many decay modes are open. The formulae for dilepton production via virtual RS graviton exchange can be gained from the above formulae for the ADD scenario via the replacement [27]

$$\frac{\lambda}{M_*^4} \to \frac{i^2}{8\Lambda_\pi^2}\sum_{n=1}^{\infty}\frac{1}{s - m_n^2 + im_n\Gamma_n}. \tag{49.102}$$

References:

1. J.F. Owens *et al.*, Phys. Rev. **D18**, 1501 (1978). Note that cross section given in previous editions of RPP for $gg \to q\overline{q}$ lacked a factor of π.
2. F. Wilczek, Phys. Rev. Lett. **39**, 1304 (1977).
3. B.L. Ioffe and V.Khoze, Leningrad Report 274, 1976; Sov. J. Nucl. Phys. **9**, 50 (1978).
4. J. Ellis *et al.*, Nucl. Phys. **B106**, 292 (1976).
5. R.N. Cahn and S. Dawson, Phys. Lett. **B136**, 196 (1984), erratum, Phys. Lett. **B138**, 464 (1984).
6. S. Dawson, Nucl. Phys. **B249**, 42 (1985).
7. M.S. Chanowitz and M.K. Gaillard, Phys. Lett. **B142**, 85 (1984).
8. R.N. Cahn, Nucl. Phys. **B255**, 341 (1985).
9. For an exhaustive treatment, see V.M. Budnev *et al.*, Phys. Reports **15C**, 181(1975).
10. See *e.g.* H. Haber, *Supersymmetry, Part I (Theory)*, this review.
11. P. R. Harrison and C. H. Llewellyn Smith, Nucl. Phys. **B213**, 223 (1983), Erratum-*ibid.*, **B223**, 542 (1983); S. Dawson, E. Eichten, and C. Quigg, Phys. Rev. **D31**, 1581 (1985); V. Barger *et al.*, Phys. Rev. **D31**, 528 (1985); H. Baer and X. Tata, Phys. Lett. **B160**, 159 (1985).
12. H. Baer, D. Karatas, and X. Tata, Phys. Rev. **D42**, 2259 (1990).
13. H. Haber and G. Kane, Phys. Rept. **117**, 75 (1985).
14. Theory and Phenomenology of Sparticles, M. Drees, R. Godbole, and P. Roy (World Scientific) 2005.

15. Weak Scale Supersymmetry: From Superfields to Scattering Events, H. Baer and X. Tata (Cambridge University Press) 2006.
16. A. Bartl, H. Fraas, and W. Majerotto, Z. Phys. **C30**, 441 (1986).
17. H. Baer *et al.*, Int. J. Mod. Phys. **A4**, 4111 (1989).
18. A. Bartl, H. Fraas, and W. Majerotto, Nucl. Phys. **B278**, 1 (1986).
19. T. Appelquist, H.C. Cheng, and B. Dobrescu, Phys. Rev. **D64**, 035002 (2001).
20. For a review of models with extra spacetime dimensions, see G. Giudice and J. Wells, *Extra Dimensions*, this *Review*.
21. J.M. Smillie and B.R. Webber, JHEP **0510**, 069 (2005).
22. C. Macesanu, C.D. McMullen, and S. Nandi, Phys. Rev. **D66**, 015009 (2002).
23. N. Arkani-Hamed, S. Dimopoulos, and G. Dvali, Phys. Lett. **B429**, 263 (1998) and Phys. Rev. **D59**, 086004 (1999).
24. J. L. Hewett, Phys. Rev. Lett. **82**, 4765 (1999).
25. G. Giudice, R. Rattazzi, and J. Wells, Nucl. Phys. **B544**, 3 (1999); E.A. Mirabelli, M. Perelstein, and M.E. Peskin, Phys. Rev. Lett. **82**, 2236 (1999); T. Han, J. Lykken, and R. Zhang, Phys. Rev. **D59**, 105006 (1999).
26. L. Randall and R.S. Sundrum, Phys. Rev. Lett. **83**, 3370 (1999).
27. H. Davoudiasl, J.L. Hewett, and T.G. Rizzo, Phys. Rev. Lett. **84**, 2080 (2000).

50. Neutrino Cross Section Measurements

Revised August 2017 by G.P. Zeller (Fermilab)

Neutrino cross sections are an essential ingredient in all neutrino experiments. Interest in neutrino scattering has recently increased due to the need for such information in the interpretation of neutrino oscillation data [1]. Historically, neutrino scattering results on both charged current (CC) and neutral current (NC) channels have been collected over many decades using a variety of targets, analysis techniques, and detector technologies. With the advent of intense neutrino sources constructed for neutrino oscillation investigations, experiments are now remeasuring these cross sections with a renewed appreciation for nuclear effects† and the importance of improved neutrino flux estimations. This work summarizes accelerator-based neutrino cross section measurements performed in the $\sim 0.1 - 300$ GeV range with an emphasis on inclusive, quasi-elastic, and pion production processes, areas where we have the most experimental input at present (Table 50.1). For a more comprehensive discussion of neutrino cross sections, including neutrino-electron elastic scattering and lower energy neutrino measurements, the reader is directed to a review of this subject [2]. Here, we survey existing experimental data on neutrino interactions and do not attempt to provide a census of the associated theoretical calculations [3], which are both important and plentiful.

50.1. Inclusive Scattering

Over the years, many experiments have measured the total inclusive charged current cross section for neutrino ($\nu_\mu N \to \mu^- X$) and antineutrino ($\overline{\nu}_\mu N \to \mu^+ X$) scattering off nucleons covering a broad range of neutrino energies. As can be seen in Fig. 50.1, the inclusive cross section approaches a linear dependence on neutrino energy. Such behavior is expected for point-like scattering of neutrinos from quarks, an assumption which breaks down at lower energies. Modern measurements of inclusive scattering cross sections and their target nuclei are summarized in Table 50.2.

To provide a more complete picture, differential cross sections for such inclusive scattering processes have also been reported – these include measurements on iron from NuTeV [18] and, more recently, at lower neutrino energies on argon from ArgoNeuT [4,5] and carbon from T2K [13]. MINERvA has also provided double differential cross sections [8] as well as ratio measurements of muon neutrino inclusive and deep inelastic scattering (DIS) cross sections on a variety of nuclear targets such as lead, iron, and carbon [6,19]. At high energy, the inclusive cross section is dominated by deep inelastic scattering. Several high energy neutrino experiments have measured the DIS cross sections for specific final states, for example opposite-sign dimuon production. The most recent dimuon cross section measurements include those from CHORUS [20], NOMAD [21], and NuTeV [22]. At lower neutrino energies, the inclusive cross section is an additionally complex combination of quasi-elastic scattering and pion production processes, two areas we discuss next.

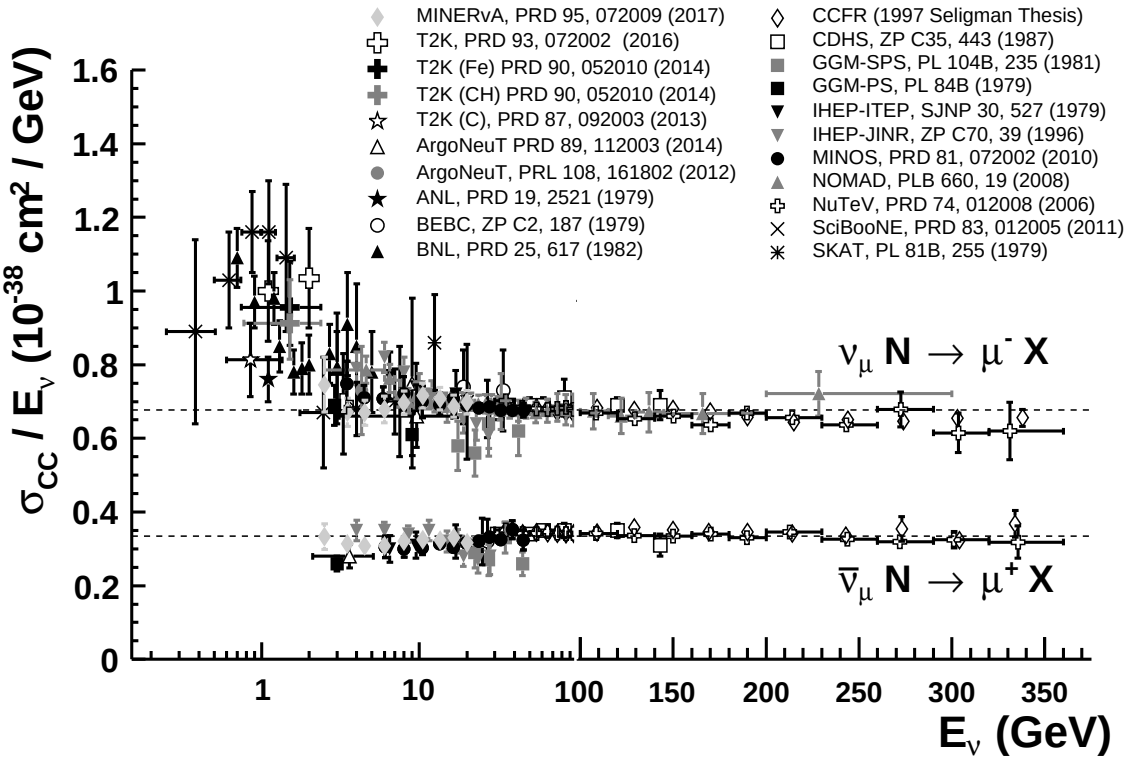

Fig. 50.1: Measurements of per nucleon ν_μ and $\overline{\nu}_\mu$ CC inclusive scattering cross sections divided by neutrino energy as a function of neutrino energy. Note the transition between logarithmic and linear scales occurring at 100 GeV. Neutrino cross sections are typically twice as large as their corresponding antineutrino counterparts, although this difference can be larger at lower energies. NC cross sections (not shown) are generally smaller compared to the CC case.

† Nuclear effects refer to kinematic and final state effects which impact neutrino scattering off nuclei. Such effects can be significant and are particularly relevant given that modern neutrino experiments make use of nuclear targets to increase their event yields.

Table 50.1: List of beam properties, nuclear targets, and durations for modern accelerator-based neutrino experiments studying neutrino scattering.

Experiment	beam	$\langle E_\nu \rangle$, $\langle E_{\overline{\nu}} \rangle$ GeV	neutrino target(s)	run period
ArgoNeuT	$\nu, \overline{\nu}$	4.3, 3.6	Ar	2009 – 2010
ICARUS (at CNGS)	ν	20.0	Ar	2010 – 2012
K2K	ν	1.3	CH, H_2O	2003 – 2004
MicroBooNE	ν	0.8	Ar	2015 –
MINERvA	$\nu, \overline{\nu}$	3.5 (LE), 5.5 (ME)	He, C, CH, H_2O, Fe, Pb	2009 –
MiniBooNE	$\nu, \overline{\nu}$	0.8, 0.7	CH_2	2002 – 2012
MINOS	$\nu, \overline{\nu}$	3.5, 6.1	Fe	2004 – 2016
NOMAD	$\nu, \overline{\nu}$	23.4, 19.7	C–based	1995 – 1998
NOvA	$\nu, \overline{\nu}$	2.0, 2.0	CH_2	2010 –
SciBooNE	$\nu, \overline{\nu}$	0.8, 0.7	CH	2007 – 2008
T2K	$\nu, \overline{\nu}$	0.6, 0.6	CH, H_2O, Fe	2010 –

Table 50.2: Summary of published measurements of neutrino CC inclusive cross sections from modern accelerator-based neutrino experiments.

experiment	measurement	target
ArgoNeuT	ν_μ CC [4,5], $\overline{\nu}_\mu$ CC [5]	Ar
MINERνA	ν_μ CC [6,7,8], $\overline{\nu}_\mu$ CC [7], $\nu_\mu/\overline{\nu}_\mu$ CC [9]	CH, C/CH, Fe/CH, Pb/CH
MINOS	ν_μ CC [10], $\overline{\nu}_\mu$ CC [10]	Fe
NOMAD	ν_μ CC [11]	C
SciBooNE	ν_μ CC [12]	CH
T2K	ν_μ CC [13,14,15], ν_e CC [16,17]	CH, H_2O, Fe

Table 50.3: Published measurements of CC and NC scattering cross sections with nucleon-only final states from modern neutrino experiments.

experiment	measurement	target
ArgoNeuT	2p [27]	Ar
K2K	M_A [28]	H_2O
MINERνA	$\frac{d\sigma}{dQ^2}$ [29,30,31], 1p [32], ν_e [33]	C, CH, Fe, Pb
MiniBooNE	$\frac{d^2\sigma}{dT_\mu d\theta_\mu}$ [23,24], M_A [34], NC [35,36]	CH_2
MINOS	M_A [37]	Fe
NOMAD	M_A, $\sigma(E_\nu)$ [38]	C
T2K	$\frac{d^2\sigma}{dT_\mu d\theta_\mu}$ [26], $\sigma(E_\nu)$ [39], M_A [40], NC [41]	CH

50.2. Quasi-elastic scattering

Quasi-elastic (QE) scattering is the dominant neutrino interaction for neutrino energies less than ~ 1 GeV and represents a large fraction of the signal samples in many neutrino oscillation experiments, which is why this process is particularly important. Historically, neutrino (antineutrino) quasi-elastic scattering refers to the process, $\nu_\mu\, n \to \mu^-\, p$ ($\overline{\nu}_\mu\, p \to \mu^+\, n$), where a charged lepton and single nucleon are ejected in the elastic interaction of a neutrino (or antineutrino) with a nucleon in the target material. This is the final state one would strictly observe, for example, in scattering off of a free nucleon target. There were many early measurements of neutrino QE scattering that span back to the 1970's [2]. In many of these initial measurements of the neutrino QE cross section, bubble chamber experiments employed light targets (H_2 or D_2) and required both the detection of the final state muon and single nucleon‡; thus the final state was clear and elastic kinematic conditions could be verified. The situation is more complicated, of course, for the heavier nuclear targets used in modern neutrino experiments. In this case, nuclear effects can impact the size and shape of the cross section as well as the final state composition, kinematics, and topology. Due to intranuclear hadron rescattering and the possible effects of correlations between target nucleons, additional nucleons may be ejected in the final state; hence, a QE interaction on a nuclear target does not necessarily imply the ejection of a *single* nucleon. One therefore needs to take some care in defining what one means by neutrino QE scattering when scattering off targets heavier than H_2 or D_2. Modern experiments tend to instead report cross sections for processes involving nucleon-only final states (often referred to as "CC 0π" or "QE-like" reactions). Such measurements are summarized in Table 50.3. Many modern experiments have also recently opted to report nucleon-only cross sections as a function of final state particle kinematics [23,24,25,26]. Such distributions can be more difficult to directly compare between experiments but are much less model-dependent and provide more stringent tests of the theory than historical cross sections as a function of neutrino energy (E_ν) or 4-momentum transfer (Q^2).

‡ In the case of D_2, many experiments additionally observed the spectator proton.

Adding to this complexity, MiniBooNE measurements of the ν_μ and $\overline{\nu}_\mu$ QE scattering cross sections on carbon near 1 GeV revealed a significantly larger cross section than originally anticipated [23,24]. Such an enhancement was observed many years prior in electron-nucleus scattering [42] and is believed to be due to the presence of correlations between target nucleons in the nucleus. As a result, the impact of such nuclear effects on neutrino QE scattering has recently been the subject of intense experimental and theoretical scrutiny with potential implications on event rates, nucleon emission, neutrino energy reconstruction, and neutrino versus antineutrino cross sections. The reader is referred to recent reviews of the situation in [3,43,44]. Additional measurements are clearly needed before a complete understanding is achieved. To help drive further progress, nucleon-only cross sections have been reported for the first time in the form of double-differential distributions in muon kinematics, $d^2\sigma/dT_\mu d\cos\theta_\mu$, by both MiniBooNE [23,24] and T2K [26] thus reducing some of the model-dependence of the reported data and allowing a more rigorous two-dimensional test of the underlying nuclear theory. Such double-differential cross sections in terms of final state particle kinematics provide the most robust measurements available. In addition, experiments such as ArgoNeuT have begun to provide the first measurements of proton multiplicities in neutrino-argon scattering [25,27], a critical ingredient in understanding the hadronic side of these interactions and the impact of final state effects. MINOS, NOvA, and T2K have also started to study nucleon-only final states in their near detectors with sizable statistics [26,37,39,40,45]. Most recently, MINERvA has produced a large body of work exploring this reaction channel, having measured differential cross sections [8,29,30], nuclear target dependencies [31], single proton emission [32], and ν_e QE scattering [33]. With the MiniBooNE results having first revealed these additional complexities in neutrino-nucleus QE scattering, measurements from other neutrino experiments are crucial for getting a better handle on the underlying nuclear physics impacting neutrino-nucleus interactions. What we once thought was "simple" QE scattering is in fact not so simple.

In addition to such charged current investigations, measurements of the neutral current counterpart of this channel have also been performed. The most recent NC elastic scattering cross section measurements include those from BNL E734 [46], MiniBooNE [35,36], and T2K [41]. A number of measurements of the Cabibbo-suppressed antineutrino QE hyperon production cross section have additionally been reported [47,48], although not in recent years.

50.3. Pion Production

In addition to such elastic processes, neutrinos can also inelastically scatter producing a nucleon excited state (Δ, N^*). Such baryonic resonances quickly decay, most often to a nucleon and single-pion final state. Historically, experiments have measured various exclusive final states associated with these reactions, the majority of which have been on hydrogen and deuterium targets [2]. There have been several recent re-analyses of this data to better understand the consistency between data sets [49], nucleon form factors [50], and non-resonant contributions [51]. Also, modern measurements of neutrino-induced pion production have since been performed on a variety of nuclear targets (Table 50.4).

In addition to resonance production processes, neutrinos can also coherently scatter off of the entire nucleus and produce a distinctly forward-scattered single pion final state. Both CC ($\nu_\mu A \to \mu^- A \pi^+$, $\overline{\nu}_\mu A \to \mu^+ A \pi^-$) and NC ($\nu_\mu A \to \nu_\mu A\pi^0, \overline{\nu}_\mu A \to \overline{\nu}_\mu A\pi^0$) processes are possible in this case. Even though the level of coherent pion production is small compared to resonant processes, observations exist across a broad energy range and on multiple nuclear targets [76]. More recently, several modern neutrino experiments have measured or set limits on coherent pion production cross sections including ArgoNeuT [52], K2K [55], MINERvA [60], MiniBooNE [68], MINOS [69], NOMAD [70], SciBooNE [71,73], and T2K [75].

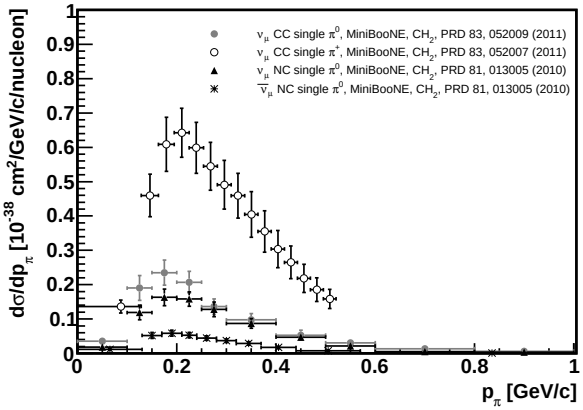

Figure 50.2: Differential cross sections for CC and NC pion production from MiniBooNE at a mean neutrino energy of 0.8 GeV. Shown here are the measurements as a function of the momentum of the outgoing pion in the interaction, a kinematic that is particularly sensitive to final state interactions. Other distributions are also available in the publications listed in the legend.

As with QE scattering, a new appreciation for the significance of nuclear effects has surfaced in pion production channels, again due to the use of heavy nuclear targets in modern neutrino experiments. Many experiments have been careful to report cross sections for various detected final states, thereby not correcting for large and uncertain nuclear effects (e.g., pion rescattering, charge exchange, and absorption) which can introduce significant sources of uncertainty and model dependence. Providing the most comprehensive survey of neutrino single-pion production to date, MiniBooNE has published a total of 16 single- and double-differential cross sections for both the final state muon (in the case of CC scattering) and pions in these interactions; thus, providing the first measurements of these distributions (Fig. 50.2) [64–67]. MINERvA has recently produced similar kinematic measurements at higher neutrino energies [59,62] and T2K at lower energies [74]. Importantly, MINERvA has been working towards an improved nuclear model that can describe all of the pion reaction channels simultaneously, an issue that many experiments have struggled with up until now [59]. Regardless of the interaction channel, such differential cross section measurements in

Table 50.4: Summary of modern measurements of NC and CC scattering cross sections involving a pion (or pions) in the final state.

experiment	$\pi^\pm$ measurement	π^0 measurement	target
ArgoNeuT	CC [52]	NC [53]	Ar
K2K	CC [54,55]	CC [56], NC [57]	CH, H_2O
MINERνA	CC [58,59,60]	CC [59,61,62], NC [63]	CH
MiniBooNE	CC [64,65]	CC [66], NC [67,68]	CH_2
MINOS	–	NC [69]	Fe
NOMAD	–	NC [70]	C
SciBooNE	CC [71]	NC [72,73]	CH
T2K	CC [74,75]	–	CH, H_2O

terms of observed final state particle kinematics are now preferred for their reduced model dependence and for the additional kinematic information they provide. Such a new direction has been the focus of modern measurements as opposed to the reporting of more model-dependent, historical cross sections as a function of E_ν or Q^2. Together with similar results for other interaction channels, a better understanding and modeling of nuclear effects will be possible moving forward.

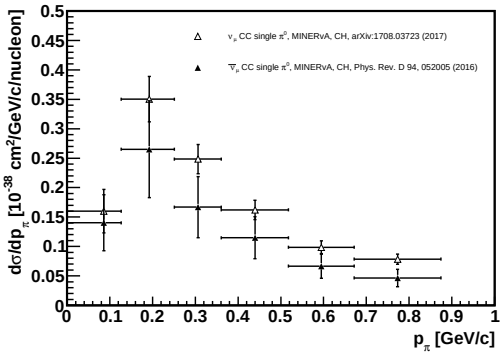

Figure 50.3: Differential cross sections for neutrino (W< 1.4 GeV) and antineutrino (W< 1.8 GeV) CC π^0 production from MINERvA at a mean neutrino energy of 3.3 GeV. Shown here are the measurements as a function of the momentum of the outgoing pion in the interaction, a kinematic that is particularly sensitive to final state interactions. Other distributions are available in the publications listed in the legend as well as for charged pion production [59].

It should be noted that baryonic resonances can also decay to multi-pion, other mesonic (K, η, ρ, etc.), and even photon final states. Experimental results for these channels are typically sparse or non-existent [2]; however, photon production processes can be an important background for $\nu_\mu \to \nu_e$ appearance searches and thus have become the focus of some recent experimental investigations; for example, in NOMAD [77]. There have also been several recent measurements of kaon final states produced in neutrino NC and CC scattering in MINERvA [78,79,80].

50.4. Outlook

Currently operating experiments will continue to produce additional neutrino cross section measurements as they accumulate additional statistics, while a few new experiments will soon be coming online. In the coming years, analysis of a broad energy range of data on a variety of targets in the MINERvA experiment will provide the most detailed analysis yet of nuclear effects in neutrino interactions. Data from ArgoNeuT, ICARUS, MicroBooNE, and SBND will probe deeper into complex neutrino final states using the superior capabilities of liquid argon time projection chambers, while the T2K and NOvA near detectors will collect high statistics samples in intense neutrino beams. Together, these investigations should significantly advance our understanding of neutrino-nucleus scattering in the next decade.

50.5. Acknowledgments

The author thanks Anne Schukraft (Fermilab) for help in updating the plots and information contained in this review.

References:

1. O. Benhar *et al.*, Phys. Rept. 700, 1 (2017).
2. J.A. Formaggio and G.P. Zeller, Rev. Mod. Phys. **84**, 1307 (2012).
3. L. Alvarez-Ruso *et al.*, `arXiv:1706.03621` [hep-ph].
4. C. Anderson *et al.*, Phys. Rev. Lett. **108**, 161802 (2012).
5. R. Acciarri *et al.*, Phys. Rev. **D89**, 112003 (2014).
6. B.G. Tice *et al.*, Phys. Rev. Lett. **112**, 231801 (2014).
7. J. DeVan *et al.*, Phys. Rev. **D94**, 112007 (2016).
8. P.A. Rodrigues *et al.*, Phys. Rev. Lett. **116**, 071802 (2016).
9. L. Ren *et al.*, Phys. Rev. **D95**, 072009 (2017).
10. P. Adamson *et al.*, Phys. Rev. **D81**, 072002 (2010).
11. Q. Wu *et al.*, Phys. Lett. **B660**, 19 (2008).
12. Y. Nakajima *et al.*, Phys. Rev. **D83**, 12005 (2011).
13. K. Abe *et al.*, Phys. Rev. **D87**, 092003 (2013).
14. K. Abe *et al.*, Phys. Rev. **D90**, 052010 (2014).
15. K. Abe *et al.*, Phys. Rev. **D93**, 072002 (2016).
16. K. Abe *et al.*, Phys. Rev. Lett. **113**, 241803 (2014).
17. K. Abe *et al.*, Phys. Rev. **D91**, 112010 (2015).
18. M. Tzanov *et al.*, Phys. Rev. **D74**, 012008 (2006).
19. J. Mousseau *et al.*, Phys. Rev. **D93**, 071101 (2016).
20. A. Kayis-Topaksu *et al.*, Nucl. Phys. **B798**, 1 (2008).
21. O. Samoylov *et al.*, Nucl. Phys. **B876**, 339 (2013).
22. D. Mason *et al.*, Phys. Rev. Lett. **99**, 192001 (2007).
23. A.A. Aguilar-Arevalo *et al.*, Phys. Rev. **D81**, 092005 (2010).
24. A.A. Aguilar-Arevalo *et al.*, Phys. Rev. **D88**, 032001 (2013).
25. O. Palamara, JPS Conf. Proc. 12, 010017 (2016).
26. K. Abe *et al.*, Phys. Rev. **D93**, 112012 (2016).
27. R. Acciarri *et al.*, Phys. Rev. **D90**, 012008 (2014).
28. R. Gran *et al.*, Phys. Rev. **D74**, 052002 (2006).
29. G.A. Fiorentini *et al.*, Phys. Rev. Lett. **111**, 022502 (2013).
30. L. Fields *et al.*, Phys. Rev. Lett. **111**, 022501 (2013).
31. M. Betancourt *et al.*, Phys. Rev. Lett. **119**, 082001 (2017).
32. T. Walton *et al.*, Phys. Rev. **D91**, 071301 (2015).
33. J. Wolcott *et al.*, Phys. Rev. Lett. **116**, 081802 (2016).
34. A.A. Aguilar-Arevalo *et al.*, Phys. Rev. Lett. **100**, 032301 (2008).
35. A.A. Aguilar-Arevalo *et al.*, Phys. Rev. **D82**, 092005 (2010).
36. A.A. Aguilar-Arevalo *et al.*, Phys. Rev. **D91**, 012004 (2015).
37. P. Adamson *et al.*, Phys. Rev. **91**, 012005 (2015).
38. V. Lyubushkin *et al.*, Eur. Phys. J. **C63**, 355 (2009).
39. K. Abe *et al.*, Phys. Rev. **D91**, 112002 (2015).
40. K. Abe *et al.*, Phys. Rev. **D92**, 112003 (2015).
41. K. Abe *et al.*, Phys. Rev. **D90**, 072012 (2014).
42. J. Carlson *et al.*, Phys. Rev. **C65**, 024002 (2002).
43. H. Gallagher *et al.*, Ann. Rev. Nucl. and Part. Sci. **61**, 355 (2011).
44. G.T. Garvey *et al.*, Phys. Reports **580**, 1 (2015).
45. M. Betancourt, Ph.D. thesis, University of Minnesota, 2013.
46. L.A. Ahrens *et al.*, Phys. Rev. **D35**, 785 (1987).
47. J. Brunner *et al.*, Z. Phys. **C45**, 551 (1990).
48. V.V. Ammosov *et al.*, Z. Phys. **C36**, 377 (1987); O. Erriques *et al.*, Phys. Lett. **70B**, 383 (1977); T. Eichten *et al.*, Phys. Lett. **40B**, 593 (1972).
49. C. Wilkinson *et al.*, Phys. Rev. **D90**, 112017 (2014).
50. A. Meyer *et al.*, Phys. Rev. **D93**, 113015 (2016).
51. P. Rodrigues *et al.*, `arXiv:1601.01888` [hep-ex].
52. R. Acciarri *et al.*, Phys. Rev. Lett. **113**, 261801 (2014).
53. R. Acciarri *et al.*, Phys. Rev. **D96**, 012006 (2017).
54. A. Rodriguez *et al.*, Phys. Rev. **D78**, 032003 (2008).
55. M. Hasegawa *et al.*, Phys. Rev. Lett. **95**, 252301 (2005).
56. C. Mariani *et al.*, Phys. Rev. **D83**, 054023 (2011).
57. S. Nakayama *et al.*, Phys. Lett. **B619**, 255 (2005).
58. B. Eberly *et al.*, Phys. Rev. **D92**, 092008 (2015).
59. C.L. McGivern *et al.*, Phys. Rev. **D94**, 052005 (2016).
60. A. Higuera *et al.*, Phys. Rev. Lett. **113**, 261802 (2014).
61. T. Le *et al.*, Phys. Lett. **B749**, 130 (2015).
62. O. Altinok *et al.*, Phys. Rev. **D96**, 072003 (2017) [`arXiv:1708.03723`].
63. J. Wolcott *et al.*, Phys. Rev. Lett. **117**, 111801 (2016).
64. A.A. Aguilar-Arevalo *et al.*, Phys. Rev. **D83**, 052007 (2011).
65. A.A. Aguilar-Arevalo *et al.*, Phys. Rev. Lett. **103**, 081801 (2009).
66. A.A. Aguilar-Arevalo *et al.*, Phys. Rev. **D83**, 052009 (2011).
67. A.A. Aguilar-Arevalo *et al.*, Phys. Rev. **D81**, 013005 (2010).
68. A.A. Aguilar-Arevalo *et al.*, Phys. Lett. **B664**, 41 (2008).
69. P. Adamson *et al.*, Phys. Rev. **D94**, 072006 (2016).
70. C.T. Kullenberg *et al.*, Phys. Lett. **B682**, 177 (2009).
71. K. Hiraide *et al.*, Phys. Rev. **D78**, 112004 (2008).
72. Y. Kurimoto *et al.*, Phys. Rev. **D81**, 033004 (2010).
73. Y. Kurimoto *et al.*, Phys. Rev. **D81**, 111102 (R)(2010).
74. K. Abe *et al.*, Phys. Rev. **D95**, 012010 (2017).
75. K. Abe *et al.*, Phys. Lett. **117**, 192501 (2016).

76. For a compilation of historical coherent pion production data, please see P. Villain *et al.*, Phys. Lett. **B313**, 267 (1993).
77. C.T. Kullenberg *et al.*, Phys. Lett. **B706**, 268 (2012).
78. C.M. Marshall *et al.*, Phys. Rev. **D94**, 012002 (2016).
79. C.M. Marshall *et al.*, Phys. Rev. Lett. **119**, 011802 (2017).
80. Z. Wang *et al.*, Phys. Rev. Lett. **117**, 061802 (2016).

51. Plots of Cross Sections and Related Quantities

Updated in 2017. See various sections for details.

This section contains a compilation of plots and tables on cross sections and related quantities that are not covered by other reviews but may be of interest to the community. The topics include:

– Pseudorapidity distributions in pp and $\overline{p}p$ interactions

– Table of average hadron multiplicities in hadronic e^+e^- annihilation events

– Cross section and R ratio in e^+e^- collisions

– R ratio in light-flavor, charm, and beauty threshold regions

– Annihilation cross section near M_Z

– Total cross section plots for hadronic (e.g. pp and $\overline{p}p$ collisions), γp, γd, and $\gamma\gamma$ processes

Pseudorapidity Distributions in pp and $\overline{p}p$ Interactions

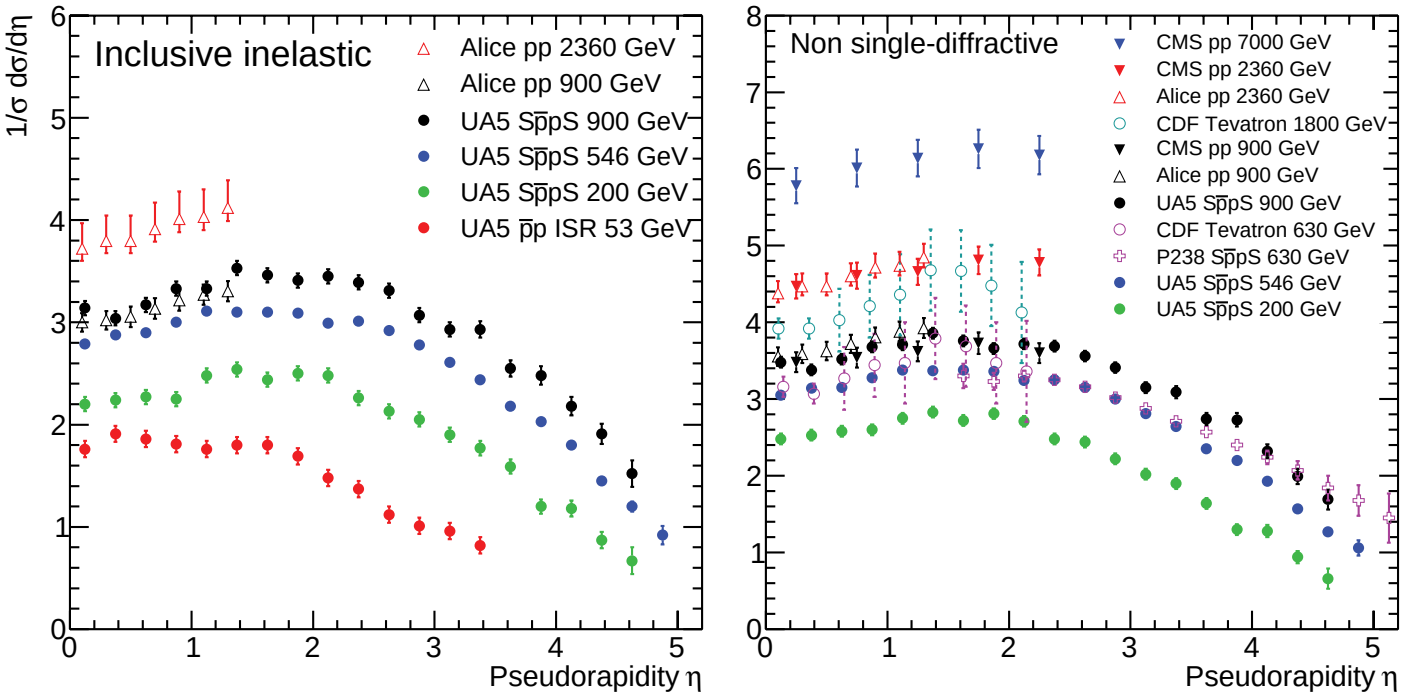

Figure 51.1: Charged particle pseudorapidity distributions in $p\overline{p}$ collisions for 53 GeV $\leq \sqrt{s} \leq$ 1800 GeV. UA5 data from the S$p\overline{p}$S are taken from G.J.Alner *et al.*, Z. Phys. **C33**, 1 (1986), and from the ISR from K.Alpgøard *et al.*, Phys.Lett. 112B 193 (1982). The UA5 data are shown for both the full inelastic cross-section and with singly diffractive events excluded. Additional non single-diffractive measurements are available from CDF at the Tevatron, F.Abe *et al.*, Phys. Rev. **D41**, 2330 (1990) and from P238 at the S$p\overline{p}$S, R.Harr *et al.*, Phys. Lett. **B401**, 176 (1997). These may be compared with both inclusive and non single-diffractive measurements in pp collisions at the LHC from ALICE, K.Aamodt *et al.*, Eur. Phys. J. **C68**, 89 (2010) and for non single-diffractive interactions from CMS , V.Khachatryan *et al.*, JHEP 1002:041 (2010), Phys. Rev. Lett. **105**, 022002 (2010). (Courtesy of D.R. Ward, Cambridge Univ., 2013)

Average Hadron Multiplicities in Hadronic e^+e^- Annihilation Events

Table 51.1: Average hadron multiplicities per hadronic e^+e^- annihilation event at $\sqrt{s} \approx 10$, 29–35, 91, and 130–200 GeV. The rates given include decay products from resonances with $c\tau < 10$ cm, and include the corresponding anti-particle state. Correlations of the systematic uncertainties were considered for the calculation of the averages. Quoted errors are not increased by scale factor S. (Updated August 2017 by O. Biebel, LMU, Munich)

Particle	$\sqrt{s} \approx 10$ GeV	$\sqrt{s} = 29$–35 GeV	$\sqrt{s} = 91$ GeV	$\sqrt{s} = 130$–200 GeV
Pseudoscalar mesons:				
π^+	6.52 ± 0.11	10.3 ± 0.4	17.02 ± 0.19	21.24 ± 0.39
π^0	3.2 ± 0.3	5.83 ± 0.28	9.42 ± 0.32	
K^+	0.953 ± 0.018	1.48 ± 0.09	2.228 ± 0.059	2.82 ± 0.19
K^0	0.91 ± 0.05	1.48 ± 0.07	2.049 ± 0.026	2.10 ± 0.12
η	0.20 ± 0.04	0.61 ± 0.07	1.049 ± 0.080	
$\eta'(958)$	0.03 ± 0.01	0.26 ± 0.10	0.152 ± 0.020	
D^+	$0.194 \pm 0.019^{(a)}$	0.17 ± 0.03	0.175 ± 0.016	
D^0	$0.446 \pm 0.032^{(a)}$	0.45 ± 0.07	0.454 ± 0.030	
D_s^+	$0.063 \pm 0.014^{(a)}$	$0.45 \pm 0.20^{(b)}$	0.131 ± 0.021	
$B^{(c)}$	—	—	$0.134 \pm 0.016^{(d)}$	
B^+	—	—	$0.141 \pm 0.004^{(d)}$	
B_s^0	—	—	$0.054 \pm 0.011^{(d)}$	
Scalar mesons:				
$f_0(980)$	0.024 ± 0.006	$0.05 \pm 0.02^{(e)}$	0.146 ± 0.012	
$a_0(980)^\pm$	—	—	$0.27 \pm 0.11^{(f)}$	
Vector mesons:				
$\rho(770)^0$	0.35 ± 0.04	0.81 ± 0.08	1.231 ± 0.098	
$\rho(770)^\pm$	—	—	$2.40 \pm 0.43^{(f)}$	
$\omega(782)$	0.30 ± 0.08	—	1.016 ± 0.065	
$K^*(892)^+$	0.27 ± 0.03	0.64 ± 0.05	0.714 ± 0.055	
$K^*(892)^0$	0.29 ± 0.03	0.56 ± 0.06	0.738 ± 0.024	
$\phi(1020)$	0.044 ± 0.003	0.085 ± 0.011	0.0963 ± 0.0032	
$D^*(2010)^+$	$0.177 \pm 0.022^{(a)}$	0.43 ± 0.07	$0.1937 \pm 0.0057^{(g)}$	
$D^*(2007)^0$	$0.168 \pm 0.019^{(a)}$	0.27 ± 0.11	—	
$D_s^*(2112)^+$	$0.048 \pm 0.014^{(a)}$	—	$0.101 \pm 0.048^{(h)}$	
$B^{*\ (i)}$	—	—	0.288 ± 0.026	
$J/\psi(1S)$	$0.00050 \pm 0.00005^{(a)}$	—	$0.0052 \pm 0.0004^{(j)}$	
$\psi(2S)$	—	—	$0.0023 \pm 0.0004^{(j)}$	
$\Upsilon(1S)$	—	—	$0.00014 \pm 0.00007^{(j)}$	
Pseudovector mesons:				
$f_1(1285)$	—	—	0.165 ± 0.051	
$f_1(1420)$	—	—	0.056 ± 0.012	
$\chi_{c1}(3510)$	—	—	$0.0041 \pm 0.0011^{(j)}$	
Tensor mesons:				
$f_2(1270)$	0.09 ± 0.02	0.14 ± 0.04	0.166 ± 0.020	
$f_2'(1525)$	—	—	0.012 ± 0.006	
$K_2^*(1430)^+$	—	0.09 ± 0.03	—	
$K_2^*(1430)^0$	—	0.12 ± 0.06	0.084 ± 0.022	
$B^{**\ (k)}$	—	—	0.118 ± 0.024	
$D_{s1}^\pm$	—	—	$0.0052 \pm 0.0011^{(\ell)}$	
$D_{s2}^{*\pm}$	—	—	$0.0083 \pm 0.0031^{(\ell)}$	
Baryons:				
p	0.266 ± 0.008	0.640 ± 0.050	1.050 ± 0.032	1.41 ± 0.18
Λ	$0.093 \pm 0.006^{(a)}$	0.205 ± 0.010	0.3915 ± 0.0065	0.39 ± 0.03
Σ^0	$0.0221 \pm 0.0018^{(a)}$	—	0.078 ± 0.010	
Σ^-	—	—	0.081 ± 0.010	
Σ^+	—	—	0.107 ± 0.011	
$\Sigma^\pm$	—	—	0.174 ± 0.009	
Ξ^-	$0.0055 \pm 0.0004^{(a)}$	0.0176 ± 0.0027	0.0262 ± 0.0009	
$\Delta(1232)^{++}$	0.040 ± 0.010	—	0.085 ± 0.014	
$\Sigma(1385)^-$	0.006 ± 0.002	0.017 ± 0.004	0.0240 ± 0.0017	
$\Sigma(1385)^+$	$0.0062 \pm 0.0011^{(a)}$	0.017 ± 0.004	0.0239 ± 0.0015	
$\Sigma(1385)^\pm$	0.0106 ± 0.0020	0.033 ± 0.008	0.0472 ± 0.0027	
$\Xi(1530)^0$	$0.00130 \pm 0.00010^{(a)}$	—	0.00694 ± 0.00049	
Ω^-	$0.00060 \pm 0.00033^{(a)}$	0.014 ± 0.007	0.00124 ± 0.00018	
Λ_c^+	$0.0479 \pm 0.0038^{(a,m)}$	0.110 ± 0.050	0.078 ± 0.017	
Λ_b^0	—	—	0.031 ± 0.016	
Σ_c^0	$0.0025 \pm 0.0004^{(a)}$	—	—	
$\Lambda(1520)$	$0.0046 \pm 0.0004^{(a)}$	—	0.0222 ± 0.0027	

Notes for Table 51.1:

(*a*) $\sigma_{\rm had} = 3.33 \pm 0.05 \pm 0.21$ nb (**CLEO**: Phys. Rev. **D29**, 1254 (1984)) has been used in converting the measured cross sections to average hadron multiplicities.

(*b*) B($D_s \to \eta\pi,\ \eta'\pi$) was used (RPP 1994).

(*c*) Comprises both charged and neutral B meson states.

(*d*) The Standard Model B($Z \to b\overline{b}$) = 0.217 was used.

(*e*) $x_p = p/p_{\rm beam} > 0.1$ only.

(*f*) Both charge states.

(*g*) B($D^*(2010)^+ \to D^0\pi^+$) × B($D^0 \to K^-\pi^+$) has been used (RPP 2000).

(*h*) B($D_s^* \to D_S^+\gamma$), B($D_s^+ \to \phi\pi^+$), B($\phi \to K^+K^-$) have been used (RPP 1998).

(*i*) Any charge state (*i.e.*, B_d^*, B_u^*, or B_s^*).

(*j*) B($Z \to$ hadrons) = 0.699 was used (RPP 1994).

(*k*) Any charge state (*i.e.*, B_d^{**}, B_u^{**}, or B_s^{**}).

(*ℓ*) Assumes B($D_{s1}^+ \to D^{*+}K^0 + D^{*0}K+$) = 100% and B($D_{s2}^+ \to D^0K^+$) = 45%.

(*m*) The value was derived from the cross section of $\Lambda_c^+ \to p\pi K$ using (*a*) and assuming the branching fraction to be (5.0 ± 1.3)% (RPP 2004).

References for Table 51.1:

RPP 1992: Phys. Rev. **D45** (1992); **RPP 1994**: Phys. Rev. **D50**, 1173 (1994); **RPP 1996**: Phys. Rev. **D54**, 1 (1996); **RPP 1998**: Eur. Phys. J. **C3**, 1 (1998); **RPP 2000**: Eur. Phys. J. **C15**, 1 (2000); **RPP 2002**: Phys. Rev. **D66**, 010001 (2002); **RPP 2004**: Phys. Lett. **B592**, 1 (2004); **RPP 2006**: J. Phys. **G33**, 1 (2006); **RPP 2008**: Phys. Lett. **B667**, 1 (2008); **RPP 2010**: J. Phys. **G37**, 075021 (2010); **RPP 2012**: Phys. Rev. D 86,010001(2012) and references therein; **RPP 2014**: Chin. Phys. C **38**, 090001 (2014) and references therein; **RPP 2016**: Chin. Phys. C **40**, 100001 (2016) and references therein.

R. Marshall, Rept. on Prog. in Phys. **52**, 1329 (1989). A. De Angelis, J. Phys. **G19**, 1233 (1993) and references therein.

ALEPH: D. Buskulic *et al.*: Phys. Lett. **B295**, 396 (1992); Z. Phys. **C64**, 361 (1994); **C69**, 15 (1996); **C69**, 379 (1996); **C73**, 409 (1997); and R. Barate *et al.*: Z. Phys. **C74**, 451 (1997); Phys. Reports **294**, 1 (1998); Eur. Phys. J. **C5**, 205 (1998); **C16**, 597 (2000); **C16**, 613 (2000); and A. Heister *et al.*: Phys. Lett. **B526**, 34 (2002); **B528**, 19 (2002).

ARGUS: H. Albrecht *et al.*: Phys. Lett. **230B**, 169 (1989); Z. Phys. **C39**, 177 (1988); **C44**, 547 (1989); **C46**, 15 (1990); **C54**, 1 (1992); **C58**, 199 (1993); **C61**, 1 (1994); Phys. Rep. **276**, 223 (1996).

BaBar: B. Aubert *et al.*: Phys. Rev. Lett. **87**, 162002 (2001); Phys. Rev. **D65**, 091104 (2002); Phys. Rev. **D75**, 012003 (2007); J.P. Lees *et al.*: Phys. Rev. **D88**, 032011 (2013).

Belle: K. Abe *et al.*, Phys. Rev. Lett. **88**, 052001 (2002); R. Seuster *et al.*, Phys. Rev. **D73**, 032002 (2006); M. Niijama *et al.*, `arXiv:1706.06791` .

CELLO: H.J. Behrend *et al.*: Z. Phys. **C46**, 397 (1990); **C47**, 1 (1990).

CLEO: S. Behrends *et al.*, Phys. Rev. **D31**, 2161 (1985); D. Bortoletto *et al.*, Phys. Rev. **D37**, 1719 (1988); erratum *ibid.* **D39**, 1471 (1989); and M. Artuso *et al.*, Phys. Rev. **D70**, 112001 (2004).

Crystal Ball: Ch. Bieler *et al.*, Z. Phys. **C49**, 225 (1991).

DELPHI: P. Abreu *et al.*: Z. Phys. **C57**, 181 (1993); **C59**, 533 (1993); **C61**, 407 (1994); **C65**, 587 (1995); **C67**, 543 (1995); **C68**, 353 (1995); **C73**, 61 (1996); Nucl. Phys. **B444**, 3 (1995); Phys. Lett. **B341**, 109 (1994); **B345**, 598 (1995); **B361**, 207 (1995); **B372**, 172 (1996); **B379**, 309 (1996); **B416**, 233 (1998); **B449**, 364 (1999); **B475**, 429 (2000); Eur. Phys. J. **C6**, 19 (1999); **C5**, 585 (1998); **C18**, 203 (2000); and J. Abdallah *et al.*, Phys. Lett. **B569**, 129 (2003); Phys. Lett. **B576**, 29 (2003); Eur. Phys. J. **C44**, 299 (2005); and W. Adam *et al.*: Z. Phys. **C69**, 561 (1996); **C70**, 371 (1996).

HRS: S. Abachi *et al.*, Phys. Rev. Lett. **57**, 1990 (1986); and M. Derrick *et al.*, Phys. Rev. **D35**, 2639 (1987).

L3: M. Acciarri *et al.*: Phys. Lett. **B328**, 223 (1994); **B345**, 589 (1995); **B371**, 126 (1996); **B371**, 137 (1996); **B393**, 465 (1997); **B404**, 390 (1997); **B407**, 351 (1997); **B407**, 389 (1997), erratum *ibid.* **B427**, 409 (1998); **B453**, 94 (1999); **B479**, 79 (2000).

MARK II: H. Schellman *et al.*, Phys. Rev. **D31**, 3013 (1985); and G. Wormser *et al.*, Phys. Rev. Lett. **61**, 1057 (1988).

JADE: W. Bartel *et al.*, Z. Phys. **C20**, 187 (1983); and D.D. Pietzl *et al.*, Z. Phys. **C46**, 1 (1990).

OPAL: R. Akers *et al.*: Z. Phys. **C63**, 181 (1994); **C66**, 555 (1995); **C67**, 389 (1995); **C68**, 1 (1995); and G. Alexander *et al.*: Phys. Lett. **B358**, 162 (1995); Z. Phys. **C70**, 197 (1996); **C72**, 1 (1996); **C72**, 191 (1996); **C73**, 569 (1997); **C73**, 587 (1997); Phys. Lett. **B370**, 185 (1996); and K. Ackerstaff *et al.*: Z. Phys. **C75**, 192 (1997); Phys. Lett. **B412**, 210 (1997); Eur. Phys. J. **C1**, 439 (1998); **C4**, 19 (1998); **C5**, 1 (1998); **C5**, 411 (1998); and G. Abbiendi *et al.*: Eur. Phys. J. **C16**, 185 (2000); **C17**, 373 (2000).

PLUTO: Ch. Berger *et al.*, Phys. Lett. **104B**, 79 (1981).

SLD: K. Abe, Phys. Rev. **D59**, 052001 (1999); Phys. Rev. **D69**, 072003 (2004).

TASSO: H. Aihara *et al.*, Z. Phys. **C27**, 27 (1985).

TPC: H. Aihara *et al.*, Phys. Rev. Lett. **53**, 2378 (1984).

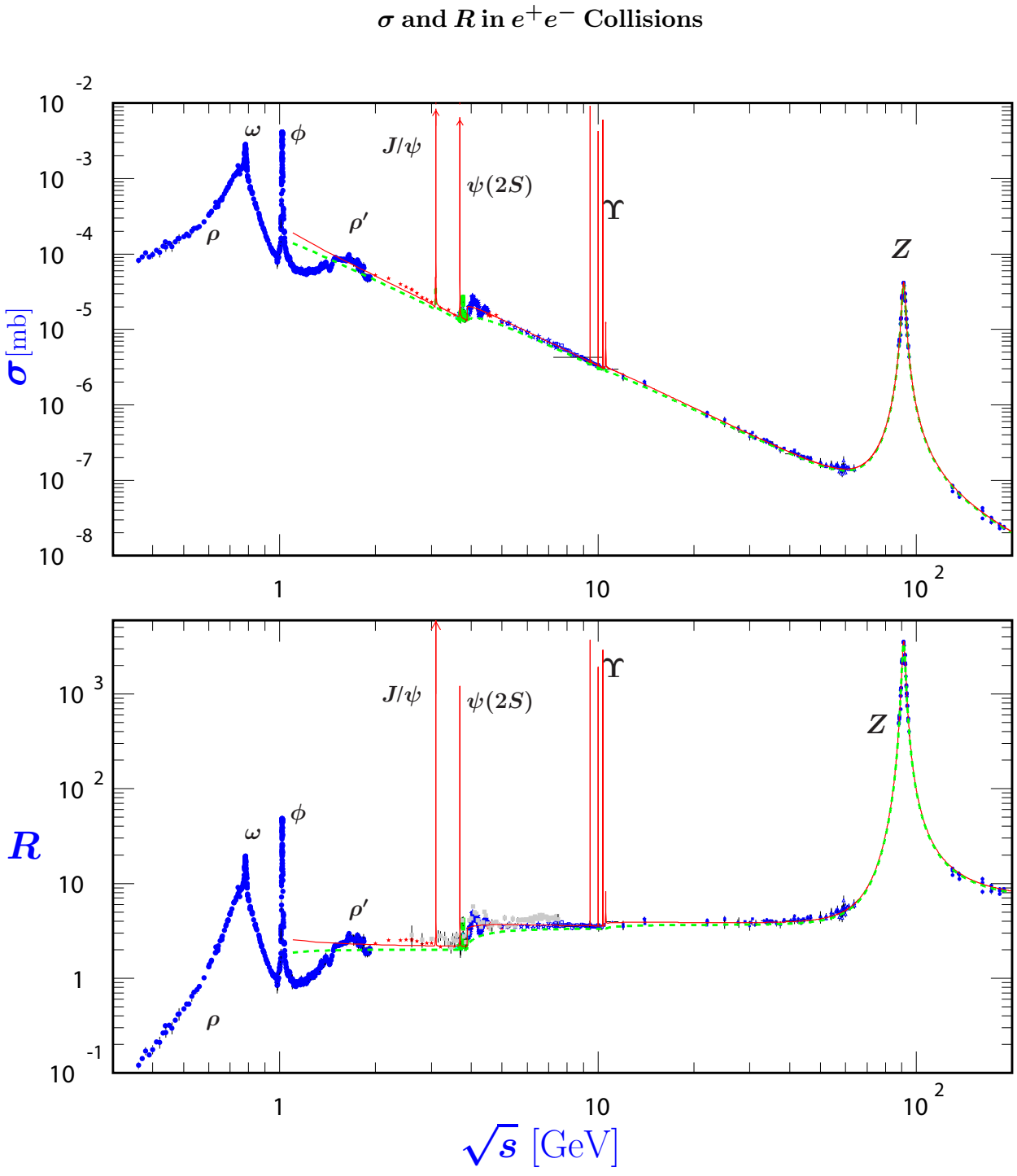

Figure 51.2: World data on the total cross section of $e^+e^- \to hadrons$ and the ratio $R(s) = \sigma(e^+e^- \to hadrons, s)/\sigma(e^+e^- \to \mu^+\mu^-, s)$. $\sigma(e^+e^- \to hadrons, s)$ is the experimental cross section corrected for initial state radiation and electron-positron vertex loops, $\sigma(e^+e^- \to \mu^+\mu^-, s) = 4\pi\alpha^2(s)/3s$. Data errors are total below 2 GeV and statistical above 2 GeV. The curves are an educative guide: the broken one (green) is a naive quark-parton model prediction, and the solid one (red) is 3-loop pQCD prediction (see "Quantum Chromodynamics" section of this *Review*, Eq. (9.7) or, for more details, K. G. Chetyrkin *et al.*, Nucl. Phys. **B586**, 56 (2000) (Erratum *ibid.* **B634**, 413 (2002)). Breit-Wigner parameterizations of J/ψ, $\psi(2S)$, and $\Upsilon(nS), n = 1, 2, 3, 4$ are also shown. The full list of references to the original data and the details of the R ratio extraction from them can be found in `[arXiv:hep-ph/0312114]`. Corresponding computer-readable data files are available at `http://pdg.lbl.gov/current/xsect/`. (Courtesy of the COMPAS (Protvino) and HEPDATA (Durham) Groups, August 2017. Corrections by P. Janot (CERN) and M. Schmitt (Northwestern U.))

R in Light-Flavor, Charm, and Beauty Threshold Regions

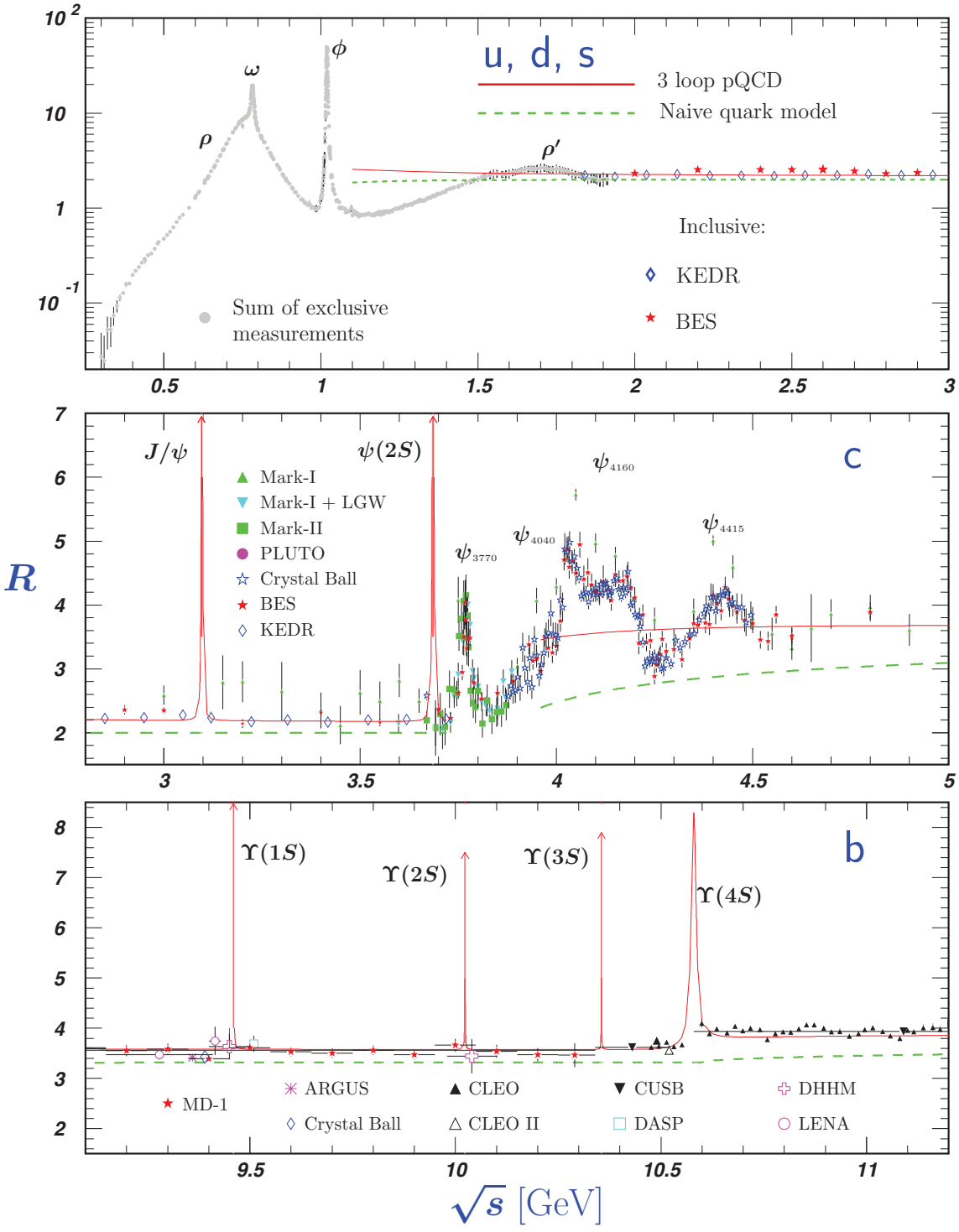

Figure 51.3: R in the light-flavor, charm, and beauty threshold regions. Data errors are total below 2 GeV and statistical above 2 GeV. The curves are the same as in Fig. 51.2. **Note:** CLEO data above $\Upsilon(4S)$ were not fully corrected for radiative effects, and we retain them on the plot only for illustrative purposes with a normalization factor of 0.8. The full list of references to the original data and the details of the R ratio extraction from them can be found in `[arXiv:hep-ph/0312114]`. The computer-readable data are available at `http://pdg.lbl.gov/current/xsect/`. (Courtesy of the COMPAS (Protvino) and HEPDATA (Durham) Groups, August 2017.)

Annihilation Cross Section Near M_Z

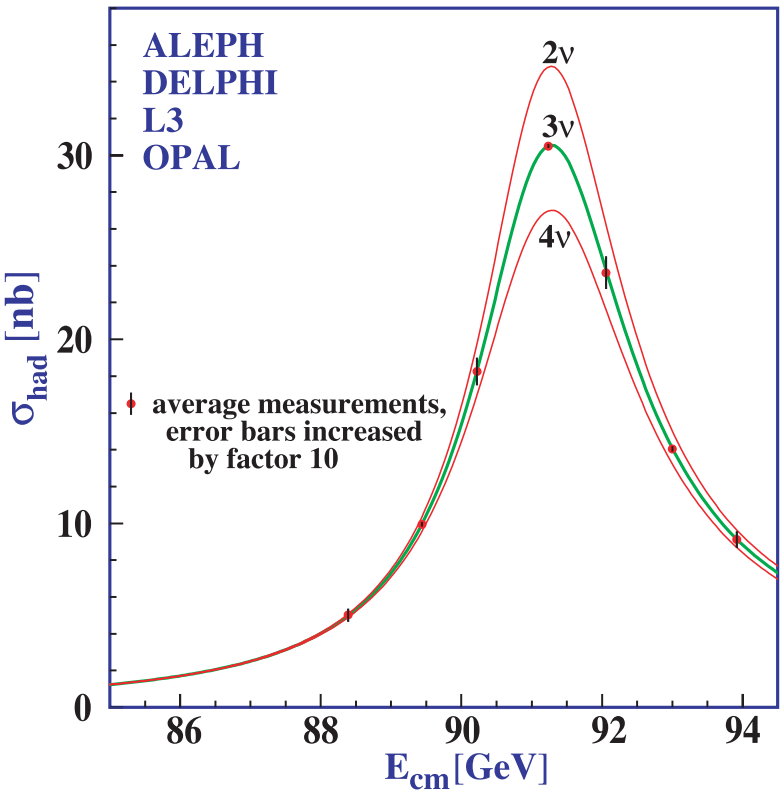

Figure 51.4: Combined data from the ALEPH, DELPHI, L3, and OPAL Collaborations for the cross section in e^+e^- annihilation into hadronic final states as a function of the center-of-mass energy near the Z pole. The curves show the predictions of the Standard Model with two, three, and four species of light neutrinos. The asymmetry of the curve is produced by initial-state radiation. Note that the error bars have been increased by a factor ten for display purposes. References:

ALEPH: R. Barate *et al.*, Eur. Phys. J. **C14**, 1 (2000).
DELPHI: P. Abreu *et al.*, Eur. Phys. J. **C16**, 371 (2000).
L3: M. Acciarri *et al.*, Eur. Phys. J. **C16**, 1 (2000).
OPAL: G. Abbiendi *et al.*, Eur. Phys. J. **C19**, 587 (2001).
Combination: The ALEPH, DELPHI, L3, OPAL, SLD Collaborations, the LEP Electroweak Working Group, and the SLD Electroweak and Heavy Flavor Groups, Phys. Rept. **427**, 257 (2006) [arXiv:hep-ex/0509008].

(Courtesy of M. Grünewald and the LEP Electroweak Working Group, 2007)

Total Hadronic Cross Sections

(Updated August 2017, COMPAS group, IHEP, Protvino)

In this section, plots of total cross section for various processes are presented. The plots include data from hadronic collisions such as pp and $\overline{p}p$, as well as γp, γd, and $\gamma\gamma$ processes. The cross section data provide crucial inputs to the study of QCD physics. In particular, to probe the non-perturbative part of QCD processes which are described by a number of diffractive models. We begin by introducing some models of diffractive scatterings and listing references for further reading.

Diffractive scattering here means scattering of hadrons at small angles and exhibiting typical diffraction pattern in angular distribution of scattered particles. Beyond purely elastic scattering diffraction phenomena include inelastic processes with large rapidity gaps: those of single and double diffractive dissociation and "central diffractive" events. In distinction from the most of other processes considered in the SM diffraction processes (DP) are related to large spatio-temporal scales growing with energy of collision. Being caused by strong interactions DP are a subject of the fundamental strong interaction theory, QCD, and hereby a part of the longstanding problem of QCD at large distances.

One of the most important basic notions and tools in general theoretical framework related to the diffractive processes is the notion of the Regge poles, or Reggeons, generalizing the simple one-particle exchange (of Yukawa type) by virtual particles of fixed spin to exchanges by states with "running spin" dependent on the transferred momenta [1,2]. The simplest case of the one-Reggeon exchange amplitude is given by the amplitude (at high c.m. energy $\sqrt{s}$ and fixed (small) transferred momentum squared, t): $T(s,t) = \beta(t)s^{\alpha(t)}$ which qualitatively exhibits many typical features of generic diffractive processes (e.g. the growth of the interaction radius with energy). In practice the single-pole Reggeon model is insufficient for many diffractive processes but still serves a building block for more sophisticated schemes. Up to now no firm results concerning Regge trajectories $\alpha(t)$ and Regge residues $\beta(t)$ were obtained from the first principles of QCD. General principles imply that both $\alpha(t)$ and $\beta(t)$are analytic functions with right cuts from some $t_0 > 0$ to positive infinity.

The theoretical requisite for analyzing diffractive phenomena is therefore represented by various model approaches. The more commonly discussed models in the literatures are:

– **Regge -Eikonal approach** [3–10]: this approach automatically satisfy the s-channel unitarity condition and generalizes the impact parameter approximation to the relativistic case.

– **Regge pole models with minimal corrections due to two-Reggeon exchanges** [11–13]: in this model, contribution of the leading trajectory is supplemented by a two-Reggeon exchange with arbitrary coefficient chosen from the fitting details.

– **U-matrix (or resonance) approach** [14, 15]: the unitarity respecting approach with the scattering amplitude defined by a reaction matrix.

– **Direct functional modelling of the amplitudes without Regge trajectories** [16, 17]: this approach appeals to only very general properties of the amplitudes leaving aside all dynamical assumptions and mostly aiming at the best phenomenological description of the data.

– **Quasi-classical approach** [18–20]: based on the observation that diffractive processes deal with high quantum numbers, in particular with large number of virtual quanta.

For readers who are interested in examples of both total and elastic cross section parametrizations and fits, see previous edition of the *Plots of Cross Sections and Related Quantities* review [21]. For the cross section plots shown in the following pages, the example fits are using parametrizations as described in [21] with the fit range starting at about $\sqrt{s} = 5$ GeV.

References:

[1] P.D.B. Collins, *An Introduction to Regge Theory and High Energy Physics*, Cambridge: Cambridge University Press, 1977.

[2] G. Pancheri and Y. N. Srivastava, Eur. Phys. J. **C77**, 150 (2017).

[3] L. A. Harland-Lang, V. A. Khoze and M. G. Ryskin, Int. J. Mod. Phys. **A30**, 1542013 (2015).

[4] V. A. Petrov and A. Prokudin, Phys. Rev. **D87**, 036003 (2013).

[5] C. Bourrely, J. Soffer and T. T. Wu, Eur. Phys. J. **C28**, 97 (2003).

[6] M. M. Block, L. Durand, P. Ha and F. Halzen, Phys. Rev. **D92**, 014030 (2015).

[7] O. V. Selyugin, Phys. Rev. **D91**, 113003 (2015); Erratum: Phys. Rev. **D92**, 099901 (2015).

[8] L. G. Dakhno and V. A. Nikonov, Eur. Phys. J. **A5**, 209 (1999).

[9] A. A. Godizov, Phys. Lett. **B735**, 57 (2014).

[10] E. Gotsman, E. M. Levin and U. Maor, Phys. Rev. **D49**, R4321 (1994).

[11] A. Donnachie and P. V. Landshoff, Phys. Lett. **B727**, 500 (2013); Erratum: Phys. Lett. **B750**, 669 (2015).

[12] E. Martynov, Phys. Rev. **D87**, 114018 (2013).

[13] L. Jenkovszky, Nuovo Cim. C **037**, 99 (2014).

[14] S. M. Troshin and N. E. Tyurin, Int. J. Mod. Phys. **A32**, 1750103 (2017).

[15] V.V. Anisovich, Phys. Usp **58**, 10 (2015).

[16] D. A. Fagundes, M. J. Menon and P. V. R. G. Silva, Nucl. Phys. **A946**, 194 (2016).

[17] E. Martynov and B. Nicolescu, Eur. Phys. J. **C56**, 57 (2008).

[18] W. Heisenberg, Z. Phys. **133**, 65 (1952).

[19] V.V. Ezhela and Yu.P. Yushchenko, Preprint IHEP/IFVE-88-198 (1988).

[20] H. Nastase and J. Sonnenschein, Phys. Rev. **D92**, 105028 (2015).

[21] C. Patrignani *et al.* (Particle Data Group), Chin. Phys. C **40**, 100001 (2016) and 2017 update.

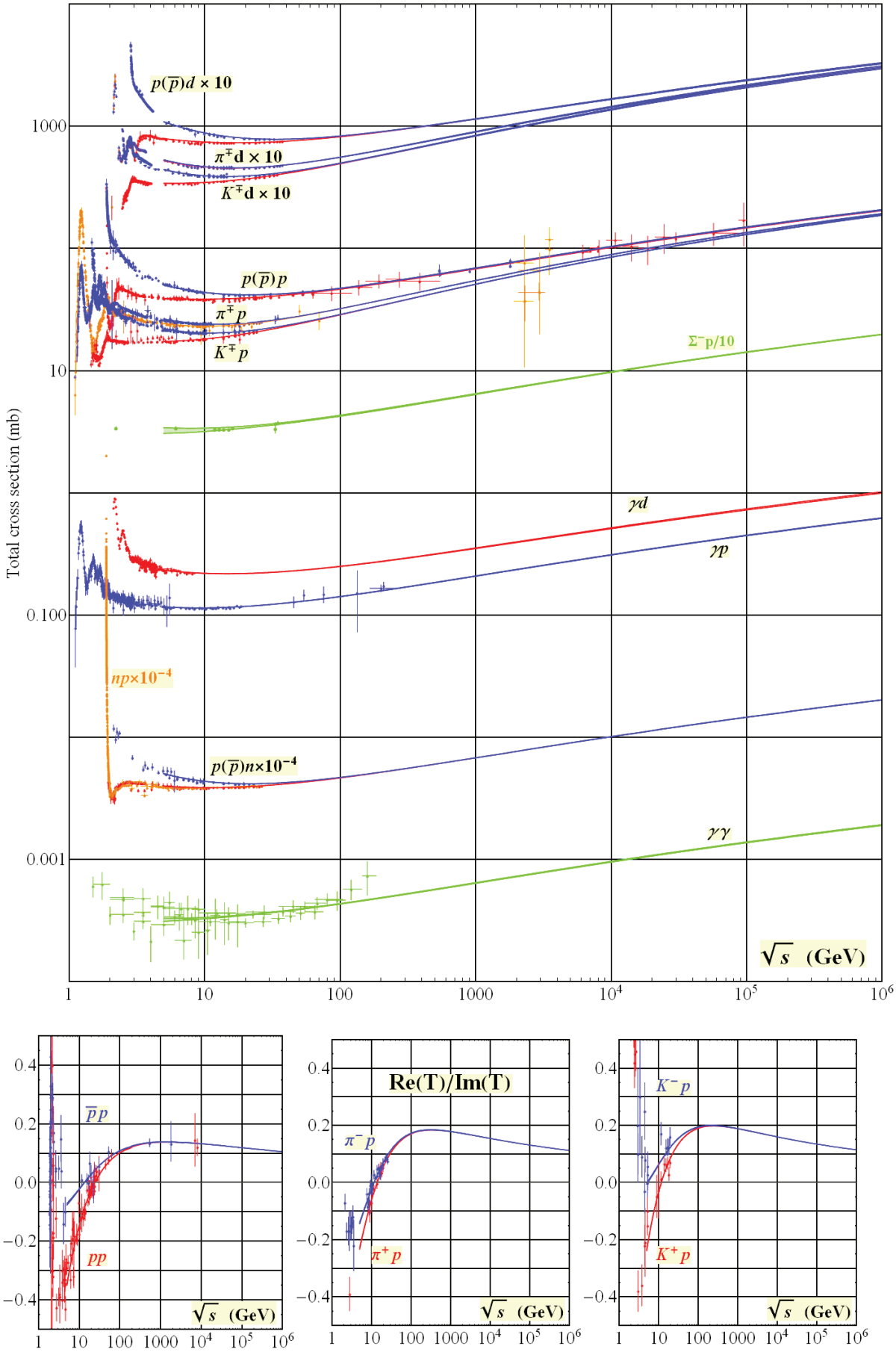

Figure 51.5: Summary of hadronic, γp, γd, and $\gamma\gamma$ total cross sections, and ratio of the real to imaginary parts of the forward hadronic amplitudes (T). Corresponding computer-readable data files may be found at `http://pdg.lbl.gov/current/xsect/`. (Courtesy of the COMPAS group, IHEP, Protvino, August 2017.)

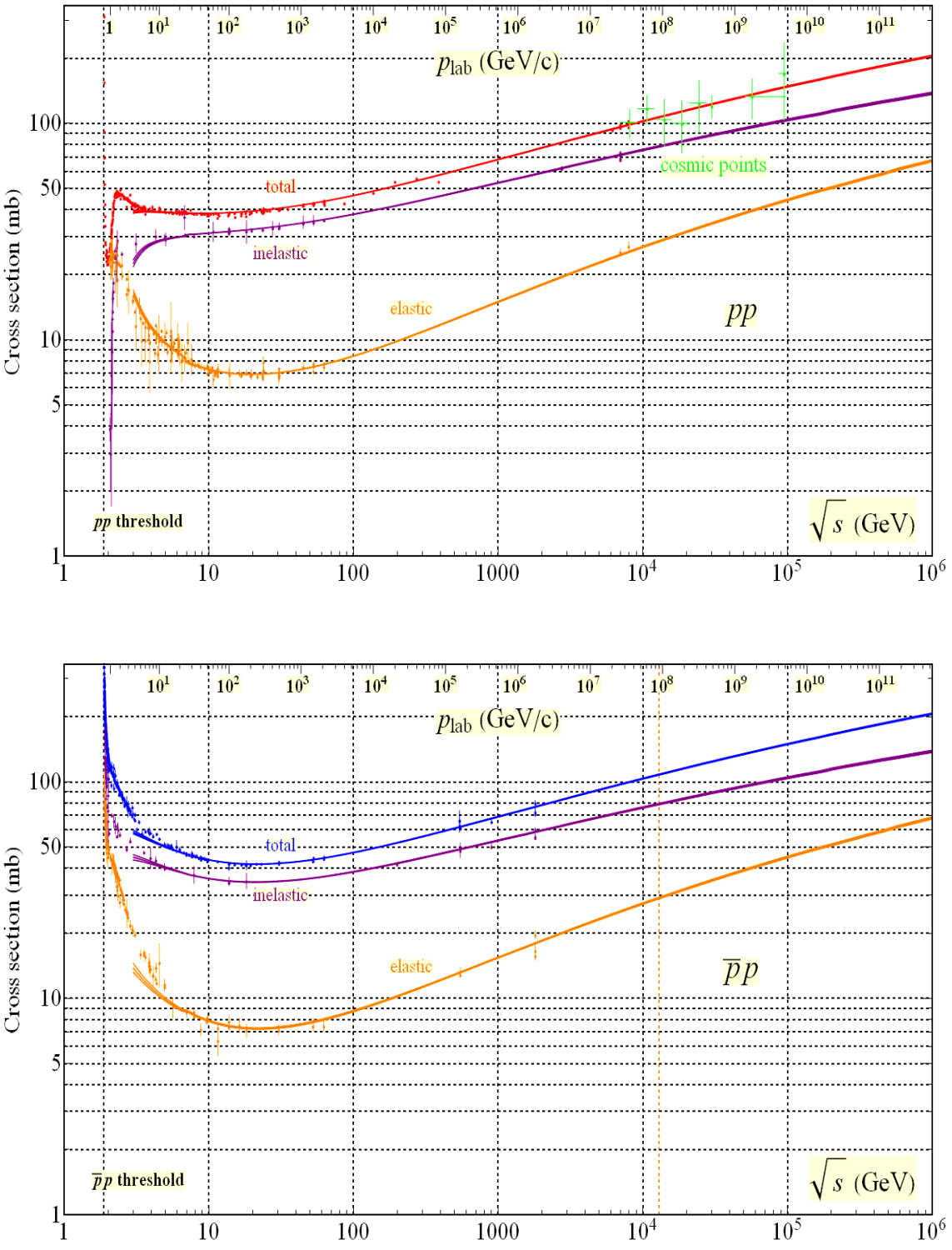

Figure 51.6: Total and elastic cross sections for pp and $\overline{p}p$ collisions as a function of laboratory beam momentum and total center-of-mass energy. Corresponding computer-readable data files may be found at `http://pdg.lbl.gov/current/xsect/`. (Courtesy of the COMPAS group, IHEP, Protvino, August 2017)

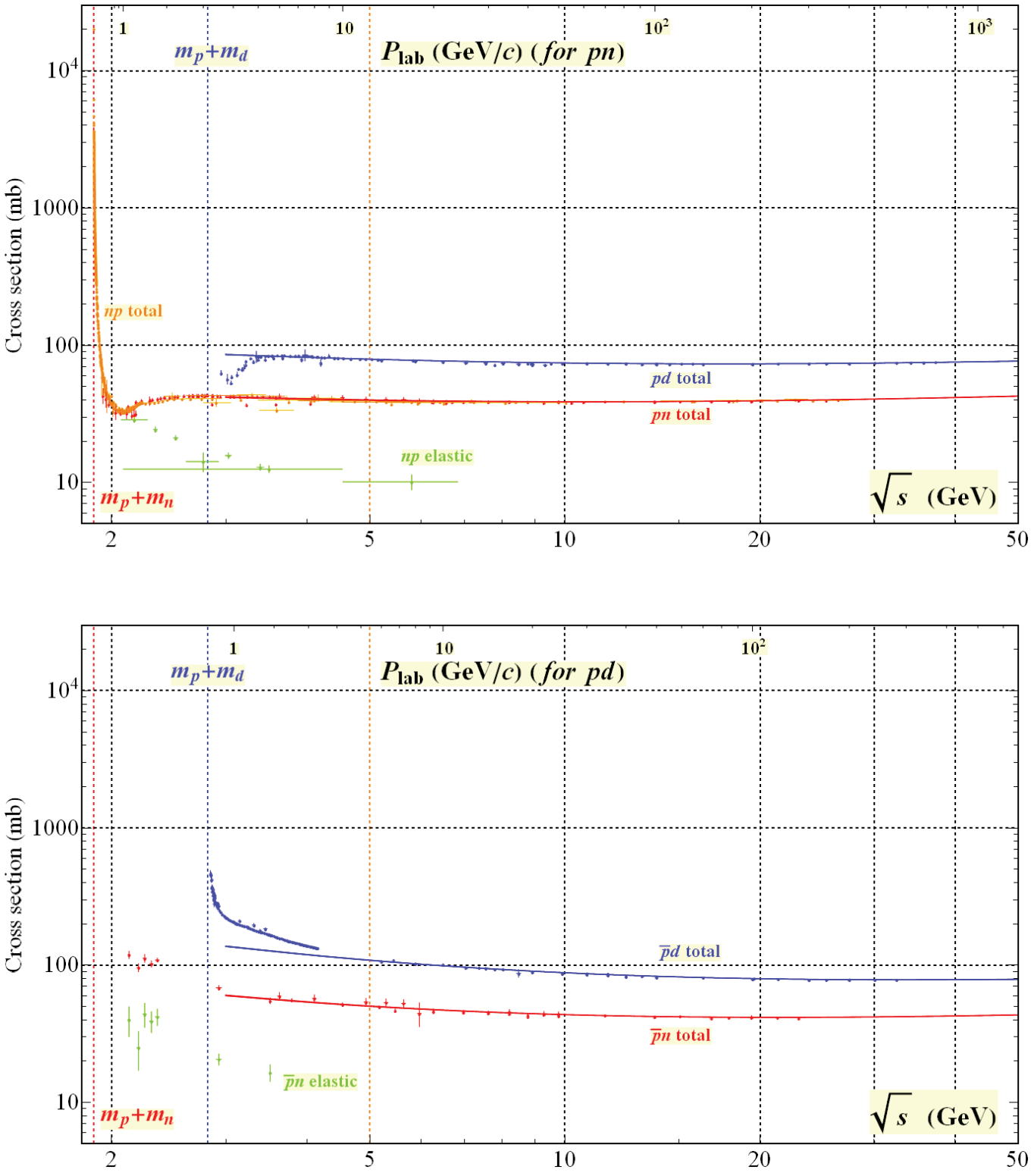

Figure 51.7: Total and elastic cross sections for pd (total only), np, $\overline{p}d$ (total only), and $\overline{p}n$ collisions as a function of laboratory beam momentum and total center-of-mass energy. Corresponding computer-readable data files may be found at `http://pdg.lbl.gov/current/xsect/`. (Courtesy of the COMPAS Group, IHEP, Protvino, August 2017)

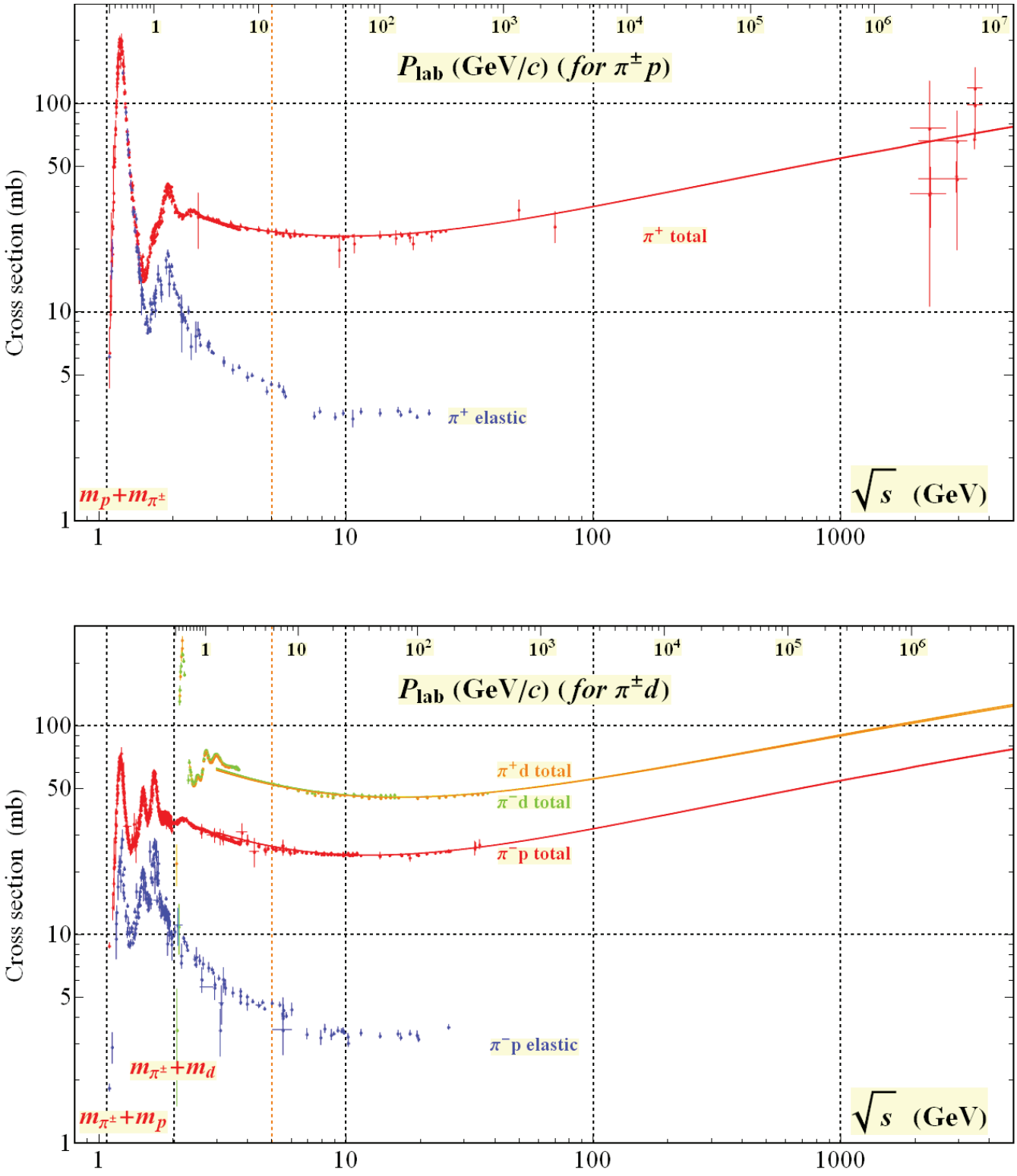

Figure 51.8: Total and elastic cross sections for $\pi^{\pm}p$ and $\pi^{\pm}d$ (total only) collisions as a function of laboratory beam momentum and total center-of-mass energy. Corresponding computer-readable data files may be found at `http://pdg.lbl.gov/current/xsect/`. (Courtesy of the COMPAS Group, IHEP, Protvino, August 2017)

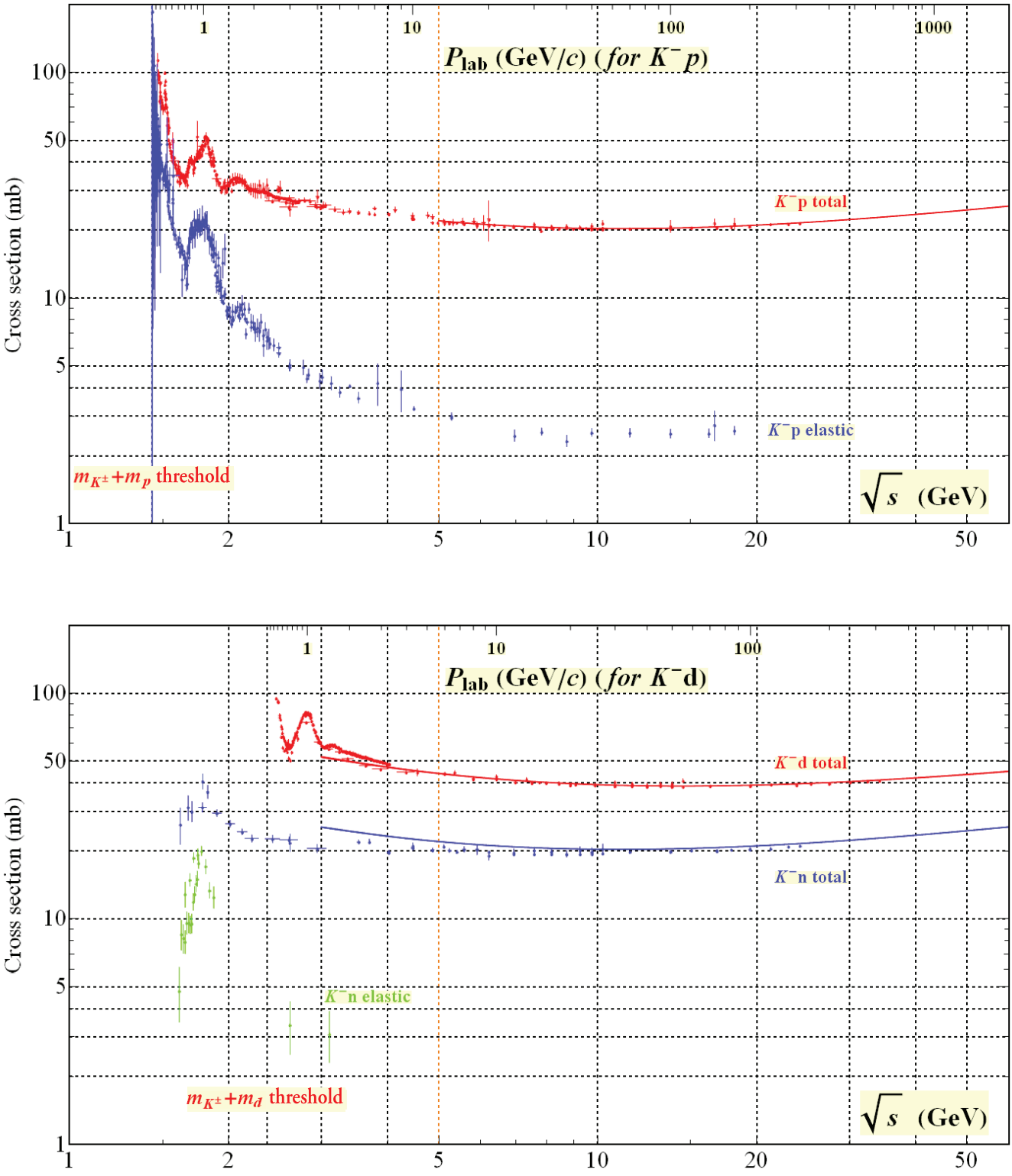

Figure 51.9: Total and elastic cross sections for K^-p and K^-d (total only), and K^-n collisions as a function of laboratory beam momentum and total center-of-mass energy. Corresponding computer-readable data files may be found at `http://pdg.lbl.gov/current/xsect/`. (Courtesy of the COMPAS Group, IHEP, Protvino, August 2017)

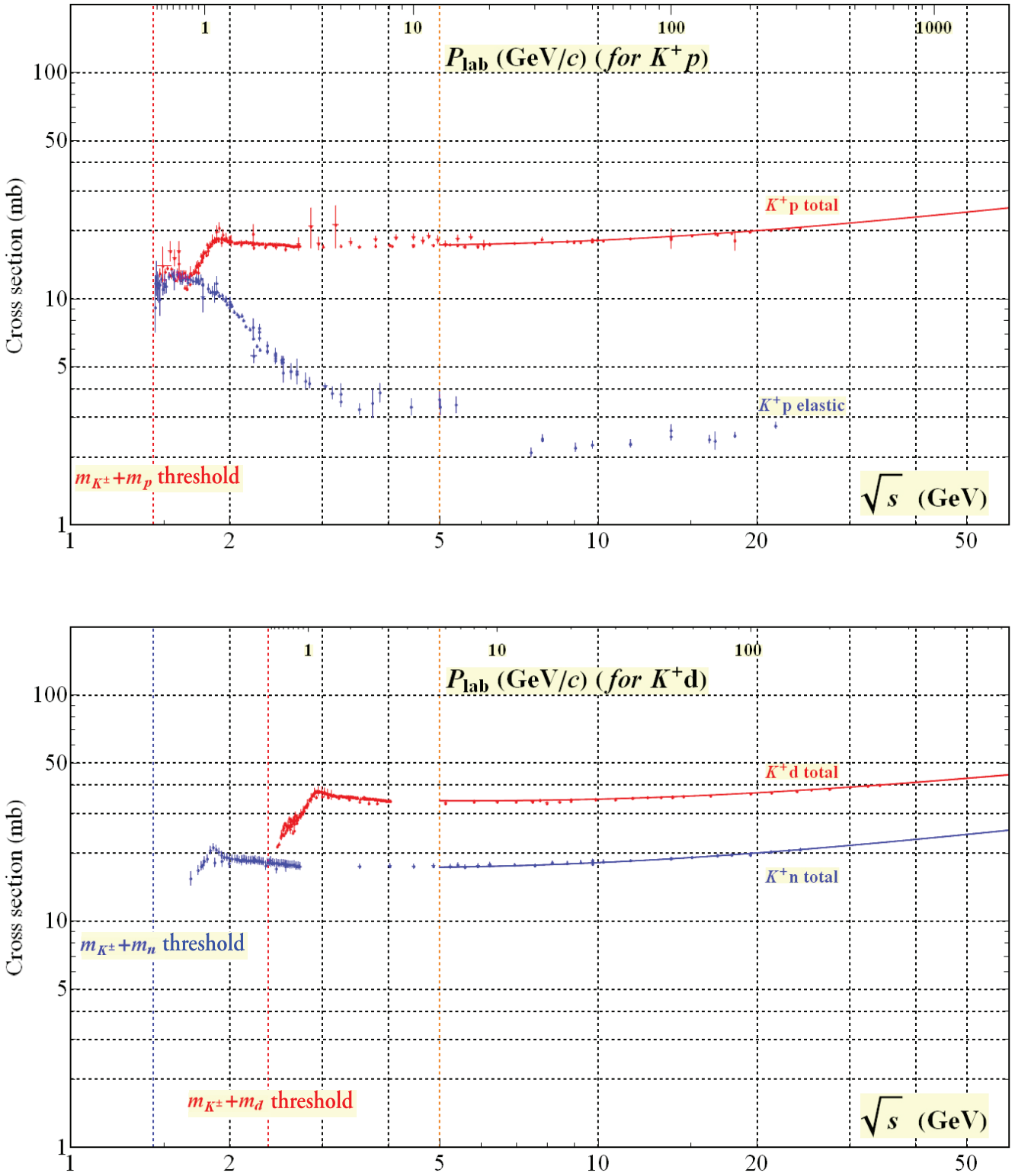

Figure 51.10: Total and elastic cross sections for K^+p and total cross sections for K^+d and K^+n collisions as a function of laboratory beam momentum and total center-of-mass energy. Corresponding computer-readable data files may be found at `http://pdg.lbl.gov/current/xsect/`. (Courtesy of the COMPAS Group, IHEP, Protvino, August 2017)

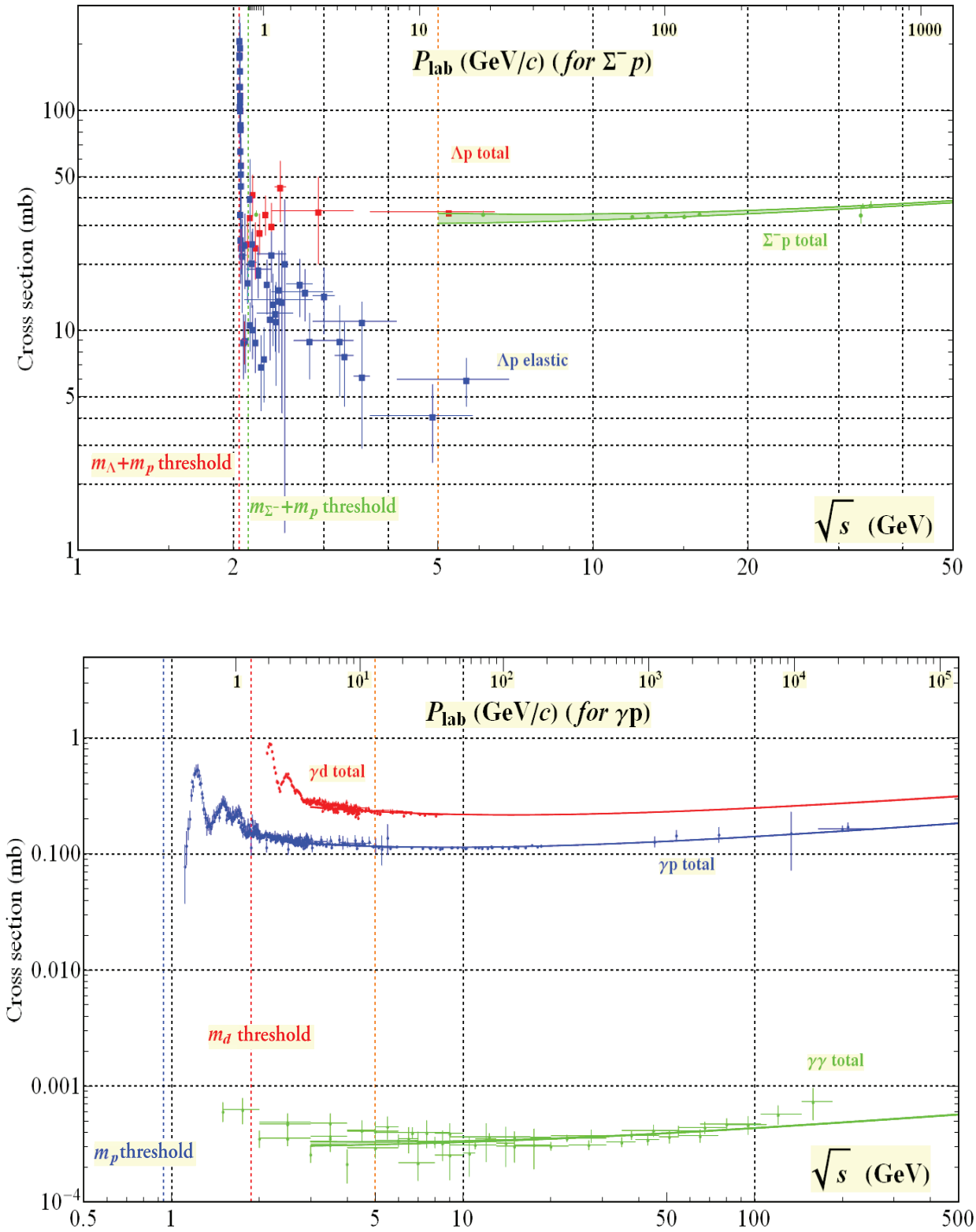

Figure 51.11: Total and elastic cross sections for Λp, total cross section for $\Sigma^- p$, and total hadronic cross sections for γd, γp, and $\gamma\gamma$ collisions as a function of laboratory beam momentum and the total center-of-mass energy. Corresponding computer-readable data files may be found at `http://pdg.lbl.gov/current/xsect/`. (Courtesy of the COMPAS group, IHEP, Protvino, August 2017)

52. Mass and Width of the W Boson

Revised March 2018 by M.W. Grünewald (U. College Dublin) and A. Gurtu (Kyung Hee U.).

Precision determination of the W-mass is of great importance in testing the internal consistency of the Standard Model. From the time of its discovery in 1983, the W-boson has been studied and its mass determined in $p\bar{p}$ and e^+e^- interactions; it is currently studied in pp interactions at the LHC. The W mass and width definition used here corresponds to a Breit-Wigner with mass-dependent width.

Production of on-shell W bosons at hadron colliders is tagged by the high p_T charged lepton from its decay. Owing to the unknown parton-parton effective energy and missing energy in the longitudinal direction, the collider experiments reconstruct the transverse mass of the W, and derive the W mass from comparing the transverse mass distribution with Monte Carlo predictions as a function of M_W. These analyses use the electron and muon decay modes of the W boson.

In the e^+e^- collider (LEP) a precise knowledge of the beam energy enables one to determine the $e^+e^- \to W^+W^-$ cross section as a function of center of mass energy, as well as to reconstruct the W mass precisely from its decay products, even if one of them decays leptonically. Close to the W^+W^- threshold (161 GeV), the dependence of the W-pair production cross section on M_W is large, and this was used to determine M_W. At higher energies (172 to 209 GeV) this dependence is much weaker and W-bosons were directly reconstructed and the mass determined as the invariant mass of its decay products, improving the resolution with a kinematic fit.

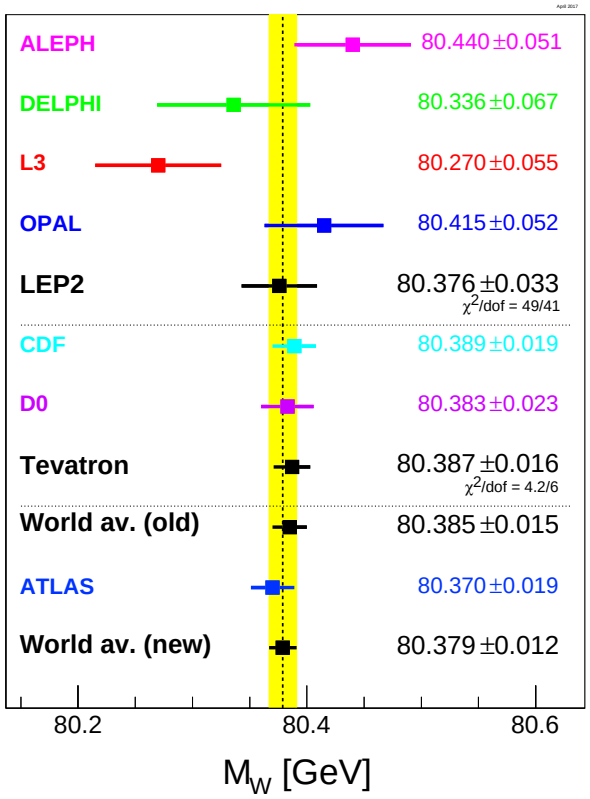

Figure 52.1: Measurements of the W-boson mass by the LEP, Tevatron and LHC experiments.

In order to compute the LEP average W mass, each experiment provided its measured W mass for the $q\bar{q}q\bar{q}$ and $q\bar{q}\ell\overline{\nu_\ell}$, $\ell = e, \mu, \tau$ channels at each center-of-mass energy, along with a detailed break-up of errors: statistical, uncorrelated, partially correlated and fully correlated systematics [1]. These have been combined to obtain a LEP W mass of $M_W = 80.376 \pm 0.033$ GeV. Errors due to uncertainties in LEP energy (9 MeV), and possible effect of color reconnection (CR) and Bose-Einstein correlations (BEC) between quarks from different W's (8 MeV) are included. The mass difference between $q\bar{q}q\bar{q}$ and $q\bar{q}\ell\overline{\nu_\ell}$ final states (due to possible CR and BEC effects) is -12 ± 45 MeV. In a similar manner, the width results obtained at LEP have been combined, resulting in $\Gamma_W = 2.195 \pm 0.083$ GeV [1].

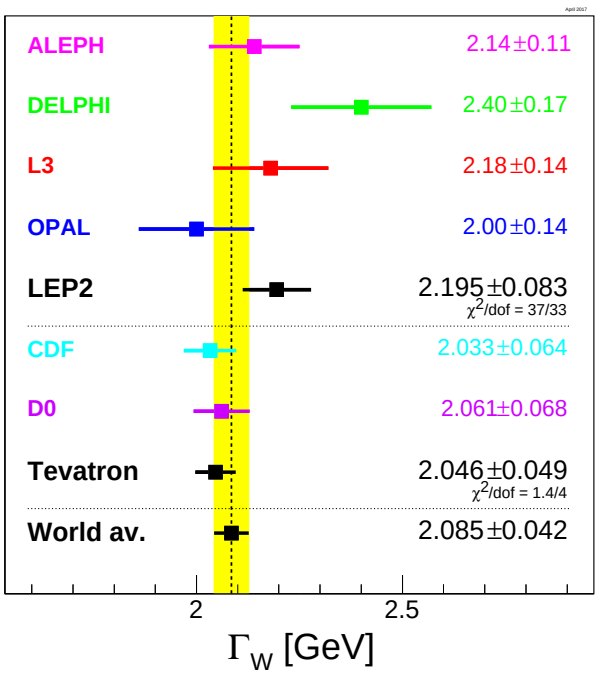

Figure 52.2: Measurements of the W-boson width by the LEP and Tevatron experiments.

The two Tevatron experiments have also identified common systematic errors. Between the two experiments, uncertainties due to the parton distribution functions, radiative corrections, and choice of mass (width) in the width (mass) measurements are treated as correlated. An average W width of $\Gamma_W = 2.046 \pm 0.049$ GeV [2] is obtained. Errors of 20 MeV and 7 MeV accounting for PDF and radiative correction uncertainties in this width combination dominate the correlated uncertainties. At the 2011/12 winter conferences, the CDF and D0 experiments have presented new results for the mass of the W boson based on $2-4$ fb^{-1} of Run-II data, 80.387 ± 0.019 GeV [3] and 80.375 ± 0.023 GeV [4], respectively. The W-mass determination from the Tevatron experiments has thus become very precise. Combining all Tevatron results from Run-I and Run-II using an improved treatment of correlations, a new average of 80.387 ± 0.016 GeV is obtained [5], with common uncertainties of 10 MeV (PDF) and 4 MeV (radiative corrections).

Good agreement between the LEP and Tevatron results is observed. Combining these results, assuming no common systematic uncertainties between the LEP and the Tevatron measurements, yields an average W mass of $M_W = 80.385 \pm 0.015$ GeV and a W width of $\Gamma_W = 2.085 \pm 0.042$ GeV.

At the 2016/17 winter conferences, the ATLAS collaboration presented a measurement of the mass of the W boson in pp collisions at $\sqrt{s} = 7$ TeV, $M_W = 80.370 \pm 0.019$ GeV, since then published [6], which is compatible with the above world average and of similar precision to the best measurements of CDF and D0. Assuming a Tevtaron/LHC common PDF uncertainty of 7 MeV [7], this results in a new world average of $M_W = 80.379 \pm 0.012$ GeV.

The LEP, Tevatron and LHC results on mass and width, which are based on all results available, are compared in Fig. 52.1 and Fig. 52.2. The Standard Model prediction from the electroweak fit, using Z-pole data plus $m_{\rm top}$ measurement, gives a W-boson mass of $M_W = 80.363 \pm 0.020$ GeV and a W-boson width of $\Gamma_W = 2.091 \pm 0.002$ GeV [1].

References:

1. The LEP Collaborations: ALEPH, DELPHI, L3, OPAL, the LEP Electroweak Working Group, CERN-PH-EP/2013-022, arXiv:1302.3415 [hep-ex], Phys.Rept. 532 (2013) 119-244.
2. The Tevatron Electroweak Working Group, for the CDF and D0 Collaborations: *Combination of CDF and D0 Results on the Width of the W Boson*, March 2010, arXiv:1003.2826 [hep-ex].
3. The CDF Collaboration, *Precise measurement of the W-boson mass with the CDF II detector*, arXiv:1203.0275 [hep-ex], Phys. Rev. Lett. **108**, 151803 (2012).
4. The D0 Collaboration, *Measurement of the W Boson Mass with the D0 Detector*, arXiv:1203.0293 [hep-ex], Phys. Rev. Lett. **108**, 151804 (2012).
5. The CDF and D0 Collabs: *Combination of CDF and D0 W-Boson Mass Measurements*, July 2013, arXiv:1307.7627 [hep-ex], Phys. Rev. **D88**, 052018 (2013).
6. The ATLAS Collaboration, *Measurement of the W-boson mass in pp collisions at* $\sqrt{s} = 7$ *TeV with the ATLAS detector*, January 2017, arXiv:1701:07240 [hep-ex], Eur.Phys.J. C78 (2018) no.2, 110.
7. Jens Erler, *Precision in EW measurements at Run 2 and beyond*, Talk presented at the *52nd Rencontres de Moriond EW*, March 2017.

53. Extraction of Triple Gauge Couplings (TGCs)

Revised April 2017 by M.W. Grünewald (U. College Dublin) and A. Gurtu (Formerly Tata Inst.).

Fourteen independent couplings, seven each for ZWW and γWW, completely describe the VWW vertices within the most general framework of the electroweak Standard Model (SM) consistent with Lorentz invariance and U(1) gauge invariance. Of each of the seven TGCs, three conserve C and P individually, three violate CP, and one violates C and P individually while conserving CP. Assumption of C and P conservation and electromagnetic gauge invariance reduces the number of independent VWW couplings to five: one common set [1,2] is $(\kappa_\gamma, \kappa_Z, \lambda_\gamma, \lambda_Z, g_1^Z)$, where $\kappa_\gamma = \kappa_Z = g_1^Z = 1$ and $\lambda_\gamma = \lambda_Z = 0$ in the Standard Model at tree level. The parameters κ_Z and λ_Z are related to the other three due to constraints of gauge invariance as follows: $\kappa_Z = g_1^Z - (\kappa_\gamma - 1)\tan^2\theta_W$ and $\lambda_Z = \lambda_\gamma$, where θ_W is the weak mixing angle. The W magnetic dipole moment, μ_W, and the W electric quadrupole moment, q_W, are expressed as $\mu_W = e\,(1 + \kappa_\gamma + \lambda_\gamma)/2M_W$ and $q_W = -e\,(\kappa_\gamma - \lambda_\gamma)/M_W^2$.

Precision measurements of suitable observables at LEP1 has already led to an exploration of much of the TGC parameter space. At LEP2, the VWW coupling arises in W-pair production via s-channel exchange, or in single W production via the radiation of a virtual photon off the incident e^+ or e^-. At the Tevatron and the LHC, hard-photon bremsstrahlung off a produced W or Z signals the presence of a triple-gauge vertex. In order to extract the value of one TGC, the others are generally kept fixed to their SM values. While most analyses use the above gauge constraints in the extraction of TGCs, one analysis of W-pair events also determines the real and imaginary parts of all 14 couplings using unconstrained single-parameter fits [3]. The results are consistent. Some experiments have determined limits on the couplings under various non-LEP scenarios and assuming different values of the form factor Λ, where the coupling parameters are scaled by $1/(1+s/\Lambda^2)^2$. For practical reasons it is not possible to quote all such determinations in the listings. For that the individual papers may be consulted. Recently, EFT-inspired sets of couplings [4,5], such as $c_{WWW}/\Lambda^2, c_W/\Lambda^2, c_B/\Lambda^2$ which are linearly related to the couplings discussed above, are also determined by the LHC experiments.

References:

1. K. Hagiwara *et al.*, Nucl. Phys. **B282**, 253 (1987).
2. G. Gounaris *et al.*, CERN 96-01 p. 525.
3. S. Schael *et al.* (ALEPH Collab.), Phys. Lett. **B614**, 7 (2005).
4. K. Hagiwara *et al.*, Phys. Rev. **D48**, 2182 (1993).
5. C. Degrande *et al.*, Annals Phys. 335 (2013) 21-32.

54. Anomalous W/Z Quartic Couplings (QGCs)

Revised November 2015 by M.W. Grünewald (U. College Dublin) and A. Gurtu (Formerly Tata Inst.).

Quartic couplings, $WWZZ$, $WWZ\gamma$, $WW\gamma\gamma$, and $ZZ\gamma\gamma$, were studied at LEP and Tevatron at energies at which the Standard Model predicts negligible contributions to multiboson production. Thus, to parametrize limits on these couplings, an effective theory approach is adopted which supplements the Standard Model Lagrangian with higher dimensional operators which include quartic couplings. The LEP collaborations chose the lowers dimensional representation of operators (dimension 6) which presumes the SU(2)×U(1) gauge symmetry is broken by means other than the conventional Higgs scalar doublet [1–3]. In this representation possible quartic couplings, a_0, a_c, a_n, are expressed in terms of the following dimension-6 operators [1,2];

$$L_6^0 = -\tfrac{e^2}{16\Lambda^2}\, a_0\, F^{\mu\nu}\, F_{\mu\nu}\vec{W^\alpha}\cdot\vec{W}_\alpha$$

$$L_6^c = -\tfrac{e^2}{16\Lambda^2}\, a_c\, F^{\mu\alpha}\, F_{\mu\beta}\vec{W^\beta}\cdot\vec{W}_\alpha$$

$$L_6^n = -i\tfrac{e^2}{16\Lambda^2}\, a_n \epsilon_{ijk}\, W_{\mu\alpha}^{(i)}\, W_\nu^{(j)}\, W^{(k)\alpha} F^{\mu\nu}$$

$$\widetilde{L}_6^0 = -\tfrac{e^2}{16\Lambda^2}\, \widetilde{a}_0\, F^{\mu\nu}\, \widetilde{F}_{\mu\nu}\vec{W^\alpha}\cdot\vec{W}_\alpha$$

$$\widetilde{L}_6^n = -i\tfrac{e^2}{16\Lambda^2}\, \widetilde{a}_n \epsilon_{ijk}\, W_{\mu\alpha}^{(i)}\, W_\nu^{(j)}\, W^{(k)\alpha} \widetilde{F}^{\mu\nu}$$

where F, W are photon and W fields, L_6^0 and L_6^c conserve C, P separately ($\widetilde{L}_6^0$ conserves only C) and generate anomalous $W^+W^-\gamma\gamma$ and $ZZ\gamma\gamma$ couplings, L_6^n violates CP ($\widetilde{L}_6^n$ violates both C and P) and generates an anomalous $W^+W^-Z\gamma$ coupling, and Λ is an energy scale for new physics. For the $ZZ\gamma\gamma$ coupling the CP-violating term represented by L_6^n does not contribute. These couplings are assumed to be real and to vanish at tree level in the Standard Model.

Within the same framework as above, a more recent description of the quartic couplings [3] treats the anomalous parts of the $WW\gamma\gamma$ and $ZZ\gamma\gamma$ couplings separately, leading to two sets parametrized as a_0^V/Λ^2 and a_c^V/Λ^2, where $V = W$ or Z.

With the discovery of a Higgs at the LHC in 2012, it is then useful to go to the next higher dimensional representation (dimension 8 operators) in which the gauge symmetry is broken by the conventional Higgs scalar doublet [3,4]. There are 14 operators which can contribute to the anomalous quartic coupling signal. Some of the operators have analogues in the dimension 6 scheme. The CMS collaboration, [5], have used this parametrization, in which the connections between the two schemes are also summarized:

$$\begin{aligned}\mathcal{L}_{AQGC} = &-\frac{e^2}{8}\frac{a_0^W}{\Lambda^2}F_{\mu\nu}F^{\mu\nu}W^{+a}W_a^- \\ &-\frac{e^2}{16}\frac{a_c^W}{\Lambda^2}F_{\mu\nu}F^{\mu a}(W^{+\nu}W_a^- + W^{-\nu}W_a^+) \\ &-e^2g^2\frac{\kappa_0^W}{\Lambda^2}F_{\mu\nu}Z^{\mu\nu}W^{+a}W_a^- \\ &-\frac{e^2g^2}{2}\frac{\kappa_c^W}{\Lambda^2}F_{\mu\nu}Z^{\mu a}(W^{+\nu}W_a^- + W^{-\nu}W_a^+) \\ &+\frac{f_{T,0}}{\Lambda^4}Tr[\widehat{W}_{\mu\nu}\widehat{W}^{\mu\nu}]\times Tr[\widehat{W}_{\alpha\beta}\widehat{W}^{\alpha\beta}]\end{aligned}$$

The energy scale of possible new physics is Λ, and $g = e/sin(\theta_W)$, e being the unit electric charge and θ_W the Weinberg angle. The field tensors are described in [3,4].

The two dimension 6 operators a_0^W/Λ^2 and a_c^W/Λ^2 are associated with the $WW\gamma\gamma$ vertex. Among dimension 8 operators, κ_0^W/Λ^2 and κ_c^W/Λ^2 are associated with the $WWZ\gamma$ vertex, whereas the parameter $f_{T,0}/\Lambda^4$ contributes to both vertices. There is a relationship between these two dimension 6 parameters and the dimension 8 parameters $f_{M,i}/\Lambda^4$ as follows [3]:

$$\frac{a_0^W}{\Lambda^2} = -\frac{4M_W^2}{g^2}\frac{f_{M,0}}{\Lambda^4} - \frac{8M_W^2}{g'^2}\frac{f_{M,2}}{\Lambda^4}$$

$$\frac{a_c^W}{\Lambda^2} = -\frac{4M_W^2}{g^2}\frac{f_{M,1}}{\Lambda^4} - \frac{8M_W^2}{g'^2}\frac{f_{M,3}}{\Lambda^4}$$

where $g' = e/cos(\theta_W)$ and M_W is the invariant mass of the W boson. This relation provides a translation between limits on dimension 6 operators $a_{0,c}^W$ and $f_{M,j}/\Lambda^4$. It is further required [4] that $f_{M,0} = 2f_{M,2}$ and $f_{M,1} = 2f_{M,3}$ which suppresses contributions to the $WWZ\gamma$ vertex. The complete set of Lagrangian contributions as presented in [4] corresponds to 19 anomalous couplings in total – $f_{S,i},\ i = 1, 2$, $f_{M,i},\ i = 0, \ldots, 8$ and $f_{T,i}, i = 0, \ldots, 9$ – each scaled by $1/\Lambda^4$.

The ATLAS collaboration [6], on the other hand, follows a K-matrix driven approach of Ref. 7 in which the anomalous couplings can be expressed in terms of two parameters α_4 and α_5, which account for all BSM effects.

It is the early stages in the determination of quartic couplings by the LHC experiments. It is hoped that the two collaborations, ATLAS and CMS, will agree to use at least one common set of parameters to express these limits to enable the reader to make a comparison and allow for a possible LHC combination.

References:

1. G. Belanger and F. Boudjema, Phys. Lett. **B288**, 201 (1992).
2. J.W. Stirling and A. Werthenbach, Eur. Phys. J. **C14**, 103 (2000); J.W. Stirling and A. Werthenbach, Phys. Lett. **B466**, 369 (1999); A. Denner *et al.*, Eur. Phys. J. **C20**, 201 (2001); G. Montagna *et al.*, Phys. Lett. **B515**, 197 (2001).
3. G. Belanger *et al.*, Eur. Phys. J. **C13**, 283 (2000).
4. O.J.P. Éboli, M.C. Gonzalez-Garcia, and S.M. Lietti, Phys. Rev. **D69**, 095005 (2004); O.J.P. Éboli, M.C. Gonzalez-Garcia, and J.K. Mizukoshi, Phys. Rev. **D77**, 073005 (2006).
5. S. Chatrchyan *et al.*, Phys. Rev. **D90**, 032008 (2014); S. Chatrchyan *et al.*, Phys. Rev. Lett. **114**, 051801 (2015).
6. G. Aad *et al.*, Phys. Rev. Lett. **113**, 141803 (2014).
7. A. Albateanu, W. Killian, and J. Reuter, JHEP **0811**, 010 (2008).

55. *Z* Boson

Revised September 2013 by M.W. Grünewald (U. College Dublin and U. Ghent) and A. Gurtu (Formerly Tata Inst.).

Precision measurements at the Z-boson resonance using electron–positron colliding beams began in 1989 at the SLC and at LEP. During 1989–95, the four LEP experiments (ALEPH, DELPHI, L3, OPAL) made high-statistics studies of the production and decay properties of the Z. Although the SLD experiment at the SLC collected much lower statistics, it was able to match the precision of LEP experiments in determining the effective electroweak mixing angle $\sin^2\overline{\theta}_W$ and the rates of Z decay to b- and c-quarks, owing to availability of polarized electron beams, small beam size, and stable beam spot.

The Z-boson properties reported in this section may broadly be categorized as:

- The standard 'lineshape' parameters of the Z consisting of its mass, M_Z, its total width, Γ_Z, and its partial decay widths, Γ(hadrons), and $\Gamma(\ell\overline{\ell})$ where $\ell = e, \mu, \tau, \nu$;
- Z asymmetries in leptonic decays and extraction of Z couplings to charged and neutral leptons;
- The b- and c-quark-related partial widths and charge asymmetries which require special techniques;
- Determination of Z decay modes and the search for modes that violate known conservation laws;
- Average particle multiplicities in hadronic Z decay;
- Z anomalous couplings.

The effective vector and axial-vector coupling constants describing the Z-to-fermion coupling are also measured in $p\bar{p}$ and ep collisions at the Tevatron and at HERA. The corresponding cross-section formulae are given in Section 39 (Cross-section formulae for specific processes) and Section 16 (Structure Functions) in this *Review*. In this minireview, we concentrate on the measurements in e^+e^- collisions at LEP and SLC.

The standard 'lineshape' parameters of the Z are determined from an analysis of the production cross sections of these final states in e^+e^- collisions. The $Z \to \nu\overline{\nu}(\gamma)$ state is identified directly by detecting single photon production and indirectly by subtracting the visible partial widths from the total width. Inclusion in this analysis of the forward-backward asymmetry of charged leptons, $A_{FB}^{(0,\ell)}$, of the τ polarization, $P(\tau)$, and its forward-backward asymmetry, $P(\tau)^{fb}$, enables the separate determination of the effective vector ($\overline{g}_V$) and axial vector ($\overline{g}_A$) couplings of the Z to these leptons and the ratio ($\overline{g}_V/\overline{g}_A$), which is related to the effective electroweak mixing angle $\sin^2\overline{\theta}_W$ (see the "Electroweak Model and Constraints on New Physics" review).

Determination of the b- and c-quark-related partial widths and charge asymmetries involves tagging the b and c quarks for which various methods are employed: requiring the presence of a high momentum prompt lepton in the event with high transverse momentum with respect to the accompanying jet; impact parameter and lifetime tagging using precision vertex measurement with high-resolution detectors; application of neural-network techniques to classify events as b or non-b on a statistical basis using event–shape variables; and using the presence of a charmed meson (D/D^*) or a kaon as a tag.

55.1. *Z*-parameter determination

LEP was run at energy points on and around the Z mass (88–94 GeV) constituting an energy 'scan.' The shape of the cross-section variation around the Z peak can be described by a Breit-Wigner *ansatz* with an energy-dependent total width [1–3]. The **three** main properties of this distribution, viz., the **position** of the peak, the **width** of the distribution, and the **height** of the peak, determine respectively the values of M_Z, Γ_Z, and $\Gamma(e^+e^-) \times \Gamma(f\overline{f})$, where $\Gamma(e^+e^-)$ and $\Gamma(f\overline{f})$ are the electron and fermion partial widths of the Z. The quantitative determination of these parameters is done by writing analytic expressions for these cross sections in terms of the parameters, and fitting the calculated cross sections to the measured ones by varying these parameters, taking properly into account all the errors. Single-photon exchange (σ^0_γ) and γ-Z interference ($\sigma^0_{\gamma Z}$) are included, and the large (∼25 %) initial-state radiation (ISR) effects are taken into account by convoluting the analytic expressions over a 'Radiator Function' [1–5] $H(s, s')$. Thus for the process $e^+e^- \to f\overline{f}$:

$$\sigma_f(s) = \int H(s, s')\ \sigma^0_f(s')\ ds' \tag{55.1}$$

$$\sigma^0_f(s) = \sigma^0_Z + \sigma^0_\gamma + \sigma^0_{\gamma Z} \tag{55.2}$$

$$\sigma^0_Z = \frac{12\pi}{M_Z^2}\ \frac{\Gamma(e^+e^-)\Gamma(f\overline{f})}{\Gamma_Z^2}\ \frac{s\ \Gamma_Z^2}{(s - M_Z^2)^2\ +\ s^2\Gamma_Z^2/M_Z^2} \tag{55.3}$$

$$\sigma^0_\gamma = \frac{4\pi\alpha^2(s)}{3s}\ Q_f^2 N_c^f \tag{55.4}$$

$$\sigma^0_{\gamma Z} = -\frac{2\sqrt{2}\alpha(s)}{3}\ (Q_f G_F N_c^f \mathcal{G}_V^e \mathcal{G}_V^f) \times \frac{(s - M_Z^2)M_Z^2}{(s - M_Z^2)^2 + s^2\Gamma_Z^2/M_Z^2} \tag{55.5}$$

where Q_f is the charge of the fermion, $N_c^f = 3$ for quarks and 1 for leptons, and $\mathcal{G}_V^f$ is the vector coupling of the Z to the fermion-antifermion pair $f\overline{f}$.

Since $\sigma^0_{\gamma Z}$ is expected to be much less than σ^0_Z, the LEP Collaborations have generally calculated the interference term in the framework of the Standard Model. This fixing of $\sigma^0_{\gamma Z}$ leads to a tighter constraint on M_Z, and consequently a smaller error on its fitted value. It is possible to relax this constraint and carry out the fit within the S-matrix framework, which is briefly described in the next section.

In the above framework, the QED radiative corrections have been explicitly taken into account by convoluting over the ISR and allowing the electromagnetic coupling constant to run [6]: $\alpha(s) = \alpha/(1 - \Delta\alpha)$. On the other hand, weak radiative corrections that depend upon the assumptions of the electroweak theory and on the values of $M_{\rm top}$ and $M_{\rm Higgs}$ are accounted for by **absorbing them into the couplings**, which are then called the *effective* couplings $\mathcal{G}_V$ and $\mathcal{G}_A$ (or alternatively the effective parameters of the $*$ scheme of Kennedy and Lynn [7].)

$\mathcal{G}_V^f$ and $\mathcal{G}_A^f$ are complex numbers with small imaginary parts. As experimental data does not allow simultaneous extraction of both real and imaginary parts of the effective couplings, the convention $g_A^f = \mathrm{Re}(\mathcal{G}_A^f)$ and $g_V^f = \mathrm{Re}(\mathcal{G}_V^f)$ is used and the imaginary parts are added in the fitting code [4].

Defining

$$A_f = 2\frac{g_V^f \cdot g_A^f}{(g_V^f)^2 + (g_A^f)^2} \tag{55.6}$$

the lowest-order expressions for the various lepton-related asymmetries on the Z pole are [8–10] $A_{FB}^{(0,\ell)} = (3/4)A_e A_f$, $P(\tau) = -A_\tau$, $P(\tau)^{fb} = -(3/4)A_e$, $A_{LR} = A_e$. The full analysis takes into account the energy-dependence of the asymmetries. Experimentally A_{LR} is defined as $(\sigma_L - \sigma_R)/(\sigma_L + \sigma_R)$, where $\sigma_{L(R)}$ are the $e^+e^- \to Z$ production cross sections with left- (right)-handed electrons.

The definition of the partial decay width of the Z to $f\overline{f}$ includes the effects of QED and QCD final-state corrections, as well as the contribution due to the imaginary parts of the couplings:

$$\Gamma(f\overline{f}) = \frac{G_F M_Z^3}{6\sqrt{2}\pi}\ N_c^f (\left|\mathcal{G}_A^f\right|^2 R_A^f + \left|\mathcal{G}_V^f\right|^2 R_V^f) + \Delta_{ew/\mathrm{QCD}} \tag{55.7}$$

where R_V^f and R_A^f are radiator factors to account for final state QED and QCD corrections, as well as effects due to nonzero fermion masses, and $\Delta_{ew/\mathrm{QCD}}$ represents the non-factorizable electroweak/QCD corrections.

55.2. S-matrix approach to the Z

While most experimental analyses of LEP/SLC data have followed the 'Breit-Wigner' approach, an alternative S-matrix-based analysis is also possible. The Z, like all unstable particles, is associated with a complex pole in the S matrix. The pole position is process-independent and gauge-invariant. The mass, $\overline{M}_Z$, and width, $\overline{\Gamma}_Z$, can be defined in terms of the pole in the energy plane via [11–14]

$$\overline{s} = \overline{M}_Z^2 - i\overline{M}_Z\overline{\Gamma}_Z \tag{55.8}$$

leading to the relations

$$\begin{aligned}\overline{M}_Z &= M_Z/\sqrt{1+\Gamma_Z^2/M_Z^2} \\ &\approx M_Z \ - 34.1 \text{ MeV} \end{aligned} \tag{55.9}$$

$$\begin{aligned}\overline{\Gamma}_Z &= \Gamma_Z/\sqrt{1+\Gamma_Z^2/M_Z^2} \\ &\approx \Gamma_Z \ - 0.9 \text{ MeV} \ . \end{aligned} \tag{55.10}$$

The LEP collaborations [15] have analyzed their data using the S–matrix approach as defined in Eq. (55.8), in addition to the conventional one. They observe a downward shift in the Z mass as expected.

55.3. Handling the large-angle e^+e^- final state

Unlike other $f\overline{f}$ decay final states of the Z, the e^+e^- final state has a contribution not only from the s-channel but also from the t-channel and s-t interference. The full amplitude is not amenable to fast calculation, which is essential if one has to carry out minimization fits within reasonable computer time. The usual procedure is to calculate the non-s channel part of the cross section separately using the Standard Model programs ALIBABA [16] or TOPAZ0 [17], with the measured value of $M_{\rm top}$, and $M_{\rm Higgs} = 150$ GeV, and add it to the s-channel cross section calculated as for other channels. This leads to two additional sources of error in the analysis: firstly, the theoretical calculation in ALIBABA itself is known to be accurate to $\sim 0.5\%$, and secondly, there is uncertainty due to the error on $M_{\rm top}$ and the unknown value of $M_{\rm Higgs}$ (100–1000 GeV). These errors are propagated into the analysis by including them in the systematic error on the e^+e^- final state. As these errors are common to the four LEP experiments, this is taken into account when performing the LEP average.

55.4. Errors due to uncertainty in LEP energy determination

The systematic errors related to the LEP energy measurement, see Refs. 18–23, can be classified as:

- The absolute energy scale error;
- Energy-point-to-energy-point errors due to the nonlinear response of the magnets to the exciting currents;
- Energy-point-to-energy-point errors due to possible higher-order effects in the relationship between the dipole field and beam energy;
- Energy reproducibility errors due to various unknown uncertainties in temperatures, tidal effects, corrector settings, RF status, *etc.*

Precise energy calibration was done outside normal data-taking using the resonant depolarization technique. Run-time energies were determined every 10 minutes by measuring the relevant machine parameters and using a model which takes into account all the known effects, including leakage currents produced by trains in the Geneva area and the tidal effects due to gravitational forces of the Sun and the Moon. The LEP Energy Working Group has provided a covariance matrix from the determination of LEP energies for the different running periods during 1993–1995 [18].

55.5. Choice of fit parameters

The LEP Collaborations have chosen the following primary set of parameters for fitting: M_Z, Γ_Z, $\sigma^0_{\rm hadron}$, R(lepton), $A_{FB}^{(0,\ell)}$, where R(lepton) $= \Gamma$(hadrons)/Γ(lepton), $\sigma^0_{\rm hadron} = 12\pi\Gamma(e^+e^-)\Gamma(\text{hadrons})/M_Z^2\Gamma_Z^2$. With a knowledge of these fitted parameters and their covariance matrix, any other parameter can be derived. The main advantage of these parameters is that they form a physics motivated set of parameters with much reduced correlations.

Thus, the most general fit carried out to cross section and asymmetry data determines the **nine parameters**: M_Z, Γ_Z, $\sigma^0_{\rm hadron}$, $R(e)$, $R(\mu)$, $R(\tau)$, $A_{FB}^{(0,e)}$, $A_{FB}^{(0,\mu)}$, $A_{FB}^{(0,\tau)}$. Assumption of lepton universality leads to a **five-parameter fit** determining M_Z, Γ_Z, $\sigma^0_{\rm hadron}$, R(lepton), $A_{FB}^{(0,\ell)}$.

55.6. Combining results from LEP and SLC experiments

With a steady increase in statistics over the years and improved understanding of the common systematic errors between LEP experiments, the procedures for combining results have evolved continuously [24]. The Line Shape Sub-group of the LEP Electroweak Working Group investigated the effects of these common errors, and devised a combination procedure for the precise determination of the Z parameters from LEP experiments. Using these procedures, this note also gives the results after combining the final parameter sets from the four experiments, and these are the results quoted as the fit results in the Z listings below. Transformation of variables leads to values of derived parameters like partial decay widths and branching ratios to hadrons and leptons. Finally, transforming the LEP combined nine parameter set to (M_Z, Γ_Z, $\sigma^\circ_{\rm hadron}$, g_A^f, g_V^f, $f = e, \mu, \tau$) using the average values of lepton asymmetry parameters (A_e, A_μ, A_τ) as constraints, leads to the best fitted values of the vector and axial-vector couplings (g_V, g_A) of the charged leptons to the Z.

Brief remarks on the handling of common errors and their magnitudes are given below. The identified common errors are those coming from

(a) LEP energy-calibration uncertainties, and

(b) the theoretical uncertainties in (i) the luminosity determination using small angle Bhabha scattering, (ii) estimating the non-s channel contribution to large angle Bhabha scattering, (iii) the calculation of QED radiative effects, and (iv) the parametrization of the cross section in terms of the parameter set used.

55.7. Common LEP energy errors

All the collaborations incorporate in their fit the full LEP energy error matrix as provided by the LEP energy group for their intersection region [18]. The effect of these errors is separated out from that of other errors by carrying out fits with energy errors scaled up and down by $\sim 10\%$ and redoing the fits. From the observed changes in the overall error matrix, the covariance matrix of the common energy errors is determined. Common LEP energy errors lead to uncertainties on M_Z, Γ_Z, and $\sigma^\circ_{\rm hadron}$ of 1.7, 1.2 MeV, and 0.011 nb, respectively.

55.8. Common luminosity errors

BHLUMI 4.04 [25] is used by all LEP collaborations for small-angle Bhabha scattering leading to a common uncertainty in their measured cross sections of 0.061% [26]. BHLUMI does not include a correction for production of light fermion pairs. OPAL explicitly corrects for this effect and reduces their luminosity uncertainty to 0.054%, which is taken fully correlated with the other experiments. The other three experiments among themselves have a common uncertainty of 0.061%.

55.9. Common non-*s* channel uncertainties

The same standard model programs ALIBABA [16] and TOPAZ0 [17] are used to calculate the non-s channel contribution to the large angle Bhabha scattering [27]. As this contribution is a function of the Z mass, which itself is a variable in the fit, it is parametrized as a function of M_Z by each collaboration to properly track this contribution as M_Z varies in the fit. The common errors on R_e and $A_{FB}^{(0,e)}$ are 0.024 and 0.0014 respectively, and are correlated between them.

55.10. Common theoretical uncertainties: QED

There are large initial-state photon and fermion pair radiation effects near the Z resonance, for which the best currently available evaluations include contributions up to $\mathcal{O}(\alpha^3)$. To estimate the remaining uncertainties, different schemes are incorporated in the standard model programs ZFITTER [5], TOPAZ0 [17], and MIZA [28]. Comparing the different options leads to error estimates of 0.3 and 0.2 MeV on M_Z and Γ_Z respectively, and of 0.02% on $\sigma^\circ_{\rm hadron}$.

55.11. Common theoretical uncertainties: parametrization of lineshape and asymmetries

To estimate uncertainties arising from ambiguities in the model-independent parametrization of the differential cross-section near the Z resonance, results from TOPAZ0 and ZFITTER were compared by using ZFITTER to fit the cross sections and asymmetries calculated using TOPAZ0. The resulting uncertainties on M_Z, Γ_Z, $\sigma^\circ_{\rm hadron}$, R(lepton), and $A_{FB}^{(0,\ell)}$ are 0.1 MeV, 0.1 MeV, 0.001 nb, 0.004, and 0.0001 respectively.

Thus, the overall theoretical errors on M_Z, Γ_Z, $\sigma^\circ_{\rm hadron}$ are 0.3 MeV, 0.2 MeV, and 0.008 nb respectively; on each R(lepton) is 0.004 and on each $A_{FB}^{(0,\ell)}$ is 0.0001. Within the set of three R(lepton)'s and the set of three $A_{FB}^{(0,\ell)}$'s, the respective errors are fully correlated.

All the theory-related errors mentioned above utilize Standard Model programs which need the Higgs mass and running electromagnetic coupling constant as inputs; uncertainties on these inputs will also lead to common errors. All LEP collaborations used the same set of inputs for Standard Model calculations: $M_Z = 91.187$ GeV, the Fermi constant $G_F = (1.16637 \pm 0.00001) \times 10^{-5}$ GeV^{-2} [29], $\alpha^{(5)}(M_Z) = 1/128.877 \pm 0.090$ [30], $\alpha_s(M_Z) = 0.119$ [31], $M_{\rm top} = 174.3 \pm 5.1$ GeV [31] and $M_{\rm Higgs} = 150$ GeV. The only observable effect, on M_Z, is due to the variation of $M_{\rm Higgs}$ between 100–1000 GeV (due to the variation of the γ/Z interference term which is taken from the Standard Model): M_Z changes by +0.23 MeV per unit change in $\log_{10} M_{\rm Higgs}/{\rm GeV}$, which is not an error but a correction to be applied once $M_{\rm Higgs}$ is determined. The effect is much smaller than the error on M_Z ($\pm$2.1 MeV).

55.12. Methodology of combining the LEP experimental results

The LEP experimental results actually used for combination are slightly modified from those published by the experiments (which are given in the Listings below). This has been done in order to facilitate the procedure by making the inputs more consistent. These modified results are given explicitly in [24]. The main differences compared to the published results are (a) consistent use of ZFITTER 6.23 and TOPAZ0 (the published ALEPH results used ZFITTER 6.10); (b) use of the combined energy-error matrix, which makes a difference of 0.1 MeV on the M_Z and Γ_Z for L3 only as at that intersection the RF modeling uncertainties are the largest.

Thus, nine-parameter sets from all four experiments with their covariance matrices are used together with all the common errors correlations. A grand covariance matrix, V, is constructed and a combined nine-parameter set is obtained by minimizing $\chi^2 = \Delta^T V^{-1} \Delta$, where Δ is the vector of residuals of the combined parameter set to the results of individual experiments. Imposing lepton universality in the combination results in the combined five parameter set.

55.13. Study of $Z \to b\overline{b}$ and $Z \to c\overline{c}$

In the sector of c- and b-physics, the LEP experiments have measured the ratios of partial widths $R_b = \Gamma(Z \to b\overline{b})/\Gamma(Z \to$ hadrons), and $R_c = \Gamma(Z \to c\overline{c})/\Gamma(Z \to$ hadrons), and the forward-backward (charge) asymmetries $A_{FB}^{b\overline{b}}$ and $A_{FB}^{c\overline{c}}$. The SLD experiment at SLC has measured the ratios R_c and R_b and, utilizing the polarization of the electron beam, was able to obtain the final state coupling parameters A_b and A_c from a measurement of the left-right forward-backward asymmetry of $b-$ and $c-$quarks. The high precision measurement of R_c at SLD was made possible owing to the small beam size and very stable beam spot at SLC, coupled with a highly precise CCD pixel detector. Several of the analyses have also determined other quantities, in particular the semileptonic branching ratios, B($b \to \ell^-$), B($b \to c \to \ell^+$), and B($c \to \ell^+$), the average time-integrated $B^0\overline{B}^0$ mixing parameter $\overline{\chi}$ and the probabilities for a c–quark to fragment into a D^+, a D_s, a D^{*+} , or a charmed baryon. The latter measurements do not concern properties of the Z boson, and hence they do not appear in the Listing below. However, for completeness, we will report at the end of this minireview their values as obtained fitting the data contained in the Z section. All these quantities are correlated with the electroweak parameters, and since the mixture of b hadrons is different from the one at the $\Upsilon(4S)$, their values might differ from those measured at the $\Upsilon(4S)$.

All the above quantities are correlated to each other since:

- Several analyses (for example the lepton fits) determine more than one parameter simultaneously;
- Some of the electroweak parameters depend explicitly on the values of other parameters (for example R_b depends on R_c);
- Common tagging and analysis techniques produce common systematic uncertainties.

The LEP Electroweak Heavy Flavour Working Group has developed [32] a procedure for combining the measurements taking into account known sources of correlation. The combining procedure determines fourteen parameters: the six parameters of interest in the electroweak sector, R_b, R_c, $A_{FB}^{b\overline{b}}$, $A_{FB}^{c\overline{c}}$, A_b and A_c and, in addition, B($b \to \ell^-$), B($b \to c \to \ell^+$), B($\overline{c} \to \ell^+$), $\overline{\chi}$, $f(D^+)$, $f(D_s)$, $f(c_{\rm baryon})$ and $P(c \to D^{*+}) \times$ B($D^{*+} \to \pi^+ D^0$), to take into account their correlations with the electroweak parameters. Before the fit both the peak and off-peak asymmetries are translated to the common energy $\sqrt{s} = 91.26$ GeV using the predicted energy-dependence from ZFITTER [5].

55.14. Summary of the measurements and of the various kinds of analysis

The measurements of R_b and R_c fall into two classes. In the first, named single-tag measurement, a method for selecting b and c events is applied and the number of tagged events is counted. A second technique, named double-tag measurement, has the advantage that the tagging efficiency is directly derived from the data thereby reducing the systematic error on the measurement.

The measurements in the b- and c-sector can be essentially grouped in the following categories:

- Lifetime (and lepton) double-tagging measurements of R_b. These are the most precise measurements of R_b and obviously dominate the combined result. The main sources of systematics come from the charm contamination and from estimating the hemisphere b-tagging efficiency correlation;
- Analyses with $D/D^{*\pm}$ to measure R_c. These measurements make use of several different tagging techniques (inclusive/exclusive double tag, exclusive double tag, reconstruction of all weakly decaying charmed states) and no assumptions are made on the energy-dependence of charm fragmentation;
- A measurement of R_c using single leptons and assuming B($b \to c \to \ell^+$);

- Lepton fits which use hadronic events with one or more leptons in the final state to measure the asymmetries $A_{FB}^{b\overline{b}}$ and $A_{FB}^{c\overline{c}}$. Each analysis usually gives several other electroweak parameters. The dominant sources of systematics are due to lepton identification, to other semileptonic branching ratios and to the modeling of the semileptonic decay;
- Measurements of $A_{FB}^{b\overline{b}}$ using lifetime tagged events with a hemisphere charge measurement. These measurements dominate the combined result;
- Analyses with $D/D^{*\pm}$ to measure $A_{FB}^{c\overline{c}}$ or simultaneously $A_{FB}^{b\overline{b}}$ and $A_{FB}^{c\overline{c}}$;
- Measurements of A_b and A_c from SLD, using several tagging methods (lepton, kaon, D/D^*, and vertex mass). These quantities are directly extracted from a measurement of the left–right forward–backward asymmetry in $c\overline{c}$ and $b\overline{b}$ production using a polarized electron beam.

55.15. Averaging procedure

All the measurements are provided by the LEP and SLD Collaborations in the form of tables with a detailed breakdown of the systematic errors of each measurement and its dependence on other electroweak parameters.

The averaging proceeds via the following steps:

- Define and propagate a consistent set of external inputs such as branching ratios, hadron lifetimes, fragmentation models *etc.* All the measurements are checked to ensure that all use a common set of assumptions (for instance, since the QCD corrections for the forward–backward asymmetries are strongly dependent on the experimental conditions, the data are corrected before combining);
- Form the full (statistical and systematic) covariance matrix of the measurements. The systematic correlations between different analyses are calculated from the detailed error breakdown in the measurement tables. The correlations relating several measurements made by the same analysis are also used;
- Take into account any explicit dependence of a measurement on the other electroweak parameters. As an example of this dependence, we illustrate the case of the double-tag measurement of R_b, where c-quarks constitute the main background. The normalization of the charm contribution is not usually fixed by the data and the measurement of R_b depends on the assumed value of R_c, which can be written as:

$$R_b = R_b^{\rm meas} + a(R_c)\frac{(R_c - R_c^{\rm used})}{R_c}\ , \qquad (55.11)$$

  where $R_b^{\rm meas}$ is the result of the analysis which assumed a value of $R_c = R_c^{\rm used}$ and $a(R_c)$ is the constant which gives the dependence on R_c;
- Perform a χ^2 minimization with respect to the combined electroweak parameters.

After the fit the average peak asymmetries $A_{FB}^{c\overline{c}}$ and $A_{FB}^{b\overline{b}}$ are corrected for the energy shift from 91.26 GeV to M_Z and for QED (initial state radiation), γ exchange, and γZ interference effects, to obtain the corresponding pole asymmetries $A_{FB}^{0,c}$ and $A_{FB}^{0,b}$.

This averaging procedure, using the fourteen parameters described above, and applied to the data contained in the Z particle listing below, gives the following results (where the last 8 parameters do not depend directly on the Z):

$$\begin{aligned}
R_b^0 &= 0.21629 \pm 0.00066 \\
R_c^0 &= 0.1721 \pm 0.0030 \\
A_{FB}^{0,b} &= 0.0992 \pm 0.0016 \\
A_{FB}^{0,c} &= 0.0707 \pm 0.0035 \\
A_b &= 0.923 \pm 0.020 \\
A_c &= 0.670 \pm 0.027 \\
B(b \to \ell^-) &= 0.1071 \pm 0.0022 \\
{\rm B}(b \to c \to \ell^+) &= 0.0801 \pm 0.0018 \\
B(c \to \ell^+) &= 0.0969 \pm 0.0031 \\
\overline{\chi} &= 0.1250 \pm 0.0039 \\
f(D^+) &= 0.235 \pm 0.016 \\
f(D_s) &= 0.126 \pm 0.026 \\
f(c_{\rm baryon}) &= 0.093 \pm 0.022 \\
P(c \to D^{*+}) \times {\rm B}(D^{*+} \to \pi^+ D^0) &= 0.1622 \pm 0.0048
\end{aligned}$$

Among the non–electroweak observables, the B semileptonic branching fraction $B(b \to \ell^-)$ is of special interest, since the dominant error source on this quantity is the dependence on the semileptonic decay model for $b \to \ell^-$, with $\Delta B(b \to \ell^-)_{b\to\ell^- -{\rm model}} = 0.0012$. Extensive studies have been made to understand the size of this error. Among the electroweak quantities, the quark asymmetries with leptons depend also on the semileptonic decay model, while the asymmetries using other methods usually do not. The fit implicitely requires that the different methods give consistent results and this effectively constrains the decay model, and thus reduces in principle the error from this source in the fit result.

To obtain a conservative estimate of the modelling error, the above fit has been repeated removing all asymmetry measurements. The results of the fit on B–decay related observables are [24]: $B(b \to \ell^-) = 0.1069 \pm 0.0022$, with $\Delta B(b \to \ell^-)_{b\to\ell^- -{\rm model}} = 0.0013$, $B(b \to c \to \ell^+) = 0.0802 \pm 0.0019$ and $\overline{\chi} = 0.1259 \pm 0.0042$.

References:

1. R.N. Cahn, Phys. Rev. **D36**, 2666 (1987).
2. F.A. Berends *et al.*, "Z Physics at LEP 1," CERN Report 89-08 (1989), Vol. 1, eds. G. Altarelli, R. Kleiss, and C. Verzegnassi, p. 89.
3. A. Borrelli *et al.*, Nucl. Phys. **B333**, 357 (1990).
4. D. Bardin and G. Passarino, "Upgrading of Precision Calculations for Electroweak Observables," `hep-ph/9803425`;
   D. Bardin, G. Passarino, and M. Grünewald, "Precision Calculation Project Report," `hep-ph/9902452`.
5. D. Bardin *et al.*, Z. Phys. **C44**, 493 (1989); Comp. Phys. Comm. **59**, 303 (1990);
   D. Bardin *et al.*, Nucl. Phys. **B351**, 1 (1991); Phys. Lett. **B255**, 290 (1991), and CERN-TH/6443/92 (1992); Comp. Phys. Comm. **133**, 229 (2001).
6. G. Burgers *et al.*, "Z Physics at LEP 1," CERN Report 89-08 (1989), Vol. 1, eds. G. Altarelli, R. Kleiss, and C. Verzegnassi, p. 55.
7. D.C. Kennedy and B.W. Lynn, Nucl. Phys. **B322**, 1 (1989).
8. M. Consoli *et al.*, "Z Physics at LEP 1," CERN Report 89-08 (1989), Vol. 1, eds. G. Altarelli, R. Kleiss, and C. Verzegnassi, p. 7.
9. M. Bohm *et al.*, *ibid*, p. 203.
10. S. Jadach *et al.*, *ibid*, p. 235.
11. R. Stuart, Phys. Lett. **B262**, 113 (1991).
12. A. Sirlin, Phys. Rev. Lett. **67**, 2127 (1991).
13. A. Leike, T. Riemann, and J. Rose, Phys. Lett. **B273**, 513 (1991).
14. See also D. Bardin *et al.*, Phys. Lett. **B206**, 539 (1988).
15. The LEP Collaborations: ALEPH, DELPHI, L3, OPAL, the LEP Electroweak Working Group, CERN-PH-EP/2013-022, `arXiv:1302.3415 [hep-ex]`, Phys.Rept. 532 (2013) 119-244.
16. W. Beenakker, F.A. Berends, and S.C. van der Marck, Nucl. Phys. **B349**, 323 (1991).

17. G. Montagna *et al.*, Nucl. Phys. **B401**, 3 (1993); Comp. Phys. Comm. **76**, 328 (1993); Comp. Phys. Comm. **93**, 120 (1996); G. Montagna *et al.*, Comp. Phys. Comm. **117**, 278 (1999).
18. R. Assmann *et al.*, (Working Group on LEP Energy), Eur. Phys. J. **C6**, 187 (1999).
19. R. Assmann *et al.*, (Working Group on LEP Energy), Z. Phys. **C66**, 567 (1995).
20. L. Arnaudon *et al.*, (Working Group on LEP Energy and LEP Collabs.), Phys. Lett. **B307**, 187 (1993).
21. L. Arnaudon *et al.*, (Working Group on LEP Energy), CERN-PPE/92-125 (1992).
22. L. Arnaudon *et al.*, Phys. Lett. **B284**, 431 (1992).
23. R. Bailey *et al.*, 'LEP Energy Calibration' CERN-SL-90-95-AP, *Proceedings of the "2nd European Particle Accelerator Conference,"* Nice, France, 12–16 June 1990, pp. 1765-1767.
24. The LEP Collabs.: ALEPH, DELPHI, L3, OPAL, the LEP Electroweak Working Group, and the SLD Heavy Flavour Group: Phys. Reports **427**, 257 (2006).
25. S. Jadach *et al.*, BHLUMI 4.04, Comp. Phys. Comm. **102**, 229 (1997);
    S. Jadach and O. Nicrosini, Event generators for Bhabha scattering, in Physics at LEP2, CERN-96-01 Vol. 2, February 1996.
26. B.F.L. Ward *et al.*, Phys. Lett. **B450**, 262 (1999).
27. W. Beenakker and G. Passarino, Phys. Lett. **B425**, 199 (1998).
28. M. Martinez *et al.*, Z. Phys. **C49**, 645 (1991);
    M. Martinez and F. Teubert, Z. Phys. **C65**, 267 (1995), updated with results summarized in S. Jadach, B. Pietrzyk, and M. Skrzypek, Phys. Lett. **B456**, 77 (1999) and Reports of the working group on precision calculations for the Z resonance, CERN 95-03, ed. D. Bardin, W. Hollik, and G. Passarino, and references therein.
29. T. van Ritbergen and R. Stuart, Phys. Lett. **B437**, 201 (1998); Phys. Rev. Lett. **82**, 488 (1999).
30. S. Eidelman and F. Jegerlehner, Z. Phys. **C67**, 585 (1995); M. Steinhauser, Phys. Lett. **B429**, 158 (1998).
31. Particle Data Group (D.E. Groom *et al.*), Eur. Phys. J. **C15**, 1 (2000).
32. The LEP Experiments: ALEPH, DELPHI, L3, and OPAL Nucl. Instrum. Methods **A378**, 101 (1996).

56. Anomalous $ZZ\gamma$, $Z\gamma\gamma$, and ZZV Couplings

Revised September 2013 by M.W. Grünewald (U. College Dublin) and A. Gurtu (Formerly Tata Inst.).

In on-shell $Z\gamma$ production, deviations from the Standard Model for the $Z\gamma\gamma^*$ and $Z\gamma Z^*$ couplings may be described in terms of eight parameters, h_i^V $(i = 1, 4;\ V = \gamma, Z)$ [1]. The parameters h_i^γ describe the $Z\gamma\gamma^*$ couplings and the parameters h_i^Z the $Z\gamma Z^*$ couplings. In this formalism h_1^V and h_2^V lead to CP-violating and h_3^V and h_4^V to CP-conserving effects. All these anomalous contributions to the cross section increase rapidly with center-of-mass energy. In order to ensure unitarity, these parameters are usually described by a form-factor representation, $h_i^V(s) = h_{i\text{o}}^V/(1 + s/\Lambda^2)^n$, where Λ is the energy scale for the manifestation of a new phenomenon and n is a sufficiently large power. By convention one uses $n = 3$ for $h_{1,3}^V$ and $n = 4$ for $h_{2,4}^V$. Usually limits on h_i^V's are put assuming some value of Λ, sometimes infinity.

In on-shell ZZ production, deviations from the Standard Model for the $ZZ\gamma^*$ and ZZZ^* couplings may be described by means of four anomalous couplings f_i^V $(i = 4, 5; V = \gamma, Z)$ [2]. As above, the parameters f_i^γ describe the $ZZ\gamma^*$ couplings and the parameters f_i^Z the ZZZ^* couplings. The anomalous couplings f_5^V lead to violation of C and P symmetries while f_4^V introduces CP violation. Also here, formfactors depending on a scale Λ are used.

All these couplings h_i^V and f_i^V are zero at tree level in the Standard Model; they are measured in e^+e^-, $p\bar{p}$ and pp collisions at LEP, Tevatron and LHC.

References:

1. U. Baur and E.L. Berger, Phys. Rev. **D47**, 4889 (1993).
2. K. Hagiwara *et al.*, Nucl. Phys. **B282**, 253 (1987).

57. Muon Anomalous Magnetic Moment

Updated August 2017 by A. Hoecker (CERN) and W.J. Marciano (BNL).

The Dirac equation predicts a muon magnetic moment, $\vec{M} = g_\mu \frac{e}{2m_\mu}\vec{S}$, with gyromagnetic ratio $g_\mu = 2$. Quantum loop effects lead to a small calculable deviation from $g_\mu = 2$, parameterized by the anomalous magnetic moment

$$a_\mu \equiv \frac{g_\mu - 2}{2} \ . \tag{57.1}$$

That quantity can be accurately measured and, within the Standard Model (SM) framework, precisely predicted. Hence, comparison of experiment and theory tests the SM at its quantum loop level. A deviation in $a_\mu^{\rm exp}$ from the SM expectation would signal effects of new physics, with current sensitivity reaching up to mass scales of $\mathcal{O}$(TeV) [1,2]. For recent and thorough muon $g-2$ reviews, see Refs. [3–5].

The E821 experiment at Brookhaven National Lab (BNL) studied the precession of μ^+ and μ^- in a constant external magnetic field as they circulated in a confining storage ring. It found [7] [1]

$$\begin{aligned} a_{\mu^+}^{\rm exp} &= 11\,659\,204(6)(5)\times 10^{-10}\,, \\ a_{\mu^-}^{\rm exp} &= 11\,659\,215(8)(3)\times 10^{-10}\,, \end{aligned} \tag{57.2}$$

where the first errors are statistical and the second systematic. Assuming CPT invariance and taking into account correlations between systematic uncertainties, one finds for their average [6,7]

$$a_\mu^{\rm exp} = 11\,659\,209.1(5.4)(3.3)\times 10^{-10} \ . \tag{57.3}$$

These results represent about a factor of 14 improvement over the classic CERN experiments of the 1970's [8]. Improvement of the measurement by a factor of four by setting up the E821 storage ring at Fermilab, and utilizing a cleaner and more intense muon beam is in progress with the commissioning of the experiment having started in 2017.

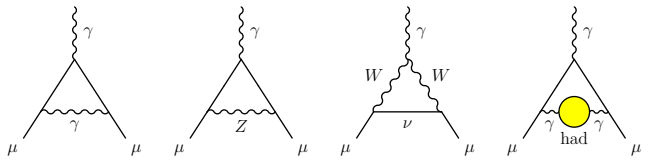

Figure 57.1: Representative diagrams contributing to $a_\mu^{\rm SM}$. From left to right: first order QED (Schwinger term), lowest-order weak, lowest-order hadronic.

The SM prediction for $a_\mu^{\rm SM}$ is generally divided into three parts (see Fig. 57.1 for representative Feynman diagrams)

$$a_\mu^{\rm SM} = a_\mu^{\rm QED} + a_\mu^{\rm EW} + a_\mu^{\rm Had} \ . \tag{57.4}$$

The QED part includes all photonic and leptonic (e,μ,τ) loops starting with the classic $\alpha/2\pi$ Schwinger contribution. It has been computed through 5 loops [9]

$$\begin{aligned} a_\mu^{\rm QED} =& \frac{\alpha}{2\pi} + 0.765\,857\,425(17)\left(\frac{\alpha}{\pi}\right)^2 + 24.050\,509\,96(32)\left(\frac{\alpha}{\pi}\right)^3 \\ &+ 130.879\,6(6\,3)\left(\frac{\alpha}{\pi}\right)^4 + 753.3(1.0)\left(\frac{\alpha}{\pi}\right)^5 + \cdots \end{aligned} \tag{57.5}$$

with no change in the coefficients since our previous update of this review in 2013. Employing[2] $\alpha^{-1} = 137.035\,999\,049(90)$, obtained [6] from the precise measurements of $h/m_{\rm Rb}$ [11], the Rydberg constant and $m_{\rm Rb}/m_e$ [6], leads to [9]

$$a_\mu^{\rm QED} = 116\,584\,718.95(0.08)\times 10^{-11}\,, \tag{57.6}$$

where the small error results mainly from the uncertainty in α.

Loop contributions involving heavy $W^\pm, Z$ or Higgs particles are collectively labeled as $a_\mu^{\rm EW}$. They are suppressed by at least a factor of $\frac{\alpha}{\pi}\frac{m_\mu^2}{m_W^2} \simeq 4\times 10^{-9}$. At 1-loop order [12]

$$\begin{aligned} a_\mu^{\rm EW}[\text{1-loop}] &= \frac{G_\mu m_\mu^2}{8\sqrt{2}\pi^2}\left[\frac{5}{3} + \frac{1}{3}\left(1 - 4\sin^2\theta_{\rm W}\right)^2\right. \\ &\quad \left. + \mathcal{O}\left(\frac{m_\mu^2}{M_W^2}\right) + \mathcal{O}\left(\frac{m_\mu^2}{m_H^2}\right)\right], \\ &= 194.8\times 10^{-11}\,, \end{aligned} \tag{57.7}$$

for $\sin^2\theta_{\rm W} \equiv 1 - M_W^2/M_Z^2 \simeq 0.223$, and where $G_\mu \simeq 1.166\times 10^{-5}$ GeV^{-2} is the Fermi coupling constant. Two-loop corrections are relatively large and negative [13]. For a Higgs boson mass of 125 GeV [13]

$$a_\mu^{\rm EW}[\text{2-loop}] = -41.2(1.0)\times 10^{-11}\,, \tag{57.8}$$

where the uncertainty stems from quark triangle loops. The 3-loop leading logarithms are negligible [13,14], $\mathcal{O}(10^{-12})$, implying in total

$$a_\mu^{\rm EW} = 153.6(1.0)\times 10^{-11} \ . \tag{57.9}$$

Hadronic (quark and gluon) loop contributions to $a_\mu^{\rm SM}$ give rise to its main theoretical uncertainties. At present, those effects are not precisely calculable from first principles, but such an approach, at least partially, may become possible as lattice QCD matures [15]. Instead, one currently relies on a dispersion relation approach to evaluate the lowest-order (*i.e.*, $\mathcal{O}(\alpha^2)$) hadronic vacuum polarization contribution $a_\mu^{\rm Had}$[LO] from corresponding cross section measurements [16]

$$a_\mu^{\rm Had}[\text{LO}] = \frac{1}{3}\left(\frac{\alpha}{\pi}\right)^2 \int_{m_\pi^2}^{\infty} ds\, \frac{K(s)}{s} R^{(0)}(s)\,, \tag{57.10}$$

where $K(s)$ is a QED kernel function [17], and where $R^{(0)}(s)$ denotes the ratio of the bare[3] cross section for e^+e^- annihilation into hadrons to the pointlike muon-pair cross section at center-of-mass energy $\sqrt{s}$. The function $K(s) \sim 1/s$ in Eq. (57.10) gives a strong weight to the low-energy part of the integral. Hence, $a_\mu^{\rm Had}$[LO] is dominated by the $\rho(770)$ resonance.

Currently, the available $\sigma(e^+e^- \to \text{hadrons})$ data give a leading-order hadronic vacuum polarization (representative) contribution of [18]

$$a_\mu^{\rm Had}[\text{LO}] = 6\,931(33)(7)\times 10^{-11}\,, \tag{57.11}$$

where the first error is experimental (dominated by systematic uncertainties), and the second due to perturbative QCD, which is used at intermediate and large energies to predict the contribution from the quark-antiquark continuum. New data in particular from the BABAR

[1] The original results reported by the experiment have been updated in Eqs. (57.2) and (57.3) to the newest value for the absolute muon-to-proton magnetic ratio $\lambda = 3.183\,345\,107(84)$ [6]. The change induced in $a_\mu^{\rm exp}$ with respect to the value of $\lambda = 3.183\,345\,39(10)$ used in Ref. 7 amounts to $+1.12\times 10^{-10}$.

[2] In early versions of this review we used the precise α value determined from the electron a_e measurement [9,10]. With the new measurement [11] of the recoil velocity of Rubidium, $h/m_{\rm Rb}$, an a_e-independent determination of α with sufficient precision is available and preferred.

[3] The bare cross section is defined as the measured cross section corrected for initial-state radiation, electron-vertex loop contributions and vacuum-polarization effects in the photon propagator. However, QED effects in the hadron vertex and final state, as photon radiation, are included.

and VEPP-2000 experiments have led to a reduction by about 20% in the uncertainty of the hadronic contribution compared to the 2013 PDG value.

Alternatively, one can use precise vector spectral functions from $\tau \to \nu_\tau$ + hadrons decays [20] that can be related to isovector e^+e^- → hadrons cross sections by isospin symmetry. Analyses replaced e^+e^- data in the two-pion and four-pion channels by the corresponding isospin-transformed τ data, and applied isospin-violating corrections [19]. Owing to the progress in the precision of the e^+e^- data, the τ data are now less precise and less reliable due to additional theoretical uncertainties. The τ-based result was therefore not updated in the most recent $a_\mu^{\rm Had}$[LO] evaluation [18].

Higher order hadronic contributions are obtained from dispersion relations using the same e^+e^- → hadrons data [28], giving $a_\mu^{\rm Had,Disp}[\rm NLO] = (-98.7 \pm 0.9) \times 10^{-11}$ and $a_\mu^{\rm Had,Disp}[\rm NNLO] = (12.4 \pm 0.1) \times 10^{-11}$ [29], along with model-dependent estimates of the hadronic light-by-light scattering contribution, $a_\mu^{\rm Had,LBL}$[NLO], motivated by large-N_C QCD [30–36]. [4] Following [34], one finds for the sum of the three terms

$$a_\mu^{\rm Had}[\rm N(N)LO] = 19(26) \times 10^{-11}\,, \qquad (57.12)$$

where the error is dominated by hadronic light-by-light uncertainty.

Adding Eqs. (57.6), (57.9), (57.11) and (57.12) gives the representative e^+e^- data based SM prediction

$$a_\mu^{\rm SM} = 116\,591\,823(1)(34)(26) \times 10^{-11}\,, \qquad (57.13)$$

where the errors are due to the electroweak, lowest-order hadronic, and higher-order hadronic contributions, respectively. The difference between experiment and theory

$$\Delta a_\mu = a_\mu^{\rm exp} - a_\mu^{\rm SM} = 268(63)(43) \times 10^{-11}\,, \qquad (57.14)$$

where the errors are from experiment and theory prediction (with all errors combined in quadrature), respectively, represents an interesting but not conclusive discrepancy of 3.5 times the combined 1σ error. All the recent estimates for the hadronic contribution compiled in Fig. 57.2 exhibit similar discrepancies.

An exciting interpretation is that Δa_μ may be a new physics signal with supersymmetric particle loops as the leading candidate explanation. Such a scenario is quite natural, since generically, supersymmetric models predict [1] an additional contribution to $a_\mu^{\rm SM}$

$$a_\mu^{\rm SUSY} \simeq \pm 130 \times 10^{-11} \cdot \left(\frac{100\ {\rm GeV}}{m_{\rm SUSY}}\right)^2 \tan\beta\,, \qquad (57.15)$$

where $m_{\rm SUSY}$ is a representative supersymmetric mass scale, $\tan\beta \simeq 3$–40 a potential enhancement factor, and ± 1 corresponds to the sign of the μ term in the supersymmetric Lagrangian. Supersymmetric particles in the mass range 100–500 GeV could be the source of the deviation Δa_μ. If so, those particles should be directly observable at the Large Hadron Collider at CERN. So far, there is however no direct evidence in support of the supersymmetry interpretation.

New physics effects [1] other than supersymmetry could also explain a non-vanishing Δa_μ. A popular scenario involves the "dark photon", a relatively light hypothetical vector boson from the dark matter sector that couples to our world of particle physics through mixing with the ordinary photon [38,39,40]. As a result, it couples to ordinary charged particles with strength $\varepsilon \cdot e$ and gives rise to an additional muon anomalous magnetic moment contribution

$$a_\mu^{\rm dark\ photon} = \frac{\alpha}{2\pi}\varepsilon^2 F(m_V/m_\mu)\,, \qquad (57.16)$$

where $F(x) = \int_0^1 2z(1-z)^2/[(1-z)^2 + x^2 z]\,dz$. For values of $\varepsilon \sim 1$–$2 \cdot 10^{-3}$ and $m_V \sim 10$–100 MeV, the dark photon, which was originally motivated by cosmology, can provide a viable solution to the muon $g-2$ discrepancy. However, recent experimental constraints disfavor such a scenario [41] under the assumption that the dark photon decays primarily into charged lepton pairs. Direct searches for the dark photon continue to be well motivated [42]; but with guidance coming from phenomena outside the muon anomalous magnetic moment discrepancy.

[4] Some representative recent estimates of the hadronic light-by-light scattering contribution, $a_\mu^{\rm Had,LBL}$[NLO], that followed after the sign correction of [32], are: $105(26) \times 10^{-11}$ [34], $110(40) \times 10^{-11}$ [30], $136(25) \times 10^{-11}$ [31].

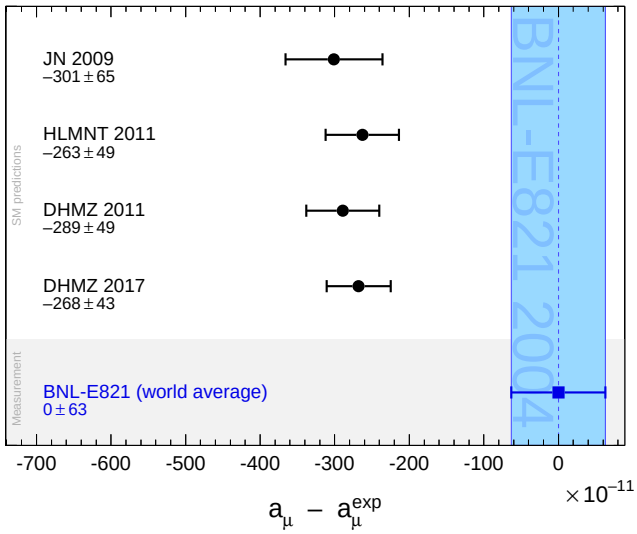

Figure 57.2: Compilation of recent published results for a_μ (in units of 10^{-11}), subtracted by the central value of the experimental average (57.3). The shaded band indicates the size of the experimental uncertainty. The SM predictions are taken from: JN 2009 [4], HLMNT 2011 [23], DHMZ 2011 [19], DHMZ 2017 [18], Note that the quoted errors in the figure do not include the uncertainty on the subtracted experimental value. To obtain for each theory calculation a result equivalent to Eq. (57.14), the errors from theory and experiment must be added in quadrature.

References:

1. A. Czarnecki and W.J. Marciano, Phys. Rev. **D64**, 013014 (2001).
2. M. Davier and W.J. Marciano, Ann. Rev. Nucl. and Part. Sci. **54**, 115 (2004).
3. J. Miller, E. de Rafael, and B. Lee Roberts, Rept. Prog. Phys. **70**, 795 (2007).
4. F. Jegerlehner and A. Nyffeler, Phys. Reports **477**, 1 (2009).
5. J.P. Miller *et al.*, Ann. Rev. Nucl. and Part. Sci. **62**, 237 (2012).
6. P.J. Mohr, B.N. Taylor, and D.B. Newell, CODATA Group, Rev. Mod. Phys. **84**, 1527 (2012).
7. G.W. Bennett *et al.*, Phys. Rev. Lett. **89**, 101804 (2002); Erratum *ibid.* Phys. Rev. Lett. **89**, 129903 (2002); G.W. Bennett *et al.*, Phys. Rev. Lett. **92**, 161802 (2004); G.W. Bennett *et al.*, Phys. Rev. **D73**, 072003 (2006).
8. J. Bailey *et al.*, Nucl. Phys. **B150**, 1 (1979).
9. T. Aoyama *et al.*, Phys. Rev. Lett. **109**, 111808 (2012); T. Aoyama *et al.*, Phys. Rev. Lett. **109**, 111807 (2012); T. Kinoshita and M. Nio, Phys. Rev. **D73**, 013003 (2006); T. Aoyama *et al.*, Phys. Rev. Lett. **99**, 110406 (2007); T. Kinoshita and M. Nio, Phys. Rev. **D70**, 113001 (2004); T. Kinoshita, Nucl. Phys. **B144**, 206 (2005)(Proc. Supp.); T. Kinoshita and M. Nio, Phys. Rev. **D73**, 053007 (2006); A. Kurz *et al.*, Phys. Rev. **D93**, 053017 (2016); A.L. Kataev, `arXiv:hep-ph/0602098` (2006); M. Passera, J. Phys. **G31**, 75 (2005).
10. G. Gabrielse et al., Phys. Rev. Lett. **97**, 030802 (2006); Erratum *ibid.* Phys. Rev. Lett. **99**, 039902 (2007); D. Hanneke, S. Fogwell, and G. Gabrielse, Phys. Rev. Lett. **100**, 120801 (2008).

11. R. Bouchendira *et al.*, Phys. Rev. Lett. **106**, 080801 (2011).
12. R. Jackiw and S. Weinberg, Phys. Rev. **D5**, 2396 (1972); G. Altarelli *et al.*, Phys. Lett. **B40**, 415 (1972); I. Bars and M. Yoshimura, Phys. Rev. **D6**, 374 (1972); K. Fujikawa, B.W. Lee, and A.I. Sanda, Phys. Rev. **D6**, 2923 (1972).
13. C. Gnendiger, D. Stöckinger, H. Stöckinger-Kim, Phys. Rev. **D88**, 053005 (2013); A. Czarnecki *et al.*, Phys. Rev. **D67**, 073006 (2003); Erratum *ibid.* Phys. Rev. **D73**, 119901 (2006); S. Heinemeyer, D. Stockinger, and G. Weiglein, Nucl. Phys. **B699**, 103 (2004); T. Gribouk and A. Czarnecki, Phys. Rev. **D72**, 053016 (2005); A. Czarnecki, B. Krause, and W.J. Marciano, Phys. Rev. Lett. **76**, 3267 (1996); A. Czarnecki, B. Krause, and W.J. Marciano, Phys. Rev. **D52**, 2619, (1995); S. Peris, M. Perrottet, and E. de Rafael, Phys. Lett. **B355**, 523 (1995); T. Kukhto et al, Nucl. Phys. **B371**, 567 (1992).
14. G. Degrassi and G.F. Giudice, Phys. Rev. **D58**, 053007 (1998).
15. B. Chakraborty *et al.*, Phys. Rev. **D96**, 034516 (2017); T. Blum *et al.*, Phys. Rev. **D96**, 034515 (2017); T. Blum, Phys. Rev. Lett. **118**, 022005 (2017); B. Chakraborty *et al.*, Phys. Rev. **D93**, 074509 (2016); C. Lehner, t arXiv:1710.06874 (2017).
16. C. Bouchiat and L. Michel, J. Phys. Radium **22**, 121 (1961); M. Gourdin and E. de Rafael, Nucl. Phys. **B10**, 667 (1969).
17. S.J. Brodsky and E. de Rafael, Phys. Rev. **168**, 1620 (1968).
18. M. Davier *et al.*, arXiv:1706.09436 (2017).
19. M. Davier *et al.*, Eur. Phys. J. **C71**, 1515 (2011).
20. R. Alemany *et al.*, Eur. Phys. J. **C2**, 123 (1998).
21. M. Davier *et al.*, Eur. Phys. J. **C66**, 127 (2010).
22. BABAR Collaboration (B. Aubert *et al.*), Phys. Rev. Lett. **103**, 231801 (2009).
23. K. Hagiwara *et al.*, J. Phys. **G38**, 085003 (2011).
24. S. Bodenstein *et al.*, Phys. Rev. **D88**, 014005 (2013).
25. M. Benayoun *et al.*, Eur. Phys. J. **C73**, 2453 (2013).
26. M. Davier, Nucl. Phys. (Proc. Suppl.), **B169**, 288 (2007).
27. M. Davier *et al.*, Eur. Phys. J. **C31**, 503 (2003); M. Davier *et al.*, Eur. Phys. J. **C27**, 497 (2003).
28. B. Krause, Phys. Lett. **B390**, 392 (1997).
29. A. Kurz *et al.*, Phys. Lett. **B734**, 144 (2014).
30. J. Bijnens and J. Prades, Mod. Phys. Lett. **A22**, 767 (2007).
31. K. Melnikov and A. Vainshtein, Phys. Rev. **D70**, 113006 (2004).
32. M. Knecht and A. Nyffeler, Phys. Rev. **D65**, 073034 (2002); M. Knecht *et al.*, Phys. Rev. Lett. **88**, 071802 (2002).
33. J. Bijnens *et al.*, Nucl. Phys. **B626**, 410 (2002).
34. J. Prades, E. de Rafael, and A. Vainshtein, Advanced series on directions in high energy physics 20, Editors B.L. Roberts and W. Marciano (2009), arXiv:0901.0306.
35. J. Hayakawa and T. Kinoshita, Erratum Phys. Rev. **D66**, 019902 (2002).
36. E. de Rafael, Phys. Lett. **B322**, 239 (1994).
37. F. Jegerlehner and R. Szafron, Eur. Phys. J. **C71**, 1632 (2011).
38. P. Fayet, Phys. Rev. **D75**, 115017 (2007).
39. M. Pospelov, Phys. Rev. **D80**, 095002 (2009).
40. D. Tucker-Smith and I. Yavin, Phys. Rev. **D83**, 101702 (R)(2011).
41. NA48/2 Collaboration (J.R. Batley et al.), Phys. Lett. **B746**, 178 (2015).
42. J. Alexander *et al.*, Dark Sectors 2016 Workshop: Community Report (2017), arXiv:1608.08632.

58. Muon Decay Parameters

Revised September 2013 by W. Fetscher and H.-J. Gerber (ETH Zürich).

58.1. Introduction:

All measurements in direct muon decay, $\mu^- \to e^- + 2$ neutrals, and its inverse, $\nu_\mu + e^- \to \mu^-$ + neutral, are successfully described by the "V-A interaction," which is a particular case of a local, derivative-free, lepton-number-conserving, four-fermion interaction [1]. As shown below, within this framework, the Standard Model assumptions, such as the V-A form and the nature of the neutrals (ν_μ and $\bar{\nu}_e$), and hence the doublet assignments $(\nu_e\ e^-)_L$ and $(\nu_\mu\ \mu^-)_L$, have been determined from experiments [2,3]. All considerations on muon decay are valid for the leptonic tau decays $\tau \to \ell + \nu_\tau + \bar{\nu}_e$ with the replacements $m_\mu \to m_\tau$, $m_e \to m_\ell$.

58.2. Parameters:

The differential decay probability to obtain an $e^\pm$ with (reduced) energy between x and $x + \mathrm{d}x$, emitted in the direction $\widehat{\boldsymbol{x}}_3$ at an angle between ϑ and $\vartheta + \mathrm{d}\vartheta$ with respect to the muon polarization vector $\boldsymbol{P}_\mu$, and with its spin parallel to the arbitrary direction $\widehat{\boldsymbol{\zeta}}$, neglecting radiative corrections, is given by

$$\begin{aligned}\frac{\mathrm{d}^2\Gamma}{\mathrm{d}x\ \mathrm{d}\cos\vartheta} =& \frac{m_\mu}{4\pi^3}\, W_{e\mu}^4\, G_\mathrm{F}^2\, \sqrt{x^2 - x_0^2} \\ & \times \left(F_\mathrm{IS}(x) \pm P_\mu \cos\vartheta\ F_\mathrm{AS}(x)\right) \\ & \times \left[1 + \widehat{\boldsymbol{\zeta}} \cdot \boldsymbol{P}_e(x,\vartheta)\right] \ . \end{aligned} \tag{58.1}$$

Here, $W_{e\mu} = \max(E_e) = (m_\mu^2 + m_e^2)/2m_\mu$ is the maximum $e^\pm$ energy, $x = E_e/W_{e\mu}$ is the reduced energy, $x_0 = m_e/W_{e\mu} = 9.67 \times 10^{-3}$, and $P_\mu = |\boldsymbol{P}_\mu|$ is the degree of muon polarization. $\widehat{\boldsymbol{\zeta}}$ is the direction in which a perfect polarization-sensitive electron detector is most sensitive. The isotropic part of the spectrum, $F_\mathrm{IS}(x)$, the anisotropic part $F_\mathrm{AS}(x)$, and the electron polarization, $\boldsymbol{P}_e(x,\vartheta)$, may be parametrized by the Michel parameter ρ [1], by η [4], by ξ and δ [5,6], *etc.* These are bilinear combinations of the coupling constants $g^\gamma_{\varepsilon\mu}$, which occur in the matrix element (given below).

If the masses of the neutrinos as well as x_0^2 are neglected, the energy and angular distribution of the electron in the rest frame of a muon ($\mu^\pm$) measured by a polarization insensitive detector, is given by

$$\begin{aligned}\frac{\mathrm{d}^2\Gamma}{\mathrm{d}x\ \mathrm{d}\cos\vartheta} \sim x^2 \cdot \Bigg\{ & 3(1-x) + \frac{2\rho}{3}(4x-3) + 3\eta\ x_0(1-x)/x \\ & \pm P_\mu \cdot \xi \cdot \cos\vartheta \left[1 - x + \frac{2\delta}{3}(4x-3)\right]\Bigg\} \ . \end{aligned} \tag{58.2}$$

Here, ϑ is the angle between the electron momentum and the muon spin, and $x \equiv 2E_e/m_\mu$. For the Standard Model coupling, we obtain $\rho = \xi\delta = 3/4$, $\xi = 1$, $\eta = 0$ and the differential decay rate is

$$\frac{\mathrm{d}^2\Gamma}{\mathrm{d}x\ \mathrm{d}\cos\vartheta} \ = \ \frac{G_\mathrm{F}^2 m_\mu^5}{192\pi^3}\ \left[3 - 2x \pm P_\mu \cos\vartheta(2x-1)\right]\ x^2 \quad . \tag{58.3}$$

The coefficient in front of the square bracket is the total decay rate.

If only the neutrino masses are neglected, and if the $e^\pm$ polarization is detected, then the functions in Eq. (58.1) become

$$\begin{aligned} F_\mathrm{IS}(x) &= x(1-x) + \tfrac{2}{9}\ \rho(4x^2 - 3x - x_0^2) + \eta \cdot x_0(1-x) \\ F_\mathrm{AS}(x) &= \tfrac{1}{3}\xi\ \sqrt{x^2 - x_0^2} \\ &\quad \times [1 - x + \tfrac{2}{3}\delta(4x - 3 + (\sqrt{1-x_0^2} - 1))] \\ \boldsymbol{P}_e(x,\vartheta) &= P_{\mathrm{T}_1} \cdot \widehat{\boldsymbol{x}}_1 + P_{\mathrm{T}_2} \cdot \widehat{\boldsymbol{x}}_2 + P_L \cdot \widehat{\boldsymbol{x}}_3 \ . \end{aligned} \tag{58.4}$$

Here $\widehat{\boldsymbol{x}}_1$, $\widehat{\boldsymbol{x}}_2$, and $\widehat{\boldsymbol{x}}_3$ are orthogonal unit vectors defined as follows:

$$\begin{aligned} \widehat{\boldsymbol{x}}_3 &\quad \text{is along the } e \text{ momentum } \boldsymbol{p}_e \\ \frac{\widehat{\boldsymbol{x}}_3 \times \boldsymbol{P}_\mu}{|\widehat{\boldsymbol{x}}_2 \times \boldsymbol{P}_\mu|} = \widehat{\boldsymbol{x}}_2 &\quad \text{is transverse to } \boldsymbol{p}_e \text{ and perpendicular to the "decay plane"} \\ \widehat{\boldsymbol{x}}_2 \times \widehat{\boldsymbol{x}}_3 = \widehat{\boldsymbol{x}}_1 &\quad \text{is transverse to the } \boldsymbol{p}_e \text{ and in the "decay plane."} \end{aligned}$$

The components of $\boldsymbol{P}_e$ then are given by

$$\begin{aligned} P_{\mathrm{T}_1}(x,\vartheta) &= P_\mu \sin\vartheta \cdot F_{\mathrm{T}_1}(x) / \left(F_\mathrm{IS}(x) \pm P_\mu \cos\vartheta \cdot F_\mathrm{AS}(x)\right) \\ P_{\mathrm{T}_2}(x,\vartheta) &= P_\mu \sin\vartheta \cdot F_{\mathrm{T}_2}(x) / \left(F_\mathrm{IS}(x) \pm P_\mu \cos\vartheta \cdot F_\mathrm{AS}(x)\right) \\ P_L(x,\vartheta) &= \Big(\pm F_\mathrm{IP}(x) + P_\mu \cos\vartheta \\ &\qquad \times F_\mathrm{AP}(x)\Big) / \left(F_\mathrm{IS}(x) \pm P_\mu \cos\vartheta \cdot F_\mathrm{AS}(x)\right) \ , \end{aligned}$$

where

$$\begin{aligned} F_{\mathrm{T}_1}(x) &= \tfrac{1}{12}\left\{-2\left[\xi'' + 12(\rho - \tfrac{3}{4})\right](1-x)x_0 \right. \\ &\qquad \left. -3\eta(x^2 - x_0^2) + \eta''(-3x^2 + 4x - x_0^2)\right\} \\ F_{\mathrm{T}_2}(x) &= \tfrac{1}{3}\sqrt{x^2 - x_0^2}\left\{3\frac{\alpha'}{A}(1-x) + 2\frac{\beta'}{A}\sqrt{1-x_0^2}\right\} \\ F_\mathrm{IP}(x) &= \tfrac{1}{54}\sqrt{x^2 - x_0^2}\left\{9\xi'\left(-2x + 2 + \sqrt{1-x_0^2}\right)\right. \\ &\qquad \left. + 4\xi(\delta - \tfrac{3}{4})(4x - 4 + \sqrt{1-x_0^2})\right\} \\ F_\mathrm{AP}(x) &= \tfrac{1}{6}\left\{\xi''(2x^2 - x - x_0^2) + 4(\rho - \tfrac{3}{4})\left(4x^2 - 3x - x_0^2\right)\right. \\ &\qquad \left. + 2\eta''(1-x)x_0\right\} \ . \end{aligned} \tag{58.5}$$

For the experimental values of the parameters ρ, ξ, ξ', ξ'', δ, η, η'', α/A, β/A, α'/A, β'/A, which are not all independent, see the Data Listings below. Experiments in the past have also been analyzed using the parameters a, b, c, a', b', c', α/A, β/A, α'/A, β'/A (and $\eta = (\alpha - 2\beta)/2A$), as defined by Kinoshita and Sirlin [5,6]. They serve as a model-independent summary of all possible measurements on the decay electron (see Listings below). The relations between the two sets of parameters are

$$\begin{aligned} \rho - \tfrac{3}{4} &= \tfrac{3}{4}(-a + 2c)/A \ , \\ \eta &= (\alpha - 2\beta)/A \ , \\ \eta'' &= (3\alpha + 2\beta)/A \ , \\ \delta - \tfrac{3}{4} &= \tfrac{9}{4} \cdot \frac{(a' - 2c')/A}{1 - [a + 3a' + 4(b + b') + 6c - 14c']/A} \ , \\ 1 - \xi\frac{\delta}{\rho} &= 4\ \frac{[(b + b') + 2(c - c')]/A}{1 - (a - 2c)/A} \ , \\ 1 - \xi' &= [(a + a') + 4(b + b') + 6(c + c')]/A \ , \\ 1 - \xi'' &= (-2a + 20c)/A \ , \end{aligned}$$

where

$$A \ = \ a \ + \ 4b \ + \ 6c \ . \tag{58.6}$$

The differential decay probability to obtain a *left-handed* ν_e with (reduced) energy between y and $y + dy$, neglecting radiative corrections as well as the masses of the electron and of the neutrinos, is given by [7]

$$\frac{\mathrm{d}\Gamma}{\mathrm{d}y} \ = \ \frac{m_\mu^5\ G_F^2}{16\pi^3} \ \cdot \ Q_L^{\nu_e} \ \cdot y^2\left\{(1-y) - \omega_L \cdot (y - \tfrac{3}{4})\right\} \ . \tag{58.7}$$

Here, $y = 2\ E_{\nu_e}/m_\mu$. $Q_L^{\nu_e}$ and ω_L are parameters. ω_L is the neutrino analog of the spectral shape parameter ρ of Michel. Since in the Standard Model, $Q_L^{\nu_e} = 1$, $\omega_L = 0$, the measurement of $d\Gamma/dy$ has allowed a null-test of the Standard Model (see Listings below).

58.3. Matrix element:

All results in direct muon decay (energy spectra of the electron and of the neutrinos, polarizations, and angular distributions), and in inverse muon decay (the reaction cross section) at energies well below $m_W c^2$, may be parametrized in terms of amplitudes $g^\gamma_{\varepsilon\mu}$ and the Fermi coupling constant G_F, using the matrix element

$$\frac{4G_F}{\sqrt{2}} \sum_{\substack{\gamma=S,V,T \\ \varepsilon,\mu=R,L}} g^\gamma_{\varepsilon\mu} \langle \bar{e}_\varepsilon | \Gamma^\gamma | (\nu_e)_n \rangle \langle (\bar{\nu}_\mu)_m | \Gamma_\gamma | \mu_\mu \rangle . \tag{58.8}$$

We use the notation of Fetscher *et al.* [2], who in turn use the sign conventions and definitions of Scheck [8]. Here, $\gamma = S, V, T$ indicates a scalar, vector, or tensor interaction; and $\varepsilon, \mu = R, L$ indicate a right- or left-handed chirality of the electron or muon. The chiralities n and m of the ν_e and $\bar{\nu}_\mu$ are then determined by the values of γ, ε, and μ. The particles are represented by fields of definite chirality [9].

As shown by Langacker and London [10], explicit lepton-number nonconservation still leads to a matrix element equivalent to Eq. (58.8). They conclude that it is not possible, even in principle, to test lepton-number conservation in (leptonic) muon decay if the final neutrinos are massless and are not observed.

The ten complex amplitudes $g^\gamma_{\varepsilon\mu}$ (g^T_{RR} and g^T_{LL} are identically zero) and G_F constitute 19 independent (real) parameters to be determined by experiment. The Standard Model interaction corresponds to one single amplitude g^V_{LL} being unity and all the others being zero.

The (direct) muon decay experiments are compatible with an arbitrary mix of the scalar and vector amplitudes g^S_{LL} and g^V_{LL} – in the extreme even with purely scalar $g^S_{LL} = 2$, $g^V_{LL} = 0$. The decision in favour of the Standard Model comes from the quantitative observation of inverse muon decay, which would be forbidden for pure g^S_{LL} [2].

58.4. Experimental determination of V–A:

In order to determine the amplitudes $g^\gamma_{\varepsilon\mu}$ uniquely from experiment, the following set of equations, where the left-hand sides represent experimental results, has to be solved.

$$
\begin{aligned}
a &= 16(|g^V_{RL}|^2 + |g^V_{LR}|^2) + |g^S_{RL} + 6g^T_{RL}|^2 + |g^S_{LR} + 6g^T_{LR}|^2 \\
a' &= 16(|g^V_{RL}|^2 - |g^V_{LR}|^2) + |g^S_{RL} + 6g^T_{RL}|^2 - |g^S_{LR} + 6g^T_{LR}|^2 \\
\alpha &= 8\mathrm{Re}\left\{g^V_{RL}(g^{S*}_{LR} + 6g^{T*}_{LR}) + g^V_{LR}(g^{S*}_{RL} + 6g^{T*}_{RL})\right\} \\
\alpha' &= 8\mathrm{Im}\left\{g^V_{LR}(g^{S*}_{RL} + 6g^{T*}_{RL}) - g^V_{RL}(g^{S*}_{LR} + 6g^{T*}_{LR})\right\} \\
b &= 4(|g^V_{RR}|^2 + |g^V_{LL}|^2) + |g^S_{RR}|^2 + |g^S_{LL}|^2 \\
b' &= 4(|g^V_{RR}|^2 - |g^V_{LL}|^2) + |g^S_{RR}|^2 - |g^S_{LL}|^2 \\
\beta &= -4\mathrm{Re}\left\{g^V_{RR}g^{S*}_{LL} + g^V_{LL}g^{S*}_{RR}\right\} \\
\beta' &= 4\mathrm{Im}\left\{g^V_{RR}g^{S*}_{LL} - g^V_{LL}g^{S*}_{RR}\right\} \\
c &= \tfrac{1}{2}\left\{|g^S_{RL} - 2g^T_{RL}|^2 + |g^S_{LR} - 2g^T_{LR}|^2\right\} \\
c' &= \tfrac{1}{2}\left\{|g^S_{RL} - 2g^T_{RL}|^2 - |g^S_{LR} - 2g^T_{LR}|^2\right\}
\end{aligned}
$$

and

$$
\begin{aligned}
Q^{\nu_e}_L &= 1 - \left\{\tfrac{1}{4}|g^S_{LR}|^2 + \tfrac{1}{4}|g^S_{LL}|^2 + |g^V_{RR}|^2 + |g^V_{RL}|^2 + 3|g^T_{LR}|^2\right\} \\
\omega_L &= \tfrac{3}{4}\,\frac{\{|g^S_{RR}|^2 + 4|g^V_{LR}|^2 + |g^S_{RL} + 2g^T_{RL}|^2\}}{|g^S_{RL}|^2 + |g^S_{RR}|^2 + 4|g^V_{LL}|^2 + 4|g^V_{LR}|^2 + 12|g^T_{RL}|^2\}}\ .
\end{aligned}
$$

It has been noted earlier by C. Jarlskog [11], that certain experiments observing the decay electron are especially informative if they yield the V-A values. The complete solution is now found as follows. Fetscher *et al.* [2] introduced four probabilities $Q_{\varepsilon\mu}(\varepsilon, \mu = R, L)$ for the decay of a μ-handed muon into an ε-handed electron, and showed that there exist upper bounds on Q_{RR}, Q_{LR}, and Q_{RL}, and a lower bound on Q_{LL}. These probabilities are given in terms of the $g^\gamma_{\varepsilon\mu}$'s by

$$
Q_{\varepsilon\mu} = \tfrac{1}{4}|g^S_{\varepsilon\mu}|^2 + |g^V_{\varepsilon\mu}|^2 + 3(1 - \delta_{\varepsilon\mu})|g^T_{\varepsilon\mu}|^2\ , \tag{58.9}
$$

where $\delta_{\varepsilon\mu} = 1$ for $\varepsilon = \mu$, and $\delta_{\varepsilon\mu} = 0$ for $\varepsilon \neq \mu$. They are related to the parameters a, b, c, a', b', and c' by

$$
\begin{aligned}
Q_{RR} &= 2(b + b')/A\ , \\
Q_{LR} &= [(a - a') + 6(c - c')]/2A\ , \\
Q_{RL} &= [(a + a') + 6(c + c')]/2A\ , \\
Q_{LL} &= 2(b - b')/A\ ,
\end{aligned} \tag{58.10}
$$

with $A = 16$. In the Standard Model, $Q_{LL} = 1$ and the others are zero.

Since the upper bounds on Q_{RR}, Q_{LR}, and Q_{RL} are found to be small, and since the helicity of the ν_μ in pion decay is known from experiment [12,13] to very high precision to be -1 [14], the cross section S of *inverse* muon decay, normalized to the V-A value, yields [2]

$$
|g^S_{LL}|^2 \leq 4(1 - S) \tag{58.11}
$$

and

$$
|g^V_{LL}|^2 \ = \ S\ . \tag{58.12}
$$

Thus the Standard Model assumption of a pure V-A leptonic charged weak interaction of e and μ is derived (within errors) from experiments at energies far below mass of the $W^\pm$: Eq. (58.12) gives a lower limit for V-A, and Eqs. (58.9) and (58.11) give upper limits for the other four-fermion interactions. The existence of such upper limits may also be seen from $Q_{RR} + Q_{RL} = (1 - \xi')/2$ and $Q_{RR} + Q_{LR} = \frac{1}{2}(1 + \xi/3 - 16\ \xi\delta/9)$. Table 58.1 gives the current experimental limits on the magnitudes of the $g^\gamma_{\varepsilon\mu}$'s. More stringent limits on the six coupling constants g^S_{LR}, g^V_{LR}, g^T_{LR}, g^S_{RL}, g^V_{RL}, and g^T_{RL} have been derived from upper limits on the neutrino mass [18]. Limits on the "charge retention" coordinates, as used in the older literature (*e.g.*, Ref. 19), are given by Burkard *et al.* [20].

Table 58.1 Coupling constants $g^\gamma_{\varepsilon\mu}$ and some combinations of them. Ninety-percent confidence level experimental limits. The limits on $|g^S_{LL}|$ and $|g^V_{LL}|$ are from Ref. 15, and the others from a general analysis of muon decay measurements. Top three rows: Ref. 22, fourth row: Ref. 16, next three rows: Ref. 17, last row: Ref. 21. The experimental uncertainty on the muon polarization in pion decay is included. Note that, by definition, $|g^S_{\varepsilon\mu}| \leq 2$, $|g^V_{\varepsilon\mu}| \leq 1$ and $|g^T_{\varepsilon\mu}| \leq 1/\sqrt{3}$.

$\lvert g^S_{RR}\rvert < 0.035$	$\lvert g^V_{RR}\rvert < 0.017$	$\lvert g^T_{RR}\rvert \equiv 0$
$\lvert g^S_{LR}\rvert < 0.050$	$\lvert g^V_{LR}\rvert < 0.023$	$\lvert g^T_{LR}\rvert < 0.015$
$\lvert g^S_{RL}\rvert < 0.420$	$\lvert g^V_{RL}\rvert < 0.105$	$\lvert g^T_{RL}\rvert < 0.105$
$\lvert g^S_{LL}\rvert < 0.550$	$\lvert g^V_{LL}\rvert > 0.960$	$\lvert g^T_{LL}\rvert \equiv 0$
$\lvert g^S_{LR} + 6g^T_{LR}\rvert < 0.143$	$\lvert g^S_{RL} + 6g^T_{RL}\rvert < 0.418$	
$\lvert g^S_{LR} + 2g^T_{LR}\rvert < 0.108$	$\lvert g^S_{RL} + 2g^T_{RL}\rvert < 0.417$	
$\lvert g^S_{LR} - 2g^T_{LR}\rvert < 0.070$	$\lvert g^S_{RL} - 2g^T_{RL}\rvert < 0.418$	
$Q_{RR} + Q_{LR} < 8.2 \times 10^{-4}$		

References:

1. L. Michel, Proc. Phys. Soc. **A63**, 514 (1950).
2. W. Fetscher, H.-J. Gerber, and K.F. Johnson, Phys. Lett. **B173**, 102 (1986).
3. P. Langacker, Comm. Nucl. Part. Phys. **19**, 1 (1989).
4. C. Bouchiat and L. Michel, Phys. Rev. **106**, 170 (1957).
5. T. Kinoshita and A. Sirlin, Phys. Rev. **107**, 593 (1957).
6. T. Kinoshita and A. Sirlin, Phys. Rev. **108**, 844 (1957).
7. W. Fetscher, Phys. Rev. **D49**, 5945 (1994).
8. F. Scheck, in *Electroweak and Strong Interactions* (Springer Verlag, 1996).
9. K. Mursula and F. Scheck, Nucl. Phys. **B253**, 189 (1985).
10. P. Langacker and D. London, Phys. Rev. **D39**, 266 (1989).
11. C. Jarlskog, Nucl. Phys. **75**, 659 (1966).

12. A. Jodidio *et al.*, Phys. Rev. **D34**, 1967 (1986); A. Jodidio *et al.*, Phys. Rev. **D37**, 237 (1988).
13. L.Ph. Roesch *et al.*, Helv. Phys. Acta **55**, 74 (1982).
14. W. Fetscher, Phys. Lett. **140B**, 117 (1984).
15. S.R. Mishra *et al.*, Phys. Lett. **B252**, 170 (1990); S.R. Mishra, private communication; See also P. Vilain *et al.*, Phys. Lett. **B364**, 121 (1995).
16. R.P. MacDonald *et al.*, Phys. Rev. **D78**, 032010 (2008).
17. C.A. Gagliardi, R.E. Tribble, and N.J. Williams, Phys. Rev. **D72**, 073002 (2005).
18. G. Prézeau and A. Kurylov, Phys. Rev. Lett. **95**, 101802 (2005).
19. S.E. Derenzo, Phys. Rev. **181**, 1854 (1969).
20. H. Burkard *et al.*, Phys. Lett. **160B**, 343 (1985).
21. R. Bayes *et al.*, Phys. Rev. Lett. **106**, 041804 (2011).
22. A. Hillairet *et al.*, Phys. Rev. **D85**, 092013 (2012).

59. τ Branching Fractions

Revised August 2017 by S. Banerjee (University of Louisville), K. Hayes (Hillsdale College), A. Lusiani (Scuola Normale Superiore and INFN, sezione di Pisa)

In order to make optimal use of the experimental data to determine the τ branching fractions, their uncertainties, and their correlations, we perform a global minimum χ^2 fit using the measured values, their uncertainties, their statistical correlations, their dependencies on external parameters and common systematics, and the relations that hold between the branching fractions, including a unitarity constraint on the sum of all the exclusive τ decay branching fractions. Starting with this edition, we use a new fit procedure, which has been elaborated by the Tau Physics Group within the Heavy Flavour Averaging Group (HFLAV) [1].

In the following, we use "branching fraction" to refer to the partial decay fraction of a particle like the τ into a specific decay mode, and "branching ratio" to refer to quantities derived from the branching fractions [2], like for instance a ratio of two branching fractions, or a ratio of two linear combinations of branching fractions.

This review contains only minor revisions with respect to the 2016 edition.

59.1. The constrained fit to τ branching fractions

The τ Listings contains 242 τ decay modes, out of which 61 are Lepton Family number, Lepton number, or Baryon number violating modes. The fit computes the branching fractions of 112 decay modes. Although no new τ branching fraction and ratio measurements have been released since the 2015 edition, the fit in this edition includes more experimental measurements (169, up from 143 in 2015) and determines in the fit several additional τ branching fractions and ratios, relying on a larger and updated set of constraints that relate the branching fractions and ratios between themselves. The measurements are treated as follows [1].

Many published measurements depend on external parameters such as the τ pair production cross-section in e^+e^- annihilations at the $\Upsilon(4S)$ peak. We compute the size and sign of these dependencies and update the measurements and their uncertainties to the current values of the external parameters. The dependencies on common systematic effects are also determined in size and sign, and all the common systematic dependencies of different measurements are used together with the published statistical and systematic uncertainties and correlations in order to compute a single all-inclusive variance and covariance matrix of the experimental measurements. All the measurements, their uncertainties, and their correlations were taken from the respective published papers. Their values and the constraints used in the fit are reported in the τ Listings section that follows this review. If only a few measurements are correlated, the correlation coefficients are listed in the footnote for each measurement (see for example $\Gamma(\text{particle}^- \geq 0\,\text{neutrals} \geq 0\,K^0\nu_\tau$ ("1-prong"))$/\Gamma_{\text{total}}$). If a large number of measurements are correlated, then the full correlation matrix is listed in the footnote to the measurement that first appears in the τ Listings. Footnotes to the other measurements refer to the first measurement. For example, the large correlation matrices for the branching fraction or ratio measurements contained in Refs. [3,4] are listed in Footnotes to the $\Gamma(e^-\overline{\nu}_e\nu_\tau)/\Gamma_{\text{total}}$ and $\Gamma(h^-\nu_\tau)/\Gamma_{\text{total}}$ measurements respectively. The constraints between the τ branching fractions and ratios include coefficients that correspond to physical quantities, like for instance the branching fractions of the η and ω mesons. All quantities are taken from the 2015 edition of the Review of Particle Physics. Their uncertainties are neglected in the fit.

Compared to the 2015 edition, the fit now includes several additional modes, mainly related to the most recent BaBar papers on high multiplicity modes [5] and $K^0_S K^0_S$ modes [6] and the Belle paper on neutral kaon modes [7]:

$$\begin{aligned}
&\mathrm{B}(\tau \to \pi^-\pi^0 K^0_S K^0_S \nu_\tau)\\
&\mathrm{B}(\tau \to K^-K^-K^+\nu_\tau)\\
&\mathrm{B}(\tau \to K^-\pi^0\eta\nu_\tau)\\
&\mathrm{B}(\tau \to \pi^-\bar{K}^0\eta\nu_\tau)\ ;
\end{aligned}$$

Also, the following components of τ-decay modes are now included [5,8,9]:

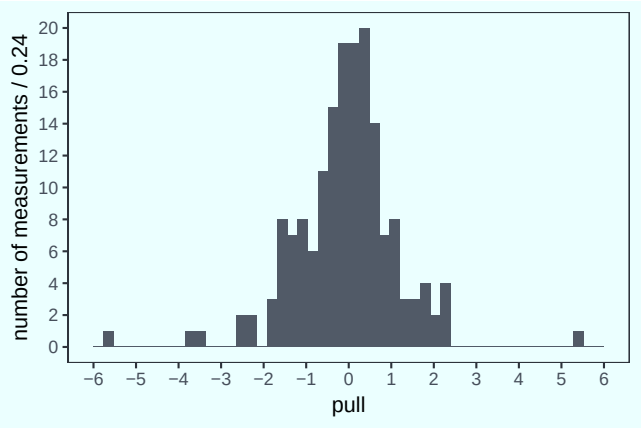

Figure 59.1: Pulls of individual measurements against the respective fitted quantity. No scale factor is used.

$$\begin{aligned}
&\mathrm{B}(\tau \to \pi^-2\pi^0\eta\nu_\tau\ (\eta \to \pi^+\pi^-\pi^0)\ (\text{ex. } K^0))\\
&\mathrm{B}(\tau \to 2\pi^-\pi^+\eta\nu_\tau\ (\eta \to \pi^+\pi^-\pi^0)\ (\text{ex. } K^0))\\
&\mathrm{B}(\tau \to 2\pi^-\pi^+\eta\nu_\tau\ (\eta \to \gamma\gamma)\ (\text{ex. } K^0))\\
&\mathrm{B}(\tau \to \pi^-2\pi^0\omega\nu_\tau\ (\text{ex. } K^0))\\
&\mathrm{B}(\tau \to 2\pi^-\pi^+\omega\nu_\tau\ (\text{ex. } K^0))\\
&\mathrm{B}(\tau \to \pi^- f_1\nu_\tau\ (f_1 \to 2\pi^-2\pi^+))\ .\\
&\mathrm{B}(\tau \to K^-\phi\nu_\tau)\ .
\end{aligned}$$

We obtain the branching fraction of $\tau \to a_1^-(\to \pi^-\gamma)\nu_\tau$ using the ALEPH estimate for $\mathrm{B}(a_1^- \to \pi^-\gamma)$ [3], which uses the measurement of $\Gamma(a_1^- \to \pi^-\gamma)$ [10]. In the fit, we assume that $\mathrm{B}(\tau^- \to a_1^-\nu_\tau)$ is equal to $\mathrm{B}(\tau \to \pi^-\pi^-\pi^+\nu_\tau\ (\text{ex. } K^0,\omega)) + \mathrm{B}(\tau \to \pi^-2\pi^0\nu_\tau\ (\text{ex. } K^0))$.

In some cases, constraints describe approximate relations that nevertheless hold within the present experimental precision. For instance, the constraint $\mathrm{B}(\tau \to K^-K^-K^+\nu_\tau) = \mathrm{B}(\tau \to K^-\phi\nu_\tau) \times \mathrm{B}(\phi \to K^+K^-)$ is justified within the current experimental evidence.

In the fit, scale factors are applied to the published uncertainties of measurements only if significant inconsistency between different measurements remain after accounting for all relevant uncertainties and correlations. After examining the data and the fit pulls, it has been decided to apply just one scale factor of 5.4 on the measurements of $\mathrm{B}(\tau \to K^-K^-K^+\nu_\tau)$. The scale factor has been computed and applied according to the standard PDG procedure. Without the scale factor applied, the χ^2 probability of the fit is about 2%. On a per-measurement basis, the pull distribution in figure 59.1 indicates that just a few measurements have more than 3σ pulls. (The uncertainties to obtain the pulls are computed using the measurements variance matrix and the variance matrix of the result, accounting for the fact that the variance matrix of the result is obtained from the measurement variance with the fit.) The pull probability distribution in figure 59.2 is reasonably flat. With many measurements some entries on the tails of the normal distribution must be expected. There are 169 pulls, one per measurement. They are partially correlated, and the effective number of independent pulls is equal to the number of degrees of freedom of the fit, 124. Only the $\tau \to K^-K^-K^+\nu_\tau$ decay mode has a pull that is inconsistent at the level of more than 3σ even if considered as the largest pull in a set of 124. This confirms the choice of adopting just that one scale factor.

After scaling the error the 2016 constrained fit has a χ^2 of 134.9 for 124 degrees of freedom, corresponding to a χ^2 probability of 24%. We use 169 measurements and 84 constraints on the branching fractions and ratios to determine 129 quantities, consisting of 112 branching fractions and 17 branching ratios. A total of 85 quantities have at least one measurement in the fit. The constraints include the unitarity constraint on the sum of all the exclusive τ decay modes, $\mathrm{B}_{\text{all}} = 1$. If the unitarity constraint is released, the fit result for B_{all} is consistent with unitarity with $1 - \mathrm{B}_{\text{all}} = (0.07 \pm 0.10)\%$.

For the convenience of summarizing the fit results, we list in the

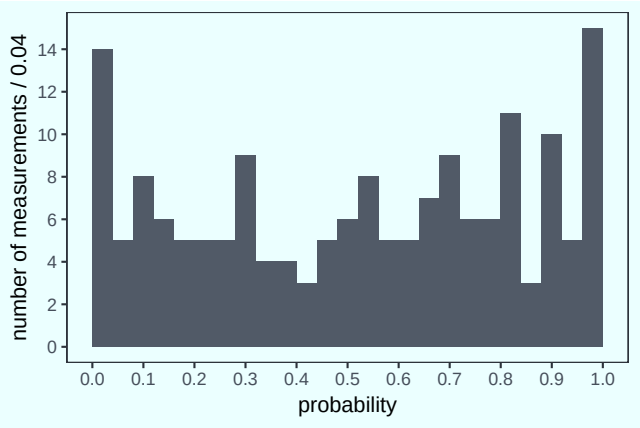

Figure 59.2: Probability of individual measurement pulls against the respective fitted quantity. No scale factor is used.

following the values and uncertainties for a set of 46 "basis" decay modes, from which all remaining branching fractions and ratios can be obtained using the constraints. Unlike in previous editions, the basis decay modes are not intended to sum up to 1. The new unitarity constraint corresponds to a linear combination of the basis modes weighted by the coefficients listed in the following. The corresponding correlation matrix is listed in the τ Listings.

decay mode	fit result (%)	coefficient
$\mu^-\bar{\nu}_\mu\nu_\tau$	17.3936 ± 0.0384	1.0000
$e^-\bar{\nu}_e\nu_\tau$	17.8174 ± 0.0399	1.0000
$\pi^-\nu_\tau$	10.8165 ± 0.0512	1.0000
$K^-\nu_\tau$	0.6964 ± 0.0096	1.0000
$\pi^-\pi^0\nu_\tau$	25.4940 ± 0.0893	1.0000
$K^-\pi^0\nu_\tau$	0.4329 ± 0.0148	1.0000
$\pi^-2\pi^0\nu_\tau$ (ex. K^0)	9.2595 ± 0.0964	1.0021
$K^-2\pi^0\nu_\tau$ (ex. K^0)	0.0648 ± 0.0218	1.0000
$\pi^-3\pi^0\nu_\tau$ (ex. K^0)	1.0428 ± 0.0707	1.0000
$K^-3\pi^0\nu_\tau$ (ex. K^0, η)	0.0478 ± 0.0212	1.0000
$h^-4\pi^0\nu_\tau$ (ex. K^0, η)	0.1119 ± 0.0391	1.0000
$\pi^-\bar{K}^0\nu_\tau$	0.8395 ± 0.0140	1.0000
$K^-K^0\nu_\tau$	0.1479 ± 0.0053	1.0000
$\pi^-\bar{K}^0\pi^0\nu_\tau$	0.3821 ± 0.0129	1.0000
$K^-\pi^0K^0\nu_\tau$	0.1503 ± 0.0071	1.0000
$\pi^-\bar{K}^0\pi^0\pi^0\nu_\tau$ (ex. K^0)	0.0263 ± 0.0226	1.0000
$\pi^-K^0_SK^0_S\nu_\tau$	0.0233 ± 0.0007	2.0000
$\pi^-K^0_SK^0_L\nu_\tau$	0.1080 ± 0.0241	1.0000
$\pi^-\pi^0K^0_SK^0_S\nu_\tau$	0.0018 ± 0.0002	2.0000
$\pi^-\pi^0K^0_SK^0_L\nu_\tau$	0.0325 ± 0.0119	1.0000
$\bar{K}^0h^-h^-h^+\nu_\tau$	0.0247 ± 0.0199	1.0000
$\pi^-\pi^-\pi^+\nu_\tau$ (ex. K^0, ω)	8.9870 ± 0.0514	1.0021
$\pi^-\pi^-\pi^+\pi^0\nu_\tau$ (ex. K^0, ω)	2.7404 ± 0.0710	1.0000
$h^-h^-h^+2\pi^0\nu_\tau$ (ex. K^0, ω, η)	0.0980 ± 0.0356	1.0000
$\pi^-K^-K^+\nu_\tau$	0.1435 ± 0.0027	1.0000
$\pi^-K^-K^+\pi^0\nu_\tau$	0.0061 ± 0.0018	1.0000
$\pi^-\pi^0\eta\nu_\tau$	0.1389 ± 0.0072	1.0000
$K^-\eta\nu_\tau$	0.0155 ± 0.0008	1.0000
$K^-\pi^0\eta\nu_\tau$	0.0048 ± 0.0012	1.0000
$\pi^-\bar{K}^0\eta\nu_\tau$	0.0094 ± 0.0015	1.0000
$\pi^-\pi^+\pi^-\eta\nu_\tau$ (ex. K^0)	0.0219 ± 0.0013	1.0000
$K^-\omega\nu_\tau$	0.0410 ± 0.0092	1.0000
$h^-\pi^0\omega\nu_\tau$	0.4085 ± 0.0419	1.0000
$K^-\phi\nu_\tau$	0.0044 ± 0.0016	0.8310
$\pi^-\omega\nu_\tau$	1.9494 ± 0.0645	1.0000
$K^-\pi^-\pi^+\nu_\tau$ (ex. K^0, ω)	0.2927 ± 0.0068	1.0000
$K^-\pi^-\pi^+\pi^0\nu_\tau$ (ex. K^0, ω, η)	0.0394 ± 0.0142	1.0000
$\pi^-2\pi^0\omega\nu_\tau$ (ex. K^0)	0.0071 ± 0.0016	1.0000
$2\pi^-\pi^+3\pi^0\nu_\tau$ (ex. K^0, η, ω, f_1)	0.0014 ± 0.0027	1.0000
$3\pi^-2\pi^+\nu_\tau$ (ex. K^0, ω, f_1)	0.0769 ± 0.0030	1.0000
$K^-2\pi^-2\pi^+\nu_\tau$ (ex. K^0)	0.0001 ± 0.0001	1.0000
$2\pi^-\pi^+\omega\nu_\tau$ (ex. K^0)	0.0084 ± 0.0006	1.0000
$3\pi^-2\pi^+\pi^0\nu_\tau$ (ex. K^0, η, ω, f_1)	0.0038 ± 0.0009	1.0000
$K^-2\pi^-2\pi^+\pi^0\nu_\tau$ (ex. K^0)	0.0001 ± 0.0001	1.0000
$\pi^-f_1\nu_\tau$ ($f_1 \to 2\pi^-2\pi^+$)	0.0052 ± 0.0004	1.0000
$\pi^-2\pi^0\eta\nu_\tau$	0.0194 ± 0.0038	1.0000

Applying the fit procedure on the PDG 2015 inputs, the fit results differ from the 2015 fit by at most 20% of their uncertainty, for fitted quantities that have measurements with asymmetric errors, and by at most 5% of their uncertainty for the other quantities. The differences originate from the different treatment of asymmetric errors. The present fit procedure symmetrizes the errors as $\sigma^2_{\rm symm} = (\sigma^2_+ + \sigma^2_-)/2$, while the PDG 2015 fit did model the asymmetric error distributions in the fit. Comparing the results of the previous edition with the current fit, there are differences up to 2.3 times the fitted quantity uncertainty (2.3σ) for quantities that have no measurement included in the fit and are derived through the constraints. Those differences arise mainly from three changes: the unitarity constraint has been updated to accomodate several additional decay modes, the definitions of the respective quantities have been updated to use the additional decay modes, and the parameters of all constraints (typically, K, η, ω branching fractions) have been updated to the values reported in the last published PDG edition. For quantities that have measurements in the fit, the fitted values changed at most by 1.1σ, reflecting the inclusion of several additional measurements, especially on high-multiplicity decay modes. The uncertainties on the fit results are generally smaller than in 2015 because only one error scale factor is used and some additional measurements have been used.

In defining the fit constraints and in selecting the modes that sum up to one we made some assumptions and choices. We assume that some channels, like $\tau^- \to \pi^-K^+\pi^- \geq 0\pi^0\nu_\tau$ and $\tau^- \to \pi^+K^-K^- \geq 0\pi^0\nu\tau$, have negligible branching fractions as expected from the Standard Model, even if the experimental limits for these branching fractions are not very stringent. The 95% confidence level upper limits are $\mathrm{B}(\tau^- \to \pi^-K^+\pi^- \geq 0\pi^0\nu_\tau) < 0.25\%$ and $\mathrm{B}(\tau^- \to \pi^+K^-K^- \geq 0\pi^0\nu\tau) < 0.09\%$, values not so different from measured branching fractions for allowed 3-prong modes containing charged kaons. For decays to final states containing one neutral kaon we assume that the branching fraction with the K^0_L are the same as the corresponding one with a K^0_S. On decays with two neutral kaons we assume that the branching fractions with $K^0_LK^0_L$ are the same as the ones with $K^0_SK^0_S$.

59.2. BaBar and Belle measure on average lower branching fractions and ratios

We compare the BaBar and Belle measurements with the results of a fit where all their measurements have been excluded. We find that that BaBar and Belle tend to measure lower τ branching fractions and ratios than the other experiments. Figure 59.3 shows histograms of the 27 normalized differences between the B-factory measurements and the respective non-B-factory fit results. The normalization is the uncertainty on the difference. The average normalized difference between the two sets of measurements is -0.8σ (-0.8σ for the 16 Belle measurements and -0.9σ for the 11 BaBar measurements).

59.3. Overconsistency of Leptonic Branching Fraction Measurements

As observed in the previous editions of this review, measurements of the leptonic branching fractions are more consistent with each other than expected from the quoted errors on the individual measurements. When fitting just a single branching fraction using just its direct measurements, the χ^2 per number of degrees of freedom is 0.31/4 for B_e and 0.038/4 for B_μ. Assuming normal errors, the probability of a smaller χ^2 is 1.1% for B_e and 0.20% for B_μ.

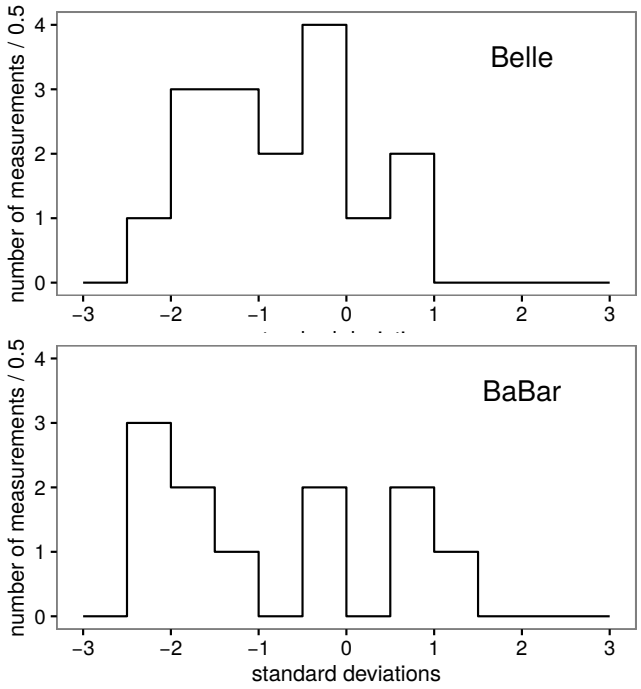

Figure 59.3: Distribution of the normalized difference between the 27 B-factory measurements and non-B-factory measurements. The list includes 16 measurements of branching fractions and ratios published by the Belle collaboration and 11 by the BaBar collaboration that are used in the fit and for which non-B-factory measurements exist.

59.4. Technical implementation of the fit

The fit computes a set of quantities denoted with q_i by minimizing a χ^2 while respecting a series of equality constraints on the q_i. The χ^2 is computed using the measurements m_i and their covariance matrix E_{ij} as $\chi^2 = (m_i - A_{ik}q_k)^t E_{ij}^{-1}(m_j - A_{jl}q_l)$ where the model matrix A_{ij} is used to get the vector of the predicted measurements m'_i from the vector of the fit parameters q_j as $m'_i = A_{ij}q_j$. In this particular implementation the measurements are grouped by the quantity that they measure, and all quantities with at least one measurement correspond to a fit parameter. Therefore, the matrix A_{ij} has one row per measurement m_i and one column per fitted quantity q_j, with unity coefficients for the rows and column that identify a measurement m_i of the quantity q_j, respectively. The constraints are equations involving the fit parameters. The fit does not impose limitations on the functional form of the constraints. In summary, the fit requires:

$$\min(m_i - A_{ik}q_k)^t E_{ij}^{-1}(m_j - A_{jl}q_l), \tag{59.1a}$$

$$\text{subjected to} \quad f_r(q_s) - c_r = 0, \tag{59.1b}$$

where the left term of Eq. (59.1b) defines the constraint expressions. Using the method of Lagrange multipliers, a set of equations is obtained by taking the derivatives with respect to the fitted quantities q_k and the Lagrange multipliers λ_r of the sum of the χ^2 and the constraint expressions multiplied by the Lagrange multipliers λ_r, one for each constraint:

$$\min\left[(A_{ik}q_k - m_i)^t E_{ij}^{-1}(A_{jl}q_l - m_j) + 2\lambda_r(f_r(q_s) - c_r)\right] \tag{59.2a}$$

$$(\partial/\partial q_k, \partial/\partial\lambda_r)[\text{expression above}] = 0 \tag{59.2b}$$

Eq. (59.2b) defines a set of equations for the vector of the unknowns (q_k, λ_r), some of which may be non-linear, in case of non-linear constraints. An iterative minimization procedure approximates at each step the non-linear constraint expressions by their first order Taylor expansion around the current values of the fitted quantities, $\bar{q}_s$:

$$f_r(q_s) - c_r = f_r(\bar{q}_s) + \left.\frac{\partial f_r(q_s)}{\partial q_s}\right|_{\bar{q}_s} (q_s - \bar{q}_s) - c_r, \tag{59.3a}$$

which can be written as

$$B_{rs}q_s - c'_r, \tag{59.3b}$$

where c'_r are the resulting constant known terms, independent of q_s at first order. After linearization, the differentiation by q_k and λ_r is trivial and leads to a set of linear equations

$$A^t_{ki}E^{-1}_{ij}A_{jl}q_l + B^t_{kr}\lambda_r = A^t_{ki}E^{-1}_{ij}m_j \tag{59.4a}$$

$$B_{rs}q_s = c'_r, \tag{59.4b}$$

which can be expressed as:

$$F_{ij}u_j = v_i \tag{59.5}$$

where $u_j = (q_k, \lambda_r)$ and v_i is the vector of the known constant terms running over the index k and then r in the right terms of Eq. (59.4a) and Eq. (59.4b), respectively. Solving the equation set in Eq. (59.5) by matrix inversion gives the the fitted quantities and their variance and covariance matrix, using the measurements and their variance and covariance matrix. The fit procedure starts by computing the linear approximation of the non-linear constraint expressions around the quantities seed values. With an iterative procedure, the unknowns are updated at each step by solving the equations and the equations are then linearized around the updated values, until the variation of the fitted unknowns is reduced below a numerically small threshold.

References:

1. D. Asner *et al.* (HFLAV), arXiv:1010.1589; Y. Amhis *et al.* (HFLAV), arXiv:1412.7515.
2. See the Introduction section of this edition of the *Review of Particle Physics*.
3. S. Schael *et al.* (ALEPH Collab.), Phys. Reports **421**, 191 (2005).
4. J. Abdallah *et al.* (DELPHI Collab.), Eur. Phys. J. **C46**, 1 (2006).
5. J.P. Lees *et al.* (BABAR Collab.), Phys. Rev. **D86**, 092010 (2012), [arXiv:1209.2734].
6. J.P. Lees *et al.* (BABAR Collab.), Phys. Rev. **D86**, 092013 (2012), [arXiv:1208.0376].
7. S. Ryu *et al.* (BELLE Collab.), Phys. Rev. **D89**, 072009 (2014).
8. B. Aubert *et al.* (BABAR Collab.), Phys. Rev. Lett. **100**, 011801 (2008).
9. K. Inami *et al.* (BELLE Collab.), Phys. Lett. **B643**, 5 (2006).
10. M. Zielinski *et al.*, Phys. Rev. Lett. **52**, 1195 (1984).

60. τ-Lepton Decay Parameters

Updated August 2011 by A. Stahl (RWTH Aachen).

The purpose of the measurements of the decay parameters (also known as Michel parameters) of the τ is to determine the structure (spin and chirality) of the current mediating its decays.

60.1. Leptonic Decays:

The Michel parameters are extracted from the energy spectrum of the charged daughter lepton $\ell = e, \mu$ in the decays $\tau \to \ell\nu_\ell\nu_\tau$. Ignoring radiative corrections, neglecting terms of order $(m_\ell/m_\tau)^2$ and $(m_\tau/\sqrt{s})^2$, and setting the neutrino masses to zero, the spectrum in the laboratory frame reads

$$\frac{d\Gamma}{dx} = \frac{G_{\tau\ell}^2\ m_\tau^5}{192\ \pi^3}\ \times$$

$$\left\{ f_0(x) + \rho f_1(x) + \eta\frac{m_\ell}{m_\tau} f_2(x) - P_\tau\left[\xi g_1(x) + \xi\delta g_2(x)\right]\right\}\ , \tag{60.1}$$

with

$$f_0(x) = 2 - 6\,x^2 + 4\,x^3$$
$$f_1(x) = -\frac{4}{9} + 4\,x^2 - \frac{32}{9}\,x^3 \qquad g_1(x) = -\frac{2}{3} + 4\,x - 6\,x^2 + \frac{8}{3}\,x^3$$
$$f_2(x) = 12\,(1-x)^2 \qquad g_2(x) = \frac{4}{9} - \frac{16}{3}\,x + 12\,x^2 - \frac{64}{9}\,x^3\ .$$

The quantity x is the fractional energy of the daughter lepton ℓ, *i.e.*, $x = E_\ell/E_{\ell,max} \approx E_\ell/(\sqrt{s}/2)$ and P_τ is the polarization of the tau leptons. The integrated decay width is given by

$$\Gamma = \frac{G_{\tau\ell}^2\ m_\tau^5}{192\ \pi^3}\left(1 + 4\,\eta\ \frac{m_\ell}{m_\tau}\right)\ . \tag{60.2}$$

The situation is similar to muon decays $\mu \to e\nu_e\nu_\mu$. The generalized matrix element with the couplings $g_{\varepsilon\mu}^\gamma$ and their relations to the Michel parameters ρ, η, ξ, and δ have been described in the "Note on Muon Decay Parameters." The Standard Model expectations are 3/4, 0, 1, and 3/4, respectively. For more details, see Ref. 1.

60.2. Hadronic Decays:

In the case of hadronic decays $\tau \to h\nu_\tau$, with $h = \pi$, ρ, or a_1, the ansatz is restricted to purely vectorial currents. The matrix element is

$$\frac{G_{\tau h}}{\sqrt{2}} \sum_{\lambda=R,L} g_\lambda\ \langle\ \overline{\Psi}_\omega(\nu_\tau)\ |\ \gamma^\mu\ |\ \Psi_\lambda(\tau)\ \rangle\quad J_\mu^h \tag{60.3}$$

with the hadronic current J_μ^h. The neutrino chirality ω is uniquely determined from λ. The spectrum depends only on a single parameter ξ_h

$$\frac{d^n\Gamma}{dx_1 dx_2 \ldots dx_n} = f(\vec{x}) + \xi_h P_\tau\, g(\vec{x})\ , \tag{60.4}$$

with f and g being channel-dependent functions of the n observables $\vec{x} = (x_1, x_2, \ldots, x_n)$ (see Ref. 2). The parameter ξ_h is related to the couplings through

$$\xi_h = |g_L|^2 - |g_R|^2\ . \tag{60.5}$$

ξ_h is the negative of the chirality of the τ neutrino in these decays. In the Standard Model, $\xi_h = 1$. Also included in the Data Listings for ξ_h are measurements of the neutrino helicity which coincide with ξ_h, if the neutrino is massless (ASNER 00 [3], ACKERSTAFF 97R [4], AKERS 95P [5], ALBRECHT 93C [6], and ALBRECHT 90I [7]) .

60.3. Combination of Measurements:

The individual measurements are combined, taking into account the correlations between the parameters. In a first fit, universality between the two leptonic decays, and between all hadronic decays, is assumed. A second fit is made without these assumptions. The results of the two fits are provided as OUR FIT in the Data Listings below in the tables whose title includes "(e or mu)" or "(all hadronic modes)," and "(e)," "(mu)" *etc.*, respectively. The measurements show good agreement with the Standard Model. The χ^2 values with respect to the Standard model predictions are 24.1 for 41 degrees of freedom and 26.8 for 56 degrees of freedom, respectively. The correlations are reduced through this combination to less than 20%, with the exception of ρ and η which are correlated by +23%, for the fit with universality and by +70% for $\tau \to \mu\nu_\mu\nu_\tau$.

60.4. Model-independent Analysis:

From the Michel parameters, limits can be derived on the couplings $g_{\varepsilon\lambda}^\kappa$ without further model assumptions. In the Standard model $g_{LL}^V = 1$ (leptonic decays), and $g_L = 1$ (hadronic decays) and all other couplings vanish. First, the partial decay widths have to be compared to the Standard Model predictions to derive limits on the normalization of the couplings $A_x = G_{\tau x}^2/G_F^2$ with Fermi's constant G_F:

$$A_e = 1.0029 \pm 0.0046\ ,$$
$$A_\mu = 0.981 \pm 0.018\ ,$$
$$A_\pi = 1.0020 \pm 0.0073\ . \tag{60.6}$$

Then limits on the couplings (95% CL) can be extracted (see Ref. 8 and Ref. 9). Without the assumption of universality, the limits given in Table 60.1 are derived.

Table 60.1: Coupling constants $g_{\varepsilon\mu}^\gamma$. 95% confidence level experimental limits. The limits include the quoted values of A_e, A_μ, and A_π and assume $A_\rho = A_{a_1} = 1$.

$\tau \to e\nu_e\nu_\tau$		
$\lvert g_{RR}^S\rvert < 0.70$	$\lvert g_{RR}^V\rvert < 0.17$	$\lvert g_{RR}^T\rvert \equiv 0$
$\lvert g_{LR}^S\rvert < 0.99$	$\lvert g_{LR}^V\rvert < 0.13$	$\lvert g_{LR}^T\rvert < 0.082$
$\lvert g_{RL}^S\rvert < 2.01$	$\lvert g_{RL}^V\rvert < 0.52$	$\lvert g_{RL}^T\rvert < 0.51$
$\lvert g_{LL}^S\rvert < 2.01$	$\lvert g_{LL}^V\rvert < 1.005$	$\lvert g_{LL}^T\rvert \equiv 0$
$\tau \to \mu\nu_\mu\nu_\tau$		
$\lvert g_{RR}^S\rvert < 0.72$	$\lvert g_{RR}^V\rvert < 0.18$	$\lvert g_{RR}^T\rvert \equiv 0$
$\lvert g_{LR}^S\rvert < 0.95$	$\lvert g_{LR}^V\rvert < 0.12$	$\lvert g_{LR}^T\rvert < 0.079$
$\lvert g_{RL}^S\rvert < 2.01$	$\lvert g_{RL}^V\rvert < 0.52$	$\lvert g_{RL}^T\rvert < 0.51$
$\lvert g_{LL}^S\rvert < 2.01$	$\lvert g_{LL}^V\rvert < 1.005$	$\lvert g_{LL}^T\rvert \equiv 0$
$\tau \to \pi\nu_\tau$		
$\lvert g_R^V\rvert < 0.15$	$\lvert g_L^V\rvert > 0.992$	
$\tau \to \rho\nu_\tau$		
$\lvert g_R^V\rvert < 0.10$	$\lvert g_L^V\rvert > 0.995$	
$\tau \to a_1\nu_\tau$		
$\lvert g_R^V\rvert < 0.16$	$\lvert g_L^V\rvert > 0.987$	

60.5. Model-dependent Interpretation:

More stringent limits can be derived assuming specific models. For example, in the framework of a two Higgs doublet model, the measurements correspond to a limit of $m_{H^\pm} > 1.9\ \text{GeV} \times \tan\beta$ on the mass of the charged Higgs boson, or a limit of 253 GeV on the mass of the second W boson in left-right symmetric models for arbitrary mixing (both 95% CL). See Ref. 9 and Ref. 10.

References:

1. F. Scheck, Phys. Reports **44**, 187 (1978);
W. Fetscher and H.J. Gerber in *Precision Tests of the Standard Model*, edited by P. Langacker, World Scientific, 1993;
A. Stahl, *Physics with τ Leptons*, Springer Tracts in Modern Physics.
2. M. Davier *et al.*, Phys. Lett. **B306**, 411 (1993).

3. CLEO Collab., D.M. Asner *et al.*, Phys. Rev. **D61**, 012002 (2000).
4. OPAL Collab., K. Ackerstaff *et al.*, Z. Phys. **C75**, 593 (1997).
5. OPAL Collab., R. Akers *et al.*, Z. Phys. **C67**, 45 (1995).
6. ARGUS Collab., H. Albrecht *et al.*, Z. Phys. **C58**, 61 (1993).
7. ARGUS Collab., H. Albrecht *et al.*, Phys. Lett. **B250**, 164 (1990).
8. OPAL Collab., K. Ackerstaff *et al.*, Eur. Phys. J. **C8**, 3 (1999).
9. A. Stahl, Nucl. Phys. (Proc. Supp.) **B76**, 173 (1999).
10. M.-T. Dova *et al.*, Phys. Rev. **D58**, 015005 (1998);
T. Hebbeker and W. Lohmann, Z. Phys. **C74**, 399 (1997);
A. Pich and J.P. Silva, Phys. Rev. **D52**, 4006 (1995).

61. Number of Light Neutrino Types from Collider Experiments

Revised March 2008 by D. Karlen (University of Victoria and TRIUMF).

The most precise measurements of the number of light neutrino types, N_ν, come from studies of Z production in e^+e^- collisions. The invisible partial width, $\Gamma_{\rm inv}$, is determined by subtracting the measured visible partial widths, corresponding to Z decays into quarks and charged leptons, from the total Z width. The invisible width is assumed to be due to N_ν light neutrino species each contributing the neutrino partial width Γ_ν as given by the Standard Model. In order to reduce the model dependence, the Standard Model value for the ratio of the neutrino to charged leptonic partial widths, $(\Gamma_\nu/\Gamma_\ell)_{\rm SM} = 1.991 \pm 0.001$, is used instead of $(\Gamma_\nu)_{\rm SM}$ to determine the number of light neutrino types:

$$N_\nu = \frac{\Gamma_{\rm inv}}{\Gamma_\ell}\left(\frac{\Gamma_\ell}{\Gamma_\nu}\right)_{\rm SM} \ . \tag{61.1}$$

The combined result from the four LEP experiments is $N_\nu = 2.984 \pm 0.008$ [1].

In the past, when only small samples of Z decays had been recorded by the LEP experiments and by the Mark II at SLC, the uncertainty in N_ν was reduced by using Standard Model fits to the measured hadronic cross sections at several center-of-mass energies near the Z resonance. Since this method is much more dependent on the Standard Model, the approach described above is favored.

Before the advent of the SLC and LEP, limits on the number of neutrino generations were placed by experiments at lower-energy e^+e^- colliders by measuring the cross section of the process $e^+e^- \to \nu\overline{\nu}\gamma$. The ASP, CELLO, MAC, MARK J, and VENUS experiments observed a total of 3.9 events above background [2], leading to a 95% CL limit of $N_\nu < 4.8$. This process has a much larger cross section at center-of-mass energies near the Z mass and has been measured at LEP by the ALEPH, DELPHI, L3, and OPAL experiments [3]. These experiments have observed several thousand such events, and the combined result is $N_\nu = 3.00 \pm 0.08$. The same process has also been measured by the LEP experiments at much higher center-of-mass energies, between 130 and 208 GeV, in searches for new physics [4]. Combined with the lower energy data, the result is $N_\nu = 2.92 \pm 0.05$.

Experiments at $p\overline{p}$ colliders also placed limits on N_ν by determining the total Z width from the observed ratio of $W^\pm \to \ell^\pm\nu$ to $Z \to \ell^+\ell^-$ events [5]. This involved a calculation that assumed Standard Model values for the total W width and the ratio of W and Z leptonic partial widths, and used an estimate of the ratio of Z to W production cross sections. Now that the Z width is very precisely known from the LEP experiments, the approach is now one of those used to determine the W width.

References:

1. ALEPH, DELPHI, L3, OPAL, and SLD Collaborations, and LEP Electroweak Working Group, and SLD Electroweak Group, and SLD Heavy Flavour Group, Phys. Reports **427**, 257 (2006).
2. VENUS: K. Abe *et al.*, Phys. Lett. **B232**, 431 (1989);
   ASP: C. Hearty *et al.*, Phys. Rev. **D39**, 3207 (1989);
   CELLO: H.J. Behrend *et al.*, Phys. Lett. **B215**, 186 (1988);
   MAC: W.T. Ford *et al.*, Phys. Rev. **D33**, 3472 (1986);
   MARK J: H. Wu, Ph.D. Thesis, Univ. Hamburg (1986).
3. L3: M. Acciarri *et al.*, Phys. Lett. **B431**, 199 (1998);
   DELPHI: P. Abreu *et al.*, Z. Phys. **C74**, 577 (1997);
   OPAL: R. Akers *et al.*, Z. Phys. **C65**, 47 (1995);
   ALEPH: D. Buskulic *et al.*, Phys. Lett. **B313**, 520 (1993).
4. DELPHI: J. Abdallah *et al.*, Eur. Phys. J. **C38**, 395 (2005);
   L3: P. Achard *et al.*, Phys. Lett. **B587**, 16 (2004);
   ALEPH: A. Heister *et al.*, Eur. Phys. J. **C28**, 1 (2003);
   OPAL: G. Abbiendi *et al.*, Eur. Phys. J. **C18**, 253 (2000).
5. UA1: C. Albajar *et al.*, Phys. Lett. **B198**, 271 (1987);
   UA2: R. Ansari *et al.*, Phys. Lett. **B186**, 440 (1987).

62. Neutrinoless Double-β decay

Revised August 2017 by P. Vogel (Caltech) and A. Piepke (University of Alabama).

Observation of neutrinoless double-beta ($0\nu\beta\beta$) decay would signal violation of total lepton number conservation. The process can be mediated by an exchange of a light Majorana neutrino, or by an exchange of other particles. However, the existence of $0\nu\beta\beta$-decay requires Majorana neutrino mass, no matter what the actual mechanism is. As long as only a limit on the lifetime is available, limits on the effective Majorana neutrino mass, on the lepton-number violating right-handed current or other possible mechanisms mediating $0\nu\beta\beta$-decay can be obtained, independently of the actual mechanism by assuming that one of these "new physics" possibilities dominates. These limits are listed in the next three tables.

In the following we assume that the exchange of light Majorana neutrinos ($m_{\nu_i} \leq 10$ MeV) contributes dominantly to the decay rate. Besides a dependence on the phase space ($G^{0\nu}$) and the nuclear matrix element ($M^{0\nu}$), the observable $0\nu\beta\beta$-decay rate is proportional to the square of the effective Majorana mass $\langle m_{\beta\beta}\rangle$, $(T^{0\nu}_{1/2})^{-1} = G^{0\nu} \cdot |M^{0\nu}|^2 \cdot \langle m_{\beta\beta}\rangle^2$, with $\langle m_{\beta\beta}\rangle^2 = |\sum_i U^2_{ei} m_{\nu_i}|^2$. The sum contains, in general, complex *CP*-phases in U^2_{ei}, *i.e.*, cancellations may occur. For three neutrino flavors, there are three physical phases for Majorana neutrinos. There is only one phase if neutrinos are Dirac particles. The two additional Majorana phase differences affect only processes to which lepton-number-changing amplitudes contribute. Given the general 3×3 mixing matrix for Majorana neutrinos, one can construct other analogous lepton number violating quantities, $\langle m_{\ell\ell'}\rangle = \sum_i U_{\ell i} U_{\ell' i} m_{\nu_i}$ (l or $l' \neq e$). However, these are currently much less constrained than $\langle m_{\beta\beta}\rangle$.

Nuclear structure calculations are needed to deduce $\langle m_{\beta\beta}\rangle$ from the decay rate. While $G^{0\nu}$ can be calculated, the computation of $M^{0\nu}$ is subject to uncertainty. Comparing different nuclear model evaluations indicates a factor $\sim$2 to 3 spread in the calculated nuclear matrix elements. In addition, if the effective value of the axial current coupling constant g_A in nuclei is substantially smaller in absolute value than its single nucleon value $g_A = -1.2723 \pm 0.0023$, the decay rate might be further reduced. The particle physics quantities to be determined are thus nuclear model-dependent, so the half-life measurements are listed first. Where possible, we reference the nuclear matrix elements used in the subsequent analysis. Since rates for the conventional $2\nu\beta\beta$ decay serve to constrain the nuclear theory models, results for this process are also given.

Oscillation experiments utilizing atmospheric-, accelerator-, solar-, and reactor-produced neutrinos and anti-neutrinos yield strong evidence that at least some neutrinos are massive. However, these findings shed no light on the mass hierarchy (*i.e.*, on the sign of Δm^2_{31}), the absolute neutrino mass values or the properties of neutrinos under CPT-conjugation (Dirac or Majorana).

All confirmed oscillation experiments can be consistently described using three interacting neutrino species with two mass splittings and three mixing angles. Full three flavor analyses such as *e.g.* Ref. 1 yield: $|\Delta m^2_{31}| = 2.55^{+0.04}_{-0.07}$ $(2.49^{+0.04}_{-0.06}) \times 10^{-3}$ eV^2 and $\sin^2\theta_{23} = 0.430^{+0.020}_{-0.018}$ $(0.596^{+0.017}_{-0.018})$ for the parameters observed in atmospheric and accelerator experiments, where the values correspond to the normal (inverted) hierarchies. Oscillations of solar ν_e and reactor $\bar{\nu}_e$ lead to $\Delta m^2_{21} = 7.56 \pm 0.19 \times 10^{-5}$ eV^2 and $\sin^2\theta_{12} = 0.321^{+0.018}_{-0.016}$. The electron type neutrinos couple only weakly to the third mass eigenstate with $\sin^2\theta_{13} = 2.155^{+0.090}_{-0.075}(2.140^{+0.082}_{-0.085}) \times 10^{-2}$. (All errors correspond to 1σ.)

Based on the 3-neutrino analysis: $\langle m_{\beta\beta}\rangle^2 = |\cos^2\theta_{13}\cos^2\theta_{12} m_1 + e^{i\Delta\alpha_{21}}\cos^2\theta_{13}\sin^2\theta_{12} m_2 + e^{i\Delta\alpha_{31}}\sin^2\theta_{13} m_3|^2$, with $\Delta\alpha_{21}, \Delta\alpha_{31}$ denoting the physically relevant Majorana *CP*-phase differences (possible Dirac phase δ is absorbed in these $\Delta\alpha$). Given the present knowledge of the neutrino oscillation parameters one can derive the relation between the effective Majorana mass and the mass of the lightest neutrino, as illustrated in the left panel of Fig. 62.1. The three mass hierarchies allowed by the oscillation data: normal ($m_1 < m_2 < m_3$), inverted ($m_3 < m_1 < m_2$), and degenerate ($m_1 \approx m_2 \approx m_3$), result in different projections. The width of the innermost hatched bands reflects the uncertainty introduced by the unknown Majorana and Dirac phases. If the experimental errors of the oscillation parameters are taken into account, then the allowed areas are widened as shown by the outer bands of Fig. 62.1. Because of the overlap of the different mass scenarios a measurement of $\langle m_{\beta\beta}\rangle$ in the degenerate or inversely hierarchical ranges would not determine the hierarchy. The middle panel of Fig. 62.1 depicts the relation of $\langle m_{\beta\beta}\rangle$ with the summed neutrino mass $m_{tot} = m_1 + m_2 + m_3$, constrained by observational cosmology. The oscillation data thus allow to test whether observed values of $\langle m_{\beta\beta}\rangle$ and m_{tot} are consistent within the 3 neutrino framework. The right hand panel of Fig. 62.1, finally, shows $\langle m_{\beta\beta}\rangle$ as a function of the average mass $\langle m_\beta\rangle = [\Sigma|U_{ei}|^2 m^2_{\nu_i}]^{1/2}$ determined through the analysis of the electron energy distribution in low energy beta decays. The rather large intrinsic width of the $\beta\beta$-decay constraint essentially does not allow to positively identify the inverted hierarchy, and thus the sign of Δm^2_{31}, even in combination with these other observables. Naturally, if the value of $\langle m_{\beta\beta}\rangle \leq 0.01$ eV, but non-zero is ever established then normal hierarchy becomes the only possible scenario.

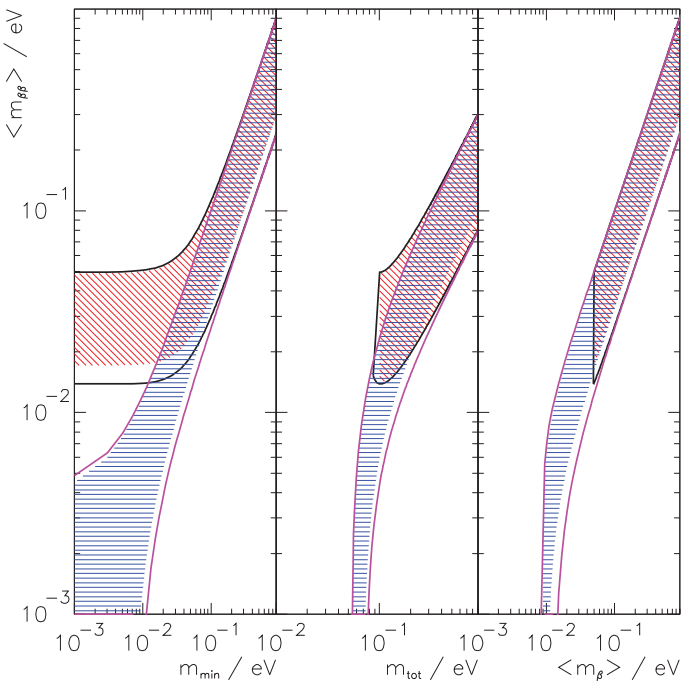

Figure 62.1: The left panel shows the dependence of $\langle m_{\beta\beta}\rangle$ on the absolute mass of the lightest neutrino m_{min}. The middle panel shows $\langle m_{\beta\beta}\rangle$ as a function of the summed neutrino mass m_{tot}, while the right panel depicts $\langle m_{\beta\beta}\rangle$ as a function of the mass $\langle m_\beta\rangle$. In all panels the width of the hatched areas is due to the unknown Majorana phases and thus irreducible. The allowed areas given by the solid lines are obtained by taking into account the errors of the oscillation parameters (at 90% confidence level [1]) . The two sets of solid lines correspond to the normal (blue) and inverted(red) hierarchies. These sets merge into each other for $\langle m_{\beta\beta}\rangle \geq 0.1$ eV, which corresponds to the degenerate mass pattern.

It should be noted that systematic uncertainties of the nuclear matrix elements are not folded into the mass projections shown in Fig. 62.1. Taking this additional uncertainty into account would further widen the allowed areas. The uncertainties in oscillation parameters affect the width of the allowed bands in an asymmetric manner, as shown in Fig. 62.1. For example, for the degenerate mass pattern ($\langle m_{\beta\beta}\rangle \geq 0.1$ eV) the upper edge is simply $\langle m_{\beta\beta}\rangle \sim m$, where m is the common mass of the degenerate multiplet, independent of the oscillation parameters, while the lower edge is $m\cos(2\theta_{12})$. Similar arguments explain the other features of Fig. 62.1. The plots in Fig. 62.1 are based on a 3-neutrino analysis. If it turns out that

additional, i.e. sterile light neutrinos exist, the allowed regions would be modified substantially.

If the neutrinoless double-beta decay is observed, it will be possible to fix a range of absolute values of the masses m_{ν_i}. Unlike the direct neutrino mass measurements, however, a limit on $\langle m_{\beta\beta}\rangle$ does not allow one to constrain the individual mass values m_{ν_i} even when the mass differences Δm^2 are known.

Neutrino oscillation data imply, for the first time, the existence of a lower limit ~ 0.014 eV for the Majorana neutrino mass for the inverted hierarchy mass pattern while $\langle m_{\beta\beta}\rangle$ could, by fine tuning, vanish in the case of the normal mass hierarchy. Several new double beta searches have been proposed to probe the interesting $\langle m_{\beta\beta}\rangle$ mass range, with the prospect of full coverage of the inverted mass hierarchy region within the next decade.

The $0\nu\beta\beta$ decay mechanism discussed so far is not the only way in which the decay can occur. Numerous other possible scenarios have been proposed, however, all of them requiring new physics. It will be a challenging task to decide which mechanism was responsible once $0\nu\beta\beta$ decay is observed. LHC experiments may reveal corresponding signatures for new physics of lepton number violation. If lepton-number-violating right-handed current weak interactions exist, their strength can be characterized by the phenomenological coupling constants η and λ (η describes the coupling between the right-handed lepton current and left-handed quark current while λ describes the coupling when both currents are right-handed). The $0\nu\beta\beta$ decay rate then depends on $\langle\eta\rangle = \eta\sum_i U_{ei}V_{ei}$ and $\langle\lambda\rangle = \lambda\sum_i U_{ei}V_{ei}$ that vanish for massless or unmixed neutrinos ($V_{\ell j}$ is a matrix analogous to $U_{\ell j}$ but describing the mixing with the hypothetical right-handed neutrinos). The observation of the single electron spectra could, in principle, allow to distinguish this mechanism of $0\nu\beta\beta$ from the light Majorana neutrino exchange driven mode. The limits on $\langle\eta\rangle$ and $\langle\lambda\rangle$ are listed in a separate table. The reader is cautioned that a number of earlier experiments did not distinguish between η and λ. In addition, see the section on Majoron searches for additional limits set by these experiments.

References:

1. P.F. de Salas *et al.*, arXiv:1708.01186 and private communication with M. Tortola.

63. Neutrino Properties

Revised August 2013 by P. Vogel (Caltech) and A. Piepke (University of Alabama).

The Neutrino Properties Listings concern measurements of various properties of neutrinos. Nearly all of the measurements, all of which so far are limits, actually concern superpositions of the mass eigenstates ν_i, which are in turn related to the weak eigenstates ν_ℓ, via the neutrino mixing matrix

$$|\nu_\ell\rangle = \sum_i U_{\ell i}\,|\nu_i\rangle\ .$$

In the analogous case of quark mixing via the CKM matrix, the smallness of the off-diagonal terms (small mixing angles) permits a "dominant eigenstate" approximation. However, the results of neutrino oscillation searches show that the mixing matrix contains two large mixing angles and a third angle that is not exceedingly small. We cannot, therefore, associate any particular state $|\nu_i\rangle$ with any particular lepton label e, μ or τ. Nevertheless, note that in the standard labeling the $|\nu_1\rangle$ has the largest $|\nu_e\rangle$ component ($\sim 2/3$), $|\nu_2\rangle$ contains $\sim 1/3$ of the $|\nu_e\rangle$ component and $|\nu_3\rangle$ contains only a small $\sim 2.5\%$ $|\nu_e\rangle$ component.

Neutrinos are produced in weak decays with a definite lepton flavor, and are typically detected by the charged current weak interaction again associated with a specific lepton flavor. Hence, the listings for the neutrino mass that follow are separated into the three associated charged lepton categories. Other properties (mean lifetime, magnetic moment, charge and charge radius) are no longer separated this way. If needed, the associated lepton flavor is reported in the footnotes.

Measured quantities (mass-squared, magnetic moments, mean lifetimes, *etc.*) all depend upon the mixing parameters $|U_{\ell i}|^2$, but to some extent also on experimental conditions (*e.g.*, on energy resolution). Most of these observables, in particular mass-squared, cannot distinguish between Dirac and Majorana neutrinos, and are unaffected by CP phases.

Direct neutrino mass measurements are usually based on the analysis of the kinematics of charged particles (leptons, pions) emitted together with neutrinos (flavor states) in various weak decays. The most sensitive neutrino mass measurement to date, involving electron type antineutrinos, is based on fitting the shape of the beta spectrum. The quantity $\langle m^2_\beta\rangle = \sum_i |U_{ei}|^2 m^2_{\nu_i}$ is determined or constrained, where the sum is over all mass eigenvalues m_{ν_i} that are too close together to be resolved experimentally. If the energy resolution is better than $\Delta m^2_{ij} \equiv m^2_{\nu_i} - m^2_{\nu_j}$, the corresponding heavier m_{ν_i} and mixing parameter could be determined by fitting the resulting spectral anomaly (step or kink).

A limit on $\langle m^2_\beta\rangle$ implies an upper limit on the minimum value m^2_{min} of $m^2_{\nu_i}$, independent of the mixing parameters U_{ei}: $m^2_{min} \le \langle m^2_\beta\rangle$. However, if and when the value of $\langle m^2_\beta\rangle$ is determined then its combination with the results derived from neutrino oscillations that give us the values of the neutrino mass-squared differences $\Delta m^2_{ij} \equiv m^2_i - m^2_j$ and the mixing parameters $|U_{ei}|^2$, the individual neutrino mass squares $m^2_{\nu_j} = \langle m^2_\beta\rangle - \sum_i |U_{ei}|^2 \Delta m^2_{ij}$ can be determined.

So far solar, reactor, atmospheric and accelerator neutrino oscillation experiments can be consistently described using three active neutrino flavors, i.e. two mass splittings and three mixing angles. However, several experiments with radioactive sources, reactors, and accelerators imply the possible existence of one or more non-interacting neutrino species that might be observable since they couple weakly to the flavor neutrinos $|\nu_l\rangle$.

Combined three neutrino analyses determine the squared mass differences and all three mixing angles to within reasonable accuracy. For given $|\Delta m^2_{ij}|$ a limit on $\langle m^2_\beta\rangle$ from beta decay defines an upper limit on the maximum value m_{max} of m_{ν_i}: $m^2_{max} \le \langle m^2_\beta\rangle + \sum_{i<j} |\Delta m^2_{ij}|$. The analysis of the low energy beta decay of tritium, combined with the oscillation results, thus limits all active neutrino masses. Traditionally, experimental neutrino mass limits obtained from pion decay $\pi^+ \to \mu^+ + \nu_\mu$ or the shape of the spectrum of decay products of the τ lepton did not distinguish between flavor and mass eigenstates. These results are reported as limits of the μ and τ based neutrino mass. After the determination of the $|\Delta m^2_{ij}|$'s and the mixing angles θ_{ij}, the corresponding neutrino mass limits are no longer competitive with those derived from low energy beta decays.

The spread of arrival times of the neutrinos from SN1987A, coupled with the measured neutrino energies, provided a time-of-flight limit on a quantity similar to $\langle m_\beta\rangle \equiv \sqrt{\langle m^2_\beta\rangle}$. This statement, clothed in various degrees of sophistication, has been the basis for a very large number of papers. The resulting limits, however, are no longer comparable with the limits from tritium beta decay.

Constraint on the sum of the neutrino masses can be obtained from the analysis of the cosmic microwave background anisotropy, combined with the galaxy redshift surveys and other data. These limits are reported in a separate table (Sum of Neutrino Masses, m_{tot}). Discussion concerning the model dependence of this limit is continuing.

64. Sum of Neutrino Masses

Revised September 2017 by K.A. Olive (University of Minnesota).

The limits on low mass ($m_\nu \lesssim$ 1 MeV) neutrinos apply to $m_{\rm tot}$ given by

$$m_{\rm tot} = \sum_\nu (g_\nu/2) m_\nu \ ,$$

where g_ν is the number of spin degrees of freedom for ν plus $\overline{\nu}$: $g_\nu = 4$ for neutrinos with Dirac masses; $g_\nu = 2$ for Majorana neutrinos. Stable neutrinos in this mass range make a contribution to the total energy density of the Universe which is given by

$$\rho_\nu = m_{\rm tot} n_\nu = m_{\rm tot}(3/11) n_\gamma \ ,$$

where the factor 3/11 is the ratio of (light) neutrinos to photons. Writing $\Omega_\nu = \rho_\nu/\rho_c$, where ρ_c is the critical energy density of the Universe, and using $n_\gamma = 412$ cm^{-3}, we have

$$\Omega_\nu h^2 = m_{\rm tot}/(94 \ {\rm eV}) \ .$$

While an upper limit to the matter density of $\Omega_m h^2 < 0.12$ would constrain $m_{\rm tot} < 11$ eV, much stronger constraints are obtained from a combination of observations of the CMB, the amplitude of density fluctuations on smaller scales from the clustering of galaxies and the Lyman-α forest, baryon acoustic oscillations, and new Hubble parameter data. These combine to give an upper limit of around 0.2 eV, and may, in the near future, be able to provide a lower bound on the sum of the neutrino masses. See Sec. 25 of this *Review* for more details.

65. Three-Neutrino Mixing Parameters

Updated August 2017 by M. Goodman (ANL).

65.1. Introduction and Notation

With the exception of possible short-baseline anomalies (such as LSND), current accelerator, reactor, solar and atmospheric neutrino data can be described within the framework of a 3×3 mixing matrix between the flavor eigenstates ν_e, ν_μ and ν_τ and mass eigenstates ν_1, ν_2 and ν_3. (See equation 14.6 of the review "Neutrino Mass, Mixing and Oscillations" by K. Nakamura and S.T. Petcov.) Whether or not this is the ultimately correct framework, it is currently widely used to parametrize neutrino mixing data and to plan new experiments.

The mass differences are called $\Delta m^2_{21} \equiv m^2_2 - m^2_1$ and $\Delta m^2_{32} \equiv m^2_3 - m^2_2$. In these listings, we assume

$$\Delta m^2_{32} \sim \Delta m^2_{31} \tag{65.1}$$

even though the experimental error is comparable to the difference $\Delta m^2_{31} - \Delta m^2_{32} = \Delta m^2_{21}$. The measurements made by ν_μ disappearance at accelerators and by ν_e disappearance at reactors are slightly different mixtures of Δm^2_{32} and Δm^2_{31}. The angles are labeled θ_{12}, θ_{23} and θ_{13}. The CP violating phase is called δ. The familiar two neutrino form for oscillations is

$$P(\nu_a \to \nu_b; a \neq b) = \sin^2(2\theta)\sin^2(\Delta m^2 L/4E). \tag{65.2}$$

Despite the fact that the mixing angles have been measured to be much larger than in the quark sector, the two neutrino form is often a very good approximation and is used in many situations.

The angles appear in the equations below in many forms. They most often appear as $\sin^2(2\theta)$. The listings currently now use $\sin^2(\theta)$ because this distinguishes whether θ_{23} is larger or smaller than 45°.

65.2. Accelerator neutrino experiments

Ignoring Δm^2_{21}, *CP* violation, and matter effects, the equations for the probability of appearance in an accelerator oscillation experiment are:

$$P(\nu_\mu \to \nu_\tau) = \sin^2(2\theta_{23})\cos^4(\theta_{13})\sin^2(\Delta m^2_{32}L/4E) \tag{65.3}$$
$$P(\nu_\mu \to \nu_e) = \sin^2(2\theta_{13})\sin^2(\theta_{23})\sin^2(\Delta m^2_{32}L/4E) \tag{65.4}$$
$$P(\nu_e \to \nu_\mu) = \sin^2(2\theta_{13})\sin^2(\theta_{23})\sin^2(\Delta m^2_{32}L/4E) \tag{65.5}$$
$$P(\nu_e \to \nu_\tau) = \sin^2(2\theta_{13})\cos^2(\theta_{23})\sin^2(\Delta m^2_{32}L/4E)\ . \tag{65.6}$$

Current and future long-baseline accelerator experiments are studying non-zero θ_{13} through $P(\nu_\mu \to \nu_e)$. Including the CP terms and low mass scale, the equation for neutrino oscillation in vacuum is:

$$\begin{aligned} P(\nu_\mu \to \nu_e) &= P1 + P2 + P3 + P4 \\ P1 &= \sin^2(\theta_{23})\sin^2(2\theta_{13})\sin^2(\Delta m^2_{32}L/4E) \\ P2 &= \cos^2(\theta_{23})\sin^2(2\theta_{13})\sin^2(\Delta m^2_{21}L/4E) \\ P3 &= -/+ J\sin(\delta)\sin(\Delta m^2_{32}L/4E) \\ P4 &= J\cos(\delta)\cos(\Delta m^2_{32}L/4E) \end{aligned} \tag{65.7}$$

where

$$\begin{aligned} J = &\cos(\theta_{13})\sin(2\theta_{12})\sin(2\theta_{13})\sin(2\theta_{23})\times \\ &\sin(\Delta m^2_{32}L/4E)\sin(\Delta m^2_{21}L/4E) \end{aligned} \tag{65.8}$$

and the sign in P3 is negative for neutrinos and positive for anti-neutrinos respectively. For most new long-baseline accelerator experiments, P2 can safely be neglected but the other three terms can all be large. Also, depending on the distance and the mass order, matter effects need to be included.

65.3. Reactor neutrino experiments

Nuclear reactors are prolific sources of $\bar{\nu}_e$ with an energy near 4 MeV. The oscillation probability can be expressed

$$\begin{aligned} P(\bar{\nu}_e \to \bar{\nu}_e) = 1 &- \cos^4(\theta_{13})\sin^2(2\theta_{12})\sin^2(\Delta m^2_{21}L/4E) \\ &- \cos^2(\theta_{12})\sin^2(2\theta_{13})\sin^2(\Delta m^2_{31}L/4E) \\ &- \sin^2(\theta_{12})\sin^2(2\theta_{13})\sin^2(\Delta m^2_{32}L/4E) \end{aligned} \tag{65.9}$$

not using the approximation in Eq. (65.1). For short distances (L<5 km) we can ignore the second term on the right and can reimpose approximation Eq. (65.1). This takes the familiar two neutrino form with θ_{13} and Δm^2_{32}:

$$P(\bar{\nu}_e \to \bar{\nu}_e) = 1 - \sin^2(2\theta_{13})\sin^2(\Delta m^2_{32}L/4E). \tag{65.10}$$

65.4. Solar and Atmospheric neutrino experiments

Solar neutrino experiments are sensitive to ν_e disappearance and have allowed the measurement of θ_{12} and Δm^2_{21}. They are also sensitive to θ_{13}. We identify $\Delta m^2_\odot = \Delta m^2_{21}$ and $\theta_\odot = \theta_{12}$.

Atmospheric neutrino experiments are primarily sensitive to ν_μ disappearance through $\nu_\mu \to \nu_\tau$ oscillations, and have allowed the measurement of θ_{23} and Δm^2_{32}. We identify $\Delta m^2_A = \Delta m^2_{32}$ and $\theta_A = \theta_{23}$. Despite the large ν_e component of the atmospheric neutrino flux, it is difficult to measure Δm^2_{21} effects. This is because of a cancellation between $\nu_\mu \to \nu_e$ and $\nu_e \to \nu_\mu$ together with the fact that the ratio of ν_μ and ν_e atmospheric fluxes, which arise from sequential π and μ decay, is near 2.

65.5. Oscillation Parameter Listings

In Section (B) we encode the three mixing angles θ_{12}, θ_{23}, θ_{13} and two mass squared differences Δm^2_{21} and Δm^2_{32}. Our knowledge of θ_{12} and Δm^2_{21} comes from the KamLAND reactor neutrino experiment together with solar neutrino experiments. Our knowledge of θ_{23} and Δm^2_{32} comes from atmospheric, reactor and long-baseline accelerator neutrino experiments. For the earlier experiments, we identified the large mass splitting as Δm^2_{32}. Now that $\sigma(\Delta m^2_{32}) \approx \Delta m^2_{21}$, some experiments report separate values for the two mass orders. Results on θ_{13} come from reactor antineutrino disappearance experiments. There are also results from long-baseline accelerator experiments looking for ν_e appearance. The interpretation of both kinds of results depends on Δm^2_{32}, and the accelerator results also depend on the mass order, θ_{23} and the CP violating phase δ.

Accelerator and atmospheric experiments have some sensitivity to the CP violation phase δ through Eq. (65.7). Note that P3 depends on the sign of Δm^2_{32} so the sensitivity depends on the mass order. For non-maximal θ_{23} mixing, it also depends on the octant of θ_{23}, i.e. whether $\theta_{23} > \pi/4$ or $\theta_{23} < \pi/4$. In this edition of the listings, we report the mean values of $\sin^2(\theta)$. If θ_{23} deviates from 45 degrees, this may not yield the correct best fit value.

66. Quark Masses

Updated March 2018 by A.V. Manohar (UC, San Diego), C.T. Sachrajda (University of Southampton), and R.M. Barnett (LBNL).

66.1. Introduction

This note discusses some of the theoretical issues relevant for the determination of quark masses, which are fundamental parameters of the Standard Model of particle physics. Unlike the leptons, quarks are confined inside hadrons and are not observed as physical particles. Quark masses therefore cannot be measured directly, but must be determined indirectly through their influence on hadronic properties. Although one often speaks loosely of quark masses as one would of the mass of the electron or muon, any quantitative statement about the value of a quark mass must make careful reference to the particular theoretical framework that is used to define it. It is important to keep this *scheme dependence* in mind when using the quark mass values tabulated in the data listings.

Historically, the first determinations of quark masses were performed using quark models. The resulting masses only make sense in the limited context of a particular quark model, and cannot be related to the quark mass parameters of the Standard Model. In order to discuss quark masses at a fundamental level, definitions based on quantum field theory must be used, and the purpose of this note is to discuss these definitions and the corresponding determinations of the values of the masses.

66.2. Mass parameters and the QCD Lagrangian

The QCD [1] Lagrangian for N_F quark flavors is

$$\mathcal{L} = \sum_{k=1}^{N_F} \overline{q}_k \left(i \not{D} - m_k\right) q_k - \tfrac{1}{4} G_{\mu\nu} G^{\mu\nu} \ , \tag{66.1}$$

where $\not{D} = \left(\partial_\mu - i g A_\mu\right) \gamma^\mu$ is the gauge covariant derivative, A_μ is the gluon field, $G_{\mu\nu}$ is the gluon field strength, m_k is the mass parameter of the k^{th} quark, and q_k is the quark Dirac field. After renormalization, the QCD Lagrangian Eq. (66.1) gives finite values for physical quantities, such as scattering amplitudes. Renormalization is a procedure that invokes a subtraction scheme to render the amplitudes finite, and requires the introduction of a dimensionful scale parameter μ. The mass parameters in the QCD Lagrangian Eq. (66.1) depend on the renormalization scheme used to define the theory, and also on the scale parameter μ. The most commonly used renormalization scheme for QCD perturbation theory is the $\overline{\text{MS}}$ scheme.

The QCD Lagrangian has a chiral symmetry in the limit that the quark masses vanish. This symmetry is spontaneously broken by dynamical chiral symmetry breaking, and explicitly broken by the quark masses. The nonperturbative scale of dynamical chiral symmetry breaking, Λ_χ, is around 1 GeV [2]. It is conventional to call quarks heavy if $m > \Lambda_\chi$, so that explicit chiral symmetry breaking dominates (c, b, and t quarks are heavy), and light if $m < \Lambda_\chi$, so that spontaneous chiral symmetry breaking dominates (the u and d are light and s quarks are considered to be light when using $\text{SU}(3)_L \times \text{SU}(3)_R$ chiral perturbation theory). The determination of light- and heavy-quark masses is considered separately in Sec. 66.4 and Sec. 66.5 below.

At high energies or short distances, nonperturbative effects, such as chiral symmetry breaking, become small and one can, in principle, determine quark masses by analyzing mass-dependent effects using QCD perturbation theory. Such computations are conventionally performed using the $\overline{\text{MS}}$ scheme at a scale $\mu \gg \Lambda_\chi$, and give the $\overline{\text{MS}}$ "running" mass $\overline{m}(\mu)$. We use the $\overline{\text{MS}}$ scheme when reporting quark masses; one can readily convert these values into other schemes using perturbation theory.

The μ dependence of $\overline{m}(\mu)$ at short distances can be calculated using the renormalization group equation,

$$\mu^2 \frac{\mathrm{d}\overline{m}\left(\mu\right)}{\mathrm{d}\mu^2} = -\gamma(\overline{\alpha}_s\left(\mu\right)) \, \overline{m}\left(\mu\right), \tag{66.2}$$

where γ is the anomalous dimension which is now known to four-loop order in perturbation theory [3,4]. $\overline{\alpha}_s$ is the coupling constant in the $\overline{\text{MS}}$ scheme. Defining the expansion coefficients γ_r by

$$\gamma\left(\overline{\alpha}_s\right) \equiv \sum_{r=1}^{\infty} \gamma_r \left(\frac{\overline{\alpha}_s}{4\pi}\right)^r ,$$

the first four coefficients are given by

$$\begin{aligned}
\gamma_1 &= 4, \\
\gamma_2 &= \frac{202}{3} - \frac{20 N_L}{9}, \\
\gamma_3 &= 1249 + \left(-\frac{2216}{27} - \frac{160}{3}\zeta\left(3\right)\right) N_L - \frac{140}{81} N_L^2, \\
\gamma_4 &= \frac{4603055}{162} + \frac{135680}{27}\zeta\left(3\right) - 8800\zeta\left(5\right) \\
&\quad + \left(-\frac{91723}{27} - \frac{34192}{9}\zeta\left(3\right) + 880\zeta\left(4\right) + \frac{18400}{9}\zeta\left(5\right)\right) N_L \\
&\quad + \left(\frac{5242}{243} + \frac{800}{9}\zeta\left(3\right) - \frac{160}{3}\zeta\left(4\right)\right) N_L^2 \\
&\quad + \left(-\frac{332}{243} + \frac{64}{27}\zeta\left(3\right)\right) N_L^3,
\end{aligned}$$

where N_L is the number of active light quark flavors at the scale μ, i.e. flavors with masses $< \mu$, and ζ is the Riemann zeta function ($\zeta(3) \simeq 1.2020569$, $\zeta(4) \simeq 1.0823232$, and $\zeta(5) \simeq 1.0369278$). In addition, as the renormalization scale crosses quark mass thresholds one needs to match the scale dependence of $\overline{m}$ below and above the threshold. There are finite threshold corrections; the necessary formulae can be found in Ref. [5].

The quark masses for light quarks discussed so far are often referred to as current quark masses. Nonrelativistic quark models use constituent quark masses, which are of order 350 MeV for the u and d quarks. Constituent quark masses model the effects of dynamical chiral symmetry breaking, and are not directly related to the quark mass parameters m_k of the QCD Lagrangian Eq. (66.1). Constituent masses are only defined in the context of a particular hadronic model.

66.3. Lattice Gauge Theory

The use of the lattice simulations for *ab initio* determinations of the fundamental parameters of QCD, including the coupling constant and quark masses (except for the top-quark mass) is a very active area of research (see the review on Lattice Quantum Chromodynamics in this *Review*). Here we only briefly recall those features which are required for the determination of quark masses. In order to determine the lattice spacing (a, i.e. the distance between neighboring points of the lattice) and quark masses, one computes a convenient and appropriate set of physical quantities (frequently chosen to be a set of hadronic masses) for a variety of input values of the quark masses. The true (physical) values of the quark masses are those which correctly reproduce the set of physical quantities being used for the calibration.

The values of the quark masses obtained directly in lattice simulations are bare quark masses, corresponding to a particular discretization of QCD and with the lattice spacing as the ultraviolet cut-off. In order for these results to be useful in phenomenological applications, it is necessary to relate them to renormalized masses defined in some standard renormalization scheme such as $\overline{\text{MS}}$. Provided that both the ultraviolet cut-off a^{-1} and the renormalization scale μ are much greater than Λ_{QCD}, the bare and renormalized masses can be related in perturbation theory. However, in order to avoid uncertainties due to the unknown higher-order coefficients in lattice perturbation theory, most results obtained recently use *non-perturbative renormalization* to relate the bare masses to those defined in renormalization schemes which can be simulated directly in lattice QCD (e.g. those obtained from quark and gluon Green functions at

specified momenta in the Landau gauge [62] or those defined using finite-volume techniques and the Schrödinger functional [63]) . The conversion to the $\overline{\rm MS}$ scheme (which cannot be simulated) is then performed using continuum perturbation theory.

The determination of quark masses using lattice simulations is well established and the current emphasis is on the reduction and control of the systematic uncertainties. With improved algorithms and access to more powerful computing resources, the precision of the results has improved immensely in recent years. Vacuum polarisation effects are included with $N_f = 2$, $2+1$ or $N_f = 2+1+1$ flavors of sea quarks. The number 2 here indicates that the up and down quarks are degenerate. In earlier *reviews*, results were presented from simulations in which vacuum polarization effects were completely neglected (this is the so-called *quenched* approximation), leading to systematic uncertainties which could not be estimated reliably. It is no longer necessary to include quenched results in compilations of quark masses. Particularly pleasing is the observation that results obtained using different formulations of lattice QCD, with different systematic uncertainties, give results which are largely consistent with each other. This gives us broad confidence in the estimates of the systematic errors. As the precision of the results approaches (or even exceeds in some cases) 1%, isospin breaking effects, including electromagnetic corrections need to be included and this is beginning to be done as will be discussed below. The results however, are still at an early stage and therefore, unless explicitly stated otherwise, the results presented below will neglect isospin breaking.

Members of the lattice QCD community have organised a Flavour Lattice Averaging Group (FLAG) which critically reviews quantities computed in lattice QCD relevant to flavor physics, including the determination of light quark masses, against stated quality criteria and presents its view of the current status of the results. The latest (2nd) edition reviewed lattice results published before November 30th 2013 [16].

66.4. Light quarks

In this section we review the determination of the masses of the light quarks u, d and s from lattice simulations and then discuss the consequences of the approximate chiral symmetry.

66.4.1. ***Lattice Gauge Theory*** : The most reliable determinations of the strange quark mass m_s and of the average of the up and down quark masses $m_{ud} = (m_u + m_d)/2$ are obtained from lattice simulations. As explained in section C above, the simulations are generally performed with degenerate up and down quarks ($m_u = m_d$) and so it is the average which is obtained directly from the computations. Below we discuss attempts to derive m_u and m_d separately using lattice results in combination with other techniques, but we start by briefly present our estimate of the current status of the latest lattice results in the isospin symmetric limit. Based largely on references [21–25], which its authors considered to have the most reliable estimates of the systematic uncertainties, the FLAG Review [16] quoted as its summary of results obtained with $N_f = 2+1$ flavors of sea quarks:

$$\overline{m}_s = (93.8 \pm 1.5 \pm 1.9)\,\text{MeV}\,, \tag{66.3}$$

$$\overline{m}_{ud} = (3.42 \pm 0.06 \pm 0.07)\,\text{MeV} \tag{66.4}$$

and

$$\frac{\overline{m}_s}{\overline{m}_{ud}} = 27.46 \pm 0.15 \pm 0.41\,. \tag{66.5}$$

The masses are given in the $\overline{\rm MS}$ scheme at a renormalization scale of 2 GeV. The first error comes from averaging the lattice results and the second is an estimate of the neglect of sea-quark effects from the charm and more massive quarks. Because of the systematic errors, these results are not simply the combinations of all the results in quadrature, but include a judgement of the remaining uncertainties. Since the different collaborations use different formulations of lattice QCD, the (relatively small) variations of the results between the groups provides important information about the reliability of the estimates.

Since the publication of the FLAG review [16] there have been a number of studies with $N_f = 2+1+1$ [26–28] and $N_f = 2+1$ [29] and a reasonable summary of the current status may be $\overline{m}_{ud} = (3.4 \pm 0.1)\,\text{MeV}$, $\overline{m}_s = (93.5 \pm 2)\,\text{MeV}$ and $\overline{m}_s/\overline{m}_{ud} = 27.5 \pm 0.3$.

To obtain the individual values of $\overline{m}_u$ and $\overline{m}_d$ requires the introduction of isospin breaking effects, including electromagnetism. In principle this can be done completely using lattice field theory. Such calculations are indeed beginning (note the recent computation of the neutron-proton mass splitting [30]) but are still at a relatively early stage. In practice therefore, $\overline{m}_u$ and $\overline{m}_d$ are extracted by combining lattice results with some elements of continuum phenomenology, most frequently based on chiral perturbation theory. Such studies include references [32,17,24,28,33,34] as well the Flavianet Lattice Averaging Group [43]. Based on these results we summarise the current status as

$$\frac{\overline{m}_u}{\overline{m}_d} = 0.46(5)\,,\ \overline{m}_u = 2.15(15)\,\text{MeV}\,,\ \overline{m}_d = 4.70(20)\,\text{MeV}\,. \tag{66.6}$$

Again the masses are given in the $\overline{\rm MS}$ scheme at a renormalization scale of 2 GeV. Of particular importance is the fact that $m_u \neq 0$ since there would have been no strong CP problem had m_u been equal to zero.

The quark mass ranges for the light quarks given in the listings combine the lattice and continuum values and use the PDG method for determining errors given in the introductory notes.

66.4.2. ***Chiral Perturbation Theory*** : For light quarks, one can use the techniques of chiral perturbation theory [6–8] to extract quark mass ratios. The mass term for light quarks in the QCD Lagrangian is

$$\overline{\Psi} M \Psi = \overline{\Psi}_L M \Psi_R + \overline{\Psi}_R M^\dagger \Psi_L, \tag{66.7}$$

where M is the light quark mass matrix,

$$M = \begin{pmatrix} m_u & 0 & 0 \\ 0 & m_d & 0 \\ 0 & 0 & m_s \end{pmatrix}, \tag{66.8}$$

$\Psi = (u, d, s)$, and L and R are the left- and right-chiral components of Ψ given by $\Psi_{L,R} = P_{L,R}\Psi$, $P_L = (1-\gamma_5)/2$, $P_R = (1+\gamma_5)/2$. The mass term is the only term in the QCD Lagrangian that mixes left- and right-handed quarks. In the limit $M \to 0$, there is an independent $SU(3) \times U(1)$ flavor symmetry for the left- and right-handed quarks. The vector $U(1)$ symmetry is baryon number; the axial $U(1)$ symmetry of the classical theory is broken in the quantum theory due to the anomaly. The remaining $G_\chi = \text{SU}(3)_L \times \text{SU}(3)_R$ chiral symmetry of the QCD Lagrangian is spontaneously broken to $SU(3)_V$, which, in the limit $M \to 0$, leads to eight massless Goldstone bosons, the π's, K's, and η.

The symmetry G_χ is only an approximate symmetry, since it is explicitly broken by the quark mass matrix M. The Goldstone bosons acquire masses which can be computed in a systematic expansion in M, in terms of low-energy constants, which are unknown nonperturbative parameters of the effective theory, and are not fixed by the symmetries. One treats the quark mass matrix M as an external field that transforms under G_χ as $M \to LMR^\dagger$, where $\Psi_L \to L\Psi_L$ and $\Psi_R \to R\Psi_R$ are the $SU(3)_L$ and $SU(3)_R$ transformations, and writes down the most general Lagrangian invariant under G_χ. Then one sets M to its given constant value Eq. (66.8), which implements the symmetry breaking. To first order in M one finds that [9]

$$\begin{aligned} m^2_{\pi^0} &= B\,(m_u + m_d)\ , \\ m^2_{\pi^\pm} &= B\,(m_u + m_d) + \Delta_{\rm em}\ , \\ m^2_{K^0} = m^2_{\overline{K}^0} &= B\,(m_d + m_s)\ , \\ m^2_{K^\pm} &= B\,(m_u + m_s) + \Delta_{\rm em}\ , \\ m^2_\eta &= \frac{1}{3} B\,(m_u + m_d + 4m_s)\ , \end{aligned} \tag{66.9}$$

with two unknown constants B and $\Delta_{\rm em}$, the electromagnetic mass difference. From Eq. (66.9), one can determine the quark mass ratios [9]

$$\frac{m_u}{m_d} = \frac{2m_{\pi^0}^2 - m_{\pi^+}^2 + m_{K^+}^2 - m_{K^0}^2}{m_{K^0}^2 - m_{K^+}^2 + m_{\pi^+}^2} = 0.56\ ,$$

$$\frac{m_s}{m_d} = \frac{m_{K^0}^2 + m_{K^+}^2 - m_{\pi^+}^2}{m_{K^0}^2 + m_{\pi^+}^2 - m_{K^+}^2} = 20.2\ , \qquad (66.10)$$

to lowest order in chiral perturbation theory, with an error which will be estimated below. Since the mass ratios extracted using chiral perturbation theory use the symmetry transformation property of M under the chiral symmetry G_χ, it is important to use a renormalization scheme for QCD that does not change this transformation law. Any mass independent subtraction scheme such as $\overline{\rm MS}$ is suitable. The ratios of quark masses are scale independent in such a scheme, and Eq. (66.10) can be taken to be the ratio of $\overline{\rm MS}$ masses. Chiral perturbation theory cannot determine the overall scale of the quark masses, since it uses only the symmetry properties of M, and any multiple of M has the same G_χ transformation law as M.

Chiral perturbation theory is a systematic expansion in powers of the light quark masses. The typical expansion parameter is $m_K^2/\Lambda_\chi^2 \sim 0.25$ if one uses $SU(3)$ chiral symmetry, and $m_\pi^2/\Lambda_\chi^2 \sim 0.02$ if instead one uses $SU(2)$ chiral symmetry. Electromagnetic effects at the few percent level also break $SU(2)$ and $SU(3)$ symmetry. The mass formulæ Eq. (66.9) were derived using $SU(3)$ chiral symmetry, and are expected to have approximately a 25% uncertainty due to second order corrections. This estimate of the uncertainty is consistent with the lattice results found in Eq. (66.3) - Eq. (66.5) and more recent calculations.

There is a subtlety which arises when one tries to determine quark mass ratios at second order in chiral perturbation theory. The second order quark mass term [10]

$$\left(M^\dagger\right)^{-1} \det M^\dagger \qquad (66.11)$$

(which can be generated by instantons) transforms in the same way under G_χ as M. Chiral perturbation theory cannot distinguish between M and $\left(M^\dagger\right)^{-1} \det M^\dagger$; one can make the replacement $M \to M(\lambda) = M + \lambda M \left(M^\dagger M\right)^{-1} \det M^\dagger$ in the chiral Lagrangian,

$$M(\lambda) = \mathrm{diag}\left(m_u(\lambda)\,,\ m_d(\lambda)\,,\ m_s(\lambda)\right)$$

$$= \mathrm{diag}\left(m_u + \lambda m_d m_s\,,\ m_d + \lambda m_u m_s\,,\ m_s + \lambda m_u m_d\right), \qquad (66.12)$$

and leave all observables unchanged.

The combination

$$\left(\frac{m_u}{m_d}\right)^2 + \frac{1}{Q^2}\left(\frac{m_s}{m_d}\right)^2 = 1 \qquad (66.13)$$

where

$$Q^2 = \frac{m_s^2 - \hat{m}^2}{m_d^2 - m_u^2}, \qquad \hat{m} = \frac{1}{2}\left(m_u + m_d\right),$$

is insensitive to the transformation in Eq. (66.12). Eq. (66.13) gives an ellipse in the $m_u/m_d - m_s/m_d$ plane. The ellipse is well-determined by chiral perturbation theory, but the exact location on the ellipse, and the absolute normalization of the quark masses, has larger uncertainties. Q is determined to be in the range 21–25 from $\eta \to 3\pi$ decay and the electromagnetic contribution to the K^+–K^0 and π^+–π^0 mass differences [11].

The absolute normalization of the quark masses cannot be determined using chiral perturbation theory. Other methods, such as lattice simulations discussed above or spectral function sum rules [12,13] for hadronic correlation functions, which we review next are necessary.

66.4.3. ***Sum Rules*** : Sum rule methods have been used extensively to determine quark masses and for illustration we briefly discuss here their application to hadronic τ decays [14]. Other applications involve very similar techniques.

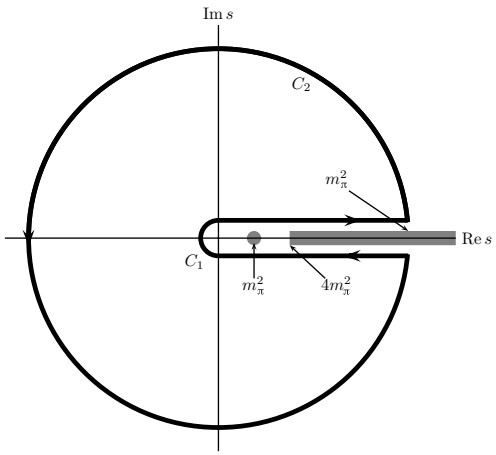

Figure 66.1: The analytic structure of $\Pi(s)$ in the complex s-plane. The contours C_1 and C_2 are the integration contours discussed in the text.

The experimentally measured quantity is R_τ,

$$\frac{{\rm d}R_\tau}{{\rm d}s} = \frac{{\rm d}\Gamma/{\rm d}s\left(\tau^- \to \text{hadrons} + \nu_\tau(\gamma)\right)}{\Gamma\left(\tau^- \to e^-\overline{\nu}_e\nu_\tau(\gamma)\right)} \qquad (66.14)$$

the hadronic invariant mass spectrum in semihadronic τ decay, normalized to the leptonic τ decay rate. It is useful to define q as the total momentum of the hadronic final state, so $s = q^2$ is the hadronic invariant mass. The total hadronic τ decay rate R_τ is then given by integrating ${\rm d}R_\tau/{\rm d}s$ over the kinematically allowed range $0 \le s \le M_\tau^2$.

R_τ can be written as

$$R_\tau = 12\pi \int_0^{M_\tau^2} \frac{{\rm d}s}{M_\tau^2}\left(1 - \frac{s}{M_\tau^2}\right)^2 \times \left[\left(1 + 2\frac{s}{M_\tau^2}\right){\rm Im}\,\Pi^T(s) + {\rm Im}\,\Pi^L(s)\right] \qquad (66.15)$$

where $s = q^2$, and the hadronic spectral functions $\Pi^{L,T}$ are defined from the time-ordered correlation function of two weak currents is the time-ordered correlator of the weak interaction current ($j^\mu(x)$ and $j^\nu(0)$) by

$$\Pi^{\mu\nu}(q) = i\int {\rm d}^4x\ e^{iq\cdot x}\left\langle 0\right| T\left(j^\mu(x) j^\nu(0)^\dagger\right)\left|0\right\rangle, \qquad (66.16)$$

$$\Pi^{\mu\nu}(q) = \left(-g^{\mu\nu} + q^\mu q^\nu\right)\Pi^T(s) + q^\mu q^\nu \Pi^L(s), \qquad (66.17)$$

and the decomposition Eq. (66.17) is the most general possible structure consistent with Lorentz invariance.

By the optical theorem, the imaginary part of $\Pi^{\mu\nu}$ is proportional to the total cross-section for the current to produce all possible states. A detailed analysis including the phase space factors leads to Eq. (66.15). The spectral functions $\Pi^{L,T}(s)$ are analytic in the complex s plane, with singularities along the real axis. There is an isolated pole at $s = m_\pi^2$, and single- and multi-particle singularities for $s \ge 4m_\pi^2$, the two-particle threshold. The discontinuity along the real axis is $\Pi^{L,T}(s + i0^+) - \Pi^{L,T}(s - i0^+) = 2i{\rm Im}\,\Pi^{L,T}(s)$. As a result, Eq. (66.15) can be rewritten with the replacement ${\rm Im}\,\Pi^{L,T}(s) \to -i\Pi^{L,T}(s)/2$, and the integration being over the contour C_1. Finally, the contour C_1 can be deformed to C_2 without crossing any singularities, and so leaving the integral unchanged. One can derive a series of sum rules analogous to Eq. (66.15) by weighting the differential τ hadronic decay rate by different powers of the hadronic invariant mass,

$$R_\tau^{kl} = \int_0^{M_\tau^2} {\rm d}s\ \left(1 - \frac{s}{M_\tau^2}\right)^k \left(\frac{s}{M_\tau^2}\right)^l \frac{{\rm d}R_\tau}{{\rm d}s} \qquad (66.18)$$

where $\mathrm{d}R_\tau/\mathrm{d}s$ is the hadronic invariant mass distribution in τ decay normalized to the leptonic decay rate. This leads to the final form of the sum rule(s),

$$R_\tau^{kl} = -6\pi i \int_{C_2} \frac{\mathrm{d}s}{M_\tau^2}\left(1-\frac{s}{M_\tau^2}\right)^{2+k}\left(\frac{s}{M_\tau^2}\right)^{l} \times \left[\left(1+2\frac{s}{M_\tau^2}\right)\Pi^T(s)+\Pi^L(s)\right]. \quad (66.19)$$

The manipulations so far are completely rigorous and exact, relying only on the general analytic structure of quantum field theory. The left-hand side of the sum rule Eq. (66.19) is obtained from experiment. The right hand-side can be computed for s far away from any physical cuts using the operator product expansion (OPE) for the time-ordered product of currents in Eq. (66.16), and QCD perturbation theory. The OPE is an expansion for the time-ordered product Eq. (66.16) in a series of local operators, and is an expansion about the $q \to \infty$ limit. It gives $\Pi(s)$ as an expansion in powers of $\alpha_s(s)$ and $\Lambda^2_{\rm QCD}/s$, and is valid when s is far (in units of $\Lambda^2_{\rm QCD}$) from any singularities in the complex s-plane.

The OPE gives $\Pi(s)$ as a series in α_s, quark masses, and various non-perturbative vacuum matrix element. By computing $\Pi(s)$ theoretically, and comparing with the experimental values of R_τ^{kl}, one determines various parameters such as α_s and the quark masses. The theoretical uncertainties in using Eq. (66.19) arise from neglected higher order corrections (both perturbative and non-perturbative), and because the OPE is no longer valid near the real axis, where Π has singularities. The contribution of neglected higher order corrections can be estimated as for any other perturbative computation. The error due to the failure of the OPE is more difficult to estimate. In Eq. (66.19), the OPE fails on the endpoints of C_2 that touch the real axis at $s = M_\tau^2$. The weight factor $(1 - s/M_\tau^2)$ in Eq. (66.19) vanishes at this point, so the importance of the endpoint can be reduced by choosing larger values of k.

66.5. Heavy quarks

For heavy-quark physics one can exploit the fact that $m_Q \gg \Lambda_{\rm QCD}$ to construct effective theories (m_Q is the mass of the heavy quark Q). The masses and decay rates of hadrons containing a single heavy quark, such as the B and D mesons can be determined using the heavy quark effective theory (HQET) [45]. The theoretical calculations involve radiative corrections computed in perturbation theory with an expansion in $\alpha_s(m_Q)$ and non-perturbative corrections with an expansion in powers of $\Lambda_{\rm QCD}/m_Q$. Due to the asymptotic nature of the QCD perturbation series, the two kinds of corrections are intimately related; an example of this are renormalon effects in the perturbative expansion which are associated with non-perturbative corrections.

Systems containing two heavy quarks such as the Υ or J/Ψ are treated using non-relativistic QCD (NRQCD) [46]. The typical momentum and energy transfers in these systems are $\alpha_s m_Q$, and $\alpha_s^2 m_Q$, respectively, so these bound states are sensitive to scales much

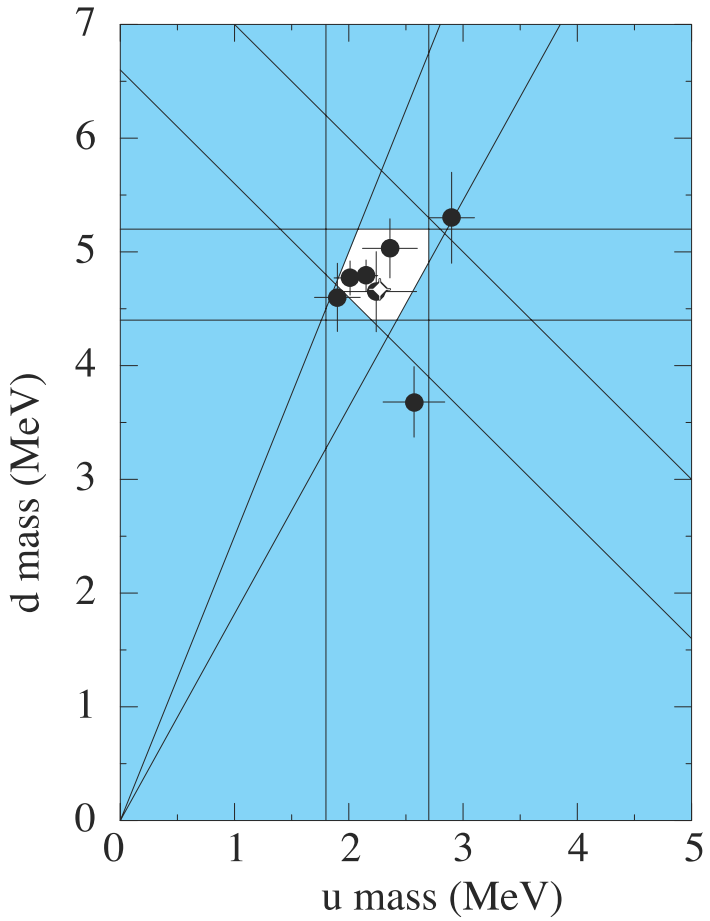

Figure 66.2: The allowed region (shown in white) for up quark and down quark masses. This region was determined in part from papers reporting values for m_u and m_d (data points shown) and in part from analysis of the allowed ranges of other mass parameters (see Fig. 66.3). The parameter $(m_u + m_d)/2$ yields the two downward-sloping lines, while m_u/m_d yields the two rising lines originating at (0,0). There are two overlapping data points, so one of them is shown as a white diamond (it has very small error bars).

smaller than m_Q. However, smeared observables, such as the cross-section for $e^+e^- \to \overline{b}b$ averaged over some range of s that includes several bound state energy levels, are better behaved and only sensitive to scales near m_Q. For this reason, most determinations of the c, b quark masses using perturbative calculations compare smeared observables with experiment [47–49].

the data. This leads to a systematic error from perturbation theory of around 20 MeV for the c quark and 25 MeV for the b quark. Electromagnetic effects, which also are important at this precision, are often not included. For this reason, we inflate the errors on the continuum extractions of m_c and m_b. The average values of m_c and m_b from continuum determinations are (see Sec. G for the 1S scheme)

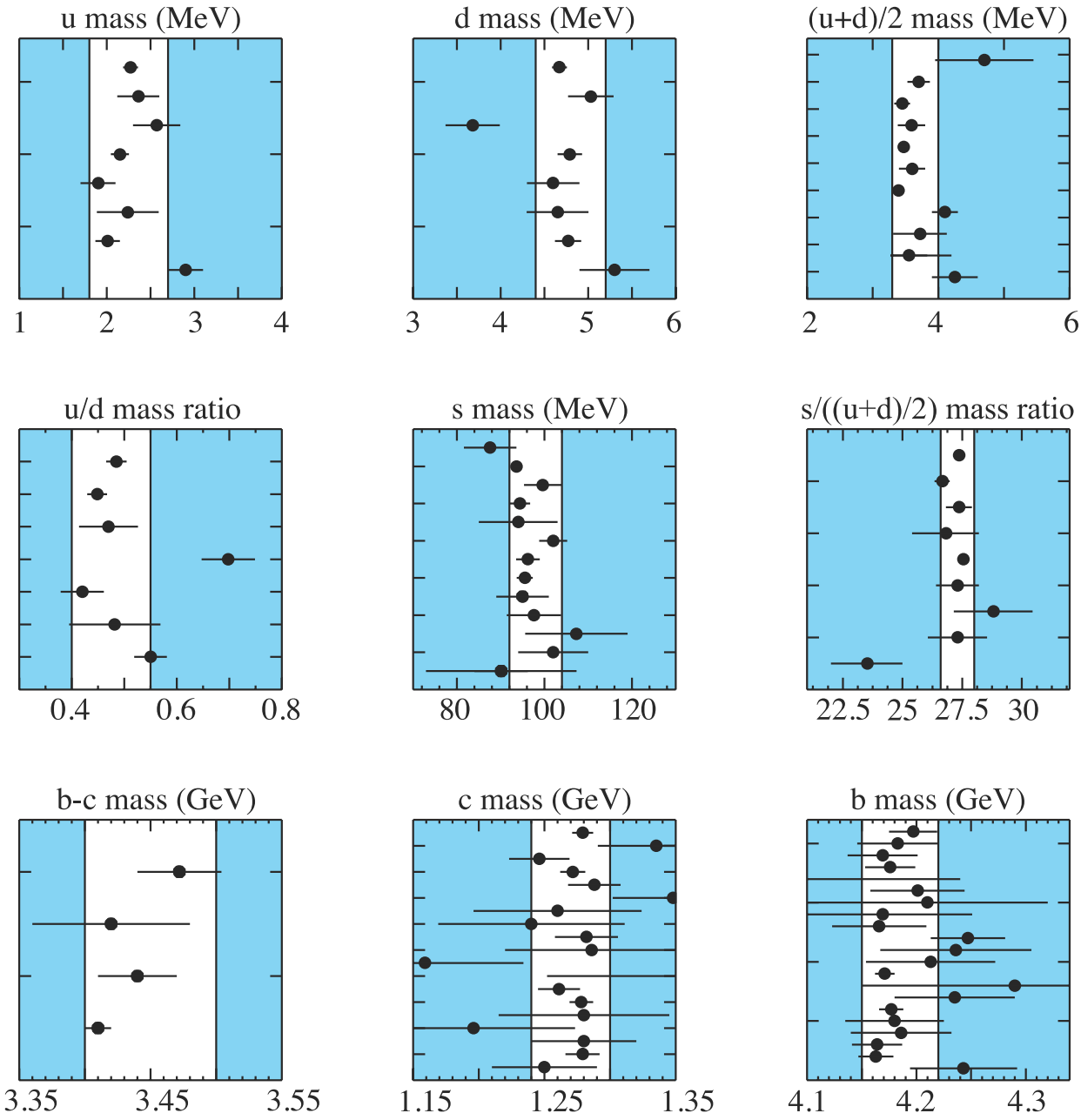

Figure 66.3: The values of each quark mass parameter taken from the Data Listings. The points are in chronological order with the more recent measurements at the top. Points from papers reporting no error bars are colored grey. The shaded regions indicate values excluded by our evaluations; some regions were determined in part through examination of Fig. 66.2.

There are many continuum extractions of the c and b quark masses, some with quoted errors of 10 MeV or smaller. There are systematic effects of comparable size, which are typically not included in these error estimates. Reference [41], for example, shows that even though the error estimate of m_c using the rapid convergence of the α_s perturbation series is only a few MeV, the central value of m_c can differ by a much larger amount depending on which algorithm (all of which are formally equally good) is used to determine m_c from

$$\overline{m}_c(\overline{m}_c) = (1.28 \pm 0.025)\,\text{GeV}$$

$$\overline{m}_b(\overline{m}_b) = (4.18 \pm 0.03)\,\text{GeV}\,, \quad m_b^{1S} = (4.65 \pm 0.03)\,\text{GeV}\,.$$

Lattice simulations of QCD lead to discretization errors which are powers of $m_Q\,a$ (modulated by logarithms); the power depends on the formulation of lattice QCD being used and in most cases is quadratic. Clearly these errors can be reduced by performing simulations at smaller lattice spacings, but also by using *improved* discretizations

of the theory. Recently, with more powerful computing resources, better algorithms and techniques, it has become possible to perform simulations in the charm quark region and beyond, also decreasing the extrapolation which has to be performed to reach the b-quark. A novel approach proposed in [64] has been to compare the lattice results for moments of correlation functions of $c\overline{c}$ quark-bilinear operators to perturbative calculations of the same quantities at 4-loop order. In this way both the strong coupling constant and the charm quark mass can be determined with remarkably small errors; in particular $\overline{m}_c(\overline{m}_c) = 1.273(6)\,\text{GeV}$ [36]. This lattice determination also uses the perturbative expression for the current-current correlator, and so has the perturbation theory systematic error discussed above. Recent updates using this correlator method, both with a very similar result, can be found in [27,37]. It should be remembered that these results were obtained in QCD with exact isospin symmetry; isospin breaking effects, including electromagnetism may well be larger or of the order of the quoted uncertainty.

As the range of heavy-quark masses which can be used in numerical simulations increases, results obtained by extrapolating the results to b-physics are becoming ever more reliable (see e.g. [27]) . Traditionally however, the main approach to controlling the discretization errors in lattice studies of heavy quark physics has been to perform simulations of the effective theories such as HQET and NRQCD. This remains an important technique, both in its own right and in providing additional information for extrapolations from lower masses to the bottom region. Using effective theories, m_b is obtained from what is essentially a computation of the difference of $M_{H_b} - m_b$, where M_{H_b} is the mass of a hadron H_b containing a b-quark. The relative error on m_b is therefore much smaller than that for $M_{H_b} - m_b$. The principal systematic errors are the matching of the effective theories to QCD and the presence of power divergences in a^{-1} in the $1/m_b$ corrections which have to be subtracted numerically. The use of HQET or NRQCD is less precise for the charm quark, but in this case, as mentioned above, direct QCD simulations are now possible.

66.6. Pole Mass

For an observable particle such as the electron, the position of the pole in the propagator is the definition of its mass. In QCD this definition of the quark mass is known as the pole mass. It is known that the on-shell quark propagator has no infrared divergences in perturbation theory [52,53], so this provides a perturbative definition of the quark mass. The pole mass cannot be used to arbitrarily high accuracy because of nonperturbative infrared effects in QCD. The full quark propagator has no pole because the quarks are confined, so that the pole mass cannot be defined outside of perturbation theory. The relation between the pole mass m_Q and the $\overline{\text{MS}}$ mass $\overline{m}_Q$ is known to three loops [54,55,56,57]

$$m_Q = \overline{m}_Q(\overline{m}_Q)\Bigg\{1 + \frac{4\overline{\alpha}_s(\overline{m}_Q)}{3\pi} + \left[-1.0414\sum_k\left(1 - \frac{4}{3}\frac{\overline{m}_{Q_k}}{\overline{m}_Q}\right) + 13.4434\right]\left[\frac{\overline{\alpha}_s(\overline{m}_Q)}{\pi}\right]^2 + \left[0.6527N_L^2 - 26.655N_L + 190.595\right]\left[\frac{\overline{\alpha}_s(\overline{m}_Q)}{\pi}\right]^3\Bigg\}, \qquad (66.20)$$

where $\overline{\alpha}_s(\mu)$ is the strong interaction coupling constants in the $\overline{\text{MS}}$ scheme, and the sum over k extends over the N_L flavors Q_k lighter than Q. The complete mass dependence of the α_s^2 term can be found in [54]; the mass dependence of the α_s^3 term is not known. For the b-quark, Eq. (66.20) reads

$$m_b = \overline{m}_b\,(\overline{m}_b)\,[1 + 0.10 + 0.05 + 0.03]\,, \qquad (66.21)$$

where the contributions from the different orders in α_s are shown explicitly. The two and three loop corrections are comparable in size and have the same sign as the one loop term. This is a signal of the asymptotic nature of the perturbation series [there is a renormalon in the pole mass]. Such a badly behaved perturbation expansion can be avoided by directly extracting the $\overline{\text{MS}}$ mass from data without extracting the pole mass as an intermediate step.

66.7. Numerical values and caveats

The quark masses in the particle data listings have been obtained by using a wide variety of methods. Each method involves its own set of approximations and uncertainties. In most cases, the errors are an estimate of the size of neglected higher-order corrections or other uncertainties. The expansion parameters for some of the approximations are not very small (for example, they are $m_K^2/\Lambda_\chi^2 \sim 0.25$ for the chiral expansion and $\Lambda_{\text{QCD}}/m_b \sim 0.1$ for the heavy-quark expansion), so an unexpectedly large coefficient in a neglected higher-order term could significantly alter the results. It is also important to note that the quark mass values can be significantly different in the different schemes.

The heavy quark masses obtained using HQET, QCD sum rules, or lattice gauge theory are consistent with each other if they are all converted into the same scheme and scale. We have specified all masses in the $\overline{\text{MS}}$ scheme. For light quarks, the renormalization scale has been chosen to be $\mu = 2\,\text{GeV}$. The light quark masses at 1 GeV are significantly different from those at 2 GeV, $\overline{m}(1\,\text{GeV})/\overline{m}(2\,\text{GeV}) \sim 1.33$. It is conventional to choose the renormalization scale equal to the quark mass for a heavy quark, so we have quoted $\overline{m}_Q(\mu)$ at $\mu = \overline{m}_Q$ for the c and b quarks. Recent analyses of inclusive B meson decays have shown that recently proposed mass definitions lead to a better behaved perturbation series than for the $\overline{\text{MS}}$ mass, and hence to more accurate mass values. We have chosen to also give values for one of these, the b quark mass in the 1S-scheme [58,59]. Other schemes that have been proposed are the PS-scheme [60] and the kinetic scheme [61].

If necessary, we have converted values in the original papers to our chosen scheme using two-loop formulæ. It is important to realized that our conversions introduce significant additional errors. In converting to the $\overline{\text{MS}}$ b-quark mass, for example, the three-loop conversions from the 1S and pole masses give values about 35 MeV and 135 MeV lower than the two-loop conversions. The uncertainty in $\alpha_s(M_Z) = 0.1181(13)$ gives an uncertainty of ± 10 MeV and ± 35 MeV respectively in the same conversions. We have not added these additional errors when we do our conversions. The α_s value in the conversion is correlated with the α_s value used in determining the quark mass, so the conversion error is not a simple additional error on the quark mass.

References:

1. See the review of QCD in this volume..
2. A.V. Manohar and H. Georgi, Nucl. Phys. **B234**, 189 (1984).
3. K.G. Chetyrkin, Phys. Lett. **B404**, 161 (1997).
4. J.A.M. Vermaseren, S.A. Larin, and T. van Ritbergen, Phys. Lett. **B405**, 327 (1997).
5. K.G. Chetyrkin, B.A. Kniehl, and M. Steinhauser, Nucl. Phys. **B510**, 61 (1998).
6. S. Weinberg, Physica **96A**, 327 (1979).
7. J. Gasser and H. Leutwyler, Ann. Phys. **158**, 142 (1984).
8. For a review, see A. Pich, Rept. on Prog. in Phys. **58**, 563 (1995).
9. S. Weinberg, Trans. N.Y. Acad. Sci. **38**, 185 (1977).
10. D.B. Kaplan and A.V. Manohar, Phys. Rev. Lett. **56**, 2004 (1986).
11. H. Leutwyler, Phys. Lett. **B374**, 163 (1996).
12. S. Weinberg, Phys. Rev. Lett. **18**, 507 (1967).
13. M.A. Shifman, A.I. Vainshtein, and V.I. Zakharov, Nucl. Phys. **B147**, 385 (1979).
14. E. Braaten, S. Narison, and A. Pich, Nucl. Phys. **B373**, 581 (1992).
15. C. Bernard *et al.*, PoS **LAT2007** (2007) 090.
16. S. Aoki *et al.* [FLAG Collab.], Eur. Phys. J. **C74**, 2890 (2014).
17. A. Bazavov *et al.*, `arXiv:0903.3598 [hep-lat]`.
18. C. Aubin *et al.* [HPQCD Collab.], Phys. Rev. **D70**, 031504 (2004).
19. C. Aubin *et al.* [MILC Collab.], Phys. Rev. **D70**, 114501 (2004).
20. B. Blossier *et al.* [ETM Collab.], Phys. Rev. **D82**, 114513 (2010).
21. A. Bazavov *et al.* [MILC Collab.], PoS **CD09** (2009) 007.
22. A. Bazavov *et al.*, PoS **LATTICE2010** (2010) 083.
23. S. Durr *et al.*, Phys. Lett. **B701**, 265 (2011).
24. S. Durr *et al.*, JHEP **1108**, 148 (2011).

25. R. Arthur *et al.* [RBC and UKQCD Collabs.], Phys. Rev. **D87**, 094514 (2013).
26. A. Bazavov *et al.* [Fermilab Lattice and MILC Collabs.], Phys. Rev. **D90**, 074509 (2014).
27. B. Chakraborty *et al.*, Phys. Rev. **D91**, 054508 (2015).
28. N. Carrasco *et al.* [European Twisted Mass Collab.], Nucl. Phys. **B887**, 19 (2014).
29. *"Domain wall QCD with physical quark masses,"* T. Blum *et al.* [RBC and UKQCD Collabs.], `arXiv:1411.7017 [hep-lat]`.
30. S. Borsanyi *et al.*, Science **347**, 1452 (2015).
31. Y. Aoki *et al.* [RBC and UKQCD Collabs.], Phys. Rev. **D83**, 074508 (2011).
32. S. Basak *et al.* [MILC Collab.], J. Phys. Conf. Ser. **640** (2015) 1, 012052.
33. T. Blum *et al.*, Phys. Rev. **D82**, 094508 (2010).
34. S. Aoki *et al.*, Phys. Rev. **D86**, 034507 (2012).
35. C.T.H. Davies *et al.*, Phys. Rev. Lett. **104**, 132003 (2010).
36. C. McNeile *et al.*, Phys. Rev. **D82**, 034512 (2010).
37. K. Nakayama, B. Fahy, and S. Hashimoto, arXiv:1511.09163 [hep-lat]..
38. C. Aubin *et al.* [MILC Collab.], Nucl. Phys. (Proc. Supp.) **140**, 231 (2005).
39. C. Aubin *et al.* [MILC Collab.], Phys. Rev. **D70**, 114501 (2004).
40. G. Colangelo *et al.*, Eur. Phys. J. **C71**, 1695 (2011).
41. B. Dehnadi *et al.*, `arXiv:1102.2264 [hep-ph]`.
42. T. Blum *et al.*, Phys. Rev. **D76**, 114508 (2007).
43. G. Colangelo *et al.*, Eur. Phys. J. **C71**, 1695 (2011).
44. A. Ali Khan *et al.* [CP-PACS Collab.], Phys. Rev. **D65**, 054505 (2002); [Erratum-ibid. D **67** (2003) 059901].
45. N. Isgur and M.B. Wise, Phys. Lett. **B232**, 113 (1989), *ibid*, **B237**, 527 (1990).
46. G.T. Bodwin, E. Braaten, and G.P. Lepage, Phys. Rev. **D51**, 1125 (1995).
47. A.H. Hoang, Phys. Rev. **D61**, 034005 (2000).
48. K. Melnikov and A. Yelkhovsky, Phys. Rev. **D59**, 114009 (1999).
49. M. Beneke and A. Signer, Phys. Lett. **B471**, 233 (1999).
50. A.X. El-Khadra, A.S. Kronfeld, and P.B. Mackenzie, Phys. Rev. **D55**, 3933 (1997).
51. S. Aoki, Y. Kuramashi, and S.i. Tominaga, Prog. Theor. Phys. **109**, 383 (2003).
52. R. Tarrach, Nucl. Phys. **B183**, 384 (1981).
53. A. Kronfeld, Phys. Rev. **D58**, 051501 (1998).
54. N. Gray *et al.*, Z. Phys. **C48**, 673 (1990).
55. D.J. Broadhurst, N. Gray, and K. Schilcher, Z. Phys. **C52**, 111 (1991).
56. K.G. Chetyrkin and M. Steinhauser, Phys. Rev. Lett. **83**, 4001 (1999).
57. K. Melnikov and T. van Ritbergen, Phys. Lett. **B482**, 99 (2000).
58. A.H. Hoang, Z. Ligeti, A.V. Manohar, Phys. Rev. Lett. **82**, 277 (1999).
59. A.H. Hoang, Z. Ligeti, A.V. Manohar, Phys. Rev. **D59**, 074017 (1999).
60. M. Beneke, Phys. Lett. **B434**, 115 (1998).
61. P. Gambino and N. Uraltsev, Eur. Phys. J. **C34**, 181 (2004).
62. G. Martinelli *et al.*, Nucl. Phys. **B445**, 81 (1995).
63. K. Jansen *et al.*, Phys. Lett. **B372**, 275 (1996).
64. I. Allison *et al.* [HPQCD Collab.], Phys. Rev. **D78**, 054513 (2008).

67. Top Quark

Updated September 2017 by T.M. Liss (The City College of New York), F. Maltoni (Univ. Catholique de Louvain), and A. Quadt (Univ. Göttingen).

67.1. Introduction

In the Standard Model (SM), the left-handed top quark is the $Q = 2/3$, $T_3 = +1/2$ member of the weak-isospin doublet containing the bottom quark, while the right-handed top is an $SU(2)_L$ singlet (see the review on the "Electroweak Model and Constraints on New Physics" for more information). Its phenomenology is driven by its large mass. Being heavier than a W boson, it is the only quark that decays semi-weakly, i.e., into a real W boson and a b quark. Therefore, it has a very short lifetime and decays before hadronization can occur. In addition, it is the only quark whose Yukawa coupling to the Higgs boson is order of unity. For these reasons, the top quark plays a special role in the Standard Model and in many extensions thereof. Its phenomenology provides a unique laboratory where our understanding of the strong interactions, both in the perturbative and non-perturbative regimes, can be tested. An accurate knowledge of its properties (mass, couplings, production cross section, decay branching ratios, *etc.*) can bring key information on fundamental interactions at the electroweak symmetry-breaking scale and beyond. This review provides a concise discussion of the experimental and theoretical issues involved in the determination the top-quark properties.

67.2. Top-quark production at the Tevatron and LHC

In hadron collisions, top quarks are produced dominantly in pairs through the processes $q\overline{q} \to t\overline{t}$ and $gg \to t\overline{t}$, at leading order in QCD. Approximately 85% of the production cross section at the Tevatron ($p\overline{p}$ at 1.96 TeV) is from $q\overline{q}$ annihilation, with the remainder from gluon-gluon fusion, while at LHC (pp) energies about 90% of the production is from the latter process at $\sqrt{s} = 14$ TeV ($\approx 80\%$ at $\sqrt{s} = 7$ TeV).

Predictions for the top-quark production total cross sections are now available at next-to-next-to leading order (NNLO) with next-to-next-to-leading-log (NNLL) soft gluon resummation [1]. Assuming a top-quark mass of 173.3 GeV/c^2, close to the Tevatron + LHC average [2], the resulting theoretical prediction of the top-quark pair cross-section at NNLO+NNLL accuracy at the Tevatron at $\sqrt{s} = 1.96$ TeV is $\sigma_{t\bar{t}} = 7.16^{+0.11+0.17}_{-0.20-0.12}$ pb where the first uncertainty is from scale dependence and the second from parton distribution functions. At the LHC, assuming a top-quark mass of 172.5 GeV/c^2 the cross sections are: $\sigma_{t\bar{t}} = 177.3^{+4.6+9.0}_{-6.0-9.0}$ pb at $\sqrt{s} = 7$ TeV, $\sigma_{t\bar{t}} = 252.9^{+6.4+11.5}_{-8.6-11.5}$ pb at $\sqrt{s} = 8$ TeV, $\sigma_{t\bar{t}} = 831.8^{+19.8+35.1}_{-29.2-35.1}$ pb at $\sqrt{s} = 13$ TeV, and $\sigma_{t\bar{t}} = 984.5^{+23.2+41.3}_{-34.7-41.3}$ pb at $\sqrt{s} = 14$ TeV [1].

Electroweak single top-quark production mechanisms, namely from $q\overline{q}' \to t\overline{b}$ [3], $qb \to q't$ [4], mediated by virtual s-channel and t-channel W-bosons, and Wt-associated production, through $bg \to W^-t$, lead to somewhat smaller cross sections. For example, t-channel production, while suppressed by the weak coupling with respect to the strong pair production, is kinematically enhanced, resulting in a sizable cross section both at Tevatron and LHC energies. At the Tevatron, the t- and s-channel cross sections of top and antitop are identical, while at the LHC they are not, due to the charge-asymmetric initial state. Approximate NNLO cross sections for t-channel single top-quark production ($t + \bar{t}$) are calculated for $m_t = 173.3$ GeV/c^2 to be $2.06^{+0.13}_{-0.13}$ pb in $p\overline{p}$ collisions at $\sqrt{s} = 1.96$ TeV (scale and parton distribution functions uncertainties are combined in quadrature) [5]. Recently, calculations at NNLO accuracy for the t-channel cross section at the LHC have appeared [6,7], predicting ($m_t = 172.5$ GeV/c^2): $\sigma_{t+\bar{t}} = 64.0^{+0.77}_{-0.38}$ pb at $\sqrt{s} = 7$ TeV, $\sigma_{t+\bar{t}} = 84.6^{+1.0}_{-0.51}$ pb at $\sqrt{s} = 8$ TeV, $\sigma_{t+\bar{t}} = 215^{+2.1}_{-1.3}$ pb at $\sqrt{s} = 13$ TeV, and $\sigma_{t+\bar{t}} = 245^{+2.7}_{-1.3}$ pb at $\sqrt{s} = 14$ TeV, where the quoted uncertainties are from scale variation only. For the s-channel, NNLO approximated calculations yield $1.03^{+0.05}_{-0.05}$ pb for the Tevatron, and $4.5^{+0.2}_{-0.2}(5.5^{+0.2}_{-0.2})$ pb for $\sqrt{s} = 7$ (8) TeV at the LHC, with 69% (31%) of top (anti-top) quarks [8]. While negligible at the Tevatron, at LHC energies the Wt-associated production becomes relevant. At $\sqrt{s} = 7$ (8) TeV, an approximate NNLO calculation gives $15.5^{+1.2}_{-1.2}(22.1^{+1.5}_{-1.5})$ pb ($t + \bar{t}$), with an equal proportion of top and anti-top quarks [9].

Assuming $|V_{tb}| \gg |V_{td}|, |V_{ts}|$ (see the review "The CKM Quark-Mixing Matrix" for more information), the cross sections for single top production are proportional to $|V_{tb}|^2$, and no extra hypothesis is needed on the number of quark families or on the unitarity of the CKM matrix in extracting $|V_{tb}|$. Separate measurements of the s- and t-channel processes provide sensitivity to physics beyond the Standard Model [10].

With a mass above the Wb threshold, and $|V_{tb}| \gg |V_{td}|$, $|V_{ts}|$, the decay width of the top quark is expected to be dominated by the two-body channel $t \to Wb$. Neglecting terms of order m_b^2/m_t^2, α_s^2, and $(\alpha_s/\pi)M_W^2/m_t^2$, the width predicted in the SM at NLO is [11]:

$$\Gamma_t = \frac{G_F m_t^3}{8\pi\sqrt{2}} \left(1 - \frac{M_W^2}{m_t^2}\right)^2 \left(1 + 2\frac{M_W^2}{m_t^2}\right) \left[1 - \frac{2\alpha_s}{3\pi}\left(\frac{2\pi^2}{3} - \frac{5}{2}\right)\right], \tag{67.1}$$

where m_t refers to the top-quark pole mass. The width for a value of $m_t = 173.3$ GeV/c^2 is 1.35 GeV/c^2 (we use $\alpha_s(M_Z) = 0.118$) and increases with mass. With its correspondingly short lifetime of $\approx 0.5 \times 10^{-24}$ s, the top quark is expected to decay before top-flavored hadrons or $t\overline{t}$-quarkonium-bound states can form [12]. In fact, since the decay time is close to the would-be-resonance binding time, a peak will be visible in e^+e^- scattering at the $t\overline{t}$ threshold [13] and it is in principle present (yet very difficult to measure) in hadron collisions, too [14]. The order α_s^2 QCD corrections to Γ_t are also available [15], thereby improving the overall theoretical accuracy to better than 1%.

The final states for the leading pair-production process can be divided into three classes:

A. $t\bar{t} \to W^+ b\, W^- \overline{b} \to q\,\overline{q}'\, b\, q''\,\overline{q}''' \,\overline{b}$, (45.7%)
B. $t\bar{t} \to W^+ b\, W^- \overline{b} \to q\,\overline{q}'\, b\, \ell^-\,\overline{\nu}_\ell\, \overline{b} + \ell^+\,\nu_\ell\, b\, q''\,\overline{q}'''\,\overline{b}$, (43.8%)
C. $t\bar{t} \to W^+ b\, W^- \overline{b} \to \ell^+\,\nu_\ell\, b\, \ell'^-\,\overline{\nu}_{\ell'}\,\overline{b}$. (10.5%)

The quarks in the final state evolve into jets of hadrons. A, B, and C are referred to as the all-jets, lepton+jets (ℓ+jets), and dilepton ($\ell\ell$) channels, respectively. Their relative contributions, including hadronic corrections, are given in parentheses assuming lepton universality. While ℓ in the above processes refers to e, μ, or τ, most of the analyses distinguish the e and μ from the τ channel, which is more difficult to reconstruct. Therefore, in what follows, we will use ℓ to refer to e or μ, unless otherwise noted. Here, typically leptonic decays of τ are included. In addition to the quarks resulting from the top-quark decays, extra QCD radiation (quarks and gluons) from the colored particles in the event can lead to extra jets.

The number of jets reconstructed in the detectors depends on the decay kinematics, as well as on the algorithm for reconstructing jets used by the analysis. Information on the transverse momenta of neutrinos is obtained from the imbalance in transverse momentum measured in each event (missing p_T, which is here also called missing E_T).

The identification of top quarks in the electroweak single top channel is much more difficult than in the QCD $t\overline{t}$ channel, due to a less distinctive signature and significantly larger backgrounds, mostly due to $t\overline{t}$ and W+jets production.

Fully exclusive predictions via Monte Carlo generators for the $t\overline{t}$ and single top production processes at NLO accuracy in QCD, including top-quark decays and possibly off-shell effects are available [16,17] through the MC@NLO [18] and POWHEG [19] methods.

Besides fully inclusive QCD or EW top-quark production, more exclusive final states can be accessed at hadron colliders, whose cross sections are typically much smaller, yet can provide key information on the properties of the top quark. For all relevant final states (*e.g.*, $t\bar{t}V$, $t\bar{t}VV$ with $V = \gamma, W, Z$, $t\bar{t}H, t\bar{t}$+jets, $t\bar{t}b\bar{b}, t\bar{t}t\bar{t}$) automatic or semi-automatic predictions at NLO accuracy in QCD also in the form of event generators, *i.e.*, interfaced to parton-shower programs, are available (see the review "Monte Carlo event generators" for more information).

67.3. Top-quark measurements

Since the discovery of the top quark, direct measurements of $t\bar{t}$ production have been made at five center-of-mass energies in pp or $p\bar{p}$ and one in pPb collisions, providing stringent tests of QCD. The first measurements were made in Run I at the Tevatron at $\sqrt{s} = 1.8$ TeV. In Run II at the Tevatron relatively precise measurements were made at $\sqrt{s} = 1.96$ TeV. Finally, beginning in 2010, measurements have been made at the LHC at $\sqrt{s} = 7$ TeV, $\sqrt{s} = 8$ TeV, and $\sqrt{s} = 13$ TeV, and recently also in a dedicated low energy run at $\sqrt{s} = 5.02$ TeV and at 8.16 TeV in pPb collisions.

Production of single top quarks through electroweak interactions has now been measured with good precision at the Tevatron at $\sqrt{s} = 1.96$ TeV, and at the LHC at $\sqrt{s} = 7$ TeV, $\sqrt{s} = 8$ TeV, and also at $\sqrt{s} = 13$ TeV. Measurements at the Tevatron have managed to separate the s- and t-channel production cross sections, and at the LHC, the Wt mechanism as well, though the t-channel is measured with best precision to date. The measurements allow an extraction of the CKM matrix element V_{tb}. Also more exclusive production modes and top-quark properties have been measured in single-top production.

With approximately 10 fb^{-1} of Tevatron data, and almost 5 fb^{-1} at 7 TeV, 20 fb^{-1} at 8 TeV and 36 fb^{-1} at 13 TeV at the LHC, many properties of the top quark have been measured with high precision. These include properties related to the production mechanism, such as $t\bar{t}$ spin correlations, forward-backward or charge asymmetries, and differential production cross sections, as well as properties related to the tWb decay vertex, such as the helicity of the W-bosons from the top-quark decay. Recently, also studies of the $t\bar{t}\gamma$ and the $t\bar{t}Z$ interactions have been made. In addition, many searches for physics beyond the Standard Model or $t\bar{t}h$ or th production are being performed with increasing reach in both production and decay channels.

In the following sections we review the current status of measurements of the characteristics of the top quark.

67.3.1. *Top-quark production* :

67.3.1.1. *$t\bar{t}$ production:*

Fig. 67.1 summarizes the $t\bar{t}$ production cross-section measurements from both the Tevatron and LHC. Please note that some cross section measurements at the LHC have luminosity-related uncertainties which have improved in the meantime [20]. The most recent measurement from DØ [21]($p\bar{p}$ at $\sqrt{s} = 1.96$ TeV), combining the measurements from the dilepton and lepton plus jets final states in 9.7 fb^{-1}, is $7.26 \pm 0.13^{+0.57}_{-0.50}$ pb.

From CDF the most precise measurement made recently [22] is in 8.8 fb^{-1} in the dilepton channel requiring at least one b-tag, yielding 7.09 ± 0.84 pb. Both of these measurements assume a top-quark mass of 172.5 GeV/c^2. The dependence of the cross-section measurements on the value chosen for the mass is less than that of the theory calculations because it only affects the determination of the acceptance. In some analyses also the shape of topological variables might be modified.

Combining the recent cross section measurements with older ones in other channels yields $\sigma_{t\bar{t}} = 7.63 \pm 0.50$ pb (6.6%) for CDF, $\sigma_{t\bar{t}} = 7.56 \pm 0.59$ pb (7.8%) for DØ and $\sigma_{t\bar{t}} = 7.60 \pm 0.41$ pb (5.4%) for the Tevatron combination [23] in good agreement with the SM expectation of $7.35^{+0.28}_{-0.33}$ pb at NNLO+NNLL in perturbative QCD [1] for a top mass of 172.5 GeV. The contributions to the uncertainty are 0.20 pb from statistical sources, 0.29 pb from systematic sources, and 0.21 pb from the uncertainty on the integrated luminosity.

CDF has measured the $t\bar{t}$ production cross section in the dilepton channel with one hadronically decaying tau in 9.0 fb^{-1}, yielding $\sigma_{t\bar{t}} = 8.1 \pm 2.1$ pb. By separately identifying the single-tau and the ditau components, they measure the branching fraction of the top quark into the tau lepton, tau neutrino, and bottom quark to be $(9.6 \pm 2.8)\%$ [24]. CDF also performs measurements of the $t\bar{t}$ production cross section normalized to the Z production cross section in order to reduce the impact of the luminosity uncertainty.

DØ has performed a measurement of differential $t\bar{t}$ cross sections in 9.7 fb^{-1} of lepton+jets data as a function of the transverse momentum and absolute value of the rapidity of the top quarks as well as of the invariant mass of the $t\bar{t}$ pair [25]. Observed differential cross sections are consistent with standard model predictions.

The LHC experiments ATLAS and CMS use similar techniques to measure the $t\bar{t}$ cross section in pp collisions. The most precise measurements come from the dilepton channel, and in particular the $e\mu$ channel. At $\sqrt{s} = 7$ TeV, ATLAS uses 4.6 fb^{-1} of $e\mu$ events in which they select an extremely clean sample and determine the $t\bar{t}$ cross section simultaneously with the efficiency to reconstruct and tag b-jets, yielding $\sigma_{t\bar{t}} = 182.9 \pm 7.1$ pb, corresponding to 3.9% precision [26]. Other measurements by ATLAS at $\sqrt{s} = 7$ TeV, include a measurement in 0.7 fb^{-1} in the lepton+jets channel [27], in the dilepton channel [28], and in 1.02 fb^{-1} in the all-hadronic channel [29], which together yield a combined value of $\sigma_{t\bar{t}} = 177 \pm 3(stat.)^{+8}_{-7}(syst.) \pm 7(lumi.)$ pb (6.2%) assuming $m_t = 172.5$ GeV/c^2 [30]. In 4.7 fb^{-1} of all-jets events, they obtain $\sigma_{t\bar{t}} = 168 \pm 62$ pb [31]. Further analyses in the hadronic τ plus jets channel in 1.67 fb^{-1} [32] and the hadronic τ + lepton channel in 2.05 fb^{-1} [33], and the all-hadronic channel in 4.7 fb^{-1} [31] yield consistent albeit less precise results. The most precise measurement from CMS is also obtained in the dilepton channel, where they measure $\sigma_{t\bar{t}} = 162 \pm 2(stat.) \pm 5(syst.) \pm 4(lumi.)$ pb, corresponding to a 4.2% precision [34]. Other measurements at $\sqrt{s} = 7$ TeV from CMS include measurements with 2.3 fb^{-1} in the e/μ+jets channel [35], dilepton channel [34], with 3.5 fb^{-1} in the all-hadronic channel [36], with 2.2 fb^{-1} in the lepton+τ channel [37], and with 3.9 fb^{-1} in the τ+jets channel [38]. ATLAS and CMS also provide a combined cross section at $\sqrt{s} = 7$ TeV of $173.3 \pm 2.3(stat.) \pm 7.6(syst.) \pm 6.3(lumi.)$ pb using slightly older results based on $0.7 - 1.1$ fb^{-1} [39].

At $\sqrt{s} = 8$ TeV, ATLAS measures the $t\bar{t}$ cross section with 20.3 fb^{-1} using $e\mu$ dilepton events, with a simultaneous measurement of the $b-$tagging efficiency, yielding $\sigma_{t\bar{t}} = 242.4 \pm 1.7(stat.) \pm 5.5(syst.) \pm 7.5(lumi.) \pm 4.2(beam\,energy)$ pb [26] assuming $m_t = 172.5$ GeV/c^2, which corresponds to a 4.7% precision. In the lepton+jets channel, they measure $\sigma_{t\bar{t}} = 260 \pm 1(stat.)^{+20}_{-23}(syst.) \pm 8(lumi.) \pm 4(beam\,energy)$ pb [41] in 20.3 fb^{-1} using a likelihood discriminant fit and b-jet identification. Very recently, ATLAS performed a new analysis in 20.2 fb^{-1} lepton+jets events. They model the W+jets background using Z+jets data and employ neural networks in three jet-multiplicity and b-jet multiplicity regions for the signal and background separation, yielding $\sigma_{t\bar{t}} = 248.3 \pm 0.7(stat.) \pm 13.4(syst.) \pm 4.7(lumi.)$ pb [42]. Recently, ATLAS also performed a cross section measurement in the hadronic τ+jets channel yielding consistent, albeit less precise results [43]. CMS performs a template fit to the M_{lb} mass distribution using 19.6 fb^{-1} in the lepton+jets channel yielding $\sigma_{t\bar{t}} = 228.5 \pm 3.8(stat.) \pm 13.7(syst.) \pm 6(lumi.)$ pb [44]. These 8 TeV measurements are in agreement with QCD predictions up to next-to-next-to-leading order. In the $e\mu$ channel, using 19.7 fb^{-1}, the cross sections are extracted using a binned likelihood fit to multi-differential final state distributions related to identified b quark and other jets in the event, yielding $\sigma_{t\bar{t}} = 244.9 \pm 1.4(stat.)^{+6.3}_{-5.5}(sys.) \pm 6.4(lumi.)$ pb [46]. The cross section and its ratio between 7 TeV and 8 TeV measurements are found to be consistent with pQCD calculations. The cross section is also measured in the hadronic τ+jets channel, yielding $\sigma_{t\bar{t}} = 257 \pm 3(stat.) \pm 24(syst.) \pm 7(lumi.)$ pb [47] and in the all-jets final state giving $\sigma_{t\bar{t}} = 275.6 \pm 6.1(stat.) \pm 37.8(syst.) \pm 7.2(lumi.)$ pb [48]. In combination of the most precise $e\mu$ measurements in $5.3 - 20.3$ fb^{-1}, ATLAS and CMS together yield at 8 TeV $\sigma_{t\bar{t}} = 241.5 \pm 1.4(stat.) \pm 5.7(syst.) \pm 6.2(lumi.)$ pb [49], which corresponds to a 3.5% precision, challenging the precision of the corresponding theoretical predictions.

The LHCb collaboration presented the first observation of top-quark production in the forward region in pp-collisions. The $W + b$ final state with $W \to \mu\nu$ is reconstructed using muons with a transverse momentum, p_T, larger than 25 GeV in the pseudorapidity range $2.0 < \eta < 4.5$. The b-jets are required to have 50 GeV $< p_T <$ 100 GeV and $2.2 < \eta < 4.2$, while the transverse component of the sum of the muon and b-jet momenta must satisfy $p_T > 20$ GeV. The results are based on data corresponding to integrated luminosities of 1.0 and 2.0 fb^{-1} collected at center-of-mass energies of 7 and 8 TeV by LHCb. The inclusive top quark production cross sections in the fiducial region are $\sigma_{t\bar{t}} = 239 \pm 53(stat.) \pm 38(syst.)$ pb at 7 TeV, and $\sigma_{t\bar{t}} = 289 \pm 43(stat.) \pm 46(syst.)$ pb at 8 TeV [50].

ATLAS and CMS have also measured the $t\bar{t}$ production cross section with early Run-II data at $\sqrt{s} = 13$ TeV in $e\mu$ events with at least one b-tag. ATLAS uses 78 pb^{-1} and obtains $\sigma_{t\bar{t}} = 825 \pm 114$ pb [51]. CMS uses 42 pb^{-1} and measures $\sigma_{t\bar{t}} = 836 \pm 27(stat.) \pm 88(syst.) \pm 100(lumi.)$ pb [52]. Very recently, ATLAS used 3.2 fb^{-1} in the $e\mu$ channel, resulting in $\sigma_{t\bar{t}} = 818 \pm 8(stat.) \pm 27(syst.) \pm 19(lumi.) \pm 12(beam)$ pb, consistent with theoretical QCD calculations at NNLO [53].

A recent 'fiducial' measurement by ATLAS, corresponding to the experimental acceptance of the leptons uses 85 pb^{-1} of lepton+jets data and a simple counting approach. ATLAS measures a cross section of $\sigma_{t\bar{t}} = 817 \pm 13(stat.) \pm 103(syst.) \pm 88(lumi)$ pb [54]. CMS uses 2.2 fb^{-1} of $e\mu$ data with two or more jets and at least one b-tag, yielding $\sigma_{t\bar{t}} = 815 \pm 9(stat.) \pm 38(syst.) \pm 19(lumi.)$ pb, in agreement with the expectation from the standard model [55]. In 2.2 fb^{-1} of lepton+jets events, CMS performs a likelihood fit to the invariant mass distribution of the isolated lepton and the b-tagged jet in categories of jet multiplicity, resulting in $\sigma_{t\bar{t}} = 888 \pm 2(stat.)^{+26}_{-28}(syst.) \pm 20(lumi.)$ pb [56], in agreement with the standard model prediction. This result is also used to extract the top-quark mass. In the all-jets channel, CMS uses 2.53 fb^{-1} of data, yielding a cross section of $\sigma_{t\bar{t}} = 834 \pm 25(stat.) \pm 23(lumi.)$ pb [57]. Also differential cross sections as a function of the leading top quark transverse momentum are measured. The measured top quark p_T spectrum is found to be significantly softer than the theory predictions.

Recently, CMS has also measured the top-quark pair production cross section in a special LHC run with $\sqrt{s} = 5.02$ TeV, accumulating 27.4 pb^{-1}. The measurement is performed by analyzing events with at least one charged lepton. The measured cross section is $\sigma_{t\bar{t}} = 69.5 \pm 8.4$ pb [58], in agreement with the expectation from the standard model. In order to test consistency of the cross-section measurements with some systematic uncertainties cancelling out while testing pQCD and PDFs, cross-section ratios between mesurements at 7 TeV and at 8 TeV are performed and cited in several cases. In other cases, the cross-section ratio between $t\bar{t}$- and Z-production is determined as that is independent of luminosity uncertainties, but keeps its sensitivity to the ratio of gluon versus quark PDFs. These experimental results should be compared to the theoretical calculations at NNLO+NNLL that yield $7.16^{+0.20}_{-0.23}$ pb for top-quark mass of 173.3 GeV/c^2 [1] at $\sqrt{s} = 1.96$ TeV, and for top-quark mass of 173.2 GeV/c^2 $\sigma_{t\bar{t}} = 173.6^{+4.5+8.9}_{-5.9-8.9}$ pb at $\sqrt{s} = 7$ TeV, $\sigma_{t\bar{t}} = 247.7^{+6.3+11.5}_{-8.5-11.5}$ pb at $\sqrt{s} = 8$ TeV, and $\sigma_{t\bar{t}} = 816.0^{+19.4+34.4}_{-28.6-34.4}$ pb at $\sqrt{s} = 13$ TeV, at the LHC [1]. CMS also performed a measurement of top-quark pair production in pPb heavy ion collisions at $\sqrt{s} = 8.16$ TeV in 174 nb^{-1} of lepton+jets events. They measure a cross section of $\sigma_{t\bar{t}} = 45 \pm 8$ pb, which is consistent with pQCD calculations and with the scaled pp data [59].

In Fig. 67.1, one sees the importance of $p\overline{p}$ at Tevatron energies where the valence antiquarks in the antiprotons contribute to the dominant $q\overline{q}$ production mechanism. At LHC energies, the dominant production mode is gluon-gluon fusion and the pp-$p\overline{p}$ difference nearly disappears. The excellent agreement of these measurements with the theory calculations is a strong validation of QCD and the soft-gluon resummation techniques employed in the calculations. The measurements reach high precision and provide stringent tests of pQCD calculations at NNLO+NNLL level including their respective PDF uncertainties.

Most of these measurements assume a $t \to Wb$ branching ratio of 100%. CDF and DØ have made direct measurements of the $t \to Wb$ branching ratio [61]. Comparing the number of events with 0, 1 and 2 tagged b jets in the lepton+jets channel, and also in the dilepton channel, using the known b-tagging efficiency, the ratio $R = B(t \to Wb)/\sum_{q=d,s,b} B(t \to Wq)$ can be extracted. In 5.4 fb^{-1} of data, DØ measures $R = 0.90 \pm 0.04$, 2.5σ from unity. The currently most precise measurement was made by CMS in 19.7 fb^{-1} at $\sqrt{s} = 8$ TeV. They find $R = 1.014 \pm 0.003(stat.) \pm 0.032(syst.)$ and $R > 0.955$ at 95% C.L. [62]. A significant deviation of R from unity would imply either non-SM top-quark decay (for example a flavor-changing neutral-current decay), or a fourth generation of quarks.

Thanks to the large available event samples, the Tevatron and the LHC experiments also performed differential cross-section measurements in $t\bar{t}$ production. Such measurements are crucial, as they allow even more stringent tests of perturbative QCD as description of the production mechanism, allow the extraction or the use of PDF fits, and enhance the sensitivity to possible new physics contributions, especially now that NNLO predictions for the main differential observables in $t\bar{t}$ prediction have become available [65]. Furthermore, such measurements reduce the uncertainty in the description of $t\bar{t}$ production as background in Higgs physics and searches for rare processes or beyond Standard Model physics. Differential cross sections are typically measured by a selection of candidate events, their kinematic reconstruction and subsequent unfolding of the obtained event counts in bins of kinematic distributions in order to correct for detector resolution effects, acceptance and migration effects. In some cases a bin-by-bin unfolding is used, while other analyses use more sophisticated techniques.

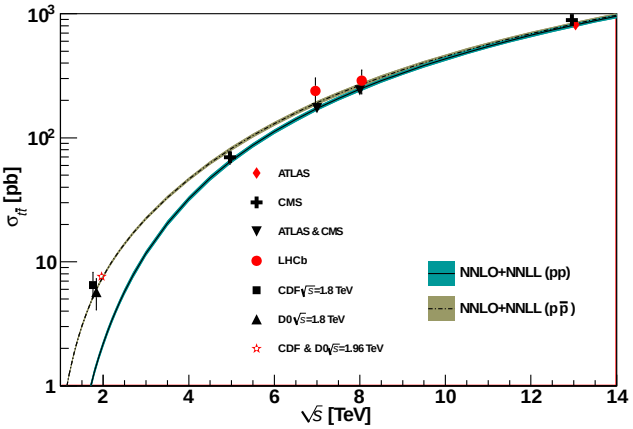

Figure 67.1: Measured and predicted $t\bar{t}$ production cross sections from Tevatron energies in $p\overline{p}$ collisions to LHC energies in pp collisions. Tevatron data points at $\sqrt{s} = 1.8$ TeV are from Refs. [63,64]. Those at $\sqrt{s} = 1.96$ TeV are from Refs. [21–23]. The ATLAS, CMS, and LHCb data points are from Refs. [26,34,39,40,45,49,50,53,56], and [58], respectively. Theory curves and uncertainties are generated using [1] for $m_t = 172.5$ GeV/c^2, the m_t value assumed in the cross-section measurements. Figure adapted from Ref. [60].

Experiments at Tevatron and LHC measure the differential cross section with respect to the $t\bar{t}$ invariant mass, $d\sigma/dM_{t\bar{t}}$. The spectra are fully corrected for detector efficiency and resolution effects and are compared to several Monte Carlo simulations as well as selected theoretical calculations.

Using 9.45 fb^{-1}, CDF measured $d\sigma/dM_{t\bar{t}}$, in the lepton+jets channel providing sensitivity to a variety of exotic particles decaying into $t\bar{t}$ pairs [66]. In 9.7 fb^{-1} of lepton+jets data, DØ measured the differential $t\bar{t}$ production cross section with respect to the transverse momentum and absolute rapidity of the top quarks as well as of the invariant mass of the $t\bar{t}$ pair [25], which are all found to be in good agreement with the SM predictions.

ATLAS measured the differential $t\bar{t}$ production cross section with respect to the top-quark transverse momentum, and of the mass, transverse momentum and rapidity of the top quark, the antitop quark as well as the $t\bar{t}$ system in 4.6 fb^{-1} at $\sqrt{s} = 7$ TeV in the lepton+jets channel [67–69]. It is found that data is softer than all predictions for higher values of the mass of the $t\bar{t}$ system as well as in the tail of the top-quark p_T spectrum beginning at 200 GeV, particularly in the case of the `Alpgen`+`Herwig` generator. The $M_{t\bar{t}}$ spectrum is not well described by NLO+NNLL calculations and there are also disagreements between the measured rapidity of the $t\bar{t}$ system spectrum and the `MC@NLO`+`Herwig` and `POWHEG`+`Herwig` generators, both evaluated with the CT10 PDF set. All distributions show a preference for HERAPDF1.5 when used for the NLO QCD predictions. In 5.0 fb^{-1} of $\sqrt{s} = 7$ TeV data in the lepton+jets and the dilepton channels, CMS measured normalised differential $t\bar{t}$ cross sections with

respect to kinematic properties of the final-state charged leptons and jets associated to b-quarks, as well as those of the top quarks and the $t\bar{t}$ system. The data are compared with several predictions from perturbative QCD calculations and found to be consistent [70].

ATLAS uses 4.6 fb^{-1} of data at 7 TeV and 20.2 fb^{-1} at 8 TeV to measure the differential $t\bar{t}$ cross section as a function of the mass, the transverse momentum and the rapidity of the $t\bar{t}$ system [71]. The results are compared with different Monte Carlo generators and theoretical calculations of $t\bar{t}$ production and found to be consistent with the majority of predictions in a wide kinematic range. Using 20.3 fb^{-1} of $t\bar{t}$ events in the lepton+jets channel, ATLAS measures the normalized differential cross sections of $t\bar{t}$ production as a function of the top-quark, $t\bar{t}$ system and event-level kinematic observables [72]. The observables have been chosen to emphasize the $t\bar{t}$ production process and to be sensitive to effects of initial- and final-state radiation, to the different parton distribution functions, and to non-resonant processes and higher-order corrections. The results are in fair agreement with the predictions over a wide kinematic range. Nevertheless, most generators predict a harder top-quark transverse momentum distribution at high values than what is observed in the data. Predictions beyond NLO accuracy improve the agreement with data at high top-quark transverse momenta. Using the current settings in the Monte Carlo programs and parton distribution functions, the rapidity distributions are not well modelled by any generator under consideration. However, the level of agreement is improved when more recent sets of parton distribution functions are used. Recently, using 20.3 fb^{-1} of 8 TeV data, ATLAS performed a dedicated differential $t\bar{t}$ cross-section measurement of highly boosted top quarks in the lepton+jets channel, where the hadronically decaying top quark has a transverse momentum above 300 GeV [73]. Jet substructure techniques are employed to identify top quarks, which are reconstructed with an anti-k_t jet with a radius parameters $R = 1.0$. The predictions of NLO and LO matrix element plus parton shower Monte Carlo generators are found to generally overestimate the measured cross sections. Using 5.0 fb^{-1} of data at 7 TeV and 19.7 fb^{-1} at 8 TeV in the lepton+jets channel, CMS reports measurements of normalized differential cross sections for $t\bar{t}$ production with respect to four kinematic event variables: the missing transverse energy; the scalar sum of the jet transverse momentum (p_T); the scalar sum of the p_T of all objects in the event; and the p_T of leptonically decaying W bosons from top quark decays [74]. No significant deviations from the predictions of several standard model event generators are observed. Using the full 19.7 fb^{-1} data in the $e\mu$ channel, CMS measures normalized double-differential cross sections for $t\bar{t}$ production as a function of various pairs of observables characterizing the kinematics of the top quark and $t\bar{t}$ system [75]. The data are compared to calculations using perturbative quantum chromodynamics at NLO and approximate NNLO orders. They are also compared to predictions of Monte Carlo event generators that complement fixed-order computations with parton showers, hadronization, and multiple-parton interactions. Overall agreement is observed with the predictions, which is improved when the latest global sets (as determined here by CMS) of proton parton distribution functions are used. The inclusion of the measured $t\bar{t}$ cross sections in a fit of parametrized parton distribution functions is shown to have significant impact on the gluon distribution [75]. Another analysis at high transverse momentum regime for the top quarks, is performed by the CMS collaboration in 19.7 fb^{-1} at $\sqrt{s} = 8$ TeV [76]. The measurement is performed for events in electron/muon plus jets final states where the hadronically decaying top quark is reconstructed as a single large-radius jet and identified as a top candidate using jet substructure techniques. The integrated cross section is measured at particle-level within a fiducial region resembling the detector-level selection as well as at parton-level. At particle-level, the fiducial cross section is measured to be $\sigma_{t\bar{t}} = 1.28 \pm 0.09(stat.+syst.) \pm 0.10(pdf) \pm 0.09(scales) \pm 0.03(lumi.)$ pb for $p_T > 400$ GeV. At parton-level, it translates to $\sigma_{t\bar{t}} = 1.44 \pm 0.10(stat.+syst.) \pm 0.13(pdf) \pm 0.15(scales) \pm 0.04(lumi.)$ pb.

At parton-level, interations between incoming partons (quarks or gluons) are considered via a gauge interation yielding final state partons. While such interactions can be well described theoretically, partons are not visible in the detector. At the particle-level, visible and measurable hadrons, i.e. bound states of quarks and anti-quarks, are considered to form jets. The hadronisation process takes us from one level to the other.

Recently, in 19.7 fb^{-1} at $\sqrt{s} = 8$ TeV, CMS repeated those measurements in the lepton+jets and in the dilepton channels [77]. While the overall precision is improved, no significant deviations from the Standard Model are found, yet a softer spectrum for the top quark at high p_T with respect to theoretical available predictions has been observed. This behaviour has been also observed in the all-jets final state [78].

In 3.2 fb^{-1} at $\sqrt{s} = 13$ TeV, ATLAS measured the differential $t\bar{t}$ cross section as a function of the transverse momentum and absolute rapidity of the top quark, and of the transverse momentum, absolute rapidity and invariant mass of the $t\bar{t}$ system [79]. The measured differential cross sections are compared to predictions of NLO generators matched to parton showers and the measurements are found to be consistent with all models within the experimental uncertainties with the exception of the Powheg-Box+ Herwig++ predictions, which differ significantly from the data in both the transverse momentum of the top quark and the mass of the $t\bar{t}$ system. Using 3.2 fb^{-1} of data in the lepton+jets channel, ATLAS measured the differential cross sections of $t\bar{t}$ production in fiducial phase-spaces as a function of top-quark and $t\bar{t}$ system kinematic observables [81]. Two separate selections are applied that each focus on different top-quark momentum regions, referred to as resolved and boosted topologies of the $t\bar{t}$ final state. The measured spectra are corrected for detector effects and are compared to several Monte Carlo simulations by means of calculated χ^2 and p-values. At a center-of-mass energy of 13 TeV, ATLAS presents a measurement of the boosted top quark differential cross section in the all-hadronic decay mode [82]. They require two top-quark candidates, one with $p_T > 500$ GeV and a second with $p_T > 350$ GeV, with each candidate reconstructed as an anti-k_T jet with radius parameter $R = 1.0$. The top-quark candidates are separated from the multijet background using the jet substructure and the presence of a b-quark tag in each jet. The observed kinematic distributions are unfolded to recover the differential cross sections in a limited phase-space region and compared with Standard Model predictions, showing agreement.

In 2.1 fb^{-1} at $\sqrt{s} = 13$ TeV, CMS measures the normalized differential cross sections for $t\bar{t}$ production in the dilepton channels as a function of the kinematic properties of the leptons, jets from bottom quark hadronization, top quarks, and top quark pairs at the particle and parton levels [83]. The results are compared to several Monte Carlo generators that implement calculations up to next-to-leading order in perturbative quantum chromodynamics interfaced with parton showering, and also to fixed-order theoretical calculations of top quark pair production up to NNLO, showing agreement. In 2.2 fb^{-1} of events in the lepton+jets channel, CMS measures the differential and double-differential cross sections for the $t\bar{t}$ production as a function of jet multiplicity and of kinematic variables of the top quarks and the $t\bar{t}$ system [84]. The differential cross sections are presented at particle level, within a phase space close to the experimental acceptance, and at parton level in the full phase space. The results are compared to several standard model predictions.

Further cross-section measurements are performed for $t\bar{t}$+ heavy flavour [85] and $t\bar{t}$+jets production as well as the differential measurement of the jet multiplicity in $t\bar{t}$ events [86,87]. Here, `MC@NLO+Herwig` MC is found to predict too few events at higher jet multiplicities. In addition, CMS measured the cross-section ratio $\sigma_{t\bar{t}b\bar{b}}/\sigma_{t\bar{t}jj}$ using 19.6 fb^{-1} of 8 TeV data [88]. This is of high relevance for top quark production as background to searches, for example for the ongoing search for $t\bar{t}h$ production. Very recently, ATLAS also measured the $t\bar{t}$ production cross section along with as the branching ratios into channels with leptons and quarks using 4.6 fb^{-1} of 7 TeV data [89]. They find agreement with the standard model at the level of a few percent.

67.3.1.2. *Single-top production:*

Single-top quark production was first observed in 2009 by DØ [90] and CDF [91,92] at the Tevatron. The production cross section at

the Tevatron is roughly half that of the $t\bar{t}$ cross section, but the final state with a single W-boson and typically two jets is less distinct than that for $t\bar{t}$ and much more difficult to distinguish from the background of W+jets and other sources. A comprehensive review of the first observation and the techniques used to extract the signal from the backgrounds can be found in [93].

The dominant production at the Tevatron is through s-channel and t-channel W-boson exchange. Associated production with a W-boson (Wt production) has a cross section that is too small to observe at the Tevatron. The t-channel process is $qb \to q't$, while the s-channel process is $q\overline{q'} \to t\bar{b}$. The s- and t-channel productions can be separated kinematically. This is of particular interest because potential physics beyond the Standard Model, such as fourth-generation quarks, heavy W and Z bosons, flavor-changing-neutral-currents [10], or a charged Higgs boson, would affect the s- and t-channels differently. However, the separation is difficult and initial observations and measurements at the Tevatron by both experiments were of combined $s+t$-channel production. The two experiments combined their measurements for maximum precision with a resulting $s+t$-channel production cross section of $2.76^{+0.58}_{-0.47}$ pb [94]. The measured value assumes a top-quark mass of 170 GeV/c^2. The mass dependence of the result comes both from the acceptance dependence and from the $t\bar{t}$ background evaluation. Also the shape of discriminating topological variables is sensitive to m_t. The dependence on m_T is therefore not necessarily a simple linear dependence but amounts to only a few tenths of picobarns over the range $170-175$ GeV/c^2. The measured value agrees well with the theoretical calculation at $m_t = 173$ GeV/c^2 of $\sigma_{s+t} = 3.12$ pb (including both top and anti-top production) [5,8].

Using the full Run-II data set of up to 9.7 fb^{-1}, CDF and DØ have measured the t-channel single-top quark production to be $\sigma_{t+\bar{t}} = 2.25^{+0.29}_{-0.31}$ pb [96]. In the same publication, they also present the simultaneously measured $s-$ and $t-$channel cross sections and the $s+t$ combined cross section measurement resulting in $\sigma_{s+t} = 3.30^{+0.52}_{-0.40}$ pb, without assuming the SM ratio of σ_s/σ_t. The modulus of the CKM matrix element obtained from the $s+t$-channel measurement is $|V_{tb}| = 1.02^{+0.06}_{-0.05}$ and its value is used to set a lower limit of $|V_{tb}| > 0.92$ at 95% C.L. Those results are in good agreement with the theoretical value at the mass 172.5 GeV/c^2 of $\sigma_t = 2.08 \pm 0.13$ pb [5]. It should be noted that the theory citations here list cross sections for t or $\bar{t}$ alone, whereas the experiments measure the sum. At the Tevatron, these cross sections are equal. The theory values quoted here already include this factor of two.

Using datasets of 9.7 fb^{-1} each, CDF and DØ combine their analyses and report the first observation of single-top-quark production in the s-channel, yielding $\sigma_s = 1.29^{+0.26}_{-0.24}$ pb [97]. The probability of observing a statistical fluctuation of the background of the given size is 1.8×10^{-10}, corresponding to a significance of 6.3 standard deviations.

At the LHC, the t-channel cross section is expected to be more than three times as large as s-channel and Wt production, combined. Both ATLAS and CMS have measured single top production cross sections at $\sqrt{s} = 7$ TeV in pp collisions (assuming $m_t = 172.5$ GeV/c^2 unless noted otherwise).

Using 4.59 fb^{-1} of data at $\sqrt{s} = 7$ TeV, ATLAS measures the t-channel single-top quark cross section in the lepton plus 2 or 3 jets channel with one b-tag by fitting the distribution of a multivariate discriminant constructed with a neural network, yielding $\sigma_t = 46 \pm 6$ pb, $\sigma_{\bar{t}} = 23 \pm 4$ pb with a ratio $R_t = \sigma_t/\sigma_{\bar{t}} = 2.04 \pm 0.18$ and $\sigma_{t+\bar{t}} = 68 \pm 8$ pb, consistent with SM expectations [98]. CMS follows two approaches in 1.6 fb^{-1} of lepton plus jets events. The first approach exploits the distributions of the pseudorapidity of the recoil jet and reconstructed top-quark mass using background estimates determined from control samples in data. The second approach is based on multivariate analysis techniques that probe the compatibility of the candidate events with the signal. They find $\sigma^{t-channel}_{t+\bar{t}} = 67.2 \pm 6.1$ pb, and $|V_{tb}| = 1.020 \pm 0.046(exp.) \pm 0.017(th.)$ [100].

At $\sqrt{s} = 8$ TeV, both experiments repeat and refine their measurements. ATLAS uses 20.2 fb^{-1} of data. Total, fiducial and differential cross-sections are measured for both top-quark and top-antiquark production [101]. An artificial neural network is employed to separate signal from background. The fiducial cross-section is measured with a precision of 5.8% (top quark) and 7.8% (top antiquark), respectively. The total cross-sections are measured to be $\sigma^{t-channel}_{t}(tq) = 56.7^{+4.3}_{-3.8}$ pb for top-quark production and $\sigma^{t-channel}_{\bar{t}}(\bar{t}q) = 32.9^{+3.0}_{-2.7}$ pb for top-antiquark production, in agreement with the Standard Model prediction. In addition, the ratio of top-quark to top-antiquark production cross-sections is determined to be $R_t = 1.72 \pm 0.09$. The total cross-section is used to extract the Wtb coupling: $f_{LV} \cdot |V_{tb}| = 1.029 \pm 0.048$, which corresponds to $|V_{tb}| > 0.92$ at the 95% confidence level, when assuming $f_{LV} = 1$ and restricting the range of $|V_{tb}|$ to the interval $[0,1]$. The differential cross-sections as a function of the transverse momentum and rapidity of both the top quark and the top antiquark are measured at both the parton and particle levels. The transverse momentum and rapidity differential cross-sections of the accompanying jet from the t-channel scattering are measured at particle level. All measurements are compared to various Monte Carlo predictions as well as to fixed-order QCD calculations where available. The SM predictions provide good descriptions of the data. CMS uses 19.7 fb^{-1} in the electron or muon plus jets channel, exploiting the pseudorapidity distribution of the recoil jet. They find $\sigma_t = 53.8 \pm 1.5(stat.) \pm 4.4(syst.)$ pb and $\sigma_{\bar{t}} = 27.6 \pm 1.3(stat.) \pm 3.7(syst.)$ pb, resulting in an inclusive t-channel cross section of $\sigma_{t+\bar{t}} = 83.6 \pm 2.3(stat.) \pm 7.4(syst.)$ [102]. They measure a cross section ratio of $R_t = \sigma_t/\sigma_{\bar{t}} = 1.95 \pm 0.10(stat.) \pm 0.19(syst.)$, in agreement with the SM. The CKM matrix element V_{tb} is extracted to be $|V_{tb}| = 0.998 \pm 0.038(exp.) \pm 0.016(th.)$. More recently, CMS has also provided a fiducial cross section measurement for t-channel single top at $\sqrt{s} = 8$ TeV with 19.7 fb^{-1} of data in signal events with exactly one muon or electron and two jets, one of which is associated with a b-hadron [103]. The definition of the fiducial phase space follows closely the constraints imposed by event-selection criteria and detector acceptance. The total fiducial cross section is measured using different generators at next-to-leading order plus parton-shower accuracy. Using as reference the `aMC@NLO` MC predictions in the four-flavour scheme a $\sigma^{\rm fid}_t = 3.38 \pm 0.25(exp.) \pm 0.20(th.)$ pb is obtained, in good agreement with the theory predictions. At 13 TeV, ATLAS uses 3.2 fb^{-1} to measurement the t-channel cross section. Using a binned maximum-likelihood fit to the discriminant distribution of a neural network, the cross-sections are determined to be $\sigma_t(tq) = 156 \pm 5(stat.) \pm 27(syst.) \pm 3(lumi.)$ pb and $\sigma(\bar{t}q) = 91 \pm 4(stat.) \pm 18(syst.) \pm 2(lumi.)$ pb [104]. The cross-section ratio is measured to be $R_t = \sigma_t/\sigma_{\bar{t}} = 1.72 \pm 0.09(stat.) \pm 0.18(syst.)$. All results are in agreement with Standard Model predictions.

A measurement of the t-channel single top-quark cross section is also available at 13 TeV with the CMS detector, corresponding to an integrated luminosity of 2.2 fb^{-1}. Fits to the transverse W-mass and the output of an artificial neural network allow the determination of the background and the signal contribution. The measured cross-section is $\sigma_t = 238 \pm 13 \pm 29$ pb [105]. The CKM matrix is determined to $|V_{tb}| = 1.05 \pm 0.07(exp.) \pm 0.02(th.)$.

The Wt process has a theoretical cross section of 15.6 ± 1.2 pb [9]. This is of interest because it probes the Wtb vertex in a different kinematic region than s- and t-channel production, and because of its similarity to the associated production of a charged-Higgs boson and a top quark. The signal is difficult to extract because of its similarity to the $t\bar{t}$ signature. Furthermore, it is difficult to uniquely define because at NLO a subset of diagrams have the same final state as $t\bar{t}$ and the two interfere [106]. The cross section is calculated using the *diagram removal* technique [107] to define the signal process. In the diagram removal technique the interfering diagrams are removed, at the amplitude level, from the signal definition (an alternative technique, *diagram subtraction* removes these diagrams at the cross-section level and yields similar results [107]) . These techniques work provided the selection cuts are defined such that the interference effects are small, which is usually the case.

Both, ATLAS and CMS, also provide evidence for the associate Wt production at $\sqrt{s} = 7$ TeV [108,109]. ATLAS uses 2.05 fb^{-1} in the dilepton plus missing E_T plus jets channel, where a template fit to the final classifier distributions resulting from boosted decision trees as signal to background separation is performed. The result is incompatible with the background-only hypothesis at the 3.3σ (3.4σ

expected) level, yielding $\sigma_{Wt} = 16.8 \pm 2.9(stat.) \pm 4.9(syst.)$ pb and $|V_{tb}| = 1.03^{+0.16}_{-0.19}$ [108]. CMS uses 4.9 fb^{-1} in the dilepton plus jets channel with at least one b-tag. A multivariate analysis based on kinematic properties is utilized to separate the $t\bar{t}$ background from the signal. The observed signal has a significance of 4.0σ and corresponds to a cross section of $\sigma_{Wt} = 16^{+5}_{-4}$ pb [109].

Both experiments repeated their Wt-analyses at $\sqrt{s} = 8$ TeV. ATLAS uses 20.3 fb^{-1} to select events with two leptons and one central b-jet. The Wt signal is separated from the backgrounds using boosted decision trees, each of which combines a number of discriminating variables into one classifier. Production of Wt events is observed with a significance of 7.7σ. The cross section is extracted in a profile likelihood fit to the classifier output distributions. The Wt cross section, inclusive of decay modes, is measured to be $\sigma_{Wt} = 23.0 \pm 1.3(stat.)^{+3.2}_{-3.5}(syst.) \pm 1.1(lumi.)$ pb, yielding a value for the CKM matrix element $|V_{tb}| = 1.01 \pm 0.10$ and a lower limit of 0.80 at the 95% C.L. [110]. A fiducial cross section is also measured. CMS uses 12.2 fb^{-1} in events with two leptons and a jet originated from a b quark. A multivariate analysis based on kinematic properties is utilized to separate the signal and background. The Wt associate production signal is observed at the level of 6.1σ, yielding $\sigma_{Wt} = 23.4 \pm 5.4$ pb and $|V_{tb}| = 1.03 \pm 0.12(exp.) \pm 0.04(th.)$ [111]. ATLAS and CMS also combine their measurements and obtain $\sigma_{Wt} = 25.0 \pm 1.4(stat.) \pm 4.4(syst.) \pm 0.7(lumi.)$ pb $= 25.0 \pm 4.7$ pb [112], in agreement with the NLO+NNLL expectation. They extract a 95% C.L. lower limit on the CKM matrix element of $|V_{tb}| > 0.79$.

At 13 TeV in the Wt-channel, ATLAS uses 3.2 fb^{-1} of events with two opposite sign isolated leptons and at least one jet; they are separated into signal and control regions based on their jet multiplicity and the number of jets with b-tags. Signal is separated from background in two regions using boosted decision trees. The cross section is extracted by fitting templates to the data distributions, and is measured to be $\sigma_{Wt} = 94 \pm 10(stat.)^{+28}_{-22}(syst.) \pm 2(lumi.)$ pb [113]. The measurement is in agreement with the Standard Model prediction. CMS uses 36 fb^{-1} of events with two opposite sign isolated leptons, one tight and one loose jet and one b-tag. Signal and background is separated in categories depending on the number of jets and the subset of b-tagged jets using a boosted decision tree. A maximum likelihood fits yields $\sigma_{Wt} = 63.1 \pm 6.6$ pb [114].

At ATLAS, a search for s-channel single top quark production is performed in 0.7 fb^{-1} at 7 TeV using events containing one lepton, missing transverse energy and two b-jets. Using a cut-based analysis, an observed (expected) upper limit at 95% C.L. on the s-channel cross-section of $\sigma_s < 26.5$ (20.5) pb is obtained [115]. In 8 TeV data, both ATLAS and CMS search for s-channel production. ATLAS uses 20.3 fb^{-1} of data with one lepton, large missing transverse momentum and exactly two b-tagged jets. They perform a maximum-likelihood fit of a discriminant based on a Matrix Element Method and optimized in order to separate single top-quark s-channel events from the main background contributions which are top-quark pair production and W boson production in association with heavy flavour jets. They find $\sigma_s = 4.8 \pm 0.8(stat.)^{+1.6}_{-1.3}(syst.)$ pb with a signal significance of 3.2 standard deviations [116], which provides first evidence for s-channel single-top production at 8 TeV. The signal is extracted through a maximum-likelihood fit to the distribution of a multivariate discriminant defined using boosted decision trees to separate the expected signal contribution from background processes. At 7 TeV and 8 TeV, CMS uses 5.1 fb^{-1} and 19.3 fb^{-1}, respectively, and analyses leptonic decay modes by performing a maximum likelihood fit to a multivariate discriminant defined using a Boosted Decision Tree, yielding cross sections of $\sigma_s = 7.1 \pm 8.1$ pb and $\sigma_s = 13.4 \pm 7.3$ pb, respectively, and a best fit value of 2.0 ± 0.9 for the combined ratio of the measured σ_s values and the ones expected in the Standard Model [117]. The signal significance is 2.5 standard deviations. Both, ATLAS and CMS, also measured the electroweak production of singel top-quarks in association with a Z-boson, see section C.2.4 of this review.

Fig. 67.2 provides a summary of all single top cross-section measurements at the Tevatron and the LHC as a function of the center-of-mass energy. All cross-section measurements are very well described by the theory calculation within their uncertainty.

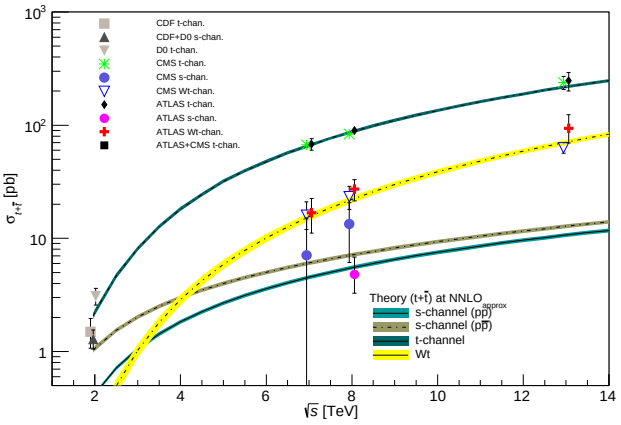

Figure 67.2: Measured and predicted single top production cross sections from Tevatron energies in $p\overline{p}$ collisions to LHC energies in pp collisions. Tevatron data points at $\sqrt{s} = 1.96$ TeV are from Refs. [96,97]. The ATLAS and CMS data points at $\sqrt{s} = 7$ TeV are from Refs. [98,100,108,109,115,117]. The ones at $\sqrt{s} = 8$ TeV are from Refs. [101,102,110,111,116,117]. The ones at $\sqrt{s} = 13$ TeV are from Refs. [104,105] Theory curves are generated using [5,8,9].

Thanks to the large statistics now available at the LHC, both CMS and ATLAS experiments also performed differential cross-section measurements in single-top t-channel production [98], [118]. Such measurements are extremely useful as they test our understanding of both QCD and EW top-quark interactions. The CMS collaboration has measured differential single top quark t-channel production cross sections as functions of the transverse momentum and the absolute value of the rapidity of the top quark. The analysis is performed in the leptonic decay channels of the top quark, with either a muon or an electron in the final state, using data collected with the CMS experiment at the LHC at $\sqrt{s} = 8$ TeV and corresponding to an integrated luminosity of 19.7 fb^{-1}. Neural networks are used to discriminate the signal process from the various background contributions. The results are found to agree with predictions from Monte Carlo generators [118]. Using the same data set and under the assumption that the spin analyzing power of a charged lepton is 100% as predicted in the SM, they are also able to measure the polarization of the top quark $P_t = 0.82 \pm 0.12(stat.) \pm 0.32(syst.)$ [119]. At 13 TeV, CMS measures the differential t-channel cross section with respect to the transverse momentum or the rapidity of the top- or the antitop-quark [120]. ATLAS has measured the differential Wt cross section in 36.1 fb^{-1} at 13 TeV with respect to the energy of the b-jet, the energy of the system of the two leptons and b-jet, and the transverse mass or mass of combinations of leptons, the b-jet and neutrinos [121].

67.3.1.3. *Top-Quark Forward-Backward & Charge Asymmetry:*

A forward-backward asymmetry in $t\bar{t}$ production at a $p\overline{p}$ collider arises starting at order α_S^3 in QCD from the interference between the Born amplitude $q\overline{q} \to t\bar{t}$ with 1-loop box production diagrams and between diagrams with initial- and final-state gluon radiation. The asymmetry, A_{FB}, is defined by

$$A_{FB} = \frac{N(\Delta y > 0) - N(\Delta y < 0)}{N(\Delta y > 0) + N(\Delta y < 0)}, \tag{67.2}$$

where $\Delta y = y_t - y_{\overline{t}}$ is the rapidity difference between the top- and the anti-top quark. Calculations at α_S^3 predict a small A_{FB} at the Tevatron. The most recent calculations up to order α_S^4, including electromagnetic and electroweak corrections, yield a predicted asymmetry of $(\approx 9.5 \pm 0.7)\%$ [122]. This is about 10% higher than the previous calculation at NLO [123,124], and improves the agreement with experiment.

Both CDF and DØ measured asymmetry values in excess of the SM prediction, fueling speculation about exotic production mechanisms

(see, for example, [125] and references therein). The first measurement of this asymmetry by DØ in 0.9 fb^{-1} [126] found an asymmetry at the detector level of $(12 \pm 8)\%$. The first CDF measurement in 1.9 fb^{-1} [127] yielded $(24 \pm 14)\%$ at parton level. Both values were higher, though statistically consistent with the SM expectation. With the addition of more data, the uncertainties have been reduced, and the central values, if somewhat smaller, have remained consistent with the first measurements. At the same time, the improved calculations from theory have increased the predicted asymmetry values to the point where the discrepancy is no longer statistically significant.

CDF and DØ have now combined results using the full Tevatron dataset at $\sqrt{s} = 1.96$ TeV [128]. Three combined asymmetries are reported: $A_{FB}^{t\bar{t}}$ as defined in Eq. 2 for fully-reconstructed $t\bar{t}$ events, a single-lepton asymmetry, A_{FB}^{ℓ} defined as in Eq. 2 but with Δy replaced by the product of the lepton charge and pseudo-rapidity, and a dilepton asymmetry, $A_{FB}^{\ell\ell}$, defined as in Eq. 2 but with Δy replaced by $\Delta\eta$ between the two leptons. The combined results are $A_{FB}^{t\bar{t}} = 0.128 \pm 0.021 \pm 0.014$, $A_{FB}^{\ell} = 0.073 \pm 0.016 \pm 0.012$, and $A_{FB}^{\ell\ell} = 0.108 \pm 0.043 \pm 0.016$. In each case the first uncertainty is statistical and the second systematic. These are to be compared to SM predictions at NNLO QCD and NLO electroweak of $A_{FB}^{t\bar{t}} = 0.095 \pm 0.007$ [122], $A_{FB}^{\ell} = 0.038 \pm 0.003$, and $A_{FB}^{\ell\ell} = 0.048 \pm 0.004$ [124], respectively. Both experiments have also measured differential asymmetries, in bins of $M_{t\bar{t}}$, Δy, $q_\ell \times \eta_\ell$, and $\Delta\eta_{\ell\ell}$, with consistent results, though the growth of $A_{FB}^{t\bar{t}}$ with increasing $M_{t\bar{t}}$ and Δy appears somewhat more rapid than the SM prediction [128].

At the LHC, where the dominant $t\bar{t}$ production mechanism is the charge-symmetric gluon-gluon fusion, the measurement is more difficult. For the sub-dominant $q\bar{q}$ production mechanism, the symmetric pp collision does not define a forward and backward direction. Instead, the charge asymmetry, A_C, is defined in terms of a positive versus a negative $t - \bar{t}$ rapidity difference, Δy

$$A_C^{t\bar{t}} = \frac{N(\Delta|y| > 0) - N(\Delta|y| < 0)}{N(\Delta|y| > 0) + N(\Delta|y| < 0)}. \qquad (67.3)$$

Both CMS and ATLAS have measured A_C in the LHC dataset. Using lepton+jets events in 4.7 fb^{-1} of data at $\sqrt{s} = 7$ TeV, ATLAS measures $A_C^{t\bar{t}} = (0.6 \pm 1.0)\%$ [129]. ATLAS has reported on the same measurement performed at $\sqrt{s} = 8$ TeV with at 20.3 fb^{-1} of data, with a result of $A_C^{t\bar{t}} = (0.009 \pm 0.005)$ [130]. In the dilepton channel at $\sqrt{s} = 8$ TeV, ATLAS measures [131] $A_C^{t\bar{t}} = 0.021 \pm 0.016$, and $A_C^{\ell\ell} = 0.008 \pm 0.006$ (defined in terms of the $\Delta\eta$ of the two leptons) in agreement with the SM predictions of $(1.11 \pm 0.04)\%$ and $(0.64 \pm 0.03)\%$, respectively [124]. CMS, in 5.0 (19.7) fb^{-1} of $\sqrt{s} = 7(8)$ TeV data uses lepton+jets events to measure $A_C^{t\bar{t}} = (0.4 \pm 1.5)\%$ ($A_C^{t\bar{t}} = (0.33 \pm 0.26(stat.) \pm 0.33(syst.))\%$) [132,133]. Both measurements are consistent with the SM expectations of $A_C^{t\bar{t}} = 1.23 \pm 0.05\%$ at $\sqrt{s} = 7$ TeV and $1.11 \pm 0.04\%$ at $\sqrt{s} = 8$ TeV [124], although the uncertainties are still too large for a precision test. In 19.5 fb^{-1} of dilepton events at $\sqrt{s} = 8$ TeV, CMS measures $A_C^{t\bar{t}} = 0.011 \pm .013$ and $A_C^{\ell\ell} = 0.003 \pm 0.007$, consistent with SM expectations [124].

In their 7 and 8 TeV analyses ATLAS and CMS also provide differential measurements as a function of $M_{t\bar{t}}$ and the transverse momentum p_T and rapidity y of the $t\bar{t}$ system. To reduce model-dependence, the CMS Collaboration has performed a measurement in a reduced fiducial phase space [134], with a result of $A_C = -0.0035 \pm 0.0072(stat.) \pm 0.0031(syst.)$, in agreement with SM expectations.

To specifically address the dependence of the asymmetry on $M_{t\bar{t}}$, ATLAS has performed a measurement in boosted $t\bar{t}$ events [135]. In 20.3 fb^{-1} of data at $\sqrt{s} = 8$ TeV, in events with $M_{t\bar{t}} > 0.75$ TeV, and $|(\Delta|y|)| < 2$, ATLAS measures $A_C^{t\bar{t}} = (4.2 \pm 3.2)\%$ compared to a NLO SM prediction of $(1.60 \pm 0.04)\%$. The measurement is also presented in three bins of $M_{t\bar{t}}$, each in agreement, though with large uncertainties, with the SM expectations.

Both ATLAS and CMS have measured asymmetries in the distribution of leptons from $t\bar{t}$ decays. ATLAS, in 4.6 fb^{-1} of $\sqrt{s} = 7$ TeV data, has measured $A^{\ell\ell} = (2.4 \pm 1.5 \pm 0.9)\%$ in dilepton events [136]. Using a neutrino weighting technique in the same dataset to reconstruct the top quarks, ATLAS measures $A_C = (2.1 \pm 2.5 \pm 1.7)\%$. CMS, in 5.0 fb^{-1} of $\sqrt{s} = 7$ TeV data, uses dilepton events to measure $A_C = (1.0 \pm 1.5 \pm 0.6)\%$, where a matrix weighting technique is used to reconstruct the top quarks, and $A^{\ell\ell} = (0.9 \pm 1.0 \pm 0.6)\%$ [137]. An earlier result using lepton+jets events from the same CMS dataset found $A_C = (0.4 \pm 1.0 \pm 1.1)\%$ [132]. Combined results from ATLAS and CMS have recently been released [138]. At $\sqrt{s} = 7$ TeV the combined result is $A_C = (0.5 \pm 0.7 \pm 0.6)\%$, and at $\sqrt{s} = 8$ TeV it is $A_C = (0.55 \pm 0.23 \pm 0.25)\%$. These results are all consistent, within their large uncertainties, with the SM expectations of $A^{\ell\ell} = (0.70 \pm 0.03)\%$ and $A_C = (1.23 \pm 0.05)\%$ [124].

A model-independent comparison of the Tevatron and LHC results is made difficult by the differing $t\bar{t}$ production mechanisms at work at the two accelerators and by the symmetric nature of the pp collisions at the LHC. Given a particular model of BSM physics, a comparison can be obtained through the resulting asymmetry predicted by the model at the two machines, see for example [135].

67.3.2. *Top-Quark Properties* :

67.3.2.1. *Top-Quark Mass Measurements:*

The most precisely studied property of the top quark is its mass. The top-quark mass has been measured in the lepton+jets, the dilepton, and the all-jets channel by all four Tevatron and LHC experiments. The latest and/or most precise results are summarized in Table 67.1. The lepton+jets channel yields the most precise single measurements because of good signal to background ratio (in particular after b-tagging) and the presence of only a single neutrino in the final state. The momentum of a single neutrino can be reconstructed (up to a quadratic ambiguity) via the missing E_T measurement and the constraint that the lepton and neutrino momenta reconstruct to the known W boson mass. In the large data samples available at the LHC, measurements in the dilepton channel can be competitive and certainly complementary to those in the lepton+jets final state.

A large number of techniques have now been applied to measuring the top-quark mass. The original 'template method' [143], in which Monte Carlo templates of reconstructed mass distributions are fit to data, has evolved into a precision tool in the lepton+jets channel, where the systematic uncertainty due to the jet energy scale (JES) uncertainty is controlled by a simultaneous, *in situ* fit to the $W \to jj$ hypothesis [144]. All the latest measurements in the lepton+jets and the all-jets channels use this technique in one way or another. In 4.6 fb^{-1} of data at $\sqrt{s} = 7$ TeV in the lepton+jets channel, ATLAS achieves a total uncertainty of 0.73% with a statistical component of 0.44% [145]. The measurement is based on a 3-dimensional template fit, determining the top-quark mass, the global jet energy scale and a b-to-light jet energy scale factor. The most precise CMS result in the lepton+jets channel uses an ideogram method and comes from a so-called 'hybrid' approach in which the prior knowledge about the jet energy scale is incorporated as a Gaussian constraint, with a width determined by the uncertainty on the jet energy corrections. In 19.7 fb^{-1} of $\sqrt{s} = 8$ TeV data, CMS achieves a total uncertainty of 0.30% with a statistical component of 0.09% with the hybrid approach [146]. Using this same method, CMS has recently released the first top-mass measurement from $\sqrt{s} = 13$ TeV data. Using 35.9 fb^{-1} of lepton+jets events they measure the top mass with a precision of 0.36%, with a statistical component of 0.05%.

The template method is complemented by the 'matrix element' method. This method was first applied by the DØ Collaboration [147], and is similar to a technique originally suggested by Kondo *et al.* [148] and Dalitz and Goldstein [149]. In the matrix element method a probability for each event is calculated as a function of the top-quark mass, using a LO matrix element for the production and decay of $t\bar{t}$ pairs. The *in situ* calibration of dijet pairs to the $W \to jj$ hypothesis is now also used with the matrix element technique to constrain the jet energy scale uncertainty. In the lepton+jets channel, DØ uses the full Tevatron dataset of 9.7 fb^{-1} and yields an uncertainty of about 0.43% [150].

In the dilepton channel, the signal to background is typically very good, but reconstruction of the mass is non-trivial because there are two neutrinos in the final state, yielding a kinematically unconstrained system. A variety of techniques have been developed to handle this. An analytic solution to the problem has been proposed [151], but this has not yet been used in the mass measurement. One of the most precise measurements in the dilepton channel comes from using the invariant mass of the charged lepton and b-quark system ($M_{\ell b}$), which is sensitive to the top-quark mass and avoids the kinematic difficulties of the two-neutrino final state. In 4.6 fb^{-1} of $\sqrt{s} = 7$ TeV data, ATLAS has measured the top-quark mass in the dilepton channel to a precision of 0.81% using a template fit to the $M_{\ell b}$ distribution [145]. Recently, using 19.7 fb^{-1} of data at $\sqrt{s} = 8$ TeV, CMS has released [152] a mass measurement in the dilepton channel based on a simultaneous fit to $M_{\ell b}$ and a transverse-mass-like variable M_{T2} [153]. The most precise result in this analysis, which comes from a linear combination of fits with the jet energy scale fixed at its nominal value and one that simultaneously determines the top mass and jet energy scale, has a total uncertainty of 0.54%. At the LHC, because of their precision, these techniques have largely displaced a number of earlier techniques in the dilepton channel, though these techniques are still included, and described, in the combined results from CMS, reported in Ref. [146].

two-dimensional template fit and achieves a precision of 1.1% [160].

The CMS Collaboration has, for the first time, extracted a top-quark mass measurement from single-top events [161], something not previously done because of the poor signal to background ratio. The mass is extracted from the invariant mass of the muon, bottom quark, and missing transverse energy. In 19.7 fb^{-1} of data at $\sqrt{s} = 8$ TeV, a precision of 0.71% is achieved.

A dominant systematic uncertainty in these methods is the understanding of the jet energy scale, and so several techniques have been developed that have little sensitivity to the jet energy scale uncertainty. In addition to Reference [157] mentioned above, these include the measurement of the top-quark mass using the following techniques: Fitting of the lepton p_T spectrum of candidate events [162]; fitting of the transverse decay length of the b-jet (L_{xy}) [163]; fitting the invariant mass of a lepton from the W-decay and a muon from the semileptonic b decay [168], kinematic properties of secondary vertices from $b-$quark fragmentation [164], the invariant mass of the $J/\psi + \ell$ system in events in which a $b-$quark fragments to a J/ψ particle [165], fitting the $b-$jet energy peak [166], and dilepton kinematics in $e\mu$ events citetopquark:CMS-PAS-TOP-16-002.

Several measurements have now been made in which the top-quark mass is extracted from the measured $t\overline{t}$ cross section using the

Table 67.1: Measurements of top-quark mass from Tevatron and LHC. $\int \mathcal{L}$dt is given in fb^{-1}. The results are a selection of both published and preliminary (not yet submitted for publication as of August 2017) measurements. For a complete set of published results see the Listings. Statistical uncertainties are listed first, followed by systematic uncertainties.

m_t (GeV/c^2)	Source	$\int \mathcal{L}$dt	Ref.	Channel
$172.99 \pm 0.48 \pm 0.78$	ATLAS	4.6	[145]	ℓ+jets+$\ell\ell$
$172.44 \pm 0.13 \pm 0.47$	CMS	19.7	[146]	ℓ+jets+$\ell\ell$+All jets
$172.35 \pm 0.16 \pm 0.48$	CMS	19.7	[146]	ℓ+jets
$172.22 \pm 0.18^{+0.89}_{-0.93}$	CMS	19.7	[152]	$\ell\ell$
$173.72 \pm 0.55 \pm 1.01$	ATLAS	20.2	[158]	All jets
$172.25 \pm 0.08 \pm 0.62$	CMS	35.9	[159]	ℓ+jets
$174.30 \pm 0.35 \pm 0.54$	CDF,DØ (I+II)	$\leq$9.7	[174]	publ. or prelim.
$173.34 \pm 0.27 \pm 0.71$	Tevatron+LHC	$\leq$8.7+$\leq$4.9	[2]	publ. or prelim.

In the neutrino weighting technique, used by CDF to analyze the full Run 2 dilepton dataset of 9.1 fb^{-1}, a weight is assigned by assuming a top-quark mass value and applying energy-momentum conservation to the top-quark decay, resulting in up to four possible pairs of solutions for the neutrino and anti-neutrino momenta. The missing E_T calculated in this way is then compared to the observed missing E_T to assign a weight [156]. The CDF result achieves a precision of 1.8% using a combination of neutrino weighting and an "alternative mass", which is insensitive to the jet energy scale [157]. The alternative mass depends on the angles between the leptons and the leading jets and the lepton four-momenta.

In the all-jets channel there is no ambiguity due to neutrino momenta, but the signal to background is significantly poorer due to the severe QCD multijets background. The emphasis therefore has been on background modeling, and reduction through event selection. The most recent measurement in the all-jets channel, by CMS in 18.2 fb^{-1} of $\sqrt{s} = 8$ TeV data [146], uses an ideogram method and a 2-dimensional simultaneous fit for m_t and the jet energy scale to extract the top-quark mass and achieves a precision of 0.56%. A recent measurement from ATLAS [158] uses a template fit to the ratio of three-jet (m_t) to two-jet (M_W) mass in the all-hadronic channel, the two-jet denominator provides an *in situ*, fit to the $W \to jj$ hypothesis. In 20.2 fb^{-1} of data at $\sqrt{s} = 8$ TeV, the result has a precision of 0.65%. A measurement from CDF in 9.3 fb^{-1} uses a

theoretical relationship between the mass and the production cross section. These determinations make use of predictions calculated at higher orders, where the top mass enters as an input parameter defined in a given scheme. At variance with the usual methods, which involve the kinematic properties of the final states and therefore the pole mass, this approach can also directly determine a short-distance mass, such as the $\overline{\rm MS}$ mass [169]. With an alternative method ATLAS recently extracted the top-quark pole mass using $t\overline{t}$ events with at least one additional jet, basing the measurement on the relationship between the differential rate of gluon radiation and the mass of the quark [170]. A similar analysis by CMS used the differential cross section as a function of the invariant mass of the $t\overline{t}$ system and the leading jet not associated with the top decays [171].

Each of the experiments has produced a measurement combining its various results. The combined measurement from CMS with up to 19.7 fb^{-1} of data achieves statistical and systematic uncertainties of 0.08% and 0.27%, respectively [146]. The combined measurement from ATLAS, with 4.6 fb^{-1} yields statistical and systematic uncertainties of 0.28% and 0.45%, respectively [145]. CDF has combined measurements with up to 9.3 fb^{-1} [172] and achieves a statistical precision of 0.33% and a systematic uncertainty of 0.43%. DØ achieves a 0.33% statistical+JES and a 0.28% systematic uncertainty by combining results in 9.7 fb^{-1} [173].

Combined measurements from the Tevatron experiments and

from the LHC experiments take into account the correlations between different measurements from a single experiment and between measurements from different experiments. The Tevatron average [174], using up to 9.7 fb^{-1} of data, now has a precision of 0.37%. The LHC combination, using up to 4.9 fb^{-1} of data, has a precision of 0.56% [175], where more work on systematic uncertainties is required. A Tevatron-LHC combination has been released, combining the results of all four experiments, using the full Tevatron dataset and the $\sqrt{s} = 7$ TeV LHC data, with a resulting precision of 0.44% [2]

The direct measurements of the top-quark mass, such as those shown in Table 67.1, correspond to the parameter used in the Monte Carlo generators, which is generally agreed to be the pole mass. The relation between the pole mass and short-distance masses, such as $\overline{\rm MS}$, is affected by non-perturbative effects. Recent calculations evaluate the size of this ambiguity to be below 250 MeV and therefore still smaller than the current measurement uncertainty [176,177].

With the discovery of a Higgs boson at the LHC with a mass of about 125 GeV/c^2 [178,179], the precision measurement of the top-quark mass takes a central role in the question of the stability of the electroweak vacuum because top-quark radiative corrections tend to drive the Higgs quartic coupling, λ, negative, potentially leading to an unstable vacuum. A recent calculation at NNLO [180] leads to the conclusion of vacuum stability for a Higgs mass satisfying $M_H \geq 129.4 \pm 5.6$ GeV/c^2 [181]. Given the uncertainty, a Higgs mass of 126 GeV/c^2 satisfies the limit, but the central values of the Higgs and top-quark masses put the electroweak vacuum squarely in the metastable region. The uncertainty is dominated by the precision of the top-quark mass measurement and its interpretation as the pole mass. For more details, see the Higgs boson review in this volume.

As a test of the CPT-symmetry, the mass difference of top- and antitop-quarks $\Delta m_t = m_t - m_{\bar{t}}$, which is expected to be zero, can be measured. CDF measures the mass difference in 8.7 fb^{-1} of 1.96 TeV data in the lepton+jets channel using a template methode to find $\Delta m_t = -1.95 \pm 1.11(stat.) \pm 0.59(syst.)$ GeV/c^2 [182] while DØ uses 3.6 fb^{-1} of lepton+jets events and the matrix element method with at least one b-tag. They find $\Delta m_t = 0.8 \pm 1.8(stat.) \pm 0.5(syst.)$ GeV/c^2 [183]. In 4.7 fb^{-1} of 7 TeV data, ATLAS measures the mass difference in lepton+jets events with a double b-tag requirement and hence very low background to find $\Delta m_t = 0.67 \pm 0.61(stat.) \pm 0.41(syst.)$ GeV/c^2 [184]. CMS measures the top-quark mass difference in 5 fb^{-1} of 7 TeV data in the lepton+jets channel and finds $\Delta m_t = -0.44 \pm 0.46(stat.) \pm 0.27(syst.)$ GeV/c^2 [185]. They repeat this measurement with 19.6 fb^{-1} of 8 TeV data to find $\Delta m_t = -0.15 \pm 0.19(stat.) \pm 0.09(syst.)$ GeV/c^2 [186]. All measurements are consistent with the SM expectation.

67.3.2.2. *Top-Quark Spin Correlations, Polarization, and Width:*

One of the unique features of the top quark is that it decays before its spin can be flipped by the strong interaction. Thus the top-quark polarization is directly observable via the angular distribution of its decay products. Hence, it is possible to define and measure observables sensitive to the top-quark spin and its production mechanism. Although the top- and antitop-quarks produced by strong interactions in hadron collisions are essentially unpolarized, the spins of t and $\bar{t}$ are correlated. For QCD production at threshold, the $t\bar{t}$ system is produced in a $^3S_1$ state with parallel spins for $q\bar{q}$ annihilation or in a $^1S_0$ state with antiparallel spins for gluon-gluon fusion. Hence, the situations at the Tevatron and at the LHC are somewhat complementary. However, at the LHC production of $t\bar{t}$ pairs at large invariant mass occurs primarily via fusion of gluons with opposite helicities, and the $t\bar{t}$ pairs so produced have parallel spins as in production at the Tevatron via $q\bar{q}$ annihilation. The direction of the top-quark spin is 100% correlated to the angular distributions of the down-type fermion (charged leptons or d-type quarks) in the decay. The joint angular distribution [187–189]

$$\frac{1}{\sigma}\frac{d^2\sigma}{d(\cos\theta_+)d(\cos\theta_-)} = \frac{1 + B_+\cos\theta_+ + B_-\cos\theta_- + \kappa\cdot\cos\theta_+\cdot\cos\theta_-}{4}, \quad (67.4)$$

where θ_+ and θ_- are the angles of the daughters in the top-quark rest frame with respect to a particular spin quantization axis (assumed here to be the same for θ_+ and θ_-), is a very sensitive observable. The maximum value for κ, 0.782 at NLO at the Tevatron [190], is found in the off-diagonal basis [187], while at the LHC the value at NLO is 0.326 in the helicity basis [190]. The coefficients B_+ and B_- are near zero in the SM because the tops are unpolarized in $t\bar{t}$ production. In place of κ, $A\alpha_+\alpha_-$ is often used, where α_i is the spin analyzing power, and A is the spin correlation coefficient, defined as

$$A = \frac{N(\uparrow\uparrow) + N(\downarrow\downarrow) - N(\uparrow\downarrow) - N(\downarrow\uparrow)}{N(\uparrow\uparrow) + N(\downarrow\downarrow) + N(\uparrow\downarrow) + N(\downarrow\uparrow)}, \quad (67.5)$$

where the first arrow represents the direction of the top-quark spin along a chosen quantization axis, and the second arrow represents the same for the antitop-quark. The spin analyzing power α_i is +0.998 for positively charged leptons, -0.966 for down-type quarks from W decays, and -0.393 for bottom quarks [191]. The sign of α flips for the respective antiparticles. The spin correlation could be modified by a new $t\bar{t}$ production mechanism such as through a Z' boson, Kaluza-Klein gluons, or a Higgs boson.

CDF used 5.1 fb^{-1} in the dilepton channel to measure the correlation coefficient in the beam axis [193]. The measurement was made using the expected distributions of $(\cos\theta_+, \cos\theta_-)$ and $(\cos\theta_b, \cos\theta_{\bar{b}})$ of the charged leptons or the b-quarks in the $t\bar{t}$ signal and background templates to calculate a likelihood of observed reconstructed distributions as a function of assumed κ. They determined the 68% confidence interval for the correlation coefficient κ as $-0.52 < \kappa < 0.61$ or $\kappa = 0.04 \pm 0.56$ assuming $m_t = 172.5$ GeV/c^2.

CDF also analyzed lepton+jets events in 5.3 fb^{-1} [194] assuming $m_t = 172.5$ GeV/c^2. They form three separate templates - the same-spin template, the opposite-spin template, and the background template for the 2-dimensional distributions in $\cos(\theta_l)\cos(\theta_d)$ vs. $\cos(\theta_l)\cos(\theta_b)$. The fit to the data in the helicity basis returns an opposite helicity fraction of $F_{OH} = 0.74 \pm 0.24(stat.) \pm 0.11(syst.)$. Converting this to the spin correlation coefficient yields $\kappa_{helicity} = 0.48 \pm 0.48(stat.) \pm 0.22(syst.)$. In the beamline basis, they find an opposite spin fraction of $F_{OS} = 0.86 \pm 0.32(stat.) \pm 0.13(syst.)$ which can be converted into a correlation coefficient of $\kappa_{beam} = 0.72 \pm 0.64(stat.) \pm 0.26(syst.)$.

DØ performed a measurement of the ratio f of events with correlated t and $\bar{t}$ spins to the total number of $t\bar{t}$ events in 5.3 fb^{-1} in the lepton+jets channel using a matrix element technique [195]. The SM expectation is $f = 1$. From 729 events, they obtain $f_{exp.} = 1.15^{+0.42}_{-0.43}(stat. + syst.)$ and can exclude values of $f < 0.420$ at the 95% C.L. In the dilepton channel [196], they also use a matrix element method and can exclude at the 97.7% C.L. the hypothesis that the spins of the t and $\bar{t}$ are uncorrelated. The combination [195] yields $f_{exp.} = 0.85 \pm 0.29$ $(stat + syst)$ and a $t\bar{t}$ production cross section which is in good agreement with the SM prediction and previous measurements. For an expected fraction of $f = 1$, they can exclude $f < 0.481$ at the 95% C.L. For the observed value of $f_{exp.} = 0.85$, they can exclude $f < 0.344(0.052)$ at the 95(99.7)% C.L. The observed fraction $f_{exp.}$ translates to a measured asymmetry value of $A_{exp.} = 0.66 \pm 0.23(stat. + syst.)$. They obtained the first evidence of SM spin correlation at 3.1 standard deviations.

Using 5.4 fb^{-1} of data, DØ measures the correlation in the dilepton channel also from the angles of the two leptons in the t and $\bar{t}$ rest frames, yielding a correlation strength $C = 0.10 \pm 0.45$ [197] (C is equivalent to negative κ in Eq. 4), in agreement with the NLO QCD prediction, but also in agreement with the no correlation hypothesis.

Spin correlations have been conclusively measured at the LHC by both the ATLAS and CMS collaborations. In the dominant gluon fusion production mode for $t\bar{t}$ pairs at the LHC, the angular distribution between the two leptons in $t\bar{t}$ decays to dileptons is sensitive to the degree of spin correlation [198].

The ATLAS collaboration has measured spin correlations in $t\bar{t}$ production at $\sqrt{s} = 7$ TeV using 4.6 fb^{-1} of data. Candidate events are selected in the dilepton and lepton plus jets topologies. Four observables are used to extract the spin correlation: The difference, $\Delta\phi$ in azimuthal angle between the two charged leptons in dilepton events or the lepton and down-quark or bottom-quark candidate from the hadronic W-decay; An observable based on the ratio matrix

elements with and without spin correlation; The double differential distribution of Eq. 4 in two different bases. The most sensitive measurement comes from using $\Delta\phi$ in dilepton events and results in $f_{\rm SM} = 1.19 \pm 0.09 \pm 0.18$. Using the helicity basis as the quantization axis, the strength of the spin correlation between the top- and antitop-quark is measured to be $A^{exp.}_{helicity} = 0.37 \pm 0.03 \pm 0.06$ [199], which is in agreement with the NLO prediction of about 0.31 [200]. Using the same events but converting $f_{exp.}$ into $A^{exp.}_{maximal}$ yields $A^{exp.}_{maximal} = 0.52 \pm 0.04 \pm 0.08$, to be compared to the NLO prediction of 0.44. In a similar analysis using 20.3 fb^{-1} of data at $\sqrt{s} = 8$ TeV, ATLAS measures $f_{\rm SM} = 1.20 \pm 0.05(stat.) \pm 0.13(syst.)$, corresponding to $A^{exp.}_{helicity} = 0.38 \pm 0.04$ [201], which compares well to the SM expectation of $A^{\rm SM}_{helicity} = 0.318 \pm 0.005$ [200]. ATLAS has released a measurement based on the correlation between the polar angles of the lepton in dilepton events [202]. The result, in the helicity basis, $A^{exp.}_{helicity} = 0.315 \pm 0.061 \pm 0.049$ is in good agreement with the SM prediction.

The CMS collaboration uses angular asymmetry variables in dilepton events, unfolded to the parton level. The most sensitive measurement is made using

$$A_{\Delta\phi} = \frac{N(\Delta\phi_{\ell^+\ell^-} > \pi/2) - N(\Delta\phi_{\ell^+\ell^-} < \pi/2)}{N(\Delta\phi_{\ell^+\ell^-} > \pi/2) + N(\Delta\phi_{\ell^+\ell^-} < \pi/2)}. \qquad (67.6)$$

In 5.0 fb^{-1} of pp collisions at $\sqrt{s} = 7$ TeV, CMS measures $A_{\Delta\phi} = 0.113 \pm 0.010 \pm 0.006 \pm 0.012$ [203], where the uncertainties are statistical, systematic, and due to the reweighting of the top p_T in the Monte Carlo to match data.

Recent results from both CMS and ATLAS top spin measurements made at $\sqrt{s} = 8$ TeV. In 19.7 fb^{-1} of data, using a matrix element technique, CMS measures $f_{\rm SM} = 0.72 \pm 0.08^{+0.15}_{-0.13}$, corresponding to $A^{exp.}_{helicity} = 0.23 \pm 0.03^{+0.05}_{-0.04}$ [204]. Corresponding results obtained by studying the dilepton final state also show consistency with the SM expectations [192]. ATLAS has published an analysis of ten top-quark spin observables [205], corresponding to the coefficients in Eq. 4, and linear combinations thereof, measured in three different bases (including measuring the coefficient κ using a different basis for the top and anti-top decay products). The spin-correlation coefficient κ is measured in the helicity basis to be $\kappa = 0.296 \pm 0.093$ in good agreement with the SM expectation of 0.318. The polarization coefficients, B, in Eq. 4 are measured, also in the helicity basis, to be $B_+ = -0.044 \pm 0.038$ and $B_- = -0.064 \pm 0.040$, consistent with the SM predictions of 0.0030 ± 0.0010 and 0.0034 ± 0.00104, respectively.

ATLAS and CMS have also produced measurements of the polarization of top quarks in $t\bar{t}$ production at $\sqrt{s} = 7$ TeV. In 4.7 fb^{-1} of data, ATLAS measures the product of the leptonic spin-analyzing power (α_ℓ) and the top quark polarization. The measurement is made in one or two lepton final states, assuming that the polarization is introduced by a CP-conserving (CPC) or maximally CP-violating (CPV) process. The results are $\alpha_\ell P_{CPC} = -0.035 \pm 0.014 \pm 0.037$ and $\alpha_\ell P_{CPV} = 0.020 \pm 0.016^{+0.013}_{-0.017}$ [206], where the uncertainties are statistical and systematic, respectively. The CMS measurement is made with 5.0 fb^{-1} of dilepton events. The polarization is extracted through an asymmetry, A_P, in the angular distribution of the two leptons, A_P, defined as

$$A_P = \frac{N(\cos\theta^*_\ell > 0) - N(\cos\theta^*_\ell < 0)}{N(\cos\theta^*_\ell > 0) + N(\cos\theta^*_\ell < 0)}, \qquad (67.7)$$

where θ^* is the angle of the charged lepton in the rest frame of its parent top quark or antiquark. The polarization, P in the helicity basis is given by $P = 2A_P$. After unfolding to the parton level, the measurement yields $A_P = 0.005 \pm 0.013 \pm 0.014 \pm 0.008$ [203], where the uncertainties are, respectively, statistical, systematic, and from top-quark p_T reweighting. Both the ATLAS and CMS results are consistent with the SM expectation of negligible polarization.

A recent DØ publication [207] presents a measurement of top-quark polarization in $t\bar{t}$ production at the Tevatron. In 9.7 fb^{-1} of $p\bar{p}$ collisions, DØ uses lepton angular distributions in lepton+jets events to measure polarization in the beam, helicity, and transverse bases. The measurements are, respectively, 0.081 ± 0.048, -0.102 ± 0.061 and, 0.040 ± 0.035, where the beam-basis result is a combination with an earlier DØ result in dilepton events [208]. These results are all consistent near-zero polarization, as predicted in the SM.

Observation of top-quark spin correlations requires a top-quark lifetime less than the spin decorrelation timescale [209]. The top-quark width, inversely proportional to its lifetime, is expected to be of order 1 GeV/c^2 (Eq. 1). The sensitivity of current experiments does not approach this level in direct measurements. Nevertheless, several measurements have been made.

CDF presents a direct measurement of the top-quark width in the lepton+jets decay channel of $t\bar{t}$ events from a data sample corresponding to 8.7 fb^{-1} of integrated luminosity. The top-quark mass and the mass of the hadronically decaying W boson that comes from the top-quark decay are reconstructed for each event and compared with templates of different top-quark widths (Γ_t) and deviations from nominal jet energy scale (ΔJES) to perform a simultaneous fit for both parameters, where ΔJES is used for the *in situ* calibration of the jet energy scale. By applying a Feldman-Cousins approach, they establish an upper limit at 95% C.L. of $\Gamma_t < 6.38$ GeV and a two-sided 68% C.L. interval of 1.10 GeV $< \Gamma_{\rm t} <$ 4.05 GeV, corresponding to a lifetime interval of $1.6 \times 10^{-15} < \tau_{top} < 6.0 \times 10^{-25}$ [210], consistent with the SM prediction. For comparison, a typical hadronization timescale is an order of magnitude larger than these limits. CMS uses partially reconstructed top-quarks in a clean sample of dilepton events to bound the top-quark width. In 12.9 fb^{-1} of data at $\sqrt{s} = 13$ TeV, CMS reports a 95% C.L. interval of $0.6 \leq \Gamma_t \leq 2.5$ GeV [211]. Recently ATLAS has provided a measurement by directly fitting reconstructed lepton+jets events in 20.2 fb^{-1} of data at $\sqrt{s} = 8$ TeV. They find $\Gamma_t = 1.76 \pm 0.33^{+0.79}_{-0.68}$ GeV [212].

The total width of the top-quark can also be determined from the partial decay width $\Gamma(t \to Wb)$ and the branching fraction $B(t \to Wb)$. DØ obtains $\Gamma(t \to Wb)$ from the measured t-channel cross section for single top-quark production in 5.4 fb^{-1}, and $B(t \to Wb)$ is extracted from a measurement of the ratio $R = B(t \to Wb)/B(t \to Wq)$ in $t\bar{t}$ events in lepton+jets channels with 0, 1 and 2 b-tags. Assuming $B(t \to Wq) = 1$, where q includes any kinematically accessible quark, the result is: $\Gamma_t = 2.00^{+0.47}_{-0.43}$ GeV which translates to a top-quark lifetime of $\tau_t = (3.29^{+0.90}_{-0.63}) \times 10^{-25}$ s. Assuming a high mass fourth generation b' quark and unitarity of the four-generation quark-mixing matrix, they set the first upper limit on $|V_{tb'}| < 0.59$ at 95% C.L. [213]. A similar analysis has performed by CMS in 19.7 fb^{-1} of $\sqrt{s} = 8$ TeV data. It provides a better determination of the total width with respect to the measurement by DØ giving $\Gamma_t = 1.36 \pm 0.02(stat.)^{+0.14}_{-0.11}(syst.)$ GeV [214].

67.3.2.3. *W-Boson Helicity in Top-Quark Decay:*

The Standard Model dictates that the top quark has the same vector-minus-axial-vector ($V - A$) charged-current weak interactions $\left(-i\frac{g}{\sqrt{2}}V_{tb}\gamma^\mu\frac{1}{2}(1-\gamma_5)\right)$ as all the other fermions. In the SM, the fraction of top-quark decays to longitudinally polarized W bosons is proportional to its Yukawa coupling and hence enhanced with respect to the weak coupling. It is expected to be [215] $\mathcal{F}_0^{\rm SM} \approx x/(1+x)$, $x = m_t^2/2M_W^2$ ($\mathcal{F}_0^{\rm SM} \sim 70\%$ for $m_t = 175$ GeV/c^2). Fractions of left-handed, right-handed, or longitudinal W bosons are denoted as $\mathcal{F}_-$, $\mathcal{F}_+$, and $\mathcal{F}_0$ respectively. In the SM, $\mathcal{F}_-$ is expected to be $\approx 30\%$ and $\mathcal{F}_+ \approx 0\%$. Predictions for the W polarization fractions at NNLO in QCD are available [216].

The Tevatron and the LHC experiments use various techniques to measure the helicity of the W boson in top-quark decays, in both the lepton+jets and in dilepton channels in $t\bar{t}$ production.

The first method uses a kinematic fit, similar to that used in the lepton+jets mass analyses, but with the top-quark mass constrained to a fixed value, to improve the reconstruction of final-state observables, and render the under-constrained dilepton channel solvable. Alternatively, in the dilepton channel the final-state momenta can also be obtained through an algebraic solution of the kinematics. The distribution of the helicity angle ($\cos\theta^*$) between the

lepton and the b quark in the W rest frame provides the most direct measure of the W helicity. In a simplified version of this approach, the $\cos\theta^*$ distribution is reduced to a forward-backward asymmetry.

The second method (p_T^ℓ) uses the different lepton p_T spectra from longitudinally or transversely polarized W-decays to determine the relative contributions.

A third method uses the invariant mass of the lepton and the b-quark in top-quark decays ($M^2_{\ell b}$) as an observable, which is directly related to $\cos\theta^*$.

At the LHC, top-quark pairs in the dilepton channels are reconstructed by solving a set of six independent kinematic equations in the missing transverse energy in x- and in y-direction, two W-masses, and the two top/antitop-quark masses. In addition, the two jets with the largest p_T in the event are interpreted as b-jets. The pairing of the jets to the charged leptons is based on the minimization of the sum of invariant masses M_{min}. Simulations show that this criterion gives the correct pairing in 68% of the events.

Finally, the Matrix Element method (ME) has also been used, in which a likelihood is formed from a product of event probabilities calculated from the ME for a given set of measured kinematic variables and assumed W-helicity fractions.

The results of recent CDF, DØ, ATLAS, and CMS analyses are summarized in Table 67.2. The datasets are now large enough to allow for a simultaneous fit of $\mathcal{F}_0$, $\mathcal{F}_-$ and $\mathcal{F}_+$, which we denote by '3-param' or $\mathcal{F}_0$ and $\mathcal{F}_+$, which we denote by '2-param' in the table. Results with either $\mathcal{F}_0$ or $\mathcal{F}_+$ fixed at its SM value are denoted '1-param'. For the simultaneous fits, the correlation coefficient between the two values is about -0.8. A complete set of published results can be found in the Listings. All results are in agreement with the SM expectation.

CDF and DØ combined their results based on $2.7 - 5.4$ fb^{-1} [217] for a top-quark mass of 172.5 GeV/c^2. ATLAS presents results from 1.04 fb^{-1} of $\sqrt{s} = 7$ TeV data using a template method for the $\cos\theta^*$ distribution and angular asymmetries from the unfolded $\cos\theta^*$ distribution in the lepton+jets and the dilepton channel [219]. CMS performs a similar measurement based on template fits to the $\cos\theta^*$ distribution with 5.0 fb^{-1} of 7 TeV data in the lepton+jets final state [220]. As the polarization of the W bosons in top-quark decays is sensitive to the Wtb vertex Lorentz structure and anomalous couplings, both experiments also derive limits on anomalous contributions to the Wtb couplings. Recently, both experiments also combined their results from 7 TeV data to obtain values on the helicity fractions as well as limits on anomalous couplings [221].

At 8 TeV, ATLAS came out with a measurement of the W-helicity fractions in 20.2 fb^{-1} in lepton+jets events with at least one b-tag [222]. Using 19.8 fb^{-1} of 8 TeV data, CMS measured the W-helicity in lepton + 4 jet events with two b-tags [223]. In $t\bar{t}$ events with two opposite-sign leptons (electron or muon) in the final state in this dataset, CMS applied six kinematic constraints on the kinematics of the produced particles [224]. Also, using the same dataset a first measurement of the W-boson helicity in top-quark decays was made in electroweak single top production [225], yielding similarly precise and consistent results.

Table 67.2: Measurement and 95% C.L. upper limits of the W helicity in top-quark decays. The table includes both preliminary, as of September 2017, and published results. A full set of published results is given in the Listings.

W Helicity	Source	$\int \mathcal{L}$dt (fb^{-1})	Ref.	Method
$\mathcal{F}_0 = 0.722 \pm 0.081$	CDF+DØ Run II	2.7-5.4	[217]	$\cos\theta^*$ 2-param
$\mathcal{F}_0 = 0.682 \pm 0.057$	CDF+DØ Run II	2.7-5.4	[217]	$\cos\theta^*$ 1-param
$\mathcal{F}_0 = 0.726 \pm 0.094$	CDF Run II	8.7	[218]	ME 2-param
$\mathcal{F}_0 = 0.67 \pm 0.07$	ATLAS (7 TeV)	1.0	[219]	$\cos\theta^*$ 3-param
$\mathcal{F}_0 = 0.682 \pm 0.045$	CMS (7 TeV)	5.0	[220]	$\cos\theta^*$ 3-param
$\mathcal{F}_0 = 0.626 \pm 0.059$	ATLAS+CMS (7 TeV)	2.2	[221]	$\cos\theta^*$ 3-param
$\mathcal{F}_0 = 0.709 \pm 0.019$	ATLAS (8 TeV)	20.2	[222]	$\cos\theta^*$ 3-param
$\mathcal{F}_0 = 0.681 \pm 0.026$	CMS (8 TeV)	19.8	[223]	$\cos\theta^*$ 3-param
$\mathcal{F}_0 = 0.653 \pm 0.029$	CMS (8 TeV)	19.7	[224]	$\cos\theta^*$ 3-param
$\mathcal{F}_0 = 0.720 \pm 0.054$	CMS (8 TeV)	19.7	[225]	$\cos\theta^*$ 3-param
$\mathcal{F}_+ = -0.033 \pm 0.046$	CDF+DØ Run II	2.7-5.4	[217]	$\cos\theta^*$ 2-param
$\mathcal{F}_+ = -0.015 \pm 0.035$	CDF+DØ Run II	2.7-5.4	[217]	$\cos\theta^*$ 1-param
$\mathcal{F}_+ = -0.045 \pm 0.073$	CDF Run II	8.7	[218]	ME 2-param
$\mathcal{F}_+ = 0.01 \pm 0.05$	ATLAS (7 TeV)	1.0	[219]	$\cos\theta^*$ 3-param
$\mathcal{F}_+ = 0.008 \pm 0.018$	CMS (7 TeV)	5.0	[220]	$\cos\theta^*$ 3-param
$\mathcal{F}_+ = 0.015 \pm 0.034$	ATLAS+CMS (7 TeV)	2.2	[221]	$\cos\theta^*$ 3-param
$\mathcal{F}_+ = -0.008 \pm 0.014$	ATLAS (8 TeV)	20.2	[222]	$\cos\theta^*$ 3-param
$\mathcal{F}_+ = -0.004 \pm 0.015$	CMS (8 TeV)	19.8	[223]	$\cos\theta^*$ 3-param
$\mathcal{F}_+ = 0.018 \pm 0.027$	CMS (8 TeV)	19.7	[224]	$\cos\theta^*$ 3-param
$\mathcal{F}_+ = -0.018 \pm 0.022$	CMS (8 TeV)	19.7	[225]	$\cos\theta^*$ 3-param

67.3.2.4. *Top-Quark Electroweak Charges:*

The top quark is the only quark whose electric charge has not been measured through production at threshold in e^+e^- collisions. Furthermore, it is the only quark whose electromagnetic coupling has not been observed and studied until recently. Since the CDF and DØ analyses on top-quark production did not associate the b, $\bar{b}$, and $W^\pm$ uniquely to the top or antitop, decays such as $t \to W^+\bar{b}, \bar{t} \to W^-b$ were not excluded. A charge 4/3 quark of this kind is consistent with current electroweak precision data. The $Z \to \ell^+\ell^-$ and $Z \to b\bar{b}$ data, in particular the discrepancy between A_{LR} from SLC at SLAC and $A_{FB}^{0,b}$ of b-quarks and $A_{FB}^{0,\ell}$ of leptons from LEP at CERN, can be fitted with a top quark of mass $m_t = 270$ GeV/c^2, provided that the right-handed b quark mixes with the isospin $+1/2$ component of an exotic doublet of charge $-1/3$ and $-4/3$ quarks, $(Q_1, Q_4)_R$ [226,227].

DØ studied the top-quark charge in double-tagged lepton+jets events, CDF did it in single tagged lepton+jets and dilepton events. Assuming the top- and antitop-quarks have equal but opposite electric charge, then reconstructing the charge of the b-quark through jet charge discrimination techniques, the $|Q_{top}| = 4/3$ and $|Q_{top}| = 2/3$ scenarios can be differentiated. For the exotic model of Chang *et al.* [227] with a top-quark charge $|Q_{top}| = 4/3$, CDF excluded the model at 99% C.L. [228] in 5.6 fb^{-1}, while DØ excluded the model at a significance greater than 5 standard deviations using 5.3 fb^{-1} and set an upper limit of 0.46 on the fraction of such quarks in the selected sample [229]. These results indicate that the observed particle is indeed consistent with being a SM $|Q| = 2/3$ quark.

In 2.05 fb^{-1} at $\sqrt{s} = 7$ TeV, ATLAS performed a similar analysis, reconstructing the b-quark charge either via a jet-charge technique or via the lepton charge in soft muon decays in combination with a kinematic likelihood fit. They measure the top-quark charge to be $0.64 \pm 0.02(stat.) \pm 0.08(syst.)$ from the charges of the top-quark decay products in single lepton $t\bar{t}$ events, and hence exclude the exotic scenario with charge $-4/3$ at more than 8σ [230].

In 4.6 fb^{-1} at $\sqrt{s} = 7$ TeV, CMS discriminates between the Standard Model and the exotic top-quark charge scenario in the muon+jets final states in $t\bar{t}$ events. They exploit the charge correlation between high-p_t muons from W-boson decays and soft muons from B-hadron decays in b-jets. Using an asymmetry technique, where $A = -1$ represent the exotic $Q = -4/3$ scenario and $A = +1$ the Standard Model $Q = +2/3$ scenario, they find $A_{meas} = 0.97 \pm 0.12(stat.) \pm 0.31(sys.)$, which agrees with the Standard Model expectation and excludes the exotic scenario at 99.9% C.L. [231].

The electromagnetic or the weak coupling of the top quark can be probed directly by investigating $t\bar{t}$ events with an additional gauge boson, such as $t\bar{t}\gamma$, $t\bar{t}W$, and $t\bar{t}Z$ events.

CDF performed a search for events containing a lepton, a photon, significant missing transverse momentum, and a jet identified as containing a b-quark and at least three jets and large total transverse energy in 6.0 fb^{-1}. They reported evidence for the observation of $t\bar{t}\gamma$ production with a cross section $\sigma_{t\bar{t}\gamma} = 0.18 \pm 0.08$ pb and a ratio of $\sigma_{t\bar{t}\gamma}/\sigma_{t\bar{t}} = 0.024 \pm 0.009$ [232].

ATLAS performed a first measurement of the $t\bar{t}\gamma$ cross section in pp collisions at $\sqrt{s} = 7$ TeV using 4.6 fb^{-1} of data. Events are selected that contain a large transverse momentum electron or muon and a large transverse momentum photon, yielding 140 and 222 events in the electron and muon samples, respectively. The production of $t\bar{t}\gamma$ events was observed with a significance of 5.3% standard deviations. The resulting cross section times branching ratio into the single lepton channel for $t\bar{t}\gamma$ production with a photon with transverse momentum above 20 GeV is $\sigma^{fid.}(t\bar{t}\gamma)\times BR = 63\pm8(stat.)^{+17}_{-13}(syst.)\pm1(lumi.)$ pb per lepton flavour [233], which is consistent with leading-order theoretical calculations. Using 19.7 fb^{-1} of data at 8 TeV, CMS performed a similar measurement of the $t\bar{t}\gamma$ production cross section in the lepton+jets decay mode with a photon transverse momentum above 25 GeV and $|\eta|$ <1.44. They obtain a normalized cross section $\mathcal{R} = \sigma_{t\bar{t}+\gamma}/\sigma_{t\bar{t}} = (5.7 \pm 1.8) \times 10^{-4}$ in e+jets and $(4.7 \pm 1.3) \times 10^{-4}$ in μ+jets. The fiducial $t\bar{t}\gamma$ cross section is obtained by multiplying by the measured $t\bar{t}$ fiducial cross section of $244.9 \pm 1.4(stat.)^{+6.3}_{-5.5}(sys.) \pm 6.4(lumi.)$pb. Extrapolating to the full phase space, the result is $\sigma_{t\bar{t}\gamma}\times$BR=$(515 \pm 108)$ fb, per lepton+jets final state [234], in good agreement with the theoretical prediction. Also at 8 TeV, ATLAS has used 20.2 fb^{-1} of data to measure the $t\bar{t}\gamma$ cross section with a photon above 15 GeV and $|\eta| < 2.37$. The fiducial cross section is measured to be 139 ± 18 fb [235], in good agreement with the NLO prediction. A precision test of the vector and axial vector couplings in $t\bar{t}\gamma$ events or searches for possible tensor couplings of top-quarks to photons will only be feasible with an integrated luminosity of several hundred fb^{-1} in the future.

ATLAS and CMS have also studied the associate production of top-antitop quark pairs along with an electroweak gauge boson, where in the Standard Model the W-boson is expected to be produced via initial state radiation, while the Z-boson can also be radiated from a final-state top-quark and hence provides sensitivity to the top-quark neutral current weak gauge coupling, which implies a sensitivity to the third component of the top-quark's weak isospin.

CMS performed measurements of the $t\bar{t}W$ and $t\bar{t}Z$ production cross section at $\sqrt{s} = 7$ TeV with 5 fb^{-1}, yielding results at about 3 standard deviations significance [236]. ATLAS performed a similar analysis with 4.7 fb^{-1} in the three-lepton channel and set an upper limit of 0.71 pb at 95% C.L. [237].

Using 20.3 fb^{-1} of 8 TeV data, ATLAS performs a simultaneous measurement of the $t\bar{t}W$ and $t\bar{t}Z$ cross section. They observe the $t\bar{t}W$ and $t\bar{t}Z$ production at the 5.0σ and 4.2σ level, respectively, yielding $\sigma_{t\bar{t}W} = 369^{+100}_{-91}$ fb and $\sigma_{t\bar{t}Z} = 176^{+58}_{-52}$ fb [238]. CMS performs an analysis where signal events are identified by matching reconstructed objects in the detector to specific final state particles from $t\bar{t}W$ and $t\bar{t}Z$ decays. using 19.5 fb^{-1} of 8 TeV data. They obtain $\sigma_{t\bar{t}W} = 382^{+117}_{-102}$ fb and $\sigma_{t\bar{t}Z} = 242^{+65}_{-55}$ fb, yielding a significance of 4.8 and 6.4 standard, respectively [239]. These measurements are used to set bounds on five anomalous dimension-six operators that would affect the $t\bar{t}W$ and $t\bar{t}Z$ cross sections.

The most recent measurements in these channels are made at 13 TeV from ATLAS and CMS in multilepton final states. Using 3.2 fb^{-1} of data, ATLAS has made measurements of the $t\bar{t}W$ and $t\bar{t}Z$ cross sections in multilepton final states. Using a likelihood technique to fit signal and control regions, ATLAS measured $t\bar{t}W$ and $t\bar{t}Z$ production cross sections of 1.5 ± 0.8 pb and 0.9 ± 0.3 pb, and significances over the background-only hypotheses of 2.2σ and 3.9σ, respectively [240]. The results are consistent with Standard Model expectations. CMS uses 35.9 fb^{-1} of data to measure $t\bar{t}W$ and $t\bar{t}Z$ production cross sections of $0.80^{+0.12}_{-0.11}\ ^{+0.13}_{-0.12}$ pb and $1.00^{+0.09}_{-0.08}\ ^{+0.12}_{-0.10}$ pb, and significances over the background-only hypotheses of 5.5σ and 9.5σ, respectively [241], firmly establishing the observation of these processes.

The electroweak couplings can also be probed in single-top production in association with a Z boson. The $pp \to tZq$ process at the LHC probes both the WWZ coupling in the case where the Z emerges from the t-channel W in single-top production and, in the case where the Z is radiated from the top quark, the tZ coupling. A CMS search at 8 TeV produced a hint of a tZq signal in tri-lepton events, with a significance compared to the background-only hypothesis of 2.4σ [242]. At 13 TeV the signal has begun to emerge. ATLAS uses 36.1 fb^{-1} of 13 TeV data in events with three leptons and two jets, at least one of which is b-tagged, to extract with a neural-network technique, a tZq cross section of $600 \pm 170 \pm 140$ fb, with a significance of 4.2σ [243]. The result is in agreement with the Standard Model NLO calculation, which predicts a production cross section of 800 fb. In the same final state, and with a BDT analysis, CMS uses 35.9 fb^{-1} of 13 TeV data to measure $\sigma(pp \to tZq \to Wb\ell^+\ell^-q) = 123^{+44}_{-39}$fb, where the leptons include electrons, muons, and taus [244]. The observed significance is 3.7σ.

67.3.3. *Searches for Physics Beyond the Standard Model* :

The top quark plays a special role in the SM. Being the only quark with a coupling to the Higgs boson of order one, it provides the most important contributions to the quadratic radiative corrections to the Higgs mass exposing the issue of the naturalness of the SM. It is therefore very common for models where the naturalness problem is addressed to have new physics associated with the top quark. In SUSY, for instance, naturalness predicts the scalar top partners to be the lightest among the squarks and to be accessible at the LHC energies (see the review "Supersymmetry: Theory"). In models where the Higgs is a pseudo-Goldstone boson, such as Little Higgs models, naturalness predicts the existence of partners of the top quarks with the same spin and color, but with different electroweak couplings, the so-called vectorial t'. Stops and t''s are expected to have sizable branching ratios to top quarks. Another intriguing prediction of SUSY models with universal couplings at the unification scale is that for a top-quark mass close to the measured value, the running of the Yukawa coupling down to 1 TeV naturally leads to the radiative breaking of the electroweak symmetry [245]. In fact, the top quark plays a role in the dynamics of electroweak symmetry breaking in many models [246]. One example is topcolor [247], where a large top-quark mass can be generated through the formation of a dynamic $t\bar{t}$ condensate, X, which is formed by a new strong gauge force coupling preferentially to the third generation. Another example is topcolor-assisted technicolor [248], predicting the existence of a heavy Z' boson that couples preferentially to the third generation of quarks. If light enough such a state might be directly accessible at the present hadron collider energies, or if too heavy, lead to four-top interactions possibly visible in the $t\bar{t}t\bar{t}$ final state, for which limits on production cross sections at the LHC $\sqrt{s} = 8$ and 13 TeV exist [249–252].

Current strategies to search for new physics in top-quark events at hadron colliders are either tailored to the discovery of specific models or model independent. They can be broadly divided in two classes. In the first class new resonant states are looked for through decay processes involving the top quarks. Current searches for bosonic resonances in $t\bar{t}$ final states, or for direct stop and t' production, or for a charged Higgs in $H^+ \to t\bar{b}$ fall in the category. On the other hand, if new states are too heavy to be directly produced, they might still give rise to deviations from the SM predictions for the strength and Lorentz form of the top-quark couplings to other SM particles. Accurate predictions and measurements are therefore needed and the results be efficiently systematized in the framework of an effective field theory [253,254]. For instance, the efforts to constrain the structure of the top couplings to vector bosons (g, γ, Z, W) and to the Higgs boson, including flavor-changing neutral currents involving the top quark, fall in this second category.

67.3.3.1. *New Physics in Top-Quark Production:*

Theoretical [255–256] and experimental efforts have been devoted to the searches of $t\bar{t}$ resonances.

At the Tevatron, both the CDF and DØ collaborations have searched for resonant production of $t\bar{t}$ pairs in the lepton+jets channel [257,258]. In both analyses, the data indicate no evidence of resonant production of $t\bar{t}$ pairs. They place upper limits on the production cross section times branching fraction to $t\bar{t}$ in comparison to the prediction for a narrow ($\Gamma_{Z'} = 0.012M_{Z'}$) leptophobic topcolor Z' boson. Within this model, they exclude Z' bosons with masses below 915 (CDF-full data set) and 835 (DØ, 5 fb^{-1}) GeV/c^2 at the 95% C.L. These limits turn out to be independent of couplings of the $t\bar{t}$ resonance (pure vector, pure axial-vector, or SM-like Z'). A similar analysis has been performed by CDF in the all-jets channel using 2.8 fb^{-1} of data [259].

At the LHC, both the CMS and ATLAS collaborations have searched for resonant production of $t\bar{t}$ pairs, employing different techniques and final-state signatures (all-jets, lepton+jets, dilepton) at $\sqrt{s} = 7$, 8 and 13 TeV. In the low mass range, from the $t\bar{t}$ threshold to about one TeV, standard techniques based on the reconstruction of each of the decay objects (lepton, jets and b-jets, missing E_T) are used to identify the top quarks, while at higher invariant mass, the top quarks are boosted and the decay products more collimated and can appear as large-radius jets with substructure. Dedicated reconstruction techniques have been developed in recent years for boosted top quarks [260] that are currently employed at the LHC. Most of the analyses are model-independent (i.e., no assumption on the quantum numbers of the resonance is made) yet they assume a small width and no signal-background interference.

Using lepton+jets and fully hadronic channels in a data set corresponding to an integrated luminosity of 2.6 fb^{-1} at 13 TeV, the CMS collaboration finds no significant deviations from the SM background [261] and improves the limits obtained at 8 TeV for resonances with masses above 2 TeV/c^2. In particular, the existence of a leptophobic topcolor particle Z' is excluded at the 95% confidence level for resonances in the mass range $0.6 < M_{Z'} < 2.5$ TeV/c^2, $0.5 < M_{Z'} < 3.9$ TeV/c^2, and $0.5 < M_{Z'} < 4.0$ TeV/c^2 for $\Gamma_{Z'} = 1\%, 10\%, 30\% M_{Z'}$, respectively [261]. Kaluza-Klein excitations of a gluon with masses between $0.5 < M_{G_{KK}} < 3.3$ TeV/c^2 (at 95% confidence level) in the Randall-Sundrum model are also excluded.

The ATLAS collaboration has performed a search for resonant $t\bar{t}$ production in the lepton+jets channel using 4.7 fb^{-1} (20.3 fb^{-1}) of proton-proton (pp) collision data collected at a center-of-mass energy $\sqrt{s} = 7(8)$ TeV [262,263]. The $t\bar{t}$ system is reconstructed using both small-radius and large-radius jets, the latter being supplemented by a jet substructure analysis. A search for local excesses in the number of data events compared to the Standard Model expectation in the $t\bar{t}$ invariant mass spectrum is performed. No evidence for a $t\bar{t}$ resonance is found and 95% confidence-level limits on the production rate are determined for massive states predicted in two benchmark models. The most stringent limits come from the sample collected at 8 TeV. The upper limits on the cross section times branching ratio of a narrow Z' boson decaying to top-quark pairs range from 4.2 pb for a resonance mass of 0.4 TeV/c^2 to 0.03 pb for a mass of 3 TeV/c^2. A narrow leptophobic topcolor Z' boson with a mass below 1.8 TeV/c^2 is excluded. Upper limits are set on the cross section times branching ratio for a broad color-octet resonance with $\Gamma/m = 15\%$ decaying to $t\bar{t}$. These range from 2.5 pb for a mass of 0.4 TeV/c^2 to 0.03 pb for a mass of 3 TeV/c^2. A Kaluza-Klein excitation of the gluon in a Randall-Sundrum model (a slightly different model is used compared to CMS) is excluded for masses below 2.2 TeV/c^2.

ATLAS has also conducted a search in the all-jet final state at 7 TeV corresponding to an integrated luminosity of 4.7 fb^{-1} [264]. The $t\bar{t}$ events are reconstructed by selecting two top quarks in their fully hadronic decay modes which are reconstructed using the Cambridge/Aachen jet finder algorithm with a radius parameter of 1.5. The substructure of the jets is analysed using the HEPTopTagger algorithm [265] to separate top-quark jets from those originating from gluons and lighter quark jets. The invariant mass spectrum of the data is compared to the SM prediction, and no evidence for resonant production of top-quark pairs is found. The data are used to set upper limits on the cross section times branching ratio for resonant $t\bar{t}$ production in two models at 95% confidence level. Leptophobic Z' bosons with masses between 700 and 1000 GeV/c^2 as well as $1280 - 1320$ GeV/c^2 and Kaluza-Klein-Gluons with masses between 700 and 1620 GeV/c^2 are excluded at the 95% confidence level.

Heavy charged bosons, such as W' or H^+, can also be searched for in $t\bar{b}, tj$ final states (for more information see the review "W'-boson searches" and "Higgs Bosons: theory and searches"), while heavy fermion resonances, such as vectorial or excited quarks, in final states such as tZ, tH, tW, bW.

CMS has performed several searches in this context, the most stringent limits coming from those at at $\sqrt{s} = 13$ TeV [266–272]. For instance, a $W' \to t\bar{b}$ has been searched for in both lepton+jets in 35.9 fb^{-1}. No evidence has been found for a right-handed W' boson and masses below 3.6 TeV/c^2 are excluded at 95% confidence level providing the most stringent limits for right-handed W' bosons in the top and bottom quark decay channel to date [266]. Single production of a vector-like quark T decaying to a Z boson and a top quark, with the Z boson decaying leptonically and the top quark decaying hadronically, has also been searched for in the same data set. At the 95% confidence level, the product of cross section and branching fraction has been excluded above values in the range 0.27-0.04 pb for vector-like quark masses in the range 0.7-1.7 TeV/c^2. In the same selection, the production of a heavy Z' boson decaying to Tt, with T decaying to tZ, has been also searched for and limits on the product of cross section and branching fractions for this process are set between 0.13 and 0.06 pb for Z' boson masses in the range from 1.5 to 2.5 TeV/c^2 [267]. Finally, a search for the production of heavy partners of the top quark with charge 5/3 decaying into a top quark and a W boson has been performed with a data sample corresponding to an integrated luminosity of 2.3 fb^{-1}, considering final states with either a pair of same-sign leptons or a single lepton plus jets. In absence of an excess, a 5/3 charged top quark with right-handed (left-handed) couplings has been excluded at 95% confidence level for masses below 1020 (990) GeV [268].

ATLAS has performed searches for heavy bosons and fermions decaying to one top quark at $\sqrt{s} = 7$ and 8 TeV. For example, t-jet resonances have been searched in the lepton+jets channel of $t\bar{t}$+ jets events in 4.7 fb^{-1} at $\sqrt{s} = 7$ TeV [273]. A heavy new particle, assumed to be produced singly in association with a $t(\bar{t})$ quark, decays to a $t(\bar{t})$ quark and a light flavor quark, leading to a color singlet (triplet) resonance in the $t(\bar{t})$+jet system. The full 2011 ATLAS pp collision dataset from the LHC (4.7 fb^{-1}) is used to select $t\bar{t}$ events. The data are consistent with the SM expectation and a new particle with mass below 350 (430) GeV/c^2 for W (color triplet) models is excluded with a 95% confidence level, assuming unit right-handed coupling. ATLAS has conducted a search for the single and pair production of a new charge +2/3 quark (T) decaying via $T \to Zt$ (and also -1/3 quark (B) decaying via $B \to Zb$) in a dataset corresponding to 20.3 fb^{-1} luminosity at $\sqrt{s} = 8$ TeV [274]. Selected events contain a high transverse momentum Z-boson candidate reconstructed from a pair of oppositely charged electrons or muons. Additionally, the presence of at least two jets possessing properties consistent with the decay of a b-hadron is required, as well as large total transverse momentum of all central jets in the event. No significant excess of events above the SM expectation is observed, and upper limits are derived for vector-like quarks of various masses in a two-dimensional plane of branching ratios. Under branching ratio assumptions corresponding to a weak-isospin singlet scenario, a T quark with mass lower than 655 GeV/c^2 is excluded at the 95% confidence level. Under branching ratio assumptions corresponding to a particular weak-isospin doublet scenario, a T quark with mass lower than 735 GeV/c^2 is excluded at the 95% confidence level.

A complementary search performed by ATLAS in the lepton+jets final state of the same dataset [250], characterized by an isolated electron or muon with moderately high transverse momentum, significant missing transverse momentum, and multiple jets is performed to look for $T(B) \to Wb, Zt, Ht(Wt, Zb, Hb)$ decays. No significant excess of events above the SM expectation is observed, and upper limits are derived for vector-like quarks of various masses under several branching ratio hypotheses. The 95% C.L. observed lower limits on the T quark mass range between 715 GeV and 950 GeV for all possible values of the branching ratios into the three decay modes. In addition this study provides limits on four top-quark production and production of two positively-charged top quarks. No significant excess of events over the background expectation is observed. The four top-quark production cross section must be less than 23 fb in the SM and less than 12 fb for production via a contact interaction; in the case of sgluon pair production decaying to $t\bar{t}$, where a sgluon is a scalar partner of the gluino [275], the mass of a sgluon must be greater than 1.06 TeV/c^2. Finally, limits in the context of models featuring two extra dimensions are also set.

In many models top-quark partners preferably decay to top quarks and weakly interacting neutral stable particles, i.e., possibly dark matter candidates, that are not detected. An observable especially

sensitive to new physics effects in $t\bar{t}$ production is therefore the missing momentum.

CMS has presented a differential cross section measurement of top-quark pair production with missing transverse energy and corresponding interpretations in the context of dark matter (effective and simplified) models at 8 and 13 TeV [276–278]. The results obtained so far are consistent with the SM expectations. In particular the search performed at 13 TeV [278] is based on 2.2 fb^{-1} of integrated luminosity and include double-leptonic, single-lepton and all-jet final states. Upper limits are derived on the production cross section and interpreted in terms of a simplified model with a scalar/pseudoscalar mediator. Cross sections larger than 1.5 (1.8) times the values predicted for a 10 GeV scalar (pseudoscalar) mediator, respectively, for couplings of $g_q = g_c = 1$ are excluded at 95% C.L.

An analogous search, at a center-of-mass energy of 7 TeV in 1.04 fb^{-1} of data has been performed by ATLAS [279]. The search is carried out in the lepton+jets channel. The results are interpreted in terms of a model where new top-quark partners are pair-produced and each decay to an on-shell top (or antitop) quark and a long-lived undetected neutral particle. The data are found to be consistent with SM expectations. A limit at 95% C.L. is set excluding a cross-section times branching ratio of 1.1 pb for a top-partner mass of 420 GeV/c^2 and a neutral particle mass less than 10 GeV/c^2. In a model of exotic fourth generation quarks, top-partner masses are excluded up to 420 GeV/c^2 and neutral particle masses up to 140 GeV/c^2.

Flavor-changing-neutral-currents (FCNC) are hugely suppressed in the SM as non zero contributions only arise at one-loop and are proportional to the splitting between the quark masses. In the case of the top quark $B(t \to Bq)$ with $B = g, \gamma, Z, H$ and $q = u, c$ are predicted to be order of 10^{-12} $(t \to cg)$ or much smaller [280]. Several observables are accessible at colliders to test and constrain such couplings.

CMS has performed several studies on the search for FCNC in top-quark production. They have considered single top quark production in the t-channel in 5 fb^{-1} integrated luminosity at 7 TeV and 19.7 fb^{-1} integrated luminosity at 8 TeV [281]. Events with the top quark decaying into a muon, neutrino and two or three jets are selected. The upper limits on effective coupling strength can be translated to the 95% upper limits on the corresponding branching ratios $B(t \to gu) \leq 2.0 \cdot 10^{-5}$, $B(t \to gc) \leq 4.1 \cdot 10^{-4}$. They have performed a search for a single top quark produced in association with a photon in 19.1 fb^{-1} integrated luminosity at 8 TeV [282]. The event selection requires the presence of one isolated muon and jets in the final state. The upper limits on effective coupling strength can be translated to the 95% upper limits on the corresponding branching ratios $B(t \to \gamma u) \leq 0.0161\%$, $B(t \to \gamma c) \leq 0.182\%$.

Recently, a search for flavor-changing neutral currents in associated production of a top quark with a Higgs boson decaying into $b\bar{b}$ has also been presented by CMS, corresponding to an integrated luminosity of 35.9 fb^{-1} at 13 TeV. Two complementary channels are considered: top quark pair production, with FCNC decay of the top quark or antiquark, and single top associated production. A final state with one isolated lepton and at least three reconstructed jets, among which at least two are identified as b quark jets, is considered. No significant deviation is observed from predicted background and upper limits at 95% confidence level are set on the branching ratios of top quark decays, $B(t \to uH) < 0.47\%$ and $B(t \to cH) < 0.47\%$ [283], which are similar to the combined limits on all decay channels obtained with the full data set at 8 TeV [284].

ATLAS has presented results on the search for single top-quark production via FCNC's in strong interactions using data collected at $\sqrt{s}$=8 TeV and corresponding to an integrated luminosity of 20.3 fb^{-1}. Flavor-changing-neutral-current events are searched for in which a light quark (u or c) interacts with a gluon to produce a single top quark, either with or without the associated production of another light quark or gluon. Candidate events of top quarks decaying into leptons and jets are selected and classified into signal- and background-like events using a neural network. The observed 95% C.L. limit is $\sigma_{qq\to t} \times B(t \to Wb) < 3.4$ pb that can be interpreted as limits on the branching ratios, $B(t \to ug) < 4 \cdot 10^{-5}$ and $B(t \to cg) < 1.7 \cdot 10^{-4}$ [285]. This result supersedes the corresponding 7 TeV analysis in 2 fb^{-1} [286].

Constraints on FCNC couplings of the top quark can also be obtained from searches for anomalous single top-quark production in e^+e^- collisions, via the process $e^+e^- \to \gamma, Z^* \to t\overline{q}$ and its charge-conjugate ($q = u, c$), or in $e^{\pm}p$ collisions, via the process $e^{\pm}u \to e^{\pm}t$. For a leptonic W decay, the topology is at least a high-p_T lepton, a high-p_T jet and missing E_T, while for a hadronic W-decay, the topology is three high-p_T jets. Limits on the cross section for this reaction have been obtained by the LEP collaborations [287] in e^+e^- collisions, and by H1 [288] and ZEUS [289] in $e^{\pm}p$ collisions. When interpreted in terms of branching ratios in top decay [290,291], the LEP limits lead to typical 95% C.L. upper bounds of $B(t \to qZ) < 0.137$. Assuming no coupling to the Z boson, the 95% C.L. limits on the anomalous FCNC coupling $\kappa_\gamma < 0.13$ and < 0.27 by ZEUS and H1, respectively, are stronger than the CDF limit of $\kappa_\gamma < 0.42$, and improve over LEP sensitivity in that domain. The H1 limit is slightly weaker than the ZEUS limit due to an observed excess of five-candidate events over an expected background of 3.2 ± 0.4. If this excess is attributed to FCNC top-quark production, this leads to a total cross section of $\sigma(ep \to e + t + X, \sqrt{s} = 319 \text{ GeV}) < 0.25$ pb [288,292].

67.3.3.2. *New Physics in Top-Quark decays:*

The large sample of top quarks produced at the Tevatron and the LHC allows to measure or set stringent limits on the branching ratios of rare top-quark decays. For example, the existence of a light H^+ can be constrained by looking for $t \to H^+b$ decay, in particular with tau-leptons in the final state (for more information see the review "Higgs Bosons: theory and searches").

A first class of searches for new physics focuses on the structure of the Wtb vertex. Using up to 2.7 fb^{-1} of data, DØ has measured the Wtb coupling form factors by combining information from the W-boson helicity in top-quark decays in $t\bar{t}$ events and single top-quark production, allowing to place limits on the left-handed and right-handed vector and tensor couplings [293–295].

ATLAS has published the results of a search for CP violation in the decay of single top quarks produced in the t-channel where the top quarks are predicted to be highly polarized, using the lepton+jets final state [296]. The data analyzed are from pp collisions at $\sqrt{s} = 7$ TeV and correspond to an integrated luminosity of 4.7 fb^{-1}. In the Standard Model, the couplings at the Wtb vertex are left-handed, right-handed couplings being absent. A forward-backward asymmetry with respect to the normal to the plane defined by the W-momentum and the top-quark polarization has been used to probe the complex phase of a possibly non-zero value of the right-handed coupling, signaling a source of CP-violation beyond the SM. The measured value of the asymmetry is $0.031 \pm 0.065(stat.)^{+0.029}_{-0.031}(syst.)$ in good agreement with the Standard Model.

A second class of searches focuses on FCNC's in the top-quark decays. Both, CDF and DØ, have provided the first limits for FCNC's in Run I and II. The most recent results from CDF give $B(t \to qZ) < 3.7\%$ and $B(t \to q\gamma) < 3.2\%$ at the 95% C.L. [297] while DØ [298,299] sets $B(t \to qZ)(q = u, c \text{ quarks }) < 3.2\%)$ at 95% C.L., $B(t \to gu) < 2.0 \cdot 10^{-4}$, and $B(t \to gc) < 3.9 \cdot 10^{-3}$ at the 95% C.L.

At the LHC, CMS has used a sample at a center-of-mass energy of 8 TeV corresponding to 19.7 fb^{-1} of integrated luminosity to perform a search for flavor changing neutral current top-quark decay $t \to Zq$. Events with a topology compatible with the decay chain $t\bar{t} \to Wb + Zq \to \ell\nu\, b + \ell\ell q$ are searched for. There is no excess seen in the observed number of events relative to the SM prediction; thus no evidence for flavor changing neutral current in top-quark decays is found. A combination with a previous search at 7 TeV excludes a $t \to Zq$ branching fraction greater than 0.05% at the 95% confidence level [300]. CMS has also performed a search for the production of a single top quark in association with a Z boson in the same data set at 8 TeV. Final states with three leptons (electrons or muons) and at least one jet are investigated. Exclusion limits at 95% confidence level on the branching fractions are found to be $B(t \to uZ) < 0.022\%$ and $B(t \to cZ) < 0.049\%$ [301].

The ATLAS collaboration has also searched for FCNC processes in 20.3 fb^{-1} of $t\bar{t}$ events with one top quark decaying through FCNC

($t \to qZ$) and the other through the SM dominant mode ($t \to bW$). Only the decays of the Z boson to charged leptons and leptonic W boson decays were considered as signal, leading to a final state topology characterized by the presence of three isolated leptons, at least two jets and missing transverse energy from the undetected neutrino. No evidence for an FCNC signal was found. An upper limit on the $t \to qZ$ branching ratio of $B(t \to qZ) < 7 \times 10^{-4}$ is set at the 95% confidence level [302], which supersedes previous results [303].

Another search for FCNCs is in the decay of a top-quark to a Higgs boson plus a light parton, $t \to qH$, $q = u, c$. The CMS collaboration has performed two searches using a sample at a center-of-mass energy of 8 TeV corresponding to 19.7 fb^{-1} of integrated luminosity, combining multi-lepton, $\gamma\gamma$ and $b\bar{b}$ final states [284]. The combined analysis sets an upper limit on the $t \to c(u)H$ branching ratios of $B(t \to c(u)H) < 0.40(0.55)\%$ at 95% confidence level. The ATLAS collaboration considers $t \to qH$, $q = u, c$ with 4.7 fb^{-1} of $t\bar{t}$ events at $\sqrt{s} = 7$ TeV and 20.3 fb^{-1} of $t\bar{t}$ events at $\sqrt{s} = 8$ TeV. A combined measurement including $H \to \gamma\gamma$ and $H \to WW*, \tau\tau$ modes yields a 95% C.L. upper limit of 0.46% and 0.45% on the branching ratios of $B(t \to cH)$ and $B(t \to uH)$, respectively [304].

67.4. Outlook

Top-quark physics at hadron colliders has developed into precision physics. Various properties of the top quark have been measured with high precision, where the LHC is about to or has already reached the precision of the Tevatron. Several $\sqrt{s}$-dependent physics quantities, such as the production cross-section, have been measured at several energies at the Tevatron and the LHC. Up to now, all measurements are consistent with the SM predictions and allow stringent tests of the underlying production mechanisms by strong and weak interactions. Given the very large event samples available at the LHC, top-quark properties will be further determined in $t\bar{t}$ as well as in electroweak single top-quark production. At the Tevatron, the $t-$ and $s-$channels for electroweak single top-quark production have been measured separately. At the LHC, significant progress has been achieved and all the three relevant channels are expected to be independently accessible in the near future. Furthermore, $t\bar{t}\gamma$, $t\bar{t}Z$, and $t\bar{t}W$ together with $t\bar{t}H$ associated production have started to or will provide further information on the top-quark electroweak couplings. At the same time various models of physics beyond the SM involving top-quark production are being constrained. With the first results from LHC Run-II at a higher center-of-mass energy and much higher luminosity starting to be released, top-quark physics has the potential to shed light on open questions and new aspects of physics at the TeV scale.

CDF note references can be retrieved from `www-cdf.fnal.gov/physics/new/top/top.html`, and DØ note references from `www-d0.fnal.gov/Run2Physics/WWW/documents/Run2Results.htm` , and ATLAS note references from `https://twiki.cern.ch/twiki/bin/view/AtlasPublic/TopPublicResults` , and CMS note references from `https://twiki.cern.ch/twiki/bin/view/CMSPublic/PhysicsResultsTOP`.

References:

1. M. Czakon, P. Fiedler, and A. Mitov, Phys. Rev. Lett. **110**, 252004 (2013).
2. ATLAS, CMS, CDF, & DØ Collabs., `arXiv:1403.4427`.
3. S. Cortese and R. Petronzio, Phys. Lett. **B253**, 494 (1991).
4. S. Willenbrock and D. Dicus, Phys. Rev. **D34**, 155 (1986).
5. N. Kidonakis, Phys. Rev. **D83**, 091503 (2011).
6. M. Brucherseifer, F. Caola, and K. Melnikov, Phys. Lett. **B736**, 58 (2014).
7. E. Berger, J. Gao, H. Xing Zhu, `arXiv:1708.09405`.
8. N. Kidonakis, Phys. Rev. **D81**, 054028 (2010).
9. N. Kidonakis, Phys. Rev. **D82**, 054018 (2010).
10. T. Tait and C.-P. Yuan. Phys. Rev. **D63**, 014018 (2001).
11. M. Jeżabek and J.H. Kühn, Nucl. Phys. **B314**, 1 (1989).
12. I.I.Y. Bigi *et al.*, Phys. Lett. **B181**, 157 (1986).
13. A.H. Hoang *et al.*, Phys. Rev. **D65**, 014014 (2002).
14. K. Hagiwara, Y. Sumino, and H. Yokoya, Phys. Lett. **B666**, 71 (2008).
15. A. Czarnecki and K. Melnikov, Nucl. Phys. **B544**, 520 (1999); K.G. Chetyrkin *et al.*, Phys. Rev. **D60**, 114015 (1999).
16. S. Frixione, P. Nason, and B. Webber, JHEP **08**, 007 (2003); S. Frixione, P. Nason, and C. Oleari, JHEP **07**, 070 (2007); S. Frixione, P. Nason, and G. Ridolfi, JHEP **07**, 126 (2007); J.M. Campbell *et al.*, JHEP **1504**, 114 (2015); T. Je?o *et al.*, Eur. Phys. J. **C76**, 691 (2016);.
17. S. Frixione *et al.*, JHEP **06**, 092 (2006); S. Frixione *et al.*, JHEP **08**, 029 (2008); S. Alioli *et al.*, JHEP **09**, 111 (2009); E. Re, Eur. Phys. J. **C71**, 1547 (2011); R. Frederix, E. Re, and P. Torrielli, JHEP **12**, 130 (2012); R. Frederix *et al.*, JHEP **06**, 027 (2016).
18. S. Frixione and B.R. Webber, JHEP **02**, 029 (2002).
19. P. Nason, JHEP **04**, 040 (2004).
20. E. Todesco and J. Wenninger, Phys. Rev. Accel. Beams **20**, 081003 (2017).
21. V.M. Abazov *et al.* (DØ Collab.), Phys. Rev. **D94**, 092004 (2016).
22. T. Aaltonen *et al.* (CDF Collab.), Phys. Rev. **D88**, 091103 (2013).
23. T. Aaltonen *et al.* (CDF and DØ Collab.), Phys. Rev. **D89**, 072001 (2014).
24. T. Aaltonen *et al.* (CDF Collab.), Phys. Rev. **D89**, 091101 (2014).
25. V.M. Abazov *et al.* (DØ Collab.), Phys. Rev. **D90**, 092006 (2014).
26. G. Aad *et al.* (ATLAS Collab.), Eur. Phys. J. **C74**, 3109 (2014).
27. ATLAS Collab., ATLAS-CONF-2011-121.
28. G. Aad *et al.* (ATLAS Collab.), JHEP **1205**, 059 (2012).
29. ATLAS Collab., ATLAS-CONF-2011-140.
30. ATLAS Collab., ATLAS-CONF-2012-024.
31. ATLAS Collab., ATLAS-CONF-2012-031.
32. G. Aad *et al.* (ATLAS Collab.), Eur. Phys. J. **C73**, 2328 (2013).
33. G. Aad *et al.* (ATLAS Collab.), Phys. Lett. **B717**, 89 (2012).
34. S. Chatrchyan *et al.* (CMS Collab.), JHEP **11**, 067 (2012).
35. S. Chatrchyan *et al.* (CMS Collab.), Phys. Lett. **B720**, 83 (2013).
36. S. Chatrchyan *et al.* (CMS Collab.), JHEP **1305**, 065 (2013).
37. S. Chatrchyan *et al.* (CMS Collab.), Phys. Rev. **D85**, 112007 (2012).
38. S. Chatrchyan *et al.* (CMS Collab.), Eur. Phys. J. **C73**, 2386 (2013).
39. ATLAS & CMS Collabs., ATLAS-CONF-2012-134, CMS PAS TOP-12-003.
40. G. Aad *et al.* (ATLAS Collab.), Eur. Phys. J. **C76**, 642 (2016).
41. G. Aad *et al.* (ATLAS Collab.), Phys. Rev. **D91**, 112013 (2015).
42. ATLAS Collab., ATLAS-CONF-2017-054.
43. G. Aad *et al.* (ATLAS Collab.), Phys. Rev. **D95**, 072003 (2017).
44. V. Khachatryan *et al.* (CMS Collab.), Eur. Phys. J. **C77**, 15 (2017).
45. S. Chatrychyan *et al.* (CMS Collab.), JHEP **02**, 024 (2014).
46. V. Khachatryan *et al.* (CMS Collab.), JHEP **08**, 029 (2016).
47. V. Khachatryan *et al.* CMS Collab., Phys. Lett. **B739**, 23 (2014).
48. V. Khachatryan *et al.* CMS Collab., Eur. Phys. J. **C76**, 128 (2016).
49. ATLAS Collab., ATLAS-CONF-2014-053, CMS Collab., CMS-PAS-TOP-14-016.
50. R. Aaij *et al.*(LHCb Collab.), Phys. Rev. Lett. **115**, 112001 (2015).
51. ATLAS Collab., ATLAS-CONF-2015-033.
52. CMS Collab., CMS-PAS-TOP-15-005.
53. M. Aaboud *et al.*(ATLAS Collab.), Phys. Rev. **B761**, 136 (2016).
54. ATLAS Collab., ATLAS-CONF-2015-049.
55. V. Khachatryan *et al.*(CMS Collab.), Eur. Phys. J. **C77**, 172 (2017).
56. A. Sirunyan *et al.*(CMS Collab.), JHEP **1709**, 051 (2017).
57. CMS Collab., CMS-PAS-TOP-16-013.
58. CMS Collab., CMS-PAS-TOP-16-023.

59. A. Sirunyan *et al.* (CMS Collab.), arXiv:1709.07411, submitted to Phys. Rev. Lett..
60. ATLAS Collab., ATLAS-CONF-2011-108.
61. V.M. Abazov *et al.* (DØ Collab.) Phys. Rev. Lett. **107**, 121802, (2011); D. Acosta *et al.* (CDF Collab.) Phys. Rev. Lett. **95**, 102002, (2005).
62. V. Khachatryan *et al.* (CMS Collab.), Phys. Lett. **B736**, 33 (2014).
63. V.M. Abazov *et al.* (DØ Collab.), Phys. Rev. **D67**, 012004 (2003).
64. T. Affolder *et al.* (CDF Collab.), Phys. Rev. **D64**, 032002 (2001).
65. M. Czakon, D. Heymes, A. Mitov, Phys. Rev. Lett. **116**, 082003 (2016).
66. T. Aaltonen *et al.* (CDF Collab.), Phys. Rev. Lett. **110**, 121802 (2013).
67. G. Aad *et al.* (ATLAS Collab.), Eur. Phys. J. **C73**, 2261 (2013).
68. G. Aad *et al.* (ATLAS Collab.), Phys. Rev. **D90**, 072004 (2014).
69. G. Aad *et al.* (ATLAS Collab.), JHEP **06**, 100 (2015).
70. S. Chatrchyan *et al.* (CMS Collab.), Eur. Phys. J. **C73**, 2339 (2013).
71. M. Aaboud *et al.* (ATLAS Collab.), Phys. Rev. **D94**, 092003 (2016).
72. G. Aad *et al.* (ATLAS Collab.), Eur. Phys. J. **C76**, 538 (2016).
73. G. Aad *et al.* (ATLAS Collab.), Phys. Rev. **D93**, 032009 (2016).
74. V. Khachatryan *et al.* (CMS Collab.), Phys. Rev. **D94**, 052006 (2016).
75. V. Khachatryan *et al.* (CMS Collab.), Eur. Phys. J. **C77**, 459 (2017).
76. V. Khachatryan *et al.* (CMS Collab.), Phys. Rev. **D94**, 072002 (2016).
77. S. Chatrchyan *et al.* (CMS Collab.), Eur. Phys. J. **C75**, 542 (2015).
78. V. Khachatryan *et al.* (CMS Collab.), Eur. Phys. J. **C76**, 128 (2016).
79. M. Aaboud *et al.* (ATLAS Collab.), Eur. Phys. J. **C77**, 292 (2017).
80. CMS Collab., CMS-PAS-TOP-15-010 (2015).
81. ATLAS Collab., arXiv:1708.00727 [hep-ex], submitted to JHEP.
82. ATLAS Collab., ATLAS-CONF-2016-100.
83. CMS Collab., CMS-TOP-16-007, submitted to JHEP.
84. V. Khachatryan *et al.* (CMS Collab.), Phys. Rev. **D95**, 092001 (2017).
85. G. Aad *et al.* (ATLAS Collab.), Eur. Phys. J. **C76**, 11 (2016).
86. G. Aad *et al.* (ATLAS Collab.), JHEP **01**, 020 (2015).
87. S. Chatrchyan *et al.* (CMS Collab.), Eur. Phys. J. **C74**, 3014 (2014).
88. S. Chatrchyan *et al.* (CMS Collab.), Phys. Lett. **B746**, 132 (2015).
89. G. Aad *et al.* (ATLAS Collab.), Phys. Rev. **D92**, 072005 (2015).
90. V.M. Abazov *et al.* (DØ Collab.), Phys. Rev. Lett. **103**, 092001 (2009); V.M. Abazov *et al.* (DØ Collab.), Phys. Rev. **D78**, 12005 (2008); V.M. Abazov *et al.* (DØ Collab.), Phys. Rev. Lett. **98**, 181802 (2007).
91. T. Aaltonen *et al.* (CDF Collab.), Phys. Rev. Lett. **103**, 092002 (2009); T. Aaltonen *et al.* (CDF Collab.), Phys. Rev. **D81**, 072003 (2010).
92. T. Aaltonen *et al.* (CDF Collab.), Phys. Rev. **D82**, 112005 (2010).
93. A. Heinson and T. Junk, Ann. Rev. Nucl. and Part. Sci. **61**, 171 (2011).
94. Tevatron Electroweak Working Group, arXiv:0908.2171 [hep-ex].
95. CDF Collab., CDF conference note 11113 (2014), DØ Collab., DØ conference note 6448 (2014).
96. T. Aaltonen *et al.* (CDF and DØ Collab.), Phys. Rev. Lett. **115**, 152003 (2015).
97. T. Aaltonen *et al.* (CDF and DØ Collab.), Phys. Rev. Lett. **112**, 231803 (2014).
98. G. Aad *et al.*, ATLAS Collab., Phys. Rev. **D90**, 112006 (2014).
99. G. Aad *et al.*, ATLAS Collab., Phys. Lett. **B717**, 330 (2012).
100. S. Chatrychan *et al.*, CMS Collab., JHEP **12**, 035 (2012).
101. M. Aaboud *et al.*, ATLAS Collab., Eur. Phys. J. **C77**, 531 (2017).
102. S. Chatrychan *et al.* (CMS Collab.), JHEP **06**, 090 (2014).
103. CMS Collab., CMS-TOP-15-007.
104. M. Aaboud *et al.* (ATLAS Collab.), JHEP **04**, 086 (2017).
105. *et al.*(CMS Collab.), arXiv:1610.00678 [hep-ex], accepted by Phys. Lett. B.
106. C.D. White *et al.*, JHEP **11**, 74 (2009).
107. S. Frixione *et al.*, JHEP **07**, 29 (2008).
108. G. Aad *et al.* (ATLAS Collab.), Phys. Lett. **B716**, 142 (2012).
109. S. Chatrychan *et al.* (CMS Collab.), Phys. Rev. Lett. **110**, 022003 (2012).
110. G. Aad *et al.*(ATLAS Collab.), JHEP **01**, 064 (2016).
111. S. Chatrychan *et al.* (CMS Collab.), Phys. Rev. Lett. **112**, 231802 (2014).
112. ATLAS Collab., ATLAS-CONF-2014-052, CMS Collab., CMS-PAS-TOP-14-009.
113. M. Aaboud *et al.* (ATLAS Collab.), arXiv:1612.07231, submitted to JHEP.
114. CMS Collab., CMS-PAS-TOP-17-018.
115. ATLAS Collab., ATLAS-CONF-2011-118.
116. G. Aad *et al.*, ATLAS Collab., Phys. Lett. **B756**, 228 (2016).
117. V. Khachatryan *et al.*(CMS Collab.), JHEP **09**, 027 (2016).
118. CMS Collab., CMS-PAS-TOP-14-004.
119. CMS Collab., CMS-PAS-TOP-13-001.
120. CMS Collab., CMS-PAS-TOP-13-004.
121. ATLAS Collab., ATLAS-CONF-2016-012.
122. M. Czakon, P. Fiedler, and A. Mitov Phys. Rev. Lett. **115**, 052001 (2015).
123. W. Hollik & D. Pagani Phys. Rev. **D84**, 093003 (2011).
124. W. Bernreuther & Z.G. Si, Phys. Rev. **D86**, 034026 (2012).
125. S. Jung, H. Murayama, A. Pierce, J.D. Wells, Phys. Rev. **D81**, 015004 (2010).
126. V.M. Abazov *et al.* (DØ Collab.), Phys. Rev. Lett. **100**, 142002 (2008).
127. T. Aaltonen *et al.* (CDF Collab.), Phys. Rev. Lett. **101**, 202001 (2008).
128. CDF & DØ Collaborations, arXiv:1709.04894.
129. G. Aad *et al.* (ATLAS Collab.), JHEP **02**, 107 (2014).
130. G. Aad *et al.* (ATLAS Collab.), Eur. Phys. J. **C76**, 87 (2016).
131. G. Aad *et al.* (ATLAS Collab.), Phys. Rev. **D94**, 032006 (2016).
132. S. Chatrchyan *et al.* (CMS Collab.), Phys. Lett. **B717**, 129 (2012).
133. V. Khachatryan *et al.* (CMS Collab.), Phys. Rev. **D93**, 034014 (2016).
134. V. Khachatryan *et al.* (CMS Collab.), Phys. Lett. **B757**, 154 (2016).
135. G. Aad *et al.* (ATLAS Collab.), Phys. Lett. **B756**, 52 (2016).
136. G. Aad *et al.* (ATLAS Collab.), JHEP **05**, 061 (2015).
137. S. Chatrchyan *et al.* (CMS Collab.), JHEP **04**, 191 (2014).
138. CMS and ATLAS Collaborations, arXiv:1709.05327.
139. V.M. Abazov *et al.* (DØ Collab.), Phys. Rev. **D90**, 072001 (2014).
140. V.M. Abazov *et al.* (DØ Collab.), Phys. Rev. **D88**, 112002 (2013).
141. T. Aaltonen *et al.* (CDF Collab.), Phys. Rev. **D88**, 072003 (2013).
142. G. Aad *et al.* (ATLAS Collab.), Eur. Phys. J. **C72**, 2039 (2012).
143. F. Abe *et al.* (CDF Collab.), Phys. Rev. **D50**, 2966 (1994).
144. A. Abulencia *et al.* (CDF Collab.), Phys. Rev. **D73**, 032003 (2006).
145. G. Aad *et al.* (ATLAS Collab.), Eur. Phys. J. **C75**, 75 (2015).
146. V. Khachatryan *et al.* (CMS Collab.), Phys. Rev. **D93**, 072004 (2016).
147. V.M. Abazov *et al.* (DØ Collab.), Nature **429**, 638 (2004).
148. K. Kondo *et al.*, J. Phys. Soc. Jpn. **G62**, 1177 (1993).

149. R.H. Dalitz and G.R. Goldstein, Phys. Rev. **D45**, 1531 (1992); Phys. Lett. **B287**, 225 (1992); Proc. Royal Soc. London **A445**, 2803 (1999).
150. V.M. Abazov *et al.* (DØ Collab.), Phys. Rev. Lett. **113**, 032002 (2014).
151. L. Sonnenschein, Phys. Rev. **D73**, 054015 (2006).
152. CMS Collab. CMS-TOP-15-008 arXiv:1704.06142.
153. C.G. Lester & D.J. Summers, Phys. Lett. **B463**, 99 (1999).
154. CMS Collab., CMS-PAS-TOP-14-014.
155. CMS Collab., CMS PAS TOP-14-010.
156. B. Abbot *et al.* (DØ Collab.), Phys. Rev. **D60**, 052001 (1999); F. Abe *et al.* (CDF Collab.), Phys. Rev. Lett. **82**, 271 (1999).
157. T. Aaltonen *et al.* (CDF Collab.), Phys. Rev. **D92**, 032003 (2015).
158. G. Aad *et al.* (ATLAS Collab.), arXiv:1702.07546.
159. CMS Collab., CMS-PAS-TOP-17-007.
160. T. Aaltonen *et al.* (CDF Collab.), Phys. Rev. **D90**, 091101R, (2014).
161. A. M. Sirunyan *et al.* (CMS Collab.), Eur. Phys. J. **C77**, 354, (2017).
162. T. Aaltonen *et al.* (CDF Collab.), Phys. Lett. **B698**, 371 (2011).
163. CMS Collab., CMS PAS TOP-12-030.
164. V. Khachatryan *et al.* (CMS Collab.), Phys. Rev. **D93**, 092006 (2016).
165. V. Khachatryan *et al.* (CMS Collab.), JHEP **12**, 123 (2016).
166. CMS Collab., CMS-PAS-TOP-15-002.
167. CMS Collab., CMS-PAS-TOP-16-002.
168. T. Aaltonen *et al.* (CDF Collab.), Phys. Rev. **D80**, 051104, (2009).
169. V.M. Abazov *et al.* (DØ Collab.) Phys. Rev. Lett. **100**, 192004, (2008); S. Chatrchyan, (CMS Collab.), Phys. Lett. **B728**, 496, (2013);
V.M. Abazov *et al.* (DØ Collab.) Phys. Lett. **B703**, 422, (2011);
ATLAS Collab., ATLAS-CONF-2011-054;
U. Langenfeld, S. Moch, and P. Uwer, Phys. Rev. **D80**, 054009 (2009).
170. G. Aad *et al.* (ATLAS Collab.) JHEP **1510**, 121 (2015).
171. CMS Collab., CMS-PAS-TOP-13-006.
172. CDF Collab., CDF conference note 11080 (2014).
173. V.M. Abazov *et al.* (DØ Collab.), Phys. Rev. **D91**, 112003 (2015).
174. The Tevatron Electroweak Working Group, For the CDF and DØ Collab., arXiv:1608.01881.
175. ATLAS & CMS Collabs., ATLAS-CONF-2013-102, CMS PAS TOP-13-005.
176. M. Beneke *et al.*, arXiv:1605.03609.
177. A. H. Hoang *et al.*, JHEP **1709**, 099 (2017).
178. G. Aad *et al.* (ATLAS Collab.), Phys. Lett. **B716**, 1 (2012).
179. S. Chatrychyan *et al.* (CMS Collab.), Phys. Lett. **B716**, 30 (2012).
180. G. Degrassi, *et al.* JHEP **08**, 98, (2012).
181. S. Alekhin, A. Djouadi, and S. Moch., Phys. Lett. **B716**, 214, (2012).
182. T. Aaltonen *et al.* (CDF Collab.), Phys. Rev. **D87**, 052013 (2013).
183. V.M. Abazov *et al.* (DØ Collab.), Phys. Rev. **D84**, 052005 (2011).
184. G. Aad *et al.* (ATLAS Collab.), Phys. Lett. **B728**, 363 (2014).
185. S. Khatrychyan *et al.* (CMS Collab.), JHEP **06**, 109 (2012).
186. S. Khatrychyan *et al.* (CMS Collab.), Phys. Lett. **B04**, 028 (2017).
187. G. Mahlon and S. Parke, Phys. Rev. **D53**, 4886 (1996);
G. Mahlon and S. Parke, Phys. Lett. **B411**, 173 (1997).
188. G.R. Goldstein, in *Spin 96: Proceedings of the 12th International Symposium on High Energy Spin Physics,* Amsterdam, 1996, ed. C.W. Jager (World Scientific, Singapore, 1997), p. 328.
189. T. Stelzer and S. Willenbrock, Phys. Lett. **B374**, 169 (1996).
190. W. Bernreuther *et al.* Nucl. Phys. **B690**, 81 (2004).
191. A. Brandenburg, Z.G. Si, & P. Uwer, Phys. Lett. **B539**, 235 (2002).
192. V. Khachatryan *et al.* (CMS Collab.) Phys. Rev. **D93**, 052007 (2016).
193. CDF Collab., CDF conference note 10719 (2011).
194. CDF Collab., CDF conference note 10211 (2010).
195. V.M. Abazov *et al.* (DØ Collab.) Phys. Rev. Lett. **108**, 032004, (2012).
196. V.M. Abazov *et al.* (DØ Collab.), Phys. Rev. Lett. **107**, 032001 (2011).
197. V.M. Abazov *et al.* (DØ Collab.), Phys. Lett. **B702**, 16 (2011).
198. G. Mahlon & S.J. Parke, Phys. Rev. **D81**, 074024,2010.
199. G. Aad *et al.* (ATLAS Collab.) Phys. Rev. **D90**, 112016 (2014).
200. W. Bernreuther & Z.G. Si, Nucl. Phys. **B837**, 90 (2010).
201. G. Aad *et al.* (ATLAS Collab.) Phys. Rev. Lett. **114**, 142001 (2015).
202. G. Aad *et al.* (ATLAS Collab.) Phys. Rev. **D93**, 12002 (2016).
203. S. Chatrchyan *et al.* (CMS Collab.) Phys. Rev. Lett. **112**, 182001 (2014).
204. V. Khachatryan *et al.* (CMS Collab.) Phys. Lett. **B758**, 321 (2016).
205. G. Aad *et al.* (ATLAS Collab.) JHEP **03**, 113 (2017).
206. G. Aad *et al.* (ATLAS Collab.) Phys. Rev. Lett. **111**, 232002 (2013).
207. V.M. Abazov (DØ Collab.) Phys. Rev. **D95**, 011101R (2017).
208. V.M. Abazov *et al.* (DØ Collab.), Phys. Rev. **D92**, 052007 (2015).
209. A. Falk and M. Peskin, Phys. Rev. **D49**, 3320 (1994).
210. T. Aaltonen *et al.* (CDF Collab.), Phys. Rev. Lett. **111**, 202001 (2013).
211. CMS Collab., CMS-PAS-TOP-16-019.
212. M. Aaboud *et al.* (ATLAS Collab.), arXiv:1709.04207.
213. V.M. Abazov *et al.* (DØ Collab.) Phys. Rev. **D85**, 091104 (2012).
214. V. Khachatryan *et al.* (CMS Collab.) Phys. Lett. **B736**, 33 (2014).
215. G.L. Kane, G.A. Ladinsky, and C.P. Yuan, Phys. Rev. **D45**, 124 (1992).
216. A. Czarnecki, J.G. Korner, and J.H. Piclum, Phys. Rev. **D81**, 111503 (2010).
217. CDF and DØ Collab., Phys. Rev. **D85**, 071106 (2012).
218. CDF Collab., Phys. Rev. **D87**, 031103 (2013).
219. ATLAS Collab., JHEP **1206**, 088 (2012).
220. S. Chatrchyan *et al.* (CMS Collab.), JHEP **10**, 167 (2013).
221. ATLAS and CMS Collab., ATLAS-CONF-2013-033, CMS-PAS-TOP-11-025.
222. M. Aaboud *et al.* (ATLAS Collab.), Eur. Phys. J. **C77**, 264 (2017).
223. V. Khachatryan *et al.* (CMS Collab.), Phys. Lett. **B762**, 512 (2017).
224. CMS Collab., CMS-PAS-TOP-14-017.
225. S. Chatrchyan *et al.* (CMS Collab.), JHEP **01**, 053 (2015).
226. D. Choudhury, T.M.P. Tait, and C.E.M. Wagner, Phys. Rev. **D65**, 053002 (2002).
227. D. Chang, W.F. Chang, and E. Ma, Phys. Rev. **D59**, 091503 (1999), Phys. Rev. **D61**, 037301 (2000).
228. T. Aaltonen *et al.* (CDF Collab.), Phys. Rev. **D88**, 032003 (2013).
229. V.M. Abazov *et al.* (DØ Collab.), Phys. Rev. **D90**, 051101 (2014).
230. G. Aad *et al.* (ATLAS Collab.), JHEP **11**, 031 (2011).
231. CMS Collab., CMS-PAS-TOP-11-031.
232. T. Aaltonen *et al.* (CDF Collab.), Phys. Rev. **D84**, 031104 (2011).
233. G. Aad *et al.* (ATLAS Collab.), Phys. Rev. **D91**, 072007 (2015).
234. CMS Collab., arXiv:1706.08128.
235. ATLAS Collab., arXiv:1706.03046.
236. S. Chatrchyan *et al.* (CMS Collab.), Phys. Rev. Lett. **110**, 172002 (2013).
237. ATLAS Collab., ATLAS-CONF-2012-126.
238. G. Aad *et al.* (ATLAS Collab.), JHEP **1511**, 172 (2015).
239. V. Khachatryan *et al.* (CMS Collab.), JHEP **2016**, 96 (2016).

240. M. Aaboud *et al.* (ATLAS Collab.) Eur. Phys. J. **C77**, 40 (2017).
241. CMS Collab., CMS-PAS-TOP-17-005.
242. A. M. Sirunyan *et al.* (CMS Collab.) JHEP **07**, 003 (2017).
243. ATLAS Collab., ATLAS-CONF-2017-052.
244. CMS Collab., CMS-PAS-TOP-16-020.
245. S.P. Martin, `hep-ph/9709356` (1997).
246. C.T. Hill and E. Simmons, Phys. Reports **381**, 235 (2003).
247. C.T. Hill, Phys. Lett. **B266**, 419 (1991).
248. C.T. Hill, Phys. Lett. **B345**, 483 (1995).
249. V. Khachatryan, *et al.* (CMS Collab.), JHEP **11**, 154 (2014).
250. G. Aad *et al.* (ATLAS Collab.), JHEP **08**, 105 (2015).
251. CMS Coll. CMS PAS TOP-17-009.
252. ATLAS Coll. ATLAS CONF-2016-020.
253. C. Zhang and S. Willenbrock, Phys. Rev. **D83**, 034006 (2011).
254. J.A. Aguilar-Saavedra, Nucl. Phys. **B843**, 638 (2011).
255. V. Barger, T. Han, and D.G.E. Walker, Phys. Rev. Lett. **100**, 031801 (2008).
256. R. Frederix and F. Maltoni, JHEP **01**, 047 (2009).
257. T. Aaltonen *et al.* (CDF Collab.), Phys. Rev. Lett. **110**, 121802 (2013).
258. D. Acosta *et al.* (DØ Collab.), Phys. Rev. Lett. **94**, 211801 (2005).
259. T. Aaltonen *et al.* (CDF Collab.), Phys. Rev. **D84**, 072003 (2011).
260. A. Altheimer *et al.*, J. Phys. **G39**, 063001 (2012).
261. A. M. Sirunyan *et al.*(CMS Collab.), JHEP **1707**, 011 (2017).
262. G. Aad *et al.* (ATLAS Collab.), Phys. Rev. **D88**, 012004 (2013).
263. G. Aad *et al.* (ATLAS Collab.), JHEP **1508**, 148 (2015).
264. G. Aad *et al.* (ATLAS Collab.), JHEP **1301**, 116 (2013).
265. T. Plehn *et al.*, JHEP **1010**, 078 (2010).
266. A. M. Sirunyan *et al.*(CMS Collab.), `arxiv:1708.08439`.
267. A. M. Sirunyan *et al.*(CMS Collab.) `arXiv:1708.01062`.
268. A. M. Sirunyan *et al.*(CMS Collab.)JHEP **1708**, 073 (2017).
269. A. M. Sirunyan *et al.*(CMS Collab.) Phys. Lett. **B772**, 634 (2017).
270. V. Khachatryan *et al.*(CMS Collab.) Phys. Lett. **B771**, 80 (2017).
271. A. M. Sirunyan *et al.*(CMS Collab.) JHEP **1704**, 136 (2017).
272. A. M. Sirunyan *et al.*(CMS Collab.) JHEP **1705**, 029 (2017).
273. G. Aad *et al.* (ATLAS Collab.), Phys. Rev. **D86**, 091103 (2012).
274. G. Aad *et al.* (ATLAS Collab.), JHEP **11**, 104 (2014).
275. T. Plehn and T.M.P. Tait, J. Phys. **G36**, 075001 (2009).
276. CMS Collab., CMS-PAS-TOP-12-042 (2013).
277. V. Khachatryan *et al.* (CMS Collab.), JHEP **06**, 121 (2015).
278. A. M. Sirunyan *et al.*(CMS Collab.) `arxiv:1706.02581`.
279. G. Aad *et al.* (ATLAS Collab.), Phys. Rev. Lett. **108**, 041805 (2012).
280. J.A. Aguilar-Saavedra, Acta Phys. Polon. **B35**, 2695 (2004).
281. V. Khachatryan *et al.*, JHEP **02**, 028 (2017).
282. CMS Collab., CMS-PAS-TOP-14-003.
283. CMS Collab. CMS-PAS-TOP-17-003.
284. V. Khachatryan *et al.*, JHEP **02**, 079 (2017).
285. G. Aad *et al.* (ATLAS Collab.), `arxiv:1509.00294`.
286. G. Aad *et al.* (ATLAS Collab.), Phys. Lett. **B712**, 351 (2012).
287. A. Heister *et al.* (ALEPH Collab.), Phys. Lett. **B543**, 173 (2002); J. Abdallah *et al.* (DELPHI Collab.), Phys. Lett. **B590**, 21 (2004); P. Achard *et al.* (L3 Collab.), Phys. Lett. **B549**, 290 (2002); G. Abbiendi *et al.* (OPAL Collab.), Phys. Lett. **B521**, 181 (2001).
288. F.D. Aaron *et al.* (H1 Collab.), Phys. Lett. **B678**, 450 (2009).
289. H. Abramowics *et al.* (ZEUS Collab.), Phys. Lett. **B708**, 27 (2012).
290. M. Beneke *et al.*, `hep-ph/0003033`, in *Proceedings of 1999 CERN Workshop on Standard Model Physics (and more) at the LHC*, G. Altarelli and M.L. Mangano eds.
291. V.F. Obraztsov, S.R. Slabospitsky, and O.P. Yushchenko, Phys. Lett. **B426**, 393 (1998).
292. T. Carli, D. Dannheim, and L. Bellagamba, Mod. Phys. Lett. **A19**, 1881 (2004).
293. V.M. Abazov *et al.* (DØ Collab.), Phys. Rev. Lett. **102**, 092002 (2009).
294. V.M. Abazov *et al.* (DØ Collab.), DØ conference note 5838 (2009).
295. V.M. Abazov *et al.* (DØ Collab.), Phys. Lett. **B708**, 21 (2012).
296. ATLAS Collab., ATLAS-CONF-2013-032.
297. T. Aaltonen *et al.* (CDF Collab.), Phys. Rev. Lett. **101**, 192002 (2009).
298. V.M. Abazov *et al.* (DØ Collab.), Phys. Lett. **B701**, 313 (2011).
299. V.M. Abazov *et al.* (DØ Collab.), Phys. Lett. **B693**, 81 (2010).
300. S. Chatrchyan*et al.*(CMS Collab.), Phys. Rev. Lett. **112**, 171802 (2014).
301. A. Sirunyan *et al.*, JHEP **07**, 003 (2017).
302. G. Aad *et al.* (ATLAS Collab.), Eur. Phys. J. **C76**, 12 (2016).
303. G. Aad *et al.* (ATLAS Collab.), JHEP **1209**, 139 (2012).
304. G. Aad *et al.* (ATLAS Collab.), JHEP **1512**, 061 (2015).

68. Form Factors for Radiative Pion and Kaon Decays

Updated August 2017 by M. Bychkov (University of Virginia) and G. D'Ambrosio (INFN Sezione di Napoli)

The radiative decays, $\pi^\pm \to l^\pm\nu\gamma$ and $K^\pm \to l^\pm\nu\gamma$, with l standing for an e or a μ, and γ for a real or virtual photon (e^+e^- pair), provide a powerful tool to investigate the hadronic structure of pions and kaons. The structure-dependent part SD_i of the amplitude describes the emission of photons from virtual hadronic states, and is parametrized in terms of form factors V, A, (vector, axial vector), in the standard description [1,2,3,4]. Note that in the Listings below and some literature, equivalent nomenclature F_V and F_A for the vector and axial form factors is often used. Exotic, non-standard contributions like $i = T, S$ (tensor, scalar) have also been considered. Apart from the SD terms, there is also the Inner Bremsstrahlung amplitude, IB, corresponding to photon radiation from external charged particles and described by Low theorem in terms of the physical decay $\pi^\pm(K^\pm) \to l^\pm\nu$. Experiments try to optimize their kinematics so as to minimize the IB part of the amplitude.

The SD amplitude in its standard form is given as

$$M(\mathrm{SD}_V) = \frac{-eG_F U_{qq'}}{\sqrt{2}m_P}\epsilon^\mu l^\nu V^P \epsilon_{\mu\nu\sigma\tau}k^\sigma q^\tau \tag{68.1}$$

$$M(\mathrm{SD}_A) = \frac{-ieG_F U_{qq'}}{\sqrt{2}m_P}\epsilon^\mu l^\nu \{A^P[(qk-k^2)g_{\mu\nu} - q_\mu k_\nu] + R^P k^2 g_{\mu\nu}\}\ , \tag{68.2}$$

which contains an additional axial form factor R^P which only can be accessed if the photon remains virtual. $U_{qq'}$ is the Cabibbo-Kobayashi-Maskawa mixing-matrix element; ϵ^μ is the polarization vector of the photon (or the effective vertex, $\epsilon^\mu = (e/k^2)\overline{u}(p_-)\gamma^\mu v(p_+)$, of the e^+e^- pair); $\ell^\nu = \overline{u}(p_\nu)\gamma^\nu(1-\gamma_5)v(p_\ell)$ is the lepton-neutrino current; q and k are the meson and photon four-momenta ($k = p_+ + p_-$ for virtual photons); and P stands for π or K.

For decay processes where the photon is real, the partial decay width can be written in analytical form as a sum of IB, SD, and IB/SD interference terms INT [1,4]:

$$\begin{aligned}\frac{d^2\Gamma_{P\to\ell\nu\gamma}}{dxdy} &= \frac{d^2\left(\Gamma_{\mathrm{IB}}+\Gamma_{\mathrm{SD}}+\Gamma_{\mathrm{INT}}\right)}{dxdy}\\ &= \frac{\alpha}{2\pi}\Gamma_{P\to\ell\nu}\frac{1}{(1-r)^2}\Bigg\{\mathrm{IB}(x,y)\\ &+\frac{1}{r}\left(\frac{m_P}{2f_P}\right)^2\Big[(V+A)^2\mathrm{SD}^+(x,y)+(V-A)^2\mathrm{SD}^-(x,y)\Big]\\ &+\epsilon_P\frac{m_P}{f_P}\Big[(V+A)\mathrm{S}^+_{\mathrm{INT}}(x,y)+(V-A)\mathrm{S}^-_{\mathrm{INT}}(x,y)\Big]\Bigg\}.\end{aligned} \tag{68.3}$$

Here

$$\begin{aligned}\mathrm{IB}(x,y) &= \left[\frac{1-y+r}{x^2(x+y-1-r)}\right]\\ &\left[x^2+2(1-x)(1-r)-\frac{2xr(1-r)}{x+y-1-r}\right]\\ \mathrm{SD}^+(x,y) &= (x+y-1-r)\Big[(x+y-1)(1-x)-r\Big]\\ \mathrm{SD}^-(x,y) &= (1-y+r)\Big[(1-x)(1-y)+r\Big]\\ \mathrm{S}^+_{\mathrm{INT}}(x,y) &= \left[\frac{1-y+r}{x(x+y-1-r)}\right]\Big[(1-x)(1-x-y)+r\Big]\\ \mathrm{S}^-_{\mathrm{INT}}(x,y) &= \left[\frac{1-y+r}{x(x+y-1-r)}\right]\Big[x^2-(1-x)(1-x-y)-r\Big]\end{aligned} \tag{68.4}$$

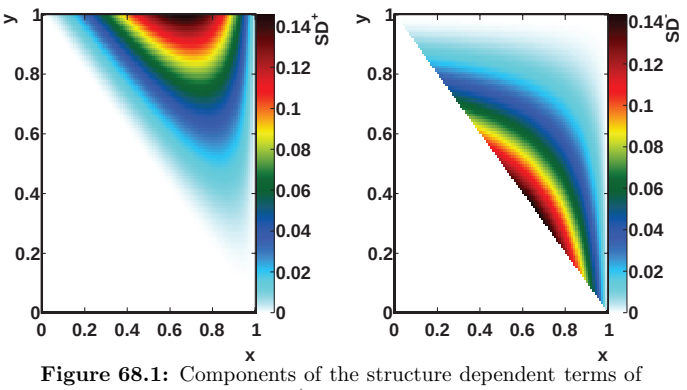

Figure 68.1: Components of the structure dependent terms of the decay width. Left: SD^+, right: SD^-

where $x = 2E_\gamma/m_P$, $y = 2E_\ell/m_P$, $r = (m_\ell/m_P)^2$, f_P is the meson decay constant, and ϵ_P is +1 for pions and -1 for kaons. The structure dependent terms SD^+ and SD^- are shown in Fig. 1. The SD^- term is maximized in the same kinematic region where overwhelming IB term dominates (along $x+y=1$ diagonal). Thus experimental yields with less background are dominated by SD^+ contribution and proportional to $A^P + V^P$ making simultaneous precise determination of the form factors difficult.

Recently, formulas (3) and (4) have been extended to describe polarized distributions in radiative meson and muon decays [7].

The "helicity" factor r is responsible for the enhancement of the SD over the IB amplitude in the decays $\pi^\pm \to e^\pm\nu\gamma$, while $\pi^\pm \to \mu^\pm\nu\gamma$ is dominated by IB. Interference terms are important for the decay $K^\pm \to \mu^\pm\nu\gamma$ [8], but contribute only a few percent correction to pion decays. However, they provide the basis for determining the signs of V and A. Radiative corrections to the decay $\pi^+ \to e^+\nu\gamma$ have to be taken into account in the analysis of the precision experiments. They make up to 4% corrections in the total decay rate [9]. In $\pi^\pm \to e^\pm\nu e^+e^-$ and $K^\pm \to \ell^\pm\nu e^+e^-$ decays, all three form factors, V^P, A^P, and R^P, can be determined [10,11].

Theoretically, the first non-trivial χPT contributions to A^P and V^P appear at $\mathcal{O}(p^4)$ [4], respectively from Gasser-Leutwyler coefficients, L_i's, and the anomalous lagrangian:

$$A^P = \frac{4\sqrt{2}M_P}{F_\pi}(L^r_9 + L^r_{10}), \quad V^P = \frac{\sqrt{2}M_P}{8\pi^2 F_\pi}. \tag{68.5}$$

In case of the kaon $A^K = 0.042$ and $V^K = 0.096$. $\mathcal{O}(p^6)$ contributions to A^K can be predicted accurately: they are flat in the momentum dependence and shift the $\mathcal{O}(p^4)$ value to 0.034. $\mathcal{O}(p^6)$ contributions to V^K are model dependent and can be approximated by a form factor linearly dependent on momentum. For example, when looking at the spread of results obtained within two different models, the constant piece of this linear form factor is shifted to 0.078 ± 0.005 [1,2,4].

We give the experimental $\pi^\pm$ form factors V^π, A^π, and R^π in the Listings below. In the $K^\pm$ Listings, we give the extracted sum $A^K + V^K$ and difference $A^K - V^K$, as well as V^K, A^K and R^K. In particular KLOE has measured for the constant piece of the form factor $A^K + V^K = 0.125 \pm 0.007 \pm 0.001$ [13] while ISTRA+, $V^K - A^K = 0.21 \pm 0.04 \pm 0.04$ [14].

The pion vector form factor, V^π, is related via CVC (Conserved Vector Current) to the $\pi^0 \to \gamma\gamma$ decay width. The constant term is given by $|V^\pi(0)| = (1/\alpha)\sqrt{2\Gamma_{\pi^0\to\gamma\gamma}/\pi m_{\pi^0}}$ [3]. The resulting value, $V^\pi(0) = 0.0259(9)$, has been confirmed by calculations based on chiral perturbation theory (χPT) [4], and by two experiments given in the Listings below. A recent experiment by the PIBETA collaboration [5] obtained a $V^\pi(0)$ that is in excellent agreement with the CVC hypothesis. It also measured the slope parameter a in $V^\pi(s) = V^\pi(0)(1 + a\cdot s)$, where $s = (1 - 2E_\gamma/m_\pi)$, and E_γ is the gamma energy in the pion rest frame: $a = 0.095 \pm 0.058$. A functional dependence on s is expected for all form factors. It becomes non-negligible in the case of $V^\pi(s)$ when a wide range of photon momenta is recorded; proper treatment in the analysis of K decays is mandatory.

The form factor, R^P, can be related to the electromagnetic radius, r_P, of the meson [2]: $R^P = \frac{1}{3} m_P f_P \langle r_P^2 \rangle$ using PCAC (Partial Conserved Axial vector Current).

In lowest order χPT, the ratio A^π/V^π is related to the pion electric polarizability $\alpha_E = [\alpha/(8\pi^2 m_\pi f_\pi^2)] \times A^\pi/V^\pi$ [6]. Direct experimental and theoretical status of pion polarizability studies currently is not settled. Most recent theoretical predictions from χPT [15] and experimental results from COMPASS collaboration [16] favor a small value of pion polarizability $\alpha_\pi \sim (2 \div 3) \times 10^{-4}\,\mathrm{fm}^3$. Dispersive analysis of $\gamma\gamma \to \pi^+\pi^-$ crossection [17] and experimental results from MAMI collaboration [18] report a much larger value of $\alpha_\pi \sim 6 \times 10^{-4}\,\mathrm{fm}^3$. Precise measurement of the pion form factors by PIBETA collaboration favors smaller values of polarizability $\alpha_\pi = 2.7^{+0.6}_{-0.5} \times 10^{-4}\,\mathrm{fm}^3$.

Several searches for the exotic form factors F_T^π, F_T^K (tensor), and F_S^K (scalar) have been pursued in the past. In particular, F_T^π has been brought into focus by experimental as well as theoretical work [12]. New high-statistics data from the PIBETA collaboration have been re-analyzed together with an additional data set optimized for low backgrounds in the radiative pion decay. In particular, lower beam rates have been used in order to reduce the accidental background, thereby making the treatment of systematic uncertainties easier and more reliable. The PIBETA analysis now restricts F_T^π to the range $-5.2 \times 10^{-4} < F_T^\pi < 4.0 \times 10^{-4}$ at a 90% confidence limit [5]. This result is in excellent agreement with the most recent theoretical work [4].

Precision measurements of radiative pion and kaon decays are effective tools to study QCD in the non-perturbative region and are of interest beyond the scope of radiative decays. Meanwhile other processes such as $\pi^+ \to e^+\nu$ that seem to be better suited to search for new physics at the precision frontier are currently studied. The advantages of such process are the very accurate and reliable theoretical predictions and the more straightforward experimental analysis.

References:

1. Phys. Reports **88**, 151 (1982). See our note on "Decay Constants of Charged Pseudoscalar Mesons" elsewhere in this *Review*;
   S.G. Brown and S.A. Bludman, Phys. Rev. **136**, B1160 (1964);
   P. DeBaenst and J. Pestieau, Nuovo Cimento **A53**, 137 (1968).
2. W.T. Chu *et al.*, Phys. Rev. **166**, 1577 (1968);
   D.Yu. Bardin and E.A. Ivanov, Sov. J. Part. Nucl. **7**, 286 (1976);
   A. Kersch and F. Scheck, Nucl. Phys. **B263**, 475 (1986).
3. V.G. Vaks and B.L. Ioffe, Nuovo Cimento **10**, 342 (1958);
   V.F. Muller, Z. Phys. **173**, 438 (1963).
4. C.Q. Geng, I-Lin Ho, and T.H. Wu, Nucl. Phys. **B684**, 281 (2004);
   J. Bijnens and P. Talavera, Nucl. Phys. **B489**, 387 (1997);
   V. Mateu and J. Portoles, Eur. Phys. J. **C52**, 325 (2007);
   R. Unterdorfer, H. Pichl, Eur. Phys. J. **C55**, 273 (2008);
   V. Cirigliano *et al.*, Rev. Mod. Phys. **84**, 399 (2012).
5. D. Počanić *et al.*, Phys. Rev. Lett. **93**, 181803 (2004);
   E. Frlež *et al.*, Phys. Rev. Lett. **93**, 181804 (2004);
   M. Bychkov *et al.*, Phys. Rev. Lett. **103**, 051802 (2009).
6. J.F. Donoghue and B.R. Holstein, Phys. Rev. **D40**, 2378 (1989).
7. E. Gabrielli and L. Trentadue, Nucl. Phys. **B792**, 48 (2008).
8. S. Adler *et al.*, Phys. Rev. Lett. **85**, 2256 (2000).
9. Yu.M. Bystritsky, E.A. Kuraev, and E.P. Velicheva, Phys. Rev. **D69**, 114004 (2004);
   R. Unterdorfer and H. Pichl have treated radiative corrections of the structure terms to lowest order within χPT for the first time. See the reference under [4].
10. S. Egli *et al.*, Phys. Lett. **B175**, 97 (1986).
11. A.A. Poblaguev *et al.*, Phys. Rev. Lett. **89**, 061803 (2002).
12. A.A. Poblaguev, Phys. Lett. **B238**, 108 (1990);
    V.N. Bolotov *et al.*, Phys. Lett. **B243**, 308 (1990);
    V.M. Belyaev and I.I. Kogan, Phys. Lett. **B280**, 238 (1992);
    A.V. Chernyshev *et al.*, Mod. Phys. Lett. **A12**, 1669 (1997);
    A.A. Poblaguev, Phys. Rev. **D68**, 054020 (2003);
    M.V. Chizhov, Phys. Part. Nucl. Lett. **2**, 193 (2005).
13. F. Ambrosino *et al.*, Eur. Phys. J. **C64**, 627 (2009).
14. V.A. Duk *et al.*, Phys. Lett. **B695**, 59 (2011).
15. J. Gasser, M.A. Ivanov, and M.E. Sainio, Nucl. Phys. B745 (2006) 84 [hep-ph/0602234].
16. C. Adolph *et al.*, Phys. Rev. Lett. **114**, 062002 (2015).
17. L.V. Fil'kov and V.L. Kashevarov, Phys. Rev. **C73**, 035210 (2006).
18. J. Ahrens *et al.*, Eur. Phys. J. A **23**, 113-127 (2005).

69. Scalar Mesons below 2 GeV

Revised March 2018 by C. Amsler (Stefan Meyer Inst. for Subatomic Physics, Vienna), S. Eidelman (Budker Institute of Nuclear Physics, Novosibirsk), T. Gutsche (University of Tübingen), C. Hanhart (Forschungszentrum Jülich), R.E. Mitchell (Indiana Univ.), S. Spanier (University of Tennessee), and N.A. Törnqvist (University of Helsinki)

69.1. Introduction

In contrast to the vector and tensor mesons, the identification of the scalar mesons is a long-standing puzzle. Scalar resonances are difficult to resolve because some of them have large decay widths which cause a strong overlap between resonances and background. In addition, several decay channels sometimes open up within a short mass interval (*e.g.* at the $K\bar{K}$ and $\eta\eta$ thresholds), producing cusps in the line shapes of the near-by resonances. Furthermore, one expects non-$q\bar{q}$ scalar objects, such as glueballs and multiquark states in the mass range below 2 GeV (for reviews see, *e.g.*, Refs. [1–5] and the mini-review on *non–$\bar{q}q$ states* in this Review of Particle Physics (RPP)).

Light scalars are produced, for example, in πN scattering on polarized/unpolarized targets, $p\bar{p}$ annihilation, central hadronic production, J/Ψ, B-, D- and K-meson decays, $\gamma\gamma$ formation, and ϕ radiative decays. Especially for the lightest scalar mesons simple parameterizations fail and more advanced theory tools are necessary to extract the resonance parameters from data. In the analyses available in the literature fundamental properties of the amplitudes such as unitarity, analyticity, Lorentz invariance, chiral and flavor symmetry are implemented at different levels of rigor. Especially, chiral symmetry implies the appearance of zeros close to the threshold in elastic S-wave scattering amplitudes involving soft pions [6,7], which may be shifted or removed in associated production processes [8]. The methods employed are the K-matrix formalism, the N/D-method, the Dalitz–Tuan ansatz, unitarized quark models with coupled channels, effective chiral field theories and the linear sigma model, *etc.* Dynamics near the lowest two-body thresholds in some analyses are described by crossed channel (t, u) meson exchange or with an effective range parameterization instead of, or in addition to, resonant features in the s-channel. Dispersion theoretical approaches are applied to pin down the location of resonance poles for the low–lying states [9–12].

The mass and width of a resonance are found from the position of the nearest pole in the process amplitude (T-matrix or S-matrix) at an unphysical sheet of the complex energy plane, traditionally labeled as

$$\sqrt{s_{\rm Pole}} = M - i\,\Gamma/2\ .$$

It is important to note that the pole of a Breit-Wigner parameterization agrees with this pole position only for narrow and well–separated resonances, far away from the opening of decay channels. For a detailed discussion of this issue we refer to the review on *Resonances* in this RPP.

In this note, we discuss the light scalars below 2 GeV organized in the listings under the entries ($I = 1/2$) $K_0^*(700)$ (or κ), $K_0^*(1430)$, ($I = 1$) $a_0(980)$, $a_0(1450)$, and ($I = 0$) $f_0(500)$ (or σ), $f_0(980)$, $f_0(1370)$, $f_0(1500)$, and $f_0(1710)$. This list is minimal and does not necessarily exhaust the list of actual resonances. The ($I = 2$) $\pi\pi$ and ($I = 3/2$) $K\pi$ phase shifts do not exhibit any resonant behavior.

69.2. The $I = 1/2$ States

The $\boldsymbol{K_0^*(1430)}$ [14] is perhaps the least controversial of the light scalar mesons. The $K\pi$ S-wave scattering has two possible isospin channels, I=1/2 and I=3/2. The I=3/2 wave is elastic and repulsive up to 1.7 GeV [15] and contains no known resonances. The I=1/2 $K\pi$ phase shift, measured from about 100 MeV above threshold in Kp production, rises smoothly, passes 90° at 1350 MeV, and continues to rise to about 170° at 1600 MeV. The first important inelastic threshold is $K\eta'(958)$. In the inelastic region the continuation of the amplitude is uncertain since the partial-wave decomposition has several solutions. The data are extrapolated towards the $K\pi$ threshold using effective range type formulas [14,16] or chiral perturbation predictions [17,18]. From analyses using unitarized amplitudes there is agreement on the presence of a resonance pole around 1410 MeV having a width of about 300 MeV. With reduced model dependence, Ref. [19] finds a larger width of 500 MeV.

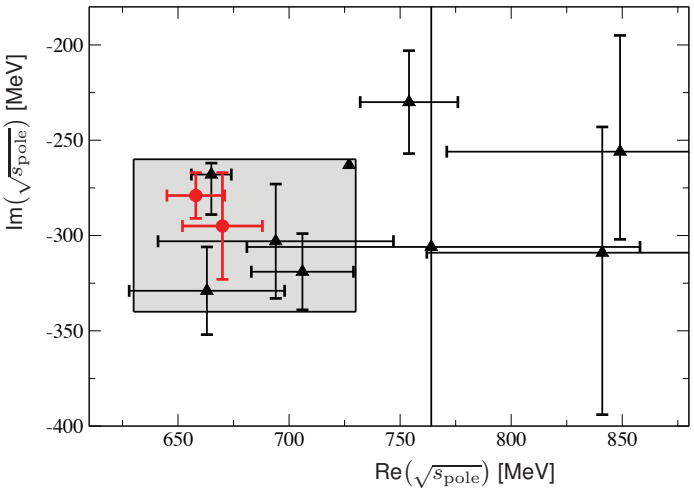

Figure 69.1: Location of the $K_0^*(700)$ (or κ) poles in the complex energy plane. Circles denote the results of the most refined analyses based on dispersion relations [44–45], while all other analyses quoted in the listings are denoted by triangles. The corresponding references are given in the listing.

Similar to the situation for the $f_0(500)$, discussed in the next section, the presence and properties of the light $\boldsymbol{K_0^*(700)}$ **(or $\boldsymbol{\kappa}$)** meson in the 700-900 MeV region are difficult to establish since it appears to have a very large width ($\Gamma \approx 500$ MeV) and resides close to the $K\pi$ threshold. Hadronic D- and B-meson decays provide additional data points in the vicinity of the $K\pi$ threshold and are discussed in detail in the *Review on Multibody Charm Analyses* in this RPP. Precision information from semileptonic D decays avoiding the theoretically more demanding final states with three strongly interacting particles is not available. BES II [20] (re-analyzed in [21]) finds a $K_0^*(700)$–like structure in J/ψ decays to $\bar{K}^{*0}(892)K^+\pi^-$ where $K_0^*(700)$ recoils against the $K^*(892)$. Also clean with respect to final-state interaction is the decay $\tau^- \to K_S^0\pi^-\nu_\tau$ studied by Belle [22], with $K_0^*(700)$ parameters fixed to those of Ref. [20].

Some authors find a $K_0^*(700)$ pole in their phenomenological analysis (see, *e.g.*, [23–34]), while others do not need to include it in their fits (see, *e.g.*, [18,35–38]). Similarly to the case of the $f_0(500)$ discussed below, all works including constraints from chiral symmetry at low energies naturally seem to find a light $K_0^*(700)$ below 800 MeV, see, *e.g.*, [39–43]. In these works the $K_0^*(700)$, $f_0(500)$, $f_0(980)$ and $a_0(980)$ appear to form a nonet [40,41]. Additional evidence for this assignment is presented in Ref. [12], where the couplings of the nine states to $\bar{q}q$ sources were compared. The same low–lying scalar nonet was also found earlier in the unitarized quark model of Ref. [42]. The analysis of Ref. [44] is based on the Roy-Steiner equations, which include analyticity and crossing symmetry. Ref. [45] uses the Padé method to extract pole parameters after refitting scattering data constrained to satisfy forward dispersion relations. Both arrive at compatible pole positions for the $K_0^*(700)$ that are consistent with the pole parameters deduced either from other theoretical methods or Breit-Wigner fits. This is illustrated in Fig. 69.1. The compilation in this figure is used as justification for the range of pole parameters of the $K_0^*(700)$ we quote as "our estimate", namely

$$\sqrt{s^{\kappa}_{\rm Pole}} = (630 - 730) - i(260 - 340)\ \text{MeV}\ .$$

69.3. The $I = 1$ States

Two isovector scalar states are known below 2 GeV, the $\boldsymbol{a_0(980)}$ and the $\boldsymbol{a_0(1450)}$. Independent of any model, the $K\bar{K}$ component

in the $a_0(980)$ wave function must be large: it lies just below the opening of the $K\bar{K}$ channel to which it strongly couples [16,47]. This generates an important cusp-like behavior in the resonant amplitude. Hence, its mass and width parameters are strongly distorted. To reveal its true coupling constants, a coupled–channel model with energy-dependent widths and mass shift contributions is necessary. All listed $a_0(980)$ measurements agree on a mass position value near 980 MeV, but the width takes values between 50 and 100 MeV, mostly due to the different models. For example, the analysis of the $p\bar{p}$-annihilation data [16] using a unitary K-matrix description finds a width as determined from the T-matrix pole of 92 ± 8 MeV, while the observed width of the peak in the $\pi\eta$ mass spectrum is about 45 MeV.

The relative coupling $K\bar{K}/\pi\eta$ is determined indirectly from $f_1(1285)$ [48–50] or $\eta(1410)$ decays [51–53], from the line shape observed in the $\pi\eta$ decay mode [54–57], or from the coupled-channel analysis of the $\pi\pi\eta$ and $K\bar{K}\pi$ final states of $p\bar{p}$ annihilation at rest [16].

The $a_0(1450)$ is seen in $p\bar{p}$ annihilation experiments with stopped and higher momenta antiprotons, with a mass of about 1450 MeV or close to the $a_2(1320)$ meson which is typically a dominant feature. A contribution from $a_0(1450)$ is also found in the analysis of the $D^{\pm} \to K^+K^-\pi^{\pm}$ [58] and $D^0 \to K^0_S K^{\pm}\pi^{\mp}$ [59] decay.

69.4. The $I = 0$ States

The $I = 0$, $J^{PC} = 0^{++}$ sector is the most complex one, both experimentally and theoretically. The data have been obtained from the $\pi\pi$, $K\bar{K}$, $\eta\eta$, 4π, and $\eta\eta'(958)$ systems produced in S-wave. Analyses based on several different production processes conclude that probably four poles are needed in the mass range from $\pi\pi$ threshold to about 1600 MeV. The claimed isoscalar resonances are found under separate entries $f_0(500)$ (or σ), $f_0(980)$, $f_0(1370)$, and $f_0(1500)$.

For discussions of the $\pi\pi$ S wave below the $K\bar{K}$ threshold and on the long history of the $f_0(500)$, which was suggested in linear sigma models more than 50 years ago, see our reviews in previous editions and the review [5].

Information on the $\pi\pi$ S-wave phase shift $\delta^I_J = \delta^0_0$ was already extracted many years ago from πN scattering [60–62], and near threshold from the K_{e4}-decay [63]. The kaon decays were later revisited leading to consistent data, however, with very much improved statistics [64,65]. The reported $\pi\pi \to K\bar{K}$ cross sections [66–69] have large uncertainties. The πN data have been analyzed in combination with high-statistics data (see entries labeled as RVUE for re-analyses of the data). The $2\pi^0$ invariant mass spectra of the $p\bar{p}$ annihilation at rest [70–72] and the central collision [73] do not show a distinct resonance structure below 900 MeV, but these data are consistently described with the standard solution for πN data [61,74], which allows for the existence of the broad $f_0(500)$. An enhancement is observed in the $\pi^+\pi^-$ invariant mass near threshold in the decays $D^+ \to \pi^+\pi^-\pi^+$ [75–103] and $J/\psi \to \omega\pi^+\pi^-$ [78,100], and in $\psi(2S) \to J/\psi\pi^+\pi^-$ with very limited phase space [80,81].

The precise **$f_0(500)$ (or σ)** pole is difficult to establish because of its large width, and because it can certainly not be modeled by a naive Breit-Wigner resonance. The $\pi\pi$ scattering amplitude shows an unusual energy dependence due to the presence of a zero in the unphysical regime close to the threshold [6–7], required by chiral symmetry, and possibly due to crossed channel exchanges, the $f_0(1370)$, and other dynamical features. However, most of the analyses listed under $f_0(500)$ agree on a pole position near $(500 - i\,250$ MeV). In particular, analyses of $\pi\pi$ data that include unitarity, $\pi\pi$ threshold behavior, strongly constrained by the K_{e4} data, and the chiral symmetry constraints from Adler zeroes and/or scattering lengths find a light $f_0(500)$, see, *e.g.*, [82,83].

Precise pole positions with an uncertainty of less than 20 MeV (see our table for the T-matrix pole) were extracted by use of Roy equations, which are twice subtracted dispersion relations derived from crossing symmetry and analyticity. In Ref. [10] the subtraction constants were fixed to the S-wave scattering lengths a^0_0 and a^2_0 derived from matching Roy equations and two-loop chiral perturbation theory [9]. The only additional relevant input to fix the $f_0(500)$ pole turned out to be the $\pi\pi$-wave phase shifts at 800 MeV. The

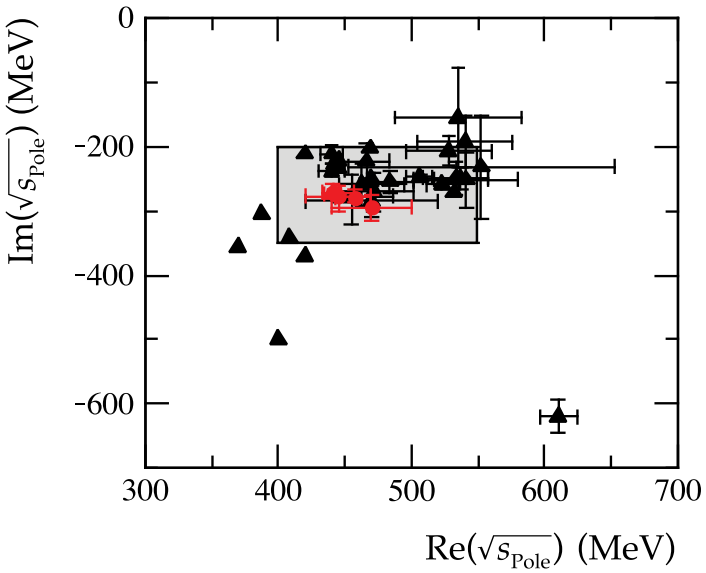

Figure 69.2: Location of the $f_0(500)$ (or σ) poles in the complex energy plane. Circles denote the recent analyses based on Roy(-like) dispersion relations [9–12], while all other analyses are denoted by triangles. The corresponding references are given in the listing.

analysis was improved further in Ref. [12]. Alternatively, in Ref. [11] only data were used as input inside Roy equations. In that reference also once-subtracted Roy–like equations, called GKPY equations, were used, since the extrapolation into the complex plane based on the twice subtracted equations leads to larger uncertainties mainly due to the limited experimental information on the isospin–2 $\pi\pi$ scattering length. Ref. [13] uses Padé approximants for the analytic continuation. All these extractions find consistent results. Using analyticity and unitarity only to describe data from $K_{2\pi}$ and K_{e4} decays, Ref. [84] finds consistent values for the pole position and the scattering length a^0_0. The importance of the $\pi\pi$ scattering data for fixing the $f_0(500)$ pole is nicely illustrated by comparing analyses of $\bar{p}p \to 3\pi^0$ omitting [70,85] or including [71,86] information on $\pi\pi$ scattering: while the former analyses find an extremely broad structure above 1 GeV, the latter find $f_0(500)$ masses of the order of 400 MeV.

As a result of the sensitivity of the extracted $f_0(500)$ pole position on the high accuracy low energy $\pi\pi$ scattering data [64,65], the currently quoted range of pole positions for the $f_0(500)$, namely

$$\sqrt{s^{\sigma}_{\rm Pole}} = (400 - 550) - i(200 - 350)\ \text{MeV}\ ,$$

in the listing was fixed including only those analyses consistent with these data, Refs. [27,30,40,42,43,56,71,80–84,87–103] as well as the advanced dispersion analyses [9–13]. The pole positions from those references are compared to the range of pole positions quoted above in Fig. 69.2. Note that this range is labeled as 'our estimate' — it is not an average over the quoted analyses but is chosen to include the bulk of the analyses consistent with the mentioned criteria. An averaging procedure is not justified, since the analyses use overlapping or identical data sets.

If one uses just the most advanced dispersive analyses of Refs. [9–12] shown as solid dots in Fig. 69.2 to determine the pole location of the $f_0(500)$ the range narrows down to [5]

$$\sqrt{s^{\sigma}_{\rm Pole}} = (449^{+22}_{-16}) - i(275 \pm 12)\ \text{MeV}\ ,$$

which is labeled as 'conservative dispersive estimate' in this reference.

Due to the large strong width of the $f_0(500)$ an extraction of its two–photon width directly from data is not possible. Thus, the

values for $\Gamma(\gamma\gamma)$ quoted in the literature as well as the listing are based on the expression in the narrow width approximation [104] $\Gamma(\gamma\gamma) \simeq \alpha^2|g_\gamma|^2/(4\mathrm{Re}(\sqrt{s^\sigma_{\mathrm{Pole}}}))$ where g_γ is derived from the residue at the $f_0(500)$ pole to two photons and α denotes the electromagnetic fine structure constant. The explicit form of the expression may vary between different authors due to different definitions of the coupling constant, however, the expression given for $\Gamma(\gamma\gamma)$ is free of ambiguities. According to Refs. [105,106], the data for $f_0(500) \to \gamma\gamma$ are consistent with what is expected for a two–step process of $\gamma\gamma \to \pi^+\pi^-$ via pion exchange in the t- and u-channel, followed by a final state interaction $\pi^+\pi^- \to \pi^0\pi^0$. The same conclusion is drawn in Ref. [107] where the bulk part of the $f_0(500) \to \gamma\gamma$ decay width is dominated by re–scattering. Therefore, it might be difficult to learn anything new about the nature of the $f_0(500)$ from its $\gamma\gamma$ coupling. For the most recent work on $\gamma\gamma \to \pi\pi$, see [108–110]. There are theoretical indications (*e.g.*, [111–114]) that the $f_0(500)$ pole behaves differently from a $q\bar{q}$-state – see next section and the mini-review on *non $q\bar{q}$-states* in this RPP for details.

The $\boldsymbol{f_0(980)}$ overlaps strongly with the background represented mainly by the $f_0(500)$ and the $f_0(1370)$. This can lead to a dip in the $\pi\pi$ spectrum at the $K\bar{K}$ threshold. It changes from a dip into a peak structure in the $\pi^0\pi^0$ invariant mass spectrum of the reaction $\pi^- p \to \pi^0\pi^0 n$ [115], with increasing four-momentum transfer to the $\pi^0\pi^0$ system, which means increasing the a_1-exchange contribution in the amplitude, while the π-exchange decreases. The $f_0(500)$ and the $f_0(980)$ are also observed in data for radiative decays ($\phi \to f_0\gamma$) from SND [116,117], CMD2 [118], and KLOE [119,120]. A dispersive analysis was used to simultaneously pin down the pole parameters of both the $f_0(500)$ and the $f_0(980)$ [11]; the uncertainty in the pole position quoted for the latter state is of the order of 10 MeV, only. We now quote for the mass

$$M_{f_0(980)} = 990 \pm 20 \text{ MeV} .$$

which is a range not an average, but is labeled as 'our estimate'.

Analyses of $\gamma\gamma \to \pi\pi$ data [121–123] underline the importance of the $K\bar{K}$ coupling of $f_0(980)$, while the resulting two-photon width of the $f_0(980)$ cannot be determined precisely [124]. The prominent appearance of the $f_0(980)$ in the semileptonic D_s decays and decays of B and B_s-mesons implies a dominant $(\bar{s}s)$ component: those decays occur via weak transitions that alternatively result in $\phi(1020)$ production. Ratios of decay rates of B and/or B_s mesons into J/ψ plus $f_0(980)$ or $f_0(500)$ were proposed to allow for an extraction of the flavor mixing angle and to probe the tetraquark nature of those mesons within a certain model [125,126]. The phenomenological fits of the LHCb collaboration using the isobar model do neither allow for a contribution of the $f_0(980)$ in the $B \to J/\psi\pi\pi$ [127] nor for an $f_0(500)$ in $B_s \to J/\psi\pi\pi$ decays [128]. From the former analysis the authors conclude that their data is incompatible with a model where $f_0(500)$ and $f_0(980)$ are formed from two quarks and two antiquarks (tetraquarks) at the eight standard deviation level. In addition, they extract an upper limit for the mixing angle of 17^o at 90% C.L. between the $f_0(980)$ and the $f_0(500)$ that would correspond to a substantial $(\bar{s}s)$ content in $f_0(980)$ [127]. However, in a dispersive analysis of the same data that allows for a model–independent inclusion of the hadronic final state interactions in Ref. [129] a substantial $f_0(980)$ contribution is also found in the B–decays putting into question the conclusions of Ref. [127].

The f_0's above 1 GeV. A meson resonance that is very well studied experimentally, is the $\boldsymbol{f_0(1500)}$ seen by the Crystal Barrel experiment in five decay modes: $\pi\pi$, $K\bar{K}$, $\eta\eta$, $\eta\eta'(958)$, and 4π [16,71,72]. Due to its interference with the $f_0(1370)$ (and $\boldsymbol{f_0(1710)}$), the peak attributed to the $f_0(1500)$ can appear shifted in invariant mass spectra. Therefore, the application of simple Breit-Wigner forms arrives at slightly different resonance masses for $f_0(1500)$. Analyses of central-production data of the likewise five decay modes Refs. [130,131] agree on the description of the S-wave with the one above. The $p\bar{p}$, $p\bar{n}/n\bar{p}$ measurements [72,132–134] show a single enhancement at 1400 MeV in the invariant 4π mass spectra, which is resolved into $f_0(1370)$ and $f_0(1500)$ [135,136]. The data on 4π from central production [137] require both resonances, too, but disagree on the relative content of $\rho\rho$ and $f_0(500)f_0(500)$ in 4π. All investigations agree that the 4π decay mode represents about half of the $f_0(1500)$ decay width and is dominant for $f_0(1370)$.

The determination of the $\pi\pi$ coupling of $\boldsymbol{f_0(1370)}$ is aggravated by the strong overlap with the broad $f_0(500)$ and $f_0(1500)$. Since it does not show up prominently in the 2π spectra, its mass and width are difficult to determine. Multichannel analyses of hadronically produced two- and three-body final states agree on a mass between 1300 MeV and 1400 MeV and a narrow $f_0(1500)$, but arrive at a somewhat smaller width for $f_0(1370)$.

69.5. Interpretation of the scalars below 1 GeV

In the literature, many suggestions are discussed, such as conventional $q\bar{q}$ mesons, compact $(qq)(\bar{q}\bar{q})$ structures (tetraquarks) or meson-meson bound states. In addition, one expects a scalar glueball in this mass range. In reality, there can be superpositions of these components, and one often depends on models to determine the dominant one. Although we have seen progress in recent years, this question remains open. Here, we mention some of the present conclusions.

The $f_0(980)$ and $a_0(980)$ are often interpreted as compact tetraquark states states [138–142] or $K\bar{K}$ bound states [143]. The insight into their internal structure using two-photon widths [117,144–150] is not conclusive. The $f_0(980)$ appears as a peak structure in $J/\psi \to \phi\pi^+\pi^-$ and in D_s decays without $f_0(500)$ background, while being nearly invisible in $J/\psi \to \omega\pi^+\pi^-$. Based on that observation it is suggested that $f_0(980)$ has a large $s\bar{s}$ component, which according to Ref. [151] is surrounded by a virtual $K\bar{K}$ cloud (see also Ref. [152]) . Data on radiative decays ($\phi \to f_0\gamma$ and $\phi \to a_0\gamma$) from SND, CMD2, and KLOE (see above) are consistent with a prominent role of kaon loops. This observation is interpreted as evidence for a compact four-quark [153] or a molecular [154,155] nature of these states. Details of this controversy are given in the comments [156,157]; see also Ref. [158]. It remains quite possible that the states $f_0(980)$ and $a_0(980)$, together with the $f_0(500)$ and the $K_0^*(700)$, form a new low-mass state nonet of predominantly four-quark states, where at larger distances the quarks recombine into a pair of pseudoscalar mesons creating a meson cloud (see, *e.g.,* Ref. [159]) . Different QCD sum rule studies [160–164] do not agree on a tetraquark configuration for the same particle group.

Models that start directly from chiral Lagrangians, either in non-linear [43,26,82,154] or in linear [165–171] realization, predict the existence of the $f_0(500)$ meson near 500 MeV. Here the $f_0(500)$, $a_0(980)$, $f_0(980)$, and $K_0^*(700)$ (in some models the $K_0^*(1430)$) would form a nonet (not necessarily $q\bar{q}$). In the linear sigma models the lightest pseudoscalars appear as their chiral partners. In these models the light $f_0(500)$ is often referred to as the "Higgs boson of strong interactions", since here the $f_0(500)$ plays a role similar to the Higgs particle in electro-weak symmetry breaking: within the linear sigma models it is important for the mechanism of chiral symmetry breaking, which generates most of the proton mass, and what is referred to as the constituent quark mass.

In the non–linear approaches of [26,82] the above resonances together with the low lying vector states are generated starting from chiral perturbation theory predictions near the first open channel, and then by extending the predictions to the resonance regions using unitarity and analyticity.

Ref. [165] uses a framework with explicit resonances that are unitarized and coupled to the light pseudoscalars in a chirally invariant way. Evidence for a non-$\bar{q}q$ nature of the lightest scalar resonances is derived from their mixing scheme. In Ref. [166] the scheme is extended and applied to the decay $\eta' \to \eta\pi\pi$, which lead to the same conclusions. To identify the nature of the resonances generated from scattering equations, in Ref. [172] the large N_c behavior of the poles was studied, with the conclusion that, while the light vector states behave consistent with what is predicted for $\bar{q}q$ states, the light scalars behave very differently. This finding provides strong support for a non-$\bar{q}q$ nature of the light scalar resonances. Note, the more refined study of Ref. [111] found, in case of the $f_0(500)$, in addition to a dominant non-$\bar{q}q$ nature, indications for a

subdominant $\bar{q}q$ component located around 1 GeV. Additional support for the non-$q\bar{q}$ nature of the $f_0(500)$ is given in Ref. [173], where the connection between the pole of resonances and their Regge trajectories is analyzed.

A model–independent method to identify hadronic molecu-les goes back to a proposal by Weinberg [174], shown to be equivalent to the pole counting arguments of [175–177] in Ref. [178]. The formalism allows one to extract the amount of molecular component in the wave function from the effective coupling constant of a physical state to a nearby continuum channel. It can be applied to near threshold states only and provided strong evidence that the $f_0(980)$ is a $\bar{K}K$ molecule, while the situation turned out to be less clear for the $a_0(980)$ (see also Refs. [150,148]). Further insights into $a_0(980)$ and $f_0(980)$ are expected from their mixing [179]. The corresponding signal predicted in Refs. [180,181] was recently observed at BES III [182]. It turned out that in order to get a quantitative understanding of those data in addition to the mixing mechanism itself, some detailed understanding of the production mechanism seems necessary [183].

In the unitarized quark model with coupled $q\bar{q}$ and meson-meson channels, the light scalars can be understood as additional manifestations of bare $q\bar{q}$ confinement states, strongly mass shifted from the 1.3 - 1.5 GeV region and very distorted due to the strong $^3P_0$ coupling to S-wave two-meson decay channels [184,185]. Thus, in these models the light scalar nonet comprising the $f_0(500)$, $f_0(980)$, $K_0^*(700)$, and $a_0(980)$, as well as the nonet consisting of the $f_0(1370)$, $f_0(1500)$ (or $f_0(1710)$), $K_0^*(1430)$, and $a_0(1450)$, respectively, are two manifestations of the same bare input states (see also Ref. [186]) .

Other models with different groupings of the observed resonances exist and may, *e.g.*, be found in earlier versions of this review.

69.6. Interpretation of the f_0's above 1 GeV

The $f_0(1370)$ and $f_0(1500)$ decay mostly into pions (2π and 4π) while the $f_0(1710)$ decays mainly into the $K\bar{K}$ final states. The $K\bar{K}$ decay branching ratio of the $f_0(1500)$ is small [130,187].

If one uses the naive quark model, it is natural to assume that the $f_0(1370)$, $a_0(1450)$, and the $K_0^*(1430)$ are in the same SU(3) flavor nonet, being the $(u\bar{u}+d\bar{d})$, $u\bar{d}$ and $u\bar{s}$ states, probably mixing with the light scalars [188], while the $f_0(1710)$ is the $s\bar{s}$ state. Indeed, the production of $f_0(1710)$ (and $f_2'(1525)$) is observed in $p\bar{p}$ annihilation [189] but the rate is suppressed compared to $f_0(1500)$ (respectively, $f_2(1270)$), as would be expected from the OZI rule for $s\bar{s}$ states. The $f_0(1500)$ would also qualify as a $(u\bar{u}+d\bar{d})$ state, although it is very narrow compared to the other states and too light to be the first radial excitation.

However, in $\gamma\gamma$ collisions leading to $K_S^0K_S^0$ [190] a spin–0 signal is observed at the $f_0(1710)$ mass (together with a dominant spin–2 component), while the $f_0(1500)$ is not observed in $\gamma\gamma \to K\bar{K}$ nor $\pi^+\pi^-$ [191]. In $\gamma\gamma$ collisions leading to $\pi^0\pi^0$ Ref. [192] reports the observation of a scalar around 1470 MeV albeit with large uncertainties on the mass and $\gamma\gamma$ couplings. This state could be the $f_0(1370)$ or the $f_0(1500)$. The upper limit from $\pi^+\pi^-$ [191] excludes a large $n\bar{n}$ (here n stands for the two lightest quarks) content for the $f_0(1500)$ and hence points to a mainly $s\bar{s}$ state [193]. This appears to contradict the small $K\bar{K}$ decay branching ratio of the $f_0(1500)$ and makes a $q\bar{q}$ assignment difficult for this state. Hence the $f_0(1500)$ could be mainly glue due the absence of a 2γ-coupling, while the $f_0(1710)$ coupling to 2γ would be compatible with an $s\bar{s}$ state. This is in accord with the recent high–statistics Belle data in $\gamma\gamma \to K_S^0K_S^0$ [194] in which the $f_0(1500)$ is absent, while a prominent peak at 1710 MeV is observed with quantum numbers 0^{++}, compatible with the formation of an $s\bar{s}$ state. However, the 2γ-couplings are sensitive to glue mixing with $q\bar{q}$ [195].

Note that an isovector scalar, possibly the $a_0(1450)$ (albeit at a lower mass of 1317 MeV) is observed in $\gamma\gamma$ collisions leading to $\eta\pi^0$ [196]. The state interferes destructively with the non-resonant background, but its $\gamma\gamma$ coupling is comparable to that of the $a_2(1320)$, in accord with simple predictions (see, *e.g.*, Ref. [193]) .

The small width of $f_0(1500)$, and its enhanced production at low transverse momentum transfer in central collisions [197–199] also favor $f_0(1500)$ to be non-$q\bar{q}$. In the mixing scheme of Ref. [195], which uses central production data from WA102 and the recent hadronic J/ψ decay data from BES [200,201], glue is shared between $f_0(1370)$, $f_0(1500)$ and $f_0(1710)$. The $f_0(1370)$ is mainly $n\bar{n}$, the $f_0(1500)$ mainly glue and the $f_0(1710)$ dominantly $s\bar{s}$. This agrees with previous analyses [202,203].

However, alternative schemes have been proposed (*e.g.*, in [204–210], for detailed reviews see, *e.g.*, Ref. [1] and the mini-review on *non–$q\bar{q}$ states* in this Review of Particle Physics (RPP)). In Ref. [210], a large K^+K^- scalar signal reported by Belle in B decays into $KK\bar{K}$ [211], compatible with the $f_0(1500)$, is explained as due to constructive interference with a broad glueball background. However, the Belle data are inconsistent with the BaBar measurements which show instead a broad scalar at this mass for B decays into both $K^\pm K^\pm K^\mp$ [212] and $K^+K^-\pi^0$ [213].

Whether the $f_0(1500)$ is observed in 'gluon rich' radiative J/ψ decays is debatable [214] because of the limited amount of data - more data for this and the $\gamma\gamma$ mode are needed.

In Ref. [215], further refined in Ref. [216], $f_0(1370)$ and $f_0(1710)$ (together with $f_2(1270)$ and $f_2'(1525)$) were interpreted as bound systems of two vector mesons. This picture could be tested in radiative J/ψ decays [217] as well as radiative decays of the states themselves [218]. The vector-vector component of the $f_0(1710)$ might also be the origin of the enhancement seen in $J/\psi \to \gamma\phi\omega$ near threshold [219] observed at BES [220]. Note that the results of Refs. [215,216] were challenged in Ref. [221] where in a covariant formalism, e.g., the $f_2(1270)$ did not not emerge as a $\rho\rho$-bound state.

References:

1. C. Amsler and N.A. Tornqvist, Phys. Reports **389**, 61 (2004).
2. D.V. Bugg, Phys. Reports **397**, 257 (2004).
3. F.E. Close and N.A. Tornqvist, J. Phys. **G28**, R249 (2002).
4. E. Klempt and A. Zaitsev, Phys. Reports **454**, 1 (2007).
5. J.R. Pelaez, Phys. Reports **658**, 1 (2016).
6. J.L. Adler, Phys. Rev. **137**, B1022 (1965).
7. J.L. Adler, Phys. Rev. **139**, B1638 (1965).
8. J.A. Oller, Phys. Rev. **D71**, 054030 (2005).
9. G. Colangelo, J. Gasser, and H. Leutwyler, Nucl. Phys. **B603**, 125 (2001).
10. I. Caprini, G. Colangelo, and H. Leutwyler, Phys. Rev. Lett. **96**, 132001 (2006).
11. R. Garcia-Martin *et al.*, Phys. Rev. Lett. **107**, 072001 (2011).
12. B. Moussallam, Eur. Phys. J. **C71**, 1814 (2011).
13. P. Masjuan, J. Ruiz de Elvira, J.J. Sanz-Cillero, Phys. Rev. **D90**, 097901 (2014).
14. D. Aston *et al.*, Nucl. Phys. **B296**, 493 (1988).
15. P.G. Estabrooks *et al.*, Nucl. Phys. **B133**, 490 (1978).
16. A. Abele *et al.*, Phys. Rev. **D57**, 3860 (1998).
17. V. Bernard, N. Kaiser, and U.-G. Meißner, Phys. Rev. **D43**, 2757 (1991).
18. S.N. Cherry and M.R. Pennington, Nucl. Phys. **A688**, 823 (2001).
19. J.M. Link *et al.*, Phys. Lett. **B648**, 156 (2007).
20. M. Ablikim *et al.*, Phys. Lett. **B633**, 681 (2006).
21. F.K. Guo *et al.*, Nucl. Phys. **A773**, 78 (2006).
22. D. Epifanov *et al.*, Phys. Lett. **B654**, 65 (2007).
23. C. Cawlfield *et al.*, Phys. Rev. **D74**, 031108R (2006).
24. A.V. Anisovich and A.V. Sarantsev, Phys. Lett. **B413**, 137 (1997).
25. R. Delbourgo *et al.*, Int. J. Mod. Phys. **A13**, 657 (1998).
26. J.A. Oller *et al.*, Phys. Rev. **D60**, 099906E (1999).
27. J.A. Oller and E. Oset, Phys. Rev. **D60**, 074023 (1999).
28. C.M. Shakin and H. Wang, Phys. Rev. **D63**, 014019 (2001).
29. M.D. Scadron *et al.*, Nucl. Phys. **A724**, 391 (2003).
30. D.V. Bugg, Phys. Lett. **B572**, 1 (2003).
31. M. Ishida, Prog. Theor. Phys. Supp. **149**, 190 (2003).
32. H.Q. Zheng *et al.*, Nucl. Phys. **A733**, 235 (2004).
33. Z.Y. Zhou and H.Q. Zheng, Nucl. Phys. **A775**, 212 (2006).
34. J.M. Link *et al.*, Phys. Lett. **B653**, 1 (2007).
35. B. Aubert *et al.*, Phys. Rev. **D76**, 011102R (2007).
36. S. Kopp *et al.*, Phys. Rev. **D63**, 092001 (2001).

37. J.M. Link *et al.*, Phys. Lett. **B535**, 43 (2002).
38. J.M. Link *et al.*, Phys. Lett. **B621**, 72 (2005).
39. M. Jamin *et al.*, Nucl. Phys. **B587**, 331 (2000).
40. D. Black, Phys. Rev. **D64**, 014031 (2001).
41. J.A. Oller, Nucl. Phys. **A727**, 353 (2003).
42. E. Van Beveren *et al.*, Z. Phys. **C30**, 615 (1986).
43. J.R. Pelaez, Mod. Phys. Lett. **A19**, 2879 (2004).
44. S. Descotes-Genon and B. Moussallam, Eur. Phys. J. **C48**, 553 (2006).
45. J.R. Pelaez, A. Rodas, J. Ruiz de Elvira, Eur. Phys. J. **C77**, 91 (2017).
46. J.J. Dudek *et al.*, Phys. Rev. Lett. **113**, 182001 (2014).
47. M. Bargiotti *et al.*, Eur. Phys. J. **C26**, 371 (2003).
48. D. Barberis *et al.*, Phys. Lett. **B440**, 225 (1998).
49. M.J. Corden *et al.*, Nucl. Phys. **B144**, 253 (1978).
50. C. Defoix *et al.*, Nucl. Phys. **B44**, 125 (1972).
51. Z. Bai *et al.*, Phys. Rev. Lett. **65**, 2507 (1990).
52. T. Bolton *et al.*, Phys. Rev. Lett. **69**, 1328 (1992).
53. C. Amsler *et al.*, Phys. Lett. **B353**, 571 (1995).
54. S.M. Flatte, Phys. Lett. **63B**, 224 (1976).
55. C. Amsler *et al.*, Phys. Lett. **B333**, 277 (1994).
56. G. Janssen *et al.*, Phys. Rev. **D52**, 2690 (1995).
57. D.V. Bugg, Phys. Rev. **D78**, 074023 (2008).
58. P. Rubin *et al.*, Phys. Rev. **D78**, 072003 (2008).
59. R. Aaij *et al.*, Phys. Rev. **D93**, 052018 (2016).
60. S.D. Protopopescu *et al.*, Phys. Rev. **D7**, 1279 (1973).
61. G. Grayer *et al.*, Nucl. Phys. **B75**, 189 (1974).
62. H. Becker *et al.*, Nucl. Phys. **B151**, 46 (1979).
63. L. Rosselet *et al.*, Phys. Rev. **D15**, 574 (1977).
64. S. Pislak *et al.*, Phys. Rev. Lett. **87**, 221801 (2001).
65. J.R. Batley *et al.*, Eur. Phys. J. **C70**, 635 (2010).
66. W. Wetzel *et al.*, Nucl. Phys. **B115**, 208 (1976).
67. V.A. Polychronakos *et al.*, Phys. Rev. **D19**, 1317 (1979).
68. D. Cohen *et al.*, Phys. Rev. **D22**, 2595 (1980).
69. A. Etkin *et al.*, Phys. Rev. **D25**, 1786 (1982).
70. C. Amsler *et al.*, Phys. Lett. **B342**, 433 (1995).
71. C. Amsler *et al.*, Phys. Lett. **B355**, 425 (1995).
72. A. Abele *et al.*, Phys. Lett. **B380**, 453 (1996).
73. D.M. Alde *et al.*, Phys. Lett. **B397**, 250 (1997).
74. R. Kaminski, L. Lesniak, and K. Rybicki, Z. Phys. **C74**, 79 (1997).
75. E.M. Aitala *et al.*, Phys. Rev. Lett. **86**, 770 (2001).
76. J.M. Link *et al.*, Phys. Lett. **B585**, 200 (2004).
77. G. Bonvicini *et al.*, Phys. Rev. **D76**, 012001 (2007).
78. J.E. Augustin and G. Cosme, Nucl. Phys. **B320**, 1 (1989).
79. M. Ablikim *et al.*, Phys. Lett. **B598**, 149 (2004).
80. A. Gallegos *et al.*, Phys. Rev. **D69**, 074033 (2004).
81. M. Ablikim *et al.*, Phys. Lett. **B645**, 19 (2007).
82. A. Dobado and J.R. Pelaez, Phys. Rev. **D56**, 3057 (1997).
83. I. Caprini, Phys. Rev. **D77**, 114019 (2008).
84. R. Garcia-Martin, J.R. Pelaez, and F.J. Yndurain, Phys. Rev. **D76**, 074034 (2007).
85. V.V. Anisovich *et al.*, Sov. Phys. Usp. **41**, 419 (1998).
86. V.V. Anisovich, Int. J. Mod. Phys. **A21**, 3615 (2006).
87. B.S. Zou and D.V. Bugg, Phys. Rev. **D48**, R3948 (1993).
88. N.A. Tornqvist and M. Roos, Phys. Rev. Lett. **76**, 1575 (1996).
89. B.S. Zou and D.V. Bugg, Phys. Rev. **D50**, 3145 (1994).
90. N.N. Achasov and G.N. Shestakov, Phys. Rev. **D49**, 5779 (1994).
91. M.P. Locher *et al.*, Eur. Phys. J. **C4**, 317 (1998).
92. J.A. Oller and E. Oset, Nucl. Phys. **A652**, 407 (1999).
93. T. Hannah, Phys. Rev. **D60**, 017502 (1999).
94. R. Kaminski *et al.*, Phys. Rev. **D50**, 3145 (1994).
95. R. Kaminski *et al.*, Phys. Lett. **B413**, 130 (1997).
96. R. Kaminski *et al.*, Eur. Phys. J. **C9**, 141 (1999).
97. M. Ishida *et al.*, Prog. Theor. Phys. **104**, 203 (2000).
98. Y.S. Surovtsev *et al.*, Phys. Rev. **D61**, 054024 (2001).
99. M. Ishida *et al.*, Phys. Lett. **B518**, 47 (2001).
100. M. Ablikim *et al.*, Phys. Lett. **B598**, 149 (2004).
101. Z.Y. Zhou *et al.*, JHEP **0502**, 043 (2005).
102. D.V. Bugg *et al.*, J. Phys. **G34**, 151 (2007).
103. G. Bonvicini *et al.*, Phys. Rev. **D76**, 012001 (2007).
104. D. Morgan and M.R. Pennington, Z. Phys. **C48**, 623 (1990).
105. M.R. Pennington, Phys. Rev. Lett. **97**, 011601 (2006).
106. M.R. Pennington, Mod. Phys. Lett. **A22**, 1439 (2007).
107. G. Mennessier, S. Narison, and W. Ochs, Phys. Lett. **B665**, 205 (2008).
108. R. Garcia-Martin and B. Moussallam, Eur. Phys. J. **C70**, 155 (2010).
109. M. Hoferichter *et al.*, Eur. Phys. J. **C71**, 1743 (2011).
110. L.Y. Dai and M.R. Pennington, Phys. Rev. **D90**, 036004 (2014).
111. J.R. Pelaez and G. Rios, Phys. Rev. Lett. **97**, 242002 (2006).
112. H.-X. Chen, A. Hosaka, and S.-L. Zhu, Phys. Lett. **B650**, 369 (2007).
113. F. Giacosa, Phys. Rev. **D75**, 054007 (2007).
114. L. Maiani *et al.*, Eur. Phys. J. **C50**, 609 (2007).
115. N.N. Achasov and G.N. Shestakov, Phys. Rev. **D58**, 054011 (1998).
116. N.N. Achasov *et al.*, Phys. Lett. **B479**, 53 (2000).
117. N.N. Achasov *et al.*, Phys. Lett. **B485**, 349 (2000).
118. R.R. Akhmetshin *et al.*, Phys. Lett. **B462**, 371 (1999).
119. A. Aloisio *et al.*, Phys. Lett. **B536**, 209 (2002).
120. F. Ambrosino *et al.*, Eur. Phys. J. **C49**, 473 (2007).
121. M. Boglione and M.R. Pennington, Eur. Phys. J. **C9**, 11 (1999).
122. T. Mori *et al.*, Phys. Rev. **D75**, 051101R (2007).
123. N.N. Achasov and G.N. Shestakov, Phys. Rev. **D77**, 074020 (2008).
124. M.R. Pennington *et al.*, Eur. Phys. J. **C56**, 1 (2008).
125. R. Fleischer *et al.*, Eur. Phys. J. **C71**, 1832 (2011).
126. S. Stone and L. Zhang, Phys. Rev. Lett. **111**, 062001 (2013).
127. R. Aaij *et al.*, Phys. Rev. **D90**, 012003 (2014).
128. R. Aaij *et al.*, Phys. Rev. **D89**, 092006 (2014).
129. J.T. Daub, C. Hanhart, and B. Kubis, JHEP **1602**, 009 (2016).
130. D. Barberis *et al.*, Phys. Lett. **B462**, 462 (1999).
131. D. Barberis *et al.*, Phys. Lett. **B479**, 59 (2000).
132. M. Gaspero, Nucl. Phys. **A562**, 407 (1993).
133. A. Adamo *et al.*, Nucl. Phys. **A558**, 13C (1993).
134. C. Amsler *et al.*, Phys. Lett. **B322**, 431 (1994).
135. A. Abele *et al.*, Eur. Phys. J. **C19**, 667 (2001).
136. A. Abele *et al.*, Eur. Phys. J. **C21**, 261 (2001).
137. D. Barberis *et al.*, Phys. Lett. **B471**, 440 (2000).
138. R. Jaffe, Phys. Rev. **D15**, 267,281 (1977).
139. M. Alford and R.L. Jaffe, Nucl. Phys. **B578**, 367 (2000).
140. L. Maiani *et al.*, Phys. Rev. Lett. **93**, 212002 (2004).
141. L. Maiani, A.D. Polosa, and V. Riquer, Phys. Lett. **B651**, 129 (2007).
142. G. 'tHooft *et al.*, Phys. Lett. **B662**, 424 (2008).
143. J. Weinstein and N. Isgur, Phys. Rev. **D41**, 2236 (1990).
144. T. Barnes, Phys. Lett. **B165**, 434 (1985).
145. Z.P. Li *et al.*, Phys. Rev. **D43**, 2161 (1991).
146. R. Delbourgo, D. Lui, and M. Scadron, Phys. Lett. **B446**, 332 (1999).
147. J.L. Lucio and M. Napsuciale, Phys. Lett. **B454**, 365 (1999).
148. C. Hanhart *et al.*, Phys. Rev. **D75**, 074015 (2007).
149. R.H. Lemmer, Phys. Lett. **B650**, 152 (2007).
150. T. Branz, T. Gutsche, and V. Lyubovitskij, Eur. Phys. J. **A37**, 303 (2008).
151. A. Deandrea *et al.*, Phys. Lett. **B502**, 79 (2001).
152. K.M. Ecklund *et al.*, Phys. Rev. **D80**, 052009 (2010).
153. N.N. Achasov, V.N. Ivanchenko, Nucl. Phys. **B315**, 465 (1989).
154. J.A. Oller *et al.*, Nucl. Phys. **A714**, 161 (2003).
155. Y.S. Kalashnikova *et al.*, Eur. Phys. J. **A24**, 437 (2005).
156. Y.S. Kalashnikova *et al.*, Phys. Rev. **D78**, 058501 (2008).
157. N.N. Achasov and A.V. Kiselev, Phys. Rev. **D78**, 058502 (2008).
158. M. Boglione and M.R. Pennington, Eur. Phys. J. **C30**, 503 (2003).
159. F. Giacosa and G. Pagliara, Phys. Rev. **C76**, 065204 (2007).
160. S. Narison, Nucl. Phys. **B96**, 244 (2001).
161. H.J. Lee, Eur. Phys. J. **A30**, 423 (2006).
162. H.X. Chen, A. Hosaka, and S.L. Zhu, Phys. Rev. **D76**, 094025 (2007).

163. J. Sugiyama *et al.*, Phys. Rev. **D76**, 114010 (2007).
164. T. Kojo and D. Jido, Phys. Rev. **D78**, 114005 (2008).
165. D. Black *et al.*, Phys. Rev. **D59**, 074026 (1999).
166. A.H. Fariborz *et al.*, Phys. Rev. **D90**, 033009 (2014).
167. M. Scadron, Eur. Phys. J. **C6**, 141 (1999).
168. M. Ishida, Prog. Theor. Phys. **101**, 661 (1999).
169. N. Tornqvist, Eur. Phys. J. **C11**, 359 (1999).
170. M. Napsuciale and S. Rodriguez, Phys. Lett. **B603**, 195 (2004).
171. M. Napsuciale and S. Rodriguez, Phys. Rev. **D70**, 094043 (2004).
172. J.R. Pelaez, Phys. Rev. Lett. **92**, 102001 (2004).
173. J.T. Londergan *et al.*, Phys. Lett. **B729**, 9 (2014).
174. S. Weinberg, Phys. Rev. **130**, 776 (1963).
175. D. Morgan and M.R. Pennington, Phys. Lett. **B258**, 444 (1991) [Phys. Lett. **B269**, 477 (1991)].
176. D. Morgan, Nucl. Phys. **A543**, 632 (1992).
177. N. Tornqvist, Phys. Rev. **D51**, 5312 (1995).
178. V. Baru *et al.*, Phys. Lett. **B586**, 53 (2004).
179. N.N. Achasov *et al.*, Phys. Lett. **B88**, 367 (1979).
180. J.-J. Wu *et al.*, Phys. Rev. **D75**, 114012 (2007).
181. C. Hanhart *et al.*, Phys. Rev. **D76**, 074028 (2007).
182. M. Ablikim *et al.*, Phys. Rev. **D83**, 032003 (2011).
183. L. Roca, Phys. Rev. **D88**, 014045 (2013).
184. N.A. Tornqvist, Z. Phys. **C68**, 647 (1995).
185. E. Van Beveren, Eur. Phys. J. **C22**, 493 (2001).
186. M. Boglione and M.R. Pennington, Phys. Rev. **D65**, 114010 (2002).
187. A. Abele *et al.*, Phys. Lett. **B385**, 425 (1996).
188. D. Black *et al.*, Phys. Rev. **D61**, 074001 (2000).
189. C. Amsler *et al.*, Phys. Lett. **B639**, 165 (2006).
190. M. Acciarri *et al.*, Phys. Lett. **B501**, 173 (2001).
191. R. Barate *et al.*, Phys. Lett. **B472**, 189 (2000).
192. S. Uehara *et al.*, Phys. Rev. **D78**, 052004 (2008).
193. C. Amsler, Phys. Lett. **B541**, 22 (2002).
194. S. Uehara, *et al.*, Prog. Theor. Exp. Phys. **2013**, 123C01 (2013).
195. F.E. Close and Q. Zhao, Phys. Rev. **D71**, 094022 (2005).
196. S. Uehara *et al.*, Phys. Rev. **D80**, 032001 (2009).
197. F.E. Close *et al.*, Phys. Lett. **B397**, 333 (1997).
198. F.E. Close, Phys. Lett. **B419**, 387 (1998).
199. A. Kirk, Phys. Lett. **B489**, 29 (2000).
200. M. Ablikim *et al.*, Phys. Lett. **B603**, 138 (2004).
201. M. Ablikim *et al.*, Phys. Lett. **B607**, 243 (2005).
202. C. Amsler and F.E. Close, Phys. Rev. **D53**, 295 (1996).
203. F.E. Close and A. Kirk, Eur. Phys. J. **C21**, 531 (2001).
204. P. Minkowski and W. Ochs, Eur. Phys. J. **C9**, 283 (1999).
205. W. Lee and D. Weingarten, Phys. Rev. **D61**, 014015 (2000).
206. M. Chanowitz, Phys. Rev. Lett. **95**, 172001 (2005).
207. F. Brünner and A. Rebhan, Phys. Rev. Lett. **115**, 131601 (2015).
208. S. Janowski *et al.*, Phys. Rev. **D90**, 114005 (2014).
209. M. Albaladejo and J.A. Oller, Phys. Rev. Lett. **101**, 252002 (2008).
210. P. Minkowski, W. Ochs, Eur. Phys. J. **C39**, 71 (2005).
211. A. Garmash *et al.*, Phys. Rev. **D71**, 092003 (2005).
212. B. Aubert *et al.*, Phys. Rev. **D74**, 032003 (2006).
213. B. Aubert *et al.*, Phys. Rev. Lett. **99**, 161802 (2007).
214. M. Ablikim *et al.*, Phys. Lett. **B642**, 441 (2006).
215. R. Molina *et al.*, Phys. Rev. **D78**, 114018 (2008).
216. C. Garcia-Recio *et al.*, Phys. Rev. **D87**, 096006 (2013).
217. L.S. Geng *et al.*, Eur. Phys. J. **A44**, 305 (2010).
218. T. Branz *et al.*, Phys. Rev. **D81**, 054037 (2010).
219. A. Martinez Torres *et al.*, Phys. Lett. **B719**, 388 (2013).
220. M. Ablikim *et al.*, Phys. Rev. Lett. **96**, 162002 (2006).
221. D. Gülmez, U.-G. Meißner, and J. A. Oller, Eur. Phys. J. **C77**, 460 (2017).

70. $\rho(770)$

Updated May 2012 by S. Eidelman (Novosibirsk) and G. Venanzoni (Frascati).

The determination of the parameters of the $\rho(770)$ is beset with many difficulties because of its large width. In physical region fits, the line shape does not correspond to a relativistic Breit-Wigner function with a P-wave width, but requires some additional shape parameter. This dependence on parameterization was demonstrated long ago [1]. Bose-Einstein correlations are another source of shifts in the $\rho(770)$ line shape, particularly in multiparticle final state systems [2].

The same model-dependence afflicts any other source of resonance parameters, such as the energy-dependence of the phase shift δ_1^1, or the pole position. It is, therefore, not surprising that a study of $\rho(770)$ dominance in the decays of the η and η' reveals the need for specific dynamical effects, in addition to the $\rho(770)$ pole [3,4].

The cleanest determination of the $\rho(770)$ mass and width comes from e^+e^- annihilation and τ-lepton decays. Analysis of ALEPH [5] showed that the charged $\rho(770)$ parameters measured from τ-lepton decays are consistent with those of the neutral one determined from e^+e^- data [6]. This conclusion is qualitatively supported by the later studies of CLEO [7] and Belle [8]. However, model-independent comparison of the two-pion mass spectrum in τ decays, and the $e^+e^- \to \pi^+\pi^-$ cross section, gave indications of discrepancies between the overall normalization: τ data are about 3% higher than e^+e^- data [7,9]. A detailed analysis using such two-pion mass spectra from τ decays measured by OPAL [10], CLEO [7], and ALEPH [11,12], as well as recent pion form factor measurements in e^+e^- annihilation by CMD-2 [13,14], showed that the discrepancy can be as high as 10% above the ρ meson [15,16]. This discrepancy remains after recent measurements of the two-pion cross section in e^+e^- annihilation at KLOE [17,18] and SND [19,20]. This effect is not accounted for by isospin breaking [21–24], but the accuracy of its calculation may be overestimated [25,26].

This problem seems to be solved after a recent analysis in [27] which showed that after correcting the τ data for the missing ρ - γ mixing contribution, besides the other known isospin symmetry violating corrections, the $\pi\pi$ I=1 part of the hadronic vacuum polarization contribution to the muon g -2 is fully compatible between τ based and e^+e^- based evaluations including more recent BaBar [28] and KLOE [29] data. Further proof of the consistency of the data on τ decays to two pions and e^+e^- annihilation is given by the global fit of the whole set of the ρ, ω, and ϕ decays, taking into account mixing effects in the hidden local symmetry model [30].

References:

1. J. Pisut and M. Roos, Nucl. Phys. **B6**, 325 (1968).
2. G.D. Lafferty, Z. Phys. **C60**, 659 (1993).
3. A. Abele *et al.*, Phys. Lett. **B402**, 195 (1997).
4. M. Benayoun *et al.*, Eur. Phys. J. **C31**, 525 (2003).
5. R. Barate *et al.*, Z. Phys. **C76**, 15 (1997).
6. L.M. Barkov *et al.*, Nucl. Phys. **B256**, 365 (1985).
7. S. Anderson *et al.*, Phys. Rev. **D61**, 112002 (2000).
8. M. Fujikawa *et al.*, Phys. Rev. **D78**, 072006 (2008).
9. S. Eidelman and V. Ivanchenko, Nucl. Phys. (Proc. Supp.) **B76**, 319 (1999).
10. K. Ackerstaff *et al.*, Eur. Phys. J. **C7**, 571 (1999).
11. M. Davier *et al.*, Nucl. Phys. (Proc. Supp.) **B123**, 47 (2003).
12. S. Schael *et al.*, Phys. Reports **421**, 191 (2005).
13. R.R. Akhmetshin *et al.*, Phys. Lett. **B527**, 161 (2002).
14. R.R. Akhmetshin *et al.*, Phys. Lett. **B578**, 285 (2004).
15. M. Davier *et al.*, Eur. Phys. J. **C27**, 497 (2003).
16. M. Davier *et al.*, Eur. Phys. J. **C31**, 503 (2003).
17. A. Aloisio *et al.*, Phys. Lett. **B606**, 12 (2005).
18. F. Ambrosino *et al.*, Phys. Lett. **B670**, 285 (2009).
19. M.N. Achasov *et al.*, Sov. Phys. JETP **101**, 1053 (2005).
20. M.N. Achasov *et al.*, Sov. Phys. JETP **103**, 380 (2006).
21. R. Alemany *et al.*, Eur. Phys. J. **C2**, 123 (1998).
22. H. Czyz and J.J. Kuhn, Eur. Phys. J. **C18**, 497 (2001).
23. V. Cirigliano *et al.*, Phys. Lett. **B513**, 361 (2001).
24. V. Cirigliano *et al.*, Eur. Phys. J. **C23**, 121 (2002).
25. K. Maltman and C.E. Wolfe, Phys. Rev. **D73**, 013004 (2006).
26. C.E. Wolfe and K. Maltman, Phys. Rev. **D80**, 114024 (2009).
27. F. Jegerlehner and R. Szafron, Eur. Phys. J. **C71**, 1632 (2011).
28. B. Aubert *et al.*, Phys. Rev. Lett. **103**, 231801 (2009).
29. F. Ambrosino *et al.*, Phys. Lett. **B700**, 102 (2011).
30. M. Benayoun *et al.*, Eur. Phys. J. **C72**, 1848 (2012).

71. Pseudoscalar and Pseudovector Mesons in the 1400 MeV Region

Revised August 2017 by C. Amsler (Stefan Meyer Institute for Subatomic Physics, Vienna) and A. Masoni (INFN Cagliari).

This minireview deals with some of the 0^{-+} and 1^{++} mesons reported in the 1200–1500 MeV region, namely the $\eta(1405)$, $\eta(1475)$, $f_1(1285)$ $f_1(1420)$, $a_1(1420)$ and $f_1(1510)$. The first observation of a pseudoscalar resonance around 1400 MeV – the $\eta(1440)$ – was made in $p\overline{p}$ annihilation at rest into $\eta(1440)\pi^+\pi^-$, $\eta(1440) \to K\overline{K}\pi$ [1]. This state was reported to decay into $a_0(980)\pi$ and $K^*(892)\overline{K}$ with roughly equal contributions. The $\eta(1440)$ was also observed in radiative $J/\psi(1S)$ decay into $K\overline{K}\pi$ [2–4] and $\gamma\rho$ [5]. However, two pseudoscalars are now reported in this mass region, the $\eta(1405)$ and $\eta(1475)$. The former decays mainly through $a_0(980)\pi$ (or direct $K\overline{K}\pi$) and the latter mainly to $K^*(892)\overline{K}$.

The simultaneous observation of two pseudoscalars is reported in three production mechanisms: $\pi^- p$ [6,7]; radiative $J/\psi(1S)$ decay [8,9]; and $\overline{p}p$ annihilation at rest [10–13]. All of them give values for the masses, widths, and decay modes that are in reasonable agreement. However, Ref. [9] favors a state decaying into $K^*(892)\overline{K}$ at a lower mass than the state decaying into $a_0(980)\pi$. In $J/\psi(1S)$ radiative decay, the $\eta(1405)$ decays into $K\overline{K}\pi$ through $a_0(980)\pi$, and hence a signal is also expected in the $\eta\pi\pi$ mass spectrum. This was indeed observed by MARK III in $\eta\pi^+\pi^-$ [14], which reported a mass of 1400 MeV, in line with the existence of the $\eta(1405)$ decaying into $a_0(980)\pi$.

BESII [15] observes an enhancement in $K^+K^-\pi^0$ around 1.44 GeV in $J/\psi(1S)$ decay, recoiling against an ω (but not a ϕ) without resolving the presence of two states nor performing a spin-parity analysis, due to low statistics. This state could also be the $f_1(1420)$ (see below). On the other hand, BESII observes $\eta(1405) \to \eta\pi\pi$ in $J/\psi(1S)$ decay, recoiling against an ω [16]. A single unresolved broad peak is also observed by BESIII in the decay $\psi(2S) \to \omega K^*K$ which could be due to $\eta(1405)$, $\eta(1475)$ and $f_1(1420)$ [17].

The $\eta(1405)$ is also observed in $\overline{p}p$ annihilation at rest into $\eta\pi^+\pi^-\pi^0\pi^0$, where it decays into $\eta\pi\pi$ [18]. The intermediate $a_0(980)\pi$ accounts for roughly half of the $\eta\pi\pi$ signal, in agreement with MARK III [14] and DM2 [4].

However, the issue remains controversial as to whether two pseudoscalar mesons really exist. According to Ref. [19] the splitting of a single state could be due to nodes in the decay amplitudes which differ in $\eta\pi\pi$ and $K^*(892)\overline{K}$. Based on the isospin-violating decay $J/\psi(1S) \to \gamma 3\pi$ observed by BESIII [20] the splitting could also be due to a triangular singularity mixing $\eta\pi\pi$ and $K^*(892)\overline{K}$ [21–22]. However, in a further paper [23], using the approach of [21], the authors concluded that the BESIII results can be reproduced either with the $\eta(1405)$ or the $\eta(1475)$, or by a mixture of these two states.

The $\eta(1295)$ has been observed by four $\pi^- p$ experiments [7,24–26], and evidence is reported in $\overline{p}p$ annihilation [27–29]. In $J/\psi(1S)$ radiative decay, the $\eta(1295)$ signal is evident in the 0^{-+} $\eta\pi\pi$ wave of the DM2 data [9]. Also BaBar [30] reports evidence for a signal around 1295 MeV in B decays into $\eta\pi\pi K$. Nonetheless, the existence of the $\eta(1295)$ is questioned in Refs. [19] and [31] in which the authors claim the existence of a single pseudoscalar meson at 1440 MeV, the first radial excitation of the η. This conclusion is mainly based on the analysis of the annihilation $\bar{p}p \to 4\pi\eta$ with Crystal Barrel data [32].

Considering that the $\eta(1295)$ has been reported by several experiments, using different production mechanisms, we shall assume that this state is established. The $\eta(1475)$ could then be the first radial excitation of the η', with the $\eta(1295)$ being the first radial excitation of the η. Ideal mixing, suggested by the $\eta(1295)$ and $\pi(1300)$ mass degeneracy, would then imply that the second isoscalar in the nonet is mainly $s\overline{s}$, and hence couples to $K^*\overline{K}$, in agreement with properties of the $\eta(1475)$. Also, its width matches the expected width for the radially excited $s\overline{s}$ state [33,34]. A study of radial excitations of pseudoscalar mesons [35] favors the $s\bar{s}$ interpretation of the $\eta(1475)$. However, due to the strong kinematical suppression the data are not sufficient to exclude a sizeable $s\bar{s}$ admixture also in the $\eta(1405)$.

The $K\overline{K}\pi$ and $\eta\pi\pi$ channels were studied in $\gamma\gamma$ collisions by L3 [36]. The analysis led to a clear $\eta(1475)$ signal in $K\overline{K}\pi$, decaying into $K^*\overline{K}$, very well identified in the untagged data sample, where contamination from spin 1 resonances is not allowed. At the same time, L3 [36] did not observe the $\eta(1405)$, neither in $K\overline{K}\pi$ nor in $\eta\pi\pi$. The observation of the $\eta(1475)$, combined with the absence of an $\eta(1405)$ signal, strengthens the two-resonances hypothesis. Since gluonium production is presumably suppressed in $\gamma\gamma$ collisions, the L3 results [36] suggest that $\eta(1405)$ has a large gluonic content (see also Refs. [37] and [38]) .

The L3 result is somewhat in disagreement with that of CLEO-II, which did not observe any pseudoscalar signal in $\gamma\gamma \to \eta(1475) \to K^0_S K^\pm\pi^\mp$ [39]. However, more data are required. Moreover, after the CLEO-II result, L3 performed a further analysis with full statistics [40], confirming their previous evidence for the $\eta(1475)$. The CLEO upper limit [39] for $\Gamma_{\gamma\gamma}(\eta(1475))$, and the L3 results [40], are consistent with the world average for the $\eta(1475)$ width.

BaBar [30] also reports the $\eta(1475)$ in B decays into $K\bar{K}^*K$ with the $\eta(1475) \to K\bar{K}^*$ recoiling against a K, but upper limits only are given for the $\eta(1405)$. As mentioned above, in B decays into $\eta\pi\pi K$ the $\eta(1295) \to \eta\pi\pi$ is observed while only upper limits are given for the $\eta(1405)$. The $f_1(1420)$ (and $f_1(1285)$) are not seen.

The gluonium interpretation for the $\eta(1405)$ is not favored by lattice gauge theories which predict the 0^{-+} state above 2 GeV [41,42] (see also the article on the "Quark model" in this issue of the Review). However, the $\eta(1405)$ is an excellent candidate for the 0^{-+} glueball in the fluxtube model [43]. In this model, the 0^{++} $f_0(1500)$ glueball is also naturally related to a 0^{-+} glueball with mass degeneracy broken in QCD. Also, Ref. [44] shows that the pseudoscalar glueball could lie at a lower mass than predicted from lattice calculation. In this model the $\eta(1405)$ appears as the natural glueball candidate, see also Refs. [45–47]. A detailed review of the experimental situation is available in Ref. 48.

Let us now deal with the 1^{++} mesons. The pseudovector nonet is believed to consist of the isovector $a_1(1260)$, the isoscalars $f_1(1285)$ and $f_1(1420)$, and the K_{1A}, which is a mixture of about 50% $K_1(1270)$ and 50% $K_1(1400)$. (This last property prevents a straightforward calculation of the nonet mixing angle via the mass formulae.) The $f_1(1285)$ could also be a $K^*\overline{K}$ molecule [49] or as a tetraquark state [50] and the $f_1(1420)$ a $K^*\overline{K}$ molecule, due to the proximity of the $K^*\overline{K}$ threshold [51]. LHCb has analyzed the decays $\overline{B}^0$ and $\overline{B}^0_s \to J/\psi(1S)f_1(1285)$ and determined the nonet mixing angle to be consistent with a mostly $u\overline{u} + d\overline{d}$ structure [52] without specifying the identity of its isoscalar partner. This is consistent with earlier determinations assuming the $f_1(1420)$ as the isoscalar partner [53] and the ratio of $\overline{B}^0/\overline{B}^0_s$ decay rates excludes the tetraquark interpretation of this state [52].

The $f_1(1420)$, decaying into $K^*\overline{K}$, was first reported in $\pi^- p$ reactions at 4 GeV/c [54]. However, later analyses found that the 1400–1500 MeV region was far more complex [55–57]. A reanalysis of the MARK III data in radiative $J/\psi(1S)$ decay into $K\overline{K}\pi$ [8] shows the $f_1(1420)$ decaying into $K^*\overline{K}$. A C=+1 state is also seen in tagged $\gamma\gamma$ collisions (*e.g.*, Ref. [58]) .

In $\pi^- p \to \eta\pi\pi n$ charge-exchange reactions at 8–9 GeV/c the $\eta\pi\pi$ mass spectrum is dominated by the $\eta(1440)$ and $\eta(1295)$ [24,59], and at 100 GeV/c Ref. [25] reports the $\eta(1295)$ and $\eta(1440)$ decaying into $\eta\pi^0\pi^0$ with a weak $f_1(1285)$ signal, and no evidence for the $f_1(1420)$.

Axial (1^{++}) mesons are not observed in $\overline{p}p$ annihilation at rest in liquid hydrogen, which proceeds dominantly through S-wave annihilation. However, in gaseous hydrogen, P-wave annihilation is enhanced and, indeed, Ref. [11] reports $f_1(1420)$ decaying into $K^*\overline{K}$. The $f_1(1420)$, decaying into $K\overline{K}\pi$, is also seen in pp central production, together with the $f_1(1285)$. The latter decays via $a_0(980)\pi$, and the former only via $K^*\overline{K}$, while the $\eta(1440)$ is absent [60,61]. The $K^0_S K^0_S\pi^0$ decay mode of the $f_1(1420)$ establishes unambiguously C=+1. On the other hand, there is no evidence for any state decaying into $\eta\pi\pi$ around 1400 MeV, and hence the $\eta\pi\pi$ mode of the $f_1(1420)$ must be suppressed [62].

The COMPASS Collaboration has recently reported an isovector state at 1414 MeV, the $a_1(1420)$ [63]. This relatively narrow state ($\simeq$150 MeV) is produced by diffractive dissociation with 190

GeV pions in $\pi N \to 3\pi N$, decays into $f_0(980)\pi \to 3\pi$ (P-wave) and has therefore the quantum numbers $(I^G)J^{PC} = (1^-)1^{++}$. The pseudovector nonet already contains the established $a_1(1260)$ as the $I = 1$ state. As mentioned above, the $f_1(1420)$ has been interpreted as a $K^*\overline{K}$ molecule [51]. The new $a_1(1420)$ could be its isovector partner. Arguments favoring the $f_1(1420)$ being a hybrid $q\overline{q}g$ meson [64] or a four-quark state [65] were also put forward. The $q\overline{q}$ state would then remain to be identified, with the $f_1(1510)$ (see below) as a candidate. However, an alternative explanation is suggested in Ref. [66] in which the authors claim a single 1^{++} isovector around 1400 MeV, leading to two peaks in the 3π mass spectrum, depending on the production mechanism, $\rho\pi$ for the $a_1(1260)$ and $f_0(980)\pi$ for the $a_1(1420)$.

We now turn to the experimental evidence for the $f_1(1510)$. The $f_1(1510)$ was seen in $K^-p \to \Lambda K\overline{K}\pi$ at 4 GeV/c [67], and at 11 GeV/c [68]. Evidence is also reported in π^-p at 8 GeV/c, based on the phase motion of the 1^{++} $K^*\overline{K}$ wave [57]. A somewhat broader 1^{++} signal is also observed in $J/\psi(1S) \to \gamma\eta\pi^+\pi^-$ [69] as well as a small signal in $J/\psi(1S) \to \gamma\eta'\pi^+\pi^-$, attributed to the $f_1(1510)$ [70].

The absence of $f_1(1420)$ in K^-p [68] argues against the $f_1(1420)$ being the $s\overline{s}$ member of the 1^{++} nonet. However, the $f_1(1420)$ was reported in K^-p but not in π^-p [71], while two experiments do not observe the $f_1(1510)$ in K^-p [71,72]. The latter is also not seen in central collisions [61], nor $\gamma\gamma$ collisions [73], although, surprisingly for an $s\overline{s}$ state, a signal is reported in 4π decays [74]. These facts led to the conclusion that $f_1(1510)$ was not well established [75].

Summarizing, there is evidence for two isovector 1^{++} states in the 1400 MeV region, the $a_1(1260)$ and $a_1(1420)$, which cannot be both $q\overline{q}$ states. These two states could stem from the same pole, or the latter be exotic (tetraquark or hybrid) or a molecular state. The $f_1(1285)$ and the $f_1(1420)$ are well known but their nature ($q\overline{q}$, tetraquark or molecular) remains to be established. In the 0^{-+} sector there is evidence for two pseudoscalars in the 1400 MeV region, the $\eta(1405)$ and $\eta(1475)$, decaying into $a_0(980)\pi$ and $K^*\overline{K}$, respectively. Alternatively, these two structures could originate from a single pole. Doubts have been expressed on the existence of the $\eta(1295)$. The $f_1(1510)$ remains to be firmly established.

References:

1. P.H. Baillon *et al.*, Nuovo Cimento **50A**, 393 (1967).
2. D.L. Scharre *et al.*, Phys. Lett. **97B**, 329 (1980).
3. C. Edwards *et al.*, Phys. Rev. Lett. **49**, 259 (1982).
4. J.E. Augustin *et al.*, Phys. Rev. **D42**, 10 (1990).
5. J.Z. Bai *et al.*, Phys. Lett. **B594**, 47 (2004).
6. M.G. Rath *et al.*, Phys. Rev. **D40**, 693 (1989).
7. G.S. Adams *et al.*, Phys. Lett. **B516**, 264 (2001).
8. J.Z. Bai *et al.*, Phys. Rev. Lett. **65**, 2507 (1990).
9. J.E. Augustin and G. Cosme, Phys. Rev. **D46**, 1951 (1992).
10. A. Bertin *et al.*, Phys. Lett. **B361**, 187 (1995).
11. A. Bertin *et al.*, Phys. Lett. **B400**, 226 (1997).
12. C. Cicalo *et al.*, Phys. Lett. **B462**, 453 (1999).
13. F. Nichitiu *et al.*, Phys. Lett. **B545**, 261 (2002).
14. T. Bolton *et al.*, Phys. Rev. Lett. **69**, 1328 (1992).
15. M. Ablikim *et al.*, Phys. Rev. **D77**, 032005 (2008).
16. M. Ablikim *et al.*, Phys. Rev. Lett. **107**, 182001 (2011).
17. M. Ablikim *et al.*, Phys. Rev. **D87**, 092006 (2013).
18. C. Amsler *et al.*, Phys. Lett. **B358**, 389 (1995).
19. E. Klempt and A. Zaitsev, Phys. Reports **454**, 1 (2007).
20. M. Ablikim *et al.*, Phys. Rev. Lett. **108**, 182001 (2012).
21. J.-J. Wu *et al.*, Phys. Rev. Lett. **108**, 081803 (2012).
22. X.-G. Wu *et al.*, Phys. Rev. **D87**, 014023 (2013).
23. F. Aceti *et al.*, Phys. Rev. **D86**, 114007 (2012).
24. S. Fukui *et al.*, Phys. Lett. **B267**, 293 (1991).
25. D. Alde *et al.*, Phys. Atom. Nucl. **60**, 386 (1997).
26. J.J. Manak *et al.*, Phys. Rev. **D62**, 012003 (2000).
27. A.V. Anisovich *et al.*, Nucl. Phys. **A690**, 567 (2001).
28. A. Abele *et al.*, Phys. Rev. **D57**, 3860 (1998).
29. C. Amsler *et al.*, Eur. Phys. J. **C33**, 23 (2004).
30. B. Aubert *et al.*, Phys. Rev. Lett. **101**, 091801 (2008).
31. E. Klempt, Int. J. Mod. Phys. **A21**, 739 (2006).
32. J. Reinnarth, PhD Thesis, University of Bonn (2003).
33. F. Close *et al.*, Phys. Lett. **B397**, 333 (1997).
34. T. Barnes *et al.*, Phys. Rev. **D55**, 4157 (1997).
35. T. Gutsche *et al.*, Phys. Rev. **D79**, 014036 (2009).
36. M. Acciarri *et al.*, Phys. Lett. **B501**, 1 (2001).
37. F. Close *et al.*, Phys. Rev. **D55**, 5749 (1997).
38. D.M. Li *et al.*, Eur. Phys. J. **C28**, 335 (2003).
39. R. Ahohe *et al.*, Phys. Rev. **D71**, 072001 (2005).
40. P. Achard *et al.*, JHEP **0703**, 018 (2007).
41. G.S. Bali *et al.*, Phys. Lett. **B309**, 378 (1993).
42. C. Morningstar and M. Peardon, Phys. Rev. **D60**, 034509 (1999).
43. L. Faddeev *et al.*, Phys. Rev. **D70**, 114033 (2004).
44. H.-Y. Cheng *et al.*, Phys. Rev. **D79**, 014024 (2009).
45. G. Li *et al.*, J. Phys. **G35**, 055002 (2008).
46. T. Gutsche *et al.*, Phys. Rev. **D80**, 014014 (2009).
47. B. Li, Phys. Rev. **D81**, 114002 (2010).
48. A. Masoni, C. Cicalo, and G.L. Usai, J. Phys. **G32**, R293 (2006).
49. F. Aceti *et al.*, Phys. Lett. **B750**, 609 (2015).
50. S. Stone and L. Zhang, Phys. Rev. Lett. **111**, 062001 (2013).
51. R.S. Longacre, Phys. Rev. **D42**, 874 (1990).
52. R. Aaij *et al.*, Phys. Rev. Lett. **112**, 091802 (2014).
53. G. Gidal *et al.*, Phys. Rev. Lett. **59**, 2012 (1987).
54. C. Dionisi *et al.*, Nucl. Phys. **B169**, 1 (1980).
55. S.U. Chung *et al.*, Phys. Rev. Lett. **55**, 779 (1985).
56. D.F. Reeves *et al.*, Phys. Rev. **D34**, 1960 (1986).
57. A. Birman *et al.*, Phys. Rev. Lett. **61**, 1557 (1988).
58. H.J. Behrend *et al.*, Z. Phys. **C42**, 367 (1989).
59. A. Ando *et al.*, Phys. Rev. Lett. **57**, 1296 (1986).
60. T.A. Armstrong *et al.*, Phys. Lett. **B221**, 216 (1989).
61. D. Barberis *et al.*, Phys. Lett. **B413**, 225 (1997).
62. T.A. Armstrong *et al.*, Z. Phys. **C52**, 389 (1991).
63. C. Adolph *et al.*, Phys. Rev. Lett. **115**, 082001 (2015).
64. S. Ishida *et al.*, Prog. Theor. Phys. **82**, 119 (1989).
65. D.O. Caldwell, *Hadron 89 Conf., Ajaccio, Corsica*, p. 127.
66. J.-L. Basdevant and E.L. Berger, Phys. Rev. Lett. **114**, 192001 (2015).
67. P. Gavillet *et al.*, Z. Phys. **C16**, 119 (1982).
68. D. Aston *et al.*, Phys. Lett. **B201**, 573 (1988).
69. J.Z. Bai *et al.*, Phys. Lett. **B446**, 356 (1999).
70. M. Ablikim *et al.*, Phys. Rev. Lett. **106**, 072002 (2011).
71. S. Bityukov *et al.*, Sov. J. Nucl. Phys. **39**, 738 (1984).
72. E. King *et al.*, Nucl. Phys. (Proc. Supp.) **B21**, 11 (1991).
73. H. Aihara *et al.*, Phys. Rev. **D38**, 1 (1988).
74. D.A. Bauer *et al.*, Phys. Rev. **D48**, 3976 (1993).
75. F.E. Close and A. Kirk, Z. Phys. **C76**, 469 (1997).

72. $\rho(1450)$ and $\rho(1700)$

Updated November 2015 by S. Eidelman (Novosibirsk), C. Hanhart (Juelich) and G. Venanzoni (Frascati).

In our 1988 edition, we replaced the $\rho(1600)$ entry with two new ones, the $\rho(1450)$ and the $\rho(1700)$, because there was emerging evidence that the 1600-MeV region actually contains two ρ-like resonances. Erkal [1] had pointed out this possibility with a theoretical analysis on the consistency of 2π and 4π electromagnetic form factors and the $\pi\pi$ scattering length. Donnachie [2], with a full analysis of data on the 2π and 4π final states in e^+e^- annihilation and photoproduction reactions, had also argued that in order to obtain a consistent picture, two resonances were necessary. The existence of $\rho(1450)$ was supported by the analysis of $\eta\rho^0$ mass spectra obtained in photoproduction and e^+e^- annihilation [3], as well as that of $e^+e^- \to \omega\pi$ [4].

The analysis of [2] was further extended by [5,6] to include new data on 4π-systems produced in e^+e^- annihilation, and in τ-decays (τ decays to 4π, and e^+e^- annihilation to 4π can be related by the Conserved Vector Current assumption). These systems were successfully analyzed using interfering contributions from two ρ-like states, and from the tail of the $\rho(770)$ decaying into two-body states. While specific conclusions on $\rho(1450) \to 4\pi$ were obtained, little could be said about the $\rho(1700)$.

Independent evidence for two 1^- states is provided by [7] in 4π electroproduction at $\langle Q^2\rangle = 1$ (GeV/c)^2, and by [8] in a high-statistics sample of the $\eta\pi\pi$ system in $\pi^- p$ charge exchange.

This scenario with two overlapping resonances is supported by other data. Bisello [9] measured the pion form factor in the interval 1.35–2.4 GeV, and observed a deep minimum around 1.6 GeV. The best fit was obtained with the hypothesis of ρ-like resonances at 1420 and 1770 MeV, with widths of about 250 MeV. Antonelli [10] found that the $e^+e^- \to \eta\pi^+\pi^-$ cross section is better fitted with two fully interfering Breit-Wigners, with parameters in fair agreement with those of [2] and [9]. These results can be considered as a confirmation of the $\rho(1450)$.

Decisive evidence for the $\pi\pi$ decay mode of both $\rho(1450)$ and $\rho(1700)$ comes from $\overline{p}p$ annihilation at rest [11]. It has been shown that these resonances also possess a $K\overline{K}$ decay mode [12–14]. High-statistics studies of the decays $\tau \to \pi\pi\nu_\tau$ [15,16], and $\tau \to 4\pi\nu_\tau$ [17] also require the $\rho(1450)$, but are not sensitive to the $\rho(1700)$, because it is too close to the τ mass. A recent very-high-statistics study of the $\tau \to \pi\pi\nu_\tau$ decay performed at Belle [18] reports the first observation of both $\rho(1450)$ and $\rho(1700)$ in τ decays. A clear picture of the two $\pi^+\pi^-$ resonances interfering with the $\rho(770)$ was also reported by BaBar using the ISR method [19].

The structure of these ρ states is not yet completely clear. Barnes [20] and Close [21] claim that $\rho(1450)$ has a mass consistent with radial $2S$, but its decays show characteristics of hybrids, and suggest that this state may be a $2S$-hybrid mixture. Donnachie [22] argues that hybrid states could have a 4π decay mode dominated by the $a_1\pi$. Such behavior has been observed by [23] in $e^+e^- \to 4\pi$ in the energy range 1.05–1.38 GeV, and by [17] in $\tau \to 4\pi$ decays. CLEO [24] and Belle [25] observe the $\rho(1450) \to \omega\pi$ decay mode in B-meson decays, however, do not find $\rho(1700) \to \omega\pi^0$. A similar conclusion is made by [26], who studied the process $e^+e^- \to \omega\pi^0$. Various decay modes of the $\rho(1450)$ and $\rho(1700)$ are observed in $\overline{p}n$ and $\overline{p}p$ annihilation [27,28], but no definite conclusions can be drawn. More data should be collected to clarify the nature of the ρ states, particularly in the energy range above 1.6 GeV.

We now list under a separate entry the $\rho(1570)$, the $\phi\pi$ state with $J^{PC} = 1^{--}$ earlier observed by [29] (referred to as $C(1480)$) and recently confirmed by [30]. While [31] shows that it may be a threshold effect, [5] and [32] suggest two independent vector states with this decay mode. The $C(1480)$ has not been seen in the $\overline{p}p$ [33] and e^+e^- [34,35] experiments. However, the sensitivity of the two latter is an order of magnitude lower than that of [30]. Note that [30] can not exclude that their observation is due to an OZI-suppressed decay mode of the $\rho(1700)$.

Several observations on the $\omega\pi$ system in the 1200-MeV region [36–42] may be interpreted in terms of either $J^P = 1^-$ $\rho(770) \to \omega\pi$ production [43], or $J^P = 1^+$ $b_1(1235)$ production [41,42]. We argue that no special entry for a $\rho(1250)$ is needed. The LASS amplitude analysis [44] showing evidence for $\rho(1270)$ is preliminary and needs confirmation. For completeness, the relevant observations are listed under the $\rho(1450)$.

Recently [45] reported a very broad 1^{--} resonance-like K^+K^- state in $J/\psi \to K^+K^-\pi^0$ decays. Its pole position corresponds to mass of 1576 MeV and width of 818 MeV. [46–48] suggest its exotic structure (molecular or multiquark), while [49] and [50] explain it by the interference between the $\rho(1450)$ and $\rho(1700)$. We quote [45] as $X(1575)$ in the section "Further States."

Evidence for ρ-like mesons decaying into 6π states was first noted by [51] in the analysis of 6π mass spectra from e^+e^- annihilation [52,53] and diffractive photoproduction [54]. Clegg [51] argued that two states at about 2.1 and 1.8 GeV exist: while the former is a candidate for the $\rho(2150)$, the latter could be a manifestation of the $\rho(1700)$ distorted by threshold effects. BaBar reported observations of the new decay modes of the $\rho(2150)$ in the channels $\eta'(958)\pi^+\pi^-$ and $f_1(1285)\pi^+\pi^-$ [55]. The relativistic quark model [56] predicts the 2^3D_1 state with $J^{PC} = 1^{--}$ at 2.15 GeV which can be identified with the $\rho(2150)$.

We no longer list under a separate particle $\rho(1900)$ various observations of irregular behavior of the cross sections near the $N\bar{N}$ threshold. Dips of various width around 1.9 GeV were reported by the E687 Collaboration (a narrow one in the $3\pi^+3\pi^-$ diffractive photoproduction [57,58]) , by the FENICE experiment (a narrow structure in the R value [59]) , by BaBar in ISR (a narrow structure in $e^+e^- \to \phi\pi$ final state [60], but much broader in $e^+e^- \to 3\pi^+3\pi^-$ and $e^+e^- \to 2(\pi^+\pi^-\pi^0)$ [61]) , by CMD-3 (also a rather broad dip in $e^+e^- \to 3\pi^+3\pi^-$ [62]) . Most probably, these structures emerge as a threshold effect due to the opening of the $N\bar{N}$ channel [63,64].

References:

1. C. Erkal, Z. Phys. **C31**, 615 (1986).
2. A. Donnachie and H. Mirzaie, Z. Phys. **C33**, 407 (1987).
3. A. Donnachie and A.B. Clegg, Z. Phys. **C34**, 257 (1987).
4. A. Donnachie and A.B. Clegg, Z. Phys. **C51**, 689 (1991).
5. A.B. Clegg and A. Donnachie, Z. Phys. **C40**, 313 (1988).
6. A.B. Clegg and A. Donnachie, Z. Phys. **C62**, 455 (1994).
7. T.J. Killian *et al.*, Phys. Rev. **D21**, 3005 (1980).
8. S. Fukui *et al.*, Phys. Lett. **B202**, 441 (1988).
9. D. Bisello *et al.*, Phys. Lett. **B220**, 321 (1989).
10. A. Antonelli *et al.*, Phys. Lett. **B212**, 133 (1988).
11. A. Abele *et al.*, Phys. Lett. **B391**, 191 (1997).
12. A. Abele *et al.*, Phys. Rev. **D57**, 3860 (1998).
13. A. Bertin *et al.*, Phys. Lett. **B434**, 180 (1998).
14. A. Abele *et al.*, Phys. Lett. **B468**, 178 (1999).
15. R. Barate *et al.*, Z. Phys. **C76**, 15 (1997).
16. S. Anderson, Phys. Rev. **D61**, 112002 (2000).
17. K.W. Edwards *et al.*, Phys. Rev. **D61**, 072003 (2000).
18. M. Fujikawa *et al.*, Phys. Rev. **D78**, 072006 (2008).
19. J.P. Lees *et al.*, Phys. Rev. **D86**, 032013 (2012).
20. T. Barnes *et al.*, Phys. Rev. **D55**, 4157 (1997).
21. F.E. Close *et al.*, Phys. Rev. **D56**, 1584 (1997).
22. A. Donnachie and Yu.S. Kalashnikova, Phys. Rev. **D60**, 114011 (1999).
23. R.R. Akhmetshin *et al.*, Phys. Lett. **B466**, 392 (1999).
24. J.P. Alexander *et al.*,Phys. Rev. **D64**, 092001 (2001).
25. D. Matvienko *et al.*,Phys. Rev. **D92**, 012013 (2015).
26. R.R. Akhmetshin *et al.*, Phys. Lett. **B562**, 173 (2003).
27. A. Abele *et al.*, Eur. Phys. J. **C21**, 261 (2001).
28. M. Bargiotti *et al.*, Phys. Lett. **B561**, 233 (2003).
29. S.I. Bityukov *et al.*, Phys. Lett. **B188**, 383 (1987).
30. B. Aubert *et al.*, Phys. Rev. **D77**, 092002 (2008).
31. N.N. Achasov and G.N. Shestakov, Phys. Atom. Nucl. **59**, 1262 (1996).
32. L.G. Landsberg, Sov. J. Nucl. Phys. **55**, 1051 (1992).
33. A. Abele *et al.*, Phys. Lett. **B415**, 280 (1997).
34. V.M. Aulchenko *et al.*, Sov. Phys. JETP Lett. **45**, 145 (1987).
35. D. Bisello *et al.*, Z. Phys. **C52**, 227 (1991).
36. P. Frenkiel *et al.*, Nucl. Phys. **B47**, 61 (1972).
37. G. Cosme *et al.*, Phys. Lett. **B63**, 352 (1976).
38. D.P. Barber *et al.*, Z. Phys. **C4**, 169 (1980).

39. D. Aston, Phys. Lett. **B92**, 211 (1980).
40. M. Atkinson *et al.*, Nucl. Phys. **B243**, 1 (1984).
41. J.E. Brau *et al.*, Phys. Rev. **D37**, 2379 (1988).
42. C. Amsler *et al.*, Phys. Lett. **B311**, 362 (1993).
43. J. Layssac and F.M. Renard, Nuovo Cimento **6A**, 134 (1971).
44. D. Aston *et al.*, Nucl. Phys. (Proc. Supp.) **B21**, 105 (1991).
45. M. Ablikim *et al.*, Phys. Rev. Lett. **97**, 142002 (2006).
46. G.-J. Ding and M.-L. Yan, Phys. Lett. **B643**, 33 (2006).
47. F.K. Guo *et al.*, Nucl. Phys. **A773**, 78 (2006).
48. A. Zhang *et al.*, Phys. Rev. **D76**, 036004 (2007).
49. B.A. Li, Phys. Rev. **D76**, 094016 (2007).
50. X. Liu *et al.*, Phys. Rev. **D75**, 074017 (2007).
51. A.B. Clegg and A. Donnachie, Z. Phys. **C45**, 677 (1990).
52. D. Bisello *et al.*, Phys. Lett. **107B**, 145 (1981).
53. A. Castro *et al.*, LAL-88-58(1988).
54. M. Atkinson *et al.*, Z. Phys. **C29**, 333 (1985).
55. B. Aubert *et al.*, Phys. Rev. **D76**, 092005 (2007).
56. S. Godfrey and N. Isgur, Phys. Rev. **D32**, 189 (1985).
57. P.L. Frabetti *et al.*, Phys. Lett. **B514**, 240 (2001).
58. P.L. Frabetti *et al.*, Phys. Lett. **B578**, 290 (2004).
59. A. Antonelli *et al.*, Phys. Lett. **B365**, 427 (1996).
60. B. Aubert *et al.*, Phys. Rev. **D77**, 092002 (2008).
61. B. Aubert *et al.*, Phys. Rev. **D73**, 052003 (2006).
62. R.R. Akhmetshin *et al.*, Phys. Lett. **B723**, 83 (2013).
63. A. Obrazovsky and S. Serednyakov, JETP Lett. **99**, 315 (2014).
64. J. Heidenauer *et al.*, Phys. Rev. **D92**, 054032 (2015).

73. Charged Kaon Mass

Revised 1994 by T.G. Trippe (LBNL).

The average of the six charged kaon mass measurements which we use in the Particle Listings is

$$m_{K^\pm} = 493.677 \pm 0.013 \text{ MeV (S = 2.4)}, \quad (73.1)$$

where the error has been increased by the scale factor S. The large scale factor indicates a serious disagreement between different input data. The average before scaling the error is

$$m_{K^\pm} = 493.677 \pm 0.005 \text{ MeV},$$
$$\chi^2 = 22.9 \text{ for 5 D.F., Prob. } = 0.04\%, \quad (73.2)$$

where the high χ^2 and correspondingly low χ^2 probability further quantify the disagreement.

The main disagreement is between the two most recent and precise results,

$$m_{K^\pm} = 493.696 \pm 0.007 \text{ MeV} \quad \text{DENISOV 91}$$
$$m_{K^\pm} = 493.636 \pm 0.011 \text{ MeV (S = 1.5)} \quad \text{GALL 88}$$
$$\text{Average} = 493.679 \pm 0.006 \text{ MeV}$$
$$\chi^2 = 21.2 \text{ for 1 D.F., Prob. } = 0.0004\%, \quad (73.3)$$

both of which are measurements of x-ray energies from kaonic atoms. Comparing the average in Eq. (73.3) with the overall average in Eq. (73.2), it is clear that DENISOV 91 [1] and GALL 88 [2] dominate the overall average, and that their disagreement is responsible for most of the high χ^2.

The GALL 88 measurement was made using four different kaonic atom transitions, K^- Pb (9 → 8), K^- Pb (11 → 10), K^- W (9 → 8), and K^- W (11 → 10). The $m_{K^\pm}$ values they obtain from each of these transitions is shown in the Particle Listings and in Fig. 1. Their K^- Pb (9 → 8) $m_{K^\pm}$is below and somewhat inconsistent with their other three transitions. The average of their four measurements is

$$m_{K^\pm} = 493.636 \pm 0.007,$$
$$\chi^2 = 7.0 \text{ for 3 D.F., Prob. } = 7.2\%. \quad (73.4)$$

This is a low but acceptable χ^2 probability so, to be conservative, GALL 88 scaled up the error on their average by S=1.5 to obtain their published error ±0.011 shown in Eq. (73.3) above and used in the Particle Listings average.

The ideogram in Fig. 73.1 shows that the DENISOV 91 measurement and the GALL 88 K^- Pb (9 → 8) measurement yield two well-separated peaks. One might suspect the GALL 88 K^- Pb (9 → 8) measurement since it is responsible both for the internal inconsistency in the GALL 88 measurements and the disagreement with DENISOV 91.

To see if the disagreement could result from a systematic problem with the K^- Pb (9 → 8) transition, we have separated the CHENG 75 [3] data, which also used K^- Pb, into its separate transitions. Figure 1 shows that the CHENG 75 and GALL 88 K^- Pb (9 → 8) values are consistent, suggesting the possibility of a common effect such as contaminant nuclear γ rays near the K^- Pb (9 → 8) transition energy, although the CHENG 75 errors are too large to make a strong conclusion. The average of all 13 measurements has a χ^2 of 52.6 as shown in Fig. 1 and the first line of Table 1, yielding an unacceptable χ^2 probability of 0.00005%. The second line of Table 1 excludes both the GALL 88 and CHENG 75 measurements of the K^- Pb (9 → 8) transition and yields a χ^2 probability of 43%. The third [fourth] line of Table 1 excludes only the GALL 88 K^- Pb (9 → 8) [DENISOV 91] measurement and yields a χ^2 probability of 20% [8.6%]. Table 1 shows that removing both measurements of the K^- Pb (9 → 8) transition produces the most consistent set of data, but that excluding only the GALL 88 K^- Pb (9 → 8) transition or DENISOV 91 also produces acceptable probabilities.

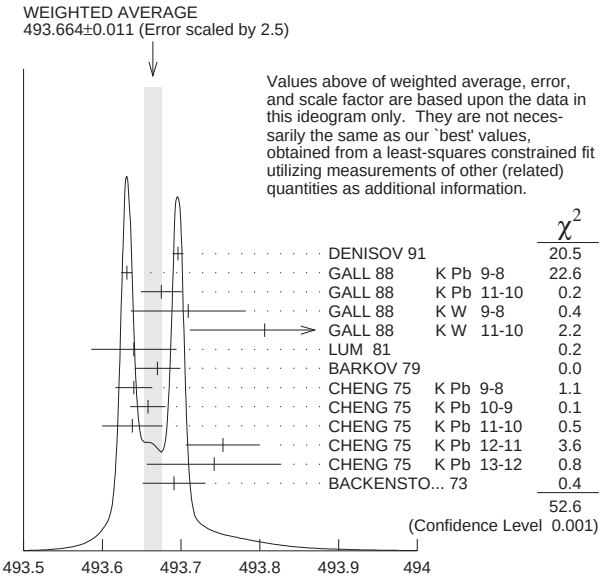

Figure 73.1: Ideogram of $m_{K^\pm}$ mass measurements. GALL 88 and CHENG 75 measurements are shown separately for each transition they measured.

Table 73.1: $m_{K^\pm}$ averages for some combinations of Fig. 1 data.

$m_{K^\pm}$ (MeV)	χ^2	D.F.	Prob. (%)	Measurements used
493.664 ± 0.004	52.6	12	0.00005	all 13 measurements
493.690 ± 0.006	10.1	10	43	no K^- Pb(9→8)
493.687 ± 0.006	14.6	11	20	no GALL 88 K^- Pb(9→8)
493.642 ± 0.006	17.8	11	8.6	no DENISOV 91

Yu.M. Ivanov, representing DENISOV 91, has estimated corrections needed for the older experiments because of improved ^{192}Ir and ^{198}Au calibration γ-ray energies. He estimates that CHENG 75 and BACKENSTOSS 73 [4] $m_{K^\pm}$ values could be raised by about 15 keV and 22 keV, respectively. With these estimated corrections, Table 1 becomes Table 2. The last line of Table 2 shows that if such corrections are assumed, then GALL 88 K^- Pb (9 → 8) is inconsistent with the rest of the data even when DENISOV 91 is excluded. Yu.M. Ivanov warns that these are rough estimates. Accordingly, we do not use Table 2 to reject the GALL 88 K^- Pb (9 → 8) transition, but we note that a future reanalysis of the CHENG 75 data could be useful because it might provide supporting evidence for such a rejection.

Table 73.2: $m_{K^\pm}$ averages for some combinations of Fig. 1 data after raising CHENG 75 and BACKENSTOSS 73 values by 0.015 and 0.022 MeV respectively.

$m_{K^\pm}$ (MeV)	χ^2	D.F.	Prob. (%)	Measurements used
493.666 ± 0.004	53.9	12	0.00003	all 13 measurements
493.693 ± 0.006	9.0	10	53	no K^- Pb(9→8)
493.690 ± 0.006	11.5	11	40	no GALL 88 K^- Pb(9→8)
493.645 ± 0.006	23.0	11	1.8	no DENISOV 91

The GALL 88 measurement uses a Ge semiconductor spectrometer which has a resolution of about 1 keV, so they run the risk of some contaminant nuclear γ rays. Studies of γ rays following stopped π^- and Σ^- absorption in nuclei (unpublished) do not show any evidence for contaminants according to GALL 88 spokesperson, B.L. Roberts. The DENISOV 91 measurement uses a crystal diffraction spectrometer with a resolution of 6.3 eV for radiation at 22.1 keV to measure the

4f-3d transition in K^- ^{12}C. The high resolution and the light nucleus reduce the probability for overlap by contaminant γ rays, compared with the measurement of GALL 88. The DENISOV 91 measurement is supported by their high-precision measurement of the 4d-2p transition energy in π^- ^{12}C, which is good agreement with the calculated energy.

While we suspect that the GALL 88 K^- Pb ($9 \rightarrow 8$) measurements could be the problem, we are unable to find clear grounds for rejecting it. Therefore, we retain their measurement in the average and accept the large scale factor until further information can be obtained from new measurements and/or from reanalysis of GALL 88 and CHENG 75 data.

We thank B.L. Roberts (Boston Univ.) and Yu.M. Ivanov (Petersburg Nuclear Physics Inst.) for their extensive help in understanding this problem.

References:

1. A.S. Denisov, *et al.* [DENISOV 91], Sov. Phys. JETP Lett. **54**, 558 (1991).
2. K.P. Gall, *et al.* [GALL 88], Phys. Rev. Lett. **60**, 186 (1988).
3. S.C. Cheng, *et al.* [CHENG 75], Nucl. Phys. **A254**, 381 (1975).
4. G. Backenstoss, *et al.* [BACKENSTOSS 73], Phys. Lett. **43B**, 431 (1973).

74. Rare Kaon Decays

Revised September 2017 by L. Littenberg (BNL) and G. Valencia (Monash University).

74.1. Introduction

There are several useful reviews on rare kaon decays and related topics [1–17]. Activity in rare kaon decays can be divided roughly into four categories:

1. Searches for explicit violations of the Standard Model (SM)
2. The golden modes: $K \to \pi\nu\bar{\nu}$
3. Other constraints on SM parameters
4. Studies of strong interactions at low energy.

The paradigm of Category 1 is the lepton flavor violating decay $K_L \to \mu e$. Category 2 includes the two modes that can be calculated with negligible theoretical uncertainty, $K^+ \to \pi^+\nu\overline{\nu}$ and $K_L \to \pi^0\nu\overline{\nu}$. These modes can lead to precision determinations of CKM parameters or, in combination with other measurements of these parameters, they can constrain new interactions. They constitute the main focus of the current experimental kaon program. Category 3 is focused on decays with charged leptons, such as $K_L \to \pi^0\ell^+\ell^-$ or $K_L \to \ell^+\ell^-$ where $\ell \equiv e, \mu$. These modes are sensitive to CKM parameters but they suffer from multiple hadronic uncertainties that can be addressed, at least in part, through a systematic study of the peripheral modes indicated in Fig. 74.1. The interplay between Categories 3-4 and their complementarity to Category 2 is illustrated in the figure. Category 4 includes reactions like $K^+ \to \pi^+\ell^+\ell^-$ where long distance contributions are dominant and which constitute a testing ground for the ideas of chiral perturbation theory. Other decays in this category are $K_L \to \pi^0\gamma\gamma$ and $K_L \to \ell^+\ell^-\gamma$. The former is important in understanding a CP-conserving contribution to $K_L \to \pi^0\ell^+\ell^-$, whereas the latter could shed light on long distance contributions to $K_L \to \mu^+\mu^-$.

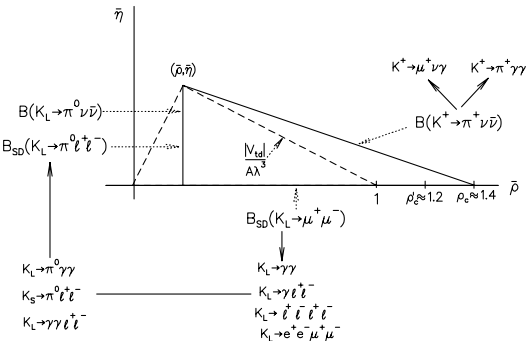

Figure 74.1: Role of rare kaon decays in determining the unitarity triangle. The solid arrows point to auxiliary modes needed to interpret the main results, or potential backgrounds to them.

74.2. Explicit violations of the Standard Model

Much activity has focussed on searches for lepton flavor violation (LFV). This is motivated by the fact that many extensions of the minimal Standard Model violate lepton flavor and by the potential to access very high energy scales. For example, the tree-level exchange of a LFV vector boson of mass M_X that couples to left-handed fermions with electroweak strength and without mixing angles yields $\mathrm{B}(K_L \to \mu e) = 4.7 \times 10^{-12}(148\ \mathrm{TeV}/M_X)^4$ [4]. This simple dimensional analysis may be used to read from Table 74.1 that the reaction $K_L \to \mu e$ is already probing scales of over 100 TeV. Table 74.1 summarizes the present experimental situation vis-à-vis LFV. The decays $K_L \to \mu^\pm e^\mp$ and $K^+ \to \pi^+ e^\mp \mu^\pm$ (or $K_L \to \pi^0 e^\mp \mu^\pm$) provide complementary information on potential family number violating interactions, since the former is sensitive to parity-odd couplings and the latter is sensitive to parity-even couplings.

Limits on certain lepton-number violating (LNV) kaon decays also have been obtained, with recent interest arising from their role in constraining possible extensions of the neutrino sector [18], and we list those in the table as well. Related searches in μ and τ processes are discussed in our section "Tests of Conservation Laws."

Table 74.1: Searches for lepton flavor and lepton number violation in K decay

LFV Mode	90% CL upper limit	Exp't	Yr./Ref.	Type
$K^+ \to \pi^+ e^- \mu^+$	1.3×10^{-11}	BNL-865	2005/Ref. 19	LFV
$K^+ \to \pi^+ e^+ \mu^-$	5.2×10^{-10}	BNL-865	2000/Ref. 20	LFV
$K_L \to \mu e$	4.7×10^{-12}	BNL-871	1998/Ref. 21	LFV
$K_L \to \pi^0 e\mu$	7.6×10^{-11}	KTeV	2008/Ref. 22	LFV
$K_L \to \pi^0\pi^0 e\mu$	1.7×10^{-10}	KTeV	2008/Ref. 22	LFV
$K^+ \to \pi^- e^+ e^+$	6.4×10^{-10}	BNL-865	2000/Ref. 20	LNV
$K^\pm \to \pi^\mp \mu^\pm \mu^\pm$	8.6×10^{-11}	NA48/2	2017/Ref. 23	LNV
$K_L \to e^\pm e^\pm \mu^\mp \mu^\mp$	4.12×10^{-11}	KTeV	2003/Ref. 24	LNV
$K^+ \to \pi^- \mu^+ e^+$	5.0×10^{-10}	BNL-865	2000/Ref. 20	LNFV

Physics beyond the SM is also pursued through the search for $K^+ \to \pi^+ X^0$, where X^0 is a new light particle. The searches cover both long-lived particles (*e.g.*, hyperphoton, axion, familon, *etc.*), and short-lived ones that decay to muon, electron or photon pairs. The 90% CL upper limit on $K^+ \to \pi^+ X^0$ is 7.3×10^{-11} [25] for the case of massless X^0; additional results as a function of the X^0 mass can be found in [26]. Recently these limits have been reinterpreted in connection with a dark photon [27] or dark Z [28]. Such vectors have also been sought in their e^+e^- decay mode by NA48/2 [29]. Additional bounds for a short lived pseudoscalar X^0 decaying to muons or photons are $B(K_L \to \pi^0\pi^0\mu^+\mu^-) < 1 \times 10^{-10}$ [30] and $B(K_L \to \pi^0\pi^0\gamma\gamma) < 2.4 \times 10^{-7}$ [31].

74.3. The golden modes: $K \to \pi\nu\bar{\nu}$

In the SM, the decay $K^+ \to \pi^+\nu\overline{\nu}$ is dominated by one-loop diagrams with top-quark intermediate states while long-distance contributions are known to be quite small [2,32,33]. This permits a precise calculation of this rate in terms of SM parameters. Studies of this process are thus motivated by the possibility of detecting non-SM physics when comparing with the results of global fits [34,35].

The branching ratio can be written in a compact form that exhibits the different ingredients that go into the calculation [36],

$$\mathrm{B}(K^+ \to \pi^+\nu\overline{\nu}(\gamma)) = \kappa_+(1+\Delta_{\mathrm{EM}})\left[\left(\frac{\mathrm{Im}(V_{ts}^*V_{td})}{\lambda^5}X_t\right)^2 + \left(\frac{\mathrm{Re}(V_{cs}^*V_{cd})}{\lambda}(P_c+\delta P_{c,u}) + \frac{\mathrm{Re}(V_{ts}^*V_{td})}{\lambda^5}X_t\right)^2\right]. \quad (74.1)$$

The parameters in Eq. (74.1) incorporate the *a priori* unknown hadronic matrix element in terms of the very well-measured K_{e3} rate [2] in κ_+; long distance QED corrections in Δ_{EM} [37]; the Inami-Lim function for the short distance top-quark contribution [38] including NLO QCD corrections [39] and the two-loop electroweak correction [36], all in X_t; and the charm-quark contributions due to short distance effects including NNLO QCD corrections [40] and NLO electroweak corrections via P_c [41], as well as certain long distance effects via $\delta P_{c,u}$ [42,33]. An interesting approximate way to cast this result in terms of the CKM parameters λ, V_{cb}, $\overline{\rho}$ and $\overline{\eta}$ (see our Section on "The Cabibbo-Kobayashi-Maskawa mixing matrix") [11] is:

$$\mathrm{B}(K^+ \to \pi^+\nu\overline{\nu}) \approx 1.6 \times 10^{-5}|V_{cb}|^4[\sigma\overline{\eta}^2 + (\rho_c - \overline{\rho})^2], \quad (74.2)$$

where $\rho_c \approx 1.45$ and $\sigma \equiv 1/(1-\frac{1}{2}\lambda^2)^2$. Thus, $\mathrm{B}(K^+ \to \pi^+\nu\overline{\nu})$ determines an ellipse in the $\overline{\rho}$, $\overline{\eta}$ plane with center $(\rho_c, 0)$ and semiaxes $\approx \frac{1}{|V_{cb}|^2}\sqrt{\frac{\mathrm{B}(K^+\to\pi^+\nu\overline{\nu})}{1.6\times10^{-5}}}$ and $\frac{1}{\sigma|V_{cb}|^2}\sqrt{\frac{\mathrm{B}(K^+\to\pi^+\nu\overline{\nu})}{1.6\times10^{-5}}}$.

BNL-787 observed two candidate events [43,44] in the clean high π^+ momentum and one event [45] in the low-momentum region. The successor experiment BNL-949 observed one more in the high-momentum region [25] and three more in the low-momentum region [46], yielding a branching ratio of $(1.73^{+1.15}_{-1.05}) \times 10^{-10}$ [26]. The NA62 experiment [47], performed with in-flight decays at CERN, aims to reach a sensitivity of $\sim 10^{-12}$/event. NA62 was commissioned in 2015 and is expected to reach SM sensitivities with the data taken in 2016. The 2017 run, presently in progress, is anticipated to produce more than 10 SM events, and the collaboration expects that the experiment will achieve its full sensitivity by the end of the 2018 run.

Our estimate for this branching ratio, using the latest CKMfitter input [34], is $\mathrm{B}(K^+ \to \pi^+\nu\overline{\nu}) = (8.3 \pm 0.4) \times 10^{-11}$, near the lower end of the measurement of BNL-787 and 949. However, current parametric uncertainty in the CKM angles can result in numbers with central values differing from this one by up to 10% [48].

The second golden mode is the neutral counterpart to our preceeding discussion: $K_L \to \pi^0\nu\overline{\nu}$. It is dominantly CP-violating and free of hadronic uncertainties [2,49,50]. In the Standard Model, this mode is dominated by an intermediate top-quark state and does not suffer from the small uncertainty associated with the charm-quark intermediate state that affects $K^+ \to \pi^+\nu\overline{\nu}$. The branching ratio is given by Ref. 11:

$$\mathrm{B}(K_L \to \pi^0\nu\overline{\nu}) = \kappa_L \left(\frac{\mathrm{Im}(V_{ts}^* V_{td})}{\lambda^5} X_t\right)^2 \approx 7.6 \times 10^{-5} |V_{cb}|^4 \overline{\eta}^2 \ . \quad (74.3)$$

As with the charged mode, the hadronic matrix element can be related to that measured in $K_{\ell 3}$ decay and is parameterized in κ_L.

Our estimate for the branching ratio, using the latest CKMfitter input [34], is $(2.9 \pm 0.2) \times 10^{-11}$. But similarly to the charged kaon case, parametric uncertainty in the CKM angles can result in a central value that differs from this one by up to almost 20% [48].

Grossman and Nir (GN) [51] pointed out that, in a nearly model-independent manner, the two golden modes satisfy the relation $\mathrm{B}(K_L \to \pi^0\nu\overline{\nu}) \lesssim 4.4\ \mathrm{B}(K^+ \to \pi^+\nu\overline{\nu})$. Using the 90% CL bound on $K^+ \to \pi^+\nu\overline{\nu}$, GN then predict $B(K_L \to \pi^0\nu\overline{\nu}) < 1.46 \times 10^{-9}$.

KEK-391a, which took data in 2004 and 2005, has published a 90% CL upper bound of $\mathrm{B}(K_L \to \pi^0\nu\overline{\nu}) \leq 2.6 \times 10^{-8}$ [52]. The KOTO experiment at J-PARC [53], whose initial goal is to observe this decay, had a short physics run in the spring of 2013, obtaining a 90% CL upper limit of 5.1×10^{-8} [54]. They resumed running in 2015 and have continued to do so each year, making incremental upgrades to the experimental configuration between runs. They expect to reach the GN bound level from the combined 2015 and 2016 data. It was pointed out in a recent paper that the GN bound quoted above applies to the three body decay $K_L \to \pi^0\nu\overline{\nu}$ and not necessarily to two body modes such as $K_L \to \pi^0 X^0$. In this case KOTO can provide interesting constraints on new physics even at the current sensitivity level [55]. Using the 2013 run, they have established a 90% CL upper limit of 3.7×10^{-8} on $K_L \to \pi^0 X^0$ for $m_{X^0} \approx m_{\pi^0}$ [54].

The current theoretical and experimental situation for the golden modes is summarized in Fig. 74.2. The red area corresponds to the 90% CL SM prediction we obtain with the latest input available from CKMfitter [34]. The dashed yellow region shows the 90% CL region established by the combined BNL-787 and BNL-949 results. The black dashed region illustrates the GN exclusion, which lies significantly above the SM expectation leaving a large window for discovery of new physics contributions by experiments seeking to measure $\mathrm{B}(K_L \to \pi^0\nu\overline{\nu})$. Much theoretical work has explored beyond the SM scenarios that can populate this window as well as their correlations with other rare processes outside kaon physics. Although it would be relatively straight forward to establish the existence of new physics by observing deviations from their SM values in the $K \to \pi\nu\overline{\nu}$ modes, it would take much more extensive global fits to pinpoint the origin of any such deviation. Partial summaries with references can be found in Refs. [14,56,57,58,59,60].

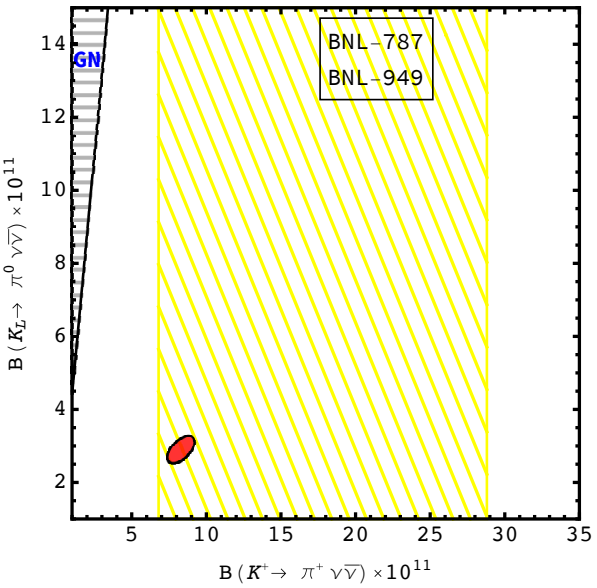

Figure 74.2: Summary of current situation for the golden modes $K \to \pi\nu\overline{\nu}$. The red and yellow regions correspond to the 90% CL SM prediction with input from CKMfitter and to the BNL measurement respectively. The black dashed region shows the GN exclusion.

Related modes with one extra pion, $K \to \pi\pi\nu\overline{\nu}$, are are similarly dominated by short distance contributions [61]. However, they occur at much lower rates with branching rations of order 10^{-13}. The current best bound comes from KEK-391a, it is $B(K_L \to \pi^0\pi^0\nu\overline{\nu}) < 8.1\times10^{-7}$ at 90% CL [62]. There is also a bound $B(K^+ \to \pi^+\pi^0\nu\overline{\nu}) < 4.3\times10^{-5}$ at 90% CL [63] from BNL-787.

74.4. Other constraints on Standard Model parameters

The decay $K_L \to \mu^+\mu^-$ has a short distance contribution sensitive to the CKM parameter $\overline{\rho}$, given by [11]:

$$\mathrm{B}_{\mathrm{SD}}(K_L \to \mu^+\mu^-) \approx 2.7 \times 10^{-4} |V_{cb}|^4 (\rho_c' - \overline{\rho})^2 \quad (74.4)$$

where ρ_c' depends on the charm quark mass and is approximately 1.2. This decay, however, is dominated by a long-distance contribution from a two-photon intermediate state. The absorptive (imaginary) part of the long-distance component is determined by the measured rate for $K_L \to \gamma\gamma$ to be $\mathrm{B}_{\mathrm{abs}}(K_L \to \mu^+\mu^-) = (6.64 \pm 0.07) \times 10^{-9}$; and it almost completely saturates the observed rate $\mathrm{B}(K_L \to \mu^+\mu^-) = (6.84 \pm 0.11) \times 10^{-9}$ [64]. The difference between the observed rate and the absorptive component can be attributed to the (coherent) sum of the short-distance amplitude and the real part of the long-distance amplitude. The latter cannot be derived directly from experiment [65], but can be estimated with certain assumptions [66,67].

By contrast, the decay $K_L \to e^+e^-$ is completely dominated by long distance physics and is easier to estimate. The result, $B(K_L \to e^+e^-) \sim 9 \times 10^{-12}$ [65,68], is in good agreement with the BNL-871 measurement, $(8.7^{+5.7}_{-4.1}) \times 10^{-12}$ [69].

The mode $K_S \to \mu^+\mu^-$ similarly has a short distance contribution proportional to the square of the CKM parameter $\overline{\eta}$ entering at the 10^{-13} level [15]. It has as well long distance contributions which arising from the two photon intermediate state which result in a rate $B(K_S \to \mu^+\mu^-)_{LD} = 5.1 \times 10^{-12}$ [15]. A 95% (90%) CL

limit $B(K_S \to \mu^+\mu^-) < 0.8(1.0) \times 10^{-9}$ was recently obtained by LHCb [70].

The decay $K_L \to \pi^0 e^+ e^-$ is sensitive to the CKM parameter η through its CP-violating component. There are both direct and indirect CP-violating amplitudes that can interfere. The direct CP-violating amplitude is short distance dominated and has been calculated in detail within the SM [8]. The indirect CP-violating amplitude can be inferred from a measurement of $K_S \to \pi^0 e^+ e^-$. The complete CP-violating contribution to the rate can be written as [71,72]:

$$\mathrm{B}_{\mathrm{CPV}} \approx 10^{-12}\left[15.7|a_S|^2 \pm 1.4\left(\frac{|V_{cb}|^2\overline{\eta}}{10^{-4}}\right)|a_S| + 0.12\left(\frac{|V_{cb}|^2\overline{\eta}}{10^{-4}}\right)^2\right] \quad (74.5)$$

where the three terms correspond to the indirect CP violation, the interference, and the direct CP violation, respectively. The parameter a_S has been extracted by NA48/1 from a measurement of $K_S \to \pi^0 e^+ e^-$ with the result $|a_S| = 1.06^{+0.26}_{-0.21} \pm 0.07$ [73], as well as from a measurement of $K_S \to \pi^0 \mu^+ \mu^-$ with the result $|a_s| = 1.54^{+0.40}_{-0.32} \pm 0.06$ [74]. With current constraints on the CKM parameters, and assuming a positive sign for the interference term [72,75], this implies that $\mathrm{B}_{\mathrm{CPV}}(K_L \to \pi^0 e^+ e^-) \approx (3.1 \pm 0.9) \times 10^{-11}$, where the three contributions to the central value from indirect, interference and direct CP violation are $(1.76, 0.9, 0.45) \times 10^{-11}$ respectively. The complete CP violating amplitude for the related mode $K_L \to \pi^0 \mu^+ \mu^-$ is predicted to be $\mathrm{B}_{\mathrm{CPV}}(K_L \to \pi^0 \mu^+ \mu^-) \approx (1.4 \pm 0.5) \times 10^{-11}$ [76,15].

$K_L \to \pi^0 e^+ e^-$ also has a CP-conserving component dominated by a two-photon intermediate state. This component can be decomposed into an absorptive and a dispersive part. The absorptive part can be extracted from the measurement of the low $m_{\gamma\gamma}$ region of the $K_L \to \pi^0\gamma\gamma$ spectrum. The rate and the shape of the distribution $d\Gamma/dm_{\gamma\gamma}$ in $K_L \to \pi^0\gamma\gamma$ are well described in chiral perturbation theory in terms of three (*a priori*) unknown parameters [77,78].

Both KTeV and NA48 have studied the mode $K_L \to \pi^0\gamma\gamma$, reporting similar results. KTeV finds $B(K_L \to \pi^0\gamma\gamma) = (1.29 \pm 0.03_{\mathrm{stat}} \pm 0.05_{\mathrm{sys}}) \times 10^{-6}$ [79], while NA48 finds $B(K_L \to \pi^0\gamma\gamma) = (1.36 \pm 0.03_{\mathrm{stat}} \pm 0.03_{\mathrm{sys}} \pm 0.03_{\mathrm{norm}}) \times 10^{-6}$ [80]. Both experiments are consistent with a negligible rate in the low $m_{\gamma\gamma}$ region, suggesting a very small CP-conserving component $B_{\mathrm{CP}}(K_L \to \pi^0 e^+ e^-) \sim \mathcal{O}(10^{-13})$ [72,78,80]. There remains some model dependence in the estimate of the dispersive part of the CP-conserving $K_L \to \pi^0 e^+ e^-$ [72].

The related process, $K_L \to \pi^0 \gamma e^+ e^-$, is potentially an additional background to $K_L \to \pi^0 e^+ e^-$ in some region of phase space [81]. This process has been observed with a branching ratio of $(1.62 \pm 0.14_{\mathrm{stat}} \pm 0.09_{\mathrm{sys}}) \times 10^{-8}$ [82].

The decay $K_L \to \gamma\gamma e^+ e^-$ constitutes the dominant background to $K_L \to \pi^0 e^+ e^-$. It was first observed by BNL-845 [83], and subsequently confirmed with a much larger sample by KTeV [84]. It has been estimated that this background will enter at about the 10^{-10} level [85,86], comparable to or larger than the signal level. Because of this, the observation of $K_L \to \pi^0 e^+ e^-$ at the SM level will depend on background subtraction with good statistics. Possible alternative strategies are discussed in Ref. 72 and references cited therein.

The 90% CL upper bound for the process $K_L \to \pi^0 e^+ e^-$ is 2.8×10^{-10} [86]. For the closely related muonic process, the published upper bound is $\mathrm{B}(K_L \to \pi^0 \mu^+ \mu^-) \leq 3.8 \times 10^{-10}$ [87], compared with the SM prediction of $(1.5 \pm 0.3) \times 10^{-11}$ [76] (assuming positive interference between the direct- and indirect-CP violating components).

A study of $K_L \to \pi^0 \mu^+ \mu^-$ has indicated that it might be possible to extract the direct CP-violating contribution by a joint study of the Dalitz plot variables and the components of the μ^+ polarization [88]. The latter tends to be quite substantial so that large statistics may not be necessary.

Combined information from $K_L \to \pi^0 \ell^+ \ell^-$ as well as $K_L \to \mu^+\mu^-$ complements the $K \to \pi\nu\overline{\nu}$ measurements in constraining physics beyond the SM [89].

74.5. Other long distance dominated modes

The decays $K^+ \to \pi^+ \ell^+ \ell^-$ ($\ell = e$ or μ) have received considerable attention. The rate and spectrum have been measured for both the electron and muon modes [90,91].

The measurements have been used to exclude new physics such as a dark photon [27]. Ref. 71 has proposed a parameterization inspired by chiral perturbation theory, which provides a successful description of data but indicates the presence of large corrections beyond leading order. More work is needed to fully understand the origin of these large corrections. The mode $K^+ \to \pi^+\pi^0 e^+ e^-$, recently analyzed by NA48/2 [92], is also dominated by long distance physics but it has been argued that measuring asymmetries can provide information on the short distance components [93]. The related mode $K_S \to \pi^+\pi^- e^+ e^-$, which was measured by NA48/1 [94], has received new interest by LHCb [95] as an important background to other rare decays.

The decay $K^+ \to \pi^+\gamma\gamma$ can be predicted in terms of one unknown parameter to leading order in χPT resulting in a correlation between the rate and the diphoton mass spectrum [96]. Certain important corrections at the next order are also known [97]. The rate was first measured by E787 [98], and more recently NA48/2 [99] has obtained a more precise result with a 6% error, as well as the corresponding spectrum fits. The most recent, and precise, result is from NA62 based on a sample of 232 events [100] but is still insufficient to distinguish between the leading order and next order χPT parameterizations.

Much information has been recorded by KTeV and NA48 on the rates and spectrum for the Dalitz pair conversion modes $K_L \to \ell^+\ell^-\gamma$ [101,102], and $K_L \to \ell^+\ell^-\ell'^+\ell'^-$ for $\ell, \ell' = e$ or μ [24,103]. More recently, LHCb has performed preliminary studies of $K_S \to \ell^+\ell^-\ell'^+\ell'^-$ [95]. All these results are used to test hadronic models and should eventually help unravel the underlying physics in $K_L \to \mu^+\mu^-$ [67,104,105].

References:

1. D. Bryman, Int. J. Mod. Phys. **A4**, 79 (1989).
2. J. Hagelin and L. Littenberg, Prog. in Part. Nucl. Phys. **23**, 1 (1989).
3. L. Littenberg and G. Valencia, Ann. Rev. Nucl. and Part. Sci. **43**, 729 (1993).
4. J. Ritchie and S. Wojcicki, Rev. Mod. Phys. **65**, 1149 (1993).
5. B. Winstein and L. Wolfenstein, Rev. Mod. Phys. **65**, 1113 (1993).
6. G. D'Ambrosio *et al.*, *Radiative Non-Leptonic Kaon Decays*, in The DAΦNE Physics Handbook (second edition), eds. L. Maiani, G. Pancheri, and N. Paver (Frascati), Vol. I, 265 (1995).
7. A. Pich, Rept. on Prog. in Phys. **58**, 563 (1995).
8. G. Buchalla, A.J. Buras, and M.E. Lautenbacher, Rev. Mod. Phys. **68**, 1125 (1996).
9. G. D'Ambrosio and G. Isidori, Int. J. Mod. Phys. **A13**, 1 (1996).
10. P. Buchholz and B. Renk Prog. in Part. Nucl. Phys. **39**, 253 (1997).
11. A.J. Buras and R. Fleischer, TUM-HEP-275-97, `hep-ph/9704376`, *Heavy Flavours II*, World Scientific, eds. A.J. Buras and M. Lindner (1997), 65–238.
12. A.J. Buras, TUM-HEP-349-99, Lectures at Lake Louise Winter Institute: Electroweak Physics, Lake Louise, Alberta, Canada, 14–20 Feb. 1999.
13. A.R. Barker and S.H. Kettell, Ann. Rev. Nucl. and Part. Sci. **50**, 249 (2000).
14. A.J. Buras, F. Schwab, and S. Uhlig, Rev. Mod. Phys. **80**, 965 (2008).
15. V. Cirigliano *et al.*, Rev. Mod. Phys. **84**, 399 (2012).
16. D. Bryman *et al.*, Ann. Rev. Nucl. and Part. Sci. **61**, 331 (2011).
17. T.K. Komatsubara, Prog. in Part. Nucl. Phys. **67**, 995 (2012).
18. A. Atre *et al.*, JHEP **0905**, 030 (2009); L.S. Littenberg and R.E. Shrock, Phys. Lett. **B491**, 285 (2000).

19. A. Sher *et al.*, Phys. Rev. **D72**, 012005 (2005).
20. R. Appel *et al.*, Phys. Rev. Lett. **85**, 2877 (2000).
21. D. Ambrose *et al.*, Phys. Rev. Lett. **81**, 5734 (1998).
22. E. Abouzaid *et al.*, Phys. Rev. Lett. **100**, 131803 (2008).
23. J.R. Batley *et al.*, Phys. Lett. **B769**, 67 (2017).
24. A. Alavi-Harati *et al.*, Phys. Rev. Lett. **90**, 141801 (2003).
25. V.V. Anisimovsky *et al.*Phys. Rev. Lett. **93**, 031801 (2004).
26. A.V. Artamonov *et al.*, Phys. Rev. **D79**, 092004 (2009).
27. M. Pospelov, Phys. Rev. **D80**, 095002 (2009).
28. H. Davoudiasl, H.S. Lee, and W.J. Marciano, Phys. Rev. **D89**, 095006 (2014).
29. J.R. Batley *et al.* [NA48/2 Collab.], Phys. Lett. **B746**, 178 (2015).
30. E. Abouzaid *et al.*, Phys. Rev. Lett. **107**, 201803 (2011); see also, D.G. Phillips II, "Search for the Rare Decay $K_L \to \pi^0\pi^0\mu^+\mu^-$," University of Virginia thesis, May 2009.
31. Y.C. Tung *et al.*, Phys. Rev. Lett. **102**, 051802 (2009).
32. M. Lu and M.B. Wise, Phys. Lett. **B324**, 461 (1994).
33. A.F. Falk, A. Lewandowski, and A.A. Petrov, Phys. Lett. **B505**, 107 (2001).
34. J. Charles *et al.* [CKMfitter Collab.], Phys. Rev. **D84**, 033005 (2011), updated results and plots available at: `http://ckmfitter.in2p3.fr`.
35. M. Bona *et al.* [UTfit Collab.] `arXiv:0707.0636`, `www.utfit.org/UTfit/`.
36. J. Brod, M. Gorbahn, and E. Stamou, Phys. Rev. **D83**, 034030 (2011).
37. F. Mescia and C. Smith, Phys. Rev. **D76**, 034017 (2007).
38. T. Inami and C.S. Lim, Prog. Theor. Phys. **65**, 297 (1981); Erratum Prog. Theor. Phys. **65**, 172 (1981).
39. G. Buchalla and A.J. Buras, Nucl. Phys. **B548**, 309 (1999); M. Misiak and J. Urban, Phys. Lett. **B451**, 161 (1999).
40. A.J. Buras *et al.*, Phys. Rev. Lett. **95**, 261805 (2005); A.J. Buras *et al.*, JHEP **0611**, 002 (2006).
41. J. Brod and M. Gorbahn, Phys. Rev. **D78**, 034006 (2008).
42. G. Isidori, F. Mescia, and C. Smith, Nucl. Phys. **B718**, 319 (2005).
43. S. Adler *et al.*, Phys. Rev. Lett. **88**, 041803 (2002).
44. S. Adler *et al.*, Phys. Rev. Lett. **84**, 3768 (2000).
45. S. Adler *et al.*, Phys. Lett. **B537**, 237 (2002).
46. A.V. Artamonov *et al.*, Phys. Rev. Lett. **101**, 191802 (2008).
47. G. Anelli *et al.*, CERN-SPSC-2005-013, 11 June 2005.
48. A.J. Buras, *et al.*, JHEP **1511**, 033 (2015).
49. L. Littenberg, Phys. Rev. **D39**, 3322 (1989).
50. G. Buchalla and G. Isidori, Phys. Lett. **B440**, 170 (1998).
51. Y. Grossman and Y. Nir, Phys. Lett. **B398**, 163 (1997).
52. J.K. Ahn *et al.*, Phys. Rev. **D81**, 072004 (2010).
53. J. Comfort *et al.*, "Proposal for $K_L^0 \to \pi^0\nu\overline{\nu}$ Experiment at J-Parc," J-PARC Proposal 14 (2006), [`koto.kek.jp/pub/p14.pdf`].
54. J.K. Ahn *et al.*, Prog. Theor. Exp. Phys. 2017, 021C01.
55. K. Fuyuto, W. S. Hou, and M. Kohda, Phys. Rev. Lett. **114**, 171802 (2015).
56. G. D'Ambrosio and G. Isidori, Phys. Lett. **B530**, 108 (2002).
57. D. Bryman *et al.*, Int. J. Mod. Phys. **A21**, 487 (2006).
58. M. Blanke, PoS KAON**13**, 10(2013), [arXiv:1305.5671].
59. A. J. Buras *et al.*, JHEP **1511**, 166 (2015).
60. M. Bordone *et al.*, arXiv:1705.10729 [hep-ph].
61. L. Littenberg and G. Valencia, Phys. Lett. **B385**, 379 (1996); C.-W. Chiang and F.J. Gilman, Phys. Rev. **D62**, 094026 (2000); C.Q. Geng, I.J. Hsu, and Y.C. Lin, Phys. Rev. **D50**, 5744 (1994).
62. R. Ogata, *et al.*, Phys. Rev. **D84**, 052009 (2011).
63. S. Adler, *et al.*, Phys. Rev. **D63**, 032004 (2001).
64. D. Ambrose *et al.*, Phys. Rev. Lett. **84**, 1389 (2000).
65. G. Valencia, Nucl. Phys. **B517**, 339 (1998).
66. G. D'Ambrosio, G. Isidori, and J. Portoles, Phys. Lett. **B423**, 385 (1998).
67. G. Isidori and R. Unterdorfer, JHEP **0401**, 009 (2004).
68. D. Gomez-Dumm and A. Pich, Phys. Rev. Lett. **80**, 4633 (1998).
69. D. Ambrose *et al.*, Phys. Rev. Lett. **81**, 4309 (1998).
70. R. Aaij *et al.* [LHCb Collab.], [`arXiv:1706.00758 [hep-ex]`].
71. G. D'Ambrosio *et al.*, JHEP **9808**, 004 (1998); C.O. Dib, I. Dunietz, and F.J. Gilman, Phys. Rev. **D39**, 2639 (1989).
72. G. Buchalla, G. D'Ambrosio, and G. Isidori, Nucl. Phys. **B672**, 387 (2003).
73. J.R. Batley *et al.*, Phys. Lett. **B576**, 43 (2003).
74. J.R. Batley *et al.*, Phys. Lett. **B599**, 197 (2004).
75. S. Friot, D. Greynat, and E. de Rafael, Phys. Lett. **B595**, 301 (2004).
76. G. Isidori, C. Smith, and R. Unterdorfer, Eur. Phys. J. **C36**, 57 (2004).
77. G. Ecker, A. Pich, and E. de Rafael, Phys. Lett. **237B**, 481 (1990); L. Cappiello, G. D'Ambrosio, and M. Miragliuolo, Phys. Lett. **B298**, 423 (1993); A. Cohen, G. Ecker, and A. Pich, Phys. Lett. **B304**, 347 (1993).
78. F. Gabbiani and G. Valencia, Phys. Rev. **D66**, 074006 (2002).
79. E. Abouzaid *et al.*, Phys. Rev. **D77**, 112004 (2008).
80. A. Lai *et al.*, Phys. Lett. **B536**, 229 (2002).
81. J. Donoghue and F. Gabbiani, Phys. Rev. **D56**, 1605 (1997).
82. E. Abouzaid *et al.*, Phys. Rev. **D76**, 052001 (2007).
83. W.M. Morse *et al.*, Phys. Rev. **D45**, 36 (1992).
84. A. Alavi-Harati *et al.*, Phys. Rev. **D64**, 012003 (2001).
85. H.B. Greenlee, Phys. Rev. **D42**, 3724 (1990).
86. A. Alavi-Harati *et al.*, Phys. Rev. Lett. **93**, 021805 (2004).
87. A. Alavi-Harati *et al.*, Phys. Rev. Lett. **84**, 5279 (2000).
88. M.V. Diwan, H. Ma, and T.L. Trueman, Phys. Rev. **D65**, 054020 (2002).
89. F. Mescia, C. Smith, and S. Trine, JHEP **0608**, 088 (2006).
90. R. Appel *et al.*, Phys. Rev. Lett. **83**, 4482 (1999); J.R. Batley *et al.*, Phys. Lett. **B677**, 246 (2009).
91. S.C. Adler *et al.*, Phys. Rev. Lett. **79**, 4756 (1997); R. Appel *et al.*, Phys. Rev. Lett. **84**, 2580 (2000); H.K. Park *et al.*, Phys. Rev. Lett. **88**, 111801 (2002); J.R. Batley *et al.*, Phys. Lett. **B697**, 107 (2011).
92. B. Bloch-Devaux *et al.* [NA48/2 Collab.], J. Phys. Conf. Ser. 800, 012029 (2017).
93. L. Cappiello *et al.*, Eur. Phys. J. **C72**, 1872 (2012) [Eur. Phys. J. **C72**, 2208 (2012)] [`arXiv:1112.5184`].
94. J. R. Batley *et al.* [NA48/1 Collab.], Phys. Lett. **B694**, 301 (2011).
95. C. Marin Benito *et al.* [LHCb Collab.] , J. Phys. Conf. Ser. 800, 012031 (2017).
96. G. Ecker, A. Pich, and E. de Rafael, Nucl. Phys. **B303**, 665 (1988).
97. G. D'Ambrosio and J. Portoles, Phys. Lett. **B386**, 403 (1996) [Phys. Lett. **B389**, 770 (1996)] [Erratum-ibid. B **395**, 390 (1997)] [`hep-ph/9606213`].
98. P. Kitching *et al.* [E787 Collab.], Phys. Rev. Lett. **79**, 4079 (1997) [`hep-ex/9708011`].
99. J.R. Batley *et al.*, Phys. Lett. **B730**, 141 (2014).
100. C. Lazzeroni *et al.*, Phys. Lett. **B732C**, 65 (2014).
101. A. Alavi-Harati *et al.*, Phys. Rev. Lett. **87**, 071801 (2001).
102. A. Abouzaid *et al.*, Phys. Rev. Lett. **99**, 051804 (2007).
103. V. Fanti *et al.*, Phys. Lett. **B458**, 458 (1999).
104. G. D'Ambrosio *et al.*, Eur. Phys. J. **C73**, 2678 (2013) [`arXiv:1309.5736`].
105. G. D'Ambrosio and T. Kitahara, [`arXiv:1707.06999 [hep-ph]`].

75. Dalitz Plot Parameters for $K \to 3\pi$ Decays

Revised 1999 by T.G. Trippe (LBNL).

The Dalitz plot distribution for $K^\pm \to \pi^\pm\pi^\pm\pi^\mp$, $K^\pm \to \pi^0\pi^0\pi^\pm$, and $K_L^0 \to \pi^+\pi^-\pi^0$ can be parameterized by a series expansion such as that introduced by Weinberg [1]. We use the form

$$\left|M\right|^2 \propto 1 + g\frac{(s_3 - s_0)}{m_{\pi^+}^2} + h\left[\frac{s_3 - s_0}{m_{\pi^+}^2}\right]^2 + j\ \frac{(s_2 - s_1)}{m_{\pi^+}^2} + k\left[\frac{s_2 - s_1}{m_{\pi^+}^2}\right]^2 + f\ \frac{(s_2 - s_1)}{m_{\pi^+}^2}\frac{(s_3 - s_0)}{m_{\pi^+}^2} + \cdots\ , \tag{75.1}$$

where $m_{\pi^+}^2$ has been introduced to make the coefficients g, h, j, and k dimensionless, and

$$s_i = (P_K - P_i)^2 = (m_K - m_i)^2 - 2m_K T_i\ ,\ i = 1, 2, 3,$$

$$s_0 = \frac{1}{3}\sum_i s_i = \frac{1}{3}(m_K^2 + m_1^2 + m_2^2 + m_3^2)\quad .$$

Here the P_i are four-vectors, m_i and T_i are the mass and kinetic energy of the i^{th} pion, and the index 3 is used for the odd pion.

The coefficient g is a measure of the slope in the variable s_3 (or T_3) of the Dalitz plot, while h and k measure the quadratic dependence on s_3 and $(s_2 - s_1)$, respectively. The coefficient j is related to the asymmetry of the plot and must be zero if CP invariance holds. Note also that if CP is good, g, h, and k must be the same for $K^+ \to \pi^+\pi^+\pi^-$ as for $K^- \to \pi^-\pi^-\pi^+$.

Since different experiments use different forms for $\left|M\right|^2$, in order to compare the experiments we have converted to g, h, j, and k whatever coefficients have been measured. Where such conversions have been done, the measured coefficient a_y, a_t, a_u, or a_v is given in the comment at the right. For definitions of these coefficients, details of this conversion, and discussion of the data, see the April 1982 version of this note [2].

References:

1. S. Weinberg, Phys. Rev. Lett. **4**, 87 (1960).
2. Particle Data Group, Phys. Lett. **111B**, 69 (1982).

76. $K^{\pm}_{\ell 3}$ and $K^0_{\ell 3}$ Form Factors

Updated September 2013 by T.G. Trippe (LBNL) and C.-J. Lin (LBNL).

Assuming that only the vector current contributes to $K \to \pi\ell\nu$ decays, we write the matrix element as

$$M \propto f_+(t)\left[(P_K+P_\pi)_\mu \overline{\ell}\gamma_\mu(1+\gamma_5)\nu\right] + f_-(t)\left[m_\ell\overline{\ell}(1+\gamma_5)\nu\right] , \quad (76.1)$$

where P_K and P_π are the four-momenta of the K and π mesons, m_ℓ is the lepton mass, and f_+ and f_- are dimensionless form factors which can depend only on $t = (P_K - P_\pi)^2$, the square of the four-momentum transfer to the leptons. If time-reversal invariance holds, f_+ and f_- are relatively real. $K_{\mu 3}$ experiments, discussed immediately below, measure f_+ and f_-, while K_{e3} experiments, discussed further below, are sensitive only to f_+ because the small electron mass makes the f_- term negligible.

76.1. $K_{\mu 3}$ Experiments

Analyses of $K_{\mu 3}$ data frequently assume a linear dependence of f_+ and f_- on t, *i.e.*,

$$f_\pm(t) = f_\pm(0)\left[1+\lambda_\pm(t/m^2_{\pi^+})\right] . \quad (76.2)$$

Most $K_{\mu 3}$ data are adequately described by Eq. (76.2) for f_+ and a constant f_- (*i.e.*, $\lambda_- = 0$).

76.1.1. *Two commonly used equivalent parametrizations* :

76.1.1.1. $\lambda_+, \xi(0)$ *parametrization:*

Older analyses of $K_{\mu 3}$ data often introduce the ratio of the two form factors

$$\xi(t) = f_-(t)/f_+(t) . \quad (76.3)$$

The $K_{\mu 3}$ decay distribution is then described by the two parameters λ_+ and $\xi(0)$ (assuming time reversal invariance and $\lambda_- = 0$).

76.1.1.2. λ_+, λ_0 *parametrization:*

More recent $K_{\mu 3}$ analyses have parametrized in terms of the form factors f_+ and f_0, which are associated with vector and scalar exchange, respectively, to the lepton pair. f_0 is related to f_+ and f_- by

$$f_0(t) = f_+(t) + \left[t/(m^2_K - m^2_\pi)\right] f_-(t) . \quad (76.4)$$

Here $f_0(0)$ must equal $f_+(0)$ unless $f_-(t)$ diverges at $t = 0$. The earlier assumption that f_+ is linear in t and f_- is constant leads to f_0 linear in t:

$$f_0(t) = f_0(0)\left[1+\lambda_0(t/m^2_{\pi^+})\right] . \quad (76.5)$$

With the assumption that $f_0(0) = f_+(0)$, the two parametrizations, $(\lambda_+, \xi(0))$ and (λ_+, λ_0) are equivalent as long as correlation information is retained. (λ_+, λ_0) correlations tend to be less strong than $(\lambda_+, \xi(0))$ correlations.

Since the 2006 edition of the *Review* [4], we no longer quote results in the $(\lambda_+, \xi(0))$ parametrization. We have removed many older low statistics results from the Listings. See the 2004 version of this note [5] for these older results, and the 1982 version [6] for additional discussion of the $K^0_{\mu 3}$ parameters, correlations, and conversion between parametrizations.

76.1.2. *Quadratic Parametrization* :

More recent high-statistics experiments have included a quadratic term in the expansion of $f_+(t)$,

$$f_+(t) = f_+(0)\left[1+\lambda'_+(t/m^2_{\pi^+}) + \frac{\lambda''_+}{2}(t/m^2_{\pi^+})^2\right] . \quad (76.6)$$

If there is a non-vanishing quadratic term, then λ_+ of Eq. (76.2) represents the average slope, which is then different from λ'_+. Our convention is to include the factor $\frac{1}{2}$ in the quadratic term, and to use m_{π^+} even for K^+_{e3} and $K^+_{\mu 3}$ decays. We have converted other's parametrizations to match our conventions, as noted in the beginning of the "$K^{\pm}_{\ell 3}$ and $K^0_{\ell 3}$ Form Factors" sections of the Listings.

76.1.3. *Pole Parametrization* :

The pole model describes the t-dependence of $f_+(t)$ and $f_0(t)$ in terms of the exchange of the lightest vector and scalar K^* mesons with masses M_v and M_s, respectively:

$$f_+(t) = f_+(0)\left[\frac{M_v^2}{M_v^2 - t}\right] , \quad f_0(t) = f_0(0)\left[\frac{M_s^2}{M_s^2 - t}\right] . \quad (76.7)$$

76.1.4. *Dispersive Parametrization* :

This approach [7,8] uses dispersive techniques and the known low-energy K-π phases to parametrize the vector and scalar form factors:

$$f_+(t) = f_+(0)\exp\left[\frac{\mathrm{t}}{\mathrm{m}^2_\pi}(\Lambda_+ + \mathrm{H(t)})\right] ; \quad (76.8)$$

$$f_0(t) = f_+(0)\exp\left[\frac{\mathrm{t}}{(\mathrm{m}^2_\mathrm{K} - \mathrm{m}^2_\pi)}(\ln[\mathrm{C}] - \mathrm{G(t)})\right] , \quad (76.9)$$

where Λ_+ is the slope of the vector form factor, and $\ln[\mathrm{C}] = \ln[\mathrm{f_0}(\mathrm{m}^2_\mathrm{K} - \mathrm{m}^2_\pi)]$ is the logarithm of the scalar form factor at the Callan-Treiman point. The functions H(t) and G(t) are dispersive integrals.

76.2. K_{e3} Experiments

Analysis of K_{e3} data is simpler than that of $K_{\mu 3}$ because the second term of the matrix element assuming a pure vector current [Eq. (76.1) above] can be neglected. Here f_+ can be assumed to be linear in t, in which case the linear coefficient λ_+ of Eq. (76.2) is determined, or quadratic, in which case the linear coefficient λ'_+ and quadratic coefficient λ''_+ of Eq. (76.6) are determined.

If we remove the assumption of a pure vector current, then the matrix element for the decay, in addition to the terms in Eq. (76.1), would contain

$$+2m_K f_S \overline{\ell}(1+\gamma_5)\nu + (2f_T/m_K)(P_K)_\lambda(P_\pi)_\mu \overline{\ell}\sigma_{\lambda\mu}(1+\gamma_5)\nu , \quad (76.10)$$

where f_S is the scalar form factor, and f_T is the tensor form factor. In the case of the K_{e3} decays where the f_- term can be neglected, experiments have yielded limits on $|f_S/f_+|$ and $|f_T/f_+|$.

76.2.1. *Fits for $K_{\ell 3}$ Form Factors* :

For K_{e3} data, we determine best values for the three parametrizations: linear (λ_+), quadratic (λ'_+, λ''_+) and pole (M_v). For $K_{\mu 3}$ data, we determine best values for the three parametrizations: linear (λ_+, λ_0), quadratic (λ'_+, λ''_+, λ_0) and pole (M_v, M_s). We then assume $\mu - e$ universality so that we can combine K_{e3} and $K_{\mu 3}$ data, and again determine best values for the three parametrizations: linear (λ_+, λ_0), quadratic (λ'_+, λ''_+, λ_0), and pole (M_v, M_s). When there is more than one parameter, fits are done including input correlations. Simple averages suffice in the two K_{e3} cases where there is only one parameter: linear (λ_+) and pole (M_v).

Both KTeV and KLOE see an improvement in the quality of their fits relative to linear fits when a quadratic term is introduced, as well as when the pole parametrization is used. The quadratic parametrization has the disadvantage that the quadratic parameter λ''_+ is highly correlated with the linear parameter λ'_+, in the neighborhood of 95%, and that neither parameter is very well determined. The pole fit has the same number of parameters as the linear fit, but yields slightly better fit probabilities, so that it would be advisable for all experiments to include the pole parametrization as one of their choices [9].

The "Kaon Particle Listings" show the results with and without assuming μ-e universality. The "Meson Summary Tables" show all of the results assuming μ-e universality, but most results not assuming μ-e universality are given only in the Listings.

References:

1. L.M. Chounet, J.M. Gaillard, and M.K. Gaillard, Phys. Reports **4C**, 199 (1972).
2. H.W. Fearing, E. Fischbach, and J. Smith, Phys. Rev. **D2**, 542 (1970).
3. N. Cabibbo and A. Maksymowicz, Phys. Lett. **9**, 352 (1964).
4. W.-M. Yao *et al.*, Particle Data Group, J. Phys. **G33**, 1 (2006).
5. S. Eidleman *et al.*, Particle Data Group, Phys. Lett. **B592**, 1 (2004).
6. M. Roos *et al.*, Particle Data Group, Phys. Lett. **111B**, 73 (1982).
7. V. Bernard *et al.*, Phys. Lett. **B638**, 48 (2006).
8. A. Lai *et al.*, Phys. Lett. **B647**, 341 (2007), and references therein.
9. We thank P. Franzini (Rome U. and Frascati) for useful discussions on this point.

77. CPT Invariance Tests in Neutral Kaon Decay

Updated October 2013 by M. Antonelli (LNF-INFN, Frascati) and G. D'Ambrosio (INFN Sezione di Napoli).

CPT theorem is based on three assumptions: quantum field theory, locality, and Lorentz invariance, and thus it is a fundamental probe of our basic understanding of particle physics. Strangeness oscillation in $K^0-\overline{K}^0$ system, described by the equation

$$i\frac{d}{dt}\begin{bmatrix}K^0\\ \overline{K}^0\end{bmatrix}=[M-i\Gamma/2]\begin{bmatrix}K^0\\ \overline{K}^0\end{bmatrix}\ ,$$

where M and Γ are hermitian matrices (see PDG review [1], references [2,3], and KLOE paper [5] for notations and previous literature), allows a very accurate test of CPT symmetry; indeed since CPT requires $M_{11}=M_{22}$ and $\Gamma_{11}=\Gamma_{22}$, the mass and width eigenstates, $K_{S,L}$, have a CPT-violating piece, δ, in addition to the usual CPT-conserving parameter ϵ:

$$K_{S,L}=\frac{1}{\sqrt{2\left(1+|\epsilon_{S,L}|^2\right)}}\left[\left(1+\epsilon_{S,L}\right)K^0\pm\left(1-\epsilon_{S,L}\right)\overline{K}^0\right]$$

$$\epsilon_{S,L}=\frac{-i\Im\left(M_{12}\right)-\frac{1}{2}\Im\left(\Gamma_{12}\right)\mp\frac{1}{2}\left[M_{11}-M_{22}-\frac{i}{2}\left(\Gamma_{11}-\Gamma_{22}\right)\right]}{m_L-m_S+i(\Gamma_S-\Gamma_L)/2}$$
$$\equiv\epsilon\pm\delta. \qquad (77.1)$$

Using the phase convention $\Im(\Gamma_{12})=0$, we determine the phase of ϵ to be $\varphi_{SW}\equiv\arctan\frac{2(m_L-m_S)}{\Gamma_S-\Gamma_L}$. Imposing unitarity to an arbitrary combination of K^0 and $\overline{K}^0$ wave functions, we obtain the Bell-Steinberger relation [4] connecting CP and CPT violation in the mass matrix to CP and CPT violation in the decay; in fact, neglecting $\mathcal{O}(\epsilon)$ corrections to the coefficient of the CPT-violating parameter, δ, we can write [5]

$$[\frac{\Gamma_S+\Gamma_L}{\Gamma_S-\Gamma_L}+i\tan\phi_{\rm SW}][\frac{\Re(\epsilon)}{1+|\epsilon|^2}-i\Im(\delta)]=$$
$$\frac{1}{\Gamma_S-\Gamma_L}\sum_f A_L(f)A_S^*(f), \qquad (77.2)$$

where $A_{L,S}(f)\equiv A(K_{L,S}\to f)$. We stress that this relation is phase-convention-independent. The advantage of the neutral kaon system is that only a few decay modes give significant contributions to the r.h.s. in Eq. (77.2); in fact, defining for the hadronic modes

$$\alpha_i\equiv\frac{1}{\Gamma_S}\langle\mathcal{A}_L(i)\mathcal{A}_S^*(i)\rangle=\eta_i\ \mathcal{B}(K_S\to i),$$
$$i=\pi^0\pi^0,\pi^+\pi^-(\gamma),3\pi^0,\pi^0\pi^+\pi^-(\gamma), \qquad (77.3)$$

the recent data from CPLEAR, KLOE, KTeV, and NA48 have led to the following determinations (the analysis described in Ref. 5 has been updated by using the recent measurements of K_L branching ratios from KTeV [6,7], NA48 [8,9], and the results described in the CP violation in K_L decays minireview, and the recent KLOE result [10])

$$\alpha_{\pi^+\pi^-}=((1.112\pm0.010)+i(1.061\pm0.010))\times10^{-3}\ ,$$
$$\alpha_{\pi^0\pi^0}=((0.493\pm0.005)+i(0.471\pm0.005))\times10^{-3}\ ,$$
$$\alpha_{\pi^+\pi^-\pi^0}=((0\pm2)+i(0\pm2))\times10^{-6},$$
$$|\alpha_{\pi^0\pi^0\pi^0}|<1.5\times10^{-6}\quad\text{at 95\% CL}\ . \qquad (77.4)$$

The semileptonic contribution to the right-handed side of Eq. (77.2) requires the determination of several observables: we define [2,3]

$$\mathcal{A}(K^0\to\pi^-l^+\nu)=\mathcal{A}_0(1-y)\ ,$$
$$\mathcal{A}(K^0\to\pi^+l^-\nu)=\mathcal{A}_0^*(1+y^*)(x_+-x_-)^*\ ,$$
$$\mathcal{A}(\overline{K}^0\to\pi^+l^-\nu)=\mathcal{A}_0^*(1+y^*)\ ,$$
$$\mathcal{A}(\overline{K}^0\to\pi^-l^+\nu)=\mathcal{A}_0(1-y)(x_++x_-)\ , \qquad (77.5)$$

where x_+ (x_-) describes the violation of the $\Delta S=\Delta Q$ rule in CPT-conserving (violating) decay amplitudes, and y parametrizes CPT violation for $\Delta S=\Delta Q$ transitions. Taking advantage of their tagged $K^0(\overline{K}^0)$ beams, CPLEAR has measured $\Im(x_+)$, $\Re(x_-)$, $\Im(\delta)$, and $\Re(\delta)$ [11]. These determinations have been improved in Ref. 5 by including the information $A_S-A_L=4[\Re(\delta)+\Re(x_-)]$, where $A_{L,S}$ are the K_L and K_S semileptonic charge asymmetries, respectively, from the PDG [12] and KLOE [13]. Here we are also including the T-violating asymmetry measurement from CPLEAR [14].

Table 77.1: Values, errors, and correlation coefficients for $\Re(\delta)$, $\Im(\delta)$, $\Re(x_-)$, $\Im(x_+)$, and A_S+A_L obtained from a combined fit, including KLOE [5] and CPLEAR [14].

	value	Correlations coefficients				
$\Re(\delta)$	$(3.0\pm2.3)\times10^{-4}$	1				
$\Im(\delta)$	$(-0.66\pm0.65)\times10^{-2}$	−0.21	1			
$\Re(x_-)$	$(-0.30\pm0.21)\times10^{-2}$	−0.21	−0.60	1		
$\Im(x_+)$	$(0.02\pm0.22)\times10^{-2}$	−0.38	−0.14	0.47	1	
A_S+A_L	$(-0.40\pm0.83)\times10^{-2}$	−0.10	−0.63	0.99	0.43	1

The value A_S+A_L in Table 77.1 can be directely included in the semileptonic contributions to the Bell Steinberger relations in Eq. (77.2)

$$\sum_{\pi\ell\nu}\langle\mathcal{A}_L(\pi\ell\nu)\mathcal{A}_S^*(\pi\ell\nu)\rangle$$
$$=2\Gamma(K_L\to\pi\ell\nu)(\Re(\epsilon)-\Re(y)-i(\Im(x_+)+\Im(\delta)))$$
$$=2\Gamma(K_L\to\pi\ell\nu)((A_S+A_L)/4-i(\Im(x_+)+\Im(\delta)))\ . \qquad (77.6)$$

Defining

$$\alpha_{\pi\ell\nu}\equiv\frac{1}{\Gamma_S}\sum_{\pi\ell\nu}\langle\mathcal{A}_L(\pi\ell\nu)\mathcal{A}_S^*(\pi\ell\nu)\rangle+2i\frac{\tau_{K_S}}{\tau_{K_L}}\mathcal{B}(K_L\to\pi\ell\nu)\Im(\delta)\ , \qquad (77.7)$$

we find:

$$\alpha_{\pi\ell\nu}=((-0.2\pm0.5)+i(0.1\pm0.5))\times10^{-5}\,.$$

Inserting the values of the α parameters into Eq. (77.2), we find

$$\Re(\epsilon)=(161.1\pm0.5)\times10^{-5},$$
$$\Im(\delta)=(-0.7\pm1.4)\times10^{-5}\,. \qquad (77.8)$$

The complete information on Eq. (77.8) is given in Table 77.2.

Table 77.2: Summary of results: values, errors, and correlation coefficients for $\Re(\epsilon)$, $\Im(\delta)$, $\Re(\delta)$, and $\Re(x_-)$.

	value	Correlations coefficients			
$\Re(\epsilon)$	$(161.1\pm0.5)\times10^{-5}$	+1			
$\Im(\delta)$	$(-0.7\pm1.4)\times10^{-5}$	+0.09	1		
$\Re(\delta)$	$(2.4\pm2.3)\times10^{-4}$	+0.08	−0.12	1	
$\Re(x_-)$	$(-4.1\pm1.7)\times10^{-3}$	+0.14	0.22	−0.43	1

Now the agreement with CPT conservation, $\Im(\delta)=\Re(\delta)=\Re(x_-)=0$, is at 18% C.L.

The allowed region in the $\Re(\epsilon)-\Im(\delta)$ plane at 68% CL and 95% C.L. is shown in the top panel of Fig. 77.1.

The process giving the largest contribution to the size of the allowed region is $K_L\to\pi^+\pi^-$, through the uncertainty on ϕ_{+-}.

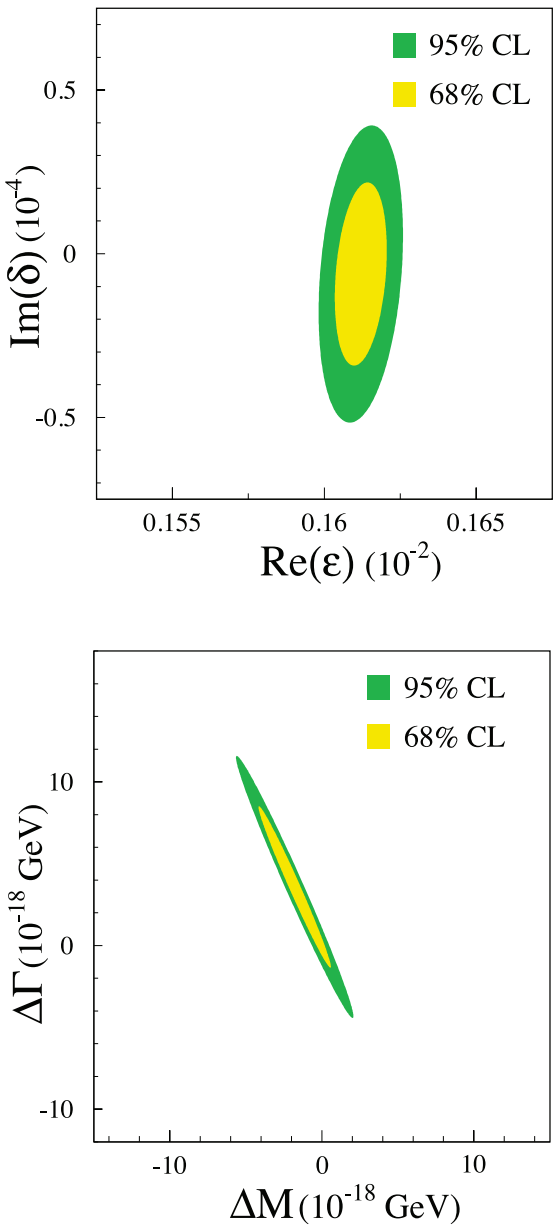

Figure 77.1: Top: allowed region at 68% and 95% C.L. in the $\Re(\epsilon)$, $\Im(\delta)$ plane. Bottom: allowed region at 68% and 95% C.L. in the $\Delta M, \Delta\Gamma$ plane.

The limits on $\Im(\delta)$ and $\Re(\delta)$ can be used to constrain the $K^0 - \overline{K}^0$ mass and width difference

$$\delta = \frac{i(m_{K^0} - m_{\overline{K}^0}) + \frac{1}{2}(\Gamma_{K^0} - \Gamma_{\overline{K}^0})}{\Gamma_S - \Gamma_L} \cos\phi_{SW} e^{i\phi_{SW}} [1 + \mathcal{O}(\epsilon)] \,.$$

The allowed region in the $\Delta M = (m_{K^0} - m_{\overline{K}^0}), \Delta\Gamma = (\Gamma_{K^0} - \Gamma_{\overline{K}^0})$ plane is shown in the bottom panel of Fig. 77.1. As a result, we improve on the previous limits (see for instance, P. Bloch in Ref. 12) and in the limit $\Gamma_{K^0} - \Gamma_{\overline{K}^0} = 0$ we obtain

$$-4.0 \times 10^{-19} \text{ GeV} < m_{K^0} - m_{\overline{K}^0} < 4.0 \times 10^{-19} \text{ GeV} \quad \text{at 95 \% C.L.}$$

References:

1. See the "CP Violation in Meson Decays," in this *Review*.
2. L. Maiani, "CP And CPT Violation in Neutral Kaon Decays," L. Maiani, G. Pancheri, and N. Paver, *The Second Daphne Physics Handbook*, Vol. 1, 2.
3. G. D'Ambrosio, G. Isidori, and A. Pugliese, "CP and CPT mesurements at DAΦNE," L. Maiani, G. Pancheri, and N. Paver, *The Second Daphne Physics Handbook*, Vol. 1, 2.
4. J. S. Bell and J. Steinberger, In Wolfenstein, L. (ed.): *CP violation,* 42-57. (In *Oxford International Symposium Conference on Elementary Particles*, September 1965, 195-208, 221-222). (See Book Index).
5. F. Ambrosino *et al.*, [KLOE Collab.], JHEP **0612**, 011 (2006) [arXiv:hep-ex/0610034].
6. T. Alexopoulos *et al.*, [KTeV Collab.], Phys. Rev. **D70**, 092006 (1998).
7. E. Abouzaid *et al.* [KTeV Collab.], Phys. Rev. **D83**, 092001 (2011).
8. A. Lai *et al.*, [NA48 Collab.], Phys. Lett. **B645**, 26 (2007); A. Lai *et al.*, [NA48 Collab.], Phys. Lett. **B602**, 41 (2004).
9. We thank G. Isidori and M. Palutan for their contribution to the original analyisis [5] performed with KLOE data.
10. D. Babusci *et al.*, [KLOE Collab.], Phys. Lett. **B723**, 54 (2013).
11. A. Angelopoulos *et al.*, [CPLEAR Collab.], Phys. Lett. **B444**, 52 (1998).
12. W. M. Yao *et al.*, [Particle Data Group], J. Phys. **G33**, 1 (2006).
13. F. Ambrosino *et al.*, [KLOE Collab.], Phys. Lett. **B636**, 173 (2006) [arXiv:hep-ex/0601026].
14. P. Bloch, M. Fidecaro, private communication of the data in a finer binning format; A. Angelopoulos *et al.*, [CPLEAR Collab.], Phys. Lett. **B444**, 43 (1998).
15. We thank M. Palutan for the collaboration in this analysis.

78. CP Violation in $K_S \to 3\pi$

Written 1996 by T. Nakada (Paul Scherrer Institute) and L. Wolfenstein (Carnegie-Mellon University).

The possible final states for the decay $K^0 \to \pi^+\pi^-\pi^0$ have isospin $I = 0$, 1, 2, and 3. The $I = 0$ and $I = 2$ states have $CP = +1$ and K_S can decay into them without violating CP symmetry, but they are expected to be strongly suppressed by centrifugal barrier effects. The $I = 1$ and $I = 3$ states, which have no centrifugal barrier, have $CP = -1$ so that the K_S decay to these requires CP violation.

In order to see CP violation in $K_S \to \pi^+\pi^-\pi^0$, it is necessary to observe the interference between K_S and K_L decay, which determines the amplitude ratio

$$\eta_{+-0} = \frac{A(K_S \to \pi^+\pi^-\pi^0)}{A(K_L \to \pi^+\pi^-\pi^0)} \ . \tag{78.1}$$

If η_{+-0} is obtained from an integration over the whole Dalitz plot, there is no contribution from the $I = 0$ and $I = 2$ final states and a nonzero value of η_{+-0} is entirely due to CP violation.

Only $I = 1$ and $I = 3$ states, which are $CP = -1$, are allowed for $K^0 \to \pi^0\pi^0\pi^0$ decays and the decay of K_S into $3\pi^0$ is an unambiguous sign of CP violation. Similarly to η_{+-0}, η_{000} is defined as

$$\eta_{000} = \frac{A(K_S \to \pi^0\pi^0\pi^0)}{A(K_L \to \pi^0\pi^0\pi^0)} \ . \tag{78.2}$$

If one assumes that CPT invariance holds and that there are no transitions to $I = 3$ (or to nonsymmetric $I = 1$ states), it can be shown that

$$\begin{aligned} \eta_{+-0} &= \eta_{000} \\ &= \epsilon + i\frac{\text{Im } a_1}{\text{Re } a_1} \ . \end{aligned} \tag{78.3}$$

With the Wu-Yang phase convention, a_1 is the weak decay amplitude for K^0 into $I = 1$ final states; ϵ is determined from CP violation in $K_L \to 2\pi$ decays. The real parts of η_{+-0} and η_{000} are equal to $\text{Re}(\epsilon)$. Since currently-known upper limits on $|\eta_{+-0}|$ and $|\eta_{000}|$ are much larger than $|\epsilon|$, they can be interpreted as upper limits on $\text{Im}(\eta_{+-0})$ and $\text{Im}(\eta_{000})$ and so as limits on the CP-violating phase of the decay amplitude a_1.

79. V_{ud}, V_{us}, the Cabibbo Angle, and CKM Unitarity

Updated February 2018 by E. Blucher (Univ. of Chicago) and W.J. Marciano (BNL)

The Cabibbo-Kobayashi-Maskawa (CKM) [1,2] three-generation quark mixing matrix written in terms of the Wolfenstein parameters (λ, A, ρ, η) [3] nicely illustrates the orthonormality constraint of unitarity and central role played by λ.

$$V_{\rm CKM} = \begin{pmatrix} V_{ud} & V_{us} & V_{ub} \\ V_{cd} & V_{cs} & V_{cb} \\ V_{td} & V_{ts} & V_{tb} \end{pmatrix}$$

$$= \begin{pmatrix} 1-\lambda^2/2 & \lambda & A\lambda^3(\rho - i\eta) \\ -\lambda & 1-\lambda^2/2 & A\lambda^2 \\ A\lambda^3(1-\rho-i\eta) & -A\lambda^2 & 1 \end{pmatrix} + \mathcal{O}(\lambda^4)\ . \quad (79.1)$$

That cornerstone is a carryover from the two-generation Cabibbo angle, $\lambda = \sin(\theta_{\rm Cabibbo}) = V_{us}$. Its value is a critical ingredient in determinations of the other parameters and in tests of CKM unitarity.

For many years, the precise value of λ was somewhat controversial, with kaon decays suggesting [4] $\lambda \simeq 0.220$, while indirect determinations via nuclear β-decays implied a somewhat larger $\lambda \simeq 0.225-0.230$. This difference resulted in a 2 – 2.5 sigma deviation from the unitarity requirement

$$|V_{ud}|^2 + |V_{us}|^2 + |V_{ub}|^2 = 1, \quad (79.2)$$

a potential signal [5] for new physics effects. Below, we discuss the current status of V_{ud}, V_{us}, and their associated unitarity test in Eq. (79.2). (Since $|V_{ub}|^2 \simeq 1.7 \times 10^{-5}$ is negligibly small, it is ignored in this discussion.) Eq. (79.2) is currently the most stringent test of unitarity in the CKM matrix.

79.1. V_{ud}

The value of V_{ud} has been obtained from superallowed nuclear, neutron, and pion decays. Currently, the most precise determination of V_{ud} comes from a set of superallowed nuclear beta-decays [5] ($0^+ \to 0^+$ transitions). Measuring their half-lives, t, and Q values that give the decay rate factor, f, leads to a precise determination of V_{ud} via the master formula [6–10]

$$|V_{ud}|^2 = \frac{2984.48(5)\,\sec}{ft(1+\Delta)}, \quad (79.3)$$

where Δ denotes the entire effect of electroweak radiative corrections (RC), nuclear structure, and isospin violating nuclear effects. Δ is nucleus-dependent, ranging from about +3.0% to +3.6% for the best measured superallowed decays. It includes a universal ±0.04% theoretical uncertainty for all beta decays coming from the radiative corrections.

The most recent analysis of 14 precisely measured superallowed transitions by Hardy and Towner [11] gives a weighted average of

$$V_{ud} = 0.97420(10)_{\rm exp.,nucl.}(18)_{\rm RC}\ \text{(superallowed)}\ , \quad (79.4)$$

which, assuming unitarity, corresponds to $\lambda = 0.2256(9)$. This recent determination of V_{ud} has shifted upward slightly compared to the 2016 value of 0.97417(21).

Combined measurements of the neutron lifetime, τ_n, and the ratio of axial-vector/vector couplings, $g_A \equiv G_A/G_V$, via neutron decay asymmetries can also be used to determine V_{ud}:

$$|V_{ud}|^2 = \frac{4908.7(1.9)\ \sec}{\tau_n(1+3g_A^2)}, \quad (79.5)$$

where the error stems from uncertainties in the electroweak radiative corrections [7,8] due to hadronic loop effects. Using the world averages from the 2016 *Review,* updated with a recent measurement [12] of $\tau_n = 877.7(7)(^{+3}_{-1})$ sec

$$\begin{aligned} \tau_n^{\rm ave} &= 879.3(9)\ \sec \quad (\times 2.1\ \text{PDG scale factor}) \\ g_A^{\rm ave} &= 1.2723(23) \quad (\times 2.2\ \text{PDG scale factor}) \end{aligned} \quad (79.6)$$

leads to

$$V_{ud} = 0.9763(5)_{\tau_n}(15)_{g_A}(2)_{\rm RC}, \quad (79.7)$$

with the error dominated by g_A uncertainties. We note that the g_A adopted in Eq. (79.6) leads to a value of V_{ud} that is somewhat high by 1.3 sigma, but roughly in accord with the superallowed nuclear beta decay result in Eq. (79.4). The value of V_{ud} in Eq. (79.4) together with the new $\tau_n^{\rm ave}$ in Eq. (79.6) suggest, via Eq. (79.5), $g_A \sim 1.276$. Future neutron studies [13] are expected to resolve any current inconsistencies and significantly reduce the uncertainties in g_A and τ_n.

The PIBETA experiment at PSI measured the very small ($\mathcal{O}(10^{-8})$) branching ratio for $\pi^+ \to \pi^o e^+ \nu_e$ with about ±0.5% precision. Their result gives [14]

$$V_{ud} = 0.9749(26)\left[\frac{BR(\pi^+ \to e^+\nu_e(\gamma))}{1.2352 \times 10^{-4}}\right]^{\frac{1}{2}} \quad (79.8)$$

which is normalized using the very precisely determined theoretical prediction for $BR(\pi^+ \to e^+\nu_e(\gamma)) = 1.2352(5) \times 10^{-4}$ [6], rather than the experimental branching ratio from this *Review* of $1.230(4) \times 10^{-4}$ which would lower the value to $V_{ud} = 0.9728(30)$. Theoretical uncertainties in the pion β-decay determination are very small; however, much higher statistics would be required to make this approach competitive with others.

79.2. V_{us}

$|V_{us}|$ may be determined from kaon decays, hyperon decays, and tau decays. Previous determinations have most often used $K\ell 3$ decays:

$$\Gamma_{K\ell 3} = \frac{G_F^2 M_K^5}{192\pi^3} S_{EW}(1+\delta_K^\ell + \delta_{SU2})C^2\,|V_{us}|^2\,f_+^2(0) I_K^\ell. \quad (79.9)$$

Here, ℓ refers to either e or μ, G_F is the Fermi constant, M_K is the kaon mass, S_{EW} is the short-distance radiative correction, δ_K^ℓ is the mode-dependent long-distance radiative correction, $f_+(0)$ is the calculated form factor at zero momentum transfer for the $\ell\nu$ system, and I_K^ℓ is the phase-space integral, which depends on measured semileptonic form factors. For charged kaon decays, δ_{SU2} is the deviation from one of the ratio of $f_+(0)$ for the charged to neutral kaon decay; it is zero for the neutral kaon. C^2 is 1 (1/2) for neutral (charged) kaon decays. Most early determinations of $|V_{us}|$ were based solely on $K \to \pi e\nu$ decays; $K \to \pi\mu\nu$ decays were not used because of large uncertainties in I_K^μ. The experimental measurements are the semileptonic decay widths (based on the semileptonic branching fractions and lifetime) and form factors (allowing calculation of the phase space integrals). Theory is needed for S_{EW}, δ_K^ℓ, δ_{SU2}, and $f_+(0)$.

Many measurements during the last decade have resulted in a significant shift in V_{us}. Most importantly, the $K \to \pi e\nu$ branching fractions are significantly different than earlier PDG averages, probably as a result of inadequate treatment of radiation in older experiments. This effect was first observed by BNL E865 [15] in the charged kaon system and then by KTeV [16,17] in the neutral kaon system; subsequent measurements were made by KLOE [18–21], NA48 [22–24], and ISTRA+ [25]. Current averages (*e.g.*, by the PDG [26] or Flavianet [27]) of the semileptonic branching fractions are based only on recent, high-statistics experiments where the treatment of radiation is clear. In addition to measurements of branching fractions, new measurements of lifetimes [28] and form factors [29–33], have resulted in improved precision for all of the experimental inputs to V_{us}. Precise measurements of form factors for $K_{\mu 3}$ decay make it possible to use both semileptonic decay modes to extract V_{us}.

Following the analysis of Moulson [34] and the Flavianet group [27], one finds, after including the isospin violating up-down mass difference effect, δ_{SU2} , the values of $|V_{us}|f_+(0)$ in Table 79.1. The average of these measurements, including correlation effects [34], gives

$$f_+(0)|V_{us}| = 0.2165(4). \quad (79.10)$$

Lattice QCD calculations of $f_+(0)$ have been carried out for 2, 2+1, and 2+1+1 quark flavors and range from about 0.96 to 0.97. Here, we use recent FLAG averages [35] for 2+1 and 2+1+1 flavors:

$$\begin{aligned} f_+(0) &= 0.9677(27) \quad N_f = 2+1 \\ f_+(0) &= 0.9704(32) \quad N_f = 2+1+1 \end{aligned} \quad (79.11)$$

One finds from Eq. (79.10) and Eq. (79.11),

$$\begin{aligned}|V_{us}| &= 0.2238(4)_{\rm exp+RC}(6)_{\rm lattice}\ (N_f = 2+1,\ K_{\ell 3}\ \text{decays})\\ &= 0.2231(4)_{\rm exp+RC}(7)_{\rm lattice}\ (N_f = 2+1+1,\ K_{\ell 3}\ \text{decays})\end{aligned} \tag{79.12}$$

Table 79.1: $|V_{us}|f_+(0)$ from $K_{\ell 3}$.

Decay Mode	$\lvert V_{us}\rvert f_+(0)$
$K^\pm e3$	0.2171 ± 0.0008
$K^\pm \mu 3$	0.2170 ± 0.0011
$K_L e3$	0.2163 ± 0.0006
$K_L \mu 3$	0.2166 ± 0.0006
$K_S e3$	0.2155 ± 0.0013
Average (including correlation effects [34])	0.2165 ± 0.0004

A value of V_{us} can also be obtained from a comparison of the radiative inclusive decay rates for $K \to \mu\nu(\gamma)$ and $\pi \to \mu\nu(\gamma)$ combined with a lattice gauge theory calculation of f_{K^+}/f_{π^+} via

$$\frac{|V_{us}|f_{K+}}{|V_{ud}|f_{\pi+}} = 0.23871(20)\left[\frac{\Gamma(K \to \mu\nu(\gamma))}{\Gamma(\pi \to \mu\nu(\gamma))}\right]^{\frac{1}{2}} \tag{79.13}$$

with the small error coming from electroweak radiative corrections and isospin breaking effects [36]. Employing

$$\frac{\Gamma(K \to \mu\nu(\gamma))}{\Gamma(\pi \to \mu\nu(\gamma))} = 1.3367(29), \tag{79.14}$$

which includes $\Gamma(K \to \mu\nu(\gamma)) = 5.134(11) \times 10^7 s^{-1}$ [34,37], leads to

$$\frac{|V_{us}|f_{K+}}{|V_{ud}|f_{\pi+}} = 0.2760(4). \tag{79.15}$$

Employing the FLAG [35] lattice QCD averages,

$$\begin{aligned}\frac{f_{K+}}{f_{\pi^+}} &= 1.192(5) \qquad N_f = 2+1\\ &= 1.1933(29) \quad N_f = 2+1+1.\end{aligned} \tag{79.16}$$

along with the value of $|V_{ud}|$ in Eq. (79.4) leads to

$$\begin{aligned}|V_{us}| &= 0.2256(10)\ (N_f = 2+1,\ K_{\mu 2}\ \text{decays})\\ &= 0.2253(7)\ (N_f = 2+1+1,\ K_{\mu 2}\ \text{decays})\end{aligned} \tag{79.17}$$

Together, weighted averages of the $K\ell 3$ (Eq. (79.12)) and $K\mu 2$ (Eq. (79.17)) values give similar results for $N_f = 2+1$ and $2+1+1$ flavors:

$$\begin{aligned}|V_{us}| &= 0.2244(6) \quad N_f = 2+1\\ |V_{us}| &= 0.2243(5) \quad N_f = 2+1+1.\end{aligned} \tag{79.18}$$

Note that the differences between $K\ell 3$ and $K\mu 2$ values for V_{us} differ by 1.5 and 2 sigma, respectively, for $N_f = 2+1$ and $2+1+1$ flavors. One might, therefore, scale the uncertainties in Eq. (79.18) accordingly.

It should be mentioned that hyperon decay fits suggest [38]

$$|V_{us}| = 0.2250(27)\ \text{(Hyperon Decays)} \tag{79.19}$$

modulo SU(3) breaking effects that could shift that value up or down. We note that a representative effort [39] that incorporates SU(3) breaking found $V_{us} = 0.226(5)$. Strangeness changing tau decays, averaging both inclusive and exclusive measurements, give [40]

$$|V_{us}| = 0.2216(15)\ \text{(Tau Decays)}\ , \tag{79.20}$$

which differs by about 2 sigma from the kaon determination discussed above, and would, if combined with V_{ud} from super-allowed beta decays, lead to a 2.4 sigma deviation from unitarity. This discrepancy results mainly from the inclusive tau decay results that rely on Finite Energy Sum Rule techniques and assumptions, as well as experimental uncertainties. Recent investigation of that approach suggests a larger value for V_{us}, which is more in accord with other determinations [41].

Employing the values of V_{ud} and V_{us} from Eq. (79.4) and Eq. (79.18), respectively, leads to the unitarity consistency check

$$|V_{ud}|^2 + |V_{us}|^2 + |V_{ub}|^2 = 0.9994(4)(2). \tag{79.21}$$

where the first error is the uncertainty from $|V_{ud}|^2$ and the second error is the uncertainty from $|V_{us}|^2$ for $N_f = 2+1+1$. For $N_f = 2+1$, the sum of the squares remains the same, but the V_{us} error increases to (3). If scale factors are included, both $|V_{us}|^2$ uncertainties roughly increase to (4).

79.3. CKM Unitarity Constraints

The current good experimental agreement with unitarity, $|V_{ud}|^2 + |V_{us}|^2 + |V_{ub}|^2 = 0.9994(5)$, provides strong confirmation of Standard Model radiative corrections (which range between 3-4% depending on the nucleus used) at better than the 50 sigma level [42]. In addition, it implies constraints on "New Physics" effects at both the tree and quantum loop levels. Those effects could be in the form of contributions to nuclear beta decays, K decays and/or muon decays, with the last of these providing normalization via the muon lifetime [43], which is used to obtain the Fermi constant, $G_\mu = 1.1663787(6) \times 10^{-5}\text{GeV}^{-2}$.

In the following sections, we illustrate the implications of CKM unitarity for (1) exotic muon decays [44](beyond ordinary muon decay $\mu^+ \to e^+\nu_e\bar{\nu}_\mu$) and (2) new heavy quark mixing V_{uD} [45]. Other examples in the literature [46,47] include Z_χ boson quantum loop effects, supersymmetry, leptoquarks, compositeness etc.

Exotic Muon Decays

If additional lepton flavor violating decays such as $\mu^+ \to e^+\bar{\nu}_e\nu_\mu$ (wrong neutrinos) occur, they would cause confusion in searches for neutrino oscillations at, for example, muon storage rings/neutrino factories or other neutrino sources from muon decays. Calling the rate for all such decays Γ(exotic μ decays), they should be subtracted before the extraction of G_μ and normalization of the CKM matrix. Since that is not done and unitarity works, one has (at one-sided 95% CL)

$$|V_{ud}|^2 + |V_{us}|^2 + |V_{ub}|^2 = 1 - BR(\text{exotic}\ \mu\ \text{decays}) \geq 0.9986 \tag{79.22}$$

or

$$BR(\text{exotic}\ \mu\ \text{decays}) \leq 0.0014\ . \tag{79.23}$$

This bound is a factor of 10 better than the direct experimental bound on $\mu^+ \to e^+\bar{\nu}_e\nu_\mu$.

New Heavy Quark Mixing

Heavy D quarks naturally occur in fourth quark generation models and some heavy quark "new physics" scenarios such as E_6 grand unification. Their mixing with ordinary quarks gives rise to V_{uD}, which is constrained by unitarity (one sided 95% CL)

$$\begin{aligned}|V_{ud}|^2 + |V_{us}|^2 + |V_{ub}|^2 = 1 - |V_{uD}|^2 \geq 0.9986\\ |V_{uD}| \leq 0.04\ .\end{aligned} \tag{79.24}$$

A similar constraint applies to heavy neutrino mixing and the couplings $V_{\mu N}$ and V_{eN}.

References:

1. N. Cabibbo, Phys. Rev. Lett. **10**, 531 (1963).
2. M. Kobayashi and T. Maskawa, Prog. Theor. Phys. **49**, 652 (1973).
3. L. Wolfenstein, Phys. Rev. Lett. **51**, 1945 (1983).
4. S. Eidelman *et al.* [Particle Data Group], Phys. Lett. **B592**, 1 (2004).
5. I.S. Towner and J.C. Hardy Rep. Prog. Phys. **73**, 046301 (2010).
6. W.J. Marciano and A. Sirlin, Phys. Rev. Lett. **71**, 3629 (1993).
7. A. Czarnecki, W.J. Marciano, and A. Sirlin, Phys. Rev. **D70**, 093006 (2004) [hep-ph/0406324].
8. W.J. Marciano and A. Sirlin, Phys. Rev. Lett. **96**, 032002 (2006) [hep-ph/0510099].
9. I.S. Towner and J.C. Hardy, Phys. Rev. **C77**, 025501 (2008).
10. J.C. Hardy and I.S. Towner, Phys. Rev. **C79**, 055502 (2009).
11. J.C. Hardy and I.S. Towner, Phys. Rev. **C91**, 0255012 (2015); PoS **CKM 2016**, 028 (2016).
12. R.W. Pattie Jr. *et al.*, arXiv:1707:01817.
13. H. Abele, Prog. in Part. Nucl. Phys. **60**, 1 (2008).
14. D. Pocanic *et al.*, Phys. Rev. Lett. **93**, 181803 (2004) [hep-ex/0312030].
15. A. Sher *et al.*, Phys. Rev. Lett. **91**, 261802 (2003).
16. T. Alexopoulos *et al.* [KTeV Collab.], Phys. Rev. Lett. **93**, 181802 (2004) [hep-ex/0406001].
17. T. Alexopoulos *et al.* [KTeV Collab.], Phys. Rev. **D70**, 092006 (2004) [hep-ex/0406002].
18. F. Ambrosino *et al.* [KLOE Collab.], Phys. Lett. **B632**, 43 (2006) [hep-ex/0508027].
19. F. Ambrosino *et al.* [KLOE Collab.], Phys. Lett. **B638**, 140 (2006) [hep-ex/0603041].
20. F. Ambrosino *et al.* [KLOE Collab.], Phys. Lett. **B636**, 173 (2006) [hep-ex/0601026].
21. F. Ambrosino *et al.* [KLOE Collab.], PoS **HEP2005**, 287 (2006) [hep-ex/0510028].
22. A. Lai *et al.* [NA48 Collab.], Phys. Lett. **B602**, 41 (2004) [hep-ex/0410059].
23. A. Lai *et al.* [NA48 Collab.], Phys. Lett. **B645**, 26 (2007) [hep-ex/0611052].
24. J.R. Batley *et al.* [NA48/2 Collab.], Eur. Phys. J. **C50**, 329 (2007) [hep-ex/0702015].
25. V.I. Romanovsky *et al.*, [hep-ex/0704.2052].
26. K.A. Olive *et al.* [Particle Data Group], Chin. Phys. C **38**, 090001 (2014).
27. Flavianet Working Group on Precise SM Tests in K Decays, http://www.lnf.infn.it/wg/vus; M. Antonelli *et al.*, Eur. Phys. J. **C69**, 399 (2010). For a detailed review, see M. Antonelli *et al.*, [hep-ph/0907.5386].
28. F. Ambrosino *et al.* [KLOE Collab.], Phys. Lett. **B626**, 15 (2005) [hep-ex/0507088].
29. T. Alexopoulos *et al.* [KTeV Collab.], Phys. Rev. **D70**, 092007 (2004) [hep-ex/0406003].
30. E. Abouzaid *et al.* [KTeV Collab.], Phys. Rev. **D74**, 097101 (2006) [hep-ex/0608058].
31. F. Ambrosino *et al.* [KLOE Collab.], Phys. Lett. **B636**, 166 (2006) [hep-ex/0601038].
32. A. Lai *et al.* [NA48 Collab.], Phys. Lett. **B604**, 1 (2004) [hep-ex/0410065].
33. O.P. Yushchenko *et al.*, Phys. Lett. **B589**, 111 (2004) [hep-ex/0404030].
34. M. Moulson, [hep-ex/1704.04104];PoS **CKM 2016**, 033 (2017).
35. S. Aoki *et al.* [FLAG], Eur. Phys. J. **C77**, 112 (2017). Averages used in this review based on A. Bazazov *et al.*, Phys. Rev. D 87, 073012 (2013); P.A. Boyle *et al.*, JHEP **1506**, 164 (2015; A. Bazazov *et al.*, Phys. Rev. Lett. **112**, 112001 (2014); E. Follana *et al.*, Phys. Rev. Lett. **100**, 062002 (2008); A. Bazazov *et al.*, PoS**LAT2010**, 074 (2010); S. Durr *et al.*, Phys. Rev. D 81,054507 (2010); R. Arthur *et al.*, Phys. Rev. D 87, 094514; A. Bazazov *et al.*, Phys. Rev. D 90, 074509 (2014); R. Dowdall *et al.*, Phys. Rev. D 88, 074504 (2013); N. Carrasco *et al.*, Phys. Rev. D 91, 054507 (2015).
36. V. Cirigliano and H. Neufeld, Phys. Lett. **B700**, 7 (2011); W.J. Marciano, Phys. Rev. Lett. **93**, 231803 (2004) [hep-ph/0402299].
37. D. Babusci *et al.* [KLOE Collab.], Phys. Lett. **B738**, 128 (2014) [arXiv:1407.2028].
38. N. Cabibbo, E.C. Swallow, and R. Winston, Phys. Rev. Lett. **92**, 251803 (2004) [hep-ph/0307214].
39. V. Mateu and A. Pich, JHEP **0510**, 041 (2005) [hep-ph/0509045].
40. Y. Amhis *et al.* [Heavy Flavor Averaging Group], Eur. Phys. J. **C77**, 895 (2017) [arXiv:1612.07233].
41. R. J. Hudspith *et al.*, [arXiv:1511.08514].
42. A. Sirlin, Rev. Mod. Phys. **50**, 573 (1978).
43. D. Webber *et al.*[MuLan Collab.], Phys. Rev. Lett. **106**, 041803 (2011); V. Tishchenko *et al.*[MuLan Collab.], Phys. Rev. **D87**, 052003 (2013).
44. K.S. Babu and S. Pakvasa, hep-ph/0204236.
45. W. Marciano and A. Sirlin, Phys. Rev. Lett. **56**, 22 (1986); P. Langacker and D. London, Phys. Rev. **D38**, 886 (1988).
46. W. Marciano and A. Sirlin, Phys. Rev. **D35**, 1672 (1987).
47. R. Barbieri *et al.*, Phys. Lett. **156B**, 348 (1985); K. Hagiwara *et al.*, Phys. Rev. Lett. **75**, 3605 (1995); A. Kurylov and M. Ramsey-Musolf, Phys. Rev. Lett. **88**, 071804 (2000).

80. CP Violation in K_L Decays

Updated April 2016 by L. Wolfenstein (Carnegie-Mellon University), C.-J. Lin (LBNL), and T.G. Trippe (LBNL).

The symmetries C (particle-antiparticle interchange) and P (space inversion) hold for strong and electromagnetic interactions. After the discovery of large C and P violation in the weak interactions, it appeared that the product CP was a good symmetry. In 1964 CP violation was observed in K^0 decays at a level given by the parameter $\epsilon \approx 2.3 \times 10^{-3}$.

A unified treatment of CP violation in K, D, B, and B_s mesons is given in "CP Violation in Meson Decays" by D. Kirkby and Y. Nir in this *Review*. A more detailed review including a thorough discussion of the experimental techniques used to determine CP violation parameters is given in a book by K. Kleinknecht [1]. Here we give a concise summary of the formalism needed to define the parameters of CP violation in K_L decays, and a description of our fits for the best values of these parameters.

80.1. Formalism for CP violation in Kaon decay

CP violation has been observed in the semi-leptonic decays $K_L^0 \to \pi^\mp \ell^\pm \nu$, and in the nonleptonic decay $K_L^0 \to 2\pi$. The experimental numbers that have been measured are

$$A_L = \frac{\Gamma(K_L^0 \to \pi^- \ell^+ \nu) - \Gamma(K_L^0 \to \pi^+ \ell^- \nu)}{\Gamma(K_L^0 \to \pi^- \ell^+ \nu) + \Gamma(K_L^0 \to \pi^+ \ell^- \nu)} \tag{80.1a}$$

$$\eta_{+-} = A(K_L^0 \to \pi^+\pi^-)/A(K_S^0 \to \pi^+\pi^-) = |\eta_{+-}|\, e^{i\phi_{+-}} \tag{80.1b}$$

$$\eta_{00} = A(K_L^0 \to \pi^0\pi^0)/A(K_S^0 \to \pi^0\pi^0) = |\eta_{00}|\, e^{i\phi_{00}} \ . \tag{80.1c}$$

CP violation can occur either in the K^0–$\overline{K}^0$ mixing or in the decay amplitudes. Assuming CPT invariance, the mass eigenstates of the K^0–$\overline{K}^0$ system can be written

$$|K_S\rangle = p|K^0\rangle + q|\overline{K}^0\rangle \ , \quad |K_L\rangle = p|K^0\rangle - q|\overline{K}^0\rangle \ . \tag{80.2}$$

If CP invariance held, we would have $q = p$ so that K_S would be CP-even and K_L CP-odd. (We define $|\overline{K}^0\rangle$ as $CP\ |K^0\rangle$). CP violation in K^0–$\overline{K}^0$ mixing is then given by the parameter $\widetilde{\epsilon}$ where

$$\frac{p}{q} = \frac{(1+\widetilde{\epsilon})}{(1-\widetilde{\epsilon})} \ . \tag{80.3}$$

CP violation can also occur in the decay amplitudes

$$A\big(K^0 \to \pi\pi(I)\big) = A_I e^{i\delta_I} \ , \quad A\big(\overline{K}^0 \to \pi\pi(I)\big) = A_I^* e^{i\delta_I} \ , \tag{80.4}$$

where I is the isospin of $\pi\pi$, δ_I is the final-state phase shift, and A_I would be real if CP invariance held. The CP-violating observables are usually expressed in terms of ϵ and ϵ' defined by

$$\eta_{+-} = \epsilon + \epsilon' \ , \quad \eta_{00} = \epsilon - 2\epsilon' \ . \tag{80.5a}$$

One can then show [2]

$$\epsilon = \widetilde{\epsilon} + i\ \big(\mathrm{Im}\ A_0/\mathrm{Re}\ A_0\big) \ , \tag{80.5b}$$

$$\sqrt{2}\epsilon' = ie^{i(\delta_2-\delta_0)}(\mathrm{Re}\ A_2/\mathrm{Re}\ A_0)\ \big(\mathrm{Im}\ A_2/\mathrm{Re}\ A_2 - \mathrm{Im}\ A_0/\mathrm{Re}\ A_0\big) \ , \tag{80.5c}$$

$$A_L = 2\mathrm{Re}\ \epsilon/(1+|\epsilon|^2) \approx 2\mathrm{Re}\ \epsilon \ . \tag{80.5d}$$

In Eqs. (80.5a), small corrections [3] of order $\epsilon' \times \mathrm{Re}\ (A_2/A_0)$ are neglected, and Eq. (80.5d) assumes the $\Delta S = \Delta Q$ rule.

The quantities Im A_0, Im A_2, and Im $\widetilde{\epsilon}$ depend on the choice of phase convention, since one can change the phases of K^0 and $\overline{K}^0$ by a transformation of the strange quark state $|s\rangle \to |s\rangle\ e^{i\alpha}$; of course, observables are unchanged. It is possible by a choice of phase convention to set Im A_0 or Im A_2 or Im $\widetilde{\epsilon}$ to zero, but none of these is zero with the usual phase conventions in the Standard Model. The choice Im $A_0 = 0$ is called the Wu-Yang phase convention [4], in which case $\epsilon = \widetilde{\epsilon}$. The value of ϵ' is independent of phase convention, and a nonzero value demonstrates CP violation in the decay amplitudes, referred to as direct CP violation. The possibility that direct CP violation is essentially zero, and that CP violation occurs only in the mixing matrix, was referred to as the superweak theory [5].

By applying CPT invariance and unitarity the phase of ϵ is given approximately by

$$\phi_\epsilon \ \approx\ \tan^{-1}\frac{2(m_{K_L} - m_{K_S})}{\Gamma_{K_S} - \Gamma_{K_L}} \approx 43.52 \pm 0.05^\circ \ , \tag{80.6a}$$

while Eq. (80.5c) gives the phase of ϵ' to be

$$\phi_{\epsilon'} = \delta_2 - \delta_0 + \frac{\pi}{2} \approx 42.3 \pm 1.5^\circ \ , \tag{80.6b}$$

where the numerical value is based on an analysis of π–π scattering using chiral perturbation theory [6]. The approximation in Eq. (80.6a) depends on the assumption that direct CP violation is very small in all K^0 decays. This is expected to be good to a few tenths of a degree, as indicated by the small value of ϵ' and of η_{+-0} and η_{000}, the CP-violation parameters in the decays $K_S \to \pi^+\pi^-\pi^0$ [7], and $K_S \to \pi^0\pi^0\pi^0$ [8]. The relation in Eq. (80.6a) is exact in the superweak theory, so this is sometimes called the superweak-phase $\phi_{\rm SW}$. An important point for the analysis is that $\cos(\phi_{\epsilon'} - \phi_\epsilon) \simeq 1$. The consequence is that only two real quantities need be measured, the magnitude of ϵ and the value of (ϵ'/ϵ), including its sign. The measured quantity $|\eta_{00}/\eta_{+-}|^2$ is very close to unity so that we can write

$$|\eta_{00}/\eta_{+-}|^2 \approx 1 - 6\mathrm{Re}\ (\epsilon'/\epsilon) \approx 1 - 6\epsilon'/\epsilon \ , \tag{80.7a}$$

$$\mathrm{Re}(\epsilon'/\epsilon) \approx \tfrac{1}{3}(1 - |\eta_{00}/\eta_{+-}|) \ . \tag{80.7b}$$

From the experimental measurements in this edition of the *Review*, and the fits discussed in the next section, one finds

$$|\epsilon| = (2.228 \pm 0.011) \times 10^{-3} \ , \tag{80.8a}$$

$$\phi_\epsilon = (43.5 \pm 0.5)^\circ \ , \tag{80.8b}$$

$$\mathrm{Re}(\epsilon'/\epsilon) \approx \epsilon'/\epsilon = (1.66 \pm 0.23) \times 10^{-3} \ , \tag{80.8c}$$

$$\phi_{+-} = (43.4 \pm 0.5)^\circ \ , \tag{80.8d}$$

$$\phi_{00} - \phi_{+-} = (0.34 \pm 0.32)^\circ \ , \tag{80.8e}$$

$$A_L = (3.32 \pm 0.06) \times 10^{-3} \ . \tag{80.8f}$$

Direct CP violation, as indicated by ϵ'/ϵ, is expected in the Standard Model. However, the numerical value cannot be reliably predicted because of theoretical uncertainties [9]. The value of A_L agrees with Eq. (80.5d). The values of ϕ_{+-} and $\phi_{00} - \phi_{+-}$ are used to set limits on CPT violation [see "Tests of Conservation Laws"].

80.2. Fits for K_L^0 CP-violation parameters

In recent years, K_L^0 CP-violation experiments have improved our knowledge of CP-violation parameters, and their consistency with the expectations of CPT invariance and unitarity. To determine the best values of the CP-violation parameters in $K_L^0 \to \pi^+\pi^-$ and $\pi^0\pi^0$ decay, we make two types of fits, one for the phases ϕ_{+-} and ϕ_{00} jointly with Δm and τ_S, and the other for the amplitudes $|\eta_{+-}|$ and $|\eta_{00}|$ jointly with the $K_L^0 \to \pi\pi$ branching fractions.

80.2.1. *Fits to ϕ_{+-}, ϕ_{00}, $\Delta\phi$, Δm, and τ_S data* :

These are joint fits to the data on ϕ_{+-}, ϕ_{00}, the phase difference $\Delta\phi = \phi_{00} - \phi_{+-}$, the K_L^0–K_S^0 mass difference Δm, and the K_S^0 mean life τ_S, including the effects of correlations.

Measurements of ϕ_{+-} and ϕ_{00} are highly correlated with Δm and τ_S. Some measurements of τ_S are correlated with Δm. The correlations are given in the footnotes of the ϕ_{+-} and ϕ_{00} sections of the K_L^0 Listings, and the τ_S section of the K_S^0 Listings.

In most cases, the correlations are quoted as 100%, *i.e.*, with the value and error of ϕ_{+-} or ϕ_{00} given at a fixed value of Δm and τ_S, with additional terms specifying the dependence of the value on Δm and τ_S. These cases lead to diagonal bands in Figs. 80.1 and 80.2. The KTeV experiment [10] quotes its results as values of Δm, τ_S, ϕ_ϵ, $\mathrm{Re}(\epsilon'/\epsilon)$, and $\mathrm{Im}(\epsilon'/\epsilon)$ with correlations, leading to the ellipses labeled "b." The correlations for the KTeV measurements are given in the $\mathrm{Im}(\epsilon'/\epsilon)$ section of the K_L^0 Listings. For small $|\epsilon'/\epsilon|$, $\phi_{+-} \approx \phi_\epsilon + \mathrm{Im}(\epsilon'/\epsilon)$.

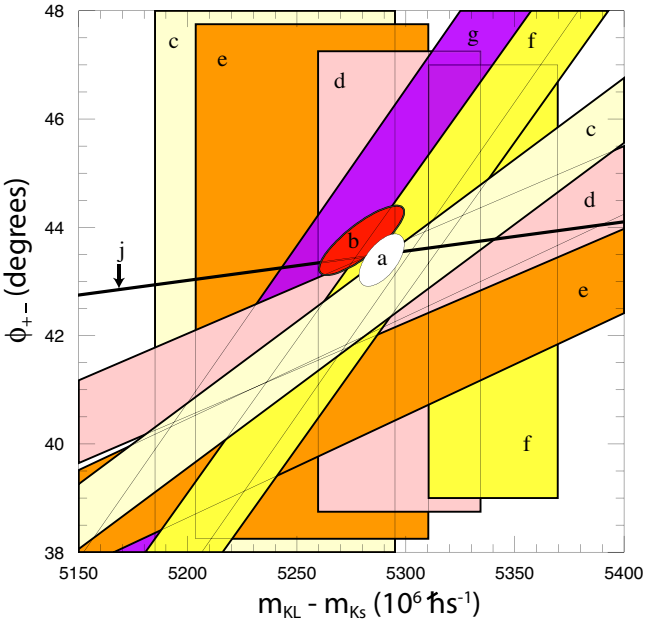

Figure 80.1: ϕ_{+-} vs Δm for experiments which do not assume CPT invariance. Δm measurements appear as vertical bands spanning $\Delta m \pm 1\sigma$, cut near the top and bottom to aid the eye. Most ϕ_{+-} measurements appear as diagonal bands spanning $\phi_{+-} \pm \sigma_\phi$. Data are labeled by letters: "b"–FNAL KTeV, "c"–CERN CPLEAR, "d"–FNAL E773, "e"–FNAL E731, "f"–CERN, "g"–CERN NA31, and are cited in Table 80.1. The narrow band "j" shows $\phi_{\rm SW}$. The ellipse "a" shows the $\chi^2 = 1$ contour of the fit result.

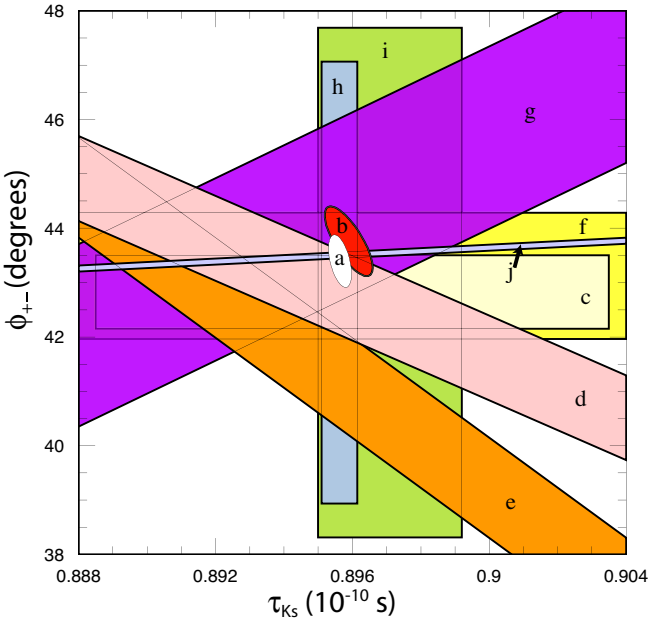

Figure 80.2: ϕ_{+-} vs τ_S. τ_S measurements appear as vertical bands spanning $\tau_S \pm 1\sigma$, some of which are cut near the top and bottom to aid the eye. Most ϕ_{+-} measurements appear as diagonal or horizontal bands spanning $\phi_{+-} \pm \sigma_\phi$. Data are labeled by letters: "b"–FNAL KTeV, "c"–CERN CPLEAR, "d"–FNAL E773, "e"–FNAL E731, "f"–CERN, "g"–CERN NA31, "h"–CERN NA48, "i"–CERN NA31, and are cited in Table 80.1. The narrow band "j" shows $\phi_{\rm SW}$. The ellipse "a" shows the fit result's $\chi^2 = 1$ contour.

Table 80.1: References, Document ID's, and sources corresponding to the letter labels in the figures. The data are given in the ϕ_{+-} and Δm sections of the K_L Listings, and the τ_S section of the K_S Listings.

Label	Source	PDG Document ID	Ref.
a	this *Review*	OUR FIT	
b	FNAL KTeV	ABOUZAID 11	[10]
c	CERN CPLEAR	APOSTOLAKIS 99C	[11]
d	FNAL E773	SCHWINGENHEUER 95	[12]
e	FNAL E731	GIBBONS 93,93C	[13,14]
f	CERN	GEWENIGER 74B,74C	[15,16]
g	CERN NA31	CAROSI 90	[17]
h	CERN NA48	LAI 02C	[18]
i	CERN NA31	BERTANZA 97	[19]
j	this *Review*	SUPERWEAK 16	

The data on τ_S, Δm, and ϕ_{+-} shown in Figs. 80.1 and 80.2 are combined with data on ϕ_{00} and $\phi_{00} - \phi_{+-}$ in two fits, one without assuming CPT, and the other with this assumption. The results without assuming CPT are shown as ellipses labeled "a." These ellipses are seen to be in good agreement with the superweak phase

$$\phi_{\rm SW} = \tan^{-1}\left(\frac{2\Delta m}{\Delta\Gamma}\right) = \tan^{-1}\left(\frac{2\Delta m \tau_S \tau_L}{\hbar(\tau_L - \tau_S)}\right) \ . \qquad (80.9)$$

In Figs. 80.1 and 80.2, $\phi_{\rm SW}$ is shown as narrow bands labeled "j."

Table 80.2 column 2, "Fit w/o CPT," gives the resulting fitted parameters, while Table 80.3 gives the correlation matrix for this fit. The white ellipses labeled "a" in Fig. 80.1 and Fig. 80.2 are the $\chi^2 = 1$ contours for this fit.

For experiments which have dependencies on unseen fit parameters, that is, parameters other than those shown on the x or y axis of the figure, their band positions are evaluated using the fit results and their band widths include the fitted uncertainty in the unseen parameters. This is also true for the $\phi_{\rm SW}$ bands.

If CPT invariance and unitarity are assumed, then by Eq. (80.6a), the phase of ϵ is constrained to be approximately equal to

$$\phi_{\rm SW} = (43.50258 \pm 0.00021)^\circ + 54.1(\Delta m - 0.5289)^\circ + 32.0(\tau_S - 0.89564) \qquad (80.10)$$

where we have linearized the Δm and τ_S dependence of Eq. (80.9). The error ± 0.00021 is due to the uncertainty in τ_L. Here Δm has units $10^{10}\,\hbar\,{\rm s}^{-1}$ and τ_S has units 10^{-10} s.

If in addition we use the observation that $Re(\epsilon'/\epsilon) \ll 1$ and $cos(\phi_{\epsilon'} - \phi_\epsilon) \simeq 1$, as well as the numerical value of $\phi_{\epsilon'}$ given in Eq. (80.6b), then Eqs. (80.5a), which are sketched in Fig. 80.3, lead to the constraint

$$\begin{aligned} \phi_{00} - \phi_{+-} &\approx -3 \ {\rm Im}\left(\frac{\epsilon'}{\epsilon}\right) \\ &\approx -3 \ {\rm Re}\left(\frac{\epsilon'}{\epsilon}\right) \tan(\phi_{\epsilon'} - \phi_\epsilon) \\ &\approx 0.006^\circ \pm 0.008^\circ \ , \end{aligned} \qquad (80.11)$$

so that $\phi_{+-} \approx \phi_{00} \approx \phi_\epsilon \approx \phi_{\rm SW}$.

In the fit assuming CPT, we constrain $\phi_\epsilon = \phi_{\rm SW}$ using the linear expression in Eq. (80.10), and constrain $\phi_{00} - \phi_{+-}$ using Eq. (80.11). These constraints are inserted into the Listings with the Document ID of SUPERWEAK 16. Some additional data for which the authors assumed CPT are added to this fit or substitute for other less precise data for which the authors did not make this assumption. See the Listings for details.

The results of this fit are shown in Table 80.2, column 3, "Fit w/CPT," and the correlation matrix is shown in Table 80.4. The Δm precision is improved by the CPT assumption.

Table 80.2: Fit results for ϕ_{+-}, Δm, τ_S, ϕ_{00}, $\Delta\phi = \phi_{00} - \phi_{+-}$, and ϕ_ϵ without and with the CPT assumption.

Quantity(units)	Fit w/o CPT	Fit w/ CPT
$\phi_{+-}(^\circ)$	43.4 ± 0.5 (S=1.2)	43.51 ± 0.05 (S=1.2)
$\Delta m(10^{10}\hbar\,\mathrm{s}^{-1})$	0.5289 ± 0.0010	0.5293 ± 0.0009 (S=1.3)
$\tau_S(10^{-10}\mathrm{s})$	0.89564 ± 0.00033	0.8954 ± 0.0004 (S=1.1)
$\phi_{00}(^\circ)$	43.7 ± 0.6 (S=1.2)	43.52 ± 0.05 (S=1.3)
$\Delta\phi(^\circ)$	0.34 ± 0.32	0.006 ± 0.014 (S=1.7)
$\phi_\epsilon(^\circ)$	43.5 ± 0.5 (S=1.3)	43.52 ± 0.05 (S=1.2)
χ^2	16.4	20.0
# Deg. Free.	14	16

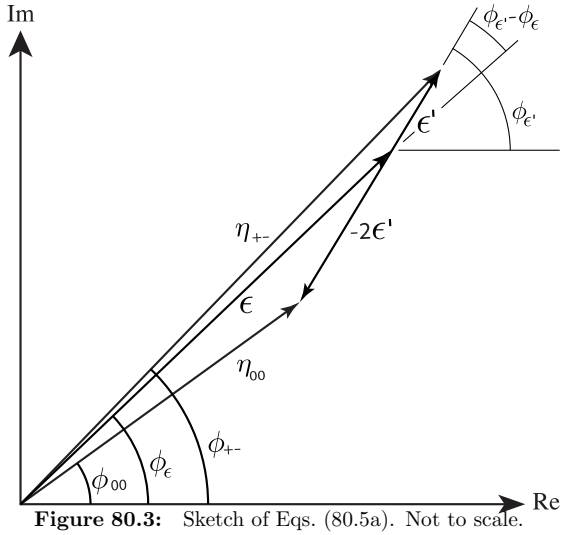

Figure 80.3: Sketch of Eqs. (80.5a). Not to scale.

Table 80.3: Correlation matrix for the results of the fit without the CPT assumption

	ϕ_{+-}	Δm	τ_S	ϕ_{00}	$\Delta\phi$	ϕ_ϵ
ϕ_{+-}	1.000	0.596	−0.488	0.827	−0.040	0.976
Δm	0.596	1.000	−0.572	0.487	−0.035	0.580
τ_S	−0.488	−0.572	1.000	−0.423	−0.014	−0.484
ϕ_{00}	0.827	0.487	−0.423	1.000	0.529	0.929
$\Delta\phi$	−0.040	−0.035	−0.014	0.529	1.000	0.178
ϕ_ϵ	0.976	0.580	−0.484	0.929	0.178	1.000

Table 80.4: Correlation matrix for the results of the fit with the CPT assumption

	ϕ_{+-}	Δm	τ_S	ϕ_{00}	$\Delta\phi$	ϕ_ϵ
ϕ_{+-}	1.000	0.972	−0.311	0.957	−0.105	0.995
Δm	0.972	1.000	−0.509	0.958	−0.007	0.977
τ_S	−0.311	−0.509	1.000	−0.306	0.004	−0.312
ϕ_{00}	0.957	0.958	−0.306	1.000	0.189	0.981
$\Delta\phi$	−0.105	−0.007	0.004	0.189	1.000	−0.006
ϕ_ϵ	0.995	0.977	−0.312	0.981	−0.006	1.000

80.2.2. *Fits for ϵ'/ϵ, $|\eta_{+-}|$, $|\eta_{00}|$, and $B(K_L \to \pi\pi)$* :

We list measurements of $|\eta_{+-}|$, $|\eta_{00}|$, $|\eta_{00}/\eta_{+-}|$, and ϵ'/ϵ. Independent information on $|\eta_{+-}|$ and $|\eta_{00}|$ can be obtained from measurements of the K_L^0 and K_S^0 lifetimes (τ_L, τ_S), and branching ratios (B) to $\pi\pi$, using the relations

$$|\eta_{+-}| = \left[\frac{\mathrm{B}(K_L^0 \to \pi^+\pi^-)}{\tau_L}\,\frac{\tau_S}{\mathrm{B}(K_S^0 \to \pi^+\pi^-)}\right]^{1/2}, \qquad (80.12a)$$

$$|\eta_{00}| = \left[\frac{\mathrm{B}(K_L^0 \to \pi^0\pi^0)}{\tau_L}\,\frac{\tau_S}{\mathrm{B}(K_S^0 \to \pi^0\pi^0)}\right]^{1/2}. \qquad (80.12b)$$

For historical reasons, the branching ratio fits and the CP-violation fits are done separately, but we want to include the influence of $|\eta_{+-}|$, $|\eta_{00}|$, $|\eta_{00}/\eta_{+-}|$, and ϵ'/ϵ measurements on $\mathrm{B}(K_L^0 \to \pi^+\pi^-)$ and $\mathrm{B}(K_L^0 \to \pi^0\pi^0)$ and vice versa. We approximate a global fit to all of these measurements by first performing two independent fits: 1) BRFIT, a fit to the K_L^0 branching ratios, rates, and mean life, and 2) ETAFIT, a fit to the $|\eta_{+-}|$, $|\eta_{00}|$, $|\eta_{+-}/\eta_{00}|$, and ϵ'/ϵ measurements. The results from fit 1, along with the K_S^0 values from this edition, are used to compute values of $|\eta_{+-}|$ and $|\eta_{00}|$, which are included as measurements in the $|\eta_{00}|$ and $|\eta_{+-}|$ sections with a document ID of BRFIT 16. Thus, the fit values of $|\eta_{+-}|$ and $|\eta_{00}|$ given in this edition include both the direct measurements and the results from the branching ratio fit.

The process is reversed in order to include the direct $|\eta|$ measurements in the branching ratio fit. The results from fit 2 above (before including BRFIT 16 values) are used along with the K_L^0 and K_S^0 mean lives and the $K_S^0 \to \pi\pi$ branching fractions to compute the K_L^0 branching ratio $\Gamma(K_L^0 \to \pi^0\pi^0)/\Gamma(K_L^0 \to \pi^+\pi^-)$. This branching ratio value is included as a measurement in the branching ratio section with a document ID of ETAFIT 16. Thus, the K_L^0 branching ratio fit values in this edition include the results of the direct measurement of $|\eta_{00}/\eta_{+-}|$ and ϵ'/ϵ. Most individual measurements of $|\eta_{+-}|$ and $|\eta_{00}|$ enter our fits directly via the corresponding measurements of $\Gamma(K_L^0 \to \pi^+\pi^-)/\Gamma(\text{total})$ and $\Gamma(K_L^0 \to \pi^0\pi^0)/\Gamma(\text{total})$, and those that do not have too large errors to have any influence on the fitted values of these branching ratios. A more detailed discussion of these fits is given in the 1990 edition of this *Review* [20].

References:

1. K. Kleinknecht, "Uncovering CP violation: experimental clarification in the neutral K meson and B meson systems," *Springer Tracts in Modern Physics*, vol. 195 (Springer Verlag 2003).
2. B. Winstein and L. Wolfenstein, Rev. Mod. Phys. **65**, 1113 (1993).
3. M.S. Sozzi, Eur. Phys. J. **C36**, 37 (2004).
4. T.T. Wu and C.N. Yang, Phys. Rev. Lett. **13**, 380 (1964).
5. L. Wolfenstein, Phys. Rev. Lett. **13**, 562 (1964);
   L. Wolfenstein, Comm. Nucl. Part. Phys. **21**, 275 (1994).
6. G. Colangelo, J. Gasser, and H. Leutwyler, Nucl. Phys. **B603**, 125 (2001).
7. R. Adler *et al.*, (CPLEAR Collab.), Phys. Lett. **B407**, 193 (1997);
   P. Bloch, *Proceedings of Workshop on K Physics* (Orsay 1996), ed. L. Iconomidou-Fayard, Edition Frontieres, Gif-sur-Yvette, France (1997) p. 307.
8. A. Lai *et al.*, Phys. Lett. **B610**, 165 (2005).
9. G. Buchalla, A.J. Buras, and M.E. Lautenbacher, Rev. Mod. Phys. **68**, 1125 (1996);
   S. Bosch *et al.*, Nucl. Phys. **B565**, 3 (2000);
   S. Bertolini, M. Fabrichesi, and J.O. Egg, Rev. Mod. Phys. **72**, 65 (2000).
10. E. Abouzaid *et al.*, Phys. Rev. **D83**, 092001 (2011).
11. A. Apostolakis *et al.*, Phys. Lett. **B458**, 545 (1999).
12. B. Schwingenheuer *et al.*, Phys. Rev. Lett. **74**, 4376 (1995).
13. L.K. Gibbons *et al.*, Phys. Rev. Lett. **70**, 1199 (1993) and footnote in Ref. 12.
14. L.K. Gibbons, Thesis, RX-1487, Univ. of Chicago, 1993.

15. C. Geweniger *et al.*, Phys. Lett. **48B**, 487 (1974).
16. C. Geweniger *et al.*, Phys. Lett. **52B**, 108 (1974).
17. R. Carosi *et al.*, Phys. Lett. **B237**, 303 (1990).
18. A. Lai *et al.*, Phys. Lett. **B537**, 28 (2002).
19. L. Bertanza *et al.*, Z. Phys. **C73**, 629 (1997).
20. J.J. Hernandez *et al.*, Particle Data Group, Phys. Lett. **B239**, 1 (1990).

81. Review of Multibody Charm Analyses

Revised 2017 by D. M. Asner (Brookhaven National Laboratory) and J. Rademacker (University of Bristol)

81.1. Kinematics & Models

The differential decay rate to a point $\mathbf{s} = (s_1, \ldots, s_n)$ in n dimensional phase space can be expressed as

$$d\Gamma = |\mathcal{M}(\mathbf{s})|^2 \left| \frac{\partial^n \phi}{\partial(s_1 \ldots s_n)} \right| d^n s \qquad (81.1)$$

where $|\partial^n \phi / \partial(s_1 \ldots s_n)|$ represents the density of states at $\mathbf{s}$, and $\mathcal{M}$ the matrix element for the decay at that point in phase space. For two-body decays, $|\partial^n \phi / \partial(s_1 \ldots s_n)|$ is a δ function, while for D decays to $3, 4, 5, \ldots$ pseudoscalars, phase space is $2, 5, 8, \ldots$ dimensional, leading to a rich phenomenology. Additional parameters are required to fully describe decays with vector particles in the initial or final state.

For the important case of a three body decay $D \to abc$, where D, a, b, c are all pseudoscalars, the decay kinematics can be represented in a two dimensional Dalitz plot [1]. This is usually parametrized in terms of invariant-mass-squared variables $s_1 = (p_a + p_b)^2$ and $s_2 = (p_b + p_c)^2$, where p_a, p_b, p_c are the four-momenta of particles a, b, c. In terms of these variables, phase-space density is constant across the kinematically allowed region, so that any structure seen in the Dalitz plot is a direct consequence of the dynamics encoded in $|\mathcal{M}|^2$. For this type of decay, the operation of parity can also be expressed as a rotation of the decay plane, so no parity violating kinematic observables can be defined (unless they also violate rotational invariance). This is not the case for decays to four or more particles, which can therefore not be unambiguously described in terms of invariant-mass-squared variables, which are parity-even. The use of parity-odd observables in four body decays is discussed below.

The matrix element $\mathcal{M}$ is usually modeled as a sum of interfering decay amplitudes, each proceeding through resonant two-body decays [2]. See Refs [2–4] for a review of resonance phenomenology. In most analyses, each resonance is described by a Breit-Wigner [5] or Flatté [6] lineshape, and the model includes a non-resonant term with a constant phase and magnitude across the Dalitz plot. This approach has well-known theoretical limitations, such as the violation of unitarity and analyticity, which can break the relationship between magnitude and phase across phase space. This motivates the use of more sophisticated descriptions, especially for broad, overlapping resonances (frequently found in S-wave components) where these limitations are particularly problematic. In charm analyses, these approaches have included the K-matrix approach [5,7,8] which respects two-body unitarity; the use of LASS scattering data [9]; dispersive methods [10,11,12,13]; methods based on chiral perturbation theory [14,15] and quasi model-independent parametrizations [16,17,18]. An important example first analyzed by CLEO [19,20,21] is $D^0 \to K_S \pi^+ \pi^-$, which is a key channel in *CP* violation and charm mixing analyses. Belle models this decay as a superposition of 18 resonances (including 4 significant doubly Cabibbo suppressed amplitudes) described by Breit-Wigner or Flatté lineshapes, plus a non-resonant component [22]. CDF's analysis follows a similar approach [23]. BaBar's model replaces the broad $\pi\pi$ and $K\pi$ S-wave resonances and the non-resonant component with a K-matrix description [24]. Belle's and BaBar's data have been re-analyzed by [25] in a QCD factorization framework, using line-shape parametrizations for the S [26,27] and P wave [11] contributions that preserve 2-body unitarity and analyticity. The measurements give compatible results for the components they share. The field of amplitudes analyses remains very active. Publications since the last update of this review two years ago include Dalitz plot analyses of $D^0 \to K^0_S K^\pm \pi^\mp$ by LHCb [28], and $D^0 \to \pi^+\pi^-\pi^0$ by BaBar [29]; and several four body amplitude analyses: $D^0 \to K^+K^-\pi^+\pi^-$ and $D^0 \to \pi^+\pi^-\pi^+\pi^-$ using CLEO data [18], and $K^-\pi^+\pi^-\pi^+$ by BES III [30].

All of the examples above remain within the confines of the "isobar" framework, which describes the decay as a series of 2-body amplitudes. While some include very sophisticated descriptions of these 2-body amplitudes, they do not respect the unitarity of the full 3 (or 4) body process and ignore long-range hadronic effects such as rescattering. Several groups work on improved models. Dispersive techniques that respect 3-body unitarity and analyticity by construction have been successfully applied to regions of the $D^+ \to K^-\pi^+\pi^+$ and $D^+ \to K_S\pi^0\pi^+$ Dalitz plots below the $\eta' K$ threshold [12,13], where they provide a good description of the data with fewer fit parameters than the isobar approach. Ref. [31] uses a unitary coupled channel approach to describe $D^+ \to K^-\pi^+\pi^+$, which has no restrictions on the kinematic range, but requires additional parameters to describe the Dalitz plot above the $\eta' K$ threshol. Ref. [14] use chiral perturbation theory to provide a description of the annihilation contribution to the decay amplitude which respects 3-body unitarity.

Limitations in the theoretical description of interfering resonances are the leading source of systematic uncertainty in many analyses. This is set to become increasingly problematic given the statistical precision achievable with the vast, clean charm samples available at the B factories, LHCb, and their upgrades. In some cases, the model uncertainty can be removed through model-independent methods, often relying on input from the charm threshold, as discussed below. At the same time, increasingly sophisticated models are being developed, and applied to data.

81.2. Applications of multibody charm analyses

The interference between the decay paths via which multibody decays proceed provides sensitivity to both relative magnitudes and phases of the contributing amplitudes. It is especially this sensitivity to phases that makes amplitude analyses such a uniquely powerful tool for studying a wide range of phenomena. Here we concentrate on their use for *CP* violation and mixing measurements in charm, and charm inputs to *CP* violation analyses in B meson decays (see also [32,33]) . The properties of light-meson resonances determined in D amplitude analyses are reported in the light-unflavored-meson section of this *Review*.

81.2.1. ***Charm Mixing and CP violation*** : Time-dependent amplitude analyses in decays to final states that are accessible to both D^0 and $\overline{D}^0$ have unique sensitivity to mixing parameters. A Dalitz plot analysis of a self-conjugate final state, such as $K_S\pi^+\pi^-$ and $K_S K^+ K^-$, allows the measurement of the phase difference between the relevant D^0 and $\overline{D}^0$ decay amplitudes, and thus a direct measurement of the mixing parameters x, y (rather than the decay-specific parameters x'^2, y' measured for example in $D^0 \to K\pi$) [21]) . These analyses are also sensitive to *CP* violation in mixing and in the interference between mixing and decay; these results are summarised in [32,33].

81.2.2. ***Measuring γ/ϕ_3*** : Neutral D mesons originating from $B^- \to DK^-$ (here denoted as D_{B^-}) are a superposition of D^0 and $\overline{D}^0$ with a relative phase that depends on γ/ϕ_3:

$$D_{B^-} \propto D^0 + r_B e^{i(\delta_B - \gamma)} \overline{D}^0,$$

where δ_B is a *CP* conserving strong phase, and $r_B \sim 0.1$. In the corresponding *CP*-conjugate expression, γ/ϕ_3 changes sign. An amplitude analysis of the subsequent decay of the $D_{B^\pm}$ to a state accessible to both D^0 and $\overline{D}^0$ allows the measurement of γ/ϕ_3 [34–39]. The method generalizes to similar B hadron decays, such as $B^0 \to DK^{*0}$. Measurements based on this technique have been reported by BaBar [40,41], Belle [22,42] and LHCb [43–49,50,51]. The most precise individual results come from the study of $D_{B^-} \to K_S\pi^+\pi^-$ and $D_{B^-} \to K_S K^+ K^-$ with an uncertainty of $\sim 15^\circ$ [22,40,42,46]; combining measurements in multiple decay modes leads to a current uncertainty on γ/ϕ_3 of less than 6°.

81.2.3. ***Time-integrated searches for CP violation in charm*** : Comparing the results of amplitude fits for *CP*-conjugate decay modes provides a measure of *CP* violation. Recent *CP* violation searches using this method include LHCb's amplitude analyses of $D^0 \to K^0_S K^\pm \pi^\mp$ [28], and amplitude analyses of $D^0 \to K^+K^-\pi^+\pi^-$ and $D^0 \to \pi^+\pi^-\pi^+\pi^-$ using CLEO data [52,18].

A widely-used model-independent technique to search for local *CP* violation is based on performing a χ^2 comparison of *CP*-conjugate phase-space distributions. This method was pioneered by BaBar [53] and developed further in [54,55,56], with recent results reported by BaBar [57] and LHCb in $D^{\pm} \to K^+K^-\pi^{\pm}$ [58,59], by CDF in $D^0 \to K_S\pi^+\pi^-$ [23], and by LHCb in $D^+ \to \pi^-\pi^+\pi^+$ [61], $D^0 \to K^+K^-\pi^+\pi^-$ and $D^0 \to \pi^+\pi^-\pi^+\pi^-$ [56]. Un-binned methods can increase the sensitivity [60] and have been applied by LHCb to $D^+ \to \pi^-\pi^+\pi^+$ [61], $D^0 \to \pi^+\pi^-\pi^0$ [62] and $D^0 \to \pi^+\pi^-\pi^+\pi$ [63].

An alternative model-independent approach, providing complementary information, is based on constructing observables in four body decays that are odd under motion reversal ("naïve T") [64–72], which is equivalent to P for scalar particles [72]. One such observable is $C_T = \vec{p}_2 \cdot (\vec{p}_3 \times \vec{p}_4) = (1/m_D)\epsilon_{\alpha\beta\gamma\delta}p_1^{\alpha}p_2^{\beta}p_3^{\gamma}p_4^{\delta}$, where $\vec{p}_i$ are the decay products' three momenta in the decay's restframe, and p_i are their four-momenta. Identical particles (as in $D^0 \to K^+\underline{\pi}^-\pi^+\underline{\pi}^-$) are ordered by momentum magnitude. Comparing the P violating asymmetry $A_T \equiv \dfrac{\Gamma(C_T>0) - \Gamma(C_T<0)}{\Gamma(C_T>0) + \Gamma(C_T<0)}$ with its C-conjugate in $\overline{D}^0$ decays, provides sensitivity to *CP* violation.

Searches for *CP* violation in this manner have been carried out by FOCUS in $D^0 \to K^+K^-\pi^+\pi^-$ [73]; by BaBar in $D^0 \to K^+K^-\pi^+\pi^-$, $D^+ \to K^+K_S\pi^+\pi^-$, and $D_s^+ \to K^+K_S\pi^+\pi^-$ [74,75]; and by LHCb in $D^0 \to K^+K^-\pi^+\pi^-$ [76], where the sensitivity of the method was improved by dividing phase space into bins.

LHCb combined these approaches and use P-odd variables to split their sample of 1M $D^0, \overline{D}^0 \to \pi^+\pi^-\pi^+\pi^-$ events into four sub-samples E, $\exists$, $\overline{E}$, $\overline{\exists}$. Samples E and $\exists$ have opposite C_T and are related by P; the over-line indicates charge conjugation. Comparing $(E + \exists)$ with $(\overline{E} + \overline{\exists})$ tests for P-even *CP* violation, while comparing $(E + \overline{E})$ with $(\exists + \overline{\exists})$ tests for P-odd *CP* violation. An unbinned method is used to compare the phase-space distributions of the samples [63].

The results of all measurements described in this section are compatible with *CP* conservation in charm. In the case of LHCb's P-odd test in $D^0, \overline{D}^0 \to \pi^+\pi^-\pi^+\pi^-$ this compatibility is, with a p-value of 0.6%, marginal.

81.3. Model Independent Methods and the Charm Threshold

The precision measurement of mixing or *CP* violation parameters (such γ/ϕ_3) from multibody charm decays requires as input both magnitude and phase of the $D^0, \overline{D}^0$ meson decay amplitudes to the final state of interest. While the magnitude is fairly easily measured, the phase information requires either amplitude models with reliable phase motion, or model-independent approaches.

The desired model-independent phase information is accessible at the charm threshold, where CLEO–c and BES III operate [32,37,77–83]. There, D mesons originate from the decay $\psi(3770) \to D\overline{D}$. Quantum-correlations between the two D mesons can be used to identify decays of well-defined $D^0 - \overline{D}^0$ superpositions to the final state of interest. The resulting interference of D^0 and $\overline{D}^0$ decay amplitudes provides observables that depend on the phase difference between those amplitudes, which is the information needed as input for γ/ϕ_3. The measurements are performed either integrated over the entire phase space of the decay, or in sub-regions/bins. The relevant results can be expressed in terms of one complex parameter $\mathcal{Z} = Re^{-i\delta} = c + is$ per pair of *CP*-conjugate bins, with magnitude $R \leq 1$. Larger R values lead to higher sensitivity to γ/ϕ_3. Amplitude models can be used to optimise the binning for sensitivity to γ/ϕ_3, without introducing a model-dependent bias in the result.

Charm mixing also results in a (time-dependent) superposition of D^0 and $\overline{D}^0$. Charm mixing measurements are therefore sensitive to the same decay-mode specific hadronic phases as γ/ϕ_3 measurements. On one hand, these phases can be seen as nuisance parameters in mixing measurements, which can be constrained at the charm threshold. This is discussed further in Ref. [32]. Conversely, charm mixing can be used to obtain the relevant decay-specific phase information needed for γ/ϕ_3 measurements, using mixing parameters x, y obtained using other charm decay modes as input. This method is particularly powerful in doubly Cabibbo-suppressed decays such as $D^0 \to K^+\pi^-\pi^+\pi^-$, and when used in combination with threshold data [84,85]. CLEO–c data have been analyzed to provide binned $\mathcal{Z}$ for the self-conjugate decays $D^0 \to K_S\pi^+\pi^-$ and $D^0 \to K_SK^+K^-$ [86,87]. For the decay modes $D^0, \overline{D}^0 \to K_SK^+\pi^-$, $K^-\pi^+\pi^0$ and $K^-\pi^+\pi^-\pi^+$, phase-space integrated analyses of CLEO–c data have yielded $\mathcal{Z}^{K_SK\pi} = (0.70 \pm 0.08)\exp(-i(0.1^\circ \pm 15.7^\circ))$, $\mathcal{Z}^{K\pi\pi^0} = (0.82 \pm 0.06)\exp(-i(199^{\circ+13^\circ}_{-14^\circ}))$, and $\mathcal{Z}^{K3\pi} = (0.53^{+0.18}_{-0.21})\exp(-i(125^{\circ+22^\circ}_{-14^\circ}))$ [88,89]. Adding input from LHCb's $D^0 \to K^+\pi^-\pi^+\pi^-$ charm mixing measurement changes the latter to $\mathcal{Z}^{K3\pi} = (0.32^{+0.17}_{-0.13})\exp(-i(128^{\circ+28^\circ}_{-17^\circ}))$ [89,90], where the increased uncertainty reported on δ is a consequence of the smaller central value for R. Restricting the analysis of the $K_SK\pi$ final state to a bin around the K^*K resonance, [88] find $R = 0.94 \pm 0.12$, illustrating the benefit in dividing phase space into bins. The above results are given following the usual convention for γ/ϕ_3-related studies where $CP|D^0\rangle = +|\overline{D}^0\rangle$; in the context of charm mixing, it is customary to take $CP|D^0\rangle = -|\overline{D}^0\rangle$, leading to a phase-shift in δ of π.

The corresponding phase space-integrated parameter for self-conjugate decays such as $D^0 \to \pi^+\pi^-\pi^0$ is the real-valued *CP*-even fraction F_+, defined such that a *CP* even eigenstate has $F_+ = 1$, while a *CP*-odd eigenstate has $F_+ = 0$ [81]. A recent analysis of CLEO–c data reveals that $D^0 \to \pi^+\pi^-\pi^0$ is compatible with being completely *CP*-even with $F_+ = 0.973 \pm 0.017$, while $D^0 \to K^+K^-\pi^0$ has $F_+ = 0.732 \pm 0.055$ and $D^0 \to \pi^+\pi^-\pi^+\pi^-$ has $F_+ = 0.737 \pm 0.028$ [82]. Comparing the latter result with the F_+ value derived from the latest $D^0 \to \pi^+\pi^-\pi^+\pi^-$ amplitude model [18], $F_+^{4\pi\ \mathrm{model}} = 0.729 \pm 0.009 \pm 0.018$, provides a useful cross check for the model.

81.4. Summary

Multibody charm decays offer a rich phenomenology, including unique sensitivity to *CP* violation and charm mixing. This is a highly dynamic field with many new results (some of which we presented here) and rapidly increasing, high quality datasets. These datasets constitute a huge opportunity, but also a challenge to improve the theoretical descriptions of soft hadronic effects in multibody decays. For some measurements, model-independent methods, many relying on input from the charm threshold, provide a way of removing model-induced uncertainties. At the same time, work is ongoing to improve the theoretical description of multibody decays.

References:

1. R.H. Dalitz, *Phil. Mag.* **44**, 1068 (1953).
2. M. Bauer, B. Stech, and M. Wirbel, Z. Phys. **C4**, 103 (1987); P. Bedaque, A. Das, and V.S. Mathur, Phys. Rev. **D49**, 269 (1994); L.-L. Chau and H.-Y. Cheng, Phys. Rev. **D36**, 137 (1987); K. Terasaki, Int. J. Mod. Phys. **A10**, 3207 (1995); F. Buccella, M. Lusignoli, and A. Pugliese, Phys. Lett. **B379**, 249 (1996).
3. J.D. Jackson, Nuovo Cimento **34**, 1644 (1964).
4. See the note on Kinematics in this *Review*.
5. E.P. Wigner, Phys. Rev. **70**, 15 (1946).
6. S. M. Flatté, Phys. Lett. **63B**, 224 (1976) Phys. Lett. **63B**, 224 (1976).
7. S.U. Chung *et al.*, Ann. Phys. **4**, 404 (1995).
8. I.J.R. Aitchison, Nucl. Phys. **A189**, 417 (1972).
9. D. Aston *et al.* (LASS Collab.), Nucl. Phys. **B296**, 493 (1988).
10. R. Omnes, Nuovo Cimento **8**, 316 (1958).
11. C. Hanhart, Phys. Lett. **B715**, 170 (2012).
12. F. Niecknig and B. Kubis, JHEP **1510**, 142 (2015).
13. F. Niecknig and B. Kubis, arXiv:1708.00446 [hep-ph] (update once published).
14. P. C. Magalhães and M. R. Robilotta, Phys. Rev. D 92,9,094005(2015).
15. P. C. Magalhães *et al.*, Phys. Rev. D 84,094001(2011).
16. E.M. Aitala *et al.* (E791 Collab.), Phys. Rev. **D73**, 032004 (2006) [Phys. Rev. **D74**, 059901 (E)(2006)].
17. G. Bonvicini *et al.* (CLEO Collab.), Phys. Rev. **D78**, 052001 (2008).
18. P. d'Argent *et al.*, JHEP **1705**, 142 (2017).

19. H. Muramatsu *et al.* (CLEO Collab.), Phys. Rev. Lett. **89**, 251802 (2002).
20. D.M. Asner *et al.* (CLEO Collab.), Phys. Rev. **D70**, 091101 (2004).
21. D.M. Asner *et al.* (CLEO Collab.), Phys. Rev. **D72**, 012001 (2005).
22. A. Poluektov *et al.* (Belle Collab.), Phys. Rev. **D81**, 112002 (2010).
23. T. Aaltonen *et al.* (CDF Collab.), Phys. Rev. **D86**, 032007 (2012).
24. P. del Amo Sanchez *et al.* (BaBar Collab.), Phys. Rev. Lett. **105**, 081803 (2010).
25. J.P. Dedonder *et al.* Phys. Rev. **D89**, 094018 (2014).
26. B. El-Bennich *et al.* Phys. Rev. **D79**, 094005 (2009) [Phys. Rev. **D83**, 039903(E) (2011)].
27. J.P. Dedonder *et al.* Acta Phys. Polon. B **42** (2011) 2013.
28. R. Aaij *et al.* [LHCb Collaboration], Phys. Rev. D 93,5,052018 (2016).
29. J. P. Lees *et al.* [BaBar Collaboration], Phys. Rev. D 93,11,112014(2016).
30. M. Ablikim *et al.* [BESIII Collaboration], Phys. Rev. D 95,7,072010(2017).
31. S. X. Nakamura, Phys. Rev. D 93,1,014005(2016).
32. See the note on D^0–$\overline{D}^0$ Mixing in this *Review*.
33. See the note CP violation in the quark sector in this *Review*.
34. M. Gronau and D. Wyler, Phys. Lett. **B265**, 172 (1991).
35. M. Gronau and D. London, Phys. Lett. **B253**, 483 (1991).
36. D. Atwood *et al.*, Phys. Rev. Lett. **78**, 17, 3257 (1997).
37. A. Giri *et al.*, Phys. Rev. **D68**, 5, 054018 (2003).
38. A. Poluektov *et al.* (Belle Collab.), Phys. Rev. **D70**, 7, 072003 (2004).
39. J. Rademacker and G. Wilkinson, Phys. Lett. **B647**, 400 (2007).
40. P. del Amo Sanchez *et al.* (BaBar Collab.), Phys. Rev. Lett. **105**, 121801 (2010).
41. J.P. Lees *et al.* (BaBar Collab.), Phys. Rev. **D84**, 012002 (2011).
42. H. Aihara *et al.* (Belle Collab.), Phys. Rev. **D85**, 112014 (2012).
43. R. Aaij *et al.* (LHCb Collab.), Phys. Lett. **B726**, 151 (2013).
44. R. Aaij *et al.* (LHCb Collab.), Phys. Lett. **B723**, 44 (2013).
45. R. Aaij *et al.* (LHCb Collab.), Phys. Lett. **B718**, 43 (2012).
46. R. Aaij *et al.* (LHCb Collab.), JHEP **1410**, 97 (2014).
47. R. Aaij *et al.* (LHCb Collab.), Phys. Lett. **B733**, 36 (2014).
48. R. Aaij *et al.* (LHCb Collab.), Nucl. Phys. **B888**, 169 (2014).
49. R. Aaij *et al.* (LHCb Collab.), Phys. Rev. **D91**, 112014 (2015).
50. R. Aaij *et al.* [LHCb Collaboration], JHEP **1606**, 131 (2016).
51. R. Aaij *et al.* [LHCb Collaboration], JHEP **1612**, 087 (2016).
52. M. Artuso *et al.* (CLEO Collab.), Phys. Rev. **D85**, 122002 (2012).
53. B. Aubert *et al.* (BABAR Collab.), Phys. Rev. **D78**, 051102 (2008).
54. I. Bediaga *et al.*, Phys. Rev. **D80**, 096006 (2009).
55. I. Bediaga *et al.*, Phys. Rev. **D86**, 036005 (2012).
56. R. Aaij *et al.* (LHCb Collab.), Phys. Lett. **B726**, 623 (2013).
57. J.P. Lees *et al.* (BaBar Collab.), Phys. Rev. **D87**, 052010 (2013).
58. R. Aaij *et al.* (LHCb Collab.), Phys. Rev. **D84**, 112008 (2011).
59. R. Aaij *et al.* (LHCb Collab.), JHEP **1306**, 112 (2013).
60. M. Williams, Phys. Rev. **D84**, 054015 (2011).
61. R. Aaij *et al.* (LHCb Collab.), Phys. Lett. **B728**, 585 (2014).
62. R. Aaij *et al.* (LHCb Collab.), Phys. Lett. **B740**, 158 (2015).
63. R. Aaij *et al.* [LHCb Collaboration], Phys. Lett. **B769**, 345 (2017).
64. E. Golowich and G. Valencia, Phys. Rev. **D40**, 112, (1989).
65. G. Valencia, Phys. Rev. **D39**, 3339 (1989).
66. W. Bensalem and D. London, Phys. Rev. **D64**, 116003 (2001).
67. I.I.Y. Bigi, `hep-ph/0107102`.
68. W. Bensalem, A. Datta, and D. London, Phys. Rev. **D66**, 094004 (2002).
69. W. Bensalem, A. Datta, and D. London, Phys. Lett. **B538**, 309 (2002).
70. A. Datta and D. London, Int. J. Mod. Phys. **A19**, 2505 (2004).
71. M. Gronau and J.L. Rosner, Phys. Rev. **D84**, 096013 (2011).
72. G. Durieux and Y. Grossman, Phys. Rev. **D92**, 076013 (2015).
73. J.M. Link *et al.* (FOCUS Collab.), Phys. Lett. **B622**, 239 (2005).
74. P. del Amo Sanchez *et al.* (BaBar Collab.), Phys. Rev. **D81**, 111103 (2010).
75. J.P. Lees *et al.* (BaBar Collab.), Phys. Rev. **D84**, 031103 (2011).
76. R. Aaij *et al.* (LHCb Collab.), JHEP **1410**, 005 (2014).
77. D. Atwood and A. Soni, Phys. Rev. **D68**, 033003 (2003).
78. S. Malde and G. Wilkinson, Phys. Lett. **B701**, 353 (2011).
79. A. Bondar *et al.*, Phys. Rev. **D82**, 034033 (2010).
80. C. Thomas and G. Wilkinson, JHEP **1210**, 184 (2012).
81. M. Nayak *et al.* Phys. Lett. **B740**, 1 (2015).
82. S. Malde *et al.* Phys. Lett. **B747**, 9 (2015).
83. S. Malde, C. Thomas, and G. Wilkinson, Phys. Rev. **D91**, 094032 (2015).
84. S. Harnew and J. Rademacker, Phys. Lett. **B728**, 296 (2014).
85. S. Harnew and J. Rademacker, JHEP **1503**, 169 (2015).
86. J. Libby *et al.* (CLEO Collab.), Phys. Rev. **D82**, 112006 (2010).
87. R.A. Briere *et al.* (CLEO Collab.), Phys. Rev. **D80**, 032002 (2009).
88. J. Insler *et al.* (CLEO Collab.), Phys. Rev. **D85**, 092016 (2012) erratum Phys. Rev. D 94,9,09905(2016).
89. T. Evans, S. Harnew, J. Libby, S. Malde, J. Rademacker and G. Wilkinson, Phys. Lett. **B757**, 520 (2017), erratum Phys. Lett. **B765**, 402, (2017).
90. R. Aaij *et al.* [LHCb Collaboration], Phys. Rev. Lett. **117**, 24,241801 (2016).

82. D^0–$\overline{D}^0$ Mixing

Revised October 2017 by D.M. Asner (Brookhaven National Laboratory)

The detailed formalism for $D^0 - \overline{D}^0$ mixing is presented in the note on "CP Violation in the Quark Sector" in this *Review*. For completeness, we present an overview here. The time evolution of the D^0–$\overline{D}^0$ system is described by the Schrödinger equation

$$i\frac{\partial}{\partial t}\begin{pmatrix} D^0(t) \\ \overline{D}^0(t) \end{pmatrix} = \left(\mathbf{M} - \tfrac{i}{2}\mathbf{\Gamma}\right)\begin{pmatrix} D^0(t) \\ \overline{D}^0(t) \end{pmatrix}, \tag{82.1}$$

where the $\mathbf{M}$ and $\mathbf{\Gamma}$ matrices are Hermitian, and CPT invariance requires that $M_{11} = M_{22} \equiv M$ and $\Gamma_{11} = \Gamma_{22} \equiv \Gamma$. The off-diagonal elements of these matrices describe the dispersive and absorptive parts of the mixing.

The two eigenstates D_1 and D_2 of the effective Hamiltonian matrix ($\mathbf{M}$ - $i\mathbf{\Gamma}$) are given by

$$|D_{1,2}\rangle = p|D^0\rangle \pm q|\overline{D}^0\rangle\,, \tag{82.2}$$

where

$$\left(\frac{q}{p}\right)^2 = \frac{M_{12}^* - \frac{i}{2}\Gamma_{12}^*}{M_{12} - \frac{i}{2}\Gamma_{12}}\,. \tag{82.3}$$

The normalization condition is $|p|^2 + |q|^2 = 1$. Our phase convention is $CP|D^0\rangle = +|\overline{D}^0\rangle$, and the sign of the square root is chosen so that D_1 is CP even, or nearly so.

The corresponding eigenvalues are

$$\omega_{1,2} \equiv m_{1,2} - \tfrac{i}{2}\Gamma_{1,2} = \left(M - \tfrac{i}{2}\Gamma\right) \pm \frac{q}{p}\left(M_{12} - \tfrac{i}{2}\Gamma_{12}\right), \tag{82.4}$$

where $m_{1,2}$ and $\Gamma_{1,2}$ are the masses and widths of the $D_{1,2}$.

We define dimensionless mixing parameters x and y by

$$x \equiv (m_1 - m_2)/\Gamma = \Delta m/\Gamma \tag{82.5}$$

and

$$y \equiv (\Gamma_1 - \Gamma_2)/2\Gamma = \Delta\Gamma/2\Gamma\,, \tag{82.6}$$

where $\Gamma \equiv (\Gamma_1 + \Gamma_2)/2$. If CP is conserved, then M_{12} and Γ_{12} are real, $\Delta m = 2M_{12}$, $\Delta\Gamma = 2\Gamma_{12}$, and $p = q = 1/\sqrt{2}$. The signs of Δm and $\Delta\Gamma$ are to be determined experimentally.

The parameters x and y are measured in several ways. The most precise values are obtained using the time dependence of D decays. Since D^0–$\overline{D}^0$ mixing is a small effect, the identifying tag of the initial particle as a D^0 or a $\overline{D}^0$ must be extremely accurate. The usual "D^*-tag" is the charge of the distinctive slow pion in the decay sequence $D^{*+} \to D^0\pi^+$ or $D^{*-} \to \overline{D}^0\pi^-$. In current experiments, the probability of mistagging is about 0.1%. The large data samples produced at the B-factories allow the production flavor to also be determined by fully reconstructing charm on the "other side" of the event—significantly reducing the mistag rate [1]. Another tag of comparable accuracy to the D^*-tag is identification of one of the D's produced from $\psi(3770) \to D^0\overline{D}^0$ decays. Although time-dependent analyses are not possible at symmetric charm-threshold facilities (the D^0 and $\overline{D}^0$ do not travel far enough), the quantum-coherent $C = -1$ $\psi(3770) \to D^0\overline{D}^0$ state provides time-integrated sensitivity [2,3].

82.1. Time-Dependent Analyses

We extend the formalism of this *Review*'s note on "CP Violation in Meson Decays." In addition to the "right-sign" instantaneous decay amplitudes $\overline{A}_f \equiv \langle f|H|\overline{D}^0\rangle$ and $A_{\overline{f}} \equiv \langle \overline{f}|H|D^0\rangle$ for final states $f = K^+\pi^-, ...$ and their CP conjugate $\overline{f} = K^-\pi^+, ...$, we include "wrong-sign" amplitudes $\overline{A}_{\overline{f}} \equiv \langle \overline{f}|H|\overline{D}^0\rangle$ and $A_f \equiv \langle f|H|D^0\rangle$.

It is conventional to normalize the wrong-sign decay distributions to the integrated rate of right-sign decays and to express time in units of the precisely measured neutral D-meson mean lifetime, $\tau_{D^0} = 1/\Gamma = 2/(\Gamma_1 + \Gamma_2)$. Starting from a pure $|D^0\rangle$ or $|\overline{D}^0\rangle$ state at $t = 0$, the time-dependent rates of decay to wrong-sign final states relative to the integrated right-sign decay rates are, to leading order:

$$r(t) \equiv \frac{\left|\langle f|H|D^0(t)\rangle\right|^2}{\left|\overline{A}_f\right|^2} = \left|\frac{q}{p}\right|^2 \left|g_+(t)\,\lambda_f^{-1} + g_-(t)\right|^2, \tag{82.7}$$

and

$$\overline{r}(t) \equiv \frac{\left|\langle \overline{f}|H|\overline{D}^0(t)\rangle\right|^2}{\left|A_{\overline{f}}\right|^2} = \left|\frac{p}{q}\right|^2 \left|g_+(t)\,\lambda_{\overline{f}} + g_-(t)\right|^2. \tag{82.8}$$

where

$$\lambda_f \equiv q\overline{A}_f/pA_f\,, \quad \lambda_{\overline{f}} \equiv q\overline{A}_{\overline{f}}/pA_{\overline{f}}\,, \tag{82.9}$$

and

$$g_\pm(t) = \frac{1}{2}\left(e^{-iz_1t} \pm e^{-iz_2t}\right), \quad z_{1,2} = \frac{\omega_{1,2}}{\Gamma}\,. \tag{82.10}$$

For multibody final states these equations apply separately to each point in phase-space. Note that a change in the convention for the relative phase of D^0 and $\overline{D}^0$ would cancel between q/p and $\overline{A}_f/A_f$ and leave λ_f unchanged. We expand $r(t)$ and $\overline{r}(t)$ to second order in x and y for modes in which the ratio of decay amplitudes, $R_D = |A_f/\overline{A}_f|^2$, is very small. Integrating over regions of phase-space leads to interesting effects. See discussion below on multibody decays and the "Review of Multibody Charm Analyses" in this *Review* [25].

82.2. Semileptonic decays

Consider the final state $f = K^+\ell^-\bar{\nu}_\ell$, where $A_f = \overline{A}_{\overline{f}} = 0$ is a very good approximation in the Standard Model. The final state f is only accessible through mixing (and tree-level second-order weak process which we neglect) and $r(t)$ is

$$r(t) = |g_-(t)|^2\left|\frac{q}{p}\right|^2 \approx \frac{e^{-t}}{4}(x^2 + y^2)\,t^2\left|\frac{q}{p}\right|^2. \tag{82.11}$$

For $\overline{r}(t)$ q/p is replaced by p/q. In the Standard Model, CP violation in charm mixing is small and $|q/p| \approx 1$. In the limit of CP conservation, $r(t) = \overline{r}(t)$, and the time-integrated mixing rate relative to the time-integrated right-sign decay rate for semileptonic decays is

$$R_M = \int_0^\infty r(t)dt = \left|\frac{q}{p}\right|^2 \frac{x^2 + y^2}{2 + x^2 - y^2} \approx \frac{1}{2}(x^2 + y^2)\,. \tag{82.12}$$

Table 82.1: Results for R_M in D^0 semileptonic decays[†].

Year	Exper.	Final state(s)	R_M ($\times 10^{-3}$)	90% C.L.
2008	Belle [4]	$K^{(*)+}e^-\overline{\nu}_e$	$0.13\pm0.22\pm0.20$	$< 0.61 \times 10^{-3}$
2007	BaBar [1]	$K^{(*)+}e^-\overline{\nu}_e$	$0.04^{+0.70}_{-0.60}$	$(-1.3, 1.2) \times 10^{-3}$
2005*	Belle [5]	$K^{(*)+}e^-\overline{\nu}_e$	$0.02\pm0.47\pm0.14$	$< 1.0 \times 10^{-3}$
2005	CLEO [6]	$K^{(*)+}e^-\overline{\nu}_e$	$1.6\pm2.9\pm2.9$	$< 7.8 \times 10^{-3}$
2004*	BaBar [7]	$K^{(*)+}e^-\overline{\nu}_e$	$2.3\pm1.2\pm0.4$	$< 4.2 \times 10^{-3}$
1996	E791 [8]	$K^+\ell^-\overline{\nu}_\ell$	$(1.1^{+3.0}_{-2.7}) \times 10^{-3}$	$< 5.0 \times 10^{-3}$
	HFLAV [9]		0.13 ± 0.27	

*These measurements are excluded from the HFLAV average. The statistical correlation of the BaBar result with Ref. 1 has not been established and the Belle result is superseded by Ref. 4. The HFLAV average of semileptonic results assumes reported statistical and systematic uncertainties are uncorrelated.

† More recently, the LHCb experiment [10] has reported the observation of charm mixing, $R_M = (9.6 \pm 3.6) \times 10^{-5}$ with 8.2σ significance, in a time dependent analysis of the ratio of $D^0 \to K^+\pi^-\pi^+\pi^-$ and $D^0 \to K^-\pi^+\pi^-\pi^+$ decay rates.

Table 82.1 summarizes results for R_M from semileptonic decays; the world average from the Heavy Flavor Averaging Group (HFLAV) [9] is $R_M = (1.30 \pm 2.69) \times 10^{-4}$.

82.3. Wrong-sign decays to hadronic non-CP eigenstates

Consider the final state $f = K^+\pi^-$, where A_f is doubly Cabibbo-suppressed. The ratio of decay amplitudes is

$$\frac{A_f}{\overline{A}_f} = -\sqrt{R_D}\, e^{-i\delta_f}, \quad \left|\frac{A_f}{\overline{A}_f}\right| \sim O(\tan^2\theta_c), \tag{82.13}$$

where R_D is the doubly Cabibbo-suppressed (DCS) decay rate relative to the Cabibbo-favored (CF) rate, δ_f is the strong phase difference between DCS and CF processes, and θ_c is the Cabibbo angle. The minus sign originates from the sign of V_{us} relative to V_{cd}.

We characterize the violation of CP with the real-valued parameters A_M, A_D, and ϕ. We adopt the parametrization (see Refs. 11 and 12)

$$\left|\frac{q}{p}\right|^2 = \sqrt{\frac{1+A_M}{1-A_M}}, \tag{82.14}$$

$$\lambda_f^{-1} \equiv \frac{pA_f}{q\overline{A}_f} = -\sqrt{R_D}\left(\frac{(1+A_D)(1-A_M)}{(1-A_D)(1+A_M)}\right)^{1/4} e^{-i(\delta_f+\phi)}, \tag{82.15}$$

$$\lambda_{\overline{f}} \equiv \frac{q\overline{A}_{\overline{f}}}{pA_{\overline{f}}} = -\sqrt{R_D}\left(\frac{(1-A_D)(1+A_M)}{(1+A_D)(1-A_M)}\right)^{1/4} e^{-i(\delta_f-\phi)}, \tag{82.16}$$

and A_D is a measure of direct CP violation, while A_M is a measure of CP violation in mixing. From these relations, we obtain

$$\sqrt{\frac{1+A_D}{1-A_D}} = \frac{|A_f/\overline{A}_f|}{|\overline{A}_{\overline{f}}/A_{\overline{f}}|}, \tag{82.17}$$

The angle ϕ measures CP violation in interference between mixing and decay. While A_M is independent of the decay process, A_D and ϕ, in general, depend on f. However, in the Standard Model the weak phase of $\frac{\overline{A}_{\overline{f}}}{A_{\overline{f}}}$ is negligible and ϕ is usually taken to be universal.

In general, $\lambda_{\overline{f}}$ and λ_f^{-1} are independent complex numbers. More detail on CP violation in meson decays can be found in Ref. 13. To leading order, for A_D, $A_M \ll 1$,

$$r(t) = e^{-t}\left[R_D(1+A_D) + \sqrt{R_D(1+A_M)(1+A_D)}\, y'_- t + \frac{1}{2}(1+A_M)R_M\, t^2\right] \tag{82.18}$$

and

$$\overline{r}(t) = e^{-t}\left[R_D(1-A_D) + \sqrt{R_D(1-A_M)(1-A_D)}\, y'_+ t + \frac{1}{2}(1-A_M)R_M\, t^2\right] \tag{82.19}$$

Here

$$y'_\pm \equiv y'\cos\phi \pm x'\sin\phi = y\cos(\delta_{K\pi}\mp\phi) - x\sin(\delta_{K\pi}\mp\phi), \tag{82.20}$$

where

$$x' \equiv x\cos\delta_{K\pi} + y\sin\delta_{K\pi},$$
$$y' \equiv y\cos\delta_{K\pi} - x\sin\delta_{K\pi}, \tag{82.21}$$

and $R_M = \left(x^2+y^2\right)/2 = \left(x'^2+y'^2\right)/2$ is the mixing rate relative to the time-integrated Cabibbo-favored rate.

The three terms in Eq. (82.18) and Eq. (82.19) probe the three fundamental types of CP violation. In the limit of CP conservation, A_M, A_D, and ϕ are all zero. Then

$$r(t) = \overline{r}(t) = e^{-t}\left(R_D + \sqrt{R_D}\, y' t + \frac{1}{2}R_M\, t^2\right), \tag{82.22}$$

Table 82.3: Results on the time-dependence of $r(t)$ in $D^0 \to K^+\pi^-$ and $\overline{D}^0 \to K^-\pi^+$ decays. The Belle 2014 and CDF results assume no CP violation. The Belle 2006 results restrict x'^2 to the physical region. The BaBar confidence intervals are obtained from the fit, whereas Belle uses a Feldman-Cousins method, and CDF uses a Bayesian method.

Year	Exper.	y' (%)	x'^2 ($\times 10^{-3}$)
2017	LHCb [14]	0.52±0.08	0.036±0.043
2014*†	Belle [15]	0.46±0.34	0.09±0.22
2013*	LHCb [16]	0.48±0.10	0.055±0.049
2013	CDF [17]	0.43±0.43	0.08±0.18
2012*	LHCb [18]	0.72±0.24	−0.09±0.13
2007*	CDF [19]	0.85±0.76	−0.12±0.35
2007	BaBar [20]	0.97±0.44±0.31	−0.22±0.30±0.21
2006†	Belle [21]	$-2.8 < y' < 2.1$	< 0.72 (95% C.L.)

*These measurements are excluded from the HFLAV average. The CDF result is superseded by Ref. 17 and the LHCb results have been superseded by Ref. 14.

† This Belle result allows for CP violation. HFLAV uses this result for the CP-violation allowed fit. This result is not superseded by Ref. 15.

*† This Belle result does not allow for CP violation. HFLAV uses this result for the CP-conserving fit. This result does not supersede Ref. 21.

and the time-integrated wrong-sign rate relative to the integrated right-sign rate is

$$R = \int_0^\infty r(t)\, dt = R_D + \sqrt{R_D}\, y' + R_M. \tag{82.23}$$

The ratio R is the most readily accessible experimental quantity. In Table 82.2 are reported the measurements of R, R_D and A_D in $D^0 \to K^+\pi^-$, and their HFLAV average [9] from a general fit that allows for both mixing and CP violation. Typically, the fit parameters are R_D, x'^2, and y'. Table 82.3 summarizes the results for x'^2 and y'. Allowing for CP violation, the separate contributions to R can be extracted by fitting the $D^0 \to K^+\pi^-$ and $\overline{D}^0 \to K^-\pi^+$ decay rates.

Table 82.2: Results for R, R_D, and A_D in $D^0 \to K^+\pi^-$.

Year	Exper.	$R(\times 10^{-3})$	$R_D(\times 10^{-3})$	$A_D(\%)$
2017	LHCb [14]	—	3.53±0.05	−1.7±1.6
2014	Belle [15]	3.86±0.06	3.53±0.13	—
2013*	LHCb [16]	—	3.57±0.07	−0.7±1.9
2013	CDF [17]	4.30±0.05	3.51±0.35	—
2012*	LHCb [18]	4.25±0.04	3.52±0.15	—
2007*	CDF [19]	4.15±0.10	3.04±0.55	—
2007	BaBar [20]	3.53±0.08±0.04	3.03±0.16±0.10	−2.1±5.2±1.5
2006*	Belle [21]	3.77±0.08±0.05	3.64±0.18	2.3±4.7
2005†	FOCUS [22]	$4.29^{+0.63}_{-0.61}$±0.28	$5.17^{+1.47}_{-1.58}$±0.76	13^{+33}_{-25}±10
2000†	CLEO [23]	$3.32^{+0.63}_{-0.65}$±0.40	4.8±1.2±0.4	-1^{+16}_{-17}±1
1998†	E791 [24]	$6.8^{+3.4}_{-3.3}$±0.7	—	—
	Average		3.485±0.035 [9]	−0.88±0.99 [9]

*These measurements are excluded from the HFLAV average of R_D. The CDF result is superseded by Ref. 17 and the LHCb results are superseded by Ref. 14. The Belle result for R and R_D is superseded by Ref. 15.

†These measurements are excluded from the HFLAV average due to poor precision.

The non trivial dependence of the efficiency as a function of decay time may explain why the values of R reported by experiments at hadron colliders are systematically larger (where online selection criteria favor D decays with longer decay times).

Extraction of the mixing parameters x and y from the results in Table 82.3 requires knowledge of the relative strong phase $\delta_{K\pi}$. An interference effect that provides useful sensitivity to $\delta_{K\pi}$ arises in the decay chain $\psi(3770)\to D^0\overline{D}^0\to(f_{CP})(K^+\pi^-)$, where f_{CP} denotes a CP-even or -odd eigenstate from D^0 decay, such as K^+K^- or $K^0_S\pi^0$, respectively [26]. Here, the amplitude relation

$$\sqrt{2}\,A(D_\pm\to K^-\pi^+) = A(D^0\to K^-\pi^+) \pm A\big(\overline{D}^0\to K^-\pi^+\big). \quad (82.24)$$

where $D_\pm$ denotes a CP-even or -odd eigenstate, implies that

$$\cos\delta_{K\pi} = \frac{|A(D_+\to K^-\pi^+)|^2 - |A(D_-\to K^-\pi^+)|^2}{2\sqrt{R_D}\,|A(D^0\to K^-\pi^+)|^2}\,. \quad (82.25)$$

This neglects CP violation.

The asymmetry of CP-tagged D decays rates to $K^-\pi^+$ is denoted as

$$A^{CP}_{K\pi} \equiv \frac{|A(D_-\to K^-\pi^+)|^2 - |A(D_+\to K^-\pi^+)|^2}{|A(D_-\to K^-\pi^+)|^2 + |A(D_+\to K^-\pi^+)|^2}. \quad (82.26)$$

To lowest order in the mixing parameters [2,3]

$$2\sqrt{R_D}\cos\delta_{K\pi} + y = (1+R)A^{CP}_{K\pi} \quad (82.27)$$

where R is the time-integrated wrong-sign rate relative to the integrated right-sign rate from Eq. (82.23).

82.3.1. *Wrong-sign decays to multibody final states* :

For multibody final states, Eqs. (82.13)–(82.23) apply separately to each point in phase-space. Although x and y do not vary across the space, knowledge of the resonant substructure is needed to extrapolate the strong phase difference δ from point to point to determine x and y. Model-independent methods to measure D mixing parameters require input related to the relative phases of the D^0 and $\overline{D}^0$ decay amplitudes across the phase-space distribution [25]. The required phase information is accessible at the charm threshold, where CLEO-c and BESIII operate [26,27].

A time-dependent analysis of the process $D^0\to K^+\pi^-\pi^0$ from BaBar [29,30] determines the *relative* strong phase variation across the Dalitz plot and reports $x'' = (2.61^{+0.57}_{-0.68}\pm0.39)\%$, and $y'' = (-0.06^{+0.55}_{-0.64}\pm0.34)\%$, where x'' and y'' are defined as

$$x'' \equiv x\cos\delta_{K\pi\pi^0} + y\sin\delta_{K\pi\pi^0}\,,$$
$$y'' \equiv y\cos\delta_{K\pi\pi^0} - x\sin\delta_{K\pi\pi^0}, \quad (82.28)$$

in analogy with x', y', and $\delta_{K\pi}$ of Eq. (82.21). Here $\delta_{K\pi\pi^0}$ is the remaining strong phase difference between the DCS $D^0\to K^+\rho^-$ and the CF $\overline{D}^0\to K^+\rho^-$ amplitudes and does not vary across the Dalitz plot. Both strong phases, $\delta_{K\pi}$ and $\delta_{K\pi\pi^0}$, can be determined from time-integrated CP asymmetries in correlated $D^0\overline{D}^0$ produced at the $\psi(3770)$ [26,27].

For the decay modes D^0 and $\overline{D}^0\to K^+\pi^-\pi^+\pi^-$, Belle observed $R = (0.324\pm0.008\pm0.007)\%$ [28]. Subsequently, a phase–space integrated analysis from LHCb using charm threshold data at CLEO-c has yielded the observation of charm mixing with 8.2σ significance.

Both the sign and magnitude of x and y without phase or sign ambiguity may be measured using the time-dependent resonant substructure of multibody D^0 decays [31,32]. In $D^0\to K^0_S\pi^+\pi^-$, the DCS and CF decay amplitudes populate the same Dalitz plot, which allows direct measurement of the relative strong phases. CLEO [33], Belle [32,35], and BaBar [34] have measured the relative phase between $D^0\to K^*(892)^-\pi^+$ and $D^0\to K^*(892)^+\pi^-$ to be $(189\pm10\pm3^{+15}_{-5})^\circ$, $(173.9\pm0.7$ (stat. only)$)^\circ$, and $(177.6\pm1.1$ (stat. only)$)^\circ$, respectively. These results are close to the 180° expected from Cabibbo factors and a small strong phase. The LHCb [36] analysis for x, y is decay-model independent. The model of resonances in the multibody final state is replaced by strong-phase measurements from CLEO-c [38]. Table 82.4 summarizes the results of time-dependent multibody analyses.

Table 82.4: Results from time-dependent multibody analyses. The errors are statistical, experimental systematic, and decay-model systematic, respectively. BaBar 2016 reports a combined systematic error. The LHCb result is decay-model independent utilizing strong-phase measurements from CLEO-c [38]

No CP Violation				
Year	Exper.	Final State(s)	$x\ \times10^{-3}$	$y\ \times10^{-3}$
2016	BaBar [37]	$\pi^+\pi^-\pi^0$	$15\pm12\pm6$	$2\pm9\pm5$
2016	LHCb [36]	$K^0_S\pi^+\pi^-$	$-8.6\pm5.3\pm1.7$	$0.3\pm4.6\pm1.3$
2014	Belle [35]	$K^0_S\pi^+\pi^-$	$5.6\pm1.9^{+0.3\,+0.6}_{-0.9\,-0.9}$	$3.0\pm1.5^{+0.4\,+0.3}_{-0.5\,-0.6}$
2010	BaBar [34]	$K^0_S\pi^+\pi^-$, $K^0_SK^+K^-$	$1.6\pm2.3\pm1.2\pm0.8$	$5.7\pm2.0\pm1.3\pm0.7$
2007	Belle [32]	$K^0_S\pi^+\pi^-$	$8.0\pm2.9^{+0.9\,+1.0}_{-0.7\,-1.4}$	$3.3\pm2.4^{+0.8\,+0.6}_{-1.2\,-0.8}$
2005	CLEO [31]	$K^0_S\pi^+\pi^-$	$19^{+32}_{-33}\pm4\pm4$	$-14\pm24\pm8\pm4$

With CP Violation				
Year	Exper.	Final State(s)	$\lvert q/p\rvert$	ϕ
2014	Belle [35]	$K^0_S\pi^+\pi^-$	$0.90^{+0.16\,+0.05\,+0.06}_{-0.15\,-0.04\,-0.05}$	$(-6\pm11\pm3^{+3}_{-4})^\circ$
2007*	Belle [32]	$K^0_S\pi^+\pi^-$	$0.86^{+0.30\,+0.06}_{-0.29\,-0.03}\pm0.08$	$(-14^{+16\,+5\,+2}_{-18\,-3\,-4})^\circ$

* This result allows for all CP violations and is superseded by Ref. [35] that assumes no direct CP violation in DCS decays.

In addition, Belle [32,35] has results for both the relative phase (statistical errors only) and ratio R (central values only) of the DCS fit fraction relative to the CF fit fractions for $K^*(892)^+\pi^-$, $K^*_0(1430)^+\pi^-$, $K^*_2(1430)^+\pi^-$, $K^*(1410)^+\pi^-$, and $K^*(1680)^+\pi^-$. Similarly, BaBar [34,39,40] has reported central values for R for $K^*(892)^+\pi^-$, $K^*_0(1430)^+\pi^-$, and $K^*_2(1430)^+\pi^-$. The systematic uncertainties on R are not evaluated. The large differences in R among these final states could point to an interesting role for hadronic effects.

82.4. Decays to CP Eigenstates

When the final state f is a CP eigenstate, there is no distinction between f and $\overline{f}$, and $A_f = A_{\overline{f}}$ and $\overline{A}_{\overline{f}} = \overline{A}_f$. We denote final states with CP eigenvalues ±1 by $f_\pm$ and write $\lambda_\pm$ for $\lambda_{f_\pm}$.

The quantity y may be measured by comparing the rate for D^0 decays to non-CP eigenstates such as $K^-\pi^+$ with decays to CP eigenstates such as K^+K^- [12]. If decays to K^+K^- have a shorter effective lifetime than those to $K^-\pi^+$, y is positive.

In the limit of slow mixing ($x, y \ll 1$) and the absence of direct CP violation ($A_D = 0$), but allowing for small indirect CP violation ($|A_M|, |\phi| \ll 1$), we can write

$$\lambda_\pm = \left|\frac{q}{p}\right| e^{\pm i\phi}\,. \quad (82.29)$$

In this scenario, to a good approximation, the decay rates for states that are initially D^0 and $\overline{D}^0$ to a CP eigenstate have exponential time dependence:

$$r_\pm(t) \propto \exp\left(-t/\tau_\pm\right)\,, \quad (82.30)$$

$$\overline{r}_\pm(t) \propto \exp\left(-t/\overline{\tau}_\pm\right)\,, \quad (82.31)$$

where τ is measured in units of $1/\Gamma$.

The effective lifetimes are given by

$$1/\tau_\pm = 1 \pm \left|\frac{q}{p}\right| (y\cos\phi - x\sin\phi)\,, \quad (82.32)$$

$$1/\overline{\tau}_\pm = 1 \pm \left|\frac{p}{q}\right| (y\cos\phi + x\sin\phi)\,. \quad (82.33)$$

The effective decay rate to a CP eigenstate combining both D^0 and $\overline{D}^0$ decays is

$$r_\pm(t) + \overline{r}_\pm(t) \propto e^{-(1\pm y_{CP})t}\,. \quad (82.34)$$

Here

$$y_{CP} = \frac{1}{2}\left(\left|\frac{q}{p}\right| + \left|\frac{p}{q}\right|\right) y\cos\phi - \frac{1}{2}\left(\left|\frac{q}{p}\right| - \left|\frac{p}{q}\right|\right) x\sin\phi \qquad (82.35)$$
$$\approx y\cos\phi - A_M x\sin\phi \ .$$

If CP is conserved, $y_{CP} = y$.

All measurements of y_{CP} are relative to the $D^0 \to K^-\pi^+$ decay rate. Table 82.5 summarizes the current status of measurements. Belle [46], BaBar [47], LHCb [48], and CDF [44] have reported y_{CP} and the decay-rate asymmetry for CP even final states (assuming $A_D = 0$)

$$A_\Gamma = \frac{\overline{\tau}_+ - \tau_+}{\overline{\tau}_+ + \tau_+} = \frac{(1/\tau_+) - (1/\overline{\tau}_+)}{(1/\tau_+) + (1/\overline{\tau}_+)} \qquad (82.36)$$
$$\approx \frac{1}{2}\left(\left|\frac{q}{p}\right| - \left|\frac{p}{q}\right|\right) y\cos\phi - \frac{1}{2}\left(\left|\frac{q}{p}\right| + \left|\frac{p}{q}\right|\right) x\sin\phi$$
$$\approx A_M y\cos\phi - x\sin\phi \ .$$

Belle [50] has also reported y_{CP} for the final state $K^0_S K^+K^-$ which is dominated by the CP odd final state $K^0_S\phi$. If CP is conserved, $A_\Gamma = 0$.

Table 82.5: Results for y_{CP} from $D^0 \to K^+K^-$ and $\pi^+\pi^-$.

Year	Exper.	final state(s)	$y_{CP}(\%)$	$A_\Gamma(\times 10^{-3})$
2016	LHCb [41]	$K^+K^-, \pi^+\pi^-$	—	$-0.13\pm0.28\pm0.10$
2016	LHCb [41]	K^+K^-	—	$-0.30\pm0.32\pm0.10$
2016	LHCb [41]	$\pi^+\pi^-$	—	$0.46\pm0.58\pm0.12$
2015	LHCb [42]	$K^+K^-, \pi^+\pi^-$	—	-1.25 ± 0.73
2015	LHCb [42]	K^+K^-	—	$-1.34\pm0.77^{+0.26}_{-0.34}$
2015	LHCb [42]	$\pi^+\pi^-$	—	$-0.92\pm1.45^{+0.25}_{-0.33}$
2015	BES III [43]	$K^0_S\pi^0, K^0_S\eta, K^0_S\omega$ $K^+K^-, \pi^+\pi^-$, $K^0_S\pi^0\pi^0$	$-2.0\pm1.3\pm0.7$	—
2014	CDF [44]	$K^+K^-, \pi^+\pi^-$	—	-1.2 ± 1.2
2014	CDF [44]	K^+K^-	—	$-1.9\pm1.5\pm0.4$
2014	CDF [44]	$\pi^+\pi^-$	—	$-0.1\pm1.8\pm0.3$
2013*	LHCb [45]	K^+K^-	—	$-0.35\pm0.62\pm0.12$
2013*	LHCb [45]	$\pi^+\pi^-$	—	$0.33\pm1.06\pm0.14$
2012	Belle [46]	$K^+K^-,\pi^+\pi^-$	$1.11\pm0.22\pm0.09$	$-0.3\pm2.0\pm0.7$
2012	BaBar [47]	$K^+K^-,\pi^+\pi^-$	$0.72\pm0.18\pm0.12$	$0.9\pm2.6\pm0.6$
2011	LHCb [48]	K^+K^-	$0.55\pm0.63\pm0.41$	$-5.9\pm5.9\pm2.1$
2009*	BaBar [49]	K^+K^-	$1.16\pm0.22\pm0.18$	—
2009	Belle [50]	$K^0_S K^+K^-$	$0.11\pm0.61\pm0.52$	—
2008*	BaBar [51]	$K^+K^-,\pi^+\pi^-$	$1.03\pm0.33\pm0.19$	$2.6\pm3.6\pm0.8$
2007*	Belle [52]	$K^+K^-,\pi^+\pi^-$	$1.31\pm0.32\pm0.25$	$0.1\pm3.0\pm1.5$
2003*	BaBar [53]	$K^+K^-,\pi^+\pi^-$	$0.8\pm0.4^{+0.5}_{-0.4}$	—
2001	CLEO [54]	$K^+K^-,\pi^+\pi^-$	$-1.2\pm2.5\pm1.4$	—
2001	Belle† [55]	K^+K^-	$-0.5\pm1.0^{+0.7}_{-0.8}$	—
2000	FOCUS [56]	K^+K^-	$3.42\pm1.39\pm0.74$	—
1999	E791 [57]	K^+K^-	$0.8\pm2.9\pm1.0$	—
	HFLAV [9]		0.835 ± 0.155	-0.32 ± 0.26

*These measurements are excluded from the HFLAV average. The BaBar results are superseded by Ref. 47 and the Belle result has been superseded by Ref. 46. The LHCb results Ref. 41 and Ref. 42 use different tagging methods, D^* and semimuonic, respectively, and thus are independent. Ref. 41 supersedes the 2013 LHCb results.

†This measurement is included in the result reported by Ref. 46.

Substantial work on the time-integrated CP asymmetries in decays to CP eigenstates are summarized in this *Review* [58]. Table 82.6 summarizes the current status of measurements of the difference in time-integrated CP asymmetries, $\Delta A_{CP} = A_K - A_\pi$, between $D^0 \to K^-K^+$ and $D^0 \to \pi^-\pi^+$. The HFLAV fit is consistent with no CP violation at the 6.5% Confidence Level [9].

Table 82.6: Results for the difference in time-integrated CP asymmetries ΔA_{CP} between $D^0 \to K^+K^-$ and $D^0 \to \pi^+\pi^-$.

Year	Exper.	$\Delta A_{CP}(\times 10^{-3})$
2016	LHCb [59]	$-1.0\pm0.8\pm0.3$
2014	LHCb [60]	$1.4\pm1.6\pm0.8$
2013	CDF [61]	$-6.2\pm2.1\pm1.0$
2012	Belle [15]	$-8.7\pm4.1\pm0.6$
2008	BaBar [62]	$2.4\pm6.2\pm2.6$

82.5. Coherent $D^0\overline{D}^0$ Analyses

Measurements of R_D, $\cos\delta_{K\pi}$, $\sin\delta_{K\pi}$, x, and y can be determined simultaneously from a combined fit to the time-integrated single-tag (ST) and double-tag (DT) yields in correlated $D^0\overline{D}^0$ produced at the $\psi(3770)$ [26,27].

Due to quantum correlations in the $C = -1$ and $C = +1$ $D^0\overline{D}^0$ pairs produced in the reactions $e^+e^- \to D^0\overline{D}^0(\pi^0)$ and $e^+e^- \to D^0\overline{D}^0\gamma(\pi^0)$, respectively, the time-integrated $D^0\overline{D}^0$ decay rates are sensitive to interference between amplitudes for indistinguishable final states. The size of this interference is governed by the relevant amplitude ratios and can include contributions from D^0–$\overline{D}^0$ mixing.

The following categories of final states are considered:

***f* or $\overline{f}$:** Hadronic states accessed from either D^0 or $\overline{D}^0$ decay but that are not CP eigenstates. An example is $K^-\pi^+$, which results from Cabibbo-favored D^0 transitions or DCS $\overline{D}^0$ transitions.

ℓ^+ or ℓ^-: Semileptonic or purely leptonic final states, which, in the absence of mixing, tag unambiguously the flavor of the parent D^0.

f_+ or f_-: CP-even and CP-odd eigenstates, respectively.

The decay rates for $D^0\overline{D}^0$ pairs to all possible combinations of the above categories of final states are calculated in Ref. 2, for both $C = -1$ and $C = +1$, reproducing the work of Ref. 3. Such $D^0\overline{D}^0$ combinations, where both D final states are specified, are double tags. In addition, the rates for single tags, where either the D^0 or $\overline{D}^0$ is identified and the other neutral D decays generically are given in Ref. 2.

BESIII has reported results using 2.92 pb^{-1} of $e^+e^- \to \psi(3770)$ data where the quantum-coherent $D^0\overline{D}^0$ pairs are in the $C = -1$ state. The values of $y_{CP} = (-2.0 \pm 1.3 \pm 0.7)\%$ [43] and $A^{CP}_{K\pi} = (12.7 \pm 1.3 \pm 0.7)\%$ [66] are determined from DT yields including a CP eigenstate vs semileptonic and vs $K\pi$, respectively. For y_{CP}, the CP eigenstates included are K^-K^+ (f_+), $\pi^+\pi^-$ (f_+), $K^0_S\pi^0\pi^0$ (f_+), $K^0_S\pi^0$ (f_-), $K^0_S\eta$ (f_-), and $K^0_S\omega$ (f_-). For $A^{CP}_{K\pi}$, the additional CP eigenstates included are $\pi^0\pi^0$ (f_+) and $\rho^0\pi^0$ (f_+). Using the external inputs of R_D and y from HFLAV [67] and R from PDG [68]- – see Eq. (82.27) — they obtain $\cos\delta_{K\pi} = 1.02 \pm 0.11 \pm 0.06 \pm 0.01$ [66] where the third uncertainty is due to the external inputs.

CLEO-c has reported results using 818 pb^{-1} of $e^+e^- \to \psi(3770)$ data [63–65]. The values of y, R_M, $\cos\delta_{K\pi}$, and $\sin\delta_{K\pi}$ are determined from a combined fit to the ST (hadronic only) and DT yields. The hadronic final states included are $K^-\pi^+$ (f), $K^+\pi^-$ ($\overline{f}$), K^-K^+ (f_+), $\pi^+\pi^-$ (f_+), $K^0_S\pi^0\pi^0$ (f_+), $K^0_L\pi^0$ (f_+), $K^0_L\eta$ (f_+), $K^0_L\omega$ (f_+), $K^0_S\pi^0$ (f_-), $K^0_S\eta$ (f_-), $K^0_S\omega$ (f_-), and $K^0_L\pi^0\pi^0$ (f_-), and $K^0_S\pi^+\pi^-$ (mixure of f,$\overline{f}$, f_+, and f_-). The two flavored final states, $K^-\pi^+$ and $K^+\pi^-$, can be reached via CF or DCS transitions.

Semileptonic DT yields are also included, where one D is fully reconstructed in one of the hadronic modes listed above, and the other D is partially reconstructed in either $D \to Ke\nu$ or $D \to K\mu\nu$. When the lepton is accompanied by a flavor tag ($D \to K^-\pi^+$ or $K^+\pi^-$), both the "right-sign" and "wrong-sign" DT samples are used, where the electron and kaon charges are the same and opposite, respectively.

The main results of the CLEO-c analysis are the determination of $\cos\delta_{K\pi} = 0.81^{+0.22+0.07}_{-0.18-0.05}$, $\sin\delta_{K\pi} = -0.01 \pm 0.49 \pm 0.04$, and world averages for the mixing parameters from an "extended" fit that combines the CLEO-c data with previous mixing and branching-ratio measurements [65]. These fits allow $\cos\delta_{K\pi}$, $\sin\delta_{K\pi}$ and x^2 to be

unphysical. Constraining $\cos\delta_{K\pi}$ and $\sin\delta_{K\pi}$ to $[-1,+1]$ — that is interpreting $\delta_{K\pi}$ as an angle — yields $\delta_{K\pi} = (18\,^{+11}_{-17} \pm 7)^\circ$. Note that measurements of y (Table 82.4 and Table 82.5) and y' (Table 82.3) dominate the determination of $\delta_{K\pi} = 15.2\,^{+7.6}_{-10.0}$ [9].

82.6. Summary of Experimental Results

Several recent results indicate that charm mixing is at the upper end of the range of Standard Model estimates.

For $D^0 \to K^+\pi^-$, LHCb [16,18], CDF [17], and Belle [15] each exclude the no-mixing hypothesis by more than 5 standard deviations.

For y_{CP} in $D^0 \to K^+K^-$ and $\pi^+\pi^-$, Belle [46] and BaBar [47] find 4.5σ and 3.3σ effects. The most sensitive measurement of x and y is in $D^0 \to K^0_S\pi^+\pi^-$ from Belle [35] and the no mixing solution is only excluded at 2.5σ. In a similar analysis using $D^0 \to K^0_S\pi^+\pi^-$ and $D^0 \to K^0_SK^+K^-$ BaBar [34] also finds the no mixing solution excluded at 1.9σ. LHCb [10] has reported the observation of charm mixing in $D^0 \to K^+\pi^-\pi^+\pi^-$ with 8.2σ significance.

The current situation would benefit from better knowledge of the strong phase difference $\delta_{K\pi}$ than provided by the current CLEO-c [65] and BESIII [66] results. This would allow one to unfold x and y from the $D^0 \to K^+\pi^-$ measurements of x'^2 and y', and directly compare them to the $D^0 \to K^0_S\pi^+\pi^-$ results.

The experimental data consistently indicate that the D^0 and $\overline{D}^0$ do mix. The mixing is presumably dominated by long-range processes. Under the assumption that the observed mixing is due entirely to non-Standard Model processes, significant constraints on a variety of new physics models are obtained [69]. A serious limitation to the interpretation of charm oscillations in terms of New Physics is the theoretical uncertainty of the Standard Model prediction [70,71].

82.7. HFLAV Averaging of Charm Mixing Results

The Heavy Flavor Averaging Group (HFLAV) has made a global fit to all mixing measurements to obtain values of x, y, $\delta_{K\pi}$, $\delta_{K\pi\pi^0}$, R_D, $A_D \equiv (R_D^+ - R_D^-)/(R_D^+ + R_D^-)$, $|q/p|$, $\mathrm{Arg}(q/p) \equiv \phi$, and the time-integrated CP asymmetries A_K and A_π. Correlations among observables are taken into account by using the error matrices from the experiments. The measurements of $D^0 \to K^{(*)+}\ell^-\overline{\nu}$, K^+K^-, $\pi^+\pi^-$, $K^+\pi^-$, $K^+\pi^-\pi^0$, $K^+\pi^-\pi^+\pi^-$, $K^0_S\pi^+\pi^-$, $K^0_SK^+K^-$, and $\pi^+\pi^-\pi^0$ decays, as well as CLEO-c and BESIII results for double-tagged branching fractions measured at the $\psi(3770)$ are used.

Table 82.7: HFLAV Charm Mixing Averages [9].

Parameter	No CP Violation	CP Violation Allowed	95% C.L. Interval CPV Allowed
$x(\%)$	$0.46\,^{+0.14}_{-0.15}$	0.32 ± 0.14	$[0.04, 0.62]$
$y(\%)$	0.62 ± 0.08	$0.69^{+0.06}_{-0.07}$	$[0.50, 0.80]$
$R_D(\%)$	$0.348\,^{+0.004}_{-0.003}$	$0.349\,^{+0.004}_{-0.003}$	$[0.342, 0.356]$
$\delta_{K\pi}(^\circ)$	$8.0\,^{+9.7}_{-11.2}$	$15.2\,^{+7.6}_{-10.0}$	$[-16.8, 30.1]$
$\delta_{K\pi\pi^0}(^\circ)$	$20.4\,^{+23.3}_{-23.8}$	$31.7\,^{+23.5}_{-24.2}$	$[-16.4, 77.7]$
$A_D(\%)$	—	-0.88 ± 0.99	$[-2.8, 1.0]$
$\lvert q/p\rvert$	—	$0.89^{+0.08}_{-0.07}$	$[0.77, 1.12]$
$\phi(^\circ)$	—	$-12.9\,^{+9.9}_{-8.7}$	$[-30.2, 10.6]$
A_K	—	-0.11 ± 0.13	$[-0.37, 0.14]$
A_π	—	0.01 ± 0.14	$[-0.25, 0.28]$

For the global fit, confidence contours in the two dimensions (x, y) and $(|q/p|, \phi)$ are obtained by letting, for any point in the two-dimensional plane, all other fit parameters take their preferred values. Figures 1 and 2 show the resulting 1 to 5 σ contours. The fits exclude the no-mixing point ($x=y=0$) at more than 11.5σ, when CP violation is allowed. The fits are consistent with no CP violation at the 40% Confidence Level. The parameters x and y differ from zero by 1.9σ and 9.1σ, respectively. One-dimensional likelihood functions for parameters are obtained by allowing, for any value of the parameter,

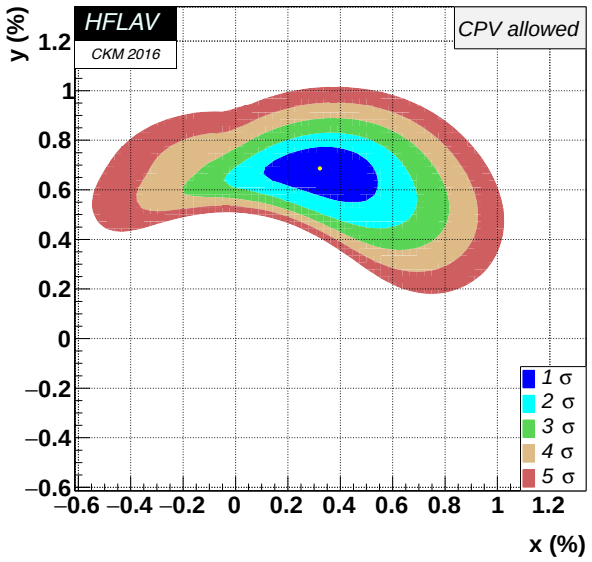

Figure 82.1: Two-dimensional 1σ-5σ contours for (x, y) from measurements of $D^0 \to K^{(*)+}\ell\nu$, h^+h^-, $K^+\pi^-$, $K^+\pi^-\pi^0$, $K^+\pi^-\pi^+\pi^-$, $K^0_S\pi^+\pi^-$, $K^0_SK^+K^-$, and $\pi^+\pi^-\pi^0$ decays, and double-tagged branching fractions measured at the $\psi(3770)$ resonance (from HFLAV [9]) .

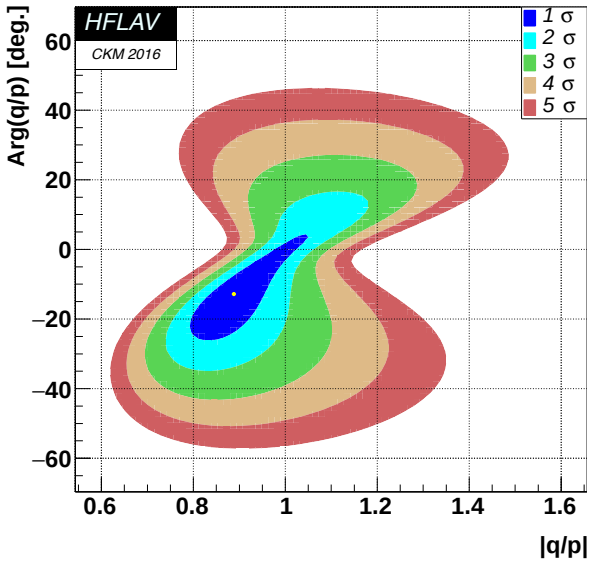

Figure 82.2: Two-dimensional 1σ-5σ contours for $(|q/p|,\mathrm{Arg}(q/p))$ from measurements of $D^0 \to K^{(*)+}\ell\nu$, h^+h^-, $K^+\pi^-$, $K^+\pi^-\pi^0$, $K^+\pi^-\pi^+\pi^-$, $K^0_S\pi^+\pi^-$, $K^0_SK^+K^-$, and $\pi^+\pi^-\pi^0$ decays, and double-tagged branching fractions measured at the $\psi(3770)$ resonance (from HFLAV [9]) .

all other fit parameters to take their preferred values. The resulting likelihood functions give central values, 68.3% C.L. intervals, and 95% C.L. intervals as listed in Table 82.7. The χ^2 for the HFLAV fit is 77 for 50 degrees of freedom, indicating some disagreement among the measurements included in the combination.

From the results of the HFLAV averaging, the following can be concluded: (1) Since CP violation is small and y_{CP} is positive, the CP-even state is shorter-lived, as in the $K^0\overline{K}^0$ system; (2) However, since x appears to be positive, the CP-even state is heavier, unlike in

the $K^0\overline{K}^0$ system; (3) The strong phase difference $\delta_{K\pi}$ is consistent with the SU(3) expectation of zero but large values are not excluded; (4) There is no evidence yet for CP-violation in $D^0\overline{D}^0$ mixing. Observing CP-violation in mixing ($|q/p| \neq 1$) at the current level of sensitivity would indicate new physics.

82.8. Future Prospects

Current results are based primarily upon CLEO-c (818 pb^{-1} of $e^+e^- \to \psi(3770)$), B-factories ($\sim$1 ab^{-1} of $e^+e^- \to \Upsilon(4S)$), and LHCb Run 1 (3 fb^{-1} of pp collisions at 3.5-4.0 TeV). Only a subset of the LHCb results reported use the full Run 1 data sample. Order of magnitude or more increases in data analyzed from each of these data types are expected.

BESIII has accumulated 2.9 fb^{-1} of $e^+e^- \to \psi(3770)$ and may integrate up to 10 fb^{-1} in the next few years. These data will provide strong phase difference measurements that enable improved model-independent determination of mixing parameters from Belle II and LHCb. In 2018, Belle II will begin to accumulate $e^+e^- \to \Upsilon(4S)$ data, 50 ab^{-1} is anticipated by 2024. The sensitivity of these data to charm mixing parameters is expected to be comparable to LHCb Run 2 [72]. LHCb Run 2 will complete in 2018 and Run 3 is planned for 2021-23, concurrent with Belle II.

The author would like to acknowledge helpful input from Bostjan Golob, Marco Gersabeck, and especially Alan Schwartz of the Heavy Flavor Averaging Group.

References:

1. B. Aubert *et al.*, (BaBar Collab.), Phys. Rev. **D76**, 014018 (2007).
2. D.M. Asner and W.M. Sun, Phys. Rev. **D73**, 034024 (2006); Erratum-*ibid*, **77**, 019901 (2008).
3. D. Atwood and A.A. Petrov, Phys. Rev. **D71**, 054032 (2005), M. Gronau, Y. Grossman, J.L. Rosner Phys. Lett. **B508**, 37 (2001), Z.Z. Xing, Phys. Rev. **D55**, 196 (1997), M. Goldhaber and J.L. Rosner, Phys. Rev. **D15**, 1254 (1977).
4. U. Bitenc *et al.*, (Belle Collab.), Phys. Rev. **D77**, 112003 (2008).
5. U. Bitenc *et al.*, (Belle Collab.), Phys. Rev. **D72**, 071101R (2005).
6. C. Cawlfield *et al.*, (CLEO Collab.), Phys. Rev. **D71**, 077101 (2005).
7. B. Aubert *et al.*, (BaBar Collab.), Phys. Rev. **D70**, 091102R (2004).
8. E.M. Aitala *et al.*, (E791 Collab.), Phys. Rev. Lett. **77**, 2384 (1996).
9. Y. Amhis *et al.*, (Heavy Flavor Averaging Group), Eur. Phys. J. **C77**, 895 (2017).
10. R. Aaij *et al.*, (LHCb Collab.), Phys. Rev. Lett. **116**, 241801 (2016).
11. Y. Nir, Lectures given at 27th SLAC Summer Institute on Particle Physics: "CP Violation in and Beyond the Standard Model (SSI 99)," Stanford, California, 7-16 July 1999. Published in Trieste 1999, *Particle Physics*, pp. 165-243.
12. S. Bergmann *et al.*, Phys. Lett. **B486**, 418 (2000).
13. See the Note on "CP Violation in Meson Decays" in this *Review*.
14. R. Aaij *et al.*, (LHCb Collab.), Phys. Rev. **D95**, 052004 (2017); Erratum-*ibid*, **96**, 099907 (2017).
15. B.R. Ko *et al.*, (Belle Collab.), Phys. Rev. Lett. **112**, 111801 (2014).
16. R. Aaij *et al.*, (LHCb Collab.), Phys. Rev. Lett. **111**, 251801 (2013).
17. T. Aaltonen *et al.*, (CDF Collab.), Phys. Rev. Lett. **111**, 231802 (2013).
18. R. Aaij *et al.*, (LHCb Collab.), Phys. Rev. Lett. **110**, 101802 (2013).
19. T. Aaltonen *et al.*, (CDF Collab.), Phys. Rev. Lett. **100**, 121802 (2008).
20. B. Aubert *et al.*, (BaBar Collab.), Phys. Rev. Lett. **98**, 211802 (2007).
21. L.M. Zhang *et al.*, (Belle Collab.), Phys. Rev. Lett. **96**, 151801 (2006).
22. J.M. Link *et al.*, (FOCUS Collab.), Phys. Lett. **B607**, 51 (2005).
23. R. Godang *et al.*, (CLEO Collab.), Phys. Rev. Lett. **84**, 5038 (2000).
24. E.M. Aitala *et al.*, (E791 Collab.), Phys. Rev. **D57**, 13 (1998).
25. See "Review of Multibody Charm Analyses" in this *Review*.
26. R.A. Briere *et al.*, (CLEO Collab.), CLNS 01-1742, (2001).
27. D. M. Asner *et al.*, (BES-III Collab.), Int. J. Mod. Phys. **A**, 24 (2009).
28. E. J. White *et al.*, (Belle Collab.) Phys. Rev. **D88**, 051101 (2013).
29. B. Aubert *et al.*, (BaBar Collab.), Phys. Rev. Lett. **97**, 221803 (2006).
30. B. Aubert *et al.*, (BaBar Collab.), Phys. Rev. Lett. **103**, 211801 (2009).
31. D.M. Asner *et al.*, (CLEO Collab.), Phys. Rev. **D72**, 012001 (2005).
32. L.M. Zhang *et al.*, (Belle Collab.), Phys. Rev. Lett. **99**, 131803 (2007).
33. H. Muramatsu *et al.*, (CLEO Collab.), Phys. Rev. Lett. **89**, 251802 (2002).
34. P. del Amo Sanchez *et al.*, (BaBar Collab.), Phys. Rev. Lett. **105**, 081803 (2010).
35. T. Peng *et al.*, (Belle Collab.), Phys. Rev. **D89**, 091103R (2014).
36. R. Aaij *et al.*, (LHCb Collab.), JHEP **1604**, 033 (2016).
37. J.P. Lees *et al.*, (BaBar Collab.), Phys. Rev. **D93**, 112014 (2016).
38. J. Libby *et al.*, (CLEO Collab.), Phys. Rev. **D82**, 112006 (2010).
39. B. Aubert *et al.*, (BaBar Collab.), Phys. Rev. Lett. **95**, 121802 (2005).
40. B. Aubert *et al.*, (BaBar Collab.), Phys. Rev. **D78**, 034023 (2008).
41. R . Aaij *et al.*. (LHCb Collab.), Phys. Rev. Lett. **118**, 261803 (2017).
42. R. Aaij *et al.*, (LHCb Collab.), JHEP **1504**, 043 (2015).
43. M. Ablikim *et al.*, (BES-III Collab.), Phys. Lett. **B744**, 339 (2015).
44. T. Aaltonen *et al.*, (CDF Collab.), Phys. Rev. **D90**, 111103R (2014).
45. R. Aaij *et al.*, (LHCb Collab.), Phys. Rev. Lett. **112**, 041801 (2014).
46. M. Staric *et al.*, (Belle Collab.), Phys. Lett. **B753**, 412 (2016).
47. B. Aubert *et al.*, (BaBar Collab.), Phys. Rev. **D87**, 012004 (2013).
48. R. Aaij *et al.*, (LHCb Collab.), JHEP **1204**, 129 (2012).
49. B. Aubert *et al.*, (BaBar Collab.), Phys. Rev. **D80**, 071103R (2009).
50. A. Zupanc *et al.*, (Belle Collab.), Phys. Rev. **D80**, 052006 (2009).
51. B. Aubert *et al.*, (BaBar Collab.), Phys. Rev. **D78**, 011105 (2008).
52. M. Staric *et al.*, (Belle Collab.), Phys. Rev. Lett. **98**, 211803 (2007).
53. B. Aubert *et al.*, (BaBar Collab.), Phys. Rev. Lett. **91**, 121801 (2003).
54. S.E. Csorna *et al.*, (CLEO Collab.), Phys. Rev. **D65**, 092001 (2002).
55. K. Abe *et al.*, (Belle Collab.), Phys. Rev. Lett. **88**, 162001 (2002).
56. J.M. Link *et al.*, (FOCUS Collab.), Phys. Lett. **B485**, 62 (2000).
57. E.M. Aitala *et al.*, (E791 Collab.), Phys. Rev. Lett. **83**, 32 (1999).
58. See the tabulation of A_{CP} results in the D^0 and D^+ Listings in this *Review*.
59. R. Aaij *et al.*, (LHCb Collab.), Phys. Rev. Lett. **116**, 191601 (2016).
60. R. Aaij *et al.*, (LHCb Collab.), JHEP **1407**, 041 (2014).
61. T. Aaltonen *et al.*, (CDF Collab.), Phys. Rev. Lett. **109**, 111801 (2012).
62. B. Aubert *et al.*, (BaBar Collab.), Phys. Rev. Lett. **100**, 061803 (2008).
63. J.L. Rosner *et al.*, (CLEO Collab.), Phys. Rev. Lett. **100**, 221801 (2008).
64. D.M. Asner *et al.*, (CLEO Collab.), Phys. Rev. **D78**, 012001 (2008).

65. D.M. Asner *et al.*, (CLEO Collab.), Phys. Rev. **D86**, 112001 (2012).
66. M. Ablikim *et al.*, (BES-III Collab.), Phys. Lett. **B734**, 227 (2014).
67. Heavy Flavor Averaging Group, `www.slac.stanford.edu/ xorg/hfag/charm/CHARM13/ results_mix_cpv.html`.
68. J. Beringer *et al.*, (Particle Data Group), Phys. Rev. **D86**, 010001 (2012).
69. E. Golowich *et al.*, Phys. Rev. **D76**, 095009 (2007).
70. G. Isidori *et al.*, Phys. Lett. **B711**, 46 (2011).
71. E. Franco *et al.*, JHEP **1205**, 140 (2012).
72. Belle II Theory Interface Platform (B2TiP) Report to be published in *Progress of Theoretical and Experimental Physics*.

83. D_s^+ Branching Fractions

Updated November 2015 by J.L. Rosner (University of Chicago) and C.G. Wohl (LBNL).

(Note added April 2018. There have been few measurements of D_s^+ branching ratios since our 2015 revision, and none at all of hadronic modes. So we run with the 2015 version.)

Figure 83.1 shows a partial breakdown of the D_s^+ branching fractions. The rest of this note is about how the figure was constructed. The values shown make heavy use of CLEO measurements of inclusive branching fractions [1]. For references to other data cited in the following, see the Listings.

83.1. Modes with leptons

The bottom $(19.9 \pm 0.9)\%$ of Fig. 83.1 shows the fractions for the modes that include leptons. Measured $Xe^+\nu_e$ semileptonic fractions have been doubled to include the $X\mu^+\nu_\mu$ fractions. The sum of the exclusive $Xe^+\nu_e$ fractions is $(6.9 \pm 0.4)\%$, consistent with an inclusive semileptonic measurement of $(6.5 \pm 0.4)\%$. There seems to be little missing here.

83.2. Inclusive hadronic $K\overline{K}$ fractions

The Cabibbo-favored $c \to s$ decay in D_s^+ decay produces a final state with both an s and an $\bar{s}$; and thus modes with a $K\overline{K}$ pair or with an η, ω, η', or ϕ predominate (as may already be seen in Fig. 83.1 in the semileptonic fractions). We consider the $K\overline{K}$ modes first. A complete picture of the exclusive $K\overline{K}$ charge modes is not yet possible, because branching fractions for many of those modes have not yet been measured. However, CLEO has measured the inclusive K^+, K^-, K_S^0, K^+K^-, $K^+K_S^0$, $K^-K_S^0$, and $2K_S^0$ fractions (these include modes with leptons) [1]. And each of these inclusive fractions with a K_S^0 is equal to the corresponding fraction with a K_L^0: $f(K^+K_L^0) = f(K^+K_S^0)$, $f(2K_L^0) = f(2K_S^0)$, *etc.* Therefore, of all inclusive fractions pairing a K^+, K_S^0, or K_L^0 with a K^-, K_S^0, or K_L^0, we know all but $f(K_S^0K_L^0)$.

We can get that fraction. The total K_S^0 fraction is

$$f(K_S^0) = f(K^+K_S^0) + f(K^-K_S^0) + 2f(2K_S^0) + f(K_S^0K_L^0) + f(\text{single } K_S^0) \ ,$$

where $f(\text{single } K_S^0)$ is the sum of the branching fractions for modes such as $K_S^0\pi^+2\pi^0$ with a K_S^0 and no second K. The $K_S^0\pi^+2\pi^0$ mode is in fact the only unmeasured single-K_S^0 mode (throughout, we shall assume that fractions for modes with a K or $K\overline{K}$ and more than three pions are negligible), and we shall take its fraction to be the same as for the $K_S^0 2\pi^+\pi^-$ mode, $(0.30 \pm 0.11)\%$. Any reasonable deviation from this value would be too small to matter much in the following. Adding the several small single-K_S^0 branching fractions, including those from semileptonic modes, we get $f(\text{single } K_S^0) = (1.65 \pm 0.26)\%$.

Using this, we have:

$$\begin{aligned} f(K_S^0K_L^0) &= f(K_S^0) - f(K^+K_S^0) - f(K^-K_S^0) \\ &\quad - 2f(2K_S^0) - f(\text{single } K_S^0) \\ &= (19.0 \pm 1.1) - (5.8 \pm 0.5) - (1.9 \pm 0.4) \\ &\quad - 2 \times (1.7 \pm 0.3) - (1.7 \pm 0.3) \\ &= (6.2 \pm 1.4)\% \ . \end{aligned}$$

Here and below we treat the errors as uncorrelated, although often they are not. However, our main aim is to get numbers for Fig. 83.1; errors are secondary.

There is a check on our result: The ϕ inclusive branching fraction is $(15.7 \pm 1.0)\%$, of which 34%, or $(5.34 \pm 0.34)\%$ of D_s^+ decays, produces a $K_S^0K_L^0$. Our $f(K_S^0K_L^0) = (6.2 \pm 1.4)\%$ has to be at least this large—and it is.

We now have all the inclusive $K\overline{K}$ fractions. We use $f(K^+\overline{K}^0) = 2\ f(K^+K_S^0)$, and likewise for $f(K^-K^0)$. For K^+K^- and $K_S^0K_L^0$,

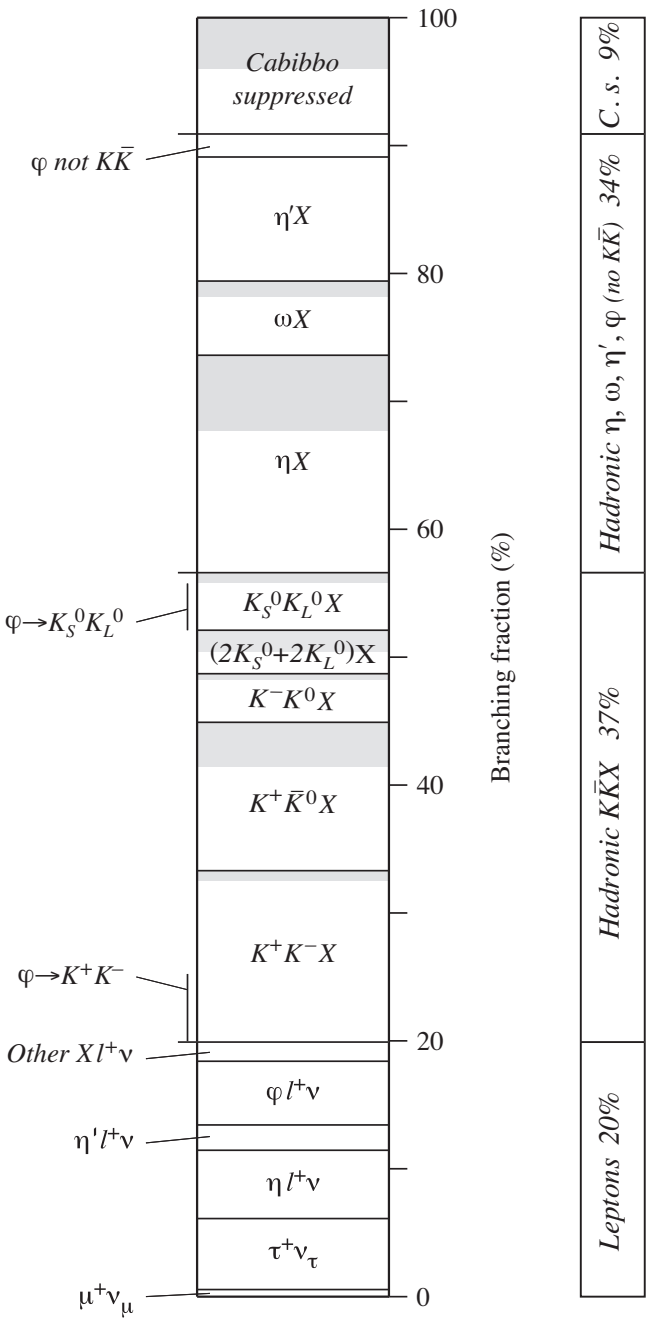

Figure 83.1: A partial breakdown of D_s^+ branching fractions. The hadronic bins in the left column show inclusive fractions. Shading within a bin shows how much of the inclusive fraction is not yet accounted for by adding up all the relevant exclusive fractions. The inclusive hadronic ϕ fraction is spread over three bins, in proportion to its decay fractions into K^+K^-, $K_S^0K_L^0$, and no-$K\bar{K}$ modes.

we subtract off the contributions from $\phi\ell^+\nu$ decay to get the purely hadronic $K\overline{K}$ inclusive fractions:

$$\begin{aligned} f(K^+K^-, \text{hadronic}) &= (15.8 \pm 0.7) - (2.44 \pm 0.14) \\ &= (13.4 \pm 0.7)\% \\ f(K^+\overline{K}^0, \text{hadronic}) &= (11.6 \pm 1.0)\% \\ f(K^-K^0, \text{hadronic}) &= (3.8 \pm 0.8)\% \\ f(2K_S^0 + 2K_L^0, \text{hadronic}) &= (3.4 \pm 0.64)\% \\ f(K_S^0K_L^0, \text{hadronic}) &= (6.2 \pm 1.4) - (1.70 \pm 0.10) \\ &= (4.5 \pm 1.4)\% \ . \end{aligned}$$

The fractions are shown in Fig. 83.1. They total $(36.7 \pm 2.1)\%$ of D_s^+ decays.

We can add more information to the figure by summing up measured branching fractions for exclusive modes within each bin:

K^+K^- *modes*—The sum of measured $K^+K^-\pi^+$, $K^+K^-\pi^+\pi^0$, and $K^+K^-2\pi^+\pi^-$ branching fractions is $(12.6 \pm 0.6)\%$. That leaves $(0.8 \pm 0.9)\%$ for the $K^+K^-\pi^+2\pi^0$ mode, which is the only other K^+K^- mode with three or fewer pions. In Fig. 83.1, this unmeasured part of the K^+K^- bin is shaded.

$K^+\overline{K}^0$ *modes*—Two times the sum of the measured $K^+K_S^0$, $K^+K_S^0\pi^0$, and $K^+K_S^0\pi^+\pi^-$ branching fractions is $(8.1 \pm 0.5)\%$. This leaves $(3.5 \pm 1.1)\%$ for the unmeasured $K^+\overline{K}^0$ modes (there are three such modes with three or fewer pions). This is shaded in the figure.

K^-K^0 *modes*—Twice the $K^-K_S^0 2\pi^+$ fraction is $(3.34 \pm 0.20)\%$, which leaves about $(0.5 \pm 0.8)\%$ for $K^-K^0 2\pi^+\pi^0$, the only other K^-K^0 mode with three or fewer pions.

$2K_S^0 + 2K_L^0$ *modes*—The $2K_S^0\pi^+$ and $2K_S^0 2\pi^+\pi^-$ fractions sum to $(0.86 \pm 0.07)\%$; this times two (for the corresponding $2K_L^0$ modes) is $(1.72 \pm 0.14)\%$. This leaves about $(1.7 \pm 0.7)\%$ for other $2K_S^0 + 2K_L^0$ modes.

$K_S^0K_L^0$ *modes*—Most of the $K_S^0K_L^0$ fraction is accounted for by ϕ decays (see below).

83.3. Inclusive hadronic η, ω, η', and ϕ fractions

These are easier. We start with the inclusive branching fractions, and then, to avoid double counting, subtract: (1) fractions for modes with leptons; (2) η mesons that are included in the inclusive η' fraction; and (3) K^+K^- and $K_S^0K_L^0$ from ϕ decays:

$$\begin{aligned}
f(\eta \text{ hadronic}) &= f(\eta \text{ inclusive}) - 0.65\, f(\eta' \text{ inclusive}) \\
-f(\eta\ell^+\nu) &= (17.0 \pm 3.1)\% \\
f(\omega \text{ hadronic}) &= f(\omega \text{ inclusive}) - 0.0275\, f(\eta' \text{ inclusive}) \\
&= (5.8 \pm 1.4)\% \\
f(\eta' \text{ hadronic}) &= f(\eta' \text{ inclusive}) - f(\eta'\ell^+\nu) \\
&= (9.7 \pm 1.9)\% \\
f(\phi \text{ hadronic}, \not\to K\overline{K}) &= 0.17\, \left[f(\phi \text{ inclusive}) - f(\phi\ell^+\nu)\right] \\
&= (1.8 \pm 0.2)\% \ .
\end{aligned}$$

The factors 0.65, 0.0275, and 0.17 are the $\eta' \to \eta$, $\eta' \to \omega$, and $\phi \not\to K\overline{K}$ branching fractions. Figure 83.1 shows the results; the sum is $(34.2 \pm 3.9)\%$, which is about equal to the hadronic $K\overline{K}$ total.

Note that the bin marked ϕ near the top of Fig. 83.1 includes neither the $\phi\ell^+\nu$ decays nor the 83% of other ϕ decays that produce a $K\overline{K}$ pair. There is twice as much ϕ in the $K_S^0K_L^0$ bin, and nearly three times as much in the K^+K^- bin. These contributions are indicated in those bins.

Again, we can show how much of each bin is accounted for by measured exclusive branching fractions:

η *modes*—The sum of $\eta\pi^+$, $\eta\rho^+$, and ηK^+ branching fractions is $(11.1 \pm 1.2)\%$, which leaves a good part of the inclusive hadronic η fraction, $(17.0 \pm 3.1)\%$, to be accounted for. This is shaded in the figure.

ω *modes*—The sum of $\omega\pi^+$, $\omega\pi^+\pi^0$, and $\omega 2\pi^+\pi^-$ fractions is $(4.6 \pm 0.9)\%$, which is nearly as large as the inclusive hadronic ω fraction, $(5.8 \pm 1.4)\%$.

η' *modes*—The sum of $\eta'\pi^+$, $\eta'\rho^+$, and $\eta' K^+$ fractions is $(9.7 \pm 1.9)\%$, which agrees with the inclusive hadronic η' fraction, $(9.7 \pm 1.9)\%$. (An old measurement of the $\eta'\rho^+$ fraction, $(12.5 \pm 2.2)\%$, has been abandoned [2].)

83.4. Cabibbo-suppressed modes

The sum of the fractions for modes with a $K\bar{K}$, η, ω, η', or leptons is $(90.8 \pm 4.5)\%$. The remaining $(9.2 \pm 4.5)\%$ is to Cabibbo-suppressed modes, mainly single-K + pions and multiple-pion modes (see below). However, it should be noted that some small parts of the modes already discussed are Cabibbo-suppressed. For example, the $(1.10 \pm 0.24)\%$ of D_s^+ decays to $K^0\ell\nu$ or $K^{*0}\ell\nu$ is already in the $X\ell\nu$ bin in Fig. 83.1. And the inclusive measurements of η, ω, and η' fractions do not distinguish between (and therefore include both) Cabibbo-allowed and -suppressed modes. We shall not try to make a separation here.

K^0 + *pions*—Above, we found that $f(\text{single } K_S^0) = (1.65 \pm 0.26)\%$. Subtracting leptonic fractions with a K_S^0 leaves $(1.22 \pm 0.28)\%$. The hadronic single-K^0 fraction is twice this, $(2.44 \pm 0.56)\%$. The sum of measured $K^0\pi^+$, $K^0\pi^+\pi^0$, and $K^0 2\pi^+\pi^-$ fractions is $(1.84 \pm 0.28)\%$.

K^+ + *pions*—The $K^+\pi^0$ and $K^+\pi^+\pi^-$ fractions sum to $(0.72 \pm 0.05)\%$. Much of the $K^+n\pi$ modes, where $n \geq 3$, is already in the η, ω, and η' bins, and the rest is not measured. The total K^+ fraction wanted here is probably in the 1-to-2% range.

Multi-pions—The $2\pi^+\pi^-$, $\pi^+2\pi^0$, and $3\pi^+2\pi^-$ fractions total $(2.54 \pm 0.16)\%$. Modes not measured might double this.

The sum of the actually measured fractions is $(5.1 \pm 0.3)\%$, which is not inconsistent with the Cabibbo-suppressed total of $(9.2 \pm 4.5)\%$.

83.5. A model

With CLEO about to publish inclusive branching fractions [1], Gronau and Rosner predicted those fractions using a "statistical isospin"model [3]. Consider, say, the $D_s^+ \to K\overline{K}\pi$ charge modes: the $K^+K^-\pi^+$ branching fraction is measured, the $K^+\overline{K}^0\pi^0$ and $K^0\overline{K}^0\pi^+$ fractions are not. The statistical isospin model assumes that all the independent isospin amplitudes for $D_s^+ \to K\overline{K}\pi$ decay are equal in magnitude and incoherent in phase—in which case, the ratio of the three fractions here is 3:3:2. (Actually, use was also made of the fact that $D_s^+ \to K\overline{K}\pi$ decay is dominated by $\phi\pi^+$, $K^+\overline{K}^{*0}$, and $K^{*+}\overline{K}^0$ submodes; but the estimated charge-mode ratios were not far from 3:3:2.) A different, quark-antiquark pair-production model was used to estimate systematic uncertainties.

In this way, unmeasured exclusive fractions were calculated from measured exclusive fractions (the latter were taken from the 2008 Review, and so did not benefit from recent results). In the hadronic sector, the measured total of 59.4% of D_s^+ decays led to an estimated total of 24.2% for unmeasured modes. Weighted counts of π^+, K_S^0, *etc.*, were then made to get the inclusive fractions.

Of interest here is that the sum of all the exclusive fractions—a way-stop in getting the inclusive values—was a nearly correct 103%. In the absence of complete measurements, the model is a way to, in effect, average over ignorance. It probably works better summed over a number of charge-mode sets than in detail. It is known to sometimes give incorrect results when there are sufficient measurements to test it.

References:

1. S. Dobbs *et al.*, Phys. Rev. **D79**, 112008 (2009).
2. P.U.E. Onyisi *et al.*, Phys. Rev. **D88**, 032009 (2013).
3. M. Gronau, J.L. Rosner, Phys. Rev. **D79**, 074022 (2009).

84. Leptonic Decays of Charged Pseudoscalar Mesons

Revised March 2016 by J. Rosner (Univ. Chicago), S. Stone (Syracuse Univ.), and R. Van de Water (FNAL).

We review the physics of purely leptonic decays of $\pi^\pm$, $K^\pm$, $D^\pm$, $D_s^\pm$, and $B^\pm$ pseudoscalar mesons. The measured decay rates are related to the product of the relevant weak-interaction-based CKM matrix element of the constituent quarks and a strong interaction parameter related to the overlap of the quark and antiquark wavefunctions in the meson, called the decay constant f_P. The leptonic decay constants for $\pi^\pm$, $K^\pm$, $D^\pm$, $D_s^\pm$, and $B^\pm$ mesons can be obtained with controlled theoretical uncertainties and high precision from *ab initio* lattice-QCD simulations. The combination of experimental leptonic decay-rate measurements and theoretical decay-constant calculations enables the determination of several elements of the CKM matrix within the standard model. These determinations are competitive with those obtained from semileptonic decays, and also complementary because they are sensitive to axial-vector (as opposed to vector) quark flavor-changing currents. They can also be used to test the unitarity of the first and second rows of the CKM matrix. Conversely, taking the CKM elements predicted by unitarity, one can infer "experimental" values for f_P that can be compared with theory. These provide tests of lattice-QCD methods, provided new-physics contributions to leptonic decays are negligible at the current level of precision. This review was prepared for the Particle Data Group's 2016 edition, updating the versions in Refs. 1–3.

84.1. Introduction

Charged mesons formed from a quark and an antiquark can decay to a charged lepton pair when these objects annihilate via a virtual W boson. Fig. 84.1 illustrates this process for the purely leptonic decay of a D^+ meson.

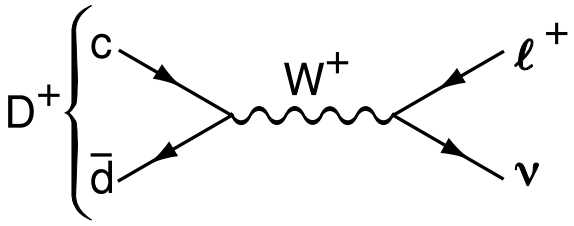

Figure 84.1: The annihilation process for pure D^+ leptonic decays in the Standard Model.

Similar quark-antiquark annihilations via a virtual W^+ to the $\ell^+\nu$ final states occur for the π^+, K^+, D_s^+, and B^+ mesons. (Whenever psuedoscalar-meson charges are specified in this article, use of the charge-conjugate particles and corresponding decays are also implied.) Let P be any of these pseudoscalar mesons. To lowest order, the decay width is

$$\Gamma(P \to \ell\nu) = \frac{G_F^2}{8\pi} f_P^2 \, m_\ell^2 M_P \left(1 - \frac{m_\ell^2}{M_P^2}\right)^2 \left|V_{q_1q_2}\right|^2 \ . \qquad (84.1)$$

Here M_P is the P mass, m_ℓ is the ℓ mass, $V_{q_1q_2}$ is the Cabibbo-Kobayashi-Maskawa (CKM) matrix element between the constituent quarks $q_1\bar{q}_2$ in P, and G_F is the Fermi coupling constant. The decay constant f_P is proportional to the matrix element of the axial current between the one-P-meson state and the vacuum:

$$\langle 0|\bar{q}_1\gamma_\mu\gamma_5 q_2|P(p)\rangle = ip_\mu f_P \, , \qquad (84.2)$$

and can be thought of as the "wavefunction overlap" of the quark and antiquark. In this article we use the convention in which $f_\pi \approx 130$ MeV.

The decay $P^\pm$ starts with a spin-0 meson, and ends up with a left-handed neutrino or right-handed antineutrino. By angular momentum conservation, the $\ell^\pm$ must then also be left-handed or right-handed, respectively. In the $m_\ell = 0$ limit, the decay is forbidden, and can only occur as a result of the finite ℓ mass. This helicity suppression is the origin of the m_ℓ^2 dependence of the decay width. Radiative corrections are needed when the final charged particle is an electron or muon; for the τ they are greatly suppressed due to the large lepton mass, and hence negligible.

Measurements of purely leptonic decay branching fractions and lifetimes allow an experimental determination of the product $\left|V_{q_1q_2}\right| f_P$. If the decay constant f_P is known to sufficient precision from theory, one can obtain the corresponding CKM element within the standard model. If, on the other hand, one takes the value of $\left|V_{q_1q_2}\right|$ assuming CKM unitarity, one can infer an "experimental measurement" of the decay constant that can then be compared with theory.

The importance of measuring $\Gamma(P \to \ell\nu)$ depends on the particle being considered. Leptonic decays of charged pseudoscalar mesons occur at tree level within the standard model. Thus one does not expect large new-physics contributions to measurements of $\Gamma(P \to \ell\nu)$ for the lighter mesons $P = \pi^+, K^+$, and these processes in principle provide clean standard-model determinations of V_{ud} and V_{us}. The situation is different for leptonic decays of charm and bottom mesons. The presence of new heavy particles such as charged Higgs bosons or leptoquarks could lead to observable effects in $\Gamma(P \to \ell\nu)$ for $P = D_{(s)}^+, B^+$ [4–8]. Thus the determination of $|V_{ub}|$ from $B^+ \to \tau\nu$ decay, in particular, should be considered a probe of new physics. More generally, the ratio of leptonic decays to $\tau\nu$ over $\mu\nu$ final states probes lepton universality [4,9].

The determinations of CKM elements from leptonic decays of charged pseudoscalar mesons provide complementary information to those from other decay processes. The decay $P \to \ell\nu$ proceeds in the standard model via the axial-vector current $\bar{q}_1\gamma_\mu\gamma_5 q_2$, whereas semileptonic pseudoscalar meson decays $P_1 \to P_2\ell\nu$ proceed via the vector current $\bar{q}_1\gamma_\mu q_2$. Thus the comparison of determinations of $\left|V_{q_1q_2}\right|$ from leptonic and semileptonic decays tests the $V-A$ structure of the standard-model electroweak charged-current interaction. More generally, a small right-handed admixture to the standard-model weak current would lead to discrepancies between $\left|V_{q_1q_2}\right|$ obtained from leptonic pseudoscalar-meson decays, exclusive semileptonic pseudoscalar-meson decays, exclusive semileptonic baryon decays, and inclusive semileptonic decays [10,11].

Both measurements of the decay rates $\Gamma(P \to \ell\nu)$ and theoretical calculations of the decay constants f_P for $P = \pi^+, K^+, D_{(s)}^+$ from numerical lattice-QCD simulations are now quite precise. As a result, the elements of the first row of the CKM matrix $|V_{ud}|$ and $|V_{us}|$ can be obtained to sub-percent precision from $\pi^+ \to \ell\nu$ and $K^+ \to \ell\nu$, where the limiting error is from theory. The elements of the second row of the CKM matrix $|V_{cd(s)}|$ can be obtained from leptonic decays of charmed pseudoscalar mesons to few-percent precision, where here the limiting error is from experiment. These enable stringent tests of the unitarity of the first and second rows of the CKM matrix.

This review is organized as follows. Because the experimental and theoretical issues associated with measurements of pions and kaons, charmed mesons, and bottom mesons differ, we discuss each one separately. We begin with the pion and kaon system in Sec. 84.2. First, in Sec. 84.2.1 we review current measurements of the experimental decay rates. We provide tables of branching-ratio measurements and determinations of the product $|V_{ud(s)}|f_{\pi^+(K^+)}$, as well as average values for these quantities including correlations and other effects needed to combine results. Then, in Sec. 84.2.2 we summarize the status of theoretical calculations of the decay constants. We provide tables of recent lattice-QCD results for f_{π^+}, f_{K^+}, and their ratio from simulations including dynamical u, d, s, and (in some cases c) quarks, and present averages for each of these quantities including correlations and strong SU(2)-isospin corrections as needed. We note that, for the leptonic decay constants in Sec. 84.2.2, Sec. 84.3.2, and Sec. 84.4.2, when available we use preliminary averages from the Flavor Lattice Averaging Group [12,13] that update the determinations in Ref. 14 to include results that have appeared since their most recent review, which dates from 2013. We next discuss the charmed meson system in

Sec. 84.3, again reviewing current experimental rate measurements in Sec. 84.3.1 and theoretical decay-constant calculations in Sec. 84.3.2. Last, we discuss the bottom meson system in Sec. 84.4, following the same organization as the two previous sections.

After having established the status of both experimental measurements and theoretical calculations of leptonic charged pseudoscalar-meson decays, we discuss some implications for phenomenology in Sec. 84.5. We combine the average $\mathcal{B}(P \to \ell\nu)$ with the average f_P to obtain the relevant CKM elements from leptonic decays, and then compare them with determinations from other processes. We also use the CKM elements obtained from leptonic decays to test the unitarity of the first and second rows of the CKM matrix. Further, as in previous reviews, we combine the experimental $\mathcal{B}(P \to \ell\nu)$s with the associated CKM elements obtained from CKM unitarity to infer "experimental" values for the decay constants; the comparison with theory provides a test of lattice and other QCD approaches assuming that new-physics contributions to these processes are not significant.

84.2. Pions and Kaons

84.2.1. *Experimental rate measurements* :

The leading-order expression for $\Gamma(P \to \ell\nu)$ in Eq. (84.1) is modified by radiative corrections arising from diagrams involving photons, in some cases with additional quark loops. These electroweak and "hadronic" contributions can be combined into an overall factor that multiplies the rate in the presence of only the strong interaction ($\Gamma^{(0)}$) as follows (cf. Refs. 15,16, and references therein):

$$\Gamma(P \to \ell\nu) = \Gamma^{(0)} \left[1 + \frac{\alpha}{\pi} C_P\right] \quad , \tag{84.3}$$

where C_P differs for $P = \pi, K$. The inclusion of these corrections is numerically important given the level of precision achieved on the experimental measurements of the $\pi^\pm \to \mu^\pm\nu$ and $K^\pm \to \mu^\pm\nu$ decay widths. The explicit expression for the term in brackets above including all known electroweak and hadronic contributions is given in Eq. (114) of Ref. 17. It includes the universal short-distance electroweak correction obtained by Sirlin [18], the universal long-distance correction for a point-like meson from Kinoshita [19], and corrections that depend on the hadronic structure [20]. We evaluate $\delta_P \equiv (\alpha/\pi)C_P$ using the latest experimentally-measured meson and lepton masses and coupling constants from the Particle Data Group [3], and taking the low-energy constants (LECs) that parameterize the hadronic contributions from Refs. 17,21,22. The finite non-logarithmic parts of the LECs were estimated within the large-N_C approximation assuming that contributions from the lowest-lying resonances dominate. We therefore conservatively assign a 100% uncertainty to the LECs, which leads to a ± 0.9 error in $C_{\pi,K}$.[1] We obtain the following correction factors to the individual charged pion and kaon decay widths:

$$\delta_\pi = 0.0176(21) \quad \text{and} \quad \delta_\mathrm{K} = 0.0107(21)\,. \tag{84.4}$$

The error on the ratio of kaon-to-pion leptonic decay widths is under better theoretical control because the hadronic contributions from low-energy constants estimated within the large-N_c framework cancel at lowest order in the chiral expansion. For the ratio, we use the correction factor

$$\delta_{K/\pi} = -0.0069(17)\,, \tag{84.5}$$

where we take the estimated error due to higher-order corrections in the chiral expansion from Ref. 24.

The sum of branching fractions for $\pi^- \to \mu^-\bar{\nu}$ and $\pi^- \to \mu^-\bar{\nu}\gamma$ is 99.98770(4)% [3]. The two modes are difficult to separate experimentally, so we use this sum. Together with the lifetime 26.033(5) ns [3] this implies $\Gamma(\pi^- \to \mu^-\bar{\nu}[\gamma]) = 3.8408(7) \times 10^7$ s^{-1}. The right-hand side of Eq. (1) is modified by the factor 1.0176 ± 0.0021 mentioned above to include photon emission and radiative corrections [23,25]. The decay rate together with the masses from the 2014 PDG review [3] gives

$$f_{\pi^-}|V_{ud}| = (127.13 \pm 0.02 \pm 0.13)\ \text{MeV}\,, \tag{84.6}$$

where the errors are from the experimental rate measurement and the radiative correction factor δ_π in Eq. (84.4), respectively. The uncertainty is dominated by that from theoretical estimate of the hadronic structure-dependent radiative corrections, which include next-to-leading order contributions of $\mathcal{O}(e^2 p^2_{\pi,K})$ in chiral perturbation theory [17].

The data on $K_{\mu 2}$ decays have been updated recently through a global fit to branching ratios and lifetime measurements [26]: $\mathcal{B}(K^- \to \mu^-\bar{\nu}[\gamma]) = 63.58(11)\%$ and $\tau_{K^\pm} = 12.384(15)$ ns. The improvement in the branching ratio is primarily due to a new measurement of $\mathcal{B}(K^\pm \to \pi^\pm\pi^+\pi^-)$ from KLOE-2 [27], which is correlated with $\mathcal{B}(K^\pm_{\mu 2})$ through the constraint that the sum of individual branching ratios must equal unity. The sum of branching fractions for $K^- \to \mu^-\bar{\nu}$ and $K^- \to \mu^-\bar{\nu}\gamma$ and the lifetime imply $\Gamma(K^- \to \mu^-\bar{\nu}[\gamma]) = 5.134(11) \times 10^7$ s^{-1}. Again taking the 2014 PDG masses [3], this decay rate implies

$$f_{K^+}|V_{us}| = (35.09 \pm 0.04 \pm 0.04)\ \text{MeV}\,, \tag{84.7}$$

where the errors are from the experimental rate measurement and the radiative correction factor δ_K, respectively.

Short-distance radiative corrections cancel in the ratio of pion-to-kaon decay rates [28]:

$$\frac{\Gamma_{K_{\ell 2[\gamma]}}}{\Gamma_{\pi_{\ell 2[\gamma]}}} = \frac{|V_{us}^2| f^2_{K^-}}{|V_{ud}|^2 f^2_{\pi^-}} \frac{m_K (1 - m_\ell^2/m_K^2)^2}{m_\pi (1 - m_\ell^2/m_\pi^2)^2} (1 + \delta_{K/\pi})\,, \tag{84.8}$$

where $\delta_{K/\pi}$ is given in Eq. (84.5). The left-hand side of Eq. (84.8) is 1.3367(28), yielding

$$\frac{|V_{us}| f_{K^-}}{|V_{ud}| f_{\pi^-}} = 0.27599 \pm 0.00029 \pm 0.00024\,, \tag{84.9}$$

where the first uncertainty is due to the branching fractions and the second is due to $\delta_{K/\pi}$. Here the estimated error on the hadronic structure-dependent radiative corrections is commensurate with the experimental error.

In summary, the main experimental results pertaining to charged pion and kaon leptonic decays are

$$|V_{ud}| f_{\pi^-} = (127.13 \pm 0.02 \pm 0.13)\ \text{MeV}\,, \tag{84.10}$$

$$|V_{us}| f_{K^+} = (35.09 \pm 0.04 \pm 0.04)\ \text{MeV}\,, \tag{84.11}$$

$$\frac{|V_{us}| f_{K^+}}{|V_{ud}| f_{\pi^-}} = 0.27599 \pm 0.00029 \pm 0.00024\,, \tag{84.12}$$

where the errors are from the experimental uncertainties in the branching fractions and the theoretical uncertainties in the radiative correction factors δ_P, respectively.

84.2.2. *Theoretical decay-constant calculations* :

Table 84.1 presents recent lattice-QCD calculations of the charged pion and kaon decay constants and their ratio from simulations with three ($N_f = 2 + 1$) or four flavors ($N_f = 2 + 1 + 1$) of dynamical quarks. The results have been obtained using several independent sets of gauge-field configurations, and a variety of lattice fermion actions that are sensitive to different systematic uncertainties.[2] The

[1] This uncertainty on $C_{\pi,K}$ is smaller than the error estimated by Marciano and Sirlin in Ref. 23, which predates the calculations of the hadronic-structure contributions in Refs. 17, 20–22. The hadronic LECs incorporate the large short-distance electroweak logarithm discussed in Ref. 23, and their dependence on the chiral renormalization scale cancels the scale-dependence induced by chiral loops, thereby removing the dominant scale uncertainty of the Marciano–Sirlin analysis [23].

[2] See the PDG mini-review on "Lattice Quantum Chromodynamics" [29] for a general review of numerical lattice-QCD simulations. Details on the different methods used in modern lattice-QCD calculations are provided in Appendix A of the FLAG "Review of lattice results concerning low energy particle physics" [14].

Table 84.1: Recent lattice-QCD results for f_{π^+}, f_{K^+}, and their ratio. The upper and lower panels show $(2+1+1)$-flavor and $(2+1)$-flavor determinations, respectively. When two errors are shown, they are statistical and systematic, respectively. Results for f_π and f_K in the isospin-symmetric limit $m_u = m_d$ are noted with an "*"; they are corrected for isospin breaking via Eq. (84.13)–Eq. (84.15) before computing the averages. Unpublished results noted with a "†" or "‡" are not included in the averages.

Reference	N_f	f_{π^+}(MeV)	f_{K^+}(MeV)	f_{K^+}/f_{π^+}
ETM 14 [31] §	2+1+1	–	154.4(1.5)(1.3)	1.184(12)(11)
Fermilab/MILC 14 [32] §	2+1+1	–	$155.92(13)(^{+42}_{-34})$	$1.1956(10)(^{+26}_{-18})$
HPQCD 13 [33] §	2+1+1	–	155.37(20)(28)	1.1916(15)(16)
FLAG 15 average [12,13] ¶	2+1+1	–	155.6(0.4)	1.193(3)
RBC/UKQCD 14 [34] *,†	2+1	130.19(89)	155.51(83)	1.1945(45)
RBC/UKQCD 12 [35] *	2+1	127(3)(3)	152(3)(2)	1.199(12)(14)
Laiho & Van de Water 11 [36] ‡	2+1	130.53(87)(210)	156.8(1.0)(1.7)	1.202(11)(9)(2)(5)
MILC 10 [37]	2+1	129.2(0.4)(1.4)	$156.1(4)(^{+6}_{-9})$	$1.197(2)(^{+3}_{-7})$
BMW 10 [38] *	2+1	–	–	1.192(7)(6)
HPQCD/UKQCD 07 [39] *	2+1	132(2)	157(2)	1.189(2)(7)
FLAG 15 average [12,13] ¶	2+1	130.2(1.4)	155.9(0.9)	1.192(5)
Our average	Both	130.2(1.7)	155.6(0.4)	1.1928(26)

§ PDG 2014 value of $f_{\pi^+} = 130.41(21)$ MeV used to set absolute lattice scale.

¶ Preliminary numbers shown here may change if further new lattice-QCD calculations are published before the deadline for inclusion in the final 2015 FLAG review.

† Preprint submitted to Phys. Rev. D. Published RBC/UKQCD 12 results included in $N_f = 2+1$ average.

‡ Lattice 2011 conference proceedings.

lattice-QCD uncertainties on both the individual decay constants and their ratio have now reached sub-percent precision. The SU(3)-breaking ratio f_{K^+}/f_{π^+} can be obtained with especially small errors because statistical errors associated with the Monte Carlo simulations are correlated between the numerator and denominator, as are some systematics. The good agreement between these largely independent determinations indicates that the lattice-QCD uncertainties are controlled and that the associated error estimates are reliable.[3]

Table 84.1 also shows the 2015 preliminary three- and four-flavor averages for the pion and kaon decay constants and their ratio from the Flavour Lattice Averaging Group (FLAG) [12,13] in the lines labeled "FLAG 15 average." These preliminary updates of the 2013 FLAG averages [14] include only those results from Table 84.1 that are published in refereed journals, or that are straightforward conference updates of published analyses. In the (2+1+1)-flavor averages, the statistical errors of HPQCD and Fermilab/MILC were conservatively treated as 100% correlated because the calculations employed some of the same gauge-field configurations. The errors have also been increased by the $\sqrt{\chi^2/\mathrm{dof}}$ to reflect a slight tension between the results. There are no four-flavor lattice-QCD results for the pion decay constant in Table 84.1 because all of the calculations listed use the quantity f_{π^+} to fix the absolute lattice scale needed to convert from lattice-spacing units to GeV [31–33].

All of the results in Table 84.1 were obtained using isospin-symmetric gauge-field configurations, *i.e.*, the dynamical up and down quarks have the same mass. Most calculations of pion and kaon decay constants now include the dominant effect of nondegenerate up- and down-quark masses by evaluating the masses of the constituent light (valence) quarks in the pion at the physical up- and down-quark masses, respectively, and evaluating the mass of the valence light quark in the kaon at the physical m_u. Those results obtained with degenerate up and down valence quarks are corrected for isospin breaking using chiral perturbation theory (χPT) before being averaged. The isospin-breaking corrections at next-to-leading order in χPT can be parameterized as [24,40]

$$f_\pi = f_{\pi^+} \ , \tag{84.13}$$

$$f_K = f_{K^+}\left(1 - \delta_{\mathrm{SU}(2)}/2\right) \ , \tag{84.14}$$

$$\frac{f_K}{f_\pi} = \frac{1}{\sqrt{\delta_{\mathrm{SU}(2)}+1}}\frac{f_{K^+}}{f_{\pi^+}} \tag{84.15}$$

where the expression for $\delta_{\mathrm{SU}(2)}$ in terms of the quark masses, meson masses, and decay constants, is given in Eq. (37) of Ref. 14. Numerically, values of $\delta_{\mathrm{SU}(2)} \approx -0.004$ were employed by FLAG to obtain the (2+1)-flavor averages in Table 84.1, but some direct lattice-QCD calculations of $\delta_{\mathrm{SU}(2)}$ give larger values [31,33,41] and further studies are needed.

To obtain the best decay-constant values for comparison with experimental rate measurements and other phenomenological applications, we combine the available $(2+1)$- and $(2+1+1)$-flavor lattice-QCD results, first accounting for the omission of charm sea quarks in the three-flavor simulations. The error introduced by omitting charm sea quarks can be roughly estimated by expanding the charm-quark determinant in powers of $1/m_c$ [42]; the resulting leading contribution is of order $\alpha_s\left(\Lambda_{\mathrm{QCD}}/2m_c\right)^2$ [43]. Taking the $\overline{\mathrm{MS}}$ values $\overline{m}_c(\overline{m}_c) = 1.275$ GeV, $\overline{\Lambda}_{\mathrm{QCD}} \sim 340$ MeV from FLAG [14], and $\overline{\alpha}(\overline{m}_c) \sim 0.4$, leads to an estimate of about 0.7% for the contribution to the decay constants from charm sea quarks. The charm sea-quark contribution to ratios of decay constants is expected to be further suppressed by the SU(3)-breaking factor $(m_s - m_d)/\Lambda_{\mathrm{QCD}}$, and hence about 0.2%.

We can compare these power-counting estimates of charm sea-quark contributions to the observed differences between the (2+1)-

[3] The recent review [30] summarizes the large body of evidence validating the methods employed in modern lattice-QCD simulations.

and (2+1+1)-flavor lattice-QCD averages for kaon, $D_{(s)}$-meson, and $B_{(s)}$-decay constants and ratios in Table 84.1, Table 84.4, and Table 84.6. Of these, the kaon decay constants have been calculated most precisely, and the and three- and four-flavor averages for f_{K^+} and f_{K^+}/f_{π^+} agree within sub-percent errors. Within present uncertainties, however, effects of this size in pseudoscalar-meson decay constants cannot be ruled out. Therefore, to be conservative, in this review we add in quadrature additional systematic errors of 0.7% and 0.2% to all (2+1)-flavor decay-constant and decay-constant-ratio averages, respectively, to account for the omission of charm sea quarks. Numerically, this increases the errors by at most about 50% for f_{K^+} and less for all other decay constants and ratios, indicating that the published (2+1)-flavor lattice-QCD results and uncertainties are reliable.

Our final preferred theoretical values for the charged pion and kaon decay constants are

$$\begin{aligned} \text{Our averages:}\quad & f_{\pi^+} = 130.2(1.7)\ \text{MeV}\,, \\ & f_{K^+} = 155.6(0.4)\ \text{MeV}\,, \\ & \frac{f_{K^+}}{f_{\pi^+}} = 1.1928(26)\,, \end{aligned} \tag{84.16}$$

where f_{π^+} is simply the (2+1)-flavor FLAG average with the error increased by the estimated 0.7% charm sea-quark contribution. For f_{K^+} and f_{K^+}/f_{π^+}, we take a simple weighted average of the (2+1)- and (2+1+1)-flavor FLAG values, because they are each obtained from a sufficient number of independent calculations that we do not expect there to be significant correlations. In practice, the addition of the charm sea-quark error has a tiny impact on our final values in Eq. (84.16), increasing the uncertainty on f_{π^+} by 0.3 MeV, and the central value for f_{K^+}/f_{π^+} by one in the last digit.

84.3. Charmed Mesons

84.3.1. *Experimental rate measurements* :

Measurements have been made for $D^+ \to \mu^+\nu$, $D_s^+ \to \mu^+\nu$, and $D_s^+ \to \tau^+\nu$. Only an upper limit has been determined for $D^+ \to \tau^+\nu$. Both CLEO-c and BES have made measurements of D^+ decay using e^+e^- collisions at the $\psi(3770)$ resonant energy where D^-D^+ pairs are copiously produced. They fully reconstruct one of the D's, say the D^-. Counting the number of these events provides the normalization for the branching fraction measurement. They then find a candidate μ^+, and then form the missing-mass squared, $MM^2 = \left(E_{\rm CM} - E_{D^-}\right)^2 - \left(\overrightarrow{p}_{\rm CM} - \overrightarrow{p}_{D^-} - \overrightarrow{p}_{\mu^+}\right)^2$, taking into account their knowledge of the center-of-mass energy, $E_{\rm CM}$, and momentum, $p_{\rm CM}$, that equals zero in e^+e^- collisions. A peak at zero MM^2 inplies the existence of a missing neutrino and hence the $\mu^+\nu$ decay of the D^+. CLEO-c does not explicitly identify the muon, so their data consists of a combination of $\mu^+\nu$ and $\tau^+\nu$, $\tau^+ \to \pi^+\nu$ events. This permits them to do two fits: in one they fit for the individual components, and in the other they fix the ratio of $\tau^+\nu/\mu^+\nu$ events to be that given by the standard-model expectation. Thus, the latter measurement should be used for standard-model comparisons and the other for new-physics searches. Our average uses the fixed ratio value. The measurements are shown in Table 84.2.

To extract the value of $|V_{cd}|f_{D^+}$ we use the well-measured D^+ lifetime of 1.040(7) ps. The $\mu^+\nu$ results include a 1% correction (lowering) of the rate due to the presence of the radiative $\mu^+\nu\gamma$ final state based on the estimate by Dobrescu and Kronfeld [8].

We now discuss the D_s^+. Measurements of the leptonic decay rate have been made by several groups and are listed in Table 84.3 [47–53]. We exclude older values obtained by normalizing to D_s^+ decay modes that are not well defined. Many measurements, for example, used the $\phi\pi^+$ mode. This decay is a subset of the $D_s^+ \to K^+K^-\pi^+$ channel which has interferences from other modes populating the K^+K^- mass region near the ϕ, the most prominent of which is the $f_0(980)$. Thus the extraction of the effective $\phi\pi^+$ rate is sensitive to the mass resolution of the experiment and the cuts used to define the ϕ mass region [54]. [4]

[4] We have not included the BaBar result for $\mathcal{B}(D_s^+ \to \mu^+\nu)$ reported in Ref. 55 because this measurement determined the ratio of the leptonic decay rate to the hadronic decay rate $\Gamma(D_s^+ \to \ell^+\nu)/\Gamma(D_s^+ \to \phi\pi^+)$.

Table 84.2: Experimental results for $\mathcal{B}(D^+ \to \mu^+\nu)$, $\mathcal{B}(D^+ \to \tau^+\nu)$, and $|V_{cd}|f_{D^+}$. Numbers for $|V_{cd}|f_{D^+}$ have been extracted using updated values for masses (see text). Radiative corrections are included. Systematic uncertainties arising from the D^+ lifetime and mass are included. For the average $\mu^+\nu$ number we use the CLEO-c result for $\mu^+\nu^+ + \tau^+\nu$.

Experiment	Mode	$\mathcal{B}$	$\lvert V_{cd}\rvert f_{D^+}$ (MeV)
CLEO-c [44,45]	$\mu^+\nu$	$(3.93 \pm 0.35 \pm 0.09) \times 10^{-4}$	$47.07 \pm 2.10 \pm 0.57$
CLEO-c [44,45]	$\mu^+\nu + \tau^+\nu$	$(3.82 \pm 0.32 \pm 0.09) \times 10^{-4}$	$46.41 \pm 1.94 \pm 0.57$
BES [46]	$\mu^+\nu$	$(3.71 \pm 0.19 \pm 0.06) \times 10^{-4}$	$45.73 \pm 1.17 \pm 0.38$
Our average	Lines 2+3	$(3.74 \pm 0.17) \times 10^{-4}$	45.91 ± 1.05
CLEO-c [47,48]	$\tau^+\nu$	$< 1.2 \times 10^{-3}$	

Table 84.3: Experimental results for $\mathcal{B}(D_s^+ \to \mu^+\nu)$, $\mathcal{B}(D_s^+ \to \tau^+\nu)$, and $|V_{cs}|f_{D_s^+}$. Numbers for $|V_{cs}|f_{D_s^+}$ have been extracted using updated values for masses (see text). The systematic uncertainty for correlated error on the D_s^+ lifetime is included. The mass uncertainties are also common, but negligible. Common systematic errors in each experiment have been taken into account in the averages.

Experiment	Mode	$\mathcal{B}$(%)	$\lvert V_{cs}\rvert f_{D_s^+}$ (MeV)
CLEO-c [47,48]	$\mu^+\nu$	$0.565 \pm 0.045 \pm 0.017$	$250.8 \pm 10.0 \pm 4.2$
BaBar[a] [53]	$\mu^+\nu$	$0.602 \pm 0.038 \pm 0.034$	$258.9 \pm 8.2 \pm 7.5$
Belle [49]	$\mu^+\nu$	$0.531 \pm 0.028 \pm 0.020$	$243.1 \pm 6.4 \pm 4.9$
Our average	$\mu^+\nu$	0.556 ± 0.024	248.8 ± 5.8
CLEO-c [47,48]	$\tau^+\nu$ $(\pi^+\overline{\nu})$	$6.42 \pm 0.81 \pm 0.18$	$270.8 \pm 17.1 \pm 4.2$
CLEO-c [50]	$\tau^+\nu$ $(\rho^+\overline{\nu})$	$5.52 \pm 0.57 \pm 0.21$	$251.1 \pm 13.0 \pm 5.1$
CLEO-c [51,52]	$\tau^+\nu$ $(e^+\nu\overline{\nu})$	$5.30 \pm 0.47 \pm 0.22$	$246.1 \pm 10.9 \pm 5.4$
BaBar [53]	$\tau^+\nu$ $(e^+(\mu^+)\nu\overline{\nu})$	$5.00 \pm 0.35 \pm 0.49$	$239.0 \pm 8.4 \pm 11.9$
Belle [49]	$\tau^+\nu$ $(\pi^+\overline{\nu})$	$6.04 \pm 0.43^{+0.46}_{-0.40}$	$262.7 \pm 9.3^{+10.2}_{-8.9}$
Belle [49]	$\tau^+\nu$ $(e^+\nu\overline{\nu})$	$5.37 \pm 0.33^{+0.35}_{-0.31}$	$247.7 \pm 7.6^{+8.3}_{-7.4}$
Belle [49]	$\tau^+\nu$ $(\mu^+\nu\overline{\nu})$	$5.86 \pm 0.37^{+0.34}_{-0.59}$	$258.7 \pm 8.2^{+7.7}_{-13.2}$
Our average	$\tau^+\nu$	5.56 ± 0.22	252.1 ± 5.2
Our average	$\mu^+\nu + \tau^+\nu$		250.9 ± 4.0

[a] We do not use a previous unpublished BaBar result from a subsample of data that uses a different technique for obtaining the branching fraction normalization [56].

To find decays in the $\mu^+\nu$ signal channels, CLEO, BaBar and Belle rely on fully reconstructing all the final state particles except for neutrinos and using a missing-mass technique to infer the existence of the neutrino. CLEO uses $e^+e^- \to D_sD_s^*$ collisions at 4170 MeV, while Babar and Belle use $e^+e^- \to DKn\pi D_s^*$ collisions at energies near the $\Upsilon(4S)$. CLEO does a similar analysis as was done for the D^+ above. Babar and Belle do a similar MM^2 calculation by using the reconstructed hadrons, the photon from the D_s^{*+} decay and a detected μ^+. To get the normalization they do a MM^2 fit without the μ^+ and use the signal at the D_s^+ mass squared to determine the total D_s^+ yield.

When selecting the $\tau^+ \to \pi^+\bar{\nu}$ and $\tau^+ \to \rho^+\bar{\nu}$ decay modes, CLEO uses both the calculation of the missing mass and the fact that there should be no extra energy in the event beyond that deposited by the measured tagged D_s^- and the τ^+ decay products. The $\tau^+ \to e^+\nu\bar{\nu}$ mode, however, uses only extra energy. Babar and Belle also use the extra energy to discriminate signal from background in their $\tau^+\nu$ measurements.

We extract the decay constant times the CKM factor from the measured branching ratios using the D_s^+ mass of 1.96830(11) GeV, the τ^+ mass of 1.77682(16) GeV, and a D_s^+ lifetime of 0.500(7) ps [3]. CLEO has included the radiative correction of 1% in the $\mu^+\nu$ rate listed in the Table [8] (the $\tau^+\nu$ rates need not be corrected). Other theoretical calculations show that the $\gamma\mu^+\nu$ rate is a factor of 40–100 below the $\mu^+\nu$ rate for charm [57–66]. As this is a small effect we do not attempt to correct the other measurements. The values for $f_{D_s^+}|V_{cs}|$ are in good agreement for the two decay modes. Our average value including both the $\mu^+\nu$ and $\tau^+\nu$ final states is 250.9 ± 4.0 MeV.

84.3.2. *Theoretical decay-constant calculations* :

Table 84.4 presents recent theoretical calculations of the charged D^+- and D_s-meson decay constants and their ratio. The upper two panels show results from lattice-QCD simulations with three ($N_f = 2+1$) or four flavors ($N_f = 2+1+1$) of dynamical quarks. Although there are fewer available results than for the pion and kaon sector, both f_{D^+} and f_{D_s} have been obtained using multiple sets of gauge-field configurations with different lattice fermion actions, providing independent confirmation. For comparison, the bottom panel of Table 84.4 shows non-lattice determinations from QCD sum rules and the light-front quark model; only results which include uncertainty estimates are shown. The lattice and non-lattice results agree, but the uncertainties on $D_{(s)}^+$-meson decay constants from lattice QCD have now reached significantly greater precision than those from other approaches.

The lattice-QCD results in Table 84.4 were all obtained using isospin-symmetric gauge-field configurations. The two calculations by the Fermilab Lattice and MILC Collaborations [69,32], however, include the dominant strong isospin-breaking contribution by evaluating the mass of the valence light quark in the D^+-meson decay constant at the physical down-quark mass. Reference 32 provides a determination of the size of this correction,

$$f_{D^+} - f_D = 0.47(1)(^{+25}_{-6})\ \text{MeV}\,, \tag{84.17}$$

where f_D is the value of the D-meson decay constant evaluated at the average up-down quark mass. Eq. (84.17) implies that the correction to the $\text{SU}(3)_f$-breaking ratio is

$$\frac{f_{D_s}}{f_{D^+}} - \frac{f_{D_s}}{f_D} = -0.0026\,, \tag{84.18}$$

taking the central values for f_{D^+} and f_{D_s} from the same work. Because the errors on the calculations listed in Table 84.4 that neglect isospin breaking are still about 5–8 × larger than the sizes of the shifts in Eqs. (84.17)–(84.18), we do not correct any results *a posteriori* for this effect in the current review. Nevertheless, we strongly encourage future lattice-QCD publications to present results for both the D^+- and D^0-meson decay constants. Including the effect of isospin breaking will be essential once lattice-QCD calculations of f_D and f_{D_s}/f_D reach the level of precision in Eqs. (84.17)–(84.18).

We average the lattice-QCD results in Table 84.4 accounting for possible correlations between them following the approach established by Laiho *et al.* [77]. Whenever we have reason to believe that a source of uncertainty is correlated between two results, we conservatively take the correlation to be 100% when calculating the average. We then construct the correlation matrix for the set of lattice-QCD results using the prescription of Schmelling [78].

We first separately average the three- and four-flavor results for the charged $D_{(s)}^+$-meson decay constants and their ratio. There have been no new three-flavor lattice-QCD calculations of f_{D^+} or $f_{D_s^+}/f_{D^+}$ since 2013, so we take the (2+1)-flavor averages from FLAG [14]. In this average, the statistical errors were treated as 100% correlated between the results of Fermilab/MILC [69] and HPQCD [68] because the calculations employed some of the same ensembles of gauge-field configurations. For f_{D_s}, we average the (2+1)-flavor results given in Table 84.4, again treating the Fermilab/MILC [69] and HPQCD [70] statistical errors as correlated, and taking the χQCD result [67] to be independent. For the (2+1+1)-flavor $D_{(s)}$-meson decay constants, we take a simple weighted average of the ETM [31] and Fermilab/MILC 14 results [32] in Table 84.4. We expect them to be independent because the calculations use different light-quark and gluon actions and different treatments of the chiral-continuum extrapolation. Our separate three- and four-flavor averages are listed in the lines labeled "Average" in Table 84.4, where the errors on the (2+1)-flavor f_{D_s} and (2+1+1)-flavor f_D averages have been rescaled by the factors $\sqrt{(\chi^2/\text{dof})} = 1.1$ and $\sqrt{(\chi^2/\text{dof})} = 1.3$, respectively.[5]

To obtain the single-best values of the $D_{(s)}^+$-meson decay constants for phenomenology applications, we combine the available (2 + 1)- and (2 + 1 + 1)-flavor lattice-QCD results, which are compatible within the current level of precision. We account for the omission of charm sea-quark contributions in the three-flavor calculations by adding to the errors on the (2+1)-flavor averages in Table 84.4 our power-counting estimates of charm sea-quark errors from Sec. 84.2.2. Because the estimated charm sea-quark errors of 0.7% for decay constants and 0.2% for decay-constant ratios are less than those on the (2+1)-flavor averages, adding them in quadrature has a small impact on the total uncertainties. The error increase is at most about 25% for f_{D_s}, and below 10% for both f_{D^+} and f_{D_s}/f_{D^+}. Our final preferred theoretical values for the charged $D_{(s)}^+$-meson decay constants are given by the weighted average of the entries in the two lines labeled "Average" in Table 84.4, after including the additional charm sea-quark errors in the (2+1)-flavor entries:

$$\begin{aligned} \text{Our averages}: \quad f_{D^+} &= 211.9(1.1)\ \text{MeV}\,, \\ f_{D_s} &= 249.0(1.2)\ \text{MeV}\,, \\ \frac{f_{D_s}}{f_{D^+}} &= 1.173(3)\,. \end{aligned} \tag{84.19}$$

In practice, the errors on the (2+1+1)-flavor averages are so much smaller than on the (2+1)-flavor averages that the combination in Eq. (84.19) is almost identical to the (2+1+1)-flavor average in Table 84.4. The most precise result from Fermilab/MILC, in particular, has a large weight in the average.

84.4. Bottom Mesons

84.4.1. *Experimental rate measurements* :

The Belle and BaBar collaborations have found evidence for $B^- \to \tau^-\overline{\nu}$ decay in $e^+e^- \to B^-B^+$ collisions at the $\Upsilon(4S)$ energy. The analysis relies on reconstructing a hadronic or semi-leptonic B decay tag, finding a τ candidate in the remaining track and photon candidates, and examining the extra energy in the event which should be close to zero for a real τ^- decay to $e^-\nu\bar{\nu}$ or $\mu^-\nu\bar{\nu}$ opposite a B^+ tag. While the BaBar results have remained unchanged, Belle reanalyzed both samples of their data. The branching fraction using hadronic tags changed from $1.79^{+0.56\,+0.46}_{-0.49\,-0.51} \times 10^{-4}$ [80] to $0.72^{+0.27}_{-0.25} \pm 0.11 \times 10^{-4}$ [81], while the corresponding change using semileptonic tags was from $1.54^{+0.38+0.29}_{-0.37-0.31}$ to $1.25 \pm 0.28 \pm 0.27$. These changes demonstrate the difficulty of the analysis. The results are listed in Table 84.5.

There are large backgrounds under the signals in all cases. The systematic errors are also quite large. Thus, the significances are not that large. Belle quotes 4.6σ for their combined hadronic and semileptonic tags, while BaBar quotes 3.3σ and 2.3 σ, for hadronic and semileptonic tags. Greater precision is necessary to determine if any effects beyond the Standard Model are present.

To extract the value of $|V_{ub}|f_{B^+}$ we use the PDG 2014 value of the B^+ lifetime of 1.638 ± 0.004 ps, and the τ^+ and B^+ masses of 1.77684 and 5.27926 GeV, respectively.

[5] After this article was submitted for review, preliminary (2+1)- and (2+1+1)-flavor FLAG averages for f_D, f_{D_s}, and f_{D_s}/f_D were presented in Ref. 79 that are identical to our separate averages in Table 84.4.

Table 84.4: Recent theoretical determinations of f_{D^+}, f_{D_s}, and their ratio. The upper panels show results from lattice-QCD simulations with (2+1+1) and (2+1) dynamical quark flavors, respectively. Statistical and systematic errors are quoted separately. Lattice-QCD results for f_D and f_{D_s}/f_D in the isospin-symmetric limit $m_u = m_d$ are noted with an "*". The bottom panel shows estimates from QCD sum rules (QCD SR) and the light-front quark model (LFQM). These are not used to obtain our preferred decay-constant values.

Reference	Method	N_f	f_{D^+}(MeV)	f_{D_s}(MeV)	f_{D_s}/f_{D^+}
ETM 14 [31] *	LQCD	2+1+1	207.4(3.7)(0.9)	247.2(3.9)(1.4)	1.192(19)(11)
Fermilab/MILC 14 [32]	LQCD	2+1+1	212.6(0.4)$(^{+1.0}_{-1.2})$	249.0(0.3)$(^{+1.1}_{-1.5})$	1.1712(10)$(^{+29}_{-32})$
Average	LQCD	2+1+1	212.2(1.5)	248.8(1.3)	1.172(3)
χQCD 14 [67] *	LQCD	2+1	–	254(2)(4)	–
HPQCD 12 [68] *	LQCD	2+1	208.3(1.0)(3.3)	–	1.187(4)(12)
Fermilab/MILC 11 [69]	LQCD	2+1	218.9(9.2)(6.6)	260.1(8.9)(6.1)	1.188(14)(21)
HPQCD 10 [70] *	LQCD	2+1	–	248.0(1.4)(2.1)	–
Average	LQCD	2+1	209.2(3.3)	249.8(2.3)	1.187(12)
Our average	LQCD	Both	211.9(1.1)	249.0(1.2)	1.173(3)
Wang 15 [71] §	QCD SR		208(10)	240(10)	1.15(6)
Gelhausen 13 [72]	QCD SR		201$\binom{+12}{-13}$	238$\binom{+13}{-23}$	1.15$\binom{+0.04}{-0.05}$
Narison 12 [73]	QCD SR		204(6)	246(6)	1.21(4)
Lucha 11 [74]	QCD SR		206.2(8.9)	245.3(16.3)	1.193(26)
Hwang 09 [75]	LFQM		–	264.5(17.5)¶	1.29(7)

§ Obtained using $m_c^{\overline{\rm MS}}$; results using $m_c^{\rm pole}$ are also given in the paper.

¶ Obtained by combining PDG value $f_D = 205.8(8.9)$ MeV [76] with f_{D_s}/f_D from this work.

Table 84.5: Experimental results for $\mathcal{B}(B^- \to \tau^- \overline{\nu})$ and $|V_{ub}|f_{B^+}$.

Experiment	Tag	$\mathcal{B}$ (units of 10^{-4})	$\lvert V_{ub}\rvert f_{B^+}$ (MeV)
Belle [81]	Hadronic	$0.72^{+0.27}_{-0.25} \pm 0.11$	
Belle [82]	Semileptonic	$1.25 \pm 0.28 \pm 0.27$	
Belle [82]	Average	0.91 ± 0.22	0.72 ± 0.09
BaBar [83]	Hadronic	$1.83^{+0.53}_{-0.49} \pm 0.24$	
BaBar [84]	Semileptonic	$1.7 \pm 0.8 \pm 0.2$	
BaBar [83]	Average	1.79 ± 0.48	1.01 ± 0.14
Our average		1.06 ± 0.20	0.77 ± 0.07

84.4.2. *Theoretical decay-constant calculations* :

Table 84.6 and Table 84.7 present theoretical calculations of the B^+-, B^0-, and B_s-meson decay constants and their ratios. (The decay constants of the neutral B^0 and B_s mesons enter the rates for the rare leptonic decays $B_{d,s} \to \mu^+\mu^-$.) The upper two panels show results from lattice-QCD simulations with three ($N_f = 2+1$) or four flavors ($N_f = 2+1+1$) of dynamical quarks. For all decay constants, calculations using different gauge-field configurations, light-quark actions, and b-quark actions provide independent confirmation. For comparison, the bottom panel of Table 84.6 shows non-lattice determinations of the $B_{(s)}$-meson decay constants which include error estimates. These are consistent with the lattice values, but with much larger uncertainties.

HPQCD and RBC/UKQCD also calculate f_{B^0} by fixing the valence light-quark mass equal to the physical down-quark mass [86,88]; they find differences between the B^+- and B^0-meson decay constants of $f_{B^0} - f_{B^+} \approx 4$ MeV and $f_{B_s}/f_{B^+} - f_{B_s}/f_{B^0} \approx 0.025$. Inspection of Table 84.6 and Table 84.7 shows that these differences are comparable to the error on the HPQCD 12 result for f_B [89], and to the errors on the Fermilab/MILC, HPQCD 12, and ETM results for f_{B_s}/f_B [69,89,85], none of which account for isospin breaking. Therefore, to enable comparison with experimental measurements, in this review we correct those lattice-QCD results for B-meson decay constants obtained with degenerate up and down valence quarks *a posteriori* for isospin breaking before computing our averages. For the correction factors, we use the differences obtained empirically by HPQCD in Ref. 86 [6]

$$f_{B^+} - f_B = -1.9(5)\ \text{MeV}\,, \tag{84.20}$$

$$\frac{f_{B_s}}{f_{B^+}} - \frac{f_{B_s}}{f_B} = 0.012(4)\,, \tag{84.21}$$

$$f_{B^0} - f_B = 1.7(5)\ \text{MeV}\,, \tag{84.22}$$

$$\frac{f_{B_s}}{f_{B^0}} - \frac{f_{B_s}}{f_B} = -0.011(4)\,. \tag{84.23}$$

The isospin-breaking correction factors in Eqs. (84.20)–(84.23) are well determined because of cancellations between correlated errors in the differences.

We first average the published (2+1)-flavor lattice-QCD results for the charged and neutral $B_{(s)}$-meson decay constants and their ratios in Table 84.6 and Table 84.7, accounting for possibly correlated uncertainties. We treat the statistical errors as correlated between the calculations of Aoki *et al.* and RBC/UKQCD because they employ the same gauge-field configurations [7] [87,88]. We also treat the statistical

[6] The correlated uncertainties were provided by HPQCD via private communication.

[7] There may be mild correlations between some sub-dominant systematic errors of Aoki *et al.* and RBC/UKQCD, who use the same determinations of the absolute lattice scale and the physical light- and strange-quark masses from Ref. 93, and who use the same power-counting estimates for the light-quark and gluon discretization errors. The effects of any correlations between these systematics, however, would be too small to impact the numerical values of the averages.

Table 84.6: Recent theoretical determinations of f_{B^+}, f_{B_s}, and their ratio. The upper panels show results from lattice-QCD simulations with $(2+1+1)$ and $(2+1)$ dynamical quark flavors, respectively. For some of the lattice-QCD results, statistical and systematic errors are quoted separately. Lattice-QCD results for f_B and f_{B_s}/f_B in the isospin-symmetric limit $m_u = m_d$ are noted with an "*"; they are corrected by the factors in Eq. (84.20) and Eq. (84.21), respectively, before computing the averages. Preliminary conference results noted with a "†" are not included in the averages. The bottom panel shows estimates from QCD sum rules and the light-front quark model, which are not used to obtain our preferred decay-constant values.

Reference	Method	N_f	f_{B^+}(MeV)	f_{B_s}(MeV)	f_{B_s}/f_{B^+}
ETM 13 [85] *,†	LQCD	2+1+1	196(9)	235(9)	1.201(25)
HPQCD 13 [86]	LQCD	2+1+1	184(4)	224(5)	1.217(8)
Average	LQCD	2+1+1	184(4)	224(5)	1.217(8)
Aoki 14 [87] *,‡	LQCD	2+1	218.8(6.5)(30.8)	263.5(4.8)(36.7)	1.193(20)(44)
RBC/UKQCD 14 [88]	LQCD	2+1	195.6(6.4)(13.3)	235.4(5.2)(11.1)	1.223(14)(70)
HPQCD 12 [89] *	LQCD	2+1	191(1)(8)	228(3)(10)	1.188(12)(13)
HPQCD 12 [89] *	LQCD	2+1	189(3)(3)*	–	–
HPQCD 11 [90]	LQCD	2+1	–	225(3)(3)	–
Fermilab/MILC 11 [69]	LQCD	2+1	196.9(5.5)(7.0)	242.0(5.1)(8.0)	1.229(13)(23)
Average	LQCD	2+1	189.9(4.2)	228.6(3.8)	1.210(15)
Our average	LQCD	Both	187.1(4.2)	227.2(3.4)	1.215(7)
Wang 15 [71] §	QCD SR		194(15)	231(16)	1.19(10)
Baker 13 [91]	QCD SR		186(14)	222 (12)	1.19(4)
Lucha 13 [92]	QCD SR		192.0(14.6)	228.0(19.8)	1.184(24)
Gelhausen 13 [72]	QCD SR		$207\binom{+17}{-9}$	$242\binom{+17}{-12}$	$1.17\binom{+3}{-4}$
Narison 12 [73]	QCD SR		206(7)	234(5)	1.14(3)
Hwang 09 [75]	LFQM		–	270.0(42.8)¶	1.32(8)

† Lattice 2013 conference proceedings.

‡ Obtained with static b quarks (*i.e.* $m_b \to \infty$).

* Obtained by combining f_{B_s} from HPQCD 11 with f_{B_s}/f_B from this work. Approximate statistical (systematic) error obtained from quadrature sum of individual statistical (systematic) errors.

§ Obtained using $m_b^{\overline{\rm MS}}$; results using $m_b^{\rm pole}$ are also given in the paper.

¶ Obtained by combining PDG value $f_B = 204(31)$ MeV [76] with f_{B_s}/f_B from this work.

errors as correlated between the HPQCD and Fermilab/MILC calculations because they analyze an overlapping set of gauge-field configurations [69,89,90]. For f_{B_s}, we include HPQCD's results from both 2011 [90] and 2012 [89], which were obtained using different b-quark actions, but on some of the same gauge-field configurations. HPQCD 11 and 12 also use the same determination of the absolute lattice scale, which is the second-largest source of systematic uncertainty in both calculations. We therefore treat the statistical and scale errors as correlated between HPQCD's (2+1)-flavor f_{B_s} results. HPQCD also presents two results for f_B in Ref. 89. The more precise value is obtained by combining the ratio f_{B_s}/f_B from this work with f_{B_s} from Ref. 90, but an associated error budget is not provided. Because this would be needed to estimate correlations between the two f_B determinations, we include only HPQCD's more precise (2+1)-flavor result for f_B in our average. Our separate three- and four-flavor averages for the B^+-, B^0-, and B_s-meson decay constants and ratios are listed in the lines labeled "Average" in Table 84.6 and Table 84.7, where the error on the (2+1)-flavor f_{B_s} average has been rescaled by the factor $\sqrt{(\chi^2/\mathrm{dof})} = 1.2$ to account for the tension among results. Our (2+1+1)-flavor "averages" are identical to the "HPQCD 13" entries in Table 84.6 and Table 84.7, whcih are the only published four-flavor results available.

To obtain the single-best values of the $B_{(s)}$-meson decay constants for phenomenology applications, we combine the available $(2+1)$- and $(2+1+1)$-flavor lattice-QCD results, which are compatible within the current level of precision. Because the four-flavor "average" is obtained from only a single result, we do not simply combine the two lines labeled "Average" in Table 84.6 and Table 84.7, which would weight the four-flavor result too heavily. Instead, we form a single average including the published (2+1)-flavor results and the (2+1+1)-flavor result from HPQCD 13. We account for the omission of charm sea-quark contributions in the three-flavor calculations by adding to the errors on the (2+1)-flavor averages in Table 84.6 and Table 84.7 our power-counting estimates of charm sea-quark errors from Sec. 84.2.2, taking charm sea-quark error to be 100% correlated between the three-flavor results. Because the estimated charm sea-quark errors of 0.7% for decay constants and 0.2% for decay-constant ratios are much less than those on the (2+1)-flavor averages, adding them in quadrature has a tiny impact on the total uncertainties. The largest observed change is an 0.3 MeV increase on the error f_{B_s} from HPQCD 11, and most are negligible. In the combined three- and four-flavor average we also consider correlations between the results of HPQCD 12 and HPQCD 13 because, although they employ different gauge-field configurations, they both use NRQCD for the b-quark action and the bottom-light axial-vector current.[8] We take both the operator-matching and relativistic errors, which are the dominant

[8] HPQCD 13 uses a 1-loop radiatively improved b-quark action, whereas HPQCD 12 uses tree-level action coefficients. Both include

uncertainties in the decay constants, to be correlated between the two calculations.

Table 84.7: Recent lattice-QCD determinations of f_{B^0} and f_{B_s}/f_{B^0}. Results obtained in the isospin-symmetric limit $m_u = m_d$ are noted with an "*", while those for the B^+-meson are noted with an "§". Although the quoted results are identical to those in Table 84.6, they are corrected by different factors in Eq. (84.20)–Eq. (84.23) before computing the averages. Other labels and descriptions are the same as in Table 84.6.

Reference	Method	N_f	f_{B^0}(MeV)	f_{B_s}/f_{B^0}
ETM 13 [85] *,†	LQCD	2+1+1	196(9)	1.201(25)
HPQCD 13 [86]	LQCD	2+1+1	188(4)	1.194(7)
Average	LQCD	2+1+1	188(4)	1.194(7)
Aoki 14 [87] *,‡	LQCD	2+1	218.8(6.5)(30.8)	1.193(20)(44)
RBC/UKQCD 14 [88]	LQCD	2+1	199.5(6.2)(12.6)	1.197(13)(49)
HPQCD 12 [89] *	LQCD	2+1	191(1)(8)	1.188(12)(13)
HPQCD 12 [89] *	LQCD	2+1	189(3)(3)*	–
Fermilab/MILC 11§ [69]	LQCD	2+1	196.9(5.5)(7.0)	1.229(13)(23)
Average	LQCD	2+1	193.6(4.2)	1.187(15)
Our average	LQCD	Both	190.9(4.1)	1.192(6)

† Lattice 2013 conference proceedings.

‡ Obtained with static b quarks (*i.e.*, $m_b \to \infty$).

* Obtained by combining f_{B_s} from HPQCD 11 with f_{B_s}/f_B from this work. Approximate statistical (systematic) error obtained from quadrature sum of individual statistical (systematic) errors.

Our final preferred theoretical values for the charged B^+ and neutral $B^0_{(s)}$-meson decay constants and their ratio are

$$\text{Our averages}: \quad f_{B^+} = 187.1(4.2)\ \text{MeV}\,,$$

$$f_{B_s} = 227.2(3.4)\ \text{MeV}\,, \quad \frac{f_{B_s}}{f_{B^+}} = 1.215(7)\,, \tag{84.24}$$

$$f_{B^0} = 190.9(4.1)\ \text{MeV}\,, \quad \frac{f_{B_s}}{f_{B^0}} = 1.192(6)\,. \tag{84.25}$$

The errors on f_B^+, f_B^0, and f_{B_s} after combining the three- and four-flavor results are only slightly smaller than those of the separate averages due to the correlations assumed.

84.5. Phenomenological Implications

84.5.1. $|V_{ud}|$, $|V_{us}|$, and status of first-row unitarity :

Using the average values for $f_{\pi^+}|V_{ud}|$, $f_{K^+}|V_{us}|$, and their ratio from Eq. (84.10)–Eq. (84.12) and for f_{π^+}, f_{K^+}, and their ratio from Eq. (84.16), we obtain the following determinations of the CKM matrix elements $|V_{ud}|$, $|V_{us}|$, and their ratio from leptonic decays within the standard model:

$$|V_{ud}| = 0.9764(2)(127)(10)\,, \quad |V_{us}| = 0.2255(3)(6)(3),$$

$$\frac{|V_{us}|}{|V_{ud}|} = 0.2314(2)(5)(2)\,, \tag{84.26}$$

where the errors are from the experimental branching fraction(s), the pseudoscalar decay constant(s), and radiative corrections, respectively. These results enable a precise test of the unitarity of the first row of the CKM matrix from leptonic decays alone (the contribution from $|V_{ub}|$ is negligible). Using the values of $|V_{ud}|$ and $|V_{us}|$ from Eq. (84.26), we find

$$|V_{ud}|^2 + |V_{us}|^2 + |V_{ub}|^2 - 1 = 0.004(25)\,, \tag{84.27}$$

which is consistent with three-generation unitarity at the sub-percent level.

The determinations of $|V_{ud}|$ and $|V_{us}|$ from leptonic decays in Eq. (84.26) can be compared to those obtained from other processes. The result above for $|V_{ud}|$ agrees with the determination from superallowed β-decay, $|V_{ud}| = 0.97417(21)$ [94], but has an error more than fifty times larger that is primarily due to the uncertainty in the theoretical determination of f_{π^+}. The CKM element $|V_{us}|$ can be determined from semileptonic $K^+ \to \pi^0 \ell^+ \nu$ decay. Here experimental measurements provide a value for the product $f_+^{K\pi}(0)|V_{us}|$, where $f_+^{K\pi}(0)$ is the form-factor at zero four-momentum transfer between the initial state kaon and the final state pion. Taking the most recent experimental determination of $|V_{us}|f_+^{K\pi}(0) = 0.2165(4)$ from Moulson [26] [9] and the preliminary 2015 (2+1+1)-flavor FLAG average for $f_+(0)^{K\pi} = 0.9704(24)(22)$ [12,13] [10] gives $|V_{us}| = 0.22310(74)_{\text{thy}}(41)_{\text{exp}}$ from $K_{\ell 3}$ decay. The determinations of $|V_{us}|$ from leptonic and semileptonic kaon decays are both quite precise (with the error from leptonic decay being about 20% smaller), but the central values differ by 2.2σ. Finally, the combination of the ratio $|V_{us}|/|V_{ud}|$ from leptonic decays [Eq. (84.26)] with $|V_{ud}|$ from β decay implies an alternative determination of $|V_{us}| = 0.2254(6)$ which agrees with the value from leptonic kaon decay, but disagrees with the $K_{\ell 3}$-decay result at the 2.2σ level. Collectively, these results indicate that that there is some tension between theoretical calculations and/or measurements of leptonic pion and kaon decays, semileptonic kaon decays, and superallowed β-decay. Although this may be due to the presence of new physics, it is also important to revisit the quoted uncertainties on both the theoretical and experimental inputs.

Finally, we combine the experimental measurements of $f_{\pi^+}|V_{ud}|$, $f_{K^+}|V_{us}|$ from leptonic pseudoscalar-meson decays in Eq. (84.10) and Eq. (84.11) with determinations of the CKM elements from other decays or unitarity to infer "experimental" values for the decay constants. Assuming that there are no significant new-physics contributions to any of the input processes, the comparison of these results with theoretical calculations of the decay constants enables a test of lattice-QCD methods. Taking $|V_{ud}|$ from superallowed β-decay [100] leads to

$$f_{\pi^-}^{\text{"exp"}} = 130.50(1)(3)(13)\ \text{MeV}\,, \tag{84.28}$$

where the uncertainties are from the errors on Γ, $|V_{ud}|$, and higher-order corrections, respectively. This agrees with the theoretical value $f_{\pi^+} = 130.2(1.7)$ MeV in Eq. (84.16) obtained from an average of recent (2+1)-flavor lattice-QCD results [39,37,35]. We take the value $|V_{us}| = 0.22534(65)$ from the most recent global unitarity-triangle fit of the UTfit Collaboration [101] because there is tension between the values of $|V_{us}|$ obtained from leptonic and semileptonic kaon decays. This implies

$$f_{K^-}^{\text{"exp"}} = 155.72(17)(45)(16)\ \text{MeV} \tag{84.29}$$

where the uncertainties are from the errors on Γ, $|V_{us}|$, and higher-order corrections, respectively. This agrees with the theoretical value $f_{K^+} = 155.6(0.4)$ MeV in Eq. (84.16) obtained from an average of recent three and four-flavor lattice-QCD results [31–33,35,37,39].

84.5.2. $|V_{cd}|$, $|V_{cs}|$, and status of second-row unitarity :

Using the average values for $|V_{cd}|f_{D^+}$ and $|V_{cs}|f_{D_s^+}$ from Table 84.2 and Table 84.3, and for f_{D^+} and $f_{D_s^+}$ from Eq. (84.19), we obtain the following determinations of the CKM matrix elements $|V_{cd}|$ and $|V_{cs}|$, and from leptonic decays within the standard model:

$$|V_{cd}| = 0.217(5)(1) \quad \text{and} \quad |V_{cs}| = 1.007(16)(5)\,, \tag{84.30}$$

the same contributions to the currents at one loop, but renormalization details differ.

[9] This is an update of the 2010 Flavianet review [28] that includes new measurements of the K_s lifetime [95,96], $\text{Re}(\epsilon'/\epsilon)$ [96], and $\mathcal{B}(K^\pm \to \pi^\pm\pi^+\pi^-)$ [27]. The latter measurement is the primary source of the reduced error on $\mathcal{B}(K_{\ell 3})$, via the constraint that the sum of all branching ratios must equal unity.

[10] This result comes from the calculation of FNAL/MILC in Ref. 97. For comparison, the 2015 preliminary (2+1)-flavor FLAG average based on the calculations of FNAL/MILC [98] and RBC/UKQCD [99] is $f_+(0)^{K\pi} = 0.9677(37)$.

where the errors are from experiment and theory, respectively, and are currently limited by the measured uncertainties on the decay rates. The central value of $|V_{cs}|$ is greater than one, but is compatible with unity within the error. The above results for $|V_{cd}|$ and $|V_{cs}|$ do not include higher-order electroweak and hadronic corrections to the rate, in analogy to Eq. (84.3). These corrections have not been computed for $D^+_{(s)}$-meson leptonic decays, but are estimated to be about to be about 1–2% for charged pion and kaon decays (see Sec. 84.2.1). Now that the uncertainties on $|V_{cd}|$ and $|V_{cs}|$ from leptonic decays are at this level, we hope that the needed theoretical calculations will be undertaken.

The CKM elements $|V_{cd}|$ and $|V_{cs}|$ can also be obtained from semileptonic $D^+ \to \pi^0 \ell^+ \nu$ and $D_s^+ \to K^0 \ell^+ \nu$ decays, respectively. Here experimental measurements determine the product of the form factor times the CKM element, and theory provides the value for the form factor at zero four-momentum transfer between the initial $D_{(s)}$ meson and the final pion or kaon. We combine the latest experimental averages for $f_+^{D\pi}(0)|V_{cd}| = 0.1425(19)$ and $f_+^{D_sK}(0)|V_{cs}| = 0.728(5)$ from the Heavy Flavor Averaging Group (HFAG) [102] with the zero-momentum-transfer form factors $f_+^{D\pi}(0) = 0.666(29)$ and $f_+^{D_sK}(0) = 0.747(19)$ calculated in (2+1)-flavor lattice QCD by the HPQCD Collaboration [103,104] to obtain $|V_{cd}| = 0.2140(97)$ and $|V_{cs}| = 0.9746(257)$ from semileptonic $D_{(s)}$-meson decays. The values of $|V_{cd}|$ from leptonic and semileptonic decays agree, while those for $|V_{cs}|$ are compatible at the 1.1σ level. The determinations of $|V_{cd}|$ and $|V_{cs}|$ from leptonic decays in Eq. (84.30), however, are 2.0× and 1.6× more precise than those from semileptonic decays, respectively.

The results for $|V_{cd}|$ and $|V_{cs}|$ from Eq. (84.30) enable a test of the unitarity of the second row of the CKM matrix. We obtain

$$|V_{cd}|^2 + |V_{cs}|^2 + |V_{cb}|^2 - 1 = 0.064(36)\,, \tag{84.31}$$

which is in slight tension with three-generation unitarity at the 2σ level. Because the contribution to Eq. (84.31) from $|V_{cb}|$ is so small, we obtain the same result taking $|V_{cb}|^{\rm incl.} \times 10^3 = 42.21(78)$ from inclusive $B \to X_c \ell\nu$ decay [105] or $|V_{cb}|^{\rm excl.} \times 10^3 = 39.04(75)$ from exclusive $B \to D^* \ell\nu$ decay at zero recoil [106].

We can also combine the experimental measurements of $f_{D^+}|V_{cd}| = 45.91(1.05)$ MeV and $f_{D_s^+}|V_{cs}| = 250.9(4.0)$ MeV from leptonic pseudoscalar-meson decays from Table 84.2 and Table 84.3 with determinations of $|V_{cd}|$ and $|V_{cs}|$ from CKM unitarity to infer "experimental" values for the decay constants within the standard model. For this purpose, we obtain the values of $|V_{cd}|$ and $|V_{cs}|$ by relating them to other CKM elements using the Wolfenstein parameterization [107]. We take $|V_{cd}|$ to equal the value of $|V_{us}|$ minus the leading correction [108]:

$$|V_{cd}| = |V_{us}| \left| -1 + \frac{|V_{cb}|^2}{2}(1 - 2(\rho + i\eta)) \right| \tag{84.32}$$

$$= |V_{us}| \left(\left[-1 + (1 - 2\rho)\frac{|V_{cb}|^2}{2} \right]^2 + \eta^2 |V_{cb}|^4 \right)^{1/2}. \tag{84.33}$$

Using $|V_{us}| = 0.2255(3)(6)(3)$ from leptonic kaon decay, Eq. (84.26), inclusive $|V_{cb}|$ as above, and $(\rho, \eta) = (0.136(24), 0.361(14))$ from CKM unitarity [101] $|V_{cd}| = 0.2254(7)$. We take $|V_{cs}| = |V_{ud}| - |V_{cb}|^2/2$ [108], using $|V_{ud}| = 0.97417(21)$ from β decay [94], giving $|V_{cs}| = 0.9733(2)$. Given these choices, we find

$$f_{D^+}^{\text{"exp"}} = 203.7(4.7)(0.6)\ \text{MeV} \quad \text{and}$$
$$f_{D_s^+}^{\text{"exp"}} = 257.8(4.1)(0.1)\ \text{MeV}\,, \tag{84.34}$$

where the uncertainties are from the errors on Γ and $|V_{us}|$ (or $|V_{ud}|$), respectively. These disagree with the theoretical values $f_{D^+} = 211.9(1.1)$ MeV and $f_{D_s^+} = 249.0(1.2)$ MeV in Eq. (84.19) obtained from averaging recently published three and four-flavor lattice-QCD results at the 1.7σ and 2.0σ levels, respectively. The significances of the tensions are sensitive, however, to the choices made for $|V_{us}|$ and $|V_{ud}|$. Thus resolving the inconsistencies between determinations of elements of the first row of the CKM matrix discussed previously in Sec. 84.5.1 may also reduce the mild tensions observed here.

84.5.3. $|V_{ub}|$ *and other applications* :

Using the average value for $|V_{ub}|f_{B^+}$ from Table 84.5, and for f_{B^+} from Eq. (84.24), we obtain the following determination of the CKM matrix element $|V_{ub}|$ from leptonic decays within the standard model:

$$|V_{ub}| = 4.12(37)(9) \times 10^{-3}\,, \tag{84.35}$$

where the errors are from experiment and theory, respectively. We note, however, that decays involving the third generation of quarks and leptons may be particularly sensitive to new physics associated with electroweak symmetry breaking due to their larger masses [4,6], so Eq. (84.35) is more likely to be influenced by new physics than the determinations of the elements of the first and second rows of the CKM matrix in the previous sections.

The CKM element $|V_{ub}|$ can also be obtained from semileptonic B-meson decays. Over the past several years there has remained a persistent 2-3σ tension between the determinations of $|V_{ub}|$ from exclusive $B \to \pi\ell\nu$ decay and from inclusive $B \to X_u\ell\nu$ decay, where X_u denotes all hadrons which contain a constituent up quark [3,102,109–111]. The currently most precise determination of $|V_{ub}|^{\rm excl} = 3.72(16) \times 10^{-3}$ is obtained from a joint z-fit of the vector and scalar form factors $f_+^{B\pi}(q^2)$ and $f_0^{B\pi}(q^2)$ calculated in (2+1)-flavor lattice QCD by the FNAL/MILC Collaboration [112] and experimental measurements of the differential decay rate from BaBar [113,114] and Belle [115,116]. On the other hand, the most recent PDG average of inclusive determinations obtained using the theoretical frameworks in Refs. 117–119 is $|V_{ub}|^{\rm incl} = 4.49(16)\left(^{+16}_{-18}\right) \times 10^{-3}$ [120]. The result for $|V_{ub}|$ from leptonic $B \to \tau\nu$ decay in Eq. (84.35) is compatible with determinations from both exclusive and inclusive semileptonic B-meson decays.

The CKM element $|V_{ub}|$ can now also be obtained from semileptonic Λ_b decays. Specifically, the recent LHCb measurement of the ratio of decay rates for $\Lambda_b \to p\ell\nu$ over $\Lambda_b \to \Lambda_c\ell\nu$ [121], when combined with the ratio of form factors from (2+1)-flavor lattice QCD [122], enables the first determination of the ratio of CKM elements $|V_{ub}|/|V_{cb}| = 0.083(4)(4)$ from baryonic decay. Taking $|V_{cb}|^{\rm incl} = 42.21(78) \times 10^{-3}$ [105] for the denominator,[11] we obtain $|V_{ub}| = 3.50(17)(17)(6) \times 10^{-3}$ from exclusive Λ_b semileptonic decays, where the errors are from experiment, the form factors, and $|V_{cb}|$, respectively. The result for $|V_{ub}|$ from leptonic $B \to \tau\nu$ decay in Eq. (84.35) is 1.4σ higher than the determination from b-baryon decays.

Given these results, the "V_{ub}" puzzle still stands, and the determination from leptonic B^+-meson decay is not yet sufficiently precise to weigh in on the discrepancy. New and improved experimental measurements and theoretical calculations of other $b \to u$ flavor-changing processes, however, are providing additional information and sharpening the picture of the various tensions. Further, the error on $|V_{ub}|$ from $B \to \tau\nu$ decay will shrink once improved rate measurements from the Belle II experiment are available.

Finally, we can combine the experimental measurement of $|V_{ub}|f_{B^+}$ from leptonic B^+-meson decays in Table 84.5 with a determination of the CKM element $|V_{ub}|$ from elsewhere to infer an "experimental" values for f_{B^+} within the standard model. This, of course, assumes that there are no significant new-physics contributions to $B^+ \to \tau\nu$, which may turn out not to be the case. Further, one does not know *a priori* what value to take for $|V_{ub}|$ given the inconsistencies between the various determinations discussed above. We therefore take the PDG weighted average of the determinations from inclusive and exclusive semileptonic B-meson decays $|V_{ub}|^{\rm excl+incl} = 4.09(39) \times 10^{-3}$ [120], where the error has been rescaled by the $\sqrt{\chi^2/\text{dof}} = 2.6$ to account

[11] This differs from the choice for $|V_{cb}|$ made by LHCb [121], who use the determination from exclusive $B \to D^{(*)}\ell\nu$ decays at zero recoil [123]. The Belle Experiment recently obtained a new measurement of the $B \to D\ell\nu$ differential decay rate [124] and determination of $|V_{cb}| = 40.83(1.13) \times 10^{-3}$. They find that the inclusion of experimental and theoretical nonzero-recoil information increases the value for $|V_{cb}|$ compared to when only zero-recoil information is used, and leads to agreement with the inclusive result.

for the disagreement. Using this result we obtain

$$f_{B^+}^{\text{"exp"}} = 188(17)(18)\ \text{MeV}\,, \tag{84.36}$$

where the uncertainties are from the errors on Γ and $|V_{ub}|$, respectively. This agrees within large uncertainties with the theoretical value $f_{B^+} = 187.1(4.2)$ MeV in Eq. (84.24) obtained from an average of recent three and four-flavor lattice-QCD results [69,86,88,89].

Acknowledgments

We thank V. Cirigliano, C. Davies, A. El Khadra, A. Khodjamirian, J. Laiho, W. Marciano, M. Moulson, S. Narison, S. Sharpe, and Z.-G. Wang for useful discussions and references. We thank P. Boyle, M. Della Morte, D. Lin and S. Simula for providing information on the preliminary FLAG-3 lattice averages. We gratefully acknowledge support of the U. S. National Science Foundation and the U. S. Department of Energy through Grant No. DE-FG02-13ER41598. The work of J. L. R. was performed in part at the Aspen Center for Physics, which is supported by National Science Foundation grant PHY-1066293. Fermilab is operated by Fermi Research Alliance, LLC, under Contract No. DE-AC02-07CH11359 with the U.S. Department of Energy.

References:

1. K. Nakamura *et al.* (PDG), J. Phys. **G37**, 075021 (2010).
2. J. Beringer *et al.* (PDG), Phys. Rev. **D86**, 010001 (2012).
3. K.A. Olive *et al.* (PDG), Chin. Phys. C **38**, 090001 (2014).
4. W.-S. Hou, Phys. Rev. **D48**, 2342 (1993).
5. A. Akeroyd and S. Recksiegel, Phys. Lett. **B554**, 38 (2003).
6. A. Akeroyd and S. Recksiegl, J. Phys. **G29**, 2311 (2003).
7. A. Akeroyd, Prog. Theor. Phys. **111**, 295 (2004).
8. B. Dobrescu and A. Kronfeld, Phys. Rev. Lett. **100**, 241802 (2008).
9. J. Hewett, arXiv:hep-ph/9505246.
10. A. Crivellin, Phys. Rev. **D81**, 031301 (2010).
11. F. Bernlochner, Z. Ligeti, and S. Turczyk, Phys. Rev. **D90**, 094003 (2014).
12. A. Jüttner, "*Light Flavour Physics*" plenary talk presented at Lattice 2015.
13. P. A. Boyle, T. Kaneko, and S. Simula (FLAG), private communication, 2015.
14. S. Aoki *et al.* (FLAG), Eur. Phys. J. **C74**, 2890 (2014).
15. W. Marciano, Phys. Rev. Lett. **93**, 231803 (2004).
16. V. Cirigliano *et al.*, Rev. Mod. Phys. **84**, 399 (2012).
17. V. Cirigliano and I. Rosell, JHEP **10**, 005 (2007).
18. A. Sirlin, Nucl. Phys. **B196**, 83 (1982).
19. T. Kinoshita, Phys. Rev. Lett. **2**, 477 (1959).
20. M. Knecht *et al.*, Eur. Phys. J. **C12**, 469 (2000).
21. B. Ananthanarayan and B. Moussallam, JHEP **06**, 047 (2004).
22. S. Descotes-Genon and B. Moussallam, Eur. Phys. J. **C42**, 403 (2005).
23. W. Marciano and A. Sirlin, Phys. Rev. Lett. **71**, 3629 (1993).
24. V. Cirigliano and H. Neufeld, Phys. Lett. **B700**, 7 (2011).
25. V.Cirigliano and I. Rosell, Phys. Rev. Lett. **99**, 231801 (2007).
26. M. Moulson, arXiv:1411.5252.
27. D. Babusci *et al.* (KLOE KLOE-2), Phys. Lett. **B738**, 128 (2014).
28. M. Antonelli *et al.* (FlaviaNet Working Group on Kaon Decays), Eur. Phys. J. **C69**, 399 (2010).
29. S. Hashimoto, J. Laiho, and S.R. Sharpe, *"Lattice Quantum Chromodynamics,"* in K.A. Olive *et al.* (PDG) Chin. Phys. C **38**, 090001 (2014) and 2015 update.
30. A. Kronfeld, Ann. Rev. Nucl. and Part. Sci. **62**, 265 (2012).
31. N. Carrasco *et al.* (ETM), Phys. Rev. **D91**, 054507 (2015).
32. A. Bazavov *et al.* (Fermilab Lattice and MILC), Phys. Rev. **D90**, 074509 (2014).
33. R.J. Dowdall *et al.* (HPQCD), Phys. Rev. **D88**, 074504 (2013).
34. T. Blum *et al.* (RBC/UKQCD), arXiv:1411.7017.
35. R. Arthur *et al.* (RBC/UKQCD), Phys. Rev. **D87**, 094514 (2013).
36. J. Laiho and R. Van de Water, PoS **LATTICE2011**, 293 (2011).
37. A. Bazavov *et al.* (MILC), PoS **LATTICE2010**, 074 (2010).
38. S. Durr *et al.* (BMW), Phys. Rev. **D81**, 054507 (2010).
39. E. Follana *et al.* (HPQCD, UKQCD), Phys. Rev. Lett. **100**, 062002 (2008).
40. J. Gasser and H. Leutwyler, Nucl. Phys. **B250**, 465 (1985).
41. G. de Divitiis *et al.* (RM123), JHEP **04**, 124 (2012).
42. M. Nobes, arXiv:hep-lat/0501009.
43. A. Bazavov *et al.*(Fermilab Lattice and MILC), arXiv:1602.03560.
44. M. Artuso *et al.* (CLEO), Phys. Rev. Lett. **95**, 251801 (2005).
45. B. Eisenstein *et al.* (CLEO), Phys. Rev. **D78**, 052003 (2008).
46. M. Ablikim *et al.* (BESIII), Phys. Rev. **D89**, 051104 (2014).
47. M. Artuso *et al.* (CLEO), Phys. Rev. Lett. **99**, 071802 (2007).
48. J. Alexander *et al.* (CLEO), Phys. Rev. **D79**, 052001 (2009).
49. A. Zupanc *et al.* (Belle), JHEP **1309**, 139 (2013).
50. P. Naik *et al.* (CLEO), Phys. Rev. **D80**, 112004 (2009).
51. K. Ecklund *et al.* (CLEO), Phys. Rev. Lett. **100**, 161801 (2008).
52. P. Oniyisi *et al.* (CLEO), Phys. Rev. **D79**, 052002 (2009).
53. P. del Amo Sanchez *et al.* (BaBar), Phys. Rev. **D82**, 091103 (2010).
54. J. Alexander *et al.* (CLEO), Phys. Rev. Lett. **100**, 161804 (2008).
55. B. Aubert *et al.* (BaBar), Phys. Rev. Lett. **98**, 141801 (2007).
56. J. Lees *et al.* (BaBar), arXiv:1003.3063.
57. G. Burdman, J. Goldman, and D. Wyler, Phys. Rev. **D51**, 111 (1995).
58. D. Atwood, G. Eilamn, and A. Soni, Mod. Phys. Lett. **A11**, 1061 (1996).
59. P. Colangelo, F. De Fazio, and G. Nardulli, Phys. Lett. **B372**, 331 (1996).
60. A. Khodjamirian, G. Stoll, and D. Wyler, Phys. Lett. **B358**, 129 (1995).
61. G. Eilam, I. Halperin, and R. Mendel, Phys. Lett. **B361**, 137 (1995).
62. C. Geng, C. Lih and W.-M. Zhang, Phys. Rev. **D57**, 5697 (1998).
63. C. Geng, C. Lih and W.-M. Zhang, Mod. Phys. Lett. **A15**, 2087 (2000).
64. G. Korchemsky, D. Pirjol, and T.-M. Yan, Phys. Rev. **D61**, 114510 (2000).
65. C.-W Hwang, Eur. Phys. J. **C46**, 379 (2006).
66. C.-D. Lu and G.-L. Song, Phys. Lett. **B562**, 75 (2003).
67. Y.-B. Yang *et al.* (χQCD), Phys. Rev. **D92**, 034517 (2015).
68. H. Na *et al.* (HPQCD), Phys. Rev. **D86**, 054510 (2012).
69. A. Bazavov *et al.* (Fermilab Lattice and MILC), Phys. Rev. **D85**, 114506 (2012).
70. C.T.H. Davies *et al.* (HPQCD), Phys. Rev. **D82**, 114504 (2010).
71. Z.-G. Wang, Eur. Phys. J. **C75**, 427 (2015).
72. P. Gelhausen *et al.*, Phys. Rev. **D88**, 014015 (2013).
73. S. Narison, Phys. Lett. **B718**, 1321 (2013).
74. W. Lucha, D. Melikhov, and S. Simula, Phys. Lett. **B701**, 82 (2011).
75. Chien-Wen Hwang, Phys. Rev. **D81**, 054022 (2010).
76. C. Amsler *et al.* (PDG), Phys. Lett. **B667**, 1 (2008), and 2009 update.
77. J. Laiho, E. Lunghi, and R. Van de Water, Phys. Rev. **D81**, 034503 (2010).
78. M. Schmelling, Phys. Scripta **51**, 676 (1995).
79. A. Vladikas, arXiv:1509.01155.
80. K. Ikado *et al.* (Belle), Phys. Rev. Lett. **97**, 251802 (2006).
81. I. Adachi *et al.* (Belle), Phys. Rev. Lett. **110**, 131801 (2013).
82. B. Kronenbitter *et al.* (Belle), Phys. Rev. **D92**, 051102 (2015).
83. J. Lees *et al.* (BaBar), Phys. Rev. **D88**, 031102 (2013).
84. B. Aubert *et al.* (BaBar), Phys. Rev. **D81**, 051101 (2010).
85. N. Carrasco *et al.* (ETM), PoS **LATTICE2013**, 313 (2014).
86. R. J. Dowdall *et al.* (HPQCD), Phys. Rev. Lett. **110**, 222003 (2013).
87. Y. Aoki *et al.*, Phys. Rev. **D91**, 114505 (2015).

88. N. Christ *et al.* (RBC/UKQCD), Phys. Rev. **D91**, 054502 (2015).
89. H. Na *et al.* (HPQCD), Phys. Rev. **D86**, 034506 (2012).
90. C. McNeile *et al.* (HPQCD), Phys. Rev. **D85**, 031503 (2012).
91. M. Baker *et al.*, JHEP **07**, 032 (2014).
92. W. Lucha, D. Melikhov, and S. Simula, Phys. Rev. **D88**, 056011 (2013).
93. Y. Aoki *et al.* (RBC/UKQCD), Phys. Rev. **D83**, 074508 (2011).
94. J. Hardy and I. Towner, Phys. Rev. **C91**, 025501 (2015).
95. F. Ambrosino *et al.* (KLOE), Eur. Phys. J. **C71**, 1604 (2011).
96. E. Abouzaid *et al.* (KTeV), Phys. Rev. **D83**, 092001 (2011).
97. A. Bazavov *et al.* (Fermilab Lattice and MILC), Phys. Rev. Lett. **112**, 112001 (2014).
98. A. Bazavov *et al.* (Fermilab Lattice and MILC), Phys. Rev. **D87**, 073012 (2013).
99. P. Boyle *et al.* (RBC/UKQCD), JHEP **06**, 164 (2015).
100. I. Towner and J. Hardy, Phys. Rev. **C91**, 015501 (2015).
101. M. Bona *et al.* (UTfit), JHEP **10**, 081 (2006).
102. Y. Amhis *et al.* (HFAG), `arXiv:1412.7515`.
103. H. Na *et al.* (HPQCD), Phys. Rev. **D82**, 114506 (2010).
104. H. Na *et al.* (HPQCD), Phys. Rev. **D84**, 114505 (2011).
105. A. Alberti *et al.*, Phys. Rev. Lett. **114**, 061802 (2015).
106. J. Bailey *et al.* (Fermilab Lattice, MILC), Phys. Rev. **D89**, 114504 (2014).
107. L. Wolfenstein, Phys. Rev. Lett. **51**, 1945 (1983).
108. J. Charles *et al.* (CKMfitter Group), Eur. Phys. J. **C41**, 1 (2005).
109. M. Antonelli *et al.*, Phys. Rev. **494**, 197 (2010).
110. J. Butler *et al.* (Quark Flavor Physics Working Group), `arXiv:1311.1076`.
111. A. Bevan *et al.* (Belle, BaBar), Eur. Phys. J. **C74**, 3026 (2014).
112. J. Bailey *et al.* (Fermilab Lattice and MILC), Phys. Rev. **D92**, 014024 (2015).
113. P. del Amo Sanchez *et al.* (BaBar), Phys. Rev. **D83**, 032007 (2011).
114. J. Lees *et al.* (BaBar), Phys. Rev. **D86**, 092004 (2012).
115. H. Ha *et al.* (Belle), Phys. Rev. **D83**, 071101 (2011).
116. A. Sibidanov *et al.* (Belle), Phys. Rev. **D88**, 032005 (2013).
117. S. Bosch *et al.*, Phys. Rev. Lett. **93**, 221801 (2004).
118. J.R. Anderson and E. Gardi, JHEP **01**, 097 (2006).
119. P. Gambino *et al.*, JHEP **10**, 058 (2007).
120. R. Kowalewski and T. Mannel, *"Semileptonic B-meson decays and the determination of V_{cb} and V_{ub},"*, in K.A. Olive *et al.* (PDG), Chin. Phys. C **38**, 090001 (2014) and 2015 update.
121. R. Aaij *et al.* (LHCb), Nat. Phys. **11**, 743 (2015).
122. W. Detmold, C. Lehner, and S. Meinel, Phys. Rev. **D92**, 034503 (2015).
123. R. Kowalewski and T. Mannel, *"Semileptonic B-meson decays and the determination of V_{cb} and V_{ub},"*, in K.A. Olive *et al.* (PDG), Chin. Phys. C **38**, 090001 (2014).
124. R. Glattauer *et al.* (Belle), Phys. Rev. **D93**, 032006 (2016).

85. Production and Decay of *b*-flavored Hadrons

Updated September 2017 by P. Eerola (U. of Helsinki, Helsinki, Finland), M. Kreps (U. of Warwick, Coventry, UK), and Y. Kwon (Yonsei U., Seoul, Korea).

The b quark belongs to the third generation of quarks and is the weak–doublet partner of the t quark. The existence of the third–generation quark doublet was proposed in 1973 by Kobayashi and Maskawa [1] in their model of the quark mixing matrix ("CKM" matrix), and confirmed four years later by the first observation of a $b\overline{b}$ meson [2]. In the KM model, CP violation is explained within the Standard Model (SM) by an irreducible phase of the 3×3 unitary matrix. The regular pattern of the three lepton and quark families is one of the most intriguing puzzles in particle physics. The existence of families gives rise to many of the free parameters in the SM, including the fermion masses, and the elements of the CKM matrix.

Since the b quark is the lighter element of the third–generation quark doublet, the decays of b-flavored hadrons occur via generation-changing processes through this matrix. Because of this, and the fact that the CKM matrix is close to a 3×3 unit matrix, many interesting features such as loop and box diagrams, flavor oscillations, as well as large CP asymmetries, can be observed in the weak decays of b-flavored hadrons.

The CKM matrix is parameterized by three real parameters and one complex phase. This complex phase can become a source of CP violation in B meson decays. A crucial milestone was the first observation of CP violation in the B meson system in 2001, by the BaBar [3] and Belle [4] collaborations. They measured a large value for the parameter $\sin 2\beta$ $(= \sin 2\phi_1)$ [5], almost four decades after the discovery of a small CP asymmetry in neutral kaons. A more detailed discussion of the CKM matrix and CP violation can be found elsewhere in this *Review* [6,7].

Recent developments in the physics of b-hadrons include the significant improvement in experimental determination of the CKM angle γ, the increased information on B_s^0, B_c^+ and Λ_b^0 decays, the precise determination of Λ_b^0 lifetime, the wealth of information in the $B^0 \to K^*(892)^0 \ell^+ \ell^-$ decays and after many years of search, the observation of $B_s^0 \to \mu^+ \mu^-$ decays along with ever increasing precision on the CKM matrix parameters.

The structure of this mini-review is organized as follows. After a discussion of b-quark production and current results on spectroscopy, we discuss lifetimes of b-flavored hadrons. We then discuss some basic properties of B-meson decays, followed by summaries of hadronic, rare, and electroweak penguin decays of B-mesons. There are separate mini-reviews for B^0–$\overline{B}^0$ mixing [8] and the extraction of the CKM matrix elements V_{cb} and V_{ub} from B-meson decays [9] in this *Review.*

85.1. Production and spectroscopy

The bound states of a $\overline{b}$ antiquark and a u, d, s, or c quark are referred to as the B_u (B^+), B_d (B^0), B_s (B_s^0), and B_c (B_c^+) mesons, respectively. The B_c^+ is the heaviest of the ground–state b-flavored mesons, and the most difficult to produce: it was observed for the first time in the semileptonic mode by CDF in 1998 [10], but its mass was accurately determined only in 2006, from the fully reconstructed mode $B_c^+ \to J/\psi \pi^+$ [11]. Many exclusive decay channels can now be used for the accurate mass measurements, given the large statistics available at the LHC. Currently the most precise measurement is made by LHCb using the $B_c^+ \to J/\psi D^0 K^+$ decay, yielding $m(B_c^+) = 6274.28 \pm 1.40 \pm 0.32$ MeV/c^2 [12].

The first excited meson is called the B^* meson, while B^{**} is the generic name for the four orbitally excited $(L = 1)$ B-meson states that correspond to the P-wave mesons in the charm system, D^{**}. Excited states of the B_s^0 meson are similarly named B_s^* and B_s^{**}. Of the possible bound $\overline{b}b$ states, the $\Upsilon(nS)$ and $\chi_{bJ}(nP)$ states are well studied.

The pseudoscalar ground state η_b has been observed for the first time by BaBar [13] indirectly through the decay $\Upsilon(3S) \to \gamma\eta_b$, and then confirmed by BaBar in $\Upsilon(2S)$ decays [14] and CLEO in $\Upsilon(3S)$ decays [15]. The most accurate mass and width measurements come now from Belle, using decays $\Upsilon(5S) \to h_b(1P)\pi^+\pi^-$, $h_b(1P) \to \gamma\eta_b(1S)$ [16] and $\Upsilon(4S) \to \eta h_b(1P)$, $h_b(1P) \to \gamma\eta_b(1S)$ [17]. Belle has also reported first evidence for the $\eta_b(2S)$ in the $h_b(2P) \to \eta_b(2S)\gamma$ transition [16]. See Ref. 18 for classification and naming of these and other states.

Experimental studies of b decays have been performed in e^+e^- collisions at the $\Upsilon(4S)$ (ARGUS, CLEO, Belle, BaBar) and $\Upsilon(5S)$ (CLEO, Belle) resonances. The full data samples of BaBar and Belle are 560 fb^{-1} and 1020 fb^{-1}, respectively, of which 433 fb^{-1} and 710 fb^{-1} are at the $\Upsilon(4S)$ resonance. The $e^+e^- \to b\overline{b}$ production cross-section at the $\Upsilon(4S)$ $(\Upsilon(5S))$ resonance is about 1.1 nb (0.3 nb). At the Z resonance (SLC, LEP) all species of b-flavored hadrons could be studied for the first time. The $e^+e^- \to b\overline{b}$ production cross-section at the Z resonance is about 6.6 nb.

High-energy $p\overline{p}$ (Tevatron) and pp collisions (LHC) produce b-flavored hadrons of all species with large cross-sections. At the Tevatron ($\sqrt{s} = 1.96$ TeV) the visible cross section $\sigma(p\overline{p} \to bX, |\eta| < 1)$ is about 30 μb. CDF and D0 experiments at the Tevatron have accumulated by the end of their running about 10 fb^{-1} each.

At the LHC pp collider at $\sqrt{s} = 7 - 13$ TeV, the visible b-hadron cross section at the LHCb experiment with pseudorapidity acceptance $2 < \eta < 5$ has been measured to be ~ 72 μb at 7 TeV and ~ 144 μb at 13 TeV [19](cross section at 13 TeV corrected in Erratum). LHCb has collected about 1 fb^{-1} at 7 TeV, 2 fb^{-1} at 8 TeV, and close to 3 fb^{-1} at 13 TeV by September 2017. CMS and ATLAS have collected each about 5 fb^{-1} of data at $\sqrt{s} = 7$, 20 fb^{-1} at 8 TeV and about 60 fb^{-1} at 13 TeV until September 2017. The LHC experiments are at the moment the only experiments taking data, and they dominate the field until Belle II becomes operational and accumulates a competitive amount of data.

In hadron collisions, production happens as $b\overline{b}$ pairs via leading order flavor creation or higher order processes such as gluon–splitting. Single b-quarks can be produced by flavor excitation. The total b-production cross section is an interesting test of our understanding of leading and higher order QCD processes. With a wealth of measurements at LHC and at Tevatron (see Ref. 19 and references therein), and improved calculations [20], there is a reasonable agreement between measurements and predictions.

Each quark of a $b\overline{b}$ pair produced in hadron collisions hadronizes separately and incoherently from the other, but it is still possible to obtain a statistical indication of the charge of a produced $b/\overline{b}$ quark ("flavor tag" or "charge tag") from the accompanying particles produced in the hadronization process, or from the decay products of the other quark. The momentum spectrum of produced b-quarks typically peaks near the b-quark mass, and extends to much higher momenta, dropping by about a decade for every ten GeV. Typical decay lengths are of the order of a centimeter at 13 TeV pp collisions; the resolution for the decay vertex must be more precise than this to resolve the fast oscillations of B_s^0 mesons.

In e^+e^- colliders, since the B mesons are very slow in the $\Upsilon(4S)$ rest frame, asymmetric beam energies are used to boost the decay products to allow time-dependent measurements that are crucial for the study of CP violation. At KEKB, the boost is $\beta\gamma = 0.43$, and the typical B-meson decay length is dilated from ≈ 20 μm to ≈ 200 μm. PEP-II used a slightly larger boost, $\beta\gamma = 0.55$. The two B mesons produced in $\Upsilon(4S)$ decay are in a coherent quantum state, which makes it easier than in hadron collisions to infer the charge state of one B meson from observation of the other; however, the coherence also requires determination of the decay time of both mesons, rather than just one, in order to perform time–dependent CP–violation measurements. For B_s^0, which can be produced at $\Upsilon(5S)$ the situation is less favourable, as boost is not high enough to provide sufficient time resolution to resolve the fast B_s^0 oscillations.

For the measurement of branching fractions, the initial composition of the data sample must be known. The $\Upsilon(4S)$ resonance decays predominantly to $B^0\overline{B}^0$ and B^+B^-; the current experimental upper limit for non-$B\overline{B}$ decays of the $\Upsilon(4S)$ is less than 4% at the 95% confidence level (CL) [21]. The observed modes of this category are decays to lower Υ states and a pion pair, measured branching fractions being of order 10^{-4} [22], and decays to $h_b(1P)\eta$ with branching fraction of order 10^{-3} [17].

The ratio f_+/f_0 of the fractions of charged to neutral B productions from $\Upsilon(4S)$ decays has been measured by CLEO, BaBar, and Belle in various ways. They typically use pairs of isospin-related decays of B^+ and B^0, such that it can be assumed that $\Gamma(B^+ \to x^+) = \Gamma(B^0 \to x^0)$. In this way, the ratio of the number of events observed in these modes is proportional to $(f_+\tau_+)/(f_0\tau_0)$ [23,24]. BaBar has also performed an independent measurement of f_0 with a different method that does not require isospin symmetry or the value of the lifetime ratio, based on the number of events with one or two reconstructed $B^0 \to D^{*-}\ell^+\nu$ decays [25]. The combined result, from the current average of τ_+/τ_0, is $f_+/f_0 = 1.058 \pm 0.024$ [26]. The result is consistent within 2.4σ with equal production of B^+B^- and $B^0\overline{B}^0$ pairs, and we assume $f_+/f_0 = 1$ in this mini-review except where explicitly stated otherwise. This assumption is also supported by the near equality of the B^+ and B^0 masses: our fit yields $m(B^0) = 5279.63 \pm 0.15$ MeV/c^2, $m(B^+) = 5279.32 \pm 0.14$ MeV/c^2, and $m(B^0) - m(B^+) = 0.31 \pm 0.06$ MeV/c^2.

Data collected at the $\Upsilon(5S)$ resonance gave CLEO, Belle and BaBar access to B_s^0 decays. In $\Upsilon(5S)$ decays there are seven possible final states including a pair of non-strange B mesons and 0, 1 or 2 pions, and three with a pair of strange B mesons ($B_s^{*0}\overline{B}_s^{*0}$, $B_s^{*0}\overline{B}_s^0$, and $B_s^0\overline{B}_s^0$). The fraction of events with a pair of B_s^0 mesons over the total number of events with a pair of b-flavored hadrons has been measured to be $f_s[\Upsilon(5S)] = 0.200^{+0.030}_{-0.031}$, of which 90% is $B_s^{*0}\bar{B}_s^{*0}$ events. However, the small boost of B_s^0 mesons produced in this way prevents resolution of their fast oscillations for time-dependent measurements; these are only accessible in hadron collisions (or at the Z peak).

In high-energy collisions, the produced b or $\bar{b}$ quarks can hadronize with different probabilities into the full spectrum of b-hadrons, either in their ground or excited states. Table 85.1 shows the measured fractions f_d, f_u, f_s, and $f_{\rm baryon}$ of B^0, B^+, B_s^0, and b baryons, respectively, in an unbiased sample of weakly decaying b hadrons produced at the Z resonance or in $p\overline{p}$ collisions [26]. The results were obtained from a fit where the sum of the fractions were constrained to equal 1.0, neglecting production of weakly decaying states made of several heavy quarks, such as B_c^+ mesons and doubly heavy baryons. The estimated production fraction of B_c^+ mesons at the Tevatron [27] is below 0.8%, with a large uncertainty coming from discrepancies in the theoretical predictions for the B_c^+ decay branching fraction. Complete measurements of b hadron production fractions at the LHC do not exist yet. LHCb has measured fractions $f_s/(f_u + f_d)$ and $f_{\Lambda_b^0}/(f_u + f_d)$ [28]. The production fractions of b hadrons are also discussed in the B^0 – $\overline{B}^0$ mixing section in this *Review* [8].

Table 85.1: Fragmentation fractions of b quarks into weakly-decaying b-hadron species in $Z \to b\overline{b}$ decay, and in $p\overline{p}$ collisions at $\sqrt{s} = 1.96$ TeV [26].

b hadron	Fraction at Z[%]	Fraction at $\overline{p}p$ [%]
B^+, B^0	41.2 ± 0.8	34.0 ± 2.1
B_s^0	8.8 ± 1.3	10.1 ± 1.5
b baryons	8.9 ± 1.2	21.8 ± 4.7

The hadronization does not have to be identical in $p\overline{p}$ or pp collisions and in Z decay, because of the different momentum distributions of the b-quark in these processes; the sample used in the $p\overline{p}$ measurements has momenta close to the b mass, rather than $m_Z/2$. Both CDF and LHCb report evidence for a strong dependence on the transverse momentum for the Λ_b^0 fraction [28,29]. LHCb and ATLAS have also investigated the transverse momentum dependence of f_s/f_d [30], but the results are inconclusive.

Excited B-meson states have been thoroughly studied by CLEO, LEP, CUSB, D0 and CDF (an admixture of B mesons) and LHCb (B^{*+}-meson). The current world average of the B^*–B mass difference is 45.42 ± 0.26 MeV/c^2. Excited B_s^*-meson states have observed in $\Upsilon(5S)$ decays by CUSB, CLEO and Belle.

For orbitally excited B meson states, with relative angular momentum L=1 of the two quarks, there exist four states $(J, j_q) = (0, 1/2), (1, 1/2), (1, 3/2), (2, 3/2)$, where j_q is the total angular momentum of the light u, d or s quark and J is the total angular momentum of the B meson. These states are collectively called as $B_{(s)}^{**}$ mesons. The $j_q = 1/2$ states are named $B_{(s)0}^*$ ($J = 0$) and $B_{(s)1}$ ($J = 1$) mesons, while the states with $j_q = 3/2$ are named $B_{(s)1}$ ($J = 1$) and $B_{(s)2}^*$ ($J = 2$) mesons. The states with $j_q = 1/2$ can decay through an S-wave transition and are expected to have a large width, but the $j_q = 3/2$ states are narrow D-wave decays. Evidence for B^{**} production has been initially obtained at LEP as a broad $B\pi$ resonance [31] or a B^+K^- enhancement [32]. Detailed results have been obtained for the narrow states $B_1(5721)^{0,+}$ and $B_2(5747)^{0,+}$ at the Tevatron and by LHCb, and clear enhancements compatible with the higher mass states $B_J(5840)^{0,+}$ and $B_J(5960)^{0,+}$ have been observed [33,34]. Also the narrow B_s^{**} states $B_{s1}(5830)^0$ and $B_{s2}(5840)^0$ have been measured at the CDF [33] and LHCb [35].

Excited states of B_c^+ mesons will provide important information about the strong potential. ATLAS has observed a $B_c^+\pi^+\pi^-$ resonance at 6842 MeV/c^2, that may be interpreted as the second S-wave state of the B_c^+ meson, $B_c^+(2S)$ [36]. The quantum numbers are to be confirmed.

Baryon states containing a b quark are labeled according to the same scheme used for non-b baryons, with the addition of a b subscript [18]. The first observed b baryon was the Λ_b^0 (quark composition udb). Thanks to the large samples accumulated at the Tevatron and specially at the LHC many new b baryons have been found. The masses of all these new baryons have been measured to a precision of a few MeV/c^2, and found to be in agreement with predictions from Heavy Quark Effective Theory (HQET).

Clear signals of four strongly–decaying baryon states, Σ_b^+, Σ_b^{*+} (uub), Σ_b^-, Σ_b^{*-} (ddb) have been obtained by CDF in $\Lambda_b^0\pi^\pm$ final states [37]. The isodublet of strange b baryons Ξ_b^0 (usb) and $\Xi_b^\pm$ (dsb) has been observed by CDF and D0 [38]. Masses, lifetimes and many decay modes have been accurately measured by LHCb [39] and CDF [40]. Other observed Ξ_b baryons are spin-3/2 states $\Xi_b(5945)^0$ (Ξ_b^{*0}) [41], and $\Xi_b(5955)^{*-}$ [42], and spin-1/2 state $\Xi_b'(5935)^-$ [42]. The doubly–strange bottom baryon Ω_b^- has been observed first by D0 and CDF [43]. Mass and mean life have been measured precisely by LHCb [44] and CDF [40].

The so-called exotic states have raised a lot of interest recently. While many exotic states were seen in the charm sector, in bottom sector there are fewer seen. The D0 Collaboration claimed narrow state $X(5568)$ decaying into $B_s^0\pi^\pm$ final state [45]. While this would be interesting addition to the observed states as first exotic state with constituent quarks with four different flavours (b, s, u, d), analysis by LHCb yields negative result [46]. Also CMS has a preliminary result finding no such state [47].

85.2. Lifetimes

Precise lifetimes are key in extracting the weak parameters that are important for understanding the role of the CKM matrix in CP violation, such as the determination of V_{cb} and $B_s^0\overline{B}_s^0$ mixing parameters. In the naive spectator model, the heavy quark can decay only via the external spectator mechanism, and thus, the lifetimes of all mesons and baryons containing b quarks would be equal. Non–spectator effects, such as the interference between contributing amplitudes, modify this simple picture and give rise to a lifetime hierarchy for b-flavored hadrons similar to the one in the charm sector. However, since the lifetime differences are expected to scale as $1/m_Q^2$, where m_Q is the mass of the heavy quark, the variations in the b system are expected to be only 10% or less [48,49]. We expect:

$$\tau(B^+) \geq \tau(B^0) \approx \tau(B_s^0) > \tau(\Lambda_b^0) \gg \tau(B_c^+)\,. \qquad (85.1)$$

For the B_c^+, both quarks decay weakly, so the lifetime is much shorter.

Measurements of the lifetimes of the different b-flavored hadrons thus provide a means to determine the importance of non-spectator mechanisms in the b sector. Availability of large samples of fully–reconstructed decays of different b-hadron species has resulted in precise measurements with small statistical and systematic uncertainties (∼1%). The world averages given in Table 85.2 have been determined by the Heavy Flavor Averaging Group (HFAG) [26].

Table 85.2: Summary of i world-average b-hadron lifetime measurements. For the B_s^0 lifetimes, see text below.

Particle	Lifetime [ps]
B^+	1.638 ± 0.004
B^0	1.520 ± 0.004
B_s^0	1.505 ± 0.005
B_{sL}^0	1.413 ± 0.006
B_{sH}^0	1.609 ± 0.010
B_c^+	0.507 ± 0.009
Λ_b^0	1.470 ± 0.010
Ξ_b^-	1.571 ± 0.040
Ξ_b^0	1.479 ± 0.031
Ω_b^-	$1.64^{+0.18}_{-0.17}$

The B_s^0 lifetime in Table 85.2 is defined as $1/\Gamma_s$, where Γ_s is the average width of the light (L) and heavy (H) mass eigenstates, $(\Gamma_L + \Gamma_H)/2$. In the absence of CP violation, the light (heavy) B_s^0 mass eigenstate is the CP-even (CP-odd) eigenstate. Thus, the lifetime of the light (heavy) mass eigenstate can be measured from CP-even (odd) final states. The lifetimes can also be obtained from time-dependent angular analysis of $B_s^0 \to J/\psi\phi$ decays.

The short B_c^+ lifetime is in good agreement with predictions [50]. With large samples of B_c^+ mesons at the LHC precision on the lifetimes can still improve. The measurement using semileptonic decays gives $\tau_{B_c^+} = 0.509 \pm 0.008 \pm 0.012$ ps [51] while using decays $B_c^+ \to J/\psi\pi^+$ yields $\tau_{B_c^+} = 0.5134 \pm 0.0110 \pm 0.0057$ ps [52]. Each of these is more precise than the combination of all previous experiments.

The recent Λ_b^0 lifetime measurements from LHC experiments and CDF are precise and favour lifetime close to the lifetime of B^0 meson, in agreement with theory.

For precision comparisons with theory, lifetime ratios are more sensitive. Experimentally it is found [26]:

$$\frac{\tau_{B^+}}{\tau_{B^0}} = 1.076 \pm 0.004\,, \quad \frac{\tau_{B_s^0}}{\tau_{B^0}} = 0.990 \pm 0.004\,,$$

$$\frac{\tau_{\Lambda_b^0}}{\tau_{B^0}} = 0.967 \pm 0.007\,,$$

while recent Heavy Quark Expansion (HQE) predictions give [49]:

$$\frac{\tau_{B^+}}{\tau_{B^0}} = 1.04^{+0.05}_{-0.01} \pm 0.02 \pm 0.01\,, \quad \frac{\tau_{B_s^0}}{\tau_{B^0}} = 1.001 \pm 0.002\,,$$

$$\frac{\tau_{\Lambda_b^0}}{\tau_{B^0}} = 0.935 \pm 0.054.$$

The ratio of B^+ to B^0 lifetimes has a precision of better than 1%, and is significantly different from 1.0, in agreement with predictions [48]. The ratio of B_s^0 to B^0 lifetimes is expected to be very close to 1.0.

For a detailed discussion on neutral B^0 and B_s^0 oscillation and relevant CP violation measurements see Ref. 8.

85.3. Features of decays

The ground states of b-flavored hadrons decay via weak interactions. In most decays of the b-flavored hadrons, where the b-quark is accompanied by lighter partner quarks (d, u, s, or c), the decay modes are well described by the decay of the b quark (spectator model) [53]. The dominant decay mode of a b quark is $b \to cW^{*-}$ (referred to as a "tree" or "spectator" decay), where the virtual W materializes either into a pair of leptons $\ell\bar{\nu}$ ("semileptonic decay"), or into a pair of quarks which then hadronizes. The transition $b \to u$ is suppressed by $|V_{ub}/V_{cb}|^2 \sim (0.1)^2$ relative to $b \to c$ transitions. The decays in which the spectator quark combines with one of the quarks from W^* to form one of the final state hadrons are suppressed by a factor $\sim (1/3)^2$, because the colors of the two quarks from different sources must match ("color–suppression").

Semileptonic B decays $B \to X_c\ell\nu$ and $B \to X_u\ell\nu$ provide an excellent way to measure the magnitude of the CKM elements $|V_{cb}|$ and $|V_{ub}|$ respectively, because the strong interaction effects are much simplified due to the two leptons in the final state. Both exclusive and inclusive decays can be used with dominant uncertainties being complementary. For exclusive decay analysis, knowledge of the form factors for the exclusive hadronic system $X_{c(u)}$ is required. For inclusive analysis, it is usually necessary to restrict the available phase-space of the decay products to suppress backgrounds; subsequently uncertainties are introduced in the extrapolation to the full phase-space. Moreover, restriction to a small corner of the phase-space may result in breakdown of the operator-product expansion scheme, thus making theoretical calculations unreliable. One of the recent unexpected results was determination of $|V_{ub}|$ using $\Lambda_b^0 \to p\mu^-\bar{\nu}_\mu$ decays by LHCb [54]. Besides, there have been measurements of inclusive semileptonic decays rates of B_s^0 [55] and B_c^+ [56] mesons. A more detailed discussion of B semileptonic decays and the extraction of $|V_{cb}|$ and $|V_{ub}|$ is given elsewhere in this *Review* [9].

On the other hand, hadronic decays of B are complicated because of strong interaction effects caused by the surrounding cloud of light quarks and gluons. While this complicates the extraction of CKM matrix elements, it also provides a great opportunity to study perturbative and non-perturbative QCD, hadronization, and Final State Interaction (FSI) effects.

Many aspects of B decays can be understood through the Heavy Quark Effective Theory (HQET) [57]. This has been particularly successful for semileptonic decays. For further discussion of HQET, see for instance Ref. 58. For hadronic decays, one typically uses effective Hamiltonian calculations that rely on a perturbative expansion with Wilson coefficients. In addition, some form of the factorization hypothesis is commonly used, where, in analogy with semileptonic decays, two-body hadronic decays of B mesons are expressed as the product of two independent hadronic currents, one describing the formation of a charm meson (in case of the dominant $b \to cW^{*-}$ decays), and the other the hadronization of the remaining $\overline{u}d$ (or $\overline{c}s$) system from the virtual W^-. Qualitatively, for B decays with a large energy release, e.g. $b \to uW^{*-}$ transitions, the $\overline{u}d$ pair (produced as a color singlet) travels fast enough to leave the interaction region without influencing the charm meson. This is known to work well for the dominant spectator decays [59]. There are several common implementations of these ideas for hadronic B decays, the most common of which are QCD factorization (QCDF) [60], perturbative QCD (pQCD) [61], and soft collinear effective theory (SCET) [62].

The transitions $b \to s$ and $b \to d$ are flavor-changing neutral-current (FCNC) processes. Although they are not allowed in the SM as a tree-process, they can occur via more complicated loop diagrams (denoted "penguin" decays). The rates for $b \to s$ penguin decays are comparable to the CKM-suppressed $b \to u$ tree processes. Pure-penguin decays were first established by the observation of $B \to K^*(892)\gamma$ [63]. Penguin processes involving $b \to d$ transitions are further suppressed by CKM, and have been observed for $B \to (\rho/\omega)\gamma$ decays [64,65]. LHCb has observed a $b \to d$ penguin transition in the $B^+ \to \pi^+\mu^+\mu^-$ mode and measured its branching fraction to be $(1.83 \pm 0.24 \pm 0.05) \times 10^{-8}$ [66].

Other decay processes discussed in this *Review* include W–exchange (a W is exchanged between initial–state quarks), penguin annihilation

(the gluon from a penguin loop attaches to the spectator quark, similar to an exchange diagram), and pure–annihilation (the initial quarks annihilate to a virtual W, which then decays). Some observed decay modes such as $B^0 \to D_s^- K^+$, may be interpreted as evidence of a W-exchange process [67]. The evidence for the purely leptonic decay $B^+ \to \tau^+\nu$ from Belle [68] and BaBar [69] is the first sign of a pure annihilation decay. The average branching fraction is $(1.09 \pm 0.24) \times 10^{-4}$, which is somewhat larger than, though consistent with, the value expected in the SM. A substantial region of parameter space of charged Higgs mass vs. $\tan\beta$ is excluded by the measurements of this mode. A dedicated discussion of purely leptonic decays of charged pseudoscalar mesons is given elsewhere in this *Review* [70].

85.4. Dominant hadronic decays

Most of the hadronic B decays involve $b \to c$ transition at the quark level, resulting in a charmed hadron or charmonium in the final state. Other types of hadronic decays are very rare and will be discussed separately in the next section. The experimental results on hadronic B decays have steadily improved over the past few years, and the measurements have reached sufficient precision to challenge our understanding of the dynamics of these decays. With good particle detection and hadron identification capabilities of B-factory detectors, a substantial fraction (roughly on the order of a few per mill) of hadronic B decay events can be fully reconstructed. In particular, good performances for detecting π^0 and other neutral particles helped Belle and BaBar make comprehensive measurements of the decays $\overline{B}^0 \to D^{(*)0}h^0$ [71], where h^0 stands for light neutral mesons such as $\pi^0, \eta^{(\prime)}, \rho^0, \omega$. These decays proceed through color-suppressed diagrams, hence they provide useful tests on the factorization models.

Because of the kinematic constraint of $\Upsilon(4S) \to B\bar{B}$, the energy sum of the final-state particles of a B meson decay is always equal to one half of the total energy in the center of mass frame. As a result, the two variables, ΔE (energy difference) and M_B (B candidate mass with a beam-energy constraint) are very effective for reducing combinatorial background both from $\Upsilon(4S)$ and $e^+e^- \to q\bar{q}$ continuum events. In particular, the energy-constraint in M_B improves the signal resolution by almost an order of magnitude.

The kinematically clean environment of B meson decays provides an excellent opportunity to search for new states. For instance, quark-level $b \to c\bar{c}s$ decays have been used to search for new charmonium and charm-strange mesons and study their properties in detail. While narrow charm-strange states $D_{s0}^*(2317)$ [72] and $D_{s1}(2460)$ [73] were discovered by BaBar and CLEO, respectively, the properties of these new states were revealed by studying the B meson decays, $B \to DD_{s0}^*(2317)$ and $B \to DD_{s1}(2460)$ by Belle [74] and BaBar [75].

In addition, a variety of exotic particles that do not fit the conventional meson spectroscopy have been discovered in B decays. Belle found the $X(3872)$ state by studying $B^+ \to J/\psi\pi^+\pi^-K^+$ [76], which was confirmed by CDF [77], D0 [78] and BaBar [79]. Production of $X(3872)$ has been studied by the LHC experiments, LHCB [80], CMS [81] and ATLAS [82].

A charged charmonium-like state $X(4430)^\pm$ that decays to $\psi(2S)\pi^\pm$ was observed by Belle in $B \to \psi(2S)K\pi^\pm$ [83]. Since it is charged, it could not be an ordinary charmonium state. A high-statistics study by LHCb confirmed the existence of the $X(4430)^\pm$ in decays $B \to \psi(2S)K\pi^\pm$ [84], demonstrated its resonance character by studying the phase motion, unambiguously determined its spin-parity, and saw evidence for another state. In a Dalitz plot analysis of $\bar{B}^0 \to J/\psi K^-\pi^+$ [85], Belle has found another state, labelled as $X(4200)^+$ in this *Review*, adding to the list of exotic charged charmonium-like states. In an amplitude analysis of the decay $\Lambda_b^0 \to J/\psi pK^-$, LHCb observed exotic structures, labelled as $P_c(4380)^+$ and $P_c(4380)^+$ in this *Review*, in the $J/\psi p$ channel [86]. They are referred to as charmonium-pentaquark states. More detailed discussions of exotic meson-like states and pentaquarks are given elsewhere in this *Review* [87].

Information on B_s^0, B_c^+ and Λ_b^0 decays have been remarkably improved with recent studies of large samples from LHCb. Noticeable additions in B_s include decay modes to $D_s^{(*)+}D_s^{(*)-}$, $\bar{D}^0\bar{K}^0$, and $J/\psi\bar{K}^*(892)^0$. The $B_s^0 \to D_s^{(*)+}D_s^{(*)-}$ decays were first observed by CDF [88], followed by Belle [89]. LHCb has improved the precision with $\mathcal{B}(B_s^0 \to D_s^{(*)+}D_s^{(*)-}) = (3.07 \pm 0.22 \pm 0.33)\%$ [90], which suggests that $B_s^0 \to D_s^{(*)+}D_s^{(*)-}$ decays do not saturate the CP-even modes of the B_s decays. The $B_s^0 \to \bar{D}^0\bar{K}^0$ decay occurs mostly via a color-suppressed tree diagram, and has a small theoretical uncertaintiy in the SM, thus this mode can significantly improve the determination of the CP-violation angle ϕ_s. LHCb has observed this decay and the branching fraction is $(4.3 \pm 0.5 \pm 0.7) \times 10^{-4}$ [91]. The $B_s^0 \to J/\psi\bar{K}^*(892)^0$ decay can be used to constrain the penguin pollution in determing ϕ_s. LHCb has updated the branching fraction and measured the CP asymmetries of this decay, thereby constraining the penguin pollution in ϕ_s [92], although a much more stringent constraint on penguin polltion can come from $B^0 \to J/\psi\rho^0$ which has been observed by BaBar [93] and LHCb [94]. The $B_c^+ \to B_s^0\pi^+$ decay is unique as the only observed mode of b-flavored hadron decays where the partner quark decays (c in this case) while the b quark remains a spectator. LHCb has observed this mode and measured $[\sigma(B_c^+)/\sigma(B_s^0)] \times \mathcal{B}(B_c^+ \to B_s^0\pi^+) = (2.37 \pm 0.31 \pm 0.11^{+0.17}_{-0.13}) \times 10^{-3}$ [95]. In addition, LHCb [96] and ATLAS [97] have measured $B_c^+ \to J/\psi D_s^{(*)+}$, which, by comparing with $B_c^+ \to B_s^0\pi^+$, provides a ratio of exclusive $b \to c$ and $c \to s$ decays of B_c^+. For $\Lambda_b^0 \to \Lambda_c^+\pi^+\pi^-\pi^-$ [98], not only the total rate is measured, but also structure involving decays through excited Λ_c and Σ_c baryons.

85.5. Rare hadronic decays

All B-meson decays that do not occur through the $b \to c$ transition are usually called rare B decays. These include both semileptonic and hadronic $b \to u$ decays that are suppressed at leading order by the small CKM matrix element V_{ub}, as well as higher-order $b \to s(d)$ processes such as electroweak and gluonic penguin decays. In this section, we review hadronic rare B decays, while electroweak penguin decays and others are discussed in the next.

Charmless B meson decays into two-body hadronic final states such as $B \to \pi\pi$ and $K\pi$ are experimentally clean, and provide good opportunities to probe new physics and search for indirect and direct CP violations. Since the final state particles in these decays tend to have larger momenta than average B decay products, the event environment is cleaner than for $b \to c$ decays. Branching fractions are typically around 10^{-5}. Over the past decade, many such modes have been observed not only by e^+e^- collider experiments such as BaBar and Belle, but also by hadron collider experiments such as CDF ($p\bar{p}$) and LHCb (pp). In the latter cases, huge data samples of the modes with all charged final-state particles have been reconstructed by triggering on the impact parameter of the charged tracks. This has also allowed observation of charmless decays of the B_s, in final states such as $\phi\phi$ [99], K^+K^- [100], and $K^-\pi^+$ [101], and of charmless decays of the Λ_b^0 baryon [101]. Charmless B_s modes are related to corresponding B^0 modes by U-spin symmetry, and are determined by similar amplitudes. Combining the observables from B_s^0 and B^0 modes is a further way of eliminating hadronic uncertainties and extracting relevant CKM information [102].

Because of relatively high-momenta for final state particles, the dominant source of background in e^+e^- collisions is $q\bar{q}$ continuum events; sophisticated background suppression techniques exploiting event shape variables are essential for these analyses. In hadron collisions, the dominant background comes from QCD or partially reconstructed heavy flavors, and is similarly suppressed by a combination of kinematic and isolation requirements. The results are in general consistent among the experiments.

Most rare decay modes including $B^0 \to K^+\pi^-$ have contributions from both $b \to u$ tree and $b \to sg$ penguin processes. If the size of the two contributions are comparable, the interference between them may result in direct CP violation, seen experimentally as a charge asymmetry in the decay rate measurement. BaBar [103], Belle [104], CDF [100], and LHCb [105] have measured the direct CP violating asymmetry in $B^0 \to K^+\pi^-$ decays. Direct CP violation

has been observed in this decay with a significance of more than 5σ. The world average value of the asymmetry is now rather precise, $A_{CP}(K^+\pi^-) = -0.082 \pm 0.006$. The CP asymmetry in $B^+ \to K^+\pi^0$ mode has been measured by BaBar [106] and Belle [104] with the average value $A_{CP}(K^+\pi^0) = 0.037 \pm 0.021$. These two asymmetries diff by more than 5σ significance, in constrast to a naive expectation based on simplified picture in the SM. For more detailed tests, there are sum rules [107] that relate the decay rates and decay-rate asymmetries between the four $K\pi$ charge states. With the future improvements via Belle II and upgraded LHCb, the measurements are expected to become precise enough to test these sum rules. The CP asymmetry in the π^+K^- mode has also been measured in B_s^0 decays, by CDF [108] and LHCb [109]. The combined value is $A_{CP}(B_s^0 \to \pi^+K^-) = 0.26 \pm 0.04$.

In addition to $B_{(s)} \to K\pi$ modes, significant ($> 3\sigma$) non-zero CP asymmetries have been measured in several other rare decay modes: $A_{CP}(B^+ \to \rho^0K^+) = 0.37 \pm 0.10$ [110], $A_{CP}(B^+ \to \eta K^+) = 0.37 \pm 0.08$ [111], $A_{CP}(B^0 \to \eta K^{*0}) = 0.19 \pm 0.05$ [112], and $A_{CP}(B^+ \to f_2(1270)K^+) = -0.68^{+0.19}_{-0.17}$ [110]. In at least the first two cases, a large direct CP violation might be expected since the penguin amplitude is suppressed so the tree and penguin amplitudes may have comparable magnitudes. There are also measurements by LHCb of CP asymmetries in several 3-body modes: $A_{CP}(B^+ \to \pi^+\pi^-\pi^+) = 0.057 \pm 0.013$, $A_{CP}(B^+ \to K^+\pi^-\pi^+) = 0.027 \pm 0.008$, $A_{CP}(B^+ \to K^+K^-\pi^+) = -0.118 \pm 0.002$, and $A_{CP}(B^+ \to K^+K^-K^+) = -0.033 \pm 0.008$ [113]. Many of these analyses now include Dalitz plot treatments with many intermediate resonances.

BaBar [114] and Belle [104,115] have observed the decays $B^+ \to \overline{K}^0K^+$ and $B^0 \to K^0\overline{K}^0$. The world-average branching fractions are $\mathcal{B}(B^0 \to K^0\overline{K}^0) = (1.21 \pm 0.16) \times 10^{-6}$ and $\mathcal{B}(B^+ \to \overline{K}^0K^+) = (1.31 \pm 0.17) \times 10^{-6}$. These are the first observations of hadronic $b \to d$ transitions, with significance bigger than 5σ for all four measurements. CP asymmetries have been measured for these modes, but with large errors. LHCb has observed $B^0 \to K^+K^-$ mode which occurs via a weak-annihilation process and is the rarest hadronic B-meson decay thus far observed, with $\mathcal{B}(B^0 \to K^+K^-) = (7.80 \pm 1.52) \times 10^{-8}$ [116]. $B_s^0 \to K^+K^-$ decay mode, which occurs mostly via $b \to s$ penguin process, has been observed by Belle [117], CDF [118] and LHCb [119]. The average branching fraction is $\mathcal{B}(B_s^0 \to K^+K^-) = (25.4 \pm 1.6) \times 10^{-6}$. Belle has also observed $B_s^0 \to K^0\overline{K}^0$ which also occurs via $b \to s$ penguin transition in the SM. The branching fraction is $(1.96^{+0.62}_{-0.56}) \times 10^{-5}$ [120].

The decay $B^0 \to \pi^+\pi^-$ can be used to extract the CKM angle α. This is complicated by the presence of significant contributions from penguin diagrams. An isospin analysis [121] can be used to untangle the penguin complications. The decay $B^0 \to \pi^0\pi^0$ is crucial in this analysis. Both BaBar and Belle have observed $B^0 \to \pi^0\pi^0$, with a mild tension in the measured branching fractions: $(1.83 \pm 0.25) \times 10^{-6}$ for BaBar [122] and $(1.31 \pm 0.26) \times 10^{-6}$ for Belle [123]. It turns out that the amount of penguin pollution in the $B \to \pi\pi$ system is rather large. In the past few years, measurements in the $B^0 \to \rho\rho$ system have produced more precise values of α, since penguin amplitudes are generally smaller for decays with vector mesons. An important ingredient in the analysis is the $B^0 \to \rho^0\rho^0$ branching fraction. The average of measurements from BaBar [124] and Belle [125] yields a branching fraction of $(0.96 \pm 0.15) \times 10^{-6}$. This is only 3% of the $\rho^+\rho^-$ branching fraction, much smaller than the corresponding ratio ($\gtrsim 20\%$) in the $\pi\pi$ system.

Since $B \to \rho\rho$ has two vector mesons in the final state, the CP eigenvalue of the final state depends on the longitudinal polarization fraction f_L for the decay. Therefore, a measurement of f_L is needed to extract the CKM angle α. Both BaBar and Belle have measured f_L for the decays $\rho^+\rho^-$ [126] and $\rho^+\rho^0$ [127] and in both cases the measurements show $f_L > 0.9$, making a complete angular analysis unnecessary. In $B^0 \to \rho^0\rho^0$, f_L is measured by BaBar [124], Belle [125] and LHCb [128], with the average value being $0.71^{+0.08}_{-0.09}$.

By analyzing the angular distributions of the B decays to two vector mesons, we can learn a lot about both weak- and strong-interaction dynamics in B decays. Decays that are penguin-dominated surprisingly have values of f_L near 0.5. The list of such decays has now grown to include $B \to \phi K^*(892)$, $B \to \rho K^*(892)$, and $B \to \omega K^*(892)$. The reasons for this "polarization puzzle" are not fully understood. A detailed description of the angular analysis of B decays to two vector mesons can be found in a separate mini-review [129] in this *Review.*

85.6. Electroweak penguin decays

Electroweak decays are one-loop FCNC decays proceeding through penguin or box Feynman diagrams with final state including real photon or pair of leptons. Such decays were first observed by CLEO experiment when it observed decay $B \to K^*(892)\gamma$ [63]. Since then significant amount of experimental information was obtained. Branching fractions for these decays are 10^{-5} or less, which makes them excellent candidates for searches for new physics beyond SM. Often several observables are available, which allows for stringent tests of the SM.

Starting with radiative decays, experimentally easiest to study are exclusive decays with a fully reconstructed final state. The best studied decay in this class is $B \to K^*(892)\gamma$ seen by CLEO, Belle, BaBar experiments [130,131] with world average branching fraction $\mathcal{B}(B^0 \to K^*(892)^0\gamma) = (43.3 \pm 1.5) \times 10^{-6}$. Decays through several other kaon resonances such as $B \to K_1(1270)\gamma$, $K_2^*(1430)\gamma$, *etc.* were studied at B-factories [132]. It is worth to mention decay $B^+ \to K^+\pi^+\pi^-\gamma$ for which besides measurements of the branching fraction [133] one can also use the angular distribution to access photon polarisation. Such a measurement was done by the LHCb experiment, which was able to clearly demonstrate that the photon in $B^+ \to K^+\pi^+\pi^-\gamma$ decay is polarised [134]. Unfortunately given non-trivial hadronic structure, more work is needed before turning this into test of the SM. The latest addition to the observed exclusive radiative decays is $B_s^0 \to \phi\gamma$, seen by the Belle and LHCb experiments [135,136] with an average branching fraction of $(35.2 \pm 3.4) \times 10^{-6}$.

Compared to $b \to s\gamma$, the $b \to d\gamma$ transitions such as $B \to \rho\gamma$, are suppressed by the CKM elements ratio $|V_{td}/V_{ts}|^2$. Both Belle and BaBar have observed these decays [64,65]. The world average $\mathcal{B}(B \to (\rho,\omega)\gamma) = (1.30 \pm 0.23) \times 10^{-6}$. This can be used to calculate $|V_{td}/V_{ts}|$ [137]; the measured values are $0.195^{+0.025}_{-0.024}$ from Belle [64] and $0.233^{+0.033}_{-0.032}$ from BaBar [65].

The observed radiative penguin branching fractions can constrain a large class of SM extensions [138]. However, due to the uncertainties in the hadronization, only the inclusive $b \to s\gamma$ rate can be reliably compared with theoretical calculations. This rate can be measured from the endpoint of the inclusive photon spectrum in B decay. By combining the measurements of $B \to X_s\gamma$ from the CLEO, BaBar, and Belle experiments [139,140,141], HFLAV obtains the new average: $\mathcal{B}(B \to X_s\gamma) = (3.32 \pm 0.15) \times 10^{-4}$ [26] for $E_\gamma \geq 1.6$ GeV, averaging over B^+ and B^0. Consistent but less precise results have been reported by ALEPH for inclusive b–hadrons produced at the Z, which includes also contribution from B_s^0 and Λ_b^0 hadrons. Using the sum of seven exclusive final states, the BaBar experiment measured the branching fraction of inclusive $b \to d\gamma$ decays to be $(9.2 \pm 2.0 \pm 2.3) \times 10^{-6}$ [142]. The measured branching fraction can be compared to theoretical calculations. Recent calculations of $\mathcal{B}(b \to s\gamma)$ at NNLO level predict for the $E_\gamma \geq 1.6$ GeV values of $(3.36 \pm 0.23) \times 10^{-4}$ for $b \to s\gamma$ and $(1.73^{+0.12}_{-0.22}) \times 10^{-5}$ for $b \to d\gamma$ decays [143].

The CP asymmetry in $b \to s\gamma$ is extensively studied theoretically both in the SM and beyond [144]. According to the SM, the CP asymmetry in $b \to s\gamma$ is smaller than 1%, but some non-SM models allow significantly larger CP asymmetry ($\sim 10\%$) without altering the branching fraction. The current world average is $A_{CP} = 0.015 \pm 0.020$, again dominated by BaBar and Belle [145]. In addition to the CP asymmetry, BaBar also measured the isospin asymmetry $\Delta_{0-} = -0.006 \pm 0.058 \pm .026$ in $b \to s\gamma$ measured using sum of exclusive decays [146]. An alternative measurement using full reconstruction of the companion B in the hadronic decay modes yields a consistent, but less precise result [147]. Both Belle and BaBar experiments measured the isospin asymmetry in exclusive $B \to K^*(892)\gamma$ decay with average of $6.5 \pm 3.0\%$ [131,148] and therefore providing evidence for the non-zero isospin asymmetry.

In addition, experiments have measured the inclusive photon energy spectrum for $b \to s\gamma$, and by analyzing the shape of the spectrum they obtain the first and second moments for photon energies. Belle has measured these moments covering the widest range in the photon energy ($1.7 < E_\gamma < 2.8$ GeV) [141]. The measurement by BaBar has slightly smaller range with lower limit at 1.8 GeV [149]. These results can be used to extract non-perturbative HQET parameters that are needed for precise determination of the CKM matrix element V_{ub}.

Additional information on FCNC processes can be obtained from $b \to s\ell^+\ell^-$ decays. These processes are studied as a function of dilepton invariant mass squared, q^2. Different q^2 regions are sensitive to different physics. Starting at the very low q^2 decays exhibit sensitivity to the same physics as the radiative decays. Then for the q^2 in region 1.1 to 6.0 GeV$^2/c^4$ the SM and new physics have best chance to compete. At the high q^2 above the $\psi(2S)$ mass, the interference of SM and new physics is to some extend complementary to that in lower q^2. Regions around J/ψ and $\psi(2S)$ is normally excluded from measurements as these are dominated by the $b \to c$ transitions to charmonia. For exclusive decays, theory predictions require calculations of hadronic form factors. With current theory predictions, the most useful are measurements within the q^2 regions 1.1 to 6.0 GeV$^2/c^4$ and from 16.0 GeV$^2/c^4$ up to the kinematic limit. From this reason in the listing we provide results mainly in those two regions.

Similar as for radiative decays, also for the $b \to s\ell^+\ell^-$ decays the inclusive measurements provide some benefits. Both Belle and BaBar performed such measurement without reconstructing hadronic part exclusively and measure a branching fraction of $(5.8 \pm 1.3) \times 10^{-6}$ [150]. Unfortunately this measurement is not trivially possible at hadron colliders and also does not easily allow the angular distributions of the decay products to be exploited. One alternative is to extract information on the inclusive decay as sum of exclusive decays. Such a measurement was performed by Belle [151], but in this case the difficulty lies in extrapolation for the missing hadronic states.

Turning to the exclusive decays, the initial measurements performed by B-factories typically averaged between charged and neutral B mesons as well as between e^+e^- and $\mu^+\mu^-$ finals states. The experiments CDF, LHCb, ATLAS and CMS are much better suited for the $\mu^+\mu^-$ finals states compared to the e^+e^- final states. As such most measurements there are done only with $\mu^+\mu^-$ decays and by separating charged and neutral B mesons. The best studied decays are $B^+ \to K^+\ell^+\ell^-$ and $B^0 \to K^*(892)^0\ell^+\ell^-$. At hadron colliders other b hadrons are produced and as such CDF and LHCb experiments did observe also $B_s^0 \to \phi\mu^+\mu^-$ [152,153], $\Lambda_b^0 \to \Lambda\mu^+\mu^-$ [152,154] and $\Lambda_b^0 \to pK^-\mu^+\mu^-$ decays [155]. The total branching fractions integrated over whole q^2 regions are $(5.5 \pm 0.7) \times 10^{-7}$ for $B^+ \to K^+e^+e^-$, $(4.43 \pm 0.24) \times 10^{-7}$ for $B^+ \to K^+\mu^+\mu^-$, $(1.03^{+0.19}_{-0.17}) \times 10^{-6}$ for $B^0 \to K^*(892)^0e^+e^-$ and $(1.03 \pm 0.06) \times 10^{-6}$ for $B^0 \to K^*(892)^0\mu^+\mu^-$ decays [156,157,158,159]. The total branching fractions for $B_s^0 \to \phi\mu^+\mu^-$ and $\Lambda_b^0 \to \Lambda\mu^+\mu^-$ decays are $(8.3 \pm 1.2) \times 10^{-7}$ [152,153] and $(1.08 \pm 0.28) \times 10^{-6}$ [152,154] respectively. With increased precision of $B^0 \to K^*(892)^0\ell^+\ell^-$ decay, there is a question on what fraction of the seen branching fraction is due to the $K^*(892)^0$ resonance and what fraction is due to the $K\pi$ in s-wave. This has been studied by LHCb which found that the $K\pi$ in s-wave fraction varies between 1% and about 10% depending on the q^2 region [159]. It should be noted, that for all relevant B meson decays the branching fractions so far studied are consistently below the SM expectation.

In the $b \to s\ell^+\ell^-$ decays angular distributions offer rich source of information. For the decays $B^+ \to K^+\ell^+\ell^-$ and $B^0 \to K^*(892)^0\ell^+\ell^-$ full angular analysis was already performed [160,161,162,163,164,165], while for other decays only partial angular analyses are available [153,166]. Recently a lot of progress was done by constructing observables, which have reduced theory uncertainties and measurements of these are done. Most notably the observable called P_5' [167] shows a discrepancy with the SM in the q^2 region which is highly sensitive to new physics [164,165]. Measurements of the CP asymmetries [157,168,155], the isospin asymmetry [156,157,158] were also performed. All these measurements are well consistent with the small A_{CP} and small isospin asymmetry expected in the SM [169]. With statistics available at the LHC, the measurement of phase difference between long- and short-distance contribution in $B^+ \to K^+\mu^+\mu^-$ decays became possible [170].

With the data samples available at LHC, the lepton universality in $b \to s\ell^+\ell^-$ can be tested. While in the SM decays to electron-positron and muon pairs are expected to be same up to small corrections due to the different masses of leptons, in extensions of the SM this does not have to hold. The angular analysis of $B^0 \to K^*(892)^0e^+e^-$ decays was performed by LHCb at low dilepton invariant masses [171] and Belle in several regions over whole q^2 range [165]. The most notable result on lepton universality test is the ratio of branching fractions between $B^+ \to K^+\mu^+\mu^-$ and $B^+ \to K^+e^+e^-$ and between $B^0 \to K^*(892)^0\mu^+\mu^-$ and $B^0 \to K^*(892)^0e^+e^-$ decays. In both cases, the measurements by LHCb show similar discrepancy from the SM, each being in the region of 2.1–2.6 σ [172,173].

While $b \to d\ell^+\ell^-$ decays are further suppressed, they recently became accessible. Signals were observed for $B^+ \to \pi^+\mu^+\mu^-$ [174], $B^0 \to \pi^+\pi^-\mu^+\mu^-$ [175] and $\Lambda_b^0 \to p\pi^-\mu^+\mu^-$ [176] decays. The total branching fractions are only quantities measured and these are about 2×10^{-8} for the meson decays and about 7×10^{-8} for the Λ_b^0 decay.

Finally the decays $B_{(s)}^0 \to e^+e^-$ and $\mu^+\mu^-$ are interesting since they only proceed at second order in weak interactions in the SM, but may have large contributions from supersymmetric loops, proportional to $(\tan\beta)^6$. First limits were published 30 years ago and since then experiments at Tevatron, B-factories and LHC gradually improved those and effectively excluded whole models of new physics and significantly constrained allowed parameter space of others. For the decays to $\mu^+\mu^-$, Tevatron experiments pushed the limits down to roughly factor of 5-10 above the SM expectation [177,178]. The long journey in the search for these decays culminated in 2012, when first evidence for $B_s^0 \to \mu^+\mu^-$ decay was seen [179]. Currently the best measurement is coming from the LHCb experiment, which observes $B_s^0 \to \mu^+\mu^-$ decay with 7.8σ and measures the branching fraction to be $(3.0 \pm 0.6^{+0.3}_{-0.2}) \times 10^{-9}$ [180]. The measurements by ATLAS [181] and CMS [182] are consistent with the LHCb measurement, although ATLAS data do not show significant signal for $B_s^0 \to \mu^+\mu^-$ decay. In experiments at hadron colliders searches for $B^0 \to \mu^+\mu^-$ decays are performed at the same time. The best limit on $B(B^0 \to \mu^+\mu^-) < 3.4 \times 10^{-10}$ at 95% C.L. [180]. The limits for the e^+e^- modes are: $< 2.8 \times 10^{-7}$ and $< 8.3 \times 10^{-8}$, respectively, for B_s^0 and B^0 [183]. The searches for decays to $\tau^+\tau^-$ are more challenging with current best limits of $B(B^0 \to \tau^+\tau^-) < 2.1 \times 10^{-3}$ and $B(B_s^0 \to \tau^+\tau^-) < 6.8 \times 10^{-3}$ at 95% C.L. [184]. All existing measurements of B^0 and B_s^0 decays to same flavour dilepton pair is consistent with SM expectation [185]. With $B_s^0 \to \mu^+\mu^-$ decay observed, it was suggested that the effective lifetime is useful further test of the decay [186]. Attempt was made by LHCb experiment, but its precision is not yet sufficient to provide test of the SM [180]. It will take couple of years until interesting precision is reached. The searches were also performed for lepton flavour violating decays to two leptons with best limits in $e^\pm\mu^\mp$ channel, where limits are $< 3.7 \times 10^{-9}$ for B^0 and $< 1.4 \times 10^{-8}$ for B_s^0, at 95% confidence level [187].

Several theory groups performed global analysis of electroweak decays with similar conclusions [188]. In those tensions with SM are observed and the tension can be relieved by new physics beyond SM. For more detailed recent review see e.g. Ref. 189.

85.7. Summary and Outlook

The study of B mesons continues to be one of the most productive fields in particle physics. With the two asymmetric B-factory experiments Belle and BaBar, we now have a combined data sample of well over 1 ab^{-1}. CP violation has been firmly established in many decays of B mesons. Evidence for direct CP violation has been observed. Many rare decays resulting from hadronic $b \to u$ transitions and $b \to s(d)$ penguin decays have been observed, and the emerging pattern is still full of surprises. Despite the remarkable successes of the B-factory experiments, many fundamental questions in the flavor sector remain unanswered.

At Fermilab, CDF and D0 each has accumulated about 10 fb^{-1}, which is the equivalent of about 10^{12} b-hadrons produced. In spite of the low trigger efficiency of hadronic experiments, a selection of modes have been reconstructed in large quantities, giving a start to a program of studies on B_s and b-flavored baryons, in which a first major step has been the determination of the B_s oscillation frequency.

As Tevatron and B-factories finished their taking data, the new experiments at the LHC have become very active. LHCb has collected about 1 fb^{-1} at 7 TeV, 2 fb^{-1} at 8 TeV, and close to 3 fb^{-1} at 13 TeV by September 2017. CMS and ATLAS have collected each about 5 fb^{-1} of data at $\sqrt{s} = 7$ TeV, 20 fb^{-1} at 8 TeV and about 60 fb^{-1} at 13 TeV until September 2017. LHCb, which is dedicated to the studies of b- and c-hadrons, has a data sample that is for many decays larger than the sum of all previous experiments. With it, we are entering to regime of precision physics even for many rare decays, which allows much more detailed measurements.

In addition, the preparation of the next generation high-luminosity B-factory at KEK is in its final stages with first physics data taking expected in 2019. The aim to increase sample to ~ 50 ab^{-1} will make it possible to explore the indirect evidence of new physics beyond the SM in the heavy-flavor particles (b, c, and τ), in a way that is complementary to the LHC. In the same time period, LHCb Collaboration is working on the upgrade of its detector, which will be installed in 2019 and 2020. The aim of the upgrade is to increase flexibility of the trigger, which will allow about a factor of five increase in instantaneous luminosity and of about a factor of two in efficiencies on triggering on purely hadronic decays. The plan is to integrate about 50 fb^{-1} of data.

These experiments promise a rich spectrum of rare and precise measurements that have the potential to fundamentally affecting our understanding of the SM and CP-violating phenomena.

References:

1. M. Kobayashi and T. Maskawa, Prog. Theor. Phys. **49**, 652 (1973).
2. S. W. Herb *et al.*, Phys. Rev. Lett. **39**, 252 (1977).
3. B. Aubert *et al.* (BaBar Collab.), Phys. Rev. Lett. **87**, 091801 (2001).
4. K. Abe *et al.* (Belle Collab.), Phys. Rev. Lett. **87**, 091802 (2001).
5. Currently two different notations (ϕ_1, ϕ_2, ϕ_3) and (α, β, γ) are used in the literature for CKM unitarity angles. In this mini-review, we use the latter notation following the other mini-reviews in this *Review*. The two notations are related by $\phi_1 = \beta$, $\phi_2 = \alpha$ and $\phi_3 = \gamma$.
6. See the "CP Violation in Meson Decays" by D. Kirkby and Y. Nir in this *Review*.
7. See the "CKM Quark Mixing Matrix," by A. Cecucci, Z. Ligeti, and Y. Sakai, in this *Review*.
8. See the note on "B^0 – $\overline{B}^0$ mixing," by O. Schneider in this *Review*.
9. See the "Determination of $|V_{cb}|$ and $|V_{ub}|$," by R. Kowalewski and T. Mannel in this *Review*.
10. F. Abe *et al.* (CDF Collab.), Phys. Rev. Lett. **81**, 2432 (1998); F. Abe *et al.* (CDF Collab.), Phys. Rev. **D58**, 112004 (1998).
11. D. Acosta *et al.* (CDF Collab.), Phys. Rev. Lett. **96**, 082002 (2006).
12. R. Aaij *et al.* (LHCb Collab.), Phys. Rev. **D95**, 032005 (2017).
13. B. Aubert *et al.* (BABAR Collab.), Phys. Rev. Lett. **101**, 071801 (2008), Erratum-Phys. Rev. Lett. **102**, 029901 (2009).
14. B. Aubert *et al.* (BABAR Collab.), Phys. Rev. Lett. **103**, 161801 (2009).
15. G. Bonvicini *et al.* (CLEO Collab.), Phys. Rev. **D81**, 031104 (2010).
16. R. Mizuk *et al.* (Belle Collab.), Phys. Rev. Lett. **109**, 232002 (2012).
17. U. Tamponi *et al.* (Belle Collab.), Phys. Rev. Lett. **115**, 142001 (2015).
18. See the note on "Naming scheme for hadrons," by M. Roos and C.G. Wohl in this *Review*.
19. R. Aaij *et al.* (LHCb Collab.), Phys. Rev. Lett. **118**, 052002 (2017), Erratum-arXiv:1612.05140v7..
20. M. Cacciari *et al.* JHEP **1210**, 137 (2012); B.A. Kniehl *et al.* Phys. Rev. **D84**, 094026 (2011); M. Cacciari, M. L. Mangano, and P. Nason, Eur. Phys. J. **C75**, 610 (2015).
21. B. Barish *et al.* (CLEO Collab.), Phys. Rev. Lett. **76**, 1570 (1996).
22. A. Sokolov *et al.* (Belle Collab.), Phys. Rev. **D75**, 071103 (R) (2007); B. Aubert *et al.* (BaBar Collab.), Phys. Rev. **D78**, 112002 (2008).
23. J.P. Alexander *et al.* (CLEO Collab.), Phys. Rev. Lett. **86**, 2737 (2001); S.B. Athar *et al.* (CLEO Collab.), Phys. Rev. **D66**, 052003 (2002).
24. N.C. Hastings *et al.* (Belle Collab.), Phys. Rev. **D67**, 052004 (2003).
25. B. Aubert *et al.* (BaBar Collab.), Phys. Rev. Lett. **95**, 042001 (2005).
26. Y. Amhis *et al.* (Heavy Flavor Averaging Group), `arXiv:1612.07233`, and online update at `http://www.slac.stanford.edu/xorg/hflav/`.
27. T. Aaltonen *et al.* (CDF Collab.), Phys. Rev. **D93**, 052001 (2016).
28. R. Aaij *et al.* (LHCb Collab.), Phys. Rev. **D85**, 032008 (2012);.
29. T. Aaltonen *et al.* (CDF Collab.), Phys. Rev. **D77**, 072003 (2008); T. Aaltonen *et al.* (CDF Collab.), Phys. Rev. **D79**, 032001 (2009); R. Aaij *et al.* (LHCb Collab.), JHEP **08**, 143 (2014).
30. R. Aaij *et al.* (LHCb Collab.), JHEP **04**, 001 (2013); G. Aad *et al.* (ATLAS Collab.), Phys. Rev. Lett. **115**, 262001 (2015).
31. P. Abreu *et al.* (DELPHI Collab.), Phys. Lett. **B345**, 598 (1995).
32. R. Akers *et al.* (OPAL Collab.), Z. Phys. **C66**, 19 (1995).
33. T. Aaltonen *et al.* (CDF Collab.), Phys. Rev. **D90**, 012013 (2014).
34. R. Aaij *et al.* (LHCb Collab.), JHEP **1504**, 024 (2015).
35. R. Aaij *et al.* (LHCb Collab.), Phys. Rev. Lett. **110**, 151803 (2013).
36. G. Aad *et al.* (ATLAS Collab.), Phys. Rev. Lett. **113**, 212004 (2014).
37. T. Aaltonen *et al.* (CDF Collab.), Phys. Rev. Lett. **99**, 202001 (2007); T. Aaltonen *et al.* (CDF Collab.), Phys. Rev. **D85**, 092011 (2012).
38. V.M. Abazov *et al.* (D0 Collab.), Phys. Rev. Lett. **99**, 052001 (2007); T. Aaltonen *et al.* (CDF Collab.), Phys. Rev. Lett. **99**, 052002 (2007).
39. R. Aaij *et al.* (LHCb Collab.), Phys. Rev. Lett. **113**, 032001 (2014); R. Aaij *et al.* (LHCb Collab.), Phys. Lett. **B**, 154 (2014); R. Aaij *et al.* (LHCb Collab.), Phys. Rev. **D89**, 032001 (2014); R. Aaij *et al.* (LHCb Collab.), Phys. Rev. Lett. **113**, 242002 (2014); R. Aaij *et al.* (LHCb Collab.), Phys. Rev. Lett. **115**, 241801 (2015); R. Aaij *et al.* (LHCb Collab.), Phys. Rev. Lett. **118**, 071801 (2017).
40. T. Aaltonen *et al.* (CDF Collab.), Phys. Rev. **D89**, 072014 (2014).
41. S. Chatrchyan *et al.* (CMS Collab.), Phys. Rev. Lett. **108**, 252002 (2012); R. Aaij *et al.* (LHCb Collab.), JHEP **1605**, 151 (2016).
42. R. Aaij *et al.* (LHCb Collab.), Phys. Rev. Lett. **114**, 062004 (2015).
43. V. M. Abazov *et al.* (D0 Collab.), Phys. Rev. Lett. **101**, 232002 (2008); T. Aaltonen *et al.* (CDF Collab.), Phys. Rev. **D80**, 072003 (2009).
44. R. Aaij *et al.* (LHCb Collab.), Phys. Rev. **D93**, 092007 (2016); R. Aaij *et al.* (LHCb Collab.), Phys. Rev. Lett. **110**, 182001 (2013); R. Aaij *et al.* (LHCb Collab.), Phys. Lett. **B**, 154 (2014).
45. V. M. Abazov *et al.* (D0 Collab.), Phys. Rev. Lett. **117**, 022003 (2016).
46. R. Aaij *et al.* (LHCb Collab.), Phys. Rev. Lett. **117**, 152003 (2016), Erratum-Phys. Rev. Lett. **118**, 109904 (2017).

47. CMS Collaboration, "Search for the $X(5568)$ state in $B_s^0\pi^\pm$ decays," CMS Physics Analysis Summary BPH-16-002 (2016), https://cds.cern.ch/record/2204918.
48. C. Tarantino, Eur. Phys. J. **C33**, S895 (2004); F. Gabbiani *et al.*, Phys. Rev. **D70**, 094031 (2004); F. Gabbiani *et al.*, Phys. Rev. **D68**, 114006 (2003).
49. A. Lenz, Int. J. Mod. Phys. A30, 1543005 (2015).
50. C.H. Chang *et al.*, Phys. Rev. **D64**, 014003 (2001); V.V. Kiselev, A.E. Kovalsky, and A.K. Likhoded, Nucl. Phys. **B585**, 353 (2000); A.Y. Anisimov *et al.*, Phys. Lett. **B452**, 129 (1999); M. Beneke and G. Buchalla, Phys. Rev. **D53**, 4991 (1996).
51. R. Aaij *et al.* (LHCb Collab.), Eur. Phys. J. **C74**, 2839 (2014).
52. R. Aaij *et al.* (LHCb Collab.), Phys. Lett. **B742**, 29 (2015).
53. The B_c is a special case, where a weak decay of the c quark is also possible, but the spectator model still applies.
54. R. Aaij *et al.* (LHCb Collab.), Nature Phys. **11**, 743 (2015).
55. J. P. Lees *et al.* (BaBar Collab.), Phys. Rev. **D85**, 011101 (2012); C. Oswald *et al.* (Belle Collab.), Phys. Rev. **D87**, 072008 (2013); C. Oswald *et al.* (Belle Collab.), Phys. Rev. **D92**, 072013 (2015).
56. T. Aaltonen *et al.* (CDF Collab.), Phys. Rev. **D93**, 052001 (2016).
57. B. Grinstein, Nucl. Phys. **B339**, 253 (1990); H. Georgi, Phys. Lett. **B240**, 447 (1990); A.F. Falk *et al.*, Nucl. Phys. **B343**, 1 (1990); E. Eichten and B. Hill, Phys. Lett. **B234**, 511 (1990).
58. "Heavy-Quark and Soft-Collinear Effective Theory" by C.W. Bauer and M. Neubert in this *Review*.
59. M. Neubert, "Aspects of QCD Factorization," hep-ph/0110093, *Proceedings of HF9*, Pasadena (2001) and references therein; Z. Ligeti *et al.*, Phys. Lett. **B507**, 142 (2001).
60. M. Beneke *et al.*, Phys. Rev. Lett. **83**, 1914 (1999); Nucl. Phys. **B591**, 313 (2000); Nucl. Phys. **B606**, 245 (2001); M. Beneke and M. Neubert, Nucl. Phys. **B675**, 333 (2003).
61. Y.Y. Keum, H-n. Li, and A.I. Sanda, Phys. Lett. **B504**, 6 (2001); Phys. Rev. **D63**, 054008 (2001); Y.Y. Keum and H-n. Li, Phys. Rev. **D63**, 074006 (2001); C.D. Lü, K. Ukai, and M.Z. Yang, Phys. Rev. **D63**, 074009 (2001); C.D. Lü and M.Z. Yang, Eur. Phys. J. **C23**, 275 (2002).
62. C.W. Bauer, S. Fleming, and M.E. Luke, Phys. Rev. **D63**, 014006 (2001); C.W. Bauer *et al.*, Phys. Rev. **D63**, 114020 (2001); C.W. Bauer and I.W. Stewart, Phys. Lett. **B516**, 134 (2001).
63. R. Ammar *et al.* (CLEO Collab.), Phys. Rev. Lett. **71**, 674 (1993).
64. N. Taniguchi *et al.* (Belle Collab.), Phys. Rev. Lett. **101**, 111801 (2008).
65. B. Aubert *et al.* (BaBar Collab.), Phys. Rev. **D78**, 112001 (2008).
66. R. Aaij *et al.* (LHCb Collab.), JHEP **1510**, 034 (2015).
67. P. Krokovny *et al.* (Belle Collab.), Phys. Rev. Lett. **89**, 231804 (2002); B. Aubert *et al.* (BaBar Collab.), Phys. Rev. Lett. **98**, 081801 (2007).
68. B. Kronenbitter *et al.* (Belle Collab.), Phys. Rev. **D92**, 051102 (2015); I. Adachi *et al.* (Belle Collab.), Phys. Rev. Lett. **110**, 131801 (2013).
69. B. Aubert *et al.* (BaBar Collab.), Phys. Rev. **D88**, 031102 (2013); B. Aubert *et al.* (BaBar Collab.), Phys. Rev. **D81**, 051101 (2010).
70. See the "Leptonic decays of charged pseudoscalar mesons," by J. Rosner, S. Stone, and R. Van de Water, in this *Review*.
71. J. P. Lees *et al.* (BaBar Collab.), Phys. Rev. **D84**, 112007 (2011); S. Blyth *et al.* (Belle Collab.), Phys. Rev. **D74**, 092002 (2006).
72. B. Aubert *et al.* (BaBar Collab.), Phys. Rev. Lett. **90**, 242001 (2003).
73. D. Besson *et al.* (CLEO Collab.), Phys. Rev. **D68**, 032002 (2003).
74. P. Krokovny *et al.* (Belle Collab.), Phys. Rev. Lett. **91**, 262002 (2003); Y. Mikami *et al.* (Belle Collab.), Phys. Rev. Lett. **92**, 012002 (2004).
75. B. Aubert *et al.* (BaBar Collab.), Phys. Rev. Lett. **93**, 181801 (2004).
76. S.-K. Choi *et al.* (Belle Collab.), Phys. Rev. Lett. **91**, 262001 (2003).
77. D. Acosta *et al.* (CDF Collab.), Phys. Rev. Lett. **93**, 072001 (2004).
78. V. M. Abazov *et al.* (D0 Collab.), Phys. Rev. Lett. **93**, 162002 (2004).
79. B. Aubert *et al.* (BaBar Collab.), Phys. Rev. **D71**, 071103 (2005).
80. R. Aaij *et al.* (LHCb Collab.), Eur. Phys. J. **C72**, 1972 (2012).
81. S. Chatrchyan *et al.* (CMS Collab.), JHEP **1304**, 154 (2013).
82. M. Aaboud *et al.* (ATLAS Collab.), JHEP **1701**, 117 (2017).
83. S.-K. Choi *et al.* (Belle Collab.), Phys. Rev. Lett. **100**, 142001 (2008); R. Mizuk *et al.* (Belle Collab.), Phys. Rev. **D80**, 031104 (2009).
84. R. Aaij *et al.*(LHCb Collab.), Phys. Rev. Lett. **112**, 222002 (2014); R. Aaij *et al.* (LHCb Collab.), Phys. Rev. **D92**, 112009 (2015).
85. K. Chilikin *et al.* (Belle Collab.), Phys. Rev. **D90**, 112009 (2014).
86. R. Aaij *et al.* (LHCb Collab.), Phys. Rev. Lett. **115**, 072001 (2015).
87. See the "Non-$q\bar{q}$ mesons," by C. Amsler and C. Hanhart, and "Pentaquarks," by M. Karliner and T. Skwarnick, in this *Review*.
88. T. Aaltonen *et al.* (CDF Collab.), Phys. Rev. Lett. **108**, 201801 (2012).
89. S. Esen *et al.* (Belle Collab.), Phys. Rev. **D87**, 031101 (2013).
90. R. Aaij *et al.* (LHCb Collab.), Phys. Rev. **D93**, 092008 (2016).
91. R. Aaij *et al.* (LHCb Collab.), Phys. Rev. Lett. **116**, 161802 (2016).
92. R. Aaij *et al.* (LHCb Collab.), JHEP **11**, 082 (2015).
93. B. Aubert *et al.* (BaBar Collab.), Phys. Rev. **D76**, 031101 (2007).
94. R. Aaij *et al.* (LHCb Collab.), Phys. Rev. **D90**, 012003 (2014).
95. R. Aaij *et al.* (LHCb Collab.), Phys. Rev. Lett. **111**, 181801 (2013).
96. R. Aaij *et al.* (LHCb Collab.), Phys. Rev. **D87**, 112012 (2013).
97. M. Aaboud *et al.* (ATLAS Collab.), Eur. Phys. J. **C76**, 4 (2016).
98. R. Aaij *et al.* (LHCb Collab.), Phys. Rev. **D84**, 092001 (2011), Erratum-Phys. Rev. **D85**, 039904 (2012); T. Aaltonen *et al.* (CDF Collab.), Phys. Rev. **D85**, 032003 (2012).
99. T. Aaltonen *et al.* (CDF Collab.), Phys. Rev. Lett. **107**, 261802 (2011).
100. T. Aaltonen *et al.* (CDF Collab.), Phys. Rev. Lett. **113**, 242001 (2014).
101. T. Aaltonen *et al.* (CDF Collab.), Phys. Rev. Lett. **103**, 031801 (2009).
102. R. Fleischer, Phys. Lett. **B459**, 306 (1999); D. London and J. Matias, Phys. Rev. **D70**, 031502 (2004).
103. J. P. Lees *et al.* (BaBar Collab.), Phys. Rev. **D87**, 052009 (2013).
104. Y.-T. Duh *et al.* (Belle Collab.), Phys. Rev. **D87**, 031103 (2013).
105. R. Aaij *et al.* (LHCb Collab.), Phys. Rev. Lett. **110**, 221601 (2013).
106. B. Aubert *et al.* (BaBar Collab.), Phys. Rev. **D76**, 091102 (2007).
107. See for example M. Gronau and J.L. Rosner, Phys. Rev. **D71**, 074019 (2005); M. Gronau, Phys. Lett. **B627**, 82 (2005).
108. T. Aaltonen *et al.* (CDF Collab.), Phys. Rev. Lett. **113**, 242001 (2013).
109. R. Aaij *et al.* (LHCb Collab.), Phys. Rev. Lett. **110**, 221601 (2013).
110. B. Aubert *et al.* (BaBar Collab.), Phys. Rev. **D78**, 012004 (2008); A. Garmash *et al.* (Belle Collab.), Phys. Rev. Lett. **96**, 251803 (2006).

111. C.-T. Hoi *et al.* (Belle Collab.), Phys. Rev. Lett. **108**, 031801 (2012); B. Aubert *et al.* (BaBar Collab.), Phys. Rev. **D80**, 112002 (2009).
112. B. Aubert *et al.* (BaBar Collab.), Phys. Rev. Lett. **97**, 201802 (2006); C.H. Wang *et al.* (Belle Collab.), Phys. Rev. **D75**, 092005 (2007).
113. R. Aaij *et al.* (LHCb Collab.), Phys. Rev. **D90**, 112004 (2014).
114. B. Aubert *et al.* (BaBar Collab.), Phys. Rev. Lett. **97**, 171805 (2006).
115. S.-W. Lin *et al.* (Belle Collab.), Phys. Rev. Lett. **98**, 181804 (2007).
116. R. Aaij *et al.* (LHCb Collab.), Phys. Rev. Lett. **118**, 081801 (2017).
117. C.-C. Peng *et al.* (Belle Collab.), Phys. Rev. **D82**, 072007 (2010).
118. T. Aaltonen *et al.* (CDF Collab.), Phys. Rev. Lett. **106**, 181802 (2011).
119. R. Aaij *et al.* (LHCb Collab.), JHEP **10**, 037 (2012).
120. B. Pal *et al.* (Belle Collab.), Phys. Rev. Lett. **116**, 161801 (2016).
121. M. Gronau and D. London, Phys. Rev. Lett. **65**, 3381 (1990).
122. J. P. Lees *et al.* (BaBar Collab.), Phys. Rev. **D87**, 052009 (2013).
123. T. Julius *et al.* (Belle Collab.), Phys. Rev. **D96**, 032007 (2017).
124. B. Aubert *et al.* (BaBar Collab.), Phys. Rev. **D78**, 071104 (2008).
125. P. Vanhoefer *et al.* (Belle Collab.), Phys. Rev. **D89**, 072008 (2014).
126. B. Aubert *et al.* (BaBar Collab.), Phys. Rev. **D76**, 052007 (2007); A. Somov *et al.* (Belle Collab.), Phys. Rev. Lett. **96**, 171801 (2006).
127. B. Aubert *et al.* (BaBar Collab.), Phys. Rev. Lett. **102**, 141802 (2009); J. Zhang *et al.* (Belle Collab.), Phys. Rev. Lett. **91**, 221801 (2003).
128. R. Aaij *et al.* (LHCb Collab.), Phys. Lett. **B747**, 468 (2015).
129. See the "Polarization in B Decays," by A. Gritsan in this *Review*.
130. T. E. Coan *et al.* (CLEO Collab.), Phys. Rev. Lett. **84**, 5283 (2000); M. Nakao *et al.* (Belle Collab.), Phys. Rev. **D69**, 112001 (2004).
131. B. Aubert *et al.* (BaBar Collab.), Phys. Rev. Lett. **103**, 211802 (2009).
132. B. Aubert *et al.* (BaBar Collab.), Phys. Rev. **D70**, 091105R (2004); H. Yang *et al.* (Belle Collab.), Phys. Rev. Lett. **94**, 111802 (2005); S. Nishida *et al.* (Belle Collab.), Phys. Lett. **B610**, 23 (2005); B. Aubert *et al.* (BaBar Collab.), Phys. Rev. **D74**, 031102R (2004).
133. H. Yang *et al.* (Belle Collab.), Phys. Rev. Lett. **94**, 111802 (2005); B. Aubert *et al.* (BaBar Collab.), Phys. Rev. Lett. **98**, 211804 (2007), Erratum-Phys. Rev. Lett. **100**, 189903 (2008), Erratum-Phys. Rev. Lett. **100**, 199905 (2008); P. del Amo Sanchez *et al.* (BaBar Collab.), Phys. Rev. **D93**, 052013 (2016).
134. R. Aaij *et al.* (LHCb Collab.), Phys. Rev. Lett. **112**, 161801 (2014).
135. J. Wicht *et al.* (Belle Collab.), Phys. Rev. Lett. **100**, 121801 (2008); D. Dutta *et al.* (Belle Collab.), Phys. Rev. **D91**, 011101 (2015).
136. R. Aaij *et al.* (LHCb Collab.), Nucl. Phys. **B867**, 1 (2013).
137. A. Ali *et al.*, Phys. Lett. **B595**, 323 (2004); P. Ball, G. Jones, and R. Zwicky, Phys. Rev. **D75**, 054004 (2007).
138. J.L. Hewett, Phys. Rev. Lett. **70**, 1045 (1993).
139. S. Chen *et al.* (CLEO Collab.), Phys. Rev. Lett. **87**, 251807 (2001).
140. J. P. Lees *et al.* (BaBar Collab.), Phys. Rev. **D86**, 112008 (2012).
141. A. Limosani *et al.* (Belle Collab.), Phys. Rev. Lett. **103**, 241801 (2009); T. Saito *et al.* (Belle Collab.), Phys. Rev. **D91**, 052004 (2015).
142. P. del Amo Sanchez *et al.* (BaBar Collab.), Phys. Rev. **D82**, 051101 (2010).
143. M. Misiak *et al.* , Phys. Rev. Lett. **114**, 221801 (2015); M. Czakon, P. Fiedler, T. Huber, M. Misiak, T. Schutzmeier and M. Steinhauser, JHEP **1504**, 168 (2015).
144. L. Wolfenstein and Y.L. Wu, Phys. Rev. Lett. **73**, 2809 (1994); H.M. Asatrian and A. Ioannisian, Phys. Rev. **D54**, 5642 (1996); M. Ciuchini *et al.*, Phys. Lett. **B388**, 353 (1996); S. Baek and P. Ko, Phys. Rev. Lett. **83**, 488 (1998); A.L. Kagan and M. Neubert, Phys. Rev. **D58**, 094012 (1998); K. Kiers *et al.*, Phys. Rev. **D62**, 116004 (2000).
145. S. Nishida *et al.* (Belle Collab.), Phys. Rev. Lett. **93**, 031803 (2004); J. P. Lees *et al.* (BaBar Collab.), Phys. Rev. **D90**, 092001 (2014).
146. B. Aubert *et al.* (BaBar Collab.), Phys. Rev. **D72**, 052004 (2005).
147. B. Aubert *et al.* (BaBar Collab.), Phys. Rev. **D77**, 051103 (2008).
148. T. Horiguchi *et al.*(Belle Collab.), arXiv:1707.00394 [hep-ex].
149. J. P. Lees *et al.* (BaBar Collab.), Phys. Rev. Lett. **109**, 191801 (2012).
150. M. Iwasaki *et al.* (Belle Collab.), Phys. Rev. **D72**, 092005 (2005); J. P. Lees *et al.* (BaBar Collab.), Phys. Rev. Lett. **112**, 211802 (2014).
151. Y. Sato *et al.* (Belle Collab.), Phys. Rev. **D93**, 032008 (2016).
152. T. Aaltonen *et al.* (CDF Collab.), Phys. Rev. Lett. **107**, 201802 (2011).
153. R. Aaij *et al.* (LHCb Collab.), JHEP **1307**, 084 (2013); R. Aaij *et al.* (LHCb Collab.), JHEP **1509**, 179 (2015).
154. R. Aaij *et al.* (LHCb Collab.), Phys. Lett. **B725**, 25 (2013).
155. R. Aaij *et al.*(LHCb Collab.), JHEP **1706**, 108 (2017).
156. J.-T. Wei *et al.* (Belle Collab.), Phys. Rev. Lett. **103**, 171801 (2009).
157. J. P. Lees *et al.* (BaBar Collab.), Phys. Rev. **D86**, 032012 (2012).
158. R. Aaij *et al.* (LHCb Collab.), JHEP **1406**, 133 (2014).
159. R. Aaij *et al.* (LHCb Collab.), JHEP **1611**, 047 (2016).
160. T. Aaltonen *et al.* (CDF Collab.), Phys. Rev. Lett. **108**, 081807 (2012).
161. R. Aaij *et al.* (LHCb Collab.), JHEP **1405**, 082 (2014).
162. S. Chatrchyan *et al.* (CMS Collab.), Phys. Lett. **B727**, 77 (2013).
163. V. Khachatryan *et al.* (CMS Collab.), Phys. Lett. **B753**, 424 (2016).
164. R. Aaij *et al.* (LHCb Collab.), JHEP **1602**, 104 (2016).
165. S. Wehle *et al.* (Belle Collab.), Phys. Rev. Lett. **118**, 111801 (2017).
166. R. Aaij *et al.*(LHCb Collab.), JHEP **1506**, 115 (2015).
167. S. Descotes-Genon, J. Matias, M. Ramon, and J. Virto, JHEP **1301**, 048 (2013).
168. R. Aaij *et al.* (LHCb Collab.), JHEP **1409**, 177 (2014).
169. J. Lyon and R. Zwicky, Phys. Rev. **D88**, 094004 (2013).
170. R. Aaij *et al.* (LHCb Collab.), Eur. Phys. J. **C77**, 161 (2017).
171. R. Aaij *et al.* (LHCb Collab.), JHEP **1504**, 064 (2015).
172. R. Aaij *et al.* (LHCb Collab.), Phys. Rev. Lett. **113**, 151601 (2014).
173. R. Aaij *et al.* (LHCb Collab.), JHEP **1708**, 055 (2017).
174. R. Aaij *et al.* (LHCb Collab.), JHEP **1510**, 034 (2015).
175. R. Aaij *et al.* (LHCb Collab.), Phys. Lett. **B743**, 46 (2015).
176. R. Aaij *et al.* (LHCb Collab.), JHEP **1704**, 029 (2017).
177. T. Aaltonen *et al.* (CDF Collab.), Phys. Rev. Lett. **107**, 239903 (2011).
178. V. M. Abazov *et al.* (D0 Collab.), Phys. Rev. **D87**, 072006 (2013).
179. R. Aaij *et al.* (LHCb Collab.), Phys. Rev. Lett. **110**, 021801 (2013).
180. R. Aaij *et al.* (LHCb Collab.), Phys. Rev. Lett. **118**, 191801 (2017).
181. M. Aaboud *et al.*. (ATLAS Collab.), Eur. Phys. J. **C76**, 513 (2016).
182. S. Chatrchyan *et al.* (CMS Collab.), Phys. Rev. Lett. **111**, 101804 (2013).

183. T. Aaltonen *et al.* (CDF Collab.), Phys. Rev. Lett. **102**, 201801 (2009).
184. R. Aaij *et al.* (LHCb Collab.), Phys. Rev. Lett. **118**, 251802 (2017).
185. C. Bobeth *et al.* , Phys. Rev. Lett. **112**, 101801 (2014).
186. K. De Bruyn *et al.*, Phys. Rev. Lett. **109**, 041801 (2012); A. J. Buras, *et al.*, JHEP **1307**, 77 (2013).
187. R. Aaij *et al.* (LHCb Collab.), Phys. Rev. Lett. **111**, 141801 (2013).
188. W. Altmannshofer and D. M. Straub, Eur. Phys. J. **C75**, 382 (2015); F. Beaujean, C. Bobeth and D. van Dyk, Eur. Phys. J. **C74**, 2897 (2014), Erratum-Eur. Phys. J. **C74**, 3179 (2014); S. Descotes-Genon, L. Hofer, J. Matias and J. Virto, JHEP **1606**, 092 (2016); T. Hurth, F. Mahmoudi and S. Neshatpour, JHEP **1412**, 053 (2014).
189. T. Blake, G. Lanfranchi and D. M. Straub, Prog. Part. Nucl. Phys. **92**, 50 (2017).

86. Heavy Flavor Averaging Group

Revised August 2017 by T. Gershon (University of Warwick) and A.J. Schwartz (University of Cincinnati)

The Heavy Flavor Averaging Group (HFLAV)* is an international collaboration of physicists from experiments measuring properties of heavy flavored particles, *i.e.*, hadrons containing b and c quarks, and τ leptons. HFLAV calculates for the HEP community world average values of quantities such as lifetimes, branching fractions, form factors, mixing parameters, and CP-violating asymmetries. Most parameters concern decays of B and D mesons, and many are related to elements of the Cabibbo-Kobayashi-Maskawa (CKM) quark mixing matrix [1,2].

HFLAV was originally formed in 2002 to continue the activities of the LEP Heavy Flavor Steering group. Since its inception a wide range of results have become available from increasingly larger data sets, and consequently HFLAV has expanded to include seven subgroups. These are as follows:

- b-hadron lifetimes and oscillations, including parameters of CP violation in b mixing;
- decay-time-dependent CP violation in B decays, and angles of the CKM Unitarity Triangle;
- semileptonic decays of b-hadrons ($B \to X\ell\nu$, $\ell = e, \mu, \tau$), including determinations of the CKM matrix elements $|V_{cb}|$ and $|V_{ub}|$;
- b-hadron decays to hadronic final states containing c-quarks (open charm and charmonium);
- (rarer) b-hadron decays to final states not containing c-quarks, including fully hadronic, semileptonic ($B \to X\ell\ell, X\nu\bar{\nu}$), leptonic, and radiative decays;
- c-hadron physics including branching fractions, CP- and T-violating asymmetries, D^0–$\bar{D}^0$ mixing, semileptonic decays, and properties of excited D states and charm baryons;
- τ-lepton physics including branching fractions, tests of lepton universality, determination of the CKM matrix element $|V_{us}|$, and searches for lepton flavor violation.

Each subgroup has one or two conveners and typically a half-dozen members representing experiments making measurements in that area. Most groups contain representatives from the Belle, BaBar, and LHCb experiments, while some groups contain representatives from the BESIII, CLEO(c), CDF, and DØ experiments. Members of HFLAV are appointed by their respective experimental collaborations. There are two co-leaders of HFLAV; these were originally appointed by the managements of the BaBar and Belle experiments and are now appointed by the managements of Belle/Belle II and LHCb.

The averaging procedures used by HFLAV are similar to those of the PDG [3]. When calculating world averages, common parameters used for different input measurements are adjusted (rescaled) to common values. The confidence level of the fit is provided to indicate the consistency of the measurements included in the average. However, unlike the PDG, in the case of obtaining a world average with a small confidence level (*i.e.*, a large χ^2 per degree of freedom), HFLAV does not usually scale the resulting uncertainty. Rather, the systematic uncertainties of the measurements are reviewed with experts from the experiments to understand the discrepancy. Unless inconsistencies among measurements are found, no correction is made to the calculated uncertainty. Close communication between representatives of the experiments and HFLAV members performing averages help ensure that measurement uncertainties, known correlations, and systematic effects are properly accounted for. If special treatment is needed to calculate an average, or if an approximation used in an average calculation might not be sufficiently accurate (*e.g.*, assuming Gaussian errors when the likelihood function is non-Gaussian), a note is included to describe this.

In general, HFLAV uses all publicly available results that have written documentation such as a journal publication, preprint, or conference note. These include preliminary results presented at conferences and workshops. However, preliminary results that remain unpublished for an extended period of time, or for which no publication is planned, are not included. A special subset of HFLAV averages are included in the PDG Listings; for these averages only measurements that are published or accepted for publication are used. The averages provided by HFLAV are listed by the PDG as "OUR EVALUATION" with a corresponding note.

All HFLAV averages and input measurements are documented in an approximately biennial preprint posted to the arXiv preprint server; the most recent version is Ref. 4. The latest results and plots are posted on an extensive set of webpages that are updated several times per year; these are available at

`http://www.slac.stanford.edu/xorg/hflav`.

References:

1. N. Cabibbo, Phys. Rev. Lett. **10**, 531 (1963).
2. M. Kobayashi and T. Maskawa, Prog. Theor. Phys. **49**, 652 (1973).
3. See Section 5 of the "Introduction" to this *Review*.
4. Y. Amhis *et al.* [HFLAV Group], `arXiv:1612.07233 [hep-ex]`.

* The group was originally referred to as "HFAG." This acronym was changed to "HFLAV" in 2017.

87. Polarization in B Decays

Revised October 2017 by A. V. Gritsan (Johns Hopkins University).

We review the notation used in polarization measurements in particle production and decay, with a particular emphasis on the B decays and the CP-violating observables in polarization measurements. We look at several examples of vector-vector and vector-tensor B meson decays, while more details about the theory and experimental results in B decays can be found in a separate mini-review [1] in this *Review*.

Figure 87.1 illustrates angular observables in an example of the sequential process $ab \to X \to P_1P_2 \to (p_{11}p_{12})(p_{21}p_{22})$ [2]. The angular distributions are of particular interest because they are sensitive to spin correlations and reveal properties of particles and their interactions, such as quantum numbers and couplings. In the case of a spin-zero particle X, such as B meson or a Higgs boson, there are no spin correlations in the production mechanism and the decay chain is to be analyzed. The angular distribution of decay products can be expressed as a function of three helicity angles which describe the alignment of the particles in the decay chain. The analyzer of the B-daughter polarization is normally chosen for two-body decays, as the direction of the daughters in the center-of-mass of the parent (*e.g.*, $\rho \to 2\pi$) [3], and for three-body decays as the normal to the decay plane (*e.g.*, $\omega \to 3\pi$) [4]. An equivalent set of transversity angles is sometimes used in polarization analyses [5]. The differential decay width depends on complex amplitudes $A_{\lambda_1\lambda_2}$, corresponding to the X-daughter helicity states λ_i.

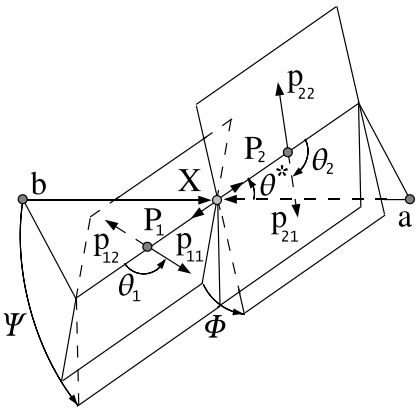

Figure 87.1: Definition of the production and helicity angles in the sequential process $ab \to X \to P_1P_2 \to (p_{11}p_{12})(p_{21}p_{22})$. The three helicity angles include θ_1 and θ_2, defined in the rest frame of the two daughters P_1 and P_2, and Φ, defined in the X frame as the angle between the two decay planes. The two production angles θ^* and Ψ are defined in the X frame, where Ψ is the angle between the production plane and the average of the two decay planes.

In the case of a spin-zero B-meson decay, its daughter helicities are constrained to $\lambda_1 = \lambda_2 = \lambda$. Therefore we simplify amplitude notation as A_λ. Moreover, most B-decay polarization analyses are limited to the case when the spin of one of the B-meson daughters is 1. In that case, there are only three independent amplitudes corresponding to $\lambda = 0$ or ± 1 [6], where the last two can be expressed in terms of parity-even and parity-odd amplitudes $A_{\parallel,\perp} = (A_{+1} \pm A_{-1})/\sqrt{2}$. The overall decay amplitude involves three complex terms proportional to the above amplitudes and the Wigner d functions of helicity angles. The exact angular dependence would depend on the quantum numbers of the B-meson daughters and of their decay products, and can be found in the literature [6,7]. The differential decay rate would involve six real quantities α_i, including interference terms,

$$\frac{d\Gamma}{\Gamma\, d\cos\theta_1\, d\cos\theta_2\, d\Phi} = \sum_i \alpha_i \;\; f_i\,(\cos\theta_1,\, \cos\theta_2,\, \Phi)\,, \qquad (87.1)$$

where each $f_i\,(\cos\theta_1,\, \cos\theta_2,\, \Phi)$ has unique angular dependence specific to particle quantum numbers, and the α_i parameters are defined as:

$$\alpha_1 = \frac{|A_0|^2}{\Sigma|A_\lambda|^2} = f_L\,, \qquad (87.2)$$

$$\alpha_2 = \frac{|A_\parallel|^2 + |A_\perp|^2}{\Sigma|A_\lambda|^2} = (1 - f_L)\,, \qquad (87.3)$$

$$\alpha_3 = \frac{|A_\parallel|^2 - |A_\perp|^2}{\Sigma|A_\lambda|^2} = (1 - f_L - 2\,f_\perp)\,, \qquad (87.4)$$

$$\alpha_4 = \frac{\Im m(A_\perp A_\parallel^*)}{\Sigma|A_\lambda|^2} = \sqrt{f_\perp(1-f_L-f_\perp)}\,\sin(\phi_\perp - \phi_\parallel)\,, \qquad (87.5)$$

$$\alpha_5 = \frac{\Re e(A_\parallel A_0^*)}{\Sigma|A_\lambda|^2} = \sqrt{f_L\,(1 - f_L - f_\perp)}\,\cos(\phi_\parallel)\,, \qquad (87.6)$$

$$\alpha_6 = \frac{\Im m(A_\perp A_0^*)}{\Sigma|A_\lambda|^2} = \sqrt{f_\perp\, f_L}\,\sin(\phi_\perp)\,, \qquad (87.7)$$

where the amplitudes have been expressed with the help of polarization parameters f_L, $f_\perp$, $\phi_\parallel$, and $\phi_\perp$ defined in Table 87.1. Note that the terms proportional to $\Re e(A_\perp A_\parallel^*)$, $\Im m(A_\parallel A_0^*)$, and $\Re e(A_\perp A_0^*)$ are absent in Eqs. (2-7). However, these terms may appear for some three-body decays of a B-meson daughter, see Ref. 7.

Table 87.1: Rate, polarization, and CP-asymmetry parameters defined for the B-meson decays to mesons with non-zero spin. Numerical examples are shown for the average of the $B^0 \to \varphi K^*(892)^0$ decay measurements obtained from BABAR [8], Belle [9], and LHCb [10]. The first six parameters are defined under the assumption of no CP violation in decay, while they are averaged between the $\overline{B}$ and B parameters in general. The last six parameters involve differences between the $\overline{B}$ and B meson decay parameters. The phase convention δ_0 is chosen with respect to a single A_{00} amplitude from a reference B decay mode, which is $B^0 \to \varphi K_0^*(1430)^0$ for numerical results.

parameter	definition	average
$\mathcal{B}$	$\Gamma/\Gamma_{\rm total}$	$(10.1^{+0.6}_{-0.5}) \times 10^{-6}$
f_L	$\lvert A_0\rvert^2/\Sigma\lvert A_\lambda\rvert^2$	0.497 ± 0.017
$f_\perp$	$\lvert A_\perp\rvert^2/\Sigma\lvert A_\lambda\rvert^2$	0.225 ± 0.015
$\phi_\parallel - \pi$	$\arg(A_\parallel/A_0) - \pi$	-0.712 ± 0.058
$\phi_\perp - \pi$	$\arg(A_\perp/A_0) - \pi$	-0.615 ± 0.056
$\delta_0 - \pi$	$\arg(A_{00}/A_0) - \pi$	-0.26 ± 0.10
A_{CP}	$(\bar\Gamma - \Gamma)/(\bar\Gamma + \Gamma)$	-0.003 ± 0.038
A_{CP}^0	$(\bar f_L - f_L)/(\bar f_L + f_L)$	-0.007 ± 0.030
$A_{CP}^\perp$	$(\bar f_\perp - f_\perp)/(\bar f_\perp + f_\perp)$	-0.014 ± 0.057
$\Delta\phi_\parallel$	$(\bar\phi_\parallel - \phi_\parallel)/2$	$+0.051 \pm 0.053$
$\Delta\phi_\perp$	$(\bar\phi_\perp - \phi_\perp - \pi)/2$	$+0.075 \pm 0.050$
$\Delta\delta_0$	$(\bar\delta_0 - \delta_0)/2$	$+0.13 \pm 0.08$

Overall, six real parameters describe three complex amplitudes A_0, $A_\parallel$, and $A_\perp$. These could be chosen to be the four polarization parameters f_L, $f_\perp$, $\phi_\parallel$, and $\phi_\perp$, one overall size normalization, such as decay rate Γ, or branching fraction $\mathcal{B}$, and one overall phase δ_0. The phase convention is arbitrary for an isolated B decay mode. However, for several B decays, the relative phase could produce meaningful and observable effects through interference with other B decays with the same final states, such as for $B \to VK_J^*$ with $J = 0, 1, 2, 3, 4, ...$ The phase could be referenced to the single $B \to VK_0^*$ amplitude A_{00} in such a case, as shown in Table 87.1. Here V stands for any spin-one vector meson.

Moreover, CP violation can be tested in the angular distribution of the decay as the difference between the B and $\overline{B}$. Each of the six real parameters describing the three complex amplitudes would have a counterpart CP-asymmetry term, corresponding to three direct-CP asymmetries in three amplitudes, and three CP-violating

phase differences, equivalent to the phase measurements from the mixing-induced *CP* asymmetries in the time evolution of B-decays [1]. In Table 87.1 and Ref. 11, these are chosen to be the direct-*CP* asymmetries in the overall decay rate $\mathcal{A}_{CP}$, in the f_L fraction $\mathcal{A}^0_{CP}$, and in the $f_\perp$ fraction $\mathcal{A}^\perp_{CP}$, and three weak phase differences:

$$\Delta\phi_\parallel = \frac{1}{2}\arg(\bar{A}_\parallel A_0/A_\parallel \bar{A}_0)\,, \tag{87.8}$$

$$\Delta\phi_\perp = \frac{1}{2}\arg(\bar{A}_\perp A_0/A_\perp \bar{A}_0) - \frac{\pi}{2}\,, \tag{87.9}$$

$$\Delta\delta_0 = \frac{1}{2}\arg(\bar{A}_{00} A_0/A_{00} \bar{A}_0)\,. \tag{87.10}$$

The $\frac{\pi}{2}$ term in Eq. (87.9) reflects the fact that $A_\perp$ and $\bar{A}_\perp$ differ in phase by π if *CP* is conserved. The two parameters $\Delta\phi_\parallel$ and $\Delta\phi_\perp$ are equivalent to triple-product asymmetries constructed from the vectors describing the decay angular distribution [12]. The *CP*-violating phase difference in the reference decay mode [11] is, in the Wolfenstein CKM quark-mixing phase convention,

$$\Delta\phi_{00} = \frac{1}{2}\arg(A_{00}/\bar{A}_{00})\,. \tag{87.11}$$

This can be measured only together with the mixing-induced phase difference for some of the neutral B-meson decays similar to other mixing-induced *CP* asymmetry measurements [1].

It may not always be possible to have a phase-reference decay mode which would define δ_0 and $\Delta\delta_0$ parameters. In that case, it may be possible to define the phase difference directly similarly to Eq. (87.11):

$$\Delta\phi_0 = \frac{1}{2}\arg(A_0/\bar{A}_0)\,. \tag{87.12}$$

One can measure the angles of the CKM unitarity triangle, assuming Standard Model contributions to the $\Delta\phi_0$ and B-mixing phases. Examples include measurements of $\beta = \phi_1$ with $B \to J/\psi K^*$ and $\alpha = \phi_2$ with $B \to \rho\rho$.

Most of the B decays that arise from tree-level $b \to c$ transitions have the amplitude hierarchy $|A_0| > |A_+| > |A_-|$ which is expected from analyses based on quark-helicity conservation [13]. The larger the mass of the vector-meson daughters, the weaker the inequality. The B meson decays to heavy vector particles with charm, such as $B \to J/\psi K^*$, $\psi(2S)K^*$, $\chi_{c1}K^*$, $D^*\rho$, D^*K^*, D^*D^*, and $D^*D_s^*$, show a substantial fraction of the amplitudes corresponding to transverse polarization of the vector mesons ($A_{\pm 1}$), in agreement with the factorization prediction. The detailed amplitude analysis of the $B \to J/\psi K^*$ decays has been performed by the BABAR [14], Belle [15], CDF [16], CLEO [17], D0 [18], and LHCb [19] collaborations. Most analyses are performed under the assumption of the absence of direct *CP* violation. The parameter values are given in the particle listing of this *Review*. The difference between the strong phases $\phi_\parallel$ and $\phi_\perp$ deviates significantly from zero. The measurements [14,15] of *CP*-violating terms similar to those in $B \to \varphi K^*$ [11] shown in Table 87.1 are consistent with zero.

In addition, the mixing-induced *CP*-violating asymmetry is measured in the $B^0 \to J/\psi K^{*0}$ decay [1,14,15] where angular analysis allows one to separate *CP*-eigenstate amplitudes. This allows one to resolve the sign ambiguity of the $\cos 2\beta$ ($\cos 2\phi_1$) term that appears in the time-dependent angular distribution due to interference of parity-even and parity-odd terms. This analysis relies on the knowledge of discrete ambiguities in the strong phases $\phi_\parallel$ and $\phi_\perp$, as discussed below. The BABAR experiment used a method based on the dependence on the $K\pi$ invariant mass of the interference between the S- and P-waves to resolve the discrete ambiguity in the determination of the strong phases $(\phi_\parallel, \phi_\perp)$ in $B \to J/\psi K^*$ decays [14]. The result is in agreement with the amplitude hierarchy expectation [13]. The CDF [20], D0 [21], and LHCb [22] experiments have studied the $B_s^0 \to J/\psi(K^+K^-)$, $J/\psi(\pi^+\pi^-)$, $\psi(K^+\pi^-)$ decays and provided the lifetime, polarization, and phase measurements.

The amplitude hierarchy $|A_0| \gg |A_+| \gg |A_-|$ was expected in B decays to light vector particles in both penguin transitions [23,24] and tree-level transitions [13]. There is confirmation by the BABAR and Belle experiments of predominantly longitudinal polarization in the tree-level $b \to u$ transition, such as $B^0 \to \rho^+\rho^-$ [25], $B^+ \to \rho^0\rho^+$ [26], and $B^+ \to \omega\rho^+$ [27]; this is consistent with the analysis of the quark helicity conservation [13]. Because the longitudinal amplitude dominates the decay, a detailed amplitude analysis is not possible with current B samples, and limits on the transverse amplitude fraction are obtained. The small branching fractions of $B^0 \to \rho^0\rho^0, \omega\rho^0, \omega\omega$ [29–31,27] indicate that $b \to d$ penguin pollution is small in the charmless, strangeless vector-vector B decays. There is a measurement of large longitudinal polarization in $B^0 \to \rho^0\rho^0$ [29–31] decays. The fraction of transverse polarization is large in decays to heavier mesons such as $B^0 \to a_1(1260)^+ a_1(1260)^-$ [28].

The interest in the polarization and *CP*-asymmetry measurements in penguin transition, such as $b \to s$ decays $B \to \varphi K^*$, ρK^*, ωK^*, or $B_s^0 \to \varphi\varphi$, K^*K^*, and $b \to d$ decay $B \to K^*\bar{K}^*$, is motivated by their potential sensitivity to physics beyond the Standard Model. The decay amplitudes for $B \to \varphi K^*$ have been measured by the BABAR, Belle, and LHCb experiments [11,9,32,33,10]. The fractions of longitudinal polarization are $f_L = 0.50 \pm 0.05$ for the $B^+ \to \varphi K^{*+}$ decay and $f_L = 0.497 \pm 0.017$ for the $B^0 \to \varphi K^{*0}$ decay. These indicate significant departure from the naive expectation of predominant longitudinal polarization, suggesting other contributions to the decay amplitude, previously neglected, either within the Standard Model, such as penguin annihilation [34] or QCD rescattering [35], or from physics beyond the Standard Model [36]. The complete set of twelve amplitude parameters measured in the $B^0 \to \varphi K^{*0}$ decay is given in Table 87.1. Several other parameters could be constructed from the above twelve parameters, as suggested in Ref. 37.

The discrete ambiguity in the phase $(\phi_\parallel, \phi_\perp, \Delta\phi_\parallel, \Delta\phi_\perp)$ measurements has been resolved by BABAR in favor of $|A_+| \gg |A_-|$ through interference between the S- and P-waves of $K\pi$. The search for vector-tensor and vector-axialvector $B \to \varphi K_J^{(*)}$ decays with $J = 1, 2, 3, 4$ revealed a large fraction of longitudinal polarization in the decay $B \to \varphi K_2^*(1430)$ with $f_L = 0.90^{+0.06}_{-0.07}$ [11,38], but large contribution of transverse amplitude in $B \to \varphi K_1(1270)$ with $f_L = 0.46^{+0.13}_{-0.15}$ [39].

Like $B \to \varphi K^*$, the decays $B \to \rho K^*$ and $B \to \omega K^*$ may be sensitive to New Physics. Measurements of the longitudinal polarization fraction in $B^+ \to \rho^0 K^{*0}$, $B^+ \to \rho^+ K^{*0}$ [40] and in both vector-vector and vector-tensor final states of $B \to \omega K_J^*$ [27] reveal a large fraction of transverse polarization, indicating an anomaly similar to $B \to \varphi K^*$ except for a different pattern in vector-tensor final states. A large transverse polarization is also observed in the $B_s^0 \to \varphi\varphi$ decay by CDF [41] and LHCb [42], $B_s^0 \to K^{*0}\bar{K}^{*0}$ decays by LHCb [43], and $B_s^0 \to \varphi K^{*0}$ decays by LHCb [44]. At the same time, measurement of the polarization in the $b \to d$ penguin decays $B \to K^*\bar{K}^*$ indicates a large fraction of longitudinal polarization [45]. The polarization pattern in penguin-dominated B-meson decays is not fully understood [34–36].

The three-body semileptonic B-meson decays, such as $B \to V\ell_1\ell_2$, share many features with the two-body $B \to VV$ decays. Their differential decay width can be parameterized with the two helicity angles defined in the V and $(\ell_1\ell_2)$ frames and with the azimuthal angle, as defined in Fig. 87.1. However, since the $(\ell_1\ell_2)$ pair does not come from an on-shell particle, the angular distribution is unique to each point in the dilepton mass $m_{\ell\ell}$ spectrum. The polarization measurements as a function of $m_{\ell\ell}$ provide complementary information on physics beyond the Standard Model, as discussed for $B \to K^*\ell^+\ell^-$ and $B_s \to \phi\ell^+\ell^-$ decays in Ref. 46. The data in these modes have been analyzed by the BABAR, Belle, CDF, CMS, and LHCb experiments [47–52].

The examples of the angular distributions and observables in $B \to K^*\ell^+\ell^-$ are discussed in Ref. 46. Two angular observables have been measured in this decay in certain ranges of the dilepton mass $m_{\ell\ell}$. One parameter is the fraction of longitudinal polarization F_L, which is determined by the K^* angular distribution and is similar to f_L defined for exclusive two-body decays. The other parameter is the forward-backward asymmetry of the lepton pair A_{FB}, which is the asymmetry of the decay rate with positive and negative values of $\cos\theta_1$. A complete set of observables and angular terms has been

adopted by the LHCb collaboration [51] following Ref. 46 with the F_L, A_{FB}, and $S_3 - S_9$ coefficients in the angular distributions. Additional set of optimized observables $P_i^{(\prime)}$ is derived from those, for example $P_2 = 2A_{FB}/(3-3F_L)$ and $P_5' = S_5/\sqrt{F_L(1-F_L)}$. These observables have the advantage that the leading form-factor uncertainties cancel. There have been hints of deviations from SM in the measurement of P_5' and lepton flavor universality [47–52].

In summary, there has been considerable interest in the polarization measurements of B-meson decays because they reveal both weak- and strong-interaction dynamics [34–36,53]. New measurements will further elucidate the pattern of spin alignment measurements in rare B decays, and further test the Standard Model and strong interaction dynamics, including the non-factorizable contributions to the B-decay amplitudes.

References:

1. M. Kreps, Y. Kwon, and P. Eerola, "Production and Decay of b-Flavored Hadrons," mini-review in this *Review*.
2. For an example and further references see Y.Y. Gao *et al.*, Phys. Rev. **D81**, 075022 (2010).
3. M. Jacob and G. C. Wick, Ann. Phys. **7**, 404 (1959).
4. S. M. Berman and M. Jacob, Phys. Rev. **139**, 1023 (1965).
5. I. Dunietz *et al.*, Phys. Rev. **D43**, 2193 (1991).
6. G. Kramer and W.F. Palmer, Phys. Rev. **D45**, 193 (1992).
7. A. Datta *et al.*, Phys. Rev. **D77**, 114025 (2008).
8. BABAR Collab., B. Aubert *et al.*, Phys. Rev. **D78**, 092008 (2008).
9. Belle Collab., M. Prim *et al.*, Phys. Rev. **D88**, 072004 (2013).
10. LHCb Collab., R. Aaij *et al.*, JHEP **05**, 069 (2014).
11. BABAR Collab., B. Aubert *et al.*, Phys. Rev. Lett. **93**, 231804 (2004); Phys. Rev. Lett. **98**, 051801 (2007); Phys. Rev. **D78**, 092008 (2008).
12. G. Valencia, Phys. Rev. **D39**, 3339 (1998); A. Datta and D. London, Int. J. Mod. Phys. **A19**, 2505 (2004).
13. A. Ali *et al.*, Z. Phys. **C1**, 269 (1979); M. Suzuki, Phys. Rev. **D64**, 117503 (2001).
14. BABAR Collab., B. Aubert *et al.*, Phys. Rev. **D71**, 032005 (2005); Phys. Rev. **D76**, 031102 (2007).
15. Belle Collab., R. Itoh *et al.*, Phys. Rev. Lett. **95**, 091601 (2005) Phys. Rev. **D88**, 072004 (2013).
16. CDF Collab., T. Affolder *et al.*, Phys. Rev. Lett. **85**, 4668 (2000); CDF Collab., D. Acosta *et al.*, Phys. Rev. Lett. **94**, 101803 (2005).
17. CLEO Collab., C. P. Jessop, Phys. Rev. Lett. **79**, 4533 (1997).
18. D0 Collab., V. M. Abazov *et al.*, Phys. Rev. Lett. **102**, 032001 (2009).
19. LHCb Collab., R. Aaij *et al.*, Phys. Rev. **D88**, 052002 (2013).
20. CDF Collab., T. Aaltonen *et al.*, Phys. Rev. Lett. **100**, 121803 (2008); Phys. Rev. **D85**, 072002 (2012).
21. D0 Collab., V. M. Abazov *et al.*, Phys. Rev. Lett. **98**, 121801 (2007); Phys. Rev. **D85**, 032006 (2012).
22. LHCb Collab., R. Aaij *et al.*, Phys. Rev. Lett. **108**, 101803 (2012); Phys. Rev. Lett. **114**, 041801 (2015); Phys. Lett. **B747**, 484 (2015); JHEP **1511**, 082 (2015); JHEP **1708**, 037 (2017).
23. H.Y. Cheng and K.C. Yang, Phys. Lett. **B511**, 40 (2001); C.H. Chen, Y.Y. Keum, and H.n. Li, Phys. Rev. **D66**, 054013 (2002).
24. A.L.Kagan, Phys. Lett. **B601**, 151 (2004); Y. Grossman, Int. J. Mod. Phys. **A19**, 907 (2004).
25. BABAR Collab., B. Aubert *et al.*, Phys. Rev. **D76**, 052007 (2007); Belle Collab., A. Somov *et al.*, Phys. Rev. **D93**, 032010 (2016).
26. Belle Collab., J. Zhang *et al.*, Phys. Rev. Lett. **91**, 221801 (2003); BABAR Collab., B. Aubert *et al.*, Phys. Rev. Lett. **102**, 141802 (2009).
27. BABAR Collab., B. Aubert *et al.*, Phys. Rev. **D74**, 051102 (2006); Phys. Rev. **D79**, 052005 (2009).
28. BABAR Collab., B. Aubert *et al.*, Phys. Rev. **D80**, 092007 (2009).
29. BABAR Collab., B. Aubert *et al.*, Phys. Rev. **D78**, 071104 (2008).
30. Belle Collab., I. Adachi *et al.*, Phys. Rev. **D89**, 072008 (2014).
31. LHCb Collab., R. Aaij *et al.*, Phys. Lett. **B747**, 468 (2015).
32. Belle Collab., K.F. Chen *et al.*, Phys. Rev. Lett. **94**, 221804 (2005).
33. BABAR Collab., B. Aubert *et al.*, Phys. Rev. Lett. **99**, 201802 (2007).
34. A.L. Kagan, Phys. Lett. **B601**, 151 (2004); H.n. Li and S. Mishima, Phys. Rev. **D71**, 054025 (2005); C.-H. Chen *et al.*, Phys. Rev. **D72**, 054011 (2005); M. Beneke *et al.*, Phys. Rev. Lett. **96**, 141801 (2006); C.-H. Chen and C.-Q. Geng, Phys. Rev. **D75**, 054010 (2007); A. Datta *et al.*, Phys. Rev. **D76**, 034015 (2007); M. Beneke, J. Rohrer, and D. Yang, Nucl. Phys. **B774**, 64 (2007); H.-Y. Cheng and K.-C. Yang, Phys. Rev. **D78**, 094001 (2008).
35. C. W. Bauer *et al.*, Phys. Rev. **D70**, 054015 (2004); P. Colangelo *et al.*, Phys. Lett. **B597**, 291 (2004); M. Ladisa *et al.*, Phys. Rev. **D70**, 114025 (2004); H. Y. Cheng *et al.*, Phys. Rev. **D71**, 014030 (2005); H. Y. Cheng and K. C. Yang, Phys. Rev. **D83**, 034001 (2011).
36. Y. Grossman, Int. J. Mod. Phys. **A19**, 907 (2004); E. Alvarez *et al.*, Phys. Rev. **D70**, 115014 (2004); P.K. Das and K.C. Yang, Phys. Rev. **D71**, 094002 (2005); C.H. Chen and C.Q. Geng, Phys. Rev. **D71**, 115004 (2005); Y.D. Yang *et al.*, Phys. Rev. **D72**, 015009 (2005); K.C. Yang, Phys. Rev. **72**, 034009 (2005); S. Baek,Phys. Rev. **D72**, 094008 (2005); C.S. Huang *et al.*, Phys. Rev. **D73**, 034026 (2006); C.H. Chen and H. Hatanaka, Phys. Rev. **D73**, 075003 (2006); A. Faessler *et al.*, Phys. Rev. **D75**, 074029 (2007).
37. D. London, N. Sinha, and R. Sinha, Phys. Rev. **D69**, 11401 (2004).
38. BABAR Collab., B. Aubert *et al.*, Phys. Rev. **D76**, 051103 (2007).
39. BABAR Collab., B. Aubert *et al.*, Phys. Rev. Lett. **101**, 161801 (2008).
40. Belle Collab., J. Zhang *et al.*, Phys. Rev. Lett. **95**, 141801 (2005); BABAR Collab., B. Aubert *et al.*, Phys. Rev. Lett. **97**, 201801 (2006); Phys. Rev. **D83**, 051101 (2011); Phys. Rev. **D85**, 072005 (2012).
41. CDF Collab., T. Aaltonen *et al.*, Phys. Rev. Lett. **107**, 261802 (2011).
42. LHCb Collab., R. Aaij *et al.*, Phys. Lett. **B713**, 369 (2012); Phys. Rev. **D90**, 052011 (2014).
43. LHCb Collab., R. Aaij *et al.*, Phys. Lett. **B709**, 50 (2012); JHEP **1507**, 166 (2015).
44. LHCb Collab., R. Aaij *et al.*, JHEP **1311**, 092 (2013).
45. BABAR Collab., B. Aubert *et al.*, Phys. Rev. Lett. **100**, 081801 (2008), Phys. Rev. **D79**, 051102 (2009).
46. G. Burdman, Phys. Rev. **D52**, 6400 (1995); F. Kruger and J. Matias, Phys. Rev. **D71**, 094009 (2005); E. Lunghi and J. Matias, JHEP **0704**, 058 (2007); W. Altmannshofer *et al.*, JHEP **0901**, 019 (2009); J. Matias *et al.*, JHEP **1204**, 104 (2012); S. Descotes-Genon *et al.*, JHEP **1301**, 048 (2013).
47. BABAR Collab., B. Aubert *et al.*, Phys. Rev. **D79**, 031102 (2009); J. P. Lees *et al.*, Phys. Rev. **D93**, 052015 (2016).
48. Belle Collab., J.-T. Wei *et al.*, Phys. Rev. Lett. **103**, 171801 (2009); S. Wehle *et al.*, Phys. Rev. Lett. **118**, 111801 (2017).
49. CDF Collab., T. Aaltonen *et al.*, Phys. Rev. Lett. **108**, 081807 (2012).
50. CMS Collab., S. Chatrchyan *et al.*, Phys. Lett. **B727**, 77 (2013); V. Khachatryan *et al.*, Phys. Lett. **B753**, 424 (2016); A. M. Sirunyan *et al.*, arXiv:1710.02846 [hep-ex].
51. LHCb Collab., R. Aaij *et al.*, JHEP **1308**, 131 (2013); JHEP **1504**, 064 (2015); JHEP **1602**, 104 (2016); JHEP **1611**, 047 (2016); JHEP **1612**, 065 (2016); JHEP **1708**, 055 (2017).
52. LHCb Collab., R. Aaij *et al.*, JHEP **1509**, 179 (2015).
53. C.H. Chen and H.n. Li, Phys. Rev. **D71**, 114008 (2005).

88. B^0–$\overline{B}^0$ Mixing

Updated March 2018 by O. Schneider (Ecole Polytechnique Fédérale de Lausanne).

There are two neutral B^0–$\overline{B}^0$ meson systems, B^0_d–$\overline{B}^0_d$ and B^0_s–$\overline{B}^0_s$ (generically denoted B^0_q–$\overline{B}^0_q$, $q = s, d$), which exhibit particle-antiparticle mixing [1]. This mixing phenomenon is described in Ref. 2. In the following, we adopt the notation introduced in Ref. 2, and assume CPT conservation throughout. In each system, the light (L) and heavy (H) mass eigenstates,

$$|B_{\rm L,H}\rangle = p|B^0_q\rangle \pm q|\overline{B}^0_q\rangle\,, \tag{88.1}$$

have a mass difference $\Delta m_q = m_{\rm H} - m_{\rm L} > 0$, a total decay width difference $\Delta\Gamma_q = \Gamma_{\rm L} - \Gamma_{\rm H}$ and an average decay width $\Gamma_q = (\Gamma_{\rm L} + \Gamma_{\rm H})/2$. In the absence of CP violation in the mixing, $|q/p| = 1$, the differences are given by $\Delta m_q = 2|M_{12}|$ and $|\Delta\Gamma_q| = 2|\Gamma_{12}|$, where M_{12} and Γ_{12} are the off-diagonal elements of the mass and decay matrices [2]. The evolution of a pure $|B^0_q\rangle$ or $|\overline{B}^0_q\rangle$ state at $t = 0$ is given by

$$|B^0_q(t)\rangle = g_+(t)\,|B^0_q\rangle + \frac{q}{p}\,g_-(t)\,|\overline{B}^0_q\rangle\,, \tag{88.2}$$

$$|\overline{B}^0_q(t)\rangle = g_+(t)\,|\overline{B}^0_q\rangle + \frac{p}{q}g_-(t)\,|B^0_q\rangle\,, \tag{88.3}$$

which means that the flavor states remain unchanged (+) or oscillate into each other (−) with time-dependent probabilities proportional to

$$|g_\pm(t)|^2 = \frac{e^{-\Gamma_q t}}{2}\left[\cosh\!\left(\frac{\Delta\Gamma_q}{2}\,t\right) \pm \cos(\Delta m_q\,t)\right]\,, \tag{88.4}$$

where $\Gamma_q = (\Gamma_{\rm H} + \Gamma_{\rm L})/2$. In the absence of CP violation, the time-integrated mixing probability $\int |g_-(t)|^2\,dt/(\int |g_-(t)|^2\,dt + \int |g_+(t)|^2\,dt)$ is given by

$$\chi_q = \frac{x_q^2 + y_q^2}{2(x_q^2+1)}\,, \quad \text{where} \quad x_q = \frac{\Delta m_q}{\Gamma_q}\,, \quad y_q = \frac{\Delta\Gamma_q}{2\Gamma_q}\,. \tag{88.5}$$

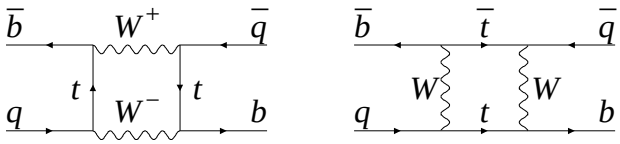

Figure 88.1: Dominant box diagrams for the B^0_q→$\overline{B}^0_q$ transitions ($q = d$ or s). Similar diagrams exist where one or both t quarks are replaced with c or u quarks.

88.1. Standard Model predictions and phenomenology

In the Standard Model, the transitions B^0_q→$\overline{B}^0_q$ and $\overline{B}^0_q$→B^0_q are due to the weak interaction. They are described, at the lowest order, by box diagrams involving two W bosons and two up-type quarks (see Fig. 88.1), as is the case for K^0–$\overline{K}^0$ mixing. However, the long range interactions arising from intermediate virtual states are negligible for the neutral B meson systems, because the large B mass is off the region of hadronic resonances. The calculation of the dispersive and absorptive parts of the box diagrams yields the following predictions for the off-diagonal element of the mass and decay matrices [3],

$$M_{12} = -\frac{G_F^2 m_W^2 \eta_B m_{B_q} B_{B_q} f_{B_q}^2}{12\pi^2}\,S_0(m_t^2/m_W^2)\,(V_{tq}^* V_{tb})^2\,, \tag{88.6}$$

$$\Gamma_{12} = \frac{G_F^2 m_b^2 \eta'_B m_{B_q} B_{B_q} f_{B_q}^2}{8\pi} \times \left[(V_{tq}^* V_{tb})^2 + V_{tq}^* V_{tb} V_{cq}^* V_{cb}\,\mathcal{O}\!\left(\frac{m_c^2}{m_b^2}\right) + (V_{cq}^* V_{cb})^2\,\mathcal{O}\!\left(\frac{m_c^4}{m_b^4}\right)\right]\,, \tag{88.7}$$

where G_F is the Fermi constant, m_W the W boson mass, and m_i the mass of quark i; m_{B_q}, f_{B_q} and B_{B_q} are the B^0_q mass, weak decay constant and bag parameter, respectively. The known function $S_0(x_t)$ can be approximated very well by $0.784\,x_t^{0.76}$ [4], and V_{ij} are the elements of the CKM matrix [5]. The QCD corrections η_B and η'_B are of order unity. The only non-negligible contributions to M_{12} are from box diagrams involving two top quarks. The phases of M_{12} and Γ_{12} satisfy

$$\phi_M - \phi_\Gamma = \pi + \mathcal{O}\left(\frac{m_c^2}{m_b^2}\right)\,, \tag{88.8}$$

implying that the mass eigenstates have mass and width differences of opposite signs. This means that, like in the K^0–$\overline{K}^0$ system, the heavy state is expected to have a smaller decay width than that of the light state: $\Gamma_{\rm H} < \Gamma_{\rm L}$. Hence, $\Delta\Gamma = \Gamma_{\rm L} - \Gamma_{\rm H}$ is expected to be positive in the Standard Model.

Furthermore, the quantity

$$\left|\frac{\Gamma_{12}}{M_{12}}\right| \simeq \frac{3\pi}{2}\frac{m_b^2}{m_W^2}\frac{1}{S_0(m_t^2/m_W^2)} \sim \mathcal{O}\left(\frac{m_b^2}{m_t^2}\right) \tag{88.9}$$

is small, and a power expansion of $|q/p|^2$ yields

$$\left|\frac{q}{p}\right|^2 = 1 + \left|\frac{\Gamma_{12}}{M_{12}}\right|\sin(\phi_M - \phi_\Gamma) + \mathcal{O}\left(\left|\frac{\Gamma_{12}}{M_{12}}\right|^2\right)\,. \tag{88.10}$$

Therefore, considering both Eqs. (88.8) and (88.9), the CP-violating parameter

$$1 - \left|\frac{q}{p}\right|^2 \simeq {\rm Im}\left(\frac{\Gamma_{12}}{M_{12}}\right) \tag{88.11}$$

is expected to be very small: $\sim \mathcal{O}(10^{-3})$ for the B^0_d–$\overline{B}^0_d$ system and $\lesssim \mathcal{O}(10^{-4})$ for the B^0_s–$\overline{B}^0_s$ system [6].

In the approximation of negligible CP violation in mixing, the ratio $\Delta\Gamma_q/\Delta m_q$ is equal to the small quantity $|\Gamma_{12}/M_{12}|$ of Eq. (88.9); it is hence independent of CKM matrix elements, *i.e.*, the same for the B^0_d–$\overline{B}^0_d$ and B^0_s–$\overline{B}^0_s$ systems. Calculations [7] yield $\sim 5 \times 10^{-3}$ with a $\sim 20\%$ uncertainty. Given the published experimental knowledge [8] on the mixing parameter x_q

$$\begin{cases} x_d = 0.770 \pm 0.004 & (B^0_d\text{–}\overline{B}^0_d \text{ system}) \\ x_s = 26.79 \pm 0.08 & (B^0_s\text{–}\overline{B}^0_s \text{ system}) \end{cases}\,, \tag{88.12}$$

the Standard Model thus predicts that $\Delta\Gamma_d/\Gamma_d$ is very small (below 1%), but $\Delta\Gamma_s/\Gamma_s$ considerably larger ($\sim 10\%$). These width differences are caused by the existence of final states to which both the B^0_q and $\overline{B}^0_q$ mesons can decay. Such decays involve $b \to c\bar{c}q$ quark-level transitions, which are Cabibbo-suppressed if $q = d$ and Cabibbo-allowed if $q = s$.

A complete set of Standard Model predictions for all mixing parameters in both the B^0_d–$\overline{B}^0_d$ and B^0_s–$\overline{B}^0_s$ systems can be found in Ref. 9.

88.2. Experimental issues and methods for oscillation analyses

Time-integrated measurements of B^0–$\overline{B}^0$ mixing were published for the first time in 1987 by UA1 [10] and ARGUS [11], and since then by many other experiments. These measurements are typically based on counting same-sign and opposite-sign lepton pairs from the semileptonic decay of the produced $b\bar{b}$ pairs. Such analyses cannot easily separate the contributions from the different b-hadron species, therefore, the clean environment of $\Upsilon(4S)$ machines (where only B^0_d and charged B_u mesons are produced) is in principle best suited to measure χ_d.

However, better sensitivity is obtained from time-dependent analyses aiming at the direct measurement of the oscillation frequencies Δm_d and Δm_s, from the proper time distributions of B^0_d or B^0_s candidates identified through their decay in (mostly) flavor-specific modes, and suitably tagged as mixed or unmixed. This is particularly true for the B^0_s–$\overline{B}^0_s$ system, where the large value of

x_s implies maximal mixing, *i.e.*, $\chi_s \simeq 1/2$. In such analyses, the B_d^0 or B_s^0 mesons are either fully reconstructed, partially reconstructed from a charm meson, selected from a lepton with the characteristics of a $b \to \ell^-$ decay, or selected from a reconstructed displaced vertex. At high-energy colliders (LEP, SLC, Tevatron, LHC), the proper time $t = \frac{m_B}{p} L$ is measured from the distance L between the production vertex and the B decay vertex, and from an estimate of the B momentum p. At asymmetric B factories (KEKB, PEP-II), producing $e^+e^- \to \Upsilon(4S) \to B_d^0\overline{B}_d^0$ events with a boost $\beta\gamma$ (= 0.425, 0.55), the proper time difference between the two B candidates is estimated as $\Delta t \simeq \frac{\Delta z}{\beta\gamma c}$, where Δz is the spatial separation between the two B decay vertices along the boost direction. In all cases, the good resolution needed on the vertex positions is obtained with silicon detectors.

The average statistical significance $\mathcal{S}$ of a B_q^0 oscillation signal can be approximated as [12]

$$\mathcal{S} \approx \sqrt{N/2}\, f_{\rm sig}\, (1-2\eta)\, e^{-(\Delta m_q\, \sigma_t)^2/2}\,, \qquad (88.13)$$

where N is the number of selected and tagged candidates, $f_{\rm sig}$ is the fraction of signal in that sample, η is the total mistag probability, and σ_t is the resolution on proper time (or proper time difference). The quantity $\mathcal{S}$ decreases very quickly as Δm_q increases; this dependence is controlled by σ_t, which is therefore a critical parameter for Δm_s analyses. At high-energy colliders, the proper time resolution $\sigma_t \sim \frac{m_B}{\langle p\rangle}\sigma_L \oplus t\frac{\sigma_p}{p}$ includes a constant contribution due to the decay length resolution σ_L (typically 0.04–0.3 ps), and a term due to the relative momentum resolution σ_p/p (typically 10–20% for partially reconstructed decays), which increases with proper time. At B factories, the boost of the B mesons is estimated from the known beam energies, and the term due to the spatial resolution dominates (typically 1–1.5 ps because of the much smaller B boost).

In order to tag a B_q^0 candidate as mixed or unmixed, it is necessary to determine its flavor both in the initial state and in the final state. The initial and final state mistag probabilities, η_i and η_f, degrade $\mathcal{S}$ by a total factor $(1-2\eta) = (1-2\eta_i)(1-2\eta_f)$. In lepton-based analyses, the final state is tagged by the charge of the lepton from $b \to \ell^-$ decays; the largest contribution to η_f is then due to $\overline{b} \to \overline{c} \to \ell^-$ decays. Alternatively, the charge of a reconstructed charm meson (D^{*-} from B_d^0 or D_s^- from B_s^0), or that of a kaon hypothesized to come from a $b \to c \to s$ decay [13], can be used. For fully-inclusive analyses based on topological vertexing, final-state tagging techniques include jet-charge [14] and charge-dipole [15,16] methods. At high-energy colliders, the methods to tag the initial state (*i.e.*, the state at production), can be divided into two groups: the ones that tag the initial charge of the $\overline{b}$ quark contained in the B_q^0 candidate itself (same-side tag), and the ones that tag the initial charge of the other b quark produced in the event (opposite-side tag). On the same side, the sign of a charged pion, kaon or proton from the primary vertex is correlated with the production state of the B_q^0 meson if that particle is a decay product of a B^{**} state or the first in the fragmentation chain [17,18]. Jet- and vertex-charge techniques work on both sides and on the opposite side, respectively. Finally, the charge of a lepton from $b \to \ell^-$, of a kaon from $b \to c \to s$ or of a charm hadron from $b \to c$ [19] can be used as an opposite-side tag, keeping in mind that its performance is degraded due to integrated mixing. At SLC, the beam polarization produced a sizeable forward-backward asymmetry in the $Z \to b\overline{b}$ decays, and provided another very interesting and effective initial state tag based on the polar angle of the B_q^0 candidate [15]. Initial state tags have also been combined to reach $\eta_i \sim 26\%$ at LEP [18,20] or 22% at SLD [15] with full efficiency. In the case $\eta_f = 0$, this corresponds to an effective tagging efficiency $Q = \epsilon D^2 = \epsilon(1-2\eta)^2$, where ϵ is the tagging efficiency, in the range $23 - 31\%$. The equivalent figure achieved by CDF during Tevatron Run I was $\sim 3.5\%$ [21], reflecting the fact that tagging is more difficult at hadron colliders. The CDF and DØ analyses of Tevatron Run II data reached $\epsilon D^2 = (1.8 \pm 0.1)\%$ [22] and $(2.5 \pm 0.2)\%$ [23] for opposite-side tagging, while same-side kaon tagging (for B_s^0 analyses) contributed an additional $3.7 - 4.8\%$ at CDF [22], and pushed the combined performance to $(4.7 \pm 0.5)\%$ at DØ [24]. LHCb, operating in the forward region at the LHC where the environment is different in terms of track multiplicity and b-hadron production kinematics, has reported $\epsilon D^2 = (2.10 \pm 0.25)\%$ [25] for opposite-side tagging, $(1.80 \pm 0.26)\%$ [26] for same-side kaon tagging, and $(2.11 \pm 0.11)\%$ [27] for same-side pion and proton tagging: the combined figure ranges typically between $(3.73 \pm 0.15)\%$ [28] and $(5.33 \pm 0.25)\%$ [29] depending on the mode in which the tagged B_s^0 meson is reconstructed, and reaches up to $(8.1 \pm 0.6)\%$ [30] for hadronic B_d^0 modes.

At B factories, the flavor of a B_d^0 meson at production cannot be determined, since the two neutral B mesons produced in a $\Upsilon(4S)$ decay evolve in a coherent P-wave state where they keep opposite flavors at any time. However, as soon as one of them decays, the other follows a time-evolution given by Eqs. (88.2) or (88.3), where t is replaced with Δt (which will take negative values half of the time). Hence, the "initial state" tag of a B can be taken as the final-state tag of the other B. Effective tagging efficiencies of 30% are achieved by BaBar and Belle [31], using different techniques including $b \to \ell^-$ and $b \to c \to s$ tags. It is worth noting that, in this case, mixing of the other B (*i.e.*, the coherent mixing occurring before the first B decay) does not contribute to the mistag probability.

Before the experimental observation of a decay-width difference, oscillation analyses typically neglected $\Delta\Gamma_q$ in Eq. (88.4), and described the time dependence with the functions $\Gamma_q e^{-\Gamma_q t}(1 \pm \cos(\Delta m_q t))/2$ (high-energy colliders) or $\Gamma_d e^{-\Gamma_d|\Delta t|}(1 \pm \cos(\Delta m_d \Delta t))/4$ (asymmetric $\Upsilon(4S)$ machines). As can be seen from Eq. (88.4), a non-zero value of $\Delta\Gamma_q$ would effectively reduce the oscillation amplitude with a small time-dependent factor that would be very difficult to distinguish from time resolution effects. Measurements of Δm_q are usually extracted from the data using a maximum likelihood fit.

88.3. Δm_d and $\Delta\Gamma_d$ measurements

Many B_d^0–$\overline{B}_d^0$ oscillations analyses have been published [32] by the ALEPH [33], DELPHI [16,34], L3 [35], OPAL [36,37] BaBar [38], Belle [39], CDF [17], DØ [23], and LHCb [40–43] collaborations. Although a variety of different techniques have been used, the individual Δm_d results obtained at LEP and Tevatron have remarkably similar precision. Their average is compatible with the recent and more precise measurements from the asymmetric B factories and the LHC. The systematic uncertainties are not negligible; they are often dominated by sample composition, mistag probability, or b-hadron lifetime contributions. Before being combined, the measurements are adjusted on the basis of a common set of input values, including the b-hadron lifetimes and fractions published in this *Review*. Some measurements are statistically correlated. Systematic correlations arise both from common physics sources (fragmentation fractions, lifetimes, branching ratios of b hadrons), and from purely experimental or algorithmic effects (efficiency, resolution, tagging, background description). Combining all measurements [16,17,23,33–43] and accounting for all identified correlations yields $\Delta m_d = 0.5065 \pm 0.0016(\text{stat}) \pm 0.0011(\text{syst})\ \text{ps}^{-1}$ [8], a result dominated by the latest LHCb measurement with $B^0 \to D^{(*)-}\mu^+\nu_\mu X$ decays [43].

On the other hand, ARGUS and CLEO have published time-integrated measurements [44–46], which average to $\chi_d = 0.182 \pm 0.015$. Following Ref. 46, the width difference $\Delta\Gamma_d$ could in principle be extracted from the measured value of Γ_d and the above averages for Δm_d and χ_d (see Eq. (88.5)), provided that $\Delta\Gamma_d$ has a negligible impact on the Δm_d measurements. However, direct time-dependent studies published by DELPHI [16], BaBar [47], Belle [48], LHCb [49] and ATLAS [50] provide stronger constraints, which can be combined to yield [8]

$$\Delta\Gamma_d/\Gamma_d = -0.002 \pm 0.010\,. \qquad (88.14)$$

Assuming $\Delta\Gamma_d = 0$ and no CP violation in mixing, and using the measured B_d^0 lifetime of 1.520 ± 0.004 ps, the Δm_d and χ_d results are combined to yield the world average

$$\Delta m_d = 0.5064 \pm 0.0019\ \text{ps}^{-1} \qquad (88.15)$$

or, equivalently,

$$\chi_d = 0.1860 \pm 0.0011\,. \tag{88.16}$$

This Δm_d value provides an estimate of $2|M_{12}|$, and can be used with Eq. (88.6) to extract $|V_{td}|$ within the Standard Model [51]. The main experimental uncertainties on the result come from m_t and Δm_d, but are still completely negligible with respect to the uncertainty due to the hadronic matrix element $f_{B_d}\sqrt{B_{B_d}} = 225 \pm 9$ MeV [52] obtained from recent three-flavor lattice QCD calculations.

88.4. Δm_s and $\Delta\Gamma_s$ measurements

After many years of intense search at LEP and SLC, B^0_s–$\overline{B}^0_s$ oscillations were first observed in 2006 by CDF using 1 fb^{-1} of Tevatron Run II data [22]. More recently LHCb observed B^0_s–$\overline{B}^0_s$ oscillations independently with $B^0_s \to D^-_s\pi^+$ [40,53], $B^0_s \to D^-_s\mu^+\nu$X [42] and even $B^0_s \to J/\psi K^+K^-$ [28] decays, using between 1 and 3 fb^{-1} of data collected at the LHC until the end of 2012. Taking systematic correlations into account, the average of all published measurements of Δm_s [22,28,40,42,53] is

$$\Delta m_s = 17.757 \pm 0.020(\text{stat}) \pm 0.007(\text{syst})\ \text{ps}^{-1}\,, \tag{88.17}$$

dominated by LHCb (see Fig. 88.2) and still statistically limited.

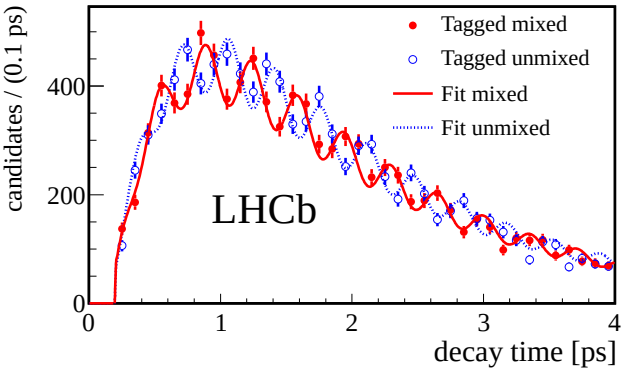

Figure 88.2: Proper time distribution of $B^0_s \to D^-_s\pi^+$ candidates tagged as mixed (red) or unmixed (blue) in the LHCb experiment, displaying B^0_s–$\overline{B}^0_s$ oscillations (from Ref. 53).

The information on $|V_{ts}|$ obtained in the framework of the Standard Model is hampered by the hadronic uncertainty, as in the B^0_d case. However, several uncertainties cancel in the frequency ratio

$$\frac{\Delta m_s}{\Delta m_d} = \frac{m_{B_s}}{m_{B_d}}\,\xi^2\left|\frac{V_{ts}}{V_{td}}\right|^2\,, \tag{88.18}$$

where $\xi = (f_{B_s}\sqrt{B_{B_s}})/(f_{B_d}\sqrt{B_{B_d}}) = 1.206 \pm 0.017$ is an SU(3) flavor-symmetry breaking factor obtained from recent three-flavor lattice QCD calculations [52]. Using the measurements of Eqs. (88.15) and (88.17), one can extract

$$\left|\frac{V_{td}}{V_{ts}}\right| = 0.2053 \pm 0.0004(\text{exp}) \pm 0.0029(\text{lattice})\,, \tag{88.19}$$

in good agreement with (but much more precise than) the value obtained from the ratio of the $b \to d\gamma$ and $b \to s\gamma$ transition rates observed at the B factories [51].

The CKM matrix can be constrained using experimental results on observables such as Δm_d, Δm_s, $|V_{ub}/V_{cb}|$, ϵ_K, and $\sin(2\beta)$ together with theoretical inputs and unitarity conditions [51,54,55]. The constraint from our knowledge on the ratio $\Delta m_s/\Delta m_d$ is more effective in limiting the position of the apex of the CKM unitarity triangle than the one obtained from the Δm_d measurements alone, due to the reduced hadronic uncertainty in Eq. (88.18). We also note that the measured value of Δm_s is consistent with the Standard Model prediction obtained from CKM fits where no experimental information on Δm_s is used, *e.g.*, 17.69 ± 0.93 ps^{-1} [54] or $16.89^{+0.47}_{-0.35}$ ps^{-1} [55].

Information on $\Delta\Gamma_s$ can be obtained from the study of the proper time distribution of untagged B^0_s samples [56]. In the case of an inclusive B^0_s selection [57], or a flavor-specific (semileptonic or hadronic) B^0_s decay selection [20,58–60], both the short- and long-lived components are present, and the proper time distribution is a superposition of two exponentials with decay constants $\Gamma_{\rm L,H} = \Gamma_s \pm \Delta\Gamma_s/2$. In principle, this provides sensitivity to both Γ_s and $(\Delta\Gamma_s/\Gamma_s)^2$. Ignoring $\Delta\Gamma_s$ and fitting for a single exponential leads to an estimate of $1/\Gamma_s$ (called effective lifetime) with a relative bias proportional to $(\Delta\Gamma_s/\Gamma_s)^2$. An alternative approach, which is directly sensitive to first order in $\Delta\Gamma_s/\Gamma_s$, is to determine the effective lifetime of untagged B^0_s candidates decaying to pure CP eigenstates; measurements exist for $B^0_s \to D^+_s D^-_s$ [59], $B^0_s \to K^+K^-$ [60,61], $B^0_s \to J/\psi\eta$ [62], $B^0_s \to J/\psi f_0(980)$ [63], $B^0_s \to J/\psi\pi^+\pi^-$ [64], $B^0_s \to J/\psi K^0_{\rm S}$ [65], and $B^0_s \to \mu^+\mu^-$ [66]. The extraction of $1/\Gamma_s$ and $\Delta\Gamma_s$ from such measurements, discussed in detail in Ref. 67, requires additional information in the form of theoretical assumptions or external inputs on weak phases and hadronic parameters. In what follows, we only use the effective lifetimes of decays to CP-even ($D^+_s D^-_s$, $J/\psi\eta$) and CP-odd ($J/\psi f_0(980)$, $J/\psi\pi^+\pi^-$) final states where CP conservation can be assumed.

The best sensitivity to $1/\Gamma_s$ and $\Delta\Gamma_s$ is achieved by the time-dependent measurements of the $B^0_s \to J/\psi K^+K^-$ (including $B^0_s \to J/\psi\phi$) and $B^0_s \to \psi(2S)\phi$ decay rates performed at CDF [68], DØ [69], ATLAS [70], CMS [71] and LHCb [28,72,73], where the CP-even and CP-odd amplitudes are separated statistically through a full angular analysis. The LHCb collaboration analyzes the $B^0_s \to J/\psi K^+K^-$ decay considering that the K^+K^- system can be in a P-wave or S-wave state, and measures the dependence of the strong phase difference between the P-wave and S-wave amplitudes as a function of the K^+K^- invariant mass [28,74]; this allows the unambiguous determination of the sign of $\Delta\Gamma_s$, which is found to be positive. All these studies use both untagged and tagged B^0_s candidates and are optimized for the measurement of the CP-violating phase $\phi_s^{c\bar{c}s}$, defined as the weak phase difference between the B^0_s–$\overline{B}^0_s$ mixing amplitude and the $b \to c\bar{c}s$ decay amplitude. As reported below in Eq. (88.28), the current experimental average of $\phi_s^{c\bar{c}s}$ is consistent with zero. Assuming no CP violation (*i.e.*, $\phi_s^{c\bar{c}s} = 0$) a combination [8] of the $B^0_s \to J/\psi K^+K^-$, $J/\psi\phi$ and $\psi(2S)\phi$ analyses [28,68–73] and of effective lifetime measurements with flavor-specific [20,58–60] and pure CP [59,62–64] final states yields

$$\Delta\Gamma_s = +0.088 \pm 0.006\ \text{ps}^{-1} \quad \text{and} \quad 1/\Gamma_s = 1.509 \pm 0.004\ \text{ps}\,, \tag{88.20}$$

or, equivalently,

$$1/\Gamma_{\rm L} = 1.415 \pm 0.006\ \text{ps} \quad \text{and} \quad 1/\Gamma_{\rm H} = 1.615 \pm 0.009\ \text{ps}\,, \tag{88.21}$$

in good agreement with the Standard Model prediction $\Delta\Gamma_s = 0.088 \pm 0.020$ ps^{-1} [9].

Estimates of $\Delta\Gamma_s/\Gamma_s$ obtained from measurements of the $B^0_s \to D^{(*)+}_s D^{(*)-}_s$ branching fractions are not included in the average, since they are based on the questionable [7] assumption that these decays account for all CP-even final states.

88.5. Average b-hadron mixing probability and b-hadron production fractions at high energy

Mixing measurements can significantly improve our knowledge on the fractions f_u, f_d, f_s, and $f_{\rm baryon}$, defined as the fractions of B_u, B^0_d, B^0_s, and b-baryons in an unbiased sample of weakly decaying b hadrons produced in high-energy collisions. Indeed, time-integrated mixing analyses using lepton pairs from $b\bar{b}$ events at high energy measure the quantity

$$\overline{\chi} = f'_d\,\chi_d + f'_s\,\chi_s\,, \tag{88.22}$$

where f'_d and f'_s are the fractions of B^0_d and B^0_s hadrons in a sample of semileptonic b-hadron decays. Assuming that all b hadrons have the same semileptonic decay width implies $f'_q = f_q/(\Gamma_q\tau_b)$ $(q = s, d)$, where τ_b is the average b-hadron lifetime. Hence $\overline{\chi}$ measurements

performed at LEP [75] and Tevatron [76,77], together with the χ_d average of Eq. (88.16) and the very good approximation $\chi_s = 1/2$ (in fact $\chi_s = 0.499307 \pm 0.000004$ from Eqs. (88.5), (88.17) and (88.20)), provide constraints on the fractions f_d and f_s.

The LEP experiments have measured $\mathcal{B}(\bar{b} \to B_s^0) \times \mathcal{B}(B_s^0 \to D_s^- \ell^+ \nu_\ell X)$ [78], $\mathcal{B}(b \to \Lambda_b^0) \times \mathcal{B}(\Lambda_b^0 \to \Lambda_c^+ \ell^- \overline{\nu}_\ell X)$ [79], and $\mathcal{B}(b \to \Xi_b^-) \times \mathcal{B}(\Xi_b^- \to \Xi^- \ell^- \overline{\nu}_\ell X)$ [80] from partially reconstructed final states including a lepton, $f_{\rm baryon}$ from protons identified in b events [81], and the production rate of charged b hadrons [82]. The b-hadron fraction ratios measured at CDF are based on double semileptonic $K^* \mu\mu$ and $\phi\mu\mu$ final states [83] and lepton-charm final states [84]; in addition CDF and DØ have both measured strange b-baryon production [85]. On the other hand, fraction ratios have been studied by LHCb using fully reconstructed hadronic B_s^0 and B_d^0 decays [86], as well as semileptonic decays [87]. ATLAS has measured f_s/f_d using $B_s^0 \to J/\psi\phi$ and $B^0 \to J/\psi K^{*0}$ decays [88]. Both CDF and LHCb observe that the ratio $f_{\Lambda_b^0}/(f_u + f_d)$ decreases with the transverse momentum of the lepton+charm system, indicating that the b-hadron fractions are not the same in different environments. We therefore provide sets of fractions separately for LEP and Tevatron (and no complete set for LHC, where strange b-baryon production has not been measured yet). A combination of all the available information under the constraints $f_u = f_d$, $f_u + f_d + f_s + f_{\rm baryon} = 1$, and Eq. (88.22), yields the averages shown in the first two columns of Table 88.1.

Table 88.1: $\overline{\chi}$ and b-hadron fractions (see text).

	in Z decays [8]	at Tevatron [8]	at LHC [86,88]
$\overline{\chi}$	0.1259 ± 0.0042	0.147 ± 0.011	
$f_u = f_d$	0.407 ± 0.007	0.343 ± 0.021	
f_s	0.101 ± 0.008	0.115 ± 0.013	
$f_{\rm baryon}$	0.085 ± 0.011	0.199 ± 0.047	
f_s/f_d	0.249 ± 0.023	0.334 ± 0.041	0.252 ± 0.012

88.6. CP-violation studies

Evidence for CP violation in B_q^0–$\overline{B}_q^0$ mixing has been searched for, both with flavor-specific and inclusive B_q^0 decays, in samples where the initial flavor state is tagged, usually with a lepton from the other b-hadron in the event. In the case of semileptonic (or other flavor-specific) decays, where the final-state tag is also available, the following asymmetry [2]

$$\mathcal{A}_{\rm SL}^q = \frac{N(\overline{B}_q^0(t) \to \ell^+ \nu_\ell X) - N(B_q^0(t) \to \ell^- \overline{\nu}_\ell X)}{N(\overline{B}_q^0(t) \to \ell^+ \nu_\ell X) + N(B_q^0(t) \to \ell^- \overline{\nu}_\ell X)} \simeq 1 - |q/p|_q^2 \tag{88.23}$$

has been measured either in time-integrated analyses at CLEO [46,89], BaBar [90], CDF [91], DØ [92–94] and LHCb [95], or in time-dependent analyses at LEP [37,96], BaBar [47,97] and Belle [98]. In the inclusive case, also investigated at LEP [96,99], no final-state tag is used, and the asymmetry [100]

$$\frac{N(\overline{B}_q^0(t) \to \text{all}) - N(B_q^0(t) \to \text{all})}{N(\overline{B}_q^0(t) \to \text{all}) + N(B_q^0(t) \to \text{all})} \simeq \mathcal{A}_{\rm SL}^q \left[\sin^2 \left(\frac{\Delta m_q\, t}{2} \right) - \frac{x_q}{2} \sin(\Delta m_q\, t) \right] \tag{88.24}$$

must be measured as a function of the proper time to extract information on CP violation. In addition LHCb has studied the time dependence of the charge asymmetry of $B^0 \to D^{(*)-} \mu^+ \nu_\mu X$ decays without tagging the initial state [101], which would be equal to

$$\frac{N(D^{(*)-} \mu^+ \nu_\mu X) - N(D^{(*)+} \mu^- \bar{\nu}_\mu X)}{N(D^{(*)-} \mu^+ \nu_\mu X) + N(D^{(*)+} \mu^- \bar{\nu}_\mu X)} = \mathcal{A}_{\rm SL}^d \frac{1 - \cos(\Delta m_d\, t)}{2} \tag{88.25}$$

in absence of detection and production asymmetries.

The DØ collaboration measured a like-sign dimuon charge asymmetry in semileptonic b decays that deviates by $2.8\,\sigma$ from the tiny Standard Model prediction and concluded, from a more refined analysis in bins of muon impact parameters, that the overall discrepancy is at the level of $3.6\,\sigma$ [92]. In all other cases, asymmetries compatible with zero (and the Standard Model [9]) have been found, with a precision limited by the available statistics. Several of the analyses at high energy don't disentangle the B_d^0 and B_s^0 contributions, and either quote a mean asymmetry or a measurement of $\mathcal{A}_{\rm SL}^d$ assuming $\mathcal{A}_{\rm SL}^s = 0$: we no longer include these in the average. An exception is the dimuon DØ analysis [92], which separates the two contributions by exploiting their dependence on the muon impact parameter cut. The resulting measurements of $\mathcal{A}_{\rm SL}^d$ and $\mathcal{A}_{\rm SL}^s$ are then both compatible with the Standard Model. They are also correlated. We therefore perform a two-dimensional average of the measurements of Refs. [46,47,89,90,92–95,97,98,101] and obtain [8]

$$\mathcal{A}_{\rm SL}^d = -0.0021 \pm 0.0017\,, \quad \text{or} \quad |q/p|_d = 1.0010 \pm 0.0008\,, \tag{88.26}$$

$$\mathcal{A}_{\rm SL}^s = -0.0006 \pm 0.0028\,, \quad \text{or} \quad |q/p|_s = 1.0003 \pm 0.0014\,, \tag{88.27}$$

with a correlation coefficient of -0.054 between $\mathcal{A}_{\rm SL}^d$ and $\mathcal{A}_{\rm SL}^s$. These results show no evidence of CP violation and don't constrain yet the Standard Model.

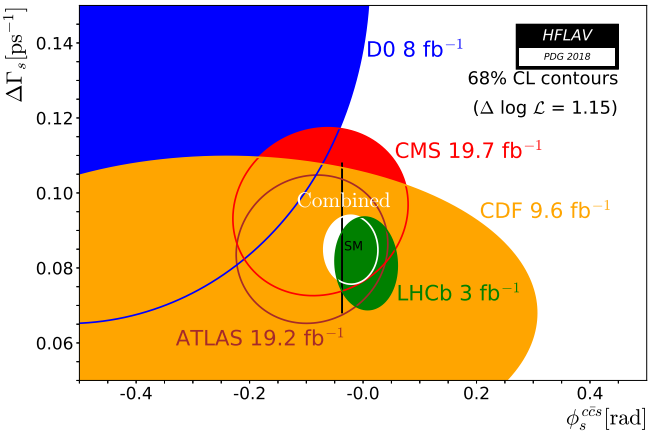

Figure 88.3: 68% CL contours in the $(\phi_s^{c\bar{c}s}, \Delta\Gamma_s)$ plane, showing the measurements from CDF [68], DØ [69], ATLAS [70], CMS [71] and LHCb [28,29,72,73,102], with their combination [8]. The thin black rectangle represents the Standard Model predictions of $\phi_s^{c\bar{c}s}$ [55] and $\Delta\Gamma_s$ [9].

CP violation induced by B_s^0–$\overline{B}_s^0$ mixing in $b \to c\bar{c}s$ decays has been a field of very active study in the past few years. In addition to the previously mentioned $B_s^0 \to J/\psi K^+ K^-$ (including $B_s^0 \to J/\psi\phi$) and $B_s^0 \to \psi(2S)\phi$ studies, the decay modes $B_s^0 \to J/\psi\pi^+\pi^-$ (including $B_s^0 \to J/\psi f_0(980)$) [102] and $B_s^0 \to D_s^+ D_s^-$ [29] have also been analyzed by LHCb to measure $\phi_s^{c\bar{c}s}$, without the need for an angular analysis. The $J/\psi\pi^+\pi^-$ final state has been shown indeed to be (very close to) a pure CP-odd state [103]. A two-dimensional fit [8] of all these results [28,29,68–73,102] in the $(\phi_s^{c\bar{c}s}, \Delta\Gamma_s)$ plane, shown on Fig. 88.3, yields

$$\phi_s^{c\bar{c}s} = -0.021 \pm 0.031\,. \tag{88.28}$$

This is consistent with the Standard Model prediction for $\phi_s^{c\bar{c}s}$, which is equal to $-2\beta_s = -2\arg(-(V_{ts}V_{tb}^*)/(V_{cs}V_{cb}^*)) = -0.0370 \pm 0.0006$ [55], assuming negligible Penguin pollution.

88.7. Summary

B^0–$\overline{B}^0$ mixing has been and still is a field of intense study. The mass differences in the B^0_d–$\overline{B}^0_d$ and B^0_s–$\overline{B}^0_s$ systems are known to relative precisions of 0.38% and 0.12%, respectively. The non-zero decay width difference in the B^0_s–$\overline{B}^0_s$ system is well established, with a relative difference of $\Delta\Gamma_s/\Gamma_s = (13.2 \pm 0.8)\%$, meaning that the heavy state of the B^0_s–$\overline{B}^0_s$ system lives $\sim 13\%$ longer than the light state. In contrast, the relative decay width difference in the B^0_d–$\overline{B}^0_d$ system, $\Delta\Gamma_d/\Gamma_d = (-0.2 \pm 1.0)\%$, is still consistent with zero. CP violation in B^0_d–$\overline{B}^0_d$ or B^0_s–$\overline{B}^0_s$ mixing has not been observed yet, with precisions on the semileptonic asymmetries below 0.3%. CP violation induced by B^0_s–$\overline{B}^0_s$ mixing in $b \to c\bar{c}s$ transitions has not yet been observed either, with an uncertainty on the $\phi_s^{c\bar{c}s}$ phase of 31 mrad. Despite the recent improvements, all observations remain consistent with the Standard Model expectations.

However, the measurements where New Physics might show up are still statistically limited. More results are awaited from the LHC experiments and Belle II, with promising prospects for the investigation of the CP-violating phase $\arg(-M_{12}/\Gamma_{12})$ and an improved determination of $\phi_s^{c\bar{c}s}$.

Mixing studies have clearly reached the stage of precision measurements, where much effort is needed, both on the experimental and theoretical sides, in particular to further reduce the hadronic uncertainties of lattice QCD calculations. In the long term, a stringent check of the consistency of the B^0_d and B^0_s mixing amplitudes (magnitudes and phases) with all other measured flavor-physics observables will be possible within the Standard Model, leading to very tight limits on (or otherwise a long-awaited surprize about) New Physics.

References:

1. T.D. Lee and C.S. Wu, Ann. Rev. Nucl. Sci. **16**, 511 (1966); I.I. Bigi and A.I. Sanda, "CP violation," Cambridge Univ. Press, 2000; G.C. Branco, L. Lavoura, and J.P. Silva, "CP violation," Clarendon Press Oxford, 1999.
2. See the review on CP violation in the quark sector by T. Gershon and Y. Nir in this publication.
3. A.J. Buras, W. Slominski, and H. Steger, Nucl. Phys. **B245**, 369 (1984).
4. T. Inami and C.S. Lim, Prog. Theor. Phys. **65**, 297 (1981); for the power-like approximation, see A.J. Buras and R. Fleischer, page 91 in "Heavy Flavours II," eds. A.J. Buras and M. Lindner, Singapore World Scientific, 1998.
5. M. Kobayashi and K. Maskawa, Prog. Theor. Phys. **49**, 652 (1973).
6. I.I. Bigi *et al.*, in "CP violation," ed. C. Jarlskog, Singapore World Scientific, 1989.
7. A. Lenz and U. Nierste, `arXiv:1102.4274 [hep-ph]`; A. Lenz and U. Nierste, JHEP **06**, 072 (2007).
8. Y. Amhis *et al.* [HFLAV Group], "Averages of b-hadron, c-hadron, and τ-lepton properties as of summer 2016," `arXiv:1612.07233 [hep-ex]`, Eur. Phys. J. **C77**, 895 (2017); the combined results on b-hadron fractions, lifetimes and mixing parameters published in this *Review* have been obtained by the B oscillations working group of the Heavy Flavor Averaging (HFLAV) Group, using the methods and procedures described in Chapter 3 of the above paper, after updating the list of inputs; for more information, see `http://www.slac.stanford.edu/xorg/hflav/osc/`.
9. T. Jubb, M. Kirk, A. Lenz, and G. Tetlalmatzi-Xolocotzi, Nucl. Phys. **B915**, 431 (2017); M. Artuso, G. Borissov, and A. Lenz, Rev. Mod. Phys. **88**, 045002 (2016).
10. C. Albajar *et al.* [UA1 Collab.], Phys. Lett. **B186**, 247 (1987).
11. H. Albrecht *et al.* [ARGUS Collab.], Phys. Lett. **B192**, 245 (1987).
12. H.-G. Moser and A. Roussarie, Nucl. Instrum. Methods **A384**, 491 (1997).
13. SLD Collab., SLAC-PUB-7228, SLAC-PUB-7229, and SLAC-PUB-7230, *28th Int. Conf. on High Energy Physics,* Warsaw, 1996; J. Wittlin, PhD thesis, SLAC-R-582, 2001.
14. ALEPH Collab., contrib. 596 to *Int. Europhysics Conf. on High Energy Physics,* Jerusalem, 1997.
15. K. Abe *et al.* [SLD Collab.], Phys. Rev. **D67**, 012006 (2003).
16. J. Abdallah *et al.* [DELPHI Collab.], Eur. Phys. J. **C28**, 155 (2003).
17. F. Abe *et al.* [CDF Collab.], Phys. Rev. Lett. **80**, 2057 (1998) and Phys. Rev. **D59**, 032001 (1999); Phys. Rev. **D60**, 051101 (1999); Phys. Rev. **D60**, 072003 (1999); T. Affolder *et al.* [CDF Collab.], Phys. Rev. **D60**, 112004 (1999).
18. R. Barate *et al.* [ALEPH Collab.], Eur. Phys. J. **C4**, 367 (1998); Eur. Phys. J. **C7**, 553 (1999).
19. R. Aaij *et al.* [LHCb Collab.], JINST **10**, P10005 (2015).
20. P. Abreu *et al.* [DELPHI Collab.], Eur. Phys. J. **C16**, 555 (2000).
21. See tagging summary on page 160 of K. Anikeev *et al.*, "B physics at the Tevatron: Run II and beyond," FERMILAB-PUB-01/97, `hep-ph/0201071`, and references therein.
22. A. Abulencia *et al.* [CDF Collab.], Phys. Rev. Lett. **97**, 242003 (2006).
23. V.M. Abazov *et al.* [DØ Collab.], Phys. Rev. **D74**, 112002 (2006).
24. V.M. Abazov *et al.* [DØ Collab.], Phys. Rev. Lett. **101**, 241801 (2008).
25. R. Aaij *et al.* [LHCb Collab.], Eur. Phys. J. **C72**, 2022 (2012).
26. R. Aaij *et al.* [LHCb Collab.], JINST **11**, P05010 (2016).
27. R. Aaij *et al.* [LHCb Collab.], Eur. Phys. J. **C77**, 238 (2017).
28. R. Aaij *et al.* [LHCb Collab.], Phys. Rev. Lett. **114**, 041801 (2015).
29. R. Aaij *et al.* [LHCb Collab.], Phys. Rev. Lett. **113**, 211801 (2014).
30. R. Aaij *et al.* [LHCb Collab.], Phys. Rev. Lett. **117**, 261801 (2016).
31. B. Aubert *et al.* [BaBar Collab.], Phys. Rev. Lett. **94**, 161803 (2005); K.-F. Chen *et al.* [Belle Collab.], Phys. Rev. **D72**, 012004 (2005).
32. Throughout this document we omit references of results that have been replaced by new published measurements.
33. D. Buskulic *et al.* [ALEPH Collab.], Z. Phys. **C75**, 397 (1997).
34. P. Abreu *et al.* [DELPHI Collab.], Z. Phys. **C76**, 579 (1997).
35. M. Acciarri *et al.* [L3 Collab.], Eur. Phys. J. **C5**, 195 (1998).
36. G. Alexander *et al.* [OPAL Collab.], Z. Phys. **C72**, 377 (1996); K. Ackerstaff *et al.* [OPAL Collab.], Z. Phys. **C76**, 417 (1997); G. Abbiendi *et al.* [OPAL Collab.], Phys. Lett. **B493**, 266 (2000).
37. K. Ackerstaff *et al.* [OPAL Collab.], Z. Phys. **C76**, 401 (1997).
38. B. Aubert *et al.* [BaBar Collab.], Phys. Rev. Lett. **88**, 221802 (2002) and Phys. Rev. **D66**, 032003 (2002); Phys. Rev. Lett. **88**, 221803 (2002); Phys. Rev. **D67**, 072002 (2003); Phys. Rev. **D73**, 012004 (2006).
39. N.C. Hastings *et al.* [Belle Collab.], Phys. Rev. **D67**, 052004 (2003); Y. Zheng *et al.* [Belle Collab.], Phys. Rev. **D67**, 092004 (2003); K. Abe *et al.* [Belle Collab.], Phys. Rev. **D71**, 072003 (2005).
40. R. Aaij *et al.* [LHCb Collab.], Phys. Lett. **B709**, 177 (2012).
41. R. Aaij *et al.* [LHCb Collab.], Phys. Lett. **B719**, 318 (2013).
42. R. Aaij *et al.* [LHCb Collab.], Eur. Phys. J. **C73**, 2655 (2013).
43. R. Aaij *et al.* [LHCb Collab.], Eur. Phys. J. **C76**, 422 (2016).
44. H. Albrecht *et al.* [ARGUS Collab.], Z. Phys. **C55**, 357 (1992); Phys. Lett. **B324**, 249 (1994).
45. J. Bartelt *et al.* [CLEO Collab.], Phys. Rev. Lett. **71**, 1680 (1993).
46. B.H. Behrens *et al.* [CLEO Collab.], Phys. Lett. **B490**, 36 (2000).
47. B. Aubert *et al.* [BaBar Collab.], Phys. Rev. Lett. **92**, 181801 (2004) and Phys. Rev. **D70**, 012007 (2004).
48. T. Higuchi *et al.* [Belle Collab.], Phys. Rev. **D85**, 071105 (2012).
49. R. Aaij *et al.* [LHCb Collab.], JHEP **04**, 114 (2014).
50. M. Aaboud *et al.* [ATLAS Collab.], JHEP **06**, 081 (2016).
51. See the review on the CKM quark-mixing matrix by A. Ceccucci, Z. Ligeti, and Y. Sakai in this publication.

52. S. Aoki *et al.* [FLAG Working Group], Eur. Phys. J. **C77**, 112 (2017); updated results at `http://itpwiki.unibe.ch/flag/`, dominated by A. Bazavov *et al.* [Fermilab Lattice and MILC Collab.], Phys. Rev. **D93**, 113016 (2016).
53. R. Aaij *et al.* [LHCb Collab.], New J. Phys. **15**, 053021 (2013).
54. M. Bona *et al.* [UTfit Collab.], JHEP **10**, 081 (2006); updated results at `http://www.utfit.org/`.
55. J. Charles *et al.* [CKMfitter Group], Phys. Rev. **D91**, 073007 (2015); updated results at `http://ckmfitter.in2p3.fr/`.
56. K. Hartkorn and H.-G. Moser, Eur. Phys. J. **C8**, 381 (1999).
57. M. Acciarri *et al.* [L3 Collab.], Phys. Lett. **B438**, 417 (1998).
58. D. Buskulic *et al.* [ALEPH Collab.], Phys. Lett. **B377**, 205 (1996); K. Ackerstaff *et al.* [OPAL Collab.], Phys. Lett. **B426**, 161 (1998); F. Abe *et al.* [CDF Collab.], Phys. Rev. **D59**, 032004 (1999); V.M. Abazov *et al.* [DØ Collab.], Phys. Rev. Lett. **114**, 062001 (2015); T. Aaltonen *et al.* [CDF Collab.], Phys. Rev. Lett. **107**, 272001 (2011); R. Aaij *et al.* [LHCb Collab.], Phys. Rev. Lett. **113**, 172001 (2014); R. Aaij *et al.* [LHCb Collab.], Phys. Rev. Lett. **119**, 101801 (2017).
59. R. Aaij *et al.* [LHCb Collab.], Phys. Rev. Lett. **112**, 111802 (2014).
60. R. Aaij *et al.* [LHCb Collab.], Phys. Lett. **B736**, 446 (2014).
61. R. Aaij *et al.* [LHCb Collab.], Phys. Lett. **B707**, 349 (2012).
62. R. Aaij *et al.* [LHCb Collab.], Phys. Lett. **B762**, 484 (2016).
63. T. Aaltonen *et al.* [CDF Collab.], Phys. Rev. **D84**, 052012 (2011); V.M. Abazov *et al.* [DØ Collab.], Phys. Rev. **D94**, 012001 (2016).
64. R. Aaij *et al.* [LHCb Collab.], Phys. Rev. **D87**, 112010 (2013).
65. R. Aaij *et al.* [LHCb Collab.], Nucl. Phys. **B873**, 275 (2013).
66. R. Aaij *et al.* [LHCb Collab.], Phys. Rev. Lett. **118**, 191801 (2017).
67. R. Fleischer and R. Knegjens, Eur. Phys. J. **C71**, 1789 (2011).
68. T. Aaltonen *et al.* [CDF Collab.], Phys. Rev. Lett. **109**, 171802 (2012).
69. V.M. Abazov *et al.* [DØ Collab.], Phys. Rev. **D85**, 032006 (2012).
70. G. Aad *et al.* [ATLAS Collab.], Phys. Rev. **D90**, 052007 (2014); JHEP **08**, 147 (2016).
71. V. Khachatryan *et al.* [CMS Collab.], Phys. Lett. **B757**, 97 (2016).
72. R. Aaij *et al.* [LHCb Collab.], JHEP **08**, 037 (2017).
73. R. Aaij *et al.* [LHCb Collab.], Phys. Lett. **B762**, 253 (2016).
74. R. Aaij *et al.* [LHCb Collab.], Phys. Rev. Lett. **108**, 241801 (2012).
75. ALEPH, DELPHI, L3, OPAL, and SLD Collabs.; Physics Reports **427**, 257 (2006); we use the $\overline{\chi}$ average given in Eq. (5.39).
76. D. Acosta *et al.* [CDF Collab.], Phys. Rev. **D69**, 012002 (2004).
77. V.M. Abazov *et al.* [DØ Collab.], Phys. Rev. **D74**, 092001 (2006).
78. P. Abreu *et al.* [DELPHI Collab.], Phys. Lett. **B289**, 199 (1992); P.D. Acton *et al.* [OPAL Collab.], Phys. Lett. **B295**, 357 (1992); D. Buskulic *et al.* [ALEPH Collab.], Phys. Lett. **B361**, 221 (1995).
79. P. Abreu *et al.* [DELPHI Collab.], Z. Phys. **C68**, 375 (1995); R. Barate *et al.* [ALEPH Collab.], Eur. Phys. J. **C2**, 197 (1998).
80. D. Buskulic *et al.* [ALEPH Collab.], Phys. Lett. **B384**, 449 (1996); J. Abdallah *et al.* [DELPHI Collab.], Eur. Phys. J. **C44**, 299 (2005).
81. R. Barate *et al.* [ALEPH Collab.], Eur. Phys. J. **C5**, 205 (1998).
82. J. Abdallah *et al.* [DELPHI Collab.], Phys. Lett. **B576**, 29 (2003).
83. F. Abe *et al.* [CDF Collab.], Phys. Rev. **D60**, 092005 (1999).
84. T. Aaltonen *et al.* [CDF Collab.], Phys. Rev. **D77**, 072003 (2008); T. Affolder *et al.* [CDF Collab.], Phys. Rev. Lett. **84**, 1663 (2000); the measurement of $f_{\rm baryon}/f_d$ in the latter paper has been updated based on T. Aaltonen *et al.* [CDF Collab.], Phys. Rev. **D79**, 032001 (2009).
85. V.M. Abazov *et al.* [DØ Collab.], Phys. Rev. Lett. **99**, 052001 (2007); V.M. Abazov *et al.* [DØ Collab.], Phys. Rev. Lett. **101**, 232002 (2008); T. Aaltonen *et al.* [CDF Collab.], Phys. Rev. **D80**, 072003 (2009).
86. R. Aaij *et al.* [LHCb Collab.], JHEP **04**, 001 (2013); the LHCb average of f_s/f_d has been updated in LHCb Collab., LHCb-CONF-2013-011 (2013).
87. R. Aaij *et al.* [LHCb Collab.], Phys. Rev. **D85**, 032008 (2012).
88. G. Aad *et al.* [ATLAS Collab.], Phys. Rev. Lett. **115**, 262001 (2015).
89. D.E. Jaffe *et al.* [CLEO Collab.], Phys. Rev. Lett. **86**, 5000 (2001).
90. J.P. Lees *et al.* [BaBar Collab.], Phys. Rev. Lett. **114**, 081801 (2015).
91. F. Abe *et al.* [CDF Collab.], Phys. Rev. **D55**, 2546 (1997).
92. V.M. Abazov *et al.* [DØ Collab.], Phys. Rev. **D89**, 012002 (2014).
93. V.M. Abazov *et al.* [DØ Collab.], Phys. Rev. **D86**, 072009 (2012).
94. V.M. Abazov *et al.* [DØ Collab.], Phys. Rev. Lett. **110**, 011801 (2013).
95. R. Aaij *et al.* [LHCb Collab.], Phys. Rev. Lett. **117**, 061803 (2016).
96. R. Barate *et al.* [ALEPH Collab.], Eur. Phys. J. **C20**, 431 (2001).
97. J.P. Lees *et al.* [BaBar Collab.], Phys. Rev. Lett. **111**, 101802 (2013).
98. E. Nakano *et al.* [Belle Collab.], Phys. Rev. **D73**, 112002 (2006).
99. G. Abbiendi *et al.* [OPAL Collab.], Eur. Phys. J. **C12**, 609 (2000).
100. M. Beneke, G. Buchalla, and I. Dunietz, Phys. Lett. **B393**, 132 (1997); I. Dunietz, Eur. Phys. J. **C7**, 197 (1999).
101. R. Aaij *et al.* [LHCb Collab.], Phys. Rev. Lett. **114**, 041601 (2015).
102. R. Aaij *et al.* [LHCb Collab.], Phys. Lett. **B736**, 186 (2014).
103. R. Aaij *et al.* [LHCb Collab.], Phys. Rev. **D86**, 052006 (2012).

89. Semileptonic b-Hadron Decays, Determination of V_{cb}, V_{ub}

Updated October 2017 by R. Kowalewski (Univ. of Victoria, Canada) and T. Mannel (Univ. of Siegen, Germany)

89.1. Introduction

Precision determinations of $|V_{ub}|$ and $|V_{cb}|$ are central to testing the CKM sector of the Standard Model, and complement the measurements of CP asymmetries in B decays. The length of the side of the unitarity triangle opposite the well-measured angle β is proportional to the ratio $|V_{ub}|/|V_{cb}|$; its precise determination is a high priority of the heavy-flavor physics program.

The semileptonic transitions $b \to c\ell\bar{\nu}_\ell$ and $b \to u\ell\bar{\nu}_\ell$ (where ℓ refers to an electron or muon) each provide two avenues for determining these CKM matrix elements, namely through inclusive and exclusive final states. Recent measurements and calculations are reflected in the values quoted in this article, which is an update of the previous review [1]. The leptonic decay $B^- \to \tau\bar{\nu}$ can also be used to extract $|V_{ub}|$; we do not use this information at present since none of the experimental measurements has reached a competitive level of precision.

The theory underlying the determination of $|V_{qb}|$ is mature, in particular for $|V_{cb}|$. Most of the theoretical approaches use the fact that the mass m_b of the b quark is large compared to the scale $\Lambda_{\rm QCD}$ that determines low-energy hadronic physics. The basis for precise calculations is a systematic expansion in powers of Λ/m_b, where $\Lambda \sim 500 - 700$ MeV is a hadronic scale of the order of $\Lambda_{\rm QCD}$, based on effective-field-theory methods described in a separate RPP mini-review [2]. The use of lattice QCD for calculations of non-perturbative quantities plays an essential role in many of the determinations discussed here; lattice methods are discussed in a separate RPP mini-review [3].

The measurements discussed in this review are of branching fractions or ratios of branching fractions. The determinations of $|V_{cb}|$ and $|V_{ub}|$ also require a measurement of the total decay widths of the corresponding b hadrons, which is the subject of a separate RPP mini-review [4]. The measurements of inclusive semileptonic decays relevant to this review come primarily from e^+e^- B factories operating at the $\Upsilon(4S)$ resonance, where $B\bar{B}$ pairs are produced nearly at rest in the center-of-mass frame. Measurements of exclusive semileptonic decays come from the e^+e^- B factories and from the LHCb experiment at CERN.

Semileptonic B meson decay amplitudes to electrons and muons are assumed to be largely free from any impact of non-Standard Model physics, since they are dominated by Standard-Model W boson exchange. The decays $\bar{B} \to D^{(*)}\tau\bar{\nu}_\tau$, however, provide sensitivity to possible non-universalities in the couplings to the third generation leptons that are present at tree level in models involving new charged mediators. For example, a charged Higgs boson, present in many models of new physics, couples to the mass of the lepton and breaks lepton universality. If the enhanced decay rates seen in recent measurements of these decay modes turn out to be robust, they are an indication of new physics.

Many of the numerical results quoted in this review have been provided by the Heavy Flavor Averaging Group (HFLAV) [5].

89.2. Determination of $|V_{cb}|$

Summary: The determination of $|V_{cb}|$ from inclusive decays has a relative uncertainty of about 2%; the limitations arise mainly from our ignorance of higher-order perturbative and non-perturbative corrections. Exclusive $\bar{B} \to D^*\ell\bar{\nu}_\ell$ decays provide a determination of $|V_{cb}|$ with a relative precision of about 2%, with comparable contributions from theory and experiment; the value determined from $\bar{B} \to D\ell\bar{\nu}_\ell$ decays is consistent and has an uncertainty of 3%. However, as discussed below, recent work has raised questions about these determinations. We choose to quote a less constraining value from exclusive decays.

The values obtained from the inclusive and exclusive determinations discussed below are:

$$|V_{cb}| = (42.2 \pm 0.8) \times 10^{-3} \quad \text{(inclusive)} \tag{89.1}$$

$$|V_{cb}| = (41.9 \pm 2.0) \times 10^{-3} \quad \text{(exclusive)}. \tag{89.2}$$

Assuming these determinations share a common 1% systematic uncertainty, their average is

$$|V_{cb}| = (42.2 \pm 0.8) \times 10^{-3} \quad \text{(average)}. \tag{89.3}$$

89.2.1. $|V_{cb}|$ *from exclusive decays* :

Exclusive determinations of $|V_{cb}|$ make use of semileptonic B decays into the ground state charmed mesons D and D^* and are based on the distribution of the variable $w \equiv v \cdot v'$, where v and v' are the four velocities of the initial and final-state hadrons. In the rest frame of the decay this variable corresponds to the Lorentz factor of the final state $D^{(*)}$ meson. Heavy Quark Symmetry (HQS) [6,7] predicts these decay rates in the infinite mass limit in terms of a single form factor, which is normalized at $w = 1$, the point of maximum momentum transfer to the leptons. Measured decay rates and calculations of the form factors are used to determine $|V_{cb}|$.

A precise determination requires corrections to the HQS prediction for the normalization as well as some information on the shape of the form factors near the point $w = 1$. These calculations utilize Heavy Quark Effective Theory, which is discussed in a separate RPP mini-review [2]. Form factors that are normalized due to HQS are protected against linear corrections [8], and thus the leading corrections are of order $\Lambda^2_{\rm QCD}/m_c^2$. For the form factors that vanish in the infinite mass limit the corrections are in general linear in $\Lambda_{\rm QCD}/m_c$. In addition to these corrections, there are perturbatively calculable radiative corrections from hard gluons and photons, which will be discussed in the relevant sections.

89.2.2. $\bar{B} \to D^*\ell\bar{\nu}_\ell$:

The decay rate for $\bar{B} \to D^*\ell\bar{\nu}_\ell$ is given by

$$\frac{d\Gamma}{dw}(\bar{B} \to D^*\ell\bar{\nu}_\ell) = \frac{G_F^2 m_B^5}{48\pi^3}|V_{cb}|^2(w^2-1)^{1/2}P(w)(\eta_{\rm ew}\mathcal{F}(w))^2, \tag{89.4}$$

where $P(w)$ is a phase space factor,

$$P(w) = r^3(1-r)^2(w+1)^2\left(1 + \frac{4w}{w+1}\frac{1-2rw+r^2}{(1-r)^2}\right).$$

with $r = m_{D^*}/m_B$. The form factor $\mathcal{F}(w)$, which at $w = 1$ is unity by HQS in the infinite-mass limit, is dominated by the axial vector form factor h_{A_1} as $w \to 1$. For the definitions of the vector and axial vector form factors as a function of w, see Eq. (2.84) of the first paper of Ref. 9. The factor $\eta_{\rm ew} = 1.0066 \pm 0.0050$ accounts for the leading electroweak corrections to the four-fermion operator mediating the semileptonic decay [10], and includes an estimated uncertainty for missing long-distance QED radiative corrections [11].

The determination of V_{cb} involves an extrapolation to the zero-recoil point, for which a parametrization of $\mathcal{F}(w)$ is needed. Convenient parametrizations make use of analyticity and unitarity constraints on the the form factors and are expressed in terms of the variable

$$z = (\sqrt{w+1} - \sqrt{2})/(\sqrt{w+1} + \sqrt{2}), \tag{89.5}$$

originating from a conformal transformation. In terms of this variable the form factors (generically denoted as F) may be written as [13]

$$F(z) = \frac{1}{P_F(z)\phi_F(z)}\sum_{n=0}^{\infty} a_n z^n \tag{89.6}$$

where the sum $\sum |a_n|^2$ is bounded. Furthermore, the function $P(z)$ takes into account the resonances in the $(\bar{c}b)$ system below the $\bar{D}B$ threshold, and the weighting functions $\phi_F(z)$ are derived from the unitarity constraint on the corresponding form factor. The values of z relevant to the decay are $0 \le z \le 0.06$, hence the series in z converges rapidly and only very few terms are needed. Eq. (89.6) will be referred to as the "BGL" expansion.

A frequently used parametrization proposed in Ref. 14,

$$F(w) = F(1) - \rho^2(w-1) + c(w-1)^2 + \cdots,$$

has the slope ρ of the form factor as the only parameter. This "CLN" parameterization imposes a relation between the curvature c and the slope ρ based on the heavy quark limit. However, this seems to be too constraining given current experimental precision. More recent analyses [15,16] take this into account and include additional parameters using the BGL expansion. Very recently it has been pointed out these BGL fits are in tension with recent lattice data and would indicate large violations of heavy-quark symmetry [32].

The theoretical analysis of $F(1)$ includes the QCD short-distance radiative correction [17] to the form factor as well as the non-perturbative $1/m^2$ corrections, which can be calculated on the lattice (see below).

Precise lattice determinations of the $B \to D^{(*)}$ form factors use heavy-quark symmetries, so all uncertainties scale with the deviation of the form factor from unity. The state-of-the-art calculations are "unquenched", i.e. calculations with realistic sea quarks using $2+1$ flavors. The relevant calculations for the form factor $\mathcal{F}(\omega)$ in Ref. 11 quote a total uncertainty at the (1-2)% level. The main contributions to this uncertainty are from the chiral extrapolation from the light quark masses used in the numerical lattice computation to realistic up and down quark masses, and from discretization errors. These sources of uncertainty will be reduced with larger lattice sizes and smaller lattice spacings. Including effects from finite quark masses to calculate the deviation of $\mathcal{F}(1)$ from unity, the current lattice prediction [11] is

$$\mathcal{F}(1) = 0.906 \pm 0.013, \tag{89.7}$$

We note that very recently an independent lattice result has been shown at a conference, indicating a lower value for $\mathcal{F}(1)$ [12].

Non-lattice estimates based on sum rules for the form factor tend to yield lower values for $\mathcal{F}(1)$ [18,19,20]. Omitting the contributions from excited states, the sum rules indicate that $\mathcal{F}(1) < 0.93$. Including an estimate for the contribution of the excited states yields $\mathcal{F}(1) = 0.86 \pm 0.01 \pm 0.02$ [20,21] where the second uncertainty accounts for the excited states.

Many experiments [22–31] have measured the differential decay rate as a function of w, employing a variety of methods: using either B^+ or B^0 decays, with or without B-tagging, and with or without explicit reconstruction of the transition pion from $D^* \to D$ decays. These measurements are input to a four-dimensional fit [5] for $\eta_{\rm ew}\mathcal{F}(1)|V_{cb}|$, $\rho^2_{A_1}$ and the form-factor ratios $R_1 \propto A_2/A_1$ and $R_2 \propto V/A_1$. The fit gives $\eta_{\rm ew}\mathcal{F}(1)\,|V_{cb}| = (35.61 \pm 0.43) \times 10^{-3}$ (LQCD, CLN) with a p-value of 0.14. The leading sources of uncertainty on $\eta_{\rm ew}\mathcal{F}(1)\,|V_{cb}|$ are due to detection efficiencies and $D^{(*)}$ decay branching fractions. Note that the $\bar{B} \to D^*\ell\bar{\nu}_\ell$ form factor in the fit is parameterized using the CLN form, which has the drawbacks discussed previously.

A safer approach is to use the more general BGL form-factor parameterization. At present, only one measurement [31] has published the unfolded fully-differential decay rate and associated covariance matrix. Using this input, two analyses [15,16] have recently shown $\sim 10\%$ shifts in $\eta_{\rm ew}\mathcal{F}(1)|V_{cb}|$ when switching from the CLN to the BGL form, well beyond the quoted experimental precision. These analyses are consistent with each other and give [15] $\eta_{\rm ew}\mathcal{F}(1)\,|V_{cb}| = (38.2\ ^{+1.7}_{-1.6}) \times 10^{-3}$. Along with the lattice value given above for $\mathcal{F}(1)$ this yields

$$|V_{cb}| = (41.9\ ^{+2.0}_{-1.9}) \times 10^{-3}\ (\bar{B} \to D^*\ell\bar{\nu}_\ell,\ \text{LQCD, BGL}). \tag{89.8}$$

It has been pointed out [32] that fits to these data with the BGL parameterization are in tension with HQET and lattice predictions for form-factor ratios. More work is needed to clarify these issues.

89.2.3. $\bar{B} \to D\ell\bar{\nu}_\ell$:

The differential rate for $\bar{B} \to D\ell\bar{\nu}_\ell$ is given by

$$\frac{d\Gamma}{dw}(\bar{B} \to D\ell\bar{\nu}_\ell) = \frac{G_F^2}{48\pi^3}|V_{cb}|^2(m_B+m_D)^2 m_D^3 (w^2-1)^{3/2}(\eta_{\rm ew}\mathcal{G}(w))^2. \tag{89.9}$$

The form factor is

$$\mathcal{G}(w) = h_+(w) - \frac{m_B - m_D}{m_B + m_D} h_-(w), \tag{89.10}$$

where h_+ is normalized to unity due to HQS and h_- vanishes in the infinite-mass limit. Thus

$$\mathcal{G}(1) = 1 + \mathcal{O}\left(\frac{m_B - m_D}{m_B + m_D}\frac{\Lambda_{\rm QCD}}{m_c}\right) \tag{89.11}$$

and the corrections to the HQET predictions are parametrically larger than was the case for $\bar{B} \to D^*\ell\bar{\nu}_\ell$.

Lattice calculations including effects beyond the heavy mass limit have become available, and hence the fact that deviations from the HQET predictions are parametrically larger than for $\bar{B} \to D^*\ell\bar{\nu}_\ell$ is irrelevant. These unquenched calculations provide information over a range of z values (see Eq. (89.5)) and can be used in a simultaneous fit, along with the differential branching fraction, in a form-factor expansion in z [13,33]. This is important, since the experimental precision near $w = 1$ is poor given the low decay rate in this region.

From lattice simulations one obtains the form factor normalization at zero recoil; the currently most precise value [34] is

$$\mathcal{G}(1) = 1.054 \pm 0.004 \pm 0.008\ . \tag{89.12}$$

The most precise measurements of $\bar{B} \to D\ell\bar{\nu}_\ell$ [29,35,36] dominate the average [5] value, $\eta_{\rm ew}\mathcal{G}(1)|V_{cb}| = (41.57 \pm 1.00) \times 10^{-3}$. Note that this average corresponds to measurements that fit to the CLN form factor parameterization; the same concerns expressed above for $\bar{B} \to D^*\ell\bar{\nu}_\ell$ apply here. Using the value from Eq. (89.12) for $\mathcal{G}(1)$ and accounting for the electroweak correction as above gives

$$|V_{cb}| = (39.18 \pm 0.94 \pm 0.36) \times 10^{-3}\ (\bar{B} \to D\ell\bar{\nu}_\ell,\ \text{LQCD, CLN}), \tag{89.13}$$

where the first uncertainty is from experiment, the second from lattice QCD and the electroweak and Coulomb corrections.

The $|V_{cb}|$ averages from $\bar{B} \to D^*\ell\bar{\nu}_\ell$ and $\bar{B} \to D\ell\bar{\nu}_\ell$ decays using the CLN form are consistent; however, these determinations need to be redone using the more general BGL parameterization. We choose to quote the result in Eq. (89.8):

$$|V_{cb}| = (41.9\ ^{+2.0}_{-1.9}) \times 10^{-3} \quad \text{(exclusive)}. \tag{89.14}$$

89.2.4. $|V_{cb}|$ *from inclusive decays* :

Measurements of the total semileptonic branching decay rate, along with moments of the lepton energy and hadronic invariant mass spectra in inclusive semileptonic $b \to c$ transitions, can be used to determine $|V_{cb}|$. The total semileptonic decay rate can be calculated quite reliably in terms of non-perturbative parameters that can be extracted from the information contained in the moments.

89.2.5. *Inclusive semileptonic rate* :

The theoretical foundation for the calculation of the total semileptonic rate is the Operator Product Expansion (OPE) which yields the Heavy Quark Expansion (HQE) [37,38]. Details can be found in the RPP mini-review on Effective Theories [2].

The OPE result for the total rate can be written schematically (details can be found, *e.g.*, in Ref. 39) as

$$\begin{aligned}\Gamma =& |V_{cb}|^2 \frac{G_F^2 m_b^5(\mu)}{192\pi^3}(1+A_{\rm ew})\times \\ & \left[z_0^{(0)}(r) + \frac{\alpha_s(\mu)}{\pi} z_0^{(1)}(r) + \left(\frac{\alpha_s(\mu)}{\pi}\right)^2 z_0^{(2)}(r) + \cdots \right. \\ & + \frac{\mu_\pi^2}{m_b^2}\left(z_2^{(0)}(r) + \frac{\alpha_s(\mu)}{\pi} z_2^{(1)}(r) + \cdots\right) \\ & + \frac{\mu_G^2}{m_b^2}\left(y_2^{(0)}(r) + \frac{\alpha_s(\mu)}{\pi} y_2^{(1)}(r) + \cdots\right) \\ & + \frac{\rho_{\rm D}^3}{m_b^3}\left(z_3^{(0)}(r) + \frac{\alpha_s(\mu)}{\pi} z_3^{(1)}(r) + \cdots\right) \\ & \left. + \frac{\rho_{\rm LS}^3}{m_b^3}\left(y_3^{(0)}(r) + \frac{\alpha_s(\mu)}{\pi} y_3^{(1)}(r) + \cdots\right) + \ldots\right] \end{aligned} \tag{89.15}$$

where $\eta_{\rm ew} = 1 + A_{\rm ew}$ denotes the electroweak corrections, r is the ratio m_c/m_b and the y_i and z_i are functions that appear in the perturbative expansion at different orders of the heavy mass expansion. The parameters μ_π, μ_G, ρ_D and ρ_{LS} constitute the non-perturbative input into the heavy quark expansion; they correspond to certain matrix elements to be discussed below. In the same way the HQE can be set up for the moments of distributions of charged-lepton energy, hadronic invariant mass and hadronic energy, e.g.

$$\langle E_e^n \rangle_{E_e > E_{\rm cut}} = \int_{E_{\rm cut}}^{E_{\rm max}} \frac{d\Gamma}{dE_e} E_e^n dE_e \Bigg/ \int_{E_{\rm cut}}^{E_{\rm max}} \frac{d\Gamma}{dE_e} dE_e \; .$$

The coefficients of the HQE are known up to order $1/m_b^5$ at tree level [40–43]. The leading term is the parton model, and is known completely to order α_s and α_s^2 [44–46]; the terms of order $\alpha_s^{n+1}\beta_0^n$ (where β_0 is the first coefficient of the QCD β function, $\beta_0 = (33 - 2n_f)/3$) have been included by the usual BLM procedure [39,47,48]. Corrections of order $\alpha_s\mu_\pi^2/m_b^2$ have been computed in Refs. 49 and 50, while the $\alpha_s\mu_G^2/m_b^2$ terms have been calculated in Refs. 51 and 52.

Starting at order $1/m_b^3$ contributions with an infrared sensitivity to the charm mass, m_c, appear [42,53,54]. At order $1/m_b^3$ this "intrinsic charm" contribution manifests as a $\log(m_c)$ in the coefficient of the Darwin term ρ_D^3. At higher orders, terms such as $1/m_b^3 \times 1/m_c^2$ and $\alpha_s(m_c)1/m_b^3 \times 1/m_c$ appear, which are comparable in size to the contributions of order $1/m_b^4$

The HQE parameters are given in terms of forward matrix elements; the parameters entering the expansion for orders up to $1/m_b^3$ are ($D_\perp^\mu = (g_{\mu\nu} - v_\mu v_\nu)D^\nu$)

$$\begin{aligned}
\overline{\Lambda} &= M_B - m_b \,, \\
\mu_\pi^2 &= -\langle B|\bar{b}(iD_\perp)^2 b|B\rangle \,, \\
\mu_G^2 &= \langle B|\bar{b}(iD_\perp^\mu)(iD_\perp^\nu)\sigma_{\mu\nu} b|B\rangle \,, \\
\rho_{\rm D}^3 &= \langle B|\bar{b}(iD_{\perp\mu})(ivD)(iD_\perp^\nu) b|B\rangle \,, \\
\rho_{\rm LS}^3 &= \langle B|\bar{b}(iD_\perp^\mu)(ivD)(iD_\perp^\nu)\sigma_{\mu\nu} b|B\rangle. \qquad (89.16)
\end{aligned}$$

These parameters still depend on the heavy quark mass. Sometimes the infinite mass limits of these parameters $\overline{\Lambda} \to \overline{\Lambda}_{\rm HQET}$, $\mu_\pi^2 \to -\lambda_1$, $\mu_G^2 \to 3\lambda_2$, $\rho_D^3 \to \rho_1$ and $\rho_{LS}^3 \to 3\rho_2$, are used instead. The hadronic parameters of the orders $1/m_b^4$ and $1/m_b^5$ have been defined and estimated in Ref. 43. The five hadronic parameters s_i of the order $1/m_b^4$ can be found in Ref. 41. These terms have not yet been included in the fits.

The rates and the spectra depend strongly on m_b (or equivalently on $\overline{\Lambda}$). This makes the discussion of renormalization issues mandatory, since the size of QCD corrections is strongly correlated with the definitions used for the quark masses. For example, it is well known (see eg. [55]) that using the pole mass definition for heavy quark masses leads to a perturbative series for the decay rates that does not converge very well, making a precision determination of $|V_{cb}|$ in such a scheme impossible.

This motivates the use of "short-distance" mass definitions, such as the kinetic scheme [18] or the 1S scheme [56]. Both schemes have been applied to semileptonic $b \to c$ transitions and yield comparable results and uncertainties. The 1S scheme eliminates the b quark pole mass by relating it to the perturbative expression for the mass of the 1S state of the Υ system. The physical mass of the $\Upsilon(1S)$ contains non-perturbative contributions, which have been estimated in Ref. 57. These non-perturbative contributions are small; nevertheless, the best determination of the b quark mass in the 1S scheme is obtained from sum rules for $e^+e^- \to b\bar{b}$ [58]. Alternatively one may use a short-distance mass definition such as the $\overline{\rm MS}$ mass, $m_b^{\overline{\rm MS}}(m_b)$. However, it has been argued that the scale m_b is unnaturally high for B decays, while for smaller scales $\mu \sim 1\,{\rm GeV}$ $m_b^{\overline{\rm MS}}(\mu)$ is under poor control. For this reason the so-called "kinetic mass" $m_b^{\rm kin}(\mu)$, has been proposed. It is the mass entering the non-relativistic expression for the kinetic energy of a heavy quark, and is defined using heavy-quark sum rules [18].

89.2.6. ***Determination of HQE Parameters and $|V_{cb}|$*** :

Several experiments have measured moments in $\bar{B} \to X_c\ell\bar{\nu}_\ell$ decays [59–67] as a function of the minimum lepton momentum. The measurements of the moments of the electron energy spectrum ($0^{\rm th}$-$3^{\rm rd}$) and of the squared hadronic mass spectrum ($0^{\rm th}$-$2^{\rm nd}$) have statistical uncertainties that are roughly equal to their systematic uncertainties. The sets of moments measured within each experiment have strong correlations; their use in a global fit requires fully specified statistical and systematic covariance matrices. Measurements of photon energy moments ($0^{\rm th}$-$2^{\rm nd}$) in $B \to X_s\gamma$ decays [68–72] as a function of the minimum accepted photon energy are also used in some fits; the dominant uncertainties on these measurements are statistical.

Global fits [67,69,73–78] to the full set of moments have been performed in the 1S and kinetic schemes. The semileptonic moments alone determine a linear combination of m_b and m_c very accurately but leave the orthogonal combination poorly determined [79]; additional input is required to allow a precise determination of m_b. This additional information can come from the radiative $B \to X_s\gamma$ moments (with the caveat that the OPE for $b \to s\gamma$ breaks down beyond leading order in $\Lambda_{\rm QCD}/m_b$), which provide complementary information on m_b and μ_π^2, or from precise determinations of the charm quark mass [80,81]. The values obtained in the kinetic scheme fits [75,77,78] with these two constraints are consistent. Based on the charm quark mass constraint $m_c^{\overline{\rm MS}}(3\,{\rm GeV}) = 0.986 \pm 0.013\,{\rm GeV}$ [82], a fit in the kinetic scheme [5] obtains

$$|V_{cb}| = (42.19 \pm 0.78) \times 10^{-3} \qquad (89.17)$$

$$m_b^{\rm kin} = 4.554 \pm 0.018\,{\rm GeV} \qquad (89.18)$$

$$\mu_\pi^2({\rm kin}) = 0.464 \pm 0.076\,{\rm GeV}^2, \qquad (89.19)$$

where the errors include experimental and theoretical uncertainties.

Theoretical uncertainties from higher orders in $1/m$ as well as in α_s are estimated and included in performing the fits. Similar values for the parameters are obtained with a variety of assumptions about the theoretical uncertainties and their correlations. The χ^2/dof is substantially below unity in all fits, which could suggest that the theoretical uncertainties may be overestimated. However, while one could obtain a satisfactory fit with smaller uncertainties, this would result in unrealistically small uncertainties on the extracted HQE parameters, which are used as input to other calculations (e.g. the determination of $|V_{ub}|$). In any case, the low χ^2 shows no evidence for duality violations at a significant level. The mass in the $\overline{\rm MS}$ scheme corresponding to Eq. (89.18) is $m_b^{\overline{\rm MS}} = 4.19 \pm 0.04\,{\rm GeV}$, where the uncertainty includes a contribution from the translation between mass schemes; this can be compared with a value obtained using relativistic sum rules [82], $m_b^{\overline{\rm MS}} = 4.163 \pm 0.016\,{\rm GeV}$, which provides a non-trivial cross-check.

A fit to the measured moments in the 1S scheme [76,5] gives

$$|V_{cb}| = (41.98 \pm 0.45) \times 10^{-3} \qquad (89.20)$$

$$m_b^{\rm 1S} = 4.691 \pm 0.037\,{\rm GeV} \qquad (89.21)$$

$$\lambda_1({\rm 1S}) = -0.362 \pm 0.067\,{\rm GeV}^2, \qquad (89.22)$$

This fit uses semileptonic and radiative moments and constrains the chromomagnetic operator using the B^*-B and D^*-D mass differences, but does not include the constraint on m_c nor the full NNLO corrections.

The fits in the two renormalization schemes give consistent results for $|V_{cb}|$ and, after translation to a common renormalization scheme, for m_b and μ_π^2. We take the fit in the kinetic scheme [78], which includes higher-order corrections and results in a more conservative uncertainty, as the inclusive determination of $|V_{cb}|$:

$$|V_{cb}| = (42.2 \pm 0.8) \times 10^{-3} \text{ (inclusive)}. \qquad (89.23)$$

The precision of the global fit results can be further improved by calculating higher-order perturbative corrections to the coefficients of the HQE parameters, in particular the still-missing $\alpha_s\mu_G^2$ corrections, which are presently only known for $B \to X_s\gamma$ [83]. The inclusion of still-higher-order moments, if they can be measured with the required precision, may improve the sensitivity of the fits to higher-order terms in the HQE.

89.3. Determination of $|V_{ub}|$

Summary: The best determinations of $|V_{ub}|$ are from $\bar{B} \to \pi \ell \bar{\nu}_\ell$ decays, where combined fits to theory and experimental data as a function of q^2 provide a precision below 5%; the uncertainties from experiment and theory are comparable in size. Determinations based on inclusive semileptonic decays are done based on different observables and using different calculational ansatzes. All determinations are consistent and provide a precision of about 6%, with comparable contributions to the uncertainty from experiment and theory.

The values obtained from inclusive and exclusive determinations are

$$|V_{ub}| = (4.49 \pm 0.15 \,^{+\,0.16}_{-\,0.17} \pm 0.17) \times 10^{-3} \quad \text{(inclusive)}, \quad (89.24)$$

$$|V_{ub}| = (3.70 \pm 0.10 \pm 0.12) \times 10^{-3} \quad \text{(exclusive)}, \quad (89.25)$$

where the last uncertainty on the inclusive result was added by the authors of this review and is discussed below. The two determinations are independent, and the dominant uncertainties are on multiplicative factors. To combine these values, the inclusive and exclusive values are weighted by their relative errors and the uncertainties are treated as normally distributed. The resulting average has $p(\chi^2) = 0.9\%$, so we scale the error by $\sqrt{\chi^2/1} = 2.6$ to find

$$|V_{ub}| = (3.94 \pm 0.36) \times 10^{-3} \quad \text{(average)}. \quad (89.26)$$

Given the poor consistency between the two determinations, this average should be treated with caution.

89.3.1. $|V_{ub}|$ *from inclusive decays* :

The theoretical description of inclusive $\bar{B} \to X_u \ell \bar{\nu}_\ell$ decays is based on the Heavy Quark Expansion, as for $\bar{B} \to X_c \ell \bar{\nu}_\ell$ decays, and leads to a predicted total decay rate with uncertainties below 5% [84,85]. Unfortunately, the total decay rate is hard to measure due to the large background from CKM-favored $\bar{B} \to X_c \ell \bar{\nu}_\ell$ transitions. Technically, the calculation of the partial decay rate in regions of phase space where $\bar{B} \to X_c \ell \bar{\nu}_\ell$ decays are suppressed requires the introduction of a non-perturbative distribution function, the "shape function" (SF) [86,87], whose form is unknown. The shape function becomes important when the light-cone momentum component $P_+ \equiv E_X - |P_X|$ is not large compared to Λ_{QCD}, as is the case near the endpoint of the $\bar{B} \to X_u \ell \bar{\nu}_\ell$ lepton spectrum. Partial rates for $\bar{B} \to X_u \ell \bar{\nu}_\ell$ are predicted and measured in a variety of kinematic regions that differ in their sensitivity to shape-function effects.

At leading order a single shape function appears, which is universal for all heavy-to-light transitions [86,87] and can be measured in $\bar{B} \to X_s \gamma$ decays. At subleading order in $1/m_b$, several shape functions appear [88]. Thus, prescriptions that relate directly the partial rates for $\bar{B} \to X_s \gamma$ and $\bar{B} \to X_u \ell \bar{\nu}_\ell$ decays [89–92] are limited to leading order in $1/m_b$.

Existing approaches have tended to use parameterizations of the leading SF that respect constraints on the normalization and on the first and second moments, which are given in terms of the HQE parameters $\overline{\Lambda} = M_B - m_b$ and μ_π^2, respectively. The relations between SF moments and HQE parameters are known to second order in α_s [93]. As a result, measurements of HQE parameters from global fits to $\bar{B} \to X_c \ell \bar{\nu}_\ell$ and $\bar{B} \to X_s \gamma$ moments can be used to constrain the SF moments, as well as to provide accurate values of m_b and other parameters for use in determining $|V_{ub}|$. Flexible parameterizations of the SF using orthogonal basis functions [94] or artificial neural networks [95] would allow global fits to inclusive B meson decay data that incorporate the known short-distance contributions and renormalization properties of the SF.

HFLAV performs fits on the basis of several approaches, with varying degrees of model dependence. We will consider here the approaches documented in Ref. 97 (BLNP), Ref. 98 (GGOU) and Ref. 99 (DGE).

The triple diffential rate in the variables

$$P_l = M_B - 2E_l, \quad P_- = E_X + |\vec{P}_X|, \quad P_+ = E_X - |\vec{P}_X| \quad (89.27)$$

is

$$\frac{d^3\Gamma}{dP_+\, dP_-\, dP_l} = \frac{G_F^2 |V_{ub}|^2}{16\pi^2}(M_B - P_+) \quad (89.28)$$

$$\Big\{(P_- - P_l)(M_B - P_- + P_l - P_+)\mathcal{F}_1$$

$$+(M_B - P_-)(P_- - P_+)\mathcal{F}_2 + (P_- - P_l)(P_l - P_+)\mathcal{F}_3\Big\}.$$

The "structure functions" $\mathcal{F}_i$ can be calculated using factorization theorems that have been proven to subleading order in the $1/m_b$ expansion [96].

The BLNP [97] calculation uses these factorization theorems to write the $\mathcal{F}_i$ in terms of perturbatively calculable hard coefficients H and jet functions J, which are convolved with the (soft) light-cone distribution functions S, the shape functions of the B meson. The calculation of $\mathcal{O}(\alpha_S^2)$ contributions [101,102] is not yet complete and is not included in the $|V_{ub}|$ determination given below.

The leading order term in the $1/m_b$ expansion of the $\mathcal{F}_i$ contains a single non-perturbative function and is calculated to subleading order in α_s, while at subleading order in the $1/m_b$ expansion there are several independent non-perturbative functions that have been calculated only at tree level in the α_s expansion.

A distinct approach (GGOU) [98] uses a hard, Wilsonian cut-off that matches the definition of the kinetic mass. The non-perturbative input is similar to what is used in BLNP, but the shape functions are defined differently. In particular, they are defined at finite m_b and depend on the light-cone component k_+ of the b quark momentum and on the momentum transfer q^2 to the leptons. These functions include subleading effects to all orders; as a result they are non-universal, with one shape function corresponding to each structure function in Eq. (89.28). Their k_+ moments can be computed in the OPE and related to observables and to the shape functions defined in Ref. 97.

Going to subleading order in α_s requires the definition of a renormalization scheme for the HQE parameters and for the SF. The relation between the moments of the SF and the forward matrix elements of local operators is plagued by ultraviolet problems and requires additional renormalization. A scheme for improving this behavior was suggested in Refs. 97 and 103, which introduce a definition of the quark mass (the so-called shape-function scheme) based on the first moment of the measured $\bar{B} \to X_s \gamma$ photon energy spectrum. Likewise, the HQE parameters can be defined from measured moments of spectra, corresponding to moments of the SF.

One can attempt to calculate the SF by using additional assumptions. One approach (DGE) is the so-called "dressed gluon exponentiation" [99], where the perturbative result is continued into the infrared regime using the renormalon structure obtained in the large β_0 limit, where β_0 has been defined following Eq. (89.15).

In order to reduce sensitivity to SF uncertainties, measurements that use a combination of cuts on the leptonic momentum transfer q^2 and the hadronic invariant mass m_X, as suggested in Ref. 100, have been made. In general, efforts to extend the experimental measurements of $\bar{B} \to X_u \ell \bar{\nu}_\ell$ into charm-dominated regions (in order to reduce SF uncertainties) lead to an increased experimental sensitivity to the modeling of $\bar{B} \to X_u \ell \bar{\nu}_\ell$ decays, resulting in measured partial rates with an undesirable level of model dependence. The measurements quoted below have used a variety of functional forms to parameterize the leading SF; a specific error budget for one determination is quoted in the next section. In no case is the parameterization uncertainty estimated to be more than a 2% on $|V_{ub}|$.

Weak Annihilation [104,105,98] (WA) can in principle contribute significantly in the high-q^2 region of $\bar{B} \to X_u \ell \bar{\nu}_\ell$ decays. Estimates based on semileptonic D_s decays [105,54,100] lead to a $\sim 2\%$ uncertainty on the total $\bar{B} \to X_u \ell \bar{\nu}_\ell$ rate from the $\Upsilon(4S)$. The q^2 spectrum of the WA contribution is not well known, but from the OPE it is expected to contribute predominantly at high q^2. More recent theoretical investigations [54,106,107] and a direct search [108] indicate that WA is a small effect, but may become a significant

source of uncertainty for $|V_{ub}|$ measurements that accept only a small fraction of the full $\bar{B} \to X_u \ell \bar{\nu}_\ell$ phase space.

89.3.2. *Measurements* :

We summarize the measurements used in the determination of $|V_{ub}|$ below. Given the improved precision and more rigorous theoretical interpretation of more recent measurements, determinations [109–112] done at LEP are not considered in this review.

Inclusive electron momentum measurements [113–115] reconstruct a single charged electron to determine a partial decay rate for $\bar{B} \to X_u \ell \bar{\nu}_\ell$ near the kinematic endpoint. This results in a selection efficiency of order 50% and only modest sensitivity to the modeling of detector response. The inclusive electron momentum spectrum from $B\bar{B}$ events, after subtraction of the $e^+e^- \to q\bar{q}$ continuum background, is fitted to a model $\bar{B} \to X_u \ell \bar{\nu}_\ell$ spectrum and several components ($D\ell\bar{\nu}_\ell$, $D^*\ell\bar{\nu}_\ell$, ...) of the $\bar{B} \to X_c \ell \bar{\nu}_\ell$ background; the dominant uncertainties are related to this subtraction and modelling. The decay rate can be cleanly extracted for $E_e > 2.3\,\mathrm{GeV}$, but this is deep in the SF region, where theoretical uncertainties are large. The resulting $|V_{ub}|$ values for various E_e cuts are given in Table 89.1; the measurements listed there do not include the most recent determination from the electron momentum spectrum,which is discussed below.

An untagged "neutrino reconstruction" measurement [116] from BABAR uses a combination [117] of a high-energy electron with a measurement of the missing momentum vector. This allows $\mathrm{S/B} \sim 0.7$ for $E_e > 2.0\,\mathrm{GeV}$ and a $\approx 5\%$ selection efficiency, but at the cost of a smaller accepted phase space for $\bar{B} \to X_u \ell \bar{\nu}_\ell$ decays and uncertainties associated with the determination of the missing momentum. The corresponding values for $|V_{ub}|$ are given in Table 89.1.

The large samples accumulated at the B factories allow studies in which one B meson is fully reconstructed and the recoiling B decays semileptonically [118–122]. The experiments can fully reconstruct a "tag" B candidate in about 0.5% (0.3%) of B^+B^- ($B^0\bar{B}^0$) events. An electron or muon with center-of-mass momentum above 1.0 GeV is required amongst the charged tracks not assigned to the tag B and the remaining particles are assigned to the X_u system. The full set of kinematic properties (E_ℓ, m_X, q^2, *etc.*) are available for studying the semileptonically decaying B, making possible selections that accept up to 90% of the full $\bar{B} \to X_u \ell \bar{\nu}_\ell$ rate; however, the sensitivity to $\bar{B} \to X_u \ell \bar{\nu}_\ell$ decays is still driven by the regions where $\bar{B} \to X_c \ell \bar{\nu}_\ell$ decays are suppressed. Despite requirements (e.g. on the square of the missing mass) aimed at rejecting events with additional missing particles, undetected or mis-measured particles from $\bar{B} \to X_c \ell \bar{\nu}_\ell$ decay (e.g., K_L^0 and additional neutrinos) remain an important source of uncertainty.

BABAR [118] and Belle [119,120] have measured partial rates with cuts on m_X, m_X and q^2, P_+ and E_ℓ using the recoil method. In each case the experimental systematics have significant contributions from the modeling of $\bar{B} \to X_u \ell \bar{\nu}_\ell$ and $\bar{B} \to X_c \ell \bar{\nu}_\ell$ decays and from the detector response to charged particles, photons and neutral hadrons. The corresponding $|V_{ub}|$ values are given in Table 89.1.

89.3.3. $|V_{ub}|$ *from inclusive partial rates* :

The measured partial rates and theoretical calculations from BLNP, GGOU and DGE described previously are used to determine $|V_{ub}|$ from all measured partial $\bar{B} \to X_u \ell \bar{\nu}_\ell$ rates [5]; selected values are given in Table 89.1. The correlations amongst the multiple BABAR recoil-based measurements [118] are fully accounted for in the average. The statistical correlations amongst the other measurements used in the average are tiny (due to small overlaps among signal events and large differences in S/B ratios) and have been ignored. Correlated systematic and theoretical errors are taken into account, both within an experiment and between experiments. As an illustration of the relative sizes of the uncertainties entering $|V_{ub}|$ we give the error breakdown for the GGOU average: statistical—2.0%; experimental—1.7%; $\bar{B} \to X_c \ell \bar{\nu}_\ell$ modeling—1.3%; $\bar{B} \to X_u \ell \bar{\nu}_\ell$ modeling—1.8%; HQE parameters (m_b) —1.4%; higher-order corrections—1.5%; q^2 modeling—1.2%; Weak Annihilation—$^{+0.0}_{-1.9}$%; SF parameterization—0.2%.

The averages quoted here are based on the following m_b values: $m_b^{SF} = 4.582 \pm 0.023 \pm 0.018$ GeV for BLNP, $m_b^{\mathrm{kin}} = 4.554 \pm 0.018$ GeV for GGOU, and $m_b^{\overline{MS}} = 4.188 \pm 0.043$ GeV for DGE. The m_b^{kin} value is determined in a global fit to moments in the kinetic scheme; this value is translated into m_b^{SF} and $m_b^{\overline{MS}}$ at fixed order in α_s. The second uncertainty quoted on m_b arises from the scheme translation.

Table 89.1: $|V_{ub}|$ (in units of 10^{-5}) from inclusive $\bar{B} \to X_u \ell \bar{\nu}_\ell$ measurements. The first uncertainty on $|V_{ub}|$ is experimental, while the second includes both theoretical and HQE parameter uncertainties. The values are listed in order of increasing kinematic acceptance f_u (0.19 to 0.90); those below the horizontal bar are based on recoil methods.

Ref.	cut (GeV)	BLNP	GGOU	DGE
[113]	$E_e > 2.1$	$422 \pm 49\ ^{+29}_{-34}$	$423 \pm 49\ ^{+22}_{-31}$	$386 \pm 45\ ^{+25}_{-27}$
[116]	$E_e - q^2$	$471 \pm 32\ ^{+33}_{-38}$	not available	$435 \pm 29\ ^{+28}_{-30}$
[115]	$E_e > 2.0$	$452 \pm 26\ ^{+26}_{-30}$	$452 \pm 26\ ^{+17}_{-24}$	$430 \pm 24\ ^{+23}_{-25}$
[114]	$E_e > 1.9$	$493 \pm 46\ ^{+26}_{-29}$	$495 \pm 46\ ^{+16}_{-21}$	$482 \pm 45\ ^{+23}_{-23}$
[118]	$q^2>8$, $m_X<1.7$	$432 \pm 23\ ^{+26}_{-28}$	$433 \pm 23\ ^{+24}_{-27}$	$424 \pm 22\ ^{+18}_{-21}$
[118]	$P_+ < 0.66$	$409 \pm 25\ ^{+25}_{-25}$	$425 \pm 26\ ^{+26}_{-27}$	$417 \pm 25\ ^{+28}_{-37}$
[118]	$m_X < 1.7$	$403 \pm 22\ ^{+22}_{-22}$	$410 \pm 23\ ^{+16}_{-17}$	$422 \pm 23\ ^{+21}_{-27}$
[118]	$E_\ell > 1$	$433 \pm 24\ ^{+19}_{-21}$	$444 \pm 24\ ^{+9}_{-10}$	$445 \pm 24\ ^{+12}_{-13}$
[120]	$E_\ell > 1$	$450 \pm 27\ ^{+20}_{-22}$	$462 \pm 28\ ^{+9}_{-10}$	$462 \pm 28\ ^{+13}_{-13}$
[5]	HFLAV	$444 \pm 15\ ^{+21}_{-22}$	$452 \pm 15\ ^{+11}_{-14}$	$452 \pm 16\ ^{+15}_{-16}$

Hadronization uncertainties also impact the $|V_{ub}|$ determination. The theoretical expressions are valid at the parton level and do not incorporate any resonant structure (*e.g.* $\bar{B} \to \pi \ell \bar{\nu}_\ell$); this must be added to the simulated $\bar{B} \to X_u \ell \bar{\nu}_\ell$ event samples, since the detailed final state multiplicity and structure impacts the estimates of experimental acceptance and efficiency. The experiments have adopted procedures to input resonant structure while preserving the appropriate behavior in the kinematic variables (q^2, E_ℓ, m_X) averaged over the sample, but these prescriptions are *ad hoc*. The resulting uncertainties have been estimated to be $\sim$ 1-2% on $|V_{ub}|$.

All calculations yield compatible $|V_{ub}|$ values and similar error estimates. The arithmetic mean of the values and errors is $|V_{ub}| = (4.49 \pm 0.15_{\mathrm{exp}}\ ^{+0.16}_{-0.17\,\mathrm{theo}}) \times 10^{-3}$. However, for reasons discussed below, we believe there is an additional uncertainty due to model dependence that is not reflected in the HFLAV averages.

A new measurement [121] from BABAR based on the inclusive electron spectrum determines the partial branching fraction and $|V_{ub}|$ for $E_e > 0.8\,\mathrm{GeV}$. This analysis shows clearly that the partial branching fraction itself has substantial model dependence when the kinematic acceptance includes regions dominated by $\bar{B} \to X_c \ell \bar{\nu}_\ell$ background. The values obtained for $|V_{ub}| \times 10^3$ are [121] $4.56 \pm 0.13\ ^{+0.28}_{-0.26}$ (BLNP), $3.96 \pm 0.10 \pm 0.17$ (GGOU) and $3.85 \pm 0.11\ ^{+0.08}_{-0.07}$ (DGE), where the first uncertainty is experimental and the second combines HQE parameter and theoretical uncertainties. The model dependence enters primarily through the partial branching fractions, and arises because the fit has sensitivity to $\bar{B} \to X_u \ell \bar{\nu}_\ell$ decays only in regions with good signal to noise (see Fig. 13 of Ref. 121). Each of the analyses shown in Table 89.1 was based on a partial branching fraction determined in a single model (i.e. the one used by that analysis when simulating $\bar{B} \to X_u \ell \bar{\nu}_\ell$ decays). The $|V_{ub}|$ value quoted by HFLAV for each model was derived from this unique partial branching fraction and the model-specific partial rate calculation. This translation from a single partial branching fraction into $|V_{ub}|$ values in different models suffers, in principle, from the difficulties made explicit in the recent BABAR measurement. The model dependence in the partial branching fraction is sensitive to how the model predictions compare in the restricted region with good signal-to-noise, not by how they compare when integrated over the full kinematic range used in the fit. This effect needs to be

accounted for by the experiments; the published results are insufficient to determine it. To try to account for this model dependence, we add in quadrature to the $|V_{ub}|$ average an additional uncertainty whose size is estimated by taking the quadrature difference, averaged over the models, between the theory errors on $|V_{ub}|$ for the regions $m_X < 1.7\,\mathrm{GeV}$ (good signal-to-noise) and $E_e > 1.0\,\mathrm{GeV}$ (more inclusive, low signal-to-noise). With this addition, the inclusive $|V_{ub}|$ average is

$$|V_{ub}| = (4.49 \pm 0.15_{\rm exp}\ ^{+0.16}_{-0.17\,\rm theo} \pm 0.17_{\Delta\rm BF}) \times 10^{-3} \quad \text{(inclusive)}. \tag{89.29}$$

89.3.4. $|V_{ub}|$ *from exclusive decays* :

Exclusive charmless semileptonic decays offer a complementary means of determining $|V_{ub}|$. For the experiments, the specification of the final state provides better background rejection, but the branching fraction to a specific final state is typically only a few percent of that for inclusive decays. For theory, the calculation of the form factors for $\bar{B} \to X_u \ell \bar{\nu}_\ell$ decays is challenging, but brings in a different set of uncertainties from those encountered in inclusive decays. In this review we focus on $\bar{B} \to \pi \ell \bar{\nu}_\ell$, as it is the most promising decay mode for both experiment and theory. Measurements of other exclusive $\bar{B} \to X_u \ell \bar{\nu}_\ell$ decays can be found in Refs. [124–131].

89.3.5. $\bar{B} \to \pi \ell \bar{\nu}_\ell$ *form factor calculations* :

The relevant form factors for the decay $\bar{B} \to \pi \ell \bar{\nu}_\ell$ are usually defined as

$$\langle \pi(p_\pi)|V^\mu|B(p_B)\rangle = \tag{89.30}$$
$$f_+(q^2)\left[p_B^\mu + p_\pi^\mu - \frac{m_B^2 - m_\pi^2}{q^2} q^\mu\right] + f_0(q^2)\frac{m_B^2 - m_\pi^2}{q^2} q^\mu$$

in terms of which the rate becomes (in the limit $m_\ell \to 0$)

$$\frac{d\Gamma}{dq^2} = \frac{G_F^2 |V_{ub}|^2}{24\pi^3} |p_\pi|^3 |f_+(q^2)|^2, \tag{89.31}$$

where p_π is the pion momentum in the B meson rest frame.

Currently available non-perturbative methods for the calculation of the form factors include lattice QCD (LQCD) and light-cone sum rules (LCSR). The two methods are complementary in phase space, since the lattice calculation is restricted to the kinematical range of high momentum transfer q^2 to the leptons, while light-cone sum rules provide information near $q^2 = 0$. Interpolations between these two regions can be constrained by unitarity and analyticity.

Unquenched simulations for heavy-to-light decays, where quark loop effects are fully incorporated, are now standard, and have been performed by the Fermilab/MILC [132], the HPQCD [133] and the RBC/UKQCD [134] collaborations. The calculations differ in the way the b quark is simulated, with HPQCD using nonrelativistic QCD, and Fermilab/MILC and RBC/UKQCD using relativistic b quarks with the Fermilab and Columbia heavy-quark forumulations; they agree within the quoted errors. The result from Ref. 132 represents a significant improvement in precision. The form factor f_+ evaluated at $q^2 = 20\,\mathrm{GeV}^2$ has an estimated uncertainty of 3.4%, where the leading contribution is due to the chiral-continuum extrapolation fit, which includes statistical and heavy-quark discretization errors. However, the lattice simulations are restricted to the region of large q^2, i.e. the region $q^2_{\rm max} > q^2 \gtrsim 15\,\mathrm{GeV}^2$.

The extrapolation to small values of q^2 is performed using guidance from analyticity and unitarity. Making use of the heavy-quark limit, stringent constraints on the shape of the form factor can be derived [135], and the conformal mapping of the kinematical variables onto the complex unit disc yields a rapidly converging series in the variable

$$z = \frac{\sqrt{t_+ - t_-} - \sqrt{t_+ - q^2}}{\sqrt{t_+ - t_-} + \sqrt{t_+ - q^2}}$$

where $t_\pm = (M_B \pm m_\pi)^2$. The use of lattice data in combination with experimental measurements of the differential decay rate provides a stringent constraint on the shape of the form factor in addition to precise determination of $|V_{ub}|$ [136].

Table 89.2: Total and partial branching fractions for $\bar{B}^0 \to \pi^+ \ell^- \bar{\nu}_\ell$. B-tagged analyses are indicated (SL *for semileptonic*, Had *for hadronic*). The first uncertainty listed is from statistics, the second from systematics. Measurements of $\mathcal{B}(B^- \to \pi^0 \ell^- \bar{\nu}_\ell)$ have been multiplied by a factor $2\tau_{B^0}/\tau_{B^+}$ to obtain the values below.

	$\mathcal{B}\times 10^4$	$\mathcal{B}(q^2 > 16) \times 10^4\,\mathrm{GeV}^2$
CLEO π^+, π^0 [129]	$1.38 \pm 0.15 \pm 0.11$	$0.41 \pm 0.08 \pm 0.04$
BABAR π^+, π^0 [130]	$1.41 \pm 0.05 \pm 0.08$	$0.32 \pm 0.02 \pm 0.03$
BABAR π^+ [131]	$1.44 \pm 0.04 \pm 0.06$	$0.37 \pm 0.02 \pm 0.02$
Belle π^+, π^0 [143]	$1.48 \pm 0.04 \pm 0.07$	$0.40 \pm 0.02 \pm 0.02$
Belle SL π^+ [144]	$1.41 \pm 0.19 \pm 0.15$	$0.37 \pm 0.10 \pm 0.04$
Belle SL π^0 [144]	$1.41 \pm 0.26 \pm 0.15$	$0.37 \pm 0.15 \pm 0.04$
Belle Had π^+ [124]	$1.49 \pm 0.09 \pm 0.07$	$0.45 \pm 0.05 \pm 0.02$
Belle Had π^0 [124]	$1.48 \pm 0.15 \pm 0.08$	$0.36 \pm 0.07 \pm 0.02$
BABAR SL π^+ [145]	$1.38 \pm 0.21 \pm 0.08$	$0.46 \pm 0.13 \pm 0.03$
BABAR SL π^0 [145]	$1.78 \pm 0.28 \pm 0.15$	$0.44 \pm 0.17 \pm 0.06$
BABAR Had π^+ [146]	$1.07 \pm 0.27 \pm 0.19$	$0.65 \pm 0.20 \pm 0.13$
BABAR Had π^0 [146]	$1.52 \pm 0.41 \pm 0.30$	$0.48 \pm 0.22 \pm 0.12$
Average [147]	$1.45 \pm 0.02 \pm 0.04$	$0.38 \pm 0.01 \pm 0.01$

Another established non-perturbative approach to obtain the form factors is through Light-Cone QCD Sum Rules (LCSR). The sum-rule approach provides an estimate for the product $f_B f_+(q^2)$, valid in the region $0 < q^2 \lesssim 12\ \mathrm{GeV}^2$. The determination of $f_+(q^2)$ itself requires knowledge of the decay constant f_B, which is usually obtained by replacing f_B by its two-point QCD (SVZ) sum rule [137] in terms of perturbative and condensate contributions. The advantage of this procedure is the approximate cancellation of various theoretical uncertainties in the ratio $(f_B f_+)/(f_B)$.

The LCSR for $f_B f_+$ is based on the light-cone OPE of the relevant vacuum-to-pion correlation function, calculated in full QCD at finite b-quark mass. The resulting expressions actually comprise a triple expansion: in the twist t of the operators near the light-cone, in α_s, and in the deviation of the pion distribution amplitudes from their asymptotic form, which is fixed from conformal symmetry. The sources of uncertainties in the LCSR calculation are discussed in Refs. 138 and 139; currently a total uncertainty slightly larger than 10% on $|V_{ub}|$ is obtained from a LCSR calculation of

$$\Delta\zeta(0, q^2_{max}) = \frac{G_F^2}{24\pi^3} \int_0^{q^2_{max}} dq^2\, p_\pi^3 |f_+(q^2)|^2$$
$$= \frac{1}{|V_{ub}|^2 \tau_{B_0}} \int_0^{q^2_{max}} dq^2\, \frac{d\mathcal{B}(B \to \pi \ell \nu)}{dq^2} \tag{89.32}$$

which gives [140]

$$\Delta\zeta(0, 12\,\mathrm{GeV}^2) = 4.59^{+1.00}_{-0.85}\,\mathrm{ps}^{-1}. \tag{89.33}$$

The recent calculation of two loop contributions to the LCSR [141] and the estimation of statistical correlations [142] results in only small changes to the central value and uncertainty.

89.3.6. $\bar{B} \to \pi \ell \bar{\nu}_\ell$ *measurements* :

The $\bar{B} \to \pi \ell \bar{\nu}_\ell$ measurements fall into two broad classes: untagged, in which case the reconstruction of the missing momentum of the event serves as an estimator for the unseen neutrino, and tagged, in which the second B meson in the event is fully reconstructed in either a hadronic or semileptonic decay mode. The tagged measurements have high and uniform acceptance and S/B as high as 10, but low statistical power. The untagged measurements have somewhat higher background (S/B < 1) and make slightly more restrictive kinematic cuts, but provide better precision on the q^2 dependence of the form factor.

CLEO has analyzed $\bar{B} \to \pi\ell\bar{\nu}_\ell$ and $\bar{B} \to \rho\ell\bar{\nu}_\ell$ using an untagged analysis [129]. Similar analyses have been done at BABAR [130,131] and Belle [143]. The leading systematic uncertainties in the untagged $\bar{B} \to \pi\ell\bar{\nu}_\ell$ analyses are associated with modeling the missing momentum reconstruction, with backgrounds from $\bar{B} \to X_u\ell\bar{\nu}_\ell$ decays and $e^+e^- \to q\bar{q}$ continuum events, and with varying the form factor used to model $\bar{B} \to \rho\ell\bar{\nu}_\ell$ decays. The values obtained for the full and partial branching fractions are listed in Table 89.2 above the horizontal line.

Analyses [144,145] based on reconstructing a B in the $\bar{D}^{(*)}\ell^+\nu_\ell$ decay mode and looking for a $\bar{B} \to \pi\ell\bar{\nu}_\ell$ or $\bar{B} \to \rho\ell\bar{\nu}_\ell$ decay amongst the remaining particles in the event make use of the fact that the B and $\bar{B}$ are back-to-back in the $\Upsilon(4S)$ frame to construct a discriminant variable that provides a signal-to-noise ratio above unity for all q^2 bins. A related technique was discussed in Ref. 148. BABAR [145] and Belle [124] have also used their samples of B mesons reconstructed in hadronic decay modes to measure exclusive charmless semileptonic decays, resulting in very clean but small samples. The corresponding full and partial branching fractions are given in Table 89.2. The averages [147] take account of correlations and common systematic uncertainties, and have $p(\chi^2) > 0.5$ in each case.

$|V_{ub}|$ can be obtained from the average $\bar{B} \to \pi\ell\bar{\nu}_\ell$ branching fraction and the measured q^2 spectrum. Fits to the q^2 spectrum using a theoretically motivated parameterization (e.g. "BCL" from Ref. 149) remove most of the model dependence from theoretical uncertainties in the shape of the spectrum. The most sensitive method for determining $|V_{ub}|$ from $\bar{B} \to \pi\ell\bar{\nu}_\ell$ decays employs a simultaneous fit [5,132,150] to measured experimental partial rates and lattice points versus q^2 (or z) to determine $|V_{ub}|$ and the first few coefficients of the expansion of the form factor in z. We quote the result from Ref. 5, which uses as experimental input an average of the measurements in Refs. [124,130,131,143] and an average [151] of the LQCD input from Refs. 132 and 134 and finds

$$|V_{ub}| = (3.70 \pm 0.10 \pm 0.12\,) \times 10^{-3} \quad \text{(exclusive)}, \tag{89.34}$$

where the first uncertainty is experimental and the second is from theory. Adding an additional constraint using input [152] from LCSR gives [5] $|V_{ub}| = (3.67{\pm}0.09{\pm}0.12\,){\times}10^{-3}$ (exclusive, LQCD + LCSR).

89.4. Semileptonic b-baryon decays and determination of $|V_{ub}|/|V_{cb}|$

Summary: A significant sample of Λ_b^0 baryons is available at the LHCb experiment, and methods have been developed to study their semileptonic decays. Both $\Lambda_b^0 \to p\mu\bar{\nu}$ and $\Lambda_b^0 \to \Lambda_c^+\mu\bar{\nu}$ decays have been measured at LHCb, and the ratio of branching fractions to these two decay modes is used to determine the ratio $|V_{ub}/V_{cb}|$. Averaging the LHCb determination with those obtained from inclusive and exclusive B meson decays, we find

$$|V_{ub}|/|V_{cb}| = 0.092 \pm 0.008 \quad \text{(average)}$$

where the average has $p(\chi^2) = 0.9\%$ and the uncertainty has been scaled by a factor $\sqrt{\chi^2/2} = 2.2$. In light of the poor consistency of the three determinations considered, the average should be treated with caution.

89.4.1. $\Lambda_b^0 \to \Lambda_c^+\mu\bar{\nu}$ and $\Lambda_b^0 \to p\mu\bar{\nu}$:

The $\Lambda_b^0 \to \Lambda_c^+$ and $\Lambda_b^0 \to p$ semileptonic transitions are described in terms of six form factors each. The three form factors corresponding to the vector current can be defined as [153]

$$\begin{aligned}\langle F(p',s')|\bar{q}\,\gamma_\mu\, b|\Lambda_b^0(p,s)\rangle = \bar{u}_F(p',s')\Big\{ & f_0(q^2)\,(M_{\Lambda_b^0} - m_F)\,\frac{q_\mu}{q^2} \\ & + f_+(q^2)\,\frac{M_{\Lambda_b^0} + m_F}{s_+}\left(p_\mu + p'_\mu - \frac{q_\mu}{q^2}\,(M^2_{\Lambda_b^0} - m_F^2)\right) \\ & + f_\perp(q^2)\left(\gamma_\mu - \frac{2m_F}{s_+}\,p_\mu - \frac{2M_{\Lambda_b^0}}{s_+}\,p'_\mu\right)\Big\}\, u_{\Lambda_b^0}(p,s)\,, \end{aligned} \tag{89.35}$$

where $F = p$ or Λ_c^+ and where we define $s_\pm = (M_{\Lambda_b^0} \pm m_F)^2 - q^2$. At vanishing momentum transfer, $q^2 \to 0$, the kinematic constraint $f_0(0) = f_+(0)$ holds. The form factors are defined in such a way that they correspond to time-like (scalar), longitudinal and transverse polarization with respect to the momentum-transfer q^μ for f_0, f_+ and $f_\perp$, respectively. Furthermore we have chosen the normalization in such a way that for $f_0, f_+, f_\perp \to 1$ one recovers the expression for point-like baryons.

Likewise, the expression for the axial-vector current is

$$\begin{aligned}\langle F(p',s')|\bar{q}\,\gamma_\mu\gamma_5\, b|\Lambda_b^0(p,s)\rangle = & -\bar{u}_F(p',s')\gamma_5 \\ & \Big\{ g_0(q^2)\,(M_{\Lambda_b^0} + m_F)\,\frac{q_\mu}{q^2} \\ & + g_+(q^2)\,\frac{M_{\Lambda_b^0} - m_F}{s_-}\left(p_\mu + p'_\mu - \frac{q_\mu}{q^2}\,(M^2_{\Lambda_b^0} - m_F^2)\right) \\ & + g_\perp(q^2)\left(\gamma_\mu + \frac{2m_F}{s_-}\,p_\mu - \frac{2M_{\Lambda_b^0}}{s_-}\,p'_\mu\right)\Big\}\, u_{\Lambda_b^0}(p,s)\,, \end{aligned} \tag{89.36}$$

with the kinematic constraint $g_0(0) = g_+(0)$ at $q^2 \to 0$.

The form factors have been discussed in the heavy quark limit; assuming both b and c as heavy, all the form factors f_i and g_i turn out to be identical [153]

$$f_0 = f_+ = f_\perp = g_0 = g_+ = g_\perp = \xi_B \tag{89.37}$$

and equal to the Isgur Wise function ξ_B for baryons. In the limit of a light baryon in the final state, the number of independent form factors is still reduced to two through the heavy quark symmetries of the Λ_b^0. It should be noted that the $\Lambda_b^0 \to (p/\Lambda_c^+)\mu\nu$ decay rates peak at high q^2, which facilitates both lattice QCD calculations and experimental measurements.

The form factors for Λ_b^0 decays have been studied on the lattice [154]. Based on these results the differential rates for both $\Lambda_b^0 \to \Lambda_c^+\mu\bar{\nu}$ as well as for $\Lambda_b^0 \to p\mu\bar{\nu}$ can be predicted in the full phase space. In particular, for the experimentally interesting region they find the ratio of decay rates to be [154]

$$\frac{\mathcal{B}(\Lambda_b^0 \to p\mu\bar{\nu})_{q^2>15\ \mathrm{GeV}^2}}{\mathcal{B}(\Lambda_b^0 \to \Lambda_c^+\mu\bar{\nu})_{q^2>7\ \mathrm{GeV}^2}} = (1.471 \pm 0.095 \pm 0.109)\left|\frac{V_{ub}}{V_{cb}}\right|^2 \tag{89.38}$$

where the first uncertainty is statistical and the second, systematic.

89.4.2. *Measurements at LHCb* :

The LHCb experiment has measured the branching fractions of the semileptonic decays $\Lambda_b^0 \to \Lambda_c^+\mu\bar{\nu}$ and $\Lambda_b^0 \to p\mu\bar{\nu}$, from which they determine $|V_{ub}|/|V_{cb}|$. This is the first such determination at a hadron collider, the first to use a b baryon decay, and the first observation of $\Lambda_b^0 \to p\mu\bar{\nu}$. Excellent vertex resolution allows the $p\mu$ and production vertices to be separated, which permits the calculation of the transverse momentum $p_\perp$ of the $p\mu$ pair relative to the Λ_b^0 flight direction. The corrected mass, $m_{\rm corr} = \sqrt{p_\perp^2 + m_{p\mu}^2} + p_\perp$, peaks at the Λ_b^0 mass for signal decays and provides good discrimination against background combinations. The topologically similar decay $\Lambda_b^0 \to \Lambda_c^+\mu\bar{\nu}$ is also measured, which eliminates the need to know the production cross-section or absolute efficiencies. Using vertex and Λ_b^0 mass constraints, q^2 can be determined up to a two-fold ambiguity. The LHCb analysis requires both solutions to be in the high q^2 region to minimise contamination from the low q^2 region. Their result [155], rescaled [5] to take into account the recent branching fraction measurement [156] $\mathcal{B}(\Lambda_c^+ \to pK^-\pi^+) = (5.84 \pm 0.27 \pm 0.23)\%$, is

$$\frac{\mathcal{B}(\Lambda_b^0 \to p\mu\bar{\nu})_{q^2>15\mathrm{GeV}^2}}{\mathcal{B}(\Lambda_b^0 \to \Lambda_c^+\mu\bar{\nu})_{q^2>7\mathrm{GeV}^2}} = (0.95 \pm 0.04 \pm 0.07) \times 10^{-2} \quad . \tag{89.39}$$

The largest systematic uncertainty is from the measured $\mathcal{B}(\Lambda_c^+ \to pK^-\pi^+)$; uncertainties due to trigger, tracking and the Λ_c^+ selection efficiency are each about 3%.

A recent LHCb analysis [157] measures the normalized q^2 spectrum and finds good agreement with the shape calculated on the lattice [154].

89.4.3. ***The ratio $|V_{ub}|/|V_{cb}|$*** :

The ratio of matrix elements, $|V_{ub}|/|V_{cb}|$, is often required when testing the compatibility of a set of measurements with theoretical predictions. It can be determined from the ratio of branching fractions measured by the LHCb experiment, quoted in the previous section. It can also be calculated based on the $|V_{ub}|$ and $|V_{cb}|$ values quoted earlier in this review.

As previously noted, the decay rate for $\Lambda_b^0 \to p\mu\bar{\nu}$ peaks at high q^2 where the calculation of the associated form factors using lattice QCD is under good control. Using the measured ratio from Eq. (89.39) along with the calculations of Ref. 154 results in [5]

$$|V_{ub}|/|V_{cb}| = 0.080 \pm 0.004 \pm 0.004 \quad \text{(LHCb)}. \tag{89.40}$$

where the first uncertainty is experimental and the second is from the LQCD calculation.

Given the similarities in the theoretical frameworks used for charmed and charmless decays, we choose to quote the ratio $|V_{ub}|/|V_{cb}|$ separately for inclusive and exclusive decays:

$$|V_{ub}|/|V_{cb}| = 0.107 \pm 0.007 \quad \text{(inclusive)}, \tag{89.41}$$
$$|V_{ub}|/|V_{cb}| = 0.088 \pm 0.006 \quad \text{(exclusive)}. \tag{89.42}$$

We average these values, along with the result in Eq. (89.40), weighting by relative errors. The average has $p(\chi^2) = 0.9\%$, so we scale the uncertainty by a factor $\sqrt{\chi^2/2} = 2.2$ to find

$$|V_{ub}|/|V_{cb}| = 0.092 \pm 0.008 \quad \text{(average)}. \tag{89.43}$$

89.5. Semitauonic decays

Summary: Semileptonic decays to third-generation leptons provide sensitivity to non-Standard Model amplitudes, such as from a charged Higgs boson [158]. The ratios of branching fractions of semileptonic decays involving tau leptons to those involving e/μ, $\mathcal{R}_{D^{(*)}} \equiv \mathcal{B}(\bar{B} \to D^{(*)}\tau\bar{\nu}_\tau)/\mathcal{B}(\bar{B} \to D^{(*)}\ell\bar{\nu}_\ell)$, are predicted with good precision in the Standard Model [34,159–163]. For $\mathcal{R}_D$ the most precise value comes from a fit to lattice and experimental data [163], while for $\mathcal{R}_{D^*}$ we use a calculation [161] based on the heavy quark expansion, combined with the measurements for $\bar{B} \to D^*\ell\bar{\nu}_\ell$

$$\mathcal{R}_D^{\rm SM} = 0.299 \pm 0.003\ ,$$
$$\mathcal{R}_{D^*}^{\rm SM} = 0.252 \pm 0.003\ . \tag{89.44}$$

Measurements [164–170] of these ratios yield higher values; averaging B-tagged measurements of $\mathcal{R}_D$ and $\mathcal{R}_{D^*}$ at the $\Upsilon(4S)$ and the LHCb measurements of $\mathcal{R}_{D^*}$ yields [171]

$$\mathcal{R}_D^{\rm meas} = 0.407 \pm 0.039 \pm 0.024$$
$$\mathcal{R}_{D^*}^{\rm meas} = 0.304 \pm 0.013 \pm 0.007 \tag{89.45}$$

with a linear correlation of -0.20. These values exceed Standard Model predictions by 2.3σ and 3.4σ, respectively. A variety of new physics models have been proposed [158,172–178] to explain this excess. Most models proposed to explain the semitauonic decays have very little impact on semileptonic decays involving muons or electrons, so they do not significantly modify the $|V_{ub}|$ or $|V_{cb}|$ determinations discussed previously in this review.

89.5.1. ***Sensitivity of $\bar{B} \to D^{(*)}\tau\bar{\nu}_\tau$ to additional amplitudes*** : In addition to the helicity amplitudes present for decays to $e\bar{\nu}_e$ and $\mu\bar{\nu}_\mu$, decays proceeding through $\tau\bar{\nu}_\tau$ include a scalar amplitude H_s. The differential decay rate is given by [179]

$$\frac{d\Gamma}{dq^2} = \frac{G_F^2\,|V_{cb}|^2\,|\mathbf{p}^*_{D^{(*)}}|q^2}{96\pi^3 m_B^2}\left(1-\frac{m_\tau^2}{q^2}\right)^2$$
$$\left[(|H_+|^2+|H_-|^2+|H_0|^2)\left(1+\frac{m_\tau^2}{2q^2}\right)+\frac{3m_\tau^2}{2q^2}|H_s|^2\right], \tag{89.46}$$

where $|\mathbf{p}^*_{D^{(*)}}|$ is the 3-momentum of the $D^{(*)}$ in the $\bar{B}$ rest frame and the helicity amplitudes H depend on the four-momentum transfer q^2. All four helicity amplitudes contribute to $\bar{B} \to D^*\tau\bar{\nu}_\tau$, while only H_0 and H_s contribute to $\bar{B} \to D\tau\bar{\nu}_\tau$; as a result, new physics contributions tend to produce larger effects in the latter mode.

The (semi)-leptonic B decays into a τ lepton provide a stringent test of the two-Higgs doublet model of type II (2HDMII), i.e. where the two Higgs doublets couple separately to up- and down-type quarks. This is also of relevance for Supersymmetry, since this corresponds to the Higgs sector of any commonly used supersymmetric model. These models involve additional charged scalar particles, which contribute at tree level to the (semi)-leptonic B decays into a τ. The distinct feature of the 2HDMII is that the contributions of the charged scalars scale as $m_\tau^2/m_{H^+}^2$, since the couplings to the charged Higgs particles are proportional to the mass of the lepton. As a consequence, one may expect visible effects in decays into a τ, but only small effects for decays into e and μ.

As discussed in the next section, the 2HDMII does not describe the observations any better than the Standard Model. To achieve a better description one has to extend the analysis to other models, where the scaling of the new contributions with the lepton mass is different.

89.5.2. ***Measurement of $\mathcal{R}_{D^{(*)}}$*** :

$\bar{B} \to D^{(*)}\tau\bar{\nu}_\tau$ decays have been studied at the $\Upsilon(4S)$ resonance and in pp collisions. At the $\Upsilon(4S)$, the experimental signature consists of a D or D^* meson, an electron or muon (denoted here by ℓ) from the decay $\tau \to \ell\nu_\tau\overline{\nu}_\ell$, a fully-reconstructed decay of the second B meson in the event, and multiple missing neutrinos. The analyses that use hadronic B tags separate signal decays from $\bar{B} \to D^{(*)}\ell\bar{\nu}_\ell$ decays using the lepton momentum and the measured missing mass squared; decays with only a single missing neutrino peak sharply at zero in this variable, while the signal is spread out to positive values. When a semileptonic B tag is used, the main discrimination between signal and $\bar{B} \to D^{(*)}\ell\bar{\nu}_\ell$ decays comes from the calorimeter energy that is unassociated with any particle used in the reconstruction of the B meson candidates and the cosine of the angle between the $D^*\ell$ system and its parent B meson, which is calculated under the assumption that only one particle (a neutrino) is missing. In both these approaches, background from $\bar{B} \to D^{**}\ell\bar{\nu}_\ell$ decays with one or more unreconstructed particles is harder to separate from signal, as is background from $\bar{B} \to D^{(*)}H_{\bar{c}}X$ (where $H_{\bar{c}}$ is a hadron containing a $\bar{c}$ quark) decays. The leading sources of systematic uncertainty are due to the limited size of simulation samples used in constructing the PDFs, the composition of the D^{**} states, efficiency corrections, and cross-feed (swapping soft particles between the signal and tag B).

A recent measurement [168] uses hadronic B tags and τ^+ decays to $\pi^+\bar{\nu}_\tau$ or $\rho^+\bar{\nu}_\tau$ to measure $\mathcal{R}_{D^*}$ and the polarization of the τ^+ lepton. The main discriminant variables are the measured missing mass squared and the unassociated calorimeter energy. This measurement provides the first determination of the τ polarization in the $\bar{B} \to D^*\tau\bar{\nu}_\tau$ decay, $\mathcal{P}(D^*) = -0.38 \pm 0.51\ ^{+0.21}_{-0.16}$, compatible with the standard model expectation [180], -0.497 ± 0.013. The main uncertainties on the $\mathcal{R}_{D^*}$ measurement come from the composition of the hadronic B background and from modeling of semileptonic B decays and mis-reconstructed D^* mesons.

The LHCb experiment has studied the decay $\bar{B} \to D^{*+}\tau\bar{\nu}_\tau$ with $D^{*+} \to D^0\pi^+$, $D^0 \to K^-\pi^+$ and $\tau \to \mu\nu_\tau\overline{\nu}_\mu$ in pp collisions. Their analysis [169] takes advantage of the measurable flight lengths of b and c hadrons and τ leptons. A multivariate discriminant is used to select decays where no additional charged particles are consistent with coming from the signal decay vertices. The separation between the primary and B decay vertices is used to calculate the momentum of the B decay products transverse to the B flight direction. The longitudinal component of the B momentum can be estimated based on the visible decay products; this allows a determination of the B rest frame, with modest resolution, and enables the calculation of the same discrimination variables available at the e^+e^- B factories. The (rest frame) muon energy, missing mass-squared and q^2 are used in a 3-d fit. The leading sources of systematic uncertainty are due to the size of the simulation sample used in constructing the fit templates, the shape of

the muon misidentification template, and uncertainties in modelling the background from $\bar{B} \to D^{**}\ell\bar{\nu}_\ell$ and $\bar{B} \to D^{(*)}H_{\bar{c}}X$ decays. The most recent LHCb preliminary result [170] on $\mathcal{R}_{D^*}$ uses three-prong decays that take advantage of their excellent vertex resolution.

Measurements from BABAR [164,165], Belle [166–168] and LHCb [169,170] result in values for $\mathcal{R}_D$ and $\mathcal{R}_{D^*}$ that exceed Standard Model predictions. Table 89.3 lists these values and their average. The simultaneous measurements of $\mathcal{R}_D$ and $\mathcal{R}_{D^*}$ have linear correlation coefficients of −0.27 (BABAR) and −0.49 (Belle); the $\mathcal{R}_D$ and $\mathcal{R}_{D^*}$ averages have a correlation of −0.20. Two untagged Belle measurements [181,182] are subject to larger systematic uncertainties; they are not included in the average. All three experiments assume the Standard Model kinematic distributions for $\bar{B} \to D^{(*)}\tau\bar{\nu}_\tau$ in their determinations of the branching fraction ratios.

Table 89.3: Measurements of $\mathcal{R}_D$ and $\mathcal{R}_{D^*}$ and their averages [171]. The correlation between the $\mathcal{R}_D$ and $\mathcal{R}_{D^*}$ averages is −0.20.

		$\mathcal{R}_D \times 10^2$	$\mathcal{R}_{D^*} \times 10^2$
BABAR [165]	B^0, B^+	$44.0 \pm 5.8 \pm 4.2$	$33.2 \pm 2.4 \pm 1.8$
Belle [166]	B^0, B^+	$37.5 \pm 6.4 \pm 2.6$	$29.3 \pm 3.8 \pm 1.5$
Belle [167]	B^0, B^+		$30.2 \pm 3.0 \pm 1.1$
Belle [168]	B^0, B^+		$27.0 \pm 3.5 \,^{+\,2.8}_{-\,2.5}$
LHCb [169]	B^0		$33.6 \pm 2.7 \pm 3.0$
LHCb [170]	B^0		$28.5 \pm 1.9 \pm 2.9$
Average	B^0, B^+	$40.7 \pm 3.9 \pm 2.4$	$30.4 \pm 1.3 \pm 0.7$

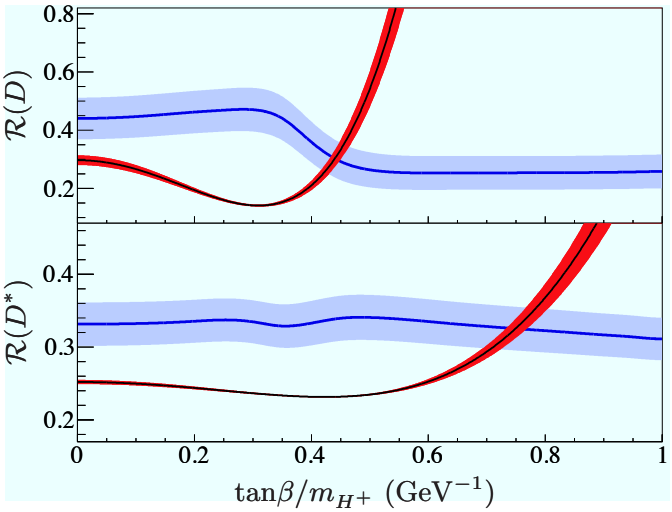

Figure 89.1: The $\mathcal{R}_{D^{(*)}}$ measured in Ref. 165 (thick bands) along with expectations in the 2HDMII (thin bands) as a function of $\tan\beta/m_{H^+}$.

The tension between the SM prediction and the measurements is at the level of 2.3σ (R_D) and 3.4σ (R_{D^*}); if one considers these deviations together the significance rises to 4.1σ. This motivates speculation on possible new physics contributions. It is striking that an interpretation in terms of the 2HDMII seems to be ruled out by the data. Fig. 89.1 shows that the interpretation of the deviation of $\mathcal{R}_D$ in terms of the 2HDMII requires vastly different values of the relevant parameter $\tan\beta/m_{H^+}$ than for $\mathcal{R}_{D^*}$, excluding this possibility. The BABAR [165] and Belle [166] analyses use kinematical distributions from the 2HDMII when comparing the compatibility of their measurements with predictions; this is why the band in Fig. 89.1 corresponding to the measurement varies with $\tan\beta/m_{H^+}$. In general, new physics contributions with a different operator structure to the SM could modify $R_{D^{(*)}}$ from the measured values, and could have a different effect in different experiments.

A more general approach has been formulated in Ref. 174 on the basis of an effective field theory. Assuming lepton-flavour-universality-violating operators of dimension six and eight, the coefficients of these operators can be fitted to the observed values. Although a detailed analysis along these lines requires more data on related decays (such as $B \to \pi\tau\bar{\nu}$, for which only a limit [183] exists at present), there are indications that the tension in $\mathcal{R}_{D^{(*)}}$ cannot be explained by a minimally flavor-violating scenario with only left-handed interactions; a better fit is obtained once right-handed and scalar currents are included.

89.6. Conclusion

The study of semileptonic B meson decays continues to be an active area for both theory and experiment. The application of HQE calculations to inclusive decays is mature, and fits to moments of $\bar{B} \to X_c\ell\bar{\nu}_\ell$ decays provide precise values for $|V_{cb}|$ and, in conjunction with input on m_c or from $B \to X_s\gamma$ decays, provide precise and consistent values for m_b.

The determination of $|V_{ub}|$ from inclusive $\bar{B} \to X_u\ell\bar{\nu}_\ell$ decays is based on multiple calculational approaches and independent measurements over a variety of kinematic regions, all of which provide consistent results. Further progress in this area is possible, but will require better theoretical control over higher-order terms, improved experimental knowledge of the $\bar{B} \to X_c\ell\bar{\nu}_\ell$ background and improvements to the modeling of the $\bar{B} \to X_u\ell\bar{\nu}_\ell$ signal distributions.

In both $b \to u$ and $b \to c$ exclusive channels there has been significant recent progress in lattice-QCD calculations, resulting in improved precision on both $|V_{ub}|$ and $|V_{cb}|$. These calculations now provide information on the form factors well away from the high q^2 region, allowing better use of experimental data. Projections for future uncertainties from lattice calculations can be found in Ref. 184.

The values from the inclusive and exclusive determinations of $|V_{ub}|$ are only marginally consistent. This is a long-standing puzzle, and the new measurement of $|V_{ub}|/|V_{cb}|$ from LHCb based on Λ_b^0 decays does not simplify the picture. The exclusive determination of $|V_{cb}|$ is currently under discussion to clarify the impact of different form-factor parameterizations.

Both $|V_{cb}|$ and $|V_{ub}|$ are indispensable inputs into unitarity triangle fits. In particular, knowing $|V_{ub}|$ with good precision allows a test of CKM unitarity in a most direct way, by comparing the length of the $|V_{ub}|$ side of the unitarity triangle with the measurement of $\sin(2\beta)$. This comparison of a "tree" process ($b \to u$) with a "loop-induced" process ($B^0 - \bar{B}^0$ mixing) provides sensitivity to possible contributions from new physics.

The observation of semileptonic decays into τ leptons has opened a new window to the physics of the third generation. The measurements indicate a tension between the data and the Standard Model prediction, which could be a hint for new physics, manifesting itself as a violation of lepton universality beyond the standard-model couplings to the Higgs. However, the most prominent and simplest candidate, the 2HDMII, cannot explain the current data. More general ansatzes fit the data, but do not provide deeper insight until measurements of related processes (such as $B \to \pi\tau\bar{\nu}$) are available. In addition, searches for a non-standard model lepton universality violation in the light lepton sector would complement the measurements of semi-tauonic decays.

The authors would like to acknowledge helpful input from M. Artuso, F. Bernlochner, G. Ricciardi and P. Urquijo.

References:

1. See R. Kowalewski and T. Mannel in C. Patrignani *et al.* (Particle Data Group), Chin. Phys. C **40**, 100001 (2016).
2. See"Heavy-Quark and Soft-Collinear Effective Theory" by C.W. Bauer and M. Neubert in this *Review*.
3. See "Lattice Quantum Chromodynamics" by S. Hashimoto, J. Laiho, and S.R. Sharpe in this *Review*.
4. See "Production and Decay of b-Flavored Hadrons" by P. Eerola, M. Kreps and Y. Kwon in this *Review*.

5. Y. Amhis *et al.* (HFLAV), arXiv:1612.07233, to appear in Eur. Phys. J. **C**.
6. N. Isgur and M.B. Wise, Phys. Lett. **B232**, 113 (1989); *ibid.* **B237**, 527 (1990).
7. M.A. Shifman and M.B. Voloshin, Sov. J. Nucl. Phys. **47**, 511 (1988) [Yad. Fiz. **47**, 801 (1988)].
8. M.E. Luke, Phys. Lett. **B252**, 447 (1990).
9. A.V. Manohar and M.B. Wise, Camb. Monogr. Part. Phys. Nucl. Phys. Cosmol. **10**, 1 (2000);
   H. Georgi, Phys. Lett. **B240**, 447 (1990);
   A.F. Falk *et al.*, Nucl. Phys. **B343**, 1 (1990);
   E. Eichten and B. Hill, Phys. Lett. **B234**, 511 (1990).
10. A. Sirlin, Nucl. Phys. **B196**, 83 (1982).
11. J.A. Bailey *et al.* [Fermilab Lattice and MILC Collab.], Phys. Rev. **D89**, 114504 (2014).
12. J. Harrison, C. Davies and M. Wingate, PoS LATTICE **2016**, 287 (2017).
13. C.G. Boyd, B. Grinstein, and R.F. Lebed, Phys. Rev. Lett. **74**, 4603 (1995); *ibid.*Phys. Rev. **D56**, 6895 (1997); B. Grinstein and A. Kobach, Phys. Lett. **B771**, 359 (2017).
14. I. Caprini *et al.*, Nucl. Phys. **B530**, 153 (1998).
15. B. Grinstein and A. Kobach, Phys. Lett. **B771**, 359 (2017).
16. D. Bigi, P. Gambino and S. Schacht, Phys. Lett. **B769**, 441 (2017).
17. A. Czarnecki and K. Melnikov, Nucl. Phys. **B505**, 65 (1997).
18. I.I.Y. Bigi *et al.*, Phys. Rev. **D52**, 196 (1995).
19. A. Kapustin *et al.*, Phys. Lett. **B375**, 327 (1996).
20. P. Gambino, T. Mannel, and N. Uraltsev, Phys. Rev. **D81**, 113002 (2010).
21. P. Gambino, T. Mannel, and N. Uraltsev, JHEP **1210**, 169 (2012).
22. D. Buskulic *et al.* (ALEPH Collab.), Phys. Lett. **B395**, 373 (1997).
23. G. Abbiendi *et al.* (OPAL Collab.), Phys. Lett. **B482**, 15 (2000).
24. P. Abreu *et al.* (DELPHI Collab.), Phys. Lett. **B510**, 55 (2001).
25. J. Abdallah *et al.* (DELPHI Collab.), Eur. Phys. J. **C33**, 213 (2004).
26. N.E. Adam *et al.* (CLEO Collab.), Phys. Rev. **D67**, 032001 (2003).
27. B. Aubert *et al.* (BABAR Collab.), Phys. Rev. **D77**, 032002 (2008).
28. B. Aubert *et al.* (BABAR Collab.), Phys. Rev. Lett. **100**, 231803 (2008).
29. B. Aubert *et al.* (BABAR Collab.), Phys. Rev. **D79**, 012002 (2009).
30. W. Dungel *et al.* (Belle Collab.), Phys. Rev. **D82**, 112007 (2010).
31. A. Abdesselam *et al.* (Belle Collab.), arXiv:1702.01521.
32. F. U. Bernlochner *et al.*, arXiv:1708.07134.
33. C. Bourrely, L. Lellouch, and I. Caprini, Phys. Rev. **D79**, 013008 (2012).
34. J. Bailey *et al.* [Fermilab Lattice and MILC Collab.], Phys. Rev. **D92**, 034506 (2015).
35. B. Aubert *et al.* (BABAR Collab.), Phys. Rev. Lett. **104**, 011802 (2010).
36. R. Glattauer *et al.* (Belle Collab.), Phys. Rev. **D93**, 032006 (2016).
37. A.V. Manohar and M.B. Wise, Phys. Rev. **D49**, 1310 (1994).
38. I.I.Y. Bigi *et al.*, Phys. Rev. Lett. **71**, 496 (1993); Phys. Lett. **B323**, 408 (1994).
39. D. Benson *et al.*, Nucl. Phys. **B665**, 367 (2003).
40. M. Gremm and A. Kapustin, Phys. Rev. **D55**, 6924 (1997).
41. B.M. Dassinger, T. Mannel, and S. Turczyk, JHEP **0703**, 087 (2007).
42. I.I. Bigi, N. Uraltsev, and R. Zwicky, Eur. Phys. J. **C50**, 539 (2007).
43. T. Mannel, S. Turczyk, and N. Uraltsev, JHEP **1011**, 109 (2010).
44. A. Pak and A. Czarnecki, Phys. Rev. **D78**, 114015 (2008).
45. S. Biswas and K. Melnikov, JHEP **1002**, 089 (2010).
46. P. Gambino, JHEP **1109**, 055 (2011).
47. P. Gambino and N. Uraltsev, Eur. Phys. J. **C34**, 181 (2004).
48. V. Aquila *et al.*, Nucl. Phys. **B719**, 77 (2005).
49. T. Becher, H. Boos, and E. Lunghi, JHEP **0712**, 062 (2007).
50. A. Alberti *et al.*, Nucl. Phys. **B870**, 16 (2013).
51. A. Alberti *et al.*, JHEP **1401**, 147 (2014).
52. T. Mannel, A.A. Pivovarov, and D. Rosenthal, Phys. Rev. **D92**, 054025 (2015).
53. C. Breidenbach *et al.*, Phys. Rev. **D78**, 014022 (2008).
54. I. Bigi *et al.*, JHEP **1004**, 073 (2010).
55. I. I. Y. Bigi, M. A. Shifman, N. G. Uraltsev and A. I. Vainshtein, Phys. Rev. D **50**, 2234 (1994).
56. A.H. Hoang *et al.*, Phys. Rev. **D59**, 074017 (1999).
57. H. Leutwyler, Phys. Lett. **B98**, 447 (1981);
   M.B. Voloshin, Sov. J. Nucl. Phys. **36**, 143 (1982).
58. A.H. Hoang, Phys. Rev. **D61**, 034005 (2000).
59. S.E. Csorna *et al.* (CLEO Collab.), Phys. Rev. **D70**, 032002 (2004).
60. A.H. Mahmood *et al.* (CLEO Collab.), Phys. Rev. **D70**, 032003 (2004).
61. B. Aubert *et al.* (BABAR Collab.), Phys. Rev. **D69**, 111103 (2004).
62. B. Aubert *et al.* (BABAR Collab.), Phys. Rev. **D69**, 111104 (2004).
63. C. Schwanda *et al.* (Belle Collab.), Phys. Rev. **D75**, 032005 (2007).
64. P. Urquijo *et al.* (Belle Collab.), Phys. Rev. **D75**, 032001 (2007).
65. J. Abdallah *et al.* (DELPHI Collab.), Eur. Phys. J. **C45**, 35 (2006).
66. D. Acosta *et al.* (CDF Collab.), Phys. Rev. **D71**, 051103 (2005).
67. B. Aubert *et al.* (BABAR Collab.), Phys. Rev. **D81**, 032003 (2010).
68. A. Limosani *et al.* [Belle Collab.], Phys. Rev. Lett. **103**, 241801 (2009).
69. C. Schwanda *et al.* (Belle Collab.), Phys. Rev. **D78**, 032016 (2008).
70. B. Aubert *et al.* (BABAR Collab.), Phys. Rev. **D72**, 052004 (2005).
71. B. Aubert *et al.* (BABAR Collab.), Phys. Rev. Lett. **97**, 171803 (2006).
72. S. Chen *et al.* (CLEO Collab.), Phys. Rev. Lett. **87**, 251807 (2001).
73. M. Battaglia *et al.* Phys. Lett. **B556**, 41 (2003).
74. B. Aubert *et al.* (BABAR Collab.), Phys. Rev. Lett. **93**, 011803 (2004).
75. O. Buchmüller and H. Flächer, hep-ph/0507253; updated in Ref. 5.
76. C.W. Bauer *et al.*, Phys. Rev. **D70**, 094017 (2004); updated in Ref. 5.
77. P. Gambino and C. Schwanda, Phys. Rev. **D89**, 014022 (2014).
78. A. Alberti *et al.*, Phys. Rev. Lett. **114**, 061802 (2015).
79. See section 5.4.2 of M. Antonelli *et al.*, Phys. Reports **494**, 197 (2010).
80. B.Dehnadi, *et al.*, JHEP **1309**, 103 (2013).
81. I. Allison *et al.* (HPQCD Collab.), Phys. Rev. **D78**, 054513 (2008).
82. K.G. Chetyrkin *et al.*, Phys. Rev. **D80**, 074010 (2009).
83. T. Ewerth, P. Gambino, and S. Nandi, Nucl. Phys. **B830**, 278 (2010).
84. A.H. Hoang *et al.*, Phys. Rev. **D59**, 074017 (1999).
85. N. Uraltsev, Int. J. Mod. Phys. **A14**, 4641 (1999).
86. M. Neubert, Phys. Rev. **D49**, 4623 (1994); *ibid.* **D49**, 3392 (1994).
87. I. Bigi *et al.*, Int. J. Mod. Phys. **A9**, 2467 (1994).
88. C. W. Bauer *et al.*, Phys. Rev. **D68**, 094001 (2003).
89. M. Neubert, Phys. Lett. **B513**, 88 (2001); Phys. Lett. **B543**, 269 (2002).
90. A.K. Leibovich *et al.*, Phys. Rev. **D61**, 053006 (2000); Phys. Rev. **D62**, 014010 (2000); Phys. Lett. **B486**, 86 (2000); Phys. Lett. **B513**, 83 (2001).

91. A.H. Hoang *et al.*, Phys. Rev. **D71**, 093007 (2005).
92. B. Lange *et al.*, JHEP **0510**, 084 (2005); B. Lange, JHEP **0601**, 104 (2006).
93. M. Neubert, Phys. Lett. **B612**, 13 (2005).
94. Z. Ligeti, I.W. Stewart, and F.J. Tackmann, Phys. Rev. **D78**, 114014 (2008).
95. P. Gambino, K. Healy, and C. Mondino, Phys. Rev. **D94**, 014031 (2016) Phys. Rev. **D78**, 114014 (2008).
96. M. Beneke, F. Campanario, T. Mannel and B. D. Pecjak, JHEP **0506**, 071 (2005).
97. B.O. Lange, M. Neubert, and G. Paz, Phys. Rev. **D72**, 073006 (2005).
98. P. Gambino *et al.*, JHEP **0710**, 058 (2007).
99. J.R. Andersen and E. Gardi, JHEP **0601**, 097 (2006).
100. C.W. Bauer, Z. Ligeti, and M. E. Luke, Phys. Rev. **D64**, 113004 (2001); Phys. Lett. **B479**, 395 (2000).
101. C. Greub, M. Neubert, and B.D. Pecjak, Eur. Phys. J. **C65**, 501 (2010).
102. M. Brucherseifer, F. Caola, and K. Melnikov, Phys. Lett. **B721**, 107 (2013).
103. T. Mannel and S. Recksiegel, Phys. Rev. **D60**, 114040 (1999).
104. I.I.Y. Bigi and N.G. Uraltsev, Nucl. Phys. **B423**, 33 (1994).
105. M.B. Voloshin, Phys. Lett. **B515**, 74 (2001).
106. Z. Ligeti, M. Luke, and A.V. Manohar, Phys. Rev. **D82**, 033003 (2010).
107. P. Gambino and J.F. Kamenik, Nucl. Phys. **B840**, 424 (2010).
108. J. Rosner *et al.* (CLEO Collab.), Phys. Rev. Lett. **96**, 121801 (2006).
109. R. Barate *et al.* (ALEPH Collab.), Eur. Phys. J. **C6**, 555 (1999).
110. M. Acciarri *et al.* (L3 Collab.), Phys. Lett. **B436**, 174 (1998).
111. G. Abbiendi *et al.* (OPAL Collab.), Eur. Phys. J. **C21**, 399 (2001).
112. P. Abreu *et al.* (DELPHI Collab.), Phys. Lett. **B478**, 14 (2000).
113. A. Bornheim *et al.* (CLEO Collab.), Phys. Rev. Lett. **88**, 231803 (2002).
114. A. Limosani *et al.* (Belle Collab.), Phys. Lett. **B621**, 28 (2005).
115. B. Aubert *et al.* (BABAR Collab.), Phys. Rev. **D73**, 012006 (2006).
116. B. Aubert *et al.* (BABAR Collab.), Phys. Rev. Lett. **95**, 111801 (2005), Erratum: Phys. Rev. Lett. **97**, 019903 (2006).
117. R. Kowalewski and S. Menke, Phys. Lett. **B541**, 29 (2002).
118. J.P. Lees *et al.* (BABAR Collab.), Phys. Rev. **D86**, 032004 (2012).
119. I. Bizjak *et al.* (Belle Collab.), Phys. Rev. Lett. **95**, 241801 (2005).
120. P. Urquijo *et al.* (Belle Collab.), Phys. Rev. Lett. **104**, 021801 (2010).
121. J. P. Lees *et al.* (BABAR Collab.), Phys. Rev. **D95**, 072001 (2017).
122. B. Aubert *et al.* (BABAR Collab.), Phys. Rev. Lett. **96**, 221801 (2006).
123. H. Kakuno *et al.* (Belle Collab.), Phys. Rev. Lett. **92**, 101801 (2004).
124. A. Sibidanov *et al.* (Belle Collab.), Phys. Rev. **D88**, 032005 (2013).
125. B. Aubert *et al.* (BABAR Collab.), Phys. Rev. Lett. **90**, 181801 (2003).
126. T. Hokuue *et al.* (Belle Collab.), Phys. Lett. **B648**, 139 (2007).
127. B. Aubert *et al.* (BABAR Collab.), Phys. Rev. **D79**, 052011 (2008);
J. P. Lees *et al.* (BaBar Collab.), Phys. Rev. **D88**, 072006 (2013);
J. P. Lees *et al.* (BaBar Collab.), Phys. Rev. **D87**, 032004 (2013).
128. C. Schwanda *et al.* (Belle Collab.), Phys. Rev. Lett. **93**, 131803 (2004).
129. N. E. Adam *et al.* (CLEO Collab.), Phys. Rev. Lett. **99**, 041802 (2007);
Phys. Rev. **D76**, 012007 (2007); supercedes Phys. Rev. **D68**, 072003 (2003).
130. P. del Amo Sanchez *et al.*, (BABAR Collab.), Phys. Rev. **D83**, 032007 (2011); supercedes B. Aubert *et al.* (BABAR Collab.), Phys. Rev. **D72**, 051102 (2005).
131. P. del Amo Sanchez *et al.*, (BABAR Collab.), Phys. Rev. **D83**, 052011 (2011); updated in J.P. Lees *et al.* (BABAR Collab.), Phys. Rev. **D86**, 092004 (2012).
132. J.A. Bailey *et al.* (Fermilab/MILC Collab.), Phys. Rev. **D92**, 014024 (2015).
133. C.M. Bouchard *et al.*, Phys. Rev. **D90**, 054506 (2014).
134. J.M. Flynn *et al.*, Phys. Rev. **D91**, 074510 (2015).
135. T. Becher and R. J. Hill, Phys. Lett. **B633**, 61 (2006).
136. M.C. Arnesen *et al.*, Phys. Rev. Lett. **95**, 071802 (2005).
137. M.A. Shifman, A.I. Vainshtein, and V.I. Zakharov, Nucl. Phys. **B147**, 385 (1979); Nucl. Phys. **B147**, 448 (1979).
138. P. Ball and R. Zwicky, Phys. Rev. **D71**, 014015 (2005).
139. G. Duplancic *et al.*, JHEP **0804**, 014 (2008).
140. A. Khodjamirian *et al.*, Phys. Rev. **D83**, 094031 (2011).
141. A. Bharucha, JHEP **1205**, 092 (2012).
142. I.S. Imsong *et al.*, JHEP **1502**, 126 (2015).
143. H. Ha *et al.* (Belle Collab.), Phys. Rev. **D83**, 071101 (2011).
144. K. Abe *et al.* (Belle Collab.), Phys. Lett. **B648**, 139 (2007).
145. B. Aubert *et al.* (BABAR Collab.), Phys. Rev. Lett. **101**, 081801 (2008).
146. B. Aubert *et al.* (BABAR Collab.), Phys. Rev. Lett. **97**, 211801 (2006).
147. Y. Amhis *et al.* (HFAG), `arXiv:1412.7515`.
148. W. Brower and H. Paar, Nucl. Instrum. Methods **A421**, 411 (1999).
149. C. Bourrely, I. Caprini, and L. Lellouch, Phys. Rev. **D79**, 013008 (2009).
150. P. Ball, `arXiv:0705.2290`;
J.M. Flynn and J. Nieves, Phys. Lett. **B649**, 269 (2007);
T. Becher and R.J. Hill, Phys. Lett. **B633**, 61 (2006);
M. Arnesen *et al.*, Phys. Rev. Lett. **95**, 071802 (2005).
151. S. Aoki *et al.*, (FLAG working group), Eur. Phys. J. **C77**, 112 (2017).
152. A. Barucha, JHEP **05**, 092 (2012).
153. T. Feldmann and M.W.Y. Yip, Phys. Rev. Lett. **85**, 014035 (2012).
154. W. Detmold, C. Lehner, and S. Meinel, Phys. Rev. **D92**, 034503 (2015).
155. The LHCb Collab., Nature Physics **11**, 743 (2015).
156. M. Ablikim *et al.*, (BESIII Collab.), Phys. Rev. Lett. **116**, 052001 (2016).
157. The LHCb Collab., `arXiv:1709.01920`.
158. M. Tanaka, Z. Phys. **C67**, 321 (1995);
H. Itoh, S. Komine, and Y. Okada, Prog. Theor. Phys. **114**, 179 (2005);
U. Nierste, S. Trine, and S. Westhoff, Phys. Rev. **D78**, 015006 (2008);
M. Tanaka and R. Watanabe, Phys. Rev. **D82**, 034027 (2010).
159. H. Na *et al.*, Phys. Rev. **D92**, 054510 (2015). Erratum ibid. **D93**, 119906 (2016).
160. J.F. Kamenik and F. Mescia, Phys. Rev. **D78**, 014003 (2008).
161. S. Fajfer, J. F. Kamenik, and I. Nišandžić, Phys. Rev. **D85**, 094025 (2012).
162. S. Aoki *et al.* (FLAG working group), Eur. Phys. J. **C77**, 112 (2017).
163. D. Bigi and P. Gambino, Phys. Rev. **D94**, 094008 (2016).
164. B. Aubert *et al.* (Babar Collab.), Phys. Rev. Lett. **100**, 021801 (2008).
165. J. Lees *et al.* (Babar Collab.), Phys. Rev. Lett. **109**, 101802 (2012); Phys. Rev. **D88**, 072012 (2013).
166. M. Huschle *et al.* (Belle Collab.), Phys. Rev. **D92**, 072014 (2015).
167. Y. Sato *et al.* (Belle Collab.), Phys. Rev. **D94**, 072007 (2016).
168. S. Hirose *et al.* (Belle Collab.), Phys. Rev. Lett. **118**, 211801 (2017).
169. The LHCb Collab., Phys. Rev. Lett. **115**, 111803 (2015).
170. The LHCb Collab., `arXiv:1708.08856`.
171. `slac.stanford.edu/xorg/hfag/semi/fpcp17/RDRDs.html`.

172. A. Datta, M. Duraisamy, and D. Ghosh, Phys. Rev. **D86**, 034027 (2012).
173. D. Becirevic, N. Kosnik, and A. Tayduganov, Phys. Lett. **B716**, 208 (2012).
174. S. Fajfer *et al.*, Phys. Rev. Lett. **109**, 161801 (2012).
175. A. Crivellin, C. Greub, and A. Kokulu, Phys. Rev. **D86**, 054014 (2012).
176. M. Bauer and M. Neubert, Phys. Rev. Lett. **116**, 141802 (2016).
177. I. Doršner et al., Phys. Rept. **641**, 1 (2016).
178. A. Celis et al., Phys. Lett. **B771**, 168 (2017).
179. J. G. Körner and G. A. Schuler, Z. Phys. **C46**, 93 (1990).
180. M. Tanaka and R. Watanabe, Phys. Rev. **D87**, 034028 (2013).
181. A. Matyja *et al.* (Belle Collab.), Phys. Rev. Lett. **99**, 191807 (2007).
182. A. Bozek *et al.* (Belle Collab.), Phys. Rev. **D82**, 072005 (2010).
183. P. Hamer *et al.* (Belle Collab.), `arXiv:1509.06521`.
184. USQCD Collab. (2011), `www.usqcd.org/documents/HiIntensityFlavor.pdf`.

90. Spectroscopy of Mesons Containing Two Heavy Quarks

Updated March 2018 by S. Eidelman (Budker Inst. and Novosibirsk State Univ.), C. Hanhart (Forschungszentrum Jülich), B.K. Heltsley (Cornell Univ.), J.J. Hernandez-Rey (Univ. Valencia–CSIC), R.E. Mitchell (Indiana Univ.), S. Navas (Univ. Granada), and C. Patrignani (Univ. Bologna, INFN).

A golden age for heavy quarkonium physics dawned at the turn of this century, initiated by the confluence of exciting advances in quantum chromodynamics (QCD) and an explosion of related experimental activity. The subsequent broad spectrum of breakthroughs, surprises, and continuing puzzles had not been anticipated. Since that time CLEO-c, BESIII and the B-factories, recently joined by ATLAS, CMS and LHCb, have continued to make groundbreaking observations. For an extensive presentation of the status of heavy quarkonium physics, the reader is referred to several reviews [1–9]. This note focuses on experimental developments in heavy quarkonium spectroscopy with very few theoretical comments. Some other comments on possible theoretical interpretations of the states not predicted by the quark model are presented in the minireview on non-$q\bar{q}$ states. Note that in this review we follow the new naming scheme for hadrons (see the review "Naming scheme for hadrons" in the current edition).

This minireview covers the newly discovered states, where "newly" is interpreted to include the period since 2002. In earlier versions of this write-up the particles were sorted according to an assumed *conventional* or *unconventional* nature with respect to the quark model. However, since this classification is not always unambiguous, we here follow Ref. [9] and sort the states into three groups, namely states below (*cf.* Table 90.1), near (*cf.* Table 90.2) and above (*cf.* Table 90.3) the lowest open-flavor thresholds.

Table 90.1 lists properties of newly observed heavy quarkonium states located below the lowest open-flavor thresholds. Those are expected to be (at least prominently) conventional quarkonia. The $h_c(1P)$ is the $^1P_1$ state of charmonium, singlet partner of the long-known χ_{cJ} triplet ^3P_J. The $\eta_c(2S)$ is the first excited state of the pseudoscalar ground state $\eta_c(1S)$, lying just below the mass of its vector counterpart, $\psi(2S)$.

Although $\eta_c(2S)$ measurements began to converge towards a mass and a width some time ago, refinements are still in progress. In particular, Belle [10] has revisited its analysis of $B \to K\eta_c(2S)$, $\eta_c(2S) \to K\overline{K}\pi$ decays with more data and methods that account for interference between the above decay chain, an equivalent one with the $\eta_c(1S)$ instead, and one with no intermediate resonance. The net effect of this interference is far from trivial; it shifts the apparent mass by $\sim$+10 MeV and blows up the apparent width by a factor of six. The updated $\eta_c(2S)$ mass and width are in better accordance with other measurements than the previous treatment [11], which did not include interference. Complementing this measurement in B-decay, BaBar [12] updated their previous [13] $\eta_c(2S)$ mass and width measurements in two-photon production, where interference effects, judging from studies of $\eta_c(1S)$, appear to be small. In combination, precision on the $\eta_c(2S)$ mass has improved dramatically.

Belle reported an observation of the $\psi_2(1D)$ decaying to $\gamma\chi_{c1}$ with J^{PC} presumed to be 2^{--} [14]. This state is listed in Table 90.1 as $\psi_2(3823)$. Its existence was confirmed with high significance by BESIII [15]. While the negative C-parity is indeed established by its observed decay channel, the assignment of $J = 2$ was done by matching to the closest quark model state. This assignment therefore requires experimental confirmation.

A new $c\bar{b}$ state was discovered by the ATLAS Collaboration [16]. Its properties are consistent with expectations for the first excited state of the $B_c^\pm$ meson, the $B_c^\pm(2S)$.

The ground state of bottomonium, $\eta_b(1S)$, was confirmed with a second observation of more than 5σ significance at Belle. In addition, the same experiment collected strong evidence for the $\eta_b(2S)$ [17], but it still needs experimental confirmation at the 5σ level.

Using dipion transitions from the $\Upsilon(10860)$ (Fig. 90.1), Belle simultaneously discovered the $h_b(1P)$, the bottomonium counterpart of the $h_c(1P)$, and the next excited state, the $h_b(2P)$ [18]. The same analysis also showed the $\Upsilon_2(1D)$, the lowest-lying D-wave triplet of the $b\bar{b}$ system. The search for the $h_b(1P)$ was directly inspired by a CLEO result [19], which found a surprisingly copious production of $e^+e^- \to \pi^+\pi^- h_c(1P)$ as well as an indication that

Table 90.1: New states below the open-flavor thresholds in the $c\bar{c}$, $b\bar{c}$, and $b\bar{b}$ regions, ordered by mass. Masses m and widths Γ represent the PDG18 weighted averages with statistical and systematic uncertainties added in quadrature. In the Production column, the state is always denoted by X. Ellipses (...) indicate inclusively selected event topologies; *i.e.*, additional particles not required by the Experiments to be present. A question mark (?) indicates an unmeasured value. The Discovery Year column gives the date of the first measurement cited. The Summary Table column indicates whether or not the state appears in the summary tables, usually requiring at least two independent experiments with significance of $>5\sigma$. Refer to the particle listings for references and further information.

PDG Name	Former/Common Name(s)	m (MeV)	Γ (MeV)	$I^G(J^{PC})$	Production	Decay	Discovery Year	Summary Table
$h_c(1P)$		3525.38 ± 0.11	0.7 ± 0.35	$0^-(1^{+-})$	$\psi(2S) \to \pi^0 X$ $p\bar{p} \to X$ $e^+e^- \to \pi\pi X$	$\gamma\eta_c(1S)$ hadrons (see listings)	2004	YES
$\eta_c(2S)$		3639.2 ± 1.2	$11.3^{+3.2}_{-2.9}$	$0^+(0^{-+})$	$B \to KX$ $e^+e^- \to e^+e^- X$ $e^+e^- \to J/\psi X$	$K^0_S K^-\pi^+$ hadrons (see listings)	2002	YES
$\psi_2(3823)$	$X(3823)$	3822.2 ± 1.2	< 16	$0^-(2^{--})$	$B \to KX$ $e^+e^- \to \pi^+\pi^- X$	$\gamma\,\chi_{c1}(1P)$	2013	YES
B_c^+		6274.9 ± 0.8	?	$0(0^-)$	$\bar{p}p \to X...$ $pp \to X...$	$\pi^+ J/\psi$ (see listings)	2007	YES
$B_c^+(2S)$		6842 ± 6	?	$0(0^-)$	$pp \to X...$	$B_c^+\pi^+\pi^-$	2014	NO
$\eta_b(1S)$		9399.0 ± 1.3	10^{+5}_{-4}	$0^+(0^{-+})$	$\Upsilon(2S,3S) \to \gamma X$ $h_b(1P,2P) \to \gamma X$		2008	YES
$h_b(1P)$		9899.3 ± 0.8	?	$0^-(1^{+-})$	$\Upsilon(10860) \to \pi^+\pi^- X$ $\Upsilon(3S) \to \pi^0 X$	$\gamma\eta_b(1S)$	2011	YES
$\eta_b(2S)$		$9999.0^{+4.5}_{-4.0}$	< 24	$0^+(0^{-+})$	$h_b(2P) \to \gamma X$	hadrons	2012	NO
$\Upsilon_2(1D)$		10163.7 ± 1.4	?	$0^-(2^{--})$	$\Upsilon(3S) \to \gamma\gamma X$ $\Upsilon(10860) \to \pi^+\pi^- X$	$\gamma\gamma\Upsilon(1S)$ $\pi^+\pi^-\Upsilon(1S)$	2004	YES
$h_b(2P)$		10259.8 ± 1.2	?	$0^-(1^{+-})$	$\Upsilon(10860) \to \pi^+\pi^- X$	$\gamma\eta_b(1S,2S)$	2011	NO
$\chi_{b1}(3P)$		10512.1 ± 2.3	?	$0^+(1^{++})$	$pp \to X...$	$\gamma\mu^+\mu^-$	2011	YES

$\psi(4260) \to \pi^+\pi^- h_c(1P)$ occurs at a comparable rate with the signature mode, $\psi(4260) \to \pi^+\pi^- J/\psi$. The presence of $\Upsilon(nS)$ peaks in Fig. 90.1 at rates two orders of magnitude larger than expected, along with separate studies with exclusive decays $\Upsilon(nS) \to \mu^+\mu^-$, allow precise calibration of the $\pi^+\pi^-$ recoil mass spectrum and very accurate measurements of $h_b(1P)$ and $h_b(2P)$ masses. Both corresponding hyperfine splittings are consistent with zero within an uncertainty of about 1.5 MeV (lowered to ±1.1 MeV for $h_b(1P)$ in Ref. [20]) .

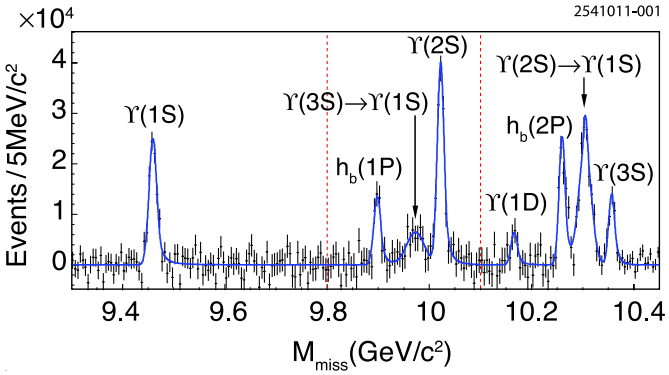

Figure 90.1: From Belle [18], the mass recoiling against $\pi^+\pi^-$ pairs, $M_{\rm miss}$, in e^+e^- collision data taken near the peak of the $\Upsilon(10860)$ (*points with error bars*). The smooth combinatorial and $K^0_S \to \pi^+\pi^-$ background contributions have been subtracted. The fit to the various labeled signal contributions is overlaid (*curve*). Adapted from [18] with kind permission, copyright (2011) The American Physical Society.

We no longer mention a hypothetical $Y_b(10888)$ state since a new analysis of the $\Upsilon(10860)$ energy range does not show evidence for an additional state with a mass different from the mass of the $\Upsilon(10860)$ [21]. After the mass of the $\eta_b(1S)$ was shifted upwards by about 10 MeV based on the new Belle measurements [17,22], all of the bottomonium states mentioned above fit into their respective spectroscopies roughly where expected. An independent experimental confirmation of the shifted masses came from the Belle observation of $\Upsilon(4S) \to \eta h_b(1P)$ [22].

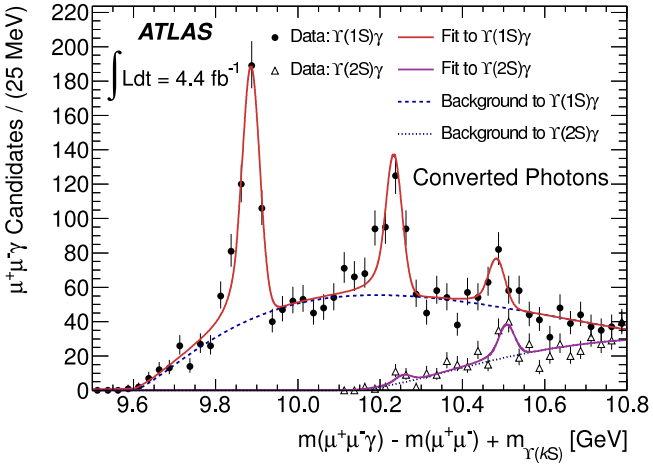

Figure 90.2: From ATLAS [23] pp collision data (*points with error bars*) taken at $\sqrt{s} = 7$ TeV, the effective mass of $\chi_{bJ}(1P, 2P, 3P) \to \gamma\Upsilon(1S, 2S)$ candidates in which $\Upsilon(1S, 2S) \to \mu^+\mu^-$ and the photon is reconstructed as an e^+e^- conversion in the tracking system. Fits (*smooth curves*) show significant signals for each triplet (J-merged) on top of a smooth background. From [23] with kind permission, copyright (2012) The American Physical Society.

The $\chi_{bJ}(nP)$ states have been observed at the LHC by ATLAS [23] and confirmed by D0 [24] for $n = 1, 2, 3$, although in each case the three J states are not distinguished from one another. Events are sought which have both a photon and an $\Upsilon(1S, 2S) \to \mu^+\mu^-$ candidate which together form a mass in the χ_b region. All three J-merged peaks are observed with a significance in excess of 6σ for both unconverted and converted photons. The mass plot for converted photons, which provide better mass resolution, is shown in Fig. 90.2. This marks the first observation of the $\chi_{bJ}(3P)$ triplet, quite near the expected mass. A precise confirmation of this result came from LHCb [25].

Table 90.2: As in Table 90.1, but for new states near the first open-flavor thresholds in the $c\bar{c}$ and $b\bar{b}$ regions, ordered by mass. Updated from [8] with kind permission, copyright (2011), Springer, and [9] with kind permission from the authors.

PDG Name	Former/Common Name(s)	m (MeV)	Γ (MeV)	$I^G(J^{PC})$	Production	Decay	Discovery Year	Summary Table
$\chi_{c1}(3872)$	$X(3872)$	3871.69±0.17	< 1.2	$0^+(1^{++})$	$B \to KX$ $p\bar{p} \to X...$ $pp \to X...$ $e^+e^- \to \gamma X$	$\pi^+\pi^- J/\psi$ $3\pi J/\psi$ $D^{*0}\overline{D}^0$ $\gamma J/\psi$ $\gamma\psi(2S)$	2003	YES
$Z_c(3900)$		3886.6 ± 2.4	28.2 ± 2.6	$1^+(1^{+-})$	$\psi(4260) \to \pi^- X$ $\psi(4260) \to \pi^0 X$	$\pi^+ J/\psi$ $\pi^0 J/\psi$ $(D\bar{D}^*)^+$ $(D\bar{D}^*)^0$	2013	YES
$X(4020)$	$Z_c(4020)$	4024.1 ± 1.9	13 ± 5	$1^+(?^{?-})$	$\psi(4260, 4360) \to \pi^- X$ $\psi(4260, 4360) \to \pi^0 X$	$\pi^+ h_c$ $\pi^0 h_c$ $(D^*\bar{D}^*)^+$ $(D^*\bar{D}^*)^0$	2013	YES
$Z_b(10610)$		10607.2 ± 2.0	18.4 ± 2.4	$1^+(1^{+-})$	$\Upsilon(10860) \to \pi^- X$ $\Upsilon(10860) \to \pi^0 X$	$\pi^+\Upsilon(1S, 2S, 3S)$ $\pi^0\Upsilon(1S, 2S, 3S)$ $\pi^+ h_b(1P, 2P)$ $(B\bar{B}^*)^+$	2011	YES
$Z_b(10650)$		10652.2 ± 1.5	11.5 ± 2.2	$1^+(1^{+-})$	$\Upsilon(10860) \to \pi^- X$	$\pi^+\Upsilon(1S, 2S, 3S)$ $\pi^+ h_b(1P, 2P)$ $(B^*\bar{B}^*)^+$	2011	YES

Table 90.3: As in Table 90.1, but for new states above the first open-flavor thresholds in the $c\bar{c}$ and $b\bar{b}$ regions, ordered by mass.

PDG Name	Former/Common Name(s)	m (MeV)	Γ (MeV)	$I^G(J^{PC})$	Production	Decay	Discovery Year	Summary Table
$\chi_{c0}(3860)$		3862^{+48}_{-35}	201^{+177}_{-106}	$0^+(0^{++})$	$e^+e^- \to J/\psi X$	$D\overline{D}$	2017	NO
$X(3915)$	$\chi_{c0}(3915)$, $Y(3940)$	3918.4 ± 1.9	20 ± 5	$0^+(0/2^{++})$	$B \to KX$ $e^+e^- \to e^+e^- X$	$\omega J/\psi$	2004	YES
$\chi_{c2}(3930)$	$\chi_{c2}(2P)$, $Z(3930)$	3927.2 ± 2.6	24 ± 6	$0^+(2^{++})$	$e^+e^- \to e^+e^- X$	$D\overline{D}$	2005	YES
$X(3940)$		3942^{+9}_{-8}	37^{+27}_{-17}	$?^?(?^{??})$	$e^+e^- \to J/\psi X$	$D\overline{D}^*$	2007	NO
$X(4050)^{\pm}$	$Z_1(4050)$	4051^{+24}_{-43}	82^{+51}_{-28}	$1^-(?^{?+})$	$B \to KX$	$\pi^+\chi_{c1}(1P)$	2008	NO
$X(4055)^{\pm}$	$Z_c(4055)$	4054 ± 3	45 ± 13	$1^+(?^{?-})$	$e^+e^- \to \pi^- X$	$\pi^+\psi(2S)$	2017	NO
$\chi_{c1}(4140)$	$Y(4140)$	4146.8 ± 2.4	22^{+8}_{-7}	$0^+(1^{++})$	$B^+ \to K^+ X$ $e^+e^- \to e^+e^- X$	$\phi J/\psi$	2009	YES
$X(4160)$		4156^{+29}_{-25}	139^{+113}_{-65}	$?^?(?^{??})$	$e^+e^- \to J/\psi X$	$D\overline{D}^*$	2007	NO
$Z_c(4200)$		4196^{+35}_{-32}	370^{+99}_{-149}	$1^+(1^{+-})$	$\bar{B}^0 \to K^- X$	$J/\psi\pi^+$	2014	NO
$\psi(4230)$	$Y(4230)$	4218^{+5}_{-4}	59^{+12}_{-10}	$0^-(1^{--})$	$e^+e^- \to X$	$\omega\chi_{c0}(1P)$ $\pi^+\pi^-\psi(2S)$ $\pi^+\pi^- h_c(1P)$	2015	NO
$R_{c0}(4240)$	$Z_c(4240)$	4239^{+48}_{-21}	220^{+118}_{-88}	$1^+(0^{--})$	$\bar{B}^0 \to K^- X$	$\pi^+\psi(2S)$	2014	NO
$X(4250)^{\pm}$	$Z_2(4250)$	$4248^{+185}_{-\ 45}$	$177^{+321}_{-\ 72}$	$1^-(?^{?+})$	$B \to KX$	$\pi^+\chi_{c1}(1P)$	2008	NO
$\psi(4260)$	$Y(4260)$	4230 ± 8	55 ± 19	$0^-(1^{--})$	$e^+e^- \to X$	$\pi\pi J/\psi$ $\gamma\chi_{c0}(3872)$	2005	YES
$\chi_{c1}(4274)$	$Y(4274)$	4274^{+8}_{-6}	49 ± 12	$0^+(1^{++})$	$B^+ \to K^+ X$	$\phi J/\psi$	2011	NO
$X(4350)$		$4350.6^{+4.6}_{-5.1}$	$13.3^{+18.4}_{-10.0}$	$0^+(?^{?+})$	$e^+e^- \to e^+e^- X$	$\phi J/\psi$	2009	NO
$\psi(4360)$	$Y(4360)$	4368 ± 13	96 ± 7	$0^-(1^{--})$	$e^+e^- \to X$	$\pi^+\pi^-\psi(2S)$	2007	YES
$\psi(4390)$	$Y(4390)$	$4391.5^{+6.4}_{-6.9}$	$139.5^{+16.2}_{-20.6}$	$0^-(1^{--})$	$e^+e^- \to X$	$\pi^+\pi^- h_c(1P)$	2017	NO
$Z_c(4430)$		4478^{+15}_{-18}	181 ± 31	$1^+(1^{+-})$	$\bar{B}^0 \to K^- X$	$\pi^+\psi(2S)$ $\pi^+ J/\psi$	2007	YES
$\chi_{c0}(4500)$	$X(4500)$	4506^{+16}_{-19}	92^{+30}_{-29}	$0^+(0^{++})$	$B^+ \to K^+ X$	$\phi J/\psi$	2017	NO
$\psi(4660)$	$X(4630)$,$Y(4660)$	4643 ± 9	72 ± 11	$0^-(1^{--})$	$e^+e^- \to X$	$\pi^+\pi^-\psi(2S)$ $\Lambda_c^+\Lambda_c^-$	2007	YES
$\chi_{c0}(4700)$	$X(4700)$	4704^{+17}_{-26}	120^{+52}_{-45}	$0^+(0^{++})$	$B^+ \to K^+ X$	$\phi J/\psi$	2017	NO
$\Upsilon(10860)$	$\Upsilon(5S)$	$10889.9^{+3.2}_{-2.6}$	51^{+6}_{-7}	$0^-(1^{--})$	$e^+e^- \to X$	$B_{(s)}^{(*)}\bar{B}_{(s)}^{(*)}(\pi)$ $\pi\pi\Upsilon(1S,2S,3S)$ $\pi^+\pi^- h_b(1P,2P)$ $\eta\Upsilon(1S,2S)$ $\pi^+\pi^-\Upsilon(1D)$	1985	YES
$\Upsilon(11020)$	$\Upsilon(6S)$	$10992.9^{+10.0}_{-3.1}$	49^{+9}_{-15}	$0^-(1^{--})$	$e^+e^- \to X$	$B_{(s)}^{(*)}\bar{B}_{(s)}^{(*)}(\pi)$ $\pi\pi\Upsilon(1S,2S,3S)$ $\pi^+\pi^- h_b(1P,2P)$	1985	YES

There is a large number of newly discovered states both near and above the lowest open-flavor thresholds. They are displayed in Table 90.2 and Table 90.3, respectively. With the exception of the tensor state located at 3930 MeV, now called $\chi_{c2}(3930)$, which has properties consistent with those expected for the $\chi_{c2}(2P)$, none of these states can easily be assigned a place in the quark model spectrum of charmonia or bottomonia. At the same time, these states have no universally accepted unconventional interpretation either. The $\chi_{c1}(3872)$, also known as $X(3872)$, is widely studied and seen in many transitions — *c.f.* Table 90.2. Yet its interpretation demands additional experimental attention: after the quantum numbers were fixed at LHCb [26,27], the next experimental challenge will be a measurement of its lineshape.

Another state (referred to here as the $X(3915)$), was discovered at 3915 MeV [28] and from a subsequent measurement its quantum numbers were determined to be $J^{PC} = 0^{++}$ [29]. This suggests it may be the $\chi_{c0}(2P)$ quark model state, but this interpretation is not generally accepted [30,31]. In addition, it was pointed out in Ref. [32] that if the assumption of helicity-2 dominance is abandoned and instead one allows for a sizable helicity-0 component, a $J^{PC} = 2^{++}$ assignment is possible. This could imply that the state at 3930 MeV (referred to here as the $\chi_{c2}(3930)$) is actually identical to the one at 3915 MeV—but to explain the large helicity-0 component a sizable portion of non-$q\bar{q}$ is necessary [32]. Because of this analysis, the name of the state was changed from $\chi_{c0}(3915)$ back to $X(3915)$. An alternative candidate for the $\chi_{c0}(2P)$ (referred to here as the $\chi_{c0}(3860)$) was reported in Ref. [33] with properties more consistent with expectation: its mass is close to the potential model expectations, it decays to $D\overline{D}$, and the preferred quantum numbers are $J^{PC} = 0^{++}$ (this hypothesis is favored over the 2^{++} one with a 2.5σ significance).

The $\psi(4260)$, also known as $Y(4260)$, and the $\psi(4360)$, also known as $Y(4360)$, are vector states decaying to $\pi^+\pi^- J/\psi$ and $\pi^+\pi^-\psi(2S)$, respectively, yet, unlike most conventional vector charmonia, they do not correspond to enhancements in the e^+e^- hadronic cross section nor decay to $D\overline{D}$. Furthermore, BESIII observed the $\chi_{c1}(3872)$, also known as $X(3872)$, in $e^+e^- \to \gamma\chi_{c1}(3872)$ in the $\psi(4260)$ mass range [34], which could allow for additional insight into the structure of both the $\psi(4260)$ as well as the $\chi_{c1}(3872)$ (*c.f.* the minireview on non-$q\bar{q}$ states). Recently BESIII produced a high-accuracy data set for $e^+e^- \to \pi^+\pi^- J/\psi$ [35], not only demonstrating that the mass of the $\psi(4260)$ is significantly lower than previously believed, but also that the lineshape is highly non-trivial. The latter observation was interpreted by the authors as the presence of two states. However, this lineshape is also consistent with other possible interpretations, such as one assuming a molecular structure for the $\psi(4260)$ [36]. Note that the data of Ref. [35] does not show any indication of the $Y(4008)$ reported by Belle – the data in this region can either be fit with a non-resonant background component or a much wider resonance at

lower mass. Also see the analysis of the $Y(4008)$ region in Ref. [37], where a wide resonance is also extracted. BESIII also performed a recent study of the process $e^+e^- \to \pi^+\pi^-\psi(2S)$ and found evidence for a lower mass state, possibly the $\psi(4260)$, in addition to the more dominant $\psi(4360)$ [38].

Another interesting question is whether a heavier $\pi^+\pi^-\psi(2S)$ state, the $\psi(4660)$, discovered by Belle [39,40] and confirmed by BaBar [41], is identical to the $\Lambda_c^+\Lambda_c^-$ state observed by Belle with a nearby mass and width [42]. Most probably it is, with $\Lambda_c^+\Lambda_c^-$ just being one more decay mode of the $\psi(4660)$ (*c.f.* the minireview on non-$q\bar{q}$ states for more detail). Note that this is the interpretation adopted in the particle listings.

Based on a full amplitude analysis of $B^0 \to K^+\pi^-\psi(2S)$ decays, Belle determined the spin-parity of the $Z_c(4430)$ to be $J^P = 1^+$ [43]. From their study of $B^0 \to K^+\pi^- J/\psi$ decays, Belle also found evidence for the decay mode $Z_c(4430) \to \pi J/\psi$ [44], which has an order of magnitude lower branching fraction than the discovery mode $Z_c(4430) \to \pi\psi(2S)$. In the same analysis, Belle also reported evidence for one more charged state, dubbed $Z_c(4200)$, decaying to $\pi J/\psi$. The existence of the $Z_c(4430)$ in $\pi\psi(2S)$ as well as its quantum number assignments were confirmed at LHCb [45] with much higher statistics. Improved values for the mass and width of the $Z_c(4430)$ from LHCb are consistent with earlier measurements; the experiment even reports a resonant behavior of the $Z_c(4430)$ amplitude. The $Z_c(4430)$ was not confirmed (or excluded) by BaBar [46].

Belle also reported an observation of two charged states decaying to $\pi\chi_{c1}$ in an analysis of $B^0 \to K^+\pi^-\chi_{c1}$ decays [47]. These were originally called the $Z_1(4050)^\pm$ and the $Z_2(4250)^\pm$, but are referred to in Table 90.3 as $X(4050)^\pm$ and $X(4250)^\pm$. These states were also not confirmed by BaBar [48]. Belle observes signals with 5.0σ significance for both the $Z_1(4050)^\pm$ and $Z_2(4250)^\pm$, whereas BABAR reports 1.1σ and 2.0σ effects, respectively, setting upper limits on product branching fractions that are not inconsistent with Belle's measured rates. The situation remains unresolved.

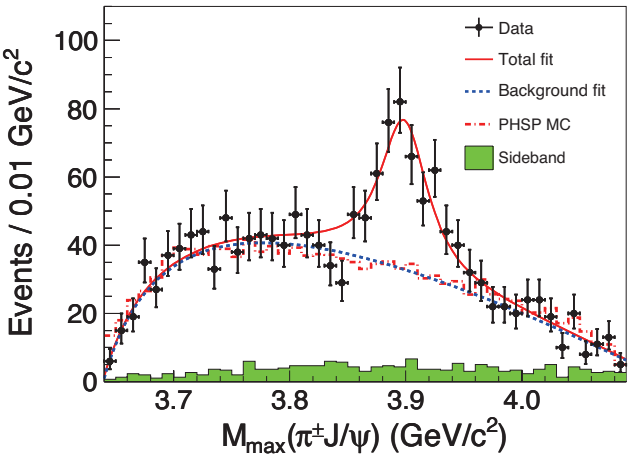

Figure 90.3: $J/\psi\pi$ invariant mass distributions from BESIII [49] e^+e^- collision data taken near the peak of the $Y(4260)$. Adapted from [49] with kind permission, copyright (2013) The American Physical Society.

In addition to the Z_c states discussed above, in 2013 a state named $Z_c(3900)$ was unearthed in the charmonium region at BESIII [49] and Belle [50]. The corresponding spectrum from BESIII is shown in Fig. 90.3. Ref. [51] confirmed this finding and also provided evidence for a neutral partner. A nearby signal was also seen in the $D\overline{D}^*$ channel [52] whose quantum numbers were fixed to 1^{+-}. BESIII reported its neutral partner in both $J/\psi\pi^0$ [53] and $D\overline{D}^*$ [54] decay modes. The masses extracted from these experiments in different decay modes have differences reaching up to 2σ. However, since the extraction of the mass and width parameters did not allow for an interference with the background and used Breit-Wigner line shapes, which is not justified near thresholds, there might be some additional systematic uncertainty in the mass values. Therefore in the RPP listings as well as Table 90.2, both structures appear under the name $Z_c(3900)$. BESIII also reported an observation of another charged state, the $X(4020)^\pm$ (originally called $Z_c(4020)^\pm$), in two decay modes — $h_c\pi^\pm$ [55] and $(D^*\overline{D}^*)^\pm$ [56]. The neutral partners have also been observed by BESIII in the $h_c\pi^0$ [57] and $(D^*\overline{D}^*)^0$ [58] final states. The Z_c states show some remarkable similarities to the Z_b states (discussed below), e.g. they decay dominantly to $D^{(*)}\bar{D}^*$ channels. However, current analyses suggest that the mass of the $Z_c(3900)$ might be somewhat above the $D\bar{D}^*$ threshold. If confirmed, this feature would clearly challenge a possible $D\bar{D}^*$–molecular interpretation. Finally, 3.5σ evidence for one more charged charmoniumlike state at 4055 MeV decaying into $\psi(2S)\pi^\pm$ was reported by Belle in their analysis of the process $e^+e^- \to \psi(2S)\pi^+\pi^-$ [40]. This state was confirmed by BESIII, although there appears to be complications in the Dalitz plot requiring further investigation [38].

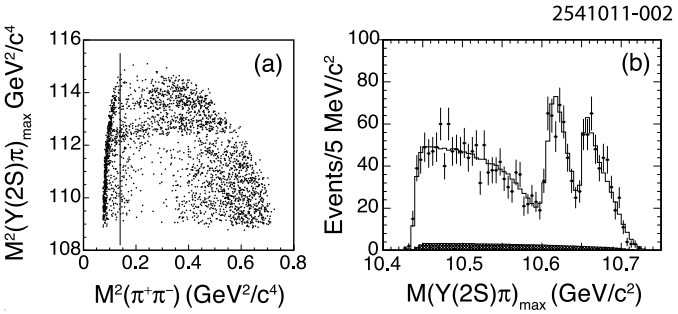

Figure 90.4: From Belle [69] e^+e^- collision data taken near the peak of the $\Upsilon(10860)$ for events with a $\pi^+\pi^-$-missing mass consistent with an $\Upsilon(2S) \to \mu^+\mu^-$, (a) the maximum of the two possible single $\pi^\pm$-missing-mass-squared combinations vs. the $\pi^+\pi^-$-mass-squared; and (b) projection of the maximum of the two possible single $\pi^\pm$-missing-mass combinations (*points with error bars*) overlaid with a fit (*curve*). Events to the left of the vertical line in (a) are excluded from amplitude analysis. The hatched histogram in (b) corresponds to the combinatorial background. The two horizontal stripes in (a) and two peaks in (b) correspond to the two Z_b states. Adapted from [69] with kind permission, copyright (2011) The American Physical Society.

The $Y(4140)$ observed in 2008 by CDF [59,60] was confirmed at D0 and CMS [61,62]. However, a second structure, the $Y(4274)$, could not be established unambiguously. Neither of the two states was seen in B decays at Belle [63], LHCb [64] and BaBar [65] or in $\gamma\gamma$ collisions at Belle [66]. The real breakthrough happened recently when LHCb performed a full amplitude analysis of $B^+ \to J/\psi\phi K^+$ with $J/\psi \to \mu^+\mu^-$, $\phi \to K^+K^-$ decays and showed that the data cannot be described in a model that contains only excited kaon states decaying into ϕK^+ [67,68]. They observe two 1^{++} states with masses close to those originally reported by CDF (the $\chi_{c1}(4140)$ and $\chi_{c1}(4274)$), but the width of the one at 4140 MeV is much larger. In addition, they find two significant 0^{++} structures at 4500 and 4700 MeV (the $\chi_{c0}(4500)$ and $\chi_{c0}(4700)$).

New results on the η_b, h_b, and Z_b mostly come from Belle [17–18], [20–22], [69–75], all from analyses of 121.4 fb^{-1} of e^+e^- collision data collected near the peak of the $\Upsilon(10860)$ resonance as well as from an additional 25 fb^{-1} of data collected during the scans of the c.m. energy range 10.63-11.05 GeV. The η_b, h_b, and Z_b appear in the decay chains: $\Upsilon(10860) \to \pi^- Z_b^+$, $Z_b^+ \to \pi^+(b\bar{b})$, and, when the $b\bar{b}$ forms an $h_b(1P)$, frequently decaying as $h_b(1P) \to \gamma\eta_b$.

Belle soon noticed that, for events in the peaks of Fig. 90.1, there seemed to be two intermediate charged states. For example, Fig. 90.4 shows a Dalitz plot for events restricted to the $\Upsilon(2S)$ region of $\pi^+\pi^-$ recoil mass, with $\Upsilon(2S) \to \mu^+\mu^-$ [69]. The two bands observed in the maximum of the two $M[\pi^\pm\Upsilon(2S)]^2$ values also appear for

$\Upsilon(1S)$, $\Upsilon(3S)$, $h_b(1P)$, and $h_b(2P)$ samples. Belle fits all subsamples to resonant plus non-resonant amplitudes, allowing for interference (notably, between $\pi^- Z_b^+$ and $\pi^+ Z_b^-$), and finds consistent pairs of Z_b masses for all bottomonium transitions, and comparable strengths of the two states. A recent angular analysis assigned $J^P = 1^+$ for both Z_b states [70], which must also have negative G-parity. Transitions through Z_b to the $h_b(nP)$ saturate the observed $\pi^+\pi^- h_b(nP)$ cross sections. While the two masses of the Z_b states as extracted from Breit-Wigner fits for the various channels are just a few MeV above the $B^*\bar{B}$ and $B^*\bar{B}^*$ thresholds, respectively, more refined analyses find pole locations right below the corresponding thresholds either on the physical [76] or the unphysical sheet [77]. Regardless of their proximity to the corresponding thresholds, both states predominantly decay into these open-flavor channels [72,78] with branching fractions that exceed 80% and 70%, respectively, at 90% CL. This feature provides strong evidence for their molecular nature.

References:

1. A. Esposito *et al.*, Int. J. Mod. Phys. A **30**, 1530002 (2015), arXiv:1411.5997 [hep-ph].
2. S.L. Olsen, Front. Phys. (Beijing) **10**, 121 (2015), arXiv:1411.7738 [hep-ex].
3. H.X. Chen, W. Chen, X. Liu, and S.L. Zhu, Phys. Rept. **639**, 1 (2016), arXiv:1601.02092 [hep-ph].
4. R.F. Lebed, R.E. Mitchell, and E.S. Swanson, Prog. Part. Nucl. Phys. **93**, 143 (2017), arXiv:1610.04528 [hep-ph].
5. A. Ali, J.S. Lange, and S. Stone, Prog. Part. Nucl. Phys. **97**, 123 (2017), arXiv:1706.00610 [hep-ph].
6. F. K. Guo *et al.*, Rev. Mod. Phys. **90**, 015004 (2018), arXiv:1705.00141 [hep-ph].
7. S. L. Olsen, T. Skwarnicki and D. Zieminska, Rev. Mod. Phys. **90**, 015003 (2018), arXiv:1708.04012 [hep-ph].
8. N. Brambilla *et al.*, Eur. Phys. J. C **71**, 1534 (2011), arXiv:1010.5827 [hep-ph].
9. N. Brambilla *et al.*, Eur. Phys. J. C **74**, 2981 (2014), arXiv:1404.3723 [hep-ph].
10. A. Vinokurova *et al.* (Belle Collab.), Phys. Lett. **B706**, 139 (2011), arXiv:1105.0978 [hep-ex].
11. S.K. Choi *et al.* (Belle Collab.), Phys. Rev. Lett. **89**, 102001 (2002), [Erratum-ibid. **89**, 129901 (2002)], arXiv:hep-ex/0206002.
12. P. del Amo Sanchez *et al.* (BaBar Collab.), Phys. Rev. **D84**, 021004 (2011), arXiv:1103.3971 [hep-ex].
13. B. Aubert *et al.* (BaBar Collab.), Phys. Rev. Lett. **92**, 142002 (2004), arXiv:hep-ex/0311038.
14. V. Bhardwaj *et al.* (Belle Collab.), Phys. Rev. Lett. **111**, 032001 (2013), arXiv:1304.3975 [hep-ex].
15. M. Ablikim *et al.* (BESIII Collab.), Phys. Rev. Lett. **115**, 011803 (2015), arXiv:1503.08203 [hep-ex].
16. G. Aad *et al.* (ATLAS Collab.), Phys. Rev. Lett. **113**, 212004 (2014), arXiv:1407.1032 [hep-ex].
17. R. Mizuk *et al.* (Belle Collab.), Phys. Rev. Lett. **109**, 232002 (2012), arXiv:1205.6351 [hep-ex].
18. I. Adachi *et al.* (Belle Collab.), Phys. Rev. Lett. **108**, 032001 (2012), arXiv:1103.3419 [hep-ex].
19. T.K. Pedlar *et al.* (CLEO Collab.), Phys. Rev. Lett. **107**, 041803 (2011), arXiv:1104.2025 [hep-ex].
20. I. Adachi *et al.* (Belle Collab.), arXiv:1110.3934 [hep-ex].
21. D. Santel *et al.* (Belle Collab.), Phys. Rev. D **93**, 011101 (2016), arXiv:1501.01137 [hep-ex].
22. U. Tamponi *et al.* (Belle Collab.), Phys. Rev. Lett. **115**, 142001 (2015), arXiv:1506.08914 [hep-ex].
23. G. Aad *et al.* (ATLAS Collab.), Phys. Rev. Lett. **108**, 152001 (2012), arXiv:1112.5154 [hep-ex].
24. V. M. Abazov (D0 Collab.), Phys.Rev. D **86**, 031103 (2012), arXiv:1203.6034 [hep-ex].
25. R. Aaij *et al.* (LHCb Collab.), JHEP **1410**, 088 (2014), arXiv:1409.1408 [hep-ex].
26. R. Aaij *et al.* (LHCb Collab.), Phys. Rev. Lett. **110**, 222001 (2013), arXiv:1302.6269 [hep-ex].
27. R. Aaij *et al.* (LHCb Collab.), Phys. Rev. D **92**, 011102 (2015), arXiv:1504.06339 [hep-ex].
28. S.-K. Choi *et al.* (Belle Collab.), Phys. Rev. Lett. **94**, 182002 (2005), arXiv:hep-ex/0408126.
29. J. P. Lees *et al.* (BaBar Collab.), Phys. Rev. D **86**, 072002 (2012), arXiv:1207.2651 [hep-ex].
30. F. -K. Guo and U.-G. Meißner, Phys. Rev. D **86**, 091501 (2012), arXiv:1208.1134 [hep-ph].
31. S.L. Olsen, Phys. Rev. D **91**, 057501 (2015), arXiv:1410.6534 [hep-ph].
32. Z. Y. Zhou, Z. Xiao and H. Q. Zhou, Phys. Rev. Lett. **115**, 022001 (2015), arXiv:1501.00879 [hep-ph].
33. K. Chilikin *et al.* (Belle Collab.), Phys. Rev. D **95**, 112003 (2017), arXiv:1704.01872 [hep-ex].
34. M. Ablikim *et al.* (BESIII Collab.), Phys. Rev. Lett. **112**, 092001 (2014), arXiv:1310.4101 [hep-ex].
35. M. Ablikim *et al.* (BESIII Collab.), Phys. Rev. Lett. **118**, 092001 (2017), arXiv:1611.01317 [hep-ex].
36. M. Cleven *et al.*, Phys. Rev. D **90**, 074039 (2014), arXiv:1310.2190 [hep-ph].
37. X. Y. Gao, C. P. Shen and C. Z. Yuan, Phys. Rev. D **95**, 092007 (2017), arXiv:1703.10351 [hep-ex].
38. M. Ablikim *et al.* (BESIII Collab.), Phys. Rev. D **96**, 032004 (2017), arXiv:1703.08787 [hep-ex].
39. X.L. Wang *et al.* (Belle Collab.), Phys. Rev. Lett. **99**, 142002 (2007), arXiv:0707.3699 [hep-ex].
40. X.L. Wang *et al.* (Belle Collab.), Phys. Rev. D **91**, 112007 (2015), arXiv:1410.7641 [hep-ex].
41. J.P. Lees *et al.* (BaBar Collab.), Phys. Rev. D **89**, 111103 (2014), arXiv:1211.6271 [hep-ex].
42. G. Pakhlova *et al.* (Belle Collab.), Phys. Rev. Lett. **101**, 172001 (2008), arXiv:0807.4458 [hep-ex].
43. K. Chilikin *et al.* (Belle Collab.), Phys.Rev. D **88**, 074026 (2013), arXiv:1306.4894 [hep-ex].
44. K. Chilikin *et al.* (Belle Collab.), Phys. Rev. D **90**, 112009 (2014), arXiv:1408.6457 [hep-ex].
45. R. Aaij *et al.* (LHCb Collab.), Phys. Rev. Lett. **112**, 222002 (2014), arXiv:1404.1903 [hep-ex].
46. B. Aubert *et al.* (BaBar Collab.), Phys. Rev. D **79**, 112001 (2009), arXiv:0811.0564 [hep-ex].
47. R. Mizuk *et al.* (Belle Collab.), Phys. Rev. **D78**, 072004 (2008), arXiv:0806.4098 [hep-ex].
48. J.P. Lees *et al.* (BaBar Collab.), Phys. Rev. **D85**, 052003 (2011), arXiv:1111.5919 [hep-ex].
49. M. Ablikim *et al.* (BESIII Collab.), Phys. Rev. Lett. **110**, 252001 (2013), arXiv:1303.5949 [hep-ex].
50. Z. Q. Liu *et al.* (Belle Collab.), Phys. Rev. Lett. **110**, 252002 (2013), arXiv:1304.0121 [hep-ex].
51. T. Xiao, S. Dobbs, A. Tomaradze and K. K. Seth, Phys. Lett. **B727**, 366 (2013), arXiv:1304.3036 [hep-ex].
52. M. Ablikim *et al.* (BESIII Collab.), Phys. Rev. Lett. **112**, 022001 (2014), arXiv:1310.1163 [hep-ex].
53. M. Ablikim *et al.* (BESIII Collab.), Phys. Rev. Lett. **115**, 112003 (2015), arXiv:1506.06018 [hep-ex].
54. M. Ablikim *et al.* (BESIII Collab.), Phys. Rev. Lett. **115**, 222002 (2015), arXiv:1509.05620 [hep-ex].
55. M. Ablikim *et al.* (BESIII Collab.), Phys. Rev. Lett. **111**, 242001 (2013), arXiv:1309.1896 [hep-ex].
56. M. Ablikim *et al.* (BESIII Collab.), Phys. Rev. Lett. **112**, 132001 (2014), arXiv:1308.2760 [hep-ex].
57. M. Ablikim *et al.* (BESIII Collab.), Phys. Rev. Lett. **113**, 212002 (2014), arXiv:1409.6577 [hep-ex].
58. M. Ablikim *et al.* (BESIII Collab.), Phys. Rev. Lett. **115**, 182002 (2015), arXiv:1507.02404 [hep-ex].
59. T. Aaltonen *et al.* (CDF Collab.), Phys. Rev. Lett. **102**, 242002 (2009), arXiv:0903.2229 [hep-ex].
60. T. Aaltonen *et al.* (CDF Collab.), Mod. Phys. Lett. **A32**, 1750139 (2017), arXiv:1101.6058 [hep-ex].
61. V. Abazov *et al.* (D0 Collab.), Phys.Rev. D **89**, 012004 (2014), arXiv:1309.6580 [hep-ex].
62. S. Chatrchyan *et al.* (CMS Collab.), Phys. Lett. B **734**, 261 (2014), arXiv:1309.6920 [hep-ex].
63. J. Brodzicka (Belle Collab.), Conf.Proc. C0908171, 299 (2009).

64. R. Aaij *et al.* (LHCb Collab.), Phys. Rev. D **85**,091103 (2012), arXiv:1202.5087 [hep-ex].
65. J.P. Lees *et al.* (BaBar Collab.), Phys. Rev. D **91**,012003 (2015), arXiv:1407.7244 [hep-ex].
66. C.P. Shen *et al.* (Belle Collab.), Phys. Rev. Lett. **104**, 112004 (2010), arXiv:0912.2383 [hep-ex].
67. R. Aaij *et al.* (LHCb Collab.), Phys. Rev. D **95**, 012002 (2017), arXiv:1606.07898 [hep-ex].
68. R. Aaij *et al.* (LHCb Collab.), Phys. Rev. Lett. **118**, 022003 (2017), arXiv:1606.07895 [hep-ex].
69. A. Bondar *et al.* (Belle Collab.), Phys. Rev. Lett. **108**, 122001 (2012), arXiv:1110.2251 [hep-ex].
70. A. Garmash *et al.* (Belle Collab.), Phys. Rev. D **91**, 072003 (2015), arXiv:1403.0992 [hep-ex].
71. P. Krokovny *et al.* (Belle Collab.), Phys.Rev. D **88**, 052016 (2013), arXiv:1308.2646 [hep-ex].
72. I. Adachi *et al.* (Belle Collab.), arXiv:1209.6450 [hep-ex].
73. K.F. Chen *et al.* (Belle Collab.), Phys. Rev. Lett. **100**, 112001 (2008), arXiv:0710.2577 [hep-ex].
74. P. Krokovny (Belle Collab.), talk given at Les Rencontres de Physique de la Vallee d'Aoste, La Thuile, Aosta Valley, Italy, 2012.
75. A. Abdesselam *et al.* (Belle Collab.), Phys. Rev. Lett. **117**, 142001 (2016), arXiv:1508.06562 [hep-ex].
76. M. Cleven *et al.*, Eur. Phys. J. A **47**, 120 (2011), arXiv:1107.0254 [hep-ph].
77. F.-K. Guo et al., Phys. Rev. D **93**, 074031 (2016), arXiv:1602.00940 [hep-ph].
78. A. Garmash *et al.* [Belle Collaboration], Phys. Rev. Lett. **116**, 212001 (2016), arXiv:1512.07419 [hep-ex].

91. Charmonium System

Updated in 2012.

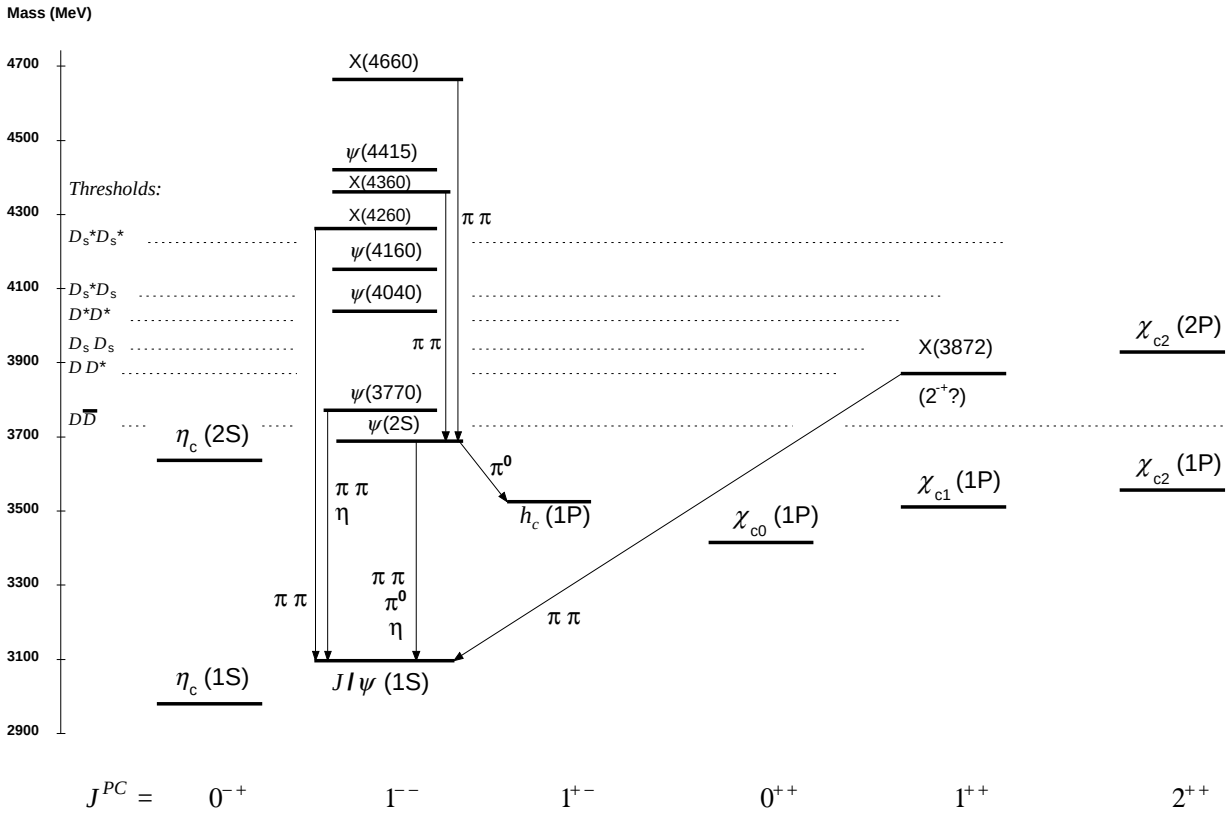

The level scheme of the $c\bar{c}$ states showing experimentally established states with solid lines. Singlet states are called η_c and h_c, triplet states ψ and χ_{cJ}, and unassigned charmonium-like states X. In parentheses it is sufficient to give the radial quantum number and the orbital angular momentum to specify the states with all their quantum numbers. Only observed hadronic transitions are shown; the single photon transitions $\psi(nS) \to \gamma\eta_c(mP)$, $\psi(nS) \to \gamma\chi_{cJ}(mP)$, and $\chi_{cJ}(1P) \to \gamma J/\psi$ are omitted for clarity.

92. Branching Ratios of $\psi(2S)$ and $\chi_{c0,1,2}$

Updated March 2018 by J.J. Hernández-Rey (IFIC, Valencia), S. Navas (U. of Granada), and C. Patrignani (Bologna Univ., INFN)

Since 2002, the treatment of the branching ratios of the $\psi(2S)$ and $\chi_{c0,1,2}$ has undergone an important restructuring.

When measuring a branching ratio experimentally, it is not always possible to normalize the number of events observed in the corresponding decay mode to the total number of particles produced. Therefore, the experimenters sometimes report the number of observed decays with respect to another decay mode of the same or another particle in the relevant decay chain. This is actually equivalent to measuring combinations of branching fractions of several decay modes.

To extract the branching ratio of a given decay mode, the collaborations use some previously reported measurements of the required branching ratios. However, the values are frequently taken from the *Review of Particle Physics* (RPP), which in turn uses the branching ratio reported by the experiment in the following edition, giving rise either to correlations or to plain vicious circles Ref. 1,Ref. 2 as discussed in more detail in earlier editions of this mini-review.

The way to avoid these dependencies and correlations is to extract the branching ratios through a fit that uses the truly measured combinations of branching fractions and partial widths. This fit, in fact, should involve decays from the four concerned particles, $\psi(2S)$, χ_{c0}, χ_{c1}, and χ_{c2}, and occasionally some combinations of branching ratios of more than one of them. This is what is done since the 2002 edition [3].

The PDG policy is to quote the results of the collaborations in a manner as close as possible to what appears in their original publications. However, in order to avoid the problems mentioned above, we had in some cases to work out the values originally measured, using the number of events and detection efficiencies given by the collaborations, or rescaling back the published results. The information was sometimes spread over several articles, and some articles referred to papers still unpublished, which in turn contained the relevant numbers in footnotes.

Even though the experimental collaborations are entitled to extract whatever branching ratios they consider appropriate by using other published results, we would like to encourage them to also quote explicitly in their articles the actual quantities measured, so that they can be used directly in averages and fits of different experimental determinations.

To inform the reader how we computed some of the values used in this edition of RPP, we use footnotes to indicate the branching ratios actually given by the experiments and the quantities they use to derive them from the true combination of branching ratios actually measured.

None of the branching ratios of the $\chi_{c0,1,2}$ are measured independently of the $\psi(2S)$ radiative decays. We tried to identify those branching ratios which can be correlated in a non-trivial way, and although we cannot preclude the existence of other cases, we are confident that the most relevant correlations have already been removed. Nevertheless, correlations in the errors of different quantities measured by the same experiment have not been taken into account.

92.1. Fit Information

This is an overall fit to 4 total widths, 1 partial width, 26 combinations of partial widths, 24 branching ratios, and 108 combinations of branching ratios. Of the latter 62 involve decays of more than one particle.

The overall fit uses 247 measurements to determine 49 parameters and has a χ^2 of 376.8 for 198 degrees of freedom.

The relatively high χ^2 of the fit, 1.9 per d.o.f., can be traced back to a few specific discrepancies in the data. No scaling factors to fit uncertainties have been applied.

In the listing we provide the inter-particle correlation coefficients $< \delta x_i \delta x_j > / (\delta x_i \cdot \delta x_j)$, in percent, from the fit to the corresponding parameter x_i.

References:

1. Y.F. Gu and X.H. Li, Phys. Lett. **B449**, 361 (1999).
2. C. Patrignani, Phys. Rev. **D64**, 034017 (2001).
3. Particle Data Group, K.Hagiwara *et al.*, Phys. Rev. **D68**, 010001 (2002).

93. Bottomonium System

Updated in 2012.

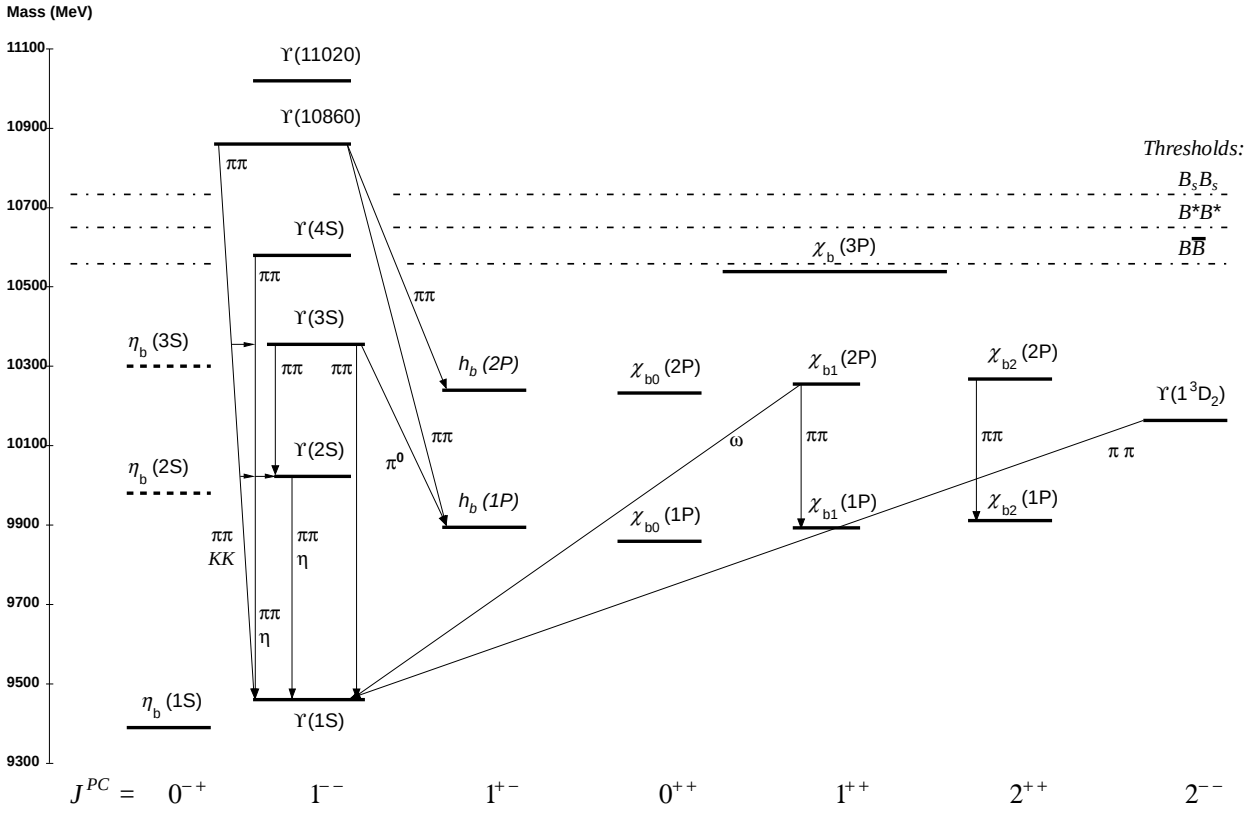

The level scheme of the $b\overline{b}$ states showing experimentally established states with solid lines. Singlet states are called η_b and h_b, triplet states Υ and χ_{bJ}. In parentheses it is sufficient to give the radial quantum number and the orbital angular momentum to specify the states with all their quantum numbers. *E.g.*, $h_b(2P)$ means 2^1P_1 with $n = 2$, $L = 1$, $S = 0$, $J = 1$, $PC = +-$. The figure shows observed hadronic transitions. The single photon transitions $\Upsilon(nS) \to \gamma\eta_b(mS)$, $\Upsilon(nS) \to \gamma\chi_{bJ}(mP)$, and $\chi_{bJ}(nP) \to \gamma\Upsilon(mS)$ are omitted for clarity.

94. Width Determinations of the Υ States

As is the case for the $J/\psi(1S)$ and $\psi(2S)$, the full widths of the $b\overline{b}$ states $\Upsilon(1S)$, $\Upsilon(2S)$, and $\Upsilon(3S)$ are not directly measurable, since they are much narrower than the energy resolution of the e^+e^- storage rings where these states are produced. The common indirect method to determine Γ starts from

$$\Gamma = \Gamma_{\ell\ell}/B_{\ell\ell} \ , \tag{94.1}$$

where $\Gamma_{\ell\ell}$ is one leptonic partial width and $B_{\ell\ell}$ is the corresponding branching fraction ($\ell = e,\ \mu,$ or τ). One then assumes e-μ-τ universality and uses

$$\begin{aligned} \Gamma_{\ell\ell} &= \Gamma_{ee} \\ B_{\ell\ell} &= \text{average of } B_{ee},\ B_{\mu\mu}, \text{ and } B_{\tau\tau} \ . \end{aligned} \tag{94.2}$$

The electronic partial width Γ_{ee} is also not directly measurable at e^+e^- storage rings, only in the combination $\Gamma_{ee}\Gamma_{\rm had}/\Gamma$, where $\Gamma_{\rm had}$ is the hadronic partial width and

$$\Gamma_{\rm had} + 3\Gamma_{ee} = \Gamma \ . \tag{94.3}$$

This combination is obtained experimentally from the energy-integrated hadronic cross section

$$\begin{aligned} &\int_{\text{resonance}} \sigma(e^+e^- \to \Upsilon \to \text{hadrons})dE \\ &= \frac{6\pi^2}{M^2}\frac{\Gamma_{ee}\Gamma_{\rm had}}{\Gamma}C_r = \frac{6\pi^2}{M^2}\frac{\Gamma_{ee}^{(0)}\Gamma_{\rm had}}{\Gamma}C_r^{(0)} \ , \end{aligned} \tag{94.4}$$

where M is the Υ mass, and C_r and $C_r^{(0)}$ are radiative correction factors. C_r is used for obtaining Γ_{ee} as defined in Eq. (94.1), and contains corrections from all orders of QED for describing $(b\overline{b}) \to e^+e^-$. The lowest order QED value $\Gamma_{ee}^{(0)}$, relevant for comparison with potential-model calculations, is defined by the lowest order QED graph (Born term) alone, and is about 7% lower than Γ_{ee}.

The Listings give experimental results on B_{ee}, $B_{\mu\mu}$, $B_{\tau\tau}$, and $\Gamma_{ee}\Gamma_{\rm had}/\Gamma$. The entries of the last quantity have been re-evaluated consistently using the correction procedure of KURAEV 85 [1]. The partial width Γ_{ee} is obtained from the average values for $\Gamma_{ee}\Gamma_{\rm had}/\Gamma$ and $B_{\ell\ell}$ using

$$\Gamma_{ee} = \frac{\Gamma_{ee}\Gamma_{\rm had}}{\Gamma(1-3B_{\ell\ell})} \ . \tag{94.5}$$

The total width Γ is then obtained from Eq. (94.1). We do not list Γ_{ee} and Γ values of individual experiments. The Γ_{ee} values in the Meson Summary Table are also those defined in Eq. (94.1).

References:

1. E.A. Kuraev, V.S. Fadin, Sov. J. Nucl. Phys. **41**, 466 (1985).

95. Non-$q\overline{q}$ Mesons

Revised March 2018 by C. Amsler (Stefan Meyer Institute for Subatomic Physics, Vienna) and C. Hanhart (Forschungszentrum Jülich).

The constituent quark model describes the observed meson spectrum as bound $q\overline{q}$ states grouped into SU(N) flavor multiplets (see our review on the 'Quark Model' in this issue of the *Review*). However, the self coupling of gluons in QCD suggests that additional mesons made of bound gluons (glueballs), or $q\overline{q}$-pairs with an excited gluon (hybrids), may exist. Furthermore, multiquark color singlet states such as $qq\overline{qq}$ (tetraquarks as compact diquark-antidiquark systems and 'molecular' bound states of two mesons) or $qqq\overline{qqq}$ (six-quark and 'baryonium' bound states of two baryons) have also been predicted.

In recent years experimental evidence for states beyond the quark model has accumulated in the heavy quark sector and elsewhere. We therefore split this minireview into three parts discussing separately light systems, heavy–light systems and heavy–heavy systems. For a more detailed discussion on exotic mesons we refer to Ref. 1 for the light meson sector and Ref. 2 for the heavy meson sector. Reviews with main focus on tetraquarks and molecular states are presented in Ref. 3 and Ref. 4, respectively. For an experimental review see Ref. 5.

95.1. Light systems

95.1.1. ***Glueball candidates*** : Among the signatures naively expected for glueballs are (i) isoscalar states that do not fit into $q\overline{q}$ nonets, (ii) enhanced production in gluon-rich channels such as central production and radiative $J/\psi(1S)$ decay, (iii) decay branching fractions incompatible with SU(N) predictions for $q\overline{q}$ states, and (iv) reduced $\gamma\gamma$ couplings. However, mixing effects with isoscalar $q\overline{q}$ mesons [6–14] and decay form factors [17] can obscure these simple signatures.

Lattice calculations, QCD sum rules, flux tube, and constituent glue models agree that the lightest glueballs have quantum numbers $J^{PC} = 0^{++}$ and 2^{++}. Lattice calculations predict for the ground state (a 0^{++} glueball) a mass around 1600 – 1700 MeV [11,18–20] with an uncertainty of about 100 MeV, while the first excited state (2^{++}) has a mass of about 2300 MeV. Hence, the low-mass glueballs lie in the same mass region as ordinary isoscalar $q\overline{q}$ states, in the mass range of the $1^3P_0(0^{++})$, $2^3P_2(2^{++})$, $3^3P_2(2^{++})$, and $1^3F_2(2^{++})$ $q\overline{q}$ states. The 0^{-+} state and exotic glueballs (with non-$q\overline{q}$ quantum numbers such as 0^{--}, 0^{+-}, 1^{-+}, 2^{+-}, *etc.*) are expected above 2 GeV [20]. The lattice calculations were performed so far in the quenched approximation. Thus neither quark loops nor mixing with conventional mesons were included, although quenching effects seem to be small [21]. For a recent comparison between quenched and unquenched lattice studies see Ref. 22.

The mixing of glueballs with nearby $q\overline{q}$ states of the same quantum numbers should lead to a supernumerary isoscalar state in the SU(3) classification of $q\overline{q}$ mesons. A lattice study in full QCD (performed at unphysical quark masses corresponding to a pion mass of 400 MeV) did not identify states with sizeable overlap with pure gluonic sources [23,24].

In the following we focus on glueball candidates in the scalar sector. For the 2^{++} sector we refer to the section on non-$q\bar{q}$ mesons in the 2006 issue of this *Review* [25], and for the 0^{-+} glueball to the note on 'The Pseudoscalar and Pseudovector Mesons in the 1400 MeV Region' in the *Meson Listings*.

Five isoscalar resonances are established: the very broad $f_0(500)$ (or σ), the $f_0(980)$, the broad $f_0(1370)$, and the comparatively narrow $f_0(1500)$ and $f_0(1710)$, see the note on 'Scalar Mesons below 2 GeV' in the *Meson Listings*, and also Ref. 26. Their isospin 1/2 and isovector partners are the $K_0^*(700)$ (or κ), the $K_0^*(1430)$, the $a_0(980)$ and the $a_0(1450)$. We shall see that none of the proposed $q\bar{q}$ ordering schemes in scalar multiplets is entirely satisfactory.

The $f_0(1370)$ and $f_0(1500)$ decay mostly into pions (2π and 4π) while the $f_0(1710)$ decays mainly into $K\overline{K}$ final states. Naively, this suggests an $n\bar{n}$ ($= u\bar{u} + d\bar{d}$) structure for the $f_0(1370)$ and $f_0(1500)$, and $s\bar{s}$ for the $f_0(1710)$. The latter is not observed in $p\overline{p}$ annihilation [27], as expected from the OZI suppression for an $s\overline{s}$ state.

In $\gamma\gamma$ collisions leading to K_SK_S [28] and K^+K^- [29] a spin-0 signal is observed at the $f_0(1710)$ mass (together with a dominant spin-2 component), while the $f_0(1500)$ is not observed in $\gamma\gamma \to K\bar{K}$ nor $\pi^+\pi^-$ [30]. The $f_0(1500)$ is also not observed by Belle in $\gamma\gamma \to \pi^0\pi^0$, although a shoulder is seen which could also be due to the $f_0(1370)$ [31]. The absence of a signal in the $\pi\pi$ channel in $\gamma\gamma$ collisions does not favor an $\overline{n}n$ interpretation for the $f_0(1500)$. The upper limit from $\pi^+\pi^-$ excludes a large $n\overline{n}$ content, and hence points to a mainly $s\overline{s}$ content [32]. This is in contradiction with the small $K\overline{K}$ decay branching ratio of the $f_0(1500)$ [33–35]. This state could be mainly glue due its absence of 2γ-coupling, while the $f_0(1710)$ coupling to 2γ would be compatible with an $s\bar{s}$ state. Indeed, Belle finds that in $\gamma\gamma \to K_SK_S$ collisions the 1500 MeV region is dominated by the $f_2'(1525)$. The $f_0(1710)$ is also observed but its production × decay rate is too large for a glueball [36]. However, the 2γ-couplings are sensitive to glue mixing with $q\bar{q}$ [37].

Since the $f_0(1370)$ does not couple strongly to $s\overline{s}$ [35], the $f_0(1370)$ or $f_0(1500)$ appear to be supernumerary. The narrow width of the $f_0(1500)$, and its enhanced production at low transverse momentum transfer in central collisions [38–40] also favor the $f_0(1500)$ to be non-$q\overline{q}$. In Ref. 6 the ground state scalar nonet is made of the $a_0(1450)$, $f_0(1370)$, $K_0^*(1430)$, and $f_0(1710)$. The isoscalars $f_0(1370)$ and $f_0(1710)$ contain a small fraction of glue, while the $f_0(1500)$ is mostly gluonic. The light scalars $f_0(500)$, $f_0(980)$, $a_0(980)$, and $K_0^*(700)$ are four-quark states or two-meson resonances (see Ref. 1 for a review). For a recent review with focus on $f_0(500)$ we refer to Ref. 41. In the mixing scheme of Ref. 37, which uses central production data from WA102 and the hadronic J/ψ decay data from BES [42,43], glue is shared between the $f_0(1370)$, $f_0(1500)$ and $f_0(1710)$. The $f_0(1370)$ is mainly $n\bar{n}$, the $f_0(1500)$ mainly glue and the $f_0(1710)$ dominantly $s\bar{s}$. This agrees with previous analyses [6,12], but, as already pointed out, alternative schemes have been proposed [6–16].

In particular, for a scalar glueball the two-gluon coupling to $n\bar{n}$ appears to be suppressed by chiral symmetry [44] and therefore $K\bar{K}$ decay could be enhanced. However, $K\bar{K}$ is naturally enhanced also in the extended linear sigma model with a dilaton as glueball [15] and in the holographic model of Ref. 16. It was argued that chiral symmetry constraints in a multichannel analysis imply that the $f_0(1710)$ is an unmixed scalar glueball [45], a view that is challenged [46].

Different mixing options have been studied in Ref. 14. In the preferred solution the ground state scalar nonet consists of the $f_0(980)$, $a_0(980)$, $K_0^*(1430)$, $f_0(1500)$ and $f_0(1710)$. The $f_0(980)$ and $f_0(1500)$ mix similarly to the η and η' in the pseudoscalar nonet, while the $f_0(1500)$ mixes with a glueball in the 500 – 1000 MeV mass range, which is identified with the $f_0(500)$ (σ). A reanalysis of the CERN-Munich data shows no signal for the $f_0(1370)$ decaying into $\pi\pi$, in contrast to Ref. 47. However, in this scheme the $K_0^*(700)$ (κ) and the $a_0(1450)$ are left out (see also our note on 'Scalar Mesons below 2 GeV' in the *Meson Listings*). The $a_0(1450)$ has recently been confirmed by LHCb data in $D^0 \to K_S^0K^\pm\pi^\mp$ [48].

The $f_0(1370)$ is not needed either in the COMPASS $\pi^-p \to \pi^-\pi^-\pi^+p$ data [49], which questions its mere existence. However, a recent analysis from CLEO-c on $D^0 \to \pi^+\pi^-\pi^+\pi^-$ decay requires a contribution from $f_0(500)f_0(1370) \to 4\pi$ [50].

The Dalitz plots of $B^\pm \to \pi^\pm\pi^\pm\pi^\mp$ have been studied by BaBar [51]. A broad 2π signal is observed around 1400 MeV which is attributed to the $f_0(1370)$, but could also be due to the $f_0(1500)$. LHCb has analyzed $\overline{B}^0$ decay into $J/\psi\,\pi^+\pi^-$ [52]. The fit to the $\pi\pi$ mass spectrum above ∼1.2 GeV does not show any significant scalar component. However, the data analysis has been challenged [53]. For $\overline{B}_s^0 \to J/\psi\,\pi^+\pi^-$ a strong scalar contribution from the $f_0(1370)$ is found [54]. Suggested by Ref. 14 the data were reanalyzed by introducing instead the $f_0(500)$ and $f_0(1500)$ [55].

In $B^\pm \to K^\pm K^\pm K^\mp$ both BaBar [56] and Belle [57] observe a strong spin-0 activity in $K\bar{K}$ around 1550 MeV. B^0 decay into $J/\psi X$ filters out the $d\overline{d}$ content of X while B_s^0 decay selects its $s\overline{s}$ component. B decay into $J/\psi X$ may therefore be the ideal environment to determine the flavor content of neutral mesons [58].

The contribution of $f_0(1500)$ production in (the supposedly gluon rich) radiative J/ψ decay is not well known. The $f_0(1500)$ is observed by BESII in $J/\psi \to \gamma\pi\pi$ [59] and by BESIII in $J/\psi \to \gamma\eta\eta$ [60] with a much smaller rate than for the $f_0(1710)$, which speaks against a

glueball interpretation for the former. However, the $f_0(1500)$ mass found by BES is significantly lower than the expected value. The overlap with the $f_0(1370)$ and $f_2'(1525)$ and the statistically limited data sample prevent a proper K-matrix analysis to be performed. Hence more data are needed in radiative J/ψ decay and in $\gamma\gamma$ collisions to clarify the spectrum of scalar mesons.

95.1.2. ***Tetraquark candidates and molecular bound states*** : The $a_0(980)$ and $f_0(980)$ could be tetraquark states [61–63] or $K\overline{K}$ molecular states [64–66] due to their strong affinity for $K\overline{K}$, in spite of their masses being very close to threshold. For $q\overline{q}$ states, the expected $\gamma\gamma$ widths [67,68] are not significantly larger than for molecular states [67,69], both predictions being consistent with data. Radiative decays of the $\phi(1020)$ into $a_0(980)$ and $f_0(980)$ were claimed to enable disentangling compact from molecular structures. Interpreting the data from DAPHNE [70,71] and VEPP - 2M [72,73] along the lines of Refs. 74,75 seems to favor these mesons to be tetraquark states. In Ref. 76 they are made of a four-quark core and a virtual $K\bar{K}$ cloud at the periphery. This is challenged in Ref. 77 showing that ϕ radiative decay data are consistent with a molecular structure of the light scalars. The $f_0(980)$ is strongly produced in D_s^+ decay [78]. This points to a large $s\overline{s}$ component, assuming Cabibbo-favored $c \to s$ decay. However, the mainly $n\bar{n}$ $f_0(1370)$ is also strongly produced in D_s^+ decay, indicating that other graphs must contribute [79].

Ratios of decay rates of B and/or B_s mesons into J/ψ plus $f_0(980)$ or $f_0(500)$ were proposed to allow for an extraction of the flavor mixing angle and to probe the tetraquark nature of those mesons within a certain model [80,81]. The phenomenological fits of the LHCb collaboration based on an isobar model do neither allow for a contribution of the $f_0(980)$ in the $B \to J/\psi\pi\pi$ [52] nor for an $f_0(500)$ in $B_s \to J/\psi\pi\pi$ decays [55]. From these analyses the authors conclude that their data are incompatible with a model where $f_0(500)$ and $f_0(980)$ are tetraquarks at the eight standard deviation level. In addition, they extract an upper limit for the mixing angle of 17^o at 90% C.L. between the $f_0(980)$ and the $f_0(500)$ that would correspond to a substantial $(\bar{s}s)$ content in $f_0(980)$ [55]. However, in a dispersive analysis of the same data that allows for a model–independent inclusion of the hadronic final state interactions in Ref. 82 a substantial $f_0(980)$ contribution is also found in the B–decays putting into question the conclusions of Ref. 55.

COMPASS reports a new 1^{++} isovector meson at 1414 MeV, decaying into $f_0(980)\pi$ [83] (called $a_1(1420)$ in the 2017 Review of Particle Physics). The resonance is observed in diffractive dissociation $\pi^- p \to \pi^-(\pi^+\pi^-)p$. Traditionally, the 1^{++} ground state nonet is believed to contain the $a_1(1260)$, $f_1(1285)$ and $f_1(1420)$ (see the mini-review on 'The Pseudoscalar and Pseudovector Mesons in the 1400 MeV Region' in the *Meson Listings*). However, a molecular $K\overline{K}\pi$ structure has been proposed for the $f_1(1420)$ [84] in view of the proximity of the $K^*\overline{K}$ threshold. The new $a_1(1420)$ could then also be a molecular state, the isovector partner of the $f_1(1420)$. Ref. [85] explains the $a_1(1420)$ not as a state but as signature of the $a_1(1260)$ distorted by a triangle singularity.

95.1.3. ***Baryonia*** :

Bound states of a baryon and an antibaryon have been predicted, but have remained elusive. The $f_2(1565)$ which is only observed in $\overline{p}p$ annihilation [86,87] is a good candidate for a 2^{++} $\bar{p}p$ bound state. Enhancements in the $\bar{p}p$ mass spectrum have also been reported below $\bar{p}p$ threshold, in $J/\psi \to \gamma\bar{p}p$ [88–90] and in $B^+ \to K^+\bar{p}p$, $B^0 \to K^0_S\bar{p}p$ [91,92] and $\bar{B}^0 \to D^0\bar{p}p$ [93]. This enhancement could be due to a 0^{-+} baryonium [94]. Note that such a pole is not necessarily a compact $qqq\bar{q}\bar{q}\bar{q}$ state but might as well be generated via non-perturbative nucleon–antinucleon final state interactions [95–98]. However, also other explanations have been proposed, such as the dynamics of the fragmentation mechanism [92]. Note that also the copious data on $e^+e^- \to n\pi$ [99,100] appear to be largely explained by the same nucleon–antinucleon final state interactions mentioned above [101].

The pronounced signal observed in $e^+e^- \to \Lambda_c^+\Lambda_c^-$ around $\sqrt{s} = 4.63$ GeV by Belle [102] was argued to be a strong evidence in favor of an interpretation of $Y(4660)$ as charmed baryonium [103]. However, this picture was challenged in Ref. 104.

95.1.4. ***Hybrid mesons*** : Hybrids may be viewed as $q\overline{q}$ mesons with a vibrating gluon flux tube. In contrast to glueballs, they can have isospin 0 or 1. The mass spectrum of hybrids with exotic (non-$q\overline{q}$) quantum numbers was predicted in Ref. 105, while Ref. 106 also deals with non-exotic quantum numbers. The ground-state hybrids with quantum numbers (0^{-+}, 1^{-+}, 1^{--}, and 2^{-+}) are expected around 1.7 to 1.9 GeV. Lattice calculations predict that the hybrid with exotic quantum numbers 1^{-+} lies at a mass of 1.9 ± 0.2 GeV [107,108]. Most hybrids are expected to be rather broad, but some can be as narrow as 100 MeV [110]. They prefer to decay into a pair of S- and P-wave mesons. The lattice study in Ref. 23 [109], based on full QCD with pion masses around 400 MeV, finds that several of the high–lying states observed in their spectrum show significant overlap with gluon rich source terms interpreted as hybrid states. For a recent experimental and theoretical review on hybrid mesons see Ref. 111.

A $J^{PC} = 1^{-+}$ exotic meson, $\pi_1(1400)$, was reported in $\pi^- p \to \eta\pi^- p$ [112,113] and in $\pi^- p \to \eta\pi^0 n$ [114]. It was observed as an interference between the angular momentum $L = 1$ and $L = 2$ $\eta\pi$ amplitudes, leading to a forward/backward asymmetry in the $\eta\pi$ angular distribution. This state has been reported earlier in $\pi^- p$ reactions [115], but ambiguous solutions in the partial wave analysis were pointed out in Ref. 116 [117]. A resonating 1^{-+} contribution to the $\eta\pi$ P-wave is also required in the Dalitz plot analysis of $\overline{p}n$ annihilation into $\pi^-\pi^0\eta$ [118], and in $\overline{p}p$ annihilation into $\pi^0\pi^0\eta$ [119]. Mass and width are consistent with the results of Ref. 112.

Another 1^{-+} state, $\pi_1(1600)$, decaying into $\rho\pi$, was reported by COMPASS with 190 GeV pions hitting a lead target [120]. It was observed earlier in $\pi^- p$ interactions in the decay modes $\eta'\pi$ [121], $f_1(1285)\pi$ [122], and $\omega\pi\pi$ [123], $b_1(1235)\pi$, but not $\eta\pi$ [124]. A strong enhancement in the 1^{-+} $\eta'\pi$ wave, compared to $\eta\pi$, was reported at this mass in [125]. Ref. 126 suggests that a Deck-generated $\eta\pi$ background from final state rescattering in $\pi_1(1600)$ decay could mimic $\pi_1(1400)$. However, this mechanism is absent in $\overline{p}p$ annihilation. The $\eta\pi\pi$ data require $\pi_1(1400)$ and cannot accommodate a state at 1600 MeV [127]. Finally, evidence for a $\pi_1(2015)$ has also been reported [122,123].

The flux tube model and the lattice concur to predict a hybrid mass of about 1.9 GeV while the $\pi_1(1400)$ and $\pi_1(1600)$ are lighter. As isovectors, $\pi_1(1400)$ and $\pi_1(1600)$ cannot be glueballs. The coupling to $\eta\pi$ of the former points to a four-quark state [128], while the strong $\eta'\pi$ coupling of the latter is favored for hybrid states [129,130]. The mass of $\pi_1(1600)$ is also not far below the lattice prediction.

Hybrid candidates with $J^{PC} = 0^{-+}$, 1^{--}, and 2^{-+} have also been reported. The $\pi(1800)$ decays mostly to a pair of S- and P-wave mesons [120,131], in line with expectations for 0^{-+} hybrid mesons. This meson is also somewhat narrow if interpreted as the second radial excitation of the pion. The evidence for 1^{--} hybrids required in e^+e^- annihilation and in τ decays has been discussed in Ref. 132. A candidate for the 2^{-+} hybrid, the $\eta_2(1870)$, was reported in $\gamma\gamma$ interactions [133], in $\overline{p}p$ annihilation [134], and in central production [135]. The near degeneracy of $\eta_2(1645)$ and $\pi_2(1670)$ suggests ideal mixing in the 2^{-+} $q\overline{q}$ nonet, and hence, the second isoscalar should be mainly $s\overline{s}$. However, $\eta_2(1870)$ decays mainly to $a_2(1320)\pi$ and $f_2(1270)\pi$ [134], with a relative rate compatible with a hybrid state [106].

95.2. Heavy-light systems

Two very narrow states, $D_{s0}^*(2317)^\pm$ and $D_{s1}(2460)^\pm$, were observed at B factories [136,137]. They lie far below the predicted masses for the two expected broad P-wave $c\overline{s}$ mesons. These states have hence been interpreted as four-quark states [138–140] or DK (DK^*) molecules [141–145]. However, strong cusp effects, due to the nearby DK (DK^*) thresholds, could shift their masses downwards and quench the observed widths, an effect similar to that occurring for the $a_0(980)$ and $f_0(980)$ mesons, which lie just below $K\overline{K}$ threshold. A hadronic width of typically 100 keV would be the unequivocal signature for a prominent molecular nature of $D_{s0}^*(2317)^\pm$ [143–145]. More

compact structures typically produce widths below 10 keV [146,147]. Currently there exists an upper bound for the width of 3.8 MeV.

It should be stressed that – akin to $q\overline{q}$ mesons – hadronic molecules also appear in multiplets. Recent studies [148–150] show that, if $D_{s0}(2317)$ were of molecular nature, the lowest non-strange scalar D-state, the $D_0^*(2400)$, would also be molecular in nature, with a two-pole structure similar to the $\Lambda(1405)$ (see the minireview "Pole structure of the $\Lambda(1405)$ region"). In Ref. 149 this assignment is demonstrated to be consistent with recent data from LHCb on $B^- \to D^+\pi^-\pi^-$ [151].

95.3. Heavy-heavy systems

Several unexpected states have been observed in the previous years in both the charmonium and the bottomonium region. With the discovery of the $X(3872)$ in $B^\pm \to K^\pm X$ ($X \to J/\psi\,\pi^+\pi^-$) by Belle [152] in 2003, soon confirmed by BaBar [153], many searches for states beyond the standard quark model were initiated both in the charm and in the bottom sectors. For an updated collection of the currently available experimental information on multiquark states we refer to the mini-review on 'Spectroscopy of mesons containing two heavy quarks' in this *Review*. Moreover, in the decay $\Lambda_b^0 \to J/\psi\,K^-p$ the LHCb collaboration has recently reported the observation of two new baryons decaying into $J/\psi\,p$, which are candidates for heavy pentaquark states [154]. Those are discussed in some depth in the mini-review on 'Pentaquarks' in this *Review*.

When restricting ourselves to confirmed states we are faced with several states that do not seem to fit into the standard quark model. This is clear for the six established charged states ($Z_c(3900)^\pm$, $Z_c(4020)^\pm$, $Z_c(4200)^\pm$ and $Z_c(4430)^\pm$ in the charmonium sector, and $Z_b(10610)^\pm$ and $Z_b(10650)^\pm$ in the bottomonium sector). The neutral ones ($X(3872)$, $Y(4260)$, $Y(4360)$, $Y(4660)$) also challenge the standard quark model since their masses and decay properties are in conflict with expectations.

The quantum numbers of the $X(3872)$ have been determined by LHCb to be $J^{PC} = 1^{++}$, first by assuming the angular momentum zero between the J/ψ and the dipion [155] and then by relaxing this constraint [156]. The $X(3872)$ can hardly be identified with the 2^3P_1 χ'_{c1} since the latter is predicted to lie about 100 MeV higher in mass [157]. Instead, the $X(3940)$ reported by Belle in $e^+e^- \to J/\psi X$, decaying into $D^*\bar{D}$ but not into $D\bar{D}$ [158], and also observed in $B \to K(X \to \omega J/\psi)$ [159] could be the χ'_{c1}. The 2^3P_2 tensor partner (χ'_{c2}) was reported by Belle at 3931 MeV in $\gamma\gamma$ interactions [160].

The $X(3872)$ lies within 200 keV of the $D^0\bar{D}^{*0}$ threshold and therefore the most natural explanation for this state is a 1^{++} $D\bar{D}^*$ molecule [161] for which strong isospin breaking is predicted [161,162] due to the nearby D^+D^{*-} threshold. Indeed, the comparable rates for $\omega J/\psi$ and $\rho^0 J/\psi$ are consistent with an interpretation of $X(3872)$ as an isoscalar $D\bar{D}^*$ molecule when the different widths of the ρ and ω are taken into account [163]. A four-quark state $cq\bar{c}\bar{q}'$ is also possible [140] but unlikely, since the charged partner of the $X(3872)$ has not been observed (e.g. in $B^- \to \bar{K}^0X^-$ nor in $B^0 \to K^+X^-$, where $X^- \to J/\psi\,\pi^-\pi^0$ [164]) — see also Ref. 165 for a possible explanation of this non-observation within the tetraquark approach. The claim that $X(3872)$ must be a compact (tetraquark) state, since it is also produced at very high p_T in $\bar{p}p$ collisions [166], was challenged in [167] which stresses the importance of rescattering, see also [168,169].

A broad structure, $Y(4260)$, decaying into $J/\psi\,\pi^+\pi^-$ was reported by BaBar in initial state radiation $e^+e^- \to \gamma(e^+e^- \to Y(4260))$ [170]. Recently a measurement with significantly improved statistics was reported from BESIII [171]. The Breit-Wigner fit of these data lead to a mass reduction of 40 MeV, but also required a second state at 4320 MeV. However, the $D_1\bar{D}$ molecular model for the $Y(4260)$ [172] is capable to describe the same data with just one single pole [173].

There are no charmonium states with the quantum numbers 1^{--} not expected in this mass region. In addition, a charmonium at this mass should have a significant coupling to $\bar{D}D$, a decay channel that is not observed for the $Y(4260)$. This state could be a hybrid charmonium with a spin-1 $\bar{c}c$ [174,175] or a spin-0 [176,177] core. However, provided that the observation of $Y(4260)$ decay into $h_c(1P)\pi\pi$ by BESIII [178] is confirmed, the hybrid hypothesis would be under pressure, since the spin of the heavy quarks (coupled to zero in the $h_c(1P)$) should be conserved in leading order in the expansion in $(\Lambda_{\rm QCD}/m_c)$. (The individual conservation of the heavy quark spin and the total angular momentum of the light quark cloud is a consequence of the heavy-quark spin symmetry, see the review on 'Heavy-Quark and Soft-Collinear Effective Theory' in this issue of the *Review*.)

The same criticism applies to the hadrocharmonium interpretation of the $Y(4260)$ which describes this state as spin-1 quarkonium surrounded by a light quark cloud [179]. To circumvent the spin-symmetry argument [180] argues that $Y(4260)$ and $Y(4360)$ could be mixtures of two hadrocharmonia with spin–triplet and spin–singlet heavy quark pairs. The same kind of mixing could also operate for a hybrid.

A dominant $D_1\bar{D}$ component in the $Y(4260)$ [181] would explain naturally why $Z_c(3900)^\pm$ (interpreted by the authors as a $\bar{D}D^*$ bound state) is seen in $Y(4260) \to \pi^\mp Z_c(3900)^\pm$. Furthermore, a prominent $D_1\bar{D}$ component of the $Y(4260)$ allowed for the prediction of a copious production of $X(3872)$ in $Y(4260)$ radiative decays [182]. This prediction was confirmed shortly after at BESIII [183]. The $Y(4360)$ as a $D_1\bar{D}^*$ bound state could be the spin partner of the $Y(4260)$ [184,185], but a detailed microscopic calculation is still lacking.

The tetraquark picture explains the observed Y states [186] and, when including a tailor-made spin-spin interaction [187], is also capable to describe the $X(3872)$, both $Z_c(3900)^{\pm,0}$ and $Z_c(4020)^\pm$ and even the recently confirmed $Z(4430)^\pm$ by Belle [188]. However, the model predicts many additional charged and neutral states which have not yet been discovered. For a possible explanation of this we refer to Ref. 165.

The charged states $Z_c(3900)^\pm$, first observed by BESIII [189] and the $Z_c(4020)^\pm$ [190] decay predominantly into $\bar{D}D^*$ and $\bar{D}^*D^*$, respectively, while $Z_b(10610)^{\pm,0}$ and $Z_b(10650)^\pm$ [191,192] decay predominantly into $\bar{B}B^*$ and $\bar{B}^*B^*$ [193], respectively, although all of them were discovered in the decay mode heavy quarkonium and pion. This suggests that the states are close relatives and their interactions are connected via heavy quark flavor symmetry. A molecular interpretation for the bottomonium states was proposed shortly after the discovery of the $Z_b^\pm$ states [194] and also shortly after that of the $Z_c(3900)^\pm$ [181]. However, some of their properties also appear to be consistent with tetraquark structures [195]. If the molecular picture were correct for the Z_b states spin, symmetry allows for the prediction of spin partner states [196] which are still to be found.

The heaviest confirmed charged state in the charmonium sector is the $Z(4430)^\pm$ observed by Belle [188]. It is interpreted as hadrocharmonium [179], $\bar{D}_1D^*$ molecule [197] as well as tetraquark state [187]. Alternatively, in Refs. 198,199 the $Z(4430)^\pm$ was explained as a cross-channel effect enhanced by a triangle singularity.

It should be stressed that the various scenarios, while describing the data, also make decisive predictions, e.g. yet unobserved quantum numbers [200,186]. The forthcoming data on heavy meson spectroscopy from various facilities should soon provide a much deeper understanding on how QCD forms matter out of quarks and gluons.

References:

1. C. Amsler and N.A. Törnqvist, Phys. Reports **389**, 61 (2004).
2. N. Brambilla *et al.*, Eur. Phys. J. **C71**, 1534 (2011).
3. A. Esposito, A. Pilloni, and A.D. Polosa, Phys. Reports **668**, 1 (2017).
4. F.-K. Guo *et al.*, Rev. Mod. Phys. **90**, 015004 (2018).
5. S.L. Olsen, Front. Phys. **10** (2015) 121.
6. C. Amsler and F.E. Close, Phys. Rev. **D53**, 295 (1996).
7. N.A. Törnqvist, Phys. Rev. Lett. **76**, 1575 (1996).
8. A.V. Anisovich and A.V. Sarantsev, Phys. Lett. **B395**, 123 (1997).
9. M. Boglione *et al.*, Phys. Rev. Lett. **79**, 1998 (1997).
10. P. Minkowski and W. Ochs, Eur. Phys. J. **C9**, 283 (1999).

11. W. Lee and D. Weingarten, Phys. Rev. **D61**, 014015 (2000).
12. F.E. Close and A. Kirk, Eur. Phys. J. **C21**, 531 (2001).
13. H.Y. Cheng *et al.*, Phys. Rev. **D92**, 094006 (2015), see also Phys. Rev. **D74**, 094005 (2006).
14. W. Ochs, J. Phys. **G40**, 043001 (2013).
15. S. Janowski *et al.*, Phys. Rev. **D90**, 114005 (2014).
16. F. Brünner and A. Rebhan, Phys. Rev. Lett. **115**, 131601 (2015).
17. T. Barnes *et al.*, Phys. Rev. **D55**, 4157 (1997).
18. G.S. Bali *et al.*, Phys. Lett. **B309**, 378 (1993).
19. C.J. Morningstar and M.J. Peardon, Phys. Rev. **D56**, 4043 (1997).
20. Y. Chen *et al.*, Phys. Rev. **D73**, 014516 (2006).
21. C.M. Richards *et al.*, Phys. Rev. **D82**, 034501 (2010).
22. E. Gregory *et al.*, JHEP **1210**, 170 (2012).
23. J.J. Dudek *et al.*, Phys. Rev. **D83**, 111502 (2011).
24. W. Sun *et al.*, arXiv:1711.00711 [hep-lat].
25. see p. 949 in W.-M. Yao *et al.*, J. Phys. **G33**, 1 (2006).
26. C. Amsler, Rev. Mod. Phys. **70**, 1293 (1998).
27. C. Amsler *et al.*, Eur. Phys. J. **C23**, 29 (2002).
28. M. Acciarri *et al.*, Phys. Lett. **B501**, 173 (2001).
29. K. Abe *et al.*, Eur. Phys. J. **C32**, 323 (2004).
30. R. Barate *et al.*, Phys. Lett. **B472**, 189 (2000).
31. S. Uehara *et al.*, Phys. Rev. **D78**, 052004 (2008).
32. C. Amsler, Phys. Lett. **B541**, 22 (2002).
33. A. Abele *et al.*, Phys. Lett. **B385**, 425 ((1996).
34. A. Abele *et al.*, Phys. Rev. **D57**, 3860 (1998).
35. D. Barberis *et al.*, Phys. Lett. **B462**, 462 (1999).
36. S. Uehara *et al.*, Prog. Theor. Exp. Phys. **2013**, 123C01 (2013).
37. F.E. Close and Q. Zhao, Phys. Rev. **D71**, 094022 (2005).
38. F.E. Close *et al.*, Phys. Lett. **B397**, 333 (1997).
39. F.E. Close , Phys. Lett. **B419**, 387 (1998).
40. A. Kirk, Phys. Lett. **B489**, 29 (2000).
41. J.R. Pelaez, , Phys. Reports **658**, 1 (2016).
42. M. Ablikim *et al.*, Phys. Lett. **B603**, 138 (2004).
43. M. Ablikim *et al.*, Phys. Lett. **B607**, 243 (2005).
44. M. Chanowitz, Phys. Rev. Lett. **95**, 172001 (2005).
45. M. Albaladejo and J.A. Oller, Phys. Rev. Lett. **101**, 252002 (2008).
46. L.S. Geng and E. Oset, Phys. Rev. **D79**, 074009 (2009).
47. D.V. Bugg, A.V. Sarantsev, B.S. Zou, Nucl. Phys. **B471**, 59 (1996).
48. R. Aaji *et al.*, Phys. Rev. **D93**, 052018 (2016).
49. C. Adolph *et al.*, Phys. Rev. **D95**, 032004 (2017).
50. P. d'Argent *et al.*, JHEP **05**, 143 (2017).
51. B. Aubert *et al.*, Phys. Rev. **D79**, 072006 (2009).
52. R. Aaij *et al.*, Phys. Rev. **D90**, 012003 (2014).
53. F.E. Close and A. Kirk, Phys. Rev. **D91**, 114015 (2015).
54. R. Aaij *et al.*, Phys. Rev. **D86**, 052006 (2012).
55. R. Aaij *et al.*, Phys. Rev. **D89**, 092006 (2014).
56. B. Aubert *et al.*, Phys. Rev. **D74**, 032003 (2006).
57. A. Garmash *et al.*, Phys. Rev. **D71**, 092003 (2005).
58. C.D. Lü *et al.*, Eur. Phys. J. **A49**, 58 (2013).
59. M. Ablikim *et al.*, Phys. Lett. **B642**, 441 (2006).
60. M. Ablikim *et al.*, Phys. Rev. **D87**, 092009 (2013).
61. R.L. Jaffe, Phys. Rev. **D15**, 267 (1977), Phys. Rev. **D15**, 281 (1977).
62. M. Alford and R.L. Jaffe, Nucl. Phys. **B578**, 367 (2000).
63. G. 't Hooft *et al.*, Phys. Lett. **B662**, 424 (2008).
64. J. Weinstein and N. Isgur, Phys. Rev. **D41**, 2236 (1990).
65. G. Janssen *et al.*, Phys. Rev. **D52**, 2690 (1995).
66. M.P. Locher *et al.*, Eur. Phys. J. **C4**, 317 (1998).
67. J.A. Oller and E. Oset, Hadron 97 Conf. AIP Conf. Proc. **432**, 413 (1997).
68. R. Delbourgo *et al.*, Phys. Lett. **B446**, 332 (1999).
69. C. Hanhart *et al.*, Phys. Rev. **D75**, 074015 (2007).
70. A. Aloisio *et al.*, Phys. Lett. **B536**, 209 (2002).
71. A. Aloisio *et al.*, Phys. Lett. **B537**, 21 (2002).
72. R.R. Akhmetshin *et al.*, Phys. Lett. **B462**, 371 (1999).
73. M.N. Achasov *et al.*, Phys. Lett. **B479**, 53 (2000).
74. F.E. Close *et al.*, Nucl. Phys. **B389**, 513 (1993).
75. N.N. Achasov *et al.*, Phys. Rev. **D56**, 203 (1997).
76. F.E. Close and N. Törnqvist, J. Phys. **G28**, R249 (2002).
77. Y.S. Kalashnikova *et al.*, Eur. Phys. J. **A24**, 437 (2005).
78. E.M. Aitala *et al.*, Phys. Rev. Lett. **86**, 765 (2001).
79. H.Y. Cheng, Phys. Rev. **D67**, 054021 (1997).
80. R. Fleischer *et al.*,Eur. Phys. J. **C71**, 1832 (2011).
81. S. Stone and L. Zhang, Phys. Rev. Lett. **111**, 062001 (2013).
82. J.T. Daub, C. Hanhart, and B. Kubis, JHEP **009**, 1602 (2016).
83. C. Adolph *et al.*, Phys. Rev. Lett. **115**, 082001 (2015).
84. R.S. Longacre, Phys. Rev. **D42**, 874 (1990).
85. M. Mikhasenko, B. Ketzer,and A. Sarantsev, Phys. Rev. **D91**, 094015 (2015).
86. B. May *et al.*, Z. Phys. **C46**, 203 (1990).
87. A. Bertin *et al.*, Phys. Rev. **D57**, 55 (1998).
88. J.Z. Bai *et al.*, Phys. Rev. Lett. **91**, 022001 (2003).
89. J.P. Alexander *et al.*, Phys. Rev. **D82**, 092002 (2010).
90. M. Ablikim *et al.*, Phys. Rev. Lett. **108**, 112003 (2012).
91. K. Abe *et al.*, Phys. Rev. Lett. **88**, 181803 (2002).
92. M.-Z. Wang *et al.*, Phys. Lett. **B617**, 141 (2005).
93. K. Abe *et al.*, Phys. Rev. Lett. **89**, 151802 (2002).
94. G.-J. Ding and M.L. Yan, Phys. Rev. **C72**, 015208 (2005).
95. B. Loiseau and S. Wycech, Phys. Rev. **C72**, 011001 (2005).
96. A. Sibirtsev *et al.*, Phys. Rev. **D71**, 054010 (2005).
97. X.W. Kang, J. Haidenbauer, and U.-G. Meißner, JHEP **1402**, 113 (2014).
98. X.W. Kang, J. Haidenbauer, and U.-G. Meißner, Phys. Rev. **D91**, 074003 (2015).
99. B. Aubert *et al.*, Phys. Rev. **D76**, 092005 (2007).
100. R.R. Akhmetshin *et al.*, Phys. Lett. **B723**, 82 (2013).
101. J. Haidenbauer *et al.*, Phys. Rev. **D92**, 054032 (2015) see also J. Haidenbauer, X.-W. Kang, and U.-G. Meißner, Nucl. Phys. **A929**, 102 (2014).
102. G. Pakhlova *et al.*, Phys. Rev. Lett. **101**, 172001 (2008).
103. G. Cotugno *et al.*, Phys. Rev. Lett. **104**, 132005 (2010).
104. F.-K. Guo *et al.*, Phys. Rev. **D82**, 094008 (2010).
105. N. Isgur *et al.*, Phys. Rev. Lett. **54**, 869 (1985).
106. F.E. Close and P.R. Page, Nucl. Phys. **B433**, 233 (1995).
107. P. Lacock *et al.*, Phys. Lett. **B401**, 308 (1997).
108. C. Bernard *et al.*, Phys. Rev. **D56**, 7039 (1997).
109. J.J. Dudek *et al.*, Phys. Rev. **D88**, 094505 (2013).
110. P.R. Page *et al.*, Phys. Rev. **D59**, 034016 (1999).
111. C.A. Meyer, E.S. Swanson, Prog. in Part. Nucl. Phys. **82**, 21 (2015).
112. D.R. Thompson *et al.*, Phys. Rev. Lett. **79**, 1630 (1997).
113. S.U. Chung *et al.*, Phys. Rev. **D60**, 092001 (1999).
114. G.S. Adams *et al.*, Phys. Lett. **B657**, 27 (2007).
115. D.M. Alde *et al.*, Phys. Lett. **B205**, 397 (1988).
116. Y.D. Prokoshkin and S.A. Sadovsky, Phys. Atom. Nucl. **58**, 606 (1995).
117. Y.D. Prokoshkin and S.A. Sadovsky, Phys. Atom. Nucl. **58**, 853 (1995).
118. A. Abele *et al.*, Phys. Lett. **B423**, 175 (1998).
119. A. Abele *et al.*, Phys. Lett. **B446**, 349 (1999).
120. M.G. Alekseev *et al.*, Phys. Rev. Lett. **104**, 241803 (2010).
121. E.I. Ivanov *et al.*, Phys. Rev. Lett. **86**, 3977 (2001).
122. J. Kuhn *et al.*, Phys. Lett. **B595**, 109 (2004).
123. M. Lu *et al.*, Phys. Rev. Lett. **94**, 032002 (2005).
124. Yu.P. Gouz *et al.*, Proc. XXVI Int. Conf. on HEP, Dallas (1992).
125. G.M. Beladidze *et al.*, Phys. Lett. **B313**, 276 (1993).
126. A. Donnachie *et al.*, Phys. Rev. **D58**, 114012 (1998).
127. W. Dünnweber, Nucl. Phys. **A663-664**, 592C (1999).
128. S.U. Chung *et al.*, Eur. Phys. J. **A15**, 539 (2002).
129. F.E. Close and H.J. Lipkin, Phys. Lett. **B196**, 245 (1987).
130. F. Iddir and A.S. Safir, Phys. Lett. **B507**, 183 (2001).
131. D.V. Amelin *et al.*, Phys. Lett. **B356**, 595 (1995).
132. A. Donnachie and Yu.S. Kalashnikova, Phys. Rev. **D60**, 114011 (1999).
133. K. Karch *et al.*, Z. Phys. **C54**, 33 (1992).
134. J. Adomeit *et al.*, Z. Phys. **C71**, 227 (1996).
135. D. Barberis *et al.*, Phys. Lett. **B413**, 217 (1997).

136. B. Aubert *et al.*, Phys. Rev. Lett. **90**, 242001 (2003).
137. D. Besson *et al.*, Phys. Rev. **D68**, 032002 (2003).
138. H.-Y. Cheng and W.-S. Hou, Phys. Lett. **B566**, 193 (2003).
139. K. Terasaki, Phys. Rev. **D68**, 011501 (2003).
140. L. Maiani *et al.*, Phys. Rev. **D71**, 014028 (2005).
141. T. Barnes *et al.*, Phys. Rev. **D68**, 054006 (2003).
142. E.E. Kolomeitsev and M.F.M. Lutz, Phys. Lett. **B582**, 39 (2004).
143. A. Faessler *et al.*, Phys. Rev. **D76**, 014005 (2007).
144. M.F.M. Lutz and M. Soyeur, Nucl. Phys. **A813**, 14 (2008).
145. L. Liu *et al.*, Phys. Rev. **D87**, 014508 (2013).
146. S. Godfrey, Phys. Lett. **B568**, 254 (2003).
147. P. Colangelo and F. De Fazio, Phys. Lett. **B570**, 180 (2003).
148. M. Albaladejo *et al.*, Phys. Lett. **B767**, 465 (2017).
149. M.L. Du *et al.*, arXiv:1712.07957 [hep-ph].
150. X.Y. Guo, Y. Heo, and M.F.M. Lutz, arXiv:1801.10122 [hep-lat].
151. R. Aaij *et al.*, Phys. Rev. **D94**, 072001 (2016).
152. S.-K. Choi *et al.*, Phys. Rev. Lett. **91**, 262001 (2003).
153. B. Aubert *et al.*, Phys. Rev. **D71**, 071103R (2005).
154. R. Aaij *et al.*, Phys. Rev. Lett. **115**, 072001 (2015).
155. R. Aaij *et al.*, Phys. Rev. Lett. **110**, 222001 (2013).
156. R. Aaij *et al.*, Phys. Rev. **D92**, 011102 (2015).
157. T. Barnes and S. Godfrey, Phys. Rev. **D69**, 054008 (2004).
158. K. Abe *et al.*, Phys. Rev. Lett. **98**, 082001 (2007).
159. S.-K. Choi *et al.*, Phys. Rev. Lett. **94**, 182002 (2005).
160. S. Uehara *et al.*, Phys. Rev. Lett. **96**, 082003 (2006).
161. N. Törnqvist, Phys. Lett. **B590**, 209 (2004).
162. E. Swanson, Phys. Lett. **B588**, 189 (2004).
163. D. Gamermann and E. Oset, Phys. Rev. **D80**, 014003 (2009).
164. B. Aubert *et al.*, Phys. Rev. **D71**, 031501R (2005).
165. L. Maiani, A.D. Polosa, and V. Riquer, Phys. Lett. **B778**, 247 (2018).
166. C. Bignamini *et al.*, Phys. Rev. Lett. **103**, 162001 (2009).
167. P. Artoisenet and E. Braaten, Phys. Rev. **D81**, 114018 (2010).
168. F.-K. Guo *et al.*, JHEP **1405**, 138 (2014).
169. M. Albaladejo *et al.*, Chin. Phys. C **41**, 121001 (2017).
170. B. Aubert *et al.*, Phys. Rev. Lett. **95**, 142001 (2005).
171. M. Ablikim *et al.*, Phys. Rev. Lett. **118**, 092001 (2017).
172. M. Cleven *et al.*, Phys. Rev. **D90**, 074039 (2014).
173. C. Hanhart, arXiv:1712.01136 [hep-ph].
174. F.E. Close and P.R. Page, Phys. Lett. **B628**, 215 (2005).
175. M. Berwein, *et al.*, Phys. Rev. **D92**, 114019 (2015).
176. E. Kou and O. Pene, Phys. Lett. **B631**, 164 (2005).
177. Yu.S. Kalashnikova and A.V. Nefediev, Phys. Rev. **D77**, 054025 (2008).
178. M. Ablikim *et al.*, Phys. Rev. Lett. **111**, 242001 (2013).
179. M.B. Voloshin, Prog. in Part. Nucl. Phys. **61**, 455 (2008).
180. X. Li, M.B. Voloshin, Mod. Phys. Lett. **A29**, 50060 (2014).
181. Q. Wang *et al.*, Phys. Rev. Lett. **111**, 132003 (2013).
182. F.K. Guo *et al.*, Phys. Lett. **B725**, 127 (2013).
183. M. Ablikim *et al.*, Phys. Rev. Lett. **112**, 092001 (2014).
184. Q. Wang *et al.*, Phys. Rev. **D89**, 034001 (2014).
185. L. Ma *et al.*, Phys. Rev. **D91**, 034002 (2015).
186. A. Ali *et al.*, Eur. Phys. J. **C78**, 29 (2018).
187. L. Maiani *et al.*, Phys. Rev. **D89**, 114010 (2014).
188. B. Chilikin *et al.*, Phys. Rev. **D88**, 074026 (2013).
189. M. Ablikim *et al.*, Phys. Rev. Lett. **110**, 252001 (2013).
190. M. Ablikim *et al.*, Phys. Rev. Lett. **111**, 242002 (2013).
191. P. Krokovny *et al.*, Phys. Rev. **D88**, 052016 (2013).
192. A. Bondar *et al.*, Phys. Rev. Lett. **108**, 122001 (2012).
193. A. Garmash *et al.*, Phys. Rev. Lett. **116**, 212001 (2016).
194. A. Bondar *et al.*, Phys. Rev. **D84**, 054010 (2011).
195. A. Ali *et al.*, Phys. Rev. **D91**, 017502 (2015).
196. V. Baru *et al.*, JHEP **1706**, 158 (2017).
197. T. Branz *et al.*, Phys. Rev. **D82**, 054025 (2010).
198. P. Pakhlov, Phys. Lett. **B702**, 139 (2011).
199. P. Pakhlov and T. Uglov, Phys. Lett. **B748**, 183 (2015).
200. M. Cleven *et al.*, Phys. Rev. **D92**, 014005 (2015).

96. Baryon Decay Parameters

Written 1996 by E.D. Commins (University of California, Berkeley).

96.1. Baryon semileptonic decays

The typical spin-1/2 baryon semileptonic decay is described by a matrix element, the hadronic part of which may be written as:

$$\overline{B}_f \left[f_1(q^2)\gamma_\lambda + i\, f_2(q^2)\sigma_{\lambda\mu}q^\mu + g_1(q^2)\gamma_\lambda\gamma_5 + g_3(q^2)\gamma_5 q_\lambda \right] B_i \ . \tag{96.1}$$

Here B_i and $\overline{B}_f$ are spinors describing the initial and final baryons, and $q = p_i - p_f$, while the terms in f_1, f_2, g_1, and g_3 account for vector, induced tensor ("weak magnetism"), axial vector, and induced pseudoscalar contributions [1]. Second-class current contributions are ignored here. In the limit of zero momentum transfer, f_1 reduces to the vector coupling constant g_V, and g_1 reduces to the axial-vector coupling constant g_A. The latter coefficients are related by Cabibbo's theory [2], generalized to six quarks (and three mixing angles) by Kobayashi and Maskawa [3]. The g_3 term is negligible for transitions in which an $e^\pm$ is emitted, and gives a very small correction, which can be estimated by PCAC [4], for $\mu^\pm$ modes. Recoil effects include weak magnetism, and are taken into account adequately by considering terms of first order in

$$\delta = \frac{m_i - m_f}{m_i + m_f} \ , \tag{96.2}$$

where m_i and m_f are the masses of the initial and final baryons.

The experimental quantities of interest are the total decay rate, the lepton-neutrino angular correlation, the asymmetry coefficients in the decay of a polarized initial baryon, and the polarization of the decay baryon in its own rest frame for an unpolarized initial baryon. Formulae for these quantities are derived by standard means [5] and are analogous to formulae for nuclear beta decay [6]. We use the notation of Ref. 6 in the Listings for neutron beta decay. For comparison with experiments at higher q^2, it is necessary to modify the form factors at $q^2 = 0$ by a "dipole" q^2 dependence, and for high-precision comparisons to apply appropriate radiative corrections [7].

The ratio g_A/g_V may be written as

$$g_A/g_V = |\, g_A/g_V \,| \, e^{i\phi_{AV}} \ . \tag{96.3}$$

The presence of a "triple correlation" term in the transition probability, proportional to $\mathrm{Im}(g_A/g_V)$ and of the form

$$\boldsymbol{\sigma}_i \cdot (\mathbf{p}_\ell \times \mathbf{p}_\nu) \tag{96.4}$$

for initial baryon polarization or

$$\boldsymbol{\sigma}_f \cdot (\mathbf{p}_\ell \times \mathbf{p}_\nu) \tag{96.5}$$

for final baryon polarization, would indicate failure of time-reversal invariance. The phase angle ϕ has been measured precisely only in neutron decay (and in ^{19}Ne nuclear beta decay), and the results are consistent with T invariance.

96.2. Hyperon nonleptonic decays

The amplitude for a spin-1/2 hyperon decaying into a spin-1/2 baryon and a spin-0 meson may be written in the form

$$M = G_F\, m_\pi^2 \cdot \overline{B}_f \,(A - B\gamma_5)\, B_i \ , \tag{96.6}$$

where A and B are constants [1]. The transition rate is proportional to

$$R = 1 + \gamma\, \widehat{\boldsymbol{\omega}}_f \cdot \widehat{\boldsymbol{\omega}}_i + (1-\gamma)(\widehat{\boldsymbol{\omega}}_f \cdot \widehat{\mathbf{n}})(\widehat{\boldsymbol{\omega}}_i \cdot \widehat{\mathbf{n}}) + \alpha(\widehat{\boldsymbol{\omega}}_f \cdot \widehat{\mathbf{n}} + \widehat{\boldsymbol{\omega}}_i \cdot \widehat{\mathbf{n}}) + \beta \widehat{\mathbf{n}} \cdot (\widehat{\boldsymbol{\omega}}_f \times \widehat{\boldsymbol{\omega}}_i) \ , \tag{96.7}$$

where $\widehat{\mathbf{n}}$ is a unit vector in the direction of the final baryon momentum, and $\widehat{\boldsymbol{\omega}}_i$ and $\widehat{\boldsymbol{\omega}}_f$ are unit vectors in the directions of the initial and final baryon spins. (The sign of the last term in the above equation was incorrect in our 1988 and 1990 editions.) The parameters α, β, and γ are defined as

$$\begin{aligned} \alpha &= 2\,\mathrm{Re}(s^* p)/(|\,s\,|^2 + |\,p\,|^2) \ , \\ \beta &= 2\,\mathrm{Im}(s^* p)/(|\,s\,|^2 + |\,p\,|^2) \ , \\ \gamma &= (|\,s\,|^2 - |\,p\,|^2)/(|\,s\,|^2 + |\,p\,|^2) \ , \end{aligned} \tag{96.8}$$

where $s = A$ and $p = |\,\mathbf{p}_f\,| B/(E_f + m_f)$; here E_f and $\mathbf{p}_f$ are the energy and momentum of the final baryon. The parameters α, β, and γ satisfy

$$\alpha^2 + \beta^2 + \gamma^2 = 1 \ . \tag{96.9}$$

If the hyperon polarization is $\mathbf{P}_Y$, the polarization $\mathbf{P}_B$ of the decay baryons is

$$\mathbf{P}_B = \frac{(\alpha + \mathbf{P}_Y \cdot \widehat{\mathbf{n}})\widehat{\mathbf{n}} + \beta(\mathbf{P}_Y \times \widehat{\mathbf{n}}) + \gamma \widehat{\mathbf{n}} \times (\mathbf{P}_Y \times \widehat{\mathbf{n}})}{1 + \alpha \mathbf{P}_Y \cdot \widehat{\mathbf{n}}} \ . \tag{96.10}$$

Here $\mathbf{P}_B$ is defined in the rest system of the baryon, obtained by a Lorentz transformation along $\widehat{\mathbf{n}}$ from the hyperon rest frame, in which $\widehat{\mathbf{n}}$ and $\mathbf{P}_Y$ are defined.

An additional useful parameter ϕ is defined by

$$\beta = (1 - \alpha^2)^{1/2} \sin\phi \ . \tag{96.11}$$

In the Listings, we compile α and ϕ for each decay, since these quantities are most closely related to experiment and are essentially uncorrelated. When necessary, we have changed the signs of reported values to agree with our sign conventions. In the Baryon Summary Table, we give α, ϕ, and Δ (defined below) with errors, and also give the value of γ without error.

Time-reversal invariance requires, in the absence of final-state interactions, that s and p be relatively real, and therefore that $\beta = 0$. However, for the decays discussed here, the final-state interaction is strong. Thus

$$s = |\,s\,|\, e^{i\delta_s} \text{ and } p = |\,p\,|\, e^{i\delta_p} \ , \tag{96.12}$$

where δ_s and δ_p are the pion-baryon s- and p-wave strong interaction phase shifts. We then have

$$\beta = \frac{-2\,|\,s\,|\,|\,p\,|}{|\,s\,|^2 + |\,p\,|^2} \sin(\delta_s - \delta_p) \ . \tag{96.13}$$

One also defines $\Delta = -\tan^{-1}(\beta/\alpha)$. If T invariance holds, $\Delta = \delta_s - \delta_p$. For $\Lambda \to p\pi^-$ decay, the value of Δ may be compared with the s- and p-wave phase shifts in low-energy $\pi^- p$ scattering, and the results are consistent with T invariance.

See also the note on "Radiative Hyperon Decays" in this *Review*.

References:

1. E.D. Commins and P.H. Bucksbaum, *Weak Interactions of Leptons and Quarks* (Cambridge University Press, Cambridge, England, 1983).
2. N. Cabibbo, Phys. Rev. Lett. **10**, 531 (1963).
3. M. Kobayashi and T. Maskawa, Prog. Theor. Phys. **49**, 652 (1973).
4. M.L. Goldberger and S.B. Treiman, Phys. Rev. **111**, 354 (1958).
5. P.H. Frampton and W.K. Tung, Phys. Rev. **D3**, 1114 (1971).
6. J.D. Jackson, S.B. Treiman, and H.W. Wyld, Jr., Phys. Rev. **106**, 517 (1957), and Nucl. Phys. **4**, 206 (1957).
7. Y. Yokoo, S. Suzuki, and M. Morita, Prog. Theor. Phys. **50**, 1894 (1973).

97. *N* and Δ Resonances

Revised February 2018 by V. Burkert (Jefferson Lab), E. Klempt (University of Bonn), U. Thoma (University of Bonn), L. Tiator (University of Mainz), and R.L. Workman (George Washington University).

97.1. Introduction

The excited states of the nucleon have been studied in a large number of formation and production experiments. Until recently, the Breit-Wigner masses and widths, the pole positions, and the elasticities of the N and Δ resonances in the Baryon Summary Table came largely from partial-wave analyses of πN total, elastic, and charge-exchange scattering data. The most comprehensive analyses were carried out by the Karlsruhe-Helsinki (KH80) [1], Carnegie Mellon-Berkeley (CMB80) [2], and George Washington U (GWU) [3] groups. Partial-wave analyses have also been performed on much smaller πN reaction data sets to get ηN, $K\Lambda$, and $K\Sigma$ branching fractions (see the Listings for references). Other branching fractions come from analyses of $\pi N \to \pi\pi N$ data.

In recent years, a large amount of data on photoproduction of many final states has been accumulated, and these data are beginning to tell us much about the properties of baryon resonances. A survey of data on photoproduction can be found in the proceedings of recent conferences [4] and workshops [5], and in recent reviews [6,7].

97.2. Naming scheme for baryon resonances

In the past, when nearly all resonance information came from elastic πN scattering, it was common to label resonances with the incoming partial wave $L_{2I,2J}$, as in $\Delta(1232)P_{33}$ and $N(1680)F_{15}$. However, most recent information has come from γN experiments. Therefore, we have replaced $L_{2I,2J}$ with the spin-parity J^P of the state, as in $\Delta(1232)3/2^+$ and $N(1680)5/2^+$; this name gives intrinsic properties of the resonance that are independent of the specific particles and reactions used to study them. This applies equally to all baryons, including Ξ resonances and charm baryons that are not produced in formation experiments. We do not, however, attach the mass or spin-parity to the names of the ground-state ("stable") baryons $N, \Lambda, \Sigma, \Xi, \Omega$, $\Lambda_c, \cdots$.

97.3. Using the *N* and Δ listings

Tables 97.1 and 97.2 list all the N and Δ entries in the Baryon Listings and give our evaluation of the overall status and the status channel by channel. Only the established resonances (overall status 3 or 4 stars) are promoted to the Baryon Summary Table. We long ago omitted from the Listings information from old analyses, prior to KH80 and CMB80, which can be found in earlier editions. A rather complete survey of older results was given in our 1982 edition [8].

As a rule, we award an overall status **** or *** only to those resonances which are derived from analyses of data sets that include precision differential cross sections and polarization observables, and are confirmed by independent analyses. All other signals are given ** or * status. New results that are not accompanied by proper error evaluation are less valuable for evaluating star ratings. The following criteria are guidelines for future error analysis.

1. Uncertainties in resonance parameters: The publication should have a detailed discussion on how the uncertainties of parameters were estimated. This requires that the error estimates go beyond the simple fit error as e.g. given by MINUIT, and the robustness of the results should be demonstrated.

2. Fit quality: Concrete measures for the fit quality should be provided. The reduced global χ^2 value of the fit, while useful, is insufficient. Other possibilities include quoting variations of local χ^2 values in kinematic regions where evidence for new resonances, or significantly improved information on resonance parameters, is claimed.

3. Weight factors in observables: Analyses sometimes use weight factors for certain data sets to either increase or reduce their impact on the results. This has been particularly important when polarization observables are involved, which often are sensitive to resonance amplitudes through interferences, but usually have much poorer statistics than differential cross section data. To evaluate sensitivities, the resulting resonance parameters should be checked against variations of the specific weight factors.

Claims of evidence for new baryon states must be based on a sufficiently complete set of partial waves in the fit. The robustness of signals must be demonstrated, e.g. by examining the effect of higher partial waves in the fit.

97.4. Properties of resonances

Resonances are defined by poles of the S-matrix, whether in scattering, production or decay matrix elements. These are poles in the complex plane in s, as discussed in the new review on *Resonances*. As is traditional, we quote here the pole positions in the complex energy $w = \sqrt{s}$ plane. Crucially, the position of the pole of the S-matrix is independent of the process, and the production and decay properties factorize. This is the rationale for listing the pole position first for each resonance.

Table 97.1. The status of the N resonances and their decays. Sub-threshold decay modes are omitted. Only resonances with an overall status of *** or **** are included in the main Baryon Summary Table.

			Status as seen in										
Particle	J^P	overall	$N\gamma$	$N\pi$	$\Delta\pi$	$N\sigma$	$N\eta$	ΛK	ΣK	$N\rho$	$N\omega$	$N\eta'$
N	$1/2^+$	****										
$N(1440)1/2^+$		****	****	****	****	***						
$N(1520)3/2^-$		****	****	****	****	**	****					
$N(1535)1/2^-$		****	****	****	***	*	****					
$N(1650)1/2^-$		****	****	****	***	*	*****					
$N(1675)5/2^-$		****	****	****	****	***	*	*	*			
$N(1680)5/2^+$		****	****	****	****	***	*	*	*			
$N(1700)3/2^-$		***	**	***	***	*	*			*		
$N(1710)1/2^+$		****	****	****	*		***	**	*	*	*	
$N(1720)3/2^+$		****	****	****	***	*	*	****	*	*	*	
$N(1860)5/2^+$		**	*	**		*	*					
$N(1875)3/2^-$		***	**	**	*	**	*	*	*	*	*	
$N(1880)1/2^+$		***	**	*	**	*	*	**	**		**	
$N(1895)1/2^-$		****	****	*	*	*	****	**	**	*	*	****
$N(1900)3/2^+$		****	****	**	**	*	*	**	**		*	**
$N(1990)7/2^+$		**	**	**			*	*	*			
$N(2000)5/2^+$		**	**	*	**	*	*				*	
$N(2040)3/2^+$		*		*								
$N(2060)5/2^-$		***	***	**	*	*	*	*	*	*	*	
$N(2100)1/2^+$		***	**	***	**	**	*	*		*	*	**
$N(2120)3/2^-$		***	***	**	**	**		**	*		*	*
$N(2190)7/2^-$		****	****	****	****	**	*	**	*	*	*	
$N(2220)9/2^+$		****	**	****			*	*	*			
$N(2250)9/2^-$		****	**	****			*	*	*			
$N(2300)1/2^+$		**		**								
$N(2570)5/2^-$		**		**								
$N(2600)11/2^-$		***		***								
$N(2700)13/2^+$		**		**								

**** Existence is certain.
*** Existence is very likely.
** Evidence of existence is fair.
* Evidence of existence is poor.

These key properties of the S-matrix pole are in contrast to other quantities related to resonance phenomena, such as Breit-Wigner parameters or any K-matrix pole. Thus, Breit-Wigner parameters depend on the formalism used, such as angular-momentum barrier factors, or cut-off parameters, and the assumed or modeled

background. However, the accurate determination of pole parameters from the analysis of data on the real energy axis is not necessarily simple or even straightforward. It requires the implementation of the correct analytic structure of the relevant (often coupled) channels. The example in the meson sector of the σ-pole highlights the need to incorporate right and left hand cut analyticity (and their relation imposed by crossing symmetry) into a dispersive analysis to obtain a robust determination of the pole position for a very short-lived state close to the lowest threshold. The development of general methods that are simpler to implement in the baryon sector is a research problem of current interest, often exploiting techniques introduced long ago when the experimental data were far poorer than those presently available for reactions like $\gamma N \to \pi N$ [9]. No consensus yet exists for the use of any particular method, beyond the need to incorporate the general properties mentioned here and discussed more fully in the review of *Resonances*.

Table 97.2. The status of the Δ resonances and their decays. Sub-threshold decay modes are omitted. Only resonances with an overall status of *** or **** are included in the main Baryon Summary Table.

		Status as seen in					
Particle J^P	overall	$N\gamma$	$N\pi$	$\Delta\pi$	ΣK	$N\rho$	$\Delta\eta$
$\Delta(1232)3/2^+$	****	****	****				
$\Delta(1600)3/2^+$	****	****	***	****			
$\Delta(1620)1/2^-$	****	****	****	****			
$\Delta(1700)3/2^-$	****	****	****	****	*	*	
$\Delta(1750)1/2^+$	*	*	*		*		
$\Delta(1900)1/2^-$	***	***	***	*	**	*	
$\Delta(1905)5/2^+$	****	****	****	**	*	*	**
$\Delta(1910)1/2^+$	****	***	****	**	**		*
$\Delta(1920)3/2^+$	***	***	***	***	**		**
$\Delta(1930)5/2^-$	***	*	***	*	*		
$\Delta(1940)3/2^-$	**	*	**	*			*
$\Delta(1950)7/2^+$	****	****	****	**	***		
$\Delta(2000)5/2^+$	**	*	**	*		*	
$\Delta(2150)1/2^-$	*		*				
$\Delta(2200)7/2^-$	***	***	**	***	**		
$\Delta(1930)5/2^-$	***	*	***	*	*		
$\Delta(1940)3/2^-$	**	*	**	*			*
$\Delta(1950)7/2^+$	****	****	****	**	***		
$\Delta(2000)5/2^+$	**	*	**	*		*	
$\Delta(2150)1/2^-$	*		*				
$\Delta(2200)7/2^-$	***	***	**	***	**		
$\Delta(2300)9/2^+$	**		**				
$\Delta(2350)5/2^-$	*		*				
$\Delta(2390)7/2^+$	*		*				
$\Delta(2400)9/2^-$	**	**	**				
$\Delta(2420)11/2^+$	****	*	****				
$\Delta(2750)13/2^-$	**		**				
$\Delta(2950)15/2^+$	**		**				

**** Existence is certain.
*** Existence is very likely.
** Evidence of existence is fair.
* Evidence of existence is poor.

97.5. Photoproduction

A new approach to the nucleon excitation spectrum is provided by dedicated facilities at the Universities of Bonn, Grenoble, and Mainz, and at the national laboratories Jefferson Lab in the US and SPring-8 in Japan. High-precision cross sections and polarization observables for the photoproduction of pseudoscalar mesons provide a data set that is approaching a "complete experiment," one that fully constrains the four complex amplitudes describing the spin-structure of the reaction [11]. A large number of photoproduction reactions has been studied.

In pseudoscalar meson photoproduction, the four independent helicity amplitudes can be expressed in terms of the four CGLN [12] amplitudes allowed by Lorentz and gauge invariance. These amplitudes can be expanded in a series of electric and magnetic multipoles. Except for $J = 1/2$, one electric and one magnetic multipole contributes to each J^P combination.

For a given state, these two amplitudes determine the resonance photo-decay helicity amplitudes $A_{1/2}$ and $A_{3/2}$. As described below, this resonance extraction has been carried out either assuming a Breit-Wigner resonance or at the pole.

If a Breit-Wigner parametrization is used, the $N\gamma$ partial width, Γ_γ, is given in terms of the helicity amplitudes $A_{1/2}$ and $A_{3/2}$ by

$$\Gamma_\gamma = \frac{k_{\rm BW}^2}{\pi}\frac{2m_N}{(2J+1)m_{\rm BW}}\Big(|A_{1/2}|^2 + |A_{3/2}|^2\Big) \ . \qquad (1)$$

Here m_N and $m_{\rm BW}$ are the nucleon and resonance masses, J is the resonance spin, and $k_{\rm BW}$ is the photon c.m. decay momentum. Most earlier analyses have provided these real quantities $A_{1/2}$ and $A_{3/2}$.

More recent studies have quoted related complex quantities, evaluated at the T-matrix pole. These complex helicity amplitudes, $\tilde{A}_{1/2}$ and $\tilde{A}_{3/2}$, can be cast onto the form

$$\tilde{A}_h = \sqrt{\frac{\pi(2J+1)w_{\rm pole}}{m_N k_{\rm pole}^2}}\,\frac{Res(T_h(\gamma N \to N\,b))}{\sqrt{Res(T\,(N\,b \to N\,b))}} \qquad (2)$$

where the residues (Res) are evaluated at the pole position, $w_{\rm pole}$, and $k_{\rm pole}^2 = (w_{\rm pole}^2 - m_N^2)^2/4w_{\rm pole}^2$ [13]. For Breit-Wigner amplitudes, $w_{\rm pole} = m_{\rm BW}$ and $\tilde{A}_h = A_h$. Similar relations for the photo and electro couplings at the pole position can be found in [14,15].

The determination of eight real numbers from four complex amplitudes (with one overall phase undetermined) requires at least seven independent measurements. At least one further measurement is required to resolve discrete ambiguities that result from the fact that data are proportional to squared amplitudes. Photon beams and nucleon targets can be polarized (with linear or circular polarization $P_\perp$, $P_\odot$ and $\vec{T}$, respectively); the recoil polarization of the outgoing baryon $\vec{R}$ can be measured. The experiments can be divided into three classes: (1) the beam and target are polarized (BT); (2) the beam is polarized and the recoil baryon polarization is measured (BR); (3) the target is polarized and the recoil polarization is measured (TR). Different sign conventions are used in the literature, as summarized in [16].

One of the best studied reactions is $\gamma p \to \Lambda K^+$. Published data include differential cross sections, the beam asymmetry Σ, the target asymmetry T, the recoil polarization P, and the BR double-polarization variables $C_{x'}, C_{z'}, O_{x'}$, and $O_{z'}$. For the photoproduction of pions and etas, off proton and neutron targets, differential cross sections, single- and double-polarization asymmetries have been measured, mainly for pions.

97.6. Electroproduction

Electroproduction of mesons provides information on the internal structure of resonances. The helicity amplitudes are functions of the (squared) momentum transfer $Q^2 = -(e - e')^2$, where e and e' are the 4-momenta of the incident and scattered electron, and a third amplitude, $S_{1/2}$, measures the resonance response to the longitudinal component of the virtual photon. Most data stem from the reactions $e^- p \to e^- n\pi^+$ and $e^- p \to e^- p\pi^0$ but also the reactions $e^- p \to e^- p\eta$, $e^- p \to e^- p\pi^+\pi^-$, and $e^- p \to e^- \Lambda(\Sigma^0)K^+$ have been studied. The data and their interpretation are reviewed in Refs. [18,19].

The transition to the $\Delta(1232)3/2^+$ is often quantified in terms of the magnetic dipole transition moment M_{1+} (or the magnetic transition form factor $G_{M,Ash}^*(Q^2)$) [20], and the electric and scalar quadrupole transition moments E_{1+} and S_{1+}. Figure 97.1 shows the

strength of the $p \to \Delta^+$ transition plotted versus the photon virtuality Q^2. At $Q^2 = 0$, M_{1+} dominates the resonance transition strength. The two amplitudes E_{1+} and S_{1+} imply a quadrupole deformation of the transition to the lowest excited state. The magnitude of $R_{EM} = E_{1+}/M_{1+}$ remains nearly constant, while the magnitude of $R_{SM} = S_{1+}/M_{1+}$ increases rapidly up to 25% at the highest Q^2 value.

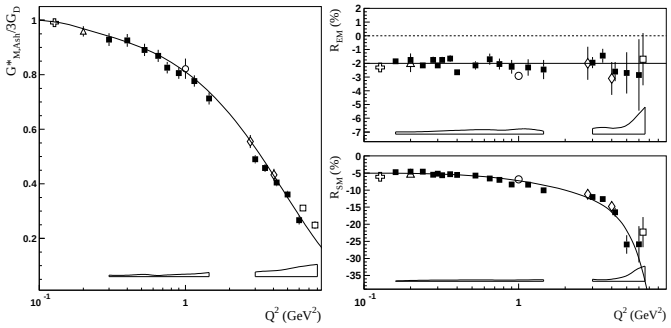

Figure 97.1: Left: The magnetic transition form factor for the $\gamma^* p \to \Delta^+(1232)$ transition versus the photon virtuality Q^2. Right: The electric and scalar quadrupole ratios R_{EM} and R_{SM}. The different symbols are results from different experiments at JLab (squares, diamonds, circle) and MAMI (triangle, cross). The boxes near the horizontal axis indicate model uncertainties of the squares. Curves to guide the eyes.

Figure 97.2 shows the transverse and scalar helicity amplitudes for the $N(1440)1/2^+$, $N(1520)3/2^-$, and $N(1535)1/2^-$ resonances from JLab [18]. Similar results have been achieved at Mainz [19]. For the states $N(1440)1/2^+$ and $N(1520)3/2^-$, helicity amplitudes and $\pi\Delta$ and ρp decays were determined at JLab in an analysis of $\pi^+\pi^- p$ electroproduction [21]. The data show distinctly different Q^2 dependencies that indicate different internal structures.

The $N(1520)3/2^-$ helicity amplitudes reveal the dominance of its three-quark nature: the $A_{3/2}$ amplitude is large at the photon point and decreases rapidly $\sim Q^{-5}$ with increasing Q^2; $A_{1/2}$ is small at the photon point, increases rapidly with Q^2 and then falls off with $\sim Q^{-3}$. Quantitative agreement with the data is, however, achieved only when meson cloud effects are included.

At high Q^2, both amplitudes for $N(1440)1/2^+$ are qualitatively described by light front quark models [22]: at short distances the resonance behaves as expected from a radial excitation of the nucleon. On the other hand, $A_{1/2}$ changes sign at about $0.6\,\mathrm{GeV}^2$. This remarkable behavior has not been observed before for any nucleon form factor or transition amplitude. Obviously, an important change in the structure occurs when the resonance is probed as a function of Q^2.

The Q^2 dependence of $A_{1/2}$ of the $N(1535)1/2^-$ resonance exhibits the expected Q^{-3} dependence, except for small Q^2 values where meson cloud effects set in.

Figure 97.3 shows the transverse and scalar amplitudes for three states in the 3rd nucleon resonance region, the $\Delta(1620)1/2^-$, the $N(1675)5/2^-$ and $N(1680)5/2^+$. The latter two states have nearly degenerate masses and are parity partners. In the quark model picture, the transverse amplitudes for $N(1675)5/2^-$ on the proton are suppressed due to the Moorhouse selection rule, allowing for a quantitative evaluation of the meson-baryon contributions. The data show significant meson-baryon strength in the $A_{1/2}$ amplitude even at quite high Q^2, while $A_{3/2}$ drops much faster with Q^2. $N(1680)5/2^+$ shows qualitatively the features predicted in constituent quark models, a dominant $A_{3/2}$ at the real photon point that drops rapidly with increasing Q^2, while $A_{1/2}$ becomes the dominant contribution at high Q^2, indicating a switch of the helicity structure in the resonance transition at short distances.

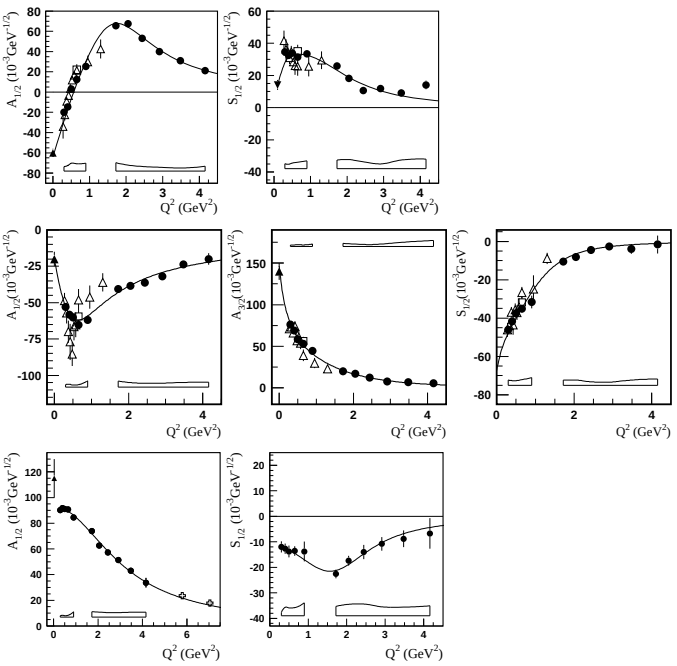

Figure 97.2: Transverse and scalar (longitudinal) helicity amplitudes for $\gamma p \to N(1440)1/2^+$ (top), $\gamma p \to N(1520)3/2^-$ (center), and $\gamma p \to N(1535)1/2^-$ (bottom) as extracted from the JLab/CLAS data in $n\pi^+$ production (full circles), MAMI/A1 data in $p\pi^0$ production (full down triangle), in $p\pi^+\pi^-$ (open triangles), and combined single and double pion production (open squares). The solid triangle is the PDG 2014 value at $Q^2 = 0$. The open boxes are the model uncertainties of the full circles.

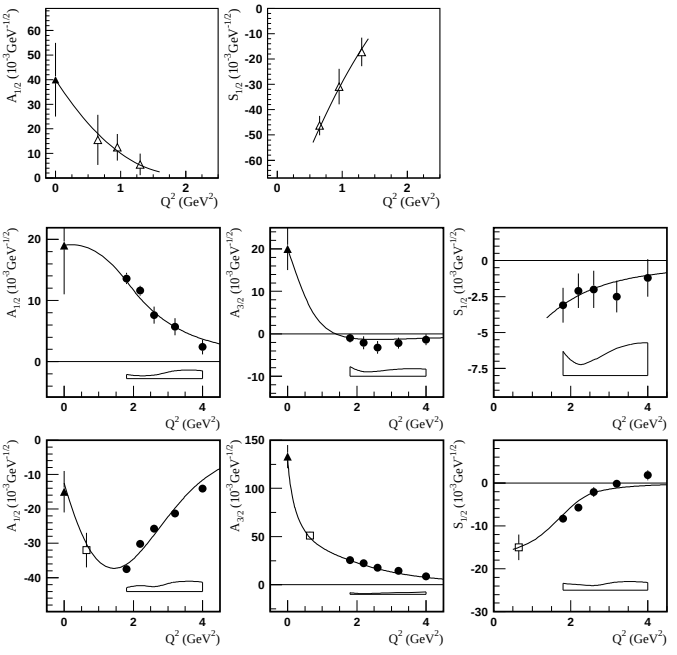

Figure 97.3: Transverse and scalar helicity amplitudes for $\gamma p \to \Delta(1620)1/2^-$ (top), $\gamma p \to N(1675)5/2^-$ (center), and $\gamma p \to N(1680)5/2^+$ (bottom) as extracted from the JLab/CLAS data in $n\pi^+$ production (full circles), $p\pi^+\pi^-$ (open triangles), combined single and double pion production (open square). The solid triangle is the 2014 PDG value at $Q^2 = 0$. The open boxes are the model uncertainties of the full circles. The curves are to guide the eye.

97.7. Partial wave analyses

Several PWA groups are now actively involved in the analysis of the new data. The GWU group maintains a nearly complete database covering reactions from πN and KN elastic scattering to $\gamma N \to N\pi$, $N\eta$, and $N\eta'$. It is presently the only group determining πN elastic amplitudes from scattering data in sliced energy bins. Given the high-precision of photoproduction data already or soon to be collected, the spectrum of N and Δ resonances will in the near future be better known.

Fits to the data are performed by various groups with the aim to understand the reaction dynamics and to identify N and Δ resonances. For practical reasons, approximations have to be made. We mention several analyses here: (1) The Mainz unitary isobar model [23] focuses on the correct treatment of the low-energy domain. Resonances are added to the unitary amplitude as a sum of Breit-Wigner amplitudes. This model also obtains resonance transition form factors and helicity amplitudes from electroproduction [19]. (2) For $N\pi$ electroproduction, the Yerevan/JLab group uses both the unitary isobar model and the dispersion relation approach developed in [22]. A phenomenological model was developed to extract resonance couplings and partial decay widths from exclusive $\pi^+\pi^- p$ electroproduction [21]. (3) Multichannel analyses using K-matrix parameterizations derive background terms from a chiral Lagrangian - providing a microscopical description of the background - (Giessen [24,25]) or from phenomenology (KSU [26,27], Bonn-Gatchina [28]) . (4.) Several groups (EBAC-Jlab [29,30], ANL-Osaka [31], Dubna-Mainz-Taipeh [32], Bonn-Jülich [33,34,35], Valencia [36]) use dynamical reaction models, driven by chiral Lagrangians, which take dispersive parts of intermediate states into account. Several other groups have made important contributions. The Giessen group pioneered multichannel analyses of large data sets on pion- and photo-induced reactions [24,25]. The Bonn-Gatchina group included recent high-statistics data and reported systematic searches for new baryon resonances in all relevant partial waves. A summary of their results can be found in [28].

References:

1. G. Höhler, Pion-Nucleon Scattering, Landolt-Börnstein Vol. I/9b2 (1983), ed. H. Schopper, Springer Verlag.
2. R.E. Cutkosky *et al.*, Baryon 1980, *IV International Conference on Baryon Resonances*, Toronto, ed. N. Isgur, p. 19.
3. R.A. Arndt *et al.*, Phys. Rev. **C74**, 045205 (2006).
4. "Hadron 2011: 14th International Conference on Hadron Spectroscopy", München, Germany, June, 13 - 17, 2011, published in eConf.
5. "NSTAR 2013: 9th International Workshop on the Physics of Excited Nucleons", 27-30 May 2013, Peñíscola, Spain.
6. E. Klempt and J.M. Richard, Rev. Mod. Phys. **82**, 1095 (2010).
7. V. Credé and W. Roberts, Rept. on Prog. in Phys. **76**, 076301 (2013).
8. M. Roos *et al.*, Phys. Lett. **B111**, 1 (1982).
9. A. Svarc *et al.*, Phys. Rev. **C88**, 035206 (2013).
10. R.H. Dalitz, R.G. Moorhouse, Proc. Royal Soc. London **A318**, 279 (1970).
11. C. G. Fasano *et al.*, Phys. Rev. **C46**, 2430 (1992).
12. G.F. Chew *et al.*, Phys. Rev. **106**, 1345 (1957).
13. R.L. Workman, L. Tiator, and A. Sarantsev, Phys. Rev. **C87**, 068201 (2013).
14. N. Suzuki, T. Sato, and T.-S.H. Lee, Phys. Rev. **C82**, 045206 (2010).
15. H. Kamano, Phys. Rev. **C88**, 045203 (2013).
16. A.M. Sandorfi *et al.*, AIP Conf. Proc. **1432**, 219 (2012).
17. R. Beck and A. Thiel, J. Phys. Conf. Ser. **295**, 012023 (2011).
18. I. G. Aznauryan and V. D. Burkert, Prog. in Part. Nucl. Phys. **67**, 1 (2012).
19. L. Tiator *et al.*, Eur. Phys. J. ST **198**, 141 (2011); S. Štajner *et al.*, Phys. Rev. Lett. **119**, 022001 (2017).
20. W.W. Ash, Phys. Lett. **B24**, 165 (1967).
21. V.I. Mokeev *et al.* [CLAS Collab.], Phys. Rev. **C86**, 035203 (2012).
22. I.G. Aznauryan, Phys. Rev. **C67**, 015209 (2003).
23. D. Drechsel, S.S. Kamalov, and L. Tiator, Eur. Phys. J. **A34**, 69 (2007).
24. G. Penner and U. Mosel, Phys. Rev. **C66**, 055211 (2002).
25. G. Penner and U. Mosel, Phys. Rev. **C66**, 055212 (2002).
26. D.M. Manley and E.M. Saleski, Phys. Rev. **D45**, 4002 (1992).
27. M. Shrestha and D.M. Manley, Phys. Rev. **C86**, 055203 (2012).
28. A.V. Anisovich *et al.*, Eur. Phys. J. **A48**, 15 (2012).
29. A. Matsuyama, T. Sato, and T.-S.H. Lee, Phys. Reports **439**, 193 (2007).
30. T. Sato and T.-S.H. Lee, J. Phys. **G36**, 073001 (2009).
31. H. Kamano *et al.*, Phys. Rev. **C88**, 035209 (2013).
32. G.Y. Chen *et al.*, Phys. Rev. **C76**, 035206 (2007).
33. M. Döring *et al.*, Phys. Lett. **B681**, 26 (2009).
34. M. Döring *et al.*, Nucl. Phys. **A829**, 170 (2009).
35. D. Rönchen *et al.*, Eur. Phys. J. **A49**, 44 (2013).
36. S. Sarkar, E. Oset, and M.J. Vicente Vacas, Nucl. Phys. **A750**, 294 (2005) [Erratum-ibid. **A780**, 78 (2006)].

98. Baryon Magnetic Moments

Written 1994 by C.G. Wohl (LBNL).

The figure below shows the measured magnetic moments of the stable baryons. It also shows the predictions of the simplest quark model, using the measured p, n, and Λ moments as input. In this model, the moments are [1]

$$\begin{aligned} \mu_p &= (4\mu_u - \mu_d)/3 & \mu_n &= (4\mu_d - \mu_u)/3 \\ \mu_{\Sigma^+} &= (4\mu_u - \mu_s)/3 & \mu_{\Sigma^-} &= (4\mu_d - \mu_s)/3 \\ \mu_{\Xi^0} &= (4\mu_s - \mu_u)/3 & \mu_{\Xi^-} &= (4\mu_s - \mu_d)/3 \\ \mu_\Lambda &= \mu_s & \mu_{\Sigma^0} &= (2\mu_u + 2\mu_d - \mu_s)/3 \\ & & \mu_{\Omega^-} &= 3\mu_s \end{aligned}$$

and the $\Sigma^0 \to \Lambda$ transition moment is

$$\mu_{\Sigma^0\Lambda} = (\mu_d - \mu_u)/\sqrt{3}\ .$$

The quark moments that result from this model are $\mu_u = +1.852\,\mu_N$, $\mu_d = -0.972\,\mu_N$, and $\mu_s = -0.613\,\mu_N$. The corresponding effective quark masses, taking the quarks to be Dirac point particles, where $\mu = q\hbar/2m$, are 338, 322, and 510 MeV. As the figure shows, the model gives a good first approximation to the experimental moments. For efforts to make a better model, we refer to the literature [2].

References:

1. See, for example, D.H. Perkins, *Introduction to High Energy Physics* (Addison-Wesley, Reading, MA, 1987), or D. Griffiths, *Introduction to Elementary Particles* (Harper & Row, New York, 1987).
2. See, for example, J. Franklin, Phys. Rev. **D29**, 2648 (1984);
H.J. Lipkin, Nucl. Phys. **B241**, 477 (1984);
K. Suzuki, H. Kumagai, and Y. Tanaka, Europhys. Lett. **2**, 109 (1986);
S.K. Gupta and S.B. Khadkikar, Phys. Rev. **D36**, 307 (1987);
M.I. Krivoruchenko, Sov. J. Nucl. Phys. **45**, 109 (1987);
L. Brekke and J.L. Rosner, Comm. Nucl. Part. Phys. **18**, 83 (1988);
K.-T. Chao, Phys. Rev. **D41**, 920 (1990) and references cited therein; Also, see references cited in discussions of results in the experimental papers..

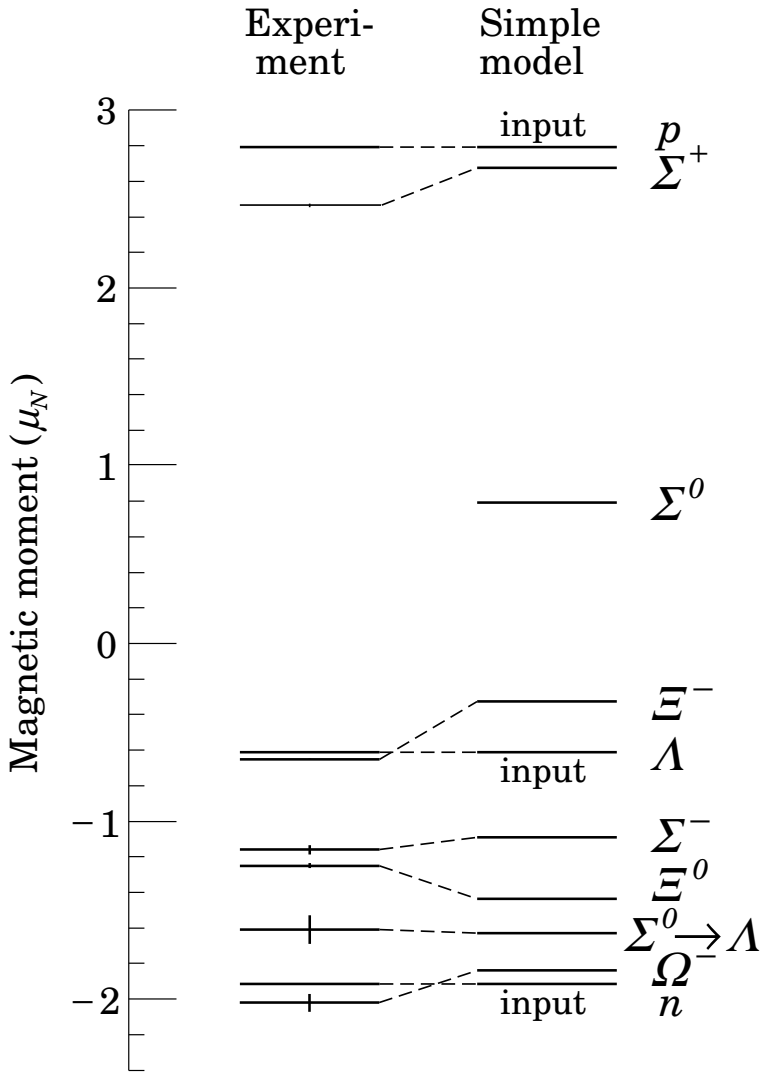

99. Λ and Σ Resonances

Revised 2016 by C.G. Wohl, (LBNL).

99.1. Introduction

Since our last edition, there have been a few measurements of properties of the lowest Λ and Σ resonances—mostly of masses and widths. But the field remains at a standstill. What follows is a much abbreviated version of the note on Λ and Σ Resonances from our 1990 edition [1]. In particular, see that edition for some representative Argand plots from partial-wave analyses.

Table 99.1 is an attempt to evaluate the status, both overall and channel by channel, of each Λ and Σ resonance in the Particle Listings. The evaluations are of course partly subjective. A blank indicates there is no evidence at all: either the relevant couplings are small or the resonance does not really exist. The main Baryon Summary Table includes only the established resonances (overall status 3 or 4 stars). A number of the 1- and 2-star entries may eventually disappear, but there are certainly many resonances yet to be discovered underlying the established ones.

99.2. Sign conventions for resonance couplings

In terms of the isospin-0 and -1 elastic scattering amplitudes A_0 and A_1, the amplitude for $K^- p \to \overline{K}^0 n$ scattering is $\pm(A_1 - A_0)/2$, where the sign depends on conventions used in conjunction with the Clebsch-Gordan coefficients (such as, is the baryon or the meson the "first" particle). If this reaction is partial-wave analyzed and if the overall phase is chosen so that, say, the $\Sigma(1775)D_{15}$ amplitude at resonance points along the positive imaginary axis (points "up"), then any Σ at resonance will point "up" and any Λ at resonance will point "down" (along the negative imaginary axis). Thus the phase at resonance determines the isospin. The above ignores background amplitudes in the resonating partial waves.

That is the basic idea. In a similar but somewhat more complicated way, the phases of the $\overline{K}N \to \Lambda\pi$ and $\overline{K}N \to \Sigma\pi$ amplitudes for a resonating wave help determine the SU(3) multiplet to which the resonance belongs. Again, a convention has to be adopted for some overall arbitrary phases: which way is "up"? Our convention is that of Levi-Setti [2] and is shown in Fig. 1, which also compares experimental results with theoretical predictions for the signs of several resonances. In the Listings, a + or − sign in front of a measurement of an inelastic resonance coupling indicates the sign (the *absence* of a sign means that the sign is not determined, *not* that it is positive). For more details, see Appendix II of our 1982 edition [3].

99.3. Errors on masses and widths

The errors quoted on resonance parameters from partial-wave analyses are often only statistical, and the parameters can change by more than these errors when a different parametrization of the waves is used. Furthermore, the different analyses use more or less the same data, so it is not really appropriate to treat the different determinations of the resonance parameters as independent or to average them together. In any case, the spread of the masses, widths, and branching fractions from the different analyses is certainly a better indication of the uncertainties than are the quoted errors. In the Baryon Summary Table, we usually give a range reflecting the spread of the values rather than a particular value with error.

For three states, the Λ(1520), the Λ(1820), and the Σ(1775), there is enough information to make an overall fit to the various branching fractions. It is then necessary to use the quoted errors, but the errors obtained from the fit should not be taken seriously.

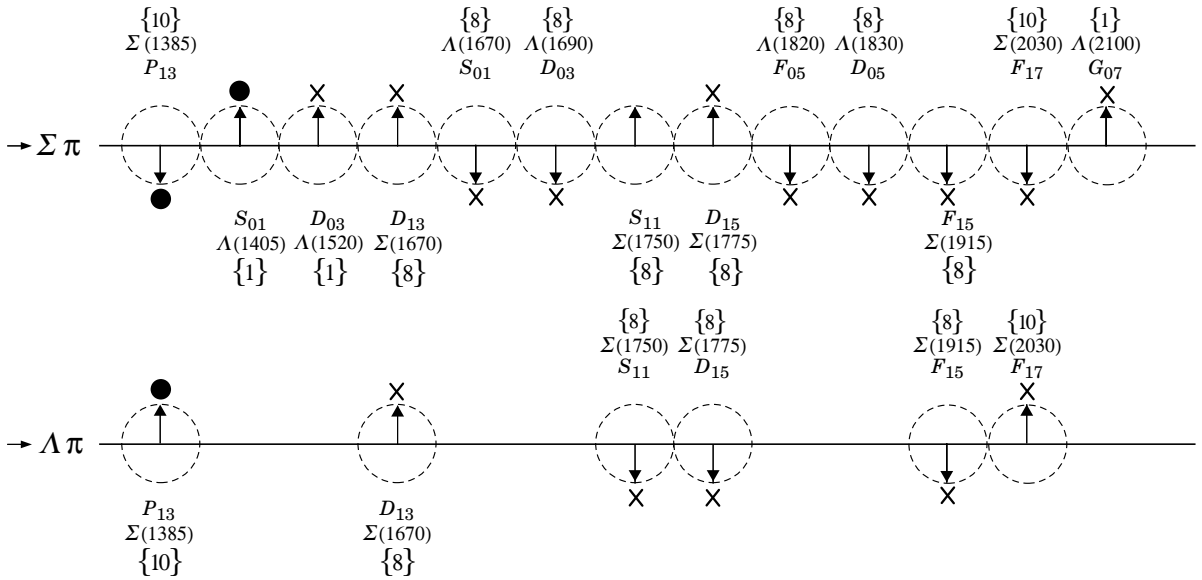

Figure 99.1: The signs of the imaginary parts of resonating amplitudes in the $\overline{K}N \to \Lambda\pi$ and $\Sigma\pi$ channels. The signs of the $\Sigma(1385)$ and $\Lambda(1405)$, marked with a •, are set by convention, and then the others are determined relative to them. The signs required by the SU(3) assignments of the resonances are shown with an arrow, and the experimentally determined signs are shown with an ×.

99.4. Production experiments

Partial-wave analyses of course separate partial waves, whereas a peak in a cross section or an invariant mass distribution usually cannot be disentangled from background and analyzed for its quantum numbers; and more than one resonance may be contributing to the peak. Results from partial-wave analyses and from production experiments are generally kept separate in the Listings, and in the Baryon Summary Table results from production experiments are used only for the low-mass states. The Σ(1385) and Λ(1405) of course lie below the $\overline{K}N$ threshold and nearly everything about them is learned from production experiments; and production and formation experiments agree quite well in the case of Λ(1520) and results have been combined. There is some disagreement between production and formation experiments in the 1600–1700 MeV region: see the note on the Σ(1670).

References:

1. Particle Data Group, Phys. Lett. **B239**, VIII.64 (1990).
2. R. Levi-Setti, in *Proceedings of the Lund International Conference on Elementary Particles* (Lund, 1969), p. 339.
3. Particle Data Group, Phys. Lett. **111B** (1982).

Table 99.1. The status of the Λ and Σ resonances. Only those with an overall status of *** or **** are included in the main Baryon Summary Table.

			Status as seen in —			
Particle	J^P	Overall status	$N\overline{K}$	$\Lambda\pi$	$\Sigma\pi$	Other channels
Λ(1116)	1/2+	****		F		$N\pi$(weakly)
Λ(1405)	1/2−	****	****	o	****	
Λ(1520)	3/2−	****	****	r	****	$\Lambda\pi\pi, \Lambda\gamma$
Λ(1600)	1/2+	***	***	b	**	
Λ(1670)	1/2−	****	****	i	****	$\Lambda\eta$
Λ(1690)	3/2−	****	****	d	****	$\Lambda\pi\pi, \Sigma\pi\pi$
Λ(1800)	1/2−	***	***	d	**	$N\overline{K}^*, \Sigma(1385)\pi$
Λ(1810)	1/2+	***	***	e	**	$N\overline{K}^*$
Λ(1820)	5/2+	****	****	n	****	$\Sigma(1385)\pi$
Λ(1830)	5/2−	****	***	F	****	$\Sigma(1385)\pi$
Λ(1890)	3/2+	****	****	o	**	$N\overline{K}^*, \Sigma(1385)\pi$
Λ(2000)		*		r	*	$\Lambda\omega, N\overline{K}^*$
Λ(2020)	7/2+	*	*	b	*	
Λ(2100)	7/2−	****	****	i	***	$\Lambda\omega, N\overline{K}^*$
Λ(2110)	5/2+	***	**	d	*	$\Lambda\omega, N\overline{K}^*$
Λ(2325)	3/2−	*	*	d		$\Lambda\omega$
Λ(2350)		***	***	e	*	
Λ(2585)		**	**	n		
Σ(1193)	1/2+	****				$N\pi$(weakly)
Σ(1385)	3/2+	****		****	****	
Σ(1480)		*	*	*	*	
Σ(1560)		**		**	**	
Σ(1580)	3/2−	*	*	*		
Σ(1620)	1/2−	**	**	*	*	
Σ(1660)	1/2+	***	***	*	**	
Σ(1670)	3/2−	****	****	****	****	several others
Σ(1690)		**	*	**	*	$\Lambda\pi\pi$
Σ(1750)	1/2−	***	***	**	*	$\Sigma\eta$
Σ(1770)	1/2+	*				
Σ(1775)	5/2−	****	****	****	***	several others
Σ(1840)	3/2+	*	*	**	*	
Σ(1880)	1/2+	**	**	**		$N\overline{K}^*$
Σ(1915)	5/2+	****	***	****	***	$\Sigma(1385)\pi$
Σ(1940)	3/2−	***	*	***	**	quasi-2-body
Σ(2000)	1/2−	*		*		$N\overline{K}^*, \Lambda(1520)\pi$
Σ(2030)	7/2+	****	****	****	**	several others
Σ(2070)	5/2+	*	*		*	
Σ(2080)	3/2+	**		**		
Σ(2100)	7/2−	*		*	*	
Σ(2250)		***	***	*	*	
Σ(2455)		**	*			
Σ(2620)		**	*			
Σ(3000)		*	*	*		
Σ(3170)		*				multi-body

**** Existence is certain, and properties are at least fairly well explored.
*** Existence ranges from very likely to certain, but further confirmation is desirable and/or quantum numbers, branching fractions, *etc.* are not well determined.
** Evidence of existence is only fair.
* Evidence of existence is poor.

100. Pole Structure of the Λ(1405) Region

Written November 2015 by Ulf-G. Meißner (Bonn Univ. / FZ Jülich) and Tetsuo Hyodo (YITP, Kyoto Univ.).

The Λ(1405) resonance emerges in the meson-baryon scattering amplitude with the strangeness $S = -1$ and isospin $I = 0$. It is the archetype of what is called a dynamically generated resonance, as pioneered by Dalitz and Tuan [1]. The most powerful and systematic approach for the low-energy regime of the strong interactions is chiral perturbation theory (ChPT), see e.g. Ref. 2. A perturbative calculation is, however, not applicable to this sector because of the existence of the Λ(1405) just below the $\bar{K}N$ threshold. In this case, ChPT has to be combined with a non-perturbative resummation technique, just as in the case of the nuclear forces. By solving the Lippmann-Schwinger equation with the interaction kernel determined by ChPT and using a particular regularization, in Ref. 3 a successful description of the low-energy K^-p scattering data as well as the mass distribution of the Λ(1405) was achieved (for further developments, see Ref. 4 and references therein).

The study of the pole structure was initiated by Ref. 5, which finds two poles of the scattering amplitude in the complex energy plane between the $\bar{K}N$ and $\pi\Sigma$ thresholds. The spectrum in experiments exhibits one effective resonance shape, while the existence of two poles results in the reaction-dependent lineshape [6]. The origin of this two-pole structure is attributed to the two attractive channels of the leading order interaction in the SU(3) basis (singlet and octet) [6] and in the isospin basis ($\bar{K}N$ and $\pi\Sigma$) [7]. It is remarkable that the sign and the strength of the leading order interaction is determined by a low-energy theorem of chiral symmetry, i.e. the so-called Weinberg-Tomozawa term. The two-pole nature of the Λ(1405) is qualitatively different from the case of the N(1440) resonance. Two poles of the N(1440) appear on different Riemann sheets of the complex energy plane separated by the $\pi\Delta$ branch point. These poles reflect a single state, with a nearby pole and a more distant shadow pole. In contrast, the two poles in the Λ(1405) region on the same Riemann sheet (where $\pi\Sigma$ channels are unphysical and all other channels physical, correspondingly to the one, connected to the real axis beween the $\pi\Sigma$ and $\bar{K}N$ thresholds) are generated from two attractive forces mentioned above [6,7].

Recently, various new experimental results on the Λ(1405) have become available [4]. Among these, the most striking measurement is the precise determination of the energy shift and width of kaonic hydrogen by the SIDDHARTA collaboration [8], [9], which provides a quantitative and stringent constraint on the K^-p amplitude at threshold through the improved Deser formula [10]. Systematic studies with error analyses based on the next-to-leading order ChPT interaction including the SIDDHARTA constraint have been performed by various groups [11–15]. All these studies confirm that the new kaonic hydrogen data are compatible with the scattering data above threshold.

The results of the pole positions of Λ(1405) in the various approaches are summarized in Table 100.1. We may regard the difference among the calculations as a systematic error, which stems from the various approximations of the Bethe-Salpeter equation, the fitting procedure, and also the inclusion of SU(3) breaking effects such as the choice of the various meson decay constants, and so on. The main component for the Λ(1405) is the pole 1, whose position converges within a relatively small region near the $\bar{K}N$ threshold. On the other hand, the position of the pole 2 shows a sizeable scatter.

Detailed studies of the $\pi\Sigma$ spectrum in various reaction processes, together with the precise experimental lineshape (see e.g. the recent precise photoproduction data from the LEPS collaboration [16] and from the CLAS collaboration [17,18], electroproduction data from the CLAS collaboration [19], and proton-proton collision data from COSY [20] and the HADES collaboration [21]) , will shed light on the position of the second pole. The $\pi\Sigma$ spectra from the CLAS data and the HADES data are analyzed in Ref. 22 and Ref. 23, respectively. Although the result of the pole positions in Ref. 22 is similar to those in Table 100.1, the pole found in Ref. 23 is not compatible with other results. Therefore, the analysis with only the $\pi\Sigma$ spectrum is not completely conclusive. It is thus desirable to perform a comprehensive analysis of $\pi\Sigma$ spectra together with the systematic error analysis of the scattering data as done in Ref. 15. It was shown there that several solutions, which agree with the scattering data are ruled out, if confronted with the recent CLAS data. The remaining solutions are collected as solution #2 and solution #4 of Ref. 15 in Table 100.1.

Table 100.1: Comparison of the pole positions of Λ(1405) in the complex energy plane from next-to-leading order chiral unitary coupled-channel approaches including the SIDDHARTA constraint.

approach	pole 1 [MeV]	pole 2 [MeV]
Refs. 11,12, NLO	$1424^{+7}_{-23} - i\ 26^{+3}_{-14}$	$1381^{+18}_{-6} - i\ 81^{+19}_{-8}$
Ref. 14, Fit II	$1421^{+3}_{-2} - i\ 19^{+8}_{-5}$	$1388^{+9}_{-9} - i\ 114^{+24}_{-25}$
Ref. 15, solution #2	$1434^{+2}_{-2} - i\ 10^{+2}_{-1}$	$1330^{+4}_{-5} - i\ 56^{+17}_{-11}$
Ref. 15, solution #4	$1429^{+8}_{-7} - i\ 12^{+2}_{-3}$	$1325^{+15}_{-15} - i\ 90^{+12}_{-18}$

References:

1. R.H. Dalitz, S.F. Tuan Phys. Rev. Lett. **2**, 425 (1959).
2. V. Bernard *et al.*, Int. J. Mod. Phys. **E4**, 193 (1995).
3. N. Kaiser *et al.*, Nucl. Phys. **A594**, 325 (1995).
4. T. Hyodo, D. Jido, Prog. in Part. Nucl. Phys. **67**, 55 (2012).
5. J.A. Oller, U.-G. Meißner, Phys. Lett. **B500**, 263 (2001).
6. D. Jido *et al.*, Nucl. Phys. **A725**, 181 (2003).
7. T. Hyodo, W. Weise, Phys. Rev. **C77**, 035204 (2008).
8. M. Bazzi *et al.*, Phys. Lett. **B704**, 113 (2011).
9. M. Bazzi *et al.*, Nucl. Phys. **A881**, 88 (2012).
10. U.-G. Meißner *et al.*, Eur. Phys. J. **C35**, 349 (2004).
11. Y. Ikeda *et al.*, Phys. Lett. **B706**, 63 (2011).
12. Y. Ikeda *et al.*, Nucl. Phys. **A881**, 98 (2012).
13. M. Mai, U.-G. Meißner, Nucl. Phys. **A900**, 51 (2013).
14. Z.-H. Guo, J. Oller, Phys. Rev. **C87**, 035202 (2013).
15. M. Mai, U.-G. Meißner, Eur. Phys. J. **A51**, 30 (2015).
16. M. Niiyama *et al.*, Phys. Rev. **C78**, 035202 (2098).
17. K. Moriya *et al.*, Phys. Rev. **C87**, 035206 (2013).
18. K. Moriya *et al.*, Phys. Rev. Lett. **112**, 082004 (2014).
19. H.Y. Lu *et al.*, Phys. Rev. **C88**, 045202 (2013).
20. I. Zychor *et al.*, Phys. Lett. **B660**, 167 (2008).
21. G. Agakishiev *et al.*, Phys. Rev. **C87**, 025201 (2013).
22. L. Roca, E. Oset, Phys. Rev. **C87**, 055201 (2013).
23. M. Hassanvand *et al.*, Phys. Rev. **C87**, 055202 (2013).

101. Σ(1670) Region

101.1. Production experiments

The measured $\Sigma\pi/\Sigma\pi\pi$ branching ratio for the Σ(1670) produced in the reaction $K^-p \to \pi^-\Sigma(1670)^+$ is strongly dependent on momentum transfer. This was first discovered by EBERHARD 69 [1], who suggested that there exist two Σ resonances with the same mass and quantum numbers: one with a large $\Sigma\pi\pi$ (mainly $\Lambda(1405)\pi$) branching fraction produced peripherally, and the other with a large $\Sigma\pi$ branching fraction produced at larger angles. The experimental results have been confirmed by AGUILAR-BENITEZ 70 [2], APSELL 74 [3], ESTES 74 [4], and TIMMERMANS 76 [5]. If, in fact, there are two resonances, the most likely quantum numbers for both the $\Sigma\pi$ and the $\Lambda(1405)\pi$ states are D_{13}. There is also possibly a third Σ in this region, the Σ(1690) in the Listings, the main evidence for which is a large $\Lambda\pi/\Sigma\pi$ branching ratio. These topics have been reviewed by EBERHARD 73 [6] and by MILLER 70 [7].

101.2. Formation experiments

Two states are also observed near this mass in formation experiments. One of these, the $\Sigma(1670)D_{13}$, has the same quantum numbers as those observed in production and has a large $\Sigma\pi/\Sigma\pi\pi$ branching ratio; it may well be the Σ(1670) produced at larger angles (see TIMMERMANS 76 [5]) . The other state, the $\Sigma(1660)P_{11}$, has different quantum numbers, its $\Sigma\pi/\Sigma\pi\pi$ branching ratio is unknown, and its relation to the produced Σ(1670) states is obscure.

References:

1. P.H. Eberhard *et al.*, Phys. Rev. Lett. **22**, 200 (1969).
2. M. Aguilar-Benitez, *et al.*, Phys. Rev. Lett. **25**, 58 (1970).
3. S.P. Apsell, *et al.*, Phys. Rev. **D10**, 1419 (1974).
4. R.D. Estes, Thesis LBL-3827 (1974).
5. J.J.M. Timmermans, *et al.*, Nucl. Phys. **B112**, 77 (1976).
6. P.H. Eberhard, Purdue Conf. 247 (1973).
7. D.H. Miller, Duke Conf. 229 (1970).

102. Radiative Hyperon Decays

Revised July 2011 by J.D. Jackson (LBNL).

The weak radiative decays of spin-1/2 hyperons, $B_i \to B_f\gamma$, yield information about matrix elements (form factors) similar to that gained from weak hadronic decays. For a polarized spin-1/2 hyperon decaying radiatively via a $\Delta Q = 0$, $\Delta S = 1$ transition, the angular distribution of the direction $\hat{\mathbf{p}}$ of the final spin-1/2 baryon in the hyperon rest frame is

$$\frac{dN}{d\Omega} = \frac{N}{4\pi}\,(1 + \alpha_\gamma\,\mathbf{P}_i{\cdot}\hat{\mathbf{p}})\ . \tag{102.1}$$

Here $\mathbf{P}_i$ is the polarization of the decaying hyperon, and α_γ is the asymmetry parameter. In terms of the form factors $F_1(q^2)$, $F_2(q^2)$, and $G(q^2)$ of the effective hadronic weak electromagnetic vertex,

$$F_1(q^2)\gamma_\lambda + iF_2(q^2)\sigma_{\lambda\mu}q^\mu + G(q^2)\gamma_\lambda\gamma_5\ ,$$

α_γ is

$$\alpha_\gamma = \frac{2\,\mathrm{Re}[G(0)F_M^*(0)]}{|G(0)|^2 + |F_M(0)|^2}\ , \tag{102.2}$$

where $F_M = (m_i - m_f)[F_2 - F_1/(m_i + m_f)]$. If the decaying hyperon is unpolarized, the decay baryon has a longitudinal polarization given by $P_f = -\alpha_\gamma$ [1].

The angular distribution for the weak hadronic decay, $B_i \to B_f\pi$, has the same form as Eq. (102.1), but of course with a different asymmetry parameter, α_π. Now, however, if the decaying hyperon is unpolarized, the decay baryon has a longitudinal polarization given by $P_f = +\alpha_\pi$ [2,3]. The difference of sign is because the spins of the pion and photon are different.

102.1. $\Xi^0 \to \Lambda\gamma$ decay

The radiative decay $\Xi^0 \to \Lambda\gamma$ of an unpolarized Ξ^0 uses the hadronic decay $\Lambda \to p\pi^-$ as the analyzer. As noted above, the longitudinal polarization of the Λ will be $P_\Lambda = -\alpha_{\Xi\Lambda\gamma}$. Let α_- be the $\Lambda \to p\pi^-$ asymmetry parameter and $\theta_{\Lambda p}$ be the angle, as seen in the Λ rest frame, between the Λ line of flight and the proton momentum. Then the hadronic version of Eq. (102.1) applied to the $\Lambda \to p\pi^-$ decay gives

$$\frac{dN}{d\cos\theta_{\Lambda p}} = \frac{N}{2}\,(1 - \alpha_{\Xi\Lambda\gamma}\,\alpha_-\cos\theta_{\Lambda p}) \tag{102.3}$$

for the angular distribution of the proton in the Λ frame. Our current value, from the CERN NA48/1 experiment [4], is $\alpha_{\Xi\Lambda\gamma} = -0.704 \pm 0.019 \pm 0.064$.

102.2. $\Xi^0 \to \Sigma^0\gamma$ decay

The asymmetry parameter here, $\alpha_{\Xi\Sigma\gamma}$, is measured by following the decay chain $\Xi^0 \to \Sigma^0\gamma$, $\Sigma^0 \to \Lambda\gamma$, $\Lambda \to p\pi^-$. Again, for an unpolarized Ξ^0, the longitudinal polarization of the Σ^0 will be $P_\Sigma = -\alpha_{\Xi\Sigma\gamma}$. In the $\Sigma^0 \to \Lambda\gamma$ decay, a parity-conserving magnetic-dipole transition, the polarization of the Σ^0 is transferred to the Λ, as may be seen as follows. Let $\theta_{\Sigma\Lambda}$ be the angle seen in the Σ^0 rest frame between the Σ^0 line of flight and the Λ momentum. For Σ^0 helicity $+1/2$, the probability amplitudes for positive and negative spin states of the Σ^0 *along the* Λ *momentum* are $\cos(\theta_{\Sigma\Lambda}/2)$ and $\sin(\theta_{\Sigma\Lambda}/2)$. Then the amplitude for a negative helicity photon and a negative helicity Λ is $\cos(\theta_{\Sigma\Lambda}/2)$, while the amplitude for positive helicities for the photon and Λ is $\sin(\theta_{\Sigma\Lambda}/2)$. For Σ^0 helicity $-1/2$, the amplitudes are interchanged. If the Σ^0 has longitudinal polarization P_Σ, the probabilities for Λ helicities $\pm 1/2$ are therefore

$$p(\pm 1/2) = \frac{1}{2}(1 \mp P_\Sigma)\cos^2(\theta_{\Sigma\Lambda}/2) + \frac{1}{2}(1 \pm P_\Sigma)\sin^2(\theta_{\Sigma\Lambda}/2)\ , \tag{102.4}$$

and the longitudinal polarization of the Λ is

$$P_\Lambda = -P_\Sigma\cos\theta_{\Sigma\Lambda} = +\alpha_{\Xi\Sigma\gamma}\cos\theta_{\Sigma\Lambda}\ . \tag{102.5}$$

Using Eq. (102.1) for the $\Lambda \to p\pi^-$ decay again, we get for the joint angular distribution of the $\Sigma^0 \to \Lambda\gamma$, $\Lambda \to p\pi^-$ chain,

$$\frac{d^2N}{d\cos\theta_{\Sigma\Lambda}\,d\cos\theta_{\Lambda p}} = \frac{N}{4}\left(1 + \alpha_{\Xi\Sigma\gamma}\cos\theta_{\Sigma\Lambda}\,\alpha_-\cos\theta_{\Lambda p}\right)\ . \tag{102.6}$$

Our current average for $\alpha_{\Xi\Sigma\gamma}$ is -0.69 ± 0.06 [4,5].

References:

1. R.E. Behrends, Phys. Rev. **111**, 1691 (1958); see Eq. (7) or (8).
2. In ancient times, the signs of the asymmetry term in the angular distributions of radiative and hadronic decays of polarized hyperons were sometimes opposite. For roughly 50 years, however, the overwhelming convention has been to make them the same. The aim, not always achieved, is to remove ambiguities.
3. For the definition of α_π, see the note on "Baryon Decay Parameters" in the Neutron Listings.
4. J.R. Batley *et al.*, Phys. Lett. **B693**, 241 (2010).
5. A. Alavi-Harati *et al.*, Phys. Rev. Lett. **86**, 3239 (2001).

103. Ξ Resonances

Revised 2004 by C.G. Wohl, (LBNL).

The accompanying table gives our evaluation of the present status of the Ξ resonances. Not much is known about Ξ resonances. This is because (1) they can only be produced as a part of a final state, and so the analysis is more complicated than if direct formation were possible, (2) the production cross sections are small (typically a few μb), and (3) the final states are topologically complicated and difficult to study with electronic techniques. Thus early information about Ξ resonances came entirely from bubble chamber experiments, where the numbers of events are small, and only in the 1980's did electronic experiments make any significant contributions. However, nothing of significance on Ξ resonances has been added since our 1988 edition.

For a detailed earlier review, see Meadows [1].

References:

1. B.T. Meadows, in *Proceedings of the IVth International Conference on Baryon Resonances* (Toronto, 1980), ed. N. Isgur, p. 283.

103.1. The status of the Ξ resonances. Only those with an overall status of *** or **** are included in the Baryon Summary Table.

			Status as seen in —				
Particle	J^P	Overall status	$\Xi\pi$	ΛK	ΣK	$\Xi(1530)\pi$	Other channels
Ξ(1318)	1/2+	****					Decays weakly
Ξ(1530)	3/2+	****	****				
Ξ(1620)		*	*				
Ξ(1690)		***		***	**		
Ξ(1820)	3/2−	***	**	***	**	**	
Ξ(1950)		***	**	**		*	
Ξ(2030)		***		**	***		
Ξ(2120)		*		*			
Ξ(2250)		**					3-body decays
Ξ(2370)		**					3-body decays
Ξ(2500)		*		*	*		3-body decays

**** Existence is certain, and properties are at least fairly well explored.
*** Existence ranges from very likely to certain, but further confirmation is desirable and/or quantum numbers, branching fractions, *etc.* are not well determined.
** Evidence of existence is only fair.
* Evidence of existence is poor.

104. Charmed Baryons

Revised March 2018 by C.G. Wohl (LBNL).

Figure 104.1(a) shows the spectrum of the charmed baryons—there are now 24 of them. The $\Lambda_c(2860)$ and the top five Ω_c^0's are new with this 2018 edition. Figure 104.1(b) shows the spectrum of the nine known bottom baryons. Since the latter set differs only by the replacement of a charm quark with a bottom quark, the spectra ought to be very similar—and they are. We discuss the charmed baryons here; nearly all we say would apply to the bottom baryons with the replacement of a c with a b.

We review briefly the theory of SU(4) multiplets, which tells what charmed baryons to expect.

104.1. SU(4) multiplets

Baryons made from u, d, s, and c quarks belong to SU(4) multiplets. The multiplet numerology, analogous to $3\times3\times3 = 10+8_1+8_2+1$ for the subset of baryons made from just u, d, and s quarks, is $4\times4\times4 = 20+20'_1+20'_2+\bar{4}$. Figure 104.2(a) shows the 20-plet whose bottom level is an SU(3) decuplet, such as the decuplet that includes the $\Delta(1232)$; each of its three sloping faces are also decuplets. Figure 104.2(b) shows the $20'$-plet whose bottom level is an SU(3) octet, such as the octet that includes the nucleon; each of its three sloping faces are also octets. Figure 104.2(c) shows the $\bar{4}$ multiplet, an inverted tetrahedron; each of its sloping faces are also triangles. The tetrahedral symmetry of the diagrams is of course what the SU(4) symmetry is about. As the masses in a multiplet are widely different, the symmetry is badly broken, but that does not spoil it as a classification scheme.

The baryons with one c quark are one level up from the bottom of each multiplet. The baryons in a given multiplet all have the same spin and parity. Each N or Δ or SU(3)-singlet-Λ resonance calls for another $20'$- or 20- or $\bar{4}$-plet, respectively. We expect to find (and do!)

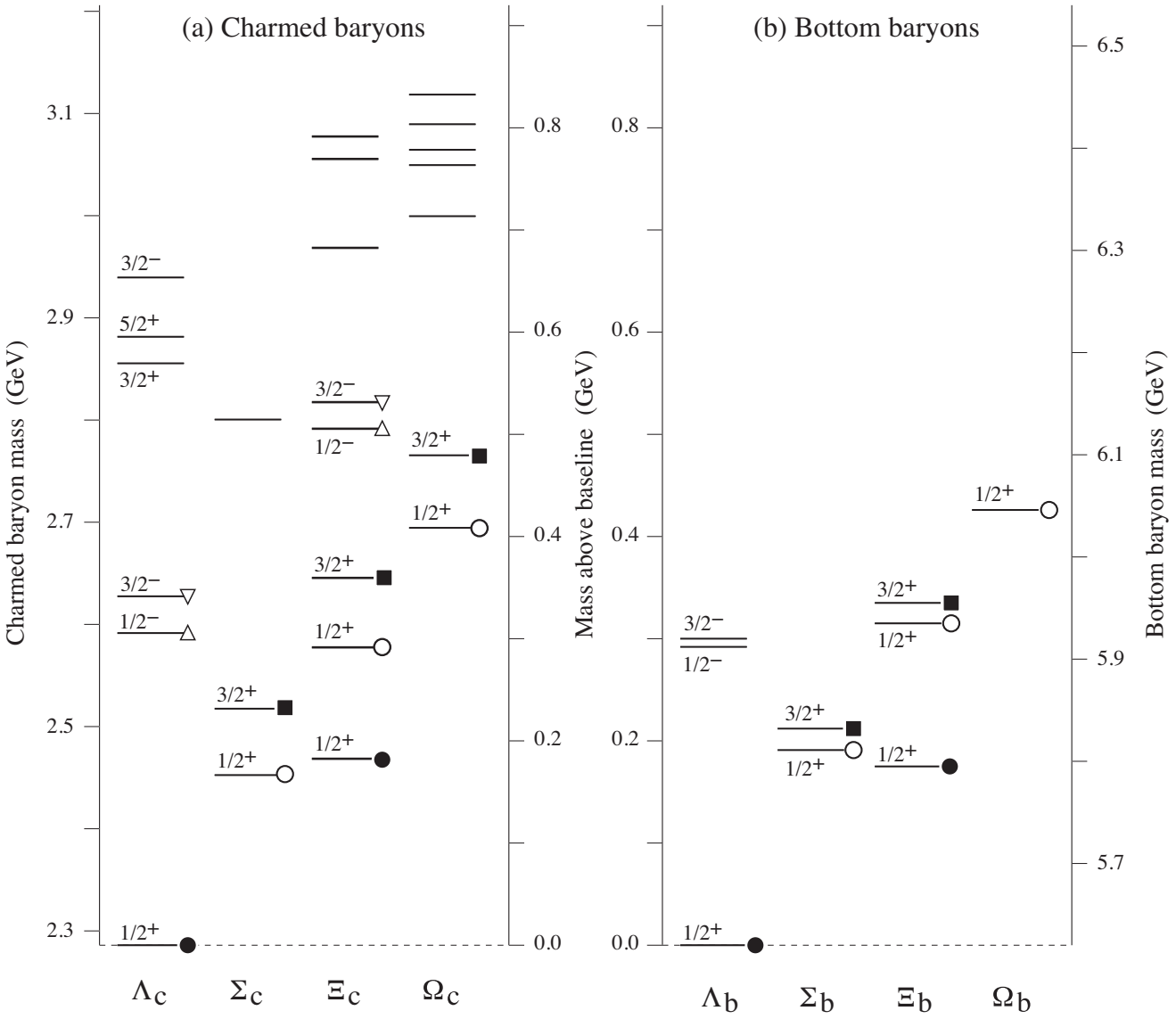

Figure 104.1: (a) The 24 known charmed baryons, and (b) the nine know bottom baryons. We discuss the charmed baryons; similar remarks would apply to the bottom baryons. The five $J^P = 1/2^+$ states, all tabbed with a circle, belong to the *udsc*-SU(4) multiplet that includes the nucleon. States with a circle with the same *fill* belong to the same SU(3) multiplet within that SU(4) multiplet (see below). The three $J^P = 3/2^+$ states tabbed with a square belong to the SU(4) multiplet that includes the $\Delta(1232)$. The $J^P = 1/2^-$ and $3/2^-$ states tabbed with triangles complete two SU(4) $\bar{4}$ multiplets.

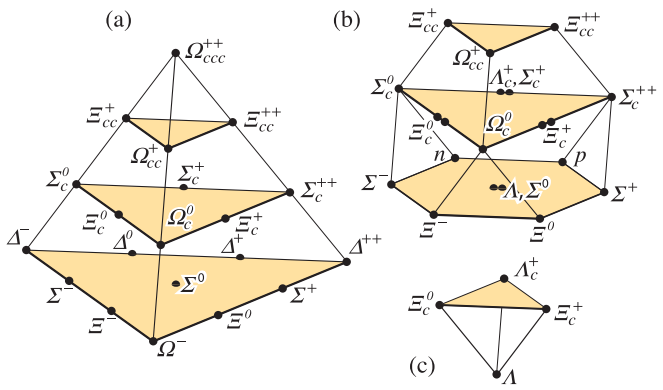

Figure 104.2: SU(4) multiplets of baryons made of u, d, s, and c quarks. (a) The 20-plet with an SU(3) decuplet on the lowest level. (b) The 20′-plet with an SU(3) octet on the lowest level. (c) The $\overline{4}$-plet. Note that here and in Fig. 104.3, but not in Fig. 104.1, each charge state is shown separately.

in the same $J^P = 1/2^+$ 20′-plet as the nucleon a Λ_c, a Σ_c, *two* Ξ_c's, and an Ω_c. Note that this Ω_c has $J^P = 1/2^+$ and is not in the same SU(4) multiplet as the famous $J^P = 3/2^+$ Ω^-.

Figure 104.3 shows in more detail the middle level of the 20′-plet of Fig. 104.2, which splits apart into two SU(3) multiplets, a $\bar{3}$ and a 6. The states of the $\bar{3}$ are antisymmetric under the interchange of the two light quarks (the u, d, and s quarks), whereas the states of the 6 are symmetric under this interchange. We use a prime to distinguish the Ξ_c in the 6 from the one in the $\bar{3}$.

The spacing in mass of the particles with open circles in Figs. 104.1(a) and (b) and with squares in Fig. 104.1(a) brings to mind an old, approximate U-spin rule for the mass differences, one to the next, between the $\Delta(1232)^-$, $\Sigma(1385)^-$, $\Xi(1530)^-$, and Ω^-, which lie along the bottom left edge of the multiplet in Fig. 104.2(a): the differences should be and are about equal.* The same rule also predicts that the mass differences along the left edges of the 6-plets on the second level of Fig. 104.2(a) and in Figure 104.3(b) should be the same. It does

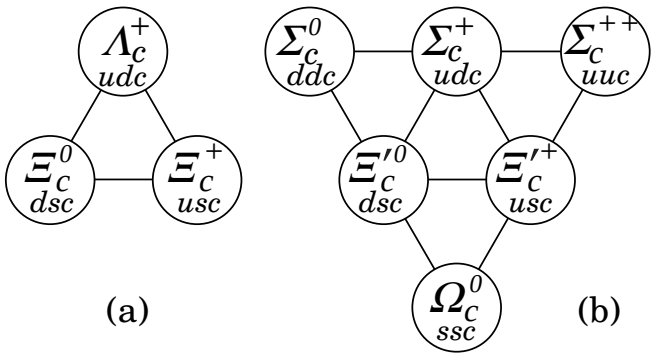

Figure 104.3: The SU(3) multiplets on the second level of the SU(4) multiplet of Fig. 104.2(b). The Λ_c and Ξ_c tabbed with closed circles in Fig. 104.1(a) complete a $J^P = 1/2^+$ SU(3) $\overline{3}$-plet, as in (a) here. The Σ_c, Ξ_c, and Ω_c tabbed with open circles in Fig. 104.1(a) complete a $J^P = 1/2^+$ SU(3) 6-plet, as in (b) here. Together the nine particles complete the charm = +1 level of a $J^P = 1/2^+$ SU(4) 20′-plet, as in Fig. 104.2(b).

not work well here:

	Particle 1	Particle 2	Mass difference (MeV)
$J = 3/2$:	$\Xi_c(2645)^0$	$\Sigma_c(2520)^0$	127.84 ± 0.37
	$\Omega_c(2770)^0$	$\Xi_c(2645)^0$	119.6 ± 2.0
$J = 1/2$:	$\Xi_c'^0$	Σ_c^0	125.1 ± 0.5
	Ω_c^0	$\Xi_c'^0$	116.4 ± 1.8
$J = 1/2$:	$\Xi_b'^0$	Σ_b^0	119.5 ± 1.8
	Ω_b^0	$\Xi_b'^0$	111.1 ± 1.7

For what it is worth, the rule *fails* by the same amount in the three cases: 8.2 ± 2.0, 8.7 ± 1.9, and 8.4 ± 2.5 MeV. This is not the place for further explorations of the mass spectra.

* Reminder: the mass is part of a particle's name if it decays strongly.

105. Pentaquarks

Written March 2016 by M. Karliner (Tel Aviv U.), T. Skwarnicki (Syracuse U.)

Experimental searches for pentaquark hadrons comprised of light flavors have a long and vivid history. No undisputed candidates have been found in 50 years. The first wave of observations of pentaquark candidates containing a strange antiquark occurred in the early seventies, see e.g. a review in the 1976 edition of Particle Data Group listings for $Z_0(1780)$, $Z_0(1865)$ and $Z_1(1900)$ [1]. The last mention of these candidates can be found in the 1992 edition [2] with the perhaps prophetic comment "the results permit no definite conclusion - the same story for 20 years. [...] The skepticism about baryons not made of three quarks, and lack of any experimental activity in this area, make it likely that another 20 years will pass before the issue is decided." A decade later, a second wave of observations occurred, possibly motivated by specific theoretical predictions for their existence [3–5]. The evidence for pentaquarks was based on observations of peaks in the invariant mass distributions of their decay products. More data, or more sensitive experiments did not confirm these claims [6]. In the last mention of the best known candidate from that period, $\Theta(1540)^+$, the 2006 Particle Data Group listing [7] included a statement: "The conclusion that pentaquarks in general, and that Θ^+, in particular, do not exist, appears compelling." which well reflected the prevailing mood in the particle physics community until a study of $\Lambda_b^0 \to J\psi p K^-$ ($J\psi \to \mu^+\mu^-$) decays by LHCb [8](charge conjugate modes are implied). In addition to many excitations of the Λ baryon (hereafter denoted as Λ^* resonances) decaying to K^-p, these data contain a narrow peak in the $J\psi p$ mass distribution, which is evident as a horizontal band in the Dalitz plot (Fig. 105.1).

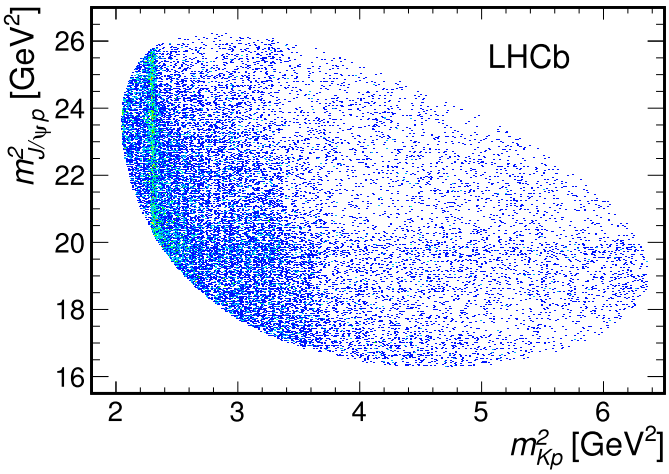

Figure 105.1: Dalitz plot distributions for $\Lambda_b^0 \to J\psi p K^-$ decays as observed by LHCb.

An amplitude analysis was performed to clarify the nature of this band that followed in the footsteps of a similar analysis of $\bar{B}^0 \to \psi(2S)\pi^+K^-$ ($\psi(2S) \to \mu^+\mu^-$) performed by the LHCb a year earlier in which the $Z(4430)^+$ tetraquark candidate [9] was confirmed and the resonant character of its amplitude was demonstrated by an Argand diagram [10]. The final states are very similar, with π^+ being replaced by p. The signal statistics, $26\,000 \pm 166$, and the background level, 5.4%, are also very comparable. The quasi-two-body amplitude model was constructed based on an isobar approximation (*i.e.* summing up Breit-Wigner amplitudes) and helicity formalism to parameterize dynamics of contributing decay processes. The amplitude fit spanned a kinematically complete, six-dimensional space of independent kinematic variables. All six dimensions of Λ_b decay kinematics were used in the amplitude fit, including invariant masses of K^-p (m_{Kp}) and $J\psi p$, ($m_{J\psi p}$) helicity angles (θ) of Λ_b, $J\psi$, Λ^* or pentaquark candidate $P_c^+ \to J\psi p$, and angles between decay planes of the particles. Fourteen reasonably well established Λ^* resonances were considered with masses and widths fixed to the values listed in 2014 PDG edition [11], and varied within their uncertainties when evaluating systematic errors. Their helicity couplings (1-6 complex numbers per resonance) were determined from the fit to the data. It was found that the Λ^* contributions alone failed to describe the data and it was necessary to add two exotic $P_c^+ \to J\psi p$ contributions to the matrix element (10 free parameters per resonance), before the narrow structure seen in $m_{J\psi p}$ could be reasonably well reproduced, as illustrated in Fig. 105.2.

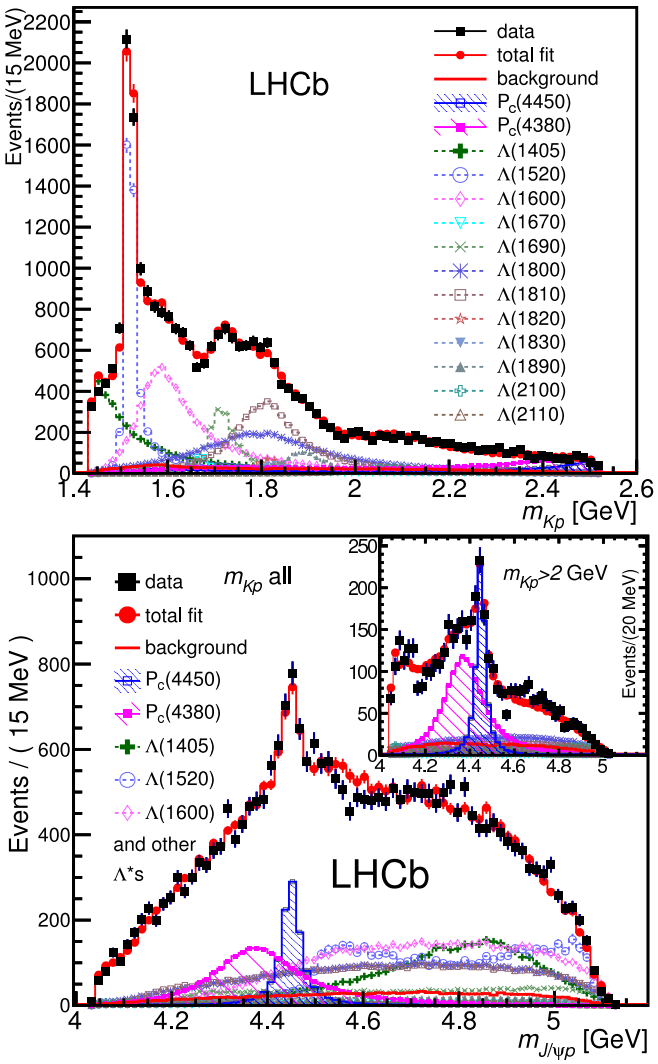

Figure 105.2: Projections of the amplitude fits with $P_c(4380)^+$ and $P_c(4450)^+$ states to the $\Lambda_b^0 \to J\psi p K^-$ data onto the invariant mass distributions of m_{Kp} (top) and $m_{J\psi p}$ (bottom).

The lower mass state, $P_c(4380)^+$, has a fitted mass of $4380 \pm 8 \pm 29$ MeV, width of $205 \pm 18 \pm 86$ MeV, fit fraction of $8.4 \pm 0.7 \pm 4.2$ % and significance of 9σ. The higher mass state, $P_c(4450)^+$, has a fitted mass of $4449.8 \pm 1.7 \pm 2.5$ MeV, narrower width of $39 \pm 5 \pm 19$ MeV, a fit fraction of $4.1 \pm 0.5 \pm 1.1$ % and significance of 12σ. The need for a second P_c^+ state becomes visually apparent in the $m_{J\psi p}$ distribution for events with high values of m_{Kp}, where Λ^* contributions are the smallest (in the inset of Fig. 105.2). Even though contributions from the two P_c^+ states are most visible in this region, they interfere destructively in this part of the Dalitz plane. The constructive P_c^+ interference makes their combined contribution the largest at the other end of their band on the Dalitz plane, corresponding to the opposite end of the $\cos\theta_{P_c^+}$ distribution (see Fig. 8b in Ref. 8). This pattern requires them to be of opposite parity. A similar interference pattern

is observed in the $\cos\theta_{\Lambda^*}$ distribution (Fig. 7 in Ref. 8), which is a consequence of parity-doublets in the Λ^* spectrum. Unfortunately, spins of the two P_c^+ states were not uniquely determined. Within the statistical and systematic ambiguities, $(3/2, 5/2)$ and $(5/2, 3/2)$ combinations with either $(-,+)$ or $(+,-)$ parities, were not well resolved. The other combinations were disfavored. The Argand diagrams for the two P_c^+ states are shown in Fig. 105.3. They were obtained by replacing the Breit-Wigner amplitude for one of the P_c^+ states at a time by a combination of independent complex amplitudes at six equidistant points in the $\pm\Gamma_0$ range (interpolated in mass for continuity) which were fit to the data simultaneously with the other parameters of the full matrix element model. While the narrower $P_c(4450)^+$ state shows the expected resonant behavior, the diagram for $P_c(4380)^+$ deviates somewhat from the expectation. The statistical errors are large, especially for the broader $P_c(4380)^+$ state. Higher statistics data might make these diagrams more conclusive. The addition of further Λ states beyond the well-established ones, of Σ excitations (expected to be suppressed) and of non-resonant contributions with a constant amplitude, did not remove the need for two pentaquark states in the model to describe the data. Yet Λ^* spectroscopy is a complex problem, from both experimental and theoretical points of view. This is illustrated by the recent reanalysis of $\bar{K}N$ scattering data [12] in which the $\Lambda(1800)$ state, which was previously considered to be "well established", is not seen, and where evidence for a few previously unidentified states is included. In fact, all theoretical models of Λ^* baryons [13–18] predict a much larger number of higher mass excitations than is established experimentally. Because of the high density of predicted states, presumably with large widths, these may be difficult to identify experimentally. Non-resonant contributions with a non-trivial K^-p mass dependence may also be present. Therefore, LHCb also inspected their data with an approach that is nearly model-independent with respect to K^-p contributions [19].

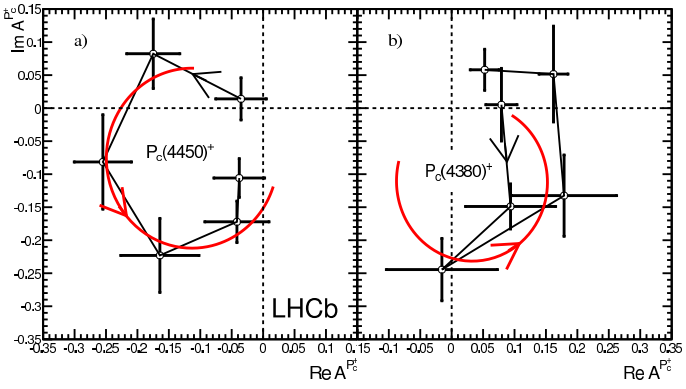

Figure 105.3: Fitted values of the real and imaginary parts of the amplitudes of the $P_c(4450)^+$ (left) and $P_c(4380)^+$ (right) states for $\Lambda_b^0 \to J\psi p K^-$ shown in the Argand diagrams as connected points with the error bars (masses increase counterclockwise). The solid red curves are the predictions from the Breit-Wigner formula, with resonance masses and widths set to the nominal fit results, scaled to the displayed points.

A representation of the Dalitz plane distribution was constructed using the observed m_{Kp} distribution and Legendre polynomial moments of the cosine of the Λ^* helicity angle determined from the data as a function of m_{Kp}. The maximal rank of the moments generated by the K^-p contributions alone cannot be higher than twice the largest total angular momentum. Since high-spin Λ^* states cannot significantly contribute at low m_{Kp} values, high rank moments were excluded from the representation (see Fig. 1 and 3 in Ref. 19). When projected onto $m_{J\psi p}$ axis of the Dalitz plane, this representation cannot describe the data as shown in Fig. 105.4. The disagreement was quantified to be at least 9σ, thus the hypothesis that only K^-p contributions can generate the observed $m_{J\psi p}$ mass structure could be rejected with very high confidence without any assumptions about number of K^-p contributions, their resonant or non-resonant character, their mass shapes or their interference patterns. This proved a need for contributions from exotic hadrons or from rescattering effects of conventional ones. However, this approach is not suitable for their characterization.

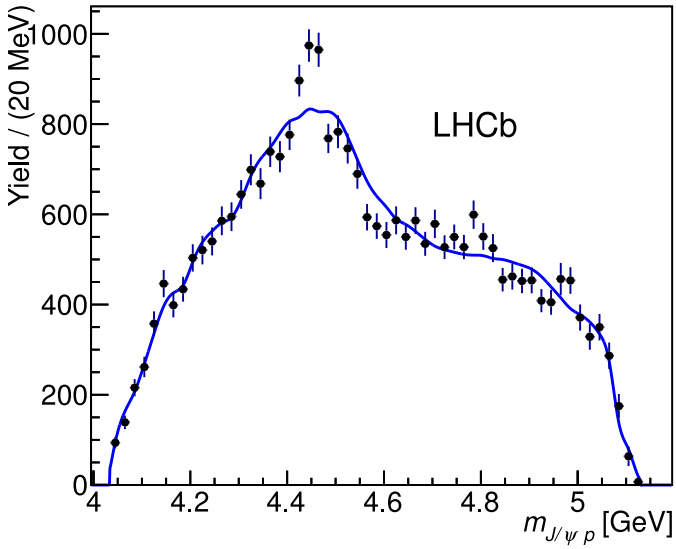

Figure 105.4: The efficiency-corrected and back-ground-subtracted distribution of $m_{J\psi p}$ for the data (black points with error bars), with the reflection of K^-p mass distribution and of the moments of the K^-p helicity angle, which can be accommodated by any plausible K^-p contribution (solid blue line) superimposed. The data and the reflection are inconsistent at $> 9\sigma$ level.

Many theoretical groups interpreted the P_c^+ states in terms of diquarks and triquarks as building blocks of a compact pentaquark [20–26]. The pair of states of opposite parity with the 3/2 spin assignment to $P_c(4380)^+$ and 5/2 to $P_c(4450)^+$ can be achieved by increasing the angular momentum between the constituents by one unit, which can also make the heavier state narrower. However, their mass splitting is too small to be only due to this mechanism [20] and requires fine-tuning of such models. It is also not clear if centrifugal barrier factor provides enough width suppression via spatial separation of c and $\bar{c}$ quarks to explain the width ratio between the two P_c^+ states and the narrowness of $P_c(4450)^+$ in absolute units as the phase space for $J/\psi p$ decay is very large (more than 400 MeV).

More effective width suppression mechanism is offered by a loosely bound charmed baryon-anticharmed meson molecular model, in which c and $\bar{c}$ can be separated to much larger distances resulting in a smaller probability of them getting close to each other in order to make a J/ψ. Since molecular binding energy cannot be large, masses of such molecules must be near the sum of the baryon and meson masses. The narrowness of $P_c(4450)^+$ and its proximity to appropriate baryon-meson mass threshold make the molecular model attractive in spite of its inability to account for other features of the LHCb results (see below).

In order to view the narrow pentaquark in a wider perspective, it is useful to consider it together with several analogous exotic states with hidden charm and bottom in the meson sector. This provides additional significant motivation for the molecular model. At least five exotic mesons are close to thresholds of two heavy-light mesons: $X(3872)$ [27–30], $Z_b(10610)$ and $Z_b(10650)$ in the bottomonium sector [31–35] and $Z_c(3900)$ [36–40] and $Z_c(4020/4025)$ [41–43] in the charmonium sector (see Table II if Ref. 44). They share several important features: a) their masses are near thresholds and their spin and parity correspond to S-wave combination of the two mesons; b) they are very narrow, despite very large phase space for decay into quarkonium + pion(s); c) the branching fractions for "fall apart"

mode into two mesons are much larger than branching fractions for decay into quarkonium and pion(s); d) there are no states at two pseudoscalar thresholds ($\bar{D}D$ and $\bar{B}B$), where there can be no binding through pseudoscalar exchange.

The above provide a strong hint that these states are deuteron-like loosely bound states of two heavy mesons [45–53]. It is then natural to conjecture that similar bound states might exist of two heavy baryons [54,55], or a meson and a baryon or a baryon and an antibaryon, leading to a rather accurate prediction of the $P_c(4450)^+$ mass as $3/2^-$ $\Sigma_c\bar{D}^*$ molecule: 4462.4 MeV [56,44]. It is essential that the two hadrons be heavy, in order to minimize the repulsive kinetic energy [54–57].

One may also consider a wider framework of doubly heavy baryon-meson hadronic molecules, which might include mixtures of various two-hadron states [58,59]. In this context it is important to keep in mind that the molecule's width cannot be smaller than the sum of its constituents' widths [60–62].

Following the LHCb discovery, several groups carried out a detailed analysis of the P_c^+ states as hadronic molecules [63–71]. The molecular picture has also been extended to a hadronic molecule built from a colored "baryon" and "meson" [72].

When trying to interpret both $P_c(4380)^+$ and $P_c(4380)^+$ as hadronic molecules, it is essential to remember that these two states have opposite parities. Thus one cannot construct both of them as S-wave bound states of a meson and a baryon with natural parities. Therefore, the interpretation of the P_c^+ states as hadronic molecules has been by no means unanimous. Moreover, the molecular model is not consistent with one of the P_c^+ states having a spin of 5/2, since S-wave combinations of baryon-meson combination that can produce such spin have thresholds which are too high in mass to be plausible. Therefore, the confirmation or disproval of the presence of this high-spin structure is a critical test of the molecular model. The large $P_c(4380)^+$ width is also difficult to accommodate in the molecular bound state model, but could have its origin in baryon-meson rescattering effects discussed below.

Shortly after the experimental discovery it has been conjectured that the observed resonances could be kinematic effects due to vicinity of thresholds and so-called triangle singularity [73–76]. While these effects might explain the large $P_c(4380)^+$ width, since such models involve S-wave rescattering of virtual baryon-meson pairs, they also cannot be reconciled with one of the P_c^+ peaks having effective spin of 5/2.

In addition to the molecular and diquark approach, the P_c^+ pentaquarks have also been analysed within the soliton picture of baryons, as a bound state of a soliton and an anticharmed meson [77]. Quite recently an interesting attempt has been made to explain the narrow width of tetraquarks and pentaquarks by extending to these states the string junction picture of baryons in QCD [78].

More extensive reviews of the theoretical issues can be found in Refs. 79,80.

So far the P_c^+ states have been observed by only one experiment in only one channel. It is essential to explore other possible experimental channels. Proposals have been made for searching for heavy pentaquarks in photoproduction [81–83], (c.f. also related work on computation of $J/\psi(\eta_c)N$ and $\Upsilon(\eta_b)N$ cross sections [84], in heavy ion collisions at LHC [85], in pA collisions [86], and in pion-induced processes [87,88].

References:

1. T.G. Trippe *et al.* (Particle Data Group), Rev. Mod. Phys. **48**, S1 (1976), [Erratum: Rev. Mod. Phys. **48**, 497 (1976)].
2. K. Hikasa *et al.* (Particle Data Group), Phys. Rev. **D45**, S1 (1992), [Erratum: Phys. Rev. **D46**, 5210 (1992)].
3. M. Praszalowicz, *Skyrmions and Anomalies, p.112, M. Jezabek Ed.*, World Scientific Publishing(1987), ISBN 9971503506.
4. D. Diakonov, V. Petrov and M.V. Polyakov, Z. Phys. **A359**, 305 (1997) [hep-ph/9703373].
5. H. Weigel, Eur. Phys. J. **A2**, 391 (1998) [hep-ph/9804260].
6. K.H. Hicks, Eur. Phys. J. **H37**, 1 (2012).
7. W.M. Yao *et al.* (Particle Data Group), J. Phys. **G33**, 1 (2006).
8. R. Aaij *et al.* (LHCb), Phys. Rev. Lett. **115**, 072001 (2015) [arXiv:1507.03414].
9. S. Choi *et al.* (Belle), Phys. Rev. Lett. **100**, 142001 (2008) [arXiv:0708.1790].
10. R. Aaij *et al.* (LHCb), Phys. Rev. Lett. **112**, 222002 (2014) [arXiv:1404.1903].
11. K. Olive *et al.* (Particle Data Group), Chin. Phys. C **38**, 090001 (2014) [arXiv:1412.1408].
12. C. Fernandez-Ramirez *et al.*, (2015), [arXiv:1510.07065].
13. R. Faustov and V. Galkin, Phys. Rev. **D92**, 054005 (2015) [arXiv:1507.04530].
14. S. Capstick and N. Isgur, Phys. Rev. **D34**, 2809 (1986).
15. U. Loring, B. Metsch and H. Petry, Eur. Phys. J. **A10**, 447 (2001).
16. T. Melde, W. Plessas and B. Sengl, Phys. Rev. **D77**, 114002 (2008).
17. E. Santopinto and J. Ferretti, Phys. Rev. **C92**, 025202 (2015) [arXiv:1412.7571].
18. G. Engel *et al.*, Phys. Rev. **D87**, 074504 (2013) [arXiv:1301.4318].
19. R. Aaij *et al.* (LHCb) (2016), arXiv:1604.05708.
20. L. Maiani, A.D. Polosa and V. Riquer, Phys. Lett. **B749**, 289 (2015) [arXiv:1507.04980].
21. R.F. Lebed, Phys. Lett. **B749**, 454 (2015) [arXiv:1507.05867].
22. V.V. Anisovich *et al.*, (2015) [arXiv:1507.07652].
23. G.-N. Li, X.-G. He and M. He, JHEP **12**, 128 (2015) [arXiv:1507.08252].
24. R. Ghosh, A. Bhattacharya and B. Chakrabarti (2015), arXiv:1508.00356.
25. Z.-G. Wang, Eur. Phys. J. **C76**, 70 (2016) [arXiv:1508.01468].
26. R. Zhu and C.-F. Qiao, Phys. Lett. **B756**, 259 (2016) [arXiv:1510.08693].
27. S.K. Choi *et al.* (Belle), Phys. Rev. Lett. **91**, 262001 (2003) [hep-ex/0309032].
28. D. Acosta *et al.* (CDF), Phys. Rev. Lett. **93**, 072001 (2004) [hep-ex/0312021].
29. B. Aubert *et al.* (BaBar), Phys. Rev. **D71**, 071103 (2005) [hep-ex/0406022].
30. V. M. Abazov *et al.* (D0), Phys. Rev. Lett. **93**, 162002 (2004) [hep-ex/0405004].
31. M. Karliner and H. J. Lipkin (2008) [arXiv:0802.0649].
32. K.F. Chen *et al.* (Belle), Phys. Rev. Lett. **100**, 112001 (2008) [arXiv:0710.2577].
33. A. Bondar *et al.* (Belle), Phys. Rev. Lett. **108**, 122001 (2012) [arXiv:1110.2251].
34. P. Krokovny *et al.* (Belle), Phys. Rev. **D88**, 052016 (2013) [arXiv:1308.2646].
35. A. Garmash *et al.* (Belle), Phys. Rev. **D91**, 072003 (2015) [arXiv:1403.0992].
36. M. Ablikim *et al.* (BES III), Phys. Rev. Lett. **110**, 252001 (2013) [arXiv:1303.5949].
37. Z. Q. Liu *et al.* (Belle), Phys. Rev. Lett. **110**, 252002 (2013) [arXiv:1304.0121].
38. T. Xiao *et al.*, Phys. Lett. **B727**, 366 (2013) [arXiv:1304.3036].
39. M. Ablikim *et al.* (BES III), Phys. Rev. Lett. **112**, 022001 (2014) [arXiv:1310.1163].
40. M. Ablikim *et al.* (BES III), Phys. Rev. Lett. **115**, 112003 (2015) [arXiv:1506.06018].
41. M. Ablikim *et al.* (BES III), Phys. Rev. Lett. **111**, 242001 (2013) [arXiv:1309.1896].
42. M. Ablikim *et al.* (BES III), Phys. Rev. Lett. **113**, 212002 (2014) [arXiv:1409.6577].
43. M. Ablikim *et al.* (BES III), Phys. Rev. Lett. **112**, 132001 (2014) [arXiv:1308.2760].
44. M. Karliner, Acta Phys. Polon. **B47**, 117 (2016).
45. M.B. Voloshin and L. B. Okun, Sov. Phys. JETP Lett. **23**, 333 (1976) [Pisma Zh. Eksp. Teor Fiz. **23**, 369 (1976)].

46. A. De Rujula, H. Georgi and S. Glashow, Phys. Rev. Lett. **38**, 317 (1977).
47. N.A. Tornqvist, Phys. Rev. Lett. **67**, 556 (1991).
48. N.A. Tornqvist, Z. Phys. **C61**, 525 (1994) [hep-ph/9310247].
49. N.A. Tornqvist, Phys. Lett. **B590**, 209 (2004) [hep-ph/0402237].
50. C.E. Thomas and F.E. Close, Phys. Rev. **D78**, 034007 (2008) [arXiv:0805.3653].
51. M. Suzuki, Phys. Rev. **D72**, 114013 (2005) [hep-ph/0508258].
52. S. Fleming *et al.*, Phys. Rev. **D76**, 034006 (2007) [hep-ph/0703168].
53. T.E.O. Ericson and G. Karl, Phys. Lett. **B309**, 426 (1993).
54. M. Karliner, H.J. Lipkin and N.A. Tornqvist, in *Proceedings, 14th International Conference on Hadron spectroscopy (Hadron 2011)*, (2011) [arXiv:1109.3472].
55. M. Karliner, H.J. Lipkin and N.A. Tornqvist, Nucl. Phys. (Proc. Supp.) **102**, 225 (2012).
56. M. Karliner and J.L. Rosner, Phys. Rev. Lett. **115**, 122001 (2015) [arXiv:1506.06386].
57. X.-Q. Li and X. Liu, Eur. Phys. J. **C74**, 3198 (2014) [arXiv:1409.3332].
58. J.-J. Wu *et al.*, Phys. Rev. Lett. **105**, 232001 (2010) [arXiv:1007.0573].
59. Z.-C. Yang *et al.*, Chin. Phys. C **36**, 6 (2012) [arXiv:1105.2901].
60. C. Hanhart, Yu.S. Kalashnikova and A.V. Nefediev, Phys. Rev. **D81**, 094028 (2010) [arXiv:1002.4097].
61. A.A. Filin *et al.*, Phys. Rev. Lett. **105**, 019101 (2010) [arXiv:1004.4789].
62. F.-K. Guo and U.-G. Meissner, Phys. Rev. **D84**, 014013 (2011) [arXiv:1102.3536].
63. R. Chen *et al.*, Phys. Rev. Lett. **115**, 132002 (2015) [arXiv:1507.03704].
64. H.-X. Chen *et al.*, Phys. Rev. Lett. **115**, 172001 (2015) [arXiv:1507.03717].
65. L. Roca, J. Nieves and E. Oset, Phys. Rev. **D92**, 094003 (2015) [arXiv:1507.04249].
66. J. He, Phys. Lett. **B753**, 547 (2016) [arXiv:1507.05200].
67. H. Huang *et al.*, (2015), arXiv:1510.04648.
68. L. Roca and E. Oset (2016), arXiv:1602.06791.
69. Q.-F. Lu and Y.-B. Dong (2016), arXiv:1603.00559.
70. Y. Shimizu, D. Suenaga and M. Harada (2016), arXiv:1603.02376.
71. C.-W. Shen *et al.*, (2016), arXiv:1603.04672.
72. A. Mironov and A. Morozov, Sov. Phys. JETP Lett. **102**, 271 (2015) [arXiv:1507.04694].
73. F.-K. Guo *et al.*, Phys. Rev. **D92**, 071502 (2015) [arXiv:1507.04950].
74. U.-G. Meissner and J. A. Oller, Phys. Lett. **B751**, 59 (2015) [arXiv:1507.07478].
75. X.-H. Liu, Q. Wang and Q. Zhao (2015), arXiv:1507.05359.
76. M. Mikhasenko (2015), arXiv:1507.06552.
77. N.N. Scoccola, D.O. Riska and M. Rho, Phys. Rev. **D92**, 051501 (2015) [arXiv:1508.01172].
78. G. Rossi and G. Veneziano (2016), arXiv:1603.05830.
79. T.J. Burns, Eur. Phys. J. **A51**, 152 (2015) [arXiv:1509.02460].
80. H.-X. Chen *et al.*, (2016), arXiv:1601.02092.
81. Q. Wang, X.-H. Liu and Q. Zhao, Phys. Rev. **D92**, 034022 (2015) [arXiv:1508.00339].
82. V. Kubarovsky and M.B. Voloshin, Phys. Rev. **D92**, 031502 (2015) [arXiv:1508.00888].
83. M. Karliner and J.L. Rosner, Phys. Lett. **B752**, 329 (2016) [arXiv:1508.01496].
84. C.W. Xiao and U.-G. Meissner, Phys. Rev. **D92**, 114002 (2015) [arXiv:1508.00924].
85. R.-Q. Wang *et al.*, (2016), arXiv:1601.02835.
86. I. Schmidt and M. Siddikov (2016), arXiv:1601.05621.
87. Q.-F. Lu *et al.*, Phys. Rev. **D93**, 034009 (2016) [arXiv:1510.06271].
88. X.-H. Liu and M. Oka (2016), arXiv:1602.07069.

106. Extra Dimensions Searches

Updated August 2017 by Yuri Gershtein (Rutgers University) and Alex Pomarol (Universitat Autònoma de Barcelona and IFAE)

106.1. Introduction

Proposals for a spacetime with more than three spatial dimensions date back to the 1920s, mainly through the work of Kaluza and Klein, in an attempt to unify the forces of nature [1]. Although their initial idea failed, the formalism that they and others developed is still useful nowadays. Around 1980, string theory proposed again to enlarge the number of space dimensions, this time as a requirement for describing a consistent theory of quantum gravity. The extra dimensions were supposed to be compactified at a scale close to the Planck scale, and thus not testable experimentally in the near future.

A different approach was given by Arkani-Hamed, Dimopoulos, and Dvali (ADD) in their seminal paper in 1998 [2], where they showed that the weakness of gravity could be explained by postulating two or more extra dimensions in which only gravity could propagate. The size of these extra dimensions should range between roughly a millimeter and ∼1/TeV, leading to possible observable consequences in current and future experiments. A year later, Randall and Sundrum (RS) [3] found a new possibility using a warped geometry, postulating a five-dimensional Anti-de Sitter (AdS) spacetime with a compactification scale of order TeV. The origin of the smallness of the electroweak scale versus the Planck scale was explained by the gravitational redshift factor present in the warped AdS metric. As in the ADD model, originally only gravity was assumed to propagate in the extra dimensions, although it was soon clear that this was not necessary in warped extra-dimensions and also the SM gauge fields [4] and SM fermions [5,6] could propagate in the five-dimensional spacetime.

The physics of warped extra-dimensional models has an alternative interpretation by means of the AdS/CFT correspondence [7]. Models with warped extra dimensions are related to four-dimensional strongly-interacting theories, allowing an understanding of the properties of five-dimensional fields as those of four-dimensional composite states [8]. This approach has opened new directions for tackling outstanding questions in particle physics, such as the flavor problem, grand unification, and the origin of electroweak symmetry breaking or supersymmetry breaking.

106.1.1. *Experimental Constraints* :

Constraints on extra-dimensional models arise from astrophysical and cosmological considerations. In addition, as we will show below, tabletop experiments exploring gravity at sub-mm distances restrict certain models. Collider limits on extra-dimensional models are dominated by LHC results. This review includes the most recent limits, most of which are published results based on LHC data collected in 2015-16 at a center-of-mass energy of 13 TeVand legacy results from 20 $\text{fb}^{-1}$of 8 TeVdata collected in Run 1. In addition, there are a few preliminary 13 TeV results, which can be found on the public WWW pages of public ATLAS [9] and CMS [10]. For most of the models, Run 2 results surpass the sensitivity of Run 1, even in the cases when the integrated luminosity is smaller.

106.1.2. *Kaluza-Klein Theories* :

Field theories with compact extra dimensions can be written as theories in ordinary four dimensions (4D) by performing a Kaluza-Klein (KK) reduction. As an illustration, consider a simple example, namely a field theory of a complex scalar in flat five-dimensional (5D) spacetime. The action will be given by †

$$S_5 = -\int d^4x\, dy\, M_5 \left[|\partial_\mu \phi|^2 + |\partial_y \phi|^2 + \lambda_5 |\phi|^4\right] , \qquad (106.1)$$

where y refers to the extra (fifth) dimension. A universal scale M_5 has been extracted in front of the action in order to keep the 5D field with the same mass-dimension as in 4D. This theory is perturbative for energies $E \lesssim \ell_5 M_5/\lambda_5$ where $\ell_5 = 24\pi^3$ [11].

† Our convention for the metric is $\eta_{MN} = \text{Diag}(-1, 1, 1, 1, 1)$.

Let us now consider that the fifth dimension is compact with the topology of a circle S^1 of radius R, which corresponds to the identification of y with $y + 2\pi R$. In such a case, the 5D complex scalar field can be expanded in a Fourier series:

$$\phi(x, y) = \frac{1}{\sqrt{2\pi R M_5}} \sum_{n=-\infty}^{\infty} e^{iny/R} \phi^{(n)}(x) ,$$

that, inserted in Eq. (106.1) and integrating over y, gives

$$S_5 = S_4^{(0)} + S_4^{(n)} ,$$

where

$$S_4^{(0)} = -\int d^4x \left[|\partial_\mu \phi^{(0)}|^2 + \lambda_4 |\phi^{(0)}|^4\right] , \text{ and} \qquad (106.2)$$

$$S_4^{(n)} = -\int d^4x \sum_{n\neq 0} \left[|\partial_\mu \phi^{(n)}|^2 + \left(\frac{n}{R}\right)^2 |\phi^{(n)}|^2\right] + \text{quartic int.}$$

The $n = 0$ mode self-coupling is given by

$$\lambda_4 = \frac{\lambda_5}{2\pi R M_5} . \qquad (106.3)$$

The above action corresponds to a 4D theory with a massless scalar $\phi^{(0)}$, referred to as the zero mode, and an infinite tower of massive modes $\phi^{(n)}$, known as KK modes. The KK reduction thus allows a treatment of 5D theories as 4D field theories with an infinite number of fields. At energies smaller than $1/R$, the KK modes can be neglected, leaving the zero-mode action of Eq. (106.2). The strength of the interaction of the zero-mode, given by Eq. (106.3), decreases as R increases. Thus, for a large extra dimension $R \gg 1/M_5$, the massless scalar is weakly coupled.

106.2. Large Extra Dimensions for Gravity

106.2.1. *The ADD Scenario* :

The ADD scenario [2,12,13] assumes a $D = 4 + \delta$ dimensional spacetime, with δ compactified spatial dimensions. The apparent weakness of gravity arises since it propagates in the higher-dimensional space. The SM is assumed to be localized in a 4D subspace, a 3-brane, as can be found in certain string constructions [14]. Gravity is described by the Einstein-Hilbert action in $D = 4 + \delta$ spacetime dimensions

$$S_D = -\frac{\bar{M}_D^{2+\delta}}{2} \int d^4x d^\delta y \sqrt{-g}\mathcal{R} + \int d^4x \sqrt{-g_{\text{ind}}}\, \mathcal{L}_{\text{SM}} , \qquad (106.4)$$

where x labels the ordinary four coordinates, y the δ extra coordinates, g refers to the determinant of the D-dimensional metric whose Ricci scalar is defined by $\mathcal{R}$, and $\bar{M}_D$ is the reduced Planck scale of the D-dimensional theory. In the second term of Eq. (106.4), which gives the gravitational interactions of SM fields, the D-dimensional metric reduces to the induced metric on the 3-brane where the SM fields propagate. The extra dimensions are assumed to be flat and compactified in a volume V_δ. As an example, consider a toroidal compactification of equal radii R and volume $V_\delta = (2\pi R)^\delta$. After a KK reduction, one finds that the fields that couple to the SM are the spin-2 gravitational field $G_{\mu\nu}(x, y)$ and a tower of spin-1 KK graviscalars [15]. The graviscalars, however, only couple to SM fields through the trace of the energy-momentum tensor, resulting in weaker couplings to the SM fields. The Fourier expansion of the spin-2 field is given by

$$G_{\mu\nu}(x, y) = G_{\mu\nu}^{(0)}(x) + \frac{1}{\sqrt{V_\delta}} \sum_{\vec{n}\neq 0} e^{i\vec{n}\cdot\vec{y}/R} G_{\mu\nu}^{(\vec{n})}(x) , \qquad (106.5)$$

where $\vec{y} = (y_1, y_2, ..., y_\delta)$ are the extra-dimensional coordinates and $\vec{n} = (n_1, n_2, ..., n_\delta)$. Eq. (106.5) contains a massless state, the 4D

graviton, and its KK tower with masses $m_{\vec{n}}^2 = |\vec{n}|^2/R^2$. At energies below $1/R$ the action is that of the zero mode

$$S_4^{(0)} = -\frac{\bar{M}_D^{2+\delta}}{2}\int d^4x\, V_\delta \sqrt{-g^{(0)}}\mathcal{R}^{(0)} + \int d^4x \sqrt{-g_{\rm ind}^{(0)}}\,\mathcal{L}_{\rm SM}\,,$$

where we can identify the 4D reduced Planck mass, $M_P \equiv G_N/\sqrt{8\pi} \simeq 2.4\times 10^{18}$ GeV, as a function of the D-dimensional parameters:

$$M_P^2 = V^\delta \bar{M}_D^{2+\delta} \equiv R^\delta M_D^{2+\delta}\,. \qquad (106.6)$$

Fixing M_D at around the electroweak scale $M_D \sim$ TeV to avoid introducing a new mass scale in the model, Eq. (106.6) gives a prediction for R:

$$\delta = 1, 2, ..., 6 \;\rightarrow\; R \sim 10^9 \text{ km}\,, 0.5 \text{ mm}\,, ...\,, 0.1 \text{ MeV}^{-1}\,. \qquad (106.7)$$

The option $\delta = 1$ is clearly ruled out, as it leads to modifications of Newton's law at solar system distances. However this is not the case for $\delta \geq 2$, and possible observable consequences can be sought in present and future experiments.

Consistency of the model requires a stabilization mechanism for the radii of the extra dimensions, to the values shown in Eq. (106.7). The fact that we need $R \gg 1/M_D$ leads to a new hierarchy problem, the solution of which might require imposing supersymmetry in the extra-dimensional bulk [16].

106.2.2. *Tests of the Gravitational Force Law at Sub-mm Distances* :

The KK modes of the graviton give rise to deviations from Newton's law of gravitation for distances $\lesssim R$. Such deviations are usually parametrized by a modified Newtonian potential of the form

$$V(r) = -G_N \frac{m_1 m_2}{r}\left[1 + \alpha\, e^{-r/\lambda}\right]\,. \qquad (106.8)$$

For a 2-torus compactification, $\alpha = 16/3$ and $\lambda = R$. Searches for deviations from Newton's law of gravitation have been performed in several experiments. Ref. [17] gives the present constraints: $R < 37\mu$m at 95% CL for $\delta = 2$, corresponding to $M_D > 3.6$ TeV.

106.2.3. *Astrophysical and Cosmological Constraints* :

The light KK gravitons could be copiously produced in stars, carrying away energy. Ensuring that the graviton luminosity is low enough to preserve the agreement of stellar models with observations provides powerful bounds on the scale M_D. The most stringent arises from supernova SN1987A, giving $M_D > 27$ (2.4) TeV for $\delta = 2$ (3) [18]. After a supernova explosion, most of the KK gravitons stay gravitationally trapped in the remnant neutron star. The requirement that neutron stars are not excessively heated by KK decays into photons leads to $M_D > 1700$ (76) TeV for $\delta = 2$ (3) [19].

Cosmological constraints are also quite stringent [20]. To avoid overclosure of the universe by relic gravitons one needs $M_D > 7$ TeV for $\delta = 2$. Relic KK gravitons decaying into photons contribute to the cosmic diffuse gamma radiation, from which one can derive the bound $M_D > 100$ TeV for $\delta = 2$.

We must mention however that bounds coming from the decays of KK gravitons into photons can be reduced if we assume that KK gravitons decay mainly into other non-SM states. This could happen, for example, if there were other 3-branes with hidden sectors residing on them [12].

106.2.4. *Collider Signals* :

106.2.4.1. *Graviton and Other Particle Production:*

Although each KK graviton has a purely gravitational coupling, suppressed by $1/M_P$, inclusive processes in which one sums over the almost continuous spectrum of available gravitons have cross sections suppressed only by powers of M_D. Processes involving gravitons are therefore detectable in collider experiments if $M_D \sim$ TeV. A number of experimental searches for evidence of large extra dimensions have been performed at colliders, and interpreted in the context of the ADD model.

One signature arises from direct graviton emission. By making a derivative expansion of Einstein gravity, one can construct an effective theory, valid for energies much lower than M_D, and use it to make predictions for graviton-emission processes at colliders [15,21,22]. Gravitons produced in the final state would escape detection, giving rise to missing transverse energy ($\not{E}_T$). The results quoted below are 95% CL lower limits on M_D for a range of values of δ between 2 and 6, with more stringent limits corresponding to lower δ values.

At hadron colliders, experimentally sensitive channels include the jet (j) + $\not{E}_T$ and γ + $\not{E}_T$ final states. ATLAS j + $\not{E}_T$ preliminary results with 36.1 fb^{-1} of 13 TeV data provide limits of $M_D > 4.79 - 7.74$ TeV [23]. A preliminary CMS analysis using 35.9 fb^{-1}of Run 2 data sets limits of $M_D > 5.2 - 10.0$ TeV [24]. For these analyses, both experiments are assuming leading order (LO) cross sections. Since the effective theory is only valid for energies much less than M_D, the results are quoted for the full space, and include the information that suppressing the graviton cross section by a factor $M_D^4/\hat{s}^2$ for $\sqrt{\hat{s}} > M_D$, where $\sqrt{\hat{s}}$ is the parton-level center-of-mass energy of the hard collision, weakens the limits on M_D by a negligible amount (∼3%) for $\delta = 2$ ($\delta = 6$). Less stringent limits are obtained by both CMS [25] and ATLAS [26] from analyses of respectively 12.9 and 3.2 fb^{-1}of 13 TeVdata in the γ + $\not{E}_T$ final state.

In models in which the ADD scenario is embedded in a string theory at the TeV scale [14], we expect the string scale M_s to be smaller than M_D, and therefore expect production of string resonances at the LHC [27]. A Run 2 result from CMS analyzing the dijet invariant mass distribution for 2.4 fb^{-1}of 13 TeV data excludes string resonances that decay predominantly to $q + g$ with masses below 7.0 TeV [28]. ATLAS dijet analysis uses 37 fb^{-1}of 13 TeV data [29], and provide their results in the context of model-independent limits on the cross section times acceptance for generic resonances of a variety of possible widths.

106.2.4.2. *Virtual graviton effects:*

One can also search for virtual graviton effects, the calculation of which however depends on the ultraviolet cut-off of the theory and is therefore very model dependent. In the literature, several different formulations exist [15,22,30] for the dimension-eight operator for gravity exchange at tree level:

$$\mathcal{L}_8 = \pm\frac{4}{M_{TT}^4}\left(T_{\mu\nu}T^{\mu\nu} - \frac{1}{\delta+2}T^\mu_\mu T^\nu_\nu\right), \qquad (106.9)$$

where $T_{\mu\nu}$ is the energy-momentum tensor and M_{TT} is related to M_D by some model-dependent coefficient [31]. The relations with the parametrizations of Refs. [30] and [15] are, respectively, $M_{TT} = M_S$ and $M_{TT} = (2/\pi)^{1/4}\Lambda_T$. The experimental results below are given as 95% CL lower limits on M_{TT}, including in some cases the possibility of both constructive or destructive interference, depending on the sign chosen in Eq. (9).

The most stringent limits arise from LHC analyses of the dijet angular distribution. Using 35.9 fb^{-1}of 13 TeV data, CMS [32] obtains results that correspond to an approximate limit of $M_{TT} > 9.5$ TeV. The next most restrictive result (6.4 TeV) is obtained by the ATLAS analysis of the di-photon mass spectrum in 37 fb^{-1}of 13 TeV data [33], followed by the combination of the dielectron and dimuon final states of Run 1 data, with both experiments providing similar limits of approximately $M_{TT} > 3.7$ TeV. The ATLAS [34](CMS [35]) dilepton results assume LO (NLO) signal cross section values.

At the one-loop level, gravitons can also generate dimension-six operators with coefficients that are also model dependent. Experimental bounds on these operators can also give stringent constraints on M_D [31].

106.2.4.3. *Black Hole Production:*

The physics at energies $\sqrt{s} \sim M_D$ is sensitive to the details of the unknown quantum theory of gravity. Nevertheless, in the transplanckian regime, $\sqrt{s} \gg M_D$, one can rely on a semiclassical description of gravity to obtain predictions. An interesting feature of

transplanckian physics is the creation of black holes [36]. A black hole is expected to be formed in a collision in which the impact parameter is smaller than the Schwarzschild radius [37]:

$$R_S = \frac{1}{M_D}\left[\frac{2^\delta \pi^{(\delta-3)/2}}{\delta+2}\Gamma\left(\frac{\delta+3}{2}\right)\frac{M_{BH}}{M_D}\right]^{1/(\delta+1)}, \qquad (106.10)$$

where M_{BH} is the mass of the black hole, which would roughly correspond to the total energy in the collision. The cross section for black hole production can be estimated to be of the same order as the geometric area $\sigma \sim \pi R_S^2$. For $M_D \sim$ TeV, this gives a production of $\sim 10^7$ black holes at the $\sqrt{s} = 14$ TeV LHC with an integrated luminosity of 30 fb^{-1} [36]. A black hole would provide a striking experimental signature since it is expected to thermally radiate with a Hawking temperature $T_H = (\delta+1)/(4\pi R_S)$, and therefore would evaporate democratically into all SM states. Nevertheless, given the present constraints on M_D, the LHC will not be able to reach energies much above M_D. This implies that predictions based on the semiclassical approximation could receive sizable modifications from model-dependent quantum-gravity effects.

The most stringent limits on microscopic black holes arise from LHC searches which observed no excesses above the SM background in high-multiplicity final states. The results are usually quoted as model-independent limits on the cross section for new physics in the final state and kinematic region analyzed. These results can then be used to provide constraints of models of low-scale gravity and weakly-coupled string theory. In addition, limits are sometimes quoted on particular implementations of models, which are used as benchmarks to illustrate the sensitivity. A Run 2 ATLAS search [38] for an excess of events with multiple high transverse momentum objects, including charged leptons and jets, using 3.2 fb^{-1}of 13 TeV data, excludes semiclassical black holes below masses of ~ 8.7 TeV for $M_D = 2$ TeV and $\delta = 6$. Another Run 2 ATLAS analysis [39], using 3.6 fb^{-1}of 13 TeV data, looks at very high transverse energy multijet events and excludes black hole masses in the range $9.0 - 9.7$ TeV, depending on M_D, for $\delta = 6$. A CMS analysis [40] of multi-object final states using 2.3 fb^{-1} of 13 TeV data provides similar limits, extending out to values of $M_D \sim 8.4 - 9.3$ TeV. The 8 TeV ATLAS analysis [41] of the track multiplicity in same-sign dimuon events provides lower mass limits of $5.1 - 5.7$ TeV for $M_D = 1.5$ TeV, with the range of the limits depending on details of the model and also the number of extra dimensions.

A complementary approach is to look for jet extinction at high transverse momenta, as we expect hard short distance scattering processes to be highly suppressed at energies above M_D [42]. CMS analysis [43] of inclusive jet p_T spectrum in 10.7 fb^{-1}of 8 TeV data set a lower limit of 3.3 TeV on the extinction mass scale.

For black hole masses near M_D, the semi-classical approximation is not valid, and one could instead expect quantum black holes (QBH) that decay primarily into two-body final states [44]. LHC Run 2 results at 13 TeV provide lower limits on QBH masses of order $2.3 - 9.0$ TeV, depending on the details of the model. Searches that consider interpretations in terms of QBH limits include the CMS multi-object [40] analysis, ATLAS dijet analysis [29], and different flavor di-lepton analyses at CMS ($e\mu$, 2.0 fb^{-1} at 13 TeV [45]) and ATLAS ($e\mu$, $e\tau$, $\mu\tau$, 3.2fb^{-1} at 13 TeV [46]) .

In weakly-coupled string models the semiclassical description of gravity fails in the energy range between M_s and M_s/g_s^2 where stringy effects are important. In this regime one expects, instead of black holes, the formation of string balls, made of highly excited long strings, that could be copiously produced at the LHC for $M_s \sim$ TeV [47], and would evaporate thermally at the Hagedorn temperature giving rise to high-multiplicity events. The same analyses used to search for black holes can be interpreted in the context of string balls. For example, for the case of $\delta = 6$ with $M_s = M_D/1.26 = 3$ TeV, the ATLAS multiple high transverse momentum object analysis [38] excludes string balls with masses below 6.5 to 9.0 TeV for values of $0.2 < g_s < 0.8$. The CMS multi-object analysis [40] excludes the production of string balls with a mass below 8 to 8.6 TeV for $0.2 < g_s < 0.5$, M_D in the range of $5.9 - 8.6$ TeV, and $1.1 < M_s < 2.0$.

106.3. TeV-Scale Extra Dimensions

106.3.1. *Warped Extra Dimensions* :

The RS model [3] is the most attractive setup of warped extra dimensions at the TeV scale, since it provides an alternative solution to the hierarchy problem. The RS model is based on a 5D theory with the extra dimension compactified in an orbifold, S^1/Z_2, a circle S^1 with the extra identification of y with $-y$. This corresponds to the segment $y \in [0, \pi R]$, a manifold with boundaries at $y = 0$ and $y = \pi R$. Let us now assume that this 5D theory has a cosmological constant in the bulk Λ, and on the two boundaries Λ_0 and $\Lambda_{\pi R}$:

$$S_5 = -\int d^4x\, dy \Big\{\sqrt{-g}\left[\frac{1}{2}M_5^3\mathcal{R} + \Lambda\right] + \sqrt{-g_0}\delta(y)\Lambda_0 + \sqrt{-g_{\pi \mathrm{R}}}\delta(y-\pi R)\Lambda_{\pi R}\Big\}, \qquad (106.11)$$

where g_0 and $g_{\pi R}$ are the values of the determinant of the induced metric on the two respective boundaries. Einstein's equations can be solved, giving in this case the metric

$$ds^2 = a(y)^2 dx^\mu dx^\nu \eta_{\mu\nu} + dy^2\ , \quad a(y) = e^{-ky}\,, \qquad (106.12)$$

where $k = \sqrt{-\Lambda/6M_5^3}$. Consistency of the solution requires $\Lambda_0 = -\Lambda_{\pi R} = -\Lambda/k$. The metric in Eq. (106.12) corresponds to a 5D AdS space. The factor $a(y)$ is called the "warp" factor and determines how 4D scales change as a function of the position in the extra dimension. In particular, this implies that energy scales for 4D fields localized at the boundary at $y = \pi R$ are red-shifted by a factor $e^{-k\pi R}$ with respect to those localized at $y = 0$. For this reason, the boundaries at $y = 0$ and $y = \pi R$ are usually referred to as the ultraviolet (UV) and infrared (IR) boundaries, respectively.

As in the ADD case, we can perform a KK reduction and obtain the low-energy effective theory of the 4D massless graviton. In this case we obtain

$$M_P^2 = \int_0^{\pi R} dy\, e^{-2ky} M_5^3 = \frac{M_5^3}{2k}\left(1 - e^{-2k\pi R}\right). \qquad (106.13)$$

Taking $M_5 \sim k \sim M_P$, we can generate an IR-boundary scale of order $ke^{-k\pi R} \sim$ TeV for an extra dimension of radius $R \simeq 11/k$. Mechanisms to stabilize R to this value have been proposed [48] that, contrary to the ADD case, do not require introducing any new small or large parameter. Therefore a natural solution to the hierarchy problem can be achieved in this framework if the Higgs field, whose vacuum expectation value (VEV) is responsible for electroweak symmetry breaking, is localized at the IR-boundary where the effective mass scales are of order TeV. The radion field is generically heavy in models with a stabilized R. Nevertheless, it has been recently discussed that under some conditions a naturally light radion can arise [49]. In these cases the radion is identified with the dilaton, the Goldstone boson associated to the spontaneous breaking of scale invariance, and its mass can be naturally below $ke^{-k\pi R} \sim$ TeV.

In the RS model [3], all the SM fields were assumed to be localized on the IR-boundary. Nevertheless, for the hierarchy problem, only the Higgs field has to be localized there. SM gauge bosons and fermions can propagate in the 5D bulk [4,5,6,50]. By performing a KK reduction from the 5D action of a gauge boson, we find [4]

$$\frac{1}{g_4^2} = \int_0^{\pi R} dy\, \frac{1}{g_5^2} = \frac{\pi R}{g_5^2}\,,$$

where g_D ($D = 4, 5$) is the gauge coupling in D-dimensions. Therefore the 4D gauge couplings can be of order one, as is the case of the SM, if one demands $g_5^2 \sim \pi R$. Using $kR \sim 10$ and $g_4 \sim 0.5$, one obtains the 5D gauge coupling

$$g_5 \sim 4/\sqrt{k}\,. \qquad (106.14)$$

Boundary kinetic terms for the gauge bosons can modify this relation, allowing for larger values of $g_5\sqrt{k}$.

Fermions propagating in a warped extra dimension have 4D massless zero-modes with wavefunctions which vary as $f_0 \sim exp[(1/2 - c_f)ky]$,

where $c_f k$ is their 5D mass [51,6]. Depending on the free parameter $c_f k$, fermions can be localized either towards the UV-boundary ($c_f > 1/2$) or IR-boundary ($c_f < 1/2$). Since the Higgs boson is localized on the IR-boundary, one can generate exponentially suppressed Yukawa couplings by having the fermion zero-modes localized towards the UV-boundary, generating naturally the light SM fermion spectrum [6]. A large overlap with the wavefunction of the Higgs is needed for the top quark, in order to generate its large mass, thus requiring it to be localized towards the IR-boundary. In conclusion, the large mass hierarchies present in the SM fermion spectrum can be easily obtained in warped models via suitable choices of the order-one parameters c_f [52]. In these scenarios, deviations in flavor physics from the SM predictions are expected to arise from flavor-changing KK gluon couplings [53], putting certain constraints on the parameters of the models and predicting new physics effects to be observed in B-physics processes [54].

The masses of the KK states can also be calculated. One finds [6]

$$m_n \simeq \left(n + \frac{\alpha}{2} - \frac{1}{4}\right) \pi k e^{-\pi k R}\,, \qquad (106.15)$$

where $n = 1, 2, ...$ and $\alpha = \{|c_f - 1/2|, 0, 1\}$ for KK fermions, KK gauge bosons and KK gravitons, respectively. Their masses are of order $ke^{-\pi kR} \sim$ TeV; the first KK state of the gauge bosons would be the lightest, while gravitons are expected to be the heaviest.

106.3.1.1. *Models of Electroweak Symmetry Breaking:*

Theories in warped extra dimensions can be used to implement symmetry breaking at low energies by boundary conditions [55]. For example, for a $U(1)$ gauge symmetry in the 5D bulk, this can be easily achieved by imposing a Dirichlet boundary condition on the IR-boundary for the gauge-boson field, $A_\mu|_{y=\pi R} = 0$. This makes the zero-mode gauge boson get a mass, given by $m_A = g_4\sqrt{2k/g_5^2}e^{-\pi kR}$. A very different situation occurs if the Dirichlet boundary condition is imposed on the UV-boundary, $A_\mu|_{y=0} = 0$. In this case the zero-mode gauge boson disappears from the spectrum. Finally, if a Dirichlet boundary condition is imposed on the two boundaries, one obtains a massless 4D scalar corresponding to the fifth component of the 5D gauge boson, A_5. Thus, different scenarios can be implemented by appropriately choosing the 5D bulk gauge symmetry, $\mathcal{G}_5$, and the symmetries to which it reduces on the UV and IR-boundary, $\mathcal{H}_{UV}$ and $\mathcal{H}_{IR}$, respectively. In all cases the KK spectrum comes in representations of the group $\mathcal{G}_5$.

The discovery of a light Higgs boson with $m_H \sim 125$ GeV [56] rules out Higgsless 5D models for electroweak symmetry breaking [57]. This discovery, however, is consistent with 5D composite Higgs models where a light Higgs boson is present in the spectrum.

Composite Higgs models: Warped extra dimensions can give rise to scenarios, often called gauge-Higgs unified models, where the Higgs boson appears as the fifth component of a 5D gauge boson, A_5. The Higgs mass is protected by the 5D gauge invariance and can only get a nonzero value from non-local one-loop effects [58]. To guarantee the relation $M_W^2 \simeq M_Z^2 \cos^2\theta_W$, a custodial $SU(2)_V$ symmetry is needed in the bulk and IR-boundary [59]. The simplest realization [60] has

$$\begin{aligned}\mathcal{G}_5 &= SU(3)_c \times SO(5) \times U(1)_X\,,\\ \mathcal{H}_{IR} &= SU(3)_c \times SO(4) \times U(1)_X\,,\\ \mathcal{H}_{UV} &= G_{SM}\,.\end{aligned}$$

The Higgs boson gets a potential at the one-loop level that triggers a VEV, breaking the electroweak symmetry. In these models there is a light Higgs boson whose mass can be around 125 GeV, as required by the discovered Higgs boson [56]. This state, as will be explained in Sec. III.2, behaves as a composite pseudo-Goldstone boson with couplings that deviate from the SM Higgs [61]. The present experimental determination of the Higgs couplings at the LHC, that agrees with the SM predictions, put important constraints on these scenarios [56]. The lightest KK modes of the model are color fermions with charges $Q = -1/3, 2/3$ and $5/3$ [62].

106.3.1.2. *Constraints from Electroweak Precision Tests:*

Models in which the SM gauge bosons propagate in 1/TeV-sized extra dimensions give generically large corrections to electroweak observables. When the SM fermions are confined on a boundary these corrections are universal and can be parametrized by four quantities: $\widehat{S}$, $\widehat{T}$, W and Y, as defined in Ref. [63]. For warped models, where the 5D gauge coupling of Eq. (106.14) is large, the most relevant parameter is $\widehat{T}$, which gives the bound $m_{KK} \gtrsim 10$ TeV [50]. When a custodial symmetry is imposed [59], the main constraint comes from the $\widehat{S}$ parameter, requiring $m_{KK} \gtrsim 3$ TeV, independent of the value of g_5. Corrections to the $Zb_L\bar{b}_L$ coupling can also be important [50], especially in warped models for electroweak symmetry breaking as the ones described above.

106.3.1.3. *Kaluza-Klein Searches:*

The main prediction of 1/TeV-sized extra dimensions is the presence of a discretized KK spectrum, with masses around the TeV scale, associated with the SM fields that propagate in the extra dimension.

In the RS model [3], only gravity propagates in the 5D bulk. Experimental searches have been performed for the lightest KK graviton through its decay to a variety of SM particle-antiparticle pairs. The results are usually interpreted in the plane of the dimensionless coupling k/M_P versus m_1, where M_P is the reduced Planck mass defined previously and m_1 is the mass of the lightest KK excitation of the graviton. Since the AdS curvature $\sim k$ cannot exceed the cut-off scale of the model, which is estimated to be $\ell_5^{1/3}M_5$ [31], one must demand $k \ll \sqrt{2\ell_5}M_P$. The results quoted below are 95% CL lower limits on the KK graviton mass for a coupling $k/M_P = 0.1$.

The most stringent limits currently arise from LHC searches for resonances in the dilepton and diphoton final states, using 13 TeV collisions. The CMS [64] dilepton analyses, combining results from the ee and $\mu\mu$ channels, exclude gravitons with masses below 3.1 TeV. ATLAS [65] analysis, while similar, does not include a RS KK graviton interpretation of the results.

Similar sensitivities are obtained in the $\gamma\gamma$ final state, which is quite powerful since it has a branching fraction twice that of any individual lepton flavor. The ATLAS $\gamma\gamma$ analysis [33] provides a lower limit on the graviton mass of 3.2 TeV, while the CMS result [66] excludes gravitons below 3.85 TeV. Less stringent limits on the KK graviton mass come from analyses of the dijet [67], HH [68,69,70], and VV [71,72] final states, where V can represent either a W or Z boson. Experimental searches for the radion [68,69], through its production via gluon fusion and decaying to HH, exclude masses from 300 to 1100 and from 1150 to 1550 GeV for a decay constant of 1 TeV.

In warped extra-dimensional models in which the SM fields propagate in the 5D bulk, the couplings of the KK graviton to $ee/\mu\mu/\gamma\gamma$ are suppressed [73], and the above bounds do not apply. Furthermore, the KK graviton is the heaviest KK state (see Eq. (106.15)), and therefore experimental searches for KK gauge bosons and fermions are more appropriate discovery channels in these scenarios. For the scenarios discussed above in which only the Higgs boson and the top quark are localized close to the IR-boundary, the KK gauge bosons mainly decay into top quarks, longitudinal W/Z bosons, and Higgs bosons. Couplings to light SM fermions are suppressed by a factor $g/\sqrt{g_5^2 k} \sim 0.2$ [6] for the value of Eq. (106.14) that is considered from now on. Searches have been made for evidence of the lightest KK excitation of the gluon, through its decay to $t\bar{t}$ pairs. The searches take into account the natural KK gluon width, which is typically $\sim 15\%$ of its mass. The decay of a heavy particle to $t\bar{t}$ would tend to produce highly boosted top (anti-)quarks in the final state. Products of the subsequent top decays would therefore tend to be close to each other in the detector. In the case of $t \to Wb \to jjb$ decays, the three jets could overlap one another and not be individually reconstructed with the standard jet algorithms, while $t \to Wb \to \ell\nu b$ decays could result in the lepton failing standard isolation requirements due to its proximity to the b-jet; in both cases, the efficiency for properly reconstructing the final state would fall as the mass of the original particle increases. To avoid the loss in sensitivity which would result, a number of techniques, known generally as "top quark tagging", have

been developed to reconstruct and identify highly boosted top quarks, for example by using a single "wide" jet to contain all the decay products of a hadronic top decay. The large backgrounds from QCD jets can then be reduced by requiring the "jet mass" be consistent with that of a top quark, and also by examining the substructure of the wide jet for indication that it resulted from the hadronic decay of a top quark. These techniques are key to extending to very high masses the range of accessible resonances decaying to $t\bar{t}$ pairs. The CMS analysis [74] of 2.6 fb^{-1} of 13 TeV data excludes KK gluons with masses below 3.3 TeV.

A gauge boson KK excitation could be also sought through its decay to longitudinal W/Z bosons. Recent analyses from ATLAS [75] and CMS [76] searching for heavy vector resonances decaying to a W or Z boson and a Higgs in the $q\bar{q}b\bar{b}$ final state have set a lower limit on the mass of these KK of ~ 2.5 TeV (warped models are equivalent to the Model B considered in the analyses with $g_V \sim g_5\sqrt{k}$). The decay to a pair of intermediate vector bosons has also been exploited to search for KK gravitons in models in which the SM fields propagate in the 5D bulk. The analyses typically reconstruct hadronic W/Z decays using variants of the boosted techniques mentioned previously. A preliminary ATLAS analysis [77] searching in the single-lepton-plus-jets final state from the KK graviton decay $G^* \to VV$, where V can represent either a W or Z boson, exclude gravitons with masses below 1.8 TeV, for a value of $k/M_P = 1$. CMS VV analyses [78] also provide cross section limits in the context of bulk gravitons; however, a maximum value of $k/M_P = 0.5$ is presented, for which no mass exclusion is possible using the combination of the full 8 TeV sample and 2.7 fb^{-1}of 13 TeV data. Less restrictive limits in these models result from searching for $G^* \to HH$ [79].

The lightest KK states are, in certain models, the partners of the top quark. For example, in 5D composite Higgs models these are colored states with charges $Q = -1/3, 2/3$ and $5/3$ (arising from $SU(2)_L$ doublets with $Y = 7/6, 1/6$), and masses expected to be below the TeV [62]. They can be either singly or pair-produced, and mainly decay into a combination of W/Z with top/bottom quarks [80]. An exhaustive review of these searches can be found in Ref. [81]. Of particular note, the $Q = 5/3$ state decays mainly into $W^+t \to W^+W^+b$, giving a pair of same-sign leptons in the final state. An analysis by ATLAS [82] searching in the lepton-plus-jets final state for evidence of pair production of the $Q = 5/3$ state provides a lower mass limit of 1.25 TeV. Their analysis requiring in addition to a pair of same-sign leptons at least one b-tagged jet in the event [83] provides a lower mass limit of 990 GeV from pair production, and also from single production, the cross section for which is model-dependent [84]. The most recent CMS analysis [85] searching for pair production of the $Q = 5/3$ state with a lepton-plus-jets final state excludes masses below 1.32 TeV. Both LHC experiments have searched for pair production of vector-like quarks T and B of charges $Q = 2/3$ and $-1/3$ respectively, assuming the allowable decays are $T \to Wb/Zt/Ht$ and $B \to Wt/Zb/Hb$. In each case, it is assumed the branching fractions of the three decay modes sum to unity, but the individual branching fractions, which are model-dependent, are allowed to vary within this constraint. Depending on the values of the individual branching fractions, CMS obtains lower limits on the mass of the T [86], [87] (B [88]) vector-like quark in the range of $720 - 940$ GeV ($740 - 900$ GeV), while ATLAS searches [82,83,89,90] provide lower limits on the T (B) mass in the range of $1000 - 1350$ GeV ($700 - 1250$ GeV).

106.3.2. *Connection with Strongly Coupled Models via the AdS/CFT Correspondence* :

The AdS/CFT correspondence [7] provides a connection between warped extra-dimensional models and strongly-coupled theories in ordinary 4D. Although the exact connection is only known for certain cases, the AdS/CFT techniques have been very useful to obtain, at the qualitative level, a 4D holographic description of the various phenomena in warped extra-dimensional models [8].

The connection goes as follows. The physics of the bulk AdS$_5$ models can be interpreted as that of a 4D conformal field theory (CFT) which is strongly coupled. The extra-dimensional coordinate y plays the role of the renormalization scale μ of the CFT by means of the identification $\mu \equiv ke^{-ky}$. Therefore the UV-boundary corresponds in the CFT to a UV cut-off scale at $\Lambda_{UV} = k \sim M_P$, breaking explicitly conformal invariance, while the IR-boundary can be interpreted as a spontaneous breaking of the conformal symmetry at energies $ke^{-k\pi R} \sim$ TeV. Fields localized on the UV-boundary are elementary fields external to the CFT, while fields localized on the IR-boundary and KK states corresponds to composite resonances of the CFT. Furthermore, local gauge symmetries in the 5D models, $\mathcal{G}_5$, correspond to global symmetries of the CFT, while the UV-boundary symmetry can be interpreted as a gauging of the subgroup $\mathcal{H}_{UV}$ of $\mathcal{G}_5$ in the CFT. Breaking gauge symmetries by IR-boundary conditions corresponds to the spontaneous breaking $\mathcal{G}_5 \to \mathcal{H}_{IR}$ in the CFT at energies $\sim ke^{-k\pi R}$. Using this correspondence one can easily derive the 4D massless spectrum of the compactified AdS$_5$ models. One also has the identification $k^3/M_5^3 \approx 16\pi^2/N^2$ and $g_5^2 k \approx 16\pi^2/N^r$ ($r = 1$ or 2 for CFT fields in the fundamental or adjoint representation of the gauge group), where N plays the role of the number of colors of the CFT. Therefore the weak-coupling limit in AdS$_5$ corresponds to a large-N expansion in the CFT.

Following the above AdS/CFT dictionary one can understand the RS solution to the hierarchy problem from a 4D viewpoint. The equivalent 4D model is a CFT with a TeV mass gap and a Higgs boson emerging as a composite state. In the particular case where the Higgs is the fifth-component of the gauge-boson, A_5 [91], this corresponds to models, similar to those proposed in Ref. [92], where the Higgs is a composite pseudo-Goldstone boson arising from the spontaneous breaking $\mathcal{G}_5 \to \mathcal{H}_{IR}$ in the CFT. The AdS/CFT dictionary tells us that KK states must behave as composite resonances. For example, if the SM gauge bosons propagate in the 5D bulk, the lowest KK $SU(2)_L$-gauge boson must have properties similar to those of the Techni-rho ρ_T [81] with a coupling to longitudinal W/Z bosons given by $g_5\sqrt{k} \approx g_{\rho_T}$, while the coupling to elementary fermions is $g^2/\sqrt{g_5^2 k} \approx g^2 F_{\rho_T}/M_{\rho_T}$.

Fermions in compactified AdS$_5$ also have a simple 4D holographic interpretation. The 4D massless mode described in Sec. III.1 corresponds to an external fermion ψ_i linearly coupled to a fermionic CFT operator $\mathcal{O}_i$: $\mathcal{L}_{\rm int} = \lambda_i \bar{\psi}_i \mathcal{O}_i + h.c.$. The dimension of the operator $\mathcal{O}_i$ is related to the 5D fermion mass according to $\mathrm{Dim}[\mathcal{O}_i] = |c_f + 1/2| - 1$. Therefore, by varying c_f one varies $\mathrm{Dim}[\mathcal{O}_i]$, making the coupling λ_i irrelevant ($c_f > 1/2$), marginal ($c_f = 1/2$) or relevant ($c_f < 1/2$). When irrelevant, the coupling is exponentially suppressed at low energies, and then the coupling of ψ_i to the CFT (and eventually to the composite Higgs) is very small. When relevant, the coupling grows in the IR and become as large as g_5 (in units of k), meaning that the fermion is as strongly coupled as the CFT states [60]. In this latter case ψ_i behaves as a composite fermion.

106.3.3. *Flat Extra Dimensions* :

Models with quantum gravity at the TeV scale, as in the ADD scenario, can have extra (flat) dimensions of 1/TeV size, as happens in string scenarios [93]. All SM fields may propagate in these extra dimensions, leading to the possibility of observing their corresponding KK states.

A simple example is to assume that the SM gauge bosons propagate in a flat five-dimensional orbifold S^1/Z_2 of radius R, with the fermions localized on a 4D boundary. The KK gauge bosons behave as sequential SM gauge bosons with a coupling to fermions enhanced by a factor $\sqrt{2}$ [93]. The experimental limits on such sequential gauge bosons could therefore be recast as limits on KK gauge bosons. Such an interpretation of the ATLAS 7 TeV dilepton analysis [94] yielded the bound $1/R > 4.16$ TeV, while a CMS 8 TeV search with a lepton and missing transverse energy in the final state [95] give $1/R > 3.4$ TeV. Indirect bounds from LEP2 require however $1/R \gtrsim 6$ TeV [96,63], a bound that can considerable improve in the future by high-energy measurements of the dilepton invariant mass spectrum from Drell-Yan processes at the LHC [97]. More recent LHC limits on leptonically decaying gauge bosons [98,99,100,35] are not interpreted as bounds on $1/R$ by the collaborations, but the published results allow for independent derivation of such bound.

An alternative scenario, known as Universal Extra Dimensions

(UED) [101], assumes that all SM fields propagate universally in a flat orbifold S^1/Z_2 with an extra Z_2 parity, called KK-parity, that interchanges the two boundaries. In this case, the lowest KK state is stable and is a Dark Matter candidate. At colliders, the KK particles would have to be created in pairs, and would then cascade decay to the lightest KK particle, which would be stable and escape detection. The UED mass-spectrum not only depend on the extra-dimensional radius R, but also on the cut-off of the 5D theory Λ, since quantum corrections sensitive to ΛR induce mass-splittings between the KK states. Experimental signatures, such as jets or leptons and $\not\!\!E_T$, would be similar to those of typical R-parity conserving SUSY searches. An interpretation of the recent LHC experimental SUSY searches for UED models has been presented in Refs. [102,103]. A lower bound $1/R > 1.4 - 1.5$ TeV was derived for $\Lambda R \sim 5 - 35$ [102].

Finally, realistic models of electroweak symmetry breaking can also be constructed with flat extra spatial dimensions, similarly to those in the warped case, requiring, however, the presence of sizeable boundary kinetic terms [104]. There is also the possibility of breaking supersymmetry by boundary conditions [105]. Models of this type could explain naturally the presence of a Higgs boson lighter than $M_D \sim$ TeV [106].

References:

1. For a comprehensive collection of the original papers see, "Modern Kaluza-Klein Theories", edited by T. Appelquist *et al.*, Addison-Wesley (1987).
2. N. Arkani-Hamed *et al.*, Phys. Lett. **B429**, 263 (1998).
3. L. Randall and R. Sundrum, Phys. Rev. Lett. **83**, 3370 (1999).
4. H. Davoudiasl *et al.*, Phys. Lett. **B473**, 43 (2000); A. Pomarol, Phys. Lett. **B486**, 153 (2000).
5. S. Chang *et al.*, Phys. Rev. **D62**, 084025 (2000).
6. T. Gherghetta and A. Pomarol, Nucl. Phys. **B586**, 141 (2000).
7. J.M. Maldacena, Adv. Theor. Math. Phys. **2**, 231 (1998); E. Witten, Adv. Theor. Math. Phys. **2**, 253 (1998); S.S. Gubser *et al.*, Phys. Lett. **B428**, 105 (1998).
8. N. Arkani-Hamed *et al.*, JHEP **0108**, 017 (2001).
9. ATLAS public results are available on WWW at `https://twiki.cern.ch/twiki/bin/view/AtlasPublic`.
10. CMS public results are available on WWW at `cms-results.web.cern.ch/cms-results/public-results/publications`.
11. Z. Chacko *et al.*, JHEP **0007**, 036 (2000).
12. N. Arkani-Hamed *et al.*, Phys. Rev. **D59**, 086004 (1999).
13. For a review see for example, R. Rattazzi, `hep-ph/0607055 (2006)`; I. Antoniadis, Yellow report CERN-2002-002 (2002).
14. I. Antoniadis *et al.*, Phys. Lett. **B436**, 257 (1998).
15. G.F. Giudice *et al.*, Nucl. Phys. **B544**, 3 (1999).
16. For the case of two extra dimensions, see for example, N. Arkani-Hamed *et al.*, Phys. Rev. **D62**, 105002 (2000).
17. E.G. Adelberger *et al.*, Prog. in Part. Nucl. Phys. **62**, 102 (2009); J. Murata and S. Tanaka, Class. Quantum Grav. **32**, 033001 (2015).
18. C. Hanhart *et al.*, Phys. Lett. **B509**, 1 (2001).
19. S. Hannestad and G.G. Raffelt, Phys. Rev. **D67**, 125008 (2003).
20. L.J. Hall and D. Tucker-Smith, Phys. Rev. **D60**, 085008 (1999).
21. E.A. Mirabelli *et al.*, Phys. Rev. Lett. **82**, 2236 (1999).
22. T. Han *et al.*, Phys. Rev. **D59**, 105006 (1999).
23. ATLAS Collab., ATLAS-CONF-2017-060.
24. CMS Collab., CMS-PAS-EXO-16-048.
25. CMS Collab., `arXiv:1706.03794`, CMS-EXO-16-039, submitted to JHEP.
26. ATLAS Collab., JHEP **1606**, 059 (2016).
27. See for example S. Cullen *et al.*, Phys. Rev. **D62**, 055012 (2000).
28. CMS Collab., CMS-PAS-EXO-16-056.
29. ATLAS Collab., `arXiv:1703.09127`, ATLAS-EXOT-2016-21.
30. J.L. Hewett, Phys. Rev. Lett. **82**, 4765 (1999).
31. G.F. Giudice and A. Strumia, Nucl. Phys. **B663**, 377 (2003).
32. CMS Collab., CMS-PAS-EXO-16-046.
33. ATLAS Collab., `arxiv:1707.04147`.
34. ATLAS Collab., Eur. Phys. J. **C74**, 3134 (2014).
35. CMS Collab., JHEP **1504**, 025 (2015).
36. S.B. Giddings and S. Thomas, Phys. Rev. **D65**, 056010 (2002); S. Dimopoulos and G. Landsberg, Phys. Rev. Lett. **87**, 161602 (2001); for a review see for example, P. Kanti, Int. J. Mod. Phys. **A19**, 4899 (2004).
37. R.C. Myers and M.J. Perry, Ann. Phys. **172**, 304 (1986).
38. ATLAS Collab., Phys. Lett. **B760**, 520 (2016).
39. ATLAS Collab., JHEP **1603**, 026 (2016).
40. CMS Collab., CMS-EXO-15-007, `arXiv:1705.01403`.
41. ATLAS Collab., Phys. Rev. **D88**, 072001 (2013).
42. C. Kilic, A. Lath, K. Rose, and S. Thomas, Phys. Rev. **D89**, 016003 (2014).
43. CMS Collab., Phys. Rev. **D90**, 032005 (2014).
44. P. Meade and L. Randall, JHEP **0805**, 003 (2008).
45. CMS Collab., Eur. Phys. J. **C76**, 317 (2016).
46. CMS Collab., Eur. Phys. J. **C76**, 541 (2016).
47. S. Dimopoulos and R. Emparan, Phys. Lett. **B526**, 393 (2002).
48. W.D. Goldberger and M.B. Wise, Phys. Rev. Lett. **83**, 4922 (1999); J. Garriga, A. Pomarol, Phys. Lett. **B560**, 91 (2003).
49. See talk by R. Rattazzi at Planck 2010, CERN; B. Bellazzini *et al.*, Eur. Phys. J. **C74**, 2790 (2014); F. Coradeschi *et al.*, JHEP **1311**, 057 (2013); E. Megias and O. Pujolas, JHEP **1408**, 081 (2014).
50. For a review see for example, H. Davoudiasl *et al.*, New J. Phys. **12**, 075011 (2010); T. Gherghetta, `arXiv:1008.2570`.
51. Y. Grossman and M. Neubert, Phys. Lett. **B474**, 361 (2000).
52. S.J. Huber and Q. Shafi, Phys. Lett. **B498**, 256 (2001).
53. A. Delgado *et al.*, JHEP **0001**, 030 (2000).
54. K. Agashe *et al.*, Phys. Rev. **D71**, 016002 (2005); for a recent analysis see for example, M. Bauer *et al.*, JHEP **1009**, 017 (2010).
55. For a review see for example, A. Pomarol, Int. J. Mod. Phys. **A24**, 61 (2009).
56. See, for example, PDG review of Higgs boson in this *Review*.
57. C. Csaki *et al.*, Phys. Rev. Lett. **92**, 101802 (2004); for a review see for example, C. Csaki *et al.*, `hep-ph/0510275`.
58. Y. Hosotani, Phys. Lett. **B126**, 309 (1983).
59. K. Agashe *et al.*, JHEP **0308**, 050 (2003).
60. K. Agashe *et al.*, Nucl. Phys. **B719**, 165 (2005); for a review see for example, R. Contino, `arXiv:1005.4269`.
61. G.F. Giudice *et al.*, JHEP **0706**, 045 (2007).
62. R. Contino *et al.*, Phys. Rev. **D75**, 055014 (2007).
63. R. Barbieri *et al.*, Nucl. Phys. **B703**, 127 (2004).
64. CMS Collab., Phys. Lett. **B768**, 57 (2017).
65. ATLAS Collab., Phys. Lett. **B761**, 372 (2016).
66. CMS Collab., Phys. Lett. **B767**, 147 (2017).
67. CMS Collab., Phys. Lett. **B769**, 520 (2017).
68. CMS Collab., Phys. Lett. **B749**, 560 (2016).
69. CMS Collab., Eur. Phys. J. **C76**, 371 (2016).
70. ATLAS Collab., Phys. Rev. **D94**, 052002 (2016).
71. ATLAS Collab., JHEP **1609**, 173 (2016).
72. CMS Collab., JHEP **1408**, 173 (2014).
73. K. Agashe *et al.*, Phys. Rev. **D76**, 036006 (2007).
74. CMS Collab., JHEP **1707**, 001 (2017).
75. ATLAS Collab., `arXiv:1707.06958`.
76. CMS Collab., `arXiv:1707.01303`.
77. ATLAS Collab., ATLAS-CONF-2017-051.
78. CMS Collab., `arXiv:1705.09171`.
79. ATLAS Collab., Eur. Phys. J. **C75**, 412 (2015).
80. R. Contino and G. Servant, JHEP **0806**, 026 (2008); J.A. Aguilar-Saavedra, JHEP **0911**, 030 (2009); J. Mrazek and A. Wulzer, Phys. Rev. **D81**, 075006 (2010); G. Dissertori *et al.*, JHEP **1009**, 019 (2010).
81. See, for example, PDG review of Technicolor searches in this volume.
82. ATLAS Collab., `arXiv:1707.03347`.
83. ATLAS Collab., ATLAS-CONF-2016-032.
84. A. De Simone *et al.*, JHEP **1304**, 004 (2013).
85. CMS Collab., CMS-PAS-B2G-17-008.
86. CMS Collab., Phys. Rev. **D93**, 012003 (2016).
87. CMS Collab., `arXiv:1706.03408`, submitted to JHEP.
88. CMS Collab., Phys. Rev. **D93**, 112009 (2016).

89. ATLAS Collab., ATLAS-CONF-16-104.
90. ATLAS Collab., arXiv:1705.10751.
91. R. Contino, Y. Nomura, and A. Pomarol, Nucl. Phys. **B671**, 148 (2003).
92. H. Georgi *et al.*, Phys. Lett. **B143**, 152 (1984); D.B. Kaplan *et al.*, Phys. Lett. **B136**, 183 (1984).
93. See for example, I. Antoniadis and K. Benakli, Int. J. Mod. Phys. **A15**, 4237 (2000).
94. ATLAS Collab., JHEP **1211**, 138 (2012).
95. CMS Collab., Phys. Rev. **D91**, 092005 (2015).
96. K. Cheung and G. L. Landsberg, Phys. Rev. **D65**, 076003 (2002).
97. M. Farina *et al.*, Phys. Lett. **B772**, 210 (2017).
98. ATLAS Collab., arXiv:1707.02424.
99. CMS Collab., Phys. Lett. **B770**, 278 (2017).
100. ATLAS Collab., arXiv:1706.04786.
101. T. Appelquist *et al.*, Phys. Rev. **D64**, 035002 (2001); for a review see for example, A. Datta *et al.*, New J. Phys. **12**, 075017 (2010).
102. N. Deutschmann, T. Flacke and J.S. Kim, Phys. Lett. **B771**, 515 (2017).
103. J. Beuria, A. Datta, D. Debnath and K. T. Matchev, arXiv:1702.00413.
104. For a review see for example, G. Panico *et al.*, JHEP **1102**, 103 (2011).
105. J. Scherk and J.H. Schwarz, Phys. Lett. **B82**, 60 (1979).
106. See for example, A. Pomarol and M. Quiros, Phys. Lett. **B438**, 255 (1998); I. Antoniadis *et al.*, Nucl. Phys. **B544**, 503 (1999); R. Barbieri *et al.*, Phys. Rev. **D63**, 105007 (2001).

107. W'-Boson Searches

Revised October 2017 by B.A. Dobrescu (Fermilab) and S. Willocq (Univ. of Massachusetts).

The W' boson is a massive hypothetical particle of spin 1 and electric charge ±1, which is a color singlet and is predicted in various extensions of the Standard Model (SM).

107.1. W' couplings to quarks and leptons.

The Lagrangian terms describing couplings of a W'^+ boson to fermions are given by

$$\frac{W'^+_\mu}{\sqrt{2}}\left[\overline{u}_i\left(C^R_{q_{ij}}P_R+C^L_{q_{ij}}P_L\right)\gamma^\mu d_j+\overline{\nu}_i\left(C^R_{\ell_{ij}}P_R+C^L_{\ell_{ij}}P_L\right)\gamma^\mu e_j\right]. \quad (107.1)$$

Here u, d, ν and e are the SM fermions in the mass eigenstate basis, $i, j = 1, 2, 3$ label the fermion generation, and $P_{R,L} = (1 \pm \gamma_5)/2$. The coefficients $C^L_{q_{ij}}$, $C^R_{q_{ij}}$, $C^L_{\ell_{ij}}$, and $C^R_{\ell_{ij}}$ are complex dimensionless parameters. If $C^R_{\ell_{ij}} \neq 0$, then the ith generation includes a right-handed neutrino. Using this notation, the SM W couplings are $C^L_q = gV_{\rm CKM}$, $C^L_\ell = g \approx 0.63$ and $C^R_q = C^R_\ell = 0$.

Unitarity considerations imply that the W' boson is associated with a spontaneously-broken gauge symmetry. This is true even when it is a composite particle (*e.g.*, $\rho^\pm$-like bound states [1]) if its mass is much smaller than the compositeness scale, or a Kaluza-Klein mode in theories where the W boson propagates in extra dimensions [2]. The simplest extension of the electroweak gauge group that includes a W' boson is $SU(2)_1 \times SU(2)_2 \times U(1)$, but larger groups are encountered in some theories. A generic property of these gauge theories is that they also include a Z' boson [3]; the Z'-to-W' mass ratio is often a free parameter.

A tree-level mass mixing may be induced between the electrically-charged gauge bosons. Upon diagonalization of their mass matrix, the $W - Z$ mass ratio and the couplings of the observed W boson are shifted from the SM values. Their measurements imply that the mixing angle between the gauge eigenstates, θ_+, must be smaller than about 10^{-2}. In certain theories the mixing is negligible (*e.g.* due to a new parity [4]), even when the W' mass is near the electroweak scale.

The W' coupling to WZ is fixed by Lorentz and gauge invariances, and to leading order in θ_+ is given by [5]

$$\frac{g\,\theta_+\,i}{\cos\theta_W}\left[W'^+_\mu\left(W^-_\nu Z^{\nu\mu}+Z_\nu W^{-\mu\nu}\right)+Z^\nu W^{-\mu}W'^+_{\nu\mu}\right]+\text{H.c.}, \quad (107.2)$$

where $W^{\mu\nu} \equiv \partial^\mu W^\nu - \partial^\nu W^\mu$, etc. The θ_W dependence shown here corrects the one given in [6], which has been referred to as the Extended Gauge Model by the experimental collaborations. The W' coupling to Wh^0, where h^0 is the SM Higgs boson, is

$$-\xi_h\, g_{W'} M_W\, W'^+_\mu\, W^{\mu-} h^0 + \text{H.c.}, \quad (107.3)$$

where $g_{W'}$ is the gauge coupling of the W' boson, and the coefficient ξ_h satisfies $\xi_h \leq 1$ in simple Higgs sectors [5].

In models based on the "left-right symmetric" gauge group [7], $SU(2)_L \times SU(2)_R \times U(1)_{B-L}$, the SM fermions that couple to the W boson transform as doublets under $SU(2)_L$ while the other fermions transform as doublets under $SU(2)_R$. Consequently, the W' boson couples primarily to right-handed fermions; its coupling to left-handed fermions arises due to the θ_+ mixing, so that C^L_q is proportional to the CKM matrix and its elements are much smaller than the diagonal elements of C^R_q. Generically, C^R_q does not need to be proportional to $V_{\rm CKM}$.

There are many other models based on the $SU(2)_1 \times SU(2)_2 \times U(1)$ gauge symmetry. In the "alternate left-right" model [8], all the couplings shown in Eq. (107.1) vanish, but there are some new fermions such that the W' boson couples to pairs involving a SM fermion and a new fermion. In the "ununified SM" [9], the left-handed quarks are doublets under one $SU(2)$, and the left-handed leptons are doublets under a different $SU(2)$, leading to a mostly leptophobic W' boson: $C^L_{\ell_{ij}} \ll C^L_{q_{ij}}$ and $C^R_{\ell_{ij}} = C^R_{q_{ij}} = 0$. Fermions of different generations may also transform as doublets under different $SU(2)$ gauge groups [10]. In particular, the couplings to third generation quarks may be enhanced [11].

It is also possible that the W' couplings to SM fermions are highly suppressed. For example, if the quarks and leptons are singlets under one $SU(2)$ [12], then the couplings are proportional to the tiny mixing angle θ_+. Similar suppressions may arise if some vectorlike fermions mix with the SM fermions [13].

Gauge groups that embed the electroweak symmetry, such as $SU(3)_W \times U(1)$ or $SU(4)_W \times U(1)$, also include one or more W' bosons [14].

107.2. Collider searches.

At LEP-II, W' bosons could have been produced in pairs via their photon and Z couplings. The production cross section is large enough to rule out $M_{W'} < \sqrt{s}/2 \approx 105$ GeV for most patterns of decay modes.

At hadron colliders, W' bosons can be detected through resonant pair production of fermions or electroweak bosons. Assuming that the W' width is much smaller than its mass, the contribution of the s-channel W' boson exchange to the total rate for $pp \to f\bar{f}'X$, where f and f' are fermions whose difference of electric charges is ±1, and X is any final state, may be approximated by the branching fraction $B(W' \to f\bar{f}')$ times the production cross section

$$\sigma\left(pp \to W'X\right) \simeq \frac{\pi}{48\,s}\sum_{i,j}\left[(C^L_{q_{ij}})^2+(C^R_{q_{ij}})^2\right] w_{ij}\left(M^2_{W'}/s, M_{W'}\right). \quad (107.4)$$

The functions w_{ij} include the information about proton structure, and are given to leading order in α_s by

$$w_{ij}(z,\mu) = \int_z^1 \frac{dx}{x}\left[u_i(x,\mu)\,\overline{d}_j\left(\frac{z}{x},\mu\right)+\overline{u}_i(x,\mu)\,d_j\left(\frac{z}{x},\mu\right)\right], \quad (107.5)$$

where $u_i(x,\mu)$ and $d_i(x,\mu)$ are the parton distributions inside the proton, at the factorization scale μ and parton momentum fraction x, for the up- and down-type quark of the ith generation, respectively. QCD corrections to W' production are sizable (they also include quark-gluon initial states), but preserve the above factorization of couplings at next-to-leading order [15].

The most commonly studied W' signal consists of a high-momentum electron or muon and large missing transverse momentum, with the transverse mass distribution forming a Jacobian peak with its endpoint at $M_{W'}$ (see Fig. 1a of [16]). Given that the branching fractions for $W' \to e\nu$ and $W' \to \mu\nu$ could be very different, the results in these channels should be presented separately. Searches in these channels often implicitly assume that the left-handed couplings vanish (no interference between W and W'), and that the right-handed neutrino is light compared to the W' boson and escapes the detector. An example of parameter values that satisfy these assumptions is $C^R_q = gV_{\rm CKM}$, $C^R_\ell = g$, $C^L_q = C^L_\ell = 0$, which define a model that preserves lepton universality and is essentially equivalent to the Sequential SM used in many W' searches. However, if a W' boson were discovered and the final state fermions have left-handed helicity, then the effects of $W - W'$ interference could be observed [17], providing useful information about the W' couplings.

In the $e\nu$ channel, the ATLAS and CMS Collaborations set limits on the W' production cross section times branching fraction (and thus indirectly on the W' couplings) when $M_{W'}$ is in the $0.15 - 6$ TeV range, based on 2–36 fb^{-1} at $\sqrt{s} = 13$ TeV [16,18], as shown in Fig. 107.1. ATLAS sets the strongest mass lower limit $M_{W'} > 5.2$ TeV in the Sequential SM (all limits in this mini-review are at the 95% CL). The coupling limits are much weaker for $M_{W'} < 150$ GeV, a range last explored with the Tevatron at $\sqrt{s} = 1.8$ TeV [19].

In the $\mu\nu$ channel, ATLAS and CMS set rate limits for $M_{W'}$ in the $0.15 - 6$ TeV range from the same analyses as mentioned above, with the strongest lower mass limit of 4.5 TeV set by ATLAS [16] using 36.1 fb^{-1} of $\sqrt{s} = 13$ TeV data. When combined with the $e\nu$ channel assuming lepton universality, the upper limit on the $\sqrt{s} = 13$ TeV

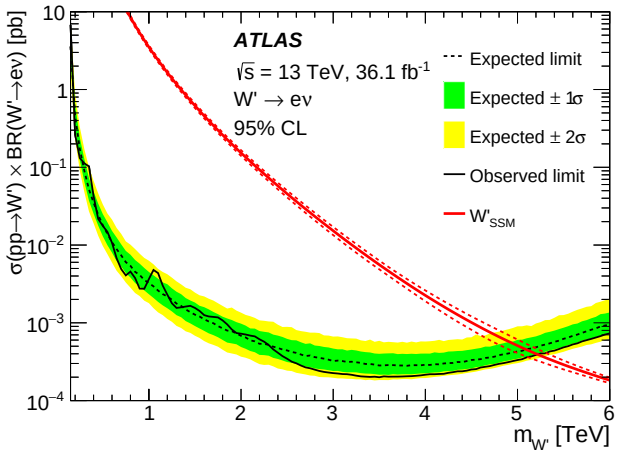

Figure 107.1: Upper limit on $\sigma(pp \to W'X)\, B(W' \to e\nu)$ from ATLAS [16], at 95% CL. The red line shows the theoretical prediction in the Sequential SM.

cross section times branching fraction to $\ell\nu$ varies between 0.2 and 4 fb for $M_{W'}$ between 1 and 5 TeV [16]. Only weak limits on $W' \to \mu\nu$ exist for $M_{W'} < 150$ GeV [20]. Note that masses of the order of the electroweak scale are interesting from a theory point of view, while lepton universality does not necessarily apply to a W' boson.

Dedicated searches for $W' \to \tau\nu$ have been performed by CMS at 8 TeV [21] and 13 TeV [22]. Limits are set on $\sigma \cdot B$ for $M_{W'}$ between 0.3 and 4 TeV for the former and between 1.0 and 5.8 TeV for the latter. A lower mass limit of 3.3 TeV is set in the Sequential SM.

The W' decay into a lepton and a right-handed neutrino, ν_R, may also be followed by the ν_R decay through a virtual W' boson into a lepton and two quark jets. The CMS [23,24] and ATLAS [25] searches in the $eejj$ and $\mu\mu jj$ channels have set limits on the cross section times branching fraction as a function of the ν_R mass or of $M_{W'}$. These searches are typically performed with same-charge lepton pairs that provide strong background reduction and are motivated by models with a left-right symmetry. However, it is also interesting to search in final states with opposite-charge lepton pairs, as done in the CMS analysis. A related W' search in the $\tau\tau jj$ channel with hadronic τ's was also performed by CMS [26].

The $t\bar{b}$ channel is particularly important because a W' boson that couples only to right-handed fermions cannot decay to leptons when the right-handed neutrinos are heavier than the W' boson (additional motivations are provided by a W' boson with enhanced couplings to the third generation [11], and by a leptophobic W' boson). The usual signature consists of a leptonically-decaying W boson and two b-jets. Recent studies have also incorporated the fully hadronic decay channel for $M_{W'} \gg m_t$ with the use of jet substructure techniques to tag highly boosted top-jets. For a detailed discussion of this channel, see [27].

Searches for dijet resonances may be used to set limits on $W' \to q\bar{q}'$. CMS [28] and ATLAS [29] provide similar coverage in the $\sim 0.75 - 7.0$ TeV mass range with data collected at $\sqrt{s} = 8$ and 13 TeV, with the most stringent lower W' mass limit in the Sequential SM set to 3.6 TeV using 37 fb^{-1} of 13 TeV data. For lower masses, the best limits on W' couplings to quarks have been set by CDF [30] in the $300 - 500$ GeV range, and by CMS [31] in the $500 - 750$ GeV range. Limits for W' masses in the $50 - 300$ GeV range can be derived from the dijet limits on Z' bosons set by CMS [32].

In some theories [4] the W' couplings to SM fermions are suppressed by discrete symmetries. W' production then occurs in pairs, through a photon or Z boson. The decay modes are model-dependent and often involve other new particles. The ensuing collider signals arise from cascade decays and typically include missing transverse momentum.

Searches for WZ resonances at the LHC have focused on the process $pp \to W' \to WZ$ with the production mainly from $u\bar{d} \to W'$ assuming SM-like couplings to quarks. ATLAS and CMS have set the strongest upper limits on the $W'WZ$ coupling for $M_{W'}$ in the $0.2 - 5.0$

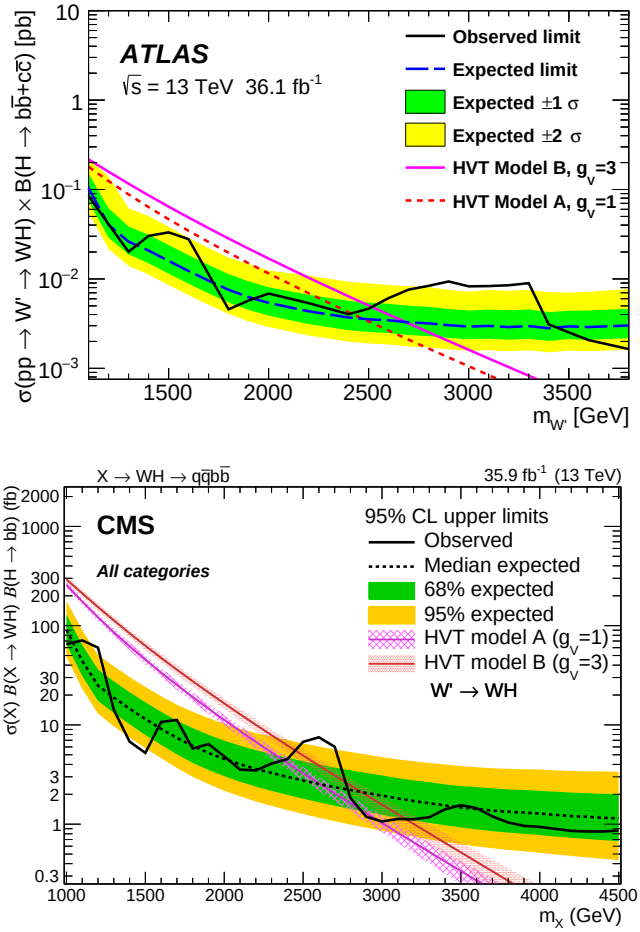

Figure 107.2: Upper limits at 95% CL on W' production cross section times branching fraction into a W and a SM Higgs boson, from [41] (top) and [44] (bottom).

TeV range with a combination of fully leptonic, semi-leptonic and fully hadronic channels (see also [27]) at both 8 and 13 TeV [33]-[37]. The strongest lower limit on the mass is set by CMS at 13 TeV with 35.5 fb^{-1} in the $WZ \to (jj)(\nu\bar{\nu})$ final state, where the parentheses represent a resonance; the limit is $M_{W'} > 3.2$ TeV in the context of the Heavy Vector Triplet (HVT) weakly-coupled scenario A [38].

A fermiophobic W' boson that couples to WZ may be produced at hadron colliders in association with a Z boson, or via WZ fusion. This would give rise to $(WZ)Z$ and $(WZ)jj$ final states [39].

W' bosons have also been searched for recently in final states with a W boson and a SM Higgs boson in the channels $W \to \ell\nu$ or $W \to qq$ and $h^0 \to b\bar{b}$ or $h^0 \to WW$ by ATLAS [40,41] and CMS [36,42,43,44] at $\sqrt{s} = 8$ and 13 TeV. Cross section limits are set for W' masses in the range between 0.4 and 4.5 TeV. The ATLAS and CMS 13 TeV analyses both set the most stringent lower limit on the mass: $M_{W'} > 2.4$ TeV for the HVT weakly-coupled scenario A, as shown in Fig. 107.2.

107.3. Low-energy constraints.

The properties of W' bosons are also constrained by measurements of processes at energies much below $M_{W'}$. The bounds on $W - W'$ mixing [45] are mostly due to the change in W properties compared to the SM. Limits on deviations in the ZWW couplings provide a leading constraint for fermiophobic W' bosons [13].

Constraints arising from low-energy effects of W' exchange are strongly model-dependent. If the W' couplings to quarks are not suppressed, then box diagrams involving a W and a W' boson contribute to neutral meson-mixing. In the case of W' couplings to right-handed quarks as in the left-right symmetric model, the limit from $K_L - K_S$ mixing is severe: $M_{W'} > 2.9$ TeV for $C_q^R = gV_{\rm CKM}$ [46].

However, if no correlation between the W' and W couplings is assumed, then the limit on $M_{W'}$ may be significantly relaxed [47].

W' exchange also contributes at tree level to various low-energy processes. In particular, it would impact the measurement of the Fermi constant G_F in muon decay, which in turn would change the predictions of many other electroweak processes. A recent test of parity violation in polarized muon decay [48] has set limits of about 600 GeV on $M_{W'}$, assuming W' couplings to right-handed leptons as in left-right symmetric models and a light ν_R. There are also W' contributions to the neutron electric dipole moment, β decays, and other processes [45].

If right-handed neutrinos have Majorana masses, then there are tree-level contributions to neutrinoless double-beta decay, and a limit on $M_{W'}$ versus the ν_R mass may be derived [49]. For ν_R masses below a few GeV, the W' boson contributes to leptonic and semileptonic B meson decays, so that limits may be placed on various combinations of W' parameters [47]. For ν_R masses below $\sim$30 MeV, the most stringent constraints on $M_{W'}$ are due to the limits on ν_R emission from supernovae.

References:

1. M. Bando, T. Kugo, and K. Yamawaki, Phys. Rept. **164**, 217 (1988).
2. H.C. Cheng *et al.*, Phys. Rev. D **64**, 065007 (2001).
3. See the Section on "Z'-boson searches" in this *Review*.
4. H.C. Cheng and I. Low, JHEP **0309**, 051 (2003).
5. B.A. Dobrescu and Z. Liu, JHEP **1510**, 118 (2015).
6. G. Altarelli, B. Mele and M. Ruiz-Altaba, Z. Phys. C **45**, 109 (1989) [Z. Phys. C **47**, 676 (1990)].
7. R.N. Mohapatra and J.C. Pati, Phys. Rev. D **11**, 566 (1975); G. Senjanovic and R.N. Mohapatra, Phys. Rev. D **12**, 1502 (1975).
8. K.S. Babu, X.G. He, and E. Ma, Phys. Rev. D **36**, 878 (1987).
9. H. Georgi, E.E. Jenkins, and E.H. Simmons, Nucl. Phys. B **331**, 541 (1990).
10. See, *e.g.*, X. Li and E. Ma, J. Phys. G **19**, 1265 (1993).
11. D.J. Muller and S. Nandi, Phys. Lett. B **383**, 345 (1996); E. Malkawi, T. Tait, and C.P. Yuan, Phys. Lett. B **385**, 304 (1996).
12. A. Donini *et al.*, Nucl. Phys. B **507**, 51 (1997).
13. R.S. Chivukula *et al.*, Phys. Rev. D **74**, 075011 (2006); H.J. He, T. Tait, and C.P. Yuan, Phys. Rev. D **62**, 011702 (2000).
14. F. Pisano and V. Pleitez, Phys. Rev. D **46**, 410 (1992); **51**, 3865 (1995).
15. Z. Sullivan, Phys. Rev. D **66**, 075011 (2002).
16. ATLAS Collab., arXiv:1706.04786.
17. T.G. Rizzo, JHEP **0705**, 037 (2007); E. Boos *et al.*, Phys. Lett. B **655**, 245 (2007).
18. CMS Collab., Phys. Lett. B **770**, 278 (2017).
19. CDF Collab., F. Abe *et al.*, Phys. Rev. Lett. **74**, 2900 (1995); D0 Collab., S. Abachi *et al.*, Phys. Lett. B **358**, 405 (1995).
20. CDF Collab., F. Abe *et al.*, Phys. Rev. Lett. **67**, 2609 (1991).
21. CMS Collab., Phys. Lett. B **755**, 196 (2016).
22. CMS Collab., PAS EXO-16-006, Mar. 2016.
23. CMS Collab., Eur. Phys. J. C **74**, 3149 (2014).
24. CMS Collab., PAS EXO-16-045, May 2017.
25. ATLAS Collab., JHEP **1507**, 162 (2015).
26. CMS Collab., JHEP **1703**, 077 (2017).
27. K.M. Black *et al.*, "Dynamical electroweak symmetry breaking" in this *Review*.
28. CMS Collab., Phys. Lett. B **769**, 520 (2017); Phys. Rev. D **91**, 052009 (2015).
29. ATLAS Collab., arXiv:1703.09127; Phys. Rev. D **91**, 052007 (2015); CONF-2016-030, June 2016.
30. CDF Collab., F. Abe *et al.*, Phys. Rev. D **55**, R5263 (1997); T. Aaltonen *et al.*, Phys. Rev. D **79**, 112002 (2009).
31. CMS Collab., Phys. Rev. Lett. **117**, 031802 (2016).
32. CMS Collab., arXiv:1705.10532; PAS-EXO-17-001, May 2017.
33. ATLAS Collab., Phys. Lett. B **755**, 285 (2016).
34. ATLAS Collab., arXiv:1708.04445; arXiv:1708.09638; CONF-2017-051, Jul. 2017.
35. CMS Collab., JHEP **1408**, 173 (2014); JHEP **1408**, 174 (2014); Phys. Lett. B **740**, 83 (2015).
36. CMS Collab., arXiv:1705.09171.
37. CMS Collab., arXiv:1708.05379; PAS EXO-15-002, Dec. 2015; PAS B2G-16-020, Aug. 2016; PAS B2G-16-022, Jan. 2017; PAS B2G-17-005, Jul. 2017.
38. D. Pappadopulo *et al.*, JHEP **1409**, 060 (2014).
39. H.J. He *et al.*, Phys. Rev. D **78**, 031701 (2008).
40. ATLAS Collab., Eur. Phys. J. C **75**, 263 (2015).
41. ATLAS Collab., arXiv:1707.06958.
42. CMS Collab., JHEP **1602**, 145 (2016).
43. CMS Collab., Phys. Lett. B **768**, 137 (2017).
44. CMS Collab., arXiv:1707.01303.
45. See the particle listings for W' in this *Review*.
46. Y. Zhang *et al.*, Phys. Rev. D **76**, 091301 (2007); S. Bertolini, A. Maiezza, and F. Nesti, Phys. Rev. D **89**, 095028 (2014).
47. P. Langacker and S.U. Sankar, Phys. Rev. D **40**, 1569 (1989).
48. TWIST Collab., J.F. Bueno *et al.*, Phys. Rev. D **84**, 032005 (2011).
49. See Fig. 5 of G. Prezeau, M. Ramsey-Musolf, and P. Vogel, Phys. Rev. D **68**, 034016 (2003).

108. Z'-Boson Searches

Revised September 2017 by B.A. Dobrescu (Fermilab) and S. Willocq (Univ. of Massachusetts).

The Z' boson is a massive, electrically-neutral and color-singlet hypothetical particle of spin 1. This particle is predicted in many extensions of the Standard Model (SM) and has been the object of extensive phenomenological studies [1].

108.1. Z' boson couplings to quarks and leptons.

The couplings of a Z' boson to the first-generation fermions are given by

$$Z'_\mu \left(g_u^L\, \overline{u}_L \gamma^\mu u_L + g_d^L\, \overline{d}_L \gamma^\mu d_L + g_u^R\, \overline{u}_R \gamma^\mu u_R + g_d^R\, \overline{d}_R \gamma^\mu d_R \right.$$
$$\left. + g_\nu^L\, \overline{\nu}_L \gamma^\mu \nu_L + g_e^L\, \overline{e}_L \gamma^\mu e_L + g_e^R\, \overline{e}_R \gamma^\mu e_R \right), \qquad (108.1)$$

where u, d, ν and e are the quark and lepton fields in the mass eigenstate basis, and the coefficients g_u^L, g_d^L, g_u^R, g_d^R, g_ν^L, g_e^L, g_e^R are real dimensionless parameters. If the Z' couplings to quarks and leptons are generation-independent, then these seven parameters describe the couplings of the Z' boson to all SM fermions. More generally, however, the Z' couplings to fermions are generation-dependent, in which case Eq. (108.1) may be written with generation indices $i, j = 1, 2, 3$ labeling the quark and lepton fields, and with the seven coefficients promoted to 3×3 Hermitian matrices (*e.g.*, $g^L_{eij}\, \overline{e}^i_L \gamma^\mu e^j_L$, where e^2_L is the left-handed muon, etc.).

These parameters describing the Z' boson interactions with quarks and leptons are subject to some theoretical constraints. Quantum field theories that include a heavy spin-1 particle are well behaved at high energies only if that particle is a gauge boson associated with a spontaneously broken gauge symmetry. Quantum effects preserve the gauge symmetry only if the couplings of the gauge boson to fermions satisfy anomaly cancellation conditions. Furthermore, the fermion charges under the new gauge symmetry are constrained by the requirement that the quarks and leptons get masses from gauge-invariant interactions with Higgs fields.

The relation between the couplings displayed in Eq. (108.1) and the gauge charges z^L_{fi} and z^R_{fi} of the fermions $f = u, d, \nu, e$ involves the unitary 3×3 matrices V^L_f and V^R_f that transform the gauge eigenstate fermions f^i_L and f^i_R, respectively, into the mass eigenstates. The Z' couplings are also modified if the new gauge boson in the gauge eigenstate basis ($\tilde{Z}'_\mu$) has a kinetic mixing $(-\chi/2) B^{\mu\nu} \tilde{Z}'_{\mu\nu}$ with the hypercharge gauge boson B^μ (χ is a dimensionless parameter), or a mass mixing $\delta M^2\, \tilde{Z}^\mu \tilde{Z}'_\mu$ with the linear combination ($\tilde{Z}_\mu$) of neutral bosons that couples as the SM Z boson [2]. Since both the kinetic and mass mixings shift the mass and couplings of the Z boson, electroweak measurements impose upper limits on χ and $\delta M^2/(M^2_{Z'} - M^2_Z)$ of the order of 10^{-3} [3]. Keeping only linear terms in these two small quantities, the couplings of the mass-eigenstate Z' boson are given by

$$g^L_{f\,ij} = g_z V^L_{fii'}\, z^L_{fi'} \left(V^L_f\right)^\dagger_{i'j} + \frac{e}{c_W} \left(\frac{s_W \chi M^2_{Z'} + \delta M^2}{2 s_W \left(M^2_{Z'} - M^2_Z\right)} \sigma^3_f - \epsilon\, Q_f \right),$$

$$g^R_{f\,ij} = g_z V^R_{fii'}\, z^R_{fi'} \left(V^R_f\right)^\dagger_{i'j} - \frac{e}{c_W}\, \epsilon\, Q_f, \qquad (108.2)$$

where g_z is the new gauge coupling, Q_f is the electric charge of f, e is the electromagnetic gauge coupling, s_W and c_W are the sine and cosine of the weak mixing angle, $\sigma^3_f = +1$ for $f = u, \nu$ and $\sigma^3_f = -1$ for $f = d, e$, and

$$\epsilon = \frac{\chi \left(M^2_{Z'} - c^2_W M^2_Z\right) + s_W \delta M^2}{M^2_{Z'} - M^2_Z}. \qquad (108.3)$$

The interaction of the Z' boson with a pair of W bosons has the form

$$\left[i \left(W^-_\mu Z'_\nu - W^-_\nu Z'_\mu \right) \partial^\mu W^{+\nu} + \text{H.c.} \right] + i \left(W^+_\mu W^-_\nu - W^+_\nu W^-_\mu \right) \partial^\mu Z'^\nu \qquad (108.4)$$

with a coefficient of order $M^2_W/M^2_{Z'}$ [4]. The Z' also couples to one SM Higgs boson and one Z boson, $Z'_\mu Z^\mu h^0$, with a coefficient of order M_Z.

108.2. $U(1)$ gauge groups.

A simple origin of a Z' boson is a new $U(1)'$ gauge symmetry. In that case, the matricial equalities $z^L_u = z^L_d$ and $z^L_\nu = z^L_e$ are required by the SM $SU(2)_W$ gauge symmetry. Given that the $U(1)'$ interaction is not asymptotically free, the theory may be well-behaved at high energies (*e.g.*, by embedding $U(1)'$ in a non-Abelian gauge group) only if the charges are commensurate numbers, *i.e.* any ratio of charges is a rational number. Satisfying the anomaly cancellation conditions (which include an equation cubic in charges) with rational numbers is highly nontrivial and in general new fermions charged under $U(1)'$ are necessary.

Table 108.1: Examples of generation-independent $U(1)'$ charges for quarks and leptons. The parameter x is an arbitrary rational number. Anomaly cancellation requires certain new fermions [5].

fermion	$U(1)_{B-xL}$	$U(1)_{10+x\bar{5}}$	$U(1)_{d-xu}$	$U(1)_{q+xu}$
(u_L, d_L)	$1/3$	$1/3$	0	$1/3$
u_R	$1/3$	$-1/3$	$-x/3$	$x/3$
d_R	$1/3$	$-x/3$	$1/3$	$(2-x)/3$
(ν_L, e_L)	$-x$	$x/3$	$(-1+x)/3$	-1
e_R	$-x$	$-1/3$	$x/3$	$-(2+x)/3$

Consider first generation-independent couplings (the V_f matrices then disappear from Eq. (108.2)) and neglect the $\tilde{Z} - \tilde{Z}'$ mixing, so that there are five commensurate couplings: g^R_u, g^R_d, g^R_e, g^L_q ($q = u$ or d), g^L_l ($l = \nu$ or e). Four sets of charges are displayed in Table 108.1, each of them spanned by a free parameter x [5]. The first set, labelled $B - xL$, has charges proportional to the baryon number minus x times the lepton number. These charges allow all SM Yukawa couplings to a Higgs doublet which is neutral under $U(1)_{B-xL}$, so that there is no tree-level $\tilde{Z} - \tilde{Z}'$ mixing. For $x = 1$ one recovers the $U(1)_{B-L}$ group, which is non-anomalous in the presence of one "right-handed neutrino" (a chiral fermion that is a singlet under the SM gauge group) per generation. For $x \neq 1$, it is necessary to include some fermions that are vectorlike (*i.e.* their mass terms are gauge invariant) with respect to the electroweak gauge group and chiral with respect to $U(1)_{B-xL}$. In the particular cases $x = 0$ or $x \gg 1$, the Z' is leptophobic or quark-phobic, respectively.

The second set, $U(1)_{10+x\bar{5}}$, has charges that commute with the representations of the $SU(5)$ grand unified group. Here x is related to the mixing angle between the two $U(1)$ bosons encountered in the $E_6 \to SU(5) \times U(1) \times U(1)$ symmetry breaking patterns of grand unified theories [1,6]. This set leads to $\tilde{Z} - \tilde{Z}'$ mass mixing at tree level, such that for a Z' mass close to the electroweak scale, the measurements at the Z-pole require some fine tuning between the charges and VEVs of the two Higgs doublets. Vectorlike fermions charged under the electroweak gauge group and also carrying color are required (except for $x = -3$) to make this set anomaly free. The particular cases $x = -3, 1, -1/2$ are usually labelled $U(1)_\chi$, $U(1)_\psi$, and $U(1)_\eta$, respectively. Under the third set, $U(1)_{d-xu}$, the weak-doublet quarks are neutral, and the ratio of u_R and d_R charges is $-x$. For $x = 1$ this is the "right-handed" group $U(1)_R$. For $x = 0$, the charges are those of the E_6-inspired $U(1)_I$ group, which requires new quarks and leptons. Other generation-independent sets of $U(1)'$ charges are given in [7].

In the absence of new fermions charged under the SM group, the most general generation-independent charge assignment is $U(1)_{q+xu}$, which is a linear combination of hypercharge and $B - L$. Many other anomaly-free solutions exist if generation-dependent charges are allowed. An example is $B - xL_e - yL_\mu + (y-3)L_\tau$, with x, y free parameters. This allows all fermion masses to be generated by Yukawa couplings to a single Higgs doublet, without inducing tree-level flavor-changing neutral current (FCNC) processes. There are also lepton-flavor dependent charges that allow neutrino masses to arise only from operators of high dimensionality [8].

If the $SU(2)_W$-doublet quarks have generation-dependent $U(1)'$ charges, then the mass eigenstate quarks have flavor off-diagonal couplings to the Z' boson (see Eq. (108.1), and note that $V_u^L \left(V_d^L\right)^\dagger$ is the CKM matrix). These are severely constrained by measurements of FCNC processes, which in this case are mediated at tree-level by Z' boson exchange [9]. The constraints are relaxed if the first and second generation charges are the same, although they are increasingly tightened by the measurements of B meson properties [10]. If only the $SU(2)_W$-singlet quarks have generation-dependent $U(1)'$ charges, there is more freedom in adjusting the flavor off-diagonal couplings because the $V_{u,d}^R$ matrices are not observable in the SM.

The anomaly cancellation conditions for $U(1)'$ could be relaxed only if there is an axion with certain dimension-5 couplings to the gauge bosons. However, such a scenario violates unitarity unless the quantum field theory description breaks down at a scale near $M_{Z'}$ [11].

108.3. Other models.

Z' bosons may also arise from larger gauge groups. These may extend the electroweak group, as in $SU(2) \times SU(2) \times U(1)$, or may embed the electroweak group, as in $SU(3)_W \times U(1)$ [12]. If the larger group is spontaneously broken down to $SU(2)_W \times U(1)_Y \times U(1)'$ at a scale $v_* \gg M_{Z'}/g_z$, then the above discussion applies up to corrections of order $M_{Z'}^2/(g_z v_*)^2$. For $v_* \sim M_{Z'}/g_z$, additional gauge bosons have masses comparable to $M_{Z'}$, including at least a W' boson [12]. If the larger gauge group breaks together with the electroweak symmetry directly to the electromagnetic $U(1)_{\rm em}$, then the left-handed fermion charges are no longer correlated ($z_u^L \neq z_d^L$, $z_\nu^L \neq z_e^L$) and a $Z'W^+W^-$ coupling is induced.

If the electroweak gauge bosons propagate in extra dimensions, then their Kaluza-Klein (KK) excitations include a series of Z' boson pairs. Each of these pairs can be associated with a different $SU(2) \times U(1)$ gauge group in four dimensions. The properties of the KK particles depend strongly on the extra-dimensional theory [13]. For example, in universal extra dimensions there is a parity that forces all couplings of Eq. (108.1) to vanish in the case of the lightest KK bosons, while allowing couplings to pairs of fermions involving a SM and a heavy vectorlike fermion. There are also 4-dimensional gauge theories (*e.g.* little Higgs with T parity) with Z' bosons exhibiting similar properties. By contrast, in a warped extra dimension, the couplings of Eq. (108.1) may be sizable even when SM fields propagate along the extra dimension.

Z' bosons may also be composite particles. For example, in confining gauge theories [14], the ρ-like bound state is a spin-1 boson that may be interpreted as arising from a spontaneously broken gauge symmetry [15].

108.4. Resonances versus cascade decays.

In the presence of the couplings shown in Eq. (108.1), the Z' boson may be produced in the s-channel at colliders, and would decay to pairs of fermions. The decay width into a pair of electrons is given by

$$\Gamma\left(Z' \to e^+e^-\right) \simeq \left[\left(g_e^L\right)^2 + \left(g_e^R\right)^2\right] \frac{M_{Z'}}{24\pi}, \qquad (108.5)$$

where small corrections from electroweak loops are not included. The decay width into $q\bar{q}$ is similar, except for an additional color factor of 3, QCD radiative corrections, and fermion mass corrections. Thus, one may compute the Z' branching fractions in terms of the couplings of Eq. (108.1). However, other decay channels, such as WW or a pair of new particles, could have large widths and need to be added to the total decay width.

As mentioned above, there are theories in which the Z' couplings are controlled by a discrete symmetry that forbids decays into a pair of SM particles. Typically, such theories involve several new particles, which may be produced only in pairs and undergo cascade decays through Z' bosons, leading to signals involving some missing (transverse) momentum. Given that the cascade decays depend on the properties of new particles other than the Z' boson, this case is not discussed further here.

108.5. LEP-II limits.

The Z' contribution to the cross sections for $e^+e^- \to f\bar{f}$ proceeds through an s-channel Z' exchange (when $f = e$, there are also t- and u-channel exchanges). For $M_{Z'} < \sqrt{s}$, the Z' appears as an $f\bar{f}$ resonance in the radiative return process where photon emission tunes the effective center-of-mass energy to $M_{Z'}$. The agreement between the LEP-II measurements and the SM predictions implies that either the Z' couplings are smaller than or of order 10^{-2}, or else $M_{Z'}$ is above 209 GeV, the maximum energy of LEP-II. In the latter case, the Z' exchange may be approximated up to corrections of order $s/M_{Z'}^2$ by the contact interactions

$$\frac{g_z^2}{M_{Z'}^2 - s}\left[\bar{e}\gamma_\mu\left(z_e^L P_L + z_e^R P_R\right) e\right]\left[\bar{f}\gamma^\mu\left(z_f^L P_L + z_f^R P_R\right) f\right], \qquad (108.6)$$

where $P_{L,R}$ are chirality projection operators, and the relation between Z' couplings and charges (see Eq. (108.2) in the limit where the mass and kinetic mixings are neglected) is used, assuming generation-independent charges. The four LEP collaborations have set limits on the coefficients of such operators for all possible chiral structures and for various combinations of fermions [16]. Thus, one may derive bounds on $(M_{Z'}/g_z)|z_e^L z_f^L|^{-1/2}$ and the analogous combinations of LR, RL and RR charges, which are typically on the order of a few TeV. LEP-II limits were derived [5] on the four sets of charges shown in Table 108.1.

Somewhat stronger bounds can be set on $M_{Z'}/g_z$ for specific sets of Z' couplings if the effects of several operators from Eq. (108.6) are combined. Dedicated analyses by the LEP collaborations have set limits on Z' bosons for particular values of the gauge coupling (see section 3.5 of [16]). For example, $M_{Z_{\rm SSM}} > 1.76$ TeV for a "sequential" Z' of same couplings as the SM Z boson, while $M_{Z_\chi} > 0.785$ TeV for the Z' associated with $U(1)_\chi$ assuming a unification condition for the gauge coupling.

108.6. Searches at hadron colliders.

Z' bosons with couplings to quarks (see Eq. (108.1)) may be produced at hadron colliders in the s-channel and would show up as resonances in the invariant mass distribution of the decay products. The cross section for producing a Z' boson at the LHC, which then decays to some $f\bar{f}$ final state, takes the form

$$\sigma\left(pp \to Z'X \to f\bar{f}X\right) \simeq \frac{\pi}{48\,s}\sum_q c_q^f\, w_q\Big(s, M_{Z'}^2\Big) \qquad (108.7)$$

for flavor-diagonal couplings to quarks. Here, we have neglected the interference with the SM contribution to $f\bar{f}$ production, which is a good approximation for a narrow Z' resonance (deviations from the narrow width approximation are discussed in [17]). The coefficients

$$c_q^f = \left[\left(g_q^L\right)^2 + \left(g_q^R\right)^2\right] B(Z' \to f\bar{f}) \qquad (108.8)$$

contain all the dependence on the Z' couplings, while the functions w_q include all the information about parton distributions and QCD corrections [5,7]. This factorization holds exactly to NLO and the deviations from it induced at NNLO are very small. Note that the w_u and w_d functions are substantially larger than the w_q functions for the other quarks. Eq. (108.7) also applies to the Tevatron, except for changing the pp initial state to $p\bar{p}$, which implies that the $w_q(s, M_{Z'}^2)$ functions are replaced by some other functions $\bar{w}_q((1.96\,\text{TeV})^2, M_{Z'}^2)$.

It is common to present results of Z' searches as limits on the cross section versus $M_{Z'}$ (see for example Fig. 108.1). An alternative is to plot exclusion curves for fixed $M_{Z'}$ values in the $c_u^f - c_d^f$ planes, allowing a simple derivation of the mass limit within any Z' model. The CMS upper limits in the $c_u^\ell - c_d^\ell$ plane ($\ell = e$ or μ) for different $M_{Z'}$ are shown in Fig. 108.2 (for Tevatron limits, see [7,18]).

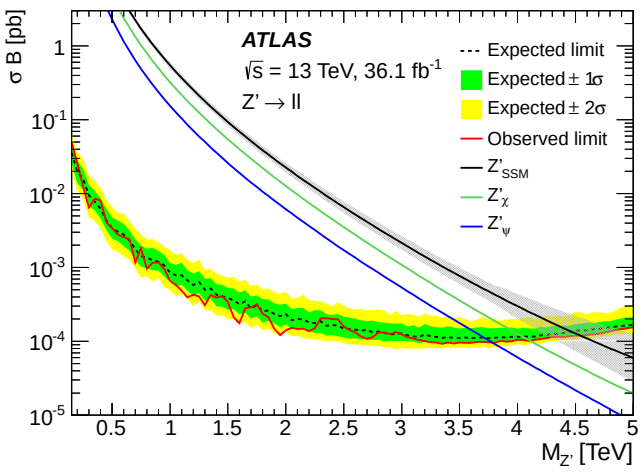

Figure 108.1: Upper limit on $\sigma(pp \to Z'X \to \ell^+\ell^-X)$ with $\ell = e$ or μ as a function of $M_{Z'}$ [24], assuming equal couplings for electrons and muons. The lines labelled by Z'_ψ and Z'_χ are theoretical predictions for the $U(1)_{10+x\bar{5}}$ models in Table 108.1 with $x = -3$ and $x = +1$, respectively, for g_z fixed by an E_6 unification condition. The $Z'_{\rm SSM}$ line corresponds to Z' couplings equal to those of the Z boson.

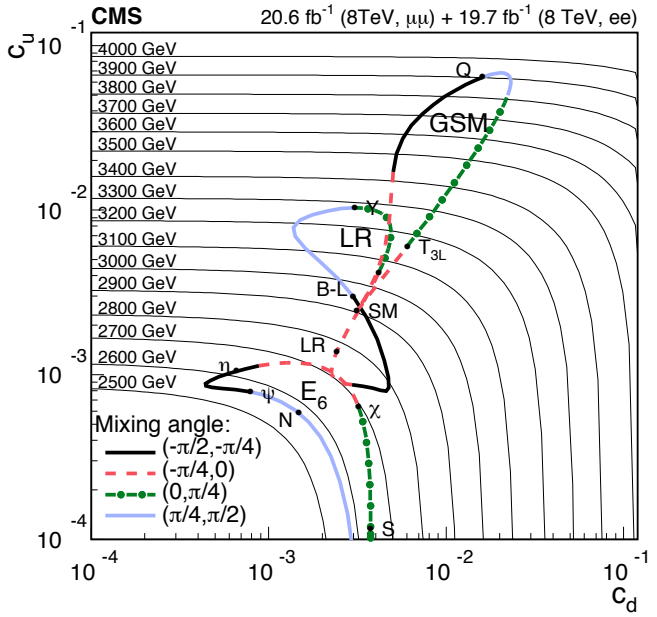

Figure 108.2: Upper limits in the c_u^ℓ–c_d^ℓ plane ($\ell = e$ or μ), set by CMS [23], are shown as thin lines for certain $M_{Z'}$ values. For specific sets of charges (labelled by E_6, GSM and LR, and described in [7]) parametrized by a mixing angle, the lower mass limit is given by the intersection of thick and thin lines. The black dots with smaller labels represent particular models.

The discovery of a dilepton resonance at the LHC would determine the Z' mass and width. A measurement of the total cross section would define a band in the $c_u^\ell - c_d^\ell$ plane. Angular distributions can be used to measure several combinations of Z' parameters (angular distributions were used in [19] to improve the Tevatron sensitivity). Even though the original quark direction in a pp collider is unknown, the leptonic forward-backward asymmetry $A_{\rm FB}^\ell$ can be extracted from the kinematics of the dilepton system, and is sensitive to parity-violating couplings. A fit to the Z' rapidity distribution can distinguish between the couplings to up and down quarks. These measurements, combined with off-peak observables, have the potential to differentiate among various Z' models [20]. In some cases, $A_{\rm FB}^\ell$ may provide discovery sensitivity that is competitive with the mass distribution [21]. With 100 fb^{-1} of data at $\sqrt{s} = 14$ TeV, the spin of the Z' boson may be determined for $M_{Z'} \leq 3$ TeV [22].

Searches for Z' decays to e^+e^- and $\mu^+\mu^-$ by the ATLAS and CMS collaborations [24,25] have set 95% C.L. upper cross-section limits as low as 0.1 fb (see Fig. 108.1), with the lower mass limits in specific models as high as 4.5 TeV. In the case of final states with taus, the lower mass limits obtained at 13 TeV are as high as ~ 2.4 TeV for the $\tau^+\tau^-$ [26] decay. Limits in the flavor-violating leptonic final states have also been reported by ATLAS and CMS [26,27], for resonances in the $e^\pm\mu^\mp$, $e^\pm\tau^\mp$ and $\mu^\pm\tau^\mp$ channels.

Final states with higher background, $t\bar{t}$, $b\bar{b}$ and jj, are also important as they probe various combinations of Z' couplings to quarks, see [28] for further discussion. Besides the improved sensitivity at masses of several TeV, the LHC searches in the dijet channel have been also extended to masses as low as 50 GeV, through the use of new techniques involving boosted topologies and initial state radiation [29].

Z' decays to Zh^0 with $Z \to \ell^+\ell^-$, $\nu\bar{\nu}$ or $q\bar{q}$ and $h^0 \to b\bar{b}$ have been studied by ATLAS [30] and CMS [31,35] using 13 TeV data. The most stringent constraint is set in the fully hadronic channel, with a lower mass limit of 2.35 TeV in the context of the Heavy Vector Triplet model weakly-coupled scenario A [32].

The $pp \to Z'X \to W^+W^-X$ process has also been searched for at the LHC. The channel where the Z' boson is produced through its couplings to quarks, and the W bosons decay hadronically, has been explored using boosted techniques to analyze the 13 TeV data [33] . The Z' boson may also be produced through its couplings to W bosons [34], which has been explored by ATLAS with the use of forward jets consistent with a vector boson fusion event topology.

At the Tevatron, the CDF and DØ collaborations have searched for Z' bosons in the e^+e^- [36], $\mu^+\mu^-$ [37], $e^\pm\mu^\mp$ [38], $\tau^+\tau^-$ [39], $t\bar{t}$ [40], jj [41] and W^+W^- [42] final states. Although these limits have been mostly superseded by the LHC results, the Tevatron limits on certain Z' couplings (especially those arising from jj resonance searches [43]) remain competitive for some mass ranges below ~ 0.4 TeV.

108.7. Low-energy constraints.

Z' boson properties are also constrained by a variety of low-energy experiments [44]. Polarized electron-nucleon scattering and atomic parity violation are sensitive to electron-quark contact interactions, which get contributions from Z' exchange that can be expressed in terms of the couplings introduced in Eq. (108.1) and M'_Z. Further corrections to the electron-quark contact interactions are induced in the presence of $\tilde{Z} - \tilde{Z}'$ mixing because of the shifts in the Z couplings to quarks and leptons [2]. Deep-inelastic neutrino-nucleon scattering is similarly affected by Z' bosons. Other low-energy observables are discussed in [3]. For Z' bosons much lighter than the Z boson, many additional experimental constraints exist [45].

In some models, the lower limits on $M_{Z'}$ set by low-energy data are above 1 TeV. For example, $M_{Z_\chi} > 1.1$ TeV and $M_{Z_\eta} > 0.43$ TeV assuming that the Higgs sectors consist of electroweak doublets and singlets only [3], while the gauge coupling is fixed by an $SO(10)$ unification condition for $U(1)_\chi$ and $U(1)_\eta$. For more general models, see [1,5,46]. The mass bounds from direct searches at the LHC [24,25] exceed the electroweak constraints by a factor of three or more for the models mentioned here. While the electroweak constraints can be slightly improved by fixing the Higgs mass to the value measured at the LHC, and the collider bounds are moderately weakened if there are open exotic decay channels [47], this conclusion will not change.

Although the LHC data are most constraining for many Z' models, one should be careful in assessing the relative reach of various experiments given the freedom in Z' couplings. For example, a Z' coupled to $B - yL_\mu + (y-3)L_\tau$ has implications for the muon $g-2$, neutrino oscillations or τ decays, and would be hard to see in processes involving first-generation fermions. Moreover, the combination of LHC searches and low-energy measurements could allow a precise determination of the Z' parameters [48].

References:

1. For reviews, see P. Langacker, Rev. Mod. Phys. **81**, 1199 (2009); A. Leike, Phys. Rept. **317**, 143 (1999); J. Hewett and T. Rizzo, Phys. Rept. **183**, 193 (1989).
2. K.S. Babu *et al.*, Phys. Rev. **D57**, 6788 (1998); B. Holdom, Phys. Lett. **B259**, 329 (1991).
3. J. Erler *et al.*, JHEP **0908**, 017 (2009).
4. B.A. Dobrescu and P.J. Fox, arXiv:1511.02148.
5. M.S. Carena *et al.*, Phys. Rev. D**70**, 093009 (2004).
6. See, *e.g.*, F. Del Aguila *et al.*, Phys. Rev. D**52**, 37 (1995).
7. E. Accomando *et al.*, Phys. Rev. D**83**, 075012 (2011).
8. M.-C. Chen *et al.*, Phys. Rev. D**75**, 055009 (2007).
9. P. Langacker and M. Plumacher, Phys. Rev. D**62**, 013006 (2000); R.S. Chivukula and E.H. Simmons, Phys. Rev. D**66**, 015006 (2002).
10. A.J. Buras *et al.*, JHEP **1302**, 116 (2013).
11. L.E. Ibanez and G.G. Ross, Phys. Lett. B**332**, 100 (1994).
12. See the Section on "W' searches" in this *Review*.
13. J. Parsons and A. Pomarol, "Extra dimensions" in this *Review*.
14. K.M. Black *et al.*, "Dynamical electroweak symmetry breaking" in this *Review*.
15. M. Bando *et al.*, Phys. Rept. **164**, 217 (1988).
16. ALEPH, DELPHI, L3, OPAL and LEP Electroweak Collab., S. Schael *et al.*, Phys. Rept. **532**, 119 (2013).
17. E. Accomando *et al.*, JHEP **1310**, 153 (2013).
18. CDF Collab., A. Abulencia *et al.*, Phys. Rev. Lett. **95**, 252001 (2005).
19. CDF Collab., A. Abulencia *et al.*, Phys. Rev. Lett. **96**, 211801 (2006).
20. F. Petriello and S. Quackenbush, Phys. Rev. D**77**, 115004 (2008).
21. E. Accomando *et al.*, JHEP **1601**, 127 (2016).
22. P. Osland *et al.*, Phys. Rev. D**79**, 115021 (2009).
23. CMS Collab., JHEP **1504**, 025 (2015).
24. ATLAS Collab., arXiv:1707.02424.
25. CMS Collab., PAS EXO-16-031, Aug. 2016.
26. ATLAS Collab., CONF-2017-050, Jul. 2017; CMS Collab., JHEP **1702**, 048 (2017).
27. ATLAS Collab., Eur. Phys. J. C **76**, 541 (2016); CMS Collab., PAS EXO-16-001, Apr. 2016.
28. See the Section on "Dynamical Electroweak Symmetry Breaking" in this *Review*.
29. CMS Collab., arXiv:1705.10532; PAS-EXO-17-001, May 2017.
30. ATLAS Collab., arXiv:1707.06958.
31. CMS Collab., Phys. Lett. B **768**, 137 (2017).
32. D. Pappadopulo *et al*, JHEP **1409**, 060 (2014).
33. ATLAS Collab., arXiv:1708.04445; arXiv:1710.07235; CONF-2016-082, Aug. 2016.
34. H.J. He *et al.*, Phys. Rev. D**78**, 031701 (2008).
35. CMS Collab., arXiv:1705.09171.
36. DØ Collab., V.M. Abazov *et al.*, Phys. Lett. B**695**, 88 (2011); CDF Collab., T. Aaltonen *et al.*, Phys. Rev. Lett. **102**, 031801 (2009).
37. CDF Collab., T. Aaltonen *et al.*, Phys. Rev. Lett. **106**, 121801 (2011).
38. CDF Collab., A. Abulencia *et al.*, Phys. Rev. Lett. **96**, 211802 (2006); DØ Collab., V.M. Abazov *et al.*, Phys. Rev. Lett. **105**, 191802 (2010).
39. CDF Collab., D. Acosta *et al.*, Phys. Rev. Lett. **95**, 131801 (2005).
40. CDF Collab., T. Aaltonen *et al.*, Phys. Rev. D**84**, 072004 (2011); DØ Collab., V.M. Abazov *et al.*, Phys. Rev. D**85**, 051101 (2012).
41. CDF Collab., T. Aaltonen *et al.*, Phys. Rev. D**79**, 112002 (2009).
42. CDF Collab., T. Aaltonen *et al.*, Phys. Rev. Lett. **104**, 241801 (2010).
43. B.A. Dobrescu and F. Yu, Phys. Rev. D**88**, 035021 (2013).
44. See, *e.g.*, V.D. Barger *et al.*, Phys. Rev. D**57**, 391 (1998); J. Erler and M.J. Ramsey-Musolf, Prog. Part. Nucl. Phys. **54**, 351 (2005).
45. R. Harnik, J. Kopp, P.A.N. Machado, JCAP **1207**, 026 (2012).
46. E. Rojas and J. Erler, JHEP **1510**, 063 (2015).
47. J. Kang and P. Langacker, Phys. Rev. **D71**, 035014 (2005); C.-F. Chang *et al.*, JHEP **1109**, 058 (2011).
48. Y. Li *et al.*, Phys. Rev. D**80**, 055018 (2009).

109. Supersymmetry, Part I (Theory)

Revised September 2017 by Howard E. Haber (UC Santa Cruz).

109.1. Introduction

Supersymmetry (SUSY) is a generalization of the space-time symmetries of quantum field theory that transforms fermions into bosons and vice versa [1]. The existence of such a non-trivial extension of the Poincaré symmetry of ordinary quantum field theory was initially surprising, and its form is highly constrained by theoretical principles [2]. Supersymmetry also provides a framework for the unification of particle physics and gravity [3–6] at the Planck energy scale, $M_{\rm P} \sim 10^{19}$ GeV, where the gravitational interactions become comparable in magnitude to the gauge interactions. Moreover, supersymmetry can provide an explanation of the large hierarchy between the energy scale that characterizes electroweak symmetry breaking, $M_{\rm EW} \sim 100$ GeV, and the Planck scale [7–10]. The stability of this large gauge hierarchy with respect to radiative quantum corrections is not possible to maintain in the Standard Model without an unnatural fine-tuning of the parameters of the fundamental theory at the Planck scale. In contrast, in a supersymmetric extension of the Standard Model, it is possible to maintain the gauge hierarchy while providing a natural framework for elementary scalar fields.

If supersymmetry were an exact symmetry of nature, then particles and their superpartners, which differ in spin by half a unit, would be degenerate in mass. Since superpartners have not (yet) been observed, supersymmetry must be a broken symmetry. Nevertheless, the stability of the gauge hierarchy can still be maintained if the supersymmetry breaking is soft [11,12], and the corresponding supersymmetry-breaking mass parameters are no larger than a few TeV. Whether this is still plausible in light of recent supersymmetry searches at the LHC [13] will be discussed in Section 109.7.

In particular, soft-supersymmetry-breaking terms of the Lagrangian involve combinations of fields with total mass dimension of three or less, with some restrictions on the dimension-three terms as elucidated in Ref. 11. The impact of the soft terms becomes negligible at energy scales much larger than the size of the supersymmetry-breaking masses. Thus, a theory of weak-scale supersymmetry, where the effective scale of supersymmetry breaking is tied to the scale of electroweak symmetry breaking, provides a natural framework for the origin and the stability of the gauge hierarchy [7–10].

At present, there is no unambiguous experimental evidence for the breakdown of the Standard Model at or below the TeV scale. The expectations for new TeV-scale physics beyond the Standard Model are based primarily on three theoretical arguments. First, in a theory with an elementary scalar field of mass m and interaction strength λ (e.g., a quartic scalar self-coupling, the square of a gauge coupling or the square of a Yukawa coupling), the stability with respect to quantum corrections requires the existence of an energy cutoff roughly of order $(16\pi^2/\lambda)^{1/2}m$, beyond which new physics must enter [14]. A significantly larger energy cutoff would require an unnatural fine-tuning of parameters that govern the low-energy theory. Applying this argument to the Standard Model leads to an expectation of new physics at the TeV scale [10].

Second, the unification of the three Standard Model gauge couplings at a very high energy close to the Planck scale is possible if new physics beyond the Standard Model (which modifies the running of the gauge couplings above the electroweak scale) is present. The minimal supersymmetric extension of the Standard Model (MSSM), where superpartner masses lie below a few TeV, provides an example of successful gauge coupling unification [15].

Third, the existence of dark matter, which makes up approximately one quarter of the energy density of the universe, cannot be explained within the Standard Model of particle physics [16]. Remarkably, a stable weakly-interacting massive particle (WIMP) whose mass and interaction rate are governed by new physics associated with the TeV-scale can be consistent with the observed density of dark matter (this is the so-called WIMP miracle, which is reviewed in Ref. 17). The lightest supersymmetric particle, if stable, is a promising (although not the unique) candidate for the dark matter [18–22]. Further aspects of dark matter can be found in Ref. 23.

109.2. Structure of the MSSM

The minimal supersymmetric extension of the Standard Model consists of the fields of the two-Higgs-doublet extension of the Standard Model and the corresponding superpartners [24,25]. A particle and its superpartner together form a supermultiplet. The corresponding field content of the supermultiplets of the MSSM and their gauge quantum numbers are shown in Table 1. The electric charge $Q = T_3 + \frac{1}{2}Y$ is determined in terms of the third component of the weak isospin (T_3) and the U(1) weak hypercharge (Y).

Table 109.1: The fields of the MSSM and their SU(3)×SU(2)×U(1) quantum numbers are listed. For simplicity, only one generation of quarks and leptons is exhibited. For each lepton, quark, and Higgs super-multiplet, there is a corresponding anti-particle multiplet of charge-conjugated fermions and their associated scalar partners [26].

Field Content of the MSSM						
Super-multiplets	Super-field	Bosonic fields	Fermionic partners	SU(3)	SU(2)	U(1)
gluon/gluino	$\widehat{V}_8$	g	$\widetilde{g}$	8	1	0
gauge boson/ gaugino	$\widehat{V}$	$W^\pm$, W^0	$\widetilde{W}^\pm$, $\widetilde{W}^0$	1	3	0
	$\widehat{V}'$	B	$\widetilde{B}$	1	1	0
slepton/ lepton	$\widehat{L}$	$(\widetilde{\nu}_L, \widetilde{e}^-_L)$	$(\nu, e^-)_L$	1	2	-1
	$\widehat{E}^c$	$\tilde{e}^+_R$	e^c_L	1	1	2
squark/ quark	$\widehat{Q}$	$(\widetilde{u}_L, \widetilde{d}_L)$	$(u, d)_L$	3	2	1/3
	$\widehat{U}^c$	$\widetilde{u}^*_R$	u^c_L	$\bar{3}$	1	$-4/3$
	$\widehat{D}^c$	$\widetilde{d}^*_R$	d^c_L	$\bar{3}$	1	2/3
Higgs/ higgsino	$\widehat{H}_d$	(H^0_d, H^-_d)	$(\widetilde{H}^0_d, \widetilde{H}^-_d)$	1	2	-1
	$\widehat{H}_u$	(H^+_u, H^0_u)	$(\widetilde{H}^+_u, \widetilde{H}^0_u)$	1	2	1

The gauge supermultiplets consist of the gluons and their gluino fermionic superpartners and the SU(2)×U(1) gauge bosons and

their gaugino fermionic superpartners. The matter supermultiplets consist of three generations of left-handed quarks and leptons and their scalar superpartners (squarks and sleptons, collectively referred to as sfermions), and the corresponding antiparticles. The Higgs supermultiplets consist of two complex Higgs doublets, their higgsino fermionic superpartners, and the corresponding antiparticles. The enlarged Higgs sector of the MSSM constitutes the minimal structure needed to guarantee the cancellation of gauge anomalies [27] generated by the higgsino superpartners that can appear as internal lines in triangle diagrams with three external electroweak gauge bosons. Moreover, without a second Higgs doublet, one cannot generate mass for both "up"-type and "down"-type quarks (and charged leptons) in a way consistent with the underlying supersymmetry [28–30].

In the most elegant treatment of supersymmetry, spacetime is extended to superspace which consists of the spacetime coordinates and new anticommuting fermionic coordinates θ and $\theta^\dagger$ [31]. Each supermultiplet is represented by a superfield that is a function of the superspace coordinates. The fields of a given supermultiplet (which are functions of the spacetime coordinates) are components of the corresponding superfield.

Vector superfields contain the gauge boson fields and their gaugino partners. Chiral superfields contain the spin-0 and spin-1/2 fields of the matter or Higgs supermultiplets. A general supersymmetric Lagrangian is determined by three functions of the chiral superfields [4]: the superpotential, the Kähler potential, and the gauge kinetic function (which can be appropriately generalized to accommodate higher derivative terms [32]). Minimal forms for the Kähler potential and gauge kinetic function, which generate canonical kinetic energy terms for all the fields, are required for renormalizable globally supersymmetric theories. A renormalizable superpotential, which is at most cubic in the chiral superfields, yields supersymmetric Yukawa couplings and mass terms. A combination of gauge invariance and supersymmetry produces couplings of gaugino fields to matter (or Higgs) fields and their corresponding superpartners. The (renormalizable) MSSM Lagrangian is then constructed by including all possible supersymmetric interaction terms (of dimension four or less) that satisfy SU(3)×SU(2)×U(1) gauge invariance and B–L conservation (where B = baryon number and L = lepton number). Finally, the most general soft-supersymmetry-breaking terms consistent with these symmetries are added [11,12,33].

Although the MSSM is the focus of much of this review, there is some motivation for considering non-minimal supersymmetric extensions of the Standard Model. For example, extra structure is needed to generate non-zero neutrino masses as discussed in Section 109.8. In addition, in order to address some theoretical issues and tensions associated with the MSSM, it has been fruitful to introduce one additional singlet Higgs superfield. The resulting next-to-minimal supersymmetric extension of the Standard Model (NMSSM) [34] is considered further in Section 109.4–Section 109.7 and Section 109.9. Finally, one is always free to add additional fields to the Standard Model along with the corresponding superpartners. However, only certain choices for the new fields (*e.g.*, the addition of complete SU(5) multiplets) will preserve the successful gauge coupling unification. Some examples will be briefly mentioned in Section 109.9.

109.2.1. *R-parity and the lightest supersymmetric particle* :

The (renormalizable) Standard Model Lagrangian possesses an accidental global B–L symmetry due to the fact that B and L-violating operators composed of Standard Model fields must have dimension $d = 5$ or larger [35]. Consequently, B and L-violating effects are suppressed by $(M_{\rm EW}/M)^{d-4}$, where M is the characteristic mass scale of the physics that generates the corresponding higher dimensional operators. Indeed, values of M of order the grand unification scale or larger yield the observed (approximate) stability of the proton and suppression of neutrino masses. Unfortunately, these results are not guaranteed in a generic supersymmetric extension of the Standard Model. For example, it is possible to construct gauge invariant supersymmetric dimension-four B and L-violating operators made up of fields of Standard Model particles and their superpartners. Such operators, if present in the theory, would yield a proton decay rate many orders of magnitude larger than the current experimental bound. It is for this reason that B–L conservation is *imposed* on the supersymmetric Lagrangian when defining the MSSM, which is sufficient for eliminating all B and L-violating operators of dimension $d \leq 4$.

As a consequence of the B–L symmetry, the MSSM possesses a multiplicative R-parity invariance, where $R = (-1)^{3(B-L)+2S}$ for a particle of spin S [36]. This implies that all the particles of the Standard Model have even R-parity, whereas the corresponding superpartners have odd R-parity. The conservation of R-parity in scattering and decay processes has a critical impact on supersymmetric phenomenology. For example, any initial state in a scattering experiment will involve ordinary (R-even) particles. Consequently, it follows that supersymmetric particles must be produced in pairs. In general, these particles are highly unstable and decay into lighter states. Moreover, R-parity invariance also implies that the lightest supersymmetric particle (LSP) is absolutely stable, and must eventually be produced at the end of a decay chain initiated by the decay of a heavy unstable supersymmetric particle.

In order to be consistent with cosmological constraints, a stable LSP is almost certainly electrically and color neutral [20]. Consequently, the LSP in an R-parity-conserving theory is weakly interacting with ordinary matter, *i.e.*, it behaves like a stable heavy neutrino and will escape collider detectors without being directly observed. Thus, the canonical signature for conventional R-parity-conserving supersymmetric theories is missing (transverse) energy, due to the escape of the LSP. Moreover, as noted in Section 109.1 and reviewed in Refs. 21 and 22, the stability of the LSP in R-parity-conserving supersymmetry makes it a promising candidate for dark matter.

The possibility of relaxing the R-parity invariance of the MSSM (which would generate new B and/or L-violating interactions) will be addressed in Section 109.8.2

109.2.2. *The goldstino and gravitino* :

In the MSSM, supersymmetry breaking is accomplished by including the most general renormalizable soft-supersymmetry-breaking terms consistent with the SU(3)×SU(2)×U(1) gauge symmetry and R-parity invariance. These terms parameterize our ignorance of the fundamental mechanism of supersymmetry breaking. If supersymmetry breaking occurs spontaneously, then a massless Goldstone fermion called the goldstino ($\widetilde{G}_{1/2}$) must exist. The goldstino would then be the LSP, and could play an important role in supersymmetric phenomenology [37].

However, the goldstino degrees of freedom are physical only in models of spontaneously-broken global supersymmetry. If supersymmetry is a local symmetry, then the theory must incorporate gravity; the resulting theory is called supergravity [5,38]. In models of spontaneously-broken supergravity, the goldstino is "absorbed" by the gravitino ($\widetilde{G}$) [often called $\widetilde{g}_{3/2}$ in the older literature], the spin-3/2 superpartner of the graviton, via the super-Higgs mechanism [39]. Consequently, the goldstino is removed from the physical spectrum and the gravitino acquires a mass (denoted by $m_{3/2}$). If $m_{3/2}$ is smaller than the mass of the lightest superpartner of the Standard Model particles, then the gravitino is the LSP.

In processes with center-of-mass energy $E \gg m_{3/2}$, the goldstino–gravitino equivalence theorem [40] states that the interactions of the helicity $\pm\frac{1}{2}$ gravitino (whose properties approximate those of the goldstino) dominate those of the helicity $\pm\frac{3}{2}$ gravitino. The interactions of gravitinos with other light fields can be described by a low-energy effective Lagrangian that is determined by fundamental principles [41].

Theories in which supersymmetry breaking is independently generated by a multiplicity of sources will yield multiple goldstino states, collectively called goldstini [42]. One linear combination of the goldstini is identified with the exactly massless goldstino $\widetilde{G}_{1/2}$ of global supersymmetry, which is absorbed by the gravitino in local supersymmetry as described above. The linear combinations of goldstini orthogonal to $\widetilde{G}_{1/2}$, sometimes called pseudo-goldstinos in the literature, acquire radiatively generated masses. Theoretical and phenomenological implications of the pseudo-goldstinos are discussed further in Ref. 42.

109.2.3. ***Hidden sectors and the structure of supersymmetry breaking*** :

It is very difficult (perhaps impossible) to construct a realistic model of spontaneously-broken weak-scale supersymmetry where the supersymmetry breaking arises solely as a consequence of the interactions of the particles of the MSSM. An alternative scheme posits a theory with at least two distinct sectors: a visible sector consisting of the particles of the MSSM [33] and a so-called hidden sector where supersymmetry breaking is generated. It is often (but not always) assumed that particles of the hidden sector are neutral with respect to the Standard Model gauge group. The effects of the hidden sector supersymmetry breaking are then transmitted to the MSSM by some mechanism (often involving the mediation by particles that comprise an additional messenger sector). Two theoretical scenarios that exhibit this structure are gravity-mediated and gauge-mediated supersymmetry breaking.

Supergravity models provide a natural mechanism for transmitting the supersymmetry breaking of the hidden sector to the particle spectrum of the MSSM. In models of gravity-mediated supersymmetry breaking, gravity is the messenger of supersymmetry breaking [43–47]. More precisely, supersymmetry breaking is mediated by effects of gravitational strength (suppressed by inverse powers of the Planck mass). The soft-supersymmetry-breaking parameters arise as model-dependent multiples of the gravitino mass $m_{3/2}$. In this scenario, $m_{3/2}$ is of order the electroweak-symmetry-breaking scale, while the gravitino couplings are roughly gravitational in strength [3,48]. However, such a gravitino typically plays no direct role in supersymmetric phenomenology at colliders (except perhaps indirectly in the case where the gravitino is the LSP [49]).

Under certain theoretical assumptions on the structure of the Kähler potential (the so-called sequestered form introduced in Ref. 50), supersymmetry breaking is due entirely to the superconformal (super-Weyl) anomaly, which is common to all supergravity models [50]. In particular, gaugino masses are radiatively generated at one-loop, and squark and slepton squared-mass matrices are flavor-diagonal. In sequestered scenarios, sfermion squared-masses arise at two-loops, which implies that gluino and sfermion masses are of the same order or magnitude. This approach is called anomaly-mediated supersymmetry breaking (AMSB). Indeed, anomaly mediation is more generic than originally conceived, and provides a ubiquitous source of supersymmetry breaking [51]. However in the simplest formulation of AMSB as applied to the MSSM, the squared-masses of the sleptons are negative (known as the so-called tachyonic slepton problem). It may be possible to cure this otherwise fatal flaw in non-minimal extensions of the MSSM [52]. Alternatively, one can assert that anomaly mediation is not the sole source of supersymmetry breaking in the sfermion sector. In non-sequestered scenarios, sfermion squared-masses can arise at tree-level, in which case squark masses would be parametrically larger than the loop-suppressed gaugino masses [53].

In gauge-mediated supersymmetry breaking (GMSB), gauge forces transmit the supersymmetry breaking to the MSSM. A typical structure of such models involves a hidden sector where supersymmetry is broken, a messenger sector consisting of particles (messengers) with nontrivial SU(3)×SU(2)×U(1) quantum numbers, and the visible sector consisting of the fields of the MSSM [54–56]. The direct coupling of the messengers to the hidden sector generates a supersymmetry-breaking spectrum in the messenger sector. Supersymmetry breaking is then transmitted to the MSSM via the virtual exchange of the messenger fields. In models of direct gauge mediation, there is no separate hidden sector. In particular, the sector in which the supersymmetry breaking originates includes fields that carry nontrivial Standard Model quantum numbers, which allows for the direct transmission of supersymmetry breaking to the MSSM [57].

In models of gauge-mediated supersymmetry breaking, the gravitino is the LSP [18], as its mass can range from a few eV (in the case of low supersymmetry breaking scales) up to a few GeV (in the case of high supersymmetry breaking scales). In particular, the gravitino is a potential dark matter candidate (for a review and guide to the literature, see Ref. 22). Big bang nucleosynthesis also provides some interesting constraints on the gravitino and the properties of the next-to-lightest supersymmetric particle that decays into the gravitino LSP [58]. The couplings of the helicity $\pm\frac{1}{2}$ components of $\widetilde{G}$ to the particles of the MSSM (which approximate those of the goldstino as previously noted in Section 109.2.2) are significantly stronger than gravitational strength and amenable to experimental collider analyses.

The concept of a hidden sector is more general than supersymmetry. Hidden valley models [59] posit the existence of a hidden sector of new particles and interactions that are very weakly coupled to particles of the Standard Model. The impact of a hidden valley on supersymmetric phenomenology at colliders can be significant if the LSP lies in the hidden sector [60].

109.2.4. ***Supersymmetry and extra dimensions*** :

Approaches to supersymmetry breaking have also been developed in the context of theories in which the number of space dimensions is greater than three. In particular, a number of supersymmetry-breaking mechanisms have been proposed that are inherently extra-dimensional [61]. The size of the extra dimensions can be significantly larger than $M_{\rm P}^{-1}$; in some cases of order $(\text{TeV})^{-1}$ or even larger [62,63].

For example, in one approach the fields of the MSSM live on some brane (a lower-dimensional manifold embedded in a higher-dimensional spacetime), while the sector of the theory that breaks supersymmetry lives on a second spatially-separated brane. Two examples of this approach are anomaly-mediated supersymmetry breaking [50] and gaugino-mediated supersymmetry breaking [64]. In both cases, supersymmetry breaking is transmitted through fields that live in the bulk (the higher-dimensional space between the two branes). This setup has some features in common with both gravity-mediated and gauge-mediated supersymmetry breaking (*e.g.*, a hidden and visible sector and messengers).

Alternatively, one can consider a higher-dimensional theory that is compactified to four spacetime dimensions. In this approach, supersymmetry is broken by boundary conditions on the compactified space that distinguish between fermions and bosons. This is the so-called Scherk-Schwarz mechanism [65]. The phenomenology of such models can be strikingly different from that of the usual MSSM [66].

109.2.5. ***Split-supersymmetry*** :

If supersymmetry is not connected with the origin of the electroweak scale, it may still be possible that some remnant of the superparticle spectrum survives down to the TeV-scale or below. This is the idea of split-supersymmetry [67,68], in which scalar superpartners of the quarks and leptons are significantly heavier (perhaps by many orders of magnitude) than 1 TeV, whereas the fermionic superpartners of the gauge and Higgs bosons have masses on the order of 1 TeV or below. With the exception of a single light neutral scalar whose properties are practically indistinguishable from those of the Standard Model Higgs boson, all other Higgs bosons are also assumed to be very heavy. Among the supersymmetric particles, only the fermionic superpartners may be kinematically accessible at the LHC.

In models of split supersymmetry, the top squark masses cannot be arbitrarily large, as these parameters enter in the radiative corrections to the observed Higgs mass. In the MSSM, a Higgs boson mass of 125 GeV [69] implies an upper bound on the top squark mass scale in the range of 10 to 10^7 TeV [70–72], depending on the value of the ratio of the two neutral Higgs field vacuum expectation values, although this mass range can be somewhat relaxed by varying other relevant MSSM parameters [72]. In some approaches, gaugino masses are one-loop suppressed relative to the sfermion masses, corresponding to the so-called mini-split supersymmetry spectrum [71,73]. The higgsino mass scale may or may not be likewise suppressed depending on the details of the model [74].

The supersymmetry breaking required to produce such a split-supersymmetry spectrum would destabilize the gauge hierarchy, and thus would not yield an explanation for the scale of electroweak symmetry breaking. Nevertheless, models of split-supersymmetry can account for the dark matter (which is assumed to be the LSP gaugino or higgsino) and gauge coupling unification, thereby preserving two of the desirable features of weak-scale supersymmetry. Finally, as a consequence of the very large squark and slepton masses, neutral

flavor changing and CP-violating effects, which can be problematic for TeV-scale supersymmetry-breaking masses, are sufficiently reduced to avoid conflict with experimental observations.

109.3. Parameters of the MSSM

The parameters of the MSSM are conveniently described by considering separately the supersymmetry-conserving and the supersymmetry-breaking sectors. A careful discussion of the conventions used here in defining the tree-level MSSM parameters can be found in Refs. 75 and 76. For simplicity, consider first the case of one generation of quarks, leptons, and their scalar superpartners.

109.3.1. *The supersymmetry-conserving parameters* :

The parameters of the supersymmetry-conserving sector consist of: (i) gauge couplings, g_s, g, and g', corresponding to the Standard Model gauge group SU(3)×SU(2)×U(1) respectively; (ii) a supersymmetry-conserving higgsino mass parameter μ; and (iii) Higgs-fermion Yukawa coupling constants, λ_u, λ_d, and λ_e, corresponding to the couplings of one generation of left- and right-handed quarks and leptons, and their superpartners to the Higgs bosons and higgsinos. Because there is no right-handed neutrino (and its superpartner) in the MSSM as defined here, a Yukawa coupling λ_ν is not included. The complex μ parameter and Yukawa couplings enter via the most general renormalizable R-parity-conserving superpotential,

$$W = \lambda_d \widehat{H}_d \widehat{Q} \widehat{D}^c - \lambda_u \widehat{H}_u \widehat{Q} \widehat{U}^c + \lambda_e \widehat{H}_d \widehat{L} \widehat{E}^c + \mu \widehat{H}_u \widehat{H}_d \,, \qquad (109.1)$$

where the superfields are defined in Table 1 and the gauge group indices are suppressed.

109.3.2. *The supersymmetry-breaking parameters* :

The supersymmetry-breaking sector contains the following sets of parameters: (i) three complex gaugino Majorana mass parameters, M_3, M_2, and M_1, associated with the SU(3), SU(2), and U(1) subgroups of the Standard Model; (ii) five diagonal sfermion squared-mass parameters, $M_{\widetilde{Q}}^2$, $M_{\widetilde{U}}^2$, $M_{\widetilde{D}}^2$, $M_{\widetilde{L}}^2$, and $M_{\widetilde{E}}^2$, corresponding to the five electroweak gauge multiplets, *i.e.*, superpartners of the left-handed fields $(u,d)_L$, u_L^c, d_L^c, $(\nu,\ e^-)_L$, and e_L^c, where the superscript c indicates a charge-conjugated fermion field [26]; and (iii) three Higgs-squark-squark and Higgs-slepton-slepton trilinear interaction terms, with complex coefficients $T_U \equiv \lambda_u A_U$, $T_D \equiv \lambda_d A_D$, and $T_E \equiv \lambda_e A_E$ (which define the so-called "A-parameters"). The notation T_U, T_D and T_E is employed in Ref. 76. Following Ref. 75, it is conventional to separate out the factors of the Yukawa couplings in defining the A-parameters (originally motivated by a simple class of gravity-mediated supersymmetry-breaking models [3,6]). If the A-parameters are parametrically of the same order (or smaller) relative to other supersymmetry-breaking mass parameters, then only the third generation A-parameters are phenomenologically relevant.

Finally, we have (iv) two real squared-mass parameters (m_1^2 and m_2^2) and one complex squared-mass parameter, $m_{12}^2 \equiv \mu B$ (the latter defines the "B-parameter"), which appear in the MSSM tree-level scalar Higgs potential [30],

$$V = (m_1^2 + |\mu|^2) H_d^\dagger H_d + (m_2^2 + |\mu|^2) H_u^\dagger H_u + (m_{12}^2 H_u H_d + \text{h.c.}) + \tfrac{1}{8}(g^2 + g'^2)(H_d^\dagger H_d - H_u^\dagger H_u)^2 + \tfrac{1}{2}|H_d^\dagger H_u|^2 \,, \qquad (109.2)$$

where the SU(2)-invariant combination, $H_u H_d \equiv H_u^+ H_d^- - H_u^0 H_d^0$. Note that the quartic Higgs couplings are related to the gauge couplings g and g' as a consequence of supersymmetry. The breaking of the electroweak symmetry SU(2)×U(1) to $\mathrm{U(1)_{EM}}$ is only possible after introducing the supersymmetry-breaking Higgs squared-mass parameters m_1^2, m_2^2 (which can be negative) and m_{12}^2. After minimizing the Higgs scalar potential, these three squared-mass parameters can be re-expressed in terms of the two Higgs vacuum expectation values, $\langle H_d^0 \rangle \equiv v_d/\sqrt{2}$ and $\langle H_u^0 \rangle \equiv v_u/\sqrt{2}$, and the CP-odd Higgs mass m_A [cf. Eqs. (109.4) and (109.5) below]. One is always free to rephase the Higgs doublet fields such that v_d and v_u (also called v_1 and v_2, respectively, in the literature) are both real and positive.

The quantity, $v_d^2 + v_u^2 = 4m_W^2/g^2 = (2G_F^2)^{-1/2} \simeq (246\ \text{GeV})^2$, is fixed by the Fermi constant, G_F, whereas the ratio

$$\tan\beta = v_u/v_d \qquad (109.3)$$

is a free parameter such that $0 \leq \beta \leq \pi/2$. The tree-level conditions for the scalar potential minimum relate the diagonal and off-diagonal Higgs squared-masses in terms of $m_Z^2 = \frac{1}{4}(g^2 + g'^2)(v_d^2 + v_u^2)$, the angle β and the CP-odd Higgs mass m_A:

$$\sin 2\beta = \frac{2m_{12}^2}{m_1^2 + m_2^2 + 2|\mu|^2} = \frac{2m_{12}^2}{m_A^2} \,, \qquad (109.4)$$

$$\tfrac{1}{2} m_Z^2 = -|\mu|^2 + \frac{m_1^2 - m_2^2 \tan^2\beta}{\tan^2\beta - 1} \,. \qquad (109.5)$$

One must also guard against the existence of charge and/or color breaking global minima due to non-zero vacuum expectation values for the squark and charged slepton fields. This possibility can be avoided if the A-parameters are not unduly large [44,77,78]. Additional constraints must also be respected to avoid the possibility of directions in scalar field space in which the full tree-level scalar potential can become unbounded from below [78].

Note that supersymmetry-breaking mass terms for the fermionic superpartners of scalar fields and non-holomorphic trilinear scalar interactions (*i.e.*, interactions that mix scalar fields and their complex conjugates) have not been included above in the soft-supersymmetry-breaking sector. These terms can potentially destabilize the gauge hierarchy [11] in models with gauge-singlet superfields. The latter are not present in the MSSM; hence as noted in Ref. 12, these so-called non-standard soft-supersymmetry-breaking terms are benign. The phenomenological impact of non-holomorphic soft supersymmetry-breaking terms has recently been considered in Refs. 79–81. However, in the most common approaches to constructing a fundamental theory of supersymmetry-breaking, the coefficients of these terms (which have dimensions of mass) are significantly suppressed compared to the TeV-scale [82]. Consequently, we follow the usual approach and omit these terms from further consideration.

109.3.3. *MSSM-124* :

The total number of independent physical parameters that define the MSSM (in its most general form) is quite large, primarily due to the soft-supersymmetry-breaking sector. In particular, in the case of three generations of quarks, leptons, and their superpartners, $M_{\widetilde{Q}}^2$, $M_{\widetilde{U}}^2$, $M_{\widetilde{D}}^2$, $M_{\widetilde{L}}^2$, and $M_{\widetilde{E}}^2$ are hermitian 3×3 matrices, and A_U, A_D, and A_E are complex 3×3 matrices. In addition, M_1, M_2, M_3, B, and μ are in general complex parameters. Finally, as in the Standard Model, the Higgs-fermion Yukawa couplings, λ_f ($f = u$, d, and e), are complex 3×3 matrices that are related to the quark and lepton mass matrices via: $M_f = \lambda_f v_f/\sqrt{2}$, where $v_e \equiv v_d$ [with v_u and v_d as defined above Eq. (109.3)].

However, not all these parameters are physical. Some of the MSSM parameters can be eliminated by expressing interaction eigenstates in terms of the mass eigenstates, with an appropriate redefinition of the MSSM fields to remove unphysical degrees of freedom. The analysis of Ref. 83 shows that the MSSM possesses 124 independent parameters. Of these, 18 correspond to Standard Model parameters (including the QCD vacuum angle $\theta_{\rm QCD}$), one corresponds to a Higgs sector parameter (the analogue of the Standard Model Higgs mass), and 105 are genuinely new parameters of the model. The latter include: five real parameters and three CP-violating phases in the gaugino/higgsino sector, 21 squark and slepton (sfermion) masses, 36 real mixing angles to define the sfermion mass eigenstates, and 40 CP-violating phases that can appear in sfermion interactions. The most general R-parity-conserving minimal supersymmetric extension of the Standard Model (without additional theoretical assumptions) will be denoted henceforth as MSSM-124 [84].

109.4. The supersymmetric-particle spectrum

The supersymmetric particles (sparticles) differ in spin by half a unit from their Standard Model partners. The superpartners of the gauge and Higgs bosons are fermions, whose names are obtained by appending "ino" to the end of the corresponding Standard Model particle name. The gluino is the color-octet Majorana fermion partner of the gluon with mass $M_{\widetilde{g}} = |M_3|$. The superpartners

of the electroweak gauge and Higgs bosons (the gauginos and higgsinos) can mix due to SU(2)×U(1) breaking effects. As a result, the physical states of definite mass are model-dependent linear combinations of the charged or neutral gauginos and higgsinos, called charginos and neutralinos, respectively (sometimes collectively called electroweakinos). The neutralinos are Majorana fermions, which can lead to some distinctive phenomenological signatures [85,86]. The superpartners of the quarks and leptons are spin-zero bosons: the squarks, charged sleptons, and sneutrinos, respectively. A complete set of Feynman rules for the sparticles of the MSSM can be found in Ref. 87. The MSSM Feynman rules also are implicitly contained in a number of Feynman diagram and amplitude generation software packages (see *e.g.*, Refs. 88–90).

It should be noted that all mass formulae quoted below in this section are tree-level results. Radiative loop corrections will modify these results and must be included in any precision study of supersymmetric phenomenology [91]. Beyond tree level, the definition of the supersymmetric parameters becomes convention-dependent. For example, one can define physical couplings or running couplings, which differ beyond the tree level. This provides a challenge to any effort that attempts to extract supersymmetric parameters from data. The Supersymmetry Les Houches Accord (SLHA) [76,92] has been adopted, which establishes a set of conventions for specifying generic file structures for supersymmetric model specifications and input parameters, supersymmetric mass and coupling spectra, and decay tables. These provide a universal interface between spectrum calculation programs, decay packages, and high energy physics event generators.

109.4.1. *The charginos and neutralinos* :

The mixing of the charged gauginos ($\widetilde{W}^{\pm}$) and charged higgsinos ($\widetilde{H}_u^+$ and $\widetilde{H}_d^-$) is described (at tree-level) by a 2×2 complex mass matrix [93,94],

$$M_C \equiv \begin{pmatrix} M_2 & \frac{1}{\sqrt{2}} g v_u \\ \frac{1}{\sqrt{2}} g v_d & \mu \end{pmatrix} . \tag{109.6}$$

To determine the physical chargino states and their masses, one must perform a singular value decomposition [95,96] of the complex matrix M_C:

$$U^* M_C V^{-1} = \mathrm{diag}(M_{\widetilde{\chi}_1^+}\,,\, M_{\widetilde{\chi}_2^+})\,, \tag{109.7}$$

where U and V are unitary matrices, and the right-hand side of Eq. (109.7) is the diagonal matrix of (real non-negative) chargino masses. The physical chargino states are denoted by $\widetilde{\chi}_1^{\pm}$ and $\widetilde{\chi}_2^{\pm}$. These are linear combinations of the charged gaugino and higgsino states determined by the matrix elements of U and V [93,94] The chargino masses correspond to the singular values [95] of M_C, *i.e.*, the positive square roots of the eigenvalues of $M_C^\dagger M_C$:

$$M^2_{\widetilde{\chi}_1^+,\widetilde{\chi}_2^+} = \tfrac{1}{2}\Big\{ |\mu|^2 + |M_2|^2 + 2m_W^2 \mp \sqrt{\left(|\mu|^2 + |M_2|^2 + 2m_W^2\right)^2 - 4|\mu M_2 - m_W^2 \sin 2\beta|^2} \Big\}\,, \tag{109.8}$$

where the states are ordered such that $M_{\widetilde{\chi}_1^+} \leq M_{\widetilde{\chi}_2^+}$. The relative phase of μ and M_2 is physical and potentially observable.

The mixing of the neutral gauginos ($\widetilde{B}$ and $\widetilde{W}^0$) and neutral higgsinos ($\widetilde{H}_d^0$ and $\widetilde{H}_u^0$) is described (at tree-level) by a 4×4 complex symmetric mass matrix [93,94],

$$M_N \equiv \begin{pmatrix} M_1 & 0 & -\frac{1}{2}g' v_d & \frac{1}{2}g' v_u \\ 0 & M_2 & \frac{1}{2} g v_d & -\frac{1}{2} g v_u \\ -\frac{1}{2}g' v_d & \frac{1}{2} g v_d & 0 & -\mu \\ \frac{1}{2}g' v_u & -\frac{1}{2} g v_u & -\mu & 0 \end{pmatrix} . \tag{109.9}$$

To determine the physical neutralino states and their masses, one must perform a Takagi-diagonalization [95–98] of the complex symmetric matrix M_N:

$$W^T M_N W = \mathrm{diag}(M_{\widetilde{\chi}_1^0}\,,\, M_{\widetilde{\chi}_2^0}\,,\, M_{\widetilde{\chi}_3^0}\,,\, M_{\widetilde{\chi}_4^0})\,, \tag{109.10}$$

where W is a unitary matrix and the right-hand side of Eq. (109.10) is the diagonal matrix of (real non-negative) neutralino masses. The physical neutralino states are denoted by $\widetilde{\chi}_i^0$ ($i = 1, \ldots 4$), where the states are ordered such that $M_{\widetilde{\chi}_1^0} \leq M_{\widetilde{\chi}_2^0} \leq M_{\widetilde{\chi}_3^0} \leq M_{\widetilde{\chi}_4^0}$. The $\widetilde{\chi}_i^0$ are the linear combinations of the neutral gaugino and higgsino states determined by the matrix elements of W (which is denoted by N^{-1} in Ref. 93). The neutralino masses correspond to the singular values of M_N, *i.e.*, the positive square roots of the eigenvalues of $M_N^\dagger M_N$. Exact formulae for these masses can be found in Refs. 99 and 100. A numerical algorithm for determining the mixing matrix W has been given in Ref. 101.

If a chargino or neutralino state approximates a particular gaugino or higgsino state, it is convenient to employ the corresponding nomenclature. Specifically, if $|M_1|$ and $|M_2|$ are small compared to m_Z and $|\mu|$, then the lightest neutralino $\widetilde{\chi}_1^0$ would be nearly a pure photino, $\widetilde{\gamma}$, the superpartner of the photon. If $|M_1|$ and m_Z are small compared to $|M_2|$ and $|\mu|$, then the lightest neutralino would be nearly a pure bino, $\widetilde{B}$, the superpartner of the weak hypercharge gauge boson. If $|M_2|$ and m_Z are small compared to $|M_1|$ and $|\mu|$, then the lightest chargino pair and neutralino would constitute a triplet of roughly mass-degenerate pure winos, $\widetilde{W}^{\pm}$, and $\widetilde{W}_3^0$, the superpartners of the weak SU(2) gauge bosons. Finally, if $|\mu|$ and m_Z are small compared to $|M_1|$ and $|M_2|$, then the lightest chargino pair and neutralino would be nearly pure higgsino states, the superpartners of the Higgs bosons. Each of the above cases leads to a strikingly different phenomenology.

In the NMSSM, an additional Higgs singlet superfield is added to the MSSM. This superfield comprises two real Higgs scalar degrees of freedom and an associated neutral higgsino degree of freedom. Consequently, there are five neutralino mass eigenstates that are obtained by a Takagi-diagonalization of the 5×5 neutralino mass matrix. In many cases, the fifth neutralino state is dominated by its SU(2)×U(1) singlet component, and thus is very weakly coupled to the Standard Model particles and their superpartners.

109.4.2. *The squarks, sleptons and sneutrinos* :

For a given Dirac fermion f, there are two superpartners, $\widetilde{f}_L$ and $\widetilde{f}_R$, where the L and R subscripts simply identify the scalar partners that are related by supersymmetry to the left-handed and right-handed fermions, $f_{L,R} \equiv \frac{1}{2}(1 \mp \gamma_5) f$, respectively. (There is no $\widetilde{\nu}_R$ in the MSSM.) However, $\widetilde{f}_L$–$\widetilde{f}_R$ mixing is possible, in which case $\widetilde{f}_L$ and $\widetilde{f}_R$ are not mass eigenstates. For three generations of squarks, one must diagonalize 6×6 matrices corresponding to the basis $(\widetilde{q}_{iL}, \widetilde{q}_{iR})$, where $i = 1, 2, 3$ are the generation labels. For simplicity, only the one-generation case is illustrated in detail below. (The effects of second and third generation squark mixing can be significant and is treated in Ref. 102.)

Using the notation of the third family, the one-generation tree-level squark squared-mass matrix is given by [103],

$$\mathcal{M}^2 = \begin{pmatrix} M_Q^2 + m_q^2 + L_q & m_q X_q^* \\ m_q X_q & M_R^2 + m_q^2 + R_q \end{pmatrix} , \tag{109.11}$$

where

$$X_q \equiv A_q - \mu^* (\cot\beta)^{2T_{3q}}\,, \tag{109.12}$$

and $T_{3q} = \frac{1}{2}$ [$-\frac{1}{2}$] for $q = t$ [b]. The diagonal squared-masses are governed by soft-supersymmetry-breaking squared-masses M_Q^2 and $M_R^2 \equiv M_U^2$ [M_D^2] for $q = t$ [b], the corresponding quark masses m_t [m_b], and electroweak correction terms:

$$L_q \equiv (T_{3q} - e_q \sin^2\theta_W) m_Z^2 \cos 2\beta\,, \qquad R_q \equiv e_q \sin^2\theta_W\, m_Z^2 \cos 2\beta\,, \tag{109.13}$$

where $e_q = \frac{2}{3}$ [$-\frac{1}{3}$] for $q = t$ [b]. The off-diagonal squark squared-masses are proportional to the corresponding quark masses and depend on $\tan\beta$, the soft-supersymmetry-breaking A-parameters and the higgsino mass parameter μ. Assuming that the A-parameters are parametrically of the same order (or smaller) relative to other supersymmetry-breaking mass parameters, it then follows that $\widetilde{q}_L$–$\widetilde{q}_R$ mixing effects are small, with the possible exception of the third

generation, where mixing can be enhanced by factors of m_t and $m_b \tan\beta$.

In the case of third generation $\widetilde{q}_L$–$\widetilde{q}_R$ mixing, the mass eigenstates (usually denoted by $\widetilde{q}_1$ and $\widetilde{q}_2$, with $m_{\widetilde{q}_1} < m_{\widetilde{q}_2}$) are determined by diagonalizing the 2×2 matrix $\mathcal{M}^2$ given by Eq. (109.11). The corresponding squared-masses and mixing angle are given by [103]:

$$m^2_{\widetilde{q}_{1,2}} = \frac{1}{2}\left[\mathrm{Tr}\,\mathcal{M}^2 \mp \sqrt{(\mathrm{Tr}\mathcal{M}^2)^2 - 4\det\mathcal{M}^2}\right],$$

$$\sin 2\theta_{\widetilde{q}} = \frac{2m_q|X_q|}{m^2_{\widetilde{q}_2} - m^2_{\widetilde{q}_1}}. \qquad (109.14)$$

The one-generation results above also apply to the charged sleptons, with the obvious substitutions: $q \to \ell$ with $T_{3\ell} = -\frac{1}{2}$ and $e_\ell = -1$, and the replacement of the supersymmetry-breaking parameters: $M^2_{\widetilde{Q}} \to M^2_{\widetilde{L}}$, $M^2_{\widetilde{D}} \to M^2_{\widetilde{E}}$, and $A_q \to A_\tau$. For the neutral sleptons, $\widetilde{\nu}_R$ does not exist in the MSSM, so $\widetilde{\nu}_L$ is a mass eigenstate.

In the case of three generations, the supersymmetry-breaking scalar-squared masses [$M^2_{\widetilde{Q}}$, $M^2_{\widetilde{U}}$, $M^2_{\widetilde{D}}$, $M^2_{\widetilde{L}}$, and $M^2_{\widetilde{E}}$] and the A-parameters [A_U, A_D, and A_E] are now 3×3 matrices as noted in Section 109.3.3 The diagonalization of the 6×6 squark mass matrices yields $\widetilde{f}_{iL}$–$\widetilde{f}_{jR}$ mixing. In practice, since the $\widetilde{f}_L$–$\widetilde{f}_R$ mixing is appreciable only for the third generation, this additional complication can often be neglected (although see Ref. 102 for examples in which the mixing between the second and third generation squarks is relevant).

109.5. The supersymmetric Higgs sector

Consider first the MSSM Higgs sector [29,30,104]. Despite the large number of potential CP-violating phases among the MSSM-124 parameters, the tree-level MSSM Higgs potential given by Eq. (109.2) is automatically CP-conserving. This follows from the fact that the only potentially complex parameter (m^2_{12}) of the MSSM Higgs potential can be chosen real and positive by rephasing the Higgs fields, in which case $\tan\beta$ is a real positive parameter. Consequently, the physical neutral Higgs scalars are CP-eigenstates. The MSSM Higgs sector contains five physical spin-zero particles: a charged Higgs boson pair ($H^\pm$), two CP-even neutral Higgs bosons (denoted by h^0 and H^0 where $m_h < m_H$), and one CP-odd neutral Higgs boson (A^0). The discovery of a Standard Model-like Higgs boson at the LHC with a mass of 125 GeV [69] strongly suggests that this state should be identified with h^0, although the possibility that the 125 GeV state should be identified with H^0 cannot be completely ruled out [105].

In the NMSSM [34], the scalar component of the singlet Higgs superfield adds two additional neutral states to the Higgs sector. In this model, the tree-level Higgs sector can exhibit explicit CP-violation. If CP is conserved, then the two extra neutral scalar states are CP-even and CP-odd, respectively. These states can potentially mix with the neutral Higgs states of the MSSM. If scalar states exist that are dominantly singlet, then they are weakly coupled to Standard Model gauge bosons and fermions through their small mixing with the MSSM Higgs scalars. Consequently, it is possible that one (or both) of the singlet-dominated states is considerably lighter than the Higgs boson that was observed at the LHC.

109.5.1. *The tree-level Higgs sector* :

The tree-level properties of the Higgs sector are determined by the Higgs potential given by Eq. (109.2). The quartic interaction terms are manifestly supersymmetric (although these are modified by supersymmetry-breaking effects at the loop level). In general, the quartic couplings arise from two sources: (i) the supersymmetric generalization of the scalar potential (the so-called "F-terms"), and (ii) interaction terms related by supersymmetry to the coupling of the scalar fields and the gauge fields, whose coefficients are proportional to the corresponding gauge couplings (the so-called "D-terms").

In the MSSM, F-term contributions to the quartic Higgs self-couplings are absent. As a result, the strengths of the MSSM quartic Higgs interactions are fixed in terms of the gauge couplings, as noted below Eq. (109.2). Consequently, all the tree-level MSSM Higgs-sector parameters depend only on two quantities: $\tan\beta$ [defined in Eq. (109.3)] and one Higgs mass usually taken to be m_A. From these two quantities, one can predict the values of the remaining Higgs boson masses, an angle α that measures the mixture of the hypercharge ± 1 scalar fields, H^0_u and H^0_d, in the physical CP-even neutral scalars, and the Higgs boson self-couplings. Moreover, the tree-level mass of the lighter CP-even Higgs boson is bounded, $m_h \leq m_Z|\cos 2\beta| \leq m_Z$ [29,30]. This bound can be substantially modified when radiative corrections are included, as discussed in Section 109.5.2.

In the NMSSM, the superpotential contains a trilinear term that couples the two $Y = \pm 1$ Higgs doublet superfields and the singlet Higgs superfield. The coefficient of this term is denoted by λ. Consequently, the tree-level bound for the mass of the lightest CP-even MSSM Higgs boson is modified [106],

$$m^2_h \leq m^2_Z \cos^2 2\beta + \tfrac{1}{2}\lambda^2 v^2 \sin^2 2\beta, \qquad (109.15)$$

where $v \equiv (v^2_u + v^2_d)^{1/2} = 246$ GeV. If one demands that λ should stay finite after renormalization-group evolution up to the Planck scale, then λ is constrained to lie below about 0.7–0.8 at the electroweak scale [34]. However, in light of the observed Higgs mass of 125 GeV, there is some motivation for considering larger values of λ [107].

The tree-level Higgs-quark and Higgs-lepton interactions of the MSSM are governed by the Yukawa couplings defined by the superpotential given in Eq. (109.1). In particular, the Higgs sector of the MSSM is a Type-II two-Higgs doublet model [108], in which one Higgs doublet (H_d) couples exclusively to the right-handed down-type quark (or lepton) fields and the second Higgs doublet (H_u) couples exclusively to the right-handed up-type quark fields. Consequently, the diagonalization of the fermion mass matrices simultaneously diagonalizes the matrix Yukawa couplings, resulting in flavor-diagonal couplings of the neutral Higgs bosons h^0, H^0 and A^0 to quark and lepton pairs.

109.5.2. *The radiatively-corrected Higgs sector* :

When radiative corrections are incorporated, additional parameters of the supersymmetric model enter via virtual supersymmetric particles that can appear in loops. The impact of these corrections can be significant [109]. The qualitative behavior of these radiative corrections can be most easily seen in the large top-squark mass limit, where in addition, both the splitting of the two diagonal entries and the off-diagonal entries of the top-squark squared-mass matrix [Eq. (109.11)] are small in comparison to the geometric mean of the two top-squark squared-masses, $M^2_{\rm S} \equiv M_{\widetilde{t}_1} M_{\widetilde{t}_2}$. In this case (assuming $m_A > m_Z$), the predicted upper bound for m_h is approximately given by

$$m^2_h \lesssim m^2_Z \cos^2 2\beta + \frac{3g^2 m^4_t}{8\pi^2 m^2_W}\left[\ln\left(\frac{M^2_{\rm S}}{m^2_t}\right) + \frac{X^2_t}{M^2_{\rm S}}\left(1 - \frac{X^2_t}{12M^2_{\rm S}}\right)\right], \qquad (109.16)$$

where $X_t \equiv A_t - \mu\cot\beta$ [cf. Eq. (109.12)] is proportional to the off-diagonal entry of the top-squark squared-mass matrix (where for simplicity, A_t and μ are taken to be real). The Higgs mass upper limit is saturated when $\tan\beta$ is large (*i.e.*, $\cos^2 2\beta \sim 1$) and $X_t = \sqrt{6}\,M_S$, which defines the so-called maximal mixing scenario.

A more complete treatment of the radiative corrections [110] shows that Eq. (109.16) somewhat overestimates the true upper bound of m_h. These more refined computations, which incorporate renormalization group improvement, the two loop and the leading three-loop contributions, yield $m_h \lesssim 135$ GeV in the region of large $\tan\beta$ (with an accuracy of a few GeV) for $m_t = 175$ GeV and $M_S \lesssim 2$ TeV [110].

In addition, one-loop radiative corrections can introduce CP-violating effects in the Higgs sector that depend on some of the CP-violating phases among the MSSM-124 parameters [111]. This phenomenon is most easily understood in a scenario where $m_A \ll M_S$ (i.e., all five physical Higgs states are significantly lighter than the supersymmetry breaking scale). In this case, one can integrate out the heavy superpartners to obtain a low-energy effective theory

with two Higgs doublets. The resulting effective two-Higgs doublet model will now contain all possible Higgs self-interaction terms (both CP-conserving and CP-violating) and Higgs-fermion interactions (beyond those of Type-II) that are consistent with electroweak gauge invariance [112].

In the NMSSM, the dominant radiative correction to Eq. (109.15) is the same as the one given in Eq. (109.16). However, in contrast to the MSSM, one does not need as large a boost from the radiative corrections to achieve a Higgs mass of 125 GeV in certain regimes of the NMSSM parameter space (*e.g.*, $\tan\beta \sim 2$ and $\lambda \sim 0.7$ [113]).

109.6. Restricting the MSSM parameter freedom

In Section 109.4 and Section 109.5, we surveyed the parameters that comprise the MSSM-124. However, without additional restrictions on the choice of parameters, a generic parameter set within the MSSM-124 framework is not phenomenologically viable. In particular, a generic point of the MSSM-124 parameter space exhibits: (i) no conservation of the separate lepton numbers L_e, L_μ, and L_τ; (ii) unsuppressed flavor-changing neutral currents (FCNCs); and (iii) new sources of CP violation that are inconsistent with the experimental bounds.

For example, the MSSM contains many new sources of CP violation [114]. Indeed, for TeV-scale sfermion and gaugino masses, some combinations of the complex phases of the gaugino-mass parameters, the A-parameters, and μ must be less than about 10^{-2}–10^{-3} to avoid generating electric dipole moments for the neutron, electron, and atoms in conflict with observed data [115–117]. The non-observation of FCNCs [118–120] places additional constraints on the off-diagonal matrix elements of the squark and slepton soft-supersymmetry-breaking squared-masses and A-parameters (see Section 109.3.3).

The MSSM-124 is also theoretically incomplete as it provides no explanation for the fundamental origin of the supersymmetry-breaking parameters. The successful unification of the Standard Model gauge couplings at very high energies close to the Planck scale [8,68,121,122] suggests that the high-energy structure of the theory may be considerably simpler than its low-energy realization. In a top-down approach, the dynamics that governs the more fundamental theory at high energies is used to derive the effective broken-supersymmetric theory at the TeV scale. A suitable choice for the high energy dynamics is one that yields a TeV-scale theory that satisfies all relevant phenomenological constraints.

In this Section, we examine a number of theoretical frameworks that potentially yield phenomenologically viable regions of the MSSM-124 parameter space. The resulting supersymmetric particle spectrum is then a function of a relatively small number of input parameters. This is accomplished by imposing a simple structure on the soft supersymmetry-breaking parameters at a common high-energy scale M_X (typically chosen to be the Planck scale, $M_{\rm P}$, the grand unification scale, $M_{\rm GUT}$, or the messenger scale, $M_{\rm mess}$). These serve as initial conditions for the MSSM renormalization group equations (RGEs), which are given in the two-loop approximation in Ref. 123 (an automated program to compute RGEs for the MSSM and other models of new physics beyond the Standard Model has been developed in Ref. 124). Solving these equations numerically, one can then derive the low-energy MSSM parameters relevant for collider physics. A number of software packages exist that numerically calculate the spectrum of supersymmetric particles, consistent with theoretical conditions on supersymmetry breaking at high energies and some experimental data at low energies [125,126].

Examples of this scenario are provided by models of gravity-mediated, anomaly mediated and gauge-mediated supersymmetry breaking, to be discussed in more detail below. In some of these approaches, one of the diagonal Higgs squared-mass parameters is driven negative by renormalization group evolution [127]. In such models, electroweak symmetry breaking is generated radiatively, and the resulting electroweak symmetry-breaking scale is intimately tied to the scale of low-energy supersymmetry breaking.

109.6.1. *Gaugino mass relations* :

One prediction of many grand unified supergravity models is the unification of the (tree-level) gaugino mass parameters at some high-energy scale, M_X,

$$M_1(M_X) = M_2(M_X) = M_3(M_X) = m_{1/2}\,. \tag{109.17}$$

Due to renormalization group running, in the one-loop approximation the effective low-energy gaugino mass parameters (at the electroweak scale) are related,

$$M_3 = (g_s^2/g^2)M_2 \simeq 3.5M_2\,, \qquad M_1 = (5g'^2/3g^2)M_2 \simeq 0.5M_2. \tag{109.18}$$

Eq. (109.18) can also arise more generally in gauge-mediated supersymmetry-breaking models where the gaugino masses are generated at the messenger scale $M_{\rm mess}$ (which typically lies significantly below the unification scale where the gauge couplings unify). In this case, the gaugino mass parameters are proportional to the corresponding squared gauge couplings at the messenger scale.

When Eq. (109.18) is satisfied, the chargino and neutralino masses and mixing angles depend only on three unknown parameters: the gluino mass, μ, and $\tan\beta$. It then follows that the lightest neutralino must be heavier than 46 GeV due to the non-observation of charginos at LEP [128]. If in addition $|\mu| \gg |M_1| \gtrsim m_Z$, then the lightest neutralino is nearly a pure bino, an assumption often made in supersymmetric particle searches at colliders. Although Eq. (109.18) is often assumed in many phenomenological studies, a truly model-independent approach would take the gaugino mass parameters, M_i, to be independent parameters to be determined by experiment. Indeed, an approximately massless neutralino *cannot* be ruled out at present by a model-independent analysis [129].

It is possible that the tree-level masses for the gauginos are zero. In this case, the gaugino mass parameters arise at one-loop and do not satisfy Eq. (109.18). For example, the gaugino masses in AMSB models arise entirely from a model-independent contribution derived from the super-conformal anomaly [50,130]. In this case, Eq. (109.18) is replaced (in the one-loop approximation) by:

$$M_i \simeq \frac{b_i g_i^2}{16\pi^2} m_{3/2}\,, \tag{109.19}$$

where $m_{3/2}$ is the gravitino mass and the b_i are the coefficients of the MSSM gauge beta-functions corresponding to the corresponding U(1), SU(2), and SU(3) gauge groups, $(b_1, b_2, b_3) = (\frac{33}{5}, 1, -3)$. Eq. (109.19) yields $M_1 \simeq 2.8M_2$ and $M_3 \simeq -8.3M_2$, which implies that the lightest chargino pair and neutralino comprise a nearly mass-degenerate triplet of winos, $\widetilde{W}^\pm$, $\widetilde{W}^0$ (cf. Table 1), over most of the MSSM parameter space. For example, if $|\mu| \gg m_Z$, $|M_2|$, then Eq. (109.19) implies that $M_{\widetilde{\chi}_1^\pm} \simeq M_{\widetilde{\chi}_1^0} \simeq M_2$ [131]. The corresponding supersymmetric phenomenology differs significantly from the standard phenomenology based on Eq. (109.18) [132,133].

Finally, it should be noted that the unification of gaugino masses (and scalar masses) can be accidental. In particular, the energy scale where unification takes place may not be directly related to any physical scale. One version of this phenomenon has been called mirage unification and can occur in certain theories of fundamental supersymmetry breaking [134].

109.6.2. *The constrained MSSM: mSUGRA, CMSSM, ...* :

In the minimal supergravity (mSUGRA) framework [3–6,43–45], a form of the Kähler potential is employed that yields minimal kinetic energy terms for the MSSM fields [47]. As a result, the soft supersymmetry-breaking parameters at the high-energy scale M_X take a particularly simple form in which the scalar squared-masses and the A-parameters are flavor-diagonal and universal [45]:

$$\begin{aligned}
&M_{\widetilde{Q}}^2(M_X) = M_{\widetilde{U}}^2(M_X) = M_{\widetilde{D}}^2(M_X) = m_0^2\mathbf{1}\,,\\
&M_{\widetilde{L}}^2(M_X) = M_{\widetilde{E}}^2(M_X) = m_0^2\mathbf{1}\,,\\
&m_1^2(M_X) = m_2^2(M_X) = m_0^2\,,\\
&A_U(M_X) = A_D(M_X) = A_E(M_X) = A_0\mathbf{1}\,,
\end{aligned} \tag{109.20}$$

where **1** is a 3×3 identity matrix in generation space. As in the Standard Model, this approach exhibits minimal flavor violation [135,136], whose unique source is the nontrivial flavor structure of the Higgs-fermion Yukawa couplings. The gaugino masses are also unified according to Eq. (109.17).

Renormalization group evolution is then used to derive the values of the supersymmetric parameters at the low-energy (electroweak) scale. For example, to compute squark masses, one must use the low-energy values for $M^2_{\widetilde{Q}}$, $M^2_{\widetilde{U}}$, and $M^2_{\widetilde{D}}$ in Eq. (109.11). Through the renormalization group running with boundary conditions specified in Eqs. (109.18) and (109.20), one can show that the low-energy values of $M^2_{\widetilde{Q}}$, $M^2_{\widetilde{U}}$, and $M^2_{\widetilde{D}}$ depend primarily on m_0^2 and $m_{1/2}^2$. A number of useful approximate analytic expressions for superpartner masses in terms of the mSUGRA parameters can be found in Ref. 137.

In the mSUGRA approach, four flavors of squarks (with two squark eigenstates per flavor) are nearly mass-degenerate. If $\tan\beta$ is not very large, $\widetilde{b}_R$ is also approximately degenerate in mass with the first two generations of squarks. The $\widetilde{b}_L$ mass and the diagonal $\widetilde{t}_L$ and $\widetilde{t}_R$ masses are typically reduced relative to the common squark mass of the first two generations. In addition, there are six flavors of nearly mass-degenerate sleptons (with two slepton eigenstates per flavor for the charged sleptons and one per flavor for the sneutrinos); the sleptons are expected to be somewhat lighter than the mass-degenerate squarks. As noted below Eq. (109.11), third-generation squark masses and tau-slepton masses are sensitive to the strength of the respective $\widetilde{f}_L$–$\widetilde{f}_R$ mixing. The LSP is typically the lightest neutralino, $\widetilde{\chi}^0_1$, which is dominated by its bino component. Regions of the mSUGRA parameter space in which the LSP is electrically charged do exist but are not phenomenologically viable [20].

One can count the number of independent parameters in the mSUGRA framework. In addition to 18 Standard Model parameters (excluding the Higgs mass), one must specify m_0, $m_{1/2}$, A_0, the Planck-scale values for μ and B-parameters (denoted by μ_0 and B_0), and the gravitino mass $m_{3/2}$. Without additional model assumptions, $m_{3/2}$ is independent of the parameters that govern the mass spectrum of the superpartners of the Standard Model [45]. In principle, A_0, B_0, μ_0, and $m_{3/2}$ can be complex, although in the mSUGRA approach, these parameters are taken (arbitrarily) to be real.

As previously noted, renormalization group evolution is used to compute the low-energy values of the mSUGRA parameters, which then fixes all the parameters of the low-energy MSSM. In particular, the two Higgs vacuum expectation values (or equivalently, m_Z and $\tan\beta$) can be expressed as a function of the Planck-scale supergravity parameters. The simplest procedure is to remove μ_0 and B_0 in favor of m_Z and $\tan\beta$ [the sign of μ_0, denoted $\mathrm{sgn}(\mu_0)$ below, is not fixed in this process]. In this case, the MSSM spectrum and its interaction strengths are determined by five parameters:

$$m_0\,,\; A_0\,,\; m_{1/2}\,,\; \tan\beta\,,\; \text{and}\;\; \mathrm{sgn}(\mu_0)\,, \tag{109.21}$$

and an independent gravitino mass $m_{3/2}$ (in addition to the 18 parameters of the Standard Model). In Ref. 138, this framework was dubbed the constrained minimal supersymmetric extension of the Standard Model (CMSSM).

In the early literature, additional conditions were obtained by assuming a simplified form for the hidden sector that provides the fundamental source of supersymmetry breaking. Two additional relations emerged among the mSUGRA parameters [43,47]: $B_0 = A_0 - m_0$ and $m_{3/2} = m_0$. These relations characterize a theory that was called minimal supergravity when first proposed. In the subsequent literature, it has been more common to omit these extra conditions in defining the mSUGRA model (in which case the mSUGRA model and the CMSSM are synonymous). The authors of Ref. 139 advocate restoring the original nomenclature in which the mSUGRA model is defined with the extra conditions as originally proposed. Additional mSUGRA variations can be considered where different relations among the CMSSM parameters are imposed.

One can also relax the universality of scalar masses by decoupling the squared-masses of the Higgs bosons and the squarks/sleptons. This leads to the non-universal Higgs mass models (NUHMs), thereby adding one or two new parameters to the CMSSM depending on whether the diagonal Higgs scalar squared-mass parameters (m_1^2 and m_2^2) are set equal (NUHM1) or taken to be independent (NUHM2) at the high energy scale M_X^2. Clearly, this modification preserves the minimal flavor violation of the mSUGRA approach. Nevertheless, the mSUGRA approach and its NUHM generalizations are probably too simplistic. Theoretical considerations suggest that the universality of Planck-scale soft supersymmetry-breaking parameters is not generic [140]. In particular, effective operators at the Planck scale exist that do not respect flavor universality, and it is difficult to find a theoretical principle that would forbid them.

In the framework of supergravity, if anomaly mediation is the sole source of supersymmetry breaking, then the gaugino mass parameters, diagonal scalar squared-mass parameters, and the supersymmetry-breaking trilinear scalar interaction terms (proportional to $\lambda_f A_F$) are determined in terms of the beta functions of the gauge and Yukawa couplings and the anomalous dimensions of the squark and slepton fields [50,130,133]. As noted in Section 109.2.3, this approach yields tachyonic sleptons in the MSSM unless additional sources of supersymmetry breaking are present. In the minimal AMSB (mAMSB) scenario, a universal squared-mass parameter, m_0^2, is added to the AMSB expressions for the diagonal scalar squared-masses [133]. Thus, the mAMSB spectrum and its interaction strengths are determined by four parameters, m_0^2, $m_{3/2}$, $\tan\beta$ and $\mathrm{sgn}(\mu_0)$.

The mAMSB scenario appears to be ruled out based on the observed value of the Higgs boson mass, assuming an upper limit on M_S of a few TeV, since the mAMSB constraint on A_F implies that the maximal mixing scenario cannot be achieved [cf. Eq. (109.16)]. Indeed, under the stated assumptions, the mAMSB Higgs mass upper bound lies below the observed Higgs mass value [141]. Thus within the AMSB scenario, either an additional supersymmetry-breaking contribution to $\lambda_f A_F$ and/or new ingredients beyond the MSSM are required.

109.6.3. *Gauge-mediated supersymmetry breaking* :

In contrast to models of gravity-mediated supersymmetry breaking, the flavor universality of the fundamental soft supersymmetry-breaking squark and slepton squared-mass parameters is guaranteed in gauge-mediated supersymmetry breaking (GMSB) because the supersymmetry breaking is communicated to the sector of MSSM fields via gauge interactions [55,56]. In GMSB models, the mass scale of the messenger sector (or its equivalent) is sufficiently below the Planck scale such that the additional supersymmetry-breaking effects mediated by supergravity can be neglected.

In the minimal GMSB approach, there is one effective mass scale, Λ, that determines all low-energy scalar and gaugino mass parameters through loop effects, while the resulting A-parameters are suppressed. In order that the resulting superpartner masses be of order 1 TeV or less, one must have $\Lambda \sim 100$ TeV. The origin of the μ and B-parameters is model-dependent, and lies somewhat outside the ansatz of gauge-mediated supersymmetry breaking [142].

The simplest GMSB models appear to be ruled out based on the observed value of the Higgs boson mass. Due to suppressed A parameters, it is difficult to boost the contributions of the radiative corrections in Eq. (109.16) to obtain a Higgs mass as large as 125 GeV. However, this conflict can be alleviated in more complicated GMSB models [143]. To analyze these generalized GMSB models, it has been especially fruitful to develop model-independent techniques that encompass all known GMSB models [144]. These techniques are well-suited for a comprehensive analysis [145] of the phenomenological profile of gauge-mediated supersymmetry breaking.

The gravitino is the LSP in GMSB models, as noted in Section 109.2.3. As a result, the next-to-lightest supersymmetric particle (NLSP) now plays a crucial role in the phenomenology of supersymmetric particle production and decays. Note that unlike the LSP, the NLSP can be charged. In GMSB models, the most likely candidates for the NLSP are $\widetilde{\chi}^0_1$ and $\widetilde{\tau}^{\pm}_R$. The NLSP will decay into its superpartner plus a gravitino (*e.g.*, $\widetilde{\chi}^0_1 \to \gamma\widetilde{G}$, $\widetilde{\chi}^0_1 \to Z\widetilde{G}$, $\widetilde{\chi}^0_1 \to h^0\widetilde{G}$ or $\widetilde{\tau}^{\pm}_R \to \tau^{\pm}\widetilde{G}$), with lifetimes and branching ratios that

depend on the model parameters. There are also GMSB scenarios in which there are several nearly degenerate co-NLSP's, any one of which can be produced at the penultimate step of a supersymmetric decay chain [146]. For example, in the slepton co-NLSP case, all three right-handed sleptons are close enough in mass and thus can each play the role of the NLSP.

Different choices for the identity of the NLSP and its decay rate lead to a variety of distinctive supersymmetric phenomenologies [56,147]. For example, a long-lived $\widetilde{\chi}_1^0$-NLSP that decays outside collider detectors leads to supersymmetric decay chains with missing energy in association with leptons and/or hadronic jets (this case is indistinguishable from the standard phenomenology of the $\widetilde{\chi}_1^0$-LSP). On the other hand, if $\widetilde{\chi}_1^0 \to \gamma\widetilde{G}$ is the dominant decay mode, and the decay occurs inside the detector, then nearly *all* supersymmetric particle decay chains would contain a photon. In contrast, in the case of a $\widetilde{\tau}_R^{\pm}$-NLSP, the $\widetilde{\tau}_R^{\pm}$ would either be long-lived or would decay inside the detector into a τ-lepton plus missing energy.

A number of attempts have been made to address the origins of the μ and B-parameters in GMSB models in the context of the MSSM (see, *e.g.*, Refs. 142 and 148). An alternative approach is to consider GMSB models based on the NMSSM [149]. The vacuum expectation value of the additional singlet Higgs superfield can be used to generate effective μ and B-parameters [150]. Such models provide an alternative GMSB framework for achieving a Higgs mass of 125 GeV, while still being consistent with LHC bounds on supersymmetric particle masses [151].

109.6.4. *The phenomenological MSSM* :

Of course, any of the theoretical assumptions described above must be tested experimentally and could turn out to be wrong. To facilitate the exploration of MSSM phenomena in a more model-independent way while respecting the constraints noted at the beginning of this Section, the phenomenological MSSM (pMSSM) has been introduced [152].

The pMSSM is governed by 19 independent real supersymmetric parameters: the three gaugino mass parameters M_1, M_2 and M_3, the Higgs sector parameters m_A and $\tan\beta$, the Higgsino mass parameter μ, five sfermion squared-mass parameters for the degenerate first and second generations ($M_{\widetilde{Q}}^2$, $M_{\widetilde{U}}^2$, $M_{\widetilde{D}}^2$, $M_{\widetilde{L}}^2$ and $M_{\widetilde{E}}^2$), the five corresponding sfermion squared-mass parameters for the third generation, and three third-generation A-parameters (A_t, A_b and A_τ). As previously noted, the first and second generation A-parameters can be neglected as their phenomenological consequences are negligible. (Recently, the pMSSM approach has been extended to include CP-violating supersymmetry-breaking parameters in Ref. 153.)

A comprehensive study of the 19-parameter pMSSM is computationally expensive. This is somewhat ameliorated in Ref. 154, where the number of pMSSM parameters is reduced to ten by assuming one common squark squared-mass parameter for the first two generations, a second common squark squared-mass parameter for the third generation, a common slepton squared-mass parameter and a common third generation A parameter. Applications of the pMSSM approach to supersymmetric particle searches, and a discussion of the implications for past and future LHC and dark matter studies can be found in Refs. 154–156.

109.6.5. *Simplified models* :

It is possible to focus on a small subset of the supersymmetric particle spectrum and study its phenomenology with minimal theoretical bias. In this simplified model approach [157], one considers the production of a pair of specific superpartners and follows their decay chains under the assumption that a limited number of decay modes dominate. Simplified models depend only on a few relevant quantities (cross sections, branching ratios and masses), and thus provide a framework for studies of supersymmetric phenomena, independently of the precise details of the theory that govern the supersymmetric parameters.

Applications of the simplified models approach to supersymmetric particle searches and a discussion of their limitations can be found in Ref. 13. A contrast between supersymmetry search limits in the context of simplified models and the corresponding constraints obtained in a more realistic pMSSM scenario is provided in Ref. 158.

109.7. Experimental data confronts the MSSM

At present, there is no significant evidence for weak-scale supersymmetry from the data analyzed by the LHC experiments. Recent LHC data has been especially effective in ruling out the existence of colored supersymmetric particles (primarily the gluino and the first generation of squarks) with masses below about 2 TeV [13]. The precise mass limits are model dependent. For example, higher mass colored superpartners have been ruled out in the context of the CMSSM. In less constrained frameworks of the MSSM, regions of parameter space can be identified in which lighter squarks and gluinos below 1 TeV cannot be definitely ruled out [13]. Additional constraints arise from limits on the contributions of virtual supersymmetric particle exchange to a variety of Standard Model processes [118–120].

In light of these negative results, one must confront the tension that exists between the theoretical expectations for the magnitude of the supersymmetry-breaking parameters and the non-observation of supersymmetric phenomena.

109.7.1. *Naturalness constraints and the little hierarchy* :

In Section 109.1, weak-scale supersymmetry was motivated as a natural solution to the hierarchy problem, which could provide an understanding of the origin of the electroweak symmetry-breaking scale without a significant fine-tuning of the fundamental parameters that govern the MSSM. In this context, the soft supersymmetry-breaking masses must be generally of the order of 1 TeV or below [159]. This requirement is most easily seen in the determination of m_Z by the scalar potential minimum condition. In light of Eq. (109.5), to avoid the fine-tuning of MSSM parameters, the soft supersymmetry-breaking squared-masses m_1^2 and m_2^2 and the higgsino squared-mass $|\mu|^2$ should all be roughly of $\mathcal{O}(m_Z^2)$. Many authors have proposed quantitative measures of fine-tuning [159–162]. One of the simplest measures is the one advocated by Barbieri and Giudice [159] (which was also introduced previously in Ref. 160),

$$\Delta_i \equiv \left| \frac{\partial \ln m_Z^2}{\partial \ln p_i} \right| , \qquad \Delta \equiv \max\ \Delta_i \,, \tag{109.22}$$

where the p_i are the MSSM parameters at the high-energy scale M_X, which are set by the fundamental supersymmetry-breaking dynamics. The theory is more fine-tuned as Δ becomes larger.

One can apply the fine-tuning measure to any explicit model of supersymmetry breaking. For example, in the approaches discussed in Section 109.6, the p_i are parameters of the model at the energy scale M_X where the soft supersymmetry-breaking operators are generated by the dynamics of supersymmetry breaking. Renormalization group evolution then determines the values of the parameters appearing in Eq. (109.5) at the electroweak scale. In this way, Δ is sensitive to all the supersymmetry-breaking parameters of the model (see e.g. Ref. 163).

As anticipated, there is a tension between the present experimental lower limits on the masses of colored supersymmetric particles [164,165] and the expectation that supersymmetry-breaking is associated with the electroweak symmetry-breaking scale. Moreover, this tension is exacerbated [166] by the observed value of the Higgs mass ($m_h \simeq 125$ GeV), which is not far from the MSSM upper bound ($m_h \lesssim 135$ GeV) [which depends on the top-squark mass and mixing as noted in Section 109.5.2].If $M_{\rm SUSY}$ characterizes the scale of supersymmetric particle masses, then one would crudely expect $\Delta \sim M_{\rm SUSY}^2/m_Z^2$. For example, if $M_{\rm SUSY} \sim 1$ TeV then there must be at least a $\Delta^{-1} \sim 1\%$ fine-tuning of the MSSM parameters to achieve the observed value of m_Z. This separation of the electroweak symmetry-breaking and supersymmetry-breaking scales is an example of the little hierarchy problem [167,168].

However, one must be very cautious when drawing conclusions about the viability of weak-scale supersymmetry to explain the origin of electroweak symmetry breaking [169]. First, one must

decide the largest tolerable value of Δ within the framework of weak-scale supersymmetry (should it be $\Delta \sim 10$? 100? 1000?). Second, the computation of Δ is often based on Eq. (109.5), which is a tree-level condition. A recent analysis given in Ref. 81 shows that the fine tuning measure can be reduced by as much as a factor of two when loop corrections are included [170]. Third, the fine-tuning parameter Δ depends quite sensitively on the structure of the supersymmetry-breaking dynamics, such as the value of M_X and relations among supersymmetry-breaking parameters in the fundamental high energy theory [171]. For example, in so-called focus point supersymmetry models [172], all squark masses can be as heavy as 5 TeV *without* significant fine-tuning. This can be attributed to a focusing behavior of the renormalization group evolution where certain relations hold among the high-energy values of the scalar squared-mass supersymmetry-breaking parameters. Although the focus point region of the CMSSM still yields an uncomfortably high value of Δ due to the observed Higgs mass of 125 GeV, one can achieve moderate values of Δ in models with NUHM2 boundary conditions for the scalar masses [166].

Among the colored superpartners, the third generation squarks generically have the most significant impact on the naturalness constraints [173], while their masses are the least constrained by the LHC data. Hence, in the absence of any relation between third generation squarks and those of the first two generations, the naturalness constraints due to present LHC data can be considerably weaker than those obtained in the CMSSM. Indeed, models with first and second generation squark masses in the multi-TeV range do not generically require significant fine tuning. Such models have the added benefit that undesirable FCNCs mediated by squark exchange are naturally suppressed [174]. Other MSSM mass spectra that are compatible with moderate fine tuning have been considered in Refs. 171 and 175.

The lower bounds on squark and gluino masses may not be as large as suggested by the experimental analyses based on the CMSSM or simplified models. For example, mass bounds for the gluino and the first and second generation squarks based on the CMSSM can often be evaded in alternative or extended MSSM models, *e.g.*, compressed supersymmetry [176] and stealth supersymmetry [177]. Moreover, the experimental upper limits for the third generation squark masses (which have a more direct impact on the fine-tuning measure) are weaker than the corresponding mass limits for other colored supersymmetric states.

Among the uncolored superpartners, the higgsinos are typically the most impacted by the naturalness constraints. Eq. (109.5) suggests that the masses of the two neutral higgsinos and charged higgsino pair (which are governed by $|\mu|$) should not be significantly larger than m_Z to avoid an unnatural fine-tuning of the supersymmetric parameters, which would imply the existence of light higgsinos (whose masses are not well constrained, as they are difficult to detect directly at the LHC due to their soft decay products). Nevertheless, it may be possible to avoid the conclusion that $\mu \sim \mathcal{O}(m_Z)$ if additional correlations among the supersymmetry breaking mass parameters and μ are present. Such a scenario can be realized in models in which the boundary conditions for supersymmetry breaking are generated by approximately conformal strong dynamics. For example, in the so-called scalar-sequestering model of Ref. 178, values of $|\mu| > 1$ TeV can be achieved while naturally maintaining the observed value of m_Z.

Finally, one can also consider extensions of the MSSM in which the degree of fine-tuning is relaxed. For example, it has already been noted in Section 109.5.2 that it is possible to accommodate the observed Higgs mass more easily in the NMSSM due to contributions to m_h^2 proportional to the parameter λ. This means that we do not have to rely on a large contribution from the radiative corrections to boost the Higgs mass sufficiently above its tree-level bound. This allows for smaller top squark masses, which are more consistent with the demands of naturalness. The reduction of the fine-tuning in various NMSSM models was initially advocated in Ref. 179, and more recently has been exhibited in Refs. 107,180. Naturalness can also be relaxed in extended supersymmetric models with vector-like quarks [181] and in gauge extensions of the MSSM [182].

Thus, it is premature to conclude that weak-scale supersymmetry is on the verge of exclusion. Nevertheless, it might be possible to sharpen the upper bounds on superpartner masses based on naturalness arguments, which ultimately will either confirm or refute the weak scale supersymmetry hypothesis [183]. Of course, if evidence for supersymmetric phenomena in the multi-TeV regime were to be established at a future collider facility (with an energy reach beyond the LHC [184]), it would be viewed as a spectacularly successful explanation of the large gauge hierarchy between the (multi-)TeV scale and Planck scale. In this case, the remaining little hierarchy, characterized by the somewhat large value of the fine-tuning parameter Δ discussed above, would perhaps be regarded as a less pressing issue.

109.7.2. *Constraints from virtual exchange of supersymmetric particles* :

There are a number of low-energy measurements that are sensitive to the effects of new physics through indirect searches via supersymmetric loop effects. For example, the virtual exchange of supersymmetric particles can contribute to the muon anomalous magnetic moment, $a_\mu \equiv \frac{1}{2}(g-2)_\mu$, as reviewed in Ref. 185. The Standard Model prediction for a_μ exhibits a deviation in the range of 3.5—4.1σ from the experimentally observed value [186]. This discrepancy is difficult to accommodate in the constrained supersymmetry models of Section 109.6.2 and Section 109.6.3 given the present sparticle mass bounds [165]. Nevertheless, there are regions of the more general pMSSM parameter space that are consistent with the observed value of a_μ [187].

The rare inclusive decay $b \to s\gamma$ also provides a sensitive probe to the virtual effects of new physics beyond the Standard Model. Recent experimental measurements of $B \to X_s + \gamma$ [188] are in very good agreement with the theoretical Standard Model predictions of Ref. 189. Since supersymmetric loop corrections can contribute an observable shift from the Standard Model predictions, the absence of any significant deviations places useful constraints on the MSSM parameter space [190].

The rare decays $B_s \to \mu^+\mu^-$ and $B_d \to \mu^+\mu^-$ are especially sensitive to supersymmetric loop effects, with some loop contributions scaling as $\tan^6\beta$ when $\tan\beta \gg 1$ [191]. At present, the observation of these rare decay modes [192] are compatible with the predicted Standard Model rates [193].

The decays $B^\pm \to \tau^\pm\nu_\tau$ and $B \to D^{(*)}\tau^-\overline{\nu}_\tau$ are noteworthy, since in models with extended Higgs sectors such as the MSSM, these processes possess tree-level charged Higgs exchange contributions that can compete with the dominant W-exchange. Experimental measurements of $B^\pm \to \tau^\pm\nu_\tau$ [194] initially suggested an enhanced rate with respect to the Standard Model, although the most recent results of the Belle Collaboration are consistent with Standard Model expectations. The BaBar Collaboration measured values of the rates for $\overline{B} \to D\tau^-\overline{\nu}_\tau$ and $\overline{B} \to D^*\tau^-\overline{\nu}_\tau$ [195] that showed a combined 3.4σ discrepancy from the Standard Model predictions, which was also not compatible with the Type-II Higgs Yukawa couplings employed by the MSSM. Subsequent measurements of the LHCb and Belle Collaborations [196] are consistent with the BaBar measurements. A recent assessment of all the data [197] concluded that the combined difference between the measured and expected values of the $\overline{B} \to D\tau^-\overline{\nu}_\tau$ and $\overline{B} \to D^*\tau^-\overline{\nu}_\tau$ decay rates relative to the corresponding Standard Model values has a significance of about four standard deviations. The possibility of accommodating these results due to supersymmetric effects has been advocated in Ref. [198].

There are a number of additional anomalies in B decay data that have recently attracted some attention, although at present the observed deviations from Standard Model expectations are typically at the level of about two standard deviations (see, *e.g.*, Ref. 199). In summary, although there are a few hints of possible deviations from the Standard Model in B decays, none of the discrepancies by themselves are significant enough to conclusively imply the existence of new physics beyond the Standard Model. Note that the absence of definitive evidence for deviations in these B-physics observables from their Standard Model predictions also places useful constraints on the MSSM parameter space [120,164,200].

Finally, we note that the constraints from precision electroweak

observables [201] are easily accommodated in models of weak-scale supersymmetry [202]. Thus, robust regions of the MSSM parameter space, compatible with the results of direct and indirect searches for supersymmetry, remain viable.

109.8. Massive neutrinos in weak-scale supersymmetry

In the minimal Standard Model and its supersymmetric extension, there are no right-handed neutrinos, and Majorana mass terms for the left-handed neutrinos are absent. However, given the overwhelming evidence for neutrino masses and mixing [203,204], any viable model of fundamental particles must provide a mechanism for generating neutrino masses [205]. In extended supersymmetric models, various mechanisms exist for producing massive neutrinos [206]. Although one can devise models for generating massive Dirac neutrinos [207], the most common approaches for incorporating neutrino masses are based on L-violating supersymmetric extensions of the MSSM, which generate massive Majorana neutrinos. Two classes of L-violating supersymmetric models will now be considered.

109.8.1. *The supersymmetric seesaw* :

Neutrino masses can be incorporated into the Standard Model by introducing SU(3)×SU(2)×U(1) singlet right-handed neutrinos (ν_R) whose mass parameters are very large, typically near the grand unification scale. In addition, one must also include a standard Yukawa couplings between the lepton doublets, the Higgs doublet, and ν_R. The Higgs vacuum expectation value then induces an off-diagonal ν_L–ν_R mass on the order of the electroweak scale. Diagonalizing the neutrino mass matrix (in the three-generation model) yields three superheavy neutrino states, and three very light neutrino states that are identified with the light neutrinos observed in nature. This is the seesaw mechanism [208].

It is straightforward to construct a supersymmetric generalization of the seesaw model of neutrino masses [209,210] by promoting the right-handed neutrino field to a superfield $\widehat{N}^c = (\widetilde{\nu}_R\,;\,\nu_R)$. Integrating out the heavy right-handed neutrino supermultiplet yields a new term in the superpotential [cf. Eq. (109.1)] of the form

$$W_{\rm seesaw} = \frac{f}{M_R}(\widehat{H}_U\widehat{L})(\widehat{H}_U\widehat{L})\,, \qquad (109.23)$$

where M_R is the mass scale of the right-handed neutrino sector and f is a dimensionless constant. Note that lepton number is broken by two units, which implies that R-parity is conserved. The supersymmetric analogue of the Majorana neutrino mass term in the sneutrino sector leads to sneutrino–antisneutrino mixing phenomena [210,211].

The Supersymmetry Les Houches Accords [76,92], mentioned at the end of the introduction to Section 109.4, have been extended to the supersymmetric seesaw (and other extensions of the MSSM) in Ref. 212.

109.8.2. *R-parity-violating supersymmetry* :

In order to incorporate massive neutrinos in renormalizable supersymmetric models while retaining the minimal particle content of the MSSM, one must relax the assumption of R-parity invariance. The most general R-parity-violating (RPV) model involving the MSSM spectrum introduces many new parameters to both the supersymmetry-conserving and the supersymmetry-breaking sectors [213,76]. Each new interaction term violates either B or L conservation. For example, starting from the MSSM superpotential given in Eq. (109.1) [suitably generalized to three generations of quarks, leptons and their superpartners], consider the effect of adding the following new terms:

$$W_{\rm RPV} = (\lambda_L)_{pmn}\widehat{L}_p\widehat{L}_m\widehat{E}^c_n + (\lambda'_L)_{pmn}\widehat{L}_p\widehat{Q}_m\widehat{D}^c_n + (\lambda_B)_{pmn}\widehat{U}^c_p\widehat{D}^c_m\widehat{D}^c_n + (\mu_L)_p\widehat{H}_u\widehat{L}_p\,, \qquad (109.24)$$

where p, m, and n are generation indices, and gauge group indices are suppressed. Eq. (109.24) yields new scalar-fermion Yukawa couplings consisting of all possible combinations involving two Standard Model fermions and one scalar superpartner.

Note that the term in Eq. (109.24) proportional to λ_B violates B, while the other three terms violate L. The L-violating term in Eq. (109.24) proportional to μ_L is the RPV generalization of the $\mu\widehat{H}_u\widehat{H}_d$ term of the MSSM superpotential, in which the $Y = -1$ Higgs/higgsino supermultiplet $\widehat{H}_d$ is replaced by the slepton/lepton supermultiplet $\widehat{L}_p$.

Phenomenological constraints derived from data on various low-energy B- and L-violating processes can be used to establish limits on each of the coefficients $(\lambda_L)_{pmn}$, $(\lambda'_L)_{pmn}$, and $(\lambda_B)_{pmn}$ taken one at a time [213,214]. If more than one coefficient is simultaneously non-zero, then the limits are in general more complicated [215]. All possible RPV terms cannot be simultaneously present and unsuppressed; otherwise the proton decay rate would be many orders of magnitude larger than the present experimental bound. One way to avoid proton decay is to impose B or L invariance (either one alone would suffice). Otherwise, one must accept the requirement that certain RPV coefficients must be extremely suppressed.

One particularly interesting class of RPV models is one in which B is conserved, but L is violated. It is possible to enforce baryon number conservation (and the stability of the proton), while allowing for lepton-number-violating interactions by imposing a discrete $\mathbf{Z_3}$ baryon triality symmetry on the low-energy theory [216], in place of the standard $\mathbf{Z_2}$ R-parity. Since the distinction between the Higgs and matter supermultiplets is lost in RPV models where L is violated, the mixing of sleptons and Higgs bosons, the mixing of neutrinos and neutralinos, and the mixing of charged leptons and charginos are now possible, leading to more complicated mass matrices and mass eigenstates than in the MSSM. The treatment of neutrino masses and mixing in this framework can be found, *e.g.*, in Ref. 217.

Alternatively, one can consider imposing a lepton parity such that all lepton superfields are odd [218,219]. In this case, only the B-violating term in Eq. (109.24) survives, and L is conserved. Models of this type have been considered in Ref. 220. Since L is conserved in these models, the mixing of the lepton and Higgs superfields is forbidden. However, one expects that lepton parity cannot be exact due to quantum gravity effects. Remarkably, the standard $\mathbf{Z_2}$ R-parity and the $\mathbf{Z_3}$ baryon triality are stable with respect to quantum gravity effects, as they can be identified as residual discrete symmetries that arise from spontaneously broken non-anomalous gauge symmetries [218].

The supersymmetric phenomenology of the RPV models exhibits features that are distinct from that of the MSSM [213]. The LSP is no longer stable, which implies that not all supersymmetric decay chains must yield missing-energy events at colliders. A comprehensive examination of the phenomenology of the MSSM extended by a single R-parity violating coupling at the unification scale and its implications for LHC searches has been given in Ref. 221. As an example, the sparticle mass bounds obtained in searches for R-parity-conserving supersymmetry can be considerably relaxed in certain RPV models due to the absence of large missing transverse energy signatures [222]. This can alleviate some of the tension with naturalness discussed in Section 109.7.1.

Nevertheless, the loss of the missing-energy signature is often compensated by other striking signals (which depend on which R-parity-violating parameters are dominant). For example, supersymmetric particles in RPV models can be singly produced (in contrast to R-parity-conserving models where supersymmetric particles must be produced in pairs). The phenomenology of pair-produced supersymmetric particles is also modified in RPV models due to new decay chains not present in R-parity-conserving supersymmetry models [213].

In RPV models with lepton number violation (these include weak-scale supersymmetry models with baryon triality mentioned above), both $\Delta L = 1$ and $\Delta L = 2$ phenomena are allowed, leading to neutrino masses and mixing [223], neutrinoless double-beta decay [224], sneutrino-antisneutrino mixing [225], and resonant s-channel production of sneutrinos in e^+e^- collisions [226] and charged sleptons in $p\bar{p}$ and pp collisions [227].

109.9. Extensions beyond the MSSM

Extensions of the MSSM have been proposed to solve a variety of theoretical problems. One such problem involves the μ parameter of the MSSM. Although μ is a supersymmetry-*preserving* parameter, it must be of order the effective supersymmetry-breaking scale of the MSSM to yield a consistent supersymmetric phenomenology [228]. Any natural solution to the so-called μ-problem must incorporate a symmetry that enforces $\mu = 0$ and a small symmetry-breaking parameter that generates a value of μ that is not parametrically larger than the effective supersymmetry-breaking scale [229]. A number of proposed mechanisms in the literature (*e.g.*, see Refs. 228–231) provide concrete examples of a natural solution to the μ-problem of the MSSM.

In extensions of the MSSM, new compelling solutions to the μ-problem are possible. For example, one can replace μ by the vacuum expectation value of a new SU(3)×SU(2)×U(1) singlet scalar field. This is the NMSSM, which yields phenomena that were briefly discussed in Section 109.4–Section 109.7. The NMSSM superpotential consists only of trilinear terms whose coefficients are dimensionless. There are some advantages to extending the NMSSM further to the USSM [98] by adding a new broken U(1) gauge symmetry [232], under which the singlet field is charged.

Alternatively, one can consider a generalized version of the NMSSM (called the GNMSSM in Ref. 180), where all possible renormalizable terms in the superpotential are allowed, which yields new supersymmetric mass terms (analogous to the μ term of the MSSM). A discussion of the parameters of the GNMSSM can be found in Ref. 76. Although the GNMSSM does not solve the μ-problem, it does exhibit regions of parameter space in which the degree of fine-tuning is relaxed, as discussed in Section 109.7.1.

The generation of the μ term may be connected with the solution to the strong CP problem [233]. Models of this type, which include new gauge singlet fields that are charged under the Peccei-Quinn (PQ) symmetry [234], were first proposed in Ref. 228. The breaking of the PQ symmetry is thus intimately tied to supersymmetry breaking, while naturally yielding a value of μ that is of order the electroweak symmetry breaking scale [235].

It is also possible to add higher dimensional Higgs multiplets, such as Higgs triplet superfields [236], provided a custodial-symmetric model (in which the ρ-parameter of precision electroweak physics is close to 1 [201]) can be formulated. Such models can provide a rich phenomenology of new signals for future LHC studies.

All supersymmetric models discussed so far in this review possess self-conjugate fermions—the Majorana gluinos and neutralinos. However, it is possible to add additional chiral superfields in the adjoint representation. The spin-1/2 components of these new superfields can pair up with the gauginos to form Dirac gauginos [237,238]. Such states appear in models of so-called supersoft supersymmetry breaking [239], in some generalized GMSB models [240] and in R-symmetric supersymmetry [241,242]. Such approaches often lead to improved naturalness and/or significantly relaxed flavor constraints. The implications of models of Dirac gauginos on the observed Higgs boson mass and its properties is addressed in Ref. 243.

For completeness, we briefly note other MSSM extensions considered in the literature. These include an enlarged electroweak gauge group beyond SU(2)×U(1) [244]; and/or the addition of new (possibly exotic) matter supermultiplets such as vector-like fermions and their superpartners [181,245].

References:

1. The early history of supersymmetry and a guide to the original literature can be found in *The Supersymmetric World—The Beginnings of the Theory*, edited by G. Kane and M. Shifman (World Scientific, Singapore, 2000).
2. R. Haag, J.T. Lopuszanski, and M. Sohnius, Nucl. Phys. **B88**, 257 (1975);
   S.R. Coleman and J. Mandula, Phys. Rev. **159**, 1251 (1967).
3. H.P. Nilles, Phys. Reports **110**, 1 (1984).
4. S. Weinberg, *The Quantum Theory of Fields, Volume III: Supersymmetry* (Cambridge University Press, Cambridge, UK, 2000);
   P. Binétruy, *Supersymmetry : Theory, Experiment, and Cosmology* (Oxford University Press, Oxford, UK, 2006).
5. P. Nath, *Supersymmetry, Supergravity, and Unification* (Cambridge University Press, Cambridge, UK, 2017).
6. S.P. Martin, in *Perspectives on Supersymmetry II*, edited by G.L. Kane (World Scientific, Singapore, 2010) pp. 1–153; see arXiv:hep-ph/9709356 for the latest version and `http://www.niu.edu/spmartin/primer/` for the most recent errata.
7. E. Witten, Nucl. Phys. **B188**, 513 (1981).
8. S. Dimopoulos and H. Georgi, Nucl. Phys. **B193**, 150 (1981).
9. N. Sakai, Z. Phys. **C11**, 153 (1981);
   R.K. Kaul, Phys. Lett. **109B**, 19 (1982);
   R.K. Kaul and M. Parthasarathi, Nucl. Phys. **B199**, 36 (1982).
10. L. Susskind, Phys. Reports **104**, 181 (1984).
11. L. Girardello and M. Grisaru, Nucl. Phys. **B194**, 65 (1982).
12. L.J. Hall and L. Randall, Phys. Rev. Lett. **65**, 2939 (1990);
    I. Jack and D.R.T. Jones, Phys. Lett. **B457**, 101 (1999).
13. O. Buchmüller and P. de Jong, *"Supersymmetry Part II (Experiment),"* and associated *Particle Listings: Other Searches–Supersymmetric Particles,* in the web edition of the *Review of Particle Physics* at `http://pdg.lbl.gov`.
14. V.F. Weisskopf, Phys. Rev. **56**, 72 (1939).
15. For a review, see *e.g.*, N. Polonsky, *Supersymmetry: Structure and phenomena. Extensions of the standard model*, Lect. Notes Phys. **M68**, 1 (2001).
16. G. Bertone, D. Hooper, and J. Silk, Phys. Reports **405**, 279 (2005).
17. D. Hooper, "TASI 2008 Lectures on Dark Matter," in *The Dawn of the LHC Era, Proceedings of the 2008 Theoretical and Advanced Study Institute in Elementary Particle Physics,* Boulder, Colorado, 2–27 June 2008, edited by Tao Han (World Scientific, Singapore, 2009).
18. H. Pagels and J.R. Primack, Phys. Rev. Lett. **48**, 223 (1982).
19. H. Goldberg, Phys. Rev. Lett. **50**, 1419 (1983) [Erratum: **103**, 099905 (2009)].
20. J. Ellis *et al.*, Nucl. Phys. **B238**, 453 (1984).
21. G. Jungman, M. Kamionkowski, and K. Griest, Phys. Reports **267**, 195 (1996);
    K. Griest and M. Kamionkowski, Phys. Reports **333**, 167 (2000).
22. F.D. Steffen, Eur. Phys. J. **C59**, 557 (2009).
23. M. Drees and G. Gerbier, *"Dark Matter,"* in the web edition of the *Review of Particle Physics* at `http://pdg.lbl.gov`.
24. H.E. Haber and G.L. Kane, Phys. Reports **117**, 75 (1985).
25. M. Drees, R. Godbole, and P. Roy, *Theory and Phenomenology of Sparticles* (World Scientific, Singapore, 2005);
    H. Baer and X. Tata, *Weak Scale Supersymmetry: from Superfields to Scattering Events* (Cambridge University Press, Cambridge, UK, 2006);
    I.J.R. Aitchison, *Supersymmetry in Particle Physics: an elementary introduction* (Cambridge University Press, Cambridge, UK, 2007).
26. Our notation for the charge-conjugated fields follows the notation of P. Langacker, *The Standard Model and Beyond*, 2nd edition (CRC Press, Boca Raton, FL, 2017).
27. H. Georgi and S.L. Glashow, Phys. Rev. **D6**, 429 (1972).
28. P. Fayet, Nucl. Phys. **B90**, 104 (1975).
29. K. Inoue *et al.*, Prog. Theor. Phys. **67**, 1889 (1982);
    R. Flores and M. Sher, Ann. Phys. (NY) **148**, 95 (1983).
30. J.F. Gunion and H.E. Haber, Nucl. Phys. **B272**, 1 (1986) [Erratum: **B402**, 567 (1993)].
31. J. Wess and J. Bagger, *Supersymmetry and Supergravity* (Princeton University Press, Princeton, NJ, 1992).
32. I. Buchbinder, S. Kuzenko, and J. Yarevskaya, Nucl. Phys. **B411**, 665 (1994);
    I. Antoniadis, E. Dudas, and D.M. Ghilencea, JHEP **0803**, 045 (2008).

33. For an overview of the theory and models of the soft-supersymmetry-breaking Lagrangian, see D.J.H. Chung *et al.*, Phys. Reports **407**, 1 (2005).
34. J. Ellis *et al.*, Phys. Rev. **D39**, 844 (1989);
U. Ellwanger and C. Hugonie, Eur. Phys. J. **C25**, 297 (2002);
U. Ellwanger, C. Hugonie, and A.M. Teixeira, Phys. Reports **496**, 1 (2010);
M. Maniatis, Int. J. Mod. Phys. **A25**, 3505 (2010).
35. S. Weinberg, Phys. Rev. Lett. **43**, 1566 (1979); Phys. Rev. **D22**, 1694 (1980);
F. Wilczek and A. Zee, Phys. Rev. Lett. **43**, 1571 (1979);
H.A. Weldon and A. Zee, Nucl. Phys. **B173**, 269 (1980).
36. P. Fayet, Phys. Lett. **69B**, 489 (1977);
G. Farrar and P. Fayet, Phys. Lett. **76B**, 575 (1978).
37. P. Fayet, Phys. Lett. **84B**, 421 (1979); Phys. Lett. **86B**, 272 (1979).
38. D.Z. Freedman and A. Van Proeyen, *Supergravity* (Cambridge University Press, Cambridge, UK, 2012).
39. S. Deser and B. Zumino, Phys. Rev. Lett. **38**, 1433 (1977);
E. Cremmer *et al.*, Phys. Lett. **79B**, 231 (1978).
40. R. Casalbuoni *et al.*, Phys. Lett. **B215**, 313 (1988); Phys. Rev. **D39**, 2281 (1989);
A.L. Maroto and J.R. Pelaez, Phys. Rev. **D62**, 023518 (2000).
41. Z. Komargodski and N. Seiberg, JHEP **0909**, 066 (2009);
I. Antoniadis *et al.*, Theor. Math. Phys. **170**, 26 (2012).
42. K. Benakli and C. Moura, Nucl. Phys. **B791**, 125 (2008);
C. Cheung, Y. Nomura, and J. Thaler, JHEP **1003**, 073 (2010);
N. Craig, J. March-Russell, and M. McCullough, JHEP **1010**, 095 (2010);
R. Argurio, Z. Komargodski and A. Mariotti, Phys. Rev. Lett. **107**, 061601 (2011).
43. A.H. Chamseddine, R. Arnowitt, and P. Nath, Phys. Rev. Lett. **49**, 970 (1982);
R. Barbieri, S. Ferrara, and C.A. Savoy, Phys. Lett. **119B**, 343 (1982);
L. Ibáñez, Nucl. Phys. **B218**, 514 (1982);
H.-P. Nilles, M. Srednicki, and D. Wyler, Phys. Lett. **120B**, 346 (1983); Phys. Lett. **124B**, 337 (1983);
E. Cremmer, P. Fayet, and L. Girardello, Phys. Lett. **122B**, 41 (1983);
N. Ohta, Prog. Theor. Phys. **70**, 542 (1983).
44. L. Alvarez-Gaumé, J. Polchinski, and M.B. Wise, Nucl. Phys. **B221**, 495 (1983).
45. L.J. Hall, J. Lykken, and S. Weinberg, Phys. Rev. **D27**, 2359 (1983).
46. S.K. Soni and H.A. Weldon, Phys. Lett. **126B**, 215 (1983);
Y. Kawamura, H. Murayama, and M. Yamaguchi, Phys. Rev. **D51**, 1337 (1995).
47. See, *e.g.*, A. Brignole, L.E. Ibáñez, and C. Munoz, in *Perspectives on Supersymmetry II*, edited by G.L. Kane (World Scientific, Singapore, 2010) pp. 244–268.
48. A.B. Lahanas and D.V. Nanopoulos, Phys. Reports **145**, 1 (1987).
49. J.L. Feng, A. Rajaraman, and F. Takayama, Phys. Rev. Lett. **91**, 011302 (2003); Phys. Rev. **D68**, 063504 (2003); Gen. Rel. Grav. **36**, 2575 (2004).
50. L. Randall and R. Sundrum, Nucl. Phys. **B557**, 79 (1999).
51. F. D'Eramo, J. Thaler, and Z. Thomas, JHEP **1206**, 151 (2012); JHEP **1309**, 125 (2013);
S.P. de Alwis, Phys. Rev. **D77**, 105020 (2008); JHEP **1301**, 006 (2013);
K. Harigaya and M. Ibe, Phys. Rev. **D90**, 085028 (2014).
52. See *e.g.*, I. Jack, D.R.T. Jones, and R. Wild, Phys. Lett. **B535**, 193 (2002);
B. Murakami and J.D. Wells, Phys. Rev. **D68**, 035006 (2003);
R. Kitano, G.D. Kribs, and H. Murayama, Phys. Rev. **D70**, 035001 (2004);
R. Hodgson *et al.*, Nucl. Phys. **B728**, 192 (2005);
D.R.T. Jones and G.G. Ross, Phys. Lett. **B642**, 540 (2006).
53. S. Asai *et al.*, Phys. Lett. **B653**, 81 (2007).
54. M. Dine, W. Fischler, and M. Srednicki, Nucl. Phys. **B189**, 575 (1981);
S. Dimopoulos and S. Raby, Nucl. Phys. **B192**, 353 (1982); Nucl. Phys. **B219**, 479 (1983);
M. Dine and W. Fischler, Phys. Lett. **110B**, 227 (1982);
C. Nappi and B. Ovrut, Phys. Lett. **113B**, 175 (1982);
L. Alvarez-Gaumé, M. Claudson, and M. Wise, Nucl. Phys. **B207**, 96 (1982).
55. M. Dine and A.E. Nelson, Phys. Rev. **D48**, 1277 (1993);
M. Dine, A.E. Nelson, and Y. Shirman, Phys. Rev. **D51**, 1362 (1995);
M. Dine *et al.*, Phys. Rev. **D53**, 2658 (1996).
56. G.F. Giudice and R. Rattazzi, Phys. Reports **322**, 419 (1999).
57. E. Poppitz and S.P. Trivedi, Phys. Rev. **D55**, 5508 (1997);
H. Murayama, Phys. Rev. Lett. **79**, 18 (1997);
M.A. Luty and J. Terning, Phys. Rev. **D57**, 6799 (1998);
K. Agashe, Phys. Lett. **B435**, 83 (1998);
N. Arkani-Hamed, J. March-Russell, and H. Murayama, Nucl. Phys. **B509**, 3 (1998);
C. Csaki, Y. Shirman, and J. Terning, JHEP **0705**, 099 (2007);
M. Ibe and R. Kitano, Phys. Rev. **D77**, 075003 (2008).
58. M. Kawasaki *et al.*, Phys. Rev. **D78**, 065011 (2008).
59. M.J. Strassler and K.M. Zurek, Phys. Lett. **B651**, 374 (2007);
T. Han *et al.*, JHEP **0807**, 008 (2008).
60. M.J. Strassler, `arXiv:hep-ph/0607160`;
K.M. Zurek, Phys. Rev. **D79**, 115002 (2009).
61. See *e.g.*, M. Quiros, in *Particle Physics and Cosmology: The Quest for Physics Beyond the Standard Model(s), Proceedings of the 2002 Theoretical Advanced Study Institute in Elementary Particle Physics (TASI 2002),* edited by H.E. Haber and A.E. Nelson (World Scientific, Singapore, 2004) pp. 549–601;
C. Csaki, in *ibid.*, pp. 605–698.
62. See, *e.g.*, J. Parsons and A. Pomarol, "Extra Dimensions," in the web edition of the *Review of Particle Physics* at `http://pdg.lbl.gov`.
63. See *e.g.*, V.A. Rubakov, Sov. Phys. Usp. **44**, 871 (2001);
J. Hewett and M. Spiropulu, Ann. Rev. Nucl. and Part. Sci. **52**, 397 (2002).
64. Z. Chacko, M.A. Luty, and E. Ponton, JHEP **0007**, 036 (2000);
D.E. Kaplan, G.D. Kribs, and M. Schmaltz, Phys. Rev. **D62**, 035010 (2000);
Z. Chacko *et al.*, JHEP **0001**, 003 (2000).
65. J. Scherk and J.H. Schwarz, Phys. Lett. **82B**, 60 (1979); Nucl. Phys. **B153**, 61 (1979).
66. See, *e.g.*, R. Barbieri, L.J. Hall, and Y. Nomura, Phys. Rev. **D66**, 045025 (2002); Nucl. Phys. **B624**, 63 (2002);
I.G. Garcia, K. Howe, and J. March-Russell, JHEP **1512**, 005 (2015).
67. J. Wells, `arXiv:hep-ph/0306127`; Phys. Rev. **D71**, 015013 (2005).
68. N. Arkani-Hamed and S. Dimopoulos, JHEP **0506**, 073 (2005);
G.F. Giudice and A. Romanino, Nucl. Phys. **B699**, 65 (2004) [Erratum: **B706**, 487 (2005)].
69. G. Aad *et al.* [ATLAS and CMS Collab.] Phys. Rev. Lett. **114**, 191803 (2015).
70. G.F. Giudice and A. Strumia, Nucl. Phys. **B858**, 63 (2012).
71. A. Arvanitaki *et al.*, JHEP **1302**, 126 (2013);
N. Arkani-Hamed *et al.*, `arXiv:1212.6971`(2012).
72. J.P. Vega and G. Villadoro, JHEP **1507**, 159 (2015).
73. Y. Kahn, M. McCullough and J. Thaler, JHEP **1311**, 161 (2013).
74. L.J. Hall and Y. Nomura, JHEP **1201**, 082 (2012);
M. Ibe and T.T. Yanagida, Phys. Lett. **B709**, 374 (2012).
75. H.E. Haber, in *Recent Directions in Particle Theory, Proceedings of the 1992 Theoretical Advanced Study Institute in Particle Physics*, edited by J. Harvey and J. Polchinski (World Scientific, Singapore, 1993) pp. 589–686.
76. B.C. Allanach *et al.*, Comp. Phys. Comm. **180**, 8 (2009).
77. J.M. Frere, D.R.T. Jones, and S. Raby, Nucl. Phys. **B222**, 11 (1983);
J.P. Derendinger and C.A. Savoy, Nucl. Phys. **B237**, 307

(1984);
J.F. Gunion, H.E. Haber, and M. Sher, Nucl. Phys. **B306**, 1 (1988);
D. Chowdhury *et al.*, JHEP **1402**, 110 (2014);
W.G. Hollik, JHEP **1608**, 126 (2016).
78. J.A. Casas, A. Lleyda, and C. Munoz, Nucl. Phys. **B471**, 3 (1996).
79. C.S. Ün *et al.*, Phys. Rev. **D91**, 105033 (2015);
U. Chattopadhyay and A. Dey, JHEP **1610**, 027 (2016).
80. G.G. Ross, K. Schmidt-Hoberg and F. Staub, Phys. Lett. **B759**, 110 (2016).
81. G.G. Ross, K. Schmidt-Hoberg and F. Staub, JHEP **1703**, 021 (2017).
82. S.P. Martin, Phys. Rev. **D61**, 035004 (2000).
83. S. Dimopoulos and D. Sutter, Nucl. Phys. **B452**, 496 (1995);
D.W. Sutter, Stanford Ph. D. thesis, arXiv:hep-ph/9704390.
84. H.E. Haber, Nucl. Phys. B (Proc. Suppl.) **62A-C**, 469 (1998).
85. R.M. Barnett, J.F. Gunion, and H.E. Haber, Phys. Lett. **B315**, 349 (1993);
H. Baer, X. Tata, and J. Woodside, Phys. Rev. **D41**, 906 (1990).
86. S.M. Bilenky, E.Kh. Khristova, and N.P. Nedelcheva, Phys. Lett. **B161**, 397 (1985); Bulg. J. Phys. **13**, 283 (1986);
G. Moortgat-Pick and H. Fraas, Eur. Phys. J. **C25**, 189 (2002).
87. J. Rosiek, Phys. Rev. **D41**, 3464 (1990) [Erratum: arXiv:hep-ph/9511250]. The most recent corrected version of this manuscript can be found on the author's webpage, www.fuw.edu.pl/~rosiek/physics/prd41.html.
88. J. Alwall *et al.*, JHEP **0709**, 028 (2007). See also the MadGraph homepage, http://madgraph.physics.illinois.edu.
89. T. Hahn, Comp. Phys. Comm. **140**, 418 (2001);
T. Hahn and C. Schappacher, Comp. Phys. Comm. **143**, 54 (2002). The FeynArts homepage is located at http://www.feynarts.de.
90. A. Pukhov *et al.*, INP MSU report 98-41/542 (arXiv:hep-ph/9908288);
E. Boos *et al.* [CompHEP Collab.], Nucl. Instrum. Methods **A534**, 50 (2004); CompHEP webpage, theory.sinp.msu.ru/dokuwiki/doku.php/comphep/news.
91. D.M. Pierce *et al.*, Nucl. Phys. **B491**, 3 (1997).
92. P. Skands *et al.*, JHEP **0407**, 036 (2004). The Supersymmetry Les Houches Accord homepage is skands.physics.monash.edu/slha/.
93. For further details, see *e.g.*, Appendix C of Ref. 24 and Appendix A of Ref. 30.
94. J.L. Kneur and G. Moultaka, Phys. Rev. **D59**, 015005 (1999).
95. R.A. Horn and C.R. Johnson, *Matrix Analysis*, 2nd Edition (Cambridge University Press, Cambridge, UK, 2003).
96. H.K. Dreiner, H.E. Haber, and S.P. Martin, Phys. Reports **494**, 1 (2010).
97. T. Takagi, Japan J. Math. **1**, 83 (1925).
98. S.Y. Choi *et al.*, Nucl. Phys. **B778**, 85 (2007).
99. S.Y. Choi *et al.*, Eur. Phys. J. **C22**, 563 (2001); Eur. Phys. J. **C23**, 769 (2002).
100. M.M. El Kheishen, A.A. Aboshousha, and A.A. Shafik, Phys. Rev. **D45**, 4345 (1992);
M. Guchait, Z. Phys. **C57**, 157 (1993) [Erratum: **C61**, 178 (1994)].
101. T. Hahn, preprint MPP-2006-85, physics/0607103.
102. K. Hikasa and M. Kobayashi, Phys. Rev. **D36**, 724 (1987);
F. Gabbiani and A. Masiero, Nucl. Phys. **B322**, 235 (1989);
Ph. Brax and C.A. Savoy, Nucl. Phys. **B447**, 227 (1995).
103. J. Ellis and S. Rudaz, Phys. Lett. **128B**, 248 (1983);
F. Browning, D. Chang, and W.Y. Keung, Phys. Rev. **D64**, 015010 (2001);
A. Bartl *et al.*, Phys. Lett. **B573**, 153 (2003); Phys. Rev. **D70**, 035003 (2004).
104. J.F. Gunion *et al.*, *The Higgs Hunter's Guide* (Westview Press, Boulder, CO, 2000);
M. Carena and H.E. Haber, Prog. in Part. Nucl. Phys. **50**, 63 (2003);
A. Djouadi, Phys. Reports **459**, 1 (2008).
105. P. Bechtle *et al.*, Eur. Phys. J. **C77**, 67 (2017).
106. H.E. Haber and M. Sher, Phys. Rev. **D35**, 2206 (1987).
107. L.J. Hall, D. Pinner, and J.T. Ruderman, JHEP **1204**, 131 (2012).
108. L.J. Hall and M.B. Wise, Nucl. Phys. **B187**, 397 (1981).
109. H.E. Haber and R. Hempfling, Phys. Rev. Lett. **66**, 1815 (1991);
Y. Okada, M. Yamaguchi, and T. Yanagida, Prog. Theor. Phys. **85**, 1 (1991);
J. Ellis, G. Ridolfi, and F. Zwirner, Phys. Lett. **B257**, 83 (1991).
110. For a recent review, see P. Draper and H. Rzehak, Phys. Reports **619**, 1 (2016).
111. A. Pilaftsis and C.E.M. Wagner, Nucl. Phys. **B553**, 3 (1999);
D.A. Demir, Phys. Rev. **D60**, 055006 (1999);
S.Y. Choi, M. Drees, and J.S. Lee, Phys. Lett. **B481**, 57 (2000);
M. Carena *et al.*, Nucl. Phys. **B586**, 92 (2000); Phys. Lett. **B495**, 155 (2000); Nucl. Phys. **B625**, 345 (2002);
M. Frank *et al.*, JHEP **0702**, 047 (2007);
S. Heinemeyer *et al.*, Phys. Lett. **B652**, 300 (2007).
112. H.E. Haber and J.D. Mason, Phys. Rev. **D77**, 115011 (2008).
113. M. Carena *et al.*, Phys. Rev. **D93**, 035013 (2016).
114. S. Khalil, Int. J. Mod. Phys. **A18**, 1697 (2003).
115. W. Fischler, S. Paban, and S. Thomas, Phys. Lett. **B289**, 373 (1992);
S.M. Barr, Int. J. Mod. Phys. **A8**, 209 (1993);
T. Ibrahim and P. Nath, Phys. Rev. **D58**, 111301 (1998) [Erratum: **D60**, 099902 (1999)];
M. Brhlik, G.J. Good, and G.L. Kane, Phys. Rev. **D59**, 115004 (1999);
V.D. Barger *et al.*, Phys. Rev. **D64**, 056007 (2001);
S. Abel, S. Khalil, and O. Lebedev, Nucl. Phys. **B606**, 151 (2001);
K.A. Olive *et al.*, Phys. Rev. **D72**, 075001 (2005);
G.F. Giudice and A. Romanino, Phys. Lett. **B634**, 307 (2006).
116. A. Masiero and L. Silvestrini, in *Perspectives on Supersymmetry*, edited by G.L. Kane (World Scientific, Singapore, 1998) pp. 423–441.
117. M. Pospelov and A. Ritz, Ann. Phys. **318**, 119 (2005).
118. See, *e.g.*, F. Gabbiani *et al.*, Nucl. Phys. **B477**, 321 (1996);
A. Masiero, and O. Vives, New J. Phys. **4**, 1 (2002).
119. For a review and references to the original literature, see: M.J. Ramsey-Musolf and S. Su, Phys. Reports **456**, 1 (2008).
120. M. Carena, A. Menon, and C.E.M. Wagner, Phys. Rev. **D79**, 075025 (2009);
S. Jager, Eur. Phys. J. **C59**, 497 (2009);
W. Altmannshofer *et al.*, Nucl. Phys. **B830**, 17 (2010).
121. M.B. Einhorn and D.R.T. Jones, Nucl. Phys. **B196**, 475 (1982).
122. For a review, see R.N. Mohapatra, in *Particle Physics 1999*, ICTP Summer School in Particle Physics, Trieste, Italy, edited by G. Senjanovic and A.Yu. Smirnov (World Scientific, Singapore, 2000) pp. 336–394;
W.J. Marciano and G. Senjanovic, Phys. Rev. **D25**, 3092 (1982).
123. R.M. Fonseca *et al.*, Nucl. Phys. **B854**, 28 (2012);
F. Staub, Comp. Phys. Comm. **182**, 808 (2011).
124. Comp. Phys. Comm. **185**, 1773 (2014); Adv. High Energy Phys. **2015**, 840780 (2015); the SARAH homepage is sarah.hepforge.org/.
125. B.C. Allanach, Comput. Phys. Commun. **143** 305 (2002); the SOFTSUSY homepage is softsusy.hepforge.org/.
126. P. Athron *et al.*, Comput. Phys. Commun. **190** 139 (2015); the FlexibleSUSY homepage is flexiblesusy.hepforge.org/.
127. L.E. Ibáñez and G.G. Ross, Phys. Lett. **B110**, 215 (1982).
128. J. Abdullah *et al.* [DELPHI Collab.], Eur. Phys. J. **C31**, 421 (2004).
129. H.K. Dreiner *et al.*, Eur. Phys. J. **C62**, 547 (2009).

130. G.F. Giudice *et al.*, JHEP **9812**, 027 (1998); A. Pomarol and R. Rattazzi, JHEP **9905**, 013 (1999); D.W. Jung and J.Y. Lee, JHEP **0903**, 123 (2009).
131. J.F. Gunion and H.E. Haber, Phys. Rev. **D37**, 2515 (1988); S.Y. Choi, M. Drees, and B. Gaissmaier, Phys. Rev. **D70**, 014010 (2004).
132. J.L. Feng *et al.*, Phys. Rev. Lett. **83**, 1731 (1999); J.F. Gunion and S. Mrenna, Phys. Rev. **D62**, 015002 (2000).
133. T. Gherghetta, G.F. Giudice, and J.D. Wells, Nucl. Phys. **B559**, 27 (1999).
134. M. Endo, M. Yamaguchi, and K. Yoshioka, Phys. Rev. **D72**, 015004 (2005); K. Choi, K.S. Jeong, and K.-I. Okumura, JHEP **0509**, 039 (2005); O. Loaiza-Brito *et al.*, AIP Conf. Proc. **805**, 198 (2006).
135. See *e.g.*, G. D'Ambrosio *et al.*, Nucl. Phys. **B465**, 155 (2002).
136. For a review of minimal flavor violation in supersymmetric theories, see C. Smith, Acta Phys. Polon. Supp. **3**, 53 (2010).
137. M. Drees and S.P. Martin, in *Electroweak Symmetry Breaking and New Physics at the TeV Scale*, edited by T. Barklow *et al.* (World Scientific, Singapore, 1996) pp. 146–215.
138. G.L. Kane *et al.*, Phys. Rev. **D49**, 6173 (1994).
139. J.R. Ellis *et al.*, Phys. Lett. **B573**, 162 (2003); Phys. Rev. **D70**, 055005 (2004).
140. L.E. Ibáñez and D. Lüst, Nucl. Phys. **B382**, 305 (1992); B. de Carlos, J.A. Casas, and C. Munoz, Phys. Lett. **B299**, 234 (1993); V. Kaplunovsky and J. Louis, Phys. Lett. **B306**, 269 (1993); A. Brignole, L.E. Ibáñez, and C. Munoz, Nucl. Phys. **B422**, 125 (1994) [Erratum: **B436**, 747 (1995)].
141. A. Arbey *et al.*, Phys. Rev. **D87**, 115020 (2013).
142. G.R. Dvali, G.F. Giudice and A. Pomarol, Nucl. Phys. **B478**, 31 (1996).
143. P. Draper *et al.*, Phys. Rev. **D85**, 095007 (2012).
144. P. Meade, N. Seiberg, and D. Shih, Prog. Theor. Phys. Supp. **177**, 143 (2009); M. Buican *et al.*, JHEP **0903**, 016 (2009).
145. A. Rajaraman *et al.*, Phys. Lett. **B678**, 367 (2009); L.M. Carpenter *et al.*, Phys. Rev. **D79**, 035002 (2009).
146. S. Ambrosanio, G.D. Kribs, and S.P. Martin, Nucl. Phys. **B516**, 55 (1998).
147. For a review and guide to the literature, see J.F. Gunion and H.E. Haber, in *Perspectives on Supersymmetry II*, edited by G.L. Kane (World Scientific, Singapore, 2010) pp. 420–445.
148. T.S. Roy and M. Schmaltz, Phys. Rev. **D77**, 095008 (2008); S. Knapen and D. Shih, JHEP **1408**, 136 (2014).
149. A. de Gouvea, A. Friedland, and H. Murayama, Phys. Rev. **D57**, 5676 (1998).
150. T. Han, D. Marfatia, and R.-J. Zhang, Phys. Rev. **D61**, 013007 (2000); Z. Chacko and E. Ponton, Phys. Rev. **D66**, 095004 (2002); A. Delgado, G.F. Giudice, and P. Slavich, Phys. Lett. **B653**, 424 (2007); T. Liu and C.E.M. Wagner, JHEP **0806**, 073 (2008).
151. B. Allanach *et al.*, Phys. Rev. **D92**, 015006 (2015).
152. A. Djouadi, J.L. Kneur, and G. Moultaka, Comp. Phys. Comm. **176**, 426 (2007); C.F. Berger *et al.*, JHEP **0902**, 023 (2009).
153. J. Berger *et al.*, Phys. Rev. **D93**, 035017 (2016).
154. K.J. de Vries *et al.*, Eur. Phys. J. **C75**, 422 (2015).
155. M. Cahill-Rowley *et al.*, Phys. Rev. **D90**, 095017 (2014); Phys. Rev. **D91**, 055002 (2015); A. Barr and J. Liu, Eur. Phys. J. **C77**, 202 (2017).
156. G. Bertone *et al.*, JCAP **1604**, 037 (2016).
157. N. Arkani-Hamed *et al.*, `arXiv:hep-ph/0703088`; J. Alwall *et al.*, Phys. Rev. **D79**, 015005 (2009); J. Alwall, P. Schuster, and N. Toro, Phys. Rev. **D79**, 075020 (2009); D.S.M. Alves, E. Izaguirre, and J.G. Wacker, Phys. Lett. **B702**, 64 (2011); JHEP **1110**, 012 (2011); D. Alves *et al.*, J. Phys. **G39**, 105005 (2012).
158. F. Ambrogi *et al.*, Eur. Phys. J. **C78**, 215 (2018).
159. R. Barbieri and G.F. Giudice, Nucl. Phys. **B305**, 63 (1988).
160. J.R. Ellis *et al.*, Mod. Phys. Lett. **A1**, 57 (1986).
161. G.W. Anderson and D.J. Castano, Phys. Lett. **B347**, 300 (1995); Phys. Rev. **D52**, 1693 (1995); Phys. Rev. **D53**, 2403 (1996); J.L. Feng, K.T. Matchev, and T. Moroi, Phys. Rev. **D61**, 075005 (2000); P. Athron and D.J. Miller, Phys. Rev. **D76**, 075010 (2007); M.E. Cabrera, J.A. Casas, and R.R. de Austri, JHEP **0903**, 075 (2009) (2009); H. Baer *et al.*, Phys. Rev. Lett. **109**, 161802 (2012).
162. D.M. Ghilencea and G.G. Ross, Nucl. Phys. **B868**, 65 (2013).
163. G.L. Kane and S.F. King, Phys. Lett. **B451**, 113 (1999); M. Bastero-Gil, G.L. Kane, and S.F. King, Phys. Lett. **B474**, 103 (2000); J.A. Casas, J.R. Espinosa, and I, Hidalgo, JHEP **0401**, 008 (2004); J. Abe, T. Kobayashi, and Y. Omura, Phys. Rev. **D76**, 015002 (2007); R. Essig and J.-F. Fortin, JHEP **0804**, 073 (2008).
164. O. Buchmüller *et al.*, Eur. Phys. J. **C74**, 2922 (2014).
165. P. Bechtle *et al.*, Eur. Phys. J. **C76**, 96 (2016).
166. H. Baer *et al.*, Phys. Rev. **D89**, 115019 (2014).
167. R. Barbieri and A. Strumia, `arXiv:hep-ph/0007265`.
168. L. Giusti, A. Romanino, and A. Strumia, Nucl. Phys. **B550**, 3 (1999); H.C. Cheng and I. Low, JHEP **0309**, 051 (2003); JHEP **0408**, 061 (2004); R. Harnik *et al.*, Phys. Rev. **D70**, 015002 (2004).
169. H. Baer, V. Barger, and D. Mickelson, Phys. Rev. **D88**, 095013 (2013).
170. B. de Carlos and J. A. Casas, Phys. Lett. **B309**, 320 (1993); S. Cassel, D.M. Ghilencea, and G.G. Ross, Nucl. Phys. **B825**, 203 (2010); **B835**, 110 (2010).
171. H. Baer *et al.*, Phys. Rev. **D87**, 035017 (2013); Phys. Rev. **D87**, 115028 (2013); Ann. Rev. Nucl. and Part. Sci. **63**, 351 (2013).
172. J. Feng, K. Matchev, and T. Moroi, Phys. Rev. Lett. **84**, 2322 (2000); Phys. Rev. **D61**, 075005 (2000); J. Feng and F. Wilczek, Phys. Lett. **B631**, 170 (2005); D. Horton and G.G. Ross, Nucl. Phys. **B830**, 221 (2010).
173. M. Drees, Phys. Rev. **D33**, 1468 (1986); S. Dimopoulos and G.F. Giudice, Phys. Lett. **B357**, 573 (1995); A. Pomarol and D. Tommasini, Nucl. Phys. **B466**, 3 (1996).
174. M. Dine, A. Kagan, and S. Samuel, Phys. Lett. **B243**, 250 (1990); A.G. Cohen, D.B. Kaplan, and A.E. Nelson, Phys. Lett. **B388**, 588 (1996).
175. C. Brust *et al.*, JHEP **1203**, 103 (2012); M. Papucci, J.T. Ruderman, and A. Weiler, JHEP **1209**, 035 (2012); H.K. Dreiner, M. Kramer, and J. Tattersall, Europhys. Lett. **99**, 61001 (2012); H. Baer *et al.*, JHEP **1205**, 109 (2012).
176. S.P. Martin, Phys. Rev. **D75**, 115005 (2007); Phys. Rev. **D78**, 055019 (2009).
177. J. Fan, M. Reece, and J.T. Ruderman, JHEP **1111**, 012 (2011); JHEP **1207**, 196 (2012).
178. H. Murayama, Y. Nomura and D. Poland, Phys. Rev. **D77**, 015005 (2008); G. Perez, T.S. Roy, and M. Schmaltz, Phys. Rev. **D79**, 095016 (2009).
179. R. Dermisek and J.F. Gunion, Phys. Rev. Lett. **95**, 041801 (2005); Phys. Rev. **D75**, 095019 (2007); Phys. Rev. **D76**, 095006 (2007).
180. G.G. Ross and K. Schmidt-Hoberg, Nucl. Phys. **B862**, 710 (2012); JHEP **1208**, 074 (2012); A. Kaminska, G.G. Ross, and K. Schmidt-Hoberg, JHEP **1311**, 209 (2013).
181. S.P. Martin and J.D. Wells, Phys. Rev. **D86**, 035017 (2012).

182. B. Bellazzini *et al.*, Phys. Rev. **D79**, 095003 (2009).
183. H. Baer, V. Barger, and M. Savoy, Phys. Rev. **D93**, 035016 (2016).
184. M.L. Mangano, editor, *Physics at the FCC-hh, a 100 TeV pp collider*, CERN Yellow Report, CERN-2017-003-M (2017).
185. D. Stockinger, J. Phys. **G34**, R45 (2007);
P. Athron *et al.*, Eur. Phys. J. **C76**, 62 (2016).
186. F. Jegerlehner, EPJ Web Conf. **166**, 00022 (2018);
M. Davier *et al.*, Eur. Phys. J. **C77**, 827 (2017);
K. Hagiwara *et al.*, Nucl. Part. Phys. Proc. **287-288**, 33 (2017).
187. M. Ibe, T. T. Yanagida, and N. Yokozaki, JHEP **1308**, 067 (2013).
188. A. Limosani *et al.* [Belle Collab.], Phys. Rev. Lett. **103**, 241801 (2009);
J.P. Lees *et al.* [BaBar Collab.], Phys. Rev. Lett. **109**, 191801 (2012); Phys. Rev. **D86**, 112008 (2012).
189. M. Misiak *et al.*, Phys. Rev. Lett. **114**, 221801 (2015);
M. Czakon *et al.*, JHEP **1504**, 168 (2015).
190. See, *e.g.*, M. Ciuchini *et al.*, Phys. Rev. **D67**, 075016 (2003);
T. Hurth, Rev. Mod. Phys. **75**, 1159 (2003);
F. Mahmoudi, JHEP **0712**, 026 (2007);
K.A. Olive and L. Velasco-Sevilla, JHEP **0805**, 052 (2008).
191. S.R. Choudhury and N. Gaur, Phys. Lett. **B451**, 86 (1999);
K.S. Babu and C.F. Kolda, Phys. Rev. Lett. **84**, 228 (2000);
G. Isidori and A. Retico, JHEP **0111**, 001 (2001); JHEP **0209**, 063 (2002).
192. The CMS and LHCb Collab., Nature **522**, 68 (2015);
ATLAS Collab., Eur. Phys. J. **C76**, 513 (2016);
LHCb Collab., Phys. Rev. Lett. **118**, 191801 (2017).
193. C. Bobeth *et al.*, Phys. Rev. Lett. **112**, 101801 (2014).
194. K. Hara *et al.* [Belle Collab.], Phys. Rev. Lett. **110**, 131801 (2013);
J.P. Lees *et al.* [BaBar Collab.], Phys. Rev. **D88**, 031102 (R)(2013).
195. J.P. Lees *et al.* [BaBar Collab.], Phys. Rev. Lett. **109**, 101802 (2012);
Phys. Rev. **D88**, 072012 (2013).
196. R. Aaij *et al.* [LHCb Collab.], Phys. Rev. Lett. **115**, 111803 (2015); Phys. Rev. Lett. **120**, 171802 (2018);
M. Huschle *et al.* [Belle Collab.], Phys. Rev. **D92**, 072014 (2015);
Y. Sato *et al.* [Belle Collab.], Phys. Rev. **D94**, 072007 (2016);
S. Hirose *et al.* [Belle Collab.], Phys. Rev. Lett. **118**, 211801 (2017); Phys. Rev. **D97**, 012004 (2018).
197. G. Ciezarek *et al.*, Nature **546**, 227 (2017).
198. D. Boubaa, S. Khalil and S. Moretti, `arXiv:1604.03416`.
199. R. Aaij *et al.* [LHCb Collaboration], JHEP **1708**, 055 (2017).
200. F. Mahmoudi, S. Neshatpour, and J. Orloff, JHEP **1208**, 092 (2012);
A. Arbey *et al.*, Phys. Rev. **D87**, 035026 (2013).
201. J. Erler and A. Freitas, "Electroweak Model and Constraints on New Physics," in the web edition of the *Review of Particle Physics* at `http://pdg.lbl.gov`.
202. J.R. Ellis *et al.*, JHEP **0708**, 083 (2007);
S. Heinemeyer *et al.*, JHEP **0808**, 087 (2008);
G.-C. Cho *et al.*, JHEP **1111**, 068 (2011).
203. See the section on neutrinos in "Particle Listings—Leptons" in the web edition of the *Review of Particle Physics* at `http://pdg.lbl.gov`;
An updated global analysis of neutrino oscillation measurements is provided by the NuFIT collaboration at `http://www.nu-fit.org`.
204. J. Bergstrom *et al.*, JHEP **1701**, 087 (2017).
205. K. Zuber, Phys. Reports **305**, 295 (1998);
S.F. King, J. Phys. **G42**, 123001 (2015).
206. For a review of neutrino masses in supersymmetry, see *e.g.*, B. Mukhopadhyaya, *Proc. Indian National Science Academy* **A70**, 239 (2004);
M. Hirsch and J.W.F. Valle, New J. Phys. **6**, 76 (2004).
207. F. Borzumati and Y. Nomura, Phys. Rev. **D64**, 053005 (2001).
208. P. Minkowski, Phys. Lett. **67B**, 421 (1977);
M. Gell-Mann, P. Ramond, and R. Slansky, in *Supergravity*, edited by D. Freedman and P. van Nieuwenhuizen (North Holland, Amsterdam, 1979) p. 315;
T. Yanagida, Prog. Theor. Phys. **64**, 1103 (1980);
R. Mohapatra and G. Senjanovic, Phys. Rev. Lett. **44**, 912 (1980); Phys. Rev. **D23**, 165 (1981).
209. J. Hisano *et al.*, Phys. Lett. **B357**, 579 (1995);
J. Hisano *et al.*, Phys. Rev. **D53**, 2442 (1996);
J.A. Casas and A. Ibarra, Nucl. Phys. **B618**, 171 (2001);
J. Ellis *et al.*, Phys. Rev. **D66**, 115013 (2002);
A. Masiero, S.K. Vempati, and O. Vives, New J. Phys. **6**, 202 (2004);
E. Arganda *et al.*, Phys. Rev. **D71**, 035011 (2005);
F.R. Joaquim and A. Rossi, Phys. Rev. Lett. **97**, 181801 (2006);
J.R. Ellis and O. Lebedev, Phys. Lett. **B653**, 411 (2007).
210. Y. Grossman and H.E. Haber, Phys. Rev. Lett. **78**, 3438 (1997);
A. Dedes, H.E. Haber, and J. Rosiek, JHEP **0711**, 059 (2007).
211. M. Hirsch, H.V. Klapdor-Kleingrothaus, and S.G. Kovalenko, Phys. Lett. **B398**, 311 (1997);
L.J. Hall, T. Moroi, and H. Murayama, Phys. Lett. **B424**, 305 (1998);
K. Choi, K. Hwang, and W.Y. Song, Phys. Rev. Lett. **88**, 141801 (2002);
T. Honkavaara, K. Huitu, and S. Roy, Phys. Rev. **D73**, 055011 (2006).
212. L. Basso *et al.*, Comp. Phys. Comm. **184**, 698 (2013).
213. M. Chemtob, Prog. in Part. Nucl. Phys. **54**, 71 (2005);
R. Barbier *et al.*, Phys. Reports **420**, 1 (2005).
214. H. Dreiner, in *Perspectives on Supersymmetry II*, edited by G.L. Kane (World Scientific, Singapore, 2010) pp. 565–583.
215. B.C. Allanach, A. Dedes, and H.K. Dreiner, Phys. Rev. **D60**, 075014 (1999).
216. L.E. Ibáñez and G.G. Ross, Nucl. Phys. **B368**, 3 (1992);
L.E. Ibáñez, Nucl. Phys. **B398**, 301 (1993).
217. A. Dedes, S. Rimmer, and J. Rosiek, JHEP **0608**, 005 (2006);
B.C. Allanach and C.H. Kom, JHEP **0804**, 081 (2008);
H.K. Dreiner *et al.*, Phys. Rev. **D84**, 113005 (2011).
218. L.E. Ibáñez and G.G. Ross, Nucl. Phys. **B368**, 3 (1992).
219. H.K. Dreiner, C. Luhn, and M. Thormeier Phys. Rev. **D73**, 075007 (2006).
220. K. Tamvakis, Phys. Lett. **B382**, 251 (1996);
G. Eyal and Y. Nir, JHEP **9906**, 024 (1999);
A. Florez *et al.*, Phys. Rev. **D87**, 095010 (2013).
221. D. Dercks *et al.*, Eur. Phys. J. **C77**, 856 (2017).
222. B.C. Allanach and B. Gripaios, JHEP **1205**, 062 (2012);
M. Asano, K. Rolbiecki, and K. Sakurai, JHEP **1301**, 128 (2013);
N. Chamoun *et al.*, JHEP **1408**, 142 (2014).
223. See *e.g.*, J.C. Romao, Nucl. Phys. (Proc. Supp.) **81**, 231 (2000);
Y. Grossman and S. Rakshit, Phys. Rev. **D69**, 093002 (2004).
224. R.N. Mohapatra, Phys. Rev. **D34**, 3457 (1986);
K.S. Babu and R.N. Mohapatra, Phys. Rev. Lett. **75**, 2276 (1995);
M. Hirsch, H.V. Klapdor-Kleingrothaus, and S.G. Kovalenko, Phys. Rev. Lett. **75**, 17 (1995); Phys. Rev. **D53**, 1329 (1996).
225. Y. Grossman and H.E. Haber, Phys. Rev. **D59**, 093008 (1999).
226. S. Dimopoulos and L.J. Hall, Phys. Lett. **B207**, 210 (1988);
J. Kalinowski *et al.*, Phys. Lett. **B406**, 314 (1997);
J. Erler, J.L. Feng, and N. Polonsky, Phys. Rev. Lett. **78**, 3063 (1997).
227. H.K. Dreiner, P. Richardson, and M.H. Seymour, Phys. Rev. **D63**, 055008 (2001).
228. J.E. Kim and H.P. Nilles, Phys. Lett. **B138**, 150 (1984).
229. J.E. Kim and H.P. Nilles, Mod. Phys. Lett. **A9**, 3575 (1994).
230. G.F. Giudice and A. Masiero, Phys. Lett. **B206**, 480 (1988).
231. J.A. Casas and C. Munoz, Phys. Lett. **B306**, 288 (1993).
232. M. Cvetič *et al.*, Phys. Rev. **D56**, 2861 (1997) [Erratum: **D58**, 119905 (1998)].

233. For a review see e.g., R. D. Peccei, Lect. Notes Phys. **741**, 3 (2008).
234. R. Peccei and H. Quinn, Phys. Rev. Lett. **38**, 1440 (1977); Phys. Rev. **D16**, 1791 (1977).
235. H. Murayama, H. Suzuki, and T. Yanagida, Phys. Lett. **B291**, 418 (1992);
T. Gherghetta, G.L. Kane, Phys. Lett. **B354**, 300 (1995);
K.J. Bae, H. Baer, and H. Serce, Phys. Rev. **D91**, 015003 (2015).
236. A. Delgado, G. Nardini, and M. Quiros, Phys. Rev. **D86**, 115010 (2012).
237. P. Fayet, Phys. Lett. **78B**, 417 (1978).
238. For a review, see *e.g.*, K. Benakli, Fortsch. Phys. **59**, 1079 (2011).
239. P.J. Fox, A.E. Nelson, and N. Weiner, JHEP **0208**, 035 (2002).
240. K. Benakli and M.D. Goodsell, Nucl. Phys. **B816**, 185 (2009); Nucl. Phys. **B840**, 1 (2010).
241. U. Sarkar and R. Adhikari, Phys. Rev. **D55**, 3836 (1997); R. Fok *et al.*, Phys. Rev. **D87**, 055018 (2013).
242. G.D. Kribs, E. Poppitz, and N. Weiner, Phys. Rev. **D78**, 055010 (2008).
243. K. Benakli, M.D. Goodsell, and F. Staub, JHEP **1306**, 073 (2013).
244. See *e.g.*, J.L. Hewett and T.G. Rizzo, Phys. Reports **183**, 193 (1989).
245. S.F. King, S. Moretti, and R. Nevzorov, Phys. Lett. **B634**, 278 (2006); Phys. Rev. **D73**, 035009 (2006).

110. Supersymmetry, Part II (Experiment)

Updated September 2017 by O. Buchmueller (Imperial College London) and P. de Jong (Nikhef and University of Amsterdam).

110.1. Introduction

Supersymmetry (SUSY), a transformation relating fermions to bosons and vice versa [1–9], is one of the most compelling possible extensions of the Standard Model of particle physics (SM).

On theoretical grounds SUSY is motivated as a generalization of space-time symmetries. A low-energy realization of SUSY, *i.e.*, SUSY at the TeV scale, is, however, not a necessary consequence. Instead, low-energy SUSY is motivated by the possible cancellation of quadratic divergences in radiative corrections to the Higgs boson mass [10–15]. Furthermore, it is intriguing that a weakly interacting, (meta)stable supersymmetric particle might make up some or all of the dark matter in the universe [16–18]. In addition, SUSY predicts that gauge couplings, as measured experimentally at the electroweak scale, unify at an energy scale $\mathcal{O}(10^{16})$ GeV ("GUT scale") near the Planck scale [19–25].

In the minimal supersymmetric extension to the Standard Model, the so called MSSM [11,26,27], a supersymmetry transformation relates every fermion and gauge boson in the SM to a supersymmetric partner with half a unit of spin difference, but otherwise with the same properties (such as mass) and quantum numbers. These are the "sfermions": squarks ($\tilde{q}$) and sleptons ($\tilde{\ell}$, $\tilde{\nu}$), and the "gauginos". The MSSM Higgs sector contains two doublets, for up-type quarks and for down-type quarks and charged leptons respectively. After electroweak symmetry breaking, five Higgs bosons arise, of which two are charged. The supersymmetric partners of the Higgs doublets are known as "higgsinos." The weak gauginos and higgsinos mix, giving rise to charged mass eigenstates called "charginos" ($\tilde{\chi}^{\pm}$), and neutral mass eigenstates called "neutralinos" ($\tilde{\chi}^0$). The SUSY partners of the gluons are known as "gluinos" ($\tilde{g}$). The fact that such particles are not yet observed leads to the conclusion that, if supersymmetry is realized, it is a broken symmetry. A description of SUSY in the form of an effective Lagrangian with only "soft" SUSY breaking terms and SUSY masses at the TeV scale maintains cancellation of quadratic divergences in particle physics models.

The phenomenology of SUSY is to a large extent determined by the SUSY breaking mechanism and the SUSY breaking scale. This determines the SUSY particle masses, the mass hierarchy, the field contents of physical particles, and their decay modes. In addition, phenomenology crucially depends on whether the multiplicative quantum number of R-parity [27], $R = (-1)^{3(B-L)+2S}$, where B and L are baryon and lepton numbers and S is the spin, is conserved or violated. If R-parity is conserved, SUSY particles (sparticles), which have odd R-parity, are produced in pairs and the decays of each SUSY particle must involve an odd number of lighter SUSY particles. The lightest SUSY particle (LSP) is then stable and often assumed to be a weakly interacting massive particle (WIMP). If R-parity is violated, new terms λ_{ijk}, λ'_{ijk} and λ''_{ijk} appear in the superpotential, where ijk are generation indices; λ-type couplings appear between lepton superfields only, λ''-type are between quark superfields only, and λ'-type couplings connect the two. R-parity violation implies lepton and/or baryon number violation. More details of the theoretical framework of SUSY are discussed elsewhere in this volume [28].

Today, low-energy data from flavor physics experiments, high-precision electroweak observables as well as astrophysical data impose strong constraints on the allowed SUSY parameter space. Recent examples of such data include measurements of the rare B-meson decay $B_s \to \mu^+\mu^-$ [29,30], measurements of the anomalous magnetic moment of the muon [31], and accurate determinations of the cosmological dark matter relic density constraint [32,33].

These indirect constraints are often more sensitive to higher SUSY mass scales than experiments searching for direct sparticle production at colliders, but the interpretation of these results is often strongly model dependent. In contrast, direct searches for sparticle production at collider experiments are less subject to interpretation ambiguities and therefore they play a crucial role in the search for SUSY.

The discovery of a Higgs boson with a mass around 125 GeV imposes constraints on SUSY, which are discussed elsewhere [28,34].

In this review we limit ourselves to direct searches, covering data analyses at LEP, HERA, the Tevatron and the LHC, with emphasis on the latter. For more details on LEP and Tevatron constraints, see earlier PDG reviews [35].

110.2. Experimental search program

The electron-positron collider LEP was operational at CERN between 1989 and 2000. In the initial phase, center-of-mass energies around the Z-peak were probed, but after 1995 the LEP experiments collected a significant amount of luminosity at higher center-of-mass energies, some 235 pb^{-1} per experiment at $\sqrt{s} \geq 204$ GeV , with a maximum $\sqrt{s}$ of 209 GeV .

Searches for new physics at e^+e^- colliders benefit from the clean experimental environment and the fact that momentum balance can be measured not only in the plane transverse to the beam, but also in the direction along the beam (up to the beam pipe holes), defined as the longitudinal direction. Searches at LEP are dominated by the data samples taken at the highest center-of-mass energies.

Constraints on SUSY have been set by the CDF and D0 experiments at the Tevatron, a proton-antiproton collider at a center-of-mass energy of up to 1.96 TeV. CDF and D0 have collected integrated luminosities between 10 and 11 fb^{-1} each up to the end of collider operations in 2011.

The electron-proton collider HERA provided collisions to the H1 and ZEUS experiments between 1992 and 2007, at a center-of-mass energy up to 318 GeV . A total integrated luminosity of approximately 0.5 fb^{-1} was collected by each experiment. Since in ep collisions no annihilation process takes place, SUSY searches at HERA typically look for R-parity violating production of single SUSY particles.

The Large Hadron Collider (LHC) at CERN started proton-proton operation at a center-of-mass energy of 7 TeV in 2010. By the end of 2011 the experiments ATLAS and CMS had collected about 5 fb^{-1} of integrated luminosity each, and the LHCb experiment had collected approximately 1 fb^{-1}. In 2012, the LHC operated at a center-of-mass energy of 8 TeV, and ATLAS and CMS collected approximately 20 fb^{-1} each, whereas LHCb collected 2 fb^{-1}. In 2015, the LHC started Run 2, with a center-of-mass energy of 13 TeV. At the end of 2016, ATLAS and CMS had both collected approximately 36 fb^{-1}, and LHCb had collected 2 fb^{-1}.

Proton-(anti)proton colliders produce interactions at higher center-of-mass energies than those available at LEP, and cross sections of QCD-mediated processes are larger, which is reflected in the higher sensitivity for SUSY particles carrying color charge: squarks and gluinos. Large background contributions from Standard Model processes, however, pose challenges to trigger and analysis. Such backgrounds are dominated by multijet production processes, including, particularly at the LHC, those of top quark production, as well as jet production in association with vector bosons. The proton momentum is shared between its parton constituents, and in each collision only a fraction of the total center-of-mass energy is available in the hard parton-parton scattering. Since the parton momenta in the

longitudinal direction are not known on an event-by-event basis, use of momentum conservation constraints in an analysis is restricted to the transverse plane, leading to the definition of transverse variables, such as the missing transverse momentum, and the transverse mass. Proton-proton collisions at the LHC differ from proton-antiproton collisions at the Tevatron in the sense that there are no valence anti-quarks in the proton, and that gluon-initiated processes play a more dominant role. The increased center-of-mass energy of the LHC compared to the Tevatron, as well as the increase at the LHC between Run 1 and Run 2, significantly extends the kinematic reach for SUSY searches. This is reflected foremost in the sensitivity for squarks and gluinos, but also for other SUSY particles.

The main production mechanisms of massive colored sparticles at hadron colliders are squark-squark, squark-gluino and gluino-gluino production; when "squark" is used "antisquark" is also implied. The typical SUSY search signature at hadron colliders contains high-p_{T} jets, which are produced in the decay chains of heavy squarks and gluinos, and significant missing momentum originating from the two LSPs produced at the end of the decay chain. Assuming R-parity conservation, the LSPs are expected to be neutral and weakly interacting massive particles, since otherwise the model contradicts standard cosmology. These particles then escape detection at colliders. Standard Model backgrounds with missing transverse momentum include leptonic W/Z-boson decays, heavy-flavor decays to neutrinos, and multijet events that may be affected by instrumental effects such as jet mismeasurement.

Selection variables designed to separate the SUSY signal from the Standard Model backgrounds include H_{T}, $E_{\mathrm{T}}^{\mathrm{miss}}$, and m_{eff}. The quantities H_{T} and $E_{\mathrm{T}}^{\mathrm{miss}}$ refer to the measured transverse energy and missing transverse momentum in the event, respectively. They are usually defined as the scalar sum of the transverse jet momenta or calorimeter clusters transverse energies measured in the event (H_{T}), or the negative vector sum of transverse momenta of reconstructed objects like jets and leptons in the event ($E_{\mathrm{T}}^{\mathrm{miss}}$). The quantity m_{eff} is referred to as the effective mass of the event and is defined as $m_{\mathrm{eff}} = H_{\mathrm{T}} + |E_{\mathrm{T}}^{\mathrm{miss}}|$. The peak of the m_{eff} distribution for SUSY signal events correlates with the SUSY mass scale, in particular with the mass difference between the primary produced SUSY particle and the LSP [36], whereas the Standard Model backgrounds dominate at low m_{eff}. Additional reduction of multijet backgrounds can be achieved by demanding isolated leptons or photons in the final states; in such events the lepton or photon transverse momentum may be added to H_{T} or m_{eff} for further signal-background separation.

At the LHC, alternative approaches have been developed to increase the sensitivity to pair production of heavy sparticles with TeV-scale masses focusing on the kinematics of their decays, and to further suppress the background from multijet production. Prominent examples of these new approaches are searches using the α_{T} [37–41], *razor* [42], *stransverse mass* (m_{T2}) [43], and *contransverse mass* (m_{CT}) [44] variables. Recently, the topological event reconstruction methods have expanded with the *super-razor* [45] and *recursive jigsaw reconstruction* [46] techniques. Furthermore, frequently the searches for massive SUSY particles attempt to identify their decay into top quarks or vector bosons, which are themselves unstable. If these are produced with a significant boost, jets from their decay will typically overlap, and such topologies are searched for with *jet-substructure* [47] techniques.

110.3. Interpretation of results

Since the mechanism by which SUSY is broken is unknown, a general approach to SUSY via the most general soft SUSY breaking Lagrangian adds a significant number of new free parameters. For the minimal supersymmetric standard model, MSSM, *i.e.*, the model with the minimal particle content, these comprise 105 new parameters. A phenomenological analysis of SUSY searches leaving all these parameters free is not feasible. For the practical interpretation of SUSY searches at colliders several approaches are taken to reduce the number of free parameters.

One approach is to assume a SUSY breaking mechanism and lower the number of free parameters through the assumption of additional constraints. Before the start of the LHC, interpretations of experimental results were predominately performed in constrained models of gravity mediated [48,49], gauge-mediated [50–52], and anomaly mediated [53,54] SUSY breaking. The most popular model was the constrained MSSM (CMSSM) [48,55,56], which in the literature is also referred to as minimal supergravity, or MSUGRA.

These constrained SUSY models are theoretically well motivated and provide a rich spectrum of experimental signatures. However, with universality relations imposed on the soft SUSY breaking parameters, they do not cover all possible kinematic signatures and mass relations of SUSY. In such scenarios the squarks are often nearly degenerate in mass, in particular for the first and second generation. The exclusion of parameter space in the CMSSM and in CMSSM-inspired models is mainly driven by first and second generation squark production together with gluino production. As shown in Fig. 110.1 [57] these processes possess the largest production cross sections in proton-proton collisions, and thus the LHC searches typically provide the tightest mass limits on these colored sparticles. This, however, implies that the allowed parameter space of constrained SUSY models today has been restrained significantly by searches from ATLAS and CMS. Furthermore, confronting the remaining allowed parameter space with other collider and non-collider measurements, which are directly or indirectly sensitive to contributions from SUSY, the overall compatibility of these models with all data is significantly worse than in the pre-LHC era (see section II.8 for further discussion), indicating that very constrained models like the CMSSM are no longer be good benchmark scenarios to solely characterize the results of SUSY searches at the LHC.

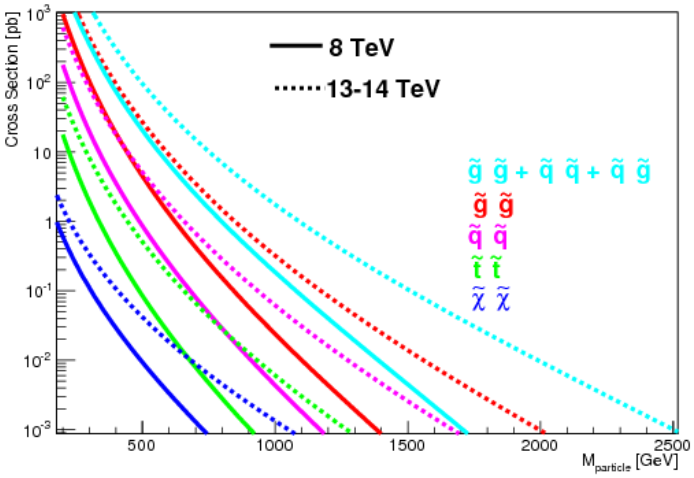

Figure 110.1: Cross sections for pair production of different sparticles as a function of their mass at the LHC for a center-of-mass energy of 8 TeV (solid curves) and 13-14 TeV (dotted curves), taken from Ref. [57]. Typically the production cross section of colored squarks and gluinos, calculated with NLL-FAST [58] at $\sqrt{s}$ =8 and 13 TeV, is several orders of magnitude larger than the one for electroweak gauginos, calculated with PROSPINO [59] at $\sqrt{s}$ =8 and 14 TeV for higgsino-like neutralinos. Except for the explicitly shown pair production of stops, production cross sections for squarks assumes mass degeneracy of left- and right-handed u, d, s, c and b squarks.

For these reasons, an effort has been made in the past years to complement the traditional constrained models with more flexible approaches.

One approach to study a broader and more comprehensive subset of the MSSM is via the phenomenological-MSSM, or pMSSM [60–62]. It is derived from the MSSM, using experimental data to eliminate parameters that are free in principle but have already been highly constrained by measurements of *e.g.*, flavor mixing and CP-violation. This effective approach reduces the number of free parameters in the

MSSM to typically 19 or even less, making it a practical compromise between the full MSSM and highly constrained models such as the CMSSM.

Even less dependent on fundamental assumptions are interpretations in terms of so-called simplified models [63–66]. Such models assume a limited set of SUSY particle production and decay modes and leave open the possibility to vary masses and other parameters freely. Therefore, simplified models enable comprehensive studies of individual SUSY topologies, and are useful for optimization of the experimental searches over a wide parameter space without limitations on fundamental kinematic properties such as masses, production cross sections, and decay modes.

As a consequence, ATLAS and CMS have adopted simplified models as the primary framework to provide interpretations of their searches. In addition to using simplified models that describe prompt decays of SUSY particles, the experiments are now also focusing more on the use simplified models that allow for decays of long-lived SUSY particles as they can arise in different SUSY scenarios (see section II.7 for further discussion). Today, almost every individual search provides interpretations of their results in one or even several simplified models that are characteristic of SUSY topologies probed by the analysis.

However, while these models are very convenient for the interpretation of individual SUSY production and decay topologies, care must be taken when applying these limits to more complex SUSY spectra. Therefore, in practice, simplified model limits are often used as an approximation of the constraints that can be placed on sparticle masses in more complex SUSY spectra. Yet, depending on the assumed SUSY spectrum, the sparticle of interest, and the considered simplified model limit, this approximation can lead to a significant mistake, typically an overestimation, in the assumed constraint on the sparticle mass (see for example [67]) . Only on a case-by-case basis can it be determined whether the limit of a given simplified model represents a good approximation of the true underlying constraint that can be applied on a sparticle mass in a complex SUSY spectrum. In the following, we will point out explicitly the assumptions that have entered the limits when quoting interpretations from simplified models.

This review covers results up to September 2017 and since none of the searches performed so far have shown significant excess above the SM background prediction, the interpretation of the presented results are exclusion limits on SUSY parameter space.

110.4. Exclusion limits on gluino and squark masses

Gluinos and squarks are the SUSY partners of gluons and quarks, and thus carry color charge. Limits on squark masses of the order 100 GeV have been set by the LEP experiments [68], in the decay to quark plus neutralino, and for a mass difference between squark and quark plus neutralino of typically at least a few GeV . However, due to the colored production of these particles at hadron colliders (see e.g. Fig. 110.1), hadron collider experiments are able to set much tighter mass limits.

Pair production of these massive colored sparticles at hadron colliders generally involve both the s-channel and t-channel parton-parton interactions. Since there is a negligible amount of bottom and top quark content in the proton, top- and bottom squark production proceeds through s-channel diagrams only. In the past, experimental analyses of squark and/or gluino production typically assumed the first and second generation squarks to be approximately degenerate in mass. However, in order to have even less model dependent interpretations of the searches, the experiments have started to also provide simplified model limits on individual first or second generation squarks.

Assuming R-parity conservation and assuming gluinos to be heavier than squarks, squarks will predominantly decay to a quark and a neutralino or chargino, if kinematically allowed. The decay may involve the lightest neutralino (typically the LSP) or chargino, but, depending on the masses of the gauginos, may involve heavier neutralinos or charginos. For pair production of first and second generation squarks, the simplest decay modes involve two jets and missing momentum, with potential extra jets stemming from initial state or final state radiation (ISR/FSR) or from decay modes with longer cascades. Similarly, gluino pair production leads to four jets and missing momentum, and possibly additional jets from ISR/FSR or cascades. Associated production of a gluino and a (anti-)squark is also possible, in particular if squarks and gluinos have similar masses, typically leading to three or more jets in the final state. In cascades, isolated photons or leptons may appear from the decays of sparticles such as neutralinos or charginos. Final states are thus characterized by significant missing transverse momentum, and at least two, and possibly many more high p_{T} jets, which can be accompanied by one or more isolated objects like photons or leptons, including τ leptons, in the final state. Table 110.1 shows a schematic overview of characteristic final state signatures of gluino and squark production for different mass hierarchy hypotheses and assuming decays involving the lightest neutralino.

Table 110.1: Typical search signatures at hadron colliders for direct gluino and first- and second-generation squark production assuming different mass hierarchies.

Mass Hierarchy	Main Production	Dominant Decay	Typical Signature
$m_{\tilde{q}} \ll m_{\tilde{g}}$	$\tilde{q}\bar{\tilde{q}}, \tilde{q}\tilde{\tilde{q}}$	$\tilde{q} \to q\tilde{\chi}_1^0$	≥ 2 jets + $E_{\mathrm{T}}^{\mathrm{miss}}$ + X
$m_{\tilde{q}} \approx m_{\tilde{g}}$	$\tilde{q}\tilde{g}, \bar{\tilde{q}}\tilde{g}$	$\tilde{q} \to q\tilde{\chi}_1^0$	≥ 3 jets + $E_{\mathrm{T}}^{\mathrm{miss}}$ + X
		$\tilde{g} \to q\bar{q}\tilde{\chi}_1^0$	
$m_{\tilde{q}} \gg m_{\tilde{g}}$	$\tilde{g}\tilde{g}$	$\tilde{g} \to q\bar{q}\tilde{\chi}_1^0$	≥ 4 jets + $E_{\mathrm{T}}^{\mathrm{miss}}$ + X

110.4.1. *Exclusion limits on the gluino mass* :

Limits set by the Tevatron experiments on the gluino mass assume the framework of the CMSSM, with $\tan\beta = 5$ (CDF) or $\tan\beta = 3$ (D0), where $\tan\beta$ is the ratio of vacuum expectation values of the Higgs fields for up-type and down-type fermions. Furthermore, $A_0 = 0$ and $\mu < 0$ is assumed, and the resulting lower mass limits are about 310 GeV for all squark masses, or 390 GeV for the case $m_{\tilde{q}} = m_{\tilde{g}}$ [69,70]. These limits have been superseded by those provided by ATLAS and CMS, and the tightest constraints have been set with up to approximately 36 fb^{-1} of data recorded at the LHC at a center-of-mass energy of 13 TeV.

Limits on the gluino mass have been established in the framework of simplified models. Assuming only gluino pair production, in particular three primary decay chains of the gluino have been considered by the LHC experiments for interpretations of their search results. The first decay chain $\tilde{g} \to q\bar{q}\tilde{\chi}_1^0$ assumes gluino mediated production of first and second generation squarks (on-shell or off-shell) which leads to four light flavor quarks in the final state. Therefore, inclusive all-hadronic analyses searching for multijet plus $E_{\mathrm{T}}^{\mathrm{miss}}$ final states are utilized to put limits on this simplified model. These limits are derived as a function of the gluino and neutralino (LSP) mass. As shown in Fig. 110.2 (upper left), using the cross section from next-to-leading order QCD corrections and the resummation of soft gluon emission at next-to-leading-logarithmic accuracy as reference [58], the ATLAS collaboration [71] excludes in this simplified model gluino masses below approximately 2000 GeV , for a massless neutralino. In scenarios where neutralinos are not very light, the efficiency of the analyses is reduced by the fact that jets are less energetic, and there is less missing transverse momentum in the event. This leads to weaker limits when the mass difference $\Delta m = m_{\tilde{g}} - m_{\tilde{\chi}_1^0}$ is reduced. For example, for neutralino masses above about 1000 GeV no limit on the gluino mass can be set for this decay chain. Therefore, limits on gluino masses are strongly affected by the assumption of the neutralino mass. Similar results for this simplified model have been obtained by CMS [72,73].

The second important decay chain of the gluino considered for interpretation in a simplified model is $\tilde{g} \to b\bar{b}\tilde{\chi}_1^0$. Here the decay is mediated via bottom squarks and thus leads to four jets from b quarks and $E_{\mathrm{T}}^{\mathrm{miss}}$ in the final state. Also for this topology inclusive all-hadronic searches provide the highest sensitivity. However, with four b quarks in the final state, the use of secondary vertex reconstruction for the identification of jets originating from b quarks provides a powerful handle on the SM background. Therefore, in addition to a multijet

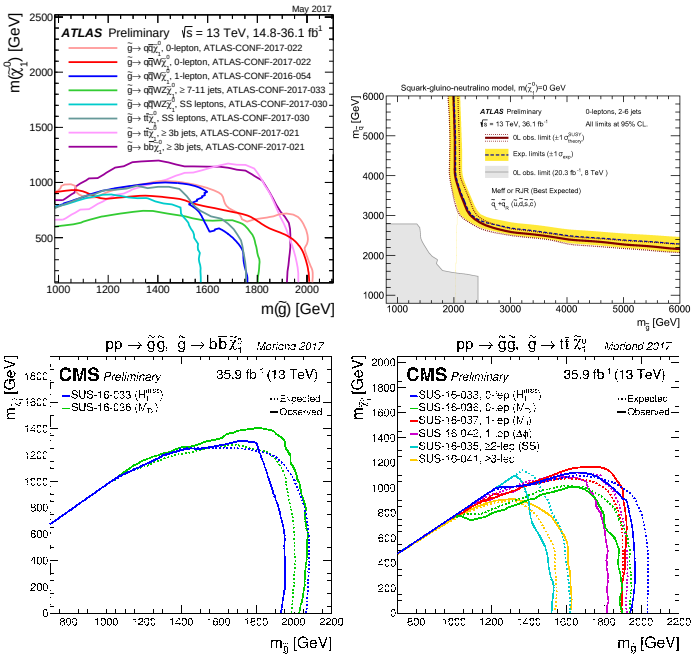

Figure 110.2: Upper left and lower left and right plots: lower mass limits, at 95% C.L., on gluino pair production for various decay chains. The upper left plot shows limits from the ATLAS collaboration; the lower plots display CMS results for the decay chains $\tilde{g} \to b\bar{b}\tilde{\chi}_1^0$ (lower left) and $\tilde{g} \to t\bar{t}\tilde{\chi}_1^0$ (lower right). The limits are defined in the framework of simplified models assuming a single decay chain, i.e. a 100% branching fraction. The upper right plot shows 95% C.L. mass limits on gluinos and squarks assuming gluino and squark production and massless neutralinos.

plus $E_{\mathrm{T}}^{\mathrm{miss}}$ signature these searches also require several jets to be tagged as b-jets. As shown in Fig. 110.2 (lower left), for this simplified model CMS [72] excludes gluino masses below ≈ 2000 GeV for a massless neutralino, while for neutralino masses above ≈ 1400 GeV no limit on the gluino mass can be set. Comparable limits for this simplified model are provided by searches from ATLAS [74].

Gluino decays are not limited to first and second generation squarks or bottom squarks, if kinematically allowed, top squarks via the decay $\tilde{g} \to \tilde{t}t$ are also possible. This leads to a "four tops" final state $ttt\bar{t}\tilde{\chi}_1^0\tilde{\chi}_1^0$ and defines the third important simplified model, $\tilde{g} \to t\bar{t}\tilde{\chi}_1^0$, characterizing gluino pair production. The topology of this decay is very rich in different experimental signatures: as many as four isolated leptons, four b-jets, several light flavor quark jets, and significant missing momentum from the neutrinos in the W decay and from the two neutralinos. As shown in Fig. 110.2 (lower right), the CMS inclusive H_{T} based search [73] and a search requiring one isolated lepton and large-radius jets [75] rule out gluinos with masses below ≈ 1900 GeV for massless neutralinos in this model. For neutralino masses above ≈ 1100 GeV , no limit can be placed on the gluino mass. The ATLAS multiple b-jets search [74] obtains similar limits.

The ATLAS collaboration also provides limits in a pMSSM-inspired model with only gluinos and first and second generation squarks, and a bino-like $\tilde{\chi}_1^0$ [71]. As shown in Fig. 110.2 (upper right), assuming $m_{\tilde{\chi}_1^0} = 0$ GeV , gluinos with masses below ≈ 2000 GeV are excluded for any squark mass and vice versa. For $m_{\tilde{q}} \approx m_{\tilde{g}}$, the mass exclusion is about 2700 GeV .

R-parity violating gluino decays are searched for in a number of final states. Searches in multilepton final states set lower mass limits of 1 to 1.4 TeV, depending on neutralino mass and lepton flavor, on decays mediated by λ and λ' couplings [76,77], assuming prompt decays. Searches for displaced vertices are sensitive to non-prompt decays [78]. Multijet final states have been used to search for fully hadronic gluino decays involving λ'', by CDF [79], ATLAS [80,81] and CMS [82,83]. Lower mass limits range between 600 and 2000 GeV depending on neutralino mass and flavor content of the final state.

110.4.2. *Exclusion limits squark masses* :

Limits on first and second generation squark masses set by the Tevatron experiments assume the CMSSM model, and amount to lower limits of about 380 GeV for all gluino masses, or 390 GeV for the case $m_{\tilde{q}} = m_{\tilde{g}}$ [69,70].

At the LHC, limits on squark masses have been set using up to approximately 36 fb^{-1} of data at 13 TeV. Interpretations in simplified models typically characterize squark pair production with only one decay chain of $\tilde{q} \to q\tilde{\chi}_1^0$. Here it is assumed that the left and right-handed $\tilde{u}$, $\tilde{d}$, $\tilde{s}$ and $\tilde{c}$ squarks are degenerate in mass. Furthermore, it is assumed that the mass of the gluino is very high and thus contributions of the corresponding t-channel diagrams to squark pair production are negligible. Therefore, the total production cross section for this simplified model is eight times the production cross section of an individual squark (e.g. $\tilde{u}_L$). The CMS collaboration provides interpretations using different all-hadronic searches for this simplified model. As displayed in the upper plot of Fig. 110.3, best observed exclusion is obtained from the analysis using the m_{T2} variable [72], which excludes squark masses just below 1550 GeV for a light neutralino. The effects of heavy neutralinos on squark limits are similar to those discussed in the gluino case (see section II.4.1) and only for neutralino masses below ≈ 800 GeV can any squark masses be excluded. Results from the ATLAS collaboration [71] for this simplified model are similar.

For the same analysis ATLAS also provides an interpretation of their search result in the aforementioned pMSSM-inspired model with only gluinos and first and second generation squarks, and a bino-like $\tilde{\chi}_1^0$ [71]. In this model, squark production can take place with non-decoupled gluinos, enhancing the squark production cross section through gluino exchange diagrams. For example, for gluinos of 6 TeV, squark masses up to 2.2 TeV are excluded, much higher than in the simplified model under consideration.

If the assumption of mass degenerate first and second generation squarks is dropped and only the production of a single light squark is assumed, the limits weaken significantly. This is shown as the much smaller exclusion region in the upper plot of Fig. 110.3, which represents the 95% C.L. limit on pair production of a single light squark, with the gluino and all other squarks decoupled to very high masses. Under this assumption, the lower limit on squark masses is only ≈ 1050 GeV for a massless neutralino, and for neutralinos heavier than ≈ 450 GeV no squark mass limit can be placed. It should be noted that this limit is not a result of a simple scaling of the above mentioned mass limits assuming eightfold mass degeneracy but it also takes into account that for an eight times lower production cross section the analyses must probe kinematic regions of phase space that are closer to the ones of SM background production. Since signal acceptance and the ratio of expected signal to SM background events of the analyses are typically worse in this region of phase space not only the 1/8 reduction in production cross section but also a worse analysis sensitivity are responsible for the much weaker limit on single squark pair production.

For single light squarks ATLAS also reports results of a dedicated search, at $\sqrt{s} = 8$ TeV, for pair production of scalar partners of charm quarks [84]. Assuming that the scalar-charm state exclusively decays into a charm quark and a neutralino, scalar-charm masses up to 490 GeV are excluded for neutralino masses below 200 GeV .

Besides placing stringent limits on first and second generation squark masses, the LHC experiments also search for the production of third generation squarks. SUSY at the TeV-scale is often motivated by naturalness arguments, most notably as a solution to stabilize quadratic divergences in radiative corrections to the Higgs boson mass. In this context, the most relevant terms for SUSY phenomenology arise from the interplay between the masses of the third generation squarks and the Yukawa coupling of the top quark to the Higgs boson. This motivates a potential constraint on the masses of the top squarks and the left-handed bottom squark. Due to the large top quark mass, significant mixing between $\tilde{t}_{\mathrm{L}}$ and $\tilde{t}_{\mathrm{R}}$ is expected, leading to a lighter mass state $\tilde{t}_1$ and a heavier mass state $\tilde{t}_2$. In the MSSM, the lightest top squark ($\tilde{t}_1$) can be the lightest squark.

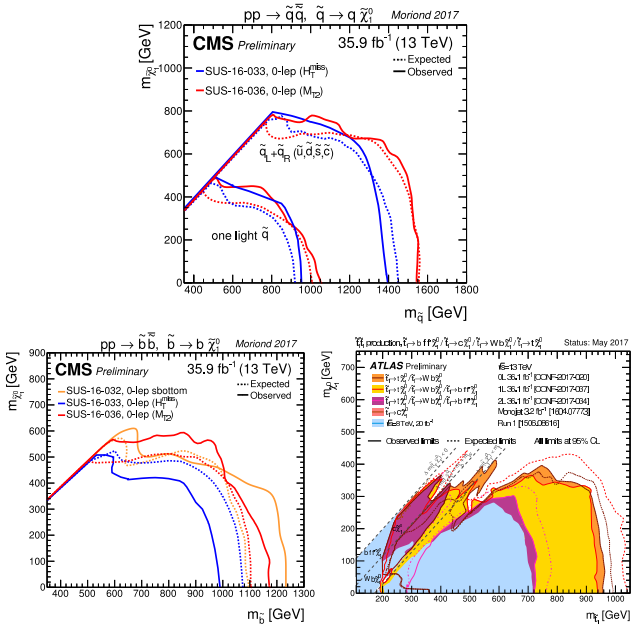

Figure 110.3: The upper plot shows 95% C.L. exclusion contours in the squark-neutralino mass plane defined in the framework of simplified models assuming a single decay chain of $\tilde{q} \to q\tilde{\chi}_1^0$ [72]. Two assumptions for the squark pair production cross sections are displayed; a) eightfold degeneracy for the masses of the first and second generation squarks and b) only one light flavor squark. The lower left plot shows the 95% C.L. exclusion contours in the sbottom-neutralino mass plane defined in the framework of a simplified model assuming a single decay chain of $\tilde{b} \to b\tilde{\chi}_1^0$ as obtained by CMS. The lower right plot shows the 95% C.L. exclusion contours in the stop-neutralino mass plane defined in various simplified models of stop decay, as obtained by ATLAS.

Bottom squarks are expected to decay predominantly to $b\tilde{\chi}^0$ giving rise to the characteristic multi b-jet and $E_{\rm T}^{\rm miss}$ signature. Direct production of bottom squark pairs has been studied at the Tevatron and at the LHC. Limits from the Tevatron are $m_{\tilde{b}} > 247$ GeV for a massless neutralino [85,86]. The LHC experiments have surpassed these limits, and the latest results are based on 36 fb^{-1} of data collected at $\sqrt{s} = 13$ TeV. As shown in the lower left plot of Fig. 110.3, using inclusive all-hadronic searches [72,73] as well as a search requiring significant $E_{\rm T}^{\rm miss}$ and two jets reconstructed as b-jets [87], CMS has set a lower limit of $m_{\tilde{b}} > \approx 1200$ GeV for massless neutralinos in this model. For $m_{\tilde{\chi}_1^0} \approx 550$ GeV or higher no limit can be placed on direct bottom squark pair production in this simplified model. Limits from ATLAS are comparable [88]. Further bottom squark decay modes have also been studied by ATLAS [88,89] and CMS [87,90].

The top squark decay modes depend on the SUSY mass spectrum, and on the $\tilde{t}_{\rm L}$-$\tilde{t}_{\rm R}$ mixture of the top squark mass eigenstate. If kinematically allowed, the two-body decays $\tilde{t} \to t\tilde{\chi}^0$ (which requires $m_{\tilde{t}} - m_{\tilde{\chi}^0} > m_t$) and $\tilde{t} \to b\tilde{\chi}^{\pm}$ (which requires $m_{\tilde{t}} - m_{\tilde{\chi}^{\pm}} > m_b$) are expected to dominate. If not, the top squark decay may proceed either via the two-body decay $\tilde{t} \to c\tilde{\chi}^0$ or through $\tilde{t} \to bf\bar{f}'\tilde{\chi}^0$ (where f and $\bar{f}'$ denote a fermion-antifermion pair with appropriate quantum numbers). For $m_{\tilde{t}} - m_{\tilde{\chi}^0} > m_b$ the latter decay chain represents a four-body decay with a W boson, charged Higgs H, slepton $\tilde{\ell}$, or light flavor squark $\tilde{q}$, exchange. If the exchanged W boson and/or sleptons are kinematically allowed to be on-shell ($m_{\tilde{t}} - m_{\tilde{\chi}^{\pm}} > m_b + m_W$ and/or $m_{\tilde{t}} - m_{\tilde{\ell}} > m_b$), the three-body decays $\tilde{t} \to Wb\tilde{\chi}^0$ and/or $\tilde{t} \to bl\tilde{\ell}$ will become dominant. For further discussion on top squark decays see for example Ref. [91].

Limits from LEP on the $\tilde{t}_1$ mass are $m_{\tilde{t}} > 96$ GeV in the charm plus neutralino final state, and > 93 GeV in the lepton, b-quark and sneutrino final state [68].

The Tevatron experiments have performed a number of searches for top squarks, often assuming direct pair production. In the $b\ell\tilde{\nu}$ decay channel, and assuming a 100% branching fraction, limits are set as $m_{\tilde{t}} > 210$ GeV for $m_{\tilde{\nu}} < 110$ GeV and $m_{\tilde{t}} - m_{\tilde{\nu}} > 30$ GeV , or $m_{\tilde{t}} > 235$ GeV for $m_{\tilde{\nu}} < 50$ GeV [92,93]. In the $\tilde{t} \to c\tilde{\chi}^0$ decay mode, a top squark with a mass below 180 GeV is excluded for a neutralino lighter than 95 GeV [94,95]. In both analyses, no limits on the top squark can be set for heavy sneutrinos or neutralinos. In the $\tilde{t} \to b\tilde{\chi}_1^{\pm}$ decay channel, searches for a relatively light top squark have been performed in the dilepton final state [96,97]. The CDF experiment sets limits in the $\tilde{t} - \tilde{\chi}_1^0$ mass plane for various branching fractions of the chargino decay to leptons and for two value of $m_{\tilde{\chi}_1^{\pm}}$. For $m_{\tilde{\chi}_1^{\pm}} = 105.8$ GeV and $m_{\tilde{\chi}_1^0} = 47.6$ GeV , top squarks between 128 and 135 GeV are excluded for W-like leptonic branching fractions of the chargino.

The LHC experiments have improved these limits substantially. As shown in the right plot of Fig. 110.3, limits on the top squark mass assuming a simplified model with a single decay chain of $\tilde{t} \to t\tilde{\chi}_1^0$ now approach or surpass 1 TeV. The most important searches for this top squark decay topology are dedicated searches requiring zero or one isolated lepton, modest $E_{\rm T}^{\rm miss}$, and four or more jets out of which at least one jet must be reconstructed as a b-jet [98–101]. For example, CMS excludes top squarks with masses below about 1100 GeV in this model for massless neutralinos, while for $m_{\tilde{\chi}_1^0} >$ 500 GeV no limits can be provided.

Assuming that the top squark decay exclusively proceeds via the chargino mediated decay chain $\tilde{t} \to b\tilde{\chi}_1^{\pm}$, $\tilde{\chi}_1^{\pm} \to W^{\pm(*)}\tilde{\chi}_1^0$ yields stop mass exclusion limits that vary strongly with the assumptions made on the $\tilde{t}-\tilde{\chi}_1^{\pm}-\tilde{\chi}_1^0$ mass hierarchy. For example, for $m_{\tilde{\chi}_1^{\pm}} = (m_{\tilde{t}}+m_{\tilde{\chi}_1^0})/2$, a stop mass below ≈ 1000 GeV for a light $\tilde{\chi}_1^0$ is excluded, while no limit can be placed for $m_{\tilde{\chi}_1^0} > 500$ GeV [98]. These limits, however, can weaken significantly when other assumptions about the mass hierarchy are imposed. For example, if the chargino becomes nearly mass degenerate with the top squark the key experimental signature turns from an all-hadronic final state with b-jets and $E_{\rm T}^{\rm miss}$ into a multi-lepton and $E_{\rm T}^{\rm miss}$ topology yielding typically weaker limits for this top squark decay (see e.g. [99,101,102]) .

If the decays $\tilde{t} \to t\tilde{\chi}_1^0$ and $\tilde{t} \to b\tilde{\chi}_1^{\pm}$, $\tilde{\chi}_1^{\pm} \to W^{\pm(*)}\tilde{\chi}_1^0$ are kinematically forbidden, the decay chains $\tilde{t} \to Wb\tilde{\chi}^0$ and $\tilde{t} \to c\tilde{\chi}^0$ can become important. As shown in the lower right plot of Fig. 110.3, the zero-lepton ATLAS search provides for the kinematic region $m_{\tilde{t}} - m_{\tilde{\chi}^{\pm}} > m_b + m_W$ lower limits on the top squark mass of ≈ 400 GeV for a neutralino lighter than ≈ 300 GeV [100], while the corresponding CMS analyses [72,73,98] push this limit to about 550 GeV for neutralino masses below ≈ 400 GeV . Furthermore, analyses with one or two lepton final states [99,101–103] also place significant constraints on this decay channel.

For the kinematic region in which even the production of real W bosons is not allowed, ATLAS and CMS improve the Tevatron limit on $\tilde{t} \to c\tilde{\chi}^0$ substantially. Based on a monojet analysis [104] ATLAS excludes top squark masses below $m_{\tilde{\chi}_1^0} \approx 450$ GeV along the kinematic boundary for the $\tilde{t} \to c\tilde{\chi}^0$ decay. The CMS collaboration uses the hadronic searches [72,98] to place constraints on this particular stop decay and excludes $m_{\tilde{t}} \approx 550$ GeV for $m_{\tilde{\chi}_1^0}$ below 450 GeV . The exclusion at the diagonal $m_{\tilde{t}} \approx m_{\tilde{\chi}_1^0}$ is also about 550 GeV .

The other decay chain relevant in this phase region is $\tilde{t} \to bf\bar{f}'\tilde{\chi}^0$. Here the ATLAS one-lepton search [101] excludes up to $m_{\tilde{t}} \approx$ 350 GeV for $m_{\tilde{\chi}_1^0}$ below 250 GeV , while the monojet analysis [104] excludes at the kinematic boundary top squarks below 400 GeV . As for the $\tilde{t} \to c\tilde{\chi}^0$ decay, CMS uses the zero-lepton searches [72,98] to also place constraints on $\tilde{t} \to bf\bar{f}'\tilde{\chi}^0$. Also in this case CMS excludes $m_{\tilde{t}} \approx 550$ GeV for $m_{\tilde{\chi}_1^0}$ below 450 GeV .

In general, the variety of top squark decay chains in the phase space region where $\tilde{t} \to t\tilde{\chi}_1^0$ is kinematically forbidden represents a

challenge for the experimental search program and more data and refined analyses will be required to further improve the sensitivity in this difficult but important region of SUSY parameter space.

R-parity violating production of single squarks via a λ'-type coupling has been studied at HERA. In such models, a lower limit on the squark mass of the order of 275 GeV has been set for electromagnetic-strength-like couplings $\lambda' = 0.3$ [105]. At the LHC, both prompt [76,77] and non-prompt [78,106] R-parity violating squark decays have been searched for, but no signal was found. Squark mass limits are very model-dependent.

R-parity violating production of single top squarks has been searched for at LEP, HERA, and the Tevatron. For example, an analysis from the ZEUS collaboration [107] makes an interpretation of its search result assuming top squarks to be produced via a λ' coupling and decay either to $b\tilde{\chi}_1^{\pm}$ or R-parity-violating to a lepton and a jet. Limits are set on λ'_{131} as a function of the top squark mass in an MSSM framework with gaugino mass unification at the GUT scale.

The search for top squark pair production in the context of R-parity violating supersymmetry has now also become a focus point for searches at the LHC. The CMS collaboration has performed a search for top squarks using a variety of multilepton final states [108]. It provides lower limits on the top squark mass in models with non-zero leptonic R-parity violating couplings λ_{122} and λ_{233}. For a bino mass of 200 GeV , these limits are 1020 GeV and 820 GeV , respectively. The analysis also provides limits in a model with the semileptonic R-parity violating coupling λ'_{233}. The λ'-mediated top squark decay $\tilde{t} \to b\ell$ has been studied by ATLAS for prompt decays [109], and by CMS for non-prompt decays [110]. CMS also searched for the λ'-mediated decay $\tilde{t} \to b\ell qq$, setting lower stop mass limits of 890 GeV (e) or 1000 GeV (μ) [111]. The fully hadronic R-parity violating top squark decays $\tilde{t} \to bs$ and $\tilde{t} \to ds$, involving λ'', have been searched for by ATLAS [112], and lower top squark mass limits between 410 and 610 GeV were set. CMS [113] have searched for a top squark decay to a bottom quark and a light-flavor quark, and excludes top squarks with masses between 200 and 385 GeV in this decay mode.

It should be noted that limits discussed in this section belong to different top and bottom squark decay channels, different sparticle mass hierarchies, and different simplified decay scenarios. Therefore, care must be taken when interpreting these limits in the context of more complete SUSY models.

110.4.3. *Summary of exclusion limits on squarks and gluinos assuming R-Parity conservation* :

A summary of the most important squark and gluino mass limits for different interpretation approaches assuming R-parity conservation is shown in Table 110.2.

For gluino masses rather similar limits of about 2 TeV are obtained from different model assumptions, indicating that the LHC is indeed probing direct gluino production at the TeV scale and beyond. However, for neutralino masses above approximately 1 to 1.4 TeV, in the best case scenarios, ATLAS and CMS searches cannot place any limits on the gluino mass.

Limits on direct squark production, on the other hand, depend strongly on the chosen model. Especially for direct production of top squarks there are still large regions in parameter space where masses below 1 TeV cannot be excluded. This is also true for first and second generation squarks when only one single squark is considered. Furthermore, for neutralino masses above ≈ 500 GeV no limit on any direct squark production scenario can be placed by the LHC.

110.5. Exclusion limits on the masses of charginos and neutralinos

Charginos and neutralinos result from mixing of the charged wino and higgsino states, and the neutral bino, wino and higgsino states, respectively. The mixing is determined by a limited number of parameters. For charginos these are the wino mass parameter M_2, the higgsino mass parameter μ, and $\tan\beta$, and for neutralinos these are the same parameters plus the bino mass parameter M_1. If any of the parameters M_1, M_2 or μ happened to be substantially smaller than the others, the chargino and neutralino composition would be dominated by specific states, which are referred to as bino-like ($M_1 \ll M_2, \mu$), wino-like ($M_2 \ll M_1, \mu$), or higgsino-like ($\mu \ll M_1, M_2$). If gaugino mass unification at the GUT scale is assumed, a relation between M_1 and M_2 at the electroweak scale follows: $M_1 = 5/3 \tan^2\theta_W M_2 \approx 0.5 M_2$, with θ_W the weak mixing angle. Charginos and neutralinos carry no color charge.

Table 110.2: Summary of squark mass and gluino mass limits using different interpretation approaches assuming R-parity conservation. Masses in this table are provided in GeV . Further details about assumption and analyses from which these limits are obtained are discussed in the corresponding sections of the text.

Model	Assumption	$m_{\tilde{q}}$	$m_{\tilde{g}}$
Simplified model	$m_{\tilde{\chi}_1^0}$= 0, $m_{\tilde{q}} \approx m_{\tilde{g}}$	$\approx$ 2700	$\approx$ 2700
$\tilde{g}\tilde{q}, \tilde{g}\bar{\tilde{q}}$	$m_{\tilde{\chi}_1^0}$= 0, all $m_{\tilde{q}}$	-	$\approx$ 2000
	$m_{\tilde{\chi}_1^0}$= 0, all $m_{\tilde{g}}$	$\approx$ 2000	-
Simplified models $\tilde{g}\tilde{g}$			
$\tilde{g} \to q\bar{q}\tilde{\chi}_1^0$	$m_{\tilde{\chi}_1^0}$ =0	-	$\approx$ 2000
	$m_{\tilde{\chi}_1^0} > \approx$ 1000	-	no limit
$\tilde{g} \to b\bar{b}\tilde{\chi}_1^0$	$m_{\tilde{\chi}_1^0}$ =0	-	$\approx$ 2000
	$m_{\tilde{\chi}_1^0} > \approx$ 1400	-	no limit
$\tilde{g} \to t\bar{t}\tilde{\chi}_1^0$	$m_{\tilde{\chi}_1^0}$ =0	-	$\approx$ 1900
	$m_{\tilde{\chi}_1^0} > \approx$ 1100	-	no limit
Simplified models $\tilde{q}\bar{\tilde{q}}$			
$\tilde{q} \to q\tilde{\chi}_1^0$	$m_{\tilde{\chi}_1^0}$ =0	$\approx$ 1550	-
	$m_{\tilde{\chi}_1^0} > \approx$ 800	no limit	-
$\tilde{u}_L \to q\tilde{\chi}_1^0$	$m_{\tilde{\chi}_1^0}$ =0	$\approx$ 1050	-
	$m_{\tilde{\chi}_1^0} > \approx$ 450	no limit	-
$\tilde{b} \to b\tilde{\chi}_1^0$	$m_{\tilde{\chi}_1^0}$ =0	$\approx$ 1200	-
	$m_{\tilde{\chi}_1^0} > \approx$ 550	no limit	-
$\tilde{t} \to t\tilde{\chi}_1^0$	$m_{\tilde{\chi}_1^0}$ =0	$\approx$ 1100	-
	$m_{\tilde{\chi}_1^0} > \approx$ 500	no limit	-
$\tilde{t} \to b\tilde{\chi}_1^{\pm}$	$m_{\tilde{\chi}_1^0}$ =0	$\approx$ 1000	-
$[m_{\tilde{\chi}_1^{\pm}} = (m_{\tilde{t}} - m_{\tilde{\chi}_1^0})/2]$	$m_{\tilde{\chi}_1^0} > \approx$ 500	no limit	-
$\tilde{t} \to Wb\tilde{\chi}_1^0$	$m_{\tilde{\chi}_1^0} < \approx$ 400	$\approx$ 550	-
$[m_W < m_{\tilde{t}} - m_{\tilde{\chi}^0} < m_t]$			
$\tilde{t} \to c\tilde{\chi}_1^0$	$m_{\tilde{\chi}_1^0} < \approx$ 450	$\approx$ 550	-
	$m_{\tilde{t}} \approx m_{\tilde{\chi}_1^0}$	$\approx$ 550	-
$\tilde{t} \to bff'\tilde{\chi}_1^0$	$m_{\tilde{\chi}_1^0} < \approx$ 450	$\approx$ 550	-
	$m_{\tilde{t}} \approx m_{\tilde{\chi}_1^0}$	$\approx$ 550	-
$[m_{\tilde{t}} - m_{\tilde{\chi}^0} < m_W]$			

110.5.1. *Exclusion limits on chargino masses* :

If kinematically allowed, two body decay modes such as $\tilde{\chi}^{\pm} \to \tilde{f}\bar{\tilde{f}}'$ (including $\ell\tilde{\nu}$ and $\tilde{\ell}\nu$) are dominant. If not, three body decay $\tilde{\chi}^{\pm} \to f\bar{f}'\tilde{\chi}^0$ are mediated through virtual W bosons or sfermions. If sfermions are heavy, the W mediation dominates, and $f\bar{f}'$ are distributed with branching fractions similar to W decay products (barring phase space effects for small mass gaps between $\tilde{\chi}^{\pm}$ and $\tilde{\chi}^0$). If, on the other hand, sleptons are light enough to play a significant role in the decay mediation, leptonic final states will be enhanced.

At LEP, charginos have been searched for in fully-hadronic, semi-leptonic and fully leptonic decay modes [114,115]. A general lower

limit on the lightest chargino mass of 103.5 GeV is derived, except in corners of phase space with low electron sneutrino mass, where destructive interference in chargino production, or two-body decay modes, play a role. The limit is also affected if the mass difference between $\tilde{\chi}_1^{\pm}$ and $\tilde{\chi}_1^0$ is small; dedicated searches for such scenarios set a lower limit of 92 GeV .

At the Tevatron, charginos have been searched for via associated production of $\tilde{\chi}_1^{\pm}\tilde{\chi}_2^0$ [116,117]. Decay modes involving multilepton final states provide the best discrimination against the large multijet background. Analyses have looked for at least three charged isolated leptons, for two leptons with missing transverse momentum, or for two leptons with the same charge. Depending on the $(\tilde{\chi}_1^{\pm} - \tilde{\chi}_1^0)$ and/or $(\tilde{\chi}_2^0 - \tilde{\chi}_1^0)$ mass differences, leptons may be soft.

At the LHC, the search strategy is similar to that at the Tevatron. As shown in Fig. 110.1, the cross section of pair production of electroweak gauginos at the LHC, for masses of several hundreds of GeV, is at least two orders of magnitude smaller than for colored SUSY particles (e.g. top squark pair production). For this reason a high statistics data sample is required to improve the sensitivity of LEP and Tevatron searches for direct chargino/neutralino production. With the full LHC Run 1 data and the first set of Run 2 data, ATLAS and CMS have started to surpass the limits from LEP and Tevatron in regions of SUSY parameter space.

Chargino pair production is searched for in the dilepton plus missing momentum final state. In the simplified model interpretation of the results, assuming mediation of the chargino decay by light sleptons, ATLAS [118] sets limits on the chargino mass up to 740 GeV for massless LSPs, but no limits on the chargino mass can be set for $\tilde{\chi}_1^0$ heavier than 350 GeV . Limits are fairly robust against variation of the slepton mass, unless the mass gap between chargino and slepton becomes small. At 8 TeV, first limits were also set on charginos decaying via a W boson [119]: chargino masses below 180 GeV are excluded for massless LSPs, but no limits are set for LSPs heavier than 25 GeV .

The trilepton plus missing momentum final state is used to set limits on $\tilde{\chi}_1^{\pm}\tilde{\chi}_2^0$ production, assuming wino-like $\tilde{\chi}^{\pm}$ and $\tilde{\chi}_2^0$, bino-like $\tilde{\chi}_1^0$, and $m_{\tilde{\chi}^{\pm}} = m_{\tilde{\chi}_2^0}$, leaving $m_{\tilde{\chi}^{\pm}}$ and $m_{\tilde{\chi}_1^0}$ free. Again, the branching fraction of leptonic final states is determined by the slepton masses. If the decay is predominantly mediated by a light $\tilde{\ell}_{\mathrm{L}}$, i.e. $\tilde{\ell}_{\mathrm{R}}$ is assumed to be heavy, the three lepton flavors will be produced in equal amounts. It is assumed that $\tilde{\ell}_{\mathrm{L}}$ and sneutrino masses are equal, and diagrams with sneutrinos are included. In this scenario, ATLAS [118] and CMS [120] exclude chargino masses below 1140 GeV for massless LSPs; no limits are set for LSP masses above 700 GeV . If the decay is dominated by a light $\tilde{\ell}_{\mathrm{R}}$, the chargino cannot be a pure wino but needs to have a large higgsino component, preferring the decays to tau leptons. Limits are set in various scenarios. If, like for $\tilde{\ell}_{\mathrm{L}}$, a flavor-democratic scenario is assumed, CMS sets limits of 1060 GeV on the chargino mass for massless LSPs, but under the assumption that both $\tilde{\chi}^{\pm}$ and $\tilde{\chi}_2^0$ decay leads to tau leptons in the final state, the chargino mass limit deteriorates to 620 GeV for massless LSPs [120]. ATLAS assumes a simplified model in which staus are significantly lighter than the other sleptons in order to search for a similar multi-tau final state, and sets a lower limit on the chargino mass of 760 GeV in this model [121].

If sleptons are heavy, the chargino is assumed to decay to a W boson plus LSP, and the $\tilde{\chi}_2^0$ into Z plus LSP or H plus LSP. In the WZ channel, ATLAS [118] and CMS [122] limits on the chargino mass reach 610 GeV for massless LSPs, but no limits are set for LSPs heavier than 250 GeV . In the WH channel, for $m_H = 125$ GeV and using Higgs decays to $b\bar{b}$, $\gamma\gamma$ and WW (ATLAS [123]) , or Higgs decays to $b\bar{b}$, $\gamma\gamma$, WW, ZZ and $\tau^+\tau^-$ (CMS [122]) , assuming a SM-like branching fraction in these final states, chargino mass limits extend up to 480 GeV for massless LSPs, but vanish for LSP masses above 100 GeV .

The results on electroweak gaugino searches interpreted in simplified models are summarized in Fig. 110.4 for the two cases of light or decoupled sleptons. For both cases, ATLAS and CMS have comparable limits.

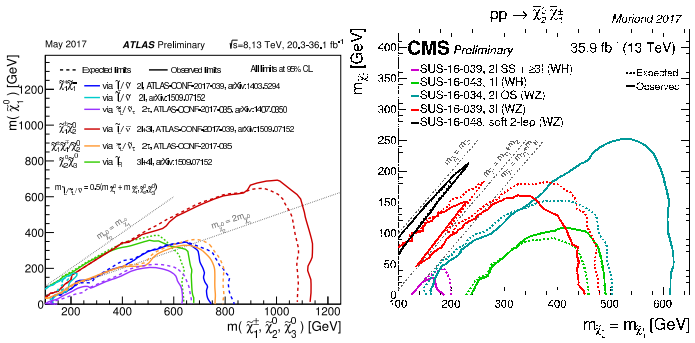

Figure 110.4: LHC exclusion limits on chargino and neutralino masses in a number of simplified models. Left: limits on chargino and neutralino masses for pair production of charginos, pair production of heavier neutralinos, or pair production of chargino and neutralino, under the assumption of light sleptons mediating the decays. Right: limits on chargino and neutralino masses for pair production of chargino and neutralino, under the assumption of decoupled sleptons, and chargino/neutralino decay through W^*, Z^* or H.

In both the wino region (a characteristic of anomaly-mediated SUSY breaking models) and the higgsino region of the MSSM, the mass splitting between $\tilde{\chi}_1^{\pm}$ and $\tilde{\chi}_1^0$ is small. The chargino decay products are very soft and may escape detection. These compressed spectra are very hard to find, and have triggered dedicated search strategies, which, however, still have limited sensitivity. Photons or jets from initial state radiation may be used to tag such decays. An alternative production mode of electroweak gauginos is provided by vector-boson-fusion, where two additional jets with a large rapidity gap can be used to select events and suppress backgrounds [124,125].

110.5.2. *Exclusion limits on neutralino masses* :

In a considerable part of the MSSM parameter space, and in particular when demanding that the LSP carries no electric or color charge, the lightest neutralino $\tilde{\chi}_1^0$ is the LSP. If R-parity is conserved, such a $\tilde{\chi}_1^0$ is stable. Since it is weakly interacting, it will typically escape detectors unseen. Limits on the invisible width of the Z boson apply to neutralinos with a mass below 45.5 GeV , but depend on the Z-neutralino coupling. Such a coupling could be small or even absent; in such a scenario there is no general lower limit on the mass of the lightest neutralino [126]. In models with gaugino mass unification and sfermion mass unification at the GUT scale, a lower limit on the neutralino mass is derived from limits from direct searches, notably for charginos and sleptons, and amounts to 47 GeV [127]. Assuming a constraining model like the CMSSM, this limit increases to 50 GeV at LEP; however the strong constraints now set by the LHC increase such CMSSM-derived $\tilde{\chi}_1^0$ mass limits to well above 200 GeV [128].

In gauge-mediated SUSY breaking models (GMSB), the LSP is typically a gravitino, and the phenomenology is determined by the nature of the next-to-lightest supersymmetric particle (NLSP). A NLSP neutralino will decay to a gravitino and a SM particle whose nature is determined by the neutralino composition. Final states with two high p_{T} photons and missing momentum are searched for, and interpreted in gauge mediation models with bino-like neutralinos [129–133].

Assuming the production of at least two neutralinos per event, neutralinos with large non-bino components can also be searched for by their decay in final states with missing momentum plus any two bosons out of the collection γ, Z, H. A number of searches at the LHC have tried to cover the rich phenomenology of the various Z and H decay modes [120,132–135].

Heavier neutralinos, in particular $\tilde{\chi}_2^0$, have been searched for in their decays to the lightest neutralino plus a γ, a Z boson or a Higgs boson. Limits on electroweak production of $\tilde{\chi}_2^0$ plus $\tilde{\chi}_1^{\pm}$ from trilepton analyses have been discussed in the section on charginos; the assumption of equal mass of $\tilde{\chi}_2^0$ and $\tilde{\chi}_1^{\pm}$ make the limits on

chargino masses apply to $\tilde{\chi}_2^0$ as well. Multilepton analyses have also been used to set limits on $\tilde{\chi}_2^0\tilde{\chi}_3^0$ production; assuming equal mass and decay through light sleptons, limits are set up to 680 GeV for massless LSPs [124]. Again, compressed spectra with small mass differences between the heavier neutralinos and the LSP form the most challenging region.

In $\tilde{\chi}_2^0$ decays to $\tilde{\chi}_1^0$ and a lepton pair, the lepton pair invariant mass distribution may show a structure that can be used to measure the $\tilde{\chi}_2^0 - \tilde{\chi}_1^0$ mass difference in case of a signal [36]. This structure, however, can also be used in the search strategy itself, as demonstrated by ATLAS [134] and CMS [136].

In models with R-parity violation, the lightest neutralino can decay even if it is the lightest supersymmetric particle. If the decay involves a non-zero λ coupling, the final state will be a multi-lepton one. Searches for events with four or more isolated charged leptons by ATLAS [76,137] and CMS [77] are interpreted in such models. With very small coupling values, the neutralino would be long-lived, leading to lepton pairs with a displaced vertex, which have also been searched for [78,106].

Searches for events with a displaced hadronic vertex, with or without a matched lepton, are interpreted in a model with R-parity violating neutralino decay involving a non-zero λ' coupling [78,138]. Neutralino decays involving non-zero λ'' lead to fully hadronic final states, and searches for jet-pair resonances are used to set limits, typically on the production of colored particles like top squarks or gluinos, which are assumed to be the primary produced sparticles in these interpretations, as discussed earlier.

The limits on weak gauginos in simplified models are summarized in Table 110.3. Interpretations of the search results outside simplified models, such as in the phenomenological MSSM [139–141], show that the simplified model limits must be interpreted with care. Electroweak gauginos in models that are compatible with the relic density of dark matter in the universe, for example, have particularly tuned mixing parameters and mass spectra, which are not always captured by the simplified models used.

Table 110.3: Summary of weak gaugino mass limits in simplified models, assuming R-parity conservation. Masses in the table are provided in GeV. Further details about assumptions and analyses from which these limits are obtained are discussed in the text.

Assumption	m_χ
$\tilde{\chi}_1^\pm$, all $\Delta m(\tilde{\chi}_1^\pm, \tilde{\chi}_1^0)$	> 92
$\tilde{\chi}_1^\pm$ $\Delta m > 5$, $m_{\tilde{\nu}} > 300$	> 103.5
$\tilde{\chi}_1^\pm$, $m_{(\tilde{\ell},\tilde{\nu})} = (m_{\tilde{\chi}_1^\pm} + m_{\tilde{\chi}_1^0})/2$	
$m_{\tilde{\chi}_1^0} \approx 0$	> 740
$\tilde{\chi}_1^\pm$, $m_{\tilde{\chi}_1^0} > 350$	no LHC limit
$\tilde{\chi}_1^\pm$, $m_{\tilde{\ell}} > m_{\tilde{\chi}_1^\pm}$	
$m_{\tilde{\chi}_1^0} \approx 0$	> 180
$\tilde{\chi}_1^\pm$, $m_{\tilde{\chi}_1^0} > 25$	no LHC limit
$m_{\tilde{\chi}_1^\pm} = m_{\tilde{\chi}_2^0}$, $m_{\tilde{\ell}_L} = (m_{\tilde{\chi}_1^\pm} + m_{\tilde{\chi}_1^0})/2$	
$m_{\tilde{\chi}_1^0} \approx 0$	> 1140
$m_{\tilde{\chi}_1^0} > 700$	no LHC limit
$m_{\tilde{\chi}_1^\pm} = m_{\tilde{\chi}_2^0}$, $m_{\tilde{\ell}_R} = (m_{\tilde{\chi}_1^\pm} + m_{\tilde{\chi}_1^0})/2$	flavor-democratic
$m_{\tilde{\chi}_1^0} \approx 0$	> 1060
$m_{\tilde{\chi}_1^0} > 600$	no LHC limit
$m_{\tilde{\chi}_1^\pm} = m_{\tilde{\chi}_2^0}$, $m_{\tilde{\tau}} = (m_{\tilde{\chi}_1^\pm} + m_{\tilde{\chi}_1^0})/2$	$\tilde{\tau}$-dominated
$m_{\tilde{\chi}_1^0} \approx 0$	> 620
$m_{\tilde{\chi}_1^0} > 260$	no LHC limit
$m_{\tilde{\chi}_1^\pm} = m_{\tilde{\chi}_2^0}$, $m_{\tilde{\ell}} > m_{\tilde{\chi}_1^\pm}$, BF$(WZ) = 1$	
$m_{\tilde{\chi}_1^0} \approx 0$	> 610
$m_{\tilde{\chi}_1^0} > 250$	no LHC limit
$m_{\tilde{\chi}_1^\pm} = m_{\tilde{\chi}_2^0}$, $m_{\tilde{\ell}} > m_{\tilde{\chi}_1^\pm}$, BF$(WH) = 1$	
$m_{\tilde{\chi}_1^0} \approx 0$	> 480
$m_{\tilde{\chi}_1^0} > 100$	no LHC limit

110.6. Exclusion limits on slepton masses

In models with slepton and gaugino mass unification at the GUT scale, the right-handed slepton, $\tilde{\ell}_R$, is expected to be lighter than the left-handed slepton, $\tilde{\ell}_L$. For tau sleptons there may be considerable mixing between the L and R states, leading to a significant mass difference between the lighter $\tilde{\tau}_1$ and the heavier $\tilde{\tau}_2$.

110.6.1. *Exclusion limits on the masses of charged sleptons* :

The most model-independent searches for selectrons, smuons and staus originate from the LEP experiments [142]. Smuon production only takes place via s-channel γ^*/Z exchange. Search results are often quoted for $\tilde{\mu}_R$, since it is typically lighter than $\tilde{\mu}_L$ and has a weaker coupling to the Z boson; limits are therefore conservative. Decays are expected to be dominated by $\tilde{\mu}_R \to \mu\tilde{\chi}_1^0$, leading to two non-back-to-back muons and missing momentum. Slepton mass limits are calculated in the MSSM under the assumption of gaugino mass unification at the GUT scale, and depend on the mass difference between the smuon and $\tilde{\chi}_1^0$. A $\tilde{\mu}_R$ with a mass below 94 GeV is excluded for $m_{\tilde{\mu}_R} - m_{\tilde{\chi}_1^0} > 10$ GeV. The selectron case is similar to the smuon case, except that an additional production mechanism is provided by t-channel neutralino exchange. The $\tilde{e}_R$ lower mass limit is 100 GeV for $m_{\tilde{\chi}_1^0} < 85$ GeV. Due to the t-channel neutralino exchange, $\tilde{e}_R\tilde{e}_L$ pair production was possible at LEP, and a lower limit of 73 GeV was set on the selectron mass regardless of the neutralino mass by scanning over MSSM parameter space [143]. The potentially large mixing between $\tilde{\tau}_L$ and $\tilde{\tau}_R$ not only makes the $\tilde{\tau}_1$ light, but can also make its coupling to the Z boson small. LEP lower limits on the $\tilde{\tau}$ mass range between 87 and 93 GeV depending on the $\tilde{\chi}_1^0$ mass, for $m_{\tilde{\tau}} - m_{\tilde{\chi}_1^0} > 7$ GeV [142].

At the LHC, pair production of sleptons is not only heavily suppressed with respect to pair production of colored SUSY particles but the cross section is also almost two orders of magnitude smaller than the one of pair production of charginos and neutralinos. Only with the full Run 1 LHC data set and the first data of Run 2, ATLAS and CMS have started to surpass the sensitivity of the LEP analyses under certain assumptions.

ATLAS and CMS have searched for direct production of selectron pairs and smuon pairs at the LHC, with each slepton decaying to its corresponding SM partner lepton and the $\tilde{\chi}_1^0$ LSP. In simplified models, ATLAS [118] and CMS [120] set lower mass limits on sleptons of 500 GeV for degenerate $\tilde{\ell}_L$ and $\tilde{\ell}_R$, for a massless $\tilde{\chi}_1^0$ and assuming equal selectron and smuon masses, as shown in Fig. 110.5. The limits deteriorate with increasing $\tilde{\chi}_1^0$ mass due to decreasing missing momentum and lepton momentum. As a consequence, no limits are set for $\tilde{\chi}_1^0$ masses above 270 GeV.

In gauge-mediated SUSY breaking models, sleptons can be (co-)NLSPs, *i.e.*, the next-to-lightest SUSY particles and almost degenerate in mass, decaying to a lepton and a gravitino. This decay can either be prompt, or the slepton can have a non-zero lifetime. Combining several analyses, lower mass limits on $\tilde{\mu}_R$ of 96.3 GeV and on $\tilde{e}_R$ of 66 GeV are set for all slepton lifetimes at LEP [144]. In a considerable part of parameter space in these models, the $\tilde{\tau}$ is the NLSP. The LEP experiments have set lower limits on the mass of such a $\tilde{\tau}$ between 87 and 97 GeV, depending on the $\tilde{\tau}$ lifetime. ATLAS has searched for final states with τs, jets and missing transverse momentum, and has interpreted the results in GMSB models setting limits on the model parameters [145]. CMS has interpreted a multilepton analysis in terms of limits on gauge mediation models with slepton NLSP [146]. CDF has put limits on gauge mediation models at high $\tan\beta$ and slepton NLSP using an analysis searching for like-charge light leptons and taus [147].

Limits also exist on sleptons in R-parity violating models, both from LEP and the Tevatron experiments. From LEP, lower limits on

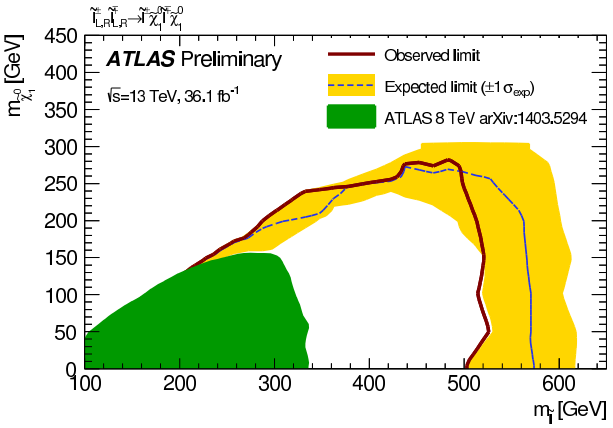

Figure 110.5: LHC exclusion limits on slepton (selectron and smuon) masses, assuming equal masses of selectrons and smuons, degeneracy of $\tilde{\ell}_{\rm L}$ and $\tilde{\ell}_{\rm R}$, and a 100% branching fraction for $\tilde{\ell} \to \ell\tilde{\chi}_1^0$ [118].

$\tilde{\mu}_{\rm R}$ and $\tilde{e}_{\rm R}$ masses in such models are 97 GeV , and the limits on the stau mass are very close: 96 GeV [148].

110.6.2. *Exclusion limits on sneutrino masses* :

The invisible width of the Z boson puts a lower limit on the sneutrino mass of about 45 GeV . Tighter limits are derived from other searches, notably for gauginos and sleptons, under the assumption of gaugino and sfermion mass universality at the GUT scale, and amount to approximately 94 GeV in the MSSM [149]. It is possible that the lightest sneutrino is the LSP; however, a left-handed sneutrino LSP is ruled out as a cold dark matter candidate [150,151].

Production of pairs of sneutrinos in R-parity violating models has been searched for at LEP [148]. Assuming fully leptonic decays via λ-type couplings, lower mass limits between 85 and 100 GeV are set. At the Tevatron [152,153] and at the LHC [154,155], searches have focused on scenarios with resonant production of a sneutrino, decaying to $e\mu$, $\mu\tau$ and $e\tau$ final states. No signal has been seen, and limits have been set on sneutrino masses as a function of the value of relevant RPV couplings. As an example, the LHC experiments exclude a resonant tau sneutrino with a mass below 1500 GeV for $\lambda_{312} > 0.07$ and $\lambda'_{311} > 0.01$.

The limits on sleptons in simplified models are summarized in Table 110.4.

Table 110.4: Summary of slepton mass limits from LEP and LHC, assuming R-parity conservation and 100% branching fraction for $\tilde{\ell} \to \ell\tilde{\chi}_1^0$. Masses in this table are provided in GeV .

Assumption	$m_{\tilde{\ell}}$
$\tilde{\mu}_{\rm R}$, $\Delta m(\tilde{\mu}_{\rm R}, \tilde{\chi}_1^0) > 10$	> 94
$\tilde{e}_{\rm R}$, $\Delta m(\tilde{e}_{\rm R}, \tilde{\chi}_1^0) > 10$	> 94
$\tilde{e}_{\rm R}$, any Δm	> 73
$\tilde{\tau}_{\rm R}$, $\Delta m((\tilde{\tau}_{\rm R}, \tilde{\chi}_1^0) > 7$	> 87
$\tilde{\nu}_e$, $\Delta m(\tilde{e}_{\rm R}, \tilde{\chi}_1^0) > 10$	> 94
$m_{\tilde{e}_{\rm L,R}} = m_{\tilde{\mu}_{\rm L,R}}$, $m_{\tilde{\chi}_1^0} \approx 0$	> 500
$m_{\tilde{\chi}_1^0} > \approx 270$	no LHC limit

110.7. Exclusion limits on long-lived sparticles

Long-lived sparticles arise in many different SUSY models. In particular in co-annihilation scenarios, where the NLSP and LSP are nearly mass-degenerate, this is rather common in order to obtain the correct Dark Matter relic density. Prominent examples are scenarios featuring $\tilde{\tau}$ co-annihilation, or models of SUSY breaking, e.g. minimal anomaly-mediated SUSY breaking, in which the appropriate Dark Matter density is obtained by co-annihilation of the LSP with an almost degenerate long-lived wino. However, in general, also other sparticles can be long-lived and it is desirable to establish a comprehensive search programme for these special long-lived cases, which lead to distinct experimental search signatures, including displaced vertices or disappearing tracks, etc.

Already in the past experiments performed dedicated searches for long-lived SUSY signatures, but with the absence of any experimental evidence for SUSY so far, it is expected that in the future even more effort and focus will be placed on SUSY scenarios involving long-lived sparticles. As for the interpretation of the canonical SUSY searches, also for long-lived scenarios simplified models are a convenient tool to benchmark these special cases (see e.g. [156,157]) .

In the following we give an overview of the most recent and relevant results for dedicated long-lived SUSY searches.

If the decay of gluinos is suppressed, for example if squark masses are high, gluinos may live longer than typical hadronization times. It is expected that such gluinos will hadronize to long-living strongly interacting particles known as R-hadrons. In particular, if the suppression of the gluino decay is highly significant, as in the case that the squark masses are much higher than the TeV scale, these R-hadrons can be (semi-)stable in collider timescales. Searches for such R-hadrons exploit the typical signature of stable charged massive particles in the detector. As shown in the upper left plot of Fig. 110.6, the CMS experiment excludes semi-stable gluino R-hadrons with masses below approximately 1.6 TeV [158]. The limits depend on the probability for gluinos to form bound states known as gluinoballs, as these are neutral and not observed in the tracking detectors. Similar limits are obtained by the ATLAS experiment [159]. Limits ranging between 1 and 1.6 TeV are set in the scenario of R-hadron decays inside the detector, using dE/dx measurements and searches for displaced vertices, for $c\tau$ ranging from 1 mm to more than 10 m, as shown in Fig. 110.6 (bottom left).

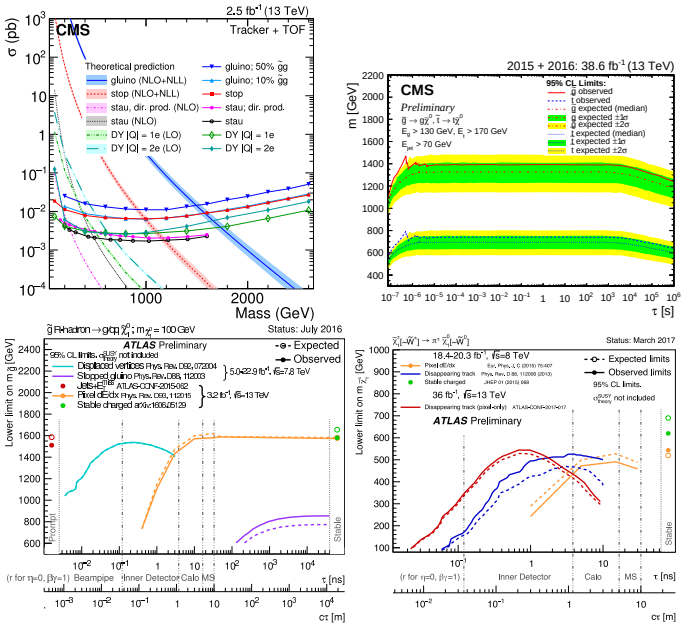

Figure 110.6: The upper left plot shows the observed 95% C.L. upper limits on the cross section for various long-lived charged sparticles. For gluinos, different fractions of gluinoball states produced after hadronization scenarios are indicated. The observed limits are compared with the predicted theoretical cross sections where the bands represent the theoretical uncertainties on the cross section values. The other plots show observed 95% C.L. lower limits on different sparticle masses in the mass-vs-lifetime plane for gluino R-hadrons (bottom left), stopped R-hadrons (top right) or charginos (bottom right).

Alternatively, since such R-hadrons are strongly interacting, they may be stopped in the calorimeter or in other material, and decay later into energetic jets. These decays are searched for by identifying the jets [160–162] or muons [163] outside the time window associated with bunch-bunch collisions. As shown in the upper right plot of Fig. 110.6, the CMS collaboration sets limits on such stopped R-hadrons over 13 orders of magnitude in gluino lifetime, up to masses of 1385 GeV [162]. A summary of a variety of different ATLAS searches for long-lived gluinos is shown in the lower left plot of Fig. 110.6. It displays constraints on the gluino mass-vs-lifetime plane for a split-supersymmetry model with the gluino R-hadron decaying into a gluon or light quarks and a neutralino with mass of 100 GeV .

Top squarks can also be long-lived and hadronize to a R-hadron, for example in the scenario where the top squark is the next-to-lightest SUSY particle (NLSP), with a small mass difference to the LSP. Searches for massive stable charged particles are sensitive to such top squarks. Displayed in the upper left plot of Fig. 110.6 are the results of the CMS analysis [158], which sets limits $m_{\tilde{t}} > 800$ GeV in such scenarios, while ATLAS [159] reports limits of $m_{\tilde{t}} > 900$ GeV . Limits from the Tevatron are about $m_{\tilde{t}} > 300$ GeV [164,165].

In addition to colored sparticles, also sparticles like charginos may be long-lived, especially in scenarios with compressed mass spectra. Charginos decaying in the detectors away from the primary vertex could lead to signatures such as kinked-tracks, or apparently disappearing tracks, since, for example, the pion in $\tilde{\chi}_1^{\pm} \to \pi^{\pm}\tilde{\chi}_1^0$ might be too soft to be reconstructed. At the LHC, searches have been performed for such disappearing tracks, and interpreted within anomaly-mediated SUSY breaking models [166–168]. The lower right plot of Fig. 110.6 shows constraints for different ATLAS searches on the chargino mass-vs-lifetime plane for an Anomaly Mediated SUSY Breaking (AMSB) model with $\tan\beta = 5$ and $\mu > 0$. It is assumed that wino-like charginos are pair-produced and decay to wino-like neutralinos and very soft charged pions. For example, for specific AMSB parameters, charginos with lifetimes between 0.1 and 10 ns are excluded for chargino masses up to 500 GeV . Within AMSB models, a lower limit on the chargino mass of 430 GeV is set, for a mass difference with the LSP of 160 MeV and a lifetime of 0.2 ns. Furthermore, charginos with a lifetime longer than the time needed to pass through the detector appear as charged stable massive particles. Limits have been derived by the LEP experiments [169], by D0 at the Tevatron [165], and by the LHC experiments [159,170,171]. For lifetimes above 100 ns, charginos below some 800 GeV are excluded.

In gauge mediation models, NLSP neutralino decays need not be prompt, and experiments have searched for late decays with photons in the final state. CDF have searched for delayed $\tilde{\chi}_1^0 \to \gamma\tilde{G}$ decays using the timing of photon signals in the calorimeter [172]. CMS has used the same technique at the LHC [173]. Results are given as upper limits on the neutralino production cross section as a function of neutralino mass and lifetime. D0 has looked at the direction of showers in the electromagnetic calorimeter with a similar goal [174], and ATLAS has searched for photon candidates that do not point back to the primary vertex, as well as for delayed photons [175].

Charged slepton decays may be kinematically suppressed, for example in the scenario of a NLSP slepton with a very small mass difference to the LSP. Such a slepton may appear to be a stable charged massive particle. Interpretation of searches at LEP for such signatures within GMSB models with stau NLSP or slepton co-NLSP exclude masses up to 99 GeV [169]. Searches of stable charged particles at the Tevatron [164,165] and at the LHC [158,159] are also interpreted in terms of limits on stable charged sleptons. The limits obtained at the LHC exclude stable staus with masses below 240 GeV when produced directly in pairs, and below 490 GeV when staus are produced both directly and indirectly in the decay of other particles in a GMSB model [158].

110.8. Global interpretations

Apart from the interpretation of direct searches for sparticle production at colliders in terms of limits on masses of individual SUSY particles, model-dependent interpretations of allowed SUSY parameter space are derived from global SUSY fits. Typically these fits combine the results from collider experiments with indirect constraints on SUSY as obtained from low-energy experiments, flavor physics, high-precision electroweak results, and astrophysical data.

In the pre-LHC era these fits were mainly dominated by indirect constraints. Even for very constrained models like the CMSSM, the allowed parameter space, in terms of squark and gluino masses, ranged from several hundreds of GeV to a few TeV. Furthermore, these global fits indicated that squarks and gluino masses in the range of 500 to 1000 GeV were the preferred region of parameter space, although values as high as few TeV were allowed with lower probabilities [176].

With ATLAS and CMS now probing mass scales around 1 TeV and even beyond, the importance of the direct searches for global analyses of allowed SUSY parameter space has strongly increased. For example, imposing the new experimental limits on constrained supergravity models pushes the most likely values of first generation squark and gluino masses significantly beyond 2 TeV, typically resulting in overall values of fit quality much worse than those in the pre-LHC era [128]. Although these constrained models are not yet ruled out, the extended experimental limits impose very tight constraints on the allowed parameter space.

For this reason, the emphasis of global SUSY fits has shifted towards less-constrained SUSY models. Especially interpretations in the pMSSM [170,139–141] but also in simplified models have been useful to generalize SUSY searches, for example to redesign experimental analyses in order to increase their sensitivity for compressed spectra, where the mass of the LSP is much closer to squark and gluino masses than predicted, for example, by the CMSSM. As shown in Table 110.2, for neutralino masses above approximately 0.5 TeV the current set of ATLAS and CMS searches, interpreted in simplified models, cannot exclude the existence of squarks or gluinos with masses only marginally above the neutralino mass. However, as these exclusion limits are defined in the context of simplified models, they are only valid for the assumptions in which these models are defined.

As an alternative approach, both ATLAS [139] and CMS [140] have performed an analysis of the impact of their searches on the parameter space of the pMSSM. Fig. 110.7 shows graphically the LHC exclusion power in the pMSSM based on searches performed at $\sqrt{s} =$ 7 and 8 TeV. The plot on the left shows the survival probability in the gluino-neutralino mass plane, which is a measure of the parameter space that remains after inclusion of the relevant CMS search results. As can be seen, gluino masses below about 1.2 TeV are almost fully excluded. This result agrees well with the typical exclusion obtained in simplified models for gluino production. However, as shown in the right plot of Fig. 110.7, when a similar analysis for other sparticles is performed it becomes apparent that exclusions on the pMSSM parameter can be significantly less stringent than simplified model limits might suggest. This is especially apparent for the electroweak sector, where even at rather low masses several of the pMSSM test points still survive the constraint of ATLAS searches at $\sqrt{s} = 7$ and 8 TeV. This again indicates that care must be taken when interpreting results from the LHC searches and there are still several scenarios where sparticles below the 1 TeV scale are not excluded, even when considering the most recent results at $\sqrt{s} = 13$ TeV.

Furthermore, the discovery of a Higgs boson with a mass around 125 GeV has triggered many studies regarding the compatibility of SUSY parameter space with this new particle. Much of it is still work in progress and it will be interesting to see how the interplay between the results from direct SUSY searches and more precise measurements of the properties of the Higgs boson will unfold in the future.

110.9. Summary and Outlook

The absence of any observation of new phenomena at the first run of the LHC at $\sqrt{s} = 7/8$ TeV, and now also during operation at $\sqrt{s} = 13$ TeV, place significant constraints on SUSY parameter space. Today, inclusive searches probe production of gluinos at about 2 TeV, first and second generation squarks in the range of about 1 to 1.6 TeV, third generation squarks at scales around 600 GeV to 1 TeV, electroweak gauginos at scales around $300 - 800$ GeV , and

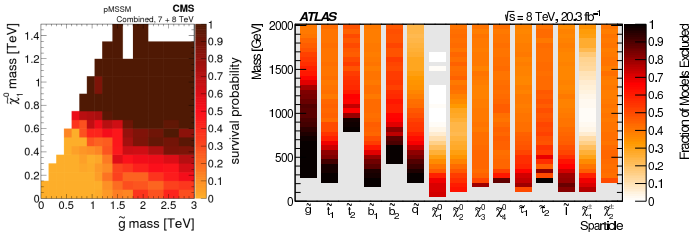

Figure 110.7: The plot on the left shows the survival probability of a pMSSM parameter space model in the gluino-neutralino mass plane after the application of the relevant CMS search results. The plot on the right shows a graphical representation of the ATLAS exclusion power in a pMSSM model. Each vertical bar is a one-dimensional projection of the fraction of models points excluded for each sparticle by ATLAS analyses. The experimental results are obtained from data taken at $\sqrt{s} = 7$ and 8 TeV.

sleptons around 500 GeV . However, depending on the assumptions made on the underlying SUSY spectrum these limits can also weaken considerably.

Fig. 110.8 shows a comparison of the results from the first run of the LHC (about 20 fb^{-1} of data at $\sqrt{s} = 7/8$ TeV) with the new results obtained from about 36 fb^{-1} taken at $\sqrt{s} = 13$ TeV. Based on the example of a selected set of simplified model limits discussed in this review, it becomes apparent that for all sparticle sectors the new LHC results push sensitivity deep into new territory. This is especially apparent for limits on colored sparticles, which typically benefit most from the energy increase, but also limits on electroweakly produced sparticles have strengthened significantly since the last run period.

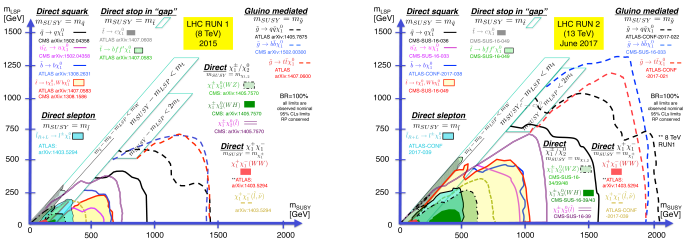

Figure 110.8: Comparison of a selected set of simplified model limits based on about 20 fb^{-1}) taken at $\sqrt{s} = 7/8$ TeV, with the same limits derived from 36 fb^{-1} taken at $\sqrt{s} = 13$ TeV. Further details about the different simplified models displaced here are provided in the text.

With the LHC having reached almost its maximum energy of about $\sqrt{s} = 14$ TeV, future sensitivity improvement will have to originate from more data and improvement of experimental analysis techniques. Therefore, it is expected that the current landscape of SUSY searches and corresponding exclusion limits at the LHC, as, for example, shown in Fig. 110.9 from the ATLAS experiment [177], will not change as rapidly anymore as it did in the past, when the LHC underwent several successive increases of collision energy.

The interpretation of results at the LHC has moved away from constrained models like the CMSSM towards a large set of simplified models, or the pMSSM. On the one hand this move is because the LHC limits have put constrained models like the CMSSM under severe pressure, while on the other hand simplified models leave more freedom to vary parameters and form a better representation of the underlying sensitivity of analyses. However, these interpretations in simplified models do not come without a price: the decomposition of a potentially complicated reality in a limited set of individual decay chains can be significantly incomplete. Therefore, quoted limits in simplified models are only valid under the explicit assumptions

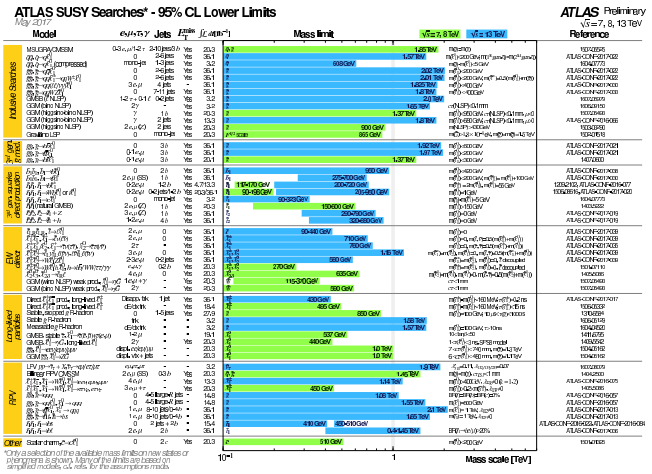

Figure 110.9: Overview of the current landscape of SUSY searches at the LHC. The plot shows exclusion mass limits of ATLAS for different searches and interpretation assumptions [177]. The corresponding results of the CMS experiment are similar [178].

made in these models. The recent addition of more comprehensive interpretations in the pMSSM will complement those derived from simplified models and, thus, will enable an even more refined understanding of the probed SUSY parameter space.

In this context, the limit range of $1.5 - 2.0$ TeV on generic colored SUSY particles only holds for light neutralinos, in the R-parity conserving MSSM. Limits on third generation squarks and electroweak gauginos also only hold for light neutralinos, and under specific assumptions for decay modes and slepton masses.

The ongoing LHC run at $\sqrt{s} = 13$ TeV, and future runs at 14 TeV with significantly larger integrated luminosities (Run 3, and the High-Luminosity LHC), will provide a large data sample for future SUSY searches. As mentioned above, the improvement in sensitivity will largely have to come from the larger statistics, and evolution of trigger and analysis techniques, since there will be no significant energy increase at the LHC anymore. Although the sensitivity for colored sparticles will increase somewhat as well, the expanded data set will be particularly beneficial for electroweak gaugino searches, and for the more difficult final states presented by compressed particle spectra, stealth SUSY, long-lived sparticles, or R-parity violating scenarios.

References:

1. H. Miyazawa, Prog. Theor. Phys. **36**, 1266 (1966).
2. Yu. A. Golfand and E.P. Likhtman, Sov. Phys. JETP Lett. **13**, 323 (1971).
3. J.L. Gervais and B. Sakita, Nucl. Phys. **B34**, 632 (1971).
4. D.V. Volkov and V.P. Akulov, Phys. Lett. **B46**, 109 (1973).
5. J. Wess and B. Zumino, Phys. Lett. **B49**, 52 (1974).
6. J. Wess and B. Zumino, Nucl. Phys. **B70**, 39 (1974).
7. A. Salam and J.A. Strathdee, Nucl. Phys. **B76**, 477 (1974).
8. H.P. Nilles, Phys. Reports **110**, 1 (1984).
9. H.E. Haber and G.L. Kane, Phys. Reports **117**, 75 (1987).
10. E. Witten, Nucl. Phys. **B188**, 513 (1981).
11. S. Dimopoulos and H. Georgi, Nucl. Phys. **B193**, 150 (1981).
12. M. Dine, W. Fischler, and M. Srednicki, Nucl. Phys. **B189**, 575 (1981).
13. S. Dimopoulos and S. Raby, Nucl. Phys. **B192**, 353 (1981).
14. N. Sakai, Z. Phys. **C11**, 153 (1981).
15. R.K. Kaul and P. Majumdar, Nucl. Phys. **B199**, 36 (1982).
16. H. Goldberg, Phys. Rev. Lett. **50**, 1419 (1983).
17. J.R. Ellis *et al.*, Nucl. Phys. **B238**, 453 (1984).
18. G. Jungman and M. Kamionkowski, Phys. Reports **267**, 195 (1996).

19. S. Dimopoulos, S. Raby, and F. Wilczek, Phys. Rev. **D24**, 1681 (1981).
20. W.J. Marciano and G. Senjanović, Phys. Rev. **D25**, 3092 (1982).
21. M.B. Einhorn and D.R.T. Jones, Nucl. Phys. **B196**, 475 (1982).
22. L.E. Ibanez and G.G. Ross, Phys. Lett. **B105**, 439 (1981).
23. N. Sakai, Z. Phys. **C11**, 153 (1981).
24. U. Amaldi, W. de Boer, and H. Furstenau, Phys. Lett. **B260**, 447 (1991).
25. P. Langacker and N. Polonsky, Phys. Rev. **D52**, 3081 (1995).
26. P. Fayet, Phys. Lett. **B64**, 159 (1976).
27. G.R. Farrar and P. Fayet, Phys. Lett. **B76**, 575 (1978).
28. H.E. Haber, *Supersymmetry, Part I (Theory)*, in this *Review*.
29. CMS Collab. and LHCb Collab., Nature **522**, 68 (2015).
30. LHCb Collab., Phys. Rev. Lett. **118**, 191801 (2017).
31. A. Höcker and W.Marciano, *The Muon Anomalous Magnetic Moment*, in this *Review*.
32. G. Hinshaw *et al.*, Astrophys. J. Supp. **208**, 19H (2013).
33. Planck Collab., Astron. & Astrophys. **594**, A13 (2016).
34. M. Carena *et al.*, *Status of Higgs Boson Physics*, in this *Review*.
35. J.F. Grivaz, *Supersymmetry, Part II (Experiment)*, in: 2010 Review of Particle Physics, K. Nakamura *et al.*, (Particle Data Group), J. Phys. **G37**, 075021 (2010).
36. I. Hinchliffe *et al.*, Phys. Rev. **D55**, 5520 (1997).
37. L. Randall and D. Tucker-Smith, Phys. Rev. Lett. **101**, 221803 (2008).
38. CMS Collab., Phys. Lett. **B698**, 196 (2011).
39. CMS Collab., Phys. Rev. Lett. **107**, 221804 (2011).
40. CMS Collab., JHEP **1301**, 077 (2013).
41. CMS Collab., Eur. Phys. J. **C73**, 2568 (2013).
42. CMS Collab., Phys. Rev. **D85**, 012004 (2012).
43. C.G. Lester and D.J. Summers, Phys. Lett. **B463**, 99 (1999).
44. D.R. Tovey, JHEP **0804**, 034 (2008).
45. M.R. Buckley *et al.*, Phys. Rev. **D89**, 055020 (2014).
46. P. Jackson, C. Rogan, and M. Sartoni, Phys. Rev. **D95**, 035031 (2017).
47. J.M. Butterworth *et al.*, Phys. Rev. Lett. **100**, 242001 (2008).
48. A.H. Chamseddine, R. Arnowitt, and P Nath, Phys. Rev. Lett. **49**, 970 (1982).
49. E. Cremmer *et al.*, Nucl. Phys. **B212**, 413 (1983).
50. P. Fayet, Phys. Lett. **B70**, 461 (1977).
51. M. Dine, A.E. Nelson, and Yu. Shirman, Phys. Rev. **D51**, 1362 (1995).
52. P. Meade, N. Seiberg, and D. Shih, Prog. Theor. Phys. Supp. **177**, 143 (2009).
53. G.F. Giudice *et al.*, JHEP **9812**, 027 (1998).
54. L. Randall and R. Sundrum, Nucl. Phys. **B557**, 79 (1999).
55. R. Arnowitt and P Nath, Phys. Rev. Lett. **69**, 725 (1992).
56. G.L. Kane *et al.*, Phys. Rev. **D49**, 6173 (1994).
57. E. Halkiadakis, G. Redlinger, and D. Shih, Ann. Rev. Nucl. and Part. Sci. **64**, 319 (2014).
58. W. Beenakker *et al.*, Int. J. Mod. Phys. **A26**, 2637 (2011).
59. W. Beenakker *et al.*, Nucl. Phys. **B492**, 51 (1997); W. Beenakker *et al.*, Nucl. Phys. **B515**, 3 (1998); W. Beenakker *et al.*, Phys. Rev. Lett. **83**, 3780 (1999), Erratum *ibid.*, **100**, 029901 (2008); M. Spira, hep-ph/0211145 (2002); T. Plehn, Czech. J. Phys. 55, B213 (2005).
60. A. Djouadi, J-L. Kneur, and G. Moultaka, Comp. Phys. Comm. **176**, 426 (2007).
61. C.F. Berger *et al.*, JHEP **0902**, 023 (2009).
62. H. Baer *et al.*, hep-ph/9305342, 1993.
63. R.M. Barnett, H.E. Haber, and G.L. Kane, Nucl. Phys. **B267**, 625 (1986).
64. H. Baer, D. Karatas, and X. Tata, Phys. Lett. **B183**, 220 (1987).
65. J. Alwall, Ph.C. Schuster, and N. Toro, Phys. Rev. **D79**, 075020 (2009).
66. J. Alwall *et al.*, Phys. Rev. **D79**, 015005 (2009).
67. O. Buchmueller and J. Marrouche, Int. J. Mod. Phys. **A29**, 1450032 (2014).
68. LEP2 SUSY Working Group, ALEPH, DELPHI, L3 and OPAL experiments, note LEPSUSYWG/04-02.1, lepsusy.web.cern.ch/lepsusy.
69. CDF Collab., Phys. Rev. Lett. **102**, 121801 (2009).
70. D0 Collab., Phys. Lett. **B660**, 449 (2008).
71. ATLAS Collab. *Search for squarks and gluinos in final states with jets and missing transverse momentum using 36 fb^{-1} of $\sqrt{s} = 13$ TeV pp collision data with the ATLAS detector*, ATLAS-CONF-2017-022 (2017).
72. CMS Collab., *Search for new phenomena with the M_{T2} variable in the all-hadronic final state produced in proton-proton collisions at $\sqrt{s}$ =13 TeV*, arXiv:1705.04650(2017).
73. CMS Collab., Phys. Rev. **D96**, 032003 (2017).
74. ATLAS Collab., *Search for production of supersymmetric particles in final states with missing transverse momentum and multiple b-jets at $\sqrt{s} = 13$ TeV proton-proton collisions with the ATLAS detector*, ATLAS-CONF-2017-021 (2017).
75. CMS Collab., *Search for supersymmetry in pp collisions at $\sqrt{s} = 13$ TeV in the single-lepton final state using the sum of masses of large-radius jets*, arXiv:1705.04673(2017).
76. ATLAS Collab., *Constraints on promptly decaying supersymmetric particles with lepton-number- and R-parity-violating interactions using Run-1 ATLAS data*, ATLAS-CONF-2015-018 (2015).
77. CMS Collab., *Search for RPV SUSY in the four-lepton final state*, CMS-PAS-SUS-13-010 (2013).
78. ATLAS Collab., Phys. Rev. **D92**, 072004 (2015).
79. CDF Collab., Phys. Rev. Lett. **107**, 042001 (2011).
80. ATLAS Collab., *Search for massive supersymmetric particles in multi-jet final states produced in pp collisions at $\sqrt{s} = 13$ TeV using the ATLAS detector at the LHC*, ATLAS-CONF-2016-057 (2016).
81. ATLAS Collab., JHEP **1709**, 088 (2017).
82. CMS Collab., Phys. Lett. **B730**, 193 (2014).
83. CMS Collab., Phys. Lett. **B770**, 257 (2017).
84. ATLAS Collab,. Phys. Rev. Lett. **114**, 161801 (2015).
85. CDF Collab., Phys. Rev. Lett. **105**, 081802 (2010).
86. D0 Collab., Phys. Lett. **B693**, 95 (2010).
87. CMS Collab., *Search for the pair production of third-generation squarks with two-body decays to a bottom or charm quark and a neutralino in proton-proton collisions at $\sqrt{s} = 13$ TeV*, arXiv:1707.07274(2017).
88. ATLAS Collab., *Search for supersymmetry in events with b-tagged jets and missing transverse momentum in pp collisions at $\sqrt{s} = 13$ TeV with the ATLAS detector*, arXiv:1708.09266(2017).
89. ATLAS Collab., Eur. Phys. J. **C75**, 510 (2015).
90. CMS Collab., Eur. Phys. J. **C77**, 578 (2017).
91. C. Boehm, A. Djouadi, and Y. Mambrini, Phys. Rev. **D61**, 095006 (2000).
92. CDF Collab., Phys. Rev. **D82**, 092001 (2010).
93. D0 Collab., Phys. Lett. **B696**, 321 (2011).
94. CDF Collab., JHEP **1210**, 158 (2012).
95. D0 Collab., Phys. Lett. **B665**, 1 (2008).
96. CDF Collab., Phys. Rev. Lett. **104**, 251801 (2010).
97. D0 Collab., Phys. Lett. **B674**, 4 (2009).
98. CMS Collab., JHEP **1710**, 005 (2017).
99. CMS Collab., JHEP **1710**, 019 (2017).
100. ATLAS Collab., *Search for a scalar partner of the top quark in the jets+E_T^{miss} final state at $\sqrt{s} = 13$ TeV with the ATLAS detector*, arXiv:1709.04183(2017).
101. ATLAS Collab., *Search for top squarks in final states with one isolated lepton, jets and missing transverse momentum using 36.1 fb^{-1} of $\sqrt{s} = 13$ TeV pp collision data with the ATLAS detector*, ATLAS-CONF-2017-037 (2017).
102. CMS Collab., *Search for direct stop pair production in the dilepton final state at $\sqrt{s} = 13$ TeV*, CMS-PAS-SUS-17-001 (2017).
103. ATLAS Collab., *Search for direct top squark pair production in final states with two leptons in $\sqrt{s} = 13$ TeV pp collisions with the ATLAS detector*, arXiv:1708.03247(2017).

104. ATLAS Collab., *Search for dark matter and other new phenomena in events with an energetic jet and large missing transverse momentum using the ATLAS detector*, ATLAS-CONF-2017-060 (2017).
105. H1 Collab., Eur. Phys. J. **C71**, 1572 (2011).
106. CMS Collab., Phys. Rev. **D91**, 052012 (2015).
107. ZEUS Collab., Eur. Phys. J. **C50**, 269 (2007).
108. CMS Collab., Phys. Rev. Lett. **111**, 221801 (2013).
109. ATLAS Collab., *A search for $B-L$ R-parity-violating scalar tops in $\sqrt{s}=13$ TeV pp collisions with the ATLAS experiment*, arXiv:1710.05544(2017).
110. CMS Collab., Phys. Rev. Lett. **114**, 061801 (2015).
111. CMS Collab., Phys. Lett. **B760**, 178 (2016).
112. ATLAS Collab., *A search for pair-produced resonances in four-jet final states at $\sqrt{s}=13$ TeV with the ATLAS detector*, ATLAS-CONF-2017-025 (2017).
113. CMS Collab., Phys. Lett. **B747**, 98 (2015).
114. LEP2 SUSY Working Group, ALEPH, DELPHI, L3 and OPAL experiments, note LEPSUSYWG/01-03.1, lepsusy.web.cern.ch/lepsusy.
115. LEP2 SUSY Working Group, ALEPH, DELPHI, L3 and OPAL experiments, note LEPSUSYWG/02-04.1, lepsusy.web.cern.ch/lepsusy.
116. CDF Collab., *Search for trilepton new physics and chargino-neutralino production at the Collider Detector at Fermilab*, CDF Note 10636 (2011).
117. D0 Collab., Phys. Lett. **B680**, 34 (2009).
118. ATLAS Collab. *Search for electroweak production of supersymmetric particles in the two and three lepton final state at $\sqrt{s}=13$ TeV with the ATLAS detector*, ATLAS-CONF-2017-039 (2017).
119. ATLAS Collab., JHEP **1405**, 071 (2014).
120. CMS Collab., *Search for electroweak production of charginos and neutralinos in multilepton final states in pp collision data at $\sqrt{s}=13$ TeV*, arXiv:1709.05406(2017).
121. ATLAS Collab., *Search for the direct production of charginos and neutralinos in $\sqrt{s}=13$ TeV pp collisions with the ATLAS detector*, arXiv:1708.07875(2017).
122. CMS Collab., *Combined search for electroweak production of charginos and neutralinos in pp collisions at $\sqrt{s}=13$ TeV*, CMS-PAS-SUS-17-004 (2017).
123. ATLAS Collab., Eur. Phys. J. **C75**, 208 (2015).
124. ATLAS Collab., Phys. Rev. **D93**, 052002 (2016).
125. CMS Collab., JHEP **1511**, 189 (2015).
126. H. Dreiner *et al.*, Eur. Phys. J. **C62**, 547 (2009).
127. LEP2 SUSY Working Group, ALEPH, DELPHI, L3 and OPAL experiments, note LEPSUSYWG/04-07.1, lepsusy.web.cern.ch/lepsusy.
128. For a sampling of recent post-LHC global analyses, see: GAMBIT Collab, arXiv:1705.07935; E.A. Bagnaschi *et al.*, Eur. Phys. J. **C77**, 268 (2017); E.A. Bagnaschi *et al.*, Eur. Phys. J. **C77**, 104 (2017); P. Bechtle *et al.*, Eur. Phys. J. **C76**, 9, (2016); E.A. Bagnaschi *et al.*, Eur. Phys. J. **C75**, 500 (2015); O. Buchmueller *et al.*, Eur. Phys. J. **C74**, 3212 (2014); O. Buchmueller *et al.*, Eur. Phys. J. **C74**, 2922 (2014); M. Citron *et al.*, Phys. Rev. **D87**, 036012 (2013); C. Strege *et al.*, JCAP **1304**, 013 (2013); A. Fowlie *et al.*, Phys. Rev. **D86**, 075010 (2012).
129. LEP2 SUSY Working Group, ALEPH, DELPHI, L3 and OPAL experiments, note LEPSUSYWG/04-09.1, lepsusy.web.cern.ch/lepsusy.
130. CDF Collab., Phys. Rev. Lett. **104**, 011801 (2010).
131. D0 Collab., Phys. Rev. Lett. **105**, 221802 (2010).
132. ATLAS Collab., Eur. Phys. J. **C76**, 517 (2016).
133. CMS Collab., *Search for supersymmetry in events with at least one photon, missing transverse momentum, and large transverse event activity in proton-proton collisions at $\sqrt{s}=13$ TeV*, arXiv:1707.06193(2017).
134. ATLAS Collab., Eur. Phys. J. **C77**, 144 (2017).
135. CMS Collab., Phys. Rev. **D90**, 092007 (2014).
136. CMS Collab., JHEP **04**, 124 (2016).
137. ATLAS Collab., *Search for supersymmetry in events with four or more leptons in $\sqrt{s}=13$ TeV pp collisions using 13.3 fb^{-1} of ATLAS data*, ATLAS-CONF-2016-075 (2016).
138. CMS Collab., Phys. Rev. **D91**, 012007 (2015).
139. ATLAS Collab., JHEP **1510**, 134 (2015).
140. CMS Collab., JHEP **1610**, 129 (2016).
141. For a sampling of recent pMSSM analyses, see: GAMBIT Collab, arXiv:1705.07917; K. de Vries *et al.*, Eur. Phys. J. **C75**, 422 (2015); C. Strege *et al.*, JHEP **1409**, 081 (2014); M. Cahill-Rowley *et al.*, Phys. Rev. **D88**, 035002 (2013); C. Boehm *et al.*, JHEP **1306**, 113, (2013); S AbdusSalam, Phys. Rev. **D87**, 115012 (2013); A. Arbey *et al.*, Eur. Phys. J. **C72**, 2169 (2012); A. Arbey *et al.*, Eur. Phys. J. **C72**, 1847 (2012); M. Carena *et al.*, Phys. Rev. **D86**, 075025 (2012); S. Sekmen *et al.*, JHEP **1202**, 075 (2012).
142. LEP2 SUSY Working Group, ALEPH, DELPHI, L3 and OPAL experiments, note LEPSUSYWG/04-01.1, lepsusy.web.cern.ch/lepsusy.
143. ALEPH Collab., Phys. Lett. **B544**, 73 (2002).
144. LEP2 SUSY Working Group, ALEPH, DELPHI, L3 and OPAL experiments, note LEPSUSYWG/02-09.2, lepsusy.web.cern.ch/lepsusy.
145. ATLAS Collab., JHEP **1409**, 103 (2014).
146. CMS Collab., Phys. Rev. **D90**, 032006 (2014).
147. CDF Collab., Phys. Rev. Lett. **110**, 201802 (2013).
148. LEP2 SUSY Working Group, ALEPH, DELPHI, L3 and OPAL experiments, note LEPSUSYWG/02-10.1, lepsusy.web.cern.ch/lepsusy.
149. DELPHI Collab., Eur. Phys. J. **C31**, 412 (2003).
150. T. Falk, K.A. Olive, and M. Srednicki, Phys. Lett. **B339**, 248 (1994).
151. C. Arina and N. Fornengo, JHEP **0711**, 029 (2007).
152. CDF Collab., Phys. Rev. Lett. **105**, 191801 (2010).
153. D0 Collab., Phys. Rev. Lett. **105**, 191802 (2010).
154. ATLAS Collab., Phys. Rev. Lett. **115**, 031801 (2015).
155. CMS Collab., Eur. Phys. J. **C76**, 317 (2016).
156. O. Buchmueller *et al.*, *Simplified Models for Displaced Dark Matter Signatures*, arXiv:1704.06515.
157. V. Khoze *et al.*, JHEP **06**, 041 (2017).
158. CMS Collab., Phys. Rev. **D94**, 112004 (2016).
159. ATLAS Collab., Phys. Lett. **B760**, 647 (2016).
160. D0 Collab., Phys. Rev. Lett. **99**, 131801 (2007).
161. ATLAS Collab., Phys. Rev. **D88**, 112003 (2013).
162. CMS Collab., *Search for stopped long-lived particles produced in pp collisions at $\sqrt{s}=13$ TeV*, CMS-PAS-EXO-16-004 (2017).
163. CMS Collab., *Search for long-lived particles that stop in the CMS detector and decay to muons at $\sqrt{s}=13$ TeV*, CMS-PAS-EXO-17-004 (2017).
164. CDF Collab., Phys. Rev. Lett. **103**, 021802 (2009).
165. D0 Collab., Phys. Rev. **D87**, 052011 (2013).
166. ATLAS Collab., Phys. Rev. **D88**, 112006 (2013).
167. ATLAS Collab., *Search for long-lived charginos based on a disappearing-track signature in pp collisions at $\sqrt{s}=13$ TeV with the ATLAS detector*, ATLAS-CONF-2017-017 (2017).
168. CMS Collab., JHEP **1501**, 096 (2015).
169. LEP2 SUSY Working Group, ALEPH, DELPHI, L3 and OPAL experiments, note LEPSUSYWG/02-05.1, lepsusy.web.cern.ch/lepsusy.
170. CMS Collab., Eur. Phys. J. **C75**, 325 (2015).
171. LHCb Collab., Eur. Phys. J. **C75**, 595 (2015).
172. CDF Collab., Phys. Rev. **D88**, 031103 (2013).
173. CMS Collab., Phys. Lett. **B722**, 273 (2013).
174. D0 Collab., Phys. Rev. Lett. **101**, 111802 (2008).
175. ATLAS Collab, Phys. Rev. **D90**, 112005 (2014).
176. For a sampling of pre-LHC global analyses, see: O. Buchmueller *et al.*, Eur. Phys. J. **C71**, 1722 (2011); E.A. Baltz and P. Gondolo, JHEP **0410**, 052 (2004); B.C. Allanach and C.G. Lester, Phys. Rev. **D73**, 015013 (2006); R.R. de Austri *et al.*, JHEP **0605**, 002 (2006); R. Lafaye *et al.*, Eur. Phys. J. **C54**, 617 (2008); S. Heinemeyer *et al.*, JHEP **0808**, 08 (2008);

R. Trotta *et al.*, JHEP **0812**, 024 (2008); P. Bechtle *et al.*, Eur. Phys. J. **C66**, 215 (2010).
177. Supersymmetry Physics Results, ATLAS experiment, http://twiki.cern.ch/twiki/bin/view/AtlasPublic/SupersymmetryPublicResults/.
178. Supersymmetry Physics Results, CMS experiment, http://cms-results.web.cern.ch/cms-results/public-results/publications/SUS/index.html.

111. Axions and Other Similar Particles

Revised October 2017 by A. Ringwald (DESY), L.J Rosenberg and G. Rybka (U. of Washington).

111.1. Introduction

In this section, we list coupling-strength and mass limits for light neutral scalar or pseudoscalar bosons that couple weakly to normal matter and radiation. Such bosons may arise from a global spontaneously broken U(1) symmetry, resulting in a massless Nambu-Goldstone (NG) boson. If there is a small explicit symmetry breaking, either already in the Lagrangian or due to quantum effects such as anomalies, the boson acquires a mass and is called a pseudo-NG boson. Typical examples are axions (A^0) [1,2], familons [3] and majorons [4], associated, respectively, with a spontaneously broken Peccei-Quinn, family and lepton-number symmetry.

A common characteristic among these light bosons ϕ is that their coupling to Standard-Model particles is suppressed by the energy scale that characterizes the symmetry breaking, *i.e.*, the decay constant f. The interaction Lagrangian is

$$\mathcal{L} = f^{-1} J^\mu \partial_\mu \phi \,, \tag{111.1}$$

where J^μ is the Noether current of the spontaneously broken global symmetry. If f is very large, these new particles interact very weakly. Detecting them would provide a window to physics far beyond what can be probed at accelerators.

Axions are of particular interest because the Peccei-Quinn (PQ) mechanism remains perhaps the most credible scheme to preserve CP in QCD. Moreover, the cold dark matter of the universe may well consist of axions and they are searched for in dedicated experiments with a realistic chance of discovery.

Originally it was assumed that the PQ scale f_A was related to the electroweak symmetry-breaking scale $v_{\rm weak} = (\sqrt{2}G_{\rm F})^{-1/2} = 247$ GeV. However, the associated "standard" and "variant" axions were quickly excluded—we refer to the Listings for detailed limits. Here we focus on "invisible axions" with $f_A \gg v_{\rm weak}$ as the main possibility.

Axions have a characteristic two-photon vertex, inherited from their mixing with π^0 and η. This coupling allows for the main search strategy based on axion-photon conversion in external magnetic fields [5], an effect that also can be of astrophysical interest. While for axions the product "$A\gamma\gamma$ interaction strength × mass" is essentially fixed by the corresponding π^0 properties, one may consider a more general class of axion-like particles (ALPs) where the two parameters (coupling and mass) are independent. A number of experiments explore this more general parameter space. ALPs populating the latter are predicted to arise generically, in addition to the axion, in low-energy effective field theories emerging from string theory [6]. The latter often contain also very light Abelian vector bosons under which the Standard-Model particles are not charged: so-called hidden-sector photons, dark photons or paraphotons. They share a number of phenomenological features with the axion and ALPs, notably the possibility of hidden photon to photon conversion. Their physics cases and the current constraints are compiled in Ref. [7].

111.2. Theory

111.2.1. *Peccei-Quinn mechanism and axions* :

The QCD Lagrangian includes a CP-violating term $\mathcal{L}_\Theta = -\bar{\Theta}\,(\alpha_s/8\pi)\,G^{\mu\nu a}\tilde{G}^a_{\mu\nu}$, where $-\pi \le \bar{\Theta} \le +\pi$ is the effective Θ parameter after diagonalizing quark masses, $G^a_{\mu\nu}$ is the color field strength tensor, and $\tilde{G}^{a,\mu\nu} \equiv \epsilon^{\mu\nu\lambda\rho}G^a_{\lambda\rho}/2$, with $\varepsilon^{0123} = 1$, its dual. Limits on the neutron electric dipole moment [8] imply $|\bar{\Theta}| \lesssim 10^{-10}$ even though $\bar{\Theta} = \mathcal{O}(1)$ is otherwise completely satisfactory. The spontaneously broken global Peccei-Quinn symmetry $\mathrm{U}(1)_{\rm PQ}$ was introduced to solve this "strong CP problem" [1], the axion being the pseudo-NG boson of $\mathrm{U}(1)_{\rm PQ}$ [2]. This symmetry is broken due to the axion's anomalous triangle coupling to gluons,

$$\mathcal{L} = \left(\frac{\phi_A}{f_A} - \bar{\Theta}\right)\frac{\alpha_s}{8\pi}\,G^{\mu\nu a}\tilde{G}^a_{\mu\nu}\,, \tag{111.2}$$

where ϕ_A is the axion field and f_A the axion decay constant. Color anomaly factors have been absorbed in the normalization of f_A which is defined by this Lagrangian. Thus normalized, f_A is the quantity that enters all low-energy phenomena [9]. Non-perturbative topological fluctuations of the gluon fields in QCD induce a potential for ϕ_A whose minimum is at $\phi_A = \bar{\Theta}\,f_A$, thereby canceling the $\bar{\Theta}$ term in the QCD Lagrangian and thus restoring CP symmetry.

The resulting axion mass, in units of the PQ scale f_A, is identical to the square root of the topological susceptibility in QCD, $m_A f_A = \sqrt{\chi}$. The latter can be evaluated further [10], exploiting the chiral limit (masses of up and down quarks much smaller than the scale of QCD), yielding $m_A f_A = \sqrt{\chi} \approx f_\pi m_\pi$, where $m_\pi = 135$ MeV and $f_\pi \approx 92$ MeV. In more detail one finds, to next-to-leading order in chiral perturbation theory [11],

$$m_A = 5.70(7)\,\left(\frac{10^9\,\mathrm{GeV}}{f_A}\right)\mathrm{meV}\,. \tag{111.3}$$

This result was recently confirmed by a direct calculation of the topological susceptibility via QCD lattice simulations [12].

Originally one assumed $f_A \sim v_{\rm weak}$ [1,2]. Tree-level flavor conservation fixes the axion properties in terms of a single parameter: the ratio of the vacuum expectation values of two Higgs fields that appear as a minimal ingredient. This "standard axion" was excluded after extensive searches [13]. A narrow peak structure observed in positron spectra from heavy ion collisions [14] suggested an axion-like particle of mass 1.8 MeV that decays into e^+e^-, but extensive follow-up searches were negative. "Variant axion models" were proposed which keep $f_A \sim v_{\rm weak}$ while relaxing the constraint of tree-level flavor conservation [15], but these models are also excluded [16].

However, axions with $f_A \gg v_{\rm weak}$ evade all current experimental limits. One generic class of models invokes "hadronic axions" where new heavy quarks carry $\mathrm{U}(1)_{\rm PQ}$ charges, leaving ordinary quarks and leptons without tree-level axion couplings. The archetype is the KSVZ model [17], where in addition the heavy quarks are electrically neutral. Another generic class requires at least two Higgs doublets and ordinary quarks and leptons carry PQ charges, the archetype being the DFSZ model [18]. All of these models contain at least one electroweak singlet scalar that acquires a vacuum expectation value and thereby breaks the PQ symmetry. The KSVZ and DFSZ models are frequently used as benchmark examples, but other models exist where both heavy quarks and Higgs doublets carry PQ charges. In supersymmetric models, the axion is part of a supermultiplet and thus inevitably accompanied by a spin-0 saxion and a spin-1 axino, which both also have couplings suppressed by f_A, and are expected to have large masses due to supersymmetry breaking [19].

111.2.2. *Model-dependent axion couplings* :

Although the generic axion interactions scale approximately with f_π/f_A from the corresponding π^0 couplings, there are non-negligible model-dependent factors and uncertainties. The axion's two-photon interaction plays a key role for many searches,

$$\mathcal{L}_{A\gamma\gamma} = -\frac{G_{A\gamma\gamma}}{4}\,F_{\mu\nu}\tilde{F}^{\mu\nu}\phi_A = G_{A\gamma\gamma}\mathbf{E}\cdot\mathbf{B}\,\phi_A\,, \tag{111.4}$$

where F is the electromagnetic field-strength tensor and $\tilde{F}^{\mu\nu} \equiv \epsilon^{\mu\nu\lambda\rho}F_{\lambda\rho}/2$, with $\varepsilon^{0123} = 1$, its dual. The coupling constant is [11]

$$G_{A\gamma\gamma} = \frac{\alpha}{2\pi f_A}\left(\frac{E}{N} - 1.92(4)\right) = \left(0.203(3)\frac{E}{N} - 0.39(1)\right)\frac{m_A}{\mathrm{GeV}^2}\,, \tag{111.5}$$

where E and N are the electromagnetic and color anomalies of the axial current associated with the axion. In grand unified models, and notably for DFSZ [18], $E/N = 8/3$, whereas for KSVZ [17] $E/N = 0$ if the electric charge of the new heavy quark is taken to vanish. In general, a broad range of E/N values is possible [20], as indicated by the yellow band in Figure 111.1. The two-photon decay width is

$$\Gamma_{A\to\gamma\gamma} = \frac{G^2_{A\gamma\gamma}m_A^3}{64\,\pi} = 1.1\times10^{-24}\ \mathrm{s}^{-1}\,\left(\frac{m_A}{\mathrm{eV}}\right)^5. \tag{111.6}$$

the second expression uses Eq. (1.5) with $E/N = 0$. Axions decay faster than the age of the universe if $m_A \gtrsim 20$ eV.

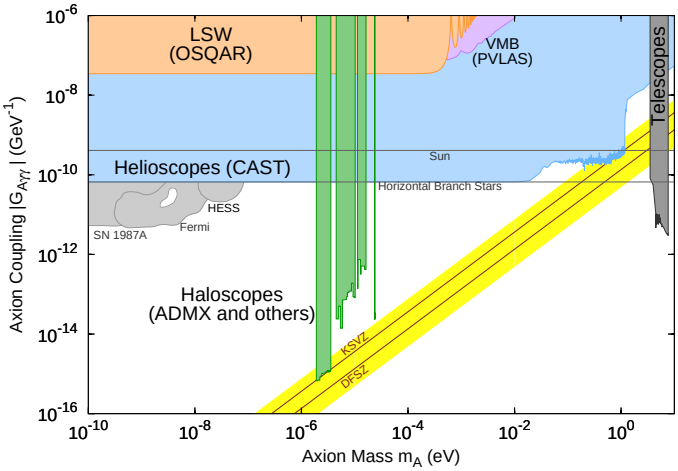

Figure 111.1: Exclusion plot for axion-like particles as described in the text.

The interaction with fermions f has derivative form and is invariant under a shift $\phi_A \to \phi_A + \phi_0$ as behooves a NG boson,

$$\mathcal{L}_{Aff} = \frac{C_f}{2f_A}\,\bar{\Psi}_f\gamma^\mu\gamma_5\Psi_f\partial_\mu\phi_A\,. \tag{111.7}$$

Here, Ψ_f is the fermion field, m_f its mass, and C_f a model-dependent coefficient. The dimensionless combination $g_{Aff} \equiv C_f m_f/f_A$ plays the role of a Yukawa coupling and $\alpha_{Aff} \equiv g^2_{Aff}/4\pi$ of a "fine-structure constant." The often-used pseudoscalar form $\mathcal{L}_{Aff} = -\mathrm{i}\,(C_f m_f/f_A)\,\bar{\Psi}_f\gamma_5\Psi_f\phi_A$ need not be equivalent to the appropriate derivative structure, for example when two NG bosons are attached to one fermion line as in axion emission by nucleon bremsstrahlung [21].

In the DFSZ model [18], the tree-level coupling coefficient to electrons is [22]

$$C_e = \frac{\sin^2\beta}{3}\,, \tag{111.8}$$

where $\tan\beta = v_u/v_d$ is the ratio of the vacuum expectation value v_u of the Higgs field H_u giving masses to the up-type quarks and the vacuum expectation value v_d of the Higgs field H_d giving masses to the down-type quarks.

For nucleons, $C_{n,p}$ have recently been determined as [11]

$$\begin{aligned} C_p &= -0.47(3) + 0.88(3)C_u - 0.39(2)C_d - 0.038(5)C_s \\ &\quad - 0.012(5)C_c - 0.009(2)C_b - 0.0035(4)C_t\,, \\ C_n &= -0.02(3) + 0.88(3)C_d - 0.39(2)C_u - 0.038(5)C_s \\ &\quad - 0.012(5)C_c - 0.009(2)C_b - 0.0035(4)C_t\,, \end{aligned} \tag{111.9}$$

in terms of the corresponding model-dependent quark couplings C_q, $q = u, d, s, c, b, t$.

Note, that the model-independent contribution of the neutron is compatible with zero. For hadronic axions $C_q = 0$, so that $C_n = -0.02(3)$. Therefore it is well possible that $C_n = 0$ whereas C_p does not vanish. In the DFSZ model, $C_u = C_c = C_t = \frac{1}{3}\cos^2\beta$ and $C_d = C_s = C_b = \frac{1}{3}\sin^2\beta$, and C_n and C_p, as functions of β,

$$\begin{aligned} C_p &= -0.435\sin^2\beta + (-0.182 \pm 0.025)\,, \\ C_n &= 0.414\sin^2\beta + (-0.16 \pm 0.025)\,, \end{aligned} \tag{111.10}$$

do not vanish simultaneously.

The axion-pion interaction is given by the Lagrangian [23]

$$\mathcal{L}_{A\pi} = \frac{C_{A\pi}}{f_\pi f_A}\left(\pi^0\pi^+\partial_\mu\pi^- + \pi^0\pi^-\partial_\mu\pi^+ - 2\pi^+\pi^-\partial_\mu\pi^0\right)\partial_\mu\phi_A\,, \tag{111.11}$$

where $C_{A\pi} = (1-z)/[3(1+z)]$ in hadronic models, with $0.38 < z = m_u/m_d < 0.58$ [24,25]. The chiral symmetry-breaking Lagrangian provides an additional term $\mathcal{L}'_{A\pi} \propto (m_\pi^2/f_\pi f_A)\,(\pi^0\pi^0 + 2\pi^-\pi^+)\,\pi^0\phi_A$. For hadronic axions it vanishes identically, in contrast to the DFSZ model (Roberto Peccei, private communication).

111.3. Laboratory Searches

111.3.1. *Light shining through walls* :

Searching for "invisible axions" is extremely challenging due to its extraordinarily feeble coupling to normal matter and radiation. Currently, the most promising approaches rely on the axion-two-photon vertex, allowing for axion-photon conversion in external electric or magnetic fields [5]. For the Coulomb field of a charged particle, the conversion is best viewed as a scattering process, $\gamma + Ze \leftrightarrow Ze + A$, called Primakoff effect [26]. In the other extreme of a macroscopic field, usually a large-scale B-field, the momentum transfer is small, the interaction coherent over a large distance, and the conversion is best viewed as an axion-photon oscillation phenomenon in analogy to neutrino flavor oscillations [27].

Photons propagating through a transverse magnetic field, with incident $\mathbf{E}_\gamma$ and magnet $\mathbf{B}$ parallel, may convert into axions. For $m_A^2 L/2\omega \ll 2\pi$, where L is the length of the B field region and ω the photon energy, the resultant axion beam is coherent with the incident photon beam and the conversion probability is $\Pi \sim (1/4)(G_{A\gamma\gamma}BL)^2$. A practical realization uses a laser beam propagating down the bore of a superconducting dipole magnet (like the bending magnets in high-energy accelerators). If another magnet is in line with the first, but shielded by an optical barrier, then photons may be regenerated from the pure axion beam [28]. The overall probability is $P(\gamma \to A \to \gamma) = \Pi^2$.

The first such experiment utilized two magnets of length $L = 4.4$ m and $B = 3.7$ T and found $|G_{A\gamma\gamma}| < 6.7 \times 10^{-7}$ GeV^{-1} at 95% CL for $m_A < 1$ meV [29]. More recently, several such experiments were performed (see Listings) [30,31]. The current best limit, $|G_{A\gamma\gamma}| < 3.5 \times 10^{-8}$ GeV^{-1} at 95% CL for $m_A \lesssim 0.3$ meV (see Figure 111.1), has been achieved by the OSQAR (Optical Search for QED Vacuum Birefringence, Axions, and Photon Regeneration) experiment, which exploited two 9 T LHC dipole magnets and an 18.5 W continuous wave laser emitting at the wavelength of 532 nm [31]. Some of these experiments have also reported limits for scalar bosons where the photon $\mathbf{E}_\gamma$ must be chosen perpendicular to the magnet $\mathbf{B}$.

The concept of resonantly enhanced photon regeneration may open unexplored regions of coupling strength [32]. In this scheme, both the production and detection magnets are within Fabry-Perot optical cavities and actively locked in frequency. The $\gamma \to A \to \gamma$ rate is enhanced by a factor $\mathcal{F}\mathcal{F}'/\pi^2$ relative to a single-pass experiment, where $\mathcal{F}$ and $\mathcal{F}'$ are the finesses of the two cavities. The resonant enhancement could be of order $10^{(10-12)}$, improving the $G_{A\gamma\gamma}$ sensitivity by $10^{(2.5-3)}$. The experiment ALPS II (Any Light Particle Search II) is based on this concept and aims at an improvement of the current laboratory bound on $G_{A\gamma\gamma}$ by a factor $\sim 10^3$ in the year 2020 [33].

Resonantly enhanced photon regeneration has already been exploited in experiments searching for "radiowaves shining through a shielding" [34,35]. For $m_A \lesssim 10^{-5}$ eV, the upper bound on $G_{A\gamma\gamma}$ established by the CROWS (CERN Resonant Weakly Interacting sub-eV Particle Search) experiment [36] is slightly less stringent than the one set by OSQAR.

111.3.2. *Photon polarization* :

An alternative to regenerating the lost photons is to use the beam itself to detect conversion: the polarization of light propagating through a transverse B field suffers dichroism and birefringence [37]. Dichroism: The $E_\parallel$ component, but not $E_\perp$, is depleted by axion production, causing a small rotation of linearly polarized light. For $m_A^2 L/2\omega \ll 2\pi$, the effect is independent of m_A. For heavier axions, it oscillates and diminishes as m_A increases, and it vanishes for $m_A > \omega$. Birefringence: This rotation occurs because there is mixing of virtual axions in the $E_\parallel$ state, but not for $E_\perp$. Hence, linearly

polarized light will develop elliptical polarization. Higher-order QED also induces vacuum magnetic birefringence (VMB). A search for these effects was performed in the same dipole magnets in the early experiment above [38]. The dichroic rotation gave a stronger limit than the ellipticity rotation: $|G_{A\gamma\gamma}| < 3.6 \times 10^{-7}$ GeV^{-1} at 95% CL for $m_A < 5 \times 10^{-4}$ eV. The ellipticity limits are better at higher masses, as they fall off smoothly and do not terminate at m_A.

In 2006 the PVLAS collaboration reported a signature of magnetically induced vacuum dichroism that could be interpreted as the effect of a pseudoscalar with $m_A = 1$–1.5 meV and $|G_{A\gamma\gamma}| = (1.6$–$5) \times 10^{-6}$ GeV^{-1} [39]. Since then, these findings are attributed to instrumental artifacts [40]. This particle interpretation is also excluded by the above photon regeneration searches that were inspired by the original PVLAS result. Recently, the fourth generation setup of the PVLAS experiment has published new results on searches for VMB (see Figure 111.1) and dichroism [41]. The bounds from the non-observation of the latter on $G_{A\gamma\gamma}$ are slightly weaker than the ones from OSQAR.

111.3.3. *Long-range forces* :

New bosons would mediate long-range forces, which are severely constrained by "fifth force" experiments [42]. Those looking for new mass-spin couplings provide significant constraints on pseudoscalar bosons [43]. Presently, the most restrictive limits are obtained from combining long-range force measurements with stellar cooling arguments [44]. For the moment, any of these limits are far from realistic values expected for axions. Still, these efforts provide constraints on more general low-mass bosons.

Recently, a method was proposed that can extend the search for axion-mediated spin-dependent forces by several orders of magnitude [45]. By combining techniques used in nuclear magnetic resonance and short-distance tests of gravity, this method appears to be sensitive to axions in the μeV – meV mass range, independent of the cosmic axion abundance, if axions have a CP-violating interaction with nuclei as large as the current experimental bound on the electric dipole moment of the neutron allows.

111.4. Axions from Astrophysical Sources

111.4.1. *Stellar energy-loss limits* :

Low-mass weakly-interacting particles (neutrinos, gravitons, axions, baryonic or leptonic gauge bosons, *etc.*) are produced in hot astrophysical plasmas, and can thus transport energy out of stars. The coupling strength of these particles with normal matter and radiation is bounded by the constraint that stellar lifetimes or energy-loss rates not conflict with observation [46–48].

We begin this discussion with our Sun and concentrate on hadronic axions. They are produced predominantly by the Primakoff process $\gamma + Ze \to Ze + A$. Integrating over a standard solar model yields the axion luminosity [49]

$$L_A = G_{10}^2\, 1.85 \times 10^{-3}\, L_\odot\,, \tag{111.12}$$

where $G_{10} = |G_{A\gamma\gamma}| \times 10^{10}$ GeV. The maximum of the spectrum is at 3.0 keV, the average at 4.2 keV, and the number flux at Earth is $G_{10}^2\ 3.75 \times 10^{11}$ cm^{-2} s^{-1}. The solar photon luminosity is fixed, so axion losses require enhanced nuclear energy production and thus enhanced neutrino fluxes. The all-flavor measurements by SNO together with a standard solar model imply $L_A \lesssim 0.10\, L_\odot$, corresponding to $G_{10} \lesssim 7$ [50], mildly superseding a similar limit from helioseismology [51]. Recently, the limit was improved to $G_{10} < 4.1$ (at $3\,\sigma$), see Figure 111.1 (Sun), exploiting a new statistical analysis that combined helioseismology (sound speed, surface helium and convective radius) and solar neutrino observations, including theoretical and observational errors, and accounting for tensions between input parameters of solar models, in particular the solar element abundances [52].

A more restrictive limit derives from globular-cluster (GC) stars that allow for detailed tests of stellar-evolution theory. The stars on the horizontal branch (HB) in the color-magnitude diagram have reached helium burning with a core-averaged energy release of about 80 erg g^{-1} s^{-1}, compared to Primakoff axion losses of $G_{10}^2\, 30$ erg g^{-1} s^{-1}. The accelerated consumption of helium reduces the HB lifetime by about $80/(80 + 30\, G_{10}^2)$. Number counts of HB stars in a large sample of 39 Galactic GCs compared with the number of red giants (that are not much affected by Primakoff losses) give a weak indication of non-standard losses which may be accounted by Primakoff-like axion emission, if the photon coupling is in the range $|G_{A\gamma\gamma}| = (2.9 \pm 1.8) \times 10^{-11}$ GeV^{-1} [53]. Still, the upper bound found in this analysis,

$$|G_{A\gamma\gamma}| < 6.6 \times 10^{-11}\,\text{GeV}^{-1}\ (95\%\,\text{CL}), \tag{111.13}$$

represents the strongest limit on $G_{A\gamma\gamma}$ for a wide mass range, see Figure 111.1.

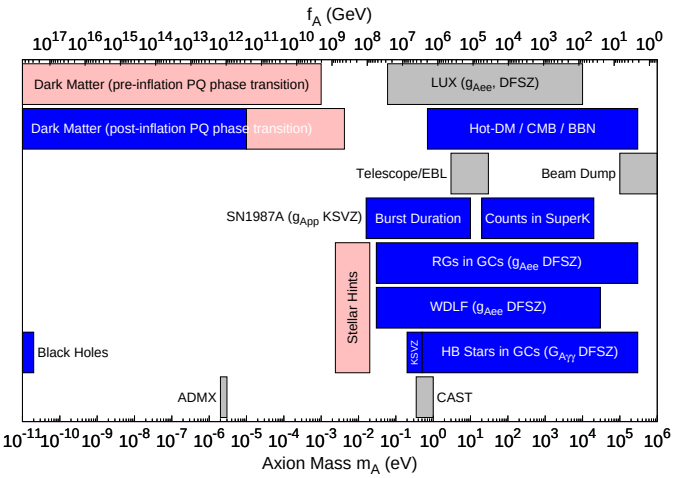

Figure 111.2: Exclusion ranges as described in the text. The intervals in the bottom row are the approximate ADMX and CAST search ranges. Limits on coupling strengths are translated into limits on m_A and f_A using the KSVZ values for the coupling strengths, if not indicated otherwise. The "Beam Dump" bar is a rough representation of the exclusion range for standard or variant axions. The limits for the axion-electron coupling are determined for the DFSZ model with an axion-electron coupling corresponding to $\sin^2\beta = 1/2$.

We translate the conservative constraint, Equation 111.13, on $G_{A\gamma\gamma}$ to $f_A > 3.4 \times 10^7$ GeV ($m_A < 0.2$ eV), using $E/N = 0$ as in the KSVZ model, and show the excluded range in Figure 111.2. For the DFSZ model with $E/N = 8/3$, the corresponding limits are slightly less restrictive, $f_A > 1.3 \times 10^7$ GeV ($m_A < 0.5$ eV).

If axions couple directly to electrons, the dominant emission processes are atomic axio-recombination and axio-deexcitation, axio-bremsstrahlung in electron-ion or electron-electron collisions, and Compton scattering [54]. Stars in the red giant (RG) branch of the color-magnitude diagram of GCs are particularly sensitive to these processes. In fact, they would lead to an extension of the latter to larger brightness. A recent analysis provided high-precision photometry for the Galactic globular cluster M5 (NGC 5904), allowing for a detailed comparison between the observed tip of the RG branch with predictions based on state-of-the-art stellar evolution theory [55]. It was found that, within the uncertainties, the observed and predicted tip of the RG branch brightness agree reasonably well within uncertainties, leading to the bound

$$\alpha_{Aee} < 1.5 \times 10^{-26} \quad (95\%\ \text{CL}), \tag{111.14}$$

implying an upper bound on the axion mass in the DFSZ model,

$$m_A \sin^2\beta < 15\ \text{meV} \quad (95\%\ \text{CL}), \tag{111.15}$$

see Figure 111.2. Intriguingly, the agreement would improve with a small amount of extra cooling that slightly postpones helium

ignition, prefering an electron coupling around $\alpha_{Aee} \sim 2.8 \times 10^{-27}$, corresponding to $m_A \sin^2\beta \sim 7$ meV.

Bremsstrahlung is also efficient in white dwarfs (WDs), where the Primakoff and Compton processes are suppressed by the large plasma frequency. A comparison of the predicted and observed luminosity function of WDs can be used to put limits on α_{Aee} [56]. A recent analysis, based on detailed WD cooling treatment and new data on the WD luminosity function (WDLF) of the Galactic Disk, found that electron couplings above $\alpha_{Aee} \gtrsim 6 \times 10^{-27}$, corresponding to a DFSZ axion mass $m_A \sin^2\beta \gtrsim 10$ meV, are disfavoured [57], see Figure 111.2. Lower couplings can not be discarded from the current knowledge of the WDLF of the Galactic Disk. On the contrary, features in some WDLFs can be interpreted as suggestions for electron couplings in the range $4.1 \times 10^{-28} \lesssim \alpha_{Aee} \lesssim 3.7 \times 10^{-27}$, corresponding to 2.5 meV $\lesssim m_A \sin^2\beta \lesssim$ 7.5 meV [57,58]. For pulsationally unstable WDs (ZZ Ceti stars), the period decrease $\dot{P}/P$ is a measure of the cooling speed. The corresponding observations of the pulsating WDs G117-B15A and R548 imply additional cooling that can be interpreted also in terms of similar axion losses [59].

Similar constraints derive from the measured duration of the neutrino signal of the supernova SN 1987A. Numerical simulations for a variety of cases, including axions and Kaluza-Klein gravitons, reveal that the energy-loss rate of a nuclear medium at the density 3×10^{14} g cm^{-3} and temperature 30 MeV should not exceed about 1×10^{19} erg g^{-1} s^{-1} [47]. The energy-loss rate from nucleon bremsstrahlung, $N + N \to N + N + A$, is $(C_N/2f_A)^2(T^4/\pi^2 m_N)\,F$. Here F is a numerical factor that represents an integral over the dynamical spin-density structure function because axions couple to the nucleon spin. For realistic conditions, even after considerable effort, one is limited to a heuristic estimate leading to $F \approx 1$ [48]. The SN 1987A limits are of particular interest for hadronic axions where the bounds on α_{Aee} are moot. Using a proton fraction of 0.3, $g_{Ann} = 0$, $F = 1$, and $T = 30$ MeV, one finds $f_A \gtrsim 4 \times 10^8$ GeV and $m_A \lesssim 16$ meV [48], see Figure 111.2. A more detailed numerical calculation [60] with state of the art SN models, again assuming $g_{Ann} = 0$, found that a coupling larger than $|g_{App}| \gtrsim 6 \times 10^{-10}$, would shorten significantly the timescale of the neutrino emission. This result is, not surprisingly, rather close to the estimate in Ref. [48].

The case of a general axion model, interacting with both protons and neutrons, is more complicated. A numerical study in Ref. [61], using the same SN models exploited in Ref. [60], inferred that the combination $g_{App}^2 + g_{Ann}^2$ would be the most appropriate to describe the axion interaction with the nuclear medium, in the regions where the axion emission rate is peaked. In combination with the results in Ref. [60], this suggests the bound

$$g_{App}^2 + g_{Ann}^2 < 3.6 \times 10^{-19}\,. \qquad (111.16)$$

Note, however, that no conclusion was drawn in Ref. [60] in terms of a robust constraint from SN 1987A, and that Equation 111.16 should be taken as an indicative result, in absence of a more definite study.

If axions interact sufficiently strongly they are trapped. Only about three orders of magnitude in g_{ANN} or m_A are excluded, a range shown somewhat schematically in Figure 111.2. For even larger couplings, the axion flux would have been negligible, yet it would have triggered additional events in the detectors, excluding a further range [62]. A possible gap between these two SN 1987A arguments was discussed as the "hadronic axion window" under the assumption that $G_{A\gamma\gamma}$ was anomalously small [63]. This range is now excluded by hot dark matter bounds (see below).

There is another hint for excessive stellar energy losses from the neutron star (NS) in the supernova remnant Cassiopeia A (Cas A): its surface temperature measured over 10 years reveals an unusually fast cooling rate. This may be interpreted as a hint for extra cooling by axion neutron bremsstrahlung, requiring a coupling to the neutron of size [64]

$$g_{Ann}^2 = (1.4 \pm 0.5) \times 10^{-19} \qquad (111.17)$$

corresponding to an axion mass

$$m_A = (2.3 \pm 0.4)\,\mathrm{meV}/C_n, \qquad (111.18)$$

see Figure 111.2. The hint is compatible with the state-of-the-art upper limit on this coupling,

$$g_{Ann}^2 < 6 \times 10^{-19}, \qquad (111.19)$$

from NS cooling [65]. In fact, as recently pointed out, the more rapid cooling of the superfluid core in the neutron star may also arise from a phase transition of the neutron condensate into a multicomponent state [66].

Recently, it has been pointed out that the hints of excessive cooling of WDs, RGs and HB stars can be explained at one stroke by an ALP coupling to electrons and photons, with couplings $g_{Aee} \sim 1.5 \times 10^{-13}$ and $|G_{A\gamma\gamma}| \sim 1.4 \times 10^{-11}\,\mathrm{GeV}^{-1}$, respectively [61,67]. Intriguingly, good fits to the data can be obtained employing the DFSZ axion with a mass in the range $2.4\,\mathrm{meV} \lesssim m_A \lesssim 20\,\mathrm{meV}$ $(2\,\sigma)$, if the SN 1987A constraint is taken into account [61], see Figure 111.2.

Finally, let us note that if the interpretation of the various hints for additional cooling of stars reported in this section in terms of emission of axions with $m_A \sim$ meV were correct, SNe would lose a large fraction of their energy as axions. This would lead to a diffuse SN axion background in the universe with an energy density comparable to the extra-galactic background light [68]. However, there is no apparent way of detecting it or the axion burst from the next nearby SN. On the other hand, neutrino detectors such as IceCube, Super-Kamiokande or a future mega-ton water Cerenkov detector will probe exactly the mass region of interest by measuring the neutrino pulse duration of the next galactic SN [60].

111.4.2. *Searches for solar axions and ALPs* :

Instead of using stellar energy losses to derive axion limits, one can also search directly for these fluxes, notably from the Sun. The main focus has been on axion-like particles with a two-photon vertex. They are produced by the Primakoff process with a flux given by Equation 111.12 and an average energy of 4.2 keV, and can be detected at Earth with the reverse process in a macroscopic B-field ("axion helioscope") [5]. In order to extend the sensitivity in mass towards larger values, one can endow the photon with an effective mass in a gas, $m_\gamma = \omega_{\rm plas}$, thus matching the axion and photon dispersion relations [69].

An early implementation of these ideas used a conventional dipole magnet, with a conversion volume of variable-pressure gas with a xenon proportional chamber as x-ray detector [70]. The conversion magnet was fixed in orientation and collected data for about 1000 s/day. Axions were excluded for $|G_{A\gamma\gamma}| < 3.6 \times 10^{-9}$ GeV^{-1} for $m_A <$ 0.03 eV, and $|G_{A\gamma\gamma}| < 7.7 \times 10^{-9}$ GeV^{-1} for $0.03 < m_A < 0.11$ eV at 95% CL.

Later, the Tokyo axion helioscope used a superconducting magnet on a tracking mount, viewing the Sun continuously. They reported $|G_{A\gamma\gamma}| < 6 \times 10^{-10}$ GeV^{-1} for $m_A < 0.3$ eV [71]. This experiment was recommissioned and a similar limit for masses around 1 eV was reported [72].

The most recent helioscope CAST (CERN Axion Solar Telescope) uses a decommissioned LHC dipole magnet on a tracking mount. The hardware includes grazing-incidence x-ray optics with solid-state x-ray detectors, as well as a novel x-ray Micromegas position-sensitive gaseous detector. CAST has established a 95% CL limit $|G_{A\gamma\gamma}| < 6.6 \times 10^{-11}$ GeV^{-1} for $m_A < 0.02$ eV [73], exploiting a IAXO (see below) pathfinder system. To cover larger masses, the magnet bores are filled with a gas at varying pressure. The runs with ^{4}He cover masses up to about 0.4 eV [74], providing the ^{4}He limits shown in Figure 111.1. To cover yet larger masses, ^{3}He was used to achieve a larger pressure at cryogenic temperatures. Limits up to 1.17 eV allowed CAST to "cross the axion line" for the KSVZ model [75], see Figure 111.1.

Dark matter direct detection experiments searching for dark matter consisting of weakly interacting massive particles, such as EDELWEISS-II, LUX, and XENON100, have also the capability to search for solar axions and ALPs [76,77]. Recently, the LUX experiment [77] has put a bound on the axion-electron coupling constant by exploiting the axio-electric effect in liquid xenon,

$$g_{Aee} < 3.5 \times 10^{-12} \quad (90\%\ \mathrm{CL}), \qquad (111.20)$$

excluding the DFSZ model with $m_A \sin^2\beta > 0.12\,\mathrm{eV}$, cf. see Figure 111.2.

Going to yet larger masses in a helioscope search is not well motivated because of the cosmic hot dark matter bound of $m_A \lesssim 1$ eV (see below). Sensitivity to significantly smaller values of $G_{A\gamma\gamma}$ can be achieved with a next-generation axion helioscope with a much larger magnetic-field cross section. Realistic design options for this "International Axion Observatory" (IAXO) have been studied in some detail [78]. Such a next-generation axion helioscope may also push the sensitivity in the product of couplings to photons and to electrons, $G_{A\gamma\gamma}g_{Aee}$, into a range beyond stellar energy-loss limits and test the hypothesis that WD, RG, and HB cooling is dominated by axion emission [61,79].

Other Primakoff searches for solar axions and ALPs have been carried out using crystal detectors, exploiting the coherent conversion of axions into photons when the axion angle of incidence satisfies a Bragg condition with a crystal plane [80]. However, none of these limits is more restrictive than the one derived from the constraint on the solar axion luminosity ($L_A \lesssim 0.10\,L_\odot$) discussed earlier.

Another idea is to look at the Sun with an x-ray satellite when the Earth is in between. Solar axions and ALPs would convert in the Earth magnetic field on the far side and could be detected [81]. The sensitivity to $G_{A\gamma\gamma}$ could be comparable to CAST, but only for much smaller m_A. Deep solar x-ray measurements with existing satellites, using the solar magnetosphere as conversion region, have reported preliminary limits on $G_{A\gamma\gamma}$ [82].

111.4.3. *Conversion of astrophysical photon fluxes* :

Large-scale B fields exist in astrophysics that can induce axion-photon oscillations. In practical cases, B is much smaller than in the laboratory, whereas the conversion region L is much larger. Therefore, while the product BL can be large, realistic sensitivities are usually restricted to very low-mass particles, far away from the "axion band" in a plot like Figure 111.1.

One example is SN 1987A, which would have emitted a burst of axion-like particles (ALPs) due to the Primakoff production in its core. They would have partially converted into γ-rays in the galactic B-field. The lack of a gamma-ray signal in the GRS instrument of the SMM satellite in coincidence with the observation of the neutrinos emitted from SN1987A therefore provides a strong bound on their coupling to photons [83]. Recently, this bound has been revisited and the underlying physics has been brought to the current state-of-the-art, as far as modelling of the supernova and the Milky-Way magnetic field are concerned, resulting in the limit [84]

$$|G_{A\gamma\gamma}| < 5.3\times10^{-12}\ \mathrm{GeV}^{-1},\ \text{for}\ \ m_A \lesssim 4.4\times10^{-10}\ \mathrm{eV}.$$

Magnetically induced oscillations between photons and axion-like particles (ALPs) can modify the photon fluxes from distant sources in various ways, featuring (i) frequency-dependent dimming, (ii) modified polarization, and (iii) avoiding absorption by propagation in the form of axions.

For example, dimming of SNe Ia could influence the interpretation in terms of cosmic acceleration [85], although it has become clear that photon-ALP conversion could only be a subdominant effect [86]. Searches for linearly polarised emission from magnetised white dwarfs [87] and changes of the linear polarisation from radio galaxies (see, e.g., Ref. [88]) provide limits close to $G_{A\gamma\gamma} \sim 10^{-11}\ \mathrm{GeV}^{-1}$, for masses $m_A \lesssim 10^{-7}$ eV and $m_A \lesssim 10^{-15}$ eV, respectively, albeit with uncertainties related to the underlying assumptions. Even stronger limits, $G_{A\gamma\gamma} \lesssim 2\times10^{-13}\ \mathrm{GeV}^{-1}$, for $m_A \lesssim 10^{-14}$ eV, have been obtained by exploiting high-precision measurements of quasar polarisations [89].

Remarkably, it appears that the universe could be too transparent to TeV γ-rays that should be absorbed by pair production on the extra-galactic background light [90]. The situation is not conclusive at present [91], but the possible role of photon-ALP oscillations in TeV γ-ray astronomy is tantalizing [92]. Fortunately, the region in ALP parameter space, $G_{A\gamma\gamma} \sim 10^{-12} - 10^{-10}\ \mathrm{GeV}^{-1}$ for $m_A \lesssim 10^{-7}$ eV [93], required to explain the anomalous TeV transparency of the universe, could be conceivably probed by the next generation of laboratory experiments (ALPS II) and helioscopes (IAXO) mentioned above. This parameter region can also be probed by searching for an irregular behavior of the gamma ray spectrum of distant active galactic nuclei (AGN), expected to arise from photon-ALP mixing in a limited energy range. The H.E.S.S. collaboration has set a limit of $|G_{A\gamma\gamma}| \lesssim 2.1\times10^{-11}\ \mathrm{GeV}^{-1}$, for $1.5\times10^{-8}\ \mathrm{eV} \lesssim m_A \lesssim 6.0\times10^{-8}$ eV, from the non-observation of an irregular behavior of the spectrum of the AGN PKS 2155 [94], see Figure 111.1. Recently, the Fermi-LAT collaboration has put an even more stringent limit on the ALP-photon coupling [95] from observations of the gamma ray spectrum of NGC 1275, the central galaxy of the Perseus cluster, see Figure 111.1.

At smaller masses, $m_A \lesssim 10^{-12}\,\mathrm{eV}$, galaxy clusters become highly efficient at interconverting ALPs and photons at x-ray energies. Constraints on spectral irregularities in the spectra of luminous x-ray sourced located in or behind galaxy clusters then lead to stringent upper limits on the ALP-photon coupling. Using Chandra and XMM-Newton observations of several local sources in galaxy clusters (Hydra A, M87, NGC 1275, NGC 3862, Seyfert galaxy 2E3140) leads to bounds $|G_{A\gamma\gamma}| \lesssim 1.5\times10^{-12}\ \mathrm{GeV}^{-1}$ [96].

111.4.4. *Superradiance of black holes* :

Light bosonic fields such as axions or ALPs can affect the dynamics and gravitational wave emission of rapidly rotating astrophysical black holes through the superradiance mechanism. When their Compton wavelength is of order of the black hole size, they form gravitational bound states around the black hole. Their occupation number grows exponentially by extracting energy and angular momentum from the black hole, forming a coherent axion or ALP bound state emitting gravitational waves. When accretion cannot replenish the spin of the black hole, superradiance dominates the black hole spin evolution; this is true for both supermassive and stellar mass black holes. The existence of destabilizing light bosonic fields thus leads to gaps in the mass vs. spin plot of rotating black holes. Stellar black hole spin measurements exploiting well-studied binaries and two independent techniques exclude a mass range $6\times10^{-13}\,\mathrm{eV} < m_A < 2\times10^{-11}\,\mathrm{eV}$ at $2\,\sigma$, which for the axion excludes $3\times10^{17}\,\mathrm{GeV} < f_A < 1\times10^{19}\,\mathrm{GeV}$ [97]. These bounds apply when gravitational interactions dominate over the axion self-interaction, which is true for the QCD axion in this mass range. Long lasting, monochromatic gravitational wave signals, which can be distinguished from ordinary astrophysical sources by their clustering in a narrow frequency range, are expected to be produced by axions or ALPs annihilating to gravitons. Gravitational waves could also be sourced by axions/ALPs transitioning between gravitationally bound levels. Accordingly, the gravitational wave detector Advanced LIGO should be sensitive to the axion in the $m_A \lesssim 10^{-10}\,\mathrm{eV}$ region. LIGO measurements of black hole spins in binary merger events could also provide statistical evidence for the presence of an axion [98]. Similar signatures could arise for supermassive black holes for particle with masses $\lesssim 10^{-15}\,\mathrm{eV}$. Gravitational waves from such sources could be detected at lower-frequency observatories such as LISA.

111.5. Cosmic Axions

111.5.1. *Cosmic axion populations* :

In the early universe, axions are produced by processes involving quarks and gluons [99]. After color confinement, the dominant thermalization process is $\pi + \pi \leftrightarrow \pi + A$ [23]. The resulting axion population would contribute a hot dark matter component in analogy to massive neutrinos. Cosmological precision data provide restrictive constraints on a possible hot dark-matter fraction that translate into $m_A \lesssim 1$ eV [100], but in detail depend on the used data set and assumed cosmological model. In the future, data from a EUCLID-like survey combined with Planck CMB data can detect hot dark matter axions with a mass $m_A \gtrsim 0.15\,\mathrm{eV}$ at very high significance [101].

For $m_A \gtrsim 20$ eV, axions decay fast on a cosmic time scale, removing the axion population while injecting photons. This excess radiation provides additional limits up to very large axion masses [102]. An anomalously small $G_{A\gamma\gamma}$ provides no loophole because suppressing

decays leads to thermal axions overdominating the mass density of the universe.

The main cosmological interest in axions derives from their possible role as cold dark matter (CDM). In addition to thermal processes, axions are abundantly produced by the "re-alignment mechanism" [103].

The axion dark matter abundance crucially depends on the cosmological history. Let us first consider the so called *pre-inflationary PQ symmetry breaking scenario*, in which the PQ symmetry is broken before and during inflation and not restored afterwards. After the breakdown of the PQ symmetry, the axion field relaxes somewhere in the bottom of the "mexican hat" potential. Near the QCD epoch, topological fluctuations of the gluon fields such as instantons explicitly break the PQ symmetry. This tilting of the"mexican hat" drives the axion field toward the CP-conserving minimum, thereby exciting coherent oscillations of the axion field that ultimately represent a condensate of CDM. The fractional cosmic mass density in this homogeneous field mode, created by this "vacuum realignment" (vr) mechanism, is [12,104,105,106],

$$\begin{aligned}\Omega_A^{\rm vr}h^2 &\approx 0.12\left(\frac{f_A}{9\times 10^{11}\ {\rm GeV}}\right)^{1.165} F\,\bar{\Theta}_{\rm i}^2\\ &\approx 0.12\left(\frac{6\ \mu{\rm eV}}{m_A}\right)^{1.165} F\,\Theta_{\rm i}^2\,,\end{aligned} \tag{111.21}$$

where h is the present-day Hubble expansion parameter in units of 100 km s^{-1} Mpc^{-1}, and $-\pi \le \Theta_{\rm i} \le \pi$ is the initial "misalignment angle" relative to the CP-conserving position attained in the causally connected region which evolved into today's observable universe. $F = F(\Theta_{\rm i}, f_A)$ is a factor accounting for anharmonicities in the axion potential. For $F\Theta_{\rm i}^2 = \mathcal{O}(1)$, m_A should be above $\sim 6\,\mu$eV in order that the cosmic axion density does not exceed the observed CDM density, $\Omega_{\rm CDM}h^2 = 0.12$. However, much smaller axion masses (much higher PQ scales) are still possible if the initial value $\Theta_{\rm i}$ just happens to be small enough in today's observable universe ("anthropic axion window" [107]) .

Since the axion field is then present during inflation and thus subject to quantum fluctuations, the non-observation of the associated isocurvature fluctuations in the CMB puts severe constraints in the (f_A, r) plane, where r is the ratio of the power in tensor to the one in scalar fluctuations [108]. In fact, isocurvature constraints, combined with a future measurement of a sizeable r, would strongly disfavor axions with [109]

$$f_A \gtrsim 1.3\times 10^{13}\,{\rm GeV}\left(\frac{r}{0.1}\right)^{1/2},\ m_A \lesssim 0.4\ \mu{\rm eV}\left(\frac{r}{0.1}\right)^{-1/2}.$$

In the *post-inflationary PQ symmetry breaking scenario*, on the other hand, $\Theta_{\rm i}$ will take on different values in different patches of the present universe. The average contribution is [12,104,105,106]

$$\Omega_A^{\rm vr}h^2 \approx 0.12\left(\frac{30\ \mu{\rm eV}}{m_A}\right)^{1.165}. \tag{111.22}$$

However, the presence of cosmic strings can decrease this quantity [106,110]. In fact, the decay of cosmic strings and domain walls gives rise to a different population of cold dark matter axions, whose abundance suffers from significant uncertainties. According to Sikivie and collaborators, these populations are comparable to the re-alignment contribution [111]. Other groups find a significantly enhanced axion density [105,106,112,113] or rather, a larger m_A value for axions providing CDM, namely

$$m_A \approx (50-200)\ \mu{\rm eV}, \tag{111.23}$$

for models with short-lived (requiring unit color anomaly $N = 1$) domain walls, such as the KSVZ model. Very recently, a value of $m_A = (26.2 \pm 3.4)\,\mu$eV was predicted from an improved calculation including the effect of the large string tension and treating the re-alignment and string-wall contribution in a unified way [110]. For models with long-lived ($N > 1$) domain walls, such as an accidental DFSZ model [114], where the PQ symmetry is broken by higher dimensional Planck suppressed operators, the mass is predicted to be significantly higher [113,115],

$$m_A \approx (0.6-4)\,{\rm meV}, \tag{111.24}$$

see Figure 111.2

In this post-inflationary PQ symmetry breakdown scenario, the spatial axion density variations are large at the QCD transition and they are not erased by free streaming. Gravitationally bound "axion miniclusters" form around and before matter-radiation equality [116]. A significant fraction of CDM axions can reside in these bound objects. Remarkably, the minicluster fraction can be bounded by gravitational lensing [117].

In the above predictions of the fractional cosmic mass density in axions, the exponent, 1.165, arises from the non-trivial temperature dependence of the topological susceptibility $\chi(T) = m_A^2(T)f_A^2$ at temperatures slighty above the QCD quark-hadron phase transition. Recent lattice QCD calculations of this exponent [12,118] found it to be remarkably close to the prediction of the dilute instanton gas approximation (see however [119]) which was previously exploited. Therefore, the state-of-the-art prediction of the axion mass relevant for dark matter for a fixed initial misalignment angle $\Theta_{\rm i}$ differs from the previous prediction by just a factor of order one.

The non-thermal production mechanisms attributed to axions are generic to light bosonic weakly interacting particles such as ALPs [120]. The relic abundance is set by the epoch when the axion mass becomes significant, $3H(t) \approx m_A(t)$, and ALP field oscillations begin. For ALPs to contribute to the dark matter density this epoch must occur before matter radiation equality. For a temperature independent ALP mass this leads to the bound:

$$m_A \gtrsim 7\times 10^{-28}\,{\rm eV}\left(\frac{\Omega_m\,h^2}{0.15}\right)^{1/2}\left(\frac{1+z_{\rm eq}}{3.4\times 10^3}\right)^{3/2}. \tag{111.25}$$

ALPs lighter than this bound are allowed if their cosmic energy density is small, but they are quite distinct from other forms of dark matter [121]. Ignoring anharmonicities in the ALP potential, and taking the ALP mass to be temperature independent, the relic density in dark matter ALPs due to re-alignment is given by

$$\Omega_{\rm ALP}^{\rm vr}h^2 = 0.12\left(\frac{m_A}{4.7\times 10^{-19}\,{\rm eV}}\right)^{1/2}\left(\frac{f_A}{10^{16}\,{\rm GeV}}\right)^2\left(\frac{\Omega_m h^2}{0.15}\right)^{3/4}\left(\frac{1+z_{\rm eq}}{3.4\times 10^3}\right)^{-3/4}\Theta_{\rm i}^2\,.$$

An ALP decay constant near the GUT scale gives the correct relic abundance for *ultralight ALPs* (ULAs), which we now define. Extended discussions of ULAs can be found in Refs. [122,123].

The standard CDM model treats dark matter as a distribution of cold, collisionless particles interacting only via gravity. Below the Compton wavelength, $\lambda_c = 2\pi/m_A$, the particle description of ALPs breaks down. For large occupation numbers we can model ALPs below the Compton wavelength as a coherent classical field. Taking as a reference length scale the Earth radius, $R_\oplus = 6371$ km, we define ULAs to be those axions with $\lambda_c > R_\oplus$, leading to the defining bound

$$m_{\rm ULA} < 2\times 10^{-13}\,{\rm eV}\,. \tag{111.26}$$

ULAs encompass the entire Earth in a single coherent field. The coherence time of the ULA field on Earth can be estimated from the crossing time of the de Broglie wavelength at the virial velocity in the Milky Way, $\tau_{\rm coh.} \sim 1/m_A v_{\rm vir.}^2$.

We notice that by the definition, Equation 111.26, an ultralight QCD axion must have a super-Planckian decay constant, $f_A > 3\times 10^{19}\,{\rm GeV}$ and would require fine tuning of θ_i to provide the relic abundance. Natural models for ULAs can be found in string and M-theory compactifications [6], in field theory with accidental symmetries [124], or new hidden strongly coupled sectors [125].

In addition to the gravitational potential energy, the ULA field also carries gradient energy. On scales where the gradient energy is non-negligible, ULAs acquire an effective pressure and do not behave as CDM. The gradient energy opposes gravitational collapse, leading to a Jeans scale below which perturbations are stable [126]. The Jeans scale suppresses linear cosmological structure formation relative to CDM [127]. The Jeans scale at matter-radiation equality in the case that ULAs make up all of CDM is:

$$k_{\rm J,eq} = 8.7\,{\rm Mpc}^{-1}\left(\frac{1+z_{\rm eq}}{3.4\times10^3}\right)^{-1/4}\left(\frac{\Omega^{\rm vr}_{\rm ALP}}{0.12}\right)^{1/4}\left(\frac{m_A}{10^{-22}\,{\rm eV}}\right)^{1/2}$$

On non-linear scales the gradient energy leads to the existence of a class of pseudo-solitons known as oscillatons, or axion stars [128].

Cosmological and astrophysical observations are consistent with the CDM model, and departures from it are only allowed on the scales of the smallest observed dark matter structures with $M \sim 10^{6-8} M_\odot$. The CMB power spectrum and galaxy auto-correlation power spectrum limit the ULA mass to $m_{\rm ULA} > 10^{-24}\,{\rm eV}$ from linear theory of structure formation [121,129]. Analytic models [130] and N-body simulations [131] for non-linear structures show that halo formation is suppressed in ULA models relative to CDM. This leads to constraints on the ULA mass of $m_{\rm ULA} > 10^{-22}\,{\rm eV}$ from observations of high-z galaxies [131,132], and $m_{\rm ULA} > 10^{-21}\,{\rm eV}$ from the Lyman-alpha forest flux power spectrum [133]. Including the effects of anharmonicities on structure formation with ALPs can weaken these bounds if the misalignment angle $\Theta_{\rm i} \approx \pi$ [134]. Cosmological simulations that treat gradient energy in the ULA field beyond the N-body approximation have just recently become available [135,136], and show, among other things, evidence for the formation of axion stars in the centres of ULA halos. These central axion stars have been conjectured to play a role in the apparently cored density profiles of dwarf spheroidal galaxies [135,137], and may have many other observational consequences [138].

111.5.2. *Telescope searches* :

The two-photon decay is extremely slow for axions with masses in the CDM regime, but could be detectable for eV masses. The signature would be a quasi-monochromatic emission line from galaxies and galaxy clusters. The expected optical line intensity for DFSZ axions is similar to the continuum night emission. An early search in three rich Abell clusters [139], and a recent search in two rich Abell clusters [140], exclude the "Telescope" range in Figure 111.1 and Figure 111.2 unless the axion-photon coupling is strongly suppressed. Of course, axions in this mass range would anyway provide an excessive hot DM contribution.

Very low-mass axions in halos produce a weak quasi-monochromatic radio line. Virial velocities in undisrupted dwarf galaxies are very low, and the axion decay line would therefore be extremely narrow. A search with the Haystack radio telescope on three nearby dwarf galaxies provided a limit $|G_{A\gamma\gamma}| < 1.0\times10^{-9}$ GeV^{-1} at 96% CL for $298 < m_A < 363$ μeV [141]. However, this combination of m_A and $G_{\rm A\gamma\gamma}$ does not exclude plausible axion models.

111.5.3. *Microwave cavity experiments* :

The limits of Figure 111.2 suggest that axions, if they exist, provide a significant fraction or even perhaps all of the cosmic CDM. In a broad range of the plausible m_A range for CDM, galactic halo axions may be detected by their resonant conversion into a quasi-monochromatic microwave signal in a high-Q electromagnetic cavity permeated by a strong static B field [5,142]. The cavity frequency is tunable, and the signal is maximized when the frequency is the total axion energy, rest mass plus kinetic energy, of $\nu = (m_A/2\pi)\,[1+\mathcal{O}(10^{-6})]$, the width above the rest mass representing the virial distribution in the galaxy. The frequency spectrum may also contain finer structure from axions more recently fallen into the galactic potential and not yet completely virialized [143].

The feasibility of this technique was established in early experiments of relatively small sensitive volume, $\mathcal{O}(1$ liter), with HFET-based amplifiers, setting limits in the range $4.5 < m_A < 16.3$ μeV [144], but lacking by 2–3 orders of magnitude the sensitivity required to detect realistic axions. Later, ADMX ($B \sim 8$ T, $V \sim 200$ liters) has achieved sensitivity to KSVZ axions, assuming they saturate the local dark matter density and are well virialized, over the mass range 1.9–3.3 μeV [145]. Should halo axions have a significant component not yet virialized, ADMX is sensitive to DFSZ axions [146]. The corresponding 90% CL exclusion regions shown in Figure 111.3 are normalized to an assumed local CDM density of 7.5×10^{-25} g cm^{-3} (450 MeV cm^{-3}). More recently the ADMX experiment commissioned an upgrade [147] that replaces the microwave HFET amplifiers by near quantum-limited low-noise dc SQUID microwave amplifiers [148], allowing for a significantly improved sensitivity. This apparatus is also sensitive to other hypothetical light bosons, such as hidden photons or chameleons, over a limited parameter space [120,149]. Recently, the HAYSTAC experiment reported on first results from a new microwave cavity search for dark matter axions with masses above 20 μeV. They exclude axions with two-photon coupling $|G_{A\gamma\gamma}| \gtrsim 2\times10^{-14}\,{\rm GeV}^{-1}$ over the range $23.55\,\mu{\rm eV} < m_A < 24.0\,\mu{\rm eV}$ [150]. Exploiting a Josephson parametric amplifier, this experiment has demonstrated total noise approaching the standard quantum limit for the first time in an axion search. A Rydberg atom single-photon detector [151] can in principle evade the standard quantum limit for coherent photon detection. The ORGAN experiment is designed to probe axions in the mass range $60\,\mu{\rm eV} < m_A < 210\,\mu{\rm eV}$. In a pathfinding run, it has set a limit on $|G_{A\gamma\gamma}| < 2\times10^{-12}\,{\rm GeV}^{-1}$ at 110 μeV, in a span of 2.5 neV [152]. There are further microwave cavity axion dark matter experiment in construction (CULTASK [153]) or proposed (KLASH [154]) .

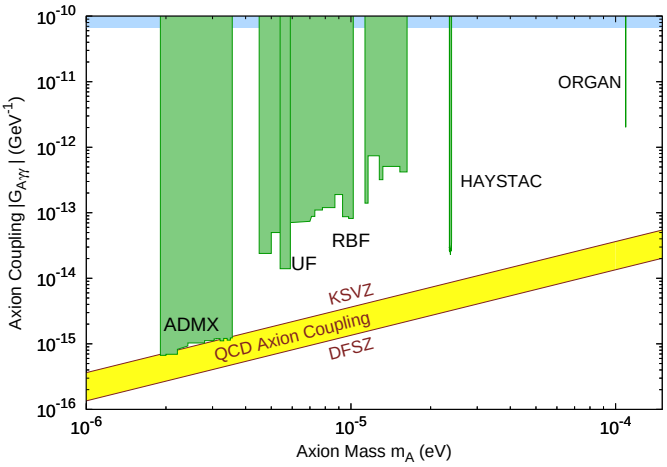

Figure 111.3: Exclusion region reported from the microwave cavity experiments RBF and UF [144], ADMX [145,147], HAYSTAC [150] and ORGAN [152]. A local dark-matter density of 450 MeV cm^{-3} is assumed.

111.5.4. *New concepts for axion dark matter direct detection* :

Other new concepts for searching for axion dark matter are also being investigated. An alternative to the microwave cavity technique is based on a novel detector architecture consisting of an open, Fabry-Perot resonator and a series of current-carrying wire planes [155]. The Orpheus detector has demonstrated this new technique, excluding dark matter ALPs with masses between 68.2 and 76.5 μeV and axion-photon couplings greater than $4\times10^{-7}\,{\rm GeV}^{-1}$. This technique may be able to probe dark matter axions in the mass range from 40 to 700 μeV. Another detector concept exploits the fact that a magnetized mirror would radiate photons in the background of axion dark matter, which could be collected like in a dish antenna [156]. Searches for hidden photon dark matter exploiting this technique are already underway [157]. The proposed MADMAX experiment will place a stack of dielectric layers in front of the magnetized mirror in

order to resonantly enhance the photon signal, aiming a sensitivity to probe the mass range $50\,\mu\text{eV} \lesssim m_A \lesssim 200\,\mu\text{eV}$ [158]. Another proposed axion dark matter search method sensitive in the 100 μeV mass range is to cool a kilogram-sized sample to mK temperatures and count axion induced atomic transitions using laser techniques [159].

The oscillating galactic dark matter axion field induces oscillating nuclear electric dipole moments (EDMs). These EDMs cause the precession of nuclear spins in a nucleon spin polarized sample in the presence of an electric field. The resulting transverse magnetization can be searched for by exploiting magnetic-resonance (MR) techniques, which are most sensitive in the range of low oscillation frequencies corresponding to sub-neV axion masses. The aim of the corresponding Cosmic Axion Spin Precession Experiment (CASPEr) [160] is to probe axion dark matter in the anthropic window, $f_A \gtrsim 10^{15}\,\text{GeV}$, corresponding to $m_A \lesssim$neV, complementary to the classic axion window probed by the RF cavity technique.

In the intermediate mass region, $\text{neV} \lesssim m_A \lesssim 0.1\,\mu\text{eV}$, one may exploit a cooled LC circuit and precision magnetometry to search for the oscillating electric current induced by dark matter axions in a strong magnetic field [161]. A similar approach is followed by the proposed ABRACADABRA [162] and DM-Radio Pathfinder [163] experiments.

An eventually non-zero axion electron coupling g_{Aee} will lead to an electron spin precession about the axion dark matter wind [164]. The QUAX (QUaerere AXions) experiment aims at exploiting MR inside a magnetized material [165]. Because of the higher Larmor frequency of the electron, it is sensitive in the classic window.

111.6. Conclusions

There is a strengthening physics case for very weakly coupled light particles beyond the Standard Model. The elegant solution of the strong CP problem proposed by Peccei and Quinn yields a particularly strong motivation for the axion. In many theoretically appealing ultraviolet completions of the Standard Model axions and axion-like particles occur automatically. Moreover, they are natural cold dark matter candidates. Perhaps the first hints of their existence have already been seen in the anomalous excessive cooling of stars and the anomalous transparency of the Universe for VHE gamma rays. Interestingly, a significant portion of previously unexplored, but phenomenologically very interesting and theoretically very well motivated axion and ALP parameter space can be tackled in the foreseeable future by a number of terrestrial experiments searching for axion/ALP dark matter, for solar axions/ALPs, and for light apparently shining through a wall.

References:

1. R.D. Peccei and H. Quinn, Phys. Rev. Lett. **38**, 1440 (1977); Phys. Rev. **D16**, 1791 (1977).
2. S. Weinberg, Phys. Rev. Lett. **40**, 223 (1978); F. Wilczek, Phys. Rev. Lett. **40**, 279 (1978).
3. F. Wilczek, Phys. Rev. Lett. **49**, 1549 (1982).
4. Y. Chikashige, R.N. Mohapatra, and R.D. Peccei, Phys. Lett. **B98**, 265 (1981); G.B. Gelmini and M. Roncadelli, Phys. Lett. **B99**, 411 (1981).
5. P. Sikivie, Phys. Rev. Lett. **51**, 1415 (1983) and Erratum *ibid.*, **52**, 695 (1984).
6. E. Witten, Phys. Lett. **B149**, 351 (1984); J.P. Conlon, JHEP **0605**, 078 (2006); P. Svrcek and E. Witten, JHEP **0606**, 051 (2006); K.-S. Choi *et al.*, Phys. Lett. **B675**, 381 (2009); A. Arvanitaki *et al.*, Phys. Rev. **D81**, 123530 (2010); B.S. Acharya, K. Bobkov, and P. Kumar, JHEP **1011**, 105 (2010); M. Cicoli, M. Goodsell, and A. Ringwald, JHEP **1210**, 146 (2012); J. Halverson, C. Long and P. Nath, Phys. Rev. **D96**, 056025 (2017).
7. J. Jaeckel and A. Ringwald, Ann. Rev. Nucl. and Part. Sci. **60**, 405 (2010); A. Ringwald, Phys. Dark Univ. **1**, 116 (2012); J. Jaeckel, Frascati Phys. Ser. **56**, 172 (2013).
8. C.A. Baker *et al.*, Phys. Rev. Lett. **97**, 131801 (2006).
9. H. Georgi, D.B. Kaplan, and L. Randall, Phys. Lett. **B169**, 73 (1986).
10. R.J. Crewther, Phys. Lett. **B70**, 349 (1977); P. Di Vecchia and G. Veneziano, Nucl. Phys. **B171**, 253 (1980).
11. G.G. di Cortona *et al.*, JHEP **1601**, 034 (2016).
12. S. Borsanyi *et al.*, Nature **539**, 69 (2016).
13. T.W. Donnelly *et al.*, Phys. Rev. **D18**, 1607 (1978); S. Barshay *et al.*, Phys. Rev. Lett. **46**, 1361 (1981); A. Barroso and N.C. Mukhopadhyay, Phys. Lett. **B106**, 91 (1981); R.D. Peccei, in *Proceedings of Neutrino '81*, Honolulu, Hawaii, Vol. 1, p. 149 (1981); L.M. Krauss and F. Wilczek, Phys. Lett. **B173**, 189 (1986).
14. J. Schweppe *et al.*, Phys. Rev. Lett. **51**, 2261 (1983); T. Cowan *et al.*, Phys. Rev. Lett. **54**, 1761 (1985).
15. R.D. Peccei, T.T. Wu, and T. Yanagida, Phys. Lett. **B172**, 435 (1986).
16. W.A. Bardeen, R.D. Peccei, and T. Yanagida, Nucl. Phys. **B279**, 401 (1987).
17. J.E. Kim, Phys. Rev. Lett. **43**, 103 (1979); M.A. Shifman, A.I. Vainstein, and V.I. Zakharov, Nucl. Phys. **B166**, 493 (1980).
18. M. Dine, W. Fischler, and M. Srednicki, Phys. Lett. **B104**, 199 (1981); A.R. Zhitnitsky, Sov. J. Nucl. Phys. **31**, 260 (1980).
19. J.E. Kim and G. Carosi, Rev. Mod. Phys. **82**, 557 (2010).
20. J.E. Kim, Phys. Rev. **D58**, 055006 (1998); L. Di Luzio, F. Mescia and E. Nardi, Phys. Rev. Lett. **118**, 031801 (2017).
21. G. Raffelt and D. Seckel, Phys. Rev. Lett. **60**, 1793 (1988); M. Carena and R.D. Peccei, Phys. Rev. **D40**, 652 (1989); K. Choi, K. Kang, and J.E. Kim, Phys. Rev. Lett. **62**, 849 (1989).
22. M. Srednicki, Nucl. Phys. **B260**, 689 (1985).
23. S. Chang and K. Choi, Phys. Lett. **B316**, 51 (1993).
24. H. Leutwyler, Phys. Lett. **B378**, 313 (1996).
25. Mini review on Quark Masses in C. Patrignani *et al.* (Particle Data Group), Chin. Phys. C **40**, 100001 (2016).
26. D.A. Dicus *et al.*, Phys. Rev. **D18**, 1829 (1978).
27. G. Raffelt and L. Stodolsky, Phys. Rev. **D37**, 1237 (1988).
28. A.A. Anselm, Yad. Fiz. **42**, 1480 (1985); K. van Bibber *et al.*, Phys. Rev. Lett. **59**, 759 (1987).
29. G. Ruoso *et al.*, Z. Phys. **C56**, 505 (1992); R. Cameron *et al.*, Phys. Rev. **D47**, 3707 (1993).
30. M. Fouche *et al.* (BMV Collab.), Phys. Rev. **D78**, 032013 (2008); P. Pugnat *et al.* (OSQAR Collab.), Phys. Rev. **D78**, 092003 (2008); A. Chou *et al.* (GammeV T-969 Collab), Phys. Rev. Lett. **100**, 080402 (2008); A. Afanasev *et al.* (LIPSS Collab.), Phys. Rev. Lett. **101**, 120401 (2008); K. Ehret *et al.* (ALPS Collab.), Phys. Lett. **B689**, 149 (2010); P. Pugnat *et al.* (OSQAR Collab.), Eur. Phys. J. **C74**, 3027 (2014).
31. R. Ballou *et al.* (OSQAR Collab.), Phys. Rev. **D92**, 092002 (2015).
32. F. Hoogeveen and T. Ziegenhagen, Nucl. Phys. **B358**, 3 (1991); P. Sikivie, D. Tanner, and K. van Bibber, Phys. Rev. Lett. **98**, 172002 (2007); G. Mueller *et al.*, Phys. Rev. **D80**, 072004 (2009).
33. R. Baehre *et al.* (ALPS Collab.), JINST **1308**, T09001 (2013).
34. F. Hoogeveen, Phys. Lett. **B288**, 195 (1992); J. Jaeckel and A. Ringwald, Phys. Lett. **B659**, 509 (2008); F. Caspers, J. Jaeckel, and A. Ringwald, JINST **0904**, P11013 (2009).
35. R. Povey, J. Hartnett, and M. Tobar, Phys. Rev. **D82**, 052003 (2010); A. Wagner *et al.*, Phys. Rev. Lett. **105**, 171801 (2010).
36. M. Betz *et al.*, Phys. Rev. **D88**, 075014 (2013).

37. L. Maiani *et al.*, Phys. Lett. **B175**, 359 (1986).
38. Y. Semertzidis *et al.*, Phys. Rev. Lett. **64**, 2988 (1990).
39. E. Zavattini *et al.* (PVLAS Collab.), Phys. Rev. Lett. **96**, 110406 (2006).
40. E. Zavattini *et al.* (PVLAS Collab.), Phys. Rev. **D77**, 032006 (2008).
41. F. Della Valle *et al.* (PVLAS Collab.), Eur. Phys. J. **C76**, 24 (2016).
42. E. Fischbach and C. Talmadge, Nature **356**, 207 (1992).
43. J.E. Moody and F. Wilczek, Phys. Rev. **D30**, 130 (1984);
A.N. Youdin *et al.*, Phys. Rev. Lett. **77**, 2170 (1996);
Wei-Tou Ni *et al.*, Phys. Rev. Lett. **82**, 2439 (1999);
D.F. Phillips *et al.*, Phys. Rev. **D63**, 111101 (2001);
B.R. Heckel *et al.* (Eöt-Wash Collab.), Phys. Rev. Lett. **97**, 021603 (2006);
S.A. Hoedl *et al.*, Phys. Rev. Lett. **106**, 041801 (2011).
44. G. Raffelt, Phys. Rev. **D86**, 015001 (2012).
45. A. Arvanitaki and A.A. Geraci, Phys. Rev. Lett. **113**, 161801 (2014).
46. M.S. Turner, Phys. Reports **197**, 67 (1990);
G.G. Raffelt, Phys. Reports **198**, 1 (1990).
47. G.G. Raffelt, *Stars as Laboratories for Fundamental Physics*, (Univ. of Chicago Press, Chicago, 1996).
48. G.G. Raffelt, Lect. Notes Phys. **741**, 51 (2008).
49. S. Andriamonje *et al.* (CAST Collab.), JCAP **0704**, 010 (2007).
50. P. Gondolo and G. Raffelt, Phys. Rev. **D79**, 107301 (2009).
51. H. Schlattl, A. Weiss, and G. Raffelt, Astropart. Phys. **10**, 353 (1999).
52. N. Vinyoles *et al.*, JCAP **1510**, 015 (2015).
53. A. Ayala *et al.*, Phys. Rev. Lett. **113**, 191302 (2014);
O. Straniero *et al.*, doi:10.3204/DESY-PROC-2015-02/straniero_oscar.
54. J. Redondo, JCAP **1312**, 008 (2013).
55. N. Viaux *et al.*, Phys. Rev. Lett. **111**, 231301 (2013).
56. G.G. Raffelt, Phys. Lett. **B166**, 402 (1986);
S.I. Blinnikov and N.V. Dunina-Barkovskaya, Mon. Not. R. Astron. Soc. **266**, 289 (1994).
57. M.M. Miller Bertolami *et al.*, JCAP **1410**, 069 (2014).
58. J. Isern *et al.*, Astrophys. J. Lett. **682**, L109 (2008);
J. Isern *et al.*, J. Phys. Conf. Ser. **172**, 012005 (2009).
59. J. Isern *et al.*, Astron. & Astrophys. **512**, A86 (2010);
A.H. Córsico *et al.*, Mon. Not. Roy. Astron. Soc. **424**, 2792 (2012);
A.H. Córsico *et al.*, JCAP **1212**, 010 (2012).
60. T. Fischer *et al.*, Phys. Rev. **D94**, 085012 (2016).
61. M. Giannotti *et al.*, JCAP **1710**, 010 (2017).
62. J. Engel, D. Seckel, and A.C. Hayes, Phys. Rev. Lett. **65**, 960 (1990).
63. T. Moroi and H. Murayama, Phys. Lett. **B440**, 69 (1998).
64. L.B. Leinson, JCAP **1408**, 031 (2014).
65. J. Keller and A. Sedrakian, Nucl. Phys. **A897**, 62 (2013);
A. Sedrakian, Phys. Rev. **D93**, 065044 (2016).
66. L.B. Leinson, Phys. Lett. **B741**, 87 (2015).
67. M. Giannotti *et al.*, JCAP **1605**, 057 (2016).
68. G.G. Raffelt, J. Redondo, and N. Viaux Maira, Phys. Rev. **D84**, 103008 (2011).
69. K. van Bibber *et al.*, Phys. Rev. **D39**, 2089 (1989).
70. D. Lazarus *et al.*, Phys. Rev. Lett. **69**, 2333 (1992).
71. S. Moriyama *et al.*, Phys. Lett. **B434**, 147 (1998);
Y. Inoue *et al.*, Phys. Lett. **B536**, 18 (2002).
72. M. Minowa *et al.*, Phys. Lett. **B668**, 93 (2008).
73. V. Anastassopoulos *et al.*, Nature Phys. **13**, 584 (2017).
74. E. Arik *et al.* (CAST Collab.), JCAP **0902**, 008 (2009).
75. S. Aune *et al.* (CAST Collab.), Phys. Rev. Lett. **107**, 261302 (2011);
M. Arik *et al.* (CAST Collab.), Phys. Rev. Lett. **112**, 091302 (2014);
M. Arik *et al.* (CAST Collab.), Phys. Rev. **D92**, 021101 (2015).
76. E. Armengaud *et al.* (EDELWEISS-II Collab.), JCAP **1311**, 067 (2013);
E. Aprile *et al.* (XENON100 Collab.), Phys. Rev. **D90**, 062009 (2014) and Erratum *ibid.*, **95**,029904(2017).
77. D. S. Akerib *et al.* (LUX Collab.), Phys. Rev. Lett. **118**, 261301 (2017).
78. E. Armengaud *et al.*, JINST **9**, T05002 (2014).
79. K. Barth *et al.*, JCAP **1305**, 010 (2013).
80. F.T. Avignone III *et al.*, Phys. Rev. Lett. **81**, 5068 (1998);
S. Cebrian *et al.*, Astropart. Phys. **10**, 397 (1999);
A. Morales *et al.* (COSME Collab.), Astropart. Phys. **16**, 325 (2002);
R. Bernabei *et al.*, Phys. Lett. **B515**, 6 (2001);
Z. Ahmed *et al.* (CDMS Collab.), Phys. Rev. Lett. **103**, 141802 (2009);
E. Armengaud *et al.* (EDELWEISS Collab.), JCAP **1311**, 067 (2013).
81. H. Davoudiasl and P. Huber, Phys. Rev. Lett. **97**, 141302 (2006).
82. H.S. Hudson *et al.*, ASP Conf. Ser. **455**, 25 (2012).
83. J.W. Brockway, E.D. Carlson, and G.G. Raffelt, Phys. Lett. **B383**, 439 (1996);
J.A. Grifols, E.Massó, and R. Toldrà, Phys. Rev. Lett. **77**, 2372 (1996).
84. A. Payez *et al.*, JCAP **1502**, 006 (2015).
85. C. Csaki, N. Kaloper, and J. Terning, Phys. Rev. Lett. **88**, 161302 (2002).
86. A. Mirizzi, G.G. Raffelt, and P.D. Serpico, Lect. Notes Phys. **741**, 115 (2008).
87. R. Gill and J. S. Heyl, Phys. Rev. **D84**, 085001 (2011).
88. D. Horns *et al.*, Phys. Rev. **D85**, 085021 (2012).
89. A. Payez, J.R. Cudell, and D. Hutsemekers, JCAP **1207**, 041 (2012).
90. D. Horns and M. Meyer, JCAP **1202**, 033 (2012).
91. J. Biteau and D.A. Williams, Astrophys. J. **812**, 60 (2015).
92. A. De Angelis, G. Galanti, and M. Roncadelli, Phys. Rev. **D84**, 105030 (2011);
M. Simet, D. Hooper, and P.D. Serpico, Phys. Rev. **D77**, 063001 (2008);
M.A. Sanchez-Conde *et al.*, Phys. Rev. **D79**, 123511 (2009).
93. M. Meyer, D. Horns, and M. Raue, Phys. Rev. **D87**, 035027 (2013).
94. A. Abramowski *et al.* (H.E.S.S. Collab.), Phys. Rev. **D88**, 102003 (2013).
95. M. Ajello *et al.* (Fermi-LAT Collab.), Phys. Rev. Lett. **116**, 161101 (2016).
96. D. Wouters and P. Brun, Astrophys. J. **772**, 44 (2013);
M. Berg *et al.*, `arXiv:1605.01043` [astro-ph.HE];
M. C. D. Marsh *et al.*, `arXiv:1703.07354` [hep-ph];
J. P. Conlon *et al.*, JCAP **1707**, 005 (2017).
97. A. Arvanitaki *et al.*, Phys. Rev. **D81**, 123530 (2010);
A. Arvanitaki and S. Dubovsky, Phys. Rev. **D83**, 044026 (2011);
A. Arvanitaki, M. Baryakhtar, and X. Huang, Phys. Rev. **D91**, 084011 (2015).
98. A. Arvanitaki *et al.*, Phys. Rev. **D95**, 043001 (2017).
99. M.S. Turner, Phys. Rev. Lett. **59**, 2489 (1987) and Erratum *ibid.*, **60**, 1101 (1988);
E. Massó, F. Rota, and G. Zsembinszki, Phys. Rev. **D66**, 023004 (2002);
P. Graf and F. D. Steffen, Phys. Rev. **D83**, 075011 (2011).
100. S. Hannestad *et al.*, JCAP **1008**, 001 (2010);
M. Archidiacono *et al.*, JCAP **1310**, 020 (2013);
E. Di Valentino *et al.*, Phys. Lett. **B752**, 182 (2016).
101. M. Archidiacono *et al.*, JCAP **1505**, 050 (2015).
102. E. Massó and R. Toldra, Phys. Rev. **D55**, 7967 (1997);
D. Cadamuro and J. Redondo, JCAP **1202**, 032 (2012).
103. J. Preskill, M.B. Wise, and F. Wilczek, Phys. Lett. **B120**, 127 (1983);
L.F. Abbott and P. Sikivie, Phys. Lett. **B120**, 133 (1983);
M. Dine and W. Fischler, Phys. Lett. **B120**, 137 (1983).
104. K.J. Bae, J.-H. Huh, and J.E. Kim, JCAP **0809**, 005 (2008).
105. O. Wantz and E.P.S. Shellard, Phys. Rev. **D82**, 123508 (2010).

106. G. Ballesteros, J. Redondo, A. Ringwald and C. Tamarit, JCAP **1708**, 001 (2017).
107. M. Tegmark *et al.*, Phys. Rev. **D73**, 023505 (2006).
108. M. Beltrán, J. García-Bellido, and J. Lesgourgues, Phys. Rev. **D75**, 103507 (2007);
M.P. Hertzberg, M. Tegmark, and F. Wilczek, Phys. Rev. **D78**, 083507 (2008);
J. Hamann *et al.*, JCAP **0906**, 022 (2009);
P.A.R. Ade *et al.* [Planck Collab.], Astron. & Astrophys. **571**, A22 (2014);
P.A.R. Ade *et al.* [Planck Collab.], Astrophys. Space Sci. **361**, 58 (2016).
109. P. Fox, A. Pierce, and S.D. Thomas, `hep-th/0409059`;
D.J.E. Marsh *et al.*, Phys. Rev. Lett. **113**, 011801 (2014);
L. Visinelli and P. Gondolo, Phys. Rev. Lett. **113**, 011802 (2014).
110. V. B. Klaer and G. D. Moore, `arXiv:1708.07521` [hep-ph].
111. S. Chang, C. Hagmann and P. Sikivie, Phys. Rev. **D59**, 023505 (1999);
C. Hagmann, S. Chang and P. Sikivie, Phys. Rev. **D63**, 125018 (2001).
112. T. Hiramatsu *et al.*, Phys. Rev. **D83**, 123531 (2011);
T. Hiramatsu *et al.*, Phys. Rev. **D85**, 105020 (2012) and Erratum *ibid.*, **86**, 089902 (2012).
113. M. Kawasaki, K. Saikawa, and T. Sekiguchi, Phys. Rev. **D91**, 065014 (2015).
114. A. Ringwald and K. Saikawa, Phys. Rev. **D94**, 049908 (2016) and Addendum *ibid.*, **94**, 049908 (2016).
115. T. Hiramatsu, M. Kawasaki, K. Saikawa and T. Sekiguchi, JCAP **1301**, 001 (2013).
116. E.W. Kolb and I.I. Tkachev, Phys. Rev. Lett. **71**, 3051 (1993);
K.M. Zurek, C.J. Hogan, and T.R. Quinn, Phys. Rev. **D75**, 043511 (2007).
117. E.W. Kolb and I.I. Tkachev, Astrophys. J. **460**, L25 (1996);
M. Fairbairn, D. J. E. Marsh and J. Quevillon, Phys. Rev. Lett. **119**, 021101 (2017).
118. E. Berkowitz, M. I. Buchoff and E. Rinaldi, Phys. Rev. **D92**, 034507 (2015);
S. Borsanyi *et al.*, Phys. Lett. **B752**, 175 (2016);
R. Kitano and N. Yamada, JHEP **1510**, 136 (2015);
P. Petreczky, H. P. Schadler and S. Sharma, Phys. Lett. **B762**, 498 (2016);
Y. Taniguchi *et al.*, Phys. Rev. **D95**, 054502 (2017).
119. C. Bonati *et al.*, JHEP **1603**, 155 (2016).
120. P. Arias *et al.*, JCAP **1206**, 013 (2012).
121. R. Hlozek *et al.*, Phys. Rev. **D91**, 103512 (2015).
122. D. J. E. Marsh, Phys. Rept. **643**, 1 (2016).
123. L. Hui, J. P. Ostriker, S. Tremaine and E. Witten, Phys. Rev. **D95**, 043541 (2017).
124. A. G. Dias *et al.*, JHEP **1406**, 037 (2014);
J. E. Kim and D. J. E. Marsh, Phys. Rev. **D93**, 025027 (2016).
125. H. Davoudiasl and C. W. Murphy, Phys. Rev. Lett. **118**, 141801 (2017).
126. M. Khlopov *et al.*, Mon. Not. Roy. Astron. Soc. **215**, 575 (1985)..
127. W. Hu, R. Barkana and A. Gruzinov, Phys. Rev. Lett. **85**, 1158 (2000);
L. Amendola and R. Barbieri, Phys. Lett. **B642**, 192 (2006);
D. J. E. Marsh and P. G. Ferreira, Phys. Rev. **D82**, 103528 (2010).
128. E. Seidel and W. M. Suen, Phys. Rev. Lett. **66**, 1659 (1991).
129. R. Hlozek, D. J. E. Marsh and D. Grin, `arXiv:1708.05681` [astro-ph.CO].
130. D. J. E. Marsh and J. Silk, Mon. Not. Roy. Astron. Soc. **437**, 2652 (2014).
131. H. Y. Schive, T. Chiueh, T. Broadhurst and K. W. Huang, Astrophys. J. 818,89(2016).
132. B. Bozek *et al.*, Mon. Not. Roy. Astron. Soc. **450**, 209 (2015);
P. S. Corasaniti, *et al.*, Phys. Rev. **D95**, 083512 (2017).
133. E. Armengaud *et al.*, Mon. Not. Roy. Astron. Soc. **471**, 4606 (2017);
V. Irsic *et al.*, Phys. Rev. Lett. **119**, 031302 (2017);
T. Kobayashi *et al.*, `arXiv:1708.00015` [astro-ph.CO].
134. H. Y. Schive and T. Chiueh, `arXiv:1706.03723` [astro-ph.CO].
135. H. Y. Schive, T. Chiueh and T. Broadhurst, Nature Phys. **10**, 496 (2014).
136. B. Schwabe, J. C. Niemeyer and J. F. Engels, Phys. Rev. **D94**, 043513 (2016);
J. Veltmaat and J. C. Niemeyer, Phys. Rev. **D94**, 123523 (2016);
P. Mocz *et al.*, `1705.05845` [astro-ph.CO].
137. D. J. E. Marsh and A. R. Pop, Mon. Not. Roy. Astron. Soc. **451**, 2479 (2015);
S. R. Chen *et al.*, Mon. Not. Roy. Astron. Soc. **468**, 1338 (2017);
A. X. Gonzles-Morales *et al.*, Mon. Not. Roy. Astron. Soc. **472**, 1346 (2017).
138. D. G. Levkov, A. G. Panin and I. I. Tkachev, Phys. Rev. Lett. **118**, 011301 (2017);
T. Helfer *et al.*, JCAP **1703**, 055 (2017);
J. Eby, M. Ma, P. Suranyi and L. C. R. Wijewardhana, `1705.05385` [hep-ph].
139. M. Bershady *et al.*, Phys. Rev. Lett. **66**, 1398 (1991);
M. Ressell, Phys. Rev. **D44**, 3001 (1991).
140. D. Grin *et al.*, Phys. Rev. **D75**, 105018 (2007).
141. B.D. Blout *et al.*, Astrophys. J. **546**, 825 (2001).
142. P. Sikivie, Phys. Rev. **D32**, 2988 (1985);
L. Krauss *et al.*, Phys. Rev. Lett. **55**, 1797 (1985);
R. Bradley *et al.*, Rev. Mod. Phys. **75**, 777 (2003).
143. P. Sikivie and J. Ipser, Phys. Lett. **B291**, 288 (1992);
P. Sikivie *et al.*, Phys. Rev. Lett. **75**, 2911 (1995).
144. S. DePanfilis *et al.*, Phys. Rev. Lett. **59**, 839 (1987);
W. Wuensch *et al.*, Phys. Rev. **D40**, 3153 (1989);
C. Hagmann *et al.*, Phys. Rev. **D42**, 1297 (1990).
145. S. Asztalos *et al.*, Phys. Rev. **D69**, 011101 (2004).
146. L. Duffy *et al.*, Phys. Rev. Lett. **95**, 091304 (2005);
J. Hoskins *et al.*, Phys. Rev. **D84**, 121302 (2011).
147. S.J. Asztalos *et al.* (ADMX Collab.), Phys. Rev. Lett. **104**, 041301 (2010).
148. S.J. Asztalos *et al.*, Nucl. Instrum. Methods **A656**, 39 (2011).
149. G. Rybka *et al.*, Phys. Rev. Lett. **105**, 051801 (2010);
A. Wagner *et al.*, Phys. Rev. Lett. **105**, 171801 (2010).
150. B. M. Brubaker *et al.*, Phys. Rev. Lett. **118**, 061302 (2017).
151. I. Ogawa, S. Matsuki, and K. Yamamoto, Phys. Rev. **D53**, 1740 (1996);
Y. Kishimoto *et al.*, Phys. Lett. **A303**, 279 (2002);
M. Tada *et al.*, Phys. Lett. **A303**, 285 (2002);
T.Haseyama *et al.*, J. Low Temp. Phys. **150**, 549 (2008).
152. B. T. McAllister *et al.*, `arXiv:1706.00209` [physics.ins-det].
153. W. Chung, PoS CORFU **2015**, 047 (2016).
154. D. Alesini *et al.*, `arXiv:1707.06010` [physics.ins-det].
155. G. Rybka *et al.*, Phys. Rev. **D91**, 011701 (2015).
156. D. Horns *et al.*, JCAP **1304**, 016 (2013).
157. J. Suzuki *et al.*, JCAP **1509**, 042 (2015);
B. Döbrich *et al.*, `arXiv:1510.05869` [physics.ins-det].
158. A. Caldwell *et al.*[MADMAX Working Group], Phys. Rev. Lett. **118**, 091801 (2017).
159. P. Sikivie, Phys. Rev. Lett. **113**, 201301 (2014).
160. D. Budker *et al.*, Phys. Rev. **X4**, 021030 (2014).
161. P. Sikivie, N. Sullivan, and D. B. Tanner, Phys. Rev. Lett. **112**, 131301 (2014).
162. Y. Kahn, B. R. Safdi and J. Thaler, Phys. Rev. Lett. **117**, 141801 (2016).
163. M. Silva-Feaver *et al.*, `arXiv:1610.09344` [astro-ph.IM].
164. L. Krauss *et al.*, Phys. Rev. Lett. **55**, 1797 (1985);
R. Barbieri *et al.*, Phys. Rev. **B226**, 357 (1989).
165. R. Barbieri *et al.*, Phys. Dark Univ. **15**, 135 (2017).

112. Searches for Quark and Lepton Compositeness

Revised 2017 by K. Hikasa (Tohoku University), M. Tanabashi (Nagoya University), K. Terashi (University of Tokyo), and N. Varelas (University of Illinois at Chicago)

112.1. Limits on contact interactions

If quarks and leptons are made of constituents, then at the scale of constituent binding energies (compositeness scale) there should appear new interactions among them. At energies much below the compositeness scale (Λ), these interactions are suppressed by inverse powers of Λ. The dominant effect of the compositeness of fermion ψ should come from the lowest dimensional interactions with four fermions (contact terms), whose most general flavor-diagonal color-singlet chirally invariant form reads [1,2]

$$\mathcal{L} = \mathcal{L}_{LL} + \mathcal{L}_{RR} + \mathcal{L}_{LR} + \mathcal{L}_{RL},$$

with

$$\mathcal{L}_{LL} = \frac{g^2_{\rm contact}}{2\Lambda^2} \sum_{i,j} \eta^{ij}_{LL} (\bar{\psi}^i_L \gamma_\mu \psi^i_L)(\bar{\psi}^j_L \gamma^\mu \psi^j_L),$$

$$\mathcal{L}_{RR} = \frac{g^2_{\rm contact}}{2\Lambda^2} \sum_{i,j} \eta^{ij}_{RR} (\bar{\psi}^i_R \gamma_\mu \psi^i_R)(\bar{\psi}^j_R \gamma^\mu \psi^j_R),$$

$$\mathcal{L}_{LR} = \frac{g^2_{\rm contact}}{2\Lambda^2} \sum_{i,j} \eta^{ij}_{LR} (\bar{\psi}^i_L \gamma_\mu \psi^i_L)(\bar{\psi}^j_R \gamma^\mu \psi^j_R),$$

$$\mathcal{L}_{RL} = \frac{g^2_{\rm contact}}{2\Lambda^2} \sum_{i,j} \eta^{ij}_{RL} (\bar{\psi}^i_R \gamma_\mu \psi^i_R)(\bar{\psi}^j_L \gamma^\mu \psi^j_L), \qquad (112.1)$$

where i, j are the indices of fermion species. Color and other indices are suppressed in Eq. (112.1). Chiral invariance provides a natural explanation why quark and lepton masses are much smaller than their inverse size Λ. Note $\eta^{ij}_{\alpha\beta} = \eta^{ji}_{\beta\alpha}$, therefore, in order to specify the contact interaction among the same fermion species $i = j$, it is enough to use η_{LL}, η_{RR} and η_{LR}. We will suppress the indices of fermion species hereafter. We may determine the scale Λ unambiguously by using the above form of the effective interactions; the conventional method [1] is to fix its scale by setting $g^2_{\rm contact}/4\pi = g^2_{\rm contact}(\Lambda)/4\pi = 1$ for the new strong interaction coupling and by setting the largest magnitude of the coefficients $\eta_{\alpha\beta}$ to be unity. In the following, we denote

$$\Lambda = \Lambda^\pm_{LL} \quad \text{for} \quad (\eta_{LL}, \eta_{RR}, \eta_{LR}) = (\pm 1, 0, 0)\ ,$$
$$\Lambda = \Lambda^\pm_{RR} \quad \text{for} \quad (\eta_{LL}, \eta_{RR}, \eta_{LR}) = (0, \pm 1, 0)\ ,$$
$$\Lambda = \Lambda^\pm_{VV} \quad \text{for} \quad (\eta_{LL}, \eta_{RR}, \eta_{LR}) = (\pm 1, \pm 1, \pm 1)\ ,$$
$$\Lambda = \Lambda^\pm_{AA} \quad \text{for} \quad (\eta_{LL}, \eta_{RR}, \eta_{LR}) = (\pm 1, \pm 1, \mp 1)\ ,$$
$$\Lambda = \Lambda^\pm_{V-A} \quad \text{for} \quad (\eta_{LL}, \eta_{RR}, \eta_{LR}) = (0, 0, \pm 1)\ . \qquad (112.2)$$

Such interactions can arise by interchanging constituents (when the fermions have common constituents), and/or by exchanging the binding quanta (whenever binding quanta couple to constituents of both particles).

Fermion scattering amplitude [2] induced from the contact interaction in Eq. (112.1) interferes with the Standard Model (SM) amplitude destructively or constructively. The sign of interference depends on the sign of $\eta_{\alpha\beta}$ ($\alpha, \beta = L, R$). For instance, in the parton level $qq \to qq$ scattering cross section in the $\Lambda^\pm_{LL}$ model, the contact interaction amplitude and the SM gluon exchange amplitude interfere destructively for $\eta_{LL} = +1$, while they interfere constructively for $\eta_{LL} = -1$. In models of quark compositeness, the quark scattering cross sections induced from the contact interactions receive sizable QCD radiative corrections. Ref. 3 provides the exact next-to-leading order (NLO) QCD corrections to the contact interaction induced quark scattering cross sections.

Over the last three decades experiments at the CERN Sp$\bar{\rm p}$S [4,5], the Fermilab Tevatron [6,7], and the CERN LHC [8–12] have searched for quark contact interactions, characterized by the four-fermion effective Lagrangian in Eq. (112.1), using jet final states. These searches have been performed primarily by studying the angular distribution of the two highest transverse momentum, $p_{\rm T}$, jets (dijets), and the inclusive jet $p_{\rm T}$ spectrum. The variable $\chi = \exp(|(y_1 - y_2)|)$ is used to measure the dijet angular distribution, where y_1 and y_2 are the rapidities of the two jets with the highest transverse momenta. For collinear massless parton scattering, χ is related to the polar scattering angle θ^* in the partonic center-of-mass frame by $\chi = (1 + |\cos\theta^*|)/(1 - |\cos\theta^*|)$. The choice of χ is motivated by the fact that the angular distribution for Rutherford scattering, which is proportional to $1/(1 - \cos\theta^*)^2$, is independent of χ. In perturbative QCD the χ distributions are relatively uniform and only mildly modified by higher-order QCD or electroweak corrections. Signatures of quark contact interactions exhibit more isotropic angular distribution than QCD and they can be identified as an excess at low values of χ. In the inclusive jet cross section measurement, quark contact interaction effects are searched as deviations from the predictions of perturbative QCD in the tails of the high-$p_{\rm T}$ jet spectrum [11].

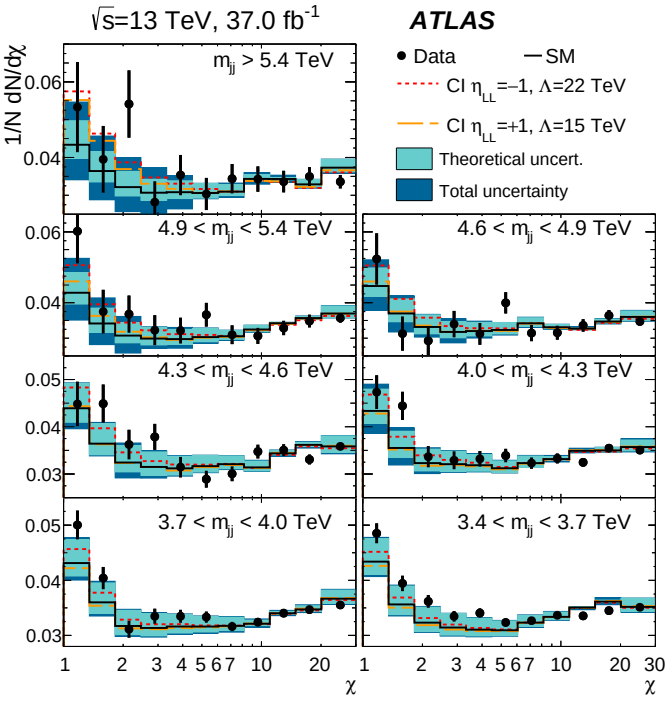

Figure 112.1: Normalized dijet angular distributions in several dijet mass (m_{jj}) ranges. The data distributions are compared to PYTHIA8 predictions with NLO and electroweak corrections applied (solid line) and with the predictions including a contact interaction (CI) term in which only left-handed quarks participate of compositeness scale $\Lambda^+_{LL} = 15$ TeV (dashed line) and $\Lambda^-_{LL} = 22$ TeV (dotted line). The theoretical uncertainties and the total theoretical and experimental uncertainties in the predictions are displayed as shaded bands around the SM prediction. Figure adopted from Ref. 9.

Recent results from the LHC, using data collected at proton-proton center-of-mass energy of $\sqrt{s} = 13$ TeV, extend previous limits on quark contact interactions. Figure 112.1 shows the normalized dijet angular distributions for several dijet mass ranges measured in ATLAS [9] at $\sqrt{s} = 13$ TeV. The data distributions are compared with SM predictions, estimated using PYTHIA8 [13] with GEANT4-based [14] ATLAS detector simulation and corrected to NLO QCD calculation provided by NLO Jet++ [15] including electroweak corrections [16],

and with predictions including a contact interaction term in which only left-handed quarks participate at compositeness scale $\Lambda^+_{LL} = 15$ TeV ($\Lambda^-_{LL} = 22$ TeV) with destructive (constructive) interference. Over a wide range of χ and dijet mass the data are well described by the SM predictions. Using the dijet angular distributions measured at high dijet masses and $\sqrt{s} = 13$ TeV, the ATLAS [9] and CMS [12] Collaborations have set 95% confidence level (C.L.) lower limits on the contact interaction scale Λ, ranging from 9.1 to 29.5 TeV for different quark contact interaction models that correspond to various combinations of (η_{LL}, η_{RR}, η_{LR}), as summarized in Figure 112.2. The contact interaction scale limits extracted using the dijet angular distributions include the exact NLO QCD corrections to dijet production induced by contact interactions [3]. In proton-proton collisions, the $\Lambda^{\pm}_{LL}$ and $\Lambda^{\pm}_{RR}$ contact interaction models result in identical tree-level cross sections and NLO QCD corrections and yield the same exclusion limits. For $\Lambda^{\pm}_{VV}$ and $\Lambda^{\pm}_{AA}$, the contact interaction predictions are identical at tree level, but exhibit different NLO QCD corrections and yield different exclusion limits.

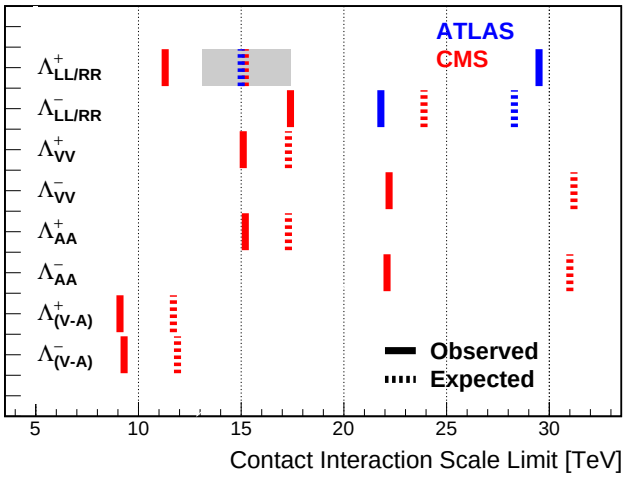

Figure 112.2: Observed (solid lines) and expected (dashed lines) 95% C.L. lower limits on the contact interaction scale Λ for different contact interaction models from ATLAS [9] and CMS preliminary [12] using the dijet angular distributions. The contact interaction models used for the dijet angular distributions include the exact NLO QCD corrections to dijet production. The shaded band for the $\Lambda^+_{LL/RR}$ model indicates the range of contact interaction scale that was not excluded in ATLAS [9] due to statistical fluctuation of observed data.

If leptons (l) and quarks (q) are composite with common constituents, the interaction of these constituents will manifest itself in the form of a $llqq$-type four-fermion contact interaction Lagrangian at energies below the compositeness scale Λ. The $llqq$ terms in the contact interaction Lagrangian can be expressed as

$$\mathcal{L}_{LL} = \frac{g^2_{\rm contact}}{\Lambda^2} \sum_{i,j} \eta^{ij}_{LL} (\bar{q}^i_L \gamma_\mu q^i_L)(\bar{l}^j_L \gamma^\mu l^j_L),$$

$$\mathcal{L}_{RR} = \frac{g^2_{\rm contact}}{\Lambda^2} \sum_{i,j} \eta^{ij}_{RR} (\bar{q}^i_R \gamma_\mu q^i_R)(\bar{l}^j_R \gamma^\mu l^j_R),$$

$$\mathcal{L}_{LR} = \frac{g^2_{\rm contact}}{\Lambda^2} \sum_{i,j} \eta^{ij}_{LR} (\bar{q}^i_L \gamma_\mu q^i_L)(\bar{l}^j_R \gamma^\mu l^j_R),$$

$$\mathcal{L}_{RL} = \frac{g^2_{\rm contact}}{\Lambda^2} \sum_{i,j} \eta^{ij}_{RL} (\bar{q}^i_R \gamma_\mu q^i_R)(\bar{l}^j_L \gamma^\mu l^j_L). \qquad (112.3)$$

Searches on quark-lepton compositeness have been reported from experiments at LEP [17–20], HERA [21,22], the Tevatron [23–24], and recently from the ATLAS [25–26] and CMS [27–28] experiments at the LHC. The most stringent searches for $llqq$ contact interactions are performed by the LHC experiments using high-mass oppositely-charged lepton pairs produced through the $q\bar{q} \to l^+l^-$ Drell-Yan process. The contact interaction amplitude of the $u\bar{u} \to l^+l^-$ process ($l = e$ or μ) interferes with the corresponding SM amplitude constructively (destructively) for $\eta^{ul}_{\alpha\beta} = -1$ ($\eta^{ul}_{\alpha\beta} = +1$). The ATLAS Collaboration has extracted limits on the $llqq$ contact interaction at $\sqrt{s} = 13$ TeV for the right-right ($\eta_{RR} = \pm 1$, $\eta_{LL} = \eta_{LR} = \eta_{RL} = 0$), left-left ($\eta_{LL} = \pm 1$, $\eta_{RR} = \eta_{LR} = \eta_{RL} = 0$), and left-right ($\eta_{LR} = \eta_{RL} = \pm 1$, $\eta_{RR} = \eta_{LL} = 0$) models. Combining the dielectron and dimuon channels, the 95% C.L. lower limits on the $llqq$ contact interaction scale Λ are 35.2 TeV (27.7 TeV) for the right-right model, 40.1 TeV (25.4 TeV) for the left-left model, and 35.7 TeV (27.5 TeV) for the left-right model, each with constructive (destructive) interference [26]. The CMS Collaboration, using the full 8-TeV dataset has set a 95% C.L. lower limit on the scale Λ of 16.9 TeV (13.1 TeV) for the benchmark left-left $llqq$ contact interaction model with constructive (destructive) interference [28].

Note that the contact interactions arising from the compositeness of quarks and leptons in Eq. (112.1) can also be regarded as a part of more general dimension six operators in the context of low energy standard model effective theory. For a complete list of these dimension six operators see Refs. 29,30.

Interactions of hypothetical dark matter candidate particles with SM particles through mediators can also be described as contact interactions at low energy. See *"Searches for WIMPs and Other Particles"* in this volume for limits on the interactions involving dark matter candidate particles.

112.2. Limits on excited fermions

Another typical consequence of compositeness is the appearance of excited leptons and quarks (l^* and q^*). Phenomenologically, an excited lepton is defined to be a heavy lepton which shares a leptonic quantum number with one of the existing leptons (an excited quark is defined similarly). For example, an excited electron e^* is characterized by a nonzero transition-magnetic coupling with electrons. Smallness of the lepton mass and the success of QED prediction for $g - 2$ suggest chirality conservation, *i.e.,* an excited lepton should not couple to both left- and right-handed components of the corresponding lepton [31–33].

Excited leptons may be classified by $SU(2) \times U(1)$ quantum numbers. Typical examples are:

1. Sequential type

$$\begin{pmatrix} \nu^* \\ l^* \end{pmatrix}_L, \qquad [\nu^*_R], \qquad l^*_R.$$

   ν^*_R is necessary unless ν^* has a Majorana mass.

2. Mirror type

$$[\nu^*_L], \qquad l^*_L, \qquad \begin{pmatrix} \nu^* \\ l^* \end{pmatrix}_R.$$

3. Homodoublet type

$$\begin{pmatrix} \nu^* \\ l^* \end{pmatrix}_L, \qquad \begin{pmatrix} \nu^* \\ l^* \end{pmatrix}_R.$$

Similar classification can be made for excited quarks.

Excited fermions can be pair produced via their minimal gauge couplings. The couplings of excited leptons with Z are given by

$$\frac{e}{2\sin\theta_W \cos\theta_W}(-1 + 2\sin^2\theta_W)\bar{l^*}\gamma^\mu l^* Z_\mu$$

$$+ \frac{e}{2\sin\theta_W \cos\theta_W}\bar{\nu^*}\gamma^\mu \nu^* Z_\mu$$

in the homodoublet model. The corresponding couplings of excited quarks can be easily obtained. Although form factor effects can be present for the gauge couplings at $q^2 \neq 0$, they are usually neglected.

Excited fermions may also be produced via the contact interactions with ordinary quarks and leptons [34]

$$\mathcal{L} = \frac{g^2_{\rm contact}}{\Lambda^2}\left[\eta'_{LL}(\bar{\psi}_L\gamma_\mu\psi_L)(\bar{\psi}^*_L\gamma^\mu\psi^*_L) + (\eta''_{LL}(\bar{\psi}_L\gamma_\mu\psi_L)(\bar{\psi}^*_L\gamma^\mu\psi_L) + \text{h.c.}) + \cdots\right]. \quad (112.4)$$

Again, the coefficient is conventionally taken $g^2_{\rm contact} = 4\pi$. It is widely assumed $\eta'_{LL} = \eta''_{LL} = 1$, $\eta'_{LR} = \eta''_{LR} = \eta'_{RL} = \eta''_{RL} = \eta'_{RR} = \eta''_{RR} = 0$ in experimental analyses for simplicity.

In addition, transition-magnetic type couplings with a gauge boson are expected. These couplings can be generally parameterized as follows:

$$\begin{aligned}\mathcal{L} =& \frac{\lambda^{(\psi^*)}_\gamma e}{2m_{\psi^*}}\bar{\psi}^*\sigma^{\mu\nu}(\eta_L\frac{1-\gamma_5}{2} + \eta_R\frac{1+\gamma_5}{2})\psi F_{\mu\nu} \\ &+ \frac{\lambda^{(\psi^*)}_Z e}{2m_{\psi^*}}\bar{\psi}^*\sigma^{\mu\nu}(\eta_L\frac{1-\gamma_5}{2} + \eta_R\frac{1+\gamma_5}{2})\psi Z_{\mu\nu} \\ &+ \frac{\lambda^{(l^*)}_W g}{2m_{l^*}}\bar{l}^*\sigma^{\mu\nu}\frac{1-\gamma_5}{2}\nu W_{\mu\nu} \\ &+ \frac{\lambda^{(\nu^*)}_W g}{2m_{\nu^*}}\bar{\nu}^*\sigma^{\mu\nu}(\eta_L\frac{1-\gamma_5}{2} + \eta_R\frac{1+\gamma_5}{2})lW^\dagger_{\mu\nu} \\ &+ \text{h.c.}, \end{aligned} \quad (112.5)$$

where $g = e/\sin\theta_W$, $\psi = \nu$ or l, $F_{\mu\nu} = \partial_\mu A_\nu - \partial_\nu A_\mu$ is the photon field strength, $Z_{\mu\nu} = \partial_\mu Z_\nu - \partial_\nu Z_\mu$, *etc.*. The normalization of the coupling is chosen such that

$$\max(|\eta_L|, |\eta_R|) = 1.$$

Chirality conservation requires

$$\eta_L\eta_R = 0. \quad (112.6)$$

These couplings in Eq. (112.5) can arise from $SU(2) \times U(1)$-invariant higher-dimensional interactions. A well-studied model is the interaction of homodoublet type l^* with the Lagrangian (see Refs. 35,36)

$$\mathcal{L} = \frac{1}{2\Lambda}\bar{L}^*\sigma^{\mu\nu}(gf\frac{\tau^a}{2}W^a_{\mu\nu} + g'f'YB_{\mu\nu})\frac{1-\gamma_5}{2}L + \text{h.c.}, \quad (112.7)$$

where L denotes the lepton doublet (ν, l), Λ is the compositeness scale, g, g' are $SU(2)$ and $U(1)_Y$ gauge couplings, and $W^a_{\mu\nu}$ and $B_{\mu\nu}$ are the field strengths for $SU(2)$ and $U(1)_Y$ gauge fields. These couplings satisfy the relation

$$\lambda_W = -\sqrt{2}\sin^2\theta_W(\lambda_Z\cot\theta_W + \lambda_\gamma), \quad (112.8)$$

with $\lambda_{W,Z,\gamma}$ being defined in Eq. (112.5) with $\lambda_{W,Z,\gamma} = \lambda^{(\ell^*)}_{W,Z,\gamma}$ or $\lambda_{W,Z,\gamma} = \lambda^{(\nu^*)}_{W,Z,\gamma}$. Here $(\eta_L, \eta_R) = (1, 0)$ is assumed. It should be noted that the electromagnetic radiative decay of l^* (ν^*) is forbidden if $f = -f'$ ($f = f'$).

Additional coupling with gluons is possible for excited quarks:

$$\mathcal{L} = \frac{1}{2\Lambda}\bar{Q}^*\sigma^{\mu\nu}\left(g_s f_s\frac{\lambda^a}{2}G^a_{\mu\nu} + gf\frac{\tau^a}{2}W^a_{\mu\nu} + g'f'YB_{\mu\nu}\right) \times \frac{1-\gamma_5}{2}Q + \text{h.c.}, \quad (112.9)$$

where Q denotes a quark doublet, g_s is the QCD gauge coupling, and $G^a_{\mu\nu}$ the gluon field strength.

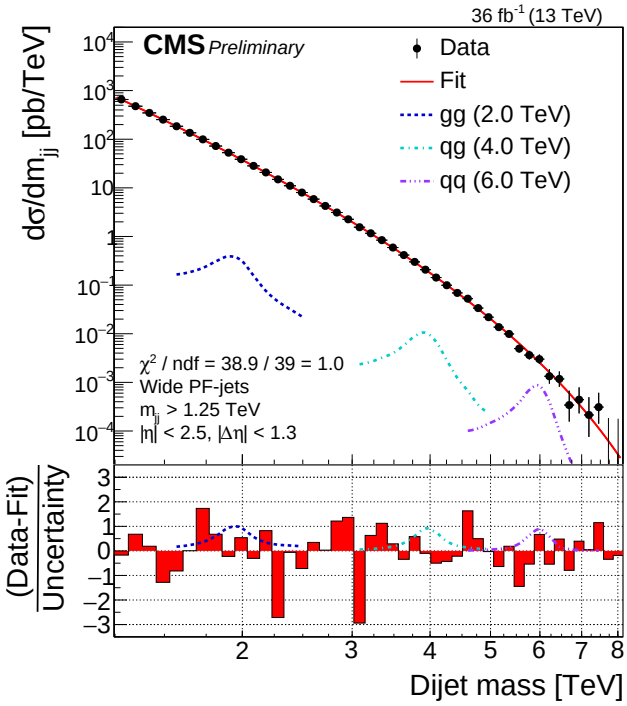

Figure 112.3: Dijet mass distribution measured by CMS using wide jets reconstructed from two highest transverse momentum jets by adding nearby jets within $\Delta R = \sqrt{\Delta\eta^2 + \Delta\phi^2} < 1.1$. The data distribution is compared to a fit representing a smooth background spectrum (solid curve). The excited quark signal with mass of 4.0 TeV (labeled as qg) is shown together with other benchmark signals. Shown at the bottom panel is the difference between the data and the fitted parametrization divided by the statistical uncertainty of the data. Figure adopted from Ref. 60.

If leptons are made of color triplet and antitriplet constituents, we may expect their color-octet partners. Transitions between the octet leptons (l_8) and the ordinary lepton (l) may take place via the dimension-five interactions

$$\mathcal{L} = \frac{1}{2\Lambda}\sum_l\{\bar{l}^\alpha_8 g_S F^\alpha_{\mu\nu}\sigma^{\mu\nu}(\eta_L l_L + \eta_R l_R) + \text{h.c.}\} \quad (112.10)$$

where the summation is over charged leptons and neutrinos. The leptonic chiral invariance implies $\eta_L\eta_R = 0$ as before.

Searches for the excited quarks and leptons have been performed over the last decades in experiments at the LEP [37–40], HERA [41–42], Tevatron [43–44], and LHC [45–67]. Most stringent constraints, which are described below at 95% confidence level, come from the LHC experiments.

The signature of excited quarks q^* at hadron colliders is characterized by a narrow resonant peak in the reconstructed invariant mass distribution of the q^* decay products. The decays via the transition-magnetic type operator in Eq. (112.9) are considered for excited quarks in LHC searches, and the final states to search for are dijet (qg) [45, 46, 57–60] or a jet in association with a photon ($q\gamma$) [47, 48, 61, 62] or a weak gauge boson (qW, qZ) [63, 64]. All analyses consider only spin-1/2 excited states of first generation quarks (u^*, d^*) with degenerate masses, expected to be predominantly produced in proton-proton collisions except for the excited b quark searches described below. Only the minimal gauge interactions and the transition-magnetic couplings with the form given in Eq. (112.9) are considered in the production process, and hence the contact interactions in Eq. (112.4) are not considered. The compositeness scale Λ is taken to be the same as the excited quark mass m_{q^*}. The transition-magnetic coupling coefficients f_s, f and f' are assumed to be equal to 1 (denoted by f).

With proton-proton collision data recorded at $\sqrt{s} = 13$ TeV at the LHC, the excited quark masses are excluded in dijet resonance searches up to 6.0 TeV in both ATLAS [46] and CMS [60]. Figure 112.3 shows the dijet mass distribution measured in CMS [60] by using the two highest p_{T} jets reconstructed with the anti-k_{T} algorithm [68] of a distance parameter of 0.4, and by combining nearby jets within $\Delta R = \sqrt{\Delta\eta^2 + \Delta\phi^2} < 1.1$ around the leading two jets. The measured dijet mass spectrum is compared to a fit with smoothly falling background shape (solid curve) to look for a narrow resonance; an excited quark signal with mass of 4.0 TeV is shown in the figure (denoted by qg) as one of the benchmark signals considered in the analysis.

The photon + jet resonance searches, targeting excited quarks decaying into a quark and a photon ($q^* \to q + \gamma$), have excluded q^* masses up to 5.3 TeV in ATLAS [48] and 5.5 TeV in CMS [62] using collision data at $\sqrt{s} = 13$ TeV. The W/Z boson + jet final states are examined to look for the $q^* \to q + W$ and $q + Z$ signal in CMS [64], exploiting jet substructure technique designed to provide sensitivity for highly-boosted hadronically decaying W and Z bosons. The lower mass limit of 5.0 (4.8) TeV is obtained from the W + jet (Z + jet) search using dataset recorded at $\sqrt{s} = 13$ TeV.

The excited b quarks (b^*) are also considered in the present searches at the LHC. Assuming the similar production processes to the first-generation excited quarks, the b^* has been searched for in final states containing at least one jet identified as originating from a b quark (b-tagging). The searches using two jets including at least one b-tagged jet have been performed at 8 and 13 TeV [49, 50, 58], resulting in b^* lower mass limits of 2.3 TeV in ATLAS using 13.3 fb^{-1} at $\sqrt{s} = 13$ TeV [49] and 1.6 TeV in CMS using 19.7 fb^{-1} at $\sqrt{s} = 8$ TeV [58]. The CMS Collaboration also performed a search for $b^* \to b + \gamma$ in events with a b-tagged jet in association with a photon using data at $\sqrt{s} = 13$ TeV [62], and excluded b^* masses up to 1.8 TeV. Excited b quarks with charged-current decay into a W-boson and a top quark ($b^* \to t + W$) were looked for in both ATLAS and CMS using the full 8 TeV data[51, 65]. ATLAS excluded b^* masses below 1.5 TeV for the b^* with left- and right-handed couplings [51] while CMS excluded the masses below 1.39(1.43) TeV for the left(right)-handed couplings [65].

Searches for excited leptons l^* are also performed at the LHC using proton-proton collision data recorded at $\sqrt{s} = 7$ and 8 TeV [53–56, 66, 67]. Considering single l^* production in contact interactions (Eq. (112.4)) and electromagnetic radiative decay to a SM lepton and a photon ($l^* \to l + \gamma$ where $l = e, \mu$), both the excited electron and excited muon masses below 2.2 TeV are excluded for $\Lambda = m_{l^*}$ using 13 fb^{-1} at $\sqrt{s} = 8$ TeV in ATLAS [54]. With the full 20.3 fb^{-1} data at $\sqrt{s} = 8$ TeV, the inclusive search on multi-lepton signatures with 3 or more charged leptons in ATLAS [55] further constrains the excited charged leptons and neutrinos. Considering both the transition-magnetic (Eq. (112.7)) and contact interaction (Eq. (112.4)) processes, the lower mass limits for the e^*, μ^*, τ^* and ν^* (for every excited neutrino flavor) are obtained to be 3.0, 3.0, 2.5 and 1.6 TeV, respectively, for $\Lambda = m_{e^*}$, m_{μ^*}, m_{τ^*} and m_{ν^*}. The rate of pair-produced excited leptons is independent of Λ for the minimal gauge interaction processes, and it allows to improve search sensitivity with multi-lepton signatures at high Λ, especially for excited neutrinos because the predominant $\nu_l^* \to l + W$ decays result in a higher acceptance for ≥ 3 charged lepton final states.

The ATLAS Collaboration performed a search [56] for single excited muons both produced and decayed in contact interaction processes (Eq. (112.4)), being characterized by the final state with two muons and two jets ($q\bar{q} \to \mu\mu^* \to \mu\mu q\bar{q}$). With the full 8 TeV data the lower mass limit of 2.8 TeV was set for the μ^* at $\Lambda = m_{\mu^*}$.

A search for excited leptons with $l^* \to l + \gamma$ decays ($l = e, \mu$) produced in contact interactions by the CMS Collaboration using the full data at $\sqrt{s} = 8$ TeV [67] resulted in mass exclusions of 2.45 TeV for the e^* and 2.47 TeV for the μ^* at $\Lambda = m_{l^*}$. The CMS Collaboration also performed an excited lepton search in the final states containing a Z boson [67], probing the excited leptons produced in contact interactions and decayed in neutral-current processes ($l^* \to l + Z$) with $f = f' = 1$ or $f = -f' = 1$. The latter ($f = -f' = 1$) is forbidden in the radiative decay $l^* \to l + \gamma$. The leptonic and hadronic decays of Z bosons have been considered in the search, and the most stringent limits are obtained from the hadronic Z decay to be 2.08 (2.34) TeV and 2.11 (2.37) TeV for the e^* and μ^*, respectively, with $f = f' = 1$ ($f = -f' = 1$) at $\Lambda = m_{l^*}$.

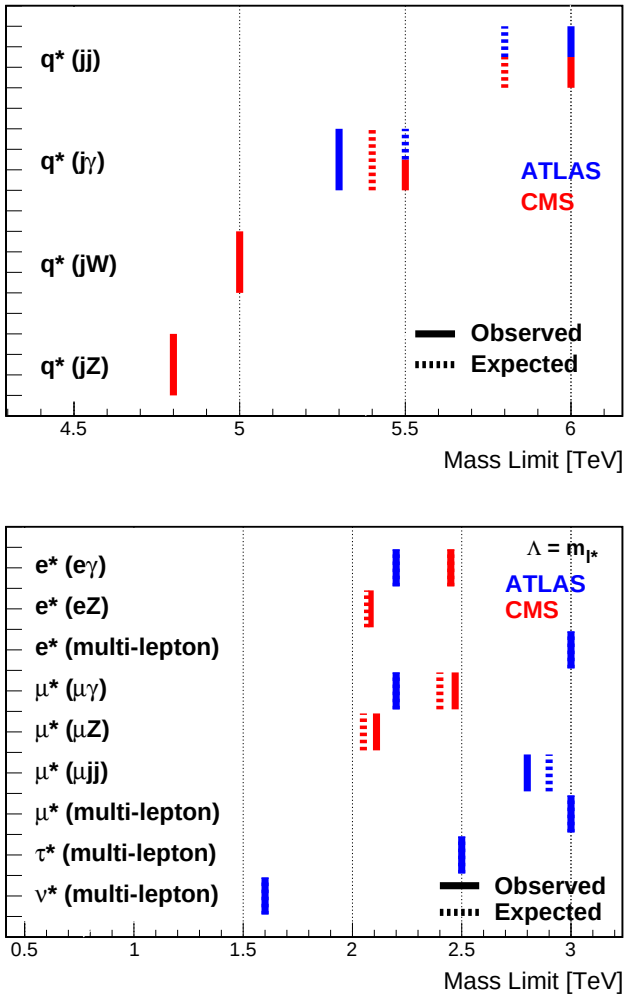

Figure 112.4: 95% C.L. lower mass limits for the excited quarks (top) and excited leptons (bottom) at ATLAS [46,48,54–56] and CMS [60,62,64] [67] experiments. Refs. [60] and [62] are CMS preliminary. Shown are the most stringent limits for each final state (denoted in parentheses) of the excited fermions from both experiments. Only first generation quarks (u, d) with transition-magnetic type interactions with $f_s = f = f' = 1$ are considered for the excited quarks. The excited lepton limits are given for the production via contact interactions with $\Lambda = m_{l^*}$. For the $q^* \to q + g$ ATLAS and CMS have the same observed and expected limits. Also, for the $q^* \to q + \gamma$ the CMS observed and ATLAS expected limits are same. For the excited leptons, the observed and expected limits are same in the ATLAS $l + \gamma$, ATLAS multi-lepton and the CMS $e + \gamma$ searches and hence the expected limit lines are not visible.

Figure 112.4 summarizes the most stringent 95% C.L. lower mass limits for excited quarks and leptons obtained from the LHC experiments.

References:

1. E.J. Eichten, K.D. Lane, and M.E. Peskin, Phys. Rev. Lett. **50**, 811 (1983).
2. E.J. Eichten *et al.*, Rev. Mod. Phys. **56**, 579 (1984); Erratum *ibid.* **58**, 1065 (1986).
3. J. Gao *et al.*, Phys. Rev. Lett. **106**, 142001 (2011).
4. G. Arnison *et al.* [UA1 Collab.], Phys. Lett. **B177**, 244 (1986).

5. J.A. Appel *et al.* [UA2 Collab.], Phys. Lett. **B160**, 349 (1985).
6. F. Abe *et al.* [CDF Collab.], Phys. Rev. Lett. **62**, 613 (1989);
F. Abe *et al.* [CDF Collab.], Phys. Rev. Lett. **69**, 2896 (1992);
F. Abe *et al.* [CDF Collab.], Phys. Rev. Lett. **77**, 5336 (1996);
F. Abe *et al.* [CDF Collab.], Erratum Phys. Rev. Lett. **78**, 4307 (1997).
7. B. Abbott *et al.* [DØ Collab.], Phys. Rev. Lett. **80**, 666 (1998);
B. Abbott *et al.* [DØ Collab.], Phys. Rev. Lett. **82**, 2457 (1999);
B. Abbott *et al.* [DØ Collab.], Phys. Rev. **D62**, 031101 (2000);
B. Abbott *et al.* [DØ Collab.], Phys. Rev. **D64**, 032003 (2001);
B. Abbott *et al.* [DØ Collab.], Phys. Rev. Lett. **103**, 191803 (2009).
8. G. Aad *et al.* [ATLAS Collab.], Phys. Lett. **B694**, 327 (2011);
G. Aad *et al.* [ATLAS Collab.], New J. Phys. **13**, 053044 (2011);
G. Aad *et al.* [ATLAS Collab.], JHEP **01**, 029 (2013);
G. Aad *et al.* [ATLAS Collab.], Phys. Rev. Lett. **114**, 221802 (2015);
G. Aad *et al.* [ATLAS Collab.], Phys. Lett. **B754**, 302 (2016).
9. G. Aad *et al.* [ATLAS Collab.], submitted to Phys. Rev. **D**, arXiv:1703.09127.
10. V. Khachatryan *et al.* [CMS Collab.], Phys. Rev. Lett. **105**, 262001 (2010);
V. Khachatryan *et al.* [CMS Collab.], Phys. Rev. Lett. **106**, 201804 (2011);
S. Chatrchyan *et al.* [CMS Collab.], JHEP **1205**, 055 (2012);
V. Khachatryan *et al.* [CMS Collab.], Phys. Lett. **B746**, 79 (2015);
A.M. Sirunyan *et al.* [CMS Collab.], JHEP **07**, 013 (2017).
11. S. Chatrchyan *et al.* [CMS Collab.], Phys. Rev. **D87**, 052017 (2013).
12. CMS Collaboration, CMS-PAS-EXO-16-046 (2017).
13. T. Sjöstrand, S. Mrenna, and P. Skands, Comp. Phys. Comm. **178**, 852 (2008).
14. S. Agostinelli *et al.* [GEANT4 Collab.], GEANT4: a simulation toolkit, Nucl. Instrum. Methods **A506**, 250 (2003).
15. Z. Nagy, Phys. Rev. Lett. **88**, 122003 (2002);
Z. Nagy, Phys. Rev. **D68**, 094002, (2003).
16. S. Dittmaier, A. Huss, and C. Speckner, JHEP **1211**, 095 (2012).
17. S. Schael *et al.* [ALEPH Collab.], Eur. Phys. J. **C49**, 411 (2007).
18. J. Abdallah *et al.* [DELPHI Collab.], Eur. Phys. J. **C45**, 589 (2006).
19. M. Acciarri *et al.* [L3 Collab.], Phys. Lett. **B489**, 81 (2000).
20. K. Ackerstaff *et al.* [OPAL Collab.], Phys. Lett. **B391**, 221 (1997);
G. Abbiendi *et al.* [OPAL Collab.], Eur. Phys. J. **C33**, 173 (2004).
21. F.D. Aaron *et al.* [H1 Collab.], Phys. Lett. **B705**, 52 (2011).
22. S. Chekanov *et al.* [ZEUS Collab.], Phys. Lett. **B591**, 23 (2004).
23. F. Abe *et al.* [CDF Collab.], Phys. Rev. Lett. **68**, 1463 (1992);
F. Abe *et al.* [CDF Collab.], Phys. Rev. Lett. **79**, 2198 (1997);
T. Affolder *et al.* [CDF Collab.], Phys. Rev. Lett. **87**, 231803 (2001);
A. Abulencia *et al.* [CDF Collab.], Phys. Rev. Lett. **96**, 211801 (2006).
24. B. Abbott *et al.* [DØ Collab.], Phys. Rev. Lett. **82**, 4769 (1999).
25. G. Aad *et al.* [ATLAS Collab.], Phys. Rev. **D84**, 011101 (2011);
G. Aad *et al.* [ATLAS Collab.], Phys. Lett. **B712**, 40 (2012);
G. Aad *et al.* [ATLAS Collab.], Phys. Rev. **D87**, 015010 (2013);
G. Aad *et al.* [ATLAS Collab.], Eur. Phys. J. **C74**, 3134 (2014);
M. Aaboud *et al.* [ATLAS Collab.], Phys. Lett. **B761**, 372 (2016).
26. M. Aaboud *et al.* [ATLAS Collab.], submitted to JHEP, arXiv:1707.02424.
27. S. Chatrchyan *et al.* [CMS Collab.], Phys. Rev. **D87**, 032001 (2013).
28. V. Khachatryan *et al.* [CMS Collab.], JHEP **04**, 025 (2015).
29. W. Buchmuller and D. Wyler, Nucl. Phys. **B268**, 621 (1986).
30. B. Grzadkowski *et al.*, JHEP **1010**, 085 (2010).
31. F.M. Renard, Phys. Lett. **B116**, 264 (1982).
32. F. del Aguila, A. Mendez, and R. Pascual, Phys. Lett. **B140**, 431 (1984).
33. M. Suzuki, Phys. Lett. **B143**, 237 (1984).
34. U. Baur, M. Spira, and P.M. Zerwas, Phys. Rev. **D42**, 815 (1990).
35. K. Hagiwara, D. Zeppenfeld, and S. Komamiya, Z. Phys. **C29**, 115 (1985).
36. N. Cabibbo, L. Maiani, and Y. Srivastava, Phys. Lett. **B139**, 459 (1984).
37. D. Decamp *et al.* [ALEPH Collab.], Phys. Reports **216**, 253 (1992);
P. Barate *et al.* [ALEPH Collab.], Eur. Phys. J. **C4**, 571 (1998).
38. P. Abreu *et al.* [DELPHI Collab.], Nucl. Phys. **B367**, 511 (1991);
J. Abdallah *et al.* [DELPHI Collab.], Eur. Phys. J. **C37**, 405 (2004).
39. O. Adriani *et al.* [L3 Collab.], Phys. Reports **236**, 1 (1993);
P. Achard *et al.* [L3 Collab.], Phys. Lett. **B531**, 28 (2002);
P. Achard *et al.* [L3 Collab.], Phys. Lett. **B568**, 23 (2003).
40. G. Abbiendi *et al.* [OPAL Collab.], Phys. Lett. **B544**, 57 (2002);
G. Abbiendi *et al.* [OPAL Collab.], Phys. Lett. **B602**, 167 (2004).
41. C. Adloff *et al.* [H1 Collab.], Phys. Lett. **B525**, 9 (2002);
F.D. Aaron *et al.* [H1 Collab.], Phys. Lett. **B663**, 382 (2008);
F.D. Aaron *et al.* [H1 Collab.], Phys. Lett. **B666**, 131 (2008).
42. S. Chekanov *et al.* [ZEUS Collab.], Phys. Lett. **B549**, 32 (2002).
43. D. Acosta *et al.* [CDF Collab.], Phys. Rev. Lett. **94**, 101802 (2005);
A. Abulencia *et al.* [CDF Collab.], Phys. Rev. Lett. **97**, 191802 (2006);
T. Aaltonen *et al.* [CDF Collab.], Phys. Rev. **D79**, 112002 (2009).
44. V.M. Abazov *et al.* [DØ Collab.], Phys. Rev. **D73**, 111102 (2006);
V.M. Abazov *et al.* [DØ Collab.], Phys. Rev. **D77**, 091102 (2008);
V.M. Abazov *et al.* [DØ Collab.], Phys. Rev. Lett. **103**, 191803 (2009).
45. G. Aad *et al.* [ATLAS Collab.], Phys. Lett. **B708**, 37 (2012);
G. Aad *et al.* [ATLAS Collab.], JHEP **1301**, 29 (2013);
G. Aad *et al.* [ATLAS Collab.], Phys. Rev. **D91**, 052007 (2015);
G. Aad *et al.* [ATLAS Collab.], Phys. Lett. **B754**, 302 (2016).
46. M. Aaboud *et al.* [ATLAS Collab.], submitted to Phys. Rev. **D**, arXiv:1703.09127.
47. G. Aad *et al.* [ATLAS Collab.], Phys. Rev. Lett. **108**, 211802 (2012);
G. Aad *et al.* [ATLAS Collab.], Phys. Lett. **B728**, 562 (2014).
48. M. Aaboud *et al.* [ATLAS Collab.], CERN-EP-2017-148.
49. ATLAS Collaboration, ATLAS-CONF-2016-060 (2016).
50. M. Aaboud *et al.* [ATLAS Collab.], Phys. Lett. **B759**, 229 (2016).
51. G. Aad *et al.* [ATLAS Collab.], JHEP **1602**, 110 (2016).
52. G. Aad *et al.* [ATLAS Collab.], Phys. Lett. **B721**, 171 (2013).
53. G. Aad *et al.* [ATLAS Collab.], Phys. Rev. **D85**, 072003 (2012).
54. G. Aad *et al.* [ATLAS Collab.], New J. Phys. **15**, 093011 (2013).
55. G. Aad *et al.* [ATLAS Collab.] JHEP **1508**, 138 (2015).
56. G. Aad *et al.* [ATLAS Collab.], New J. Phys. **18**, 073021 (2016).
57. S. Chatrchyan *et al.* [CMS Collab.], Phys. Lett. **B704**, 123 (2011);
S. Chatrchyan *et al.* [CMS Collab.], JHEP **1301**, 13 (2013);
S. Chatrchyan *et al.* [CMS Collab.], Phys. Rev. **D87**, 114015 (2013).
58. V. Khachatryan *et al.* [CMS Collab.], Phys. Rev. **D91**, 052009 (2015).
59. V. Khachatryan *et al.* [CMS Collab.], Phys. Rev. Lett. **116**, 071801 (2016);
V. Khachatryan *et al.* [CMS Collab.], Phys. Rev. Lett. **117**, 031802 (2016);
A.M. Sirunyan *et al.* [CMS Collab.], Phys. Lett. **B769**, 520 (2017).
60. CMS Collaboration, CMS-PAS-EXO-16-056 (2017).
61. V. Khachatryan *et al.* [CMS Collab.], Phys. Lett. **B738**, 274 (2014).
62. CMS Collaboration, CMS-PAS-EXO-17-002 (2017).

63. S. Chatrchyan *et al.* [CMS Collab.], Phys. Lett. **B722**, 28 (2013);
S. Chatrchyan *et al.* [CMS Collab.], Phys. Lett. **B723**, 280 (2013);
V. Khachatryan *et al.* [CMS Collab.], JHEP **1408**, 173 (2014).
64. A.M. Sirunyan *et al.* [CMS Collab.], submitted to Phys. Rev. **D**, arXiv:1708.05379.
65. V. Khachatryan *et al.* [CMS Collab.], JHEP **1601**, 166 (2016).
66. S. Chatrchyan *et al.* [CMS Collab.], Phys. Lett. **B704**, 143 (2011);
S. Chatrchyan *et al.* [CMS Collab.], Phys. Lett. **B720**, 309 (2013).
67. V. Khachatryan *et al.* [CMS Collab.], JHEP **1603**, 125 (2016).
68. M. Cacciari, G.P. Salam, and G. Soyez, JHEP **0804**, 063 (2008).
69. T. Sjöstrand *et al.*, Comp. Phys. Comm. **135**, 238 (2001).

113. Dynamical Electroweak Symmetry Breaking: Implications of the H^0

Updated August 2017 by K.M. Black (Boston University), R.S. Chivukula (Michigan State University), and M. Narain (Brown University).

113.1. Introduction and Phenomenology

In theories of dynamical electroweak symmetry breaking, the electroweak interactions are broken to electromagnetism by the vacuum expectation value of a composite operator, typically a fermion bilinear. In these theories, the longitudinal components of the massive weak bosons are identified with composite Nambu-Goldstone bosons arising from dynamical symmetry breaking in a strongly-coupled extension of the standard model. Viable theories of dynamical electroweak symmetry breaking must also explain (or at least accommodate) the presence of an additional composite scalar state to be identified with the H^0 scalar boson [1,2] – a state unlike any other observed so far.

Theories of dynamical electroweak symmetry breaking can be classified by the nature of the composite singlet state to be associated with the H^0, and the corresponding dimensional scales f, the analog of the pion decay-constant in QCD, and Λ, the scale of the underlying strong dynamics.[1] Of particular importance is the ratio v/f, where $v^2 = 1/(\sqrt{2}G_F) \approx (246\,\text{GeV})^2$, since this ratio measures the expected size of the deviations of the couplings of a composite Higgs boson from those expected in the standard model. The basic possibilities, and the additional states that they predict, are described below.

113.1.1. *Technicolor, $v/f \simeq 1$, $\Lambda \simeq 1$ TeV*:

Technicolor models [8–10] incorporate a new asymptotically free gauge theory ("technicolor") and additional massless fermions ("technifermions" transforming under a vectorial representation of the gauge group). The global chiral symmetry of the fermions is spontaneously broken by the formation of a technifermion condensate, just as the approximate chiral symmetry in QCD is broken down to isospin by the formation of a quark condensate. The $SU(2)_W \times U(1)_Y$ interactions are embedded in the global technifermion chiral symmetries in such a way that the only unbroken gauge symmetry after chiral symmetry breaking is $U(1)_{em}$.[2] These theories naturally provide the Nambu-Goldstone bosons "eaten" by the W and Z boson. There would also typically be additional heavy states (e.g. vector mesons, analogous to the ρ and ω mesons in QCD) with TeV masses [14,15], and the WW and ZZ scattering amplitudes would be expected to be strong at energies of order 1 TeV.

There are various possibilities for the scalar H^0 in technicolor models, as described below.[3] In all of these cases, however, to the extent that the H^0 has couplings consistent with those of the standard model [16], these theories are very highly constrained.

a) H^0 **as a singlet scalar resonance:** The strongly-interacting fermions which make up the Nambu-Goldstone bosons eaten by the weak bosons would naturally be expected to also form an isoscalar neutral bound state, analogous to the σ particle expected in pion-scattering in QCD [17]. However, in this case, there is no symmetry protecting the mass of such a particle – which would therefore generically be of order the energy scale of the underlying strong dynamics Λ. In the simplest theories of this kind – those with a global $SU(2)_L \times SU(2)_R$ chiral symmetry which is spontaneously broken to $SU(2)_V$ – the natural dynamical scale Λ would be of order a TeV, resulting in a particle too heavy and broad to be identified with the H^0. The scale of the underlying interactions could naturally be smaller than 1 TeV if the global symmetries of the theory are larger than $SU(2)_L \times SU(2)_R$, but in this case there would be additional (pseudo-)Nambu-Goldstone bosons (more on this below). A theory of this kind would only be viable, therefore, if some choice of the parameters of the high energy theory could give rise to sufficiently light state without the appearance of additional particles that should have already been observed. Furthermore, while a particle with these quantum numbers could have Higgs-like couplings to any electrically neutral spin-zero state made of quarks, leptons, or gauge-bosons, there is no symmetry insuring that the coupling strengths of such a composite singlet scalar state would be precisely the same as those of the standard model Higgs [18].

b) H^0 **as a dilaton:** It is possible that the underlying strong dynamics is approximately scale-invariant, as inspired by theories of "walking technicolor" [19–23], and that both the scale and electroweak symmetries are spontaneously broken at the TeV energy scale [24]. In this case, due to the spontaneous breaking of approximate scale invariance, one might expect a corresponding (pseudo-) Nambu-Goldstone boson [20] with a mass less than a TeV, the dilaton.[4] A dilaton couples to the trace of the energy momentum tensor, which leads to a similar pattern of two-body couplings as the couplings of the standard model Higgs boson [29–31]. Scale-invariance is a space-time symmetry, however, and is unrelated to the global symmetries that we can identify with the electroweak group. Therefore the decay-constants associated with the breaking of the scale and electroweak symmetries will not, in general, be the same.[5] In other words, if there are no large anomalous dimensions associated with the W- and Z-bosons or the top- or bottom-quarks, the ratios of the couplings of the dilaton to these particles would be the same as the ratios of the same couplings for the standard model Higgs boson, but the overall strength of the dilaton couplings would be expected to be different [32,33]. Furthermore, the couplings of the dilaton to gluon- and photon-pairs can be related to the beta functions of the corresponding gauge interactions in the underlying high-energy theory, and will not in general yield couplings with the exactly the same strengths as the standard model [34,35].

c) H^0 **as a singlet Pseudo-Nambu-Goldstone Boson:** If the global symmetries of the technicolor theory are larger than $SU(2)_L \times SU(2)_R$, there can be extra singlet (pseudo-) Nambu-Goldstone bosons which could be identified with the H^0. In this case, however, the coupling strength of the singlet state to WW and ZZ pairs would be comparable to the couplings to gluon and photon pairs, and these would all arise from loop-level couplings in the underlying technicolor theory [36]. This pattern of couplings is not supported by the data.

113.1.2. *The Higgs doublet as a pseudo-Nambu-Goldstone Boson, $v/f < 1$, $\Lambda > 1$ TeV*:

In technicolor models, the symmetry-breaking properties of the underlying strong dynamics necessarily breaks the electroweak gauge symmetries. An alternative possibility is that the underlying strong dynamics itself does not break the electroweak interactions, and that the entire quartet of bosons in the Higgs doublet (including the state associated with the H^0) are composite (pseudo-) Nambu-Goldstone particles [37,38], In this case, the underlying dynamics can occur at energies larger than 1 TeV and additional interactions with the top-quark mass generating sector (and possibly with additional weakly-coupled gauge bosons) cause the vacuum energy to be minimized when the composite Higgs doublet gains a vacuum expectation value [39,40]. In these theories, the couplings of the remaining singlet scalar state would naturally be equal to that of the standard model Higgs boson up to corrections of order $(v/f)^2$ and, therefore, constraints on the

[1] In a strongly interacting theory "Naive Dimensional Analysis" [3,4] implies that, in the absence of fine-tuning, $\Lambda \simeq g^* f$ where $g^* \simeq 4\pi$ is the typical size of a strong coupling in the low-energy theory [5,6]. This estimate is modified in the presence of multiple flavors or colors [7].

[2] For a review of technicolor models, see [11–13].

[3] In these models, the self-coupling of the H^0 scalar is not related to its mass, as it is in the SM – though there are currently no experimental constraints on this coupling.

[4] Even in this case, however, a dilaton associated with electroweak symmetry breaking will likely not *generically* be as light as the H^0 [25–28].

[5] If both the electroweak symmetry and the approximate scale symmetry are broken only by electroweak doublet condensate(s), then the decay-constants for scale and electroweak symmetry breaking may be approximately equal – differing only by terms formally proportional to the amount of explicit scale-symmetry breaking.

size of deviations of the H^0 couplings from that of the standard model Higgs [16] give rise to lower bounds on the scales f and Λ.[6]

The electroweak gauge interactions, as well as the interactions responsible for the top-quark mass, explicitly break the chiral symmetries of the composite Higgs model, and lead generically to sizable corrections to the mass-squared of the Higgs-doublet – the so-called "Little Hierarchy Problem" [41]. "Little Higgs" theories [42–45] are examples of composite Higgs models in which the (collective) symmetry-breaking structure is selected so as to suppress these contributions to the Higgs mass-squared.

Composite Higgs models typically require a larger global symmetry of the underlying theory, and hence additional relatively light (compared to Λ) scalar particles, extra electroweak vector bosons (e.g. an additional $SU(2) \times U(1)$ gauge group), and vector-like partners of the top-quark of charge $+2/3$ and possibly also $+5/3$ [46]. In addition to these states, one would expect the underlying dynamics to yield additional scalar and vector resonances with masses of order Λ. If the theory respects a custodial symmetry [47], the couplings of these additional states to the electroweak and Higgs boson will be related – and, for example, one might expect a charged vector resonance to have similar branching ratios to WZ and WH. Different composite Higgs models utilize different mechanisms for arranging for the hierarchy of scales $v < f$ and arranging for a scalar Higgs self-coupling small enough to produce an H^0 of mass of order 125 GeV, for a review see [48]. If the additional states in these models carry color, they can provide additional contributions to Higgs production via gluon fusion [49]. The extent to which Higgs production at the LHC conforms with standard model predictions provides additional constraints (typically lower bounds on the masses of the additional colored states of order 0.7 TeV) on these models.

In addition, if the larger symmetry of the underlying composite Higgs theory does not commute with the standard model gauge group, then the additional states found in those models – especially those related to the top-quark, which tend to have the largest couplings to the electroweak sector – may be *colorless*. For example, in twin Higgs models [50], the top-partners carry no standard model charges. The phenomenology of the additional states such theories are rather different, since lacking color the production these particles at the LHC will be suppressed – and, their decays may occur only via the electroweak symmetry breaking sector, leading to their being long-lived.

113.1.3. *Top-Condensate, Top-Color, Top-Seesaw and related theories, $v/f < 1$, $\Lambda > 1$ TeV* :

A final alternative is to consider a strongly interacting theory with a high (compared to a TeV) underlying dynamical scale that *would* naturally break the electroweak interactions, but whose strength is adjusted ("fine-tuned") to produce electroweak symmetry breaking at 1 TeV. This alternative is possible if the electroweak (quantum) phase transition is continuous (second order) in the strength of the strong dynamics [51]. If the fine tuning can be achieved, the underlying strong interactions will produce a light composite Higgs bound state with couplings equal to that of the standard model Higgs boson up to corrections of order $(1\ \text{TeV}/\Lambda)^2$. As in theories in which electroweak symmetry breaking occurs through vacuum alignment, therefore, constraints on the size of deviations of the H^0 couplings from that of the standard model Higgs give rise to lower bounds on the scale Λ. Formally, in the limit $\Lambda \to \infty$ (a limit which requires arbitrarily fine adjustment of the strength of the high-energy interactions), these theories are equivalent to a theory with a fundamental Higgs boson – and the fine adjustment of the coupling strength is a manifestation of the hierarchy problem of theories with a fundamental scalar particle.

In many of these theories the top-quark itself interacts strongly (at high energies), potentially through an extended color gauge sector [52–56]. In these theories, top-quark condensation (or the condensation of an admixture of the top with additional vector-like quarks) is responsible for electroweak symmetry breaking, and the H^0 is identified with a bound state involving the third generation of quarks. These theories typically include an extra set of massive color-octet vector bosons (top-gluons), and an extra $U(1)$ interaction (giving rise to a top-color Z') which couple preferentially to the third generation and whose masses define the scale Λ of the underlying physics.

113.1.4. *Flavor* :

In addition to the electroweak symmetry breaking dynamics described above, which gives rise to the masses of the W and Z particles, additional interactions must be introduced to produce the masses of the standard model fermions. Two general avenues have been suggested for these new interactions. In one case, e.g. "extended technicolor" (ETC) theories [57,58], the gauge interactions in the underlying strongly interacting theory are extended to incorporate flavor. This extended gauge symmetry is broken down (possibly sequentially, at several different mass scales) to the residual strong interaction responsible for electroweak symmetry breaking. The massive gauge-bosons corresponding to the broken symmetries then mediate interactions between mass operators for the quarks/leptons and the corresponding bilinears of the strongly-interacting fermions, giving rise to the masses of the ordinary fermions after electroweak symmetry breaking. An an alternative proposal, "partial compositeness" [59], the additional interactions giving rise to mixing between the ordinary quarks and leptons and massive composite fermions in the strongly-interacting underlying theory. Theories incorporating partial compositeness include additional vector-like partners of the ordinary quarks and leptons, typically with masses of order a TeV or less.

In both cases, the effects of these flavor interactions on the electroweak properties of the ordinary quarks and leptons are likely to be most pronounced in the third generation of fermions.[7] The additional particles present, especially the additional scalars, often couple more strongly to heavier fermions.

Moreover, since the flavor interactions must give rise to quark mixing, we expect that a generic theory of this kind could give rise to large flavor-changing neutral-currents [58]. In ETC theories, these constraints are typically somewhat relaxed if the theory incorporates approximate generational flavor symmetries [60], the theory "walks" [19–23], or if $\Lambda > 1$ TeV [61]. In theories of partial compositeness, the masses of the ordinary fermions depend on the scaling-dimension of the operators corresponding to the composite fermions with which they mix. This leads to a new mechanism for generating the mass-hierarchy of the observed quarks and leptons that, potentially, ameliorates flavor-changing neutral current problems and can provide new contributions to the composite Higgs potential which allows for $v/f < 1$ [62–66].

Alternatively, one can assume that the underlying flavor dynamics respects flavor symmetries ("minimal" [67,68] or "next-to-minimal" [69] flavor violation) which suppress flavor-changing neutral currents in the two light generations. Additional considerations apply when extending these arguments to potential explanation of neutrino masses (see, for example, [70,71]) .

Since the underlying high-energy dynamics in these theories are strongly coupled, there are no reliable calculation techniques that can be applied to analyze their properties. Instead, most phenomenological studies depend on the construction of a "low-energy" effective theory describing additional scalar, fermion, or vector

[6] In these models v/f is an adjustable parameter, and in the limit $v/f \to 1$ they reduce, essentially, to the technicolor models discussed in the previous subsection. Our discussion here is consistent with that given there, since we expect corrections to the SM Higgs couplings to be large for $v/f \simeq 1$. Current measurements constrain the couplings of the H^0 to equal those predicted for the Higgs in the standard model to about the 10% level [16], suggesting that f must have values of order a TeV or higher and, therefore, a dynamical scale Λ of at least several TeV.

[7] Indeed, from this point of view, the vector-like partners of the top-quark in top-seesaw and little Higgs models can be viewed as incorporating partial compositeness to explain the origin of the top quark's large mass.

boson degrees of freedom, which incorporates the relevant symmetries and, when available, dynamical principles. In some cases, motivated by the AdS/CFT correspondence [72], the strongly-interacting theories described above have been investigated by analyzing a dual compactified five-dimensional gauge theory. In these cases, the AdS/CFT "dictionary" is used to map the features of the underlying strongly coupled high-energy dynamics onto the low-energy weakly coupled dual theory [73].

More recently, progress has been made in investigating strongly-coupled models using lattice gauge theory [74]. These calculations offer the prospect of establishing which strongly coupled theories of electroweak symmetry breaking have a particle with properties consistent with those observed for the H^0 – and for establishing concrete predictions for these theories at the LHC [75].

113.2. Experimental Searches

As discussed above, the extent to which the couplings of the H^0 conform to the expectations for a standard model Higgs boson constrains the viability of each of these models. Measurements of the H^0 couplings, and their interpretation in terms of effective field theory, are summarized in the H^0 review in this volume. In what follows, we will focus on searches for the additional particles that might be expected to accompany the singlet scalar: extra scalars, fermions, and vector bosons. In some cases, detailed model-specific searches have been made for the particles described above (though generally not yet taking account of the demonstrated existence of the H^0 boson).

In most cases, however, generic searches (e.g. for extra W' or Z' particles, extra scalars in the context of multi-Higgs models, or for fourth-generation quarks) are quoted that can be used – when appropriately translated – to derive bounds on a specific model of interest.

The mass scale of the new particles implied by the interpretations of the low mass of H^0 discussed above, and existing studies from the Tevatron and lower-energy colliders, suggests that only the Large Hadron Collider has any real sensitivity. A number of analyses already carried out by ATLAS and CMS use relevant final states and might have been expected to observe a deviation from standard model expectations – in no case so far has any such deviation been reported. The detailed implications of these searches in various model frameworks are described below.

Except where otherwise noted, all limits in this section are quoted at a confidence level of 95%. The searches at $\sqrt{s}$ = 8 TeV (Run 1) are based on 20.3 fb^{-1} of data recorded by ATLAS, and an integrated luminosity of 19.7 fb^{-1} analyzed by CMS. The datasets collected at $\sqrt{s}$ = 13 TeV during Run 2 of the LHC since 2015 are based on analyses with varied integrated luminosities ranging between ∼2-36fb^{-1}.

113.2.1. *Searches for Z′ or W′ Bosons* :

Massive vector bosons or particles with similar decay channels would be expected to arise in Little Higgs theories, in theories of Technicolor, or models involving a dilaton, adjusted to produce a light Higgs boson, consistent with the observed H^0. These particles would be expected to decay to pairs of vector bosons, to third generation quarks, or to leptons. The generic searches for W' and Z' vector bosons listed below can, therefore, be used to constrain models incorporating a composite Higgs-like boson.

A general review of searches for Z' and W' bosons is also included in this volume [76,77]. In the context of the dynamical electroweak symmetry breaking models, we emphasize their decays to third generation fermions by including a detailed overview, while also briefly summarizing the other searches.

$Z' \to \ell\ell$:

ATLAS [78] and CMS [79] have both searched for Z' production with $Z' \to ee$ or $\mu\mu$. No deviation from the standard model prediction was seen in the dielectron and dimuon invariant mass spectra, by either the ATLAS or the CMS analysis, and lower limits on possible Z' boson masses were set. A $Z'_{\rm SSM}$ with couplings equal to the standard model Z (a "sequential standard model" Z') and a mass below 4.5 TeV was excluded by ATLAS, while CMS set a lower mass limit of 4.0 TeV. The experiments also place limits on the parameters of extra dimension models and in the case of ATLAS on the parameters of a minimal walking technicolor model [19–23], consistent with a 125 GeV Higgs boson [80]. For a general review of searches in these channels see the PDG review of Z prime in this volume [76].

In addition, both experiments have also searched for Z' decaying to a ditau final state [81,82]. While less sensitive than dielectron or dimuon final states, an excess in $\tau^+\tau^-$ could have interesting implications for models in which lepton universality is not a requirement and enhanced couplings to the third generation are allowed. This analysis led to lower limits on the mass of a $Z'_{\rm SSM}$ of 2.4 and 2.1 TeV from ATLAS and CMS respectively.

$Z' \to q\overline{q}$:

The ability to relatively cleanly select $t\bar{t}$ pairs at the LHC together with the existence of enhanced couplings to the third generation in many models makes it worthwhile to search for new particles decaying in this channel. Both ATLAS [84] and CMS [83] have carried out searches for new particles decaying into $t\bar{t}$.

ATLAS focused on the lepton plus jets final state, where the top quark pair decays as $t\bar{t} \to WbWb$ with one W boson decaying leptonically and the other hadronically; CMS used final states where both, one or neither W decays leptonically and then combined the results. The $t\bar{t}$ invariant mass spectrum was analyzed for any excess, and no evidence for any resonance was seen. ATLAS excluded a narrow (Γ/m = 1.2%) leptophobic top-color Z' boson with masses between 0.7 and 2.1 TeV and with Γ/m = 3% between 0.7 and 3.2 TeV. CMS set limits on leptophobic Z' bosons for three different assumed widths Γ/m = 1.0% , Γ/m = 10.0%, and Γ/m = 30.0% of 3.9 TeV to 4.0 TeV and exclude RS KK gluons up to 3.3 TeV.

Both ATLAS [85] and CMS [86] have also searched for resonances decaying into $q\overline{q}$, qg or gg using the dijet invariant mass spectrum. Model-independent upper limits on cross sections were set; ATLAS excluded Z' bosons below 2.1 TeV, W' bosons below 3.6 TeV and chiral W^* bosons below 3.4 TeV. CMS was able to exclude W' bosons below 2.7 TeV; Z' bosons below 2.1 TeV and between 2.3 and 2.6 TeV; color octet scalars below 3.0 TeV; and g_{KK} gravitons below 1.9 TeV. Searches were also carried out for wide resonances, assuming Γ/m up to 30%, and excluded axigluons and colorons with mass below 5.5 TeV. Additionally ATLAS [87] and CMS [88] searched for $Z' \to b\bar{b}$ selecting events where at least one of the jets is b-tagged. ATLAS excluded Z' bosons in the range of 1.1 to 1.5 TeV while CMS excluded masses between 1.2 and 1.68 TeV.

$W' \to \ell\nu$:

Both LHC experiments have also searched for massive charged vector bosons. In this section we include a summary of the results, with emphasis on final states with third generation fermions, while the details on other decays are discussed in the mini-review of W' [77]. ATLAS searched for a heavy W' decaying to $e\nu$ or $\mu\nu$ and find no excess over the standard model expectation. A sequential standard model (SSM) W' boson (assuming zero branching ratio to WZ) with mass less than 5.1 TeV was excluded [89] using 36 fb^{-1} dataset at $\sqrt{s}$ = 13 TeV, and excited chiral bosons W^* excluded up to 3.21 TeV [90](20.3 fb^{-1}, $\sqrt{}$ = 8 TeV). Based on a smaller dataset, the CMS experiment excluded a SSM W' boson with mass up to 4.1 TeV [91] and presented the upper limits on the production of generic W' bosons decaying into this final state using a model-independent approach.

CMS [92] has carried out a complementary search in the $\tau\nu$ final state. As noted above, such searches place interesting limits on models with enhanced couplings to the third generation. No excess was observed and limits between 2.0 and 2.7 TeV were set on the mass of a W' decaying preferentially to the third generation; a W' with universal fermion couplings was also excluded for masses less than 2.7 TeV.

$W' \to t\overline{b}$:

Heavy new gauge bosons can couple to left-handed fermions like the SM W boson or to right-handed fermions. W' bosons that couple only to right-handed fermions (W'_R) may not have leptonic decay modes, depending on the mass of the right-handed neutrino. For these W' bosons, the tb ($t\overline{b} + \overline{t}b$) decay mode is especially important because in many models the W' boson is expected to have enhanced couplings

to the third generation of quarks relative to those in the first and second generations. It is also the hadronic decay mode with the best signal-to-background. ATLAS and CMS have performed searches for W' bosons via the $W' \to$ tb decay channel in the lepton+jets and all-hadronic final state.

The CMS lepton+jets search [93,94,95,96], $W' \to$ tb $\to$ Wbb $\to \ell\nu$bb, proceeded via selecting events with an isolated lepton (electron or muon), and at least two jets, one of which is identified to originate from a b-quark. The mass of the W' boson ($M_{\rm tb}$) was reconstructed using the four-momentum vectors of the final state objects (bb$\ell\nu$). The distribution of $M_{\rm tb}$ is used as the search discriminant. A search [96] using 35.9fb^{-1} of data, collected at $\sqrt{s} = 13$ TeV, led to an exclusion of W'_R bosons with masses below 3.4 TeV (3.6 TeV) if $M_{W'_R} >> M_{\nu_R}$ ($M_{W'_R} < M_{\nu_R}$), where M_{ν_R} is the mass of the right-handed neutrino.

The CMS search for $W' \to$tb decays using the all-hadronic final state focused on W' masses above 1 TeV [95]. In this region, the top quark gets a large Lorentz boost and hence the three hadronic products from its decay merge into a single large-radius jet. Techniques which rely on substructure information of the jets [97] are employed to identify boosted W and top quark jets and compute the mass of the jet. W' candidate mass was computed from back-to-back boosted top tagged jet and a low mass b tagged jet. From this all-hadronic search, W' bosons were excluded for masses up to 2.02 TeV.

ATLAS has searched for W'_R bosons in the $t\bar{b}$ final state both for lepton+jets [98] and all-hadronic [99] decays of the top. No significant deviations from the standard model were seen in either analysis and limits were set on the $W' \to t\bar{b}$ cross section times branching ratio and W' bosons with purely left-handed (right-handed) couplings to fermions were excluded for masses below 1.70 (1.92) TeV.

In addition, the above studies also provided upper limits on the W' effective couplings to right- and left-handed fermions. In Fig. 113.1 (bottom) the upper limits on W' couplings normalized to the SM W couplings derived by ATLAS [98] are shown. The top panel of Fig. 113.1 shows the upper limits for arbitrary combinations of left- and right-handed couplings of the W' boson to fermions set using a model independent approach by CMS [96].

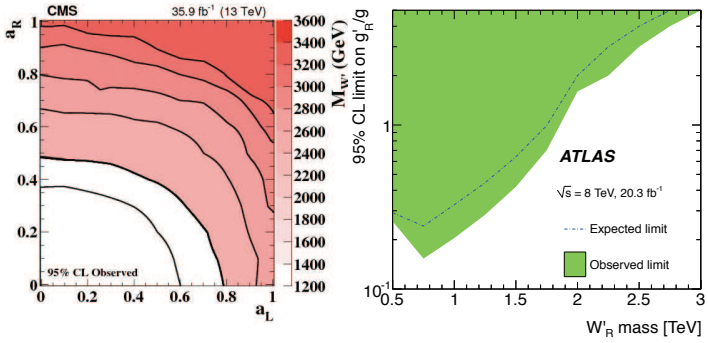

Figure 113.1: Left panel: Observed limits on the W' boson mass as function of the left-handed ($a_{\rm L}$) and right-handed ($a_{\rm R}$) couplings. Black lines represent contours of equal W' boson mass [96]. Right panel: Observed and expected regions, on the g$'$/g vs mass of the W' -boson plane, that are excluded at 95% CL, for right-handed W' bosons [98].

113.2.2. *Searches for Resonances decaying to Vector Bosons and/or Higgs Bosons* :

$X \to WW, WZ, ZZ$:

Both the ATLAS and CMS experiments have used the data collected at $\sqrt{s} = 8$ TeV and $\sqrt{s} = 13$ TeV to search for resonances decaying to pairs of bosons. Overall no significant excesses were seen in the full datasets that were analyzed and the results are interpreted in models with heavy vector triplets (HVT) [100], models with strong gravity and extra spatial dimensions, as well as setting model independent limits as a function of mass. For a full review of models including extra spatial dimensions including the interpretation of many of these results in that context please see the review of extra dimensions in this volume [73].

Utilizing data collected at $\sqrt{s} = 8$ TeV, ATLAS [101] and CMS [102] have both looked for a resonant state (such as a W') decaying to WZ in the fully-leptonic channel, $\ell\nu\ell'\ell'$ (where $\ell, \ell' = e, \mu$). The WZ invariant mass distribution reconstructed from the observed lepton momenta missing transverse energy. The backgrounds arise mainly from standard model WZ, ZZ and $t\bar{t} + W/Z$ production. No significant deviation from the standard model prediction is observed by either experiment. A W' with mass less than 1.55 (1.52) TeV is excluded by CMS (ATLAS); ATLAS also sets limits on the production cross section for HVT particles, and CMS sets limits on the production of low-scale technimesons ρ_{TC} from the reconstructed WZ mass spectrum and cross section.

ATLAS [103,104] and CMS [105] have also searched for narrow resonances decaying to WW, WZ or ZZ in $\ell\nu jj$ and $\ell\ell jj$ final states (where one boson decays leptonically and the other to jets) in data recorded at $\sqrt{s} = 13$ TeV. No deviation from the standard model is seen by either experiment; resonance masses below 2.750 TeV for a HVT model decaying into WW and 2.820 TeV decaying into WZ by ATLAS and below 2.4 TeV by CMS.

Searches have also been conducted in fully hadronic final states. ATLAS [106] and CMS [107] have searched for massive resonance in dijet systems with one or both jets identified as a W or a Z boson using jet-substructure techniques. Limits are set by both experiments on the production cross section times branching ratio for new HVT particles decaying to WZ and ZZ and for g_{KK} gravitons decaying to WW or ZZ. ATLAS excludes HVT particles between 1.2 and 3.5 TeV while CMS excludes W' bosons below 3.6 TeV and Z' bosons below 2.7 TeV.

$X \to W/Z + H^0$ and $X \to H^0H^0$:

With the existence and decay properties of the Higgs boson established, and the significant datasets now available, it is possible to use searches for anomalous production of the Higgs as a potential signature for new physics. ATLAS [108,109] and CMS [110,111] have both searched in the data collected at $\sqrt{s} = 13$ TeV for new particles decaying to a vector boson plus a Higgs boson, where the vector boson decays leptonically or hadronically and the Higgs boson to $b\bar{b}$. No deviation from the standard model is seen in any of these final states and limits can be placed on the allowed production cross section times branching ratio for resonances on a heavy vector triplet model. The exact limits depend on the parameters considered but exclude HVT particles with a mass up to 3.8 TeV. Both experiments also place model-independent limits on the production cross-section as a function of mass.

Both experiments [112,113,114] have also searched for resonant production of Higgs boson pairs $X \to H^0H^0$ with $H^0 \to b\bar{b}$. No signal is observed and limits are placed on the possible production cross section for any new resonance and cross-section limits are placed between 1000 fb and 2 fb for masses between 0.3and 3.0 TeV on resonant production. ATLAS places additionally places limits on non-resonant Standard Model Higgs production constrained to be less than 330 fb.

$Y \to W/Z + X$ with $X \to jj$:

ATLAS has searched for a dijet resonance [115] with an invariant mass in the range $130 - 300$ GeV, produced in association with a W or a Z boson. The analysis used 20.3 fb^{-1} of data recorded at $\sqrt{s} = 8$ TeV. The W or Z boson is required to decay leptonically ($\ell = e, \mu$). No significant deviation from the standard model prediction is observed and limits are set on the production cross section times branching ratio for a hypothetical technipion produced in association with a W or Z boson from the decay of a technirho particle in the context of Low Scale Technicolor models.

ATLAS [116] has searched for a resonance (Y) decaying into XH where $H \to bb$ and a new particle X decays into dijet pairs ($X \to jj$). A two dimensional scan in both Y, between 1 and 4 TeV, and X masses, between 0.05 and 1 TeV is performed. No significant excesses are seen and upper limits on the cross-section of this process are set as a function of X and Y.

Summary of Searches with Diboson Final States:

Both ATLAS [117] and CMS [118] provide plots summarizing the various searches results and limits. The results are shown in the context of HVT models and models of strong gravity with extra spatial dimensions. No excess is seen in any search and limits on the W' are placed up to 3.5 TeV and 2.7 TeV on Z' particles in the HVT model as seen in Fig. 113.2

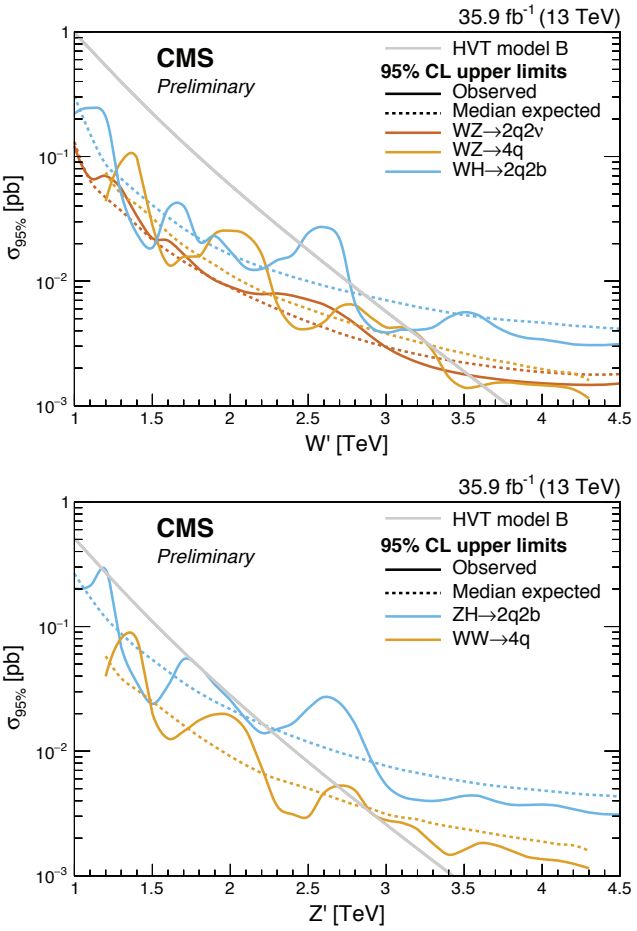

Figure 113.2: Top panel: Observed limits from W' to diboson from CMS [118]. Bottom panel: Observed limits from Z' to diboson decays from CMS [118]. Note in both cases ATLAS provides similar summary plots which are available [117].

113.2.3. *Vector-like third generation quarks* :

Vector-like quarks (VLQ) have non-chiral couplings to W bosons, i.e. their left- and right-handed components couple in the same way. They therefore have vectorial couplings to W bosons. Vector-like quarks arise in Little Higgs theories, top-coloron-models, and theories of a composite Higgs boson with partial compositeness. In the following, the notation T quark refers to a vector-like quark with charge 2/3 and the notation B quark refers to a vector-like quark with charge $-1/3$, the same charges as the SM top and b quarks respectively. The X and Y have charges 5/3, and $-4/3$ respectively. Vector-like quarks couple with SM quarks with Yukawa interactions and may exist as SU(2) singlets (T, and B), doublets $[(X,T),(T,B),(B,Y)]$, or triplets $[(X,T,B),\ (T,B,Y)]$. At the LHC, VLQs can be pair produced via the dominant gluon-gluon fusion. VLQs can also be produced singly by their electroweak effective couplings to a weak boson and a standard model quark. Single production rate is expected to dominate over the rate of pair production at large VLQ masses. T quarks can decay to bW, tZ, or tH^0. Weak isospin singlets are expected to decay to all three final states with (asymptotic) branching fractions of 50%, 25%, 25%, respectively. Weak isospin doublets are expected to decay exclusively to tZ and to tH^0 [119] with equal branching ratios. Analogously, B quarks can decay to tW, bZ, or bH^0. The Y and X quarks decay exclusively to bW and to tW. While these are taken as the benchmark scenarios, other representations are possible and hence the final results are interpreted for many allowed branching fraction combinations.

Given the multiple decay modes of the VLQs, the final state signatures of both pair produced and the singly produced VLQs are fairly rich with leptons, jets, b-jets, and missing energy. Depending on the mass of the VLQ, the top quarks and $W/Z/H^0$ bosons may be Lorentz boosted and identified using jet substructure techniques. Thus the searches are performed using lepton+jets signatures, multi-lepton and all-hadronic decays. In addition, T or B quarks with their antiparticles can result in events with same-sign leptons, for example if the decay $T \to tH \to bWW^+W^-$ is present, followed by leptonic decays of two same-sign W bosons. In the following subsections, while we describe the searches for each of the decay modes of the VLQs, the same analysis can be re-interpreted to obtain the sensitivity to a combination with varied branching fractions to the different decay modes.

In the following sections, the results obtained for T (B) quarks assuming 100% branching ratio to Wb (Wt) are also applicable to heavy vector-like Y (X) with charge 4/3 (5/3).

113.2.3.1. *Searches for T quarks that decay to W, Z and H^0 bosons:*

$T/Y \to bW$:

CMS has searched for pair production of heavy T quarks that decay exclusively to bW [120,121,122]. The analysis selected events with exactly one charged lepton, assuming that the W boson from the second T quark decays hadronically. Under this hypothesis, a 2-constraint kinematic fit can be performed to reconstruct the mass of the T quark. In Ref. 121 and Ref. 122, the two-dimensional distribution of reconstructed mass vs S_T was used to test for the signal. S_T is the scalar sum of the missing p_T and the transverse momenta of the lepton and the leading four jets. This analysis, when combined with the search in the fully hadronic final state [123] excluded new quarks that decay 100% to bW for masses below 0.89 TeV [122]. At times the hadronically-decaying W boson is produced with a large Lorentz boost, leading to the W decay products merged into a wide single jet also known as a fat jet. Algorithms such as jet pruning [124] were used to resolve the substructure of the fat jets from the decays of the heavy particles. If the mass of the boosted jet was compatible with the W boson mass, then the W boson candidate jet and its subjets were used in the kinematic reconstruction of the T quark. No excess over standard model backgrounds was observed. Upper limits on the production cross section as a function of the mass of T quarks were measured. By comparing them with the predicted cross section for vector like quark pair production, the strong pair production of T quarks was excluded for masses below 1.30 TeV (1.28 TeV expected) [120].

An analogous search has been carried out by ATLAS [125], [126] for the pair production of heavy T quarks. It used the lepton+jets final state with an isolated electron or muon and at least four jets, including a b-jet and required reconstruction of the T quark mass. Given the mass range of the T quark being explored was from a 0.4 TeV to a couple of TeV, the W boson from the T quark may fall in two categories: those with a high boost leading to merged decay products, and others where the two jets from the W boson were resolved. In addition, the selection was optimized to require large angular separation between the high p_T W bosons and the b-jets. The $T \to Wb$ candidates were constructed from both the leptonically and hadronically decaying W bosons by pairing them with the two highest p_T b-tagged jets in the event. The pairing of b-jets with W bosons which minimizes the difference between the masses of leptonically decaying T ($m_{lep}(T)$) and the hadronic T ($m_{had}(T)$) was chosen. Finally, $m_{lep}(T)$ was used as the discriminating variable in a signal region defined by high S_T, the scalar sum of the missing p_T, the p_T of the lepton and jets, and the opening angle between the lepton and the neutrino ($\Delta\ R(e,\nu)$). With the 36.1fb^{-1} data collected during

Run 2 at $\sqrt{s}$ = 13 TeV, assuming 100% branching ratio to the Wb decay, the observed lower limit on the T mass was 1.35 TeV, and in the SU(2) singlet scenario, the lower mass limit was obtained to be 1.17 TeV [125].

A targeted search for a T quark, produced singly in association with a light flavor quark and a b quark and decaying into bW, was carried out by CMS at $\sqrt{s}$=13 teV and a dataset corresponding to 2.3fb^{-1} [127]. The anlaysis used lepton+jets events, with at least one b-tagged jet with large transverse momentum, and a jet in the forward η region. Selected events were required to have $S_T > 500$ GeV, where S_T is defined as the scalar sum of the transverse momenta of the lepton, the leading central jet, and the missing transverse momentum. The invariant mass of the T candidate was used as the discriminating variable and was reconstructed using the four-vectors of the leptonically decaying W boson and the leading central jet. No excess over the standard model prediction was observed. As the VLQ width is proportional to the square of the coupling, upper limits were set on the production cross section assuming a narrow width VLQ with coupling greater than 0.5. For Y/T quarks with a coupling of 0.5 and a 100% branching fraction for the decay to bW the excluded masses were in the range from 0.85 to 1.40 TeV [127]. A similar search [128,129] performed by ATLAS, for singlet T quarks, with coupling of $\sqrt{(c_L{}^{Wb})2 + (c_R{}^{Wb})^2} = \frac{1}{\sqrt{2}}$, and $\mathcal{B}(T \to bW) = 0.5$, led to exclusion limits on T/Y masses below 1.44 TeV. This search also provided limits, as a function of the Y quark mass, on the coupling of the Y quark to bW, and the mixing parameter $|sin\theta_R|$ for a (Y,B) doublet model [128]. For a VLQ mass around 1 TeV, the smallest excluded coupling-strength values are obtained, with $|c_L^{Wb}|$=0.45 for a T quark and $\sqrt{(c_L{}^{Wb})2 + (c_R{}^{Wb})^2}$=0.33 for a Y quark. The limit on $|sin\theta_R|$ is around 0.23, and close to the constraints from electroweak precision observables.

$T \to tH^0$:

ATLAS has performed a search for $T\overline{T}$ production with $T \to tH^0$ [126], [130]. Given the dominant decay mode $H^0 \to b\overline{b}$, these events are characterized by a large number of jets, many of which are b-jets. Thus the event selection required one isolated electron or muon and high jet multicplicity (including b tagged jets). The sample is categorized by the jet multiplicity (5 and ≥6 jets in the 1-lepton channel; 6 and ≥7 jets in the 0-lepton channel), b-tag multiplicity (2, 3 and ≥4) and mass-tagged jet multiplicity (0, 1 and ≥2). The distribution of $m_{\rm eff}$, defined as the scalar sum of the lepton and jet p_Ts and the missing E_T, for each category were used as the discriminant for the final signal and background separation. No excess of events were found. Weak isospin doublet T quarks were excluded below 1.16 TeV.

The CMS search for $T\overline{T}$ production, with $T \to tH^0$ decays has been performed in both lepton+jets, multilepton and all hadronic final states. The lepton+jets analysis [131] emphasizes the presence of large number of b-tagged jets, and combined with other kinematic variables in a Boosted Decision Tree (BDT) for enhancing signal to background discrimination. The multilepton analysis [131] was optimized for the presence of b-jets and the large hadronic activity. For $\mathcal{B}(T \to Wb) = 1$, the combined lepton+jets and multilepton analyses led to a lower limit on T quark masses of 0.71 TeV. A search for $T \to tH^0$ in all hadronic decays [132], optimized for a high mass T quark, and based on identifying boosted top quark jets has been carried out by CMS. This search aimed to resolve sub-jets within the jets arising from boosted top quark decays, including b-tagging of the sub-jets. A likelihood discriminator was defined based on the distributions of H_T, and the invariant mass of the two b-jets in the events for signal and background. No excess above background expectations was observed. Assuming 100% branching ratio for $T \to tH^0$, this analysis led to a lower limit of 0.75 TeV on the mass of the T quark.

Searches for T quarks at $\sqrt{s}$=13 TeV, based on a 2.6fb^{-1} dataset [133] have been performed by CMS using the lepton+jets final state. This search has been optimized for high mass T quarks by exploiting techniques to identify W or Higgs bosons decaying hadronically with large transverse momenta. The boosted W channel excluded T quarks decaying only to bW with masses below 0.91 TeV, and the boosted tH channel excluded T quarks decaying only to tH for masses below 0.89 TeV.

A CMS search for $T \to tH^0$ with $H^0 \to \gamma\gamma$ decays has been performed [134] in pair production of T quarks. To identify the Higgs boson produced in the decay of the heavy T quark, and the subsequent $H^0 \to \gamma\gamma$ decay, the analysis focused on identification of two photons in events with one or more high p_T lepton+jets or events with no leptons and large hadronic activity. A search for a resonance in the invariant mass distribution of the two photons in events with large hadronic activity defined by the H_T variable showed no excess above the prediction from standard model processes. The analysis resulted in exclusion of T quark masses below 0.54 TeV.

A search for electroweak single production of T quark decaying to tH^0 using boosted topologies in fully hadronic [135] and lepton+jets [136] in the final states has been performed by CMS. The electroweak couplings of the T quarks to the SM third generation quarks are highly model dependent and hence these couplings determine the rates of the single T quark production. In both analyses, T quark candidate invariant mass was reconstructed using the boosted Higgs boson jets and the top quark. Higgs boson jets were identified using jet substructure techniques and subjet b tagging. For the lepton+jets analysis the top quark was reconstructed from the leptonically decaying W and the b jet, while in the all hadronic analysis the top quark jet was tagged using substructure analysis. There was no excess of events observed above background. Exclusion limits on the product of the production cross section and the branching fraction ($\sigma(pp \to Tqt/b) \times \mathcal{B}(T \to tH^0)$ were derived for the T quark masses in the range 0.70-1.8 TeV. From the lepton+jets analysis, for a mass of 1.0 TeV, values of ($\sigma(pp \to Tqt/b) \times \mathcal{B}(T \to tH^0)$ greater than 0.8 and 0.7 pb were excluded assuming left- and right-handed coupling of the T quark to standard model fermions, respectively [136]. For the all-hadronic analysis, upper limits between 0.31 and 0.93 pb were obtained on ($\sigma(pp \to Tqt/b) \times \mathcal{B}(T \to tH^0)$ for T quark masses in the range 1.0-1.8 TeV [135].

$T \to tZ$:

Both ATLAS and CMS search for T quarks that decay exclusively into tZ in pp collisons at $\sqrt{s}$ = 13 TeV. No excesses were found in either search.

ATLAS performed a search [137] for optimized pair production of vector-like top quarks decaying into tZ where the Z boson subsequently decays into neutrino pairs utilizing 36.1 fb^{-1} of data. The search selected events with one lepton, multiple jets, and significant missing transverse momentum. No significant excesses were found and lower limits on the mass of a vector like top quark were placed, excluding masses below 0.87 TeV (weak-isopsin singlet) , 1.05 TeV (weak-isospin doublet), and 1.16 TeV (pure Zt mode). CMS searched [138] for single production of T quarks decaying into tZ with the Z boson decaying to pairs of charged leptons (electrons and muons) and the top quark decaying hadronically usig 35.9 fb^{-1} of data. Limits were placed on T quarks with masses between 0.7 and 1.7 TeV excluding the product of cross-section and branching fraction above values of 0.27 to 0.04 pb. Additionally, limits on a Z' boson decaying into tZ were set.

Combined searches for $T \to bW/tZ/tH^0$:

Most of the analyses described above targeted an individual decay mode of the T quark, with 100% branching ratio to either bW, tZ or tH^0 and were optimized accordingly. However, they have varied sensitivity to all three decay modes and the results can be interpreted as a function of branching ratios to each of the three decay modes, with the total adding up to unity ($\mathcal{B}(tH) + \mathcal{B}(tZ) + \mathcal{B}(Wb) = 1$).

Combinations of analyses are performed by both ATLAS and CMS. The limits set by ATLAS searches in lepton+jets, dileptons with same-sign charge, and final states with Z boson have been combined and the results obtained for various sets of branching fractions for T quark decays to bW, tH^0 and tZ are shown in Fig. 113.3. In the combined analysis, ATLAS set lower T quarks mass limits that ranged from 0.6 to 1.35 TeV for all possible values of the branching fractions to the three decay modes [125,139]. In Fig. 113.3, exclusion is shown in the plane of $\mathcal{B}(T \to Ht)$ versus $\mathcal{B}(T \to Wb)$, for different values of

the T quark mass from the lepton+jets analyses optimized for bW, tH, Zt modes and the same-sign leptons analysis. The grey (light shaded) area in the figure corresponds to the unphysical region where the sum of branching ratios exceeds unity, or is smaller than zero. The default branching ratio values for the weak-isospin singlet and doublet cases are also shown in Fig. 113.3 as cross and square symbols respectively. A similar combination was also performed by CMS.

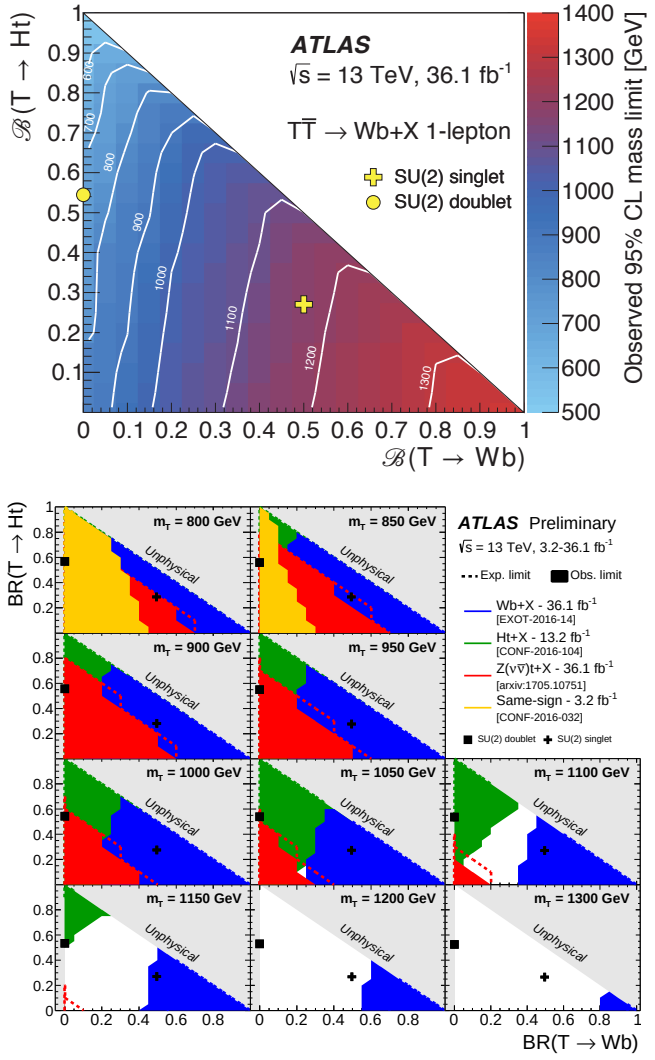

Figure 113.3: Observed limits on the mass of the T quark in the plane of $\mathcal{B}(T \to tH^0)$ versus $\mathcal{B}(T \to bW)$ from all ATLAS searches for TT production. The markers indicate the default branching ratios for the SU(2) singlet and doublet scenarios with masses above 0.8 TeV, where they are approximately independent of the VLQ T mass. Top panel: Summary from the $T \to Wb$ analysis [125]. Bottom panel: Exclusions for different values of the T quark mass for the Wb+X (blue), the tH^0+X (green), the $Z(\nu\bar{\nu})t$+X (red) and the same-sign leptons (yellow) analyses. Similar combination plots are also made by CMS.

An inclusive search by CMS targeted at heavy T quarks decaying to any combination of bW, tZ, or tH^0 is described in Ref. 131. Selected events have at least one isolated charged lepton. Events were categorized according to number and flavour of the leptons, the number of jets, and the presence of hadronic vector boson and top quark decays that are merged into a single jet. The use of jet substructure to identify hadronic decays significantly increases the acceptance for high T quark masses. No excess above standard model backgrounds was observed. Limits on the pair production cross section of the new quarks are set, combining all event categories, for all combinations of branching fractions into the three final states. For T quarks that exclusively decay to $bW/tZ/tH^0$, masses below 0.70/0.78/0.71 TeV are excluded.

113.2.3.2. *Searches for B quarks that decay to W, Z and H^0 bosons:*

ATLAS and CMS have performed searches for pair production of heavy B quarks which subsequently decay to Wt, bZ or bH^0. The searches have been carried out in final states with single leptons, di-leptons (with same charge or opposite charge), multileptons, as well as in fully hadronic final states.

$B \to WtX$:

A search for $B \to tW$ has been performed by the ATLAS experiment [125] using lepton+jets events with one hadronically decaying W and one leptonically decaying W utilizing 36.1 fb^{-1} of data at $\sqrt{s} = 13$ TeV. The search was optimized for T production decaying into Wb. Since the analysis was optimized for $T \to Wb$ rather than Wt decays the analysis does not reconstruct the full B mass. As discussed earlier, the hadronically and leptonically decaying heavy quarks were required to have similar reconstructed masses (within 300 GeV). The interpretation of the $T \to Wb$ in the context of $B \to tW$ production led to the exclusion of Heavy B like VLQs for masses less than 1.25 TeV and 1.08 TeV, assuming a 100% branching fraction to tW or SU(2) singlet B scenario, respectively.

A similar search by CMS [140], using 19.8 fb^{-1} of $\sqrt{s} = 8$ TeV data, selected events with one lepton and four or more jets, with at least one b-tagged jet, significant missing p_T, and further categorizes them based on the number of jets tagged as arising from the decay of boosted W, Z or H^0 bosons. The S_T distributions of the events in different categories showed no excess of events above the expected background and yielded a lower limit on the B quark mass of 0.73 TeV for $BR(B \to Wt) = 1$.

CMS [133] also searches for pair production of both TT and BB with collisions from 2.5 fb^{-1} of $\sqrt{s} = 13$ TeV data. The analysis searches for events with one high p_T lepton , multiple jets, and highly boosted W or Higgs bosons decaying hadronically. The analysis focuses on pair production and selects events with either a boosted W or Higgs candidate and then proceeds to search for anomalous production in excess of standard model production. Seeing no significant excesses CMS then proceeded to set limits in many different interpretations. The strongest was from the the $B \to Wt$ interpretation leading to excluding heavy vector like B's less than 0.73 TeV.

$B \to bZX$:

A search by CMS [141] for the pair-production of a heavy B quark and its antiparticle, one of which decays to bZ, selected events with a Z-boson decay to e^+e^- or $\mu^+\mu^-$ and a jet identified as originating from a b quark. The signal from $B \to bZ$ decays would appear as a local enhancement in the bZ mass distribution. No such enhancement was found and B quarks that decay 100% into bZ are excluded below 0.70 TeV. This analysis also set upper limits on the branching fraction for $B \to bZ$ decays of 30-100% in the B quark mass range 0.45-0.70 TeV. A complementary search has been carried out by ATLAS for new heavy quarks decaying into a Z boson and a b-quark [142]. Selected dilepton events contain a high transverse momentum Z boson that decays leptonically, together with two b-jets. If the dilepton events have an extra lepton in addition to those from the Z boson, then only one b-jet is required. No significant excess of events above the standard model expectation was observed, and mass limits were set depending on the assumed branching ratios, see Fig. 113.4. In a weak-isospin singlet scenario, a B quark with mass lower than 0.65 TeV was excluded, while for a particular weak-isospin doublet scenario, a B quark with mass lower than 0.73 TeV was ruled out.

ATLAS has searched for the electroweak production of single B quarks, which is accompanied by a b-jet and a light jet [142]. The dilepton selection for double B production was modified for the single B production study by requiring the presence of an additional energetic jet in the forward region. An upper limit of 200 fb was

obtained for the process $\sigma(pp \to B\bar{b}q) \times B(B \to Zb)$ with a heavy B quark mass at 0.70 TeV. This search indicated that the electroweak mixing parameter X_{Bb} below 0.5 is neither expected or observed to be excluded for any values of B quark mass.

Combination $B \to tW/bZ/bH^0$:

The ATLAS experiment has combined the various analyses targeted for specific decay modes to obtain the most sensitive limits on the pair production of B quarks [126]. The analyses using single lepton events, same sign charge dilepton events, events with opposite sign dilepton events, and multilepton events are combined to obtain lower limits on the mass of the B quark in the plane of $BR(B \to Wt)$ vs $BR(B \to bH)$. The searches were optimized for 100% branching fractions and hence are most sensitive at large $BR(B \to Wt)$, and also at large $BR(B \to bH^0)$. For all possible values of branching ratios in the three decay modes tW, bZ, or bH^0, the lower limits on the B quark mass was found to be between 0.58 TeV and 0.81 TeV and as shown in Fig. 113.4. Analyses were also combined by the ATLAS experiment to provide the most sensitive limits on the pair production of B quarks to produce limits as a function of both B mass and branching ratio [125]. CMS provided similar combinations of their analyses.

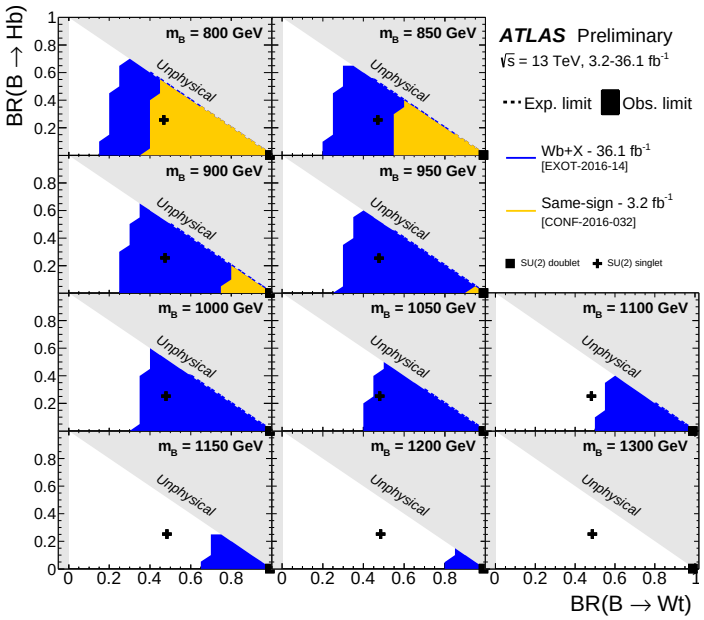

Figure 113.4: Observed limits on the mass of the B quark in the plane of $BR(B \to bH^0)$ versus $BR(B \to tW)$ from ATLAS searches for BB production [125]. Exclusion limits are drawn sequentially for each of the analyses and overlaid (rather than combined).

113.2.3.3. *Searches for top-partner quark X:*

Searches for a heavy top vector-like quark X, with exotic charge 5/3, such as that proposed in Refs. 143,144, have been performed by both ATLAS and CMS [125,145].

The analyses assumed pair-production or single-production of X with X decaying with 100% branching fraction to to tW. Searches for X have been performed using two final state signatures: same-sign leptons and lepton+jets.

The analysis based on searching for same-sign leptons, from the two W bosons from one of the X, has smaller backgrounds compared to the lepton+jets signature. Requiring same-sign leptons eliminates most of the standard model background processes, leaving those with smaller cross sections: $t\bar{t}$, W, $t\bar{t}Z$, WWW, and same-sign WW. In addition, backgrounds from instrumental effects due to charge misidentification were considered. Assuming pair production of X, the analyses by CMS using H_T as the discriminating variable restrict the X mass to be higher than 1.16 (1.10) TeV for a right (left) handed chirality particle [145,146,147]. The limits obtained by ATLAS, by classifying the signal region by number of b-jets, H_T, and missing p_T in the event, corresponded to a lower mass limit on X of 0.99 TeV [148,149].

Searches for X using leptons+jets final state signatures are based on either full or partial reconstruction of the T mass from the lepton, jets (including b jets) and missing p_T. The CMS search [145,150] also utilized jet substructure techniques to identify boosted X topologies. The discriminating variable used was the mass constructed from the lepton and b-tagged jet, $M_{(\ell,b)}$, which corresponds to the visible mass of leptonically decaying top quark. To optimize the search sensitivity, the events were further separated into categories based on lepton flavor (e, μ), the number of b-tagged jets, the number of W-tagged jets, and the number of t-tagged jets. In the absence of a signal, the CMS analysis excluded X quark masses with right-handed (left-handed) couplings below 1.32 (1.30) TeV [150].

The ATLAS lepton+jets search for X utilized events with high p_T W bosons and b-jets. The search described earlier for T pair production, with $T \to Wb$ decays, can be reinterpreted as a search for $X \to tW$. This analysis excluded X with masses below 1.25 TeV [125].

The single X production cross section depends on the coupling constant λ of the tWX vertex. ATLAS has performed an analysis of same-sign dileptons which includes both the single and pair production. This analysis led to a lower limit on the mass of the X of 0.75 TeV for both values of $\lambda = 0.5$ and 1.0 [151].

113.2.4. ***Colorons and Colored Scalars*** : These particles are associated with top-condensate and top-seesaw models, which involve an enlarged color gauge group. The new particles decay to dijets, $t\bar{t}$, and $b\bar{b}$.

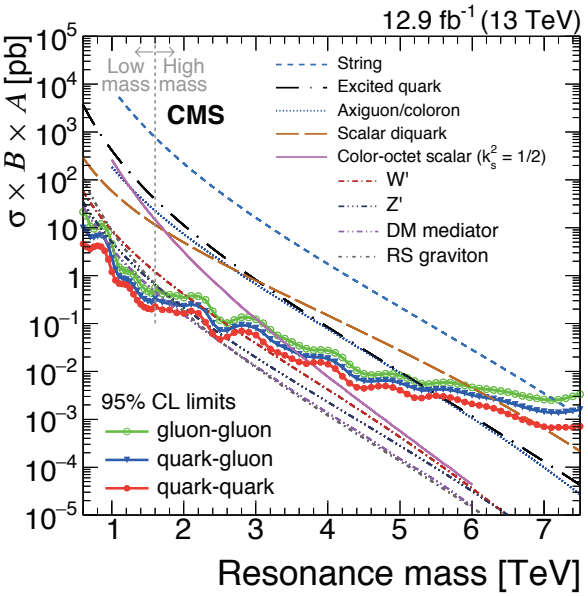

Figure 113.5: Observed 95% C.L. limits on $\sigma \times B \times A$ for string resonances, excited quarks, axigluons, colorons, E6 diquarks, s8 resonances, W' and Z' bosons, and Randall-Sundrum gravitons g_{KK} from [156].

Direct searches for colorons, color-octect scalars and other heavy objects decaying to $q\bar{q}$, qg, qq, or gg has been performed using LHC data from pp collisions at $\sqrt{s}$ =7, 8 and 13 TeV. Based on the analysis of dijet events from a data sample corresponding to a luminosity of 19.6 fb^{-1}, at $\sqrt{s}$ = 8 TeV the CMS experiment excluded pair production of colorons with mass between $1.20 - 3.60$ and $3.90 - 4.08$ TeV [152]. Analyses of inclusive 8- and 10-jet final states with low missing transverse momentum by CMS [153], set limits in several benchmark models. Colorons (axigluons) with masses

between 0.6 and 0.75 (up to 1.15) TeV were excluded, and gluinos in R-parity violating supersymmetric scenarios were ruled out from 0.6 up to 1.1 TeV.

A search for pair-produced colorons based on an integrated luminosity of 5.0 fb^{-1} at $\sqrt{s} = 7$ TeV by CMS excluded colorons with masses between 0.25 TeV and 0.74 TeV, assuming colorons decay 100% into $q\overline{q}$ [154]. This analysis was based on events with at least four jets and two dijet combinations with similar dijet mass. Color-octet scalars (s8) with masses between $1.20 - 2.79$ TeV were excluded by CMS [152], and below 2.7 TeV by ATLAS [155].

These studies have now been extended to take advantage of the increased center-of-mass energy during Run 2 of the LHC. Using the 12.6fb^{-1} of data collected at $\sqrt{s}$ =13 TeV, searches for narrow resonances have been performed by CMS. An analysis of the dijet invariant mass spectrum formed using wide jets [156,157], separated by $\Delta\eta_{jj} \leq 1.3$, led to limits on new particles decaying to parton pairs (qq, qg, gg). Specific exclusions on the masses of colorons and color-octet scalars were obtained and are shown in Fig. 113.5.

113.3. Conclusions

As the above analyses have demonstrated, there is already substantial sensitivity to possible new particles predicted to accompany the H^0 in dynamical frameworks of electroweak symmetry breaking. No hints of any deviations from the standard model have been observed, and limits typically at the scale of a few hundred GeV to a few TeV are set.

Given the need to better understand the H^0 and to determine in detail how it behaves, such analyses continue to be a major theme of Run 2 the LHC, and we look forward to increased sensitivity as a result of the higher luminosity at the increased centre of mass energy of collisions.

References:

1. ATLAS Collab., Phys. Lett. **B716**, 1 (2012).
2. CMS Collab., Phys. Lett. **B716**, 30 (2012).
3. S. Weinberg, Physica A **96**, 327 (1979).
4. A. Manohar and H. Georgi, Nucl. Phys. **B234**, 189 (1984).
5. H. Georgi, Nucl. Phys. **B266**, 274 (1986).
6. R.S. Chivukula, hep-ph/0011264 (2000).
7. R.S. Chivukula, M.J. Dugan, and M. Golden, Phys. Rev. **D47**, 2930 (1993).
8. S. Weinberg, Phys. Rev. **D13**, 974 (1976).
9. S. Weinberg, Phys. Rev. **D19**, 1277 (1979).
10. L. Susskind, Phys. Rev. **D20**, 2619 (1979).
11. K. Lane, hep-ph/0202255 (2002).
12. C.T. Hill and E.H. Simmons, Phys. Reports **381**, 235 (2003), [Erratum-ibid. **390**, 553 (2004)].
13. R. Shrock, hep-ph/0703050 (2007).
14. E. Eichten *et al.*, Rev. Mod. Phys. **56**, 579 (1984) [Addendum-ibid. **58**, 1065 (1986)].
15. E. Eichten *et al.*, Phys. Rev. **D34**, 1547 (1986).
16. See "Status of Higgs Boson Physics" review in this volume..
17. R.S. Chivukula and V. Koulovassilopoulos, Phys. Lett. **B309**, 371 (1993).
18. R. Foadi, M.T. Frandsen, and F. Sannino, Phys. Rev. **D87**, 095001 (2013).
19. B. Holdom, Phys. Lett. **B150**, 301 (1985).
20. K. Yamawaki, M. Bando, and K.-i. Matumoto, Phys. Rev. Lett. **56**, 1335 (1986).
21. T.W. Appelquist, D. Karabali, and L.C.R. Wijewardhana, Phys. Rev. Lett. **57**, 957 (1986).
22. T. Appelquist and L.C.R. Wijewardhana, Phys. Rev. **D35**, 774 (1987).
23. T. Appelquist and L.C.R. Wijewardhana, Phys. Rev. **D36**, 568 (1987).
24. E. Gildener and S. Weinberg, Phys. Rev. **D13**, 3333 (1976).
25. Z. Chacko, R. Franceschini and R. K. Mishra, JHEP **1304**, 015 (2013).
26. B. Bellazzini *et al.*, Eur. Phys. J. **C73**, 2333 (2013).
27. B. Bellazzini *et al.*, Eur. Phys. J. **C74**, 2790 (2014).
28. Z. Chacko, R.K. Mishra, and D. Stolarski, JHEP **1309**, 121 (2013).
29. J.R. Ellis, M.K. Gaillard, and D.V. Nanopoulos, Nucl. Phys. **B106**, 292 (1976).
30. M.A. Shifman *et al.*, Sov. J. Nucl. Phys. **30**, 711 (1979) [Yad. Fiz. **30**, 1368 (1979)].
31. A.I. Vainshtein, V.I. Zakharov, and M.A. Shifman, Sov. Phys. Usp. **23**, 429 (1980) [Usp. Fiz. Nauk **131**, 537 (1980)].
32. M. Bando, K.-i. Matumoto, and K. Yamawaki, Phys. Lett. **B178**, 308 (1986).
33. W.D. Goldberger, B. Grinstein, and W. Skiba, Phys. Rev. Lett. **100**, 111802 (2008).
34. S. Matsuzaki and K. Yamawaki, Phys. Rev. **D85**, 095020 (2012).
35. S. Matsuzaki and K. Yamawaki, Phys. Rev. **D86**, 035025 (2012).
36. E. Eichten, K. Lane, and A. Martin, arXiv:1210.5462 (2012).
37. D.B. Kaplan and H. Georgi, Phys. Lett. **B136**, 183 (1984).
38. D.B. Kaplan, H. Georgi, and S. Dimopoulos, Phys. Lett. **B136**, 187 (1984).
39. M.E. Peskin, Nucl. Phys. **B175**, 197 (1980).
40. J. Preskill, Nucl. Phys. **B177**, 21 (1981).
41. R. Barbieri and A. Strumia, hep-ph/0007265 (2000).
42. N. Arkani-Hamed, A.G. Cohen, and H. Georgi, Phys. Lett. **B513**, 232 (2001).
43. N. Arkani-Hamed *et al.*, JHEP **0208**, 020 (2002).
44. N. Arkani-Hamed *et al.*, JHEP **0207**, 034 (2002).
45. M. Schmaltz and D. Tucker-Smith, Ann. Rev. Nucl. and Part. Sci. **55**, 229 (2005).
46. K. Agashe *et al.*, Phys. Lett. **B641**, 62 (2006).
47. P. Sikivie *et al.*, Nucl. Phys. **B173**, 189 (1980).
48. B. Bellazzini, C. Csaki, and J. Serra, Eur. Phys. J. **C74**, 2766 (2014).
49. R. Essig *et al.*, arxiv:1707.03399.
50. Z. Chacko, H. S. Goh and R. Harnik, Phys. Rev. Lett. **96**, 231802 (2006).
51. R.S. Chivukula, A.G. Cohen, and K.D. Lane, Nucl. Phys. **B343**, 554 (1990).
52. V.A. Miransky, M. Tanabashi, and K. Yamawaki, Phys. Lett. **B221**, 177 (1989) and Mod. Phys. Lett. **A4**, 1043 (1989).
53. W.A. Bardeen, C.T. Hill, and M. Lindner, Phys. Rev. **D41**, 1647 (1990).
54. C.T. Hill, Phys. Lett. **B266**, 419 (1991).
55. B.A. Dobrescu and C.T. Hill, Phys. Rev. Lett. **81**, 2634 (1998).
56. R.S. Chivukula *et al.*, Phys. Rev. **D59**, 075003 (1999).
57. S. Dimopoulos and L. Susskind, Nucl. Phys. **B155**, 237 (1979).
58. E. Eichten and K.D. Lane, Phys. Lett. **B90**, 125 (1980).
59. D.B. Kaplan, Nucl. Phys. **B365**, 259 (1991).
60. T. Appelquist, M. Piai, and R. Shrock, Phys. Rev. **D69**, 015002 (2004).
61. R.S. Chivukula, B.A. Dobrescu, and E.H. Simmons, Phys. Lett. **B401**, 74 (1997).
62. Y. Grossman and M. Neubert, Phys. Lett. **B474**, 361 (2000).
63. S.J. Huber and Q. Shafi, Phys. Lett. **B498**, 256 (2001).
64. T. Gherghetta and A. Pomarol, Nucl. Phys. **B586**, 141 (2000).
65. K. Agashe, R. Contino, and A. Pomarol, Nucl. Phys. **B719**, 165 (2005).
66. G.F. Giudice *et al.*, JHEP **0706**, 045 (2007).
67. R.S. Chivukula and H. Georgi, Phys. Lett. **B188**, 99 (1987).
68. G. D'Ambrosio *et al.*, Nucl. Phys. **B645**, 155 (2002).
69. K. Agashe *et al.*, hep-ph/0509117 (2005).
70. T. Appelquist and R. Shrock, Phys. Lett. **B548**, 204 (2002).
71. B. Keren-Zur *et al.*, Nucl. Phys. **B867**, 429 (2013).
72. J.M. Maldacena, Adv. Theor. Math. Phys. **2**, 231 (1998).
73. For a review, see C. Csaki, J. Hubisz, and P. Meade, hep-ph/0510275 (2005), and "Extra Dimensions" review in this volume.
74. C. Pica, PoS LATTICE **2016**, 015 (2016), arXiv:1701.07782.
75. T. Appelquist *et al.*, Phys. Rev. **D93**, 114514 (2016).
76. PDG review of Zprime boson in this volume.
77. PDG review of Wprime boson in this volume.

78. ATLAS Collab., arXiv:1707.02424 [hep-ex] , submitted to JHEP.
79. CMS Collab., CMS-PAS-EXO-16-031 (2016).
80. ATLAS Collab., Phys. Rev. **D90**, 052005 (2014).
81. ATLAS Collab., arXiv:1709.07242 [hep-ex] (2017).
82. CMS Collab., JHEP **0217**, 48 (2017).
83. CMS Collab., JHEP **0717**, 001 (2016).
84. ATLAS Collab., ATLAS-CONF-2016-014 (2016).
85. ATLAS Collab.,arXiv:1703.09127 [hep-ex], submitted to PRD.
86. CMS Collab., Phys. Lett. B 769,520(2017).
87. ATLAS Collab., Phys. Lett. B 759, 229 (2016).
88. CMS Collab., CMS-PAS-EXO-12-023 (2014).
89. ATLAS Collab., arXiv:1706.04786 [hep-ex] (2017).
90. ATLAS Collab., JHEP **1409**, 037 (2014).
91. CMS Collab., Phys. Lett. **B770**, 278 (2017).
92. CMS Collab., Phys. Lett. **B755**, 196 (2016).
93. CMS Collab., JHEP **1405**, 108 (2014).
94. CMS Collab., JHEP **1602**, 122 (2016).
95. CMS Collab., JHEP **1708**, 029 (2017).
96. CMS Collab., arXiv:arXiv:1708.08539 , submitted to Phys. Lett. B.
97. CMS Collab., CMS-PAS-JME-15-002, (2015), cds.cern.ch/record/2126325.
98. ATLAS Collab., Phys. Lett. **B743**, 235 (2015).
99. ATLAS Collab., Eur. Phys. J. **C75**, 165 (2015).
100. D. Pappadopulo, A. Thamm,R. Torre, and A. Wulzer, JHEP **1409**, 060 (2014).
101. ATLAS Collab., Phys. Lett. **B737**, 223 (2014).
102. CMS Collab., Phys. Lett. **B740**, 83 (2015).
103. ATLAS Collab., JHEP **1609**, 173 (2016).
104. ATLAS Collab., ATLAS-CONF-2017-051.
105. CMS Collab., arXiv:1705.09171 [hep-ex], submitted to Phys. Lett. B.
106. ATLAS Collab., arXiv:1708.04445 [hep-ex], submitted to Phys. Lett. B.
107. CMS Collab., arXiv:1708.05379 [hep-ex], submitted to Physical Review D.
108. ATLAS Collab., Phys. Lett. **B765**, 32 (2016).
109. ATLAS Collab., arXiv:1707.06958 [hep-ex], submitted to Phys. Lett. B.
110. CMS Collab., Phys. Lett. **B768**, 137 (2017).
111. CMS Collab., Eur. Phys. J. **C77**, 636 (2017).
112. ATLAS Collab., Eur. Phys. J. **C75**, 412 (2015).
113. ATLAS Collab., ATLAS-CONF-2016-049 (2016).
114. CMS Collab., CMS-EXO-12-053 (2015).
115. ATLAS Collab., ATLAS-CONF-2013-074 (2013).
116. ATLAS Collab., arXiv:1709.06783 [hep-ex], submitted to PLB (2017).
117. ATLAS Collab., atlas.web.cern.ch/Atlas/GROUPS/PHYSICS/CombinedSummaryPlots/EXOTICS/index.html.
118. CMS Collab., twiki.cern.ch/twiki/bin/view/CMSPublic/PhysicsResultsB2GDibosons.
119. F. del Aguila *et al.*, Nucl. Phys. **B334**, 1 (1990).
120. CMS Collab., CMS-PAS-B2G-17-003 (2017).
121. CMS Collab., CMS-PAS-B2G-12-017 (2014).
122. CMS Collab., Phys. Rev. **D93**, 012003 (2016) arXiv:1509.04177.
123. CMS Collab., CMS-PAS-B2G-12-013 (2015).
124. S.D. Ellis, C.K. Vermilion, and J.R. Walsh, Phys. Rev. **D80**, 051501 (2009).
125. ATLAS Collab., arXiv:1707.03347 [hep-ex].
126. ATLAS Collab., JHEP **1508**, 105 (2015).
127. CMS Collab., Phys. Lett. **B772**, 634 (2017).
128. ATLAS Collab., ATLAS-CONF-16-072 (2016), http://cds.cern.ch/record/1480052.
129. ATLAS Collab., Eur. Phys. J. **C76**, 442 (2016).
130. ATLAS Collab., ATLAS-CONF-2016-104 (2016), http://cds.cern.ch/record/2220371.
131. CMS Collab., Phys. Lett. **B729**, 149 (2014).
132. CMS Collab., JHEP **1506**, 080 (2015).
133. CMS Collab., arXiv:1706.03408 [hep-ex].
134. CMS Collab., cds.cern.ch/record/1709129 (2014).
135. CMS Collab, JHEP **1704**, 136 (2017).
136. CMS Collab, Phys. Lett. **B771**, 80 (2017).
137. ATLAS Collab., JHEP **1700**, 052 (2017) CERN-EP-2017-075, submitted to JHEP.
138. CMS Collab., arXiv:1708.01062 [hep-ex], Submitted to Phys. Lett. B.
139. ATLAS Collab., JHEP **1708**, 052, (2017).
140. CMS Collab., CMS-PAS-B2G-12-019 (2012), http://cds.cern.ch/record/1599436.
141. CMS Collab., Phys. Rev. **D93**, 112009 (2016) arXiv:1507.07129.
142. ATLAS Collab., JHEP **1411**, 104 (2014).
143. R. Contino and G. Servant, JHEP **0806**, 026 (2008).
144. J. Mrazek, A. Wulzer, Phys. Rev. **D81**, 075006 (2010).
145. CMS Collab., JHEP **1708**, 073 (2017).
146. CMS Collab., CMS-PAS-B2G-16-019 (2017), https://cds.cern.ch/record/2256747.
147. CMS Collab., Phys. Rev. Lett. **112**, 171801 (2014).
148. ATLAS Collab., ATLAS-CONF-16-03 (2016), http://cds.cern.ch/record/2161545.
149. ATLAS Collab., Phys. Rev. **D91**, 112011 (2015).
150. CMS Collab., CMS-PAS-B2G-17-008 (2017), http://cds.cern.ch/record/2264686.
151. ATLAS Collab., JHEP **1510**, 150 (2015).
152. V. Khachatryan *et al.* [CMS Collab.], Phys. Rev. **D91**, 052009 (2015).
153. CMS Collaboration, Phys. Lett. **B770**, 257 (2017).
154. CMS Collab., Phys. Rev. Lett. **110**, 141802 (2013).
155. ATLAS Collab., Phys. Rev. **D91**, 052007 (2015).
156. CMS Collaboration, Phys. Lett. **B769**, 520 (2017).
157. CMS Collab., CMS-PAS-EXO-15-001 (2015), https://cds.cern.ch/record/2048099.

114. Grand Unified Theories

Revised August 2017 by A. Hebecker (U. Heidelberg) and J. Hisano (Nagoya U.)

114.1. The standard model

The Standard Model (SM) may be defined as the renormalizable field theory with gauge group $G_{SM} = SU(3)_C \times SU(2)_L \times U(1)_Y$, with 3 generations of fermions in the representation

$$(\mathbf{3},\mathbf{2})_{1/3} + (\bar{\mathbf{3}},\mathbf{1})_{-4/3} + (\bar{\mathbf{3}},\mathbf{1})_{2/3} + (\mathbf{1},\mathbf{2})_{-1} + (\mathbf{1},\mathbf{1})_{2}\ , \quad (114.1)$$

and a scalar Higgs doublet H transforming as $(\mathbf{1},\mathbf{2})_1$. Here and below we use boldface numbers to specify the dimension of representations of non-Abelian groups (in this case fundamental and antifundamental) and lower indices for $U(1)$ charges. The fields of Eq. (114.1) should also be familiar as $[Q, u^c, d^c, L, e^c]$, with $Q = (u, d)$ and $L = (\nu, e)$ being the quark and lepton $SU(2)$-doublets and u^c, d^c, e^c charge conjugate $SU(2)$-singlets.† Especially after the recent discovery of the Higgs, this model is remarkably complete and consistent with almost all experimental data.

A notable exception are neutrino masses, which are known to be non-zero but are absent in the SM even after the Higgs acquires its vacuum expectation value (VEV). The minimalist attitude is to allow for the dimension-five operator $(HL)^2$, which induces (Majorana) neutrino masses. In the seesaw mechanism [1,2,3] this operator is generated by integrating out heavy singlet fermions (right-handed (r.h.) neutrinos). Alternatively, neutrinos can have Dirac masses if light singlet neutrinos are added to the SM spectrum.

Conceptual problems of the SM include the absence of a Dark Matter candidate, of a mechanism for generating the baryon asymmetry of the universe, and of any reason for the observed smallness of the θ parameter of QCD (θ_{QCD}). In addition, the apparently rather complex group-theoretic data of Eq. (114.1) remains unexplained. Together with the abundance of seemingly arbitrary coupling constants, this disfavors the SM as a candidate fundamental theory, even before quantum gravity problems arise at energies near the Planck mass M_P.

To be precise, there are 19 SM parameters which have to be fitted to data: Three gauge couplings* g_3, g_2 and g_1, 13 parameters associated with the Yukawa couplings (9 charged fermion masses, three mixing angles and one CP phase in the CKM matrix.), the Higgs mass and quartic coupling, and θ_{QCD}. In addition, Majorana neutrinos introduce 3 more masses and 6 mixing angles and phases. As we will see, the paradigm of grand unification addresses mainly the group theoretic data of Eq. (114.1) and the values of the three gauge couplings. In many concrete realizations, it then impacts also the other mentioned issues of the SM, such as the family structure and fermion mass hierarchy.

More specifically, after precision measurements of the Weinberg angle θ_W in the LEP experiments, supersymmetric GUTs (SUSY GUTs) have become the leading candidates in the search for 'Physics beyond the SM'. Supersymmetry (SUSY) is a symmetry between bosons and fermions which requires the addition of superpartners to the SM spectrum, thereby leading to the noted prediction of θ_W [4]. The measured Higgs mass ($\sim$ 125 GeV) is in principle consistent with this picture, assuming superpartners in the region of roughly 10 TeV. Such heavy superpartners then induce radiative corrections raising the Higgs mass above the Z boson mass m_Z [5,6]. However, if SUSY is motivated as a solution to the gauge hierarchy problem (i.e. to the naturalness problem of the Higgs mass) [7], its minimal incarnation in terms of the MSSM is becoming questionable. Indeed, compared to expectations based on the minimal SUSY SM (MSSM) with superpartner masses below about 1 TeV, the Higgs mass is somewhat too high [8]. Independently, the LHC has disfavored light colored superpartners. These facts represent new hints for future work on SUSY GUTs or on GUTs without TeV-scale supersymmetry.

† In our convention the electric charge is $Q = T_3 + Y/2$ and all our spinor fields are left-handed (l.h.).

* Equivalently, the $SU(2)_L$ and $U(1)_Y$ couplings are denoted as $g = g_2$ and $g' = \sqrt{3/5}\ g_1$. One also uses $\alpha_s = \alpha_3 = (g_3^2/4\pi)$, $\alpha_{\rm EM} = (e^2/4\pi)$ with $e = g\ \sin\theta_W$ and $\sin^2\theta_W = (g')^2/(g^2 + (g')^2)$.

114.2. Basic group theory and charge quantization

Historically, the first attempt at unification was the Pati-Salam model with gauge group $G_{PS} = SU(4)_C \times SU(2)_L \times SU(2)_R$ [9]. It unifies SM fermions in the sense that one generation (plus an extra SM singlet) now comes from the $(\mathbf{4},\mathbf{2},\mathbf{1}) + (\bar{\mathbf{4}},\mathbf{1},\mathbf{2})$ of G_{PS}. This is easy to verify from the breaking pattern $SU(4)_C \to SU(3)_C \times U(1)_{B-L}$ together with the identification of SM hypercharge as a linear combination between $B - L$ (baryon minus lepton number) and the T_3 generator of $SU(2)_R$. This model explains charge quantization, that is, why all electric charges are integer multiples of some smallest charge in the SM. However, G_{PS} is not simple (containing three simple factors), and thus it does not predict gauge coupling unification.

Since G_{SM} has rank four (two for $SU(3)_C$ and one for $SU(2)_L$ and $U(1)_Y$, respectively), the rank-four group $SU(5)$ is the minimal choice for unification in a simple group [10]. The three SM gauge coupling constants derive from a universal coupling α_G at the GUT scale M_G. Explicitly embedding G_{SM} in $SU(5)$ is straightforward, with $SU(3)_C$ and $SU(2)_L$ corresponding e.g. to the upper-left 3×3 and lower-right 2×2 blocks, respectively, in traceless 5×5 matrices for $SU(5)$ generators of the fundamental representation. The $U(1)_Y$ corresponds to matrices generated by $\mathrm{diag}(-2/3, -2/3, -2/3, 1, 1)$ and hence commutes with $SU(3)_C \times SU(2)_L \subset SU(5)$. It is then easy to derive how one SM generation precisely comes from the $\mathbf{10} + \bar{\mathbf{5}}$ of $SU(5)$ (where $\mathbf{10}$ is the antisymmetric rank-2 tensor):

$$\mathbf{10}: \begin{pmatrix} 0 & u_b^c & -u_g^c & u_r & d_r \\ -u_b^c & 0 & u_r^c & u_g & d_g \\ u_g^c & -u_r^c & 0 & u_b & d_b \\ -u_r & -u_g & -u_b & 0 & e^c \\ -d_r & -d_g & -d_b & -e^c & 0 \end{pmatrix} \quad \text{and} \quad \bar{\mathbf{5}}: \begin{pmatrix} d_r^c \\ d_g^c \\ d_b^c \\ e \\ -\nu_e \end{pmatrix}. \quad (114.2)$$

Since $SU(5)$ has 24 generators, $SU(5)$ GUTs have 12 new gauge bosons known as X bosons (or X/Y bosons) in addition to the SM. X bosons form an $SU(3)_C$-triplet and $SU(2)_L$-doublet. Their interaction connects quarks and leptons such that baryon and lepton numbers are not conserved and nucleon decay is predicted. Furthermore, $U(1)_Y$ hypercharge is automatically quantized since it is embedded in $SU(5)$.

In order to break the electroweak symmetry at the weak scale and give mass to quarks and leptons, Higgs doublets are needed. In the minimal $SU(5)$ model, they can sit in either a $\mathbf{5_H}$ or $\bar{\mathbf{5}}_\mathbf{H}$. The three additional states are referred to as color-triplet Higgs scalars. Their couplings also violate baryon and lepton numbers, inducing nucleon decay. In order not to violently disagree with the non-observation of nucleon decay, the triplet mass must be greater than $\sim 10^{11}$ GeV [11]. Moreover, in SUSY GUTs [12], in order to cancel anomalies as well as give mass to both up and down quarks, both Higgs multiplets $\mathbf{5_H}$ and $\bar{\mathbf{5}}_\mathbf{H}$ are required. As we shall discuss later, nucleon decay now constrains the Higgs triplets to have mass significantly greater than M_G in the minimal SUSY $SU(5)$ GUT since integrating out the Higgs triplets generates dimension-five baryon-number-violating operators [13]. The mass splitting between doublet and triplet in the $\mathbf{5_H}$ (and $\bar{\mathbf{5}}_\mathbf{H}$) comes from their interaction with the $SU(5)$ breaking sector.

While $SU(5)$ allows for the minimal GUT models, unification is not complete: Two independent representations, $\mathbf{10}$ and $\bar{\mathbf{5}}$, are required for one SM generation. A further representation, an SU(5) singlet, has to be added to serve as r.h. neutrino in the seesaw mechanism. In this case, the r.h. neutrino masses are not necessarily related to the GUT scale. By contrast, a single $\mathbf{16}$-dimensional spinor representation of $SO(10)$ accommodates a full SM generation together with an extra singlet, potentially providing a r.h. neutrino [14]. This is most easily understood from the breaking pattern $SO(10) \to SU(5) \times U(1)_X$ and the associated branching rule* $\mathbf{16} = \mathbf{10}_{-5} + \bar{\mathbf{5}}_3 + \mathbf{1}_{-1}$. Here the indices refer to charges under the $U(1)_X$ subgroup, which is orthogonal to $SU(5)$ and reflects the fact that $SO(10)$ has rank five. From the above, it is easy to see that $U(1)_X$ charges can be given as $2Y - 5(B - L)$. Intriguingly, all representations of $SO(10)$ are anomaly free in four

* Useful references on group theory in the present context include [15] and refs. therein.

dimensions (4d). Thus, the absence of anomalies in an $SU(5)$-GUT or a SM generation can be viewed as deriving from this feature.

Table 114.1 presents the states of one family of quarks and leptons, as they appear in the **16**. To understand this, recall that the Γ-matrices of the 10d Clifford algebra give rise to five independent, anticommuting 'creation-annihilation' operators $\Gamma^{a\pm} = (\Gamma^{2a-1} \pm i\Gamma^{2a})/2$ with $a = 1, ..., 5$. These correspond to five fermionic harmonic oscillators or "spin" 1/2 systems. The 32-dimensional tensor product of those is reducible since the 10d rotation generators $M_{mn} = -i[\Gamma^m, \Gamma^n]/4$ $(m, n = 1, ..., 10)$ always flip an even number of "spins". This gives rise to the **16** as displayed in Table 114.1.

Next, one also recalls that the natural embedding of $SU(5)$ in $SO(10)$ relies on 'pairing up' real dimensions, $R^{10} \equiv C^5$, similarly to the paring up of Γ^ms used above. This makes it clear how to associate one $|\pm>$ system to each complex dimension of $SU(5)$, which explains the labeling of the "spin" columns in Table 114.1: The first three and last two "spins" correspond to $SU(3)_C$ and $SU(2)_L$, respectively. In fact, an $SU(3)_C$ rotation just raises one color index and lowers another, changing colors $\{r,\ g,\ b\}$, or changes relative phases between the three spin states. Similarly, an $SU(2)_L$ rotation raises one weak index and lowers another, thereby flipping the weak isospin from up to down or vice versa, or changes the relative phase between the two spin states. In this representation $U(1)_Y$ hypercharge is simply given by $Y = -2/3(\sum$ color spins$) + (\sum$ weak spins$)$. $SU(5)$ rotations corresponding to X bosons then raise (or lower) a color index, while at the same time lowering (or raising) a weak index. It is easy to see that such rotations can mix the states $\{Q,\ u^c,\ e^c\}$ and $\{d^c, L\}$ among themselves and ν^c is a singlet. Since $SO(10)$ has 45 generators, additional 21 gauge bosons are introduced including the $U(1)_X$ above. The 20 new $SO(10)$ rotations not in $SU(5)$ are then given by either raising any two spins or lowering them. With these rotations, **1** and **5** are connected with **10**. The last $SO(10)$ rotation changes phases of states with weight $2(\sum$ color spins$) + 2(\sum$ weak spins$)$, which corresponds to $U(1)_X$.

Table 114.1: Quantum numbers of **16**-dimensional representation of $SO(10)$.

state	Y	Color	Weak	$SU(5)$	$SO(10)$
ν^c	0	− − −	− −	**1**	
e^c	2	− − −	+ +		
u_r	1/3	+ − −	− +		
d_r	1/3	+ − −	+ −		
u_g	1/3	− + −	− +		
d_g	1/3	− + −	+ −	**10**	
u_b	1/3	− − +	− +		
d_b	1/3	− − +	+ −		**16**
u_r^c	−4/3	− + +	− −		
u_g^c	−4/3	+ − +	− −		
u_b^c	−4/3	+ + −	− −		
d_r^c	2/3	− + +	+ +		
d_g^c	2/3	+ − +	+ +		
d_b^c	2/3	+ + −	+ +	$\overline{\mathbf{5}}$	
ν	−1	+ + +	− +		
e	−1	+ + +	+ −		

$SO(10)$ has two inequivalent maximal subgroups and hence breaking patterns, $SO(10) \to SU(5) \times U(1)_X$ and $SO(10) \to SU(4)_C \times SU(2)_L \times SU(2)_R$. In the first case, one can carry on breaking to $G_{SM} \subset SU(5)$ precisely as in the minimal $SU(5)$ case above. Alternatively, one can identify $U(1)_Y$ as an appropriate linear combination of $U(1)_X$ and the $U(1)$ factor from $SU(5)$, leading to the so-called flipped $SU(5)$ [16] as an intermediate step in breaking $SO(10)$ to G_{SM}. In the second case, we have an intermediate Pati-Salam model thanks to the branching rule $\mathbf{16} = (\mathbf{4}, \mathbf{2}, \mathbf{1}) + (\overline{\mathbf{4}}, \mathbf{1}, \mathbf{2})$. Finally, $SO(10)$ can break directly to the SM at M_G. Gauge coupling unification remains intact in the case of this 'direct' breaking and for the breaking pattern $SO(10) \to SU(5) \to G_{SM}$ (with $SU(5)$ broken at M_G). In the case of intermediate-scale Pati-Salam or flipped $SU(5)$ models, gauge coupling predictions are modified. The Higgs multiplets in the minimal $SO(10)$ come from the fundamental representation, $\mathbf{10_H} = \mathbf{5_H} + \overline{\mathbf{5}}_\mathbf{H}$. Note, only in $SO(10)$ does the representation type distinguish SM matter from Higgs fields.

Finally, larger symmetry groups can be considered. For example, the exceptional group E_6 has maximal subgroup $SO(10) \times U(1)$ [17]. Its fundamental representation branches as $\mathbf{27} = \mathbf{16}_1 + \mathbf{10}_{-2} + \mathbf{1}_4$. Another maximal subgroup is $SU(3)_C \times SU(3)_L \times SU(3)_R \subset E_6$ with branching rule $\mathbf{27} = (\mathbf{3}, \mathbf{3}, \mathbf{1}) + (\overline{\mathbf{3}}, \mathbf{1}, \overline{\mathbf{3}}) + (\mathbf{1}, \overline{\mathbf{3}}, \mathbf{3})$. Independently of any underlying E_6, the group $[SU(3)]^3$ with additional permutation symmetry Z_3 interchanging the three factors can be considered. This is known as "trinification" [18]. The $E_6 \to [SU(3)]^3$ breaking pattern has been used in phenomenological analyses of the heterotic string [19]. However, in larger symmetry groups, such as E_6, $SU(6)$, etc., there are now many more states which have not been observed and must be removed from the effective low-energy theory.

Intriguingly, the logic by which G_{SM} is a maximal subgroup of $SU(5)$, which together with $U(1)_X$ is a maximal subgroup of $SO(10)$, continues in a very elegant and systematic way up to the largest exceptional group. The resulting famous breaking chain $E_8 \to E_7 \to E_6 \to SO(10) \to SU(5) \to G_{SM}$ together with the special role played by E_8 in group and in string theory is a tantalizing hint at deeper structures. However, since all representations of E_8 and E_7 are real and can not lead to 4d chiral fermions, this is necessarily outside the 4d GUT framework.

114.3. GUT breaking and doublet-triplet splitting

In the standard, 4d field-theoretic approach to GUTs, the unified gauge group is broken spontaneously by an appropriate GUT Higgs sector. Scalar potentials (or superpotentials in SUSY GUTs) exist whose vacua spontaneously break $SU(5)$ or $SO(10)$. While these potentials are ad hoc (just like the Higgs potential in the SM), the most naive expectation is that all their dimensionful parameters are $O(M_G)$. In the simplest case of $SU(5)$, the **24** (adjoint) GUT Higgs develops a VEV along the G_{SM}-singlet direction as $\langle\Phi\rangle \propto \mathrm{diag}(-2/3, -2/3, -2/3, 1, 1)$. In order for $SO(10)$ to break to $SU(5)$, the **16** or **126**, which have a G_{SM}-singlet with non-zero $U(1)_X$ charge, get a VEV.

The masses of doublet and triplet in the $\mathbf{5_H}$ (and $\overline{\mathbf{5}}_\mathbf{H}$) generically split due to their coupling to the GUT Higgs. In addition, both the doublet and the triplet masses also get an equal contribution from an $SU(5)$-invariant GUT-scale mass term. Without any further structure, an extreme fine-tuning between two large effects is then necessary to keep the doublet mass at the electroweak scale. Supersymmetry plays an important role in forbidding large radiative correction to the doublet mass due to the non-renormalization theorem [7]. However, even in this case we have to fine tune parameters at tree level. This is the doublet-triplet splitting problem which, in the SUSY context, is clearly related the μ-term problem of the MSSM (the smallness of the coefficient of $\mu H_u\ H_d$).

Several mechanisms for natural doublet-triplet splitting have been suggested under the assumption of supersymmetry, such as the sliding singlet [20], missing partner [21] missing VEV [22], and pseudo-Nambu-Goldstone boson mechanisms [23]. Particular examples of the missing partner mechanism for $SU(5)$ [24], the missing VEV mechanism for $SO(10)$ [25,26] and the pseudo-Nambu-Goldstone boson mechanism for $SU(6)$ [27] have been shown to be consistent with gauge coupling unification and nucleon decay. From the GUT-scale perspective, one is satisfied if the triplets are naturally heavy and the doublets are massless ($\mu \simeq 0$). There are also several mechanisms for

resolving the subsequent issue of why μ is of order the SUSY breaking scale [28]. * For a review of the μ problem and some suggested solutions in SUSY GUTs and string theory, see [29,30,31,32] and references therein.

In general, GUT-breaking sectors successfully resolving the doublet-triplet splitting problem, dynamically stabilizing all GUT-scale VEVs and allowing for realistic neutrino masses and Yukawa couplings (including the GUT-symmetry violation in the latter) require a number of ingredients. However, for validity of the effective theory, introduction of higher or many representations is limited, otherwise a Landau pole may appear below the Planck scale. In addition, GUTs are only effective theories below the Planck scale in the 4d field-theoretic approach. Since M_G is close to this scale, the effects of higher-dimension operators are not obviously negligible. In particular, operators including the GUT-breaking Higgs may affect low-energy predictions, such as quark and lepton masses.

Thus, especially in the context of GUT breaking and doublet-triplet splitting, models beyond 4d field theory appear attractive. While this is mainly the subject of the next section, some advantages can already be noted: In models with extra dimensions, in particular string constructions, GUT breaking may occur due to boundary conditions in the compactified dimensions [33,34,35,36]. No complicated GUT breaking sector is then required. Moreover, boundary conditions can give mass only to the triplet, leaving the doublet massless. This is similar to the 'missing partner mechanism' since the effective mass term does not 'pair up' the triplets from $\mathbf{5_H}$ and $\overline{\mathbf{5}}_\mathbf{H}$ but rather each of them with further fields which are automatically present in the higher-dimensional theory. This can eliminate dimension-five nucleon decay (cf. Sec. 114.6).

114.4. String-theoretic and higher-dimensional unified models

As noted earlier, the GUT scale is dangerously close to the scale of quantum gravity. It may hence be necessary to discuss unified models of particle physics in the latter, more ambitious context. Among the models of quantum gravity, superstring or M-theory stands out as the best-studied and technically most developed proposal, possessing in particular a high level internal, mathematical consistency. For our purposes, it is sufficient to know that five 10d and one 11d low-energy effective supergravity theories arise in this setting (cf. [37] and refs. therein).

Grand unification is realized most naturally in the context of the two 'heterotic' theories with gauge groups $\mathrm{E_8}\times\mathrm{E_8}$ and $SO(32)$, respectively [35] (see [38] for some of the more recent results). Justified in part by the intriguing breaking path $\mathrm{E_8} \to \cdots \to G_{SM}$ mentioned above, the focus has historically largely been on $\mathrm{E_8}\times\mathrm{E_8}$. To describe particle physics, solutions of the 10d theory with geometry $R^{1,3} \times M_6$ are considered, where M_6 is a Calabi-Yau (CY) 3-fold (with 6 real dimensions). The background solution involves expectation values of higher-dimensional components of the $\mathrm{E_8}\times\mathrm{E_8}$ gauge fields. This includes both Wilson lines [33] and non-vanishing field-strength and leads, in general, to a reduced gauge symmetry and to chirality in the resulting 4d effective theory. The 4d fermions arise from 10d gauginos.

Given an appropriate embedding of G_{SM} in $\mathrm{E_8}\times\mathrm{E_8}$, gauge coupling unification is automatic at leading order. Corrections arise mainly through (string)-loop effects and are similar to the familiar field-theory thresholds of 4d GUTs [39]. Thus, one may say that coupling unification is a generic prediction in spite of the complete absence* of a 4d GUT at any energy scale. This absence is both an advantage and a weakness. On the up side, GUT breaking and doublet-triplet splitting [41] are more naturally realized and dimension-five nucleon decay is relatively easy to avoid. On the down side, there is no reason to expect full GUT representations in the matter sector and flavor model building is much less tied to the GUT structure than in 4d.

One technical problem of heterotic constructions is the dependence on the numerous size and shape parameters of M_6 (the so-called moduli), the stabilization of which is poorly understood (see [42] for recent developments). Another is the sheer mathematical complexity of the analysis, involving in particular the study of (non-Abelian) gauge-bundles on CY spaces [43] (see however [44]) .

An interesting sub-chapter of heterotic string constructions is represented by orbifold models [34]. Here the internal space is given by a six-torus, modded out by a discrete symmetry group (e.g. T^6/Z_n). More recent progress is reported in [45,46], including in particular the systematic exploration of the phenomenological advantages of so-called 'non-prime' (referring to n) orbifolds. The symmetry breaking to G_{SM} as well as the survival of Higgs doublets without triplet partners is ensured by the appropriate embedding of the discrete orbifold group in $\mathrm{E_8}\times\mathrm{E_8}$. String theory on such spaces, which are locally flat but include singularities, is much more calculable than in the CY case. The orbifold geometries can be viewed as singular limits of CYs.

An even simpler approach to unified models, which includes many of the advantages of full-fledged string constructions, is provided by Orbifold GUTs [36]. These are (mostly) 5d or 6d SUSY field theories with unified gauge group (e.g. $SU(5)$ or $SO(10)$), broken in the process of compactifying to 4d. To give a particularly simple example, consider $SU(5)$ on $R^{1,3}\times S^1/(Z_2 \times Z_2')$. Here the compact space is an interval of length $\pi R/2$ and the embedding of Z_2' in the hypercharge direction of $SU(5)$ realizes the breaking to G_{SM}. Concretely, 5d X bosons are given Dirichlet BCs at one endpoint of the interval and thus have no Kaluza-Klein (KK) zero mode. Their lightest modes have mass $\sim 1/R$, making the KK-scale the effective GUT scale. As an implication, the boundary theory has no $SU(5)$ invariance. Nevertheless, since the $SU(5)$-symmetric 5d bulk dominates 4d gauge couplings, unification remains a prediction. Many other features but also problems of 4d GUTs can be circumvented, especially doublet-triplet splitting is easily realized.

With the advent of the string-theory 'flux landscape' [47], which is best understood in 10d type-IIB supergravity, the focus in string model building has shifted to this framework. While type II string theories have no gauge group in 10d, brane-stacks support gauge dynamics. A particularly appealing setting (see e.g. [48]) is provided by type IIB models with D7 branes (defining 8d submanifolds). However, in the $SO(10)$ context the **16** is not available and, for $SU(5)$, the top-Yukawa coupling vanishes at leading order [49]. As a crucial insight, this can be overcome on the non-perturbative branch of type IIB, also known as F-theory [50,51]. This setting allows for more general branes, thus avoiding constraints of the Dp-brane framework. GUT breaking can be realized using hypercharge flux (the VEV of the $\mathrm{U}(1)_Y$ field strength), an option not available in heterotic models. The whole framework combines the advantages of the heterotic or higher-dimensional unification approach with the more recent progress in understanding moduli stabilization. It thus represents at this moment the most active and promising branch of theory-driven GUT model building (see e.g. [52] and refs. therein).

As a result of the flux-breaking, a characteristic 'type IIB' or 'F-theoretic' tree-level correction to gauge unification arises [53]. The fact that this correction can be rather significant numerically is occasionally held against the framework of F-theory GUTs. However, at a parametric level, this correction nevertheless behaves like a 4d threshold, i.e., it provides $\mathcal{O}(1)$ additive contributions to the inverse 4d gauge coupling $\alpha_i^{-1}(M_G)$.

A final important issue in string GUTs is the so-called string-scale/GUT-scale problem [54]. It arises since, in heterotic compactifications, the Planck scale and the high-scale value of the gauge coupling unambiguously fix the string-scale to about 10^{18} GeV. As the compactification radius R is raised above the string length, the GUT scale (identified with $1/R$) goes down and the string coupling goes up. Within the domain of perturbative string theory, a gap of about a factor ~ 20 remains between the lowest GUT scale achievable in this way and the phenomenological goal of 2×10^{16} GeV. The situation

* The solution of [28] relies on the absence of the fundamental superpotential term $\mu H_u\, H_d$ (or $\mu\, \mathbf{5}_H \overline{\mathbf{5}}_H$). This is ensured by a $U(1)_R$. The latter clashes with typical superpotentials for the GUT breaking sector. However, higher-dimensional or stringy GUTs, where the triplet Higgs is simply projected out, can be consistent with the $U(1)_R$ symmetry.

* See however [40].

can be improved by venturing into the non-perturbative regime [54] or by considering 'anisotropic' geometries with hierarchically different radii R [54,55].

In F-theory GUTs, the situation is dramatically improved since the gauge theory lives only in four out of the six compact dimensions. This allows for models with a 'decoupling limit', where the GUT scale is parametrically below the Planck scale [51]. However, moduli stabilization may not be without problems in such constructions, in part due to a tension between the required large volume and the desirable low SUSY breaking scale.

114.5. Gauge coupling unification

The quantitative unification of the three SM gauge couplings at the energy scale M_G is one of the cornerstones of the GUT paradigm. It is obviously of direct phenomenological relevance. Gauge coupling unification is best understood in the framework of effective field theory (EFT) [56]. In the simplest case, the relevant EFT at energies $\mu \gg M_G$ has a unified gauge symmetry (say $SU(5)$ for definiteness) and a single running gauge coupling $\alpha_G(\mu)$. At energies $\mu \ll M_G$, states with mass $\sim M_G$ (such as X bosons, GUT Higgs, color-triplet Higgs) have to be integrated out. The EFT now has three independent couplings and SM (or SUSY SM) matter content. One-loop renormalization group equations readily allow for an extrapolation to the weak scale,

$$\alpha_i^{-1}(m_Z) = \alpha_G^{-1}(M_G) + \frac{b_i}{2\pi}\log\left(\frac{M_G}{m_Z}\right) + \delta_i\,, \qquad (114.3)$$

(i = 1-3). Here we defined δ_i to absorb all sub-leading effects, including threshold corrections at or near the weak scale (e.g. from superpartners and the additional Higgs bosons in the case of the MSSM). We will discuss them momentarily.

It is apparent from Eq. (114.3) that the three low-scale couplings can be very different. This is due to the large energy range $m_Z \ll \mu \ll M_G$ and the non-universal β-function coefficients ($b_i^{\rm SM} = \{41/10, -19/6, -7\}$ or $b_i^{\rm MSSM} = \{33/5, 1, -3\}$). Incomplete GUT multiplets, such as gauge and Higgs bosons in the SM and also their superpartners and the additional Higgs bosons in the MSSM, contribute to the differences between the β functions. Inverting the argument, one expects that extrapolating the measured couplings to the high scale, we find quantitative unification at $\mu \sim M_G$. While this fails in the SM, it works intriguingly well in the MSSM (cf. Fig. 1).

The three equations contained in (Eq. (114.3)) can be used to determine the three 'unknowns' $\alpha_3(m_Z)$, $\alpha_G(M_G)$ and M_G, assuming that all other parameters entering the equations are given. Focusing on the SUSY case and using the $\overline{\rm MS}$ coupling constants $\alpha_{\rm EM}^{-1}(m_Z)$ and $\sin^2\theta_W(m_Z)$ from [57],

$$\alpha_{\rm EM}^{-1}(m_Z) = 127.950 \pm 0.017\,, \qquad (114.4)$$

$$\sin^2\theta_W(m_Z) = 0.23129 \pm 0.00005\,, \qquad (114.5)$$

as input, one determines $\alpha_{1,2}^{-1}(m_Z)$, which then gives

$$\alpha_G^{-1}(M_G) \simeq 24.3 \qquad \text{and} \qquad M_G \simeq 2\times 10^{16}\ \text{GeV}\,. \qquad (114.6)$$

Here we have set $\delta_i = 0$ for simplicity. Crucially, one in addition obtains a prediction for the low-energy observable α_3,

$$\alpha_3^{-1}(m_Z) = -\frac{5}{7}\alpha_1^{-1}(m_Z) + \frac{12}{7}\alpha_2^{-1}(m_Z) + \Delta_3\,, \qquad (114.7)$$

where

$$\Delta_3 = \frac{5}{7}\delta_1 - \frac{12}{7}\delta_2 + \delta_3\,. \qquad (114.8)$$

Here we followed the elegant formulation in Ref. [58] of the classical analyses of [4]. Of course, it is a matter of convention which of the three low-energy gauge coupling parameters one 'predicts' and indeed, early works on the subject discussed the prediction of $\sin^2\theta_W$ in terms of $\alpha_{\rm EM}$ and α_3 [59,60].

Remarkably, the leading order result (i.e. Eq. (114.7) with $\delta_i = 0$) is in excellent agreement with experiments [57]:

$$\alpha_3^{\rm LO}(m_Z) = 0.117 \qquad \text{vs.} \qquad \alpha_3^{\rm EXP}(m_Z) = 0.1181 \pm 0.0011\,. \qquad (114.9)$$

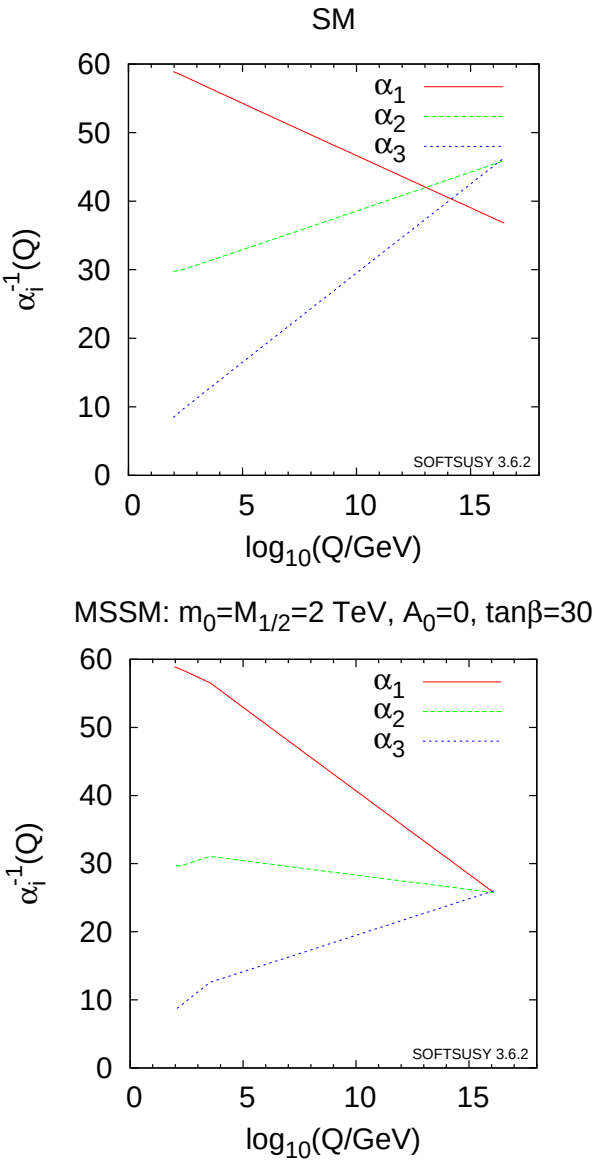

Figure 114.1: Running couplings in SM and MSSM using two-loop RG evolution. The SUSY threshold at 2 TeV is clearly visible on the MSSM side. (We thank Ben Allanach for providing the plots created using SOFTSUSY [62].)

However, this near perfection is to some extent accidental. To see this, we now discuss the various contributions to the δ_i (and hence to Δ_3).

The two-loop running correction from the gauge sector $\Delta_3^{(2)}$ and the low-scale threshold correction $\Delta_3^{(l)}$ from superpartners can be summarized as [58]

$$\Delta_3^{(2)} \simeq -0.82 \qquad \text{and} \qquad \Delta_3^{(l)} \simeq \frac{19}{28\pi}\log\left(\frac{m_{\rm SUSY}}{m_Z}\right)\,. \qquad (114.10)$$

The relevant scale $m_{\rm SUSY}$ can be estimated as [61]

$$m_{\rm SUSY} \;\to\; m_H^{3/19} m_{\widetilde{H}}^{12/19} m_{\widetilde{W}}^{4/19} \times \left(\frac{m_{\widetilde{W}}}{m_{\widetilde{g}}}\right)^{28/19}\left(\frac{m_{\widetilde{l}}}{m_{\widetilde{q}}}\right)^{3/19}\,, \qquad (114.11)$$

where m_H stands for the masses of non-SM Higgs states and superpartner masses are given in self-evident notation. Detailed analyses including the above effects are best done using appropriate software packages, such as SOFTSUSY [62], (or alternatively SuSpect [63] or SPheno [64]) . See also [62] for references to the underlying theoretical two-loop analyses.

To get a very rough feeling for these effects, let us assume that all superpartners are degenerate at $m_{\rm SUSY} = 1$ TeV, except for heavier gluinos: $m_{\widetilde{W}}/m_{\widetilde{g}} \simeq 1/3$. This gives $\Delta_3^{(l)} \simeq -0.35 + 0.22\ln(m_{\rm SUSY}/m_Z) \simeq 0.18$. The resulting prediction of $\alpha_3(m_Z) \simeq 0.126$ significantly upsets the perfect one-loop agreement found earlier. Before discussing this issue further, it is useful to introduce yet another important type of correction, the high or GUT scale thresholds.

To discuss high scale thresholds, let us set all other corrections to zero for the moment and write down a version of Eq. (114.3) that captures the running near and above the GUT scale more correctly. The threshold correction at one-loop level can be evaluated accurately by the simple step-function approximation for the β functions in the $\overline{\rm DR}$ scheme* [68],

$$\alpha_i^{-1}(m_Z) = \alpha_G^{-1}(\mu) + \frac{1}{2\pi}\left[b_i \ln\frac{\mu}{m_Z} + b_i^C \ln\frac{\mu}{M_C} + b_i^X \ln\frac{\mu}{M_X} + b_i^\Phi \ln\frac{\mu}{M_\Phi}\right] . \quad (114.12)$$

Here we started the running at some scale $\mu \gg M_G$, including the contribution of the minimal set of states relevant for the transition from the high-scale $SU(5)$ model to the MSSM. These are the color-triplet Higgs multiplets with mass M_C, massive vector multiplets of X-bosons with mass M_X (including GUT Higgs degrees of freedom), and the remaining GUT-Higgs fields and superpartners with mass M_Φ. The coefficients $b_i^{C,X,\Phi}$ can be found in Ref. [69]. Crucially, the b_i in Eq. (114.12) conspire to make the running GUT-universal at high scales, such that the resulting prediction for α_3 does not depend on the value of μ.

To relate this to our previous discussion, we can, for example, define $M_G \equiv M_X$ and then choose $\mu = M_G$ in Eq. (114.12). This gives the high-scale threshold corrections

$$\delta_i^{(h)} = \frac{1}{2\pi}\left[b_i^C \ln\frac{M_G}{M_C} + b_i^\Phi \ln\frac{M_G}{M_\Phi}\right] , \quad (114.13)$$

and a corresponding correction $\Delta_3^{(h)}$. To get some intuition for the magnitude, one can furthermore assume $M_\Phi = M_G$, finding (with $b_i^C = \{2/5, 0, 1\}$)

$$\Delta_3^{(h)} = \frac{9}{14\pi}\ln\left(\frac{M_G}{M_C}\right) . \quad (114.14)$$

To obtain the desired effect of $-\Delta_3^{(2)} - \Delta_3^{(l)} \simeq +0.64$, the triplet Higgs would have to be by about a factor 20 lighter than the GUT scale. While this is ruled out by nucleon decay in the minimal model [70] as will be discussed Sec. 114.6, it is also clear that threshold corrections of this order of magnitude can, in general, be realized with a certain amount of GUT-scale model building, e.g. in specific $SU(5)$ [24] or $SO(10)$ [25,26] constructions. It is, however, a significant constraint on the 4d GUT sector of the theory.

The above analysis implicitly assumes universal soft SUSY breaking masses at the GUT scale, which directly affect the spectrum of SUSY particles at the weak scale. In the simplest case we have a universal gaugino mass $M_{1/2}$, a universal mass for squarks and sleptons m_{16} and a universal Higgs mass m_{10}, as motivated by $SO(10)$. In some cases, threshold corrections to gauge coupling unification can be exchanged for threshold corrections to soft SUSY parameters (see [71] and refs. therein). For example, if gaugino masses were not unified at M_G and, in particular, gluinos were lighter than winos at the weak scale (cf. Eq. (114.11))), then it is possible that, due to weak scale threshold corrections, a much smaller or even slightly negative threshold correction at the GUT scale would be consistent with gauge coupling unification [72].

It is also noteworthy that perfect unification can be realized without significant GUT-scale corrections, simply by slightly raising the (universal) SUSY breaking scale. In this case the dark matter abundance produced by thermal processes in the early universe (if the lightest neutralino is the dark matter particle) is too high. However, even if the gaugino mass in the MSSM is about 1 TeV to explain the dark matter abundance, if the Higgsino and the non-SM Higgs boson masses are about 10-100 TeV, the effective SUSY scale can be raised [73]. This setup is realized in split SUSY [74] or the pure gravity mediation model [75] based on anomaly mediation [76]. Since the squarks and sleptons are much heavier than the gaugino masses in those setups, a gauge hierarchy problem is reintroduced. The facts that no superpartners have so far been seen at the LHC and that the observed Higgs mass favors heavier stop masses than about 1 TeV force one to accept a certain amount of fine-tuning anyway.

For non-SUSY GUTs or GUTs with a very high SUSY breaking scale to fit the data, new light states in incomplete GUT multiplets or multiple GUT breaking scales are required. For example, non-SUSY models $SO(10) \to SU(4)_C \times SU(2)_L \times SU(2)_R \to$ SM, with the second breaking scale of order an intermediate scale, determined by light neutrino masses using the see-saw mechanism, can fit the low-energy data for gauge couplings [77] and at the same time survive nucleon decay bounds [78]. Alternatively, one can appeal to string-theoretic corrections discussed in Sec. 114.4 to compensate for a high SUSY breaking scale. This has, for example, been concretely analyzed in the context of F-theory GUTs in [79].

In 5d or 6d orbifold GUTs, certain "GUT scale" threshold corrections come from the Kaluza-Klein modes between the compactification scale, $M_c \sim 1/R$, and the effective cutoff scale M_*. In string theory, this cutoff scale is the string scale. Gauge coupling unification at two loops then constrains the values of M_c and M_*.* Typically, one finds M_c to be lower than the 4d GUT scale. Since the X-bosons, responsible for nucleon decay, get mass at the compactification scale, this has significant consequences for nucleon decay.

Finally, it has been shown that non-supersymmetric GUTs in warped 5d orbifolds can be consistent with gauge coupling unification. This assumes (in 4d language) that the r.h. top quark and the Higgs doublets are composite-like objects with a compositeness scale in the TeV range [81].

114.6. Nucleon decay

Quarks and leptons are indistinguishable in any 4d GUT, and both the baryon (B) and lepton number (L) are not conserved. This leads to baryon-number-violating nucleon decay. In addition to baryon-number violation, lepton-number violation is also required for nucleon decay since, in the SM, leptons are the only free fermions which are lighter than nucleons. The lowest-dimension operators relevant for nucleon decay are $(B+L)$ violating dimension-six four-fermion-terms in the SM, and all baryon-violating operators with dimension less than seven preserve $(B-L)$ [82]. In $SU(5)$ GUTs, the dimension-six operators are induced by X boson exchange. These operators are suppressed by $(1/M_G^2)$, and the nucleon lifetime is given by $\tau_N \propto M_G^4/(\alpha_G^2\, m_p^5)$ (m_p is proton mass). The dominant decay mode of the proton (and the baryon-violating decay mode of the neutron), via X boson exchange, is $p \to e^+\,\pi^0$ ($n \to e^+\,\pi^-$). In any simple gauge symmetry, with one universal GUT coupling α_G and scale M_G, the nucleon lifetime from gauge boson exchange is calculable. Hence, the GUT scale may be directly observed via the extremely rare decay of the nucleon. Experimental searches for nucleon decay began with the Kolar Gold Mine, Homestake, Soudan, NUSEX, Frejus, HPW, IMB, and Kamiokande detectors [59]. The present experimental bounds come from Super-Kamiokande. The null result on search for $p \to e^+\pi^0$ constrains M_G to be be larger than $O(10^{15})$ GeV. Non-SUSY GUTs are constrained by the non-observation of nucleon decay, while a precise and general statement is hard to make. The reason is that gauge couplings do not unify with just the SM particle content. Once extra states or large thresholds are included to ensure precision unification, a certain range of unification scales is allowed. By contrast,

* The $\overline{\rm DR}$ scheme is frequently used in a supersymmetric regularization [65]. The renormalization transformation of the gauge coupling constants from $\overline{\rm MS}$ to $\overline{\rm DR}$ scheme is given in Ref. [66]. For an alternative treatment using holomorphic gauge couplings and NSVZ β-functions see e.g. [67].

* It is interesting to note that a ratio $M_*/M_c \sim 100$, needed for gauge coupling unification to work in orbifold GUTs, is typically the maximum value for this ratio consistent with perturbativity [80].

in SUSY GUTs one generically has $M_G \sim 2\times10^{16}$ GeV from the gauge coupling unification. Hence dimension-six baryon-number-violating operators are predicted to induce a lifetime of about $\tau_p \sim 10^{36}$ years.

However, in SUSY GUTs there are additional sources for baryon and/or lepton-number violation – dimension-four and five operators [13]. These arise since, in the SUSY SM, quarks and leptons have scalar partners (squarks and sleptons). Although our notation does not change, when discussing SUSY models our fields are chiral superfields and both fermionic and bosonic matter is implicitly represented by those. In this language, baryon- and/or lepton-number-violating dimension-four and five operators are given as so-called F terms of products of chiral superfields, which contain two fermionic components and the rest scalars or products of scalars. Within the context of $SU(5)$ the dimension-four and five operators have the form

$$(\mathbf{10}\,\bar{\mathbf{5}}\,\bar{\mathbf{5}}) \supset (u^c\,d^c\,d^c) + (Q\,L\,d^c) + (e^c\,L\,L),$$

$$(\mathbf{10}\,\mathbf{10}\,\mathbf{10}\,\bar{\mathbf{5}}) \supset (Q\,Q\,Q\,L) + (u^c\,u^c\,d^c\,e^c)$$

$$+B\text{- and } L\text{-conserving terms},$$

respectively. The dimension-four operators are renormalizable, with dimensionless couplings similar to Yukawa couplings. By contrast, the dimension-five operators have a dimensionful coupling of order $(1/M_G)$. They are generated by integrating out the color-triplet Higgs with GUT-scale mass. Note that both triplet Higgsinos (due to their fermionic nature) and Higgs scalars (due to their mass-enhanced trilinear coupling with matter) contribute to the operators.

The dimension-four operators violate either baryon number or lepton number. The nucleon lifetime is extremely short if both types of dimension-four operators are present in the SUSY SM since squark or slepton exchange induces the dangerous dimension-six SM operators. Even in the case that they violate baryon number or lepton number only but not both, they are constrained by various phenomena [83]. For example, the primordial baryon number in the universe is washed out unless the dimensionless coupling constants are less than 10^{-7}. Both types of operators can be eliminated by requiring R parity, which distinguishes Higgs from ordinary matter multiplets. R parity [84] or its cousin, matter parity [12,85], act as $F \to -F$, $H \to H$ with $F = \{\mathbf{10},\,\bar{\mathbf{5}}\}$, $H = \{\bar{\mathbf{5}}_\mathbf{H},\,\mathbf{5}_\mathbf{H}\}$ in $SU(5)$. This forbids the dimension-four operator $(\mathbf{10}\,\bar{\mathbf{5}}\,\bar{\mathbf{5}})$, but allows the Yukawa couplings for quark and lepton masses of the form $(\mathbf{10}\,\bar{\mathbf{5}}\,\bar{\mathbf{5}}_\mathbf{H})$ and $(\mathbf{10}\,\mathbf{10}\,\mathbf{5}_\mathbf{H})$. It also forbids the dimension-three, lepton-number-violating operator $(\bar{\mathbf{5}}\,\mathbf{5}_\mathbf{H}) \supset (L\,H_u)$ as well as the dimension-five, baryon-number-violating operator $(\mathbf{10}\,\mathbf{10}\,\mathbf{10}\,\bar{\mathbf{5}}_\mathbf{H}) \supset (Q\,Q\,Q\,H_d) + \cdots$. In $SU(5)$, the Higgs multiplet $\bar{\mathbf{5}}_\mathbf{H}$ and the matter multiplets $\bar{\mathbf{5}}$ have identical gauge quantum numbers. In E_6, Higgs and matter multiplets could be unified within the fundamental **27** representation. Only in $SO(10)$ are Higgs and matter multiplets distinguished by their gauge quantum numbers. The Z_4 center of $SO(10)$ distinguishes **10**s from **16**s and can be associated with R parity [86].

The dimension-five baryon-number-violating operators may also be forbidden at tree level by certain symmetries consistent with $SU(5)$ [13]. However, these symmetries are typically broken by the VEVs responsible for the color-triplet Higgs masses. Consequently the dimension-five operators are generically generated via the triplet Higgs exchange in SUSY $SU(5)$ GUTs, as mentioned above. Hence, the triplet partners of Higgs doublets must necessarily obtain mass of order the GUT scale. In addition, it is also important to note that Planck or string scale physics may independently generate the dimension-five operators, even without a GUT. These contributions must be suppressed by some underlying symmetry; for example, the same flavor symmetry which may be responsible for hierarchical fermion Yukawa matrices.

Dimension-five operators include squarks and/or sleptons. To allow for nucleon decay, these must be converted to light quarks or leptons by exchange of a gaugino or Higgsino in the SUSY SM. The nucleon lifetime is proportional to $M_G^2\,m_{\rm SUSY}^2/m_p^5$, where $m_{\rm SUSY}$ is the SUSY breaking scale. Thus, dimension-five operators may predict a shorter nucleon lifetime than dimension-six operators. Unless accidental cancellations are present, the dominant decay modes from dimension-five operators include a K meson, such as $p \to K^+\,\bar{\nu}$ ($n \to K^0\,\bar{\nu}$). This is due to a simple symmetry argument: The operators are given as $(Q_i\,Q_j\,Q_k\,L_l)$ and $(u_i^c\,u_j^c\,d_k^c\,e_l^c)$, where i, j, k, l (= 1–3) are family indices and color and weak indices are implicit. They must be invariant under $SU(3)_C$ and $SU(2)_L$ so that their color and weak doublet indices must be anti-symmetrized. Since these operators are given by bosonic superfields, they must be totally symmetric under interchange of all indices. Thus the first operator vanishes for $i = j = k$ and the second vanishes for $i = j$. Hence a second or third generation member exists in the dominant modes of nucleon decay unless these modes are accidentally suppressed [85].

Recent Super-Kamiokande bounds on the proton lifetime severely constrain the dimension-six and five operators. With 306 kton-years of data they find $\tau_p/{\rm Br}(p \to e^+\pi^0) > 1.67\times10^{34}$ years and $\tau_p/{\rm Br}(p \to K^+\bar{\nu}) > 6.61\times10^{33}$ years at 90% CL [87]. The hadronic matrix elements for baryon-number-violating operators are evaluated with lattice QCD simulations [88]. The lower bound on the X boson mass from null results in nucleon decay searches is approaching 10^{16} GeV in SUSY $SU(5)$ GUTs [89]. In the minimal SUSY $SU(5)$, $\tau_p/{\rm Br}(p \to K^+\bar{\nu})$ is smaller than about 10^{31} years if the triplet Higgs mass is 10^{16} GeV and $m_{\rm SUSY} = 1$ TeV [90]. The triplet Higgs mass bound from nucleon decay is then in conflict with gauge coupling unification so that this model is considered to be ruled out [70].

Since nucleon decay induced by the triplet Higgs is a severe problem in SUSY GUTs, various proposals for its suppression have been made. First, some accidental symmetry or accidental structure in non-minimal Higgs sectors in $SU(5)$ or $SO(10)$ theories may suppress the dimension-five operators [25,26,21,91]. As mentioned above, the triplet Higgs mass term violates symmetries which forbid the dimension-five operators. In other words, the nucleon decay is suppressed if the Higgs triplets in $\bar{\mathbf{5}}_\mathbf{H}$ and $\mathbf{5}_\mathbf{H}$ do not have a common mass term but, instead, their mass terms involve partners from other $SU(5)$ multiplets. Second, the SUSY breaking scale may be around $\mathcal{O}$(10–100) TeV in order to explain the observed Higgs boson mass at the LHC. In this case, nucleon decay is automatically suppressed [74,92,93]. Third, accidental cancellations among diagrams due to a fine-tuned structure of squark and slepton flavor mixing might suppress nucleon decay [94]. Last, we have also implicitly assumed a hierarchical structure for Yukawa matrices in the analysis. It is however possible to fine-tune a hierarchical structure for quarks and leptons which baffles the family structure so that the nucleon decay is suppressed [95]. The upper bound on the proton lifetime from some of these theories is approximately a factor of 10 above the experimental bounds. Future experiments with larger neutrino detectors, such as JUNO [96], Hyper-Kamiokande [97] and DUNE [98], are planned and will have higher sensitivities to nucleon decay.

Appealing to global symmetries to suppress specific interactions may not always be as straightforward as it naively seems, as a general remark, while global symmetries are introduced to control the dimension-four and five operators in SUSY GUTs. Indeed, there are two possibilities: On the one hand, the relevant symmetry might be gauged at a higher scale. Effects of the VEVs responsible for the spontaneous breaking are then in principle dangerous and need to be quantified. On the other hand, the symmetry might be truly only global. This must e.g. be the case for anomalous symmetries, which are then also violated by field-theoretic non-perturbative effects. The latter can in principle be exponentially small. It is, however, widely believed that global symmetries are always broken in quantum gravity (see e.g. [99]). One then needs to understand which power or functional form the Planck scale suppression of the relevant interaction has. For example, dimension-five baryon number violating operators suppressed by just one unit of the Planck or string scale are completely excluded.

In view of the above, it is also useful to recall that in string models 4d global symmetries generally originate in higher-dimensional gauge symmetries. Here 'global' implies that the gauge boson has acquired a Stückelberg-mass. This is a necessity in the anomalous case (Green-Schwarz mechanism) but can also happen to non-anomalous symmetries. One expects no symmetry violation beyond the well-understood non-perturbative effects. Discrete symmetries arise as

subgroups of continuous gauge symmetries, such as $Z_N \subset U(1)$. In particular, non-anomalous subgroups of Stückelberg-massive $U(1)$s represent unbroken discrete gauge symmetries and as such are non-perturbatively exact (see e.g. [100]). Of course, such discrete gauge symmetries may also arise as remnants of continuous gauge symmetries after conventional 4d spontaneous breaking.

Are there ways to avoid the stringent predictions for proton decay discussed above? Orbifold GUTs and string theories, see Sec. 114.4, contain grand unified symmetries realized in higher dimensions. In the process of compactification and GUT symmetry breaking, the triplet Higgs states may be removed (projected out of the massless sector of the theory). In such models, the nucleon decay due to dimension-five operators can be severely suppressed or eliminated completely. However, nucleon decay due to dimension-six operators may be enhanced, since the gauge-bosons mediating proton decay obtain mass at the compactification scale, M_c, which is typically less than the 4d GUT scale (cf. Sec. 114.5). Alternatively, the same projections which eliminate the triplet Higgs may rearrange the quark and lepton states such that the massless states of one family come from different higher-dimensional GUT multiplets. This can suppress or completely eliminate even dimension-six proton decay. Thus, enhancement or suppression of dimension-six proton decay is model-dependent. In some complete 5d orbifold GUT models [101,58] the lifetime for the decay $\tau_p/\mathrm{Br}(p \to e^+\pi^0)$ can be near the bound of 1×10^{34} years with, however, large model-dependence and/or theoretical uncertainties. In other cases, the modes $p \to K^+\bar{\nu}$ and $p \to K^0\mu^+$ may be dominant [58]. Thus, interestingly, the observation of nucleon decay may distinguish string or higher-dimensional GUTs from 4d ones.

In orbifold GUTs or string theory, new discrete symmetries consistent with SUSY GUTs can forbid all dimension-three and four baryon- and lepton-number-violating operators. Even the μ term and dimension-five baryon- and lepton-number-violating operators can be forbidden to all orders in perturbation theory [32]. The μ term and dimension-five baryon- and lepton-number-violating operators may then be generated, albeit sufficiently suppressed, via non-perturbative effects. The simplest example of this is a Z_4^R symmetry which is the unique discrete R symmetry consistent with $SO(10)$ [32]. Even though it forbids the dimension-five proton decay operator to the desired level, it allows the required dimension-five neutrino mass term. In this case, proton decay is dominated by dimension-six operators, leading to decays such as $p \to e^+\pi^0$.

114.7. Yukawa coupling unification

In the SM, masses and mixings for quarks and leptons come from the Yukawa couplings with the Higgs doublet, but the values of these couplings remain a mystery. GUTs provide at least a partial understanding since each generation is embedded in unified multiplet(s). Specifically, since quarks and leptons are two sides of the same coin, the GUT symmetry relates the Yukawa couplings (and hence the masses) of quarks and leptons.

In $SU(5)$, there are two types of independent renormalizable Yukawa interactions given by $\lambda_{ij}\ (\mathbf{10}_i\ \mathbf{10}_j\ \mathbf{5_H}) + \lambda'_{ij}\ (\mathbf{10}_i\ \bar{\mathbf{5}}_j\ \bar{\mathbf{5}}_{\mathbf{H}})$. These contain the SM interactions $\lambda_{ij}\ (Q_i\ u^c_j\ H_u) + \lambda'_{ij}\ (Q_i\ d^c_j\ H_d\ + e^c_i\ L_j\ H_d)$. Here $i, j\,(=1\text{–}3)$ are, as before, family indices. Hence, at the GUT scale we have tree-level relations between Yukawa coupling constants for charged lepton and down quark masses, such as $\lambda_b = \lambda_\tau$ in which $\lambda_{b/\tau}$ are the bottom quark /τ lepton Yukawa coupling constants [102,103]. In $SO(10)$, there is only one type of independent renormalizable Yukawa interaction given by $\lambda_{ij}\ (\mathbf{16}_i\ \mathbf{16}_j\ \mathbf{10_H})$, leading to relations among all Yukawa coupling constants and quark and lepton masses within one generation [104,105] (such as $\lambda_t = \lambda_b = \lambda_\tau$, with λ_t the top quark Yukawa coupling constant).

114.7.1. *The third generation, b–τ or t–b–τ unification* :

Third generation Yukawa couplings are larger than those of the first two generations. Hence, the fermion mass relations predicted from renormalizable GUT interactions which we introduced above are expected to be more reliable. In order to compare them with data, we have to include the radiative correction to these relations from the RG evolution between GUT and fermion mass scale, from integrating out heavy particles at the GUT scale, and from weak scale thresholds.

Since testing Yukawa coupling unification is only possible in models with successful gauge coupling unification, we here focus on SUSY GUTs. In the MSSM, top and bottom quark and τ lepton masses are related to the Yukawa coupling constants at the scale m_Z as

$$m_t(m_Z) = \lambda_t(m_Z)\ v_u(1 + \delta m_t/m_t),$$

$$m_{b/\tau}(m_Z) = \lambda_{b/\tau}(m_Z)\ v_d(1 + \delta m_{b/\tau}/m_{b/\tau}),$$

where $\langle H^0_u\rangle \equiv v_u = \sin\beta\ v/\sqrt{2}$, $\langle H^0_d\rangle \equiv v_d = \cos\beta\ v/\sqrt{2}$, $v_u/v_d \equiv \tan\beta$ and $v \sim 246$ GeV is fixed by the Fermi constant, G_μ. Here, $\delta m_f/m_f$ $(f = t, b, \tau)$ represents the threshold correction due to integrating out SUSY partners. For the bottom quark mass, it is found [106] that the dominant corrections come from the gluino-sbottom and from the Higgsino-stop loops,

$$\left(\frac{\delta m_b}{m_b}\right)_{g_3} \sim \frac{g_3^2}{6\pi^2}\frac{m_{\tilde{g}}\mu}{m^2_{\mathrm{SUSY}}}\tan\beta$$

and

$$\left(\frac{\delta m_b}{m_b}\right)_{\lambda_t} \sim \frac{\lambda_t^2}{16\pi^2}\frac{A_t\mu}{m^2_{\mathrm{SUSY}}}\tan\beta\,, \qquad (114.15)$$

where $m_{\tilde{g}}$, μ, and A_t stand for gluino and Higgsino masses and trilinear stop coupling, respectively. Note that Eq. (114.15) only illustrates the structure of the corrections – non-trivial functional dependences on several soft parameters $\sim m_{\mathrm{SUSY}}$ have been suppressed. For the full one-loop correction to the bottom quark mass see, for example, Ref. [107].

Note also that the corrections do not go to zero as SUSY particles become much heavier than m_Z. They may change the bottom quark mass at the $\mathcal{O}(10)\%$ level for $\tan\beta = \mathcal{O}(10)$. The total effect is sensitive to the relative phase between gluino and Higgsino masses since $A_t \sim -m_{\tilde{g}}$ due to the infrared fixed point nature of the RG equation for A_t [108] in settings where SUSY breaking terms come from Planck scale dynamics, such as gravity mediation. The τ lepton mass also receives a similar correction, though only at the few % level. The top quark mass correction, not being proportional to $\tan\beta$, is at most 10% [109].

Including one loop threshold corrections at m_Z and additional RG running, one finds the top, bottom and τ pole masses. In SUSY GUTs, b–τ unification has two possible solutions with $\tan\beta \sim 1$ or $\mathcal{O}(10)$. The small $\tan\beta$ solution may be realized in the MSSM if superpartner masses are $\mathcal{O}(10)$ TeV, as suggested by the observed Higgs mass [92]. The large $\tan\beta$ limit such as $\tan\beta \sim 40$–50 overlaps the $SO(10)$ symmetry relation [109]. When $\tan\beta$ is large, there are significant threshold corrections to down quark masses as mentioned above, and Yukawa unification is only consistent with low-energy data in a restricted region of SUSY parameter space, with important consequences for SUSY searches [109,110]. More recent analyses of Yukawa unification after LHC Run-I are found in Ref. [111].

Gauge coupling unification is also successful in the scenario of split supersymmetry [74], in which squarks and sleptons have mass at a scale $\tilde{m} \gg m_Z$, while gauginos and/or Higgsinos have masses of order the weak scale. Unification of b–τ Yukawa couplings requires $\tan\beta$ to be fine-tuned close to 1 [92]. If by contrast, $\tan\beta \gtrsim 1.5$, b–τ Yukawa unification only works for $\tilde{m} \lesssim 10^4$ GeV. This is because the effective theory between the gaugino mass scale and $\tilde{m}$ includes only one Higgs doublet, as in the standard model. As a result, the large top quark Yukawa coupling tends to increase the ratio λ_b/λ_τ due to the vertex correction, which is absent in supersymmetric theories, as one runs down in energy below $\tilde{m}$. This is opposite to what happens in the MSSM where the large top quark Yukawa coupling lowers the ratio λ_b/λ_τ [103].

114.7.2. *Beyond leading order: three-family models* :

Simple Yukawa unification is not possible for the first two generations. Indeed, $SU(5)$ implies $\lambda_s = \lambda_\mu$, $\lambda_d = \lambda_e$ and hence $\lambda_s/\lambda_d = \lambda_\mu/\lambda_e$. This is an RG-invariant relation which extrapolates to $m_s/m_d = m_\mu/m_e$ at the weak scale, in serious disagreement with data ($m_s/m_d \sim 20$ and $m_\mu/m_e \sim 200$). An elegant solution to this

problem was given by Georgi and Jarlskog [112] (for a recent analysis in the SUSY context see [113]) .

More generally, we have to recall that in all of the previous discussion of Yukawa couplings, we assumed renormalizable interactions as well as the minimal matter and Higgs content. Since the GUT scale is close to the Planck scale, higher-dimension operators involving the GUT-breaking Higgs may modify the predictions, especially for lower generations. An example is provided by the operators $\mathbf{10}\ \bar{\mathbf{5}}\ \bar{\mathbf{5}}_{\mathbf{H}}\ \mathbf{24}_{\mathbf{H}}$ with $\mathbf{24}_{\mathbf{H}}$ the GUT-breaking Higgs of $SU(5)$. We can fit parameters to the observed fermion masses with these operators, though some fine-tuning is introduced in doing so. The SM Higgs doublet may come in part from higher representations of the GUT group. For example, the **45** of $SU(5)$ includes an $SU(2)_L$ doublet with appropriate $U(1)_Y$ charge [112]. This **45** can, in turn, come from the **120** or **126** of $SO(10)$ after its breaking to $SU(5)$ [114]. These fields may also have renormalizable couplings with quarks and leptons. The relations among the Yukawa coupling constants in the SM are modified if the SM Higgs doublet is a linear combination of several such doublets from different $SU(5)$ multiplets. Finally, the SM fermions may not be embedded in GUT multiplets in the minimal way. Indeed, if all quarks and leptons are embedded in **16**s of $SO(10)$, the renormalizable interactions with $\mathbf{10}_{\mathbf{H}}$ cannot explain the observed CKM mixing angles. This situation improves when extra matter multiplets, such as **10**, are introduced: After $U(1)_X$, which distinguishes the $\bar{\mathbf{5}}$s coming from the **16** and the **10** of $SO(10)$, is broken (e.g. by a VEV of $\mathbf{16}_{\mathbf{H}}$ or $\mathbf{126}_{\mathbf{H}}$), the r.h. down quarks and l.h. leptons in the SM can be linear combinations of components in **16**s and **10**s. As a result, $\lambda \neq \lambda'$ in $SU(5)$ [115].

To construct realistic three-family models, some or all of the above effects can be used. Even so, to achieve significant predictions for fermion masses and mixing angles grand unification alone is not sufficient. Other ingredients, for example additional global family symmetries are needed (in particular, non-abelian symmetries can strongly reduce the number of free parameters). These family symmetries constrain the set of effective higher-dimensional fermion mass operators discussed above. In addition, sequential breaking of the family symmetry can be correlated with the hierarchy of fermion masses. One simple, widely known idea in this context is to ensure that each $\mathbf{10}_i$ enters Yukawa interactions together with a suppression factor ϵ^{3-i} (ϵ being a small parameter). This way one automatically generates a stronger hierarchy in up-type quark Yukawas as compared to down-type quark and lepton Yukawas and no hierarchy for neutrinos, which agrees with observations at the $\mathcal{O}(1)$-level. Three-family models exist which fit all the data, including neutrino masses and mixing [26,116].

Finally, a particularly ambitious variant of unification is to require that the fermions of all three generations come from a single representation of a large gauge group. A somewhat weaker assumption is that the flavor group (e.g. $SU(3)$) unifies with the SM gauge group in a simple gauge group at some energy scale $M \geq M_G$. Early work on such 'flavor-unified GUTs', see e.g. [117], has been reviewed in [118,119]. For a selection of more recent papers see [120]. In such settings, Yukawa couplings are generally determined by gauge couplings together with symmetry breaking VEVs. This is reminiscent of heterotic string GUTs, where all couplings come from the 10d gauge coupling. However, while the $\mathrm{E}_8 \to SU(3)\times\mathrm{E}_6$ branching rule $\mathbf{248} = (\mathbf{8},\mathbf{1}) + (\mathbf{1},\mathbf{78}) + (\mathbf{3},\mathbf{27}) + (\bar{\mathbf{3}},\bar{\mathbf{27}})$ looks very suggestive in this context, the way in which most modern heterotic models arrive at three generations is actually more complicated.

114.7.3. *Flavor violation* :

Yukawa interactions of GUT-scale particles with quarks and leptons may leave imprints on the flavor violation induced by SUSY breaking parameters [121]. To understand this, focus first on the MSSM with universal Planck-scale boundary conditions (as e.g. in gravity mediation). Working in a basis where up-quark and lepton Yukawas are diagonal, one finds that the large top-quark Yukawa coupling reduces the l.h. squark mass squareds in the third generation radiatively. It turns out that only the l.h. down-type squark mass matrix has sizable off-diagonal terms in the flavor basis after CKM-rotation. However, in GUTs the color-triplet Higgs has flavor violating interactions from the Yukawa coupling λ_{ij} ($\mathbf{10}_i\ \mathbf{10}_j\ \mathbf{5}_{\mathbf{H}}$), such that flavor-violating r.h. slepton mass terms are radiatively generated in addition [122]. If r.h. neutrinos are introduced as $SU(5)$ singlets with interactions λ''_{ij} ($\mathbf{1}_i\ \bar{\mathbf{5}}_j\ \mathbf{5}_{\mathbf{H}}$), the doublet and color-triplet Higgses acquire another type of Yukawa coupling, respectively. They then radiatively generate flavor-violating l.h. slepton [123] and r.h. down squark masses [124]. These flavor-violating SUSY breaking terms induce new contributions to FCNC processes in quark and lepton sectors, such as $\mu \to e\gamma$ and K^0–$\bar{K}^0$ and B^0–$\bar{B}^0$ mixing. EDMs are also induced when both l.h. and r.h. squarks/sleptons have flavor-violating mass terms with relative phases, as discussed for $SO(10)$ in [125] or for $SU(5)$ with r.h. neutrinos in [126]. Thus, such low-energy observables constrain GUT-scale interactions.

114.8. Neutrino masses

We see from atmospheric and solar neutrino oscillation observations, along with long baseline accelerator and reactor experiments, that neutrinos have finite masses. By adding three "sterile" neutrinos ν_i^c with Yukawa couplings $\lambda_{\nu,ij}$ ($\nu_i^c\ L_j\ H_u$) (i,j = 1–3), one easily obtains three massive Dirac neutrinos with mass $m_\nu = \lambda_\nu\ v_u$, analogously to quark and charged lepton masses. However, in order to obtain a τ neutrino with mass of order 0.1 eV, one requires the exceedingly small coupling ratio $\lambda_{\nu_\tau}/\lambda_\tau \lesssim 10^{-10}$. By contrast, the seesaw mechanism *naturally* explains such tiny neutrino masses as follows [1,2,3]: The sterile neutrinos have no SM gauge quantum numbers so that there is no symmetry other than global lepton number which forbids the Majorana mass term $\frac{1}{2}M_{ij}\ \nu_i^c\ \nu_j^c$. Note also that sterile neutrinos can be identified with the r.h. neutrinos necessarily contained in complete families of $SO(10)$ or Pati-Salam models. Since the Majorana mass term violates $U(1)_X$ in $SO(10)$, one might expect $M_{ij} \sim M_G$. The heavy sterile neutrinos can be integrated out, defining an effective low-energy theory with only three light active Majorana neutrinos with the effective dimension-five operator

$$-\mathcal{L}_{eff} = \frac{1}{2}c_{ij}\ (L_i\ H_u)\ (L_j\ H_u)\,, \tag{114.16}$$

where $c = \lambda_\nu^T\ M^{-1}\ \lambda_\nu$. This then leads to a 3×3 Majorana neutrino mass matrix $m = m_\nu^T\ M^{-1}\ m_\nu$.

Atmospheric neutrino oscillations require neutrino masses with $\Delta m_\nu^2 \sim 2.5\times 10^{-3}$ eV^2 with maximal mixing, in the simplest scenario of two neutrino dominance. With hierarchical neutrino masses this implies $m_{\nu_\tau} = \sqrt{\Delta m_\nu^2} \sim 0.05$ eV. Next, we can try to relate the neutrino Yukawa coupling to the top quark Yukawa coupling, $\lambda_{\nu_\tau} = \lambda_t$ at the GUT scale, as in $SO(10)$ or $SU(4)\times SU(2)_L \times SU(2)_R$ models. This gives $M \sim 10^{14}$ GeV, which is remarkably close to the GUT scale.

Neutrinos pose a special problem for SUSY GUTs. The question is why the quark mixing angles in the CKM matrix are small while there are two large lepton mixing angles in the PMNS matrix (cf. however the comment at the end of Sec. 114.7). Discussions of neutrino masses and mixing angles can, for example, be found in Refs. [127] and [128]. For SUSY GUT models which fit quark and lepton masses, see Ref. [25]. Finally, for a compilation of the range of SUSY GUT predictions for neutrino mixing, see [129].

The seesaw mechanism implemented by r.h. neutrinos is sometimes called the type-I seesaw model. There are variant models in which the dimension-five operator for neutrino masses is induced in different ways: In the type-II model, an $SU(2)_L$ triplet Higgs boson Σ is introduced to have couplings ΣL^2 and also ΣH_u^2 [130]. In the type-III model, an $SU(2)_L$ triplet of fermions $\tilde{\Sigma}$ with a Yukawa coupling $\tilde{\Sigma}LH_u$ is introduced [131]. In these models, the dimension-five operator is induced by integrating out the triplet Higgs boson or fermions. Such models can also be implemented in GUTs by introducing Higgs bosons in the **15** or fermions in the **24** in $SU(5)$ GUTs or the **126** in $SO(10)$ GUTs. Notice that the gauge non-singlet fields in the type-II and III models have masses at the intermediate scale. Thus, gauge coupling unification is not automatic if they are implemented in SUSY GUTs.

114.9. Selected topics

114.9.1. ***Magnetic monopoles*** :

In the broken phase of a GUT there are typically localized classical solutions carrying magnetic charge under an unbroken $U(1)$ symmetry [132]. These magnetic monopoles with mass of order M_G/α_G can be produced during a possible GUT phase transition in the early universe. The flux of magnetic monopoles is experimentally found to be less than $\sim 10^{-16}$ cm^{-2} s^{-1} sr^{-1} [133]. Many more are however predicted, hence the GUT monopole problem. In fact, one of the original motivations for inflation was to solve the monopole problem by exponential expansion after the GUT phase transition [134] and hence dilution of the monopole density. Other possible solutions to the monopole problem include: sweeping them away by domain walls [135], $U(1)$ electromagnetic symmetry breaking at high temperature [136] or GUT symmetry non-restoration [137]. Parenthetically, it was also shown that GUT monopoles can catalyze nucleon decay [138]. A significantly stronger bound on the monopole flux can then be obtained by considering X-ray emission from radio pulsars due to monopole capture and the subsequent nucleon decay catalysis [139].

Note that the present upper bound on the inflationary vacuum energy density is very close to the GUT scale, $V_{inf}^{1/4} = (1.88 \times 10^{16}\,\text{GeV}) \times (r/0.10)^{1/4}$, with the scalar-to-tensor ratio constraint to $r < 0.11$ [140]. This guarantees that reheating does not lead to temperatures above M_G and hence the monopole problem is solved by inflation (unless M_G is unexpectedly low).

114.9.2. ***Anomaly constraints vs. GUT paradigm*** :

As emphasized at the very beginning, the fact that the SM fermions of one generation fill out the $\mathbf{10} + \overline{\mathbf{5}}$ of $SU(5)$ appears to provide overwhelming evidence for some form of GUT embedding. However, one should be aware that a counterargument can be made which is related to the issue of 'charge quantization by anomaly cancellation' (see [141,142] for some early papers and [143] for a more detailed reference list): Imagine we only knew that the low-energy gauge group were G_{SM} and the matter content included the $(\mathbf{3},\mathbf{2})_Y$, i.e. a 'quark doublet' with $U(1)$-charge Y. One can then ask which possibilities exist of adding further matter to ensure the cancellation of all triangle anomalies. It turns out that this problem has only three different, minimal* solutions [142]. One of those is precisely a single SM generation, with the apparent '$SU(5)$-ness' emerging accidentally. Thus, if one randomly picks models from the set of consistent gauge theories, preconditioning on G_{SM} and $(\mathbf{3},\mathbf{2})_Y$, one may easily end up with '$\mathbf{10} + \overline{\mathbf{5}}$' of an $SU(5)$ that is in no way dynamically present. This is precisely what happens in the context of non-GUT string model building [144].

114.9.3. ***GUT baryogenesis and leptogenesis*** :

During inflation, any conserved quantum number is extremely diluted. Thus, one expects the observed baryon asymmetry of the universe to originate at reheating or in the subsequent cosmological evolution. In detail, the situation is slightly more involved: Both baryon number B and lepton number L are global symmetries of the SM. However, $(B+L)$ is anomalous and violated by thermal fluctuations in the early universe, via so-called sphaleron processes. Moreover, it is violated in GUT models, as is most apparent in proton decay. By contrast, $(B-L)$ is anomaly free and preserved by both the SM as well as $SU(5)$ or $SO(10)$ gauge interactions.

Now, the old idea of GUT baryogenesis [145,146] is to generate a $(B+L)$ and hence a baryon asymmetry by the out-of-equilibrium decay of the color-triplet Higgs. However such an asymmetry, generated at GUT temperatures, is washed out by sphalerons. This can be overcome [147] using lepton-number violating interaction of neutrinos to create a $(B-L)$ from the $(B+L)$ asymmetry, before sphaleron processes become sufficiently fast at $T < 10^{12}$ GeV. This $(B-L)$ asymmetry can then survive the subsequent sphaleron dominated phase. Note that this does not work in the minimal SUSY GUT setting, with the triplet Higgs above the GUT scale. The reason is that a correspondingly high reheating temperature would be required which, as explained above, is ruled out by Planck data.

However, the most widely accepted simple way out of the dilemma is to directly generate a net $(B-L)$ asymmetry dynamically in the early universe, also using r.h. neutrinos. Indeed, we have seen that neutrino oscillations suggest a new scale of physics of order 10^{14} GeV. This scale is associated with heavy Majorana neutrinos in the seesaw mechanism. If in the early universe, the decay of the heavy neutrinos is out of equilibrium and violates both lepton number and CP, then a net lepton number may be generated. This lepton number will then be partially converted into baryon number via electroweak processes [148]. This mechanism is called leptogenesis.

If the three heavy Majorana neutrino masses are hierarchical, the net lepton number is produced by decay of the lightest one, and it is proportional to the CP asymmetry in the decay, ϵ_1. The CP asymmetry is bounded from above, and the lightest neutrino mass is required to be larger than 10^9 GeV in order to explain the observed baryon asymmetry [149]. This implies that the reheating temperature after inflation should be larger than 10^9 GeV so that the heavy neutrinos are thermally produced. In supersymmetric models, there is a tension between leptogenesis and Big Bang Nucleosynthesis (BBN) if gravitinos decay in the BBN era. The gravitino problem gives a constraint on the reheating temperature $\lesssim 10^{6-10}$ GeV though the precise value depends on the SUSY breaking parameters [150]. Recent reviews of leptogenesis can be found in Ref. [151].

114.10. Conclusion

Most conservatively, grand unification means that (some of) the SM gauge interactions of $U(1)_Y$, $SU(2)_L$ and $SU(3)_C$ become part of a larger, unifying gauge symmetry at a high energy scale. In most models, especially in the simplest and most appealing variants of $SU(5)$ and $SO(10)$ unification, the statement is much stronger: One expects the three gauge couplings to unify (up to small threshold corrections) at a unique scale, M_G, and the proton to be unstable due to exchange of gauge bosons of the larger symmetry group. Supersymmetric grand unified theories provide, by far, the most predictive and economical framework allowing for perturbative unification. For a selection of reviews, with many more details than could be discussed in the present article, see [118,152].

Thus, the three classical pillars of GUTs are gauge coupling unification at $M_G \sim 2 \times 10^{16}$ GeV, low-energy supersymmetry (with a large SUSY desert), and nucleon decay. The first of these may be viewed as predicting the value of the strong coupling – a prediction which has already been verified (see Fig. 114.1). Numerically, this prediction remains intact even if SUSY partner masses are somewhat above the weak scale. However, at the conceptual level a continuously increasing lower bound on the SUSY scale is nevertheless problematic for the GUT paradigm: Indeed, if the independent, gauge-hierarchy-based motivation for SUSY is completely abandoned, the SUSY scale and hence α_3 become simply free parameters and the first two pillars crumble. Thus, it is important to keep pushing bounds on proton decay which, although again not completely universal in all GUT constructions, is arguably a more generic part of the GUT paradigm than low-energy SUSY.

Whether or not Yukawa couplings unify is more model dependent. However, irrespective of possible (partial) Yukawa unification, there certainly exists a very interesting and potentially fruitful interplay between flavor model building and grand unification. Especially in the neutrino sector this is strongly influenced by the developing experimental situation.

Another phenomenological signature of grand unification is the strength of the direct coupling of the QCD axion to photons, relative to its coupling to gluons. It is quantified by the predicted anomaly ratio $E/N = 8/3$ (see [153,154]). This arises in field-theoretic axion models consistent with GUT symmetry (such as DFSZ [155]) and in string-theoretic GUTs [154]. In the latter, the axion does not come from the phase of a complex scalar but is a fundamental shift-symmetric real field, coupling through a higher-dimension operator

* Adding extra vector-like sets of fields, e.g. two fermions which only transform under $U(1)$ and have charges Y and $-Y$, is considered to violate minimality.

directly to the product of the GUT field-strength and its dual.

It is probably fair to say that, due to limitations of the 4d approach, including especially remaining ambiguities (free parameters or ad hoc assumptions) in models of flavor and GUT breaking, the string theoretic approach has become more important in GUT model building. In this framework, challenges include learning how to deal with the many vacua of the 'landscape' as well as, for each vacuum, developing the tools for reliably calculating detailed, phenomenological observables. Finally, due to limitations of space, the present article has barely touched on the interesting cosmological implications of GUTs. They may become more important in the future, especially in the case that a high inflationary energy scale is established observationally.

References:

1. P. Minkowski, Phys. Lett. **B67**, 421 (1977).
2. T. Yanagida, in *Proceedings of the Workshop on the Unified Theory and the Baryon Number of the Universe*, eds. O. Sawada and A. Sugamoto, KEK report No. 79-18, Tsukuba, Japan, 1979;
   S. Glashow, Quarks and leptons, published in *Proceedings of the Carg'ese Lectures*, M. Levy (ed.), Plenum Press, New York, (1980);
   M. Gell-Mann, P. Ramond and R. Slansky, in *Supergravity*, ed. P. van Nieuwenhuizen *et al.*, North-Holland, Amsterdam, (1979), p. 315 [arXiv:1306.4669].
3. F. Wilczek, eConf C **790823**, 437 (1979);
   E. Witten, Phys. Lett. **B91**, 81 (1980);
   R.N. Mohapatra and G. Senjanovic, Phys. Rev. Lett. **44**, 912 (1980).
4. U. Amaldi, W. de Boer and H. Furstenau, Phys. Lett. **B260**, 447 (1991);
   J.R. Ellis, S. Kelley and D.V. Nanopoulos, Phys. Lett. **B260**, 131 (1991);
   P. Langacker and M. Luo, Phys. Rev. **D44**, 817 (1991);
   C. Giunti, C.W. Kim and U.W. Lee, Mod. Phys. Lett. **A6**, 1745 (1991);
   P. Langacker and N. Polonsky, Phys. Rev. **D47**, 4028 (1993), [hep-ph/9210235];
   M. Carena, S. Pokorski and C.E.M. Wagner, Nucl. Phys. **B406**, 59 (1993) [hep-ph/9303202];
   See also the review by S. Dimopoulos, S.A. Raby and F. Wilczek, Physics Today, p. 25 October (1991).
5. Y. Okada, M. Yamaguchi and T. Yanagida, Prog. Theor. Phys. **85**, 1 (1991);
   J.R. Ellis, G. Ridolfi and F. Zwirner, Phys. Lett. **B257**, 83 (1991);
   H.E. Haber and R. Hempfling, Phys. Rev. Lett. **66**, 1815 (1991).
6. M.S. Carena *et al.*, Phys. Lett. **B355**, 209 (1995) [hep-ph/9504316];
   G. Degrassi *et al.*, Eur. Phys. J. **C28**, 133 (2003) [arXiv:hep-ph/0212020];
   P. Kant *et al.*, JHEP **1008**, 104 (2010) [arXiv:1005.5709].
7. M.J.G. Veltman, Acta Phys. Pol. **B12**, 437 (1981);
   L. Maiani, Gif-sur-Yvette Summer School on Particle Physics, 11th, Gif-sur-Yvette, France, 1979 (Inst. Nat. Phys. Nucl. Phys. Particules, Paris, 1979);
   E. Witten, Nucl. Phys. **B188**, 513 (1981).
8. J.L. Feng *et al.*, Phys. Rev. Lett. **111**, 131802 (2013) [arXiv:1306.2318];
   S. Heinemeyer, Lecture at 42nd ITEP winter school, Moscow, arXiv:1405.3781;
   P. Draper and H. Rzehak, Phys. Rept. **619**, 1 (2016) [arXiv:1601.01890].
9. J. Pati and A. Salam, Phys. Rev. **D8**, 1240 (1973);
   For more discussion on the standard charge assignments in this formalism, see A. Davidson, Phys. Rev. **D20**, 776 (1979) and R.N Mohapatra and R.E. Marshak, Phys. Lett. **B91**, 222 (1980); see also J. C. Pati, Int. J. Mod. Phys. A **32**, 1741013 (2017), arXiv:1706.09531 for a recent account.
10. H. Georgi and S.L Glashow, Phys. Rev. Lett. **32**, 438 (1974).
11. J.R. Ellis, M.K. Gaillard and D.V. Nanopoulos, Phys. Lett. **B80**, 360 (1979) [Phys. Lett. **B82**, 464 (1979)];
    E. Golowich, Phys. Rev. **D24**, 2899 (1981).
12. S. Dimopoulos, S. Raby, and F. Wilczek, Phys. Rev. **D24**, 1681 (1981);
    S. Dimopoulos and H. Georgi, Nucl. Phys. **B193**, 150 (1981);
    L. Ibanez and G.G. Ross, Phys. Lett. **B105**, 439 (1981);
    N. Sakai, Z. Phys. **C11**, 153 (1981);
    M.B. Einhorn and D.R.T. Jones, Nucl. Phys. **B196**, 475 (1982);
    W.J. Marciano and G. Senjanovic, Phys. Rev. **D25**, 3092 (1982).
13. S. Weinberg, Phys. Rev. **D26**, 287 (1982);
    N. Sakai and T. Yanagida, Nucl. Phys. **B197**, 533 (1982).
14. H. Georgi, Particles and Fields, *Proceedings of the APS Div. of Particles and Fields*, ed. C. Carlson, p. 575 (1975);
    H Fritzsch and P. Minkowski, Ann. Phys. **93**, 193 (1975).
15. R. Slansky, Phys. Reports **79**, 1 (1981);
    H. Georgi, Front. Phys. **54**, 1 (1982);
    R. Feger and T.W. Kephart, Comp. Phys. Comm. **192**, 166 (2015) [arXiv:1206.6379];
    N. Yamatsu, PTEP, no.4, 043B02 (2016) [arXiv:1512.05559].
16. S.M. Barr, Phys. Lett. **B112**, 219 (1982);
    J.P. Derendinger, J.E. Kim and D.V. Nanopoulos, Phys. Lett. **B139**, 170 (1984);
    I. Antoniadis *et al.*, Phys. Lett. **B194**, 231 (1987) and Phys. Lett. **B231**, 65 (1989).
17. F. Gursey, P. Ramond and P. Sikivie, Phys. Lett. **B60**, 177 (1976).
18. A. de Rujula, H. Georgi and S. L. Glashow, *5th Workshop on Grand Unification*, ed. K. Kang, H. Fried and P. Frampton, World Scientific, Singapore (1984), p. 88;
    See also earlier paper by Y. Achiman and B. Stech, p. 303, "New Phenomena in Lepton-Hadron Physics," ed. D.E.C. Fries and J. Wess, Plenum, NY (1979).
19. B.R. Greene *et al.*, Nucl. Phys. **B278**, 667 (1986) and Nucl. Phys. **B292**, 606 (1987);
    B.R. Greene, C.A. Lutken and G.G. Ross, Nucl. Phys. **B325**, 101 (1989);
    J.E. Kim, Phys. Lett. **B591**, 119 (2004) [hep-ph/0403196].
20. E. Witten, Phys. Lett. **B105**, 267 (1981).
21. A. Masiero *et al.*, Phys. Lett. **B115**, 380 (1982);
    B. Grinstein, Nucl. Phys. **B206**, 387 (1982).
22. S. Dimopoulos and F. Wilczek, *Proceedings Erice Summer School*, ed. A. Zichichi (1981);
    M. Srednicki, Nucl. Phys. **B202**, 327 (1982).
23. K. Inoue, A. Kakuto and H. Takano, Prog. Theor. Phys. **75**, 664 (1986).
24. Y. Yamada, Z. Phys. **C60**, 83 (1993);
    J. Hisano *et al.*, Phys. Lett. **B342**, 138 (1995) [hep-ph/9406417];
    G. Altarelli, F. Feruglio and I. Masina, JHEP **0011**, 040 (2000) [hep-ph/0007254].
25. K.S. Babu and S.M. Barr, Phys. Rev. **D48**, 5354 (1993) [hep-ph/9306242];
    K.S. Babu and S.M. Barr, Phys. Rev. **D50**, 3529 (1994) [hep-ph/9402291];
    K.S. Babu, J.C. Pati and Z. Tavartkiladze, JHEP **1006**, 084 (2010) [arXiv:1003.2625].
26. K.S. Babu and R.N. Mohapatra, Phys. Rev. Lett. **74**, 2418 (1995) [hep-ph/9410326];
    V. Lucas and S. Raby, Phys. Rev. **D54**, 2261 (1996) [hep-ph/9601303];
    T. Blažek *et al.*, Phys. Rev. **D56**, 6919 (1997) [hep-ph/9611217];
    S.M. Barr and S. Raby, Phys. Rev. Lett. **79**, 4748 (1997) [hep-ph/9705366];
    K.S. Babu, J.C. Pati and F. Wilczek, Nucl. Phys. **B566**, 33 (2000) [hep-ph/9812538];
    R. Dermíšek, A. Mafi and S. Raby, Phys. Rev. **D63**, 035001 (2001) [hep-ph/0007213].
27. R. Barbieri, G.R. Dvali and A. Strumia, Nucl. Phys. **B391**, 487 (1993);

Z. Berezhiani, C. Csaki and L. Randall, Nucl. Phys. **B444**, 61 (1995) [hep-ph/9501336];
Q. Shafi and Z. Tavartkiladze, Phys. Lett. **B522**, 102 (2001) [hep-ph/0105140].
28. G.F. Giudice and A. Masiero, Phys. Lett. **B206**, 480 (1988); J.E. Kim and H.P. Nilles, Mod. Phys. Lett. **A9**, 3575 (1994) [hep-ph/9406296].
29. L. Randall and C. Csaki, in *Palaiseau 1995, SUSY 95* 99-109 [hep-ph/9508208].
30. E. Witten, in *Hamburg 2002, SUSY 02* [hep-ph/0201018]; M. Dine, Y. Nir and Y. Shadmi, Phys. Rev. **D66**, 115001 (2002) [hep-ph/0206268].
31. A. Hebecker, J. March-Russell and R. Ziegler, JHEP **0908**, 064 (2009) [arXiv:0801.4101]; F. Brümmer *et al.*, JHEP **0908**, 011 (2009) [arXiv:0906.2957]; F. Brümmer *et al.*, JHEP **1004**, 006 (2010) [arXiv:1003.0084].
32. H.M. Lee *et al.*, Phys. Lett. **B694**, 491 (2011) [arXiv:1009.0905]; R. Kappl *et al.*, Nucl. Phys. **B847**, 325 (2011) [arXiv:1012.4574];
H.M. Lee *et al.*, Nucl. Phys. **B850**, 1 (2011) [arXiv:1102.3595].
33. Y. Hosotani, Phys. Lett. **B126**, 309 (1983).
34. L.J. Dixon *et al.*, Nucl. Phys. **B261**, 678 (1985) and Nucl. Phys. **B274**, 285 (1986);
L.E. Ibanez, H.P. Nilles and F. Quevedo, Phys. Lett. **B187**, 25 (1987);
L.E. Ibanez *et al.*, Phys. Lett. **B191**, 282 (1987).
35. P. Candelas *et al.*, Nucl. Phys. **B258**, 46 (1985).
36. Y. Kawamura, Prog. Theor. Phys. **103**, 613 (2000) [hep-ph/9902423] and Prog. Theor. Phys. **105**, 999 (2001) [hep-ph/0012125];
G. Altarelli and F. Feruglio, Phys. Lett. **B511**, 257 (2001) [hep-ph/0102301];
L.J. Hall and Y. Nomura, Phys. Rev. **D64**, 055003 (2001) [hep-ph/0103125];
A. Hebecker and J. March-Russell, Nucl. Phys. **B613**, 3 (2001) [hep-ph/0106166];
T. Asaka, W. Buchmuller and L. Covi, Phys. Lett. **B523**, 199 (2001) [hep-ph/0108021];
L.J. Hall *et al.*, Phys. Rev. **D65**, 035008 (2002) [hep-ph/0108071];
R. Dermisek and A. Mafi, Phys. Rev. **D65**, 055002 (2002) [hep-ph/0108139];
H.D. Kim and S. Raby, JHEP **0301**, 056 (2003) [hep-ph/0212348].
37. L.E. Ibanez and A.M. Uranga, "String theory and particle physics: An introduction to string phenomenology," Cambridge University Press 2012;
K.S. Choi and J.E. Kim, Lect. Notes Phys. **696**, 1 (2006);
R. Blumenhagen *et al.*, Phys. Reports **445**, 1 (2007) [hep-th/0610327].
38. V. Braun *et al.*, JHEP **0605**, 043 (2006) [hep-th/0512177];
V. Bouchard and R. Donagi, Phys. Lett. **B633**, 783 (2006) [hep-th/0512149];
L.B. Anderson *et al.*, Phys. Rev. **D84**, 106005 (2011) [arXiv:1106.4804].
39. L.J. Dixon, V. Kaplunovsky and J. Louis, Nucl. Phys. **B355**, 649 (1991).
40. G. Aldazabal *et al.*, Nucl. Phys. **B452**, 3 (1995) [hep-th/9410206];
Z. Kakushadze *et al.*, Int. J. Mod. Phys. **A13**, 2551 (1998) [hep-th/9710149].
41. E. Witten, Nucl. Phys. **B258**, 75 (1985).
42. S. Gukov *et al.*, Phys. Rev. **D69**, 086008 (2004) [hep-th/0310159];
G. Curio, A. Krause and D. Lust, Fortsch. Phys. **54**, 225 (2006) [hep-th/0502168];
L.B. Anderson *et al.*, Phys. Rev. **D83**, 106011 (2011) [arXiv:1102.0011].
43. R. Friedman, J. Morgan and E. Witten, Commun. Math. Phys. **187**, 679 (1997) [hep-th/9701162].
44. R. Blumenhagen, G. Honecker and T. Weigand, JHEP **0508**, 009 (2005) [hep-th/0507041];
L. B. Anderson *et al.*, JHEP **1401** (2014) 047 [arXiv:1307.4787].
45. T. Kobayashi, S. Raby and R.J. Zhang, Phys. Lett. **B593**, 262 (2004) [hep-ph/0403065].
46. S. Forste *et al.*, Phys. Rev. **D70**, 106008 (2004) [hep-th/0406208];
T. Kobayashi, S. Raby and R.J. Zhang, Nucl. Phys. **B704**, 3 (2005) [hep-ph/0409098];
W. Buchmuller *et al.*, Nucl. Phys. **B712**, 139 (2005) [hep-ph/0412318];
W. Buchmuller *et al.*, Phys. Rev. Lett. **96**, 121602 (2006) [hep-ph/0511035], and Nucl. Phys. **B785**, 149 (2007) [hep-th/0606187];
O. Lebedev, *et al.*, Phys. Lett. **B645**, 88 (2007) [hep-th/0611095];
J.E. Kim, J.H. Kim and B. Kyae, JHEP **0706**, 034 (2007) [hep-ph/0702278];
O. Lebedev, *et al.*, Phys. Rev. **D77**, 046013 (2008) [arXiv:0708.2691].
47. S.B. Giddings, S. Kachru and J. Polchinski, Phys. Rev. **D66**, 106006 (2002) [hep-th/0105097];
S. Kachru *et al.*, Phys. Rev. **D68**, 046005 (2003) [hep-th/0301240].
48. R. Blumenhagen *et al.*, Nucl. Phys. **B815**, 1 (2009) [arXiv:0811.2936].
49. R. Blumenhagen *et al.*, Nucl. Phys. **B616**, 3 (2001) [hep-th/0107138].
50. R. Donagi and M. Wijnholt, Adv. Theor. Math. Phys. **15**, 1237 (2011) [arXiv:0802.2969].
51. C. Beasley, J.J. Heckman and C. Vafa, JHEP **0901**, 058 (2009) [arXiv:0802.3391], and JHEP **0901**, 059 (2009) [arXiv:0806.0102].
52. T. Weigand, Class. Quantum Grav. **27**, 214004 (2010) [arXiv:1009.3497];
J.J. Heckman, Ann. Rev. Nucl. and Part. Sci. **160**, 237 (2010) [arXiv:1001.0577];
M. Cvetic, I. Garcia-Etxebarria and J. Halverson, JHEP **1101**, 073 (2011) [arXiv:1003.5337];
A. Maharana and E. Palti, Int. J. Mod. Phys. **A28**, 1330005 (2013) [arXiv:1212.0555];
S. Krippendorf, S. Schafer-Nameki and J.M. Wong, JHEP **1511**, 008 (2015) [arXiv:1507.05961].
53. R. Donagi and M. Wijnholt, Adv. Theor. Math. Phys. **15**, 1523 (2011) [arXiv:0808.2223];
R. Blumenhagen, Phys. Rev. Lett. **102**, 071601 (2009) [arXiv:0812.0248];
K. S. Choi and J. E. Kim, Phys. Rev. **D83**, 065016 (2011) [arXiv:1012.0847];
C. Mayrhofer, E. Palti and T. Weigand, JHEP **1309**, 082 (2013) [arXiv:1303.3589];
G. K. Leontaris and Q. Shafi, Phys. Rev. **D96**, 066023 (2017) [arXiv:1706.08372].
54. E. Witten, Nucl. Phys. **B471**, 135 (1996) [hep-th/9602070].
55. A. Hebecker and M. Trapletti, Nucl. Phys. **B713**, 173 (2005) [hep-th/0411131].
56. H. Georgi, H. R. Quinn and S. Weinberg, Phys. Rev. Lett. **33**, 451 (1974);
See also the definition of effective field theories by S. Weinberg, Phys. Lett. **B91**, 51 (1980).
57. C. Patrignani *et al.* [Particle Data Group], Chin. Phys. C **40**, 100001 (2016).
58. M.L. Alciati *et al.*, JHEP **0503**, 054 (2005) [hep-ph/0501086].
59. See talks on proposed and running nucleon decay experiments, and theoretical talks by P. Langacker, p. 131, and W.J. Marciano and A. Sirlin, p. 151, in *The Second Workshop on Grand Unification*, eds. J.P. Leveille *et al.*, Birkhäuser, Boston (1981).
60. W.J. Marciano, p. 190, *Eighth Workshop on Grand Unification*, ed. K. Wali, World Scientific Publishing Co., Singapore (1987).
61. M.S. Carena *et al.*, in Ref. [4].

62. B.C. Allanach, Comp. Phys. Comm. **143**, 305 (2002) [hep-ph/0104145].
63. A. Djouadi, J. L. Kneur and G. Moultaka, Comp. Phys. Comm. **176**, 426 (2007) [hep-ph/0211331].
64. W. Porod and F. Staub, Comp. Phys. Comm. **183**, 2458 (2012) [arXiv:1104.1573].
65. W. Siegel, Phys. Lett. **B94**, 37 (1980).
66. I. Antoniadis, C. Kounnas, and R. Lacaze, Nucl. Phys. **B221**, 377 (1983).
67. M.A. Shifman, Int. J. Mod. Phys. **A11**, 5761 (1996) [arXiv:hep-ph/9606281];
N. Arkani-Hamed and H. Murayama, JHEP **0006**, 030 (2000) [arXiv:hep-th/9707133];
I. Jack, D.R.T. Jones and A. Pickering, Phys. Lett. **B435**, 61 (1998) [arXiv:hep-ph/9805482].
68. M.B. Einhorn and D.R.T. Jones in Ref. [12];
I. Antoniadis, C. Kounnas, and K. Tamvakis, Phys. Lett. **B119**, 377 (1982).
69. J. Hisano, H. Murayama and T. Yanagida, Phys. Rev. Lett. **69**, 1014 (1992) and Nucl. Phys. **B402**, 46 (1993) [hep-ph/9207279].
70. H. Murayama and A. Pierce, Phys. Rev. **D65**, 055009 (2002) [hep-ph/0108104].
71. G. Anderson *et al.*, eConf **C960625**, SUP107 (1996) [hep-ph/9609457].
72. S. Raby, M. Ratz and K. Schmidt-Hoberg, Phys. Lett. **B687**, 342 (2010) [arXiv:0911.4249].
73. J. Hisano, T. Kuwahara and N. Nagata, Phys. Lett. **B723**, 324 (2013) [arXiv:1304.0343].
74. N. Arkani-Hamed, A. Delgado and G.F. Giudice, Nucl. Phys. **B741**, 108 (2006) [hep-ph/0601041].
75. M. Ibe, T. Moroi and T.T. Yanagida, Phys. Lett. **B644**, 355 (2007) [hep-ph/0610277].
76. G.F. Giudice *et al.*, JHEP **9812**, 027 (1998) [hep-ph/9810442]; L. Randall and R. Sundrum, Nucl. Phys. **B557**, 79 (1999) [hep-th/9810155].
77. R.N. Mohapatra and M.K. Parida, Phys. Rev. **D47**, 264 (1993) [hep-ph/9204234].
78. D.G. Lee *et al.*, Phys. Rev. **D51**, 229 (1995) [hep-ph/9404238].
79. L.E. Ibanez *et al.*, JHEP **1207**, 195 (2012) [arXiv:1206.2655].
80. K.R. Dienes, E. Dudas and T. Gherghetta, Phys. Rev. Lett. **91**, 061601 (2003) [hep-th/0210294].
81. K. Agashe, R. Contino and R. Sundrum, Phys. Rev. Lett. **95**, 171804 (2005) [hep-ph/0502222].
82. S. Weinberg, Phys. Rev. Lett. **43**, 1566 (1979);
F. Wilczek and A. Zee, Phys. Rev. Lett. **43**, 1571 (1979).
83. R. Barbier *et al.*, Phys. Rev. **420**, 1 (2005) [hep-ph/0406039].
84. G. Farrar and P. Fayet, Phys. Lett. **B76**, 575 (1978).
85. S. Dimopoulos, S. Raby and F. Wilczek, Phys. Lett. **B112**, 133 (1982);
J. Ellis, D.V. Nanopoulos and S. Rudaz, Nucl. Phys. **B202**, 43 (1982).
86. For a recent discussion, see C.S. Aulakh *et al.*, Nucl. Phys. **B597**, 89 (2001) [hep-ph/0004031].
87. K. Abe *et al.* [Super-Kamiokande Collaboration], Phys. Rev. **D95**, 012004 (2017) [arXiv:1610.03597];
S. Mine for the Super Kamiokande Collaboration, J. Phys. Conf. Ser. **718**, 062044 (2016).
88. Y. Aoki, T. Izubuchi, E. Shintani and A. Soni, Phys. Rev. **D96**, 014506 (2017) [arXiv:1705.01338 [hep-lat]].
89. For recent analysis, see J. Hisano, T. Kuwahara and Y. Omura, Nucl. Phys. **B898**, 1 (2015) [arXiv:1503.08561].
90. T. Goto and T. Nihei, Phys. Rev. **D59**, 115009 (1999) [hep-ph/9808255].
91. J.L. Chkareuli and I.G. Gogoladze, Phys. Rev. **D58**, 055011 (1998) [hep-ph/9803335].
92. G.F. Giudice and A. Romanino, Nucl. Phys. **B699**, 65 (2004) [hep-ph/0406088], [Erratum: *ibid.*, Nucl. Phys. **B706**, 65 (2005)].
93. J. Hisano *et al.*, JHEP **1307**, 038 (2013) [arXiv:1304.3651].
94. B. Bajc, P. Fileviez Perez and G. Senjanovic, Phys. Rev. **D66**, 075005 (2002) [hep-ph/0204311].
95. K.S. Choi, Phys. Lett. **B668**, 392 (2008) [arXiv:0807.2766].
96. F. An *et al.* [JUNO Collab.], J. Phys. G **43**, 030401 (2016) [arXiv:1507.05613].
97. Hyper-Kamiokande Collab., 'Hyper-Kamiokande Design Report', KEK-PREPRINT-2016-21, ICRR-REPORT-701-2016-1 (2016).
98. R. Acciarri *et al.* [DUNE Collaboration], 'The Physics Program for DUNE at LBNF', arXiv:1512.06148.
99. R. Kallosh *et al.*, Phys. Rev. **D52**, 912 (1995) [hep-th/9502069].
100. L.E. Ibanez and G.G. Ross, Nucl. Phys. **B368**, 3 (1992);
M. Berasaluce-Gonzalez *et al.*, JHEP **1112**, 113 (2011) [arXiv:1106.4169 [hep-th]].
101. L.J. Hall and Y. Nomura, Phys. Rev. **D66**, 075004 (2002) [hep-ph/0205067];
H.D. Kim, S. Raby and L. Schradin, JHEP **0505**, 036 (2005) [hep-ph/0411328].
102. M.S. Chanowitz, J.R. Ellis and M.K. Gaillard, Nucl. Phys. **B128**, 506 (1977);
A.J. Buras *et al.*, Nucl. Phys. **B135**, 66 (1978).
103. K. Inoue *et al.*, Prog. Theor. Phys. **67**, 1889 (1982);
L.E. Ibanez and C. Lopez, Phys. Lett. **B126**, 54 (1983) and Nucl. Phys. **B233**, 511 (1984).
104. H. Georgi and D.V. Nanopoulos, Nucl. Phys. **B159**, 16 (1979);
J. Harvey, P. Ramond and D.B. Reiss, Phys. Lett. **B92**, 309 (1980) and Nucl. Phys. **B199**, 223 (1982).
105. T. Banks, Nucl. Phys. **B303**, 172 (1988);
M. Olechowski and S. Pokorski, Phys. Lett. **B214**, 393 (1988);
S. Pokorski, Nucl. Phys. (Proc. Supp.) **B13**, 606 (1990);
B. Ananthanarayan, G. Lazarides and Q. Shafi, Phys. Rev. **D44**, 1613 (1991);
Q. Shafi and B. Ananthanarayan, ICTP Summer School lectures (1991);
S. Dimopoulos, L.J. Hall and S. Raby, Phys. Rev. Lett. **68**, 1984 (1992) and Phys. Rev. **D45**, 4192 (1992);
G. Anderson *et al.*, Phys. Rev. **D47**, 3702 (1993) [hep-ph/9209250];
B. Ananthanarayan, G. Lazarides and Q. Shafi, Phys. Lett. **B300**, 245 (1993);
G. Anderson *et al.*, Phys. Rev. **D49**, 3660 (1994) [hep-ph/9308333];
B. Ananthanarayan, Q. Shafi and X.M. Wang, Phys. Rev. **D50**, 5980 (1994) [hep-ph/9311225].
106. L.J. Hall, R. Rattazzi and U. Sarid, Phys. Rev. **D50**, 7048 (1994) [hep-ph/9306309, hep-ph/9306309];
M. Carena *et al.*, Nucl. Phys. **B426**, 269 (1994) [hep-ph/9402253].
107. A. Anandakrishnan, B.C. Bryant and S. Raby, JHEP **1505**, 088 (2015) [arXiv:1411.7035]..
108. M. Lanzagorta and G.G. Ross, Phys. Lett. **B364**, 163 (1995) [hep-ph/9507366].
109. K. Tobe and J.D. Wells, Nucl. Phys. **B663**, 123 (2003) [hep-ph/0301015].
110. T. Blazek, R. Dermisek and S. Raby, Phys. Rev. Lett. **88**, 111804 (2002) and Phys. Rev. **D65**, 115004 (2002) [hep-ph/0107097];
D. Auto, *et al.*, JHEP **0306**, 023 (2003) [hep-ph/0302155];
R. Dermisek *et al.*, JHEP **0304**, 037 (2003) and JHEP **0509**, 029 (2005) [hep-ph/0304101].
111. A. Anandakrishnan, S. Raby and A. Wingerter, Phys. Rev. **D87**, 055005 (2013) [arXiv:1212.0542];
M. Adeel Ajaib *et al.*, JHEP **1307**, 139 (2013) [arXiv:1303.6964];
Z. Poh and S. Raby, Phys. Rev. **D92**, 015017 (2015) [arXiv:1505.00264];
M. Badziak, M. Olechowski and S. Pokorski, JHEP **1310**, 088 (2013) [arXiv:1307.7999].
112. H. Georgi and C. Jarlskog, Phys. Lett. **B86**, 297 (1979).
113. S. Antusch and M. Spinrath, Phys. Rev. **D79**, 095004 (2009) [arXiv:0902.4644].
114. G. Lazarides, Q. Shafi and C. Wetterich, Nucl. Phys. **B181**, 287 (1981);

T.E. Clark, T.K. Kuo and N. Nakagawa, Phys. Lett. **B115**, 26 (1982);
K.S. Babu and R.N. Mohapatra, Phys. Rev. Lett. **70**, 2845 (1993) [hep-ph/9209215].
115. R. Barbieri and D.V. Nanopoulos, Phys. Lett. **B91**, 369 (1980).
116. R. Barbieri and A. Strumia, Nucl. Phys. **B493**, 3 (1997) [hep-ph/9704402];
T. Blazek, S. Raby and K. Tobe, Phys. Rev. **D60**, 113001 (1999) and Phys. Rev. **D62**, 055001 (2000) [hep-ph/9903340];
Q. Shafi and Z. Tavartkiladze, Phys. Lett. **B487**, 145 (2000) [hep-ph/0002150];
C.H. Albright and S.M. Barr, Phys. Rev. Lett. **85**, 244 (2000) [hep-ph/0002155];
Z. Berezhiani and A. Rossi, Nucl. Phys. **B594**, 113 (2001) [hep-ph/0003084];
C.H. Albright and S.M. Barr, Phys. Rev. **D64**, 073010 (2001) [hep-ph/0104294];
M.-C. Chen, K.T. Mahanthappa, Int. J. Mod. Phys. **A18**, 5819 (2003) [hep-ph/0305088];
R. Dermisek and S. Raby, Phys. Lett. **B622**, 327 (2005) [hep-ph/0507045].
117. H. Georgi, Nucl. Phys. **B156**, 126 (1979);
P.H. Frampton, Phys. Lett. **B88**, 299 (1979);
P. Frampton and S. Nandi, Phys. Rev. Lett. **43**, 1460 (1979);
J.E. Kim, Phys. Rev. Lett. **45**, 1916 (1980), Phys. Rev. **D23**, 2706 (1981) and Phys. Rev. **D26**, 674 (1982);
R. Barbieri and D.V. Nanopoulos, Phys. Lett. **B91**, 369 (1980);
Y. Fujimoto, Phys. Rev. **D26**, 3183 (1982).
118. P. Langacker, Phys. Reports **72**, 185 (1981).
119. H. Georgi, Conf. Proc. C **820726**, 705 (1982).
120. S.M. Barr, Phys. Rev. **D78**, 055008 (2008) [arXiv:0805.4808];
Y. Goto, Y. Kawamura and T. Miura, Phys. Rev. **D88**, 055016 (2013) [arXiv:1307.2631];
J.E. Kim, JHEP **1506**, 114 (2015) [arXiv:1503.03104];
C.H. Albright, R.P. Feger and T.W. Kephart, arXiv:1601.07523;
M. Reig, J. W. F. Valle, C. A. Vaquera-Araujo and F. Wilczek, arXiv:1706.03116.
121. L.J. Hall, V.A. Kostelecky and S. Raby, Nucl. Phys. **B267**, 415 (1986).
122. R. Barbieri and L.J. Hall, Phys. Lett. **B338**, 212 (1994) [hep-ph/9408406];
R. Barbieri, L.J. Hall and A. Strumia, Nucl. Phys. **B445**, 219 (1995) [hep-ph/9501334].
123. F. Borzumati and A. Masiero, Phys. Rev. Lett. **57**, 961 (1986);
J. Hisano *et al.*, Phys. Lett. **B357**, 579 (1995) [hep-ph/9501407];
J. Hisano *et al.*, Phys. Rev. **D53**, 2442 (1996) [hep-ph/9501407];
J. Hisano and D. Nomura, Phys. Rev. **D59**, 116005 (1999) [hep-ph/9810479].
124. T. Moroi, JHEP **0003**, 019 (2000) [hep-ph/0002208];
D. Chang, A. Masiero and H. Murayama, Phys. Rev. **D67**, 075013 (2003) [hep-ph/0205111].
125. S. Dimopoulos and L.J. Hall, Phys. Lett. **B344**, 185 (1995) [hep-ph/9411273].
126. J. Hisano *et al.*, Phys. Lett. **B604**, 216 (2004) [hep-ph/0407169].
127. G.L. Fogli *et al.*, Phys. Rev. **D84**, 053007 (2011) [arXiv:1106.6028].
128. T. Schwetz, M. Tortola, and J.W.F. Valle, New J. Phys. **13**, 109401 (2011) [arXiv:1108.1376].
129. C.H. Albright and M.-C. Chen, Phys. Rev. **D74**, 113006 (2006) [hep-ph/0608137].
130. M. Magg and C. Wetterich, Phys. Lett. **B94**, 61 (1980);
J. Schechter and J.W.F. Valle, Phys. Rev. **D22**, 2227 (1980);
G. Lazarides, Q. Shafi and C. Wetterich, Nucl. Phys. **B181**, 287 (1981);
R.N. Mohapatra and G. Senjanovic, Phys. Rev. **D23**, 165 (1981);
G.B. Gelmini and M. Roncadelli, Phys. Lett. **B99**, 411 (1981).
131. R. Foot, *et al.*, Z. Phys. **C44**, 441 (1989).
132. G. 't Hooft, Nucl. Phys. **B79**, 276 (1974) A.M. Polyakov, Pis'ma Zh. Eksp. Teor. Fiz. **20**, 430 (1974) [Sov. Phys. JETP Lett. **20**, 194 (1974)];
For a pedagogical introduction, see S. Coleman, in *Aspects of Symmetry*, Selected Erice Lectures, Cambridge University Press, Cambridge, (1985), and P. Goddard and D. Olive, Rept. on Prog. in Phys. **41**, 1357 (1978).
133. M. Ambrosio *et al.* [MACRO Collaboration], Eur. Phys. J. C **25** (2002) 511 [hep-ex/0207020];
S. Balestra *et al.* 'Magnetic Monopole Bibliography-II,' arXiv:1105.5587;
L. Patrizii and M. Spurio, Ann. Rev. Nucl. Part. Sci. **65** (2015) 279 [arXiv:1510.07125].
134. For a review, see A.D. Linde, *Particle Physics and Inflationary Cosmology*, Harwood Academic, Switzerland (1990).
135. G.R. Dvali, H. Liu and T. Vachaspati, Phys. Rev. Lett. **80**, 2281 (1998) [hep-ph/9710301].
136. P. Langacker and S.Y. Pi, Phys. Rev. Lett. **45**, 1 (1980).
137. G.R. Dvali, A. Melfo and G. Senjanovic, Phys. Rev. Lett. **75**, 4559 (1995) [hep-ph/9507230].
138. V. Rubakov, Nucl. Phys. **B203**, 311 (1982) and Institute of Nuclear Research Report No. P-0211, Moscow (1981), unpublished;
C. Callan, Phys. Rev. **D26**, 2058 (1982);
F. Wilczek, Phys. Rev. Lett. **48**, 1146 (1982);
See also, S. Dawson and A.N. Schellekens, Phys. Rev. **D27**, 2119 (1983).
139. K. Freese, M. S. Turner and D. N. Schramm, Phys. Rev. Lett. **51**, 1625 (1983).
140. P.A.R. Ade *et al.* [BICEP2 and Planck Collabs.], Phys. Rev. Lett. **114**, 101301 (2015) [arXiv:1502.00612];
P.A.R. Ade *et al.* [Planck Collab.], Astron. Astrophys. **594**, A20 (2016) [arXiv:1502.02114].
141. N.G. Deshpande, OITS-107;
C.Q. Geng and R.E. Marshak, Phys. Rev. **D39**, 693 (1989);
A. Font, L.E. Ibanez and F. Quevedo, Phys. Lett. **B228**, 79 (1989);
K.S. Babu and R.N. Mohapatra, Phys. Rev. Lett. **63**, 938 (1989).
142. R. Foot *et al.*, Phys. Rev. **D39**, 3411 (1989).
143. M. Nowakowski and A. Pilaftsis, Phys. Rev. **D48**, 259 (1993) [hep-ph/9304312].
144. T.P. T. Dijkstra, L.R. Huiszoon and A.N. Schellekens, Phys. Lett. **B609**, 408 (2005) [hep-th/0403196];
F. Gmeiner *et al.*, JHEP **0601**, 004 (2006) [hep-th/0510170];
B. Gato-Rivera and A.N. Schellekens, Nucl. Phys. **B883**, 529 (2014) [arXiv:1401.1782].
145. A.Y. Ignatiev *et al.*, Phys. Lett. **B76**, 436 (1978);
M. Yoshimura, Phys. Rev. Lett. **41**, 281 (1978) [Phys. Rev. Lett. **42**, 746 (1979)].
146. D. Toussaint *et al.*, Phys. Rev. **D19**, 1036 (1979);
S. Weinberg, Phys. Rev. Lett. **42**, 850 (1979);
M. Yoshimura, Phys. Lett. **B88**, 294 (1979);
S.M. Barr, G. Segre and H.A. Weldon, Phys. Rev. **D20**, 2494 (1979);
D.V. Nanopoulos and S. Weinberg, Phys. Rev. **D20**, 2484 (1979);
A. Yildiz and P.H. Cox, Phys. Rev. **D21**, 906 (1980).
147. M. Fukugita and T. Yanagida, Phys. Rev. Lett. **89**, 131602 (2002) [hep-ph/0203194].
148. M. Fukugita and T. Yanagida, Phys. Lett. **B174**, 45 (1986).
149. S. Davidson and A. Ibarra, Phys. Lett. **B535**, 25 (2002) [hep-ph/0202239];
K. Hamaguchi, H. Murayama and T. Yanagida, Phys. Rev. **D65**, 043512 (2002) [hep-ph/0109030].
150. M. Kawasaki *et al.*, Phys. Rev. **D78**, 065011 (2008) [arXiv:0804.3745].
151. W. Buchmuller, R.D. Peccei and T. Yanagida, Ann. Rev. Nucl. and Part. Sci. **55**, 311 (2005) [hep-ph/0502169];
C.S. Fong, E. Nardi and A. Riotto, Adv. High Energy Phys. **2012**, 158303 (2012) [arXiv:1301.3062].
152. G.G. Ross, "Grand Unified Theories", Benjamin/Cummings, 1984.;
K.R. Dienes, Phys. Reports **287**, 447 (1997) [hep-th/9602045];

P. Nath and P. Fileviez Perez, Phys. Reports **441**, 191 (2007) [hep-ph/0601023];
S. Raby, "Supersymmetric Grand Unified Theories" Lect. Notes Phys. **939** 1 (2017).
153. A. Ringwald, L.J. Rosenberg and G. Rybka, Review of 'Axions and other Very Light Bosons' in Ref. [57].
154. P. Svrcek and E. Witten, JHEP **0606** 051 (2006) [hep-th/0605206].
155. M. Dine, W. Fischler and M. Srednicki, Phys. Lett. **104B** 199 (1981);
A. R. Zhitnitsky, Sov. J. Nucl. Phys. **31** 260 (1980).

115. Leptoquarks

Updated August 2017 by S. Rolli (US Department of Energy) and M. Tanabashi (Nagoya U.)

Leptoquarks are hypothetical particles carrying both baryon number (B) and lepton number (L). The possible quantum numbers of leptoquark states can be restricted by assuming that their direct interactions with the ordinary SM fermions are dimensionless and invariant under the standard model (SM) gauge group. Table 115.1 shows the list of all possible quantum numbers with this assumption [1]. The columns of $SU(3)_C$, $SU(2)_W$, and $U(1)_Y$ in Table 115.1 indicate the QCD representation, the weak isospin representation, and the weak hypercharge, respectively. The spin of a leptoquark state is taken to be 1 (vector leptoquark) or 0 (scalar leptoquark).

Table 115.1: Possible leptoquarks and their quantum numbers.

Spin	$3B+L$	$SU(3)_c$	$SU(2)_W$	$U(1)_Y$	Allowed coupling
0	-2	$\bar{3}$	1	1/3	$\bar{q}_L^c \ell_L$ or $\bar{u}_R^c e_R$
0	-2	$\bar{3}$	1	4/3	$\bar{d}_R^c e_R$
0	-2	$\bar{3}$	3	1/3	$\bar{q}_L^c \ell_L$
1	-2	$\bar{3}$	2	5/6	$\bar{q}_L^c \gamma^\mu e_R$ or $\bar{d}_R^c \gamma^\mu \ell_L$
1	-2	$\bar{3}$	2	$-1/6$	$\bar{u}_R^c \gamma^\mu \ell_L$
0	0	3	2	7/6	$\bar{q}_L e_R$ or $\bar{u}_R \ell_L$
0	0	3	2	1/6	$\bar{d}_R \ell_L$
1	0	3	1	2/3	$\bar{q}_L \gamma^\mu \ell_L$ or $\bar{d}_R \gamma^\mu e_R$
1	0	3	1	5/3	$\bar{u}_R \gamma^\mu e_R$
1	0	3	3	2/3	$\bar{q}_L \gamma^\mu \ell_L$

If we do not require leptoquark states to couple directly with SM fermions, different assignments of quantum numbers become possible [2,3].

Leptoquark states are expected to exist in various extensions of SM. The Pati-Salam model [4] is an example predicting the existence of a leptoquark state. Leptoquark states also exist in grand unification theories based on $SU(5)$ [5], $SO(10)$ [6], which includes Pati-Salam color $SU(4)$, and larger gauge groups. Scalar quarks in supersymmetric models with R-parity violation may also have leptoquark-type Yukawa couplings. The bounds on the leptoquark states can therefore be applied to constrain R-parity-violating supersymmetric models. Scalar leptoquarks are expected to exist at TeV scale in extended technicolor models [7,8] where leptoquark states appear as the bound states of techni-fermions. Compositeness of quarks and leptons also provides examples of models which may have light leptoquark states [9].

Bounds on leptoquark states are obtained both directly and indirectly. Direct limits are from their production cross sections at colliders, while indirect limits are calculated from the bounds on the leptoquark-induced four-fermion interactions, which are obtained from low-energy experiments, or from collider experiments below threshold. These four-fermion interactions often cause lepton-flavor non-universalities in heavy quark decays. Anomalies observed recently in the R_K and R_D ratios [10,11] in the semi-leptonic B decays may be explained in models with TeV scale leptoquarks.

If a leptoquark couples to quarks (leptons) belonging to more than a single generation in the mass eigenbasis, it can induce four-fermion interactions causing flavor-changing neutral currents (lepton-family-number violations). The quantum number assignment of Table 1 allows several leptoquark states to couple to both left- and right-handed quarks simultaneously. Such leptoquark states are called non-chiral and may cause four-fermion interactions affecting the $(\pi \to e\nu)/(\pi \to \mu\nu)$ ratio [12]. Non-chiral scalar leptoquarks also contribute to the muon anomalous magnetic moment [13,14]. Since indirect limits provide more stringent constraints on these types of leptoquarks, it is often assumed that a leptoquark state couples only to a single generation of quarks and a single generation of leptons in a chiral interaction, for which indirect limits become much weaker. Additionally, this assumption gives strong constraints on concrete models of leptoquarks.

Refs. [15,16,17] give extensive lists of the bounds on the leptoquark-induced four-fermion interactions. For the isoscalar scalar and vector leptoquarks S_0 and V_0, for example, which couple with the first- (second-) generation left-handed quark, and the first-generation left-handed lepton, the bounds of Ref. 17 read $\lambda^2 < 0.07 \times (M_{\rm LQ}/1\ {\rm TeV})^2$ for S_0, and $\lambda^2 < 0.4 \times (M_{\rm LQ}/1\ {\rm TeV})^2$ for V_0 ($\lambda^2 < 0.7 \times (M_{\rm LQ}/1\ {\rm TeV})^2$ for S_0, and $\lambda^2 < 0.5 \times (M_{\rm LQ}/1\ {\rm TeV})^2$ for V_0) with λ being the leptoquark coupling strength. The e^+e^- experiments are sensitive to the indirect effects coming from t- and u-channel exchanges of leptoquarks in the $e^+e^- \to q\bar{q}$ process. The HERA experiments give bounds on the leptoquark-induced four-fermion interaction. For detailed bounds obtained in this way, see the Boson Particle Listings for "Indirect Limits for Leptoquarks" and its references.

Collider experiments provide direct limits on the leptoquark states through limits on the pair- and single-production cross sections. The leading-order cross sections of the parton processes

$$\begin{aligned} &q + \bar{q} \to LQ + \overline{LQ} \\ &g + g \to LQ + \overline{LQ} \\ &e + q \to LQ \end{aligned} \tag{115.1}$$

may be written as [18]

$$\begin{aligned} \hat{\sigma}_{\rm LO}\Big[q\bar{q} \to {\rm LQ} + \overline{\rm LQ}\Big] &= \frac{2\alpha_s^2\pi}{27\hat{s}}\beta^3, \\ \hat{\sigma}_{\rm LO}\Big[gg \to {\rm LQ} + \overline{\rm LQ}\Big] &= \frac{\alpha_s^2\pi}{96\hat{s}} \\ &\quad \times \Big[\beta(41 - 31\beta^2) + (18\beta^2 - \beta^4 - 17)\log\frac{1+\beta}{1-\beta}\Big], \\ \hat{\sigma}_{\rm LO}\Big[eq \to {\rm LQ}\Big] &= \frac{\pi\lambda^2}{4}\delta(\hat{s} - M_{\rm LQ}^2) \end{aligned} \tag{115.2}$$

for a scalar leptoquark. Here $\sqrt{\hat{s}}$ is the invariant energy of the parton subprocess, and $\beta \equiv \sqrt{1 - 4M_{\rm LQ}^2/\hat{s}}$. The leptoquark Yukawa coupling is given by λ. Leptoquarks are also produced singly at hadron colliders through $g + q \to LQ + \ell$ [19], which allows extending to higher masses the collider reach in the leptoquark search [20], depending on the leptoquark Yukawa coupling. See also Ref. [21] for a comprehensive review on the leptoquark phenomenology in precision experiments and particle colliders.

Leptoquark states which couple only to left- or right-handed quarks are called chiral leptoquarks. Leptoquark states which couple only to the first (second, third) generation are referred as the first- (second-, third-) generation leptoquarks.

The LHC, Tevatron and LEP experiments search for pair production of the leptoquark states, which arises from the leptoquark gauge interaction. The searches are carried on in signatures including high P_T leptons, E_T jets and large missing transverse energy, due to the typical decay of the leptoquark. The gauge couplings of a scalar leptoquark are determined uniquely according to its quantum numbers in Table 115.1. Since all of the leptoquark states belong to color-triplet representation, the scalar leptoquark pair-production cross section at the Tevatron and LHC can be determined solely as a function of the leptoquark mass without making further assumptions. This is in contrast to the indirect or single-production limits, which give constraints in the leptoquark mass-coupling plane.

Older results from the Tevatron run can be found here: [23], [24], [25] and [26].

Current results from the LHC proton-proton collider, running at a center of mass energies of 7, 8 TeV and 13 TeV, extend previous mass limits for scalar leptoquarks to > 1130 GeV (first generation, CMS, $\beta = 1$, $\sqrt{s} = 13$ TeV) and > 920 GeV(first generation, CMS, $\beta = 0.5$, $\sqrt{s} = 13$ TeV) [27]; > 1100 GeV (first generation, ATLAS, $\beta = 1$, $\sqrt{s} = 13$ TeV) [28] and > 900 GeV (first generation, ATLAS, $\beta = 0.5$, $\sqrt{s} = 8$ TeV - no update at 13 TeV is available at this time) [29]; > 1165 GeV (second generation, CMS, $\beta = 1$, $\sqrt{s} =$

13 TeV) [30] and > 960 GeV (second generation, CMS, $\beta = 0.5$, $\sqrt{s}$ = 13 TeV) [30]; and > 1050 GeV (second generation, ATLAS, $\beta = 1$, $\sqrt{s}$ = 13 TeV) [28] and > 850 GeV (second generation, ATLAS, β = 0.5, $\sqrt{s}$ = 8 TeV - no update at 13 TeV is available at this time) [29]. All limits at 95% C.L.

As for third generation leptoquarks, CMS results are the following (using both 8 and 13 TeV run data): 1) assuming that all leptoquarks decay to a top quark and a τ lepton, the existence of pair produced, third-generation leptoquarks up to a mass of 685 GeV (β =1, 8 TeV) is excluded at 95% confidence level [31]; 2) assuming that all leptoquarks decay to a bottom quark and a τ lepton, the existence of pair produced, third-generation leptoquarks up to a mass of 850 GeV (β =1, 13 TeV) is excluded at 95% confidence level [32]; 3)assuming that all leptoquarks decay to a bottom quark and a τ neutrino, the existence of pair produced, third-generation leptoquarks up to a mass of 450 GeV (β =0.5, 8 TeV)is excluded at 95% confidence level [33].

The ATLAS collaboration has a limit on third generation scalar leptoquark for the case of β =1 of 525 GeV [34] and 625 GeV for third-generation leptoquarks in the bottom τ neutrino channel, and 200 $< m_{LQ} <$ 640 GeV in the top τ neutrino channel [34].

It is also possible to consider leptoquark states which couple only with the i-th generation quarks and the j-th generation leptons ($i \neq j$) without causing conflicts with severe indirect constraints. See Ref. [35] for collider search strategies and present limits on the pair production cross sections of this class of leptoquark states.

The magnetic-dipole-type and the electric-quadrupole-type interactions of a vector leptoquark are not determined even if we fix its gauge quantum numbers as listed in the Table [36]. The production of vector leptoquarks depends in general on additional assumptions that the leptoquark couplings and their pair-production cross sections are enhanced relative to the scalar leptoquark contributions. The leptoquark pair-production cross sections in e^+e^- collisions depend on the leptoquark $SU(2) \times U(1)$ quantum numbers and Yukawa coupling with electron [37].

The most stringent searches for the leptoquark single production were performed by the HERA experiments. Since the leptoquark single-production cross section depends on its Yukawa coupling, the leptoquark mass limits from HERA are usually displayed in the mass-coupling plane. For leptoquark Yukawa coupling $\lambda = 0.1$, the ZEUS bounds on the first-generation leptoquarks range from 248 to 290 GeV, depending on the leptoquark species [39]. The H1 Collaboration released a comprehensive summary of searches for first generation leptoquarks using the full data sample collected in ep collisions at HERA (446 pb^{-1}). No evidence of production of leptoquarks was observed in final states with a large transverse momentum electron or large missing transverse momentum. For a coupling strength $\lambda = 0.3$, first generation leptoquarks with masses up to 800 GeV are excluded at 95% C.L. [41]. The CMS collaboration performed a search for single production of first and second geneation leptoquarks [42], which is complementary to the HERA searches in the high λ region (for coupling strenght $\lambda = 1.0$, first generation leptoquarks are excluded for masses up to 1.75 TeV).

The search for LQ will continue with more LHC data. Early feasability studies by the LHC experiments ATLAS [44] and CMS [45] indicate that clear signals can be established for masses up to about $M_{\rm LQ}$ 1.3 to 1.4 TeV for first- and second-generation scalar LQ, with a likely final reach 1.5 TeV, for collisions at 14 TeV in the center of mass.

References:

1. W. Buchmüller, R. Rückl, and D. Wyler, Phys. Lett. **B191**, 442 (1987).
2. K.S. Babu, C.F. Kolda, and J. March-Russell, Phys. Lett. **B408**, 261 (1997).
3. J.L. Hewett and T.G. Rizzo, Phys. Rev. **D58**, 055005 (1998).
4. J.C. Pati and A. Salam, Phys. Rev. **D10**, 275 (1974).
5. H. Georgi and S.L. Glashow, Phys. Rev. Lett. **32**, 438 (1974).
6. H. Georgi, AIP Conf. Proc. **23**, 575 (1975);
   H. Fritzsch and P. Minkowski, Ann. Phys. **93**, 193 (1975).
7. For a review, see, E. Farhi and L. Susskind, Phys. Reports **74**, 277 (1981).
8. K. Lane and M. Ramana, Phys. Rev. **D44**, 2678 (1991).
9. See, for example, B. Schremp and F. Schremp, Phys. Lett. **153B**, 101 (1985).
10. R. Aaij *et al.* [LHCb Collab.], Phys. Rev. Lett. **113**, 151601 (2014);
    R. Aaij *et al.* [LHCb Collab.], arXiv:1705.05802.
11. Y. Amhis *et al.*, arXiv:1612.07233.
12. O. Shanker, Nucl. Phys. **B204**, 375, (1982).
13. U. Mahanta, Eur. Phys. J. **C21**, 171 (2001) [Phys. Lett. **B515**, 111 (2001)].
14. K. Cheung, Phys. Rev. **D64**, 033001 (2001).
15. S. Davidson, D.C. Bailey, and B.A. Campbell, Z. Phys. **C61**, 613 (1994).
16. M. Leurer, Phys. Rev. **D49**, 333 (1994);
    Phys. Rev. **D50**, 536 (1994).
17. M. Carpentier and S. Davidson, Eur. Phys. J. **C70**, 1071 (2010).
18. T. Plehn *et al.*, Z. Phys. **C74**, 611 (1997);
    M. Kramer *et al.*, Phys. Rev. Lett. **79**, 341 (1997); and references therein.
19. J.L. Hewett and S. Pakvasa, Phys. Rev. **D37**, 3165 (1988);
    O.J.P. Eboli and A.V. Olinto, Phys. Rev. **D38**, 3461 (1988);
    A. Dobado, M.J. Herrero, and C. Muñoz, Phys. Lett. **207B**, 97 (1988);
    V.D. Barger *et al.*, Phys. Lett. **B220**, 464 (1989);
    M. De Montigny and L. Marleau, Phys. Rev. **D40**, 2869 (1989) [Erratum-*ibid.* **D56**, 3156 (1997)].
20. A. Belyaev *et al.*, JHEP **0509**, 005 (2005).
21. I. Doršner *et al.*, Phys. Reports **641**, 1 (2016).
22. D. Acosta *et al.* [CDF Collab.], Phys. Rev. **D72**, 051107 (2005).
23. V.M. Abazov *et al.* [DØCollab.], Phys. Lett. **B681**, 224 (2009).
24. A. Abulencia *et al.* [CDF Collab.], Phys. Rev. **D73**, 051102 (2006).
25. V.M. Abazov *et al.* [DØCollab.], Phys. Lett. **B671**, 224 (2009).
26. V.Abazov *et al.* [DØCollab.], Phys. Lett. **B693**, 95 (2010).
27. [CMS Collab.], CMS PAS EXO-16-043 (2016).
28. M. Aaboud, *et al.* [ATLAS Collab.], New J. Phys. **18**, 093016 (2016).
29. G.Aad *et al.* [ATLAS Collab.], arXiv:1508.04735v1.
30. [CMS Collab.], CMS PAS EXO-16-007 (2016).
31. V. Khachatryan *et al.* [CMS Collab.], JHEP **1507**, 042 (2015).
32. A.M. Sirunyan, *et al.* [CMS Collab.], JHEP **1707**, 121 (2017).
33. S. Chatrchyan *et al.* [CMS Collab.], JHEP **1212**, 055 (2012).
34. G. Aad *et al.* [ATLAS Collab.], Eur. Phys. J. **C76**, 5 (2016).
35. B. Diaz, M. Schmaltz, and Y. M. Zhong, arXiv:1706.05033.
36. J. Blümlein, E. Boos, and A. Kryukov, Z. Phys. **C76**, 137 (1997).
37. J. Blümlein and R. Ruckl, Phys. Lett. **B304**, 337 (1993).
38. G. Abbiendi *et al.* [OPAL Collab.], Eur. Phys. J. **C31**, 281 (2003).
39. S. Chekanov *et al.* [ZEUS Collab.], Phys. Rev. **D68**, 052004 (2003).
40. A. Aktas *et al.* [H1 Collab.], Phys. Lett. **B629**, 9 (2005).
41. F.D. Aaron *et al.* [H1 Collab.], Phys. Lett. **B704**, 388 (2011).
42. V. Khachatryan *et al.* [CMS Collab.], Phys. Rev. **D93**, 032005 (2016).
43. T. Aalton *et al.* [CDF Collab.], Phys. Rev. **D77**, 091105 (2008).
44. V.A. Mitsou *et al.*, Czech. J. Phys. **55**, B659 (2005).
45. S. Abdulin and F. Charles, Phys. Lett. **B464**, 223 (1999).

116. Magnetic Monopoles

Updated August 2017 by D. Milstead (Stockholm Univ.) and E.J. Weinberg (Columbia Univ.).

The symmetry between electric and magnetic fields in the source-free Maxwell's equations naturally suggests that electric charges might have magnetic counterparts, known as magnetic monopoles. Although the greatest interest has been in the supermassive monopoles that are a firm prediction of all grand unified theories, one cannot exclude the possibility of lighter monopoles, even though there is at present no strong theoretical motivation for these.

In either case, the magnetic charge is constrained by a quantization condition first found by Dirac [1]. Consider a monopole with magnetic charge Q_M and a Coulomb magnetic field

$$\mathbf{B} = \frac{Q_M}{4\pi}\frac{\hat{\mathbf{r}}}{r^2}\,. \tag{116.1}$$

Any vector potential $\mathbf{A}$ whose curl is equal to $\mathbf{B}$ must be singular along some line running from the origin to spatial infinity. This Dirac string singularity could potentially be detected through the extra phase that the wavefunction of a particle with electric charge Q_E would acquire if it moved along a loop encircling the string. For the string to be unobservable, this phase must be a multiple of 2π. Requiring that this be the case for any pair of electric and magnetic charges gives the condition that all charges be integer multiples of minimum charges $Q_E^{\rm min}$ and $Q_M^{\rm min}$ obeying

$$Q_E^{\rm min}Q_M^{\rm min} = 2\pi\,. \tag{116.2}$$

(For monopoles which also carry an electric charge, called dyons, the quantization conditions on their electric charges can be modified. However, the constraints on magnetic charges, as well as those on all purely electric particles, will be unchanged.)

Another way to understand this result is to note that the conserved orbital angular momentum of a point electric charge moving in the field of a magnetic monopole has an additional component, with

$$\mathbf{L} = m\mathbf{r}\times\mathbf{v} - 4\pi Q_E Q_M\hat{\mathbf{r}} \tag{116.3}$$

Requiring the radial component of $\mathbf{L}$ to be quantized in half-integer units yields Eq. (116.2).

If there are unbroken gauge symmetries in addition to the U(1) of electromagnetism, the above analysis must be modified [2,3]. For example, a monopole could have both a U(1) magnetic charge and a color magnetic charge. The latter could combine with the color charge of a quark to give an additional contribution to the phase factor associated with a loop around the Dirac string, so that the U(1) charge could be the Dirac charge $Q_M^D \equiv 2\pi/e$, the result that would be obtained by substituting the electron charge into Eq. (116.2). On the other hand, for monopoles without color-magnetic charge, one would simply insert the quark electric charges into Eq. (116.2) and conclude that Q_M must be a multiple of $6\pi/e$.

The prediction of GUT monopoles arises from the work of 't Hooft [4] and Polyakov [5], who showed that certain spontaneously broken gauge theories have nonsingular classical solutions that lead to magnetic monopoles in the quantum theory. The simplest example occurs in a theory where the vacuum expectation value of a triplet Higgs field ϕ breaks an SU(2) gauge symmetry down to the U(1) of electromagnetism and gives a mass M_V to two of the gauge bosons. In order to have finite energy, ϕ must approach a vacuum value at infinity. However, there is a continuous family of possible vacua, since the scalar field potential determines only the magnitude v of $\langle\phi\rangle$, but not its orientation in the internal SU(2) space. In the monopole solution, the direction of ϕ in internal space is correlated with the position in physical space; *i.e.*, $\phi^a \sim v\hat{r}^a$. The stability of the solution follows from the fact that this twisting Higgs field cannot be smoothly deformed to a spatially uniform vacuum configuration. Reducing the energetic cost of the spatial variation of ϕ requires a nonzero gauge potential, which turns out to yield the magnetic field corresponding to a charge $Q_M = 4\pi/e$. Numerical solution of the classical field equations shows that the mass of this monopole is

$$M_{\rm mon} \sim \frac{4\pi M_V}{e^2}\,. \tag{116.4}$$

The essential ingredient here was the fact that the Higgs fields at spatial infinity could be arranged in a topologically nontrivial configuration. A discussion of the general conditions under which this is possible is beyond the scope of this review, so we restrict ourselves to the two phenomenologically most important cases.

The first is the electroweak theory, with SU(2) × U(1) broken to U(1). There are no topologically nontrivial configurations of the Higgs field, and hence no topologically stable monopole solutions.

The second is when any simple Lie group is broken to a subgroup with a U(1) factor, a case that includes all grand unified theories. The monopole mass is determined by the mass scale of the symmetry breaking that allows nontrivial topology. For example, an SU(5) model with

$$\mathrm{SU(5)} \xrightarrow{M_X} \mathrm{SU(3)\times SU(2)\times U(1)} \xrightarrow{M_W} \mathrm{SU(3)\times U(1)} \tag{116.5}$$

has a monopole [6] with $Q_M = 2\pi/e$ and mass

$$M_{\rm mon} \sim \frac{4\pi M_{\rm X}}{g^2}\,, \tag{116.6}$$

where g is the SU(5) gauge coupling. For a unification scale of 10^{16} GeV, these monopoles would have a mass $M_{\rm mon} \sim 10^{17}$ – 10^{18} GeV.

In theories with several stages of symmetry breaking, monopoles of different mass scales can arise. In an SO(10) theory with

$$\mathrm{SO(10)} \xrightarrow{M_1} \mathrm{SU(4)\times SU(2)\times SU(2)} \xrightarrow{M_2} \mathrm{SU(3)\times SU(2)\times U(1)} \tag{116.7}$$

there is monopole with $Q_M = 2\pi/e$ and mass $\sim 4\pi M_1/g^2$ and a much lighter monopole with $Q_M = 4\pi/e$ and mass $\sim 4\pi M_2/g^2$ [7].

The central core of a GUT monopole contains the fields of the superheavy gauge bosons that mediate baryon number violation, so one might expect that baryon number conservation could be violated in baryon–monopole scattering. The surprising feature, pointed out by Callan [8] and Rubakov [9], is that these processes are not suppressed by powers of the gauge boson mass. Instead, the cross-sections for catalysis processes such as p + monopole → $e^+ + \pi^0$ + monopole are essentially geometric; *i.e.*, $\sigma_{\Delta B}\beta \sim 10^{-27}$ cm^2, where $\beta = v/c$. Note, however, that intermediate mass monopoles arising at later stages of symmetry breakings, such as the doubly charged monopoles of the SO(10) theory, do not catalyze baryon number violation.

116.1. Production and Annihilation

GUT monopoles are far too massive to be produced in any foreseeable accelerator. However, they could have been produced in the early universe as topological defects arising via the Kibble mechanism [10] in a symmetry-breaking phase transition. Estimates of the initial monopole abundance, and of the degree to which it can be reduced by monopole-antimonopole annihilation, predict a present-day monopole abundance that exceeds by many orders of magnitude the astrophysical and experimental bounds described below [11]. Cosmological inflation and other proposed solutions to this primordial monopole problem generically lead to present-day abundances exponentially smaller than could be plausibly detected, although potentially observable abundances can be obtained in scenarios with carefully tuned parameters.

If monopoles light enough to be produced at colliders exist, one would expect that these could be produced by analogs of the electromagnetic processes that produce pairs of electrically charged particles. Because of the large size of the magnetic charge, this is a strong coupling problem for which perturbation theory cannot be trusted. Indeed, the problem of obtaining reliable quantitative estimates of the production cross-sections remains an open one, on which there is no clear consensus.

116.2. Astrophysical and Cosmological Bounds

If there were no galactic magnetic field, one would expect monopoles in the galaxy to have typical velocities of the order of $10^{-3}c$, comparable to the virial velocity in the galaxy (relevant if the monopoles cluster with the galaxy) and the peculiar velocity of the galaxy with respect to the CMB rest frame (relevant if the monopoles are not bound to the galaxy). This situation is modified by the existence of a galactic magnetic field $B \sim 3\mu$G. A monopole with the Dirac charge and mass M would be accelerated by this field to a velocity

$$v_{\rm mag} \sim \begin{cases} c, & M \lesssim 10^{11}{\rm GeV}\ , \\ 10^{-3}c\left(\frac{10^{17}\,{\rm GeV}}{M}\right)^{1/2}, & M \gtrsim 10^{11}{\rm GeV}\ . \end{cases} \tag{116.8}$$

Accelerating these monopoles drains energy from the magnetic field. Parker [12] obtained an upper bound on the flux of monopoles in the galaxy by requiring that the rate of this energy loss be small compared to the time scale on which the galactic field can be regenerated. With reasonable choices for the astrophysical parameters (see Ref. 13 for details), this Parker bound is

$$F < \begin{cases} 10^{-15}\,{\rm cm}^{-2}\,{\rm sr}^{-1}\,{\rm sec}^{-1}\,, & M \lesssim 10^{17}\,{\rm GeV}\ , \\ 10^{-15}\left(\frac{M}{10^{17}\,{\rm GeV}}\right){\rm cm}^{-2}\,{\rm sr}^{-1}\,{\rm sec}^{-1}\,, & M \gtrsim 10^{17}\,{\rm GeV}\ . \end{cases} \tag{116.9}$$

Applying similar arguments to an earlier seed field that was the progenitor of the current galactic field leads to a tighter bound [14],

$$F < \left[\frac{M}{10^{17}{\rm GeV}} + (3\times 10^{-6})\right] 10^{-16}\,{\rm cm}^{-2}{\rm sr}^{-1}{\rm sec}^{-1}. \tag{116.10}$$

Considering magnetic fields in galactic clusters gives a bound [15] which, although less secure, is about three orders of magnitude lower than the Parker bound.

A flux bound can also be inferred from the total mass of monopoles in the universe. If the monopole mass density is a fraction Ω_M of the critical density, and the monopoles were uniformly distributed throughout the universe, there would be a monopole flux

$$F_{\rm uniform} = 1.3\times 10^{-16}\Omega_M \left(\frac{10^{17}\,{\rm GeV}}{M}\right)\left(\frac{v}{10^{-3}c}\right){\rm cm}^{-2}{\rm sr}^{-1}{\rm sec}^{-1}. \tag{116.11}$$

If we assume that $\Omega_M \sim 0.1$, this gives a stronger constraint than the Parker bound for $M \sim 10^{15}$ GeV. However, monopoles with masses $\sim 10^{17}$ GeV are not ejected by the galactic field and can be gravitationally bound to the galaxy. In this case their flux within the galaxy is increased by about five orders of magnitude for a given value of Ω_M, and the mass density bound only becomes stronger than the Parker bound for $M \sim 10^{18}$ GeV.

A much more stringent flux bound applies to GUT monopoles that catalyze baryon number violation. The essential idea is that compact astrophysical objects would capture monopoles at a rate proportional to the galactic flux. These monopoles would then catalyze proton decay, with the energy released in the decay leading to an observable increase in the luminosity of the object. A variety of bounds, based on neutron stars [16–20], white dwarfs [21], and Jovian planets [22] have been obtained. These depend in the obvious manner on the catalysis cross section, but also on the details of the astrophysical scenarios; *e.g.*, on how much the accumulated density is reduced by monopole-antimonopole annihilation, and on whether monopoles accumulated in the progenitor star survive its collapse to a white dwarf or neutron star. The bounds obtained in this manner lie in the range

$$F\left(\frac{\sigma_{\Delta B}\beta}{10^{-27}{\rm cm}^2}\right) \sim (10^{-18} - 10^{-29}){\rm cm}^{-2}{\rm sr}^{-1}{\rm sec}^{-1}. \tag{116.12}$$

It is important to remember that not all GUT monopoles catalyze baryon number nonconservation. In particular, the intermediate mass monopoles that arise in some GUTs at later stages of symmetry-breaking are examples of theoretically motivated monopoles that are exempt from the bound of Eq. (116.12).

116.3. Searches for Magnetic Monopoles

To date there have been no confirmed observations of exotic particles possessing magnetic charge. Precision measurements of the properties of known particles have led to tight limits on the values of magnetic charge they may possess. Using the induction method (see below), the electron's magnetic charge has been found to be $Q_e^m < 10^{-24}Q_M^D$ [23](where Q_M^D is the Dirac charge). Furthermore, measurements of the anomalous magnetic moment of the muon have been used to place a model dependent lower limit of 120 GeV on the monopole mass [1] [24]. Nevertheless, guided mainly by Dirac's argument and the predicted existence of monopoles from spontaneous symmetry breaking mechanisms, searches have been routinely made for monopoles produced at accelerators, in cosmic rays, and bound in matter [25]. Although the resultant limits from such searches are usually made under the assumption of a particle possessing only magnetic charge, most of the searches are also sensitive to dyons.

116.4. Search Techniques

Search strategies are determined by the expected interactions of monopoles as they pass through matter. These would give rise to a number of striking characteristic signatures. Since a complete description of monopole search techniques falls outside of the scope of this minireview, only the most common methods are described below. More comprehensive descriptions of search techniques can be found in Refs. [26,27].

The induction method exploits the long-ranged electromagnetic interaction of the monopole with the quantum state of a superconducting ring which would lead to a monopole which passes through such a ring inducing a permanent current. The induction technique typically uses Superconducting Quantum Interference Devices (SQUID) technology for detection and is employed for searches for monopoles in cosmic rays and matter. Another approach is to exploit the electromagnetic energy loss of monopoles. Monopoles with Dirac charge would typically lose energy at a rate which is several thousand times larger than that expected from particles possessing the elementary electric charge. Consequently, scintillators, gas chambers and nuclear track detectors (NTDs) have been used in cosmic ray and collider experiments. A further approach, which has been used at colliders, is to search for particles describing a non-helical path in a uniform magnetic field.

116.4.1. *Searches for Monopoles Bound in Matter* :

Monopoles have been sought in a range of bulk materials which it is assumed would have absorbed incident cosmic ray monopoles over a long exposure time of order million years. Materials which have been studied include moon rock, meteorites, manganese modules, and sea water [28]. A stringent upper limit on the monopoles per nucleon ratio of $\sim 10^{-29}$ has been obtained [28].

116.4.2. ***Searches in Cosmic Rays*** : Direct searches for monopoles in cosmic rays refer to those experiments in which the passage of the monopole is measured by an active detector. Searches made assuming a catalysis processes in which GUT monopoles could induce nucleon decay are discussed in the next section. To interpret the results of the non-catalysis searches, the cross section for the catalysis process is typically either set to zero [29] or assigned a modest value (1mb) [30].

Although early cosmic ray searches using the induction technique [31] and NTDs [32] observed monopole candidates, none of these apparent observations have been confirmed. Recent experiments have typically employed large scale detectors. The MACRO experiment at the Gran Sasso underground laboratory comprised three different types of detector: liquid scintillator, limited stream tubes, and NTDs, which provided a total acceptance of $\sim 10000{\rm m}^2$ for an isotropic flux. As shown in Fig. 116.1, this experiment has so far provided the most extensive β-dependent flux limits for GUT monopoles with Dirac charge [30]. Also shown are limits from an experiment at the OHYA mine in Japan [29], which used a $2000{\rm m}^2$ array of NTDs.

[1] Where no ambiguity is likely to arise, a reference to a monopole implies a particle possessing Dirac charge.

In Fig. 116.1, upper flux limits are also shown as a function of mass for monopole speed $\beta > 0.05$. In addition to MACRO and OYHA flux limits, results from the SLIM [33] high-altitude experiment are shown. The SLIM experiment provided a good sensitivity to intermediate mass monopoles ($10^5 \lesssim M \lesssim 10^{12}$ GeV). In addition to the results shown in Fig. 116.1, limits as low as $\sim 3 \times 10^{-18}$ cm^{-2}s^{-1}sr^{-1} and $\sim 10^{-17}$ cm^{-2}s^{-1}sr^{-1} were obtained for monopoles with $\beta > 0.8$ and $\beta > 0.625$ by the IceCube [34] and Antares [35] experiments, respectively. Stringent constraints on the flux of ultra-relativistic monopoles have been obtained at the Pierre Auger Observatory [36] which was sensitive to monopoles with γ values ranging from 10^9 to 10^{12}, leading to flux limits in the range $10^{-15} - 2.5 \times 10^{-21}$ cm^{-2}s^{-1}sr^{-1}. The RICE [37] and ANITA-II experiments [38] at the South Pole have also sought ultra-relativistic monopoles with γ values of $10^7 \lesssim \gamma \lesssim 10^{12}$ and $10^9 \lesssim \gamma \lesssim 10^{13}$, respectively, and which produced flux limits as low as 2.5×10^{-21} cm^{-2}s^{-1}sr^{-1}.

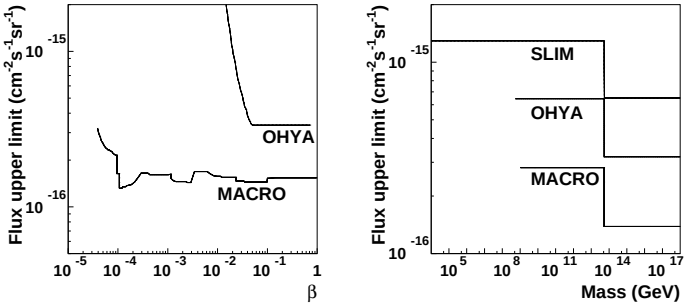

Figure 116.1: Upper flux limits for (a) GUT monopoles as a function of β (b) Monopoles as a function of mass for $\beta > 0.05$.

116.4.3. *Searches via the Catalysis of Nucleon-Decay* :

Searches have been performed for evidence of the catalysed decay of a nucleon by a monopole, as predicted by the Callan-Rubakov mechanism. The searches are thus sensitive to the assumed value of the catalysis decay cross section. Searches have been made with the Soudan [39] and Macro [40] experiments, using tracking detectors. Searches at IMB [41], the underwater Lake Baikal experiment [42] and the The IceCube experiment [43] which exploit the Cerenkov effect have also been made. The resulting β-dependent flux limits from these experiments typically vary between $\sim 10^{-18}$ and $\sim 10^{-14}$cm^{-2}sr^{-1}s^{-1}. A recent search for low energy neutrinos (assumed to be produced from induced proton decay in the sun) was made at Super-Kamiokande [44]. A model- and β-dependent of limit of $6.3 \times 10^{-24}(\frac{\beta}{10^{-3}})^2$cm^{-2}sr^{-1}s^{-1} was obtained.

116.4.4. *Searches at Colliders* :

Searches have been performed at hadron-hadron, electron-positron and lepton-hadron experiments. Collider searches can be broadly classed as being direct or indirect. In a direct search, evidence of the passage of a monopole through material, such as a charged particle track, is sought. In indirect searches, virtual monopole processes are assumed to influence the production rates of certain final states.

116.4.4.1. *Direct Searches at Colliders:*

Collider experiments typically express their results in terms of upper limits on a production cross section and/or monopole mass. To calculate these limits, ansatzes are used to model the kinematics of monopole-antimonopole pair production processes since perturbative field theory cannot be used to calculate the rate and kinematic properties of produced monopoles. Limits therefore suffer from a degree of model-dependence, implying that a comparison between the results of different experiments can be problematic, in particular when this concerns excluded mass regions. A conservative approach with as little model-dependence as possible is thus to present the upper cross-section limits as a function of one half the centre-of-mass energy of the collisions, as shown in Fig. 116.2 for recent results from high energy colliders.

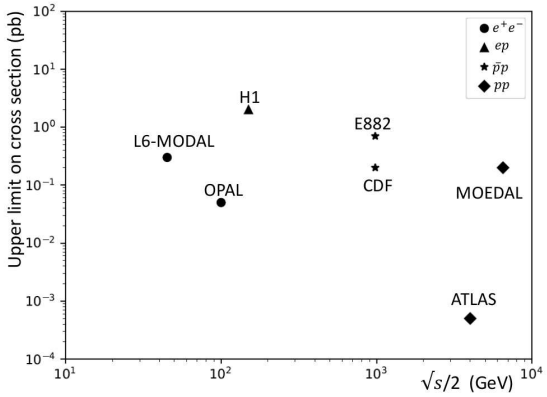

Figure 116.2: Upper limits on the production cross sections of monopoles from various collider-based experiments.

Searches for monopoles produced at the highest available energies in hadron-hadron collisions were made in pp collisions at the LHC by the ATLAS [45] and MOEDAL [46] experiments. The experiments looked for highly ionising particles leaving characteristic energy deposition profiles and stopped monopoles with the induction method, respectively. Tevatron searches have also been carried out by the CDF [47] and E882 [48] experiments. The CDF experiment used a dedicated time-of-flight system whereas the E882 experiment employed the induction technique to search for stopped monopoles in discarded detector material which had been part of the CDF and D0 detectors using periods of luminosity. Earlier searches at the Tevatron, such as [49], used NTDs and were based on comparatively modest amounts of integrated luminosity. Lower energy hadron-hadron experiments have employed a variety of search techniques including plastic track detectors [50] and searches for trapped monopoles [51].

The only LEP-2 search was made by OPAL [52] which quoted cross section limits for the production of monopoles possessing masses up to around 103 GeV. At LEP-1, searches were made with NTDs deployed around an interaction region. This allowed a range of charges to be sought for masses up to ~ 45 GeV. The L6-MODAL experiment [53] gave limits for monopoles with charges in the range $0.9Q_M^D$ and $3.6Q_M^D$, whilst an earlier search by the MODAL experiment was sensitive to monopoles with charges as low as $0.1Q_M^D$ [54]. The deployment of NTDs around the beam interaction point was also used at earlier e^+e^- colliders such as KEK [55] and PETRA [56]. Searches at e^+e^- facilities have also been made for particles following non-helical trajectories [57,58].

There has so far been one search for monopole production in lepton-hadron scattering. Using the induction method, monopoles were sought which could have stopped in the aluminium beampipe which had been used by the H1 experiment at HERA [59]. Cross section limits were set for monopoles with charges in the range $Q_M^D - 6Q_M^D$ for masses up to around 140 GeV.

116.4.4.2. *Indirect Searches at Colliders:*

It has been proposed that virtual monopoles can mediate processes which give rise to multi-photon final-states [60,61]. Photon-based searches were made by the D0 [62] and L3 [63] experiments. The D0 work led to spin-dependent lower mass limits of between 610 and 1580 GeV, while L3 reported a lower mass limit of 510 GeV. However, it should be stressed that uncertainties on the theoretical calculations which were used to derive these limits are difficult to estimate.

References:

1. P.A.M.Dirac, Proc. Royal Soc. London **A133**, 60 (1931).
2. F. Englert and P. Windey, Phys. Rev. **D14**, 2728 (1976).
3. P. Goddard, J. Nuyts, and D.I. Olive, Nucl. Phys. **B125**, 1 (1977).
4. G.'t Hooft, Nucl. Phys. **B79**, 276 (1974).

5. A.M. Polyakov, Pisma Zh. Eksp. Teor. Fiz. **20**, 194 (1974) [Pisma Zh. Eksp. Teor. Fiz. **20**, 430 (1974)].
6. C.P. Dokos and T.N. Tomaras, Phys. Rev. **D21**, 2940 (1980).
7. G. Lazarides and Q. Shafi, Phys. Lett. **B94**, 149 (1980).
8. C.G. Callan, Phys. Rev. **D26**, 2058 (1982).
9. V.A. Rubakov, Nucl. Phys. **B203**, 311 (1982).
10. T.W.B. Kibble, J. Phys. **A9**, 1387 (1976).
11. J. Preskill, Phys. Rev. Lett. **43**, 1365 (1979).
12. E.N. Parker, Astrophys. J. **160**, 383 (1970).
13. M.S. Turner, E.N. Parker, and T.J. Bogdan, Phys. Rev. **D26**, 1296 (1982).
14. F.C. Adams *et al.*, Phys. Rev. Lett. **70**, 2511 (1993).
15. Y. Rephaeli and M.S. Turner, Phys. Lett. **B121**, 115 (1983).
16. E.W. Kolb, S.A. Colgate, and J.A. Harvey, Phys. Rev. Lett. **49**, 1373 (1982).
17. S. Dimopoulos, J. Preskill, and F. Wilczek, Phys. Lett. **B119**, 320 (1982).
18. K. Freese, M.S. Turner, and D.N. Schramm, Phys. Rev. Lett. **51**, 1625 (1983).
19. E.W. Kolb and M.S. Turner, Astrophys. J. **286**, 702 (1984).
20. J.A. Harvey, Nucl. Phys. **B236**, 255 (1984).
21. K. Freese and E. Krasteva, Phys. Rev. **D59**, 063007 (1999).
22. J. Arafune, M. Fukugita, and S. Yanagita, Phys. Rev. **D32**, 2586 (1985).
23. L.L. Vant-Hull, Phys. Rev. **173**, 1412 (1968).
24. S. Graf, A. Schaefer, and W. Greiner, Phys. Lett. **B262**, 463 (1991).
25. Review of Particle Physics 2012 (*this Review*), listing on *Searches for Magnetic Monopoles*.
26. G. Giacomelli and L. Patrizii, `arXiv:hep-ex/0506014`.
27. M. Fairbairn *et al.*, Phys. Reports **438**, 1 (2007).
28. J.M. Kovalik and J.L. Kirschvink, Phys. Rev. **A33**, 1183 (1986); H. Jeon and M. J. Longo, Phys. Rev. Lett. **75**, 1443 (1995) [Erratum-ibid. **76**, 159 (1996)].
29. S. Orito *et al.*, Phys. Rev. Lett. **66**, 1951 (1991).
30. M. Ambrosio *et al.* [MACRO Collab.], Eur. Phys. J. **C25**, 511 (2002).
31. B. Cabrera, Phys. Rev. Lett. **48**, 1378 (1982).
32. P.B. Price *et al.*, Phys. Rev. Lett. **35**, 487 (1975).
33. S. Balestra *et al.*, Eur. Phys. J. **C55**, 57 (2008).
34. R. Abbasi *et al.* [IceCube Collab.], Phys. Rev. **D87**, 022001 (2013).
35. S. Adrian-Martinez *et al.* [ANTARES Collab.], Astropart. Phys. **35**, 634 (2012).
36. A. Aab *et al.* [Pierre Auger Collab.], Phys. Rev. **D98**, 082002 (2016).
37. D.P. Hogan *et al.*, Phys. Rev. **D78**, 075031 (2008).
38. M. Detrixhe *et al.*, Phys. Rev. **D83**, 023513 (2011).
39. J.E. Bartelt *et al.*, Phys. Rev. **D36**, 1990 (1987) [Erratum-ibid. **D40**, 1701 (1989)].
40. M. Ambrosio *et al.*, Eur. Phys. J. **C26**, 163 (2002).
41. R. Becker-Szendy *et al.*, Phys. Rev. **D49**, 2169 (1994).
42. V. A. Balkanov *et al.*, Prog. in Part. Nucl. Phys. **40**, 391 (1998).
43. M.G. Aartsen *et al.* [IceCube Collab.], Eur. Phys. J. **C74**, 2938 (2014).
44. K. Ueno *et al.* [Super-Kamiokande Collab.], Astropart. Phys. **36**, 131 (2012).
45. G. Aad *et al.* [ATLAS Collab.], Phys. Rev. **D93**, 052009 (2016).
46. B. Acharya *et al.*[MoEDAL Collab.], Phys. Rev. Lett. **118**, 061801 (2017).
47. A. Abulencia *et al.* [CDF Collab.], Phys. Rev. Lett. **96**, 201801 (2006).
48. G.R. Kalbfleisch *et al.*, Phys. Rev. **D69**, 052002 (2004).
49. P.B. Price, G.X. Ren, and K. Kinoshita, Phys. Rev. Lett. **59**, 2523 (1987).
50. B. Aubert *et al.*, Phys. Lett. **B120**, 465 (1983).
51. R.A. Carrigan, F.A. Nezrick, and B.P. Strauss, Phys. Rev. **D8**, 3717 (1973).
52. G. Abbiendi *et al.* [OPAL Collab.], Phys. Lett. **B663**, 37 (2008).
53. J.L. Pinfold *et al.*, Phys. Lett. **B316**, 407 (1993).
54. K. Kinoshita *et al.*, Phys. Rev. **D46**, 881 (1992).
55. K. Kinoshita *et al.*, Phys. Lett. **B228**, 543 (1989).
56. P. Musset *et al.*, Phys. Lett. **B128**, 333 (1983).
57. T. Gentile *et al.* [Cleo Collab.], Phys. Rev. **D35**, 1081 (1987).
58. W. Braunschweig *et al.* [TASSO Collab.], Z. Phys. **C38**, 543 (1988).
59. A. Aktas *et al.* [H1 Collab.], Eur. Phys. J. **C41**, 133 (2005).
60. A. De Rujula, Nucl. Phys. **B435**, 257 (1995).
61. I.F. Ginzburg and A. Schiller, Phys. Rev. **D60**, 075016 (1999).
62. B. Abbott *et al.* [D0 Collab.], Phys. Rev. Lett. **81**, 524 (1998).
63. M. Acciarri *et al.* [L3 Collab.], Phys. Lett. **B345**, 609 (1995).

INDEX

Greek letters are alphabetized by their English-language spelling. Bold page numbers signify entries in the Particle Properties Summary Tables.

Greek letters are alphabetized by their English-language spelling. Bold page numbers signify entries in the Particle Properties Summary Tables.

Greek letters are alphabetized by their English-language spelling. Bold page numbers signify entries in the Particle Properties Summary Tables.

Greek letters are alphabetized by their English-language spelling. Bold page numbers signify entries in the Particle Properties Summary Tables.

Greek letters are alphabetized by their English-language spelling. Bold page numbers signify entries in the Particle Properties Summary Tables.

Greek letters are alphabetized by their English-language spelling. Bold page numbers signify entries in the Particle Properties Summary Tables.

Greek letters are alphabetized by their English-language spelling. Bold page numbers signify entries in the Particle Properties Summary Tables.

Greek letters are alphabetized by their English-language spelling. Bold page numbers signify entries in the Particle Properties Summary Tables.

Greek letters are alphabetized by their English-language spelling. Bold page numbers signify entries in the Particle Properties Summary Tables.

Greek letters are alphabetized by their English-language spelling. Bold page numbers signify entries in the Particle Properties Summary Tables.

Greek letters are alphabetized by their English-language spelling. Bold page numbers signify entries in the Particle Properties Summary Tables.

VOLUME II: TABLE OF CONTENTS

PARTICLE LISTINGS*

*The divider sheets give more detailed indices for each main section of the Particle Listings.

INTRODUCTION TO THE PARTICLE LISTINGS

Illustrative Key to the Particle Listings

Name of particle. "Old" name used before 1986 renaming scheme also given if different. See the section "Naming Scheme for Hadrons" for details.

Particle quantum numbers (where known).

Indicates particle omitted from Particle Physics Summary Table, implying particle's existence is not confirmed.

Quantity tabulated below.

General comments on particle.

Top line gives our best value (and error) of quantity tabulated here, based on weighted average of measurements used. Could also be from fit, best limit, estimate, or other evaluation. See next page for details.

"Document id" for this result; full reference given below.

Footnote number linking measurement to text of footnote.

Measurement technique. (See abbreviations on next page.)

Number of events *above background*.

Scale factor > 1 indicates possibly inconsistent data.

Measured value used in averages, fits, limits, etc.

Reaction producing particle, or general comments.

Error in measured value (often statistical only; followed by systematic if separately known; the two are combined in quadrature for averaging and fitting.)

"Change bar" indicates result added or changed since previous edition.

Measured value *not used* in averages, fits, limits, etc. See the Introductory Text for explanations.

Charge(s) of particle(s) detected.

Arrow points to weighted average.

Ideogram to display possibly inconsistent data. Curve is sum of Gaussians, one for each experiment (area of Gaussian = 1/error; width of Gaussian = ±error). See Introductory Text for discussion.

Shaded pattern extends $\pm 1\sigma$ (scaled by "scale factor" S) from weighted average.

Value and error for each experiment.

Contribution of experiment to χ^2 (if no entry present, experiment not used in calculating χ^2 or scale factor because of very large error).

Partial decay mode (labeled by Γ_i).

Our best value for branching fraction as determined from data averaging, fitting, evaluating, limit selection, etc. This list is basically a compact summary of results in the Branching Ratio section below.

Branching ratio.

Our best value (and error) of quantity tabulated, as determined from constrained fit (using *all significant* measured branching ratios for this particle).

Weighted average of measurements of this ratio only.

Footnote (referring to LYNCH 81).

Branching ratio in terms of partial decay mode(s) Γ_i above.

Confidence level for measured upper limit.

References, ordered inversely by year, then author.

Partial list of author(s) in addition to first author.

"Document id" used on data entries above.

Quantum number determinations in this reference.

Journal, report, preprint, etc. (See abbreviations on next page.)

Institution(s) of author(s). (See abbreviations on next page.)

$a_0(1200)$

$I^G(J^{PC}) = 1^-(0^{++})$

OMITTED FROM SUMMARY TABLE

Evidence not compelling, may be a kinematic effect.

$a_0(1200)$ MASS

VALUE (MeV)	EVTS	DOCUMENT ID		TECN	CHG	COMMENT
1206± 7 OUR AVERAGE						
1210± 8±9	3000	FENNER	87	MMS	−	3.5 $\pi^- p$
1198±10		PIERCE	83	ASPK	+	2.1 $K^- p$
1216±11±9	1500	[1] MERRILL	81	HBC	0	3.2 $K^- p$
• • • We do not use the following data for averages, fits, limits, etc. • • •						
1192±16	200	LYNCH	81	HBC	±	2.7 $\pi^- p$

[1] Systematic error was added quadratically by us in our 1986 edition.

$a_0(1200)$ WIDTH

VALUE (MeV)	EVTS	DOCUMENT ID		TECN	CHG	COMMENT
41±11 OUR AVERAGE Error includes scale factor of 1.8. See the ideogram below.						
50± 8		PIERCE	83	ASPK	+	2.1 $K^- p$
70^{+30}_{-20}	200	LYNCH	81	HBC	±	2.7 $\pi^- p$
25± 5±7		MERRILL	81	HBC	0	3.2 $K^- p$
• • • We do not use the following data for averages, fits, limits, etc. • • •						
<60		FENNER	87	MMS	−	3.5 $\pi^- p$

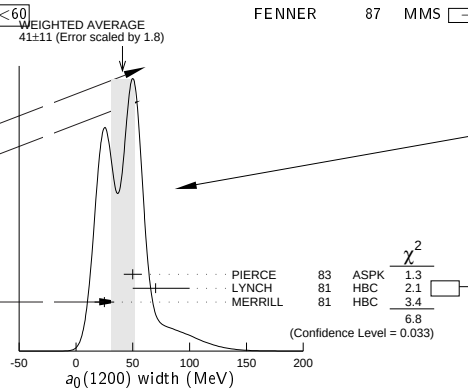

$a_0(1200)$ DECAY MODES

Mode		Fraction (Γ_i/Γ)	Scale factor/ Confidence level
Γ_1	3π	(65.2±1.3) %	S=1.7
Γ_2	$K\overline{K}$	(34.8±1.3) %	S=1.7
Γ_3	$\eta\pi^\pm$	< 5 $\times 10^{-4}$	CL=95%

$a_0(1200)$ BRANCHING RATIOS

$\Gamma(3\pi)/\Gamma_{total}$ Γ_1/Γ

VALUE	DOCUMENT ID		TECN	CHG	COMMENT
0.652±0.013 OUR FIT Error includes scale factor of 1.7.					
0.643±0.010 OUR AVERAGE					
0.64 ±0.01	PIERCE	83	ASPK	+	2.1 $K^- p$
0.74 ±0.06	MERRILL	81	HBC	0	3.2 $K^- p$
• • • We do not use the following data for averages, fits, limits, etc. • • •					
0.48 ±0.15	[2] LYNCH	81	HBC	±	2.7 $\pi^- p$

[2] Data has questionable background subtraction.

$\Gamma(K\overline{K})/\Gamma_{total}$ Γ_2/Γ

VALUE	DOCUMENT ID		TECN	CHG	COMMENT
0.348±0.013 OUR FIT Error includes scale factor of 1.7.					
0.35 ±0.05	PIERCE	83	ASPK	+	2.1 $K^- p$

$\Gamma(K\overline{K})/\Gamma(3\pi)$ Γ_2/Γ_1

VALUE	DOCUMENT ID		TECN	CHG	COMMENT
0.535±0.030 OUR FIT Error includes scale factor of 1.7.					
0.50 ±0.03	MERRILL	81	HBC	0	3.2 $K^- p$

$\Gamma(\eta(\text{neutral decay})\pi^\pm)/\Gamma_{total}$ $0.71\Gamma_3/\Gamma$

VALUE (units 10^{-4})	CL%	DOCUMENT ID		TECN	CHG	COMMENT
<3.5	95	PIERCE	83	ASPK	+	2.1 $K^- p$

$a_0(1200)$ REFERENCES

FENNER	87	PRL 55 14	H. Fenner *et al.*	(SLAC)	
PIERCE	83	PL 123B 230	J.H. Pierce	(FNAL)	UP
LYNCH	81	PR D24 610	G.R. Lynch *et al.*	(CLEO Collab.)	
MERRILL	81	PRL 47 143	D.W. Merrill *et al.*	(SACL, CERN)	

Abbreviations Used in the Particle Listings

Indicator of Procedure Used to Obtain Our Result

OUR AVERAGE	From a weighted average of selected data.
OUR FIT	From a constrained or overdetermined multiparameter fit of selected data.
OUR EVALUATION	Not from a direct measurement, but evaluated from measurements of other quantities.
OUR ESTIMATE	Based on the observed range of the data. Not from a formal statistical procedure.
OUR LIMIT	For special cases where the limit is evaluated by us from measured ratios or other data. Not from a direct measurement.

Measurement Techniques (i.e., Detectors and Methods of Analysis)

A1	A1 Collaboration at MAMI
A2MM	A2 spectrometer at the Mainz Microtron, MAMI
ACCM	ACCMOR Collaboration
ADMX	Axion Dark Matter Experiment
AEMS	Argonne effective mass spectrometer
ALEP	ALEPH – CERN LEP detector
ALPS	Photon regeneration experiment
AMND	AMANDA South Pole neutrino detector
AMY	AMY detector at KEK-TRISTAN
ANIT	Antarctic Impulsive Transient Antenna balloon mission
ANTR	ANTARES underwater neutrino telescope in the Western Mediterranean Sea
APEX	FNAL APEX Collab.
ARG	ARGUS detector at DORIS
ARGD	Fit to semicircular amplitude path on Argand diagram
ASP	Anomalous single-photon detector
ASPK	Automatic spark chambers
ASTE	ASTERIX detector at LEAR
ASTR	Astronomy
ATLS	ATLAS detector at CERN LHC
AUGE	Pierre Auger Observatory
AURG	Resonant-mass gravitational wave AURIGA detector
B787	BNL experiment 787 detector
B791	BNL experiment 791 detector
B845	BNL experiment 845 detector
B852	BNL E-852
B865	BNL E865 detector
B871	BNL experiment 871 detector
B949	BNL E949 detector at AGS
BABR	BaBar Collab.
BAIK	Lake Baikal neutrino telescope
BAKS	Baksan underground scintillation telescope
BC	Bubble chamber
BDMP	Beam dump
BEAT	CERN BEATRICE Collab.
BEBC	Big European bubble chamber at CERN
BELL	Belle Collab.
BES	BES Beijing Spectrometer at Beijing Electron-Positron Collider
BES2	BES Beijing Spectrometer at Beijing Electron-Positron Collider
BES3	BES Beijing Spectrometer at Beijing Electron-Positron Collider
BIS2	BIS-2 spectrometer at Serpukhov
BKEI	BENKEI spectrometer system at KEK Proton Synchroton
BOLO	Bolometer, a cryogenic thermal detector
BONA	Bonanza nonmagnetic detector at DORIS
BORX	BOREXINO
BPWA	Barrelet-zero partial-wave analysis
CALO	Calorimeter
CAST	CAST experiment at CERN
CBAL	Crystal Ball detector at SLAC-SPEAR or DORIS
CBAR	Crystal Barrel detector at CERN-LEAR
CBOX	Crystal Box at LAMPF
CBTP	CBELSA/TAPS Collaboration
CC	Cloud chamber
CCFR	Columbia-Chicago-Fermilab-Rochester detector
CDEX	China Dark Matter Experiment
CDF	Collider detector at Fermilab
CDF2	CDF-II Collab.
CDHS	CDHS neutrino detector at CERN
CDM2	CDMS II, Cryogenic Dark Matter Search at Soudan Underground Lab.
CDMS	CDMS Collaboration
CELL	CELLO detector at DESY
CGNT	CoGeNT dark matter search experiment
CHER	Cherenkov detector
CHM2	CHARM-II neutrino detector (glass) at CERN
CHOZ	Nuclear Power Station near Chooz, France
CHRM	CHARM neutrino detector (marble) at CERN
CHRS	CHORUS Collaboration – CERNS SPS
CIB	Cosmic Infrared Background
CIBS	CERN-IHEP boson spectrometer
CLAS	Jefferson CLAS Collab.
CLE2	CLEO II detector at CESR
CLE3	CLEO III detector at CESR
CLEC	CLEO-c detector at CESR
CLEO	Cornell magnetic detector at CESR
CMB	Cosmic Microwave Background
CMD	Cryogenic magnetic detector at VEPP-2M, Novosibirsk
CMD2	Cryogenic magnetic detector 2 at VEPP-2M, Novosibirsk
CMD3	Cryogenic magnetic detector 3 at VEPP-2000, Novosibirsk
CMS	CMS detector at CERN LHC
CNTR	Counters
COMB	Combined analysis of data from independent experiments.
COMP	COMPASS experiment at the CERN SPS
COSM	Cosmology and astrophysics
COSY	COSY-TOF Collaboration
COUP	COUPP (the Chicagoland Observatory for Underground Particle Physics) Collab.
CPLR	CPLEAR Collaboration
CRBT	Crystal Ball and TAPS detector at MAMI
CRES	CRESST cryogenic detector
CRYB	Crystal Ball at BNL
CRYM	Crystal Ball detector at Mainz Microtron MAMI
CSB2	Columbia U. - Stony Brook BGO calorimeter inserted in NaI array
CSME	COSME Collaboration
CUOR	CUORICINO experiment at Gran Sasso Laboratory.
CUSB	Columbia U. - Stony Brook segmented NaI detector at CESR
D0	D0 detector at Fermilab Tevatron Collider
DAMA	DAMA, dark matter detector at Gran Sasso National Lab.
DASP	DESY double-arm spectrometer
DAYA	Daya Bay Collaboration
DBC	Deuterium bubble chamber
DCHZ	Double Chooz Collaboration
DISP	Graviton mass measurement based on dispersion measure
DLCO	DELCO detector at SLAC-SPEAR or SLAC-PEP
DLPH	DELPHI detector at LEP
DM1	Magnetic detector no. 1 at Orsay DCI collider
DM2	Magnetic detector no. 2 at Orsay DCI collider
DMIC	DAMIC Dark Matter in CCD experiment at Fermilab
DMTP	Dark Matter Time Projection Chamber (DMTPC) directional detection experiment
DONU	DONUT Collab.
DPWA	Energy-dependent partial-wave analysis
DRFT	Directional dark matter detector at Boulby Underground Science Facility
DS50	DarkSide-50 Liquid Argon TPC at Gran Sasso National Laboratory
E621	Fermilab E621 detector
E653	Fermilab E653 detector
E665	Fermilab E665 detector
E687	Fermilab E687 detector
E691	Fermilab E691 detector
E705	Fermilab E705 Spectrometer-Calorimeter
E731	Fermilab E731 Spectrometer-Calorimeter
E756	Fermilab E756 detector
E760	Fermilab E760 detector
E761	Fermilab E761 detector
E771	Fermilab E771 detector
E773	Fermilab E773 Spectrometer-Calorimeter
E789	Fermilab E789 detector
E791	Fermilab E791 detector
E799	Fermilab E799 Spectrometer-Calorimeter
E835	Fermilab E835 detector
EDE2	EDELWEISS II dark matter search Collaboration
EDE3	EDELWEISS III dark matter search Collaboration
EDEL	EDELWEISS dark matter search Collaboration
EHS	Four-pi detector at CERN
ELEC	Electronic combination
EMC	European muon collaboration detector at CERN
EMUL	Emulsions
ESR	Electron spin resonance spectroscopy
FAST	Fiber Active Scintillator Target detector at PSI
FBC	Freon bubble chamber

Abbreviations Used in the Particle Listings

FENI FENICE (at the ADONE collider of Frascati)
FIT Fit to previously existing data
FLAT Large Area Telescope onboard the Fermi Gamma-Ray Space Telescope (Fermi-LAT)
FMPS Fermilab Multiparticle Spectrometer
FOCS FNAL E831 FOCUS Collab.
FRAB ADONE $B\overline{B}$ group detector
FRAG ADONE $\gamma\gamma$ group detector
FRAM ADONE MEA group detector
FREJ FREJUS Collaboration – modular flash chamber detector (calorimeter)
GA24 Hodoscope Cherenkov γ calorimeter (IHEP GAMS-2000) (CERN GAMS-4000)
GALX GALLEX solar neutrino detector in the Gran Sasso Underground Lab.
GAM2 IHEP hodoscope Cherenkov γ calorimeter GAMS-2000
GAM4 CERN hodoscope Cherenkov γ calorimeter GAMS-4000
GAMS IHEP hodoscope Cherenkov γ calorimeter GAMS-4π
GNO Gallium Neutrino Observatory in the Gran Sasso Underground Lab.
GOLI CERN Goliath spectrometer
GRAL GRAAL Collaboration
H1 H1 detector at DESY/HERA
HBC Hydrogen bubble chamber
HDBC Hydrogen and deuterium bubble chambers
HDES HADES Collaboration at GSI in Darmstadt
HDMO Heidelberg-Moscow Experiment
HDMS Heidelberg Dark Matter Search Experiment
HEBC Helium bubble chamber
HEPT Helium proportional tubes
HERA H1 and ZEUS Collaborations at DESY/HERA
HERB HERA-B detector at DESY/HERA
HERM HERMES detector at DESY/HERA
HESS High Energy Stereoscopic System gamma-ray instrument
HFS Hyperfine structure
HLBC Heavy-liquid bubble chamber
HOME Homestake underground scintillation detector
HPGE High-purity Germanium detector
HPW Harvard-Pennsylvania-Wisconsin detector
HRS SLAC high-resolution spectrometer
HYBR Hybrid: bubble chamber + electronics
HYCP HyperCP Collab. (FNAL E-871)
IACT Imaging Air Cherenkov Telescope
ICAR ICARUS experiment at Gran Sasso Laboratory.
ICCB IceCube neutrino detector at South Pole
IGEX IGEX Collab.
IMB Irvine-Michigan-Brookhaven underground Cherenkov detector
IMB3 Irvine-Michigan-Brookhaven underground Cherenkov detector
INDU Magnetic induction
IPWA Energy-independent partial-wave analysis
ISTR IHEP ISTRA+ spectrometer-calorimeter
JADE JADE detector at DESY
K246 KEK E246 detector with polarimeter
K2K KEK to Super-Kamiokande
K391 KEK E391a detector
K470 KEK-E470 Stopping K detector
KAM2 KAMIOKANDE-II underground Cherenkov detector
KAMI KAMIOKANDE underground Cherenkov detector
KAR2 KARMEN2 calorimeter at the ISIS neutron spallation source at Rutherford
KARM KARMEN calorimeter at the ISIS neutron spallation source at Rutherford
KEDR detector operating at VEPP-4M collider (Novosibirsk)
KIMS Korea Invisible Mass Search experiment at YangYang, Korea
KLND KamLand Collab. (Japan)
KLOE KLOE detector at DAFNE (the Frascati e+e- collider Italy)
KOLR Kolar Gold Field underground detector
KOTO KOTO experiment with K_L^0 beam at J-PARC
KTEV KTeV Collaboration
L3 L3 detector at LEP
LASR Laser
LASS Large-angle superconducting solenoid spectrometer at SLAC
LATT Lattice calculations
LEBC Little European bubble chamber at CERN
LEGS BNL LEGS Collab.
LENA Nonmagnetic lead-glass NaI detector at DORIS
LEP From combination of all 4 LEP experiments: ALEPH, DELPHI, L3, OPAL
LEPS Low-Energy Pion Spectrometer at the Paul Scherrer Institute
LGW Lead Glass Wall collaboration at SPEAR/SLAC
LHC Combined analysis of LHC experiments
LHCB LHCb detector at CERN LHC
L+P Multichannel L + P model fit
LSD Mont Blanc liquid scintillator detector
LSND Liquid Scintillator Neutrino Detector
LSW Light Shining through a Wall
LUX Large Underground Xenon experiment at SURF
MAC MAC detector at PEP/SLAC
MBNE Fermilab MiniBooNE neutrino experiment
MBR Molecular beam resonance technique
MCRO MACRO detector in Gran Sasso
MD1 Magnetic detector at VEPP-4, Novosibirsk
MDRP Millikan drop measurement
MEG Muon to electron conversion detector at PSI
MGFL MAGIC and Fermi-LAT Collaborations
MGIC MAGIC Telescopes gamma-ray observatory.
MICA Underground mica deposits
MINS Fermilab MINOS experiment
MIRA MIRABELLE Liquid-hydrogen bubble chamber
MLEV Magnetic levitation
MLS Modified Laurent Series
MMS Missing mass spectrometer
MOED MoEDAL magnetic monopoles search experiment at LHC
MPS Multiparticle spectrometer at BNL
MPS2 Multiparticle spectrometer upgrade at BNL
MPSF Multiparticle spectrometer at Fermilab
MPWA Model-dependent partial-wave analysis
MRK1 SLAC Mark-I detector
MRK2 SLAC Mark-II detector
MRK3 SLAC Mark-III detector
MRKJ Mark-J detector at DESY
MRS Magnetic resonance spectrometer
MUG2 MUON(g-2)
MWPC Multi-Wire Proportional Chamber
NA14 CERN NA14
NA31 CERN NA31 Spectrometer-Calorimeter
NA32 CERN NA32 Spectrometer
NA48 CERN NA48 Collaboration
NA49 CERN NA49 Collaboration
NA60 CERN NA60 Collaboration
NA62 CERN NA62 Experiment
NA64 CERN SPS NA64 Experiment
NAGE NEWAGE, New generation WIMP-search experiment with advanced gaseous tracking
NAIA NAIAD (NaI Advanced Detector) dark matter search experiment
ND NaI detector at VEPP-2M, Novosibirsk
NEOS NEOS Collaboration
NICE Serpukhov nonmagnetic precision spectrometer
NMR Nuclear magnetic resonance
NOMD NOMAD Collaboration, CERN SPS
NOVA NOvA experiment with Fermilabs NuMI neutrino beam
NTEV NuTeV Collab. at Fermilab
nTRV neutron Time-Reversal Violation
NUSX Mont Blanc NUSEX underground detector
OBLX OBELIX detector at LEAR
OLYA Detector at VEPP-2M and VEPP-4, Novosibirsk
OMEG CERN OMEGA spectrometer
OPAL OPAL detector at LEP
OPER OPERA experiment with emulsion tracking at Gran Sasso
OSPK Optical spark chamber
PIBE The PIBETA detector at the Paul Scherrer Institute (PSI), Switzerland.
PICA PICASSO dark matter search experiment
PICO PICO bubble chamber experiment in SNOLAB underground laboratory
PIE3 πE3 beam-line of Paul Scherrer Institute
PLAS Plastic detector
PLUT DESY PLUTO detector
PMLA PAMELA space spectrometer on Resurs-DK1 satellite
PNDX PandaX dual-phase liquid xenon dark matter experiment at Jin-Ping
PRMX The PRIMEX detector in Hall B at TJNAF
PWA Partial-wave analysis
RDK2 NIST rare radioactive decay experiment

Abbreviations Used in the Particle Listings

REDE Resonance depolarization
RENO RENO Collaboration
RICE Radio Ice Cherenkov Experiment
RVUE Review of previous data
SAGE US - Russian Gallium Experiment
SCDM SuperCDMS experiment at Soudan Underground Lab.
SELX FNAL SELEX Collab.
SFM CERN split-field magnet
SHF SLAC Hybrid Facility Photon Collaboration
SIGM Serpukhov CERN-IHEP magnetic spectrometer (SIGMA)
SILI Silicon detector
SIMP SIMPLE, dark matter detector at Laboratori Nazionali del Sud
SKAM Super-Kamiokande Collab.
SLAX Solar Axion Experiment in Canfranc Underground Laboratory
SLD SLC Large Detector for $e^+ e^-$ colliding beams at SLAC
SMPL SIMPLE, Superheated Instrument for Massive ParticLe Experiments
SND Novosibirisk Spherical neutral detector at VEPP-2M
SNDR SINDRUM spectrometer at PSI
SNO SNO Collaboration (Sudbury Neutrino Observatory)
SOU2 Soudan 2 underground detector
SOUD Soudan underground detector
SPEC Spectrometer
SPED From maximum of speed plot or resonant amplitude
SPHR Bonn SAPHIR Collab.
SPNX SPHINX spectrometer at IHEP accelerator
SPRK Spark chamber
SQID SQUID device
STRC Streamer chamber
SVD2 SVD-2 experiment at IHEP, Protvino
T2K T2K Collaboration
TASS DESY TASSO detector
TEVA Combined analysis of CDF and DØ experiments
TEXO TEXONO Collab., ultra low energy Ge detector at Kuo-Sheng Laboratory
THEO Theoretical or heavily model-dependent result
TNF TNF-IHEP facility at 70 GeV IHEP accelerator
TOF Time-of-flight
TOPZ TOPAZ detector at KEK-TRISTAN
TPC TPC detector at PEP/SLAC
TPS Tagged photon spectrometer at Fermilab
TRAP Penning trap
TWST TWIST spectrometer at TRIUMF
UA1 UA1 detector at CERN
UA2 UA2 detector at CERN
UA5 UA5 detector at CERN
UCNA UCNA collaboration using polarizeed ultracold neutrons at LANSCE
UKDM UK Dark Matter Collab.
VES Vertex Spectrometer Facility at 70 GeV IHEP accelerator
VLBI Very Long Baseline Interferometer
VNS VENUS detector at KEK-TRISTAN
VRTS Very Energetic Radiation Imaging Telescope Array System (VERITAS)
WA75 CERN WA75 experiment
WA82 CERN WA82 experiment
WA89 CERN WA89 experiment
WARP Liquid argon detector for CDM searches at Gran Sasso
WASA WASA detector at CELSIUS, Uppsala and at COSY, Juelich
WIRE Wire chamber
X100 XENON100 dark matter search experiment at Gran Sasso National Laboratory
XE10 XENON10 experiment at Gran Sasso National Laboratory
XE1T XENON1T dark matter search experiment at Gran Sasso National Laboratory
XEBC Xenon bubble chamber
XMAS XMASS, liquid xenon scintillation detector at Kamioka Observatory
YUKA Graviton mass measurement based on Yukawa potential
ZEP2 ZEPLIN-II dark matter detector
ZEP3 ZEPLIN-III dark matter detector at Palmer Underground Lab.
ZEPL ZEPLIN-I galactic dark matter detector
ZEUS ZEUS detector at DESY/HERA

Conferences

Conferences are generally referred to by the location at which they were held (e.g., HAMBURG, TORONTO, CORNELL, BRIGHTON, etc.).

Journals

AA Astronomy and Astrophysics
ADVP Advances in Physics
AFIS Anales de Fisica
AJP American Journal of Physics
AL Astronomy Letters
ANP Annals of Physics
ANPL Annals of Physics (Leipzig)
ANYAS Annals of the New York Academy of Sciences
AP Atomic Physics
APAH Acta Physica Academiae Scientiarum Hungaricae
APJ Astrophysical Journal
APJS Astrophysical Journal Suppl.
APP Acta Physica Polonica
APS Acta Physica Slovaca
ARNPS Annual Review of Nuclear and Particle Science
ARNS Annual Review of Nuclear Science
ASP Astroparticle Physics
AST American Statistician
BAPS Bulletin of the American Physical Society
BASUP Bulletin of the Academy of Science, USSR (Physics)
CJNP Chinese Journal of Nuclear Physics
CJP Canadian Journal of Physics
CNPP Comments on Nuclear and Particle Physics
CP Chinese Physics
CPC Chinese Physics C
CTP Communications in Theoretical Physics
CZJP Czechoslovak Journal of Physics
DANS Doklady Akademii nauk SSSR
DP Doklady Physics (Magazine)
EPJ The European Physical Journal
EPL Europhysics Letters
FECAY Fizika Elementarnykh Chastits i Atomnogo Yadra
HADJ Hadronic Journal
IJMP International Journal of Modern Physics
JAP Journal of Applied Physics
JCAP Journal of Cosmology and Astroparticle Physics
JETP English Translation of Soviet Physics ZETF
JETPL English Translation of Soviet Physics ZETF Letters
JHEP Journal of High Energy Physics
JINR Joint Inst. for Nuclear Research
JINRRC JINR Rapid Communications
JP Journal of Physics
JPA Journal of Physics, A
JPB Journal of Physics, B
JPCRD Journal of Physical and Chemical Reference Data
JPCS Journal of Physics: Conference Series
JPG Journal of Physics, G
JPSJ Journal of the Physical Society of Japan
LNC Lettere Nuovo Cimento
MNRAS Monthly Notices of the Royal Astronomical Society
MPL Modern Physics Letters
NAST New Astronomy
NAT Nature
NATC Nature Communications (NCAOBW)
NATP Nature Physics
NC Nuovo Cimento
NIM Nuclear Instruments and Methods
NJP New Journal of Physics
NP Nuclear Physics
NPBPS Nuclear Physics B Proceedings Supplement
NPPP Nuclear and Particle Physics Proceedings
PAN Physics of Atomic Nuclei (formerly SJNP)
PD Physics Doklady (Magazine)
PDAT Physik Daten
PL Physics Letters
PN Particles and Nuclei
PPCF Plasma Physics and Controlled Fusion
PPN Physics of Particles and Nuclei (formerly SJPN)
PPNL Physics of Particles and Nuclei Letters
PPNP Progress in Particles and Nuclear Physics
PPSL Proc. of the Physical Society of London
PR Physical Review
PRAM Pramana
PRL Physical Review Letters
PRPL Physics Reports (Physics Letters C)

PRSE	Proc. of the Royal Society of Edinburgh
PRSL	Proc. of the Royal Society of London, Section A
PS	Physica Scripta
PTEP	Progress of Theoretical and Experimental Physics
PTP	Progress of Theoretical Physics
PTPS	Progress of Theoretical Physics Supplement
PTRSL	Phil. Trans. Royal Society of London
RA	Radiochimica Acta
RMP	Reviews of Modern Physics
RNC	La Rivista del Nuovo Cimento
RPP	Reports on Progress in Physics
RRP	Revue Roumaine de Physique
SCI	Science
SJNP	Soviet Journal of Nuclear Physics
SJPN	Soviet Journal of Particles and Nuclei
SPD	Soviet Physics Doklady (Magazine)
SPU	Soviet Physics - Uspekhi
UFN	Usp. Fiz. Nauk – Russian version of SPU
YAF	Yadernaya Fizika
ZETF	Zhurnal Eksperimental'noi i Teoreticheskoi Fiziki
ZETFP	Zhurnal Eksperimental'noi i Teoreticheskoi Fiziki, Pis'ma v Redakts
ZNAT	Zeitschrift fur Naturforschung
ZPHY	Zeitschrift fur Physik

Institutions

AACH	Phys. Inst. der Techn. Hochschule **Aachen** (Historical, use for general Inst. der Techn. Hochschule)	Aachen, Germany
AACH1	I Phys. Inst. B, RWTH **Aachen**	Aachen, Germany
AACH3	III Phys. Inst. A, RWTH **Aachen** Univ.	Aachen, Germany
AACHT	Inst. für Theoretische Teilchenphysik & Kosmologie, RWTH **Aachen**	Aachen, Germany
AARH	Univ. of **Aarhus**	Aarhus C, Denmark
ABO	**Åbo** Akademi Univ.	Turku, Finland
ADEL	**Adelphi** Univ.	Garden City, NY, USA
ADLD	The Univ. of **Adelaide**	Adelaide, SA, Australia
AERE	Atomic Energy Research Estab.	Didcot, United Kingdom
AFRR	**Armed Forces** Radiobiology Res. Inst.	Bethesda, MD, USA
AHMED	Physical Research Lab.	**Ahmedabad**, Gujarat, India
AICH	**Aichi** Univ. of Education	Aichi, Japan
AKIT	**Akita** Univ.	Akita, Japan
ALAH	Univ. of **Alabama (Huntsville)**	Huntsville, AL, USA
ALAT	Univ. of **Alabama (Tuscaloosa)**	Tuscaloosa, AL, USA
ALBA	**SUNY at Albany**	Albany, NY, USA
ALBE	Univ. of **Alberta**	Edmonton, AB, Canada
AMES	**Ames Lab.**	Ames, IA, USA
AMHT	**Amherst** College	Amherst, MA, USA
AMST	Univ. van **Amsterdam**	GL Amsterdam, The Netherlands
ANIK	**NIKHEF**	**Amsterdam**, The Netherlands
ANKA	**Middle East** Technical Univ.; Dept. of Physics; Experimental HEP Lab	Ankara, Turkey
ANL	**Argonne** National Lab.; High Energy Physics Division, Bldg. 362; Physics Division, Bldg. 203	Argonne, IL, USA
ANSM	**St. Anselm** Coll.	Manchester, NH, USA
ARCBO	**Arecibo** Observatory	Arecibo, PR, USA
ARIZ	Univ. of **Arizona**	Tucson, AZ, USA
ARZS	**Arizona State** Univ.	Tempe, AZ, USA
ASCI	Russian Academy of Sciences	**Moscow**, Russian Federation
AST	**Academia Sinica**	Nankang, Taipei, Taiwan
ATEN	NCSR **"Demokritos"**	**Aghia** Paraskevi , Greece
ATHU	Univ. of **Athens**	Athens, Greece
AUCK	Univ. of **Auckland**	Auckland, New Zealand
BAKU	**Natl. Azerbaijan Academy of Sciences**, Inst. of Physics	**Baku**, Azerbaijan
BANG	Indian Inst. of Science	**Bangalore**, India
BANGB	**Bangabasi** College	Calcutta, India
BARC	Univ. Autónoma de **Barcelona**	Bellaterra (Barcelona), Spain
BARI	Univ. e del Politecnico di **Bari**	Bari, Italy
BART	Univ. of **Delaware**; **Bartol** Research Inst.	Newark, DE, USA
BASL	Inst. für Physik der Univ. **Basel**	Basel, Switzerland
BAYR	Univ. **Bayreuth**	Bayreuth, Germany
BCEN	Centre d'Etudes Nucleaires de **Bordeaux-Gradignan**	Gradignan, France
BCIP	Natl. Inst. for Physics & Nuclear Eng. "Horia Hulubei" **(IFIN-HH)**	**Bucharest**-Magurele, Romania
BEIJ	**Beijing** Univ.	Beijing, China
BEIJT	**Inst. of Theoretical Physics**	**Beijing**, China
BELG	Inter-University Inst. for High Energies (ULB-VUB)	**Brussel**, Belgium
BELL	AT & T **Bell** Labs	Murray Hill, NJ, USA
BERG	Univ. of **Bergen**	Bergen, Norway
BERL	**DESY**, Deutsches Elektronen-Synchrotron	**Zeuthen**, Germany
BERN	Univ. of **Berne**	Berne, Switzerland
BGNA	Univ. di **Bologna**, & **INFN**, Sezione di Bologna; Via Irnerio, 46, I-40126 Bologna; Viale C. Berti Pichat, n. 6/2	Bologna, Italy
BHAB	**Bhabha Atomic** Research Center	Trombay, Bombay, India
BHEP	**Inst. of High Energy Physics**	**Beijing**, China
BIEL	Univ. **Bielefeld**	Bielefeld, Germany
BING	**SUNY at Binghamton**	Binghamton, NY, USA
BIRK	**Birkbeck** College, Univ. of London	London, United Kingdom
BIRM	Univ. of **Birmingham**	Edgbaston, Birmingham, United Kingdom
BLSU	**Bloomsburg** Univ.	Bloomsburg, PA, USA
BNL	**Brookhaven National Lab.**	Upton, NY, USA
BOCH	**Ruhr** Univ. **Bochum**	Bochum, Germany
BOHR	**Niels Bohr Inst.**	Copenhagen Ø, Denmark
BOIS	**Boise** State Univ.	Boise, ID, USA
BOMB	Univ. of **Bombay**	Bombay, India
BONN	**Univ. of Bonn**	Bonn, Germany
BORD	Centre d'Etudes Nucléaires de **Bordeaux** Gradignan **(CENBG)**	Gradignan, France
BOSE	S.N. **Bose** National Centre for Basis Sciences	Calcutta, India
BOSK	**"Rudjer Bošković"** Inst.	Zagreb, Croatia
BOST	**Boston** Univ.	Boston, MA, USA
BRAN	**Brandeis** Univ.	Waltham, MA, USA
BRCO	Univ. of **British Columbia**	Vancouver, BC, Canada
BRIS	Univ. of **Bristol**	Bristol, United Kingdom
BROW	**Brown** Univ.	Providence, RI, USA
BRUN	**Brunel** Univ.	Uxbridge, Middlesex, United Kingdom
BRUX	Univ. Libre de **Bruxelles**; Physique des Particules Elémentaires	Bruxelles, Belgium
BRUXT	Univ. Libre de **Bruxelles**; Physique Théorique	Bruxelles, Belgium
BUCH	Univ. of **Bucharest**	Bucharest-Magurele, Romania
BUDA	**Wigner** Research Centre for Physics	**Budapest**, Hungary
BUFF	**SUNY at Buffalo**	Buffalo, NY, USA
BURE	Inst. des Hautes Etudes Scientifiques	**Bures-sur-Yvette**, France
CAEN	Lab. de Physique Corpusculaire, **ENSICAEN**	**Caen**, France
CAGL	Univ. degli Studi di **Cagliari**	Monserrato (CA), Italy
CAIR	**Cairo** University	Orman, Giza, Cairo, Egypt
CAIW	**Carnegie Inst.** of Washington	Washington, DC, USA
CALB	Univ. della **Calabria**	Cosenza, Italy
CALC	Univ. of **Calcutta**	Calcutta, India
CAMB	**DAMTP**	Cambridge, United Kingdom

Abbreviations Used in the Particle Listings

CAMP	Univ. Estadual de **Campinas** (UNICAMP)	**Campinas**, SP, Brasil
CANB	**Australian National Univ.**	Canberra, ACT, Australia
CANTB	Inst. de Física de Cantabria (CSIC–Univ. **Cantabria**)	Santander, Spain
CAPE	University of **Cape Town**	Rondebosch, Cape Town, South Africa
CARA	Univ. Central de **Venezuela**	Caracas, Venezuela
CARL	**Carleton** Univ.	Ottawa, ON, Canada
CARLC	**Carleton** College	Northfield, MN, USA
CASE	**Case** Western Reserve Univ.	Cleveland, OH, USA
CAST	**China** Center of Advanced Science and Technology	Beijing, China
CATA	Univ. di **Catania**	Catania, Italy
CATH	**Catholic** Univ. of America	Washington, DC, USA
CAVE	**Cavendish** Lab.	Cambridge, United Kingdom
CBNM	CBNM	**Geel**, Belgium
CBPF	Centro Brasileiro de Pesquisas Físicas – **BIB/CDI/CBPF**	**Rio de Janeiro**, RJ, Brasil
CCAC	**Allegheny** College	Meadville, PA, USA
CDEF	**Univ. Paris VII, Denis Diderot**	Paris, France
CEA	Cambridge Electron Accelerator (Historical in *Review*)	**Cambridge, MA**, USA
CEADE	Center for Apl. Studies for Nuclear Physics	Havana, Cuba
CEBAF	**Jefferson Lab—Thomas Jefferson National Accelerator Facility**	**Newport News**, VA, USA
CENG	Centre d'Etudes Nucleaires	**Grenoble**, France
CERN	**CERN**, European Organization for Nuclear Research	Genève, Switzerland
CFPA	Univ. of **California, (Berkeley)**	Berkeley, CA, USA
CHIC	Univ. of **Chicago**	Chicago, IL, USA
CIAE	**State Nuclear Power Research Inst.**	**Beijing**, China
CINC	Univ. of **Cincinnati**	Cincinnati, OH, USA
CINV	**CINVESTAV-IPN** Centro de Investigacion y de Estudios Avanzados del IPN	**México**, DF, Mexico
CIT	**California Inst. of Tech.**	Pasadena, CA, USA
CLER	Univ. de **Clermont-Ferrand**	Aubière, France
CLEV	**Cleveland** State Univ.	Cleveland, OH, USA
CMNS	**Comenius** Univ. (FMFI UK)	**Bratislava**, Slovakia
CMU	**Carnegie Mellon** Univ.	Pittsburgh, PA, USA
CNEA	**Comisión Nacional de Energía Atómica**	Buenos Aires, Argentina
CNRC	Centre for Research in Particle Physics	Ottawa, ON, Canada
COIM	Univ. de Coimbra	**Coimbra**, Portugal
COLO	Univ. of **Colorado**	Boulder, CO, USA
COLU	**Columbia** Univ.	New York, NY, USA
CONC	**Concordia** University	Montreal, PQ, Canada
CORN	**Cornell** Univ.	Ithaca, NY, USA
COSU	**Colorado State** Univ.	Fort Collins, CO, USA
CPPM	Centre National de la Recherche Scientifique, Luminy	**Marseille**, France
CRAC	Henryk Niewodnicza'nski Inst. of Nuclear Physics	**Kraków**, Poland
CRNL	**Chalk River** Labs.	Chalk River, ON, Canada
CSOK	**Oklahoma** Central State Univ.	Edmond, OK, USA
CST	Univ. of **Science and Technology** of China	**Hefei**, Anhui 230026, China
CSULB	**California** State Univ.	Long Beach, CA, USA
CSUS	**California** State Univ.	Sacramento, CA, USA
CUNY	**City College** of **New York**	New York, NY, USA
CURCP	**Univ. Pierre et Marie Curie** (Paris VI), LCP	Paris, France
CURIN	**Univ. Pierre et Marie Curie** (Paris VI), LPNHE	Paris, France
CURIT	**Univ. Pierre et Marie Curie** (Paris VI), LPTHE	Paris, France
DALH	**Dalhousie** Univ.	Halifax, NS, Canada
DALI	**Dalian** Univ. of Tech.	Dalian, China
DARE	**Daresbury** Lab	Cheshire, United Kingdom
DARM	Tech. Hochschule **Darmstadt**	Darmstadt, Germany
DELA	Univ. of **Delaware**; Dept. of Physics & Astronomy	Newark, DE, USA
DELH	Univ. of **Delhi**	Delhi, India
DESY	**DESY**, Deutsches Elektronen-Synchrotron	**Hamburg**, Germany
DFAB	Escuela de Ingenieros	**Bilbao**, Spain
DOE	**Department of Energy**	Washington, DC, USA
DORT	Technische Univ. **Dortmund**	Dortmund, Germany
DUKE	**Duke** Univ.	Durham, NC, USA
DURH	Univ. of **Durham**	Durham , United Kingdom
DUUC	**University College** Dublin	Dublin, Ireland
EDIN	Univ. of **Edinburgh**	Edinburgh, United Kingdom
EFI	Univ. of Chicago, **The Enrico Fermi Inst.**	**Chicago**, IL, USA
ELMT	**Elmhurst** College	Elmhurst, IL, USA
ENSP	**l'Ecole Normale Supérieure**	**Paris**, France
EOTV	**Eötvös** University	Budapest, Hungary
EPOL	**École Polytechnique**	**Palaiseau**, France
ERLA	Univ. **Erlangen-Nurnberg**	Erlangen, Germany
ETH	**Univ. Zürich**	Zürich, Switzerland
FERR	Univ. di **Ferrara**	Ferrara, Italy
FIRZ	Univ. degli Studi di **Firenze**	Sesto Fiorentino, Italy
FISK	**Fisk** Univ.	Nashville, TN, USA
FLOR	Univ. of **Florida**	Gainesville, FL, USA
FNAL	**Fermilab**	Batavia, IL, USA
FOM	**FOM**, Stichting voor Fundamenteel Onderzoek der Materie	JP **Utrecht**, The Netherlands
FRAN	**Frankfurt Inst. for Advanced Studies (FIAS)**	Frankfurt am Main, Germany
FRAS	Lab. Nazionali di **Frascati** dell'**INFN**	Frascati (Roma), Italy
FREIB	**Albert-Ludwigs** Univ.	**Freiburg**, Germany
FREIE	**Freie Univ. Berlin**	Berlin, Germany
FRIB	Univ. de **Fribourg**	Fribourg, Switzerland
FSU	**Florida State** Univ.; High Energy Physics	Tallahassee, FL, USA
FSUSC	**Florida State** Univ.; SCS (School of Computational Science)	Tallahassee, FL, USA
FUKI	**Fukui** Univ.	Fukui, Japan
FUKU	**Fukushima** Univ.	Fukushima, Japan
GENO	Univ. di **Genova**	Genova, Italy
GEOR	**E. Andronikashvili Inst. of Physics**	Tbilisi, Republic of Georgia
GESC	**General Electric** Co.	Schenectady, NY, USA
GEVA	Univ. de **Genève**	Genève, Switzerland
GIES	Univ. **Giessen**	Giessen, Germany
GIFU	**Gifu** Univ.	Gifu, Japan
GLAS	Univ. of **Glasgow**	Glasgow, United Kingdom
GMAS	**George Mason** Univ.	Fairfax, VA, USA
GOET	Univ. **Göttingen**	Göttingen, Germany
GRAN	Univ. de **Granada**	Granada, Spain
GRAZ	Univ. **Graz**	Graz, Austria
GRON	Univ. of **Groningen**	Groningen, The Netherlands
GSCO	**Geological Survey of Canada**	Ottawa, ON, Canada
GSI	GSI Helmholtzzentrum für Schwerionenforschung GmbH	**Darmstadt**, Germany
GUAN	Univ. de **Guanajuato**	León, Gto., Mexico
GUEL	Univ. of **Guelph**	Guelph, ON, Canada
GWU	**George Washington** Univ.	Washington, DC, USA
HAHN	**Hahn-Meitner** Inst. Berlin GmbH	Berlin, Germany
HAIF	**Technion** – Israel Inst. of Tech.	Technion, Haifa, Israel
HAMB	Univ. **Hamburg**	Hamburg, Germany
HANN	Univ. **Hannover**	Hannover, Germany
HARC	**Houston Advanced Research Ctr.**	The Woodlands, TX, USA
HARV	**Harvard** Univ.	Cambridge, MA, USA
HARV	**Harvard** Univ. (LPPC)	Cambridge, MA, USA
HAWA	Univ. of **Hawai'i**	Honolulu, HI, USA
HEBR	**Hebrew** Univ.	Jerusalem, Israel
HEID	Univ. **Heidelberg**; (unspecified division) (Historical in *Review*)	Heidelberg, Germany

Abbreviations Used in the Particle Listings

HEIDH	Ruprecht-Karls Univ. **Heidelberg**	Heidelberg, Germany
HEIDP	Univ. **Heidelberg**; Physics Inst.	Heidelberg, Germany
HEIDT	Ruprecht-Karls-Univ. **Heidelberg**	Heidelberg, Germany
HELS	Univ. of **Helsinki**	University of Helsinki, Finland
HIRO	**Hiroshima** Univ.	Higashi-Hiroshima, Japan
HOUS	Univ. of **Houston**	Houston, TX, USA
HPC	**Hewlett-Packard** Corp.	Cupertino, CA, USA
HSCA	**Harvard-Smithsonian** Center for Astrophysics	Cambridge, MA, USA
IAS	**Inst. for Advanced Study**	Princeton, NJ, USA
IASD	**Dublin** Inst. for Advanced Studies	Dublin, Ireland
IBAR	**Ibaraki** Univ.	Ibaraki, Japan
IBM	**IBM** Corp.	Palo Alto, CA, USA
IBMY	**IBM**	Yorktown Heights, NY, USA
IBS	Inst. for **Boson Studies**	Pasadena, CA, USA
ICEPP	The Univ. of **Tokyo**	Tokyo, Japan
ICRR	Univ. of **Tokyo**	Chiba, Japan
ICTP	**Abdus Salam** International Centre for Theoretical Physics	**Trieste**, Italy
IFIC	**IFIC** (Instituto de Física Corpuscular)	**Paterna (Valencia)**, Spain
IFRJ	Univ. Federal do **Rio de Janeiro**	Rio de Janeiro, RJ, Brasil
IIT	**Illinois Inst. of Tech.**	Chicago, IL, USA
ILL	Univ. of **Illinois at Urbana-Champaign**	Urbana, IL, USA
ILLC	Univ. of **Illinois at Chicago**	Chicago, IL, USA
ILLG	Inst. **Laue-Langevin**	Grenoble, France
IND	**Indiana** Univ.	Bloomington, IN, USA
INEL	E G and G **Idaho**, Inc.	Idaho Falls, ID, USA
INFN	Ist. Nazionale di Fisica Nuclear (Generic INFN, unknown location)	Various places, Italy
INNS	Univ. of **Innsbruck**	**Innsbruck**, Austria
INPK	Henryk Niewodniczański Inst. of Nuclear Physics	**Kraków**, Poland
INRM	**INR**, Inst. for Nucl. Research	**Moscow**, Russian Federation
INUS	**KEK**, High Energy Accelerator Research Organization	Tokyo, Japan
IOAN	Univ. of **Ioannina**	Ioannina, Greece
IOFF	A.F. **Ioffe** Phys. Tech. Inst.	St. **Petersburg**, Russian Federation
IOWA	Univ. of **Iowa**	Iowa City, IA, USA
IPN	**IPN**, Inst. de Phys. Nucl.	**Orsay**, France
IPNP	Univ. Pierre et Marie Curie (**Paris** VI)	Paris, France
IRAD	Inst. du Radium (Historical)	**Paris**, France
ISNG	Lab. de Physique Subatomique et de Cosmologie **(LPSC)**	**Grenoble**, France
ISU	**Iowa State** Univ.	Ames, IA, USA
ISUT	Isfahan University of Technology	Isfahan, Iran
ITEP	**ITEP**, Inst. of Theor. and Exp. Physics	**Moscow**, Russian Federation
ITHA	**Ithaca** College	Ithaca, NY, USA
IUPU	**Indiana** Univ., **Purdue** Univ. **Indianapolis**	Indianapolis, IN, USA
JADA	**Jadavpur** Univ.	Calcutta, India
JAGL	**Jagiellonian** Univ.	Kraków, Poland
JHU	**Johns Hopkins** Univ.	Baltimore, MD, USA
JINR	**JINR**, Joint Inst. for Nucl. Research	**Dubna**, Russian Federation
JULI	Forschungszentrum **Jülich**	Jülich, Germany
JYV	Univ. of **Jyväskylä**	Jyväskylä, Finland
KAGO	Univ. of **Kagoshima**	Kagoshima-shi, Japan
KAIST	**Korea** Advanced Inst. of Science and Technology	Yusung ku, Daejon, Republic of Korea
KANS	Univ. of **Kansas**	Lawrence, KS, USA
KARL	Univ. **Karlsruhe** (Historical in *Review*)	Karlsruhe, Germany
KARLE	**Karlsruhe** Inst. of Technology (KIT); Inst. for Experimental Nuclear Physics	Karlsruhe, Germany
KARLK	**Karlsruhe** Inst. of Technology (KIT)	Eggenstein-Leopoldshafen, Germany
KARLT	**Karlsruhe** Inst. of Technology (KIT); Inst. for Theoretical Physics	Karlsruhe, Germany
KAZA	**Kazakh** Inst. of High Energy Physics	Alma Ata, Kazakhstan
KEK	**KEK**, High Energy Accelerator Research Organization	Ibaraki-ken, Japan
KENT	Univ. of **Kent**	Canterbury, United Kingdom
KEYN	**Open** Univ.	Milton Keynes, United Kingdom
KFTI	**Kharkov** Inst. of Physics and Tech. (NSC KIPT)	Kharkov, Ukraine
KIAE	**Kurchatov** Inst.	**Moscow**, Russian Federation
KIAM	**Keldysh** Inst. of Applied Math., Acad. Sci., Russia	Moscow, Russian Federation
KIDR	**Vinča Inst. of Nuclear Sciences**	Belgrade, Serbia
KIEV	**Institute for Nuclear Research**	**Kyiv**, Ukraine
KINK	**Kinki** Univ.	Osaka, Japan
KNTY	Univ. of **Kentucky**	Lexington, KY, USA
KOBE	**Kobe** Univ.	Kobe, Japan
KOMAB	Univ. of **Tokyo, Komaba**	Tokyo, Japan
KONAN	**Konan** Univ.	Kobe, Japan
KOSI	Inst. of Experimental Physics SAS	**Košice**, Slovakia
KYOT	**Kyoto** Univ.; Dept. of Physics, Graduate School of Science	Kyoto, Japan
KYOTU	**Kyoto** Univ.; **Yukawa** Inst. for Theor. Physics	Kyoto, Japan
KYUN	**Kyungpook** National Univ.	Daegu, Republic of Korea
KYUSH	**Kyushu** Univ.; Elementary ParticleTheory Group; Exp. Particle Physics Group; Research Center for Advanced Particle Physics	Fukuoka, Japan
LALO	**LAL**, Laboratoire de l'Accélérateur Linéaire	**Orsay**, France
LANC	**Lancaster** Univ.	Lancaster, United Kingdom
LANL	**Los Alamos National Lab.** (LANL)	Los Alamos, NM, USA
LAPL	Univ. Nacional de **La Plata**	La Plata, Argentina
LAPP	**LAPP**, Lab. d'Annecy-le-Vieux de Phys. des Particules	**Annecy-le-Vieux**, France
LASL	U.C. **Los Alamos Scientific** Lab. (Old name for LANL)	Los Alamos, NM, USA
LATV	**Latvian** State Univ.	Riga, Latvia
LAUS	EPFL **Lausanne**	Lausanne, Switzerland
LAVL	Univ. **Laval**	Quebec, QC, Canada
LBL	**Lawrence Berkeley National Lab.**	Berkeley, CA, USA
LCGT	Univ. di **Torino**	Turin, Italy
LEBD	**Lebedev** Physical Inst.	**Moscow**, Russian Federation
LECE	Univ. di **Lecce**	Lecce, Italy
LEED	Univ. of **Leeds**	Leeds, United Kingdom
LEGN	Lab. Naz. di Legnaro	**Legnaro**, Italy
LEHI	**Lehigh** Univ.	Bethlehem, PA, USA
LEHM	**Lehman** College of CUNY	Bronx, NY, USA
LEID	Univ. **Leiden**	Leiden, The Netherlands
LEMO	**Le Moyne** Coll.	Syracuse, NY, USA
LEUV	Katholieke Univ. **Leuven**	Leuven, Belgium
LIEG	Univ. de **Liège**	Liège, Belgium
LINZ	Univ. **Linz**	Linz, Austria
LISB	Inst. Nacional de Investigacion Cientifica	**Lisboa** CODEX, Portugal
LISBT	Centro de Física Teórica de Partículas **(CFTP)**	**Lisboa**, Portugal
LIVP	Univ. of **Liverpool**	Liverpool, United Kingdom
LLL	**Lawrence Livermore Lab.** (Old name for LLNL)	Livermore, CA, USA
LLNL	**Lawrence Livermore National Lab.**	Livermore, CA, USA
LOCK	**Lockheed** Palo Alto Res. Lab	Palo Alto, CA, USA
LOIC	**Imperial** College of Science Tech. & Medicine	London, United Kingdom

Abbreviations Used in the Particle Listings

LOQM	Queen Mary, **Univ. of London**	London, United Kingdom
LOUC	**University College** London	London, United Kingdom
LOUV	Univ. Catholique de **Louvain**	Louvain-la-Neuve, Belgium
LOWC	**Westfield** College (Historical, see LOQM (Queen Mary and Westfield joined))	London, United Kingdom
LRL	U.C. Lawrence Radiation Lab. (Old name for LBL)	**Berkeley**, CA, USA
LSU	**Louisiana** State Univ.	Baton Rouge, LA, USA
LUND	**Fysiska Institutionen**	**Lund**, Sweden
LUND	**Lund** Univ.	Lund, Sweden
LYON	Institute de Physique Nucléaire de **Lyon** (IPN)	Villeurbanne, France
MADE	**UAM/CSIC**, Inst. de Física Teórica	**Madrid**, Cantoblanco, Spain
MADR	**C.I.E.M.A.T**	**Madrid**, Spain
MADRA	Univ. of **Madras**	Madras, India
MADU	Univ. Autónoma de **Madrid**	Cantoblanco, Madrid, Spain
MANI	Univ. of **Manitoba**	Winnipeg, MB, Canada
MANZ	**Johannes-Gutenberg-Univ.**; Inst. für Kernphysik, J.-J.-Becher-Weg 45; Inst. für Physik, Staudingerweg 7	**Mainz**, Germany
MARB	Univ. **Marburg**	Marburg, Germany
MARS	Centre de Physique des Particules de **Marseille**	Marseille, France
MASA	Univ. of **Massachusetts** Amherst	**Amherst**, MA, USA
MASB	Univ. of **Massachusetts** Boston	**Boston**, MA, USA
MASD	Univ. of **Massachusetts** Dartmouth	North **Dartmouth**, MA, USA
MCGI	**McGill** Univ.	Montreal, QC, Canada
MCHS	Univ. of **Manchester**	Manchester, United Kingdom
MCMS	**McMaster** Univ.	Hamilton, ON, Canada
MEHTA	**Harish-Chandra** Research Inst.	Allahabad, India
MEIS	**Meisei** Univ.	Tokyo, Japan
MELB	Univ. of **Melbourne**	Victoria, Australia
MEUD	Observatoire de **Meudon**	Meudon, France
MICH	Univ. of **Michigan**	Ann Arbor, MI, USA
MILA	Univ. di **Milano**	Milano, Italy
MILAI	**INFN**, Sez. di **Milano**	Milano, Italy
MINN	Univ. of **Minnesota**	Minneapolis, MN, USA
MIPT	Moscow Institute of Physics and Technology	Moscow, Russian Federation
MISS	Univ. of **Mississippi**	University, MS, USA
MISSR	Univ. of **Missouri**	Rolla, MO, USA
MIT	**MIT Massachusetts Inst. of Technology**	Cambridge, MA, USA
MIU	**Maharishi** International Univ.	Fairfield, IA, USA
MIYA	**Miyazaki** Univ.	Miyazaki-shi, Japan
MONP	Univ. de **Montpellier** II	Montpellier, France
MONS	Univ. of **Mons**	**Mons**, Belgium
MONT	Univ. de **Montréal**; Pavillon René-J.-A.-Lévesque	Montréal, PQ, Canada
MONTC	Univ. de **Montréal**; Centre de recherches mathématiques	Montréal, PQ, Canada
MOSU	**Skobeltsyn** Inst. of Nuclear Physics, Lomonosov Moscow State Univ.; Experimental HEP Division; Theoretical HEP Division	**Moscow**, Russian Federation
MPCM	Max Planck Inst. fur Chemie	**Mainz**, Germany
MPEI	**Moscow Physical Engineering** Inst.	Moscow, Russian Federation
MPIG	**Max-Planck**-Institute für Astrophysik	Garching, Germany
MPIH	**Max-Planck-Inst.** für Kernphysik	**Heidelberg**, Germany
MPIM	**Max-Planck-Inst.** für Physik	**München**, Germany
MSST	Mississippi State University	Mississippi State, MS, USA
MSU	**Michigan State** Univ.	East Lansing, MI, USA
MTHO	**Mount Holyoke** College	South Hadley, MA, USA
MULH	Centre Univ. du **Haut-Rhin**	Mulhouse, France
MUNI	**Ludwig-Maximilians-Univ. München**	Garching, Germany
MUNT	Tech. Univ. **München**	Garching, Germany
MURA	**Midwestern** Univ. Research Assoc. (Historical in *Review*)	Stroughton, WI, USA
MURC	Univ. of Murcia	Murcia, Spain
NAAS	North Americal Aviation Science Center (Historical in *Review*)	Thousand Oaks, CA, USA
NAGO	**Nagoya** Univ.	Nagoya, Japan
NANJ	**Nanjing** Univ.	Nanjing, China
NAPL	Univ. di **Napoli** "Federico II"	Napoli, Italy
NASA	**NASA**	Greenbelt, MD, USA
NBS	U.S **National Bureau of Standards** (Old name for NIST)	Gaithersburg, MD, USA
NBSB	**National Inst. Standards Tech.**	Boulder, CO, USA
NCAR	**National Center for Atmospheric Research**	Boulder, CO, USA
NCSU	**North Carolina** State Univ.	**Raleigh**, NC, USA
NDAM	Univ. of **Notre Dame**	Notre Dame, IN, USA
NEAS	**Northeastern** Univ.	Boston, MA, USA
NEBR	Univ. of **Nebraska**	Lincoln, NE, USA
NEUC	Univ. de **Neuchâtel**	Neuchâtel, Switzerland
NICEA	Univ. de **Nice**	Nice, France
NICEO	Observatoire de **Nice**	Nice, France
NIHO	**Nihon** Univ.	Tokyo, Japan
NIIG	**Niigata** Univ.	Niigata, Japan
NIJM	**Radboud** Univ. Nijmegen	AJ **Nijmegen**, The Netherlands
NIRS	Nat. Inst. Radiological Sciences	**Chiba**, Japan
NIST	**National Institute of Standards & Technology**	Gaithersburg, MD, USA
NIU	**Northern Illinois** Univ.	De Kalb, IL, USA
NMSU	**New Mexico** State Univ.; Dept. of Physics, MSC 3D; Part. & Nucl. Phys. Group, Box 30001/Dept.	Las Cruces, NM, USA
NORD	**Nordita**	Stockholm, Sweden
NOTT	Univ. of **Nottingham**	Nottingham, United Kingdom
NOVM	Inst. of Mathematics	**Novosibirsk**, Russian Federation
NOVO	BINP, **Budker** Inst. of Nuclear Physics	**Novosibirsk**, Russian Federation
NPOL	Polytechnic of **North London**	London, United Kingdom
NRL	**Naval Research** Lab	Washington, DC, USA
NSF	**National Science Foundation**	Arlington, VA, USA
NTHU	**National Tsing Hua** Univ.	Hsinchu, Taiwan
NTUA	**National Tech. Univ. of Athens**	Athens, Greece
NWES	**Northwestern** Univ.	Evanston, IL, USA
NYU	**New York** Univ.	New York, NY, USA
OBER	**Oberlin** College	Oberlin, OH, USA
OCH	**Ochanomizu** Univ.	Tokyo, Japan
OHIO	**Ohio** Univ.	Athens, OH, USA
OKAY	**Okayama** Univ.	Okayama, Japan
OKLA	Univ. of **Oklahoma**	Norman, OK, USA
OKSU	**Oklahoma State** Univ.	Stillwater, OK, USA
OREG	Univ. of **Oregon**; Inst. of Theoretical Science; U.O. Center for High Energy Physics	Eugene, OR, USA
ORNL	**Oak Ridge** National Laboratory	Oak Ridge, TN, USA
ORSAY	Univ. de **Paris Sud** 11	**Orsay** CEDEX, France
ORST	**Oregon State** Univ.	Corvallis, OR, USA
OSAK	**Osaka** Univ.	Osaka, Japan
OSKC	**Osaka City** Univ.	Osaka, Japan
OSLO	Univ. of **Oslo**	Oslo, Norway
OSU	**Ohio State** Univ.	Columbus, OH, USA
OTTA	Univ. of **Ottawa**	Ottawa, ON, Canada
OXF	University of **Oxford**	Oxford, United Kingdom
OXFTP	Univ. of **Oxford**	Oxford, United Kingdom
PADO	Univ. degli Studi di **Padova**	Padova, Italy
PARIN	**LPNHE**, IN^2P^3/CNRS	Paris, France
PARIS	Univ. de Paris (Historical)	**Paris**, France

Abbreviations Used in the Particle Listings

PARIT	**Univ. Paris VII**, LPTHE	Paris, France
PARM	**INFN**, Gruppo Collegato di **Parma**	Parma, Italy
PAST	Institut **Pasteur**	**Paris**, France
PATR	Univ. of **Patras**	Patras, Greece
PAVI	Univ. di **Pavia**	Pavia, Italy
PAVII	INFN, Sez. di **Pavia**	**Pavia**, Italy
PENN	Univ. of **Pennsylvania**	Philadelphia, PA, USA
PGIA	**INFN**, Sezione di **Perugia**	Perugia, Italy
PISA	Univ. di **Pisa**	Pisa, Italy
PISAI	**INFN**, Sez. di **Pisa**	Pisa, Italy
PITT	Univ. of **Pittsburgh**	Pittsburgh, PA, USA
PLAT	**SUNY at Plattsburgh**	Plattsburgh, NY, USA
PLRM	Univ. di **Palermo**	Palermo, Italy
PNL	**Battelle Memorial** Inst.	Richland, WA, USA
PNPI	**Petersburg** Nuclear Physics Inst. of Russian Academy of Sciences	Gatchina, Russian Federation
PPA	Princeton-Penn. Proton Accelerator (Historical in *Review*)	Princeton, NJ, USA
PRAG	Inst. of Physics, **ASCR**	**Prague**, Czech Republic
PRIN	**Princeton** Univ.	Princeton, NJ, USA
PSI	Paul Scherrer Inst.	**Villigen** PSI, Switzerland
PSLL	**Physical Science Lab**	Las Cruces, NM, USA
PSU	**Penn State** Univ.	University Park, PA, USA
PUCB	**Pontifícia Univ. Católica do Rio de Janeiro**	Rio de Janeiro, RJ, Brasil
PUEB	Univ. Autonoma de **Puebla**	**Puebla**, Pue, Mexico
PURD	**Purdue** Univ.	West Lafayette, IN, USA
QUKI	**Queen's** Univ.	Kingston, ON, Canada
RAL	**STFC Rutherford Appleton** Lab.	Chilton, Didcot, Oxfordshire, United Kingdom
REGE	Univ. **Regensburg**	Regensburg, Germany
REHO	**Weizmann** Inst. of Science	Rehovot, Israel
REZ	Nuclear Physics Inst. **AVČR**	**Řež**, Czech Republic
RGSUL	Univ. Federal do **Rio Grande do Sul** (UFRGS)	Porto Alegre, RS, Brasil
RHBL	**Royal Holloway, Univ. of London**	Egham, Surrey, United Kingdom
RHEL	**Rutherford** High Energy Lab (Old name for RAL)	Chilton, Didcot, Oxon., United Kingdom
RICE	**Rice** Univ.	Houston, TX, USA
RIKEN	**Riken** Nishina Center for Accelerator-Based Science	Saitama, Japan
RIKK	**Rikkyo** Univ.	Tokyo, Japan
RIS	**Rowland** Inst. for Science	Cambridge, MA, USA
RISC	**Rockwell** International	Thousand Oaks, CA, USA
RISL	**Universities Research Reactor**	**Risley**, Warrington, United Kingdom
RISO	**Riso** National Laboratory	Roskilde, Denmark
RL	**Rutherford** High Energy Lab (Old name for RAL)	Chilton, Didcot, Oxon., United Kingdom
RMCS	**Royal Military** Coll. of Science	Swindon, Wilts., United Kingdom
ROCH	Univ. of **Rochester**	Rochester, NY, USA
ROCK	**Rockefeller** Univ.	New York, NY, USA
ROMA	Univ. di **Roma** (Historical)	**Roma**, Italy
ROMA2	Univ. di **Roma**, "Tor Vergata"	Roma, Italy
ROMA3	**INFN, Sez. di Roma Tre**	**Roma**, Italy
ROMAI	**INFN, Sez. di Roma**	Roma, Italy
ROSE	**Rose-Hulman** Inst. of Technology	Terre Haute, IN, USA
RPI	**Rensselaer Polytechnic** Inst.	Troy, NY, USA
RUTG	**Rutgers**, the State Univ. of New Jersey	Piscataway, NJ, USA
S0GA	**Sogang** University	Seoul, Republic of Korea
SACL	**CEA Saclay**, IRFU	Gif-sur-Yvette, France
SACL5	**CEA Saclay** – IPhT	Gif-sur-Yvette, France
SACLD	**CEA Saclay** (Essonne)	Gif-sur-Yvette, France
SAGA	**Saga** Univ.	Saga-shi, Japan
SAHA	**Saha** Inst. of Nuclear Physics	Bidhan Nagar, Calcutta, India
SANG	**Kyoto Sangyo** Univ.	Kyoto-shi, Japan
SANI	Ist. Superiore di Sanità	**Roma**, Italy
SASK	Univ. of **Saskatchewan**	Saskatoon, SK, Canada
SASSO	Lab. Naz. **Gran Sasso** dell'INFN	**Assergi** (AQ), Italy
SAVO	Univ. de **Savoie**	Chambery, France
SBER	**California** State Univ.	**San Bernardino**, CA, USA
SCHAF	W.J. **Schafer** Assoc.	Livermore, DA, USA
SCIT	**Science** Univ. of **Tokyo**	Tokyo, Japan
SCOT	**Scottish** Univ. Research and Reactor Ctr.	Glasgow, United Kingdom
SCUC	Univ. of **South Carolina**	Columbia, SC, USA
SEAT	**Seattle Pacific** Coll.	Seattle, WA, USA
SEIB	Austrian Research Center, **Seibersdorf** LTD.	Seibersdorf, Austria
SEOU	**Korea** Univ.; Dept. of Physics; HEP Group	Seoul, Republic of Korea
SEOUL	**Seoul** National Univ.; Center for Theoretical Physics; Dept. of Physics & Astronomy, Coll. of Natural Sciences	Seoul, Republic of Korea
SERP	**IHEP**, Inst. for High Energy Physics	Protvino, Russian Federation
SETO	**Seton Hall** Univ.	South Orange, NJ, USA
SFLA	Univ. of **South Florida**	Tampa, FL, USA
SFRA	**Simon Fraser University**	Burnaby, BC, Canada
SFSU	**California** State Univ.	**San Francisco**, CA, USA
SHAMS	**Ain Shams** University	Abbassia, Cairo, Egypt
SHDN	**Shandong** Univ.	Jinan, Shandong, China
SHEF	Univ. of **Sheffield**	Sheffield, United Kingdom
SHMP	Univ. of **Southampton**	Southampton, United Kingdom
SHRZ	**Shiraz** Univ.	Shiraz, Iran
SIEG	Univ. **Siegen**	Siegen, Germany
SILES	Univ. of **Silesia**	Katowice, Poland
SIN	Swiss Inst. of Nuclear Research (Old name for VILL)	**Villigen**, Switzerland
SING	**National Univ.** of Singapore	Kent Ridge, Singapore
SISSA	Scuola Internazionale Superiore di Studi Avanzati	**Trieste**, Italy
SLAC	**SLAC National Accelerator Laboratory**	Menlo Park, CA, USA
SLOV	Inst. of Physics, Slovak Acad. of Sciences	**Bratislava** 45, Slovakia
SMU	**Southern Methodist** Univ.	Dallas, TX, USA
SNSP	**Scuola Normale Superiore**	**Pisa**, Italy
SOFI	Inst. for Nuclear Research and Nuclear Energy	**Sofia**, Bulgaria
SOFU	Univ. of **Sofia** "St. Kliment Ohridski"	Sofia, Bulgaria
SPAUL	Univ. de **São Paulo**	São Paulo, SP, Brasil
SPIFT	Inst. de Física Teórica (**IFT**)	**São Paulo**, SP, Brasil
SSL	Univ. of **California (Berkeley)**	Berkeley, CA, USA
STAN	**Stanford** Univ.	Stanford, CA, USA
STEV	**Stevens** Inst. of Tech.	Hoboken, NJ, USA
STFN	**Jožef Stefan** Institute	**Ljubljana**, Slovenia
STLO	**St. Louis** Univ.	St. Louis, MO, USA
STOH	**Stockholm** Univ.	Stockholm, Sweden
STON	**SUNY at Stony Brook**	Stony Brook, NY, USA
STRB	Inst. Pluridisciplinaire Hubert Curien (**CNRS**)	**Strasbourg**, France
STUT	Univ. **Stuttgart**	Stuttgart, Germany
STUTM	Max-Planck-Inst.	**Stuttgart**, Germany
SUGI	**Sugiyama Jogakuen** Univ.	Aichi, Japan
SURR	Univ. of **Surrey**	Guildford, Surrey, United Kingdom
SUSS	Univ. of **Sussex**	Brighton, United Kingdom
SVR	**Savannah** River Labs.	Aiken, SC, USA
SYDN	Univ. of **Sydney**	Sydney, NSW, Australia
SYRA	**Syracuse** Univ.	Syracuse, NY, USA
TAJK	Acad. Sci., Tadzhik SSR	**Dushanbe**, Tadzhikstan
TAMU	**Texas A&M** Univ.	College Station, TX, USA
TATA	**Tata** Inst. of Fundamental Research	Bombay, India
TBIL	**Tbilisi State University**	Tbilisi, Republic of Georgia
TELA	**Tel-Aviv** Univ.	Tel Aviv, Israel
TELE	**Teledyne Brown** Engineering	Huntsville, AL, USA
TEMP	**Temple** Univ.	Philadelphia, PA, USA
TENN	Univ. of **Tennessee**	Knoxville, TN, USA
TEXA	Univ. of **Texas** at **Austin**	Austin, TX, USA
TGAK	**Tokyo Gakugei** Univ.	Tokyo, Japan
TGU	**Tohoku Gakuin** Univ.	Miyagi, Japan

Abbreviations Used in the Particle Listings

THES	Aristotle Univ. of **Thessaloniki** (AUTh)	Thessaloniki, Greece
TINT	**Tokyo Inst. of Technology**	Tokyo, Japan
TISA	**Sagamihara** Inst. of Space & Astronautical Sci.	Kanagawa, Japan
TMSK	**Tomsk** Polytechnic Univ.	**Tomsk**, Russian Federation
TMTC	**Tokyo Metropolitan** Coll. Tech.	Tokyo, Japan
TMU	**Tokyo Metropolitan Univ.**	Tokyo, Japan
TNTO	Univ. of **Toronto**	Toronto, ON, Canada
TOHO	**Toho** Univ.	Chiba, Japan
TOHOK	**Tohoku** Univ.	Sendai, Japan
TOKA	**Tokai** Univ.	Shimizu, Japan
TOKAH	**Tokai** Univ.	Hiratsuka, Japan
TOKMS	Univ. of **Tokyo**; Meson Science Laboratory	Tokyo, Japan
TOKU	Univ. of **Tokushima**	Tokushima-shi, Japan
TOKY	Univ. of **Tokyo**; High-Energy Physics Theory Group	Tokyo, Japan
TOKYC	Univ. of **Tokyo**; Dept. of Chemistry	Tokyo, Japan
TORI	Univ. degli Studi di **Torino**	Torino, Italy
TPTI	**Uzbek** Academy of Sciences	**Tashkent**, Republic of Uzbekistan
TRIN	Trinity College **Dublin**	Dublin, Ireland
TRIU	**TRIUMF**	Vancouver, BC, Canada
TRST	Univ. di **Trieste**	Trieste, Italy
TRSTI	**INFN**, Sez. di **Trieste**	Trieste, Italy
TRSTT	Univ. degli Studi di **Trieste**	**Trieste**, Italy
TSUK	Univ. of **Tsukuba**	Ibaraki-ken, Japan
TTAM	**Tamagawa** Univ.	Tokyo, Japan
TUAT	**Tokyo** Univ. of Agriculture Tech.	Tokyo, Japan
TUBIN	Univ. **Tübingen**	Tübingen, Germany
TUFTS	**Tufts** Univ.	Medford, MA, USA
TUW	**Technische** Univ. **Wien**	Vienna, Austria
TUZL	**Tuzla** Univ.	Tuzla, Argentina
UBA	Univ. de **Buenos Aires**	Buenos Aires, Argentina
UCB	Univ. of **California (Berkeley)**	Berkeley, CA, USA
UCD	Univ. of **California (Davis)**	Davis, CA, USA
UCI	Univ. of **California (Irvine)**	Irvine, CA, USA
UCLA	Univ. of **California (Los Angeles)**	Los Angeles, CA, USA
UCND	**Union Carbide** Corp.	Oak Ridge, TN, USA
UCR	Univ. of **California (Riverside)**	Riverside, CA, USA
UCSB	Univ. of **California (Santa Barbara)**; Physics Dept., High Energy Physics Experiment	Santa Barbara, CA, USA
UCSBT	Univ. of **California (Santa Barbara)**; Kavli Inst. for Theoretical Physics	Santa Barbara, CA, USA
UCSC	Univ. of **California (Santa Cruz)**	Santa Cruz, CA, USA
UCSD	Univ. of **California (San Diego)**	La Jolla, CA, USA
UGAZ	Univ. of **Gaziantep**	Gaziantep, Turkey
UMD	Univ. of **Maryland**	College Park, MD, USA
UNAM	Univ. Nac. Autónoma de México (**UNAM**)	**México**, DF, Mexico
UNAM	Univ. Nacional Autónoma de México (**UNAM**)	**México**, DF, Mexico
UNC	Univ. of **North Carolina**	Greensboro, NC, USA
UNCCH	Univ. of **North Carolina** at **Chapel Hill**	Chapel Hill, NC, USA
UNCS	**Union** College	Schenectady, NY, USA
UNESP	UNESP	Botucatu, Brasil
UNH	Univ. of **New Hampshire**	Durham, NH, USA
UNM	Univ. of **New Mexico**	Albuquerque, NM, USA
UOEH	Univ. of Occupational and Environmental Health	**Kitakyushu**, Japan
UPNJ	**Upsala** College	East Orange, NJ, USA
UPPS	**Uppsala** Univ.	**Uppsala**, Sweden
UPR	Univ. of **Puerto Rico**	**San Juan**, PR, USA
URI	Univ. of **Rhode Island**	Kingston, RI, USA
USC	Univ. of **Southern California**	Los Angeles, CA, USA
USF	Univ. of **San Francisco**	San Francisco, CA, USA
UTAH	Univ. of **Utah**	Salt Lake City, UT, USA
UTRE	Univ. of **Utrecht**	Utrecht, The Netherlands
UTRO	**Norwegian Univ. of Science & Technology**	Trondheim, Norway
UVA	Univ. of **Virginia**	Charlottesville, VA, USA
UZINR	Acad. Sci., **Ukrainian** SSR	**Uzhgorod**, Ukraine
VALE	Univ. de **Valencia**	Burjassot, **Valencia**, Spain
VALP	**Valparaiso** Univ.	Valparaiso, IN, USA
VAND	**Vanderbilt** Univ.	Nashville, TN, USA
VASS	**Vassar** College	Poughkeepsie, NY, USA
VICT	Univ. of **Victoria**	Victoria, BC, Canada
VIEN	Inst. für Hochenergiephysik (HEPHY)	**Vienna**, Austria
VILL	**ETH Zürich**	Zürich, Switzerland
VPI	**Virginia Tech.**	Blacksburg, VA, USA
VRIJ	**Vrije** Univ.	HV **Amsterdam**, The Netherlands
WABRN	Eidgenossisches Amt für Messwesen	**Waber**, Switzerland
WARS	Univ. of **Warsaw**	Warsaw, Poland
WASCR	**Waseda** Univ.; Cosmic Ray Division	Tokyo, Japan
WASH	Univ. of **Washington**; Elem. Particle Experiment (EPE); Particle Astrophysics (PA)	Seattle, WA, USA
WASU	**Waseda** Univ.; Dept. of Physics, High Energy Physics Group	Tokyo, Japan
WAYN	**Wayne** State Univ.	Detroit, MI, USA
WESL	**Wesleyan** Univ.	Middletown, CT, USA
WIEN	Univ. **Wien**	Vienna, Austria
WILL	Coll. of **William and Mary**	Williamsburg, VA, USA
WINR	National Centre for Nuclear Research	**Warsaw**, Poland
WISC	Univ. of **Wisconsin**	Madison, WI, USA
WITW	Univ. of the **Witwatersrand**	Wits, South Africa
WMIU	**Western Michigan** Univ.	Kalamazoo, MI, USA
WONT	The Univ. of **Western Ontario**	London, ON, Canada
WOOD	**Woodstock** College (No longer in existence)	Woodstock, MD, USA
WUPP	**Bergische** Univ. Wuppertal	**Wuppertal**, Germany
WURZ	Univ. **Würzburg**	Würzburg, Germany
WUSL	**Washington** Univ.	St. Louis, MO, USA
WYOM	Univ. of **Wyoming**	Laramie, WY, USA
YALE	**Yale** Univ.	New Haven, CT, USA
YARO	**Yaroslavl** State Univ.	Yaroslavl, Russian Federation
YCC	**Yokohama** Coll. of Commerce	Yokohama, Japan
YERE	**Yerevan** Physics Inst.	Yerevan, Armenia
YOKO	**Yokohama National** Univ.	Yokohama-shi, Japan
YORKC	**York** Univ.	Toronto, Canada
ZAGR	**Zagreb** Univ.	Zagreb, Croatia
ZARA	Univ. de **Zaragoza**	Zaragoza, Spain
ZEEM	Univ. van **Amsterdam**	TV Amsterdam, The Netherlands
ZHON	**Zhongshan** (Sun Yat-Sen) Univ.	Guangzhou, China
ZHZH	**Zhengzhou** Univ.	Zhengzhou, Henan, China
ZURI	Univ. **Zürich**	Zürich, Switzerland

GAUGE AND HIGGS BOSONS

Related Reviews in Volume 1

GAUGE AND HIGGS BOSONS

γ (photon)

$I(J^{PC}) = 0,1(1^{--})$

γ MASS

Results prior to 2008 are critiqued in GOLDHABER 10. All experimental results published prior to 2005 are summarized in detail by TU 05.

The following conversions are useful: 1 eV = 1.783×10^{-33} g = 1.957×10^{-6} m_e; $\lambda\!\!\!^{-}_C = (1.973 \times 10^{-7}$ m)$\times$(1 eV/m_γ).

VALUE (eV)	CL%	DOCUMENT ID		COMMENT
<1 $\times 10^{-18}$		[1] RYUTOV	07	MHD of solar wind
• • • We do not use the following data for averages, fits, limits, etc. • • •				
$<2.2 \times 10^{-14}$		[2] BONETTI	17	Fast Radio Bursts, FRB 121102
$<1.8 \times 10^{-14}$		[3] BONETTI	16	Fast Radio Bursts, FRB 150418
$<1.9 \times 10^{-15}$		[4] RETINO	16	Ampere's Law in solar wind
$<2.3 \times 10^{-9}$	95	[5] EGOROV	14	Lensed quasar position
		[6] ACCIOLY	10	Anomalous magn. mom.
$<1 \times 10^{-26}$		[7] ADELBERGER	07A	Proca galactic field
no limit feasible		[7] ADELBERGER	07A	γ as Higgs particle
$<1 \times 10^{-19}$		[8] TU	06	Torque on rotating magnetized toroid
$<1.4 \times 10^{-7}$		ACCIOLY	04	Dispersion of GHz radio waves by sun
$<2 \times 10^{-16}$		[9] FULLEKRUG	04	Speed of 5-50 Hz radiation in atmosphere
$<7 \times 10^{-19}$		[10] LUO	03	Torque on rotating magnetized toroid
$<1 \times 10^{-17}$		[11] LAKES	98	Torque on toroid balance
$<6 \times 10^{-17}$		[12] RYUTOV	97	MHD of solar wind
$<8 \times 10^{-16}$	90	[13] FISCHBACH	94	Earth magnetic field
$<5 \times 10^{-13}$		[14] CHERNIKOV	92	Ampere's Law null test
$<1.5 \times 10^{-9}$	90	[15] RYAN	85	Coulomb's Law null test
$<3 \times 10^{-27}$		[16] CHIBISOV	76	Galactic magnetic field
$<6 \times 10^{-16}$	99.7	[17] DAVIS	75	Jupiter's magnetic field
$<7.3 \times 10^{-16}$		HOLLWEG	74	Alfven waves
$<6 \times 10^{-17}$		[18] FRANKEN	71	Low freq. res. circuit
$<2.4 \times 10^{-13}$		[19] KROLL	71A	Dispersion in atmosphere
$<1 \times 10^{-14}$		[20] WILLIAMS	71	Tests Coulomb's Law
$<2.3 \times 10^{-15}$		GOLDHABER	68	Satellite data

[1] RYUTOV 07 extends the method of RYUTOV 97 to the radius of Pluto's orbit.

[2] BONETTI 17 uses frequency-dependent time delays of repeating FRB with well-determined redshift, assuming the DM is caused by expected dispersion in IGM. There are several uncertainties, leading to mass limit 2.2×10^{-14} eV.

[3] BONETTI 16 uses frequency-dependent time delays of FRB, assuming the DM is caused by expected dispersion in IGM. There are several uncertainties, leading to mass limit 1.8×10^{-14} eV, if indeed the FRB is at the initially reported redshift.

[4] RETINO 16 looks for deviations from Ampere's law in the solar wind, using Cluster four spacecraft data. Authors quote a range of limits from 1.9×10^{-15} eV to 7.9×10^{-14} eV depending on the assumptions of the vector potential from the interplanetary magnetic field.

[5] EGOROV 14 studies chromatic dispersion of lensed quasar positions ("gravitational rainbows") that could be produced by any of several mechanisms, among them via photon mass. Limit not competitive but obtained on cosmological distance scales.

[6] ACCIOLY 10 limits come from possible alterations of anomalous magnetic moment of electron and gravitational deflection of electromagnetic radiation. Reported limits are not "claimed" by the authors and in any case are not competitive.

[7] When trying to measure m one must distinguish between measurements performed on large and small scales. If the photon acquires mass by the Higgs mechanism, the large-scale behavior of the photon might be effectively Maxwellian. If, on the other hand, one postulates the Proca regime for all scales, the very existence of the galactic field implies $m < 10^{-26}$ eV, as correctly calculated by YAMAGUCHI 59 and CHIBISOV 76.

[8] TU 06 continues the work of LUO 03, with extended LAKES 98 method, reporting the improved limit $\mu^2 A = (0.7 \pm 1.7) \times 10^{-13}$ T/m if $A = 0.2$ μG out to 4×10^{22} m. Reported result $\mu = (0.9 \pm 1.5) \times 10^{-52}$ g reduces to the frequentist mass limit 1.2×10^{-19} eV (FELDMAN 98).

[9] FULLEKRUG 04 adopted KROLL 71A method with newer and better Schumann resonance data. Result questionable because assumed frequency shift with photon mass is assumed to be linear. It is quadratic according to theorem by GOLDHABER 71B, KROLL 71, and PARK 71.

[10] LUO 03 extends LAKES 98 technique to set a limit on $\mu^2 A$, where μ^{-1} is the Compton wavelength $\lambda\!\!\!^{-}_C$ of the massive photon and A is the ambient vector potential. The important departure is that the apparatus rotates, removing sensitivity to the direction of A. They take $A = 10^{12}$ Tm, due to "cluster level fields." But see comment of GOLDHABER 03 and reply by LUO 03B.

[11] LAKES 98 reports limits on torque on a toroid Cavendish balance, obtaining a limit on $\mu^2 A < 2 \times 10^{-9}$ Tm/m^2 via the Maxwell-Proca equations, where μ^{-1} is the characteristic length associated with the photon mass and A is the ambient vector potential in the Lorentz gauge. Assuming $A \approx 1 \times 10^{12}$ Tm due to cluster fields he obtains $\mu^{-1} > 2 \times 10^{10}$ m, corresponding to $\mu < 1 \times 10^{-17}$ eV. A more conservative limit, using $A \approx (1$ μG)$\times$(600 pc) based on the galactic field, is $\mu^{-1} > 1 \times 10^{9}$ m or $\mu < 2 \times 10^{-16}$ eV.

[12] RYUTOV 97 uses a magnetohydrodynamics argument concerning survival of the Sun's field to the radius of the Earth's orbit. "To reconcile observations to theory, one has to reduce [the photon mass] by approximately an order of magnitude compared with" per DAVIS 75. "Secure limit, best by this method" (per GOLDHABER 10).

[13] FISCHBACH 94 analysis is based on terrestrial magnetic fields; approach analogous to DAVIS 75. Similar result based on a much smaller planet probably follows from more precise B field mapping. "Secure limit, best by this method" (per GOLDHABER 10).

[14] CHERNIKOV 92, motivated by possibility that photon exhibits mass only below some unknown critical temperature, searches for departure from Ampere's Law at 1.24 K. See also RYAN 85.

[15] RYAN 85, motivated by possibility that photon exhibits mass only below some unknown critical temperature, sets mass limit at $< (1.5 \pm 1.4) \times 10^{-42}$ g based on Coulomb's Law departure limit at 1.36 K. We report the result as frequentist 90% CL (FELDMAN 98).

[16] CHIBISOV 76 depends in critical way on assumptions such as applicability of virial theorem. Some of the arguments given only in unpublished references.

[17] DAVIS 75 analysis of Pioneer-10 data on Jupiter's magnetic field. "Secure limit, best by this method" (per GOLDHABER 10).

[18] FRANKEN 71 method is of dubious validity (KROLL 71A, JACKSON 99, GOLDHABER 10, and references therein).

[19] KROLL 71A used low frequency Schumann resonances in cavity between the conducting earth and resistive ionosphere, overcoming objections to resonant-cavity methods (JACKSON 99, GOLDHABER 10, and references therein). "Secure limit, best by this method" (per GOLDHABER 10).

[20] WILLIAMS 71 is landmark test of Coulomb's law. "Secure limit, best by this method" (per GOLDHABER 10).

γ CHARGE

OKUN 06 has argued that schemes in which all photons are charged are inconsistent. He says that if a neutral photon is also admitted to avoid this problem, then other problems emerge, such as those connected with the emission and absorption of charged photons by charged particles. He concludes that in the absence of a self-consistent phenomenological basis, interpretation of experimental data is at best difficult.

VALUE (e)	CHARGE	DOCUMENT ID		TECN	COMMENT
<1 $\times 10^{-46}$	**mixed**	[1] ALTSCHUL	07B	VLBI	Aharonov-Bohm effect
<1 $\times 10^{-35}$	**single**	[2] CAPRINI	05	CMB	Isotropy constraint
• • • We do not use the following data for averages, fits, limits, etc. • • •					
$<1 \times 10^{-32}$	single	[1] ALTSCHUL	07B	VLBI	Aharonov-Bohm effect
$<3 \times 10^{-33}$	mixed	[3] KOBYCHEV	05	VLBI	Smear as function of B·E_γ
$<4 \times 10^{-31}$	single	[3] KOBYCHEV	05	VLBI	Deflection as function of B·E_γ
$<8.5 \times 10^{-17}$		[4] SEMERTZIDIS	03		Laser light deflection in B-field
$<3 \times 10^{-28}$	single	[5] SIVARAM	95	CMB	For $\Omega_M = 0.3$, $h^2 = 0.5$
$<5 \times 10^{-30}$		[6] RAFFELT	94	TOF	Pulsar $f_1 - f_2$
$<2 \times 10^{-28}$		[7] COCCONI	92		VLBA radio telescope resolution
$<2 \times 10^{-32}$		COCCONI	88	TOF	Pulsar $f_1 - f_2$ TOF

[1] ALTSCHUL 07B looks for Aharonov-Bohm phase shift in addition to geometric phase shift in radio interference fringes (VSOP mission).

[2] CAPRINI 05 uses isotropy of the cosmic microwave background to place stringent limits on possible charge asymmetry of the Universe. Charge limits are set on the photon, neutrino, and dark matter particles. Valid if charge asymmetries produced by different particles are not anticorrelated.

[3] KOBYCHEV 05 considers a variety of observable effects of photon charge for extragalactic compact radio sources. Best limits if source observed through a foreground cluster of galaxies.

[4] SEMERTZIDIS 03 reports the first laboratory limit on the photon charge in the last 30 years. Straightforward improvements in the apparatus could attain a sensitivity of 10^{-20} e.

[5] SIVARAM 95 requires that CMB photon charge density not overwhelm gravity. Result scales as $\Omega_M h^2$.

[6] RAFFELT 94 notes that COCCONI 88 neglects the fact that the time delay due to dispersion by free electrons in the interstellar medium has the same photon energy dependence as that due to bending of a charged photon in the magnetic field. His limit is based on the assumption that the entire observed dispersion is due to photon charge. It is a factor of 200 less stringent than the COCCONI 88 limit.

[7] See COCCONI 92 for less stringent limits in other frequency ranges. Also see RAFFELT 94 note.

γ REFERENCES

BONETTI	17	PL B768 326	L. Bonetti *et al.*	(ORLEANS, CERN)
BONETTI	16	PL B757 548	L. Bonetti *et al.*	
RETINO	16	ASP 82 49	A. Retino, A.D.A.M. Spallicci, A. Vaivads	(CURCP+)
EGOROV	14	MNRAS 437 L90	P. Egorov *et al.*	(MOSU, MIPT, INRM)
ACCIOLY	10	PR D82 065026	A. Accioly, J. Helayel-Neto, E. Scatena	(LABEX+)
GOLDHABER	10	RMP 82 939	A.S. Goldhaber, M.M. Nieto	(STON, LANL)
ADELBERGER	07A	PRL 98 010402	E. Adelberger, G. Dvali, A. Gruzinov	(WASH, NYU)
ALTSCHUL	07B	PRL 98 261801	B. Altschul	(IND)
Also		ASP 29 290	B. Altschul	(SCUC)
RYUTOV	07	PPCF 49 B429	D.D. Ryutov	(LLNL)
OKUN	06	APP B37 565	L.B. Okun	(ITEP)
TU	06	PL A352 267	L.-C. Tu *et al.*	
CAPRINI	05	JCAP 0502 006	C. Caprini, P.G. Ferreira	(GEVA, OXFTP)
KOBYCHEV	05	AL 31 147	V.V. Kobychev, S.B. Popov	(KIEV, PADO)
TU	05	RPP 68 77	L.-C. Tu, J. Luo, G.T. Gillies	
ACCIOLY	04	PR D69 107501	A. Accioly, R. Paszko	
FULLEKRUG	04	PRL 93 043901	M. Fullekrug	
GOLDHABER	03	PRL 91 149101	A.S. Goldhaber, M.M. Nieto	
LUO	03	PRL 90 081801	J. Luo *et al.*	
LUO	03B	PRL 91 149102	J. Luo *et al.*	
SEMERTZIDIS	03	PR D67 017701	Y.K. Semertzidis, G.T. Danby, D.M. Lazarus	
JACKSON	99	Classical Electrodynamics	J.D. Jackson	(3rd ed., J. Wiley and Sons (1999))
FELDMAN	98	PR D57 3873	G.J. Feldman, R.D. Cousins	
LAKES	98	PRL 80 1826	R. Lakes	(WISC)
RYUTOV	97	PPCF 39 A73	D.D. Ryutov	(LLNL)

Gauge & Higgs Boson Particle Listings

γ, g, graviton, W

SIVARAM	95	AJP 63 473	C. Sivaram	(BANG)
FISCHBACH	94	PRL 73 514	E. Fischbach *et al.*	(PURD, JHU+)
RAFFELT	94	PR D50 7729	G. Raffelt	(MPIM)
CHERNIKOV	92	PRL 68 3383	M.A. Chernikov *et al.*	(ETH)
Also		PRL 69 2999 (erratum)	M.A. Chernikov *et al.*	(ETH)
COCCONI	92	AJP 60 750	G. Cocconi	(CERN)
COCCONI	88	PL B206 705	G. Cocconi	(CERN)
RYAN	85	PR D32 802	J.J. Ryan, F. Accetta, R.H. Austin	(PRIN)
CHIBISOV	76	SPU 19 624 Translated from UFN 119 551.	G.V. Chibisov	(LEBD)
DAVIS	75	PRL 35 1402	L. Davis, A.S. Goldhaber, M.M. Nieto	(CIT, STON+)
HOLLWEG	74	PRL 32 961	J.V. Hollweg	(NCAR)
FRANKEN	71	PRL 26 115	P.A. Franken, G.W. Ampulski	(MICH)
GOLDHABER	71B	RMP 43 277	A.S. Goldhaber, M.M. Nieto	(STON, BOHR, UCSB)
KROLL	71	PRL 26 1395	N.M. Kroll	(SLAC)
KROLL	71A	PRL 27 340	N.M. Kroll	(SLAC)
PARK	71	PRL 26 1393	D. Park, E.R. Williams	(WILC)
WILLIAMS	71	PRL 26 721	E.R. Williams, J.E. Faller, H.A. Hill	(WESL)
GOLDHABER	68	PRL 21 567	A.S. Goldhaber, M.M. Nieto	(STON)
YAMAGUCHI	59	PTPS 11 37	Y. Yamaguchi	

g or gluon

$I(J^P) = 0(1^-)$

SU(3) color octet

Mass $m = 0$. Theoretical value. A mass as large as a few MeV may not be precluded, see YNDURAIN 95.

VALUE	DOCUMENT ID		TECN	COMMENT
• • • We do not use the following data for averages, fits, limits, etc. • • •				
	ABREU	92E	DLPH	Spin 1, not 0
	ALEXANDER	91H	OPAL	Spin 1, not 0
	BEHREND	82D	CELL	Spin 1, not 0
	BERGER	80D	PLUT	Spin 1, not 0
	BRANDELIK	80C	TASS	Spin 1, not 0

gluon REFERENCES

YNDURAIN	95	PL B345 524	F.J. Yndurain	(MADU)
ABREU	92E	PL B274 498	P. Abreu *et al.*	(DELPHI Collab.)
ALEXANDER	91H	ZPHY C52 543	G. Alexander *et al.*	(OPAL Collab.)
BEHREND	82D	PL B110 329	H.J. Behrend *et al.*	(CELLO Collab.)
BERGER	80D	PL B97 459	C. Berger *et al.*	(PLUTO Collab.)
BRANDELIK	80C	PL B97 453	R. Brandelik *et al.*	(TASSO Collab.)

graviton

$J = 2$

graviton MASS

Van Dam and Veltman (VANDAM 70), Iwasaki (IWASAKI 70), and Zakharov (ZAKHAROV 70) almost simultanously showed that "... there is a discrete difference between the theory with zero-mass and a theory with finite mass, no matter how small as compared to all external momenta." The resolution of this "vDVZ discontinuity" has to do with whether the linear approximation is valid. De Rham *etal*. (DE-RHAM 11) have shown that nonlinear effects not captured in their linear treatment can give rise to a screening mechanism, allowing for massive gravity theories. See also GOLDHABER 10 and DE-RHAM 17 and references therein. Experimental limits have been set based on a Yukawa potential or signal dispersion. h_0 is the Hubble constant in units of 100 km s^{-1} Mpc^{-1}.

The following conversions are useful: 1 eV = 1.783×10^{-33} g = 1.957×10^{-6} m_e; $\lambda\!\!\!^{-}_C = (1.973 \times 10^{-7}\ \text{m}) \times (1\ \text{eV}/m_g)$.

VALUE (eV)		DOCUMENT ID		TECN	COMMENT
<6 $\times 10^{-32}$	[1]	CHOUDHURY 04		YUKA	Weak gravitational lensing
• • • We do not use the following data for averages, fits, limits, etc. • • •					
$<7 \times 10^{-23}$	[2]	ABBOTT	17	DISP	Combined dispersion limit from three BH mergers
$<1.2 \times 10^{-22}$	[2]	ABBOTT	16	DISP	Combined dispersion limit from two BH mergers
$<5 \times 10^{-23}$	[3]	BRITO	13		Spinning black holes bounds
$<4 \times 10^{-25}$	[4]	BASKARAN	08		Graviton phase velocity fluctuations
$<6 \times 10^{-32}$	[5]	GRUZINOV	05	YUKA	Solar System observations
$<9.0 \times 10^{-34}$	[6]	GERSHTEIN	04		From Ω_{tot} value assuming RTG
$>6 \times 10^{-34}$	[7]	DVALI	03		Horizon scales
$<8 \times 10^{-20}$	[8,9]	FINN	02	DISP	Binary pulsar orbital period decrease
	[9,10]	DAMOUR	91		Binary pulsar PSR 1913+16
$<7 \times 10^{-23}$		TALMADGE	88	YUKA	Solar system planetary astrometric data
$< 2 \times 10^{-29}\ h_0^{-1}$		GOLDHABER	74		Rich clusters
$<7 \times 10^{-28}$		HARE	73		Galaxy
$<8 \times 10^{4}$		HARE	73		2γ decay

[1] CHOUDHURY 04 concludes from a study of weak-lensing data that masses heavier than about the inverse of 100 Mpc seem to be ruled out if the gravitation field has the Yukawa form.

[2] ABBOTT 16 and ABBOTT 17 assumed a dispersion relation for gravitational waves modified relative to GR.

[3] BRITO 13 explore massive graviton (spin-2) fluctuations around rotating black holes.

[4] BASKARAN 08 consider fluctuations in pulsar timing due to photon interactions ("surfing") with background gravitational waves.

[5] GRUZINOV 05 uses the DGP model (DVALI 00) showing that non-perturbative effects restore continuity with Einstein's equations as the gravition mass approaches 0, then bases his limit on Solar System observations.

[6] GERSHTEIN 04 use non-Einstein field relativistic theory of gravity (RTG), with a massive graviton, to obtain the 95% CL mass limit implied by the value of $\Omega_{tot} = 1.02 \pm 0.02$ current at the time of publication.

[7] DVALI 03 suggest scale of horizon distance via DGP model (DVALI 00). For a horizon distance of 3×10^{26} m (about age of Universe/c; GOLDHABER 10) this graviton mass limit is implied.

[8] FINN 02 analyze the orbital decay rates of PSR B1913+16 and PSR B1534+12 with a possible graviton mass as a parameter. The combined frequentist mass limit is at 90%CL.

[9] As of 2014, limits on dP/dt are now about 0.1% (see T. Damour, "Experimental tests of gravitational theory," in this *Review*).

[10] DAMOUR 91 is an analysis of the orbital period change in binary pulsar PSR 1913+16, and confirms the general relativity prediction to 0.8%. "The theoretical importance of the [rate of orbital period decay] measurement has long been recognized as a direct confirmation that the gravitational interaction propagates with velocity c (which is the immediate cause of the appearance of a damping force in the binary pulsar system) and thereby as a test of the existence of gravitational radiation and of its quadrupolar nature." TAYLOR 93 adds that orbital parameter studies now agree with general relativity to 0.5%, and set limits on the level of scalar contribution in the context of a family of tensor [spin 2]-biscalar theories.

graviton REFERENCES

ABBOTT	17	PRL 118 221101	B.P. Abbot *et al.*	(LIGO and Virgo Collabs.)
DE-RHAM	17	RMP 89 025004	C. de Rham *et al.*	
ABBOTT	16	PRL 116 061102	B.P. Abbott *et al.*	(LIGO and Virgo Collabs.)
BRITO	13	PR D88 023514	R. Brito, V. Cardoso, P. Pani	(LISB, MISS, HSCA+)
DE-RHAM	11	PRL 106 231101	C. de Rham, G. Gabadadze, A.J. Tolley	
GOLDHABER	10	RMP 82 939	A.S. Goldhaber, M.M. Nieto	(STON, LANL)
BASKARAN	08	PR D78 044018	D. Baskaran *et al.*	
GRUZINOV	05	NAST 10 311	A. Gruzinov	(NYU)
CHOUDHURY	04	ASP 21 559	S.R. Choudhury *et al.*	(DELPH, MELB)
GERSHTEIN	04	PAN 67 1596 Translated from YAF 67 1618.	S.S. Gershtein *et al.*	(SERP)
DVALI	03	PR D68 024012	G.R. Dvali, A. Grizinov, M. Zaldarriaga	(NYU)
FINN	02	PR D65 044022	L.S. Finn, P.J. Sutton	
DVALI	00	PL B485 208	G.R. Dvali, G. Gabadadze, M. Porrati	(NYU)
TAYLOR	93	NAT 355 132	J.N. Taylor *et al.*	(PRIN, ARCBO, BURE+)
DAMOUR	91	APJ 366 501	T. Damour, J.H. Taylor	(BURE, MEUD, PRIN)
TALMADGE	88	PRL 61 1159	C. Talmadge *et al.*	(JPL)
GOLDHABER	74	PR D9 1119	A.S. Goldhaber, M.M. Nieto	(LANL, STON)
HARE	73	CJP 51 431	M.G. Hare	(SASK)
IWASAKI	70	PR D2 2255	Y. Iwasaki	
VANDAM	70	NP B22 397	H. van Dam, M. Veltman	(UTRE)
ZAKHAROV	70	JETPL 12 312	V.I. Zakharov *et al.*	

W

$J = 1$

See the related review(s):
Mass and Width of the W Boson

W MASS

The W-mass listed here corresponds to the mass parameter in a Breit-Wigner distribution with mass-dependent width. To obtain the world average, common systematic uncertainties between experiments are properly taken into account. The LEP-2 average W mass based on published results is 80.376 ± 0.033 GeV [SCHAEL 13A]. The combined Tevatron data yields an average W mass of 80.387 ± 0.016 GeV [AALTONEN 13N]. A combination of the LEP average with this Tevatron average and the ATLAS value [AABOUD 18J], assuming a common systematic error of 7 MeV between the latter two [Jens Erler, 52nd Rencontres de Moriond EW, March 2017], the world average W mass of 80.379 ± 0.012 GeV is obtained. OUR FIT quotes this value for the W mass.

VALUE (GeV)	EVTS		DOCUMENT ID		TECN	COMMENT
80.379± 0.012 OUR FIT						
80.370± 0.007±0.017	13.7M	[1]	AABOUD	18J	ATLS	$E_{\rm cm}^{pp} = 7$ TeV
80.375± 0.023	2177k	[2]	ABAZOV	14N	D0	$E_{\rm cm}^{p\overline{p}} = 1.96$ TeV
80.387± 0.019	1095k	[3]	AALTONEN	12E	CDF	$E_{\rm cm}^{p\overline{p}} = 1.96$ TeV
80.336± 0.055±0.039	10.3k	[4]	ABDALLAH	08A	DLPH	$E_{\rm cm}^{ee} = 161$–209 GeV
80.415± 0.042±0.031	11830	[5]	ABBIENDI	06	OPAL	$E_{\rm cm}^{ee} = 170$–209 GeV
80.270± 0.046±0.031	9909	[6]	ACHARD	06	L3	$E_{\rm cm}^{ee} = 161$–209 GeV
80.440± 0.043±0.027	8692	[7]	SCHAEL	06	ALEP	$E_{\rm cm}^{ee} = 161$–209 GeV
80.483± 0.084	49247	[8]	ABAZOV	02D	D0	$E_{\rm cm}^{p\overline{p}} = 1.8$ TeV
80.433± 0.079	53841	[9]	AFFOLDER	01E	CDF	$E_{\rm cm}^{p\overline{p}} = 1.8$ TeV
• • • We do not use the following data for averages, fits, limits, etc. • • •						
80.367± 0.026	1677k	[10]	ABAZOV	12F	D0	$E_{\rm cm}^{p\overline{p}} = 1.96$ TeV
80.401± 0.043	500k	[11]	ABAZOV	09AB	D0	$E_{\rm cm}^{p\overline{p}} = 1.96$ TeV
80.413± 0.034±0.034	115k	[12]	AALTONEN	07F	CDF	$E_{\rm cm}^{p\overline{p}} = 1.96$ TeV
82.87 ± 1.82 $^{+0.30}_{-0.16}$	1500	[13]	AKTAS	06	H1	$e^{\pm}p \to \overline{\nu}_e(\nu_e)X$, $\sqrt{s} \approx 300$ GeV
80.3 ± 2.1 ± 1.2 ± 1.0	645	[14]	CHEKANOV	02C	ZEUS	$e^-p \to \nu_e X$, $\sqrt{s} =$ 318 GeV
81.4 $^{+2.7}_{-2.6}$ ± 2.0 $^{+3.3}_{-3.0}$	1086	[15]	BREITWEG	00D	ZEUS	$e^+p \to \overline{\nu}_e X$, $\sqrt{s} \approx$ 300 GeV
80.84 ± 0.22 ±0.83	2065	[16]	ALITTI	92B	UA2	See W/Z ratio below

80.79	± 0.31	±0.84		[17] ALITTI	90B	UA2	$E_{cm}^{p\overline{p}}$ = 546,630 GeV
80.0	± 3.3	±2.4	22	[18] ABE	89I	CDF	$E_{cm}^{p\overline{p}}$ = 1.8 TeV
82.7	± 1.0	±2.7	149	[19] ALBAJAR	89	UA1	$E_{cm}^{p\overline{p}}$ = 546,630 GeV
81.8	$^{+\ 6.0}_{-\ 5.3}$	±2.6	46	[20] ALBAJAR	89	UA1	$E_{cm}^{p\overline{p}}$ = 546,630 GeV
89	± 3	±6	32	[21] ALBAJAR	89	UA1	$E_{cm}^{p\overline{p}}$ = 546,630 GeV
81.	± 5.		6	ARNISON	83	UA1	$E_{cm}^{e\overline{e}}$ = 546 GeV
80.	$^{+10.}_{-\ 6.}$		4	BANNER	83B	UA2	Repl. by ALITTI 90B

[1] AABOUD 18J select 4.61M $W^+ \to \mu^+\nu_\mu$, 3.40M $W^+ \to e^+\nu_e$, 3.23M $W^- \to \mu^-\overline{\nu}_\mu$ and 2.49M $W^- \to e^-\overline{\nu}_e$ events in 4.6 fb^{-1} pp data at 7 TeV. The W mass is determined using the transverse mass and transverse lepton momentum distributions, accounting for correlations. The systematic error includes 0.011 GeV experimental and 0.014 GeV modelling uncertainties.

[2] ABAZOV 14N is a combination of ABAZOV 09AB and ABAZOV 12F, also giving more details on the analysis.

[3] AALTONEN 12E select 470k $W \to e\nu$ decays and 625k $W \to \mu\nu$ decays in 2.2 fb^{-1} of Run-II data. The mass is determined using the transverse mass, transverse lepton momentum and transverse missing energy distributions, accounting for correlations. This result supersedes AALTONEN 07F. AALTONEN 14D gives more details on the procedures followed by the authors.

[4] ABDALLAH 08A use direct reconstruction of the kinematics of $W^+W^- \to q\overline{q}\ell\nu$ and $W^+W^- \to q\overline{q}q\overline{q}$ events for energies 172 GeV and above. The W mass was also extracted from the dependence of the WW cross section close to the production threshold and combined appropriately to obtain the final result. The systematic error includes ±0.025 GeV due to final state interactions and ±0.009 GeV due to LEP energy uncertainty.

[5] ABBIENDI 06 use direct reconstruction of the kinematics of $W^+W^- \to q\overline{q}\ell\nu_\ell$ and $W^+W^- \to q\overline{q}q\overline{q}$ events. The result quoted here is obtained combining this mass value with the results using $W^+W^- \to \ell\nu_\ell\ell'\nu_{\ell'}$ events in the energy range 183–207 GeV (ABBIENDI 03C) and the dependence of the WW production cross-section on m_W at threshold. The systematic error includes ±0.009 GeV due to the uncertainty on the LEP beam energy.

[6] ACHARD 06 use direct reconstruction of the kinematics of $W^+W^- \to q\overline{q}\ell\nu_\ell$ and $W^+W^- \to q\overline{q}q\overline{q}$ events in the C.M. energy range 189–209 GeV. The result quoted here is obtained combining this mass value with the results obtained from a direct W mass reconstruction at 172 and 183 GeV and with those from the dependence of the WW production cross-section on m_W at 161 and 172 GeV (ACCIARRI 99).

[7] SCHAEL 06 use direct reconstruction of the kinematics of $W^+W^- \to q\overline{q}\ell\nu_\ell$ and $W^+W^- \to q\overline{q}q\overline{q}$ events in the C.M. energy range 183–209 GeV. The result quoted here is obtained combining this mass value with those obtained from the dependence of the W pair production cross-section on m_W at 161 and 172 GeV (BARATE 97 and BARATE 97S respectively). The systematic error includes ±0.009 GeV due to possible effects of final state interactions in the $q\overline{q}q\overline{q}$ channel and ±0.009 GeV due to the uncertainty on the LEP beam energy.

[8] ABAZOV 02D improve the measurement of the W-boson mass including $W \to e\nu_e$ events in which the electron is close to a boundary of a central electromagnetic calorimeter module. Properly combining the results obtained by fitting $m_T(W)$, $p_T(e)$, and $p_T(\nu)$, this sample provides a mass value of 80.574 ± 0.405 GeV. The value reported here is a combination of this measurement with all previous DØ W-boson mass measurements.

[9] AFFOLDER 01E fit the transverse mass spectrum of 30115 $W \to e\nu_e$ events (M_W= 80.473 ± 0.065 ± 0.092 GeV) and of 14740 $W \to \mu\nu_\mu$ events (M_W= 80.465 ± 0.100 ± 0.103 GeV) obtained in the run IB (1994-95). Combining the electron and muon results, accounting for correlated uncertainties, yields M_W= 80.470 ± 0.089 GeV. They combine this value with their measurement of ABE 95P reported in run IA (1992-93) to obtain the quoted value.

[10] ABAZOV 12F select 1677k $W \to e\nu$ decays in 4.3 fb^{-1} of Run-II data. The mass is determined using the transverse mass and transverse lepton momentum distributions, accounting for correlations.

[11] ABAZOV 09AB study the transverse mass, transverse electron momentum, and transverse missing energy in a sample of 0.5 million $W \to e\nu$ decays selected in Run-II data. The quoted result combines all three methods, accounting for correlations.

[12] AALTONEN 07F obtain high purity $W \to e\nu_e$ and $W \to \mu\nu_\mu$ candidate samples totaling 63,964 and 51,128 events respectively. The W mass value quoted above is derived by simultaneously fitting the transverse mass and the lepton, and neutrino p_T distributions.

[13] AKTAS 06 fit the Q^2 dependence ($300 < Q^2 < 30{,}000$ GeV^2) of the charged-current differential cross section with a propagator mass. The first error is experimental and the second corresponds to uncertainties due to input parameters and model assumptions.

[14] CHEKANOV 02C fit the Q^2 dependence ($200 < Q^2 < 60000$ GeV^2) of the charged-current differential cross sections with a propagator mass fit. The last error is due to the uncertainty on the probability density functions.

[15] BREITWEG 00D fit the Q^2 dependence ($200 < Q^2 < 22500$ GeV^2) of the charged-current differential cross sections with a propagator mass fit. The last error is due to the uncertainty on the probability density functions.

[16] ALITTI 92B result has two contributions to the systematic error (±0.83); one (±0.81) cancels in m_W/m_Z and one (±0.17) is noncancelling. These were added in quadrature. We choose the ALITTI 92B value without using the LEP m_Z value, because we perform our own combined fit.

[17] There are two contributions to the systematic error (±0.84): one (±0.81) which cancels in m_W/m_Z and one (±0.21) which is non-cancelling. These were added in quadrature.

[18] ABE 89I systematic error dominated by the uncertainty in the absolute energy scale.

[19] ALBAJAR 89 result is from a total sample of 299 $W \to e\nu$ events.

[20] ALBAJAR 89 result is from a total sample of 67 $W \to \mu\nu$ events.

[21] ALBAJAR 89 result is from $W \to \tau\nu$ events.

W/*Z* MASS RATIO

VALUE	EVTS	DOCUMENT ID		TECN	COMMENT
0.88153±0.00017		[1] PDG	16		
• • • We do not use the following data for averages, fits, limits, etc. • • •					
0.8821 ±0.0011 ±0.0008	28323	[2] ABBOTT	98N	D0	$E_{cm}^{p\overline{p}}$ = 1.8 TeV
0.88114±0.00154±0.00252	5982	[3] ABBOTT	98P	D0	$E_{cm}^{p\overline{p}}$ = 1.8 TeV
0.8813 ±0.0036 ±0.0019	156	[4] ALITTI	92B	UA2	$E_{cm}^{p\overline{p}}$ = 630 GeV

[1] PDG 16 is the PDG average using the world average m_W and m_Z values as quoted in this edition of *Review of Particle Physics*. The directly measured values of m_W/m_Z are not used as their correlation with the Tevatron measured m_W is unknown.

[2] ABBOTT 98N obtain this from a study of 28323 $W \to e\nu_e$ and 3294 $Z \to e^+e^-$ decays. Of this latter sample, 2179 events are used to calibrate the electron energy scale.

[3] ABBOTT 98P obtain this from a study of 5982 $W \to e\nu_e$ events. The systematic error includes an uncertainty of ±0.00175 due to the electron energy scale.

[4] Scale error cancels in this ratio.

$m_Z - m_W$

VALUE (GeV)	DOCUMENT ID		TECN	COMMENT
10.803±0.015 OUR AVERAGE				
10.803±0.015	[1] PDG	16		
10.4 ±1.4 ±0.8	ALBAJAR	89	UA1	$E_{cm}^{p\overline{p}}$ = 546,630 GeV
• • • We do not use the following data for averages, fits, limits, etc. • • •				
11.3 ±1.3 ±0.9	ANSARI	87	UA2	$E_{cm}^{p\overline{p}}$ = 546,630 GeV

[1] PDG 16 value was obtained using the world average values of m_Z and m_W as listed in this publication.

$m_{W^+} - m_{W^-}$

Test of *CPT* invariance.

VALUE (GeV)	EVTS	DOCUMENT ID		TECN	COMMENT
−0.029±0.028 OUR AVERAGE					
−0.029±0.013±0.025	13.7M	[1] AABOUD	18J	ATLS	E_{cm}^{pp} = 7 TeV
−0.19 ±0.58	1722	ABE	90G	CDF	$E_{cm}^{p\overline{p}}$ = 1.8 TeV

[1] AABOUD 18J select 4.61M $W^+ \to \mu^+\nu_\mu$, 3.40M $W^+ \to e^+\nu_e$, 3.23M $W^- \to \mu^-\overline{\nu}_\mu$ and 2.49M $W^- \to e^-\overline{\nu}_e$ events in 4.6 fb^{-1} pp data at 7 TeV. The W mass is determined using the transverse mass and transverse lepton momentum distributions, accounting for correlations. The systematic error includes 0.007 GeV experimental and 0.024 GeV modelling uncertainties.

W WIDTH

The W width listed here corresponds to the width parameter in a Breit-Wigner distribution with mass-dependent width. To obtain the world average, common systematic uncertainties between experiments are properly taken into account. The LEP-2 average W width based on published results is 2.195 ± 0.083 GeV [SCHAEL 13A]. The combined Tevatron data yields an average W width of 2.046±0.049 GeV [FERMILAB-TM-2460-E].

OUR FIT uses these average LEP and Tevatron width values and combines them assuming no correlations.

VALUE (GeV)	EVTS	DOCUMENT ID		TECN	COMMENT
2.085±0.042 OUR FIT					
2.028±0.072	5272	[1] ABAZOV	09AK	D0	$E_{cm}^{p\overline{p}}$ = 1.96 GeV
2.032±0.045±0.057	6055	[2] AALTONEN	08B	CDF	$E_{cm}^{p\overline{p}}$ = 1.96 TeV
2.404±0.140±0.101	10.3k	[3] ABDALLAH	08A	DLPH	E_{cm}^{ee} = 183–209 GeV
1.996±0.096±0.102	10729	[4] ABBIENDI	06	OPAL	E_{cm}^{ee} = 170–209 GeV
2.18 ±0.11 ±0.09	9795	[5] ACHARD	06	L3	E_{cm}^{ee} = 172–209 GeV
2.14 ±0.09 ±0.06	8717	[6] SCHAEL	06	ALEP	E_{cm}^{ee} = 183–209 GeV
2.23 $^{+0.15}_{-0.14}$ ±0.10	294	[7] ABAZOV	02E	D0	$E_{cm}^{p\overline{p}}$ = 1.8 TeV
2.05 ±0.10 ±0.08	662	[8] AFFOLDER	00M	CDF	$E_{cm}^{p\overline{p}}$ = 1.8 TeV
• • • We do not use the following data for averages, fits, limits, etc. • • •					
2.152±0.066	79176	[9] ABBOTT	00B	D0	Extracted value
2.064±0.060±0.059		[10] ABE	95W	CDF	Extracted value
2.10 $^{+0.14}_{-0.13}$ ±0.09	3559	[11] ALITTI	92	UA2	Extracted value
2.18 $^{+0.26}_{-0.24}$ ±0.04		[12] ALBAJAR	91	UA1	Extracted value

[1] ABAZOV 09AK obtain this result fitting the high-end tail (100-200 GeV) of the transverse mass spectrum in $W \to e\nu$ decays.

[2] AALTONEN 08B obtain this result fitting the high-end tail (90–200 GeV) of the transverse mass spectrum in semileptonic $W \to e\nu_e$ and $W \to \mu\nu_\mu$ decays.

[3] ABDALLAH 08A use direct reconstruction of the kinematics of $W^+W^- \to q\overline{q}\ell\nu$ and $W^+W^- \to q\overline{q}q\overline{q}$ events. The systematic error includes ±0.065 GeV due to final state interactions.

[4] ABBIENDI 06 use direct reconstruction of the kinematics of $W^+W^- \to q\overline{q}\ell\nu_\ell$ and $W^+W^- \to q\overline{q}q\overline{q}$ events. The systematic error includes ±0.003 GeV due to the uncertainty on the LEP beam energy.

[5] ACHARD 06 use direct reconstruction of the kinematics of $W^+W^- \to q\overline{q}\ell\nu_\ell$ and $W^+W^- \to q\overline{q}q\overline{q}$ events in the C.M. energy range 189–209 GeV. The result quoted

here is obtained combining this value of the width with the result obtained from a direct W mass reconstruction at 172 and 183 GeV (ACCIARRI 99).

[6] SCHAEL 06 use direct reconstruction of the kinematics of $W^+W^- \to q\overline{q}\ell\nu_\ell$ and $W^+W^- \to q\overline{q}q\overline{q}$ events. The systematic error includes ±0.05 GeV due to possible effects of final state interactions in the $q\overline{q}q\overline{q}$ channel and ±0.01 GeV due to the uncertainty on the LEP beam energy.

[7] ABAZOV 02E obtain this result fitting the high-end tail (90–200 GeV) of the transverse-mass spectrum in semileptonic $W \to e\nu_e$ decays.

[8] AFFOLDER 00M fit the high transverse mass (100–200 GeV) $W \to e\nu_e$ and $W \to \mu\nu_\mu$ events to obtain $\Gamma(W) = 2.04 \pm 0.11(\text{stat}) \pm 0.09(\text{syst})$ GeV. This is combined with the earlier CDF measurement (ABE 95C) to obtain the quoted result.

[9] ABBOTT 00B measure $R = 10.43 \pm 0.27$ for the $W \to e\nu_e$ decay channel. They use the SM theoretical predictions for $\sigma(W)/\sigma(Z)$ and $\Gamma(W \to e\nu_e)$ and the world average for $B(Z \to ee)$. The value quoted here is obtained combining this result (2.169 ± 0.070 GeV) with that of ABBOTT 99H.

[10] ABE 95W measured $R = 10.90 \pm 0.32 \pm 0.29$. They use m_W=80.23 ± 0.18 GeV, $\sigma(W)/\sigma(Z) = 3.35 \pm 0.03$, $\Gamma(W \to e\nu) = 225.9 \pm 0.9$ MeV, $\Gamma(Z \to e^+e^-) = 83.98 \pm 0.18$ MeV, and $\Gamma(Z) = 2.4969 \pm 0.0038$ GeV.

[11] ALITTI 92 measured $R = 10.4^{+0.7}_{-0.6} \pm 0.3$. The values of $\sigma(Z)$ and $\sigma(W)$ come from $O(\alpha_s^2)$ calculations using $m_W = 80.14 \pm 0.27$ GeV, and $m_Z = 91.175 \pm 0.021$ GeV along with the corresponding value of $\sin^2\theta_W = 0.2274$. They use $\sigma(W)/\sigma(Z) = 3.26 \pm 0.07 \pm 0.05$ and $\Gamma(Z) = 2.487 \pm 0.010$ GeV.

[12] ALBAJAR 91 measured $R = 9.5^{+1.1}_{-1.0}$ (stat. + syst.). $\sigma(W)/\sigma(Z)$ is calculated in QCD at the parton level using $m_W = 80.18 \pm 0.28$ GeV and $m_Z = 91.172 \pm 0.031$ GeV along with $\sin^2\theta_W = 0.2322 \pm 0.0014$. They use $\sigma(W)/\sigma(Z) = 3.23 \pm 0.05$ and $\Gamma(Z) = 2.498 \pm 0.020$ GeV. This measurement is obtained combining both the electron and muon channels.

W^+ DECAY MODES

W^- modes are charge conjugates of the modes below.

	Mode		Fraction (Γ_i/Γ)		Confidence level
Γ_1	$\ell^+\nu$	[a]	(10.86± 0.09) %		
Γ_2	$e^+\nu$		(10.71± 0.16) %		
Γ_3	$\mu^+\nu$		(10.63± 0.15) %		
Γ_4	$\tau^+\nu$		(11.38± 0.21) %		
Γ_5	hadrons		(67.41± 0.27) %		
Γ_6	$\pi^+\gamma$		< 7	$\times 10^{-6}$	95%
Γ_7	$D_s^+\gamma$		< 1.3	$\times 10^{-3}$	95%
Γ_8	cX		(33.3 ± 2.6) %		
Γ_9	$c\overline{s}$		(31 $^{+13}_{-11}$) %		
Γ_{10}	invisible	[b]	(1.4 ± 2.9) %		

[a] ℓ indicates each type of lepton (e, μ, and τ), not sum over them.

[b] This represents the width for the decay of the W boson into a charged particle with momentum below detectability, p< 200 MeV.

W PARTIAL WIDTHS

Γ(invisible) Γ_{10}

This represents the width for the decay of the W boson into a charged particle with momentum below detectability, p< 200 MeV.

VALUE (MeV)	DOCUMENT ID		TECN	COMMENT
$30^{+52}_{-48} \pm 33$	[1] BARATE	99I	ALEP	E_{cm}^{ee}= 161+172+183 GeV
• • • We do not use the following data for averages, fits, limits, etc. • • •				
	[2] BARATE	99L	ALEP	E_{cm}^{ee}= 161+172+183 GeV

[1] BARATE 99I measure this quantity using the dependence of the total cross section σ_{WW} upon a change in the total width. The fit is performed to the WW measured cross sections at 161, 172, and 183 GeV. This partial width is < 139 MeV at 95%CL.

[2] BARATE 99L use W-pair production to search for effectively invisible W decays, tagging with the decay of the other W boson to Standard Model particles. The partial width for effectively invisible decay is < 27 MeV at 95%CL.

W BRANCHING RATIOS

Overall fits are performed to determine the branching ratios of the W boson. Averages on $W \to e\nu$, $W \to \mu\nu$, and $W \to \tau\nu$, and their correlations are obtained by combining results from the four LEP experiments properly taking into account the common systematic uncertainties and their correlations [SCHAEL 13A]. A first fit determines the three individual leptonic braching ratios $B(W \to e\nu)$, $B(W \to \mu\nu)$, and $B(W \to \tau\nu)$. This fit has a $\chi^2 = 6.3$ for 9 degrees of freedom. The correlation coefficients between the branching fractions are 0.14 $(e-\mu)$, −0.20 $(e-\tau)$, −0.12 $(\mu-\tau)$. A second fit assumes lepton universality and determines the leptonic branching ratio br$W \to \ell\nu$ and the hadronic branching ratio is derived as $B(W \to \text{hadrons}) = 1\text{–}3\ \text{br}W \to \ell$. This fit has a $\chi^2 = 15.4$ for 11 degrees of freedom.

$\Gamma(\ell^+\nu)/\Gamma_{total}$ Γ_1/Γ

ℓ indicates average over e, μ, and τ modes, not sum over modes.

VALUE (units 10^{-2})	EVTS	DOCUMENT ID		TECN	COMMENT
10.86±0.09 OUR FIT					
10.86±0.12±0.08	16438	ABBIENDI	07A	OPAL	E_{cm}^{ee}= 161–209 GeV
10.85±0.14±0.08	13600	ABDALLAH	04G	DLPH	E_{cm}^{ee}= 161–209 GeV
10.83±0.14±0.10	11246	ACHARD	04J	L3	E_{cm}^{ee}= 161–209 GeV
10.96±0.12±0.05	16116	SCHAEL	04A	ALEP	E_{cm}^{ee}= 183–209 GeV
• • • We do not use the following data for averages, fits, limits, etc. • • •					
11.02±0.52	11858	[1] ABBOTT	99H	D0	$E_{cm}^{p\overline{p}}$= 1.8 TeV
10.4 ±0.8	3642	[2] ABE	92I	CDF	$E_{cm}^{p\overline{p}}$= 1.8 TeV

[1] ABBOTT 99H measure $R \equiv [\sigma_W B(W \to \ell\nu_\ell)]/[\sigma_Z B(Z \to \ell\ell)] = 10.90 \pm 0.52$ combining electron and muon channels. They use $M_W = 80.39 \pm 0.06$ GeV and the SM theoretical predictions for $\sigma(W)/\sigma(Z)$ and $B(Z \to \ell\ell)$.

[2] $1216 \pm 38^{+27}_{-31}$ $W \to \mu\nu$ events from ABE 92I and 2426 $W \to e\nu$ events of ABE 91C. ABE 92I give the inverse quantity as 9.6 ± 0.7 and we have inverted.

$\Gamma(e^+\nu)/\Gamma_{total}$ Γ_2/Γ

VALUE (units 10^{-2})	EVTS	DOCUMENT ID		TECN	COMMENT
10.71±0.16 OUR FIT					
10.71±0.25±0.11	2374	ABBIENDI	07A	OPAL	E_{cm}^{ee}= 161–209 GeV
10.55±0.31±0.14	1804	ABDALLAH	04G	DLPH	E_{cm}^{ee}= 161–209 GeV
10.78±0.29±0.13	1576	ACHARD	04J	L3	E_{cm}^{ee}= 161–209 GeV
10.78±0.27±0.10	2142	SCHAEL	04A	ALEP	E_{cm}^{ee}= 183–209 GeV
• • • We do not use the following data for averages, fits, limits, etc. • • •					
10.61±0.28		[1] ABAZOV	04D	TEVA	$E_{cm}^{p\overline{p}}$= 1.8 TeV

[1] ABAZOV 04D take into account all correlations to properly combine the CDF (ABE 95W) and DØ (ABBOTT 00B) measurements of the ratio R in the electron channel. The ratio R is defined as $[\sigma_W \cdot B(W \to e\nu_e)] / [\sigma_Z \cdot B(Z \to ee)]$. The combination gives $R^{Tevatron} = 10.59 \pm 0.23$. σ_W / σ_Z is calculated at next–to–next–to–leading order (3.360 ± 0.051). The branching fraction $B(Z \to ee)$ is taken from this *Review* as (3.363 ± 0.004)%.

$\Gamma(\mu^+\nu)/\Gamma_{total}$ Γ_3/Γ

VALUE (units 10^{-2})	EVTS	DOCUMENT ID		TECN	COMMENT
10.63±0.15 OUR FIT					
10.78±0.24±0.10	2397	ABBIENDI	07A	OPAL	E_{cm}^{ee}= 161–209 GeV
10.65±0.26±0.08	1998	ABDALLAH	04G	DLPH	E_{cm}^{ee}= 161–209 GeV
10.03±0.29±0.12	1423	ACHARD	04J	L3	E_{cm}^{ee} = 161–209 GeV
10.87±0.25±0.08	2216	SCHAEL	04A	ALEP	E_{cm}^{ee} = 183–209 GeV

$\Gamma(\mu^+\nu)/\Gamma(e^+\nu)$ Γ_3/Γ_2

VALUE	EVTS	DOCUMENT ID		TECN	COMMENT
0.986±0.013 OUR AVERAGE					
0.980±0.018		[1] AAIJ	16AJ	LHCB	E_{cm}^{pp}= 8 TeV
0.993±0.019		SCHAEL	13A	LEP	E_{cm}^{ee}= 130–209 GeV
0.89 ±0.10	13k	[2] ABACHI	95D	D0	$E_{cm}^{p\overline{p}}$= 1.8 TeV
1.02 ±0.08	1216	[3] ABE	92I	CDF	$E_{cm}^{p\overline{p}}$= 1.8 TeV
1.00 ±0.14 ±0.08	67	ALBAJAR	89	UA1	$E_{cm}^{p\overline{p}}$= 546,630 GeV
• • • We do not use the following data for averages, fits, limits, etc. • • •					
1.24 $^{+0.6}_{-0.4}$	14	ARNISON	84D	UA1	Repl. by ALBAJAR 89

[1] AAIJ 16AJ make precise measurements of forward $W \to e\nu$ and $W \to \mu\nu$ production in proton-proton collisions at 8 TeV and determine the ratio of the W branching fractions $B(W \to e\nu)/B(W \to \mu\nu) = 1.020 \pm 0.002 \pm 0.019$.

[2] ABACHI 95D obtain this result from the measured $\sigma_W B(W \to \mu\nu) = 2.09 \pm 0.23 \pm 0.11$ nb and $\sigma_W B(W \to e\nu) = 2.36 \pm 0.07 \pm 0.13$ nb in which the first error is the combined statistical and systematic uncertainty, the second reflects the uncertainty in the luminosity.

[3] ABE 92I obtain $\sigma_W B(W \to \mu\nu) = 2.21 \pm 0.07 \pm 0.21$ and combine with ABE 91C $\sigma_W B((W \to e\nu))$ to give a ratio of the couplings from which we derive this measurement.

$\Gamma(\tau^+\nu)/\Gamma_{total}$ Γ_4/Γ

VALUE (units 10^{-2})	EVTS	DOCUMENT ID		TECN	COMMENT
11.38±0.21 OUR FIT					
11.14±0.31±0.17	2177	ABBIENDI	07A	OPAL	E_{cm}^{ee}= 161–209 GeV
11.46±0.39±0.19	2034	ABDALLAH	04G	DLPH	E_{cm}^{ee} = 161–209 GeV
11.89±0.40±0.20	1375	ACHARD	04J	L3	E_{cm}^{ee} = 161–209 GeV
11.25±0.32±0.20	2070	SCHAEL	04A	ALEP	E_{cm}^{ee} = 183–209 GeV

$\Gamma(\tau^+\nu)/\Gamma(e^+\nu)$ Γ_4/Γ_2

VALUE	EVTS	DOCUMENT ID		TECN	COMMENT
1.043±0.024 OUR AVERAGE					
1.063±0.027		SCHAEL	13A	LEP	E_{cm}^{ee}= 130–209 GeV
0.961±0.061	980	[1] ABBOTT	00D	D0	$E_{cm}^{p\overline{p}}$= 1.8 TeV
0.94 ±0.14	179	[2] ABE	92E	CDF	$E_{cm}^{p\overline{p}}$= 1.8 TeV
1.04 ±0.08 ±0.08	754	[3] ALITTI	92F	UA2	$E_{cm}^{p\overline{p}}$= 630 GeV
1.02 ±0.20 ±0.12	32	ALBAJAR	89	UA1	$E_{cm}^{p\overline{p}}$= 546,630 GeV

• • • We do not use the following data for averages, fits, limits, etc. • • •

0.995±0.112±0.083	198	ALITTI	91C	UA2	Repl. by ALITTI 92F
1.02 ±0.20 ±0.10	32	ALBAJAR	87	UA1	Repl. by ALBAJAR 89

[1] ABBOTT 00D measure $\sigma_W \times B(W \to \tau\nu_\tau) = 2.22 \pm 0.09 \pm 0.10 \pm 0.10$ nb. Using the ABBOTT 00B result $\sigma_W \times B(W \to e\nu_e) = 2.31 \pm 0.01 \pm 0.05 \pm 0.10$ nb, they quote the ratio of the couplings from which we derive this measurement.

[2] ABE 92E use two procedures for selecting $W \to \tau\nu_\tau$ events. The missing E_T trigger leads to $132 \pm 14 \pm 8$ events and the τ trigger to $47 \pm 9 \pm 4$ events. Proper statistical and systematic correlations are taken into account to arrive at $\sigma B(W \to \tau\nu) = 2.05 \pm 0.27$ nb. Combined with ABE 91C result on $\sigma B(W \to e\nu)$, ABE 92E quote a ratio of the couplings from which we derive this measurement.

[3] This measurement is derived by us from the ratio of the couplings of ALITTI 92F.

$\Gamma(\tau^+\nu)/\Gamma(\mu^+\nu)$ Γ_4/Γ_3

VALUE	DOCUMENT ID		TECN	COMMENT
1.070±0.026	SCHAEL	13A	LEP	E_{cm}^{ee} = 130–209 GeV

$\Gamma(\text{hadrons})/\Gamma_{\text{total}}$ Γ_5/Γ

OUR FIT value is obtained by a fit to the lepton branching ratio data assuming lepton universality.

VALUE (units 10^{-2})	EVTS	DOCUMENT ID		TECN	COMMENT
67.41±0.27 OUR FIT					
67.41±0.37±0.23	16438	ABBIENDI	07A	OPAL	E_{cm}^{ee} = 161–209 GeV
67.45±0.41±0.24	13600	ABDALLAH	04G	DLPH	E_{cm}^{ee} = 161–209 GeV
67.50±0.42±0.30	11246	ACHARD	04J	L3	E_{cm}^{ee} = 161–209 GeV
67.13±0.37±0.15	16116	SCHAEL	04A	ALEP	E_{cm}^{ee} = 183–209 GeV

$\Gamma(\pi^+\gamma)/\Gamma(e^+\nu)$ Γ_6/Γ_2

VALUE	CL%	DOCUMENT ID		TECN	COMMENT
< 6.4 × 10^{-5}	95	AALTONEN	12W	CDF	$E_{cm}^{p\overline{p}}$ = 1.96 Tev
< 7 × 10^{-4}	95	ABE	98H	CDF	$E_{cm}^{p\overline{p}}$ = 1.8 TeV
< 4.9 × 10^{-3}	95	[1] ALITTI	92D	UA2	$E_{cm}^{p\overline{p}}$ = 630 GeV
<58 × 10^{-3}	95	[2] ALBAJAR	90	UA1	$E_{cm}^{p\overline{p}}$ = 546, 630 GeV

[1] ALITTI 92D limit is 3.8×10^{-3} at 90%CL.
[2] ALBAJAR 90 obtain < 0.048 at 90%CL.

$\Gamma(D_s^+\gamma)/\Gamma(e^+\nu)$ Γ_7/Γ_2

VALUE	CL%	DOCUMENT ID		TECN	COMMENT
<1.2 × 10^{-2}	95	ABE	98P	CDF	$E_{cm}^{p\overline{p}}$ = 1.8 TeV

$\Gamma(cX)/\Gamma(\text{hadrons})$ Γ_8/Γ_5

VALUE	EVTS	DOCUMENT ID		TECN	COMMENT
0.49 ±0.04 OUR AVERAGE					
0.481±0.042±0.032	3005	[1] ABBIENDI	00V	OPAL	E_{cm}^{ee} = 183 + 189 GeV
0.51 ±0.05 ±0.03	746	[2] BARATE	99M	ALEP	E_{cm}^{ee} = 172 + 183 GeV

[1] ABBIENDI 00V tag $W \to cX$ decays using measured jet properties, lifetime information, and leptons produced in charm decays. From this result, and using the additional measurements of $\Gamma(W)$ and $B(W \to \text{hadrons})$, $|V_{cs}|$ is determined to be $0.969 \pm 0.045 \pm 0.036$.

[2] BARATE 99M tag c jets using a neural network algorithm. From this measurement $|V_{cs}|$ is determined to be $1.00 \pm 0.11 \pm 0.07$.

$R_{cs} = \Gamma(c\overline{s})/\Gamma(\text{hadrons})$ Γ_9/Γ_5

VALUE	DOCUMENT ID		TECN	COMMENT
$0.46^{+0.18}_{-0.14}$ ±0.07	[1] ABREU	98N	DLPH	E_{cm}^{ee} = 161+172 GeV

[1] ABREU 98N tag c and s jets by identifying a charged kaon as the highest momentum particle in a hadronic jet. They also use a lifetime tag to independently identify a c jet, based on the impact parameter distribution of charged particles in a jet. From this measurement $|V_{cs}|$ is determined to be $0.94^{+0.32}_{-0.26} \pm 0.13$.

AVERAGE PARTICLE MULTIPLICITIES IN HADRONIC *W* DECAY

Summed over particle and antiparticle, when appropriate.

$\langle N_{\pi^\pm} \rangle$

VALUE	DOCUMENT ID		TECN	COMMENT
15.70±0.35	[1] ABREU,P	00F	DLPH	E_{cm}^{ee} = 189 GeV

[1] ABREU,P 00F measure $\langle N_{\pi^\pm} \rangle = 31.65 \pm 0.48 \pm 0.76$ and $15.51 \pm 0.38 \pm 0.40$ in the fully hadronic and semileptonic final states respectively. The value quoted is a weighted average without assuming any correlations.

$\langle N_{K^\pm} \rangle$

VALUE	DOCUMENT ID		TECN	COMMENT
2.20±0.19	[1] ABREU,P	00F	DLPH	E_{cm}^{ee} = 189 GeV

[1] ABREU,P 00F measure $\langle N_{K^\pm} \rangle = 4.38 \pm 0.42 \pm 0.12$ and $2.23 \pm 0.32 \pm 0.17$ in the fully hadronic and semileptonic final states respectively. The value quoted is a weighted average without assuming any correlations.

$\langle N_p \rangle$

VALUE	DOCUMENT ID		TECN	COMMENT
0.92±0.14	[1] ABREU,P	00F	DLPH	E_{cm}^{ee} = 189 GeV

[1] ABREU,P 00F measure $\langle N_p \rangle = 1.82 \pm 0.29 \pm 0.16$ and $0.94 \pm 0.23 \pm 0.06$ in the fully hadronic and semileptonic final states respectively. The value quoted is a weighted average without assuming any correlations.

$\langle N_{\text{charged}} \rangle$

VALUE	DOCUMENT ID		TECN	COMMENT
19.39±0.08 OUR AVERAGE				
19.38±0.05±0.08	[1] ABBIENDI	06A	OPAL	E_{cm}^{ee} = 189–209 GeV
19.44±0.17	[2] ABREU,P	00F	DLPH	E_{cm}^{ee} = 183+189 GeV
19.3 ±0.3 ±0.3	[3] ABBIENDI	99N	OPAL	E_{cm}^{ee} = 183 GeV
19.23±0.74	[4] ABREU	98C	DLPH	E_{cm}^{ee} = 172 GeV

[1] ABBIENDI 06A measure $\langle N_{\text{charged}} \rangle = 38.74 \pm 0.12 \pm 0.26$ when both W bosons decay hadronically and $\langle N_{\text{charged}} \rangle = 19.39 \pm 0.11 \pm 0.09$ when one W boson decays semileptonically. The value quoted here is obtained under the assumption that there is no color reconnection between W bosons; the value is a weighted average taking into account correlations in the systematic uncertainties.

[2] ABREU,P 00F measure $\langle N_{\text{charged}} \rangle = 39.12 \pm 0.33 \pm 0.36$ and $38.11 \pm 0.57 \pm 0.44$ in the fully hadronic final states at 189 and 183 GeV respectively, and $\langle N_{\text{charged}} \rangle = 19.49 \pm 0.31 \pm 0.27$ and $19.78 \pm 0.49 \pm 0.43$ in the semileptonic final states. The value quoted is a weighted average without assuming any correlations.

[3] ABBIENDI 99N use the final states $W^+W^- \to q\overline{q}\ell\overline{\nu}_\ell$ to derive this value.

[4] ABREU 98C combine results from both the fully hadronic as well semileptonic WW final states after demonstrating that the W decay charged multiplicity is independent of the topology within errors.

TRIPLE GAUGE COUPLINGS (TGC'S)

See the related review(s):
Extraction of Triple Gauge Couplings (TGC's)

g_1^Z

OUR FIT below is taken from [SCHAEL 13A].

VALUE	EVTS	DOCUMENT ID		TECN	COMMENT
$0.984^{+0.018}_{-0.020}$ OUR FIT					
$0.975^{+0.033}_{-0.030}$	7872	[1] ABDALLAH	10	DLPH	E_{cm}^{ee} = 189–209 GeV
1.001±0.027±0.013	9310	[2] SCHAEL	05A	ALEP	E_{cm}^{ee} = 183–209 GeV
$0.987^{+0.034}_{-0.033}$	9800	[3] ABBIENDI	04D	OPAL	E_{cm}^{ee} = 183–209 GeV
$0.966^{+0.034}_{-0.032}$±0.015	8325	[4] ACHARD	04D	L3	E_{cm}^{ee} = 161–209 GeV

• • • We do not use the following data for averages, fits, limits, etc. • • •

		[5] AABOUD	17S	ATLS	E_{cm}^{pp} = 7+8 TeV
		[6] AABOUD	17U	ATLS	E_{cm}^{pp} = 8 TeV
		[7] KHACHATRY...	17O	CMS	E_{cm}^{pp} = 8 TeV
		[8] SIRUNYAN	17X		E_{cm}^{pp} = 8 TeV
		[9] AAD	16AR	ATLS	E_{cm}^{pp} = 8 TeV
		[10] AAD	16P	ATLS	E_{cm}^{pp} = 8 TeV
		[11] AAD	14Y	ATLS	E_{cm}^{pp} = 8 TeV
		[12] AAD	13AL	ATLS	E_{cm}^{pp} = 7 TeV
		[13] CHATRCHYAN	13BF	CMS	E_{cm}^{pp} = 7 TeV
		[14] AAD	12CD	ATLS	E_{cm}^{pp} = 7 TeV
		[15] AALTONEN	12AC	CDF	$E_{cm}^{p\overline{p}}$ = 1.96 TeV
		[16] ABAZOV	12AG	D0	$E_{cm}^{p\overline{p}}$ = 1.96 TeV
	34	[17] ABAZOV	11	D0	$E_{cm}^{p\overline{p}}$ = 1.96 TeV
	334	[18] AALTONEN	10K	CDF	$E_{cm}^{p\overline{p}}$ = 1.96 TeV
1.04 ±0.09		[19] ABAZOV	09AD	D0	$E_{cm}^{p\overline{p}}$ = 1.96 TeV
		[20] ABAZOV	09AJ	D0	$E_{cm}^{p\overline{p}}$ = 1.96 TeV
1.07 $^{+0.08}_{-0.12}$	1880	[21] ABDALLAH	08C	DLPH	Superseded by ABDALLAH 10
	13	[22] ABAZOV	07Z	D0	$E_{cm}^{p\overline{p}}$ = 1.96 TeV
	2.3	[23] ABAZOV	05S	D0	$E_{cm}^{p\overline{p}}$ = 1.96 TeV
0.98 ±0.07 ±0.01	2114	[24] ABREU	01I	DLPH	E_{cm}^{ee} = 183+189 GeV
	331	[25] ABBOTT	99I	D0	$E_{cm}^{p\overline{p}}$ = 1.8 TeV

[1] ABDALLAH 10 use data on the final states $e^+e^- \to jj\ell\nu$, $jjjj$, jjX, ℓX, at center-of-mass energies between 189–209 GeV at LEP2, where j = jet, ℓ = lepton, and X represents missing momentum. The fit is carried out keeping all other parameters fixed at their SM values.

[2] SCHAEL 05A study single–photon, single–W, and WW–pair production from 183 to 209 GeV. The result quoted here is derived from the WW–pair production sample. Each parameter is determined from a single–parameter fit in which the other parameters assume their Standard Model values.

[3] ABBIENDI 04D combine results from W^+W^- in all decay channels. Only CP-conserving couplings are considered and each parameter is determined from a single-parameter fit in which the other parameters assume their Standard Model values. The 95% confidence interval is $0.923 < g_1^Z < 1.054$.

[4] ACHARD 04D study WW–pair production, single–W production and single–photon production with missing energy from 189 to 209 GeV. The result quoted here is obtained from the WW–pair production sample including data from 161 to 183 GeV, ACCIARRI 99Q. Each parameter is determined from a single–parameter fit in which the other parameters assume their Standard Model values.

[5] AABOUD 17S analyze electroweak production of a W boson in association with two jets at high dijet invariant mass, with the W boson decaying to electron or muon plus neutrino. In the signal region of dijet mass larger than 1 TeV and leading-jet transverse momentum larger than 600 GeV, 30 events are observed in the data with 39 ± 4 events expected in the Standard Model, yielding the following limit at 95% CL for the form factor cut-off scale $\Lambda_{FF} \to \infty$: $0.87 < g_1^Z < 1.12$.

[6] AABOUD 17U analyze production of WW or WZ boson pairs with one W boson decaying to electron or muon plus neutrino, and the other W or Z boson decaying hadronically. The hadronic decay system is reconstructed as either a resolved two-jet system or as a single large jet. Analysing the transverse momentum distribution of the hadronic system above 100 GeV yields the following limit at 95% CL for the form factor cut-off scale $\Lambda_{FF} \to \infty$: $0.979 < g_1^Z < 1.024$.

[7] KHACHATRYAN 17O analyse WZ production where each boson decays into electrons or muons. Events are required to have a tri-lepton invariant mass larger than 100 GeV, with one of the lepton pairs having an invariant mass within 20 GeV of the Z boson mass. The Z transverse momentum spectrum is analyzed to set a 95% C.L. limit of: $0.982 < g_1^Z < 1.035$.

[8] SIRUNYAN 17X study $pp \to WW/WZ \to \ell\nu q\overline{q}$ production at 8 TeV where ℓ is an electron or muon with $p_T > 30$ or 25 GeV respectively. Suitable cuts are put on the p_T of the dijet system and the missing E_T of the event yielding a total of 285 and 204 WV events observed in the electron and muon channels. The following 95% C.L. limit is obtained: $0.9913 < g_1^Z < 1.024$.

[9] AAD 16AR study WW production in pp collisions and select 6636 WW candidates in decay modes with electrons or muons with an expected background of 1546 ± 157 events. Assuming the LEP formulation and setting the form-factor Λ to infinity, a fit to the transverse momentum distribution of the leading charged lepton, leads to a 95% C.L. range of $0.984 < g_1^Z < 1.027$.

[10] AAD 16P study WZ production in pp collisions and select 2091 WZ candidates in 4 decay modes with electrons and muons, with an expected background of 1825 ± 7 events. Analyzing the WZ transverse momentum distribution, the resulting 95% C.L. limit is: $0.981 < g_1^Z < 1.029$.

[11] AAD 14Y determine the electroweak Z-dijet cross section in 8 TeV pp collisions. $Z \to ee$ and $Z \to \mu\mu$ decays are selected with the di-lepton $p_T > 20$ GeV and mass in the 81–101 GeV range. Minimum two jets are required with $p_T > 55$ and 45 GeV and no additional jets with $p_T > 25$ GeV in the rapidity interval between them. The normalized p_T balance between the Z and the two jets is required to be < 0.15. This leads to a selection of 900 events with dijet mass > 1 TeV. The number of signal and background events expected is 261 and 592 respectively. A Poisson likelihood method is used on an event by event basis to obtain the 95% CL limit $0.5 < g_1^Z < 1.26$ for a form factor value $\Lambda = \infty$.

[12] AAD 13AL study WW production in pp collisions and select 1325 WW candidates in decay modes with electrons or muons with an expected background of 369 ± 61 events. Assuming the LEP formulation and setting the form-factor Λ = infinity, a fit to the transverse momentum distribution of the leading charged lepton, leads to a 95% C.L. range of $0.961 < g_1^Z < 1.052$. Supersedes AAD 12AC.

[13] CHATRCHYAN 13BF determine the W^+W^- production cross section using unlike sign di-lepton (e or μ) events with high $\not{p}_T$. The leptons have $p_T > 20$ GeV/c and are isolated. 1134 candidate events are observed with an expected SM background of 247 ± 34. The p_T distribution of the leading lepton is fitted to obtain 95% C.L. limits of $0.905 \leq g_1^Z \leq 1.095$.

[14] AAD 12CD study WZ production in pp collisions and select 317 WZ candidates in three $\ell\nu$ decay modes with an expected background of 68.0 ± 10.0 events. The resulting 95% C.L. range is: $0.943 < g_1^Z < 1.093$. Supersedes AAD 12V.

[15] AALTONEN 12AC study WZ production in $p\overline{p}$ collisions and select 63 WZ candidates in three $\ell\nu$ decay modes with an expected background of 7.9 ± 1.0 events. Based on the cross section and shape of the Z transverse momentum spectrum, the following 95% C.L. range is reported: $0.92 < g_1^Z < 1.20$ for a form factor of $\Lambda = 2$ TeV.

[16] ABAZOV 12AG combine new results with already published results on $W\gamma$, WW and WZ production in order to determine the couplings with increased precision, superseding ABAZOV 08R, ABAZOV 11AC, ABAZOV 09AJ, ABAZOV 09AD. The 68% C.L. result for a formfactor cutoff of $\Lambda = 2$ TeV is $g_1^Z = 1.022^{+0.032}_{-0.030}$.

[17] ABAZOV 11 study the $p\overline{p} \to 3\ell\nu$ process arising in WZ production. They observe 34 WZ candidates with an estimated background of 6 events. An analysis of the p_T spectrum of the Z boson leads to a 95% C.L. limit of $0.944 < g_1^Z < 1.154$, for a form factor $\Lambda = 2$ TeV.

[18] AALTONEN 10K study $p\overline{p} \to W^+W^-$ with $W \to e/\mu\nu$. The p_T of the leading (second) lepton is required to be > 20 (10) GeV. The final number of events selected is 654 of which 320 ± 47 are estimated to be background. The 95% C.L. interval is $0.76 < g_1^Z < 1.34$ for $\Lambda = 1.5$ TeV and $0.78 < g_1^Z < 1.30$ for $\Lambda = 2$ TeV.

[19] ABAZOV 09AD study the $p\overline{p} \to \ell\nu 2$jet process arising in WW and WZ production. They select 12,473 (14,392) events in the electron (muon) channel with an expected di-boson signal of 436 (527) events. The results on the anomalous couplings are derived from an analysis of the p_T spectrum of the 2-jet system and quoted at 68% C.L. and for a form factor of 2 TeV. This measurement is not used for obtaining the mean as it is for a specific form factor. The 95% confidence interval is $0.88 < g_1^Z < 1.20$.

[20] ABAZOV 09AJ study the $p\overline{p} \to 2\ell 2\nu$ process arising in WW production. They select 100 events with an expected WW signal of 65 events. An analysis of the p_T spectrum of the two charged leptons leads to 95% C.L. limits of $0.86 < g_1^Z < 1.3$, for a form factor $\Lambda = 2$ TeV.

[21] ABDALLAH 08C determine this triple gauge coupling from the measurement of the spin density matrix elements in $e^+e^- \to W^+W^- \to (q\overline{q})(\ell\nu)$, where $\ell = e$ or μ. Values of all other couplings are fixed to their standard model values.

[22] ABAZOV 07Z set limits on anomalous TGCs using the measured cross section and $p_T(Z)$ distribution in WZ production with both the W and the Z decaying leptonically into electrons and muons. Setting the other couplings to their standard model values, the 95% C.L. limit for a form factor scale $\Lambda = 2$ TeV is $0.86 < g_1^Z < 1.35$.

[23] ABAZOV 05S study $p\overline{p} \to WZ$ production with a subsequent trilepton decay to $\ell\nu\ell'\overline{\ell}'$ (ℓ and $\ell' = e$ or μ). Three events (estimated background 0.71 ± 0.08 events) with WZ decay characteristics are observed from which they derive limits on the anomalous WWZ couplings. The 95% CL limit for a form factor scale $\Lambda = 1.5$ TeV is $0.51 < g_1^Z < 1.66$, fixing λ_Z and κ_Z to their Standard Model values.

[24] ABREU 01I combine results from e^+e^- interactions at 189 GeV leading to W^+W^- and $We\nu_e$ final states with results from ABREU 99L at 183 GeV. The 95% confidence interval is $0.84 < g_1^Z < 1.13$.

[25] ABBOTT 99I perform a simultaneous fit to the $W\gamma$, $WW \to$ dilepton, $WW/WZ \to e\nu jj$, $WW/WZ \to \mu\nu jj$, and $WZ \to$ trilepton data samples. For $\Lambda = 2.0$ TeV, the 95%CL limits are $0.63 < g_1^Z < 1.57$, fixing λ_Z and κ_Z to their Standard Model values, and assuming Standard Model values for the $WW\gamma$ couplings.

κ_γ

OUR FIT below is taken from [SCHAEL 13A].

VALUE	EVTS	DOCUMENT ID		TECN	COMMENT
0.982±0.042 OUR FIT					
$1.024^{+0.077}_{-0.081}$	7872	[1] ABDALLAH	10	DLPH	E_{cm}^{ee}= 189–209 GeV
$0.971 \pm 0.055 \pm 0.030$	10689	[2] SCHAEL	05A	ALEP	E_{cm}^{ee}= 183–209 GeV
$0.88\ ^{+0.09}_{-0.08}$	9800	[3] ABBIENDI	04D	OPAL	E_{cm}^{ee}= 183–209 GeV
$1.013^{+0.067}_{-0.064} \pm 0.026$	10575	[4] ACHARD	04D	L3	E_{cm}^{ee}= 161–209 GeV
• • • We do not use the following data for averages, fits, limits, etc. • • •					
		[5] AABOUD	17U	ATLS	E_{cm}^{pp} = 8 TeV
		[6] SIRUNYAN	17X		E_{cm}^{pp} = 8 TeV
		[7] CHATRCHYAN	14AB	CMS	E_{cm}^{pp} = 7 TeV
		[8] AAD	13AN	ATLS	E_{cm}^{pp} = 7 TeV
		[9] CHATRCHYAN	13BF	CMS	E_{cm}^{pp} = 7 TeV
		[10] ABAZOV	12AG	D0	$E_{cm}^{p\overline{p}}$ = 1.96 TeV
		[11] ABAZOV	11AC	D0	$E_{cm}^{p\overline{p}}$ = 1.96 TeV
		[12] CHATRCHYAN	11M	CMS	E_{cm}^{pp} = 7 TeV
	334	[13] AALTONEN	10K	CDF	$E_{cm}^{p\overline{p}}$ = 1.96 TeV
	53	[14] AARON	09B	H1	E_{cm}^{ep} = 0.3 TeV
$1.07\ ^{+0.26}_{-0.29}$		[15] ABAZOV	09AD	D0	$E_{cm}^{p\overline{p}}$ = 1.96 TeV
		[16] ABAZOV	09AJ	D0	$E_{cm}^{p\overline{p}}$ = 1.96 TeV
		[17] ABAZOV	08R	D0	$E_{cm}^{p\overline{p}}$ = 1.96 TeV
$0.68\ ^{+0.17}_{-0.15}$	1880	[18] ABDALLAH	08C	DLPH	Superseded by ABDALLAH 10
	1617	[19] AALTONEN	07L	CDF	$E_{cm}^{p\overline{p}}$ = 1.96 GeV
	17	[20] ABAZOV	06H	D0	$E_{cm}^{p\overline{p}}$ = 1.96 TeV
	141	[21] ABAZOV	05J	D0	$E_{cm}^{p\overline{p}}$ = 1.96 TeV
$1.25\ ^{+0.21}_{-0.20} \pm 0.06$	2298	[22] ABREU	01I	DLPH	E_{cm}^{ee}= 183+189 GeV
		[23] BREITWEG	00	ZEUS	$e^+p \to e^+W^\pm X$, $\sqrt{s} \approx$ 300 GeV
0.92 ± 0.34	331	[24] ABBOTT	99I	D0	$E_{cm}^{p\overline{p}}$= 1.8 TeV

[1] ABDALLAH 10 use data on the final states $e^+e^- \to jj\ell\nu$, $jjjj$, jjX, ℓX, at center-of-mass energies between 189–209 GeV at LEP2, where j = jet, ℓ = lepton, and X represents missing momentum. The fit is carried out keeping all other parameters fixed at their SM values.

[2] SCHAEL 05A study single–photon, single–W, and WW–pair production from 183 to 209 GeV. Each parameter is determined from a single–parameter fit in which the other parameters assume their Standard Model values.

[3] ABBIENDI 04D combine results from W^+W^- in all decay channels. Only *CP*-conserving couplings are considered and each parameter is determined from a single-parameter fit in which the other parameters assume their Standard Model values. The 95% confidence interval is $0.73 < \kappa_\gamma < 1.07$.

[4] ACHARD 04D study WW–pair production, single–W production and single–photon production with missing energy from 189 to 209 GeV. The result quoted here is obtained including data from 161 to 183 GeV, ACCIARRI 99Q. Each parameter is determined from a single–parameter fit in which the other parameters assume their Standard Model values.

[5] AABOUD 17U analyze production of WW or WZ boson pairs with one W boson decaying to electron or muon plus neutrino, and the other W or Z boson decaying hadronically. The hadronic decay system is reconstructed as either a resolved two-jet system or as a single large jet. Analysing the transverse momentum distribution of the hadronic system above 100 GeV yields the following limit at 95% CL for the form factor cut-off scale $\Lambda_{FF} \to \infty$: $0.939 < \kappa_\gamma < 1.064$.

[6] SIRUNYAN 17X study $pp \to WW/WZ \to \ell\nu q\overline{q}$ production at 8 TeV where ℓ is an electron or muon with $p_T > 30$ or 25 GeV respectively. Suitable cuts are put on the p_T of the dijet system and the missing E_T of the event yielding a total of 285 and 204 WV events observed in the electron and muon channels. The following 95% C.L. limit is obtained: $0.956 < \kappa_\gamma < 1.063$.

[7] CHATRCHYAN 14AB measure $W\gamma$ production cross section for $p_T^\gamma > 15$ GeV and $R(\ell\gamma) > 0.7$, which is the separation between the γ and the final state charged lepton (e or μ) in the azimuthal angle-pseudorapidity ($\phi - \eta$) plane. After background subtraction the number of $e\nu\gamma$ and $\mu\nu\gamma$ events is determined to be 3200 ± 325 and 4970 ± 543 respectively, compatible with expectations from the SM. This leads to a 95% CL limit of $0.62 < \kappa_\gamma < 1.29$, assuming other parameters have SM values.

[8] AAD 13AN study $W\gamma$ production in pp collisions. In events with no additional jet, 4449 (6578) W decays to electron (muon) are selected, with an expected background of

1662 ± 262 (2538 ± 362) events. Analysing the photon p_T spectrum above 100 GeV yields a 95% C.L. limit of $0.59 < \kappa_\gamma < 1.46$. Supersedes AAD 12BX.

[9] CHATRCHYAN 13BF determine the W^+W^- production cross section using unlike sign di-lepton (e or μ) events with high $\not{p}_T$. The leptons have $p_T > 20$ GeV/c and are isolated. 1134 candidate events are observed with an expected SM background of 247 ± 34. The p_T distribution of the leading lepton is fitted to obtain 95% C.L. limits of $0.79 \leq k_\gamma \leq 1.22$.

[10] ABAZOV 12AG combine new results with already published results on $W\gamma$, WW and WZ production in order to determine the couplings with increased precision, superseding ABAZOV 08R, ABAZOV 11AC, ABAZOV 09AJ, ABAZOV 09AD. The 68% C.L. result for a formfactor cutoff of $\Lambda = 2$ TeV is $\kappa_\gamma = 1.048^{+0.106}_{-0.105}$.

[11] ABAZOV 11AC study $W\gamma$ production in $p\overline{p}$ collisions at 1.96 TeV, with the W decay products containing an electron or a muon. They select 196 (363) events in the electron (muon) mode, with a SM expectation of 190 (372) events. A likelihood fit to the photon E_T spectrum above 15 GeV yields at 95% C.L. the result: $0.6 < \kappa_\gamma < 1.4$ for a formfactor $\Lambda = 2$ TeV.

[12] CHATRCHYAN 11M study $W\gamma$ production in pp collisions at $\sqrt{s} = 7$ TeV using 36 pb^{-1} pp data with the W decaying to electron and muon. The total cross section is measured for photon transverse energy $E_T^\gamma > 10$ GeV and spatial separation from charged leptons in the plane of pseudo rapidity and azimuthal angle $\Delta R(\ell,\gamma) > 0.7$. The number of candidate (background) events is 452 (228 ± 21) for the electron channel and 520 (277 ± 25) for the muon channel. Setting other couplings to their standard model value, they derive a 95% CL limit of $-0.11 < \kappa_\gamma < 2.04$.

[13] AALTONEN 10K study $p\overline{p} \rightarrow W^+W^-$ with $W \rightarrow e/\mu\nu$. The p_T of the leading (second) lepton is required to be > 20 (10) GeV. The final number of events selected is 654 of which 320 ± 47 are estimated to be background. The 95% C.L. interval is $0.37 < \kappa_\gamma < 1.72$ for $\Lambda = 1.5$ TeV and $0.43 < \kappa_\gamma < 1.65$ for $\Lambda = 2$ TeV.

[14] AARON 09B study single-W production in ep collisions at 0.3 TeV C.M. energy. They select 53 $W \rightarrow e/\mu$ events with a standard model expectation of 54.1 ± 7.4 events. Fitting the transverse momentum spectrum of the hadronic recoil system they obtain a 95% C.L. limit of $-3.7 < \kappa_\gamma < -1.5$ or $0.3 < \kappa_\gamma < 1.5$, where the ambiguity is due to the quadratic dependence of the cross section to the coupling parameter.

[15] ABAZOV 09AD study the $p\overline{p} \rightarrow \ell\nu$ 2jet process arising in WW and WZ production. They select 12,473 (14,392) events in the electron (muon) channel with an expected di-boson signal of 436 (527) events. The results on the anomalous couplings are derived from an analysis of the p_T spectrum of the 2-jet system and quoted at 68% C.L. and for a form factor of 2 TeV. This measurement is not used for obtaining the mean as it is for a specific form factor. The 95% confidence interval is $0.56 < \kappa_\gamma < 1.55$.

[16] ABAZOV 09AJ study the $p\overline{p} \rightarrow 2\ell 2\nu$ process arising in WW production. They select 100 events with an expected WW signal of 65 events. An analysis of the p_T spectrum of the two charged leptons leads to 95% C.L. limits of $0.46 < \kappa_\gamma < 1.83$, for a form factor $\Lambda = 2$ TeV.

[17] ABAZOV 08R use 0.7 fb^{-1} $p\overline{p}$ data at $\sqrt{s} = 1.96$ TeV to select 263 $W\gamma + X$ events, of which 187 constitute signal, with the W decaying into an electron or a muon, which is required to be well separated from a photon with $E_T > 9$ GeV. A likelihood fit to the photon E_T spectrum yields a 95% CL limit $0.49 < \kappa_\gamma < 1.51$ with other couplings fixed to their Standard Model values.

[18] ABDALLAH 08C determine this triple gauge coupling from the measurement of the spin density matrix elements in $e^+e^- \rightarrow W^+W^- \rightarrow (qq)(\ell\nu)$, where $\ell = e$ or μ. Values of all other couplings are fixed to their standard model values.

[19] AALTONEN 07L set limits on anomalous TGCs using the $p_T(W)$ distribution in WW and WZ production with the W decaying to an electron or muon and the Z to 2 jets. Setting other couplings to their standard model value, the 95% C.L. limits are $0.54 < \kappa_\gamma < 1.39$ for a form factor scale $\Lambda = 1.5$ TeV.

[20] ABAZOV 06H study $\overline{p}p \rightarrow WW$ production with a subsequent decay $WW \rightarrow e^+\nu_e e^-\overline{\nu}_e$, $WW \rightarrow e^\pm\nu_e\mu^\mp\nu_\mu$ or $WW \rightarrow \mu^+\nu_\mu\mu^-\overline{\nu}_\mu$. The 95% C.L. limit for a form factor scale $\Lambda = 1$ TeV is $-0.05 < \kappa_\gamma < 2.29$, fixing λ_γ=0. With the assumption that the $WW\gamma$ and WWZ couplings are equal the 95% C.L. one-dimensional limit ($\Lambda = 2$ TeV) is $0.68 < \kappa < 1.45$.

[21] ABAZOV 05J perform a likelihood fit to the photon E_T spectrum of $W\gamma$ + X events, where the W decays to an electron or muon which is required to be well separated from the photon. For $\Lambda = 2.0$ TeV the 95% CL limits are $0.12 < \kappa_\gamma < 1.96$. In the fit λ_γ is kept fixed to its Standard Model value.

[22] ABREU 01I combine results from e^+e^- interactions at 189 GeV leading to W^+W^-, $We\nu_e$, and $\nu\overline{\nu}\gamma$ final states with results from ABREU 99L at 183 GeV. The 95% confidence interval is $0.87 < \kappa_\gamma < 1.68$.

[23] BREITWEG 00 search for W production in events with large hadronic p_T. For p_T >20 GeV, the upper limit on the cross section gives the 95%CL limit $-3.7 < \kappa_\gamma < 2.5$ (for λ_γ=0).

[24] ABBOTT 99I perform a simultaneous fit to the $W\gamma$, $WW \rightarrow$ dilepton, $WW/WZ \rightarrow e\nu jj$, $WW/WZ \rightarrow \mu\nu jj$, and $WZ \rightarrow$ trilepton data samples. For $\Lambda = 2.0$ TeV, the 95%CL limits are $0.75 < \kappa_\gamma < 1.39$.

λ_γ

OUR FIT below is taken from [SCHAEL 13A].

VALUE	EVTS	DOCUMENT ID		TECN	COMMENT
−0.022±0.019 OUR FIT					
0.002±0.035	7872	[1] ABDALLAH	10	DLPH	E_{cm}^{ee}= 189–209 GeV
−0.012±0.027±0.011	10689	[2] SCHAEL	05A	ALEP	E_{cm}^{ee}= 183–209 GeV
$-0.060^{+0.034}_{-0.033}$	9800	[3] ABBIENDI	04D	OPAL	E_{cm}^{ee}= 183–209 GeV
$-0.021^{+0.035}_{-0.034}$±0.017	10575	[4] ACHARD	04D	L3	E_{cm}^{ee}= 161–209 GeV
• • • We do not use the following data for averages, fits, limits, etc. • • •					
0.00 ±0.06	53	[5] CHATRCHYAN	14AB	CMS	E_{cm}^{pp} = 7 TeV
		[6] AAD	13AN	ATLS	E_{cm}^{pp} = 7 TeV
		[7] ABAZOV	12AG	D0	$E_{cm}^{p\overline{p}}$ = 1.96 TeV
		[8] ABAZOV	11AC	D0	$E_{cm}^{p\overline{p}}$ = 1.96 TeV
		[9] CHATRCHYAN	11M	CMS	E_{cm}^{pp} = 7 TeV
		[10] AARON	09B	H1	E_{cm}^{ep} = 0.3 TeV
0.00 ±0.06		[11] ABAZOV	09AD	D0	$E_{cm}^{p\overline{p}}$ = 1.96 TeV
		[12] ABAZOV	09AJ	D0	$E_{cm}^{p\overline{p}}$ = 1.96 TeV
		[13] ABAZOV	08R	D0	$E_{cm}^{p\overline{p}}$ = 1.96 TeV
$0.16\ ^{+0.12}_{-0.13}$	1880	[14] ABDALLAH	08C	DLPH	Superseded by ABDALLAH 10
	1617	[15] AALTONEN	07L	CDF	$E_{cm}^{p\overline{p}}$ = 1.96 GeV
	17	[16] ABAZOV	06H	D0	$E_{cm}^{p\overline{p}}$ = 1.96 TeV
	141	[17] ABAZOV	05J	D0	$E_{cm}^{p\overline{p}}$ = 1.96 TeV
0.05 ±0.09 ±0.01	2298	[18] ABREU	01I	DLPH	E_{cm}^{ee}= 183+189 GeV
		[19] BREITWEG	00	ZEUS	$e^+p \rightarrow e^+W^\pm$X, $\sqrt{s} \approx$ 300 GeV
$0.00\ ^{+0.10}_{-0.09}$	331	[20] ABBOTT	99I	D0	$E_{cm}^{p\overline{p}}$ = 1.8 TeV

[1] ABDALLAH 10 use data on the final states $e^+e^- \rightarrow jj\ell\nu$, $jjjj$, jjX, ℓX, at center-of-mass energies between 189–209 GeV at LEP2, where j = jet, ℓ = lepton, and X represents missing momentum. The fit is carried out keeping all other parameters fixed at their SM values.

[2] SCHAEL 05A study single–photon, single–W, and WW–pair production from 183 to 209 GeV. Each parameter is determined from a single–parameter fit in which the other parameters assume their Standard Model values.

[3] ABBIENDI 04D combine results from W^+W^- in all decay channels. Only CP-conserving couplings are considered and each parameter is determined from a single-parameter fit in which the other parameters assume their Standard Model values. The 95% confidence interval is $-0.13 < \lambda_\gamma < 0.01$.

[4] ACHARD 04D study WW–pair production, single–W production and single–photon production with missing energy from 189 to 209 GeV. The result quoted here is obtained including data from 161 to 183 GeV, ACCIARRI 99Q. Each parameter is determined from a single–parameter fit in which the other parameters assume their Standard Model values.

[5] CHATRCHYAN 14AB measure $W\gamma$ production cross section for $p_T^\gamma > 15$ GeV and R($\ell\gamma$) > 0.7, which is the separation between the γ and the final state charged lepton (e or μ) in the azimuthal angle-pseudorapidity ($\phi - \eta$) plane. After background subtraction the number of $e\nu\gamma$ and $\mu\nu\gamma$ events is determined to be 3200 ± 325 and 4970 ± 543 respectively, compatible with expectations from the SM. This leads to a 95% CL limit of $-0.050 < \lambda_\gamma < 0.037$, assuming all other parameters have SM values.

[6] AAD 13AN study $W\gamma$ production in pp collisions. In events with no additional jet, 4449 (6578) W decays to electron (muon) are selected, with an expected background of 1662 ± 262 (2538 ± 362) events. Analysing the photon p_T spectrum above 100 GeV yields a 95% C.L. limit of $-0.065 < \lambda_\gamma < 0.061$. Supersedes AAD 12BX.

[7] ABAZOV 12AG combine new results with already published results on $W\gamma$, WW and WZ production in order to determine the couplings with increased precision, superseding ABAZOV 08R, ABAZOV 11AC, ABAZOV 09AJ, ABAZOV 09AD. The 68% C.L. result for a formfactor cutoff of $\Lambda = 2$ TeV is $\lambda_\gamma = 0.007^{+0.021}_{-0.022}$.

[8] ABAZOV 11AC study $W\gamma$ production in $p\overline{p}$ collisions at 1.96 TeV, with the W decay products containing an electron or a muon. They select 196 (363) events in the electron (muon) mode, with a SM expectation of 190 (372) events. A likelihood fit to the photon E_T spectrum above 15 GeV yields at 95% C.L. the result: $-0.08 < \lambda_\gamma < 0.07$ for a formfactor $\Lambda = 2$ TeV.

[9] CHATRCHYAN 11M study $W\gamma$ production in pp collisions at $\sqrt{s} = 7$ TeV using 36 pb^{-1} pp data with the W decaying to electron and muon. The total cross section is measured for photon transverse energy $E_T^\gamma > 10$ GeV and spatial separation from charged leptons in the plane of pseudo rapidity and azimuthal angle $\Delta R(\ell,\gamma) > 0.7$. The number of candidate (background) events is 452 (228 ± 21) for the electron channel and 520 (277 ± 25) for the muon channel. Setting other couplings to their standard model value, they derive a 95% CL limit of $-0.18 < \lambda_\gamma < 0.17$.

[10] AARON 09B study single-W production in ep collisions at 0.3 TeV C.M. energy. They select 53 $W \rightarrow e/\mu$ events with a standard model expectation of 54.1 ± 7.4 events. Fitting the transverse momentum spectrum of the hadronic recoil system they obtain a 95% C.L. limit of $-2.5 < \lambda_\gamma < 2.5$.

[11] ABAZOV 09AD study the $p\overline{p} \rightarrow \ell\nu$ 2jet process arising in WW and WZ production. They select 12,473 (14,392) events in the electron (muon) channel with an expected di-boson signal of 436 (527) events. The results on the anomalous couplings are derived from an analysis of the p_T spectrum of the 2-jet system and quoted at 68% C.L. and for a form factor of 2 TeV. This measurement is not used for obtaining the mean as it is for a specific form factor. The 95% confidence interval is $-0.10 < \lambda_\gamma < 0.11$.

[12] ABAZOV 09AJ study the $p\overline{p} \rightarrow 2\ell 2\nu$ process arising in WW production. They select 100 events with an expected WW signal of 65 events. An analysis of the p_T spectrum of the two charged leptons leads to 95% C.L. limits of $-0.14 < \lambda_\gamma < 0.18$, for a form factor $\Lambda = 2$ TeV.

[13] ABAZOV 08R use 0.7 fb^{-1} $p\overline{p}$ data at $\sqrt{s} = 1.96$ TeV to select 263 $W\gamma + X$ events, of which 187 constitute signal, with the W decaying into an electron or a muon, which is required to be well separated from a photon with $E_T > 9$ GeV. A likelihood fit to the photon E_T spectrum yields a 95% CL limit $-0.12 < \lambda_\gamma < 0.13$ with other couplings fixed to their Standard Model values.

[14] ABDALLAH 08C determine this triple gauge coupling from the measurement of the spin density matrix elements in $e^+e^- \rightarrow W^+W^- \rightarrow (qq)(\ell\nu)$, where $\ell = e$ or μ. Values of all other couplings are fixed to their standard model values.

[15] AALTONEN 07L set limits on anomalous TGCs using the $p_T(W)$ distribution in WW and WZ production with the W decaying to an electron or muon and the Z to 2 jets. Setting other couplings to their standard model value, the 95% C.L. limits are $-0.18 < \lambda_\gamma < 0.17$ for a form factor scale $\Lambda = 1.5$ TeV.

[16] ABAZOV 06H study $\overline{p}p \rightarrow WW$ production with a subsequent decay $WW \rightarrow e^+\nu_e e^-\overline{\nu}_e$, $WW \rightarrow e^\pm\nu_e\mu^\mp\nu_\mu$ or $WW \rightarrow \mu^+\nu_\mu\mu^-\overline{\nu}_\mu$. The 95% C.L. limit for a form factor scale $\Lambda = 1$ TeV is $-0.97 < \lambda_\gamma < 1.04$, fixing κ_γ=1. With the assumption that the $WW\gamma$ and WWZ couplings are equal the 95% C.L. one-dimensional limit ($\Lambda = 2$ TeV) is $-0.29 < \lambda < 0.30$.

[17] ABAZOV 05J perform a likelihood fit to the photon E_T spectrum of $W\gamma$ + X events, where the W decays to an electron or muon which is required to be well separated from

the photon. For $\Lambda = 2.0$ TeV the 95% CL limits are $-0.20 < \lambda_\gamma < 0.20$. In the fit κ_γ is kept fixed to its Standard Model value.

[18] ABREU 01I combine results from e^+e^- interactions at 189 GeV leading to W^+W^-, $We\nu_e$, and $\nu\overline{\nu}\gamma$ final states with results from ABREU 99L at 183 GeV. The 95% confidence interval is $-0.11 < \lambda_\gamma < 0.23$.

[19] BREITWEG 00 search for W production in events with large hadronic p_T. For p_T >20 GeV, the upper limit on the cross section gives the 95%CL limit $-3.2 < \lambda_\gamma < 3.2$ for κ_γ fixed to its Standard Model value.

[20] ABBOTT 99I perform a simultaneous fit to the $W\gamma$, $WW \to$ dilepton, $WW/WZ \to e\nu jj$, $WW/WZ \to \mu\nu jj$, and $WZ \to$ trilepton data samples. For $\Lambda = 2.0$ TeV, the 95%CL limits are $-0.18 < \lambda_\gamma < 0.19$.

κ_Z

This coupling is *CP*-conserving (*C*- and *P*- separately conserving).

VALUE	EVTS	DOCUMENT ID		TECN	COMMENT
$\mathbf{0.924^{+0.059}_{-0.056} \pm 0.024}$	7171	[1] ACHARD	04D	L3	$E^{ee}_{\rm cm}$ = 189–209 GeV

• • • We do not use the following data for averages, fits, limits, etc. • • •

		[2] AABOUD	17S	ATLS	$E^{pp}_{\rm cm}$ = 7+8 TeV
		[3] KHACHATRY...17O		CMS	$E^{pp}_{\rm cm}$ = 8 TeV
		[4] AAD	16AR	ATLS	$E^{pp}_{\rm cm}$ = 8 TeV
		[5] AAD	16P	ATLS	$E^{pp}_{\rm cm}$ = 8 TeV
		[6] AAD	13AL	ATLS	$E^{pp}_{\rm cm}$ = 7 TeV
		[7] AAD	12CD	ATLS	$E^{pp}_{\rm cm}$ = 7 TeV
		[8] AALTONEN	12AC	CDF	$E^{p\overline{p}}_{\rm cm}$ = 1.96 TeV
34		[9] ABAZOV	11	D0	$E^{p\overline{p}}_{\rm cm}$ = 1.96 TeV
17		[10] ABAZOV	06H	D0	$E^{p\overline{p}}_{\rm cm}$ = 1.96 TeV
2.3		[11] ABAZOV	05S	D0	$E^{p\overline{p}}_{\rm cm}$ = 1.96 TeV

[1] ACHARD 04D study WW–pair production, single–W production and single–photon production with missing energy from 189 to 209 GeV. The result quoted here is obtained using the WW–pair production sample. Each parameter is determined from a single–parameter fit in which the other parameters assume their Standard Model values.

[2] AABOUD 17S analyze electroweak production of a W boson in association with two jets at high dijet invariant mass, with the W boson decaying to electron or muon plus neutrino. In the signal region of dijet mass larger than 1 TeV and leading-jet transverse momentum larger than 600 GeV, 30 events are observed in the data with 39 ± 4 events expected in the Standard Model, yielding the following limit at 95% CL for the form factor cut-off scale $\Lambda_{FF} \to \infty$: $0.85 < \kappa_Z < 1.16$.

[3] KHACHATRYAN 17O analyse WZ production where each boson decays into electrons or muons. Events are required to have a tri-lepton invariant mass larger than 100 GeV, with one of the lepton pairs having an invariant mass within 20 GeV of the Z boson mass. The Z transverse momentum spectrum is analyzed to set a 95% C.L. limit of: $0.79 < \kappa_Z < 1.25$.

[4] AAD 16AR study WW production in pp collisions and select 6636 WW candidates in decay modes with electrons or muons with an expected background of 1546 ± 157 events. Assuming the LEP formulation and setting the form-factor Λ to infinity, a fit to the transverse momentum distribution of the leading charged lepton, leads to a 95% C.L. range of $0.975 < \kappa_Z < 1.020$.

[5] AAD 16P study WZ production in pp collisions and select 2091 WZ candidates in 4 decay modes with electrons and muons, with an expected background of 1825 ± 7 events. Analyzing the WZ transverse momentum distribution, the resulting 95% C.L. limit is: $0.81 < \kappa_Z < 1.30$.

[6] AAD 13AL study WW production in pp collisions and select 1325 WW candidates in decay modes with electrons or muons with an expected background of 369 ± 61 events. Assuming the LEP formulation and setting the form-factor Λ = infinity, a fit to the transverse momentum distribution of the leading charged lepton, leads to a 95% C.L. range of $0.957 < \kappa_Z < 1.043$. Supersedes AAD 12AC.

[7] AAD 12CD study WZ production in pp collisions and select 317 WZ candidates in three $\ell\nu$ decay modes with an expected background of 68.0 ± 10.0 events. The resulting 95% C.L. range is: $0.63 < \kappa_Z < 1.57$. Supersedes AAD 12V.

[8] AALTONEN 12AC study WZ production in $p\overline{p}$ collisions and select 63 WZ candidates in three $\ell\nu$ decay modes with an expected background of 7.9 ± 1.0 events. Based on the cross section and shape of the Z transverse momentum spectrum, the following 95% C.L. range is reported: $0.61 < \kappa_Z < 1.90$ for a form factor of $\Lambda = 2$ TeV.

[9] ABAZOV 11 study the $p\overline{p} \to 3\ell\nu$ process arising in WZ production. They observe 34 WZ candidates with an estimated background of 6 events. An analysis of the p_T spectrum of the Z boson leads to a 95% C.L. limit of $0.600 < \kappa_Z < 1.675$, for a form factor $\Lambda = 2$ TeV.

[10] ABAZOV 06H study $\overline{p}p \to WW$ production with a subsequent decay $WW \to e^+\nu_e e^-\overline{\nu}_e$, $WW \to e^\pm\nu_e\mu^\mp\nu_\mu$ or $WW \to \mu^+\nu_\mu\mu^-\overline{\nu}_\mu$. The 95% C.L. limit for a form factor scale $\Lambda = 2$ TeV is $0.55 < \kappa_Z < 1.55$, fixing λ_Z=0. With the assumption that the $WW\gamma$ and WWZ couplings are equal the 95% C.L. one-dimensional limit ($\Lambda = 2$ TeV) is $0.68 < \kappa < 1.45$.

[11] ABAZOV 05S study $\overline{p}p \to WZ$ production with a subsequent trilepton decay to $\ell\nu\ell'\overline{\ell}'$ (ℓ and $\ell' = e$ or μ). Three events (estimated background 0.71 ± 0.08 events) with WZ decay characteristics are observed from which they derive limits on the anomalous WWZ couplings. The 95% CL limit for a form factor scale $\Lambda = 1$ TeV is $-1.0 < \kappa_Z < 3.4$, fixing λ_Z and g_1^Z to their Standard Model values.

λ_Z

This coupling is *CP*-conserving (*C*- and *P*- separately conserving).

VALUE	EVTS	DOCUMENT ID		TECN	COMMENT
$\mathbf{-0.088^{+0.060}_{-0.057} \pm 0.023}$	7171	[1] ACHARD	04D	L3	$E^{ee}_{\rm cm}$ = 189–209 GeV

• • • We do not use the following data for averages, fits, limits, etc. • • •

		[2] AABOUD	17S	ATLS	$E^{pp}_{\rm cm}$ = 7+8 TeV
		[3] AABOUD	17U	ATLS	$E^{pp}_{\rm cm}$ = 8 TeV
		[4] KHACHATRY...17O		CMS	$E^{pp}_{\rm cm}$ = 8 TeV
		[5] SIRUNYAN	17X		$E^{pp}_{\rm cm}$ = 8 TeV
		[6] AAD	16AR	ATLS	$E^{pp}_{\rm cm}$ = 8 TeV
		[7] AAD	16P	ATLS	$E^{pp}_{\rm cm}$ = 8 TeV
		[8] AAD	14Y	ATLS	$E^{pp}_{\rm cm}$ = 8 TeV
		[9] AAD	13AL	ATLS	$E^{pp}_{\rm cm}$ = 7 TeV
		[10] CHATRCHYAN	13BF	CMS	$E^{pp}_{\rm cm}$ = 7 TeV
		[11] AAD	12CD	ATLS	$E^{pp}_{\rm cm}$ = 7 TeV
		[12] AALTONEN	12AC	CDF	$E^{p\overline{p}}_{\rm cm}$ = 1.96 TeV
34		[13] ABAZOV	11	D0	$E^{p\overline{p}}_{\rm cm}$ = 1.96 TeV
334		[14] AALTONEN	10K	CDF	$E^{p\overline{p}}_{\rm cm}$ = 1.96 TeV
13		[15] ABAZOV	07Z	D0	$E^{p\overline{p}}_{\rm cm}$ = 1.96 TeV
17		[16] ABAZOV	06H	D0	$E^{p\overline{p}}_{\rm cm}$ = 1.96 TeV
2.3		[17] ABAZOV	05S	D0	$E^{p\overline{p}}_{\rm cm}$ = 1.96 TeV

[1] ACHARD 04D study WW–pair production, single–W production and single–photon production with missing energy from 189 to 209 GeV. The result quoted here is obtained using the WW–pair production sample. Each parameter is determined from a single–parameter fit in which the other parameters assume their Standard Model values.

[2] AABOUD 17S analyze electroweak production of a W boson in association with two jets at high dijet invariant mass, with the W boson decaying to electron or muon plus neutrino. In the signal region of dijet mass larger than 1 TeV and leading-jet transverse momentum larger than 600 GeV, 30 events are observed in the data with 39 ± 4 events expected in the Standard Model, yielding the following limit at 95% CL for the form factor cut-off scale $\Lambda_{FF} \to \infty$: $-0.053 < \lambda_Z < 0.042$.

[3] AABOUD 17U analyze production of WW or WZ boson pairs with one W boson decaying to electron or muon plus neutrino, and the other W or Z boson decaying hadronically. The hadronic decay system is reconstructed as either a resolved two-jet system or as a single large jet. Analysing the transverse momentum distribution of the hadronic system above 100 GeV yields the following limit at 95% CL for the form factor cut-off scale $\Lambda_{FF} \to \infty$: $-0.013 < \lambda_Z < 0.013$.

[4] KHACHATRYAN 17O analyse WZ production where each boson decays into electrons or muons. Events are required to have a tri-lepton invariant mass larger than 100 GeV, with one of the lepton pairs having an invariant mass within 20 GeV of the Z boson mass. The Z transverse momentum spectrum is analyzed to set a 95% C.L. limit of: $-0.018 < \lambda_Z < 0.016$.

[5] SIRUNYAN 17X study $pp \to WW/WZ \to \ell\nu q\overline{q}$ production at 8 TeV where ℓ is an electron or muon with p_T > 30 or 25 GeV respectively. Suitable cuts are put on the p_T of the dijet system and the missing E_T of the event yielding a total of 285 and 204 WV events observed in the electron and muon channels. The following 95% C.L. limit is obtained: $-0.011 < \lambda_Z < 0.011$.

[6] AAD 16AR study WW production in pp collisions and select 6636 WW candidates in decay modes with electrons or muons with an expected background of 1546 ± 157 events. Assuming the LEP formulation and setting the form-factor Λ to infinity, a fit to the transverse momentum distribution of the leading charged lepton, leads to a 95% C.L. range of $-0.019 < \lambda_Z < 0.019$.

[7] AAD 16P study WZ production in pp collisions and select 2091 WZ candidates in 4 decay modes with electrons and muons, with an expected background of 1825 ± 7 events. Analyzing the WZ transverse momentum distribution, the resulting 95% C.L. limit is: $-0.016 < \lambda_Z < 0.016$.

[8] AAD 14Y determine the electroweak Z-dijet cross section in 8 TeV pp collisions. $Z \to ee$ and $Z \to \mu\mu$ decays are selected with the di-lepton $p_T > 20$ GeV and mass in the 81–101 GeV range. Minimum two jets are required with $p_T > 55$ and 45 GeV and no additional jets with $p_T > 25$ GeV in the rapidity interval between them. The normalized p_T balance between the Z and the two jets is required to be < 0.15. This leads to a selection of 900 events with dijet mass > 1 TeV. The number of signal and background events expected is 261 and 592 respectively. A Poisson likelihood method is used on an event by event basis to obtain the 95% CL limit $-0.15 < \lambda_Z < 0.13$ for a form factor value $\Lambda = \infty$.

[9] AAD 13AL study WW production in pp collisions and select 1325 WW candidates in decay modes with electrons or muons with an expected background of 369 ± 61 events. Assuming the LEP formulation and setting the form-factor Λ = infinity, a fit to the transverse momentum distribution of the leading charged lepton, leads to a 95% C.L. range of $-0.062 < \lambda_Z < 0.059$. Supersedes AAD 12AC.

[10] CHATRCHYAN 13BF determine the W^+W^- production cross section using unlike sign di-lepton (e or μ) events with high $\not{p}_T$. The leptons have $p_T > 20$ GeV/c and are isolated. 1134 candidate events are observed with an expected SM background of 247 ± 34. The p_T distribution of the leading lepton is fitted to obtain 95% C.L. limits of $-0.048 \leq \lambda_Z \leq 0.048$.

[11] AAD 12CD study WZ production in pp collisions and select 317 WZ candidates in three $\ell\nu$ decay modes with an expected background of 68.0 ± 10.0 events. The resulting 95% C.L. range is: $-0.046 < \lambda_Z < 0.047$. Supersedes AAD 12V.

[12] AALTONEN 12AC study WZ production in $p\overline{p}$ collisions and select 63 WZ candidates in three $\ell\nu$ decay modes with an expected background of 7.9 ± 1.0 events. Based on the cross section and shape of the Z transverse momentum spectrum, the following 95% C.L. range is reported: $-0.08 < \lambda_Z < 0.10$ for a form factor of $\Lambda = 2$ TeV.

[13] ABAZOV 11 study the $p\overline{p} \to 3\ell\nu$ process arising in WZ production. They observe 34 WZ candidates with an estimated background of 6 events. An analysis of the p_T spectrum of the Z boson leads to a 95% C.L. limit of $-0.077 < \lambda_Z < 0.093$, for a form factor $\Lambda = 2$ TeV.

[14] AALTONEN 10K study $p\overline{p} \to W^+W^-$ with $W \to e/\mu\nu$. The p_T of the leading (second) lepton is required to be > 20 (10) GeV. The final number of events selected is 654 of which 320 ± 47 are estimated to be background. The 95% C.L. interval is $-0.16 < \lambda_Z < 0.16$ for $\Lambda = 1.5$ TeV and $-0.14 < \lambda_Z < 0.15$ for $\Lambda = 2$ TeV.

[15] ABAZOV 07Z set limits on anomalous TGCs using the measured cross section and $p_T(Z)$ distribution in WZ production with both the W and the Z decaying leptonically into electrons and muons. Setting the other couplings to their standard model values, the 95% C.L. limit for a form factor scale $\Lambda = 2$ TeV is $-0.17 < \lambda_Z < 0.21$.

[16] ABAZOV 06H study $\overline{p}p \to WW$ production with a subsequent decay $WW \to e^+\nu_e e^-\overline{\nu}_e$, $WW \to e^\pm\nu_e\mu^\mp\nu_\mu$ or $WW \to \mu^+\nu_\mu\mu^-\overline{\nu}_\mu$. The 95% C.L. limit for

a form factor scale $\Lambda = 2$ TeV is $-0.39 < \lambda_Z < 0.39$, fixing κ_Z=1. With the assumption that the $WW\gamma$ and WWZ couplings are equal the 95% C.L. one-dimensional limit ($\Lambda = 2$ TeV) is $-0.29 < \lambda < 0.30$.

[17] ABAZOV 05S study $\overline{p}p \to WZ$ production with a subsequent trilepton decay to $\ell\nu\ell'\overline{\ell}'$ (ℓ and $\ell' = e$ or μ). Three events (estimated background 0.71 ± 0.08 events) with WZ decay characteristics are observed from which they derive limits on the anomalous WWZ couplings. The 95% CL limit for a form factor scale $\Lambda = 1.5$ TeV is $-0.48 < \lambda_Z < 0.48$, fixing g_1^Z and κ_Z to their Standard Model values.

g_5^Z

This coupling is *CP*-conserving but *C*- and *P*-violating.

VALUE	EVTS	DOCUMENT ID		TECN	COMMENT
-0.07 ± 0.09 OUR AVERAGE		Error includes scale factor of 1.1.			
$-0.04^{+0.13}_{-0.12}$	9800	[1] ABBIENDI	04D	OPAL	$E_{\rm cm}^{ee} = 183$–209 GeV
$0.00 \pm 0.13 \pm 0.05$	7171	[2] ACHARD	04D	L3	$E_{\rm cm}^{ee} = 189$–209 GeV
$-0.44^{+0.23}_{-0.22} \pm 0.12$	1154	[3] ACCIARRI	99Q	L3	$E_{\rm cm}^{ee} = 161+172+183$ GeV
• • • We do not use the following data for averages, fits, limits, etc. • • •					
-0.31 ± 0.23		[4] EBOLI	00	THEO	LEP1, SLC+ Tevatron

[1] ABBIENDI 04D combine results from W^+W^- in all decay channels. Only *CP*-conserving couplings are considered and each parameter is determined from a single-parameter fit in which the other parameters assume their Standard Model values. The 95% confidence interval is $-0.28 < g_5^Z < +0.21$.

[2] ACHARD 04D study WW–pair production, single–W production and single–photon production with missing energy from 189 to 209 GeV. The result quoted here is obtained using the WW–pair production sample. Each parameter is determined from a single–parameter fit in which the other parameters assume their Standard Model values.

[3] ACCIARRI 99Q study W-pair, single-W, and single photon events.

[4] EBOLI 00 extract this indirect value of the coupling studying the non-universal one-loop contributions to the experimental value of the $Z \to b\overline{b}$ width (Λ=1 TeV is assumed).

g_4^Z

This coupling is *CP*-violating (*C*-violating and *P*-conserving).

VALUE	EVTS	DOCUMENT ID		TECN	COMMENT
-0.30 ± 0.17 OUR AVERAGE					
$-0.39^{+0.19}_{-0.20}$	1880	[1] ABDALLAH	08C	DLPH	$E_{\rm cm}^{ee} = 189$–209 GeV
$-0.02^{+0.32}_{-0.33}$	1065	[2] ABBIENDI	01H	OPAL	$E_{\rm cm}^{ee} = 189$ GeV

[1] ABDALLAH 08C determine this triple gauge coupling from the measurement of the spin density matrix elements in $e^+e^- \to W^+W^- \to (q\overline{q})(\ell\nu)$, where $\ell = e$ or μ. Values of all other couplings are fixed to their standard model values.

[2] ABBIENDI 01H study W-pair events, with one leptonically and one hadronically decaying W. The coupling is extracted using information from the W production angle together with decay angles from the leptonically decaying W.

$\tilde{\kappa}_Z$

This coupling is *CP*-violating (*C*-conserving and *P*-violating).

VALUE	EVTS	DOCUMENT ID		TECN	COMMENT
$-0.12^{+0.06}_{-0.04}$ OUR AVERAGE					
$-0.09^{+0.08}_{-0.05}$	1880	[1] ABDALLAH	08C	DLPH	$E_{\rm cm}^{ee} = 189$–209 GeV
$-0.20^{+0.10}_{-0.07}$	1065	[2] ABBIENDI	01H	OPAL	$E_{\rm cm}^{ee} = 189$ GeV
• • • We do not use the following data for averages, fits, limits, etc. • • •					
		[3] AABOUD	17S	ATLS	$E_{\rm cm}^{pp} = 7+8$ TeV
		[4] BLINOV	11	LEP	$E_{\rm cm}^{ee} = 183$–207 GeV

[1] ABDALLAH 08C determine this triple gauge coupling from the measurement of the spin density matrix elements in $e^+e^- \to W^+W^- \to (q\overline{q})(\ell\nu)$, where $\ell = e$ or μ. Values of all other couplings are fixed to their standard model values.

[2] ABBIENDI 01H study W-pair events, with one leptonically and one hadronically decaying W. The coupling is extracted using information from the W production angle together with decay angles from the leptonically decaying W.

[3] AABOUD 17S analyze electroweak production of a W boson in association with two jets at high dijet invariant mass, with the W boson decaying to electron or muon plus neutrino. In the signal region of dijet mass larger than 1 TeV and leading-jet transverse momentum larger than 600 GeV, 30 events are observed in the data with 39 ± 4 events expected in the Standard Model, yielding the following limit at 95% CL for the form factor cut-off scale $\Lambda_{FF} \to \infty$: $-0.56 < \tilde{\kappa}_Z < 0.56$.

[4] BLINOV 11 use the LEP-average $e^+e^- \to W^+W^-$ cross section data for $\sqrt{s} =$ 183–207 GeV to determine an upper limit on the TGC $\tilde{\kappa}_Z$. The average values of the cross sections as well as their correlation matrix, and standard model expectations of the cross sections are taken from the LEPEWWG note hep-ex/0612034. At 95% confidence level $|\tilde{\kappa}_Z| < 0.13$.

$\tilde{\lambda}_Z$

This coupling is *CP*-violating (*C*-conserving and *P*-violating).

VALUE	EVTS	DOCUMENT ID		TECN	COMMENT
-0.09 ± 0.07 OUR AVERAGE					
-0.08 ± 0.07	1880	[1] ABDALLAH	08C	DLPH	$E_{\rm cm}^{ee} = 189$–209 GeV
$-0.18^{+0.24}_{-0.16}$	1065	[2] ABBIENDI	01H	OPAL	$E_{\rm cm}^{ee} = 189$ GeV
• • • We do not use the following data for averages, fits, limits, etc. • • •					
		[3] AABOUD	17S	ATLS	$E_{\rm cm}^{pp} = 7+8$ TeV
		[4] BLINOV	11	LEP	$E_{\rm cm}^{ee} = 183$–207 GeV

[1] ABDALLAH 08C determine this triple gauge coupling from the measurement of the spin density matrix elements in $e^+e^- \to W^+W^- \to (q\overline{q})(\ell\nu)$, where $\ell = e$ or μ. Values of all other couplings are fixed to their standard model values.

[2] ABBIENDI 01H study W-pair events, with one leptonically and one hadronically decaying W. The coupling is extracted using information from the W production angle together with decay angles from the leptonically decaying W.

[3] AABOUD 17S analyze electroweak production of a W boson in association with two jets at high dijet invariant mass, with the W boson decaying to electron or muon plus neutrino. In the signal region of dijet mass larger than 1 TeV and leading-jet transverse momentum larger than 600 GeV, 30 events are observed in the data with 39 ± 4 events expected in the Standard Model, yielding the following limit at 95% CL for the form factor cut-off scale $\Lambda_{FF} \to \infty$: $-0.047 < \tilde{\lambda}_Z < 0.046$.

[4] BLINOV 11 use the LEP-average $e^+e^- \to W^+W^-$ cross section data for $\sqrt{s} =$ 183–207 GeV to determine an upper limit on the TGC $\tilde{\lambda}_Z$. The average values of the cross sections as well as their correlation matrix, and standard model expectations of the cross sections are taken from the LEPEWWG note hep-ex/0612034. At 95% confidence level $|\tilde{\lambda}_Z| < 0.31$.

W ANOMALOUS MAGNETIC MOMENT

The full magnetic moment is given by $\mu_W = e(1+\kappa+\lambda)/2m_W$. In the Standard Model, at tree level, $\kappa = 1$ and $\lambda = 0$. Some papers have defined $\Delta\kappa = 1-\kappa$ and assume that $\lambda = 0$. Note that the electric quadrupole moment is given by $-e(\kappa-\lambda)/m_W^2$. A description of the parameterization of these moments and additional references can be found in HAGIWARA 87 and BAUR 88. The parameter Λ appearing in the theoretical limits below is a regularization cutoff which roughly corresponds to the energy scale where the structure of the W boson becomes manifest.

VALUE ($e/2m_W$)	EVTS	DOCUMENT ID		TECN	COMMENT
$2.22^{+0.20}_{-0.19}$	2298	[1] ABREU	01I	DLPH	$E_{\rm cm}^{ee} = 183+189$ GeV
• • • We do not use the following data for averages, fits, limits, etc. • • •					
		[2] ABE	95G	CDF	
		[3] ALITTI	92C	UA2	
		[4] SAMUEL	92	THEO	
		[5] SAMUEL	91	THEO	
		[6] GRIFOLS	88	THEO	
		[7] GROTCH	87	THEO	
		[8] VANDERBIJ	87	THEO	
		[9] GRAU	85	THEO	
		[10] SUZUKI	85	THEO	
		[11] HERZOG	84	THEO	

[1] ABREU 01I combine results from e^+e^- interactions at 189 GeV leading to W^+W^-, $We\nu_e$, and $\nu\overline{\nu}\gamma$ final states with results from ABREU 99L at 183 GeV to determine Δg_1^Z, $\Delta\kappa_\gamma$, and λ_γ. $\Delta\kappa_\gamma$ and λ_γ are simultaneously floated in the fit to determine μ_W.

[2] ABE 95G report $-1.3 < \kappa < 3.2$ for λ=0 and $-0.7 < \lambda < 0.7$ for κ=1 in $p\overline{p} \to e\nu_e\gamma$X and $\mu\nu_\mu\gamma$X at $\sqrt{s} = 1.8$ TeV.

[3] ALITTI 92C measure $\kappa = 1^{+2.6}_{-2.2}$ and $\lambda = 0^{+1.7}_{-1.8}$ in $p\overline{p} \to e\nu\gamma+$ X at $\sqrt{s} = 630$ GeV. At 95%CL they report $-3.5 < \kappa < 5.9$ and $-3.6 < \lambda < 3.5$.

[4] SAMUEL 92 use preliminary CDF and UA2 data and find $-2.4 < \kappa < 3.7$ at 96%CL and $-3.1 < \kappa < 4.2$ at 95%CL respectively. They use data for $W\gamma$ production and radiative W decay.

[5] SAMUEL 91 use preliminary CDF data for $p\overline{p} \to W\gamma$X to obtain $-11.3 \leq \Delta\kappa \leq 10.9$. Note that their $\kappa = 1-\Delta\kappa$.

[6] GRIFOLS 88 uses deviation from ρ parameter to set limit $\Delta\kappa \lesssim 65\ (M_W^2/\Lambda^2)$.

[7] GROTCH 87 finds the limit $-37 < \Delta\kappa < 73.5$ (90% CL) from the experimental limits on $e^+e^- \to \nu\overline{\nu}\gamma$ assuming three neutrino generations and $-19.5 < \Delta\kappa < 56$ for four generations. Note their $\Delta\kappa$ has the opposite sign as our definition.

[8] VANDERBIJ 87 uses existing limits to the photon structure to obtain $|\Delta\kappa| < 33\ (m_W/\Lambda)$. In addition VANDERBIJ 87 discusses problems with using the ρ parameter of the Standard Model to determine $\Delta\kappa$.

[9] GRAU 85 uses the muon anomaly to derive a coupled limit on the anomalous magnetic dipole and electric quadrupole (λ) moments $1.05 > \Delta\kappa\ \ln(\Lambda/m_W) + \lambda/2 > -2.77$. In the Standard Model $\lambda = 0$.

[10] SUZUKI 85 uses partial-wave unitarity at high energies to obtain $|\Delta\kappa| \lesssim 190\ (m_W/\Lambda)^2$. From the anomalous magnetic moment of the muon, SUZUKI 85 obtains $|\Delta\kappa| \lesssim 2.2/\ln(\Lambda/m_W)$. Finally SUZUKI 85 uses deviations from the ρ parameter and obtains a very qualitative, order-of-magnitude limit $|\Delta\kappa| \lesssim 150\ (m_W/\Lambda)^4$ if $|\Delta\kappa| \ll 1$.

[11] HERZOG 84 consider the contribution of W-boson to muon magnetic moment including anomalous coupling of $WW\gamma$. Obtain a limit $-1 < \Delta\kappa < 3$ for $\Lambda \gtrsim 1$ TeV.

c_{WWW}/Λ^2, c_W/Λ^2, c_B/Λ^2

These couplings are used in EFT-based approaches to anomalous couplings. They are linearly related to the couplings discussed above.

VALUE	DOCUMENT ID		TECN	COMMENT
• • • We do not use the following data for averages, fits, limits, etc. • • •				
	[1] AABOUD	17S	ATLS	$E_{\rm cm}^{pp} = 7+8$ TeV
	[2] AABOUD	17U	ATLS	$E_{\rm cm}^{pp} = 8$ TeV
	[3] KHACHATRY...	17O	CMS	$E_{\rm cm}^{pp} = 8$ TeV
	[4] SIRUNYAN	17X		$E_{\rm cm}^{pp} = 8$ TeV
	[5] AAD	16AR	ATLS	$E_{\rm cm}^{pp} = 8$ TeV
	[6] AAD	16P	ATLS	$E_{\rm cm}^{pp} = 8$ TeV
	[7] KHACHATRY...	16BI	CMS	$E_{\rm cm}^{pp} = 8$ TeV

[1] AABOUD 17S analyze electroweak production of a W boson in association with two jets at high dijet invariant mass, with the W boson decaying to electron or muon plus neutrino. In the signal region of dijet mass larger than 1 TeV and leading-jet transverse momentum larger than 600 GeV, 30 events are observed in the data with 39 ± 4 events expected in the Standard Model, yielding the following limits at 95% CL for the form factor cut-off scale $\Lambda_{FF} \to \infty$: $-33 < c_W/\Lambda^2 < 30$, $-170 < c_B/\Lambda^2 < 160$, $-13 < c_{WWW}/\Lambda^2 < 9$, $-580 < c_{\widetilde{W}}/\Lambda^2 < 580$, $-11 < c_{\widetilde{W}WW}/\Lambda^2 < 11$, in units of TeV^{-2}.

[2] AABOUD 17U analyze production of WW or WZ boson pairs with one W boson decaying to electron or muon plus neutrino, and the other W or Z boson decaying hadronically. The hadronic decay system is reconstructed as either a resolved two-jet system or as a single large jet. Analysing the transverse momentum distribution of the hadronic system above 100 GeV yields the following limits at 95% CL for the form factor cut-off scale $\Lambda_{FF} \to \infty$: $-3.1 < c_{WWW}/\Lambda^2 < 3.1$, $-19 < c_B/\Lambda^2 < 20$, $-5.1 < c_W/\Lambda^2 < 5.8$, in units of TeV^{-2}.

[3] KHACHATRYAN 17O analyse WZ production where each boson decays into electrons or muons. Events are required to have a tri-lepton invariant mass larger than 100 GeV, with one of the lepton pairs having an invariant mass within 20 GeV of the Z boson mass. The Z transverse momentum spectrum is analyzed to set 95% C.L. limits of: $-260 < c_B/\Lambda^2 < 210$, $-4.2 < c_W/\Lambda^2 < 8.0$, $-4.6 < c_{WWW}/\Lambda^2 < 4.2$, in units of TeV^{-2}.

[4] SIRUNYAN 17X study $pp \to WW/WZ \to \ell\nu q\overline{q}$ production at 8 TeV where ℓ is an electron or muon with $p_T > 30$ or 25 GeV respectively. Suitable cuts are put on the p_T of the dijet system and the missing E_T of the event yielding a total of 285 and 204 WV events observed in the electron and muon channels. The following 95% C.L. limits in units of TeV^{-2} are obtained: $-2.7 < c_{WWW}/\Lambda^2 < 2.7$, $-14 < c_B/\Lambda^2 < 17$, $-2.0 < c_W/\Lambda^2 < 5.7$.

[5] AAD 16AR study WW production in pp collisions and select 6636 WW candidates in decay modes with electrons or muons with an expected background of 1546 ± 157 events. Assuming an EFT formulation, a fit to the transverse momentum distribution of the leading charged lepton, leads to 95% C.L. ranges of: $-4.61 < c_{WWW}/\Lambda^2 < 4.60$, $-5.87 < c_W/\Lambda^2 < 10.54$ and $-20.9 < c_B/\Lambda^2 < 26.3$,in units of TeV^{-2}.

[6] AAD 16P study WZ production in pp collisions and select 2091 WZ candidates in 4 decay modes with electrons and muons, with an expected background of 1825 ± 7 events. Analyzing the WZ transverse momentum distribution, the resulting 95% C.L. limits are: $-3.9 < c_{WWW}/\Lambda^2 < 4.0$, $-4.3 < c_W/\Lambda^2 < 6.8$, and $-320 < c_B/\Lambda^2 < 210$, in units of TeV^{-2}.

[7] KHACHATRYAN 16BI determine the W^+W^- production cross section using unlike sign di-lepton (e or μ) events with high p_T. The leptons have $p_T > 20$ GeV/c and are isolated. Events are required to have no jets above p_T of 30 GeV/c. 4847 (2233) events are selected with different (same) flavor leptons, with an expected total background of 1179 ± 123 (643 ± 73) events. Analysing the di-lepton invariant mass spectrum, the following values are obtained: $c_{WWW}/\Lambda^2 = 0.1 \pm 3.2$, $c_W/\Lambda^2 = -3.6^{+5.0}_{-4.5}$ and $c_B/\Lambda^2 = -3.2^{+15.0}_{-14.5}$, in units of TeV^{-2}. The limits at 95% C.L. are: $-5.7 < c_{WWW}/\Lambda^2 < 5.9$, $-11.4 < c_W/\Lambda^2 < 5.4$ and $-29.2 < c_B/\Lambda^2 < 23.9$, in units of TeV^{-2}.

[8] CHATRCHYAN 14Q CMS
[9] ABAZOV 13D D0
[10] CHATRCHYAN 13AA CMS
[11] ABBIENDI 04B OPAL
[12] ABBIENDI 04L OPAL
[13] HEISTER 04A ALEP
[14] ABDALLAH 03I DLPH
[15] ACHARD 02F L3

[1] AABOUD 17AA analyze $W^\pm W^\pm$ production in association with two jets and W decay modes with electrons or muons. In the kinematic region of VBS the effect of anomalous QGCs is enhanced by requiring the transverse mass of the WW system to be larger than 400 GeV. In the data, 8 events are selected with a total background expected from SM processes of 3.8 ± 0.6 events. Assuming the other QGC coupling to have the SM value of zero, the observed event yield is used to determine 95% CL limits on the QGCs: $-0.14 < \alpha_4 < 0.15$ and $-0.22 < \alpha_5 < 0.22$. Supersedes AAD 14AM.

[2] AABOUD 17AG determine the $WW\gamma$ and $WZ\gamma$ cross sections in 8 TeV pp interactions by studying the final states $e\nu\mu\nu\gamma$ and $e\nu jj\gamma$ or $\mu\nu jj\gamma$. Upper limits on the production cross sections are derived in a fiducial region optimized for BSM physics. These are used to derive the following 95% C.L. upper limits for quartic couplings assuming the form scale factor, $\Lambda_{FF} = \infty$ (all in units of 10^3 TeV^{-4}): $-0.3 < f_{M,0}/\Lambda^4 < 0.3$, $-0.5 < f_{M,1}/\Lambda^4 < 0.5$, $-1.8 < f_{M,2}/\Lambda^4 < 1.8$, $-1.1 < f_{M,4}/\Lambda^4 < 1.1$, $-1.7 < f_{M,5}/\Lambda^4 < 1.7$, $-0.6 < f_{M,6}/\Lambda^4 < 0.6$, $-1.1 < f_{M,7}/\Lambda^4 < 1.1$, $-0.1 < f_{T,0}/\Lambda^4 < 0.1$, $-0.2 < f_{T,1}/\Lambda^4 < 0.2$, $-0.4 < f_{T,4}/\Lambda^4 < 0.4$, $-1.5 < f_{T,5}/\Lambda^4 < 1.6$, $-1.9 < f_{T,6}/\Lambda^4 < 1.9$, $-4.3 < f_{T,7}/\Lambda^4 < 4.3$.

[3] AABOUD 17D analyze electroweak diboson (WV, $V = W, Z$) production in association with a high-mass dijet system. In the data, 32 events are selected with an expected total background of 32 ± 12 events. Analysing the transverse mass distribution of the WV system, the following limits are set at 95% C.L.: $-0.024 < \alpha_4 < 0.030$ and $-0.028 < \alpha_5 < 0.033$.

[4] AABOUD 17J analyze the $Z\gamma$ production in association with a high-mass dijet system, with the Z boson decaying into a pair of electrons, muons, or neutrinos. In the charged lepton (neutrino) channel, events are selected with a dijet mass larger than 500 (600) GeV and a transverse photon energy larger than 250 (150) GeV, with 2 (4) events selected in the data and 0.30 ± 0.08 (1.6 ± 0.5) expected background events. The observed event yield is used to determine 95% CL limits as follows: $-4.1 \times 10^3 < f_{T,9}/\Lambda^4 < 4.2 \times 10^3$, $-1.9 \times 10^3 < f_{T,8}/\Lambda^4 < 2.1 \times 10^3$, $-1.9 \times 10^1 < f_{T,0}/\Lambda^4 < 1.6 \times 10^1$, $-1.6 \times 10^2 < f_{M,0}/\Lambda^4 < 1.8 \times 10^2$, $-3.5 \times 10^2 < f_{M,1}/\Lambda^4 < 3.4 \times 10^2$, $-8.9 \times 10^2 < f_{M,2}/\Lambda^4 < 8.9 \times 10^2$, $-1.7 \times 10^3 < f_{M,3}/\Lambda^4 < 1.7 \times 10^3$, in units of TeV^{-4} and without application of a form factor.

[5] AABOUD 17M analyze tri-boson $W^\pm W^\pm W^\mp$ production in decay channels with three charged leptons or two like-sign charged leptons with two jets, where the lepton can be an electron or muon. In the data, 24 tri-lepton events and 21 di-lepton plus jets events are selected, compared to a total event yield expected in the SM of 30.8 ± 3.0 and 21.9 ± 2.0, respectively. Analysing the tri-lepton transverse mass or the transverse momentum sum of the two leptons, two jets and the missing transverse energy, the following limits at 95% CL are derived for the form factor cut-off scale $\Lambda_{FF} \to \infty$: $-0.13 < f_{S,0}/\Lambda^4 < 0.18$, $-0.21 < f_{S,1}/\Lambda^4 < 0.27$, in units of 10^4 TeV^{-4}, which are converted into the following limits: $-0.49 < \alpha_4 < 0.75$ and $-0.48 < \alpha_5 < 0.62$.

[6] KHACHATRYAN 17AA analyse electroweak production of $Z\gamma$ in association with two hadronic jets, with the Z boson decaying to electron or muon pairs. Events with photon transverse momentum larger than 60 GeV and di-jet invariant mass larger than 400 GeV are selected. The $Z\gamma$ inavariant mass spectrum is analysed to set 95% C.L. limits as follows: $-71 < f_{M,0}/\Lambda^4 < 75$, $-190 < f_{M,1}/\Lambda^4 < 182$, $-32 < f_{M,2}/\Lambda^4 < 31$, $-58 < f_{M,3}/\Lambda^4 < 59$, $-3.8 < f_{T,0}/\Lambda^4 < 3.4$, $-4.4 < f_{T,1}/\Lambda^4 < 4.4$, $-9.9 < f_{T,2}/\Lambda^4 < 9.0$, $-1.8 < f_{T,8}/\Lambda^4 < 1.8$, $-4.0 < f_{T,9}/\Lambda^4 < 4.0$, in units of TeV^{-4} and without application of a form factor.

[7] KHACHATRYAN 17M analyse electroweak production of $W\gamma$ in association with two hadronic jets, with the W boson decaying to electrons or muons. Events with photon transverse momentum larger than 200 GeV and di-jet invariant mass larger than 200 GeV are selected. The W transverse momentum spectrum is analysed to set 95% C.L. limits as follows: $-77 < f_{M,0}/\Lambda^4 < 74$, $-125 < f_{M,1}/\Lambda^4 < 129$, $-26 < f_{M,2}/\Lambda^4 < 26$, $-43 < f_{M,3}/\Lambda^4 < 44$, $-40 < f_{M,4}/\Lambda^4 < 40$, $-65 < f_{M,5}/\Lambda^4 < 65$, $-129 < f_{M,6}/\Lambda^4 < 129$, $-164 < f_{M,7}/\Lambda^4 < 162$, $-5.4 < f_{T,0}/\Lambda^4 < 5.6$, $-3.7 < f_{T,1}/\Lambda^4 < 4.0$, $-11 < f_{T,2}/\Lambda^4 < 12$, $-3.8 < f_{T,5}/\Lambda^4 < 3.8$, $-2.8 < f_{T,6}/\Lambda^4 < 3.0$, $-7.3 < f_{T,7}/\Lambda^4 < 7.7$, in units of TeV^{-4} and without application of a form factor.

[8] SIRUNYAN 17AD study pp collisions at $\sqrt{s} = 13$ TeV to determine the cross section of $ZZjj$ with the Z decaying to ee or $\mu\mu$. The ZZ mass distribution is used to set upper limits on the anomalous quartic couplings. The 95% upper limits for the relevant quartic couplings in units of TeV^{-4} are: $-0.46 < f_{T,0}/\Lambda^4 < 0.44$, $-0.61 < f_{T,1}/\Lambda^4 < 0.61$, $-1.2 < f_{T,2}/\Lambda^4 < 1.2$, $-0.84 < f_{T,8}/\Lambda^4 < 0.84$, $-1.8 < f_{T,9}/\Lambda^4 < 1.8$.

[9] SIRUNYAN 17AR study pp collisions at $\sqrt{s} = 8$ TeV to determine the cross section of $pp \to WV\gamma\gamma$ and $pp \to Z\gamma\gamma$ where $W \to \ell\nu$ and $Z \to \ell^+\ell^-$, ℓ being an electron or a muon. The number of W events in the e and μ channels is 63 and 108 respectively, and the number of Z events in the e and μ channels is 117 and 141. To increase sensitivity, the transverse momentum of the leading photon is required to be larger than 70 GeV. The 95% C.L. upper limits in units of TeV^{-4} are $-701 < f_{M,2}/\Lambda^4 < 683$, $-1170 < f_{M,3}/\Lambda^4 < 1220$, $-33.5 < f_{T,0}/\Lambda^4 < 34.0$, $-44.3 < f_{T,1}/\Lambda^4 < 44.8$, $-93.8 < f_{T,2}/\Lambda^4 < 93.2$.

ANOMALOUS W/Z QUARTIC COUPLINGS

See the related review(s):
Anomalous W/Z Quartic Couplings (QGCs)

a_0/Λ^2, a_C/Λ^2, a_n/Λ^2, κ_0^W/Λ^2, κ_C^W/Λ^2, $f_{T,0}/\Lambda^4$, $f_{M,i}/\Lambda^4$, α_4, α_5, $F_{S,i}/\Lambda^4$, $F_{M,i}/\Lambda^4$, $F_{T,i}/\Lambda^4$

Anomalous W quartic couplings are measured by the experiments at LEP, the Tevatron, and the LHC. Some of the recent results from the Tevatron and LHC experiments individually surpass the combined LEP-2 results in precision (see below). As discussed in the review on the "Anomalous W/Z quartic couplings (QGCS)," the measurements are typically done using different operator expansions which then do not allow the results to be compared and averaged. At least one common framework should be agreed upon for the use in the future publications by the experiments.

Some publications from LHC experiments derive limits for various assumed values of the form-factor cutoff Λ_{FF}. The values quoted below are for $\Lambda_{FF} \to \infty$.

VALUE	DOCUMENT ID		TECN	COMMENT
• • • We do not use the following data for averages, fits, limits, etc. • • •				
[1] AABOUD	17AA	ATLS		$E_{cm}^{pp} = 8$ TeV
[2] AABOUD	17AG			$E_{cm}^{pp} = 8$ TeV
[3] AABOUD	17D	ATLS		$E_{cm}^{pp} = 8$ TeV
[4] AABOUD	17J	ATLS		$E_{cm}^{pp} = 8$ TeV
[5] AABOUD	17M	ATLS		$E_{cm}^{pp} = 8$ TeV
[6] KHACHATRY...	17AA	CMS		$E_{cm}^{pp} = 8$ TeV
[7] KHACHATRY...	17M	CMS		$E_{cm}^{pp} = 8$ TeV
[8] SIRUNYAN	17AD			$E_{cm}^{pp} = 13$ TeV
[9] SIRUNYAN	17AR			$E_{cm}^{pp} = 8$ TeV
[10] AABOUD	16E	ATLS		
[11] AAD	16Q	ATLS		$E_{cm}^{pp} = 8$ TeV
[12] KHACHATRY...	16AX	CMS		$E_{cm}^{pp} = 8$ TeV
[13] AAD	15N	ATLS		
[14] KHACHATRY...	15D	CMS		
[15] AAD	14AM	ATLS		

[10] AABOUD 16E study WW production in two-photon mediated pp collisions at 8 TeV where the W boson decays into an electron or muon, probing the $\gamma\gamma WW$ vertex for anomalous quartic gauge couplings. The lepton p_T is required to be larger than 30 GeV. Limits on anomalous couplings are determined from events with p_T larger than 120 GeV where the aQGC effect is enhanced and the SM background reduced; in the data corresponding to an integrated luminosity of 20.2fb^{-1}, 1 event is selected with an expected SM background of 0.37 ± 0.13 events. The 95% C.L. limits without a form-factor cutoff ($\Lambda_{\text{cutoff}} \to \infty$) are as follows: $-1.7 < a_0^W/\Lambda^2 < 1.7$ and $-6.4 < a_C^W/\Lambda^2 < 6.3$ in units of 10^{-6} GeV^{-2}. In terms of another set of variables: $-6.6 < f_{M,0}/\Lambda^4 < 6.6$ and $-24 < f_{M,1}/\Lambda^4 < 25$ in units of 10^{-11} GeV^{-4}.

[11] AAD 16Q study $Z\gamma\gamma$ production in pp collisions. In events with no additional jets, 29 (22) Z decays to electron (muon) pairs are selected, with an expected background of 3.3 ± 1.1 (6.5 ± 2.0) events, as well as 19 Z decays to netrino pairs with an expected background of 8.3 ± 4.4 events. Analysing the photon transverse momentum distribution for $m_{\gamma\gamma}$ above 200 GeV (300 GeV) for lepton (neutrino) events, yields the 95% C.L. limits: $-1.6\times10^4 < f_{M,2}/\Lambda^4 < 1.6\times10^4$, $-2.9\times10^4 < f_{M,3}/\Lambda^4 < 2.7\times10^4$, $-0.86\times10^2 < f_{T,0}/\Lambda^4 < 1.03\times10^2$, $-0.69\times10^3 < f_{T,5}/\Lambda^4 < 0.68\times10^3$, $-0.74\times10^4 < f_{T,9}/\Lambda^4 < 0.74\times10^4$ in units of TeV^{-4} and without application of a form factor Λ_{FF}.

[12] KHACHATRYAN 16AX searches for anomalous $WW\gamma\gamma$ quartic gauge couplings in the two-photon-mediated process $pp \to ppWW$, assuming the $WW\gamma$ triple gauge boson couplings to be at their Standard Model values. 13 events containing an $e^\pm\mu^\mp$ pair with $p_T(e,\mu) > 30$ GeV are selected in a total luminosity of 19.7 fb^{-1}, with an expected $\gamma\gamma \to WW$ signal of 5.3 ± 0.1 events and an expected background of 3.9 ± 0.5 events. When combining with the data collected at 7 TeV (CHATRCHYAN 13AA), and not assuming a form factor, the following 1-parameter limits at 95% C.L. are obtained from the $p_T(e,\mu)$ spectrum: $|a_0^W/\Lambda^2| < 1.1\times10^{-6}$ GeV^{-2} ($a_C^W = 0$), and $|a_C^W/\Lambda^2| < 4.1\times10^{-6}$ GeV^{-2} ($a_0^W = 0$). In terms of another set of variables: $|f_{M,0}/\Lambda^4| < 4.2\times10^{-12}$ GeV^{-4}, $|f_{M,1}/\Lambda^4| < 16\times10^{-12}$ GeV^{-4}, $|f_{M,2}/\Lambda^4| < 2.1\times10^{-12}$ GeV^{-4}, $|f_{M,3}/\Lambda^4| < 7.8\times10^{-12}$ GeV^{-4}.

[13] AAD 15N study $WW\gamma\gamma$ events in 8 TeV pp interactions, where the W decays into an electron or a muon. The events are characterized by an isolated lepton, a missing transverse energy due to the decay neutrino, and two isolated photons, with the p_T of the lepton and the photons being > 20 GeV. The number of candidate events observed in the electron channel for N(jet) ≥ 0 and N(jet) = 0 is 47 and 15, the corresponding numbers for the muon channel being 110 and 53. The backgrounds expected are 30.2 ± 7.4, 8.7 ± 3.0, 52.1 ± 12.2, and 24.4 ± 8.3 respectively. The 95% C.L. limits on the values of the parameters $f_{T,0}/\Lambda^4$, $f_{M,2}/\Lambda^4$ and $f_{M,3}/\Lambda^4$ are -0.9–0.9×10^2, -0.8–0.8×10^4, and -1.5–1.4×10^4 respectively, without application of a form factor Λ_{FF}.

[14] KHACHATRYAN 15D study vector-boson-scattering tagged by two jets, requiring two same-sign charged leptons arising from $W^\pm W^\pm$ production and decay. The two jets must have a transverse momentum larger than 30 GeV, while the leptons, electrons or muons, must have a transverse momentum > 20 GeV. The dijet mass is required to be > 500 GeV, the dilepton mass > 50 GeV, with additional requirement of differing from the Z mass by > 15 GeV. In the two categories W^+W^+ and W^-W^-, 10 and 2 data events are observed in a data sample corresponding to an integrated luminosity of 19.4 fb^{-1}, with an expected background of 3.1 ± 0.6 and 2.6 ± 0.5 events. Analysing the distribution of the dilepton invariant mass, the following limits at 95% C.L. are obtained, in units of TeV^{-4}: $-38 < F_{S,0}/\Lambda^4 < 40$, $-118 < F_{S,1}/\Lambda^4 < 120$, $-33 < F_{M,0}/\Lambda^4 < 32$, $-44 < F_{M,1}/\Lambda^4 < 47$, $-65 < F_{M,6}/\Lambda^4 < 63$, $-70 < F_{M,7}/\Lambda^4 < 66$, $-4.2 < F_{T,0}/\Lambda^4 < 4.6$, $-1.9 < F_{T,1}/\Lambda^4 < 2.2$, $-5.2 < F_{T,2}/\Lambda^4 < 6.4$.

[15] AAD 14AM analyze electroweak production of WW jet jet same-charge diboson plus two jets production, with the W bosons decaying to electron or muon, to study the quartic $WWWW$ coupling. In a kinematic region enhancing the electroweak production over the strong production, 34 events are observed in the data while 29.8 ± 2.4 events are expected with a backgound of 15.9 ± 1.9 events. Assuming the other QGC coupling to have the SM value of zero, the observed event yield is used to determine 95% CL limits on the quartic gauge couplings: $-0.14 < \alpha_4 < 0.16$ and $-0.23 < \alpha_5 < 0.24$.

[16] CHATRCHYAN 14Q study $WV\gamma$ production in 8 TeV pp collisions, in the single lepton final state, with $W \to \ell\nu$, $Z \to$ dijet or $W \to \ell\nu$, $W \to$ dijet, the dijet mass resolution precluding differentiation between the W and Z. p_T and pseudo-rapidity cuts are put on the lepton, the photon and the two jets to minimize backgrounds. The dijet mass is required to be between 70–100 GeV and $|\Delta\eta_{jj}| < 1.4$. The selected number of muon (electron) events are 183 (139), with SM expectation being 194.2 ± 11.5 (147.9 ± 10.7) including signal and background. The photon E_T distribution is used to set limits on the anomalous quartic couplings. The following 95% CL limits are deduced (all in units of TeV^{-2} or TeV^{-4}): $-21 < a_0^W/\Lambda^2 < 20$, $-34 < a_c^W/\Lambda^2 < 32$, $-12 < \kappa_0^W/\Lambda^2 < 10$ and $-18 < \kappa_c^W/\Lambda^2 < 17$; and $-25 < f_{T,0}/\Lambda^4 < 24$ TeV^{-4}.

[17] ABAZOV 13D searches for anomalous $WW\gamma\gamma$ quartic gauge couplings in the two-photon-mediated process $pp \to ppWW$, assuming the $WW\gamma$ triple gauge boson couplings to be at their Standard Model values. 946 events containing an e^+e^- pair with missing energy are selected in a total luminosity of 9.7 fb^{-1}, with an expectation of 983 ± 108 events from Standard-Model processes. The following 1-parameter limits at 95% CL are otained: $|a_0^W/\Lambda^2| < 4.3\times10^{-4}$ GeV^{-2} ($a_c^W = 0$), $|a_c^W/\Lambda^2| < 1.5\times10^{-3}$ GeV^{-2} ($a_0^W = 0$).

[18] CHATRCHYAN 13AA searches for anomalous $WW\gamma\gamma$ quartic gauge couplings in the two-photon-mediated process $pp \to ppWW$, assuming the $WW\gamma$ triple gauge boson couplings to be at their Standard Model values. 2 events containing an $e^\pm\mu^\mp$ pair with $p_T(e,\mu) > 30$ GeV are selected in a total luminosity of 5.05 fb^{-1}, with an expected $ppWW$ signal of 2.2 ± 0.4 events and an expected background of 0.84 ± 0.15 events. The following 1-parameter limits at 95% CL are otained from the $p_T(e,\mu)$ spectrum: $|a_0^W/\Lambda^2| < 4.0\times10^{-6}$ GeV^{-2} ($a_c^W = 0$), $|a_c^W/\Lambda^2| < 1.5\times10^{-5}$ GeV^{-2} ($a_0^W = 0$).

[19] ABBIENDI 04B select 187 $e^+e^- \to W^+W^-\gamma$ events in the C.M. energy range 180–209 GeV, where $E_\gamma > 2.5$ GeV, the photon has a polar angle $|\cos\theta_\gamma| < 0.975$ and is well isolated from the nearest jet and charged lepton, and the effective masses of both fermion-antifermion systems agree with the W mass within 3 Γ_W. The measured differential cross section as a function of the photon energy and photon polar angle is used to extract the 95% CL limits: -0.020 GeV$^{-2} < a_0/\Lambda^2 < 0.020$ GeV^{-2}, -0.053 GeV$^{-2} < a_c/\Lambda^2 < 0.037$ GeV^{-2} and -0.16 GeV$^{-2} < a_n/\Lambda^2 < 0.15$ GeV^{-2}.

[20] ABBIENDI 04L select 20 $e^+e^- \to \nu\overline{\nu}\gamma\gamma$ acoplanar events in the energy range 180–209 GeV and 176 $e^+e^- \to q\overline{q}\gamma\gamma$ events in the energy range 130–209 GeV. These samples are used to constrain possible anomalous $W^+W^-\gamma\gamma$ and $ZZ\gamma\gamma$ quartic couplings. Further combining with the $W^+W^-\gamma$ sample of ABBIENDI 04B the following one–parameter 95% CL limits are obtained: $-0.007 < a_0^Z/\Lambda^2 < 0.023$ GeV^{-2}, $-0.029 < a_c^Z/\Lambda^2 < 0.029$ GeV^{-2}, $-0.020 < a_0^W/\Lambda^2 < 0.020$ GeV^{-2}, $-0.052 < a_c^W/\Lambda^2 < 0.037$ GeV^{-2}.

[21] In the CM energy range 183 to 209 GeV HEISTER 04A select 30 $e^+e^- \to \nu\overline{\nu}\gamma\gamma$ events with two acoplanar, high energy and high transverse momentum photons. The photon–photon acoplanarity is required to be > 5°, $E_\gamma/\sqrt{s} > 0.025$ (the more energetic photon having energy > 0.2 $\sqrt{s}$), $p_{T_\gamma}/E_{\text{beam}} > 0.05$ and $|\cos\theta_\gamma| < 0.94$. A likelihood fit to the photon energy and recoil missing mass yields the following one–parameter 95% CL limits: $-0.012 < a_0^Z/\Lambda^2 < 0.019$ GeV^{-2}, $-0.041 < a_c^Z/\Lambda^2 < 0.044$ GeV^{-2}, $-0.060 < a_0^W/\Lambda^2 < 0.055$ GeV^{-2}, $-0.099 < a_c^W/\Lambda^2 < 0.093$ GeV^{-2}.

[22] ABDALLAH 03I select 122 $e^+e^- \to W^+W^-\gamma$ events in the C.M. energy range 189–209 GeV, where $E_\gamma > 5$ GeV, the photon has a polar angle $|\cos\theta_\gamma| < 0.95$ and is well isolated from the nearest charged fermion. A fit to the photon energy spectra yields $a_c/\Lambda^2 = 0.000^{+0.019}_{-0.040}$ GeV^{-2}, $a_0/\Lambda^2 = -0.004^{+0.018}_{-0.010}$ GeV^{-2}, $\tilde{a}_0/\Lambda^2 = -0.007^{+0.019}_{-0.008}$ GeV^{-2}, $a_n/\Lambda^2 = -0.09^{+0.16}_{-0.05}$ GeV^{-2}, and $\tilde{a}_n/\Lambda^2 = +0.05^{+0.07}_{-0.15}$ GeV^{-2}, keeping the other parameters fixed to their Standard Model values (0). The 95% CL limits are: -0.063 GeV$^{-2} < a_c/\Lambda^2 < +0.032$ GeV^{-2}, -0.020 GeV$^{-2} < a_0/\Lambda^2 < +0.020$ GeV^{-2}, -0.020 GeV$^{-2} < \tilde{a}_0/\Lambda^2 < +0.020$ GeV^{-2}, -0.18 GeV$^{-2} < a_n/\Lambda^2 < +0.14$ GeV^{-2}, -0.16 GeV$^{-2} < \tilde{a}_n/\Lambda^2 < +0.17$ GeV^{-2}.

[23] ACHARD 02F select 86 $e^+e^- \to W^+W^-\gamma$ events at 192–207 GeV, where $E_\gamma > 5$ GeV and the photon is well isolated. They also select 43 acoplanar $e^+e^- \to \nu\overline{\nu}\gamma\gamma$ events in this energy range, where the photon energies are >5 GeV and >1 GeV and the photon polar angles are between 14° and 166°. All these 43 events are in the recoil mass region corresponding to the Z (75–110 GeV). Using the shape and normalization of the photon spectra in the $W^+W^-\gamma$ events, and combining with the 42 event sample from 189 GeV data (ACCIARRI 00T), they obtain: $a_0/\Lambda^2 = 0.000 \pm 0.010$ GeV^{-2}, $a_c/\Lambda^2 = -0.013 \pm 0.023$ GeV^{-2}, and $a_n/\Lambda^2 = -0.002 \pm 0.076$ GeV^{-2}. Further combining the analyses of $W^+W^-\gamma$ events with the low recoil mass region of $\nu\overline{\nu}\gamma\gamma$ events (including samples collected at 183 + 189 GeV), they obtain the following one-parameter 95% CL limits: -0.015 GeV$^{-2} < a_0/\Lambda^2 < 0.015$ GeV^{-2}, -0.048 GeV$^{-2} < a_c/\Lambda^2 < 0.026$ GeV^{-2}, and -0.14 GeV$^{-2} < a_n/\Lambda^2 < 0.13$ GeV^{-2}.

W REFERENCES

AABOUD	18J	EPJ C78 110	M. Aaboud *et al.*	(ATLAS Collab.)
AABOUD	17AA	PR D96 012007	M. Aaboud *et al.*	(ATLAS Collab.)
AABOUD	17AG	EPJ C77 646	M. Aaboud *et al.*	(ATLAS Collab.)
AABOUD	17D	PR D95 032001	M. Aaboud *et al.*	(ATLAS Collab.)
AABOUD	17J	JHEP 1707 107	M. Aaboud *et al.*	(ATLAS Collab.)
AABOUD	17M	EPJ C77 141	M. Aaboud *et al.*	(ATLAS Collab.)
AABOUD	17S	EPJ C77 474	M. Aaboud *et al.*	(ATLAS Collab.)
AABOUD	17U	EPJ C77 563	M. Aaboud *et al.*	(ATLAS Collab.)
KHACHATRY...	17AA	PL B770 380	V. Khachatryan *et al.*	(CMS Collab.)
KHACHATRY...	17M	JHEP 1706 106	V. Khachatryan *et al.*	(CMS Collab.)
KHACHATRY...	17O	EPJ C77 236	V. Khachatryan *et al.*	(CMS Collab.)
SIRUNYAN	17AD	PL B774 682	A.M. Sirunyan *et al.*	(CMS Collab.)
SIRUNYAN	17AR	JHEP 1710 072	A.M. Sirunyan *et al.*	(CMS Collab.)
SIRUNYAN	17X	PL B772 21	A.M. Sirunyan *et al.*	(CMS Collab.)
AABOUD	16E	PR D94 032011	M. Aaboud *et al.*	(ATLAS Collab.)
AAD	16AR	JHEP 1609 029	G. Aad *et al.*	(ATLAS Collab.)
AAD	16P	PR D93 092004	G. Aad *et al.*	(ATLAS Collab.)
AAD	16Q	PR D93 112002	G. Aad *et al.*	(ATLAS Collab.)
AAIJ	16AJ	JHEP 1610 030	R. Aaij *et al.*	(LHCb Collab.)
KHACHATRY...	16AX	JHEP 1608 119	V. Khachatryan *et al.*	(CMS Collab.)
KHACHATRY...	16BI	EPJ C76 401	V. Khachatryan *et al.*	(CMS Collab.)
PDG	16	CP C40 100001	C. Patrignani *et al.*	(PDG Collab.)
AAD	15N	PRL 115 031802	G. Aad *et al.*	(ATLAS Collab.)
KHACHATRY...	15D	PRL 114 051801	V. Khachatryan *et al.*	(CMS Collab.)
AAD	14AM	PRL 113 141803	G. Aad *et al.*	(ATLAS Collab.)
AAD	14Y	JHEP 1404 031	G. Aad *et al.*	(ATLAS Collab.)
AALTONEN	14D	PR D89 072003	T. Aaltonen *et al.*	(CDF Collab.)
ABAZOV	14N	PR D89 012005	V.M. Abazov *et al.*	(D0 Collab.)
CHATRCHYAN	14AB	PR D89 092005	S. Chatrchyan *et al.*	(CMS Collab.)
CHATRCHYAN	14Q	PR D90 032008	S. Chatrchyan *et al.*	(CMS Collab.)
AAD	13AL	PR D87 112001	G. Aad *et al.*	(ATLAS Collab.)
Also		PR D88 079906 (errat.)	G. Aad *et al.*	(ATLAS Collab.)
AAD	13AN	PR D87 112003	G. Aad *et al.*	(ATLAS Collab.)
Also		PR D91 119901 (errat.)	G. Aad *et al.*	(ATLAS Collab.)
AALTONEN	13N	PR D88 052018	T. Aaltonen *et al.*	(CDF and D0 Collabs.)
ABAZOV	13D	PR D88 012005	V.M. Abazov *et al.*	(D0 Collab.)
CHATRCHYAN	13AA	JHEP 1307 116	S. Chatrchyan *et al.*	(CMS Collab.)
CHATRCHYAN	13BF	EPJ C73 2610	S. Chatrchyan *et al.*	(CMS Collab.)
SCHAEL	13A	PRPL 532 119	S. Schael *et al.*	(ALEPH Collab., DELPHI, L3+)
AAD	12AC	PL B712 289	G. Aad *et al.*	(ATLAS Collab.)
AAD	12BX	PL B717 49	G. Aad *et al.*	(ATLAS Collab.)
AAD	12CD	EPJ C72 2173	G. Aad *et al.*	(ATLAS Collab.)
AAD	12V	PL B709 341	G. Aad *et al.*	(ATLAS Collab.)
AALTONEN	12AC	PR D86 031104	T. Aaltonen *et al.*	(CDF Collab.)
AALTONEN	12E	PRL 108 151803	T. Aaltonen *et al.*	(CDF Collab.)
AALTONEN	12W	PR D85 032001	T. Aaltonen *et al.*	(CDF Collab.)
ABAZOV	12AG	PL B718 451	V.M. Abazov *et al.*	(D0 Collab.)
ABAZOV	12F	PRL 108 151804	V.M. Abazov *et al.*	(D0 Collab.)
ABAZOV	11	PL B695 67	V.M. Abazov *et al.*	(D0 Collab.)
ABAZOV	11AC	PRL 107 241803	V.M. Abazov *et al.*	(D0 Collab.)
BLINOV	11	PL B699 287	A.E. Blinov, A.S. Rudenko	(NOVO)
CHATRCHYAN	11M	PL B701 535	S. Chatrchyan *et al.*	(CMS Collab.)
AALTONEN	10K	PRL 104 201801	T. Aaltonen *et al.*	(CDF Collab.)
Also		PRL 105 019905(errat.)	T. Aaltonen *et al.*	(CDF Collab.)
ABDALLAH	10	EPJ C66 35	J. Abdallah *et al.*	(DELPHI Collab.)
AARON	09B	EPJ C64 251	F.D. Aaron *et al.*	(H1 Collab.)
ABAZOV	09AB	PRL 103 141801	V.M. Abazov *et al.*	(D0 Collab.)
ABAZOV	09AD	PR D80 053012	V.M. Abazov *et al.*	(D0 Collab.)
ABAZOV	09AJ	PRL 103 191801	V.M. Abazov *et al.*	(D0 Collab.)

ABAZOV	09AK	PRL 103 231802	V.M. Abazov *et al.*	(D0 Collab.)
AALTONEN	08B	PRL 100 071801	T. Aaltonen *et al.*	(CDF Collab.)
ABAZOV	08R	PRL 100 241805	V.M. Abazov *et al.*	(D0 Collab.)
ABDALLAH	08A	EPJ C55 1	J. Abdallah *et al.*	(DELPHI Collab.)
ABDALLAH	08C	EPJ C54 345	J. Abdallah *et al.*	(DELPHI Collab.)
AALTONEN	07F	PRL 99 151801	T. Aaltonen *et al.*	(CDF Collab.)
Also		PR D77 112001	T. Aaltonen *et al.*	(CDF Collab.)
AALTONEN	07L	PR D76 111103	T. Aaltonen *et al.*	(CDF Collab.)
ABAZOV	07Z	PR D76 111104	V.M. Abazov *et al.*	(D0 Collab.)
ABBIENDI	07A	EPJ C52 767	G. Abbiendi *et al.*	(OPAL Collab.)
ABAZOV	06H	PR D74 057101	V.M. Abazov *et al.*	(D0 Collab.)
Also		PR D74 059904(errat.)	V.M. Abazov *et al.*	(D0 Collab.)
ABBIENDI	06	EPJ C45 307	G. Abbiendi *et al.*	(OPAL Collab.)
ABBIENDI	06A	EPJ C45 291	G. Abbiendi *et al.*	(OPAL Collab.)
ACHARD	06	EPJ C45 569	P. Achard *et al.*	(L3 Collab.)
AKTAS	06	PL B632 35	A. Aktas *et al.*	(H1 Collab.)
SCHAEL	06	EPJ C47 309	S. Schael *et al.*	(ALEPH Collab.)
ABAZOV	05J	PR D71 091108	V.M. Abazov *et al.*	(D0 Collab.)
ABAZOV	05S	PRL 95 141802	V.M. Abazov *et al.*	(D0 Collab.)
SCHAEL	05A	PL B614 7	S. Schael *et al.*	(ALEPH Collab.)
ABAZOV	04D	PR D70 092008	V.M. Abazov *et al.*	(D0 Collab., D0 Collab.)
ABBIENDI	04B	PL B580 17	G. Abbiendi *et al.*	(OPAL Collab.)
ABBIENDI	04D	EPJ C33 463	G. Abbiendi *et al.*	(OPAL Collab.)
ABBIENDI	04L	PR D70 032005	G. Abbiendi *et al.*	(OPAL Collab.)
ABDALLAH	04G	EPJ C34 127	J. Abdallah *et al.*	(DELPHI Collab.)
ACHARD	04D	PL B586 151	P. Achard *et al.*	(L3 Collab.)
ACHARD	04J	PL B600 22	P. Achard *et al.*	(L3 Collab.)
HEISTER	04A	PL B602 31	A. Heister *et al.*	(ALEPH Collab.)
SCHAEL	04A	EPJ C38 147	S. Schael *et al.*	(ALEPH Collab.)
ABBIENDI	03C	EPJ C26 321	G. Abbiendi *et al.*	(OPAL Collab.)
ABDALLAH	03I	EPJ C31 139	J. Abdallah *et al.*	(DELPHI Collab.)
ABAZOV	02D	PR D66 012001	V.M. Abazov *et al.*	(D0 Collab.)
ABAZOV	02E	PR D66 032008	V.M. Abazov *et al.*	(D0 Collab.)
ACHARD	02F	PL B527 29	P. Achard *et al.*	(L3 Collab.)
CHEKANOV	02C	PL B539 197	S. Chekanov *et al.*	(ZEUS Collab.)
ABBIENDI	01H	EPJ C19 229	G. Abbiendi *et al.*	(OPAL Collab.)
ABREU	01I	PL B502 9	P. Abreu *et al.*	(DELPHI Collab.)
AFFOLDER	01E	PR D64 052001	T. Affolder *et al.*	(CDF Collab.)
ABBIENDI	00V	PL B490 71	G. Abbiendi *et al.*	(OPAL Collab.)
ABBOTT	00B	PR D61 072001	B. Abbott *et al.*	(D0 Collab.)
ABBOTT	00D	PRL 84 5710	B. Abbott *et al.*	(D0 Collab.)
ABREU,P	00F	EPJ C18 203	P. Abreu *et al.*	(DELPHI Collab.)
Also		EPJ C25 493 (errat.)	P. Abreu *et al.*	(DELPHI Collab.)
ACCIARRI	00T	PL B490 187	M. Acciarri *et al.*	(L3 Collab.)
AFFOLDER	00M	PRL 85 3347	T. Affolder *et al.*	(CDF Collab.)
BREITWEG	00	PL B471 411	J. Breitweg *et al.*	(ZEUS Collab.)
BREITWEG	00D	EPJ C12 411	J. Breitweg *et al.*	(ZEUS Collab.)
EBOLI	00	MPL A15 1	O. Eboli, M. Gonzalez-Garcia, S. Novaes	
ABBIENDI	99N	PL B453 153	G. Abbiendi *et al.*	(OPAL Collab.)
ABBOTT	99H	PR D60 052003	B. Abbott *et al.*	(D0 Collab.)
ABBOTT	99I	PR D60 072002	B. Abbott *et al.*	(D0 Collab.)
ABREU	99L	PL B459 382	P. Abreu *et al.*	(DELPHI Collab.)
ACCIARRI	99	PL B454 386	M. Acciarri *et al.*	(L3 Collab.)
ACCIARRI	99Q	PL B467 171	M. Acciarri *et al.*	(L3 Collab.)
BARATE	99I	PL B453 107	R. Barate *et al.*	(ALEPH Collab.)
BARATE	99L	PL B462 389	R. Barate *et al.*	(ALEPH Collab.)
BARATE	99M	PL B465 349	R. Barate *et al.*	(ALEPH Collab.)
ABBOTT	98N	PR D58 092003	B. Abbott *et al.*	(D0 Collab.)
ABBOTT	98P	PR D58 012002	B. Abbott *et al.*	(D0 Collab.)
ABE	98H	PR D58 031101	F. Abe *et al.*	(CDF Collab.)
ABE	98P	PR D58 091101	F. Abe *et al.*	(CDF Collab.)
ABREU	98C	PL B416 233	P. Abreu *et al.*	(DELPHI Collab.)
ABREU	98N	PL B439 209	P. Abreu *et al.*	(DELPHI Collab.)
BARATE	97	PL B401 347	R. Barate *et al.*	(ALEPH Collab.)
BARATE	97S	PL B415 435	R. Barate *et al.*	(ALEPH Collab.)
ABACHI	95D	PRL 75 1456	S. Abachi *et al.*	(D0 Collab.)
ABE	95C	PRL 74 341	F. Abe *et al.*	(CDF Collab.)
ABE	95G	PRL 74 1936	F. Abe *et al.*	(CDF Collab.)
ABE	95P	PRL 75 11	F. Abe *et al.*	(CDF Collab.)
Also		PR D52 4784	F. Abe *et al.*	(CDF Collab.)
ABE	95W	PR D52 2624	F. Abe *et al.*	(CDF Collab.)
Also		PRL 73 220	F. Abe *et al.*	(CDF Collab.)
ABE	92E	PRL 68 3398	F. Abe *et al.*	(CDF Collab.)
ABE	92I	PRL 69 28	F. Abe *et al.*	(CDF Collab.)
ALITTI	92	PL B276 365	J. Alitti *et al.*	(UA2 Collab.)
ALITTI	92B	PL B276 354	J. Alitti *et al.*	(UA2 Collab.)
ALITTI	92C	PL B277 194	J. Alitti *et al.*	(UA2 Collab.)
ALITTI	92D	PL B277 203	J. Alitti *et al.*	(UA2 Collab.)
ALITTI	92F	PL B280 137	J. Alitti *et al.*	(UA2 Collab.)
SAMUEL	92	PL B280 124	M.A. Samuel *et al.*	(OKSU, CARL)
ABE	91C	PR D44 29	F. Abe *et al.*	(CDF Collab.)
ALBAJAR	91	PL B253 503	C. Albajar *et al.*	(UA1 Collab.)
ALITTI	91C	ZPHY C52 209	J. Alitti *et al.*	(UA2 Collab.)
SAMUEL	91	PRL 67 9	M.A. Samuel *et al.*	(OKSU, CARL)
Also		PRL 67 2920 (erratum)	M.A. Samuel *et al.*	
ABE	90G	PRL 65 2243	F. Abe *et al.*	(CDF Collab.)
Also		PR D43 2070	F. Abe *et al.*	(CDF Collab.)
ALBAJAR	90	PL B241 283	C. Albajar *et al.*	(UA1 Collab.)
ALITTI	90B	PL B241 150	J. Alitti *et al.*	(UA2 Collab.)
ABE	89I	PRL 62 1005	F. Abe *et al.*	(CDF Collab.)
ALBAJAR	89	ZPHY C44 15	C. Albajar *et al.*	(UA1 Collab.)
BAUR	88	NP B308 127	U. Baur, D. Zeppenfeld	(FSU, WISC)
GRIFOLS	88	IJMP A3 225	J.A. Grifols, S. Peris, J. Sola	(BARC, DESY)
Also		PL B197 437	J.A. Grifols, S. Peris, J. Sola	(BARC, DESY)
ALBAJAR	87	PL B185 233	C. Albajar *et al.*	(UA1 Collab.)
ANSARI	87	PL B186 440	R. Ansari *et al.*	(UA2 Collab.)
GROTCH	87	PR D36 2153	H. Grotch, R.W. Robinett	(PSU)
HAGIWARA	87	NP B282 253	K. Hagiwara *et al.*	(KEK, UCLA, FSU)
VANDERBIJ	87	PR D35 1088	J.J. van der Bij	(FNAL)
GRAU	85	PL 154B 283	A. Grau, J.A. Grifols	(BARC)
SUZUKI	85	PL 153B 289	M. Suzuki	(LBL)
ARNISON	84D	PL 134B 469	G.T.J. Arnison *et al.*	(UA1 Collab.)
HERZOG	84	PL 148B 355	F. Herzog	(WISC)
Also		PL 155B 468 (erratum)	F. Herzog	(WISC)
ARNISON	83	PL 122B 103	G.T.J. Arnison *et al.*	(UA1 Collab.)
BANNER	83B	PL 122B 476	M. Banner *et al.*	(UA2 Collab.)

Z

$J = 1$

See the related review(s):
Z Boson

Z MASS

OUR FIT is obtained using the fit procedure and correlations as determined by the LEP Electroweak Working Group (see the note "The *Z* boson" and ref. LEP-SLC 06). The fit is performed using the *Z* mass and width, the *Z* hadronic pole cross section, the ratios of hadronic to leptonic partial widths, and the *Z* pole forward-backward lepton asymmetries. This set is believed to be most free of correlations.

The *Z*-boson mass listed here corresponds to the mass parameter in a Breit-Wigner distribution with mass dependent width. The value is 34 MeV greater than the real part of the position of the pole (in the energy-squared plane) in the *Z*-boson propagator. Also the LEP experiments have generally assumed a fixed value of the $\gamma - Z$ interferences term based on the standard model. Keeping this term as free parameter leads to a somewhat larger error on the fitted *Z* mass. See ACCIARRI 00Q and ABBIENDI 04G for a detailed investigation of both these issues.

VALUE (GeV)	*EVTS*	*DOCUMENT ID*		*TECN*	*COMMENT*
91.1876±0.0021 OUR FIT					
91.1852±0.0030	4.57M	[1] ABBIENDI	01A	OPAL	E_{cm}^{ee} = 88–94 GeV
91.1863±0.0028	4.08M	[2] ABREU	00F	DLPH	E_{cm}^{ee} = 88–94 GeV
91.1898±0.0031	3.96M	[3] ACCIARRI	00C	L3	E_{cm}^{ee} = 88–94 GeV
91.1885±0.0031	4.57M	[4] BARATE	00C	ALEP	E_{cm}^{ee} = 88–94 GeV
• • • We do not use the following data for averages, fits, limits, etc. • • •					
91.1872±0.0033		[5] ABBIENDI	04G	OPAL	E_{cm}^{ee} = LEP1 + 130–209 GeV
91.272 ±0.032 ±0.033		[6] ACHARD	04C	L3	E_{cm}^{ee} = 183–209 GeV
91.1875±0.0039	3.97M	[7] ACCIARRI	00Q	L3	E_{cm}^{ee} = LEP1 + 130–189 GeV
91.151 ±0.008		[8] MIYABAYASHI	95	TOPZ	E_{cm}^{ee} = 57.8 GeV
91.74 ±0.28 ±0.93	156	[9] ALITTI	92B	UA2	$E_{cm}^{p\overline{p}}$ = 630 GeV
90.9 ±0.3 ±0.2	188	[10] ABE	89C	CDF	$E_{cm}^{p\overline{p}}$ = 1.8 TeV
91.14 ±0.12	480	[11] ABRAMS	89B	MRK2	E_{cm}^{ee} = 89–93 GeV
93.1 ±1.0 ±3.0	24	[12] ALBAJAR	89	UA1	$E_{cm}^{p\overline{p}}$ = 546,630 GeV

[1] ABBIENDI 01A error includes approximately 2.3 MeV due to statistics and 1.8 MeV due to LEP energy uncertainty.
[2] The error includes 1.6 MeV due to LEP energy uncertainty.
[3] The error includes 1.8 MeV due to LEP energy uncertainty.
[4] BARATE 00C error includes approximately 2.4 MeV due to statistics, 0.2 MeV due to experimental systematics, and 1.7 MeV due to LEP energy uncertainty.
[5] ABBIENDI 04G obtain this result using the S–matrix formalism for a combined fit to their cross section and asymmetry data at the *Z* peak and their data at 130–209 GeV. The authors have corrected the measurement for the 34 MeV shift with respect to the Breit–Wigner fits.
[6] ACHARD 04C select $e^+e^- \to Z\gamma$ events with hard initial–state radiation. Z decays to $q\overline{q}$ and muon pairs are considered. The fit results obtained in the two samples are found consistent to each other and combined considering the uncertainty due to ISR modelling as fully correlated.
[7] ACCIARRI 00Q interpret the *s*-dependence of the cross sections and lepton forward-backward asymmetries in the framework of the S-matrix formalism. They fit to their cross section and asymmetry data at high energies, using the results of S-matrix fits to *Z*-peak data (ACCIARRI 00C) as constraints. The 130–189 GeV data constrains the γ/Z interference term. The authors have corrected the measurement for the 34.1 MeV shift with respect to the Breit-Wigner fits. The error contains a contribution of ±2.3 MeV due to the uncertainty on the γZ interference.
[8] MIYABAYASHI 95 combine their low energy total hadronic cross-section measurement with the ACTON 93D data and perform a fit using an S-matrix formalism. As expected, this result is below the mass values obtained with the standard Breit-Wigner parametrization.
[9] Enters fit through W/Z mass ratio given in the *W* Particle Listings. The ALITTI 92B systematic error (±0.93) has two contributions: one (±0.92) cancels in m_W/m_Z and one (±0.12) is noncancelling. These were added in quadrature.
[10] First error of ABE 89 is combination of statistical and systematic contributions; second is mass scale uncertainty.
[11] ABRAMS 89B uncertainty includes 35 MeV due to the absolute energy measurement.
[12] ALBAJAR 89 result is from a total sample of 33 $Z \to e^+e^-$ events.

Z WIDTH

OUR FIT is obtained using the fit procedure and correlations as determined by the LEP Electroweak Working Group (see the note "The *Z* boson" and ref. LEP-SLC 06).

VALUE (GeV)	*EVTS*	*DOCUMENT ID*		*TECN*	*COMMENT*
2.4952±0.0023 OUR FIT					
2.4948±0.0041	4.57M	[1] ABBIENDI	01A	OPAL	E_{cm}^{ee} = 88–94 GeV
2.4876±0.0041	4.08M	[2] ABREU	00F	DLPH	E_{cm}^{ee} = 88–94 GeV
2.5024±0.0042	3.96M	[3] ACCIARRI	00C	L3	E_{cm}^{ee} = 88–94 GeV
2.4951±0.0043	4.57M	[4] BARATE	00C	ALEP	E_{cm}^{ee} = 88–94 GeV

• • • We do not use the following data for averages, fits, limits, etc. • • •

2.4943 ± 0.0041			[5] ABBIENDI	04G	OPAL	E_{cm}^{ee} = LEP1 + 130–209 GeV
2.5025 ± 0.0041		3.97M	[6] ACCIARRI	00Q	L3	E_{cm}^{ee} = LEP1 + 130–189 GeV
2.50	± 0.21	± 0.06	[7] ABREU	96R	DLPH	E_{cm}^{ee} = 91.2 GeV
3.8	± 0.8	± 1.0	188	ABE	89C	CDF	$E_{cm}^{p\overline{p}}$ = 1.8 TeV
2.42	$^{+0.45}_{-0.35}$		480	[8] ABRAMS	89B	MRK2	E_{cm}^{ee} = 89–93 GeV
2.7	$^{+1.2}_{-1.0}$	± 1.3	24	[9] ALBAJAR	89	UA1	$E_{cm}^{p\overline{p}}$ = 546,630 GeV
2.7	± 2.0	± 1.0	25	[10] ANSARI	87	UA2	$E_{cm}^{p\overline{p}}$ = 546,630 GeV

[1] ABBIENDI 01A error includes approximately 3.6 MeV due to statistics, 1 MeV due to event selection systematics, and 1.3 MeV due to LEP energy uncertainty.

[2] The error includes 1.2 MeV due to LEP energy uncertainty.

[3] The error includes 1.3 MeV due to LEP energy uncertainty.

[4] BARATE 00C error includes approximately 3.8 MeV due to statistics, 0.9 MeV due to experimental systematics, and 1.3 MeV due to LEP energy uncertainty.

[5] ABBIENDI 04G obtain this result using the S–matrix formalism for a combined fit to their cross section and asymmetry data at the Z peak and their data at 130–209 GeV. The authors have corrected the measurement for the 1 MeV shift with respect to the Breit–Wigner fits.

[6] ACCIARRI 00Q interpret the s-dependence of the cross sections and lepton forward-backward asymmetries in the framework of the S-matrix formalism. They fit to their cross section and asymmetry data at high energies, using the results of S-matrix fits to Z-peak data (ACCIARRI 00C) as constraints. The 130–189 GeV data constrains the γ/Z interference term. The authors have corrected the measurement for the 0.9 MeV shift with respect to the Breit-Wigner fits.

[7] ABREU 96R obtain this value from a study of the interference between initial and final state radiation in the process $e^+e^- \to Z \to \mu^+\mu^-$.

[8] ABRAMS 89B uncertainty includes 50 MeV due to the miniSAM background subtraction error.

[9] ALBAJAR 89 result is from a total sample of 33 $Z \to e^+e^-$ events.

[10] Quoted values of ANSARI 87 are from direct fit. Ratio of Z and W production gives either $\Gamma(Z) < (1.09 \pm 0.07) \times \Gamma(W)$, CL = 90% or $\Gamma(Z) = (0.82^{+0.19}_{-0.14} \pm 0.06) \times \Gamma(W)$. Assuming Standard-Model value $\Gamma(W) = 2.65$ GeV then gives $\Gamma(Z) < 2.89 \pm 0.19$ or $= 2.17^{+0.50}_{-0.37} \pm 0.16$.

Z DECAY MODES

	Mode		Fraction (Γ_i/Γ)			Scale factor/ Confidence level
Γ_1	e^+e^-	[a]	(3.3632 ± 0.0042)		%	
Γ_2	$\mu^+\mu^-$	[a]	(3.3662 ± 0.0066)		%	
Γ_3	$\tau^+\tau^-$	[a]	(3.3696 ± 0.0083)		%	
Γ_4	$\ell^+\ell^-$	[a,b]	(3.3658 ± 0.0023)		%	
Γ_5	$\ell^+\ell^-\ell^+\ell^-$	[c]	(4.45 ± 0.32)		$\times 10^{-6}$	
Γ_6	invisible	[a]	(20.000 ± 0.055)		%	
Γ_7	hadrons	[a]	(69.911 ± 0.056)		%	
Γ_8	$(u\overline{u}+c\overline{c})/2$		(11.6 ± 0.6)		%	
Γ_9	$(d\overline{d}+s\overline{s}+b\overline{b})/3$		(15.6 ± 0.4)		%	
Γ_{10}	$c\overline{c}$		(12.03 ± 0.21)		%	
Γ_{11}	$b\overline{b}$		(15.12 ± 0.05)		%	
Γ_{12}	$b\overline{b}b\overline{b}$		(3.6 ± 1.3)		$\times 10^{-4}$	
Γ_{13}	ggg		< 1.1		%	CL=95%
Γ_{14}	$\pi^0\gamma$		< 2.01		$\times 10^{-5}$	CL=95%
Γ_{15}	$\eta\gamma$		< 5.1		$\times 10^{-5}$	CL=95%
Γ_{16}	$\omega\gamma$		< 6.5		$\times 10^{-4}$	CL=95%
Γ_{17}	$\eta'(958)\gamma$		< 4.2		$\times 10^{-5}$	CL=95%
Γ_{18}	$\phi\gamma$		< 8.3		$\times 10^{-6}$	CL=95%
Γ_{19}	$\gamma\gamma$		< 1.46		$\times 10^{-5}$	CL=95%
Γ_{20}	$\pi^0\pi^0$		< 1.52		$\times 10^{-5}$	CL=95%
Γ_{21}	$\gamma\gamma\gamma$		< 2.2		$\times 10^{-6}$	CL=95%
Γ_{22}	$\pi^\pm W^\mp$	[d]	< 7		$\times 10^{-5}$	CL=95%
Γ_{23}	$\rho^\pm W^\mp$	[d]	< 8.3		$\times 10^{-5}$	CL=95%
Γ_{24}	$J/\psi(1S)$X		(3.51	$^{+0.23}_{-0.25}$)	$\times 10^{-3}$	S=1.1
Γ_{25}	$J/\psi(1S)\gamma$		< 2.6		$\times 10^{-6}$	CL=95%
Γ_{26}	$\psi(2S)$X		(1.60 ± 0.29)		$\times 10^{-3}$	
Γ_{27}	$\chi_{c1}(1P)$X		(2.9 ± 0.7)		$\times 10^{-3}$	
Γ_{28}	$\chi_{c2}(1P)$X		< 3.2		$\times 10^{-3}$	CL=90%
Γ_{29}	$\Upsilon(1S)$ X + $\Upsilon(2S)$ X + $\Upsilon(3S)$ X		(1.0 ± 0.5)		$\times 10^{-4}$	
Γ_{30}	$\Upsilon(1S)$X		< 3.4		$\times 10^{-6}$	CL=95%
Γ_{31}	$\Upsilon(2S)$X		< 6.5		$\times 10^{-6}$	CL=95%
Γ_{32}	$\Upsilon(3S)$X		< 5.4		$\times 10^{-6}$	CL=95%
Γ_{33}	$(D^0/\overline{D}^0)$ X		(20.7 ± 2.0)		%	
Γ_{34}	$D^\pm$X		(12.2 ± 1.7)		%	
Γ_{35}	$D^*(2010)^\pm$X	[d]	(11.4 ± 1.3)		%	
Γ_{36}	$D_{s1}(2536)^\pm$X		(3.6 ± 0.8)		$\times 10^{-3}$	
Γ_{37}	$D_{sJ}(2573)^\pm$X		(5.8 ± 2.2)		$\times 10^{-3}$	
Γ_{38}	$D^{*\prime}(2629)^\pm$X		searched for			
Γ_{39}	BX					
Γ_{40}	B^*X					
Γ_{41}	B^+X	[e]	(6.08 ± 0.13)		%	
Γ_{42}	B^0_sX	[e]	(1.59 ± 0.13)		%	
Γ_{43}	B^+_cX		searched for			
Γ_{44}	Λ^+_cX		(1.54 ± 0.33)		%	
Γ_{45}	Ξ^0_cX		seen			
Γ_{46}	Ξ_bX		seen			
Γ_{47}	b-baryon X	[e]	(1.38 ± 0.22)		%	
Γ_{48}	anomalous γ+ hadrons	[f]	< 3.2		$\times 10^{-3}$	CL=95%
Γ_{49}	$e^+e^-\gamma$	[f]	< 5.2		$\times 10^{-4}$	CL=95%
Γ_{50}	$\mu^+\mu^-\gamma$	[f]	< 5.6		$\times 10^{-4}$	CL=95%
Γ_{51}	$\tau^+\tau^-\gamma$	[f]	< 7.3		$\times 10^{-4}$	CL=95%
Γ_{52}	$\ell^+\ell^-\gamma\gamma$	[g]	< 6.8		$\times 10^{-6}$	CL=95%
Γ_{53}	$q\overline{q}\gamma\gamma$	[g]	< 5.5		$\times 10^{-6}$	CL=95%
Γ_{54}	$\nu\overline{\nu}\gamma\gamma$	[g]	< 3.1		$\times 10^{-6}$	CL=95%
Γ_{55}	$e^\pm\mu^\mp$	LF [d]	< 7.5		$\times 10^{-7}$	CL=95%
Γ_{56}	$e^\pm\tau^\mp$	LF [d]	< 9.8		$\times 10^{-6}$	CL=95%
Γ_{57}	$\mu^\pm\tau^\mp$	LF [d]	< 1.2		$\times 10^{-5}$	CL=95%
Γ_{58}	pe	L,B	< 1.8		$\times 10^{-6}$	CL=95%
Γ_{59}	$p\mu$	L,B	< 1.8		$\times 10^{-6}$	CL=95%

[a] This parameter is not directly used in the overall fit but is derived using the fit results; see the note "The Z boson" and ref. LEP-SLC 06 (Physics Reports (Physics Letters C) **427** 257 (2006)).

[b] ℓ indicates each type of lepton (e, μ, and τ), not sum over them.

[c] Here ℓ indicates e or μ.

[d] The value is for the sum of the charge states or particle/antiparticle states indicated.

[e] This value is updated using the product of (i) the $Z \to b\overline{b}$ fraction from this listing and (ii) the b-hadron fraction in an unbiased sample of weakly decaying b-hadrons produced in Z-decays provided by the Heavy Flavor Averaging Group (HFLAV, http://www.slac.stanford.edu/xorg/hflav/osc/PDG_2009/#FRACZ).

[f] See the Particle Listings below for the γ energy range used in this measurement.

[g] For $m_{\gamma\gamma} = (60 \pm 5)$ GeV.

Z PARTIAL WIDTHS

$\Gamma(e^+e^-)$ Γ_1

For the LEP experiments, this parameter is not directly used in the overall fit but is derived using the fit results; see the note "The Z boson" and ref. LEP-SLC 06.

VALUE (MeV)	EVTS	DOCUMENT ID		TECN	COMMENT
83.91 ± 0.12 OUR FIT					
83.66 ± 0.20	137.0K	ABBIENDI	01A	OPAL	E_{cm}^{ee} = 88–94 GeV
83.54 ± 0.27	117.8k	ABREU	00F	DLPH	E_{cm}^{ee} = 88–94 GeV
84.16 ± 0.22	124.4k	ACCIARRI	00C	L3	E_{cm}^{ee} = 88–94 GeV
83.88 ± 0.19		BARATE	00C	ALEP	E_{cm}^{ee} = 88–94 GeV
82.89 ± 1.20 ± 0.89	[1]	ABE	95J	SLD	E_{cm}^{ee} = 91.31 GeV

[1] ABE 95J obtain this measurement from Bhabha events in a restricted fiducial region to improve systematics. They use the values 91.187 and 2.489 GeV for the Z mass and total decay width to extract this partial width.

$\Gamma(\mu^+\mu^-)$ Γ_2

This parameter is not directly used in the overall fit but is derived using the fit results; see the note "The Z boson" and ref. LEP-SLC 06.

VALUE (MeV)	EVTS	DOCUMENT ID		TECN	COMMENT
83.99 ± 0.18 OUR FIT					
84.03 ± 0.30	182.8K	ABBIENDI	01A	OPAL	E_{cm}^{ee} = 88–94 GeV
84.48 ± 0.40	157.6k	ABREU	00F	DLPH	E_{cm}^{ee} = 88–94 GeV
83.95 ± 0.44	113.4k	ACCIARRI	00C	L3	E_{cm}^{ee} = 88–94 GeV
84.02 ± 0.28		BARATE	00C	ALEP	E_{cm}^{ee} = 88–94 GeV

$\Gamma(\tau^+\tau^-)$ Γ_3

This parameter is not directly used in the overall fit but is derived using the fit results; see the note "The Z boson" and ref. LEP-SLC 06.

VALUE (MeV)	EVTS	DOCUMENT ID		TECN	COMMENT
84.08 ± 0.22 OUR FIT					
83.94 ± 0.41	151.5K	ABBIENDI	01A	OPAL	E_{cm}^{ee} = 88–94 GeV
83.71 ± 0.58	104.0k	ABREU	00F	DLPH	E_{cm}^{ee} = 88–94 GeV
84.23 ± 0.58	103.0k	ACCIARRI	00C	L3	E_{cm}^{ee} = 88–94 GeV
84.38 ± 0.31		BARATE	00C	ALEP	E_{cm}^{ee} = 88–94 GeV

Gauge & Higgs Boson Particle Listings

Z

$\Gamma(\ell^+\ell^-)$ Γ_4

ℓ indicates each type of lepton (e, μ, and τ), not sum over them.

In our fit $\Gamma(\ell^+\ell^-)$ is defined as the partial Z width for the decay into a pair of massless charged leptons. This parameter is not directly used in the 5-parameter fit assuming lepton universality but is derived using the fit results. See the note "The Z boson" and ref. LEP-SLC 06.

VALUE (MeV)	EVTS	DOCUMENT ID		TECN	COMMENT
83.984±0.086 OUR FIT					
83.82 ±0.15	471.3K	ABBIENDI	01A	OPAL	E_{cm}^{ee}= 88–94 GeV
83.85 ±0.17	379.4k	ABREU	00F	DLPH	E_{cm}^{ee}= 88–94 GeV
84.14 ±0.17	340.8k	ACCIARRI	00C	L3	E_{cm}^{ee}= 88–94 GeV
84.02 ±0.15	500k	BARATE	00C	ALEP	E_{cm}^{ee}= 88–94 GeV

Γ(invisible) Γ_6

We use only direct measurements of the invisible partial width using the single photon channel to obtain the average value quoted below. OUR FIT value is obtained as a difference between the total and the observed partial widths assuming lepton universality.

VALUE (MeV)	EVTS	DOCUMENT ID		TECN	COMMENT
499.0± 1.5 OUR FIT					
503 ±16 OUR AVERAGE Error includes scale factor of 1.2.					
498 ±12 ±12	1791	ACCIARRI	98G	L3	E_{cm}^{ee}= 88–94 GeV
539 ±26 ±17	410	AKERS	95C	OPAL	E_{cm}^{ee}= 88–94 GeV
450 ±34 ±34	258	BUSKULIC	93L	ALEP	E_{cm}^{ee}= 88–94 GeV
540 ±80 ±40	52	ADEVA	92	L3	E_{cm}^{ee}= 88–94 GeV
• • • We do not use the following data for averages, fits, limits, etc. • • •					
498.1± 2.6		[1] ABBIENDI	01A	OPAL	E_{cm}^{ee}= 88–94 GeV
498.1± 3.2		[1] ABREU	00F	DLPH	E_{cm}^{ee}= 88–94 GeV
499.1± 2.9		[1] ACCIARRI	00C	L3	E_{cm}^{ee}= 88–94 GeV
499.1± 2.5		[1] BARATE	00C	ALEP	E_{cm}^{ee}= 88–94 GeV

[1] This is an indirect determination of Γ(invisible) from a fit to the visible Z decay modes.

Γ(hadrons) Γ_7

This parameter is not directly used in the 5-parameter fit assuming lepton universality, but is derived using the fit results. See the note "The Z boson" and ref. LEP-SLC 06.

VALUE (MeV)	EVTS	DOCUMENT ID		TECN	COMMENT
1744.4±2.0 OUR FIT					
1745.4±3.5	4.10M	ABBIENDI	01A	OPAL	E_{cm}^{ee}= 88–94 GeV
1738.1±4.0	3.70M	ABREU	00F	DLPH	E_{cm}^{ee}= 88–94 GeV
1751.1±3.8	3.54M	ACCIARRI	00C	L3	E_{cm}^{ee}= 88–94 GeV
1744.0±3.4	4.07M	BARATE	00C	ALEP	E_{cm}^{ee}= 88–94 GeV

Z BRANCHING RATIOS

OUR FIT is obtained using the fit procedure and correlations as determined by the LEP Electroweak Working Group (see the note "The Z boson" and ref. LEP-SLC 06).

$\Gamma(\mu^+\mu^-)/\Gamma(e^+e^-)$ Γ_2/Γ_1

This parameter is not directly used in the overall fit but is derived using the fit results; see the note "The Z boson" and ref. LEP-SLC 06.

VALUE	DOCUMENT ID
1.0009±0.0028 OUR FIT	

$\Gamma(\tau^+\tau^-)/\Gamma(e^+e^-)$ Γ_3/Γ_1

This parameter is not directly used in the overall fit but is derived using the fit results; see the note "The Z boson" and ref. LEP-SLC 06.

VALUE	DOCUMENT ID
1.0019±0.0032 OUR FIT	

$\Gamma(\ell^+\ell^-\ell^+\ell^-)/\Gamma_{total}$ Γ_5/Γ

Here ℓ indicates either e or μ. The branching fractions in this node are given within the phase-space defined by the requirements that (i) the 4-lepton invariant mass is between 80 GeV and 100 GeV, and (ii) any opposite-sign same-flavor lepton pair has a di-lepton invariant mass larger than 4 GeV.

VALUE (units 10^{-6})	EVTS	DOCUMENT ID		TECN	COMMENT
4.45±0.32 OUR AVERAGE					
$4.9\ ^{+0.8}_{-0.7}\ ^{+0.4}_{-0.2}$	39	[1] KHACHATRY...16CC		CMS	E_{cm}^{pp} = 13 TeV
4.31±0.34±0.17	172	AAD	14N	ATLS	E_{cm}^{pp} = 7, 8 TeV
$4.6\ ^{+1.0}_{-0.9}$ ±0.2	28	[2] CHATRCHYAN	12BN	CMS	E_{cm}^{pp} = 7 TeV

[1] KHACHATRYAN 16CC reports $(4.9\ ^{+0.8}_{-0.7}\ ^{+0.3}_{-0.2}\ ^{+0.2}_{-0.1}\ ^{+0.1}_{-0.1}) \times 10^{-6}$ value, where the uncertainties are statistical, systematic, theory, and due to luminosity. We have combined uncertainties in quadrature.

[2] CHATRCHYAN 12BN reports $(4.2^{+0.9}_{-0.8} \pm 0.2) \times 10^{-6}$ value. Their result (both central value and uncertainties) is scaled up by 10% to account for the different phase-space definition used here (see RAINBOLD 18, arXiv:1805.05791 (2018)).

Γ(hadrons)/$\Gamma(e^+e^-)$ Γ_7/Γ_1

VALUE	EVTS	DOCUMENT ID		TECN	COMMENT
20.804± 0.050 OUR FIT					
20.902± 0.084	137.0K	[1] ABBIENDI	01A	OPAL	E_{cm}^{ee}= 88–94 GeV
20.88 ± 0.12	117.8k	ABREU	00F	DLPH	E_{cm}^{ee}= 88–94 GeV
20.816± 0.089	124.4k	ACCIARRI	00C	L3	E_{cm}^{ee}= 88–94 GeV
20.677± 0.075		[2] BARATE	00C	ALEP	E_{cm}^{ee}= 88–94 GeV
• • • We do not use the following data for averages, fits, limits, etc. • • •					
$27.0\ ^{+11.7}_{-\ 8.8}$	12	[3] ABRAMS	89D	MRK2	E_{cm}^{ee}= 89–93 GeV

[1] ABBIENDI 01A error includes approximately 0.067 due to statistics, 0.040 due to event selection systematics, 0.027 due to the theoretical uncertainty in t-channel prediction, and 0.014 due to LEP energy uncertainty.

[2] BARATE 00C error includes approximately 0.062 due to statistics, 0.033 due to experimental systematics, and 0.026 due to the theoretical uncertainty in t-channel prediction.

[3] ABRAMS 89D have included both statistical and systematic uncertainties in their quoted errors.

Γ(hadrons)/$\Gamma(\mu^+\mu^-)$ Γ_7/Γ_2

OUR FIT is obtained using the fit procedure and correlations as determined by the LEP Electroweak Working Group (see the note "The Z boson" and ref. LEP-SLC 06).

VALUE	EVTS	DOCUMENT ID		TECN	COMMENT
20.785±0.033 OUR FIT					
20.811±0.058	182.8K	[1] ABBIENDI	01A	OPAL	E_{cm}^{ee}= 88–94 GeV
20.65 ±0.08	157.6k	ABREU	00F	DLPH	E_{cm}^{ee}= 88–94 GeV
20.861±0.097	113.4k	ACCIARRI	00C	L3	E_{cm}^{ee}= 88–94 GeV
20.799±0.056		[2] BARATE	00C	ALEP	E_{cm}^{ee}= 88–94 GeV
• • • We do not use the following data for averages, fits, limits, etc. • • •					
$18.9\ ^{+7.1}_{-5.3}$	13	[3] ABRAMS	89D	MRK2	E_{cm}^{ee}= 89–93 GeV

[1] ABBIENDI 01A error includes approximately 0.050 due to statistics and 0.027 due to event selection systematics.

[2] BARATE 00C error includes approximately 0.053 due to statistics and 0.021 due to experimental systematics.

[3] ABRAMS 89D have included both statistical and systematic uncertainties in their quoted errors.

Γ(hadrons)/$\Gamma(\tau^+\tau^-)$ Γ_7/Γ_3

OUR FIT is obtained using the fit procedure and correlations as determined by the LEP Electroweak Working Group (see the note "The Z boson" and ref. LEP-SLC 06).

VALUE	EVTS	DOCUMENT ID		TECN	COMMENT
20.764±0.045 OUR FIT					
20.832±0.091	151.5K	[1] ABBIENDI	01A	OPAL	E_{cm}^{ee}= 88–94 GeV
20.84 ±0.13	104.0k	ABREU	00F	DLPH	E_{cm}^{ee}= 88–94 GeV
20.792±0.133	103.0k	ACCIARRI	00C	L3	E_{cm}^{ee}= 88–94 GeV
20.707±0.062		[2] BARATE	00C	ALEP	E_{cm}^{ee}= 88–94 GeV
• • • We do not use the following data for averages, fits, limits, etc. • • •					
$15.2\ ^{+4.8}_{-3.9}$	21	[3] ABRAMS	89D	MRK2	E_{cm}^{ee}= 89–93 GeV

[1] ABBIENDI 01A error includes approximately 0.055 due to statistics and 0.071 due to event selection systematics.

[2] BARATE 00C error includes approximately 0.054 due to statistics and 0.033 due to experimental systematics.

[3] ABRAMS 89D have included both statistical and systematic uncertainties in their quoted errors.

Γ(hadrons)/$\Gamma(\ell^+\ell^-)$ Γ_7/Γ_4

ℓ indicates each type of lepton (e, μ, and τ), not sum over them.

Our fit result is obtained requiring lepton universality.

VALUE	EVTS	DOCUMENT ID		TECN	COMMENT
20.767±0.025 OUR FIT					
20.823±0.044	471.3K	[1] ABBIENDI	01A	OPAL	E_{cm}^{ee}= 88–94 GeV
20.730±0.060	379.4k	ABREU	00F	DLPH	E_{cm}^{ee}= 88–94 GeV
20.810±0.060	340.8k	ACCIARRI	00C	L3	E_{cm}^{ee}= 88–94 GeV
20.725±0.039	500k	[2] BARATE	00C	ALEP	E_{cm}^{ee}= 88–94 GeV
• • • We do not use the following data for averages, fits, limits, etc. • • •					
$18.9\ ^{+3.6}_{-3.2}$	46	ABRAMS	89B	MRK2	E_{cm}^{ee}= 89–93 GeV

[1] ABBIENDI 01A error includes approximately 0.034 due to statistics and 0.027 due to event selection systematics.

[2] BARATE 00C error includes approximately 0.033 due to statistics, 0.020 due to experimental systematics, and 0.005 due to the theoretical uncertainty in t-channel prediction.

$\Gamma((u\overline{u}+c\overline{c})/2)/\Gamma$(hadrons) Γ_8/Γ_7

This quantity is the branching ratio of $Z \to$ "up-type" quarks to $Z \to$ hadrons. Except ACKERSTAFF 97T the values of $Z \to$ "up-type" and $Z \to$ "down-type" branchings are extracted from measurements of Γ(hadrons), and $\Gamma(Z \to \gamma+$ jets) where γ is a high-energy (>5 or 7 GeV) isolated photon. As the experiments use different procedures and slightly different values of M_Z, Γ(hadrons) and α_s in their extraction procedures, our average has to be taken with caution.

VALUE	DOCUMENT ID		TECN	COMMENT
0.166±0.009 OUR AVERAGE				
$0.172\ ^{+0.011}_{-0.010}$	[1] ABBIENDI	04E	OPAL	E_{cm}^{ee} = 91.2 GeV
0.160±0.019±0.019	[2] ACKERSTAFF	97T	OPAL	E_{cm}^{ee}= 88–94 GeV
$0.137\ ^{+0.038}_{-0.054}$	[3] ABREU	95X	DLPH	E_{cm}^{ee}= 88–94 GeV
0.137±0.033	[4] ADRIANI	93	L3	E_{cm}^{ee}= 91.2 GeV

[1] ABBIENDI 04E select photons with energy > 7 GeV and use Γ(hadrons) = 1744.4 ± 2.0 MeV and $\alpha_s = 0.1172 \pm 0.002$ to obtain $\Gamma_u = 300^{+19}_{-18}$ MeV.

[2] ACKERSTAFF 97T measure $\Gamma_{u\overline{u}}/(\Gamma_{d\overline{d}}+\Gamma_{u\overline{u}}+\Gamma_{s\overline{s}}) = 0.258 \pm 0.031 \pm 0.032$. To obtain this branching ratio authors use $R_c+R_b = 0.380 \pm 0.010$. This measurement is fully negatively correlated with the measurement of $\Gamma_{d\overline{d},s\overline{s}}/(\Gamma_{d\overline{d}}+\Gamma_{u\overline{u}}+\Gamma_{s\overline{s}})$ given in the next data block.

[3] ABREU 95X use $M_Z = 91.187 \pm 0.009$ GeV, Γ(hadrons) = 1725 ± 12 MeV and $\alpha_s = 0.123 \pm 0.005$. To obtain this branching ratio we divide their value of $C_{2/3} = 91^{+0.25}_{-0.36}$ by their value of $(3C_{1/3} + 2C_{2/3}) = 6.66 \pm 0.05$.

[4] ADRIANI 93 use $M_Z = 91.181 \pm 0.022$ GeV, Γ(hadrons) = 1742 ± 19 MeV and $\alpha_s = 0.125 \pm 0.009$. To obtain this branching ratio we divide their value of $C_{2/3} = 0.92 \pm 0.22$ by their value of $(3C_{1/3} + 2C_{2/3}) = 6.720 \pm 0.076$.

$\Gamma((d\overline{d}+s\overline{s}+b\overline{b})/3)/\Gamma$(hadrons) — Γ_9/Γ_7

This quantity is the branching ratio of $Z \to$ "down-type" quarks to $Z \to$ hadrons. Except ACKERSTAFF 97T the values of $Z \to$ "up-type" and $Z \to$ "down-type" branchings are extracted from measurements of Γ(hadrons), and $\Gamma(Z \to \gamma +$ jets) where γ is a high-energy (>5 or 7 GeV) isolated photon. As the experiments use different procedures and slightly different values of M_Z, Γ(hadrons) and α_s in their extraction procedures, our average has to be taken with caution.

VALUE	DOCUMENT ID		TECN	COMMENT
0.223±0.006 OUR AVERAGE				
0.218±0.007	[1] ABBIENDI	04E	OPAL	$E^{ee}_{\rm cm}$ = 91.2 GeV
0.230±0.010±0.010	[2] ACKERSTAFF	97T	OPAL	$E^{ee}_{\rm cm}$= 88–94 GeV
$0.243^{+0.036}_{-0.026}$	[3] ABREU	95X	DLPH	$E^{ee}_{\rm cm}$= 88–94 GeV
0.243±0.022	[4] ADRIANI	93	L3	$E^{ee}_{\rm cm}$= 91.2 GeV

[1] ABBIENDI 04E select photons with energy > 7 GeV and use Γ(hadrons) = 1744.4 ± 2.0 MeV and $\alpha_s = 0.1172 \pm 0.002$ to obtain $\Gamma_d = 381 \pm 12$ MeV.

[2] ACKERSTAFF 97T measure $\Gamma_{d\overline{d},s\overline{s}}/(\Gamma_{d\overline{d}}+\Gamma_{u\overline{u}}+\Gamma_{s\overline{s}}) = 0.371 \pm 0.016 \pm 0.016$. To obtain this branching ratio authors use $R_c+R_b = 0.380 \pm 0.010$. This measurement is fully negatively correlated with the measurement of $\Gamma_{u\overline{u}}/(\Gamma_{d\overline{d}}+\Gamma_{u\overline{u}}+\Gamma_{s\overline{s}})$ presented in the previous data block.

[3] ABREU 95X use $M_Z = 91.187 \pm 0.009$ GeV, Γ(hadrons) = 1725 ± 12 MeV and $\alpha_s = 0.123 \pm 0.005$. To obtain this branching ratio we divide their value of $C_{1/3} = 1.62^{+0.24}_{-0.17}$ by their value of $(3C_{1/3} + 2C_{2/3}) = 6.66 \pm 0.05$.

[4] ADRIANI 93 use $M_Z = 91.181 \pm 0.022$ GeV, Γ(hadrons) = 1742 ± 19 MeV and $\alpha_s = 0.125 \pm 0.009$. To obtain this branching ratio we divide their value of $C_{1/3} = 1.63 \pm 0.15$ by their value of $(3C_{1/3} + 2C_{2/3}) = 6.720 \pm 0.076$.

$R_c = \Gamma(c\overline{c})/\Gamma$(hadrons) — Γ_{10}/Γ_7

OUR FIT is obtained by a simultaneous fit to several c- and b-quark measurements as explained in the note "The Z boson" and ref. LEP-SLC 06.

The Standard Model predicts $R_c = 0.1723$ for $m_t = 174.3$ GeV and $M_H = 150$ GeV.

VALUE	DOCUMENT ID		TECN	COMMENT
0.1721±0.0030 OUR FIT				
0.1744±0.0031±0.0021	[1] ABE	05F	SLD	$E^{ee}_{\rm cm}$=91.28 GeV
0.1665±0.0051±0.0081	[2] ABREU	00	DLPH	$E^{ee}_{\rm cm}$= 88–94 GeV
0.1698±0.0069	[3] BARATE	00B	ALEP	$E^{ee}_{\rm cm}$= 88–94 GeV
0.180 ±0.011 ±0.013	[4] ACKERSTAFF	98E	OPAL	$E^{ee}_{\rm cm}$= 88–94 GeV
0.167 ±0.011 ±0.012	[5] ALEXANDER	96R	OPAL	$E^{ee}_{\rm cm}$= 88–94 GeV
• • • We do not use the following data for averages, fits, limits, etc. • • •				
0.1623±0.0085±0.0209	[6] ABREU	95D	DLPH	$E^{ee}_{\rm cm}$= 88–94 GeV

[1] ABE 05F use hadronic Z decays collected during 1996–98 to obtain an enriched sample of $c\overline{c}$ events using a double tag method. The single c-tag is obtained with a neural network trained to perform flavor discrimination using as input several signatures (corrected secondary vertex mass, vertex decay length, multiplicity and total momentum of the hemisphere). A multitag approach is used, defining 4 regions of the output value of the neural network and R_c is extracted from a simultaneous fit to the count rates of the 4 different tags. The quoted systematic error includes an uncertainty of ±0.0006 due to the uncertainty on R_b.

[2] ABREU 00 obtain this result properly combining the measurement from the D^{*+} production rate (R_c= 0.1610 ± 0.0104 ± 0.0077 ± 0.0043 (BR)) with that from the overall charm counting (R_c= 0.1692 ± 0.0047 ± 0.0063 ± 0.0074 (BR)) in $c\overline{c}$ events. The systematic error includes an uncertainty of ±0.0054 due to the uncertainty on the charmed hadron branching fractions.

[3] BARATE 00B use exclusive decay modes to independently determine the quantities $R_c \times$f($c \to$ X), X=D^0, D^+, D_s^+, and Λ_c. Estimating $R_c \times$f($c \to \Xi_c/\Omega_c$)= 0.0034, they simply sum over all the charm decays to obtain R_c= 0.1738 ± 0.0047 ± 0.0088 ± 0.0075(BR). This is combined with all previous ALEPH measurements (BARATE 98T and BUSKULIC 94G, R_c= 0.1681 ± 0.0054 ± 0.0062) to obtain the quoted value.

[4] ACKERSTAFF 98E use an inclusive/exclusive double tag. In one jet $D^{*\pm}$ mesons are exclusively reconstructed in several decay channels and in the opposite jet a slow pion (opposite charge inclusive $D^{*\pm}$) tag is used. The b content of this sample is measured by the simultaneous detection of a lepton in one jet and an inclusively reconstructed $D^{*\pm}$ meson in the opposite jet. The systematic error includes an uncertainty of ±0.006 due to the external branching ratios.

[5] ALEXANDER 96R obtain this value via direct charm counting, summing the partial contributions from D^0, D^+, D_s^+, and Λ_c^+, and assuming that strange-charmed baryons account for the 15% of the Λ_c^+ production. An uncertainty of ±0.005 due to the uncertainties in the charm hadron branching ratios is included in the overall systematics.

[6] ABREU 95D perform a maximum likelihood fit to the combined p and p_T distributions of single and dilepton samples. The second error includes an uncertainty of ±0.0124 due to models and branching ratios.

$R_b = \Gamma(b\overline{b})/\Gamma$(hadrons) — Γ_{11}/Γ_7

OUR FIT is obtained by a simultaneous fit to several c- and b-quark measurements as explained in the note "The Z boson" and ref. LEP-SLC 06.

The Standard Model predicts R_b=0.21581 for m_t=174.3 GeV and M_H=150 GeV.

VALUE	DOCUMENT ID		TECN	COMMENT
0.21629±0.00066 OUR FIT				
0.21594±0.00094±0.00075	[1] ABE	05F	SLD	$E^{ee}_{\rm cm}$=91.28 GeV
0.2174 ±0.0015 ±0.0028	[2] ACCIARRI	00	L3	$E^{ee}_{\rm cm}$= 89–93 GeV
0.2178 ±0.0011 ±0.0013	[3] ABBIENDI	99B	OPAL	$E^{ee}_{\rm cm}$= 88–94 GeV
0.21634±0.00067±0.00060	[4] ABREU	99B	DLPH	$E^{ee}_{\rm cm}$= 88–94 GeV
0.2159 ±0.0009 ±0.0011	[5] BARATE	97F	ALEP	$E^{ee}_{\rm cm}$= 88–94 GeV
• • • We do not use the following data for averages, fits, limits, etc. • • •				
0.2145 ±0.0089 ±0.0067	[6] ABREU	95D	DLPH	$E^{ee}_{\rm cm}$= 88–94 GeV
0.219 ±0.006 ±0.005	[7] BUSKULIC	94G	ALEP	$E^{ee}_{\rm cm}$= 88–94 GeV
0.251 ±0.049 ±0.030	[8] JACOBSEN	91	MRK2	$E^{ee}_{\rm cm}$= 91 GeV

[1] ABE 05F use hadronic Z decays collected during 1996–98 to obtain an enriched sample of $b\overline{b}$ events using a double tag method. The single b–tag is obtained with a neural network trained to perform flavor discrimination using as input several signatures (corrected secondary vertex mass, vertex decay length, multiplicity and total momentum of the hemisphere; the key tag is obtained requiring the secondary vertex corrected mass to be above the D–meson mass). ABE 05F obtain R_b =0.21604 ± 0.00098 ± 0.00074 where the systematic error includes an uncertainty of ±0.00012 due to the uncertainty on R_c. The value reported here is obtained properly combining with ABE 98D. The quoted systematic error includes an uncertainty of ±0.00012 due to the uncertainty on R_c.

[2] ACCIARRI 00 obtain this result using a double-tagging technique, with a high p_T lepton tag and an impact parameter tag in opposite hemispheres.

[3] ABBIENDI 99B tag $Z \to b\overline{b}$ decays using leptons and/or separated decay vertices. The b-tagging efficiency is measured directly from the data using a double-tagging technique.

[4] ABREU 99B obtain this result combining in a multivariate analysis several tagging methods (impact parameter and secondary vertex reconstruction, complemented by event shape variables). For R_c different from its Standard Model value of 0.172, R_b varies as $-0.024\times(R_c-0.172)$.

[5] BARATE 97F combine the lifetime-mass hemisphere tag (BARATE 97E) with event shape information and lepton tag to identify $Z \to b\overline{b}$ candidates. They further use c- and $u\,d\,s$-selection tags to identify the background. For R_c different from its Standard Model value of 0.172, R_b varies as $-0.019\times(R_c - 0.172)$.

[6] ABREU 95D perform a maximum likelihood fit to the combined p and p_T distributions of single and dilepton samples. The second error includes an uncertainty of ±0.0023 due to models and branching ratios.

[7] BUSKULIC 94G perform a simultaneous fit to the p and p_T spectra of both single and dilepton events.

[8] JACOBSEN 91 tagged $b\overline{b}$ events by requiring coincidence of ≥ 3 tracks with significant impact parameters using vertex detector. Systematic error includes lifetime and decay uncertainties (±0.014).

$\Gamma(b\overline{b}b\overline{b})/\Gamma$(hadrons) — Γ_{12}/Γ_7

VALUE (units 10^{-4})	DOCUMENT ID		TECN	COMMENT
5.2±1.9 OUR AVERAGE				
3.6±1.7±2.7	[1] ABBIENDI	01G	OPAL	$E^{ee}_{\rm cm}$= 88–94 GeV
6.0±1.9±1.4	[2] ABREU	99U	DLPH	$E^{ee}_{\rm cm}$= 88–94 GeV

[1] ABBIENDI 01G use a sample of four-jet events from hadronic Z decays. To enhance the $b\overline{b}b\overline{b}$ signal, at least three of the four jets are required to have a significantly detached secondary vertex.

[2] ABREU 99U force hadronic Z decays into 3 jets to use all the available phase space and require a b tag for every jet. This decay mode includes primary and secondary $4b$ production, *e.g.* from gluon splitting to $b\overline{b}$.

$\Gamma(ggg)/\Gamma$(hadrons) — Γ_{13}/Γ_7

VALUE	CL%	DOCUMENT ID		TECN	COMMENT
<1.6 × 10⁻²	95	[1] ABREU	96S	DLPH	$E^{ee}_{\rm cm}$= 88–94 GeV

[1] This branching ratio is slightly dependent on the jet-finder algorithm. The value we quote is obtained using the JADE algorithm, while using the DURHAM algorithm ABREU 96S obtain an upper limit of 1.5×10^{-2}.

$\Gamma(\pi^0\gamma)/\Gamma_{\rm total}$ — Γ_{14}/Γ

VALUE	CL%	DOCUMENT ID		TECN	COMMENT
<2.01 × 10⁻⁵	95	AALTONEN	14E	CDF	$E^{p\overline{p}}_{\rm cm}$ = 1.96 TeV
$<5.2 \times 10^{-5}$	95	[1] ACCIARRI	95G	L3	$E^{ee}_{\rm cm}$= 88–94 GeV
$<5.5 \times 10^{-5}$	95	ABREU	94B	DLPH	$E^{ee}_{\rm cm}$= 88–94 GeV
$<2.1 \times 10^{-4}$	95	DECAMP	92	ALEP	$E^{ee}_{\rm cm}$= 88–94 GeV
$<1.4 \times 10^{-4}$	95	AKRAWY	91F	OPAL	$E^{ee}_{\rm cm}$= 88–94 GeV

[1] This limit is for both decay modes $Z \to \pi^0\gamma/\gamma\gamma$ which are indistinguishable in ACCIARRI 95G.

$\Gamma(\eta\gamma)/\Gamma_{\rm total}$ — Γ_{15}/Γ

VALUE	CL%	DOCUMENT ID		TECN	COMMENT
$<7.6 \times 10^{-5}$	95	ACCIARRI	95G	L3	$E^{ee}_{\rm cm}$= 88–94 GeV
$<8.0 \times 10^{-5}$	95	ABREU	94B	DLPH	$E^{ee}_{\rm cm}$= 88–94 GeV
<5.1 × 10⁻⁵	95	DECAMP	92	ALEP	$E^{ee}_{\rm cm}$= 88–94 GeV
$<2.0 \times 10^{-4}$	95	AKRAWY	91F	OPAL	$E^{ee}_{\rm cm}$= 88–94 GeV

$\Gamma(\omega\gamma)/\Gamma_{\rm total}$ — Γ_{16}/Γ

VALUE	CL%	DOCUMENT ID		TECN	COMMENT
<6.5 × 10⁻⁴	95	ABREU	94B	DLPH	$E^{ee}_{\rm cm}$= 88–94 GeV

Gauge & Higgs Boson Particle Listings

Z

$\Gamma(\eta'(958)\gamma)/\Gamma_{total}$ Γ_{17}/Γ

VALUE	CL%	DOCUMENT ID		TECN	COMMENT
$<4.2\times10^{-5}$	95	DECAMP	92	ALEP	E_{cm}^{ee}= 88–94 GeV

$\Gamma(\phi\gamma)/\Gamma_{total}$ Γ_{18}/Γ

VALUE	CL%	EVTS	DOCUMENT ID		TECN	COMMENT
$<8.3\times10^{-6}$	95	1065	[1] AABOUD	16K	ATLS	E_{cm}^{pp} = 13 TeV

[1] AABOUD 16K search for the $Z\to\phi\gamma$ decay mode where the ϕ is identified through its decay into K^+K^-. In the data corresponding to a total luminosity of 2.7 fb^{-1}, 1065 events are selected and their $K^+K^-\gamma$ invariant mass spectrum is analyzed.

$\Gamma(\gamma\gamma)/\Gamma_{total}$ Γ_{19}/Γ

This decay would violate the Landau-Yang theorem.

VALUE	CL%	DOCUMENT ID		TECN	COMMENT
$<1.46\times10^{-5}$	95	AALTONEN	14E	CDF	$E_{cm}^{p\overline{p}}$ = 1.96 TeV
$<5.2\times10^{-5}$	95	[1] ACCIARRI	95G	L3	E_{cm}^{ee}= 88–94 GeV
$<5.5\times10^{-5}$	95	ABREU	94B	DLPH	E_{cm}^{ee}= 88–94 GeV
$<1.4\times10^{-4}$	95	AKRAWY	91F	OPAL	E_{cm}^{ee}= 88–94 GeV

[1] This limit is for both decay modes $Z\to\pi^0\gamma/\gamma\gamma$ which are indistinguishable in ACCIARRI 95G.

$\Gamma(\pi^0\pi^0)/\Gamma_{total}$ Γ_{20}/Γ

VALUE	CL%	DOCUMENT ID	TECN	COMMENT
$<1.52\times10^{-5}$	95	AALTONEN 14E	CDF	$E_{cm}^{p\overline{p}}$ = 1.96 TeV

$\Gamma(\gamma\gamma\gamma)/\Gamma_{total}$ Γ_{21}/Γ

VALUE	CL%	DOCUMENT ID		TECN	COMMENT
$<2.2\times10^{-6}$	95	AAD	16L	ATLS	E_{cm}^{pp} = 8 TeV
• • • We do not use the following data for averages, fits, limits, etc. • • •					
$<1.0\times10^{-5}$	95	[1] ACCIARRI	95C	L3	E_{cm}^{ee}= 88–94 GeV
$<1.7\times10^{-5}$	95	[1] ABREU	94B	DLPH	E_{cm}^{ee}= 88–94 GeV
$<6.6\times10^{-5}$	95	AKRAWY	91F	OPAL	E_{cm}^{ee}= 88–94 GeV

[1] Limit derived in the context of composite Z model.

$\Gamma(\pi^\pm W^\mp)/\Gamma_{total}$ Γ_{22}/Γ

The value is for the sum of the charge states indicated.

VALUE	CL%	DOCUMENT ID		TECN	COMMENT
$<7\times10^{-5}$	95	DECAMP	92	ALEP	E_{cm}^{ee}= 88–94 GeV

$\Gamma(\rho^\pm W^\mp)/\Gamma_{total}$ Γ_{23}/Γ

The value is for the sum of the charge states indicated.

VALUE	CL%	DOCUMENT ID		TECN	COMMENT
$<8.3\times10^{-5}$	95	DECAMP	92	ALEP	E_{cm}^{ee}= 88–94 GeV

$\Gamma(J/\psi(1S)X)/\Gamma_{total}$ Γ_{24}/Γ

VALUE (units 10^{-3})	EVTS	DOCUMENT ID		TECN	COMMENT
$3.51^{+0.23}_{-0.25}$ OUR AVERAGE		Error includes scale factor of 1.1.			
$3.21\pm0.21^{+0.19}_{-0.28}$	553	[1] ACCIARRI	99F	L3	E_{cm}^{ee}= 88–94 GeV
$3.9\ \pm0.2\ \pm0.3$	511	[2] ALEXANDER	96B	OPAL	E_{cm}^{ee}= 88–94 GeV
$3.73\pm0.39\pm0.36$	153	[3] ABREU	94P	DLPH	E_{cm}^{ee}= 88–94 GeV

[1] ACCIARRI 99F combine $\mu^+\mu^-$ and e^+e^- $J/\psi(1S)$ decay channels. The branching ratio for prompt $J/\psi(1S)$ production is measured to be $(2.1\pm0.6\pm0.4^{+0.4}_{-0.2}(\text{theor.}))\times10^{-4}$.

[2] ALEXANDER 96B identify $J/\psi(1S)$ from the decays into lepton pairs. (4.8 ± 2.4)% of this branching ratio is due to prompt $J/\psi(1S)$ production (ALEXANDER 96N).

[3] Combining $\mu^+\mu^-$ and e^+e^- channels and taking into account the common systematic errors. $(7.7^{+6.3}_{-5.4})$% of this branching ratio is due to prompt $J/\psi(1S)$ production.

$\Gamma(J/\psi(1S)\gamma)/\Gamma_{total}$ Γ_{25}/Γ

VALUE	CL%	DOCUMENT ID		TECN	COMMENT
$<2.6\times10^{-6}$	95	[1] AAD	15I	ATLS	E_{cm}^{pp} = 8 TeV

[1] AAD 15I use events with the highest p_T muon in the pair required to have $p_T>20$ GeV, the dimuon mass required to be within 0.2 GeV of the $J/\psi(1S)$ mass and it's transverse momentum required to be >36 GeV. The photon is also required to have it's $p_T>36$ GeV.

$\Gamma(\psi(2S)X)/\Gamma_{total}$ Γ_{26}/Γ

VALUE (units 10^{-3})	EVTS	DOCUMENT ID		TECN	COMMENT
1.60±0.29 OUR AVERAGE					
$1.6\ \pm0.5\ \pm0.3$	39	[1] ACCIARRI	97J	L3	E_{cm}^{ee}= 88–94 GeV
$1.6\ \pm0.3\ \pm0.2$	46.9	[2] ALEXANDER	96B	OPAL	E_{cm}^{ee}= 88–94 GeV
$1.60\pm0.73\pm0.33$	5.4	[3] ABREU	94P	DLPH	E_{cm}^{ee}= 88–94 GeV

[1] ACCIARRI 97J measure this branching ratio via the decay channel $\psi(2S)\to\ell^+\ell^-$ ($\ell=\mu$, e).

[2] ALEXANDER 96B measure this branching ratio via the decay channel $\psi(2S)\to J/\psi\pi^+\pi^-$, with $J/\psi\to\ell^+\ell^-$.

[3] ABREU 94P measure this branching ratio via decay channel $\psi(2S)\to J/\psi\pi^+\pi^-$, with $J/\psi\to\mu^+\mu^-$.

$\Gamma(\chi_{c1}(1P)X)/\Gamma_{total}$ Γ_{27}/Γ

VALUE (units 10^{-3})	EVTS	DOCUMENT ID		TECN	COMMENT
2.9±0.7 OUR AVERAGE					
$2.7\pm0.6\pm0.5$	33	[1] ACCIARRI	97J	L3	E_{cm}^{ee}= 88–94 GeV
$5.0\pm2.1^{+1.5}_{-0.9}$	6.4	[2] ABREU	94P	DLPH	E_{cm}^{ee}= 88–94 GeV

[1] ACCIARRI 97J measure this branching ratio via the decay channel $\chi_{c1}\to J/\psi+\gamma$, with $J/\psi\to\ell^+\ell^-$ ($\ell=\mu$, e). The $M(\ell^+\ell^-\gamma)$–$M(\ell^+\ell^-)$ mass difference spectrum is fitted with two gaussian shapes for χ_{c1} and χ_{c2}.

[2] This branching ratio is measured via the decay channel $\chi_{c1}\to J/\psi+\gamma$, with $J/\psi\to\mu^+\mu^-$.

$\Gamma(\chi_{c2}(1P)X)/\Gamma_{total}$ Γ_{28}/Γ

VALUE	CL%	DOCUMENT ID		TECN	COMMENT
$<3.2\times10^{-3}$	90	[1] ACCIARRI	97J	L3	E_{cm}^{ee}= 88–94 GeV

[1] ACCIARRI 97J derive this limit via the decay channel $\chi_{c2}\to J/\psi+\gamma$, with $J/\psi\to\ell^+\ell^-$ ($\ell=\mu$, e). The $M(\ell^+\ell^-\gamma)$–$M(\ell^+\ell^-)$ mass difference spectrum is fitted with two gaussian shapes for χ_{c1} and χ_{c2}.

$\Gamma(\Upsilon(1S)X+\Upsilon(2S)X+\Upsilon(3S)X)/\Gamma_{total}$ $\Gamma_{29}/\Gamma=(\Gamma_{30}+\Gamma_{31}+\Gamma_{32})/\Gamma$

VALUE (units 10^{-4})	EVTS	DOCUMENT ID		TECN	COMMENT
1.0±0.4±0.22	6.4	[1] ALEXANDER	96F	OPAL	E_{cm}^{ee}= 88–94 GeV

[1] ALEXANDER 96F identify the Υ (which refers to any of the three lowest bound states) through its decay into e^+e^- and $\mu^+\mu^-$. The systematic error includes an uncertainty of ±0.2 due to the production mechanism.

$\Gamma(\Upsilon(1S)X)/\Gamma_{total}$ Γ_{30}/Γ

VALUE	CL%	DOCUMENT ID		TECN	COMMENT
$<3.4\times10^{-6}$	95	[1] AAD	15I	ATLS	E_{cm}^{pp} = 8 TeV
• • • We do not use the following data for averages, fits, limits, etc. • • •					
$<4.4\times10^{-5}$	95	[2] ACCIARRI	99F	L3	E_{cm}^{ee}= 88–94 GeV

[1] AAD 15I use events with the highest p_T muon in the pair required to have $p_T>20$ GeV, the dimuon mass required to be in the range 8–12 GeV and it's transverse momentum required to be >36 GeV. The photon is also required to have it's $p_T>36$ GeV.

[2] ACCIARRI 99F search for $\Upsilon(1S)$ through its decay into $\ell^+\ell^-$ ($\ell=e$ or μ).

$\Gamma(\Upsilon(2S)X)/\Gamma_{total}$ Γ_{31}/Γ

VALUE	CL%	DOCUMENT ID		TECN	COMMENT
$<6.5\times10^{-6}$	95	[1] AAD	15I	ATLS	E_{cm}^{pp} = 8 TeV
• • • We do not use the following data for averages, fits, limits, etc. • • •					
$<13.9\times10^{-5}$	95	[2] ACCIARRI	97R	L3	E_{cm}^{ee}= 88–94 GeV

[1] AAD 15I use events with the highest p_T muon in the pair required to have $p_T>20$ GeV, the dimuon mass required to be in the range 8–12 GeV and it's transverse momentum required to be >36 GeV. The photon is also required to have it's $p_T>36$ GeV.

[2] ACCIARRI 97R search for $\Upsilon(2S)$ through its decay into $\ell^+\ell^-$ ($\ell=e$ or μ).

$\Gamma(\Upsilon(3S)X)/\Gamma_{total}$ Γ_{32}/Γ

VALUE	CL%	DOCUMENT ID		TECN	COMMENT
$<5.4\times10^{-6}$	95	[1] AAD	15I	ATLS	E_{cm}^{pp} = 8 TeV
• • • We do not use the following data for averages, fits, limits, etc. • • •					
$<9.4\times10^{-5}$	95	[2] ACCIARRI	97R	L3	E_{cm}^{ee}= 88–94 GeV

[1] AAD 15I use events with the highest p_T muon in the pair required to have $p_T>20$ GeV, the dimuon mass required to be in the range 8–12 GeV and it's transverse momentum required to be >36 GeV. The photon is also required to have it's $p_T>36$ GeV.

[2] ACCIARRI 97R search for $\Upsilon(3S)$ through its decay into $\ell^+\ell^-$ ($\ell=e$ or μ).

$\Gamma((D^0/\overline{D}^0)X)/\Gamma(\text{hadrons})$ Γ_{33}/Γ_7

VALUE	EVTS	DOCUMENT ID		TECN	COMMENT
0.296±0.019±0.021	369	[1] ABREU	93I	DLPH	E_{cm}^{ee}= 88–94 GeV

[1] The $(D^0/\overline{D}^0)$ states in ABREU 93I are detected by the $K\pi$ decay mode. This is a corrected result (see the erratum of ABREU 93I).

$\Gamma(D^\pm X)/\Gamma(\text{hadrons})$ Γ_{34}/Γ_7

VALUE	EVTS	DOCUMENT ID		TECN	COMMENT
0.174±0.016±0.018	539	[1] ABREU	93I	DLPH	E_{cm}^{ee}= 88–94 GeV

[1] The $D^\pm$ states in ABREU 93I are detected by the $K\pi\pi$ decay mode. This is a corrected result (see the erratum of ABREU 93I).

$\Gamma(D^*(2010)^\pm X)/\Gamma(\text{hadrons})$ Γ_{35}/Γ_7

The value is for the sum of the charge states indicated.

VALUE	EVTS	DOCUMENT ID		TECN	COMMENT
0.163±0.019 OUR AVERAGE		Error includes scale factor of 1.3.			
$0.155\pm0.010\pm0.013$	358	[1] ABREU	93I	DLPH	E_{cm}^{ee}= 88–94 GeV
$0.21\ \pm0.04$	362	[2] DECAMP	91J	ALEP	E_{cm}^{ee}= 88–94 GeV

[1] $D^*(2010)^\pm$ in ABREU 93I are reconstructed from $D^0\pi^\pm$, with $D^0\to K^-\pi^+$. The new CLEO II measurement of $B(D^{*\pm}\to D^0\pi^\pm)=(68.1\pm1.6)$ % is used. This is a corrected result (see the erratum of ABREU 93I).

[2] DECAMP 91J report $B(D^*(2010)^+\to D^0\pi^+)\ B(D^0\to K^-\pi^+)\ \Gamma(D^*(2010)^\pm X)\ /\ \Gamma(\text{hadrons})=(5.11\pm0.34)\times10^{-3}$. They obtained the above number assuming $B(D^0\to K^-\pi^+)=(3.62\pm0.34\pm0.44)$% and $B(D^*(2010)^+\to D^0\pi^+)=(55\pm4)$%. We have rescaled their original result of 0.26 ± 0.05 taking into account the new CLEO II branching ratio $B(D^*(2010)^+\to D^0\pi^+)=(68.1\pm1.6)$%.

$\Gamma(D_{s1}(2536)^{\pm}X)/\Gamma(\text{hadrons})$ Γ_{36}/Γ_7

$D_{s1}(2536)^{\pm}$ is an expected orbitally-excited state of the D_s meson.

VALUE (%)	EVTS	DOCUMENT ID		TECN	COMMENT
0.52±0.09±0.06	92	[1] HEISTER	02B	ALEP	E_{cm}^{ee}= 88–94 GeV

[1] HEISTER 02B reconstruct this meson in the decay modes $D_{s1}(2536)^{\pm} \to D^{*\pm} K^0$ and $D_{s1}(2536)^{\pm} \to D^{*0} K^{\pm}$. The quoted branching ratio assumes that the decay width of the $D_{s1}(2536)$ is saturated by the two measured decay modes.

$\Gamma(D_{sJ}(2573)^{\pm}X)/\Gamma(\text{hadrons})$ Γ_{37}/Γ_7

$D_{sJ}(2573)^{\pm}$ is an expected orbitally-excited state of the D_s meson.

VALUE (%)	EVTS	DOCUMENT ID		TECN	COMMENT
$0.83\pm0.29^{+0.07}_{-0.13}$	64	[1] HEISTER	02B	ALEP	E_{cm}^{ee}= 88–94 GeV

[1] HEISTER 02B reconstruct this meson in the decay mode $D_{s2}^{*}(2573)^{\pm} \to D^0 K^{\pm}$. The quoted branching ratio assumes that the detected decay mode represents 45% of the full decay width.

$\Gamma(D^{*\prime}(2629)^{\pm}X)/\Gamma(\text{hadrons})$ Γ_{38}/Γ_7

$D^{*\prime}(2629)^{\pm}$ is a predicted radial excitation of the $D^*(2010)^{\pm}$ meson.

VALUE	DOCUMENT ID		TECN	COMMENT
searched for	[1] ABBIENDI	01N	OPAL	E_{cm}^{ee}= 88–94 GeV

[1] ABBIENDI 01N searched for the decay mode $D^{*\prime}(2629)^{\pm} \to D^{*\pm}\pi^+\pi^-$ with $D^{*+} \to D^0\pi^+$, and $D^0 \to K^-\pi^+$. They quote a 95% CL limit for $Z \to D^{*\prime}(2629)^{\pm}\times B(D^{*\prime}(2629)^+ \to D^{*+}\pi^+\pi^-) < 3.1\times10^{-3}$.

$\Gamma(B^*X)/[\Gamma(BX)+\Gamma(B^*X)]$ $\Gamma_{40}/(\Gamma_{39}+\Gamma_{40})$

As the experiments assume different values of the b-baryon contribution, our average should be taken with caution.

VALUE	EVTS	DOCUMENT ID		TECN	COMMENT
0.75 ±0.04 OUR AVERAGE					
0.760±0.036±0.083		[1] ACKERSTAFF	97M	OPAL	E_{cm}^{ee}= 88–94 GeV
0.771±0.026±0.070		[2] BUSKULIC	96D	ALEP	E_{cm}^{ee}= 88–94 GeV
0.72 ±0.03 ±0.06		[3] ABREU	95R	DLPH	E_{cm}^{ee}= 88–94 GeV
0.76 ±0.08 ±0.06	1378	[4] ACCIARRI	95B	L3	E_{cm}^{ee}= 88–94 GeV

[1] ACKERSTAFF 97M use an inclusive B reconstruction method and assume a (13.2 ± 4.1)% b-baryon contribution. The value refers to a b-flavored meson mixture of B_u, B_d, and B_s.

[2] BUSKULIC 96D use an inclusive reconstruction of B hadrons and assume a (12.2 ± 4.3)% b-baryon contribution. The value refers to a b-flavored mixture of B_u, B_d, and B_s.

[3] ABREU 95R use an inclusive B-reconstruction method and assume a (10 ± 4)% b-baryon contribution. The value refers to a b-flavored meson mixture of B_u, B_d, and B_s.

[4] ACCIARRI 95B assume a 9.4% b-baryon contribution. The value refers to a b-flavored mixture of B_u, B_d, and B_s.

$\Gamma(B^+X)/\Gamma(\text{hadrons})$ Γ_{41}/Γ_7

"OUR EVALUATION" is obtained using our current values for $f(\overline{b} \to B^+)$ and $R_b = \Gamma(b\overline{b})/\Gamma(\text{hadrons})$. We calculate $\Gamma(B^+ X)/\Gamma(\text{hadrons}) = R_b \times f(\overline{b} \to B^+)$. The decay fraction $f(\overline{b} \to B^+)$ was provided by the Heavy Flavor Averaging Group (HFLAV, http://www.slac.stanford.edu/xorg/hflav/osc/PDG_2009/#FRACZ).

VALUE	DOCUMENT ID		TECN	COMMENT
0.0869±0.0019 OUR EVALUATION				
0.0887±0.0030	[1] ABDALLAH	03K	DLPH	E_{cm}^{ee} = 88–94 GeV

[1] ABDALLAH 03K measure the production fraction of B^+ mesons in hadronic Z decays $f(B^+) = (40.99 \pm 0.82 \pm 1.11)\%$. The value quoted here is obtained multiplying this production fraction by our value of $R_b = \Gamma(\overline{b}b)/\Gamma(\text{hadrons})$.

$\Gamma(B_s^0X)/\Gamma(\text{hadrons})$ Γ_{42}/Γ_7

"OUR EVALUATION" is obtained using our current values for $f(\overline{b} \to B_s^0)$ and $R_b = \Gamma(b\overline{b})/\Gamma(\text{hadrons})$. We calculate $\Gamma(B_s^0)/\Gamma(\text{hadrons}) = R_b \times f(\overline{b} \to B_s^0)$. The decay fraction $f(\overline{b} \to B_s^0)$ was provided by the Heavy Flavor Averaging Group (HFLAV, http://www.slac.stanford.edu/xorg/hflav/osc/PDG_2009/#FRACZ).

VALUE	DOCUMENT ID		TECN	COMMENT
0.0227±0.0019 OUR EVALUATION				
seen	[1] ABREU	92M	DLPH	E_{cm}^{ee}= 88–94 GeV
seen	[2] ACTON	92N	OPAL	E_{cm}^{ee}= 88–94 GeV
seen	[3] BUSKULIC	92E	ALEP	E_{cm}^{ee}= 88–94 GeV

[1] ABREU 92M reported value is $\Gamma(B_s^0X)*B(B_s^0 \to D_s\mu\nu_\mu X)*B(D_s \to \phi\pi)/\Gamma(\text{hadrons}) = (18 \pm 8)\times10^{-5}$.

[2] ACTON 92N find evidence for B_s^0 production using D_s-ℓ correlations, with $D_s^+ \to \phi\pi^+$ and $K^*(892)\,K^+$. Assuming R_b from the Standard Model and averaging over the e and μ channels, authors measure the product branching fraction to be $f(\overline{b} \to B_s^0)\times B(B_s^0 \to D_s^-\ell^+\nu_\ell X)\times B(D_s^- \to \phi\pi^-) = (3.9 \pm 1.1 \pm 0.8)\times10^{-4}$.

[3] BUSKULIC 92E find evidence for B_s^0 production using D_s-ℓ correlations, with $D_s^+ \to \phi\pi^+$ and $K^*(892)\,K^+$. Using $B(D_s^+ \to \phi\pi^+) = (2.7 \pm 0.7)\%$ and summing up the e and μ channels, the weighted average product branching fraction is measured to be $B(\overline{b} \to B_s^0)\times B(B_s^0 \to D_s^-\ell^+\nu_\ell X) = 0.040 \pm 0.011^{+0.010}_{-0.012}$.

$\Gamma(B_c^+X)/\Gamma(\text{hadrons})$ Γ_{43}/Γ_7

VALUE	DOCUMENT ID		TECN	COMMENT
searched for	[1] ACKERSTAFF	98O	OPAL	E_{cm}^{ee}= 88–94 GeV
searched for	[2] ABREU	97E	DLPH	E_{cm}^{ee}= 88–94 GeV
searched for	[3] BARATE	97H	ALEP	E_{cm}^{ee}= 88–94 GeV

[1] ACKERSTAFF 98O searched for the decay modes $B_c \to J/\psi\pi^+$, $J/\psi a_1^+$, and $J/\psi\ell^+\nu_\ell$, with $J/\psi \to \ell^+\ell^-$, $\ell = e,\mu$. The number of candidates (background) for the three decay modes is 2 (0.63 ± 0.2), 0 (1.10 ± 0.22), and 1 (0.82 ± 0.19) respectively. Interpreting the 2 $B_c \to J/\psi\pi^+$ candidates as signal, they report $\Gamma(B_c^+X)\times B(B_c \to J/\psi\pi^+)/\Gamma(\text{hadrons}) = (3.8^{+5.0}_{-2.4} \pm 0.5)\times10^{-5}$. Interpreted as background, the 90% CL bounds are $\Gamma(B_c^+X)*B(B_c \to J/\psi\pi^+)/\Gamma(\text{hadrons}) < 1.06\times10^{-4}$, $\Gamma(B_c^+X)*B(B_c \to J/\psi a_1^+)/\Gamma(\text{hadrons}) < 5.29\times10^{-4}$, $\Gamma(B_c^+X)*B(B_c \to J/\psi\ell^+\nu_\ell)/\Gamma(\text{hadrons}) < 6.96\times10^{-5}$.

[2] ABREU 97E searched for the decay modes $B_c \to J/\psi\pi^+$, $J/\psi\ell^+\nu_\ell$, and $J/\psi(3\pi)^+$, with $J/\psi \to \ell^+\ell^-$, $\ell = e,\mu$. The number of candidates (background) for the three decay modes is 1 (1.7), 0 (0.3), and 1 (2.3) respectively. They report the following 90% CL limits: $\Gamma(B_c^+X)*B(B_c \to J/\psi\pi^+)/\Gamma(\text{hadrons}) < (1.05\text{–}0.84)\times10^{-4}$, $\Gamma(B_c^+X)*B(B_c \to J/\psi\ell\nu_\ell)/\Gamma(\text{hadrons}) < (5.8\text{–}5.0)\times10^{-5}$, $\Gamma(B_c^+X)*B(B_c \to J/\psi(3\pi)^+)/\Gamma(\text{hadrons}) < 1.75\times10^{-4}$, where the ranges are due to the predicted B_c lifetime (0.4–1.4) ps.

[3] BARATE 97H searched for the decay modes $B_c \to J/\psi\pi^+$ and $J/\psi\ell^+\nu_\ell$ with $J/\psi \to \ell^+\ell^-$, $\ell = e,\mu$. The number of candidates (background) for the two decay modes is 0 (0.44) and 2 (0.81) respectively. They report the following 90% CL limits: $\Gamma(B_c^+X)*B(B_c \to J/\psi\pi^+)/\Gamma(\text{hadrons}) < 3.6\times10^{-5}$ and $\Gamma(B_c^+X)*B(B_c \to J/\psi\ell^+\nu_\ell)/\Gamma(\text{hadrons}) < 5.2\times10^{-5}$.

$\Gamma(\Lambda_c^+X)/\Gamma(\text{hadrons})$ Γ_{44}/Γ_7

VALUE	DOCUMENT ID		TECN	COMMENT
0.022±0.005 OUR AVERAGE				
0.024±0.005±0.006	[1] ALEXANDER	96R	OPAL	E_{cm}^{ee} = 88–94 GeV
0.021±0.003±0.005	[2] BUSKULIC	96Y	ALEP	E_{cm}^{ee} = 88–94 GeV

[1] ALEXANDER 96R measure $R_b \times f(b \to \Lambda_c^+ X) \times B(\Lambda_c^+ \to pK^-\pi^+) = (0.122 \pm 0.023 \pm 0.010)\%$ in hadronic Z decays; the value quoted here is obtained using our best value $B(\Lambda_c^+ \to pK^-\pi^+) = (5.0 \pm 1.3)\%$. The first error is the total experiment's error and the second error is the systematic error due to the branching fraction uncertainty.

[2] BUSKULIC 96Y obtain the production fraction of Λ_c^+ baryons in hadronic Z decays $f(b \to \Lambda_c^+ X) = 0.110 \pm 0.014 \pm 0.006$ using $B(\Lambda_c^+ \to pK^-\pi^+) = (4.4 \pm 0.6)\%$; we have rescaled using our best value $B(\Lambda_c^+ \to pK^-\pi^+) = (5.0 \pm 1.3)\%$ obtaining $f(b \to \Lambda_c^+ X) = 0.097 \pm 0.013 \pm 0.025$ where the first error is their total experiment's error and the second error is the systematic error due to the branching fraction uncertainty. The value quoted here is obtained multiplying this production fraction by our value of $R_b = \Gamma(b\overline{b})/\Gamma(\text{hadrons})$.

$\Gamma(\Xi_c^0X)/\Gamma(\text{hadrons})$ Γ_{45}/Γ_7

VALUE	DOCUMENT ID		TECN	COMMENT
• • • We do not use the following data for averages, fits, limits, etc. • • •				
seen	[1] ABDALLAH	05C	DLPH	E_{cm}^{ee} = 88–94 GeV

[1] ABDALLAH 05C searched for the charmed strange baryon Ξ_c^0 in the decay channel $\Xi_c^0 \to \Xi^-\pi^+$ ($\Xi^- \to \Lambda\pi^-$). The production rate is measured to be $f_{\Xi_c^0} \times B(\Xi_c^0 \to \Xi^-\pi^+) = (4.7 \pm 1.4 \pm 1.1)\times10^{-4}$ per hadronic Z decay.

$\Gamma(\Xi_bX)/\Gamma(\text{hadrons})$ Γ_{46}/Γ_7

Here Ξ_b is used as a notation for the strange b-baryon states Ξ_b^- and Ξ_b^0.

VALUE	DOCUMENT ID		TECN	COMMENT
• • • We do not use the following data for averages, fits, limits, etc. • • •				
seen	[1] ABDALLAH	05C	DLPH	E_{cm}^{ee} = 88–94 GeV
seen	[2] BUSKULIC	96T	ALEP	E_{cm}^{ee} = 88–94 GeV
seen	[3] ABREU	95V	DLPH	E_{cm}^{ee} = 88–94 GeV

[1] ABDALLAH 05C searched for the beauty strange baryon Ξ_b in the inclusive semileptonic decay channel $\Xi_b \to \Xi^-\ell^-\overline{\nu}_\ell X$. Evidence for the Ξ_b production is seen from the observation of $\Xi^{\mp}$ production accompanied by a lepton of the same sign. From the excess of "right-sign" pairs $\Xi^{\mp}\ell^{\mp}$ compared to "wrong-sign" pairs $\Xi^{\mp}\ell^{\pm}$ the production rate is measured to be $B(b \to \Xi_b) \times B(\Xi_b \to \Xi^-\ell^-X) = (3.0 \pm 1.0 \pm 0.3)\times10^{-4}$ per lepton species, averaged over electrons and muons.

[2] BUSKULIC 96T investigate Ξ-lepton correlations and find a significant excess of "right–sign" pairs $\Xi^{\mp}\ell^{\mp}$ compared to "wrong–sign" pairs $\Xi^{\mp}\ell^{\pm}$. This excess is interpreted as evidence for Ξ_b semileptonic decay. The measured product branching ratio is $B(b \to \Xi_b) \times B(\Xi_b \to X_c X\ell^-\overline{\nu}_\ell) \times B(X_c \to \Xi^-X') = (5.4 \pm 1.1 \pm 0.8)\times10^{-4}$ per lepton species, averaged over electrons and muons, with X_c a charmed baryon.

[3] ABREU 95V observe an excess of "right-sign" pairs $\Xi^{\mp}\ell^{\mp}$ compared to "wrong-sign" pairs $\Xi^{\mp}\ell^{\pm}$ in jets: this excess is interpreted as evidence for the beauty strange baryon Ξ_b production, with $\Xi_b \to \Xi^-\ell^-\overline{\nu}_\ell X$. They find that the probability for this signal to come from non b-baryon decays is less than 5×10^{-4} and that Λ_b decays can account for less than 10% of these events. The Ξ_b production rate is then measured to be $B(b \to \Xi_b) \times B(\Xi_b \to \Xi^-\ell^-X) = (5.9 \pm 2.1 \pm 1.0)\times10^{-4}$ per lepton species, averaged over electrons and muons.

Gauge & Higgs Boson Particle Listings

Z

$\Gamma(b\text{-baryon X})/\Gamma(\text{hadrons})$ Γ_{47}/Γ_7

"OUR EVALUATION" is obtained using our current values for $f(b \to b\text{-baryon})$ and $R_b = \Gamma(b\overline{b})/\Gamma(\text{hadrons})$. We calculate $\Gamma(b\text{-baryon X})/\Gamma(\text{hadrons}) = R_b \times f(b \to b\text{-baryon})$. The decay fraction $f(b \to b\text{-baryon})$ was provided by the Heavy Flavor Averaging Group (HFLAV, http://www.slac.stanford.edu/xorg/hflav/osc/PDG_2009).

VALUE	DOCUMENT ID		TECN	COMMENT
0.0197±0.0032 OUR EVALUATION				
0.0221±0.0015±0.0058	[1] BARATE	98V	ALEP	E_{cm}^{ee}= 88–94 GeV

[1] BARATE 98V use the overall number of identified protons in b-hadron decays to measure $f(b \to b\text{-baryon}) = 0.102 \pm 0.007 \pm 0.027$. They assume $BR(b\text{-baryon} \to pX) = (58 \pm 6)\%$ and $BR(B_s^0 \to pX) = (8.0 \pm 4.0)\%$. The value quoted here is obtained multiplying this production fraction by our value of $R_b = \Gamma(b\overline{b})/\Gamma(\text{hadrons})$.

$\Gamma(\text{anomalous } \gamma + \text{hadrons})/\Gamma_{\text{total}}$ Γ_{48}/Γ

Limits on additional sources of prompt photons beyond expectations for final-state bremsstrahlung.

VALUE	CL%	DOCUMENT ID		TECN	COMMENT
$\mathbf{<3.2\times10^{-3}}$	95	[1] AKRAWY	90J	OPAL	E_{cm}^{ee}= 88–94 GeV

[1] AKRAWY 90J report $\Gamma(\gamma X) <$ 8.2 MeV at 95%CL. They assume a three-body $\gamma q\overline{q}$ distribution and use $E(\gamma) > 10$ GeV.

$\Gamma(e^+e^-\gamma)/\Gamma_{\text{total}}$ Γ_{49}/Γ

VALUE	CL%	DOCUMENT ID		TECN	COMMENT
$\mathbf{<5.2\times10^{-4}}$	95	[1] ACTON	91B	OPAL	E_{cm}^{ee}= 91.2 GeV

[1] ACTON 91B looked for isolated photons with E>2% of beam energy (> 0.9 GeV).

$\Gamma(\mu^+\mu^-\gamma)/\Gamma_{\text{total}}$ Γ_{50}/Γ

VALUE	CL%	DOCUMENT ID		TECN	COMMENT
$\mathbf{<5.6\times10^{-4}}$	95	[1] ACTON	91B	OPAL	E_{cm}^{ee}= 91.2 GeV

[1] ACTON 91B looked for isolated photons with E>2% of beam energy (> 0.9 GeV).

$\Gamma(\tau^+\tau^-\gamma)/\Gamma_{\text{total}}$ Γ_{51}/Γ

VALUE	CL%	DOCUMENT ID		TECN	COMMENT
$\mathbf{<7.3\times10^{-4}}$	95	[1] ACTON	91B	OPAL	E_{cm}^{ee}= 91.2 GeV

[1] ACTON 91B looked for isolated photons with E>2% of beam energy (> 0.9 GeV).

$\Gamma(\ell^+\ell^-\gamma\gamma)/\Gamma_{\text{total}}$ Γ_{52}/Γ

The value is the sum over $\ell = e, \mu, \tau$.

VALUE	CL%	DOCUMENT ID		TECN	COMMENT
$\mathbf{<6.8\times10^{-6}}$	95	[1] ACTON	93E	OPAL	E_{cm}^{ee}= 88–94 GeV

[1] For $m_{\gamma\gamma} = 60 \pm 5$ GeV.

$\Gamma(q\overline{q}\gamma\gamma)/\Gamma_{\text{total}}$ Γ_{53}/Γ

VALUE	CL%	DOCUMENT ID		TECN	COMMENT
$\mathbf{<5.5\times10^{-6}}$	95	[1] ACTON	93E	OPAL	E_{cm}^{ee}= 88–94 GeV

[1] For $m_{\gamma\gamma} = 60 \pm 5$ GeV.

$\Gamma(\nu\overline{\nu}\gamma\gamma)/\Gamma_{\text{total}}$ Γ_{54}/Γ

VALUE	CL%	DOCUMENT ID		TECN	COMMENT
$\mathbf{<3.1\times10^{-6}}$	95	[1] ACTON	93E	OPAL	E_{cm}^{ee}= 88–94 GeV

[1] For $m_{\gamma\gamma} = 60 \pm 5$ GeV.

$\Gamma(e^\pm\mu^\mp)/\Gamma_{\text{total}}$ Γ_{55}/Γ

Test of lepton family number conservation. The value is for the sum of the charge states indicated.

VALUE	CL%	DOCUMENT ID		TECN	COMMENT
$\mathbf{<7.5\times10^{-7}}$	95	AAD	14AU	ATLS	E_{cm}^{pp} = 8 TeV
$<2.5\times10^{-6}$	95	ABREU	97C	DLPH	E_{cm}^{ee}= 88–94 GeV
$<1.7\times10^{-6}$	95	AKERS	95W	OPAL	E_{cm}^{ee}= 88–94 GeV
$<0.6\times10^{-5}$	95	ADRIANI	93I	L3	E_{cm}^{ee}= 88–94 GeV
$<2.6\times10^{-5}$	95	DECAMP	92	ALEP	E_{cm}^{ee}= 88–94 GeV

$\Gamma(e^\pm\mu^\mp)/\Gamma(e^+e^-)$ Γ_{55}/Γ_1

Test of lepton family number conservation. The value is for the sum of the charge states indicated.

VALUE	CL%	DOCUMENT ID		TECN	COMMENT
<0.07	90	ALBAJAR	89	UA1	$E_{cm}^{p\overline{p}}$= 546,630 GeV

$\Gamma(e^\pm\tau^\mp)/\Gamma_{\text{total}}$ Γ_{56}/Γ

Test of lepton family number conservation. The value is for the sum of the charge states indicated.

VALUE	CL%	DOCUMENT ID		TECN	COMMENT
$<2.2\times10^{-5}$	95	ABREU	97C	DLPH	E_{cm}^{ee}= 88–94 GeV
$\mathbf{<9.8\times10^{-6}}$	95	AKERS	95W	OPAL	E_{cm}^{ee}= 88–94 GeV
$<1.3\times10^{-5}$	95	ADRIANI	93I	L3	E_{cm}^{ee}= 88–94 GeV
$<1.2\times10^{-4}$	95	DECAMP	92	ALEP	E_{cm}^{ee}= 88–94 GeV

$\Gamma(\mu^\pm\tau^\mp)/\Gamma_{\text{total}}$ Γ_{57}/Γ

Test of lepton family number conservation. The value is for the sum of the charge states indicated.

VALUE	CL%	DOCUMENT ID		TECN	COMMENT
$<1.69\times10^{-5}$	95	AAD	17	ATLS	E_{cm}^{pp} = 8 TeV
$\mathbf{<1.2\times10^{-5}}$	95	ABREU	97C	DLPH	E_{cm}^{ee}= 88–94 GeV
$<1.7\times10^{-5}$	95	AKERS	95W	OPAL	E_{cm}^{ee}= 88–94 GeV
$<1.9\times10^{-5}$	95	ADRIANI	93I	L3	E_{cm}^{ee}= 88–94 GeV
$<1.0\times10^{-4}$	95	DECAMP	92	ALEP	E_{cm}^{ee}= 88–94 GeV

$\Gamma(pe)/\Gamma_{\text{total}}$ Γ_{58}/Γ

Test of baryon number and lepton number conservations. Charge conjugate states are implied.

VALUE	CL%	DOCUMENT ID		TECN	COMMENT
$\mathbf{<1.8\times10^{-6}}$	95	[1] ABBIENDI	99I	OPAL	E_{cm}^{ee}= 88–94 GeV

[1] ABBIENDI 99I give the 95%CL limit on the partial width $\Gamma(Z^0 \to pe) < 4.6$ KeV and we have transformed it into a branching ratio.

$\Gamma(p\mu)/\Gamma_{\text{total}}$ Γ_{59}/Γ

Test of baryon number and lepton number conservations. Charge conjugate states are implied.

VALUE	CL%	DOCUMENT ID		TECN	COMMENT
$\mathbf{<1.8\times10^{-6}}$	95	[1] ABBIENDI	99I	OPAL	E_{cm}^{ee}= 88–94 GeV

[1] ABBIENDI 99I give the 95%CL limit on the partial width $\Gamma(Z^0 \to p\mu) < 4.4$ KeV and we have transformed it into a branching ratio.

AVERAGE PARTICLE MULTIPLICITIES IN HADRONIC Z DECAY

Summed over particle and antiparticle, when appropriate.

$\langle N_\gamma \rangle$

VALUE	DOCUMENT ID		TECN	COMMENT
20.97±0.02±1.15	ACKERSTAFF	98A	OPAL	E_{cm}^{ee}= 91.2 GeV

$\langle N_{\pi^\pm} \rangle$

VALUE	DOCUMENT ID		TECN	COMMENT
17.03 ±0.16 OUR AVERAGE				
17.007±0.209	ABE	04C	SLD	E_{cm}^{ee}= 91.2 GeV
17.26 ±0.10 ±0.88	ABREU	98L	DLPH	E_{cm}^{ee}= 91.2 GeV
17.04 ±0.31	BARATE	98V	ALEP	E_{cm}^{ee}= 91.2 GeV
17.05 ±0.43	AKERS	94P	OPAL	E_{cm}^{ee}= 91.2 GeV

$\langle N_{\pi^0} \rangle$

VALUE	DOCUMENT ID		TECN	COMMENT
9.76±0.26 OUR AVERAGE				
9.55±0.06±0.75	ACKERSTAFF	98A	OPAL	E_{cm}^{ee}= 91.2 GeV
9.63±0.13±0.63	BARATE	97J	ALEP	E_{cm}^{ee}= 91.2 GeV
9.90±0.02±0.33	ACCIARRI	96	L3	E_{cm}^{ee}= 91.2 GeV
9.2 ±0.2 ±1.0	ADAM	96	DLPH	E_{cm}^{ee}= 91.2 GeV

$\langle N_\eta \rangle$

VALUE	DOCUMENT ID		TECN	COMMENT
1.01±0.08 OUR AVERAGE Error includes scale factor of 1.3. See the ideogram below.				
1.20±0.04±0.11	HEISTER	02C	ALEP	E_{cm}^{ee}= 91.2 GeV
0.97±0.03±0.11	ACKERSTAFF	98A	OPAL	E_{cm}^{ee}= 91.2 GeV
0.93±0.01±0.09	ACCIARRI	96	L3	E_{cm}^{ee}= 91.2 GeV

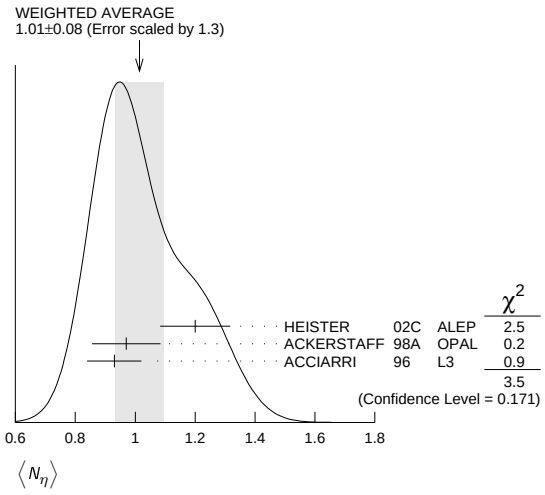

$\langle N_{\rho^\pm} \rangle$

VALUE	DOCUMENT ID		TECN	COMMENT
2.57±0.15 OUR AVERAGE				
2.59±0.03±0.16	[1] BEDDALL	09		ALEPH archive, E_{cm}^{ee} = 91.2 GeV
2.40±0.06±0.43	ACKERSTAFF	98A	OPAL	E_{cm}^{ee} = 91.2 GeV

[1] BEDDALL 09 analyse 3.2 million hadronic Z decays as archived by ALEPH collaboration and report a value of 2.59 ± 0.03 ± 0.15 ± 0.04. The first error is statistical, the second systematic, and the third arises from extrapolation to full phase space. We combine the systematic errors in quadrature.

$\langle N_{\rho^0} \rangle$

VALUE	DOCUMENT ID		TECN	COMMENT
1.24±0.10 OUR AVERAGE Error includes scale factor of 1.1.				
1.19±0.10	ABREU	99J	DLPH	E_{cm}^{ee} = 91.2 GeV
1.45±0.06±0.20	BUSKULIC	96H	ALEP	E_{cm}^{ee} = 91.2 GeV

$\langle N_\omega \rangle$

VALUE	DOCUMENT ID		TECN	COMMENT
1.02±0.06 OUR AVERAGE				
1.00±0.03±0.06	HEISTER	02C	ALEP	E_{cm}^{ee} = 91.2 GeV
1.04±0.04±0.14	ACKERSTAFF	98A	OPAL	E_{cm}^{ee} = 91.2 GeV
1.17±0.09±0.15	ACCIARRI	97D	L3	E_{cm}^{ee} = 91.2 GeV

$\langle N_{\eta'} \rangle$

VALUE	DOCUMENT ID		TECN	COMMENT
0.17 ±0.05 OUR AVERAGE Error includes scale factor of 2.4.				
0.14 ±0.01 ±0.02	ACKERSTAFF	98A	OPAL	E_{cm}^{ee} = 91.2 GeV
0.25 ±0.04	[1] ACCIARRI	97D	L3	E_{cm}^{ee} = 91.2 GeV
• • • We do not use the following data for averages, fits, limits, etc. • • •				
0.068±0.018±0.016	[2] BUSKULIC	92D	ALEP	E_{cm}^{ee} = 91.2 GeV

[1] ACCIARRI 97D obtain this value averaging over the two decay channels $\eta' \to \pi^+\pi^-\eta$ and $\eta' \to \rho^0\gamma$.

[2] BUSKULIC 92D obtain this value for $x > 0.1$.

$\langle N_{f_0(980)} \rangle$

VALUE	DOCUMENT ID		TECN	COMMENT
0.147±0.011 OUR AVERAGE				
0.164±0.021	ABREU	99J	DLPH	E_{cm}^{ee} = 91.2 GeV
0.141±0.007±0.011	ACKERSTAFF	98Q	OPAL	E_{cm}^{ee} = 91.2 GeV

$\langle N_{a_0(980)^\pm} \rangle$

VALUE	DOCUMENT ID		TECN	COMMENT
0.27±0.04±0.10	ACKERSTAFF	98A	OPAL	E_{cm}^{ee} = 91.2 GeV

$\langle N_\phi \rangle$

VALUE	DOCUMENT ID		TECN	COMMENT
0.098±0.006 OUR AVERAGE Error includes scale factor of 2.0. See the ideogram below.				
0.105±0.008	ABE	99E	SLD	E_{cm}^{ee} = 91.2 GeV
0.091±0.002±0.003	ACKERSTAFF	98Q	OPAL	E_{cm}^{ee} = 91.2 GeV
0.104±0.003±0.007	ABREU	96U	DLPH	E_{cm}^{ee} = 91.2 GeV
0.122±0.004±0.008	BUSKULIC	96H	ALEP	E_{cm}^{ee} = 91.2 GeV

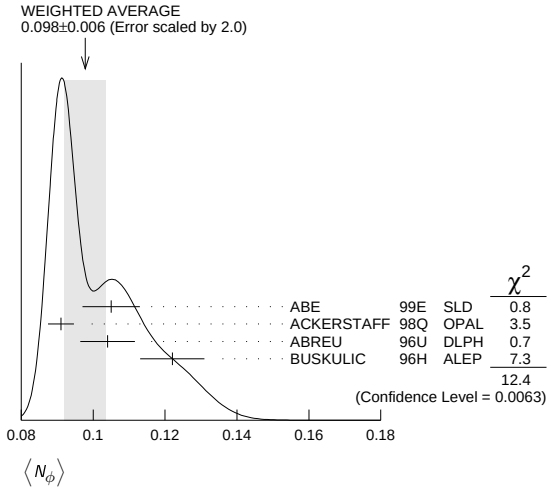

$\langle N_{f_2(1270)} \rangle$

VALUE	DOCUMENT ID		TECN	COMMENT
0.169±0.025 OUR AVERAGE Error includes scale factor of 1.4.				
0.214±0.038	ABREU	99J	DLPH	E_{cm}^{ee} = 91.2 GeV
0.155±0.011±0.018	ACKERSTAFF	98Q	OPAL	E_{cm}^{ee} = 91.2 GeV

$\langle N_{f_1(1285)} \rangle$

VALUE	DOCUMENT ID		TECN	COMMENT
0.165±0.051	[1] ABDALLAH	03H	DLPH	E_{cm}^{ee} = 91.2 GeV

[1] ABDALLAH 03H assume a $K\overline{K}\pi$ branching ratio of (9.0 ± 0.4)%.

$\langle N_{f_1(1420)} \rangle$

VALUE	DOCUMENT ID		TECN	COMMENT
0.056±0.012	[1] ABDALLAH	03H	DLPH	E_{cm}^{ee} = 91.2 GeV

[1] ABDALLAH 03H assume a $K\overline{K}\pi$ branching ratio of 100%.

$\langle N_{f_2'(1525)} \rangle$

VALUE	DOCUMENT ID		TECN	COMMENT
0.012±0.006	ABREU	99J	DLPH	E_{cm}^{ee} = 91.2 GeV

$\langle N_{K^\pm} \rangle$

VALUE	DOCUMENT ID		TECN	COMMENT
2.24 ±0.04 OUR AVERAGE				
2.203±0.071	ABE	04C	SLD	E_{cm}^{ee} = 91.2 GeV
2.21 ±0.05 ±0.05	ABREU	98L	DLPH	E_{cm}^{ee} = 91.2 GeV
2.26 ±0.12	BARATE	98V	ALEP	E_{cm}^{ee} = 91.2 GeV
2.42 ±0.13	AKERS	94P	OPAL	E_{cm}^{ee} = 91.2 GeV

$\langle N_{K^0} \rangle$

VALUE	DOCUMENT ID		TECN	COMMENT
2.039±0.025 OUR AVERAGE Error includes scale factor of 1.3. See the ideogram below.				
2.093±0.004±0.029	BARATE	00O	ALEP	E_{cm}^{ee} = 91.2 GeV
2.01 ±0.08	ABE	99E	SLD	E_{cm}^{ee} = 91.2 GeV
2.024±0.006±0.042	ACCIARRI	97L	L3	E_{cm}^{ee} = 91.2 GeV
1.962±0.022±0.056	ABREU	95L	DLPH	E_{cm}^{ee} = 91.2 GeV
1.99 ±0.01 ±0.04	AKERS	95U	OPAL	E_{cm}^{ee} = 91.2 GeV

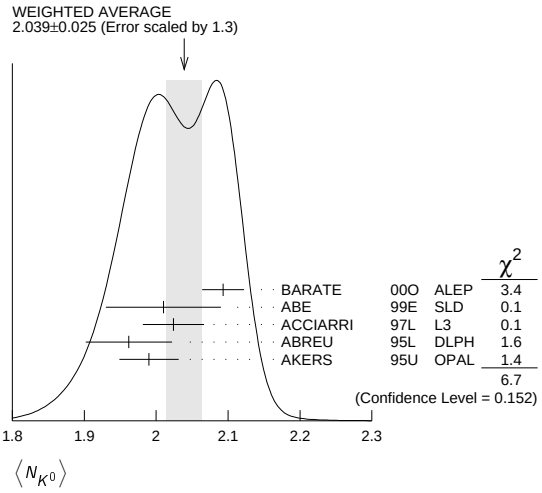

$\langle N_{K^*(892)^\pm} \rangle$

VALUE	DOCUMENT ID		TECN	COMMENT
0.72 ±0.05 OUR AVERAGE				
0.712±0.031±0.059	ABREU	95L	DLPH	E_{cm}^{ee} = 91.2 GeV
0.72 ±0.02 ±0.08	ACTON	93	OPAL	E_{cm}^{ee} = 91.2 GeV

$\langle N_{K^*(892)^0} \rangle$

VALUE	DOCUMENT ID		TECN	COMMENT
0.739±0.022 OUR AVERAGE				
0.707±0.041	ABE	99E	SLD	E_{cm}^{ee} = 91.2 GeV
0.74 ±0.02 ±0.02	ACKERSTAFF	97S	OPAL	E_{cm}^{ee} = 91.2 GeV
0.77 ±0.02 ±0.07	ABREU	96U	DLPH	E_{cm}^{ee} = 91.2 GeV
0.83 ±0.01 ±0.09	BUSKULIC	96H	ALEP	E_{cm}^{ee} = 91.2 GeV
0.97 ±0.18 ±0.31	ABREU	93	DLPH	E_{cm}^{ee} = 91.2 GeV

$\langle N_{K_2^*(1430)} \rangle$

VALUE	DOCUMENT ID		TECN	COMMENT
0.073±0.023	ABREU	99J	DLPH	E_{cm}^{ee} = 91.2 GeV
• • • We do not use the following data for averages, fits, limits, etc. • • •				
0.19 ±0.04 ±0.06	[1] AKERS	95X	OPAL	E_{cm}^{ee} = 91.2 GeV

[1] AKERS 95X obtain this value for $x < 0.3$.

$\langle N_{D^\pm} \rangle$

VALUE	DOCUMENT ID		TECN	COMMENT
0.187±0.020 OUR AVERAGE	Error includes scale factor of 1.5.			See the ideogram below.
0.170±0.009±0.014	ALEXANDER	96R	OPAL	E_{cm}^{ee} = 91.2 GeV
0.251±0.026±0.025	BUSKULIC	94J	ALEP	E_{cm}^{ee} = 91.2 GeV
0.199±0.019±0.024	[1] ABREU	93I	DLPH	E_{cm}^{ee} = 91.2 GeV

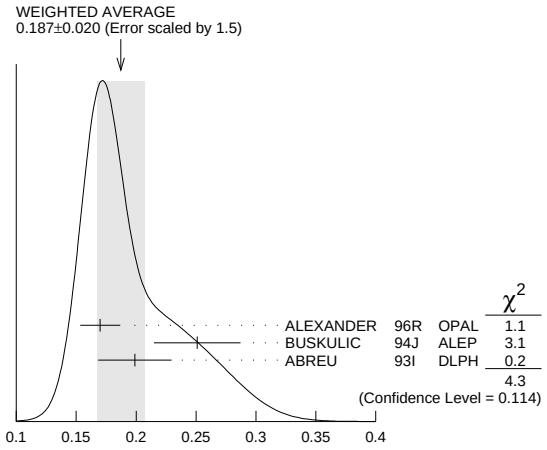

[1] See ABREU 95 (erratum).

$\langle N_{D^\pm} \rangle$

$\langle N_{D^0} \rangle$

VALUE	DOCUMENT ID		TECN	COMMENT
0.462±0.026 OUR AVERAGE				
0.465±0.017±0.027	ALEXANDER	96R	OPAL	E_{cm}^{ee} = 91.2 GeV
0.518±0.052±0.035	BUSKULIC	94J	ALEP	E_{cm}^{ee} = 91.2 GeV
0.403±0.038±0.044	[1] ABREU	93I	DLPH	E_{cm}^{ee} = 91.2 GeV

[1] See ABREU 95 (erratum).

$\langle N_{D_s^\pm} \rangle$

VALUE	DOCUMENT ID		TECN	COMMENT
0.131±0.010±0.018	ALEXANDER	96R	OPAL	E_{cm}^{ee} = 91.2 GeV

$\langle N_{D^*(2010)^\pm} \rangle$

VALUE	DOCUMENT ID		TECN	COMMENT
0.183 ±0.008 OUR AVERAGE				
0.1854±0.0041±0.0091	[1] ACKERSTAFF	98E	OPAL	E_{cm}^{ee} = 91.2 GeV
0.187 ±0.015 ±0.013	BUSKULIC	94J	ALEP	E_{cm}^{ee} = 91.2 GeV
0.171 ±0.012 ±0.016	[2] ABREU	93I	DLPH	E_{cm}^{ee} = 91.2 GeV

[1] ACKERSTAFF 98E systematic error includes an uncertainty of ±0.0069 due to the branching ratios $B(D^{*+} \to D^0\pi^+) = 0.683\pm0.014$ and $B(D^0 \to K^-\pi^+) = 0.0383\pm0.0012$.
[2] See ABREU 95 (erratum).

$\langle N_{D_{s1}(2536)^+} \rangle$

VALUE (units 10^{-3})	DOCUMENT ID		TECN	COMMENT
• • • We do not use the following data for averages, fits, limits, etc. • • •				
$2.9^{+0.7}_{-0.6}\pm0.2$	[1] ACKERSTAFF	97W	OPAL	E_{cm}^{ee} = 91.2 GeV

[1] ACKERSTAFF 97W obtain this value for $x > 0.6$ and with the assumption that its decay width is saturated by the D^*K final states.

$\langle N_{B^*} \rangle$

VALUE	DOCUMENT ID		TECN	COMMENT
0.28±0.01±0.03	[1] ABREU	95R	DLPH	E_{cm}^{ee} = 91.2 GeV

[1] ABREU 95R quote this value for a flavor-averaged excited state.

$\langle N_{J/\psi(1S)} \rangle$

VALUE	DOCUMENT ID		TECN	COMMENT
0.0056±0.0003±0.0004	[1] ALEXANDER	96B	OPAL	E_{cm}^{ee} = 91.2 GeV

[1] ALEXANDER 96B identify $J/\psi(1S)$ from the decays into lepton pairs.

$\langle N_{\psi(2S)} \rangle$

VALUE	DOCUMENT ID		TECN	COMMENT
0.0023±0.0004±0.0003	ALEXANDER	96B	OPAL	E_{cm}^{ee} = 91.2 GeV

$\langle N_p \rangle$

VALUE	DOCUMENT ID		TECN	COMMENT
1.046±0.026 OUR AVERAGE				
1.054±0.035	ABE	04C	SLD	E_{cm}^{ee} = 91.2 GeV
1.08 ±0.04 ±0.03	ABREU	98L	DLPH	E_{cm}^{ee} = 91.2 GeV
1.00 ±0.07	BARATE	98V	ALEP	E_{cm}^{ee} = 91.2 GeV
0.92 ±0.11	AKERS	94P	OPAL	E_{cm}^{ee} = 91.2 GeV

$\langle N_{\Delta(1232)^{++}} \rangle$

VALUE	DOCUMENT ID		TECN	COMMENT
0.087±0.033 OUR AVERAGE	Error includes scale factor of 2.4.			
0.079±0.009±0.011	ABREU	95W	DLPH	E_{cm}^{ee} = 91.2 GeV
0.22 ±0.04 ±0.04	ALEXANDER	95D	OPAL	E_{cm}^{ee} = 91.2 GeV

$\langle N_\Lambda \rangle$

VALUE	DOCUMENT ID		TECN	COMMENT
0.388±0.009 OUR AVERAGE	Error includes scale factor of 1.7.			See the ideogram below.
0.404±0.002±0.007	BARATE	00O	ALEP	E_{cm}^{ee} = 91.2 GeV
0.395±0.022	ABE	99E	SLD	E_{cm}^{ee} = 91.2 GeV
0.364±0.004±0.017	ACCIARRI	97L	L3	E_{cm}^{ee} = 91.2 GeV
0.374±0.002±0.010	ALEXANDER	97D	OPAL	E_{cm}^{ee} = 91.2 GeV
0.357±0.003±0.017	ABREU	93L	DLPH	E_{cm}^{ee} = 91.2 GeV

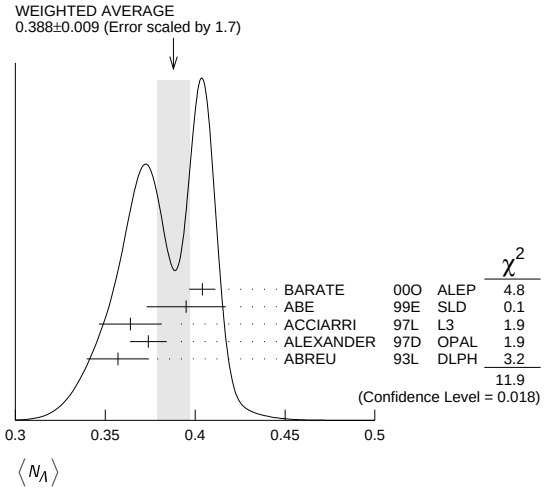

$\langle N_\Lambda \rangle$

$\langle N_{\Lambda(1520)} \rangle$

VALUE	DOCUMENT ID		TECN	COMMENT
0.0224±0.0027 OUR AVERAGE				
0.029 ±0.005 ±0.005	ABREU	00P	DLPH	E_{cm}^{ee} = 91.2 GeV
0.0213±0.0021±0.0019	ALEXANDER	97D	OPAL	E_{cm}^{ee} = 91.2 GeV

$\langle N_{\Sigma^+} \rangle$

VALUE	DOCUMENT ID		TECN	COMMENT
0.107±0.010 OUR AVERAGE				
0.114±0.011±0.009	ACCIARRI	00J	L3	E_{cm}^{ee} = 91.2 GeV
0.099±0.008±0.013	ALEXANDER	97E	OPAL	E_{cm}^{ee} = 91.2 GeV

$\langle N_{\Sigma^-} \rangle$

VALUE	DOCUMENT ID		TECN	COMMENT
0.082±0.007 OUR AVERAGE				
0.081±0.002±0.010	ABREU	00P	DLPH	E_{cm}^{ee} = 91.2 GeV
0.083±0.006±0.009	ALEXANDER	97E	OPAL	E_{cm}^{ee} = 91.2 GeV

$\langle N_{\Sigma^+ + \Sigma^-} \rangle$

VALUE	DOCUMENT ID		TECN	COMMENT
0.181±0.018 OUR AVERAGE				
0.182±0.010±0.016	[1] ALEXANDER	97E	OPAL	E_{cm}^{ee} = 91.2 GeV
0.170±0.014±0.061	ABREU	95O	DLPH	E_{cm}^{ee} = 91.2 GeV

[1] We have combined the values of $\langle N_{\Sigma^+} \rangle$ and $\langle N_{\Sigma^-} \rangle$ from ALEXANDER 97E adding the statistical and systematic errors of the two final states separately in quadrature. If isospin symmetry is assumed this value becomes 0.174 ± 0.010 ± 0.015.

$\langle N_{\Sigma^0} \rangle$

VALUE	DOCUMENT ID		TECN	COMMENT
0.076±0.010 OUR AVERAGE				
0.095±0.015±0.013	ACCIARRI	00J	L3	E_{cm}^{ee} = 91.2 GeV
0.071±0.012±0.013	ALEXANDER	97E	OPAL	E_{cm}^{ee} = 91.2 GeV
0.070±0.010±0.010	ADAM	96B	DLPH	E_{cm}^{ee} = 91.2 GeV

$\langle N_{(\Sigma^+ + \Sigma^- + \Sigma^0)/3} \rangle$

VALUE	DOCUMENT ID		TECN	COMMENT
0.084 ± 0.005 ± 0.008	ALEXANDER	97E	OPAL	E_{cm}^{ee} = 91.2 GeV

$\langle N_{\Sigma(1385)^+} \rangle$

VALUE	DOCUMENT ID		TECN	COMMENT
0.0239 ± 0.0009 ± 0.0012	ALEXANDER	97D	OPAL	E_{cm}^{ee} = 91.2 GeV

$\langle N_{\Sigma(1385)^-} \rangle$

VALUE	DOCUMENT ID		TECN	COMMENT
0.0240 ± 0.0010 ± 0.0014	ALEXANDER	97D	OPAL	E_{cm}^{ee} = 91.2 GeV

$\langle N_{\Sigma(1385)^+ + \Sigma(1385)^-} \rangle$

VALUE	DOCUMENT ID		TECN	COMMENT
0.046 ± 0.004 OUR AVERAGE Error includes scale factor of 1.6.				
0.0479 ± 0.0013 ± 0.0026	ALEXANDER	97D	OPAL	E_{cm}^{ee} = 91.2 GeV
0.0382 ± 0.0028 ± 0.0045	ABREU	95O	DLPH	E_{cm}^{ee} = 91.2 GeV

$\langle N_{\Xi^-} \rangle$

VALUE	DOCUMENT ID		TECN	COMMENT
0.0258 ± 0.0009 OUR AVERAGE				
0.0247 ± 0.0009 ± 0.0025	ABDALLAH	06E	DLPH	E_{cm}^{ee} = 91.2 GeV
0.0259 ± 0.0004 ± 0.0009	ALEXANDER	97D	OPAL	E_{cm}^{ee} = 91.2 GeV

$\langle N_{\Xi(1530)^0} \rangle$

VALUE	DOCUMENT ID		TECN	COMMENT
0.0059 ± 0.0011 OUR AVERAGE Error includes scale factor of 2.3.				
0.0045 ± 0.0005 ± 0.0006	ABDALLAH	05C	DLPH	E_{cm}^{ee} = 91.2 GeV
0.0068 ± 0.0005 ± 0.0004	ALEXANDER	97D	OPAL	E_{cm}^{ee} = 91.2 GeV

$\langle N_{\Omega^-} \rangle$

VALUE	DOCUMENT ID		TECN	COMMENT
0.00164 ± 0.00028 OUR AVERAGE				
0.0018 ± 0.0003 ± 0.0002	ALEXANDER	97D	OPAL	E_{cm}^{ee} = 91.2 GeV
0.0014 ± 0.0002 ± 0.0004	ADAM	96B	DLPH	E_{cm}^{ee} = 91.2 GeV

$\langle N_{\Lambda_c^+} \rangle$

VALUE	DOCUMENT ID		TECN	COMMENT
0.078 ± 0.012 ± 0.012	ALEXANDER	96R	OPAL	E_{cm}^{ee} = 91.2 GeV

$\langle N_{\overline{D}} \rangle$

VALUE (units 10^{-6})	DOCUMENT ID		TECN	COMMENT
• • • We do not use the following data for averages, fits, limits, etc. • • •				
5.9 ± 1.8 ± 0.5	[1] SCHAEL	06A	ALEP	E_{cm}^{ee} = 91.2 GeV

[1] SCHAEL 06A obtain this anti-deuteron production rate per hadronic Z decay in the anti-deuteron momentum range from 0.62 to 1.03 GeV/c.

$\langle N_{charged} \rangle$

VALUE	DOCUMENT ID		TECN	COMMENT
20.76 ± 0.16 OUR AVERAGE Error includes scale factor of 2.1. See the ideogram below.				
20.46 ± 0.01 ± 0.11	ACHARD	03G	L3	E_{cm}^{ee} = 91.2 GeV
21.21 ± 0.01 ± 0.20	ABREU	99	DLPH	E_{cm}^{ee} = 91.2 GeV
21.05 ± 0.20	AKERS	95Z	OPAL	E_{cm}^{ee} = 91.2 GeV
20.91 ± 0.03 ± 0.22	BUSKULIC	95R	ALEP	E_{cm}^{ee} = 91.2 GeV
21.40 ± 0.43	ACTON	92B	OPAL	E_{cm}^{ee} = 91.2 GeV
20.71 ± 0.04 ± 0.77	ABREU	91H	DLPH	E_{cm}^{ee} = 91.2 GeV
20.7 ± 0.7	ADEVA	91I	L3	E_{cm}^{ee} = 91.2 GeV
20.1 ± 1.0 ± 0.9	ABRAMS	90	MRK2	E_{cm}^{ee} = 91.1 GeV

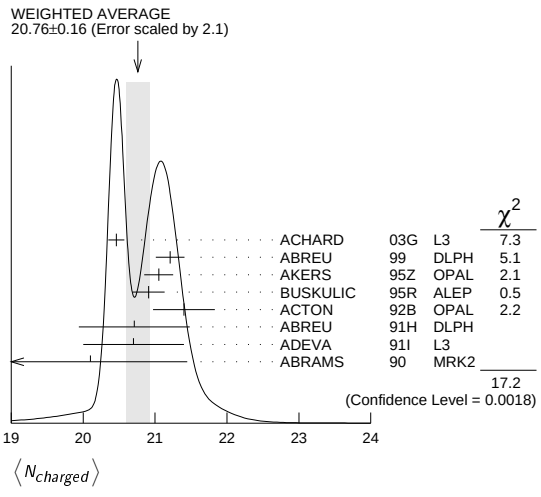

Z HADRONIC POLE CROSS SECTION

OUR FIT is obtained using the fit procedure and correlations as determined by the LEP Electroweak Working Group (see the note "The Z boson" and ref. LEP-SLC 06). This quantity is defined as

$$\sigma_h^0 = \frac{12\pi}{M_Z^2} \frac{\Gamma(e^+e^-)\,\Gamma(\text{hadrons})}{\Gamma_Z^2}$$

It is one of the parameters used in the Z lineshape fit.

VALUE (nb)	EVTS	DOCUMENT ID		TECN	COMMENT
41.541 ± 0.037 OUR FIT					
41.501 ± 0.055	4.10M	[1] ABBIENDI	01A	OPAL	E_{cm}^{ee} = 88–94 GeV
41.578 ± 0.069	3.70M	ABREU	00F	DLPH	E_{cm}^{ee} = 88–94 GeV
41.535 ± 0.055	3.54M	ACCIARRI	00C	L3	E_{cm}^{ee} = 88–94 GeV
41.559 ± 0.058	4.07M	[2] BARATE	00C	ALEP	E_{cm}^{ee} = 88–94 GeV
• • • We do not use the following data for averages, fits, limits, etc. • • •					
42 ± 4	450	ABRAMS	89B	MRK2	E_{cm}^{ee} = 89.2–93.0 GeV

[1] ABBIENDI 01A error includes approximately 0.031 due to statistics, 0.033 due to event selection systematics, 0.029 due to uncertainty in luminosity measurement, and 0.011 due to LEP energy uncertainty.
[2] BARATE 00C error includes approximately 0.030 due to statistics, 0.026 due to experimental systematics, and 0.025 due to uncertainty in luminosity measurement.

Z VECTOR COUPLINGS

These quantities are the effective vector couplings of the Z to charged leptons. Their magnitude is derived from a measurement of the Z lineshape and the forward-backward lepton asymmetries as a function of energy around the Z mass. The relative sign among the vector to axial-vector couplings is obtained from a measurement of the Z asymmetry parameters, A_e, A_μ, and A_τ. By convention the sign of g_A^e is fixed to be negative (and opposite to that of g^{ν_e} obtained using ν_e scattering measurements). For the light quarks, the sign of the couplings is assigned consistently with this assumption. The fit values quoted below correspond to global nine- or five-parameter fits to lineshape, lepton forward-backward asymmetry, and A_e, A_μ, and A_τ measurements. See the note "The Z boson" and ref. LEP-SLC 06 for details. Where $p\overline{p}$ and ep data is quoted, OUR FIT value corresponds to a weighted average of this with the LEP/SLD fit result.

g_V^e

VALUE	EVTS	DOCUMENT ID		TECN	COMMENT
−0.03817 ± 0.00047 OUR FIT					
−0.058 ± 0.016 ± 0.007	5026	[1] ACOSTA	05M	CDF	$E_{cm}^{p\overline{p}}$ = 1.96 TeV
−0.0346 ± 0.0023	137.0K	[2] ABBIENDI	01O	OPAL	E_{cm}^{ee} = 88–94 GeV
−0.0412 ± 0.0027	124.4k	[3] ACCIARRI	00C	L3	E_{cm}^{ee} = 88–94 GeV
−0.0400 ± 0.0037		BARATE	00C	ALEP	E_{cm}^{ee} = 88–94 GeV
−0.0414 ± 0.0020		[4] ABE	95J	SLD	E_{cm}^{ee} = 91.31 GeV

[1] ACOSTA 05M determine the forward–backward asymmetry of e^+e^- pairs produced via $q\overline{q} \to Z/\gamma^* \to e^+e^-$ in 15 M(e^+e^-) effective mass bins ranging from 40 GeV to 600 GeV. These results are used to obtain the vector and axial–vector couplings of the Z to e^+e^-, assuming the quark couplings are as predicted by the standard model. Higher order radiative corrections have not been taken into account.
[2] ABBIENDI 01O use their measurement of the τ polarization in addition to the lineshape and forward-backward lepton asymmetries.
[3] ACCIARRI 00C use their measurement of the τ polarization in addition to forward-backward lepton asymmetries.
[4] ABE 95J obtain this result combining polarized Bhabha results with the A_{LR} measurement of ABE 94C. The Bhabha results alone give $-0.0507 \pm 0.0096 \pm 0.0020$.

g_V^μ

VALUE	EVTS	DOCUMENT ID		TECN	COMMENT
−0.0367 ± 0.0023 OUR FIT					
$-0.0388^{+0.0060}_{-0.0064}$	182.8K	[1] ABBIENDI	01O	OPAL	E_{cm}^{ee} = 88–94 GeV
−0.0386 ± 0.0073	113.4k	[2] ACCIARRI	00C	L3	E_{cm}^{ee} = 88–94 GeV
−0.0362 ± 0.0061		BARATE	00C	ALEP	E_{cm}^{ee} = 88–94 GeV
• • • We do not use the following data for averages, fits, limits, etc. • • •					
−0.0413 ± 0.0060	66143	[3] ABBIENDI	01K	OPAL	E_{cm}^{ee} = 89–93 GeV

[1] ABBIENDI 01O use their measurement of the τ polarization in addition to the lineshape and forward-backward lepton asymmetries.
[2] ACCIARRI 00C use their measurement of the τ polarization in addition to forward-backward lepton asymmetries.
[3] ABBIENDI 01K obtain this from an angular analysis of the muon pair asymmetry which takes into account effects of initial state radiation on an event by event basis and of initial-final state interference.

g_V^τ

VALUE	EVTS	DOCUMENT ID		TECN	COMMENT
−0.0366 ± 0.0010 OUR FIT					
−0.0365 ± 0.0023	151.5K	[1] ABBIENDI	01O	OPAL	E_{cm}^{ee} = 88–94 GeV
−0.0384 ± 0.0026	103.0k	[2] ACCIARRI	00C	L3	E_{cm}^{ee} = 88–94 GeV
−0.0361 ± 0.0068		BARATE	00C	ALEP	E_{cm}^{ee} = 88–94 GeV

[1] ABBIENDI 01O use their measurement of the τ polarization in addition to the lineshape and forward-backward lepton asymmetries.
[2] ACCIARRI 00C use their measurement of the τ polarization in addition to forward-backward lepton asymmetries.

g_V^ℓ

VALUE	EVTS	DOCUMENT ID		TECN	COMMENT
−0.03783±0.00041 OUR FIT					
−0.0358 ±0.0014	471.3K	[1] ABBIENDI	01O	OPAL	E_{cm}^{ee}= 88–94 GeV
−0.0397 ±0.0020	379.4k	[2] ABREU	00F	DLPH	E_{cm}^{ee}= 88–94 GeV
−0.0397 ±0.0017	340.8k	[3] ACCIARRI	00C	L3	E_{cm}^{ee}= 88–94 GeV
−0.0383 ±0.0018	500k	BARATE	00C	ALEP	E_{cm}^{ee}= 88–94 GeV

[1] ABBIENDI 01O use their measurement of the τ polarization in addition to the lineshape and forward-backward lepton asymmetries.
[2] Using forward-backward lepton asymmetries.
[3] ACCIARRI 00C use their measurement of the τ polarization in addition to forward-backward lepton asymmetries.

g_V^u

VALUE	EVTS	DOCUMENT ID		TECN	COMMENT
0.18 ±0.05 OUR AVERAGE					
$0.144^{+0.066}_{-0.058}$		[1] ABT	16		
0.201±0.112	156k	[2] ABAZOV	11D	D0	$E_{cm}^{p\overline{p}}$ = 1.97 TeV
$0.24\ ^{+0.28}_{-0.11}$		[3] LEP-SLC	06		E_{cm}^{ee} = 88–94 GeV
$0.399^{+0.152}_{-0.188}\pm0.066$	5026	[4] ACOSTA	05M	CDF	$E_{cm}^{p\overline{p}}$= 1.96 TeV
• • • We do not use the following data for averages, fits, limits, etc. • • •					
$0.14\ ^{+0.09}_{-0.09}$		[5] ABRAMOWICZ	16A	ZEUS	
0.27 ±0.13	1500	[6] AKTAS	06	H1	$e^{\pm}p \to \overline{\nu}_e(\nu_e)X$, $\sqrt{s}\approx 300$ GeV

[1] ABT 16 determine the Z^0 couplings to u- and d-quarks using the same techniques and data as ABRAMOWICZ 16A but additionally use the published H1 polarised data.
[2] ABAZOV 11D study $p\overline{p} \to Z/\gamma^* e^+e^-$ events using 5 fb^{-1} data at $\sqrt{s}$ = 1.96 TeV. The candidate events are selected by requiring two isolated electromagnetic showers with $E_T > 25$ GeV, at least one electron in the central region and the di-electron mass in the range 50–1000 GeV. From the forward-backward asymmetry, determined as a function of the di-electron mass, they derive the axial and vector couplings of the u- and d- quarks and the value of $\sin^2\theta^\ell_{eff}$ = 0.2309 ± 0.0008(stat)±0.0006(syst).
[3] LEP-SLC 06 is a combination of the results from LEP and SLC experiments using light quark tagging. s- and d-quark couplings are assumed to be identical.
[4] ACOSTA 05M determine the forward-backward asymmetry of e^+e^- pairs produced via $q\overline{q} \to Z/\gamma^* \to e^+e^-$ in 15 M(e^+e^-) effective mass bins ranging from 40 GeV to 600 GeV. These results are used to obtain the vector and axial-vector couplings of the Z to the light quarks, assuming the electron couplings are as predicted by the Standard Model. Higher order radiative corrections have not been taken into account.
[5] ABRAMOWICZ 16A determine the Z^0 couplings to u- and d-quarks using the ZEUS polarised data from Run II together with the unpolarised data from both ZEUS and H1 Collaborations for Run I and unpolarised H1 data from Run II.
[6] AKTAS 06 fit the neutral current ($1.5 \le Q^2 \le 30{,}000$ GeV^2) and charged current ($1.5 \le Q^2 \le 15{,}000$ GeV^2) differential cross sections. In the determination of the u-quark couplings the electron and d-quark couplings are fixed to their standard model values.

g_V^d

VALUE	EVTS	DOCUMENT ID		TECN	COMMENT
$\mathbf{-0.35\ ^{+0.05}_{-0.06}}$ **OUR AVERAGE**					
$-0.503^{+0.171}_{-0.103}$		[1] ABT	16		
−0.351±0.251	156k	[2] ABAZOV	11D	D0	$E_{cm}^{p\overline{p}}$ = 1.97 TeV
$-0.33\ ^{+0.05}_{-0.07}$		[3] LEP-SLC	06		E_{cm}^{ee} = 88–94 GeV
$-0.226^{+0.635}_{-0.290}\pm0.090$	5026	[4] ACOSTA	05M	CDF	$E_{cm}^{p\overline{p}}$= 1.96 TeV
• • • We do not use the following data for averages, fits, limits, etc. • • •					
$-0.41\ ^{+0.25}_{-0.20}$		[5] ABRAMOWICZ	16A	ZEUS	
−0.33 ±0.33	1500	[6] AKTAS	06	H1	$e^{\pm}p \to \overline{\nu}_e(\nu_e)X$, $\sqrt{s}\approx 300$ GeV

[1] ABT 16 determine the Z^0 couplings to u- and d-quarks using the same techniques and data as ABRAMOWICZ 16A but additionally use the published H1 polarised data.
[2] ABAZOV 11D study $p\overline{p} \to Z/\gamma^* e^+e^-$ events using 5 fb^{-1} data at $\sqrt{s}$ = 1.96 TeV. The candidate events are selected by requiring two isolated electromagnetic showers with $E_T > 25$ GeV, at least one electron in the central region and the di-electron mass in the range 50–1000 GeV. From the forward-backward asymmetry, determined as a function of the di-electron mass, they derive the axial and vector couplings of the u- and d- quarks and the value of $\sin^2\theta^\ell_{eff}$ = 0.2309 ± 0.0008(stat)±0.0006(syst).
[3] LEP-SLC 06 is a combination of the results from LEP and SLC experiments using light quark tagging. s- and d-quark couplings are assumed to be identical.
[4] ACOSTA 05M determine the forward-backward asymmetry of e^+e^- pairs produced via $q\overline{q} \to Z/\gamma^* \to e^+e^-$ in 15 M(e^+e^-) effective mass bins ranging from 40 GeV to 600 GeV. These results are used to obtain the vector and axial-vector couplings of the Z to the light quarks, assuming the electron couplings are as predicted by the Standard Model. Higher order radiative corrections have not been taken into account.
[5] ABRAMOWICZ 16A determine the Z^0 couplings to u- and d-quarks using the ZEUS polarised data from Run II together with the unpolarised data from both ZEUS and H1 Collaborations for Run I and unpolarised H1 data from Run II.
[6] AKTAS 06 fit the neutral current ($1.5 \le Q^2 \le 30{,}000$ GeV^2) and charged current ($1.5 \le Q^2 \le 15{,}000$ GeV^2) differential cross sections. In the determination of the d-quark couplings the electron and u-quark couplings are fixed to their standard model values.

Z AXIAL-VECTOR COUPLINGS

These quantities are the effective axial-vector couplings of the Z to charged leptons. Their magnitude is derived from a measurement of the Z lineshape and the forward-backward lepton asymmetries as a function of energy around the Z mass. The relative sign among the vector to axial-vector couplings is obtained from a measurement of the Z asymmetry parameters, A_e, A_μ, and A_τ. By convention the sign of g_A^e is fixed to be negative (and opposite to that of g^{ν_e} obtained using ν_e scattering measurements). For the light quarks, the sign of the couplings is assigned consistently with this assumption. The fit values quoted below correspond to global nine- or five-parameter fits to lineshape, lepton forward-backward asymmetry, and A_e, A_μ, and A_τ measurements. See the note "The Z boson" and ref. LEP-SLC 06 for details. Where $p\overline{p}$ and ep data is quoted, our FIT value corresponds to a weighted average of this with the LEP/SLD fit result.

g_A^e

VALUE	EVTS	DOCUMENT ID		TECN	COMMENT
−0.50111±0.00035 OUR FIT					
−0.528 ±0.123 ±0.059	5026	[1] ACOSTA	05M	CDF	$E_{cm}^{p\overline{p}}$= 1.96 TeV
−0.50062±0.00062	137.0K	[2] ABBIENDI	01O	OPAL	E_{cm}^{ee}= 88–94 GeV
−0.5015 ±0.0007	124.4k	[3] ACCIARRI	00C	L3	E_{cm}^{ee}= 88–94 GeV
−0.50166±0.00057		BARATE	00C	ALEP	E_{cm}^{ee}= 88–94 GeV
−0.4977 ±0.0045		[4] ABE	95J	SLD	E_{cm}^{ee}= 91.31 GeV

[1] ACOSTA 05M determine the forward–backward asymmetry of e^+e^- pairs produced via $q\overline{q} \to Z/\gamma^* \to e^+e^-$ in 15 M(e^+e^-) effective mass bins ranging from 40 GeV to 600 GeV. These results are used to obtain the vector and axial–vector couplings of the Z to e^+e^-, assuming the quark couplings are as predicted by the standard model. Higher order radiative corrections have not been taken into account.
[2] ABBIENDI 01O use their measurement of the τ polarization in addition to the lineshape and forward-backward lepton asymmetries.
[3] ACCIARRI 00C use their measurement of the τ polarization in addition to forward-backward lepton asymmetries.
[4] ABE 95J obtain this result combining polarized Bhabha results with the A_{LR} measurement of ABE 94C. The Bhabha results alone give −0.4968 ± 0.0039 ± 0.0027.

g_A^μ

VALUE	EVTS	DOCUMENT ID		TECN	COMMENT
−0.50120±0.00054 OUR FIT					
−0.50117±0.00099	182.8K	[1] ABBIENDI	01O	OPAL	E_{cm}^{ee}= 88–94 GeV
−0.5009 ±0.0014	113.4k	[2] ACCIARRI	00C	L3	E_{cm}^{ee}= 88–94 GeV
−0.50046±0.00093		BARATE	00C	ALEP	E_{cm}^{ee}= 88–94 GeV
• • • We do not use the following data for averages, fits, limits, etc. • • •					
−0.520 ±0.015	66143	[3] ABBIENDI	01K	OPAL	E_{cm}^{ee}= 89–93 GeV

[1] ABBIENDI 01O use their measurement of the τ polarization in addition to the lineshape and forward-backward lepton asymmetries.
[2] ACCIARRI 00C use their measurement of the τ polarization in addition to forward-backward lepton asymmetries.
[3] ABBIENDI 01K obtain this from an angular analysis of the muon pair asymmetry which takes into account effects of initial state radiation on an event by event basis and of initial-final state interference.

g_A^τ

VALUE	EVTS	DOCUMENT ID		TECN	COMMENT
−0.50204±0.00064 OUR FIT					
−0.50165±0.00124	151.5K	[1] ABBIENDI	01O	OPAL	E_{cm}^{ee}= 88–94 GeV
−0.5023 ±0.0017	103.0k	[2] ACCIARRI	00C	L3	E_{cm}^{ee}= 88–94 GeV
−0.50216±0.00100		BARATE	00C	ALEP	E_{cm}^{ee}= 88–94 GeV

[1] ABBIENDI 01O use their measurement of the τ polarization in addition to the lineshape and forward-backward lepton asymmetries.
[2] ACCIARRI 00C use their measurement of the τ polarization in addition to forward-backward lepton asymmetries.

g_A^ℓ

VALUE	EVTS	DOCUMENT ID		TECN	COMMENT
−0.50123±0.00026 OUR FIT					
−0.50089±0.00045	471.3K	[1] ABBIENDI	01O	OPAL	E_{cm}^{ee}= 88–94 GeV
−0.5007 ±0.0005	379.4k	ABREU	00F	DLPH	E_{cm}^{ee}= 88–94 GeV
−0.50153±0.00053	340.8k	[2] ACCIARRI	00C	L3	E_{cm}^{ee}= 88–94 GeV
−0.50150±0.00046	500k	BARATE	00C	ALEP	E_{cm}^{ee}= 88–94 GeV

[1] ABBIENDI 01O use their measurement of the τ polarization in addition to the lineshape and forward-backward lepton asymmetries.
[2] ACCIARRI 00C use their measurement of the τ polarization in addition to forward-backward lepton asymmetries.

g_A^u

VALUE	EVTS	DOCUMENT ID		TECN	COMMENT
$\mathbf{0.50\ ^{+0.04}_{-0.05}}$ **OUR AVERAGE**					
$0.532^{+0.107}_{-0.063}$		[1] ABT	16		
0.501±0.110	156k	[2] ABAZOV	11D	D0	$E_{cm}^{p\overline{p}}$ = 1.97 TeV
$0.47\ ^{+0.05}_{-0.33}$		[3] LEP-SLC	06		E_{cm}^{ee} = 88–94 GeV
$0.441^{+0.207}_{-0.173}\pm0.067$	5026	[4] ACOSTA	05M	CDF	$E_{cm}^{p\overline{p}}$= 1.96 TeV

• • • We do not use the following data for averages, fits, limits, etc. • • •

$0.50\ ^{+0.12}_{-0.05}$		[5] ABRAMOWICZ	16A	ZEUS		
$0.57\ \pm0.08$	1500	[6] AKTAS	06	H1	$e^{\pm}p \to \overline{\nu}_e(\nu_e)X$, $\sqrt{s} \approx 300$ GeV	

[1] ABT 16 determine the Z^0 couplings to u- and d-quarks using the same techniques and data as ABRAMOWICZ 16A but additionally use the published H1 polarised data.

[2] ABAZOV 11D study $p\overline{p} \to Z/\gamma^* e^+e^-$ events using 5 fb^{-1} data at $\sqrt{s} = 1.96$ TeV. The candidate events are selected by requiring two isolated electromagnetic showers with $E_T > 25$ GeV, at least one electron in the central region and the di-electron mass in the range 50–1000 GeV. From the forward-backward asymmetry, determined as a function of the di-electron mass, they derive the axial and vector couplings of the u- and d- quarks and the value of $\sin^2\theta^\ell_{eff} = 0.2309 \pm 0.0008(\text{stat}) \pm 0.0006(\text{syst})$.

[3] LEP-SLC 06 is a combination of the results from LEP and SLC experiments using light quark tagging. s- and d-quark couplings are assumed to be identical.

[4] ACOSTA 05M determine the forward-backward asymmetry of e^+e^- pairs produced via $q\overline{q} \to Z/\gamma^* \to e^+e^-$ in 15 M(e^+e^-) effective mass bins ranging from 40 GeV to 600 GeV. These results are used to obtain the vector and axial-vector couplings of the Z to the light quarks, assuming the electron couplings are as predicted by the Standard Model. Higher order radiative corrections have not been taken into account.

[5] ABRAMOWICZ 16A determine the Z^0 couplings to u- and d-quarks using the ZEUS polarised data from Run II together with the unpolarised data from both ZEUS and H1 Collaborations for Run I and unpolarised H1 data from Run II.

[6] AKTAS 06 fit the neutral current ($1.5 \le Q^2 \le 30{,}000$ GeV^2) and charged current ($1.5 \le Q^2 \le 15{,}000$ GeV^2) differential cross sections. In the determination of the u-quark couplings the electron and d-quark couplings are fixed to their standard model values.

g^d_A

VALUE	EVTS	DOCUMENT ID		TECN	COMMENT
$-0.514\ ^{+0.050}_{-0.029}$ OUR AVERAGE					
$-0.409\ ^{+0.373}_{-0.213}$		[1] ABT	16		
-0.497 ± 0.165	156k	[2] ABAZOV	11D	D0	$E^{p\overline{p}}_{\text{cm}} = 1.97$ TeV
$-0.52\ ^{+0.05}_{-0.03}$		[3] LEP-SLC	06		$E^{ee}_{\text{cm}} = 88$–94 GeV
$-0.016\ ^{+0.346}_{-0.536} \pm 0.091$	5026	[4] ACOSTA	05M	CDF	$E^{p\overline{p}}_{\text{cm}} = 1.96$ TeV
• • • We do not use the following data for averages, fits, limits, etc. • • •					
$-0.56\ ^{+0.41}_{-0.15}$		[5] ABRAMOWICZ	16A	ZEUS	
$-0.80\ \pm0.24$	1500	[6] AKTAS	06	H1	$e^{\pm}p \to \overline{\nu}_e(\nu_e)X$, $\sqrt{s} \approx 300$ GeV

[1] ABT 16 determine the Z^0 couplings to u- and d-quarks using the same techniques and data as ABRAMOWICZ 16A but additionally use the published H1 polarised data.

[2] ABAZOV 11D study $p\overline{p} \to Z/\gamma^* e^+e^-$ events using 5 fb^{-1} data at $\sqrt{s} = 1.96$ TeV. The candidate events are selected by requiring two isolated electromagnetic showers with $E_T > 25$ GeV, at least one electron in the central region and the di-electron mass in the range 50–1000 GeV. From the forward-backward asymmetry, determined as a function of the di-electron mass, they derive the axial and vector couplings of the u- and d- quarks and the value of $\sin^2\theta^\ell_{eff} = 0.2309 \pm 0.0008(\text{stat}) \pm 0.0006(\text{syst})$.

[3] LEP-SLC 06 is a combination of the results from LEP and SLC experiments using light quark tagging. s- and d-quark couplings are assumed to be identical.

[4] ACOSTA 05M determine the forward-backward asymmetry of e^+e^- pairs produced via $q\overline{q} \to Z/\gamma^* \to e^+e^-$ in 15 M(e^+e^-) effective mass bins ranging from 40 GeV to 600 GeV. These results are used to obtain the vector and axial-vector couplings of the Z to the light quarks, assuming the electron couplings are as predicted by the Standard Model. Higher order radiative corrections have not been taken into account.

[5] ABRAMOWICZ 16A determine the Z^0 couplings to u- and d-quarks using the ZEUS polarised data from Run II together with the unpolarised data from both ZEUS and H1 Collaborations for Run I and unpolarised H1 data from Run II.

[6] AKTAS 06 fit the neutral current ($1.5 \le Q^2 \le 30{,}000$ GeV^2) and charged current ($1.5 \le Q^2 \le 15{,}000$ GeV^2) differential cross sections. In the determination of the d-quark couplings the electron and u-quark couplings are fixed to their standard model values.

Z COUPLINGS TO NEUTRAL LEPTONS

Averaging over neutrino species, the invisible Z decay width determines the effective neutrino coupling g^{ν_ℓ}. For g^{ν_e} and g^{ν_μ}, $\nu_e e$ and $\nu_\mu e$ scattering results are combined with g^e_A and g^e_V measurements at the Z mass to obtain g^{ν_e} and g^{ν_μ} following NOVIKOV 93C.

g^{ν_ℓ}

VALUE	DOCUMENT ID			TECN	COMMENT
0.50076 ± 0.00076	[1] LEP-SLC	06			$E^{ee}_{\text{cm}} = 88$–94 GeV

[1] From invisible Z-decay width.

g^{ν_e}

VALUE	DOCUMENT ID		TECN	COMMENT
0.528 ± 0.085	[1] VILAIN	94	CHM2	From $\nu_\mu e$ and $\nu_e e$ scattering

[1] VILAIN 94 derive this value from their value of g^{ν_μ} and their ratio $g^{\nu_e}/g^{\nu_\mu} = 1.05\ ^{+0.15}_{-0.18}$.

g^{ν_μ}

VALUE	DOCUMENT ID		TECN	COMMENT
0.502 ± 0.017	[1] VILAIN	94	CHM2	From $\nu_\mu e$ scattering

[1] VILAIN 94 derive this value from their measurement of the couplings $g_A^{e\nu_\mu} = -0.503 \pm 0.017$ and $g_V^{e\nu_\mu} = -0.035 \pm 0.017$ obtained from $\nu_\mu e$ scattering. We have re-evaluated this value using the current PDG values for g^e_A and g^e_V.

Z ASYMMETRY PARAMETERS

For each fermion-antifermion pair coupling to the Z these quantities are defined as

$$A_f = \frac{2g_V^f g_A^f}{(g_V^f)^2 + (g_A^f)^2}$$

where g_V^f and g_A^f are the effective vector and axial-vector couplings. For their relation to the various lepton asymmetries see the note "The Z boson" and ref. LEP-SLC 06.

A_e

Using polarized beams, this quantity can also be measured as $(\sigma_L - \sigma_R)/(\sigma_L + \sigma_R)$, where σ_L and σ_R are the e^+e^- production cross sections for Z bosons produced with left-handed and right-handed electrons respectively.

VALUE	EVTS	DOCUMENT ID		TECN	COMMENT
0.1515 ± 0.0019 OUR AVERAGE					
$0.1454 \pm 0.0108 \pm 0.0036$	144810	[1] ABBIENDI	01O	OPAL	$E^{ee}_{\text{cm}} = 88$–94 GeV
0.1516 ± 0.0021	559000	[2] ABE	01B	SLD	$E^{ee}_{\text{cm}} = 91.24$ GeV
$0.1504 \pm 0.0068 \pm 0.0008$		[3] HEISTER	01	ALEP	$E^{ee}_{\text{cm}} = 88$–94 GeV
$0.1382 \pm 0.0116 \pm 0.0005$	105000	[4] ABREU	00E	DLPH	$E^{ee}_{\text{cm}} = 88$–94 GeV
$0.1678 \pm 0.0127 \pm 0.0030$	137092	[5] ACCIARRI	98H	L3	$E^{ee}_{\text{cm}} = 88$–94 GeV
$0.162\ \pm 0.041\ \pm 0.014$	89838	[6] ABE	97	SLD	$E^{ee}_{\text{cm}} = 91.27$ GeV
$0.202\ \pm 0.038\ \pm 0.008$		[7] ABE	95J	SLD	$E^{ee}_{\text{cm}} = 91.31$ GeV

[1] ABBIENDI 01O fit for A_e and A_τ from measurements of the τ polarization at varying τ production angles. The correlation between A_e and A_τ is less than 0.03.

[2] ABE 01B use the left-right production and left-right forward-backward decay asymmetries in leptonic Z decays to obtain a value of 0.1544 ± 0.0060. This is combined with left-right production asymmetry measurement using hadronic Z decays (ABE 00B) to obtain the quoted value.

[3] HEISTER 01 obtain this result fitting the τ polarization as a function of the polar production angle of the τ.

[4] ABREU 00E obtain this result fitting the τ polarization as a function of the polar τ production angle. This measurement is a combination of different analyses (exclusive τ decay modes, inclusive hadronic 1-prong reconstruction, and a neural network analysis).

[5] Derived from the measurement of forward-backward τ polarization asymmetry.

[6] ABE 97 obtain this result from a measurement of the observed left-right charge asymmetry, $A_Q^{\text{obs}} = 0.225 \pm 0.056 \pm 0.019$, in hadronic Z decays. If they combine this value of A_Q^{obs} with their earlier measurement of A_{LR}^{obs} they determine A_e to be $0.1574 \pm 0.0197 \pm 0.0067$ independent of the beam polarization.

[7] ABE 95J obtain this result from polarized Bhabha scattering.

A_μ

This quantity is directly extracted from a measurement of the left-right forward-backward asymmetry in $\mu^+\mu^-$ production at SLC using a polarized electron beam. This double asymmetry eliminates the dependence on the Z-e-e coupling parameter A_e.

VALUE	EVTS	DOCUMENT ID		TECN	COMMENT
0.142 ± 0.015	16844	[1] ABE	01B	SLD	$E^{ee}_{\text{cm}} = 91.24$ GeV
• • • We do not use the following data for averages, fits, limits, etc. • • •					
0.153 ± 0.012	1.7M	[2] AAD	15BT	ATLS	$E^{pp}_{\text{cm}} = 7$ TeV

[1] ABE 01B obtain this direct measurement using the left-right production and left-right forward-backward polar angle asymmetries in $\mu^+\mu^-$ decays of the Z boson obtained with a polarized electron beam.

[2] AAD 15BT study $pp \to Z \to \ell^+\ell^-$ events where ℓ is an electron or a muon in the dilepton mass region 70–1000 GeV. The background in the Z peak region is estimated to be < 1% for the muon channel. The muon asymmetry parameter is derived from the measured forward-backward asymmetry assuming the value of the quark asymmetry parameter from the SM. For this reason it is not used in the average.

A_τ

The LEP Collaborations derive this quantity from the measurement of the τ polarization in $Z \to \tau^+\tau^-$. The SLD Collaboration directly extracts this quantity from its measured left-right forward-backward asymmetry in $Z \to \tau^+\tau^-$ produced using a polarized e^- beam. This double asymmetry eliminates the dependence on the Z-e-e coupling parameter A_e.

VALUE	EVTS	DOCUMENT ID		TECN	COMMENT
0.143 ± 0.004 OUR AVERAGE					
$0.1456 \pm 0.0076 \pm 0.0057$	144810	[1] ABBIENDI	01O	OPAL	$E^{ee}_{\text{cm}} = 88$–94 GeV
$0.136\ \pm 0.015$	16083	[2] ABE	01B	SLD	$E^{ee}_{\text{cm}} = 91.24$ GeV
$0.1451 \pm 0.0052 \pm 0.0029$		[3] HEISTER	01	ALEP	$E^{ee}_{\text{cm}} = 88$–94 GeV
$0.1359 \pm 0.0079 \pm 0.0055$	105000	[4] ABREU	00E	DLPH	$E^{ee}_{\text{cm}} = 88$–94 GeV
$0.1476 \pm 0.0088 \pm 0.0062$	137092	ACCIARRI	98H	L3	$E^{ee}_{\text{cm}} = 88$–94 GeV

[1] ABBIENDI 01O fit for A_e and A_τ from measurements of the τ polarization at varying τ production angles. The correlation between A_e and A_τ is less than 0.03.

[2] ABE 01B obtain this direct measurement using the left-right production and left-right forward-backward polar angle asymmetries in $\tau^+\tau^-$ decays of the Z boson obtained with a polarized electron beam.

[3] HEISTER 01 obtain this result fitting the τ polarization as a function of the polar production angle of the τ.
[4] ABREU 00E obtain this result fitting the τ polarization as a function of the polar τ production angle. This measurement is a combination of different analyses (exclusive τ decay modes, inclusive hadronic 1-prong reconstruction, and a neural network analysis).

A_s

The SLD Collaboration directly extracts this quantity by a simultaneous fit to four measured s-quark polar angle distributions corresponding to two states of e^- polarization (positive and negative) and to the K^+K^- and $K^\pm K^0_S$ strange particle tagging modes in the hadronic final states.

VALUE	EVTS	DOCUMENT ID		TECN	COMMENT
0.895±0.066±0.062	2870	[1] ABE	00D	SLD	E^{ee}_{cm}= 91.2 GeV

[1] ABE 00D tag $Z \to s\overline{s}$ events by an absence of B or D hadrons and the presence in each hemisphere of a high momentum $K^\pm$ or K^0_S.

A_c

This quantity is directly extracted from a measurement of the left-right forward-backward asymmetry in $c\overline{c}$ production at SLC using polarized electron beam. This double asymmetry eliminates the dependence on the Z-e-e coupling parameter A_e. OUR FIT is obtained by a simultaneous fit to several c- and b-quark measurements as explained in the note "The Z boson" and ref. LEP-SLC 06.

VALUE	DOCUMENT ID		TECN	COMMENT
0.670 ±0.027 OUR FIT				
0.6712±0.0224±0.0157	[1] ABE	05	SLD	E^{ee}_{cm}= 91.24 GeV
• • • We do not use the following data for averages, fits, limits, etc. • • •				
0.583 ±0.055 ±0.055	[2] ABE	02G	SLD	E^{ee}_{cm}= 91.24 GeV
0.688 ±0.041	[3] ABE	01C	SLD	E^{ee}_{cm}= 91.25 GeV

[1] ABE 05 use hadronic Z decays collected during 1996–98 to obtain an enriched sample of $c\overline{c}$ events tagging on the invariant mass of reconstructed secondary decay vertices. The charge of the underlying c–quark is obtained with an algorithm that takes into account the net charge of the vertex as well as the charge of tracks emanating from the vertex and identified as kaons. This yields (9970 events) A_c = 0.6747 ± 0.0290 ± 0.0233. Taking into account all correlations with earlier results reported in ABE 02G and ABE 01C, they obtain the quoted overall SLD result.
[2] ABE 02G tag b and c quarks through their semileptonic decays into electrons and muons. A maximum likelihood fit is performed to extract simultaneously A_b and A_c.
[3] ABE 01C tag $Z \to c\overline{c}$ events using two techniques: exclusive reconstruction of D^{*+}, D^+ and D^0 mesons and the soft pion tag for $D^{*+} \to D^0\pi^+$. The large background from D mesons produced in $b\overline{b}$ events is separated efficiently from the signal using precision vertex information. When combining the A_c values from these two samples, care is taken to avoid double counting of events common to the two samples, and common systematic errors are properly taken into account.

A_b

This quantity is directly extracted from a measurement of the left-right forward-backward asymmetry in $b\overline{b}$ production at SLC using polarized electron beam. This double asymmetry eliminates the dependence on the Z-e-e coupling parameter A_e. OUR FIT is obtained by a simultaneous fit to several c- and b-quark measurements as explained in the note "The Z boson" and ref. LEP-SLC 06.

VALUE	EVTS	DOCUMENT ID		TECN	COMMENT
0.923 ±0.020 OUR FIT					
0.9170±0.0147±0.0145		[1] ABE	05	SLD	E^{ee}_{cm}= 91.24 GeV
• • • We do not use the following data for averages, fits, limits, etc. • • •					
0.907 ±0.020 ±0.024	48028	[2] ABE	03F	SLD	E^{ee}_{cm}= 91.24 GeV
0.919 ±0.030 ±0.024		[3] ABE	02G	SLD	E^{ee}_{cm}= 91.24 GeV
0.855 ±0.088 ±0.102	7473	[4] ABE	99L	SLD	E^{ee}_{cm}= 91.27 GeV

[1] ABE 05 use hadronic Z decays collected during 1996–98 to obtain an enriched sample of $b\overline{b}$ events tagging on the invariant mass of reconstructed secondary decay vertices. The charge of the underlying b–quark is obtained with an algorithm that takes into account the net charge of the vertex as well as the charge of tracks emanating from the vertex and identified as kaons. This yields (25917 events) A_b = 0.9173 ± 0.0184 ± 0.0173. Taking into account all correlations with earlier results reported in ABE 03F, ABE 02G and ABE 99L, they obtain the quoted overall SLD result.
[2] ABE 03F obtain an enriched sample of $b\overline{b}$ events tagging on the invariant mass of a 3-dimensional topologically reconstructed secondary decay. The charge of the underlying b quark is obtained using a self-calibrating track-charge method. For the 1996–1998 data sample they measure A_b = 0.906 ± 0.022 ± 0.023. The value quoted here is obtained combining the above with the result of ABE 98I (1993–1995 data sample).
[3] ABE 02G tag b and c quarks through their semileptonic decays into electrons and muons. A maximum likelihood fit is performed to extract simultaneously A_b and A_c.
[4] ABE 99L obtain an enriched sample of $b\overline{b}$ events tagging with an inclusive vertex mass cut. For distinguishing b and $\overline{b}$ quarks they use the charge of identified $K^\pm$.

TRANSVERSE SPIN CORRELATIONS IN $Z \to \tau^+\tau^-$

The correlations between the transverse spin components of $\tau^+\tau^-$ produced in Z decays may be expressed in terms of the vector and axial-vector couplings:

$$C_{TT} = \frac{|g^\tau_A|^2 - |g^\tau_V|^2}{|g^\tau_A|^2 + |g^\tau_V|^2}$$

$$C_{TN} = -2\frac{|g^\tau_A||g^\tau_V|}{|g^\tau_A|^2 + |g^\tau_V|^2}\sin(\Phi_{g^\tau_V} - \Phi_{g^\tau_A})$$

C_{TT} refers to the transverse-transverse (within the collision plane) spin correlation and C_{TN} refers to the transverse-normal (to the collision plane) spin correlation.

The longitudinal τ polarization P_τ ($= -A_\tau$) is given by:

$$P_\tau = -2\frac{|g^\tau_A||g^\tau_V|}{|g^\tau_A|^2 + |g^\tau_V|^2}\cos(\Phi_{g^\tau_V} - \Phi_{g^\tau_A})$$

Here Φ is the phase and the phase difference $\Phi_{g^\tau_V} - \Phi_{g^\tau_A}$ can be obtained using both the measurements of C_{TN} and P_τ.

C_{TT}

VALUE	EVTS	DOCUMENT ID		TECN	COMMENT
1.01±0.12 OUR AVERAGE					
$0.87\pm0.20^{+0.10}_{-0.12}$	9.1k	ABREU	97G	DLPH	E^{ee}_{cm}= 91.2 GeV
1.06±0.13±0.05	120k	BARATE	97D	ALEP	E^{ee}_{cm}= 91.2 GeV

C_{TN}

VALUE	EVTS	DOCUMENT ID		TECN	COMMENT
0.08±0.13±0.04	120k	[1] BARATE	97D	ALEP	E^{ee}_{cm}= 91.2 GeV

[1] BARATE 97D combine their value of C_{TN} with the world average $P_\tau = -0.140 \pm 0.007$ to obtain $\tan(\Phi_{g^\tau_V} - \Phi_{g^\tau_A}) = -0.57 \pm 0.97$.

FORWARD-BACKWARD $e^+e^- \to f\overline{f}$ CHARGE ASYMMETRIES

These asymmetries are experimentally determined by tagging the respective lepton or quark flavor in e^+e^- interactions. Details of heavy flavor (c- or b-quark) tagging at LEP are described in the note on "The Z boson" and ref. LEP-SLC 06. The Standard Model predictions for LEP data have been (re)computed using the ZFITTER package (version 6.36) with input parameters M_Z=91.187 GeV, M_{top}=174.3 GeV, M_{Higgs}=150 GeV, α_S=0.119, $\alpha^{(5)}$ (M_Z)= 1/128.877 and the Fermi constant G_F= 1.16637×10^{-5} GeV^{-2} (see the note on "The Z boson" for references). For non-LEP data the Standard Model predictions are as given by the authors of the respective publications.

$A^{(0,e)}_{FB}$ CHARGE ASYMMETRY IN $e^+e^- \to e^+e^-$

OUR FIT is obtained using the fit procedure and correlations as determined by the LEP Electroweak Working Group (see the note "The Z boson" and ref. LEP-SLC 06). For the Z peak, we report the pole asymmetry defined by $(3/4)A^2_e$ as determined by the nine-parameter fit to cross-section and lepton forward-backward asymmetry data.

ASYMMETRY (%)	STD. MODEL	$\sqrt{s}$ (GeV)	DOCUMENT ID		TECN
1.45±0.25 OUR FIT					
0.89±0.44	1.57	91.2	[1] ABBIENDI	01A	OPAL
1.71±0.49	1.57	91.2	ABREU	00F	DLPH
1.06±0.58	1.57	91.2	ACCIARRI	00C	L3
1.88±0.34	1.57	91.2	[2] BARATE	00C	ALEP

[1] ABBIENDI 01A error includes approximately 0.38 due to statistics, 0.16 due to event selection systematics, and 0.18 due to the theoretical uncertainty in t-channel prediction.
[2] BARATE 00C error includes approximately 0.31 due to statistics, 0.06 due to experimental systematics, and 0.13 due to the theoretical uncertainty in t-channel prediction.

$A^{(0,\mu)}_{FB}$ CHARGE ASYMMETRY IN $e^+e^- \to \mu^+\mu^-$

OUR FIT is obtained using the fit procedure and correlations as determined by the LEP Electroweak Working Group (see the note "The Z boson" and ref. LEP-SLC 06). For the Z peak, we report the pole asymmetry defined by $(3/4)A_eA_\mu$ as determined by the nine-parameter fit to cross-section and lepton forward-backward asymmetry data.

ASYMMETRY (%)	STD. MODEL	$\sqrt{s}$ (GeV)	DOCUMENT ID		TECN
1.69± 0.13 OUR FIT					
1.59± 0.23	1.57	91.2	[1] ABBIENDI	01A	OPAL
1.65± 0.25	1.57	91.2	ABREU	00F	DLPH
1.88± 0.33	1.57	91.2	ACCIARRI	00C	L3
1.71± 0.24	1.57	91.2	[2] BARATE	00C	ALEP
• • • We do not use the following data for averages, fits, limits, etc. • • •					
9 ±30	−1.3	20	[3] ABREU	95M	DLPH
7 ±26	−8.3	40	[3] ABREU	95M	DLPH
−11 ±33	−24.1	57	[3] ABREU	95M	DLPH
−62 ±17	−44.6	69	[3] ABREU	95M	DLPH
−56 ±10	−63.5	79	[3] ABREU	95M	DLPH
−13 ± 5	−34.4	87.5	[3] ABREU	95M	DLPH
$-29.0\ ^{+\ 5.0}_{-\ 4.8}\ \pm0.5$	−32.1	56.9	[4] ABE	90I	VNS
− 9.9 ± 1.5 ±0.5	−9.2	35	HEGNER	90	JADE
0.05± 0.22	0.026	91.14	[5] ABRAMS	89D	MRK2
−43.4 ±17.0	−24.9	52.0	[6] BACALA	89	AMY
−11.0 ±16.5	−29.4	55.0	[6] BACALA	89	AMY
−30.0 ±12.4	−31.2	56.0	[6] BACALA	89	AMY
−46.2 ±14.9	−33.0	57.0	[6] BACALA	89	AMY
−29 ±13	−25.9	53.3	ADACHI	88C	TOPZ
+ 5.3 ± 5.0 ±0.5	−1.2	14.0	ADEVA	88	MRKJ
−10.4 ± 1.3 ±0.5	−8.6	34.8	ADEVA	88	MRKJ

$-12.3 \pm 5.3 \pm 0.5$	-10.7	38.3	ADEVA	88	MRKJ
$-15.6 \pm 3.0 \pm 0.5$	-14.9	43.8	ADEVA	88	MRKJ
-1.0 ± 6.0	-1.2	13.9	BRAUNSCH...	88D	TASS
$-9.1 \pm 2.3 \pm 0.5$	-8.6	34.5	BRAUNSCH...	88D	TASS
$-10.6 \pm {}^{2.2}_{2.3} \pm 0.5$	-8.9	35.0	BRAUNSCH...	88D	TASS
$-17.6 \pm {}^{4.4}_{4.3} \pm 0.5$	-15.2	43.6	BRAUNSCH...	88D	TASS
$-4.8 \pm 6.5 \pm 1.0$	-11.5	39	BEHREND	87C	CELL
$-18.8 \pm 4.5 \pm 1.0$	-15.5	44	BEHREND	87C	CELL
$+2.7 \pm 4.9$	-1.2	13.9	BARTEL	86C	JADE
$-11.1 \pm 1.8 \pm 1.0$	-8.6	34.4	BARTEL	86C	JADE
$-17.3 \pm 4.8 \pm 1.0$	-13.7	41.5	BARTEL	86C	JADE
$-22.8 \pm 5.1 \pm 1.0$	-16.6	44.8	BARTEL	86C	JADE
$-6.3 \pm 0.8 \pm 0.2$	-6.3	29	ASH	85	MAC
$-4.9 \pm 1.5 \pm 0.5$	-5.9	29	DERRICK	85	HRS
-7.1 ± 1.7	-5.7	29	LEVI	83	MRK2
-16.1 ± 3.2	-9.2	34.2	BRANDELIK	82C	TASS

[1] ABBIENDI 01A error is almost entirely on account of statistics.
[2] BARATE 00C error is almost entirely on account of statistics.
[3] ABREU 95M perform this measurement using radiative muon-pair events associated with high-energy isolated photons.
[4] ABE 90I measurements in the range $50 \leq \sqrt{s} \leq 60.8$ GeV.
[5] ABRAMS 89D asymmetry includes both 9 $\mu^+\mu^-$ and 15 $\tau^+\tau^-$ events.
[6] BACALA 89 systematic error is about 5%.

$A_{FB}^{(0,\tau)}$ CHARGE ASYMMETRY IN $e^+e^- \to \tau^+\tau^-$

OUR FIT is obtained using the fit procedure and correlations as determined by the LEP Electroweak Working Group (see the note "The Z boson" and ref. LEP-SLC 06). For the Z peak, we report the pole asymmetry defined by $(3/4)A_eA_\tau$ as determined by the nine-parameter fit to cross-section and lepton forward-backward asymmetry data.

ASYMMETRY (%)	STD. MODEL	$\sqrt{s}$ (GeV)	DOCUMENT ID		TECN
1.88± 0.17 OUR FIT					
1.45± 0.30	1.57	91.2	[1] ABBIENDI	01A	OPAL
2.41± 0.37	1.57	91.2	ABREU	00F	DLPH
2.60± 0.47	1.57	91.2	ACCIARRI	00C	L3
1.70± 0.28	1.57	91.2	[2] BARATE	00C	ALEP
• • • We do not use the following data for averages, fits, limits, etc. • • •					
$-32.8 \pm {}^{6.4}_{6.2} \pm 1.5$	-32.1	56.9	[3] ABE	90I	VNS
$-8.1 \pm 2.0 \pm 0.6$	-9.2	35	HEGNER	90	JADE
-18.4 ± 19.2	-24.9	52.0	[4] BACALA	89	AMY
-17.7 ± 26.1	-29.4	55.0	[4] BACALA	89	AMY
-45.9 ± 16.6	-31.2	56.0	[4] BACALA	89	AMY
-49.5 ± 18.0	-33.0	57.0	[4] BACALA	89	AMY
-20 ± 14	-25.9	53.3	ADACHI	88C	TOPZ
$-10.6 \pm 3.1 \pm 1.5$	-8.5	34.7	ADEVA	88	MRKJ
$-8.5 \pm 6.6 \pm 1.5$	-15.4	43.8	ADEVA	88	MRKJ
$-6.0 \pm 2.5 \pm 1.0$	8.8	34.6	BARTEL	85F	JADE
$-11.8 \pm 4.6 \pm 1.0$	14.8	43.0	BARTEL	85F	JADE
$-5.5 \pm 1.2 \pm 0.5$	-0.063	29.0	FERNANDEZ	85	MAC
-4.2 ± 2.0	0.057	29	LEVI	83	MRK2
-10.3 ± 5.2	-9.2	34.2	BEHREND	82	CELL
-0.4 ± 6.6	-9.1	34.2	BRANDELIK	82C	TASS

[1] ABBIENDI 01A error includes approximately 0.26 due to statistics and 0.14 due to event selection systematics.
[2] BARATE 00C error includes approximately 0.26 due to statistics and 0.11 due to experimental systematics.
[3] ABE 90I measurements in the range $50 \leq \sqrt{s} \leq 60.8$ GeV.
[4] BACALA 89 systematic error is about 5%.

$A_{FB}^{(0,\ell)}$ CHARGE ASYMMETRY IN $e^+e^- \to \ell^+\ell^-$

For the Z peak, we report the pole asymmetry defined by $(3/4)A_\ell^2$ as determined by the five-parameter fit to cross-section and lepton forward-backward asymmetry data assuming lepton universality. For details see the note "The Z boson" and ref. LEP-SLC 06.

ASYMMETRY (%)	STD. MODEL	$\sqrt{s}$ (GeV)	DOCUMENT ID		TECN
1.71±0.10 OUR FIT					
1.45±0.17	1.57	91.2	[1] ABBIENDI	01A	OPAL
1.87±0.19	1.57	91.2	ABREU	00F	DLPH
1.92±0.24	1.57	91.2	ACCIARRI	00C	L3
1.73±0.16	1.57	91.2	[2] BARATE	00C	ALEP

[1] ABBIENDI 01A error includes approximately 0.15 due to statistics, 0.06 due to event selection systematics, and 0.03 due to the theoretical uncertainty in t-channel prediction.
[2] BARATE 00C error includes approximately 0.15 due to statistics, 0.04 due to experimental systematics, and 0.02 due to the theoretical uncertainty in t-channel prediction.

$A_{FB}^{(0,u)}$ CHARGE ASYMMETRY IN $e^+e^- \to u\overline{u}$

ASYMMETRY (%)	STD. MODEL	$\sqrt{s}$ (GeV)	DOCUMENT ID		TECN
4.0±6.7±2.8	**7.2**	**91.2**	[1] ACKERSTAFF	97T	OPAL

[1] ACKERSTAFF 97T measure the forward-backward asymmetry of various fast hadrons made of light quarks. Then using SU(2) isospin symmetry and flavor independence for down and strange quarks authors solve for the different quark types.

$A_{FB}^{(0,s)}$ CHARGE ASYMMETRY IN $e^+e^- \to s\overline{s}$

The s-quark asymmetry is derived from measurements of the forward-backward asymmetry of fast hadrons containing an s quark.

ASYMMETRY (%)	STD. MODEL	$\sqrt{s}$ (GeV)	DOCUMENT ID		TECN
9.8 ±1.1 OUR AVERAGE					
10.08±1.13±0.40	10.1	91.2	[1] ABREU	00B	DLPH
6.8 ±3.5 ±1.1	10.1	91.2	[2] ACKERSTAFF	97T	OPAL

[1] ABREU 00B tag the presence of an s quark requiring a high-momentum-identified charged kaon. The s-quark pole asymmetry is extracted from the charged-kaon asymmetry taking the expected d- and u-quark asymmetries from the Standard Model and using the measured values for the c- and b-quark asymmetries.
[2] ACKERSTAFF 97T measure the forward-backward asymmetry of various fast hadrons made of light quarks. Then using SU(2) isospin symmetry and flavor independence for down and strange quarks authors solve for the different quark types. The value reported here corresponds then to the forward-backward asymmetry for "down-type" quarks.

$A_{FB}^{(0,c)}$ CHARGE ASYMMETRY IN $e^+e^- \to c\overline{c}$

OUR FIT, which is obtained by a simultaneous fit to several c- and b-quark measurements as explained in the note "The Z boson" and ref. LEP-SLC 06, refers to the **Z pole** asymmetry. The experimental values, on the other hand, correspond to the measurements carried out at the respective energies.

ASYMMETRY (%)	STD. MODEL	$\sqrt{s}$ (GeV)	DOCUMENT ID		TECN
7.07± 0.35 OUR FIT					
6.31± 0.93±0.65	6.35	91.26	[1] ABDALLAH	04F	DLPH
5.68± 0.54±0.39	6.3	91.25	[2] ABBIENDI	03P	OPAL
6.45± 0.57±0.37	6.10	91.21	[3] HEISTER	02H	ALEP
6.59± 0.94±0.35	6.2	91.235	[4] ABREU	99Y	DLPH
6.3 ± 0.9 ±0.3	6.1	91.22	[5] BARATE	98O	ALEP
6.3 ± 1.2 ±0.6	6.1	91.22	[6] ALEXANDER	97C	OPAL
8.3 ± 3.8 ±2.7	6.2	91.24	[7] ADRIANI	92D	L3
• • • We do not use the following data for averages, fits, limits, etc. • • •					
3.1 ± 3.5 ±0.5	−3.5	89.43	[1] ABDALLAH	04F	DLPH
11.0 ± 2.8 ±0.7	12.3	92.99	[1] ABDALLAH	04F	DLPH
−6.8 ± 2.5 ±0.9	−3.0	89.51	[2] ABBIENDI	03P	OPAL
14.6 ± 2.0 ±0.8	12.2	92.95	[2] ABBIENDI	03P	OPAL
−12.4 ±15.9 ±2.0	−9.6	88.38	[3] HEISTER	02H	ALEP
−2.3 ± 2.6 ±0.2	−3.8	89.38	[3] HEISTER	02H	ALEP
−0.3 ± 8.3 ±0.6	0.9	90.21	[3] HEISTER	02H	ALEP
10.6 ± 7.7 ±0.7	9.6	92.05	[3] HEISTER	02H	ALEP
11.9 ± 2.1 ±0.6	12.2	92.94	[3] HEISTER	02H	ALEP
12.1 ±11.0 ±1.0	14.2	93.90	[3] HEISTER	02H	ALEP
−4.96± 3.68±0.53	−3.5	89.434	[4] ABREU	99Y	DLPH
11.80± 3.18±0.62	12.3	92.990	[4] ABREU	99Y	DLPH
−1.0 ± 4.3 ±1.0	−3.9	89.37	[5] BARATE	98O	ALEP
11.0 ± 3.3 ±0.8	12.3	92.96	[5] BARATE	98O	ALEP
3.9 ± 5.1 ±0.9	−3.4	89.45	[6] ALEXANDER	97C	OPAL
15.8 ± 4.1 ±1.1	12.4	93.00	[6] ALEXANDER	97C	OPAL
−12.9 ± 7.8 ±5.5	−13.6	35	BEHREND	90D	CELL
7.7 ±13.4 ±5.0	−22.1	43	BEHREND	90D	CELL
−12.8 ± 4.4 ±4.1	−13.6	35	ELSEN	90	JADE
−10.9 ±12.9 ±4.6	−23.2	44	ELSEN	90	JADE
−14.9 ± 6.7	−13.3	35	OULD-SAADA	89	JADE

[1] ABDALLAH 04F tag b– and c–quarks using semileptonic decays combined with charge flow information from the hemisphere opposite to the lepton. Enriched samples of $c\overline{c}$ and $b\overline{b}$ events are obtained using lifetime information.
[2] ABBIENDI 03P tag heavy flavors using events with one or two identified leptons. This allows the simultaneous fitting of the b and c quark forward-backward asymmetries as well as the average B^0-$\overline{B}^0$ mixing.
[3] HEISTER 02H measure simultaneously b and c quark forward-backward asymmetries using their semileptonic decays to tag the quark charge. The flavor separation is obtained with a discriminating multivariate analysis.
[4] ABREU 99Y tag $Z \to b\overline{b}$ and $Z \to c\overline{c}$ events by an exclusive reconstruction of several D meson decay modes (D^{*+}, D^0, and D^+ with their charge-conjugate states).
[5] BARATE 98O tag $Z \to c\overline{c}$ events requiring the presence of high-momentum reconstructed D^{*+}, D^+, or D^0 mesons.
[6] ALEXANDER 97C identify the b and c events using a D/D^* tag.
[7] ADRIANI 92D use both electron and muon semileptonic decays.

$A_{FB}^{(0,b)}$ CHARGE ASYMMETRY IN $e^+e^- \to b\overline{b}$

OUR FIT, which is obtained by a simultaneous fit to several c- and b-quark measurements as explained in the note "The Z boson" and ref. LEP-SLC 06, refers to the **Z pole** asymmetry. The experimental values, on the other hand, correspond to the measurements carried out at the respective energies.

ASYMMETRY (%)	STD. MODEL	$\sqrt{s}$ (GeV)	DOCUMENT ID		TECN
9.92± 0.16 OUR FIT					
9.58± 0.32± 0.14	9.68	91.231	[1] ABDALLAH	05	DLPH
10.04± 0.56± 0.25	9.69	91.26	[2] ABDALLAH	04F	DLPH
9.72± 0.42± 0.15	9.67	91.25	[3] ABBIENDI	03P	OPAL
9.77± 0.36± 0.18	9.69	91.26	[4] ABBIENDI	02I	OPAL
9.52± 0.41± 0.17	9.59	91.21	[5] HEISTER	02H	ALEP
10.00± 0.27± 0.11	9.63	91.232	[6] HEISTER	01D	ALEP
7.62± 1.94± 0.85	9.64	91.235	[7] ABREU	99Y	DLPH
9.60± 0.66± 0.33	9.69	91.26	[8] ACCIARRI	99D	L3
9.31± 1.01± 0.55	9.65	91.24	[9] ACCIARRI	98U	L3
9.4 ± 2.7 ± 2.2	9.61	91.22	[10] ALEXANDER	97C	OPAL
• • • We do not use the following data for averages, fits, limits, etc. • • •					
6.37± 1.43± 0.17	5.8	89.449	[1] ABDALLAH	05	DLPH
10.41± 1.15± 0.24	12.1	92.990	[1] ABDALLAH	05	DLPH
6.7 ± 2.2 ± 0.2	5.7	89.43	[2] ABDALLAH	04F	DLPH
11.2 ± 1.8 ± 0.2	12.1	92.99	[2] ABDALLAH	04F	DLPH
4.7 ± 1.8 ± 0.1	5.9	89.51	[3] ABBIENDI	03P	OPAL
10.3 ± 1.5 ± 0.2	12.0	92.95	[3] ABBIENDI	03P	OPAL
5.82± 1.53± 0.12	5.9	89.50	[4] ABBIENDI	02I	OPAL
12.21± 1.23± 0.25	12.0	92.91	[4] ABBIENDI	02I	OPAL
−13.1 ±13.5 ± 1.0	3.2	88.38	[5] HEISTER	02H	ALEP
5.5 ± 1.9 ± 0.1	5.6	89.38	[5] HEISTER	02H	ALEP
− 0.4 ± 6.7 ± 0.8	7.5	90.21	[5] HEISTER	02H	ALEP
11.1 ± 6.4 ± 0.5	11.0	92.05	[5] HEISTER	02H	ALEP
10.4 ± 1.5 ± 0.3	12.0	92.94	[5] HEISTER	02H	ALEP
13.8 ± 9.3 ± 1.1	12.9	93.90	[5] HEISTER	02H	ALEP
4.36± 1.19± 0.11	5.8	89.472	[6] HEISTER	01D	ALEP
11.72± 0.97± 0.11	12.0	92.950	[6] HEISTER	01D	ALEP
5.67± 7.56± 1.17	5.7	89.434	[7] ABREU	99Y	DLPH
8.82± 6.33± 1.22	12.1	92.990	[7] ABREU	99Y	DLPH
6.11± 2.93± 0.43	5.9	89.50	[8] ACCIARRI	99D	L3
13.71± 2.40± 0.44	12.2	93.10	[8] ACCIARRI	99D	L3
4.95± 5.23± 0.40	5.8	89.45	[9] ACCIARRI	98U	L3
11.37± 3.99± 0.65	12.1	92.99	[9] ACCIARRI	98U	L3
− 8.6 ±10.8 ± 2.9	5.8	89.45	[10] ALEXANDER	97C	OPAL
− 2.1 ± 9.0 ± 2.6	12.1	93.00	[10] ALEXANDER	97C	OPAL
$-71 \pm 34 \,{}^{+\,7}_{-\,8}$	−58	58.3	SHIMONAKA	91	TOPZ
−22.2 ± 7.7 ± 3.5	−26.0	35	BEHREND	90D	CELL
−49.1 ±16.0 ± 5.0	−39.7	43	BEHREND	90D	CELL
−28 ±11	−23	35	BRAUNSCH...	90	TASS
−16.6 ± 7.7 ± 4.8	−24.3	35	ELSEN	90	JADE
−33.6 ±22.2 ± 5.2	−39.9	44	ELSEN	90	JADE
3.4 ± 7.0 ± 3.5	−16.0	29.0	BAND	89	MAC
−72 ±28 ±13	−56	55.2	SAGAWA	89	AMY

[1] ABDALLAH 05 obtain an enriched samples of $b\overline{b}$ events using lifetime information. The quark (or antiquark) charge is determined with a neural network using the secondary vertex charge, the jet charge and particle identification.

[2] ABDALLAH 04F tag b– and c–quarks using semileptonic decays combined with charge flow information from the hemisphere opposite to the lepton. Enriched samples of $c\overline{c}$ and $b\overline{b}$ events are obtained using lifetime information.

[3] ABBIENDI 03P tag heavy flavors using events with one or two identified leptons. This allows the simultaneous fitting of the b and c quark forward-backward asymmetries as well as the average B^0-$\overline{B}^0$ mixing.

[4] ABBIENDI 02I tag $Z^0 \to b\overline{b}$ decays using a combination of secondary vertex and lepton tags. The sign of the b-quark charge is determined using an inclusive tag based on jet, vertex, and kaon charges.

[5] HEISTER 02H measure simultaneously b and c quark forward-backward asymmetries using their semileptonic decays to tag the quark charge. The flavor separation is obtained with a discriminating multivariate analysis.

[6] HEISTER 01D tag $Z \to b\overline{b}$ events using the impact parameters of charged tracks complemented with information from displaced vertices, event shape variables, and lepton identification. The b-quark direction and charge is determined using the hemisphere charge method along with information from fast kaon tagging and charge estimators of primary and secondary vertices. The change in the quoted value due to variation of A_{FB}^c and R_b is given as $+0.103\ (A_{FB}^c - 0.0651) - 0.440\ (R_b - 0.21585)$.

[7] ABREU 99Y tag $Z \to b\overline{b}$ and $Z \to c\overline{c}$ events by an exclusive reconstruction of several D meson decay modes (D^{*+}, D^0, and D^+ with their charge-conjugate states).

[8] ACCIARRI 99D tag $Z \to b\overline{b}$ events using high p and p_T leptons. The analysis determines simultaneously a mixing parameter $\chi_b = 0.1192 \pm 0.0068 \pm 0.0051$ which is used to correct the observed asymmetry.

[9] ACCIARRI 98U tag $Z \to b\overline{b}$ events using lifetime and measure the jet charge using the hemisphere charge.

[10] ALEXANDER 97C identify the b and c events using a D/D^* tag.

CHARGE ASYMMETRY IN $e^+e^- \to q\overline{q}$

Summed over five lighter flavors.

Experimental and Standard Model values are somewhat event-selection dependent. Standard Model expectations contain some assumptions on B^0-$\overline{B}^0$ mixing and on other electroweak parameters.

ASYMMETRY (%)	STD. MODEL	$\sqrt{s}$ (GeV)	DOCUMENT ID		TECN
• • • We do not use the following data for averages, fits, limits, etc. • • •					
− 0.76±0.12±0.15		91.2	[1] ABREU	92I	DLPH
4.0 ±0.4 ±0.63	4.0	91.3	[2] ACTON	92L	OPAL
9.1 ±1.4 ±1.6	9.0	57.9	ADACHI	91	TOPZ
− 0.84±0.15±0.04		91	DECAMP	91B	ALEP
8.3 ±2.9 ±1.9	8.7	56.6	STUART	90	AMY
11.4 ±2.2 ±2.1	8.7	57.6	ABE	89L	VNS
6.0 ±1.3	5.0	34.8	GREENSHAW	89	JADE
8.2 ±2.9	8.5	43.6	GREENSHAW	89	JADE

[1] ABREU 92I has 0.14 systematic error due to uncertainty of quark fragmentation.

[2] ACTON 92L use the weight function method on 259k selected $Z \to$ hadrons events. The systematic error includes a contribution of 0.2 due to B^0-$\overline{B}^0$ mixing effect, 0.4 due to Monte Carlo (MC) fragmentation uncertainties and 0.3 due to MC statistics. ACTON 92L derive a value of $\sin^2\theta_W^{\rm eff}$ to be $0.2321 \pm 0.0017 \pm 0.0028$.

CHARGE ASYMMETRY IN $p\overline{p} \to Z \to e^+e^-$

ASYMMETRY (%)	STD. MODEL	$\sqrt{s}$ (GeV)	DOCUMENT ID		TECN
• • • We do not use the following data for averages, fits, limits, etc. • • •					
5.2±5.9±0.4		91	ABE	91E	CDF

ANOMALOUS $ZZ\gamma$, $Z\gamma\gamma$, AND ZZV COUPLINGS

See the related review(s):
Anomalous $ZZ\gamma$, $Z\gamma\gamma$, and ZZV Couplings

h_i^V

Combining the LEP-2 results taking into account the correlations, the following 95% CL limits are derived [SCHAEL 13A]:

$$-0.12 < h_1^Z < +0.11, \quad -0.07 < h_2^Z < +0.07,$$
$$-0.19 < h_3^Z < +0.06, \quad -0.04 < h_4^Z < +0.13,$$
$$-0.05 < h_1^\gamma < +0.05, \quad -0.04 < h_2^\gamma < +0.02,$$
$$-0.05 < h_3^\gamma < +0.00, \quad +0.01 < h_4^\gamma < +0.05.$$

Some of the recent results from the Tevatron and LHC experiments individually surpass the combined LEP-2 results in precision (see below).

VALUE	DOCUMENT ID		TECN	COMMENT
• • • We do not use the following data for averages, fits, limits, etc. • • •				
[1] AAD	16Q	ATLS		$E_{\rm cm}^{pp} = 8$ TeV
[2] KHACHATRY...	16AE	CMS		$E_{\rm cm}^{pp} = 8$ TeV
[3] KHACHATRY...	15AC	CMS		$E_{\rm cm}^{pp} = 8$ TeV
[4] CHATRCHYAN	14AB	CMS		$E_{\rm cm}^{pp} = 7$ TeV
[5] AAD	13AN	ATLS		$E_{\rm cm}^{pp} = 7$ TeV
[6] CHATRCHYAN	13BI	CMS		$E_{\rm cm}^{pp} = 7$ TeV
[7] ABAZOV	12S	D0		$E_{\rm cm}^{p\overline{p}} = 1.96$ TeV
[8] AALTONEN	11S	CDF		$E_{\rm cm}^{p\overline{p}} = 1.96$ TeV
[9] CHATRCHYAN	11M	CMS		$E_{\rm cm}^{pp} = 7$ TeV
[10] ABAZOV	09L	D0		$E_{\rm cm}^{p\overline{p}} = 1.96$ TeV
[11] ABAZOV	07M	D0		$E_{\rm cm}^{p\overline{p}} = 1.96$ TeV
[12] ABDALLAH	07C	DLPH		$E_{\rm cm}^{ee} = 183$–208 GeV
[13] ACHARD	04H	L3		$E_{\rm cm}^{ee} = 183$–208 GeV
[14] ABBIENDI,G	00C	OPAL		$E_{\rm cm}^{ee} = 189$ GeV
[15] ABBOTT	98M	D0		$E_{\rm cm}^{p\overline{p}} = 1.8$ TeV
[16] ABREU	98K	DLPH		$E_{\rm cm}^{ee} = 161, 172$ GeV

[1] AAD 16Q study $Z\gamma$ production in pp collisions. In events with no additional jets, 10268 (12738) Z decays to electron (muon) pairs are selected, with an expected background of 1291 ± 340 (1537 ± 408) events, as well as 1039 Z decays to neutrino pairs with an expected background of 450 ± 96 events. Analyzing the photon transverse momentum distribution above 250 GeV (400 GeV) for lepton (neutrino) events, yields the 95% C.L. limits: $-7.8\times10^{-4} < h_3^Z < 8.6\times10^{-4}$, $-3.0\times10^{-6} < h_4^Z < 2.9\times10^{-6}$, $-9.5\times10^{-4} < h_3^\gamma < 9.9\times10^{-4}$, $-3.2\times10^{-6} < h_4^\gamma < 3.2\times10^{-6}$.

[2] KHACHATRYAN 16AE determine the $Z\gamma \to \nu\overline{\nu}\gamma$ cross section by selecting events with a photon of $E_T > 145$ GeV and $\not{E}_T > 140$ GeV. 630 candidate events are observed with an expected SM background of 269 ± 26. The E_T spectrum of the photon is used to set 95% C.L. limits as follows: $-1.5\times10^{-3} < h_3^Z < 1.6\times10^{-3}$, $-3.9\times10^{-6} < h_4^Z < 4.5\times10^{-6}$, $-1.1\times10^{-3} < h_3^\gamma < 0.9\times10^{-3}$, $-3.8\times10^{-6} < h_4^\gamma < 4.3\times10^{-6}$.

[3] KHACHATRYAN 15AC study $Z\gamma$ events in 8 TeV pp interactions, where the Z decays into 2 same-flavor, opposite sign leptons (e or μ) and a photon with $p_T > 15$ GeV. The p_T of a lepton is required to be > 20 GeV/c, their effective mass > 50 GeV, and the photon should have a separation $\Delta R > 0.7$ with each lepton. The observed p_T distribution of the photons is used to extract the 95% C.L. limits: $-3.8\times10^{-3} < h_3^Z < 3.7\times10^{-3}$, $-3.1\times10^{-5} < h_4^Z < 3.0\times10^{-5}$, $-4.6\times10^{-3} < h_3^\gamma < 4.6\times10^{-3}$, $-3.6\times10^{-5} < h_4^\gamma < 3.5\times10^{-5}$.

[4] CHATRCHYAN 14AB measure $Z\gamma$ production cross section for $p_T^\gamma > 15$ GeV and $R(\ell\gamma) > 0.7$, which is the separation between the γ and the final state charged lepton (e or μ) in the azimuthal angle-pseudorapidity ($\phi - \eta$) plane. The di-lepton mass is required to be > 50 GeV. After background subtraction the number of $ee\gamma$ and $\mu\mu\gamma$ events is determined to be 3160 ± 120 and 5030 ± 233 respectively, compatible with expectations from the SM. This leads to a 95% CL limits of $-1\times10^{-2} < h_3^\gamma < 1\times10^{-2}$, $-9\times10^{-5} < h_4^\gamma < 9\times10^{-5}$, $-9\times10^{-3} < h_3^Z < 9\times10^{-3}$, $-8\times10^{-5} < h_4^Z < 8\times10^{-5}$, assuming h_1^V and h_2^V have SM values, $V = \gamma$ or Z.

[5] AAD 13AN study $Z\gamma$ production in pp collisions. In events with no additional jet, 1417 (2031) Z decays to electron (muon) pairs are selected, with an expected background of 156 ± 54 (244 ± 64) events, as well as 662 Z decays to neutrino pairs with an expected background of 302 ± 42 events. Analysing the photon p_T spectrum above 100 GeV yields the 95% C.L. limts: $-0.013 < h_3^Z < 0.014$, $-8.7\times10^{-5} < h_4^Z < 8.7\times10^{-5}$, $-0.015 < h_3^\gamma < 0.016$, $-9.4\times10^{-5} < h_4^\gamma < 9.2\times10^{-5}$. Supersedes AAD 12BX.

[6] CHATRCHYAN 13BI determine the $Z\gamma \to \nu\overline{\nu}\gamma$ cross section by selecting events with a photon of $E_T > 145$ GeV and a $\not{E}_T > 130$ GeV. 73 candidate events are observed with an expected SM background of 30.2 ± 6.5. The E_T spectrum of the photon is used to set 95% C.L. limits as follows: $|h_3^Z| < 2.7\times10^{-3}$, $|h_4^Z| < 1.3\times10^{-5}$, $|h_3^\gamma| < 2.9\times10^{-3}$, $|h_4^\gamma| < 1.5\times10^{-5}$.

[7] ABAZOV 12S study $Z\gamma$ production in $p\overline{p}$ collisions at $\sqrt{s} = 1.96$ TeV using 6.2 fb^{-1} of data where the Z decays to electron (muon) pairs and the photon has at least 10 GeV of transverse momentum. In data, 304 (308) di-electron (di-muon) events are observed with an expected background of 255 ± 16 (285 ± 24) events. Based on the photon p_T spectrum, and including also earlier data and the $Z \to \nu\overline{\nu}$ decay mode (from ABAZOV 09L), the following 95% C.L. limits are reported: $|h_{03}^Z| < 0.026$, $|h_{04}^Z| < 0.0013$, $|h_{03}^\gamma| < 0.027$, $|h_{04}^\gamma| < 0.0014$ for a form factor scale of $\Lambda = 1.5$ TeV.

[8] AALTONEN 11S study $Z\gamma$ events in $p\overline{p}$ interactions at $\sqrt{s} = 1.96$ TeV with integrated luminosity 5.1 fb^{-1} for $Z \to e^+e^-/\mu^+\mu^-$ and 4.9 fb^{-1} for $Z \to \nu\overline{\nu}$. For the charged lepton case, the two leptons must be of the same flavor with the transverse momentum/energy of one > 20 GeV and the other > 10 GeV. The isolated photon must have $E_T > 50$ GeV. They observe 91 events with 87.2 ± 7.8 events expected from standard model processes. For the $\nu\overline{\nu}$ case they require solitary photons with $E_T > 25$ GeV and missing $E_T > 25$ GeV and observe 85 events with standard model expectation of 85.9 ± 5.6 events. Taking the form factor $\Lambda = 1.5$ TeV they derive 95% C.L. limits as $|h_3^{\gamma,Z}| < 0.022$ and $|h_4^{\gamma,Z}| < 0.0009$.

[9] CHATRCHYAN 11M study $Z\gamma$ production in pp collisions at $\sqrt{s} = 7$ TeV using 36 pb^{-1} pp data, where the Z decays to e^+e^- or $\mu^+\mu^-$. The total cross sections are measured for photon transverse energy $E_T^\gamma > 10$ GeV and spatial separation from charged leptons in the plane of pseudo rapidity and azimuthal angle $\Delta R(\ell,\gamma) > 0.7$ with the dilepton invariant mass requirement of $M_{\ell\ell} > 50$ GeV. The number of $e^+e^-\gamma$ and $\mu^+\mu^-\gamma$ candidates is 81 and 90 with estimated backgrounds of 20.5 ± 2.5 and 27.3 ± 3.2 events respectively. The 95% CL limits for $ZZ\gamma$ couplings are $-0.05 < h_3^Z < 0.06$ and $-0.0005 < h_4^Z < 0.0005$, and for $Z\gamma\gamma$ couplings are $-0.07 < h_3^\gamma < 0.07$ and $-0.0005 < h_4^\gamma < 0.0006$.

[10] ABAZOV 09L study $Z\gamma$, $Z \to \nu\overline{\nu}$ production in $p\overline{p}$ collisions at 1.96 TeV C.M. energy. They select 51 events with a photon of transverse energy E_T larger than 90 GeV, with an expected background of 17 events. Based on the photon E_T spectrum and including also Z decays to charged leptons (from ABAZOV 07M), the following 95% CL limits are reported: $|h_{30}^\gamma| < 0.033$, $|h_{40}^\gamma| < 0.0017$, $|h_{30}^Z| < 0.033$, $|h_{40}^Z| < 0.0017$.

[11] ABAZOV 07M use 968 $p\overline{p} \to e^+e^-/\mu^+\mu^-\gamma X$ candidates, at 1.96 TeV center of mass energy, to tag $p\overline{p} \to Z\gamma$ events by requiring $E_T(\gamma) > 7$ GeV, lepton-gamma separation $\Delta R_{\ell\gamma} > 0.7$, and di-lepton invariant mass > 30 GeV. The cross section is in agreement with the SM prediction. Using these $Z\gamma$ events they obtain 95% C.L. limits on each h_i^V, keeping all others fixed at their SM values. They report: $-0.083 < h_{30}^Z < 0.082$, $-0.0053 < h_{40}^Z < 0.0054$, $-0.085 < h_{30}^\gamma < 0.084$, $-0.0053 < h_{40}^\gamma < 0.0054$, for the form factor scale $\Lambda = 1.2$ TeV.

[12] Using data collected at $\sqrt{s} = 183$–208, ABDALLAH 07C select 1,877 $e^+e^- \to Z\gamma$ events with $Z \to q\overline{q}$ or $\nu\overline{\nu}$, 171 $e^+e^- \to ZZ$ events with $Z \to q\overline{q}$ or lepton pair (except an explicit τ pair), and 74 $e^+e^- \to Z\gamma^*$ events with a $q\overline{q}\mu^+\mu^-$ or $q\overline{q}e^+e^-$ signature, to derive 95% CL limits on h_i^V. Each limit is derived with other parameters set to zero. They report: $-0.23 < h_1^Z < 0.23$, $-0.30 < h_3^Z < 0.16$, $-0.14 < h_1^\gamma < 0.14$, $-0.049 < h_3^\gamma < 0.044$.

[13] ACHARD 04H select 3515 $e^+e^- \to Z\gamma$ events with $Z \to q\overline{q}$ or $\nu\overline{\nu}$ at $\sqrt{s} = 189$–209 GeV to derive 95% CL limits on h_i^V. For deriving each limit the other parameters are fixed at zero. They report: $-0.153 < h_1^Z < 0.141$, $-0.087 < h_2^Z < 0.079$, $-0.220 < h_3^Z < 0.112$, $-0.068 < h_4^Z < 0.148$, $-0.057 < h_1^\gamma < 0.057$, $-0.050 < h_2^\gamma < 0.023$, $-0.059 < h_3^\gamma < 0.004$, $-0.004 < h_4^\gamma < 0.042$.

[14] ABBIENDI,G 00C study $e^+e^- \to Z\gamma$ events (with $Z \to q\overline{q}$ and $Z \to \nu\overline{\nu}$) at 189 GeV to obtain the central values (and 95% CL limits) of these couplings: $h_1^Z = 0.000 \pm 0.100$ $(-0.190, 0.190)$, $h_2^Z = 0.000 \pm 0.068$ $(-0.128, 0.128)$, $h_3^Z = -0.074^{+0.102}_{-0.103}$ $(-0.269, 0.119)$, $h_4^Z = 0.046 \pm 0.068$ $(-0.084, 0.175)$, $h_1^\gamma = 0.000 \pm 0.061$ $(-0.115, 0.115)$, $h_2^\gamma = 0.000 \pm 0.041$ $(-0.077, 0.077)$, $h_3^\gamma = -0.080^{+0.039}_{-0.041}$ $(-0.164, -0.006)$, $h_4^\gamma = 0.064^{+0.033}_{-0.030}$ $(+0.007, +0.134)$. The results are derived assuming that only one coupling at a time is different from zero.

[15] ABBOTT 98M study $p\overline{p} \to Z\gamma + X$, with $Z \to e^+e^-$, $\mu^+\mu^-$, $\overline{\nu}\nu$ at 1.8 TeV, to obtain 95% CL limits at $\Lambda = 750$ GeV: $|h_{30}^Z| < 0.36$, $|h_{40}^Z| < 0.05$ (keeping $h_i^\gamma = 0$), and $|h_{30}^\gamma| < 0.37$, $|h_{40}^\gamma| < 0.05$ (keeping $h_i^Z = 0$). Limits on the *CP*-violating couplings are $|h_{10}^Z| < 0.36$, $|h_{20}^Z| < 0.05$ (keeping $h_i^\gamma = 0$), and $|h_{10}^\gamma| < 0.37$, $|h_{20}^\gamma| < 0.05$ (keeping $h_i^Z = 0$).

[16] ABREU 98K determine a 95% CL upper limit on $\sigma(e^+e^- \to \gamma +$ invisible particles$) < 2.5$ pb using 161 and 172 GeV data. This is used to set 95% CL limits on $|h_{30}^\gamma| < 0.8$ and $|h_{30}^Z| < 1.3$, derived at a scale $\Lambda = 1$ TeV and with $n = 3$ in the form factor representation.

f_i^V

Combining the LEP-2 results taking into account the correlations, the following 95% CL limits are derived [SCHAEL 13A]:

$$-0.28 < f_4^Z < +0.32, \qquad -0.34 < f_5^Z < +0.35,$$
$$-0.17 < f_4^\gamma < +0.19, \qquad -0.35 < f_5^\gamma < +0.32.$$

Some of the recent results from the Tevatron and LHC experiments individually surpass the combined LEP-2 results in precision (see below).

VALUE	*DOCUMENT ID*		*TECN*	*COMMENT*
• • • We do not use the following data for averages, fits, limits, etc. • • •				
	[1] KHACHATRY...15B	CMS		$E_{\rm cm}^{pp} = 8$ TeV
	[2] KHACHATRY...15BC	CMS		$E_{\rm cm}^{pp} = 7,\ 8$ TeV
	[3] AAD	13Z	ATLS	$E_{\rm cm}^{pp} = 7$ TeV
	[4] CHATRCHYAN	13B	CMS	$E_{\rm cm}^{pp} = 7$ TeV
	[5] SCHAEL	09	ALEP	$E_{\rm cm}^{ee} = 192$–209 GeV
	[6] ABAZOV	08K	D0	$E_{\rm cm}^{p\overline{p}} = 1.96$ TeV
	[7] ABDALLAH	07C	DLPH	$E_{\rm cm}^{ee} = 183$–208 GeV
	[8] ABBIENDI	04C	OPAL	
	[9] ACHARD	03D	L3	

[1] KHACHATRYAN 15B study ZZ production in 8 TeV pp collisions. In the decay modes $ZZ \to 4e$, 4μ, $2e2\mu$, 54, 75, 148 events are observed, with an expected background of 2.2 ± 0.9, 1.2 ± 0.6, and 2.4 ± 1.0 events, respectively. Analysing the 4-lepton invariant mass spectrum in the range from 110 GeV to 1200 GeV, the following 95% C.L. limits are obtained: $|f_4^Z| < 0.004$, $|f_5^Z| < 0.004$, $|f_4^\gamma| < 0.005$, $|f_5^\gamma| < 0.005$.

[2] KHACHATRYAN 15BC use the cross section measurement of the final state $pp \to ZZ \to 2\ell2\nu$, (ℓ being an electron or a muon) at 7 and 8 TeV to put limits on these triple gauge couplings. Effective mass of the charged lepton pair is required to be in the range 83.5–98.5 GeV and the dilepton $p_T > 45$ GeV. The reduced missing E_T is required to be > 65 GeV, which takes into account the fake missing E_T due to detector effects. The numbers of e^+e^- and $\mu^+\mu^-$ events selected are 35 and 40 at 7 TeV and 176 and 271 at 8 TeV respectively. The production cross sections so obtained are in agreement with SM predictions. The following 95% C.L. limits are set: $-0.0028 < f_4^Z < 0.0032$, $-0.0037 < f_4^\gamma < 0.0033$, $-0.0029 < f_5^Z < 0.0031$, $-0.0033 < f_5^\gamma < 0.0037$. Combining with previous results (KHACHATRYAN 15B and CHATRCHYAN 13B) which include 7 TeV and 8 TeV data on the final states $pp \to ZZ \to 2\ell2\ell'$ where ℓ and ℓ' are an electron or a muon, the best limits are $-0.0022 < f_4^Z < 0.0026$, $-0.0029 < f_4^\gamma < 0.0026$, $-0.0023 < f_5^Z < 0.0023$, $-0.0026 < f_5^\gamma < 0.0027$.

[3] AAD 13Z study ZZ production in pp collisions at $\sqrt{s} = 7$ TeV. In the $ZZ \to \ell^+\ell^-\ell'^+\ell'^-$ final state they observe a total of 66 events with an expected background of 0.9 ± 1.3. In the $ZZ \to \ell^+\ell^-\nu\nu$ final state they observe a total of 87 events with an expected background of 46.9 ± 5.2. The limits on anomalous TGCs are determined using the observed and expected numbers of these ZZ events binned in p_T^Z. The 95% C.L. are as follows: for form factor scale $\Lambda = \infty$, $-0.015 < f_4^\gamma < 0.015$, $-0.013 < f_4^Z < 0.013$, $-0.016 < f_5^\gamma < 0.015$, $-0.013 < f_5^Z < 0.013$; for form factor scale $\Lambda = 3$ TeV, $-0.022 < f_4^\gamma < 0.023$, $-0.019 < f_4^Z < 0.019$, $-0.023 < f_5^\gamma < 0.023$, $-0.020 < f_5^Z < 0.019$.

[4] CHATRCHYAN 13B study ZZ production in pp collisions and select 54 ZZ candidates in the Z decay channel with electrons or muons with an expected background of 1.4 ± 0.5 events. The resulting 95% C.L. ranges are: $-0.013 < f_4^\gamma < 0.015$, $-0.011 < f_4^Z < 0.012$, $-0.014 < f_5^\gamma < 0.014$, $-0.012 < f_5^Z < 0.012$.

[5] Using data collected in the center of mass energy range 192–209 GeV, SCHAEL 09 select 318 $e^+e^- \to ZZ$ events with 319.4 expected from the standard model. Using this data they derive the following 95% CL limits: $-0.321 < f_4^\gamma < 0.318$, $-0.534 < f_4^Z < 0.534$, $-0.724 < f_5^\gamma < 0.733$, $-1.194 < f_5^Z < 1.190$.

[6] ABAZOV 08K search for ZZ and $Z\gamma^*$ events with 1 fb^{-1} $p\overline{p}$ data at $\sqrt{s} = 1.96$ TeV in $(ee)(ee)$, $(\mu\mu)(\mu\mu)$, $(ee)(\mu\mu)$ final states requiring the lepton pair masses to be > 30 GeV. They observe 1 event, which is consistent with an expected signal of 1.71 ± 0.15 events and a background of 0.13 ± 0.03 events. From this they derive the following limits, for a form factor (Λ) value of 1.2 TeV: $-0.28 < f_{40}^Z < 0.28$, $-0.31 < f_{50}^Z < 0.29$, $-0.26 < f_{40}^\gamma < 0.26$, $-0.30 < f_{50}^\gamma < 0.28$.

[7] Using data collected at $\sqrt{s} = 183$–208 GeV, ABDALLAH 07C select 171 $e^+e^- \to ZZ$ events with $Z \to q\overline{q}$ or lepton pair (except an explicit τ pair), and 74 $e^+e^- \to Z\gamma^*$ events with a $q\overline{q}\mu^+\mu^-$ or $q\overline{q}e^+e^-$ signature, to derive 95% CL limits on f_i^V. Each limit is derived with other parameters set to zero. They report: $-0.40 < f_4^Z < 0.42$, $-0.38 < f_5^Z < 0.62$, $-0.23 < f_4^\gamma < 0.25$, $-0.52 < f_5^\gamma < 0.48$.

[8] ABBIENDI 04C study ZZ production in e^+e^- collisions in the C.M. energy range 190–209 GeV. They select 340 events with an expected background of 180 events. Including the ABBIENDI 00N data at 183 and 189 GeV (118 events with an expected background of 65 events) they report the following 95% CL limits: $-0.45 < f_4^Z < 0.58$, $-0.94 < f_5^Z < 0.25$, $-0.32 < f_4^\gamma < 0.33$, and $-0.71 < f_5^\gamma < 0.59$.

[9] ACHARD 03D study Z-boson pair production in e^+e^- collisions in the C.M. energy range 200–209 GeV. They select 549 events with an expected background of 432 events. Including the ACCIARRI 99G and ACCIARRI 99O data (183 and 189 GeV respectively, 286

events with an expected background of 241 events) and the 192–202 GeV ACCIARRI 01I results (656 events, expected background of 512 events), they report the following 95% CL limits: $-0.48 \leq f_4^Z \leq 0.46$, $-0.36 \leq f_5^Z \leq 1.03$, $-0.28 \leq f_4^\gamma \leq 0.28$, and $-0.40 \leq f_5^\gamma \leq 0.47$.

ANOMALOUS W/Z QUARTIC COUPLINGS

See the related review(s):
Anomalous W/Z Quartic Couplings (QGCs)

a_0/Λ^2, a_C/Λ^2

Combining published and unpublished preliminary LEP results the following 95% CL intervals for the QGCs associated with the $ZZ\gamma\gamma$ vertex are derived (CERN-PH-EP/2005-051 or hep-ex/0511027):

$$-0.008 < a_0^Z/\Lambda^2 < +0.021$$
$$-0.029 < a_C^Z/\Lambda^2 < +0.039$$

Anomalous Z quartic couplings have also been measured by the Tevatron and LHC experiments. As discussed in the review on "Anomalous W/Z quartic couplings," the coupling parameters in the Anomalous QGC Lagrangian may relate to processes involving only the W or only to the Z or to both. Thus, results on all other AQGCs are reported together in the W listings.

VALUE	DOCUMENT ID	TECN
• • • We do not use the following data for averages, fits, limits, etc. • • •		
	[1] ABBIENDI 04L	OPAL
	[2] HEISTER 04A	ALEP
	[3] ACHARD 02G	L3

[1] ABBIENDI 04L select 20 $e^+e^- \to \nu\overline{\nu}\gamma\gamma$ acoplanar events in the energy range 180–209 GeV and 176 $e^+e^- \to q\overline{q}\gamma\gamma$ events in the energy range 130–209 GeV. These samples are used to constrain possible anomalous $W^+W^-\gamma\gamma$ and $ZZ\gamma\gamma$ quartic couplings. Further combining with the $W^+W^-\gamma$ sample of ABBIENDI 04B the following one–parameter 95% CL limits are obtained: $-0.007 < a_0^Z/\Lambda^2 < 0.023$ GeV^{-2}, $-0.029 < a_C^Z/\Lambda^2 < 0.029$ GeV^{-2}, $-0.020 < a_0^W/\Lambda^2 < 0.020$ GeV^{-2}, $-0.052 < a_C^W/\Lambda^2 < 0.037$ GeV^{-2}.

[2] In the CM energy range 183 to 209 GeV HEISTER 04A select 30 $e^+e^- \to \nu\overline{\nu}\gamma\gamma$ events with two acoplanar, high energy and high transverse momentum photons. The photon–photon acoplanarity is required to be $> 5^\circ$, $E_\gamma/\sqrt{s} > 0.025$ (the more energetic photon having energy $> 0.2\sqrt{s}$), $p_{T_\gamma}/E_{beam} > 0.05$ and $|\cos\theta_\gamma| < 0.94$. A likelihood fit to the photon energy and recoil missing mass yields the following one–parameter 95% CL limits: $-0.012 < a_0^Z/\Lambda^2 < 0.019$ GeV^{-2}, $-0.041 < a_C^Z/\Lambda^2 < 0.044$ GeV^{-2}, $-0.060 < a_0^W/\Lambda^2 < 0.055$ GeV^{-2}, $-0.099 < a_C^W/\Lambda^2 < 0.093$ GeV^{-2}.

[3] ACHARD 02G study $e^+e^- \to Z\gamma\gamma \to q\overline{q}\gamma\gamma$ events using data at center-of-mass energies from 200 to 209 GeV. The photons are required to be isolated, each with energy >5 GeV and $|\cos\theta| < 0.97$, and the di-jet invariant mass to be compatible with that of the Z boson (74–111 GeV). Cuts on Z velocity ($\beta < 0.73$) and on the energy of the most energetic photon reduce the backgrounds due to non-resonant production of the $q\overline{q}\gamma\gamma$ state and due to ISR respectively, yielding a total of 40 candidate events of which 8.6 are expected to be due to background. The energy spectra of the least energetic photon are fitted for all ten center-of-mass energy values from 130 GeV to 209 GeV (as obtained adding to the present analysis 130–202 GeV data of ACCIARRI 01E, for a total of 137 events with an expected background of 34.1 events) to obtain the fitted values $a_0/\Lambda^2 = 0.00^{+0.02}_{-0.01}$ GeV^{-2} and $a_C/\Lambda^2 = 0.03^{+0.01}_{-0.02}$ GeV^{-2}, where the other parameter is kept fixed to its Standard Model value (0). A simultaneous fit to both parameters yields the 95% CL limits -0.02 GeV$^{-2} < a_0/\Lambda^2 < 0.03$ GeV^{-2} and -0.07 GeV$^{-2} < a_C/\Lambda^2 < 0.05$ GeV^{-2}.

Z REFERENCES

RAINBOLD	18	arXiv:1805.05791	J.L. Rainbolt, M. Schmitt	(NWES)
AAD	17	EPJ C77 70	G. Aad *et al.*	(ATLAS Collab.)
AABOUD	16K	PRL 117 111802	M. Aaboud *et al.*	(ATLAS Collab.)
AAD	16L	EPJ C76 210	G. Aad *et al.*	(ATLAS Collab.)
AAD	16Q	PR D93 112002	G. Aad *et al.*	(ATLAS Collab.)
ABRAMOWICZ	16A	PR D93 092002	H. Abramowicz *et al.*	(ZEUS Collab.)
ABT	16	PR D94 052007	I. Abt *et al.*	(MPIM, OXF, HAMB, DESY)
KHACHATRY...	16AE	PL B760 448	V. Khachatryan *et al.*	(CMS Collab.)
KHACHATRY...	16CC	PL B763 280	V. Khachatryan *et al.*	(CMS Collab.)
AAD	15BT	JHEP 1509 049	G. Aad *et al.*	(ATLAS Collab.)
AAD	15I	PRL 114 121801	G. Aad *et al.*	(ATLAS Collab.)
KHACHATRY...	15AC	JHEP 1504 164	V. Khachatryan *et al.*	(CMS Collab.)
KHACHATRY...	15B	PL B740 250	V. Khachatryan *et al.*	(CMS Collab.)
KHACHATRY...	15BC	EPJ C75 511	V. Khachatryan *et al.*	(CMS Collab.)
AAD	14AU	PR D90 072010	G. Aad *et al.*	(ATLAS Collab.)
AAD	14N	PRL 112 231806	G. Aad *et al.*	(ATLAS Collab.)
AALTONEN	14E	PRL 112 111803	T. Aaltonen *et al.*	(CDF Collab.)
CHATRCHYAN	14AB	PR D89 092005	S. Chatrchyan *et al.*	(CMS Collab.)
AAD	13AN	PR D87 112003	G. Aad *et al.*	(ATLAS Collab.)
Also		PR D91 119901 (errat.)	G. Aad *et al.*	(ATLAS Collab.)
AAD	13Z	JHEP 1303 128	G. Aad *et al.*	(ATLAS Collab.)
CHATRCHYAN	13B	JHEP 1301 063	S. Chatrchyan *et al.*	(CMS Collab.)
CHATRCHYAN	13BI	JHEP 1310 164	S. Chatrchyan *et al.*	(CMS Collab.)
SCHAEL	13A	PRPL 532 119	S. Schael *et al.*	(ALEPH Collab., DELPHI, L3+)
AAD	12BX	PL B717 49	G. Aad *et al.*	(ATLAS Collab.)
ABAZOV	12S	PR D85 052001	V.M. Abazov *et al.*	(D0 Collab.)
CHATRCHYAN	12BN	JHEP 1212 034	S. Chatrchyan *et al.*	(CMS Collab.)
AALTONEN	11S	PRL 107 051802	T. Aaltonen *et al.*	(CDF Collab.)
ABAZOV	11D	PR D84 012007	V.M. Abazov *et al.*	(D0 Collab.)
CHATRCHYAN	11M	PL B701 535	S. Chatrchyan *et al.*	(CMS Collab.)
ABAZOV	09L	PRL 102 201802	V.M. Abazov *et al.*	(D0 Collab.)
BEDDALL	09	PL B670 300	A. Beddall, A. Beddall, A. Bingul	(UGAZ)
SCHAEL	09	JHEP 0904 124	S. Schael *et al.*	(ALEPH Collab.)
ABAZOV	08K	PRL 100 131801	V.M. Abazov *et al.*	(D0 Collab.)
ABAZOV	07M	PL B653 378	V.M. Abazov *et al.*	(D0 Collab.)
ABDALLAH	07C	EPJ C51 525	J. Abdallah *et al.*	(DELPHI Collab.)
ABDALLAH	06E	PL B639 179	J. Abdallah *et al.*	(DELPHI Collab.)
AKTAS	06	PL B632 35	A. Aktas *et al.*	(H1 Collab.)
LEP-SLC	06	PRPL 427 257	ALEPH, DELPHI, L3, OPAL, SLD and working groups	
SCHAEL	06A	PL B639 192	S. Schael *et al.*	(ALEPH Collab.)
ABDALLAH	05	EPJ C40 1	J. Abdallah *et al.*	(DELPHI Collab.)
ABDALLAH	05C	EPJ C44 299	J. Abdallah *et al.*	(DELPHI Collab.)
ABE	05	PRL 94 091801	K. Abe *et al.*	(SLD Collab.)
ABE	05F	PR D71 112004	K. Abe *et al.*	(SLD Collab.)
ACOSTA	05M	PR D71 052002	D. Acosta *et al.*	(CDF Collab.)
ABBIENDI	04B	PL B580 17	G. Abbiendi *et al.*	(OPAL Collab.)
ABBIENDI	04C	EPJ C32 303	G. Abbiendi *et al.*	(OPAL Collab.)
ABBIENDI	04E	PL B586 167	G. Abbiendi *et al.*	(OPAL Collab.)
ABBIENDI	04G	EPJ C33 173	G. Abbiendi *et al.*	(OPAL Collab.)
ABBIENDI	04L	PR D70 032005	G. Abbiendi *et al.*	(OPAL Collab.)
ABDALLAH	04F	EPJ C34 109	J. Abdallah *et al.*	(DELPHI Collab.)
ABE	04C	PR D69 072003	K. Abe *et al.*	(SLD Collab.)
ACHARD	04C	PL B585 42	P. Achard *et al.*	(L3 Collab.)
ACHARD	04H	PL B597 119	P. Achard *et al.*	(L3 Collab.)
HEISTER	04A	PL B602 31	A. Heister *et al.*	(ALEPH Collab.)
ABBIENDI	03P	PL B577 18	G. Abbiendi *et al.*	(OPAL Collab.)
ABDALLAH	03H	PL B569 129	J. Abdallah *et al.*	(DELPHI Collab.)
ABDALLAH	03K	PL B576 29	J. Abdallah *et al.*	(DELPHI Collab.)
ABE	03F	PRL 90 141804	K. Abe *et al.*	(SLD Collab.)
ACHARD	03D	PL B572 133	P. Achard *et al.*	(L3 Collab.)
ACHARD	03G	PL B577 109	P. Achard *et al.*	(L3 Collab.)
ABBIENDI	02I	PL B546 29	G. Abbiendi *et al.*	(OPAL Collab.)
ABE	02G	PRL 88 151801	K. Abe *et al.*	(SLD Collab.)
ACHARD	02G	PL B540 43	P. Achard *et al.*	(L3 Collab.)
HEISTER	02B	PL B526 34	A. Heister *et al.*	(ALEPH Collab.)
HEISTER	02C	PL B528 19	A. Heister *et al.*	(ALEPH Collab.)
HEISTER	02H	EPJ C24 177	A. Heister *et al.*	(ALEPH Collab.)
ABBIENDI	01A	EPJ C19 587	G. Abbiendi *et al.*	(OPAL Collab.)
ABBIENDI	01G	EPJ C18 447	G. Abbiendi *et al.*	(OPAL Collab.)
ABBIENDI	01K	PL B516 1	G. Abbiendi *et al.*	(OPAL Collab.)
ABBIENDI	01N	EPJ C20 445	G. Abbiendi *et al.*	(OPAL Collab.)
ABBIENDI	01O	EPJ C21 1	G. Abbiendi *et al.*	(OPAL Collab.)
ABE	01B	PRL 86 1162	K. Abe *et al.*	(SLD Collab.)
ABE	01C	PR D63 032005	K. Abe *et al.*	(SLD Collab.)
ACCIARRI	01E	PL B505 47	M. Acciarri *et al.*	(L3 Collab.)
ACCIARRI	01I	PL B497 23	M. Acciarri *et al.*	(L3 Collab.)
HEISTER	01	EPJ C20 401	A. Heister *et al.*	(ALEPH Collab.)
HEISTER	01D	EPJ C22 201	A. Heister *et al.*	(ALEPH Collab.)
ABBIENDI	00N	PL B476 256	G. Abbiendi *et al.*	(OPAL Collab.)
ABBIENDI,G	00C	EPJ C17 553	G. Abbiendi *et al.*	(OPAL Collab.)
ABE	00B	PRL 84 5945	K. Abe *et al.*	(SLD Collab.)
ABE	00D	PRL 85 5059	K. Abe *et al.*	(SLD Collab.)
ABREU	00	EPJ C12 225	P. Abreu *et al.*	(DELPHI Collab.)
ABREU	00B	EPJ C14 613	P. Abreu *et al.*	(DELPHI Collab.)
ABREU	00E	EPJ C14 585	P. Abreu *et al.*	(DELPHI Collab.)
ABREU	00F	EPJ C16 371	P. Abreu *et al.*	(DELPHI Collab.)
ABREU	00P	PL B475 429	P. Abreu *et al.*	(DELPHI Collab.)
ACCIARRI	00	EPJ C13 47	M. Acciarri *et al.*	(L3 Collab.)
ACCIARRI	00C	EPJ C16 1	M. Acciarri *et al.*	(L3 Collab.)
ACCIARRI	00J	PL B479 79	M. Acciarri *et al.*	(L3 Collab.)
ACCIARRI	00Q	PL B489 93	M. Acciarri *et al.*	(L3 Collab.)
BARATE	00B	EPJ C16 597	R. Barate *et al.*	(ALEPH Collab.)
BARATE	00C	EPJ C14 1	R. Barate *et al.*	(ALEPH Collab.)
BARATE	00O	EPJ C16 613	R. Barate *et al.*	(ALEPH Collab.)
ABBIENDI	99B	EPJ C8 217	G. Abbiendi *et al.*	(OPAL Collab.)
ABBIENDI	99I	PL B447 157	G. Abbiendi *et al.*	(OPAL Collab.)
ABE	99E	PR D59 052001	K. Abe *et al.*	(SLD Collab.)
ABE	99L	PRL 83 1902	K. Abe *et al.*	(SLD Collab.)
ABREU	99	EPJ C6 19	P. Abreu *et al.*	(DELPHI Collab.)
ABREU	99B	EPJ C10 415	P. Abreu *et al.*	(DELPHI Collab.)
ABREU	99J	PL B449 364	P. Abreu *et al.*	(DELPHI Collab.)
ABREU	99U	PL B462 425	P. Abreu *et al.*	(DELPHI Collab.)
ABREU	99Y	EPJ C10 219	P. Abreu *et al.*	(DELPHI Collab.)
ACCIARRI	99D	PL B448 152	M. Acciarri *et al.*	(L3 Collab.)
ACCIARRI	99F	PL B453 94	M. Acciarri *et al.*	(L3 Collab.)
ACCIARRI	99G	PL B450 281	M. Acciarri *et al.*	(L3 Collab.)
ACCIARRI	99O	PL B465 363	M. Acciarri *et al.*	(L3 Collab.)
ABBOTT	98M	PR D57 3817	B. Abbott *et al.*	(D0 Collab.)
ABE	98D	PRL 80 660	K. Abe *et al.*	(SLD Collab.)
ABE	98I	PRL 81 942	K. Abe *et al.*	(SLD Collab.)
ABREU	98K	PL B423 194	P. Abreu *et al.*	(DELPHI Collab.)
ABREU	98L	EPJ C5 585	P. Abreu *et al.*	(DELPHI Collab.)
ACCIARRI	98G	PL B431 199	M. Acciarri *et al.*	(L3 Collab.)
ACCIARRI	98H	PL B429 387	M. Acciarri *et al.*	(L3 Collab.)
ACCIARRI	98U	PL B439 225	M. Acciarri *et al.*	(L3 Collab.)
ACKERSTAFF	98A	EPJ C5 411	K. Ackerstaff *et al.*	(OPAL Collab.)
ACKERSTAFF	98E	EPJ C1 439	K. Ackerstaff *et al.*	(OPAL Collab.)
ACKERSTAFF	98O	PL B420 157	K. Ackerstaff *et al.*	(OPAL Collab.)
ACKERSTAFF	98Q	EPJ C4 19	K. Ackerstaff *et al.*	(OPAL Collab.)
BARATE	98O	PL B434 415	R. Barate *et al.*	(ALEPH Collab.)
BARATE	98T	EPJ C4 557	R. Barate *et al.*	(ALEPH Collab.)
BARATE	98V	EPJ C5 205	R. Barate *et al.*	(ALEPH Collab.)
ABE	97	PRL 78 17	K. Abe *et al.*	(SLD Collab.)
ABREU	97C	ZPHY C73 243	P. Abreu *et al.*	(DELPHI Collab.)
ABREU	97E	PL B398 207	P. Abreu *et al.*	(DELPHI Collab.)
ABREU	97G	PL B404 194	P. Abreu *et al.*	(DELPHI Collab.)
ACCIARRI	97D	PL B393 465	M. Acciarri *et al.*	(L3 Collab.)
ACCIARRI	97J	PL B407 351	M. Acciarri *et al.*	(L3 Collab.)
ACCIARRI	97L	PL B407 389	M. Acciarri *et al.*	(L3 Collab.)
ACCIARRI	97R	PL B413 167	M. Acciarri *et al.*	(L3 Collab.)
ACKERSTAFF	97M	ZPHY C74 413	K. Ackerstaff *et al.*	(OPAL Collab.)
ACKERSTAFF	97S	PL B412 210	K. Ackerstaff *et al.*	(OPAL Collab.)
ACKERSTAFF	97T	ZPHY C76 387	K. Ackerstaff *et al.*	(OPAL Collab.)
ACKERSTAFF	97W	ZPHY C76 425	K. Ackerstaff *et al.*	(OPAL Collab.)
ALEXANDER	97C	ZPHY C73 379	G. Alexander *et al.*	(OPAL Collab.)
ALEXANDER	97D	ZPHY C73 569	G. Alexander *et al.*	(OPAL Collab.)
ALEXANDER	97E	ZPHY C73 587	G. Alexander *et al.*	(OPAL Collab.)
BARATE	97D	PL B405 191	R. Barate *et al.*	(ALEPH Collab.)
BARATE	97E	PL B401 150	R. Barate *et al.*	(ALEPH Collab.)
BARATE	97F	PL B401 163	R. Barate *et al.*	(ALEPH Collab.)
BARATE	97H	PL B402 213	R. Barate *et al.*	(ALEPH Collab.)
BARATE	97J	ZPHY C74 451	R. Barate *et al.*	(ALEPH Collab.)
ABREU	96R	ZPHY C72 31	P. Abreu *et al.*	(DELPHI Collab.)
ABREU	96S	PL B389 405	P. Abreu *et al.*	(DELPHI Collab.)
ABREU	96U	ZPHY C73 61	P. Abreu *et al.*	(DELPHI Collab.)
ACCIARRI	96	PL B371 126	M. Acciarri *et al.*	(L3 Collab.)
ADAM	96	ZPHY C69 561	W. Adam *et al.*	(DELPHI Collab.)
ADAM	96B	ZPHY C70 371	W. Adam *et al.*	(DELPHI Collab.)
ALEXANDER	96B	ZPHY C70 197	G. Alexander *et al.*	(OPAL Collab.)
ALEXANDER	96F	PL B370 185	G. Alexander *et al.*	(OPAL Collab.)
ALEXANDER	96N	PL B384 343	G. Alexander *et al.*	(OPAL Collab.)
ALEXANDER	96R	ZPHY C72 1	G. Alexander *et al.*	(OPAL Collab.)
BUSKULIC	96D	ZPHY C69 393	D. Buskulic *et al.*	(ALEPH Collab.)
BUSKULIC	96H	ZPHY C69 379	D. Buskulic *et al.*	(ALEPH Collab.)
BUSKULIC	96T	PL B384 449	D. Buskulic *et al.*	(ALEPH Collab.)
BUSKULIC	96Y	PL B388 648	D. Buskulic *et al.*	(ALEPH Collab.)
ABE	95J	PRL 74 2880	K. Abe *et al.*	(SLD Collab.)

ABREU	95	ZPHY C65 709 (erratum)	P. Abreu *et al.*	(DELPHI Collab.)
ABREU	95D	ZPHY C66 323	P. Abreu *et al.*	(DELPHI Collab.)
ABREU	95L	ZPHY C65 587	P. Abreu *et al.*	(DELPHI Collab.)
ABREU	95M	ZPHY C65 603	P. Abreu *et al.*	(DELPHI Collab.)
ABREU	95O	ZPHY C67 543	P. Abreu *et al.*	(DELPHI Collab.)
ABREU	95R	ZPHY C68 353	P. Abreu *et al.*	(DELPHI Collab.)
ABREU	95V	ZPHY C68 541	P. Abreu *et al.*	(DELPHI Collab.)
ABREU	95W	PL B361 207	P. Abreu *et al.*	(DELPHI Collab.)
ABREU	95X	ZPHY C69 1	P. Abreu *et al.*	(DELPHI Collab.)
ACCIARRI	95B	PL B345 589	M. Acciarri *et al.*	(L3 Collab.)
ACCIARRI	95C	PL B345 609	M. Acciarri *et al.*	(L3 Collab.)
ACCIARRI	95G	PL B353 136	M. Acciarri *et al.*	(L3 Collab.)
AKERS	95C	ZPHY C65 47	R. Akers *et al.*	(OPAL Collab.)
AKERS	95U	ZPHY C67 389	R. Akers *et al.*	(OPAL Collab.)
AKERS	95W	ZPHY C67 555	R. Akers *et al.*	(OPAL Collab.)
AKERS	95X	ZPHY C68 1	R. Akers *et al.*	(OPAL Collab.)
AKERS	95Z	ZPHY C68 203	R. Akers *et al.*	(OPAL Collab.)
ALEXANDER	95D	PL B358 162	G. Alexander *et al.*	(OPAL Collab.)
BUSKULIC	95R	ZPHY C69 15	D. Buskulic *et al.*	(ALEPH Collab.)
MIYABAYASHI	95	PL B347 171	K. Miyabayashi *et al.*	(TOPAZ Collab.)
ABE	94C	PRL 73 25	K. Abe *et al.*	(SLD Collab.)
ABREU	94B	PL B327 386	P. Abreu *et al.*	(DELPHI Collab.)
ABREU	94P	PL B341 109	P. Abreu *et al.*	(DELPHI Collab.)
AKERS	94P	ZPHY C63 181	R. Akers *et al.*	(OPAL Collab.)
BUSKULIC	94G	ZPHY C62 179	D. Buskulic *et al.*	(ALEPH Collab.)
BUSKULIC	94J	ZPHY C62 1	D. Buskulic *et al.*	(ALEPH Collab.)
VILAIN	94	PL B320 203	P. Vilain *et al.*	(CHARM II Collab.)
ABREU	93	PL B298 236	P. Abreu *et al.*	(DELPHI Collab.)
ABREU	93I	ZPHY C59 533	P. Abreu *et al.*	(DELPHI Collab.)
Also		ZPHY C65 709 (erratum)	P. Abreu *et al.*	(DELPHI Collab.)
ABREU	93L	PL B318 249	P. Abreu *et al.*	(DELPHI Collab.)
ACTON	93	PL B305 407	P.D. Acton *et al.*	(OPAL Collab.)
ACTON	93D	ZPHY C58 219	P.D. Acton *et al.*	(OPAL Collab.)
ACTON	93E	PL B311 391	P.D. Acton *et al.*	(OPAL Collab.)
ADRIANI	93	PL B301 136	O. Adriani *et al.*	(L3 Collab.)
ADRIANI	93I	PL B316 427	O. Adriani *et al.*	(L3 Collab.)
BUSKULIC	93L	PL B313 520	D. Buskulic *et al.*	(ALEPH Collab.)
NOVIKOV	93C	PL B298 453	V.A. Novikov, L.B. Okun, M.I. Vysotsky	(ITEP)
ABREU	92I	PL B277 371	P. Abreu *et al.*	(DELPHI Collab.)
ABREU	92M	PL B289 199	P. Abreu *et al.*	(DELPHI Collab.)
ACTON	92B	ZPHY C53 539	D.P. Acton *et al.*	(OPAL Collab.)
ACTON	92L	PL B294 436	P.D. Acton *et al.*	(OPAL Collab.)
ACTON	92N	PL B295 357	P.D. Acton *et al.*	(OPAL Collab.)
ADEVA	92	PL B275 209	B. Adeva *et al.*	(L3 Collab.)
ADRIANI	92D	PL B292 454	O. Adriani *et al.*	(L3 Collab.)
ALITTI	92B	PL B276 354	J. Alitti *et al.*	(UA2 Collab.)
BUSKULIC	92D	PL B292 210	D. Buskulic *et al.*	(ALEPH Collab.)
BUSKULIC	92E	PL B294 145	D. Buskulic *et al.*	(ALEPH Collab.)
DECAMP	92	PRPL 216 253	D. Decamp *et al.*	(ALEPH Collab.)
ABE	91E	PRL 67 1502	F. Abe *et al.*	(CDF Collab.)
ABREU	91H	ZPHY C50 185	P. Abreu *et al.*	(DELPHI Collab.)
ACTON	91B	PL B273 338	D.P. Acton *et al.*	(OPAL Collab.)
ADACHI	91	PL B255 613	I. Adachi *et al.*	(TOPAZ Collab.)
ADEVA	91I	PL B259 199	B. Adeva *et al.*	(L3 Collab.)
AKRAWY	91F	PL B257 531	M.Z. Akrawy *et al.*	(OPAL Collab.)
DECAMP	91B	PL B259 377	D. Decamp *et al.*	(ALEPH Collab.)
DECAMP	91J	PL B266 218	D. Decamp *et al.*	(ALEPH Collab.)
JACOBSEN	91	PRL 67 3347	R.G. Jacobsen *et al.*	(Mark II Collab.)
SHIMONAKA	91	PL B268 457	A. Shimonaka *et al.*	(TOPAZ Collab.)
ABE	90I	ZPHY C48 13	K. Abe *et al.*	(VENUS Collab.)
ABRAMS	90	PRL 64 1334	G.S. Abrams *et al.*	(Mark II Collab.)
AKRAWY	90J	PL B246 285	M.Z. Akrawy *et al.*	(OPAL Collab.)
BEHREND	90D	ZPHY C47 333	H.J. Behrend *et al.*	(CELLO Collab.)
BRAUNSCH...	90	ZPHY C48 433	W. Braunschweig *et al.*	(TASSO Collab.)
ELSEN	90	ZPHY C46 349	E. Elsen *et al.*	(JADE Collab.)
HEGNER	90	ZPHY C46 547	S. Hegner *et al.*	(JADE Collab.)
STUART	90	PRL 64 983	D. Stuart *et al.*	(AMY Collab.)
ABE	89	PRL 62 613	F. Abe *et al.*	(CDF Collab.)
ABE	89C	PRL 63 720	F. Abe *et al.*	(CDF Collab.)
ABE	89L	PL B232 425	K. Abe *et al.*	(VENUS Collab.)
ABRAMS	89B	PRL 63 2173	G.S. Abrams *et al.*	(Mark II Collab.)
ABRAMS	89D	PRL 63 2780	G.S. Abrams *et al.*	(Mark II Collab.)
ALBAJAR	89	ZPHY C44 15	C. Albajar *et al.*	(UA1 Collab.)
BACALA	89	PL B218 112	A. Bacala *et al.*	(AMY Collab.)
BAND	89	PL B218 369	H.R. Band *et al.*	(MAC Collab.)
GREENSHAW	89	ZPHY C42 1	T. Greenshaw *et al.*	(JADE Collab.)
OULD-SAADA	89	ZPHY C44 567	F. Ould-Saada *et al.*	(JADE Collab.)
SAGAWA	89	PRL 63 2341	H. Sagawa *et al.*	(AMY Collab.)
ADACHI	88C	PL B208 319	I. Adachi *et al.*	(TOPAZ Collab.)
ADEVA	88	PR D38 2665	B. Adeva *et al.*	(Mark-J Collab.)
BRAUNSCH...	88D	ZPHY C40 163	W. Braunschweig *et al.*	(TASSO Collab.)
ANSARI	87	PL B186 440	R. Ansari *et al.*	(UA2 Collab.)
BEHREND	87C	PL B191 209	H.J. Behrend *et al.*	(CELLO Collab.)
BARTEL	86C	ZPHY C30 371	W. Bartel *et al.*	(JADE Collab.)
Also		ZPHY C26 507	W. Bartel *et al.*	(JADE Collab.)
Also		PL 108B 140	W. Bartel *et al.*	(JADE Collab.)
ASH	85	PRL 55 1831	W.W. Ash *et al.*	(MAC Collab.)
BARTEL	85F	PL 161B 188	W. Bartel *et al.*	(JADE Collab.)
DERRICK	85	PR D31 2352	M. Derrick *et al.*	(HRS Collab.)
FERNANDEZ	85	PRL 54 1624	E. Fernandez *et al.*	(MAC Collab.)
LEVI	83	PRL 51 1941	M.E. Levi *et al.*	(Mark II Collab.)
BEHREND	82	PL 114B 282	H.J. Behrend *et al.*	(CELLO Collab.)
BRANDELIK	82C	PL 110B 173	R. Brandelik *et al.*	(TASSO Collab.)

H^0

$J = 0$

In the following H^0 refers to the signal that has been discovered in the Higgs searches. Whereas the observed signal is labeled as a spin 0 particle and is called a Higgs Boson, the detailed properties of H^0 and its role in the context of electroweak symmetry breaking need to be further clarified. These issues are addressed by the measurements listed below.

Concerning mass limits and cross section limits that have been obtained in the searches for neutral and charged Higgs bosons, see the sections "Searches for Neutral Higgs Bosons" and "Searches for Charged Higgs Bosons ($H^{\pm}$ and $H^{\pm\pm}$)", respectively.

H^0 MASS

VALUE (GeV)	DOCUMENT ID		TECN	COMMENT
125.18±0.16 OUR AVERAGE				
125.26±0.20±0.08	[1] SIRUNYAN	17AV	CMS	pp, 13 TeV, $ZZ^* \to 4\ell$
125.09±0.21±0.11	[2,3] AAD	15B	LHC	pp, 7, 8 TeV
• • • We do not use the following data for averages, fits, limits, etc. • • •				
125.07±0.25±0.14	[3] AAD	15B	LHC	pp, 7, 8 TeV, $\gamma\gamma$
125.15±0.37±0.15	[3] AAD	15B	LHC	pp, 7, 8 TeV, $ZZ^* \to 4\ell$
126.02±0.43±0.27	AAD	15B	ATLS	pp, 7, 8 TeV, $\gamma\gamma$
124.51±0.52±0.04	AAD	15B	ATLS	pp, 7, 8 TeV, $ZZ^* \to 4\ell$
125.59±0.42±0.17	AAD	15B	CMS	pp, 7, 8 TeV, $ZZ^* \to 4\ell$
$125.02^{+0.26}_{-0.27}{}^{+0.14}_{-0.15}$	[4] KHACHATRY...	15AM	CMS	pp, 7, 8 TeV
125.36±0.37±0.18	[2,5] AAD	14W	ATLS	pp, 7, 8 TeV
125.98±0.42±0.28	[5] AAD	14W	ATLS	pp, 7, 8 TeV, $\gamma\gamma$
124.51±0.52±0.06	[5] AAD	14W	ATLS	pp, 7, 8 TeV, $ZZ^* \to 4\ell$
125.6 ±0.4 ±0.2	[6] CHATRCHYAN	14AA	CMS	pp, 7, 8 TeV, $ZZ^* \to 4\ell$
122 ±7	[7] CHATRCHYAN	14K	CMS	pp, 7, 8 TeV, $\tau\tau$
124.70±0.31±0.15	[8] KHACHATRY...	14P	CMS	pp, 7, 8 TeV, $\gamma\gamma$
$125.5 \pm 0.2\ ^{+0.5}_{-0.6}$	[2,9] AAD	13AK	ATLS	pp, 7, 8 TeV
126.8 ±0.2 ±0.7	[9] AAD	13AK	ATLS	pp, 7, 8 TeV, $\gamma\gamma$
$124.3\ ^{+0.6}_{-0.5}\ ^{+0.5}_{-0.3}$	[9] AAD	13AK	ATLS	pp, 7, 8 TeV, $ZZ^* \to 4\ell$
125.8 ±0.4 ±0.4	[2,10] CHATRCHYAN	13J	CMS	pp, 7, 8 TeV
126.2 ±0.6 ±0.2	[10] CHATRCHYAN	13J	CMS	pp, 7, 8 TeV, $ZZ^* \to 4\ell$
126.0 ±0.4 ±0.4	[2,11] AAD	12AI	ATLS	pp, 7, 8 TeV
125.3 ±0.4 ±0.5	[2,12] CHATRCHYAN	12N	CMS	pp, 7, 8 TeV

[1] SIRUNYAN 17AV use 35.9 fb^{-1} of pp collisions at $E_{cm} = 13$ TeV with $pp \to ZZ^* \to 4\ell$ where $\ell = e,\ \mu$.

[2] Combined value from $\gamma\gamma$ and $ZZ^* \to 4\ell$ final states.

[3] ATLAS and CMS data are fitted simultaneously.

[4] KHACHATRYAN 15AM use up to 5.1 fb^{-1} of pp collisions at $E_{cm} = 7$ TeV and up to 19.7 fb^{-1} at $E_{cm} = 8$ TeV.

[5] AAD 14W use 4.5 fb^{-1} of pp collisions at $E_{cm} = 7$ TeV and 20.3 fb^{-1} at 8 TeV.

[6] CHATRCHYAN 14AA use 5.1 fb^{-1} of pp collisions at $E_{cm} = 7$ TeV and 19.7 fb^{-1} at $E_{cm} = 8$ TeV.

[7] CHATRCHYAN 14K use 4.9 fb^{-1} of pp collisions at $E_{cm} = 7$ TeV and 19.7 fb^{-1} at $E_{cm} = 8$ TeV.

[8] KHACHATRYAN 14P use 5.1 fb^{-1} of pp collisions at $E_{cm} = 7$ TeV and 19.7 fb^{-1} at $E_{cm} = 8$ TeV.

[9] AAD 13AK use 4.7 fb^{-1} of pp collisions at E_{cm}=7 TeV and 20.7 fb^{-1} at E_{cm}=8 TeV. Superseded by AAD 14W.

[10] CHATRCHYAN 13J use 5.1 fb^{-1} of pp collisions at $E_{cm} = 7$ TeV and 12.2 fb^{-1} at $E_{cm} = 8$ TeV.

[11] AAD 12AI obtain results based on 4.6–4.8 fb^{-1} of pp collisions at $E_{cm} = 7$ TeV and 5.8–5.9 fb^{-1} at $E_{cm} = 8$ TeV. An excess of events over background with a local significance of 5.9 σ is observed at $m_{H^0} = 126$ GeV. See also AAD 12DA.

[12] CHATRCHYAN 12N obtain results based on 4.9–5.1 fb^{-1} of pp collisions at $E_{cm} = 7$ TeV and 5.1–5.3 fb^{-1} at $E_{cm} = 8$ TeV. An excess of events over background with a local significance of 5.0 σ is observed at about $m_{H^0} = 125$ GeV. See also CHATRCHYAN 12BY and CHATRCHYAN 13Y.

H^0 SPIN AND CP PROPERTIES

The observation of the signal in the $\gamma\gamma$ final state rules out the possibility that the discovered particle has spin 1, as a consequence of the Landau-Yang theorem. This argument relies on the assumptions that the decaying particle is an on-shell resonance and that the decay products are indeed two photons rather than two pairs of boosted photons, which each could in principle be misidentified as a single photon.

Concerning distinguishing the spin 0 hypothesis from a spin 2 hypothesis, some care has to be taken in modelling the latter in order to ensure that the discriminating power is actually based on the spin properties rather than on unphysical behavior that may affect the model of the spin 2 state.

Under the assumption that the observed signal consists of a single state rather than an overlap of more than one resonance, it is sufficient to discriminate between distinct hypotheses in the spin analyses. On the other hand, the determination of the CP properties is in general much more difficult since in principle the observed state could consist of any admixture of CP-even and CP-odd components. As a first step, the compatibility of the data with distinct hypotheses of pure CP-even and pure CP-odd states with different spin assignments has been investigated. In order to treat the case of a possible mixing of different CP states, certain cross section ratios are considered. Those cross section ratios need to be distinguished from the amount of mixing between a CP-even and a CP-odd state, as the cross section ratios depend in addition also on the coupling strengths of the CP-even and CP-odd components to the involved particles. A small relative coupling implies a small sensitivity of the corresponding cross section ratio to effects of CP mixing.

VALUE	DOCUMENT ID		TECN	COMMENT
• • • We do not use the following data for averages, fits, limits, etc. • • •				
	[1] SIRUNYAN	17AM	CMS	$pp \to H^0 + \geq 2j$, $H^0 \to 4\ell$ ($\ell = e,\ \mu$)
	[2] AAD	16	ATLS	$H^0 \to \gamma\gamma$
	[3] AAD	16BL	ATLS	$pp \to H^0 jjX$ (VBF), $H^0 \to \tau\tau$, 8 TeV
	[4] KHACHATRY...	16AB	CMS	$pp \to WH^0$, ZH^0, $H^0 \to b\overline{b}$, 8 TeV
	[5] AAD	15AX	ATLS	$H^0 \to WW^*$

Gauge & Higgs Boson Particle Listings

H^0

[6] AAD 15CI ATLS $H^0 \to ZZ^*, WW^*, \gamma\gamma$
[7] AALTONEN 15 TEVA $p\overline{p} \to WH^0, ZH^0, H^0 \to b\overline{b}$
[8] AALTONEN 15B CDF $p\overline{p} \to WH^0, ZH^0, H^0 \to b\overline{b}$
[9] KHACHATRY...15Y CMS $H^0 \to 4\ell, WW^*, \gamma\gamma$
[10] ABAZOV 14F D0 $p\overline{p} \to WH^0, ZH^0, H^0 \to b\overline{b}$
[11] CHATRCHYAN 14AA CMS $H^0 \to ZZ^*$
[12] CHATRCHYAN 14G CMS $H^0 \to WW^*$
[13] KHACHATRY...14P CMS $H^0 \to \gamma\gamma$
[14] AAD 13AJ ATLS $H^0 \to \gamma\gamma, ZZ^* \to 4\ell, WW^* \to \ell\nu\ell\nu$
[15] CHATRCHYAN 13J CMS $H^0 \to ZZ^* \to 4\ell$

[1] SIRUNYAN 17AM constrain anomalous couplings of the Higgs boson with 5.1 fb^{-1} of pp collisions at $E_{cm} = 7$ TeV, 19.7 fb^{-1} at $E_{cm} = 8$ TeV, and 38.6 fb^{-1} at $E_{cm} = 13$ TeV. See their Table 3 and Fig. 3, which show 68% CL and 95% CL intervals. A CP violation parameter f_{a3} is set to be $f_{a3}\cos(\phi_{a3}) = [-0.38, 0.46]$ at 95% CL ($\phi_{a3} = 0$ or π).

[2] AAD 16 study $H^0 \to \gamma\gamma$ with an effective Lagrangian including CP even and odd terms in 20.3 fb^{-1} of pp collisions at $E_{cm} = 8$ TeV. The data is consistent with the expectations for the Higgs boson of the Standard Model. Limits on anomalous couplings are also given.

[3] AAD 16BL study VBF $H^0 \to \tau\tau$ with an effective Lagrangian including a CP odd term in 20.3 fb^{-1} of pp collisions at $E_{cm} = 8$ TeV. The measurement is consistent with the expectation of the Standard Model. The CP-mixing parameter $\tilde{d}$ (a dimensionless coupling $\tilde{d} = -(m_W^2/\Lambda^2) f_{\widetilde{W}W}$) is constrained to the interval of $(-0.11, 0.05)$ at 68% CL under the assumption of $d = \tilde{d}_B$.

[4] KHACHATRYAN 16AB search for anomalous pseudoscalar couplings of the Higgs boson to W and Z with 18.9 fb^{-1} of pp collisions at $E_{cm} = 8$ TeV. See their Table 5 and Figs 5 and 6 for limits on possible anomalous pseudoscalar coupling parameters.

[5] AAD 15AX compare the $J^{CP} = 0^+$ Standard Model assignment with other J^{CP} hypotheses in 20.3 fb^{-1} of pp collisions at $E_{cm} = 8$ TeV, using the process $H^0 \to WW^* \to e\nu\mu\nu$. 2^+ hypotheses are excluded at 84.5–99.4%CL, 0^- at 96.5%CL, 0^+ (field strength coupling) at 70.8%CL. See their Fig. 19 for limits on possible CP mixture parameters.

[6] AAD 15CI compare the $J^{CP} = 0^+$ Standard Model assignment with other J^{CP} hypotheses in 4.5 fb^{-1} of pp collisions at $E_{cm} = 7$ TeV and 20.3 fb^{-1} at $E_{cm} = 8$ TeV, using the processes $H^0 \to ZZ^* \to 4\ell$. $H^0 \to \gamma\gamma$ and combine with AAD 15AX data. 0^+ (field strength coupling), 0^- and several 2^+ hypotheses are excluded at more than 99.9% CL. See their Tables 7–9 for limits on possible CP mixture parameters.

[7] AALTONEN 15 combine AALTONEN 15B and ABAZOV 14F data. An upper limit of 0.36 of the Standard Model production rate at 95% CL is obtained both for a 0^- and a 2^+ state. Assuming the SM event rate, the $J^{CP} = 0^-$ (2^+) hypothesis is excluded at the 5.0σ (4.9σ) level.

[8] AALTONEN 15B compare the $J^{CP} = 0^+$ Standard Model assignment with other J^{CP} hypotheses in 9.45 fb^{-1} of $p\overline{p}$ collisions at $E_{cm} = 1.96$ TeV, using the processes $ZH^0 \to \ell\ell b\overline{b}$, $WH^0 \to \ell\nu b\overline{b}$, and $ZH^0 \to \nu\nu b\overline{b}$. Bounds on the production rates of 0^- and 2^+ (graviton-like) states are set, see their tables II and III.

[9] KHACHATRYAN 15Y compare the $J^{CP} = 0^+$ Standard Model assignment with other J^{CP} hypotheses in up to 5.1 fb^{-1} of pp collisions at $E_{cm} = 7$ TeV and up to 19.7 fb^{-1} at $E_{cm} = 8$ TeV, using the processes $H^0 \to 4\ell$, $H^0 \to WW^*$, and $H^0 \to \gamma\gamma$. 0^- is excluded at 99.98% CL, and several 2^+ hypotheses are excluded at more than 99% CL. Spin 1 models are excluded at more than 99.999% CL in ZZ^* and WW^* modes. Limits on anomalous couplings and several cross section fractions, treating the case of CP-mixed states, are also given.

[10] ABAZOV 14F compare the $J^{CP} = 0^+$ Standard Model assignment with $J^{CP} = 0^-$ and 2^+ (graviton-like coupling) hypotheses in up to 9.7 fb^{-1} of $p\overline{p}$ collisions at $E_{cm} = 1.96$ TeV. They use kinematic correlations between the decay products of the vector boson and the Higgs boson in the final states $ZH \to \ell\ell b\overline{b}$, $WH \to \ell\nu b\overline{b}$, and $ZH \to \nu\nu b\overline{b}$. The 0^- (2^+) hypothesis is excluded at 97.6% CL (99.0% CL). In order to treat the case of a possible mixture of a 0^+ state with another J^{CP} state, the cross section fractions $f_X = \sigma_X/(\sigma_{0^+} + \sigma_X)$ are considered, where $X = 0^-, 2^+$. Values for f_{0^-} (f_{2^+}) above 0.80 (0.67) are excluded at 95% CL under the assumption that the total cross section is that of the SM Higgs boson.

[11] CHATRCHYAN 14AA compare the $J^{CP} = 0^+$ Standard Model assignment with various J^{CP} hypotheses in 5.1 fb^{-1} of pp collisions at $E_{cm} = 7$ TeV and 19.7 fb^{-1} at $E_{cm} = 8$ TeV. $J^{CP} = 0^-$ and $1^\pm$ hypotheses are excluded at 99% CL, and several $J = 2$ hypotheses are excluded at 95% CL. In order to treat the case of a possible mixture of a 0^+ state with another J^{CP} state, the cross section fraction $f_{a3} = |a_3|^2\sigma_3 / (|a_1|^2\sigma_1 + |a_2|^2\sigma_2 + |a_3|^2\sigma_3)$ is considered, where the case $a_3 = 1$, $a_1 = a_2 = 0$ corresponds to a pure CP-odd state. Assuming $a_2 = 0$, a value for f_{a3} above 0.51 is excluded at 95% CL.

[12] CHATRCHYAN 14G compare the $J^{CP} = 0^+$ Standard Model assignment with $J^{CP} = 0^-$ and 2^+ (graviton-like coupling) hypotheses in 4.9 fb^{-1} of pp collisions at $E_{cm} = 7$ TeV and 19.4 fb^{-1} at $E_{cm} = 8$ TeV. Varying the fraction of the production of the 2^+ state via gg and $q\overline{q}$, 2^+ hypotheses are disfavored at CL between 83.7 and 99.8%. The 0^- hypothesis is disfavored against 0^+ at the 65.3% CL.

[13] KHACHATRYAN 14P compare the $J^{CP} = 0^+$ Standard Model assignment with a 2^+ (graviton-like coupling) hypothesis in 5.1 fb^{-1} of pp collisions at $E_{cm} = 7$ TeV and 19.7 fb^{-1} at $E_{cm} = 8$ TeV. Varying the fraction of the production of the 2^+ state via gg and $q\overline{q}$, 2^+ hypotheses are disfavored at CL between 71 and 94%.

[14] AAD 13AJ compare the spin 0, CP-even hypothesis with specific alternative hypotheses of spin 0, CP-odd, spin 1, CP-even and CP-odd, and spin 2, CP-even models using the Higgs boson decays $H \to \gamma\gamma$, $H \to ZZ^* \to 4\ell$ and $H \to WW^* \to \ell\nu\ell\nu$ and combinations thereof. The data are compatible with the spin 0, CP-even hypothesis, while all other tested hypotheses are excluded at confidence levels above 97.8%.

[15] CHATRCHYAN 13J study angular distributions of the lepton pairs in the ZZ^* channel where both Z bosons decay to e or μ pairs. Under the assumption that the observed particle has spin 0, the data are found to be consistent with the pure CP-even hypothesis, while the pure CP-odd hypothesis is disfavored.

H^0 DECAY WIDTH

The total decay width for a light Higgs boson with a mass in the observed range is not expected to be directly observable at the LHC. For the case of the Standard Model the prediction for the total width is about 4 MeV, which is three orders of magnitude smaller than the experimental mass resolution. There is no indication from the results observed so far that the natural width is broadened by new physics effects to such an extent that it could be directly observable. Furthermore, as all LHC Higgs channels rely on the identification of Higgs decay products, the total Higgs width cannot be measured indirectly without additional assumptions. The different dependence of on-peak and off-peak contributions on the total width in Higgs decays to ZZ^* and interference effects between signal and background in Higgs decays to $\gamma\gamma$ can provide additional information in this context. Constraints on the total width from the combination of on-peak and off-peak contributions in Higgs decays to ZZ^* rely on the assumption of equal on- and off-shell effective couplings. Without an experimental determination of the total width or further theoretical assumptions, only ratios of couplings can be determined at the LHC rather than absolute values of couplings.

VALUE (GeV)	CL%	DOCUMENT ID		TECN	COMMENT
<1.10	95	[1] SIRUNYAN	17AV	CMS	pp, 13 TeV, $ZZ^* \to 4\ell$
<0.013	95	[2] KHACHATRY...	16BA	CMS	pp, 7, 8 TeV, $ZZ^{(*)}, WW^{(*)}$
<1.7	95	[3] KHACHATRY...	15AM	CMS	pp, 7, 8 TeV
>3.5 $\times 10^{-12}$	95	[4] KHACHATRY...	15BA	CMS	pp, 7, 8 TeV, flight distance
<5.0	95	[5] AAD	14W	ATLS	pp, 7, 8 TeV, $\gamma\gamma$
<2.6	95	[5] AAD	14W	ATLS	pp, 7, 8 TeV, $ZZ^* \to 4\ell$
• • • We do not use the following data for averages, fits, limits, etc. • • •					
<0.026	95	[6] KHACHATRY...	16BA	CMS	pp, 7, 8 TeV, $WW^{(*)}$
<0.0227	95	[7] AAD	15BE	ATLS	pp, 8 TeV, $ZZ^{(*)}, WW^{(*)}$
<0.046	95	[8] KHACHATRY...	15BA	CMS	pp, 7, 8 TeV, $ZZ^{(*)} \to 4\ell$
<3.4	95	[9] CHATRCHYAN	14AA	CMS	pp, 7, 8 TeV, $ZZ^* \to 4\ell$
<0.022	95	[10] KHACHATRY...	14D	CMS	pp, 7, 8 TeV, $ZZ^{(*)}$
<2.4	95	[11] KHACHATRY...	14P	CMS	pp, 7, 8 TeV, $\gamma\gamma$

[1] SIRUNYAN 17AV obtain an upper limit on the width from the $m_{4\ell}$ distribution in $ZZ^* \to 4\ell$ ($\ell = e$, μ) decays. Data of 35.9 fb^{-1} pp collisions at $E_{cm} = 13$ TeV is used. The expected limit is 1.60 GeV.

[2] KHACHATRYAN 16BA combine the $WW^{(*)}$ result with $ZZ^{(*)}$ results of KHACHATRYAN 15BA and KHACHATRYAN 14D.

[3] KHACHATRYAN 15AM combine $\gamma\gamma$ and $ZZ^* \to 4\ell$ results. The expected limit is 2.3 GeV.

[4] KHACHATRYAN 15BA derive a lower limit on the total width from an upper limit on the decay flight distance $\tau < 1.9 \times 10^{-13}$ s. 5.1 fb^{-1} of pp collisions at $E_{cm} = 7$ TeV and 19.7 fb^{-1} at 8 TeV are used.

[5] AAD 14W use 4.5 fb^{-1} of pp collisions at $E_{cm} = 7$ TeV and 20.3 fb^{-1} at 8 TeV. The expected limit is 6.2 GeV.

[6] KHACHATRYAN 16BA derive constraints on the total width from comparing $WW^{(*)}$ production via on-shell and off-shell H^0 using 4.9 fb^{-1} of pp collisions at $E_{cm} = 7$ TeV and 19.4 fb^{-1} at 8 TeV.

[7] AAD 15BE derive constraints on the total width from comparing $ZZ^{(*)}$ and $WW^{(*)}$ production via on-shell and off-shell H^0 using 20.3 fb^{-1} of pp collisions at $E_{cm} = 8$ TeV. The K factor for the background processes is assumed to be equal to that for the signal.

[8] KHACHATRYAN 15BA derive constraints on the total width from comparing $ZZ^{(*)}$ production via on-shell and off-shell H^0 with an unconstrained anomalous coupling. 4ℓ final states in 5.1 fb^{-1} of pp collisions at $E_{cm} = 7$ TeV and 19.7 fb^{-1} at $E_{cm} = 8$ TeV are used.

[9] CHATRCHYAN 14AA use 5.1 fb^{-1} of pp collisions at $E_{cm} = 7$ TeV and 19.7 fb^{-1} at $E_{cm} = 8$ TeV. The expected limit is 2.8 GeV.

[10] KHACHATRYAN 14D derive constraints on the total width from comparing $ZZ^{(*)}$ production via on-shell and off-shell H^0. 4ℓ and $\ell\ell\nu\nu$ final states in 5.1 fb^{-1} of pp collisions at $E_{cm} = 7$ TeV and 19.7 fb^{-1} at $E_{cm} = 8$ TeV are used.

[11] KHACHATRYAN 14P use 5.1 fb^{-1} of pp collisions at $E_{cm} = 7$ TeV and 19.7 fb^{-1} at $E_{cm} = 8$ TeV. The expected limit is 3.1 GeV.

H^0 DECAY MODES

	Mode	Fraction (Γ_i/Γ)	Confidence level
Γ_1	WW^*		
Γ_2	ZZ^*		
Γ_3	$\gamma\gamma$		
Γ_4	$b\overline{b}$		
Γ_5	e^+e^-	$< 1.9 \times 10^{-3}$	95%
Γ_6	$\mu^+\mu^-$		
Γ_7	$\tau^+\tau^-$		
Γ_8	$Z\gamma$		
Γ_9	$J/\psi\gamma$	$< 1.5 \times 10^{-3}$	95%
Γ_{10}	$\Upsilon(1S)\gamma$	$< 1.3 \times 10^{-3}$	95%
Γ_{11}	$\Upsilon(2S)\gamma$	$< 1.9 \times 10^{-3}$	95%
Γ_{12}	$\Upsilon(3S)\gamma$	$< 1.3 \times 10^{-3}$	95%
Γ_{13}	$\phi(1020)\gamma$	$< 1.4 \times 10^{-3}$	95%
Γ_{14}	$e\mu$	$< 3.5 \times 10^{-4}$	95%
Γ_{15}	$e\tau$	$< 6.9 \times 10^{-3}$	95%

Γ_{16}	$\mu\tau$	< 1.43 %	95%
Γ_{17}	invisible	<24 %	95%

H^0 BRANCHING RATIOS

$\Gamma(e^+e^-)/\Gamma_{total}$ Γ_5/Γ

VALUE	CL%	DOCUMENT ID		TECN
$<1.9\times10^{-3}$	95	[1] KHACHATRY...15H		CMS

[1] KHACHATRYAN 15H use 5.0 fb^{-1} of pp collisions at E_{cm} = 7 TeV and 19.7 fb^{-1} at 8 TeV.

$\Gamma(J/\psi\gamma)/\Gamma_{total}$ Γ_9/Γ

VALUE	CL%	DOCUMENT ID		TECN	COMMENT
$<1.5\times10^{-3}$	95	[1] KHACHATRY...16B		CMS	8 TeV
$<1.5\times10^{-3}$	95	[2] AAD	15I	ATLS	8 TeV

[1] KHACHATRYAN 16B use 19.7 fb^{-1} of pp collision data at 8 TeV.
[2] AAD 15I use 19.7 fb^{-1} of pp collision data at 8 TeV.

$\Gamma(\Upsilon(1S)\gamma)/\Gamma_{total}$ Γ_{10}/Γ

VALUE	CL%	DOCUMENT ID		TECN	COMMENT
$<1.3\times10^{-3}$	95	[1] AAD	15I	ATLS	8 TeV

[1] AAD 15I use 19.7 fb^{-1} of pp collision data at 8 TeV.

$\Gamma(\Upsilon(2S)\gamma)/\Gamma_{total}$ Γ_{11}/Γ

VALUE	CL%	DOCUMENT ID		TECN	COMMENT
$<1.9\times10^{-3}$	95	[1] AAD	15I	ATLS	8 TeV

[1] AAD 15I use 19.7 fb^{-1} of pp collision data at 8 TeV.

$\Gamma(\Upsilon(3S)\gamma)/\Gamma_{total}$ Γ_{12}/Γ

VALUE	CL%	DOCUMENT ID		TECN	COMMENT
$<1.3\times10^{-3}$	95	[1] AAD	15I	ATLS	8 TeV

[1] AAD 15I use 19.7 fb^{-1} of pp collision data at 8 TeV.

$\Gamma(\phi(1020)\gamma)/\Gamma_{total}$ Γ_{13}/Γ

VALUE	CL%	DOCUMENT ID		TECN	COMMENT
$<1.4\times10^{-3}$	95	[1] AABOUD	16K	ATLS	pp at 13 TeV

[1] AABOUD 16K use 2.7 fb^{-1} of pp collision data at 13 TeV.

$\Gamma(e\mu)/\Gamma_{total}$ Γ_{14}/Γ

VALUE	CL%	DOCUMENT ID		TECN	COMMENT
$<3.5\times10^{-4}$	95	[1] KHACHATRY...16CD		CMS	pp, 8 TeV

[1] KHACHATRYAN 16CD search for $H^0 \to e\mu$ in 19.7 fb^{-1} of pp collisions at E_{cm} = 8 TeV. The limit constrains the $Y_{e\mu}$ Yukawa coupling to $\sqrt{|Y_{e\mu}|^2+|Y_{\mu e}|^2} < 5.4\times10^{-4}$ at 95% CL (see their Fig. 6).

$\Gamma(e\tau)/\Gamma_{total}$ Γ_{15}/Γ

VALUE	CL%	DOCUMENT ID		TECN	COMMENT
$<6.9\times10^{-3}$	95	[1] KHACHATRY...16CD		CMS	pp, 8 TeV
• • • We do not use the following data for averages, fits, limits, etc. • • •					
$<1.04\times10^{-2}$	95	[2] AAD	17	ATLS	pp, 8 TeV

[1] KHACHATRYAN 16CD search for $H^0 \to e\tau$ in 19.7 fb^{-1} of pp collisions at E_{cm} = 8 TeV. The limit constrains the $Y_{e\tau}$ Yukawa coupling to $\sqrt{|Y_{e\tau}|^2+|Y_{\tau e}|^2} < 2.4\times10^{-3}$ at 95% CL (see their Fig. 6).
[2] AAD 17 search for $H^0 \to e\tau$ in 20.3 fb^{-1} of pp collisions at E_{cm} = 8 TeV.

$\Gamma(\mu\tau)/\Gamma_{total}$ Γ_{16}/Γ

VALUE	CL%	DOCUMENT ID		TECN	COMMENT
$<1.43\times10^{-2}$	95	[1] AAD	17	ATLS	pp, 8 TeV
• • • We do not use the following data for averages, fits, limits, etc. • • •					
$<1.51\times10^{-2}$	95	[2] KHACHATRY...15Q		CMS	pp, 8 TeV

[1] AAD 17 search for $H^0 \to \mu\tau$ in 20.3 fb^{-1} of pp collisions at E_{cm} = 8 TeV.
[2] KHACHATRYAN 15Q search for $H^0 \to \mu\tau$ with τ decaying electronically or hadronically in 19.7 fb^{-1} of pp collisions at E_{cm} = 8 TeV. The fit gives B($H^0 \to \mu\tau$) = $(0.84^{+0.39}_{-0.37})$% with a significance of 2.4 σ.

$\Gamma(\text{invisible})/\Gamma_{total}$ Γ_{17}/Γ

Invisible final states.

VALUE	CL%	DOCUMENT ID		TECN	COMMENT
<0.24	95	[1] KHACHATRY...17F		CMS	pp, 7, 8, 13 TeV
<0.28	95	[2] AAD	16AF	ATLS	$pp \to qqH^0X$, 8 TeV
<0.34	95	[3] AAD	16AN	LHC	pp, 7, 8 TeV
• • • We do not use the following data for averages, fits, limits, etc. • • •					
<0.67	95	[4] AABOUD	18	ATLS	$pp \to H^0ZX$, $H^0 \to$ inv., 13 TeV
<0.46	95	[5] AABOUD	17BD	ATLS	$pp \to gH^0X, qqH^0X$, $H^0 \to$ inv, 13 TeV
<0.78	95	[6] AAD	15BD	ATLS	$pp \to H^0W/ZX$, 8 TeV
<0.75	95	[7] AAD	14O	ATLS	$pp \to H^0ZX$, 7, 8 TeV
<0.58	95	[8] CHATRCHYAN	14B	CMS	$pp \to H^0ZX, qqH^0X$
<0.81	95	[9] CHATRCHYAN	14B	CMS	$pp \to H^0ZX$, 7, 8 TeV
<0.65	95	[10] CHATRCHYAN	14B	CMS	$pp \to qqH^0X$, 8 TeV

[1] KHACHATRYAN 17F search for H^0 decaying to invisible final states with gluon fusion, VBF, ZH, and WH productions using 2.3 fb^{-1} of pp collisions at E_{cm} = 13 TeV, 19.7 fb^{-1} at 8 TeV, and 5.1 fb^{-1} at 7 TeV. The quoted limit is given for m_{H^0} = 125 GeV and assumes the Standard Model rates for gluon fusion, VBF, ZH, and WH productions.
[2] AAD 16AF search for $pp \to qqH^0X$ (VBF) with H^0 decaying to invisible final states in 20.3 fb^{-1} at E_{cm} = 8 TeV. The quoted limit on the branching ratio is given for m_{H^0} = 125 GeV and assumes the Standard Model rates for VBF and gluon-fusion production.
[3] AAD 16AN perform fits to the ATLAS and CMS data at E_{cm} = 7 and 8 TeV. The branching fraction of decays into BSM particles that are invisible or into undetected decay modes is measured for m_{H^0} = 125.09 GeV.
[4] AABOUD 18 search for $pp \to H^0ZX$, $Z \to ee$, $\mu\mu$ with H^0 decaying to invisible final states in 36.1 fb^{-1} at E_{cm} = 13 TeV. The quoted limit on the branching ratio is given for m_{H^0} = 125 GeV and assumes the Standard Model rate for H^0Z production.
[5] AABOUD 17BD search for H^0 decaying to invisible final states with $\geq$ 1 jet and VBF events using 3.2 fb^{-1} of pp collisions at E_{cm} = 13 TeV. A cross-section ratio R^{miss} is used in the measurement. The quoted limit is given for m_{H^0} = 125 GeV.
[6] AAD 15BD search for $pp \to H^0WX$ and $pp \to H^0ZX$ with W or Z decaying hadronically and H^0 decaying to invisible final states using data at E_{cm} = 8 TeV. The quoted limit is given for m_{H^0} = 125 GeV, assumes the Standard Model rates for the production processes and is based on a combination of the contributions from H^0W, H^0Z and the gluon-fusion process.
[7] AAD 14O search for $pp \to H^0ZX$, $Z \to \ell\ell$, with H^0 decaying to invisible final states in 4.5 fb^{-1} at E_{cm} = 7 TeV and 20.3 fb^{-1} at E_{cm} = 8 TeV. The quoted limit on the branching ratio is given for m_{H^0} = 125.5 GeV and assumes the Standard Model rate for H^0Z production.
[8] CHATRCHYAN 14B search for $pp \to H^0ZX$, $Z \to \ell\ell$ and $Z \to b\overline{b}$, and also $pp \to qqH^0X$ with H^0 decaying to invisible final states using data at E_{cm} = 7 and 8 TeV. The quoted limit on the branching ratio is obtained from a combination of the limits from H^0Z and qqH^0. It is given for m_{H^0} = 125 GeV and assumes the Standard Model rates for the two production processes.
[9] CHATRCHYAN 14B search for $pp \to H^0ZX$ with H^0 decaying to invisible final states and $Z \to \ell\ell$ in 4.9 fb^{-1} at E_{cm} = 7 TeV and 19.7 fb^{-1} at E_{cm} = 8 TeV, and also with $Z \to b\overline{b}$ in 18.9 fb^{-1} at E_{cm} = 8 TeV. The quoted limit on the branching ratio is given for m_{H^0} = 125 GeV and assumes the Standard Model rate for H^0Z production.
[10] CHATRCHYAN 14B search for $pp \to qqH^0X$ (vector boson fusion) with H^0 decaying to invisible final states in 19.5 fb^{-1} at E_{cm} = 8 TeV. The quoted limit on the branching ratio is given for m_{H^0} = 125 GeV and assumes the Standard Model rate for qqH^0 production.

H^0 SIGNAL STRENGTHS IN DIFFERENT CHANNELS

The H^0 signal strength in a particular final state xx is given by the cross section times branching ratio in this channel normalized to the Standard Model (SM) value, $\sigma \cdot$ B($H^0 \to xx$) / $(\sigma \cdot$ B($H^0 \to xx$))$_{SM}$, for the specified mass value of H^0. For the SM predictions, see DITTMAIER 11, DITTMAIER 12, and HEINEMEYER 13A. Results for fiducial and differential cross sections are also listed below.

Combined Final States

VALUE	DOCUMENT ID		TECN	COMMENT
1.10±0.11 OUR AVERAGE				
$1.09\pm0.07\pm0.04\pm0.03^{+0.07}_{-0.06}$	[1,2] AAD	16AN	LHC	pp, 7, 8 TeV
$1.44^{+0.59}_{-0.56}$	[3] AALTONEN	13M	TEVA	$p\overline{p} \to H^0X$, 1.96 TeV
• • • We do not use the following data for averages, fits, limits, etc. • • •				
$1.20\pm0.10\pm0.06\pm0.04^{+0.08}_{-0.07}$	[2] AAD	16AN	ATLS	pp, 7, 8 TeV
$0.97\pm0.09\pm0.05^{+0.04}_{-0.03}{}^{+0.07}_{-0.06}$	[2] AAD	16AN	CMS	pp, 7, 8 TeV
$1.18\pm0.10\pm0.07^{+0.08}_{-0.07}$	[4] AAD	16K	ATLS	pp, 7, 8 TeV
$0.75^{+0.28}_{-0.26}{}^{+0.13}_{-0.11}{}^{+0.08}_{-0.05}$	[4] AAD	16K	ATLS	pp, 7 TeV
$1.28\pm0.11^{+0.08}_{-0.07}{}^{+0.10}_{-0.08}$	[4] AAD	16K	ATLS	pp, 8 TeV
	[5] AAD	15P	ATLS	pp, 8 TeV, cross section
$1.00\pm0.09\pm0.07^{+0.08}_{-0.07}$	[6] KHACHATRY...15AM		CMS	pp, 7, 8 TeV
$1.33^{+0.14}_{-0.10}\pm0.15$	[7] AAD	13AK	ATLS	pp, 7 and 8 TeV
$1.54^{+0.77}_{-0.73}$	[8] AALTONEN	13L	CDF	$p\overline{p} \to H^0X$, 1.96 TeV
$1.40^{+0.92}_{-0.88}$	[9] ABAZOV	13L	D0	$p\overline{p} \to H^0X$, 1.96 TeV
$1.4\ \pm0.3$	[10] AAD	12AI	ATLS	$pp \to H^0X$, 7, 8 TeV
$1.2\ \pm0.4$	[10] AAD	12AI	ATLS	$pp \to H^0X$, 7 TeV
$1.5\ \pm0.4$	[10] AAD	12AI	ATLS	$pp \to H^0X$, 8 TeV
0.87 ± 0.23	[11] CHATRCHYAN	12N	CMS	$pp \to H^0X$, 7, 8 TeV

[1] AAD 16AN perform fits to the ATLAS and CMS data at E_{cm} = 7 and 8 TeV. The signal strengths for individual production processes are $1.03^{+0.16}_{-0.14}$ for gluon fusion, $1.18^{+0.25}_{-0.23}$ for vector boson fusion, $0.89^{+0.40}_{-0.38}$ for WH^0 production, $0.79^{+0.38}_{-0.36}$ for ZH^0 production, and $2.3^{+0.7}_{-0.6}$ for $t\overline{t}H^0$ production.

Gauge & Higgs Boson Particle Listings

H^0

[2] AAD 16AN: The uncertainties represent statistics, experimental systematics, theory systematics on the background, and theory systematics on the signal. The quoted signal strengths are given for $m_{H^0} = 125.09$ GeV. In the fit, relative branching ratios and relative production cross sections are fixed to those in the Standard Model.

[3] AALTONEN 13M combine all Tevatron data from the CDF and D0 Collaborations with up to 10.0 fb^{-1} and 9.7 fb^{-1}, respectively, of $p\overline{p}$ collisions at $E_{cm} = 1.96$ TeV. The quoted signal strength is given for $m_{H^0} = 125$ GeV.

[4] AAD 16K use up to 4.7 fb^{-1} of pp collisions at $E_{cm} = 7$ TeV and up to 20.3 fb^{-1} at $E_{cm} = 8$ TeV. The third uncertainty in the measurement is theory systematics. The signal strengths for individual production modes are $1.23 \pm 0.14^{+0.09}_{-0.08}{}^{+0.16}_{-0.12}$ for gluon fusion, $1.23^{+0.28}_{-0.27}{}^{+0.13}_{-0.12}{}^{+0.11}_{-0.09}$ for vector boson fusion, $0.80^{+0.31}_{-0.30} \pm 0.17^{+0.10}_{-0.05}$ for W/ZH^0 production, and $1.81^{+0.52}_{-0.50}{}^{+0.58}_{-0.55}{}^{+0.31}_{-0.12}$ for $t\overline{t}H^0$ production. The quoted signal strengths are given for $m_{H^0} = 125.36$ GeV.

[5] AAD 15P measure total and differential cross sections of the process $pp \to H^0X$ at $E_{cm} = 8$ TeV with 20.3 fb^{-1}. $\gamma\gamma$ and 4ℓ final states are used. $\sigma(pp \to H^0X) = 33.0 \pm 5.3 \pm 1.6$ pb is given. See their Figs. 2 and 3 for data on differential cross sections.

[6] KHACHATRYAN 15AM use up to 5.1 fb^{-1} of pp collisions at $E_{cm} = 7$ TeV and up to 19.7 fb^{-1} at $E_{cm} = 8$ TeV. The third uncertainty in the measurement is theory systematics. Fits to each production mode give the value of $0.85^{+0.19}_{-0.16}$ for gluon fusion, $1.16^{+0.37}_{-0.34}$ for vector boson fusion, $0.92^{+0.38}_{-0.36}$ for WH^0, ZH^0 production, and $2.90^{+1.08}_{-0.94}$ for $t\overline{t}H^0$ production.

[7] AAD 13AK use 4.7 fb^{-1} of pp collisions at $E_{cm} = 7$ TeV and 20.7 fb^{-1} at $E_{cm} = 8$ TeV. The combined signal strength is based on the $\gamma\gamma$, $ZZ^* \to 4\ell$, and $WW^* \to \ell\nu\ell\nu$ channels. The quoted signal strength is given for $m_{H^0} = 125.5$ GeV. Reported statistical error value modified following private communication with the experiment.

[8] AALTONEN 13L combine all CDF results with 9.45–10.0 fb^{-1} of $p\overline{p}$ collisions at $E_{cm} = 1.96$ TeV. The quoted signal strength is given for $m_{H^0} = 125$ GeV.

[9] ABAZOV 13L combine all D0 results with up to 9.7 fb^{-1} of $p\overline{p}$ collisions at $E_{cm} = 1.96$ TeV. The quoted signal strength is given for $m_{H^0} = 125$ GeV.

[10] AAD 12AI obtain results based on 4.6–4.8 fb^{-1} of pp collisions at $E_{cm} = 7$ TeV and 5.8–5.9 fb^{-1} at $E_{cm} = 8$ TeV. An excess of events over background with a local significance of 5.9 σ is observed at $m_{H^0} = 126$ GeV. The quoted signal strengths are given for $m_{H^0} = 126$ GeV. See also AAD 12DA.

[11] CHATRCHYAN 12N obtain results based on 4.9–5.1 fb^{-1} of pp collisions at $E_{cm} = 7$ TeV and 5.1–5.3 fb^{-1} at $E_{cm} = 8$ TeV. An excess of events over background with a local significance of 5.0 σ is observed at about $m_{H^0} = 125$ GeV. The combined signal strength is based on the $\gamma\gamma$, ZZ^*, WW^*, $\tau^+\tau^-$, and $b\overline{b}$ channels. The quoted signal strength is given for $m_{H^0} = 125.5$ GeV. See also CHATRCHYAN 13Y.

WW^* Final State

VALUE	DOCUMENT ID		TECN	COMMENT
$1.08^{+0.18}_{-0.16}$ OUR AVERAGE				
$1.09^{+0.18}_{-0.16}$	[1,2] AAD	16AN	LHC	pp, 7, 8 TeV
$0.94^{+0.85}_{-0.83}$	[3] AALTONEN	13M	TEVA	$p\overline{p} \to H^0X$, 1.96 TeV
• • • We do not use the following data for averages, fits, limits, etc. • • •				
$1.22^{+0.23}_{-0.21}$	[2] AAD	16AN	ATLS	pp, 7, 8 TeV
$0.90^{+0.23}_{-0.21}$	[2] AAD	16AN	CMS	pp, 7, 8 TeV
	[4] AAD	16AO	ATLS	pp, 8 TeV, cross sections
$1.18 \pm 0.16^{+0.17}_{-0.14}$	[5] AAD	16K	ATLS	pp, 7, 8 TeV
$1.09^{+0.16}_{-0.15}{}^{+0.17}_{-0.14}$	[6] AAD	15AA	ATLS	pp, 7, 8 TeV
$3.0\ ^{+1.3}_{-1.1}\ ^{+1.0}_{-0.7}$	[7] AAD	15AQ	ATLS	$pp \to H^0 W/ZX$, 7, 8 TeV
$1.16^{+0.16}_{-0.15}{}^{+0.18}_{-0.15}$	[8] AAD	15AQ	ATLS	pp, 7, 8 TeV
$0.72 \pm 0.12 \pm 0.10^{+0.12}_{-0.10}$	[9] CHATRCHYAN	14G	CMS	pp, 7, 8 TeV
$0.99^{+0.31}_{-0.28}$	[10] AAD	13AK	ATLS	pp, 7 and 8 TeV
$0.00^{+1.78}_{-0.00}$	[11] AALTONEN	13L	CDF	$p\overline{p} \to H^0X$, 1.96 TeV
$1.90^{+1.63}_{-1.52}$	[12] ABAZOV	13L	D0	$p\overline{p} \to H^0X$, 1.96 TeV
1.3 ± 0.5	[13] AAD	12AI	ATLS	$pp \to H^0X$, 7, 8 TeV
0.5 ± 0.6	[13] AAD	12AI	ATLS	$pp \to H^0X$, 7 TeV
1.9 ± 0.7	[13] AAD	12AI	ATLS	$pp \to H^0X$, 8 TeV
$0.60^{+0.42}_{-0.37}$	[14] CHATRCHYAN	12N	CMS	$pp \to H^0X$, 7, 8 TeV

[1] AAD 16AN perform fits to the ATLAS and CMS data at $E_{cm} = 7$ and 8 TeV. The signal strengths for individual production processes are 0.84 ± 0.17 for gluon fusion, 1.2 ± 0.4 for vector boson fusion, $1.6^{+1.2}_{-1.0}$ for WH^0 production, $5.9^{+2.6}_{-2.2}$ for ZH^0 production, and $5.0^{+1.8}_{-1.7}$ for $t\overline{t}H^0$ production.

[2] AAD 16AN: In the fit, relative production cross sections are fixed to those in the Standard Model. The quoted signal strength is given for $m_{H^0} = 125.09$ GeV.

[3] AALTONEN 13M combine all Tevatron data from the CDF and D0 Collaborations with up to 10.0 fb^{-1} and 9.7 fb^{-1}, respectively, of $p\overline{p}$ collisions at $E_{cm} = 1.96$ TeV. The quoted signal strength is given for $m_{H^0} = 125$ GeV.

[4] AAD 16AO measure fiducial total and differential cross sections of gluon fusion process at $E_{cm} = 8$ TeV with 20.3 fb^{-1} using $H^0 \to WW^* \to e\nu\mu\nu$. The measured fiducial total cross section is 36.0 ± 9.7 fb in their fiducial region (Table 7). See their Fig. 6 for fiducial differential cross sections. The results are given for $m_{H^0} = 125$ GeV.

[5] AAD 16K use up to 4.7 fb^{-1} of pp collisions at $E_{cm} = 7$ TeV and up to 20.3 fb^{-1} at $E_{cm} = 8$ TeV. The quoted signal strength is given for $m_{H^0} = 125.36$ GeV.

[6] AAD 15AA use 4.5 fb^{-1} of pp collisions at $E_{cm} = 7$ TeV and 20.3 fb^{-1} at $E_{cm} = 8$ TeV. The signal strength for the gluon fusion and vector boson fusion mode is $1.02 \pm 0.19^{+0.22}_{-0.18}$ and $1.27^{+0.44}_{-0.40}{}^{+0.30}_{-0.21}$, respectively. The quoted signal strengths are given for $m_{H^0} = 125.36$ GeV.

[7] AAD 15AQ use 4.5 fb^{-1} of pp collisions at $E_{cm} = 7$ TeV and 20.3 fb^{-1} at $E_{cm} = 8$ TeV. The quoted signal strength is given for $m_{H^0} = 125.36$ GeV.

[8] AAD 15AQ combine their result on W/ZH^0 production with the results of AAD 15AA (gluon fusion and vector boson fusion, slightly updated). The quoted signal strength is given for $m_{H^0} = 125.36$ GeV.

[9] CHATRCHYAN 14G use 4.9 fb^{-1} of pp collisions at $E_{cm} = 7$ TeV and 19.4 fb^{-1} at $E_{cm} = 8$ TeV. The last uncertainty in the measurement is theory systematics. The quoted signal strength is given for $m_{H^0} = 125.6$ GeV.

[10] AAD 13AK use 4.7 fb^{-1} of pp collisions at $E_{cm} = 7$ TeV and 20.7 fb^{-1} at $E_{cm} = 8$ TeV. The quoted signal strength is given for $m_{H^0} = 125.5$ GeV. Superseded by AAD 15AA.

[11] AALTONEN 13L combine all CDF results with 9.45–10.0 fb^{-1} of $p\overline{p}$ collisions at $E_{cm} = 1.96$ TeV. The quoted signal strength is given for $m_{H^0} = 125$ GeV.

[12] ABAZOV 13L combine all D0 results with up to 9.7 fb^{-1} of $p\overline{p}$ collisions at $E_{cm} = 1.96$ TeV. The quoted signal strength is given for $m_{H^0} = 125$ GeV.

[13] AAD 12AI obtain results based on 4.7 fb^{-1} of pp collisions at $E_{cm} = 7$ TeV and 5.8 fb^{-1} at $E_{cm} = 8$ TeV. The quoted signal strengths are given for $m_{H^0} = 126$ GeV. See also AAD 12DA.

[14] CHATRCHYAN 12N obtain results based on 4.9 fb^{-1} of pp collisions at $E_{cm} = 7$ TeV and 5.1 fb^{-1} at $E_{cm} = 8$ TeV. The quoted signal strength is given for $m_{H^0} = 125.5$ GeV. See also CHATRCHYAN 13Y.

ZZ^* Final State

VALUE	DOCUMENT ID		TECN	COMMENT
$1.14^{+0.15}_{-0.13}$ OUR AVERAGE				
$1.05^{+0.15}_{-0.14}{}^{+0.11}_{-0.09}$	[1] SIRUNYAN	17AV	CMS	pp, 13 TeV
$1.29^{+0.26}_{-0.23}$	[2,3] AAD	16AN	LHC	pp, 7, 8 TeV
• • • We do not use the following data for averages, fits, limits, etc. • • •				
$1.52^{+0.40}_{-0.34}$	[3] AAD	16AN	ATLS	pp, 7, 8 TeV
$1.04^{+0.32}_{-0.26}$	[3] AAD	16AN	CMS	pp, 7, 8 TeV
$1.46^{+0.35}_{-0.31}{}^{+0.19}_{-0.13}$	[4] AAD	16K	ATLS	pp, 7, 8 TeV
	[5] KHACHATRY...	16AR	CMS	pp, 7, 8 TeV cross sections
$1.44^{+0.34}_{-0.31}{}^{+0.21}_{-0.11}$	[6] AAD	15F	ATLS	$pp \to H^0X$, 7, 8 TeV
	[7] AAD	14AR	ATLS	pp, 8 TeV, differential cross section
$0.93^{+0.26}_{-0.23}{}^{+0.13}_{-0.09}$	[8] CHATRCHYAN	14AA	CMS	pp, 7, 8 TeV
$1.43^{+0.40}_{-0.35}$	[9] AAD	13AK	ATLS	pp, 7 and 8 TeV
$0.80^{+0.35}_{-0.28}$	[10] CHATRCHYAN	13J	CMS	$pp \to H^0X$, 7, 8 TeV
1.2 ± 0.6	[11] AAD	12AI	ATLS	$pp \to H^0X$, 7, 8 TeV
1.4 ± 1.1	[11] AAD	12AI	ATLS	$pp \to H^0X$, 7 TeV
1.1 ± 0.8	[11] AAD	12AI	ATLS	$pp \to H^0X$, 8 TeV
$0.73^{+0.45}_{-0.33}$	[12] CHATRCHYAN	12N	CMS	$pp \to H^0X$, 7, 8 TeV

[1] SIRUNYAN 17AV use 35.9 fb^{-1} of pp collisions at $E_{cm} = 13$ TeV. The quoted signal strength, obtained from the analysis of $H^0 \to ZZ^* \to 4\ell$ ($\ell = e,\ \mu$) decays, is given for $m_{H^0} = 125.09$ GeV. The signal strengths for different production modes are given in their Table 3. The fiducial and differential cross sections are shown in their Fig. 10.

[2] AAD 16AN perform fits to the ATLAS and CMS data at $E_{cm} = 7$ and 8 TeV. The signal strengths for individual production processes are $1.13^{+0.34}_{-0.31}$ for gluon fusion and $0.1^{+1.1}_{-0.6}$ for vector boson fusion.

[3] AAD 16AN: In the fit, relative production cross sections are fixed to those in the Standard Model. The quoted signal strength is given for $m_{H^0} = 125.09$ GeV.

[4] AAD 16K use up to 4.7 fb^{-1} of pp collisions at $E_{cm} = 7$ TeV and up to 20.3 fb^{-1} at $E_{cm} = 8$ TeV. The quoted signal strength is given for $m_{H^0} = 125.36$ GeV.

[5] KHACHATRYAN 16AR use data of 5.1 fb^{-1} at $E_{cm} = 7$ TeV and 19.7 fb^{-1} at 8 TeV. The fiducial cross sections for the production of 4 leptons via $H^0 \to 4\ell$ decays are measured to be $0.56^{+0.67}_{-0.44}{}^{+0.21}_{-0.06}$ fb at 7 TeV and $1.11^{+0.41}_{-0.35}{}^{+0.14}_{-0.10}$ fb at 8 TeV in their fiducial region (Table 2). The differential cross sections at $E_{cm} = 8$ TeV are also shown in Figs. 4 and 5. The results are given for $m_{H^0} = 125$ GeV.

[6] AAD 15F use 4.5 fb^{-1} of pp collisions at $E_{cm} = 7$ TeV and 20.3 fb^{-1} at $E_{cm} = 8$ TeV. The quoted signal strength is given for $m_{H^0} = 125.36$ GeV. The signal strength for the gluon fusion production mode is $1.66^{+0.45}_{-0.41}{}^{+0.25}_{-0.15}$, while the signal strength for the vector boson fusion production mode is $0.26^{+1.60}_{-0.91}{}^{+0.36}_{-0.23}$.

[7] AAD 14AR measure the cross section for $pp \to H^0X$, $H^0 \to ZZ^*$ using 20.3 fb^{-1} at $E_{cm} = 8$ TeV. They give $\sigma \cdot B = 2.11^{+0.53}_{-0.47} \pm 0.08$ fb in their fiducial region, where 1.30 ± 0.13 fb is expected in the Standard Model for $m_{H^0} = 125.4$ GeV. Various differential cross sections are also given, which are in agreement with the Standard Model expectations.

[8] CHATRCHYAN 14AA use 5.1 fb^{-1} of pp collisions at $E_{cm} = 7$ TeV and 19.7 fb^{-1} at $E_{cm} = 8$ TeV. The quoted signal strength is given for $m_{H^0} = 125.6$ GeV. The signal

strength for the gluon fusion and $t\bar{t}H$ production mode is $0.80^{+0.46}_{-0.36}$, while the signal strength for the vector boson fusion and WH^0, ZH^0 production mode is $1.7^{+2.2}_{-2.1}$.

[9] AAD 13AK use 4.7 fb^{-1} of pp collisions at E_{cm} = 7 TeV and 20.7 fb^{-1} at E_{cm} = 8 TeV. The quoted signal strength is given for m_{H^0} = 125.5 GeV.

[10] CHATRCHYAN 13J obtain results based on $ZZ \to 4\ell$ final states in 5.1 fb^{-1} of pp collisions at E_{cm} = 7 TeV and 12.2 fb^{-1} at E_{cm} = 8 TeV. The quoted signal strength is given for m_{H^0} = 125.8 GeV. Superseded by CHATRCHYAN 14AA.

[11] AAD 12AI obtain results based on 4.7–4.8 fb^{-1} of pp collisions at E_{cm} = 7 TeV and 5.8 fb^{-1} at E_{cm} = 8 TeV. The quoted signal strengths are given for m_{H^0} = 126 GeV. See also AAD 12DA.

[12] CHATRCHYAN 12N obtain results based on 4.9–5.1 fb^{-1} of pp collisions at E_{cm} = 7 TeV and 5.1–5.3 fb^{-1} at E_{cm} = 8 TeV. An excess of events over background with a local significance of 5.0 σ is observed at about m_{H^0} = 125 GeV. The quoted signal strengths are given for m_{H^0} = 125.5 GeV. See also CHATRCHYAN 12BY and CHATRCHYAN 13Y.

$\gamma\gamma$ Final State

VALUE	DOCUMENT ID		TECN	COMMENT
1.16±0.18 OUR AVERAGE				
$1.14^{+0.19}_{-0.18}$	[1,2] AAD	16AN	LHC	pp, 7, 8 TeV
$5.97^{+3.39}_{-3.12}$	[3] AALTONEN	13M	TEVA	$p\bar{p} \to H^0X$, 1.96 TeV
• • • We do not use the following data for averages, fits, limits, etc. • • •				
$1.14^{+0.27}_{-0.25}$	[2] AAD	16AN	ATLS	pp, 7, 8 TeV
$1.11^{+0.25}_{-0.23}$	[2] AAD	16AN	CMS	pp, 7, 8 TeV
	[4] KHACHATRY...	16B	CMS	$H^0 \to \gamma^*\gamma \to \ell^+\ell^-\gamma$
	[5] KHACHATRY...	16G	CMS	differential cross section
$1.17\pm0.23^{+0.10+0.12}_{-0.08-0.08}$	[6] AAD	14BC	ATLS	$pp \to H^0X$, 7, 8 TeV
	[7] AAD	14BJ	ATLS	pp, 8 TeV, differential cross section
$1.14\pm0.21^{+0.09+0.13}_{-0.05-0.09}$	[8] KHACHATRY...	14P	CMS	pp, 7, 8 TeV
$1.55^{+0.33}_{-0.28}$	[9] AAD	13AK	ATLS	pp, 7 and 8 TeV
$7.81^{+4.61}_{-4.42}$	[10] AALTONEN	13L	CDF	$p\bar{p} \to H^0X$, 1.96 TeV
$4.20^{+4.60}_{-4.20}$	[11] ABAZOV	13L	D0	$p\bar{p} \to H^0X$, 1.96 TeV
1.8 ±0.5	[12] AAD	12AI	ATLS	$pp \to H^0X$, 7, 8 TeV
2.2 ±0.7	[12] AAD	12AI	ATLS	$pp \to H^0X$, 7 TeV
1.5 ±0.6	[12] AAD	12AI	ATLS	$pp \to H^0X$, 8 TeV
$1.54^{+0.46}_{-0.42}$	[13] CHATRCHYAN	12N	CMS	$pp \to H^0X$, 7, 8 TeV

[1] AAD 16AN perform fits to the ATLAS and CMS data at E_{cm} = 7 and 8 TeV. The signal strengths for individual production processes are $1.10^{+0.23}_{-0.22}$ for gluon fusion, 1.3 ± 0.5 for vector boson fusion, $0.5^{+1.3}_{-1.2}$ for WH^0 production, $0.5^{+3.0}_{-2.5}$ for ZH^0 production, and $2.2^{+1.6}_{-1.3}$ for $t\bar{t}H^0$ production.

[2] AAD 16AN: In the fit, relative production cross sections are fixed to those in the Standard Model. The quoted signal strength is given for m_{H^0} = 125.09 GeV.

[3] AALTONEN 13M combine all Tevatron data from the CDF and D0 Collaborations with up to 10.0 fb^{-1} and 9.7 fb^{-1}, respectively, of $p\bar{p}$ collisions at E_{cm} = 1.96 TeV. The quoted signal strength is given for m_{H^0} = 125 GeV.

[4] KHACHATRYAN 16B search for $H^0 \to \gamma^*\gamma \to e^+e^-\gamma$ and $\mu^+\mu^-\gamma$ (with m($\ell^+\ell^-$) < 20 GeV) in 19.7 fb^{-1} of pp collisions at E_{cm} = 8 TeV. An upper limit of 6.7 times the Standard Model expectation is obtained at 95% CL. See their Fig. 6 for limits on individual channels.

[5] KHACHATRYAN 16G measure fiducial and differential cross sections of the process $pp \to H^0X$, $H^0 \to \gamma\gamma$ at E_{cm} = 8 TeV with 19.7 fb^{-1}. See their Figs. 4–6 and Table 1 for data.

[6] AAD 14BC use 4.5 fb^{-1} of pp collisions at E_{cm} = 7 TeV and 20.3 fb^{-1} at E_{cm} = 8 TeV. The last uncertainty in the measurement is theory systematics. The quoted signal strength is given for m_{H^0} = 125.4 GeV. The signal strengths for the individual production modes are: 1.32 ± 0.38 for gluon fusion, 0.8 ± 0.7 for vector boson fusion, 1.0 ± 1.6 for WH^0 production, $0.1^{+3.7}_{-0.1}$ for ZH^0 production, and $1.6^{+2.7}_{-1.8}$ for $t\bar{t}H^0$ production.

[7] AAD 14BJ measure fiducial and differential cross sections of the process $pp \to H^0X$, $H^0 \to \gamma\gamma$ at E_{cm} = 8 TeV with 20.3 fb^{-1}. See their Table 3 and Figs. 3–12 for data.

[8] KHACHATRYAN 14P use 5.1 fb^{-1} of pp collisions at E_{cm} = 7 TeV and 19.7 fb^{-1} at E_{cm} = 8 TeV. The last uncertainty in the measurement is theory systematics. The quoted signal strength is given for m_{H^0} = 124.7 GeV. The signal strength for the gluon fusion and $t\bar{t}H$ production mode is $1.13^{+0.37}_{-0.31}$, while the signal strength for the vector boson fusion and WH^0, ZH^0 production mode is $1.16^{+0.63}_{-0.58}$.

[9] AAD 13AK use 4.7 fb^{-1} of pp collisions at E_{cm} = 7 TeV and 20.7 fb^{-1} at E_{cm} = 8 TeV. The quoted signal strength is given for m_{H^0} = 125.5 GeV.

[10] AALTONEN 13L combine all CDF results with 9.45–10.0 fb^{-1} of $p\bar{p}$ collisions at E_{cm} = 1.96 TeV. The quoted signal strength is given for m_{H^0} = 125 GeV.

[11] ABAZOV 13L combine all D0 results with up to 9.7 fb^{-1} of $p\bar{p}$ collisions at E_{cm} = 1.96 TeV. The quoted signal strength is given for m_{H^0} = 125 GeV.

[12] AAD 12AI obtain results based on 4.8 fb^{-1} of pp collisions at E_{cm} = 7 TeV and 5.9 fb^{-1} at E_{cm} = 8 TeV. The quoted signal strengths are given for m_{H^0} = 126 GeV. See also AAD 12DA.

[13] CHATRCHYAN 12N obtain results based on 5.1 fb^{-1} of pp collisions at E_{cm}=7 TeV and 5.3 fb^{-1} at E_{cm}=8 TeV. The quoted signal strength is given for m_{H^0}=125.5 GeV. See also CHATRCHYAN 13Y.

$b\bar{b}$ Final State

VALUE	DOCUMENT ID		TECN	COMMENT
0.95±0.22 OUR AVERAGE				
$1.20^{+0.24+0.34}_{-0.23-0.28}$	[1] AABOUD	17BA	ATLS	$pp \to H^0W/ZX$, $H^0 \to b\bar{b}$, 13 TeV
$0.70^{+0.29}_{-0.27}$	[2,3] AAD	16AN	LHC	pp, 7, 8 TeV
$1.59^{+0.69}_{-0.72}$	[4] AALTONEN	13M	TEVA	$p\bar{p} \to H^0X$, 1.96 TeV
• • • We do not use the following data for averages, fits, limits, etc. • • •				
$2.3\ ^{+1.8}_{-1.6}$	[5] SIRUNYAN	18E	CMS	$pp \to H^0X$, boosted, 13 TeV
$0.90\pm0.18^{+0.21}_{-0.19}$	[6] AABOUD	17BA	ATLS	$pp \to H^0W/ZX$, $H^0 \to b\bar{b}$, 7, 8, 13 TeV
$-0.8\ \pm1.3\ ^{+1.8}_{-1.9}$	[7] AABOUD	16X	ATLS	$pp \to H^0X$, VBF, 8 TeV
0.62±0.37	[3] AAD	16AN	ATLS	pp, 7, 8 TeV
$0.81^{+0.45}_{-0.43}$	[3] AAD	16AN	CMS	pp, 7, 8 TeV
$0.63^{+0.31+0.24}_{-0.30-0.23}$	[8] AAD	16K	ATLS	pp, 7, 8 TeV
0.52±0.32±0.24	[9] AAD	15G	ATLS	$pp \to H^0W/ZX$, 7, 8 TeV
$2.8\ ^{+1.6}_{-1.4}$	[10] KHACHATRY...	15Z	CMS	$pp \to H^0X$, VBF, 8 TeV
$1.03^{+0.44}_{-0.42}$	[11] KHACHATRY...	15Z	CMS	pp, 8 TeV, combined
1.0 ±0.5	[12] CHATRCHYAN	14AI	CMS	$pp \to H^0W/ZX$, 7, 8 TeV
$1.72^{+0.92}_{-0.87}$	[13] AALTONEN	13L	CDF	$p\bar{p} \to H^0X$, 1.96 TeV
$1.23^{+1.24}_{-1.17}$	[14] ABAZOV	13L	D0	$p\bar{p} \to H^0X$, 1.96 TeV
0.5 ±2.2	[15] AAD	12AI	ATLS	$pp \to H^0W/ZX$, 7 TeV
	[16] AALTONEN	12T	TEVA	$p\bar{p} \to H^0W/ZX$, 1.96 TeV
$0.48^{+0.81}_{-0.70}$	[17] CHATRCHYAN	12N	CMS	$pp \to H^0W/ZX$, 7, 8 TeV

[1] AABOUD 17BA use 36.1 fb^{-1} at E_{cm} = 13 TeV. The quoted signal strength is given for m_{H^0} = 125 GeV. They give σ(W H)·$B(H^0 \to b\bar{b})$ = $1.08^{+0.54}_{-0.47}$ pb and σ(Z H)·$B(H^0 \to b\bar{b})$ = $0.57^{+0.26}_{-0.23}$ pb.

[2] AAD 16AN perform fits to the ATLAS and CMS data at E_{cm} = 7 and 8 TeV. The signal strengths for individual production processes are 1.0 ± 0.5 for WH^0 production, 0.4 ± 0.4 for ZH^0 production, and 1.1 ± 1.0 for $t\bar{t}H^0$ production.

[3] AAD 16AN: In the fit, relative production cross sections are fixed to those in the Standard Model. The quoted signal strength is given for m_{H^0} = 125.09 GeV.

[4] AALTONEN 13M combine all Tevatron data from the CDF and D0 Collaborations with up to 10.0 fb^{-1} and 9.7 fb^{-1}, respectively, of $p\bar{p}$ collisions at E_{cm} = 1.96 TeV. The quoted signal strength is given for m_{H^0} = 125 GeV.

[5] SIRUNYAN 18E use 35.9 fb^{-1} at E_{cm} = 13 TeV. The quoted signal strength is given for m_{H^0} = 125 GeV. They measure $\sigma \cdot B$ for gluon fusion production of $H^0 \to b\bar{b}$ with p_T >450 GeV, $|\eta|$ <2.5 to be 74 ± 48^{+17}_{-10} fb.

[6] AABOUD 17BA combine 7, 8 and 13 TeV analyses. The quoted signal strength is given for m_{H^0} = 125 GeV.

[7] AABOUD 16X search for vector-boson fusion production of H^0 decaying to $b\bar{b}$ in 20.2 fb^{-1} of pp collisions at E_{cm} = 8 TeV. The quoted signal strength is given for m_{H^0} = 125 GeV.

[8] AAD 16K use up to 4.7 fb^{-1} of pp collisions at E_{cm} = 7 TeV and up to 20.3 fb^{-1} at E_{cm} = 8 TeV. The quoted signal strength is given for m_{H^0} = 125.36 GeV.

[9] AAD 15G use 4.7 fb^{-1} of pp collisions at E_{cm} = 7 TeV and 20.3 fb^{-1} at E_{cm} = 8 TeV. The quoted signal strength is given for m_{H^0} = 125.36 GeV.

[10] KHACHATRYAN 15Z search for vector-boson fusion production of H^0 decaying to $b\bar{b}$ in up to 19.8 fb^{-1} of pp collisions at E_{cm} = 8 TeV. The quoted signal strength is given for m_{H^0} = 125 GeV.

[11] KHACHATRYAN 15Z combined vector boson fusion, WH^0, ZH^0 production, and $t\bar{t}H^0$ production results. The quoted signal strength is given for m_{H^0} = 125 GeV.

[12] CHATRCHYAN 14AI use up to 5.1 fb^{-1} of pp collisions at E_{cm} = 7 TeV and up to 18.9 fb^{-1} at E_{cm} = 8 TeV. The quoted signal strength is given for m_{H^0} = 125 GeV. See also CHATRCHYAN 14AJ.

[13] AALTONEN 13L combine all CDF results with 9.45–10.0 fb^{-1} of $p\bar{p}$ collisions at E_{cm} = 1.96 TeV. The quoted signal strength is given for m_{H^0} = 125 GeV.

[14] ABAZOV 13L combine all D0 results with up to 9.7 fb^{-1} of $p\bar{p}$ collisions at E_{cm} = 1.96 TeV. The quoted signal strength is given for m_{H^0} = 125 GeV.

[15] AAD 12AI obtain results based on 4.6–4.8 fb^{-1} of pp collisions at E_{cm} = 7 TeV. The quoted signal strengths are given in their Fig. 10 for m_{H^0} = 126 GeV. See also Fig. 13 of AAD 12DA.

[16] AALTONEN 12T combine AALTONEN 12Q, AALTONEN 12R, AALTONEN 12S, ABAZOV 12O, ABAZOV 12P, and ABAZOV 12K. An excess of events over background is observed which is most significant in the region m_{H^0} = 120–135 GeV, with a local significance of up to 3.3 σ. The local significance at m_{H^0} = 125 GeV is 2.8 σ, which corresponds to $(\sigma(H^0W) + \sigma(H^0Z)) \cdot B(H^0 \to b\bar{b}) = (0.23^{+0.09}_{-0.08})$ pb, compared to the Standard Model expectation at m_{H^0} = 125 GeV of 0.12 ± 0.01 pb. Superseded by AALTONEN 13M.

[17] CHATRCHYAN 12N obtain results based on 5.0 fb^{-1} of pp collisions at E_{cm}=7 TeV and 5.1 fb^{-1} at E_{cm}=8 TeV. The quoted signal strength is given for m_{H^0}=125.5 GeV. See also CHATRCHYAN 13Y.

$\mu^+\mu^-$ Final State

VALUE	CL%	DOCUMENT ID		TECN	COMMENT
0.0±1.3 OUR AVERAGE					
−0.1±1.4		[1] AABOUD	17Y	ATLS	pp, 7, 8, 13 TeV

Gauge & Higgs Boson Particle Listings

H^0

$0.9^{+3.6}_{-3.5}$		[2] AAD	16AN	CMS	pp, 7, 8 TeV

• • • We do not use the following data for averages, fits, limits, etc. • • •

-0.1 ± 1.5		[1] AABOUD	17Y	ATLS	pp, 13 TeV
0.1 ± 2.5		[2] AAD	16AN	LHC	pp, 7, 8 TeV
-0.6 ± 3.6		[2] AAD	16AN	ATLS	pp, 7, 8 TeV
$<$ 7.4	95	[3] KHACHATRY...	15H	CMS	$pp \to H^0X$, 7, 8 TeV
$<$ 7.0	95	[4] AAD	14AS	ATLS	$pp \to H^0X$, 7, 8 TeV

[1] AABOUD 17Y use 36.1 fb^{-1} of pp collisions at E_{cm} = 13 TeV, 20.3 fb^{-1} at 8 TeV and 4.5 fb^{-1} at 7 TeV. The quoted signal strength is given for m_{H^0} = 125 GeV.

[2] AAD 16AN: In the fit, relative production cross sections are fixed to those in the Standard Model. The quoted signal strength is given for m_{H^0} = 125.09 GeV.

[3] KHACHATRYAN 15H use 5.0 fb^{-1} of pp collisions at E_{cm} = 7 TeV and 19.7 fb^{-1} at 8 TeV. The quoted signal strength is given for m_{H^0} = 125 GeV.

[4] AAD 14AS search for $H^0 \to \mu^+\mu^-$ in 4.5 fb^{-1} of pp collisions at E_{cm} = 7 TeV and 20.3 fb^{-1} at E_{cm} = 8 TeV. The quoted signal strength is given for m_{H^0} = 125.5 GeV.

$\tau^+\tau^-$ Final State

VALUE		DOCUMENT ID		TECN	COMMENT
1.12±0.23 OUR AVERAGE					
$1.11^{+0.24}_{-0.22}$	[1,2]	AAD	16AN	LHC	pp, 7, 8 TeV
$1.68^{+2.28}_{-1.68}$	[3]	AALTONEN	13M	TEVA	$p\overline{p} \to H^0X$, 1.96 TeV

• • • We do not use the following data for averages, fits, limits, etc. • • •

2.3 ±1.6	[4]	AAD	16AC	ATLS	$pp \to H^0 W/ZX$, 8 TeV
$1.41^{+0.40}_{-0.36}$	[2]	AAD	16AN	ATLS	pp, 7, 8 TeV
$0.88^{+0.30}_{-0.28}$	[2]	AAD	16AN	CMS	pp, 7, 8 TeV
$1.44^{+0.30}_{-0.29}{}^{+0.29}_{-0.23}$	[5]	AAD	16K	ATLS	pp, 7, 8 TeV
$1.43^{+0.27}_{-0.26}{}^{+0.32}_{-0.25}\pm0.09$	[6]	AAD	15AH	ATLS	$pp \to H^0X$, 7, 8 TeV
0.78 ± 0.27	[7]	CHATRCHYAN	14K	CMS	$pp \to H^0X$, 7, 8 TeV
$0.00^{+8.44}_{-0.00}$	[8]	AALTONEN	13L	CDF	$p\overline{p} \to H^0X$, 1.96 TeV
$3.96^{+4.11}_{-3.38}$	[9]	ABAZOV	13L	D0	$p\overline{p} \to H^0X$, 1.96 TeV
$0.4^{+1.6}_{-2.0}$	[10]	AAD	12AI	ATLS	$pp \to H^0X$, 7 TeV
$0.09^{+0.76}_{-0.74}$	[11]	CHATRCHYAN	12N	CMS	$pp \to H^0X$, 7, 8 TeV

[1] AAD 16AN perform fits to the ATLAS and CMS data at E_{cm} = 7 and 8 TeV. The signal strengths for individual production processes are 1.0 ± 0.6 for gluon fusion, 1.3 ± 0.4 for vector boson fusion, -1.4 ± 1.4 for WH^0 production, $2.2^{+2.2}_{-1.8}$ for ZH^0 production, and $-1.9^{+3.7}_{-3.3}$ for $t\overline{t}H^0$ production.

[2] AAD 16AN: In the fit, relative production cross sections are fixed to those in the Standard Model. The quoted signal strength is given for m_{H^0} = 125.09 GeV.

[3] AALTONEN 13M combine all Tevatron data from the CDF and D0 Collaborations with up to 10.0 fb^{-1} and 9.7 fb^{-1}, respectively, of $p\overline{p}$ collisions at E_{cm} = 1.96 TeV. The quoted signal strength is given for m_{H^0} = 125 GeV.

[4] AAD 16AC measure the signal strength with $pp \to H^0 W/ZX$ processes using 20.3 fb^{-1} of E_{cm} = 8 TeV. The quoted signal strength is given for m_{H^0} = 125 GeV.

[5] AAD 16K use up to 4.7 fb^{-1} of pp collisions at E_{cm} = 7 TeV and up to 20.3 fb^{-1} at E_{cm} = 8 TeV. The quoted signal strength is given for m_{H^0} = 125.36 GeV.

[6] AAD 15AH use 4.5 fb^{-1} of pp collisions at E_{cm} = 7 TeV and 20.3 fb^{-1} at E_{cm} = 8 TeV. The third uncertainty in the measurement is theory systematics. The signal strength for the gluon fusion mode is $2.0 \pm 0.8^{+1.2}_{-0.8} \pm 0.3$ and that for vector boson fusion and W/ZH^0 production modes is $1.24^{+0.49}_{-0.45}{}^{+0.31}_{-0.29} \pm 0.08$. The quoted signal strength is given for m_{H^0} = 125.36 GeV.

[7] CHATRCHYAN 14K use 4.9 fb^{-1} of pp collisions at E_{cm} = 7 TeV and 19.7 fb^{-1} at E_{cm} = 8 TeV. The quoted signal strength is given for m_{H^0} = 125 GeV. See also CHATRCHYAN 14AJ.

[8] AALTONEN 13L combine all CDF results with 9.45–10.0 fb^{-1} of $p\overline{p}$ collisions at E_{cm} = 1.96 TeV. The quoted signal strength is given for m_{H^0} = 125 GeV.

[9] ABAZOV 13L combine all D0 results with up to 9.7 fb^{-1} of $p\overline{p}$ collisions at E_{cm} = 1.96 TeV. The quoted signal strength is given for m_{H^0} = 125 GeV.

[10] AAD 12AI obtain results based on 4.7 fb^{-1} of pp collisions at E_{cm} = 7 TeV. The quoted signal strengths are given in their Fig. 10 for m_{H^0} = 126 GeV. See also Fig. 13 of AAD 12DA.

[11] CHATRCHYAN 12N obtain results based on 4.9 fb^{-1} of pp collisions at E_{cm}=7 TeV and 5.1 fb^{-1} at E_{cm}=8 TeV. The quoted signal strength is given for m_{H^0}=125.5 GeV. See also CHATRCHYAN 13Y .

$Z\gamma$ Final State

VALUE	CL%	DOCUMENT ID		TECN	COMMENT
< 6.6	95	[1] AABOUD	17AW	ATLS	$pp \to H^0X$, 13 TeV
<11	95	[2] AAD	14J	ATLS	$pp \to H^0X$, 7, 8 TeV
< 9.5	95	[3] CHATRCHYAN	13BK	CMS	$pp \to H^0X$, 7, 8 TeV

[1] AABOUD 17AW search for $H^0 \to Z\gamma$, $Z \to ee$, $\mu\mu$ in 36.1 fb^{-1} of pp collisions at E_{cm} = 13 TeV. The quoted signal strength is given for m_{H^0} = 125.09 GeV. The upper limit on the branching ratio of $H^0 \to Z\gamma$ is 1.0% at 95% CL assuming the SM Higgs boson production.

[2] AAD 14J search for $H^0 \to Z\gamma \to \ell\ell\gamma$ in 4.5 fb^{-1} of pp collisions at E_{cm} = 7 TeV and 20.3 fb^{-1} at E_{cm} = 8 TeV. The quoted signal strength is given for m_{H^0} = 125.5 GeV.

[3] CHATRCHYAN 13BK search for $H^0 \to Z\gamma \to \ell\ell\gamma$ in 5.0 fb^{-1} of pp collisions at E_{cm} = 7 TeV and 19.6 fb^{-1} at E_{cm} = 8 TeV. A limit on cross section times branching ratio which corresponds to (4–25) times the expected Standard Model cross section is given in the range m_{H^0} = 120–160 GeV at 95% CL. The quoted limit is given for m_{H^0} = 125 GeV, where 10 is expected for no signal.

$t\overline{t}H^0$ Production

Signal strengh relative to the Standard Model cross section.

VALUE	CL%	DOCUMENT ID		TECN	COMMENT
2.3 $^{+0.7}_{-0.6}$	[1,2]	AAD	16AN	LHC	pp, 7, 8 TeV

• • • We do not use the following data for averages, fits, limits, etc. • • •

1.7 ±0.8	[3]	AAD	16AL	ATLS	$pp \to H^0 t\overline{t}X$, 7, 8 TeV
$1.9^{+0.8}_{-0.7}$	[2]	AAD	16AN	ATLS	pp, 7, 8 TeV
$2.9^{+1.0}_{-0.9}$	[2]	AAD	16AN	CMS	pp, 7, 8 TeV
$1.81^{+0.52}_{-0.50}{}^{+0.58}_{-0.55}{}^{+0.31}_{-0.12}$	[4]	AAD	16K	ATLS	pp, 7, 8 TeV
$1.4^{+2.1}_{-1.4}{}^{+0.6}_{-0.3}$	[5]	AAD	15	ATLS	pp, 7, 8 TeV
1.5 ±1.1	[6]	AAD	15BC	ATLS	pp, 8 TeV
$2.1^{+1.4}_{-1.2}$	[7]	AAD	15T	ATLS	pp, 8 TeV
$1.2^{+1.6}_{-1.5}$	[8]	KHACHATRY...	15AN	CMS	pp, 8 TeV
$2.8^{+1.0}_{-0.9}$	[9]	KHACHATRY...	14H	CMS	pp, 7, 8 TeV
$9.49^{+6.60}_{-6.28}$	[10]	AALTONEN	13L	CDF	$p\overline{p}$, 1.96 TeV
<5.8	95	[11] CHATRCHYAN	13X	CMS	$pp \to H^0 t\overline{t}X$

[1] AAD 16AN perform fits to the ATLAS and CMS data at E_{cm} = 7 and 8 TeV.

[2] AAD 16AN: In the fit, relative branching ratios are fixed to those in the Standard Model. The quoted signal strength is given for m_{H^0} = 125.09 GeV.

[3] AAD 16AL search for $t\overline{t}H^0$ production with H^0 decaying to $\gamma\gamma$ in 4.5 fb^{-1} of pp collisions at E_{cm} = 7 TeV and $b\overline{b}$, $\tau\tau$, $\gamma\gamma$, WW^*, and ZZ^* in 20.3 fb^{-1} at E_{cm} = 8 TeV. The quoted signal strength is given for m_{H^0} = 125 GeV. This paper combines the results of previous papers, and the new result of this paper only is: $\mu = 1.6 \pm 2.6$.

[4] AAD 16K use up to 4.7 fb^{-1} of pp collisions at E_{cm} = 7 TeV and up to 20.3 fb^{-1} at E_{cm} = 8 TeV. The third uncertainty in the measurement is theory systematics. The quoted signal strength is given for m_{H^0} = 125.36 GeV.

[5] AAD 15 search for $t\overline{t}H^0$ production with H^0 decaying to $\gamma\gamma$ in 4.5 fb^{-1} of pp collisions at E_{cm} = 7 TeV and 20.3 fb^{-1} at E_{cm} = 8 TeV. The quoted result on the signal strength is equivalent to an upper limit of 6.7 at 95% CL and is given for m_{H^0} = 125.4 GeV.

[6] AAD 15BC search for $t\overline{t}H^0$ production with H^0 decaying to $b\overline{b}$ in 20.3 fb^{-1} of pp collisions at E_{cm} = 8 TeV. The corresponding upper limit is 3.4 at 95% CL. The quoted signal strength is given for m_{H^0} = 125 GeV.

[7] AAD 15T search for $t\overline{t}H^0$ production with H^0 resulting in multilepton final states (mainly from WW^*, $\tau\tau$, ZZ^*) in 20.3 fb^{-1} of pp collisions at E_{cm} = 8 TeV. The quoted result on the signal strength is given for m_{H^0} = 125 GeV and corresponds to an upper limit of 4.7 at 95% CL. The data sample is independent from AAD 15 and AAD 15BC.

[8] KHACHATRYAN 15AN search for $t\overline{t}H^0$ production with H^0 decaying to $b\overline{b}$ in 19.5 fb^{-1} of pp collisions at E_{cm} = 8 TeV. The quoted result on the signal strength is equivalent to an upper limit of 4.2 at 95% CL and is given for m_{H^0} = 125 GeV.

[9] KHACHATRYAN 14H search for $t\overline{t}H^0$ production with H^0 decaying to $b\overline{b}$, $\tau\tau$, $\gamma\gamma$, WW^*, and ZZ^*, in 5.1 fb^{-1} of pp collisions at E_{cm} = 7 TeV and 19.7 fb^{-1} at E_{cm} = 8 TeV. The quoted signal strength is given for m_{H^0} = 125.6 GeV.

[10] AALTONEN 13L combine all CDF results with 9.45–10.0 fb^{-1} of $p\overline{p}$ collisions at E_{cm} = 1.96 TeV. The quoted signal strength is given for m_{H^0} = 125 GeV.

[11] CHATRCHYAN 13X search for $t\overline{t}H^0$ production followed by $H^0 \to b\overline{b}$, one top decaying to $\ell\nu$ and the other to either $\ell\nu$ or $q\overline{q}$ in 5.0 fb^{-1} and 5.1 fb^{-1} of pp collisions at E_{cm} = 7 and 8 TeV. A limit on cross section times branching ratio which corresponds to (4.0–8.6) times the expected Standard Model cross section is given for m_{H^0} = 110–140 GeV at 95% CL. The quoted limit is given for m_{H^0} = 125 GeV, where 5.2 is expected for no signal.

H^0H^0 Production

The limits are for the scaling factor relative to the SM prediction.

VALUE	CL%	DOCUMENT ID		TECN	COMMENT
• • • We do not use the following data for averages, fits, limits, etc. • • •					
< 30	95	[1] SIRUNYAN	18A	CMS	$pp \to H^0H^0$, 13 TeV, $b\overline{b}\tau\tau$
< 43	95	[2] SIRUNYAN	17CN	CMS	$pp \to H^0H^0$, 8 TeV, $b\overline{b}\tau\tau$, $\gamma\gamma b\overline{b}$, $b\overline{b}b\overline{b}$
<108	95	[3] AABOUD	16I	ATLS	$pp \to H^0H^0$, 13 TeV, $b\overline{b}b\overline{b}$
< 74	95	[4] KHACHATRY...	16BQ	CMS	$pp \to H^0H^0$, 8 TeV, $\gamma\gamma b\overline{b}$
< 70	95	[5] AAD	15CE	ATLS	$pp \to H^0H^0$, 8 TeV, $b\overline{b}b\overline{b}$, $b\overline{b}\tau\tau$, $\gamma\gamma b\overline{b}$, $\gamma\gamma WW$

[1] SIRUNYAN 18A search for H^0H^0 production using $H^0H^0 \to b\overline{b}\tau\tau$ with data of 35.9 fb^{-1} at E_{cm} = 13 TeV. The upper limit on the $gg \to H^0H^0 \to b\overline{b}\tau\tau$ production cross section is measured to be 75.4 fb, which corresponds to about 30 times the SM prediction. Limits on Higgs-boson trilinear coupling λ_{HHH} and top Yukawa coupling y_t are also given (see their Fig. 6).

[2] SIRUNYAN 17CN search for H^0H^0 production using $H^0H^0 \to b\overline{b}\tau\tau$ with data of 18.3 fb^{-1} at E_{cm} = 8 TeV. Results are then combined with the published results of the $H^0H^0 \to \gamma\gamma b\overline{b}$ and $H^0H^0 \to b\overline{b}b\overline{b}$, which use data of up to 19.7 fb^{-1} at E_{cm} = 8 TeV. The upper limit on the $gg \to H^0H^0$ production cross section is measured to be 0.59 pb from $b\overline{b}\tau\tau$, which corresponds to about 59 times the SM prediction (gluon fusion). The combined upper limit is 0.43 pb, which is about 43 times the SM prediction. The quoted values are given for m_{H^0} = 125 GeV.

[3] AABOUD 16I search for H^0H^0 production using $H^0H^0 \to b\overline{b}b\overline{b}$ with data of 3.2 fb^{-1} at E_{cm} = 13 TeV. The upper limit on the $pp \to H^0H^0 \to b\overline{b}b\overline{b}$ production cross section is measured to be 1.22 pb. This result corresponds to about 108 times the SM prediction (gluon fusion), which is $11.3^{+0.9}_{-1.0}$ fb (NNLO+NNLL) including top quark mass effects. The quoted values are given for m_{H^0} = 125 GeV .

[4] KHACHATRYAN 16BQ search for H^0H^0 production using $H^0H^0 \to \gamma\gamma b\overline{b}$ with data of 19.7 fb^{-1} at E_{cm} = 8 TeV. The upper limit on the $gg \to H^0H^0 \to \gamma\gamma b\overline{b}$ production is measured to be 1.85 fb, which corresponds to 0.71 pb for $gg \to H^0H^0$ production cross section. The upper limit of 74 is for the scaling factor relative to the SM prediction. Limits on Higgs-boson trilinear coupling λ are also given.

[5] AAD 15CE search for H^0H^0 production using $H^0H^0 \to b\overline{b}\tau\tau$ and $H^0H^0 \to \gamma\gamma WW$ with data of 20.3 fb^{-1} at E_{cm} = 8 TeV. These results are then combined with the published results of the $H^0H^0 \to \gamma\gamma b\overline{b}$ and $H^0H^0 \to b\overline{b}b\overline{b}$, which use data of up to 20.3 fb^{-1} at E_{cm} = 8 TeV. The upper limits on the $gg \to H^0H^0$ production cross section are measured to be 1.6 pb, 11.4 pb, 2.2 pb and 0.62 pb from $b\overline{b}\tau\tau$, $\gamma\gamma WW$, $\gamma\gamma b\overline{b}$ and $b\overline{b}b\overline{b}$, respectively. The combined upper limit is 0.69 pb, which corresponds to about 70 times the SM prediction. The quoted results are given for m_{H^0} = 125.4 GeV. See their Table 4.

tH^0 associated production cross section

VALUE	CL%	DOCUMENT ID	TECN	COMMENT
• • • We do not use the following data for averages, fits, limits, etc. • • •				
	95	[1] KHACHATRY...16AU	CMS	pp, 8 TeV

[1] KHACHATRYAN 16AU search for the tH^0 associated production in 19.7 fb^{-1} at E_{cm} = 8 TeV. The 95% CL upper limits on the tH^0 associated production cross section is measured to be 600–1000 fb depending on the assumed $\gamma\gamma$ branching ratios of the Higgs boson. The $\gamma\gamma$ branching ratio is varied to be by a factor of 0.5–3.0 of the Standard Model Higgs boson (m_{H^0} = 125 GeV). The results of the signal strengths for a negative Higgs-boson trilinear coupling are given. The results are given for m_{H^0} = 125 GeV.

H^0 REFERENCES

AABOUD	18	PL B776 318	M. Aaboud *et al.*	(ATLAS Collab.)
SIRUNYAN	18A	PL B778 101	A.M. Sirunyan *et al.*	(CMS Collab.)
SIRUNYAN	18E	PRL 120 071802	A.M. Sirunyan *et al.*	(CMS Collab.)
AABOUD	17AW	JHEP 1710 112	M. Aaboud *et al.*	(ATLAS Collab.)
AABOUD	17BA	JHEP 1712 024	M. Aaboud *et al.*	(ATLAS Collab.)
AABOUD	17BD	EPJ C77 765	M. Aaboud *et al.*	(ATLAS Collab.)
AABOUD	17Y	PRL 119 051802	M. Aaboud *et al.*	(ATLAS Collab.)
AAD	17	EPJ C77 70	G. Aad *et al.*	(ATLAS Collab.)
KHACHATRY...	17F	JHEP 1702 135	V. Khachatryan *et al.*	(CMS Collab.)
SIRUNYAN	17AM	PL B775 1	A.M. Sirunyan *et al.*	(CMS Collab.)
SIRUNYAN	17AV	JHEP 1711 047	A.M. Sirunyan *et al.*	(CMS Collab.)
SIRUNYAN	17CN	PR D96 072004	A.M. Sirunyan *et al.*	(CMS Collab.)
AABOUD	16I	PR D94 052002	M. Aaboud *et al.*	(ATLAS Collab.)
AABOUD	16K	PRL 117 111802	M. Aaboud *et al.*	(ATLAS Collab.)
AABOUD	16X	JHEP 1611 112	M. Aaboud *et al.*	(ATLAS Collab.)
AAD	16	PL B753 69	G. Aad *et al.*	(ATLAS Collab.)
AAD	16AC	PR D93 092005	G. Aad *et al.*	(ATLAS Collab.)
AAD	16AF	JHEP 1601 172	G. Aad *et al.*	(ATLAS Collab.)
AAD	16AL	JHEP 1605 160	G. Aad *et al.*	(ATLAS Collab.)
AAD	16AN	JHEP 1608 045	G. Aad *et al.*	(ATLAS and CMS Collabs.)
AAD	16AO	JHEP 1608 104	G. Aad *et al.*	(ATLAS Collab.)
AAD	16BL	EPJ C76 658	G. Aad *et al.*	(ATLAS Collab.)
AAD	16K	EPJ C76 6	G. Aad *et al.*	(ATLAS Collab.)
KHACHATRY...	16AB	PL B759 672	V. Khachatryan *et al.*	(CMS Collab.)
KHACHATRY...	16AR	JHEP 1604 005	V. Khachatryan *et al.*	(CMS Collab.)
KHACHATRY...	16AU	JHEP 1606 177	V. Khachatryan *et al.*	(CMS Collab.)
KHACHATRY...	16B	PL B753 341	V. Khachatryan *et al.*	(CMS Collab.)
KHACHATRY...	16BA	JHEP 1609 051	V. Khachatryan *et al.*	(CMS Collab.)
KHACHATRY...	16BQ	PR D94 052012	V. Khachatryan *et al.*	(CMS Collab.)
KHACHATRY...	16CD	PL B763 472	V. Khachatryan *et al.*	(CMS Collab.)
KHACHATRY...	16G	EPJ C76 13	V. Khachatryan *et al.*	(CMS Collab.)
AAD	15	PL B740 222	G. Aad *et al.*	(ATLAS Collab.)
AAD	15AA	PR D92 012006	G. Aad *et al.*	(ATLAS Collab.)
AAD	15AH	JHEP 1504 117	G. Aad *et al.*	(ATLAS Collab.)
AAD	15AQ	JHEP 1508 137	G. Aad *et al.*	(ATLAS Collab.)
AAD	15AX	EPJ C75 231	G. Aad *et al.*	(ATLAS Collab.)
AAD	15B	PRL 114 191803	G. Aad *et al.*	(ATLAS and CMS Collabs.)
AAD	15BC	EPJ C75 349	G. Aad *et al.*	(ATLAS Collab.)
AAD	15BD	EPJ C75 337	G. Aad *et al.*	(ATLAS Collab.)
AAD	15BE	EPJ C75 335	G. Aad *et al.*	(ATLAS Collab.)
AAD	15CE	PR D92 092004	G. Aad *et al.*	(ATLAS Collab.)
AAD	15CI	EPJ C75 476	G. Aad *et al.*	(ATLAS Collab.)
Also		EPJ C76 152 (errat.)	G. Aad *et al.*	(ATLAS Collab.)
AAD	15F	PR D91 012006	G. Aad *et al.*	(ATLAS Collab.)
AAD	15G	JHEP 1501 069	G. Aad *et al.*	(ATLAS Collab.)
AAD	15I	PRL 114 121801	G. Aad *et al.*	(ATLAS Collab.)
AAD	15P	PRL 115 091801	G. Aad *et al.*	(ATLAS Collab.)
AAD	15T	PL B749 519	G. Aad *et al.*	(ATLAS Collab.)
AALTONEN	15	PRL 114 151802	T. Aaltonen *et al.*	(CDF and D0 Collabs.)
AALTONEN	15B	PRL 114 141802	T. Aaltonen *et al.*	(CDF Collab.)
KHACHATRY...	15AM	EPJ C75 212	V. Khachatryan *et al.*	(CMS Collab.)
KHACHATRY...	15AN	EPJ C75 251	V. Khachatryan *et al.*	(CMS Collab.)
KHACHATRY...	15BA	PR D92 072010	V. Khachatryan *et al.*	(CMS Collab.)
KHACHATRY...	15H	PL B744 184	V. Khachatryan *et al.*	(CMS Collab.)
KHACHATRY...	15Q	PL B749 337	V. Khachatryan *et al.*	(CMS Collab.)
KHACHATRY...	15Y	PR D92 012004	V. Khachatryan *et al.*	(CMS Collab.)
KHACHATRY...	15Z	PR D92 032008	V. Khachatryan *et al.*	(CMS Collab.)
AAD	14AR	PL B738 234	G. Aad *et al.*	(ATLAS Collab.)
AAD	14AS	PL B738 68	G. Aad *et al.*	(ATLAS Collab.)
AAD	14BC	PR D90 112015	G. Aad *et al.*	(ATLAS Collab.)
AAD	14BJ	JHEP 1409 112	G. Aad *et al.*	(ATLAS Collab.)
AAD	14J	PL B732 8	G. Aad *et al.*	(ATLAS Collab.)
AAD	14O	PRL 112 201802	G. Aad *et al.*	(ATLAS Collab.)
AAD	14W	PR D90 052004	G. Aad *et al.*	(ATLAS Collab.)
ABAZOV	14F	PRL 113 161802	V.M. Abazov *et al.*	(D0 Collab.)
CHATRCHYAN	14AA	PR D89 092007	S. Chatrchyan *et al.*	(CMS Collab.)
CHATRCHYAN	14AI	PR D89 012003	S. Chatrchyan *et al.*	(CMS Collab.)
CHATRCHYAN	14AJ	NATP 10 557	S. Chatrchyan *et al.*	(CMS Collab.)
CHATRCHYAN	14B	EPJ C74 2980	S. Chatrchyan *et al.*	(CMS Collab.)
CHATRCHYAN	14G	JHEP 1401 096	S. Chatrchyan *et al.*	(CMS Collab.)
CHATRCHYAN	14K	JHEP 1405 104	S. Chatrchyan *et al.*	(CMS Collab.)
KHACHATRY...	14D	PL B736 64	V. Khachatryan *et al.*	(CMS Collab.)
KHACHATRY...	14H	JHEP 1409 087	V. Khachartryan *et al.*	(CMS Collab.)
KHACHATRY...	14P	EPJ C74 3076	V. Khachatryan *et al.*	(CMS Collab.)
AAD	13AJ	PL B726 120	G. Aad *et al.*	(ATLAS Collab.)
AAD	13AK	PL B726 88	G. Aad *et al.*	(ATLAS Collab.)
Also		PL B734 406 (errat.)	G. Aad *et al.*	(ATLAS Collab.)
AALTONEN	13L	PR D88 052013	T. Aaltonen *et al.*	(CDF Collab.)
AALTONEN	13M	PR D88 052014	T. Aaltonen *et al.*	(CDF and D0 Collabs.)
ABAZOV	13L	PR D88 052011	V.M. Abazov *et al.*	(D0 Collab.)
CHATRCHYAN	13BK	PL B726 587	S. Chatrchyan *et al.*	(CMS Collab.)
CHATRCHYAN	13J	PRL 110 081803	S. Chatrchyan *et al.*	(CMS Collab.)
CHATRCHYAN	13X	JHEP 1305 145	S. Chatrchyan *et al.*	(CMS Collab.)
CHATRCHYAN	13Y	JHEP 1306 081	S. Chatrchyan *et al.*	(CMS Collab.)
HEINEMEYER	13A	arXiv:1307.1347	S. Heinemeyer *et al.*	(LHC Higgs CS Working Group)
AAD	12AI	PL B716 1	G. Aad *et al.*	(ATLAS Collab.)
AAD	12DA	SCI 338 1576	G. Aad *et al.*	(ATLAS Collab.)
AALTONEN	12Q	PRL 109 111803	T. Aaltonen *et al.*	(CDF Collab.)
AALTONEN	12R	PRL 109 111804	T. Aaltonen *et al.*	(CDF Collab.)
AALTONEN	12S	PRL 109 111805	T. Aaltonen *et al.*	(CDF Collab.)
AALTONEN	12T	PRL 109 071804	T. Aaltonen *et al.*	(CDF and D0 Collabs.)
ABAZOV	12K	PL B716 285	V.M. Abazov *et al.*	(D0 Collab.)
ABAZOV	12O	PRL 109 121803	V.M. Abazov *et al.*	(D0 Collab.)
ABAZOV	12P	PRL 109 121804	V.M. Abazov *et al.*	(D0 Collab.)
CHATRCHYAN	12BY	SCI 338 1569	S. Chatrchyan *et al.*	(CMS Collab.)
CHATRCHYAN	12N	PL B716 30	S. Chatrchyan *et al.*	(CMS Collab.)
DITTMAIER	12	arXiv:1201.3084	S. Dittmaier *et al.*	(LHC Higgs CS Working Group)
DITTMAIER	11	arXiv:1101.0593	S. Dittmaier *et al.*	(LHC Higgs CS Working Group)

Neutral Higgs Bosons, Searches for

CONTENTS:

MASS LIMITS FOR NEUTRAL HIGGS BOSONS IN SUPERSYMMETRIC MODELS

The minimal supersymmetric model has two complex doublets of Higgs bosons. The resulting physical states are two scalars [H_1^0 and H_2^0, where we define $m_{H_1^0} < m_{H_2^0}$], a pseudoscalar (A^0), and a charged Higgs pair ($H^\pm$). H_1^0 and H_2^0 are also called h and H in the literature. There are two free parameters in the Higgs sector which can be chosen to be m_{A^0} and $\tan\beta = v_2/v_1$, the ratio of vacuum expectation values of the two Higgs doublets. Tree-level Higgs masses are constrained by the model to be $m_{H_1^0} \leq m_Z$, $m_{H_2^0} \geq m_Z$, $m_{A^0} \geq m_{H_1^0}$, and $m_{H^\pm} \geq m_W$. However, as described in the review on "Status of Higgs Boson Physics" in this Volume these relations are violated by radiative corrections.

Unless otherwise noted, the experiments in e^+e^- collisions search for the processes $e^+e^- \to H_1^0 Z^0$ in the channels used for the Standard Model Higgs searches and $e^+e^- \to H_1^0 A^0$ in the final states $b\overline{b}b\overline{b}$ and $b\overline{b}\tau^+\tau^-$. In $p\overline{p}$ and pp collisions the experiments search for a variety of processes, as explicitly specified for each entry. Limits on the A^0 mass arise from these direct searches, as well as from the relations valid in the minimal supersymmetric model between m_{A^0} and $m_{H_1^0}$. As discussed in the review on "Status of Higgs Boson Physics" in this Volume, these relations depend, via potentially large radiative corrections, on the mass of the t quark and on the supersymmetric parameters, in particular those of the stop sector. These indirect limits are weaker for larger t and $\bar{t}$ masses. To include the radiative corrections to the Higgs masses, unless otherwise stated, the listed papers use theoretical predictions incorporating two-loop corrections, and the results are given for the m_h^{max} benchmark scenario, which gives rise to the most conservative upper bound on the mass of H_1^0 for given values of m_{A^0} and $\tan\beta$, see CARENA 99B, CARENA 03, and CARENA 13.

Limits in the low-mass region of H_1^0, as well as other by now obsolete limits from different techniques, have been removed from this compilation, and can be found in earlier editions of this Review. Unless otherwise stated, the following results assume no invisible H_1^0 or A^0 decays.

The observed signal at about 125 GeV, see section "H^0", can be interpreted as one of the neutral Higgs bosons of supersymmetric models.

Gauge & Higgs Boson Particle Listings

Neutral Higgs Bosons, Searches for

Mass Limits for H_1^0 (Higgs Boson) in Supersymmetric Models

VALUE (GeV)	CL%	DOCUMENT ID		TECN	COMMENT
>89.7		[1] ABDALLAH	08B	DLPH	$E_{cm} \leq 209$ GeV
>92.8	95	[2] SCHAEL	06B	LEP	$E_{cm} \leq 209$ GeV
>84.5	95	[3,4] ABBIENDI	04M	OPAL	$E_{cm} \leq 209$ GeV
>86.0	95	[3,5] ACHARD	02H	L3	$E_{cm} \leq 209$ GeV, $\tan\beta > 0.4$
• • • We do not use the following data for averages, fits, limits, etc. • • •					
		[6] AABOUD	16AA	ATLS	$H_2^0 \to \tau^+\tau^-$
		[7] KHACHATRY...	16A	CMS	$H_{1,2}^0/A^0 \to \mu^+\mu^-$
		[8] AAD	15CE	ATLS	$H_2^0 \to H^0H^0$
		[9] KHACHATRY...	15AY	CMS	$pp \to H_{1,2}^0/A^0 + b + X$, $H_{1,2}^0/A^0 \to b\overline{b}$
		[10] AAD	14AW	ATLS	$pp \to H_{1,2}^0/A^0 + X$, $H_{1,2}^0/A^0 \to \tau\tau$
		[11] KHACHATRY...	14M	CMS	$pp \to H_{1,2}^0/A^0 + X$, $H_{1,2}^0/A^0 \to \tau\tau$
		[12] AAD	13O	ATLS	$pp \to H_{1,2}^0/A^0 + X$, $H_{1,2}^0/A^0 \to \tau^+\tau^-, \mu^+\mu^-$
		[13] AAIJ	13T	LHCB	$pp \to H_{1,2}^0/A^0 + X$, $H_{1,2}^0/A^0 \to \tau^+\tau^-$
		[14] CHATRCHYAN	13AG	CMS	$pp \to H_{1,2}^0/A^0 + b + X$, $H_{1,2}^0/A^0 \to b\overline{b}$
		[15] AALTONEN	12AQ	TEVA	$p\overline{p} \to H_{1,2}^0/A^0 + b + X$, $H_{1,2}^0/A^0 \to b\overline{b}$
		[16] AALTONEN	12X	CDF	$p\overline{p} \to H_{1,2}^0/A^0 + b + X$, $H_{1,2}^0/A^0 \to b\overline{b}$
		[17] ABAZOV	12G	D0	$p\overline{p} \to H_{1,2}^0/A^0 + X$, $H_{1,2}^0/A^0 \to \tau^+\tau^-$
		[18] CHATRCHYAN	12K	CMS	$pp \to H_{1,2}^0/A^0 + X$, $H_{1,2}^0/A^0 \to \tau^+\tau^-$
		[19] ABAZOV	11K	D0	$p\overline{p} \to H_{1,2}^0/A^0 + b + X$, $H_{1,2}^0/A^0 \to b\overline{b}$
		[20] ABAZOV	11W	D0	$p\overline{p} \to H_{1,2}^0/A^0 + b + X$, $H_{1,2}^0/A^0 \to \tau^+\tau^-$
		[21] AALTONEN	09AR	CDF	$p\overline{p} \to H_{1,2}^0/A^0 + X$, $H_{1,2}^0/A^0 \to \tau^+\tau^-$
		[22] ABBIENDI	03G	OPAL	$H_1^0 \to A^0A^0$
>89.8	95	[3,23] HEISTER	02	ALEP	$E_{cm} \leq 209$ GeV, $\tan\beta > 0.5$

[1] ABDALLAH 08B give limits in eight *CP*-conserving benchmark scenarios and some *CP*-violating scenarios. See paper for excluded regions for each scenario. Supersedes ABDALLAH 04.

[2] SCHAEL 06B make a combined analysis of the LEP data. The quoted limit is for the m_h^{max} scenario with $m_t = 174.3$ GeV. In the *CP*-violating CPX scenario no lower bound on $m_{H_1^0}$ can be set at 95% CL. See paper for excluded regions in various scenarios. See Figs. 2–6 and Tabs. 14–21 for limits on $\sigma(ZH^0)\cdot$ B($H^0 \to b\overline{b}, \tau^+\tau^-$) and $\sigma(H_1^0H_2^0)\cdot$ B($H_1^0, H_2^0 \to b\overline{b}, \tau^+\tau^-$).

[3] Search for $e^+e^- \to H_1^0A^0$ in the final states $b\overline{b}b\overline{b}$ and $b\overline{b}\tau^+\tau^-$, and $e^+e^- \to H_1^0Z$. Universal scalar mass of 1 TeV, SU(2) gaugino mass of 200 GeV, and $\mu = -200$ GeV are assumed, and two-loop radiative corrections incorporated. The limits hold for m_t=175 GeV, and for the m_h^{max} scenario.

[4] ABBIENDI 04M exclude $0.7 < \tan\beta < 1.9$, assuming $m_t = 174.3$ GeV. Limits for other MSSM benchmark scenarios, as well as for *CP* violating cases, are also given.

[5] ACHARD 02H also search for the final state $H_1^0Z \to 2A^0q\overline{q}$, $A^0 \to q\overline{q}$. In addition, the MSSM parameter set in the "large-μ" and "no-mixing" scenarios are examined.

[6] AABOUD 16AA search for production of a Higgs boson in gluon fusion and in association with a $b\overline{b}$ pair followed by the decay $H_2^0 \to \tau^+\tau^-$ in 3.2 fb^{-1} of pp collisions at E_{cm} = 13 TeV. See their Fig. 5(a, b) for limits on cross section times branching ratio for $m_{H_2^0}$ = 200–1200 GeV, and Fig. 5(c, d) for the excluded region in the MSSM parameter space in the m_h^{mod+} and hMSSM scenarios.

[7] KHACHATRYAN 16A search for production of a Higgs boson in gluon fusion and in association with a $b\overline{b}$ pair followed by the decay $H_{1,2}^0/A^0 \to \mu^+\mu^-$ in 5.1 fb^{-1} of pp collisions at $E_{cm} = 7$ TeV and 19.3 fb^{-1} at $E_{cm} = 8$ TeV. See their Fig. 7 for the excluded region in the MSSM parameter space in the m_h^{mod+} benchmark scenario and Fig. 9 for limits on cross section times branching ratio.

[8] AAD 15CE search for production of H_2^0 decaying to H^0H^0 in the final states $b\overline{b}\tau^+\tau^-$ and $\gamma\gamma WW^*$ in 20.3 fb^{-1} of pp collisions at $E_{cm} = 8$ TeV and combine with data from AAD 15H ($\gamma\gamma b\overline{b}$) and AAD 15BK ($b\overline{b}b\overline{b}$). See their Fig. 7 for excluded regions in the parameter space in several scenarios.

[9] KHACHATRYAN 15AY search for production of a Higgs boson in association with a b quark in the decay $H_{1,2}^0/A^0 \to b\overline{b}$ in 19.7 fb^{-1} of pp collisions at $E_{cm} = 8$ TeV and combine with CHATRCHYAN 13AG 7 TeV data. See their Fig. 6 for the limits on cross section times branching ratio for m_{A^0} = 100–900 GeV and Figs. 7–9 for the excluded region in the MSSM parameter space in various benchmark scenarios.

[10] AAD 14AW search for production of a Higgs boson followed by the decay $H_{1,2}^0/A^0 \to \tau^+\tau^-$ in 19.5–20.3 fb^{-1} of pp collisions at $E_{cm} = 8$ TeV. See their Fig. 11 for the limits on cross section times branching ratio and their Figs. 9 and 10 for the excluded region in the MSSM parameter space. For $m_{A^0} = 140$ GeV, the region $\tan\beta > 5.4$ is excluded at 95% CL in the m_h^{max} scenario.

[11] KHACHATRYAN 14M search for production of a Higgs boson in gluon fusion and in association with a b quark followed by the decay $H_{1,2}^0/A^0 \to \tau^+\tau^-$ in 4.9 fb^{-1} of pp collisions at $E_{cm} = 7$ TeV and 19.7 fb^{-1} at $E_{cm} = 8$ TeV. See their Figs. 7 and 8 for one- and two-dimensional limits on cross section times branching ratio and their Figs. 5 and 6 for the excluded region in the MSSM parameter space. For $m_{A^0} = 140$ GeV, the region $\tan\beta > 3.8$ is excluded at 95% CL in the m_h^{max} scenario.

[12] AAD 13O search for production of a Higgs boson in the decay $H_{1,2}^0/A^0 \to \tau^+\tau^-$ and $\mu^+\mu^-$ with 4.7–4.8 fb^{-1} of pp collisions at $E_{cm} = 7$ TeV. See their Fig. 6 for the excluded region in the MSSM parameter space and their Fig. 7 for the limits on cross section times branching ratio. For $m_{A^0} = 110$–170 GeV, $\tan\beta \gtrsim 10$ is excluded, and for $\tan\beta = 50$, m_{A^0} below 470 GeV is excluded at 95% CL in the m_h^{max} scenario.

[13] AAIJ 13T search for production of a Higgs boson in the forward region in the decay $H_{1,2}^0/A^0 \to \tau^+\tau^-$ in 1.0 fb^{-1} of pp collisions at $E_{cm} = 7$ TeV. See their Fig. 2 for the limits on cross section times branching ratio and the excluded region in the MSSM parameter space.

[14] CHATRCHYAN 13AG search for production of a Higgs boson in association with a b quark in the decay $H_{1,2}^0/A^0 \to b\overline{b}$ in 2.7–4.8 fb^{-1} of pp collisions at $E_{cm} = 7$ TeV. See their Fig. 6 for the excluded region in the MSSM parameter space and Fig. 5 for the limits on cross section times branching ratio. For $m_{A^0} = 90$–350 GeV, upper bounds on $\tan\beta$ of 18–42 at 95% CL are obtained in the m_h^{max} scenario with $\mu = +200$ GeV.

[15] AALTONEN 12AQ combine AALTONEN 12X and ABAZOV 11K. See their Table I and Fig. 1 for the limit on cross section times branching ratio and Fig. 2 for the excluded region in the MSSM parameter space.

[16] AALTONEN 12X search for associated production of a Higgs boson and a b quark in the decay $H_{1,2}^0/A^0 \to b\overline{b}$, with 2.6 fb^{-1} of $p\overline{p}$ collisions at $E_{cm} = 1.96$ TeV. See their Table III and Fig. 15 for the limit on cross section times branching ratio and Figs. 17, 18 for the excluded region in the MSSM parameter space.

[17] ABAZOV 12G search for production of a Higgs boson in the decay $H_{1,2}^0/A^0 \to \tau^+\tau^-$ with 7.3 fb^{-1} of $p\overline{p}$ collisions at $E_{cm} = 1.96$ TeV and combine with ABAZOV 11W and ABAZOV 11K. See their Figs. 4, 5, and 6 for the excluded region in the MSSM parameter space. For $m_{A^0} = 90$–180 GeV, $\tan\beta \gtrsim 30$ is excluded at 95% CL. in the m_h^{max} scenario.

[18] CHATRCHYAN 12K search for production of a Higgs boson in the decay $H_{1,2}^0/A^0 \to \tau^+\tau^-$ with 4.6 fb^{-1} of pp collisions at $E_{cm} = 7$ TeV. See their Fig. 3 and Table 4 for the excluded region in the MSSM parameter space. For $m_{A^0} = 160$ GeV, the region $\tan\beta > 7.1$ is excluded at 95% CL in the m_h^{max} scenario. Superseded by KHACHATRYAN 14M.

[19] ABAZOV 11K search for associated production of a Higgs boson and a b quark, followed by the decay $H_{1,2}^0/A^0 \to b\overline{b}$, in 5.2 fb^{-1} of $p\overline{p}$ collisions at $E_{cm} = 1.96$ TeV. See their Fig. 5/Table 2 for the limit on cross section times branching ratio and Fig. 6 for the excluded region in the MSSM parameter space for $\mu = -200$ GeV.

[20] ABAZOV 11W search for associated production of a Higgs boson and a b quark, followed by the decay $H_{1,2}^0/A^0 \to \tau\tau$, in 7.3 fb^{-1} of $p\overline{p}$ collisions at $E_{cm} = 1.96$ TeV. See their Fig. 2 for the limit on cross section times branching ratio and for the excluded region in the MSSM parameter space.

[21] AALTONEN 09AR search for Higgs bosons decaying to $\tau^+\tau^-$ in two doublet models in 1.8 fb^{-1} of $p\overline{p}$ collisions at $E_{cm} = 1.96$ TeV. See their Fig. 2 for the limit on $\sigma\cdot$ B($H_{1,2}^0/A^0 \to \tau^+\tau^-$) for different Higgs masses, and see their Fig. 3 for the excluded region in the MSSM parameter space.

[22] ABBIENDI 03G search for $e^+e^- \to H_1^0Z$ followed by $H_1^0 \to A^0A^0$, $A^0 \to c\overline{c}$, gg, or $\tau^+\tau^-$. In the no-mixing scenario, the region $m_{H_1^0}$ = 45–85 GeV and m_{A^0} = 2–9.5 GeV is excluded at 95% CL.

[23] HEISTER 02 excludes the range 0.7 <$\tan\beta$ < 2.3. A wider range is excluded with different stop mixing assumptions. Updates BARATE 01C.

Mass Limits for A^0 (Pseudoscalar Higgs Boson) in Supersymmetric Models

VALUE (GeV)	CL%	DOCUMENT ID		TECN	COMMENT
>90.4		[1] ABDALLAH	08B	DLPH	$E_{cm} \leq 209$ GeV
>93.4	95	[2] SCHAEL	06B	LEP	$E_{cm} \leq 209$ GeV
>85.0	95	[3,4] ABBIENDI	04M	OPAL	$E_{cm} \leq 209$ GeV
>86.5	95	[3,5] ACHARD	02H	L3	$E_{cm} \leq 209$ GeV, $\tan\beta > 0.4$
>90.1	95	[3,6] HEISTER	02	ALEP	$E_{cm} \leq 209$ GeV, $\tan\beta > 0.5$
• • • We do not use the following data for averages, fits, limits, etc. • • •					
		[7] AABOUD	18G	ATLS	$H_2^0/A^0 \to \tau^+\tau^-$
		[8] SIRUNYAN	18A	CMS	$H_2^0/A^0 \to H^0H^0$
		[9] AABOUD	16AA	ATLS	$A^0 \to \tau^+\tau^-$
		[10] KHACHATRY...	16A	CMS	$H_{1,2}^0/A^0 \to \mu^+\mu^-$
		[11] KHACHATRY...	16P	CMS	$H_2^0 \to H^0H^0$, $A^0 \to ZH^0$
		[12] KHACHATRY...	15AY	CMS	$pp \to H_{1,2}^0/A^0 + b + X$, $H_{1,2}^0/A^0 \to b\overline{b}$
		[13] AAD	14AW	ATLS	$pp \to H_{1,2}^0/A^0 + X$, $H_{1,2}^0/A^0 \to \tau\tau$
		[14] KHACHATRY...	14M	CMS	$pp \to H_{1,2}^0/A^0 + X$, $H_{1,2}^0/A^0 \to \tau\tau$

[15] AAD	13O	ATLS	$pp \to H^0_{1,2}/A^0 + X$,	$H^0_{1,2}/A^0 \to \tau^+\tau^-, \mu^+\mu^-$
[16] AAIJ	13T	LHCB	$pp \to H^0_{1,2}/A^0 + X$,	$H^0_{1,2}/A^0 \to \tau^+\tau^-$
[17] CHATRCHYAN	13AG	CMS	$pp \to H^0_{1,2}/A^0 + b + X$,	$H^0_{1,2}/A^0 \to b\overline{b}$
[18] AALTONEN	12AQ	TEVA	$p\overline{p} \to H^0_{1,2}/A^0 + b + X$,	$H^0_{1,2}/A^0 \to b\overline{b}$
[19] AALTONEN	12X	CDF	$p\overline{p} \to H^0_{1,2}/A^0 + b + X$,	$H^0_{1,2}/A^0 \to b\overline{b}$
[20] ABAZOV	12G	D0	$p\overline{p} \to H^0_{1,2}/A^0 + X$,	$H^0_{1,2}/A^0 \to \tau^+\tau^-$
[21] CHATRCHYAN	12K	CMS	$pp \to H^0_{1,2}/A^0 + X$,	$H^0_{1,2}/A^0 \to \tau^+\tau^-$
[22] ABAZOV	11K	D0	$p\overline{p} \to H^0_{1,2}/A^0 + b + X$,	$H^0_{1,2}/A^0 \to b\overline{b}$
[23] ABAZOV	11W	D0	$p\overline{p} \to H^0_{1,2}/A^0 + b + X$,	$H^0_{1,2}/A^0 \to \tau^+\tau^-$
[24] AALTONEN	09AR	CDF	$p\overline{p} \to H^0_{1,2}/A^0 + X$,	$H^0_{1,2}/A^0 \to \tau^+\tau^-$
[25] ACOSTA	05Q	CDF	$p\overline{p} \to H^0_{1,2}/A^0 + X$	
[26] ABBIENDI	03G	OPAL	$H^0_1 \to A^0A^0$	
[27] AKEROYD	02	RVUE		

[1] ABDALLAH 08B give limits in eight *CP*-conserving benchmark scenarios and some *CP*-violating scenarios. See paper for excluded regions for each scenario. Supersedes ABDALLAH 04.

[2] SCHAEL 06B make a combined analysis of the LEP data. The quoted limit is for the m_h^{max} scenario with $m_t = 174.3$ GeV. In the *CP*-violating CPX scenario no lower bound on $m_{H^0_1}$ can be set at 95% CL. See paper for excluded regions in various scenarios. See Figs. 2–6 and Tabs. 14–21 for limits on $\sigma(ZH^0)\cdot B(H^0 \to b\overline{b}, \tau^+\tau^-)$ and $\sigma(H^0_1H^0_2)\cdot B(H^0_1,H^0_2 \to b\overline{b},\tau^+\tau^-)$.

[3] Search for $e^+e^- \to H^0_1A^0$ in the final states $b\overline{b}b\overline{b}$ and $b\overline{b}\tau^+\tau^-$, and $e^+e^- \to H^0_1Z$. Universal scalar mass of 1 TeV, SU(2) gaugino mass of 200 GeV, and $\mu = -200$ GeV are assumed, and two-loop radiative corrections incorporated. The limits hold for m_t=175 GeV, and for the m_h^{max} scenario.

[4] ABBIENDI 04M exclude $0.7 < \tan\beta < 1.9$, assuming $m_t = 174.3$ GeV. Limits for other MSSM benchmark scenarios, as well as for *CP* violating cases, are also given.

[5] ACHARD 02H also search for the final state $H^0_1Z \to 2A^0q\overline{q}$, $A^0 \to q\overline{q}$. In addition, the MSSM parameter set in the "large-μ" and "no-mixing" scenarios are examined.

[6] HEISTER 02 excludes the range $0.7 < \tan\beta < 2.3$. A wider range is excluded with different stop mixing assumptions. Updates BARATE 01C.

[7] AABOUD 18G search for production of $H^0_2/A^0 \to \tau^+\tau^-$ by gluon fusion and b-associated prodution in 36.1 fb^{-1} of pp collisions at $E_{cm} = 13$ TeV. See their Fig. 7 for the limits on cross section times branching ratio for $m_{H^0_2}$, $m_{A^0} = 0.2$–2.25 TeV, and Fig. 10 for excluded regions in the m_{A^0}– $\tan\beta$ plane in several MSSM scenarios.

[8] SIRUNYAN 18A search for production of a scalar resonance decaying to $H^0H^0 \to b\overline{b}\tau^+\tau^-$ in 35.9 fb^{-1} of pp collisions at $E_{cm} = 13$ TeV. See their Fig. 5 for the limits on cross section times branching ratio for the resonance mass = 250–900 GeV and also for excluded regions in the $m_{A^0} - \tan(\beta)$ plane in the hMSSM scenario.

[9] AABOUD 16AA search for production of a Higgs boson in gluon fusion and in association with a $b\overline{b}$ pair followed by the decay $A^0 \to \tau^+\tau^-$ in 3.2 fb^{-1} of pp collisions at $E_{cm} = 13$ TeV. See their Fig. 5(a, b) for limits on cross section times branching ratio for $m_{A^0} = 200$–1200 GeV, and Fig. 5(c, d) for the excluded region in the MSSM parameter space in the m_h^{mod+} and hMSSM scenarios.

[10] KHACHATRYAN 16A search for production of a Higgs boson in gluon fusion and in association with a $b\overline{b}$ pair followed by the decay $H^0_{1,2}/A^0 \to \mu^+\mu^-$ in 5.1 fb^{-1} of pp collisions at $E_{cm} = 7$ TeV and 19.3 fb^{-1} at $E_{cm} = 8$ TeV. See their Fig. 7 for the excluded region in the MSSM parameter space in the m_h^{mod+} benchmark scenario and Fig. 9 for limits on cross section times branching ratio.

[11] KHACHATRYAN 16P search for gluon fusion production of an H^0_2 decaying to $H^0H^0 \to b\overline{b}\tau^+\tau^-$ and an A^0 decaying to $ZH^0 \to \ell^+\ell^-\tau^+\tau^-$ in 19.7 fb^{-1} of pp collisions at $E_{cm} = 8$ TeV. See their Fig. 12 for excluded region in the $\tan\beta - \cos(\beta-\alpha)$ plane for $m_{H^0_2} = m_{A^0} = 300$ GeV.

[12] KHACHATRYAN 15AY search for production of a Higgs boson in association with a b quark in the decay $H^0_{1,2}/A^0 \to b\overline{b}$ in 19.7 fb^{-1} of pp collisions at $E_{cm} = 8$ TeV and combine with CHATRCHYAN 13AG 7 TeV data. See their Fig. 6 for the limits on cross section times branching ratio for $m_{A^0} = 100$–900 GeV and Figs. 7–9 for the excluded region in the MSSM parameter space in various benchmark scenarios.

[13] AAD 14AW search for production of a Higgs boson followed by the decay $H^0_{1,2}/A^0 \to \tau^+\tau^-$ in 19.5–20.3 fb^{-1} of pp collisions at $E_{cm} = 8$ TeV. See their Fig. 11 for the limits on cross section times branching ratio and their Figs. 9 and 10 for the excluded region in the MSSM parameter space. For $m_{A^0} = 140$ GeV, the region $\tan\beta > 5.4$ is excluded at 95% CL in the m_h^{max} scenario.

[14] KHACHATRYAN 14M search for production of a Higgs boson in gluon fusion and in association with a b quark followed by the decay $H^0_{1,2}/A^0 \to \tau^+\tau^-$ in 4.9 fb^{-1} of pp collisions at $E_{cm} = 7$ TeV and 19.7 fb^{-1} at $E_{cm} = 8$ TeV. See their Figs. 7 and 8 for one- and two-dimensional limits on cross section times branching ratio and their Figs. 5 and 6 for the excluded region in the MSSM parameter space. For $m_{A^0} = 140$ GeV, the region $\tan\beta > 3.8$ is excluded at 95% CL in the m_h^{max} scenario.

[15] AAD 13O search for production of a Higgs boson in the decay $H^0_{1,2}/A^0 \to \tau^+\tau^-$ and $\mu^+\mu^-$ with 4.7–4.8 fb^{-1} of pp collisions at $E_{cm} = 7$ TeV. See their Fig. 6 for the excluded region in the MSSM parameter space and their Fig. 7 for the limits on cross section times branching ratio. For $m_{A^0} = 110$–170 GeV, $\tan\beta \gtrsim 10$ is excluded, and for $\tan\beta = 50$, m_{A^0} below 470 GeV is excluded at 95% CL in the m_h^{max} scenario.

[16] AAIJ 13T search for production of a Higgs boson in the forward region in the decay $H^0_{1,2}/A^0 \to \tau^+\tau^-$ in 1.0 fb^{-1} of pp collisions at $E_{cm} = 7$ TeV. See their Fig. 2 for the limits on cross section times branching ratio and the excluded region in the MSSM parameter space.

[17] CHATRCHYAN 13AG search for production of a Higgs boson in association with a b quark in the decay $H^0_{1,2}/A^0 \to b\overline{b}$ in 2.7–4.8 fb^{-1} of pp collisions at $E_{cm} = 7$ TeV. See their Fig. 6 for the excluded region in the MSSM parameter space and Fig. 5 for the limits on cross section times branching ratio. For $m_{A^0} = 90$–350 GeV, upper bounds on $\tan\beta$ of 18–42 at 95% CL are obtained in the m_h^{max} scenario with $\mu = +200$ GeV.

[18] AALTONEN 12AQ combine AALTONEN 12X and ABAZOV 11K. See their Table I and Fig. 1 for the limit on cross section times branching ratio and Fig. 2 for the excluded region in the MSSM parameter space.

[19] AALTONEN 12X search for associated production of a Higgs boson and a b quark in the decay $H^0_{1,2}/A^0 \to b\overline{b}$, with 2.6 fb^{-1} of $p\overline{p}$ collisions at $E_{cm} = 1.96$ TeV. See their Table III and Fig. 15 for the limit on cross section times branching ratio and Figs. 17, 18 for the excluded region in the MSSM parameter space.

[20] ABAZOV 12G search for production of a Higgs boson in the decay $H^0_{1,2}/A^0 \to \tau^+\tau^-$ with 7.3 fb^{-1} of $p\overline{p}$ collisions at $E_{cm} = 1.96$ TeV and combine with ABAZOV 11W and ABAZOV 11K. See their Figs. 4, 5, and 6 for the excluded region in the MSSM parameter space. For $m_{A^0} = 90$–180 GeV, $\tan\beta \gtrsim 30$ is excluded at 95% CL. in the m_h^{max} scenario.

[21] CHATRCHYAN 12K search for production of a Higgs boson in the decay $H^0_{1,2}/A^0 \to \tau^+\tau^-$ with 4.6 fb^{-1} of pp collisions at $E_{cm} = 7$ TeV. See their Fig. 3 and Table 4 for the excluded region in the MSSM parameter space. For $m_{A^0} = 160$ GeV, the region $\tan\beta > 7.1$ is excluded at 95% CL in the m_h^{max} scenario. Superseded by KHACHATRYAN 14M.

[22] ABAZOV 11K search for associated production of a Higgs boson and a b quark, followed by the decay $H^0_{1,2}/A^0 \to b\overline{b}$, in 5.2 fb^{-1} of $p\overline{p}$ collisions at $E_{cm} = 1.96$ TeV. See their Fig. 5/Table 2 for the limit on cross section times branching ratio and Fig. 6 for the excluded region in the MSSM parameter space for $\mu = -200$ GeV.

[23] ABAZOV 11W search for associated production of a Higgs boson and a b quark, followed by the decay $H^0_{1,2}/A^0 \to \tau\tau$, in 7.3 fb^{-1} of $p\overline{p}$ collisions at $E_{cm} = 1.96$ TeV. See their Fig. 2 for the limit on cross section times branching ratio and for the excluded region in the MSSM parameter space.

[24] AALTONEN 09AR search for Higgs bosons decaying to $\tau^+\tau^-$ in two doublet models in 1.8 fb^{-1} of $p\overline{p}$ collisions at $E_{cm} = 1.96$ TeV. See their Fig. 2 for the limit on $\sigma \cdot B(H^0_{1,2}/A^0 \to \tau^+\tau^-)$ for different Higgs masses, and see their Fig. 3 for the excluded region in the MSSM parameter space.

[25] ACOSTA 05Q search for $H^0_{1,2}/A^0$ production in $p\overline{p}$ collisions at $E_{cm} = 1.8$ TeV with $H^0_{1,2}/A^0 \to \tau^+\tau^-$. At $m_{A^0} = 100$ GeV, the obtained cross section upper limit is above theoretical expectation.

[26] ABBIENDI 03G search for $e^+e^- \to H^0_1Z$ followed by $H^0_1 \to A^0A^0$, $A^0 \to c\overline{c}$, gg, or $\tau^+\tau^-$. In the no-mixing scenario, the region $m_{H^0_1} = 45$–85 GeV and $m_{A^0} = 2$–9.5 GeV is excluded at 95% CL.

[27] AKEROYD 02 examine the possibility of a light A^0 with $\tan\beta < 1$. Electroweak measurements are found to be inconsistent with such a scenario.

MASS LIMITS FOR NEUTRAL HIGGS BOSONS IN EXTENDED HIGGS MODELS

This Section covers models which do not fit into either the Standard Model or its simplest minimal Supersymmetric extension (MSSM), leading to anomalous production rates, or nonstandard final states and branching ratios. In particular, this Section covers limits which may apply to generic two-Higgs-doublet models (2HDM), or to special regions of the MSSM parameter space where decays to invisible particles or to photon pairs are dominant (see the review on "Status of Higgs Boson Physics"). Concerning the mass limits for H^0 and A^0 listed below, see the footnotes or the comment lines for details on the nature of the models to which the limits apply.

The observed signal at about 125 GeV, see section "H^0", can be interpreted as one of the neutral Higgs bosons of an extended Higgs sector.

Mass Limits in General two-Higgs-doublet Models

VALUE (GeV)	CL%	DOCUMENT ID	TECN	COMMENT
• • • We do not use the following data for averages, fits, limits, etc. • • •				
[1] AABOUD		17AN ATLS		$H^0_2, A^0 \to t\overline{t}$
[2] SIRUNYAN		17AX CMS		$A^0b\overline{b}, A^0 \to \mu^+\mu^-$
[3] AAD		16AX ATLS		$H^0_2 \to ZZ$
[4] KHACHATRY...16P		CMS		$H^0_2 \to H^0H^0, A^0 \to ZH^0$
[5] KHACHATRY...16W		CMS		$A^0b\overline{b}, A^0 \to \tau^+\tau^-$

Gauge & Higgs Boson Particle Listings

Neutral Higgs Bosons, Searches for

		[6] KHACHATRY...16Z	CMS	$H_2^0 \to Z A^0$ or $A^0 \to Z H_2^0$
		[7] AAD	15BK ATLS	$H_2^0 \to H^0 H^0$
		[8] AAD	15S ATLS	$A^0 \to Z H^0$
		[9] KHACHATRY...15BB	CMS	H_2^0, $A^0 \to \gamma\gamma$
		[10] KHACHATRY...15N	CMS	$A^0 \to Z H^0$
		[11] AAD	14M ATLS	$H_2^0 \to H^\pm W^\mp \to H^0 W^\pm W^\mp$, $H^0 \to b\overline{b}$
		[12] KHACHATRY...14Q	CMS	$H_2^0 \to H^0 H^0$, $A^0 \to Z H^0$
		[13] AALTONEN	09AR CDF	$p\overline{p} \to H_{1,2}^0/A^0 + X$, $H_{1,2}^0/A^0 \to \tau^+\tau^-$
none 1–55	95	[14] ABBIENDI	05A OPAL	H_1^0, Type II model
>110.6	95	[15] ABDALLAH	05D DLPH	$H^0 \to$ 2 jets
		[16] ABDALLAH	04O DLPH	$Z \to f\overline{f}H$
		[17] ABDALLAH	04O DLPH	$e^+e^- \to H^0 Z$, $H^0 A^0$
		[18] ABBIENDI	02D OPAL	$e^+e^- \to b\overline{b}H$
none 1–44	95	[19] ABBIENDI	01E OPAL	H_1^0, Type-II model
> 68.0	95	[20] ABBIENDI	99E OPAL	$\tan\beta > 1$
		[21] ABREU	95H DLPH	$Z \to H^0 Z^*$, $H^0 A^0$
		[22] PICH	92 RVUE	Very light Higgs

[1] AABOUD 17AN search for production of a heavy H_2^0 and/or A^0 decaying to $t\overline{t}$ in 20.3 fb^{-1} of pp collisions at E_{cm} = 8 TeV. See their Fig. 3 and Table III for excluded parameter regions in Type II Two-Higgs-Doublet-Models.

[2] SIRUNYAN 17AX search for $A^0 b\overline{b}$ production followed by the decay $A^0 \to \mu^+\mu^-$ in 19.7 fb^{-1} of pp collisions at E_{cm} = 8 TeV. Limits are set in the range m_{A^0} = 25–60 GeV. See their Fig. 5 for upper limits on $\sigma(A^0 b\overline{b})\cdot B(A^0 \to \mu^+\mu^-)$.

[3] AAD 16AX search for production of a heavy H^0 state decaying to ZZ in the final states $\ell^+\ell^-\ell^+\ell^-$, $\ell^+\ell^-\nu\overline{\nu}$, $\ell^+\ell^- q\overline{q}$, and $\nu\overline{\nu}q\overline{q}$ in 20.3 fb^{-1} of pp collisions at E_{cm} = 8 TeV. See their Figs. 13 and 14 for excluded parameter regions in Type I and II models.

[4] KHACHATRYAN 16P search for gluon fusion production of an H_2^0 decaying to $H^0 H^0 \to b\overline{b}\tau^+\tau^-$ and an A^0 decaying to $ZH^0 \to \ell^+\ell^-\tau^+\tau^-$ in 19.7 fb^{-1} of pp collisions at E_{cm} = 8 TeV. See their Fig. 11 for limits on $\tan\beta$ for m_{A^0} = 230–350 GeV.

[5] KHACHATRYAN 16W search for $A^0 b\overline{b}$ production followed by the decay $A^0 \to \tau^+\tau^-$ in 19.7 fb^{-1} of pp collisions at E_{cm} = 8 TeV. See their Fig. 3 for upper limits on $\sigma(A^0 b\overline{b})\cdot B(A^0 \to \tau^+\tau^-)$.

[6] KHACHATRYAN 16Z search for $H_2^0 \to Z A^0$ followed by $A^0 \to b\overline{b}$ or $\tau^+\tau^-$, and $A^0 \to Z H_2^0$ followed by $H_2^0 \to b\overline{b}$ or $\tau^+\tau^-$, in 19.8 fb^{-1} of pp collisions at E_{cm} = 8 TeV. See their Fig. 4 for cross section limits and Fig. 5 for excluded region in the parameter space.

[7] AAD 15BK search for production of a heavy H_2^0 decaying to $H^0 H^0$ in the final state $b\overline{b}b\overline{b}$ in 19.5 fb^{-1} of pp collisions at E_{cm} = 8 TeV. See their Figs. 15–18 for excluded regions in the parameter space.

[8] AAD 15S search for production of A^0 decaying to $ZH^0 \to \ell^+\ell^- b\overline{b}$, $\nu\overline{\nu}b\overline{b}$ and $\ell^+\ell^-\tau^+\tau^-$ in 20.3 fb^{-1} of pp collisions at E_{cm} = 8 TeV. See their Figs. 4 and 5 for excluded regions in the parameter space.

[9] KHACHATRYAN 15BB search for H_2^0, $A^0 \to \gamma\gamma$ in 19.7 fb^{-1} of pp collisions at E_{cm} = 8 TeV. See their Fig. 10 for excluded regions in the two-Higgs-doublet model parameter space.

[10] KHACHATRYAN 15N search for production of A^0 decaying to $ZH^0 \to \ell^+\ell^- b\overline{b}$ in 19.7 fb^{-1} of pp collisions at E_{cm} = 8 TeV. See their Fig. 5 for excluded regions in the $\tan\beta - \cos(\beta-\alpha)$ plane for m_{A^0} = 300 GeV.

[11] AAD 14M search for the decay cascade $H_2^0 \to H^\pm W^\mp \to H^0 W^\pm W^\mp$, H^0 decaying to $b\overline{b}$ in 20.3 fb^{-1} of pp collisions at E_{cm} = 8 TeV. See their Table IV for limits in a two-Higgs-doublet model for $m_{H_2^0}$= 325–1025 GeV and m_{H^+}= 225–825 GeV.

[12] KHACHATRYAN 14Q search for $H_2^0 \to H^0 H^0$ and $A^0 \to Z H^0$ in 19.5 fb^{-1} of pp collisions at E_{cm} = 8 TeV. See their Figs. 4 and 5 for limits on cross section times branching ratio for m_{H_2,A^0}= 260–360 GeV and their Figs. 7–9 for limits in two-Higgs-doublet models.

[13] AALTONEN 09AR search for Higgs bosons decaying to $\tau^+\tau^-$ in two doublet models in 1.8 fb^{-1} of $p\overline{p}$ collisions at E_{cm} = 1.96 TeV. See their Fig. 2 for the limit on $\sigma \cdot B(H_{1,2}^0/A^0 \to \tau^+\tau^-)$ for different Higgs masses, and see their Fig. 3 for the excluded region in the MSSM parameter space.

[14] ABBIENDI 05A search for $e^+e^- \to H_1^0 A^0$ in general Type-II two-doublet models, with decays $H_1^0 \to q\overline{q}$, gg, $\tau^+\tau^-$, and $H_1^0 \to A^0 A^0$.

[15] ABDALLAH 05D search for $e^+e^- \to H^0 Z$ and $H^0 A^0$ with H^0, A^0 decaying to two jets of any flavor including gg. The limit is for SM $H^0 Z$ production cross section with $B(H^0 \to jj) = 1$.

[16] ABDALLAH 04O search for $Z \to b\overline{b}H^0$, $b\overline{b}A^0$, $\tau^+\tau^- H^0$ and $\tau^+\tau^- A^0$ in the final states $4b$, $b\overline{b}\tau^+\tau^-$, and 4τ. See paper for limits on Yukawa couplings.

[17] ABDALLAH 04O search for $e^+e^- \to H^0 Z$ and $H^0 A^0$, with H^0, A^0 decaying to $b\overline{b}$, $\tau^+\tau^-$, or $H^0 \to A^0 A^0$ at E_{cm} = 189–208 GeV. See paper for limits on couplings.

[18] ABBIENDI 02D search for $Z \to b\overline{b}H_1^0$ and $b\overline{b}A^0$ with $H_1^0/A^0 \to \tau^+\tau^-$, in the range $4 < m_H < 12$ GeV. See their Fig. 8 for limits on the Yukawa coupling.

[19] ABBIENDI 01E search for neutral Higgs bosons in general Type-II two-doublet models, at $E_{cm} \leq 189$ GeV. In addition to usual final states, the decays H_1^0, $A^0 \to q\overline{q}$, gg are searched for. See their Figs. 15,16 for excluded regions.

[20] ABBIENDI 99E search for $e^+e^- \to H^0 A^0$ and $H^0 Z$ at E_{cm} = 183 GeV. The limit is with $m_H = m_A$ in general two Higgs-doublet models. See their Fig. 18 for the exclusion limit in the m_H–m_A plane. Updates the results of ACKERSTAFF 98S.

[21] See Fig. 4 of ABREU 95H for the excluded region in the $m_{H^0} - m_{A^0}$ plane for general two-doublet models. For $\tan\beta > 1$, the region $m_{H^0} + m_{A^0} \lesssim 87$ GeV, $m_{H^0} < 47$ GeV is excluded at 95% CL.

[22] PICH 92 analyse H^0 with $m_{H^0} < 2m_\mu$ in general two-doublet models. Excluded regions in the space of mass-mixing angles from LEP, beam dump, and $\pi^\pm$, η rare decays are shown in Figs. 3,4. The considered mass region is not totally excluded.

Mass Limits for H^0 with Vanishing Yukawa Couplings

These limits assume that H^0 couples to gauge bosons with the same strength as the Standard Model Higgs boson, but has no coupling to quarks and leptons (this is often referred to as "fermiophobic").

VALUE (GeV)	CL%	DOCUMENT ID		TECN	COMMENT
• • • We do not use the following data for averages, fits, limits, etc. • • •					
	95	[1] AALTONEN	13K	CDF	$H^0 \to WW^{(*)}$
none 100–113	95	[2] AALTONEN	13L	CDF	$H^0 \to \gamma\gamma$, WW^*, ZZ^*
none 100–116	95	[3] AALTONEN	13M	TEVA	$H^0 \to \gamma\gamma$, WW^*, ZZ^*
		[4] ABAZOV	13G	D0	$H^0 \to WW^{(*)}$
none 100–113	95	[5] ABAZOV	13H	D0	$H^0 \to \gamma\gamma$
		[6] ABAZOV	13I	D0	$H^0 \to WW^{(*)}$
		[7] ABAZOV	13J	D0	$H^0 \to WW^{(*)}$, $ZZ^{(*)}$
none 100–114	95	[8] ABAZOV	13L	D0	$H^0 \to \gamma\gamma$, WW^*, ZZ^*
none 110–147	95	[9] CHATRCHYAN	13AL	CMS	$H^0 \to \gamma\gamma$
none 110–118, 119.5–121	95	[10] AAD	12N	ATLS	$H^0 \to \gamma\gamma$
none 100–114	95	[11] AALTONEN	12AN	CDF	$H^0 \to \gamma\gamma$
none 110–194	95	[12] CHATRCHYAN	12AO	CMS	$H^0 \to \gamma\gamma$, $WW^{(*)}$, $ZZ^{(*)}$
none 70–106	95	[13] AALTONEN	09AB	CDF	$H^0 \to \gamma\gamma$
none 70–100	95	[14] ABAZOV	08U	D0	$H^0 \to \gamma\gamma$
>105.8	95	[15] SCHAEL	07	ALEP	$e^+e^- \to H^0 Z$, $H^0 \to WW^*$
>104.1	95	[16,17] ABDALLAH	04L	DLPH	$e^+e^- \to H^0 Z$, $H^0 \to \gamma\gamma$
>107	95	[18] ACHARD	03C	L3	$H^0 \to WW^*, ZZ^*, \gamma\gamma$
>105.5	95	[16,19] ABBIENDI	02F	OPAL	$H^0 \to \gamma\gamma$
>105.4	95	[20] ACHARD	02C	L3	$H^0 \to \gamma\gamma$
none 60–82	95	[21] AFFOLDER	01H	CDF	$p\overline{p} \to H^0 W/Z$, $H^0 \to \gamma\gamma$
> 94.9	95	[22] ACCIARRI	00S	L3	$e^+e^- \to H^0 Z$, $H^0 \to \gamma\gamma$
>100.7	95	[23] BARATE	00L	ALEP	$e^+e^- \to H^0 Z$, $H^0 \to \gamma\gamma$
> 96.2	95	[24] ABBIENDI	99O	OPAL	$e^+e^- \to H^0 Z$, $H^0 \to \gamma\gamma$
> 78.5	95	[25] ABBOTT	99B	D0	$p\overline{p} \to H^0 W/Z$, $H^0 \to \gamma\gamma$
		[26] ABREU	99P	DLPH	$e^+e^- \to H^0\gamma$ and/or $H^0 \to \gamma\gamma$

[1] AALTONEN 13K search for $H^0 \to WW^{(*)}$ in 9.7 fb^{-1} of $p\overline{p}$ collisions at E_{cm} = 1.96 TeV. A limit on cross section times branching ratio which corresponds to (1.3–6.6) times the expected cross section is given in the range m_{H^0} = 110–200 GeV at 95% CL.

[2] AALTONEN 13L combine all CDF searches with 9.45–10.0 fb^{-1} of $p\overline{p}$ collisions at E_{cm} = 1.96 TeV.

[3] AALTONEN 13M combine all Tevatron data from the CDF and D0 Collaborations of $p\overline{p}$ collisions at E_{cm} = 1.96 TeV.

[4] ABAZOV 13G search for $H^0 \to WW^{(*)}$ in 9.7 fb^{-1} of $p\overline{p}$ collisions at E_{cm} = 1.96 TeV. A limit on cross section times branching ratio which corresponds to (2–9) times the expected cross section is given for m_{H^0} = 100–200 GeV at 95% CL.

[5] ABAZOV 13H search for $H^0 \to \gamma\gamma$ in 9.6 fb^{-1} of $p\overline{p}$ collisions at E_{cm} = 1.96 TeV.

[6] ABAZOV 13I search for H^0 production in the final state with one lepton and two or more jets plus missing E_T in 9.7 fb^{-1} of $p\overline{p}$ collisions at E_{cm} = 1.96 TeV. The search is sensitive to WH^0, ZH^0 and vector-boson fusion Higgs production with $H^0 \to WW^{(*)}$. A limit on cross section times branching ratio which corresponds to (8–30) times the expected cross section is given in the range m_{H^0} = 100–200 GeV at 95% CL.

[7] ABAZOV 13J search for H^0 production in the final states $ee\mu$, $e\mu\mu$, $\mu\tau\tau$, and $e^\pm\mu^\pm$ in 8.6–9.7 fb^{-1} of $p\overline{p}$ collisions at E_{cm} = 1.96 TeV. The search is sensitive to WH^0, ZH^0 production with $H^0 \to WW^{(*)}$, $ZZ^{(*)}$, decaying to leptonic final states. A limit on cross section times branching ratio which corresponds to (2.4–13.0) times the expected cross section is given in the range m_{H^0} = 100–200 GeV at 95% CL.

[8] ABAZOV 13L combine all D0 results with up to 9.7 fb^{-1} of $p\overline{p}$ collisions at E_{cm} = 1.96 TeV.

[9] CHATRCHYAN 13AL search for $H^0 \to \gamma\gamma$ in 5.1 fb^{-1} and 5.3 fb^{-1} of pp collisions at E_{cm} = 7 and 8 TeV.

[10] AAD 12N search for $H^0 \to \gamma\gamma$ with 4.9 fb^{-1} of pp collisions at E_{cm} = 7 TeV in the mass range m_{H^0} = 110–150 GeV.

[11] AALTONEN 12AN search for $H^0 \to \gamma\gamma$ with 10 fb^{-1} of $p\overline{p}$ collisions at E_{cm} = 1.96 TeV in the mass range m_{H^0} = 100–150 GeV.

[12] CHATRCHYAN 12AO use data from CHATRCHYAN 12G, CHATRCHYAN 12E, CHATRCHYAN 12H, CHATRCHYAN 12I, CHATRCHYAN 12D, and CHATRCHYAN 12C.

[13] AALTONEN 09AB search for $H^0 \to \gamma\gamma$ in 3.0 fb^{-1} of $p\overline{p}$ collisions at E_{cm} = 1.96 TeV in the mass range m_{H^0} = 70–150 GeV. Associated $H^0 W$, $H^0 Z$ production and WW, ZZ fusion are considered.

[14] ABAZOV 08U search for $H^0 \to \gamma\gamma$ in $p\overline{p}$ collisions at E_{cm} = 1.96 TeV in the mass range m_{H^0} = 70–150 GeV. Associated $H^0 W$, $H^0 Z$ production and WW, ZZ fusion are considered. See their Tab. 1 for the limit on $\sigma \cdot B(H^0 \to \gamma\gamma)$, and see their Fig. 3 for the excluded region in the m_{H^0} — $B(H^0 \to \gamma\gamma)$ plane.

[15] SCHAEL 07 search for Higgs bosons in association with a fermion pair and decaying to WW^*. The limit is from this search and HEISTER 02L for a H^0 with SM production cross section.

[16] Search for associated production of a $\gamma\gamma$ resonance with a Z boson, followed by $Z \to q\overline{q}$, $\ell^+\ell^-$, or $\nu\overline{\nu}$, at $E_{cm} \leq 209$ GeV. The limit is for a H^0 with SM production cross section.

[17] Updates ABREU 01F.

[18] ACHARD 03C search for $e^+e^- \to ZH^0$ followed by $H^0 \to WW^*$ or ZZ^* at E_{cm}= 200-209 GeV and combine with the ACHARD 02C result. The limit is for a H^0 with SM

production cross section. For B($H^0 \to WW^*$) + B($H^0 \to ZZ^*$) = 1, $m_{H^0} > 108.1$ GeV is obtained. See fig. 6 for the limits under different BR assumptions.

[19] For B($H^0 \to \gamma\gamma$)=1, m_{H^0} >117 GeV is obtained.

[20] ACHARD 02C search for associated production of a $\gamma\gamma$ resonance with a Z boson, followed by $Z \to q\overline{q}$, $\ell^+\ell^-$, or $\nu\overline{\nu}$, at $E_{cm} \leq 209$ GeV. The limit is for a H^0 with SM production cross section. For B($H^0 \to \gamma\gamma$)=1, m_{H^0} >114 GeV is obtained.

[21] AFFOLDER 01H search for associated production of a $\gamma\gamma$ resonance and a W or Z (tagged by two jets, an isolated lepton, or missing E_T). The limit assumes Standard Model values for the production cross section and for the couplings of the H^0 to W and Z bosons. See their Fig. 11 for limits with B($H^0 \to \gamma\gamma$)< 1.

[22] ACCIARRI 00S search for associated production of a $\gamma\gamma$ resonance with a $q\overline{q}$, $\nu\overline{\nu}$, or $\ell^+\ell^-$ pair in e^+e^- collisions at E_{cm}= 189 GeV. The limit is for a H^0 with SM production cross section. For B($H^0 \to \gamma\gamma$)=1, $m_{H^0} > 98$ GeV is obtained. See their Fig. 5 for limits on B($H \to \gamma\gamma$)·$\sigma(e^+e^- \to Hf\overline{f})/\sigma(e^+e^- \to Hf\overline{f})$ (SM).

[23] BARATE 00L search for associated production of a $\gamma\gamma$ resonance with a $q\overline{q}$, $\nu\overline{\nu}$, or $\ell^+\ell^-$ pair in e^+e^- collisions at E_{cm}= 88–202 GeV. The limit is for a H^0 with SM production cross section. For B($H^0 \to \gamma\gamma$)=1, $m_{H^0} > 109$ GeV is obtained. See their Fig. 3 for limits on B($H \to \gamma\gamma$)·$\sigma(e^+e^- \to Hf\overline{f})/\sigma(e^+e^- \to Hf\overline{f})$ (SM).

[24] ABBIENDI 99O search for associated production of a $\gamma\gamma$ resonance with a $q\overline{q}$, $\nu\overline{\nu}$, or $\ell^+\ell^-$ pair in e^+e^- collisions at 189 GeV. The limit is for a H^0 with SM production cross section. See their Fig. 4 for limits on $\sigma(e^+e^- \to H^0Z^0)$×B($H^0 \to \gamma\gamma$)×B($X^0 \to f\overline{f}$) for various masses. Updates the results of ACKERSTAFF 98Y.

[25] ABBOTT 99B search for associated production of a $\gamma\gamma$ resonance and a dijet pair. The limit assumes Standard Model values for the production cross section and for the couplings of the H^0 to W and Z bosons. Limits in the range of $\sigma(H^0 + Z/W)$·B($H^0 \to \gamma\gamma$)= 0.80–0.34 pb are obtained in the mass range m_{H^0}= 65–150 GeV.

[26] ABREU 99P search for $e^+e^- \to H^0\gamma$ with $H^0 \to b\overline{b}$ or $\gamma\gamma$, and $e^+e^- \to H^0q\overline{q}$ with $H^0 \to \gamma\gamma$. See their Fig. 4 for limits on σ×B. Explicit limits within an effective interaction framework are also given.

Mass Limits for H^0 Decaying to Invisible Final States

These limits are for a neutral scalar H^0 which predominantly decays to invisible final states. Standard Model values are assumed for the couplings of H^0 to ordinary particles unless otherwise stated.

VALUE (GeV)	CL%	DOCUMENT ID		TECN	COMMENT
• • • We do not use the following data for averages, fits, limits, etc. • • •					
		[1] AAD	15BD	ATLS	$pp \to H^0WX$, H^0ZX
		[2] AAD	15BH	ATLS	jet + missing E_T
		[3] AAD	14BA	ATLS	secondary vertex
		[4] AAD	14O	ATLS	$pp \to H^0ZX$
		[5] CHATRCHYAN	14B	CMS	$pp \to H^0ZX$, qqH^0X
		[6] AAD	13AG	ATLS	secondary vertex
		[7] AAD	13AT	ATLS	electron jets
		[8] CHATRCHYAN	13BJ	CMS	
		[9] AAD	12AQ	ATLS	secondary vertex
		[10] AALTONEN	12AB	CDF	secondary vertex
		[11] AALTONEN	12U	CDF	secondary vertex
>108.2	95	[12] ABBIENDI	10	OPAL	
		[13] ABBIENDI	07	OPAL	large width
>112.3	95	[14] ACHARD	05	L3	
>112.1	95	[14] ABDALLAH	04B	DLPH	
>114.1	95	[14] HEISTER	02	ALEP	$E_{cm} \leq 209$ GeV
>106.4	95	[14] BARATE	01C	ALEP	$E_{cm} \leq 202$ GeV
> 89.2	95	[15] ACCIARRI	00M	L3	

[1] AAD 15BD search for $pp \to H^0WX$ and $pp \to H^0ZX$ with W or Z decaying hadronically and H^0 decaying to invisible final states in 20.3 fb^{-1} at E_{cm} = 8TeV. See their Fig. 6 for a limit on the cross section times branching ratio for m_{H^0} = 115–300 GeV.

[2] AAD 15BH search for events with a jet and missing E_T in 20.3 fb^{-1} of pp collisions at E_{cm} = 8 TeV. Limits on $\sigma(H'^0)$ B($H'^0 \to$ invisible) < (44–10) pb (95%CL) is given for $m_{H'^0}$ = 115–300 GeV.

[3] AAD 14BA search for H^0 production in the decay mode $H^0 \to X^0X^0$, where X^0 is a long-lived particle which decays to collimated pairs of e^+e^-, $\mu^+\mu^-$, or $\pi^+\pi^-$ plus invisible particles, in 20.3 fb^{-1} of pp collisions at E_{cm} = 8 TeV. See their Figs. 15 and 16 for limits on cross section times branching ratio.

[4] AAD 14O search for $pp \to H^0ZX$, $Z \to \ell\ell$, with H^0 decaying to invisible final states in 4.5 fb^{-1} at E_{cm} = 7 TeV and 20.3 fb^{-1} at E_{cm} = 8 TeV. See their Fig. 3 for a limit on the cross section times branching ratio for m_{H^0} = 110–400 GeV.

[5] CHATRCHYAN 14B search for $pp \to H^0ZX$, $Z \to \ell\ell$ and $Z \to b\overline{b}$, and also $pp \to qqH^0X$ with H^0 decaying to invisible final states using data at E_{cm} = 7 and 8 TeV. See their Figs. 10, 11 for limits on the cross section times branching ratio for m_{H^0} = 100–400 GeV.

[6] AAD 13AG search for H^0 production in the decay mode $H^0 \to X^0X^0$, where X^0 is a long-lived particle which decays to $\mu^+\mu^-X'^0$, in 1.9 fb^{-1} of pp collisions at E_{cm} = 7 TeV. See their Fig. 7 for limits on cross section times branching ratio.

[7] AAD 13AT search for H^0 production in the decay $H^0 \to X^0X^0$, where X^0 eventually decays to clusters of collimated e^+e^- pairs, in 2.04 fb^{-1} of pp collisions at E_{cm} = 7 TeV. See their Fig. 3 for limits on cross section times branching ratio.

[8] CHATRCHYAN 13BJ search for H^0 production in the decay chain $H^0 \to X^0X^0$, $X^0 \to \mu^+\mu^-X'^0$ in 5.3 fb^{-1} of pp collisions at E_{cm} = 7 TeV. See their Fig. 2 for limits on cross section times branching ratio.

[9] AAD 12AQ search for H^0 production in the decay mode $H^0 \to X^0X^0$, where X^0 is a long-lived particle which decays mainly to $b\overline{b}$ in the muon detector, in 1.94 fb^{-1} of pp collisions at E_{cm} = 7 TeV. See their Fig. 3 for limits on cross section times branching ratio for m_{H^0} = 120, 140 GeV, m_{X^0} = 20, 40 GeV in the $c\tau$ range of 0.5–35 m.

[10] AALTONEN 12AB search for H^0 production in the decay $H^0 \to X^0X^0$, where X^0 eventually decays to clusters of collimated $\ell^+\ell^-$ pairs, in 5.1 fb^{-1} of $p\overline{p}$ collisions at E_{cm} = 1.96 TeV. Cross section limits are provided for a benchmark MSSM model incorporating the parameters given in Table VI.

[11] AALTONEN 12U search for H^0 production in the decay mode $H^0 \to X^0X^0$, where X^0 is a long-lived particle with $c\tau \approx 1$ cm which decays mainly to $b\overline{b}$, in 3.2 fb^{-1} of $p\overline{p}$ collisions at E_{cm} = 1.96 TeV. See their Figs. 9 and 10 for limits on cross section times branching ratio for m_{H^0} = (130–170) GeV, m_{X^0} = 20, 40 GeV.

[12] ABBIENDI 10 search for $e^+e^- \to H^0Z$ with H^0 decaying invisibly. The limit assumes SM production cross section and B($H^0 \to$ invisible) = 1.

[13] ABBIENDI 07 search for $e^+e^- \to H^0Z$ with $Z \to q\overline{q}$ and H^0 decaying to invisible final states. The H^0 width is varied between 1 GeV and 3 TeV. A limit σ·B($H^0 \to$ invisible) < (0.07–0.57) pb (95%CL) is obtained at E_{cm} = 206 GeV for m_{H^0} = 60–114 GeV.

[14] Search for $e^+e^- \to H^0Z$ with H^0 decaying invisibly. The limit assumes SM production cross section and B($H^0 \to$ invisible) = 1.

[15] ACCIARRI 00M search for $e^+e^- \to ZH^0$ with H^0 decaying invisibly at E_{cm}=183–189 GeV. The limit assumes SM production cross section and B($H^0 \to$ invisible)=1. See their Fig. 6 for limits for smaller branching ratios.

Mass Limits for Light A^0

These limits are for a pseudoscalar A^0 in the mass range below $\mathcal{O}(10)$ GeV.

VALUE (GeV)	DOCUMENT ID		TECN	COMMENT
• • • We do not use the following data for averages, fits, limits, etc. • • •				
	[1] KHACHATRY...17AZ		CMS	$H^0 \to A^0A^0$
	[2] ABLIKIM	16E	BES3	$J/\psi \to A^0\gamma$
	[3] KHACHATRY...16F		CMS	$H^0 \to A^0A^0$
	[4] LEES	15H	BABR	$\Upsilon(1S) \to A^0\gamma$
	[5] LEES	13C	BABR	$\Upsilon(1S) \to A^0\gamma$
	[6] LEES	13L	BABR	$\Upsilon(1S) \to A^0\gamma$
	[7] LEES	13R	BABR	$\Upsilon(1S) \to A^0\gamma$
	[8] ABLIKIM	12	BES3	$J/\psi \to A^0\gamma$
	[9] CHATRCHYAN	12V	CMS	$A^0 \to \mu^+\mu^-$
	[10] AALTONEN	11P	CDF	$t \to bH^+$, $H^+ \to W^+A^0$
	[11,12] ABOUZAID	11A	KTEV	$K_L \to \pi^0\pi^0A^0$, $A^0 \to \mu^+\mu^-$
	[13] DEL-AMO-SA...	11J	BABR	$\Upsilon(1S) \to A^0\gamma$
	[14] LEES	11H	BABR	$\Upsilon(2S,3S) \to A^0\gamma$
	[15] ANDREAS	10	RVUE	
	[12,16] HYUN	10	BELL	$B^0 \to K^{*0}A^0$, $A^0 \to \mu^+\mu^-$
	[12,17] HYUN	10	BELL	$B^0 \to \rho^0A^0$, $A^0 \to \mu^+\mu^-$
	[18] AUBERT	09P	BABR	$\Upsilon(3S) \to A^0\gamma$
	[19] AUBERT	09Z	BABR	$\Upsilon(2S) \to A^0\gamma$
	[20] AUBERT	09Z	BABR	$\Upsilon(3S) \to A^0\gamma$
	[12,21] TUNG	09	K391	$K_L \to \pi^0\pi^0A^0$, $A^0 \to \gamma\gamma$
	[22] LOVE	08	CLEO	$\Upsilon(1S) \to A^0\gamma$
	[23] BESSON	07	CLEO	$\Upsilon(1S) \to \eta_b\gamma$
	[24] PARK	05	HYCP	$\Sigma^+ \to pA^0$, $A^0 \to \mu^+\mu^-$
	[25] BALEST	95	CLE2	$\Upsilon(1S) \to A^0\gamma$
	[26] ANTREASYAN	90C	CBAL	$\Upsilon(1S) \to A^0\gamma$

[1] KHACHATRYAN 17AZ search for the decay $H^0 \to A^0A^0 \to \tau^+\tau^-\tau^+\tau^-$, $\mu^+\mu^-b\overline{b}$, and $\mu^+\mu^-\tau^+\tau^-$ in 19.7 fb^{-1} of pp collisions at E_{cm} = 8 TeV. See their Figs. 4, 5, and 6 for cross section limits in the range m_{A^0} = 5–62.5 GeV. See also their Figs. 7, 8, and 9 for interpretation of the data in terms of models with two Higgs doublets and a singlet.

[2] ABLIKIM 16E search for the process $J/\psi \to A^0\gamma$ with A^0 decaying to $\mu^+\mu^-$ and give limits on B($J/\psi \to A^0\gamma$)·B($A^0 \to \mu^+\mu^-$) in the range 2.8×10^{-8}–5.0×10^{-6} (90% CL) for $0.212 \leq m_{A^0} \leq 3.0$ GeV. See their Fig. 5.

[3] KHACHATRYAN 16F search for the decay $H^0 \to A^0A^0 \to \tau^+\tau^-\tau^+\tau^-$ in 19.7 fb^{-1} of pp collisions at E_{cm} = 8 TeV. See their Fig. 8 for cross section limits for m_{A^0} = 4–8 GeV.

[4] LEES 15H search for the process $\Upsilon(2S) \to \Upsilon(1S)\pi^+\pi^- \to A^0\gamma\pi^+\pi^-$ with A^0 decaying to $c\overline{c}$ and give limits on B($\Upsilon(1S) \to A^0\gamma$)·B($A^0 \to c\overline{c}$) in the range 7.4×10^{-5}–2.4×10^{-3} (90% CL) for $4.00 \leq m_{A^0} \leq 8.95$ and $9.10 \leq m_{A^0} \leq 9.25$ GeV. See their Fig. 6.

[5] LEES 13C search for the process $\Upsilon(2S,3S) \to \Upsilon(1S)\pi^+\pi^- \to A^0\gamma\pi^+\pi^-$ with A^0 decaying to $\mu^+\mu^-$ and give limits on B($\Upsilon(1S) \to A^0\gamma$)·B($A^0 \to \mu^+\mu^-$) in the range $(0.3–9.7)\times10^{-6}$ (90% CL) for $0.212 \leq m_{A^0} \leq 9.20$ GeV. See their Fig. 5(e) for limits on the $b-A^0$ Yukawa coupling derived by combining this result with AUBERT 09Z.

[6] LEES 13L search for the process $\Upsilon(2S) \to \Upsilon(1S)\pi^+\pi^- \to A^0\gamma\pi^+\pi^-$ with A^0 decaying to gg or $s\overline{s}$ and give limits on B($\Upsilon(1S) \to A^0\gamma$)·B($A^0 \to gg$) between 1×10^{-6} and 2×10^{-2} (90% CL) for $0.5 \leq m_{A^0} \leq 9.0$ GeV, and B($\Upsilon(1S) \to A^0\gamma$)·B($A^0 \to s\overline{s}$) between 4×10^{-6} and 1×10^{-3} (90%CL) for $1.5 \leq m_{A^0} \leq 9.0$ GeV. See their Fig. 4.

[7] LEES 13R search for the process $\Upsilon(2S) \to \Upsilon(1S)\pi^+\pi^- \to A^0\gamma\pi^+\pi^-$ with A^0 decaying to $\tau^+\tau^-$ and give limits on B($\Upsilon(1S) \to A^0\gamma$)·B($A^0 \to \tau^+\tau^-$) in the range $0.9–13\times10^{-5}$ (90% CL) for $3.6 \leq m_{A^0} \leq 9.2$ GeV. See their Fig. 4 for limits on the $b-A^0$ Yukawa coupling derived by combining this result with AUBERT 09P.

[8] ABLIKIM 12 searches for the process $\psi(3686) \to \pi\pi J/\psi$, $J/\psi \to A^0\gamma$ with A^0 decaying to $\mu^+\mu^-$. It gives mass dependent limits on B($J/\psi \to A^0\gamma$)·B($A^0 \to \mu^+\mu^-$) in the range 4×10^{-7}–2.1×10^{-5} (90% C.L.) for $0.212 \leq m_{A^0} \leq 3.0$ GeV. See their Fig. 2.

[9] CHATRCHYAN 12V search for A^0 production in the decay $A^0 \to \mu^+\mu^-$ with 1.3 fb^{-1} of pp collisions at E_{cm} = 7 TeV. A limit on $\sigma(A^0)$·B($A^0 \to \mu^+\mu^-$) in the range (1.5–7.5) pb is given for m_{A^0} = (5.5–8.7) and (11.5–14) GeV at 95% CL.

Gauge & Higgs Boson Particle Listings

Neutral Higgs Bosons, Searches for

[10] AALTONEN 11P search in 2.7 fb^{-1} of $p\overline{p}$ collisions at E_{cm} = 1.96 TeV for the decay chain $t \to bH^+$, $H^+ \to W^+A^0$, $A^0 \to \tau^+\tau^-$ with m_{A^0} between 4 and 9 GeV. See their Fig. 4 for limits on B($t \to bH^+$) for $90 < m_{H^+} < 160$ GeV.

[11] ABOUZAID 11A search for the decay chain $K_L \to \pi^0\pi^0A^0$, $A^0 \to \mu^+\mu^-$ and give a limit B($K_L \to \pi^0\pi^0A^0$) · B($A^0 \to \mu^+\mu^-$) $< 1.0\times10^{-10}$ at 90% CL for m_{A^0} = 214.3 MeV.

[12] The search was motivated by PARK 05.

[13] DEL-AMO-SANCHEZ 11J search for the process $\Upsilon(2S) \to \Upsilon(1S)\pi^+\pi^-$ → $A^0\gamma\pi^+\pi^-$ with A^0 decaying to invisible final states. They give limits on B($\Upsilon(1S) \to A^0\gamma$)·B($A^0 \to$ invisible) in the range (1.9–4.5) $\times10^{-6}$ (90% CL) for $0 \le m_{A^0} \le$ 8.0 GeV, and (2.7–37) $\times10^{-6}$ for $8.0 \le m_{A^0} \le$ 9.2 GeV.

[14] LEES 11H search for the process $\Upsilon(2S,3S) \to A^0\gamma$ with A^0 decaying hadronically and give limits on B($\Upsilon(2S,3S) \to A^0\gamma$)·B($A^0 \to$ hadrons) in the range 1×10^{-6}–8×10^{-5} (90% CL) for $0.3 < m_{A^0} < 7$ GeV. The decay rates for $\Upsilon(2S)$ and $\Upsilon(3S)$ are assumed to be equal up to the phase space factor. See their Fig. 5.

[15] ANDREAS 10 analyze constraints from rare decays and other processes on a light A^0 with $m_{A^0} < 2m_\mu$ and give limits on its coupling to fermions at the level of 10^{-4} times the Standard Model value.

[16] HYUN 10 search for the decay chain $B^0 \to K^{*0}A^0$, $A^0 \to \mu^+\mu^-$ and give a limit on B($B^0 \to K^{*0}A^0$) · B($A^0 \to \mu^+\mu^-$) in the range (2.26–5.53) $\times10^{-8}$ at 90%CL for m_{A^0} = 212–300 MeV. The limit for m_{A^0} = 214.3 MeV is 2.26×10^{-8}.

[17] HYUN 10 search for the decay chain $B^0 \to \rho^0A^0$, $A^0 \to \mu^+\mu^-$ and give a limit on B($B^0 \to \rho^0A^0$) · B($A^0 \to \mu^+\mu^-$) in the range (1.73–4.51) $\times10^{-8}$ at 90%CL for m_{A^0} = 212–300 MeV. The limit for m_{A^0} = 214.3 MeV is 1.73×10^{-8}.

[18] AUBERT 09P search for the process $\Upsilon(3S) \to A^0\gamma$ with $A^0 \to \tau^+\tau^-$ for 4.03 $< m_{A^0} <$ 9.52 and 9.61 $< m_{A^0} <$ 10.10 GeV, and give limits on B($\Upsilon(3S) \to A^0\gamma$)·B($A^0 \to \tau^+\tau^-$) in the range (1.5–16) $\times10^{-5}$ (90% CL).

[19] AUBERT 09Z search for the process $\Upsilon(2S) \to A^0\gamma$ with $A^0 \to \mu^+\mu^-$ for 0.212 $< m_{A^0} <$ 9.3 GeV and give limits on B($\Upsilon(2S) \to A^0\gamma$)·B($A^0 \to \mu^+\mu^-$) in the range (0.3–8) $\times10^{-6}$ (90% CL).

[20] AUBERT 09Z search for the process $\Upsilon(3S) \to A^0\gamma$ with $A^0 \to \mu^+\mu^-$ for 0.212 $< m_{A^0} <$ 9.3 GeV and give limits on B($\Upsilon(3S) \to A^0\gamma$)·B($A^0 \to \mu^+\mu^-$) in the range (0.3–5) $\times10^{-6}$ (90% CL).

[21] TUNG 09 search for the decay chain $K_L \to \pi^0\pi^0A^0$, $A^0 \to \gamma\gamma$ and give a limit on B($K_L \to \pi^0\pi^0A^0$) · B($A^0 \to \gamma\gamma$) in the range (2.4–10.7) $\times10^{-7}$ at 90%CL for m_{A^0} = 194.3–219.3 MeV. The limit for m_{A^0} = 214.3 MeV is 2.4×10^{-7}.

[22] LOVE 08 search for the process $\Upsilon(1S) \to A^0\gamma$ with $A^0 \to \mu^+\mu^-$ (for $m_{A^0} < 2m_\tau$) and $A^0 \to \tau^+\tau^-$. Limits on B($\Upsilon(1S) \to A^0\gamma$) · B($A^0 \to \ell^+\ell^-$) in the range 10^{-6}–10^{-4} (90% CL) are given.

[23] BESSON 07 give a limit B($\Upsilon(1S) \to \eta_b\gamma$) · B($\eta_b \to \tau^+\tau^-$) < 0.27% (95% CL), which constrains a possible A^0 exchange contribution to the η_b decay.

[24] PARK 05 found three candidate events for $\Sigma^+ \to p\mu^+\mu^-$ in the HyperCP experiment. Due to a narrow spread in dimuon mass, they hypothesize the events as a possible signal of a new boson. It can be interpreted as a neutral particle with $m_{A^0} = 214.3 \pm 0.5$ MeV and the branching fraction B($\Sigma^+ \to pA^0$)·B($A^0 \to \mu^+\mu^-$) = $(3.1^{+2.4}_{-1.9}\pm1.5)\times10^{-8}$.

[25] BALEST 95 give limits B($\Upsilon(1S) \to A^0\gamma$) ¡ 1.5×10^{-5} at 90% CL for $m_{A^0} <$ 5 GeV. The limit becomes $< 10^{-4}$ for $m_{A^0} <$ 7.7 GeV.

[26] ANTREASYAN 90C give limits B($\Upsilon(1S) \to A^0\gamma$) ¡ 5.6×10^{-5} at 90% CL for $m_{A^0} <$ 7.2 GeV. A^0 is assumed not to decay in the detector.

Other Mass Limits

We use a symbol H^0_1 if mass < 125 GeV or H^0_2 if mass > 125 GeV. The notation H^0 is reserved for the 125 GeV particle.

VALUE (GeV)	CL%	DOCUMENT ID		TECN	COMMENT
• • • We do not use the following data for averages, fits, limits, etc. • • •					
		[1] SIRUNYAN	18F	CMS	pp, 13 TeV, $H^0_2 \to H^0H^0$
		[2] AABOUD	17	ATLS	$H^0_2 \to Z\gamma$
		[3] AABOUD	17AW	ATLS	$H^0_2 \to Z\gamma$
		[4] KHACHATRY...	17D	CMS	pp, 8, 13 TeV, $H^0_2 \to Z\gamma$
		[5] KHACHATRY...	17R	CMS	$H^0_2 \to \gamma\gamma$
		[6] SIRUNYAN	17CN	CMS	pp, 8 TeV, $H^0_2 \to H^0H^0$
		[7] SIRUNYAN	17Y	CMS	pp, 8, 13 TeV, $H^0_2 \to Z\gamma$
		[8] AABOUD	16AB	ATLS	$H^0 \to A^0A^0$
		[9] AABOUD	16AE	ATLS	$H^0_2 \to W^+W^-, ZZ$
		[10] AABOUD	16H	ATLS	$H^0_2 \to \gamma\gamma$
		[11] AABOUD	16I	ATLS	$H^0_2 \to H^0H^0$
		[12] AAD	16AX	ATLS	$H^0 \to ZZ$
		[13] AAD	16C	ATLS	$H^0 \to W^+W^-$
		[14] AAD	16L	ATLS	$H^0 \to A^0A^0$
		[15] AAD	16L	ATLS	$H^0_2 \to A^0A^0$
		[16] AALTONEN	16C	CDF	$H^0_1H^\pm \to H^0_1H^0_1W^*$, $H^0_1 \to \gamma\gamma$
		[17] KHACHATRY...	16BG	CMS	$H^0_2 \to H^0H^0$
		[18] KHACHATRY...	16BQ	CMS	pp, 8 TeV, $H^0_2 \to H^0H^0$
		[19] KHACHATRY...	16F	CMS	$H^0 \to H^0_1H^0_1$
		[20] KHACHATRY...	16M	CMS	$H^0_2 \to \gamma\gamma$
		[21] KHACHATRY...	16P	CMS	$H^0_2 \to H^0H^0$
		[22] KHACHATRY...	16P	CMS	$A^0 \to ZH^0$
		[23] AAD	15BK	ATLS	$H^0_2 \to H^0H^0$
		[24] AAD	15BZ	ATLS	$H^0 \to A^0A^0$
		[25] AAD	15BZ	ATLS	$H^0_2 \to A^0A^0$
		[26] AAD	15CE	ATLS	$H^0_2 \to H^0H^0$
		[27] AAD	15H	ATLS	$H^0_2 \to H^0H^0$
		[28] AAD	15S	ATLS	$A^0 \to ZH^0$
		[29] KHACHATRY...	15AW	CMS	$H^0_2 \to W^+W^-, ZZ$
		[30] KHACHATRY...	15BB	CMS	$H^0 \to \gamma\gamma$
		[31] KHACHATRY...	15N	CMS	$A^0 \to ZH^0$
		[32] KHACHATRY...	15O	CMS	$A^0 \to ZH^0$
		[33] KHACHATRY...	15R	CMS	$H^0_2 \to H^0H^0$
		[34] AAD	14AP	ATLS	$H^0 \to \gamma\gamma$
		[35] AAD	14M	ATLS	$H^0_2 \to H^\pm W^\mp \to H^0W^\pm W^\mp$, $H^0 \to b\overline{b}$
		[36] CHATRCHYAN	14G	CMS	$H^0 \to WW^{(*)}$
		[37] KHACHATRY...	14P	CMS	$H^0 \to \gamma\gamma$
		[38] AALTONEN	13P	CDF	$H'^0 \to H^\pm W^\mp \to H^0W^+W^-$
		[39] CHATRCHYAN	13BJ	CMS	$H^0 \to A^0A^0$
		[40] AALTONEN	11P	CDF	$t \to bH^+$, $H^+ \to W^+A^0$
		[41] ABBIENDI	10	OPAL	$H^0 \to \widetilde{\chi}^0_1\widetilde{\chi}^0_2$
		[42] SCHAEL	10	ALEP	$H^0 \to A^0A^0$
		[43] ABAZOV	09V	D0	$H^0 \to A^0A^0$
none 3–63	95	[44] ABBIENDI	05A	OPAL	A^0, Type II model
>104	95	[45] ABBIENDI	04K	OPAL	$H^0 \to$ 2 jets
		[46] ABDALLAH	04	DLPH	H^0VV couplings
>110.3	95	[47] ACHARD	04B	L3	$H^0 \to$ 2 jets
		[48] ACHARD	04F	L3	Anomalous coupling
		[49] ABBIENDI	03F	OPAL	$e^+e^- \to H^0Z$, $H^0 \to$ any
		[50] ABBIENDI	03G	OPAL	$H^0_1 \to A^0A^0$
>105.4	95	[51,52] HEISTER	02L	ALEP	$H^0_1 \to \gamma\gamma$
>109.1	95	[53] HEISTER	02M	ALEP	$H^0 \to$ 2 jets or $\tau^+\tau^-$
none 12–56	95	[54] ABBIENDI	01E	OPAL	A^0, Type-II model
		[55] ACCIARRI	00R	L3	$e^+e^- \to H^0\gamma$ and/or $H^0 \to \gamma\gamma$
		[56] ACCIARRI	00R	L3	$e^+e^- \to e^+e^-H^0$
		[57] GONZALEZ...	98B	RVUE	Anomalous coupling
		[58] KRAWCZYK	97	RVUE	$(g-2)_\mu$
		[59] ALEXANDER	96H	OPAL	$Z \to H^0\gamma$

[1] SIRUNYAN 18F search for a narrow scalar resonance decaying to $H^0H^0 \to WWb\overline{b}$ or $ZZb\overline{b}$ in the final state $\ell\ell\nu\nu b\overline{b}$ in 35.9 fb^{-1} of pp collisions at E_{cm} = 13 TeV. See their Fig. 7 for limits on cross section times branching ratios for $m_{H^0_2}$ = 250–900 GeV.

[2] AABOUD 17 search for production of a scalar resonance decaying to $Z\gamma$ in 3.2 fb^{-1} of pp collisions at E_{cm} = 13 TeV. See their Fig. 4 for the limits on cross section times branching ratio for $m_{H^0_2}$ = 0.25–3.0 TeV.

[3] AABOUD 17AW search for production of a scalar resonance decaying to $Z\gamma$ in 36.1 fb^{-1} of pp collisions at E_{cm} = 13 TeV. See their Fig. 7 for limits on cross section times branching ratio for $m_{H^0_2}$ = 0.25–2.4 TeV.

[4] KHACHATRYAN 17D search for production of a scalar resonance decaying to $Z\gamma$ in 19.7 fb^{-1} of pp collisions at E_{cm} = 8 TeV and 2.7 fb^{-1} at E_{cm} = 13 TeV. See their Figs. 3 and 4 for the limits on cross section times branching ratio for $m_{H^0_2}$ = 0.2–2.0 TeV.

[5] KHACHATRYAN 17R search for production of a narrow scalar resonance decaying to $\gamma\gamma$ in 12.9 fb^{-1} (taken in 2016) of pp collisions at E_{cm} = 13 TeV. See their Fig. 2 for limits on cross section times branching ratio for $m_{H^0_2}$ = 0.5–4.5 TeV for several values of its width-to-mass ratio. Limits from combination with KHACHATRYAN 16M are shown in their Figs. 4 and 6.

[6] SIRUNYAN 17CN search for a narrow scalar resonance decaying to $H^0H^0 \to b\overline{b}\tau^+\tau^-$ in 18.3 fb^{-1} of pp collisions at E_{cm} = 8 TeV. See their Fig. 5 (above) and Table II for limits on the cross section times branching ratios for $m_{H^0_2}$ = 0.3–1 TeV, and Fig. 6 (above) and Table III for the corresponding limits by combining with data from KHACHATRYAN 16BQ and KHACHATRYAN 15R.

[7] SIRUNYAN 17Y search for production of a scalar resonance decaying to $Z\gamma$ in 19.7 fb^{-1} of pp collisions at E_{cm} = 8 TeV and 2.7 fb^{-1} at E_{cm} = 13 TeV. See their Figs. 3, 4 and Table 3 for limits on cross section times branching ratio for $m_{H^0_2}$ = 0.7–3.0 TeV, and Fig. 5 for the corresponding limits for $m_{H^0_2}$ = 0.2–3.0 TeV from combination with KHACHATRYAN 17D data.

[8] AABOUD 16AB search for associated production of WH^0 with the decay $H^0 \to A^0A^0 \to b\overline{b}b\overline{b}$ in 3.2 fb^{-1} of pp collisions at E_{cm} = 13 TeV. See their Fig. 8 for limits on cross section times branching ratios for m_{A^0} = 20–60 GeV.

[9] AABOUD 16AE search for production of a narrow scalar resonance decaying to W^+W^- and ZZ in 3.2 fb^{-1} of pp collisions at E_{cm} = 13 TeV. See their Fig. 4 for limits on cross section times branching ratio for $m_{H^0_2}$ = 0.5–3 TeV.

[10] AABOUD 16H search for production of a scalar resonance decaying to $\gamma\gamma$ in 3.2 fb^{-1} of pp collisions at E_{cm} = 13 TeV. See their Fig. 12 for limits on cross section times branching ratio for $m_{H^0_2}$ = 0.2–2 TeV with different assumptions on the width.

[11] AABOUD 16I search for a narrow scalar resonance decaying to $H^0H^0 \to b\overline{b}b\overline{b}$ in 3.2 fb^{-1} of pp collisions at E_{cm} = 13 TeV. See their Fig. 10(c) for limits on cross section times branching ratios for $m_{H^0_2}$ = 0.5–3 TeV.

[12] AAD 16AX search for production of a heavy H^0 state decaying to ZZ in the final states $\ell^+\ell^-\ell^+\ell^-$, $\ell^+\ell^-\nu\overline{\nu}$, $\ell^+\ell^- q\overline{q}$, and $\nu\overline{\nu}q\overline{q}$ in 20.3 fb^{-1} of pp collisions at E_{cm} = 8 TeV. See their Fig.12 for upper limits on $\sigma(H^0)$ B($H^0 \to ZZ$) for m_{H^0} ranging from 140 GeV to 1000 GeV.

[13] AAD 16C search for production of a heavy H^0 state decaying to W^+W^- in the final states $\ell\nu\ell\nu$ and $\ell\nu qq$ in 20.3 fb^{-1} of pp collisions at E_{cm} = 8 TeV. See their Figs. 12, 13, and 16 for upper limits on $\sigma(H^0)$ B($H^0 \to W^+W^-$) for m_{H^0} ranging from 300 GeV to 1000 or 1500 GeV with various assumptions on the total width of H^0.

[14] AAD 16L search for the decay $H^0 \to A^0A^0 \to \gamma\gamma\gamma\gamma$ in 20.3 fb^{-1} of pp collisions at E_{cm} = 8 TeV. See their Fig. 4 (upper right) for limits on cross section times branching ratios (normalized to the SM H^0 cross section) for m_{A^0} = 10–60 GeV.

[15] AAD 16L search for the decay $H_2^0 \to A^0A^0 \to \gamma\gamma\gamma\gamma$ in 20.3 fb^{-1} of pp collisions at E_{cm} = 8 TeV. See their Fig. 4 (lower right) for limits on cross section times branching ratios for $m_{H_2^0}$ = 600 GeV and m_{A^0} = 10–245 GeV, and Table 5 for limits for $m_{H_2^0}$= 300 and 900 GeV.

[16] AALTONEN 16C search for electroweak associated production of $H_1^0H^\pm$ followed by the decays $H^\pm \to H_1^0W^*$, $H_1^0 \to \gamma\gamma$ for $m_{H_1^0}$ = 10–105 GeV and $m_{H^\pm}$ = 30–300 GeV. See their Fig. 3 for excluded parameter region in a two-doublet model in which H_1^0 has no direct decay to fermions.

[17] KHACHATRYAN 16BG search for a narrow scalar resonance decaying to $H^0H^0 \to b\overline{b}b\overline{b}$ in 19.7 fb^{-1} of pp collisions at E_{cm} = 8 TeV. See their Fig. 6 for limits on the cross section times branching ratios for $m_{H_2^0}$ = 1.15–3 TeV.

[18] KHACHATRYAN 16BQ search for a resonance decaying to $H^0H^0 \to \gamma\gamma b\overline{b}$ in 19.7 fb^{-1} of pp collisions at E_{cm} = 8 TeV. See their Fig. 9 for limits on the cross section times branching ratios for $m_{H_2^0}$ = 0.26–1.1 TeV.

[19] KHACHATRYAN 16F search for the decay $H^0 \to H_1^0H_1^0 \to \tau^+\tau^-\tau^+\tau^-$ in 19.7 fb^{-1} of pp collisions at E_{cm} = 8 TeV. See their Fig. 8 for cross section limits for $m_{H_1^0}$ = 4–8 GeV.

[20] KHACHATRYAN 16M search for production of a narrow resonance decaying to $\gamma\gamma$ in 19.7 fb^{-1} of pp collisions at E_{cm} = 8 TeV and 3.3 fb^{-1} at E_{cm} = 13 TeV. See their Fig. 3 (top) for limits on cross section times branching ratio for $m_{H_2^0}$ = 0.5–4 TeV.

[21] KHACHATRYAN 16P search for gluon fusion production of an H_2^0 decaying to $H^0H^0 \to b\overline{b}\tau^+\tau^-$ in 19.7 fb^{-1} of pp collisions at E_{cm} = 8 TeV. See their Fig. 8 (lower right) for cross section limits for $m_{H_2^0}$ = 260–350 GeV.

[22] KHACHATRYAN 16P search for gluon fusion production of an A^0 decaying to $ZH^0 \to \ell^+\ell^-\tau^+\tau^-$ in 19.7 fb^{-1} of pp collisions at E_{cm} = 8 TeV. See their Fig. 10 for cross section limits for $m_{H_2^0}$ = 220–350 GeV.

[23] AAD 15BK search for production of a heavy H_2^0 decaying to H^0H^0 in the final state $b\overline{b}b\overline{b}$ in 19.5 fb^{-1} of pp collisions at E_{cm} = 8 TeV. See their Fig. 14(c) for $\sigma(H_2^0)$ B($H_2^0 \to H^0H^0$) for $m_{H_2^0}$ = 500–1500 GeV with $\Gamma_{H_2^0}$ = 1 GeV.

[24] AAD 15BZ search for the decay $H^0 \to A^0A^0 \to \mu^+\mu^-\tau^+\tau^-$ (m_{H^0} = 125 GeV) in 20.3 fb^{-1} of pp collisions at E_{cm} = 8 TeV. See their Fig. 6 for limits on cross section times branching ratio for m_{A^0} = 3.7–50 GeV.

[25] AAD 15BZ search for a state H_2^0 via the decay $H_2^0 \to A^0A^0 \to \mu^+\mu^-\tau^+\tau^-$ in 20.3 fb^{-1} of pp collisions at E_{cm} = 8 TeV. See their Fig. 6 for limits on cross section times branching ratio for $m_{H_2^0}$ = 100–500 GeV and m_{A^0} = 5 GeV.

[26] AAD 15CE search for production of a heavy H_2^0 decaying to H^0H^0 in the final states $b\overline{b}\tau^+\tau^-$ and $\gamma\gamma WW^*$ in 20.3 fb^{-1} of pp collisions at E_{cm} = 8 TeV and combine with data from AAD 15H and AAD 15BK. A limit $\sigma(H_2^0)$ B($H_2^0 \to H^0H^0$) < 2.1–0.011 pb (95% CL) is given for $m_{H_2^0}$ = 260–1000 GeV. See their Fig. 6.

[27] AAD 15H search for production of a heavy H_2^0 decaying to H^0H^0 in the finalstate $\gamma\gamma b\overline{b}$ in 20.3 fb^{-1} of pp collisions at E_{cm} = 8 TeV.A limit of $\sigma(H_2^0)$ B($H_2^0 \to H^0H^0$) < 3.5–0.7 pb is given for $m_{H_2^0}$ = 260–500 GeV at 95% CL. See their Fig. 3.

[28] AAD 15S search for production of A^0 decaying to $ZH^0 \to \ell^+\ell^-b\overline{b}$, $\nu\overline{\nu}b\overline{b}$ and $\ell^+\ell^-\tau^+\tau^-$ in 20.3 fb^{-1} of pp collisions at E_{cm} = 8 TeV. See their Fig. 3 for cross section limits for m_{A^0} = 200–1000 GeV.

[29] KHACHATRYAN 15AW search for production of a heavy state H_2^0 of an electroweak singlet extension of the Standard Model via the decays of H_2^0 to W^+W^- and ZZ in up to 5.1 fb^{-1} of pp collisions at E_{cm} = 7 TeV and up to 19.7 fb^{-1} at E_{cm} = 8 TeV in the range $m_{H_2^0}$ = 145–1000 GeV. See their Figs. 8 and 9 for limits in the parameter space of the model.

[30] KHACHATRYAN 15BB search for production of a resonance H^0 decaying to $\gamma\gamma$ in 19.7 fb^{-1} of pp collisions at E_{cm} = 8 TeV. See their Fig. 7 for limits on cross section times branching ratio for m_{H^0} = 150–850 GeV.

[31] KHACHATRYAN 15N search for production of A^0 decaying to $ZH^0 \to \ell^+\ell^-b\overline{b}$ in 19.7 fb^{-1} of pp collisions at E_{cm} = 8 TeV. See their Fig. 3 for limits on cross section times branching ratios for m_{A^0} = 225–600 GeV.

[32] KHACHATRYAN 15O search for production of a high-mass narrow resonance A^0 decaying to $ZH^0 \to q\overline{q}\tau^+\tau^-$ in 19.7 fb^{-1} of pp collisions at E_{cm} = 8 TeV. See their Fig. 6 for limits on cross section times branching ratios for m_{A^0} = 800–2500 GeV.

[33] KHACHATRYAN 15R search for a narrow scalar resonance decaying to $H^0H^0 \to b\overline{b}b\overline{b}$ in 17.9 fb^{-1} of pp collisions at E_{cm} = 8 TeV. See their Fig. 5 (top) for limits on cross section times branching ratios for $m_{H_2^0}$ = 0.27–1.1 TeV.

[34] AAD 14AP search for a second H^0 state decaying to $\gamma\gamma$ in addition to the state at about 125 GeV in 20.3 fb^{-1} of pp collisions at E_{cm} = 8 TeV. See their Fig. 4 for limits on cross section times branching ratio for m_{H^0} = 65–600 GeV.

[35] AAD 14M search for the decay cascade $H_2^0 \to H^\pm W^\mp \to H^0W^\pm W^\mp$, H^0 decaying to $b\overline{b}$ in 20.3 fb^{-1} of pp collisions at E_{cm} = 8 TeV. See their Table III for limits on cross section times branching ratio for $m_{H_2^0}$= 325–1025 GeV and m_{H^+}= 225–925 GeV.

[36] CHATRCHYAN 14G search for a second H^0 state decaying to $WW^{(*)}$ in addition to the observed signal at about 125 GeV using 4.9 fb^{-1} of pp collisions at E_{cm} = 7 TeV and 19.4 fb^{-1} at E_{cm} = 8 TeV. See their Fig. 21 (right) for cross section limits in the mass range 110–600 GeV.

[37] KHACHATRYAN 14P search for a second H^0 state decaying to $\gamma\gamma$ in addition to the observed signal at about 125 GeV using 5.1 fb^{-1} of pp collisions at E_{cm} = 7 TeV and 19.7 fb^{-1} at E_{cm} = 8 TeV. See their Figs. 27 and 28 for cross section limits in the mass range 110–150 GeV.

[38] AALTONEN 13P search for production of a heavy Higgs boson H'^0 that decays into a charged Higgs boson $H^\pm$ and a lighter Higgs boson H^0 via the decay chain $H'^0 \to H^\pm W^\mp$, $H^\pm \to W^\pm H^0$, $H^0 \to b\overline{b}$ in the final state $\ell\nu$ plus 4 jets in 8.7 fb^{-1} of $p\overline{p}$ collisions at E_{cm} = 1.96 TeV. See their Fig. 4 for limits on cross section times branching ratio in the $m_{H^\pm}$–$m_{H'^0}$ plane for m_{H^0} = 126 GeV.

[39] CHATRCHYAN 13BJ search for H^0 production in the decay chain $H^0 \to A^0A^0$, $A^0 \to \mu^+\mu^-$ in 5.3 fb^{-1} of pp collisions at E_{cm} = 7 TeV. See their Fig. 2 for limits on cross section times branching ratio.

[40] AALTONEN 11P search in 2.7 fb^{-1} of $p\overline{p}$ collisions at E_{cm} = 1.96 TeV for the decay chain $t \to bH^+$, $H^+ \to W^+A^0$, $A^0 \to \tau^+\tau^-$ with m_{A^0} between 4 and 9 GeV. See their Fig. 4 for limits on B($t \to bH^+$) for $90 < m_{H^+} < 160$ GeV.

[41] ABBIENDI 10 search for $e^+e^- \to ZH^0$ with the decay chain $H^0 \to \tilde{\chi}_1^0\tilde{\chi}_2^0$, $\tilde{\chi}_2^0 \to \tilde{\chi}_1^0 + (\gamma$ or $Z^*)$, when $\tilde{\chi}_1^0$ and $\tilde{\chi}_2^0$ are nearly degenerate. For a mass difference of 2 (4) GeV, a lower limit on m_{H^0} of 108.4 (107.0) GeV (95% CL) is obtained for SM ZH^0 cross section and B($H^0 \to \tilde{\chi}_1^0\tilde{\chi}_2^0$) = 1.

[42] SCHAEL 10 search for the process $e^+e^- \to H^0Z$ followed by the decay chain $H^0 \to A^0A^0 \to \tau^+\tau^-\tau^+\tau^-$ with $Z \to \ell^+\ell^-$, $\nu\overline{\nu}$ at E_{cm} = 183–209 GeV. For a H^0ZZ coupling equal to the SM value, B($H^0 \to A^0A^0$) = B($A^0 \to \tau^+\tau^-$) = 1, and m_{A^0} = 4–10 GeV, m_{H^0} up to 107 GeV is excluded at 95% CL.

[43] ABAZOV 09V search for H^0 production followed by the decay chain $H^0 \to A^0A^0 \to \mu^+\mu^-\mu^+\mu^-$ or $\mu^+\mu^-\tau^+\tau^-$ in 4.2 fb^{-1} of $p\overline{p}$ collisions at E_{cm} = 1.96 TeV. See their Fig. 3 for limits on $\sigma(H^0)$·B($H^0 \to A^0A^0$) for m_{A^0} = 3.6–19 GeV.

[44] ABBIENDI 05A search for $e^+e^- \to H_1^0A^0$ in general Type-II two-doublet models, with decays H_1^0, $A^0 \to q\overline{q}$, gg, $\tau^+\tau^-$, and $H_1^0 \to A^0A^0$.

[45] ABBIENDI 04K search for $e^+e^- \to H^0Z$ with H^0 decaying to two jets of any flavor including gg. The limit is for SM production cross section with B($H^0 \to jj$) = 1.

[46] ABDALLAH 04 consider the full combined LEP and LEP2 datasets to set limits on the Higgs coupling to W or Z bosons, assuming SM decays of the Higgs. Results in Fig. 26.

[47] ACHARD 04B search for $e^+e^- \to H^0Z$ with H^0 decaying to $b\overline{b}$, $c\overline{c}$, or gg. The limit is for SM production cross section with B($H^0 \to jj$) = 1.

[48] ACHARD 04F search for H^0 with anomalous coupling to gauge boson pairs in the processes $e^+e^- \to H^0\gamma$, $e^+e^-H^0$, H^0Z with decays $H^0 \to f\overline{f}$, $\gamma\gamma$, $Z\gamma$, and W^*W at E_{cm} = 189–209 GeV. See paper for limits.

[49] ABBIENDI 03F search for $H^0 \to$ anything in $e^+e^- \to H^0Z$, using the recoil mass spectrum of $Z \to e^+e^-$ or $\mu^+\mu^-$. In addition, it searched for $Z \to \nu\overline{\nu}$ and $H^0 \to e^+e^-$ or photons. Scenarios with large width or continuum H^0 mass distribution are considered. See their Figs. 11–14 for the results.

[50] ABBIENDI 03G search for $e^+e^- \to H_1^0Z$ followed by $H_1^0 \to A^0A^0$, $A^0 \to c\overline{c}$, gg, or $\tau^+\tau^-$ in the region $m_{H_1^0}$ = 45-86 GeV and m_{A^0} = 2-11 GeV. See their Fig. 7 for the limits.

[51] Search for associated production of a $\gamma\gamma$ resonance with a Z boson, followed by $Z \to q\overline{q}$, $\ell^+\ell^-$, or $\nu\overline{\nu}$, at $E_{cm} \leq$ 209 GeV. The limit is for a H^0 with SM production cross section and B($H^0 \to f\overline{f}$)=0 for all fermions f.

[52] For B($H^0 \to \gamma\gamma$)=1, $m_{H^0} > 113.1$ GeV is obtained.

[53] HEISTER 02M search for $e^+e^- \to H^0Z$, assuming that H^0 decays to $q\overline{q}$, gg, or $\tau^+\tau^-$ only. The limit assumes SM production cross section.

[54] ABBIENDI 01E search for neutral Higgs bosons in general Type-II two-doublet models, at $E_{cm} \leq$ 189 GeV. In addition to usual final states, the decays H_1^0, $A^0 \to q\overline{q}$, gg are searched for. See their Figs. 15,16 for excluded regions.

[55] ACCIARRI 00R search for $e^+e^- \to H^0\gamma$ with $H^0 \to b\overline{b}$, $Z\gamma$, or $\gamma\gamma$. See their Fig. 3 for limits on σ·B. Explicit limits within an effective interaction framework are also given, for which the Standard Model Higgs search results are used in addition.

[56] ACCIARRI 00R search for the two-photon type processes $e^+e^- \to e^+e^-H^0$ with $H^0 \to b\overline{b}$ or $\gamma\gamma$. See their Fig. 4 for limits on $\Gamma(H^0 \to \gamma\gamma)$·B($H^0 \to \gamma\gamma$ or $b\overline{b}$) for m_{H^0}=70–170 GeV.

[57] GONZALEZ-GARCIA 98B use DØ limit for $\gamma\gamma$ events with missing E_T in $p\overline{p}$ collisions (ABBOTT 98) to constrain possible ZH or WH production followed by unconventional $H \to \gamma\gamma$ decay which is induced by higher-dimensional operators. See their Figs. 1 and 2 for limits on the anomalous couplings.

[58] KRAWCZYK 97 analyse the muon anomalous magnetic moment in a two-doublet Higgs model (with type II Yukawa couplings) assuming no H_1^0ZZ coupling and obtain $m_{H_1^0} \gtrsim$ 5 GeV or $m_{A^0} \gtrsim$ 5 GeV for $\tan\beta > 50$. Other Higgs bosons are assumed to be much heavier.

[59] ALEXANDER 96H give B($Z \to H^0\gamma$)×B($H^0 \to q\overline{q}$) < 1–4 × 10^{-5} (95%CL) and B($Z \to H^0\gamma$)×B($H^0 \to b\overline{b}$) < 0.7–2 × 10^{-5} (95%CL) in the range $20 < m_{H^0} < 80$ GeV.

Gauge & Higgs Boson Particle Listings

Neutral Higgs Bosons, Searches for

SEARCHES FOR A HIGGS BOSON WITH STANDARD MODEL COUPLINGS

These listings are based on experimental searches for a scalar boson whose couplings to W, Z and fermions are precisely those of the Higgs boson predicted by the three-generation Standard Model with the minimal Higgs sector.

For a review and a bibliography, see the review on "Status of Higgs Boson Physics."

Direct Mass Limits for H^0

The mass limits shown below apply to a Higgs boson H^0 with Standard Model couplings whose mass is a priori unknown. These mass limits are compatible with and independent of the observed signal at about 125 GeV. In particular, the symbol H^0 employed below does not in general refer to the observed signal at about 125 GeV.

The cross section times branching ratio limits quoted in the footnotes below are typically given relative to those of a Standard Model Higgs boson of the relevant mass. These limits can be reinterpreted in terms of more general models (e.g. extended Higgs sectors) in which the Higgs couplings to W, Z and fermions are re-scaled from their Standard Model values.

All data that have been superseded by newer results are marked as "not used" or have been removed from this compilation, and are documented in previous editions of this *Review* of Particle Physics.

VALUE (GeV)	CL%	DOCUMENT ID		TECN	COMMENT
> 122 and none 128–1000 (CL = 95%)					
none 145–1000	95	[1] KHACHATRY..15AW		CMS	$pp \to H^0 X$ combined
none 90–102, 149–172	95	[2] AALTONEN	13L	CDF	$p\overline{p} \to H^0 X$, combined
none 90–109, 149–182	95	[3] AALTONEN	13M	TEVA	Tevatron combined
none 90–101, 157–178	95	[4] ABAZOV	13L	D0	$p\overline{p} \to H^0 X$, combined
none 110–121.5, 128–145	95	[5] CHATRCHYAN	12N	CMS	$pp \to H^0 X$ combined
>114.1	95	[6] ABDALLAH	04	DLPH	$e^+e^- \to H^0 Z$
>112.7	95	[6] ABBIENDI	03B	OPAL	$e^+e^- \to H^0 Z$
>114.4	95	[6,7] HEISTER	03D	LEP	$e^+e^- \to H^0 Z$
>111.5	95	[6,8] HEISTER	02	ALEP	$e^+e^- \to H^0 Z$
>112.0	95	[6] ACHARD	01C	L3	$e^+e^- \to H^0 Z$
• • • We do not use the following data for averages, fits, limits, etc. • • •					
none 132–200	95	[9] AAD	15AA	ATLS	$pp \to H^0 X, H^0 \to WW^{(*)}$
		[10] AAD	15G	ATLS	$pp \to H^0 W/ZX, H^0 \to b\overline{b}$
		[11] AAD	14AS	ATLS	$pp \to H^0 X, H^0 \to \mu\mu$
		[12] AAD	14J	ATLS	$pp \to H^0 X, H^0 \to Z\gamma$
none 114.5–119, 129.5–832	95	[13] CHATRCHYAN	14AA	CMS	$pp \to H^0 X, H^0 \to 4\ell$
		[14] CHATRCHYAN	14AI	CMS	$pp \to H^0 W/ZX, H^0 \to b\overline{b}$
none 127–600	95	[15] CHATRCHYAN	14G	CMS	$pp \to H^0 X, H^0 \to WW^{(*)}$
		[16] AALTONEN	13B	CDF	$p\overline{p} \to H^0 W/ZX, H^0 \to b\overline{b}$
		[17] AALTONEN	13C	CDF	$p\overline{p} \to H^0 X, H^0 \to b\overline{b}$
none 149–172	95	[18] AALTONEN	13K	CDF	$p\overline{p} \to H^0 X, H^0 \to WW^{(*)}$
		[19] ABAZOV	13E	D0	$p\overline{p} \to H^0 X, 4\ell$
		[20] ABAZOV	13F	D0	$p\overline{p} \to H^0 X, \ell\tau jj$
none 159–176	95	[21] ABAZOV	13G	D0	$p\overline{p} \to H^0 X, H^0 \to WW^{(*)}$
		[22] ABAZOV	13H	D0	$p\overline{p} \to H^0 X, H^0 \to \gamma\gamma$
		[23] ABAZOV	13I	D0	$p\overline{p} \to H^0 X, \ell\nu jj$
		[24] ABAZOV	13J	D0	$p\overline{p} \to H^0 X$, leptonic
		[25] ABAZOV	13K	D0	$p\overline{p} \to H^0 ZX$
		[26] CHATRCHYAN	13AL	CMS	$pp \to H^0 X, H^0 \to \tau\tau$, $WW^{(*)}, ZZ^{(*)}$
		[27] CHATRCHYAN	13BK	CMS	$pp \to H^0 X, H^0 \to Z\gamma$
none 145–710	95	[28] CHATRCHYAN	13Q	CMS	$pp \to H^0 X$ combined
		[29] CHATRCHYAN	13X	CMS	$pp \to H^0 t\overline{t} X$
none 113–122, 128–133, 138–149	95	[30] CHATRCHYAN	13Y	CMS	$pp \to H^0 X, H^0 \to \gamma\gamma$
none 130–164, 170–180	95	[31] CHATRCHYAN	13Y	CMS	$pp \to H^0 X, H^0 \to ZZ^*$
none 129–160	95	[32] CHATRCHYAN	13Y	CMS	$pp \to H^0 X, H^0 \to WW^*$
none 111–122, 131–559	95	[33] AAD	12AI	ATLS	$pp \to H^0 X$ combined
none 133–261	95	[34] AAD	12AJ	ATLS	$pp \to H^0 X, H^0 \to WW^{(*)}$
		[35] AAD	12BU	ATLS	$pp \to H^0 X, H^0 \to \tau^+\tau^-$
none 319–558	95	[36] AAD	12BZ	ATLS	$pp \to H^0 X, H^0 \to ZZ$
none 300–322, 353–410	95	[37] AAD	12CA	ATLS	$pp \to H^0 X, H^0 \to ZZ$
		[38] AAD	12CN	ATLS	$pp \to H^0 W/ZX, H^0 \to b\overline{b}$
		[39] AAD	12CO	ATLS	$pp \to H^0 X, H^0 \to WW$
none 134–156, 182–233, 256–265, 268–415	95	[40] AAD	12D	ATLS	$pp \to H^0 X, H^0 \to ZZ^{(*)}$
none 113–115, 134.5–136	95	[41] AAD	12G	ATLS	$pp \to H^0 X, H^0 \to \gamma\gamma$
		[42] AALTONEN	12AK	CDF	$p\overline{p} \to H^0 t\overline{t} X$
		[43] AALTONEN	12AM	CDF	$p\overline{p} \to H^0 X$, inclusive 4ℓ
		[44] AALTONEN	12AN	CDF	$p\overline{p} \to H^0 X, H^0 \to \gamma\gamma$
		[45] AALTONEN	12J	CDF	$p\overline{p} \to H^0 X, H^0 \to \tau\tau$
		[46] AALTONEN	12Q	CDF	$p\overline{p} \to H^0 ZX, H^0 \to b\overline{b}$
none 100–106	95	[47] AALTONEN	12T	TEVA	$p\overline{p} \to H^0 W/ZX, H^0 \to b\overline{b}$
		[48] ABAZOV	12K	D0	$p\overline{p} \to H^0 W/ZX, H^0 \to b\overline{b}$
		[49,50] CHATRCHYAN	12AY	CMS	$pp \to H^0 WX, H^0 ZX$
		[51] CHATRCHYAN	12C	CMS	$pp \to H^0 X, H^0 \to ZZ$
		[52] CHATRCHYAN	12D	CMS	$pp \to H^0 X, H^0 \to ZZ^{(*)}$
none 129–270	95	[53] CHATRCHYAN	12E	CMS	$pp \to H^0 X, H^0 \to WW^{(*)}$
		[54] CHATRCHYAN	12F	CMS	$pp \to H^0 WX, H^0 ZX$
none 128–132	95	[55] CHATRCHYAN	12G	CMS	$pp \to H^0 X, H^0 \to \gamma\gamma$
none 134–158, 180–305, 340–465	95	[56] CHATRCHYAN	12H	CMS	$pp \to H^0 X, H^0 \to ZZ^{(*)}$
none 270–440	95	[57] CHATRCHYAN	12I	CMS	$pp \to H^0 X, H^0 \to ZZ$
		[58] CHATRCHYAN	12K	CMS	$pp \to H^0 X, H^0 \to \tau^+\tau^-$
		[59] ABAZOV	11G	D0	$p\overline{p} \to H^0 X, H^0 \to WW^{(*)}$
		[60] CHATRCHYAN	11J	CMS	$pp \to H^0 X, H^0 \to WW$
none 162–166	95	[61] AALTONEN	10F	TEVA	$p\overline{p} \to H^0 X, H^0 \to WW^{(*)}$
		[62] AALTONEN	10M	TEVA	$p\overline{p} \to ggX \to H^0 X, H^0 \to WW^{(*)}$
		[63] AALTONEN	09A	CDF	$p\overline{p} \to H^0 X, H^0 \to WW^{(*)}$
		[64] ABAZOV	09U	D0	$H^0 \to \tau^+\tau^-$
		[65] ABAZOV	06	D0	$p\overline{p} \to H^0 X, H^0 \to WW^*$
		[66] ABAZOV	06O	D0	$p\overline{p} \to H^0 WX, H^0 \to WW^*$

[1] KHACHATRYAN 15AW search for H^0 production in the decays $H^0 \to W^+W^- \to \ell\nu\ell\nu$, $\ell\nu qq$, and $H^0 \to ZZ \to 4\ell$, $\ell\ell\tau\tau$, $\ell\ell\nu\nu$, and $\ell\ell qq$ in up to 5.1 fb^{-1} of pp collisions at E_{cm} = 7 TeV and up to 19.7 fb^{-1} at E_{cm}=8 TeV in the range m_{H^0} = 145–1000 GeV. See their Fig. 7 for limits on cross section times branching ratio.

[2] AALTONEN 13L combine all CDF searches with 9.45–10.0 fb^{-1} of $p\overline{p}$ collisions at E_{cm} = 1.96 TeV. A limit on cross section times branching ratio which corresponds to (0.45–4.8) times the expected Standard Model cross section is given for m_{H^0} = 90–200 GeV at 95 %CL. An excess of events over background is observed with a local significance of 2.0 σ at m_{H^0} = 125 GeV. In the Standard Model with an additional generation of heavy quarks and leptons which receive their masses via the Higgs mechanism, m_{H^0} values between 124 and 203 GeV are excluded at 95% CL.

[3] AALTONEN 13M combine all Tevatron data from the CDF and D0 Collaborations. A limit on cross section times branching ratio which corresponds to (0.37–3.1) times the expected Standard Model cross section is given for m_{H^0} = 90–200 GeV at 95% CL. An excess of events over background is observed with a local significance of 3.0σ at m_{H^0} = 125 GeV. In the Standard Model with an additional generation of heavy quarks and leptons which receive their masses via the Higgs mechanism, m_{H^0} values between 121 and 225 GeV are excluded at 95% CL.

[4] ABAZOV 13L combine all D0 results with up to 9.7 fb^{-1} of $p\overline{p}$ collisions at E_{cm} = 1.96 TeV. A limit on cross section times branching ratio which corresponds to (0.66–3.1) times the expected Standard Model cross section is given in the range m_{H^0} = 90–200 GeV at 95% CL. An excess of events over background is observed with a local significance of 1.7σ at m_{H^0} = 125 GeV. In the Standard Model with an additional generation of heavy quarks and leptons which receive their masses via the Higgs mechanism, m_{H^0} values between 125 and 218 GeV are excluded at 95% CL.

[5] CHATRCHYAN 12N search for H^0 production in the decays $H \to \gamma\gamma$, $ZZ^* \to 4\ell$, $WW^* \to \ell\nu\ell\nu$, $\tau\tau$, and $b\overline{b}$ in 4.9–5.1 fb^{-1} of pp collisions at E_{cm} = 7 TeV and 5.1–5.3 fb^{-1} at E_{cm} = 8 TeV. The expected exclusion region for no signal is 110–145 GeV at 99.9% CL. See also CHATRCHYAN 13Y.

[6] Search for $e^+e^- \to H^0 Z$ at $E_{cm} \leq$ 209 GeV in the final states $H^0 \to b\overline{b}$ with $Z \to \ell\overline{\ell}$, $\nu\overline{\nu}$, $q\overline{q}$, $\tau^+\tau^-$ and $H^0 \to \tau^+\tau^-$ with $Z \to q\overline{q}$.

[7] Combination of the results of all LEP experiments.

[8] A 3σ excess of candidate events compatible with m_{H^0} near 114 GeV is observed in the combined channels $q\overline{q}q\overline{q}$, $q\overline{q}\ell\overline{\ell}$, $q\overline{q}\tau^+\tau^-$.

[9] AAD 15AA search for $H^0 \to WW^{(*)}$ in 4.5 fb^{-1} of pp collisions at E_{cm} = 7 TeV and 20.3 fb^{-1} at E_{cm} = 8 TeV. A limit on cross section times branching ratio which corresponds to (0.2–6) times the expected Standard Model cross section is given for m_{H^0} = 110–200 GeV at 95% CL.

[10] AAD 15G search for WH^0 and ZH^0 production followed by $H^0 \to b\overline{b}$ in 4.7 fb^{-1} of pp collisions at E_{cm} = 7 TeV and 20.3 fb^{-1} at E_{cm} = 8 TeV. A limit on the cross section times branching ratio which corresponds to (0.8–2.6) times the expected Standard Model cross section is given for m_{H^0} = 110–140 GeV at 95% CL.

[11] AAD 14AS search for $H^0 \to \mu^+\mu^-$ in 4.5 fb^{-1} of pp collisions at E_{cm} = 7 TeV and 20.3 fb^{-1} at E_{cm} = 8 TeV. A limit on the cross section times branching ratio which corresponds to (6.5–16.8) times the expected Standard Model cross section is given for m_{H^0} = 120–150 GeV at 95% CL.

[12] AAD 14J search for $H^0 \to Z\gamma \to \ell\ell\gamma$ in 4.5 fb^{-1} of pp collisions at E_{cm} = 7 TeV and 20.3 fb^{-1} at E_{cm} = 8 TeV. A limit on cross section times branching ratio which corresponds to (4–18) times the expected Standard Model cross section is given for m_{H^0} = 120–150 GeV at 95% CL.

[13] CHATRCHYAN 14AA search for H^0 production in the decay mode $H^0 \to ZZ^{(*)} \to 4\ell$ in 5.1 fb^{-1} of pp collisions at E_{cm} = 7 TeV and 19.7 fb^{-1} at E_{cm} = 8 TeV. The expected exclusion region for no signal is 115–740 GeV at the 95% CL. See their Fig. 18 for cross section limits for m_{H^0} = 110–1000 GeV.

[14] CHATRCHYAN 14AI search for WH^0 and ZH^0 production followed by $H^0 \to b\overline{b}$ in up to 5.1 fb^{-1} of pp collisions at E_{cm} = 7 TeV and up to 18.9 fb^{-1} at E_{cm} = 8 TeV. A limit on the cross section times branching ratio which corresponds to (1–3) times the expected Standard Model cross section is given for m_{H^0} = 110–135 GeV at 95% CL.

[15] CHATRCHYAN 14G search for H^0 production in the decay mode $H^0 \to WW^{(*)} \to \ell\nu\ell\nu$ in 4.9 fb^{-1} of pp collisions at E_{cm} = 7 TeV and 19.4 fb^{-1} at E_{cm} = 8 TeV. The expected exclusion region for no signal is 115–600 GeV at the 95% CL. See their Fig. 21 (left) for cross section limits for m_{H^0} = 110–600 GeV.

[16] AALTONEN 13B search for associated $H^0 Z$ production in the final state $H^0 \to b\overline{b}$, $Z \to \nu\overline{\nu}$, and $H^0 W$ production in $H^0 \to b\overline{b}$, $W \to \ell\nu$ (ℓ not identified) with an improved b identification algorithm in 9.45 fb^{-1} of $p\overline{p}$ collisions at $E_{\rm cm} = 1.96$ TeV. A limit on cross section times branching ratio which corresponds to (0.72–11.8) times the expected Standard Model cross section is given for $m_{H^0} = 90$–150 GeV at 95%CL. The limit for $m_{H^0} = 125$ GeV is 3.06, where 3.33 is expected for no signal.

[17] AALTONEN 13C search for associated $H^0 W$ and $H^0 Z$ as well as vector-boson fusion $H^0 q\overline{q}'$ production in the final state $H^0 \to b\overline{b}$, $W/Z \to q\overline{q}$ with 9.45 fb^{-1} of $p\overline{p}$ collisions at $E_{\rm cm} = 1.96$ TeV. A limit on cross section times branching ratio which is (7.0–64.6) times larger than the expected Standard Model cross section is given in the range $m_{H^0} = 100$–150 GeV at 95% CL. The limit for $m_{H^0} = 125$ GeV is 9.0, where 11.0 is expected for no signal.

[18] AALTONEN 13K search for H^0 production (with a possible additional W or Z) in the final state $H^0 \to WW^{(*)} \to \ell\nu\ell\nu$ in 9.7 fb^{-1} of $p\overline{p}$ collisions at $E_{\rm cm} = 1.96$ TeV. A limit on cross section times branching ratio which corresponds to (0.49–14.1) times the expected Standard Model cross section is given in the range $m_{H^0} = 110$–200 GeV at 95% CL. The limit at $m_{H^0} = 125$ GeV is 3.26, where 3.25 is expected for no signal. In the Standard Model with an additional generation of heavy quarks and leptons which receive their masses via the Higgs mechanism, m_{H^0} values between 124 and 200 GeV are excluded at 95% CL.

[19] ABAZOV 13E search for H^0 production in four-lepton final states from $H^0 \to ZZ^{(*)}$ and $H^0 Z$ in 9.6–9.8 fb^{-1} of $p\overline{p}$ collisions at $E_{\rm cm} = 1.96$ TeV. A limit on cross section times branching ratio which corresponds to (8.6–78.9) times the expected Standard Model cross section is given in the range $m_{H^0} = 115$–200 GeV at 95% CL. The limit for $m_{H^0} = 125$ GeV is 42.3, where 42.8 is expected for no signal.

[20] ABAZOV 13F search for H^0 production in final states $e\tau jj$ and $\mu\tau jj$ in 9.7 fb^{-1} of $p\overline{p}$ collisions at $E_{\rm cm} = 1.96$ TeV. The search is sensitive to $H \to \tau\tau$ and $H \to WW^{(*)}$. A limit on cross section times branching ratio which corresponds to (9.4–17.9) times the expected Standard Model cross section is given in the range $m_{H^0} = 105$–150 GeV at 95% CL. The limit for $m_{H^0} = 125$ GeV is 11.3, where 9.0 is expected for no signal.

[21] ABAZOV 13G search for H^0 production in final states $H^0 \to WW^{(*)} \to \ell^+\nu\ell^-\nu$ in 9.7 fb^{-1} of $p\overline{p}$ collisions at $E_{\rm cm} = 1.96$ TeV and give a limit on cross section times branching ratio for $m_{H^0} = 100$–150 GeV at 95% CL. The limit for $m_{H^0} = 125$ GeV is 4.1, where 3.4 is expected for no signal. In the Standard Model with an additional generation of heavy quarks and leptons which receive their masses via the Higgs mechanism, m_{H^0} values between 125 and 218 GeV are excluded at 95% CL.

[22] ABAZOV 13H search for H^0 production with the decay $H^0 \to \gamma\gamma$ in 9.6 fb^{-1} of $p\overline{p}$ collisions at $E_{\rm cm} = 1.96$ TeV. A limit on cross section times branching ratio which corresponds to (8.3–25.4) times the expected Standard Model cross section is given in the range $m_{H^0} = 100$–150 GeV at 95% CL. The limit for $m_{H^0} = 125$ GeV is 12.8, where 8.7 is expected for no signal.

[23] ABAZOV 13I search for H^0 production in the final state with one lepton and two or more jets plus missing E_T with b identification in 9.7 fb^{-1} of $p\overline{p}$ collisions at $E_{\rm cm} = 1.96$ TeV. The search is mainly sensitive to $H^0 W \to b\overline{b}\ell\nu$, $H^0 \to WW^{(*)} \to \ell\nu q\overline{q}$, and $H^0 V \to VWW^{(*)} \to \ell\nu q\overline{q}q\overline{q}$ ($V = W, Z$). A limit on cross section times branching ratio which corresponds to (1.3–11.4) times the expected Standard Model cross section is given in the range $m_{H^0} = 90$–200 GeV at 95% CL. The limit for $m_{H^0} = 125$ GeV is 5.8, where 4.7 is expected for no signal. In the Standard Model with an additional generation of heavy quarks and leptons which receive their masses via the Higgs mechanism, m_{H^0} values between 150 and 188 GeV are excluded at 95% CL.

[24] ABAZOV 13J search for H^0 production in the final states $ee\mu$, $e\mu\mu$, $\mu\tau\tau$, and $e^\pm\mu^\pm$ in 8.6–9.7 fb^{-1} of $p\overline{p}$ collisions at $E_{\rm cm} = 1.96$ TeV. The search is sensitive to WH^0, ZH^0 and gluon fusion production with $H^0 \to WW^{(*)}$, $ZZ^{(*)}$, decaying to leptonic final states, and to WH^0, ZH^0 production with $H^0 \to \tau^+\tau^-$. A limit on cross section times branching ratio which corresponds to (4.4–12.7) times the expected Standard Model cross section is given in the range $m_{H^0} = 100$–200 GeV at 95% CL. The limit for $m_{H^0} = 125$ GeV is 8.4, where 6.3 is expected for no signal.

[25] ABAZOV 13K search for associated $H^0 Z$ production in the final states $\ell\ell bb$ with b identification in 9.7 fb^{-1} of $p\overline{p}$ collisions at $E_{\rm cm} = 1.96$ TeV. A limit on cross section times branching ratio which corresponds to (1.8–53) times the expected Standard Model cross section is given for $m_{H^0} = 90$–150 GeV at 95% CL. The limit for $m_{H^0} = 125$ GeV is 7.1, where 5.1 is expected for no signal.

[26] CHATRCHYAN 13AL search for $H^0 \to \tau^+\tau^-$, $WW^{(*)}$, and $ZZ^{(*)}$ in 5.1 fb^{-1} and 5.3 fb^{-1} of pp collisions at $E_{\rm cm} = 7$ and 8 TeV. In the Standard Model with an additional generation of heavy quarks and leptons which receive their masses via the Higgs mechanism, m_{H^0} values between 110 and 600 GeV are excluded at 99% CL.

[27] CHATRCHYAN 13BK search for $H^0 \to Z\gamma \to \ell\ell\gamma$ in 5.0 fb^{-1} of pp collisions at $E_{\rm cm} = 7$ TeV and 19.6 fb^{-1} at $E_{\rm cm} = 8$ TeV. A limit on cross section times branching ratio which corresponds to (4–25) times the expected Standard Model cross section is given in the range $m_{H^0} = 120$–160 GeV at 95% CL. The limit for $m_{H^0} = 125$ GeV is 9.5, where 10 is expected for no signal.

[28] CHATRCHYAN 13Q search for H^0 production in the decays $H^0 \to W^+W^- \to \ell\nu\ell\nu$, $\ell\nu qq$ and $H^0 \to ZZ \to 4\ell$, $\ell\ell\tau\tau$, $\ell\ell\nu\nu$, and $\ell\ell qq$ in up to 5.1 fb^{-1} of pp collisions at $E_{\rm cm} = 7$ TeV and up to 5.3 fb^{-1} at $E_{\rm cm} = 8$ TeV in the range $m_{H^0} = 145$–1000 GeV. Superseded by KHACHATRYAN 15AW.

[29] CHATRCHYAN 13X search for $H^0 t\overline{t}$ production followed by $H^0 \to b\overline{b}$, one top decaying to $\ell\nu$ and the other to either $\ell\nu$ or $q\overline{q}$ in 5.0 fb^{-1} and 5.1 fb^{-1} of pp collisions at $E_{\rm cm} = 7$ and 8 TeV. A limit on cross section times branching ratio which corresponds to (4.0–8.6) times the expected Standard Model cross section is given for $m_{H^0} = 110$–140 GeV at 95% CL. The limit for $m_{H^0} = 125$ GeV is 5.8, where 5.2 is expected for no signal.

[30] CHATRCHYAN 13Y search for H^0 production in the decay $H \to \gamma\gamma$ in 5.1 fb^{-1} of pp collisions at $E_{\rm cm} = 7$ TeV and 5.3 fb^{-1} at $E_{\rm cm} = 8$ TeV. The expected exclusion region for no signal is 110–144 GeV at 95% CL.

[31] CHATRCHYAN 13Y search for H^0 production in the decay $H \to ZZ^* \to 4\ell$ in 5.0 fb^{-1} of pp collisions at $E_{\rm cm} = 7$ TeV and 5.3 fb^{-1} at $E_{\rm cm} = 8$ TeV. The expected exclusion region for no signal is 120–180 GeV at 95% CL.

[32] CHATRCHYAN 13Y search for H^0 production in the decay $H \to WW^* \to \ell\nu\ell\nu$ in 4.9 fb^{-1} of pp collisions at $E_{\rm cm} = 7$ TeV and 5.3 fb^{-1} at $E_{\rm cm} = 8$ TeV. The expected exclusion region for no signal is 122–160 GeV at 95% CL.

[33] AAD 12AI search for H^0 production in pp collisions for the final states $H^0 \to ZZ^{(*)}$, $\gamma\gamma$, $WW^{(*)}$, $b\overline{b}$, $\tau\tau$ with 4.6–4.8 fb^{-1} at $E_{\rm cm} = 7$ TeV, and $H^0 \to ZZ^{(*)} \to 4\ell$, $\gamma\gamma$, $WW^{(*)} \to e\nu\mu\nu$ with 5.8–5.9 fb^{-1} at $E_{\rm cm} = 8$ TeV. The 99% CL excluded range is 113–114, 117–121, and 132–527 GeV. An excess of events over background with a local significance of 5.9 σ is observed at $m_{H^0} = 126$ GeV.

[34] AAD 12AJ search for H^0 production in the decay $H^0 \to WW^{(*)} \to \ell\nu\ell\nu$ with 4.7 fb^{-1} of pp collisions at $E_{\rm cm} = 7$ TeV. A limit on cross section times branching ratio which corresponds to (0.2–10) times the expected Standard Model cross section is given for $m_{H^0} = 110$–600 GeV at 95% CL.

[35] AAD 12BU search for H^0 production in the decay $H \to \tau^+\tau^-$ with 4.7 fb^{-1} of pp collisions at $E_{\rm cm} = 7$ TeV. A limit on cross section times branching ratio which is (2.9–11.7) times larger than the expected Standard Model cross section is given for $m_{H^0} = 100$–150 GeV at 95% CL.

[36] AAD 12BZ search for H^0 production in the decay $H \to ZZ \to \ell^+\ell^-\nu\overline{\nu}$ with 4.7 fb^{-1} of pp collisions at $E_{\rm cm} = 7$ TeV. A limit on cross section times branching ratio which corresponds to (0.2–4) times the expected Standard Model cross section is given for $m_{H^0} = 200$–600 GeV at 95% CL.

[37] AAD 12CA search for H^0 production in the decay $H \to ZZ \to \ell^+\ell^- q\overline{q}$ with 4.7 fb^{-1} of pp collisions at $E_{\rm cm} = 7$ TeV. A limit on cross section times branching ratio which corresponds to (0.7–9) times the expected Standard Model cross section is given for $m_{H^0} = 200$–600 GeV at 95% CL.

[38] AAD 12CN search for associated $H^0 W$ and $H^0 Z$ production in the channels $W \to \ell\nu$, $Z \to \ell^+\ell^-$, $\nu\overline{\nu}$, and $H^0 \to b\overline{b}$, with 4.7 fb^{-1} of pp collisions at $E_{\rm cm} = 7$ TeV. A limit on cross section times branching ratio which is (2.5–5.5) times larger than the expected Standard Model cross section is given for $m_{H^0} = 110$–130 GeV at 95% CL.

[39] AAD 12CO search for H^0 production in the decay $H \to WW \to \ell\nu q\overline{q}$ with 4.7 fb^{-1} of pp collisions at $E_{\rm cm} = 7$ TeV. A limit on cross section times branching ratio which is (1.9–10) times larger than the expected Standard Model cross section is given for $m_{H^0} = 300$–600 GeV at 95% CL.

[40] AAD 12D search for H^0 production with $H \to ZZ^{(*)} \to 4\ell$ in 4.8 fb^{-1} of pp collisions at $E_{\rm cm} = 7$ TeV in the mass range $m_{H^0} = 110$–600 GeV. An excess of events over background with a local significance of 2.1 σ is observed at 125 GeV.

[41] AAD 12G search for H^0 production with $H \to \gamma\gamma$ in 4.9 fb^{-1} of pp collisions at $E_{\rm cm} = 7$ TeV in the mass range $m_{H^0} = 110$–150 GeV. An excess of events over background with a local significance of 2.8 σ is observed at 126.5 GeV.

[42] AALTONEN 12AK search for associated $H^0 t\overline{t}$ production in the decay chain $t\overline{t} \to WWbb \to \ell\nu qqbb$ with 9.45 fb^{-1} of $p\overline{p}$ collisions at $E_{\rm cm} = 1.96$ TeV. A limit on cross section times branching ratio which is (10–40) times larger than the expected Standard Model cross section is given for $m_{H^0} = 100$–150 GeV at 95% CL. The limit for $m_{H^0} = 125$ GeV is 20.5, where 12.6 is expected.

[43] AALTONEN 12AM search for H^0 production in inclusive four-lepton final states coming from $H^0 \to ZZ$, $H^0 Z \to WW^{(*)}\ell\ell$, or $H^0 Z \to \tau\tau\ell\ell$, with 9.7 fb^{-1} of $p\overline{p}$ collisions at $E_{\rm cm} = 1.96$ TeV. A limit on cross section times branching ratio which is (7.2–42.4) times larger than the expected Standard Model cross section is given for $m_{H^0} = 120$–300 GeV at 95% CL. The best limit is for $m_{H^0} = 200$ GeV.

[44] AALTONEN 12AN search for H^0 production in the decay $H^0 \to \gamma\gamma$ with 10 fb^{-1} of $p\overline{p}$ collisions at $E_{\rm cm} = 1.96$ TeV. A limit on cross section times branching ratio which is (7.7–21.3) times larger than the expected Standard Model cross section is given for $m_{H^0} = 100$–150 GeV at 95% CL. The limit for $m_{H^0} = 125$ GeV is 17.0, where 9.9 is expected.

[45] AALTONEN 12J search for H^0 production in the decay $H^0 \to \tau^+\tau^-$ (one leptonic, the other hadronic) with 6.0 fb^{-1} of $p\overline{p}$ collisions at $E_{\rm cm} = 1.96$ TeV. A limit on cross section times branching ratio which is (14.6–70.2) times larger than the expected Standard Model cross section is given for $m_{H^0} = 100$–150 GeV at 95% CL. The best limit is for $m_{H^0} = 120$ GeV.

[46] AALTONEN 12Q search for associated $H^0 Z$ production in the final state $H^0 \to b\overline{b}$, $Z \to \ell^+\ell^-$ with 9.45 fb^{-1} of $p\overline{p}$ collisions at $E_{\rm cm} = 1.96$ TeV. A limit on cross section times branching ratio which corresponds to (1.0–37.5) times the expected Standard Model cross section is given for $m_{H^0} = 90$–150 GeV at 95% CL. The limit for $m_{H^0} = 125$ GeV is 7.1, where 3.9 is expected. A broad excess of events for $m_{H^0} > 110$ GeV is observed, with a local significance of 2.4 σ at $m_{H^0} = 135$ GeV.

[47] AALTONEN 12T combine AALTONEN 12Q, AALTONEN 12R, AALTONEN 12S, ABAZOV 12O, ABAZOV 12P, and ABAZOV 12K. An excess of events over background is observed which is most significant in the region $m_{H^0} = 120$–135 GeV, with a local significance of up to 3.3 σ. The local significance at $m_{H^0} = 125$ GeV is 2.8 σ, which corresponds to $(\sigma(H^0 W) + \sigma(H^0 Z))\ {\rm B}(H^0 \to b\overline{b})) = (0.23^{+0.09}_{-0.08})$ pb, compared to the Standard Model expectation at $m_{H^0} = 125$ GeV of 0.12 ± 0.01 pb.

[48] ABAZOV 12K search for associated $H^0 Z$ production in the final state $H^0 \to b\overline{b}$, $Z \to \nu\overline{\nu}$, and $H^0 W$ production with $W \to \ell\nu$ (ℓ not identified) with 9.5 fb^{-1} of $p\overline{p}$ collisions at $E_{\rm cm} = 1.96$ TeV. A limit on cross section times branching ratio which is (1.9–16.8) times larger than the expected Standard Model cross section is given for $m_{H^0} = 100$–150 GeV at 95% CL. The limit for $m_{H^0} = 125$ GeV is 4.3, where 3.9 is expected.

[49] CHATRCHYAN 12AY search for associated $H^0 W$ and $H^0 Z$ production in the channels $W \to \ell\nu$, $Z \to \ell^+\ell^-$, and $H^0 \to \tau\tau$, $WW^{(*)}$, with 5 fb^{-1} of pp collisions at $E_{\rm cm} = 7$ TeV. A limit on cross section times branching ratio which is (3.1–9.1) times larger than the expected Standard Model cross section is given for $m_{H^0} = 110$–200 GeV at 95% CL.

[50] CHATRCHYAN 12AY combine CHATRCHYAN 12F and CHATRCHYAN 12AO in addition and give a limit on cross section times branching ratio which is (2.1–3.7) times larger than the expected Standard Model cross section for $m_{H^0} = 110$–170 GeV at 95% CL. The limit for $m_{H^0} = 125$ GeV is 3.3.

[51] CHATRCHYAN 12C search for H^0 production with $H \to ZZ \to \ell^+\ell^-\tau^+\tau^-$ in 4.7 fb^{-1} of pp collisions at $E_{\rm cm} = 7$ TeV. A limit on cross section times branching ratio

which is (4–12) times larger than the expected Standard Model cross section is given for m_{H^0} = 190–600 GeV at 95% CL. The best limit is at m_{H^0} = 200 GeV.

[52] CHATRCHYAN 12D search for H^0 production with $H \to ZZ^{(*)} \to \ell^+\ell^- q\overline{q}$ in 4.6 fb^{-1} of pp collisions at E_{cm} = 7 TeV. A limit on cross section times branching ratio which corresponds to (1–22) times the expected Standard Model cross section is given for m_{H^0} = 130–164 GeV, 200–600 GeV at 95% CL. The best limit is at m_{H^0} = 230 GeV. In the Standard Model with an additional generation of heavy quarks and leptons which receive their masses via the Higgs mechanism, m_{H^0} values in the ranges m_{H^0} = 154–161 GeV and 200–470 GeV are excluded at 95% CL.

[53] CHATRCHYAN 12E search for H^0 production with $H \to WW^{(*)} \to \ell^+\nu\ell^-\overline{\nu}$ in 4.6 fb^{-1} of pp collisions at E_{cm} = 7 TeV in the mass range m_{H^0} = 110–600 GeV.

[54] CHATRCHYAN 12F search for associated $H^0 W$ and $H^0 Z$ production followed by $W \to \ell\nu$, $Z \to \ell^+\ell^-$, $\nu\overline{\nu}$, and $H^0 \to b\overline{b}$, in 4.7 fb^{-1} of pp collisions at E_{cm} = 7 TeV. A limit on cross section times branching ratio which is (3.1–9.0) times larger than the expected Standard Model cross section is given for m_{H^0} = 110–135 GeV at 95% CL. The best limit is at m_{H^0} = 110 GeV.

[55] CHATRCHYAN 12G search for H^0 production with $H \to \gamma\gamma$ in 4.8 fb^{-1} of pp collisions at E_{cm} = 7 TeV in the mass range m_{H^0} = 110–150 GeV. An excess of events over background with a local significance of 3.1 σ is observed at 124 GeV.

[56] CHATRCHYAN 12H search for H^0 production with $H \to ZZ^{(*)} \to 4\ell$ in 4.7 fb^{-1} of pp collisions at E_{cm} = 7 TeV in the mass range m_{H^0} = 110–600 GeV. Excesses of events over background are observed around 119, 126 and 320 GeV. The region m_{H^0} = 114.4–134 GeV remains consistent with the expectation for the production of a SM-like Higgs boson.

[57] CHATRCHYAN 12I search for H^0 production with $H \to ZZ \to \ell^+\ell^-\nu\overline{\nu}$ in 4.6 fb^{-1} of pp collisions at E_{cm} = 7 TeV in the mass range m_{H^0} = 250–600 GeV.

[58] CHATRCHYAN 12K search for H^0 production in the decay $H \to \tau^+\tau^-$ with 4.6 fb^{-1} of pp collisions at E_{cm} = 7 TeV. A limit on cross section times branching ratio which is (3.2–7.0) times larger than the expected Standard Model cross section is given for m_{H^0} = 110–145 GeV at 95% CL.

[59] ABAZOV 11G search for H^0 production in 5.4 fb^{-1} of $p\overline{p}$ collisions at E_{cm} = 1.96 TeV in the decay mode $H^0 \to WW^{(*)} \to \ell\nu q\overline{q}'$ (and processes with similar final states). A limit on cross section times branching ratio which is (3.9–37) times larger than the expected Standard Model cross section is given for m_{H^0} = 115–200 GeV at 95% CL. The best limit is at m_{H^0} = 160 GeV.

[60] CHATRCHYAN 11J search for H^0 production with $H \to W^+W^- \to \ell\ell\nu\nu$ in 36 pb^{-1} of pp collisions at E_{cm} = 7 TeV. See their Fig. 6 for a limit on cross section times branching ratio for m_{H^0} = 120–600 GeV at 95% CL. In the Standard Model with an additional generation of heavy quarks and leptons which receive their masses via the Higgs mechanism, m_{H^0} values between 144 and 207 GeV are excluded at 95% CL.

[61] AALTONEN 10F combine searches for H^0 decaying to W^+W^- in $p\overline{p}$ collisions at E_{cm} = 1.96 TeV with 4.8 fb^{-1} (CDF) and 5.4 fb^{-1} (DØ).

[62] AALTONEN 10M combine searches for H^0 decaying to W^+W^- in $p\overline{p}$ collisions at E_{cm} = 1.96 TeV with 4.8 fb^{-1} (CDF) and 5.4 fb^{-1} (DØ) and derive limits $\sigma(p\overline{p} \to H^0)\cdot$ B($H^0 \to W^+W^-$) < (1.75–0.38) pb for m_H = 120–165 GeV, where H^0 is produced in gg fusion. In the Standard Model with an additional generation of heavy quarks, m_{H^0} between 131 and 204 GeV is excluded at 95% CL.

[63] AALTONEN 09A search for H^0 production in $p\overline{p}$ collisions at E_{cm} =1.96 TeV in the decay mode $H^0 \to WW^{(*)} \to \ell^+\ell^-\nu\overline{\nu}$. A limit on $\sigma(H^0)\cdot$B($H^0 \to WW^{(*)}$) between 0.7 and 2.5 pb (95% CL) is given for m_{H^0} = 110–200 GeV, which is 1.7–45 times larger than the expected Standard Model cross section. The best limit is obtained for m_{H^0} = 160 GeV.

[64] ABAZOV 09U search for $H^0 \to \tau^+\tau^-$ with $\tau \to$ hadrons in 1 fb^{-1} of $p\overline{p}$ collisions at E_{cm} = 1.96 TeV. The production mechanisms include associated $W/Z+H^0$ production, weak boson fusion, and gluon fusion. A limit (95% CL) is given for m_{H^0} = 105–145 GeV, which is 20–82 times larger than the expected Standard Model cross section. The limit for m_{H^0} = 115 GeV is 29 times larger than the expected Standard Model cross section.

[65] ABAZOV 06 search for Higgs boson production in $p\overline{p}$ collisions at E_{cm} = 1.96 TeV with the decay chain $H^0 \to WW^* \to \ell^\pm\nu\ell'^\mp\overline{\nu}$. A limit $\sigma(H^0)\cdot$B($H^0 \to WW^*$) < (5.6–3.2) pb (95 %CL) is given for m_{H^0} = 120–200 GeV, which far exceeds the expected Standard Model cross section.

[66] ABAZOV 06O search for associated $H^0 W$ production in $p\overline{p}$ collisions at E_{cm} = 1.96 TeV with the decay $H^0 \to WW^*$, in the final states $\ell^\pm\ell'^\mp\nu\nu' X$ where ℓ = e, μ. A limit $\sigma(H^0 W)\cdot$ B($H^0 \to WW^*$) < (3.2–2.8) pb (95 %CL) is given for m_{H^0} = 115–175 GeV, which far exceeds the expected Standard Model cross section.

Indirect Mass Limits for H^0 from Electroweak Analysis

The mass limits shown below apply to a Higgs boson H^0 with Standard Model couplings whose mass is a priori unknown.

For limits obtained before the direct measurement of the top quark mass, see the 1996 (Physical Review **D54** 1 (1996)) Edition of this Review. Other studies based on data available prior to 1996 can be found in the 1998 Edition (The European Physical Journal **C3** 1 (1998)) of this Review.

VALUE (GeV)	DOCUMENT ID		TECN
$\mathbf{94^{+25}_{-22}}$	[1] BAAK	12A	RVUE
• • • We do not use the following data for averages, fits, limits, etc. • • •			
91^{+30}_{-23}	[2] BAAK	12	RVUE
91^{+31}_{-24}	[3] ERLER	10A	RVUE
129^{+74}_{-49}	[4] LEP-SLC	06	RVUE

[1] BAAK 12A make Standard Model fits to Z and neutral current parameters, m_t, m_W, and Γ_W measurements available in 2012 (using also preliminary data). The quoted result is obtained from a fit that does not include the measured mass value of the signal observed at the LHC and also no limits from direct Higgs searches.

[2] BAAK 12 make Standard Model fits to Z and neutral current parameters, m_t, m_W, and Γ_W measurements available in 2010 (using also preliminary data). The quoted result is obtained from a fit that does not include the limit from the direct Higgs searches. The result including direct search data from LEP2, the Tevatron and the LHC is 120^{+12}_{-5} GeV.

[3] ERLER 10A makes Standard Model fits to Z and neutral current parameters, m_t, m_W measurements available in 2009 (using also preliminary data). The quoted result is obtained from a fit that does not include the limits from the direct Higgs searches. With direct search data from LEP2 and Tevatron added to the fit, the 90% CL (99% CL) interval is 115–148 (114–197) GeV.

[4] LEP-SLC 06 make Standard Model fits to Z parameters from LEP/SLC and m_t, m_W, and Γ_W measurements available in 2005 with $\Delta\alpha^{(5)}_{had}(m_Z) = 0.02758 \pm 0.00035$. The 95% CL limit is 285 GeV.

SEARCHES FOR NEUTRAL HIGGS BOSONS REFERENCES

AABOUD	18G	JHEP 1801 055	M. Aaboud *et al.*	(ATLAS Collab.)
SIRUNYAN	18A	PL B778 101	A.M. Sirunyan *et al.*	(CMS Collab.)
SIRUNYAN	18F	JHEP 1801 054	A.M. Sirunyan *et al.*	(CMS Collab.)
AABOUD	17	PL B764 11	M. Aaboud *et al.*	(ATLAS Collab.)
AABOUD	17AN	PRL 119 191803	M. Aaboud *et al.*	(ATLAS Collab.)
AABOUD	17AW	JHEP 1710 112	M. Aaboud *et al.*	(ATLAS Collab.)
KHACHATRY...	17AZ	JHEP 1710 076	V. Khachatryan *et al.*	(CMS Collab.)
KHACHATRY...	17D	JHEP 1701 076	V. Khachatryan *et al.*	(CMS Collab.)
KHACHATRY...	17R	PL B767 147	V. Khachatryan *et al.*	(CMS Collab.)
SIRUNYAN	17AX	JHEP 1711 010	A.M. Sirunyan *et al.*	(CMS Collab.)
SIRUNYAN	17CN	PR D96 072004	A.M. Sirunyan *et al.*	(CMS Collab.)
SIRUNYAN	17Y	PL B772 363	A.M. Sirunyan *et al.*	(CMS Collab.)
AABOUD	16AA	EPJ C76 585	M. Aaboud *et al.*	(ATLAS Collab.)
AABOUD	16AB	EPJ C76 605	M. Aaboud *et al.*	(ATLAS Collab.)
AABOUD	16AE	JHEP 1609 173	M. Aaboud *et al.*	(ATLAS Collab.)
AABOUD	16H	JHEP 1609 001	M. Aaboud *et al.*	(ATLAS Collab.)
AABOUD	16I	PR D94 052002	M. Aaboud *et al.*	(ATLAS Collab.)
AAD	16AX	EPJ C76 45	G. Aad *et al.*	(ATLAS Collab.)
AAD	16C	JHEP 1601 032	G. Aad *et al.*	(ATLAS Collab.)
AAD	16L	EPJ C76 210	G. Aad *et al.*	(ATLAS Collab.)
AALTONEN	16C	PR D93 112010	T. Aaltonen *et al.*	(CDF Collab.)
ABLIKIM	16E	PR D93 052005	M. Ablikim *et al.*	(BES III Collab.)
KHACHATRY...	16A	PL B752 221	V. Khachatryan *et al.*	(CMS Collab.)
KHACHATRY...	16BG	EPJ C76 371	V. Khachatryan *et al.*	(CMS Collab.)
KHACHATRY...	16BQ	PR D94 052012	V. Khachatryan *et al.*	(CMS Collab.)
KHACHATRY...	16F	JHEP 1601 079	V. Khachatryan *et al.*	(CMS Collab.)
KHACHATRY...	16M	PRL 117 051802	V. Khachatryan *et al.*	(CMS Collab.)
KHACHATRY...	16P	PL B755 217	V. Khachatryan *et al.*	(CMS Collab.)
KHACHATRY...	16W	PL B758 296	V. Khachatryan *et al.*	(CMS Collab.)
KHACHATRY...	16Z	PL B759 369	V. Khachatryan *et al.*	(CMS Collab.)
AAD	15AA	PR D92 012006	G. Aad *et al.*	(ATLAS Collab.)
AAD	15BD	EPJ C75 337	G. Aad *et al.*	(ATLAS Collab.)
AAD	15BH	EPJ C75 299	G. Aad *et al.*	(ATLAS Collab.)
Also		EPJ C75 408 (errat.)	G. Aad *et al.*	(ATLAS Collab.)
AAD	15BK	EPJ C75 412	G. Aad *et al.*	(ATLAS Collab.)
AAD	15BZ	PR D92 052002	G. Aad *et al.*	(ATLAS Collab.)
AAD	15CE	PR D92 092004	G. Aad *et al.*	(ATLAS Collab.)
AAD	15G	JHEP 1501 069	G. Aad *et al.*	(ATLAS Collab.)
AAD	15H	PRL 114 081802	G. Aad *et al.*	(ATLAS Collab.)
AAD	15S	PL B744 163	G. Aad *et al.*	(ATLAS Collab.)
KHACHATRY...	15AW	JHEP 1510 144	V. Khachatryan *et al.*	(CMS Collab.)
KHACHATRY...	15AY	JHEP 1511 071	V. Khachatryan *et al.*	(CMS Collab.)
KHACHATRY...	15BB	PL B750 494	V. Khachatryan *et al.*	(CMS Collab.)
KHACHATRY...	15N	PL B748 221	V. Khachatryan *et al.*	(CMS Collab.)
KHACHATRY...	15O	PL B748 255	V. Khachatryan *et al.*	(CMS Collab.)
KHACHATRY...	15R	PL B749 560	V. Khachatryan *et al.*	(CMS Collab.)
LEES	15H	PR D91 071102	J.P. Lees *et al.*	(BABAR Collab.)
AAD	14AP	PRL 113 171801	G. Aad *et al.*	(ATLAS Collab.)
AAD	14AS	PL B738 68	G. Aad *et al.*	(ATLAS Collab.)
AAD	14AW	JHEP 1411 056	G. Aad *et al.*	(ATLAS Collab.)
AAD	14BA	JHEP 1411 088	G. Aad *et al.*	(ATLAS Collab.)
AAD	14J	PL B732 8	G. Aad *et al.*	(ATLAS Collab.)
AAD	14M	PR D89 032002	G. Aad *et al.*	(ATLAS Collab.)
AAD	14O	PRL 112 201802	G. Aad *et al.*	(ATLAS Collab.)
CHATRCHYAN	14AA	PR D89 092007	S. Chatrchyan *et al.*	(CMS Collab.)
CHATRCHYAN	14AI	PR D89 012003	S. Chatrchyan *et al.*	(CMS Collab.)
CHATRCHYAN	14B	EPJ C74 2980	S. Chatrchyan *et al.*	(CMS Collab.)
CHATRCHYAN	14G	JHEP 1401 096	S. Chatrchyan *et al.*	(CMS Collab.)
KHACHATRY...	14M	JHEP 1410 160	V. Khachatryan *et al.*	(CMS Collab.)
KHACHATRY...	14P	EPJ C74 3076	V. Khachatryan *et al.*	(CMS Collab.)
KHACHATRY...	14Q	PR D90 112013	V. Khachatryan *et al.*	(CMS Collab.)
AAD	13AG	PL B721 32	G. Aad *et al.*	(ATLAS Collab.)
AAD	13AT	NJP 15 043009	G. Aad *et al.*	(ATLAS Collab.)
AAD	13O	JHEP 1302 095	G. Aad *et al.*	(ATLAS Collab.)
AAIJ	13T	JHEP 1305 132	R. Aaij *et al.*	(LHCb Collab.)
AALTONEN	13B	PR D87 052008	T. Aaltonen *et al.*	(CDF Collab.)
AALTONEN	13C	JHEP 1302 004	T. Aaltonen *et al.*	(CDF Collab.)
AALTONEN	13K	PR D88 052012	T. Aaltonen *et al.*	(CDF Collab.)
AALTONEN	13L	PR D88 052013	T. Aaltonen *et al.*	(CDF Collab.)
AALTONEN	13M	PR D88 052014	T. Aaltonen *et al.*	(CDF and D0 Collabs.)
AALTONEN	13P	PRL 110 121801	T. Aaltonen *et al.*	(CDF Collab.)
ABAZOV	13E	PR D88 032008	V.M. Abazov *et al.*	(D0 Collab.)
ABAZOV	13F	PR D88 052005	V.M. Abazov *et al.*	(D0 Collab.)
ABAZOV	13G	PR D88 052006	V.M. Abazov *et al.*	(D0 Collab.)
ABAZOV	13H	PR D88 052007	V.M. Abazov *et al.*	(D0 Collab.)
ABAZOV	13I	PR D88 052008	V.M. Abazov *et al.*	(D0 Collab.)
ABAZOV	13J	PR D88 052009	V.M. Abazov *et al.*	(D0 Collab.)
ABAZOV	13K	PR D88 052010	V.M. Abazov *et al.*	(D0 Collab.)
ABAZOV	13L	PR D88 052011	V.M. Abazov *et al.*	(D0 Collab.)
CARENA	13	EPJ C73 2552	M. Carena *et al.*	
CHATRCHYAN	13AG	PL B722 207	S. Chatrchyan *et al.*	(CMS Collab.)
CHATRCHYAN	13AL	PL B725 36	S. Chatrchyan *et al.*	(CMS Collab.)
CHATRCHYAN	13BJ	PL B726 564	S. Chatrchyan *et al.*	(CMS Collab.)
CHATRCHYAN	13BK	PL B726 587	S. Chatrchyan *et al.*	(CMS Collab.)
CHATRCHYAN	13Q	EPJ C73 2469	S. Chatrchyan *et al.*	(CMS Collab.)
CHATRCHYAN	13X	JHEP 1305 145	S. Chatrchyan *et al.*	(CMS Collab.)
CHATRCHYAN	13Y	JHEP 1306 081	S. Chatrchyan *et al.*	(CMS Collab.)
LEES	13C	PR D87 031102	J.P. Lees *et al.*	(BABAR Collab.)
LEES	13L	PR D88 031701	J.P. Lees *et al.*	(BABAR Collab.)
LEES	13R	PR D88 071102	J.P. Lees *et al.*	(BABAR Collab.)
AAD	12AI	PL B716 1	G. Aad *et al.*	(ATLAS Collab.)
AAD	12AJ	PL B716 62	G. Aad *et al.*	(ATLAS Collab.)
AAD	12AQ	PRL 108 251801	G. Aad *et al.*	(ATLAS Collab.)
AAD	12BU	JHEP 1209 070	G. Aad *et al.*	(ATLAS Collab.)
AAD	12BZ	PL B717 29	G. Aad *et al.*	(ATLAS Collab.)
AAD	12CA	PL B717 70	G. Aad *et al.*	(ATLAS Collab.)
AAD	12CN	PL B718 369	G. Aad *et al.*	(ATLAS Collab.)
AAD	12CO	PL B718 391	G. Aad *et al.*	(ATLAS Collab.)

AAD 12D PL B710 383 G. Aad *et al.* (ATLAS Collab.)
AAD 12G PRL 108 111803 G. Aad *et al.* (ATLAS Collab.)
AAD 12N EPJ C72 2157 G. Aad *et al.* (ATLAS Collab.)
AALTONEN 12AB PR D85 092001 T. Aaltonen *et al.* (CDF Collab.)
AALTONEN 12AK PRL 109 181802 T. Aaltonen *et al.* (CDF Collab.)
AALTONEN 12AM PR D86 072012 T. Aaltonen *et al.* (CDF Collab.)
AALTONEN 12AN PL B717 173 T. Aaltonen *et al.* (CDF Collab.)
AALTONEN 12AQ PR D86 091101 T. Aaltonen *et al.* (CDF and D0 Collabs.)
AALTONEN 12J PRL 108 181804 T. Aaltonen *et al.* (CDF Collab.)
AALTONEN 12Q PRL 109 111803 T. Aaltonen *et al.* (CDF Collab.)
AALTONEN 12R PRL 109 111804 T. Aaltonen *et al.* (CDF Collab.)
AALTONEN 12S PRL 109 111805 T. Aaltonen *et al.* (CDF Collab.)
AALTONEN 12T PRL 109 071804 T. Aaltonen *et al.* (CDF and D0 Collabs.)
AALTONEN 12U PR D85 012007 T. Aaltonen *et al.* (CDF Collab.)
AALTONEN 12X PR D85 032005 T. Aaltonen *et al.* (CDF Collab.)
ABAZOV 12G PL B710 569 V.M. Abazov *et al.* (D0 Collab.)
ABAZOV 12K PL B716 285 V.M. Abazov *et al.* (D0 Collab.)
ABAZOV 12O PRL 109 121803 V.M. Abazov *et al.* (D0 Collab.)
ABAZOV 12P PRL 109 121804 V.M. Abazov *et al.* (D0 Collab.)
ABLIKIM 12 PR D85 092012 M. Ablikim *et al.* (BES III Collab.)
BAAK 12 EPJ C72 2003 M. Baak *et al.* (Gfitter Group)
BAAK 12A EPJ C72 2205 M. Baak *et al.* (Gfitter Group)
CHATRCHYAN 12AO JHEP 1209 111 S. Chatrchyan *et al.* (CMS Collab.)
CHATRCHYAN 12AY JHEP 1211 088 S. Chatrchyan *et al.* (CMS Collab.)
CHATRCHYAN 12C JHEP 1203 081 S. Chatrchyan *et al.* (CMS Collab.)
CHATRCHYAN 12D JHEP 1204 036 S. Chatrchyan *et al.* (CMS Collab.)
CHATRCHYAN 12E PL B710 91 S. Chatrchyan *et al.* (CMS Collab.)
CHATRCHYAN 12F PL B710 284 S. Chatrchyan *et al.* (CMS Collab.)
CHATRCHYAN 12G PL B710 403 S. Chatrchyan *et al.* (CMS Collab.)
CHATRCHYAN 12H PRL 108 111804 S. Chatrchyan *et al.* (CMS Collab.)
CHATRCHYAN 12I JHEP 1203 040 S. Chatrchyan *et al.* (CMS Collab.)
CHATRCHYAN 12K PL B713 68 S. Chatrchyan *et al.* (CMS Collab.)
CHATRCHYAN 12N PL B716 30 S. Chatrchyan *et al.* (CMS Collab.)
CHATRCHYAN 12V PRL 109 121801 S. Chatrchyan *et al.* (CMS Collab.)
AALTONEN 11P PRL 107 031801 T. Aaltonen *et al.* (CDF Collab.)
ABAZOV 11G PRL 106 171802 V.M. Abazov *et al.* (D0 Collab.)
ABAZOV 11K PL B698 97 V.M. Abazov *et al.* (D0 Collab.)
ABAZOV 11W PRL 107 121801 V.M. Abazov *et al.* (D0 Collab.)
ABOUZAID 11A PRL 107 201803 E. Abouzaid *et al.* (KTeV Collab.)
CHATRCHYAN 11J PL B699 25 S. Chatrchyan *et al.* (CMS Collab.)
DEL-AMO-SA... 11J PRL 107 021804 P. del Amo Sanchez *et al.* (BABAR Collab.)
LEES 11H PRL 107 221803 J.P. Lees *et al.* (BABAR Collab.)
AALTONEN 10F PRL 104 061802 T. Aaltonen *et al.* (CDF and D0 Collabs.)
AALTONEN 10M PR D82 011102 T. Aaltonen *et al.* (CDF and D0 Collabs.)
ABBIENDI 10 PL B682 381 G. Abbiendi *et al.* (OPAL Collab.)
ANDREAS 10 JHEP 1008 003 S. Andreas *et al.* (DESY)
ERLER 10A PR D81 051301 J. Erler (UNAM)
HYUN 10 PRL 105 091801 H.J. Hyun *et al.* (BELLE Collab.)
SCHAEL 10 JHEP 1005 049 S. Schael *et al.* (ALEPH Collab.)
AALTONEN 09A PRL 102 021802 T. Aaltonen *et al.* (CDF Collab.)
AALTONEN 09AB PRL 103 061803 T. Aaltonen *et al.* (CDF Collab.)
AALTONEN 09AR PRL 103 201801 T. Aaltonen *et al.* (CDF Collab.)
ABAZOV 09U PRL 102 251801 V.M. Abazov *et al.* (D0 Collab.)
ABAZOV 09V PRL 103 061801 V.M. Abazov *et al.* (D0 Collab.)
AUBERT 09P PRL 103 181801 B. Aubert *et al.* (BABAR Collab.)
AUBERT 09Z PRL 103 081803 B. Aubert *et al.* (BABAR Collab.)
TUNG 09 PRL 102 051802 Y.C. Tung *et al.* (KEK E391a Collab.)
ABAZOV 08U PRL 101 051801 V.M. Abazov *et al.* (D0 Collab.)
ABDALLAH 08B EPJ C54 1 J. Abdallah *et al.* (DELPHI Collab.)
Also EPJ C56 165 (errat.) J. Abdallah *et al.* (DELPHI Collab.)
LOVE 08 PRL 101 151802 W. Love *et al.* (CLEO Collab.)
ABBIENDI 07 EPJ C49 457 G. Abbiendi *et al.* (OPAL Collab.)
BESSON 07 PRL 98 052002 D. Besson *et al.* (CLEO Collab.)
SCHAEL 07 EPJ C49 439 S. Schael *et al.* (ALEPH Collab.)
ABAZOV 06 PRL 96 011801 V.M. Abazov *et al.* (D0 Collab.)
ABAZOV 06O PRL 97 151804 V.M. Abazov *et al.* (D0 Collab.)
LEP-SLC 06 PRPL 427 257 ALEPH, DELPHI, L3, OPAL, SLD and working groups
SCHAEL 06B EPJ C47 547 S. Schael *et al.* (LEP Collabs.)
ABBIENDI 05A EPJ C40 317 G. Abbiendi *et al.* (OPAL Collab.)
ABDALLAH 05D EPJ C44 147 J. Abdallah *et al.* (DELPHI Collab.)
ACHARD 05 PL B609 35 P. Achard *et al.* (L3 Collab.)
ACOSTA 05Q PR D72 072004 D. Acosta *et al.* (CDF Collab.)
PARK 05 PRL 94 021801 H.K. Park *et al.* (FNAL HyperCP Collab.)
ABBIENDI 04K PL B597 11 G. Abbiendi *et al.* (OPAL Collab.)
ABBIENDI 04M EPJ C37 49 G. Abbiendi *et al.* (OPAL Collab.)
ABDALLAH 04 EPJ C32 145 J. Abdallah *et al.* (DELPHI Collab.)
ABDALLAH 04B EPJ C32 475 J. Abdallah *et al.* (DELPHI Collab.)
ABDALLAH 04L EPJ C35 313 J. Abdallah *et al.* (DELPHI Collab.)
ABDALLAH 04O EPJ C38 1 J. Abdallah *et al.* (DELPHI Collab.)
ACHARD 04B PL B583 14 P. Achard *et al.* (L3 Collab.)
ACHARD 04F PL B589 89 P. Achard *et al.* (L3 Collab.)
ABBIENDI 03B EPJ C26 479 G. Abbiendi *et al.* (OPAL Collab.)
ABBIENDI 03F EPJ C27 311 G. Abbiendi *et al.* (OPAL Collab.)
ABBIENDI 03G EPJ C27 483 G. Abbiendi *et al.* (OPAL Collab.)
ACHARD 03C PL B568 191 P. Achard *et al.* (L3 Collab.)
CARENA 03 EPJ C26 601 M.S. Carena *et al.*
HEISTER 03D PL B565 61 A. Heister *et al.* (ALEPH, DELPHI, L3+)
ALEPH, DELPHI, L3, OPAL, LEP Higgs Working Group
ABBIENDI 02D EPJ C23 397 G. Abbiendi *et al.* (OPAL Collab.)
ABBIENDI 02F PL B544 44 G. Abbiendi *et al.* (OPAL Collab.)
ACHARD 02C PL B534 28 P. Achard *et al.* (L3 Collab.)
ACHARD 02H PL B545 30 P. Achard *et al.* (L3 Collab.)
AKEROYD 02 PR D66 037702 A.G. Akeroyd *et al.*
HEISTER 02 PL B526 191 A. Heister *et al.* (ALEPH Collab.)
HEISTER 02L PL B544 16 A. Heister *et al.* (ALEPH Collab.)
HEISTER 02M PL B544 25 A. Heister *et al.* (ALEPH Collab.)
ABBIENDI 01E EPJ C18 425 G. Abbiendi *et al.* (OPAL Collab.)
ABREU 01F PL B507 89 P. Abreu *et al.* (DELPHI Collab.)
ACHARD 01C PL B517 319 P. Achard *et al.* (L3 Collab.)
AFFOLDER 01H PR D64 092002 T. Affolder *et al.* (CDF Collab.)
BARATE 01C PL B499 53 R. Barate *et al.* (ALEPH Collab.)
ACCIARRI 00M PL B485 85 M. Acciarri *et al.* (L3 Collab.)
ACCIARRI 00R PL B489 102 M. Acciarri *et al.* (L3 Collab.)
ACCIARRI 00S PL B489 115 M. Acciarri *et al.* (L3 Collab.)
BARATE 00L PL B487 241 R. Barate *et al.* (ALEPH Collab.)
ABBIENDI 99E EPJ C7 407 G. Abbiendi *et al.* (OPAL Collab.)
ABBIENDI 99O PL B464 311 G. Abbiendi *et al.* (OPAL Collab.)
ABBOTT 99B PRL 82 2244 B. Abbott *et al.* (D0 Collab.)
ABREU 99P PL B458 431 P. Abreu *et al.* (DELPHI Collab.)
CARENA 99B hep-ph/9912223 M.S. Carena *et al.*
CERN-TH/99-374
ABBOTT 98 PRL 80 442 B. Abbott *et al.* (D0 Collab.)
ACKERSTAFF 98S EPJ C5 19 K. Ackerstaff *et al.* (OPAL Collab.)
ACKERSTAFF 98Y PL B437 218 K. Ackerstaff *et al.* (OPAL Collab.)
GONZALEZ... 98B PR D57 7045 M.C. Gonzalez-Garcia, S.M. Lietti, S.F. Novaes
PDG 98 EPJ C3 1 C. Caso *et al.* (PDG Collab.)
KRAWCZYK 97 PR D55 6968 M. Krawczyk, J. Zochowski (WARS)
ALEXANDER 96H ZPHY C71 1 G. Alexander *et al.* (OPAL Collab.)
PDG 96 PR D54 1 R. M. Barnett *et al.* (PDG Collab.)
ABREU 95H ZPHY C67 69 P. Abreu *et al.* (DELPHI Collab.)
BALEST 95 PR D51 2053 R. Balest *et al.* (CLEO Collab.)
PICH 92 NP B388 31 A. Pich, J. Prades, P. Yepes (CERN, CPPM)
ANTREASYAN 90C PL B251 204 D. Antreasyan *et al.* (Crystal Ball Collab.)

Charged Higgs Bosons ($H^\pm$ and $H^{\pm\pm}$), Searches for

CONTENTS:

$H^\pm$ (Charged Higgs) MASS LIMITS

Unless otherwise stated, the limits below assume $B(H^+ \to \tau^+\nu)+B(H^+ \to c\overline{s})=1$, and hold for all values of $B(H^+ \to \tau^+\nu_\tau)$, and assume H^+ weak isospin of $T_3=+1/2$. In the following, $\tan\beta$ is the ratio of the two vacuum expectation values in two-doublet models (2HDM).

The limits are also applicable to point-like technipions. For a discussion of technipparticles, see the Review of Dynamical Electroweak Symmetry Breaking in this Review.

For limits obtained in hadronic collisions before the observation of the top quark, and based on the top mass values inconsistent with the current measurements, see the 1996 (Physical Review **D54** 1 (1996)) Edition of this Review.

Searches in e^+e^- collisions at and above the Z pole have conclusively ruled out the existence of a charged Higgs in the region $m_{H^+} \lesssim 45$ GeV, and are meanwhile superseded by the searches in higher energy e^+e^- collisions at LEP. Results that are by now obsolete are therefore not included in this compilation, and can be found in a previous Edition (The European Physical Journal **C15** 1 (2000)) of this Review.

In the following, and unless otherwise stated, results from the LEP experiments (ALEPH, DELPHI, L3, and OPAL) are assumed to derive from the study of the $e^+e^- \to H^+H^-$ process. Limits from $b \to s\gamma$ decays are usually stronger in generic 2HDM models than in Supersymmetric models.

VALUE (GeV)	*CL%*	*DOCUMENT ID*		*TECN*	*COMMENT*
> 80	95	[1] LEP	13	LEP	$e^+e^- \to H^+H^-, E_{\rm cm} \leq 209$GeV
> 76.3	95	[2] ABBIENDI	12	OPAL	$e^+e^- \to H^+H^-, E_{\rm cm} \leq 209$GeV
> 74.4	95	ABDALLAH	04I	DLPH	$E_{\rm cm} \leq 209$ GeV
> 76.5	95	ACHARD	03E	L3	$E_{\rm cm} \leq 209$ GeV
> 79.3	95	HEISTER	02P	ALEP	$E_{\rm cm} \leq 209$ GeV
• • • We do not use the following data for averages, fits, limits, etc. • • •					
		[3] MISIAK	17	RVUE	$b \to s(d)\gamma$
		[4] SIRUNYAN	17AE	CMS	$H^\pm \to W^\pm Z$
		[5] AABOUD	16A	ATLS	$t(b)\ H^+,\ H^+ \to \tau^+\nu$
		[6] AAD	16AJ	ATLS	$t(b)\ H^+,\ H^+ \to t\overline{b}$
		[7] AAD	16AJ	ATLS	$qq \to H^+,\ H^+ \to t\overline{b}$
		[8] AAD	15AF	ATLS	$t \to bH^+$
		[9] AAD	15AF	ATLS	$tH^\pm$
		[10] AAD	15M	ATLS	$H^\pm \to W^\pm Z$
		[11] KHACHATRY...	15AX	CMS	$t \to bH^+,\ H^+ \to \tau^+\nu$
		[12] KHACHATRY...	15AX	CMS	$tH^+,\ H^+ \to t\overline{b}$
		[13] KHACHATRY...	15AX	CMS	$tH^+,\ H^\pm \to \tau^\pm\nu$
		[14] KHACHATRY...	15BF	CMS	$t \to bH^+,\ H^+ \to c\overline{s}$
		[15] AAD	14M	ATLS	$H_2^0 \to H^\pm W^\mp \to H^0 W^\pm W^\mp,\ H^0 \to b\overline{b}$
		[16] AALTONEN	14A	CDF	$t \to b\tau\nu$
		[17] AAD	13AC	ATLS	$t \to bH^+$
		[18] AAD	13V	ATLS	$t \to bH^+$, lepton non-universality
		[19] AAD	12BH	ATLS	$t \to bH^+$
		[20] CHATRCHYAN	12AA	CMS	$t \to bH^+$
		[21] AALTONEN	11P	CDF	$t \to bH^+,\ H^+ \to W^+A^0$
>316	95	[22] DESCHAMPS	10	RVUE	Type II, flavor physics data
		[23] AALTONEN	09AJ	CDF	$t \to bH^+$
		[24] ABAZOV	09AC	D0	$t \to bH^+$
		[25] ABAZOV	09AG	D0	$t \to bH^+$
		[26] ABAZOV	09AI	D0	$t \to bH^+$
		[27] ABAZOV	09P	D0	$H^+ \to t\overline{b}$
		[28] ABULENCIA	06E	CDF	$t \to bH^+$
> 92.0	95	ABBIENDI	04	OPAL	$B(\tau\nu) = 1$
> 76.7	95	[29] ABDALLAH	04I	DLPH	Type I
		[30] ABBIENDI	03	OPAL	$\tau \to \mu\overline{\nu}\nu,\ e\overline{\nu}\nu$
		[31] ABAZOV	02B	D0	$t \to bH^+,\ H \to \tau\nu$
		[32] BORZUMATI	02	RVUE	

Gauge & Higgs Boson Particle Listings

Charged Higgs Bosons ($H^\pm$ and $H^{\pm\pm}$), Searches for

		[33] ABBIENDI	01Q	OPAL	$B \to \tau\nu_\tau X$
		[34] BARATE	01E	ALEP	$B \to \tau\nu_\tau$
>315	99	[35] GAMBINO	01	RVUE	$b \to s\gamma$
		[36] AFFOLDER	00I	CDF	$t \to bH^+$, $H \to \tau\nu$
> 59.5	95	ABBIENDI	99E	OPAL	$E_{cm} \leq 183$ GeV
		[37] ABBOTT	99E	D0	$t \to bH^+$
		[38] ACKERSTAFF	99D	OPAL	$\tau \to e\nu\nu$, $\mu\nu\nu$
		[39] ACCIARRI	97F	L3	$B \to \tau\nu_\tau$
		[40] AMMAR	97B	CLEO	$\tau \to \mu\nu\nu$
		[41] COARASA	97	RVUE	$B \to \tau\nu_\tau X$
		[42] GUCHAIT	97	RVUE	$t \to bH^+$, $H \to \tau\nu$
		[43] MANGANO	97	RVUE	$B_{u(c)} \to \tau\nu_\tau$
		[44] STAHL	97	RVUE	$\tau \to \mu\nu\nu$
>244	95	[45] ALAM	95	CLE2	$b \to s\gamma$
		[46] BUSKULIC	95	ALEP	$b \to \tau\nu_\tau X$

[1] LEP 13 give a limit that refers to the Type II scenario. The limit for $B(H^+ \to \tau\nu) = 1$ is 94 GeV (95% CL), and for $B(H^+ \to cs) = 1$ the region below 80.5 as well as the region 83–88 GeV is excluded (95% CL). LEP 13 also search for the decay mode $H^+ \to A^0 W^*$ with $A^0 \to b\overline{b}$, which is not negligible in Type I models. The limit in Type I models is 72.5 GeV (95% CL) if $m_{A^0} > 12$ GeV.

[2] ABBIENDI 12 also search for the decay mode $H^+ \to A^0 W^*$ with $A^0 \to b\overline{b}$.

[3] MISIAK 17 give 95% CL lower limits on m_{H^+} between 570 and 800 GeV in type II two Higgs doublet model from combined data (including an unpublished BELLE result) for $B(b \to s(d)\gamma)$.

[4] SIRUNYAN 17AE search for vector boson fusion production of $H^\pm$ decaying to $H^\pm \to W^\pm Z \to \ell^\pm\nu\ell^+\ell^-$ in 15.2 fb^{-1} of pp collisions at $E_{cm} = 13$ TeV. See their Fig. 3 for limits on cross section times branching ratio for $m_{H^\pm} = 0.2$–2.0 TeV, and also for limits on the triplet vacuum expectation value fraction in the Georgi-Machacek model.

[5] AABOUD 16A search for $t(b)\,H^\pm$ associated production followed by $H^+ \to \tau^+\nu$ in 3.2 fb^{-1} of pp collisions at $E_{cm} = 13$ TeV. Upper limits on $\sigma(t(b)\,H^\pm)\,B(H^+ \to \tau\nu)$ between 1.9 pb and 15 fb (95% CL) are given for $m_{H^+} = 200$–2000 GeV, see their Fig. 6. See their Fig. 7 for the excluded regions in the hMSSM scenario.

[6] AAD 16AJ search for $t(b)\,H^\pm$ associated production followed by $H^\pm \to tb$ in 20.3 fb^{-1} of pp collisions at $E_{cm} = 8$ TeV. See their Fig. 6 for upper limits on $\sigma(t(b)\,H^\pm)\,B(H^+ \to tb)$ for $m_{H^+} = 200$–600 GeV.

[7] AAD 16AJ search for $H^\pm$ production from quark-antiquark annihilation, followed by $H^\pm \to tb$, in 20.3 fb^{-1} of pp collisions at $E_{cm} = 8$ TeV. See their Fig. 10 for upper limits on $\sigma(H^\pm)\,B(H^+ \to tb)$ for $m_{H^+} = 400$–3000 GeV.

[8] AAD 15AF search for $t\overline{t}$ production followed by $t \to bH^+$, $H^+ \to \tau^+\nu$ in 19.5 fb^{-1} of pp collisions at $E_{cm} = 8$ TeV. Upper limits on $B(t \to bH^+)\,B(H^+ \to \tau\nu)$ between 2.3×10^{-3} and 1.3×10^{-2} (95% CL) are given for $m_{H^+} = 80$–160 GeV. See their Fig. 8 for the excluded regions in different benchmark scenarios of the MSSM. The region $m_{H^+} < 140$ GeV is excluded for $\tan\beta > 1$ in the considered scenarios.

[9] AAD 15AF search for $tH^\pm$ associated production followed by $H^\pm \to \tau^\pm\nu$ in 19.5 fb^{-1} of pp collisions at $E_{cm} = 8$ TeV. Upper limits on $\sigma(tH^\pm)\,B(H^+ \to \tau\nu)$ between 760 and 4.5 fb (95% CL) are given for $m_{H^+} = 180$–1000 GeV. See their Fig. 8 for the excluded regions in different benchmark scenarios of the MSSM.

[10] AAD 15M search for vector boson fusion production of $H^\pm$ decaying to $H^\pm \to W^\pm Z \to q\overline{q}\ell^+\ell^-$ in 20.3 fb^{-1} of pp collisions at $E_{cm} = 8$ TeV. See their Fig. 2 for limits on cross section times branching ratio for $m_{H^\pm} = 200$–1000 GeV, and Fig. 3 for limits on thetriplet vacuum expectation value fraction in the Georgi-Machacek model.

[11] KHACHATRYAN 15AX search for $t\overline{t}$ production followed by $t \to bH^+$, $H^+ \to \tau^+\nu$ in 19.7 fb^{-1} of pp collisions at $E_{cm} = 8$ TeV. Upper limits on $B(t \to bH^+)\,B(H^+ \to \tau\nu)$ between 1.2×10^{-2} and 1.5×10^{-3} (95% CL) are given for $m_{H^+} = 80$–160 GeV. See their Fig. 11 for the excluded regions in different benchmark scenarios of the MSSM. The region $m_{H^+} < 155$ GeV is excluded for $\tan\beta > 1$ in the considered scenarios.

[12] KHACHATRYAN 15AX search for $tH^\pm$ associated production followed by $H^\pm \to tb$ in 19.7 fb^{-1} of pp collisions at $E_{cm} = 8$ TeV. Upper limits on $\sigma(tH^\pm)\,B(H^+ \to t\overline{b})$ between 2.0 and 0.13 pb (95% CL) are given for $m_{H^+} = 180$–600 GeV. See their Fig. 11 for the excluded regions in different benchmark scenarios of the MSSM.

[13] KHACHATRYAN 15AX search for $tH^\pm$ associated production followed by $H^\pm \to \tau^\pm\nu$ in 19.7 fb^{-1} of pp collisions at $E_{cm} = 8$ TeV. Upper limits on $\sigma(tH^\pm)\,B(H^+ \to \tau\nu)$ between 380 and 25 fb (95% CL) are given for $m_{H^+} = 180$–600 GeV. See their Fig. 11 for the excluded regions in different benchmark scenarios of the MSSM.

[14] KHACHATRYAN 15BF search for $t\overline{t}$ production followed by $t \to bH^+$, $H^+ \to c\overline{s}$ in 19.7 fb^{-1} of pp collisions at $E_{cm} = 8$ TeV. Upper limits on $B(t \to bH^+)\,B(H^+ \to c\overline{s})$ between 1.2×10^{-2} and 6.5×10^{-2} (95% CL) are given for $m_{H^+} = 90$–160 GeV.

[15] AAD 14M search for the decay cascade $H_2^0 \to H^\pm W^\mp \to H^0 W^\pm W^\mp$, H^0 decaying to $b\overline{b}$ in 20.3 fb^{-1} of pp collisions at $E_{cm} = 8$ TeV. See their Table III for limits on cross section times branching ratio for $m_{H_2^0} = 325$–1025 GeV and $m_{H^+} = 225$–925 GeV.

[16] AALTONEN 14A measure $B(t \to b\tau\nu) = 0.096 \pm 0.028$ using 9 fb^{-1} of $p\overline{p}$ collisions at $E_{cm} = 1.96$ TeV. For $m_{H^+} = 80$–140 GeV, this measured value is translated to a limit $B(t \to bH^+) < 0.059$ at 95% CL assuming $B(H^+ \to \tau^+\nu) = 1$.

[17] AAD 13AC search for $t\overline{t}$ production followed by $t \to bH^+$, $H^+ \to c\overline{s}$ (flavor unidentified) in 4.7 fb^{-1} of pp collisions at $E_{cm} = 7$ TeV. Upper limits on $B(t \to bH^+)$ between 0.05 and 0.01 (95%CL) are given for m_{H^+}=90–150 GeV and $B(H^+ \to c\overline{s})$=1.

[18] AAD 13V search for $t\overline{t}$ production followed by $t \to bH^+$, $H^+ \to \tau^+\nu$ through violation of lepton universality with 4.6 fb^{-1} of pp collisions at $E_{cm} = 7$ TeV. Upper limits on $B(t \to bH^+)$ between 0.032 and 0.044 (95% CL) are given for $m_{H^+} = 90$–140 GeV and $B(H^+ \to \tau^+\nu) = 1$. By combining with AAD 12BH, the limits improve to 0.008 to 0.034 for $m_{H^+} = 90$–160 GeV. See their Fig. 7 for the excluded region in the $m_h^{\max}$ scenario of the MSSM.

[19] AAD 12BH search for $t\overline{t}$ production followed by $t \to bH^+$, $H^+ \to \tau^+\nu$ with 4.6 fb^{-1} of pp collisions at $E_{cm} = 7$ TeV. Upper limits on $B(t \to bH^+)$ between 0.01 and 0.05 (95% CL) are given for $m_{H^+} = 90$–160 GeV and $B(H^+ \to \tau^+\nu) = 1$. See their Fig. 8 for the excluded region in the $m_h^{\max}$ scenario of the MSSM.

[20] CHATRCHYAN 12AA search for $t\overline{t}$ production followed by $t \to bH^+$, $H^+ \to \tau^+\nu$ with 2 fb^{-1} of pp collisions at $E_{cm} = 7$ TeV. Upper limits on $B(t \to bH^+)$ between 0.019 and 0.041 (95% CL) are given for $m_{H^+} = 80$–160 GeV and $B(H^+ \to \tau^+\nu)$=1.

[21] AALTONEN 11P search in 2.7 fb^{-1} of $p\overline{p}$ collisions at $E_{cm} = 1.96$ TeV for the decay chain $t \to bH^+$, $H^+ \to W^+A^0$, $A^0 \to \tau^+\tau^-$ with m_{A^0} between 4 and 9 GeV. See their Fig. 4 for limits on $B(t \to bH^+)$ for $90 < m_{H^+} < 160$ GeV.

[22] DESCHAMPS 10 make Type II two Higgs doublet model fits to weak leptonic and semileptonic decays, $b \to s\gamma$, B, B_s mixings, and $Z \to b\overline{b}$. The limit holds irrespective of $\tan\beta$.

[23] AALTONEN 09AJ search for $t \to bH^+$, $H^+ \to c\overline{s}$ in $t\overline{t}$ events in 2.2 fb^{-1} of $p\overline{p}$ collisions at $E_{cm} = 1.96$ TeV. Upper limits on $B(t \to bH^+)$ between 0.08 and 0.32 (95% CL) are given for $m_{H^+} = 60$–150 GeV and $B(H^+ \to c\overline{s}) = 1$.

[24] ABAZOV 09AC search for $t \to bH^+$, $H^+ \to \tau^+\nu$ in $t\overline{t}$ events in 0.9 fb^{-1} of $p\overline{p}$ collisions at $E_{cm} = 1.96$ TeV. Upper limits on $B(t \to bH^+)$ between 0.19 and 0.25 (95% CL) are given for $m_{H^+} = 80$–155 GeV and $B(H^+ \to \tau^+\nu) = 1$. See their Fig. 4 for an excluded region in a MSSM scenario.

[25] ABAZOV 09AG measure $t\overline{t}$ cross sections in final states with ℓ + jets ($\ell = e$, μ), $\ell\ell$, and $\tau\ell$ in 1 fb^{-1} of $p\overline{p}$ collisions at $E_{cm} = 1.96$ TeV, which constrains possible $t \to bH^+$ branching fractions. Upper limits (95% CL) on $B(t \to bH^+)$ between 0.15 and 0.40 (0.48 and 0.57) are given for $B(H^+ \to \tau^+\nu) = 1$ ($B(H^+ \to c\overline{s}) = 1$) for m_{H^+} = 80–155 GeV.

[26] ABAZOV 09AI search for $t \to bH^+$ in $t\overline{t}$ events in 1 fb^{-1} of $p\overline{p}$ collisions at E_{cm} = 1.96 TeV. Final states with ℓ + jets ($\ell = e$, μ), $\ell\ell$, and $\tau\ell$ are examined. Upper limits on $B(t \to bH^+)$ (95% CL) between 0.15 and 0.19 (0.19 and 0.22) are given for $B(H^+ \to \tau^+\nu) = 1$ ($B(H^+ \to c\overline{s}) = 1$) for $m_{H^+} = 80$–155 GeV. For $B(H^+ \to \tau^+\nu) = 1$ also a simultaneous extraction of $B(t \to bH^+)$ and the $t\overline{t}$ cross section is performed, yielding a limit on $B(t \to bH^+)$ between 0.12 and 0.26 for $m_{H^+} = 80$–155 GeV. See their Figs. 5–8 for excluded regions in several MSSM scenarios.

[27] ABAZOV 09P search for H^+ production by $q\overline{q}'$ annihilation followed by $H^+ \to t\overline{b}$ decay in 0.9 fb^{-1} of $p\overline{p}$ collisions at $E_{cm} = 1.96$ TeV. Cross section limits in several two-doublet models are given for $m_{H^+} = 180$–300 GeV. A region with $20 \lesssim \tan\beta \lesssim 70$ is excluded (95% CL) for 180 GeV $\lesssim m_{H^+} \lesssim$ 184 GeV in type-I models.

[28] ABULENCIA 06E search for associated $H^0 W$ production in $p\overline{p}$ collisions at $E_{cm} = 1.96$ TeV. A fit is made for $t\overline{t}$ production processes in dilepton, lepton + jets, and lepton + τ final states, with the decays $t \to W^+b$ and $t \to H^+b$ followed by $H^+ \to \tau^+\nu$, $c\overline{s}$, $t^*\overline{b}$, or W^+H^0. Within the MSSM the search is sensitive to the region $\tan\beta < 1$ or > 30 in the mass range $m_{H^+} = 80$–160 GeV. See Fig. 2 for the excluded region in a certain MSSM scenario.

[29] ABDALLAH 04I search for $e^+e^- \to H^+H^-$ with $H^\pm$ decaying to $\tau\nu$, cs, or W^*A^0 in Type-I two-Higgs-doublet models.

[30] ABBIENDI 03 give a limit $m_{H^+} > 1.28\tan\beta$ GeV (95%CL) in Type II two-doublet models.

[31] ABAZOV 02B search for a charged Higgs boson in top decays with $H^+ \to \tau^+\nu$ at E_{cm}=1.8 TeV. For m_{H^+}=75 GeV, the region $\tan\beta > 32.0$ is excluded at 95%CL. The excluded mass region extends to over 140 GeV for $\tan\beta$ values above 100.

[32] BORZUMATI 02 point out that the decay modes such as $b\overline{b}\,W$, $A^0\,W$, and supersymmetric ones can have substantial branching fractions in the mass range explored at LEP II and Tevatron.

[33] ABBIENDI 01Q give a limit $\tan\beta/m_{H^+} < 0.53$ GeV^{-1} (95%CL) in Type II two-doublet models.

[34] BARATE 01E give a limit $\tan\beta/m_{H^+} < 0.40$ GeV^{-1} (90% CL) in Type II two-doublet models. An independent measurement of $B \to \tau\nu_\tau X$ gives $\tan\beta/m_{H^+} < 0.49$ GeV^{-1} (90% CL).

[35] GAMBINO 01 use the world average data in the summer of 2001 $B(b \to s\gamma) = (3.23 \pm 0.42) \times 10^{-4}$. The limit applies for Type-II two-doublet models.

[36] AFFOLDER 00I search for a charged Higgs boson in top decays with $H^+ \to \tau^+\nu$ in $p\overline{p}$ collisions at E_{cm}=1.8 TeV. The excluded mass region extends to over 120 GeV for $\tan\beta$ values above 100 and $B(\tau\nu) = 1$. If $B(t \to bH^+) \gtrsim 0.6$, m_{H^+} up to 160 GeV is excluded. Updates ABE 97L.

[37] ABBOTT 99E search for a charged Higgs boson in top decays in $p\overline{p}$ collisions at E_{cm}=1.8 TeV, by comparing the observed $t\overline{t}$ cross section (extracted from the data assuming the dominant decay $t \to bW^+$) with theoretical expectation. The search is sensitive to regions of the domains $\tan\beta \lesssim 1$, $50 < m_{H^+}$(GeV) $\lesssim 120$ and $\tan\beta \gtrsim 40$, $50 < m_{H^+}$ (GeV) $\lesssim 160$. See Fig. 3 for the details of the excluded region.

[38] ACKERSTAFF 99D measure the Michel parameters ρ, ξ, η, and $\xi\delta$ in leptonic τ decays from $Z \to \tau\tau$. Assuming e-μ universality, the limit $m_{H^+} > 0.97\tan\beta$ GeV (95%CL) is obtained for two-doublet models in which only one doublet couples to leptons.

[39] ACCIARRI 97F give a limit $m_{H^+} > 2.6\tan\beta$ GeV (90% CL) from their limit on the exclusive $B \to \tau\nu_\tau$ branching ratio.

[40] AMMAR 97B measure the Michel parameter ρ from $\tau \to e\nu\nu$ decays and assumes e/μ universality to extract the Michel η parameter from $\tau \to \mu\nu\nu$ decays. The measurement is translated to a lower limit on m_{H^+} in a two-doublet model $m_{H^+} > 0.97\tan\beta$ GeV (90% CL).

[41] COARASA 97 reanalyzed the constraint on the ($m_{H^\pm}$,$\tan\beta$) plane derived from the inclusive $B \to \tau\nu_\tau X$ branching ratio in GROSSMAN 95B and BUSKULIC 95. They show that the constraint is quite sensitive to supersymmetric one-loop effects.

[42] GUCHAIT 97 studies the constraints on m_{H^+} set by Tevatron data on $\ell\tau$ final states in $t\overline{t} \to (Wb)(Hb)$, $W \to \ell\nu$, $H \to \tau\nu_\tau$. See Fig. 2 for the excluded region.

[43] MANGANO 97 reconsiders the limit in ACCIARRI 97F including the effect of the potentially large $B_c \to \tau\nu_\tau$ background to $B_u \to \tau\nu_\tau$ decays. Stronger limits are obtained.

[44] STAHL 97 fit τ lifetime, leptonic branching ratios, and the Michel parameters and derive limit $m_{H^+} > 1.5 \tan\beta$ GeV (90% CL) for a two-doublet model. See also STAHL 94.

[45] ALAM 95 measure the inclusive $b \to s\gamma$ branching ratio at $\Upsilon(4S)$ and give $B(b \to s\gamma) < 4.2 \times 10^{-4}$ (95% CL), which translates to the limit $m_{H^+} > [244 + 63/(\tan\beta)^{1.3}]$ GeV in the Type II two-doublet model. Light supersymmetric particles can invalidate this bound.

[46] BUSKULIC 95 give a limit $m_{H^+} > 1.9 \tan\beta$ GeV (90% CL) for Type-II models from $b \to \tau\nu_\tau X$ branching ratio, as proposed in GROSSMAN 94.

MASS LIMITS for $H^{\pm\pm}$ (doubly-charged Higgs boson)

This section covers searches for a doubly-charged Higgs boson with couplings to lepton pairs. Its weak isospin T_3 is thus restricted to two possibilities depending on lepton chiralities: $T_3(H^{\pm\pm}) = \pm 1$, with the coupling $g_{\ell\ell}$ to $\ell_L^- \ell_L'^-$ and $\ell_R^+ \ell_R'^+$ ("left-handed") and $T_3(H^{\pm\pm}) = 0$, with the coupling to $\ell_R^- \ell_R'^-$ and $\ell_L^+ \ell_L'^+$ ("right-handed"). These Higgs bosons appear in some left-right symmetric models based on the gauge group $SU(2)_L \times SU(2)_R \times U(1)$, the type-II seesaw model, and the Zee-Babu model. The two cases are listed separately in the following. Unless noted, one of the lepton flavor combinations is assumed to be dominant in the decay.

LIMITS for $H^{\pm\pm}$ with $T_3 = \pm 1$

VALUE (GeV)	CL%	DOCUMENT ID		TECN	COMMENT
>551	95	[1] AAD	15AG	ATLS	ee
>468	95	[1] AAD	15AG	ATLS	$e\mu$
>516	95	[1] AAD	15AG	ATLS	$\mu\mu$
>400	95	[2] AAD	15AP	ATLS	$e\tau$
>400	95	[2] AAD	15AP	ATLS	$\mu\tau$
>169	95	[3] CHATRCHYAN	12AU	CMS	$\tau\tau$
>300	95	[3] CHATRCHYAN	12AU	CMS	$\mu\tau$
>293	95	[3] CHATRCHYAN	12AU	CMS	$e\tau$
>395	95	[3] CHATRCHYAN	12AU	CMS	$\mu\mu$
>391	95	[3] CHATRCHYAN	12AU	CMS	$e\mu$
>382	95	[3] CHATRCHYAN	12AU	CMS	ee
> 98.1	95	[4] ABDALLAH	03	DLPH	$\tau\tau$
> 99.0	95	[5] ABBIENDI	02C	OPAL	$\tau\tau$
• • • We do not use the following data for averages, fits, limits, etc. • • •					
		[6] KANEMURA	15	RVUE	$W^{(*)\pm} W^{(*)\pm}$
		[7] KHACHATRY...	15D	CMS	$W^{\pm} W^{\pm}$
		[8] KANEMURA	14	RVUE	$W^{(*)\pm} W^{(*)\pm}$
>330	95	[9] AAD	13Y	ATLS	$\mu\mu$
>237	95	[9] AAD	13Y	ATLS	$\mu\tau$
>355	95	[10] AAD	12AY	ATLS	$\mu\mu$
>398	95	[11] AAD	12CQ	ATLS	$\mu\mu$
>375	95	[11] AAD	12CQ	ATLS	$e\mu$
>409	95	[11] AAD	12CQ	ATLS	ee
>128	95	[12] ABAZOV	12A	D0	$\tau\tau$
>144	95	[12] ABAZOV	12A	D0	$\mu\tau$
>245	95	[13] AALTONEN	11AF	CDF	$\mu\mu$
>210	95	[13] AALTONEN	11AF	CDF	$e\mu$
>225	95	[13] AALTONEN	11AF	CDF	ee
>114	95	[14] AALTONEN	08AA	CDF	$e\tau$
>112	95	[14] AALTONEN	08AA	CDF	$\mu\tau$
>168	95	[15] ABAZOV	08V	D0	$\mu\mu$
		[16] AKTAS	06A	H1	single $H^{\pm\pm}$
>133	95	[17] ACOSTA	05L	CDF	stable
>118.4	95	[18] ABAZOV	04E	D0	$\mu\mu$
		[19] ABBIENDI	03Q	OPAL	$E_{cm} \leq 209$ GeV, single $H^{\pm\pm}$
		[20] GORDEEV	97	SPEC	muonium conversion
		[21] ASAKA	95	THEO	
> 45.6	95	[22] ACTON	92M	OPAL	
> 30.4	95	[23] ACTON	92M	OPAL	
none 6.5–36.6	95	[24] SWARTZ	90	MRK2	

[1] AAD 15AG search for $H^{++}H^{--}$ production in 20.3 fb^{-1} of pp collisions at $E_{cm} = 8$ TeV. The limit assumes 100% branching ratio to the specified final state. See their Fig. 5 for limits for arbitrary branching ratios.

[2] AAD 15AP search for $H^{++}H^{--}$ production in 20.3 fb^{-1} of pp collisions at $E_{cm} = 8$ TeV. The limit assumes 100% branching ratio to the specified final state.

[3] CHATRCHYAN 12AU search for $H^{++}H^{--}$ production with 4.9 fb^{-1} of pp collisions at $E_{cm} = 7$ TeV. The limit assumes 100% branching ratio to the specified final state. See their Table 6 for limits including associated $H^{++}H^{-}$ production or assuming different scenarios.

[4] ABDALLAH 03 search for $H^{++}H^{--}$ pair production either followed by $H^{++} \to \tau^+\tau^+$, or decaying outside the detector.

[5] ABBIENDI 02C searches for pair production of $H^{++}H^{--}$, with $H^{\pm\pm} \to \ell^{\pm}\ell^{\pm}$ (ℓ,ℓ' = e,μ,τ). The limit holds for ℓ=ℓ'=τ, and becomes stronger for other combinations of leptonic final states. To ensure the decay within the detector, the limit only applies for $g(H\ell\ell) \gtrsim 10^{-7}$.

[6] KANEMURA 15 examine the case where H^{++} decays preferentially to $W^{(*)}W^{(*)}$ and estimate that a lower mass limit of $\sim$ 84 GeV can be derived from the same-sign dilepton data of AAD 15AG if H^{++} decays with 100% branching ratio to $W^{(*)}W^{(*)}$.

[7] KHACHATRYAN 15D search for $H^{\pm\pm}$ production by vector boson fusion followed by the decay $H^{\pm\pm} \to W^{\pm}W^{\pm}$ in 19.4 fb^{-1} of pp collisions at $E_{cm} = 8$ TeV. See their Fig. 4 for limits on cross section times branching ratio for $m_{H^{++}}$ between 160 and 800 GeV.

[8] KANEMURA 14 examine the case where H^{++} decays preferentially to $W^{(*)}W^{(*)}$ and estimate that a lower mass limit of $\sim$ 60 GeV can be derived from the same-sign dilepton data of AAD 12CY.

[9] AAD 13Y search for $H^{++}H^{--}$ production in a generic search of events with three charged leptons in 4.6 fb^{-1} of pp collisions at $E_{cm} = 7$ TeV. The limit assumes 100% branching ratio to the specified final state.

[10] AAD 12AY search for $H^{++}H^{--}$ production with 1.6 fb^{-1} of pp collisions at $E_{cm} = 7$ TeV. The limit assumes 100% branching ratio to the specified final state.

[11] AAD 12CQ search for $H^{++}H^{--}$ production with 4.7 fb^{-1} of pp collisions at $E_{cm} = 7$ TeV. The limit assumes 100% branching ratio to the specified final state. See their Table 1 for limits assuming smaller branching ratios.

[12] ABAZOV 12A search for $H^{++}H^{--}$ production in 7.0 fb^{-1} of $p\overline{p}$ collisions at $E_{cm} = 1.96$ TeV.

[13] AALTONEN 11AF search for $H^{++}H^{--}$ production in 6.1 fb^{-1} of $p\overline{p}$ collisions at $E_{cm} = 1.96$ TeV.

[14] AALTONEN 08AA search for $H^{++}H^{--}$ production in $p\overline{p}$ collisions at $E_{cm} = 1.96$ TeV. The limit assumes 100% branching ratio to the specified final state.

[15] ABAZOV 08V search for $H^{++}H^{--}$ production in $p\overline{p}$ collisions at $E_{cm} = 1.96$ TeV. The limit is for $B(H \to \mu\mu) = 1$. The limit is updated in ABAZOV 12A.

[16] AKTAS 06A search for single $H^{\pm\pm}$ production in ep collisions at HERA. Assuming that H^{++} only couples to $e^+\mu^+$ with $g_{e\mu} = 0.3$ (electromagnetic strength), a limit $m_{H^{++}} > 141$ GeV (95% CL) is derived. For the case where H^{++} couples to $e\tau$ only the limit is 112 GeV.

[17] ACOSTA 05L search for $H^{++}H^{--}$ pair production in $p\overline{p}$ collisions. The limit is valid for $g_{\ell\ell'} < 10^{-8}$ so that the Higgs decays outside the detector.

[18] ABAZOV 04E search for $H^{++}H^{--}$ pair production in $H^{\pm\pm} \to \mu^{\pm}\mu^{\pm}$. The limit is valid for $g_{\mu\mu} \gtrsim 10^{-7}$.

[19] ABBIENDI 03Q searches for single $H^{\pm\pm}$ via direct production in $e^+e^- \to e^{\mp}e^{\mp}H^{\pm\pm}$, and via t-channel exchange in $e^+e^- \to e^+e^-$. In the direct case, and assuming $B(H^{\pm\pm} \to \ell^{\pm}\ell^{\pm}) = 1$, a 95% CL limit on $h_{ee} < 0.071$ is set for $m_{H^{\pm\pm}} < 160$ GeV (see Fig. 6). In the second case, indirect limits on h_{ee} are set for $m_{H^{\pm\pm}} < 2$ TeV (see Fig. 8).

[20] GORDEEV 97 search for muonium-antimuonium conversion and find $G_{M\overline{M}}/G_F < 0.14$ (90% CL), where $G_{M\overline{M}}$ is the lepton-flavor violating effective four-fermion coupling. This limit may be converted to $m_{H^{++}} > 210$ GeV if the Yukawa couplings of H^{++} to ee and $\mu\mu$ are as large as the weak gauge coupling. For similar limits on muonium-antimuonium conversion, see the muon Particle Listings.

[21] ASAKA 95 point out that H^{++} decays dominantly to four fermions in a large region of parameter space where the limit of ACTON 92M from the search of dilepton modes does not apply.

[22] ACTON 92M limit assumes $H^{\pm\pm} \to \ell^{\pm}\ell^{\pm}$ or $H^{\pm\pm}$ does not decay in the detector. Thus the region $g_{\ell\ell} \approx 10^{-7}$ is not excluded.

[23] ACTON 92M from $\Delta\Gamma_Z < 40$ MeV.

[24] SWARTZ 90 assume $H^{\pm\pm} \to \ell^{\pm}\ell^{\pm}$ (any flavor). The limits are valid for the Higgs-lepton coupling $g(H\ell\ell) \gtrsim 7.4 \times 10^{-7}/[m_H/\text{GeV}]^{1/2}$. The limits improve somewhat for ee and $\mu\mu$ decay modes.

LIMITS for $H^{\pm\pm}$ with $T_3 = 0$

VALUE (GeV)	CL%	DOCUMENT ID		TECN	COMMENT
>374	95	[1] AAD	15AG	ATLS	ee
>402	95	[1] AAD	15AG	ATLS	$e\mu$
>438	95	[1] AAD	15AG	ATLS	$\mu\mu$
>290	95	[2] AAD	15AP	ATLS	$e\tau$
>290	95	[2] AAD	15AP	ATLS	$\mu\tau$
> 97.3	95	[3] ABDALLAH	03	DLPH	$\tau\tau$
> 97.3	95	[4] ACHARD	03F	L3	$\tau\tau$
> 98.5	95	[5] ABBIENDI	02C	OPAL	$\tau\tau$
• • • We do not use the following data for averages, fits, limits, etc. • • •					
>251	95	[6] AAD	12AY	ATLS	$\mu\mu$
>306	95	[7] AAD	12CQ	ATLS	$\mu\mu$
>310	95	[7] AAD	12CQ	ATLS	$e\mu$
>322	95	[7] AAD	12CQ	ATLS	ee
>113	95	[8] ABAZOV	12A	D0	$\mu\tau$
>205	95	[9] AALTONEN	11AF	CDF	$\mu\mu$
>190	95	[9] AALTONEN	11AF	CDF	$e\mu$
>205	95	[9] AALTONEN	11AF	CDF	ee
>145	95	[10] ABAZOV	08V	D0	$\mu\mu$
		[11] AKTAS	06A	H1	single $H^{\pm\pm}$
>109	95	[12] ACOSTA	05L	CDF	stable
> 98.2	95	[13] ABAZOV	04E	D0	$\mu\mu$
		[14] ABBIENDI	03Q	OPAL	$E_{cm} \leq 209$ GeV, single $H^{\pm\pm}$
		[15] GORDEEV	97	SPEC	muonium conversion
> 45.6	95	[16] ACTON	92M	OPAL	
> 25.5	95	[17] ACTON	92M	OPAL	
none 7.3–34.3	95	[18] SWARTZ	90	MRK2	

[1] AAD 15AG search for $H^{++}H^{--}$ production in 20.3 fb^{-1} of pp collisions at $E_{cm} = 8$ TeV. The limit assumes 100% branching ratio to the specified final state. See their Fig. 5 for limits for arbitrary branching ratios.

[2] AAD 15AP search for $H^{++}H^{--}$ production in 20.3 fb^{-1} of pp collisions at $E_{cm} = 8$ TeV. The limit assumes 100% branching ratio to the specified final state.

[3] ABDALLAH 03 search for $H^{++}H^{--}$ pair production either followed by $H^{++} \to \tau^+\tau^+$, or decaying outside the detector.

[4] ACHARD 03F search for $e^+e^- \to H^{++}H^{--}$ with $H^{\pm\pm} \to \ell^{\pm}\ell'^{\pm}$. The limit holds for $\ell = \ell' = \tau$, and slightly different limits apply for other flavor combinations. The limit is valid for $g_{\ell\ell'} \gtrsim 10^{-7}$.

[5] ABBIENDI 02C searches for pair production of $H^{++}H^{--}$, with $H^{\pm\pm} \to \ell^{\pm}\ell^{\pm}$ (ℓ,ℓ' = e,μ,τ). the limit holds for ℓ=ℓ'=τ, and becomes stronger for other combinations of

Gauge & Higgs Boson Particle Listings

Charged Higgs Bosons ($H^\pm$ and $H^{\pm\pm}$), Searches for, New Heavy Bosons

leptonic final states. To ensure the decay within the detector, the limit only applies for $g(H\ell\ell) \gtrsim 10^{-7}$.

[6] AAD 12AY search for $H^{++}H^{--}$ production with 1.6 fb^{-1} of pp collisions at E_{cm} = 7 TeV. The limit assumes 100% branching ratio to the specified final state.

[7] AAD 12CQ search for $H^{++}H^{--}$ production with 4.7 fb^{-1} of pp collisions at E_{cm} = 7 TeV. The limit assumes 100% branching ratio to the specified final state. See their Table 1 for limits assuming smaller branching ratios.

[8] ABAZOV 12A search for $H^{++}H^{--}$ production in 7.0 fb^{-1} of $p\overline{p}$ collisions at E_{cm} = 1.96 TeV.

[9] AALTONEN 11AF search for $H^{++}H^{--}$ production in 6.1 fb^{-1} of $p\overline{p}$ collisions at E_{cm} = 1.96 TeV.

[10] ABAZOV 08V search for $H^{++}H^{--}$ production in $p\overline{p}$ collisions at E_{cm}= 1.96 TeV. The limit is for B($H \to \mu\mu$) = 1. The limit is updated in ABAZOV 12A.

[11] AKTAS 06A search for single $H^{\pm\pm}$ production in ep collisions at HERA. Assuming that H^{++} only couples to $e^+\mu^+$ with $g_{e\mu} = 0.3$ (electromagnetic strength), a limit $m_{H^{++}} > 141$ GeV (95% CL) is derived. For the case where H^{++} couples to $e\tau$ only the limit is 112 GeV.

[12] ACOSTA 05L search for $H^{++}H^{--}$ pair production in $p\overline{p}$ collisions. The limit is valid for $g_{\ell\ell'} < 10^{-8}$ so that the Higgs decays outside the detector.

[13] ABAZOV 04E search for $H^{++}H^{--}$ pair production in $H^{\pm\pm} \to \mu^\pm\mu^\pm$. The limit is valid for $g_{\mu\mu} \gtrsim 10^{-7}$.

[14] ABBIENDI 03Q searches for single $H^{\pm\pm}$ via direct production in $e^+e^- \to e^\mp e^\mp H^{\pm\pm}$, and via t-channel exchange in $e^+e^- \to e^+e^-$. In the direct case, and assuming B($H^{\pm\pm} \to \ell^\pm\ell^\pm$) = 1, a 95% CL limit on $h_{ee} < 0.071$ is set for $m_{H^{\pm\pm}} < 160$ GeV (see Fig. 6). In the second case, indirect limits on h_{ee} are set for $m_{H^{\pm\pm}} < 2$ TeV (see Fig. 8).

[15] GORDEEV 97 search for muonium-antimuonium conversion and find $G_{M\overline{M}}/G_F < 0.14$ (90% CL), where $G_{M\overline{M}}$ is the lepton-flavor violating effective four-fermion coupling. This limit may be converted to $m_{H^{++}} > 210$ GeV if the Yukawa couplings of H^{++} to ee and $\mu\mu$ are as large as the weak gauge coupling. For similar limits on muonium-antimuonium conversion, see the muon Particle Listings.

[16] ACTON 92M limit assumes $H^{\pm\pm} \to \ell^\pm\ell^\pm$ or $H^{\pm\pm}$ does not decay in the detector. Thus the region $g_{\ell\ell} \approx 10^{-7}$ is not excluded.

[17] ACTON 92M from $\Delta\Gamma_Z$ <40 MeV.

[18] SWARTZ 90 assume $H^{\pm\pm} \to \ell^\pm\ell^\pm$ (any flavor). The limits are valid for the Higgs-lepton coupling g($H\ell\ell$) $\gtrsim 7.4\times10^{-7}/[m_H/\text{GeV}]^{1/2}$. The limits improve somewhat for ee and $\mu\mu$ decay modes.

$H^\pm$ and $H^{\pm\pm}$ REFERENCES

MISIAK	17	EPJ C77 201	M. Misiak, M. Steinhauser	
SIRUNYAN	17AE	PRL 119 141802	A.M. Sirunyan *et al.*	(CMS Collab.)
AABOUD	16A	PL B759 555	M. Aaboud *et al.*	(ATLAS Collab.)
AAD	16AJ	JHEP 1603 127	G. Aad *et al.*	(ATLAS Collab.)
AAD	15AF	JHEP 1503 088	G. Aad *et al.*	(ATLAS Collab.)
AAD	15AG	JHEP 1503 041	G. Aad *et al.*	(ATLAS Collab.)
AAD	15AP	JHEP 1508 138	G. Aad *et al.*	(ATLAS Collab.)
AAD	15M	PRL 114 231801	G. Aad *et al.*	(ATLAS Collab.)
KANEMURA	15	PTEP 2015 051B02	S. Kanemura *et al.*	
KHACHATRY...	15AX	JHEP 1511 018	V. Khachatryan *et al.*	(CMS Collab.)
KHACHATRY...	15BF	JHEP 1512 178	V. Khachatryan *et al.*	(CMS Collab.)
KHACHATRY...	15D	PRL 114 051801	V. Khachatryan *et al.*	(CMS Collab.)
AAD	14M	PR D89 032002	G. Aad *et al.*	(ATLAS Collab.)
AALTONEN	14A	PR D89 091101	T. Aaltonen *et al.*	(CDF Collab.)
KANEMURA	14	PR D90 115018	S. Kanemura *et al.*	
AAD	13AC	EPJ C73 2465	G. Aad *et al.*	(ATLAS Collab.)
AAD	13V	JHEP 1303 076	G. Aad *et al.*	(ATLAS Collab.)
AAD	13Y	PR D87 052002	G. Aad *et al.*	(ATLAS Collab.)
LEP	13	EPJ C73 2463	LEP Collabs	(ALEPH, DELPHI, L3, OPAL, LEP)
AAD	12AY	PR D85 032004	G. Aad *et al.*	(ATLAS Collab.)
AAD	12BH	JHEP 1206 039	G. Aad *et al.*	(ATLAS Collab.)
AAD	12CQ	EPJ C72 2244	G. Aad *et al.*	(ATLAS Collab.)
AAD	12CY	JHEP 1212 007	G. Aad *et al.*	(ATLAS Collab.)
ABAZOV	12A	PRL 108 021801	V.M. Abazov *et al.*	(D0 Collab.)
ABBIENDI	12	EPJ C72 2076	G. Abbiendi *et al.*	(OPAL Collab.)
CHATRCHYAN	12AA	JHEP 1207 143	S. Chatrchyan *et al.*	(CMS Collab.)
CHATRCHYAN	12AU	EPJ C72 2189	S. Chatrchyan *et al.*	(CMS Collab.)
AALTONEN	11AF	PRL 107 181801	T. Aaltonen *et al.*	(CDF Collab.)
AALTONEN	11P	PRL 107 031801	T. Aaltonen *et al.*	(CDF Collab.)
DESCHAMPS	10	PR D82 073012	O. Deschamps *et al.*	(CLER, ORSAY, LAPP)
AALTONEN	09AJ	PRL 103 101803	T. Aaltonen *et al.*	(CDF Collab.)
ABAZOV	09AC	PR D80 051107	V.M. Abazov *et al.*	(D0 Collab.)
ABAZOV	09AG	PR D80 071102	V.M. Abazov *et al.*	(D0 Collab.)
ABAZOV	09AI	PL B682 278	V.M. Abazov *et al.*	(D0 Collab.)
ABAZOV	09P	PRL 102 191802	V.M. Abazov *et al.*	(D0 Collab.)
AALTONEN	08AA	PRL 101 121801	T. Aaltonen *et al.*	(CDF Collab.)
ABAZOV	08V	PRL 101 071803	V.M. Abazov *et al.*	(D0 Collab.)
ABULENCIA	06E	PRL 96 042003	A. Abulencia *et al.*	(CDF Collab.)
AKTAS	06A	PL B638 432	A. Aktas *et al.*	(H1 Collab.)
ACOSTA	05L	PRL 95 071801	D. Acosta *et al.*	(CDF Collab.)
ABAZOV	04E	PRL 93 141801	V.M. Abazov *et al.*	(D0 Collab.)
ABBIENDI	04	EPJ C32 453	G. Abbiendi *et al.*	(OPAL Collab.)
ABDALLAH	04I	EPJ C34 399	J. Abdallah *et al.*	(DELPHI Collab.)
ABBIENDI	03	PL B551 35	G. Abbiendi *et al.*	(OPAL Collab.)
ABBIENDI	03Q	PL B577 93	G. Abbiendi *et al.*	(OPAL Collab.)
ABDALLAH	03	PL B552 127	J. Abdallah *et al.*	(DELPHI Collab.)
ACHARD	03E	PL B575 208	P. Achard *et al.*	(L3 Collab.)
ACHARD	03F	PL B576 18	P. Achard *et al.*	(L3 Collab.)
ABAZOV	02B	PRL 88 151803	V.M. Abazov *et al.*	(D0 Collab.)
ABBIENDI	02C	PL B526 221	G. Abbiendi *et al.*	(OPAL Collab.)
BORZUMATI	02	PL B549 170	F.M. Borzumati, A. Djouadi	
HEISTER	02P	PL B543 1	A. Heister *et al.*	(ALEPH Collab.)
ABBIENDI	01Q	PL B520 1	G. Abbiendi *et al.*	(OPAL Collab.)
BARATE	01E	EPJ C19 213	R. Barate *et al.*	(ALEPH Collab.)
GAMBINO	01	NP B611 338	P. Gambino, M. Misiak	
AFFOLDER	00I	PR D62 012004	T. Affolder *et al.*	(CDF Collab.)
PDG	00	EPJ C15 1	D.E. Groom *et al.*	(PDG Collab.)
ABBIENDI	99E	EPJ C7 407	G. Abbiendi *et al.*	(OPAL Collab.)
ABBOTT	99E	PRL 82 4975	B. Abbott *et al.*	(D0 Collab.)
ACKERSTAFF	99D	EPJ C8 3	K. Ackerstaff *et al.*	(OPAL Collab.)
ABE	97L	PRL 79 357	F. Abe *et al.*	(CDF Collab.)
ACCIARRI	97F	PL B396 327	M. Acciarri *et al.*	(L3 Collab.)
AMMAR	97B	PRL 78 4686	R. Ammar *et al.*	(CLEO Collab.)
COARASA	97	PL B406 337	J.A. Coarasa, R.A. Jimenez, J. Sola	
GORDEEV	97	PAN 60 1164	V.A. Gordeev *et al.*	(PNPI)
		Translated from YAF 60 1291.		
GUCHAIT	97	PR D55 7263	M. Guchait, D.P. Roy	(TATA)
MANGANO	97	PL B410 299	M. Mangano, S. Slabospitsky	
STAHL	97	ZPHY C74 73	A. Stahl, H. Voss	(BONN)
PDG	96	PR D54 1	R. M. Barnett *et al.*	(PDG Collab.)
ALAM	95	PRL 74 2885	M.S. Alam *et al.*	(CLEO Collab.)
ASAKA	95	PL B345 36	T. Asaka, K.I. Hikasa	(TOHOK)
BUSKULIC	95	PL B343 444	D. Buskulic *et al.*	(ALEPH Collab.)
GROSSMAN	95B	PL B357 630	Y. Grossman, H. Haber, Y. Nir	
GROSSMAN	94	PL B332 373	Y. Grossman, Z. Ligeti	
STAHL	94	PL B324 121	A. Stahl	(BONN)
ACTON	92M	PL B295 347	P.D. Acton *et al.*	(OPAL Collab.)
SWARTZ	90	PRL 64 2877	M.L. Swartz *et al.*	(Mark II Collab.)

New Heavy Bosons (W', Z', leptoquarks, etc.), Searches for

We list here various limits on charged and neutral heavy vector bosons (other than W's and Z's), heavy scalar bosons (other than Higgs bosons), vector or scalar leptoquarks, and axigluons. The latest unpublished results are described in "W' Searches" and "Z' Searches" reviews. For recent searches on scalar bosons which could be identified as Higgs bosons, see the listings in the Higgs boson section.

CONTENTS:

See the related review(s):

W'-Boson Searches

MASS LIMITS for W' (Heavy Charged Vector Boson Other Than W) in Hadron Collider Experiments

Couplings of W' to quarks and leptons are taken to be identical with those of W. The following limits are obtained from $p\overline{p}$ or $pp \to W'X$ with W' decaying to the mode indicated in the comments. New decay channels (*e.g.*, $W' \to WZ$) are assumed to be suppressed. The most recent preliminary results can be found in the "W'-boson searches" review above.

VALUE (GeV)	*CL%*	*DOCUMENT ID*		*TECN*	*COMMENT*
none 1200–3300	95	[1] AABOUD	18F	ATLS	$W' \to WZ$
none 1000–3600	95	[2] SIRUNYAN	18	CMS	$W' \to tb$
>3600	95	[3] AABOUD	17AK	ATLS	$W' \to q\overline{q}$
none 1100–2500	95	[4] AABOUD	17AO	ATLS	$W' \to hW$
>2220	95	[5] AABOUD	17B	ATLS	$W' \to hW$
>2300	95	[6] KHACHATRY...	17J	CMS	$W' \to N_\tau\tau \to \tau\tau jj$
none 600–2700	95	[7] KHACHATRY...	17W	CMS	$W' \to q\overline{q}$
>4100	95	[8] KHACHATRY...	17Z	CMS	$W' \to e\nu,\ \mu\nu$
>2200	95	[9] SIRUNYAN	17A	CMS	$W' \to WZ$
>2300	95	[10] SIRUNYAN	17AK	CMS	$W' \to WZ,\ hW$
>2900	95	[11] SIRUNYAN	17H	CMS	$W' \to \tau N$
>2600	95	[12] SIRUNYAN	17I	CMS	$W' \to tb$
>2450	95	[13] SIRUNYAN	17R	CMS	$W' \to hW$
none 2780–3150	95	[13] SIRUNYAN	17R	CMS	$W' \to hW$
>2600	95	[14] AABOUD	16AE	ATLS	$W' \to WZ$
>4070	95	[15] AABOUD	16V	ATLS	$W' \to e\nu,\ \mu\nu$
>1810	95	[16] AAD	16R	ATLS	$W' \to WZ$
>2600	95	[17] AAD	16S	ATLS	$W' \to q\overline{q}$
>2150	95	[18] KHACHATRY...	16AO	CMS	$W' \to tb$
none 1000–1600	95	[19] KHACHATRY...	16AP	CMS	$W' \to hW$

none 800–1500	95	[20] KHACHATRY...16BD	CMS	$W' \to hW \to b\bar{b}\ell\nu$	
none 1500–2600	95	[21] KHACHATRY...16K	CMS	$W' \to q\bar{q}$	
none 500–1600	95	[22] KHACHATRY...16L	CMS	$W' \to q\bar{q}$	
none 300–2700	95	[23] KHACHATRY...16O	CMS	$W' \to \tau\nu$	
none 400–1590	95	[24] AAD	15AU ATLS	$W' \to WZ$	
none 1500–1760	95	[25] AAD	15AV ATLS	$W' \to tb$	
none 300–1490	95	[26] AAD	15AZ ATLS	$W' \to WZ$	
none 1300–1500	95	[27] AAD	15CP ATLS	$W' \to WZ$	
none 500–1920	95	[28] AAD	15R ATLS	$W' \to tb$	
none 800–2450	95	[29] AAD	15V ATLS	$W' \to q\bar{q}$	
>1470	95	[30] KHACHATRY...15C	CMS	$W' \to WZ$	
>3710	95	[31] KHACHATRY...15T	CMS	$W' \to e\nu, \mu\nu$	
none 1000–3010	95	[32] KHACHATRY...14O	CMS	$W' \to N\ell \to \ell\ell jj$	
• • • We do not use the following data for averages, fits, limits, etc. • • •					
		[33] KHACHATRY...17U	CMS	$W' \to hW$	
		[34] AAD	15BB ATLS	$W' \to Wh$	
none 300–880	95	[35] AALTONEN	15C CDF	$W' \to tb$	
none 1200–1900 and 2000–2200	95	[36] KHACHATRY...15V	CMS	$W' \to q\bar{q}$	
>3240	95	AAD	14AI ATLS	$W' \to e\nu, \mu\nu$	
		[37] AAD	14AT ATLS	$W' \to W\gamma$	
none 200–1520	95	AAD	14S ATLS	$W' \to WZ$	
none 1000–1700	95	[39] KHACHATRY...14	CMS	$W' \to WZ$	
		[40] KHACHATRY...14A	CMS	$W' \to WZ$	
none 500–950	95	[41] AAD	13AO ATLS	$W' \to WZ$	
none 1100–1680	95	AAD	13D ATLS	$W' \to q\bar{q}$	
none 1000–1920	95	CHATRCHYAN	13A CMS	$W' \to q\bar{q}$	
		[42] CHATRCHYAN	13AJ CMS	$W' \to WZ$	
>2900	95	[43] CHATRCHYAN	13AQ CMS	$W' \to e\nu, \mu\nu$	
none 800–1510	95	[44] CHATRCHYAN	13E CMS	$W' \to tb$	
none 700–940	95	[45] CHATRCHYAN	13U CMS	$W' \to WZ$	
none 700–1130	95	[46] AAD	12AV ATLS	$W' \to tb$	
none 200–760	95	[47] AAD	12BB ATLS	$W' \to WZ$	
		[48] AAD	12CK ATLS	$W' \to \bar{t}q$	
>2550	95	[49] AAD	12CR ATLS	$W' \to e\nu, \mu\nu$	
		[50] AAD	12M ATLS	$W' \to N\ell \to \ell\ell jj$	
		[51] AALTONEN	12N CDF	$W' \to \bar{t}q$	
none 200–1143	95	[47] CHATRCHYAN	12AF CMS	$W' \to WZ$	
		[52] CHATRCHYAN	12AR CMS	$W' \to \bar{t}q$	
		[53] CHATRCHYAN	12BG CMS	$W' \to N\ell \to \ell\ell jj$	
>1120	95	AALTONEN	11C CDF	$W' \to e\nu$	
none 180–690	95	[54] ABAZOV	11H D0	$W' \to WZ$	
none 600–863	95	[55] ABAZOV	11L D0	$W' \to tb$	
none 285–516	95	[56] AALTONEN	10N CDF	$W' \to WZ$	
none 280–840	95	[57] AALTONEN	09AC CDF	$W' \to q\bar{q}$	
>1000	95	ABAZOV	08C D0	$W' \to e\nu$	
none 300–800	95	ABAZOV	04C D0	$W' \to q\bar{q}$	
none 225–536	95	[58] ACOSTA	03B CDF	$W' \to tb$	
none 200–480	95	[59] AFFOLDER	02C CDF	$W' \to WZ$	
> 786	95	[60] AFFOLDER	01I CDF	$W' \to e\nu, \mu\nu$	
none 300–420	95	[61] ABE	97G CDF	$W' \to q\bar{q}$	
> 720	95	[62] ABACHI	96C D0	$W' \to e\nu$	
> 610	95	[63] ABACHI	95E D0	$W' \to e\nu, \tau\nu$	
none 260–600	95	[64] RIZZO	93 RVUE	$W' \to q\bar{q}$	

[1] AABOUD 18F search for resonances decaying to WZ in pp collisions at $\sqrt{s} = 13$ TeV. The quoted limit is for heavy-vector-triplet W' with $g_V = 3$. The limit becomes $M_{W'} > 3000$ GeV for $g_V = 1$. If we assume $M_{Z'} = M_{W'}$, the limit increases $M_{W'} > 3500$ GeV and $M_{W'} > 3100$ GeV for $g_V = 3$ and $g_V = 1$, respectively. See their Fig.5 for limits on $\sigma \cdot B$.

[2] SIRUNYAN 18 limit is for right-handed W' using pp collisions at $\sqrt{s} = 13$ TeV. $W' \to \ell\nu_R$ decay is assumed to be forbidden. The limit becomes $M_{W'} > 3.4$ TeV if $M_{\nu_R} \ll M_{W'}$. See their Fig. 5 for exclusion limits on W' models having both left- and right-handed couplings.

[3] AABOUD 17AK search for a new resonance decaying to dijets in pp collisions at $\sqrt{s} = 13$ TeV. The limit above is for a W' boson having axial-vector SM couplings and decaying to quarks with 75% branching fraction.

[4] AABOUD 17AO search for resonances decaying to hW in pp collisions at $\sqrt{s} = 13$ TeV. The limit quoted above is for a W' in the heavy-vector-triplet model with $g_V = 3$. See their Fig.4 for limits on $\sigma \cdot B$.

[5] AABOUD 17B search for resonances decaying to hW ($h \to b\bar{b}$, $c\bar{c}$; $W \to \ell\nu$) in pp collisions at $\sqrt{s} = 13$ TeV. The quoted limit is for heavy-vector-triplet W' with $g_V = 3$. The limit becomes $M_{W'} > 1750$ GeV for $g_V = 1$. If we assume $M_{W'} = M_{Z'}$, the limit increases $M_{W'} > 2310$ GeV and $M_{W'} > 1730$ GeV for $g_V = 3$ and $g_V = 1$, respectively. See their Fig.3 for limits on $\sigma \cdot B$.

[6] KHACHATRYAN 17J search for right-handed W_R in pp collisions at $\sqrt{s} = 13$ TeV. W_R is assumed to decay into τ and hypothetical heavy neutrino N_τ, with N_τ decaying into τjj. The quoted limit is for $M_{N_\tau} = M_{W_R}/2$. The limit becomes $M_{W_R} > 2350$ GeV (1630 GeV) for $M_{W_R}/M_{N_\tau} = 0.8$ (0.2). See their Fig. 4 for excluded regions in the $M_{W_R} - M_{N_\tau}$ plane.

[7] KHACHATRYAN 17W search for resonances decaying to dijets in pp collisions at $\sqrt{s} = 13$ TeV.

[8] KHACHATRYAN 17Z limit is for W' with SM-like coupling using pp collisions at $\sqrt{s} = 13$ TeV. The bosonic decays of W' and the interference with SM W process are neglected.

[9] SIRUNYAN 17A search for resonances decaying to WZ with $WZ \to \ell\nu q\bar{q}$, $q\bar{q}q\bar{q}$ in pp collisions at $\sqrt{s} = 13$ TeV. The quoted limit is for heavy-vector-triplet W' with $g_V = 3$. The limit becomes $M_{W'} > 2000$ GeV for $g_V = 1$. If we assume $M_{Z'} = M_{W'}$, the limit increases $M_{W'} > 2400$ GeV and $M_{W'} > 2300$ GeV for $g_V = 3$ and $g_V = 1$, respectively. See their Fig.6 for limits on $\sigma \cdot B$.

[10] SIRUNYAN 17AK search for resonances decaying to WZ or hW in pp collisions at $\sqrt{s} = 8$ and 13 TeV. The quoted limit is for heavy-vector-triplet W' with $g_V = 3$. The limit becomes $M_{W'} > 2300$ GeV for $g_V = 1$. If we assume $M_{W'} = M_{Z'}$, the limit increases $M_{W'} > 2400$ GeV for both $g_V = 3$ and $g_V = 1$. See their Fig.1 and 2 for limits on $\sigma \cdot B$.

[11] SIRUNYAN 17H search for right-handed W' in pp collisions at $\sqrt{s} = 13$ TeV. W' is assumed to decay into τ and a heavy neutrino N, with N decaying to $\tau q\bar{q}$. The limit above assumes $M_N = M_{W'}/2$.

[12] SIRUNYAN 17I limit is for a right-handed W' using pp collisions at $\sqrt{s} = 13$ TeV. The limit becomes $M_{W'} > 2400$ GeV for $M_{\nu_R} \ll M_{W'}$.

[13] SIRUNYAN 17R search for resonances decaying to hW in pp collisions at $\sqrt{s} = 13$ TeV. The quoted limit is for heavy-vector-triplet W' with $g_V = 3$. Mass regions $M_{W'} < 2370$ GeV and $2870 < M_{W'} < 2970$ GeV are excluded for $g_V = 1$. If we assume $M_{Z'} = M_{W'}$, the excluded mass regions are $1000 < M_{W'} < 2500$ GeV and $2760 < M_{W'} < 3300$ GeV for $g_V = 3$; $1000 < M_{W'} < 2430$ GeV and $2810 < M_{W'} < 3130$ GeV for $g_V = 1$. See their Fig.5 for limits on $\sigma \cdot B$.

[14] AABOUD 16AE search for resonances decaying to VV ($V = W$ or Z) in pp collisions at $\sqrt{s} = 13$ TeV. Results from $\nu\nu qq$, $\nu\ell qq$, $\ell\ell qq$ and $qqqq$ final states are combined. The quoted limit is for a heavy-vector-triplet W' with $g_V = 3$ and $M_{W'} = M_{Z'}$.

[15] AABOUD 16V limit is for W' with SM-like coupling using pp collisions at $\sqrt{s} = 13$ TeV. The bosonic decays of W' and the interference with SM W process are neglected.

[16] AAD 16R search for $W' \to WZ$ in pp collisions at $\sqrt{s} = 8$ TeV. $\ell\nu\ell'\ell'$, $\ell\ell q\bar{q}$, $\ell\nu q\bar{q}$, and all hadronic channels are combined. The quoted limit assumes $g_{W'WZ}/g_{WWZ} = (M_W/M_{W'})^2$.

[17] AAD 16S search for a new resonance decaying to dijets in pp collisions at $\sqrt{s} = 13$ TeV. The limit quoted above is for a W' having SM-like couplings to quarks.

[18] KHACHATRYAN 16AO limit is for a SM-like right-handed W' using pp collisions at $\sqrt{s} = 8$ TeV. The quoted limit combines $t \to qqb$ and $t \to \ell\nu b$ events.

[19] KHACHATRYAN 16AP search for a resonance decaying to hW in pp collisions at $\sqrt{s} = 8$ TeV. Both h and W are assumed to decay to fat jets. The quoted limit is for heavy-vector-triplet W' with $g_V = 3$.

[20] KHACHATRYAN 16BD search for resonance decaying to hW in pp collisions at $\sqrt{s} = 8$ TeV. The quoted limit is for heavy-vector-triplet (HVT) W' with $g_V = 3$. The HVT model $m_{W'} = m_{Z'} > 1.8$ TeV is also obtained by combining $W'/Z' \to Wh/Zh \to \ell\nu b\bar{b}$, $qq\tau\tau$, $qq\bar{b}\bar{b}$, and $qqqqqq$ channels.

[21] KHACHATRYAN 16K search for resonances decaying to dijets in pp collisions at $\sqrt{s} = 13$ TeV.

[22] KHACHATRYAN 16L search for resonances decaying to dijets in pp collisions at $\sqrt{s} = 8$ TeV with the data scouting technique, increasing the sensitivity to the low mass resonances.

[23] KHACHATRYAN 16O limit is for W' having universal couplings. Interferences with the SM amplitudes are assumed to be absent.

[24] AAD 15AU search for W' decaying into the WZ final state with $W \to q\bar{q}'$, $Z \to \ell^+\ell^-$ using pp collisions at $\sqrt{s} = 8$ TeV. The quoted limit assumes $g_{W'WZ}/g_{WWZ} = (M_W/M_{W'})^2$.

[25] AAD 15AV limit is for a SM like right-handed W' using pp collisions at $\sqrt{s} = 8$ TeV. $W' \to \ell\nu$ decay is assumed to be forbidden.

[26] AAD 15AZ search for W' decaying into the WZ final state with $W \to \ell\nu$, $Z \to q\bar{q}$ using pp collisions at $\sqrt{s} = 8$ TeV. The quoted limit assumes $g_{W'WZ}/g_{WWZ} = (M_W/M_{W'})^2$.

[27] AAD 15CP search for W' decaying into the WZ final state with $W \to q\bar{q}$, $Z \to q\bar{q}$ using pp collisions at $\sqrt{s} = 8$ TeV. The quoted limit assumes $g_{W'WZ}/g_{WWZ} = (M_W/M_{W'})^2$.

[28] AAD 15R limit is for a SM like right-handed W' using pp collisions at $\sqrt{s} = 8$ TeV. $W' \to \ell\nu$ decay is assumed to be forbidden.

[29] AAD 15V search for new resonance decaying to dijets in pp collisions at $\sqrt{s} = 8$ TeV.

[30] KHACHATRYAN 15C search for W' decaying via WZ to fully leptonic final states using pp collisions at $\sqrt{s}$=8 TeV. The quoted limit assumes $g_{W'WZ}/g_{WWZ} = M_W M_Z/M^2_{W'}$.

[31] KHACHATRYAN 15T limit is for W' with SM-like coupling which interferes the SM W boson constructively using pp collisions at $\sqrt{s} = 8$ TeV. For W' without interference, the limit becomes > 3280 GeV.

[32] KHACHATRYAN 14O search for right-handed W_R in pp collisions at $\sqrt{s} = 8$ TeV. W_R is assumed to decay into ℓ and hypothetical heavy neutrino N, with N decaying into ℓjj. The quoted limit is for $M_{\nu_{eR}} = M_{\nu_{\mu R}} = M_{W_R}/2$. See their Fig. 3 and Fig. 5 for excluded regions in the $M_{W_R} - M_\nu$ plane.

[33] KHACHATRYAN 17U search for resonances decaying to hW ($h \to b\bar{b}$; $W \to \ell\nu$) in pp collisions at $\sqrt{s} = 13$ TeV. The limit on the heavy-vector-triplet model is $M_{Z'} = M_{W'} > 2$ TeV for $g_V = 3$, in which constraints from the $Z' \to hZ$ ($h \to b\bar{b}$; $Z \to \ell^+\ell^-$, $\nu\bar{\nu}$) are combined. See their Fig.3 and Fig.4 for limits on $\sigma \cdot B$.

[34] AAD 15BB search for W' decaying into Wh with $W \to \ell\nu$, $h \to b\bar{b}$. See their Fig. 4 for the exclusion limits in the heavy vector triplet benchmark model parameter space.

[35] AALTONEN 15C limit is for a SM-like right-handed W' assuming $W' \to \ell\nu$ decays are forbidden, using $p\bar{p}$ collisions at $\sqrt{s}$=1.96 TeV. See their Fig. 3 for limit on $g_{W'}/g_W$.

[36] KHACHATRYAN 15V search new resonance decaying to dijets in pp collisions at $\sqrt{s} = 8$ TeV.

[37] AAD 14AT search for a narrow charged vector boson decaying to $W\gamma$. See their Fig. 3a for the exclusion limit in $m_{W'} - \sigma B$ plane.

Gauge & Higgs Boson Particle Listings

New Heavy Bosons

[38] AAD 14S search for W' decaying into the WZ final state with $W \to \ell\nu$, $Z \to \ell\ell$ using pp collisions at $\sqrt{s}$=8 TeV. The quoted limit assumes $g_{W'WZ}/g_{WWZ} = (M_W/M_{W'})^2$.

[39] KHACHATRYAN 14 search for W' decaying into WZ final state with $W \to q\overline{q}$, $Z \to q\overline{q}$ using pp collisions at $\sqrt{s}$=8 TeV. The quoted limit assumes $g_{W'WZ}/g_{WWZ} = (M_W/M_{W'})^2$.

[40] KHACHATRYAN 14A search for W' decaying into the WZ final state with $W \to \ell\nu$, $Z \to q\overline{q}$, or $W \to q\overline{q}$, $Z \to \ell\ell$. pp collisions data at $\sqrt{s}$=8 TeV are used for the search. See their Fig. 13 for the exclusion limit on the number of events in the mass−width plane.

[41] AAD 13AO search for W' decaying into the WZ final state with $W \to \ell\nu$, $Z \to 2j$ using pp collisions at $\sqrt{s}$=7 TeV. The quoted limit assumes $g_{W'WZ}/g_{WWZ} = (M_W/M_{W'})^2$.

[42] CHATRCHYAN 13AJ search for resonances decaying to WZ pair, using the hadronic decay modes of W and Z, in pp collisions at $\sqrt{s}$=7 TeV. See their Fig. 7 for the limit on the cross section.

[43] CHATRCHYAN 13AQ limit is for W' with SM-like coupling which interferes with the SM W boson using pp collisions at $\sqrt{s}$=7 TeV.

[44] CHATRCHYAN 13E limit is for W' with SM-like coupling which intereferes with the SM W boson using pp collisions at $\sqrt{s}$=7 TeV. For W' with right-handed coupling, the bound becomes >1850 GeV (>1910 GeV) if W' decays to both leptons and quarks (only to quarks). If both left- and right-handed couplings are present, the limit becomes >1640 GeV.

[45] CHATRCHYAN 13U search for W' decaying to the WZ final state, with W decaying into jets, in pp collisions at $\sqrt{s}$=7 TeV. The quoted limit assumes $g_{W'WZ}/g_{WWZ} = (M_W/M_{W'})^2$.

[46] The AAD 12AV quoted limit is for a SM-like right-handed W' using pp collisions at $\sqrt{s}$=7 TeV. $W' \to \ell\nu$ decay is assumed to be forbidden.

[47] AAD 12BB use pp collisions data at $\sqrt{s}$=7 TeV. The quoted limit assumes $g_{W'WZ}/g_{WWZ} = (M_W/M_{W'})^2$.

[48] AAD 12CK search for $pp \to tW'$, $W' \to \overline{t}q$ events in pp collisions. See their Fig. 5 for the limit on $\sigma \cdot$B.

[49] AAD 12CR use pp collisions at $\sqrt{s}$=7 TeV.

[50] AAD 12M search for right-handed W_R in pp collisions at $\sqrt{s}$ = 7 TeV. W_R is assumed to decay into ℓ and hypothetical heavy neutrino N, with N decaying into ℓjj. See their Fig. 4 for the limit in the m_N−$m_{W'}$ plane.

[51] AALTONEN 12N search for $p\overline{p} \to tW'$, $W' \to \overline{t}d$ events in $p\overline{p}$ collisions. See their Fig. 3 for the limit on $\sigma \cdot$B.

[52] CHATRCHYAN 12AR search for $pp \to tW'$, $W' \to \overline{t}d$ events in pp collisions. See their Fig. 2 for the limit on $\sigma \cdot$B.

[53] CHATRCHYAN 12BG search for right-handed W_R in pp collisions $\sqrt{s}$ = 7 TeV. W_R is assumed to decay into ℓ and hypothetical heavy neutrino N, with N decaying into ℓjj. See their Fig. 3 for the limit in the m_N−$m_{W'}$ plane.

[54] ABAZOV 11H use data from $p\overline{p}$ collisions at $\sqrt{s}$=1.96 TeV. The quoted limit is obtained assuming $W'WZ$ coupling strength is the same as the ordinary WWZ coupling strength in the Standard Model.

[55] ABAZOV 11L limit is for W' with SM-like coupling which interferes with the SM W boson, using $p\overline{p}$ collisions at $\sqrt{s}$=1.96 TeV. For W' with right-handed coupling, the bound becomes >885 GeV (>890 GeV) if W' decays to both leptons and quarks (only to quarks). If both left- and right-handed couplings present, the limit becomes >916 GeV.

[56] AALTONEN 10N use $p\overline{p}$ collision data at $\sqrt{s}$=1.96 TeV. The quoted limit assumes $g_{W'WZ}/g_{WWZ} = (M_W/M_{W'})^2$. See their Fig. 4 for limits in mass-coupling plane.

[57] AALTONEN 09AC search for new particle decaying to dijets using $p\overline{p}$ collisions at $\sqrt{s}$=1.96 TeV.

[58] The ACOSTA 03B quoted limit is for $M_{W'} \gg M_{\nu_R}$, using $p\overline{p}$ collisions at $\sqrt{s}$=1.8 TeV. For $M_{W'} < M_{\nu_R}$, $M_{W'}$ between 225 and 566 GeV is excluded.

[59] The quoted limit is obtained assuming $W'WZ$ coupling strength is the same as the ordinary WWZ coupling strength in the Standard Model, using $p\overline{p}$ collisions at $\sqrt{s}$=1.8 TeV. See their Fig. 2 for the limits on the production cross sections as a function of the W' width.

[60] AFFOLDER 01I combine a new bound on $W' \to e\nu$ of 754 GeV, using $p\overline{p}$ collisions at $\sqrt{s}$=1.8 TeV, with the bound of ABE 00 on $W' \to \mu\nu$ to obtain quoted bound.

[61] ABE 97G search for new particle decaying to dijets using $p\overline{p}$ collisions at $\sqrt{s}$=1.8 TeV.

[62] For bounds on W_R with nonzero right-handed mass, see Fig. 5 from ABACHI 96C.

[63] ABACHI 95E assume that the decay $W' \to WZ$ is suppressed and that the neutrino from W' decay is stable and has a mass significantly less $m_{W'}$.

[64] RIZZO 93 analyses CDF limit on possible two-jet resonances. The limit is sensitive to the inclusion of the assumed K factor.

W_R (Right-Handed W Boson) MASS LIMITS

Assuming a light right-handed neutrino, except for BEALL 82, LANGACKER 89B, and COLANGELO 91. $g_R = g_L$ assumed. [Limits in the section MASS LIMITS for W' below are also valid for W_R if $m_{\nu_R} \ll m_{W_R}$.] Some limits assume manifest left-right symmetry, *i.e.*, the equality of left- and right Cabibbo-Kobayashi-Maskawa matrices. For a comprehensive review, see LANGACKER 89B. Limits on the W_L-W_R mixing angle ζ are found in the next section. Values in brackets are from cosmological and astrophysical considerations and assume a light right-handed neutrino.

VALUE (GeV)	CL%	DOCUMENT ID		TECN	COMMENT
> 592	90	[1] BUENO	11	TWST	μ decay
> 715	90	[2] CZAKON	99	RVUE	Electroweak
• • • We do not use the following data for averages, fits, limits, etc. • • •					
> 235	90	[3] PRIEELS	14	PIE3	μ decay
> 245	90	[4] WAUTERS	10	CNTR	^{60}Co β decay
>2500		[5] ZHANG	08	THEO	$m_{K_L^0} - m_{K_S^0}$
> 180	90	[6] MELCONIAN	07	CNTR	^{37}K β^+ decay
> 290.7	90	[7] SCHUMANN	07	CNTR	Polarized neutron decay
[> 3300]	95	[8] CYBURT	05	COSM	Nucleosynthesis; light ν_R
> 310	90	[9] THOMAS	01	CNTR	β^+ decay
> 137	95	[10] ACKERSTAFF	99D	OPAL	τ decay
>1400	68	[11] BARENBOIM	98	RVUE	Electroweak, Z-Z' mixing
> 549	68	[12] BARENBOIM	97	RVUE	μ decay
> 220	95	[13] STAHL	97	RVUE	τ decay
> 220	90	[14] ALLET	96	CNTR	β^+ decay
> 281	90	[15] KUZNETSOV	95	CNTR	Polarized neutron decay
> 282	90	[16] KUZNETSOV	94B	CNTR	Polarized neutron decay
> 439	90	[17] BHATTACH...	93	RVUE	Z-Z' mixing
> 250	90	[18] SEVERIJNS	93	CNTR	β^+ decay
		[19] IMAZATO	92	CNTR	K^+ decay
> 475	90	[20] POLAK	92B	RVUE	μ decay
> 240	90	[21] AQUINO	91	RVUE	Neutron decay
> 496	90	[21] AQUINO	91	RVUE	Neutron and muon decay
> 700		[22] COLANGELO	91	THEO	$m_{K_L^0} - m_{K_S^0}$
> 477	90	[23] POLAK	91	RVUE	μ decay
[none 540–23000]		[24] BARBIERI	89B	ASTR	SN 1987A; light ν_R
> 300	90	[25] LANGACKER	89B	RVUE	General
> 160	90	[26] BALKE	88	CNTR	$\mu \to e\nu\overline{\nu}$
> 406	90	[27] JODIDIO	86	ELEC	Any ζ
> 482	90	[27] JODIDIO	86	ELEC	$\zeta = 0$
> 800		MOHAPATRA	86	RVUE	$SU(2)_L \times SU(2)_R \times U(1)$
> 400	95	[28] STOKER	85	ELEC	Any ζ
> 475	95	[28] STOKER	85	ELEC	ζ <0.041
		[29] BERGSMA	83	CHRM	$\nu_\mu e \to \mu\nu_e$
> 380	90	[30] CARR	83	ELEC	μ^+ decay
>1600		[31] BEALL	82	THEO	$m_{K_L^0} - m_{K_S^0}$

[1] The quoted limit is for manifest left-right symmetric model.

[2] CZAKON 99 perform a simultaneous fit to charged and neutral sectors.

[3] PRIEELS 14 limit is from $\mu^+ \to e^+\nu\overline{\nu}$ decay parameter ξ'', which is determined by the positron polarization measurement.

[4] WAUTERS 10 limit is from a measurement of the asymmetry parameter of polarized ^{60}Co β decays. The listed limit assumes no mixing.

[5] ZHANG 08 limit uses a lattice QCD calculation of the relevant hadronic matrix elements, while BEALL 82 limit used the vacuum saturation approximation.

[6] MELCONIAN 07 measure the neutrino angular asymmetry in β^+-decays of polarized ^{37}K, stored in a magneto-optical trap. Result is consistent with SM prediction and does not constrain the $W_L - W_R$ mixing angle appreciably.

[7] SCHUMANN 07 limit is from measurements of the asymmetry $\langle \vec{p}_\nu \cdot \sigma_n \rangle$ in the β decay of polarized neutrons. Zero mixing is assumed.

[8] CYBURT 05 limit follows by requiring that three light ν_R's decouple when $T_{dec} > 140$ MeV. For different T_{dec}, the bound becomes $M_{W_R} > 3.3$ TeV $(T_{dec} / 140\ \text{MeV})^{3/4}$.

[9] THOMAS 01 limit is from measurement of β^+ polarization in decay of polarized ^{12}N. The listed limit assumes no mixing.

[10] ACKERSTAFF 99D limit is from τ decay parameters. Limit increase to 145 GeV for zero mixing.

[11] BARENBOIM 98 assumes minimal left-right model with Higgs of $SU(2)_R$ in $SU(2)_L$ doublet. For Higgs in $SU(2)_L$ triplet, m_{W_R} >1100 GeV. Bound calculated from effect of corresponding Z_{LR} on electroweak data through Z–Z_{LR} mixing.

[12] The quoted limit is from μ decay parameters. BARENBOIM 97 also evaluate limit from K_L-K_S mass difference.

[13] STAHL 97 limit is from fit to τ-decay parameters.

[14] ALLET 96 measured polarization-asymmetry correlation in ^{12}N β^+ decay. The listed limit assumes zero L-R mixing.

[15] KUZNETSOV 95 limit is from measurements of the asymmetry $\langle \vec{p}_\nu \cdot \sigma_n \rangle$ in the β decay of polarized neutrons. Zero mixing assumed. See also KUZNETSOV 94B.

[16] KUZNETSOV 94B limit is from measurements of the asymmetry $\langle \vec{p}_\nu \cdot \sigma_n \rangle$ in the β decay of polarized neutrons. Zero mixing assumed.

[17] BHATTACHARYYA 93 uses Z-Z' mixing limit from LEP '90 data, assuming a specific Higgs sector of $SU(2)_L \times SU(2)_R \times U(1)$ gauge model. The limit is for m_t=200 GeV and slightly improves for smaller m_t.

[18] SEVERIJNS 93 measured polarization-asymmetry correlation in ^{107}In β^+ decay. The listed limit assumes zero L-R mixing. Value quoted here is from SEVERIJNS 94 erratum.

[19] IMAZATO 92 measure positron asymmetry in $K^+ \to \mu^+\nu_\mu$ decay and obtain $\xi P_\mu > 0.990$ (90% CL). If W_R couples to $u\overline{s}$ with full weak strength (V^R_{us}=1), the result corresponds to m_{W_R} >653 GeV. See their Fig. 4 for m_{W_R} limits for general $|V^R_{us}|^2 = 1 - |V^R_{ud}|^2$.

[20] POLAK 92B limit is from fit to muon decay parameters and is essentially determined by JODIDIO 86 data assuming ζ=0. Supersedes POLAK 91.

[21] AQUINO 91 limits obtained from neutron lifetime and asymmetries together with unitarity of the CKM matrix. Manifest left-right symmetry assumed. Stronger of the two limits also includes muon decay results.

[22] COLANGELO 91 limit uses hadronic matrix elements evaluated by QCD sum rule and is less restrictive than BEALL 82 limit which uses vacuum saturation approximation. Manifest left-right symmetry assumed.

[23] POLAK 91 limit is from fit to muon decay parameters and is essentially determined by JODIDIO 86 data assuming ζ=0. Superseded by POLAK 92B.

[24] BARBIERI 89B limit holds for $m_{\nu_R} \leq 10$ MeV.

[25] LANGACKER 89B limit is for any ν_R mass (either Dirac or Majorana) and for a general class of right-handed quark mixing matrices.

[26] BALKE 88 limit is for $m_{\nu_{eR}} = 0$ and $m_{\nu_{\mu R}} \leq 50$ MeV. Limits come from precise measurements of the muon decay asymmetry as a function of the positron energy.

[27] JODIDIO 86 is the same TRIUMF experiment as STOKER 85 (and CARR 83); however, it uses a different technique. The results given here are combined results of the two techniques. The technique here involves precise measurement of the end-point e^+ spectrum in the decay of the highly polarized μ^+.

[28] STOKER 85 is same TRIUMF experiment as CARR 83. Here they measure the decay e^+ spectrum asymmetry above 46 MeV/c using a muon-spin-rotation technique. Assumed a light right-handed neutrino. Quoted limits are from combining with CARR 83.

[29] BERGSMA 83 set limit m_{W_2}/m_{W_1} >1.9 at CL = 90%.

[30] CARR 83 is TRIUMF experiment with a highly polarized μ^+ beam. Looked for deviation from $V-A$ at the high momentum end of the decay e^+ energy spectrum. Limit from previous world-average muon polarization parameter is m_{W_R} >240 GeV. Assumes a light right-handed neutrino.

[31] BEALL 82 limit is obtained assuming that W_R contribution to K_L^0-K_S^0 mass difference is smaller than the standard one, neglecting the top quark contributions. Manifest left-right symmetry assumed.

Limit on W_L-W_R Mixing Angle ζ

Lighter mass eigenstate $W_1 = W_L\cos\zeta - W_R\sin\zeta$. Light ν_R assumed unless noted. Values in brackets are from cosmological and astrophysical considerations.

VALUE	CL%	DOCUMENT ID		TECN	COMMENT
• • • We do not use the following data for averages, fits, limits, etc. • • •					
−0.020 to 0.017	90	BUENO	11	TWST	$\mu \to e\nu\overline{\nu}$
< 0.022	90	MACDONALD	08	TWST	$\mu \to e\nu\overline{\nu}$
< 0.12	95	[1] ACKERSTAFF	99D	OPAL	τ decay
< 0.013	90	[2] CZAKON	99	RVUE	Electroweak
< 0.0333		[3] BARENBOIM	97	RVUE	μ decay
< 0.04	90	[4] MISHRA	92	CCFR	νN scattering
−0.0006 to 0.0028	90	[5] AQUINO	91	RVUE	
[none 0.00001–0.02]		[6] BARBIERI	89B	ASTR	SN 1987A
< 0.040	90	[7] JODIDIO	86	ELEC	μ decay
−0.056 to 0.040	90	[7] JODIDIO	86	ELEC	μ decay

[1] ACKERSTAFF 99D limit is from τ decay parameters.

[2] CZAKON 99 perform a simultaneous fit to charged and neutral sectors.

[3] The quoted limit is from μ decay parameters. BARENBOIM 97 also evaluate limit from K_L-K_S mass difference.

[4] MISHRA 92 limit is from the absence of extra large-x, large-y $\overline{\nu}_\mu N \to \overline{\nu}_\mu X$ events at Tevatron, assuming left-handed ν and right-handed $\overline{\nu}$ in the neutrino beam. The result gives $\zeta^2(1-2m^2_{W_1}/m^2_{W_2})< 0.0015$. The limit is independent of ν_R mass.

[5] AQUINO 91 limits obtained from neutron lifetime and asymmetries together with unitarity of the CKM matrix. Manifest left-right asymmetry is assumed.

[6] BARBIERI 89B limit holds for $m_{\nu_R} \leq 10$ MeV.

[7] First JODIDIO 86 result assumes $m_{W_R}=\infty$, second is for unconstrained m_{W_R}.

See the related review(s):

Z′-Boson Searches

MASS LIMITS for Z' (Heavy Neutral Vector Boson Other Than Z)

Limits for Z'_{SM}

Z'_{SM} is assumed to have couplings with quarks and leptons which are identical to those of Z, and decays only to known fermions. The most recent preliminary results can be found in the "Z'-boson searches" review above.

VALUE (GeV)	CL%	DOCUMENT ID		TECN	COMMENT
>2420	95	[1] AABOUD	18G	ATLS	pp; $Z'_{SM} \to \tau^+\tau^-$
>4500	95	[2] AABOUD	17AT	ATLS	pp; $Z'_{SM} \to e^+e^-, \mu^+\mu^-$
>2100	95	[3] KHACHATRY...17H		CMS	pp; $Z'_{SM} \to \tau^+\tau^-$
>3370	95	[4] KHACHATRY...17T		CMS	pp; $Z'_{SM} \to e^+e^-, \mu^+\mu^-$
none 600–2100, 2300–2600	95	[5] KHACHATRY...17W		CMS	pp; $Z'_{SM} \to q\overline{q}$
>3360	95	[6] AABOUD	16U	ATLS	pp; $Z'_{SM} \to e^+e^-, \mu^+\mu^-$
>2900	95	[7] KHACHATRY...15AE		CMS	pp; $Z'_{SM} \to e^+e^-, \mu^+\mu^-$
none 1200–1700	95	[8] KHACHATRY...15V		CMS	pp; $Z'_{SM} \to q\overline{q}$
>2900	95	[9] AAD	14V	ATLS	pp; $Z'_{SM} \to e^+e^-, \mu^+\mu^-$
• • • We do not use the following data for averages, fits, limits, etc. • • •					
>1900	95	[10] AABOUD	16AA	ATLS	pp; $Z'_{SM} \to \tau^+\tau^-$
>2020	95	[11] AAD	15AM	ATLS	pp; $Z'_{SM} \to \tau^+\tau^-$
>1400	95	[12] AAD	13S	ATLS	pp; $Z'_{SM} \to \tau^+\tau^-$
>1470	95	[13] CHATRCHYAN	13A	CMS	pp; $Z'_{SM} \to q\overline{q}$
>2590	95	[14] CHATRCHYAN	13AF	CMS	pp; $Z'_{SM} \to e^+e^-, \mu^+\mu^-$
>2220	95	[15] AAD	12CC	ATLS	pp; $Z'_{SM} \to e^+e^-, \mu^+\mu^-$
>1400	95	[16] CHATRCHYAN	12O	CMS	pp; $Z'_{SM} \to \tau^+\tau^-$
>1071	95	[17] AALTONEN	11I	CDF	$p\overline{p}$; $Z'_{SM} \to \mu^+\mu^-$
>1023	95	[18] ABAZOV	11A	D0	$p\overline{p}$, $Z'_{SM} \to e^+e^-$
none 247–544	95	[19] AALTONEN	10N	CDF	$Z' \to WW$
none 320–740	95	[20] AALTONEN	09AC	CDF	$Z' \to q\overline{q}$
> 963	95	[18] AALTONEN	09T	CDF	$p\overline{p}$, $Z'_{SM} \to e^+e^-$
>1403	95	[21] ERLER	09	RVUE	Electroweak
>1305	95	[22] ABDALLAH	06C	DLPH	e^+e^-
> 399	95	[23] ACOSTA	05R	CDF	$p\overline{p}$: $Z'_{SM} \to \tau^+\tau^-$
none 400–640	95	ABAZOV	04C	D0	$p\overline{p}$: $Z'_{SM} \to q\overline{q}$
>1018	95	[24] ABBIENDI	04G	OPAL	e^+e^-
> 670	95	[25] ABAZOV	01B	D0	$p\overline{p}$, $Z'_{SM} \to e^+e^-$
>1500	95	[26] CHEUNG	01B	RVUE	Electroweak
> 710	95	[27] ABREU	00S	DLPH	e^+e^-
> 898	95	[28] BARATE	00I	ALEP	e^+e^-
> 809	95	[29] ERLER	99	RVUE	Electroweak
> 690	95	[30] ABE	97S	CDF	$p\overline{p}$; $Z'_{SM} \to e^+e^-, \mu^+\mu^-$
> 398	95	[31] VILAIN	94B	CHM2	$\nu_\mu e \to \nu_\mu e$ and $\overline{\nu}_\mu e \to \overline{\nu}_\mu e$
> 237	90	[32] ALITTI	93	UA2	$p\overline{p}$; $Z'_{SM} \to q\overline{q}$
none 260–600	95	[33] RIZZO	93	RVUE	$p\overline{p}$; $Z'_{SM} \to q\overline{q}$
> 426	90	[34] ABE	90F	VNS	e^+e^-

[1] AABOUD 18G search for resonances decaying to $\tau^+\tau^-$ in pp collisions at $\sqrt{s}$ = 13 TeV.

[2] AABOUD 17AT search for resonances decaying to $\ell^+\ell^-$ in pp collisions at $\sqrt{s}$ = 13 TeV.

[3] KHACHATRYAN 17H search for resonances decaying to $\tau^+\tau^-$ in pp collisions at $\sqrt{s}$ = 13 TeV.

[4] KHACHATRYAN 17T search for resonances decaying to e^+e^-, $\mu^+\mu^-$ in pp collisions at $\sqrt{s}$ = 8, 13 TeV.

[5] KHACHATRYAN 17W search for resonances decaying to dijets in pp collisions at $\sqrt{s}$ = 13 TeV.

[6] AABOUD 16U search for resonances decaying to $\ell^+\ell^-$ in pp collisions at $\sqrt{s}$ = 13 TeV.

[7] KHACHATRYAN 15AE search for resonances decaying to e^+e^-, $\mu^+\mu^-$ in pp collisions at $\sqrt{s}$ = 8 TeV.

[8] KHACHATRYAN 15V search for resonances decaying to dijets in pp collisions at $\sqrt{s}$ = 8 TeV.

[9] AAD 14V search for resonances decaying to e^+e^-, $\mu^+\mu^-$ in pp collisions at $\sqrt{s}$ = 8 TeV.

[10] AABOUD 16AA search for resonances decaying to $\tau^+\tau^-$ in pp collisions at $\sqrt{s}$ = 13 TeV.

[11] AAD 15AM search for resonances decaying to $\tau^+\tau^-$ in pp collisions at $\sqrt{s}$ = 8 TeV.

[12] AAD 13S search for resonances decaying to $\tau^+\tau^-$ in pp collisions at $\sqrt{s}$ = 7 TeV.

[13] CHATRCHYAN 13A use pp collisions at $\sqrt{s}$=7 TeV.

[14] CHATRCHYAN 13AF search for resonances decaying to e^+e^-, $\mu^+\mu^-$ in pp collisions at $\sqrt{s}$ = 7 TeV and 8 TeV.

[15] AAD 12CC search for resonances decaying to e^+e^-, $\mu^+\mu^-$ in pp collisions at $\sqrt{s}$ = 7 TeV.

[16] CHATRCHYAN 12O search for resonances decaying to $\tau^+\tau^-$ in pp collisions at $\sqrt{s}$ = 7 TeV.

[17] AALTONEN 11I search for resonances decaying to $\mu^+\mu^-$ in $p\overline{p}$ collisions at $\sqrt{s}$ = 1.96 TeV.

[18] ABAZOV 11A, AALTONEN 09T, AALTONEN 07H, and ABULENCIA 06L search for resonances decaying to e^+e^- in $p\overline{p}$ collisions at $\sqrt{s}$ = 1.96 TeV.

[19] The quoted limit assumes $g_{WWZ'}/g_{WWZ} = (M_W/M_{Z'})^2$. See their Fig. 4 for limits in mass-coupling plane.

[20] AALTONEN 09AC search for new particle decaying to dijets.

[21] ERLER 09 give 95% CL limit on the Z-Z' mixing $-0.0026 < \theta < 0.0006$.

[22] ABDALLAH 06C use data $\sqrt{s}$ = 130–207 GeV.

[23] ACOSTA 05R search for resonances decaying to tau lepton pairs in $\overline{p}p$ collisions at $\sqrt{s}$ = 1.96 TeV.

[24] ABBIENDI 04G give 95% CL limit on Z-Z' mixing $-0.00422 < \theta < 0.00091$. $\sqrt{s}$ = 91 to 207 GeV.

[25] ABAZOV 01B search for resonances in $p\overline{p} \to e^+e^-$ at $\sqrt{s}$=1.8 TeV. They find $\sigma \cdot B(Z' \to ee) < 0.06$ pb for $M_{Z'} > 500$ GeV.

[26] CHEUNG 01B limit is derived from bounds on contact interactions in a global electroweak analysis.

[27] ABREU 00S uses LEP data at $\sqrt{s}$=90 to 189 GeV.

[28] BARATE 00I search for deviations in cross section and asymmetries in $e^+e^- \to$ fermions at $\sqrt{s}$=90 to 183 GeV. Assume θ=0. Bounds in the mass-mixing plane are shown in their Figure 18.

[29] ERLER 99 give 90%CL limit on the Z-Z' mixing $-0.0041 < \theta < 0.0003$. ρ_0=1 is assumed.

[30] ABE 97S find $\sigma(Z') \times B(e^+e^-, \mu^+\mu^-) < 40$ fb for $m_{Z'} > 600$ GeV at $\sqrt{s}$= 1.8 TeV.

[31] VILAIN 94B assume m_t = 150 GeV.

[32] ALITTI 93 search for resonances in the two-jet invariant mass. The limit assumes $B(Z' \to q\overline{q})$=0.7. See their Fig. 5 for limits in the $m_{Z'}$–$B(q\overline{q})$ plane.

[33] RIZZO 93 analyses CDF limit on possible two-jet resonances.

[34] ABE 90F use data for R, $R_{\ell\ell}$, and $A_{\ell\ell}$. They fix $m_W = 80.49 \pm 0.43 \pm 0.24$ GeV and m_Z = 91.13 ± 0.03 GeV.

Limits for Z_{LR}

Z_{LR} is the extra neutral boson in left-right symmetric models. $g_L = g_R$ is assumed unless noted. Values in parentheses assume stronger constraint on the Higgs sector, usually motivated by specific left-right symmetric models (see the Note on the W'). Values in brackets are from cosmological and astrophysical considerations and assume a light right-handed neutrino. Direct search bounds assume decays to Standard Model fermions only, unless noted.

VALUE (GeV)	CL%	DOCUMENT ID		TECN	COMMENT
>1162	95	[1] DEL-AGUILA	10	RVUE	Electroweak
> 630	95	[2] ABE	97S	CDF	$p\overline{p}$; $Z'_{LR} \to e^+e^-, \mu^+\mu^-$
• • • We do not use the following data for averages, fits, limits, etc. • • •					
> 998	95	[3] ERLER	09	RVUE	Electroweak
> 600	95	SCHAEL	07A	ALEP	e^+e^-
> 455	95	[4] ABDALLAH	06C	DLPH	e^+e^-
> 518	95	[5] ABBIENDI	04G	OPAL	e^+e^-

Gauge & Higgs Boson Particle Listings

New Heavy Bosons

> 860	95	[6] CHEUNG	01B	RVUE	Electroweak
> 380	95	[7] ABREU	00S	DLPH	e^+e^-
> 436	95	[8] BARATE	00I	ALEP	Repl. by SCHAEL 07A
> 550	95	[9] CHAY	00	RVUE	Electroweak
		[10] ERLER	00	RVUE	Cs
		[11] CASALBUONI	99	RVUE	Cs
(> 1205)	90	[12] CZAKON	99	RVUE	Electroweak
> 564	95	[13] ERLER	99	RVUE	Electroweak
(> 1673)	95	[14] ERLER	99	RVUE	Electroweak
(> 1700)	68	[15] BARENBOIM	98	RVUE	Electroweak
> 244	95	[16] CONRAD	98	RVUE	$\nu_\mu N$ scattering
> 253	95	[17] VILAIN	94B	CHM2	$\nu_\mu e \to \nu_\mu e$ and $\overline{\nu}_\mu e \to \overline{\nu}_\mu e$
none 200–600	95	[18] RIZZO	93	RVUE	$p\overline{p}$; Z_{LR} → $q\overline{q}$
[> 2000]		WALKER	91	COSM	Nucleosynthesis; light ν_R
none 200–500		[19] GRIFOLS	90	ASTR	SN 1987A; light ν_R
none 350–2400		[20] BARBIERI	89B	ASTR	SN 1987A; light ν_R

[1] DEL-AGUILA 10 give 95% CL limit on the Z-Z' mixing $-0.0012 < \theta < 0.0004$.

[2] ABE 97S find $\sigma(Z')\times B(e^+e^-,\mu^+\mu^-) < 40$ fb for $m_{Z'} > 600$ GeV at $\sqrt{s} = 1.8$ TeV.

[3] ERLER 09 give 95% CL limit on the Z-Z' mixing $-0.0013 < \theta < 0.0006$.

[4] ABDALLAH 06C give 95% CL limit $|\theta| < 0.0028$. See their Fig. 14 for limit contours in the mass-mixing plane.

[5] ABBIENDI 04G give 95% CL limit on Z-Z' mixing $-0.00098 < \theta < 0.00190$. See their Fig. 20 for the limit contour in the mass-mixing plane. $\sqrt{s} = 91$ to 207 GeV.

[6] CHEUNG 01B limit is derived from bounds on contact interactions in a global electroweak analysis.

[7] ABREU 00S give 95% CL limit on Z-Z' mixing $|\theta| < 0.0018$. See their Fig. 6 for the limit contour in the mass-mixing plane. $\sqrt{s}$=90 to 189 GeV.

[8] BARATE 00I search for deviations in cross section and asymmetries in $e^+e^- \to$ fermions at $\sqrt{s}$=90 to 183 GeV. Assume θ=0. Bounds in the mass-mixing plane are shown in their Figure 18.

[9] CHAY 00 also find $-0.0003 < \theta < 0.0019$. For g_R free, $m_{Z'} > 430$ GeV.

[10] ERLER 00 discuss the possibility that a discrepancy between the observed and predicted values of Q_W(Cs) is due to the exchange of Z'. The data are better described in a certain class of the Z' models including Z_{LR} and Z_χ.

[11] CASALBUONI 99 discuss the discrepancy between the observed and predicted values of Q_W(Cs). It is shown that the data are better described in a class of models including the Z_{LR} model.

[12] CZAKON 99 perform a simultaneous fit to charged and neutral sectors. Assumes manifest left-right symmetric model. Finds $|\theta| < 0.0042$.

[13] ERLER 99 give 90% CL limit on the Z-Z' mixing $-0.0009 < \theta < 0.0017$.

[14] ERLER 99 assumes 2 Higgs doublets, transforming as 10 of SO(10), embedded in E_6.

[15] BARENBOIM 98 also gives 68% CL limits on the Z-Z' mixing $-0.0005 < \theta < 0.0033$. Assumes Higgs sector of minimal left-right model.

[16] CONRAD 98 limit is from measurements at CCFR, assuming no Z-Z' mixing.

[17] VILAIN 94B assume $m_t = 150$ GeV and θ=0. See Fig. 2 for limit contours in the mass-mixing plane.

[18] RIZZO 93 analyses CDF limit on possible two-jet resonances.

[19] GRIFOLS 90 limit holds for $m_{\nu_R} \lesssim 1$ MeV. A specific Higgs sector is assumed. See also GRIFOLS 90D, RIZZO 91.

[20] BARBIERI 89B limit holds for $m_{\nu_R} \leq 10$ MeV. Bounds depend on assumed supernova core temperature.

Limits for Z_χ

Z_χ is the extra neutral boson in SO(10) → SU(5) × U(1)$_\chi$. $g_\chi = e/\cos\theta_W$ is assumed unless otherwise stated. We list limits with the assumption $\rho = 1$ but with no further constraints on the Higgs sector. Values in parentheses assume stronger constraint on the Higgs sector motivated by superstring models. Values in brackets are from cosmological and astrophysical considerations and assume a light right-handed neutrino.

VALUE (GeV)	CL%	DOCUMENT ID		TECN	COMMENT
>4100	95	[1] AABOUD	17AT	ATLS	pp; $Z'_\chi \to e^+e^-, \mu^+\mu^-$
• • • We do not use the following data for averages, fits, limits, etc. • • •					
>3050	95	[2] AABOUD	16U	ATLS	pp; $Z'_\chi \to e^+e^-, \mu^+\mu^-$
>2620	95	[3] AAD	14V	ATLS	pp, $Z'_\chi \to e^+e^-, \mu^+\mu^-$
>1970	95	[4] AAD	12CC	ATLS	pp, $Z'_\chi \to e^+e^-, \mu^+\mu^-$
> 930	95	[5] AALTONEN	11I	CDF	$p\overline{p}$; $Z'_\chi \to \mu^+\mu^-$
> 903	95	[6] ABAZOV	11A	D0	$p\overline{p}$, $Z'_\chi \to e^+e^-$
>1022	95	[7] DEL-AGUILA	10	RVUE	Electroweak
> 862	95	[6] AALTONEN	09T	CDF	$p\overline{p}$, $Z'_\chi \to e^+e^-$
> 892	95	[8] AALTONEN	09V	CDF	Repl. by AALTONEN 11I
>1141	95	[9] ERLER	09	RVUE	Electroweak
> 822	95	[6] AALTONEN	07H	CDF	Repl. by AALTONEN 09T
> 680	95	SCHAEL	07A	ALEP	e^+e^-
> 545	95	[10] ABDALLAH	06C	DLPH	e^+e^-
> 740		[6] ABULENCIA	06L	CDF	Repl. by AALTONEN 07H
> 690	95	[11] ABULENCIA	05A	CDF	$p\overline{p}$; $Z'_\chi \to e^+e^-, \mu^+\mu^-$
> 781	95	[12] ABBIENDI	04G	OPAL	e^+e^-
>2100		[13] BARGER	03B	COSM	Nucleosynthesis; light ν_R
> 680	95	[14] CHEUNG	01B	RVUE	Electroweak
> 440	95	[15] ABREU	00S	DLPH	e^+e^-
> 533	95	[16] BARATE	00I	ALEP	Repl. by SCHAEL 07A
> 554	95	[17] CHO	00	RVUE	Electroweak
		[18] ERLER	00	RVUE	Cs
		[19] ROSNER	00	RVUE	Cs
> 545	95	[20] ERLER	99	RVUE	Electroweak
(> 1368)	95	[21] ERLER	99	RVUE	Electroweak
> 215	95	[22] CONRAD	98	RVUE	$\nu_\mu N$ scattering
> 595	95	[23] ABE	97S	CDF	$p\overline{p}$; $Z'_\chi \to e^+e^-, \mu^+\mu^-$
> 190	95	[24] ARIMA	97	VNS	Bhabha scattering
> 262	95	[25] VILAIN	94B	CHM2	$\nu_\mu e \to \nu_\mu e$; $\overline{\nu}_\mu e \to \overline{\nu}_\mu e$
[>1470]		[26] FARAGGI	91	COSM	Nucleosynthesis; light ν_R
> 231	90	[27] ABE	90F	VNS	e^+e^-
[> 1140]		[28] GONZALEZ...	90D	COSM	Nucleosynthesis; light ν_R
[> 2100]		[29] GRIFOLS	90	ASTR	SN 1987A; light ν_R

[1] AABOUD 17AT search for resonances decaying to $\ell^+\ell^-$ in pp collisions at $\sqrt{s} = 13$ TeV.

[2] AABOUD 16U search for resonances decaying to $\ell^+\ell^-$ in pp collisions at $\sqrt{s} = 13$ TeV.

[3] AAD 14V search for resonances decaying to e^+e^-, $\mu^+\mu^-$ in pp collisions at $\sqrt{s} = 8$ TeV.

[4] AAD 12CC search for resonances decaying to e^+e^-, $\mu^+\mu^-$ in pp collisions at $\sqrt{s} = 7$ TeV.

[5] AALTONEN 11I search for resonances decaying to $\mu^+\mu^-$ in $p\overline{p}$ collisions at $\sqrt{s} = 1.96$ TeV.

[6] ABAZOV 11A, AALTONEN 09T, AALTONEN 07H, and ABULENCIA 06L search for resonances decaying to e^+e^- in $p\overline{p}$ collisions at $\sqrt{s} = 1.96$ TeV.

[7] DEL-AGUILA 10 give 95% CL limit on the Z-Z' mixing $-0.0011 < \theta < 0.0007$.

[8] AALTONEN 09V search for resonances decaying to $\mu^+\mu^-$ in $p\overline{p}$ collisions at $\sqrt{s} =$ 1.96 TeV.

[9] ERLER 09 give 95% CL limit on the Z-Z' mixing $-0.0016 < \theta < 0.0006$.

[10] ABDALLAH 06C give 95% CL limit $|\theta| < 0.0031$. See their Fig. 14 for limit contours in the mass-mixing plane.

[11] ABULENCIA 05A search for resonances decaying to electron or muon pairs in $p\overline{p}$ collisions at $\sqrt{s} = 1.96$ TeV.

[12] ABBIENDI 04G give 95% CL limit on Z-Z' mixing $-0.00099 < \theta < 0.00194$. See their Fig. 20 for the limit contour in the mass-mixing plane. $\sqrt{s} = 91$ to 207 GeV.

[13] BARGER 03B limit is from the nucleosynthesis bound on the effective number of light neutrino δN_ν <1. The quark-hadron transition temperature T_c=150 MeV is assumed. The limit with T_c=400 MeV is >4300 GeV.

[14] CHEUNG 01B limit is derived from bounds on contact interactions in a global electroweak analysis.

[15] ABREU 00S give 95% CL limit on Z-Z' mixing $|\theta| < 0.0017$. See their Fig. 6 for the limit contour in the mass-mixing plane. $\sqrt{s}$=90 to 189 GeV.

[16] BARATE 00I search for deviations in cross section and asymmetries in $e^+e^- \to$ fermions at $\sqrt{s}$=90 to 183 GeV. Assume θ=0. Bounds in the mass-mixing plane are shown in their Figure 18.

[17] CHO 00 use various electroweak data to constrain Z' models assuming m_H=100 GeV. See Fig. 3 for limits in the mass-mixing plane.

[18] ERLER 00 discuss the possibility that a discrepancy between the observed and predicted values of Q_W(Cs) is due to the exchange of Z'. The data are better described in a certain class of the Z' models including Z_{LR} and Z_χ.

[19] ROSNER 00 discusses the possibility that a discrepancy between the observed and predicted values of Q_W(Cs) is due to the exchange of Z'. The data are better described in a certain class of the Z' models including Z_χ.

[20] ERLER 99 give 90% CL limit on the Z-Z' mixing $-0.0020 < \theta < 0.0015$.

[21] ERLER 99 assumes 2 Higgs doublets, transforming as 10 of SO(10), embedded in E_6.

[22] CONRAD 98 limit is from measurements at CCFR, assuming no Z-Z' mixing.

[23] ABE 97S find $\sigma(Z')\times B(e^+e^-,\mu^+\mu^-) < 40$ fb for $m_{Z'} > 600$ GeV at $\sqrt{s} = 1.8$ TeV.

[24] Z-Z' mixing is assumed to be zero. $\sqrt{s} = 57.77$ GeV.

[25] VILAIN 94B assume $m_t = 150$ GeV and θ=0. See Fig. 2 for limit contours in the mass-mixing plane.

[26] FARAGGI 91 limit assumes the nucleosynthesis bound on the effective number of neutrinos $\Delta N_\nu < 0.5$ and is valid for $m_{\nu_R} < 1$ MeV.

[27] ABE 90F use data for R, $R_{\ell\ell}$, and $A_{\ell\ell}$. ABE 90F fix $m_W = 80.49 \pm 0.43 \pm 0.24$ GeV and $m_Z = 91.13 \pm 0.03$ GeV.

[28] Assumes the nucleosynthesis bound on the effective number of light neutrinos ($\delta N_\nu < 1$) and that ν_R is light ($\lesssim 1$ MeV).

[29] GRIFOLS 90 limit holds for $m_{\nu_R} \lesssim 1$ MeV. See also GRIFOLS 90D, RIZZO 91.

Limits for Z_ψ

Z_ψ is the extra neutral boson in $E_6 \to$ SO(10) × U(1)$_\psi$. $g_\psi = e/\cos\theta_W$ is assumed unless otherwise stated. We list limits with the assumption $\rho = 1$ but with no further constraints on the Higgs sector. Values in brackets are from cosmological and astrophysical considerations and assume a light right-handed neutrino.

VALUE (GeV)	CL%	DOCUMENT ID		TECN	COMMENT
>3800	95	[1] AABOUD	17AT	ATLS	pp; $Z'_\psi \to e^+e^-, \mu^+\mu^-$
>2820	95	[2] KHACHATRY...17T		CMS	pp; $Z'_\psi \to e^+e^-, \mu^+\mu^-$
>1100	95	[3] CHATRCHYAN	12O	CMS	pp, $Z'_\psi \to \tau^+\tau^-$
• • • We do not use the following data for averages, fits, limits, etc. • • •					
>2740	95	[4] AABOUD	16U	ATLS	pp; $Z'_\psi \to e^+e^-, \mu^+\mu^-$
>2570	95	[5] KHACHATRY...15AE		CMS	pp; $Z'_\psi \to e^+e^-, \mu^+\mu^-$
>2510	95	[6] AAD	14V	ATLS	pp, $Z'_\psi \to e^+e^-, \mu^+\mu^-$
>2260	95	[7] CHATRCHYAN	13AF	CMS	pp, $Z'_\psi \to e^+e^-, \mu^+\mu^-$
>1790	95	[8] AAD	12CC	ATLS	pp, $Z'_\psi \to e^+e^-, \mu^+\mu^-$
>2000	95	[9] CHATRCHYAN	12M	CMS	Repl. by CHATRCHYAN 13AF
> 917	95	[10] AALTONEN	11I	CDF	$p\overline{p}$; $Z'_\psi \to \mu^+\mu^-$
> 891	95	[11] ABAZOV	11A	D0	$p\overline{p}$, $Z'_\psi \to e^+e^-$
> 476	95	[12] DEL-AGUILA	10	RVUE	Electroweak
> 851	95	[11] AALTONEN	09T	CDF	$p\overline{p}$, $Z'_\psi \to e^+e^-$

[1] AABOUD 17AT search for resonances decaying to $\ell^+\ell^-$ in pp collisions at $\sqrt{s} = 13$ TeV.

[2] AABOUD 16U search for resonances decaying to $\ell^+\ell^-$ in pp collisions at $\sqrt{s} = 13$ TeV.

[3] AAD 14V search for resonances decaying to e^+e^-, $\mu^+\mu^-$ in pp collisions at $\sqrt{s} = 8$ TeV.

[4] AAD 12CC search for resonances decaying to e^+e^-, $\mu^+\mu^-$ in pp collisions at $\sqrt{s} = 7$ TeV.

[5] AALTONEN 11I search for resonances decaying to $\mu^+\mu^-$ in $p\overline{p}$ collisions at $\sqrt{s} = 1.96$ TeV.

[6] ABAZOV 11A, AALTONEN 09T, AALTONEN 07H, and ABULENCIA 06L search for resonances decaying to e^+e^- in $p\overline{p}$ collisions at $\sqrt{s} = 1.96$ TeV.

[7] DEL-AGUILA 10 give 95% CL limit on the Z-Z' mixing $-0.0011 < \theta < 0.0007$.

[8] AALTONEN 09V search for resonances decaying to $\mu^+\mu^-$ in $p\overline{p}$ collisions at $\sqrt{s} =$ 1.96 TeV.

[9] ERLER 09 give 95% CL limit on the Z-Z' mixing $-0.0016 < \theta < 0.0006$.

[10] ABDALLAH 06C give 95% CL limit $|\theta| < 0.0031$. See their Fig. 14 for limit contours in the mass-mixing plane.

[11] ABULENCIA 05A search for resonances decaying to electron or muon pairs in $p\overline{p}$ collisions at $\sqrt{s} = 1.96$ TeV.

[12] ABBIENDI 04G give 95% CL limit on Z-Z' mixing $-0.00099 < \theta < 0.00194$. See their Fig. 20 for the limit contour in the mass-mixing plane. $\sqrt{s} = 91$ to 207 GeV.

[13] BARGER 03B limit is from the nucleosynthesis bound on the effective number of light neutrino δN_ν <1. The quark-hadron transition temperature T_c=150 MeV is assumed. The limit with T_c=400 MeV is >4300 GeV.

[14] CHEUNG 01B limit is derived from bounds on contact interactions in a global electroweak analysis.

[15] ABREU 00S give 95% CL limit on Z-Z' mixing $|\theta| < 0.0017$. See their Fig. 6 for the limit contour in the mass-mixing plane. $\sqrt{s}$=90 to 189 GeV.

[16] BARATE 00I search for deviations in cross section and asymmetries in $e^+e^- \to$ fermions at $\sqrt{s}$=90 to 183 GeV. Assume θ=0. Bounds in the mass-mixing plane are shown in their Figure 18.

[17] CHO 00 use various electroweak data to constrain Z' models assuming m_H=100 GeV. See Fig. 3 for limits in the mass-mixing plane.

[18] ERLER 00 discuss the possibility that a discrepancy between the observed and predicted values of Q_W(Cs) is due to the exchange of Z'. The data are better described in a certain class of the Z' models including Z_{LR} and Z_χ.

[19] ROSNER 00 discusses the possibility that a discrepancy between the observed and predicted values of Q_W(Cs) is due to the exchange of Z'. The data are better described in a certain class of the Z' models including Z_χ.

[20] ERLER 99 give 90% CL limit on the Z-Z' mixing $-0.0020 < \theta < 0.0015$.

[21] ERLER 99 assumes 2 Higgs doublets, transforming as 10 of SO(10), embedded in E_6.

[22] CONRAD 98 limit is from measurements at CCFR, assuming no Z-Z' mixing.

[23] ABE 97S find $\sigma(Z')\times B(e^+e^-,\mu^+\mu^-) < 40$ fb for $m_{Z'} > 600$ GeV at $\sqrt{s} = 1.8$ TeV.

[24] Z-Z' mixing is assumed to be zero. $\sqrt{s} = 57.77$ GeV.

[25] VILAIN 94B assume $m_t = 150$ GeV and θ=0. See Fig. 2 for limit contours in the mass-mixing plane.

[26] FARAGGI 91 limit assumes the nucleosynthesis bound on the effective number of neutrinos $\Delta N_\nu < 0.5$ and is valid for $m_{\nu_R} < 1$ MeV.

[27] ABE 90F use data for R, $R_{\ell\ell}$, and $A_{\ell\ell}$. ABE 90F fix $m_W = 80.49 \pm 0.43 \pm 0.24$ GeV and $m_Z = 91.13 \pm 0.03$ GeV.

[28] Assumes the nucleosynthesis bound on the effective number of light neutrinos ($\delta N_\nu < 1$) and that ν_R is light ($\lesssim 1$ MeV).

[29] GRIFOLS 90 limit holds for $m_{\nu_R} \lesssim 1$ MeV. See also GRIFOLS 90D, RIZZO 91.

> 878	95	[13] AALTONEN	09V	CDF	Repl. by AALTONEN 11I	
> 147	95	[14] ERLER	09	RVUE	Electroweak	
> 822	95	[11] AALTONEN	07H	CDF	Repl. by AALTONEN 09T	
> 410	95	SCHAEL	07A	ALEP	e^+e^-	
> 475	95	[15] ABDALLAH	06C	DLPH	e^+e^-	
> 725		[11] ABULENCIA	06L	CDF	Repl. by AALTONEN 07H	
> 675	95	[16] ABULENCIA	05A	CDF	Repl. by AALTONEN 11I and AALTONEN 09T	
> 366	95	[17] ABBIENDI	04G	OPAL	e^+e^-	
> 600		[18] BARGER	03B	COSM	Nucleosynthesis; light ν_R	
> 350	95	[19] ABREU	00S	DLPH	e^+e^-	
> 294	95	[20] BARATE	00I	ALEP	Repl. by SCHAEL 07A	
> 137	95	[21] CHO	00	RVUE	Electroweak	
> 146	95	[22] ERLER	99	RVUE	Electroweak	
> 54	95	[23] CONRAD	98	RVUE	$\nu_\mu N$ scattering	
> 590	95	[24] ABE	97S	CDF	$p\overline{p}$; $Z'_\psi \to e^+e^-, \mu^+\mu^-$	
> 135	95	[25] VILAIN	94B	CHM2	$\nu_\mu e \to \nu_\mu e$; $\overline{\nu}_\mu e \to \overline{\nu}_\mu e$	
> 105	90	[26] ABE	90F	VNS	e^+e^-	
[> 160]		[27] GONZALEZ...	90D	COSM	Nucleosynthesis; light ν_R	
[> 2000]		[28] GRIFOLS	90D	ASTR	SN 1987A; light ν_R	

[1] AABOUD 17AT search for resonances decaying to $\ell^+\ell^-$ in pp collisions at $\sqrt{s}$ = 13 TeV.
[2] KHACHATRYAN 17T search for resonances decaying to e^+e^-, $\mu^+\mu^-$ in pp collisions at $\sqrt{s}$ = 8, 13 TeV.
[3] CHATRCHYAN 12O search for resonances decaying to $\tau^+\tau^-$ in pp collisions at $\sqrt{s}$ = 7 TeV.
[4] AABOUD 16U search for resonances decaying to $\ell^+\ell^-$ in pp collisions at $\sqrt{s}$ = 13 TeV.
[5] KHACHATRYAN 15AE search for resonances decaying to e^+e^-, $\mu^+\mu^-$ in pp collisions at $\sqrt{s}$ = 8 TeV.
[6] AAD 14V search for resonances decaying to e^+e^-, $\mu^+\mu^-$ in pp collisions at $\sqrt{s}$ = 8 TeV.
[7] CHATRCHYAN 13AF search for resonances decaying to e^+e^-, $\mu^+\mu^-$ in pp collisions at $\sqrt{s}$ = 7 TeV and 8 TeV.
[8] AAD 12CC search for resonances decaying to e^+e^-, $\mu^+\mu^-$ in pp collisions at $\sqrt{s}$ = 7 TeV.
[9] CHATRCHYAN 12M search for resonances decaying to e^+e^- or $\mu^+\mu^-$ in pp collisions at $\sqrt{s}$ = 7 TeV.
[10] AALTONEN 11I search for resonances decaying to $\mu^+\mu^-$ in $p\overline{p}$ collisions at $\sqrt{s}$ = 1.96 TeV.
[11] ABAZOV 11A, AALTONEN 09T, AALTONEN 07H, and ABULENCIA 06L search for resonances decaying to e^+e^- in $p\overline{p}$ collisions at $\sqrt{s}$ = 1.96 TeV.
[12] DEL-AGUILA 10 give 95% CL limit on the Z-Z' mixing $-0.0019 < \theta < 0.0007$.
[13] AALTONEN 09V search for resonances decaying to $\mu^+\mu^-$ in $p\overline{p}$ collisions at $\sqrt{s}$ = 1.96 TeV.
[14] ERLER 09 give 95% CL limit on the Z-Z' mixing $-0.0018 < \theta < 0.0009$.
[15] ABDALLAH 06C give 95% CL limit $|\theta| < 0.0027$. See their Fig. 14 for limit contours in the mass-mixing plane.
[16] ABULENCIA 05A search for resonances decaying to electron or muon pairs in $p\overline{p}$ collisions at $\sqrt{s}$ = 1.96 TeV.
[17] ABBIENDI 04G give 95% CL limit on Z-Z' mixing $-0.00129 < \theta < 0.00258$. See their Fig. 20 for the limit contour in the mass-mixing plane. $\sqrt{s}$ = 91 to 207 GeV.
[18] BARGER 03B limit is from the nucleosynthesis bound on the effective number of light neutrino δN_ν <1. The quark-hadron transition temperature T_c=150 MeV is assumed. The limit with T_c=400 MeV is >1100 GeV.
[19] ABREU 00S give 95% CL limit on Z-Z' mixing $|\theta| < 0.0018$. See their Fig. 6 for the limit contour in the mass-mixing plane. $\sqrt{s}$=90 to 189 GeV.
[20] BARATE 00I search for deviations in cross section and asymmetries in $e^+e^- \to$ fermions at $\sqrt{s}$=90 to 183 GeV. Assume θ=0. Bounds in the mass-mixing plane are shown in their Figure 18.
[21] CHO 00 use various electroweak data to constrain Z' models assuming m_H=100 GeV. See Fig. 3 for limits in the mass-mixing plane.
[22] ERLER 99 give 90% CL limit on the Z-Z' mixing $-0.0013 < \theta < 0.0024$.
[23] CONRAD 98 limit is from measurements at CCFR, assuming no Z-Z' mixing.
[24] ABE 97S find $\sigma(Z')\times$B(e^+e^-,$\mu^+\mu^-$)< 40 fb for $m_{Z'} > 600$ GeV at $\sqrt{s}$= 1.8 TeV.
[25] VILAIN 94B assume m_t = 150 GeV and θ=0. See Fig. 2 for limit contours in the mass-mixing plane.
[26] ABE 90F use data for R, $R_{\ell\ell}$, and $A_{\ell\ell}$. ABE 90F fix $m_W = 80.49 \pm 0.43 \pm 0.24$ GeV and $m_Z = 91.13 \pm 0.03$ GeV.
[27] Assumes the nucleosynthesis bound on the effective number of light neutrinos ($\delta N_\nu < 1$) and that ν_R is light ($\lesssim$ 1 MeV).
[28] GRIFOLS 90D limit holds for $m_{\nu_R} \lesssim 1$ MeV. See also RIZZO 91.

Limits for Z_η

Z_η is the extra neutral boson in E_6 models, corresponding to $Q_\eta = \sqrt{3/8}\, Q_\chi - \sqrt{5/8}\, Q_\psi$. $g_\eta = e/\cos\theta_W$ is assumed unless otherwise stated. We list limits with the assumption $\rho = 1$ but with no further constraints on the Higgs sector. Values in parentheses assume stronger constraint on the Higgs sector motivated by superstring models. Values in brackets are from cosmological and astrophysical considerations and assume a light right-handed neutrino.

VALUE (GeV)	CL%	DOCUMENT ID		TECN	COMMENT
>3900	95	[1] AABOUD	17AT	ATLS	pp; $Z'_\eta \to e^+e^-, \mu^+\mu^-$
• • • We do not use the following data for averages, fits, limits, etc. • • •					
>2810	95	[2] AABOUD	16U	ATLS	pp; $Z'_\eta \to e^+e^-, \mu^+\mu^-$
>1870	95	[3] AAD	12CC	ATLS	pp, $Z'_\eta \to e^+e^-, \mu^+\mu^-$
> 938	95	[4] AALTONEN	11I	CDF	$p\overline{p}$; $Z'_\eta \to \mu^+\mu^-$
> 923	95	[5] ABAZOV	11A	D0	$p\overline{p}$, $Z'_\eta \to e^+e^-$
> 488	95	[6] DEL-AGUILA	10	RVUE	Electroweak
> 877	95	[5] AALTONEN	09T	CDF	$p\overline{p}$, $Z'_\eta \to e^+e^-$
> 904	95	[7] AALTONEN	09V	CDF	Repl. by AALTONEN 11I
> 427	95	[8] ERLER	09	RVUE	Electroweak
> 891	95	[5] AALTONEN	07H	CDF	Repl. by AALTONEN 09T
> 350	95	SCHAEL	07A	ALEP	e^+e^-
> 360	95	[9] ABDALLAH	06C	DLPH	e^+e^-
> 745		[5] ABULENCIA	06L	CDF	Repl. by AALTONEN 07H
> 720	95	[10] ABULENCIA	05A	CDF	Repl. by AALTONEN 11I and AALTONEN 09T
> 515	95	[11] ABBIENDI	04G	OPAL	e^+e^-
>1600		[12] BARGER	03B	COSM	Nucleosynthesis; light ν_R
> 310	95	[13] ABREU	00S	DLPH	e^+e^-
> 329	95	[14] BARATE	00I	ALEP	Repl. by SCHAEL 07A
> 619	95	[15] CHO	00	RVUE	Electroweak
> 365	95	[16] ERLER	99	RVUE	Electroweak
> 87	95	[17] CONRAD	98	RVUE	$\nu_\mu N$ scattering
> 620	95	[18] ABE	97S	CDF	$p\overline{p}$; $Z'_\eta \to e^+e^-, \mu^+\mu^-$
> 100	95	[19] VILAIN	94B	CHM2	$\nu_\mu e \to \nu_\mu e$; $\overline{\nu}_\mu e \to \overline{\nu}_\mu e$
> 125	90	[20] ABE	90F	VNS	e^+e^-
[> 820]		[21] GONZALEZ...	90D	COSM	Nucleosynthesis; light ν_R
[> 3300]		[22] GRIFOLS	90	ASTR	SN 1987A; light ν_R
[> 1040]		[21] LOPEZ	90	COSM	Nucleosynthesis; light ν_R

[1] AABOUD 17AT search for resonances decaying to $\ell^+\ell^-$ in pp collisions at $\sqrt{s}$ = 13 TeV.
[2] AABOUD 16U search for resonances decaying to $\ell^+\ell^-$ in pp collisions at $\sqrt{s}$ = 13 TeV.
[3] AAD 12CC search for resonances decaying to e^+e^-, $\mu^+\mu^-$ in pp collisions at $\sqrt{s}$ = 7 TeV.
[4] AALTONEN 11I search for resonances decaying to $\mu^+\mu^-$ in $p\overline{p}$ collisions at $\sqrt{s}$ = 1.96 TeV.
[5] ABAZOV 11A, AALTONEN 09T, AALTONEN 07H, and ABULENCIA 06L search for resonances decaying to e^+e^- in $p\overline{p}$ collisions at $\sqrt{s}$ = 1.96 TeV.
[6] DEL-AGUILA 10 give 95% CL limit on the Z-Z' mixing $-0.0023 < \theta < 0.0027$.
[7] AALTONEN 09V search for resonances decaying to $\mu^+\mu^-$ in $p\overline{p}$ collisions at $\sqrt{s}$ = 1.96 TeV.
[8] ERLER 09 give 95% CL limit on the Z-Z' mixing $-0.0047 < \theta < 0.0021$.
[9] ABDALLAH 06C give 95% CL limit $|\theta| < 0.0092$. See their Fig. 14 for limit contours in the mass-mixing plane.
[10] ABULENCIA 05A search for resonances decaying to electron or muon pairs in $p\overline{p}$ collisions at $\sqrt{s}$ = 1.96 TeV.
[11] ABBIENDI 04G give 95% CL limit on Z-Z' mixing $-0.00447 < \theta <$0.00331. See their Fig. 20 for the limit contour in the mass-mixing plane. $\sqrt{s}$ = 91 to 207 GeV.
[12] BARGER 03B limit is from the nucleosynthesis bound on the effective number of light neutrino δN_ν <1. The quark-hadron transition temperature T_c=150 MeV is assumed. The limit with T_c=400 MeV is >3300 GeV.
[13] ABREU 00S give 95% CL limit on Z-Z' mixing $|\theta| < 0.0024$. See their Fig. 6 for the limit contour in the mass-mixing plane. $\sqrt{s}$=90 to 189 GeV.
[14] BARATE 00I search for deviations in cross section and asymmetries in $e^+e^- \to$ fermions at $\sqrt{s}$=90 to 183 GeV. Assume θ=0. Bounds in the mass-mixing plane are shown in their Figure 18.
[15] CHO 00 use various electroweak data to constrain Z' models assuming m_H=100 GeV. See Fig. 3 for limits in the mass-mixing plane.
[16] ERLER 99 give 90% CL limit on the Z-Z' mixing $-0.0062 < \theta < 0.0011$.
[17] CONRAD 98 limit is from measurements at CCFR, assuming no Z-Z' mixing.
[18] ABE 97S find $\sigma(Z')\times$B(e^+e^-,$\mu^+\mu^-$)< 40 fb for $m_{Z'} > 600$ GeV at $\sqrt{s}$= 1.8 TeV.
[19] VILAIN 94B assume m_t = 150 GeV and θ=0. See Fig. 2 for limit contours in the mass-mixing plane.
[20] ABE 90F use data for R, $R_{\ell\ell}$, and $A_{\ell\ell}$. ABE 90F fix $m_W = 80.49 \pm 0.43 \pm 0.24$ GeV and $m_Z = 91.13 \pm 0.03$ GeV.
[21] These authors claim that the nucleosynthesis bound on the effective number of light neutrinos ($\delta N_\nu < 1$) constrains Z' masses if ν_R is light ($\lesssim$ 1 MeV).
[22] GRIFOLS 90 limit holds for $m_{\nu_R} \lesssim 1$ MeV. See also GRIFOLS 90D, RIZZO 91.

Limits for other Z'

VALUE (GeV)	CL%	DOCUMENT ID		TECN	COMMENT
>1300	95	[1] AABOUD	18B	ATLS	$Z' \to WW$
none 1200–2800	95	[2] AABOUD	18F	ATLS	$Z' \to WW$
>2900	95	[3] AABOUD	17AK	ATLS	$Z' \to q\overline{q}$
none 1100–2600	95	[4] AABOUD	17AO	ATLS	$Z' \to hZ$
>2300	95	[5] SIRUNYAN	17AK	CMS	$Z' \to WW$, hZ
>2500	95	[6] SIRUNYAN	17Q	CMS	$Z' \to t\overline{t}$
>1190	95	[7] SIRUNYAN	17R	CMS	$Z' \to hZ$
none 1210–2260	95	[7] SIRUNYAN	17R	CMS	$Z' \to hZ$
• • • We do not use the following data for averages, fits, limits, etc. • • •					
		[8] SIRUNYAN	18G	CMS	$Z' \to q\overline{q}$
>1580	95	[9] AABOUD	17B	ATLS	$Z' \to hZ$
		[10] KHACHATRY...	17AX	CMS	$Z' \to \ell\ell\ell\ell$
		[11] KHACHATRY...	17U	CMS	$Z' \to hZ$
>1700	95	[12] SIRUNYAN	17A	CMS	$Z' \to WW$
		[13] SIRUNYAN	17AP	CMS	$Z' \to hA$
		[14] SIRUNYAN	17T	CMS	$Z' \to q\overline{q}$
		[15] SIRUNYAN	17V	CMS	$Z' \to Tt$
none 1100–1500	95	[16] AABOUD	16	ATLS	$Z' \to b\overline{b}$
		[17] AAD	16L	ATLS	$Z' \to a\gamma$, $a \to \gamma\gamma$
none 1500–2600	95	[18] AAD	16S	ATLS	$Z' \to q\overline{q}$

Gauge & Higgs Boson Particle Listings

New Heavy Bosons

none 1000–1100, none 1300–1500	95	[19] KHACHATRY...	16AP	CMS	$Z' \to hZ$
>2400	95	[20] KHACHATRY...	16E	CMS	$Z' \to t\bar{t}$
		[21] AAD	15AO	ATLS	$Z' \to t\bar{t}$
		[22] AAD	15AT	ATLS	monotop
		[23] AAD	15CD	ATLS	$h \to ZZ'$, $Z'Z'$; $Z' \to \ell^+\ell^-$
		[24] KHACHATRY...	15F	CMS	monotop
		[25] KHACHATRY...	15O	CMS	$Z' \to hZ$
		[26] AAD	14AT	ATLS	$Z' \to Z\gamma$
		[27] KHACHATRY...	14A	CMS	$Z' \to VV$
		[28] MARTINEZ	14	RVUE	Electroweak
none 500–1740	95	[29] AAD	13AQ	ATLS	$Z' \to t\bar{t}$
>1320 or 1000–1280	95	[30] AAD	13G	ATLS	$Z' \to t\bar{t}$
> 915	95	[30] AALTONEN	13A	CDF	$Z' \to t\bar{t}$
>1300	95	[31] CHATRCHYAN	13AP	CMS	$Z' \to t\bar{t}$
>2100	95	[30] CHATRCHYAN	13BM	CMS	$Z' \to t\bar{t}$
		[32] AAD	12BV	ATLS	$Z' \to t\bar{t}$
		[33] AAD	12K	ATLS	$Z' \to t\bar{t}$
		[34] AALTONEN	12AR	CDF	Chromophilic
		[35] AALTONEN	12N	CDF	$Z' \to \bar{t}u$
> 835	95	[36] ABAZOV	12R	D0	$Z' \to t\bar{t}$
		[37] CHATRCHYAN	12AI	CMS	$Z' \to t\bar{u}$
		[38] CHATRCHYAN	12AQ	CMS	$Z' \to t\bar{t}$
>1490	95	[30] CHATRCHYAN	12BL	CMS	$Z' \to t\bar{t}$
		[39] AALTONEN	11AD	CDF	$Z' \to t\bar{t}$
		[40] AALTONEN	11AE	CDF	$Z' \to t\bar{t}$
		[41] CHATRCHYAN	11O	CMS	$pp \to tt$
		[42] AALTONEN	08D	CDF	$Z' \to t\bar{t}$
		[42] AALTONEN	08Y	CDF	$Z' \to t\bar{t}$
		[42] ABAZOV	08AA	D0	$Z' \to t\bar{t}$
		[43] ABAZOV	04A	D0	Repl. by ABAZOV 08AA
		[44] BARGER	03B	COSM	Nucleosynthesis; light ν_R
		[45] CHO	00	RVUE	E_6-motivated
		[46] CHO	98	RVUE	E_6-motivated
		[47] ABE	97G	CDF	$Z' \to \bar{q}q$

[1] AABOUD 18B search for resonances decaying to WW in pp collisions at $\sqrt{s} = 13$ TeV. The quoted limit is for heavy-vector-triplet Z' with $g_V = 1$. See their Fig.11 for limits on $\sigma \cdot B$.

[2] AABOUD 18F search for resonances decaying to WW in pp collisions at $\sqrt{s} = 13$ TeV. The quoted limit is for heavy-vector-triplet Z' with $g_V = 3$. The limit becomes $M_{Z'} > 2200$ GeV for $g_V = 1$. If we assume $M_{Z'} = M_{W'}$, the limit increases $M_{Z'} > 3500$ GeV and $M_{Z'} > 3100$ GeV for $g_V = 3$ and $g_V = 1$, respectively. See their Fig.5 for limits on $\sigma \cdot B$.

[3] AABOUD 17AK search for a new resonance decaying to dijets in pp collisions at $\sqrt{s} = 13$ TeV. The limit quoted above is for a leptophobic Z' boson having axial-vector coupling strength with quarks $g_q = 0.2$. The limit is 2100 GeV if $g_q = 0.1$.

[4] AABOUD 17AO search for resonances decaying to hZ in pp collisions at $\sqrt{s} = 13$ TeV. The limit quoted above is for a Z' in the heavy-vector-triplet model with $g_V = 3$. See their Fig.4 for limits on $\sigma \cdot B$.

[5] SIRUNYAN 17AK search for resonances decaying to WW or hZ in pp collisions at $\sqrt{s} = 8$ and 13 TeV. The quoted limit is for heavy-vector-triplet Z' with $g_V = 3$. The limit becomes $M_{Z'} > 2200$ GeV for $g_V = 1$. If we assume $M_{Z'} = M_{W'}$, the limit increases $M_{Z'} > 2400$ GeV for both $g_V = 3$ and $g_V = 1$. See their Fig.1 and 2 for limits on $\sigma \cdot B$.

[6] SIRUNYAN 17Q search for a resonance decaying to $t\bar{t}$ in pp collisions at $\sqrt{s} = 13$ TeV. The limit quoted above is for a resonance with relative width $\Gamma_{Z'} / M_{Z'} = 0.01$. Limits for wider resonances are available. See their Fig.6 for limits on $\sigma \cdot B$.

[7] SIRUNYAN 17R search for resonances decaying to hZ in pp collisions at $\sqrt{s} = 13$ TeV. The quoted limit is for heavy-vector-triplet Z' with $g_V = 3$. Mass regions $M_{Z'} < 1150$ GeV and 1250 GeV $< M_{Z'} < 1670$ GeV are excluded for $g_V = 1$. If we assume $M_{Z'} = M_{W'}$, the excluded mass regions are $1000 < M_{Z'} < 2500$ GeV and $2760 < M_{Z'} < 3300$ GeV for $g_V = 3$; $1000 < M_{Z'} < 2430$ GeV and $2810 < M_{Z'} < 3130$ GeV for $g_V = 1$. See their Fig.5 for limits on $\sigma \cdot B$.

[8] SIRUNYAN 18G search for a new resonance decaying to dijets in pp collisions at $\sqrt{s} = 13$ TeV in the mass range 50–300 GeV. See their Fig.7 for limits in the mass-coupling plane.

[9] AABOUD 17B search for resonances decaying to hZ ($h \to b\bar{b}$, $c\bar{c}$; $Z \to \ell^+\ell^-$, $\nu\bar{\nu}$) in pp collisions at $\sqrt{s} = 13$ TeV. The quoted limit is for heavy-vector-triplet Z' with $g_V = 3$. The limit becomes $M_{Z'} > 1490$ GeV for $g_V = 1$. If we assume $M_{Z'} = M_{W'}$, the limit increases $M_{Z'} > 2310$ GeV and $M_{Z'} > 1730$ GeV for $g_V = 3$ and $g_V = 1$, respectively. See their Fig.3 for limits on $\sigma \cdot B$.

[10] KHACHATRYAN 17AX search for lepto-phobic resonances decaying to four leptons in pp collisions at $\sqrt{s} = 8$ TeV.

[11] KHACHATRYAN 17U search for resonances decaying to hZ ($h \to b\bar{b}$; $Z \to \ell^+\ell^-$, $\nu\bar{\nu}$) in pp collisions at $\sqrt{s} = 13$ TeV. The limit on the heavy-vector-triplet model is $M_{Z'} = M_{W'} > 2$ TeV for $g_V = 3$, in which constraints from the $W' \to hW$ ($h \to b\bar{b}$; $W \to \ell\nu$) are combined. See their Fig.3 and Fig.4 for limits on $\sigma \cdot B$.

[12] SIRUNYAN 17A search for resonances decaying to WW with $WW \to \ell\nu q\bar{q}$, $q\bar{q}q\bar{q}$ in pp collisions at $\sqrt{s} = 13$ TeV. The quoted limit is for heavy-vector-triplet Z' with $g_V = 3$. The limit becomes $M_{Z'} > 1600$ GeV for $g_V = 1$. If we assume $M_{Z'} = M_{W'}$, the limit increases $M_{Z'} > 2400$ GeV and $M_{Z'} > 2300$ GeV for $g_V = 3$ and $g_V = 1$, respectively. See their Fig.6 for limits on $\sigma \cdot B$.

[13] SIRUNYAN 17AP search for resonances decaying into a SM-like Higgs scalar h and a light pseudo scalar A. A is assumed to decay invisibly. See their Fig.9 for limits on $\sigma \cdot B$.

[14] SIRUNYAN 17T search for a new resonance decaying to dijets in pp collisions at $\sqrt{s} = 13$ TeV in the mass range 100–300 GeV. See their Fig.3 for limits in the mass-coupling plane.

[15] SIRUNYAN 17V search for a new resonance decaying to a top quark and a heavy vector-like top partner T in pp collisions at $\sqrt{s} = 13$ TeV. See their table 5 for limits on the Z' production cross section for various values of $M_{Z'}$ and M_T in the range of $M_{Z'} =$ 1500–2500 GeV and $M_T =$ 700–1500 GeV.

[16] AABOUD 16 search for a narrow resonance decaying into $b\bar{b}$ in pp collisions at $\sqrt{s} = 13$ TeV. The limit quoted above is for a leptophobic Z' with SM-like couplings to quarks. See their Fig.6 for limits on $\sigma \cdot B$.

[17] AAD 16L search for $Z' \to a\gamma$, $a \to \gamma\gamma$ in pp collisions at $\sqrt{s} = 8$ TeV. See their Table 6 for limits on $\sigma \cdot B$.

[18] AAD 16S search for a new resonance decaying to dijets in pp collisions at $\sqrt{s} = 13$ TeV. The limit quoted above is for a leptophobic Z' having coupling strength with quark $g_q = 0.3$ and is taken from their Figure 3.

[19] KHACHATRYAN 16AP search for a resonance decaying to hZ in pp collisions at $\sqrt{s} = 8$ TeV. Both h and Z are assumed to decay to fat jets. The quoted limit is for heavy-vector-triplet Z' with $g_V = 3$.

[20] KHACHATRYAN 16E search for a leptophobic top-color Z' decaying to $t\bar{t}$ using pp collisions at $\sqrt{s} = 8$ TeV. The quoted limit assumes that $\Gamma_{Z'}/m_{Z'} = 0.012$. Also $m_{Z'} < 2.9$ TeV is excluded for wider topcolor Z' with $\Gamma_{Z'}/m_{Z'} = 0.1$.

[21] AAD 15AO search for narrow resonance decaying to $t\bar{t}$ using pp collisions at $\sqrt{s} = 8$ TeV. See Fig. 11 for limit on σB.

[22] AAD 15AT search for monotop production plus large missing E_T events in pp collisions at $\sqrt{s} = 8$ TeV and give constraints on a Z' model having $Z'u\bar{t}$ coupling. Z' is assumed to decay invisibly. See their Fig. 6 for limits on $\sigma \cdot B$.

[23] AAD 15CD search for decays of Higgs bosons to 4 ℓ states via Z' bosons, $h \to ZZ' \to 4\ell$ or $h \to Z'Z' \to 4\ell$. See Fig. 5 for the limit on the signal strength of the $h \to ZZ' \to 4\ell$ process and Fig. 16 for the limit on $h \to Z'Z' \to 4\ell$.

[24] KHACHATRYAN 15F search for monotop production plus large missing E_T events in pp collisions at $\sqrt{s} = 8$ TeV and give constraints on a Z' model having $Z'u\bar{t}$ coupling. Z' is assumed to decay invisibly. See Fig. 3 for limits on σB.

[25] KHACHATRYAN 15O search for narrow Z' resonance decaying to Zh in pp collisions at $\sqrt{s} = 8$ TeV. See their Fig. 6 for limit on σB.

[26] AAD 14AT search for a narrow neutral vector boson decaying to $Z\gamma$. See their Fig. 3b for the exclusion limit in $m_{Z'} - \sigma B$ plane.

[27] KHACHATRYAN 14A search for new resonance in the WW ($\ell\nu q\bar{q}$) and the ZZ ($\ell\ell q\bar{q}$) channels using pp collisions at $\sqrt{s}$=8 TeV. See their Fig.13 for the exclusion limit on the number of events in the mass-width plane.

[28] MARTINEZ 14 use various electroweak data to constrain the Z' boson in the 3-3-1 models.

[29] AAD 13AQ search for a leptophobic top-color Z' decaying to $t\bar{t}$. The quoted limit assumes that $\Gamma_{Z'}/m_{Z'} = 0.012$.

[30] CHATRCHYAN 13BM search for top-color Z' decaying to $t\bar{t}$ using pp collisions at $\sqrt{s}$=8 TeV. The quoted limit is for $\Gamma_{Z'}/m_{Z'} = 0.012$.

[31] CHATRCHYAN 13AP search for top-color leptophobic Z' decaying to $t\bar{t}$ using pp collisions at $\sqrt{s}$=7 TeV. The quoted limit is for $\Gamma_{Z'}/m_{Z'} = 0.012$.

[32] AAD 12BV search for narrow resonance decaying to $t\bar{t}$ using pp collisions at $\sqrt{s}$=7 TeV. See their Fig. 7 for limit on $\sigma \cdot$ B.

[33] AAD 12K search for narrow resonance decaying to $t\bar{t}$ using pp collisions at $\sqrt{s}$=7 TeV. See their Fig. 5 for limit on $\sigma \cdot$ B.

[34] AALTONEN 12AR search for chromophilic Z' in $p\bar{p}$ collisions at $\sqrt{s} = 1.96$ TeV. See their Fig. 5 for limit on $\sigma \cdot$ B.

[35] AALTONEN 12N search for $p\bar{p} \to tZ'$, $Z' \to \bar{t}u$ events in $p\bar{p}$ collisions. See their Fig. 3 for the limit on $\sigma \cdot$ B.

[36] ABAZOV 12R search for top-color Z' boson decaying exclusively to $t\bar{t}$. The quoted limit is for $\Gamma_{Z'}/m_{Z'}$= 0.012.

[37] CHATRCHYAN 12AI search for $pp \to tt$ events and give constraints on a Z' model having $Z'\bar{u}t$ coupling. See their Fig. 4 for the limit in mass-coupling plane.

[38] Search for resonance decaying to $t\bar{t}$. See their Fig. 6 for limit on $\sigma \cdot$ B.

[39] Search for narrow resonance decaying to $t\bar{t}$. See their Fig. 4 for limit on $\sigma \cdot$ B.

[40] Search for narrow resonance decaying to $t\bar{t}$. See their Fig. 3 for limit on $\sigma \cdot$ B.

[41] CHATRCHYAN 11O search for same-sign top production in pp collisions induced by a hypothetical FCNC Z' at $\sqrt{s} = 7$ TeV. See their Fig. 3 for limit in mass-coupling plane.

[42] Search for narrow resonance decaying to $t\bar{t}$. See their Fig. 3 for limit on $\sigma \cdot$ B.

[43] Search for narrow resonance decaying to $t\bar{t}$. See their Fig. 2 for limit on $\sigma \cdot$ B.

[44] BARGER 03B use the nucleosynthesis bound on the effective number of light neutrino δN_ν. See their Figs. 4–5 for limits in general E_6 motivated models.

[45] CHO 00 use various electroweak data to constrain Z' models assuming m_H=100 GeV. See Fig. 2 for limits in general E_6-motivated models.

[46] CHO 98 study constraints on four-Fermi contact interactions obtained from low-energy electroweak experiments, assuming no Z-Z' mixing.

[47] Search for Z' decaying to dijets at $\sqrt{s}$=1.8 TeV. For Z' with electromagnetic strength coupling, no bound is obtained.

Searches for Z' with Lepton-Flavor-Violating decays

The following limits are obtained from $p\bar{p}$ or $pp \to Z'X$ with Z' decaying to the mode indicated in the comments.

VALUE	DOCUMENT ID		TECN	COMMENT
• • • We do not use the following data for averages, fits, limits, etc. • • •				
	[1] AABOUD	16P	ATLS	$Z' \to e\mu$, $e\tau$, $\mu\tau$
	[2] KHACHATRY...	16BE	CMS	$Z' \to e\mu$
	[3] AAD	15O	ATLS	$Z' \to e\mu$, $e\tau$, $\mu\tau$
	[4] AAD	11H	ATLS	$Z' \to e\mu$
	[5] AAD	11Z	ATLS	$Z' \to e\mu$
	[6] ABULENCIA	06M	CDF	$Z' \to e\mu$

[1] AABOUD 16P search for new particle with lepton flavor violating decay in pp collisions at $\sqrt{s} = 13$ TeV. See their Figs.2, 3, and 4 for limits on $\sigma \cdot B$.

[2] KHACHATRYAN 16BE search for new particle Z' with lepton flavor violating decay in pp collisions at $\sqrt{s}$ = 8 TeV in the range of 200 GeV < $M_{Z'}$ < 2000 GeV. See their Fig.4 for limits on $\sigma \cdot B$ and their Table 5 for bounds on various masses.

[3] AAD 15O search for new particle Z' with lepton flavor violating decay in pp collisions at $\sqrt{s}$ = 8 TeV in the range of 500 GeV < $M_{Z'}$ < 3000 GeV. See their Fig. 2 for limits on σB.

[4] AAD 11H search for new particle Z' with lepton flavor violating decay in pp collisions at $\sqrt{s}$ = 7 TeV in the range of 700 GeV < $M_{Z'}$ < 1000 GeV. See their Fig. 3 for limits on $\sigma \cdot B$.

[5] AAD 11Z search for new particle Z' with lepton flavor violating decay in pp collisions at $\sqrt{s}$ = 7 TeV in the range 700 GeV < $M_{Z'}$ < 2000 GeV. See their Fig. 3 for limits on $\sigma \cdot B$.

[6] ABULENCIA 06M search for new particle Z' with lepton flavor violating decay in $p\overline{p}$ collisions at $\sqrt{s}$ = 1.96 TeV in the range of 100 GeV < $M_{Z'}$ < 800 GeV. See their Fig. 4 for limits in the mass-coupling plane.

Indirect Constraints on Kaluza-Klein Gauge Bosons

Bounds on a Kaluza-Klein excitation of the Z boson or photon in d=1 extra dimension. These bounds can also be interpreted as a lower bound on $1/R$, the size of the extra dimension. Unless otherwise stated, bounds assume all fermions live on a single brane and all gauge fields occupy the 4+d-dimensional bulk. See also the section on "Extra Dimensions" in the "Searches" Listings in this *Review*.

VALUE (TeV)	CL%	DOCUMENT ID		TECN	COMMENT
• • • We do not use the following data for averages, fits, limits, etc. • • •					
> 4.7		[1] MUECK	02	RVUE	Electroweak
> 3.3	95	[2] CORNET	00	RVUE	$e\nu qq'$
>5000		[3] DELGADO	00	RVUE	ϵ_K
> 2.6	95	[4] DELGADO	00	RVUE	Electroweak
> 3.3	95	[5] RIZZO	00	RVUE	Electroweak
> 2.9	95	[6] MARCIANO	99	RVUE	Electroweak
> 2.5	95	[7] MASIP	99	RVUE	Electroweak
> 1.6	90	[8] NATH	99	RVUE	Electroweak
> 3.4	95	[9] STRUMIA	99	RVUE	Electroweak

[1] MUECK 02 limit is 2σ and is from global electroweak fit ignoring correlations among observables. Higgs is assumed to be confined on the brane and its mass is fixed. For scenarios of bulk Higgs, of brane-SU(2)$_L$, bulk-U(1)$_Y$, and of bulk-SU(2)$_L$, brane-U(1)$_Y$, the corresponding limits are > 4.6 TeV, > 4.3 TeV and > 3.0 TeV, respectively.

[2] Bound is derived from limits on $e\nu qq'$ contact interaction, using data from HERA and the Tevatron.

[3] Bound holds only if first two generations of quarks lives on separate branes. If quark mixing is not complex, then bound lowers to 400 TeV from Δm_K.

[4] See Figs. 1 and 2 of DELGADO 00 for several model variations. Special boundary conditions can be found which permit KK states down to 950 GeV and that agree with the measurement of Q_W(Cs). Quoted bound assumes all Higgs bosons confined to brane; placing one Higgs doublet in the bulk lowers bound to 2.3 TeV.

[5] Bound is derived from global electroweak analysis assuming the Higgs field is trapped on the matter brane. If the Higgs propagates in the bulk, the bound increases to 3.8 TeV.

[6] Bound is derived from global electroweak analysis but considering only presence of the KK W bosons.

[7] Global electroweak analysis used to obtain bound independent of position of Higgs on brane or in bulk.

[8] Bounds from effect of KK states on G_F, α, M_W, and M_Z. Hard cutoff at string scale determined using gauge coupling unification. Limits for d=2,3,4 rise to 3.5, 5.7, and 7.8 TeV.

[9] Bound obtained for Higgs confined to the matter brane with m_H=500 GeV. For Higgs in the bulk, the bound increases to 3.5 TeV.

See the related review(s):

Leptoquarks

MASS LIMITS for Leptoquarks from Pair Production

These limits rely only on the color or electroweak charge of the leptoquark.

VALUE (GeV)	CL%	DOCUMENT ID		TECN	COMMENT
> 740	95	[1] KHACHATRY...	17J	CMS	Third generation
> 850	95	[2] SIRUNYAN	17H	CMS	Third generation
>1050	95	[3] AAD	16G	ATLS	First generation
>1000	95	[4] AAD	16G	ATLS	Second generation
> 625	95	[5] AAD	16G	ATLS	Third generation
none 200–640	95	[6] AAD	16G	ATLS	Third generation
>1010	95	[7] KHACHATRY...	16AF	CMS	First generation
>1080	95	[8] KHACHATRY...	16AF	CMS	Second generation
> 685	95	[9] KHACHATRY...	15AJ	CMS	Third generation
> 740	95	[10] KHACHATRY...	14T	CMS	Third generation
• • • We do not use the following data for averages, fits, limits, etc. • • •					
> 534	95	[11] AAD	13AE	ATLS	Third generation
> 525	95	[12] CHATRCHYAN	13M	CMS	Third generation
> 660	95	[13] AAD	12H	ATLS	First generation
> 685	95	[14] AAD	12O	ATLS	Second generation
> 830	95	[15] CHATRCHYAN	12AG	CMS	First generation
> 840	95	[16] CHATRCHYAN	12AG	CMS	Second generation
> 450	95	[17] CHATRCHYAN	12BO	CMS	Third generation
> 376	95	[18] AAD	11D	ATLS	Superseded by AAD 12H
> 422	95	[19] AAD	11D	ATLS	Superseded by AAD 12O
> 326	95	[20] ABAZOV	11V	D0	First generation
> 339	95	[21] CHATRCHYAN	11N	CMS	Superseded by CHATRCHYAN 12AG
> 384	95	[22] KHACHATRY...	11D	CMS	Superseded by CHATRCHYAN 12AG
> 394	95	[23] KHACHATRY...	11E	CMS	Superseded by CHATRCHYAN 12AG
> 247	95	[24] ABAZOV	10L	D0	Third generation
> 316	95	[25] ABAZOV	09	D0	Second generation
> 299	95	[26] ABAZOV	09AF	D0	Superseded by ABAZOV 11V
		[27] AALTONEN	08P	CDF	Third generation
> 153	95	[28] AALTONEN	08Z	CDF	Third generation
> 205	95	[29] ABAZOV	08AD	D0	All generations
> 210	95	[28] ABAZOV	08AN	D0	Third generation
> 229	95	[30] ABAZOV	07J	D0	Superseded by ABAZOV 10L
> 251	95	[31] ABAZOV	06A	D0	Superseded by ABAZOV 09
> 136	95	[32] ABAZOV	06L	D0	Superseded by ABAZOV 08AD
> 226	95	[33] ABULENCIA	06T	CDF	Second generation
> 256	95	[34] ABAZOV	05H	D0	First generation
> 117	95	[29] ACOSTA	05I	CDF	First generation
> 236	95	[35] ACOSTA	05P	CDF	First generation
> 99	95	[36] ABBIENDI	03R	OPAL	First generation
> 100	95	[36] ABBIENDI	03R	OPAL	Second generation
> 98	95	[36] ABBIENDI	03R	OPAL	Third generation
> 98	95	[37] ABAZOV	02	D0	All generations
> 225	95	[38] ABAZOV	01D	D0	First generation
> 85.8	95	[39] ABBIENDI	00M	OPAL	Superseded by ABBIENDI 03R
> 85.5	95	[39] ABBIENDI	00M	OPAL	Superseded by ABBIENDI 03R
> 82.7	95	[39] ABBIENDI	00M	OPAL	Superseded by ABBIENDI 03R
> 200	95	[40] ABBOTT	00C	D0	Second generation
> 123	95	[41] AFFOLDER	00K	CDF	Second generation
> 148	95	[42] AFFOLDER	00K	CDF	Third generation
> 160	95	[43] ABBOTT	99J	D0	Second generation
> 225	95	[44] ABBOTT	98E	D0	First generation
> 94	95	[45] ABBOTT	98J	D0	Third generation
> 202	95	[46] ABE	98S	CDF	Second generation
> 242	95	[47] GROSS-PILCH..	98		First generation
> 99	95	[48] ABE	97F	CDF	Third generation
> 213	95	[49] ABE	97X	CDF	First generation
> 45.5	95	[50,51] ABREU	93J	DLPH	First + second generation
> 44.4	95	[52] ADRIANI	93M	L3	First generation
> 44.5	95	[52] ADRIANI	93M	L3	Second generation
> 45	95	[52] DECAMP	92	ALEP	Third generation
none 8.9–22.6	95	[53] KIM	90	AMY	First generation
none 10.2–23.2	95	[53] KIM	90	AMY	Second generation
none 5–20.8	95	[54] BARTEL	87B	JADE	
none 7–20.5	95	[55] BEHREND	86B	CELL	

[1] KHACHATRYAN 17J search for scalar leptoquarks decaying to τb using pp collisions at $\sqrt{s}$ = 13 TeV. The limit above assumes B(τb) = 1.

[2] SIRUNYAN 17H search for scalar leptoquarks using $\tau\tau bb$ events in pp collisions at $\sqrt{s}$ = 8 TeV. The limit above assumes B(τb) = 1.

[3] AAD 16G search for scalar leptoquarks using $eejj$ events in collisions at $\sqrt{s}$ = 8 TeV. The limit above assumes $B(eq)$ = 1.

[4] AAD 16G search for scalar leptoquarks using $\mu\mu jj$ events in collisions at $\sqrt{s}$ = 8 TeV. The limit above assumes $B(\mu q)$ = 1.

[5] AAD 16G search for scalar leptoquarks decaying to $b\nu$. The limit above assumes $B(b\nu)$ = 1.

[6] AAD 16G search for scalar leptoquarks decaying to $t\nu$. The limit above assumes $B(t\nu)$ = 1.

[7] KHACHATRYAN 16AF search for scalar leptoquarks using $eejj$ and $e\nu jj$ events in pp collisions at $\sqrt{s}$ = 8 TeV. The limit above assumes B(eq)= 1. For B(eq) = 0.5, the limit becomes 850 GeV.

[8] KHACHATRYAN 16AF search for scalar leptoquarks using $\mu\mu jj$ and $\mu\nu jj$ events in pp collisions at $\sqrt{s}$ = 8 TeV. The limit above assumes B(μq) = 1. For B(μq) = 0.5, the limit becomes 760 GeV.

[9] KHACHATRYAN 15AJ search for scalar leptoquarks using $\tau\tau tt$ events in pp collisions at $\sqrt{s}$ = 8 TeV. The limit above assumes $B(\tau t)$ = 1.

[10] KHACHATRYAN 14T search for scalar leptoquarks decaying to τb using pp collisions at $\sqrt{s}$ = 8 TeV. The limit above assumes B(τb) = 1. See their Fig. 5 for the exclusion limit as function of B(τb).

[11] AAD 13AE search for scalar leptoquarks using $\tau\tau bb$ events in pp collisions at E_{cm} = 7 TeV. The limit above assumes B(τb) = 1.

[12] CHATRCHYAN 13M search for scalar and vector leptoquarks decaying to τb in pp collisions at E_{cm} = 7 TeV. The limit above is for scalar leptoquarks with B(τb) = 1.

[13] AAD 12H search for scalar leptoquarks using $eejj$ and $e\nu jj$ events in pp collisions at E_{cm} = 7 TeV. The limit above assumes B(eq) = 1. For B(eq) = 0.5, the limit becomes 607 GeV.

[14] AAD 12O search for scalar leptoquarks using $\mu\mu jj$ and $\mu\nu jj$ events in pp collisions at E_{cm} = 7 TeV. The limit above assumes B(μq) = 1. For B(μq) = 0.5, the limit becomes 594 GeV.

[15] CHATRCHYAN 12AG search for scalar leptoquarks using $eejj$ and $e\nu jj$ events in pp collisions at E_{cm} = 7 TeV. The limit above assumes B(eq) = 1. For B(eq) = 0.5, the limit becomes 640 GeV.

[16] CHATRCHYAN 12AG search for scalar leptoquarks using $\mu\mu jj$ and $\mu\nu jj$ events in pp collisions at E_{cm} = 7 TeV. The limit above assumes B(μq) = 1. For B(μq) = 0.5, the limit becomes 650 GeV.

[17] CHATRCHYAN 12BO search for scalar leptoquarks decaying to νb in pp collisions at $\sqrt{s}$ = 7 TeV. The limit above assumes B(νb) = 1.

[18] AAD 11D search for scalar leptoquarks using $eejj$ and $e\nu jj$ events in pp collisions at E_{cm} = 7 TeV.The limit above assumes B(eq) = 1. For B(eq) = 0.5, the limit becomes 319 GeV.

[19] AAD 11D search for scalar leptoquarks using $\mu\mu jj$ and $\mu\nu jj$ events in pp collisions at E_{cm} = 7 TeV. The limit above assumes B(μq) = 1. For B(μq) = 0.5, the limit becomes 362 GeV.

[20] ABAZOV 11V search for scalar leptoquarks using $e\nu jj$ events in $p\overline{p}$ collisions at E_{cm} = 1.96 TeV. The limit above assumes B(eq) = 0.5.

[21] CHATRCHYAN 11N search for scalar leptoquarks using $e\nu jj$ events in pp collisions at E_{cm} = 7 TeV. The limit above assumes B(eq) = 0.5.

[22] KHACHATRYAN 11D search for scalar leptoquarks using $eejj$ events in pp collisions at E_{cm} = 7 TeV. The limit above assumes B(eq) = 1.

[23] KHACHATRYAN 11E search for scalar leptoquarks using $\mu\mu jj$ events in pp collisions at E_{cm} = 7 TeV. The limit above assumes B(μq) = 1.
[24] ABAZOV 10L search for pair productions of scalar leptoquark state decaying to νb in $p\overline{p}$ collisions at E_{cm} = 1.96 TeV. The limit above assumes B(νb) = 1.
[25] ABAZOV 09 search for scalar leptoquarks using $\mu\mu jj$ and $\mu\nu jj$ events in $p\overline{p}$ collisions at E_{cm} = 1.96 TeV. The limit above assumes B(μq) = 1. For B(μq) = 0.5, the limit becomes 270 GeV.
[26] ABAZOV 09AF search for scalar leptoquarks using $eejj$ and $e\nu jj$ events in $p\overline{p}$ collisions at E_{cm} = 1.96 TeV. The limit above assumes B(eq) = 1. For B(eq) = 0.5 the bound becomes 284 GeV.
[27] AALTONEN 08P search for vector leptoquarks using $\tau^+\tau^- b\overline{b}$ events in $p\overline{p}$ collisions at E_{cm} = 1.96 TeV. Assuming Yang-Mills (minimal) couplings, the mass limit is >317 GeV (251 GeV) at 95% CL for B(τb) = 1.
[28] Search for pair production of scalar leptoquark state decaying to τb in $p\overline{p}$ collisions at E_{cm}= 1.96 TeV. The limit above assumes B(τb) = 1.
[29] Search for scalar leptoquarks using $\nu\nu jj$ events in $\overline{p}p$ collisions at E_{cm} = 1.96 TeV. The limit above assumes B(νq) = 1.
[30] ABAZOV 07J search for pair productions of scalar leptoquark state decaying to νb in $p\overline{p}$ collisions at E_{cm} = 1.96 TeV. The limit above assumes B(νb) = 1.
[31] ABAZOV 06A search for scalar leptoquarks using $\mu\mu jj$ events in $p\overline{p}$ collisions at E_{cm} = 1.8 TeV and 1.96 TeV. The limit above assumes B(μq) = 1. For B(μq) = 0.5, the limit becomes 204 GeV.
[32] ABAZOV 06L search for scalar leptoquarks using $\nu\nu jj$ events in $p\overline{p}$ collisions at E_{cm} = 1.8 TeV and at 1.96 TeV. The limit above assumes B(νq) = 1.
[33] ABULENCIA 06T search for scalar leptoquarks using $\mu\mu jj$, $\mu\nu jj$, and $\nu\nu jj$ events in $p\overline{p}$ collisions at E_{cm} = 1.96 TeV. The quoted limit assumes B(μq) = 1. For B(μq) = 0.5 or 0.1, the bound becomes 208 GeV or 143 GeV, respectively. See their Fig. 4 for the exclusion limit as a function of B(μq).
[34] ABAZOV 05H search for scalar leptoquarks using $eejj$ and $e\nu jj$ events in $\overline{p}p$ collisions at E_{cm} = 1.8 TeV and 1.96 TeV. The limit above assumes B(eq) = 1. For B(eq) = 0.5 the bound becomes 234 GeV.
[35] ACOSTA 05P search for scalar leptoquarks using $eejj$, $e\nu jj$ events in $\overline{p}p$ collisions at E_{cm} = 1.96TeV. The limit above assumes B(eq) = 1. For B(eq) = 0.5 and 0.1, the bound becomes 205 GeV and 145 GeV, respectively.
[36] ABBIENDI 03R search for scalar/vector leptoquarks in e^+e^- collisions at $\sqrt{s}$ = 189–209 GeV. The quoted limits are for charge $-4/3$ isospin 0 scalar-leptoquark with B(ℓq) = 1. See their table 12 for other cases.
[37] ABAZOV 02 search for scalar leptoquarks using $\nu\nu jj$ events in $\overline{p}p$ collisions at E_{cm}=1.8 TeV. The bound holds for all leptoquark generations. Vector leptoquarks are likewise constrained to lie above 200 GeV.
[38] ABAZOV 01D search for scalar leptoquarks using $e\nu jj$, $eejj$, and $\nu\nu jj$ events in $p\overline{p}$ collisions at E_{cm}=1.8 TeV. The limit above assumes B(eq)=1. For B(eq)=0.5 and 0, the bound becomes 204 and 79 GeV, respectively. Bounds for vector leptoquarks are also given. Supersedes ABBOTT 98E.
[39] ABBIENDI 00M search for scalar/vector leptoquarks in e^+e^- collisions at $\sqrt{s}$=183 GeV. The quoted limits are for charge $-4/3$ isospin 0 scalar-leptoquarks with B(ℓq)=1. See their Table 8 and Figs. 6–9 for other cases.
[40] ABBOTT 00C search for scalar leptoquarks using $\mu\mu jj$, $\mu\nu jj$, and $\nu\nu jj$ events in $p\overline{p}$ collisions at E_{cm}=1.8 TeV. The limit above assumes B(μq)=1. For B(μq)=0.5 and 0, the bound becomes 180 and 79 GeV respectively. Bounds for vector leptoquarks are also given.
[41] AFFOLDER 00K search for scalar leptoquark using $\nu\nu cc$ events in $p\overline{p}$ collisions at E_{cm}=1.8 TeV. The quoted limit assumes B(νc)=1. Bounds for vector leptoquarks are also given.
[42] AFFOLDER 00K search for scalar leptoquark using $\nu\nu bb$ events in $p\overline{p}$ collisions at E_{cm}=1.8 TeV. The quoted limit assumes B(νb)=1. Bounds for vector leptoquarks are also given.
[43] ABBOTT 99J search for leptoquarks using $\mu\nu jj$ events in $p\overline{p}$ collisions at E_{cm}= 1.8TeV. The quoted limit is for a scalar leptoquark with B(μq) = B(νq) = 0.5. Limits on vector leptoquarks range from 240 to 290 GeV.
[44] ABBOTT 98E search for scalar leptoquarks using $e\nu jj$, $eejj$, and $\nu\nu jj$ events in $p\overline{p}$ collisions at E_{cm}=1.8 TeV. The limit above assumes B(eq)=1. For B(eq)=0.5 and 0, the bound becomes 204 and 79 GeV, respectively.
[45] ABBOTT 98J search for charge $-1/3$ third generation scalar and vector leptoquarks in $p\overline{p}$ collisions at E_{cm}= 1.8 TeV. The quoted limit is for scalar leptoquark with B(νb)=1.
[46] ABE 98S search for scalar leptoquarks using $\mu\mu jj$ events in $p\overline{p}$ collisions at E_{cm}= 1.8 TeV. The limit is for B(μq)= 1. For B(μq)=B(νq)=0.5, the limit is > 160 GeV.
[47] GROSS-PILCHER 98 is the combined limit of the CDF and DØ Collaborations as determined by a joint CDF/DØ working group and reported in this FNAL Technical Memo. Original data published in ABE 97X and ABBOTT 98E.
[48] ABE 97F search for third generation scalar and vector leptoquarks in $p\overline{p}$ collisions at E_{cm} = 1.8 TeV. The quoted limit is for scalar leptoquark with B(τb) = 1.
[49] ABE 97X search for scalar leptoquarks using $eejj$ events in $p\overline{p}$ collisions at E_{cm}=1.8 TeV. The limit is for B(eq)=1.
[50] Limit is for charge $-1/3$ isospin-0 leptoquark with B(ℓq) = 2/3.
[51] First and second generation leptoquarks are assumed to be degenerate. The limit is slightly lower for each generation.
[52] Limits are for charge $-1/3$, isospin-0 scalar leptoquarks decaying to $\ell^- q$ or νq with any branching ratio. See paper for limits for other charge-isospin assignments of leptoquarks.
[53] KIM 90 assume pair production of charge 2/3 scalar-leptoquark via photon exchange. The decay of the first (second) generation leptoquark is assumed to be any mixture of de^+ and $u\overline{\nu}$ ($s\mu^+$ and $c\overline{\nu}$). See paper for limits for specific branching ratios.
[54] BARTEL 87B limit is valid when a pair of charge 2/3 spinless leptoquarks X is produced with point coupling, and when they decay under the constraint B(X $\rightarrow$ $c\overline{\nu}_\mu$) + B(X $\rightarrow$ $s\mu^+$) = 1.
[55] BEHREND 86B assumed that a charge 2/3 spinless leptoquark, χ, decays either into $s\mu^+$ or $c\overline{\nu}$. B($\chi \rightarrow s\mu^+$) + B($\chi \rightarrow c\overline{\nu}$) = 1.

MASS LIMITS for Leptoquarks from Single Production

These limits depend on the q-ℓ-leptoquark coupling g_{LQ}. It is often assumed that $g^2_{LQ}/4\pi$=1/137. Limits shown are for a scalar, weak isoscalar, charge $-1/3$ leptoquark.

VALUE (GeV)	CL%	DOCUMENT ID		TECN	COMMENT
>1755	95	[1] KHACHATRY...16AG		CMS	First generation
> 660	95	[2] KHACHATRY...16AG		CMS	Second generation
> 304	95	[3] ABRAMOWICZ	12A	ZEUS	First generation
> 73	95	[4] ABREU	93J	DLPH	Second generation
• • • We do not use the following data for averages, fits, limits, etc. • • •					
		[5] DEY	16	ICCB	$\nu q \rightarrow$ LQ $\rightarrow \nu q$
		[6] AARON	11A	H1	Lepton-flavor violation
> 300	95	[7] AARON	11B	H1	First generation
		[8] ABAZOV	07E	D0	Second generation
> 295	95	[9] AKTAS	05B	H1	First generation
		[10] CHEKANOV	05A	ZEUS	Lepton-flavor violation
> 298	95	[11] CHEKANOV	03B	ZEUS	First generation
> 197	95	[12] ABBIENDI	02B	OPAL	First generation
		[13] CHEKANOV	02	ZEUS	Repl. by CHEKANOV 05A
> 290	95	[14] ADLOFF	01C	H1	First generation
> 204	95	[15] BREITWEG	01	ZEUS	First generation
		[16] BREITWEG	00E	ZEUS	First generation
> 161	95	[17] ABREU	99G	DLPH	First generation
> 200	95	[18] ADLOFF	99	H1	First generation
		[19] DERRICK	97	ZEUS	Lepton-flavor violation
> 168	95	[20] DERRICK	93	ZEUS	First generation

[1] KHACHATRYAN 16AG search for single production of charge $\pm 1/3$ scalar leptoquarks using eej events in pp collisions at $\sqrt{s}$ = 8 TeV. The limit above assumes B(eq) = 1 and the leptoquark coupling strength λ = 1.
[2] KHACHATRYAN 16AG search for single production of charge $\pm 1/3$ scalar leptoquarks using $\mu\mu j$ events in pp collisions at $\sqrt{s}$ = 8 TeV. The limit above assumes B(μq) = 1 and the leptoquark coupling strength λ = 1.
[3] ABRAMOWICZ 12A limit is for a scalar, weak isoscalar, charge $-1/3$ leptoquark coupled with e_R. See their Figs. 12–17 and Table 4 for states with different quantum numbers.
[4] Limit from single production in Z decay. The limit is for a leptoquark coupling of electromagnetic strength and assumes B(ℓq) = 2/3. The limit is 77 GeV if first and second leptoquarks are degenerate.
[5] DEY 16 use the 2010-2012 IceCube PeV energy data set to constrain the leptoquark production cross section through the $\nu q \rightarrow$ LQ $\rightarrow \nu q$ process. See their Figure 4 for the exclusion limit in the mass-coupling plane.
[6] AARON 11A search for various leptoquarks with lepton-flavor violating couplings. See their Figs. 2–3 and Tables 1–4 for detailed limits.
[7] The quoted limit is for a scalar, weak isoscalar, charge $-1/3$ leptoquark coupled with e_R. See their Figs. 3–5 for limits on states with different quantum numbers.
[8] ABAZOV 07E search for leptoquark single production through qg fusion process in $p\overline{p}$ collisions. See their Fig. 4 for exclusion plot in mass-coupling plane.
[9] AKTAS 05B limit is for a scalar, weak isoscalar, charge $-1/3$ leptoquark coupled with e_R. See their Fig. 3 for limits on states with different quantum numbers.
[10] CHEKANOV 05 search for various leptoquarks with lepton-flavor violating couplings. See their Figs.6–10 and Tables 1–8 for detailed limits.
[11] CHEKANOV 03B limit is for a scalar, weak isoscalar, charge $-1/3$ leptoquark coupled with e_R. See their Figs. 11–12 and Table 5 for limits on states with different quantum numbers.
[12] For limits on states with different quantum numbers and the limits in the mass-coupling plane, see their Fig. 4 and Fig. 5.
[13] CHEKANOV 02 search for various leptoquarks with lepton-flavor violating couplings. See their Figs. 6–7 and Tables 5–6 for detailed limits.
[14] For limits on states with different quantum numbers and the limits in the mass-coupling plane, see their Fig. 3.
[15] See their Fig. 14 for limits in the mass-coupling plane.
[16] BREITWEG 00E search for F=0 leptoquarks in e^+p collisions. For limits in mass-coupling plane, see their Fig. 11.
[17] ABREU 99G limit obtained from process $e\gamma \rightarrow LQ+q$. For limits on vector and scalar states with different quantum numbers and the limits in the coupling-mass plane, see their Fig. 4 and Table 2.
[18] For limits on states with different quantum numbers and the limits in the mass-coupling plane, see their Fig. 13 and Fig. 14. ADLOFF 99 also search for leptoquarks with lepton-flavor violating couplings. ADLOFF 99 supersedes AID 96B.
[19] DERRICK 97 search for various leptoquarks with lepton-flavor violating couplings. See their Figs. 5–8 and Table 1 for detailed limits.
[20] DERRICK 93 search for single leptoquark production in ep collisions with the decay eq and νq. The limit is for leptoquark coupling of electromagnetic strength and assumes B(eq) = B(νq) = 1/2. The limit for B(eq) = 1 is 176 GeV. For limits on states with different quantum numbers, see their Table 3.

Indirect Limits for Leptoquarks

VALUE (TeV)	CL%	DOCUMENT ID		TECN	COMMENT
• • • We do not use the following data for averages, fits, limits, etc. • • •					
		[1] BARRANCO	16	RVUE	D decays
		[2] KUMAR	16	RVUE	neutral K mixing, rare K decays
		[3] BESSAA	15	RVUE	$q\overline{q} \rightarrow e^+e^-$
> 14	95	[4] SAHOO	15A	RVUE	$B_{s,d} \rightarrow \mu^+\mu^-$
		[5] SAKAKI	13	RVUE	$B \rightarrow D^{(*)}\tau\overline{\nu}$, $B \rightarrow X_s\nu\overline{\nu}$
		[6] KOSNIK	12	RVUE	$b \rightarrow s\ell^+\ell^-$
> 2.5	95	[7] AARON	11C	H1	First generation
		[8] DORSNER	11	RVUE	scalar, weak singlet, charge 4/3
		[9] AKTAS	07A	H1	Lepton-flavor violation
> 0.49	95	[10] SCHAEL	07A	ALEP	$e^+e^- \rightarrow q\overline{q}$
		[11] SMIRNOV	07	RVUE	$K \rightarrow e\mu$, $B \rightarrow e\tau$
		[12] CHEKANOV	05A	ZEUS	Lepton-flavor violation
> 1.7	96	[13] ADLOFF	03	H1	First generation
> 46	90	[14] CHANG	03	BELL	Pati-Salam type
		[15] CHEKANOV	02	ZEUS	Repl. by CHEKANOV 05A
> 1.7	95	[16] CHEUNG	01B	RVUE	First generation
> 0.39	95	[17] ACCIARRI	00P	L3	$e^+e^- \rightarrow qq$

>	1.5	95	[18] ADLOFF	00	H1	First generation
>	0.2	95	[19] BARATE	00I	ALEP	Repl. by SCHAEL 07A
			[20] BARGER	00	RVUE	Cs
			[21] GABRIELLI	00	RVUE	Lepton flavor violation
>	0.74	95	[22] ZARNECKI	00	RVUE	S_1 leptoquark
			[23] ABBIENDI	99	OPAL	
>	19.3	95	[24] ABE	98V	CDF	$B_s \to e^\pm\mu^\mp$, Pati-Salam type
			[25] ACCIARRI	98J	L3	$e^+e^- \to q\overline{q}$
			[26] ACKERSTAFF	98V	OPAL	$e^+e^- \to q\overline{q}$, $e^+e^- \to b\overline{b}$
>	0.76	95	[27] DEANDREA	97	RVUE	$\tilde{R}_2$ leptoquark
			[28] DERRICK	97	ZEUS	Lepton-flavor violation
			[29] GROSSMAN	97	RVUE	$B \to \tau^+\tau^-$(X)
			[30] JADACH	97	RVUE	$e^+e^- \to q\overline{q}$
>1200			[31] KUZNETSOV	95B	RVUE	Pati-Salam type
			[32] MIZUKOSHI	95	RVUE	Third generation scalar leptoquark
>	0.3	95	[33] BHATTACH...	94	RVUE	Spin-0 leptoquark coupled to $\overline{e}_R\, t_L$
			[34] DAVIDSON	94	RVUE	
>	18		[35] KUZNETSOV	94	RVUE	Pati-Salam type
>	0.43	95	[36] LEURER	94	RVUE	First generation spin-1 leptoquark
>	0.44	95	[36] LEURER	94B	RVUE	First generation spin-0 leptoquark
			[37] MAHANTA	94	RVUE	P and T violation
>	1		[38] SHANKER	82	RVUE	Nonchiral spin-0 leptoquark
>	125		[38] SHANKER	82	RVUE	Nonchiral spin-1 leptoquark

[1] BARRANCO 16 give bounds on leptoquark induced four-fermion interactions from $D \to K\ell\nu$ and $D_s \to \ell\nu$.

[2] KUMAR 16 gives bound on SU(2) singlet scalar leptoquark with chrge $-1/3$ from $K^0 - \overline{K}^0$ mixing, $K \to \pi\nu\overline{\nu}$, $K_L^0 \to \mu^+\mu^-$, and $K_L^0 \to \mu^\pm e^\mp$ decays.

[3] BESSAA 15 obtain limit on leptoquark induced four-fermion interactions from the ATLAS and CMS limit on the $\overline{q}q\overline{e}e$ contact interactions.

[4] SAHOO 15A obtain limit on leptoquark induced four-fermion interactions from $B_{s,d} \to \mu^+\mu^-$ for $\lambda \simeq O(1)$.

[5] SAKAKI 13 explain the $B \to D^{(*)}\tau\overline{\nu}$ anomaly using Wilson coefficients of leptoquark-induced four-fermion operators.

[6] KOSNIK 12 obtains limits on leptoquark induced four-fermion interactions from $b \to s\ell^+\ell^-$ decays.

[7] AARON 11C limit is for weak isotriplet spin-0 leptoquark at strong coupling $\lambda = \sqrt{4\pi}$. For the limits of leptoquarks with different quantum numbers, see their Table 3. Limits are derived from bounds of eq contact intereractions.

[8] DORSNER 11 give bounds on scalar, weak singlet, charge 4/3 leptoquark from K, B, τ decays, meson mixings, LFV, $g-2$ and $Z \to b\overline{b}$.

[9] AKTAS 07A search for lepton-flavor violation in ep collision. See their Tables 4–7 for limits on lepton-flavor violating four-fermion interactions induced by various leptoquarks.

[10] SCHAEL 07A limit is for the weak-isoscalar spin-0 left-handed leptoquark with the coupling of electromagnetic strength. For the limits of leptoquarks with different quantum numbers, see their Table 35.

[11] SMIRNOV 07 obtains mass limits for the vector and scalar chiral leptoquark states from $K \to e\mu$, $B \to e\tau$ decays.

[12] CHEKANOV 05 search for various leptoquarks with lepton-flavor violating couplings. See their Figs.6–10 and Tables 1–8 for detailed limits.

[13] ADLOFF 03 limit is for the weak isotriplet spin-0 leptoquark at strong coupling $\lambda=\sqrt{4\pi}$. For the limits of leptoquarks with different quantum numbers, see their Table 3. Limits are derived from bounds on $e^\pm q$ contact interactions.

[14] The bound is derived from $B(B^0 \to e^\pm\mu^\mp) < 1.7 \times 10^{-7}$.

[15] CHEKANOV 02 search for lepton-flavor violation in ep collisions. See their Tables 1–4 for limits on lepton-flavor violating and four-fermion interactions induced by various leptoquarks.

[16] CHEUNG 01B quoted limit is for a scalar, weak isoscalar, charge $-1/3$ leptoquark with a coupling of electromagnetic strength. The limit is derived from bounds on contact interactions in a global electroweak analysis. For the limits of leptoquarks with different quantum numbers, see Table 5.

[17] ACCIARRI 00P limit is for the weak isoscalar spin-0 leptoquark with the coupling of electromagnetic strength. For the limits of leptoquarks with different quantum numbers, see their Table 4.

[18] ADLOFF 00 limit is for the weak isotriplet spin-0 leptoquark at strong coupling, $\lambda=\sqrt{4\pi}$. For the limits of leptoquarks with different quantum numbers, see their Table 2. ADLOFF 00 limits are from the Q^2 spectrum measurement of $e^+p \to e^+$X.

[19] BARATE 00I search for deviations in cross section and jet-charge asymmetry in $e^+e^- \to \overline{q}q$ due to t-channel exchange of a leptoquark at $\sqrt{s}$=130 to 183 GeV. Limits for other scalar and vector leptoquarks are also given in their Table 22.

[20] BARGER 00 explain the deviation of atomic parity violation in cesium atoms from prediction is explained by scalar leptoquark exchange.

[21] GABRIELLI 00 calculate various process with lepton flavor violation in leptoquark models.

[22] ZARNECKI 00 limit is derived from data of HERA, LEP, and Tevatron and from various low-energy data including atomic parity violation. Leptoquark coupling with electromagnetic strength is assumed.

[23] ABBIENDI 99 limits are from $e^+e^- \to q\overline{q}$ cross section at 130–136, 161–172, 183 GeV. See their Fig. 8 and Fig. 9 for limits in mass-coupling plane.

[24] ABE 98V quoted limit is from $B(B_s \to e^\pm\mu^\mp) < 8.2 \times 10^{-6}$. ABE 98V also obtain a similar limit on $M_{LQ} > 20.4$ TeV from $B(B_d \to e^\pm\mu^\mp) < 4.5 \times 10^{-6}$. Both bounds assume the non-canonical association of the b quark with electrons or muons under SU(4).

[25] ACCIARRI 98J limit is from $e^+e^- \to q\overline{q}$ cross section at $\sqrt{s}$= 130–172 GeV which can be affected by the t- and u-channel exchanges of leptoquarks. See their Fig. 4 and Fig. 5 for limits in the mass-coupling plane.

[26] ACKERSTAFF 98V limits are from $e^+e^- \to q\overline{q}$ and $e^+e^- \to b\overline{b}$ cross sections at $\sqrt{s}$ = 130–172 GeV, which can be affected by the t- and u-channel exchanges of leptoquarks. See their Fig. 21 and Fig. 22 for limits of leptoquarks in mass-coupling plane.

[27] DEANDREA 97 limit is for $\tilde{R}_2$ leptoquark obtained from atomic parity violation (APV). The coupling of leptoquark is assumed to be electromagnetic strength. See Table 2 for limits of the four-fermion interactions induced by various scalar leptoquark exchange. DEANDREA 97 combines APV limit and limits from Tevatron and HERA. See Fig. 1–4 for combined limits of leptoquark in mass-coupling plane.

[28] DERRICK 97 search for lepton-flavor violation in ep collision. See their Tables 2–5 for limits on lepton-flavor violating four-fermion interactions induced by various leptoquarks.

[29] GROSSMAN 97 estimate the upper bounds on the branching fraction $B \to \tau^+\tau^-$(X) from the absence of the B decay with large missing energy. These bounds can be used to constrain leptoquark induced four-fermion interactions.

[30] JADACH 97 limit is from $e^+e^- \to q\overline{q}$ cross section at $\sqrt{s}$=172.3 GeV which can be affected by the t- and u-channel exchanges of leptoquarks. See their Fig. 1 for limits on vector leptoquarks in mass-coupling plane.

[31] KUZNETSOV 95B use π, K, B, τ decays and μe conversion and give a list of bounds on the leptoquark mass and the fermion mixing matrix in the Pati-Salam model. The quoted limit is from $K_L \to \mu e$ decay assuming zero mixing.

[32] MIZUKOSHI 95 calculate the one-loop radiative correction to the Z-physics parameters in various scalar leptoquark models. See their Fig. 4 for the exclusion plot of third generation leptoquark models in mass-coupling plane.

[33] BHATTACHARYYA 94 limit is from one-loop radiative correction to the leptonic decay width of the Z. m_H=250 GeV, $\alpha_s(m_Z)$=0.12, m_t=180 GeV, and the electroweak strength of leptoquark coupling are assumed. For leptoquark coupled to $\overline{e}_L\, t_R$, $\overline{\mu}t$, and $\overline{\tau}t$, see Fig. 2 in BHATTACHARYYA 94B erratum and Fig. 3.

[34] DAVIDSON 94 gives an extensive list of the bounds on leptoquark-induced four-fermion interactions from π, K, D, B, μ, τ decays and meson mixings, *etc.* See Table 15 of DAVIDSON 94 for detail.

[35] KUZNETSOV 94 gives mixing independent bound of the Pati-Salam leptoquark from the cosmological limit on $\pi^0 \to \overline{\nu}\nu$.

[36] LEURER 94, LEURER 94B limits are obtained from atomic parity violation and apply to any chiral leptoquark which couples to the first generation with electromagnetic strength. For a nonchiral leptoquark, universality in $\pi_{\ell 2}$ decay provides a much more stringent bound.

[37] MAHANTA 94 gives bounds of P- and T-violating scalar-leptoquark couplings from atomic and molecular experiments.

[38] From $(\pi \to e\nu)/(\pi \to \mu\nu)$ ratio. SHANKER 82 assumes the leptoquark induced four-fermion coupling $4g^2/M^2\ (\overline{\nu}_{eL}\ u_R)\ (\overline{d}_L\, e_R)$with g=0.004 for spin-0 leptoquark and $g^2/M^2\ (\overline{\nu}_{eL}\ \gamma_\mu u_L)\ (\overline{d}_R\ \gamma^\mu e_R)$ with $g\simeq$ 0.6 for spin-1 leptoquark.

MASS LIMITS for Diquarks

VALUE (GeV)	CL%	DOCUMENT ID		TECN	COMMENT
>6000 (CL = 95%) OUR LIMIT					
none 600–6900	95	[1] KHACHATRY...17W		CMS	E_6 diquark
none 1500–6000	95	[2] KHACHATRY...16K		CMS	E_6 diquark
none 500–1600	95	[3] KHACHATRY...16L		CMS	E_6 diquark
none 1200–4700	95	[4] KHACHATRY...15V		CMS	E_6 diquark
• • • We do not use the following data for averages, fits, limits, etc. • • •					
>3750	95	[5] CHATRCHYAN 13A		CMS	E_6 diquark
none 1000–4280	95	[6] CHATRCHYAN 13AS		CMS	Superseded by KHACHATRYAN 15V
>3520	95	[7] CHATRCHYAN 11Y		CMS	Superseded by CHATRCHYAN 13A
none 970–1080, 1450–1600	95	[8] KHACHATRY...10		CMS	Superseded by CHATRCHYAN 13A
none 290–630	95	[9] AALTONEN	09AC	CDF	E_6 diquark
none 290–420	95	[10] ABE	97G	CDF	E_6 diquark
none 15–31.7	95	[11] ABREU	94O	DLPH	SUSY E_6 diquark

[1] KHACHATRYAN 17W search for resonances decaying to dijets in pp collisions at $\sqrt{s}$ = 13 TeV.

[2] KHACHATRYAN 16K search for resonances decaying to dijets in pp collisions at $\sqrt{s}$ = 13 TeV.

[3] KHACHATRYAN 16L search for resonances decaying to dijets in pp collisions at $\sqrt{s}$ = 8 TeV with the data scouting technique, increasing the sensitivity to the low mass resonances.

[4] KHACHATRYAN 15V search for resonances decaying to dijets in pp collisions at $\sqrt{s}$ = 8 TeV.

[5] CHATRCHYAN 13A search for new resonance decaying to dijets in pp collisions at $\sqrt{s}$ = 7 TeV.

[6] CHATRCHYAN 13AS search for new resonance decaying to dijets in pp collisions at $\sqrt{s}$ = 8 TeV.

[7] CHATRCHYAN 11Y search for new resonance decaying to dijets in pp collisions at $\sqrt{s}$ = 7 TeV.

[8] KHACHATRYAN 10 search for new resonance decaying to dijets in pp collisions at $\sqrt{s}$ = 7 TeV.

[9] AALTONEN 09AC search for new narrow resonance decaying to dijets.

[10] ABE 97G search for new particle decaying to dijets.

[11] ABREU 94O limit is from $e^+e^- \to \overline{cs}cs$. Range extends up to 43 GeV if diquarks are degenerate in mass.

MASS LIMITS for g_A (axigluon) and Other Color-Octet Gauge Bosons

Axigluons are massive color-octet gauge bosons in chiral color models and have axial-vector coupling to quarks with the same coupling strength as gluons.

VALUE (GeV)	CL%	DOCUMENT ID		TECN	COMMENT
>5500 (CL = 95%) OUR LIMIT					
none 600–5500	95	[1] KHACHATRY...17W		CMS	$pp \to g_A X$, $g_A \to 2j$
none 1500–5100	95	[2] KHACHATRY...16K		CMS	$pp \to g_A X$, $g_A \to 2j$
none 500–1600	95	[3] KHACHATRY...16L		CMS	$pp \to g_A X$, $g_A \to 2j$
none 1300–3600	95	[4] KHACHATRY...15V		CMS	$pp \to g_A X$, $g_A \to 2j$
• • • We do not use the following data for averages, fits, limits, etc. • • •					
		[5] KHACHATRY...17Y		CMS	$pp \to g_A g_A \to 8j$
		[6] AAD	16W	ATLS	$pp \to g_A X$, $g_A \to b\overline{b}\,b\overline{b}$

Gauge & Higgs Boson Particle Listings

New Heavy Bosons

>2800	95	[7] KHACHATRY...16E	CMS	$pp \to g_{KK}X$, $g_{KK} \to t\bar{t}$	
		[8] KHACHATRY...15AV	CMS	$pp \to \Theta^0\Theta^0 \to b\bar{b}Zg$	
		[9] AALTONEN 13R	CDF	$p\bar{p} \to g_A X$, $g_A \to \sigma\sigma$, $\sigma \to 2j$	
>3360	95	[10] CHATRCHYAN 13A	CMS	$pp \to g_A X$, $g_A \to 2j$	
none 1000–3270	95	[11] CHATRCHYAN 13AS	CMS	Superseded by KHACHATRYAN 15V	
none 250–740	95	[12] CHATRCHYAN 13AU	CMS	$pp \to 2g_A X$, $g_A \to 2j$	
> 775	95	[13] ABAZOV 12R	D0	$p\bar{p} \to g_A X$, $g_A \to t\bar{t}$	
>2470	95	[14] CHATRCHYAN 11Y	CMS	Superseded by CHATRCHYAN 13A	
		[15] AALTONEN 10L	CDF	$p\bar{p} \to g_A X$, $g_A \to t\bar{t}$	
none 1470–1520	95	[16] KHACHATRY...10	CMS	Superseded by CHATRCHYAN 13A	
none 260–1250	95	[17] AALTONEN 09AC	CDF	$p\bar{p} \to g_A X$, $g_A \to 2j$	
> 910	95	[18] CHOUDHURY 07	RVUE	$p\bar{p} \to t\bar{t}X$	
> 365	95	[19] DONCHESKI 98	RVUE	$\Gamma(Z \to$ hadron)	
none 200–980	95	[20] ABE 97G	CDF	$p\bar{p} \to g_A X$, $g_A \to 2j$	
none 200–870	95	[21] ABE 95N	CDF	$p\bar{p} \to g_A X$, $g_A \to q\bar{q}$	
none 240–640	95	[22] ABE 93G	CDF	$p\bar{p} \to g_A X$, $g_A \to 2j$	
> 50	95	[23] CUYPERS 91	RVUE	$\sigma(e^+e^- \to$ hadrons)	
none 120–210	95	[24] ABE 90H	CDF	$p\bar{p} \to g_A X$, $g_A \to 2j$	
> 29		[25] ROBINETT 89	THEO	Partial-wave unitarity	
none 150–310	95	[26] ALBAJAR 88B	UA1	$p\bar{p} \to g_A X$, $g_A \to 2j$	
> 20		BERGSTROM 88	RVUE	$p\bar{p} \to \Upsilon X$ via $g_A g$	
> 9		[27] CUYPERS 88	RVUE	Υ decay	
> 25		[28] DONCHESKI 88B	RVUE	Υ decay	

[1] KHACHATRYAN 17W search for resonances decaying to dijets in pp collisions at $\sqrt{s}$ = 13 TeV.

[2] KHACHATRYAN 16K search for resonances decaying to dijets in pp collisions at $\sqrt{s}$ = 13 TeV.

[3] KHACHATRYAN 16L search for resonances decaying to dijets in pp collisions at $\sqrt{s}$ = 8 TeV with the data scouting technique, increasing the sensitivity to the low mass resonances.

[4] KHACHATRYAN 15V search for resonances decaying to dijets in pp collisions at $\sqrt{s}$ = 8 TeV.

[5] KHACHATRYAN 17Y search for pair production of color-octet gauge boson g_A each decaying to $4j$ in pp collisions at $\sqrt{s}$ = 8 TeV.

[6] AAD 16W search for a new resonance decaying to a pair of b and B_H in pp collisions at $\sqrt{s}$ = 8 TeV. The vector-like quark B_H is assumed to decay to bH. See their Fig. 3 and Fig. 4 for limits on $\sigma \cdot B$.

[7] KHACHATRYAN 16E search for KK gluon decaying to $t\bar{t}$ in pp collisions at $\sqrt{s}$ = 8 TeV.

[8] KHACHATRYAN 15AV search for pair productions of neutral color-octet weak-triplet scalar particles (Θ^0), decaying to $b\bar{b}$, Zg or γg, in pp collisions at $\sqrt{s}$ = 8 TeV. The Θ^0 particle is often predicted in coloron (G', color-octet gauge boson) models and appear in the pp collisions through $G' \to \Theta^0\Theta^0$ decays. Assuming B($\Theta^0 \to b\bar{b}$) = 0.5, they give limits $m_{\Theta^0} > 623$ GeV (426 GeV) for $m_{G'} = 2.3\, m_{\Theta^0}$ ($m_{G'} = 5\, m_{\Theta^0}$).

[9] AALTONEN 13R search for new resonance decaying to $\sigma\sigma$, with hypothetical strongly interacting σ particle subsequently decaying to 2 jets, in $p\bar{p}$ collisions at $\sqrt{s}$ = 1.96 TeV, using data corresponding to an integrated luminosity of 6.6 fb^{-1}. For 50 GeV $< m_\sigma <$ $m_{g_A}/2$, axigluons in mass range 150–400 GeV are excluded.

[10] CHATRCHYAN 13A search for new resonance decaying to dijets in pp collisions at $\sqrt{s}$ = 7 TeV.

[11] CHATRCHYAN 13AS search for new resonance decaying to dijets in pp collisions at $\sqrt{s}$ = 8 TeV.

[12] CHATRCHYAN 13AU search for the pair produced color-octet vector bosons decaying to $q\bar{q}$ pairs in pp collisions. The quoted limit is for B($g_A \to q\bar{q}$) = 1.

[13] ABAZOV 12R search for massive color octet vector particle decaying to $t\bar{t}$. The quoted limit assumes g_A couplings with light quarks are suppressed by 0.2.

[14] CHATRCHYAN 11Y search for new resonance decaying to dijets in pp collisions at $\sqrt{s}$ = 7 TeV.

[15] AALTONEN 10L search for massive color octet non-chiral vector particle decaying into $t\bar{t}$ pair with mass in the range 400 GeV < M < 800 GeV. See their Fig. 6 for limit in the mass-coupling plane.

[16] KHACHATRYAN 10 search for new resonance decaying to dijets in pp collisions at $\sqrt{s}$ = 7 TeV.

[17] AALTONEN 09AC search for new narrow resonance decaying to dijets.

[18] CHOUDHURY 07 limit is from the $t\bar{t}$ production cross section measured at CDF.

[19] DONCHESKI 98 compare α_s derived from low-energy data and that from $\Gamma(Z \to$ hadrons$)/\Gamma(Z \to$ leptons).

[20] ABE 97G search for new particle decaying to dijets.

[21] ABE 95N assume axigluons decaying to quarks in the Standard Model only.

[22] ABE 93G assume $\Gamma(g_A) = N\alpha_s m_{g_A}/6$ with N = 10.

[23] CUYPERS 91 compare α_s measured in Υ decay and that from R at PEP/PETRA energies.

[24] ABE 90H assumes $\Gamma(g_A) = N\alpha_s m_{g_A}/6$ with $N = 5$ ($\Gamma(g_A) = 0.09 m_{g_A}$). For N = 10, the excluded region is reduced to 120–150 GeV.

[25] ROBINETT 89 result demands partial-wave unitarity of $J = 0$ $t\bar{t} \to t\bar{t}$ scattering amplitude and derives a limit $m_{g_A} > 0.5\, m_t$. Assumes $m_t > 56$ GeV.

[26] ALBAJAR 88B result is from the nonobservation of a peak in two-jet invariant mass distribution. $\Gamma(g_A) < 0.4\, m_{g_A}$ assumed. See also BAGGER 88.

[27] CUYPERS 88 requires $\Gamma(\Upsilon \to g g g_A) < \Gamma(\Upsilon \to ggg)$. A similar result is obtained by DONCHESKI 88.

[28] DONCHESKI 88B requires $\Gamma(\Upsilon \to g q\bar{q})/\Gamma(\Upsilon \to ggg) < 0.25$, where the former decay proceeds via axigluon exchange. A more conservative estimate of < 0.5 leads to $m_{g_A} > 21$ GeV.

MASS LIMITS for Color-Octet Scalar Bosons

VALUE (GeV)	CL%	DOCUMENT ID		TECN	COMMENT
• • • We do not use the following data for averages, fits, limits, etc. • • •					
		[1] KHACHATRY...15AV	CMS		$pp \to \Theta^0\Theta^0 \to b\bar{b}Zg$
none 150–287	95	[2] AAD 13K	ATLS		$pp \to S_8 S_8 X$, $S_8 \to 2$ jets

[1] KHACHATRYAN 15AV search for pair productions of neutral color-octet weak-triplet scalar particles (Θ^0), decaying to $b\bar{b}$, Zg or γg, in pp collisions at $\sqrt{s}$ = 8 TeV. The Θ^0 particle is often predicted in coloron (G', color-octet gauge boson) models and appear in the pp collisions through $G' \to \Theta^0\Theta^0$ decays. Assuming B($\Theta^0 \to b\bar{b}$) = 0.5, they give limits $m_{\Theta^0} > 623$ GeV (426 GeV) for $m_{G'} = 2.3\, m_{\Theta^0}$ ($m_{G'} = 5\, m_{\Theta^0}$).

[2] AAD 13K search for pair production of color-octet scalar particles in pp collisions at $\sqrt{s}$ = 7 TeV. Cross section limits are interpreted as mass limits on scalar partners of a Dirac gluino.

X^0 (Heavy Boson) Searches in Z Decays

Searches for radiative transition of Z to a lighter spin-0 state X^0 decaying to hadrons, a lepton pair, a photon pair, or invisible particles as shown in the comments. The limits are for the product of branching ratios.

VALUE	CL%	DOCUMENT ID		TECN	COMMENT
• • • We do not use the following data for averages, fits, limits, etc. • • •					
		[1] BARATE 98U	ALEP		$X^0 \to \ell\bar{\ell}$, $q\bar{q}$, gg, $\gamma\gamma$, $\nu\bar{\nu}$
		[2] ACCIARRI 97Q	L3		$X^0 \to$ invisible particle(s)
		[3] ACTON 93E	OPAL		$X^0 \to \gamma\gamma$
		[4] ABREU 92D	DLPH		$X^0 \to$ hadrons
		[5] ADRIANI 92F	L3		$X^0 \to$ hadrons
		[6] ACTON 91	OPAL		$X^0 \to$ anything
$<1.1 \times 10^{-4}$	95	[7] ACTON 91B	OPAL		$X^0 \to e^+e^-$
$<9 \times 10^{-5}$	95	[7] ACTON 91B	OPAL		$X^0 \to \mu^+\mu^-$
$<1.1 \times 10^{-4}$	95	[7] ACTON 91B	OPAL		$X^0 \to \tau^+\tau^-$
$<2.8 \times 10^{-4}$	95	[8] ADEVA 91D	L3		$X^0 \to e^+e^-$
$<2.3 \times 10^{-4}$	95	[8] ADEVA 91D	L3		$X^0 \to \mu^+\mu^-$
$<4.7 \times 10^{-4}$	95	[9] ADEVA 91D	L3		$X^0 \to$ hadrons
$<8 \times 10^{-4}$	95	[10] AKRAWY 90J	OPAL		$X^0 \to$ hadrons

[1] BARATE 98U obtain limits on B($Z \to \gamma X^0$)B($X^0 \to \ell\bar{\ell}$, $q\bar{q}$, gg, $\gamma\gamma$, $\nu\bar{\nu}$). See their Fig. 17.

[2] See Fig. 4 of ACCIARRI 97Q for the upper limit on B($Z \to \gamma X^0$; $E_\gamma > E_{\min}$) as a function of $E_{\min}$.

[3] ACTON 93E give $\sigma(e^+e^- \to X^0\gamma)\cdot$B($X^0 \to \gamma\gamma$)< 0.4 pb (95%CL) for m_{X^0}=60 ± 2.5 GeV. If the process occurs via s-channel γ exchange, the limit translates to $\Gamma(X^0)\cdot$B($X^0 \to \gamma\gamma$)^2 <20 MeV for $m_{X^0} = 60 \pm 1$ GeV.

[4] ABREU 92D give $\sigma_Z \cdot$ B($Z \to \gamma X^0$) · B($X^0 \to$ hadrons) <(3–10) pb for m_{X^0} = 10–78 GeV. A very similar limit is obtained for spin-1 X^0.

[5] ADRIANI 92F search for isolated γ in hadronic Z decays. The limit $\sigma_Z \cdot$ B($Z \to \gamma X^0$) · B($X^0 \to$ hadrons) <(2–10) pb (95%CL) is given for m_{X^0} = 25–85 GeV.

[6] ACTON 91 searches for $Z \to Z^* X^0$, $Z^* \to e^+e^-$, $\mu^+\mu^-$, or $\nu\bar{\nu}$. Excludes any new scalar X^0 with $m_{X^0} < 9.5$ GeV/c if it has the same coupling to ZZ^* as the MSM Higgs boson.

[7] ACTON 91B limits are for m_{X^0} = 60–85 GeV.

[8] ADEVA 91D limits are for m_{X^0} = 30–89 GeV.

[9] ADEVA 91D limits are for m_{X^0} = 30–86 GeV.

[10] AKRAWY 90J give $\Gamma(Z \to \gamma X^0)\cdot$B($X^0 \to$ hadrons) < 1.9 MeV (95%CL) for m_{X^0} = 32–80 GeV. We divide by $\Gamma(Z)$ = 2.5 GeV to get product of branching ratios. For nonresonant transitions, the limit is B($Z \to \gamma q\bar{q}$) < 8.2 MeV assuming three-body phase space distribution.

MASS LIMITS for a Heavy Neutral Boson Coupling to e^+e^-

VALUE (GeV)	CL%	DOCUMENT ID		TECN	COMMENT
• • • We do not use the following data for averages, fits, limits, etc. • • •					
none 55–61		[1] ODAKA 89	VNS		$\Gamma(X^0 \to e^+e^-)\cdot$ B($X^0 \to$ had.) $\gtrsim$ 0.2 MeV
>45	95	[2] DERRICK 86	HRS		$\Gamma(X^0 \to e^+e^-)$=6 MeV
>46.6	95	[3] ADEVA 85	MRKJ		$\Gamma(X^0 \to e^+e^-)$=10 keV
>48	95	[3] ADEVA 85	MRKJ		$\Gamma(X^0 \to e^+e^-)$=4 MeV
		[4] BERGER 85B	PLUT		
none 39.8–45.5		[5] ADEVA 84	MRKJ		$\Gamma(X^0 \to e^+e^-)$=10 keV
>47.8	95	[5] ADEVA 84	MRKJ		$\Gamma(X^0 \to e^+e^-)$=4 MeV
none 39.8–45.2		[5] BEHREND 84C	CELL		
>47	95	[5] BEHREND 84C	CELL		$\Gamma(X^0 \to e^+e^-)$=4 MeV

[1] ODAKA 89 looked for a narrow or wide scalar resonance in $e^+e^- \to$ hadrons at $E_{\rm cm}$ = 55.0–60.8 GeV.

[2] DERRICK 86 found no deviation from the Standard Model Bhabha scattering at $E_{\rm cm}$= 29 GeV and set limits on the possible scalar boson e^+e^- coupling. See their figure 4 for excluded region in the $\Gamma(X^0 \to e^+e^-)$-m_{X^0} plane. Electronic chiral invariance requires a parity doublet of X^0, in which case the limit applies for $\Gamma(X^0 \to e^+e^-)$ = 3 MeV.

[3] ADEVA 85 first limit is from 2γ, $\mu^+\mu^-$, hadrons assuming X^0 is a scalar. Second limit is from e^+e^- channel. $E_{\rm cm}$ = 40–47 GeV. Supersedes ADEVA 84.

[4] BERGER 85B looked for effect of spin-0 boson exchange in $e^+e^- \to e^+e^-$ and $\mu^+\mu^-$ at $E_{\rm cm}$ = 34.7 GeV. See Fig. 5 for excluded region in the $m_{X^0} - \Gamma(X^0)$ plane.

[5] ADEVA 84 and BEHREND 84C have E_{cm} = 39.8–45.5 GeV. MARK-J searched X^0 in $e^+e^- \to$ hadrons, 2γ, $\mu^+\mu^-$, e^+e^- and CELLO in the same channels plus τ pair. No narrow or broad X^0 is found in the energy range. They also searched for the effect of X^0 with $m_X > E_{cm}$. The second limits are from Bhabha data and for spin-0 singlet. The same limits apply for $\Gamma(X^0 \to e^+e^-) = 2$ MeV if X^0 is a spin-0 doublet. The second limit of BEHREND 84C was read off from their figure 2. The original papers also list limits in other channels.

Search for X^0 Resonance in e^+e^- Collisions

The limit is for $\Gamma(X^0 \to e^+e^-) \cdot B(X^0 \to f)$, where f is the specified final state. Spin 0 is assumed for X^0.

VALUE (keV)	CL%	DOCUMENT ID		TECN	COMMENT
• • • We do not use the following data for averages, fits, limits, etc. • • •					
$<10^3$	95	[1] ABE	93C	VNS	$\Gamma(ee)$
<(0.4–10)	95	[2] ABE	93C	VNS	$f = \gamma\gamma$
<(0.3–5)	95	[3,4] ABE	93D	TOPZ	$f = \gamma\gamma$
<(2–12)	95	[3,4] ABE	93D	TOPZ	$f =$ hadrons
<(4–200)	95	[4,5] ABE	93D	TOPZ	$f = ee$
<(0.1–6)	95	[4,5] ABE	93D	TOPZ	$f = \mu\mu$
<(0.5–8)	90	[6] STERNER	93	AMY	$f = \gamma\gamma$

[1] Limit is for $\Gamma(X^0 \to e^+e^-)$ m_{X^0} = 56–63.5 GeV for $\Gamma(X^0)$ = 0.5 GeV.

[2] Limit is for m_{X^0} = 56–61.5 GeV and is valid for $\Gamma(X^0) \ll 100$ MeV. See their Fig. 5 for limits for Γ = 1,2 GeV.

[3] Limit is for m_{X^0} = 57.2–60 GeV.

[4] Limit is valid for $\Gamma(X^0) \ll 100$ MeV. See paper for limits for Γ = 1 GeV and those for J = 2 resonances.

[5] Limit is for m_{X^0} = 56.6–60 GeV.

[6] STERNER 93 limit is for m_{X^0} = 57–59.6 GeV and is valid for $\Gamma(X^0)$<100 MeV. See their Fig. 2 for limits for Γ = 1,3 GeV.

Search for X^0 Resonance in ep Collisions

VALUE	DOCUMENT ID		TECN	COMMENT
• • • We do not use the following data for averages, fits, limits, etc. • • •				
	[1] CHEKANOV	02B	ZEUS	$X \to jj$

[1] CHEKANOV 02B search for photoproduction of X decaying into dijets in ep collisions. See their Fig. 5 for the limit on the photoproduction cross section.

Search for X^0 Resonance in $e^+e^- \to X^0\gamma$

VALUE (GeV)	DOCUMENT ID		TECN	COMMENT
• • • We do not use the following data for averages, fits, limits, etc. • • •				
	[1] ABBIENDI	03D	OPAL	$X^0 \to \gamma\gamma$
	[2] ABREU	00Z	DLPH	X^0 decaying invisibly
	[3] ADAM	96C	DLPH	X^0 decaying invisibly

[1] ABBIENDI 03D measure the $e^+e^- \to \gamma\gamma\gamma$ cross section at $\sqrt{s}$=181–209 GeV. The upper bound on the production cross section, $\sigma(e^+e^- \to X^0\gamma)$ times the branching ratio for $X^0 \to \gamma\gamma$, is less than 0.03 pb at 95%CL for X^0 masses between 20 and 180 GeV. See their Fig. 9b for the limits in the mass-cross section plane.

[2] ABREU 00Z is from the single photon cross section at $\sqrt{s}$=183, 189 GeV. The production cross section upper limit is less than 0.3 pb for X^0 mass between 40 and 160 GeV. See their Fig. 4 for the limit in mass-cross section plane.

[3] ADAM 96C is from the single photon production cross at $\sqrt{s}$=130, 136 GeV. The upper bound is less than 3 pb for X^0 masses between 60 and 130 GeV. See their Fig. 5 for the exact bound on the cross section $\sigma(e^+e^- \to \gamma X^0)$.

Search for X^0 Resonance in $Z \to f\overline{f}X^0$

The limit is for $B(Z \to f\overline{f}X^0) \cdot B(X^0 \to F)$ where f is a fermion and F is the specified final state. Spin 0 is assumed for X^0.

VALUE	CL%	DOCUMENT ID		TECN	COMMENT
• • • We do not use the following data for averages, fits, limits, etc. • • •					
		[1] ABREU	96T	DLPH	f=e,μ,τ; F=$\gamma\gamma$
$<3.7 \times 10^{-6}$	95	[2] ABREU	96T	DLPH	f=ν; F=$\gamma\gamma$
		[3] ABREU	96T	DLPH	f=q; F=$\gamma\gamma$
$<6.8 \times 10^{-6}$	95	[2] ACTON	93E	OPAL	f=e,μ,τ; F=$\gamma\gamma$
$<5.5 \times 10^{-6}$	95	[2] ACTON	93E	OPAL	f=q; F=$\gamma\gamma$
$<3.1 \times 10^{-6}$	95	[2] ACTON	93E	OPAL	f=ν; F=$\gamma\gamma$
$<6.5 \times 10^{-6}$	95	[2] ACTON	93E	OPAL	f=e,μ; F=$\ell\overline{\ell}$, $q\overline{q}$, $\nu\overline{\nu}$
$<7.1 \times 10^{-6}$	95	[2] BUSKULIC	93F	ALEP	f=e,μ; F=$\ell\overline{\ell}$, $q\overline{q}$, $\nu\overline{\nu}$
		[4] ADRIANI	92F	L3	f=q; F=$\gamma\gamma$

[1] ABREU 96T obtain limit as a function of m_{X^0}. See their Fig. 6.

[2] Limit is for m_{X^0} around 60 GeV.

[3] ABREU 96T obtain limit as a function of m_{X^0}. See their Fig. 15.

[4] ADRIANI 92F give $\sigma_Z \cdot B(Z \to q\overline{q}X^0) \cdot B(X^0 \to \gamma\gamma)$<(0.75–1.5) pb (95%CL) for m_{X^0} = 10–70 GeV. The limit is 1 pb at 60 GeV.

Search for X^0 Resonance in WX^0 final state

VALUE (MeV)	DOCUMENT ID		TECN	COMMENT
• • • We do not use the following data for averages, fits, limits, etc. • • •				
	[1] AALTONEN	13AA	CDF	$X^0 \to jj$
	[2] CHATRCHYAN	12BR	CMS	$X^0 \to jj$
	[3] ABAZOV	11I	D0	$X^0 \to jj$
	[4] ABE	97W	CDF	$X^0 \to b\overline{b}$

[1] AALTONEN 13AA search for X^0 production associated with W (or Z) in $p\overline{p}$ collisions at E_{cm} = 1.96 TeV. The upper limit on the cross section $\sigma(p\overline{p} \to WX^0)$ is 2.2 pb for M_{X^0} = 145 GeV.

[2] CHATRCHYAN 12BR search for X^0 production associated with W in pp collisions at E_{cm} = 7 TeV. The upper limit on the cross section is 5.0 pb at 95% CL for m_{X^0} = 150 GeV.

[3] ABAZOV 11I search for X^0 production associated with W in $p\overline{p}$ collisions at E_{cm} = 1.96 TeV. The 95% CL upper limit on the cross section ranges from 2.57 to 1.28 pb for X^0 mass between 110 and 170 GeV.

[4] ABE 97W search for X^0 production associated with W in $p\overline{p}$ collisions at E_{cm}=1.8 TeV. The 95%CL upper limit on the production cross section times the branching ratio for $X^0 \to b\overline{b}$ ranges from 14 to 19 pb for X^0 mass between 70 and 120 GeV. See their Fig. 3 for upper limits of the production cross section as a function of m_{X^0}.

Search for X^0 Resonance in Quarkonium Decays

Limits are for branching ratios to modes shown. Spin 1 is assumed for X^0.

VALUE	CL%	DOCUMENT ID		TECN	COMMENT
• • • We do not use the following data for averages, fits, limits, etc. • • •					
$< 3 \times 10^{-5} - 6 \times 10^{-3}$	90	[1] BALEST	95	CLE2	$\Upsilon(1S) \to X^0\overline{X}^0\gamma$, $m_{X^0} < 3.9$ GeV

[1] BALEST 95 three-body limit is for phase-space photon energy distribution and angular distribution same as for $\Upsilon \to gg\gamma$.

REFERENCES FOR Searches for New Heavy Bosons (W', Z', leptoquarks, etc.)

AABOUD	18B	EPJ C78 24	M. Aaboud *et al.*	(ATLAS Collab.)
AABOUD	18F	PL B777 91	M. Aaboud *et al.*	(ATLAS Collab.)
AABOUD	18G	JHEP 1801 055	M. Aaboud *et al.*	(ATLAS Collab.)
SIRUNYAN	18	PL B777 39	A.M. Sirunyan *et al.*	(CMS Collab.)
SIRUNYAN	18G	JHEP 1801 097	A.M. Sirunyan *et al.*	(CMS Collab.)
AABOUD	17AK	PR D96 052004	M. Aaboud *et al.*	(ATLAS Collab.)
AABOUD	17AO	PL B774 494	M. Aaboud *et al.*	(ATLAS Collab.)
AABOUD	17AT	JHEP 1710 182	M. Aaboud *et al.*	(ATLAS Collab.)
AABOUD	17B	PL B765 32	M. Aaboud *et al.*	(ATLAS Collab.)
KHACHATRY...	17AX	PL B773 563	V. Khachatryan *et al.*	(CMS Collab.)
KHACHATRY...	17H	JHEP 1702 048	V. Khachatryan *et al.*	(CMS Collab.)
KHACHATRY...	17J	JHEP 1703 077	V. Khachatryan *et al.*	(CMS Collab.)
KHACHATRY...	17T	PL B768 57	V. Khachatryan *et al.*	(CMS Collab.)
KHACHATRY...	17U	PL B768 137	V. Khachatryan *et al.*	(CMS Collab.)
KHACHATRY...	17W	PL B769 520	V. Khachatryan *et al.*	(CMS Collab.)
KHACHATRY...	17Y	PL B770 257	V. Khachatryan *et al.*	(CMS Collab.)
KHACHATRY...	17Z	PL B770 278	V. Khachatryan *et al.*	(CMS Collab.)
SIRUNYAN	17A	JHEP 1703 162	A.M. Sirunyan *et al.*	(CMS Collab.)
SIRUNYAN	17AK	PL B774 533	A.M. Sirunyan *et al.*	(CMS Collab.)
SIRUNYAN	17AP	JHEP 1710 180	A.M. Sirunyan *et al.*	(CMS Collab.)
SIRUNYAN	17H	JHEP 1707 121	A.M. Sirunyan *et al.*	(CMS Collab.)
SIRUNYAN	17I	JHEP 1708 029	A.M. Sirunyan *et al.*	(CMS Collab.)
SIRUNYAN	17Q	JHEP 1707 001	A.M. Sirunyan *et al.*	(CMS Collab.)
SIRUNYAN	17R	EPJ C77 636	A.M. Sirunyan *et al.*	(CMS Collab.)
SIRUNYAN	17T	PRL 119 111802	A.M. Sirunyan *et al.*	(CMS Collab.)
SIRUNYAN	17V	JHEP 1709 053	A.M. Sirunyan *et al.*	(CMS Collab.)
AABOUD	16	PL B759 229	M. Aaboud *et al.*	(ATLAS Collab.)
AABOUD	16AA	EPJ C76 585	M. Aaboud *et al.*	(ATLAS Collab.)
AABOUD	16AE	JHEP 1609 173	M. Aaboud *et al.*	(ATLAS Collab.)
AABOUD	16P	EPJ C76 541	M. Aaboud *et al.*	(ATLAS Collab.)
AABOUD	16U	PL B761 372	M. Aaboud *et al.*	(ATLAS Collab.)
AABOUD	16V	PL B762 334	M. Aaboud *et al.*	(ATLAS Collab.)
AAD	16G	EPJ C76 5	G. Aad *et al.*	(ATLAS Collab.)
AAD	16L	EPJ C76 210	G. Aad *et al.*	(ATLAS Collab.)
AAD	16R	PL B755 285	G. Aad *et al.*	(ATLAS Collab.)
AAD	16S	PL B754 302	G. Aad *et al.*	(ATLAS Collab.)
AAD	16W	PL B758 249	G. Aad *et al.*	(ATLAS Collab.)
BARRANCO	16	JP G43 115004	J. Barranco *et al.*	
DEY	16	JHEP 1604 187	U.K. Dey, S. Mohanty	
KHACHATRY...	16AF	PR D93 032004	V. Khachatryan *et al.*	(CMS Collab.)
KHACHATRY...	16AG	PR D93 032005	V. Khachatryan *et al.*	(CMS Collab.)
Also		PR D95 039906 (errat.)	V. Khachatryan *et al.*	(CMS Collab.)
KHACHATRY...	16AO	JHEP 1602 122	V. Khachatryan *et al.*	(CMS Collab.)
KHACHATRY...	16AP	JHEP 1602 145	V. Khachatryan *et al.*	(CMS Collab.)
KHACHATRY...	16BD	EPJ C76 237	V. Khachatryan *et al.*	(CMS Collab.)
KHACHATRY...	16BE	EPJ C76 317	V. Khachatryan *et al.*	(CMS Collab.)
KHACHATRY...	16E	PR D93 012001	V. Khachatryan *et al.*	(CMS Collab.)
KHACHATRY...	16K	PRL 116 071801	V. Khachatryan *et al.*	(CMS Collab.)
KHACHATRY...	16L	PRL 117 031802	V. Khachatryan *et al.*	(CMS Collab.)
KHACHATRY...	16O	PL B755 196	V. Khachatryan *et al.*	(CMS Collab.)
KUMAR	16	PR D94 014022	G. Kumar	
AAD	15AM	JHEP 1507 157	G. Aad *et al.*	(ATLAS Collab.)
AAD	15AO	JHEP 1508 148	G. Aad *et al.*	(ATLAS Collab.)
AAD	15AT	EPJ C75 79	G. Aad *et al.*	(ATLAS Collab.)
AAD	15AU	EPJ C75 69	G. Aad *et al.*	(ATLAS Collab.)
AAD	15AV	EPJ C75 165	G. Aad *et al.*	(ATLAS Collab.)
AAD	15AZ	EPJ C75 209	G. Aad *et al.*	(ATLAS Collab.)
Also		EPJ C75 370 (errat.)	G. Aad *et al.*	(ATLAS Collab.)
AAD	15BB	EPJ C75 263	G. Aad *et al.*	(ATLAS Collab.)
AAD	15CD	PR D92 092001	G. Aad *et al.*	(ATLAS Collab.)
AAD	15CP	JHEP 1512 055	G. Aad *et al.*	(ATLAS Collab.)
AAD	15O	PRL 115 031801	G. Aad *et al.*	(ATLAS Collab.)
AAD	15R	PL B743 235	G. Aad *et al.*	(ATLAS Collab.)
AAD	15V	PR D91 052007	G. Aad *et al.*	(ATLAS Collab.)
AALTONEN	15C	PRL 115 061801	T. Aaltonen *et al.*	(CDF Collab.)
BESSAA	15	EPJ C75 97	A. Bessaa, S. Davidson	
KHACHATRY...	15AE	JHEP 1504 025	V. Khachatryan *et al.*	(CMS Collab.)
KHACHATRY...	15AJ	JHEP 1507 042	V. Khachatryan *et al.*	(CMS Collab.)
KHACHATRY...	15AV	JHEP 1509 201	V. Khachatryan *et al.*	(CMS Collab.)
KHACHATRY...	15C	PL B740 83	V. Khachatryan *et al.*	(CMS Collab.)
KHACHATRY...	15F	PRL 114 101801	V. Khachatryan *et al.*	(CMS Collab.)
KHACHATRY...	15O	PL B748 255	V. Khachatryan *et al.*	(CMS Collab.)
KHACHATRY...	15T	PR D91 092005	V. Khachatryan *et al.*	(CMS Collab.)
KHACHATRY...	15V	PR D91 052009	V. Khachatryan *et al.*	(CMS Collab.)

Gauge & Higgs Boson Particle Listings

New Heavy Bosons

SAHOO 15A PR D91 094019 S. Sahoo, R. Mohanta
AAD 14AI JHEP 1409 037 G. Aad *et al.* (ATLAS Collab.)
AAD 14AT PL B738 428 G. Aad *et al.* (ATLAS Collab.)
AAD 14S PL B737 223 G. Aad *et al.* (ATLAS Collab.)
AAD 14V PR D90 052005 G. Aad *et al.* (ATLAS Collab.)
KHACHATRY... 14 JHEP 1408 173 V. Khachatryan *et al.* (CMS Collab.)
KHACHATRY... 14A JHEP 1408 174 V. Khachatryan *et al.* (CMS Collab.)
KHACHATRY... 14O EPJ C74 3149 V. Khachatryan *et al.* (CMS Collab.)
KHACHATRY... 14T PL B739 229 V. Khachatryan *et al.* (CMS Collab.)
MARTINEZ 14 PR D90 015028 R. Martinez, F. Ochoa
PRIEELS 14 PR D90 112003 R. Prieels *et al.* (LOUV, ETH, PSI+)
AAD 13AE JHEP 1306 033 G. Aad *et al.* (ATLAS Collab.)
AAD 13AO PR D87 112006 G. Aad *et al.* (ATLAS Collab.)
AAD 13AQ PR D88 012004 G. Aad *et al.* (ATLAS Collab.)
AAD 13D JHEP 1301 029 G. Aad *et al.* (ATLAS Collab.)
AAD 13G JHEP 1301 116 G. Aad *et al.* (ATLAS Collab.)
AAD 13K EPJ C73 2263 G. Aad *et al.* (ATLAS Collab.)
AAD 13S PL B719 242 G. Aad *et al.* (ATLAS Collab.)
AALTONEN 13A PRL 110 121802 T. Aaltonen *et al.* (CDF Collab.)
AALTONEN 13AA PR D88 092004 T. Aaltonen *et al.* (CDF Collab.)
AALTONEN 13R PRL 111 031802 T. Aaltonen *et al.* (CDF Collab.)
CHATRCHYAN 13A JHEP 1301 013 S. Chatrchyan *et al.* (CMS Collab.)
CHATRCHYAN 13AF PL B720 63 S. Chatrchyan *et al.* (CMS Collab.)
CHATRCHYAN 13AJ PL B723 280 S. Chatrchyan *et al.* (CMS Collab.)
CHATRCHYAN 13AP PR D87 072002 S. Chatrchyan *et al.* (CMS Collab.)
CHATRCHYAN 13AQ PR D87 072005 S. Chatrchyan *et al.* (CMS Collab.)
CHATRCHYAN 13AS PR D87 114015 S. Chatrchyan *et al.* (CMS Collab.)
CHATRCHYAN 13AU PRL 110 141802 S. Chatrchyan *et al.* (CMS Collab.)
CHATRCHYAN 13BM PRL 111 211804 S. Chatrchyan *et al.* (CMS Collab.)
Also PRL 112 119903 (errat.) S. Chatrchyan *et al.* (CMS Collab.)
CHATRCHYAN 13E PL B718 1229 S. Chatrchyan *et al.* (CMS Collab.)
CHATRCHYAN 13M PRL 110 081801 S. Chatrchyan *et al.* (CMS Collab.)
CHATRCHYAN 13U JHEP 1302 036 S. Chatrchyan *et al.* (CMS Collab.)
SAKAKI 13 PR D88 094012 Y. Sakaki *et al.*
AAD 12AV PRL 109 081801 G. Aad *et al.* (ATLAS Collab.)
AAD 12BB PR D85 112012 G. Aad *et al.* (ATLAS Collab.)
AAD 12BV JHEP 1209 041 G. Aad *et al.* (ATLAS Collab.)
AAD 12CC JHEP 1211 138 G. Aad *et al.* (ATLAS Collab.)
AAD 12CK PR D86 091103 G. Aad *et al.* (ATLAS Collab.)
AAD 12CR EPJ C72 2241 G. Aad *et al.* (ATLAS Collab.)
AAD 12H PL B709 158 G. Aad *et al.* (ATLAS Collab.)
Also PL B711 442 (errat.) G. Aad *et al.* (ATLAS Collab.)
AAD 12K EPJ C72 2083 G. Aad *et al.* (ATLAS Collab.)
AAD 12M EPJ C72 2056 G. Aad *et al.* (ATLAS Collab.)
AAD 12O EPJ C72 2151 G. Aad *et al.* (ATLAS Collab.)
AALTONEN 12AR PR D86 112002 T. Aaltonen *et al.* (CDF Collab.)
AALTONEN 12N PRL 108 211805 T. Aaltonen *et al.* (CDF Collab.)
ABAZOV 12R PR D85 051101 V.M. Abazov *et al.* (D0 Collab.)
ABRAMOWICZ 12A PR D86 012005 H. Abramowicz *et al.* (ZEUS Collab.)
CHATRCHYAN 12AF PRL 109 141801 S. Chatrchyan *et al.* (CMS Collab.)
CHATRCHYAN 12AG PR D86 052013 S. Chatrchyan *et al.* (CMS Collab.)
CHATRCHYAN 12AI JHEP 1208 110 S. Chatrchyan *et al.* (CMS Collab.)
CHATRCHYAN 12AQ JHEP 1209 029 S. Chatrchyan *et al.* (CMS Collab.)
Also JHEP 1403 132 (errat.) S. Chatrchyan *et al.* (CMS Collab.)
CHATRCHYAN 12AR PL B717 351 S. Chatrchyan *et al.* (CMS Collab.)
CHATRCHYAN 12BG PRL 109 261802 S. Chatrchyan *et al.* (CMS Collab.)
CHATRCHYAN 12BL JHEP 1212 015 S. Chatrchyan *et al.* (CMS Collab.)
CHATRCHYAN 12BO JHEP 1212 055 S. Chatrchyan *et al.* (CMS Collab.)
CHATRCHYAN 12BR PRL 109 251801 S. Chatrchyan *et al.* (CMS Collab.)
CHATRCHYAN 12M PL B714 158 S. Chatrchyan *et al.* (CMS Collab.)
CHATRCHYAN 12O PL B716 82 S. Chatrchyan *et al.* (CMS Collab.)
KOSNIK 12 PR D86 055004 N. Kosnik (LALO, STFN)
AAD 11D PR D83 112006 G. Aad *et al.* (ATLAS Collab.)
AAD 11H PRL 106 251801 G. Aad *et al.* (ATLAS Collab.)
AAD 11Z EPJ C71 1809 G. Aad *et al.* (ATLAS Collab.)
AALTONEN 11AD PR D84 072003 T. Aaltonen *et al.* (CDF Collab.)
AALTONEN 11AE PR D84 072004 T. Aaltonen *et al.* (CDF Collab.)
AALTONEN 11C PR D83 031102 T. Aaltonen *et al.* (CDF Collab.)
AALTONEN 11I PRL 106 121801 T. Aaltonen *et al.* (CDF Collab.)
AARON 11A PL B701 20 F. D. Aaron *et al.* (H1 Collab.)
AARON 11B PL B704 388 F. D. Aaron *et al.* (H1 Collab.)
AARON 11C PL B705 52 F. D. Aaron *et al.* (H1 Collab.)
ABAZOV 11A PL B695 88 V.M. Abazov *et al.* (D0 Collab.)
ABAZOV 11H PRL 107 011801 V.M. Abazov *et al.* (D0 Collab.)
ABAZOV 11I PRL 107 011804 V.M. Abazov *et al.* (D0 Collab.)
ABAZOV 11L PL B699 145 V.M. Abazov *et al.* (D0 Collab.)
ABAZOV 11V PR D84 071104 V.M. Abazov *et al.* (D0 Collab.)
BUENO 11 PR D84 032005 J.F. Bueno *et al.* (TWIST Collab.)
Also PR D85 039908 (errat.) J.F. Bueno *et al.* (TWIST Collab.)
CHATRCHYAN 11N PL B703 246 S. Chatrchyan *et al.* (CMS Collab.)
CHATRCHYAN 11O JHEP 1108 005 S. Chatrchyan *et al.* (CMS Collab.)
CHATRCHYAN 11Y PL B704 123 S. Chatrchyan *et al.* (CMS Collab.)
DORSNER 11 JHEP 1111 002 I. Dorsner *et al.*
KHACHATRY... 11D PRL 106 201802 V. Khachatryan *et al.* (CMS Collab.)
KHACHATRY... 11E PRL 106 201803 V. Khachatryan *et al.* (CMS Collab.)
AALTONEN 10L PL B691 183 T. Aaltonen *et al.* (CDF Collab.)
AALTONEN 10N PRL 104 241801 T. Aaltonen *et al.* (CDF Collab.)
ABAZOV 10L PL B693 95 V.M. Abazov *et al.* (D0 Collab.)
DEL-AGUILA 10 JHEP 1009 033 F. del Aguila, J. de Blas, M. Perez-Victoria (GRAN)
KHACHATRY... 10 PRL 105 211801 V. Khachatryan *et al.* (CMS Collab.)
Also PRL 106 029902 V. Khachatryan *et al.* (CMS Collab.)
WAUTERS 10 PR C82 055502 F. Wauters *et al.* (REZ, TAMU)
AALTONEN 09AC PR D79 112002 T. Aaltonen *et al.* (CDF Collab.)
AALTONEN 09T PRL 102 031801 T. Aaltonen *et al.* (CDF Collab.)
AALTONEN 09V PRL 102 091805 T. Aaltonen *et al.* (CDF Collab.)
ABAZOV 09 PL B671 224 V.M. Abazov *et al.* (D0 Collab.)
ABAZOV 09AF PL B681 224 V.M. Abazov *et al.* (D0 Collab.)
ERLER 09 JHEP 0908 017 J. Erler *et al.*
AALTONEN 08D PR D77 051102 T. Aaltonen *et al.* (CDF Collab.)
AALTONEN 08P PR D77 091105 T. Aaltonen *et al.* (CDF Collab.)
AALTONEN 08Y PRL 100 231801 T. Aaltonen *et al.* (CDF Collab.)
AALTONEN 08Z PRL 101 071802 T. Aaltonen *et al.* (CDF Collab.)
ABAZOV 08AA PL B668 98 V.M. Abazov *et al.* (D0 Collab.)
ABAZOV 08AD PL B668 357 V.M. Abazov *et al.* (D0 Collab.)
ABAZOV 08AN PRL 101 241802 V.M. Abazov *et al.* (D0 Collab.)
ABAZOV 08C PRL 100 031804 V.M. Abazov *et al.* (D0 Collab.)
MACDONALD 08 PR D78 032010 R.P. MacDonald *et al.* (TWIST Collab.)
ZHANG 08 NP B802 247 Y. Zhang *et al.* (PKGU, UMD)
AALTONEN 07H PRL 99 171802 T. Aaltonen *et al.* (CDF Collab.)
ABAZOV 07E PL B647 74 V.M. Abazov *et al.* (D0 Collab.)
ABAZOV 07J PRL 99 061801 V.M. Abazov *et al.* (D0 Collab.)
AKTAS 07A EPJ C52 833 A. Aktas *et al.* (H1 Collab.)
CHOUDHURY 07 PL B657 69 D. Choudhury *et al.*
MELCONIAN 07 PL B649 370 D. Melconian *et al.* (TRIUMF)
SCHAEL 07A EPJ C49 411 S. Schael *et al.* (ALEPH Collab.)
SCHUMANN 07 PRL 99 191803 M. Schumann *et al.* (HEID, ILLG, KARL+)
SMIRNOV 07 MPL A22 2353 A.D. Smirnov
ABAZOV 06A PL B636 183 V.M. Abazov *et al.* (D0 Collab.)
ABAZOV 06L PL B640 230 V.M. Abazov *et al.* (D0 Collab.)
ABDALLAH 06C EPJ C45 589 J. Abdallah *et al.* (DELPHI Collab.)
ABULENCIA 06L PRL 96 211801 A. Abulencia *et al.* (CDF Collab.)
ABULENCIA 06M PRL 96 211802 A. Abulencia *et al.* (CDF Collab.)
ABULENCIA 06T PR D73 051102 A. Abulencia *et al.* (CDF Collab.)
ABAZOV 05H PR D71 071104 V.M. Abazov *et al.* (D0 Collab.)
ABULENCIA 05A PRL 95 252001 A. Abulencia *et al.* (CDF Collab.)
ACOSTA 05I PR D71 112001 D. Acosta *et al.* (CDF Collab.)
ACOSTA 05P PR D72 051107 D. Acosta *et al.* (CDF Collab.)
ACOSTA 05R PRL 95 131801 D. Acosta *et al.* (CDF Collab.)
AKTAS 05B PL B629 9 A. Aktas *et al.* (H1 Collab.)
CHEKANOV 05 PL B610 212 S. Chekanov *et al.* (HERA ZEUS Collab.)
CHEKANOV 05A EPJ C44 463 S. Chekanov *et al.* (ZEUS Collab.)
CYBURT 05 ASP 23 313 R.H. Cyburt *et al.*
ABAZOV 04A PRL 92 221801 V.M. Abazov *et al.* (D0 Collab.)
ABAZOV 04C PR D69 111101 V.M. Abazov *et al.* (D0 Collab.)
ABBIENDI 04G EPJ C33 173 G. Abbiendi *et al.* (OPAL Collab.)
ABBIENDI 03D EPJ C26 331 G. Abbiendi *et al.* (OPAL Collab.)
ABBIENDI 03R EPJ C31 281 G. Abbiendi *et al.* (OPAL)
ACOSTA 03B PRL 90 081802 D. Acosta *et al.* (CDF Collab.)
ADLOFF 03 PL B568 35 C. Adloff *et al.* (H1 Collab.)
BARGER 03B PR D67 075009 V. Barger, P. Langacker, H. Lee
CHANG 03 PR D68 111101 M.-C. Chang *et al.* (BELLE Collab.)
CHEKANOV 03B PR D68 052004 S. Chekanov *et al.* (ZEUS Collab.)
ABAZOV 02 PRL 88 191801 V.M. Abazov *et al.* (D0 Collab.)
ABBIENDI 02B PL B526 233 G. Abbiendi *et al.* (OPAL Collab.)
AFFOLDER 02C PRL 88 071806 T. Affolder *et al.* (CDF Collab.)
CHEKANOV 02 PR D65 092004 S. Chekanov *et al.* (ZEUS Collab.)
CHEKANOV 02B PL B531 9 S. Chekanov *et al.* (ZEUS Collab.)
MUECK 02 PR D65 085037 A. Mueck, A. Pilaftsis, R. Rueckl
ABAZOV 01B PRL 87 061802 V.M. Abazov *et al.* (D0 Collab.)
ABAZOV 01D PR D64 092004 V.M. Abazov *et al.* (D0 Collab.)
ADLOFF 01C PL B523 234 C. Adloff *et al.* (H1 Collab.)
AFFOLDER 01I PRL 87 231803 T. Affolder *et al.* (CDF Collab.)
BREITWEG 01 PR D63 052002 J. Breitweg *et al.* (ZEUS Collab.)
CHEUNG 01B PL B517 167 K. Cheung
THOMAS 01 NP A694 559 E. Thomas *et al.*
ABBIENDI 00M EPJ C13 15 G. Abbiendi *et al.* (OPAL Collab.)
ABBOTT 00C PRL 84 2088 B. Abbott *et al.* (D0 Collab.)
ABE 00 PRL 84 5716 F. Abe *et al.* (CDF Collab.)
ABREU 00S PL B485 45 P. Abreu *et al.* (DELPHI Collab.)
ABREU 00Z EPJ C17 53 P. Abreu *et al.* (DELPHI Collab.)
ACCIARRI 00P PL B489 81 M. Acciarri *et al.* (L3 Collab.)
ADLOFF 00 PL B479 358 C. Adloff *et al.* (H1 Collab.)
AFFOLDER 00K PRL 85 2056 T. Affolder *et al.* (CDF Collab.)
BARATE 00I EPJ C12 183 R. Barate *et al.* (ALEPH Collab.)
BARGER 00 PL B480 149 V. Barger, K. Cheung
BREITWEG 00E EPJ C16 253 J. Breitweg *et al.* (ZEUS Collab.)
CHAY 00 PR D61 035002 J. Chay, K.Y. Lee, S. Nam
CHO 00 MPL A15 311 G. Cho
CORNET 00 PR D61 037701 F. Cornet, M. Relano, J. Rico
DELGADO 00 JHEP 0001 030 A. Delgado, A. Pomarol, M. Quiros
ERLER 00 PR 84 212 J. Erler, P. Langacker
GABRIELLI 00 PR D62 055009 E. Gabrielli
RIZZO 00 PR D61 016007 T.G. Rizzo, J.D. Wells
ROSNER 00 PR D61 016006 J.L. Rosner
ZARNECKI 00 EPJ C17 695 A. Zarnecki
ABBIENDI 99 EPJ C6 1 G. Abbiendi *et al.* (OPAL Collab.)
ABBOTT 99J PRL 83 2896 B. Abbott *et al.* (D0 Collab.)
ABREU 99G PL B446 62 P. Abreu *et al.* (DELPHI Collab.)
ACKERSTAFF 99D EPJ C8 3 K. Ackerstaff *et al.* (OPAL Collab.)
ADLOFF 99 EPJ C11 447 C. Adloff *et al.* (H1 Collab.)
Also EPJ C14 553 (errat.) C. Adloff *et al.* (H1 Collab.)
CASALBUONI 99 PL B460 135 R. Casalbuoni *et al.*
CZAKON 99 PL B458 355 M. Czakon, J. Gluza, M. Zralek
ERLER 99 PL B456 68 J. Erler, P. Langacker
MARCIANO 99 PR D60 093006 W. Marciano
MASIP 99 PR D60 096005 M. Masip, A. Pomarol
NATH 99 PR D60 116004 P. Nath, M. Yamaguchi
STRUMIA 99 PL B466 107 A. Strumia
ABBOTT 98E PRL 80 2051 B. Abbott *et al.* (D0 Collab.)
ABBOTT 98J PRL 81 38 B. Abbott *et al.* (D0 Collab.)
ABE 98S PRL 81 4806 F. Abe *et al.* (CDF Collab.)
ABE 98V PRL 81 5742 F. Abe *et al.* (CDF Collab.)
ACCIARRI 98J PL B433 163 M. Acciarri *et al.* (L3 Collab.)
ACKERSTAFF 98V EPJ C2 441 K. Ackerstaff *et al.* (OPAL Collab.)
BARATE 98U EPJ C4 571 R. Barate *et al.* (ALEPH Collab.)
BARENBOIM 98 EPJ C1 369 G. Barenboim
CHO 98 EPJ C5 155 G. Cho, K. Hagiwara, S. Matsumoto
CONRAD 98 RMP 70 1341 J.M. Conrad, M.H. Shaevitz, T. Bolton
DONCHESKI 98 PR D58 097702 M.A. Doncheski, R.W. Robinett
GROSS-PILCH... 98 hep-ex/9810015 C. Grosso-Pilcher, G. Landsberg, M. Paterno
ABE 97F PRL 78 2906 F. Abe *et al.* (CDF Collab.)
ABE 97G PR D55 5263 F. Abe *et al.* (CDF Collab.)
ABE 97S PRL 79 2192 F. Abe *et al.* (CDF Collab.)
ABE 97W PRL 79 3819 F. Abe *et al.* (CDF Collab.)
ABE 97X PRL 79 4327 F. Abe *et al.* (CDF Collab.)
ACCIARRI 97Q PL B412 201 M. Acciarri *et al.* (L3 Collab.)
ARIMA 97 PR D55 19 T. Arima *et al.* (VENUS Collab.)
BARENBOIM 97 PR D55 4213 G. Barenboim *et al.* (VALE, IFIC)
DEANDREA 97 PL B409 277 A. Deandrea (MARS)
DERRICK 97 ZPHY C73 613 M. Derrick *et al.* (ZEUS Collab.)
GROSSMAN 97 PR D55 2768 Y. Grossman, Z. Ligeti, E. Nardi (REHO, CIT)
JADACH 97 PL B408 281 S. Jadach, B.F.L. Ward, Z. Was (CERN, INPK+)
STAHL 97 ZPHY C74 73 A. Stahl, H. Voss (BONN)
ABACHI 96C PRL 76 3271 S. Abachi *et al.* (D0 Collab.)
ABREU 96T ZPHY C72 179 P. Abreu *et al.* (DELPHI Collab.)
ADAM 96C PL B380 471 W. Adam *et al.* (DELPHI Collab.)
AID 96B PL B369 173 S. Aid *et al.* (H1 Collab.)
ALLET 96 PL B383 139 M. Allet *et al.* (VILL, LEUV, LOUV, WISC)
ABACHI 95E PL B358 405 S. Abachi *et al.* (D0 Collab.)
ABE 95N PRL 74 3538 F. Abe *et al.* (CDF Collab.)
BALEST 95 PR D51 2053 R. Balest *et al.* (CLEO Collab.)
KUZNETSOV 95 PRL 75 794 I.A. Kuznetsov *et al.* (PNPI, KIAE, HARV+)
KUZNETSOV 95B PAN 58 2113 A.V. Kuznetsov, N.V. Mikheev (YARO)
Translated from YAF 58 2228.
MIZUKOSHI 95 NP B443 20 J.K. Mizukoshi, O.J.P. Eboli, M.C. Gonzalez-Garcia
ABREU 94O ZPHY C64 183 P. Abreu *et al.* (DELPHI Collab.)
BHATTACH... 94 PL B336 100 G. Bhattacharyya, J. Ellis, K. Sridhar (CERN)
Also PL B338 522 (erratum) G. Bhattacharyya, J. Ellis, K. Sridhar (CERN)
BHATTACH... 94B PL B338 522 (erratum) G. Bhattacharyya, J. Ellis, K. Sridhar (CERN)
DAVIDSON 94 ZPHY C61 613 S. Davidson, D. Bailey, B.A. Campbell (CFPA+)
KUZNETSOV 94 PL B329 295 A.V. Kuznetsov, N.V. Mikheev (YARO)
KUZNETSOV 94B JETPL 60 315 I.A. Kuznetsov *et al.* (PNPI, KIAE, HARV+)
Translated from ZETFP 60 311.
LEURER 94 PR D50 536 M. Leurer (REHO)
LEURER 94B PR D49 333 M. Leurer (REHO)
Also PRL 71 1324 M. Leurer (REHO)
MAHANTA 94 PL B337 128 U. Mahanta (MEHTA)
SEVERIJNS 94 PRL 73 611 (erratum) N. Severijns *et al.* (LOUV, WISC, LEUV+)
VILAIN 94B PL B332 465 P. Vilain *et al.* (CHARM II Collab.)
ABE 93C PL B302 119 K. Abe *et al.* (VENUS Collab.)
ABE 93D PL B304 373 T. Abe *et al.* (TOPAZ Collab.)
ABE 93G PRL 71 2542 F. Abe *et al.* (CDF Collab.)
ABREU 93J PL B316 620 P. Abreu *et al.* (DELPHI Collab.)
ACTON 93E PL B311 391 P.D. Acton *et al.* (OPAL Collab.)

ADRIANI	93M	PRPL 236 1	O. Adriani *et al.*	(L3 Collab.)
ALITTI	93	NP B400 3	J. Alitti *et al.*	(UA2 Collab.)
BHATTACH...	93	PR D47 3693	G. Bhattacharyya *et al.*	(CALC, JADA, ICTP+)
BUSKULIC	93F	PL B308 425	D. Buskulic *et al.*	(ALEPH Collab.)
DERRICK	93	PL B306 173	M. Derrick *et al.*	(ZEUS Collab.)
RIZZO	93	PR D48 4470	T.G. Rizzo	(ANL)
SEVERIJNS	93	PRL 70 4047	N. Severijns *et al.*	(LOUV, WISC, LEUV+)
Also		PRL 73 611 (erratum)	N. Severijns *et al.*	(LOUV, WISC, LEUV+)
STERNER	93	PL B303 385	K.L. Sterner *et al.*	(AMY Collab.)
ABREU	92D	ZPHY C53 555	P. Abreu *et al.*	(DELPHI Collab.)
ADRIANI	92F	PL B292 472	O. Adriani *et al.*	(L3 Collab.)
DECAMP	92	PRPL 216 253	D. Decamp *et al.*	(ALEPH Collab.)
IMAZATO	92	PRL 69 877	J. Imazato *et al.*	(KEK, INUS, TOKY+)
MISHRA	92	PRL 68 3499	S.R. Mishra *et al.*	(COLU, CHIC, FNAL+)
POLAK	92B	PR D46 3871	J. Polak, M. Zralek	(SILES)
ACTON	91	PL B268 122	D.P. Acton *et al.*	(OPAL Collab.)
ACTON	91B	PL B273 338	D.P. Acton *et al.*	(OPAL Collab.)
ADEVA	91D	PL B262 155	B. Adeva *et al.*	(L3 Collab.)
AQUINO	91	PL B261 280	M. Aquino, A. Fernandez, A. Garcia	(CINV, PUEB)
COLANGELO	91	PL B253 154	P. Colangelo, G. Nardulli	(BARI)
CUYPERS	91	PL B259 173	F. Cuypers, A.F. Falk, P.H. Frampton	(DURH, HARV+)
FARAGGI	91	MPL A6 61	A.E. Faraggi, D.V. Nanopoulos	(TAMU)
POLAK	91	NP B363 385	J. Polak, M. Zralek	(SILES)
RIZZO	91	PR D44 202	T.G. Rizzo	(WISC, ISU)
WALKER	91	APJ 376 51	T.P. Walker *et al.*	(HSCA, OSU, CHIC+)
ABE	90F	PL B246 297	K. Abe *et al.*	(VENUS Collab.)
ABE	90H	PR D41 1722	F. Abe *et al.*	(CDF Collab.)
AKRAWY	90J	PL B246 285	M.Z. Akrawy *et al.*	(OPAL Collab.)
GONZALEZ...	90D	PL B240 163	M.C. Gonzalez-Garcia, J.W.F. Valle	(VALE)
GRIFOLS	90	NP B331 244	J.A. Grifols, E. Masso	(BARC)
GRIFOLS	90D	PR D42 3293	J.A. Grifols, E. Masso, T.G. Rizzo	(BARC, CERN+)
KIM	90	PL B240 243	G.N. Kim *et al.*	(AMY Collab.)
LOPEZ	90	PL B241 392	J.L. Lopez, D.V. Nanopoulos	(TAMU)
BARBIERI	89B	PR D39 1229	R. Barbieri, R.N. Mohapatra	(PISA, UMD)
LANGACKER	89B	PR D40 1569	P. Langacker, S. Uma Sankar	(PENN)
ODAKA	89	JPSJ 58 3037	S. Odaka *et al.*	(VENUS Collab.)
ROBINETT	89	PR D39 834	R.W. Robinett	(PSU)
ALBAJAR	88B	PL B209 127	C. Albajar *et al.*	(UA1 Collab.)
BAGGER	88	PR D37 1188	J. Bagger, C. Schmidt, S. King	(HARV, BOST)
BALKE	88	PR D37 587	B. Balke *et al.*	(LBL, UCB, COLO, NWES+)
BERGSTROM	88	PL B212 386	L. Bergstrom	(STOH)
CUYPERS	88	PRL 60 1237	F. Cuypers, P.H. Frampton	(UNCCH)
DONCHESKI	88	PL B206 137	M.A. Doncheski, H. Grotch, R. Robinett	(PSU)
DONCHESKI	88B	PR D38 412	M.A. Doncheski, H. Grotch, R.W. Robinett	(PSU)
BARTEL	87B	ZPHY C36 15	W. Bartel *et al.*	(JADE Collab.)
BEHREND	86B	PL B178 452	H.J. Behrend *et al.*	(CELLO Collab.)
DERRICK	86	PL 166B 463	M. Derrick *et al.*	(HRS Collab.)
Also		PR D34 3286	M. Derrick *et al.*	(HRS Collab.)
JODIDIO	86	PR D34 1967	A. Jodidio *et al.*	(LBL, NWES, TRIU)
Also		PR D37 237 (erratum)	A. Jodidio *et al.*	(LBL, NWES, TRIU)
MOHAPATRA	86	PR D34 909	R.N. Mohapatra	(UMD)
ADEVA	85	PL 152B 439	B. Adeva *et al.*	(Mark-J Collab.)
BERGER	85B	ZPHY C27 341	C. Berger *et al.*	(PLUTO Collab.)
STOKER	85	PRL 54 1887	D.P. Stoker *et al.*	(LBL, NWES, TRIU)
ADEVA	84	PRL 53 134	B. Adeva *et al.*	(Mark-J Collab.)
BEHREND	84C	PL 140B 130	H.J. Behrend *et al.*	(CELLO Collab.)
BERGSMA	83	PL 122B 465	F. Bergsma *et al.*	(CHARM Collab.)
CARR	83	PRL 51 627	J. Carr *et al.*	(LBL, NWES, TRIU)
BEALL	82	PRL 48 848	G. Beall, M. Bander, A. Soni	(UCI, UCLA)
SHANKER	82	NP B204 375	O. Shanker	(TRIU)

Axions (A^0) and Other Very Light Bosons, Searches for

See the related review(s):
Axions and Other Similar Particles

A^0 (Axion) MASS LIMITS from Astrophysics and Cosmology

These bounds depend on model-dependent assumptions (i.e. — on a combination of axion parameters).

VALUE (MeV)	DOCUMENT ID		TECN	COMMENT
• • • We do not use the following data for averages, fits, limits, etc. • • •				
>0.2	BARROSO	82	ASTR	Standard Axion
>0.25	[1] RAFFELT	82	ASTR	Standard Axion
>0.2	[2] DICUS	78C	ASTR	Standard Axion
	MIKAELIAN	78	ASTR	Stellar emission
>0.3	[2] SATO	78	ASTR	Standard Axion
>0.2	VYSOTSKII	78	ASTR	Standard Axion

[1] Lower bound from 5.5 MeV γ-ray line from the sun.
[2] Lower bound from requiring the red giants' stellar evolution not be disrupted by axion emission.

A^0 (Axion) and Other Light Boson (X^0) Searches in Hadron Decays

Limits are for branching ratios.

VALUE	CL%	DOCUMENT ID		TECN	COMMENT
• • • We do not use the following data for averages, fits, limits, etc. • • •					
$<2 \times 10^{-10}$	95	[1] AAIJ	17AQ	LHCB	$B^+ \to K^+ X^0$ ($X^0 \to \mu^+\mu^-$)
$<3.7 \times 10^{-8}$	90	[2] AHN	17	KOTO	$K_L^0 \to \pi^0 X^0$, $m_{X^0} = 135$ MeV
$<6 \times 10^{-11}$	90	[3] BATLEY	17	NA48	$K^\pm \to \pi^\pm X^0$ ($X^0 \to \mu^+\mu^-$)
		[4] WON	16	BELL	$\eta \to \gamma X^0$ ($X^0 \to \pi^+\pi^-$)
$<1 \times 10^{-9}$	95	[5] AAIJ	15AZ	LHCB	$B^0 \to K^{*0} X^0$ ($X^0 \to \mu^+\mu^-$)
$<1.5 \times 10^{-6}$	90	[6] ADLARSON	13	WASA	$\pi^0 \to \gamma X^0$ ($X^0 \to e^+e^-$), $m_{X^0} = 100$ MeV
$<2 \times 10^{-8}$	90	[7] BABUSCI	13B	KLOE	$\phi \to \eta X^0$ ($X^0 \to e^+e^-$)
		[8] ARCHILLI	12	KLOE	$\phi \to \eta X^0$, $X^0 \to e^+e^-$
$<2 \times 10^{-15}$	90	[9] GNINENKO	12A	BDMP	$\pi^0 \to \gamma X^0$ ($X^0 \to e^+e^-$)
$<3 \times 10^{-14}$	90	[10] GNINENKO	12B	BDMP	$\eta(\eta') \to \gamma X^0$ ($X^0 \to e^+e^-$)
$<7 \times 10^{-10}$	90	[11] ADLER	04	B787	$K^+ \to \pi^+ X^0$
$<7.3 \times 10^{-11}$	90	[12] ANISIMOVSK...04	B949		$K^+ \to \pi^+ X^0$
$<4.5 \times 10^{-11}$	90	[13] ADLER	02C	B787	$K^+ \to \pi^+ X^0$
$<4 \times 10^{-5}$	90	[14] ADLER	01	B787	$K^+ \to \pi^+ \pi^0 A^0$
$<4.9 \times 10^{-5}$	90	AMMAR	01B	CLEO	$B^\pm \to \pi^\pm (K^\pm) X^0$
$<5.3 \times 10^{-5}$	90	AMMAR	01B	CLEO	$B^0 \to K_S^0 X^0$
$<3.3 \times 10^{-5}$	90	[15] ALTEGOER	98	NOMD	$\pi^0 \to \gamma X^0$, $m_{X^0} < 120$ MeV
$<5.0 \times 10^{-8}$	90	[16] KITCHING	97	B787	$K^+ \to \pi^+ X^0$ ($X^0 \to \gamma\gamma$)
$<5.2 \times 10^{-10}$	90	[17] ADLER	96	B787	$K^+ \to \pi^+ X^0$
$<2.8 \times 10^{-4}$	90	[18] AMSLER	96B	CBAR	$\pi^0 \to \gamma X^0$, $m_{X^0} < 65$ MeV
$<3 \times 10^{-4}$	90	[18] AMSLER	96B	CBAR	$\eta \to \gamma X^0$, $m_{X^0} = 50$–200 MeV
$<4 \times 10^{-5}$	90	[18] AMSLER	96B	CBAR	$\eta' \to \gamma X^0$, $m_{X^0} = 50$–925 MeV
$<6 \times 10^{-5}$	90	[18] AMSLER	94B	CBAR	$\pi^0 \to \gamma X^0$, $m_{X^0} = 65$–125 MeV
$<6 \times 10^{-5}$	90	[18] AMSLER	94B	CBAR	$\eta \to \gamma X^0$, $m_{X^0} = 200$–525 MeV
$<7 \times 10^{-3}$	90	[19] MEIJERDREES	94	CNTR	$\pi^0 \to \gamma X^0$, $m_{X^0} = 25$ MeV
$<2 \times 10^{-3}$	90	[19] MEIJERDREES	94	CNTR	$\pi^0 \to \gamma X^0$, $m_{X^0} = 100$ MeV
$<2 \times 10^{-7}$	90	[20] ATIYA	93B	B787	Sup. by ADLER 04
$<3 \times 10^{-13}$		[21] NG	93	COSM	$\pi^0 \to \gamma X^0$
$<1.1 \times 10^{-8}$	90	[22] ALLIEGRO	92	SPEC	$K^+ \to \pi^+ X^0$ ($X^0 \to e^+e^-$)
$<5 \times 10^{-4}$	90	[23] ATIYA	92	B787	$\pi^0 \to \gamma X^0$
$<1 \times 10^{-12}$	95	[24] BARABASH	92	BDMP	$\pi^\pm \to e^\pm \nu X^0$($X^0 \to e^+e^-$, $\gamma\gamma$), $m_{X^0} = 8$ MeV
$<1 \times 10^{-12}$	95	[25] BARABASH	92	BDMP	$K^\pm \to \pi^\pm X^0$($X^0 \to e^+e^-$, $\gamma\gamma$), $m_{X^0} = 10$ MeV
$<1 \times 10^{-11}$	95	[26] BARABASH	92	BDMP	$K_L^0 \to \pi^0 X^0$($X^0 \to e^+e^-$, $\gamma\gamma$), $m_{X^0} = 10$ MeV
$<1 \times 10^{-14}$	95	[27] BARABASH	92	BDMP	$\eta' \to \eta X^0$($X^0 \to e^+e^-, \gamma\gamma$), $m_{X^0} = 10$ MeV
$<4 \times 10^{-6}$	90	[28] MEIJERDREES	92	SPEC	$\pi^0 \to \gamma X^0$ ($X^0 \to e^+e^-$), $m_{X^0} = 100$ MeV
$<1 \times 10^{-7}$	90	[29] ATIYA	90B	B787	Sup. by KITCHING 97
$<1.3 \times 10^{-8}$	90	[30] KORENCHE...	87	SPEC	$\pi^+ \to e^+ \nu A^0$ ($A^0 \to e^+e^-$)
$<1 \times 10^{-9}$	90	[31] EICHLER	86	SPEC	Stopped $\pi^+ \to e^+ \nu A^0$
$<2 \times 10^{-5}$	90	[32] YAMAZAKI	84	SPEC	For $160 < m < 260$ MeV
$<(1.5–4) \times 10^{-6}$	90	[32] YAMAZAKI	84	SPEC	K decay, $m_{X^0} \ll 100$ MeV
		[33] ASANO	82	CNTR	Stopped $K^+ \to \pi^+ X^0$
		[34] ASANO	81B	CNTR	Stopped $K^+ \to \pi^+ X^0$
		[35] ZHITNITSKII	79		Heavy axion

[1] The limit is for $\tau_{X^0} = 10$ ps. See their Fig. 4 for limits in the range of $m_{X^0} = 250$–4700 MeV and $\tau_{X^0} = 0.1$–1000 ps.
[2] The limit as a function of m_{X^0} from 0 to 250 MeV is provided in their Fig. 5 .
[3] The limit is for $m_{X^0} = 216$ MeV and $\tau_{X^0} \leq 10$ ps. See their Fig. 4(c) for limits in the range of $m_{X^0} = 211$–354 MeV and longer lifetimes.
[4] WON 16 look for a vector boson coupled to baryon number. Derived limits on $\alpha' < 10^{-3}$–10^{-2} for $m_{X^0} = 290$–520 MeV at 95% CL. See their Fig. 4 for mass-dependent limits.
[5] The limit is for $\tau_{X^0} = 10$ ps and $m_{X^0} = 214$–4350 MeV. See their Fig. 4 for mass- and lifetime-dependent limits.
[6] Limits between 2.0×10^{-5} and 1.5×10^{-6} are obtained for $m_{X^0} = 20$–100 MeV (see their Fig. 8). Angular momentum conservation requires that X^0 has spin ≥ 1.
[7] The limit is for $B(\phi \to \eta X^0) \cdot B(X^0 \to e^+e^-)$ and applies to $m_{X^0} = 410$ MeV. It is derived by analyzing $\eta \to \pi^0\pi^0\pi^0$ and $\pi^-\pi^+\pi^0$. Limits between 1×10^{-6} and 2×10^{-8} are obtained for $m_{X^0} \leq 450$ MeV (see their Fig. 6).
[8] ARCHILLI 12 analyzed $\eta \to \pi^+\pi^-\pi^0$ decays. Derived limits on $\alpha'/\alpha < 2 \times 10^{-5}$ for $m_{X^0} = 50$–420 MeV at 90% CL. See their Fig. 8 for mass-dependent limits.
[9] This limit is for $B(\pi^0 \to \gamma X^0) \cdot B(X^0 \to e^+e^-)$ and applies for $m_{X^0} = 90$ MeV and $\tau_{X^0} \simeq 1 \times 10^{-8}$ sec. Limits between 10^{-8} and 2×10^{-15} are obtained for $m_{X^0} = 3$–120 MeV and $\tau_{X^0} = 1 \times 10^{-11}$–1 sec. See their Fig. 3 for limits at different masses and lifetimes.
[10] This limit is for $B(\eta \to \gamma X^0) \cdot B(X^0 \to e^+e^-)$ and applies for $m_{X^0} = 100$ MeV and $\tau_{X^0} \simeq 6 \times 10^{-9}$ sec. Limits between 10^{-5} and 3×10^{-14} are obtained for $m_{X^0} \lesssim 550$ MeV and $\tau_{X^0} = 10^{-10}$–10 sec. See their Fig. 5 for limits at different mass and lifetime and for η' decays.
[11] This limit applies for a mass near 180 MeV. For other masses in the range $m_{X^0} = 150$–250 MeV the limit is less restrictive, but still improves ADLER 02C and ATIYA 93B.
[12] ANISIMOVSKY 04 bound is for $m_{X^0} = 0$.
[13] ADLER 02C bound is for $m_{X^0} < 60$ MeV. See Fig. 2 for limits at higher masses.
[14] The quoted limit is for $m_{X^0} = 0$–80 MeV. See their Fig. 5 for the limit at higher mass. The branching fraction limit assumes pure phase space decay distributions.
[15] ALTEGOER 98 looked for X^0 from π^0 decay which penetrate the shielding and convert to π^0 in the external Coulomb field of a nucleus.
[16] KITCHING 97 limit is for $B(K^+ \to \pi^+ X^0) \cdot B(X^0 \to \gamma\gamma)$ and applies for $m_{X^0} \simeq 50$ MeV, $\tau_{X^0} < 10^{-10}$ s. Limits are provided for $0 < m_{X^0} < 100$ MeV, $\tau_{X^0} < 10^{-8}$ s.
[17] ADLER 96 looked for a peak in missing-mass distribution. This work is an update of ATIYA 93. The limit is for massless stable X^0 particles and extends to $m_{X^0} = 80$ MeV at the same level. See paper for dependence on finite lifetime.
[18] AMSLER 94B and AMSLER 96B looked for a peak in missing-mass distribution.
[19] The MEIJERDREES 94 limit is based on inclusive photon spectrum and is independent of X^0 decay modes. It applies to $\tau(X^0) > 10^{-23}$ sec.

Gauge & Higgs Boson Particle Listings

Axions (A^0) and Other Very Light Bosons

[20] ATIYA 93B looked for a peak in missing mass distribution. The bound applies for stable X^0 of m_{X^0}=150–250 MeV, and the limit becomes stronger (10^{-8}) for m_{X^0}=180–240 MeV.

[21] NG 93 studied the production of X^0 via $\gamma\gamma \to \pi^0 \to \gamma X^0$ in the early universe at $T \simeq 1$ MeV. The bound on extra neutrinos from nucleosynthesis $\Delta N_\nu < 0.3$ (WALKER 91) is employed. It applies to $m_{X^0} \ll 1$ MeV in order to be relativistic down to nucleosynthesis temperature. See paper for heavier X^0.

[22] ALLIEGRO 92 limit applies for m_{X^0}=150–340 MeV and is the branching ratio times the decay probability. Limit is $< 1.5 \times 10^{-8}$ at 99%CL.

[23] ATIYA 92 looked for a peak in missing mass distribution. The limit applies to m_{X^0}=0–130 MeV in the narrow resonance limit. See paper for the dependence on lifetime. Covariance requires X^0 to be a vector particle.

[24] BARABASH 92 is a beam dump experiment that searched for a light Higgs. Limits between 1×10^{-12} and 1×10^{-7} are obtained for $3 < m_{X^0} < 40$ MeV.

[25] Limits between 1×10^{-12} and 1 are obtained for $4 < m_{X^0} < 69$ MeV.

[26] Limits between 1×10^{-11} and 5×10^{-3} are obtained for $4 < m_{X^0} < 63$ MeV.

[27] Limits between 1×10^{-14} and 1 are obtained for $3 < m_{X^0} < 82$ MeV.

[28] MEIJERDREES 92 limit applies for $\tau_{X^0} = 10^{-23}$–10^{-11} sec. Limits between 2×10^{-4} and 4×10^{-6} are obtained for m_{X^0} = 25–120 MeV. Angular momentum conservation requires that X^0 has spin ≥ 1.

[29] ATIYA 90B limit is for $B(K^+ \to \pi^+ X^0) \cdot B(X^0 \to \gamma\gamma)$ and applies for $m_{X^0} = 50$ MeV, $\tau_{X^0} < 10^{-10}$ s. Limits are also provided for $0 < m_{X^0} < 100$ MeV, $\tau_{X^0} < 10^{-8}$ s.

[30] KORENCHENKO 87 limit assumes $m_{A^0} = 1.7$ MeV, $\tau_{A^0} \lesssim 10^{-12}$ s, and $B(A^0 \to e^+ e^-) = 1$.

[31] EICHLER 86 looked for $\pi^+ \to e^+ \nu A^0$ followed by $A^0 \to e^+ e^-$. Limits on the branching fraction depend on the mass and and lifetime of A^0. The quoted limits are valid when $\tau(A^0) \gtrsim 3. \times 10^{-10}$s if the decays are kinematically allowed.

[32] YAMAZAKI 84 looked for a discrete line in $K^+ \to \pi^+$ X. Sensitive to wide mass range (5–300 MeV), independent of whether X decays promptly or not.

[33] ASANO 82 at KEK set limits for $B(K^+ \to \pi^+ X^0)$ for m_{X^0} <100 MeV as BR $< 4. \times 10^{-8}$ for $\tau(X^0 \to n\gamma\text{'s}) > 1. \times 10^{-9}$ s, BR $< 1.4 \times 10^{-6}$ for $\tau < 1. \times 10^{-9}$s.

[34] ASANO 81B is KEK experiment. Set $B(K^+ \to \pi^+ X^0) < 3.8 \times 10^{-8}$ at CL = 90%.

[35] ZHITNITSKII 79 argue that a heavy axion predicted by YANG 78 ($3 < m < 40$ MeV) contradicts experimental muon anomalous magnetic moments.

A^0 (Axion) Searches in Quarkonium Decays

Decay or transition of quarkonium. Limits are for branching ratio.

VALUE	CL%	DOCUMENT ID		TECN	COMMENT
• • • We do not use the following data for averages, fits, limits, etc. • • •					
$<2.8 \times 10^{-8}$	90	[1] ABLIKIM	16E	BES3	$J/\psi \to A^0\gamma$ ($A^0 \to \mu^+\mu^-$)
$<4 \times 10^{-7}$	90	[2] ABLIKIM	12	BES3	$J/\psi \to A^0\gamma$ ($A^0 \to \mu^+\mu^-$)
$<4.0 \times 10^{-5}$	90	[3] ANTREASYAN	90C	CBAL	$\Upsilon(1S) \to A^0\gamma$
$<5 \times 10^{-5}$	90	[4] DRUZHININ	87	ND	$\phi \to A^0\gamma$ ($A^0 \to e^+e^-$)
$<2 \times 10^{-3}$	90	[5] DRUZHININ	87	ND	$\phi \to A^0\gamma$ ($A^0 \to \gamma\gamma$)
$<7 \times 10^{-6}$	90	[6] DRUZHININ	87	ND	$\phi \to A^0\gamma$ ($A^0 \to$ missing)
$<1.4 \times 10^{-5}$	90	[7] EDWARDS	82	CBAL	$J/\psi \to A^0\gamma$

[1] ABLIKIM 16E limits between 2.8–495.3×10^{-8} were obtained for 0.212 GeV $< m_{A^0} <$ 3.0 GeV. See their Fig. 5 for mass-dependent limits.

[2] ABLIKIM 12 derived limits between 4×10^{-7}–2.1×10^{-5} for 0.212 GeV $< m_{A^0} <$ 3.0 GeV. See their Fig. 2(c) for mass-dependent limits.

[3] ANTREASYAN 90C assume that A^0 does not decay in the detector.

[4] The first DRUZHININ 87 limit is valid when $\tau_{A^0}/m_{A^0} < 3 \times 10^{-13}$ s/MeV and $m_{A^0} < 20$ MeV.

[5] The second DRUZHININ 87 limit is valid when $\tau_{A^0}/m_{A^0} < 5 \times 10^{-13}$ s/MeV and $m_{A^0} < 20$ MeV.

[6] The third DRUZHININ 87 limit is valid when $\tau_{A^0}/m_{A^0} > 7 \times 10^{-12}$ s/MeV and $m_{A^0} < 200$ MeV.

[7] EDWARDS 82 looked for $J/\psi \to \gamma A^0$ decays by looking for events with a single γ [of energy $\sim 1/2$ the $J/\psi(1S)$ mass], plus nothing else in the detector. The limit is inconsistent with the axion interpretation of the FAISSNER 81B result.

A^0 (Axion) Searches in Positronium Decays

Decay or transition of positronium. Limits are for branching ratio.

VALUE	CL%	DOCUMENT ID		TECN	COMMENT
• • • We do not use the following data for averages, fits, limits, etc. • • •					
$<4.4 \times 10^{-5}$	90	[1] BADERT...	02	CNTR	o-Ps $\to \gamma X_1 X_2$, $m_{X_1}+m_{X_2} \leq$ 900 keV
$<2 \times 10^{-4}$	90	MAENO	95	CNTR	o-Ps $\to A^0\gamma$ m_{A^0}=850–1013 keV
$<3.0 \times 10^{-4}$	90	[2] ASAI	94	CNTR	o-Ps $\to A^0\gamma$ m_{A^0}=30–500 keV
$<2.8 \times 10^{-5}$	90	[3] AKOPYAN	91	CNTR	o-Ps $\to A^0\gamma$ ($A^0 \to \gamma\gamma$), $m_{A^0} < 30$ keV
$<1.1 \times 10^{-6}$	90	[4] ASAI	91	CNTR	o-Ps $\to A^0\gamma$, $m_{A^0} < 800$ keV
$<3.8 \times 10^{-4}$	90	GNINENKO	90	CNTR	o-Ps $\to A^0\gamma$, $m_{A^0} < 30$ keV
$<(1$–$5) \times 10^{-4}$	95	[5] TSUCHIAKI	90	CNTR	o-Ps $\to A^0\gamma$, m_{A^0} = 300–900 keV
$<6.4 \times 10^{-5}$	90	[6] ORITO	89	CNTR	o-Ps $\to A^0\gamma$, $m_{A^0} < 30$ keV
		[7] AMALDI	85	CNTR	Ortho-positronium
		[8] CARBONI	83	CNTR	Ortho-positronium

[1] BADERTSCHER 02 looked for a three-body decay of ortho-positronium into a photon and two penetrating (neutral or milli-charged) particles.

[2] The ASAI 94 limit is based on inclusive photon spectrum and is independent of A^0 decay modes.

[3] The AKOPYAN 91 limit applies for a short-lived A^0 with $\tau_{A^0} < 10^{-13}\ m_{A^0}$ [keV]s.

[4] ASAI 91 limit translates to $g^2_{A^0 e^+ e^-}/4\pi < 1.1 \times 10^{-11}$ (90% CL) for $m_{A^0} < 800$ keV.

[5] The TSUCHIAKI 90 limit is based on inclusive photon spectrum and is independent of A^0 decay modes.

[6] ORITO 89 limit translates to $g^2_{A^0 ee}/4\pi < 6.2 \times 10^{-10}$. Somewhat more sensitive limits are obtained for larger m_{A^0}: $B < 7.6 \times 10^{-6}$ at 100 keV.

[7] AMALDI 85 set limits $B(A^0\gamma)$ / $B(\gamma\gamma\gamma) < (1$–$5) \times 10^{-6}$ for m_{A^0} = 900–100 keV which are about 1/10 of the CARBONI 83 limits.

[8] CARBONI 83 looked for orthopositronium $\to A^0\gamma$. Set limit for A^0 electron coupling squared, $g(eeA^0)^2/(4\pi) < 6. \times 10^{-10}$–$7. \times 10^{-9}$ for m_{A^0} from 150–900 keV (CL = 99.7%). This is about 1/10 of the bound from $g-2$ experiments.

A^0 (Axion) Search in Photoproduction

VALUE	DOCUMENT ID		COMMENT
• • • We do not use the following data for averages, fits, limits, etc. • • •			
	[1] BASSOMPIE...	95	$m_{A^0} = 1.8 \pm 0.2$ MeV

[1] BASSOMPIERRE 95 is an extension of BASSOMPIERRE 93. They looked for a peak in the invariant mass of e^+e^- pairs in the region $m_{e^+e^-} = 1.8 \pm 0.2$ MeV. They obtained bounds on the production rate A^0 for $\tau(A^0) = 10^{-18}$–10^{-9} sec. They also found an excess of events in the range $m_{e^+e^-} = 2.1$–3.5 MeV.

A^0 (Axion) Production in Hadron Collisions

Limits are for $\sigma(A^0)$ / $\sigma(\pi^0)$.

VALUE	CL%	EVTS	DOCUMENT ID		TECN	COMMENT
• • • We do not use the following data for averages, fits, limits, etc. • • •						
			[1] JAIN	07	CNTR	$A^0 \to e^+e^-$
			[2] AHMAD	97	SPEC	e^+ production
			[3] LEINBERGER	97	SPEC	$A^0 \to e^+e^-$
			[4] GANZ	96	SPEC	$A^0 \to e^+e^-$
			[5] KAMEL	96	EMUL	^{32}S emulsion, $A^0 \to e^+e^-$
			[6] BLUEMLEIN	92	BDMP	$A^0 N_Z \to \ell^+\ell^- N_Z$
			[7] MEIJERDREES	92	SPEC	$\pi^- p \to nA^0$, $A^0 \to e^+e^-$
			[8] BLUEMLEIN	91	BDMP	$A^0 \to e^+e^-$, 2γ
			[9] FAISSNER	89	OSPK	Beam dump, $A^0 \to e^+e^-$
			[10] DEBOER	88	RVUE	$A^0 \to e^+e^-$
			[11] EL-NADI	88	EMUL	$A^0 \to e^+e^-$
			[12] FAISSNER	88	OSPK	Beam dump, $A^0 \to 2\gamma$
			[13] BADIER	86	BDMP	$A^0 \to e^+e^-$
$<2. \times 10^{-11}$	90	0	[14] BERGSMA	85	CHRM	CERN beam dump
$<1. \times 10^{-13}$	90	0	[14] BERGSMA	85	CHRM	CERN beam dump
		24	[15] FAISSNER	83	OSPK	Beam dump, $A^0 \to 2\gamma$
			[16] FAISSNER	83B	RVUE	LAMPF beam dump
			[17] FRANK	83B	RVUE	LAMPF beam dump
			[18] HOFFMAN	83	CNTR	$\pi p \to nA^0$ ($A^0 \to e^+e^-$)
			[19] FETSCHER	82	RVUE	See FAISSNER 81B
		12	[20] FAISSNER	81	OSPK	CERN PS ν wideband
		15	[21] FAISSNER	81B	OSPK	Beam dump, $A^0 \to 2\gamma$
		8	[22] KIM	81	OSPK	26 GeV $pN \to A^0$X
		0	[23] FAISSNER	80	OSPK	Beam dump, $A^0 \to e^+e^-$
$<1. \times 10^{-8}$	90		[24] JACQUES	80	HLBC	28 GeV protons
$<1. \times 10^{-14}$	90		[24] JACQUES	80	HLBC	Beam dump
			[25] SOUKAS	80	CALO	28 GeV p beam dump
			[26] BECHIS	79	CNTR	
$<1. \times 10^{-8}$	90		[27] COTEUS	79	OSPK	Beam dump
$<1. \times 10^{-3}$	95		[28] DISHAW	79	CALO	400 GeV pp
$<1. \times 10^{-8}$	90		ALIBRAN	78	HYBR	Beam dump
$<6. \times 10^{-9}$	95		ASRATYAN	78B	CALO	Beam dump
$<1.5 \times 10^{-8}$	90		[29] BELLOTTI	78	HLBC	Beam dump
$<5.4 \times 10^{-14}$	90		[29] BELLOTTI	78	HLBC	m_{A^0}=1.5 MeV
$<4.1 \times 10^{-9}$	90		[29] BELLOTTI	78	HLBC	m_{A^0}=1 MeV
$<1. \times 10^{-8}$	90		[30] BOSETTI	78B	HYBR	Beam dump
			[31] DONNELLY	78		
$<0.5 \times 10^{-8}$	90		HANSL	78D	WIRE	Beam dump
			[32] MICELMAC...	78		
			[33] VYSOTSKII	78		

[1] JAIN 07 claims evidence for $A^0 \to e^+e^-$ produced in ^{207}Pb collision on nuclear emulsion (Ag/Br) for $m(A^0) = 7 \pm 1$ or 19 ± 1 MeV and $\tau(A^0) \leq 10^{-13}$ s.

[2] AHMAD 97 reports a result of APEX Collaboration which studied positron production in ^{238}U+^{232}Ta and ^{238}U+^{181}Ta collisions, without requiring a coincident electron. No narrow lines were found for $250 < E_{e^+} < 750$ keV.

[3] LEINBERGER 97 (ORANGE Collaboration) at GSI looked for a narrow sum-energy e^+e^--line at $\sim$ 635 keV in ^{238}U+^{181}Ta collision. Limits on the production probability for a narrow sum-energy e^+e^- line are set. See their Table 2.

[4] GANZ 96 (EPOS II Collaboration) has placed upper bounds on the production cross section of e^+e^- pairs from ^{238}U+^{181}Ta and ^{238}U+^{232}Th collisions at GSI. See Table 2 for limits both for back-to-back and isotropic configurations of e^+e^- pairs. These limits rule out the existence of peaks in the e^+e^- sum-energy distribution, reported by an earlier version of this experiment.

[5] KAMEL 96 looked for e^+e^- pairs from the collision of ^{32}S (200 GeV/nucleon) and emulsion. No evidence of mass peaks is found in the region of sensitivity $m_{ee} > 2$ MeV.

[6] BLUEMLEIN 92 is a proton beam dump experiment at Serpukhov with a secondary target to induce Bethe-Heitler production of e^+e^- or $\mu^+\mu^-$ from the produce A^0. See Fig. 5 for the excluded region in m_{A^0}-x plane. For the standard axion, $0.3 < x < 25$ is excluded at 95% CL. If combined with BLUEMLEIN 91, $0.008 < x < 32$ is excluded.

[7] MEIJERDREES 92 give $\Gamma(\pi^- p \to n A^0)\cdot B(A^0 \to e^+e^-)/\Gamma(\pi^- p \to \text{all}) < 10^{-5}$ (90% CL) for $m_{A^0} = 100$ MeV, $\tau_{A^0} = 10^{-11}$–10^{-23} sec. Limits ranging from 2.5×10^{-3} to 10^{-7} are given for $m_{A^0} = 25$–136 MeV.

[8] BLUEMLEIN 91 is a proton beam dump experiment at Serpukhov. No candidate event for $A^0 \to e^+e^-, 2\gamma$ are found. Fig. 6 gives the excluded region in m_{A^0}-x plane ($x = \tan\beta = v_2/v_1$). Standard axion is excluded for $0.2 < m_{A^0} < 3.2$ MeV for most $x > 1$, 0.2–11 MeV for most $x < 1$.

[9] FAISSNER 89 searched for $A^0 \to e^+e^-$ in a proton beam dump experiment at SIN. No excess of events was observed over the background. A standard axion with mass $2m_e$–20 MeV is excluded. Lower limit on f_{A^0} of $\simeq 10^4$ GeV is given for $m_{A^0} = 2m_e$–20 MeV.

[10] DEBOER 88 reanalyze EL-NADI 88 data and claim evidence for three distinct states with mass ~ 1.1, ~ 2.1, and ~ 9 MeV, lifetimes 10^{-16}–10^{-15} s decaying to e^+e^- and note the similarity of the data with those of a cosmic-ray experiment by Bristol group (B.M. Anand, Proc. of the Royal Society of London, Section A **A22** 183 (1953)). For a criticism see PERKINS 89, who suggests that the events are compatible with π^0 Dalitz decay. DEBOER 89B is a reply which contests the criticism.

[11] EL-NADI 88 claim the existence of a neutral particle decaying into e^+e^- with mass 1.60 ± 0.59 MeV, lifetime $(0.15 \pm 0.01) \times 10^{-14}$ s, which is produced in heavy ion interactions with emulsion nuclei at ~ 4 GeV/c/nucleon.

[12] FAISSNER 88 is a proton beam dump experiment at SIN. They found no candidate event for $A^0 \to \gamma\gamma$. A standard axion decaying to 2γ is excluded except for a region $x \simeq 1$. Lower limit on f_{A^0} of 10^2–10^3 GeV is given for $m_{A^0} = 0.1$–1 MeV.

[13] BADIER 86 did not find long-lived A^0 in 300 GeV π^- Beam Dump Experiment that decays into e^+e^- in the mass range $m_{A^0} = (20$–$200)$ MeV, which excludes the A^0 decay constant $f(A^0)$ in the interval (60–600) GeV. See their figure 6 for excluded region on $f(A^0)$-m_{A^0} plane.

[14] BERGSMA 85 look for $A^0 \to 2\gamma$, e^+e^-, $\mu^+\mu^-$. First limit above is for $m_{A^0} = 1$ MeV; second is for 200 MeV. See their figure 4 for excluded region on f_{A^0}–m_{A^0} plane, where f_{A^0} is A^0 decay constant. For Peccei-Quinn PECCEI 77 A^0, $m_{A^0} < 180$ keV and $\tau > 0.037$ s. (CL = 90%). For the axion of FAISSNER 81B at 250 keV, BERGSMA 85 expect 15 events but observe zero.

[15] FAISSNER 83 observed 19 1-γ and 12 2-γ events where a background of 4.8 and 2.3 respectively is expected. A small-angle peak is observed even if iron wall is set in front of the decay region.

[16] FAISSNER 83B extrapolate SIN γ signal to LAMPF ν experimental condition. Resulting 370 γ's are not at variance with LAMPF upper limit of 450 γ's. Derived from LAMPF limit that $[d\sigma(A^0)/d\omega$ at $90^\circ] m_{A^0}/\tau_{A^0} < 14 \times 10^{-35}$ cm^2 sr^{-1} MeV ms^{-1}. See comment on FRANK 83B.

[17] FRANK 83B stress the importance of LAMPF data bins with negative net signal. By statistical analysis say that LAMPF and SIN-A0 are at variance when extrapolation by phase-space model is done. They find LAMPF upper limit is 248 not 450 γ's. See comment on FAISSNER 83B.

[18] HOFFMAN 83 set CL = 90% limit $d\sigma/dt\, B(e^+e^-) < 3.5 \times 10^{-32}$ cm^2/GeV^2 for $140 < m_{A^0} < 160$ MeV. Limit assumes $\tau(A^0) < 10^{-9}$ s.

[19] FETSCHER 82 reanalyzes SIN beam-dump data of FAISSNER 81. Claims no evidence for axion since 2-γ peak rate remarkably decreases if iron wall is set in front of the decay region.

[20] FAISSNER 81 see excess μe events. Suggest axion interactions.

[21] FAISSNER 81B is SIN 590 MeV proton beam dump. Observed 14.5 ± 5.0 events of 2γ decay of long-lived neutral penetrating particle with $m_{2\gamma} \lesssim 1$ MeV. Axion interpretation with η-A^0 mixing gives $m_{A^0} = 250 \pm 25$ keV, $\tau(2\gamma) = (7.3 \pm 3.7) \times 10^{-3}$ s from above rate. See critical remarks below in comments of FETSCHER 82, FAISSNER 83, FAISSNER 83B, FRANK 83B, and BERGSMA 85. Also see in the next subsection ALEKSEEV 82B, CAVAIGNAC 83, and ANANEV 85.

[22] KIM 81 analyzed 8 candidates for $A^0 \to 2\gamma$ obtained by Aachen-Padova experiment at CERN with 26 GeV protons on Be. Estimated axion mass is about 300 keV and lifetime is $(0.86 \sim 5.6) \times 10^{-3}$ s depending on models. Faissner (private communication), says axion production underestimated and mass overestimated. Correct value around 200 keV.

[23] FAISSNER 80 is SIN beam dump experiment with 590 MeV protons looking for $A^0 \to e^+e^-$ decay. Assuming $A^0/\pi^0 = 5.5 \times 10^{-7}$, obtained decay rate limit $20/(A^0$ mass) MeV/s (CL = 90%), which is about 10^{-7} below theory and interpreted as upper limit to $m_{A^0} < 2m_{e^-}$.

[24] JACQUES 80 is a BNL beam dump experiment. First limit above comes from nonobservation of excess neutral-current-type events $[\sigma(\text{production})\sigma(\text{interaction}) < 7. \times 10^{-68}$ cm^4, CL = 90%]. Second limit is from nonobservation of axion decays into 2γ's or e^+e^-, and for axion mass a few MeV.

[25] SOUKAS 80 at BNL observed no excess of neutral-current-type events in beam dump.

[26] BECHIS 79 looked for the axion production in low energy electron Bremsstrahlung and the subsequent decay into either 2γ or e^+e^-. No signal found. CL = 90% limits for model parameter(s) are given.

[27] COTEUS 79 is a beam dump experiment at BNL.

[28] DISHAW 79 is a calorimetric experiment and looks for low energy tail of energy distributions due to energy lost to weakly interacting particles.

[29] BELLOTTI 78 first value comes from search for $A^0 \to e^+e^-$. Second value comes from search for $A^0 \to 2\gamma$, assuming mass $< 2m_{e^-}$. For any mass satisfying this, limit is above value$\times$(mass^{-4}). Third value uses data of PL 60B 401 and quotes σ(production)σ(interaction) $< 10^{-67}$ cm^4.

[30] BOSETTI 78B quotes σ(production)σ(interaction) $< 2. \times 10^{-67}$ cm^4.

[31] DONNELLY 78 examines data from reactor neutrino experiments of REINES 76 and GURR 74 as well as SLAC beam dump experiment. Evidence is negative.

[32] MICELMACHER 78 finds no evidence of axion existence in reactor experiments of REINES 76 and GURR 74. (See reference under DONNELLY 78 below).

[33] VYSOTSKII 78 derived lower limit for the axion mass 25 keV from luminosity of the sun and 200 keV from red supergiants.

A^0 (Axion) Searches in Reactor Experiments

VALUE		DOCUMENT ID		TECN	COMMENT
• • • We do not use the following data for averages, fits, limits, etc. • • •					
		[1] CHANG	07		Primakoff or Compton
		[2] ALTMANN	95	CNTR	Reactor; $A^0 \to e^+e^-$
		[3] KETOV	86	SPEC	Reactor, $A^0 \to \gamma\gamma$
		[4] KOCH	86	SPEC	Reactor; $A^0 \to \gamma\gamma$
		[5] DATAR	82	CNTR	Light water reactor
		[6] VUILLEUMIER	81	CNTR	Reactor, $A^0 \to 2\gamma$

[1] CHANG 07 looked for monochromatic photons from Primakoff or Compton conversion of axions from the Kuo-Sheng reactor due to axion coupling to photon or electron, respectively. The search places model-independent limits on the products $G_{A\gamma\gamma}G_{ANN}$ and $G_{Aee}G_{ANN}$ for $m(A^0)$ less than the MeV range.

[2] ALTMANN 95 looked for A^0 decaying into e^+e^- from the Bugey 5 nuclear reactor. They obtain an upper limit on the A^0 production rate of $\omega(A^0)/\omega(\gamma) \times B(A^0 \to e^+e^-) < 10^{-16}$ for $m_{A^0} = 1.5$ MeV at 90% CL. The limit is weaker for heavier A^0. In the case of a standard axion, this limit excludes a mass in the range $2m_e < m_{A^0} < 4.8$ MeV at 90% CL. See Fig. 5 of their paper for exclusion limits of axion-like resonances Z^0 in the (m_{X^0}, f_{X^0}) plane.

[3] KETOV 86 searched for A^0 at the Rovno nuclear power plant. They found an upper limit on the A^0 production probability of 0.8 $[100 \text{ keV}/m_{A^0}]^6 \times 10^{-6}$ per fission. In the standard axion model, this corresponds to $m_{A^0} > 150$ keV. Not valid for $m_{A^0} \gtrsim 1$ MeV.

[4] KOCH 86 searched for $A^0 \to \gamma\gamma$ at nuclear power reactor Biblis A. They found an upper limit on the A^0 production rate of $\omega(A^0)/\omega(\gamma(M1)) < 1.5 \times 10^{-10}$ (CL=95%). Standard axion with $m_{A^0} = 250$ keV gives 10^{-5} for the ratio. Not valid for $m_{A^0} > 1022$ keV.

[5] DATAR 82 looked for $A^0 \to 2\gamma$ in neutron capture ($np \to dA^0$) at Tarapur 500 MW reactor. Sensitive to sum of $I = 0$ and $I = 1$ amplitudes. With ZEHNDER 81 $[(I = 0) - (I = 1)]$ result, assert nonexistence of standard A^0.

[6] VUILLEUMIER 81 is at Grenoble reactor. Set limit $m_{A^0} < 280$ keV.

A^0 (Axion) and Other Light Boson (X^0) Searches in Nuclear Transitions

Limits are for branching ratio.

VALUE	CL%	DOCUMENT ID		TECN	COMMENT
• • • We do not use the following data for averages, fits, limits, etc. • • •					
$< 8.5 \times 10^{-6}$	90	[1] DERBIN	02	CNTR	^{125m}Te decay
		[2] DEBOER	97C	RVUE	M1 transitions
$< 5.5 \times 10^{-10}$	95	[3] TSUNODA	95	CNTR	^{252}Cf fission, $A^0 \to ee$
$< 1.2 \times 10^{-6}$	95	[4] MINOWA	93	CNTR	^{139}La$^* \to {}^{139}$LaA^0
$< 2 \times 10^{-4}$	90	[5] HICKS	92	CNTR	^{35}S decay, $A^0 \to \gamma\gamma$
$< 1.5 \times 10^{-9}$	95	[6] ASANUMA	90	CNTR	^{241}Am decay
$< (0.4$–$10) \times 10^{-3}$	95	[7] DEBOER	90	CNTR	^{8}Be$^* \to {}^8$BeA^0, $A^0 \to e^+e^-$
$< (0.2$–$1) \times 10^{-3}$	90	[8] BINI	89	CNTR	^{16}O$^* \to {}^{16}$OX^0, $X^0 \to e^+e^-$
		[9] AVIGNONE	88	CNTR	Cu$^* \to$ CuA^0 ($A^0 \to 2\gamma$, $A^0 e \to \gamma e$, $A^0 Z \to \gamma Z$)
$< 1.5 \times 10^{-4}$	90	[10] DATAR	88	CNTR	^{12}C$^* \to {}^{12}$CA^0, $A^0 \to e^+e^-$
$< 5 \times 10^{-3}$	90	[11] DEBOER	88C	CNTR	^{16}O$^* \to {}^{16}$OX^0, $X^0 \to e^+e^-$
$< 3.4 \times 10^{-5}$	95	[12] DOEHNER	88	SPEC	^{2}H*, $A^0 \to e^+e^-$
$< 4 \times 10^{-4}$	95	[13] SAVAGE	88	CNTR	Nuclear decay (isovector)
$< 3 \times 10^{-3}$	95	[13] SAVAGE	88	CNTR	Nuclear decay (isoscalar)
$< 10.6 \times 10^{-2}$	90	[14] HALLIN	86	SPEC	^{6}Li isovector decay
< 10.8	90	[14] HALLIN	86	SPEC	^{10}B isoscalar decays
< 2.2	90	[14] HALLIN	86	SPEC	^{14}N isoscalar decays
$< 4 \times 10^{-4}$	90	[15] SAVAGE	86B	CNTR	^{14}N*
		[16] ANANEV	85	CNTR	Li*, deut* $A^0 \to 2\gamma$
		[17] CAVAIGNAC	83	CNTR	^{97}Nb*, deut* transition $A^0 \to 2\gamma$
		[18] ALEKSEEV	82B	CNTR	Li*, deut* transition $A^0 \to 2\gamma$
		[19] LEHMANN	82	CNTR	Cu$^* \to$ CuA^0 ($A^0 \to 2\gamma$)
		[20] ZEHNDER	82	CNTR	Li*, Nb* decay, n-capt.
		[21] ZEHNDER	81	CNTR	Ba$^* \to$ BaA^0 ($A^0 \to 2\gamma$)
		[22] CALAPRICE	79		Carbon

[1] DERBIN 02 looked for the axion emission in an M1 transition in ^{125m}Te decay. They looked for a possible presence of a shifted energy spectrum in gamma rays due to the undetected axion.

[2] DEBOER 97C reanalyzed the existent data on Nuclear M1 transitions and find that a 9 MeV boson decaying into e^+e^- would explain the excess of events with large opening angles. See also DEBOER 01 for follow-up experiments.

[3] TSUNODA 95 looked for axion emission when ^{252}Cf undergoes a spontaneous fission, with the axion decaying into e^+e^-. The bound is for m_{A^0}=40 MeV. It improves to 2.5×10^{-5} for m_{A^0}=200 MeV.

[4] MINOWA 93 studied chain process, ^{139}Ce $\rightarrow$ ^{139}La* by electron capture and M1 transition of ^{139}La* to the ground state. It does not assume decay modes of A^0. The bound applies for $m_{A^0}<166$ keV.

[5] HICKS 92 bound is applicable for $\tau_{X^0}<4\times10^{-11}$ sec.

[6] The ASANUMA 90 limit is for the branching fraction of X^0 emission per ^{241}Am α decay and valid for $\tau_{X^0}<3\times10^{-11}$ s.

[7] The DEBOER 90 limit is for the branching ratio ^{8}Be* (18.15 MeV, 1^+) $\rightarrow$ ^{8}BeA^0, $A^0\rightarrow e^+e^-$ for the mass range m_{A^0} = 4–15 MeV.

[8] The BINI 89 limit is for the branching fraction of ^{16}O*(6.05 MeV, 0^+) $\rightarrow$ ^{16}OX^0, $X^0\rightarrow e^+e^-$ for m_X = 1.5–3.1 MeV. $\tau_{X^0}\lesssim10^{-11}$ s is assumed. The spin-parity of X is restricted to 0^+ or 1^-.

[9] AVIGNONE 88 looked for the 1115 keV transition C* $\rightarrow$ CuA^0, either from $A^0\rightarrow 2\gamma$ in-flight decay or from the secondary A^0 interactions by Compton and by Primakoff processes. Limits for axion parameters are obtained for $m_{A^0}<1.1$ MeV.

[10] DATAR 88 rule out light pseudoscalar particle emission through its decay $A^0\rightarrow e^+e^-$ in the mass range 1.02–2.5 MeV and lifetime range 10^{-13}–10^{-8} s. The above limit is for $\tau=5\times10^{-13}$ s and m = 1.7 MeV; see the paper for the τ-m dependence of the limit.

[11] The limit is for the branching fraction of ^{16}O*(6.05 MeV, 0^+) $\rightarrow$ ^{16}OX^0, $X^0\rightarrow e^+e^-$ against internal pair conversion for m_{X^0} = 1.7 MeV and $\tau_{X^0}<10^{-11}$ s. Similar limits are obtained for m_{X^0} = 1.3–3.2 MeV. The spin parity of X^0 must be either 0^+ or 1^-. The limit at 1.7 MeV is translated into a limit for the X^0-nucleon coupling constant: $g^2_{X^0NN}/4\pi<2.3\times10^{-9}$.

[12] The DOEHNER 88 limit is for m_{A^0} = 1.7 MeV, $\tau(A^0)<10^{-10}$ s. Limits less than 10^{-4} are obtained for m_{A^0} = 1.2–2.2 MeV.

[13] SAVAGE 88 looked for A^0 that decays into e^+e^- in the decay of the 9.17 MeV $J^P=2^+$ state in ^{14}N, 17.64 MeV state $J^P=1^+$ in ^{8}Be, and the 18.15 MeV state $J^P=1^+$ in ^{8}Be. This experiment constrains the isovector coupling of A^0 to hadrons, if m_{A^0} = (1.1 $\rightarrow$ 2.2) MeV and the isoscalar coupling of A^0 to hadrons, if m_{A^0} = (1.1 $\rightarrow$ 2.6) MeV. Both limits are valid only if $\tau(A^0)\lesssim1\times10^{-11}$ s.

[14] Limits are for $\Gamma(A^0(1.8\text{ MeV}))/\Gamma(\pi\text{M1})$; i.e., for 1.8 MeV axion emission normalized to the rate for internal emission of e^+e^- pairs. Valid for $\tau_{A^0}<2\times10^{-11}$s. ^{6}Li isovector decay data strongly disfavor PECCEI 86 model I, whereas the ^{10}B and ^{14}N isoscalar decay data strongly reject PECCEI 86 model II and III.

[15] SAVAGE 86B looked for A^0 that decays into e^+e^- in the decay of the 9.17 MeV $J^P=2^+$ state in ^{14}N. Limit on the branching fraction is valid if $\tau_{A^0}\lesssim1.\times10^{-11}$s for m_{A^0} = (1.1–1.7) MeV. This experiment constrains the iso-vector coupling of A^0 to hadrons.

[16] ANANEV 85 with IBR-2 pulsed reactor exclude standard A^0 at CL = 95% masses below 470 keV (Li* decay) and below $2m_e$ for deuteron* decay.

[17] CAVAIGNAC 83 at Bugey reactor exclude axion at any m_{97}Nb*decay and axion with m_{A^0} between 275 and 288 keV (deuteron* decay).

[18] ALEKSEEV 82 with IBR-2 pulsed reactor exclude standard A^0 at CL = 95% mass-ranges m_{A^0} <400 keV (Li* decay) and 330 keV <m_{A^0} <2.2 MeV. (deuteron* decay).

[19] LEHMANN 82 obtained $A^0\rightarrow 2\gamma$ rate $<6.2\times10^{-5}$/s (CL = 95%) excluding m_{A^0} between 100 and 1000 keV.

[20] ZEHNDER 82 used Gosgen 2.8GW light-water reactor to check A^0 production. No 2γ peak in Li*, Nb* decay (both single p transition) nor in n capture (combined with previous Ba* negative result) rules out standard A^0. Set limit m_{A^0} <60 keV for any A^0.

[21] ZEHNDER 81 looked for Ba* $\rightarrow$ A^0Ba transition with $A^0\rightarrow 2\gamma$. Obtained 2γ coincidence rate $<2.2\times10^{-5}$/s (CL = 95%) excluding m_{A^0} >160 keV (or 200 keV depending on Higgs mixing). However, see BARROSO 81.

[22] CALAPRICE 79 saw no axion emission from excited states of carbon. Sensitive to axion mass between 1 and 15 MeV.

A^0 (Axion) Limits from Its Electron Coupling

Limits are for $\tau(A^0\rightarrow e^+e^-)$.

VALUE (s)	CL%	DOCUMENT ID		TECN	COMMENT
• • • We do not use the following data for averages, fits, limits, etc. • • •					
none 4×10^{-16}–4.5×10^{-12}	90	[1] BROSS	91	BDMP	$eN\rightarrow eA^0N$ ($A^0\rightarrow ee$)
		[2] GUO	90	BDMP	$eN\rightarrow eA^0N$ ($A^0\rightarrow ee$)
		[3] BJORKEN	88	CALO	$A\rightarrow e^+e^-$ or 2γ
		[4] BLINOV	88	MD1	$ee\rightarrow eeA^0$ ($A^0\rightarrow ee$)
none 1×10^{-14}–1×10^{-10}	90	[5] RIORDAN	87	BDMP	$eN\rightarrow eA^0N$ ($A^0\rightarrow ee$)
none 1×10^{-14}–1×10^{-11}	90	[6] BROWN	86	BDMP	$eN\rightarrow eA^0N$ ($A^0\rightarrow ee$)
none 6×10^{-14}–9×10^{-11}	95	[7] DAVIER	86	BDMP	$eN\rightarrow eA^0N$ ($A^0\rightarrow ee$)
none 3×10^{-13}–1×10^{-7}	90	[8] KONAKA	86	BDMP	$eN\rightarrow eA^0N$ ($A^0\rightarrow ee$)

[1] The listed BROSS 91 limit is for m_{A^0} = 1.14 MeV. B($A^0\rightarrow e^+e^-$) = 1 assumed. Excluded domain in the τ_{A^0}–m_{A^0} plane extends up to $m_{A^0}\approx$ 7 MeV (see Fig. 5). Combining with electron $g-2$ constraint, axions coupling only to e^+e^- ruled out for $m_{A^0}<4.8$ MeV (90% CL).

[2] GUO 90 use the same apparatus as BROWN 86 and improve the previous limit in the shorter lifetime region. Combined with $g-2$ constraint, axions coupling only to e^+e^- are ruled out for $m_{A^0}<2.7$ MeV (90% CL).

[3] BJORKEN 88 reports limits on axion parameters (f_A, m_A, τ_A) for $m_{A^0}<200$ MeV from electron beam-dump experiment with production via Primakoff photoproduction, bremsstrahlung from electrons, and resonant annihilation of positrons on atomic electrons.

[4] BLINOV 88 assume zero spin, m = 1.8 MeV and lifetime $<5\times10^{-12}$ s and find $\Gamma(A^0\rightarrow\gamma\gamma)$B($A^0\rightarrow e^+e^-$) < 2 eV (CL=90%).

[5] Assumes $A^0\gamma\gamma$ coupling is small and hence Primakoff production is small. Their figure 2 shows limits on axions for $m_{A^0}<15$ MeV.

[6] Uses electrons in hadronic showers from an incident 800 GeV proton beam. Limits for $m_{A^0}<15$ MeV are shown in their figure 3.

[7] m_{A^0} = 1.8 MeV assumed. The excluded domain in the τ_{A^0}–m_{A^0} plane extends up to $m_{A^0}\approx$ 14 MeV, see their figure 4.

[8] The limits are obtained from their figure 3. Also given is the limit on the $A^0\gamma\gamma$–$A^0e^+e^-$ coupling plane by assuming Primakoff production.

Search for A^0 (Axion) Resonance in Bhabha Scattering

The limit is for $\Gamma(A^0)$[B($A^0\rightarrow e^+e^-$)]^2.

VALUE (10^{-3} eV)	CL%	DOCUMENT ID		TECN	COMMENT
• • • We do not use the following data for averages, fits, limits, etc. • • •					
< 1.3	97	[1] HALLIN	92	CNTR	m_{A^0} = 1.75–1.88 MeV
none 0.0016–0.47	90	[2] HENDERSON	92C	CNTR	m_{A^0}= 1.5–1.86 MeV
< 2.0	90	[3] WU	92	CNTR	m_{A^0}= 1.56–1.86 MeV
< 0.013	95	TSERTOS	91	CNTR	m_{A^0} = 1.832 MeV
none 0.19–3.3	95	[4] WIDMANN	91	CNTR	m_{A^0}= 1.78–1.92 MeV
< 5	97	BAUER	90	CNTR	m_{A^0} = 1.832 MeV
none 0.09–1.5	95	[5] JUDGE	90	CNTR	m_{A^0} = 1.832 MeV, elastic
< 1.9	97	[6] TSERTOS	89	CNTR	m_{A^0} = 1.82 MeV
<(10–40)	97	[6] TSERTOS	89	CNTR	m_{A^0} = 1.51–1.65 MeV
<(1–2.5)	97	[6] TSERTOS	89	CNTR	m_{A^0} = 1.80–1.86 MeV
< 31	95	LORENZ	88	CNTR	m_{A^0} = 1.646 MeV
< 94	95	LORENZ	88	CNTR	m_{A^0} = 1.726 MeV
< 23	95	LORENZ	88	CNTR	m_{A^0} = 1.782 MeV
< 19	95	LORENZ	88	CNTR	m_{A^0} = 1.837 MeV
< 3.8	97	[7] TSERTOS	88	CNTR	m_{A^0} = 1.832 MeV
		[8] VANKLINKEN	88	CNTR	
		[9] MAIER	87	CNTR	
<2500	90	MILLS	87	CNTR	m_{A^0} = 1.8 MeV
		[10] VONWIMMER..	87	CNTR	

[1] HALLIN 92 quote limits on lifetime, $8\times10^{-14}-5\times10^{-13}$ sec depending on mass, assuming B($A^0\rightarrow e^+e^-$) = 100%. They say that TSERTOS 91 overstated their sensitivity by a factor of 3.

[2] HENDERSON 92C exclude axion with lifetime τ_{A^0}=$1.4\times10^{-12}-4.0\times10^{-10}$ s, assuming B($A^0\rightarrow e^+e^-$)=100%. HENDERSON 92C also exclude a vector boson with τ=$1.4\times10^{-12}-6.0\times10^{-10}$ s.

[3] WU 92 quote limits on lifetime $>3.3\times10^{-13}$s assuming B($A^0\rightarrow e^+e^-$)=100%. They say that TSERTOS 89 overestimate the limit by a factor of $\pi/2$. WU 92 also quote a bound for vector boson, $\tau>8.2\times10^{-13}$s.

[4] WIDMANN 91 bound applies exclusively to the case B($A^0\rightarrow e^+e^-$)=1, since the detection efficiency varies substantially as $\Gamma(A^0)_{\text{total}}$ changes. See their Fig. 6.

[5] JUDGE 90 excludes an elastic pseudoscalar e^+e^- resonance for 4.5×10^{-13} s < $\tau(A^0)$ < 7.5×10^{-12} s (95% CL) at m_{A^0} = 1.832 MeV. Comparable limits can be set for m_{A^0} = 1.776–1.856 MeV.

[6] See also TSERTOS 88B in references.

[7] The upper limit listed in TSERTOS 88 is too large by a factor of 4. See TSERTOS 88B, footnote 3.

[8] VANKLINKEN 88 looked for relatively long-lived resonance ($\tau=10^{-10}$–10^{-12} s). The sensitivity is not sufficient to exclude such a narrow resonance.

[9] MAIER 87 obtained limits $R\Gamma\lesssim$ 60 eV (100 eV) at $m_{A^0}\simeq$ 1.64 MeV (1.83 MeV) for energy resolution $\Delta E_{\text{cm}}\simeq$ 3 keV, where R is the resonance cross section normalized to that of Bhabha scattering, and $\Gamma=\Gamma^2_{ee}/\Gamma_{\text{total}}$. For a discussion implying that $\Delta E_{\text{cm}}\simeq$ 10 keV, see TSERTOS 89.

[10] VONWIMMERSPERG 87 measured Bhabha scattering for E_{cm} = 1.37–1.86 MeV and found a possible peak at 1.73 with $\int\sigma dE_{\text{cm}}=14.5\pm6.8$ keV·b. For a comment and a reply, see VANKLINKEN 88B and VONWIMMERSPERG 88. Also see CONNELL 88.

Search for A^0 (Axion) Resonance in $e^+e^-\rightarrow\gamma\gamma$

The limit is for $\Gamma(A^0\rightarrow e^+e^-)\cdot\Gamma(A^0\rightarrow\gamma\gamma)/\Gamma_{\text{total}}$

VALUE (10^{-3} eV)	CL%	DOCUMENT ID		TECN	COMMENT
• • • We do not use the following data for averages, fits, limits, etc. • • •					
< 0.18	95	VO	94	CNTR	m_{A^0}=1.1 MeV
< 1.5	95	VO	94	CNTR	m_{A^0}=1.4 MeV
<12	95	VO	94	CNTR	m_{A^0}=1.7 MeV
< 6.6	95	[1] TRZASKA	91	CNTR	m_{A^0} = 1.8 MeV
< 4.4	95	WIDMANN	91	CNTR	m_{A^0}= 1.78–1.92 MeV

See key on page 885

Gauge & Higgs Boson Particle Listings

Axions (A^0) and Other Very Light Bosons

		[2] FOX	89	CNTR	
< 0.11	95	[3] MINOWA	89	CNTR	m_{A^0} = 1.062 MeV
<33	97	CONNELL	88	CNTR	m_{A^0} = 1.580 MeV
<42	97	CONNELL	88	CNTR	m_{A^0} = 1.642 MeV
<73	97	CONNELL	88	CNTR	m_{A^0} = 1.782 MeV
<79	97	CONNELL	88	CNTR	m_{A^0} = 1.832 MeV

[1] TRZASKA 91 also give limits in the range (6.6–30) $\times 10^{-3}$ eV (95%CL) for m_{A^0} = 1.6–2.0 MeV.
[2] FOX 89 measured positron annihilation with an electron in the source material into two photons and found no signal at 1.062 MeV ($< 9\times10^{-5}$ of two-photon annihilation at rest).
[3] Similar limits are obtained for m_{A^0} = 1.045–1.085 MeV.

Search for X^0 (Light Boson) Resonance in $e^+e^- \to \gamma\gamma\gamma$

The limit is for $\Gamma(X^0 \to e^+e^-)\cdot\Gamma(X^0 \to \gamma\gamma\gamma)/\Gamma_{\text{total}}$. C invariance forbids spin-0 X^0 coupling to both e^+e^- and $\gamma\gamma\gamma$.

VALUE (10^{-3} eV)	CL%	DOCUMENT ID		TECN	COMMENT
• • • We do not use the following data for averages, fits, limits, etc. • • •					
< 0.2	95	[1] VO	94	CNTR	m_{X^0}=1.1–1.9 MeV
< 1.0	95	[2] VO	94	CNTR	m_{X^0}=1.1 MeV
< 2.5	95	[2] VO	94	CNTR	m_{X^0}=1.4 MeV
<120	95	[2] VO	94	CNTR	m_{X^0}=1.7 MeV
< 3.8	95	[3] SKALSEY	92	CNTR	m_{X^0}= 1.5 MeV

[1] VO 94 looked for $X^0 \to \gamma\gamma\gamma$ decaying at rest. The precise limits depend on m_{X^0}. See Fig. 2(b) in paper.
[2] VO 94 looked for $X^0 \to \gamma\gamma\gamma$ decaying in flight.
[3] SKALSEY 92 also give limits 4.3 for m_{X^0} = 1.54 and 7.5 for 1.64 MeV. The spin of X^0 is assumed to be one.

Light Boson (X^0) Search in Nonresonant e^+e^- Annihilation at Rest

Limits are for the ratio of $n\gamma + X^0$ production relative to $\gamma\gamma$.

VALUE (units 10^{-6})	CL%	DOCUMENT ID		TECN	COMMENT
• • • We do not use the following data for averages, fits, limits, etc. • • •					
< 4.2	90	[1] MITSUI	96	CNTR	γX^0
< 4	68	[2] SKALSEY	95	CNTR	γX^0
<40	68	[3] SKALSEY	95	RVUE	γX^0
< 0.18	90	[4] ADACHI	94	CNTR	$\gamma\gamma X^0$, $X^0 \to \gamma\gamma$
< 0.26	90	[5] ADACHI	94	CNTR	$\gamma\gamma X^0$, $X^0 \to \gamma\gamma$
< 0.33	90	[6] ADACHI	94	CNTR	γX^0, $X^0 \to \gamma\gamma\gamma$

[1] MITSUI 96 looked for a monochromatic γ. The bound applies for a vector X^0 with C=−1 and m_{X^0} <200 keV. They derive an upper bound on eeX^0 coupling and hence on the branching ratio B(o-Ps $\to \gamma\gamma X^0$)< 6.2×10^{-6}. The bounds weaken for heavier X^0.
[2] SKALSEY 95 looked for a monochromatic γ without an accompanying γ in e^+e^- annihilation. The bound applies for scalar and vector X^0 with $C=-1$ and m_{X^0} = 100–1000 keV.
[3] SKALSEY 95 reinterpreted the bound on γA^0 decay of o-Ps by ASAI 91 where 3% of delayed annihilations are not from $^3S_1$ states. The bound applies for scalar and vector X^0 with $C=-1$ and m_{X^0} = 0–800 keV.
[4] ADACHI 94 looked for a peak in the $\gamma\gamma$ invariant mass distribution in $\gamma\gamma\gamma$ production from e^+e^- annihilation. The bound applies for m_{X^0} = 70–800 keV.
[5] ADACHI 94 looked for a peak in the missing-mass mass distribution in $\gamma\gamma$ channel, using $\gamma\gamma\gamma$ production from e^+e^- annihilation. The bound applies for m_{X^0} <800 keV.
[6] ADACHI 94 looked for a peak in the missing mass distribution in $\gamma\gamma\gamma$ channel, using $\gamma\gamma\gamma$ production from e^+e^- annihilation. The bound applies for m_{X^0} = 200–900 keV.

Searches for Goldstone Bosons (X^0)

(Including Horizontal Bosons and Majorons.) Limits are for branching ratios.

VALUE	CL%	DOCUMENT ID		TECN	COMMENT
• • • We do not use the following data for averages, fits, limits, etc. • • •					
$<9\times10^{-6}$	90	[1] BAYES	15	TWST	$\mu^+ \to e^+X^0$, Familon
		[2] LATTANZI	13	COSM	Majoron dark matter decay
		[3] LESSA	07	RVUE	Meson, ℓ decays to Majoron
		[4] DIAZ	98	THEO	$H^0 \to X^0X^0$, $A^0 \to X^0X^0X^0$, Majoron
		[5] BOBRAKOV	91		Electron quasi-magnetic interaction
$<3.3\times10^{-2}$	95	[6] ALBRECHT	90E	ARG	$\tau \to \mu X^0$. Familon
$<1.8\times10^{-2}$	95	[6] ALBRECHT	90E	ARG	$\tau \to eX^0$. Familon
$<6.4\times10^{-9}$	90	[7] ATIYA	90	B787	$K^+ \to \pi^+X^0$. Familon
$<1.4\times10^{-5}$	90	[8] BALKE	88	CNTR	$\mu^+ \to e^+X^0$. Familon
$<1.1\times10^{-9}$	90	[9] BOLTON	88	CBOX	$\mu^+ \to e^+\gamma X^0$. Familon
		[10] CHANDA	88	ASTR	Sun, Majoron
		[11] CHOI	88	ASTR	Majoron, SN 1987A
$<5\times10^{-6}$	90	[12] PICCIOTTO	88	CNTR	$\pi \to e\nu X^0$, Majoron
$<1.3\times10^{-9}$	90	[13] GOLDMAN	87	CNTR	$\mu \to e\gamma X^0$. Familon
$<3\times10^{-4}$	90	[14] BRYMAN	86B	RVUE	$\mu \to eX^0$. Familon
$<1\times10^{-10}$	90	[15] EICHLER	86	SPEC	$\mu^+ \to e^+X^0$. Familon
$<2.6\times10^{-6}$	90	[16] JODIDIO	86	SPEC	$\mu^+ \to e^+X^0$. Familon
		[17] BALTRUSAIT...	85	MRK3	$\tau \to \ell X^0$. Familon
		[18] DICUS	83	COSM	ν(hvy) $\to \nu$(light)X^0

[1] BAYES 15 limits are the average over m_{X^0} = 13–80 MeV for the isotropic decay distribution of positrons. See their Fig. 4 and Table II for the mass-dependent limits as well as the dependence on the decay anisotropy. In particular, they find a limit $< 58\times10^{-6}$ at 90% CL for massless familons and for the same asymmetry as normal muon decay, a case not covered by JODIDIO 86.
[2] LATTANZI 13 use WMAP 9 year data as well as X-ray and γ-ray observations to derive limits on decaying majoron dark matter. A limit on the decay width $\Gamma(X^0 \to \nu\overline{\nu})$ $< 6.4\times10^{-19}$ s^{-1} at 95% CL is found if majorons make up all of the dark matter.
[3] LESSA 07 consider decays of the form Meson $\to \ell\nu$Majoron and $\ell \to \ell'\nu\overline{\nu}$Majoron and use existing data to derive limits on the neutrino-Majoron Yukawa couplings $g_{\alpha\beta}$ ($\alpha,\beta=e,\mu,\tau$). Their best limits are $|g_{e\alpha}|^2 < 5.5\times10^{-6}$, $|g_{\mu\alpha}|^2 < 4.5\times10^{-5}$, $|g_{\tau\alpha}|^2 < 5.5\times10^{-2}$ at CL = 90%.
[4] DIAZ 98 studied models of spontaneously broken lepton number with both singlet and triplet Higgses. They obtain limits on the parameter space from invisible decay $Z \to H^0A^0 \to X^0X^0X^0X^0X^0$ and $e^+e^- \to ZH^0$ with $H^0 \to X^0X^0$.
[5] BOBRAKOV 91 searched for anomalous magnetic interactions between polarized electrons expected from the exchange of a massless pseudoscalar boson (arion). A limit $x_e^2 < 2\times10^{-4}$ (95%CL) is found for the effective anomalous magneton parametrized as $x_e(G_F/8\pi\sqrt{2})^{1/2}$.
[6] ALBRECHT 90E limits are for B($\tau \to \ell X^0$)/B($\tau \to \ell\nu\overline{\nu}$). Valid for m_{X^0} < 100 MeV. The limits rise to 7.1% (for μ), 5.0% (for e) for m_{X^0} = 500 MeV.
[7] ATIYA 90 limit is for m_{X^0} = 0. The limit B $< 1\times10^{-8}$ holds for m_{X^0} < 95 MeV. For the reduction of the limit due to finite lifetime of X^0, see their Fig. 3.
[8] BALKE 88 limits are for B($\mu^+ \to e^+X^0$). Valid for m_{X^0} <80 MeV and $\tau_{X^0} > 10^{-8}$ sec.
[9] BOLTON 88 limit corresponds to $F > 3.1\times10^9$ GeV, which does not depend on the chirality property of the coupling.
[10] CHANDA 88 find v_T < 10 MeV for the weak-triplet Higgs vacuum expectation value in Gelmini-Roncadelli model, and $v_S > 5.8\times10^6$ GeV in the singlet Majoron model.
[11] CHOI 88 used the observed neutrino flux from the supernova SN1987A to exclude the neutrino Majoron Yukawa coupling h in the range $2\times10^{-5} < h < 3\times10^{-4}$ for the interaction $L_{\text{int}} = \frac{1}{2}ih\overline{\psi^c_\nu}\gamma_5\psi_\nu\phi_X$. For several families of neutrinos, the limit applies for $(\Sigma h_i^4)^{1/4}$.
[12] PICCIOTTO 88 limit applies when m_{X^0} < 55 MeV and $\tau_{X^0} > 2$ns, and it decreases to 4×10^{-7} at m_{X^0} = 125 MeV, beyond which no limit is obtained.
[13] GOLDMAN 87 limit corresponds to $F > 2.9\times10^9$ GeV for the family symmetry breaking scale from the Lagrangian $L_{\text{int}} = (1/F)\overline{\psi}_\mu\gamma^\mu(a+b\gamma_5)\psi_e\partial_\mu\phi_{X^0}$ with $a^2+b^2=1$. This is not as sensitive as the limit $F > 9.9\times10^9$ GeV derived from the search for $\mu^+ \to e^+X^0$ by JODIDIO 86, but does not depend on the chirality property of the coupling.
[14] Limits are for $\Gamma(\mu \to eX^0)/\Gamma(\mu \to e\nu\overline{\nu})$. Valid when m_{X^0} = 0–93.4, 98.1–103.5 MeV.
[15] EICHLER 86 looked for $\mu^+ \to e^+X^0$ followed by $X^0 \to e^+e^-$. Limits on the branching fraction depend on the mass and and lifetime of X^0. The quoted limits are valid when $\tau_{X^0} \lesssim 3.\times10^{-10}$ s if the decays are kinematically allowed.
[16] JODIDIO 86 corresponds to $F > 9.9\times10^9$ GeV for the family symmetry breaking scale with the parity-conserving effective Lagrangian $L_{\text{int}} = (1/F)\ \overline{\psi}_\mu\gamma^\mu\psi_e\partial^\mu\phi_{X^0}$.
[17] BALTRUSAITIS 85 search for light Goldstone boson(X^0) of broken U(1). CL = 95% limits are B($\tau \to \mu^+X^0$)/B($\tau \to \mu^+\nu\nu$) <0.125 and B($\tau \to e^+X^0$)/B($\tau \to e^+\nu\nu$) <0.04. Inferred limit for the symmetry breaking scale is m >3000 TeV.
[18] The primordial heavy neutrino must decay into ν and familon, f_A, early so that the red-shifted decay products are below critical density, see their table. In addition, $K \to \pi f_A$ and $\mu \to e f_A$ are unseen. Combining these excludes $m_{\text{heavy}\nu}$ between 5×10^{-5} and 5×10^{-4} MeV (μ decay) and $m_{\text{heavy}\nu}$ between 5×10^{-5} and 0.1 MeV (K-decay).

Majoron Searches in Neutrinoless Double β Decay

Limits are for the half-life of neutrinoless $\beta\beta$ decay with a Majoron emission. No experiment currently claims any such evidence. Only the best or comparable limits for each isotope are reported. Also see the reviews ZUBER 98 and FAESSLER 98B.

$t_{1/2}$(10^{21} yr)	CL%	ISOTOPE	TRANSITION	METHOD	DOCUMENT ID	
>7200	**90**	**^{128}Te**		**CNTR**	[1] BERNATOW...	92
• • • We do not use the following data for averages, fits, limits, etc. • • •						
> 420	90	^{76}Ge	$0\nu1\chi$	GERDA	[2] AGOSTINI	15A
> 400	90	^{100}Mo	$0\nu1\chi$	NEMO-3	[3] ARNOLD	15
>1200	90	^{136}Xe	$0\nu1\chi$	EXO-200	[4] ALBERT	14A
>2600	90	^{136}Xe	$0\nu1\chi$	KamLAND-Zen	[5] GANDO	12
> 16	90	^{130}Te	$0\nu1\chi$	NEMO-3	[6] ARNOLD	11
> 1.9	90	^{96}Zr	$2\nu1\chi$	NEMO-3	[7] ARGYRIADES	10
> 1.52	90	^{150}Nd	$0\nu1\chi$	NEMO-3	[8] ARGYRIADES	09
> 27	90	^{100}Mo	$0\nu1\chi$	NEMO-3	[9] ARNOLD	06
> 15	90	^{82}Se	$0\nu1\chi$	NEMO-3	[10] ARNOLD	06
> 14	90	^{100}Mo	$0\nu1\chi$	NEMO-3	[11] ARNOLD	04
> 12	90	^{82}Se	$0\nu1\chi$	NEMO-3	[12] ARNOLD	04
> 2.2	90	^{130}Te	$0\nu1\chi$	Cryog. det.	[13] ARNABOLDI	03
> 0.9	90	^{130}Te	$0\nu2\chi$	Cryog. det.	[14] ARNABOLDI	03
> 8	90	^{116}Cd	$0\nu1\chi$	$CdWO_4$ scint.	[15] DANEVICH	03
> 0.8	90	^{116}Cd	$0\nu2\chi$	$CdWO_4$ scint.	[16] DANEVICH	03

Gauge & Higgs Boson Particle Listings

Axions (A^0) and Other Very Light Bosons

> 500	90	^{136}Xe	$0\nu1\chi$	Liquid Xe Scint.	[17] BERNABEI	02D
> 5.8	90	^{100}Mo	$0\nu1\chi$	ELEGANT V	[18] FUSHIMI	02
> 0.32	90	^{100}Mo	$0\nu1\chi$	Liq. Ar ioniz.	[19] ASHITKOV	01
> 0.0035	90	^{160}Gd	$0\nu1\chi$	$^{160}Gd_2SiO_5$:Ce	[20] DANEVICH	01
> 0.013	90	^{160}Gd	$0\nu2\chi$	$^{160}Gd_2SiO_5$:Ce	[21] DANEVICH	01
> 2.3	90	^{82}Se	$0\nu1\chi$	NEMO 2	[22] ARNOLD	00
> 0.31	90	^{96}Zr	$0\nu1\chi$	NEMO 2	[23] ARNOLD	00
> 0.63	90	^{82}Se	$0\nu2\chi$	NEMO 2	[24] ARNOLD	00
> 0.063	90	^{96}Zr	$0\nu2\chi$	NEMO 2	[24] ARNOLD	00
> 0.16	90	^{100}Mo	$0\nu2\chi$	NEMO 2	[24] ARNOLD	00
> 2.4	90	^{82}Se	$0\nu1\chi$	NEMO 2	[25] ARNOLD	98
> 7.2	90	^{136}Xe	$0\nu2\chi$	TPC	[26] LUESCHER	98
> 7.91	90	^{76}Ge		SPEC	[27] GUENTHER	96
> 17	90	^{76}Ge		CNTR	BECK	93

[1] BERNATOWICZ 92 studied double-β decays of ^{128}Te and ^{130}Te, and found the ratio $\tau(^{130}\text{Te})/\tau(^{128}\text{Te}) = (3.52 \pm 0.11) \times 10^{-4}$ in agreement with relatively stable theoretical predictions. The bound is based on the requirement that Majoron-emitting decay cannot be larger than the observed double-beta rate of ^{128}Te of $(7.7 \pm 0.4) \times 10^{24}$ year. We calculated 90% CL limit as $(7.7\text{–}1.28 \times 0.4{=}7.2) \times 10^{24}$.

[2] AGOSTINI 15A analyze a 20.3 kg yr of data set of the GERDA calorimeter to determine $g_{\nu\chi} < 3.4\text{–}8.7 \times 10^{-5}$ on the Majoron-neutrino coupling constant. The range reflects the spread of the nuclear matrix elements.

[3] ARNOLD 15 use the NEMO-3 tracking calorimeter with 3.43 kg yr exposure to determine the limit on Majoron emission. The limit corresponds to $g_{\nu\chi} < 1.6\text{–}3.0 \times 10^{-4}$. The spread reflects different nuclear matrix elements. Supersedes ARNOLD 06.

[4] ALBERT 14A utilize 100 kg yr of exposure of the EXO-200 tracking calorimeter to place a limit on the $g_{\nu\chi} < 0.8\text{–}1.7 \times 10^{-5}$ on the Majoron-neutrino coupling constant. The range reflects the spread of the nuclear matrix elements.

[5] GANDO 12 use the KamLAND-Zen detector to obtain the limit on the $0\nu\chi$ decay with Majoron emission. It implies that the coupling constant $g_{\nu\chi} < 0.8\text{–}1.6 \times 10^{-5}$ depending on the nuclear matrix elements used.

[6] ARNOLD 11 use the NEMO-3 detector to obtain the reported limit on Majoron emission. It implies that the coupling constant $g_{\nu\chi} < 0.6\text{–}1.6 \times 10^{-4}$ depending on the nuclear matrix element used. Supercedes ARNABOLDI 03.

[7] ARGYRIADES 10 use the NEMO-3 tracking detector and ^{96}Zr to derive the reported limit. No limit for the Majoron electron coupling is given.

[8] ARGYRIADES 09 use ^{150}Nd data taken with the NEMO-3 tracking detector. The reported limit corresponds to $\langle g_{\nu\chi} \rangle < 1.7\text{–}3.0 \times 10^{-4}$ using a range of nuclear matrix elements that include the effect of nuclear deformation.

[9] ARNOLD 06 use ^{100}Mo data taken with the NEMO-3 tracking detector. The reported limit corresponds to $\langle g_{\nu\chi} \rangle < (0.4\text{–}1.8) \times 10^{-4}$ using a range of matrix element calculations. Superseded by ARNOLD 15.

[10] NEMO-3 tracking calorimeter is used in ARNOLD 06 . Reported half-life limit for ^{82}Se corresponds to $\langle g_{\nu\chi} \rangle < (0.66\text{–}1.9) \times 10^{-4}$ using a range of matrix element calculations. Supersedes ARNOLD 04.

[11] ARNOLD 04 use the NEMO-3 tracking detector. The limit corresponds to $\langle g_{\nu\chi} \rangle < (0.5\text{–}0.9)10^{-4}$ using the matrix elements of SIMKOVIC 99, STOICA 01 and CIVITARESE 03. Superseded by ARNOLD 06.

[12] ARNOLD 04 use the NEMO-3 tracking detector. The limit corresponds to $\langle g_{\nu\chi} \rangle < (0.7\text{–}1.6)10^{-4}$ using the matrix elements of SIMKOVIC 99, STOICA 01 and CIVITARESE 03.

[13] Supersedes ALESSANDRELLO 00. Array of TeO_2 crystals in high resolution cryogenic calorimeter. Some enriched in ^{130}Te. Derive $\langle g_{\nu\chi} \rangle < 17\text{–}33 \times 10^{-5}$ depending on matrix element.

[14] Supersedes ALESSANDRELLO 00. Cryogenic calorimeter search.

[15] Limit for the $0\nu\chi$ decay with Majoron emission of ^{116}Cd using enriched $CdWO_4$ scintillators. $\langle g_{\nu\chi} \rangle < 4.6\text{–}8.1 \times 10^{-5}$ depending on the matrix element. Supersedes DANEVICH 00.

[16] Limit for the $0\nu2\chi$ decay of ^{116}Cd. Supersedes DANEVICH 00.

[17] BERNABEI 02D obtain limit for $0\nu\chi$ decay with Majoron emission of ^{136}Xe using liquid Xe scintillation detector. They derive $\langle g_{\nu\chi} \rangle < 2.0\text{–}3.0 \times 10^{-5}$ with several nuclear matrix elements.

[18] Replaces TANAKA 93. FUSHIMI 02 derive half-life limit for the $0\nu\chi$ decay by means of tracking calorimeter ELEGANT V. Considering various matrix element calculations, a range of limits for the Majoron-neutrino coupling is given: $\langle g_{\nu\chi} \rangle < (6.3\text{–}360) \times 10^{-5}$.

[19] ASHITKOV 01 result for $0\nu\chi$ of ^{100}Mo is less stringent than ARNOLD 00.

[20] DANEVICH 01 obtain limit for the $0\nu\chi$ decay with Majoron emission of ^{160}Gd using Gd_2SiO_5:Ce crystal scintillators.

[21] DANEVICH 01 obtain limit for the $0\nu2\chi$ decay with 2 Majoron emission of ^{160}Gd.

[22] ARNOLD 00 reports limit for the $0\nu\chi$ decay with Majoron emission derived from tracking calorimeter NEMO 2. Using ^{82}Se source: $\langle g_{\nu\chi} \rangle < 1.6 \times 10^{-4}$. Matrix element from GUENTHER 96.

[23] Using ^{96}Zr source: $\langle g_{\nu\chi} \rangle < 2.6 \times 10^{-4}$. Matrix element from ARNOLD 99.

[24] ARNOLD 00 reports limit for the $0\nu2\chi$ decay with two Majoron emission derived from tracking calorimeter NEMO 2.

[25] ARNOLD 98 determine the limit for $0\nu_\chi$ decay with Majoron emission of ^{82}Se using the NEMO-2 tracking detector. They derive $\langle g_{\nu_\chi} \rangle < 2.3\text{–}4.3 \times 10^{-4}$ with several nuclear matrix elements.

[26] LUESCHER 98 report a limit for the 0ν decay with Majoron emission of ^{136}Xe using Xe TPC. This result is more stringent than BARABASH 89. Using the matrix elements of ENGEL 88, they obtain a limit on $\langle g_{\nu\chi} \rangle$ of 2.0×10^{-4}.

[27] See Table 1 in GUENTHER 96 for limits on the Majoron coupling in different models.

Invisible A^0 (Axion) MASS LIMITS from Astrophysics and Cosmology

$v_1 = v_2$ is usually assumed (v_i = vacuum expectation values). For a review of these limits, see RAFFELT 91 and TURNER 90. In the comment lines below, D and K refer to DFSZ and KSVZ axion types, discussed in the above minireview.

VALUE (eV)	CL%	DOCUMENT ID		TECN	COMMENT
• • • We do not use the following data for averages, fits, limits, etc. • • •					
< 0.67	95	[1] ARCHIDIACO...	13A	COSM	K, hot dark matter
none 0.7–3×10^5		[2] CADAMURO	11	COSM	D abundance
<105	90	[3] DERBIN	11A	CNTR	D, solar axion
		[4] ANDRIAMON...	10	CAST	K, solar axions
< 0.72	95	[5] HANNESTAD	10	COSM	K, hot dark matter
		[6] ANDRIAMON...	09	CAST	K, solar axions
<191	90	[7] DERBIN	09A	CNTR	K, solar axions
<334	95	[8] KEKEZ	09	HPGE	K, solar axions
< 1.02	95	[9] HANNESTAD	08	COSM	K, hot dark matter
< 1.2	95	[10] HANNESTAD	07	COSM	K, hot dark matter
< 0.42	95	[11] MELCHIORRI	07A	COSM	K, hot dark matter
< 1.05	95	[12] HANNESTAD	05A	COSM	K, hot dark matter
3 to 20		MOROI	98	COSM	K, hot dark matter
< 0.007		[13] BORISOV	97	ASTR	D, neutron star
< 4		[14] KACHELRIESS	97	ASTR	D, neutron star cooling
<(0.5–6) $\times 10^{-3}$		[15] KEIL	97	ASTR	SN 1987A
< 0.018		[16] RAFFELT	95	ASTR	D, red giant
< 0.010		[17] ALTHERR	94	ASTR	D, red giants, white dwarfs
		[18] CHANG	93	ASTR	K, SN 1987A
< 0.01		WANG	92	ASTR	D, white dwarf
< 0.03		WANG	92C	ASTR	D, C-O burning
none 3–8		[19] BERSHADY	91	ASTR	D, K, intergalactic light
< 10		[20] KIM	91C	COSM	D, K, mass density of the universe, supersymmetry
		[21] RAFFELT	91B	ASTR	D,K, SN 1987A
< 1 $\times 10^{-3}$		[22] RESSELL	91	ASTR	K, intergalactic light
none 10^{-3}–3		BURROWS	90	ASTR	D,K, SN 1987A
		[23] ENGEL	90	ASTR	D,K, SN 1987A
< 0.02		[24] RAFFELT	90D	ASTR	D, red giant
< 1 $\times 10^{-3}$		[25] BURROWS	89	ASTR	D,K, SN 1987A
<(1.4–10) $\times 10^{-3}$		[26] ERICSON	89	ASTR	D,K, SN 1987A
< 3.6 $\times 10^{-4}$		[27] MAYLE	89	ASTR	D,K, SN 1987A
< 12		CHANDA	88	ASTR	D, Sun
< 1 $\times 10^{-3}$		RAFFELT	88	ASTR	D,K, SN 1987A
		[28] RAFFELT	88B	ASTR	red giant
< 0.07		FRIEMAN	87	ASTR	D, red giant
< 0.7		[29] RAFFELT	87	ASTR	K, red giant
< 2–5		TURNER	87	COSM	K, thermal production
< 0.01		[30] DEARBORN	86	ASTR	D, red giant
< 0.06		RAFFELT	86	ASTR	D, red giant
< 0.7		[31] RAFFELT	86	ASTR	K, red giant
< 0.03		RAFFELT	86B	ASTR	D, white dwarf
< 1		[32] KAPLAN	85	ASTR	K, red giant
< 0.003–0.02		IWAMOTO	84	ASTR	D, K, neutron star
> 1 $\times 10^{-5}$		ABBOTT	83	COSM	D,K, mass density of the universe
> 1 $\times 10^{-5}$		DINE	83	COSM	D,K, mass density of the universe
< 0.04		ELLIS	83B	ASTR	D, red giant
> 1 $\times 10^{-5}$		PRESKILL	83	COSM	D,K, mass density of the universe
< 0.1		BARROSO	82	ASTR	D, red giant
< 1		[33] FUKUGITA	82	ASTR	D, stellar cooling
< 0.07		FUKUGITA	82B	ASTR	D, red giant

[1] ARCHIDIACONO 13A is analogous to HANNESTAD 05A. The limit is based on the CMB temperature power spectrum of the Planck data, the CMB polarization from the WMAP 9-yr data, the matter power spectrum from SDSS-DR7, and the local Hubble parameter measurement by the Carnegie Hubble program.

[2] CADAMURO 11 use the deuterium abundance to show that the m_{A^0} range 0.7 eV – 300 keV is excluded for axions, complementing HANNESTAD 10.

[3] DERBIN 11A look for solar axions produced by Compton and bremsstrahlung processes, in the resonant excitation of ^{169}Tm, constraining the axion-electron × axion nucleon couplings.

[4] ANDRIAMONJE 10 search for solar axions produced from ^{7}Li (478 keV) and D$(p,\gamma)^3$He (5.5 MeV) nuclear transitions. They show limits on the axion-photon coupling for two reference values of the axion-nucleon coupling for $m_A < 100$ eV.

[5] This is an update of HANNESTAD 08 including 7 years of WMAP data.

[6] ANDRIAMONJE 09 look for solar axions produced from the thermally excited 14.4 keV level of ^{57}Fe. They show limits on the axion-nucleon × axion-photon coupling assuming $m_A < 0.03$ eV.

[7] DERBIN 09A look for Primakoff-produced solar axions in the resonant excitation of ^{169}Tm, constraining the axion-photon × axion-nucleon couplings.

[8] KEKEZ 09 look at axio-electric effect of solar axions in HPGe detectors. The one-loop axion-electron coupling for hadronic axions is used.

[9] This is an update of HANNESTAD 07 including 5 years of WMAP data.

[10] This is an update of HANNESTAD 05A with new cosmological data, notably WMAP (3 years) and baryon acoustic oscillations (BAO). Lyman-α data are left out, in contrast to HANNESTAD 05A and MELCHIORRI 07A, because it is argued that systematic errors are large. It uses Bayesian statistics and marginalizes over a possible neutrino hot dark matter component.

[11] MELCHIORRI 07A is analogous to HANNESTAD 05A, with updated cosmological data, notably WMAP (3 years). Uses Bayesian statistics and marginalizes over a possible

neutrino hot dark matter component. Leaving out Lyman-α data, a conservative limit is 1.4 eV.

[12] HANNESTAD 05A puts an upper limit on the mass of hadronic axion because in this mass range it would have been thermalized and contribute to the hot dark matter component of the universe. The limit is based on the CMB anisotropy from WMAP, SDSS large scale structure, Lyman α, and the prior Hubble parameter from HST Key Project. A χ^2 statistic is used. Neutrinos are assumed not to contribute to hot dark matter.

[13] MOROI 98 points out that a KSVZ axion of this mass range (see CHANG 93) can be a viable hot dark matter of Universe, as long as the model-dependent $g_{A\gamma}$ is accidentally small enough as originally emphasized by KAPLAN 85; see Fig. 1.

[14] BORISOV 97 bound is on the axion-electron coupling $g_{ae} < 1\times10^{-13}$ from the photo-production of axions off of magnetic fields in the outer layers of neutron stars.

[15] KACHELRIESS 97 bound is on the axion-electron coupling $g_{ae} < 1\times10^{-10}$ from the production of axions in strongly magnetized neutron stars. The authors also quote a stronger limit, $g_{ae} < 9\times10^{-13}$ which is strongly dependent on the strength of the magnetic field in white dwarfs.

[16] KEIL 97 uses new measurements of the axial-vector coupling strength of nucleons, as well as a reanalysis of many-body effects and pion-emission processes in the core of the neutron star, to update limits on the invisible-axion mass.

[17] RAFFELT 95 reexamined the constraints on axion emission from red giants due to the axion-electron coupling. They improve on DEARBORN 86 by taking into proper account degeneracy effects in the bremsstrahlung rate. The limit comes from requiring the red giant core mass at helium ignition not to exceed its standard value by more than 5% (0.025 solar masses).

[18] ALTHERR 94 bound is on the axion-electron coupling $g_{ae} < 1.5\times10^{-13}$, from energy loss via axion emission.

[19] CHANG 93 updates ENGEL 90 bound with the Kaplan-Manohar ambiguity in $z=m_u/m_d$ (see the Note on the Quark Masses in the Quark Particle Listings). It leaves the window f_A=3×10^5–3×10^6 GeV open. The constraint from Big-Bang Nucleosynthesis is satisfied in this window as well.

[20] BERSHADY 91 searched for a line at wave length from 3100–8300 Å expected from 2γ decays of relic thermal axions in intergalactic light of three rich clusters of galaxies.

[21] KIM 91C argues that the bound from the mass density of the universe will change drastically for the supersymmetric models due to the entropy production of saxion (scalar component in the axionic chiral multiplet) decay. Note that it is an *upperbound* rather than a lowerbound.

[22] RAFFELT 91B argue that previous SN 1987A bounds must be relaxed due to corrections to nucleon bremsstrahlung processes.

[23] RESSELL 91 uses absence of any intracluster line emission to set limit.

[24] ENGEL 90 rule out $10^{-10} \lesssim g_{AN} \lesssim 10^{-3}$, which for a hadronic axion with EMC motivated axion-nucleon couplings corresponds to 2.5×10^{-3} eV $\lesssim m_{A^0} \lesssim 2.5\times10^4$ eV. The constraint is loose in the middle of the range, i.e. for $g_{AN} \sim 10^{-6}$.

[25] RAFFELT 90D is a re-analysis of DEARBORN 86.

[26] The region $m_{A^0} \gtrsim 2$ eV is also allowed.

[27] ERICSON 89 considered various nuclear corrections to axion emission in a supernova core, and found a reduction of the previous limit (MAYLE 88) by a large factor.

[28] MAYLE 89 limit based on naive quark model couplings of axion to nucleons. Limit based on couplings motivated by EMC measurements is 2–4 times weaker. The limit from axion-electron coupling is weak: see HATSUDA 88B.

[29] RAFFELT 88B derives a limit for the energy generation rate by exotic processes in helium-burning stars $\epsilon < 100$ erg g^{-1} s^{-1}, which gives a firmer basis for the axion limits based on red giant cooling.

[30] RAFFELT 87 also gives a limit $g_{A\gamma} < 1\times10^{-10}$ GeV^{-1}.

[31] DEARBORN 86 also gives a limit $g_{A\gamma} < 1.4\times10^{-11}$ GeV^{-1}.

[32] RAFFELT 86 gives a limit $g_{A\gamma} < 1.1\times10^{-10}$ GeV^{-1} from red giants and $< 2.4\times10^{-9}$ GeV^{-1} from the sun.

[33] KAPLAN 85 says $m_{A^0} < 23$ eV is allowed for a special choice of model parameters.

[34] FUKUGITA 82 gives a limit $g_{A\gamma} < 2.3\times10^{-10}$ GeV^{-1}.

Search for Relic Invisible Axions

Limits are for $[G_{A\gamma\gamma}/m_{A^0}]^2\rho_A$ where $G_{A\gamma\gamma}$ denotes the axion two-photon coupling, $L_{\rm int} = -\frac{G_{A\gamma\gamma}}{4}\phi_A F_{\mu\nu}\tilde{F}^{\mu\nu} = G_{A\gamma\gamma}\phi_A \mathbf{E}\cdot\mathbf{B}$, and ρ_A is the axion energy density near the earth.

VALUE	CL%	DOCUMENT ID		TECN	COMMENT
• • • We do not use the following data for averages, fits, limits, etc. • • •					
		[1] BRANCA	17	AURG	m_{S^0} = 3.5–3.9 peV
$<3\times10^{-42}$	90	[2] BRUBAKER	17		m_{A^0} = 23.55–24.0 μeV
$<1.0\times10^{-29}$	95	[3] CHOI	17		m_{A^0} = 24.7–29.1 μeV
$<8.6\times10^{-42}$	90	[4] HOSKINS	16	ADMX	m_{A^0} =3.36–3.52 or 3.55–3.69 μeV
		[5] BECK	13		m_{A^0} = 0.11 meV
$<3.5\times10^{-43}$		[6] HOSKINS	11	ADMX	$m_{A^0} = 3.3$–3.69×10^{-6} eV
$<2.9\times10^{-43}$	90	[7] ASZTALOS	10	ADMX	$m_{A^0} = 3.34$–3.53×10^{-6} eV
$<1.9\times10^{-43}$	97.7	[8] DUFFY	06	ADMX	$m_{A^0} = 1.98$–2.17×10^{-6} eV
$<5.5\times10^{-43}$	90	[9] ASZTALOS	04	ADMX	$m_{A^0} = 1.9$–3.3×10^{-6} eV
		[10] KIM	98	THEO	
$<2\times10^{-41}$		[11] HAGMANN	90	CNTR	m_{A^0} = (5.4–5.9)10^{-6} eV
$<6.3\times10^{-42}$	95	[12] WUENSCH	89	CNTR	m_{A^0} = (4.5–10.2)10^{-6} eV
$<5.4\times10^{-41}$	95	[12] WUENSCH	89	CNTR	m_{A^0} = (11.3–16.3)10^{-6} eV

[1] BRANCA 17 look for modulations of the fine-structure constant and the electron mass due to moduli dark matter by using the cryogenic resonant-mass AURIGA detector. The limit on the assumed dilatonic coupling implies $G_{S\gamma\gamma} < 1.5\times10^{-24}$ GeV^{-1} for the scalar to two-photon coupling. See Fig. 5 for the mass-dependent limits.

[2] BRUBAKER 17 used a microwave cavity detector at the Yale Wright Laboratory to search for dark matter axions. See Fig. 3 for the mass-dependent limits.

[3] CHOI 17 used a microwave cavity detector with toroidal geometry. See Fig. 4 for their mass-dependent limits.

[4] HOSKINS 16 is analogous to DUFFY 06. See Fig. 12 for mass-dependent limits in terms of the local dark matter density.

[5] BECK 13 argues that dark-matter axions passing through Earth may generate a small observable signal in resonant S/N/S Josephson junctions. A measurement by HOFFMANN 04 [Physical Review **B70** 180503 (2004)] is interpreted in terms of subdominant dark matter axions with m_{A^0} = 0.11 meV.

[6] HOSKINS 11 is analogous to DUFFY 06. See Fig. 4 for the mass-dependent limit in terms of the local density.

[7] ASZTALOS 10 used the upgraded detector of ASZTALOS 04 to search for halo axions. See their Fig. 5 for the m_{A^0} dependence of the limit.

[8] DUFFY 06 used the upgraded detector of ASZTALOS 04, while assuming a smaller velocity dispersion than the isothermal model as in Eq. (8) of their paper. See Fig. 10 of their paper on the axion mass dependence of the limit.

[9] ASZTALOS 04 looked for a conversion of halo axions to microwave photons in magnetic field. At 90% CL, the KSVZ axion cannot have a local halo density more than 0.45 GeV/cm^3 in the quoted mass range. See Fig. 7 of their paper on the axion mass dependence of the limit.

[10] KIM 98 calculated the axion-to-photon couplings for various axion models and compared them to the HAGMANN 90 bounds. This analysis demonstrates a strong model dependence of $G_{A\gamma\gamma}$ and hence the bound from relic axion search.

[11] HAGMANN 90 experiment is based on the proposal of SIKIVIE 83.

[12] WUENSCH 89 looks for condensed axions near the earth that could be converted to photons in the presence of an intense electromagnetic field via the Primakoff effect, following the proposal of SIKIVIE 83. The theoretical prediction with $[G_{A\gamma\gamma}/m_{A^0}]^2 = 2\times10^{-14}$ MeV^{-4} (the three generation DFSZ model) and ρ_A = 300 MeV/cm^3 that makes up galactic halos gives $(G_{A\gamma\gamma}/m_{A^0})^2\,\rho_A = 4\times10^{-44}$. Note that our definition of $G_{A\gamma\gamma}$ is $(1/4\pi)$ smaller than that of WUENSCH 89.

Invisible A^0 (Axion) Limits from Photon Coupling

Limits are for the modulus of the axion-two-photon coupling $G_{A\gamma\gamma}$ defined by $L = -G_{A\gamma\gamma}\phi_A \mathbf{E}\cdot\mathbf{B}$. For scalars S^0 the limit is on the coupling constant in $L = G_{S\gamma\gamma}\phi_S(\mathbf{E}^2-\mathbf{B}^2)$. The relation between $G_{A\gamma\gamma}$ and m_{A^0} is not used unless stated otherwise, i.e., many of these bounds apply to low-mass axion-like particles (ALPs), not to QCD axions.

VALUE (GeV^{-1})	CL%	DOCUMENT ID		TECN	COMMENT
• • • We do not use the following data for averages, fits, limits, etc. • • •					
		[1] ADE	17	CMB	Axion-like particles
$<6.6\times10^{-11}$	95	[2] ANASTASSO...	17	CAST	$m_{A^0} < 0.02$ eV
		[3] DOLAN	17	RVUE	Axion-like particles
$<2.51\times10^{-4}$	95	[4] INADA	17	LSW	$m_{A^0} < 0.1$ eV
$>1.5\times10^{-11}$	95	[5] KOHRI	17	ASTR	m_{A^0} = 0.7–50 neV
$<2.6\times10^{-12}$	95	[6] MARSH	17	ASTR	$m_{A^0} \le 10^{-13}$ eV
$<6\times10^{-13}$		[7] TIWARI	17	COSM	$m_{A^0} \le 10^{-15}$ eV
$<5\times10^{-12}$	95	[8] AJELLO	16	ASTR	m_{A^0} = 0.5–5 neV
$<1.2\times10^{-7}$	95	[9] DELLA-VALLE	16	LASR	m_{A^0} = 1.3 meV
$<7.2\times10^{-8}$	95	[10] DELLA-VALLE	16	LASR	$m_{A^0} < 0.5$ meV
$<8\times10^{-4}$		[11] JAECKEL	16	ALPS	m_{A^0} = 0.1–100 GeV
$<6\times10^{-21}$		[12] LEEFER	16		$m_{S^0} < 10^{-18}$ eV
		[13] ANASTASSO...	15	CAST	Chameleons
$<1.47\times10^{-10}$	95	[14] ARIK	15	CAST	m_{A^0} = 0.39–0.42 eV
$<3.5\times10^{-8}$	95	[15] BALLOU	15	LSW	$m_{A^0} < 2\times10^{-4}$ eV
		[16] BRAX	15	ASTR	$m_{S^0} < 4\times10^{-12}$ eV
$<5.42\times10^{-4}$	95	[17] HASEBE	15	LASR	m_{A^0} = 0.15 eV
		[18] MILLEA	15	COSM	Axion-like particles
		[19] VANTILBURG	15		Dilaton-like dark matter
$<4.1\times10^{-10}$	99.7	[20] VINYOLES	15	ASTR	m_{A^0} = 0.6–185 eV
$<3.3\times10^{-10}$	95	[21] ARIK	14	CAST	m_{A^0} = 0.64–1.17 eV
$<6.6\times10^{-11}$	95	[22] AYALA	14	ASTR	Globular clusters
$<1.4\times10^{-7}$	95	[23] DELLA-VALLE	14	LASR	m_{A^0} = 1 meV
		[24] EJLLI	14	COSM	m_{A^0} = 2.66–48.8 μeV
$<8\times10^{-8}$	95	[25] PUGNAT	14	LSW	$m_{A^0} < 0.3$ meV
$<1\times10^{-11}$		[26] REESMAN	14	ASTR	$m_{A^0} < 1\times10^{-10}$ eV
$<2.1\times10^{-11}$	95	[27] ABRAMOWSKI	13A	IACT	m_{A^0} = 15–60 neV
$<2.15\times10^{-9}$	95	[28] ARMENGAUD	13	EDEL	$m_{A^0} < 200$ eV
$<4.5\times10^{-8}$	95	[29] BETZ	13	LSW	$m_{A^0} = 7.2\times10^{-6}$ eV
$<8\times10^{-11}$		[30] FRIEDLAND	13	ASTR	Red giants
$>2\times10^{-11}$		[31] MEYER	13	ASTR	$m_{A^0} < 1\times10^{-7}$ eV
$<8.3\times10^{-12}$	95	[32] WOUTERS	13	ASTR	$m_{A^0} < 7\times10^{-12}$ eV
		[33] CADAMURO	12	COSM	Axion-like particles
$<2.5\times10^{-13}$	95	[34] PAYEZ	12	ASTR	$m_{A^0} < 4.2\times10^{-14}$ eV
$<2.3\times10^{-10}$	95	[35] ARIK	11	CAST	m_{A^0} = 0.39–0.64 eV
$<6.5\times10^{-8}$	95	[36] EHRET	10	ALPS	$m_{A^0} < 0.7$ meV
$<2.4\times10^{-9}$	95	[37] AHMED	09A	CDMS	$m_{A^0} < 100$ eV
<1.2–2.8×10^{-10}	95	[38] ARIK	09	CAST	m_{A^0} = 0.02–0.39 eV
		[39] CHOU	09		Chameleons
$<7\times10^{-10}$		[40] GONDOLO	09	ASTR	$m_{A^0} <$ few keV
$<1.3\times10^{-6}$	95	[41] AFANASEV	08		$m_{S^0} < 1$ meV

Gauge & Higgs Boson Particle Listings

Axions (A^0) and Other Very Light Bosons

$<3.5 \times 10^{-7}$	99.7	[42] CHOU	08		$m_{A^0} < 0.5$ meV
$<1.1 \times 10^{-6}$	99.7	[43] FOUCHE	08		$m_{A^0} < 1$ meV
< 5.6–13.4×10^{-10}	95	[44] INOUE	08		$m_{A^0} = 0.84$–1.00 eV
$<5 \times 10^{-7}$		[45] ZAVATTINI	08		$m_{A^0} < 1$ meV
$<8.8 \times 10^{-11}$	95	[46] ANDRIAMON...07		CAST	$m_{A^0} < 0.02$ eV
$<1.25 \times 10^{-6}$	95	[47] ROBILLIARD	07		$m_{A^0} < 1$ meV
2–5×10^{-6}		[48] ZAVATTINI	06		$m_{A^0} = 1$–1.5 meV
$<1.1 \times 10^{-9}$	95	[49] INOUE	02		$m_{A^0} = 0.05$–0.27 eV
$<2.78 \times 10^{-9}$	95	[50] MORALES	02B		$m_{A^0} <1$ keV
$<1.7 \times 10^{-9}$	90	[51] BERNABEI	01B		$m_{A^0} <100$ eV
$<1.5 \times 10^{-4}$	90	[52] ASTIER	00B	NOMD	$m_{A^0} <40$ eV
		[53] MASSO	00	THEO	induced γ coupling
$<2.7 \times 10^{-9}$	95	[54] AVIGNONE	98	SLAX	$m_{A^0} < 1$ keV
$<6.0 \times 10^{-10}$	95	[55] MORIYAMA	98		$m_{A^0} < 0.03$ eV
$<3.6 \times 10^{-7}$	95	[56] CAMERON	93		$m_{A^0} < 10^{-3}$ eV, optical rotation
$<6.7 \times 10^{-7}$	95	[57] CAMERON	93		$m_{A^0} < 10^{-3}$ eV, photon regeneration
$<3.6 \times 10^{-9}$	99.7	[58] LAZARUS	92		$m_{A^0} < 0.03$ eV
$<7.7 \times 10^{-9}$	99.7	[58] LAZARUS	92		$m_{A^0} = 0.03$–0.11 eV
$<7.7 \times 10^{-7}$	99	[59] RUOSO	92		$m_{A^0} < 10^{-3}$ eV
$<2.5 \times 10^{-6}$		[60] SEMERTZIDIS	90		$m_{A^0} < 7 \times 10^{-4}$ eV

[1] ADE 17 look for cosmic birefringence from axion-like particles using CMB polarization data taken by the BICEP2 and Keck Array experiments. They set a limit $G_{A\gamma\gamma} H_I < 7.2 \times 10^{-2}$ at 95 %CL for $m_{A^0} < 10^{-28}$ eV, where H_I is the Hubble parameter during inflation.

[2] ANASTASSOPOULOS 17 looked for solar axions by the CAST axion helioscope in the vacuum phase, and supersedes ANDRIAMONJE 07.

[3] DOLAN 17 update existing limits on $G_{A\gamma\gamma}$ for axion-like particles. See their Fig. 2 for mass-dependent limits.

[4] INADA 17 search for axions with an x-ray LSW at Spring-8. See their Fig. 4 for mass-dependent limits.

[5] KOHRI 17 attributed to axion-photon oscillations the excess of cosmic infrared background observed by the CIBER experiment. See their Fig. 5 for the region preferred by their scenario.

[6] MARSH 17 is similar to WOUTERS 13, using Chandra observations of M87. See their Fig. 6 for mass-dependent limits.

[7] TIWARI 17 use observed limits of the cosmic distance-duality relation to constrain the photon-ALP mixing based on 3D simulations of the magnetic field configuration. The quoted value is for the averaged magnetic field of 1nG with a coherent length of 1 Mpc. See their Fig. 5 for mass-dependent limits.

[8] AJELLO 16 look for irregularities in the energy spectrum of the NGC1275 measured by Fermi LAT, assuming photon-ALP mixing in the intra-cluster and Galactic magnetic felds. See their Fig. 2 for mass-dependent limits.

[9] DELLA-VALLE 16 look for the birefringence induced by axion-like particles. See their Fig. 14 for mass-dependent limits.

[10] DELLA-VALLE 16 look for the dichroism induced by axion-like particles. See their Fig. 14 for mass-dependent limits.

[11] JAECKEL 16 use the LEP data of $Z \to 2\gamma$ and $Z \to 3\gamma$ to constrain the ALP production via $e^+ e^- \to Z \to A^0 \gamma$ ($A^0 \to \gamma\gamma$), assuming the ALP coupling with two hypercharge bosons. See their Fig. 4 for mass-dependent limits.

[12] LEEFER 16 derived limits by using radio-frequency spectroscopy of dysprosium and atomic clock measurements. See their Fig. 1 for mass-dependent limits as well as limits on Yukawa-type couplings of the scalar to the electron and nucleons.

[13] ANASTASSOPOULOS 15 search for solar chameleons with CAST and derived limits on the chameleon coupling to photons and matter. See their Fig. 12 for the exclusion region.

[14] ARIK 15 is analogous to ARIK 09, and search for solar axions for m_{A^0} around 0.2 and 0.4 eV. See their Figs. 1 and 3 for the mass-dependent limits.

[15] Based on OSQAR photon regeneration experiment. See their Fig. 6 for mass-dependent limits on scalar and pseudoscalar bosons.

[16] BRAX 15 derived limits on conformal and disformal couplings of a scalar to photons by searching for a chaotic absorption pattern in the X-ray and UV bands of the Hydra A galaxy cluster and a BL lac object, respectively. See their Fig. 8.

[17] HASEBE 15 look for an axion via a four-wave mixing process at quasi-parallel colliding laser beams. They also derived limits on a scalar coupling to photons $G_{S\gamma\gamma} < 2.62 \times 10^{-4}$ GeV^{-1} at $m_{S^0} = 0.15$ eV. See their Figs. 11 and 12 for mass-dependent limits.

[18] MILLEA 15 is similar to CADAMURO 12, including the Planck data and the latest inferences of primordial deuterium abundance. See their Fig. 3 for mass-dependent limits.

[19] VANTILBURG 15 look for harmonic variations in the dyprosium transition frequency data, induced by coherent oscillations of the fine-structure constant due to dilaton-like dark matter, and set the limits, $G_{S\gamma\gamma} < 6 \times 10^{-27}$ GeV^{-1} at $m_{S^0} = 6 \times 10^{-23}$ eV. See their Fig. 4 for mass-dependent limits between $1 \times 10^{-24} < m_{S^0} < 1 \times 10^{-15}$ eV.

[20] VINYOLES 15 performed a global fit analysis based on helioseismology and solar neutrino observations. See their Fig. 9.

[21] ARIK 14 is similar to ARIK 11. See their Fig. 2 for mass-dependent limits.

[22] AYALA 14 derived the limit from the helium-burning lifetime of horizontal-branch stars based on number counts in globular clusters.

[23] DELLA-VALLE 14 use the new PVLAS apparatus to set a limit on vacuum magnetic birefringence induced by axion-like particles. See their Fig. 6 for the mass-dependent limits.

[24] EJLLI 14 set limits on a product of primordial magnetic field and the axion mass using CMB distortion induced by resonant axion production from CMB photons. See their Fig. 1 for limits applying specifically to the DFSZ and KSVZ axion models.

[25] PUGNAT 14 is analogous to EHRET 10. See their Fig. 5 for mass-dependent limits on scalar and pseudoscalar bosons.

[26] REESMAN 14 derive limits by requiring effects of axion-photon interconversion on gamma-ray spectra from distant blazars to be no larger than errors in the best-fit optical depth based on a certain extragalactic background light model. See their Fig. 5 for mass-dependent limits.

[27] ABRAMOWSKI 13A look for irregularities in the energy spectrum of the BL Lac object PKS 2155–304 measured by H.E.S.S. The limits depend on assumed magnetic field around the source. See their Fig. 7 for mass-dependent limits.

[28] ARMENGAUD 13 is analogous to AVIGNONE 98. See Fig. 6 for the limit.

[29] BETZ 13 performed a microwave-based light shining through the wall experiment. See their Fig. 13 for mass-dependent limits.

[30] FRIEDLAND 13 derived the limit by considering blue-loop suppression of the evolution of red giants with 7–12 solar masses.

[31] MEYER 13 attributed to axion-photon oscillations the observed excess of very high-energy γ-rays with respect to predictions based on extragalactic background light models. See their Fig.4 for mass-dependent lower limits for various magnetic field configurations.

[32] WOUTERS 13 look for irregularities in the X-ray spectrum of the Hydra cluster observed by Chandra. See their Fig. 4 for mass-dependent limits.

[33] CADAMURO 12 derived cosmological limits on $G_{A\gamma\gamma}$ for axion-like particles. See their Fig. 1 for mass-dependent limits.

[34] PAYEZ 12 derive limits from polarization measurements of quasar light (see their Fig. 3). The limits depend on assumed magnetic field strength in galaxy clusters. The limits depend on assumed magnetic field and electron density in the local galaxy supercluster.

[35] ARIK 11 search for solar axions using ^{3}He buffer gas in CAST, continuing from the ^{4}He version of ARIK 09. See Fig. 2 for the exact mass-dependent limits.

[36] ALPS is a photon regeneration experiment. See their Fig. 4 for mass-dependent limits on scalar and pseudoscalar bosons.

[37] AHMED 09A is analogous to AVIGNONE 98.

[38] ARIK 09 is the ^{4}He filling version of the CAST axion helioscope in analogy to INOUE 02 and INOUE 08. See their Fig. 7 for mass-dependent limits.

[39] CHOU 09 use the GammeV apparatus in the afterglow mode to search for chameleons, (pseudo)scalar bosons with a mass depending on the environment. For pseudoscalars they exclude at 3σ the range 2.6×10^{-7} GeV$^{-1} < G_{A\gamma\gamma} < 4.2 \times 10^{-6}$ GeV^{-1} for vacuum m_{A^0} roughly below 6 meV for density scaling index exceeding 0.8.

[40] GONDOLO 09 use the all-flavor measured solar neutrino flux to constrain solar interior temperature and thus energy losses.

[41] LIPSS photon regeneration experiment, assuming scalar particle S^0. See Fig. 4 for mass-dependent limits.

[42] CHOU 08 perform a variable-baseline photon regeneration experiment. See their Fig. 3 for mass-dependent limits. Excludes the PVLAS result of ZAVATTINI 06.

[43] FOUCHE 08 is an update of ROBILLIARD 07. See their Fig. 12 for mass-dependent limits.

[44] INOUE 08 is an extension of INOUE 02 to larger axion masses, using the Tokyo axion helioscope. See their Fig. 4 for mass-dependent limits.

[45] ZAVATTINI 08 is an upgrade of ZAVATTINI 06, see their Fig. 8 for mass-dependent limits. They now exclude the parameter range where ZAVATTINI 06 had seen a positive signature.

[46] ANDRIAMONJE 07 looked for Primakoff conversion of solar axions in 9T superconducting magnet into X-rays. Supersedes ZIOUTAS 05.

[47] ROBILLIARD 07 perform a photon regeneration experiment with a pulsed laser and pulsed magnetic field. See their Fig. 4 for mass-dependent limits. Excludes the PVLAS result of ZAVATTINI 06 with a CL exceeding 99.9%.

[48] ZAVATTINI 06 propagate a laser beam in a magnetic field and observe dichroism and birefringence effects that could be attributed to an axion-like particle. This result is now excluded by ROBILLIARD 07, ZAVATTINI 08, and CHOU 08.

[49] INOUE 02 looked for Primakoff conversion of solar axions in 4T superconducting magnet into X ray.

[50] MORALES 02B looked for the coherent conversion of solar axions to photons via the Primakoff effect in Germanium detector.

[51] BERNABEI 01B looked for Primakoff coherent conversion of solar axions into photons via Bragg scattering in NaI crystal in DAMA dark matter detector.

[52] ASTIER 00B looked for production of axions from the interaction of high-energy photons with the horn magnetic field and their subsequent re-conversion to photons via the interaction with the NOMAD dipole magnetic field.

[53] MASSO 00 studied limits on axion-proton coupling using the induced axion-photon coupling through the proton loop and CAMERON 93 bound on the axion-photon coupling using optical rotation. They obtained the bound $g_p^2/4\pi < 1.7 \times 10^{-9}$ for the coupling $g_p \overline{p} \gamma_5 p \phi_A$.

[54] AVIGNONE 98 result is based on the coherent conversion of solar axions to photons via the Primakoff effect in a single crystal germanium detector.

[55] Based on the conversion of solar axions to X-rays in a strong laboratory magnetic field.

[56] Experiment based on proposal by MAIANI 86.

[57] Experiment based on proposal by VANBIBBER 87.

[58] LAZARUS 92 experiment is based on proposal found in VANBIBBER 89.

[59] RUOSO 92 experiment is based on the proposal by VANBIBBER 87.

[60] SEMERTZIDIS 90 experiment is based on the proposal of MAIANI 86. The limit is obtained by taking the noise amplitude as the upper limit. Limits extend to $m_{A^0} = 4 \times 10^{-3}$ where $G_{A\gamma\gamma} < 1 \times 10^{-4}$ GeV^{-1}.

Limit on Invisible A^0 (Axion) Electron Coupling

The limit is for $g_{Aee}\, \phi_A\, \overline{e}(i\gamma_5)e$, or equivalently, the dipole-dipole potential $-\frac{g_{Aee}^2}{16\pi m_e^2}((\boldsymbol{\sigma}_1 \cdot \boldsymbol{\sigma}_2) - 3(\boldsymbol{\sigma}_1 \cdot \boldsymbol{n})(\boldsymbol{\sigma}_2 \cdot \boldsymbol{n}))/r^3$ where $\boldsymbol{n} = \boldsymbol{r}/r$ and the sign of the potential was corrected based on DAIDO 17.

VALUE	CL%	DOCUMENT ID		TECN	COMMENT
• • • We do not use the following data for averages, fits, limits, etc. • • •					
$<4.5 \times 10^{-13}$	90	[1] ABGRALL	17	HPGE	$m_{A^0} = 11.8$ keV
$<3.5 \times 10^{-12}$	90	[2] AKERIB	17B	LUX	Solar axions
$<4.2 \times 10^{-13}$	90	[3] AKERIB	17B	LUX	$m_{A^0} = 1$–16 keV
$<2.3 \times 10^{-13}$	90	[4] APRILE	17B	X100	$m_{A^0} = 6$ keV

$<4 \times 10^{-4}$	90	[5] FICEK	17		$m_{A^0} < 1$ keV
$<4.35 \times 10^{-12}$	90	[6] FU	17A	PNDX	Solar axions
$<4.3 \times 10^{-14}$	90	[7] FU	17A	PNDX	$m_{A^0} = 2$ keV
$<5 \times 10^{-13}$	90	[8] LIU	17A	CDEX	$m_{A^0} = 13$ keV
$<2.5 \times 10^{-11}$	90	[9] LIU	17A	CDEX	Solar axions
<0.15	95	[10] LUO	17		$m_{A^0} = 300$ eV
$<3.3 \times 10^{-13}$	68	[11] BATTICH	16	ASTR	White dwarf cooling
$<7 \times 10^{-13}$		[12] CORSICO	16	ASTR	White dwarf cooling
$<1.39 \times 10^{-11}$	90	[13] YOON	16	KIMS	Solar axions
$<7.4 \times 10^{-9}$	95	[14] TERRANO	15		$m_{A^0} < 30$ μeV
$<8 \times 10^{-13}$	90	[15] ABE	14F	XMAS	$m_{A^0} = 60$ keV
$<7.7 \times 10^{-12}$	90	[16] APRILE	14B	X100	Solar axions
		[17] APRILE	14B	X100	$m_{A^0} = 5$–7 keV
< 0.96–8.2×10^{-8}	90	[18] DERBIN	14	CNTR	$m_{A^0} = 0.1$–1 MeV
$<2.8 \times 10^{-13}$	99	[19] MILLER-BER...	14	ASTR	White dwarf cooling
$<5.4 \times 10^{-11}$	90	[20] ABE	13D	XMAS	Solar axions
$<1.07 \times 10^{-12}$	90	[21] ARMENGAUD	13	EDEL	$m_{A^0} = 12.5$ keV
$<2.59 \times 10^{-11}$	90	[22] ARMENGAUD	13	EDEL	Solar axions
		[23] BARTH	13	CAST	Solar axions
< 1.4–9.7×10^{-7}	90	[24] DERBIN	13	CNTR	$m_{A^0} = 0.1$–1 MeV
$<1.5 \times 10^{-8}$	68	[25] HECKEL	13		$m_{A^0} \leq 0.1$ μeV
$<4.3 \times 10^{-13}$	95	[26] VIAUX	13A	ASTR	Low-mass red giants
$<7 \times 10^{-13}$	95	[27] CORSICO	12	ASTR	White dwarf cooling
$<2.2 \times 10^{-10}$	90	[28] DERBIN	12	CNTR	Solar axions
< 0.02–1×10^{-10}	90	[29] AALSETH	11	CNTR	$m_{A^0} = 0.3$–8 keV
$<1.4 \times 10^{-12}$	90	[30] AHMED	09A	CDMS	$m_{A^0} = 2.5$ keV
$<4 \times 10^{-9}$		[31] DAVOUDIASL	09	ASTR	Earth cooling
$<2.7 \times 10^{-8}$	66	[32] NI	94		Induced magnetism
		[32] CHUI	93		Induced magnetism
$<3.6 \times 10^{-7}$	66	[33] PAN	92		Torsion pendulum
$<2.9 \times 10^{-8}$	95	[32] BOBRAKOV	91		Induced magnetism
$<1.9 \times 10^{-6}$	66	[34] WINELAND	91	NMR	
$<7 \times 10^{-7}$	66	[33] RITTER	90		Torsion pendulum
$<6.6 \times 10^{-8}$	95	[32] VOROBYOV	88		Induced magnetism

[1] ABGRALL 17 is analogous to AHMED 09A using the MAJORANA DEMONSTRATOR. See their Fig. 2 for limits between 6 keV $< m_{A^0} <$ 97 keV.

[2] AKERIB 17B is analogous to LIU 17A.

[3] AKERIB 17B is analogous to AHMED 09A. See their Fig. 7 for mass-dependent limits.

[4] APRILE 17B is analogous to AHMED 09A. They found a bug in their code and needed to correct the limits in Fig. 7 of APRILE 14B. See their Fig. 1 for the corrected limits between 1 keV $< m_{A^0} <$ 40 keV.

[5] FICEK 17 look for spin-dependent interactions between electrons by comparing precision spectroscopic measurements in ^{4}He with theoretical calculations. See their Fig. 1 for limits up to $m_{A^0} = 10$ keV.

[6] FU 17A is analogous to LIU 17A. See their Fig. 3 for mass-dependent limits.

[7] FU 17A is analogous to AHMED 09A. See their Fig. 4 for mass-dependent limits.

[8] LIU 17A is analogous to AHMED 09A. See their Fig. 9 for limits between 0.25 keV $< m_{A^0} <$ 20 keV.

[9] LIU 17A look for solar axions produced from Compton, bremsstrahlung, atomic-recombination and deexcitation channels, and set a limit for $m_{A^0} < 1$ keV.

[10] LUO 17 use a recent measurement of the dipole-dipole interaction between two iron atoms at the nanometer scale and set a limit for $m_{A^0} < 1$ keV. See their Fig. 3 for mass-dependent limits.

[11] BATTICH 16 is analogous to CORSICO 16 and used the pulsating DB white dwarf PG 1351+489.

[12] CORSICO 16 studied the cooling rate of the pulsating DA white dwarf L19-2 based on an asteroseismic model.

[13] YOON 16 look for solar axions with the axio-electric effect in CsI(Tl) crystals and set a limit for $m_{A^0} < 1$ keV.

[14] TERRANO 15 used a torsion pendulum and rotating attractor with 20-pole electron-spin distributions. See their Fig. 4 for a mass-dependent limit up to $m_{A^0} = 500$ μeV.

[15] ABE 14F set limits on the axioelectric effect in the XMASS detector assuming the pseudoscalar constitutes all the local dark matter. See their Fig. 3 for limits between m_{A^0} = 40–120 keV.

[16] APRILE 14B look for solar axions using the XENON100 detector.

[17] APRILE 14B is analogous to AHMED 09A. Their Fig. 7 was later found to be incorrect due to a bug in their code. See Fig. 1 in APRILE 17B for the corrected limits.

[18] DERBIN 14 is an update of DERBIN 13 with a BGO scintillating bolometer. See their Fig. 3 for mass-dependent limits.

[19] MILLER-BERTOLAMI 14 studied the impact of axion emission on white dwarf cooling in a self-consistent way.

[20] ABE 13D is analogous to DERBIN 12, using the XMASS detector.

[21] ARMENGAUD 13 is similar to AALSETH 11. See their Fig. 10 for limits between 3 keV $< m_{A^0} <$ 100 keV.

[22] ARMENGAUD 13 is similar to DERBIN 12, and take account of axio-recombination and axio-deexcitation effects. See their Fig. 12 for mass-dependent limits.

[23] BARTH 13 search for solar axions produced by axion-electron coupling, and obtained the limit, $g_{Aee} \cdot G_{A\gamma\gamma} < 8.1 \times 10^{-23}$ GeV^{-1} at 95%CL.

[24] DERBIN 13 looked for 5.5 MeV solar axions produced in $pd \rightarrow {}^3\mathrm{He}\ A^0$ in a BGO detector through the axioelectric effect. See their Fig. 4 for mass-dependent limits.

[25] HECKEL 13 studied the influence of 2 or 4 stationary sources each containing 6.0×10^{24} polarized electrons, on a rotating torsion pendulum containing 9.8×10^{24} polarized electrons. See their Fig. 4 for mass-dependent limits.

[26] VIAUX 13A constrain axion emission using the observed brightness of the tip of the red-giant branch in the globular cluster M5.

[27] CORSICO 12 attributed the excessive cooling rate of the pulsating white dwarf R548 to emission of axions with $g_{Aee} \simeq 4.8 \times 10^{-13}$.

[28] DERBIN 12 look for solar axions with the axio-electric effect in a Si(Li) detector. The solar production is based on Compton and bremsstrahlung processes.

[29] AALSETH 11 is analogous to AHMED 09A. See their Fig. 4 for mass-dependent limits.

[30] AHMED 09A assume keV-mass pseudoscalars are the local dark matter and constrain the axio-electric effect in the CDMS detector. See their Fig. 5 for mass-dependent limits.

[31] DAVOUDIASL 09 use geophysical constraints on Earth cooling by axion emission.

[32] These experiments measured induced magnetization of a bulk material by the spin-dependent potential generated from other bulk material with aligned electron spins, where the magnetic field is shielded with superconductor. The sign of the limit set by CHUI 93 is opposite to that of the axion-mediated dipole-dipole potential.

[33] These experiments used a torsion pendulum to measure the potential between two bulk matter objects where the spins are polarized but without a net magnetic field in either of them. The limits reflect the corrected sign of the dipole-dipole potential.

[34] WINELAND 91 looked for an effect of bulk matter with aligned electron spins on atomic hyperfine splitting using nuclear magnetic resonance.

Invisible A^0 (Axion) Limits from Nucleon Coupling

Limits are for the axion mass in eV.

VALUE (eV)	CL%	DOCUMENT ID		TECN	COMMENT
• • • We do not use the following data for averages, fits, limits, etc. • • •					
		[1] ABEL	17		Neutron EDM
< 93	90	[2] ABGRALL	17	HPGE	Solar axion
< 70	90	[3] FU	17A	PNDX	Solar axion
		[4] KLIMCHITSK...	17A		Casimir effect
<177	90	[5] LIU	17A	CDEX	Solar axion
$< 1 \times 10^2$	95	[6] GAVRILYUK	15	CNTR	Solar axion
		[7] KLIMCHITSK...	15		Casimir-less
		[8] BEZERRA	14		Casimir effect
		[9] BEZERRA	14A		Casimir effect
		[10] BEZERRA	14B		Casimir effect
		[11] BEZERRA	14C		Casimir effect
		[12] BLUM	14	COSM	^{4}He abundance
		[13] LEINSON	14	ASTR	Neutron star cooling
$< 2.50 \times 10^2$	95	[14] ALESSANDRIA	13	CNTR	Solar axion
$< 1.55 \times 10^2$	90	[15] ARMENGAUD	13	EDEL	Solar axion
$< 8.6 \times 10^3$	90	[16] BELLI	12	CNTR	Solar axion
$< 1.4 \times 10^4$	90	[17] BELLINI	12B	BORX	Solar axion
$< 1.45 \times 10^2$	95	[18] DERBIN	11	CNTR	Solar axion
		[19] BELLINI	08	CNTR	Solar axion
		[20] ADELBERGER	07		Test of Newton's law

[1] ABEL 17 look for a time-oscillating neutron EDM and an axion-wind spin-precession effect respectively induced by axion dark matter couplings to gluons and nucleons. See their Fig. 4 for limits in the range of $m_{A^0} = 10^{-24}$–10^{-17} eV.

[2] ABGRALL 17 limit assumes the hadronic axion model used in ALESSANDRIA 13. See their Fig. 4 for the limit on product of axion couplings to electrons and nucleons.

[3] FU 17A look for the 14.4 keV ^{57}Fe solar axions. The limit assumes the DFSZ axion model. See their Fig. 3 for mass-dependent limits on the axion-electron coupling.

[4] KLIMCHITSKAYA 17A use the differential measurement of the Casimir force between a Ni-coated sphere and Au and Ni sectors of the structured disc to constrain the axion coupling to nucleons for 2.61 meV $< m_{A^0} <$ 0.9 eV. See their Figs. 1 and 2 for mass dependent limits.

[5] LIU 17 is analogous to ALESSANDRIA 13. The limit assumes the hadronic axion model. See their Fig. 6(b) for the limit on product of axion couplings to electrons and nucleons.

[6] GAVRILYUK 15 look for solar axions emitted by the M1 transition of ^{83}Kr (9.4 keV). The mass bound assumes $m_u/m_d = 0.56$ and $S = 0.5$.

[7] KLIMCHITSKAYA 15 use the measurement of differential forces between a test mass and rotating source masses of Au and Si to constrain the force due to two-axion exchange for $1.7 \times 10^{-3} < m_{A^0} <$ 0.9 eV. See their Figs. 1 and 2 for mass dependent limits.

[8] BEZERRA 14 use the measurement of the thermal Casimir-Polder force between a Bose-Einstein condensate of ^{87}Rb atoms and a SiO_2 plate to constrain the force mediated by exchange of two pseudoscalars for 0.1 meV $< m_{A^0} <$ 0.3 eV. See their Fig. 2 for the mass-dependent limit on pseudoscalar coupling to nucleons.

[9] BEZERRA 14A is analogous to BEZERRA 14. They use the measurement of the Casimir pressure between two Au-coated plates to constrain pseudoscalar coupling to nucleons for 1×10^{-3} eV $< m_{A^0} <$ 15 eV. See their Figs. 1 and 2 for the mass-dependent limit.

[10] BEZERRA 14B is analogous to BEZERRA 14. BEZERRA 14B use the measurement of the normal and lateral Casimir forces between sinusoidally corrugated surfaces of a sphere and a plate to constrain pseudoscalar coupling to nucleons for 1 eV $< m_{A^0} <$ 20 eV. See their Figs. 1–3 for mass-dependent limits.

[11] BEZERRA 14C is analogous to BEZERRA 14. They use the measurement of the gradient of the Casimir force between Au- and Ni-coated surfaces of a sphere and a plate to constrain pseudoscalar coupling to nucleons for 3×10^{-5} eV $< m_{A_0} <$ 1 eV. See their Figs. 1, 3, and 4 for the mass-dependent limits.

[12] BLUM 14 studied effects of an oscillating strong CP phase induced by axion dark matter on the primordial ^{4}He abundance. See their Fig. 1 for mass-dependent limits.

[13] LEINSON 14 attributes the excessive cooling rate of the neutron star in Cassiopeia A to axion emission from the superfluid core, and found $C_n^2\, m_{A^0}^2 \simeq 5.7 \times 10^{-6}$ eV^2, where C_n is the effective Peccei-Quinn charge of the neutron.

[14] ALESSANDRIA 13 used the CUORE experiment to look for 14.4 keV solar axions produced from the M1 transition of thermally excited ^{57}Fe nuclei in the solar core, using the axio-electric effect. The limit assumes the hadronic axion model. See their Fig. 4 for the limit on product of axion couplings to electrons and nucleons.

[15] ARMENGAUD 13 is analogous to ALESSANDRIA 13. The limit assumes the hadronic axion model. See their Fig. 8 for the limit on product of axion couplings to electrons and nucleons.

[16] BELLI 12 looked for solar axions emitted by the M1 transition of ^{7}Li* (478 keV) after the electron capture of ^{7}Be, using the resonant excitation ^{7}Li in the LiF crystal. The mass bound assumes $m_u/m_d = 0.55$, $m_u/m_s = 0.029$, and the flavor-singlet axial vector matrix element $S = 0.4$.

[17] BELLINI 12B looked for 5.5 MeV solar axions produced in the $pd \rightarrow {}^3\mathrm{He}\ A^0$.The limit assumes the hadronic axion model. See their Figs. 6 and 7 for mass-dependent limits on productsof axion couplings to photons, electrons, and nucleons.

[18] DERBIN 11 looked for solar axions emitted by the M1 transition of thermally excited ^{57}Fe nuclei in the Sun, using their possible resonant capture on ^{57}Fe in the laboratory. The mass bound assumes $m_u/m_d = 0.56$ and the flavor-singlet axial vector matrix element $S = 3F - D \simeq 0.5$.

[19] BELLINI 08 consider solar axions emitted in the M1 transition of ^{7}Li* (478 keV) and look for a peak at 478 keV in the energy spectra of the Counting Test Facility (CTF), a Borexino prototype. For $m_{A^0} < 450$ keV they find mass-dependent limits on products of axion couplings to photons, electrons, and nucleons.

[20] ADELBERGER 07 use precision tests of Newton's law to constrain a force contribution from the exchange of two pseudoscalars. See their Fig. 5 for limits on the pseudoscalar coupling to nucleons, relevant for m_{A^0} below about 1 meV.

Axion Limits from *T*-violating Medium-Range Forces

The limit is for the coupling $g = g_p\ g_s$ in a *T*-violating potential between nucleons or nucleon and electron of the form $V = \frac{g\hbar^2}{8\pi m_p}(\boldsymbol{\sigma}\cdot\hat{\boldsymbol{r}})\ (\frac{1}{r^2} + \frac{1}{\lambda r})\ e^{-r/\lambda}$, where g_p and g_s are dimensionless scalar and pseudoscalar coupling constants and $\lambda = \hbar/(m_A c)$ is the range of the force.

VALUE	DOCUMENT ID		TECN	COMMENT
• • • We do not use the following data for averages, fits, limits, etc. • • •				
	[1] STADNIK	18	THEO	atomic and molecular EDMs
	[2] CRESCINI	17	SQID	paramagnetic GSO crystal
	[3] AFACH	15		ultracold neutrons
	[4] STADNIK	15	THEO	nucleon spin contributions for nuclei
	[5] TERRANO	15		torsion pendulum
	[6] BULATOWICZ	13	NMR	polarized ^{129}Xe and ^{131}Xe
	[7] CHU	13		polarized ^{3}He
	[8] TULLNEY	13	SQID	polarized ^{3}He and ^{129}Xe
	[9] RAFFELT	12		stellar energy loss
	[10] HOEDL	11		torsion pendulum
	[11] PETUKHOV	10		polarized ^{3}He
	[12] SEREBROV	10		ultracold neutrons
	[13] IGNATOVICH	09	RVUE	ultracold neutrons
	[14] SEREBROV	09	RVUE	ultracold neutrons
	[15] BAESSLER	07		ultracold neutrons
	[16] HECKEL	06		torsion pendulum
	[17] NI	99		paramagnetic Tb F_3
	[18] POSPELOV	98	THEO	neutron EDM
	[19] YOUDIN	96		
	[20] RITTER	93		torsion pendulum
	[21] VENEMA	92		nuclear spin-precession frequencies
	[22] WINELAND	91	NMR	

[1] STADNIK 18 used atomic and molecular EDM experiments to derive limits on the product of the pseudoscalar couplings to electron and the scalar coupling to nucleon and electron. See their Fig. 2 for mass-dependent limits, which improved on the laboratory bounds for $m_{A^0} > 0.01$ eV.

[2] CRESCINI 17 use the QUAX-$g_p g_s$ experiment to look for variation of a paramagnetic GSO crystal magnetization when rotating lead disks are positioned near the crystal, and find $g = g_p^e g_s^N < 4.3 \times 10^{-30}$ for $\lambda = 0.1$–0.2 m at 95% CL. See their Fig. 6 for limits as a function of λ.

[3] AFACH 15 look for a change of spin precession frequency of ultracold neutrons when a magnetic field with opposite directions is applied, and find $g < 2.2 \times 10^{-27}\ (\mathrm{m}/\lambda)^2$ at 95% CL for $1\ \mu\mathrm{m} < \lambda < 5$ mm. See their Fig. 3 for their limits.

[4] STADNIK 15 studied proton and neutron spin contributions for nuclei and derive the limits $g < 10^{-28}$–10^{-23} for $\lambda > 3 \times 10^{-4}$ m using the data of TULLNEY 13. See their Figs. 1 and 2 for λ-dependent limits.

[5] TERRANO 15 used a torsion pendulum and rotating attractor, and derived a restrictive limit on the product of the pseudoscalar coupling to electron and the scalar coupling to nucleons, $g < 9 \times 10^{-29}$–5×10^{-26} for $m_{A^0} < 1.5$–$400\ \mu$eV. See their Fig. 5 for mass-dependent limits.

[6] BULATOWICZ 13 looked for NMR frequency shifts in polarized ^{129}Xe and ^{131}Xe when a zirconia rod is positioned near the NMR cell, and find $g < 1 \times 10^{-19}$–1×10^{-24} for $\lambda = 0.01$–1 cm. See their Fig. 4 for their limits.

[7] CHU 13 look for a shift of the spin precession frequency of polarized ^{3}He in the presence of an unpolarized mass, in analogy to YOUDIN 96. See Fig. 3 for limits on g in the approximate m_{A^0} range 0.02–2 meV.

[8] TULLNEY 13 look for a shift of the precession frequency difference between the colocated ^{3}He and ^{129}Xe in the presence an unpolarized mass, and derive limits $g < 3 \times 10^{-29}$–2×10^{-22} for $\lambda > 3 \times 10^{-4}$ m. See their Fig. 3 for λ-dependent limits.

[9] RAFFELT 12 show that the pseudoscalar couplings to electron and nucleon and the scalar coupling to nucleon are individually constrained by stellar energy-loss arguments and searches for anomalous monopole-monopole forces, together providing restrictive constraints on g. See their Figs. 2 and 3 for results.

[10] HOEDL 11 use a novel torsion pendulum to study the force by the polarized electrons of an external magnet. In their Fig. 3 they show restrictive limits on g in the approximate m_{A^0} range 0.03–10 meV.

[11] PETUKHOV 10 use spin relaxation of polarized ^{3}He and find $g < 3 \times 10^{-23}\ (\mathrm{cm}/\lambda)^2$ at 95% CL for the force range $\lambda = 10^{-4}$–1 cm.

[12] SEREBROV 10 use spin precession of ultracold neutrons close to bulk matter and find $g < 2 \times 10^{-21}\ (\mathrm{cm}/\lambda)^2$ at 95% CL for the force range $\lambda = 10^{-4}$–1 cm.

[13] IGNATOVICH 09 use data on depolarization of ultracold neutrons in material traps. They show λ-dependent limits in their Fig. 1.

[14] SEREBROV 09 uses data on depolarization of ultracold neutrons stored in material traps and finds $g < 2.96 \times 10^{-21}\ (\mathrm{cm}/\lambda)^2$ for the force range $\lambda = 10^{-3}$–1 cm and $g < 3.9 \times 10^{-22}\ (\mathrm{cm}/\lambda)^2$ for $\lambda = 10^{-4}$–10^{-3} cm, each time at 95% CL, significantly improving on BAESSLER 07.

[15] BAESSLER 07 use the observation of quantum states of ultracold neutrons in the Earth's gravitational field to constrain g for an interaction range 1 μm–a few mm. See their Fig. 3 for results.

[16] HECKEL 06 studied the influence of unpolarized bulk matter, including the laboratory's surroundings or the Sun, on a torsion pendulum containing about 9×10^{22} polarized electrons. See their Fig. 4 for limits on g as a function of interaction range.

[17] NI 99 searched for a *T*-violating medium-range force acting on paramagnetic Tb F_3 salt. See their Fig. 1 for the result.

[18] POSPELOV 98 studied the possible contribution of *T*-violating Medium-Range Force to the neutron electric dipole moment, which is possible when axion interactions violate *CP*. The size of the force among nucleons must be smaller than gravity by a factor of $2 \times 10^{-10}\ (1\,\mathrm{cm}/\lambda_A)$, where $\lambda_A = \hbar/m_A c$.

[19] YOUDIN 96 compared the precession frequencies of atomic ^{199}Hg and Cs when a large mass is positioned near the cells, relative to an applied magnetic field. See Fig. 3 for their limits.

[20] RITTER 93 studied the influence of bulk mass with polarized electrons on an unpolarized torsion pendulum, providing limits in the interaction range from 1 to 100 cm.

[21] VENEMA 92 looked for an effect of Earth's gravity on nuclear spin-precession frequencies of ^{199}Hg and ^{201}Hg atoms.

[22] WINELAND 91 looked for an effect of bulk matter with aligned electron spins on atomic hyperfine resonances in stored ^{9}Be$^+$ ions using nuclear magnetic resonance.

Hidden Photons: Kinetic Mixing Parameter Limits

Hidden photons limits are listed for the first time, including only the most recent papers. Suggestions for previous important results are welcome. Limits are on the kinetic mixing parameter χ which is defined by the Lagrangian

$$L = -\frac{1}{4} F_{\mu\nu}F^{\mu\nu} - \frac{1}{4} F'_{\mu\nu}F'^{\mu\nu} - \frac{\chi}{2} F_{\mu\nu}F'^{\mu\nu} + \frac{m^2_{\gamma'}}{2} A'_\mu A'^\mu,$$

where A_μ and A'_μ are the photon and hidden-photon fields with field strengths $F_{\mu\nu}$ and $F'_{\mu\nu}$, respectively, and $m_{\gamma'}$ is the hidden-photon mass.

VALUE	CL%	DOCUMENT ID		TECN	COMMENT
• • • We do not use the following data for averages, fits, limits, etc. • • •					
$<3.1 \times 10^{-14}$	90	[1] ABGRALL	17	HPGE	$m_{\gamma'} = 11.8$ keV
$<6 \times 10^{-4}$	90	[2] ABLIKIM	17AA	BES3	$m_{\gamma'} = 1.5$–3.4 GeV
$<7 \times 10^{-15}$	90	[3] ANGLOHER	17	CRES	$m_{\gamma'} = 0.3$–0.7 keV
$<1.2 \times 10^{-4}$	90	[4] BANERJEE	17	NA64	$m_{\gamma'} = 0.002$–0.4 GeV
$<2 \times 10^{-11}$		[5] CHANG	17	ASTR	$m_{\gamma'} = 15$ MeV
$<4.5 \times 10^{-3}$	90	[6] DUBININA	17	EMUL	$m_{\gamma'} = 1.1$–24 MeV
$<4 \times 10^{-4}$	90	[7] LEES	17E	BABR	$m_{\gamma'} = 4.7$ GeV
		[8] AAD	16AG	ATLS	$m_{\gamma'} = 0.1$–2 GeV
$<4.4 \times 10^{-4}$	90	[9] ANASTASI	16	KLOE	$m_{\gamma'} = 527$–987 MeV
$<1.7 \times 10^{-6}$	95	[10] KHACHATRY...16		CMS	$m_{\gamma'} = 2$ GeV
$<7 \times 10^{-4}$	90	[11] LEES	16F	BABR	$m_{\gamma'} = 0.212$–10 GeV
$<4 \times 10^{-2}$	95	[12] AAD	15CD	ATLS	$m_{\gamma'} = 15$–55 GeV
$<1.4 \times 10^{-3}$	90	[13] ADARE	15		$m_{\gamma'} = 30$–90 MeV
		[14] AN	15A		$m_{\gamma'} = 12$ eV - 40 keV
		[15] ANASTASI	15	KLOE	$m_{\gamma'} = 2m_\mu$ - 1 GeV
$<1.7 \times 10^{-3}$	90	[16] ANASTASI	15A	KLOE	$m_{\gamma'} = 5$–320 MeV
$<4.2 \times 10^{-4}$	90	[17] BATLEY	15A	NA48	$m_{\gamma'} = 36$ MeV
		[18] JAEGLE	15	BELL	$m_{\gamma'} = 0.1$–3.5 GeV
$<3 \times 10^{-13}$		[19] KAZANAS	15	ASTR	$m_{\gamma'} = 2m_e$ – 100 MeV
		[20] SUZUKI	15		$m_{\gamma'} = 1.9$–4.3 eV
$<2.3 \times 10^{-13}$	99.7	[21] VINYOLES	15	ASTR	$m_{\gamma'} = 8$ eV
		[22] ABE	14F	XMAS	$m_{\gamma'} = 40$–120 keV
$<1.8 \times 10^{-3}$	90	[23] AGAKISHIEV	14	HDES	$m_{\gamma'} = 63$ MeV
$<9.0 \times 10^{-4}$	90	[24] BABUSCI	14	KLOE	$m_{\gamma'} = 969$ MeV
		[25] BATELL	14	BDMP	$m_{\gamma'} = 10^{-3}$–1 GeV
$<1.3 \times 10^{-7}$	95	[26] BLUEMLEIN	14	BDMP	$m_{\gamma'} = 0.6$ GeV
$<3 \times 10^{-18}$		[27] FRADETTE	14	COSM	$m_{\gamma'} = 50$–300 MeV
$<3.5 \times 10^{-4}$	90	[28] LEES	14J	BABR	$m_{\gamma'} = 0.2$ GeV
$<9 \times 10^{-4}$	95	[29] MERKEL	14	A1	$m_{\gamma'} = 40$–300 MeV
$<3 \times 10^{-15}$		[30] AN	13B	ASTR	$m_{\gamma'} = 2$ keV
$<7 \times 10^{-14}$		[31] AN	13C	XE10	$m_{\gamma'} = 100$ eV
$<8 \times 10^{-4}$		[32] DIAMOND	13	BDMP	$m_{\gamma'} = 30$–250 MeV
$<2.2 \times 10^{-13}$		[33] HORVAT	13	HPGE	$m_{\gamma'} = 230$ eV
$<8.06 \times 10^{-5}$	95	[34] INADA	13	LSW	$m_{\gamma'} = 0.04$ eV–26 keV
$<2 \times 10^{-10}$	95	[35] MIZUMOTO	13		$m_{\gamma'} = 1$ eV

$<1.7 \times 10^{-7}$		[36] PARKER	13	LSW	$m_{\gamma'} = 53$ μeV	
$<5.32 \times 10^{-15}$		[37] PARKER	13		$m_{\gamma'} = 53$ μeV	
$<1 \times 10^{-15}$		[38] REDONDO	13	ASTR	$m_{\gamma'} = 2$ keV	
$<8 \times 10^{-8}$	90	[39] GNINENKO	12A	BDMP	$m_{\gamma'} = 1$–135 MeV	
$<1 \times 10^{-7}$	90	[40] GNINENKO	12B	CHRM	$m_{\gamma'} = 1$–500 MeV	
$<1 \times 10^{-3}$	90	[41] ABRAHAMY...	11		$m_{\gamma'} = 175$–250 MeV	
$<9 \times 10^{-8}$	95	[42] BLUEMLEIN	11	BDMP	$m_{\gamma'} = 70$ MeV	
$<1 \times 10^{-7}$		[43] BJORKEN	09	BDMP	$m_{\gamma'} = 2$–400 MeV	
$<5 \times 10^{-9}$		[44] BJORKEN	09	ASTR	$m_{\gamma'} = 2$–50 MeV	

[1] ABGRALL 17 is analogous to ABE 14F using the MAJORANA DEMONSTRATOR. See their Fig. 3 for limits between 6 keV $< m_{\gamma'} <$ 97 keV.

[2] ABLIKIM 17AA look for $e^+e^- \to \gamma\gamma'$ ($\gamma' \to e^+e^-$ or $\mu^+\mu^-$) . Limits between 10^{-3} and 10^{-4} are obtained (see their Fig. 3).

[3] ANGLOHER 17 is analogous to ABE 14F. The quoted limit is at $m_{\gamma'} = 0.7$ keV. See their Fig. 8 for mass-dependent limits.

[4] BANERJEE 17 look for invisible decays of hidden photons produced in the reaction $e^- Z \to e^- Z\gamma'$. The quoted limit applies to $m_{\gamma'} = 2$ MeV. See their Fig. 3 for mass-dependent limits.

[5] CHANG 17 examine the hidden photon emission from SN1987A, including the effects of finite temperature and density on χ and obtain limits $\chi\,(m_{\gamma'}/\text{MeV}) \lesssim 3 \times 10^{-9}$ for $m_{\gamma'} <$ 15 MeV and $\chi \lesssim 10^{-9}$ for $m_{\gamma'} =$ 15–120 MeV.

[6] DUBININA 17 look for $\mu^+ \to e^+ \overline{\nu}_\mu \nu_e \gamma'$ ($\gamma' \to e^+e^-$) in a nuclear photoemulsion. The quoted limit applies to $m_{\gamma'} = 1.1$ MeV. Limits between 4.5×10^{-3} and 10^{-2} are obtained (see their Fig. 3).

[7] LEES 17E look for invisible decays of hidden photons produced in the reaction $e^+e^- \to \gamma\gamma'$. See their Fig. 5 for limits in the mass range $m_{\gamma'} \leq 8$ GeV.

[8] AAD 16AG look for hidden photons promptly decaying into collimated electrons and/or muons, assuming that they are produced in the cascade decays of squarks or the Higgs boson. See their Fig. 10 and Fig.13 for their limits on the cross section times branching fractions.

[9] ANASTASI 16 look for the decay $\gamma' \to \pi^+\pi^-$ in the reaction $e^+e^- \to \gamma\gamma'$. Limits between 4.3×10^{-3} and 4.4×10^{-4} are obtained for $527 < m_{\gamma'} <$ 987 MeV (see their Fig. 9).

[10] KHACHATRYAN 16 look for $\gamma' \to \mu^+\mu^-$ in a dark SUSY scenario where the SM-like Higgs boson decays into a pair of the visible lightest neutralinos with mass 10 GeV, both of which decay into γ' and a hidden neutralino with mass 1 GeV. See the right panel in their Fig. 2.

[11] LEES 16F looked for a hidden photon coupled only to the second and third generations of leptons in the reaction $e^+e^- \to \mu^+\mu^-\gamma'$ ($\gamma' \to \mu^+\mu^-$) using data collected by BABAR detector, and derived limits on the hidden photon gauge coupling as low as 7×10^{-4} for $m_{\gamma'} = 0.212$–10 GeV. See their Fig. 5 for the mass-dependent limits.

[12] AAD 15CD look for $H \to Z\gamma' \to 4\ell$ with the ATLAS detector at LHC and find $\chi <$ 4–17 $\times 10^{-2}$ for $m_{\gamma'} =$ 15–55 GeV. See their Fig. 6.

[13] ADARE 15 look for a hidden photon in $\pi^0, \eta^0 \to \gamma e^+e^-$ at the PHENIX experiment. See their Fig. 4 for mass-dependent limits.

[14] AN 15A derived limits from the absence of ionization signals in the XENON10 and XENON100 experiments, assuming hidden photons constitute all the local dark matter. Their best limit is $\chi < 1.3 \times 10^{-15}$ at $m_{\gamma'} = 18$ eV. See their Fig. 1 for mass-dependent limits.

[15] ANASTASI 15 look for a production of a hidden photon and a hidden Higgs boson with the KLOE detector at DAΦNE, where the hidden photon decays into a pair of muons and the hidden Higgs boson lighter than $m_{\gamma'}$ escape detection. See their Figs. 6 and 7 for mass-dependent limits on a product of the hidden fine structure constant and the kinetic mixing.

[16] ANASTASI 15A look for the decay $\gamma' \to e^+e^-$ in the reaction $e^+e^- \to e^+e^-\gamma$. Limits between 1.7×10^{-3} and 1×10^{-2} are obtained for $m_{\gamma'} =$ 5–320 MeV (see their Fig. 7).

[17] BATLEY 15A look for $\pi^0 \to \gamma\gamma'$ ($\gamma' \to e^+e^-$) at the NA48/2 experiment. Limits between 4.2×10^{-4} and 8.8×10^{-3} are obtained for $m_{\gamma'} =$ 9–120 MeV (see their Fig. 4).

[18] JAEGLE 15 look for the decay $\gamma' \to e^+e^-, \mu^+\mu^-$, or $\pi^+\pi^-$ in the dark Higgstrahlung channel, $e^+e^- \to \gamma' H'$ ($H' \to \gamma'\gamma'$) at the BELLE experiment. They set limits on a product of the branching fraction and the Born cross section as well as a product of the hidden fine structure constant and the kinetic mixing. See their Figs. 3 and 4.

[19] KAZANAS 15 set limits by studying the decay of hidden photons $\gamma' \to e^+e^-$ inside and near the progenitor star of SN1987A. See their Fig. 6 for mass-dependent limits.

[20] SUZUKI 15 looked for hidden-photon dark matter with a dish antenna and derived limits assuming they constitute all the local dark matter. Their limits are $\chi < 6 \times 10^{-12}$ for $m_{\gamma'} =$ 1.9–4.3 eV. See their Fig. 7 for mass-dependent limits.

[21] VINYOLES 15 performed a global fit analysis based on helioseismology and solar neutrino observations, and set the limits $\chi m_{\gamma'} < 1.8 \times 10^{-12}$ eV for $m_{\gamma'} = 3 \times 10^{-5}$–8 eV. See their Fig. 11.

[22] ABE 14F look for the photoelectric-like interaction in the XMASS detector assuming the hidden photon constitutes all the local dark matter. Limits between 2×10^{-13} and 1×10^{-12} are obtained. See their Fig. 3 for mass-dependent limits.

[23] AGAKISHIEV 14 look for hidden photons $\gamma' \to e^+e^-$ at the HADES experiment, and set limits on χ for $m_{\gamma'} =$ 0.02–0.6 GeV. See their Fig. 5 for mass-dependent limits.

[24] BABUSCI 14 look for the decay $\gamma' \to \mu^+\mu^-$ in the reaction $e^+e^- \to \mu^+\mu^-\gamma$. Limits between 4×10^{-3} and 9.0×10^{-4} are obtained for 520 MeV $< m_{\gamma'} <$ 980 MeV (see their Fig. 7).

[25] BATELL 14 derived limits from the electron beam dump experiment at SLAC (E-137) by searching for events with recoil electrons by sub-GeV dark matter produced from the decay of the hidden photon. Limits at the level of 10^{-4}–10^{-1} are obtained for $m_{\gamma'} = 10^{-3}$–1 GeV, depending on the dark matter mass and the hidden gauge coupling (see their Fig. 2).

[26] BLUEMLEIN 14 analyzed the beam dump data taken at the U-70 accelerator to look for γ'-bremsstrahlung and the subsequent decay into muon pairs and hadrons. See their Fig. 4 for mass-dependent excluded region.

[27] FRADETTE 14 studied effects of decay of relic hidden photons on BBN and CMB to set constraints on very small values of the kinetic mixing. See their Figs. 4 and 7 for mass-dependent excluded regions.

[28] LEES 14J look for hidden photons in the reaction $e^+e^- \to \gamma\gamma'$ ($\gamma' \to e^+e^-, \mu^+\mu^-$). Limits at the level of 10^{-4}–10^{-3} are obtained for 0.02 GeV $< m_{\gamma'} <$ 10.2 GeV. See their Fig. 4 for mass-dependent limits.

[29] MERKEL 14 look for $\gamma' \to e^+e^-$ at the A1 experiment at the Mainz Microtron (MAMI). See their Fig. 3 for mass-dependent limits.

[30] AN 13B examined the stellar production of hidden photons, correcting an important error of the production rate of the longitudinal mode which now dominates. See their Fig. 2 for mass-dependent limits based on solar energy loss.

[31] AN 13C use the solar flux of hidden photons to set a limit on the atomic ionization rate in the XENON10 experiment. They find $\chi\, m_{\gamma'} < 3 \times 10^{-12}$ eV for $m_{\gamma'} <$ 1 eV. See their Fig. 2 for mass-dependent limits.

[32] DIAMOND 13 analyzed the beam dump data taken at the SLAC millicharge experiment to constrain a hidden photon invisibly decaying into lighter long-lived particles, which undergo elastic scattering off nuclei in the detector. Limits between 8×10^{-4}–2×10^{-2} are obtained. The quoted limit is applied when the dark gauge coupling is set equal to the electromagnetic coupling. See their Fig.4 for mass-dependent limits.

[33] HORVAT 13 look for hidden-photo-electric effect in HPGe detectors induced by solar hidden photons. See their Fig. 3 for mass-dependent limits.

[34] INADA 13 search for hidden photons using an intense X-ray beamline at SPring-8. See their Fig. 4 for mass-dependent limits.

[35] MIZUMOTO 13 look for solar hidden photons. See their Fig. 5 for mass-dependent limits.

[36] PARKER 13 look for hidden photons using a cryogenic resonant microwave cavity. See their Fig.5 for mass-dependent limits.

[37] PARKER 13 derived a limit for the hidden photon CDM with a randomly oriented hidden photon field.

[38] REDONDO 13 examined the solar emission of hidden photons including the enhancement factor for the longitudinal mode pointed out by AN 13B, and also updated stellar-energy loss arguments. See their Fig.3 for mass-dependent limits, including a review of the currently best limits from other arguments.

[39] GNINENKO 12A obtained bounds on $B(\pi^0 \to \gamma\gamma') \cdot B(\gamma' \to e^+e^-)$ from the NOMAD and PS191 neutrino experiments, and derived limits between 8×10^{-8}–2×10^{-4}. See their Fig.4 for mass-dependent excluded regions.

[40] GNINENKO 12B used the data taken at the CHARM experiment to constrain the decay, $\eta(\eta') \to \gamma\gamma'$ ($\gamma' \to e^+e^-$), and derived limits between 1×10^{-7}–1×10^{-4}. See their Fig.4 for mass-dependent excluded region.

[41] ABRAHAMYAN 11 look for $\gamma' \to e^+e^-$ in the electron-nucelon fixed-target experiment at the Jefferson Laboratory (APEX). See their Fig. 5 for mass-dependent limits.

[42] BLUEMLEIN 11 analyzed the beam dump data taken at the U-70 accelerator to look for $\pi^0 \to \gamma\gamma'$ ($\gamma' \to e^+e^-$). See their Fig. 5 for mass-dependent limits.

[43] BJORKEN 09 analyzed the beam dump data taken at E137, E141, and E774 to constrain a hidden photon produced by bremsstrahlung, subsequently decaying into e^+e^-, and derived limits between 10^{-7} and 10^{-2}. See their Fig. 1 for mass-dependent excluded region.

[44] BJORKEN 09 required the energy loss in the γ' emission from the core of SN1987A not to exceed 10^{53} erg/s, and derived limits between 5×10^{-9} and 2×10^{-6}. See their Fig. 1 for mass-dependent excluded region.

REFERENCES FOR Searches for Axions (A^0) and Other Very Light Bosons

STADNIK	18	PRL 120 013202	Y.V. Stadnik, V.A. Dzuba, V.V. Flambaum
AAIJ	17AQ	PR D95 071101	R. Aaij *et al.* (LHCb Collab.)
ABEL	17	PR X7 041034	C. Abel *et al.* (nEDM Collab.)
ABGRALL	17	PRL 118 161801	N. Abgrall *et al.* (MAJORANA Collab.)
ABLIKIM	17AA	PL B774 252	M. Ablikim *et al.* (BES III Collab.)
ADE	17	PR D96 102003	P.A.R. Ade *et al.* (BICEP2/Keck Array Collab.)
AHN	17	PTEP 2017 021C01	J.K. Ahn *et al.* (KOTO Collab.)
AKERIB	17B	PRL 118 261301	D.S. Akerib *et al.* (LUX Collab.)
ANASTASSO...	17	NATP 13 584	V. Anastassopoulos *et al.* (CAST Collab.)
ANGLOHER	17	EPJ C77 299	G. Angloher *et al.* (CRESST-II Collab.)
APRILE	17B	PR D95 029904	E. Aprile *et al.* (XENON100 Collab.)
BANERJEE	17	PRL 118 011802	D. Banerjee *et al.* (NA64 Collab.)
BATLEY	17	PL B769 67	J.R. Batley *et al.* (NA48/2 Collab.)
BRANCA	17	PRL 118 021302	A. Branca *et al.* (AURIGA Collab.)
BRUBAKER	17	PRL 118 061302	B.M. Brubaker *et al.* (YALE, UCB, NIST+)
CHANG	17	JHEP 1701 107	J.H. Chang, R. Essig, S.D. McDermott (STON)
CHOI	17	PR D96 061102	J. Choi *et al.* (CAPP-ACTION Collab.)
CRESCINI	17	PL B773 677	N. Crescini *et al.* (QUAX-gpgs Collab.)
DAIDO	17	PL B772 127	R. Daido, F. Takahashi
DOLAN	17	JHEP 1712 094	Matthew J. Dolan *et al.*
DUBININA	17	PAN 80 461	V.V. Dubinina *et al.*
FICEK	17	PR A95 032505	F. Ficek *et al.*
FU	17A	PRL 119 181806	C. Fu *et al.* (PandaX-II Collab.)
INADA	17	PRL 118 071803	T. Inada *et al.*
KLIMCHITSK...	17A	PR D95 123013	G.L. Klimchitskaya, V.M. Mostepanenko
KOHRI	17	PR D96 051701	K. Kohri, H. Kodama (KEK, KYOT)
LEES	17E	PRL 119 131804	J.P. Lees *et al.* (BABAR Collab.)
LIU	17	PL B766 117	X.-H. Liu (TINT)
LIU	17A	PR D95 052006	S.K. Liu *et al.* (CDEX Collab.)
LUO	17	PR D96 055028	P. Luo *et al.*
MARSH	17	JCAP 1712 036	M.C.D. Marsh *et al.*
TIWARI	17	PR D95 023005	P. Tiwari (Technion)
AAD	16AG	JHEP 1602 062	G. Aad *et al.* (ATLAS Collab.)
ABLIKIM	16E	PR D93 052005	M. Ablikim *et al.* (BES III Collab.)
AJELLO	16	PRL 116 161101	M. Ajello *et al.* (Fermi-LAT Collab.)
ANASTASI	16	PL B757 356	A. Anastasi *et al.* (KLOE-2 Collab.)
BATTICH	16	JCAP 1608 062	T. Battich *et al.*
CORSICO	16	JCAP 1607 036	A.H. Corsico *et al.*
DELLA-VALLE	16	EPJ C76 24	F. Della Valle *et al.* (PVLAS Collab.)
HOSKINS	16	PR D94 082001	J. Hoskins *et al.* (ADMX Collab.)

Gauge & Higgs Boson Particle Listings

Axions (A^0) and Other Very Light Bosons

JAECKEL 16 PL B753 482 J. Jaeckel, M. Spannowsky (HEID, DURH)
KHACHATRY... 16 PL B752 146 V. Khachatryan *et al.* (CMS Collab.)
LEEFER 16 PRL 117 271601 N. Leefer *et al.* (MAINZ, BONN, LBL, UCB+)
LEES 16F PR D94 011102 J.P. Lees *et al.* (BABAR Collab.)
WON 16 PR D94 092006 E. Won *et al.* (BELLE Collab.)
YOON 16 JHEP 1606 011 Y.S. Yoon *et al.* (KIMS Collab.)
AAD 15CD PR D92 092001 G. Aad *et al.* (ATLAS Collab.)
AAIJ 15AZ PRL 115 161802 R. Aaij *et al.* (LHCb Collab.)
ADARE 15 PR C91 031901 A. Adare *et al.* (PHENIX Collab.)
AFACH 15 PL B745 58 S. Afach *et al.* (ETH, PSI, CAEN, +)
AGOSTINI 15A EPJ C75 416 M. Agostini *et al.* (GERDA Collab.)
AN 15A PL B747 331 H. An *et al.* (CIT, VICT, VIEN)
ANASTASI 15 PL B747 365 A. Anastasi *et al.* (KLOE-2 Collab.)
ANASTASI 15A PL B750 633 A. Anastasi *et al.* (KLOE-2 Collab.)
ANASTASSO... 15 PL B749 172 V. Anastassopoulos *et al.* (CAST Collab.)
ARIK 15 PR D92 021101 M. Arik *et al.* (CAST Collab.)
ARNOLD 15 PR D92 072011 R. Arnold *et al.* (NEMO-3 Collab.)
BALLOU 15 PR D92 092002 R. Ballou *et al.* (OSQAR Collab.)
BATLEY 15A PL B746 178 J.R. Batley *et al.* (NA48/2 Collab.)
BAYES 15 PR D91 052020 R. Bayes *et al.* (TWIST Collab.)
BRAX 15 PR D92 083501 P. Brax, P. Brun, D. Wouters (SACL, SACL5)
GAVRILYUK 15 JETPL 101 664 Yu.M. Gavrilyuk *et al.*
Translated from ZETFP 101 739.
HASEBE 15 PTEP 2015 073C01 T. Hasebe *et al.*
JAEGLE 15 PRL 114 211801 I. Jaegle *et al.* (BELLE Collab.)
KAZANAS 15 NP B890 17 D. Kazanas *et al.*
KLIMCHITSK... 15 EPJ C75 164 G.L. Klimchitskaya, V.M. Mostepanenko
MILLEA 15 PR D92 023010 M. Millea, L. Knox, B. Fields (UCD, ILL)
STADNIK 15 EPJ C75 110 Y.V. Stadnik, V.V. Flambaum (SYDN)
SUZUKI 15 JCAP 1509 042 J. Suzuki *et al.*
TERRANO 15 PRL 115 201801 W.A. Terrano *et al.* (WASH)
VANTILBURG 15 PRL 115 011802 K. Van Tilburg *et al.*
VINYOLES 15 JCAP 1510 015 N. Vinyoles *et al.*
ABE 14F PRL 113 121301 K. Abe *et al.* (XMASS Collab.)
AGAKISHIEV 14 PL B731 265 G. Agakishiev *et al.* (HADES Collab.)
ALBERT 14A PR D90 092004 J.B. Albert *et al.* (EXO-200 Collab.)
APRILE 14B PR D90 062009 E. Aprile *et al.* (XENON100 Collab.)
ARIK 14 PRL 112 091302 M. Arik *et al.* (CAST Collab.)
AYALA 14 PRL 113 191302 A. Ayala *et al.*
BABUSCI 14 PL B736 459 D. Babusci *et al.* (KLOE-2 Collab.)
BATELL 14 PRL 113 171802 B. Batell, R. Essig, Z. Surujon (EFI, STON)
BEZERRA 14 PR D89 035010 V.B. Bezerra *et al.*
BEZERRA 14A EPJ C74 2859 V.B. Bezerra *et al.*
BEZERRA 14B PR D90 055013 V.B. Bezerra *et al.*
BEZERRA 14C PR D89 075002 V.B. Bezerra *et al.*
BLUEMLEIN 14 PL B731 320 J. Bluemlein, J. Brunner (CPPM, DESY)
BLUM 14 PL B737 30 K. Blum *et al.* (IAS, PRIN)
DELLA-VALLE 14 PR D90 092003 F. Della Valle *et al.* (PVLAS Collab.)
DERBIN 14 EPJ C74 3035 A.V. Derbin *et al.*
EJLLI 14 PR D90 123527 D. Ejlli
FRADETTE 14 PR D90 035022 A. Fradette *et al.*
LEES 14J PRL 113 201801 J.P. Lees *et al.* (BABAR Collab.)
LEINSON 14 JCAP 1408 031 L. Leinson
MERKEL 14 PRL 112 221802 H. Merkel *et al.* (A1 at MAMI)
MILLER-BER... 14 JCAP 1410 069 M.M. Miller Bertolami *et al.*
PUGNAT 14 EPJ C74 3027 P. Pugnat *et al.* (OSQAR Collab.)
REESMAN 14 JCAP 1408 021 R. Reesman *et al.* (OSU)
ABE 13D PL B724 46 K. Abe *et al.* (XMASS Collab.)
ABRAMOWSKI 13A PR D88 102003 A. Abramowski *et al.* (H.E.S.S. Collab.)
ADLARSON 13 PL B726 187 P. Adlarson *et al.* (WASA-at-COSY Collab.)
ALESSANDRIA 13 JCAP 1305 007 F. Alessandria *et al.* (CUORE Collab.)
AN 13B PL B725 190 H. An, M. Pospelov, J. Pradler
AN 13C PRL 111 041302 H. An, M. Pospelov, J. Pradler
ARCHIDIACO... 13A JCAP 1310 020 M. Archidiacono *et al.*
ARMENGAUD 13 JCAP 1311 067 E. Armengaud *et al.* (EDELWEISS-II Collab.)
BABUSCI 13B PL B720 111 D. Babusci *et al.* (KLOE-2 Collab.)
BARTH 13 JCAP 1305 010 K. Barth *et al.* (CAST Collab.)
BECK 13 PRL 111 231801 C. Beck
BETZ 13 PR D88 075014 M. Betz *et al.* (CROWS Collab.)
BULATOWICZ 13 PRL 111 102001 M. Bulatowicz *et al.*
CHU 13 PR D87 011105 P.-H. Chu *et al.* (DUKE, IND, SJTU)
DERBIN 13 EPJ C73 2490 A. V. Derbin *et al.*
DIAMOND 13 PRL 111 221803 M.D. Diamond, P. Schuster
FRIEDLAND 13 PRL 110 061101 A. Friedland, M. Giannotti, M. Wise
HECKEL 13 PRL 111 151802 B. R. Heckel *et al.*
HORVAT 13 PL B721 220 R. Horvat *et al.*
INADA 13 PL B722 301 T. Inada *et al.*
LATTANZI 13 PR D88 063528 M. Lattanzi *et al.*
MEYER 13 PR D87 035027 M. Meyer, D. Horns, M. Raue
MIZUMOTO 13 JCAP 1307 013 T. Mizumoto *et al.*
PARKER 13 PR D88 112004 S. Parker *et al.*
REDONDO 13 JCAP 1308 034 J. Redondo, G. Raffelt
TULLNEY 13 PRL 111 100801 K. Tullney *et al.*
VIAUX 13A PRL 111 231301 N. Viaux *et al.*
WOUTERS 13 APJ 772 44 D. Wouters, P. Brun (SACL)
ABLIKIM 12 PR D85 092012 M. Ablikim *et al.* (BES III Collab.)
ARCHILLI 12 PL B706 251 F. Archilli *et al.* (KLOE-2 Collab.)
BELLI 12 PL B711 41 P. Belli *et al.* (DAMA-KIEV)
BELLINI 12B PR D85 092003 G. Bellini *et al.* (Borexino Collab.)
CADAMURO 12 JCAP 1202 032 D. Cadamuro *et al.* (MPIM)
CORSICO 12 JCAP 1212 010 A.H. Corsico *et al.* (LAPL, RGSUL, WASH+)
DERBIN 12 JETPL 95 339 A.V. Derbin *et al.* (PNPI)
Translated from ZETFP 95 379.
GANDO 12 PR C86 021601 A. Gando *et al.* (KamLAND-Zen Collab.)
GNINENKO 12A PR D85 055027 S.N. Gninenko (INRM)
GNINENKO 12B PL B713 244 S.N. Gninenko (INRM)
PAYEZ 12 JCAP 1207 041 A. Payez *et al.* (LIEG)
RAFFELT 12 PR D86 015001 G. Raffelt (MPIM)
AALSETH 11 PRL 106 131301 C.E. Aalseth *et al.* (CoGeNT Collab.)
ABRAHAMY... 11 PRL 107 191804 S. Abrahamyan *et al.*
ARIK 11 PRL 107 261302 M. Arik *et al.* (CAST Collab.)
ARNOLD 11 PRL 107 062504 R. Arnold *et al.* (NEMO-3 Collab.)
BLUEMLEIN 11 PL B701 155 J. Bluemlein, J. Brunner (DESY)
CADAMURO 11 JCAP 1102 003 D. Cadamuro *et al.* (MPIM, AARHUS)
DERBIN 11 PAN 74 596 A.V. Derbin *et al.* (PNPI)
Translated from YAF 74 620.
DERBIN 11A PR D83 023505 A.V. Derbin *et al.* (PNPI)
HOEDL 11 PRL 106 041801 S.A. Hoedl *et al.* (WASH)
HOSKINS 11 PR D84 121302 J. Hoskins *et al.* (ADMX Collab.)
ANDRIAMON... 10 JCAP 1003 032 S. Andriamonje *et al.* (CAST Collab.)
ARGYRIADES 10 NP A847 168 J. Argyriades *et al.* (NEMO-3 Collab.)
ASZTALOS 10 PRL 104 041301 S.J. Asztalos *et al.* (ADMX Collab.)
EHRET 10 PL B689 149 K. Ehret *et al.* (ALPS Collab.)
HANNESTAD 10 JCAP 1008 001 S. Hannestad *et al.*
PETUKHOV 10 PRL 105 170401 A.K. Petukhov *et al.*
SEREBROV 10 JETPL 91 6 A. Serebrov *et al.*
Translated from ZETFP 91 8.
AHMED 09A PRL 103 141802 Z. Ahmed *et al.* (CDMS Collab.)
ANDRIAMON... 09 JCAP 0912 002 S. Andriamonje *et al.*
ARGYRIADES 09 PR C80 032501 J. Argyriades *et al.* (NEMO-3 Collab.)
ARIK 09 JCAP 0902 008 E. Arik *et al.* (CAST Collab.)
BJORKEN 09 PR D80 075018 J. Bjorken *et al.*
CHOU 09 PRL 102 030402 A.S. Chou *et al.* (GammeV Collab.)
DAVOUDIASL 09 PR D79 095024 H. Davoudiasl, P. Huber
DERBIN 09A PL B678 181 A.V. Derbin *et al.*
GONDOLO 09 PR D79 107301 P. Gondolo, G. Raffelt (UTAH, MPIM)
IGNATOVICH 09 EPJ C64 19 V.K. Ignatovich, Y.N. Pokotilovski (JINR)
KEKEZ 09 PL B671 345 D. Kekez *et al.*
SEREBROV 09 PL B680 423 A. Serebrov (PNPI)
AFANASEV 08 PRL 101 120401 A. Afanasev *et al.*
BELLINI 08 EPJ C54 61 G. Bellini *et al.* (Borexino Collab.)
CHOU 08 PRL 100 080402 A.S. Chou *et al.* (GammeV Collab.)
FOUCHE 08 PR D78 032013 M. Fouche *et al.*
HANNESTAD 08 JCAP 0804 019 S. Hannestad *et al.*
INOUE 08 PL B668 93 Y. Inoue *et al.*
ZAVATTINI 08 PR D77 032006 E. Zavattini *et al.* (PVLAS Collab.)
ADELBERGER 07 PRL 98 131104 E.G. Adelberger *et al.*
ANDRIAMON... 07 JCAP 0704 010 S. Andriamonje *et al.* (CAST Collab.)
BAESSLER 07 PR D75 075006 S. Baessler *et al.*
CHANG 07 PR D75 052004 H.M. Chang *et al.* (TEXONO Collab.)
HANNESTAD 07 JCAP 0708 015 S. Hannestad *et al.*
JAIN 07 JP G34 129 P.L. Jain, G. Singh
LESSA 07 PR D75 094001 A.P. Lessa, O.L.G. Peres
MELCHIORRI 07A PR D76 041303 A. Melchiorri, O. Mena, A. Slosar
ROBILLIARD 07 PRL 99 190403 C. Robilliard *et al.*
ARNOLD 06 NP A765 483 R. Arnold *et al.* (NEMO-3 Collab.)
DUFFY 06 PR D74 012006 L.D. Duffy *et al.*
HECKEL 06 PRL 97 021603 B.R. Heckel *et al.*
ZAVATTINI 06 PRL 96 110406 E. Zavattini *et al.* (PVLAS Collab.)
HANNESTAD 05A JCAP 0507 002 S. Hannestad, A. Mirizzi, G. Raffelt
ZIOUTAS 05 PRL 94 121301 K. Zioutas *et al.* (CAST Collab.)
ADLER 04 PR D70 037102 S. Adler *et al.* (BNL E787 Collab.)
ANISIMOVSK... 04 PRL 93 031801 V.V. Anisimovsky *et al.* (BNL E949 Collab.)
ARNOLD 04 JETPL 80 377 R. Arnold *et al.* (NEMO-3 Collab.)
Translated from ZETFP 80 429.
ASZTALOS 04 PR D69 011101 S.J. Asztalos *et al.*
HOFFMANN 04 PR B70 180503 C. Hoffmann *et al.*
ARNABOLDI 03 PL B557 167 C. Arnaboldi *et al.*
CIVITARESE 03 NP A729 867 O. Civitarese, J. Suhonen
DANEVICH 03 PR C68 035501 F.A. Danevich *et al.*
ADLER 02C PL B537 211 S. Adler *et al.* (BNL E787 Collab.)
BADERT... 02 PL B542 29 A. Badertscher *et al.*
BERNABEI 02D PL B546 23 R. Bernabei *et al.* (DAMA Collab.)
DERBIN 02 PAN 65 1302 A.V. Derbin *et al.*
Translated from YAF 65 1335.
FUSHIMI 02 PL B531 190 K. Fushimi *et al.* (ELEGANT V Collab.)
INOUE 02 PL B536 18 Y. Inoue *et al.*
MORALES 02B ASP 16 325 A. Morales *et al.* (COSME Collab.)
ADLER 01 PR D63 032004 S. Adler *et al.* (BNL E787 Collab.)
AMMAR 01B PRL 87 271801 R. Ammar *et al.* (CLEO Collab.)
ASHITKOV 01 JETPL 74 529 V.D. Ashitkov *et al.*
Translated from ZETFP 74 601.
BERNABEI 01B PL B515 6 R. Bernabei *et al.* (DAMA Collab.)
DANEVICH 01 NP A694 375 F.A. Danevich *et al.*
DEBOER 01 JP G27 L29 F.W.N. de Boer *et al.*
STOICA 01 NP A694 269 S. Stoica, H.V. Klapdor-Kleingrothous
ALESSAND... 00 PL B486 13 A. Alessandrello *et al.*
ARNOLD 00 NP A678 341 R. Arnold *et al.*
ASTIER 00B PL B479 371 P. Astier *et al.* (NOMAD Collab.)
DANEVICH 00 PR C62 045501 F.A. Danevich *et al.*
MASSO 00 PR D61 011701 E. Masso
ARNOLD 99 NP A658 299 R. Arnold *et al.* (NEMO Collab.)
NI 99 PRL 82 2439 W.-T. Ni *et al.*
SIMKOVIC 99 PR C60 055502 F. Simkovic *et al.*
ALTEGOER 98 PL B428 197 J. Altegoer *et al.*
ARNOLD 98 NP A636 209 R. Arnold *et al.* (NEMO-2 Collab.)
AVIGNONE 98 PRL 81 5068 F.T. Avignone *et al.* (Solar Axion Experiment)
DIAZ 98 NP B527 44 M.A. Diaz *et al.*
FAESSLER 98B JP G24 2139 A. Faessler, F. Simkovic
KIM 98 PR D58 055006 J.E. Kim
LUESCHER 98 PL B434 407 R. Luescher *et al.*
MORIYAMA 98 PL B434 147 S. Moriyama *et al.*
MOROI 98 PL B440 69 T. Moroi, H. Murayama
POSPELOV 98 PR D58 097703 M. Pospelov
ZUBER 98 PRPL 305 295 K. Zuber
AHMAD 97 PRL 78 618 I. Ahmad *et al.* (APEX Collab.)
BORISOV 97 JETP 83 868 A.V. Borisov, V.Y. Grishinia (MOSU)
DEBOER 97C JP G23 L85 F.W.N. de Boer *et al.*
KACHELRIESS 97 PR D56 1313 M. Kachelriess, C. Wilke, G. Wunner (BOCH)
KEIL 97 PR D56 2419 W. Keil *et al.*
KITCHING 97 PRL 79 4079 P. Kitching *et al.* (BNL E787 Collab.)
LEINBERGER 97 PL B394 16 U. Leinberger *et al.* (ORANGE Collab.)
ADLER 96 PRL 76 1421 S. Adler *et al.* (BNL E787 Collab.)
AMSLER 96B ZPHY C70 219 C. Amsler *et al.* (Crystal Barrel Collab.)
GANZ 96 PL B389 4 R. Ganz *et al.* (GSI, HEID, FRAN, JAGL+)
GUENTHER 96 PR D54 3641 M. Gunther *et al.* (MPIH, SASSO)
KAMEL 96 PL B368 291 S. Kamel (SHAMS)
MITSUI 96 EPL 33 111 T. Mitsui *et al.* (TOKY)
YOUDIN 96 PRL 77 2170 A.N. Youdin *et al.* (AMHT, WASH)
ALTMANN 95 ZPHY C68 221 M. Altmann *et al.* (MUNT, LAPP, CPPM)
BASSOMPIE... 95 PL B355 584 G. Bassompierre *et al.* (LAPP, LCGT, LYON)
MAENO 95 PL B351 574 T. Maeno *et al.* (TOKY)
RAFFELT 95 PR D51 1495 G. Raffelt, A. Weiss (MPIM, MPIG)
SKALSEY 95 PR D51 6292 M. Skalsey, R.S. Conti (MICH)
TSUNODA 95 EPL 30 273 T. Tsunoda *et al.* (TOKY)
ADACHI 94 PR A49 3201 S. Adachi *et al.* (TMU)
ALTHERR 94 ASP 2 175 T. Altherr, E. Petitgirard, T. del Rio Gaztelurrutia
AMSLER 94B PL B333 271 C. Amsler *et al.* (Crystal Barrel Collab.)
ASAI 94 PL B323 90 S. Asai *et al.* (TOKY)
MEIJERDREES 94 PR D49 4937 M.R. Drees *et al.* (BRCO, OREG, TRIU)
NI 94 Physica B194 153 W.T. Ni *et al.* (NTHU)
VO 94 PR C49 1551 D.T. Vo *et al.* (ISU, LBL, LLNL, UCD)
ATIYA 93 PRL 70 2521 M.S. Atiya *et al.* (BNL E787 Collab.)
Also PRL 71 305 (erratum) M.S. Atiya *et al.* (BNL E787 Collab.)
ATIYA 93B PR D48 1 M.S. Atiya *et al.* (BNL E787 Collab.)
BASSOMPIE... 93 EPL 22 239 G. Bassompierre *et al.* (LAPP, TORI, LYON)
BECK 93 PRL 70 2853 M. Beck *et al.* (MPIH, KIAE, SASSO)
CAMERON 93 PR D47 3707 R.E. Cameron *et al.* (ROCH, BNL, FNAL+)
CHANG 93 PL B316 51 S. Chang, K. Choi
CHUI 93 PRL 71 3247 T.C.P. Chui, W.T. Ni (NTHU)
MINOWA 93 PRL 71 4120 M. Minowa *et al.* (TOKY)
NG 93 PR D48 2941 K.W. Ng (AST)
RITTER 93 PRL 70 701 R.C. Ritter *et al.*
TANAKA 93 PR D48 5412 J. Tanaka, H. Ejiri (OSAK)
ALLIEGRO 92 PRL 68 278 C. Alliegro *et al.* (BNL, FNAL, PSI+)
ATIYA 92 PRL 69 733 M.S. Atiya *et al.* (BNL, LANL, PRIN+)
BARABASH 92 PL B295 154 L.S. Barabash *et al.* (JINR, CERN, SERP+)
BERNATOW... 92 PRL 69 2341 T. Bernatowicz *et al.* (WUSL, TATA)
BLUEMLEIN 92 IJMP A7 3835 J. Bluemlein *et al.* (BERL, BUDA, JINR+)
HALLIN 92 PR D45 3955 A.L. Hallin *et al.* (PRIN)
HENDERSON 92C PRL 69 1733 S.D. Henderson *et al.* (YALE, BNL)
HICKS 92 PL B276 423 K.H. Hicks, D.E. Alburger (OHIO, BNL)
LAZARUS 92 PRL 69 2333 D.M. Lazarus *et al.* (BNL, ROCH, FNAL)
MEIJERDREES 92 PRL 68 3845 R. Meijer Drees *et al.* (SINDRUM I Collab.)
PAN 92 MPL A7 1287 S.S. Pan, W.T. Ni, S.C. Chen (NTHU)

See key on page 885

Gauge & Higgs Boson Particle Listings

Axions (A^0) and Other Very Light Bosons

RUOSO 92 ZPHY C56 505 G. Ruoso *et al.* (ROCH, BNL, FNAL, TRST)
SKALSEY 92 PRL 68 456 M. Skalsey, J.J. Kolata (MICH, NDAM)
VENEMA 92 PRL 68 135 B.J. Venema *et al.*
WANG 92 MPL A7 1497 J. Wang (ILL)
WANG 92C PL B291 97 J. Wang (ILL)
WU 92 PRL 69 1729 X.Y. Wu *et al.* (BNL, YALE, CUNY)
AKOPYAN 91 PL B272 443 M.V. Akopyan *et al.* (INRM)
ASAI 91 PRL 66 2440 S. Asai *et al.* (ICEPP)
BERSHADY 91 PRL 66 1398 M.A. Bershady, M.T. Ressell, M.S. Turner (CHIC+)
BLUEMLEIN 91 ZPHY C51 341 J. Bluemlein *et al.* (BERL, BUDA, JINR+)
BOBRAKOV 91 JETPL 53 294 V.F. Bobrakov *et al.* (PNPI)
Translated from ZETFP 53 283.
BROSS 91 PRL 67 2942 A.D. Bross *et al.* (FNAL, ILL)
KIM 91C PRL 67 3465 J.E. Kim (SEOUL)
RAFFELT 91 PRPL 198 1 G.G. Raffelt (MPIM)
RAFFELT 91B PRL 67 2605 G. Raffelt, D. Seckel (MPIM, BART)
RESSELL 91 PR D44 3001 M.T. Ressell (CHIC, FNAL)
TRZASKA 91 PL B269 54 W.H. Trzaska *et al.* (TAMU)
TSERTOS 91 PL B266 259 H. Tsertos *et al.* (ILLG, GSI)
WALKER 91 APJ 376 51 T.P. Walker *et al.* (HSCA, OSU, CHIC+)
WIDMANN 91 ZPHY A340 209 E. Widmann *et al.* (STUT, GSI, STUTM)
WINELAND 91 PRL 67 1735 D.J. Wineland *et al.* (NBSB)
ALBRECHT 90E PL B246 278 H. Albrecht *et al.* (ARGUS Collab.)
ANTREASYAN 90C PL B251 204 D. Antreasyan *et al.* (Crystal Ball Collab.)
ASANUMA 90 PL B237 588 T. Asanuma *et al.* (TOKY)
ATIYA 90 PRL 64 21 M.S. Atiya *et al.* (BNL E787 Collab.)
ATIYA 90B PRL 65 1188 M.S. Atiya *et al.* (BNL E787 Collab.)
BAUER 90 NIM B50 300 W. Bauer *et al.* (STUT, VILL, GSI)
BURROWS 90 PR D42 3297 A. Burrows, M.T. Ressell, M.S. Turner (ARIZ+)
DEBOER 90 JP G16 L1 F.W.N. de Boer, J. Lehmann, J. Steyaert (LOUV)
ENGEL 90 PRL 65 960 J. Engel, D. Seckel, A.C. Hayes (BART, LANL)
GNINENKO 90 PL B237 287 S.N. Gninenko *et al.* (INRM)
GUO 90 PR D41 2924 R. Guo *et al.* (NIU, LANL, FNAL, CASE+)
HAGMANN 90 PR D42 1297 C. Hagmann *et al.* (FLOR)
JUDGE 90 PRL 65 972 S.M. Judge *et al.* (ILLG, GSI)
RAFFELT 90D PR D41 1324 G.G. Raffelt (MPIM)
RITTER 90 PR D42 977 R.C. Ritter *et al.* (UVA)
SEMERTZIDIS 90 PRL 64 2988 Y.K. Semertzidis *et al.* (ROCH, BNL, FNAL+)
TSUCHIAKI 90 PL B236 81 M. Tsuchiaki *et al.* (ICEPP)
TURNER 90 PRPL 197 67 M.S. Turner (FNAL)
BARABASH 89 PL B223 273 A.S. Barabash *et al.* (ITEP, INRM)
BINI 89 PL B221 99 M. Bini *et al.* (FIRZ, CERN, AARH)
BURROWS 89 PR D39 1020 A. Burrows, M.S. Turner, R.P. Brinkmann (ARIZ+)
Also PRL 60 1797 M.S. Turner (FNAL, EFI)
DEBOER 89B PRL 62 2639 F.W.N. de Boer, R. van Dantzig (ANIK)
ERICSON 89 PL B219 507 T.E.O. Ericson, J.F. Mathiot (CERN, IPN)
FAISSNER 89 ZPHY C44 557 H. Faissner *et al.* (AACH3, BERL, PSI)
FOX 89 PR C39 288 J.D. Fox *et al.* (FSU)
MAYLE 89 PL B219 515 R. Mayle *et al.* (LLL, CERN, MINN, FNAL+)
Also PL B203 188 R. Mayle *et al.* (LLL, CERN, MINN, FNAL+)
MINOWA 89 PRL 62 1091 H. Minowa *et al.* (ICEPP)
ORITO 89 PRL 63 597 S. Orito *et al.* (ICEPP)
PERKINS 89 PRL 62 2638 D.H. Perkins (OXF)
TSERTOS 89 PR D40 1397 H. Tsertos *et al.* (GSI, ILLG)
VANBIBBER 89 PR D39 2089 K. van Bibber *et al.* (LLL, TAMU, LBL)
WUENSCH 89 PR D40 3153 W.U. Wuensch *et al.* (ROCH, BNL, FNAL)
Also PRL 59 839 S. de Panfilis *et al.* (ROCH, BNL, FNAL)
AVIGNONE 88 PR D37 618 F.T. Avignone *et al.* (PRIN, SCUC, ORNL+)
BALKE 88 PR D37 587 B. Balke *et al.* (LBL, UCB, COLO, NWES+)
BJORKEN 88 PR D38 3375 J.D. Bjorken *et al.* (FNAL, SLAC, VPI)
BLINOV 88 SJNP 47 563 A.E. Blinov *et al.* (NOVO)
Translated from YAF 47 889.
BOLTON 88 PR D38 2077 R.D. Bolton *et al.* (LANL, STAN, CHIC+)
Also PRL 56 2461 R.D. Bolton *et al.* (LANL, STAN, CHIC+)
Also PRL 57 3241 D. Grosnick *et al.* (CHIC, LANL, STAN+)
CHANDA 88 PR D37 2714 R. Chanda, J.F. Nieves, P.B. Pal (UMD, UPR+)
CHOI 88 PR D37 3225 K. Choi *et al.* (JHU)
CONNELL 88 PRL 60 2242 S.H. Connell *et al.* (WITW)
DATAR 88 PR C37 250 V.M. Datar *et al.* (IPN)
DEBOER 88 PRL 61 1274 F.W.N. de Boer, R. van Dantzig (ANIK)
Also PRL 62 2644 (erratum) F.W.N. de Boer, R. van Dantzig (ANIK)
Also PRL 62 2638 D.H. Perkins (OXF)
Also PRL 62 2639 F.W.N. de Boer, R. van Dantzig (ANIK)
DEBOER 88C JP G14 L131 F.W.N. de Boer *et al.* (LOUV)
DOEHNER 88 PR D38 2722 J. Dohner *et al.* (HEIDP, ANL, ILLG)
EL-NADI 88 PRL 61 1271 M. el Nadi, O.E. Badawy (CAIR)
ENGEL 88 PR C37 731 J. Engel, P. Vogel, M.R. Zirnbauer
FAISSNER 88 ZPHY C37 231 H. Faissner *et al.* (AACH3, BERL, SIN)
HATSUDA 88B PL B203 469 T. Hatsuda, M. Yoshimura (KEK)
LORENZ 88 PL B214 10 E. Lorenz *et al.* (MPIM, PSI)
MAYLE 88 PL B203 188 R. Mayle *et al.* (LLL, CERN, MINN, FNAL+)
PICCIOTTO 88 PR D37 1131 C.E. Picciotto *et al.* (TRIU, CNRC)
RAFFELT 88 PRL 60 1793 G. Raffelt, D. Seckel (UCB, LLL, UCSC)
RAFFELT 88B PR D37 549 G.G. Raffelt, D.S.P. Dearborn (UCB, LLL)
SAVAGE 88 PR D37 1134 M.J. Savage, B.W. Filippone, L.W. Mitchell (CIT)
TSERTOS 88 PL B207 273 A. Tsertos *et al.* (GSI, ILLG)
TSERTOS 88B ZPHY A331 103 A. Tsertos *et al.* (GSI, ILLG)
VANKLINKEN 88 PL B205 223 J. van Klinken *et al.* (GRON, GSI)
VANKLINKEN 88B PRL 60 2442 J. van Klinken (GRON)
VONWIMMER...88 PRL 60 2443 U. von Wimmersperg (BNL)
VOROBYOV 88 PL B208 146 P.V. Vorobiev, Y.I. Gitarts (NOVO)
DRUZHININ 87 ZPHY C37 1 V.P. Druzhinin *et al.* (NOVO)
FRIEMAN 87 PR D36 2201 J.A. Frieman, S. Dimopoulos, M.S. Turner (SLAC+)
GOLDMAN 87 PR D36 1543 T. Goldman *et al.* (LANL, CHIC, STAN+)
KORENCHE... 87 SJNP 46 192 S.M. Korenchenko *et al.* (JINR)
Translated from YAF 46 313.
MAIER 87 ZPHY A326 527 K. Maier *et al.* (STUT, GSI)
MILLS 87 PR D36 707 A.P. Mills, J. Levy (BELL)
RAFFELT 87 PR D36 2211 G.G. Raffelt, D.S.P. Dearborn (LLL, UCB)
RIORDAN 87 PRL 59 755 E.M. Riordan *et al.* (ROCH, CIT+)
TURNER 87 PRL 59 2489 M.S. Turner (FNAL, EFI)
VANBIBBER 87 PRL 59 759 K. van Bibber *et al.* (LLL, CIT, MIT+)
VONWIMMER...87 PRL 59 266 U. von Wimmersperg *et al.* (WITW)
BADIER 86 ZPHY C31 21 J. Badier *et al.* (NA3 Collab.)
BROWN 86 PRL 57 2101 C.N. Brown *et al.* (FNAL, WASH, KYOT+)
BRYMAN 86B PRL 57 2787 D.A. Bryman, E.T.H. Clifford (TRIU)
DAVIER 86 PL B180 295 M. Davier, J. Jeanjean, H. Nguyen Ngoc (LALO)
DEARBORN 86 PRL 56 26 D.S.P. Dearborn, D.N. Schramm, G. Steigman (LLL+)
EICHLER 86 PL B175 101 R.A. Eichler *et al.* (SINDRUM Collab.)
HALLIN 86 PRL 57 2105 A.L. Hallin *et al.* (PRIN)
JODIDIO 86 PR D34 1967 A. Jodidio *et al.* (LBL, NWES, TRIU)
Also PR D37 237 (erratum) A. Jodidio *et al.* (LBL, NWES, TRIU)
KETOV 86 JETPL 44 146 S.N. Ketov *et al.* (KIAE)
Translated from ZETFP 44 114.
KOCH 86 NC 96A 182 H.R. Koch, O.W.B. Schult (JULI)
KONAKA 86 PRL 57 659 A. Konaka *et al.* (KYOT, KEK)
MAIANI 86 PL B175 359 L. Maiani, R. Petronzio, E. Zavattini (CERN)
PECCEI 86 PL B172 435 R.D. Peccei, T.T. Wu, T. Yanagida (DESY)
RAFFELT 86 PR D33 897 G.G. Raffelt (MPIM)
RAFFELT 86B PL 166B 402 G.G. Raffelt (MPIM)
SAVAGE 86B PRL 57 178 M.J. Savage *et al.* (CIT)
AMALDI 85 PL 153B 444 U. Amaldi *et al.* (CERN)
ANANEV 85 SJNP 41 585 V.D. Ananev *et al.* (JINR)
Translated from YAF 41 912.
BALTRUSAIT... 85 PRL 55 1842 R.M. Baltrusaitis *et al.* (Mark III Collab.)
BERGSMA 85 PL 157B 458 F. Bergsma *et al.* (CHARM Collab.)
KAPLAN 85 NP B260 215 D.B. Kaplan (HARV)
IWAMOTO 84 PRL 53 1198 N. Iwamoto (UCSB, WUSL)
YAMAZAKI 84 PRL 52 1089 T. Yamazaki *et al.* (INUS, KEK)
ABBOTT 83 PL 120B 133 L.F. Abbott, P. Sikivie (BRAN, FLOR)
CARBONI 83 PL 123B 349 G. Carboni, W. Dahme (CERN, MUNI)
CAVAIGNAC 83 PL 121B 193 J.F. Cavaignac *et al.* (ISNG, LAPP)
DICUS 83 PR D28 1778 D.A. Dicus, V.L. Teplitz (TEXA, UMD)
DINE 83 PL 120B 137 M. Dine, W. Fischler (IAS, PENN)
ELLIS 83B NP B223 252 J. Ellis, K.A. Olive (CERN)
FAISSNER 83 PR D28 1198 H. Faissner *et al.* (AACH)
FAISSNER 83B PR D28 1787 H. Faissner *et al.* (AACH3)
FRANK 83B PR D28 1790 J.S. Frank *et al.* (LANL, YALE, LBL+)
HOFFMAN 83 PR D28 660 C.M. Hoffman *et al.* (LANL, ARZS)
PRESKILL 83 PL 120B 127 J. Preskill, M.B. Wise, F. Wilczek (HARV, UCSBT)
SIKIVIE 83 PRL 51 1415 P. Sikivie (FLOR)
Also PRL 52 695 (erratum) P. Sikivie (FLOR)
ALEKSEEV 82 JETP 55 591 E.A. Alekseeva *et al.* (KIAE)
Translated from ZETF 82 1007.
ALEKSEEV 82B JETPL 36 116 G.D. Alekseev *et al.* (MOSU, JINR)
Translated from ZETFP 36 94.
ASANO 82 PL 113B 195 Y. Asano *et al.* (KEK, TOKY, INUS, OSAK)
BARROSO 82 PL 116B 247 A. Barroso, G.C. Branco (LISB)
DATAR 82 PL 114B 63 V.M. Datar *et al.* (BHAB)
EDWARDS 82 PRL 48 903 C. Edwards *et al.* (Crystal Ball Collab.)
FETSCHER 82 JP G8 L147 W. Fetscher (ETH)
FUKUGITA 82 PRL 48 1522 M. Fukugita, S. Watamura, M. Yoshimura (KEK)
FUKUGITA 82B PR D26 1840 M. Fukugita, S. Watamura, M. Yoshimura (KEK)
LEHMANN 82 PL 115B 270 P. Lehmann *et al.* (SACL)
RAFFELT 82 PL 119B 323 G. Raffelt, L. Stodolsky (MPIM)
ZEHNDER 82 PL 110B 419 A. Zehnder, K. Gabathuler, J.L. Vuilleumier (ETH+)
ASANO 81B PL 107B 159 Y. Asano *et al.* (KEK, TOKY, INUS, OSAK)
BARROSO 81 PL 106B 91 A. Barroso, N.C. Mukhopadhyay (SIN)
FAISSNER 81 ZPHY C10 95 H. Faissner *et al.* (AACH3)
FAISSNER 81B PL 103B 234 H. Faissner *et al.* (AACH3)
KIM 81 PL 105B 55 B.R. Kim, C. Stamm (AACH3)
VUILLEUMIER 81 PL 101B 341 J.L. Vuilleumier *et al.* (CIT, MUNI)
ZEHNDER 81 PL 104B 494 A. Zehnder (ETH)
FAISSNER 80 PL 96B 201 H. Faissner *et al.* (AACH3)
JACQUES 80 PR D21 1206 P.F. Jacques *et al.* (RUTG, STEV, COLU)
SOUKAS 80 PRL 44 564 A. Soukas *et al.* (BNL, HARV, ORNL, PENN)
BECHIS 79 PRL 42 1511 D.J. Bechis *et al.* (UMD, COLU, AFRR)
CALAPRICE 79 PR D20 2708 F.P. Calaprice *et al.* (PRIN)
COTEUS 79 PRL 42 1438 P. Coteus *et al.* (COLU, ILL, BNL)
DISHAW 79 PL 85B 142 J.P. Dishaw *et al.* (SLAC, CIT)
ZHITNITSKII 79 SJNP 29 517 A.R. Zhitnitsky, Y.I. Skovpen (NOVO)
Translated from YAF 29 1001.
ALIBRAN 78 PL 74B 134 P. Alibran *et al.* (Gargamelle Collab.)
ASRATYAN 78B PL 79B 497 A.E. Asratyan *et al.* (ITEP, SERP)
BELLOTTI 78 PL 76B 223 E. Bellotti, E. Fiorini, L. Zanotti (MILA)
BOSETTI 78B PL 74B 143 P.C. Bosetti *et al.* (BEBC Collab.)
DICUS 78C PR D18 1829 D.A. Dicus *et al.* (TEXA, VPI, STAN)
DONNELLY 78 PR D18 1607 T.W. Donnelly *et al.* (STAN)
Also PRL 37 315 F. Reines, H.S. Gurr, H.W. Sobel (UCI)
Also PRL 33 179 H.S. Gurr, F. Reines, H.W. Sobel (UCI)
HANSL 78D PL 74B 139 T. Hansl *et al.* (CDHS Collab.)
MICELMAC... 78 LNC 21 441 G.V. Mitselmakher, B. Pontecorvo (JINR)
MIKAELIAN 78 PR D18 3605 K.O. Mikaelian (FNAL, NWES)
SATO 78 PTP 60 1942 K. Sato (KYOT)
VYSOTSKII 78 JETPL 27 502 M.I. Vysotsky *et al.* (ASCI)
Translated from ZETFP 27 533.
YANG 78 PRL 41 523 T.C. Yang (MASA)
PECCEI 77 PR D16 1791 R.D. Peccei, H.R. Quinn (STAN, SLAC)
Also PRL 38 1440 R.D. Peccei, H.R. Quinn (STAN, SLAC)
REINES 76 PRL 37 315 F. Reines, H.S. Gurr, H.W. Sobel (UCI)
GURR 74 PR 33 179 H.S. Gurr, F. Reines, H.W. Sobel (UCI)
ANAND 53 PRSL A22 183 B.M. Anand

OTHER RELATED PAPERS

SREDNICKI 85 NP B260 689 M. Srednicki (UCSB)
BARDEEN 78 PL 74B 229 W.A. Bardeen, S.-H.H. Tye (FNAL)

LEPTONS

Related Reviews in Volume 1

LEPTONS

e

$J = \frac{1}{2}$

e MASS (atomic mass units u)

The primary determination of an electron's mass comes from measuring the ratio of the mass to that of a nucleus, so that the result is obtained in u (atomic mass units). The conversion factor to MeV is more uncertain than the mass of the electron in u; indeed, the recent improvements in the mass determination are not evident when the result is given in MeV. In this datablock we give the result in u, and in the following datablock in MeV.

VALUE (10^{-6} u)		DOCUMENT ID		TECN	COMMENT
548.579909070±0.000000016		MOHR	16	RVUE	2014 CODATA value
• • • We do not use the following data for averages, fits, limits, etc. • • •					
548.57990946	±0.00000022	MOHR	12	RVUE	2010 CODATA value
548.57990943	±0.00000023	MOHR	08	RVUE	2006 CODATA value
548.57990945	±0.00000024	MOHR	05	RVUE	2002 CODATA value
548.5799092	±0.0000004	[1] BEIER	02	CNTR	Penning trap
548.5799110	±0.0000012	MOHR	99	RVUE	1998 CODATA value
548.5799111	±0.0000012	[2] FARNHAM	95	CNTR	Penning trap
548.579903	±0.000013	COHEN	87	RVUE	1986 CODATA value

[1] BEIER 02 compares Larmor frequency of the electron bound in a $^{12}C^{5+}$ ion with the cyclotron frequency of a single trapped $^{12}C^{5+}$ ion.
[2] FARNHAM 95 compares cyclotron frequency of trapped electrons with that of a single trapped $^{12}C^{6+}$ ion.

e MASS

2010 CODATA (MOHR 12) gives the conversion factor from u (atomic mass units, see the above datablock) to MeV as 931.494 061 (21). Earlier values use the then-current conversion factor. The conversion error dominates the uncertainty of the masses given below.

VALUE (MeV)		DOCUMENT ID		TECN	COMMENT
0.510998946 1±0.0000000031		MOHR	16	RVUE	2014 CODATA value
• • • We do not use the following data for averages, fits, limits, etc. • • •					
0.510998928	±0.000000011	MOHR	12	RVUE	2010 CODATA value
0.510998910	±0.000000013	MOHR	08	RVUE	2006 CODATA value
0.510998918	±0.000000044	MOHR	05	RVUE	2002 CODATA value
0.510998901	±0.000000020	[1,2] BEIER	02	CNTR	Penning trap
0.510998902	±0.000000021	MOHR	99	RVUE	1998 CODATA value
0.510998903	±0.000000020	[1,3] FARNHAM	95	CNTR	Penning trap
0.510998895	±0.000000024	[1] COHEN	87	RVUE	1986 CODATA value
0.5110034	±0.0000014	COHEN	73	RVUE	1973 CODATA value

[1] Converted to MeV using the 1998 CODATA value of the conversion constant, 931.494013 ± 0.000037 MeV/u.
[2] BEIER 02 compares Larmor frequency of the electron bound in a $^{12}C^{5+}$ ion with the cyclotron frequency of a single trapped $^{12}C^{5+}$ ion.
[3] FARNHAM 95 compares cyclotron frequency of trapped electrons with that of a single trapped $^{12}C^{6+}$ ion.

$(m_{e^+} - m_{e^-})$ / $m_{average}$

A test of CPT invariance.

VALUE	CL%	DOCUMENT ID		TECN	COMMENT
$<8\times10^{-9}$	90	[1] FEE	93	CNTR	Positronium spectroscopy
• • • We do not use the following data for averages, fits, limits, etc. • • •					
$<4\times10^{-23}$	90	[2] DOLGOV	14		From photon mass limit
$<4\times10^{-8}$	90	CHU	84	CNTR	Positronium spectroscopy

[1] FEE 93 value is obtained under the assumption that the positronium Rydberg constant is exactly half the hydrogen one.
[2] DOLGOV 14 result is obtained under the assumption that any mass difference between electron and positron would lead to a non-zero photon mass. The PDG 12 limit of 1×10^{-18} eV on the photon mass is in turn used to derive the value quoted here.

$|q_{e^+} + q_{e^-}|/e$

A test of CPT invariance. See also similar tests involving the proton.

VALUE	DOCUMENT ID		TECN	COMMENT
$<4\times10^{-8}$	[1] HUGHES	92	RVUE	
• • • We do not use the following data for averages, fits, limits, etc. • • •				
$<2\times10^{-18}$	[2] SCHAEFER	95	THEO	Vacuum polarization
$<1\times10^{-18}$	[3] MUELLER	92	THEO	Vacuum polarization

[1] HUGHES 92 uses recent measurements of Rydberg-energy and cyclotron-frequency ratios.
[2] SCHAEFER 95 removes model dependency of MUELLER 92.
[3] MUELLER 92 argues that an inequality of the charge magnitudes would, through higher-order vacuum polarization, contribute to the net charge of atoms.

e MAGNETIC MOMENT ANOMALY

$\mu_e/\mu_B - 1 = (g-2)/2$

VALUE (units 10^{-6})	DOCUMENT ID		TECN	CHG	COMMENT
1159.65218091±0.00000026	MOHR	16	RVUE		2014 CODATA value
• • • We do not use the following data for averages, fits, limits, etc. • • •					
1159.65218076±0.00000027	MOHR	12	RVUE		2010 CODATA value
1159.65218073±0.00000028	HANNEKE	08	MRS		Single electron
1159.65218111±0.00000074	[1] MOHR	08	RVUE		2006 CODATA value
1159.65218085±0.00000076	[2] ODOM	06	MRS	−	Single electron
1159.65218 59 ±0.0000038	MOHR	05	RVUE		2002 CODATA value
1159.65218 69 ±0.0000041	MOHR	99	RVUE		1998 CODATA value
1159.652193 ±0.000010	COHEN	87	RVUE		1986 CODATA value
1159.65218 84 ±0.0000043	VANDYCK	87	MRS	−	Single electron
1159.65218 79 ±0.0000043	VANDYCK	87	MRS	+	Single positron

[1] MOHR 08 average is dominated by ODOM 06.
[2] Superseded by HANNEKE 08 per private communication with Gerald Gabrielse.

$(g_{e^+} - g_{e^-})$ / $g_{average}$

A test of CPT invariance.

VALUE (units 10^{-12})	CL%	DOCUMENT ID		TECN	COMMENT
− 0.5± 2.1		[1] VANDYCK	87	MRS	Penning trap
• • • We do not use the following data for averages, fits, limits, etc. • • •					
< 12	95	[2] VASSERMAN	87	CNTR	Assumes $m_{e^+} = m_{e^-}$
22 ±64		SCHWINBERG	81	MRS	Penning trap

[1] VANDYCK 87 measured $(g_-/g_+)-1$ and we converted it.
[2] VASSERMAN 87 measured $(g_+ - g_-)/(g-2)$. We multiplied by $(g-2)/g = 1.2\times10^{-3}$.

e ELECTRIC DIPOLE MOMENT (d)

A nonzero value is forbidden by both T invariance and P invariance.

VALUE (10^{-28} ecm)	CL%	DOCUMENT ID		TECN	COMMENT
< 0.87	90	[1] BARON	14	CNTR	ThO molecules
• • • We do not use the following data for averages, fits, limits, etc. • • •					
< 1.3	90	[2] CAIRNCROSS	17	ESR	$^{180}Hf^{19}F$ molecules
− 5570 ± 7980 ±120		KIM	15	CNTR	$Gd_3Ga_5O_{12}$ molecules
< 6050	90	[3] ECKEL	12	CNTR	$Eu_{0.5}Ba_{0.5}TiO_3$ molecules
< 10.5	90	[4] HUDSON	11	NMR	YbF molecules
6.9 ± 7.4		REGAN	02	MRS	^{205}Tl beams
18 ± 12 ± 10		[5] COMMINS	94	MRS	^{205}Tl beams
− 27 ± 83		[5] ABDULLAH	90	MRS	^{205}Tl beams
− 1400 ± 2400		CHO	89	NMR	TlF molecules
− 150 ± 550 ±150		MURTHY	89		Cs, no B field
− 5000 ±11000		LAMOREAUX	87	NMR	^{199}Hg
19000 ±34000	90	SANDARS	75	MRS	Thallium
7000 ±22000	90	PLAYER	70	MRS	Xenon
< 30000	90	WEISSKOPF	68	MRS	Cesium

[1] BARON 14 gives a measurement corresponding to this limit as $(-0.21\pm0.37\pm0.25)\times10^{-28}$ ecm.
[2] CAIRNCROSS 17 gives a measurement corresponding to this limit as $(0.09\pm0.77\pm0.17)\times10^{-28}$ ecm.
[3] ECKEL 12 gives a measurement corresponding to this limit as $(-1.07\pm3.06\pm1.74)\times10^{-25}$ ecm.
[4] HUDSON 11 gives a measurement corresponding to this limit as $(-2.4\pm5.7\pm1.5)\times10^{-28}$ ecm.
[5] ABDULLAH 90, COMMINS 94, and REGAN 02 use the relativistic enhancement of a valence electron's electric dipole moment in a high-Z atom.

e^- MEAN LIFE / BRANCHING FRACTION

A test of charge conservation. See the "Note on Testing Charge Conservation and the Pauli Exclusion Principle" following this section in our 1992 edition (Physical Review **D45** S1 (1992), p. VI.10).

Most of these experiments are one of three kinds: Attempts to observe (a) the 255.5 keV gamma ray produced in $e^- \to \nu_e\gamma$, (b) the (K) shell x ray produced when an electron decays without additional energy deposit, e.g., $e^- \to \nu_e\overline{\nu}_e\nu_e$ ("disappearance" experiments), and (c) nuclear de-excitation gamma rays after the electron disappears from an atomic shell and the nucleus is left in an excited state. The last can include both weak boson and photon mediating processes. We use the best $e^- \to \nu_e\gamma$ limit for the Summary Tables.

Note that we use the mean life rather than the half life, which is often reported.

$e \to \nu_e\gamma$ and astrophysical limits

VALUE (yr)	CL%	DOCUMENT ID		TECN	COMMENT
>6.6 $\times10^{28}$	90	AGOSTINI	15B	BORX	$e^- \to \nu\gamma$

• • • We do not use the following data for averages, fits, limits, etc. • • •

$>1.2 \times 10^{24}$	90		ABGRALL	17	HPGE	electron decay to invisible
$>1.22 \times 10^{26}$	68	[1]	KLAPDOR-K...	07	CNTR	$e^- \to \nu\gamma$
$>4.6 \times 10^{26}$	90		BACK	02	BORX	$e^- \to \nu\gamma$
$>3.4 \times 10^{26}$	68		BELLI	00B	DAMA	$e^- \to \nu\gamma$, liquid Xe
$>3.7 \times 10^{25}$	68		AHARONOV	95B	CNTR	$e^- \to \nu\gamma$
$>2.35 \times 10^{25}$	68		BALYSH	93	CNTR	$e^- \to \nu\gamma$, ^{76}Ge detector
$>1.5 \times 10^{25}$	68		AVIGNONE	86	CNTR	$e^- \to \nu\gamma$
$>1 \times 10^{39}$		[2]	ORITO	85	ASTR	Astrophysical argument
$>3 \times 10^{23}$	68		BELLOTTI	83B	CNTR	$e^- \to \nu\gamma$

[1] The authors of A. Derbin et al, arXiv:0704.2047v1 argue that this limit is overestimated by at least a factor of 5.
[2] ORITO 85 assumes that electromagnetic forces extend out to large enough distances and that the age of our galaxy is 10^{10} years.

Disappearance and nuclear-de-excitation experiments

VALUE (yr)	CL%		DOCUMENT ID		TECN	COMMENT
$>6.4 \times 10^{24}$	68	[1]	BELLI	99B	DAMA	De-excitation of ^{129}Xe

• • • We do not use the following data for averages, fits, limits, etc. • • •

$>4.2 \times 10^{24}$	68		BELLI	99	DAMA	Iodine L-shell disappearance
$>2.4 \times 10^{23}$	90	[2]	BELLI	99D	DAMA	De-excitation of ^{127}I (in NaI)
$>4.3 \times 10^{23}$	68		AHARONOV	95B	CNTR	Ge K-shell disappearance
$>2.7 \times 10^{23}$	68		REUSSER	91	CNTR	Ge K-shell disappearance
$>2 \times 10^{22}$	68		BELLOTTI	83B	CNTR	Ge K-shell disappearance

[1] BELLI 99B limit on charge nonconserving e^- capture involving excitation of the 236.1 keV nuclear state of ^{129}Xe; the 90% CL limit is 3.7×10^{24} yr. Less stringent limits for other states are also given.
[2] BELLI 99D limit on charge nonconserving e^- capture involving excitation of the 57.6 keV nuclear state of ^{127}I. Less stringent limits for the other states and for the state of ^{23}Na are also given.

LIMITS ON LEPTON-FLAVOR VIOLATION IN PRODUCTION

Forbidden by lepton family number conservation.

This section was added for the 2008 edition of this *Review* and is not complete. For a list of further measurements see references in the papers listed below.

$\sigma(e^+e^- \to e^\pm\tau^\mp) / \sigma(e^+e^- \to \mu^+\mu^-)$

VALUE	CL%	DOCUMENT ID		TECN	COMMENT
$<8.9 \times 10^{-6}$	95	AUBERT	07P	BABR	e^+e^- at $E_{cm} = 10.58$ GeV

• • • We do not use the following data for averages, fits, limits, etc. • • •

$<1.8 \times 10^{-3}$	95	GOMEZ-CAD...	91	MRK2	e^+e^- at $E_{cm} = 29$ GeV

$\sigma(e^+e^- \to \mu^\pm\tau^\mp) / \sigma(e^+e^- \to \mu^+\mu^-)$

VALUE	CL%	DOCUMENT ID		TECN	COMMENT
$<4.0 \times 10^{-6}$	95	AUBERT	07P	BABR	e^+e^- at $E_{cm} = 10.58$ GeV

• • • We do not use the following data for averages, fits, limits, etc. • • •

$<6.1 \times 10^{-3}$	95	GOMEZ-CAD...	91	MRK2	e^+e^- at $E_{cm} = 29$ GeV

e REFERENCES

ABGRALL	17	PRL 118 161801	N. Abgrall *et al.* (MAJORANA Collab.)
CAIRNCROSS	17	PRL 119 153001	W.B. Cairncross *et al.* (NIST,COLO)
MOHR	16	RMP 88 035009	P.J. Mohr, D.B. Newell, B.N. Taylor (NIST)
AGOSTINI	15B	PRL 115 231802	M. Agostini *et al.* (BOREXINO Collab.)
KIM	15	PR D91 102004	Y.J. Kim *et al.* (IND, YALE, LANL)
BARON	14	SCIENCE 343 269	J. Baron *et al.* (ACME Collab.)
DOLGOV	14	PL B732 244	A.D. Dolgov, V.A. Novikov
ECKEL	12	PRL 109 193003	S. Eckel, A.O. Sushkov, S.K. Lamoreaux (YALE)
MOHR	12	RMP 84 1527	P.J. Mohr, B.N. Taylor, D.B. Newell (NIST)
PDG	12	PR D86 010001	J. Beringer *et al.* (PDG Collab.)
HUDSON	11	NAT 473 493	J.J. Hudson *et al.* (LOIC)
HANNEKE	08	PRL 100 120801	D. Hanneke, S. Fogwell, G. Gabrielse (HARV)
MOHR	08	RMP 80 633	P.J. Mohr, B.N. Taylor, D.B. Newell (NIST)
AUBERT	07P	PR D75 031103	B. Aubert *et al.* (BABAR Collab.)
KLAPDOR-K...	07	PL B644 109	H.V. Klapdor-Kleingrothaus, I.V. Krivosheina, I.V. Titkova
ODOM	06	PRL 97 030801	B. Odom *et al.* (HARV)
MOHR	05	RMP 77 1	P.J. Mohr, B.N. Taylor (NIST)
BACK	02	PL B525 29	H.O. Back *et al.* (BOREXINO/SASSO Collab.)
BEIER	02	PRL 88 011603	T. Beier *et al.*
REGAN	02	PRL 88 071805	B.C. Regan *et al.*
BELLI	00B	PR D61 117301	P. Belli *et al.* (DAMA Collab.)
BELLI	99	PL B460 236	P. Belli *et al.* (DAMA Collab.)
BELLI	99B	PL B465 315	P. Belli *et al.* (DAMA Collab.)
BELLI	99D	PR C60 065501	P. Belli *et al.* (DAMA Collab.)
MOHR	99	JPCRD 28 1713	P.J. Mohr, B.N. Taylor (NIST)
Also		RMP 72 351	P.J. Mohr, B.N. Taylor (NIST)
AHARONOV	95B	PR D52 3785	Y. Aharonov *et al.* (SCUC, PNL, ZARA+)
Also		PL B353 168	Y. Aharonov *et al.* (SCUC, PNL, ZARA+)
FARNHAM	95	PRL 75 3598	D.L. Farnham, R.S. van Dyck, P.B. Schwinberg (WASH)
SCHAEFER	95	PR A51 838	A. Schaefer, J. Reinhardt (FRAN)
COMMINS	94	PR A50 2960	E.D. Commins *et al.*
BALYSH	93	PL B298 278	A. Balysh *et al.* (KIAE, MPIH, SASSO)
FEE	93	PR A48 192	M.S. Fee *et al.*
HUGHES	92	PRL 69 578	R.J. Hughes, B.I. Deutch (LANL, AARH)
MUELLER	92	PRL 69 3432	B. Muller, M.H. Thoma (DUKE)
PDG	92	PR D45 S1	K. Hikasa *et al.* (KEK, LBL, BOST+)
GOMEZ-CAD...	91	PRL 66 1007	J.J. Gomez-Cadenas *et al.* (SLAC MARK-2 Collab.)
REUSSER	91	PL B255 143	D. Reusser *et al.* (NEUC, CIT, PSI)
ABDULLAH	90	PRL 65 2347	K. Abdullah *et al.* (LBL, UCB)
CHO	89	PRL 63 2559	D. Cho, K. Sangster, E.A. Hinds (YALE)
MURTHY	89	PRL 63 965	S.A. Murthy *et al.* (AMHT)
COHEN	87	RMP 59 1121	E.R. Cohen, B.N. Taylor (RISC, NBS)
LAMOREAUX	87	PRL 59 2275	S.K. Lamoreaux *et al.* (WASH)
VANDYCK	87	PRL 59 26	R.S. van Dyck, P.B. Schwinberg, H.G. Dehmelt (WASH)
VASSERMAN	87	PL B198 302	I.B. Vasserman *et al.* (NOVO)
Also		PL B187 172	I.B. Vasserman *et al.* (NOVO)
AVIGNONE	86	PR D34 97	F.T. Avignone *et al.* (PNL, SCUC)
ORITO	85	PRL 54 2457	S. Orito, M. Yoshimura (TOKY, KEK)
CHU	84	PRL 52 1689	S. Chu, A.P. Mills, J.L. Hall (BELL, NBS, COLO)
BELLOTTI	83B	PL 124B 435	E. Bellotti *et al.* (MILA)
SCHWINBERG	81	PRL 47 1679	P.B. Schwinberg, R.S. van Dyck, H.G. Dehmelt (WASH)
SANDARS	75	PR A11 473	P.G.H. Sandars, D.M. Sternheimer (OXF, BNL)
COHEN	73	JPCRD 2 664	E.R. Cohen, B.N. Taylor (RISC, NBS)
PLAYER	70	JP B3 1620	M.A. Player, P.G.H. Sandars (OXF)
WEISSKOPF	68	PRL 21 1645	M.C. Weisskopf *et al.* (BRAN)

μ

$J = \frac{1}{2}$

μ MASS (atomic mass units u)

The muon's mass is obtained from the muon-electron mass ratio as determined from the measurement of Zeeman transition frequencies in muonium (μ^+e^- atom). Since the electron's mass is most accurately known in u, the muon's mass is also most accurately known in u. The conversion factor to MeV has approximately the same relative uncertainty as the mass of the muon in u. In this datablock we give the result in u, and in the following datablock in MeV.

VALUE (u)	DOCUMENT ID		TECN	COMMENT
0.1134289257±0.0000000025	MOHR	16	RVUE	2014 CODATA value

• • • We do not use the following data for averages, fits, limits, etc. • • •

0.1134289267±0.0000000029	MOHR	12	RVUE	2010 CODATA value
0.1134289256±0.0000000029	MOHR	08	RVUE	2006 CODATA value
0.1134289264±0.0000000030	MOHR	05	RVUE	2002 CODATA value
0.1134289168±0.0000000034	[1] MOHR	99	RVUE	1998 CODATA value
0.113428913 ±0.000000017	[2] COHEN	87	RVUE	1986 CODATA value

[1] MOHR 99 make use of other 1998 CODATA entries below.
[2] COHEN 87 make use of other 1986 CODATA entries below.

μ MASS

2010 CODATA (MOHR 12) gives the conversion factor from u (atomic mass units, see the above datablock) to MeV as 931.494 061 (21). Earlier values use the then-current conversion factor. The conversion error contributes significantly to the uncertainty of the masses given below.

VALUE (MeV)	DOCUMENT ID		TECN	CHG	COMMENT
105.6583745±0.0000024	MOHR	16	RVUE		2014 CODATA value

• • • We do not use the following data for averages, fits, limits, etc. • • •

105.6583715±0.0000035	MOHR	12	RVUE		2010 CODATA value
105.6583668±0.0000038	MOHR	08	RVUE		2006 CODATA value
105.6583692±0.0000094	MOHR	05	RVUE		2002 CODATA value
105.6583568±0.0000052	MOHR	99	RVUE		1998 CODATA value
105.658353 ±0.000016	[1] COHEN	87	RVUE		1986 CODATA value
105.658386 ±0.000044	[2] MARIAM	82	CNTR	+	
105.65836 ±0.00026	[3] CROWE	72	CNTR		
105.65865 ±0.00044	[4] CRANE	71	CNTR		

[1] Converted to MeV using the 1998 CODATA value of the conversion constant, 931.494013 ± 0.000037 MeV/u.
[2] MARIAM 82 give $m_\mu/m_e = 206.768259(62)$.
[3] CROWE 72 give $m_\mu/m_e = 206.7682(5)$.
[4] CRANE 71 give $m_\mu/m_e = 206.76878(85)$.

μ MEAN LIFE τ

Measurements with an error $> 0.001 \times 10^{-6}$ s have been omitted.

VALUE (10^{-6} s)	DOCUMENT ID		TECN	CHG	COMMENT
2.1969811±0.0000022 OUR AVERAGE					
2.1969803±0.0000021±0.0000007	[1] TISHCHENKO	13	CNTR	+	Surface μ^+ at PSI
2.197083 ±0.000032 ±0.000015	BARCZYK	08	CNTR	+	Muons from π^+ decay at rest
2.197013 ±0.000021 ±0.000011	CHITWOOD	07	CNTR	+	Surface μ^+ at PSI
2.197078 ±0.000073	BARDIN	84	CNTR	+	
2.197025 ±0.000155	BARDIN	84	CNTR	−	
2.19695 ±0.00006	GIOVANETTI	84	CNTR	+	
2.19711 ±0.00008	BALANDIN	74	CNTR	+	
2.1973 ±0.0003	DUCLOS	73	CNTR	+	

• • • We do not use the following data for averages, fits, limits, etc. • • •

2.1969803±0.0000022	WEBBER	11	CNTR	+	Surface μ^+ at PSI

[1] TISHCHENKO 13 uses 1.6×10^{12} μ^+ events and supersedes WEBBER 11.

$\tau_{\mu^+}/\tau_{\mu^-}$ MEAN LIFE RATIO

A test of CPT invariance.

VALUE	DOCUMENT ID		TECN	COMMENT
1.000024±0.000078	BARDIN	84	CNTR	

• • • We do not use the following data for averages, fits, limits, etc. • • •

1.0008	±0.0010	BAILEY	79	CNTR	Storage ring
1.000	±0.001	MEYER	63	CNTR	Mean life μ^+/μ^-

$(\tau_{\mu^+} - \tau_{\mu^-}) / \tau_{\text{average}}$

A test of CPT invariance. Calculated from the mean-life ratio, above.

VALUE	DOCUMENT ID
(2±8) × 10^{-5} OUR EVALUATION	

μ/p MAGNETIC MOMENT RATIO

This ratio is used to obtain a precise value of the muon mass and to reduce experimental muon Larmor frequency measurements to the muon magnetic moment anomaly. Measurements with an error > 0.00001 have been omitted. By convention, the minus sign on this ratio is omitted. CODATA values were fitted using their selection of data, plus other data from multiparameter fits.

VALUE	DOCUMENT ID		TECN	CHG	COMMENT
3.183345142±0.000000071	MOHR	16	RVUE		2014 CODATA value
• • • We do not use the following data for averages, fits, limits, etc. • • •					
3.183345107±0.000000084	MOHR	12	RVUE		2010 CODATA value
3.183345137±0.000000085	MOHR	08	RVUE		2006 CODATA value
3.183345118±0.000000089	MOHR	05	RVUE		2002 CODATA value
3.18334513 ±0.00000039	LIU	99	CNTR	+	HFS in muonium
3.18334539 ±0.00000010	MOHR	99	RVUE		1998 CODATA value
3.18334547 ±0.00000047	COHEN	87	RVUE		1986 CODATA value
3.1833441 ±0.0000017	KLEMPT	82	CNTR	+	Precession strob
3.1833461 ±0.0000011	MARIAM	82	CNTR	+	HFS splitting
3.1833448 ±0.0000029	CAMANI	78	CNTR	+	See KLEMPT 82
3.1833403 ±0.0000044	CASPERSON	77	CNTR	+	HFS splitting
3.1833402 ±0.0000072	COHEN	73	RVUE		1973 CODATA value
3.1833467 ±0.0000082	CROWE	72	CNTR	+	Precession phase

See the related review(s):
Muon Anomalous Magnetic Moment

μ MAGNETIC MOMENT ANOMALY

The parity-violating decay of muons in a storage ring is observed. The difference frequency ω_a between the muon spin precision and the orbital angular frequency $(e/m_\mu c)\langle B\rangle$ is measured, as is the free proton NMR frequency ω_p, thus determining the ratio $R=\omega_a/\omega_p$. Given the magnetic moment ratio $\lambda=\mu_\mu/\mu_p$ (from hyperfine structure in muonium), $(g-2)/2 = R/(\lambda-R)$.

$\mu_\mu/(e\hbar/2m_\mu)-1 = (g_\mu-2)/2$

VALUE (units 10^{-10})	DOCUMENT ID		TECN	CHG	COMMENT
11659208.9± 5.4±3.3	[1] BENNETT	06	MUG2		Average μ^+ and μ^-
• • • We do not use the following data for averages, fits, limits, etc. • • •					
11659208 ± 6	BENNETT	04	MUG2		Average μ^+ and μ^-
11659214 ± 8 ±3	BENNETT	04	MUG2	−	Storage ring
11659203 ± 6 ±5	BENNETT	04	MUG2	+	Storage ring
11659204 ± 7 ±5	BENNETT	02	MUG2	+	Storage ring
11659202 ± 14 ±6	BROWN	01	MUG2	+	Storage ring
11659191 ± 59	BROWN	00	MUG2	+	
11659100 ± 110	[2] BAILEY	79	CNTR	+	Storage ring
11659360 ± 120	[2] BAILEY	79	CNTR	−	Storage ring
11659230 ± 85	[2] BAILEY	79	CNTR	±	Storage ring
11620000 ±5000	CHARPAK	62	CNTR	+	

[1] BENNETT 06 reports $(g_\mu-2)/2 = (11659208.0 \pm 5.4 \pm 3.3) \times 10^{-10}$. We rescaled this value using μ/p magnetic moment ratio of 3.183345137(85) from MOHR 08.
[2] BAILEY 79 values recalculated by HUGHES 99 using the COHEN 87 μ/p magnetic moment. The improved MOHR 99 value does not change the result.

$(g_{\mu^+} - g_{\mu^-}) / g_{\text{average}}$

A test of CPT invariance.

VALUE (units 10^{-8})	DOCUMENT ID		TECN
−0.11±0.12	BENNETT	04	MUG2
• • • We do not use the following data for averages, fits, limits, etc. • • •			
−2.6 ±1.6	BAILEY	79	CNTR

μ ELECTRIC DIPOLE MOMENT (d)

A nonzero value is forbidden by both T invariance and P invariance.

VALUE (10^{-19} e cm)	DOCUMENT ID		TECN	CHG	COMMENT
−0.1±0.9	[1] BENNETT	09	MUG2	±	Storage ring
• • • We do not use the following data for averages, fits, limits, etc. • • •					
−0.1±1.0	BENNETT	09	MUG2	+	Storage ring
−0.1±0.7	BENNETT	09	MUG2	−	Storage ring
−3.7±3.4	[2] BAILEY	78	CNTR	±	Storage ring
8.6±4.5	BAILEY	78	CNTR	+	Storage ring
0.8±4.3	BAILEY	78	CNTR	−	Storage ring

[1] This is the combination of the two BENNETT 09 results quoted here separately for μ^+ and μ^-. BENNETT 09 uses the convention $d = 1/2 \cdot (d_{\mu^-} - d_{\mu^+})$.
[2] This is the combination of the two BAILEY 78 results quoted here separately for μ^+ and μ^-. BAILEY 78 uses the convention $d = 1/2 \cdot (d_{\mu^+} - d_{\mu^-})$ and reports 3.7 ± 3.4. We convert their result to use the same convention as BENNETT 09.

MUON-ELECTRON CHARGE RATIO ANOMALY $q_{\mu^+}/q_{e^-} + 1$

VALUE	DOCUMENT ID		TECN	CHG	COMMENT
(1.1±2.1) × 10^{-9}	[1] MEYER	00	CNTR	+	1s–2s muonium interval

[1] MEYER 00 measure the 1s–2s muonium interval, and then interpret the result in terms of muon-electron charge ratio q_{μ^+}/q_{e^-}.

μ^- DECAY MODES

μ^+ modes are charge conjugates of the modes below.

	Mode		Fraction (Γ_i/Γ)		Confidence level
Γ_1	$e^-\overline{\nu}_e\nu_\mu$		≈ 100%		
Γ_2	$e^-\overline{\nu}_e\nu_\mu\gamma$		[a] $(6.0\pm0.5)\times10^{-8}$		
Γ_3	$e^-\overline{\nu}_e\nu_\mu e^+e^-$		[b] $(3.4\pm0.4)\times10^{-5}$		
	Lepton Family number (LF) violating modes				
Γ_4	$e^-\nu_e\overline{\nu}_\mu$	LF	[c] < 1.2	%	90%
Γ_5	$e^-\gamma$	LF	< 4.2	$\times10^{-13}$	90%
Γ_6	$e^-e^+e^-$	LF	< 1.0	$\times10^{-12}$	90%
Γ_7	$e^-2\gamma$	LF	< 7.2	$\times10^{-11}$	90%

[a] This only includes events with energy of $e > 45$ MeV and energy of $\gamma > 40$ MeV. Since the $e^-\overline{\nu}_e\nu_\mu$ and $e^-\overline{\nu}_e\nu_\mu\gamma$ modes cannot be clearly separated, we regard the latter mode as a subset of the former.
[b] See the Particle Listings below for the energy limits used in this measurement.
[c] A test of additive vs. multiplicative lepton family number conservation.

μ^- BRANCHING RATIOS

$\Gamma(e^-\overline{\nu}_e\nu_\mu\gamma)/\Gamma_{\text{total}}$ Γ_2/Γ

VALUE	EVTS	DOCUMENT ID		TECN	COMMENT
(6.03±0.14±0.53) × 10^{-8}	13k	[1] BALDINI	16A	SPEC	γ KE > 40 MeV
• • • We do not use the following data for averages, fits, limits, etc. • • •					
	862	BOGART	67	CNTR	γ KE > 14.5 MeV
(3.3 ±1.3) × 10^{-3}		CRITTENDEN	61	CNTR	γ KE > 20 MeV
(1.4 ±0.4) × 10^{-2}		CRITTENDEN	61	CNTR	γ KE > 10 MeV
	27	ASHKIN	59	CNTR	

[1] BALDINI 16 measurement refers to $\mu^+ \to e^+\nu\overline{\nu}\gamma$ decay and requires energy of $e^+ >$ 45 MeV and energy $\gamma > 40$ MeV.

$\Gamma(e^-\overline{\nu}_e\nu_\mu e^+e^-)/\Gamma_{\text{total}}$ Γ_3/Γ

VALUE (units 10^{-5})	EVTS	DOCUMENT ID		TECN	CHG	COMMENT
3.4±0.2±0.3	7443	[1] BERTL	85	SPEC	+	SINDRUM
• • • We do not use the following data for averages, fits, limits, etc. • • •						
2.2±1.5	7	[2] CRITTENDEN	61	HLBC	+	E(e^+e^-) > 10 MeV
2	1	[3] GUREVICH	60	EMUL	+	
1.5±1.0	3	[4] LEE	59	HBC	+	

[1] BERTL 85 has transverse momentum cut $p_T > 17$ MeV/c. Systematic error was increased by us.
[2] CRITTENDEN 61 count only those decays where total energy of either (e^+, e^-) combination is >10 MeV.
[3] GUREVICH 60 interpret their event as either virtual or real photon conversion. e^+ and e^- energies not measured.
[4] In the three LEE 59 events, the sum of energies E(e^+) + E(e^-) + E(e^+) was 51 MeV, 55 MeV, and 33 MeV.

$\Gamma(e^-\nu_e\overline{\nu}_\mu)/\Gamma_{\text{total}}$ Γ_4/Γ

Forbidden by the additive conservation law for lepton family number. A multiplicative law predicts this branching ratio to be 1/2. For a review see NEMETHY 81.

VALUE	CL%	DOCUMENT ID		TECN	CHG	COMMENT
< 0.012	90	[1] FREEDMAN	93	CNTR	+	ν oscillation search
• • • We do not use the following data for averages, fits, limits, etc. • • •						
< 0.018	90	KRAKAUER	91B	CALO	+	
< 0.05	90	[2] BERGSMA	83	CALO		$\overline{\nu}_\mu e \to \mu^-\overline{\nu}_e$
< 0.09	90	JONKER	80	CALO		See BERGSMA 83
−0.001±0.061		WILLIS	80	CNTR	+	
0.13 ±0.15		BLIETSCHAU	78	HLBC	±	Avg. of 4 values
< 0.25	90	EICHTEN	73	HLBC	+	

[1] FREEDMAN 93 limit on $\overline{\nu}_e$ observation is here interpreted as a limit on lepton family number violation.
[2] BERGSMA 83 gives a limit on the inverse muon decay cross-section ratio $\sigma(\overline{\nu}_\mu e^- \to \mu^- \overline{\nu}_e)/\sigma(\nu_\mu e^- \to \mu^- \nu_e)$, which is essentially equivalent to $\Gamma(e^- \nu_e \overline{\nu}_\mu)/\Gamma_{\text{total}}$ for small values like that quoted.

$\Gamma(e^-\gamma)/\Gamma_{\text{total}}$ Γ_5/Γ

Forbidden by lepton family number conservation.

VALUE (units 10^{-11})	CL%	DOCUMENT ID		TECN	CHG	COMMENT
< 0.042	90	BALDINI	16	SPEC	+	MEG at PSI
• • • We do not use the following data for averages, fits, limits, etc. • • •						
< 0.057	90	ADAM	13B	SPEC	+	MEG at PSI
< 0.24	90	ADAM	11	SPEC	+	MEG at PSI
< 2.8	90	ADAM	10	SPEC	+	MEG at PSI
< 1.2	90	AHMED	02	SPEC	+	MEGA
< 1.2	90	BROOKS	99	SPEC	+	LAMPF
< 4.9	90	BOLTON	88	CBOX	+	LAMPF
<100	90	AZUELOS	83	CNTR	+	TRIUMF
< 17	90	KINNISON	82	SPEC	+	LAMPF
<100	90	SCHAAF	80	ELEC	+	SIN

$\Gamma(e^-e^+e^-)/\Gamma_{\text{total}}$ Γ_6/Γ

Forbidden by lepton family number conservation.

VALUE (units 10^{-12})	CL%	DOCUMENT ID		TECN	CHG	COMMENT
< 1.0	90	[1] BELLGARDT	88	SPEC	+	SINDRUM
• • • We do not use the following data for averages, fits, limits, etc. • • •						
< 36	90	BARANOV	91	SPEC	+	ARES
< 35	90	BOLTON	88	CBOX	+	LAMPF
< 2.4	90	[1] BERTL	85	SPEC	+	SINDRUM
<160	90	[1] BERTL	84	SPEC	+	SINDRUM
<130	90	[1] BOLTON	84	CNTR		LAMPF

[1] These experiments assume a constant matrix element.

$\Gamma(e^-2\gamma)/\Gamma_{\text{total}}$ Γ_7/Γ

Forbidden by lepton family number conservation.

VALUE (units 10^{-11})	CL%	DOCUMENT ID		TECN	CHG	COMMENT
< 7.2	90	BOLTON	88	CBOX	+	LAMPF
• • • We do not use the following data for averages, fits, limits, etc. • • •						
< 840	90	[1] AZUELOS	83	CNTR	+	TRIUMF
<5000	90	[2] BOWMAN	78	CNTR		DEPOMMIER 77 data

[1] AZUELOS 83 uses the phase space distribution of BOWMAN 78.
[2] BOWMAN 78 assumes an interaction Lagrangian local on the scale of the inverse μ mass.

LIMIT ON $\mu^- \to e^-$ CONVERSION

Forbidden by lepton family number conservation.

$\sigma(\mu^- {}^{32}\text{S} \to e^- {}^{32}\text{S}) / \sigma(\mu^- {}^{32}\text{S} \to \nu_\mu {}^{32}\text{P}^*)$

VALUE	CL%	DOCUMENT ID		TECN	COMMENT
$<7 \times 10^{-11}$	90	BADERT...	80	STRC	SIN
• • • We do not use the following data for averages, fits, limits, etc. • • •					
$<4 \times 10^{-10}$	90	BADERT...	77	STRC	SIN

$\sigma(\mu^- \text{Cu} \to e^- \text{Cu}) / \sigma(\mu^- \text{Cu} \to \text{capture})$

VALUE	CL%	DOCUMENT ID		TECN
• • • We do not use the following data for averages, fits, limits, etc. • • •				
$<1.6 \times 10^{-8}$	90	BRYMAN	72	SPEC

$\sigma(\mu^- \text{Ti} \to e^- \text{Ti}) / \sigma(\mu^- \text{Ti} \to \text{capture})$

VALUE	CL%	DOCUMENT ID		TECN	COMMENT
$<4.3 \times 10^{-12}$	90	[1] DOHMEN	93	SPEC	SINDRUM II
• • • We do not use the following data for averages, fits, limits, etc. • • •					
$<4.6 \times 10^{-12}$	90	AHMAD	88	TPC	TRIUMF
$<1.6 \times 10^{-11}$	90	BRYMAN	85	TPC	TRIUMF

[1] DOHMEN 93 assumes $\mu^- \to e^-$ conversion leaves the nucleus in its ground state, a process enhanced by coherence and expected to dominate.

$\sigma(\mu^- \text{Pb} \to e^- \text{Pb}) / \sigma(\mu^- \text{Pb} \to \text{capture})$

VALUE	CL%	DOCUMENT ID		TECN	COMMENT
$<4.6 \times 10^{-11}$	90	HONECKER	96	SPEC	SINDRUM II
• • • We do not use the following data for averages, fits, limits, etc. • • •					
$<4.9 \times 10^{-10}$	90	AHMAD	88	TPC	TRIUMF

$\sigma(\mu^- \text{Au} \to e^- \text{Au}) / \sigma(\mu^- \text{Au} \to \text{capture})$

VALUE	CL%	DOCUMENT ID		TECN	CHG	COMMENT
$<7 \times 10^{-13}$	90	BERTL	06	SPEC	–	SINDRUM II

LIMIT ON $\mu^- \to e^+$ CONVERSION

Forbidden by total lepton number conservation.

$\sigma(\mu^- {}^{32}\text{S} \to e^+ {}^{32}\text{Si}^*) / \sigma(\mu^- {}^{32}\text{S} \to \nu_\mu {}^{32}\text{P}^*)$

VALUE	CL%	DOCUMENT ID		TECN	COMMENT
$<9 \times 10^{-10}$	90	BADERT...	80	STRC	SIN
• • • We do not use the following data for averages, fits, limits, etc. • • •					
$<1.5 \times 10^{-9}$	90	BADERT...	78	STRC	SIN

$\sigma(\mu^- {}^{127}\text{I} \to e^+ {}^{127}\text{Sb}^*) / \sigma(\mu^- {}^{127}\text{I} \to \text{anything})$

VALUE	CL%	DOCUMENT ID		TECN	COMMENT
$<3 \times 10^{-10}$	90	[1] ABELA	80	CNTR	Radiochemical tech.

[1] ABELA 80 is upper limit for $\mu^- e^+$ conversion leading to particle-stable states of ^{127}Sb. Limit for total conversion rate is higher by a factor less than 4 (G. Backenstoss, private communication).

$\sigma(\mu^- \text{Cu} \to e^+ \text{Co}) / \sigma(\mu^- \text{Cu} \to \nu_\mu \text{Ni})$

VALUE	CL%	DOCUMENT ID		TECN
• • • We do not use the following data for averages, fits, limits, etc. • • •				
$<2.6 \times 10^{-8}$	90	BRYMAN	72	SPEC
$<2.2 \times 10^{-7}$	90	CONFORTO	62	OSPK

$\sigma(\mu^- \text{Ti} \to e^+ \text{Ca}) / \sigma(\mu^- \text{Ti} \to \text{capture})$

VALUE	CL%	EVTS	DOCUMENT ID		TECN	CHG	COMMENT
$<3.6 \times 10^{-11}$	90	1	[1,2] KAULARD	98	SPEC	–	SINDRUM II
• • • We do not use the following data for averages, fits, limits, etc. • • •							
$<1.7 \times 10^{-12}$	90	1	[2,3] KAULARD	98	SPEC	–	SINDRUM II
$<4.3 \times 10^{-12}$	90		[3] DOHMEN	93	SPEC		SINDRUM II
$<8.9 \times 10^{-11}$	90		[1] DOHMEN	93	SPEC		SINDRUM II
$<1.7 \times 10^{-10}$	90		[4] AHMAD	88	TPC		TRIUMF

[1] This limit assumes a giant resonance excitation of the daughter Ca nucleus (mean energy and width both 20 MeV).
[2] KAULARD 98 obtained these same limits using the unified classical analysis of FELDMAN 98.
[3] This limit assumes the daughter Ca nucleus is left in the ground state. However, the probability of this is unknown.
[4] Assuming a giant-resonance-excitation model.

LIMIT ON MUONIUM → ANTIMUONIUM CONVERSION

Forbidden by lepton family number conservation.

$R_g = G_C / G_F$

The effective Lagrangian for the $\mu^+ e^- \to \mu^- e^+$ conversion is assumed to be

$$\mathcal{L} = 2^{-1/2}\, G_C\, [\overline{\psi}_\mu \gamma_\lambda (1-\gamma_5)\, \psi_e]\, [\overline{\psi}_\mu \gamma_\lambda (1-\gamma_5)\, \psi_e] + \text{h.c.}$$

The experimental result is then an upper limit on G_C/G_F, where G_F is the Fermi coupling constant.

VALUE	CL%	EVTS	DOCUMENT ID		TECN	CHG	COMMENT
< 0.0030	90	1	[1] WILLMANN	99	SPEC	+	μ^+ at 26 GeV/c
• • • We do not use the following data for averages, fits, limits, etc. • • •							
< 0.14	90	1	[2] GORDEEV	97	SPEC	+	JINR phasotron
< 0.018	90	0	[3] ABELA	96	SPEC	+	μ^+ at 24 MeV
< 6.9	90		NI	93	CBOX		LAMPF
< 0.16	90		MATTHIAS	91	SPEC		LAMPF
< 0.29	90		HUBER	90B	CNTR		TRIUMF
<20	95		BEER	86	CNTR		TRIUMF
<42	95		MARSHALL	82	CNTR		

[1] WILLMANN 99 quote both probability $P_{M\overline{M}} < 8.3 \times 10^{-11}$ at 90%CL in a 0.1 T field and $R_g = G_C/G_F$.
[2] GORDEEV 97 quote limits on both $f = G_{MM}/GF$ and the probability $W_{MM} < 4.7 \times 10^{-7}$ (90% CL).
[3] ABELA 96 quote both probability $P_{M\overline{M}} < 8 \times 10^{-9}$ at 90% CL and $R_g = G_C/G_F$.

See the related review(s):
Muon Decay Parameters

μ DECAY PARAMETERS

ρ PARAMETER

$(V-A)$ theory predicts $\rho = 0.75$.

VALUE	EVTS	DOCUMENT ID		TECN	CHG	COMMENT
0.74979±0.00026 OUR AVERAGE						
0.74977±0.00012±0.00023		[1] BAYES	11	TWST	+	Surface μ^+
0.7518 ±0.0026		DERENZO	69	RVUE		
• • • We do not use the following data for averages, fits, limits, etc. • • •						
0.75014±0.00017±0.00045		[2] MACDONALD	08	TWST	+	Surface μ^+
0.75080±0.00032±0.00100	6G	[3] MUSSER	05	TWST	+	Surface μ^+
0.72 ±0.06 ±0.08		AMORUSO	04	ICAR		Liquid Ar TPC
0.762 ±0.008	170k	[4] FRYBERGER	68	ASPK	+	25–53 MeV e^+
0.760 ±0.009	280k	[4] SHERWOOD	67	ASPK	+	25–53 MeV e^+
0.7503 ±0.0026	800k	[4] PEOPLES	66	ASPK	+	20–53 MeV e^+

[1] The quoted systematic error includes a contribution of 0.00013 (added in quadrature) from uncertainties on radiative corrections and on the Michel parameter η.
[2] The quoted systematic error includes a contribution of 0.00011 (added in quadrature) from the dependence on the Michel parameter η.
[3] The quoted systematic error includes a contribution of 0.00023 (added in quadrature) from the dependence on the Michel parameter η.
[4] η constrained = 0. These values incorporated into a two parameter fit to ρ and η by DERENZO 69.

η PARAMETER

($V-A$) theory predicts $\eta = 0$.

VALUE	EVTS	DOCUMENT ID		TECN	CHG	COMMENT
0.057 ±0.034 OUR AVERAGE						
0.071 ±0.037 ±0.005	30M	DANNEBERG	05	CNTR	+	7–53 MeV e^+
0.011 ±0.081 ±0.026	5.3M	[1] BURKARD	85B	CNTR	+	9–53 MeV e^+
−0.12 ±0.21	6346	DERENZO	69	HBC	+	1.6–6.8 MeV e^+
• • • We do not use the following data for averages, fits, limits, etc. • • •						
−0.0021±0.0070±0.0010	30M	[2] DANNEBERG	05	CNTR	+	7–53 MeV e^+
−0.012 ±0.015 ±0.003	5.3M	[2] BURKARD	85B	CNTR	+	9–53 MeV e^+
−0.007 ±0.013	5.3M	[3] BURKARD	85B	FIT	+	9–53 MeV e^+
−0.7 ±0.5	170k	[4] FRYBERGER	68	ASPK	+	25–53 MeV e^+
−0.7 ±0.6	280k	[4] SHERWOOD	67	ASPK	+	25–53 MeV e^+
0.05 ±0.5	800k	[4] PEOPLES	66	ASPK	+	20–53 MeV e^+
−2.0 ±0.9	9213	[5] PLANO	60	HBC	+	Whole spectrum

[1] Previously we used the global fit result from BURKARD 85B in OUR AVERAGE, we now only include their actual measurement.
[2] $\alpha = \alpha' = 0$ assumed.
[3] Global fit to all measured parameters. The fit correlation coefficients are given in BURKARD 85B.
[4] ρ constrained = 0.75.
[5] Two parameter fit to ρ and η; PLANO 60 discounts value for η.

δ PARAMETER

($V-A$) theory predicts $\delta = 0.75$.

VALUE	EVTS	DOCUMENT ID		TECN	CHG	COMMENT
0.75047±0.00034 OUR AVERAGE						
0.75049±0.00021±0.00027		[1] BAYES	11	TWST	+	Surface μ^+
0.7486 ±0.0026 ±0.0028		[2] BALKE	88	SPEC	+	Surface μ^+
• • • We do not use the following data for averages, fits, limits, etc. • • •						
0.75067±0.00030±0.00067		MACDONALD	08	TWST	+	Surface μ^+
0.74964±0.00066±0.00112	6G	GAPONENKO	05	TWST	+	Surface μ^+
		[3] VOSSLER	69			
0.752 ±0.009	490k	FRYBERGER	68	ASPK	+	25–53 MeV e^+
0.782 ±0.031		KRUGER	61			
0.78 ±0.05	8354	PLANO	60	HBC	+	Whole spectrum

[1] The quoted systematic error includes a contribution of 0.00006 (added in quadrature) from uncertainties on radiative corrections and on the Michel parameter η.
[2] BALKE 88 uses $\rho = 0.752 \pm 0.003$.
[3] VOSSLER 69 has measured the asymmetry below 10 MeV. See comments about radiative corrections in VOSSLER 69.

|(ξ PARAMETER)×(μ LONGITUDINAL POLARIZATION)|

($V-A$) theory predicts $\xi = 1$, longitudinal polarization = 1.

VALUE	DOCUMENT ID		TECN	CHG	COMMENT
1.0009 $^{+0.0016}_{-0.0007}$ OUR AVERAGE					
1.00084±0.00029$^{+0.00165}_{-0.00063}$	BUENO	11	TWST		Surface μ^+ beam
1.0027 ±0.0079 ±0.0030	BELTRAMI	87	CNTR		SIN, π decay in flight
• • • We do not use the following data for averages, fits, limits, etc. • • •					
1.0003 ±0.0006 ±0.0038	JAMIESON	06	TWST	+	surface μ^+ beam
1.0013 ±0.0030 ±0.0053	[1] IMAZATO	92	SPEC	+	$K^+ \to \mu^+ \nu_\mu$
0.975 ±0.015	AKHMANOV	68	EMUL		140 kG
0.975 ±0.030	GUREVICH	64	EMUL		See AKHMANOV 68
0.903 ±0.027	[2] ALI-ZADE	61	EMUL	+	27 kG
0.93 ±0.06	PLANO	60	HBC	+	8.8 kG
0.97 ±0.05	BARDON	59	CNTR		Bromoform target

[1] The corresponding 90% confidence limit from IMAZATO 92 is $|\xi P_\mu| > 0.990$. This measurement is of K^+ decay, not π^+ decay, so we do not include it in an average, nor do we yet set up a separate data block for K results.
[2] Depolarization by medium not known sufficiently well.

ξ × (μ LONGITUDINAL POLARIZATION) × δ / ρ

VALUE	CL%	DOCUMENT ID		TECN	CHG	COMMENT
1.00179$^{+0.00156}_{-0.00071}$		[1] BAYES	11	TWST	+	Surface μ^+ beam
• • • We do not use the following data for averages, fits, limits, etc. • • •						
>0.99682	90	[2] JODIDIO	86	SPEC	+	TRIUMF
>0.9966	90	[3] STOKER	85	SPEC	+	μ-spin rotation
>0.9959	90	CARR	83	SPEC	+	11 kG

[1] BAYES 11 obtains the limit > 0.99909 (90% CL) with the constraint that $\xi\times(\mu$ LONGITUDINAL POLARIZATION$) \times \delta/\rho \leq 1.0$.
[2] JODIDIO 86 includes data from CARR 83 and STOKER 85. The value here is from the erratum.
[3] STOKER 85 find ($\xi P_\mu \delta/\rho$) >0.9955 and >0.9966, where the first limit is from new μ spin-rotation data and the second is from combination with CARR 83 data. In $V-A$ theory, $(\delta/\rho) = 1.0$.

ξ′ = LONGITUDINAL POLARIZATION OF e^+

($V-A$) theory predicts the longitudinal polarization = ±1 for $e^\pm$, respectively. We have flipped the sign for e^- so our programs can average.

VALUE	EVTS	DOCUMENT ID		TECN	CHG	COMMENT
1.00 ±0.04 OUR AVERAGE						
0.998±0.045	1M	BURKARD	85	CNTR	+	Bhabha + annihil
0.89 ±0.28	29k	SCHWARTZ	67	OSPK	−	Moller scattering
0.94 ±0.38		BLOOM	64	CNTR	+	Brems. transmiss.
1.04 ±0.18		DUCLOS	64	CNTR	+	Bhabha scattering
1.05 ±0.30		BUHLER	63	CNTR	+	Annihilation

ξ″ PARAMETER

VALUE	EVTS	DOCUMENT ID		TECN	CHG	COMMENT
0.98 ±0.04 OUR AVERAGE						
0.981±0.045±0.003	3.87M	PRIEELS	14	CNTR	+	Bhabha + annihil
0.65 ±0.36	326k	[1] BURKARD	85	CNTR	+	Bhabha + annihil

[1] BURKARD 85 measure $(\xi''-\xi\xi')/\xi$ and ξ' and set $\xi = 1$.

TRANSVERSE e^+ POLARIZATION IN PLANE OF μ SPIN, e^+ MOMENTUM

VALUE (units 10^{-3})	EVTS	DOCUMENT ID		TECN	CHG	COMMENT
7 ± 8 OUR AVERAGE						
6.3± 7.7± 3.4	30M	DANNEBERG	05	CNTR	+	7–53 MeV e^+
16 ±21 ±10	5.3M	BURKARD	85B	CNTR	+	Annihil 9–53 MeV

TRANSVERSE e^+ POLARIZATION NORMAL TO PLANE OF μ SPIN, e^+ MOMENTUM

Zero if T invariance holds.

VALUE (units 10^{-3})	EVTS	DOCUMENT ID		TECN	CHG	COMMENT
−2 ± 8 OUR AVERAGE						
−3.7± 7.7±3.4	30M	DANNEBERG	05	CNTR	+	7–53 MeV e^+
7 ±22 ±7	5.3M	BURKARD	85B	CNTR	+	Annihil 9–53 MeV

α/A

VALUE (units 10^{-3})	EVTS	DOCUMENT ID		TECN	CHG	COMMENT
0.4± 4.3		[1] BURKARD	85B	FIT		
• • • We do not use the following data for averages, fits, limits, etc. • • •						
15 ±50 ±14	5.3M	BURKARD	85B	CNTR	+	9–53 MeV e^+

[1] Global fit to all measured parameters. Correlation coefficients are given in BURKARD 85B.

α′/A

Zero if T invariance holds.

VALUE (units 10^{-3})	EVTS	DOCUMENT ID		TECN	CHG	COMMENT
−10 ±20 OUR AVERAGE						
− 3.4±21.3± 4.9	30M	DANNEBERG	05	CNTR	+	7–53 MeV e^+
−47 ±50 ±14	5.3M	[1] BURKARD	85B	CNTR	+	9–53 MeV e^+
• • • We do not use the following data for averages, fits, limits, etc. • • •						
− 0.2± 4.3		[2] BURKARD	85B	FIT		

[1] Previously we used the global fit result from BURKARD 85B in OUR AVERAGE, we now only include their actual measurement. BURKARD 85B measure e^+ polarizations P_{T_1} and P_{T_2} versus e^+ energy.
[2] Global fit to all measured parameters. The fit correlation coefficients are given in BURKARD 85B.

β/A

VALUE (units 10^{-3})	EVTS	DOCUMENT ID		TECN	CHG	COMMENT
3.9± 6.2		[1] BURKARD	85B	FIT		
• • • We do not use the following data for averages, fits, limits, etc. • • •						
2 ±17 ±6	5.3M	BURKARD	85B	CNTR	+	9–53 MeV e^+

[1] Global fit to all measured parameters. The fit correlation coefficients are given in BURKARD 85B.

β′/A

Zero if T invariance holds.

VALUE (units 10^{-3})	EVTS	DOCUMENT ID		TECN	CHG	COMMENT
2 ± 7 OUR AVERAGE						
− 0.5± 7.8±1.8	30M	DANNEBERG	05	CNTR	+	7–53 MeV e^+
17 ±17 ±6	5.3M	[1] BURKARD	85B	CNTR	+	9–53 MeV e^+
• • • We do not use the following data for averages, fits, limits, etc. • • •						
− 1.3± 3.5±0.6	30M	[2] DANNEBERG	05	CNTR	+	7–53 MeV e^+
1.5± 6.3		[3] BURKARD	85B	FIT		

[1] Previously we used the global fit result from BURKARD 85B in OUR AVERAGE, we now only include their actual measurement. BURKARD 85B measure e^+ polarizations P_{T_1} and P_{T_2} versus e^+ energy.
[2] $\alpha = \alpha' = 0$ assumed.
[3] Global fit to all measured parameters. The fit correlation coefficients are given in BURKARD 85B.

Lepton Particle Listings

μ, τ

a/A

This comes from an alternative parameterization to that used in the Summary Table (see the "Note on Muon Decay Parameters" above).

VALUE (units 10^{-3})	CL%	DOCUMENT ID		TECN
• • • We do not use the following data for averages, fits, limits, etc. • • •				
<15.9	90	[1] BURKARD	85B	FIT

[1] Global fit to all measured parameters. Correlation coefficients are given in BURKARD 85B.

a'/A

This comes from an alternative parameterization to that used in the Summary Table (see the "Note on Muon Decay Parameters" above).

VALUE (units 10^{-3})	DOCUMENT ID			TECN
• • • We do not use the following data for averages, fits, limits, etc. • • •				
5.3 ± 4.1	[1] BURKARD		85B	FIT

[1] Global fit to all measured parameters. Correlation coefficients are given in BURKARD 85B.

(b'+b)/A

This comes from an alternative parameterization to that used in the Summary Table (see the "Note on Muon Decay Parameters" above).

VALUE (units 10^{-3})	CL%	DOCUMENT ID		TECN
• • • We do not use the following data for averages, fits, limits, etc. • • •				
<1.04	90	[1] BURKARD	85B	FIT

[1] Global fit to all measured parameters. Correlation coefficients are given in BURKARD 85B.

c/A

This comes from an alternative parameterization to that used in the Summary Table (see the "Note on Muon Decay Parameters" above).

VALUE (units 10^{-3})	CL%	DOCUMENT ID		TECN
• • • We do not use the following data for averages, fits, limits, etc. • • •				
<6.4	90	[1] BURKARD	85B	FIT

[1] Global fit to all measured parameters. Correlation coefficients are given in BURKARD 85B.

c'/A

This comes from an alternative parameterization to that used in the Summary Table (see the "Note on Muon Decay Parameters" above).

VALUE (units 10^{-3})	DOCUMENT ID			TECN
• • • We do not use the following data for averages, fits, limits, etc. • • •				
3.5 ± 2.0	[1] BURKARD		85B	FIT

[1] Global fit to all measured parameters. Correlation coefficients are given in BURKARD 85B.

$\overline{\eta}$ PARAMETER

($V-A$) theory predicts $\overline{\eta} = 0$. $\overline{\eta}$ affects spectrum of radiative muon decay.

VALUE	DOCUMENT ID		TECN	CHG	COMMENT
0.02 ±0.08 OUR AVERAGE					
-0.014 ± 0.090	EICHENBER...	84	ELEC	+	ρ free
$+0.09 \pm 0.14$	BOGART	67	CNTR	+	
• • • We do not use the following data for averages, fits, limits, etc. • • •					
-0.035 ± 0.098	EICHENBER...	84	ELEC	+	ρ=0.75 assumed

μ REFERENCES

BALDINI	16	EPJ C76 434	A.M. Baldini *et al.*	(MEG Collab.)
BALDINI	16A	EPJ C76 108	A.M. Baldini *et al.*	(MEG Collab.)
MOHR	16	RMP 88 035009	P.J. Mohr, D.B. Newell, B.N. Taylor	(NIST)
PRIEELS	14	PR D90 112003	R. Prieels *et al.*	(LOUV, ETH, PSI+)
ADAM	13B	PRL 110 201801	J. Adam *et al.*	(MEG Collab.)
TISHCHENKO	13	PR D87 052003	V. Tishchenko *et al.*	(MuLan Collab.)
MOHR	12	RMP 84 1527	P.J. Mohr, B.N. Taylor, D.B. Newell	(NIST)
ADAM	11	PRL 107 171801	J. Adam *et al.*	(MEG Collab.)
BAYES	11	PRL 106 041804	R. Bayes *et al.*	(TWIST Collab.)
Also		PR D85 092013	A. Hillairet *et al.*	(TWIST Collab.)
BUENO	11	PR D84 032005	J.F. Bueno *et al.*	(TWIST Collab.)
Also		PR D85 039908 (errat.)	J.F. Bueno *et al.*	(TWIST Collab.)
WEBBER	11	PRL 106 041803	D.M. Webber *et al.*	(MuLan Collab.)
Also		PRL 106 079901 (errat.)	D.M. Webber *et al.*	(MuLan Collab.)
ADAM	10	NP B834 1	J. Adam *et al.*	(MEG Collab.)
BENNETT	09	PR D80 052008	G.W. Bennett *et al.*	(MUG-2 Collab.)
BARCZYK	08	PL B663 172	A. Barczyk *et al.*	(FAST Collab.)
MACDONALD	08	PR D78 032010	R.P. MacDonald *et al.*	(TWIST Collab.)
MOHR	08	RMP 80 633	P.J. Mohr, B.N. Taylor, D.B. Newell	(NIST)
CHITWOOD	07	PRL 99 032001	D.B. Chitwood *et al.*	(MULAN Collab.)
BENNETT	06	PR D73 072003	G.W. Bennett *et al.*	(MUG-2 Collab.)
BERTL	06	EPJ C47 337	W. Bertl *et al.*	(SINDRUM II Collab.)
JAMIESON	06	PR D74 072007	B. Jamieson *et al.*	(TWIST Collab.)
DANNEBERG	05	PRL 94 021802	N. Danneberg *et al.*	(ETH, JAGL, PSI+)
GAPONENKO	05	PR D71 071101	A. Gaponenko *et al.*	(TWIST Collab.)
MOHR	05	RMP 77 1	P.J. Mohr, B.N. Taylor	(NIST)
MUSSER	05	PRL 94 101805	J.R. Musser *et al.*	(TWIST Collab.)
AMORUSO	04	EPJ C33 233	S. Amoruso *et al.*	(ICARUS Collab.)
BENNETT	04	PRL 92 161802	G.W. Bennett *et al.*	(Muon(g-2) Collab.)
AHMED	02	PR D65 112002	M. Ahmed *et al.*	(MEGA Collab.)
BENNETT	02	PRL 89 101804	G.W. Bennett *et al.*	(Muon(g-2) Collab.)
BROWN	01	PRL 86 2227	H.N. Brown *et al.*	(Muon(g-2) Collab.)
BROWN	00	PR D62 091101	H.N. Brown *et al.*	(BNL/G-2 Collab.)
MEYER	00	PRL 84 1136	V. Meyer *et al.*	
BROOKS	99	PRL 83 1521	M.L. Brooks *et al.*	(MEGA/LAMPF Collab.)
HUGHES	99	RMP 71 S133	V.W. Hughes, T. Kinoshita	
LIU	99	PRL 82 711	W. Liu *et al.*	(LAMPF Collab.)
MOHR	99	JPCRD 28 1713	P.J. Mohr, B.N. Taylor	(NIST)
Also		RMP 72 351	P.J. Mohr, B.N. Taylor	(NIST)
WILLMANN	99	PRL 82 49	L. Willmann *et al.*	
FELDMAN	98	PR D57 3873	G.J. Feldman, R.D. Cousins	
KAULARD	98	PL B422 334	J. Kaulard *et al.*	(SINDRUM-II Collab.)
GORDEEV	97	PAN 60 1164	V.A. Gordeev *et al.*	(PNPI)
		Translated from YAF 60 1291.		
ABELA	96	PRL 77 1950	R. Abela *et al.*	(PSI, ZURI, HEIDH, TBIL+)
HONECKER	96	PRL 76 200	W. Honecker *et al.*	(SINDRUM II Collab.)
DOHMEN	93	PL B317 631	C. Dohmen *et al.*	(PSI SINDRUM-II Collab.)
FREEDMAN	93	PR D47 811	S.J. Freedman *et al.*	(LAMPF E645 Collab.)
NI	93	PR D48 1976	B. Ni *et al.*	(LAMPF Crystal-Box Collab.)
IMAZATO	92	PRL 69 877	J. Imazato *et al.*	(KEK, INUS, TOKY+)
BARANOV	91	SJNP 53 802	V.A. Baranov *et al.*	(JINR)
		Translated from YAF 53 1302.		
KRAKAUER	91B	PL B263 534	D.A. Krakauer *et al.*	(UMD, UCI, LANL)
MATTHIAS	91	PRL 66 2716	B.E. Matthias *et al.*	(YALE, HEIDP, WILL+)
Also		PRL 67 932 (erratum)	B.E. Matthias *et al.*	(YALE, HEIDP, WILL+)
HUBER	90B	PR D41 2709	T.M. Huber *et al.*	(WYOM, VICT, ARIZ+)
AHMAD	88	PR D38 2102	S. Ahmad *et al.*	(TRIU, VICT, VPI, BRCO+)
Also		PRL 59 970	S. Ahmad *et al.*	(TRIU, VPI, VICT, BRCO+)
BALKE	88	PR D37 587	B. Balke *et al.*	(LBL, UCB, COLO, NWES+)
BELLGARDT	88	NP B299 1	U. Bellgardt *et al.*	(SINDRUM Collab.)
BOLTON	88	PR D38 2077	R.D. Bolton *et al.*	(LANL, STAN, CHIC+)
Also		PRL 56 2461	R.D. Bolton *et al.*	(LANL, STAN, CHIC+)
Also		PRL 57 3241	D. Grosnick *et al.*	(CHIC, LANL, STAN+)
BELTRAMI	87	PL B194 326	I. Beltrami *et al.*	(ETH, SIN, MANZ)
COHEN	87	RMP 59 1121	E.R. Cohen, B.N. Taylor	(RISC, NBS)
BEER	86	PRL 57 671	G.A. Beer *et al.*	(VICT, TRIU, WYOM)
JODIDIO	86	PR D34 1967	A. Jodidio *et al.*	(LBL, NWES, TRIU)
Also		PR D37 237 (erratum)	A. Jodidio *et al.*	(LBL, NWES, TRIU)
BERTL	85	NP B260 1	W. Bertl *et al.*	(SINDRUM Collab.)
BRYMAN	85	PRL 55 465	D.A. Bryman *et al.*	(TRIU, CNRC, BRCO+)
BURKARD	85	PL 150B 242	H. Burkhardt *et al.*	(ETH, SIN, MANZ)
BURKARD	85B	PL 160B 343	H. Burkhardt *et al.*	(ETH, SIN, MANZ)
Also		PR D24 2004	F. Corriveau *et al.*	(ETH, SIN, MANZ)
Also		PL 129B 260	F. Corriveau *et al.*	(ETH, SIN, MANZ)
STOKER	85	PRL 54 1887	D.P. Stoker *et al.*	(LBL, NWES, TRIU)
BARDIN	84	PL 137B 135	G. Bardin *et al.*	(SACL, CERN, BGNA, FIRZ)
BERTL	84	PL 140B 299	W. Bertl *et al.*	(SINDRUM Collab.)
BOLTON	84	PRL 53 1415	R.D. Bolton *et al.*	(LANL, CHIC, STAN+)
EICHENBER...	84	NP A412 523	W. Eichenberger, R. Engfer, A. van der Schaff	
GIOVANETTI	84	PR D29 343	K.L. Giovanetti *et al.*	(WILL)
AZUELOS	83	PRL 51 164	G. Azuelos *et al.*	(MONT, TRIU, BRCO)
Also		PRL 39 1113	P. Depommier *et al.*	(MONT, BRCO, TRIU+)
BERGSMA	83	PL 122B 465	F. Bergsma *et al.*	(CHARM Collab.)
CARR	83	PRL 51 627	J. Carr *et al.*	(LBL, NWES, TRIU)
KINNISON	82	PR D25 2846	W.W. Kinnison *et al.*	(EFI, STAN, LANL)
Also		PRL 42 556	J.D. Bowman *et al.*	(LASL, EFI, STAN)
KLEMPT	82	PR D25 652	E. Klempt *et al.*	(MANZ, ETH)
MARIAM	82	PRL 49 993	F.G. Mariam *et al.*	(YALE, HEIDH, BERN)
MARSHALL	82	PR D25 1174	G.M. Marshall *et al.*	(BRCO)
NEMETHY	81	CNPP 10 147	P. Nemethy, V.W. Hughes	(LBL, YALE)
ABELA	80	PL 95B 318	R. Abela *et al.*	(BASL, KARLK, KARLE)
BADERT...	80	LNC 28 401	A. Badertscher *et al.*	(BERN)
Also		NP A377 406	A. Badertscher *et al.*	(BERN)
JONKER	80	PL 93B 203	M. Jonker *et al.*	(CHARM Collab.)
SCHAAF	80	NP A340 249	A. van der Schaaf *et al.*	(ZURI, ETH+)
Also		PL 72B 183	H.P. Povel *et al.*	(ZURI, ETH, SIN)
WILLIS	80	PRL 44 522	S.E. Willis *et al.*	(YALE, LBL, LASL+)
Also		PRL 45 1370	S.E. Willis *et al.*	(YALE, LBL, LASL+)
BAILEY	79	NP B150 1	J.M. Bailey	(CERN, DARE, MANZ)
BADERT...	78	PL 79B 371	A. Badertscher *et al.*	(BERN)
BAILEY	78	JP G4 345	J.M. Bailey (DARE, BERN, SHEF, MANZ, RMCS+)	
Also		NP B150 1	J.M. Bailey	(CERN, DARE, MANZ)
BLIETSCHAU	78	NP B133 205	J. Blietschau *et al.*	(Gargamelle Collab.)
BOWMAN	78	PRL 41 442	J.D. Bowman *et al.*	(LASL, IAS, CMU+)
CAMANI	78	PL 77B 326	M. Camani *et al.*	(ETH, MANZ)
BADERT...	77	PRL 39 1385	A. Badertscher *et al.*	(BERN)
CASPERSON	77	PRL 38 956	D.E. Casperson *et al.*	(BERN, HEIDH, LASL+)
DEPOMMIER	77	PRL 39 1113	P. Depommier *et al.*	(MONT, BRCO, TRIU+)
BALANDIN	74	JETP 40 811	M.P. Balandin *et al.*	(JINR)
		Translated from ZETF 67 1631.		
COHEN	73	JPCRD 2 664	E.R. Cohen, B.N. Taylor	(RISC, NBS)
DUCLOS	73	PL 47B 491	J. Duclos, A. Magnon, J. Picard	(SACL)
EICHTEN	73	PL 46B 281	T. Eichten *et al.*	(Gargamelle Collab.)
BRYMAN	72	PRL 28 1469	D.A. Bryman *et al.*	(VPI)
CROWE	72	PR D5 2145	K.M. Crowe *et al.*	(LBL, WASH)
CRANE	71	PRL 27 474	T. Crane *et al.*	(YALE)
DERENZO	69	PR 181 1854	S.E. Derenzo	(EFI)
VOSSLER	69	NC 63A 423	C. Vossler	(EFI)
AKHMANOV	68	SJNP 6 230	V.V. Akhmanov *et al.*	(KIAE)
		Translated from YAF 6 316.		
FRYBERGER	68	PR 166 1379	D. Fryberger	(EFI)
BOGART	67	PR 156 1405	E. Bogart *et al.*	(COLU)
SCHWARTZ	67	PR 162 1306	D.M. Schwartz	(EFI)
SHERWOOD	67	PR 156 1475	B.A. Sherwood	(EFI)
PEOPLES	66	Nevis 147 unpub.	J. Peoples	(COLU)
BLOOM	64	PL 8 87	S. Bloom *et al.*	(CERN)
DUCLOS	64	PL 9 62	J. Duclos *et al.*	(CERN)
GUREVICH	64	PL 11 185	I.I. Gurevich *et al.*	(KIAE)
BUHLER	63	PL 7 368	A. Buhler-Broglin *et al.*	(CERN)
MEYER	63	PR 132 2693	S.L. Meyer *et al.*	(COLU)
CHARPAK	62	PL 1 16	G. Charpak *et al.*	(CERN)
CONFORTO	62	NC 26 261	G. Conforto *et al.*	(INFN, ROMA, CERN)
ALI-ZADE	61	JETP 13 313	S.A. Ali-Zade, I.I. Gurevich, B.A. Nikolsky	
		Translated from ZETF 40 452.		
CRITTENDEN	61	PR 121 1823	R.R. Crittenden, W.D. Walker, J. Ballam	(WISC+)
KRUGER	61	UCRL 9322 unpub.	H. Kruger	(LRL)
GUREVICH	60	JETP 10 225	I.I. Gurevich, B.A. Nikolsky, L.V. Surkova	(ITEP)
		Translated from ZETF 37 318.		
PLANO	60	PR 119 1400	R.J. Plano	(COLU)
ASHKIN	59	NC 14 1266	J. Ashkin *et al.*	(CERN)
BARDON	59	PRL 2 56	M. Bardon, D. Berley, L.M. Lederman	(COLU)
LEE	59	PRL 3 55	J. Lee, N.P. Samios	(COLU)

τ

$J = \frac{1}{2}$

τ discovery paper was PERL 75. $e^+e^- \to \tau^+\tau^-$ cross-section threshold behavior and magnitude are consistent with pointlike spin-1/2 Dirac particle. BRANDELIK 78 ruled out pointlike spin-0 or spin-1 particle. FELDMAN 78 ruled out $J = 3/2$. KIRKBY 79 also ruled out J=integer, $J = 3/2$.

τ MASS

VALUE (MeV)	EVTS	DOCUMENT ID		TECN	COMMENT
1776.86±0.12 OUR AVERAGE					
1776.91±0.12$^{+0.10}_{-0.13}$	1171	[1] ABLIKIM	14D	BES3	23.3 pb^{-1}, E^{ee}_{cm}= 3.54–3.60 GeV
1776.68±0.12±0.41	682k	[2] AUBERT	09AK	BABR	423 fb^{-1}, E^{ee}_{cm}=10.6 GeV
1776.81$^{+0.25}_{-0.23}$±0.15	81	ANASHIN	07	KEDR	6.7 pb^{-1}, E^{ee}_{cm}= 3.54–3.78 GeV
1776.61±0.13±0.35		[2] BELOUS	07	BELL	414 fb^{-1} E^{ee}_{cm}=10.6 GeV
1775.1 ±1.6 ±1.0	13.3k	[3] ABBIENDI	00A	OPAL	1990–1995 LEP runs
1778.2 ±0.8 ±1.2		ANASTASSOV	97	CLEO	E^{ee}_{cm}= 10.6 GeV
1776.96$^{+0.18+0.25}_{-0.21-0.17}$	65	[4] BAI	96	BES	E^{ee}_{cm}= 3.54–3.57 GeV
1776.3 ±2.4 ±1.4	11k	[5] ALBRECHT	92M	ARG	E^{ee}_{cm}= 9.4–10.6 GeV
1783 $^{+3}_{-4}$	692	[6] BACINO	78B	DLCO	E^{ee}_{cm}= 3.1–7.4 GeV
• • • We do not use the following data for averages, fits, limits, etc. • • •					
1777.8 ±0.7 ±1.7	35k	[7] BALEST	93	CLEO	Repl. by ANASTASSOV 97
1776.9 $^{+0.4}_{-0.5}$ ±0.2	14	[8] BAI	92	BES	Repl. by BAI 96

[1] ABLIKIM 14D fit $\sigma(e^+e^- \to \tau^+\tau^-)$ at different energies near threshold.
[2] AUBERT 09AK and BELOUS 07 fit τ pseudomass spectrum in $\tau \to \pi\pi^+\pi^-\nu_\tau$ decays. Result assumes $m_{\nu_\tau} = 0$.
[3] ABBIENDI 00A fit τ pseudomass spectrum in $\tau \to \pi^\pm \leq 2\pi^0\nu_\tau$ and $\tau \to \pi^\pm\pi^+\pi^- \leq 1\pi^0\nu_\tau$ decays. Result assumes m_{ν_τ}=0.
[4] BAI 96 fit $\sigma(e^+e^- \to \tau^+\tau^-)$ at different energies near threshold.
[5] ALBRECHT 92M fit τ pseudomass spectrum in $\tau^- \to 2\pi^-\pi^+\nu_\tau$ decays. Result assumes m_{ν_τ}=0.
[6] BACINO 78B value comes from $e^\pm X^\mp$ threshold. Published mass 1782 MeV increased by 1 MeV using the high precision $\psi(2S)$ mass measurement of ZHOLENTZ 80 to eliminate the absolute SPEAR energy calibration uncertainty.
[7] BALEST 93 fit spectra of minimum kinematically allowed τ mass in events of the type $e^+e^- \to \tau^+\tau^- \to (\pi^+ n\pi^0\nu_\tau)(\pi^- m\pi^0\nu_\tau)$ $n \leq 2$, $m \leq 2$, $1 \leq n+m \leq 3$. If $m_{\nu_\tau} \neq 0$, result increases by $(m^2_{\nu_\tau}/1100$ MeV).
[8] BAI 92 fit $\sigma(e^+e^- \to \tau^+\tau^-)$ near threshold using $e\mu$ events.

$(m_{\tau^+} - m_{\tau^-})/m_{\text{average}}$

A test of CPT invariance.

VALUE	CL%	DOCUMENT ID		TECN	COMMENT
$<2.8\times10^{-4}$	90	BELOUS	07	BELL	414 fb^{-1}, E^{ee}_{cm}=10.6 GeV
• • • We do not use the following data for averages, fits, limits, etc. • • •					
$<5.5\times10^{-4}$	90	[1] AUBERT	09AK	BABR	423 fb^{-1}, E^{ee}_{cm}=10.6 GeV
$<3.0\times10^{-3}$	90	ABBIENDI	00A	OPAL	1990–1995 LEP runs

[1] AUBERT 09AK quote both the listed upper limit and $(m_{\tau^+} - m_{\tau^-})/m_{\text{average}} = (-3.4 \pm 1.3 \pm 0.3)\times10^{-4}$.

τ MEAN LIFE

VALUE (10^{-15} s)	EVTS	DOCUMENT ID		TECN	COMMENT
290.3 ± 0.5 OUR AVERAGE					
290.17± 0.53± 0.33	1.1M	BELOUS	14	BELL	711 fb^{-1} E^{ee}_{cm}=10.6 GeV
290.9 ± 1.4 ± 1.0		ABDALLAH	04T	DLPH	1991-1995 LEP runs
293.2 ± 2.0 ± 1.5		ACCIARRI	00B	L3	1991–1995 LEP runs
290.1 ± 1.5 ± 1.1		BARATE	97R	ALEP	1989–1994 LEP runs
289.2 ± 1.7 ± 1.2		ALEXANDER	96E	OPAL	1990–1994 LEP runs
289.0 ± 2.8 ± 4.0	57.4k	BALEST	96	CLEO	E^{ee}_{cm}= 10.6 GeV
• • • We do not use the following data for averages, fits, limits, etc. • • •					
291.2 ± 2.0 ± 1.2		BARATE	97I	ALEP	Repl. by BARATE 97R
291.4 ± 3.0		ABREU	96B	DLPH	Repl. by ABDALLAH 04T
290.1 ± 4.0	34k	ACCIARRI	96K	L3	Repl. by ACCIARRI 00B
297 ± 9 ± 5	1671	ABE	95Y	SLD	1992–1993 SLC runs
304 ±14 ± 7	4100	BATTLE	92	CLEO	E^{ee}_{cm}= 10.6 GeV
301 ±29	3780	KLEINWORT	89	JADE	E^{ee}_{cm}= 35–46 GeV
288 ±16 ±17	807	AMIDEI	88	MRK2	E^{ee}_{cm}= 29 GeV
306 ±20 ±14	695	BRAUNSCH...	88C	TASS	E^{ee}_{cm}= 36 GeV
299 ±15 ±10	1311	ABACHI	87C	HRS	E^{ee}_{cm}= 29 GeV
295 ±14 ±11	5696	ALBRECHT	87P	ARG	E^{ee}_{cm}= 9.3–10.6 GeV
309 ±17 ± 7	3788	BAND	87B	MAC	E^{ee}_{cm}= 29 GeV
325 ±14 ±18	8470	BEBEK	87C	CLEO	E^{ee}_{cm}= 10.5 GeV
460 ± 190	102	FELDMAN	82	MRK2	E^{ee}_{cm}= 29 GeV

$(\tau_{\tau^+} - \tau_{\tau^-}) / \tau_{\text{average}}$

Test of CPT invariance.

VALUE	CL%	DOCUMENT ID		TECN	COMMENT
$<7.0\times10^{-3}$	90	[1] BELOUS	14	BELL	711 fb^{-1} E^{ee}_{cm} = 10.6 GeV

[1] BELOUS 14 quote limit on the absolute value of the relative lifetime difference.

τ MAGNETIC MOMENT ANOMALY

The q^2 dependence is expected to be small providing no thresholds are nearby.

$\mu_\tau/(e\hbar/2m_\tau) - 1 = (g_\tau - 2)/2$

For a theoretical calculation [$(g_\tau - 2)/2 = 117\,721(5)\times10^{-8}$], see EIDELMAN 07.

VALUE	CL%	DOCUMENT ID		TECN	COMMENT
> -0.052 and < 0.013 (CL = 95%) OUR LIMIT					
> -0.052 and < 0.013	95	[1] ABDALLAH	04K	DLPH	$e^+e^- \to e^+e^-\tau^+\tau^-$ at LEP2
• • • We do not use the following data for averages, fits, limits, etc. • • •					
<0.107	95	[2] ACHARD	04G	L3	$e^+e^- \to e^+e^-\tau^+\tau^-$ at LEP2
> -0.007 and < 0.005	95	[3] GONZALEZ-S...00		RVUE	$e^+e^- \to \tau^+\tau^-$ and $W \to \tau\nu_\tau$
> -0.052 and < 0.058	95	[4] ACCIARRI	98E	L3	1991–1995 LEP runs
> -0.068 and < 0.065	95	[5] ACKERSTAFF	98N	OPAL	1990–1995 LEP runs
> -0.004 and < 0.006	95	[6] ESCRIBANO	97	RVUE	$Z \to \tau^+\tau^-$ at LEP
<0.01	95	[7] ESCRIBANO	93	RVUE	$Z \to \tau^+\tau^-$ at LEP
<0.12	90	GRIFOLS	91	RVUE	$Z \to \tau\tau\gamma$ at LEP
<0.023	95	[8] SILVERMAN	83	RVUE	$e^+e^- \to \tau^+\tau^-$ at PETRA

[1] ABDALLAH 04K limit is derived from $e^+e^- \to e^+e^-\tau^+\tau^-$ total cross-section measurements at $\sqrt{s}$ between 183 and 208 GeV. In addition to the limits, the authors also quote a value of -0.018 ± 0.017.
[2] ACHARD 04G limit is derived from $e^+e^- \to e^+e^-\tau^+\tau^-$ total cross-section measurements at $\sqrt{s}$ between 189 and 206 GeV, and is on the absolute value of the magnetic moment anomaly.
[3] GONZALEZ-SPRINBERG 00 use data on tau lepton production at LEP1, SLC, and LEP2, and data from colliders and LEP2 to determine limits. Assume imaginary component is zero.
[4] ACCIARRI 98E use $Z \to \tau^+\tau^-\gamma$ events. In addition to the limits, the authors also quote a value of $0.004 \pm 0.027 \pm 0.023$.
[5] ACKERSTAFF 98N use $Z \to \tau^+\tau^-\gamma$ events. The limit applies to an average of the form factor for off-shell τ's having p^2 ranging from m^2_τ to $(M_Z - m_\tau)^2$.
[6] ESCRIBANO 97 use preliminary experimental results.
[7] ESCRIBANO 93 limit derived from $\Gamma(Z \to \tau^+\tau^-)$, and is on the absolute value of the magnetic moment anomaly.
[8] SILVERMAN 83 limit is derived from $e^+e^- \to \tau^+\tau^-$ total cross-section measurements for q^2 up to $(37\text{ GeV})^2$.

τ ELECTRIC DIPOLE MOMENT (d_τ)

A nonzero value is forbidden by both T invariance and P invariance.

The q^2 dependence is expected to be small providing no thresholds are nearby.

Re(d_τ)

VALUE (10^{-16} ecm)	CL%	DOCUMENT ID		TECN	COMMENT
− 0.22 to 0.45	95	[1] INAMI	03	BELL	E^{ee}_{cm}= 10.6 GeV
• • • We do not use the following data for averages, fits, limits, etc. • • •					
< 2.3	90	[2] GROZIN	09A	RVUE	From e EDM limit
< 3.7	95	[3] ABDALLAH	04K	DLPH	$e^+e^- \to e^+e^-\tau^+\tau^-$ at LEP2
< 11.4	95	[4] ACHARD	04G	L3	$e^+e^- \to e^+e^-\tau^+\tau^-$ at LEP2
< 4.6	95	[5] ALBRECHT	00	ARG	E^{ee}_{cm}= 10.4 GeV
> -3.1 and < 3.1	95	ACCIARRI	98E	L3	1991–1995 LEP runs
> -3.8 and < 3.6	95	[6] ACKERSTAFF	98N	OPAL	1990–1995 LEP runs
< 0.11	95	[7,8] ESCRIBANO	97	RVUE	$Z \to \tau^+\tau^-$ at LEP
< 0.5	95	[9] ESCRIBANO	93	RVUE	$Z \to \tau^+\tau^-$ at LEP
< 7	90	GRIFOLS	91	RVUE	$Z \to \tau\tau\gamma$ at LEP
< 1.6	90	DELAGUILA	90	RVUE	$e^+e^- \to \tau^+\tau^-$ E^{ee}_{cm}= 35 GeV

[1] INAMI 03 use $e^+e^- \to \tau^+\tau^-$ events.
[2] GROZIN 09A calculate the contribution to the electron electric dipole moment from the τ electric dipole moment appearing in loops, which is $\Delta d_e = 6.9\times10^{-12}\ d_\tau$. Dividing the REGAN 02 upper limit $|d_e| \leq 1.6\times10^{-27}$ e cm at CL=90% by 6.9×10^{-12} gives this limit.
[3] ABDALLAH 04K limit is derived from $e^+e^- \to e^+e^-\tau^+\tau^-$ total cross-section measurements at $\sqrt{s}$ between 183 and 208 GeV and is on the absolute value of d_τ.
[4] ACHARD 04G limit is derived from $e^+e^- \to e^+e^-\tau^+\tau^-$ total cross-section measurements at $\sqrt{s}$ between 189 and 206 GeV, and is on the absolute value of d_τ.
[5] ALBRECHT 00 use $e^+e^- \to \tau^+\tau^-$ events. Limit is on the absolute value of Re(d_τ).
[6] ACKERSTAFF 98N use $Z \to \tau^+\tau^-\gamma$ events. The limit applies to an average of the form factor for off-shell τ's having p^2 ranging from m^2_τ to $(M_Z - m_\tau)^2$.
[7] ESCRIBANO 97 derive the relationship $|d_\tau| = \cot\theta_W\,|d^W_\tau|$ using effective Lagrangian methods, and use a conference result $|d^W_\tau| < 5.8\times10^{-18}$ e cm at 95% CL (L. Silvestris, ICHEP96) to obtain this result.
[8] ESCRIBANO 97 use preliminary experimental results.
[9] ESCRIBANO 93 limit derived from $\Gamma(Z \to \tau^+\tau^-)$, and is on the absolute value of the electric dipole moment.

Lepton Particle Listings

τ

Im(d_τ)

VALUE (10^{-16} e cm)	CL%	DOCUMENT ID		TECN	COMMENT
−0.25 to 0.008	95	[1] INAMI	03	BELL	E_{cm}^{ee}= 10.6 GeV
• • • We do not use the following data for averages, fits, limits, etc. • • •					
< 1.8	95	[2] ALBRECHT	00	ARG	E_{cm}^{ee}= 10.4 GeV

[1] INAMI 03 use $e^+e^- \to \tau^+\tau^-$ events.
[2] ALBRECHT 00 use $e^+e^- \to \tau^+\tau^-$ events. Limit is on the absolute value of Im(d_τ).

τ WEAK DIPOLE MOMENT (d_τ^W)

A nonzero value is forbidden by *CP* invariance.

The q^2 dependence is expected to be small providing no thresholds are nearby.

Re(d_τ^W)

VALUE (10^{-17} e cm)	CL%	DOCUMENT ID		TECN	COMMENT
<0.50	95	[1] HEISTER	03F	ALEP	1990–1995 LEP runs
• • • We do not use the following data for averages, fits, limits, etc. • • •					
<3.0	90	[1] ACCIARRI	98C	L3	1991–1995 LEP runs
<0.56	95	ACKERSTAFF	97L	OPAL	1991–1995 LEP runs
<0.78	95	[2] AKERS	95F	OPAL	Repl. by ACKERSTAFF 97L
<1.5	95	[2] BUSKULIC	95C	ALEP	Repl. by HEISTER 03F
<7.0	95	[2] ACTON	92F	OPAL	$Z \to \tau^+\tau^-$ at LEP
<3.7	95	[2] BUSKULIC	92J	ALEP	Repl. by BUSKULIC 95C

[1] Limit is on the absolute value of the real part of the weak dipole moment.
[2] Limit is on the absolute value of the real part of the weak dipole moment, and applies for $q^2 = m_Z^2$.

Im(d_τ^W)

VALUE (10^{-17} e cm)	CL%	DOCUMENT ID		TECN	COMMENT
<1.1	95	[1] HEISTER	03F	ALEP	1990–1995 LEP runs
• • • We do not use the following data for averages, fits, limits, etc. • • •					
<1.5	95	ACKERSTAFF	97L	OPAL	1991–1995 LEP runs
<4.5	95	[2] AKERS	95F	OPAL	Repl. by ACKERSTAFF 97L

[1] HEISTER 03F limit is on the absolute value of the imaginary part of the weak dipole moment.
[2] Limit is on the absolute value of the imaginary part of the weak dipole moment, and applies for $q^2 = m_Z^2$.

τ WEAK ANOMALOUS MAGNETIC DIPOLE MOMENT (a_τ^W)

Electroweak radiative corrections are expected to contribute at the 10^{-6} level. See BERNABEU 95.

The q^2 dependence is expected to be small providing no thresholds are nearby.

Re(a_τ^W)

VALUE		CL%	DOCUMENT ID		TECN	COMMENT
$<1.1 \times 10^{-3}$		95	[1] HEISTER	03F	ALEP	1990–1995 LEP runs
• • • We do not use the following data for averages, fits, limits, etc. • • •						
> -0.0024 and < 0.0025		95	[2] GONZALEZ-S...00		RVUE	$e^+e^- \to \tau^+\tau^-$ and $W \to \tau\nu_\tau$
$<4.5 \times 10^{-3}$		90	[1] ACCIARRI	98C	L3	1991–1995 LEP runs

[1] Limit is on the absolute value of the real part of the weak anomalous magnetic dipole moment.
[2] GONZALEZ-SPRINBERG 00 use data on tau lepton production at LEP1, SLC, and LEP2, and data from colliders and LEP2 to determine limits. Assume imaginary component is zero.

Im(a_τ^W)

VALUE	CL%	DOCUMENT ID		TECN	COMMENT
$<2.7 \times 10^{-3}$	95	[1] HEISTER	03F	ALEP	1990–1995 LEP runs
• • • We do not use the following data for averages, fits, limits, etc. • • •					
$<9.9 \times 10^{-3}$	90	[1] ACCIARRI	98C	L3	1991–1995 LEP runs

[1] Limit is on the absolute value of the imaginary part of the weak anomalous magnetic dipole moment.

τ^- DECAY MODES

τ^+ modes are charge conjugates of the modes below. "$h^\pm$" stands for $\pi^\pm$ or $K^\pm$. "ℓ" stands for e or μ. "Neutrals" stands for γ's and/or π^0's.

	Mode	Fraction (Γ_i/Γ)	Scale factor/ Confidence level
	Modes with one charged particle		
Γ_1	particle$^- \geq 0$ neutrals $\geq 0 K^0 \nu_\tau$ ("1-prong")	(85.24 ± 0.06) %	
Γ_2	particle$^- \geq 0$ neutrals $\geq 0 K_L^0 \nu_\tau$	(84.58 ± 0.06) %	
Γ_3	$\mu^- \overline{\nu}_\mu \nu_\tau$	[a] (17.39 ± 0.04) %	
Γ_4	$\mu^- \overline{\nu}_\mu \nu_\tau \gamma$	[b] (3.67 ± 0.08) $\times 10^{-3}$	
Γ_5	$e^- \overline{\nu}_e \nu_\tau$	[a] (17.82 ± 0.04) %	
Γ_6	$e^- \overline{\nu}_e \nu_\tau \gamma$	[b] (1.83 ± 0.05) %	
Γ_7	$h^- \geq 0 K_L^0 \nu_\tau$	(12.03 ± 0.05) %	
Γ_8	$h^- \nu_\tau$	(11.51 ± 0.05) %	
Γ_9	$\pi^- \nu_\tau$	[a] (10.82 ± 0.05) %	
Γ_{10}	$K^- \nu_\tau$	[a] (6.96 ± 0.10) $\times 10^{-3}$	
Γ_{11}	$h^- \geq 1$ neutrals ν_τ	(37.00 ± 0.09) %	
Γ_{12}	$h^- \geq 1\pi^0 \nu_\tau$ (ex.K^0)	(36.51 ± 0.09) %	
Γ_{13}	$h^- \pi^0 \nu_\tau$	(25.93 ± 0.09) %	
Γ_{14}	$\pi^- \pi^0 \nu_\tau$	[a] (25.49 ± 0.09) %	
Γ_{15}	$\pi^- \pi^0$ non-$\rho(770)\, \nu_\tau$	(3.0 ± 3.2) $\times 10^{-3}$	
Γ_{16}	$K^- \pi^0 \nu_\tau$	[a] (4.33 ± 0.15) $\times 10^{-3}$	
Γ_{17}	$h^- \geq 2\pi^0 \nu_\tau$	(10.81 ± 0.09) %	
Γ_{18}	$h^- 2\pi^0 \nu_\tau$	(9.48 ± 0.10) %	
Γ_{19}	$h^- 2\pi^0 \nu_\tau$ (ex.K^0)	(9.32 ± 0.10) %	
Γ_{20}	$\pi^- 2\pi^0 \nu_\tau$ (ex.K^0)	[a] (9.26 ± 0.10) %	
Γ_{21}	$\pi^- 2\pi^0 \nu_\tau$ (ex.K^0), scalar	< 9 $\times 10^{-3}$	CL=95%
Γ_{22}	$\pi^- 2\pi^0 \nu_\tau$ (ex.K^0), vector	< 7 $\times 10^{-3}$	CL=95%
Γ_{23}	$K^- 2\pi^0 \nu_\tau$ (ex.K^0)	[a] (6.5 ± 2.2) $\times 10^{-4}$	
Γ_{24}	$h^- \geq 3\pi^0 \nu_\tau$	(1.34 ± 0.07) %	
Γ_{25}	$h^- \geq 3\pi^0 \nu_\tau$ (ex. K^0)	(1.25 ± 0.07) %	
Γ_{26}	$h^- 3\pi^0 \nu_\tau$	(1.18 ± 0.07) %	
Γ_{27}	$\pi^- 3\pi^0 \nu_\tau$ (ex.K^0)	[a] (1.04 ± 0.07) %	
Γ_{28}	$K^- 3\pi^0 \nu_\tau$ (ex.K^0, η)	[a] (4.8 ± 2.1) $\times 10^{-4}$	
Γ_{29}	$h^- 4\pi^0 \nu_\tau$ (ex.K^0)	(1.6 ± 0.4) $\times 10^{-3}$	
Γ_{30}	$h^- 4\pi^0 \nu_\tau$ (ex.K^0,η)	[a] (1.1 ± 0.4) $\times 10^{-3}$	
Γ_{31}	$a_1(1260)\nu_\tau \to \pi^- \gamma \nu_\tau$	(3.8 ± 1.5) $\times 10^{-4}$	
Γ_{32}	$K^- \geq 0\pi^0 \geq 0 K^0 \geq 0\gamma\ \nu_\tau$	(1.552 ± 0.029) %	
Γ_{33}	$K^- \geq 1$ (π^0 or K^0 or γ) ν_τ	(8.59 ± 0.28) $\times 10^{-3}$	
	Modes with K^0's		
Γ_{34}	K_S^0 (particles)$^- \nu_\tau$	(9.44 ± 0.28) $\times 10^{-3}$	
Γ_{35}	$h^- \overline{K}^0 \nu_\tau$	(9.87 ± 0.14) $\times 10^{-3}$	
Γ_{36}	$\pi^- \overline{K}^0 \nu_\tau$	[a] (8.40 ± 0.14) $\times 10^{-3}$	
Γ_{37}	$\pi^- \overline{K}^0$ (non-$K^*(892)^-$) ν_τ	(5.4 ± 2.1) $\times 10^{-4}$	
Γ_{38}	$K^- K^0 \nu_\tau$	[a] (1.48 ± 0.05) $\times 10^{-3}$	
Γ_{39}	$K^- K^0 \geq 0\pi^0 \nu_\tau$	(2.98 ± 0.08) $\times 10^{-3}$	
Γ_{40}	$h^- \overline{K}^0 \pi^0 \nu_\tau$	(5.32 ± 0.13) $\times 10^{-3}$	
Γ_{41}	$\pi^- \overline{K}^0 \pi^0 \nu_\tau$	[a] (3.82 ± 0.13) $\times 10^{-3}$	
Γ_{42}	$\overline{K}^0 \rho^- \nu_\tau$	(2.2 ± 0.5) $\times 10^{-3}$	
Γ_{43}	$K^- K^0 \pi^0 \nu_\tau$	[a] (1.50 ± 0.07) $\times 10^{-3}$	
Γ_{44}	$\pi^- \overline{K}^0 \geq 1\pi^0 \nu_\tau$	(4.08 ± 0.25) $\times 10^{-3}$	
Γ_{45}	$\pi^- \overline{K}^0 \pi^0 \pi^0 \nu_\tau$ (ex.K^0)	[a] (2.6 ± 2.3) $\times 10^{-4}$	
Γ_{46}	$K^- K^0 \pi^0 \pi^0 \nu_\tau$	< 1.6 $\times 10^{-4}$	CL=95%
Γ_{47}	$\pi^- K^0 \overline{K}^0 \nu_\tau$	(1.55 ± 0.24) $\times 10^{-3}$	
Γ_{48}	$\pi^- K_S^0 K_S^0 \nu_\tau$	[a] (2.33 ± 0.07) $\times 10^{-4}$	
Γ_{49}	$\pi^- K_S^0 K_L^0 \nu_\tau$	[a] (1.08 ± 0.24) $\times 10^{-3}$	
Γ_{50}	$\pi^- K_L^0 K_L^0 \nu_\tau$	(2.33 ± 0.07) $\times 10^{-4}$	
Γ_{51}	$\pi^- K^0 \overline{K}^0 \pi^0 \nu_\tau$	(3.6 ± 1.2) $\times 10^{-4}$	
Γ_{52}	$\pi^- K_S^0 K_S^0 \pi^0 \nu_\tau$	[a] (1.82 ± 0.21) $\times 10^{-5}$	
Γ_{53}	$K^{*-} K^0 \pi^0 \nu_\tau \to \pi^- K_S^0 K_S^0 \pi^0 \nu_\tau$	(1.08 ± 0.21) $\times 10^{-5}$	
Γ_{54}	$f_1(1285)\pi^- \nu_\tau \to \pi^- K_S^0 K_S^0 \pi^0 \nu_\tau$	(6.8 ± 1.5) $\times 10^{-6}$	
Γ_{55}	$f_1(1420)\pi^- \nu_\tau \to \pi^- K_S^0 K_S^0 \pi^0 \nu_\tau$	(2.4 ± 0.8) $\times 10^{-6}$	
Γ_{56}	$\pi^- K_S^0 K_L^0 \pi^0 \nu_\tau$	[a] (3.2 ± 1.2) $\times 10^{-4}$	
Γ_{57}	$\pi^- K_L^0 K_L^0 \pi^0 \nu_\tau$	(1.82 ± 0.21) $\times 10^{-5}$	
Γ_{58}	$K^- K_S^0 K_S^0 \nu_\tau$	< 6.3 $\times 10^{-7}$	CL=90%
Γ_{59}	$K^- K_S^0 K_S^0 \pi^0 \nu_\tau$	< 4.0 $\times 10^{-7}$	CL=90%
Γ_{60}	$K^0 h^+ h^- h^- \geq 0$ neutrals ν_τ	< 1.7 $\times 10^{-3}$	CL=95%
Γ_{61}	$K^0 h^+ h^- h^- \nu_\tau$	[a] (2.5 ± 2.0) $\times 10^{-4}$	
	Modes with three charged particles		
Γ_{62}	$h^- h^- h^+ \geq 0$ neutrals $\geq 0 K_L^0 \nu_\tau$	(15.21 ± 0.06) %	
Γ_{63}	$h^- h^- h^+ \geq 0$ neutrals ν_τ (ex. $K_S^0 \to \pi^+\pi^-$) ("3-prong")	(14.55 ± 0.06) %	
Γ_{64}	$h^- h^- h^+ \nu_\tau$	(9.80 ± 0.05) %	
Γ_{65}	$h^- h^- h^+ \nu_\tau$ (ex.K^0)	(9.46 ± 0.05) %	
Γ_{66}	$h^- h^- h^+ \nu_\tau$ (ex.K^0,ω)	(9.43 ± 0.05) %	
Γ_{67}	$\pi^- \pi^+ \pi^- \nu_\tau$	(9.31 ± 0.05) %	
Γ_{68}	$\pi^- \pi^+ \pi^- \nu_\tau$ (ex.K^0)	(9.02 ± 0.05) %	
Γ_{69}	$\pi^- \pi^+ \pi^- \nu_\tau$ (ex.K^0), non-axial vector	< 2.4 %	CL=95%

Γ_{70}	$\pi^-\pi^+\pi^-\nu_\tau$ (ex.K^0,ω)	[a]	(8.99 ± 0.05) %		
Γ_{71}	$h^-h^-h^+ \geq 1$ neutrals ν_τ		(5.29 ± 0.05) %		
Γ_{72}	$h^-h^-h^+ \geq 1\pi^0\nu_\tau$ (ex. K^0)		(5.09 ± 0.05) %		
Γ_{73}	$h^-h^-h^+\pi^0\nu_\tau$		(4.76 ± 0.05) %		
Γ_{74}	$h^-h^-h^+\pi^0\nu_\tau$ (ex.K^0)		(4.57 ± 0.05) %		
Γ_{75}	$h^-h^-h^+\pi^0\nu_\tau$ (ex. K^0, ω)		(2.79 ± 0.07) %		
Γ_{76}	$\pi^-\pi^+\pi^-\pi^0\nu_\tau$		(4.62 ± 0.05) %		
Γ_{77}	$\pi^-\pi^+\pi^-\pi^0\nu_\tau$ (ex.K^0)		(4.49 ± 0.05) %		
Γ_{78}	$\pi^-\pi^+\pi^-\pi^0\nu_\tau$ (ex.K^0,ω)	[a]	(2.74 ± 0.07) %		
Γ_{79}	$h^-\rho\pi^0\nu_\tau$				
Γ_{80}	$h^-\rho^+h^-\nu_\tau$				
Γ_{81}	$h^-\rho^-h^+\nu_\tau$				
Γ_{82}	$h^-h^-h^+ \geq 2\pi^0\nu_\tau$ (ex. K^0)		(5.17 ± 0.31) $\times 10^{-3}$		
Γ_{83}	$h^-h^-h^+2\pi^0\nu_\tau$		(5.05 ± 0.31) $\times 10^{-3}$		
Γ_{84}	$h^-h^-h^+2\pi^0\nu_\tau$ (ex.K^0)		(4.95 ± 0.31) $\times 10^{-3}$		
Γ_{85}	$h^-h^-h^+2\pi^0\nu_\tau$ (ex.K^0,ω,η)	[a]	(10 ± 4) $\times 10^{-4}$		
Γ_{86}	$h^-h^-h^+3\pi^0\nu_\tau$		(2.12 ± 0.30) $\times 10^{-4}$		
Γ_{87}	$2\pi^-\pi^+3\pi^0\nu_\tau$ (ex.K^0)		(1.94 ± 0.30) $\times 10^{-4}$		
Γ_{88}	$2\pi^-\pi^+3\pi^0\nu_\tau$ (ex.K^0, η, $f_1(1285)$)		(1.7 ± 0.4) $\times 10^{-4}$		
Γ_{89}	$2\pi^-\pi^+3\pi^0\nu_\tau$ (ex.K^0, η, ω, $f_1(1285)$)	[a]	(1.4 ± 2.7) $\times 10^{-5}$		
Γ_{90}	$K^-h^+h^- \geq 0$ neutrals ν_τ		(6.29 ± 0.14) $\times 10^{-3}$		
Γ_{91}	$K^-h^+\pi^-\nu_\tau$ (ex.K^0)		(4.37 ± 0.07) $\times 10^{-3}$		
Γ_{92}	$K^-h^+\pi^-\pi^0\nu_\tau$ (ex.K^0)		(8.6 ± 1.2) $\times 10^{-4}$		
Γ_{93}	$K^-\pi^+\pi^- \geq 0$ neutrals ν_τ		(4.77 ± 0.14) $\times 10^{-3}$		
Γ_{94}	$K^-\pi^+\pi^- \geq 0\pi^0\nu_\tau$ (ex.K^0)		(3.73 ± 0.13) $\times 10^{-3}$		
Γ_{95}	$K^-\pi^+\pi^-\nu_\tau$		(3.45 ± 0.07) $\times 10^{-3}$		
Γ_{96}	$K^-\pi^+\pi^-\nu_\tau$ (ex.K^0)		(2.93 ± 0.07) $\times 10^{-3}$		
Γ_{97}	$K^-\pi^+\pi^-\nu_\tau$ (ex.K^0,ω)	[a]	(2.93 ± 0.07) $\times 10^{-3}$		
Γ_{98}	$K^-\rho^0\nu_\tau \rightarrow K^-\pi^+\pi^-\nu_\tau$		(1.4 ± 0.5) $\times 10^{-3}$		
Γ_{99}	$K^-\pi^+\pi^-\pi^0\nu_\tau$		(1.31 ± 0.12) $\times 10^{-3}$		
Γ_{100}	$K^-\pi^+\pi^-\pi^0\nu_\tau$ (ex.K^0)		(7.9 ± 1.2) $\times 10^{-4}$		
Γ_{101}	$K^-\pi^+\pi^-\pi^0\nu_\tau$ (ex.K^0,η)		(7.6 ± 1.2) $\times 10^{-4}$		
Γ_{102}	$K^-\pi^+\pi^-\pi^0\nu_\tau$ (ex.K^0,ω)		(3.7 ± 0.9) $\times 10^{-4}$		
Γ_{103}	$K^-\pi^+\pi^-\pi^0\nu_\tau$ (ex.K^0,ω,η)	[a]	(3.9 ± 1.4) $\times 10^{-4}$		
Γ_{104}	$K^-\pi^+K^- \geq 0$ neut. ν_τ		< 9	$\times 10^{-4}$	CL=95%
Γ_{105}	$K^-K^+\pi^- \geq 0$ neut. ν_τ		(1.496± 0.033) $\times 10^{-3}$		
Γ_{106}	$K^-K^+\pi^-\nu_\tau$	[a]	(1.435± 0.027) $\times 10^{-3}$		
Γ_{107}	$K^-K^+\pi^-\pi^0\nu_\tau$	[a]	(6.1 ± 1.8) $\times 10^{-5}$		
Γ_{108}	$K^-K^+K^-\nu_\tau$		(2.2 ± 0.8) $\times 10^{-5}$		S=5.4
Γ_{109}	$K^-K^+K^-\nu_\tau$ (ex. ϕ)		< 2.5	$\times 10^{-6}$	CL=90%
Γ_{110}	$K^-K^+K^-\pi^0\nu_\tau$		< 4.8	$\times 10^{-6}$	CL=90%
Γ_{111}	$\pi^-K^+\pi^- \geq 0$ neut. ν_τ		< 2.5	$\times 10^{-3}$	CL=95%
Γ_{112}	$e^-e^-e^+\overline{\nu}_e\nu_\tau$		(2.8 ± 1.5) $\times 10^{-5}$		
Γ_{113}	$\mu^-e^-e^+\overline{\nu}_\mu\nu_\tau$		< 3.6	$\times 10^{-5}$	CL=90%

Modes with five charged particles

Γ_{114}	$3h^-2h^+ \geq 0$ neutrals ν_τ (ex. $K^0_S \rightarrow \pi^-\pi^+$) ("5-prong")		(9.9 ± 0.4) $\times 10^{-4}$		
Γ_{115}	$3h^-2h^+\nu_\tau$ (ex.K^0)		(8.22 ± 0.32) $\times 10^{-4}$		
Γ_{116}	$3\pi^-2\pi^+\nu_\tau$ (ex.K^0, ω)		(8.21 ± 0.31) $\times 10^{-4}$		
Γ_{117}	$3\pi^-2\pi^+\nu_\tau$ (ex.K^0, ω, $f_1(1285)$)	[a]	(7.69 ± 0.30) $\times 10^{-4}$		
Γ_{118}	$K^-2\pi^-2\pi^+\nu_\tau$ (ex.K^0)	[a]	(6 ±12) $\times 10^{-7}$		
Γ_{119}	$K^+3\pi^-\pi^+\nu_\tau$		< 5.0	$\times 10^{-6}$	CL=90%
Γ_{120}	$K^+K^-2\pi^-\pi^+\nu_\tau$		< 4.5	$\times 10^{-7}$	CL=90%
Γ_{121}	$3h^-2h^+\pi^0\nu_\tau$ (ex.K^0)		(1.64 ± 0.11) $\times 10^{-4}$		
Γ_{122}	$3\pi^-2\pi^+\pi^0\nu_\tau$ (ex.K^0)		(1.62 ± 0.11) $\times 10^{-4}$		
Γ_{123}	$3\pi^-2\pi^+\pi^0\nu_\tau$ (ex.K^0, η, $f_1(1285)$)		(1.11 ± 0.10) $\times 10^{-4}$		
Γ_{124}	$3\pi^-2\pi^+\pi^0\nu_\tau$ (ex.K^0, η, ω, $f_1(1285)$)	[a]	(3.8 ± 0.9) $\times 10^{-5}$		
Γ_{125}	$K^-2\pi^-2\pi^+\pi^0\nu_\tau$ (ex.K^0)	[a]	(1.1 ± 0.6) $\times 10^{-6}$		
Γ_{126}	$K^+3\pi^-\pi^+\pi^0\nu_\tau$		< 8	$\times 10^{-7}$	CL=90%
Γ_{127}	$3h^-2h^+2\pi^0\nu_\tau$		< 3.4	$\times 10^{-6}$	CL=90%

Miscellaneous other allowed modes

Γ_{128}	$(5\pi)^-\nu_\tau$		(7.8 ± 0.5) $\times 10^{-3}$		
Γ_{129}	$4h^-3h^+ \geq 0$ neutrals ν_τ ("7-prong")		< 3.0	$\times 10^{-7}$	CL=90%
Γ_{130}	$4h^-3h^+\nu_\tau$		< 4.3	$\times 10^{-7}$	CL=90%
Γ_{131}	$4h^-3h^+\pi^0\nu_\tau$		< 2.5	$\times 10^{-7}$	CL=90%
Γ_{132}	$X^-(S=-1)\nu_\tau$		(2.92 ± 0.04) %		
Γ_{133}	$K^*(892)^- \geq 0$ neutrals $\geq 0K^0_L\nu_\tau$		(1.42 ± 0.18) %		S=1.4
Γ_{134}	$K^*(892)^-\nu_\tau$		(1.20 ± 0.07) %		S=1.8
Γ_{135}	$K^*(892)^-\nu_\tau \rightarrow \pi^-\overline{K}^0\nu_\tau$		(7.83 ± 0.26) $\times 10^{-3}$		
Γ_{136}	$K^*(892)^0K^- \geq 0$ neutrals ν_τ		(3.2 ± 1.4) $\times 10^{-3}$		
Γ_{137}	$K^*(892)^0K^-\nu_\tau$		(2.1 ± 0.4) $\times 10^{-3}$		
Γ_{138}	$\overline{K}^*(892)^0\pi^- \geq 0$ neutrals ν_τ		(3.8 ± 1.7) $\times 10^{-3}$		
Γ_{139}	$\overline{K}^*(892)^0\pi^-\nu_\tau$		(2.2 ± 0.5) $\times 10^{-3}$		
Γ_{140}	$(\overline{K}^*(892)\pi)^-\nu_\tau \rightarrow \pi^-\overline{K}^0\pi^0\nu_\tau$		(1.0 ± 0.4) $\times 10^{-3}$		
Γ_{141}	$K_1(1270)^-\nu_\tau$		(4.7 ± 1.1) $\times 10^{-3}$		
Γ_{142}	$K_1(1400)^-\nu_\tau$		(1.7 ± 2.6) $\times 10^{-3}$		S=1.7
Γ_{143}	$K^*(1410)^-\nu_\tau$		(1.5 $^{+\ 1.4}_{-\ 1.0}$) $\times 10^{-3}$		
Γ_{144}	$K^*_0(1430)^-\nu_\tau$		< 5	$\times 10^{-4}$	CL=95%
Γ_{145}	$K^*_2(1430)^-\nu_\tau$		< 3	$\times 10^{-3}$	CL=95%
Γ_{146}	$a_0(980)^- \geq 0$ neutrals ν_τ				
Γ_{147}	$\eta\pi^-\nu_\tau$		< 9.9	$\times 10^{-5}$	CL=95%
Γ_{148}	$\eta\pi^-\pi^0\nu_\tau$	[a]	(1.39 ± 0.07) $\times 10^{-3}$		
Γ_{149}	$\eta\pi^-\pi^0\pi^0\nu_\tau$	[a]	(1.9 ± 0.4) $\times 10^{-4}$		
Γ_{150}	$\eta K^-\nu_\tau$	[a]	(1.55 ± 0.08) $\times 10^{-4}$		
Γ_{151}	$\eta K^*(892)^-\nu_\tau$		(1.38 ± 0.15) $\times 10^{-4}$		
Γ_{152}	$\eta K^-\pi^0\nu_\tau$	[a]	(4.8 ± 1.2) $\times 10^{-5}$		
Γ_{153}	$\eta K^-\pi^0$(non-$K^*(892)$)ν_τ		< 3.5	$\times 10^{-5}$	CL=90%
Γ_{154}	$\eta\overline{K}^0\pi^-\nu_\tau$	[a]	(9.4 ± 1.5) $\times 10^{-5}$		
Γ_{155}	$\eta\overline{K}^0\pi^-\pi^0\nu_\tau$		< 5.0	$\times 10^{-5}$	CL=90%
Γ_{156}	$\eta K^-K^0\nu_\tau$		< 9.0	$\times 10^{-6}$	CL=90%
Γ_{157}	$\eta\pi^+\pi^-\pi^- \geq 0$ neutrals ν_τ		< 3	$\times 10^{-3}$	CL=90%
Γ_{158}	$\eta\pi^-\pi^+\pi^-\nu_\tau$ (ex.K^0)	[a]	(2.19 ± 0.13) $\times 10^{-4}$		
Γ_{159}	$\eta\pi^-\pi^+\pi^-\nu_\tau$ (ex.K^0,$f_1(1285)$)		(9.9 ± 1.6) $\times 10^{-5}$		
Γ_{160}	$\eta a_1(1260)^-\nu_\tau \rightarrow \eta\pi^-\rho^0\nu_\tau$		< 3.9	$\times 10^{-4}$	CL=90%
Γ_{161}	$\eta\eta\pi^-\nu_\tau$		< 7.4	$\times 10^{-6}$	CL=90%
Γ_{162}	$\eta\eta\pi^-\pi^0\nu_\tau$		< 2.0	$\times 10^{-4}$	CL=95%
Γ_{163}	$\eta\eta K^-\nu_\tau$		< 3.0	$\times 10^{-6}$	CL=90%
Γ_{164}	$\eta'(958)\pi^-\nu_\tau$		< 4.0	$\times 10^{-6}$	CL=90%
Γ_{165}	$\eta'(958)\pi^-\pi^0\nu_\tau$		< 1.2	$\times 10^{-5}$	CL=90%
Γ_{166}	$\eta'(958)K^-\nu_\tau$		< 2.4	$\times 10^{-6}$	CL=90%
Γ_{167}	$\phi\pi^-\nu_\tau$		(3.4 ± 0.6) $\times 10^{-5}$		
Γ_{168}	$\phi K^-\nu_\tau$	[a]	(4.4 ± 1.6) $\times 10^{-5}$		
Γ_{169}	$f_1(1285)\pi^-\nu_\tau$		(3.9 ± 0.5) $\times 10^{-4}$		S=1.9
Γ_{170}	$f_1(1285)\pi^-\nu_\tau \rightarrow \eta\pi^-\pi^+\pi^-\nu_\tau$		(1.18 ± 0.07) $\times 10^{-4}$		S=1.3
Γ_{171}	$f_1(1285)\pi^-\nu_\tau \rightarrow 3\pi^-2\pi^+\nu_\tau$	[a]	(5.2 ± 0.4) $\times 10^{-5}$		
Γ_{172}	$\pi(1300)^-\nu_\tau \rightarrow (\rho\pi)^-\nu_\tau \rightarrow (3\pi)^-\nu_\tau$		< 1.0	$\times 10^{-4}$	CL=90%
Γ_{173}	$\pi(1300)^-\nu_\tau \rightarrow ((\pi\pi)_{S-\text{wave}}\,\pi)^-\nu_\tau \rightarrow (3\pi)^-\nu_\tau$		< 1.9	$\times 10^{-4}$	CL=90%
Γ_{174}	$h^-\omega \geq 0$ neutrals ν_τ		(2.40 ± 0.08) %		
Γ_{175}	$h^-\omega\nu_\tau$		(1.99 ± 0.06) %		
Γ_{176}	$\pi^-\omega\nu_\tau$	[a]	(1.95 ± 0.06) %		
Γ_{177}	$K^-\omega\nu_\tau$	[a]	(4.1 ± 0.9) $\times 10^{-4}$		
Γ_{178}	$h^-\omega\pi^0\nu_\tau$	[a]	(4.1 ± 0.4) $\times 10^{-3}$		
Γ_{179}	$h^-\omega2\pi^0\nu_\tau$		(1.4 ± 0.5) $\times 10^{-4}$		
Γ_{180}	$\pi^-\omega2\pi^0\nu_\tau$	[a]	(7.1 ± 1.6) $\times 10^{-5}$		
Γ_{181}	$h^-2\omega\nu_\tau$		< 5.4	$\times 10^{-7}$	CL=90%
Γ_{182}	$2h^-h^+\omega\nu_\tau$		(1.20 ± 0.22) $\times 10^{-4}$		
Γ_{183}	$2\pi^-\pi^+\omega\nu_\tau$ (ex.K^0)	[a]	(8.4 ± 0.6) $\times 10^{-5}$		

Lepton Family number (LF), Lepton number (L), or Baryon number (B) violating modes

L means lepton number violation (*e.g.* $\tau^- \rightarrow e^+\pi^-\pi^-$). Following common usage, *LF* means lepton family violation *and not* lepton number violation (*e.g.* $\tau^- \rightarrow e^-\pi^+\pi^-$). *B* means baryon number violation.

Γ_{184}	$e^-\gamma$	LF	< 3.3	$\times 10^{-8}$	CL=90%
Γ_{185}	$\mu^-\gamma$	LF	< 4.4	$\times 10^{-8}$	CL=90%
Γ_{186}	$e^-\pi^0$	LF	< 8.0	$\times 10^{-8}$	CL=90%
Γ_{187}	$\mu^-\pi^0$	LF	< 1.1	$\times 10^{-7}$	CL=90%
Γ_{188}	$e^-K^0_S$	LF	< 2.6	$\times 10^{-8}$	CL=90%
Γ_{189}	$\mu^-K^0_S$	LF	< 2.3	$\times 10^{-8}$	CL=90%
Γ_{190}	$e^-\eta$	LF	< 9.2	$\times 10^{-8}$	CL=90%
Γ_{191}	$\mu^-\eta$	LF	< 6.5	$\times 10^{-8}$	CL=90%
Γ_{192}	$e^-\rho^0$	LF	< 1.8	$\times 10^{-8}$	CL=90%
Γ_{193}	$\mu^-\rho^0$	LF	< 1.2	$\times 10^{-8}$	CL=90%
Γ_{194}	$e^-\omega$	LF	< 4.8	$\times 10^{-8}$	CL=90%
Γ_{195}	$\mu^-\omega$	LF	< 4.7	$\times 10^{-8}$	CL=90%

Γ_{196}	$e^- K^*(892)^0$	LF	<	3.2	$\times 10^{-8}$	CL=90%
Γ_{197}	$\mu^- K^*(892)^0$	LF	<	5.9	$\times 10^{-8}$	CL=90%
Γ_{198}	$e^- \overline{K}^*(892)^0$	LF	<	3.4	$\times 10^{-8}$	CL=90%
Γ_{199}	$\mu^- \overline{K}^*(892)^0$	LF	<	7.0	$\times 10^{-8}$	CL=90%
Γ_{200}	$e^- \eta'(958)$	LF	<	1.6	$\times 10^{-7}$	CL=90%
Γ_{201}	$\mu^- \eta'(958)$	LF	<	1.3	$\times 10^{-7}$	CL=90%
Γ_{202}	$e^- f_0(980) \rightarrow e^- \pi^+ \pi^-$	LF	<	3.2	$\times 10^{-8}$	CL=90%
Γ_{203}	$\mu^- f_0(980) \rightarrow \mu^- \pi^+ \pi^-$	LF	<	3.4	$\times 10^{-8}$	CL=90%
Γ_{204}	$e^- \phi$	LF	<	3.1	$\times 10^{-8}$	CL=90%
Γ_{205}	$\mu^- \phi$	LF	<	8.4	$\times 10^{-8}$	CL=90%
Γ_{206}	$e^- e^+ e^-$	LF	<	2.7	$\times 10^{-8}$	CL=90%
Γ_{207}	$e^- \mu^+ \mu^-$	LF	<	2.7	$\times 10^{-8}$	CL=90%
Γ_{208}	$e^+ \mu^- \mu^-$	LF	<	1.7	$\times 10^{-8}$	CL=90%
Γ_{209}	$\mu^- e^+ e^-$	LF	<	1.8	$\times 10^{-8}$	CL=90%
Γ_{210}	$\mu^+ e^- e^-$	LF	<	1.5	$\times 10^{-8}$	CL=90%
Γ_{211}	$\mu^- \mu^+ \mu^-$	LF	<	2.1	$\times 10^{-8}$	CL=90%
Γ_{212}	$e^- \pi^+ \pi^-$	LF	<	2.3	$\times 10^{-8}$	CL=90%
Γ_{213}	$e^+ \pi^- \pi^-$	L	<	2.0	$\times 10^{-8}$	CL=90%
Γ_{214}	$\mu^- \pi^+ \pi^-$	LF	<	2.1	$\times 10^{-8}$	CL=90%
Γ_{215}	$\mu^+ \pi^- \pi^-$	L	<	3.9	$\times 10^{-8}$	CL=90%
Γ_{216}	$e^- \pi^+ K^-$	LF	<	3.7	$\times 10^{-8}$	CL=90%
Γ_{217}	$e^- \pi^- K^+$	LF	<	3.1	$\times 10^{-8}$	CL=90%
Γ_{218}	$e^+ \pi^- K^-$	L	<	3.2	$\times 10^{-8}$	CL=90%
Γ_{219}	$e^- K^0_S K^0_S$	LF	<	7.1	$\times 10^{-8}$	CL=90%
Γ_{220}	$e^- K^+ K^-$	LF	<	3.4	$\times 10^{-8}$	CL=90%
Γ_{221}	$e^+ K^- K^-$	L	<	3.3	$\times 10^{-8}$	CL=90%
Γ_{222}	$\mu^- \pi^+ K^-$	LF	<	8.6	$\times 10^{-8}$	CL=90%
Γ_{223}	$\mu^- \pi^- K^+$	LF	<	4.5	$\times 10^{-8}$	CL=90%
Γ_{224}	$\mu^+ \pi^- K^-$	L	<	4.8	$\times 10^{-8}$	CL=90%
Γ_{225}	$\mu^- K^0_S K^0_S$	LF	<	8.0	$\times 10^{-8}$	CL=90%
Γ_{226}	$\mu^- K^+ K^-$	LF	<	4.4	$\times 10^{-8}$	CL=90%
Γ_{227}	$\mu^+ K^- K^-$	L	<	4.7	$\times 10^{-8}$	CL=90%
Γ_{228}	$e^- \pi^0 \pi^0$	LF	<	6.5	$\times 10^{-6}$	CL=90%
Γ_{229}	$\mu^- \pi^0 \pi^0$	LF	<	1.4	$\times 10^{-5}$	CL=90%
Γ_{230}	$e^- \eta \eta$	LF	<	3.5	$\times 10^{-5}$	CL=90%
Γ_{231}	$\mu^- \eta \eta$	LF	<	6.0	$\times 10^{-5}$	CL=90%
Γ_{232}	$e^- \pi^0 \eta$	LF	<	2.4	$\times 10^{-5}$	CL=90%
Γ_{233}	$\mu^- \pi^0 \eta$	LF	<	2.2	$\times 10^{-5}$	CL=90%
Γ_{234}	$p \mu^- \mu^-$	L,B	<	4.4	$\times 10^{-7}$	CL=90%
Γ_{235}	$\overline{p} \mu^+ \mu^-$	L,B	<	3.3	$\times 10^{-7}$	CL=90%
Γ_{236}	$\overline{p} \gamma$	L,B	<	3.5	$\times 10^{-6}$	CL=90%
Γ_{237}	$\overline{p} \pi^0$	L,B	<	1.5	$\times 10^{-5}$	CL=90%
Γ_{238}	$\overline{p} 2\pi^0$	L,B	<	3.3	$\times 10^{-5}$	CL=90%
Γ_{239}	$\overline{p} \eta$	L,B	<	8.9	$\times 10^{-6}$	CL=90%
Γ_{240}	$\overline{p} \pi^0 \eta$	L,B	<	2.7	$\times 10^{-5}$	CL=90%
Γ_{241}	$\Lambda \pi^-$	L,B	<	7.2	$\times 10^{-8}$	CL=90%
Γ_{242}	$\overline{\Lambda} \pi^-$	L,B	<	1.4	$\times 10^{-7}$	CL=90%
Γ_{243}	e^- light boson	LF	<	2.7	$\times 10^{-3}$	CL=95%
Γ_{244}	μ^- light boson	LF	<	5	$\times 10^{-3}$	CL=95%

[a] Basis mode for the τ.

[b] See the Particle Listings below for the energy limits used in this measurement.

CONSTRAINED FIT INFORMATION

An overall fit to 85 branching ratios uses 169 measurements and one constraint to determine 46 parameters. The overall fit has a $\chi^2 = 134.9$ for 124 degrees of freedom.

The following *off-diagonal* array elements are the correlation coefficients $\langle \delta x_i \delta x_j \rangle / (\delta x_i \cdot \delta x_j)$, in percent, from the fit to the branching fractions, $x_i \equiv \Gamma_i / \Gamma_{\text{total}}$.

x_5	18									
x_9	2	−1								
x_{10}	3	4	5							
x_{14}	−18	−19	−17	−5						
x_{16}	−1	−1	1	−2	−9					
x_{20}	−11	−11	−14	−4	−46	−1				
x_{23}	−1	0	−2	−3	−1	−14	−10			
x_{27}	−6	−5	−10	−1	0	0	−39	1		
x_{28}	−1	−1	−1	−2	0	−13	−3	−23	−11	
x_{30}	−4	−4	−11	−1	−9	0	7	−2	−44	2
x_{36}	−2	−2	−3	−1	−1	0	−2	0	−1	0
x_{38}	0	0	0	0	0	−2	0	−3	0	−3
x_{41}	−2	−2	−2	−1	−1	0	−2	0	−1	0
x_{43}	−1	−1	−1	−1	0	−3	0	−5	0	−5
x_{45}	−5	−5	−5	−2	−3	−1	−5	−2	−1	−2
x_{48}	0	0	0	0	0	0	0	0	0	0
x_{49}	−5	−5	−5	−2	−3	−1	−5	−2	−1	−2
x_{52}	0	0	0	0	0	0	0	−1	0	−1
x_{56}	−2	−2	−2	−1	−1	−1	−2	−1	−1	−1
x_{61}	−5	−5	−5	−2	−3	−1	−4	−2	−1	−2
x_{70}	−7	−9	4	−2	−6	3	−12	−2	−7	−1
x_{78}	−4	−4	−5	0	−9	0	1	1	−1	1
x_{85}	0	0	−2	0	−2	0	0	0	2	0
x_{89}	0	0	0	0	0	0	0	0	0	0
x_{97}	−2	−2	−1	−1	−1	−1	−4	−1	−2	−1
x_{103}	1	1	0	−1	1	−1	−1	−1	0	−1
x_{106}	−2	−2	2	−1	−1	2	−2	−1	−1	−1
x_{107}	0	0	0	0	0	0	0	0	0	0
x_{117}	−1	0	0	0	0	0	−1	0	−1	0
x_{118}	0	0	0	0	0	0	0	0	0	0
x_{124}	0	0	0	0	0	0	0	0	0	0
x_{125}	0	0	0	0	0	0	0	0	0	0
x_{148}	−1	−1	−1	0	−1	0	−2	−1	0	−1
x_{149}	−1	−1	−1	0	0	0	−1	0	0	0
x_{150}	0	0	0	0	0	0	0	−1	0	−1
x_{152}	0	0	0	0	0	0	0	0	0	0
x_{154}	0	0	0	0	0	0	0	0	0	0
x_{158}	−1	−1	−1	0	0	0	−1	0	0	0
x_{168}	0	0	0	0	0	0	0	0	0	0
x_{171}	0	0	0	0	0	0	−1	0	0	0
x_{176}	−3	−3	−3	−1	−4	−1	−1	0	−1	0
x_{177}	0	0	0	0	0	0	0	0	0	0
x_{178}	−2	−2	−5	−1	−3	0	−2	−1	2	−1
x_{180}	0	0	0	0	0	0	0	0	0	0
x_{183}	−1	0	0	0	0	0	−1	0	0	0
	x_3	x_5	x_9	x_{10}	x_{14}	x_{16}	x_{20}	x_{23}	x_{27}	x_{28}

See key on page 885

	x_{30}	x_{36}	x_{38}	x_{41}	x_{43}	x_{45}	x_{48}	x_{49}	x_{52}	x_{56}
x_{36}	0									
x_{38}	0	−22								
x_{41}	0	−13	4							
x_{43}	0	2	−21	−20						
x_{45}	0	−3	0	−6	0					
x_{48}	0	−1	1	−4	1	0				
x_{49}	0	−5	0	−4	−1	−10	0			
x_{52}	0	0	7	0	5	0	−7	0		
x_{56}	0	−2	0	−2	−1	−4	0	−8	0	
x_{61}	0	−2	0	−2	0	−4	0	−4	0	−2
x_{70}	−5	−2	0	−1	0	−4	1	−4	0	−2
x_{78}	3	1	0	1	0	2	0	2	0	1
x_{85}	2	0	0	0	0	0	0	0	0	0
x_{89}	0	0	0	0	0	0	0	0	−1	0
x_{97}	−1	−1	0	−1	0	−2	0	−2	0	−1
x_{103}	−1	−1	0	−1	0	−1	0	−1	0	−1
x_{106}	−1	−1	0	0	0	−1	0	−1	0	0
x_{107}	0	0	0	0	0	0	0	0	0	0
x_{117}	−1	0	0	0	0	−1	0	−1	0	0
x_{118}	0	0	0	0	0	0	0	0	0	0
x_{124}	0	0	0	0	0	0	0	0	0	0
x_{125}	0	0	0	0	0	0	0	0	0	0
x_{148}	−2	0	0	0	0	−1	1	−1	0	0
x_{149}	0	0	0	0	0	−1	0	−1	0	0
x_{150}	0	0	0	0	0	0	1	0	0	0
x_{152}	0	0	0	0	0	0	0	0	0	0
x_{154}	0	0	0	0	0	0	0	−1	0	0
x_{158}	−1	0	0	0	0	−1	0	−1	0	0
x_{168}	0	0	0	0	0	0	0	0	0	0
x_{171}	0	0	0	0	0	0	0	0	0	0
x_{176}	1	−1	0	0	0	−1	0	−1	0	0
x_{177}	0	0	0	0	0	0	0	0	0	0
x_{178}	2	−1	0	0	0	−1	0	−1	0	0
x_{180}	0	0	0	0	0	0	0	0	0	0
x_{183}	−1	0	0	0	0	0	0	0	0	0

	x_{61}	x_{70}	x_{78}	x_{85}	x_{89}	x_{97}	x_{103}	x_{106}	x_{107}	x_{117}
x_{70}	−4									
x_{78}	2	−19								
x_{85}	0	−1	−8							
x_{89}	0	−1	−1	0						
x_{97}	−2	19	−6	0	0					
x_{103}	−1	−4	−14	−1	0	−1				
x_{106}	−1	15	−4	0	0	0	−1			
x_{107}	0	−1	−1	0	0	0	−3	0		
x_{117}	−1	0	0	0	−4	0	0	0	0	
x_{118}	0	0	0	0	0	0	0	0	0	−1
x_{124}	0	0	0	0	0	0	0	0	0	3
x_{125}	0	0	0	0	0	0	0	0	0	−1
x_{148}	−1	0	0	−5	0	0	0	0	0	0
x_{149}	−1	−1	0	0	−11	0	0	0	0	10
x_{150}	0	2	0	0	0	0	−1	1	0	0
x_{152}	0	0	0	−1	0	0	0	0	0	0
x_{154}	0	0	0	0	−2	0	0	0	0	0
x_{158}	−1	−1	0	0	−8	0	0	0	0	47
x_{168}	0	−1	0	0	0	1	0	1	0	0
x_{171}	0	0	0	0	−2	0	0	0	0	35
x_{176}	−1	−9	−67	−3	0	−2	10	−2	0	0
x_{177}	0	0	12	0	0	−2	−58	0	0	0
x_{178}	−1	−2	−11	−64	−1	−1	−1	−1	0	0
x_{180}	0	0	0	0	−16	0	0	0	0	8
x_{183}	0	0	0	0	−4	0	0	0	0	39

	x_{118}	x_{124}	x_{125}	x_{148}	x_{149}	x_{150}	x_{152}	x_{154}	x_{158}	x_{168}
x_{124}	0									
x_{125}	0	−1								
x_{148}	0	0	0							
x_{149}	0	2	0	0						
x_{150}	0	0	0	4	0					
x_{152}	0	0	0	1	0	1				
x_{154}	0	0	0	2	−1	1	0			
x_{158}	−1	3	−1	0	25	0	0	0		
x_{168}	0	0	0	0	0	0	0	0	0	
x_{171}	−1	1	0	0	4	0	0	0	20	0
x_{176}	0	0	0	0	0	0	0	0	0	0
x_{177}	0	0	0	0	0	0	0	0	0	0
x_{178}	0	0	0	0	0	0	0	0	0	0
x_{180}	0	2	0	0	10	0	0	−1	20	0
x_{183}	−1	−2	−1	0	17	0	0	0	39	0

	x_{171}	x_{176}	x_{177}	x_{178}	x_{180}
x_{176}	0				
x_{177}	0	−14			
x_{178}	0	−4	0		
x_{180}	3	0	0	0	
x_{183}	17	0	0	0	14

See the related review(s):

τ Branching Fractions

$(\Gamma(\tau^+) - \Gamma(\tau^-)) / (\Gamma(\tau^+) + \Gamma(\tau^-))$

$\tau^\pm \to \pi^\pm K^0_S \nu_\tau$ (RATE DIFFERENCE) / (RATE SUM)

VALUE (%)	DOCUMENT ID		TECN	COMMENT
−0.36 ± 0.23 ± 0.11	LEES	12M	BABR	476 fb^{-1} $E^{ee}_{\rm cm}$ = 10.6 GeV

τ^- BRANCHING RATIOS

$\Gamma(\text{particle}^- \geq 0 \text{ neutrals} \geq 0 K^0 \nu_\tau(\text{"1-prong"}))/\Gamma_{\text{total}}$ Γ_1/Γ

$\Gamma_1/\Gamma = (\Gamma_3+\Gamma_5+\Gamma_9+\Gamma_{10}+\Gamma_{14}+\Gamma_{16}+\Gamma_{20}+\Gamma_{23}+\Gamma_{27}+\Gamma_{28}+\Gamma_{30}+\Gamma_{36}+\Gamma_{38}+\Gamma_{41}+\Gamma_{43}+\Gamma_{45}+\Gamma_{48}+\Gamma_{49}+\Gamma_{50}+\Gamma_{52}+\Gamma_{56}+\Gamma_{57}+0.7212\Gamma_{148}+0.7212\Gamma_{150}+0.7212\Gamma_{152}+0.7212\Gamma_{154}+0.340\Gamma_{168}+0.0840\Gamma_{176}+0.0840\Gamma_{177}+0.0840\Gamma_{178})/\Gamma$

The charged particle here can be e, μ, or hadron. In many analyses, the sum of the topological branching fractions (1, 3, and 5 prongs) is constrained to be unity. Since the 5-prong fraction is very small, the measured 1-prong and 3-prong fractions are highly correlated and cannot be treated as independent quantities in our overall fit. We arbitrarily choose to use the 3-prong fraction in our fit, and leave the 1-prong fraction out. We do, however, use these 1-prong measurements in our average below.

VALUE (%)	EVTS	DOCUMENT ID		TECN	COMMENT
85.24 ± 0.06 OUR FIT					
85.26 ± 0.13 OUR AVERAGE		Error includes scale factor of 1.6. See the ideogram below.			
• • • We use the following data for averages but not for fits. • • •					
85.316 ± 0.093 ± 0.049	78k	[1] ABREU	01M	DLPH	1992–1995 LEP runs
85.274 ± 0.105 ± 0.073		[2] ACHARD	01D	L3	1992–1995 LEP runs
84.48 ± 0.27 ± 0.23		ACTON	92H	OPAL	1990–1991 LEP runs
• • • We do not use the following data for averages, fits, limits, etc. • • •					
85.45 $^{+0.69}_{-0.73}$ ± 0.65		DECAMP	92C	ALEP	Repl. by SCHAEL 05C

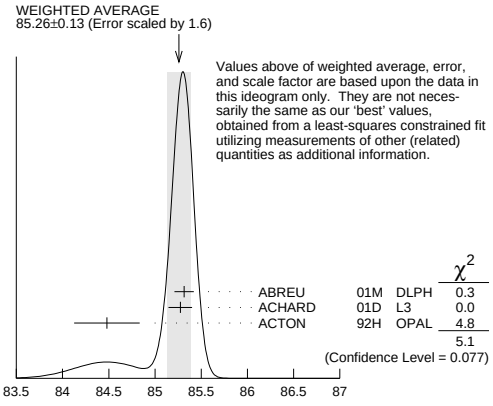

$\Gamma(\text{particle}^- \geq 0 \text{ neutrals} \geq 0 K^0 \nu_\tau(\text{"1-prong"}))/\Gamma_{\text{total}}$ (%)

[1] The correlation coefficients between this measurement and the ABREU 01M measurements of B($\tau \to$ 3-prong) and B($\tau \to$ 5-prong) are −0.98 and −0.08 respectively.

[2] The correlation coefficients between this measurement and the ACHARD 01D measurements of B($\tau \to$ "3-prong") and B($\tau \to$ "5-prong") are -0.978 and -0.082 respectively.

$\Gamma(\text{particle}^- \geq 0 \text{ neutrals} \geq 0K^0_L\nu_\tau)/\Gamma_{\text{total}}$ Γ_2/Γ

$\Gamma_2/\Gamma = (\Gamma_3+\Gamma_5+\Gamma_9+\Gamma_{10}+\Gamma_{14}+\Gamma_{16}+\Gamma_{20}+\Gamma_{23}+\Gamma_{27}+\Gamma_{28}+\Gamma_{30}+0.6534\Gamma_{36}+0.6534\Gamma_{38}+0.6534\Gamma_{41}+0.6534\Gamma_{43}+0.6534\Gamma_{45}+0.0942\Gamma_{48}+0.3069\Gamma_{49}+\Gamma_{50}+0.0942\Gamma_{52}+0.3069\Gamma_{56}+\Gamma_{57}+0.7212\Gamma_{148}+0.7212\Gamma_{150}+0.7212\Gamma_{152}+0.4712\Gamma_{154}+0.1049\Gamma_{168}+0.0840\Gamma_{176}+0.0840\Gamma_{177}+0.0840\Gamma_{178})/\Gamma$

VALUE (%)	EVTS	DOCUMENT ID		TECN	COMMENT
84.58±0.06 OUR FIT					
85.1 ±0.4 OUR AVERAGE					
• • • We use the following data for averages but not for fits. • • •					
85.6 ±0.6 ±0.3	3300	[1] ADEVA	91F	L3	E^{ee}_{cm}= 88.3–94.3 GeV
84.9 ±0.4 ±0.3		BEHREND	89B	CELL	E^{ee}_{cm}= 14–47 GeV
84.7 ±0.8 ±0.6		[2] AIHARA	87B	TPC	E^{ee}_{cm}= 29 GeV
• • • We do not use the following data for averages, fits, limits, etc. • • •					
86.4 ±0.3 ±0.3		ABACHI	89B	HRS	E^{ee}_{cm}= 29 GeV
87.1 ±1.0 ±0.7		[3] BURCHAT	87	MRK2	E^{ee}_{cm}= 29 GeV
87.2 ±0.5 ±0.8		SCHMIDKE	86	MRK2	E^{ee}_{cm}= 29 GeV
84.7 ±1.1 $^{+1.6}_{-1.3}$	169	[4] ALTHOFF	85	TASS	E^{ee}_{cm}= 34.5 GeV
86.1 ±0.5 ±0.9		BARTEL	85F	JADE	E^{ee}_{cm}= 34.6 GeV
87.8 ±1.3 ±3.9		[5] BERGER	85	PLUT	E^{ee}_{cm}= 34.6 GeV
86.7 ±0.3 ±0.6		FERNANDEZ	85	MAC	E^{ee}_{cm}= 29 GeV

[1] Not independent of ADEVA 91F $\Gamma(h^-h^-h^+ \geq 0 \text{ neutrals} \geq 0K^0_L\nu_\tau)/\Gamma_{\text{total}}$ value.

[2] Not independent of AIHARA 87B $\Gamma(\mu^-\overline{\nu}_\mu\nu_\tau)/\Gamma_{\text{total}}$, $\Gamma(e^-\overline{\nu}_e\nu_\tau)/\Gamma_{\text{total}}$, and $\Gamma(h^- \geq 0 \text{ neutrals} \geq 0K^0_L\nu_\tau)/\Gamma_{\text{total}}$ values.

[3] Not independent of SCHMIDKE 86 value (also not independent of BURCHAT 87 value for $\Gamma(h^-h^-h^+ \geq 0 \text{ neutrals} \geq 0K^0_L\nu_\tau)/\Gamma_{\text{total}}$.

[4] Not independent of ALTHOFF 85 $\Gamma(\mu^-\overline{\nu}_\mu\nu_\tau)/\Gamma_{\text{total}}$, $\Gamma(e^-\overline{\nu}_e\nu_\tau)/\Gamma_{\text{total}}$, $\Gamma(h^- \geq 0 \text{ neutrals} \geq 0K^0_L\nu_\tau)/\Gamma_{\text{total}}$, and $\Gamma(h^-h^-h^+ \geq 0 \text{ neutrals} \geq 0K^0_L\nu_\tau)/\Gamma_{\text{total}}$ values.

[5] Not independent of (1-prong + $0\pi^0$) and (1-prong + $\geq 1\pi^0$) values.

$\Gamma(\mu^-\overline{\nu}_\mu\nu_\tau)/\Gamma_{\text{total}}$ Γ_3/Γ

To minimize the effect of experiments with large systematic errors, we exclude experiments which together would contribute 5% of the weight in the average.

VALUE (%)	EVTS	DOCUMENT ID		TECN	COMMENT
17.39 ±0.04 OUR FIT					
17.33 ±0.05 OUR AVERAGE					
17.319±0.070±0.032	54k	[1] SCHAEL	05C	ALEP	1991-1995 LEP runs
17.34 ±0.09 ±0.06	31.4k	ABBIENDI	03	OPAL	1990-1995 LEP runs
17.342±0.110±0.067	21.5k	[2] ACCIARRI	01F	L3	1991-1995 LEP runs
17.325±0.095±0.077	27.7k	ABREU	99X	DLPH	1991-1995 LEP runs
• • • We use the following data for averages but not for fits. • • •					
17.37 ±0.08 ±0.18		[3] ANASTASSOV	97	CLEO	E^{ee}_{cm}= 10.6 GeV
• • • We do not use the following data for averages, fits, limits, etc. • • •					
17.31 ±0.11 ±0.05	20.7k	BUSKULIC	96C	ALEP	Repl. by SCHAEL 05C
17.02 ±0.19 ±0.24	6586	ABREU	95T	DLPH	Repl. by ABREU 99X
17.36 ±0.27	7941	AKERS	95I	OPAL	Repl. by ABBIENDI 03
17.6 ±0.4 ±0.4	2148	ADRIANI	93M	L3	Repl. by ACCIARRI 01F
17.4 ±0.3 ±0.5		[4] ALBRECHT	93G	ARG	E^{ee}_{cm}= 9.4–10.6 GeV
17.35 ±0.41 ±0.37		DECAMP	92C	ALEP	1989-1990 LEP runs
17.7 ±0.8 ±0.4	568	BEHREND	90	CELL	E^{ee}_{cm}= 35 GeV
17.4 ±1.0	2197	ADEVA	88	MRKJ	E^{ee}_{cm}= 14–16 GeV
17.7 ±1.2 ±0.7		AIHARA	87B	TPC	E^{ee}_{cm}= 29 GeV
18.3 ±0.9 ±0.8		BURCHAT	87	MRK2	E^{ee}_{cm}= 29 GeV
18.6 ±0.8 ±0.7	558	[5] BARTEL	86D	JADE	E^{ee}_{cm}= 34.6 GeV
12.9 ±1.7 $^{+0.7}_{-0.5}$		ALTHOFF	85	TASS	E^{ee}_{cm}= 34.5 GeV
18.0 ±0.9 ±0.5	473	[5] ASH	85B	MAC	E^{ee}_{cm}= 29 GeV
18.0 ±1.0 ±0.6		[6] BALTRUSAIT...85		MRK3	E^{ee}_{cm}= 3.77 GeV
19.4 ±1.6 ±1.7	153	BERGER	85	PLUT	E^{ee}_{cm}= 34.6 GeV
17.6 ±2.6 ±2.1	47	BEHREND	83C	CELL	E^{ee}_{cm}= 34 GeV
17.8 ±2.0 ±1.8		BERGER	81B	PLUT	E^{ee}_{cm}= 9–32 GeV

[1] See footnote to SCHAEL 05C $\Gamma(\tau^- \to e^-\overline{\nu}_e\nu_\tau)/\Gamma_{\text{total}}$ measurement for correlations with other measurements.

[2] The correlation coefficient between this measurement and the ACCIARRI 01F measurement of B($\tau^- \to e^-\overline{\nu}_e\nu_\tau$) is 0.08.

[3] The correlation coefficients between this measurement and the ANASTASSOV 97 measurements of B($e\overline{\nu}_e\nu_\tau$), B($\mu\overline{\nu}_\mu\nu_\tau$)/B($e\overline{\nu}_e\nu_\tau$), B($h^-\nu_\tau$), and B($h^-\nu_\tau$)/B($e\overline{\nu}_e\nu_\tau$) are 0.50, 0.58, 0.50, and 0.08 respectively.

[4] Not independent of ALBRECHT 92D $\Gamma(\mu^-\overline{\nu}_\mu\nu_\tau)/\Gamma(e^-\overline{\nu}_e\nu_\tau)$ and ALBRECHT 93G $\Gamma(\mu^-\overline{\nu}_\mu\nu_\tau) \times \Gamma(e^-\overline{\nu}_e\nu_\tau)/\Gamma^2_{\text{total}}$ values.

[5] Modified using B($e^-\overline{\nu}_e\nu_\tau$)/B("1 prong") and B("1 prong") ,= 0.855.

[6] Error correlated with BALTRUSAITIS 85 $e\nu\overline{\nu}$ value.

$\Gamma(\mu^-\overline{\nu}_\mu\nu_\tau\gamma)/\Gamma_{\text{total}}$ Γ_4/Γ

VALUE (%)	EVTS	DOCUMENT ID		TECN	COMMENT
0.367±0.008 OUR AVERAGE					
0.363±0.002±0.015	22K	[1] SHIMIZU	18A	BELL	711 fb^{-1} E^{ee}_{cm}=10.6 GeV
0.369±0.003±0.010	16k	[2] LEES	15G	BABR	431 fb^{-1} E^{ee}_{cm}=10.6 GeV
0.361±0.016±0.035		[3] BERGFELD	00	CLEO	E^{ee}_{cm}= 10.6 GeV
• • • We do not use the following data for averages, fits, limits, etc. • • •					
0.30 ±0.04 ±0.05	116	[4] ALEXANDER	96S	OPAL	1991–1994 LEP runs
0.23 ±0.10	10	[5] WU	90	MRK2	E^{ee}_{cm}= 29 GeV

[1] SHIMIZU 18A impose requirements on detected γ's corresponding to a τ-rest-frame energy cutoff $E^*_\gamma > 10$ MeV.

[2] LEES 15G impose requirements on detected γ's corresponding to a τ-rest-frame energy cutoff $E^*_\gamma > 10$ MeV.

[3] BERGFELD 00 impose requirements on detected γ's corresponding to a τ-rest-frame energy cutoff $E^*_\gamma > 10$ MeV. For $E^*_\gamma > 20$ MeV, they quote $(3.04 \pm 0.14 \pm 0.30) \times 10^{-3}$.

[4] ALEXANDER 96S impose requirements on detected γ's corresponding to a τ-rest-frame energy cutoff E_γ >20 MeV.

[5] WU 90 reports $\Gamma(\mu^-\overline{\nu}_\mu\nu_\tau\gamma)/\Gamma(\mu^-\overline{\nu}_\mu\nu_\tau) = 0.013 \pm 0.006$, which is converted to $\Gamma(\mu^-\overline{\nu}_\mu\nu_\tau\gamma)/\Gamma_{\text{total}}$ using $\Gamma(\mu^-\overline{\nu}_\mu\nu_\tau\gamma)/\Gamma_{\text{total}} = 17.35\%$. Requirements on detected γ's correspond to a τ rest frame energy cutoff $E_\gamma > 37$ MeV.

$\Gamma(e^-\overline{\nu}_e\nu_\tau)/\Gamma_{\text{total}}$ Γ_5/Γ

To minimize the effect of experiments with large systematic errors, we exclude experiments which together would contribute 5% of the weight in the average.

VALUE (%)	EVTS	DOCUMENT ID		TECN	COMMENT
17.82 ±0.04 OUR FIT					
17.82 ±0.05 OUR AVERAGE					
17.837±0.072±0.036	56k	[1] SCHAEL	05C	ALEP	1991-1995 LEP runs
17.806±0.104±0.076	24.7k	[2] ACCIARRI	01F	L3	1991–1995 LEP runs
17.81 ±0.09 ±0.06	33.1k	ABBIENDI	99H	OPAL	1991–1995 LEP runs
17.877±0.109±0.110	23.3k	ABREU	99X	DLPH	1991–1995 LEP runs
17.76 ±0.06 ±0.17		[3] ANASTASSOV	97	CLEO	E^{ee}_{cm}= 10.6 GeV
• • • We do not use the following data for averages, fits, limits, etc. • • •					
17.78 ±0.10 ±0.09	25.3k	ALEXANDER	96D	OPAL	Repl. by ABBIENDI 99H
17.79 ±0.12 ±0.06	20.6k	BUSKULIC	96C	ALEP	Repl. by SCHAEL 05C
17.51 ±0.23 ±0.31	5059	ABREU	95T	DLPH	Repl.. by ABREU 99X
17.9 ±0.4 ±0.4	2892	ADRIANI	93M	L3	Repl. by ACCIARRI 01F
17.5 ±0.3 ±0.5		[4] ALBRECHT	93G	ARG	E^{ee}_{cm}= 9.4–10.6 GeV
17.97 ±0.14 ±0.23	3970	AKERIB	92	CLEO	Repl. by ANASTASSOV 97
19.1 ±0.4 ±0.6	2960	[5] AMMAR	92	CLEO	E^{ee}_{cm}= 10.5–10.9 GeV
18.09 ±0.45 ±0.45		DECAMP	92C	ALEP	Repl. by SCHAEL 05C
17.0 ±0.5 ±0.6	1.7k	ABACHI	90	HRS	E^{ee}_{cm}= 29 GeV
18.4 ±0.8 ±0.4	644	BEHREND	90	CELL	E^{ee}_{cm}= 35 GeV
16.3 ±0.3 ±3.2		JANSSEN	89	CBAL	E^{ee}_{cm}= 9.4–10.6 GeV
18.4 ±1.2 ±1.0		AIHARA	87B	TPC	E^{ee}_{cm}= 29 GeV
19.1 ±0.8 ±1.1		BURCHAT	87	MRK2	E^{ee}_{cm}= 29 GeV
16.8 ±0.7 ±0.9	515	[5] BARTEL	86D	JADE	E^{ee}_{cm}= 34.6 GeV
20.4 ±3.0 $^{+1.4}_{-0.9}$		ALTHOFF	85	TASS	E^{ee}_{cm}= 34.5 GeV
17.8 ±0.9 ±0.6	390	[5] ASH	85B	MAC	E^{ee}_{cm}= 29 GeV
18.2 ±0.7 ±0.5		[6] BALTRUSAIT...85		MRK3	E^{ee}_{cm}= 3.77 GeV
13.0 ±1.9 ±2.9		BERGER	85	PLUT	E^{ee}_{cm}= 34.6 GeV
18.3 ±2.4 ±1.9	60	BEHREND	83C	CELL	E^{ee}_{cm}= 34 GeV
16.0 ±1.3	459	[7] BACINO	78B	DLCO	E^{ee}_{cm}= 3.1–7.4 GeV

[1] Correlation matrix for SCHAEL 05C branching fractions, in percent:

(1) $\Gamma(\tau^- \to e^-\overline{\nu}_e\nu_\tau)/\Gamma_{\text{total}}$
(2) $\Gamma(\tau^- \to \mu^-\overline{\nu}_\mu\nu_\tau)/\Gamma_{\text{total}}$
(3) $\Gamma(\tau^- \to \pi^-\nu_\tau)/\Gamma_{\text{total}}$
(4) $\Gamma(\tau^- \to \pi^-\pi^0\nu_\tau)/\Gamma_{\text{total}}$
(5) $\Gamma(\tau^- \to \pi^-2\pi^0\nu_\tau(\text{ex.}K^0))/\Gamma_{\text{total}}$
(6) $\Gamma(\tau^- \to \pi^-3\pi^0\nu_\tau(\text{ex.}K^0))/\Gamma_{\text{total}}$
(7) $\Gamma(\tau^- \to h^-4\pi^0\nu_\tau(\text{ex.}K^0,\eta))/\Gamma_{\text{total}}$
(8) $\Gamma(\tau^- \to \pi^-\pi^+\pi^-\nu_\tau(\text{ex.}K^0,\omega))/\Gamma_{\text{total}}$
(9) $\Gamma(\tau^- \to \pi^-\pi^+\pi^-\pi^0\nu_\tau(\text{ex.}K^0))/\Gamma_{\text{total}}$
(10) $\Gamma(\tau^- \to h^-h^-h^+2\pi^0\nu_\tau(\text{ex.}K^0))/\Gamma_{\text{total}}$
(11) $\Gamma(\tau^- \to h^-h^-h^+3\pi^0\nu_\tau)/\Gamma_{\text{total}}$
(12) $\Gamma(\tau^- \to 3h^-2h^+\nu_\tau(\text{ex.}K^0))/\Gamma_{\text{total}}$
(13) $\Gamma(\tau^- \to 3h^-2h^+\pi^0\nu_\tau(\text{ex.}K^0))/\Gamma_{\text{total}}$

	(1)	(2)	(3)	(4)	(5)	(6)	(7)	(8)	(9)	(10)	(11)	(12)
(2)	-20											
(3)	-9	-6										
(4)	-16	-12	2									
(5)	-5	-5	-17	-37								
(6)	0	-4	-15	2	-27							
(7)	-2	-4	-24	-15	20	-47						
(8)	-14	-9	15	-5	-17	-14	-8					

(9)	–13	–12	–25	–30	4	–2	16	–15			
(10)	0	–2	–23	–14	4	10	13	–6	–17		
(11)	1	0	–5	1	4	6	0	–9	–2	–11	
(12)	0	1	9	4	–8	–4	–6	9	–5	–4	–2
(13)	1	–4	–3	–5	3	2	–4	–3	–1	4	1 –24

[2] The correlation coefficient between this measurement and the ACCIARRI 01F measurement of $B(\tau^- \to \mu^- \overline{\nu}_\mu \nu_\tau)$ is 0.08.

[3] The correlation coefficients between this measurement and the ANASTASSOV 97 measurements of $B(\mu\overline{\nu}_\mu\nu_\tau)$, $B(\mu\overline{\nu}_\mu\nu_\tau)/B(e\overline{\nu}_e\nu_\tau)$, $B(h^-\nu_\tau)$, and $B(h^-\nu_\tau)/B(e\overline{\nu}_e\nu_\tau)$ are 0.50, −0.42, 0.48, and −0.39 respectively.

[4] Not independent of ALBRECHT 92D $\Gamma(\mu^-\overline{\nu}_\mu\nu_\tau)/\Gamma(e^-\overline{\nu}_e\nu_\tau)$ and ALBRECHT 93G $\Gamma(\mu^-\overline{\nu}_\mu\nu_\tau)\times\Gamma(e^-\overline{\nu}_e\nu_\tau)/\Gamma^2_{\rm total}$ values.

[5] Modified using $B(e^-\overline{\nu}_e\nu_\tau)/B(\text{“1 prong”})$ and $B(\text{“1 prong”})$,= 0.855.

[6] Error correlated with BALTRUSAITIS 85 $\Gamma(\mu^-\overline{\nu}_\mu\nu_\tau)/\Gamma_{\rm total}$.

[7] BACINO 78B value comes from fit to events with $e^\pm$ and one other nonelectron charged prong.

$\Gamma(\mu^-\overline{\nu}_\mu\nu_\tau)/\Gamma(e^-\overline{\nu}_e\nu_\tau)$ Γ_3/Γ_5

Standard Model prediction including mass effects is 0.9726.

VALUE (units 10^{-2})	EVTS	DOCUMENT ID		TECN	COMMENT
97.62±0.28 OUR FIT					
97.9 ±0.4 OUR AVERAGE					
97.96±0.16±0.36	731k	[1] AUBERT	10F	BABR	467 fb^{-1} $E^{ee}_{\rm cm}$= 10.6 GeV
97.77±0.63±0.87		[2] ANASTASSOV	97	CLEO	$E^{ee}_{\rm cm}$= 10.6 GeV
99.7 ±3.5 ±4.0		ALBRECHT	92D	ARG	$E^{ee}_{\rm cm}$= 9.4–10.6 GeV

[1] Correlation matrix for AUBERT 10F branching fractions:

(1) $\Gamma(\tau^- \to \mu^- \overline{\nu}_\mu \nu_\tau)$ / $\Gamma(\tau^- \to e^- \overline{\nu}_e \nu_\tau)$
(2) $\Gamma(\tau^- \to \pi^- \nu_\tau)$ / $\Gamma(\tau^- \to e^- \overline{\nu}_e \nu_\tau)$
(3) $\Gamma(\tau^- \to K^- \nu_\tau)$ / $\Gamma(\tau^- \to e^- \overline{\nu}_e \nu_\tau)$

	(1)	(2)
(2)	0.25	
(3)	0.12	0.33

[2] The correlation coefficients between this measurement and the ANASTASSOV 97 measurements of $B(\mu\overline{\nu}_\mu\nu_\tau)$, $B(e\overline{\nu}_e\nu_\tau)$, $B(h^-\nu_\tau)$, and $B(h^-\nu_\tau)/B(e\overline{\nu}_e\nu_\tau)$ are 0.58, −0.42, 0.07, and 0.45 respectively.

$\Gamma(e^-\overline{\nu}_e\nu_\tau\gamma)/\Gamma_{\rm total}$ Γ_6/Γ

VALUE (%)	EVTS	DOCUMENT ID		TECN	COMMENT
1.83 ±0.05 OUR AVERAGE					
1.79 ±0.02 ±0.10	12K	[1] SHIMIZU	18A	BELL	711 fb^{-1} $E^{ee}_{\rm cm}$=10.6 GeV
1.847±0.015±0.052	18k	[2] LEES	15G	BABR	431 fb^{-1} $E^{ee}_{\rm cm}$=10.6 GeV
1.75 ±0.06 ±0.17		[3] BERGFELD	00	CLEO	$E^{ee}_{\rm cm}$= 10.6 GeV

[1] SHIMIZU 18A impose requirements on detected γ's corresponding to a τ-rest-frame energy cutoff $E^*_\gamma > 10$ MeV.

[2] LEES 15G impose requirements on detected γ's corresponding to a τ-rest-frame energy cutoff $E^*_\gamma > 10$ MeV.

[3] BERGFELD 00 impose requirements on detected γ's corresponding to a τ-rest-frame energy cutoff $E^*_\gamma > 10$ MeV.

$\Gamma(h^- \geq 0K^0_L\,\nu_\tau)/\Gamma_{\rm total}$ Γ_7/Γ

$\Gamma_7/\Gamma = (\Gamma_9+\Gamma_{10}+\frac{1}{2}\Gamma_{36}+\frac{1}{2}\Gamma_{38}+\Gamma_{50})/\Gamma$

VALUE (%)	EVTS	DOCUMENT ID		TECN	COMMENT
12.03±0.05 OUR FIT					
12.2 ±0.4 OUR AVERAGE					
12.47±0.26±0.43	2967	[1] ACCIARRI	95	L3	1992 LEP run
12.4 ±0.7 ±0.7	283	[2] ABREU	92N	DLPH	1990 LEP run
12.1 ±0.7 ±0.5	309	ALEXANDER	91D	OPAL	1990 LEP run
• • • We use the following data for averages but not for fits. • • •					
11.3 ±0.5 ±0.8	798	[3] FORD	87	MAC	$E^{ee}_{\rm cm}$= 29 GeV
• • • We do not use the following data for averages, fits, limits, etc. • • •					
12.44±0.11±0.11	15k	[4] BUSKULIC	96	ALEP	Repl. by SCHAEL 05C
11.7 ±0.6 ±0.8		[5] ALBRECHT	92D	ARG	$E^{ee}_{\rm cm}$= 9.4–10.6 GeV
12.98±0.44±0.33		[6] DECAMP	92C	ALEP	Repl. by SCHAEL 05C
12.3 ±0.9 ±0.5	1338	BEHREND	90	CELL	$E^{ee}_{\rm cm}$= 35 GeV
11.1 ±1.1 ±1.4		[7] BURCHAT	87	MRK2	$E^{ee}_{\rm cm}$= 29 GeV
12.3 ±0.6 ±1.1	328	[8] BARTEL	86D	JADE	$E^{ee}_{\rm cm}$= 34.6 GeV
13.0 ±2.0 ±4.0		BERGER	85	PLUT	$E^{ee}_{\rm cm}$= 34.6 GeV
11.2 ±1.7 ±1.2	34	[9] BEHREND	83C	CELL	$E^{ee}_{\rm cm}$= 34 GeV

[1] ACCIARRI 95 with 0.65% added to remove their correction for $\pi^- K^0_L$ backgrounds.

[2] ABREU 92N with 0.5% added to remove their correction for $K^*(892)^-$ backgrounds.

[3] FORD 87 result for $B(\pi^-\nu_\tau)$ with 0.67% added to remove their K^- correction and adjusted for 1992 B(“1 prong”).

[4] BUSKULIC 96 quote 11.78 ± 0.11 ± 0.13 We add 0.66 to undo their correction for unseen K^0_L and modify the systematic error accordingly.

[5] Not independent of ALBRECHT 92D $\Gamma(\mu^-\overline{\nu}_\mu\nu_\tau)/\Gamma(e^-\overline{\nu}_e\nu_\tau)$, $\Gamma(\mu^-\overline{\nu}_\mu\nu_\tau)\times\Gamma(e^-\overline{\nu}_e\nu_\tau)$, and $\Gamma(h^-\geq 0K^0_L\nu_\tau)/\Gamma(e^-\overline{\nu}_e\nu_\tau)$ values.

[6] DECAMP 92C quote $B(h^-\geq 0K^0_L\geq 0(K^0_S\to\pi^+\pi^-)\,\nu_\tau) = 13.32\pm0.44\pm0.33$. We subtract 0.35 to correct for their inclusion of the K^0_S decays.

[7] BURCHAT 87 with 1.1% added to remove their correction for K^- and $K^*(892)^-$ backgrounds.

[8] BARTEL 86D result for $B(\pi^-\nu_\tau)$ with 0.59% added to remove their K^- correction and adjusted for 1992 B(“1 prong”).

[9] BEHREND 83C quote $B(\pi^-\nu_\tau) = 9.9\pm1.7\pm1.3$ after subtracting 1.3 ± 0.5 to correct for $B(K^-\nu_\tau)$.

$\Gamma(h^-\nu_\tau)/\Gamma_{\rm total}$ $\Gamma_8/\Gamma = (\Gamma_9+\Gamma_{10})/\Gamma$

VALUE (%)	EVTS	DOCUMENT ID		TECN	COMMENT
11.51 ±0.05 OUR FIT					
11.63 ±0.12 OUR AVERAGE		Error includes scale factor of 1.4. See the ideogram below.			
11.571±0.120±0.114	19k	[1] ABDALLAH	06A	DLPH	1992–1995 LEP runs
11.98 ±0.13 ±0.16		ACKERSTAFF	98M	OPAL	1991–1995 LEP runs
11.52 ±0.05 ±0.12		[2] ANASTASSOV	97	CLEO	$E^{ee}_{\rm cm}$= 10.6 GeV

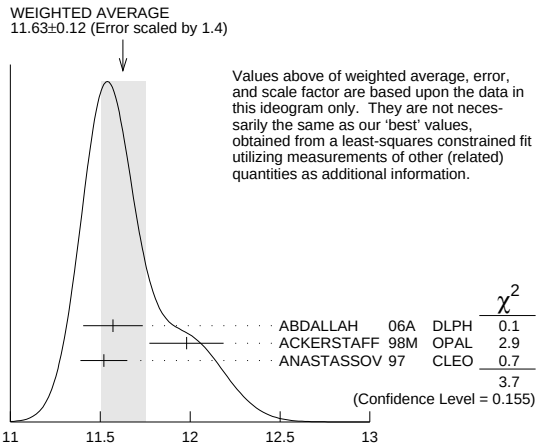

[1] Correlation matrix for ABDALLAH 06A branching fractions, in percent:

(1) $\Gamma(\tau^- \to h^-\nu_\tau)/\Gamma_{\rm total}$
(2) $\Gamma(\tau^- \to h^-\pi^0\nu_\tau)/\Gamma_{\rm total}$
(3) $\Gamma(\tau^- \to h^- \geq 1\pi^0\nu_\tau(\text{ex. }K^0))/\Gamma_{\rm total}$
(4) $\Gamma(\tau^- \to h^-2\pi^0\nu_\tau(\text{ex. }K^0))/\Gamma_{\rm total}$
(5) $\Gamma(\tau^- \to h^- \geq 3\pi^0\nu_\tau(\text{ex. }K^0))/\Gamma_{\rm total}$
(6) $\Gamma(\tau^- \to h^-h^-h^+\nu_\tau(\text{ex. }K^0))/\Gamma_{\rm total}$
(7) $\Gamma(\tau^- \to h^-h^-h^+\pi^0\nu_\tau(\text{ex. }K^0))/\Gamma_{\rm total}$
(8) $\Gamma(\tau^- \to h^-h^-h^+ \geq 1\pi^0\nu_\tau(\text{ex. }K^0))/\Gamma_{\rm total}$
(9) $\Gamma(\tau^- \to h^-h^-h^+ \geq 2\pi^0\nu_\tau(\text{ex. }K^0))/\Gamma_{\rm total}$
(10) $\Gamma(\tau^- \to 3h^-2h^+\nu_\tau(\text{ex. }K^0))/\Gamma_{\rm total}$
(11) $\Gamma(\tau^- \to 3h^-2h^+\pi^0\nu_\tau(\text{ex. }K^0))/\Gamma_{\rm total}$

	(1)	(2)	(3)	(4)	(5)	(6)	(7)	(8)	(9)	(10)
(2)	–34									
(3)	–47	56								
(4)	6	–66	15							
(5)	–6	38	11	–86						
(6)	–7	–8	15	0	–2					
(7)	–2	–1	–5	–3	3	–53				
(8)	–4	–4	–13	–4	–2	–56	75			
(9)	–1	–1	–4	3	–6	26	–78	–16		
(10)	–1	–1	1	0	0	–2	–3	–1	3	
(11)	0	0	0	0	0	1	0	–5	5	–57

[2] The correlation coefficients between this measurement and the ANASTASSOV 97 measurements of $B(\mu\overline{\nu}_\mu\nu_\tau)$, $B(e\overline{\nu}_e\nu_\tau)$, $B(\mu\overline{\nu}_\mu\nu_\tau)/B(e\overline{\nu}_e\nu_\tau)$, and $B(h^-\nu_\tau)/B(e\overline{\nu}_e\nu_\tau)$ are 0.50, 0.48, 0.07, and 0.63 respectively.

$\Gamma(h^-\nu_\tau)/\Gamma_{\rm total}$ (%)

$\Gamma(h^-\nu_\tau)/\Gamma(e^-\overline{\nu}_e\nu_\tau)$ $\Gamma_8/\Gamma_5 = (\Gamma_9+\Gamma_{10})/\Gamma_5$

VALUE (units 10^{-2})	EVTS	DOCUMENT ID		TECN	COMMENT
64.62±0.33 OUR FIT					
64.0 ±0.7 OUR AVERAGE		Error includes scale factor of 1.6.			
• • • We use the following data for averages but not for fits. • • •					
63.33±0.14±0.61	394k	[1] AUBERT	10F	BABR	467 fb^{-1} $E^{ee}_{\rm cm}$=10.6 GeV
64.84±0.41±0.60		[2] ANASTASSOV	97	CLEO	$E^{ee}_{\rm cm}$= 10.6 GeV

[1] Not independent of AUBERT 10F $\Gamma(\tau^- \to \pi^-\nu_\tau)/\Gamma(\tau^- \to e^-\overline{\nu}_e\nu_\tau)$ and $\Gamma(\tau^- \to K^-\nu_\tau)/\Gamma(\tau^- \to e^-\overline{\nu}_e\nu_\tau)$.

[2] The correlation coefficients between this measurement and the ANASTASSOV 97 measurements of $B(\mu\overline{\nu}_\mu\nu_\tau)$, $B(e\overline{\nu}_e\nu_\tau)$, $B(\mu\overline{\nu}_\mu\nu_\tau)/B(e\overline{\nu}_e\nu_\tau)$, and $B(h^-\nu_\tau)$ are 0.08, −0.39, 0.45, and 0.63 respectively.

$\Gamma(\pi^-\nu_\tau)/\Gamma_{\rm total}$ Γ_9/Γ

VALUE (%)	EVTS	DOCUMENT ID		TECN	COMMENT
10.82 ±0.05 OUR FIT					
10.828±0.070±0.078	38k	[1] SCHAEL	05C	ALEP	1991-1995 LEP runs
• • • We do not use the following data for averages, fits, limits, etc. • • •					
11.06 ±0.11 ±0.14		[2] BUSKULIC	96	ALEP	Repl. by SCHAEL 05C
11.7 ±0.4 ±1.8	1138	BLOCKER	82D	MRK2	$E^{ee}_{\rm cm}$= 3.5–6.7 GeV

[1] See footnote to SCHAEL 05C $\Gamma(\tau^- \to e^-\overline{\nu}_e\nu_\tau)/\Gamma_{\rm total}$ measurement for correlations with other measurements.
[2] Not independent of BUSKULIC 96 B($h^-\nu_\tau$) and B($K^-\nu_\tau$) values.

$\Gamma(\pi^-\nu_\tau)/\Gamma(e^-\overline{\nu}_e\nu_\tau)$ Γ_9/Γ_5

VALUE (units 10^{-2})	EVTS	DOCUMENT ID		TECN	COMMENT
60.71±0.32 OUR FIT					
59.45±0.14±0.61	369k	[1] AUBERT	10F	BABR	467 fb^{-1} $E^{ee}_{\rm cm}$= 10.6 GeV

[1] See footnote to AUBERT 10F $\Gamma(\tau^- \to \mu^-\overline{\nu}_\mu\nu_\tau)/\Gamma(\tau^- \to e^-\overline{\nu}_e\nu_\tau)$ for correlations with other measurements.

$\Gamma(K^-\nu_\tau)/\Gamma_{\rm total}$ Γ_{10}/Γ

VALUE (%)	EVTS	DOCUMENT ID		TECN	COMMENT
0.696±0.010 OUR FIT					
0.685±0.023 OUR AVERAGE					
0.658±0.027±0.029		[1] ABBIENDI	01J	OPAL	1990–1995 LEP runs
0.696±0.025±0.014	2032	BARATE	99K	ALEP	1991–1995 LEP runs
0.85 ±0.18	27	ABREU	94K	DLPH	LEP 1992 Z data
0.66 ±0.07 ±0.09	99	BATTLE	94	CLEO	$E^{ee}_{\rm cm}\approx$ 10.6 GeV
• • • We do not use the following data for averages, fits, limits, etc. • • •					
0.72 ±0.04 ±0.04	728	BUSKULIC	96	ALEP	Repl. by BARATE 99K
0.59 ±0.18	16	MILLS	84	DLCO	$E^{ee}_{\rm cm}$= 29 GeV
1.3 ±0.5	15	BLOCKER	82B	MRK2	$E^{ee}_{\rm cm}$= 3.9–6.7 GeV

[1] The correlation coefficient between this measurement and the ABBIENDI 01J B($\tau^- \to K^- \geq 0\pi^0 \geq 0K^0 \geq 0\gamma\ \nu_\tau$) is 0.60.

$\Gamma(K^-\nu_\tau)/\Gamma(e^-\overline{\nu}_e\nu_\tau)$ Γ_{10}/Γ_5

VALUE (units 10^{-2})	EVTS	DOCUMENT ID		TECN	COMMENT
3.91 ±0.05 OUR FIT					
3.882±0.032±0.057	25k	[1] AUBERT	10F	BABR	467 fb^{-1} $E^{ee}_{\rm cm}$= 10.6 GeV

[1] See footnote to AUBERT 10F $\Gamma(\tau^- \to \mu^-\overline{\nu}_\mu\nu_\tau)/\Gamma(\tau^- \to e^-\overline{\nu}_e\nu_\tau)$ for correlations with other measurements.

$\Gamma(K^-\nu_\tau)/\Gamma(\pi^-\nu_\tau)$ Γ_{10}/Γ_9

VALUE (units 10^{-2})	DOCUMENT ID		TECN	COMMENT
6.44 ±0.09 OUR FIT				
• • • We use the following data for averages but not for fits. • • •				
6.531±0.056±0.093	[1] AUBERT	10F	BABR	467 fb^{-1} $E^{ee}_{\rm cm}$= 10.6 GeV

[1] Not independent of AUBERT 10F $\Gamma(\tau^- \to \pi^-\nu_\tau)/\Gamma(\tau^- \to e^-\overline{\nu}_e\nu_\tau)$ and $\Gamma(\tau^- \to K^-\nu_\tau)/\Gamma(\tau^- \to e^-\overline{\nu}_e\nu_\tau)$.

$\Gamma(h^- \geq 1\ \text{neutrals}\ \nu_\tau)/\Gamma_{\rm total}$ Γ_{11}/Γ

$\Gamma_{11}/\Gamma = (\Gamma_{14}+\Gamma_{16}+\Gamma_{20}+\Gamma_{23}+\Gamma_{27}+\Gamma_{28}+\Gamma_{30}+0.15344\Gamma_{36}+0.15344\Gamma_{38}+0.15344\Gamma_{41}+0.15344\Gamma_{43}+0.0942\Gamma_{48}+0.0942\Gamma_{52}+0.7212\Gamma_{148}+0.7212\Gamma_{150}+0.7212\Gamma_{152}+0.1107\Gamma_{154}+0.0840\Gamma_{176}+0.0840\Gamma_{177}+0.0840\Gamma_{178})/\Gamma$

VALUE (%)	DOCUMENT ID		TECN	COMMENT
37.00±0.09 OUR FIT				
• • • We do not use the following data for averages, fits, limits, etc. • • •				
36.14±0.33±0.58	[1] AKERS	94E	OPAL	1991–1992 LEP runs
38.4 ±1.2 ±1.0	[2] BURCHAT	87	MRK2	$E^{ee}_{\rm cm}$= 29 GeV
42.7 ±2.0 ±2.9	BERGER	85	PLUT	$E^{ee}_{\rm cm}$= 34.6 GeV

[1] Not independent of ACKERSTAFF 98M B($h^-\pi^0\nu_\tau$) and B($h^- \geq 2\pi^0\nu_\tau$) values.
[2] BURCHAT 87 quote for B($\pi^\pm \geq 1$ neutralν_τ) = 0.378 ± 0.012 ± 0.010. We add 0.006 to account for contribution from ($K^{*-}\nu_\tau$) which they fixed at BR = 0.013.

$\Gamma(h^- \geq 1\pi^0\nu_\tau\,(\text{ex.}K^0))/\Gamma_{\rm total}$ Γ_{12}/Γ

$\Gamma_{12}/\Gamma = (\Gamma_{14}+\Gamma_{16}+\Gamma_{20}+\Gamma_{23}+\Gamma_{27}+\Gamma_{28}+\Gamma_{30}+0.3268\Gamma_{148}+0.3268\Gamma_{150}+0.3268\Gamma_{152})/\Gamma$

VALUE (%)	EVTS	DOCUMENT ID		TECN	COMMENT
36.51 ±0.09 OUR FIT					
• • • We use the following data for averages but not for fits. • • •					
36.641±0.155±0.127	45k	[1] ABDALLAH	06A	DLPH	1992–1995 LEP runs

[1] See footnote to ABDALLAH 06A $\Gamma(\tau^- \to h^-\nu_\tau)/\Gamma_{\rm total}$ measurement for correlations with other measurements.

$\Gamma(h^-\pi^0\nu_\tau)/\Gamma_{\rm total}$ $\Gamma_{13}/\Gamma = (\Gamma_{14}+\Gamma_{16})/\Gamma$

VALUE (%)	EVTS	DOCUMENT ID		TECN	COMMENT
25.93 ±0.09 OUR FIT					
25.73 ±0.16 OUR AVERAGE					
25.67 ±0.01 ±0.39	5.4M	FUJIKAWA	08	BELL	72 fb^{-1} $E^{ee}_{\rm cm}$=10.6GeV
25.740±0.201±0.138	35k	[1] ABDALLAH	06A	DLPH	1992–1995 LEP runs
25.89 ±0.17 ±0.29		ACKERSTAFF	98M	OPAL	1991–1995 LEP runs
25.05 ±0.35 ±0.50	6613	ACCIARRI	95	L3	1992 LEP run
25.87 ±0.12 ±0.42	51k	[2] ARTUSO	94	CLEO	$E^{ee}_{\rm cm}$= 10.6 GeV
• • • We do not use the following data for averages, fits, limits, etc. • • •					
25.76 ±0.15 ±0.13	31k	BUSKULIC	96	ALEP	Repl. by SCHAEL 05C
25.98 ±0.36 ±0.52		[3] AKERS	94E	OPAL	Repl. by ACKER-STAFF 98M
22.9 ±0.8 ±1.3	283	[4] ABREU	92N	DLPH	$E^{ee}_{\rm cm}$= 88.2–94.2 GeV
23.1 ±0.4 ±0.9	1249	[5] ALBRECHT	92Q	ARG	$E^{ee}_{\rm cm}$= 10 GeV
25.02 ±0.64 ±0.88	1849	DECAMP	92C	ALEP	1989–1990 LEP runs
22.0 ±0.8 ±1.9	779	ANTREASYAN	91	CBAL	$E^{ee}_{\rm cm}$= 9.4–10.6 GeV
22.6 ±1.5 ±0.7	1101	BEHREND	90	CELL	$E^{ee}_{\rm cm}$= 35 GeV
23.1 ±1.9 ±1.6		BEHREND	84	CELL	$E^{ee}_{\rm cm}$= 14,22 GeV

[1] See footnote to ABDALLAH 06A $\Gamma(\tau^- \to h^-\nu_\tau)/\Gamma_{\rm total}$ measurement for correlations with other measurements.
[2] ARTUSO 94 reports the combined result from three independent methods, one of which (23% of the $\tau^- \to h^-\pi^0\nu_\tau$) is normalized to the inclusive one-prong branching fraction, taken as 0.854 ± 0.004. Renormalization to the present value causes negligible change.
[3] AKERS 94E quote $(26.25 \pm 0.36 \pm 0.52)\times10^{-2}$; we subtract 0.27% from their number to correct for $\tau^- \to h^- K^0_L\nu_\tau$.
[4] ABREU 92N with 0.5% added to remove their correction for $K^*(892)^-$ backgrounds.
[5] ALBRECHT 92Q with 0.5% added to remove their correction for $\tau^- \to K^*(892)^-\nu_\tau$ background.

$\Gamma(\pi^-\pi^0\nu_\tau)/\Gamma_{\rm total}$ Γ_{14}/Γ

VALUE (%)	EVTS	DOCUMENT ID		TECN	COMMENT
25.49 ±0.09 OUR FIT					
25.46 ±0.12 OUR AVERAGE					
25.471±0.097±0.085	81k	[1] SCHAEL	05C	ALEP	1991-1995 LEP runs
• • • We use the following data for averages but not for fits. • • •					
25.36 ±0.44		[2] ARTUSO	94	CLEO	$E^{ee}_{\rm cm}$= 10.6 GeV
• • • We do not use the following data for averages, fits, limits, etc. • • •					
25.30 ±0.15 ±0.13		[3] BUSKULIC	96	ALEP	Repl. by SCHAEL 05C
21.5 ±0.4 ±1.9	4400	[4,5] ALBRECHT	88L	ARG	$E^{ee}_{\rm cm}$= 10 GeV
23.0 ±1.3 ±1.7	582	ADLER	87B	MRK3	$E^{ee}_{\rm cm}$= 3.77 GeV
25.8 ±1.7 ±2.5		[6] BURCHAT	87	MRK2	$E^{ee}_{\rm cm}$= 29 GeV
22.3 ±0.6 ±1.4	629	[5] YELTON	86	MRK2	$E^{ee}_{\rm cm}$= 29 GeV

[1] See footnote to SCHAEL 05C $\Gamma(\tau^- \to e^-\overline{\nu}_e\nu_\tau)/\Gamma_{\rm total}$ measurement for correlations with other measurements.
[2] Not independent of ARTUSO 94 B($h^-\pi^0\nu_\tau$) and BATTLE 94 B($K^-\pi^0\nu_\tau$) values.
[3] Not independent of BUSKULIC 96 B($h^-\pi^0\nu_\tau$) and B($K^-\pi^0\nu_\tau$) values.
[4] The authors divide by ($\Gamma_3+\Gamma_5+\Gamma_9+\Gamma_{10}$)/Γ = 0.467 to obtain this result.
[5] Experiment had no hadron identification. Kaon corrections were made, but insufficient information is given to permit their removal.
[6] BURCHAT 87 value is not independent of YELTON 86 value. Nonresonant decays included.

$\Gamma(\pi^-\pi^0\,\text{non-}\rho(770)\nu_\tau)/\Gamma_{\rm total}$ Γ_{15}/Γ

VALUE (%)	DOCUMENT ID		TECN	COMMENT
0.3±0.1±0.3	[1] BEHREND	84	CELL	$E^{ee}_{\rm cm}$= 14,22 GeV

[1] BEHREND 84 assume a flat nonresonant mass distribution down to the $\rho(770)$ mass, using events with mass above 1300 to set the level.

$\Gamma(K^-\pi^0\nu_\tau)/\Gamma_{\rm total}$ Γ_{16}/Γ

VALUE (%)	EVTS	DOCUMENT ID		TECN	COMMENT
0.433±0.015 OUR FIT					
0.426±0.016 OUR AVERAGE					
0.416±0.003±0.018	78k	AUBERT	07AP	BABR	230 fb^{-1} $E^{ee}_{\rm cm}$= 10.6 GeV
0.471±0.059±0.023	360	ABBIENDI	04J	OPAL	1991-1995 LEP runs
0.444±0.026±0.024	923	BARATE	99K	ALEP	1991-1995 LEP runs
0.51 ±0.10 ±0.07	37	BATTLE	94	CLEO	$E^{ee}_{\rm cm}\approx$ 10.6 GeV
• • • We do not use the following data for averages, fits, limits, etc. • • •					
0.52 ±0.04 ±0.05	395	BUSKULIC	96	ALEP	Repl. by BARATE 99K

$\Gamma(h^- \geq 2\pi^0\nu_\tau)/\Gamma_{\rm total}$ Γ_{17}/Γ

$\Gamma_{17}/\Gamma = (\Gamma_{20}+\Gamma_{23}+\Gamma_{27}+\Gamma_{28}+\Gamma_{30}+0.15344\Gamma_{36}+0.15344\Gamma_{38}+0.15344\Gamma_{41}+0.15344\Gamma_{43}+0.09419\Gamma_{48}+0.0942\Gamma_{52}+0.3268\Gamma_{148}+0.3268\Gamma_{150}+0.3268\Gamma_{152})/\Gamma$

VALUE (%)	EVTS	DOCUMENT ID		TECN	COMMENT
10.81±0.09 OUR FIT					
9.91±0.31±0.27		ACKERSTAFF	98M	OPAL	1991–1995 LEP runs
• • • We do not use the following data for averages, fits, limits, etc. • • •					
9.89±0.34±0.55		[1] AKERS	94E	OPAL	Repl. by ACKER-STAFF 98M
14.0 ±1.2 ±0.6	938	[2] BEHREND	90	CELL	$E^{ee}_{\rm cm}$= 35 GeV
12.0 ±1.4 ±2.5		[3] BURCHAT	87	MRK2	$E^{ee}_{\rm cm}$= 29 GeV
13.9 ±2.0 $^{+1.9}_{-2.2}$		[4] AIHARA	86E	TPC	$E^{ee}_{\rm cm}$= 29 GeV

[1] AKERS 94E not independent of AKERS 94E B($h^- \geq 1\pi^0\nu_\tau$) and B($h^-\pi^0\nu_\tau$) measurements.
[2] No independent of BEHREND 90 $\Gamma(h^-2\pi^0\nu_\tau(\text{exp. } K^0))$ and $\Gamma(h^- \geq 3\pi^0\nu_\tau)$.
[3] Error correlated with BURCHAT 87 $\Gamma(\rho^-\nu_e)/\Gamma$(total) value.
[4] AIHARA 86E (TPC) quote B($2\pi^0\pi^-\nu_\tau$) + 1.6B($3\pi^0\pi^-\nu_\tau$) + 1.1B($\pi^0\eta\pi^-\nu_\tau$).

$\Gamma(h^-2\pi^0\nu_\tau)/\Gamma_{total}$ Γ_{18}/Γ

$\Gamma_{18}/\Gamma = (\Gamma_{20}+\Gamma_{23}+0.15344\Gamma_{36}+0.15344\Gamma_{38})/\Gamma$

VALUE (%)	EVTS	DOCUMENT ID		TECN	COMMENT
9.48±0.10 OUR FIT					
• • • We do not use the following data for averages, fits, limits, etc. • • •					
9.48±0.13±0.10	12k	[1] BUSKULIC	96	ALEP	Repl. by SCHAEL 05C

[1] BUSKULIC 96 quote 9.29 ± 0.13 ± 0.10. We add 0.19 to undo their correction for $\tau^- \to h^- K^0 \nu_\tau$.

$\Gamma(h^-2\pi^0\nu_\tau(\text{ex.}K^0))/\Gamma_{total}$ Γ_{19}/Γ

$\Gamma_{19}/\Gamma = (\Gamma_{20}+\Gamma_{23})/\Gamma$

VALUE (%)	EVTS	DOCUMENT ID		TECN	COMMENT
9.32 ±0.10 OUR FIT					
9.17 ±0.27 OUR AVERAGE					
9.498±0.320±0.275	9.5k	[1] ABDALLAH	06A	DLPH	1992–1995 LEP runs
8.88 ±0.37 ±0.42	1060	ACCIARRI	95	L3	1992 LEP run
• • • We use the following data for averages but not for fits. • • •					
8.96 ±0.16 ±0.44		[2] PROCARIO	93	CLEO	$E^{ee}_{cm} \approx$ 10.6 GeV
• • • We do not use the following data for averages, fits, limits, etc. • • •					
10.38 ±0.66 ±0.82	809	[3] DECAMP	92C	ALEP	Repl. by SCHAEL 05C
5.7 ±0.5 $^{+1.7}_{-1.0}$	133	[4] ANTREASYAN	91	CBAL	E^{ee}_{cm}= 9.4–10.6 GeV
10.0 ±1.5 ±1.1	333	[5] BEHREND	90	CELL	E^{ee}_{cm}= 35 GeV
8.7 ±0.4 ±1.1	815	[6] BAND	87	MAC	E^{ee}_{cm}= 29 GeV
6.2 ±0.6 ±1.2		[7] GAN	87	MRK2	E^{ee}_{cm}= 29 GeV
6.0 ±3.0 ±1.8		BEHREND	84	CELL	E^{ee}_{cm}= 14,22 GeV

[1] See footnote to ABDALLAH 06A $\Gamma(\tau^- \to h^-\nu_\tau)/\Gamma_{total}$ measurement for correlations with other measurements.
[2] PROCARIO 93 entry is obtained from $B(h^-2\pi^0\nu_\tau)/B(h^-\pi^0\nu_\tau)$ using ARTUSO 94 result for $B(h^-\pi^0\nu_\tau)$.
[3] We subtract 0.0015 to account for $\tau^- \to K^*(892)^-\nu_\tau$ contribution.
[4] ANTREASYAN 91 subtract 0.001 to account for the $\tau^- \to K^*(892)^-\nu_\tau$ contribution.
[5] BEHREND 90 subtract 0.002 to account for the $\tau^- \to K^*(892)^-\nu_\tau$ contribution.
[6] BAND 87 assume $B(\pi^-3\pi^0\nu_\tau) = 0.01$ and $B(\pi^-\pi^0\eta\nu_\tau) = 0.005$.
[7] GAN 87 analysis use photon multiplicity distribution.

$\Gamma(h^-2\pi^0\nu_\tau(\text{ex.}K^0))/\Gamma(h^-\pi^0\nu_\tau)$ Γ_{19}/Γ_{13}

$\Gamma_{19}/\Gamma_{13} = (\Gamma_{20}+\Gamma_{23})/(\Gamma_{14}+\Gamma_{16})$

VALUE (units 10^{-2})	DOCUMENT ID		TECN	COMMENT
36.0±0.4 OUR FIT				
34.2±0.6±1.6	[1] PROCARIO	93	CLEO	$E^{ee}_{cm} \approx$ 10.6 GeV

[1] PROCARIO 93 quote 0.345 ± 0.006 ± 0.016 after correction for 2 kaon backgrounds assuming $B(K^{*-}\nu_\tau)$=1.42 ± 0.18% and $B(h^-K^0\pi^0\nu_\tau)$=0.48 ± 0.48%. We multiply by 0.990 ± 0.010 to remove these corrections to $B(h^-\pi^0\nu_\tau)$.

$\Gamma(\pi^-2\pi^0\nu_\tau(\text{ex.}K^0))/\Gamma_{total}$ Γ_{20}/Γ

VALUE (%)	EVTS	DOCUMENT ID		TECN	COMMENT
9.26 ±0.10 OUR FIT					
9.239±0.086±0.090	31k	[1] SCHAEL	05C	ALEP	1991–1995 LEP runs
• • • We do not use the following data for averages, fits, limits, etc. • • •					
9.21 ±0.13 ±0.11		[2] BUSKULIC	96	ALEP	Repl. by SCHAEL 05C

[1] See footnote to SCHAEL 05C $\Gamma(\tau^- \to e^-\overline{\nu}_e\nu_\tau)/\Gamma_{total}$ measurement for correlations with other measurements.
[2] Not independent of BUSKULIC 96 $B(h^-2\pi^0\nu_\tau(\text{ex. } K^0))$ and $B(K^-2\pi^0\nu_\tau(\text{ex. } K^0))$ values.

$\Gamma(\pi^-2\pi^0\nu_\tau(\text{ex.}K^0),\text{scalar})/\Gamma(\pi^-2\pi^0\nu_\tau(\text{ex.}K^0))$ Γ_{21}/Γ_{20}

VALUE	CL%	DOCUMENT ID		TECN	COMMENT
<0.094	95	[1] BROWDER	00	CLEO	4.7 fb^{-1} E^{ee}_{cm}= 10.6 GeV

[1] Model-independent limit from structure function analysis on contribution to $B(\tau^- \to \pi^-2\pi^0\nu_\tau(\text{ex. } K^0))$ from scalars.

$\Gamma(\pi^-2\pi^0\nu_\tau(\text{ex.}K^0),\text{vector})/\Gamma(\pi^-2\pi^0\nu_\tau(\text{ex.}K^0))$ Γ_{22}/Γ_{20}

VALUE	CL%	DOCUMENT ID		TECN	COMMENT
<0.073	95	[1] BROWDER	00	CLEO	4.7 fb^{-1} E^{ee}_{cm}= 10.6 GeV

[1] Model-independent limit from structure function analysis on contribution to $B(\tau^- \to \pi^-2\pi^0\nu_\tau(\text{ex. } K^0))$ from vectors.

$\Gamma(K^-2\pi^0\nu_\tau(\text{ex.}K^0))/\Gamma_{total}$ Γ_{23}/Γ

VALUE (units 10^{-4})	EVTS	DOCUMENT ID		TECN	COMMENT
6.5± 2.2 OUR FIT					
5.8± 2.4 OUR AVERAGE					
5.6± 2.0±1.5	131	BARATE	99K	ALEP	1991–1995 LEP runs
9 ±10 ±3	3	[1] BATTLE	94	CLEO	$E^{ee}_{cm} \approx$ 10.6 GeV
• • • We do not use the following data for averages, fits, limits, etc. • • •					
8 ± 2 ±2	59	BUSKULIC	96	ALEP	Repl. by BARATE 99K

[1] BATTLE 94 quote $(14 \pm 10 \pm 3) \times 10^{-4}$ or $< 30 \times 10^{-4}$ at 90% CL. We subtract $(5 \pm 2) \times 10^{-4}$ to account for $\tau^- \to K^-(K^0 \to \pi^0\pi^0)\nu_\tau$ background.

$\Gamma(h^- \geq 3\pi^0\nu_\tau)/\Gamma_{total}$ Γ_{24}/Γ

$\Gamma_{24}/\Gamma = (\Gamma_{27}+\Gamma_{28}+\Gamma_{30}+0.15344\Gamma_{41}+0.15344\Gamma_{43}+0.0942\Gamma_{48}+0.0942\Gamma_{52}+0.3268\Gamma_{148}+0.3268\Gamma_{150}+0.3268\Gamma_{152}+0.0501\Gamma_{154})/\Gamma$

VALUE (%)	EVTS	DOCUMENT ID		TECN	COMMENT
1.34±0.07 OUR FIT					
• • • We do not use the following data for averages, fits, limits, etc. • • •					
1.53±0.40±0.46	186	DECAMP	92C	ALEP	Repl. by SCHAEL 05C
3.2 ±1.0 ±1.0		BEHREND	90	CELL	E^{ee}_{cm}= 35 GeV

$\Gamma(h^- \geq 3\pi^0\nu_\tau(\text{ex. } K^0))/\Gamma_{total}$ Γ_{25}/Γ

$\Gamma_{25}/\Gamma = (\Gamma_{27}+\Gamma_{28}+\Gamma_{30}+0.3268\Gamma_{148}+0.3268\Gamma_{150}+0.3268\Gamma_{152})/\Gamma$

VALUE (%)	EVTS	DOCUMENT ID		TECN	COMMENT
1.25 ±0.07 OUR FIT					
1.403±0.214±0.224	1.1k	[1] ABDALLAH	06A	DLPH	1992–1995 LEP runs

[1] See footnote to ABDALLAH 06A $\Gamma(\tau^- \to h^-\nu_\tau)/\Gamma_{total}$ measurement for correlations with other measurements.

$\Gamma(h^-3\pi^0\nu_\tau)/\Gamma_{total}$ Γ_{26}/Γ

$\Gamma_{26}/\Gamma = (\Gamma_{27}+\Gamma_{28}+0.15344\Gamma_{41}+0.15344\Gamma_{43}+0.3268\Gamma_{150})/\Gamma$

VALUE (%)	EVTS	DOCUMENT ID		TECN	COMMENT
1.18±0.07 OUR FIT					
1.21±0.17 OUR AVERAGE Error includes scale factor of 1.2.					
1.70±0.24±0.38	293	ACCIARRI	95	L3	1992 LEP run
• • • We use the following data for averages but not for fits. • • •					
1.15±0.08±0.13		[1] PROCARIO	93	CLEO	$E^{ee}_{cm} \approx$ 10.6 GeV
• • • We do not use the following data for averages, fits, limits, etc. • • •					
1.24±0.09±0.11	2.3k	[2] BUSKULIC	96	ALEP	Repl. by SCHAEL 05C
0.0 $^{+1.4}_{-0.1}$ $^{+1.1}_{-0.1}$		[3] GAN	87	MRK2	E^{ee}_{cm}= 29 GeV

[1] PROCARIO 93 entry is obtained from $B(h^-3\pi^0\nu_\tau)/B(h^-\pi^0\nu_\tau)$ using ARTUSO 94 result for $B(h^-\pi^0\nu_\tau)$.
[2] BUSKULIC 96 quote $B(h^-3\pi^0\nu_\tau(\text{ex. } K^0)) = 1.17 \pm 0.09 \pm 0.11$. We add 0.07 to remove their correction for K^0 backgrounds.
[3] Highly correlated with GAN 87 $\Gamma(\eta\pi^-\pi^0\nu_\tau)/\Gamma_{total}$ value. Authors quote $B(\pi^\pm3\pi^0\nu_\tau) + 0.67B(\pi^\pm\eta\pi^0\nu_\tau) = 0.047 \pm 0.010 \pm 0.011$.

$\Gamma(h^-3\pi^0\nu_\tau)/\Gamma(h^-\pi^0\nu_\tau)$ Γ_{26}/Γ_{13}

$\Gamma_{26}/\Gamma_{13} = (\Gamma_{27}+\Gamma_{28}+0.15344\Gamma_{41}+0.15344\Gamma_{43}+0.3268\Gamma_{150})/(\Gamma_{14}+\Gamma_{16})$

VALUE (units 10^{-2})	DOCUMENT ID		TECN	COMMENT
4.54±0.28 OUR FIT				
4.4 ±0.3 ±0.5	[1] PROCARIO	93	CLEO	$E^{ee}_{cm} \approx$ 10.6 GeV

[1] PROCARIO 93 quote 0.041 ± 0.003 ± 0.005 after correction for 2 kaon backgrounds assuming $B(K^{*-}\nu_\tau)$=1.42 ± 0.18% and $B(h^-K^0\pi^0\nu_\tau)$=0.48 ± 0.48%. We add 0.003 ± 0.003 and multiply the sum by 0.990 ± 0.010 to remove these corrections.

$\Gamma(\pi^-3\pi^0\nu_\tau(\text{ex.}K^0))/\Gamma_{total}$ Γ_{27}/Γ

VALUE (%)	EVTS	DOCUMENT ID		TECN	COMMENT
1.04 ±0.07 OUR FIT					
0.977±0.069±0.058	6.1k	[1] SCHAEL	05C	ALEP	1991–1995 LEP runs

[1] See footnote to SCHAEL 05C $\Gamma(\tau^- \to e^-\overline{\nu}_e\nu_\tau)/\Gamma_{total}$ measurement for correlations with other measurements.

$\Gamma(K^-3\pi^0\nu_\tau(\text{ex.}K^0,\eta))/\Gamma_{total}$ Γ_{28}/Γ

VALUE (units 10^{-4})	EVTS	DOCUMENT ID		TECN	COMMENT
4.8± 2.1 OUR FIT					
3.7± 2.1±1.1	22	BARATE	99K	ALEP	1991–1995 LEP runs
• • • We do not use the following data for averages, fits, limits, etc. • • •					
5 ±13		[1] BUSKULIC	94E	ALEP	Repl. by BARATE 99K

[1] BUSKULIC 94E quote $B(K^- \geq 0\pi^0 \geq 0K^0\nu_\tau) - [B(K^-\nu_\tau) + B(K^-\pi^0\nu_\tau) + B(K^-K^0\nu_\tau) + B(K^-\pi^0\pi^0\nu_\tau) + B(K^-\pi^0K^0\nu_\tau)] = (5 \pm 13) \times 10^{-4}$ accounting for common systematic errors in BUSKULIC 94E and BUSKULIC 94F measurements of these modes. We assume $B(K^- \geq 2K^0\nu_\tau)$ and $B(K^- \geq 4\pi^0\nu_\tau)$ are negligible.

$\Gamma(h^-4\pi^0\nu_\tau(\text{ex.}K^0))/\Gamma_{total}$ Γ_{29}/Γ

$\Gamma_{29}/\Gamma = (\Gamma_{30}+0.3268\Gamma_{148}+0.3268\Gamma_{152})/\Gamma$

VALUE (%)	EVTS	DOCUMENT ID		TECN	COMMENT
0.16±0.04 OUR FIT					
0.16±0.05±0.05		[1] PROCARIO	93	CLEO	$E^{ee}_{cm} \approx$ 10.6 GeV
• • • We do not use the following data for averages, fits, limits, etc. • • •					
0.16±0.04±0.09	232	[2] BUSKULIC	96	ALEP	Repl. by SCHAEL 05C

[1] PROCARIO 93 quotes $B(h^-4\pi^0\nu_\tau)/B(h^-\pi^0\nu_\tau)$ =0.006±0.002±0.002. We multiply by the ARTUSO 94 result for $B(h^-\pi^0\nu_\tau)$ to obtain $B(h^-4\pi^0\nu_\tau)$. PROCARIO 93 assume $B(h^- \geq 5\ \pi^0\nu_\tau)$ is small and do not correct for it.
[2] BUSKULIC 96 quote result for $\tau^- \to h^- \geq 4\pi^0\nu_\tau$. We assume $B(h^- \geq 5\pi^0\nu_\tau)$ is negligible.

$\Gamma(h^-4\pi^0\nu_\tau(\text{ex.}K^0,\eta))/\Gamma_{total}$ Γ_{30}/Γ

VALUE (%)	EVTS	DOCUMENT ID		TECN	COMMENT
0.11 ±0.04 OUR FIT					
0.112±0.037±0.035	957	[1] SCHAEL	05C	ALEP	1991–1995 LEP runs

[1] See footnote to SCHAEL 05C $\Gamma(\tau^- \to e^-\overline{\nu}_e\nu_\tau)/\Gamma_{total}$ measurement for correlations with other measurements.

$\Gamma(a_1(1260)\nu_\tau \to \pi^-\gamma\nu_\tau)/\Gamma_{total}$ $\Gamma_{31}/\Gamma = (0.0021\Gamma_{20}+0.0021\Gamma_{70})/\Gamma$

The uncertainty on $\Gamma(\tau^- \to a_1(1260)\nu_\tau \to \pi^-\gamma\nu_\tau)/\Gamma_{total}$ is the sum in quadrature of the uncertainty on the fit result for $\Gamma(\tau^- \to a_1(1260)\nu_\tau \to \pi^-\gamma\nu_\tau)/\Gamma_{total}$ and of the uncertainty on $\Gamma(a_1(1260) \to \pi\gamma)/\Gamma_{total}^{a_1(1260)} = ((2.1 \pm 0.8)\times 10^{-3})$ as reported in SCHAEL 05C, which is the coefficient of the relationship that defines $\Gamma(\tau^- \to a_1(1260)\nu_\tau \to \pi^-\gamma\nu_\tau)/\Gamma_{total}$ in terms of $\Gamma(\tau^- \to \pi^-2\pi^0\nu_\tau(\text{ex.}K^0))/\Gamma_{total}$ and $\Gamma(\tau^- \to \pi^-\pi^+\pi^-\nu_\tau(\text{ex.}K^0,\omega))/\Gamma_{total}$.

VALUE (units 10^{-4})	DOCUMENT ID
3.8±1.5 OUR FIT	

$\Gamma(K^- \geq 0\pi^0 \geq 0K^0 \geq 0\gamma\,\nu_\tau)/\Gamma_{total}$ Γ_{32}/Γ

$\Gamma_{32}/\Gamma = (\Gamma_{10}+\Gamma_{16}+\Gamma_{23}+\Gamma_{28}+\Gamma_{38}+\Gamma_{43}+0.7212\Gamma_{150}+0.1049\Gamma_{168})/\Gamma$

VALUE (%)	EVTS	DOCUMENT ID		TECN	COMMENT
1.552±0.029 OUR FIT					
1.53 ±0.04 OUR AVERAGE					
1.528±0.039±0.040		[1] ABBIENDI	01J	OPAL	1990–1995 LEP runs
1.54 ±0.24		ABREU	94K	DLPH	LEP 1992 Z data
1.70 ±0.12 ±0.19	202	[2] BATTLE	94	CLEO	$E_{cm}^{ee} \approx$ 10.6 GeV
• • • We use the following data for averages but not for fits. • • •					
1.520±0.040±0.041	4006	[3] BARATE	99K	ALEP	1991–1995 LEP runs
• • • We do not use the following data for averages, fits, limits, etc. • • •					
1.70 ±0.05 ±0.06	1610	[4] BUSKULIC	96	ALEP	Repl. by BARATE 99K
1.6 ±0.4 ±0.2	35	AIHARA	87B	TPC	E_{cm}^{ee}= 29 GeV
1.71 ±0.29	53	MILLS	84	DLCO	E_{cm}^{ee}= 29 GeV

[1] The correlation coefficient between this measurement and the ABBIENDI 01J $B(\tau^- \to K^-\nu_\tau)$ is 0.60.
[2] BATTLE 94 quote 1.60 ± 0.12 ± 0.19. We add 0.10 ± 0.02 to correct for their rejection of $K_S^0 \to \pi^+\pi^-$ decays.
[3] Not independent of BARATE 99K $B(K^-\nu_\tau)$, $B(K^-\pi^0\nu_\tau)$, $B(K^-2\pi^0\nu_\tau(\text{ex. }K^0))$, $B(K^-3\pi^0\nu_\tau(\text{ex. }K^0))$, $B(K^-K^0\nu_\tau)$, and $B(K^-K^0\pi^0\nu_\tau)$ values.
[4] Not independent of BUSKULIC 96 $B(K^-\nu_\tau)$, $B(K^-\pi^0\nu_\tau)$, $B(K^-2\pi^0\nu_\tau)$, $B(K^-K^0\nu_\tau)$, and $B(K^-K^0\pi^0\nu_\tau)$ values.

$\Gamma(K^- \geq 1(\pi^0 \text{ or } K^0 \text{ or } \gamma)\,\nu_\tau)/\Gamma_{total}$ Γ_{33}/Γ

$\Gamma_{33}/\Gamma = (\Gamma_{16}+\Gamma_{23}+\Gamma_{28}+\Gamma_{38}+\Gamma_{43}+0.7212\Gamma_{150}+0.7212\Gamma_{152}+0.1049\Gamma_{168})/\Gamma$

VALUE (%)	EVTS	DOCUMENT ID		TECN	COMMENT
0.859±0.028 OUR FIT					
0.86 ±0.05 OUR AVERAGE					
• • • We use the following data for averages but not for fits. • • •					
0.869±0.031±0.034		[1] ABBIENDI	01J	OPAL	1990–1995 LEP runs
0.69 ±0.25		[2] ABREU	94K	DLPH	LEP 1992 Z data
• • • We do not use the following data for averages, fits, limits, etc. • • •					
1.2 ±0.5 $^{+0.2}_{-0.4}$	9	AIHARA	87B	TPC	E_{cm}^{ee}= 29 GeV

[1] Not independent of ABBIENDI 01J $B(\tau^- \to K^-\nu_\tau)$ and $B(\tau^- \to K^- \geq 0\pi^0 \geq 0K^0 \geq 0\gamma\ \nu_\tau)$ values.
[2] Not independent of ABREU 94K $B(K^-\nu_\tau)$ and $B(K^- \geq 0 \text{ neutrals}\nu_\tau)$ measurements.

$\Gamma(K_S^0(\text{particles})^-\nu_\tau)/\Gamma_{total}$ Γ_{34}/Γ

$\Gamma_{34}/\Gamma = (\frac{1}{2}\Gamma_{36}+\frac{1}{2}\Gamma_{38}+\frac{1}{2}\Gamma_{41}+\frac{1}{2}\Gamma_{43}+\frac{1}{2}\Gamma_{45}+\Gamma_{48}+\Gamma_{49}+\Gamma_{52}+\Gamma_{56}+0.3606\Gamma_{154}+0.340\Gamma_{168})/\Gamma$

VALUE (%)	EVTS	DOCUMENT ID		TECN	COMMENT
0.944±0.028 OUR FIT					
0.918±0.015 OUR AVERAGE					
0.970±0.058±0.062	929	BARATE	98E	ALEP	1991–1995 LEP runs
0.97 ±0.09 ±0.06	141	AKERS	94G	OPAL	E_{cm}^{ee}= 88–94 GeV
• • • We use the following data for averages but not for fits. • • •					
0.915±0.001±0.015	398k	[1] RYU	14	BELL	669 fb^{-1} E_{cm}^{ee}=10.6 GeV

[1] Not independent of RYU 14 measurements of $B(\tau^- \to \pi^-\overline{K}^0\nu_\tau)$, $B(\tau^- \to K^-K^0\nu_\tau)$, $B(\tau^- \to \pi^-\overline{K}^0\pi^0\nu_\tau)$, $B(\tau^- \to K^-K^0\pi^0\nu_\tau)$, $B(\tau^- \to \pi^-K_S^0K_S^0\nu_\tau)$, and $B(\tau^- \to \pi^-K_S^0K_S^0\pi^0\nu_\tau)$.

$\Gamma(h^-\overline{K}^0\nu_\tau)/\Gamma_{total}$ $\Gamma_{35}/\Gamma = (\Gamma_{36}+\Gamma_{38})/\Gamma$

VALUE (%)	EVTS	DOCUMENT ID		TECN	COMMENT
0.987±0.014 OUR FIT					
0.90 ±0.07 OUR AVERAGE					
0.855±0.036±0.073	1242	COAN	96	CLEO	$E_{cm}^{ee} \approx$ 10.6 GeV
• • • We use the following data for averages but not for fits. • • •					
1.01 ±0.11 ±0.07	555	[1] BARATE	98E	ALEP	1991–1995 LEP runs

[1] Not independent of BARATE 98E $B(\tau^- \to \pi^-\overline{K}^0\nu_\tau)$ and $B(\tau^- \to K^-K^0\nu_\tau)$ values.

$\Gamma(\pi^-\overline{K}^0\nu_\tau)/\Gamma_{total}$ Γ_{36}/Γ

VALUE (units 10^{-3})	EVTS	DOCUMENT ID		TECN	COMMENT
8.40±0.14 OUR FIT					
8.39±0.22 OUR AVERAGE Error includes scale factor of 1.5. See the ideogram below.					
8.32±0.02±0.16	158k	[1] RYU	14	BELL	669 fb^{-1} E_{cm}^{ee}=10.6 GeV
9.33±0.68±0.49	377	ABBIENDI	00C	OPAL	1991–1995 LEP runs
9.28±0.45±0.34	937	[2] BARATE	99K	ALEP	1991–1995 LEP runs
9.5 ±1.5 ±0.6		[3] ACCIARRI	95F	L3	1991–1993 LEP runs
• • • We use the following data for averages but not for fits. • • •					
8.55±1.17±0.66	509	[4] BARATE	98E	ALEP	1991–1995 LEP runs
7.04±0.41±0.72		[5] COAN	96	CLEO	$E_{cm}^{ee} \approx$ 10.6 GeV
• • • We do not use the following data for averages, fits, limits, etc. • • •					
8.08±0.04±0.26	53k	EPIFANOV	07	BELL	Repl. by RYU 14
7.9 ±1.0 ±0.9	98	[6] BUSKULIC	96	ALEP	Repl. by BARATE 99K

[1] RYU 14 reconstruct K^0's using $K_S^0 \to \pi^+\pi^-$ decays.
[2] BARATE 99K measure K^0's by detecting K_L^0's in their hadron calorimeter.
[3] ACCIARRI 95F do not identify π^-/K^- and assume $B(K^-K^0\nu_\tau) = (0.29 \pm 0.12)\%$.
[4] BARATE 98E reconstruct K^0's using $K_S^0 \to \pi^+\pi^-$ decays. Not independent of BARATE 98E $B(K^0 \text{particles}^-\nu_\tau)$ value.
[5] Not independent of COAN 96 $B(h^-K^0\nu_\tau)$ and $B(K^-K^0\nu_\tau)$ measurements.
[6] BUSKULIC 96 measure K^0's by detecting K_L^0's in their hadron calorimeter.

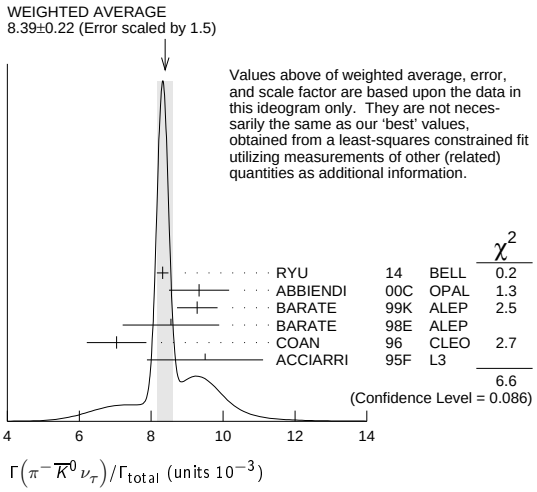

$\Gamma(\pi^-\overline{K}^0(\text{non-}K^*(892)^-)\nu_\tau)/\Gamma_{total}$ Γ_{37}/Γ

VALUE (units 10^{-4})	CL%	DOCUMENT ID		TECN	COMMENT
5.4±2.1		[1] EPIFANOV	07	BELL	351 fb^{-1} E_{cm}^{ee}= 10.6 GeV
• • • We do not use the following data for averages, fits, limits, etc. • • •					
<17	95	ACCIARRI	95F	L3	1991–1993 LEP runs

[1] EPIFANOV 07 quote $B(\tau^- \to K^*(892)^-\nu_\tau)\ B(K^*(892)^- \to K_S^0\pi^-)\ /\ B(\tau^- \to K_S^0\pi^-\nu_\tau) = 0.933 \pm 0.027$. We multiply their $B(\tau^- \to \overline{K}^0\pi^-\nu_\tau)$ by [1−(0.933 ± 0.027)] to obtain this result.

$\Gamma(K^-K^0\nu_\tau)/\Gamma_{total}$ Γ_{38}/Γ

VALUE (units 10^{-4})	EVTS	DOCUMENT ID		TECN	COMMENT
14.8 ±0.5 OUR FIT					
14.9 ±0.5 OUR AVERAGE					
14.80±0.14±0.54	33k	[1] RYU	14	BELL	669 fb^{-1} E_{cm}^{ee}=10.6 GeV
16.2 ±2.1 ±1.1	150	[2] BARATE	99K	ALEP	1991–1995 LEP runs
15.8 ±4.2 ±1.7	46	[3] BARATE	98E	ALEP	1991–1995 LEP runs
15.1 ±2.1 ±2.2	111	COAN	96	CLEO	$E_{cm}^{ee} \approx$ 10.6 GeV
• • • We do not use the following data for averages, fits, limits, etc. • • •					
26 ±9 ±2	13	[4] BUSKULIC	96	ALEP	Repl. by BARATE 99K

[1] RYU 14 reconstruct K^0's using $K_S^0 \to \pi^+\pi^-$ decays.
[2] BARATE 99K measure K^0's by detecting K_L^0's in their hadron calorimeter.
[3] BARATE 98E reconstruct K^0's using $K_S^0 \to \pi^+\pi^-$ decays.
[4] BUSKULIC 96 measure K^0's by detecting K_L^0's in their hadron calorimeter.

$\Gamma(K^-K^0 \geq 0\pi^0\nu_\tau)/\Gamma_{total}$ $\Gamma_{39}/\Gamma = (\Gamma_{38}+\Gamma_{43})/\Gamma$

VALUE (%)	EVTS	DOCUMENT ID		TECN	COMMENT
0.298±0.008 OUR FIT					
0.330±0.055±0.039	124	ABBIENDI	00C	OPAL	1991–1995 LEP runs

$\Gamma(h^-\overline{K}^0\pi^0\nu_\tau)/\Gamma_{total}$ $\Gamma_{40}/\Gamma = (\Gamma_{41}+\Gamma_{43})/\Gamma$

VALUE (%)	EVTS	DOCUMENT ID		TECN	COMMENT
0.532±0.013 OUR FIT					
0.50 ±0.06 OUR AVERAGE Error includes scale factor of 1.2.					
0.562±0.050±0.048	264	COAN	96	CLEO	$E_{cm}^{ee} \approx$ 10.6 GeV
• • • We use the following data for averages but not for fits. • • •					
0.446±0.052±0.046	157	[1] BARATE	98E	ALEP	1991–1995 LEP runs

[1] Not independent of BARATE 98E $B(\tau^- \to \pi^-\overline{K}^0\pi^0\tau)$ and $B(\tau^- \to K^-K^0\pi^0\nu_\tau)$ values.

$\Gamma(\pi^-\overline{K}^0\pi^0\nu_\tau)/\Gamma_{total}$ Γ_{41}/Γ

VALUE (%)	EVTS	DOCUMENT ID		TECN	COMMENT
0.382±0.013 OUR FIT					
0.383±0.014 OUR AVERAGE					
0.386±0.004±0.014	27k	[1] RYU	14	BELL	669 fb^{-1} E_{cm}^{ee}=10.6 GeV
0.347±0.053±0.037	299	[2] BARATE	99K	ALEP	1991–1995 LEP runs
0.294±0.073±0.037	142	[3] BARATE	98E	ALEP	1991–1995 LEP runs
0.41 ±0.12 ±0.03		[4] ACCIARRI	95F	L3	1991–1993 LEP runs
• • • We use the following data for averages but not for fits. • • •					
0.417±0.058±0.044		[5] COAN	96	CLEO	$E_{cm}^{ee}\approx$ 10.6 GeV
• • • We do not use the following data for averages, fits, limits, etc. • • •					
0.32 ±0.11 ±0.05	23	[6] BUSKULIC	96	ALEP	Repl. by BARATE 99K

[1] RYU 14 reconstruct K^0's using $K_S^0\to\pi^+\pi^-$ decays.
[2] BARATE 99K measure K^0's by detecting K_L^0's in their hadron calorimeter.
[3] BARATE 98E reconstruct K^0's using $K_S^0\to\pi^+\pi^-$ decays.
[4] ACCIARRI 95F do not identify π^-/K^- and assume B($K^-K^0\pi^0\nu_\tau$) = (0.05 ± 0.05)%.
[5] Not independent of COAN 96 B($h^-K^0\pi^0\nu_\tau$) and B($K^-K^0\pi^0\nu_\tau$) measurements.
[6] BUSKULIC 96 measure K^0's by detecting K_L^0's in their hadron calorimeter.

$\Gamma(\overline{K}^0\rho^-\nu_\tau)/\Gamma_{total}$ Γ_{42}/Γ

VALUE (%)	DOCUMENT ID		TECN	COMMENT
0.22 ±0.05 OUR AVERAGE				
0.250±0.057±0.044	[1] BARATE	99K	ALEP	1991–1995 LEP runs
0.188±0.054±0.038	[2] BARATE	98E	ALEP	1991–1995 LEP runs

[1] BARATE 99K measure K^0's by detecting K_L^0's in hadron calorimeter. They determine the $\overline{K}^0\rho^-$ fraction in $\tau^-\to\pi^-\overline{K}^0\pi^0\nu_\tau$ decays to be (0.72 ± 0.12 ± 0.10) and multiply their B($\pi^-\overline{K}^0\pi^0\nu_\tau$) measurement by this fraction to obtain the quoted result.
[2] BARATE 98E reconstruct K^0's using $K_S^0\to\pi^+\pi^-$ decays. They determine the $\overline{K}^0\rho^-$ fraction in $\tau^-\to\pi^-\overline{K}^0\pi^0\nu_\tau$ decays to be (0.64 ± 0.09 ± 0.10) and multiply their B($\pi^-\overline{K}^0\pi^0\nu_\tau$) measurement by this fraction to obtain the quoted result.

$\Gamma(K^-K^0\pi^0\nu_\tau)/\Gamma_{total}$ Γ_{43}/Γ

VALUE (units 10^{-4})	EVTS	DOCUMENT ID		TECN	COMMENT
15.0 ±0.7 OUR FIT					
14.9 ±0.7 OUR AVERAGE					
14.96±0.20±0.74	8.3k	[1] RYU	14	BELL	669 fb^{-1} E_{cm}^{ee}=10.6 GeV
14.3 ±2.5 ±1.5	78	[2] BARATE	99K	ALEP	1991–1995 LEP runs
15.2 ±7.6 ±2.1	15	[3] BARATE	98E	ALEP	1991–1995 LEP runs
14.5 ±3.6 ±2.0	32	COAN	96	CLEO	$E_{cm}^{ee}\approx$ 10.6 GeV
• • • We do not use the following data for averages, fits, limits, etc. • • •					
10 ±5 ±3	5	[4] BUSKULIC	96	ALEP	Repl. by BARATE 99K

[1] RYU 14 reconstruct K^0's using $K_S^0\to\pi^+\pi^-$ decays.
[2] BARATE 99K measure K^0's by detecting K_L^0's in their hadron calorimeter.
[3] BARATE 98E reconstruct K^0's using $K_S^0\to\pi^+\pi^-$ decays.
[4] BUSKULIC 96 measure K^0's by detecting K_L^0's in their hadron calorimeter.

$\Gamma(\pi^-\overline{K}^0\geq 1\pi^0\nu_\tau)/\Gamma_{total}$ $\Gamma_{44}/\Gamma=(\Gamma_{41}+\Gamma_{45})/\Gamma$

VALUE (%)	EVTS	DOCUMENT ID		TECN	COMMENT
0.408±0.025 OUR FIT					
0.324±0.074±0.066	148	ABBIENDI	00C	OPAL	1991–1995 LEP runs

$\Gamma(\pi^-\overline{K}^0\pi^0\pi^0\nu_\tau\,(\text{ex.}K^0))/\Gamma_{total}$ Γ_{45}/Γ

VALUE (units 10^{-3})	CL%	EVTS	DOCUMENT ID		TECN	COMMENT
0.26±0.23 OUR FIT						
0.26±0.24			[1] BARATE	99R	ALEP	1991–1995 LEP runs
• • • We do not use the following data for averages, fits, limits, etc. • • •						
<0.66	95	17	[2] BARATE	99K	ALEP	1991–1995 LEP runs
0.58±0.33±0.14		5	[3] BARATE	98E	ALEP	1991–1995 LEP runs

[1] BARATE 99R combine the BARATE 98E and BARATE 99K measurements to obtain this value.
[2] BARATE 99K measure K^0's by detecting K_L^0's in their hadron calorimeter.
[3] BARATE 98E reconstruct K^0's using $K_S^0\to\pi^+\pi^-$ decays.

$\Gamma(K^-K^0\pi^0\pi^0\nu_\tau)/\Gamma_{total}$ Γ_{46}/Γ

VALUE	CL%	DOCUMENT ID		TECN	COMMENT
<0.16 × 10^{-3}	95	[1] BARATE	99R	ALEP	1991–1995 LEP runs
• • • We do not use the following data for averages, fits, limits, etc. • • •					
<0.18 × 10^{-3}	95	[2] BARATE	99K	ALEP	1991–1995 LEP runs
<0.39 × 10^{-3}	95	[3] BARATE	98E	ALEP	1991–1995 LEP runs

[1] BARATE 99R combine the BARATE 98E and BARATE 99K bounds to obtain this value.
[2] BARATE 99K measure K^0's by detecting K_L^0's in hadron calorimeter.
[3] BARATE 98E reconstruct K^0's by using $K_S^0\to\pi^+\pi^-$ decays.

$\Gamma(\pi^-K^0\overline{K}^0\nu_\tau)/\Gamma_{total}$ $\Gamma_{47}/\Gamma=(\Gamma_{48}+\Gamma_{49}+\Gamma_{50})/\Gamma$

VALUE (%)	EVTS	DOCUMENT ID		TECN	COMMENT
0.155±0.024 OUR FIT					
• • • We use the following data for averages but not for fits. • • •					
0.153±0.030±0.016	74	[1] BARATE	98E	ALEP	1991–1995 LEP runs
• • • We do not use the following data for averages, fits, limits, etc. • • •					
0.31 ±0.12 ±0.04		[2] ACCIARRI	95F	L3	1991–1993 LEP runs

[1] BARATE 98E obtain this value by adding twice their B($\pi^-K_S^0K_S^0\nu_\tau$) value to their B($\pi^-K_S^0K_L^0\nu_\tau$) value.
[2] ACCIARRI 95F assume B($\pi^-K_S^0K_S^0\nu$)= B($\pi^-K_S^0K_L^0\nu$) = 1/2B($\pi^-K_S^0K_L^0\nu$).

$\Gamma(\pi^-K_S^0K_S^0\nu_\tau)/\Gamma_{total}$ Γ_{48}/Γ

Bose-Einstein correlations might make the mixing fraction different than 1/4.

VALUE (units 10^{-4})	EVTS	DOCUMENT ID		TECN	COMMENT
2.33±0.07 OUR FIT					
2.32±0.06 OUR AVERAGE					
2.33±0.03±0.09	6.7k	RYU	14	BELL	669 fb^{-1} E_{cm}^{ee}=10.6 GeV
2.31±0.04±0.08	5.0k	LEES	12Y	BABR	468 fb^{-1} E_{cm}^{ee}=10.6 GeV
2.6 ±1.0 ±0.5	6	BARATE	98E	ALEP	1991–1995 LEP runs
2.3 ±0.5 ±0.3	42	COAN	96	CLEO	$E_{cm}^{ee}\approx$ 10.6 GeV

$\Gamma(\pi^-K_S^0K_L^0\nu_\tau)/\Gamma_{total}$ Γ_{49}/Γ

VALUE (units 10^{-4})	EVTS	DOCUMENT ID		TECN	COMMENT
10.8±2.4 OUR FIT					
10.1±2.3±1.3	68	BARATE	98E	ALEP	1991–1995 LEP runs

$\Gamma(\pi^-K_L^0K_L^0\nu_\tau)/\Gamma_{total}$ $\Gamma_{50}/\Gamma=\Gamma_{48}/\Gamma$

VALUE (units 10^{-4})	DOCUMENT ID
2.33±0.07 OUR FIT	

$\Gamma(\pi^-K^0\overline{K}^0\pi^0\nu_\tau)/\Gamma_{total}$ $\Gamma_{51}/\Gamma=(\Gamma_{52}+\Gamma_{56}+\Gamma_{57})/\Gamma$

VALUE (units 10^{-4})	DOCUMENT ID		TECN	COMMENT
3.6±1.2 OUR FIT				
• • • We use the following data for averages but not for fits. • • •				
3.1±2.3	[1] BARATE	99R	ALEP	1991–1995 LEP runs

[1] BARATE 99R combine BARATE 98E $\Gamma(\pi^-K_S^0K_S^0\pi^0\nu_\tau)/\Gamma_{total}$ and $\Gamma(\pi^-K_S^0K_L^0\pi^0\nu_\tau)/\Gamma_{total}$ measurements to obtain this value.

$\Gamma(\pi^-K_S^0K_S^0\pi^0\nu_\tau)/\Gamma_{total}$ Γ_{52}/Γ

VALUE (units 10^{-5})	CL%	EVTS	DOCUMENT ID		TECN	COMMENT
1.82±0.21 OUR FIT						
1.80±0.21 OUR AVERAGE						
2.00±0.22±0.20		303	RYU	14	BELL	669 fb^{-1} E_{cm}^{ee}=10.6 GeV
1.60±0.20±0.22		409	LEES	12Y	BABR	468 fb^{-1} E_{cm}^{ee}=10.6 GeV
• • • We do not use the following data for averages, fits, limits, etc. • • •						
<20	95		BARATE	98E	ALEP	1991–1995 LEP runs

$\Gamma(K^{*-}K^0\pi^0\nu_\tau\to\pi^-K_S^0K_S^0\pi^0\nu_\tau)/\Gamma_{total}$ Γ_{53}/Γ

VALUE (units 10^{-6})	DOCUMENT ID		TECN	COMMENT
10.8±1.4±1.5	RYU	14	BELL	669 fb^{-1} E_{cm}^{ee}=10.6 GeV

$\Gamma(f_1(1285)\pi^-\nu_\tau\to\pi^-K_S^0K_S^0\pi^0\nu_\tau)/\Gamma_{total}$ Γ_{54}/Γ

VALUE (units 10^{-6})	DOCUMENT ID		TECN	COMMENT
6.8±1.3±0.7	RYU	14	BELL	669 fb^{-1} E_{cm}^{ee}=10.6 GeV

$\Gamma(f_1(1420)\pi^-\nu_\tau\to\pi^-K_S^0K_S^0\pi^0\nu_\tau)/\Gamma_{total}$ Γ_{55}/Γ

VALUE (units 10^{-6})	DOCUMENT ID		TECN	COMMENT
2.4±0.5±0.6	RYU	14	BELL	669 fb^{-1} E_{cm}^{ee}=10.6 GeV

$\Gamma(\pi^-K_S^0K_L^0\pi^0\nu_\tau)/\Gamma_{total}$ Γ_{56}/Γ

VALUE (units 10^{-4})	EVTS	DOCUMENT ID		TECN	COMMENT
3.2±1.2 OUR FIT					
3.1±1.1±0.5	11	BARATE	98E	ALEP	1991–1995 LEP runs

$\Gamma(\pi^-K_L^0K_L^0\pi^0\nu_\tau)/\Gamma_{total}$ $\Gamma_{57}/\Gamma=\Gamma_{52}/\Gamma$

VALUE (units 10^{-5})	DOCUMENT ID
1.82±0.21 OUR FIT	

$\Gamma(K^-K_S^0K_S^0\nu_\tau)/\Gamma_{total}$ Γ_{58}/Γ

VALUE	CL%	DOCUMENT ID		TECN	COMMENT
<6.3 × 10^{-7}	90	LEES	12Y	BABR	468 fb^{-1} E_{cm}^{ee}=10.6 GeV

$\Gamma(K^-K_S^0K_S^0\pi^0\nu_\tau)/\Gamma_{total}$ Γ_{59}/Γ

VALUE	CL%	DOCUMENT ID		TECN	COMMENT
<4.0 × 10^{-7}	90	LEES	12Y	BABR	468 fb^{-1} E_{cm}^{ee}=10.6 GeV

$\Gamma(K^0h^+h^-h^-\geq 0\text{ neutrals }\nu_\tau)/\Gamma_{total}$ Γ_{60}/Γ

VALUE (%)	CL%	DOCUMENT ID		TECN	COMMENT
<0.17	95	TSCHIRHART	88	HRS	E_{cm}^{ee}= 29 GeV
• • • We do not use the following data for averages, fits, limits, etc. • • •					
<0.27	90	BELTRAMI	85	HRS	E_{cm}^{ee}= 29 GeV

$\Gamma(K^0h^+h^-h^-\nu_\tau)/\Gamma_{total}$ Γ_{61}/Γ

VALUE (units 10^{-4})	EVTS	DOCUMENT ID		TECN	COMMENT
2.5±2.0 OUR FIT					
2.3±1.9±0.7	6	[1] BARATE	98E	ALEP	1991–1995 LEP runs

[1] BARATE 98E reconstruct K^0's using $K_S^0\to\pi^+\pi^-$ decays.

$\Gamma(h^-h^-h^+ \geq 0 \text{ neutrals } \geq 0K^0_L\nu_\tau)/\Gamma_{\text{total}}$ Γ_{62}/Γ

$\Gamma_{62}/\Gamma = (0.34598\Gamma_{36}+0.34598\Gamma_{38}+0.34598\Gamma_{41}+0.34598\Gamma_{43}+0.4247\Gamma_{48}+0.6920\Gamma_{49}+0.4247\Gamma_{52}+0.6920\Gamma_{56}+0.6534\Gamma_{61}+\Gamma_{70}+\Gamma_{78}+\Gamma_{85}+\Gamma_{86}+\Gamma_{97}+\Gamma_{103}+\Gamma_{106}+\Gamma_{107}+0.2810\Gamma_{148}+0.2810\Gamma_{150}+0.2810\Gamma_{152}+0.2628\Gamma_{154}+0.7259\Gamma_{168}+0.9078\Gamma_{176}+0.9078\Gamma_{177}+0.9078\Gamma_{178})/\Gamma$

VALUE (%)	EVTS	DOCUMENT ID		TECN	COMMENT
15.21± 0.06 OUR FIT					
14.8 ± 0.4 OUR AVERAGE					
14.4 ± 0.6 ±0.3		ADEVA	91F	L3	E^{ee}_{cm}= 88.3–94.3 GeV
15.0 ± 0.4 ±0.3		BEHREND	89B	CELL	E^{ee}_{cm}= 14–47 GeV
15.1 ± 0.8 ±0.6		AIHARA	87B	TPC	E^{ee}_{cm}= 29 GeV
• • • We do not use the following data for averages, fits, limits, etc. • • •					
13.5 ± 0.3 ±0.3		ABACHI	89B	HRS	E^{ee}_{cm}= 29 GeV
12.8 ± 1.0 ±0.7		[1] BURCHAT	87	MRK2	E^{ee}_{cm}= 29 GeV
12.1 ± 0.5 ±1.2		RUCKSTUHL	86	DLCO	E^{ee}_{cm}= 29 GeV
12.8 ± 0.5 ±0.8	1420	SCHMIDKE	86	MRK2	E^{ee}_{cm}= 29 GeV
15.3 ± 1.1 $^{+1.3}_{-1.6}$	367	ALTHOFF	85	TASS	E^{ee}_{cm}= 34.5 GeV
13.6 ± 0.5 ±0.8		BARTEL	85F	JADE	E^{ee}_{cm}= 34.6 GeV
12.2 ± 1.3 ±3.9		[2] BERGER	85	PLUT	E^{ee}_{cm}= 34.6 GeV
13.3 ± 0.3 ±0.6		FERNANDEZ	85	MAC	E^{ee}_{cm}= 29 GeV
24 ± 6	35	BRANDELIK	80	TASS	E^{ee}_{cm}= 30 GeV
32 ± 5	692	[3] BACINO	78B	DLCO	E^{ee}_{cm}= 3.1–7.4 GeV
35 ±11		[3] BRANDELIK	78	DASP	Assumes $V-A$ decay
18 ± 6.5	33	[3] JAROS	78	LGW	$E^{ee}_{\text{cm}} > 6$ GeV

[1] BURCHAT 87 value is not independent of SCHMIDKE 86 value.
[2] Not independent of BERGER 85 $\Gamma(\mu^-\overline{\nu}_\mu\nu_\tau)/\Gamma_{\text{total}}$, $\Gamma(e^-\overline{\nu}_e\nu_\tau)/\Gamma_{\text{total}}$, $\Gamma(h^- \geq 1 \text{ neutrals}\,\nu_\tau)/\Gamma_{\text{total}}$, and $\Gamma(h^- \geq 0K^0_L\,\nu_\tau)/\Gamma_{\text{total}}$, and therefore not used in the fit.
[3] Low energy experiments are not in average or fit because the systematic errors in background subtraction are judged to be large.

$\Gamma(h^-h^-h^+ \geq 0 \text{ neutrals } \nu_\tau(\text{ex. } K^0_S \to \pi^+\pi^-)(\text{"3-prong"}))/\Gamma_{\text{total}}$ Γ_{63}/Γ

$\Gamma_{63}/\Gamma = (\Gamma_{70}+\Gamma_{78}+\Gamma_{85}+\Gamma_{86}+\Gamma_{97}+\Gamma_{103}+\Gamma_{106}+\Gamma_{107}+0.2810\Gamma_{148}+0.2810\Gamma_{150}+0.2810\Gamma_{152}+0.492\Gamma_{168}+0.9078\Gamma_{176}+0.9078\Gamma_{177}+0.9078\Gamma_{178})/\Gamma$

VALUE (%)	EVTS	DOCUMENT ID		TECN	COMMENT
14.55 ±0.06 OUR FIT					
14.61 ±0.06 OUR AVERAGE					
14.556±0.105±0.076		[1] ACHARD	01D	L3	1992–1995 LEP runs
14.96 ±0.09 ±0.22	10.4k	AKERS	95Y	OPAL	1991–1994 LEP runs
• • • We use the following data for averages but not for fits. • • •					
14.652±0.067±0.086		SCHAEL	05C	ALEP	1991–1995 LEP runs
14.569±0.093±0.048	23k	[2] ABREU	01M	DLPH	1992–1995 LEP runs
14.22 ±0.10 ±0.37		[3] BALEST	95C	CLEO	$E^{ee}_{\text{cm}} \approx 10.6$ GeV
• • • We use the following data for averages, fits, limits, etc. • • •					
15.26 ±0.26 ±0.22		ACTON	92H	OPAL	Repl. by AKERS 95Y
13.3 ±0.3 ±0.8		[4] ALBRECHT	92D	ARG	E^{ee}_{cm}= 9.4–10.6 GeV
14.35 $^{+0.40}_{-0.45}$ ±0.24		DECAMP	92C	ALEP	1989–1990 LEP runs

[1] The correlation coefficients between this measurement and the ACHARD 01D measurements of B($\tau \to$ "1-prong") and B($\tau \to$ "5-prong") are -0.978 and -0.19 respectively.
[2] The correlation coefficients between this measurement and the ABREU 01M measurements of B($\tau \to$ 1-prong) and B($\tau \to$ 5-prong) are -0.98 and -0.08 respectively.
[3] Not independent of BALEST 95C B($h^-h^-h^+\nu_\tau$) and B($h^-h^-h^+\pi^0\nu_\tau$) values, and BORTOLETTO 93 B($h^-h^-h^+2\pi^0\nu_\tau$)/B($h^-h^-h^+ \geq 0$ neutrals ν_τ) value.
[4] This ALBRECHT 92D value is not independent of their $\Gamma(\mu^-\overline{\nu}_\mu\nu_\tau)\Gamma(e^-\overline{\nu}_e\nu_\tau)/\Gamma^2_{\text{total}}$ value.

$\Gamma(h^-h^-h^+\nu_\tau)/\Gamma_{\text{total}}$ Γ_{64}/Γ

$\Gamma_{64}/\Gamma = (0.34598\Gamma_{36}+0.34598\Gamma_{38}+\Gamma_{70}+\Gamma_{97}+\Gamma_{106}+0.492\Gamma_{168}+0.0153\Gamma_{176}+0.0153\Gamma_{177})/\Gamma$

VALUE (%)	EVTS	DOCUMENT ID		TECN	COMMENT
9.80±0.05 OUR FIT					
• • • We use the following data for averages but not for fits. • • •					
7.6 ±0.1 ±0.5	7.5k	[1] ALBRECHT	96E	ARG	E^{ee}_{cm}= 9.4–10.6 GeV
• • • We do not use the following data for averages, fits, limits, etc. • • •					
9.92±0.10±0.09	11.2k	[2] BUSKULIC	96	ALEP	Repl. by SCHAEL 05C
9.49±0.36±0.63		DECAMP	92C	ALEP	Repl. by SCHAEL 05C
8.7 ±0.7 ±0.3	694	[3] BEHREND	90	CELL	E^{ee}_{cm}= 35 GeV
7.0 ±0.3 ±0.7	1566	[4] BAND	87	MAC	E^{ee}_{cm}= 29 GeV
6.7 ±0.8 ±0.9		[5] BURCHAT	87	MRK2	E^{ee}_{cm}= 29 GeV
6.4 ±0.4 ±0.9		[6] RUCKSTUHL	86	DLCO	E^{ee}_{cm}= 29 GeV
7.8 ±0.5 ±0.8	890	SCHMIDKE	86	MRK2	E^{ee}_{cm}= 29 GeV
8.4 ±0.4 ±0.7	1255	[6] FERNANDEZ	85	MAC	E^{ee}_{cm}= 29 GeV
9.7 ±2.0 ±1.3		BEHREND	84	CELL	E^{ee}_{cm}= 14,22 GeV

[1] ALBRECHT 96E not independent of ALBRECHT 93C $\Gamma(h^-h^-h^+\nu_\tau(\text{ex. } K^0) \times \Gamma(\text{particle}^- \geq 0 \text{ neutrals } \geq 0K^0_L\nu_\tau)/\Gamma^2_{\text{total}}$ value.
[2] BUSKULIC 96 quote B($h^-h^-h^+\nu_\tau$(ex. K^0)) = 9.50 ± 0.10 ± 0.11. We add 0.42 to remove their K^0 correction and reduce the systematic error accordingly.
[3] BEHREND 90 subtract 0.3% to account for the $\tau^- \to K^*(892)^-\nu_\tau$ contribution to measured events.
[4] BAND 87 subtract for charged kaon modes; not independent of FERNANDEZ 85 value.
[5] BURCHAT 87 value is not independent of SCHMIDKE 86 value.
[6] Value obtained by multiplying paper's R = B($h^-h^-h^+\nu_\tau$)/B(3-prong) by B(3-prong) = 0.143 and subtracting 0.3% for $K^*(892)$ background.

$\Gamma(h^-h^-h^+\nu_\tau(\text{ex.}K^0))/\Gamma_{\text{total}}$ Γ_{65}/Γ

$\Gamma_{65}/\Gamma = (\Gamma_{70}+\Gamma_{97}+\Gamma_{106}+0.492\Gamma_{168}+0.0153\Gamma_{176}+0.0153\Gamma_{177})/\Gamma$

VALUE (%)	EVTS	DOCUMENT ID		TECN	COMMENT
9.46 ±0.05 OUR FIT					
9.44 ±0.14 OUR AVERAGE		Error includes scale factor of 1.4. See the ideogram below.			
9.317±0.090±0.082	12.2k	[1] ABDALLAH	06A	DLPH	1992–1995 LEP runs
9.51 ±0.07 ±0.20	37.7k	BALEST	95C	CLEO	$E^{ee}_{\text{cm}} \approx 10.6$ GeV
• • • We use the following data for averages but not for fits. • • •					
9.87 ±0.10 ±0.24		[2] AKERS	95Y	OPAL	1991–1994 LEP runs
• • • We do not use the following data for averages, fits, limits, etc. • • •					
9.50 ±0.10 ±0.11	11.2k	[3] BUSKULIC	96	ALEP	Repl. by SCHAEL 05C

[1] See footnote to ABDALLAH 06A $\Gamma(\tau^- \to h^-\nu_\tau)/\Gamma_{\text{total}}$ measurement for correlations with other measurements.
[2] Not independent of AKERS 95Y B($h^-h^-h^+ \geq 0$ neutrals ν_τ(ex. $K^0_S \to \pi^+\pi^-$)) and B($h^-h^-h^+\nu_\tau$(ex. K^0))/B($h^-h^-h^+ \geq 0$ neutrals ν_τ(ex. $K^0_S \to \pi^+\pi^-$)) values.
[3] Not independent of BUSKULIC 96 B($h^-h^-h^+\nu_\tau$) value.

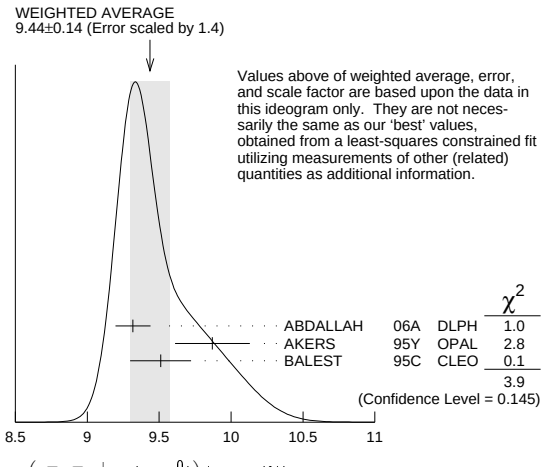

$\Gamma(h^-h^-h^+\nu_\tau(\text{ex.}K^0))/\Gamma(h^-h^-h^+ \geq 0 \text{ neutrals } \nu_\tau(\text{ex. } K^0_S \to \pi^+\pi^-)$ ("3-prong")) Γ_{65}/Γ_{63}

$\Gamma_{65}/\Gamma_{63} = (\Gamma_{70}+\Gamma_{97}+\Gamma_{106}+0.492\Gamma_{168}+0.0153\Gamma_{176}+0.0153\Gamma_{177})/(0.4247\Gamma_{52}+\Gamma_{70}+\Gamma_{78}+\Gamma_{85}+\Gamma_{89}+\Gamma_{97}+\Gamma_{103}+\Gamma_{106}+\Gamma_{107}+0.2810\Gamma_{148}+0.2292\Gamma_{149}+0.2810\Gamma_{150}+0.2810\Gamma_{152}+0.1131\Gamma_{154}+0.3268\Gamma_{158}+0.492\Gamma_{168}+0.9078\Gamma_{176}+0.9078\Gamma_{177}+0.9078\Gamma_{178}+0.892\Gamma_{180})$

VALUE (units 10^{-2})	DOCUMENT ID		TECN	COMMENT
64.98±0.31 OUR FIT				
66.0 ±0.4 ±1.4	AKERS	95Y	OPAL	1991–1994 LEP runs

$\Gamma(h^-h^-h^+\nu_\tau(\text{ex.}K^0,\omega))/\Gamma_{\text{total}}$ Γ_{66}/Γ

$\Gamma_{66}/\Gamma = (\Gamma_{70}+\Gamma_{97}+\Gamma_{106}+0.492\Gamma_{168})/\Gamma$

VALUE (%)	DOCUMENT ID
9.43±0.05 OUR FIT	

$\Gamma(\pi^-\pi^+\pi^-\nu_\tau)/\Gamma_{\text{total}}$ $\Gamma_{67}/\Gamma = (0.34598\Gamma_{36}+\Gamma_{70}+0.0153\Gamma_{176})/\Gamma$

VALUE (%)	DOCUMENT ID
9.31±0.05 OUR FIT	

$\Gamma(\pi^-\pi^+\pi^-\nu_\tau(\text{ex.}K^0))/\Gamma_{\text{total}}$ $\Gamma_{68}/\Gamma = (\Gamma_{70}+0.0153\Gamma_{176})/\Gamma$

VALUE (%)	EVTS	DOCUMENT ID		TECN	COMMENT
9.02±0.05 OUR FIT					
8.77±0.13 OUR AVERAGE		Error includes scale factor of 1.1.			
8.42±0.00 $^{+0.26}_{-0.25}$	8.9M	[1] LEE	10	BELL	666 fb^{-1} E^{ee}_{cm} = 10.6 GeV
8.83±0.01±0.13	1.6M	[2] AUBERT	08	BABR	342 fb^{-1} E^{ee}_{cm} = 10.6 GeV
9.13±0.05±0.46	43k	[3] BRIERE	03	CLE3	E^{ee}_{cm}= 10.6 GeV

[1] Quoted statistical error is 0.003%. Correlation matrix for LEE 10 branching fractions:
(1) $\Gamma(\tau^- \to \pi^-\pi^+\pi^-\nu_\tau(\text{ex.}K^0))/\Gamma_{\text{total}}$
(2) $\Gamma(\tau^- \to K^-\pi^+\pi^-\nu_\tau(\text{ex.}K^0))/\Gamma_{\text{total}}$
(3) $\Gamma(\tau^- \to K^-K^+\pi^-\nu_\tau)/\Gamma_{\text{total}}$
(4) $\Gamma(\tau^- \to K^-K^+K^-\nu_\tau)/\Gamma_{\text{total}}$

	(1)	(2)	(3)
(2)	0.175		
(3)	0.049	0.080	
(4)	–0.053	0.035	–0.008

[2] Correlation matrix for AUBERT 08 branching fractions:
(1) $\Gamma(\tau^- \to \pi^-\pi^+\pi^-\nu_\tau(\text{ex.}K^0))/\Gamma_{\text{total}}$
(2) $\Gamma(\tau^- \to K^-\pi^+\pi^-\nu_\tau(\text{ex.}K^0))/\Gamma_{\text{total}}$
(3) $\Gamma(\tau^- \to K^-K^+\pi^-\nu_\tau)/\Gamma_{\text{total}}$

(4) $\Gamma(\tau^- \to K^- K^+ K^- \nu_\tau)/\Gamma_{\rm total}$

	(1)	(2)	(3)
(2)	0.544		
(3)	0.390	0.177	
(4)	0.031	0.093	0.087

[3] 47% correlated with BRIERE 03 $\tau^- \to K^-\pi^+\pi^-\nu_\tau$ and 71% correlated with $\tau^- \to K^- K^+ \pi^-\nu_\tau$ because of a common 5% normalization error.

$\Gamma(\pi^-\pi^+\pi^-\nu_\tau$ (ex.K^0), non-axial vector)/$\Gamma(\pi^-\pi^+\pi^-\nu_\tau$ (ex.K^0)) Γ_{69}/Γ_{68}

$\Gamma_{69}/\Gamma_{68} = \Gamma_{69}/(\Gamma_{70}+0.0153\Gamma_{175})$

VALUE	CL%	DOCUMENT ID		TECN	COMMENT
<0.261	95	[1] ACKERSTAFF	97R	OPAL	1992–1994 LEP runs

[1] Model-independent limit from structure function analysis on contribution to B($\tau^- \to \pi^-\pi^+\pi^-\nu_\tau$(ex. K^0)) from non-axial vectors.

$\Gamma(\pi^-\pi^+\pi^-\nu_\tau$ (ex.K^0,ω))/$\Gamma_{\rm total}$ Γ_{70}/Γ

VALUE (%)	EVTS	DOCUMENT ID		TECN	COMMENT
8.99 ±0.05 OUR FIT					
9.041±0.060±0.076	29k	[1] SCHAEL	05C	ALEP	1991-1995 LEP runs

[1] See footnote to SCHAEL 05C $\Gamma(\tau^- \to e^-\overline{\nu}_e\nu_\tau)/\Gamma_{\rm total}$ measurement for correlations with other measurements.

$\Gamma(h^-h^-h^+ \geq 1$ neutrals $\nu_\tau)/\Gamma_{\rm total}$ Γ_{71}/Γ

$\Gamma_{71}/\Gamma = (0.34598\Gamma_{41}+0.34598\Gamma_{43}+0.4247\Gamma_{48}+0.4247\Gamma_{52}+\Gamma_{78}+\Gamma_{85}+\Gamma_{86}+\Gamma_{103}+\Gamma_{107}+0.2810\Gamma_{148}+0.2810\Gamma_{150}+0.2810\Gamma_{152}+0.2926\Gamma_{154}+0.892\Gamma_{176}+0.892\Gamma_{177}+0.9078\Gamma_{178})/\Gamma$

VALUE (%)	EVTS	DOCUMENT ID		TECN	COMMENT
5.29±0.05 OUR FIT					
• • • We do not use the following data for averages, fits, limits, etc. • • •					
5.6 ±0.7 ±0.3	352	[1] BEHREND	90	CELL	$E^{ee}_{\rm cm}$= 35 GeV
4.2 ±0.5 ±0.9	203	[2] ALBRECHT	87L	ARG	$E^{ee}_{\rm cm}$= 10 GeV
6.1 ±0.8 ±0.9		[3] BURCHAT	87	MRK2	$E^{ee}_{\rm cm}$= 29 GeV
7.6 ±0.4 ±0.9		[4,5] RUCKSTUHL	86	DLCO	$E^{ee}_{\rm cm}$= 29 GeV
4.7 ±0.5 ±0.8	530	[6] SCHMIDKE	86	MRK2	$E^{ee}_{\rm cm}$= 29 GeV
5.6 ±0.4 ±0.7		[5] FERNANDEZ	85	MAC	$E^{ee}_{\rm cm}$= 29 GeV
6.2 ±2.3 ±1.7		BEHREND	84	CELL	$E^{ee}_{\rm cm}$= 14,22 GeV

[1] BEHREND 90 value is not independent of BEHREND 90 B($3h\nu_\tau \geq 1$ neutrals) + B(5-prong).
[2] ALBRECHT 87L measure the product of branching ratios B($3\pi^\pm\pi^0\nu_\tau$) B(($e\overline{\nu}$or$\mu\overline{\nu}$orπor$K$or$\rho)\nu_\tau$) = 0.029 and use the PDG 86 values for the second branching ratio which sum to 0.69 ± 0.03 to get the quoted value.
[3] BURCHAT 87 value is not independent of SCHMIDKE 86 value.
[4] Contributions from kaons and from $>1\pi^0$ are subtracted. Not independent of (3-prong + $0\pi^0$) and (3-prong + $\geq 0\pi^0$) values.
[5] Value obtained using paper's R = B($h^-h^-h^+\nu_\tau$)/B(3-prong) and current B(3-prong) = 0.143.
[6] Not independent of SCHMIDKE 86 $h^-h^-h^+\nu_\tau$ and $h^-h^-h^+(\geq 0\pi^0)\nu_\tau$ values.

$\Gamma(h^-h^-h^+ \geq 1\pi^0\nu_\tau$ (ex. K^0))/$\Gamma_{\rm total}$ Γ_{72}/Γ

$\Gamma_{72}/\Gamma = (\Gamma_{78}+\Gamma_{85}+\Gamma_{86}+\Gamma_{103}+\Gamma_{107}+0.2292\Gamma_{148}+0.2292\Gamma_{150}+0.2292\Gamma_{152}+0.892\Gamma_{176}+0.892\Gamma_{177}+0.9078\Gamma_{178})/\Gamma$

VALUE (%)	EVTS	DOCUMENT ID		TECN	COMMENT
5.09 ±0.05 OUR FIT					
5.10 ±0.12 OUR AVERAGE					
• • • We use the following data for averages but not for fits. • • •					
5.106±0.083±0.103	10.1k	[1] ABDALLAH	06A	DLPH	1992–1995 LEP runs
5.09 ±0.10 ±0.23		[2] AKERS	95Y	OPAL	1991–1994 LEP runs
• • • We do not use the following data for averages, fits, limits, etc. • • •					
4.95 ±0.29 ±0.65	570	DECAMP	92C	ALEP	Repl. by SCHAEL 05C

[1] See footnote to ABDALLAH 06A $\Gamma(\tau^- \to h^-\nu_\tau)/\Gamma_{\rm total}$ measurement for correlations with other measurements.
[2] Not independent of AKERS 95Y B($h^-h^-h^+ \geq 0$ neutralsν_τ(ex. $K^0_S \to \pi^+\pi^-$)) and B($h^-h^-h^+ \geq 0$ neutralsν_τ(ex. K^0))/B($h^-h^-h^+ \geq 0$ neutralsν_τ(ex. $K^0_S \to \pi^+\pi^-$)) values.

$\Gamma(h^-h^-h^+\pi^0\nu_\tau)/\Gamma_{\rm total}$ Γ_{73}/Γ

$\Gamma_{73}/\Gamma = (0.34598\Gamma_{41}+0.34598\Gamma_{43}+\Gamma_{78}+\Gamma_{103}+\Gamma_{107}+0.2292\Gamma_{150}+0.892\Gamma_{176}+0.892\Gamma_{177}+0.0153\Gamma_{178})/\Gamma$

VALUE (%)	EVTS	DOCUMENT ID		TECN	COMMENT
4.76±0.05 OUR FIT					
• • • We do not use the following data for averages, fits, limits, etc. • • •					
4.45±0.09±0.07	6.1k	[1] BUSKULIC	96	ALEP	Repl. by SCHAEL 05C

[1] BUSKULIC 96 quote B($h^-h^-h^+\pi^0\nu_\tau$(ex. K^0)) = 4.30 ± 0.09 ± 0.09. We add 0.15 to remove their K^0 correction and reduce the systematic error accordingly.

$\Gamma(h^-h^-h^+\pi^0\nu_\tau$ (ex.K^0))/$\Gamma_{\rm total}$ Γ_{74}/Γ

$\Gamma_{74}/\Gamma = (\Gamma_{78}+\Gamma_{103}+\Gamma_{107}+0.2292\Gamma_{150}+0.892\Gamma_{176}+0.892\Gamma_{177}+0.0153\Gamma_{178})/\Gamma$

VALUE (%)	EVTS	DOCUMENT ID		TECN	COMMENT
4.57 ±0.05 OUR FIT					
4.45 ±0.14 OUR AVERAGE	Error includes scale factor of 1.2.				
4.545±0.106±0.103	8.9k	[1] ABDALLAH	06A	DLPH	1992–1995 LEP runs
4.23 ±0.06 ±0.22	7.2k	BALEST	95C	CLEO	$E^{ee}_{\rm cm} \approx$ 10.6 GeV

[1] See footnote to ABDALLAH 06A $\Gamma(\tau^- \to h^-\nu_\tau)/\Gamma_{\rm total}$ measurement for correlations with other measurements.

$\Gamma(h^-h^-h^+\pi^0\nu_\tau$(ex. K^0,ω))/$\Gamma_{\rm total}$ $\Gamma_{75}/\Gamma = (\Gamma_{78}+\Gamma_{103}+\Gamma_{107}+0.2292\Gamma_{150})/\Gamma$

VALUE (%)	DOCUMENT ID
2.79±0.07 OUR FIT	

$\Gamma(\pi^-\pi^+\pi^-\pi^0\nu_\tau)/\Gamma_{\rm total}$ Γ_{76}/Γ

$\Gamma_{76}/\Gamma = (0.34598\Gamma_{41}+\Gamma_{78}+0.892\Gamma_{176}+0.0153\Gamma_{178})/\Gamma$

VALUE (%)	DOCUMENT ID
4.62±0.05 OUR FIT	

$\Gamma(\pi^-\pi^+\pi^-\pi^0\nu_\tau$ (ex.K^0))/$\Gamma_{\rm total}$ Γ_{77}/Γ

$\Gamma_{77}/\Gamma = (\Gamma_{78}+0.892\Gamma_{176}+0.0153\Gamma_{178})/\Gamma$

VALUE (%)	EVTS	DOCUMENT ID		TECN	COMMENT
4.49 ±0.05 OUR FIT					
4.55 ±0.13 OUR AVERAGE	Error includes scale factor of 1.6.				
4.598±0.057±0.064	16k	[1] SCHAEL	05C	ALEP	1991-1995 LEP runs
4.19 ±0.10 ±0.21		[2] EDWARDS	00A	CLEO	4.7 fb^{-1} $E^{ee}_{\rm cm}$= 10.6 GeV

[1] SCHAEL 05C quote (4.590 ± 0.057 ± 0.064)%. We add 0.008% to remove their correction for $\tau^- \to \pi^-\pi^0\omega\nu_\tau \to \pi^-\pi^0\pi^+\pi^-\nu_\tau$ decays. See footnote to SCHAEL 05C $\Gamma(\tau^- \to e^-\overline{\nu}_e\nu_\tau)/\Gamma_{\rm total}$ measurement for correlations with other measurements.
[2] EDWARDS 00A quote (4.19 ± 0.10) × 10^{-2} with a 5% systematic error.

$\Gamma(\pi^-\pi^+\pi^-\pi^0\nu_\tau$ (ex.K^0,ω))/$\Gamma_{\rm total}$ Γ_{78}/Γ

VALUE (%)	DOCUMENT ID
2.74±0.07 OUR FIT	

$\Gamma(h^-\rho\pi^0\nu_\tau)/\Gamma(h^-h^-h^+\pi^0\nu_\tau)$ Γ_{79}/Γ_{73}

VALUE	EVTS	DOCUMENT ID		TECN	COMMENT
• • • We do not use the following data for averages, fits, limits, etc. • • •					
0.30±0.04±0.02	393	ALBRECHT	91D	ARG	$E^{ee}_{\rm cm}$= 9.4–10.6 GeV

$\Gamma(h^-\rho^+h^-\nu_\tau)/\Gamma(h^-h^-h^+\pi^0\nu_\tau)$ Γ_{80}/Γ_{73}

VALUE	EVTS	DOCUMENT ID		TECN	COMMENT
• • • We do not use the following data for averages, fits, limits, etc. • • •					
0.10±0.03±0.04	142	ALBRECHT	91D	ARG	$E^{ee}_{\rm cm}$= 9.4–10.6 GeV

$\Gamma(h^-\rho^-h^+\nu_\tau)/\Gamma(h^-h^-h^+\pi^0\nu_\tau)$ Γ_{81}/Γ_{73}

VALUE	EVTS	DOCUMENT ID		TECN	COMMENT
• • • We do not use the following data for averages, fits, limits, etc. • • •					
0.26±0.05±0.01	370	ALBRECHT	91D	ARG	$E^{ee}_{\rm cm}$= 9.4–10.6 GeV

$\Gamma(h^-h^-h^+ \geq 2\pi^0\nu_\tau$(ex. K^0))/$\Gamma_{\rm total}$ Γ_{82}/Γ

$\Gamma_{82}/\Gamma = (\Gamma_{85}+\Gamma_{86}+0.2292\Gamma_{148}+0.2292\Gamma_{152}+0.892\Gamma_{178})/\Gamma$

VALUE (%)	EVTS	DOCUMENT ID		TECN	COMMENT
0.517±0.031 OUR FIT					
0.561±0.068±0.095	1.3k	[1] ABDALLAH	06A	DLPH	1992–1995 LEP runs

[1] See footnote to ABDALLAH 06A $\Gamma(\tau^- \to h^-\nu_\tau)/\Gamma_{\rm total}$ measurement for correlations with other measurements.

$\Gamma(h^-h^-h^+2\pi^0\nu_\tau)/\Gamma_{\rm total}$ Γ_{83}/Γ

$\Gamma_{83}/\Gamma = (0.4247\Gamma_{48}+\Gamma_{85}+0.2292\Gamma_{148}+0.2292\Gamma_{152}+0.892\Gamma_{178})/\Gamma$

VALUE (%)	DOCUMENT ID
0.505±0.031 OUR FIT	

$\Gamma(h^-h^-h^+2\pi^0\nu_\tau$(ex.$K^0$))/$\Gamma_{\rm total}$ Γ_{84}/Γ

$\Gamma_{84}/\Gamma = (\Gamma_{85}+0.2292\Gamma_{148}+0.2292\Gamma_{152}+0.892\Gamma_{178})/\Gamma$

VALUE (%)	EVTS	DOCUMENT ID		TECN	COMMENT
0.495±0.031 OUR FIT					
0.435±0.030±0.035	2.6k	[1] SCHAEL	05C	ALEP	1991-1995 LEP runs
• • • We do not use the following data for averages, fits, limits, etc. • • •					
0.50 ±0.07 ±0.07	1.8k	BUSKULIC	96	ALEP	Repl. by SCHAEL 05C

[1] SCHAEL 05C quote (0.392 ± 0.030 ± 0.035)%. We add 0.043% to remove their correction for $\tau^- \to \pi^-\eta\pi^0\nu_\tau \to \pi^-\pi^+\pi^-2\pi^0\nu_\tau$ and $\tau^- \to K^*(892)^-\eta\nu_\tau \to K^-\pi^+\pi^-2\pi^0\nu_\tau$ decays. See footnote to SCHAEL 05C $\Gamma(\tau^- \to e^-\overline{\nu}_e\nu_\tau)/\Gamma_{\rm total}$ measurement for correlations with other measurements.

$\Gamma(h^-h^-h^+2\pi^0\nu_\tau$(ex.$K^0$))/$\Gamma(h^-h^-h^+ \geq 0$ neutrals $\geq 0K^0_L\nu_\tau)$ Γ_{84}/Γ_{62}

$\Gamma_{84}/\Gamma_{62} = (\Gamma_{85}+0.2292\Gamma_{148}+0.2292\Gamma_{152}+0.892\Gamma_{178})/(0.34598\Gamma_{36}+0.34598\Gamma_{38}+0.34598\Gamma_{41}+0.34598\Gamma_{43}+0.4247\Gamma_{48}+0.6920\Gamma_{49}+0.8494\Gamma_{52}+0.6920\Gamma_{56}+0.6534\Gamma_{61}+\Gamma_{70}+\Gamma_{78}+\Gamma_{85}+\Gamma_{89}+\Gamma_{97}+\Gamma_{103}+\Gamma_{106}+\Gamma_{107}+0.2810\Gamma_{148}+0.2292\Gamma_{149}+0.2810\Gamma_{150}+0.2810\Gamma_{152}+0.3759\Gamma_{154}+0.3268\Gamma_{158}+0.7259\Gamma_{168}+0.9078\Gamma_{176}+0.9078\Gamma_{177}+0.9078\Gamma_{178}+0.892\Gamma_{180})$

VALUE (units 10^{-2})	EVTS	DOCUMENT ID		TECN	COMMENT
3.26±0.20 OUR FIT					
3.4 ±0.2 ±0.3	668	BORTOLETTO	93	CLEO	$E^{ee}_{\rm cm} \approx$ 10.6 GeV

$\Gamma(h^-h^-h^+2\pi^0\nu_\tau$ (ex.K^0,ω,η))/$\Gamma_{\rm total}$ Γ_{85}/Γ

VALUE (units 10^{-4})	DOCUMENT ID
10±4 OUR FIT	

$\Gamma(h^-h^-h^+3\pi^0\nu_\tau)/\Gamma_{total}$ $\Gamma_{86}/\Gamma = (0.4247\Gamma_{52}+\Gamma_{87}+0.1131\Gamma_{154})/\Gamma$

VALUE (units 10^{-4})	CL%	EVTS	DOCUMENT ID		TECN	COMMENT
2.12±0.30 OUR FIT						
2.2 ±0.3 ±0.4		139	ANASTASSOV	01	CLEO	E^{ee}_{cm}= 10.6 GeV
• • • We do not use the following data for averages, fits, limits, etc. • • •						
< 4.9	95		SCHAEL	05C	ALEP	1991–1995 LEP runs
2.85±0.56±0.51		57	ANDERSON	97	CLEO	Repl. by ANASTASSOV 01
11 ±4 ±5		440	[1] BUSKULIC	96	ALEP	Repl. by SCHAEL 05C

[1] BUSKULIC 96 state their measurement is for B($h^-h^-h^+ \geq 3\pi^0\nu_\tau$). We assume that B($h^-h^-h^+ \geq 4\pi^0\nu_\tau$) is very small.

$\Gamma(2\pi^-\pi^+3\pi^0\nu_\tau(ex.K^0))/\Gamma_{total}$ Γ_{87}/Γ

$\Gamma_{87}/\Gamma = (\Gamma_{89}+0.2292\Gamma_{149}+0.3268\Gamma_{158}+0.892\Gamma_{180})/\Gamma$

VALUE (units 10^{-4})	DOCUMENT ID		TECN	COMMENT
1.94±0.30 OUR FIT				
• • • We use the following data for averages but not for fits. • • •				
2.07±0.18±0.37	[1] LEES	12X	BABR	468 fb^{-1} E^{ee}_{cm} = 10.6 GeV

[1] Not independent of LEES 12X $\Gamma(\tau^- \to \eta\pi^-\pi^+\pi^-\nu_\tau(ex.K^0))/\Gamma$, $\Gamma(\tau^- \to \eta\pi^-\pi^0\pi^0\nu_\tau)/\Gamma$, $\Gamma(\tau^- \to \pi^-\omega2\pi^0\nu_\tau)/\Gamma$, and $\Gamma(\tau^- \to f_1(1285)\pi^-\nu_\tau \to \eta\pi^-\pi^+\pi^-\nu_\tau)/\Gamma$ values.

$\Gamma(2\pi^-\pi^+3\pi^0\nu_\tau(ex.K^0,\eta,f_1(1285)))/\Gamma_{total}$ Γ_{88}/Γ

VALUE (units 10^{-4})	DOCUMENT ID		TECN	COMMENT
1.69±0.08±0.43	LEES	12X	BABR	468 fb^{-1} E^{ee}_{cm} = 10.6 GeV

$\Gamma(2\pi^-\pi^+3\pi^0\nu_\tau(ex.K^0,\eta,\omega,f_1(1285)))/\Gamma_{total}$ Γ_{89}/Γ

VALUE (units 10^{-5})	DOCUMENT ID		TECN	COMMENT
1.4±2.7 OUR FIT				
1.0±0.8±3.0	[1] LEES	12X	BABR	468 fb^{-1} E^{ee}_{cm} = 10.6 GeV

[1] LEES 12X meaurement corresponds to the lower limit of $< 5.8 \times 10^{-5}$ at 90% CL.

$\Gamma(K^-h^+h^- \geq 0 \text{ neutrals } \nu_\tau)/\Gamma_{total}$ Γ_{90}/Γ

$\Gamma_{90}/\Gamma = (0.34598\Gamma_{38}+0.34598\Gamma_{43}+\Gamma_{97}+\Gamma_{103}+\Gamma_{106}+\Gamma_{107}+0.2810\Gamma_{150}+0.492\Gamma_{168}+0.9078\Gamma_{177})/\Gamma$

VALUE (%)	CL%	DOCUMENT ID		TECN	COMMENT
0.629±0.014 OUR FIT					
<0.6	90	AIHARA	84C	TPC	E^{ee}_{cm}= 29 GeV

$\Gamma(K^-h^+\pi^-\nu_\tau(ex.K^0))/\Gamma_{total}$ $\Gamma_{91}/\Gamma = (\Gamma_{97}+\Gamma_{106}+0.0153\Gamma_{177})/\Gamma$

VALUE (%)	DOCUMENT ID
0.437±0.007 OUR FIT	

$\Gamma(K^-h^+\pi^-\nu_\tau(ex.K^0))/\Gamma(\pi^-\pi^+\pi^-\nu_\tau(ex.K^0))$ Γ_{91}/Γ_{68}

$\Gamma_{91}/\Gamma_{68} = (\Gamma_{97}+\Gamma_{106}+0.0153\Gamma_{177})/(\Gamma_{70}+0.0153\Gamma_{176})$

VALUE (%)	EVTS	DOCUMENT ID		TECN	COMMENT
4.84±0.08 OUR FIT					
5.44±0.21±0.53	7.9k	RICHICHI	99	CLEO	E^{ee}_{cm}= 10.6 GeV

$\Gamma(K^-h^+\pi^-\pi^0\nu_\tau(ex.K^0))/\Gamma_{total}$ Γ_{92}/Γ

$\Gamma_{92}/\Gamma = (\Gamma_{103}+\Gamma_{107}+0.2292\Gamma_{150}+0.892\Gamma_{177})/\Gamma$

VALUE (units 10^{-4})	DOCUMENT ID
8.6±1.2 OUR FIT	

$\Gamma(K^-h^+\pi^-\pi^0\nu_\tau(ex.K^0))/\Gamma(\pi^-\pi^+\pi^-\pi^0\nu_\tau(ex.K^0))$ Γ_{92}/Γ_{77}

$\Gamma_{92}/\Gamma_{77} = (\Gamma_{103}+\Gamma_{107}+0.2292\Gamma_{150}+0.892\Gamma_{177})/(\Gamma_{78}+0.892\Gamma_{176}+0.0153\Gamma_{178})$

VALUE (%)	EVTS	DOCUMENT ID		TECN	COMMENT
1.91±0.26 OUR FIT					
2.61±0.45±0.42	719	RICHICHI	99	CLEO	E^{ee}_{cm}= 10.6 GeV

$\Gamma(K^-\pi^+\pi^- \geq 0 \text{ neutrals } \nu_\tau)/\Gamma_{total}$ Γ_{93}/Γ

$\Gamma_{93}/\Gamma = (0.34598\Gamma_{38}+0.34598\Gamma_{43}+\Gamma_{97}+\Gamma_{103}+0.2810\Gamma_{150}+0.9078\Gamma_{177})/\Gamma$

VALUE (%)	EVTS	DOCUMENT ID		TECN	COMMENT
0.477±0.014 OUR FIT					
0.58 $^{+0.15}_{-0.13}$ ±0.12	20	[1] BAUER	94	TPC	E^{ee}_{cm}= 29 GeV
• • • We do not use the following data for averages, fits, limits, etc. • • •					
0.22 $^{+0.16}_{-0.13}$ ±0.05	9	[2] MILLS	85	DLCO	E^{ee}_{cm}= 29 GeV

[1] We multiply 0.58% by 0.20, the relative systematic error quoted by BAUER 94, to obtain the systematic error.
[2] Error correlated with MILLS 85 ($KK\pi\nu$) value. We multiply 0.22% by 0.23, the relative systematic error quoted by MILLS 85, to obtain the systematic error.

$\Gamma(K^-\pi^+\pi^- \geq 0\pi^0\nu_\tau(ex.K^0))/\Gamma_{total}$ Γ_{94}/Γ

$\Gamma_{94}/\Gamma = (\Gamma_{97}+\Gamma_{103}+0.2292\Gamma_{150}+0.9078\Gamma_{177})/\Gamma$

VALUE (%)	DOCUMENT ID		TECN	COMMENT
0.373±0.013 OUR FIT				
0.30 ±0.05 OUR AVERAGE				
• • • We use the following data for averages but not for fits. • • •				
0.343±0.073±0.031	ABBIENDI	00D	OPAL	1990–1995 LEP runs
0.275±0.064	[1] BARATE	98	ALEP	1991–1995 LEP runs

[1] Not independent of BARATE 98 $\Gamma(\tau^- \to K^-\pi^+\pi^-\nu_\tau)/\Gamma_{total}$ and $\Gamma(\tau^- \to K^-\pi^+\pi^-\pi^0\nu_\tau)/\Gamma_{total}$ values.

$\Gamma(K^-\pi^+\pi^-\nu_\tau)/\Gamma_{total}$ $\Gamma_{95}/\Gamma = (0.34598\Gamma_{38}+\Gamma_{97}+0.0153\Gamma_{177})/\Gamma$

VALUE (%)	DOCUMENT ID
0.345±0.007 OUR FIT	

$\Gamma(K^-\pi^+\pi^-\nu_\tau(ex.K^0))/\Gamma_{total}$ $\Gamma_{96}/\Gamma = (\Gamma_{97}+0.0153\Gamma_{177})/\Gamma$

VALUE (%)	EVTS	DOCUMENT ID		TECN	COMMENT
0.293±0.007 OUR FIT					
0.290±0.018 OUR AVERAGE		Error includes scale factor of 2.4. See the ideogram below.			
0.330±0.001 $^{+0.016}_{-0.017}$	794k	[1] LEE	10	BELL	666 fb^{-1} E^{ee}_{cm}=10.6 GeV
0.273±0.002±0.009	70k	[2] AUBERT	08	BABR	342 fb^{-1} E^{ee}_{cm}=10.6 GeV
0.415±0.053±0.040	269	ABBIENDI	04J	OPAL	1991–1995 LEP runs
0.384±0.014±0.038	3.5k	[3] BRIERE	03	CLE3	E^{ee}_{cm}= 10.6 GeV
0.214±0.037±0.029		BARATE	98	ALEP	1991–1995 LEP runs
• • • We use the following data for averages but not for fits. • • •					
0.346±0.023±0.056	158	[4] RICHICHI	99	CLEO	E^{ee}_{cm}= 10.6 GeV
• • • We do not use the following data for averages, fits, limits, etc. • • •					
0.360±0.082±0.048		ABBIENDI	00D	OPAL	1990–1995 LEP runs

[1] See footnote to LEE 10 $\Gamma(\tau^- \to \pi^-\pi^+\pi^-\nu_\tau(ex.K^0))/\Gamma_{total}$ measurement for correlations with other measurements. Not independent of LEE 10 $\Gamma(\tau^- \to K^-\pi^+\pi^-\nu_\tau(ex.K^0))/\Gamma(\tau^- \to \pi^-\pi^+\pi^-\nu_\tau(ex.K^0))$ value.
[2] See footnote to AUBERT 08 $\Gamma(\tau^- \to \pi^-\pi^+\pi^-\nu_\tau(ex.K^0))/\Gamma_{total}$ measurement for correlations with other measurements.
[3] 47% correlated with BRIERE 03 $\tau^- \to \pi^-\pi^+\pi^-\nu_\tau$ and 34% correlated with $\tau^- \to K^-K^+\pi^-\nu_\tau$ because of a common 5% normalization error.
[4] Not independent of RICHICHI 99 $\Gamma(\tau^- \to K^-h^+\pi^-\nu_\tau(ex.K^0))/\Gamma(\tau^- \to \pi^-\pi^+\pi^-\nu_\tau(ex.K^0))$, $\Gamma(\tau^- \to K^-K^+\pi^-\nu_\tau)/\Gamma(\tau^- \to \pi^-\pi^+\pi^-\nu_\tau(ex.K^0))$ and BALEST 95C $\Gamma(\tau^- \to h^-h^-h^+\nu_\tau(ex.K^0))/\Gamma_{total}$ values.

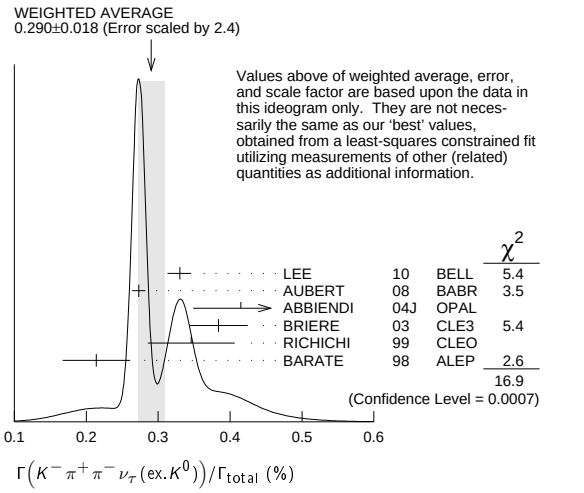

$\Gamma(K^-\pi^+\pi^-\nu_\tau(ex.K^0))/\Gamma(\pi^-\pi^+\pi^-\nu_\tau(ex.K^0))$ Γ_{96}/Γ_{68}

$\Gamma_{96}/\Gamma_{68} = (\Gamma_{97}+0.0153\Gamma_{177})/(\Gamma_{70}+0.0153\Gamma_{176})$

VALUE (units 10^{-2})	EVTS	DOCUMENT ID		TECN	COMMENT
3.25±0.07 OUR FIT					
• • • We use the following data for averages but not for fits. • • •					
3.92±0.02 $^{+0.15}_{-0.16}$	794k	[1] LEE	10	BELL	666 fb^{-1} E^{ee}_{cm} = 10.6 GeV

[1] Not independent of LEE 10 $\Gamma(\tau^- \to K^-\pi^+\pi^-\nu_\tau(ex.K^0))/\Gamma_{total}$ and $\Gamma(\tau^- \to \pi^-\pi^+\pi^-\nu_\tau(ex.K^0))/\Gamma_{total}$ values.

$\Gamma(K^-\pi^+\pi^-\nu_\tau(ex.K^0,\omega))/\Gamma_{total}$ Γ_{97}/Γ

VALUE (units 10^{-3})	DOCUMENT ID
2.93±0.07 OUR FIT	

$\Gamma(K^-\rho^0\nu_\tau \to K^-\pi^+\pi^-\nu_\tau)/\Gamma(K^-\pi^+\pi^-\nu_\tau(ex.K^0))$ Γ_{98}/Γ_{96}

VALUE	DOCUMENT ID		TECN	COMMENT
0.48±0.14±0.10	[1] ASNER	00B	CLEO	E^{ee}_{cm}= 10.6 GeV
• • • We do not use the following data for averages, fits, limits, etc. • • •				
0.39±0.14	[2] BARATE	99R	ALEP	1991–1995 LEP runs

[1] ASNER 00B assume $\tau^- \to K^-\pi^+\pi^-\nu_\tau$ (ex. K^0) decays proceed only through $K\rho$ and $K^*\pi$ intermediate states. They assume the resonance structure of $\tau^- \to K^-\pi^+\pi^-\nu_\tau$ (ex. K^0) decays is dominated by $K_1(1270)^-$ and $K_1(1400)^-$ resonances, and assume B($K_1(1270) \to K^*(892)\pi$) = (16 ± 5)%, B($K_1(1270) \to K\rho$) = (42 ± 6)%, and B($K_1(1400) \to K\rho$) = 0.
[2] BARATE 99R assume $\tau^- \to K^-\pi^+\pi^-\nu_\tau$ (ex. K^0) decays proceed only through $K\rho$ and $K^*\pi$ intermediate states. The quoted error is statistical only.

$\Gamma(K^-\pi^+\pi^-\pi^0\nu_\tau)/\Gamma_{total}$ Γ_{99}/Γ

$\Gamma_{99}/\Gamma = (0.34598\Gamma_{43}+\Gamma_{103}+0.2292\Gamma_{150}+0.892\Gamma_{177})/\Gamma$

VALUE (units 10^{-4})	DOCUMENT ID
13.1±1.2 OUR FIT	

$\Gamma(K^-\pi^+\pi^-\pi^0\nu_\tau(\mathrm{ex.}K^0))/\Gamma_{total}$ Γ_{100}/Γ

$\Gamma_{100}/\Gamma = (\Gamma_{103}+0.2292\Gamma_{150}+0.892\Gamma_{177})/\Gamma$

VALUE (units 10^{-4})	CL%	DOCUMENT ID		TECN	COMMENT
7.9±1.2 OUR FIT					
7.3±1.2 OUR AVERAGE					
7.4±0.8±1.1		[1] ARMS	05	CLE3	7.6 fb^{-1}, E^{ee}_{cm}= 10.6 GeV
6.1±3.9±1.8		BARATE	98	ALEP	1991–1995 LEP runs
• • • We use the following data for averages but not for fits. • • •					
7.5±2.6±1.8		[2] RICHICHI	99	CLEO	E^{ee}_{cm}= 10.6 GeV
• • • We do not use the following data for averages, fits, limits, etc. • • •					
<17	95	ABBIENDI	00D	OPAL	1990–1995 LEP runs

[1] Not independent of ARMS 05 $\Gamma(\tau^- \to K^-\pi^+\pi^-\pi^0\nu_\tau(\mathrm{ex.}K^0,\omega))$ / Γ_{total} and $\Gamma(\tau^- \to K^-\omega\nu_\tau)$ / Γ_{total} values.

[2] Not independent of RICHICHI 99 $\Gamma(\tau^- \to K^-h^+\pi^-\nu_\tau(\mathrm{ex.}K^0))/\Gamma(\tau^- \to \pi^-\pi^+\pi^-\nu_\tau(\mathrm{ex.}K^0))$, $\Gamma(\tau^- \to K^-K^+\pi^-\nu_\tau)/\Gamma(\tau^- \to \pi^-\pi^+\pi^-\nu_\tau(\mathrm{ex.}K^0))$ and BALEST 95C $\Gamma(\tau^- \to h^-h^-h^+\nu_\tau(\mathrm{ex.}K^0))/\Gamma_{total}$ values.

$\Gamma(K^-\pi^+\pi^-\pi^0\nu_\tau(\mathrm{ex.}K^0,\eta))/\Gamma_{total}$ $\Gamma_{101}/\Gamma = (\Gamma_{103}+0.892\Gamma_{177})/\Gamma$

VALUE (units 10^{-4})	DOCUMENT ID
7.6±1.2 OUR FIT	

$\Gamma(K^-\pi^+\pi^-\pi^0\nu_\tau(\mathrm{ex.}K^0,\omega))/\Gamma_{total}$ Γ_{102}/Γ

VALUE (units 10^{-4})	EVTS	DOCUMENT ID		TECN	COMMENT
3.7±0.5±0.8	833	ARMS	05	CLE3	7.6 fb^{-1}, E^{ee}_{cm}= 10.6 GeV

$\Gamma(K^-\pi^+\pi^-\pi^0\nu_\tau(\mathrm{ex.}K^0,\omega,\eta))/\Gamma_{total}$ Γ_{103}/Γ

VALUE (units 10^{-4})	DOCUMENT ID
3.9±1.4 OUR FIT	

$\Gamma(K^-\pi^+K^- \geq 0\ \mathrm{neut.}\ \nu_\tau)/\Gamma_{total}$ Γ_{104}/Γ

VALUE (%)	CL%	DOCUMENT ID		TECN	COMMENT
<0.09	95	BAUER	94	TPC	E^{ee}_{cm}= 29 GeV

$\Gamma(K^-K^+\pi^- \geq 0\ \mathrm{neut.}\ \nu_\tau)/\Gamma_{total}$ $\Gamma_{105}/\Gamma = (\Gamma_{106}+\Gamma_{107})/\Gamma$

VALUE (%)	EVTS	DOCUMENT ID		TECN	COMMENT
0.1496±0.0033 OUR FIT					
0.203 ±0.031 OUR AVERAGE					
0.159 ±0.053 ±0.020		ABBIENDI	00D	OPAL	1990–1995 LEP runs
0.15 $^{+0.09}_{-0.07}$ ±0.03	4	[1] BAUER	94	TPC	E^{ee}_{cm}= 29 GeV
• • • We use the following data for averages but not for fits. • • •					
0.238 ±0.042		[2] BARATE	98	ALEP	1991–1995 LEP runs

[1] We multiply 0.15% by 0.20, the relative systematic error quoted by BAUER 94, to obtain the systematic error.

[2] Not independent of BARATE 98 $\Gamma(\tau^- \to K^-K^+\pi^-\nu_\tau)/\Gamma_{total}$ and $\Gamma(\tau^- \to K^-K^+\pi^-\pi^0\nu_\tau)/\Gamma_{total}$ values.

$\Gamma(K^-K^+\pi^-\nu_\tau)/\Gamma_{total}$ Γ_{106}/Γ

VALUE (units 10^{-3})	EVTS	DOCUMENT ID		TECN	COMMENT
1.435±0.027 OUR FIT					
1.43 ±0.07 OUR AVERAGE		Error includes scale factor of 2.4. See the ideogram below.			
1.55 ±0.01 $^{+0.06}_{-0.05}$	108k	[1] LEE	10	BELL	666 fb^{-1} E^{ee}_{cm}=10.6 GeV
1.346±0.010±0.036	18k	[2] AUBERT	08	BABR	342 fb^{-1} E^{ee}_{cm}= 10.6 GeV
1.55 ±0.06 ±0.09	932	[3] BRIERE	03	CLE3	E^{ee}_{cm}= 10.6 GeV
1.63 ±0.21 ±0.17		BARATE	98	ALEP	1991–1995 LEP runs
• • • We use the following data for averages but not for fits. • • •					
0.87 ±0.56 ±0.40		ABBIENDI	00D	OPAL	1990–1995 LEP runs
1.45 ±0.13 ±0.28	2.3k	[4] RICHICHI	99	CLEO	E^{ee}_{cm}= 10.6 GeV
• • • We do not use the following data for averages, fits, limits, etc. • • •					
2.2 $^{+1.7}_{-1.1}$ ±0.5	9	[5] MILLS	85	DLCO	E^{ee}_{cm}= 29 GeV

[1] See footnote to LEE 10 $\Gamma(\tau^- \to \pi^-\pi^+\pi^-\nu_\tau(\mathrm{ex.}K^0))/\Gamma_{total}$ measurement for correlations with other measurements. Not independent of LEE 10 $\Gamma(\tau^- \to K^-K^+\pi^-\nu_\tau)/\Gamma(\tau^- \to \pi^-\pi^+\pi^-\nu_\tau(\mathrm{ex.}K^0))$ value.

[2] See footnote to AUBERT 08 $\Gamma(\tau^- \to \pi^-\pi^+\pi^-\nu_\tau(\mathrm{ex.}K^0))/\Gamma_{total}$ measurement for correlations with other measurements.

[3] 71% correlated with BRIERE 03 $\tau^- \to \pi^-\pi^+\pi^-\nu_\tau$ and 34% correlated with $\tau \to K^-\pi^+\pi^-\nu_\tau$ because of a common 5% normalization error.

[4] Not independent of RICHICHI 99 $\Gamma(\tau^- \to K^-K^+\pi^-\nu_\tau)/\Gamma(\tau^- \to \pi^-\pi^+\pi^-\nu_\tau(\mathrm{ex.}K^0))$ and BALEST 95C $\Gamma(\tau^- \to h^-h^-h^+\nu_\tau(\mathrm{ex.}K^0))/\Gamma_{total}$ values.

[5] Error correlated with MILLS 85 ($K\pi\pi\pi^0\nu$) value. We multiply 0.22% by 0.23, the relative systematic error quoted by MILLS 85, to obtain the systematic error.

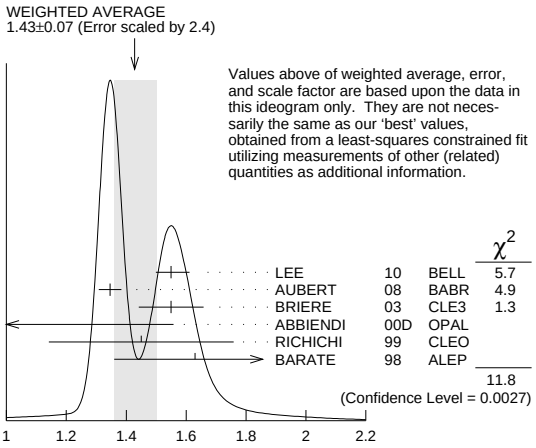

$\Gamma(K^-K^+\pi^-\nu_\tau)/\Gamma(\pi^-\pi^+\pi^-\nu_\tau(\mathrm{ex.}K^0))$ Γ_{106}/Γ_{68}

$\Gamma_{106}/\Gamma_{68} = \Gamma_{106}/(\Gamma_{70}+0.0153\Gamma_{176})$

VALUE (%)	EVTS	DOCUMENT ID		TECN	COMMENT
1.592±0.030 OUR FIT					
1.83 ±0.05 OUR AVERAGE					
1.60 ±0.15 ±0.30	2.3k	RICHICHI	99	CLEO	E^{ee}_{cm}= 10.6 GeV
• • • We use the following data for averages but not for fits. • • •					
1.84 ±0.01 ±0.05	108k	[1] LEE	10	BELL	666 fb^{-1} E^{ee}_{cm}= 10.6 GeV

[1] Not independent of LEE 10 $\Gamma(\tau^- \to K^-K^+\pi^-\nu_\tau)/\Gamma_{total}$ and $\Gamma(\tau^- \to \pi^-\pi^+\pi^-\nu_\tau(\mathrm{ex.}K^0))/\Gamma_{total}$ values.

$\Gamma(K^-K^+\pi^-\pi^0\nu_\tau)/\Gamma_{total}$ Γ_{107}/Γ

VALUE (units 10^{-4})	CL%	EVTS	DOCUMENT ID		TECN	COMMENT
0.61±0.18 OUR FIT						
0.60±0.18 OUR AVERAGE						
0.55±0.14±0.12		48	ARMS	05	CLE3	7.6 fb^{-1}, E^{ee}_{cm}=10.6 GeV
7.5 ±2.9 ±1.5			BARATE	98	ALEP	1991–1995 LEP runs
• • • We use the following data for averages but not for fits. • • •						
3.3 ±1.8 ±0.7		158	[1] RICHICHI	99	CLEO	E^{ee}_{cm}= 10.6 GeV
• • • We do not use the following data for averages, fits, limits, etc. • • •						
<27	95		ABBIENDI	00D	OPAL	1990–1995 LEP runs

[1] Not independent of RICHICHI 99 $\Gamma(\tau^- \to K^-K^+\pi^-\nu_\tau)/\Gamma(\tau^- \to \pi^-\pi^+\pi^-\nu_\tau(\mathrm{ex.}K^0))$ and BALEST 95C $\Gamma(\tau^- \to h^-h^-h^+\nu_\tau(\mathrm{ex.}K^0))/\Gamma_{total}$ values.

$\Gamma(K^-K^+\pi^-\pi^0\nu_\tau)/\Gamma(\pi^-\pi^+\pi^-\pi^0\nu_\tau(\mathrm{ex.}K^0))$ Γ_{107}/Γ_{77}

$\Gamma_{107}/\Gamma_{77} = \Gamma_{107}/(\Gamma_{78}+0.892\Gamma_{176}+0.0153\Gamma_{178})$

VALUE (%)	EVTS	DOCUMENT ID		TECN	COMMENT
0.14±0.04 OUR FIT					
0.79±0.44±0.16	158	[1] RICHICHI	99	CLEO	E^{ee}_{cm}= 10.6 GeV

[1] RICHICHI 99 also quote a 95%CL upper limit of 0.0157 for this measurement.

$\Gamma(K^-K^+K^-\nu_\tau)/\Gamma_{total}$ $\Gamma_{108}/\Gamma = 0.492\Gamma_{168}/\Gamma$

VALUE (units 10^{-5})	CL%	EVTS	DOCUMENT ID		TECN	COMMENT
2.2 ±0.8 OUR FIT			Error includes scale factor of 5.4.			
2.1 ±0.8 OUR AVERAGE			Error includes scale factor of 5.4.			
3.29±0.17 $^{+0.19}_{-0.20}$		3.2k	[1] LEE	10	BELL	666 fb^{-1} E^{ee}_{cm} = 10.6 GeV
1.58±0.13±0.12		275	[2] AUBERT	08	BABR	342 fb^{-1} E^{ee}_{cm}= 10.6 GeV
• • • We do not use the following data for averages, fits, limits, etc. • • •						
< 3.7	90		BRIERE	03	CLE3	E^{ee}_{cm}= 10.6 GeV
< 19	90		BARATE	98	ALEP	1991–1995 LEP runs

[1] See footnote to LEE 10 $\Gamma(\tau^- \to \pi^-\pi^+\pi^-\nu_\tau(\mathrm{ex.}K^0))/\Gamma_{total}$ measurement for correlations with other measurements. Not independent of LEE 10 $\Gamma(\tau^- \to K^-K^+K^-\nu_\tau)/\Gamma(\tau^- \to \pi^-\pi^+\pi^-\nu_\tau(\mathrm{ex.}K^0))$ value.

[2] See footnote to AUBERT 08 $\Gamma(\tau^- \to \pi^-\pi^+\pi^-\nu_\tau(\mathrm{ex.}K^0))/\Gamma_{total}$ measurement for correlations with other measurements.

$\Gamma(K^-K^+K^-\nu_\tau)/\Gamma(\pi^-\pi^+\pi^-\nu_\tau(\mathrm{ex.}K^0))$ Γ_{108}/Γ_{68}

VALUE (units 10^{-4})	EVTS	DOCUMENT ID		TECN	COMMENT
• • • We do not use the following data for averages, fits, limits, etc. • • •					
3.90±0.02 $^{+0.22}_{-0.23}$	3.2k	[1] LEE	10	BELL	666 fb^{-1} E^{ee}_{cm} = 10.6 GeV

[1] Not independent of LEE 10 $\Gamma(\tau^- \to K^-K^+K^-\nu_\tau)/\Gamma_{total}$ and $\Gamma(\tau^- \to \pi^-\pi^+\pi^-\nu_\tau(\mathrm{ex.}K^0))/\Gamma_{total}$ values.

Lepton Particle Listings

τ

$\Gamma(K^-K^+K^-\nu_\tau(\text{ex. }\phi))/\Gamma_{\text{total}}$ Γ_{109}/Γ

VALUE	CL%	DOCUMENT ID		TECN	COMMENT
$<2.5\times10^{-6}$	90	AUBERT	08	BABR	342 fb^{-1} $E_{\text{cm}}^{ee}=10.6$ GeV

$\Gamma(K^-K^+K^-\pi^0\nu_\tau)/\Gamma_{\text{total}}$ Γ_{110}/Γ

VALUE	CL%	DOCUMENT ID		TECN	COMMENT
$<4.8\times10^{-6}$	90	ARMS	05	CLE3	7.6 fb^{-1}, $E_{\text{cm}}^{ee}=10.6$ GeV

$\Gamma(\pi^-K^+\pi^-\geq0\text{ neut. }\nu_\tau)/\Gamma_{\text{total}}$ Γ_{111}/Γ

VALUE (%)	CL%	DOCUMENT ID		TECN	COMMENT
<0.25	95	BAUER	94	TPC	$E_{\text{cm}}^{ee}=29$ GeV

$\Gamma(e^-e^-e^+\overline{\nu}_e\nu_\tau)/\Gamma_{\text{total}}$ Γ_{112}/Γ

VALUE (units 10^{-5})	EVTS	DOCUMENT ID		TECN	COMMENT
2.8±1.4±0.4	5	ALAM	96	CLEO	$E_{\text{cm}}^{ee}=10.6$ GeV

$\Gamma(\mu^-e^-e^+\overline{\nu}_\mu\nu_\tau)/\Gamma_{\text{total}}$ Γ_{113}/Γ

VALUE (units 10^{-5})	CL%	DOCUMENT ID		TECN	COMMENT
<3.6	90	ALAM	96	CLEO	$E_{\text{cm}}^{ee}=10.6$ GeV

$\Gamma(3h^-2h^+\geq0\text{ neutrals }\nu_\tau(\text{ex. }K^0_S\to\pi^-\pi^+)(\text{"5-prong"}))/\Gamma_{\text{total}}$ Γ_{114}/Γ

$\Gamma_{114}/\Gamma=(\Gamma_{115}+\Gamma_{121})/\Gamma$

VALUE (%)	EVTS	DOCUMENT ID		TECN	COMMENT
0.099±0.004 OUR FIT					
0.107±0.007 OUR AVERAGE		Error includes scale factor of 1.1.			
0.170±0.022±0.026		[1] ACHARD	01D	L3	1992–1995 LEP runs
0.097±0.005±0.011	419	GIBAUT	94B	CLEO	$E_{\text{cm}}^{ee}=10.6$ GeV
0.102±0.029	13	BYLSMA	87	HRS	$E_{\text{cm}}^{ee}=29$ GeV
• • • We use the following data for averages but not for fits. • • •					
0.093±0.009±0.012		SCHAEL	05C	ALEP	1991–1995 LEP runs
0.115±0.013±0.006	112	[2] ABREU	01M	DLPH	1992–1995 LEP runs
0.119±0.013±0.008	119	[3] ACKERSTAFF	99E	OPAL	1991–1995 LEP runs
• • • We do not use the following data for averages, fits, limits, etc. • • •					
0.26 ±0.06 ±0.05		ACTON	92H	OPAL	$E_{\text{cm}}^{ee}=88.2$–94.2 GeV
$0.10\ ^{+0.05}_{-0.04}$ ±0.03		DECAMP	92C	ALEP	1989–1990 LEP runs
0.16 ±0.13 ±0.04		BEHREND	89B	CELL	$E_{\text{cm}}^{ee}=14$–47 GeV
0.3 ±0.1 ±0.2		BARTEL	85F	JADE	$E_{\text{cm}}^{ee}=34.6$ GeV
0.13 ±0.04	10	BELTRAMI	85	HRS	Repl. by BYLSMA 87
0.16 ±0.08 ±0.04	4	BURCHAT	85	MRK2	$E_{\text{cm}}^{ee}=29$ GeV
1.0 ±0.4	10	BEHREND	82	CELL	Repl. by BEHREND 89B

[1] The correlation coefficients between this measurement and the ACHARD 01D measurements of B($\tau\to$ "1-prong") and B($\tau\to$ "3-prong") are -0.082 and -0.19 respectively.
[2] The correlation coefficients between this measurement and the ABREU 01M measurements of B($\tau\to$ 1-prong) and B($\tau\to$ 3-prong) are -0.08 and -0.08 respectively.
[3] Not independent of ACKERSTAFF 99E B($\tau^-\to 3h^-2h^+\nu_\tau$(ex. K^0)) and B($\tau^-\to 3h^-2h^+\pi^0\nu_\tau$(ex. K^0)) measurements.

$\Gamma(3h^-2h^+\nu_\tau(\text{ex.}K^0))/\Gamma_{\text{total}}$ $\Gamma_{115}/\Gamma=(\Gamma_{116}+\Gamma_{118}+0.0153\Gamma_{183})/\Gamma$

VALUE (units 10^{-4})	EVTS	DOCUMENT ID		TECN	COMMENT
8.22±0.32 OUR FIT					
8.32±0.35 OUR AVERAGE					
9.7 ±1.5 ±0.5	96	[1] ABDALLAH	06A	DLPH	1992–1995 LEP runs
7.2 ±0.9 ±1.2	165	[2] SCHAEL	05C	ALEP	1991-1995 LEP runs
9.1 ±1.4 ±0.6	97	ACKERSTAFF	99E	OPAL	1991–1995 LEP runs
7.7 ±0.5 ±0.9	295	GIBAUT	94B	CLEO	$E_{\text{cm}}^{ee}=10.6$ GeV
6.4 ±2.3 ±1.0	12	ALBRECHT	88B	ARG	$E_{\text{cm}}^{ee}=10$ GeV
5.1 ±2.0	7	BYLSMA	87	HRS	$E_{\text{cm}}^{ee}=29$ GeV
• • • We use the following data for averages but not for fits. • • •					
8.56±0.05±0.42	34k	AUBERT,B	05W	BABR	232 fb^{-1}, $E_{\text{cm}}^{ee}=10.6$ GeV
• • • We do not use the following data for averages, fits, limits, etc. • • •					
8.0 ±1.1 ±1.3	58	BUSKULIC	96	ALEP	Repl. by SCHAEL 05C
6.7 ±3.0	5	[3] BELTRAMI	85	HRS	Repl. by BYLSMA 87

[1] See footnote to ABDALLAH 06A $\Gamma(\tau^-\to h^-\nu_\tau)/\Gamma_{\text{total}}$ measurement for correlations with other measurements.
[2] See footnote to SCHAEL 05C $\Gamma(\tau^-\to e^-\overline{\nu}_e\nu_\tau)/\Gamma_{\text{total}}$ measurement for correlations with other measurements.
[3] The error quoted is statistical only.

$\Gamma(3\pi^-2\pi^+\nu_\tau(\text{ex.}K^0,\omega))/\Gamma_{\text{total}}$ $\Gamma_{116}/\Gamma=(\Gamma_{117}+\Gamma_{171})/\Gamma$

VALUE (units 10^{-4})	DOCUMENT ID		TECN	COMMENT
8.21±0.31 OUR FIT				
• • • We use the following data for averages but not for fits. • • •				
8.33±0.04±0.43	[1] LEES	12X	BABR	468 fb^{-1} $E_{\text{cm}}^{ee}=10.6$ GeV

[1] Not independent of LEES 12X $\Gamma(\tau^-\to f_1(1285)\,\pi^-\nu_\tau\to 3\pi^-2\pi^+\nu_\tau)/\Gamma$ and $\Gamma(\tau^-\to 3\pi^-2\pi^+\nu_\tau$(ex. K^0, ω, $f_1(1285)$))$/\Gamma$ values.

$\Gamma(3\pi^-2\pi^+\nu_\tau(\text{ex.}K^0,\omega,f_1(1285)))/\Gamma_{\text{total}}$ Γ_{117}/Γ

VALUE (units 10^{-4})	EVTS	DOCUMENT ID		TECN	COMMENT
7.69±0.30 OUR FIT					
7.68±0.04±0.40	69k	LEES	12X	BABR	468 fb^{-1} $E_{\text{cm}}^{ee}=10.6$ GeV

$\Gamma(K^-2\pi^-2\pi^+\nu_\tau(\text{ex.}K^0))/\Gamma_{\text{total}}$ Γ_{118}/Γ

VALUE (units 10^{-6})	DOCUMENT ID		TECN	COMMENT
0.6±1.2 OUR FIT				
0.6±0.5±1.1	[1] LEES	12X	BABR	468 fb^{-1} $E_{\text{cm}}^{ee}=10.6$ GeV

[1] LEES 12X meaurement corresponds to the lower limit of $<2.4\times10^{-6}$ at 90% CL.

$\Gamma(K^+3\pi^-\pi^+\nu_\tau)/\Gamma_{\text{total}}$ Γ_{119}/Γ

VALUE	CL%	DOCUMENT ID		TECN	COMMENT
$<5.0\times10^{-6}$	90	LEES	12X	BABR	468 fb^{-1} $E_{\text{cm}}^{ee}=10.6$ GeV

$\Gamma(K^+K^-2\pi^-\pi^+\nu_\tau)/\Gamma_{\text{total}}$ Γ_{120}/Γ

VALUE	CL%	DOCUMENT ID		TECN	COMMENT
$<4.5\times10^{-7}$	90	LEES	12X	BABR	468 fb^{-1} $E_{\text{cm}}^{ee}=10.6$ GeV

$\Gamma(3h^-2h^+\pi^0\nu_\tau(\text{ex.}K^0))/\Gamma_{\text{total}}$ $\Gamma_{121}/\Gamma=(\Gamma_{122}+\Gamma_{125})/\Gamma$

VALUE (units 10^{-4})	EVTS	DOCUMENT ID		TECN	COMMENT
1.64±0.11 OUR FIT					
1.74±0.27 OUR AVERAGE					
1.6 ±1.2 ±0.6	13	[1] ABDALLAH	06A	DLPH	1992–1995 LEP runs
2.1 ±0.7 ±0.9	95	[2] SCHAEL	05C	ALEP	1991-1995 LEP runs
1.7 ±0.2 ±0.2	231	ANASTASSOV	01	CLEO	$E_{\text{cm}}^{ee}=10.6$ GeV
2.7 ±1.8 ±0.9	23	ACKERSTAFF	99E	OPAL	1991–1995 LEP runs
• • • We do not use the following data for averages, fits, limits, etc. • • •					
1.8 ±0.7 ±1.2	18	BUSKULIC	96	ALEP	Repl. by SCHAEL 05C
1.9 ±0.4 ±0.4	31	GIBAUT	94B	CLEO	Repl. by ANASTASSOV 01
5.1 ±2.2	6	BYLSMA	87	HRS	$E_{\text{cm}}^{ee}=29$ GeV
6.7 ±3.0	5	[3] BELTRAMI	85	HRS	Repl. by BYLSMA 87

[1] See footnote to ABDALLAH 06A $\Gamma(\tau^-\to h^-\nu_\tau)/\Gamma_{\text{total}}$ measurement for correlations with other measurements.
[2] SCHAEL 05C quote $(1.4\pm0.7\pm0.9)\times10^{-4}$. We add 0.7×10^{-4} to remove their correction for $\tau^-\to\eta\pi^-\pi^+\pi^-\nu_\tau\to 3\pi^-2\pi^+\pi^0\nu_\tau$ and $\tau^-\to K^*(892)^-\eta\nu_\tau\to 3\pi^-2\pi^+\pi^0\nu_\tau$ decays. See footnote to SCHAEL 05C $\Gamma(\tau^-\to e^-\overline{\nu}_e\nu_\tau)/\Gamma_{\text{total}}$ measurement for correlations with other measurements.
[3] The error quoted is statistical only.

$\Gamma(3\pi^-2\pi^+\pi^0\nu_\tau(\text{ex.}K^0))/\Gamma_{\text{total}}$ Γ_{122}/Γ

$\Gamma_{122}/\Gamma=(\Gamma_{124}+0.2292\Gamma_{158}+0.892\Gamma_{183})/\Gamma$

VALUE (units 10^{-4})	DOCUMENT ID		TECN	COMMENT
1.62±0.11 OUR FIT				
• • • We use the following data for averages but not for fits. • • •				
1.65±0.05±0.09	[1] LEES	12X	BABR	468 fb^{-1} $E_{\text{cm}}^{ee}=10.6$ GeV

[1] Not independent of LEES 12X measurements of $\Gamma(\tau^-\to 2\pi^-\pi^+\omega\nu_\tau(\text{ex.}K^0))/\Gamma$, $\Gamma(\tau^-\to\eta\pi^-\pi^+\pi^-\nu_\tau(\text{ex.}K^0))/\Gamma$, and $\Gamma(\tau^-\to 3\pi^-2\pi^+\pi^0\nu_\tau$(ex.$K^0$, η, ω, $f_1(1285)$))$/\Gamma$.

$\Gamma(3\pi^-2\pi^+\pi^0\nu_\tau(\text{ex.}K^0,\eta,f_1(1285)))/\Gamma_{\text{total}}$ Γ_{123}/Γ

VALUE (units 10^{-4})	DOCUMENT ID		TECN	COMMENT
1.11±0.04±0.09	[1] LEES	12X	BABR	468 fb^{-1} $E_{\text{cm}}^{ee}=10.6$ GeV

[1] Not independent of LEES 12X $\Gamma(\tau^-\to 2\pi^-\pi^+\omega\nu_\tau(\text{ex.}K^0))/\Gamma$ and $\Gamma(\tau^-\to 3\pi^-2\pi^+\pi^0\nu_\tau$(ex.$K^0$, η, ω, $f_1(1285)$))$/\Gamma$ values.

$\Gamma(3\pi^-2\pi^+\pi^0\nu_\tau(\text{ex.}K^0,\eta,\omega,f_1(1285)))/\Gamma_{\text{total}}$ Γ_{124}/Γ

VALUE (units 10^{-4})	EVTS	DOCUMENT ID		TECN	COMMENT
0.38±0.09 OUR FIT					
0.36±0.03±0.09	7.3k	LEES	12X	BABR	468 fb^{-1} $E_{\text{cm}}^{ee}=10.6$ GeV

$\Gamma(K^-2\pi^-2\pi^+\pi^0\nu_\tau(\text{ex.}K^0))/\Gamma_{\text{total}}$ Γ_{125}/Γ

VALUE (units 10^{-6})	DOCUMENT ID		TECN	COMMENT
1.1±0.6 OUR FIT				
1.1±0.4±0.4	[1] LEES	12X	BABR	468 fb^{-1} $E_{\text{cm}}^{ee}=10.6$ GeV

[1] LEES 12X meaurement corresponds to the lower limit of $<1.9\times10^{-6}$ at 90% CL.

$\Gamma(K^+3\pi^-\pi^+\pi^0\nu_\tau)/\Gamma_{\text{total}}$ Γ_{126}/Γ

VALUE	CL%	DOCUMENT ID		TECN	COMMENT
$<8\times10^{-7}$	90	LEES	12X	BABR	468 fb^{-1} $E_{\text{cm}}^{ee}=10.6$ GeV

$\Gamma(3h^-2h^+2\pi^0\nu_\tau)/\Gamma_{\text{total}}$ Γ_{127}/Γ

VALUE	CL%	DOCUMENT ID		TECN	COMMENT
$<3.4\times10^{-6}$	90	AUBERT,B	06	BABR	232 fb^{-1} $E_{\text{cm}}^{ee}=10.6$ GeV
• • • We do not use the following data for averages, fits, limits, etc. • • •					
$<1.1\times10^{-4}$	90	GIBAUT	94B	CLEO	$E_{\text{cm}}^{ee}=10.6$ GeV

$\Gamma((5\pi)^-\nu_\tau)/\Gamma_{\text{total}}$ Γ_{128}/Γ

$\Gamma_{128}/\Gamma=(\Gamma_{30}+\frac{1}{2}\Gamma_{45}+\Gamma_{48}+\frac{1}{2}\Gamma_{61}+\Gamma_{85}+\Gamma_{115}+0.5559\Gamma_{148}+0.892\Gamma_{178})/\Gamma$

VALUE (%)	DOCUMENT ID		TECN	COMMENT
0.78±0.05 OUR FIT				
• • • We use the following data for averages but not for fits. • • •				
0.61±0.06±0.08	[1] GIBAUT	94B	CLEO	$E_{\text{cm}}^{ee}=10.6$ GeV

[1] Not independent of GIBAUT 94B B($3h^-2h^+\nu_\tau$), PROCARIO 93 B($h^-4\pi^0\nu_\tau$), and BORTOLETTO 93 B($2h^-h^+2\pi^0\nu_\tau$)/B("3prong") measurements. Result is corrected for η contributions.

$\Gamma(4h^-3h^+ \geq 0$ neutrals ν_τ ("7-prong"))/Γ_{total} Γ_{129}/Γ

VALUE	CL%	DOCUMENT ID		TECN	COMMENT
$<3.0\times10^{-7}$	90	AUBERT,B	05F	BABR	232 fb^{-1}, E_{cm}^{ee}= 10.6 GeV
• • • We do not use the following data for averages, fits, limits, etc. • • •					
$<1.8\times10^{-5}$	95	ACKERSTAFF	97J	OPAL	1990–1995 LEP runs
$<2.4\times10^{-6}$	90	EDWARDS	97B	CLEO	E_{cm}^{ee}= 10.6 GeV
$<2.9\times10^{-4}$	90	BYLSMA	87	HRS	E_{cm}^{ee}= 29 GeV

$\Gamma(4h^-3h^+\nu_\tau)/\Gamma_{total}$ Γ_{130}/Γ

VALUE	CL%	DOCUMENT ID		TECN	COMMENT
$<4.3\times10^{-7}$	90	AUBERT,B	05F	BABR	232 fb^{-1}, E_{cm}^{ee}= 10.6 GeV

$\Gamma(4h^-3h^+\pi^0\nu_\tau)/\Gamma_{total}$ Γ_{131}/Γ

VALUE	CL%	DOCUMENT ID		TECN	COMMENT
$<2.5\times10^{-7}$	90	AUBERT,B	05F	BABR	232 fb^{-1}, E_{cm}^{ee}= 10.6 GeV

$\Gamma(X^-(S=-1)\nu_\tau)/\Gamma_{total}$ Γ_{132}/Γ

$\Gamma_{132}/\Gamma=(\Gamma_{10}+\Gamma_{16}+\Gamma_{23}+\Gamma_{28}+\Gamma_{36}+\Gamma_{41}+\Gamma_{45}+\Gamma_{61}+\Gamma_{97}+\Gamma_{103}+\Gamma_{118}+\Gamma_{125}+\Gamma_{150}+\Gamma_{152}+\Gamma_{154}+0.8312\Gamma_{168}+\Gamma_{177})/\Gamma$

VALUE (%)	DOCUMENT ID		TECN	COMMENT
2.92±0.04 OUR FIT				
• • • We use the following data for averages but not for fits. • • •				
2.87±0.12	[1] BARATE	99R	ALEP	1991–1995 LEP runs

[1] BARATE 99R perform a combined analysis of all ALEPH LEP 1 data on τ branching fraction measurements for decay modes having total strangeness equal to -1.

$\Gamma(K^*(892)^-\geq 0$ neutrals $\geq 0K_L^0\nu_\tau)/\Gamma_{total}$ Γ_{133}/Γ

VALUE (%)	EVTS	DOCUMENT ID		TECN	COMMENT
1.42±0.18 OUR AVERAGE		Error includes scale factor of 1.4. See the ideogram below.			
$1.19\pm0.15^{+0.13}_{-0.18}$	104	ALBRECHT	95H	ARG	E_{cm}^{ee}= 9.4–10.6 GeV
1.94±0.27±0.15	74	[1] AKERS	94G	OPAL	E_{cm}^{ee}= 88–94 GeV
1.43±0.11±0.13	475	[2] GOLDBERG	90	CLEO	E_{cm}^{ee}= 9.4–10.9 GeV

[1] AKERS 94G reject events in which a K_S^0 accompanies the $K^*(892)^-$. We do not correct for them.
[2] GOLDBERG 90 estimates that 10% of observed $K^*(892)$ are accompanied by a π^0.

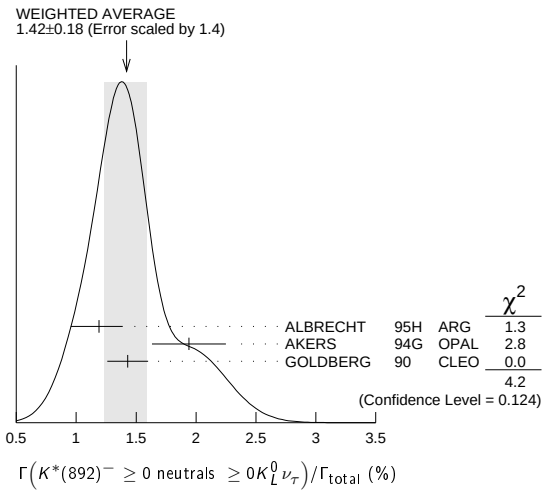

$\Gamma(K^*(892)^-\nu_\tau)/\Gamma_{total}$ Γ_{134}/Γ

VALUE (%)	EVTS	DOCUMENT ID		TECN	COMMENT
1.20 ±0.07 OUR AVERAGE		Error includes scale factor of 1.8. See the ideogram below.			
1.131±0.006±0.051	49k	[1] EPIFANOV	07	BELL	351 fb^{-1} E_{cm}^{ee}=10.6 GeV
1.326±0.063		BARATE	99R	ALEP	1991–1995 LEP runs
1.11 ±0.12		[2] COAN	96	CLEO	$E_{cm}^{ee}\approx$ 10.6 GeV
1.42 ±0.22 ±0.09		[3] ACCIARRI	95F	L3	1991–1993 LEP runs
• • • We do not use the following data for averages, fits, limits, etc. • • •					
1.39 ±0.09 ±0.10		[4] BUSKULIC	96	ALEP	Repl. by BARATE 99R
1.45 ±0.13 ±0.11	273	[5] BUSKULIC	94F	ALEP	Repl. by BUSKULIC 96
1.23 ±0.21 $^{+0.11}_{-0.21}$	54	[6] ALBRECHT	88L	ARG	E_{cm}^{ee}= 10 GeV
1.9 ±0.3 ±0.4	44	[7] TSCHIRHART	88	HRS	E_{cm}^{ee}= 29 GeV
1.5 ±0.4 ±0.4	15	[8] AIHARA	87C	TPC	E_{cm}^{ee}= 29 GeV
1.3 ±0.3 ±0.3	31	YELTON	86	MRK2	E_{cm}^{ee}= 29 GeV
1.7 ±0.7	11	DORFAN	81	MRK2	E_{cm}^{ee}= 4.2–6.7 GeV

[1] EPIFANOV 07 quote B($\tau^-\to K^*(892)^-\nu_\tau$) B($K^*(892)^-\to K_S^0\pi^-$) = (3.77 ± 0.02(stat) ±0.12(syst) ±0.12(mod)) × 10^{-3}. We add the systematic and model uncertainties in quadrature and divide by B($K^*(892)^-\to K_S^0\pi^-$) = 0.3333.
[2] Not independent of COAN 96 B($\pi^-\overline{K}^0\nu_\tau$) and BATTLE 94 B($K^-\pi^0\nu_\tau$) measurements. $K\pi$ final states are consistent with and assumed to originate from $K^*(892)^-$ production.
[3] This result is obtained from their B($\pi^-\overline{K}^0\nu_\tau$) assuming all those decays originate in $K^*(892)^-$ decays.
[4] Not independent of BUSKULIC 96 B($\pi^-\overline{K}^0\nu_\tau$) and B($K^-\pi^0\nu_\tau$) measurements.
[5] BUSKULIC 94F obtain this result from BUSKULIC 94F B($\overline{K}^0\pi^-\nu_\tau$) and BUSKULIC 94E B($K^-\pi^0\nu_\tau$) assuming all of those decays originate in $K^*(892)^-$ decays.
[6] The authors divide by Γ_2/Γ = 0.865 to obtain this result.
[7] Not independent of TSCHIRHART 88 $\Gamma(\tau^-\to h^-\overline{K}^0\geq 0$ neutrals $\geq 0K_L^0\nu_\tau)$ / Γ.
[8] Decay π^- identified in this experiment, is assumed in the others.

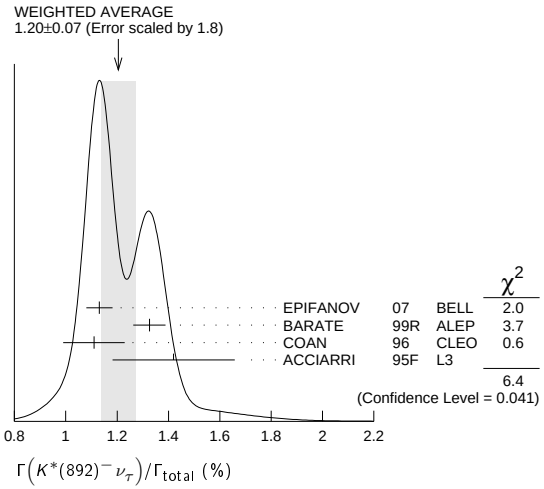

$\Gamma(K^*(892)^-\nu_\tau)/\Gamma(\pi^-\pi^0\nu_\tau)$ Γ_{134}/Γ_{14}

VALUE	DOCUMENT ID		TECN	COMMENT
0.075±0.027	[1] ABREU	94K	DLPH	LEP 1992 Z data

[1] ABREU 94K quote B($\tau^-\to K^*(892)^-\nu_\tau$)B($K^*(892)^-\to K^-\pi^0$)/B($\tau^-\to\rho^-\nu_\tau$) = 0.025 ± 0.009. We divide by B($K^*(892)^-\to K^-\pi^0$) = 0.333 to obtain this result.

$\Gamma(K^*(892)^-\nu_\tau\to\pi^-\overline{K}^0\nu_\tau)/\Gamma(\pi^-\overline{K}^0\nu_\tau)$ Γ_{135}/Γ_{36}

VALUE	EVTS	DOCUMENT ID		TECN	COMMENT
0.933±0.027	49k	EPIFANOV	07	BELL	351 fb^{-1} E_{cm}^{ee}= 10.6 GeV

$\Gamma(K^*(892)^0K^-\geq 0$ neutrals $\nu_\tau)/\Gamma_{total}$ Γ_{136}/Γ

VALUE (%)	EVTS	DOCUMENT ID		TECN	COMMENT
0.32±0.08±0.12	119	GOLDBERG	90	CLEO	E_{cm}^{ee}= 9.4–10.9 GeV

$\Gamma(K^*(892)^0K^-\nu_\tau)/\Gamma_{total}$ Γ_{137}/Γ

VALUE (%)	EVTS	DOCUMENT ID		TECN	COMMENT
0.21 ±0.04 OUR AVERAGE					
0.213±0.048		[1] BARATE	98	ALEP	1991–1995 LEP runs
0.20 ±0.05 ±0.04	47	ALBRECHT	95H	ARG	E_{cm}^{ee}= 9.4–10.6 GeV

[1] BARATE 98 measure the K^- ($\rho^0\to\pi^+\pi^-$) fraction in $\tau^-\to K^-\pi^+\pi^-\nu_\tau$ decays to be (35 ± 11)% and derive this result from their measurement of $\Gamma(\tau^-\to K^-\pi^+\pi^-\nu_\tau)/\Gamma_{total}$ assuming the intermediate states are all $K^-\rho$ and $K^-K^*(892)^0$.

$\Gamma(\overline{K}^*(892)^0\pi^-\geq 0$ neutrals $\nu_\tau)/\Gamma_{total}$ Γ_{138}/Γ

VALUE (%)	EVTS	DOCUMENT ID		TECN	COMMENT
0.38±0.11±0.13	105	GOLDBERG	90	CLEO	E_{cm}^{ee}= 9.4–10.9 GeV

$\Gamma(\overline{K}^*(892)^0\pi^-\nu_\tau)/\Gamma_{total}$ Γ_{139}/Γ

VALUE (%)	EVTS	DOCUMENT ID		TECN	COMMENT
0.22 ±0.05 OUR AVERAGE					
0.209±0.058		[1] BARATE	98	ALEP	1991–1995 LEP runs
0.25 ±0.10 ±0.05	27	ALBRECHT	95H	ARG	E_{cm}^{ee}= 9.4–10.6 GeV

[1] BARATE 98 measure the $K^-K^*(892)^0$ fraction in $\tau^-\to K^-K^+\pi^-\nu_\tau$ decays to be (87 ± 13)% and derive this result from their measurement of $\Gamma(\tau^-\to K^-K^+\pi^-\nu_\tau)/\Gamma_{total}$.

$\Gamma((\overline{K}^*(892)\pi)^-\nu_\tau\to\pi^-\overline{K}^0\pi^0\nu_\tau)/\Gamma_{total}$ Γ_{140}/Γ

VALUE (%)	DOCUMENT ID		TECN	COMMENT
0.10 ±0.04 OUR AVERAGE				
0.097±0.044±0.036	[1] BARATE	99K	ALEP	1991–1995 LEP runs
0.106±0.037±0.032	[2] BARATE	98E	ALEP	1991–1995 LEP runs

[1] BARATE 99K measure K^0's by detecting K_L^0's in their hadron calorimeter. They determine the $\overline{K}^0\rho^-$ fraction in $\tau^-\to\pi^-\overline{K}^0\pi^0\nu_\tau$ decays to be (0.72 ± 0.12 ± 0.10) and multiply their B($\pi^-\overline{K}^0\pi^0\nu_\tau$) measurement by one minus this fraction to obtain the quoted result.
[2] BARATE 98E reconstruct K^0's using $K_S^0\to\pi^+\pi^-$ decays. They determine the $\overline{K}^0\rho^-$ fraction in $\tau^-\to\pi^-\overline{K}^0\pi^0\nu_\tau$ decays to be (0.64 ± 0.09 ± 0.10) and multiply their B($\pi^-\overline{K}^0\pi^0\nu_\tau$) measurement by one minus this fraction to obtain the quoted result.

$\Gamma(K_1(1270)^-\nu_\tau)/\Gamma_{total}$ Γ_{141}/Γ

VALUE (%)	EVTS	DOCUMENT ID		TECN	COMMENT
0.47±0.11 OUR AVERAGE					
0.48±0.11		BARATE	99R	ALEP	1991–1995 LEP runs
$0.41^{+0.41}_{-0.35}\pm0.10$	5	[1] BAUER	94	TPC	E^{ee}_{cm}= 29 GeV

[1] We multiply 0.41% by 0.25, the relative systematic error quoted by BAUER 94, to obtain the systematic error.

$\Gamma(K_1(1400)^-\nu_\tau)/\Gamma_{total}$ Γ_{142}/Γ

VALUE (%)	EVTS	DOCUMENT ID		TECN	COMMENT
0.17±0.26 OUR AVERAGE Error includes scale factor of 1.7.					
0.05±0.17		BARATE	99R	ALEP	1991–1995 LEP runs
$0.76^{+0.40}_{-0.33}\pm0.20$	11	[1] BAUER	94	TPC	E^{ee}_{cm}= 29 GeV

[1] We multiply 0.76% by 0.25, the relative systematic error quoted by BAUER 94, to obtain the systematic error.

$[\Gamma(K_1(1270)^-\nu_\tau)+\Gamma(K_1(1400)^-\nu_\tau)]/\Gamma_{total}$ $(\Gamma_{141}+\Gamma_{142})/\Gamma$

VALUE (%)	EVTS	DOCUMENT ID		TECN	COMMENT
$\mathbf{1.17^{+0.41}_{-0.37}\pm0.29}$	16	[1] BAUER	94	TPC	E^{ee}_{cm}= 29 GeV

[1] We multiply 1.17% by 0.25, the relative systematic error quoted by BAUER 94, to obtain the systematic error. Not independent of BAUER 94 B($K_1(1270)^-\nu_\tau$) and BAUER 94 B($K_1(1400)^-\nu_\tau$) measurements.

$\Gamma(K_1(1270)^-\nu_\tau)/[\Gamma(K_1(1270)^-\nu_\tau)+\Gamma(K_1(1400)^-\nu_\tau)]$ $\Gamma_{141}/(\Gamma_{141}+\Gamma_{142})$

VALUE	DOCUMENT ID		TECN	COMMENT
0.69±0.15 OUR AVERAGE				
0.71±0.16±0.11	[1] ABBIENDI	00D	OPAL	1990–1995 LEP runs
0.66±0.19±0.13	[2] ASNER	00B	CLEO	E^{ee}_{cm}= 10.6 GeV

[1] ABBIENDI 00D assume the resonance structure of $\tau^- \to K^-\pi^+\pi^-\nu_\tau$ decays is dominated by the $K_1(1270)^-$ and $K_1(1400)^-$ resonances.

[2] ASNER 00B assume the resonance structure of $\tau^- \to K^-\pi^+\pi^-\nu_\tau$ (ex. K^0) decays is dominated by $K_1(1270)^-$ and $K_1(1400)^-$ resonances.

$\Gamma(K^*(1410)^-\nu_\tau)/\Gamma_{total}$ Γ_{143}/Γ

VALUE (units 10^{-3})	DOCUMENT ID		TECN	COMMENT
$\mathbf{1.5^{+1.4}_{-1.0}}$	BARATE	99R	ALEP	1991–1995 LEP runs

$\Gamma(K_0^*(1430)^-\nu_\tau)/\Gamma_{total}$ Γ_{144}/Γ

VALUE (units 10^{-3})	CL%	DOCUMENT ID		TECN	COMMENT
<0.5	95	BARATE	99R	ALEP	1991–1995 LEP runs

$\Gamma(K_2^*(1430)^-\nu_\tau)/\Gamma_{total}$ Γ_{145}/Γ

VALUE (%)	CL%	EVTS	DOCUMENT ID		TECN	COMMENT
<0.3	95		TSCHIRHART	88	HRS	E^{ee}_{cm}= 29 GeV
• • • We do not use the following data for averages, fits, limits, etc. • • •						
<0.33	95		[1] ACCIARRI	95F	L3	1991–1993 LEP runs
<0.9	95	0	DORFAN	81	MRK2	E^{ee}_{cm}= 4.2–6.7 GeV

[1] ACCIARRI 95F quote B($\tau^- \to K^*(1430)^- \to \pi^-\overline{K}^0\nu_\tau$) < 0.11%. We divide by B($K^*(1430)^- \to \pi^-\overline{K}^0$) = 0.33 to obtain the limit shown.

$\Gamma(a_0(980)^- \geq 0 \text{ neutrals } \nu_\tau)/\Gamma_{total} \times B(a_0(980) \to K^0K^-)$ $\Gamma_{146}/\Gamma \times B$

VALUE (units 10^{-4})	CL%	DOCUMENT ID		TECN	COMMENT
<2.8	90	GOLDBERG	90	CLEO	E^{ee}_{cm}= 9.4–10.9 GeV

$\Gamma(\eta\pi^-\nu_\tau)/\Gamma_{total}$ Γ_{147}/Γ

VALUE (units 10^{-4})	CL%	EVTS	DOCUMENT ID		TECN	COMMENT
< 0.99	95		[1] DEL-AMO-SA...11E		BABR	470 fb^{-1} E^{ee}_{cm}= 10.6 GeV
• • • We do not use the following data for averages, fits, limits, etc. • • •						
< 6.2	95		BUSKULIC	97C	ALEP	1991–1994 LEP runs
< 1.4	95	0	BARTELT	96	CLEO	$E^{ee}_{cm} \approx$ 10.6 GeV
< 3.4	95		ARTUSO	92	CLEO	$E^{ee}_{cm} \approx$ 10.6 GeV
< 90	95		ALBRECHT	88M	ARG	$E^{ee}_{cm} \approx$ 10 GeV
<140	90		BEHREND	88	CELL	E^{ee}_{cm}= 14–46.8 GeV
<180	95		BARINGER	87	CLEO	E^{ee}_{cm}= 10.5 GeV
<250	90	0	COFFMAN	87	MRK3	E^{ee}_{cm}= 3.77 GeV
510 ±100±120	65		DERRICK	87	HRS	E^{ee}_{cm}= 29 GeV
<100	95		GAN	87B	MRK2	E^{ee}_{cm}= 29 GeV

[1] DEL-AMO-SANCHEZ 11E also quote B($\tau^- \to \eta\pi^-\nu_\tau$) = (3.4 ± 3.4 ± 2.1) × 10^{-5}.

$\Gamma(\eta\pi^-\pi^0\nu_\tau)/\Gamma_{total}$ Γ_{148}/Γ

VALUE (units 10^{-3})	CL%	EVTS	DOCUMENT ID		TECN	COMMENT
1.39± 0.07 OUR FIT						
1.38± 0.09 OUR AVERAGE Error includes scale factor of 1.2.						
1.35± 0.03± 0.07	6.0k		INAMI	09	BELL	490 fb^{-1} E^{ee}_{cm}= 10.6 GeV
1.8 ± 0.4 ± 0.2			BUSKULIC	97C	ALEP	1991–1994 LEP runs
1.7 ± 0.2 ± 0.2		125	ARTUSO	92	CLEO	$E^{ee}_{cm} \approx$ 10.6 GeV
• • • We do not use the following data for averages, fits, limits, etc. • • •						
< 11.0	95		ALBRECHT	88M	ARG	$E^{ee}_{cm} \approx$ 10 GeV
< 21.0	95		BARINGER	87	CLEO	E^{ee}_{cm}= 10.5 GeV
$42.0\ ^{+\ 7.0}_{-12.0}\pm16.0$		[1] GAN	87	MRK2	E^{ee}_{cm}= 29 GeV	

[1] Highly correlated with GAN 87 $\Gamma(\pi^-3\pi^0\nu_\tau)/\Gamma$(total) value.

$\Gamma(\eta\pi^-\pi^0\pi^0\nu_\tau)/\Gamma_{total}$ Γ_{149}/Γ

VALUE (units 10^{-4})	CL%	EVTS	DOCUMENT ID		TECN	COMMENT
1.9 ±0.4 OUR FIT						
1.81±0.31 OUR AVERAGE						
2.01±0.34±0.22		381	LEES	12X	BABR	468 fb^{-1} E^{ee}_{cm} = 10.6 GeV
• • • We use the following data for averages but not for fits. • • •						
1.5 ±0.5		30	[1] ANASTASSOV	01	CLEO	E^{ee}_{cm}= 10.6 GeV
• • • We do not use the following data for averages, fits, limits, etc. • • •						
1.4 ±0.6 ±0.3		15	[2] BERGFELD	97	CLEO	Repl. by ANASTASSOV 01
< 4.3	95		ARTUSO	92	CLEO	$E^{ee}_{cm} \approx$ 10.6 GeV
<120	95		ALBRECHT	88M	ARG	$E^{ee}_{cm} \approx$ 10 GeV

[1] Weighted average of BERGFELD 97 and ANASTASSOV 01 value of (1.5 ± 0.6 ± 0.3) × 10^{-4} obtained using η's reconstructed from $\eta \to \pi^+\pi^-\pi^0$ decays.

[2] BERGFELD 97 reconstruct η's using $\eta \to \gamma\gamma$ decays.

$\Gamma(\eta K^-\nu_\tau)/\Gamma_{total}$ Γ_{150}/Γ

VALUE (units 10^{-4})	CL%	EVTS	DOCUMENT ID		TECN	COMMENT
1.55±0.08 OUR FIT						
1.54±0.08 OUR AVERAGE						
1.42±0.11±0.07		690	DEL-AMO-SA...11E		BABR	470 fb^{-1} E^{ee}_{cm}= 10.6 GeV
1.58±0.05±0.09		1.6k	INAMI	09	BELL	490 fb^{-1} E^{ee}_{cm}= 10.6 GeV
$2.9\ ^{+1.3}_{-1.2}\pm0.7$			BUSKULIC	97C	ALEP	1991–1994 LEP runs
2.6 ±0.5 ±0.5		85	BARTELT	96	CLEO	$E^{ee}_{cm} \approx$ 10.6 GeV
• • • We do not use the following data for averages, fits, limits, etc. • • •						
< 4.7	95		ARTUSO	92	CLEO	$E^{ee}_{cm} \approx$ 10.6 GeV

$\Gamma(\eta K^*(892)^-\nu_\tau)/\Gamma_{total}$ Γ_{151}/Γ

VALUE (units 10^{-4})	EVTS	DOCUMENT ID		TECN	COMMENT
1.38±0.15 OUR AVERAGE					
1.34±0.12±0.09	245	[1] INAMI	09	BELL	490 fb^{-1} E^{ee}_{cm}= 10.6 GeV
2.90±0.80±0.42	25	BISHAI	99	CLEO	E^{ee}_{cm}= 10.6 GeV

[1] Not independent of INAMI 09 B($\tau^- \to \eta K^-\pi^0\nu_\tau$) and B($\tau^- \to \eta\overline{K}^0\pi^-\nu_\tau$) values.

$\Gamma(\eta K^-\pi^0\nu_\tau)/\Gamma_{total}$ Γ_{152}/Γ

VALUE (units 10^{-4})	EVTS	DOCUMENT ID		TECN	COMMENT
0.48±0.12 OUR FIT					
0.48±0.12 OUR AVERAGE					
0.46±0.11±0.04	270	INAMI	09	BELL	490 fb^{-1} E^{ee}_{cm}= 10.6 GeV
1.77±0.56±0.71	36	BISHAI	99	CLEO	E^{ee}_{cm}= 10.6 GeV

$\Gamma(\eta K^-\pi^0(\text{non-}K^*(892))\nu_\tau)/\Gamma_{total}$ Γ_{153}/Γ

VALUE	CL%	DOCUMENT ID		TECN	COMMENT
<3.5 × 10^{-5}	90	INAMI	09	BELL	490 fb^{-1} E^{ee}_{cm}= 10.6 GeV

$\Gamma(\eta\overline{K}^0\pi^-\nu_\tau)/\Gamma_{total}$ Γ_{154}/Γ

VALUE (units 10^{-4})	EVTS	DOCUMENT ID		TECN	COMMENT
0.94±0.15 OUR FIT					
0.93±0.15 OUR AVERAGE					
0.88±0.14±0.06	161	[1] INAMI	09	BELL	490 fb^{-1} E^{ee}_{cm}= 10.6 GeV
2.20±0.70±0.22	15	[2] BISHAI	99	CLEO	E^{ee}_{cm}= 10.6 GeV

[1] We multiply the INAMI 09 measurement B($\tau^- \to \eta K^0_S\pi^-\nu_\tau$) = (0.44 ± 0.07 ± 0.03) × 10^{-4} by 2 to obtain the listed value.

[2] We multiply the BISHAI 99 measurement B($\tau^- \to \eta K^0_S\pi^-\nu_\tau$) = (1.10 ± 0.35 ± 0.11) × 10^{-4} by 2 to obtain the listed value.

$\Gamma(\eta\overline{K}^0\pi^-\pi^0\nu_\tau)/\Gamma_{total}$ Γ_{155}/Γ

VALUE	CL%	DOCUMENT ID		TECN	COMMENT
<5.0 × 10^{-5}	90	[1] INAMI	09	BELL	490 fb^{-1} E^{ee}_{cm}= 10.6 GeV

[1] We multiply the INAMI 09 measurement B($\tau^- \to \eta K^0_S\pi^-\pi^0\nu_\tau$) < 2.5 × 10^{-5} by 2 to obtain the listed value.

$\Gamma(\eta K^-K^0\nu_\tau)/\Gamma_{total}$ Γ_{156}/Γ

VALUE	CL%	DOCUMENT ID		TECN	COMMENT
<9.0 × 10^{-6}	90	[1] INAMI	09	BELL	490 fb^{-1} E^{ee}_{cm}= 10.6 GeV

[1] We multiply the INAMI 09 measurement B($\tau^- \to \eta K^-K^0_S\nu_\tau$) < 4.5 × 10^{-6} by 2 to obtain the listed value.

$\Gamma(\eta\pi^+\pi^-\pi^- \geq 0$ neutrals $\nu_\tau)/\Gamma_{total}$ Γ_{157}/Γ

VALUE (%)	CL%	DOCUMENT ID		TECN	COMMENT
<0.3	90	ABACHI	87B	HRS	E_{cm}^{ee} = 29 GeV

$\Gamma(\eta\pi^-\pi^+\pi^-\nu_\tau$ (ex.K^0))/Γ_{total} Γ_{158}/Γ

VALUE (units 10^{-4})	EVTS	DOCUMENT ID		TECN	COMMENT
2.19±0.13 OUR FIT					
2.23±0.12 OUR AVERAGE					
2.10±0.09±0.13	2.9k	[1] LEES	12X	BABR	$\eta \to \gamma\gamma$
2.37±0.12±0.18	1.4k	[1] LEES	12X	BABR	$\eta \to \pi^+\pi^-\pi^0$
2.54±0.27±0.25	315	[1] LEES	12X	BABR	$\eta \to 3\pi^0$
• • • We use the following data for averages but not for fits. • • •					
2.3 ±0.5	170	[2] ANASTASSOV	01	CLEO	E_{cm}^{ee} = 10.6 GeV
• • • We do not use the following data for averages, fits, limits, etc. • • •					
1.60±0.05±0.11	1.8 k	AUBERT	08AE	BABR	Repl. by LEES 12X
3.4 $^{+0.6}_{-0.5}$ ±0.6	89	[3] BERGFELD	97	CLEO	Repl. by ANASTASSOV 01

[1] LEES 12X uses 468 fb^{-1} of data taken at $E_{cm}^{ee} = 10.6$ GeV. It gives the average of the three measurements listed here as $(2.25 \pm 0.07 \pm 0.12) \times 10^{-4}$.

[2] Weighted average of BERGFELD 97 and ANASTASSOV 01 measurements using η's reconstructed from $\eta \to \pi^+\pi^-\pi^0$ and $\eta \to 3\pi^0$ decays.

[3] BERGFELD 97 reconstruct η's using $\eta \to \gamma\gamma$ and $\eta \to 3\pi^0$ decays.

$\Gamma(\eta\pi^-\pi^+\pi^-\nu_\tau$ (ex.K^0,$f_1(1285)$))/Γ_{total} Γ_{159}/Γ

VALUE (units 10^{-4})	DOCUMENT ID		TECN	COMMENT
0.99±0.09±0.13	[1] LEES	12X	BABR	468 fb^{-1} E_{cm}^{ee} = 10.6 GeV

[1] LEES 12X obtain this result by subtracting their B($\tau^- \to f_1(1285)\pi^-\nu_\tau \to \eta\pi^-\pi^+\pi^-\nu_\tau$) measurement from their B($\tau^- \to \eta\pi^-\pi^+\pi^-\nu_\tau$(ex.$K^0$)) measurement.

$\Gamma(\eta a_1(1260)^-\nu_\tau \to \eta\pi^-\rho^0\nu_\tau)/\Gamma_{total}$ Γ_{160}/Γ

VALUE	CL%	DOCUMENT ID		TECN	COMMENT
<3.9 × 10^{-4}	90	BERGFELD	97	CLEO	E_{cm}^{ee} = 10.6 GeV

$\Gamma(\eta\eta\pi^-\nu_\tau)/\Gamma_{total}$ Γ_{161}/Γ

VALUE	CL%	DOCUMENT ID		TECN	COMMENT
<7.4 × 10^{-6}	90	INAMI	09	BELL	490 fb^{-1} E_{cm}^{ee} = 10.6 GeV
• • • We do not use the following data for averages, fits, limits, etc. • • •					
<1.1 × 10^{-4}	95	ARTUSO	92	CLEO	$E_{cm}^{ee} \approx$ 10.6 GeV
<8.3 × 10^{-3}	95	ALBRECHT	88M	ARG	$E_{cm}^{ee} \approx$ 10 GeV

$\Gamma(\eta\eta\pi^-\pi^0\nu_\tau)/\Gamma_{total}$ Γ_{162}/Γ

VALUE (units 10^{-4})	CL%	DOCUMENT ID		TECN	COMMENT
< 2.0	95	ARTUSO	92	CLEO	$E_{cm}^{ee} \approx$ 10.6 GeV
• • • We do not use the following data for averages, fits, limits, etc. • • •					
<90	95	ALBRECHT	88M	ARG	$E_{cm}^{ee} \approx$ 10 GeV

$\Gamma(\eta\eta K^-\nu_\tau)/\Gamma_{total}$ Γ_{163}/Γ

VALUE	CL%	DOCUMENT ID		TECN	COMMENT
<3.0 × 10^{-6}	90	INAMI	09	BELL	490 fb^{-1} E_{cm}^{ee} = 10.6 GeV

$\Gamma(\eta'(958)\pi^-\nu_\tau)/\Gamma_{total}$ Γ_{164}/Γ

VALUE	CL%	DOCUMENT ID		TECN	COMMENT
<4.0 × 10^{-6}	90	LEES	12X	BABR	468 fb^{-1} E_{cm}^{ee} = 10.6 GeV
• • • We do not use the following data for averages, fits, limits, etc. • • •					
<7.2 × 10^{-6}	90	AUBERT	08AE	BABR	384 fb^{-1}, E_{cm}^{ee} = 10.6 GeV
<7.4 × 10^{-5}	90	BERGFELD	97	CLEO	E_{cm}^{ee} = 10.6 GeV

$\Gamma(\eta'(958)\pi^-\pi^0\nu_\tau)/\Gamma_{total}$ Γ_{165}/Γ

VALUE	CL%	DOCUMENT ID		TECN	COMMENT
<1.2 × 10^{-5}	90	LEES	12X	BABR	468 fb^{-1} E_{cm}^{ee} = 10.6 GeV
• • • We do not use the following data for averages, fits, limits, etc. • • •					
<8.0 × 10^{-5}	90	BERGFELD	97	CLEO	E_{cm}^{ee} = 10.6 GeV

$\Gamma(\eta'(958)K^-\nu_\tau)/\Gamma_{total}$ Γ_{166}/Γ

VALUE	CL%	DOCUMENT ID		TECN	COMMENT
<2.4 × 10^{-6}	90	LEES	12X	BABR	468 fb^{-1} E_{cm}^{ee} = 10.6 GeV

$\Gamma(\phi\pi^-\nu_\tau)/\Gamma_{total}$ Γ_{167}/Γ

VALUE (units 10^{-5})	CL%	EVTS	DOCUMENT ID		TECN	COMMENT
3.42±0.55±0.25		344	AUBERT	08	BABR	342 fb^{-1} E_{cm}^{ee} = 10.6 GeV
• • • We do not use the following data for averages, fits, limits, etc. • • •						
< 20	90		[1] AVERY	97	CLEO	E_{cm}^{ee} = 10.6 GeV
< 35	90		ALBRECHT	95H	ARG	E_{cm}^{ee} = 9.4–10.6 GeV

[1] AVERY 97 limit varies from (1.2–2.0) × 10^{-4} depending on decay model assumptions.

$\Gamma(\phi K^-\nu_\tau)/\Gamma_{total}$ Γ_{168}/Γ

VALUE (units 10^{-5})	CL%	EVTS	DOCUMENT ID		TECN	COMMENT
4.4 ±1.6 OUR FIT						
3.70±0.33 OUR AVERAGE Error includes scale factor of 1.3.						
• • • We use the following data for averages but not for fits. • • •						
3.39±0.20±0.28		274	AUBERT	08	BABR	342 fb^{-1} E_{cm}^{ee} = 10.6 GeV
4.05±0.25±0.26		551	INAMI	06	BELL	401 fb^{-1} E_{cm}^{ee} =10.6 GeV
• • • We do not use the following data for averages, fits, limits, etc. • • •						
<6.7	90		[1] AVERY	97	CLEO	E_{cm}^{ee} = 10.6 GeV

[1] AVERY 97 limit varies from (5.4–6.7) × 10^{-5} depending on decay model assumptions.

$\Gamma(f_1(1285)\pi^-\nu_\tau)/\Gamma_{total}$ Γ_{169}/Γ

VALUE (units 10^{-4})	EVTS	DOCUMENT ID		TECN	COMMENT
3.9 ±0.5 OUR AVERAGE Error includes scale factor of 1.9.					
4.73±0.28±0.45	3.7k	[1] LEES	12X	BABR	468 fb^{-1} E_{cm}^{ee} = 10.6 GeV
3.60±0.18±0.23	2.5k	[2] LEES	12X	BABR	468 fb^{-1} E_{cm}^{ee} = 10.6 GeV
• • • We do not use the following data for averages, fits, limits, etc. • • •					
3.19±0.18±1.00	1.3 k	[3] AUBERT	08AE	BABR	Repl. by LEES 12X
3.9 ±0.7 ±0.5	1.4 k	[4] AUBERT,B	05W	BABR	Repl. by LEES 12X
5.8 $^{+1.4}_{-1.3}$ ±1.8	54	[5] BERGFELD	97	CLEO	E_{cm}^{ee} = 10.6 GeV

[1] LEES 12X obtain this value by dividing their B($\tau^- \to f_1(1285)\pi^-\nu_\tau \to 3\pi^-2\pi^+\nu_\tau$) measurement by the PDG 12 value of B($f_1(1285) \to 2\pi^+2\pi^-$) = 0.111 $^{+0.007}_{-0.006}$.

[2] LEES 12X obtain this value by dividing their B($\tau^- \to f_1(1285)\pi^-\nu_\tau \to \eta\pi^-\pi^+\pi^-\nu_\tau$) measurement by 2/3 of the PDG 12 value of B($f_1(1285) \to \eta\pi\pi$) = 0.524 $^{+0.019}_{-0.021}$.

[3] AUBERT 08AE obtain this value by dividing their B($\tau^- \to f_1(1285)\pi^-\nu_\tau \to \eta\pi^-\pi^+\pi^-\nu_\tau$) measurement by the PDG 06 value of B($f_1(1285) \to \eta\pi^-\pi^+$) = 0.35 ± 0.11. The quote $(3.19 \pm 0.18 \pm 0.16 \pm 0.99) \times 10^{-4}$ where the final error is due to the uncertainty on B($f_1(1285) \to \eta\pi^-\pi^+$). We combine the two systematic errors in quadrature.

[4] AUBERT,B 05W use the $f_1(1285) \to 2\pi^+2\pi^-$ decay mode and the PDG 04 value of B($f_1(1285) \to 2\pi^+2\pi^-$) = 0.110 $^{+0.007}_{-0.006}$.

[5] BERGFELD 97 use the $f_1(1285) \to \eta\pi^+\pi^-$ decay mode.

$\Gamma(f_1(1285)\pi^-\nu_\tau \to \eta\pi^-\pi^+\pi^-\nu_\tau)/\Gamma_{total}$ Γ_{170}/Γ

VALUE (units 10^{-4})	EVTS	DOCUMENT ID		TECN	COMMENT
1.18±0.07 OUR AVERAGE Error includes scale factor of 1.3.					
1.26±0.06±0.06	2.5k	LEES	12X	BABR	468 fb^{-1} E_{cm}^{ee} = 10.6 GeV
1.11±0.06±0.05	1.3 k	AUBERT	08AE	BABR	384 fb^{-1}, E_{cm}^{ee} = 10.6 GeV

$\Gamma(f_1(1285)\pi^-\nu_\tau \to \eta\pi^-\pi^+\pi^-\nu_\tau)/\Gamma(\eta\pi^-\pi^+\pi^-\nu_\tau$(ex.$K^0$)) $\Gamma_{170}/\Gamma_{158}$

VALUE	DOCUMENT ID		TECN	COMMENT
0.69±0.01±0.05	[1] AUBERT	08AE	BABR	384 fb^{-1}, E_{cm}^{ee} = 10.6 GeV
• • • We do not use the following data for averages, fits, limits, etc. • • •				
0.55±0.14	BERGFELD	97	CLEO	E_{cm}^{ee} = 10.6 GeV

[1] Not independent of AUBERT 08AE B($\tau^- \to f_1(1285)\pi^-\nu_\tau \to \eta\pi^-\pi^+\pi^-\nu_\tau$) and B($\tau^- \to \eta\pi^-\pi^+\pi^-\nu_\tau$(ex.$K^0$)) values.

$\Gamma(f_1(1285)\pi^-\nu_\tau \to 3\pi^-2\pi^+\nu_\tau)/\Gamma_{total}$ Γ_{171}/Γ

VALUE (units 10^{-4})	EVTS	DOCUMENT ID		TECN	COMMENT
0.52 ±0.04 OUR FIT					
0.520±0.031±0.037	3.7k	LEES	12X	BABR	468 fb^{-1} E_{cm}^{ee}=10.6 GeV

$\Gamma(\pi(1300)^-\nu_\tau \to (\rho\pi)^-\nu_\tau \to (3\pi)^-\nu_\tau)/\Gamma_{total}$ Γ_{172}/Γ

VALUE	CL%	DOCUMENT ID		TECN	COMMENT
<1.0 × 10^{-4}	90	ASNER	00	CLEO	E_{cm}^{ee} = 10.6 GeV

$\Gamma(\pi(1300)^-\nu_\tau \to ((\pi\pi)_{S-wave}\,\pi)^-\nu_\tau \to (3\pi)^-\nu_\tau)/\Gamma_{total}$ Γ_{173}/Γ

VALUE	CL%	DOCUMENT ID		TECN	COMMENT
<1.9 × 10^{-4}	90	ASNER	00	CLEO	E_{cm}^{ee} = 10.6 GeV

$\Gamma(h^-\omega \geq 0$ neutrals $\nu_\tau)/\Gamma_{total}$ Γ_{174}/Γ

$\Gamma_{174}/\Gamma = (\Gamma_{176}+\Gamma_{177}+\Gamma_{178})/\Gamma$

VALUE (%)	EVTS	DOCUMENT ID		TECN	COMMENT
2.40±0.08 OUR FIT					
• • • We use the following data for averages but not for fits. • • •					
1.65±0.3 ±0.2	1513	ALBRECHT	88M	ARG	$E_{cm}^{ee} \approx$ 10 GeV

$\Gamma(h^-\omega\nu_\tau)/\Gamma_{total}$ $\Gamma_{175}/\Gamma = (\Gamma_{176}+\Gamma_{177})/\Gamma$

VALUE (%)	EVTS	DOCUMENT ID		TECN	COMMENT
1.99±0.06 OUR FIT					
1.92±0.07 OUR AVERAGE					
1.91±0.07±0.06	5803	BUSKULIC	97C	ALEP	1991–1994 LEP runs
1.60±0.27±0.41	139	BARINGER	87	CLEO	E_{cm}^{ee} = 10.5 GeV
• • • We use the following data for averages but not for fits. • • •					
1.95±0.07±0.11	2223	[1] BALEST	95C	CLEO	$E_{cm}^{ee} \approx$ 10.6 GeV

[1] Not independent of BALEST 95C B($\tau^- \to h^-\omega\nu_\tau$)/B($\tau^- \to h^-h^-h^+\pi^0\nu_\tau$) value.

Lepton Particle Listings

τ

$[\Gamma(\pi^-\omega\nu_\tau)+\Gamma(K^-\omega\nu_\tau)]/\Gamma(h^-h^-h^+\pi^0\nu_\tau(\text{ex.}K^0))$ $(\Gamma_{176}+\Gamma_{177})/\Gamma_{74}$

$(\Gamma_{176}+\Gamma_{177})/\Gamma_{74}=(\Gamma_{176}+\Gamma_{177})/(\Gamma_{78}+\Gamma_{103}+\Gamma_{107}+0.2292\Gamma_{150}+0.892\Gamma_{176}+0.892\Gamma_{177}+0.0153\Gamma_{178})$

VALUE (units 10^{-2})	EVTS	DOCUMENT ID		TECN	COMMENT
43.5±1.4 OUR FIT					
45.3±1.9 OUR AVERAGE					
43.1±3.3	2350	[1] BUSKULIC	96	ALEP	LEP 1991–1993 data
46.4±1.6±1.7	2223	[2] BALEST	95C	CLEO	$E^{ee}_{cm}\approx$ 10.6 GeV
• • • We do not use the following data for averages, fits, limits, etc. • • •					
37 ±5 ±2	458	[3] ALBRECHT	91D	ARG	E^{ee}_{cm}= 9.4–10.6 GeV

[1] BUSKULIC 96 quote the fraction of $\tau\to h^-h^-h^+\pi^0\nu_\tau$(ex. K^0) decays which originate in a $h^-\omega$ final state = 0.383 ± 0.029. We divide this by the $\omega(782)\to\pi^+\pi^-\pi^0$ branching fraction (0.888).

[2] BALEST 95C quote the fraction of $\tau^-\to h^-h^-h^+\pi^0\nu_\tau$ (ex. K^0) decays which originate in a $h^-\omega$ final state equals 0.412 ± 0.014 ± 0.015. We divide this by the $\omega(782)\to\pi^+\pi^-\pi^0$ branching fraction (0.888).

[3] ALBRECHT 91D quote the fraction of $\tau^-\to h^-h^-h^+\pi^0\nu_\tau$ decays which originate in a $\pi^-\omega$ final state equals 0.33 ± 0.04 ± 0.02. We divide this by the $\omega(782)\to\pi^+\pi^-\pi^0$ branching fraction (0.888).

$\Gamma(\pi^-\omega\nu_\tau)/\Gamma_{total}$ Γ_{176}/Γ

VALUE (%)	DOCUMENT ID
1.95±0.06 OUR FIT	

$\Gamma(K^-\omega\nu_\tau)/\Gamma_{total}$ Γ_{177}/Γ

VALUE (units 10^{-4})	EVTS	DOCUMENT ID		TECN	COMMENT
4.1±0.9 OUR FIT					
4.1±0.6±0.7	500	ARMS	05	CLE3	7.6 fb^{-1}, E^{ee}_{cm}= 10.6 GeV

$\Gamma(h^-\omega\pi^0\nu_\tau)/\Gamma_{total}$ Γ_{178}/Γ

VALUE (%)	EVTS	DOCUMENT ID		TECN	COMMENT
0.41±0.04 OUR FIT					
0.43±0.06±0.05	7283	BUSKULIC	97C	ALEP	1991–1994 LEP runs

$\Gamma(h^-\omega\pi^0\nu_\tau)/\Gamma(h^-h^-h^+\geq 0\text{ neutrals }\geq 0K^0_L\nu_\tau)$ Γ_{178}/Γ_{62}

$\Gamma_{178}/\Gamma_{62}=\Gamma_{178}/(0.34598\Gamma_{36}+0.34598\Gamma_{38}+0.34598\Gamma_{41}+0.34598\Gamma_{43}+0.4247\Gamma_{48}+0.6920\Gamma_{49}+0.8494\Gamma_{52}+0.6920\Gamma_{56}+0.6534\Gamma_{61}+\Gamma_{70}+\Gamma_{78}+\Gamma_{85}+\Gamma_{89}+\Gamma_{97}+\Gamma_{103}+\Gamma_{106}+\Gamma_{107}+0.2810\Gamma_{148}+0.2292\Gamma_{149}+0.2810\Gamma_{150}+0.2810\Gamma_{152}+0.3759\Gamma_{154}+0.3268\Gamma_{158}+0.7259\Gamma_{168}+0.9078\Gamma_{176}+0.9078\Gamma_{177}+0.9078\Gamma_{178}+0.892\Gamma_{180})$

VALUE	EVTS	DOCUMENT ID		TECN	COMMENT
(2.69 ±0.28) × 10^{-2} OUR FIT					
• • • We use the following data for averages but not for fits. • • •					
0.028±0.003±0.003	430	[1] BORTOLETTO	93	CLEO	$E^{ee}_{cm}\approx$ 10.6 GeV

[1] Not independent of BORTOLETTO 93 $\Gamma(\tau^-\to h^-\omega\pi^0\nu_\tau)/\Gamma(\tau^-\to h^-h^-h^+2\pi^0\nu_\tau(\text{ex.}K^0))$ value.

$\Gamma(h^-\omega\pi^0\nu_\tau)/\Gamma(h^-h^-h^+2\pi^0\nu_\tau(\text{ex.}K^0))$ Γ_{178}/Γ_{84}

$\Gamma_{178}/\Gamma_{84}=\Gamma_{178}/(\Gamma_{85}+0.2292\Gamma_{148}+0.2292\Gamma_{152}+0.892\Gamma_{178})$

VALUE (units 10^{-2})	DOCUMENT ID		TECN	COMMENT
82±8 OUR FIT				
81±6±6	BORTOLETTO	93	CLEO	$E^{ee}_{cm}\approx$ 10.6 GeV

$\Gamma(h^-\omega 2\pi^0\nu_\tau)/\Gamma_{total}$ Γ_{179}/Γ

VALUE (units 10^{-4})	EVTS	DOCUMENT ID		TECN	COMMENT
1.4 ±0.4 ±0.3	53	ANASTASSOV	01	CLEO	E^{ee}_{cm}= 10.6 GeV
• • • We do not use the following data for averages, fits, limits, etc. • • •					
$1.89^{+0.74}_{-0.67}\pm0.40$	19	ANDERSON	97	CLEO	Repl. by ANASTASSOV 01

$\Gamma(\pi^-\omega 2\pi^0\nu_\tau)/\Gamma_{total}$ Γ_{180}/Γ

VALUE (units 10^{-4})	EVTS	DOCUMENT ID		TECN	COMMENT
0.71±0.16 OUR FIT					
0.73±0.12±0.12	1.1k	LEES	12X	BABR	468 fb^{-1} E^{ee}_{cm} = 10.6 GeV

$\Gamma(h^-2\omega\nu_\tau)/\Gamma_{total}$ Γ_{181}/Γ

VALUE	CL%	DOCUMENT ID		TECN	COMMENT
<5.4 × 10^{-7}	90	AUBERT,B	06	BABR	232 fb^{-1} E^{ee}_{cm} = 10.6 GeV

$\Gamma(2h^-h^+\omega\nu_\tau)/\Gamma_{total}$ Γ_{182}/Γ

VALUE (units 10^{-4})	EVTS	DOCUMENT ID		TECN	COMMENT
1.2±0.2±0.1	110	ANASTASSOV	01	CLEO	E^{ee}_{cm}= 10.6 GeV

$\Gamma(2\pi^-\pi^+\omega\nu_\tau(\text{ex.}K^0))/\Gamma_{total}$ Γ_{183}/Γ

VALUE (units 10^{-4})	EVTS	DOCUMENT ID		TECN	COMMENT
0.84±0.06 OUR FIT					
0.84±0.04±0.06	2.4k	LEES	12X	BABR	468 fb^{-1} E^{ee}_{cm} = 10.6 GeV

$\Gamma(e^-\gamma)/\Gamma_{total}$ Γ_{184}/Γ

Test of lepton family number conservation.

VALUE	CL%	DOCUMENT ID		TECN	COMMENT
<3.3 × 10^{-8}	90	AUBERT	10B	BABR	516 fb^{-1}, E^{ee}_{cm}=10.6 GeV
• • • We do not use the following data for averages, fits, limits, etc. • • •					
<1.2 × 10^{-7}	90	HAYASAKA	08	BELL	535 fb^{-1}, E^{ee}_{cm}= 10.6 GeV
<1.1 × 10^{-7}	90	AUBERT	06C	BABR	232 fb^{-1}, E^{ee}_{cm}= 10.6 GeV
<3.9 × 10^{-7}	90	HAYASAKA	05	BELL	86.7 fb^{-1}, E^{ee}_{cm}=10.6 GeV
<2.7 × 10^{-6}	90	EDWARDS	97	CLEO	
<1.1 × 10^{-4}	90	ABREU	95U	DLPH	1990–1993 LEP runs
<1.2 × 10^{-4}	90	ALBRECHT	92K	ARG	E^{ee}_{cm}= 10 GeV
<2.0 × 10^{-4}	90	KEH	88	CBAL	E^{ee}_{cm}= 10 GeV
<6.4 × 10^{-4}	90	HAYES	82	MRK2	E^{ee}_{cm}= 3.8–6.8 GeV

$\Gamma(\mu^-\gamma)/\Gamma_{total}$ Γ_{185}/Γ

Test of lepton family number conservation.

VALUE	CL%	DOCUMENT ID		TECN	COMMENT
< 4.4 × 10^{-8}	90	AUBERT	10B	BABR	516 fb^{-1}, E^{ee}_{cm}=10.6 GeV
• • • We do not use the following data for averages, fits, limits, etc. • • •					
< 4.5 × 10^{-8}	90	HAYASAKA	08	BELL	535 fb^{-1}, E^{ee}_{cm} = 10.6 GeV
< 6.8 × 10^{-8}	90	AUBERT,B	05A	BABR	232 fb^{-1}, E^{ee}_{cm}= 10.6 GeV
< 3.1 × 10^{-7}	90	ABE	04B	BELL	86.3 fb^{-1}, E^{ee}_{cm} = 10.6 GeV
< 1.1 × 10^{-6}	90	AHMED	00	CLEO	E^{ee}_{cm}= 10.6 GeV
< 3.0 × 10^{-6}	90	EDWARDS	97	CLEO	
< 6.2 × 10^{-5}	90	ABREU	95U	DLPH	1990–1993 LEP runs
< 0.42 × 10^{-5}	90	BEAN	93	CLEO	E^{ee}_{cm}= 10.6 GeV
< 3.4 × 10^{-5}	90	ALBRECHT	92K	ARG	E^{ee}_{cm}= 10 GeV
<55 × 10^{-5}	90	HAYES	82	MRK2	E^{ee}_{cm}= 3.8–6.8 GeV

$\Gamma(e^-\pi^0)/\Gamma_{total}$ Γ_{186}/Γ

Test of lepton family number conservation.

VALUE	CL%	DOCUMENT ID		TECN	COMMENT
< 8.0 × 10^{-8}	90	MIYAZAKI	07	BELL	401 fb^{-1}, E^{ee}_{cm}=10.6 GeV
• • • We do not use the following data for averages, fits, limits, etc. • • •					
< 1.3 × 10^{-7}	90	AUBERT	07I	BABR	339 fb^{-1}, E^{ee}_{cm}=10.6 GeV
< 1.9 × 10^{-7}	90	ENARI	05	BELL	154 fb^{-1}, E^{ee}_{cm}= 10.6 GeV
< 3.7 × 10^{-6}	90	BONVICINI	97	CLEO	E^{ee}_{cm}= 10.6 GeV
< 17 × 10^{-5}	90	ALBRECHT	92K	ARG	E^{ee}_{cm}= 10 GeV
< 14 × 10^{-5}	90	KEH	88	CBAL	E^{ee}_{cm}= 10 GeV
<210 × 10^{-5}	90	HAYES	82	MRK2	E^{ee}_{cm}= 3.8–6.8 GeV

$\Gamma(\mu^-\pi^0)/\Gamma_{total}$ Γ_{187}/Γ

Test of lepton family number conservation.

VALUE	CL%	DOCUMENT ID		TECN	COMMENT
< 1.1 × 10^{-7}	90	AUBERT	07I	BABR	339 fb^{-1}, E^{ee}_{cm}=10.6 GeV
• • • We do not use the following data for averages, fits, limits, etc. • • •					
< 1.2 × 10^{-7}	90	MIYAZAKI	07	BELL	401 fb^{-1}, E^{ee}_{cm}=10.6 GeV
< 4.1 × 10^{-7}	90	ENARI	05	BELL	154 fb^{-1}, E^{ee}_{cm}= 10.6 GeV
< 4.0 × 10^{-6}	90	BONVICINI	97	CLEO	E^{ee}_{cm}= 10.6 GeV
< 4.4 × 10^{-5}	90	ALBRECHT	92K	ARG	E^{ee}_{cm}= 10 GeV
<82 × 10^{-5}	90	HAYES	82	MRK2	E^{ee}_{cm}= 3.8–6.8 GeV

$\Gamma(e^-K^0_S)/\Gamma_{total}$ Γ_{188}/Γ

Test of lepton family number conservation.

VALUE	CL%	DOCUMENT ID		TECN	COMMENT
<2.6 × 10^{-8}	90	MIYAZAKI	10A	BELL	671 fb^{-1} E^{ee}_{cm} = 10.6 GeV
• • • We do not use the following data for averages, fits, limits, etc. • • •					
<3.3 × 10^{-8}	90	AUBERT	09D	BABR	469 fb^{-1} E^{ee}_{cm} = 10.6 GeV
<5.6 × 10^{-8}	90	MIYAZAKI	06A	BELL	281 fb^{-1} E^{ee}_{cm} = 10.6 GeV
<9.1 × 10^{-7}	90	CHEN	02C	CLEO	E^{ee}_{cm}= 10.6 GeV
<1.3 × 10^{-3}	90	HAYES	82	MRK2	E^{ee}_{cm}= 3.8–6.8 GeV

$\Gamma(\mu^-K^0_S)/\Gamma_{total}$ Γ_{189}/Γ

Test of lepton family number conservation.

VALUE	CL%	DOCUMENT ID		TECN	COMMENT
<2.3 × 10^{-8}	90	MIYAZAKI	10A	BELL	671 fb^{-1} E^{ee}_{cm} = 10.6 GeV
• • • We do not use the following data for averages, fits, limits, etc. • • •					
<4.0 × 10^{-8}	90	AUBERT	09D	BABR	469 fb^{-1} E^{ee}_{cm} = 10.6 GeV
<4.9 × 10^{-8}	90	MIYAZAKI	06A	BELL	281 fb^{-1} E^{ee}_{cm} = 10.6 GeV
<9.5 × 10^{-7}	90	CHEN	02C	CLEO	E^{ee}_{cm}= 10.6 GeV
<1.0 × 10^{-3}	90	HAYES	82	MRK2	E^{ee}_{cm}= 3.8–6.8 GeV

$\Gamma(e^-\eta)/\Gamma_{total}$ Γ_{190}/Γ

Test of lepton family number conservation.

VALUE	CL%	DOCUMENT ID		TECN	COMMENT
< 9.2 × 10^{-8}	90	MIYAZAKI	07	BELL	401 fb^{-1}, E^{ee}_{cm}=10.6 GeV

• • • We do not use the following data for averages, fits, limits, etc. • • •

$< 1.6 \times 10^{-7}$	90	AUBERT	07I	BABR	339 fb^{-1}, E_{cm}^{ee}=10.6 GeV
$< 2.4 \times 10^{-7}$	90	ENARI	05	BELL	154 fb^{-1}, E_{cm}^{ee}= 10.6 GeV
$< 8.2 \times 10^{-6}$	90	BONVICINI	97	CLEO	E_{cm}^{ee}= 10.6 GeV
$< 6.3 \times 10^{-5}$	90	ALBRECHT	92K	ARG	E_{cm}^{ee}= 10 GeV
$<24 \times 10^{-5}$	90	KEH	88	CBAL	E_{cm}^{ee}= 10 GeV

$\Gamma(\mu^-\eta)/\Gamma_{total}$ Γ_{191}/Γ

Test of lepton family number conservation.

VALUE	CL%	DOCUMENT ID		TECN	COMMENT
$<6.5 \times 10^{-8}$	90	MIYAZAKI	07	BELL	401 fb^{-1}, E_{cm}^{ee}=10.6 GeV

• • • We do not use the following data for averages, fits, limits, etc. • • •

$<1.5 \times 10^{-7}$	90	AUBERT	07I	BABR	339 fb^{-1}, E_{cm}^{ee}=10.6 GeV
$<1.5 \times 10^{-7}$	90	ENARI	05	BELL	154 fb^{-1}, E_{cm}^{ee}= 10.6 GeV
$<3.4 \times 10^{-7}$	90	ENARI	04	BELL	84.3 fb^{-1}, E_{cm}^{ee}=10.6 GeV
$<9.6 \times 10^{-6}$	90	BONVICINI	97	CLEO	E_{cm}^{ee}= 10.6 GeV
$<7.3 \times 10^{-5}$	90	ALBRECHT	92K	ARG	E_{cm}^{ee}= 10 GeV

$\Gamma(e^-\rho^0)/\Gamma_{total}$ Γ_{192}/Γ

Test of lepton family number conservation.

VALUE	CL%	DOCUMENT ID		TECN	COMMENT
$< 1.8 \times 10^{-8}$	90	MIYAZAKI	11	BELL	854 fb^{-1} E_{cm}^{ee} = 10.6 GeV

• • • We do not use the following data for averages, fits, limits, etc. • • •

$< 4.6 \times 10^{-8}$	90	AUBERT	09W	BABR	451 fb^{-1} E_{cm}^{ee} = 10.6 GeV
$< 6.3 \times 10^{-8}$	90	NISHIO	08	BELL	543 fb^{-1} E_{cm}^{ee} = 10.6 GeV
$< 6.5 \times 10^{-7}$	90	YUSA	06	BELL	158 fb^{-1} E_{cm}^{ee} = 10.6 GeV
$< 2.0 \times 10^{-6}$	90	BLISS	98	CLEO	E_{cm}^{ee}= 10.6 GeV
$< 4.2 \times 10^{-6}$	90	[1] BARTELT	94	CLEO	Repl. by BLISS 98
$< 1.9 \times 10^{-5}$	90	ALBRECHT	92K	ARG	E_{cm}^{ee}= 10 GeV
$<37 \times 10^{-5}$	90	HAYES	82	MRK2	E_{cm}^{ee}= 3.8–6.8 GeV

[1] BARTELT 94 assume phase space decays.

$\Gamma(\mu^-\rho^0)/\Gamma_{total}$ Γ_{193}/Γ

Test of lepton family number conservation.

VALUE	CL%	DOCUMENT ID		TECN	COMMENT
$< 1.2 \times 10^{-8}$	90	MIYAZAKI	11	BELL	854 fb^{-1} E_{cm}^{ee} = 10.6 GeV

• • • We do not use the following data for averages, fits, limits, etc. • • •

$< 2.6 \times 10^{-8}$	90	AUBERT	09W	BABR	451 fb^{-1} E_{cm}^{ee} = 10.6 GeV
$< 6.8 \times 10^{-8}$	90	NISHIO	08	BELL	543 fb^{-1} E_{cm}^{ee} = 10.6 GeV
$< 2.0 \times 10^{-7}$	90	YUSA	06	BELL	158 fb^{-1} E_{cm}^{ee} = 10.6 GeV
$< 6.3 \times 10^{-6}$	90	BLISS	98	CLEO	E_{cm}^{ee}= 10.6 GeV
$< 5.7 \times 10^{-6}$	90	[1] BARTELT	94	CLEO	Repl. by BLISS 98
$< 2.9 \times 10^{-5}$	90	ALBRECHT	92K	ARG	E_{cm}^{ee}= 10 GeV
$<44 \times 10^{-5}$	90	HAYES	82	MRK2	E_{cm}^{ee}= 3.8–6.8 GeV

[1] BARTELT 94 assume phase space decays.

$\Gamma(e^-\omega)/\Gamma_{total}$ Γ_{194}/Γ

VALUE	CL%	DOCUMENT ID		TECN	COMMENT
$<4.8 \times 10^{-8}$	90	MIYAZAKI	11	BELL	854 fb^{-1} E_{cm}^{ee} = 10.6 GeV

• • • We do not use the following data for averages, fits, limits, etc. • • •

$<1.1 \times 10^{-7}$	90	AUBERT	08K	BABR	384 fb^{-1} E_{cm}^{ee} = 10.6 GeV
$<1.8 \times 10^{-7}$	90	NISHIO	08	BELL	543 fb^{-1} E_{cm}^{ee} = 10.6 GeV

$\Gamma(\mu^-\omega)/\Gamma_{total}$ Γ_{195}/Γ

VALUE	CL%	DOCUMENT ID		TECN	COMMENT
$<4.7 \times 10^{-8}$	90	MIYAZAKI	11	BELL	854 fb^{-1} E_{cm}^{ee} = 10.6 GeV

• • • We do not use the following data for averages, fits, limits, etc. • • •

$<1.0 \times 10^{-7}$	90	AUBERT	08K	BABR	384 fb^{-1} E_{cm}^{ee} = 10.6 GeV
$<8.9 \times 10^{-8}$	90	NISHIO	08	BELL	543 fb^{-1} E_{cm}^{ee} = 10.6 GeV

$\Gamma(e^- K^*(892)^0)/\Gamma_{total}$ Γ_{196}/Γ

Test of lepton family number conservation.

VALUE	CL%	DOCUMENT ID		TECN	COMMENT
$<3.2 \times 10^{-8}$	90	MIYAZAKI	11	BELL	854 fb^{-1} E_{cm}^{ee} = 10.6 GeV

• • • We do not use the following data for averages, fits, limits, etc. • • •

$<5.9 \times 10^{-8}$	90	AUBERT	09W	BABR	451 fb^{-1} E_{cm}^{ee} = 10.6 GeV
$<7.8 \times 10^{-8}$	90	NISHIO	08	BELL	543 fb^{-1} E_{cm}^{ee} = 10.6 GeV
$<3.0 \times 10^{-7}$	90	YUSA	06	BELL	158 fb^{-1} E_{cm}^{ee} = 10.6 GeV
$<5.1 \times 10^{-6}$	90	BLISS	98	CLEO	E_{cm}^{ee}= 10.6 GeV
$<6.3 \times 10^{-6}$	90	[1] BARTELT	94	CLEO	Repl. by BLISS 98
$<3.8 \times 10^{-5}$	90	ALBRECHT	92K	ARG	E_{cm}^{ee}= 10 GeV

[1] BARTELT 94 assume phase space decays.

$\Gamma(\mu^- K^*(892)^0)/\Gamma_{total}$ Γ_{197}/Γ

Test of lepton family number conservation.

VALUE	CL%	DOCUMENT ID		TECN	COMMENT
$<5.9 \times 10^{-8}$	90	NISHIO	08	BELL	543 fb^{-1} E_{cm}^{ee} = 10.6 GeV

• • • We do not use the following data for averages, fits, limits, etc. • • •

$<7.2 \times 10^{-8}$	90	MIYAZAKI	11	BELL	854 fb^{-1} E_{cm}^{ee} = 10.6 GeV
$<1.7 \times 10^{-7}$	90	AUBERT	09W	BABR	451 fb^{-1} E_{cm}^{ee} = 10.6 GeV
$<3.9 \times 10^{-7}$	90	YUSA	06	BELL	158 fb^{-1} E_{cm}^{ee} = 10.6 GeV
$<7.5 \times 10^{-6}$	90	BLISS	98	CLEO	E_{cm}^{ee}= 10.6 GeV
$<9.4 \times 10^{-6}$	90	[1] BARTELT	94	CLEO	Repl. by BLISS 98
$<4.5 \times 10^{-5}$	90	ALBRECHT	92K	ARG	E_{cm}^{ee}= 10 GeV

[1] BARTELT 94 assume phase space decays.

$\Gamma(e^-\overline{K}^*(892)^0)/\Gamma_{total}$ Γ_{198}/Γ

Test of lepton family number conservation.

VALUE	CL%	DOCUMENT ID		TECN	COMMENT
$<3.4 \times 10^{-8}$	90	MIYAZAKI	11	BELL	854 fb^{-1} E_{cm}^{ee} = 10.6 GeV

• • • We do not use the following data for averages, fits, limits, etc. • • •

$<4.6 \times 10^{-8}$	90	AUBERT	09W	BABR	451 fb^{-1} E_{cm}^{ee} = 10.6 GeV
$<7.7 \times 10^{-8}$	90	NISHIO	08	BELL	543 fb^{-1} E_{cm}^{ee} = 10.6 GeV
$<4.0 \times 10^{-7}$	90	YUSA	06	BELL	158 fb^{-1} E_{cm}^{ee} = 10.6 GeV
$<7.4 \times 10^{-6}$	90	BLISS	98	CLEO	E_{cm}^{ee}= 10.6 GeV
$<1.1 \times 10^{-5}$	90	[1] BARTELT	94	CLEO	Repl. by BLISS 98

[1] BARTELT 94 assume phase space decays.

$\Gamma(\mu^-\overline{K}^*(892)^0)/\Gamma_{total}$ Γ_{199}/Γ

Test of lepton family number conservation.

VALUE	CL%	DOCUMENT ID		TECN	COMMENT
$<7.0 \times 10^{-8}$	90	MIYAZAKI	11	BELL	854 fb^{-1} E_{cm}^{ee} = 10.6 GeV

• • • We do not use the following data for averages, fits, limits, etc. • • •

$<7.3 \times 10^{-8}$	90	AUBERT	09W	BABR	451 fb^{-1} E_{cm}^{ee} = 10.6 GeV
$<1.0 \times 10^{-7}$	90	NISHIO	08	BELL	543 fb^{-1} E_{cm}^{ee} = 10.6 GeV
$<4.0 \times 10^{-7}$	90	YUSA	06	BELL	158 fb^{-1} E_{cm}^{ee} = 10.6 GeV
$<7.5 \times 10^{-6}$	90	BLISS	98	CLEO	E_{cm}^{ee}= 10.6 GeV
$<8.7 \times 10^{-6}$	90	[1] BARTELT	94	CLEO	Repl. by BLISS 98

[1] BARTELT 94 assume phase space decays.

$\Gamma(e^-\eta'(958))/\Gamma_{total}$ Γ_{200}/Γ

VALUE	CL%	DOCUMENT ID		TECN	COMMENT
$< 1.6 \times 10^{-7}$	90	MIYAZAKI	07	BELL	401 fb^{-1}, E_{cm}^{ee}=10.6 GeV

• • • We do not use the following data for averages, fits, limits, etc. • • •

$< 2.4 \times 10^{-7}$	90	AUBERT	07I	BABR	339 fb^{-1}, E_{cm}^{ee}=10.6 GeV
$<10. \times 10^{-7}$	90	ENARI	05	BELL	154 fb^{-1}, E_{cm}^{ee}= 10.6 GeV

$\Gamma(\mu^-\eta'(958))/\Gamma_{total}$ Γ_{201}/Γ

VALUE	CL%	DOCUMENT ID		TECN	COMMENT
$<1.3 \times 10^{-7}$	90	MIYAZAKI	07	BELL	401 fb^{-1}, E_{cm}^{ee}=10.6 GeV

• • • We do not use the following data for averages, fits, limits, etc. • • •

$<1.4 \times 10^{-7}$	90	AUBERT	07I	BABR	339 fb^{-1}, E_{cm}^{ee}=10.6 GeV
$<4.7 \times 10^{-7}$	90	ENARI	05	BELL	154 fb^{-1}, E_{cm}^{ee}= 10.6 GeV

$\Gamma(e^- f_0(980) \to e^-\pi^+\pi^-)/\Gamma_{total}$ Γ_{202}/Γ

VALUE	CL%	DOCUMENT ID		TECN	COMMENT
$<3.2 \times 10^{-8}$	90	MIYAZAKI	09	BELL	671 fb^{-1} E_{cm}^{ee}= 10.6 GeV

$\Gamma(\mu^- f_0(980) \to \mu^-\pi^+\pi^-)/\Gamma_{total}$ Γ_{203}/Γ

VALUE	CL%	DOCUMENT ID		TECN	COMMENT
$<3.4 \times 10^{-8}$	90	MIYAZAKI	09	BELL	671 fb^{-1} E_{cm}^{ee}= 10.6 GeV

$\Gamma(e^-\phi)/\Gamma_{total}$ Γ_{204}/Γ

Test of lepton family number conservation.

VALUE	CL%	DOCUMENT ID		TECN	COMMENT
$<3.1 \times 10^{-8}$	90	MIYAZAKI	11	BELL	854 fb^{-1} E_{cm}^{ee} = 10.6 GeV
$<3.1 \times 10^{-8}$	90	AUBERT	09W	BABR	451 fb^{-1} E_{cm}^{ee} = 10.6 GeV

• • • We do not use the following data for averages, fits, limits, etc. • • •

$<7.3 \times 10^{-8}$	90	NISHIO	08	BELL	543 fb^{-1} E_{cm}^{ee} = 10.6 GeV
$<7.3 \times 10^{-7}$	90	YUSA	06	BELL	158 fb^{-1} E_{cm}^{ee} = 10.6 GeV
$<6.9 \times 10^{-6}$	90	BLISS	98	CLEO	E_{cm}^{ee}= 10.6 GeV

$\Gamma(\mu^-\phi)/\Gamma_{total}$ Γ_{205}/Γ

Test of lepton family number conservation.

VALUE	CL%	DOCUMENT ID		TECN	COMMENT
$<8.4 \times 10^{-8}$	90	MIYAZAKI	11	BELL	854 fb^{-1} E_{cm}^{ee} = 10.6 GeV

• • • We do not use the following data for averages, fits, limits, etc. • • •

$<1.9 \times 10^{-7}$	90	AUBERT	09W	BABR	451 fb^{-1} E_{cm}^{ee} = 10.6 GeV
$<1.3 \times 10^{-7}$	90	NISHIO	08	BELL	543 fb^{-1} E_{cm}^{ee} = 10.6 GeV
$<7.7 \times 10^{-7}$	90	YUSA	06	BELL	158 fb^{-1} E_{cm}^{ee} = 10.6 GeV
$<7.0 \times 10^{-6}$	90	BLISS	98	CLEO	E_{cm}^{ee}= 10.6 GeV

$\Gamma(e^- e^+ e^-)/\Gamma_{total}$ Γ_{206}/Γ

Test of lepton family number conservation.

VALUE	CL%	DOCUMENT ID		TECN	COMMENT
$< 2.7 \times 10^{-8}$	90	HAYASAKA	10	BELL	782 fb^{-1} E_{cm}^{ee}= 10.6 GeV

• • • We do not use the following data for averages, fits, limits, etc. • • •

$< 2.9 \times 10^{-8}$	90	LEES	10A	BABR	468 fb^{-1} E_{cm}^{ee}= 10.6 GeV
$< 3.6 \times 10^{-8}$	90	MIYAZAKI	08	BELL	535 fb^{-1} E_{cm}^{ee}= 10.6 GeV

$< 4.3 \times 10^{-8}$	90	AUBERT	07BK	BABR	376 fb^{-1}	E_{cm}^{ee} = 10.6 GeV
$< 2.0 \times 10^{-7}$	90	AUBERT	04J	BABR	91.5 fb^{-1}	E_{cm}^{ee} = 10.6 GeV
$< 3.5 \times 10^{-7}$	90	YUSA	04	BELL	87.1 fb^{-1}	E_{cm}^{ee} = 10.6 GeV
$< 2.9 \times 10^{-6}$	90	BLISS	98	CLEO	E_{cm}^{ee} = 10.6 GeV	
$< 0.33 \times 10^{-5}$	90	[1] BARTELT	94	CLEO	Repl. by BLISS 98	
$< 1.3 \times 10^{-5}$	90	ALBRECHT	92K	ARG	E_{cm}^{ee} = 10 GeV	
$< 2.7 \times 10^{-5}$	90	BOWCOCK	90	CLEO	E_{cm}^{ee} = 10.4–10.9	
$<40 \times 10^{-5}$	90	HAYES	82	MRK2	E_{cm}^{ee} = 3.8–6.8 GeV	

[1] BARTELT 94 assume phase space decays.

$\Gamma(e^-\mu^+\mu^-)/\Gamma_{total}$ Γ_{207}/Γ

Test of lepton family number conservation.

VALUE	CL%	DOCUMENT ID		TECN	COMMENT
$< 2.7 \times 10^{-8}$	90	HAYASAKA	10	BELL	782 fb^{-1} E_{cm}^{ee} = 10.6 GeV
• • • We do not use the following data for averages, fits, limits, etc. • • •					
$< 3.2 \times 10^{-8}$	90	LEES	10A	BABR	468 fb^{-1} E_{cm}^{ee} = 10.6 GeV
$< 4.1 \times 10^{-8}$	90	MIYAZAKI	08	BELL	535 fb^{-1} E_{cm}^{ee} = 10.6 GeV
$< 3.7 \times 10^{-8}$	90	AUBERT	07BK	BABR	376 fb^{-1} E_{cm}^{ee} = 10.6 GeV
$< 3.3 \times 10^{-7}$	90	AUBERT	04J	BABR	91.5 fb^{-1} E_{cm}^{ee} = 10.6 GeV
$< 2.0 \times 10^{-7}$	90	YUSA	04	BELL	87.1 fb^{-1} E_{cm}^{ee} = 10.6 GeV
$< 1.8 \times 10^{-6}$	90	BLISS	98	CLEO	E_{cm}^{ee} = 10.6 GeV
$< 0.36 \times 10^{-5}$	90	[1] BARTELT	94	CLEO	Repl. by BLISS 98
$< 1.9 \times 10^{-5}$	90	ALBRECHT	92K	ARG	E_{cm}^{ee} = 10 GeV
$< 2.7 \times 10^{-5}$	90	BOWCOCK	90	CLEO	E_{cm}^{ee} = 10.4–10.9
$<33 \times 10^{-5}$	90	HAYES	82	MRK2	E_{cm}^{ee} = 3.8–6.8 GeV

[1] BARTELT 94 assume phase space decays.

$\Gamma(e^+\mu^-\mu^-)/\Gamma_{total}$ Γ_{208}/Γ

Test of lepton family number conservation.

VALUE	CL%	DOCUMENT ID		TECN	COMMENT
$<1.7 \times 10^{-8}$	90	HAYASAKA	10	BELL	782 fb^{-1} E_{cm}^{ee} = 10.6 GeV
• • • We do not use the following data for averages, fits, limits, etc. • • •					
$<2.6 \times 10^{-8}$	90	LEES	10A	BABR	468 fb^{-1} E_{cm}^{ee} = 10.6 GeV
$<2.3 \times 10^{-8}$	90	MIYAZAKI	08	BELL	535 fb^{-1} E_{cm}^{ee} = 10.6 GeV
$<5.6 \times 10^{-8}$	90	AUBERT	07BK	BABR	376 fb^{-1} E_{cm}^{ee} = 10.6 GeV
$<1.3 \times 10^{-7}$	90	AUBERT	04J	BABR	91.5 fb^{-1} E_{cm}^{ee} = 10.6 GeV
$<2.0 \times 10^{-7}$	90	YUSA	04	BELL	87.1 fb^{-1} E_{cm}^{ee} = 10.6 GeV
$<1.5 \times 10^{-6}$	90	BLISS	98	CLEO	E_{cm}^{ee} = 10.6 GeV
$<0.35 \times 10^{-5}$	90	[1] BARTELT	94	CLEO	Repl. by BLISS 98
$<1.8 \times 10^{-5}$	90	ALBRECHT	92K	ARG	E_{cm}^{ee} = 10 GeV
$<1.6 \times 10^{-5}$	90	BOWCOCK	90	CLEO	E_{cm}^{ee} = 10.4–10.9

[1] BARTELT 94 assume phase space decays.

$\Gamma(\mu^- e^+ e^-)/\Gamma_{total}$ Γ_{209}/Γ

Test of lepton family number conservation.

VALUE	CL%	DOCUMENT ID		TECN	COMMENT
$< 1.8 \times 10^{-8}$	90	HAYASAKA	10	BELL	782 fb^{-1} E_{cm}^{ee} = 10.6 GeV
• • • We do not use the following data for averages, fits, limits, etc. • • •					
$< 2.2 \times 10^{-8}$	90	LEES	10A	BABR	468 fb^{-1} E_{cm}^{ee} = 10.6 GeV
$< 2.7 \times 10^{-8}$	90	MIYAZAKI	08	BELL	535 fb^{-1} E_{cm}^{ee} = 10.6 GeV
$< 8.0 \times 10^{-8}$	90	AUBERT	07BK	BABR	376 fb^{-1} E_{cm}^{ee} = 10.6 GeV
$< 2.7 \times 10^{-7}$	90	AUBERT	04J	BABR	91.5 fb^{-1} E_{cm}^{ee} = 10.6 GeV
$< 1.9 \times 10^{-7}$	90	YUSA	04	BELL	87.1 fb^{-1} E_{cm}^{ee} = 10.6 GeV
$< 1.7 \times 10^{-6}$	90	BLISS	98	CLEO	E_{cm}^{ee} = 10.6 GeV
$< 0.34 \times 10^{-5}$	90	[1] BARTELT	94	CLEO	Repl. by BLISS 98
$< 1.4 \times 10^{-5}$	90	ALBRECHT	92K	ARG	E_{cm}^{ee} = 10 GeV
$< 2.7 \times 10^{-5}$	90	BOWCOCK	90	CLEO	E_{cm}^{ee} = 10.4–10.9
$<44 \times 10^{-5}$	90	HAYES	82	MRK2	E_{cm}^{ee} = 3.8–6.8 GeV

[1] BARTELT 94 assume phase space decays.

$\Gamma(\mu^+ e^- e^-)/\Gamma_{total}$ Γ_{210}/Γ

Test of lepton family number conservation.

VALUE	CL%	DOCUMENT ID		TECN	COMMENT
$<1.5 \times 10^{-8}$	90	HAYASAKA	10	BELL	782 fb^{-1} E_{cm}^{ee} = 10.6 GeV
• • • We do not use the following data for averages, fits, limits, etc. • • •					
$<1.8 \times 10^{-8}$	90	LEES	10A	BABR	468 fb^{-1} E_{cm}^{ee} = 10.6 GeV
$<2.0 \times 10^{-8}$	90	MIYAZAKI	08	BELL	535 fb^{-1} E_{cm}^{ee} = 10.6 GeV
$<5.8 \times 10^{-8}$	90	AUBERT	07BK	BABR	376 fb^{-1} E_{cm}^{ee} = 10.6 GeV
$<1.1 \times 10^{-7}$	90	AUBERT	04J	BABR	91.5 fb^{-1} E_{cm}^{ee} = 10.6 GeV
$<2.0 \times 10^{-7}$	90	YUSA	04	BELL	87.1 fb^{-1} E_{cm}^{ee} = 10.6 GeV
$<1.5 \times 10^{-6}$	90	BLISS	98	CLEO	E_{cm}^{ee} = 10.6 GeV
$<0.34 \times 10^{-5}$	90	[1] BARTELT	94	CLEO	Repl. by BLISS 98
$<1.4 \times 10^{-5}$	90	ALBRECHT	92K	ARG	E_{cm}^{ee} = 10 GeV
$<1.6 \times 10^{-5}$	90	BOWCOCK	90	CLEO	E_{cm}^{ee} = 10.4–10.9

[1] BARTELT 94 assume phase space decays.

$\Gamma(\mu^-\mu^+\mu^-)/\Gamma_{total}$ Γ_{211}/Γ

Test of lepton family number conservation.

VALUE	CL%	DOCUMENT ID		TECN	COMMENT
$< 2.1 \times 10^{-8}$	90	HAYASAKA	10	BELL	782 fb^{-1} E_{cm}^{ee} = 10.6 GeV
• • • We do not use the following data for averages, fits, limits, etc. • • •					
$< 3.8 \times 10^{-7}$	90	AAD	16BA	ATLS	20.3 fb^{-1} $\sqrt{s}$ = 8 TeV
$< 4.6 \times 10^{-8}$	90	AAIJ	15AI	LHCB	3.0 fb^{-1} $\sqrt{s}$ = 7, 8 TeV
$< 8.0 \times 10^{-8}$	90	[1] AAIJ	13AH	LHCB	1.0 fb^{-1}, $\sqrt{s}$ = 7 TeV
$< 3.3 \times 10^{-8}$	90	LEES	10A	BABR	468 fb^{-1} E_{cm}^{ee} = 10.6 GeV
$< 3.2 \times 10^{-8}$	90	MIYAZAKI	08	BELL	535 fb^{-1} E_{cm}^{ee} = 10.6 GeV
$< 5.3 \times 10^{-8}$	90	AUBERT	07BK	BABR	376 fb^{-1} E_{cm}^{ee} = 10.6 GeV
$< 1.9 \times 10^{-7}$	90	AUBERT	04J	BABR	91.5 fb^{-1} E_{cm}^{ee} = 10.6 GeV
$< 2.0 \times 10^{-7}$	90	YUSA	04	BELL	87.1 fb^{-1} E_{cm}^{ee} = 10.6 GeV
$< 1.9 \times 10^{-6}$	90	BLISS	98	CLEO	E_{cm}^{ee} = 10.6 GeV
$< 0.43 \times 10^{-5}$	90	[2] BARTELT	94	CLEO	Repl. by BLISS 98
$< 1.9 \times 10^{-5}$	90	ALBRECHT	92K	ARG	E_{cm}^{ee} = 10 GeV
$< 1.7 \times 10^{-5}$	90	BOWCOCK	90	CLEO	E_{cm}^{ee} = 10.4–10.9
$<49 \times 10^{-5}$	90	HAYES	82	MRK2	E_{cm}^{ee} = 3.8–6.8 GeV

[1] Repl. by AAIJ 15AI.
[2] BARTELT 94 assume phase space decays.

$\Gamma(e^-\pi^+\pi^-)/\Gamma_{total}$ Γ_{212}/Γ

Test of lepton family number conservation.

VALUE	CL%	DOCUMENT ID		TECN	COMMENT
$<2.3 \times 10^{-8}$	90	MIYAZAKI	13	BELL	854 fb^{-1} E_{cm}^{ee} = 10.6 GeV
• • • We do not use the following data for averages, fits, limits, etc. • • •					
$<4.4 \times 10^{-8}$	90	MIYAZAKI	10	BELL	Repl. by MIYAZAKI 13
$<7.3 \times 10^{-7}$	90	YUSA	06	BELL	158 fb^{-1} E_{cm}^{ee} = 10.6 GeV
$<1.2 \times 10^{-7}$	90	AUBERT,BE	05D	BABR	221 fb^{-1}, E_{cm}^{ee} = 10.6 GeV
$<2.2 \times 10^{-6}$	90	BLISS	98	CLEO	E_{cm}^{ee} = 10.6 GeV
$<4.4 \times 10^{-6}$	90	[1] BARTELT	94	CLEO	Repl. by BLISS 98
$<2.7 \times 10^{-5}$	90	ALBRECHT	92K	ARG	E_{cm}^{ee} = 10 GeV
$<6.0 \times 10^{-5}$	90	BOWCOCK	90	CLEO	E_{cm}^{ee} = 10.4–10.9

[1] BARTELT 94 assume phase space decays.

$\Gamma(e^+\pi^-\pi^-)/\Gamma_{total}$ Γ_{213}/Γ

Test of lepton number conservation.

VALUE	CL%	DOCUMENT ID		TECN	COMMENT
$<2.0 \times 10^{-8}$	90	MIYAZAKI	13	BELL	854 fb^{-1} E_{cm}^{ee} = 10.6 GeV
• • • We do not use the following data for averages, fits, limits, etc. • • •					
$<8.8 \times 10^{-8}$	90	MIYAZAKI	10	BELL	Repl. by MIYAZAKI 13
$<2.0 \times 10^{-7}$	90	YUSA	06	BELL	158 fb^{-1} E_{cm}^{ee} = 10.6 GeV
$<2.7 \times 10^{-7}$	90	AUBERT,BE	05D	BABR	221 fb^{-1}, E_{cm}^{ee} = 10.6 GeV
$<1.9 \times 10^{-6}$	90	BLISS	98	CLEO	E_{cm}^{ee} = 10.6 GeV
$<4.4 \times 10^{-6}$	90	[1] BARTELT	94	CLEO	Repl. by BLISS 98
$<1.8 \times 10^{-5}$	90	ALBRECHT	92K	ARG	E_{cm}^{ee} = 10 GeV
$<1.7 \times 10^{-5}$	90	BOWCOCK	90	CLEO	E_{cm}^{ee} = 10.4–10.9

[1] BARTELT 94 assume phase space decays.

$\Gamma(\mu^-\pi^+\pi^-)/\Gamma_{total}$ Γ_{214}/Γ

Test of lepton family number conservation.

VALUE	CL%	DOCUMENT ID		TECN	COMMENT
$<2.1 \times 10^{-8}$	90	MIYAZAKI	13	BELL	854 fb^{-1} E_{cm}^{ee} = 10.6 GeV
• • • We do not use the following data for averages, fits, limits, etc. • • •					
$<3.3 \times 10^{-8}$	90	MIYAZAKI	10	BELL	Repl. by MIYAZAKI 13
$<4.8 \times 10^{-7}$	90	YUSA	06	BELL	158 fb^{-1} E_{cm}^{ee} = 10.6 GeV
$<2.9 \times 10^{-7}$	90	AUBERT,BE	05D	BABR	221 fb^{-1}, E_{cm}^{ee} = 10.6 GeV
$<8.2 \times 10^{-6}$	90	BLISS	98	CLEO	E_{cm}^{ee} = 10.6 GeV
$<7.4 \times 10^{-6}$	90	[1] BARTELT	94	CLEO	Repl. by BLISS 98
$<3.6 \times 10^{-5}$	90	ALBRECHT	92K	ARG	E_{cm}^{ee} = 10 GeV
$<3.9 \times 10^{-5}$	90	BOWCOCK	90	CLEO	E_{cm}^{ee} = 10.4–10.9

[1] BARTELT 94 assume phase space decays.

$\Gamma(\mu^+\pi^-\pi^-)/\Gamma_{total}$ Γ_{215}/Γ

Test of lepton number conservation.

VALUE	CL%	DOCUMENT ID		TECN	COMMENT
$<3.9 \times 10^{-8}$	90	MIYAZAKI	13	BELL	854 fb^{-1} E_{cm}^{ee} = 10.6 GeV
• • • We do not use the following data for averages, fits, limits, etc. • • •					
$<3.7 \times 10^{-8}$	90	MIYAZAKI	10	BELL	Repl. by MIYAZAKI 13
$<3.4 \times 10^{-7}$	90	YUSA	06	BELL	158 fb^{-1} E_{cm}^{ee} = 10.6 GeV
$<7 \times 10^{-8}$	90	AUBERT,BE	05D	BABR	221 fb^{-1}, E_{cm}^{ee} = 10.6 GeV
$<3.4 \times 10^{-6}$	90	BLISS	98	CLEO	E_{cm}^{ee} = 10.6 GeV
$<6.9 \times 10^{-6}$	90	[1] BARTELT	94	CLEO	Repl. by BLISS 98
$<6.3 \times 10^{-5}$	90	ALBRECHT	92K	ARG	E_{cm}^{ee} = 10 GeV
$<3.9 \times 10^{-5}$	90	BOWCOCK	90	CLEO	E_{cm}^{ee} = 10.4–10.9

[1] BARTELT 94 assume phase space decays.

$\Gamma(e^-\pi^+K^-)/\Gamma_{total}$ Γ_{216}/Γ

Test of lepton family number conservation.

VALUE	CL%	DOCUMENT ID		TECN	COMMENT
$<3.7\times10^{-8}$	90	MIYAZAKI	13	BELL	854 fb^{-1} E^{ee}_{cm} = 10.6 GeV
• • • We do not use the following data for averages, fits, limits, etc. • • •					
$<5.8\times10^{-8}$	90	MIYAZAKI	10	BELL	Repl. by MIYAZAKI 13
$<7.2\times10^{-7}$	90	YUSA	06	BELL	158 fb^{-1} E^{ee}_{cm} = 10.6 GeV
$<3.2\times10^{-7}$	90	AUBERT,BE	05D	BABR	221 fb^{-1}, E^{ee}_{cm} = 10.6 GeV
$<6.4\times10^{-6}$	90	BLISS	98	CLEO	E^{ee}_{cm} = 10.6 GeV
$<7.7\times10^{-6}$	90	[1] BARTELT	94	CLEO	Repl. by BLISS 98
$<2.9\times10^{-5}$	90	ALBRECHT	92K	ARG	E^{ee}_{cm} = 10 GeV
$<5.8\times10^{-5}$	90	BOWCOCK	90	CLEO	E^{ee}_{cm} = 10.4–10.9

[1] BARTELT 94 assume phase space decays.

$\Gamma(e^-\pi^-K^+)/\Gamma_{total}$ Γ_{217}/Γ

Test of lepton family number conservation.

VALUE	CL%	DOCUMENT ID		TECN	COMMENT
$<3.1\times10^{-8}$	90	MIYAZAKI	13	BELL	854 fb^{-1} E^{ee}_{cm} = 10.6 GeV
• • • We do not use the following data for averages, fits, limits, etc. • • •					
$<5.2\times10^{-8}$	90	MIYAZAKI	10	BELL	Repl. by MIYAZAKI 13
$<1.6\times10^{-7}$	90	YUSA	06	BELL	158 fb^{-1} E^{ee}_{cm} = 10.6 GeV
$<1.7\times10^{-7}$	90	AUBERT,BE	05D	BABR	221 fb^{-1}, E^{ee}_{cm} = 10.6 GeV
$<3.8\times10^{-6}$	90	BLISS	98	CLEO	E^{ee}_{cm} = 10.6 GeV
$<4.6\times10^{-6}$	90	[1] BARTELT	94	CLEO	Repl. by BLISS 98
$<5.8\times10^{-5}$	90	BOWCOCK	90	CLEO	E^{ee}_{cm} = 10.4–10.9

[1] BARTELT 94 assume phase space decays.

$\Gamma(e^+\pi^-K^-)/\Gamma_{total}$ Γ_{218}/Γ

Test of lepton number conservation.

VALUE	CL%	DOCUMENT ID		TECN	COMMENT
$<3.2\times10^{-8}$	90	MIYAZAKI	13	BELL	854 fb^{-1} E^{ee}_{cm} = 10.6 GeV
• • • We do not use the following data for averages, fits, limits, etc. • • •					
$<6.7\times10^{-8}$	90	MIYAZAKI	10	BELL	Repl. by MIYAZAKI 13
$<1.9\times10^{-7}$	90	YUSA	06	BELL	158 fb^{-1} E^{ee}_{cm} = 10.6 GeV
$<1.8\times10^{-7}$	90	AUBERT,BE	05D	BABR	221 fb^{-1}, E^{ee}_{cm} = 10.6 GeV
$<2.1\times10^{-6}$	90	BLISS	98	CLEO	E^{ee}_{cm} = 10.6 GeV
$<4.5\times10^{-6}$	90	[1] BARTELT	94	CLEO	Repl. by BLISS 98
$<2.0\times10^{-5}$	90	ALBRECHT	92K	ARG	E^{ee}_{cm} = 10 GeV
$<4.9\times10^{-5}$	90	BOWCOCK	90	CLEO	E^{ee}_{cm} = 10.4–10.9

[1] BARTELT 94 assume phase space decays.

$\Gamma(e^-K^0_SK^0_S)/\Gamma_{total}$ Γ_{219}/Γ

Test of lepton family number conservation.

VALUE	CL%	DOCUMENT ID		TECN	COMMENT
$<7.1\times10^{-8}$	90	MIYAZAKI	10A	BELL	671 fb^{-1} E^{ee}_{cm} = 10.6 GeV
• • • We do not use the following data for averages, fits, limits, etc. • • •					
$<2.2\times10^{-6}$	90	CHEN	02C	CLEO	E^{ee}_{cm} = 10.6 GeV

$\Gamma(e^-K^+K^-)/\Gamma_{total}$ Γ_{220}/Γ

Test of lepton family number conservation.

VALUE	CL%	DOCUMENT ID		TECN	COMMENT
$<3.4\times10^{-8}$	90	MIYAZAKI	13	BELL	854 fb^{-1} E^{ee}_{cm} = 10.6 GeV
• • • We do not use the following data for averages, fits, limits, etc. • • •					
$<5.4\times10^{-8}$	90	MIYAZAKI	10	BELL	Repl. by MIYAZAKI 13
$<3.0\times10^{-7}$	90	YUSA	06	BELL	158 fb^{-1} E^{ee}_{cm} = 10.6 GeV
$<1.4\times10^{-7}$	90	AUBERT,BE	05D	BABR	221 fb^{-1}, E^{ee}_{cm} = 10.6 GeV
$<6.0\times10^{-6}$	90	BLISS	98	CLEO	E^{ee}_{cm} = 10.6 GeV

$\Gamma(e^+K^-K^-)/\Gamma_{total}$ Γ_{221}/Γ

Test of lepton number conservation.

VALUE	CL%	DOCUMENT ID		TECN	COMMENT
$<3.3\times10^{-8}$	90	MIYAZAKI	13	BELL	854 fb^{-1} E^{ee}_{cm} = 10.6 GeV
• • • We do not use the following data for averages, fits, limits, etc. • • •					
$<6.0\times10^{-8}$	90	MIYAZAKI	10	BELL	Repl. by MIYAZAKI 13
$<3.1\times10^{-7}$	90	YUSA	06	BELL	158 fb^{-1} E^{ee}_{cm} = 10.6 GeV
$<1.5\times10^{-7}$	90	AUBERT,BE	05D	BABR	221 fb^{-1}, E^{ee}_{cm} = 10.6 GeV
$<3.8\times10^{-6}$	90	BLISS	98	CLEO	E^{ee}_{cm} = 10.6 GeV

$\Gamma(\mu^-\pi^+K^-)/\Gamma_{total}$ Γ_{222}/Γ

Test of lepton family number conservation.

VALUE	CL%	DOCUMENT ID		TECN	COMMENT
$< 8.6\times10^{-8}$	90	MIYAZAKI	13	BELL	854 fb^{-1} E^{ee}_{cm} = 10.6 GeV
• • • We do not use the following data for averages, fits, limits, etc. • • •					
$< 1.6\times10^{-7}$	90	MIYAZAKI	10	BELL	Repl. by MIYAZAKI 13
$< 2.7\times10^{-7}$	90	YUSA	06	BELL	158 fb^{-1} E^{ee}_{cm} = 10.6 GeV
$< 2.6\times10^{-7}$	90	AUBERT,BE	05D	BABR	221 fb^{-1}, E^{ee}_{cm} = 10.6 GeV
$< 7.5\times10^{-6}$	90	BLISS	98	CLEO	E^{ee}_{cm} = 10.6 GeV
$< 8.7\times10^{-6}$	90	[1] BARTELT	94	CLEO	Repl. by BLISS 98
$<11\times10^{-5}$	90	ALBRECHT	92K	ARG	E^{ee}_{cm} = 10 GeV
$< 7.7\times10^{-5}$	90	BOWCOCK	90	CLEO	E^{ee}_{cm} = 10.4–10.9

[1] BARTELT 94 assume phase space decays.

$\Gamma(\mu^-\pi^-K^+)/\Gamma_{total}$ Γ_{223}/Γ

Test of lepton family number conservation.

VALUE	CL%	DOCUMENT ID		TECN	COMMENT
$<4.5\times10^{-8}$	90	MIYAZAKI	13	BELL	854 fb^{-1} E^{ee}_{cm} = 10.6 GeV
• • • We do not use the following data for averages, fits, limits, etc. • • •					
$<1.0\times10^{-7}$	90	MIYAZAKI	10	BELL	Repl. by MIYAZAKI 13
$<7.3\times10^{-7}$	90	YUSA	06	BELL	158 fb^{-1} E^{ee}_{cm} = 10.6 GeV
$<3.2\times10^{-7}$	90	AUBERT,BE	05D	BABR	221 fb^{-1}, E^{ee}_{cm} = 10.6 GeV
$<7.4\times10^{-6}$	90	BLISS	98	CLEO	E^{ee}_{cm} = 10.6 GeV
$<1.5\times10^{-5}$	90	[1] BARTELT	94	CLEO	Repl. by BLISS 98
$<7.7\times10^{-5}$	90	BOWCOCK	90	CLEO	E^{ee}_{cm} = 10.4–10.9

[1] BARTELT 94 assume phase space decays.

$\Gamma(\mu^+\pi^-K^-)/\Gamma_{total}$ Γ_{224}/Γ

Test of lepton number conservation.

VALUE	CL%	DOCUMENT ID		TECN	COMMENT
$<4.8\times10^{-8}$	90	MIYAZAKI	13	BELL	854 fb^{-1} E^{ee}_{cm} = 10.6 GeV
• • • We do not use the following data for averages, fits, limits, etc. • • •					
$<9.4\times10^{-8}$	90	MIYAZAKI	10	BELL	Repl. by MIYAZAKI 13
$<2.9\times10^{-7}$	90	YUSA	06	BELL	158 fb^{-1} E^{ee}_{cm} = 10.6 GeV
$<2.2\times10^{-7}$	90	AUBERT,BE	05D	BABR	221 fb^{-1}, E^{ee}_{cm} = 10.6 GeV
$<7.0\times10^{-6}$	90	BLISS	98	CLEO	E^{ee}_{cm} = 10.6 GeV
$<2.0\times10^{-5}$	90	[1] BARTELT	94	CLEO	Repl. by BLISS 98
$<5.8\times10^{-5}$	90	ALBRECHT	92K	ARG	E^{ee}_{cm} = 10 GeV
$<4.0\times10^{-5}$	90	BOWCOCK	90	CLEO	E^{ee}_{cm} = 10.4–10.9

[1] BARTELT 94 assume phase space decays.

$\Gamma(\mu^-K^0_SK^0_S)/\Gamma_{total}$ Γ_{225}/Γ

VALUE	CL%	DOCUMENT ID		TECN	COMMENT
$<8.0\times10^{-8}$	90	MIYAZAKI	10A	BELL	671 fb^{-1} E^{ee}_{cm} = 10.6 GeV
• • • We do not use the following data for averages, fits, limits, etc. • • •					
$<3.4\times10^{-6}$	90	CHEN	02C	CLEO	E^{ee}_{cm} = 10.6 GeV

$\Gamma(\mu^-K^+K^-)/\Gamma_{total}$ Γ_{226}/Γ

Test of lepton family number conservation.

VALUE	CL%	DOCUMENT ID		TECN	COMMENT
$< 4.4\times10^{-8}$	90	MIYAZAKI	13	BELL	854 fb^{-1} E^{ee}_{cm} = 10.6 GeV
• • • We do not use the following data for averages, fits, limits, etc. • • •					
$< 6.8\times10^{-8}$	90	MIYAZAKI	10	BELL	Repl. by MIYAZAKI 13
$< 8.0\times10^{-7}$	90	YUSA	06	BELL	158 fb^{-1} E^{ee}_{cm} = 10.6 GeV
$< 2.5\times10^{-7}$	90	AUBERT,BE	05D	BABR	221 fb^{-1}, E^{ee}_{cm} = 10.6 GeV
$<15\times10^{-6}$	90	BLISS	98	CLEO	E^{ee}_{cm} = 10.6 GeV

$\Gamma(\mu^+K^-K^-)/\Gamma_{total}$ Γ_{227}/Γ

Test of lepton number conservation.

VALUE	CL%	DOCUMENT ID		TECN	COMMENT
$<4.7\times10^{-8}$	90	MIYAZAKI	13	BELL	854 fb^{-1} E^{ee}_{cm} = 10.6 GeV
• • • We do not use the following data for averages, fits, limits, etc. • • •					
$<9.6\times10^{-8}$	90	MIYAZAKI	10	BELL	Repl. by MIYAZAKI 13
$<4.4\times10^{-7}$	90	YUSA	06	BELL	158 fb^{-1} E^{ee}_{cm} = 10.6 GeV
$<4.8\times10^{-7}$	90	AUBERT,BE	05D	BABR	221 fb^{-1}, E^{ee}_{cm} = 10.6 GeV
$<6.0\times10^{-6}$	90	BLISS	98	CLEO	E^{ee}_{cm} = 10.6 GeV

$\Gamma(e^-\pi^0\pi^0)/\Gamma_{total}$ Γ_{228}/Γ

Test of lepton family number conservation.

VALUE	CL%	DOCUMENT ID		TECN	COMMENT
$<6.5\times10^{-6}$	90	BONVICINI	97	CLEO	E^{ee}_{cm} = 10.6 GeV

$\Gamma(\mu^-\pi^0\pi^0)/\Gamma_{total}$ Γ_{229}/Γ

Test of lepton family number conservation.

VALUE	CL%	DOCUMENT ID		TECN	COMMENT
$<14\times10^{-6}$	90	BONVICINI	97	CLEO	E^{ee}_{cm} = 10.6 GeV

$\Gamma(e^-\eta\eta)/\Gamma_{total}$ Γ_{230}/Γ

Test of lepton family number conservation.

VALUE	CL%	DOCUMENT ID		TECN	COMMENT
$<35\times10^{-6}$	90	BONVICINI	97	CLEO	E^{ee}_{cm} = 10.6 GeV

$\Gamma(\mu^-\eta\eta)/\Gamma_{total}$ Γ_{231}/Γ

Test of lepton family number conservation.

VALUE	CL%	DOCUMENT ID		TECN	COMMENT
$<60\times10^{-6}$	90	BONVICINI	97	CLEO	E^{ee}_{cm} = 10.6 GeV

$\Gamma(e^-\pi^0\eta)/\Gamma_{total}$ Γ_{232}/Γ

Test of lepton family number conservation.

VALUE	CL%	DOCUMENT ID		TECN	COMMENT
$<24\times10^{-6}$	90	BONVICINI	97	CLEO	E^{ee}_{cm} = 10.6 GeV

$\Gamma(\mu^-\pi^0\eta)/\Gamma_{total}$ Γ_{233}/Γ

Test of lepton family number conservation.

VALUE	CL%	DOCUMENT ID		TECN	COMMENT
$<22\times10^{-6}$	90	BONVICINI	97	CLEO	E^{ee}_{cm} = 10.6 GeV

$\Gamma(p\mu^-\mu^-)/\Gamma_{total}$ Γ_{234}/Γ

VALUE	CL%	DOCUMENT ID		TECN	COMMENT
$<4.4\times10^{-7}$	90	AAIJ	13AH	LHCB	1.0 fb^{-1}, $\sqrt{s}=7$ TeV

$\Gamma(\overline{p}\mu^+\mu^-)/\Gamma_{total}$ Γ_{235}/Γ

VALUE	CL%	DOCUMENT ID		TECN	COMMENT
$<3.3\times10^{-7}$	90	AAIJ	13AH	LHCB	1.0 fb^{-1}, $\sqrt{s}=7$ TeV

$\Gamma(\overline{p}\gamma)/\Gamma_{total}$ Γ_{236}/Γ

Test of lepton number and baryon number conservation.

VALUE	CL%	DOCUMENT ID		TECN	COMMENT
$<3.5\times10^{-6}$	90	GODANG	99	CLEO	$E_{cm}^{ee}=10.6$ GeV
• • • We do not use the following data for averages, fits, limits, etc. • • •					
$<29\ \times10^{-5}$	90	ALBRECHT	92K	ARG	$E_{cm}^{ee}=10$ GeV

$\Gamma(\overline{p}\pi^0)/\Gamma_{total}$ Γ_{237}/Γ

Test of lepton number and baryon number conservation.

VALUE	CL%	DOCUMENT ID		TECN	COMMENT
$<15\times10^{-6}$	90	GODANG	99	CLEO	$E_{cm}^{ee}=10.6$ GeV
• • • We do not use the following data for averages, fits, limits, etc. • • •					
$<66\times10^{-5}$	90	ALBRECHT	92K	ARG	$E_{cm}^{ee}=10$ GeV

$\Gamma(\overline{p}2\pi^0)/\Gamma_{total}$ Γ_{238}/Γ

Test of lepton number and baryon number conservation.

VALUE	CL%	DOCUMENT ID		TECN	COMMENT
$<33\times10^{-6}$	90	GODANG	99	CLEO	$E_{cm}^{ee}=10.6$ GeV

$\Gamma(\overline{p}\eta)/\Gamma_{total}$ Γ_{239}/Γ

Test of lepton number and baryon number conservation.

VALUE	CL%	DOCUMENT ID		TECN	COMMENT
$<8.9\times10^{-6}$	90	GODANG	99	CLEO	$E_{cm}^{ee}=10.6$ GeV
• • • We do not use the following data for averages, fits, limits, etc. • • •					
$<130\ \times10^{-5}$	90	ALBRECHT	92K	ARG	$E_{cm}^{ee}=10$ GeV

$\Gamma(\overline{p}\pi^0\eta)/\Gamma_{total}$ Γ_{240}/Γ

Test of lepton number and baryon number conservation.

VALUE	CL%	DOCUMENT ID		TECN	COMMENT
$<27\times10^{-6}$	90	GODANG	99	CLEO	$E_{cm}^{ee}=10.6$ GeV

$\Gamma(\Lambda\pi^-)/\Gamma_{total}$ Γ_{241}/Γ

Test of lepton number and baryon number conservation.

VALUE	CL%	DOCUMENT ID		TECN	COMMENT
$<0.72\times10^{-7}$	90	MIYAZAKI	06	BELL	154 fb^{-1}, $E_{cm}^{ee}=10.6$ GeV

$\Gamma(\overline{\Lambda}\pi^-)/\Gamma_{total}$ Γ_{242}/Γ

Test of lepton number and baryon number conservation.

VALUE	CL%	DOCUMENT ID		TECN	COMMENT
$<1.4\times10^{-7}$	90	MIYAZAKI	06	BELL	154 fb^{-1}, $E_{cm}^{ee}=10.6$ GeV

$\Gamma(e^-\text{light boson})/\Gamma(e^-\overline{\nu}_e\nu_\tau)$ Γ_{243}/Γ_5

Test of lepton family number conservation.

VALUE	CL%	DOCUMENT ID		TECN	COMMENT
<0.015	95	[1] ALBRECHT	95G	ARG	$E_{cm}^{ee}=9.4$–10.6 GeV
• • • We do not use the following data for averages, fits, limits, etc. • • •					
<0.018	95	[2] ALBRECHT	90E	ARG	$E_{cm}^{ee}=9.4$–10.6 GeV
<0.040	95	[3] BALTRUSAIT...85		MRK3	$E_{cm}^{ee}=3.77$ GeV

[1] ALBRECHT 95G limit holds for bosons with mass <0.4 GeV. The limit rises to 0.036 for a mass of 1.0 GeV, then falls to 0.006 at the upper mass limit of 1.6 GeV.
[2] ALBRECHT 90E limit applies for spinless boson with mass <100 MeV, and rises to 0.050 for mass $=500$ MeV.
[3] BALTRUSAITIS 85 limit applies for spinless boson with mass <100 MeV.

$\Gamma(\mu^-\text{light boson})/\Gamma(e^-\overline{\nu}_e\nu_\tau)$ Γ_{244}/Γ_5

Test of lepton family number conservation.

VALUE	CL%	DOCUMENT ID		TECN	COMMENT
<0.026	95	[1] ALBRECHT	95G	ARG	$E_{cm}^{ee}=9.4$–10.6 GeV
• • • We do not use the following data for averages, fits, limits, etc. • • •					
<0.033	95	[2] ALBRECHT	90E	ARG	$E_{cm}^{ee}=9.4$–10.6 GeV
<0.125	95	[3] BALTRUSAIT...85		MRK3	$E_{cm}^{ee}=3.77$ GeV

[1] ALBRECHT 95G limit holds for bosons with mass <1.3 GeV. The limit rises to 0.034 for a mass of 1.4 GeV, then falls to 0.003 at the upper mass limit of 1.6 GeV.
[2] ALBRECHT 90E limit applies for spinless boson with mass <100 MeV, and rises to 0.071 for mass $=500$ MeV.
[3] BALTRUSAITIS 85 limit applies for spinless boson with mass <100 MeV.

τ-DECAY PARAMETERS

See the related review(s):
τ-Lepton Decay Parameters

$\rho(e$ or $\mu)$ PARAMETER

($V-A$) theory predicts $\rho=0.75$.

VALUE	EVTS	DOCUMENT ID		TECN	COMMENT
0.745 ± 0.008 OUR FIT					
0.749 ± 0.008 OUR AVERAGE					
$0.742\pm0.014\pm0.006$	81k	HEISTER	01E	ALEP	1991–1995 LEP runs
$0.775\pm0.023\pm0.020$	36k	ABREU	00L	DLPH	1992–1995 runs
$0.781\pm0.028\pm0.018$	46k	ACKERSTAFF	99D	OPAL	1990–1995 LEP runs
0.762 ± 0.035	54k	ACCIARRI	98R	L3	1991–1995 LEP runs
0.731 ± 0.031		[1] ALBRECHT	98	ARG	$E_{cm}^{ee}=9.5$–10.6 GeV
$0.72\ \pm0.09\ \pm0.03$		[2] ABE	97O	SLD	1993–1995 SLC runs
$0.747\pm0.010\pm0.006$	55k	ALEXANDER	97F	CLEO	$E_{cm}^{ee}=10.6$ GeV
$0.79\ \pm0.10\ \pm0.10$	3732	FORD	97B	MAC	$E_{cm}^{ee}=29$ GeV
$0.71\ \pm0.09\ \pm0.03$	1426	BEHRENDS	85	CLEO	e^+e^- near $\Upsilon(4S)$
• • • We do not use the following data for averages, fits, limits, etc. • • •					
$0.735\pm0.013\pm0.008$	31k	AMMAR	97B	CLEO	Repl. by ALEXANDER 97F
$0.794\pm0.039\pm0.031$	18k	ACCIARRI	96H	L3	Repl. by ACCIARRI 98R
$0.732\pm0.034\pm0.020$	8.2k	[3] ALBRECHT	95	ARG	$E_{cm}^{ee}=9.5$–10.6 GeV
0.738 ± 0.038		[4] ALBRECHT	95C	ARG	Repl. by ALBRECHT 98
$0.751\pm0.039\pm0.022$		BUSKULIC	95D	ALEP	Repl. by HEISTER 01E
$0.742\pm0.035\pm0.020$	8000	ALBRECHT	90E	ARG	$E_{cm}^{ee}=9.4$–10.6 GeV

[1] Combined fit to ARGUS tau decay parameter measurements in ALBRECHT 98, ALBRECHT 95C, ALBRECHT 93G, and ALBRECHT 94E. ALBRECHT 98 use tau pair events of the type $\tau^-\tau^+\to(\ell^-\overline{\nu}_\ell\nu_\tau)(\pi^+\pi^0\overline{\nu}_\tau)$, and their charged conjugates.
[2] ABE 97O assume $\eta=0$ in their fit. Letting η vary in the fit gives a ρ value of $0.69\pm0.13\pm0.05$.
[3] Value is from a simultaneous fit for the ρ and η decay parameters to the lepton energy spectrum. Not independent of ALBRECHT 90E $\rho(e$ or $\mu)$ value which assumes $\eta=0$. Result is strongly correlated with ALBRECHT 95C.
[4] Combined fit to ARGUS tau decay parameter measurements in ALBRECHT 95C, ALBRECHT 93G, and ALBRECHT 94E.

$\rho(e)$ PARAMETER

($V-A$) theory predicts $\rho=0.75$.

VALUE	EVTS	DOCUMENT ID		TECN	COMMENT
0.747 ± 0.010 OUR FIT					
0.744 ± 0.010 OUR AVERAGE					
$0.747\pm0.019\pm0.014$	44k	HEISTER	01E	ALEP	1991–1995 LEP runs
$0.744\pm0.036\pm0.037$	17k	ABREU	00L	DLPH	1992–1995 runs
$0.779\pm0.047\pm0.029$	25k	ACKERSTAFF	99D	OPAL	1990–1995 LEP runs
$0.68\ \pm0.04\ \pm0.07$		[1] ALBRECHT	98	ARG	$E_{cm}^{ee}=9.5$–10.6 GeV
$0.71\ \pm0.14\ \pm0.05$		ABE	97O	SLD	1993–1995 SLC runs
$0.747\pm0.012\pm0.004$	34k	ALEXANDER	97F	CLEO	$E_{cm}^{ee}=10.6$ GeV
$0.735\pm0.036\pm0.020$	4.7k	[2] ALBRECHT	95	ARG	$E_{cm}^{ee}=9.5$–10.6 GeV
$0.79\ \pm0.08\ \pm0.06$	3230	[3] ALBRECHT	93G	ARG	$E_{cm}^{ee}=9.4$–10.6 GeV
$0.64\ \pm0.06\ \pm0.07$	2753	JANSSEN	89	CBAL	$E_{cm}^{ee}=9.4$–10.6 GeV
$0.62\ \pm0.17\ \pm0.14$	1823	FORD	87B	MAC	$E_{cm}^{ee}=29$ GeV
$0.60\ \pm0.13$	699	BEHRENDS	85	CLEO	e^+e^- near $\Upsilon(4S)$
$0.72\ \pm0.10\ \pm0.11$	594	BACINO	79B	DLCO	$E_{cm}^{ee}=3.5$–7.4 GeV
• • • We do not use the following data for averages, fits, limits, etc. • • •					
$0.732\pm0.014\pm0.009$	19k	AMMAR	97B	CLEO	Repl. by ALEXANDER 97F
$0.793\pm0.050\pm0.025$		BUSKULIC	95D	ALEP	Repl. by HEISTER 01E
$0.747\pm0.045\pm0.028$	5106	ALBRECHT	90E	ARG	Repl. by ALBRECHT 95

[1] ALBRECHT 98 use tau pair events of the type $\tau^-\tau^+\to(\ell^-\overline{\nu}_\ell\nu_\tau)(\pi^+\pi^0\overline{\nu}_\tau)$, and their charged conjugates.
[2] ALBRECHT 95 use tau pair events of the type $\tau^-\tau^+\to(\ell^-\overline{\nu}_\ell\nu_\tau)(h^+h^-h^+(\pi^0)\overline{\nu}_\tau)$ and their charged conjugates.
[3] ALBRECHT 93G use tau pair events of the type $\tau^-\tau^+\to(\mu^-\overline{\nu}_\mu\nu_\tau)(e^+\nu_e\overline{\nu}_\tau)$ and their charged conjugates.

$\rho(\mu)$ PARAMETER

($V-A$) theory predicts $\rho=0.75$.

VALUE	EVTS	DOCUMENT ID		TECN	COMMENT
0.763 ± 0.020 OUR FIT					
0.770 ± 0.022 OUR AVERAGE					
$0.776\pm0.045\pm0.019$	46k	HEISTER	01E	ALEP	1991–1995 LEP runs
$0.999\pm0.098\pm0.045$	22k	ABREU	00L	DLPH	1992–1995 runs
$0.777\pm0.044\pm0.016$	27k	ACKERSTAFF	99D	OPAL	1990–1995 LEP runs
$0.69\ \pm0.06\ \pm0.06$		[1] ALBRECHT	98	ARG	$E_{cm}^{ee}=9.5$–10.6 GeV
$0.54\ \pm0.28\ \pm0.14$		ABE	97O	SLD	1993–1995 SLC runs
$0.750\pm0.017\pm0.045$	22k	ALEXANDER	97F	CLEO	$E_{cm}^{ee}=10.6$ GeV
$0.76\ \pm0.07\ \pm0.08$	3230	ALBRECHT	93G	ARG	$E_{cm}^{ee}=9.4$–10.6 GeV
$0.734\pm0.055\pm0.027$	3041	ALBRECHT	90E	ARG	$E_{cm}^{ee}=9.4$–10.6 GeV
$0.89\ \pm0.14\ \pm0.08$	1909	FORD	87B	MAC	$E_{cm}^{ee}=29$ GeV
$0.81\ \pm0.13$	727	BEHRENDS	85	CLEO	e^+e^- near $\Upsilon(4S)$
• • • We do not use the following data for averages, fits, limits, etc. • • •					
$0.747\pm0.048\pm0.044$	13k	AMMAR	97B	CLEO	Repl. by ALEXANDER 97F
$0.693\pm0.057\pm0.028$		BUSKULIC	95D	ALEP	Repl. by HEISTER 01E

[1] ALBRECHT 98 use tau pair events of the type $\tau^-\tau^+\to(\ell^-\overline{\nu}_\ell\nu_\tau)(\pi^+\pi^0\overline{\nu}_\tau)$, and their charged conjugates.

$\xi(e$ or $\mu)$ PARAMETER

($V-A$) theory predicts $\xi = 1$.

VALUE	EVTS	DOCUMENT ID		TECN	COMMENT
0.985±0.030 OUR FIT					
0.981±0.031 OUR AVERAGE					
0.986±0.068±0.031	81k	HEISTER	01E	ALEP	1991–1995 LEP runs
0.929±0.070±0.030	36k	ABREU	00L	DLPH	1992–1995 runs
0.98 ±0.22 ±0.10	46k	ACKERSTAFF	99D	OPAL	1990–1995 LEP runs
0.70 ±0.16	54k	ACCIARRI	98R	L3	1991–1995 LEP runs
1.03 ±0.11		[1] ALBRECHT	98	ARG	E^{ee}_{cm}= 9.5–10.6 GeV
1.05 ±0.35 ±0.04		[2] ABE	97O	SLD	1993–1995 SLC runs
1.007±0.040±0.015	55k	ALEXANDER	97F	CLEO	E^{ee}_{cm}= 10.6 GeV
• • • We do not use the following data for averages, fits, limits, etc. • • •					
0.94 ±0.21 ±0.07	18k	ACCIARRI	96H	L3	Repl. by ACCIARRI 98R
0.97 ±0.14		[3] ALBRECHT	95C	ARG	Repl. by ALBRECHT 98
1.18 ±0.15 ±0.16		BUSKULIC	95D	ALEP	Repl. by HEISTER 01E
0.90 ±0.15 ±0.10	3230	[4] ALBRECHT	93G	ARG	E^{ee}_{cm}= 9.4–10.6 GeV

[1] Combined fit to ARGUS tau decay parameter measurements in ALBRECHT 98, ALBRECHT 95C, ALBRECHT 93G, and ALBRECHT 94E. ALBRECHT 98 use tau pair events of the type $\tau^-\tau^+ \to (\ell^-\overline{\nu}_\ell\nu_\tau)(\pi^+\pi^0\overline{\nu}_\tau)$, and their charged conjugates.

[2] ABE 97O assume $\eta = 0$ in their fit. Letting η vary in the fit gives a ξ value of 1.02 ± 0.36 ± 0.05.

[3] Combined fit to ARGUS tau decay parameter measurements in ALBRECHT 95C, ALBRECHT 93G, and ALBRECHT 94E. ALBRECHT 95C uses events of the type $\tau^-\tau^+ \to (\ell^-\overline{\nu}_\ell\nu_\tau)\ (h^+h^-h^+\overline{\nu}_\tau)$ and their charged conjugates.

[4] ALBRECHT 93G measurement determines $|\xi|$ for the case $\xi(e) = \xi(\mu)$, but the authors point out that other LEP experiments determine the sign to be positive.

$\xi(e)$ PARAMETER

($V-A$) theory predicts $\xi = 1$.

VALUE	EVTS	DOCUMENT ID		TECN	COMMENT
0.994±0.040 OUR FIT					
1.00 ±0.04 OUR AVERAGE					
1.011±0.094±0.038	44k	HEISTER	01E	ALEP	1991–1995 LEP runs
1.01 ±0.12 ±0.05	17k	ABREU	00L	DLPH	1992–1995 runs
1.13 ±0.39 ±0.14	25k	ACKERSTAFF	99D	OPAL	1990–1995 LEP runs
1.11 ±0.20 ±0.08		[1] ALBRECHT	98	ARG	E^{ee}_{cm}= 9.5–10.6 GeV
1.16 ±0.52 ±0.06		ABE	97O	SLD	1993–1995 SLC runs
0.979±0.048±0.016	34k	ALEXANDER	97F	CLEO	E^{ee}_{cm}= 10.6 GeV
• • • We do not use the following data for averages, fits, limits, etc. • • •					
1.03 ±0.23 ±0.09		BUSKULIC	95D	ALEP	Repl. by HEISTER 01E

[1] ALBRECHT 98 use tau pair events of the type $\tau^-\tau^+ \to (\ell^-\overline{\nu}_\ell\nu_\tau)(\pi^+\pi^0\overline{\nu}_\tau)$, and their charged conjugates.

$\xi(\mu)$ PARAMETER

($V-A$) theory predicts $\xi = 1$.

VALUE	EVTS	DOCUMENT ID		TECN	COMMENT
1.030±0.059 OUR FIT					
1.06 ±0.06 OUR AVERAGE					
1.030±0.120±0.050	46k	HEISTER	01E	ALEP	1991–1995 LEP runs
1.16 ±0.19 ±0.06	22k	ABREU	00L	DLPH	1992–1995 runs
0.79 ±0.41 ±0.09	27k	ACKERSTAFF	99D	OPAL	1990–1995 LEP runs
1.26 ±0.27 ±0.14		[1] ALBRECHT	98	ARG	E^{ee}_{cm}= 9.5–10.6 GeV
0.75 ±0.50 ±0.14		ABE	97O	SLD	1993–1995 SLC runs
1.054±0.069±0.047	22k	ALEXANDER	97F	CLEO	E^{ee}_{cm}= 10.6 GeV
• • • We do not use the following data for averages, fits, limits, etc. • • •					
1.23 ±0.22 ±0.10		BUSKULIC	95D	ALEP	Repl. by HEISTER 01E

[1] ALBRECHT 98 use tau pair events of the type $\tau^-\tau^+ \to (\ell^-\overline{\nu}_\ell\nu_\tau)(\pi^+\pi^0\overline{\nu}_\tau)$, and their charged conjugates.

$\eta(e$ or $\mu)$ PARAMETER

($V-A$) theory predicts $\eta = 0$.

VALUE	EVTS	DOCUMENT ID		TECN	COMMENT
0.013±0.020 OUR FIT					
0.015±0.021 OUR AVERAGE					
0.012±0.026±0.004	81k	HEISTER	01E	ALEP	1991–1995 LEP runs
−0.005±0.036±0.037		ABREU	00L	DLPH	1992–1995 runs
0.027±0.055±0.005	46k	ACKERSTAFF	99D	OPAL	1990–1995 LEP runs
0.27 ±0.14	54k	ACCIARRI	98R	L3	1991–1995 LEP runs
−0.13 ±0.47 ±0.15		ABE	97O	SLD	1993–1995 SLC runs
−0.015±0.061±0.062	31k	AMMAR	97B	CLEO	E^{ee}_{cm}= 10.6 GeV
0.03 ±0.18 ±0.12	8.2k	ALBRECHT	95	ARG	E^{ee}_{cm}= 9.5–10.6 GeV
• • • We do not use the following data for averages, fits, limits, etc. • • •					
0.25 ±0.17 ±0.11	18k	ACCIARRI	96H	L3	Repl. by ACCIARRI 98R
−0.04 ±0.15 ±0.11		BUSKULIC	95D	ALEP	Repl. by HEISTER 01E

$\eta(\mu)$ PARAMETER

($V-A$) theory predicts $\eta = 0$.

VALUE	EVTS	DOCUMENT ID		TECN	COMMENT
0.094±0.073 OUR FIT					
0.17 ±0.15 OUR AVERAGE Error includes scale factor of 1.2.					
0.160±0.150±0.060	46k	HEISTER	01E	ALEP	1991–1995 LEP runs
0.72 ±0.32 ±0.15		ABREU	00L	DLPH	1992–1995 runs
−0.59 ±0.82 ±0.45		[1] ABE	97O	SLD	1993–1995 SLC runs
0.010±0.149±0.171	13k	[2] AMMAR	97B	CLEO	E^{ee}_{cm}= 10.6 GeV
• • • We do not use the following data for averages, fits, limits, etc. • • •					
0.010±0.065±0.001	27k	[3] ACKERSTAFF	99D	OPAL	1990–1995 LEP runs
−0.24 ±0.23 ±0.18		BUSKULIC	95D	ALEP	Repl. by HEISTER 01E

[1] Highly correlated (corr. = 0.92) with ABE 97O $\rho(\mu)$ measurement.

[2] Highly correlated (corr. = 0.949) with AMMAR 97B $\rho(\mu)$ value.

[3] ACKERSTAFF 99D result is dominated by a constraint on η from the OPAL measurements of the τ lifetime and B($\tau^- \to \mu^-\overline{\nu}_\mu\nu_\tau$) assuming lepton universality for the total coupling strength.

$(\delta\xi)(e$ or $\mu)$ PARAMETER

($V-A$) theory predicts $(\delta\xi) = 0.75$.

VALUE	EVTS	DOCUMENT ID		TECN	COMMENT
0.746±0.021 OUR FIT					
0.744±0.022 OUR AVERAGE					
0.776±0.045±0.024	81k	HEISTER	01E	ALEP	1991–1995 LEP runs
0.779±0.070±0.028	36k	ABREU	00L	DLPH	1992–1995 runs
0.65 ±0.14 ±0.07	46k	ACKERSTAFF	99D	OPAL	1990–1995 LEP runs
0.70 ±0.11	54k	ACCIARRI	98R	L3	1991–1995 LEP runs
0.63 ±0.09		[1] ALBRECHT	98	ARG	E^{ee}_{cm}= 9.5–10.6 GeV
0.88 ±0.27 ±0.04		[2] ABE	97O	SLD	1993–1995 SLC runs
0.745±0.026±0.009	55k	ALEXANDER	97F	CLEO	E^{ee}_{cm}= 10.6 GeV
• • • We do not use the following data for averages, fits, limits, etc. • • •					
0.81 ±0.14 ±0.06	18k	ACCIARRI	96H	L3	Repl. by ACCIARRI 98R
0.65 ±0.12		[3] ALBRECHT	95C	ARG	Repl. by ALBRECHT 98
0.88 ±0.11 ±0.07		BUSKULIC	95D	ALEP	Repl. by HEISTER 01E

[1] Combined fit to ARGUS tau decay parameter measurements in ALBRECHT 98, ALBRECHT 95C, ALBRECHT 93G, and ALBRECHT 94E. ALBRECHT 98 use tau pair events of the type $\tau^-\tau^+ \to (\ell^-\overline{\nu}_\ell\nu_\tau)(\pi^+\pi^0\overline{\nu}_\tau)$, and their charged conjugates.

[2] ABE 97O assume $\eta = 0$ in their fit. Letting η vary in the fit gives a $(\delta\xi)$ value of 0.87 ± 0.27 ± 0.04.

[3] Combined fit to ARGUS tau decay parameter measurements in ALBRECHT 95C, ALBRECHT 93G, and ALBRECHT 94E. ALBRECHT 95C uses events of the type $\tau^-\tau^+ \to (\ell^-\overline{\nu}_\ell\nu_\tau)\ (h^+h^-h^+\overline{\nu}_\tau)$ and their charged conjugates.

$(\delta\xi)(e)$ PARAMETER

($V-A$) theory predicts $(\delta\xi) = 0.75$.

VALUE	EVTS	DOCUMENT ID		TECN	COMMENT
0.734±0.028 OUR FIT					
0.731±0.029 OUR AVERAGE					
0.778±0.066±0.024	44k	HEISTER	01E	ALEP	1991–1995 LEP runs
0.85 ±0.12 ±0.04	17k	ABREU	00L	DLPH	1992–1995 runs
0.72 ±0.31 ±0.14	25k	ACKERSTAFF	99D	OPAL	1990–1995 LEP runs
0.56 ±0.14 ±0.06		[1] ALBRECHT	98	ARG	E^{ee}_{cm}= 9.5–10.6 GeV
0.85 ±0.43 ±0.08		ABE	97O	SLD	1993–1995 SLC runs
0.720±0.032±0.010	34k	ALEXANDER	97F	CLEO	E^{ee}_{cm}= 10.6 GeV
• • • We do not use the following data for averages, fits, limits, etc. • • •					
1.11 ±0.17 ±0.07		BUSKULIC	95D	ALEP	Repl. by HEISTER 01E

[1] ALBRECHT 98 use tau pair events of the type $\tau^-\tau^+ \to (\ell^-\overline{\nu}_\ell\nu_\tau)(\pi^+\pi^0\overline{\nu}_\tau)$, and their charged conjugates.

$(\delta\xi)(\mu)$ PARAMETER

($V-A$) theory predicts $(\delta\xi) = 0.75$.

VALUE	EVTS	DOCUMENT ID		TECN	COMMENT
0.778±0.037 OUR FIT					
0.79 ±0.04 OUR AVERAGE					
0.786±0.066±0.028	46k	HEISTER	01E	ALEP	1991–1995 LEP runs
0.86 ±0.13 ±0.04	22k	ABREU	00L	DLPH	1992–1995 runs
0.63 ±0.23 ±0.05	27k	ACKERSTAFF	99D	OPAL	1990–1995 LEP runs
0.73 ±0.18 ±0.10		[1] ALBRECHT	98	ARG	E^{ee}_{cm}= 9.5–10.6 GeV
0.82 ±0.32 ±0.07		ABE	97O	SLD	1993–1995 SLC runs
0.786±0.041±0.032	22k	ALEXANDER	97F	CLEO	E^{ee}_{cm}= 10.6 GeV
• • • We do not use the following data for averages, fits, limits, etc. • • •					
0.71 ±0.14 ±0.06		BUSKULIC	95D	ALEP	Repl. by HEISTER 01E

[1] ALBRECHT 98 use tau pair events of the type $\tau^-\tau^+ \to (\ell^-\overline{\nu}_\ell\nu_\tau)(\pi^+\pi^0\overline{\nu}_\tau)$, and their charged conjugates.

$\xi(\pi)$ PARAMETER

($V-A$) theory predicts $\xi(\pi) = 1$.

VALUE	EVTS	DOCUMENT ID		TECN	COMMENT
0.993±0.022 OUR FIT					
0.994±0.023 OUR AVERAGE					
0.994±0.020±0.014	27k	HEISTER	01E	ALEP	1991–1995 LEP runs
0.81 ±0.17 ±0.02		ABE	97O	SLD	1993–1995 SLC runs
1.03 ±0.06 ±0.04	2.0k	COAN	97	CLEO	E^{ee}_{cm}= 10.6 GeV
• • • We do not use the following data for averages, fits, limits, etc. • • •					
0.987±0.057±0.027		BUSKULIC	95D	ALEP	Repl. by HEISTER 01E
0.95 ±0.11 ±0.05		[1] BUSKULIC	94D	ALEP	1990+1991 LEP run

[1] Superseded by BUSKULIC 95D.

$\xi(\rho)$ PARAMETER

($V-A$) theory predicts $\xi(\rho) = 1$.

VALUE	EVTS	DOCUMENT ID		TECN	COMMENT
0.994±0.008 OUR FIT					
0.994±0.009 OUR AVERAGE					
0.987±0.012±0.011	59k	HEISTER	01E	ALEP	1991–1995 LEP runs
0.99 ±0.12 ±0.04		ABE	97O	SLD	1993–1995 SLC runs
0.995±0.010±0.003	66k	ALEXANDER	97F	CLEO	E^{ee}_{cm}= 10.6 GeV
1.022±0.028±0.030	1.7k	[1] ALBRECHT	94E	ARG	E^{ee}_{cm}= 9.4–10.6 GeV
• • • We do not use the following data for averages, fits, limits, etc. • • •					
1.045±0.058±0.032		BUSKULIC	95D	ALEP	Repl. by HEISTER 01E
1.03 ±0.11 ±0.05		[2] BUSKULIC	94D	ALEP	1990+1991 LEP run

[1] ALBRECHT 94E measure the square of this quantity and use the sign determined by ALBRECHT 90I to obtain the quoted result.
[2] Superseded by BUSKULIC 95D.

$\xi(a_1)$ PARAMETER

($V-A$) theory predicts $\xi(a_1) = 1$.

VALUE	EVTS	DOCUMENT ID		TECN	COMMENT
1.001±0.027 OUR FIT					
1.002±0.028 OUR AVERAGE					
1.000±0.016±0.024	35k	[1] HEISTER	01E	ALEP	1991–1995 LEP runs
1.02 ±0.13 ±0.03	17.2k	ASNER	00	CLEO	E_{cm}^{ee}= 10.6 GeV
1.29 ±0.26 ±0.11	7.4k	[2] ACKERSTAFF	97R	OPAL	1992–1994 LEP runs
0.85 $^{+0.15}_{-0.17}$ ±0.05		ALBRECHT	95C	ARG	E_{cm}^{ee}= 9.5–10.6 GeV
1.25 ±0.23 $^{+0.15}_{-0.08}$	7.5k	ALBRECHT	93C	ARG	E_{cm}^{ee}= 9.4–10.6 GeV
• • • We do not use the following data for averages, fits, limits, etc. • • •					
1.08 $^{+0.46}_{-0.41}$ $^{+0.14}_{-0.25}$	2.6k	[3] AKERS	95P	OPAL	Repl. by ACKERSTAFF 97R
0.937±0.116±0.064		BUSKULIC	95D	ALEP	Repl. by HEISTER 01E

[1] HEISTER 01E quote 1.000 ± 0.016 ± 0.013 ± 0.020 where the errors are statistical, systematic, and an uncertainty due to the final state model. We combine the systematic error and model uncertainty.
[2] ACKERSTAFF 97R obtain this result with a model independent fit to the hadronic structure functions. Fitting with the model of Kuhn and Santamaria (ZPHY **C48**, 445 (1990)) gives 0.87 ± 0.16 ± 0.04, and with the model of of Isgur *et al.* (PR **D39**,1357 (1989)) they obtain 1.20 ± 0.21 ± 0.14.
[3] AKERS 95P obtain this result with a model independent fit to the hadronic structure functions. Fitting with the model of Kuhn and Santamaria (ZPHY **C48**, 445 (1990)) gives 0.87 ± 0.27 $^{+0.05}_{-0.06}$, and with the model of of Isgur *et al.* (PR **D39**,1357 (1989)) they obtain 1.10 ± 0.31 $^{+0.13}_{-0.14}$.

ξ(all hadronic modes) PARAMETER

($V-A$) theory predicts $\xi = 1$.

VALUE	EVTS	DOCUMENT ID		TECN	COMMENT
0.995±0.007 OUR FIT					
0.997±0.007 OUR AVERAGE					
0.992±0.007±0.008	102k	[1] HEISTER	01E	ALEP	1991–1995 LEP runs
0.997±0.027±0.011	39k	[2] ABREU	00L	DLPH	1992–1995 runs
1.02 ±0.13 ±0.03	17.2k	[3] ASNER	00	CLEO	E_{cm}^{ee}= 10.6 GeV
1.032±0.031	37k	[4] ACCIARRI	98R	L3	1991–1995 LEP runs
0.93 ±0.10 ±0.04		ABE	97O	SLD	1993–1995 SLC runs
1.29 ±0.26 ±0.11	7.4k	[5] ACKERSTAFF	97R	OPAL	1992–1994 LEP runs
0.995±0.010±0.003	66k	[6] ALEXANDER	97F	CLEO	E_{cm}^{ee}= 10.6 GeV
1.03 ±0.06 ±0.04	2.0k	[7] COAN	97	CLEO	E_{cm}^{ee}= 10.6 GeV
1.017±0.039		[8] ALBRECHT	95C	ARG	E_{cm}^{ee}= 9.5–10.6 GeV
1.25 ±0.23 $^{+0.15}_{-0.08}$	7.5k	[9] ALBRECHT	93C	ARG	E_{cm}^{ee}= 9.4–10.6 GeV
• • • We do not use the following data for averages, fits, limits, etc. • • •					
0.970±0.053±0.011	14k	[10] ACCIARRI	96H	L3	Repl. by ACCIARRI 98R
1.08 $^{+0.46}_{-0.41}$ $^{+0.14}_{-0.25}$	2.6k	[11] AKERS	95P	OPAL	Repl. by ACKERSTAFF 97R
1.006±0.032±0.019		[12] BUSKULIC	95D	ALEP	Repl. by HEISTER 01E
1.022±0.028±0.030	1.7k	[13] ALBRECHT	94E	ARG	E_{cm}^{ee}= 9.4–10.6 GeV
0.99 ±0.07 ±0.04		[14] BUSKULIC	94D	ALEP	1990+1991 LEP run
1.14 ±0.34 $^{+0.34}_{-0.17}$	3.9k	[9] ALBRECHT	90I	ARG	Repl. by ALBRECHT 93C

[1] HEISTER 01E quote 0.992 ± 0.007 ± 0.006 ± 0.005 where the errors are statistical, systematic, and an uncertainty due to the final state model. We combine the systematic error and model uncertainty. They use $\tau \to \pi\nu_\tau$, $\tau \to K\nu_\tau$, $\tau \to \rho\nu_\tau$, and $\tau \to a_1\nu_\tau$ decays.
[2] ABREU 00L use $\tau^- \to h^- \geq 0\pi^0\nu_\tau$ decays.
[3] ASNER 00 use $\tau^- \to \pi^- 2\pi^0\nu_\tau$ decays.
[4] ACCIARRI 98R use $\tau \to \pi\nu_\tau$, $\tau \to K\nu_\tau$, and $\tau \to \rho\nu_\tau$ decays.
[5] ACKERSTAFF 97R use $\tau \to a_1\nu_\tau$ decays.
[6] ALEXANDER 97F use $\tau \to \rho\nu_\tau$ decays.
[7] COAN 97 use h^+h^- energy correlations.
[8] Combined fit to ARGUS tau decay parameter measurements in ALBRECHT 95C, ALBRECHT 93G, and ALBRECHT 94E.
[9] Uses $\tau \to a_1\nu_\tau$ decays. Replaced by ALBRECHT 95C.
[10] ACCIARRI 96H use $\tau \to \pi\nu_\tau$, $\tau \to K\nu_\tau$, and $\tau \to \rho\nu_\tau$ decays.
[11] AKERS 95P use $\tau \to a_1\nu_\tau$ decays.
[12] BUSKULIC 95D use $\tau \to \pi\nu_\tau$, $\tau \to \rho\nu_\tau$, and $\tau \to a_1\nu_\tau$ decays.
[13] ALBRECHT 94E measure the square of this quantity and use the sign determined by ALBRECHT 90I to obtain the quoted result. Uses $\tau \to a_1\nu_\tau$ decays. Replaced by ALBRECHT 95C.
[14] BUSKULIC 94D use $\tau \to \pi\nu_\tau$ and $\tau \to \rho\nu_\tau$ decays. Superseded by BUSKULIC 95D.

$\overline{\eta}(\mu)$ PARAMETER

($V-A$) theory predicts $\overline{\eta}(\mu) = 0$.

VALUE	EVTS	DOCUMENT ID		TECN	COMMENT
−1.3±1.5±0.8	71K	[1] SHIMIZU	18A	BELL	$\tau^- \to \nu_\tau\mu^-\overline{\nu}_\mu\gamma$

[1] The measurement procedure fits a distribution affected by $\overline{\eta}(\mu)$, $\xi_\kappa(\mu)$ and $\eta''(\mu)$, floating $\overline{\eta}(\mu)$ and $\xi_\kappa(\mu)$ and fixing $\eta''(\mu)$=0. The contribution of $\eta''(\mu)$ is suppressed by m_μ/m_τ.

$\xi_\kappa(e)$ PARAMETER

($V-A$) theory predicts $\xi_\kappa(e) = 0$.

VALUE	EVTS	DOCUMENT ID		TECN	COMMENT
−0.4±0.8±0.9	78K	[1] SHIMIZU	18A	BELL	$\tau^- \to \nu_\tau e^-\overline{\nu}_e\gamma$

[1] The measurement procedure fits a distribution affected by $\overline{\eta}(e)$, $\xi_\kappa(e)$ and $\eta''(e)$, floating $\xi_\kappa(e)$ and fixing $\overline{\eta}(e)$=0 and $\eta''(e)$=0. The contribution of $\eta''(e)$ is suppressed by m_e/m_τ.

$\xi_\kappa(\mu)$ PARAMETER

($V-A$) theory predicts $\xi_\kappa(\mu) = 0$.

VALUE	EVTS	DOCUMENT ID		TECN	COMMENT
0.8±0.5±0.3	71K	[1] SHIMIZU	18A	BELL	$\tau^- \to \nu_\tau\mu^-\overline{\nu}_\mu\gamma$

[1] The measurement procedure fits a distribution affected by $\overline{\eta}(\mu)$, $\xi_\kappa(\mu)$ and $\eta''(\mu)$, floating $\overline{\eta}(\mu)$ and $\xi_\kappa(\mu)$ and fixing $\eta''(\mu)$=0. The contribution of $\eta''(\mu)$ is suppressed by m_μ/m_τ.

τ REFERENCES

SHIMIZU	18A	PTEP 2018 023C01	N. Shimizu *et al.*	(BELLE Collab.)
AAD	16BA	EPJ C76 232	G.Aad *et al.*	(ATLAS Collab.)
AAIJ	15AI	JHEP 1502 121	R. Aaij *et al.*	(LHCb Collab.)
LEES	15G	PR D91 051103	J.P. Lees *et al.*	(Babar)
ABLIKIM	14D	PR D90 012001	M. Ablikim *et al.*	(BES III Collab.)
BELOUS	14	PRL 112 031801	K. Belous *et al.*	(BELLE Collab.)
RYU	14	PR D89 072009	S. Ryu *et al.*	(BELLE Collab.)
AAIJ	13AH	PL B724 36	R. Aaij *et al.*	(LHCb Collab.)
MIYAZAKI	13	PL B719 346	Y. Miyazaki *et al.*	(BELLE Collab.)
LEES	12M	PR D85 031102	J.P. Lees *et al.*	(BABAR Collab.)
Also		PR D85 099904 (errat.)	J.P. Lees *et al.*	(BABAR Collab.)
LEES	12X	PR D86 092010	J.P. Lees *et al.*	(BABAR Collab.)
LEES	12Y	PR D86 092013	J.P. Lees *et al.*	(BABAR Collab.)
PDG	12	PR D86 010001	J. Beringer *et al.*	(PDG Collab.)
DEL-AMO-SA...	11E	PR D83 032002	P. del Amo Sanchez *et al.*	(BABAR Collab.)
MIYAZAKI	11	PL B699 251	Y. Miyazaki *et al.*	(BELLE Collab.)
AUBERT	10B	PRL 104 021802	B. Aubert *et al.*	(BABAR Collab.)
AUBERT	10F	PRL 105 051602	B. Aubert *et al.*	(BABAR Collab.)
HAYASAKA	10	PL B687 139	K. Hayasaka *et al.*	(BELLE Collab.)
LEE	10	PR D81 113007	M.J. Lee *et al.*	(BELLE Collab.)
LEES	10A	PR D81 111101	J.P. Lees *et al.*	(BABAR Collab.)
MIYAZAKI	10	PL B682 355	Y. Miyazaki *et al.*	(BELLE Collab.)
MIYAZAKI	10A	PL B692 4	Y. Miyazaki *et al.*	(BELLE Collab.)
AUBERT	09AK	PR D80 092005	B. Aubert *et al.*	(BABAR Collab.)
AUBERT	09D	PR D79 012004	B. Aubert *et al.*	(BABAR Collab.)
AUBERT	09W	PRL 103 021801	B. Aubert *et al.*	(BABAR Collab.)
GROZIN	09A	PAN 72 1203	A.G. Grozin, I.B. Khriplovich, A.S. Rudenko	(NOVO)
INAMI	09	PL B672 209	K. Inami *et al.*	(BELLE Collab.)
MIYAZAKI	09	PL B672 317	Y. Miyazaki *et al.*	(BELLE Collab.)
AUBERT	08	PRL 100 011801	B. Aubert *et al.*	(BABAR Collab.)
AUBERT	08AE	PR D77 112002	B. Aubert *et al.*	(BABAR Collab.)
AUBERT	08K	PRL 100 071802	B. Aubert *et al.*	(BABAR Collab.)
FUJIKAWA	08	PR D78 072006	M. Fujikawa *et al.*	(BELLE Collab.)
HAYASAKA	08	PL B666 16	K. Hayasaka *et al.*	(BELLE Collab.)
MIYAZAKI	08	PL B660 154	Y. Miyazaki *et al.*	(BELLE Collab.)
NISHIO	08	PL B664 35	Y. Nishio *et al.*	(BELLE Collab.)
ANASHIN	07	JETPL 85 347 Translated from ZETFP 85 429.	V.V. Anashin *et al.*	(KEDR Collab.)
AUBERT	07AP	PR D76 051104	B. Aubert *et al.*	(BABAR Collab.)
AUBERT	07BK	PRL 99 251803	B. Aubert *et al.*	(BABAR Collab.)
AUBERT	07I	PRL 98 061803	B. Aubert *et al.*	(BABAR Collab.)
BELOUS	07	PRL 99 011801	K. Belous *et al.*	(BELLE Collab.)
EIDELMAN	07	MPL A22 159	S. Eidelman, M. Passera	(NOVO, PADO)
EPIFANOV	07	PL B654 65	D. Epifanov *et al.*	(BELLE Collab.)
MIYAZAKI	07	PL B648 341	Y. Miyazaki *et al.*	(BELLE Collab.)
ABDALLAH	06A	EPJ C46 1	J. Abdallah *et al.*	(DELPHI Collab.)
AUBERT	06C	PRL 96 041801	B. Aubert *et al.*	(BABAR Collab.)
AUBERT,B	06	PR D73 112003	B. Aubert *et al.*	(BABAR Collab.)
INAMI	06	PL B643 5	K. Inami *et al.*	(BELLE Collab.)
MIYAZAKI	06	PL B632 51	Y. Miyazaki *et al.*	(BELLE Collab.)
MIYAZAKI	06A	PL B639 159	Y. Miyazaki *et al.*	(BELLE Collab.)
PDG	06	JP G33 1	W.-M. Yao *et al.*	(PDG Collab.)
YUSA	06	PL B640 138	Y. Yusa *et al.*	(BELLE Collab.)
ARMS	05	PRL 94 241802	K. Arms *et al.*	(CLEO Collab.)
AUBERT,B	05A	PRL 95 041802	B. Aubert *et al.*	(BABAR Collab.)
AUBERT,B	05F	PR D72 012003	B. Aubert *et al.*	(BABAR Collab.)
AUBERT,B	05W	PR D72 072001	B. Aubert *et al.*	(BABAR Collab.)
AUBERT,BE	05D	PRL 95 191801	B. Aubert *et al.*	(BABAR Collab.)
ENARI	05	PL B622 218	Y. Enari *et al.*	(BELLE Collab.)
HAYASAKA	05	PL B613 20	K. Hayasaka *et al.*	(BELLE Collab.)
SCHAEL	05C	PRPL 421 191	S. Schael *et al.*	(ALEPH Collab.)
ABBIENDI	04J	EPJ C35 437	G. Abbiendi *et al.*	(OPAL Collab.)
ABDALLAH	04K	EPJ C35 159	J. Abdallah *et al.*	(DELPHI Collab.)
ABDALLAH	04T	EPJ C36 283	J. Abdallah *et al.*	(DELPHI Collab.)
ABE	04B	PRL 92 171802	K. Abe *et al.*	(BELLE Collab.)
ACHARD	04G	PL B585 53	P. Achard *et al.*	(L3 Collab.)
AUBERT	04J	PRL 92 121801	B. Aubert *et al.*	(BABAR Collab.)
ENARI	04	PRL 93 081803	Y. Enari *et al.*	(BELLE Collab.)
PDG	04	PL B592 1	S. Eidelman *et al.*	(PDG Collab.)
YUSA	04	PL B589 103	Y. Yusa *et al.*	(BELLE Collab.)
ABBIENDI	03	PL B551 35	G. Abbiendi *et al.*	(OPAL Collab.)
BRIERE	03	PRL 90 181802	R. A. Briere *et al.*	(CLEO Collab.)
HEISTER	03F	EPJ C30 291	A. Heister *et al.*	(ALEPH Collab.)
INAMI	03	PL B551 16	K. Inami *et al.*	(BELLE Collab.)
CHEN	02C	PR D66 071101	S. Chen *et al.*	(CLEO Collab.)
REGAN	02	PRL 88 071805	B.C. Regan *et al.*	
ABBIENDI	01J	EPJ C19 653	G. Abbiendi *et al.*	(OPAL Collab.)
ABREU	01M	EPJ C20 617	P. Abreu *et al.*	(DELPHI Collab.)
ACCIARRI	01F	PL B507 47	M. Acciarri *et al.*	(L3 Collab.)
ACHARD	01D	PL B519 189	P. Achard *et al.*	(L3 Collab.)
ANASTASSOV	01	PRL 86 4467	A. Anastassov *et al.*	(CLEO Collab.)
HEISTER	01E	EPJ C22 217	A. Heister *et al.*	(ALEPH Collab.)
ABBIENDI	00A	PL B492 23	G. Abbiendi *et al.*	(OPAL Collab.)
ABBIENDI	00C	EPJ C13 213	G. Abbiendi *et al.*	(OPAL Collab.)
ABBIENDI	00D	EPJ C13 197	G. Abbiendi *et al.*	(OPAL Collab.)
ABREU	00L	EPJ C16 229	P. Abreu *et al.*	(DELPHI Collab.)
ACCIARRI	00B	PL B479 67	M. Acciarri *et al.*	(L3 Collab.)
AHMED	00	PR D61 071101	S. Ahmed *et al.*	(CLEO Collab.)
ALBRECHT	00	PL B485 37	H. Albrecht *et al.*	(ARGUS Collab.)
ASNER	00	PR D61 012002	D.M. Asner *et al.*	(CLEO Collab.)
ASNER	00B	PR D62 072006	D.M. Asner *et al.*	(CLEO Collab.)
BERGFELD	00	PRL 84 830	T. Bergfeld *et al.*	(CLEO Collab.)
BROWDER	00	PR D61 052004	T.E. Browder *et al.*	(CLEO Collab.)
EDWARDS	00A	PR D61 072003	K.W. Edwards *et al.*	(CLEO Collab.)
GONZALEZ-S...	00	NP B582 3	G.A. Gonzalez-Sprinberg *et al.*	
ABBIENDI	99H	PL B447 134	G. Abbiendi *et al.*	(OPAL Collab.)

ABREU 99X EPJ C10 201 P. Abreu *et al.* (DELPHI Collab.)
ACKERSTAFF 99D EPJ C8 3 K. Ackerstaff *et al.* (OPAL Collab.)
ACKERSTAFF 99E EPJ C8 183 K. Ackerstaff *et al.* (OPAL Collab.)
BARATE 99K EPJ C10 1 R. Barate *et al.* (ALEPH Collab.)
BARATE 99R EPJ C11 599 R. Barate *et al.* (ALEPH Collab.)
BISHAI 99 PRL 82 281 M. Bishai *et al.* (CLEO Collab.)
GODANG 99 PR D59 091303 R. Godang *et al.* (CLEO Collab.)
RICHICHI 99 PR D60 112002 S.J. Richichi *et al.* (CLEO Collab.)
ACCIARRI 98C PL B426 207 M. Acciarri *et al.* (L3 Collab.)
ACCIARRI 98E PL B434 169 M. Acciarri *et al.* (L3 Collab.)
ACCIARRI 98R PL B438 405 M. Acciarri *et al.* (L3 Collab.)
ACKERSTAFF 98M EPJ C4 193 K. Ackerstaff *et al.* (OPAL Collab.)
ACKERSTAFF 98N PL B431 188 K. Ackerstaff *et al.* (OPAL Collab.)
ALBRECHT 98 PL B431 179 H. Albrecht *et al.* (ARGUS Collab.)
BARATE 98 EPJ C1 65 R. Barate *et al.* (ALEPH Collab.)
BARATE 98E EPJ C4 29 R. Barate *et al.* (ALEPH Collab.)
BLISS 98 PR D57 5903 D.W. Bliss *et al.* (CLEO Collab.)
ABE 97O PRL 78 4691 K. Abe *et al.* (SLD Collab.)
ACKERSTAFF 97J PL B404 213 K. Ackerstaff *et al.* (OPAL Collab.)
ACKERSTAFF 97L ZPHY C74 403 K. Ackerstaff *et al.* (OPAL Collab.)
ACKERSTAFF 97R ZPHY C75 593 K. Ackerstaff *et al.* (OPAL Collab.)
ALEXANDER 97F PR D56 5320 J.P. Alexander *et al.* (CLEO Collab.)
AMMAR 97B PRL 78 4686 R. Ammar *et al.* (CLEO Collab.)
ANASTASSOV 97 PR D55 2559 A. Anastassov *et al.* (CLEO Collab.)
Also PR D58 119903 (erratum) A. Anastassov *et al.* (CLEO Collab.)
ANDERSON 97 PRL 79 3814 S. Anderson *et al.* (CLEO Collab.)
AVERY 97 PR D55 1119 P. Avery *et al.* (CLEO Collab.)
BARATE 97I ZPHY C74 387 R. Barate *et al.* (ALEPH Collab.)
BARATE 97R PL B414 362 R. Barate *et al.* (ALEPH Collab.)
BERGFELD 97 PRL 79 2406 T. Bergfeld *et al.* (CLEO Collab.)
BONVICINI 97 PRL 79 1221 G. Bonvicini *et al.* (CLEO Collab.)
BUSKULIC 97C ZPHY C74 263 D. Buskulic *et al.* (ALEPH Collab.)
COAN 97 PR D55 7291 T.E. Coan *et al.* (CLEO Collab.)
EDWARDS 97 PR D55 3919 K.W. Edwards *et al.* (CLEO Collab.)
EDWARDS 97B PR D56 5297 K.W. Edwards *et al.* (CLEO Collab.)
ESCRIBANO 97 PL B395 369 R. Escribano, E. Masso (BARC, PARIT)
ABREU 96B PL B365 448 P. Abreu *et al.* (DELPHI Collab.)
ACCIARRI 96H PL B377 313 M. Acciarri *et al.* (L3 Collab.)
ACCIARRI 96K PL B389 187 M. Acciarri *et al.* (L3 Collab.)
ALAM 96 PRL 76 2637 M.S. Alam *et al.* (CLEO Collab.)
ALBRECHT 96E PRPL 276 223 H. Albrecht *et al.* (ARGUS Collab.)
ALEXANDER 96D PL B369 163 G. Alexander *et al.* (OPAL Collab.)
ALEXANDER 96E PL B374 341 G. Alexander *et al.* (OPAL Collab.)
ALEXANDER 96S PL B388 437 G. Alexander *et al.* (OPAL Collab.)
BAI 96 PR D53 20 J.Z. Bai *et al.* (BES Collab.)
BALEST 96 PL B388 402 R. Balest *et al.* (CLEO Collab.)
BARTELT 96 PRL 76 4119 J.E. Bartelt *et al.* (CLEO Collab.)
BUSKULIC 96 ZPHY C70 579 D. Buskulic *et al.* (ALEPH Collab.)
BUSKULIC 96C ZPHY C70 561 D. Buskulic *et al.* (ALEPH Collab.)
COAN 96 PR D53 6037 T.E. Coan *et al.* (CLEO Collab.)
ABE 95Y PR D52 4828 K. Abe *et al.* (SLD Collab.)
ABREU 95T PL B357 715 P. Abreu *et al.* (DELPHI Collab.)
ABREU 95U PL B359 411 P. Abreu *et al.* (DELPHI Collab.)
ACCIARRI 95 PL B345 93 M. Acciarri *et al.* (L3 Collab.)
ACCIARRI 95F PL B352 487 M. Acciarri *et al.* (L3 Collab.)
AKERS 95F ZPHY C66 31 R. Akers *et al.* (OPAL Collab.)
AKERS 95I ZPHY C66 543 R. Akers *et al.* (OPAL Collab.)
AKERS 95P ZPHY C67 45 R. Akers *et al.* (OPAL Collab.)
AKERS 95Y ZPHY C68 555 R. Akers *et al.* (OPAL Collab.)
ALBRECHT 95 PL B341 441 H. Albrecht *et al.* (ARGUS Collab.)
ALBRECHT 95C PL B349 576 H. Albrecht *et al.* (ARGUS Collab.)
ALBRECHT 95G ZPHY C68 25 H. Albrecht *et al.* (ARGUS Collab.)
ALBRECHT 95H ZPHY C68 215 H. Albrecht *et al.* (ARGUS Collab.)
BALEST 95C PRL 75 3809 R. Balest *et al.* (CLEO Collab.)
BERNABEU 95 NP B436 474 J. Bernabeu *et al.*
BUSKULIC 95C PL B346 371 D. Buskulic *et al.* (ALEPH Collab.)
BUSKULIC 95D PL B346 379 D. Buskulic *et al.* (ALEPH Collab.)
Also PL B363 265 (erratum) D. Buskulic *et al.* (ALEPH Collab.)
ABREU 94K PL B334 435 P. Abreu *et al.* (DELPHI Collab.)
AKERS 94E PL B328 207 R. Akers *et al.* (OPAL Collab.)
AKERS 94G PL B339 278 R. Akers *et al.* (OPAL Collab.)
ALBRECHT 94E PL B337 383 H. Albrecht *et al.* (ARGUS Collab.)
ARTUSO 94 PRL 72 3762 M. Artuso *et al.* (CLEO Collab.)
BARTELT 94 PRL 73 1890 J.E. Bartelt *et al.* (CLEO Collab.)
BATTLE 94 PRL 73 1079 M. Battle *et al.* (CLEO Collab.)
BAUER 94 PR D50 13 D.A. Bauer *et al.* (TPC/2gamma Collab.)
BUSKULIC 94D PL B321 168 D. Buskulic *et al.* (ALEPH Collab.)
BUSKULIC 94E PL B332 209 D. Buskulic *et al.* (ALEPH Collab.)
BUSKULIC 94F PL B332 219 D. Buskulic *et al.* (ALEPH Collab.)
GIBAUT 94B PRL 73 934 D. Gibaut *et al.* (CLEO Collab.)
ADRIANI 93M PRPL 236 1 O. Adriani *et al.* (L3 Collab.)
ALBRECHT 93C ZPHY C58 61 H. Albrecht *et al.* (ARGUS Collab.)
ALBRECHT 93G PL B316 608 H. Albrecht *et al.* (ARGUS Collab.)
BALEST 93 PR D47 3671 R. Balest *et al.* (CLEO Collab.)
BEAN 93 PRL 70 138 A. Bean *et al.* (CLEO Collab.)
BORTOLETTO 93 PRL 71 1791 D. Bortoletto *et al.* (CLEO Collab.)
ESCRIBANO 93 PL B301 419 R. Escribano, E. Masso (BARC)
PROCARIO 93 PRL 70 1207 M. Procario *et al.* (CLEO Collab.)
ABREU 92N ZPHY C55 555 P. Abreu *et al.* (DELPHI Collab.)
ACTON 92F PL B281 405 D.P. Acton *et al.* (OPAL Collab.)
ACTON 92H PL B288 373 P.D. Acton *et al.* (OPAL Collab.)
AKERIB 92 PRL 69 3610 D.S. Akerib *et al.* (CLEO Collab.)
Also PRL 71 3395 (erratum) D.S. Akerib *et al.* (CLEO Collab.)
ALBRECHT 92D ZPHY C53 367 H. Albrecht *et al.* (ARGUS Collab.)
ALBRECHT 92K ZPHY C55 179 H. Albrecht *et al.* (ARGUS Collab.)
ALBRECHT 92M PL B292 221 H. Albrecht *et al.* (ARGUS Collab.)
ALBRECHT 92Q ZPHY C56 339 H. Albrecht *et al.* (ARGUS Collab.)
AMMAR 92 PR D45 3976 R. Ammar *et al.* (CLEO Collab.)
ARTUSO 92 PRL 69 3278 M. Artuso *et al.* (CLEO Collab.)
BAI 92 PRL 69 3021 J.Z. Bai *et al.* (BES Collab.)
BATTLE 92 PL B291 488 M. Battle *et al.* (CLEO Collab.)
BUSKULIC 92J PL B297 459 D. Buskulic *et al.* (ALEPH Collab.)
DECAMP 92C ZPHY C54 211 D. Decamp *et al.* (ALEPH Collab.)
ADEVA 91F PL B265 451 B. Adeva *et al.* (L3 Collab.)
ALBRECHT 91D PL B260 259 H. Albrecht *et al.* (ARGUS Collab.)
ALEXANDER 91D PL B266 201 G. Alexander *et al.* (OPAL Collab.)
ANTREASYAN 91 PL B259 216 D. Antreasyan *et al.* (Crystal Ball Collab.)
GRIFOLS 91 PL B255 611 J.A. Grifols, A. Mendez (BARC)
ABACHI 90 PR D41 1414 S. Abachi *et al.* (HRS Collab.)
ALBRECHT 90E PL B246 278 H. Albrecht *et al.* (ARGUS Collab.)
ALBRECHT 90I PL B250 164 H. Albrecht *et al.* (ARGUS Collab.)
BEHREND 90 ZPHY C46 537 H.J. Behrend *et al.* (CELLO Collab.)
BOWCOCK 90 PR D41 805 T.J.V. Bowcock *et al.* (CLEO Collab.)
DELAGUILA 90 PL B252 116 F. del Aguila, M. Sher (BARC, WILL)
GOLDBERG 90 PL B251 223 M. Goldberg *et al.* (CLEO Collab.)
WU 90 PR D41 2339 D.Y. Wu *et al.* (Mark II Collab.)
ABACHI 89B PR D40 902 S. Abachi *et al.* (HRS Collab.)
BEHREND 89B PL B222 163 H.J. Behrend *et al.* (CELLO Collab.)
JANSSEN 89 PL B228 273 H. Janssen *et al.* (Crystal Ball Collab.)
KLEINWORT 89 ZPHY C42 7 C. Kleinwort *et al.* (JADE Collab.)
ADEVA 88 PR D38 2665 B. Adeva *et al.* (Mark-J Collab.)
ALBRECHT 88B PL B202 149 H. Albrecht *et al.* (ARGUS Collab.)
ALBRECHT 88L ZPHY C41 1 H. Albrecht *et al.* (ARGUS Collab.)
ALBRECHT 88M ZPHY C41 405 H. Albrecht *et al.* (ARGUS Collab.)
AMIDEI 88 PR D37 1750 D. Amidei *et al.* (Mark II Collab.)
BEHREND 88 PL B200 226 H.J. Behrend *et al.* (CELLO Collab.)
BRAUNSCH... 88C ZPHY C39 331 W. Braunschweig *et al.* (TASSO Collab.)
KEH 88 PL B212 123 S. Keh *et al.* (Crystal Ball Collab.)
TSCHIRHART 88 PL B205 407 R. Tschirhart *et al.* (HRS Collab.)
ABACHI 87B PL B197 291 S. Abachi *et al.* (HRS Collab.)
ABACHI 87C PRL 59 2519 S. Abachi *et al.* (HRS Collab.)
ADLER 87B PRL 59 1527 J. Adler *et al.* (Mark III Collab.)
AIHARA 87B PR D35 1553 H. Aihara *et al.* (TPC Collab.)
AIHARA 87C PRL 59 751 H. Aihara *et al.* (TPC Collab.)
ALBRECHT 87L PL B185 223 H. Albrecht *et al.* (ARGUS Collab.)
ALBRECHT 87P PL B199 580 H. Albrecht *et al.* (ARGUS Collab.)
BAND 87 PL B198 297 H.R. Band *et al.* (MAC Collab.)
BAND 87B PRL 59 415 H.R. Band *et al.* (MAC Collab.)
BARINGER 87 PRL 59 1993 P. Baringer *et al.* (CLEO Collab.)
BEBEK 87C PR D36 690 C. Bebek *et al.* (CLEO Collab.)
BURCHAT 87 PR D35 27 P.R. Burchat *et al.* (Mark II Collab.)
BYLSMA 87 PR D35 2269 B.G. Bylsma *et al.* (HRS Collab.)
COFFMAN 87 PR D36 2185 D.M. Coffman *et al.* (Mark III Collab.)
DERRICK 87 PL B189 260 M. Derrick *et al.* (HRS Collab.)
FORD 87 PR D35 408 W.T. Ford *et al.* (MAC Collab.)
FORD 87B PR D36 1971 W.T. Ford *et al.* (MAC Collab.)
GAN 87 PRL 59 411 K.K. Gan *et al.* (Mark II Collab.)
GAN 87B PL B197 561 K.K. Gan *et al.* (Mark II Collab.)
AIHARA 86E PRL 57 1836 H. Aihara *et al.* (TPC Collab.)
BARTEL 86D PL B182 216 W. Bartel *et al.* (JADE Collab.)
PDG 86 PL 170B 1 M. Aguilar-Benitez *et al.* (CERN, CIT+)
RUCKSTUHL 86 PRL 56 2132 W. Ruckstuhl *et al.* (DELCO Collab.)
SCHMIDKE 86 PRL 57 527 W.B. Schmidke *et al.* (Mark II Collab.)
YELTON 86 PRL 56 812 J.M. Yelton *et al.* (Mark II Collab.)
ALTHOFF 85 ZPHY C26 521 M. Althoff *et al.* (TASSO Collab.)
ASH 85B PRL 55 2118 W.W. Ash *et al.* (MAC Collab.)
BALTRUSAIT... 85 PRL 55 1842 R.M. Baltrusaitis *et al.* (Mark III Collab.)
BARTEL 85F PL 161B 188 W. Bartel *et al.* (JADE Collab.)
BEHRENDS 85 PR D32 2468 S. Behrends *et al.* (CLEO Collab.)
BELTRAMI 85 PRL 54 1775 I. Beltrami *et al.* (HRS Collab.)
BERGER 85 ZPHY C28 1 C. Berger *et al.* (PLUTO Collab.)
BURCHAT 85 PRL 54 2489 P.R. Burchat *et al.* (Mark II Collab.)
FERNANDEZ 85 PRL 54 1624 E. Fernandez *et al.* (MAC Collab.)
MILLS 85 PRL 54 624 G.B. Mills *et al.* (DELCO Collab.)
AIHARA 84C PR D30 2436 H. Aihara *et al.* (TPC Collab.)
BEHREND 84 ZPHY C23 103 H.J. Behrend *et al.* (CELLO Collab.)
MILLS 84 PRL 52 1944 G.B. Mills *et al.* (DELCO Collab.)
BEHREND 83C PL 127B 270 H.J. Behrend *et al.* (CELLO Collab.)
SILVERMAN 83 PR D27 1196 D.J. Silverman, G.L. Shaw (UCI)
BEHREND 82 PL 114B 282 H.J. Behrend *et al.* (CELLO Collab.)
BLOCKER 82B PRL 48 1586 C.A. Blocker *et al.* (Mark II Collab.)
BLOCKER 82D PL 109B 119 C.A. Blocker *et al.* (Mark II Collab.) J
FELDMAN 82 PRL 48 66 G.J. Feldman *et al.* (Mark II Collab.)
HAYES 82 PR D25 2869 K.G. Hayes *et al.* (Mark II Collab.)
BERGER 81B PL 99B 489 C. Berger *et al.* (PLUTO Collab.)
DORFAN 81 PRL 46 215 J.M. Dorfan *et al.* (Mark II Collab.)
BRANDELIK 80 PL 92B 199 R. Brandelik *et al.* (TASSO Collab.)
ZHOLENTZ 80 PL 96B 214 A.A. Zholents *et al.* (NOVO)
Also SJNP 34 814 A.A. Zholents *et al.* (NOVO)
Translated from YAF 34 1471.
BACINO 79B PRL 42 749 W.J. Bacino *et al.* (DELCO Collab.)
KIRKBY 79 SLAC-PUB-2419 J. Kirkby (SLAC) J
Batavia Lepton Photon Conference.
BACINO 78B PRL 41 13 W.J. Bacino *et al.* (DELCO Collab.) J
Also Tokyo Conf. 249 J. Kirz (STON)
Also PL 96B 214 A.A. Zholents *et al.* (NOVO)
BRANDELIK 78 PL 73B 109 R. Brandelik *et al.* (DASP Collab.) J
FELDMAN 78 Tokyo Conf. 777 G.J. Feldman (SLAC) J
JAROS 78 PRL 40 1120 J. Jaros *et al.* (LGW Collab.)
PERL 75 PRL 35 1489 M.L. Perl *et al.* (LBL, SLAC)

OTHER RELATED PAPERS

DAVIER 06 RMP 78 1043 M. Davier, A. Hocker, Z. Zhang (LALO, PARIN+)
RAHAL-CAL... 98 IJMP A13 695 G. Rahal-Callot (ETH)
GENTILE 96 PRPL 274 287 S. Gentile, M. Pohl (ROMAI, ETH)
WEINSTEIN 93 ARNPS 43 457 A.J. Weinstein, R. Stroynowski (CIT, SMU)
PERL 92 RPP 55 653 M.L. Perl (SLAC)
PICH 90 MPL A5 1995 A. Pich (VALE)
BARISH 88 PRPL 157 1 B.C. Barish, R. Stroynowski (CIT)
GAN 88 IJMP A3 531 K.K. Gan, M.L. Perl (SLAC)
HAYES 88 PR D38 3351 K.G. Hayes, M.L. Perl (SLAC)
PERL 80 ARNPS 30 299 M.L. Perl (SLAC)

Heavy Charged Lepton Searches

Charged Heavy Lepton MASS LIMITS

Sequential Charged Heavy Lepton ($L^{\pm}$) MASS LIMITS

These experiments assumed that a fourth generation $L^{\pm}$ decayed to a fourth generation ν_L (or L^0) where ν_L was stable, or that $L^{\pm}$ decays to a light ν_ℓ via mixing.

See the "Quark and Lepton Compositeness, Searches for" Listings for limits on radiatively decaying excited leptons, *i.e.* $\ell^* \to \ell\gamma$. See the "WIMPs and other Particle Searches" section for heavy charged particle search limits in which the charged particle could be a lepton.

VALUE (GeV)	*CL%*	*DOCUMENT ID*		*TECN*	*COMMENT*
>100.8	95	ACHARD	01B	L3	Decay to νW
>101.9	95	ACHARD	01B	L3	$m_L - m_{L^0} > 15$ GeV
• • • We do not use the following data for averages, fits, limits, etc. • • •					
> 81.5	95	ACKERSTAFF	98C	OPAL	Assumed $m_{L^\pm} - m_{L^0} > 8.4$ GeV
> 80.2	95	ACKERSTAFF	98C	OPAL	$m_{L^0} > m_{L^\pm}$ and $L^\pm \to \nu W$
< 48 or > 61	95	[1] ACCIARRI	96G	L3	
> 63.9	95	ALEXANDER	96P	OPAL	Decay to massless ν's
> 63.5	95	BUSKULIC	96S	ALEP	$m_L - m_{L^0} > 7$ GeV
> 65	95	BUSKULIC	96S	ALEP	Decay to massless ν's
none 10–225		[2] AHMED	94	CNTR	H1 Collab. at HERA

Lepton Particle Listings

Heavy Charged Lepton Searches, Neutrino Properties

none 12.6–29.6	95	KIM	91B	AMY	Massless ν assumed
$>$ 44.3	95	AKRAWY	90G	OPAL	
none 0.5–10	95	[3] RILES	90	MRK2	For $(m_{L^0}$-$m_{L^0})>$ 0.25–0.4GeV
$>$ 8		[4] STOKER	89	MRK2	For $(m_{L^+} - m_{L^0})=$ 0.4 GeV
$>$ 12		[4] STOKER	89	MRK2	For m_{L^0}=0.9 GeV
none 18.4–27.6	95	[5] ABE	88	VNS	
$>$ 25.5	95	[6] ADACHI	88B	TOPZ	
none 1.5–22.0	95	BEHREND	88C	CELL	
$>$ 41	90	[7] ALBAJAR	87B	UA1	
$>$ 22.5	95	[8] ADEVA	85	MRKJ	
$>$ 18.0	95	[9] BARTEL	83	JADE	
none 4–14.5	95	[10] BERGER	81B	PLUT	
$>$ 15.5	95	[11] BRANDELIK	81	TASS	
$>$ 13.		[12] AZIMOV	80		
$>$ 16.	95	[13] BARBER	80B	CNTR	
$>$ 0.490		[14] ROTHE	69	RVUE	

[1] ACCIARRI 96G assumes LEP result that the associated neutral heavy lepton mass $>$ 40 GeV.

[2] The AHMED 94 limits are from a search for neutral and charged sequential heavy leptons at HERA via the decay channels $L^- \to e\gamma$, $L^- \to \nu W^-$, $L^- \to eZ$; and $L^0 \to \nu\gamma$, $L^0 \to e^- W^+$, $L^- \to \nu Z$, where the W decays to $\ell\nu_\ell$, or to jets, and Z decays to $\ell^+\ell^-$ or jets.

[3] RILES 90 limits were the result of a special analysis of the data in the case where the mass difference $m_{L^-} - m_{L^0}$ was allowed to be quite small, where L^0 denotes the neutrino into which the sequential charged lepton decays. With a slightly reduced $m_{L^\pm}$ range, the mass difference extends to about 4 GeV.

[4] STOKER 89 (Mark II at PEP) gives bounds on charged heavy lepton (L^+) mass for the generalized case in which the corresponding neutral heavy lepton (L^0) in the SU(2) doublet is not of negligible mass.

[5] ABE 88 search for L^+ and $L^- \to$ hadrons looking for acoplanar jets. The bound is valid for $m_\nu < 10$ GeV.

[6] ADACHI 88B search for hadronic decays giving acoplanar events with large missing energy. $E_{cm}{}^{ee} = 52$ GeV.

[7] Assumes associated neutrino is approximately massless.

[8] ADEVA 85 analyze one-isolated-muon data and sensitive to τ $<$10 nanosec. Assume B(lepton) = 0.30. E_{cm} = 40–47 GeV.

[9] BARTEL 83 limit is from PETRA e^+e^- experiment with average E_{cm} = 34.2 GeV.

[10] BERGER 81B is DESY DORIS and PETRA experiment. Looking for $e^+e^- \to L^+L^-$.

[11] BRANDELIK 81 is DESY-PETRA experiment. Looking for $e^+e^- \to L^+L^-$.

[12] AZIMOV 80 estimated probabilities for $M+N$ type events in $e^+e^- \to L^+L^-$ deducing semi-hadronic decay multiplicities of L from e^+e^- annihilation data at $E_{cm} = (2/3)m_L$. Obtained above limit comparing these with e^+e^- data (BRANDELIK 80).

[13] BARBER 80B looked for $e^+e^- \to L^+L^-$, $L \to \nu_L^+ X$ with MARK-J at DESY-PETRA.

[14] ROTHE 69 examines previous data on μ pair production and π and K decays.

Stable Charged Heavy Lepton ($L^\pm$) MASS LIMITS

VALUE (GeV)	CL%	DOCUMENT ID		TECN
>102.6	95	ACHARD	01B	L3
• • • We do not use the following data for averages, fits, limits, etc. • • •				
$>$ 28.2	95	[15] ADACHI	90C	TOPZ
none 18.5–42.8	95	AKRAWY	90O	OPAL
$>$ 26.5	95	DECAMP	90F	ALEP
none m_μ–36.3	95	SODERSTROM	90	MRK2

[15] ADACHI 90C put lower limits on the mass of stable charged particles with electric charge Q satisfying $2/3 < Q/e < 4/3$ and with spin 0 or 1/2. We list here the special case for a stable charged heavy lepton.

Charged Long-Lived Heavy Lepton MASS LIMITS

VALUE (GeV)	CL%	DOCUMENT ID		TECN	CHG	COMMENT
• • • We do not use the following data for averages, fits, limits, etc. • • •						
>574	95	CHATRCHYAN	13AB	CMS		Leptons singlet model
>102.0	95	ABBIENDI	03L	OPAL		pair produced in e^+e^-
$>$ 0.1		[16] ANSORGE	73B	HBC	–	Long-lived
none 0.55–4.5		[17] BUSHNIN	73	CNTR	–	Long-lived
none 0.2–0.92		[18] BARNA	68	CNTR	–	Long-lived
none 0.97–1.03		[18] BARNA	68	CNTR	–	Long-lived

[16] ANSORGE 73B looks for electron pair production and electron-like Bremsstrahlung.

[17] BUSHNIN 73 is SERPUKHOV 70 GeV p experiment. Masses assume mean life above 7×10^{-10} and 3×10^{-8} respectively. Calculated from cross section (see "Charged Quasi-Stable Lepton Production Differential Cross Section" below) and 30 GeV muon pair production data.

[18] BARNA 68 is SLAC photoproduction experiment.

Doubly-Charged Heavy Lepton MASS LIMITS

VALUE (GeV)	CL%	DOCUMENT ID		TECN	CHG
• • • We do not use the following data for averages, fits, limits, etc. • • •					
none 1–9 GeV	90	[19] CLARK	81	SPEC	++

[19] CLARK 81 is FNAL experiment with 209 GeV muons. Bounds apply to μ_P which couples with full weak strength to muon. See also section on "Doubly-Charged Lepton Production Cross Section."

Doubly-Charged Lepton Production Cross Section (μN Scattering)

VALUE (cm^2)	EVTS	DOCUMENT ID		TECN	CHG
• • • We do not use the following data for averages, fits, limits, etc. • • •					
$<6. \times 10^{-38}$	0	[20] CLARK	81	SPEC	++

[20] CLARK 81 is FNAL experiment with 209 GeV muon. Looked for μ^+ nucleon $\to \overline{\mu}_P^0 X$, $\overline{\mu}_P^0 \to \mu^+\mu^-\overline{\nu}_\mu$ and $\mu^+ n \to \mu_P^{++} X$, $\mu_P^{++} \to 2\mu^+\nu_\mu$. Above limits are for $\sigma\times$BR taken from their mass-dependence plot figure 2.

REFERENCES FOR Heavy Charged Lepton Searches

CHATRCHYAN	13AB	JHEP 1307 122	S. Chatrchyan *et al.*	(CMS Collab.)
ABBIENDI	03L	PL B572 8	G. Abbiendi *et al.*	(OPAL Collab.)
ACHARD	01B	PL B517 75	P. Achard *et al.*	(L3 Collab.)
ACKERSTAFF	98C	EPJ C1 45	K. Ackerstaff *et al.*	(OPAL Collab.)
ACCIARRI	96G	PL B377 304	M. Acciarri *et al.*	(L3 Collab.)
ALEXANDER	96P	PL B385 433	G. Alexander *et al.*	(OPAL Collab.)
BUSKULIC	96S	PL B384 439	D. Buskulic *et al.*	(ALEPH Collab.)
AHMED	94	PL B340 205	T. Ahmed *et al.*	(H1 Collab.)
KIM	91B	IJMP A6 2583	G.N. Kim *et al.*	(AMY Collab.)
ADACHI	90C	PL B244 352	I. Adachi *et al.*	(TOPAZ Collab.)
AKRAWY	90G	PL B240 250	M.Z. Akrawy *et al.*	(OPAL Collab.)
AKRAWY	90O	PL B252 290	M.Z. Akrawy *et al.*	(OPAL Collab.)
DECAMP	90F	PL B236 511	D. Decamp *et al.*	(ALEPH Collab.)
RILES	90	PR D42 1	K. Riles *et al.*	(Mark II Collab.)
SODERSTROM	90	PRL 64 2980	E. Soderstrom *et al.*	(Mark II Collab.)
STOKER	89	PR D39 1811	D.P. Stoker *et al.*	(Mark II Collab.)
ABE	88	PRL 61 915	K. Abe *et al.*	(VENUS Collab.)
ADACHI	88B	PR D37 1339	I. Adachi *et al.*	(TOPAZ Collab.)
BEHREND	88C	ZPHY C41 7	H.J. Behrend *et al.*	(CELLO Collab.)
ALBAJAR	87B	PL B185 241	C. Albajar *et al.*	(UA1 Collab.)
ADEVA	85	PL 152B 439	B. Adeva *et al.*	(Mark-J Collab.)
Also		PRPL 109 131	B. Adeva *et al.*	(Mark-J Collab.)
BARTEL	83	PL 123B 353	W. Bartel *et al.*	(JADE Collab.)
BERGER	81B	PL 99B 489	C. Berger *et al.*	(PLUTO Collab.)
BRANDELIK	81	PL 99B 163	R. Brandelik *et al.*	(TASSO Collab.)
CLARK	81	PRL 46 299	A.R. Clark *et al.*	(UCB, LBL, FNAL+)
Also		PR D25 2762	W.H. Smith *et al.*	(LBL, FNAL, PRIN)
AZIMOV	80	JETPL 32 664	Y.I. Azimov, V.A. Khoze	(PNPI)
		Translated from ZETFP 32 677.		
BARBER	80B	PRL 45 1904	D.P. Barber *et al.*	(Mark-J Collab.)
BRANDELIK	80	PL 92B 199	R. Brandelik *et al.*	(TASSO Collab.)
ANSORGE	73B	PR D7 26	R.E. Ansorge *et al.*	(CAVE)
BUSHNIN	73	NP B58 476	Y.B. Bushnin *et al.*	(SERP)
Also		PL 42B 136	S.V. Golovkin *et al.*	(SERP)
ROTHE	69	NP B10 241	K.W. Rothe, A.M. Wolsky	(PENN)
BARNA	68	PR 173 1391	A. Barna *et al.*	(SLAC, STAN)

OTHER RELATED PAPERS

PERL	81	SLAC-PUB-2752	M.L. Perl	(SLAC)
Physics in Collision Conference.				

Neutrino Properties

See the related review(s):
Neutrino Properties

$\overline{\nu}$ MASS (electron based)

Those limits given below are for the square root of $m_{\nu_e}^{2(\text{eff})} \equiv \sum_i |U_{ei}|^2 m_{\nu_i}^2$. Limits that come from the kinematics of $^3\text{H}\,\beta^-\overline{\nu}$ decay are the square roots of the limits for $m_{\nu_e}^{2(\text{eff})}$. Obtained from the measurements reported in the Listings for "$\overline{\nu}$ Mass Squared," below.

VALUE (eV)	CL%	DOCUMENT ID		TECN	COMMENT
< 2 OUR EVALUATION					
< 2.05	95	[1] ASEEV	11	SPEC	^{3}H β decay
< 2.3	95	[2] KRAUS	05	SPEC	^{3}H β decay
• • • We do not use the following data for averages, fits, limits, etc. • • •					
< 5.8	95	[3] PAGLIAROLI	10	ASTR	SN1987A
<21.7	90	[4] ARNABOLDI	03A	BOLO	^{187}Re β-decay
< 5.7	95	[5] LOREDO	02	ASTR	SN1987A
< 2.5	95	[6] LOBASHEV	99	SPEC	^{3}H β decay
< 2.8	95	[7] WEINHEIMER	99	SPEC	^{3}H β decay
< 4.35	95	[8] BELESEV	95	SPEC	^{3}H β decay
<12.4	95	[9] CHING	95	SPEC	^{3}H β decay
<92	95	[10] HIDDEMANN	95	SPEC	^{3}H β decay
15 $^{+32}_{-15}$		HIDDEMANN	95	SPEC	^{3}H β decay
<19.6	95	KERNAN	95	ASTR	SN 1987A
< 7.0	95	[11] STOEFFL	95	SPEC	^{3}H β decay
< 7.2	95	[12] WEINHEIMER	93	SPEC	^{3}H β decay
<11.7	95	[13] HOLZSCHUH	92B	SPEC	^{3}H β decay
<13.1	95	[14] KAWAKAMI	91	SPEC	^{3}H β decay
< 9.3	95	[15] ROBERTSON	91	SPEC	^{3}H β decay
<14	95	AVIGNONE	90	ASTR	SN 1987A
<16		SPERGEL	88	ASTR	SN 1987A
17 to 40		[16] BORIS	87	SPEC	^{3}H β decay

[1] ASEEV 11 report the analysis of the entire beta endpoint data, taken with the Troitsk integrating electrostatic spectrometer between 1997 and 2002 (some of the earlier runs were rejected), using a windowless gaseous tritium source. The fitted value of m_ν, based on the method of Feldman and Cousins, is obtained from the upper limit of the fit for m_ν^2. Previous analysis problems were resolved by careful monitoring of the tritium gas column density. Supersedes LOBASHEV 99 and BELESEV 95.

[2] KRAUS 05 is a continuation of the work reported in WEINHEIMER 99. This result represents the final analysis of data taken from 1997 to 2001. Various sources of systematic uncertainties have been identified and quantified. The background has been reduced

compared to the initial running period. A spectral anomaly at the endpoint, reported in LOBASHEV 99, was not observed.

[3] PAGLIAROLI 10 is critical of the likelihood method used by LOREDO 02.

[4] ARNABOLDI 03A *et al.* report kinematical neutrino mass limit using β-decay of ^{187}Re. Bolometric $AgReO_4$ micro-calorimeters are used. Mass bound is substantially weaker than those derived from tritium β-decays but has different systematic uncertainties.

[5] LOREDO 02 updates LOREDO 89.

[6] LOBASHEV 99 report a new measurement which continues the work reported in BELESEV 95. This limit depends on phenomenological fit parameters used to derive their best fit to m_ν^2, making unambiguous interpretation difficult. See the footnote under "$\overline{\nu}$ Mass Squared."

[7] WEINHEIMER 99 presents two analyses which exclude the spectral anomaly and result in an acceptable m_ν^2. We report the most conservative limit, but the other is nearly the same. See the footnote under "$\overline{\nu}$ Mass Squared."

[8] BELESEV 95 (Moscow) use an integral electrostatic spectrometer with adiabatic magnetic collimation and a gaseous tritium sources. A fit to a normal Kurie plot above 18300–18350 eV (to avoid a low-energy anomaly) plus a monochromatic line 7–15 eV below the endpoint yields $m_\nu^2 = -4.1 \pm 10.9$ eV^2, leading to this Bayesian limit.

[9] CHING 95 quotes results previously given by SUN 93; no experimental details are given. A possible explanation for consistently negative values of m_ν^2 is given.

[10] HIDDEMANN 95 (Munich) experiment uses atomic tritium embedded in a metal-dioxide lattice. Bayesian limit calculated from the weighted mean $m_\nu^2 = 221 \pm 4244$ eV^2 from the two runs listed below.

[11] STOEFFL 95 (LLNL) result is the Bayesian limit obtained from the m_ν^2 errors given below but with m_ν^2 set equal to 0. The anomalous endpoint accumulation leads to a value of m_ν^2 which is negative by more than 5 standard deviations.

[12] WEINHEIMER 93 (Mainz) is a measurement of the endpoint of the tritium β spectrum using an electrostatic spectrometer with a magnetic guiding field. The source is molecular tritium frozen onto an aluminum substrate.

[13] HOLZSCHUH 92B (Zurich) result is obtained from the measurement $m_\nu^2 = -24 \pm 48 \pm 61$ (1σ errors), in eV^2, using the PDG prescription for conversion to a limit in m_ν.

[14] KAWAKAMI 91 (Tokyo) experiment uses tritium-labeled arachidic acid. This result is the Bayesian limit obtained from the m_ν^2 limit with the errors combined in quadrature. This was also done in ROBERTSON 91, although the authors report a different procedure.

[15] ROBERTSON 91 (LANL) experiment uses gaseous molecular tritium. The result is in strong disagreement with the earlier claims by the ITEP group [LUBIMOV 80, BORIS 87 (+ BORIS 88 erratum)] that m_ν lies between 17 and 40 eV. However, the probability of a positive m^2 is only 3% if statistical and systematic error are combined in quadrature.

[16] See also comment in BORIS 87B and erratum in BORIS 88.

$\overline{\nu}$ MASS SQUARED (electron based)

Given troubling systematics which result in improbably negative estimators of $m^{2(\text{eff})}_{\nu_e} \equiv \sum_i |U_{ei}|^2\ m^2_{\nu_i}$, in many experiments, we use only KRAUS 05 and LOBASHEV 99 for our average.

VALUE (eV^2)				CL%	DOCUMENT ID		TECN	COMMENT
− 0.6	**±**	**1.9**	**OUR AVERAGE**					
− 0.67	±	2.53			[1] ASEEV	11	SPEC	^{3}H β decay
− 0.6	±	2.2	± 2.1		[2] KRAUS	05	SPEC	^{3}H β decay
• • • We do not use the following data for averages, fits, limits, etc. • • •								
− 1.9	±	3.4	± 2.2		[3] LOBASHEV	99	SPEC	^{3}H β decay
− 3.7	±	5.3	± 2.1		[4] WEINHEIMER	99	SPEC	^{3}H β decay
− 22	±	4.8			[5] BELESEV	95	SPEC	^{3}H β decay
129	±6010				[6] HIDDEMANN	95	SPEC	^{3}H β decay
313	±5994				[6] HIDDEMANN	95	SPEC	^{3}H β decay
−130	± 20	±15		95	[7] STOEFFL	95	SPEC	^{3}H β decay
− 31	± 75	±48			[8] SUN	93	SPEC	^{3}H β decay
− 39	± 34	±15			[9] WEINHEIMER	93	SPEC	^{3}H β decay
− 24	± 48	±61			[10] HOLZSCHUH	92B	SPEC	^{3}H β decay
− 65	± 85	±65			[11] KAWAKAMI	91	SPEC	^{3}H β decay
−147	± 68	±41			[12] ROBERTSON	91	SPEC	^{3}H β decay

[1] ASEEV 11 report the analysis of the entire beta endpoint data, taken with the Troitsk integrating electrostatic spectrometer between 1997 and 2002, using a windowless gaseous tritium source. The analysis does not use the two additional fit parameters (see LOBASHEV 99) for a step-like structure near the endpoint. Using only the runs where the tritium gas column density was carefully monitored the need for such parameters was eliminated. Supersedes LOBASHEV 99 and BELESEV 95.

[2] KRAUS 05 is a continuation of the work reported in WEINHEIMER 99. This result represents the final analysis of data taken from 1997 to 2001. Problems with significantly negative squared neutrino masses, observed in some earlier experiments, have been resolved in this work.

[3] LOBASHEV 99 report a new measurement which continues the work reported in BELESEV 95. The data were corrected for electron trapping effects in the source, eliminating the dependence of the fitted neutrino mass on the fit interval. The analysis assuming a pure beta spectrum yields significantly negative fitted $m_\nu^2 \approx -(20\text{–}10)$ eV^2. This problem is attributed to a discrete spectral anomaly of about 6×10^{-11} intensity with a time-dependent energy of 5–15 eV below the endpoint. The data analysis accounts for this anomaly by introducing two extra phenomenological fit parameters resulting in a best fit of $m_\nu^2 = -1.9 \pm 3.4 \pm 2.2$ eV^2 which is used to derive a neutrino mass limit. However, the introduction of phenomenological fit parameters which are correlated with the derived m_ν^2 limit makes unambiguous interpretation of this result difficult.

[4] WEINHEIMER 99 is a continuation of the work reported in WEINHEIMER 93 . Using a lower temperature of the frozen tritium source eliminated the dewetting of the T_2 film, which introduced a dependence of the fitted neutrino mass on the fit interval in the earlier work. An indication for a spectral anomaly reported in LOBASHEV 99 has been seen, but its time dependence does not agree with LOBASHEV 99. Two analyses, which exclude the spectral anomaly either by choice of the analysis interval or by using a particular data set which does not exhibit the anomaly, result in acceptable m_ν^2 fits and are used to derive the neutrino mass limit published by the authors. We list the most conservative of the two.

[5] BELESEV 95 (Moscow) use an integral electrostatic spectrometer with adiabatic magnetic collimation and a gaseous tritium sources. This value comes from a fit to a normal Kurie plot above 18300–18350 eV (to avoid a low-energy anomaly), including the effects of an apparent peak 7–15 eV below the endpoint.

[6] HIDDEMANN 95 (Munich) experiment uses atomic tritium embedded in a metal-dioxide lattice. They quote measurements from two data sets.

[7] STOEFFL 95 (LLNL) uses a gaseous source of molecular tritium. An anomalous pileup of events at the endpoint leads to the negative value for m_ν^2. The authors acknowledge that "the negative value for the best fit of m_ν^2 has no physical meaning" and discuss possible explanations for this effect.

[8] SUN 93 uses a tritiated hydrocarbon source. See also CHING 95.

[9] WEINHEIMER 93 (Mainz) is a measurement of the endpoint of the tritium β spectrum using an electrostatic spectrometer with a magnetic guiding field. The source is molecular tritium frozen onto an aluminum substrate.

[10] HOLZSCHUH 92B (Zurich) source is a monolayer of tritiated hydrocarbon.

[11] KAWAKAMI 91 (Tokyo) experiment uses tritium-labeled arachidic acid.

[12] ROBERTSON 91 (LANL) experiment uses gaseous molecular tritium. The result is in strong disagreement with the earlier claims by the ITEP group [LUBIMOV 80, BORIS 87 (+ BORIS 88 erratum)] that m_ν lies between 17 and 40 eV. However, the probability of a positive m_ν^2 is only 3% if statistical and systematic error are combined in quadrature.

ν MASS (electron based)

These are measurement of m_ν (in contrast to $m_{\overline{\nu}}$, given above). The masses can be different for a Dirac neutrino in the absence of *CPT* invariance. The possible distinction between ν and $\overline{\nu}$ properties is usually ignored elsewhere in these Listings.

VALUE (eV)	CL%	DOCUMENT ID		TECN	COMMENT
<460	68	YASUMI	94	CNTR	^{163}Ho decay
<225	95	SPRINGER	87	CNTR	^{163}Ho decay

ν MASS (muon based)

Limits given below are for the square root of $m^{2(\text{eff})}_{\nu_\mu} \equiv \sum_i |U_{\mu i}|^2\ m^2_{\nu_i}$.

In some of the COSM papers listed below, the authors did not distinguish between weak and mass eigenstates.

OUR EVALUATION is based on OUR AVERAGE for the $\pi^\pm$ mass and the ASSAMAGAN 96 value for the muon momentum for the π^+ decay at rest. The limit is calculated using the unified classical analysis of FELDMAN 98 for a Gaussian distribution near a physical boundary. WARNING: since $m^{2(\text{eff})}_{\nu_\mu}$ is calculated from the differences of large numbers, it and the corresponding limits are extraordinarily sensitive to small changes in the pion mass, the decay muon momentum, and their errors. For example, the limits obtained using JECKELMANN 94, LENZ 98, and the weighted averages are 0.15, 0.29, and 0.19 MeV, respectively.

VALUE (MeV)	CL%	DOCUMENT ID		TECN	COMMENT
<0.19 (CL = 90%) OUR EVALUATION					
<0.17	90	[1] ASSAMAGAN	96	SPEC	$m_\nu^2 = -0.016 \pm 0.023$
• • • We do not use the following data for averages, fits, limits, etc. • • •					
<0.15		[2] DOLGOV	95	COSM	Nucleosynthesis
<0.48		[3] ENQVIST	93	COSM	Nucleosynthesis
<0.3		[4] FULLER	91	COSM	Nucleosynthesis
<0.42		[4] LAM	91	COSM	Nucleosynthesis
<0.50	90	[5] ANDERHUB	82	SPEC	$m_\nu^2 = -0.14 \pm 0.20$
<0.65	90	CLARK	74	ASPK	$K_{\mu 3}$ decay

[1] ASSAMAGAN 96 measurement of p_μ from $\pi^+ \to \mu^+\nu$ at rest combined with JECKELMANN 94 Solution B pion mass yields $m_\nu^2 = -0.016 \pm 0.023$ with corresponding Bayesian limit listed above. If Solution A is used, $m_\nu^2 = -0.143 \pm 0.024$ MeV^2. Replaces ASSAMAGAN 94.

[2] DOLGOV 95 removes earlier assumptions (DOLGOV 93) about thermal equilibrium below T_{QCD} for wrong-helicity Dirac neutrinos (ENQVIST 93, FULLER 91) to set more stringent limits.

[3] ENQVIST 93 bases limit on the fact that thermalized wrong-helicity Dirac neutrinos would speed up expansion of early universe, thus reducing the primordial abundance. FULLER 91 exploits the same mechanism but in the older calculation obtains a larger production rate for these states, and hence a lower limit. Neutrino lifetime assumed to exceed nucleosynthesis time, ~ 1 s.

[4] Assumes neutrino lifetime >1 s. For Dirac neutrinos only. See also ENQVIST 93.

[5] ANDERHUB 82 kinematics is insensitive to the pion mass.

ν MASS (tau based)

The limits given below are the square roots of limits for $m^{2(\text{eff})}_{\nu_\tau} \equiv \sum_i |U_{\tau i}|^2\ m^2_{\nu_i}$.

In some of the ASTR and COSM papers listed below, the authors did not distinguish between weak and mass eigenstates.

VALUE (MeV)	CL%	EVTS	DOCUMENT ID		TECN	COMMENT
< 18.2	95		[1] BARATE	98F	ALEP	1991–1995 LEP runs

Lepton Particle Listings

Neutrino Properties

• • • We do not use the following data for averages, fits, limits, etc. • • •

< 28	95		[2] ATHANAS	00	CLEO	E_{cm}^{ee} = 10.6 GeV
< 27.6	95		[3] ACKERSTAFF	98T	OPAL	1990–1995 LEP runs
< 30	95	473	[4] AMMAR	98	CLEO	E_{cm}^{ee} = 10.6 GeV
< 60	95		[5] ANASTASSOV	97	CLEO	E_{cm}^{ee} = 10.6 GeV
< 0.37 or >22			[6] FIELDS	97	COSM	Nucleosynthesis
< 68	95		[7] SWAIN	97	THEO	m_τ, τ_τ, τ partial widths
< 29.9	95		[8] ALEXANDER	96M	OPAL	1990–1994 LEP runs
<149			[9] BOTTINO	96	THEO	π, μ, τ leptonic decays
<1 or >25			[10] HANNESTAD	96C	COSM	Nucleosynthesis
< 71	95		[11] SOBIE	96	THEO	m_τ, τ_τ, B($\tau^- \to e^- \overline{\nu}_e \nu_\tau$)
< 24	95	25	[12] BUSKULIC	95H	ALEP	1991–1993 LEP runs
< 0.19			[13] DOLGOV	95	COSM	Nucleosynthesis
< 3			[14] SIGL	95	ASTR	SN 1987A
< 0.4 or > 30			[15] DODELSON	94	COSM	Nucleosynthesis
< 0.1 or > 50			[16] KAWASAKI	94	COSM	Nucleosynthesis
155–225			[17] PERES	94	THEO	π,K,μ,τ weak decays
< 32.6	95	113	[18] CINABRO	93	CLEO	$E_{cm}^{ee} \approx$ 10.6 GeV
< 0.3 or > 35			[19] DOLGOV	93	COSM	Nucleosynthesis
< 0.74			[20] ENQVIST	93	COSM	Nucleosynthesis
< 31	95	19	[21] ALBRECHT	92M	ARG	E_{cm}^{ee} = 9.4–10.6 GeV
< 0.3			[22] FULLER	91	COSM	Nucleosynthesis
< 0.5 or > 25			[23] KOLB	91	COSM	Nucleosynthesis
< 0.42			[22] LAM	91	COSM	Nucleosynthesis

[1] BARATE 98F result based on kinematics of 2939 $\tau^- \to 2\pi^-\pi^+\nu_\tau$ and 52 $\tau^- \to 3\pi^- 2\pi^+ (\pi^0)\nu_\tau$ decays. If possible 2.5% excited a_1 decay is included in 3-prong sample analysis, limit increases to 19.2 MeV.

[2] ATHANAS 00 bound comes from analysis of $\tau^- \to \pi^-\pi^+\pi^-\pi^0\nu_\tau$ decays.

[3] ACKERSTAFF 98T use $\tau \to 5\pi^\pm\nu_\tau$ decays to obtain a limit of 43.2 MeV (95%CL). They combine this with ALEXANDER 96M value using $\tau \to 3h^\pm\nu_\tau$ decays to obtain quoted limit.

[4] AMMAR 98 limit comes from analysis of $\tau^- \to 3\pi^- 2\pi^+\nu_\tau$ and $\tau^- \to 2\pi^-\pi^+ 2\pi^0\nu_\tau$ decay modes.

[5] ANASTASSOV 97 derive limit by comparing their m_τ measurement (which depends on m_{ν_τ}) to BAI 96 m_τ threshold measurement.

[6] FIELDS 97 limit for a Dirac neutrino. For a Majorana neutrino the mass region < 0.93 or >31 MeV is excluded. These bounds assume N_ν <4 from nucleosynthesis; a wider excluded region occurs with a smaller N_ν upper limit.

[7] SWAIN 97 derive their limit from the Standard Model relationships between the tau mass, lifetime, branching fractions for $\tau^- \to e^-\overline{\nu}_e\nu_\tau$, $\tau^- \to \mu^-\overline{\nu}_\mu\nu_\tau$, $\tau^- \to \pi^-\nu_\tau$, and $\tau^- \to K^-\nu_\tau$, and the muon mass and lifetime by assuming lepton universality and using world average values. Limit is reduced to 48 MeV when the CLEO τ mass measurement (BALEST 93) is included; see CLEO's more recent m_{ν_τ} limit (ANASTASSOV 97). Consideration of mixing with a fourth generation heavy neutrino yields $\sin^2\theta_L < 0.016$ (95%CL).

[8] ALEXANDER 96M bound comes from analyses of $\tau^- \to 3\pi^- 2\pi^+\nu_\tau$ and $\tau^- \to h^- h^- h^+\nu_\tau$ decays.

[9] BOTTINO 96 assumes three generations of neutrinos with mixing, finds consistency with massless neutrinos with no mixing based on 1995 data for masses, lifetimes, and leptonic partial widths.

[10] HANNESTAD 96C limit is on the mass of a Majorana neutrino. This bound assumes $N_\nu < 4$ from nucleosynthesis. A wider excluded region occurs with a smaller N_ν upper limit. This paper is the corrected version of HANNESTAD 96; see the erratum: HANNESTAD 96B.

[11] SOBIE 96 derive their limit from the Standard Model relationship between the tau mass, lifetime, and leptonic branching fraction, and the muon mass and lifetime, by assuming lepton universality and using world average values.

[12] BUSKULIC 95H bound comes from a two-dimensional fit of the visible energy and invariant mass distribution of $\tau \to 5\pi(\pi^0)\nu_\tau$ decays. Replaced by BARATE 98F.

[13] DOLGOV 95 removes earlier assumptions (DOLGOV 93) about thermal equilibrium below T_{QCD} for wrong-helicity Dirac neutrinos (ENQVIST 93, FULLER 91) to set more stringent limits. DOLGOV 96 argues that a possible window near 20 MeV is excluded.

[14] SIGL 95 exclude massive Dirac or Majorana neutrinos with lifetimes between 10^{-3} and 10^8 seconds if the decay products are predominantly γ or e^+e^-.

[15] DODELSON 94 calculate constraints on ν_τ mass and lifetime from nucleosynthesis for 4 generic decay modes. Limits depend strongly on decay mode. Quoted limit is valid for all decay modes of Majorana neutrinos with lifetime greater than about 300 s. For Dirac neutrinos limits change to < 0.3 or > 33.

[16] KAWASAKI 94 excluded region is for Majorana neutrino with lifetime >1000 s. Other limits are given as a function of ν_τ lifetime for decays of the type $\nu_\tau \to \nu_\mu\phi$ where ϕ is a Nambu-Goldstone boson.

[17] PERES 94 used PDG 92 values for parameters to obtain a value consistent with mixing. Reexamination by BOTTINO 96 which included radiative corrections and 1995 PDG parameters resulted in two allowed regions, m_3 < 70 MeV and 140 MeV m_3 < 149 MeV.

[18] CINABRO 93 bound comes from analysis of $\tau^- \to 3\pi^- 2\pi^+\nu_\tau$ and $\tau^- \to 2\pi^-\pi^+ 2\pi^0\nu_\tau$ decay modes.

[19] DOLGOV 93 assumes neutrino lifetime >100 s. For Majorana neutrinos, the low mass limit is 0.5 MeV. KAWANO 92 points out that these bounds can be overcome for a Dirac neutrino if it possesses a magnetic moment. See also DOLGOV 96.

[20] ENQVIST 93 bases limit on the fact that thermalized wrong-helicity Dirac neutrinos would speed up expansion of early universe, thus reducing the primordial abundance. FULLER 91 exploits the same mechanism but in the older calculation obtains a larger production rate for these states, and hence a lower limit. Neutrino lifetime assumed to exceed nucleosynthesis time, $\sim$ 1 s.

[21] ALBRECHT 92M reports measurement of a slightly lower τ mass, which has the effect of reducing the ν_τ mass reported in ALBRECHT 88B. Bound is from analysis of $\tau^- \to 3\pi^- 2\pi^+\nu_\tau$ mode.

[22] Assumes neutrino lifetime >1 s. For Dirac neutrinos. See also ENQVIST 93.

[23] KOLB 91 exclusion region is for Dirac neutrino with lifetime >1 s; other limits are given.

See the related review(s):
Sum of Neutrino Masses

SUM OF THE NEUTRINO MASSES, m_{tot}

(Defined in the above note), of effectively stable neutrinos (i.e., those with mean lives greater than or equal to the age of the universe). These papers assumed Dirac neutrinos. When necessary, we have generalized the results reported so they apply to m_{tot}. For other limits, see SZALAY 76, VYSOTSKY 77, BERNSTEIN 81, FREESE 84, SCHRAMM 84, and COWSIK 85.

VALUE (eV)	CL%	DOCUMENT ID		TECN	COMMENT
• • • We do not use the following data for averages, fits, limits, etc. • • •					
< 0.151	95	[1] VAGNOZZI	17	COSM	
< 0.14	95	[2] YECHE	17	COSM	BOSS and XQ-100
< 0.0926	90	[3] DIVALENTINO	16	COSM	
< 0.18	95	[4] HUANG	16	COSM	Normal mass hierarchy
< 0.14	95	[5] ROSSI	15	COSM	
< 0.23	95	[6] ADE	14	COSM	Planck
0.320 $\pm$0.081		[7] BATTYE	14	COSM	
0.35 $\pm$0.10		[8] BEUTLER	14	COSM	BOSS
0.22 $^{+0.09}_{-0.10}$		[9] COSTANZI	14	COSM	
< 0.22	95	[10] GIUSARMA	14	COSM	
0.32 $\pm$0.11		[11] HOU	14	COSM	
< 0.26	95	[12] LEISTEDT	14	COSM	
< 0.18	95	[13] RIEMER-SOR...	14	COSM	
< 0.24	68	[14] MORESCO	12	COSM	
< 0.29	95	[15] XIA	12	COSM	
< 0.81	95	[16] SAITO	11	COSM	SDSS
< 0.44	95	[17] HANNESTAD	10	COSM	
< 0.6	95	[18] SEKIGUCHI	10	COSM	
< 0.28	95	[19] THOMAS	10	COSM	
< 1.1		[20] ICHIKI	09	COSM	
< 1.3	95	[21] KOMATSU	09	COSM	WMAP
< 1.2		[22] TERENO	09	COSM	
< 0.33		[23] VIKHLININ	09	COSM	
< 0.28		[24] BERNARDIS	08	COSM	
< 0.17–2.3		[25] FOGLI	07	COSM	
< 0.42	95	[26] KRISTIANSEN	07	COSM	
< 0.63–2.2		[27] ZUNCKEL	07	COSM	
< 0.24	95	[28] CIRELLI	06	COSM	
< 0.62	95	[29] HANNESTAD	06	COSM	
< 1.2		[30] SANCHEZ	06	COSM	
< 0.17	95	[28] SELJAK	06	COSM	
< 2.0	95	[31] ICHIKAWA	05	COSM	
< 0.75		[32] BARGER	04	COSM	
< 1.0		[33] CROTTY	04	COSM	
< 0.7		[34] SPERGEL	03	COSM	WMAP
< 0.9		[35] LEWIS	02	COSM	
< 4.2		[36] WANG	02	COSM	CMB
< 2.7		[37] FUKUGITA	00	COSM	
< 5.5		[38] CROFT	99	ASTR	Ly α power spec
<180		SZALAY	74	COSM	
<132		COWSIK	72	COSM	
<280		MARX	72	COSM	
<400		GERSHTEIN	66	COSM	

[1] Combines temperature anisotropies of the CMB from Planck with data on baryon acoustic oscillations and the optical depth to reionization. Limit is strengthened to 0.118 when high multipole polarization data is included. Updates GIUSARMA 16.

[2] Constrains the total mass of neutrinos using the Lyman-alpha forest power spectrum with BOSS (mid-resolution), XQ-100 (high-resolution) and CMB. Without the CMB data, the limit relaxes to 0.8 eV. Supersedes PALANQUE-DELABROUILLE 15A.

[3] Constrains the total mass of neutrinos from Planck CMB data combined with baryon acoustic oscillation and Planck cluster data.

[4] Constrains the total mass of neutrinos from BAO data from SDSS-III/BOSS combined with CMB data from Planck. Limit quoted for normal mass hierarchy. The limit for the inverted mass hierarchy is 0.20 eV and for the degenerate mass hierarchy it is 0.15 eV.

[5] ROSSI 15 sets limits on the sum of neutrino masses using BOSS Lyman alpha forest data combined with Planck CMB data and baryon acoustic oscillations.

[6] Constrains the total mass of neutrinos from Planck CMB data along with WMAP polarization, high L, and BAO data.

[7] Finite neutrino mass fit to resolve discrepancy between CMB and lensing measurements.

[8] Fit to the total mass of neutrinos from BOSS data along with WMAP CMB data and data from other BAO constraints and weak lensing.

[9] Fit to the total mass of neutrinos from Planck CMB data along with BAO.

[10] Constrains the total mass of neutrinos from Planck CMB data combined with baryon acoustic oscillation data from BOSS and HST data on the Hubble parameter.

[11] Fit based on the SPT-SZ survey combined with CMB, BAO, and H_0 data.

[12] Constraints the total mass of neutrinos (marginalizing over the effective number of neutrino species) from CMB, CMB lensing, BAO, and galaxy clustering data.

[13] Constrains the total mass of neutrinos from Planck CMB data combined with baryon acoustic oscillation data from BOSS, 6dFGS, SDSS, WiggleZ data on the galaxy power

spectrum, and HST data on the Hubble parameter. The limit is increased to 0.25 eV if a lower bound to the sum of neutrino masses of 0.04 eV is assumed.

[14] Constrains the total mass of neutrinos from observational Hubble parameter data with seven-year WMAP data and the most recent estimate of H_0.

[15] Constrains the total mass of neutrinos from the CFHTLS combined with seven-year WMAP data and a prior on the Hubble parameter. Limit is relaxed to 0.41 eV when small scales affected by non-linearities are removed.

[16] Constrains the total mass of neutrinos from the Sloan Digital Sky Survey and the five-year WMAP data.

[17] Constrains the total mass of neutrinos from the 7-year WMAP data including SDSS and HST data. Limit relaxes to 1.19 eV when CMB data is used alone. Supersedes HANNESTAD 06.

[18] Constrains the total mass of neutrinos from a combination of CMB data, a recent measurement of H_0 (SHOES), and baryon acoustic oscillation data from SDSS.

[19] Constrains the total mass of neutrinos from SDSS MegaZ LRG DR7 galaxy clustering data combined with CMB, HST, supernovae and baryon acoustic oscillation data. Limit relaxes to 0.47 eV when the equation of state parameter, $w \neq 1$.

[20] Constrains the total mass of neutrinos from weak lensing measurements when combined with CMB. Limit improves to 0.54 eV when supernovae and baryon acoustic oscillation observations are included. Assumes ΛCDM model.

[21] Constrains the total mass of neutrinos from five-year WMAP data. Limit improves to 0.67 eV when supernovae and baryon acoustic oscillation observations are included. Limits quoted assume the ΛCDM model. Supersedes SPERGEL 07.

[22] Constrains the total mass of neutrinos from weak lensing measurements when combined with CMB. Limit improves to $0.03 < \Sigma m_\nu < 0.54$ eV when supernovae and baryon acoustic oscillation observations are included. The slight preference for massive neutrinos at the two-sigma level disappears when systematic errors are taken into account. Assumes ΛCDM model.

[23] Constrains the total mass of neutrinos from recent Chandra X-ray observations of galaxy clusters when combined with CMB, supernovae, and baryon acoustic oscillation measurements. Assumes flat universe and constant dark-energy equation of state, w.

[24] Constraints the total mass of neutrinos from recent CMB and SOSS LRG power spectrum data along with bias mass relations from SDSS, DEEP2, and Lyman-Break Galaxies. It assumes ΛCDM model. Limit degrades to 0.59 eV in a more general wCDM model.

[25] Constrains the total mass of neutrinos from neutrino oscillation experiments and cosmological data. The most conservative limit uses only WMAP three-year data, while the most stringent limit includes CMB, large-scale structure, supernova, and Lyman-alpha data.

[26] Constrains the total mass of neutrinos from recent CMB, large scale structure, SN1a, and baryon acoustic oscillation data. The limit relaxes to 1.75 when WMAP data alone is used with no prior. Paper shows results with several combinations of data sets. Supersedes KRISTIANSEN 06.

[27] Constrains the total mass of neutrinos from the CMB and the large scale structure data. The most conservative limit is obtained when generic initial conditions are allowed.

[28] Constrains the total mass of neutrinos from recent CMB, large scale structure, Lyman-alpha forest, and SN1a data.

[29] Constrains the total mass of neutrinos from recent CMB and large scale structure data. See also GOOBAR 06. Superseded by HANNESTAD 10.

[30] Constrains the total mass of neutrinos from the CMB and the final 2dF Galaxy Redshift Survey.

[31] Constrains the total mass of neutrinos from the CMB experiments alone, assuming ΛCDM Universe. FUKUGITA 06 show that this result is unchanged by the 3-year WMAP data.

[32] Constrains the total mass of neutrinos from the power spectrum of fluctuations derived from the Sloan Digital Sky Survey and the 2dF galaxy redshift survey, WMAP and 27 other CMB experiments and measurements by the HST Key project.

[33] Constrains the total mass of neutrinos from the power spectrum of fluctuations derived from the Sloan Digital Sky Survey, the 2dF galaxy redshift survey, WMAP and ACBAR. The limit is strengthened to 0.6 eV when measurements by the HST Key project and supernovae data are included.

[34] Constrains the fractional contribution of neutrinos to the total matter density in the Universe from WMAP data combined with other CMB measurements, the 2dfGRS data, and Lyman α data. The limit does not noticeably change if the Lyman α data are not used.

[35] LEWIS 02 constrains the total mass of neutrinos from the power spectrum of fluctuations derived from the CMB, HST Key project, 2dF galaxy redshift survey, supernovae type Ia, and BBN.

[36] WANG 02 constrains the total mass of neutrinos from the power spectrum of fluctuations derived from the CMB and other cosmological data sets such as galaxy clustering and the Lyman α forest.

[37] FUKUGITA 00 is a limit on neutrino masses from structure formation. The constraint is based on the clustering scale σ_8 and the COBE normalization and leads to a conservative limit of 0.9 eV assuming 3 nearly degenerate neutrinos. The quoted limit is on the sum of the light neutrino masses.

[38] CROFT 99 result based on the power spectrum of the Ly α forest. If $\Omega_{\text{matter}} < 0.5$, the limit is improved to $m_\nu < 2.4\ (\Omega_{\text{matter}}/0.17\text{–}1)$ eV.

Limits on MASSES of Light Stable Right-Handed ν (with necessarily suppressed interaction strengths)

VALUE (eV)	DOCUMENT ID		TECN	COMMENT
• • • We do not use the following data for averages, fits, limits, etc. • • •				
<100–200	[1] OLIVE	82	COSM	Dirac ν
<200–2000	[1] OLIVE	82	COSM	Majorana ν

[1] Depending on interaction strength G_R where $G_R < G_F$.

Limits on MASSES of Heavy Stable Right-Handed ν (with necessarily suppressed interaction strengths)

VALUE (GeV)	DOCUMENT ID		TECN	COMMENT
• • • We do not use the following data for averages, fits, limits, etc. • • •				
> 10	[1] OLIVE	82	COSM	G_R/G_F <0.1
>100	[1] OLIVE	82	COSM	G_R/G_F <0.01

[1] These results apply to heavy Majorana neutrinos and are summarized by the equation: m_ν >1.2 GeV (G_F/G_R). The bound saturates, and if G_R is too small no mass range is allowed.

ν CHARGE

VALUE (units: electron charge)	CL%	DOCUMENT ID		TECN	COMMENT
• • • We do not use the following data for averages, fits, limits, etc. • • •					
$<3 \times 10^{-8}$	95	[1] DELLA-VALLE	16	LASR	Magnetic dichroism
$<2.1 \times 10^{-12}$	90	[2] CHEN	14A	TEXO	Nuclear reactor
$<1.5 \times 10^{-12}$	90	[3] STUDENIKIN	14		Nuclear reactor
$<3.7 \times 10^{-12}$	90	[4] GNINENKO	07	RVUE	Nuclear reactor
$<2 \times 10^{-14}$		[5] RAFFELT	99	ASTR	Red giant luminosity
$<6 \times 10^{-14}$		[6] RAFFELT	99	ASTR	Solar cooling
$<4 \times 10^{-4}$		[7] BABU	94	RVUE	BEBC beam dump
$<3 \times 10^{-4}$		[8] DAVIDSON	91	RVUE	SLAC e^- beam dump
$<2 \times 10^{-15}$		[9] BARBIELLINI	87	ASTR	SN 1987A
$<1 \times 10^{-13}$		[10] BERNSTEIN	63	ASTR	Solar energy losses

[1] DELLA-VALLE 16 obtain a limit on the charge of neutrinos valid for masses of less than 10 meV. For heavier neutrinos the limit increases as a power of mass, reaching 10^{-6} e for $m = 100$ meV.

[2] CHEN 14A use the Multi-Configuration RRPA method to analyze reactor $\overline{\nu}_e$ scattering on Ge atoms with 300 eV recoil energy threshold to obtain this limit.

[3] STUDENIKIN 14 uses the limit on μ_ν from BEDA 13 and the 2.8 keV threshold of the electron recoil energy to obtain this limit.

[4] GNINENKO 07 use limit on $\overline{\nu}_e$ magnetic moment from LI 03B to derive this result. The limit is considerably weaker than the limits on the charge of ν_e and $\overline{\nu}_e$ from various astrophysics considerations.

[5] This RAFFELT 99 limit applies to all neutrino flavors which are light enough (<5 keV) to be emitted from globular-cluster red giants.

[6] This RAFFELT 99 limit is derived from the helioseismological limit on a new energy-loss channel of the Sun, and applies to all neutrino flavors which are light enough (<1 keV) to be emitted from the sun.

[7] BABU 94 use COOPER-SARKAR 92 limit on ν magnetic moment to derive quoted result. It applies to ν_τ.

[8] DAVIDSON 91 use data from early SLAC electron beam dump experiment to derive charge limit as a function of neutrino mass. It applies to ν_τ.

[9] Exact BARBIELLINI 87 limit depends on assumptions about the intergalactic or galactic magnetic fields and about the direct distance and time through the field. It applies to ν_e.

[10] The limit applies to all flavors.

ν (MEAN LIFE) / MASS

Measures $\left[\sum |U_{\ell j}|^2\ \Gamma_j\ m_j\right]^{-1}$, where the sum is over mass eigenstates which cannot be resolved experimentally. Some of the limits constrain the radiative decay and are based on the limit of the corresponding photon flux. Other apply to the decay of a heavier neutrino into the lighter one and a Majoron or other invisible particle. Many of these limits apply to any ν within the indicated mass range.

Limits on the radiative decay are either directly based on the limits of the corresponding photon flux, or are derived from the limits on the neutrino magnetic moments. In the later case the transition rate for $\nu_i \to \nu_j + \gamma$ is constrained by $\Gamma_{ij} = \frac{1}{\tau_{ij}} = \frac{(m_i^2 - m_j^2)^3}{m_i^3}\ \mu_{ij}^2$ where μ_{ij} is the neutrino transition moment in the mass eigenstates basis. Typically, the limits on lifetime based on the magnetic moments are many orders of magnitude more restrictive than limits based on the nonobservation of photons.

VALUE (s/eV)	CL%	DOCUMENT ID		TECN	COMMENT
> 15.4	90	[1] KRAKAUER	91	CNTR	ν_μ, $\overline{\nu}_\mu$ at LAMPF
> 7 $\times 10^9$		[2] RAFFELT	85	ASTR	
> 300	90	[3] REINES	74	CNTR	$\overline{\nu}_e$
• • • We do not use the following data for averages, fits, limits, etc. • • •					
$> 10^5 - 10^{10}$	95	[4] CECCHINI	11	ASTR	$\nu_2 \to \nu_1$ radiative decay
	90	[5] MIRIZZI	07	CMB	radiative decay
	90	[6] MIRIZZI	07	CIB	radiative decay
		[7] WONG	07	CNTR	Reactor $\overline{\nu}_e$
> 0.11	90	[8] XIN	05	CNTR	Reactor ν_e
		[9] XIN	05	CNTR	Reactor ν_e
> 0.004	90	[10] AHARMIM	04	SNO	quasidegen. ν masses
> 4.4 $\times 10^{-5}$	90	[10] AHARMIM	04	SNO	hierarchical ν masses
$\gtrsim$ 100	95	[11] CECCHINI	04	ASTR	Radiative decay for ν mass > 0.01 eV
> 0.067	90	[12] EGUCHI	04	KLND	quasidegen. ν masses
> 1.1 $\times 10^{-3}$	90	[12] EGUCHI	04	KLND	hierarchical ν masses
> 8.7 $\times 10^{-5}$	99	[13] BANDYOPA...	03	FIT	nonradiative decay
$\geq$ 4200	90	[14] DERBIN	02B	CNTR	Solar pp and Be ν
> 2.8 $\times 10^{-5}$	99	[15] JOSHIPURA	02B	FIT	nonradiative decay
		[16] DOLGOV	99	COSM	
		[17] BILLER	98	ASTR	m_ν= 0.05–1 eV
> 2.8 $\times 10^{15}$		[18,19] BLUDMAN	92	ASTR	$m_\nu < 50$ eV
none 10^{-12} – 5×10^4		[20] DODELSON	92	ASTR	m_ν=1–300 keV
$< 10^{-12}$ or $> 5 \times 10^4$		[20] DODELSON	92	ASTR	m_ν=1–300 keV
		[21] GRANEK	91	COSM	Decaying L^0
> 6.4	90	[22] KRAKAUER	91	CNTR	ν_e at LAMPF
> 1.1 $\times 10^{15}$		[23] WALKER	90	ASTR	m_ν= 0.03 – ~ 2 MeV
> 6.3 $\times 10^{15}$		[19,24] CHUPP	89	ASTR	$m_\nu < 20$ eV
> 1.7 $\times 10^{15}$		[19] KOLB	89	ASTR	$m_\nu < 20$ eV
		[25] RAFFELT	89	RVUE	$\overline{\nu}$ (Dirac, Majorana)

>	8.3	$\times 10^{14}$	
>	22		68
>	38		68
>	59		68
>	30		68
>	20		68
>	0.11		90
>	2	$\times 10^{21}$	
>	1.0	$\times 10^{-2}$	90
>	1.7	$\times 10^{-2}$	90
<	3	$\times 10^{-11}$	
>	2.2	$\times 10^{-3}$	90
>	3.	$\times 10^{-3}$	90
>	1.3	$\times 10^{-2}$	90

[1] KRAKAUER 91 quotes the limit $\tau/m_{\nu_1} > (0.75a^2 + 21.65a + 26.3)$ s/eV, where a is a parameter describing the asymmetry in the neutrino decay defined as $dN_\gamma/d\cos\theta = (1/2)(1 + a\cos\theta)$ The parameter $a = 0$ for a Majorana neutrino, but can vary from -1 to 1 for a Dirac neutrino. The bound given by the authors is the most conservative (which applies for $a = -1$).

[2] RAFFELT 85 limit on the radiative decay is from solar x- and γ-ray fluxes. Limit depends on ν flux from pp, now established from GALLEX and SAGE to be > 0.5 of expectation.

[3] REINES 74 looked for ν of nonzero mass decaying radiatively to a neutral of lesser mass + γ. Used liquid scintillator detector near fission reactor. Finds lab lifetime 6×10^7 s or more. Above value of (mean life)/mass assumes average effective neutrino energy of 0.2 MeV. To obtain the limit 6×10^7 s REINES 74 assumed that the full $\overline{\nu}_e$ reactor flux could be responsible for yielding decays with photon energies in the interval 0.1 MeV – 0.5 MeV. This represents some overestimate so their lower limit is an over-estimate of the lab lifetime (VOGEL 84). If so, OBERAUER 87 may be comparable or better.

[4] CECCHINI 11 search for radiative decays of solar neutrinos into visible photons during the 2006 total solar eclipse. The range of (mean life)/mass values corresponds to a range of ν_1 masses between 10^{-4} and 0.1 eV.

[5] MIRIZZI 07 determine a limit on the neutrino radiative decay from analysis of the maximum allowed distortion of the CMB spectrum as measured by the COBE/FIRAS. For the decay $\nu_2 \to \nu_1$ the lifetime limit is $\lesssim 4 \times 10^{20}$ s for $m_{min} \lesssim 0.14$ eV. For transition with the $|\Delta m_{31}|$ mass difference the lifetime limit is $\sim 2 \times 10^{19}$ s for $m_{min} \lesssim 0.14$ eV and $\sim 5 \times 10^{20}$ s for $m_{min} \gtrsim 0.14$ eV.

[6] MIRIZZI 07 determine a limit on the neutrino radiative decay from analysis of the cosmic infrared background (CIB) using the Spitzer Observatory data. For transition with the $|\Delta m_{31}|$ mass difference they obtain the lifetime limit $\sim 10^{20}$ s for $m_{min} \lesssim 0.14$ eV.

[7] WONG 07 use their limit on the neutrino magnetic moment together with the assumed experimental value of $\Delta m^2_{13} \sim 2\times10^{-3}$ eV^2 to obtain $\tau_{13}/m_1^3 > 3.2\times10^{27}$ s/eV^3 for the radiative decay in the case of the inverted mass hierarchy. Similarly to RAFFELT 89 this limit can be violated if electric and magnetic moments are equal to each other. Analogous, but numerically somewhat different limits are obtained for τ_{23} and τ_{21}.

[8] XIN 05 search for the γ from radiative decay of ν_e produced by the electron capture on ^{51}Cr. No events were seen and the limit on τ/m_ν was derived. This is a weaker limit on the decay of ν_e than KRAKAUER 91.

[9] XIN 05 use their limit on the neutrino magnetic moment of ν_e together with the assumed experimental value of $\Delta m^2_{1,3} \sim 2\times10^{-3}$ eV^2 to obtain $\tau_{13}/m_1^3 > 1\times10^{23}$ s/eV^3 for the radiative decay in the case of the inverted mass hierarchy. Similarly to RAFFELT 89 this limit can be violated if electric and magnetic moments are equal to each other. Analogous, but numerically somewhat different limits are obtained for τ_{23} and τ_{21}. Again, this limit is specific for ν_e.

[10] AHARMIM 04 obtained these results from the solar $\overline{\nu}_e$ flux limit set by the SNO measurement assuming ν_2 decay through nonradiative process $\nu_2 \to \overline{\nu}_1 X$, where X is a Majoron or other invisible particle. Limits are given for the cases of quasidegenerate and hierarchical neutrino masses.

[11] CECCHINI 04 obtained this bound through the observations performed on the occasion of the 21 June 2001 total solar eclipse, looking for visible photons from radiative decays of solar neutrinos. Limit is a τ/m_{ν_2} in $\nu_2 \to \nu_1\gamma$. Limit ranges from $\sim$ 100 to 10^7 s/eV for $0.01 < m_{\nu_1} < 0.1$ eV.

[12] EGUCHI 04 obtained these results from the solar $\overline{\nu}_e$ flux limit set by the KamLAND measurement assuming ν_2 decay through nonradiative process $\nu_2 \to \overline{\nu}_1 X$, where X is a Majoron or other invisible particle. Limits are given for the cases of quasidegenerate and hierarchical neutrino masses.

[13] The ratio of the lifetime over the mass derived by BANDYOPADHYAY 03 is for ν_2. They obtained this result using the following solar-neutrino data: total rates measured in Cl and Ga experiments, the Super-Kamiokande's zenith-angle spectra, and SNO's day and night spectra. They assumed that ν_1 is the lowest mass, stable or nearly stable neutrino state and ν_2 decays through nonradiative Majoron emission process, $\nu_2 \to \overline{\nu}_1 + J$, or through nonradiative process with all the final state particles being sterile. The best fit is obtained in the region of the LMA solution.

[14] DERBIN 02B (also BACK 03B) obtained this bound for the radiative decay from the results of background measurements with Counting Test Facility (the prototype of the Borexino detector). The laboratory gamma spectrum is given as $dN_\gamma/d\cos\theta = (1/2)(1 + \alpha\cos\theta)$ with α=0 for a Majorana neutrino, and α varying to -1 to 1 for a Dirac neutrino. The listed bound is for the case of α=0. The most conservative bound 1.5×10^3 s eV^{-1} is obtained for the case of α=-1.

[15] The ratio of the lifetime over the mass derived by JOSHIPURA 02B is for ν_2. They obtained this result from the total rates measured in all solar neutrino experiments. They assumed that ν_1 is the lowest mass, stable or nearly stable neutrino state and ν_2 decays through nonradiative process like Majoron emission decay, $\nu_2 \to \nu_1' + J$ where ν_1' state is sterile. The exact limit depends on the specific solution of the solar neutrino problem. The quoted limit is for the LMA solution.

[16] DOLGOV 99 places limits in the (Majorana) τ-associated ν mass-lifetime plane based on nucleosynthesis. Results would be considerably modified if neutrino oscillations exist.

[26] RAFFELT	89B	ASTR		
[27] VONFEILIT...	88	ASTR		
[28] OBERAUER	87		$\overline{\nu}_R$ (Dirac)	
[28] OBERAUER	87		$\overline{\nu}$ (Majorana)	
[28] OBERAUER	87		$\overline{\nu}_L$ (Dirac)	
KETOV	86	CNTR	$\overline{\nu}$ (Dirac)	
KETOV	86	CNTR	$\overline{\nu}$ (Majorana)	
[29] BINETRUY	84	COSM	$m_\nu \sim$ 1 MeV	
[30] FRANK	81	CNTR	$\nu\overline{\nu}$ LAMPF	
[31] STECKER	80	ASTR	m_ν= 10–100 eV	
[30] BLIETSCHAU	78	HLBC	ν_μ, CERN GGM	
[30] BLIETSCHAU	78	HLBC	$\overline{\nu}_\mu$, CERN GGM	
[32] FALK	78	ASTR	m_ν <10 MeV	
[30] BARNES	77	DBC	ν, ANL 12-ft	
[33] COWSIK	77	ASTR		
[30] BELLOTTI	76	HLBC	ν, CERN GGM	
[30] BELLOTTI	76	HLBC	$\overline{\nu}$, CERN GGM	

[17] BILLER 98 use the observed TeV γ-ray spectra to set limits on the mean life of any radiatively decaying neutrino between 0.05 and 1 eV. Curve shows $\tau_\nu/B_\gamma > 0.15\times10^{21}$ s at 0.05 eV, $> 1.2\times10^{21}$ s at 0.17 eV, $> 3\times10^{21}$ s at 1 eV, where B_γ is the branching ratio to photons.

[18] BLUDMAN 92 sets additional limits by this method for higher mass ranges. Cosmological limits are also obtained.

[19] Limit on the radiative decay based on nonobservation of γ's in coincidence with ν's from SN 1987A.

[20] DODELSON 92 range is for wrong-helicity keV mass Dirac ν's from the core of neutron star in SN 1987A decaying to ν's that would have interacted in KAM2 or IMB detectors.

[21] GRANEK 91 considers heavy neutrino decays to $\gamma\nu_L$ and $3\nu_L$, where m_{ν_L} <100 keV. Lifetime is calculated as a function of heavy neutrino mass, branching ratio into $\gamma\nu_L$, and m_{ν_L}.

[22] KRAKAUER 91 quotes the limit for ν_e, $\tau/m_\nu > (0.3a^2 + 9.8a + 15.9)$ s/eV, where a is a parameter describing the asymmetry in the radiative neutrino decay defined as $dN_\gamma/d\cos\theta = (1/2)(1 + a\cos\theta)$ $a = 0$ for a Majorana neutrino, but can vary from -1 to 1 for a Dirac neutrino. The bound given by the authors is the most conservative (which applies for $a = -1$).

[23] WALKER 90 uses SN 1987A γ flux limits after 289 days.

[24] CHUPP 89 should be multiplied by a branching ratio (about 1) and a detection efficiency (about 1/4), and pertains to radiative decay of any neutrino to a lighter or sterile neutrino.

[25] RAFFELT 89 uses KYULDJIEV 84 to obtain $\tau m^3 > 3\times10^{18}$ s eV^3 (based on $\overline{\nu}_e e^-$ cross sections). The bound for the radiative decay is not valid if electric and magnetic transition moments are equal for Dirac neutrinos.

[26] RAFFELT 89B analyze stellar evolution and exclude the region $3\times10^{12} < \tau m^3 < 3\times10^{21}$ s eV^3.

[27] Model-dependent theoretical analysis of SN 1987A neutrinos. Quoted limit is for $\left[\sum_j |U_{\ell j}|^2\ \Gamma_j\ m_j\right]^{-1}$, where $\ell = \mu, \tau$. Limit is 3.3×10^{14} s/eV for $\ell = e$.

[28] OBERAUER 87 looks for photons and e^+e^- pairs from radiative decays of reactor neutrinos.

[29] BINETRUY 84 finds $\tau < 10^8$ s for neutrinos in a radiation-dominated universe.

[30] These experiments look for $\nu_k \to \nu_j\gamma$ or $\overline{\nu}_k \to \overline{\nu}_j\gamma$.

[31] STECKER 80 limit based on UV background; result given is $\tau > 4\times10^{22}$ s at m_ν=20 eV.

[32] FALK 78 finds lifetime constraints based on supernova energetics.

[33] COWSIK 77 considers variety of scenarios. For neutrinos produced in the big bang, present limits on optical photon flux require $\tau > 10^{23}$ s for $m_\nu \sim$ 1 eV. See also COWSIK 79 and GOLDMAN 79.

ν MAGNETIC MOMENT

The coupling of neutrinos to an electromagnetic field is a characterized by a 3×3 matrix λ of the magnetic (μ) and electric (d) dipole moments ($\lambda = \mu - id$). For Majorana neutrinos the matrix λ is antisymmetric and only transition moments are allowed, while for Dirac neutrinos λ is a general 3×3 matrix. In the standard electroweak theory extended to include neutrino masses (see FUJIKAWA 80) $\mu_\nu = 3eG_F m_\nu/(8\pi^2\sqrt{2}) = 3.2\times10^{-19}(m_\nu/\text{eV})\mu_B$, i.e. it is unobservably small given the known small neutrino masses. In more general models there is no longer a proportionality between neutrino mass and its magnetic moment, even though only massive neutrinos have nonvanishing magnetic moments without fine tuning.

Laboratory bounds on λ are obtained via elastic ν-e scattering, where the scattered neutrino is not observed. The combinations of matrix elements of λ that are constrained by various experiments depend on the initial neutrino flavor and on its propagation between source and detector (e.g., solar ν_e and reactor $\overline{\nu}_e$ do not constrain the same combinations). The listings below therefore identify the initial neutrino flavor.

Other limits, e.g. from various stellar cooling processes, apply to all neutrino flavors. Analogous flavor independent, but weaker, limits are obtained from the analysis of $e^+e^- \to \nu\overline{\nu}\gamma$ collider experiments.

VALUE (10^{-10} μ_B)	CL%	DOCUMENT ID		TECN	COMMENT
< 0.28	90	[1] AGOSTINI	17A	BORX	Solar ν spectrum
< 0.29	90	[2] BEDA	13	CNTR	Reactor $\overline{\nu}_e$
< 6.8	90	[3] AUERBACH	01	LSND	$\nu_e e$, $\nu_\mu e$ scattering
< 3900	90	[4] SCHWIENHO...	01	DONU	$\nu_\tau e^- \to \nu_\tau e^-$
• • • We do not use the following data for averages, fits, limits, etc. • • •					
< 0.022	90	[5] ARCEO-DIAZ	15	ASTR	Red giants
< 0.1	95	[6] CORSICO	14	ASTR	
< 0.05	95	[7] MILLER-BER...	14B	ASTR	
< 0.045	95	[8] VIAUX	13A	ASTR	Globular cluster M5
< 0.32	90	[9] BEDA	10	CNTR	Reactor $\overline{\nu}_e$
< 2.2	90	[10] DENIZ	10	TEXO	Reactor $\overline{\nu}_e$
< 0.011–0.027		[11] KUZNETSOV	09	ASTR	$\nu_L \to \nu_R$ in SN1987A
< 0.54	90	[12] ARPESELLA	08A	BORX	Solar ν spectrum
< 0.58	90	[13] BEDA	07	CNTR	Reactor $\overline{\nu}_e$
< 0.74	90	[14] WONG	07	CNTR	Reactor $\overline{\nu}_e$
< 0.9	90	[15] DARAKTCH...	05		Reactor $\overline{\nu}_e$
< 130	90	[16] XIN	05	CNTR	Reactor ν_e
< 37	95	[17] GRIFOLS	04	FIT	Solar ^{8}B ν (SNO NC)
< 3.6	90	[18] LIU	04	SKAM	Solar ν spectrum
< 1.1	90	[19] LIU	04	SKAM	Solar ν spectrum (LMA region)
< 5.5	90	[20] BACK	03B	CNTR	Solar pp and Be ν
< 1.0	90	[21] DARAKTCH...	03		Reactor $\overline{\nu}_e$
< 1.3	90	[22] LI	03B	CNTR	Reactor $\overline{\nu}_e$
< 2	90	[23] GRIMUS	02	FIT	solar + reactor (Majorana ν)

<80000	90	[24] TANIMOTO	00	RVUE	$e^+e^- \to \nu\overline{\nu}\gamma$
< 0.01–0.04		[25] AYALA	99	ASTR	$\nu_L \to \nu_R$ in SN1987A
< 1.5	90	[26] BEACOM	99	SKAM	Solar ν spectrum
< 0.03		[27] RAFFELT	99	ASTR	Red giant luminosity
< 4		[28] RAFFELT	99	ASTR	Solar cooling
<44000	90	ABREU	97J	DLPH	$e^+e^- \to \nu\overline{\nu}\gamma$ at LEP
<33000	90	[29] ACCIARRI	97Q	L3	$e^+e^- \to \nu\overline{\nu}\gamma$ at LEP
< 0.62		[30] ELMFORS	97	COSM	Depolarization in early universe plasma
<27000	95	[31] ESCRIBANO	97	RVUE	$\Gamma(Z \to \nu\nu)$ at LEP
< 30	90	VILAIN	95B	CHM2	$\nu_\mu e \to \nu_\mu e$
<55000	90	GOULD	94	RVUE	$e^+e^- \to \nu\overline{\nu}\gamma$ at LEP
< 1.9	95	[32] DERBIN	93	CNTR	Reactor $\overline{\nu}e \to \overline{\nu}e$
< 5400	90	[33] COOPER-...	92	BEBC	$\nu_\tau e^- \to \nu_\tau e^-$
< 2.4	90	[34] VIDYAKIN	92	CNTR	Reactor $\overline{\nu}e \to \overline{\nu}e$
<56000	90	DESHPANDE	91	RVUE	$e^+e^- \to \nu\overline{\nu}\gamma$
< 100	95	[35] DORENBOS...	91	CHRM	$\nu_\mu e \to \nu_\mu e$
< 8.5	90	AHRENS	90	CNTR	$\nu_\mu e \to \nu_\mu e$
< 10.8	90	[36] KRAKAUER	90	CNTR	LAMPF $\nu e \to \nu e$
< 7.4	90	[36] KRAKAUER	90	CNTR	LAMPF $(\nu_\mu, \overline{\nu}_\mu)e$ elast.
< 0.02		[37] RAFFELT	90	ASTR	Red giant luminosity
< 0.1		[38] RAFFELT	89B	ASTR	Cooling helium stars
		[39] FUKUGITA	88	COSM	Primordial magn. fields
<40000	90	[40] GROTCH	88	RVUE	$e^+e^- \to \nu\overline{\nu}\gamma$
≤ .3		[38] RAFFELT	88B	ASTR	He burning stars
< 0.11		[38] FUKUGITA	87	ASTR	Cooling helium stars
< 0.0006		[41] NUSSINOV	87	ASTR	Cosmic EM backgrounds
< 0.1–0.2		MORGAN	81	COSM	^{4}He abundance
< 0.85		BEG	78	ASTR	Stellar plasmons
< 0.6		[42] SUTHERLAND	76	ASTR	Red giants + degenerate dwarfs
< 81		[43] KIM	74	RVUE	$\overline{\nu}_\mu e \to \overline{\nu}_\mu e$
< 1		BERNSTEIN	63	ASTR	Solar cooling
< 14		COWAN	57	CNTR	Reactor $\overline{\nu}$

[1] AGOSTINI 17A obtained this limit using the shape of the recoil electron energy spectrum from the Borexino Phase-II 1291.5 live days of solar neutrino data and the constraints on the sum of the solar neutrino fluxes from the radiochemical gallium experiments SAGE, Gallex, and GNO. Without radiochemical constraints, the 90% C.L. limit of $< 4.0 \times 10^{-11} \mu_B$ is obtained.

[2] BEDA 13 report $\overline{\nu}_e e^-$ scattering results, using the Kalinin Nuclear Power Plant and a shielded Ge detector. The recoil electron spectrum is analyzed between 2.5 and 55 keV. Supersedes BEDA 07. Supersedes BEDA 10. This is the most stringent limit on the magnetic moment of reactor $\overline{\nu}_e$.

[3] AUERBACH 01 limit is based on the LSND ν_e and ν_μ electron scattering measurements. The limit is slightly more stringent than KRAKAUER 90.

[4] SCHWIENHORST 01 quote an experimental sensitivity of 4.9×10^{-7}.

[5] ARCEO-DIAZ 15 constrains the neutrino magnetic moment from observation of the tip of the red giant branch in the globular cluster ω-Centauri.

[6] CORSICO 14 constrains the neutrino magnetic moment from observations of white drarf pulsations.

[7] MILLER-BERTOLAMI 14B constrains the neutrino magnetic moment from observations of the white dwarf luminosity function of the Galactic disk.

[8] VIAUX 13A constrains the neutrino magnetic moment from observations of the globular cluster M5.

[9] BEDA 10 report $\overline{\nu}_e e^-$ scattering results, using the Kalinin Nuclear Power Plant and a shielded Ge detector. The recoil electron spectrum is analyzed between 2.9 and 45 keV. Supersedes BEDA 07. Superseded by BEDA 13.

[10] DENIZ 10 observe reactor $\overline{\nu}_e e$ scattering with recoil kinetic energies 3–8 MeV using CsI(Tl) detectors. The observed rate and spectral shape are consistent with the Standard Model prediction, leading to the reported constraint on $\overline{\nu}_e$ magnetic moment.

[11] KUZNETSOV 09 obtain a limit on the flavor averaged magnetic moment of Dirac neutrinos from the time averaged neutrino signal of SN1987A. Improves and supersedes the analysis of BARBIERI 88 and AYALA 99.

[12] ARPESELLA 08A obtained this limit using the shape of the recoil electron energy spectrum from the Borexino 192 live days of solar neutrino data.

[13] BEDA 07 performed search for electromagnetic $\overline{\nu}_e$-e scattering at Kalininskaya nuclear reactor. A Ge detector with active and passive shield was used and the electron recoil spectrum between 3.0 and 61.3 keV analyzed. Superseded by BEDA 10.

[14] WONG 07 performed search for non-standard $\overline{\nu}_e$-e scattering at the Kuo-Sheng nuclear reactor. Ge detector equipped with active anti-Compton shield is used. Most stringent laboratory limit on magnetic moment of reactor $\overline{\nu}_e$. Supersedes LI 03B.

[15] DARAKTCHIEVA 05 present the final analysis of the search for non-standard $\overline{\nu}_e$-e scattering component at Bugey nuclear reactor. Full kinematical event reconstruction of both the kinetic energy above 700 keV and scattering angle of the recoil electron, by use of TPC. Most stringent laboratory limit on magnetic moment. Supersedes DARAKTCHIEVA 03.

[16] XIN 05 evaluated the ν_e flux at the Kuo-Sheng nuclear reactor and searched for non-standard ν_e-e scattering. Ge detector equipped with active anti-Compton shield was used. This laboratory limit on magnetic moment is considerably less stringent than the limits for reactor $\overline{\nu}_e$, but is specific to ν_e.

[17] GRIFOLS 04 obtained this bound using the SNO data of the solar ^{8}B neutrino flux measured with deuteron breakup. This bound applies to $\mu_{\rm eff} = (\mu_{21}^2 + \mu_{22}^2 + \mu_{23}^2)^{1/2}$.

[18] LIU 04 obtained this limit using the shape of the recoil electron energy spectrum from the Super-Kamiokande-I 1496 days of solar neutrino data. Neutrinos are assumed to have only diagonal magnetic moments, $\mu_{\nu 1} = \mu_{\nu 2}$. This limit corresponds to the oscillation parameters in the vacuum oscillation region.

[19] LIU 04 obtained this limit using the shape of the recoil electron energy spectrum from the Super-Kamiokande-I 1496 live-day solar neutrino data, by limiting the oscillation parameter region in the LMA region allowed by solar neutrino experiments plus KamLAND. $\mu_{\nu 1} = \mu_{\nu 2}$ is assumed. In the LMA region, the same limit would be obtained even if neutrinos have off-diagonal magnetic moments.

[20] BACK 03B obtained this bound from the results of background measurements with Counting Test Facility (the prototype of the Borexino detector). Standard Solar Model flux was assumed. This μ_ν can be different from the reactor μ_ν in certain oscillation scenarios (see BEACOM 99).

[21] DARAKTCHIEVA 03 searched for non-standard $\overline{\nu}_e$-e scattering component at Bugey nuclear reactor. Full kinematical event reconstruction by use of TPC. Superseded by DARAKTCHIEVA 05.

[22] LI 03B used Ge detector in active shield near nuclear reactor to test for nonstandard $\overline{\nu}_e$-e scattering.

[23] GRIMUS 02 obtain stringent bounds on all Majorana neutrino transition moments from a simultaneous fit of LMA-MSW oscillation parameters and transition moments to global solar neutrino data + reactor data. Using only solar neutrino data, a 90% CL bound of $6.3 \times 10^{-10} \mu_B$ is obtained.

[24] TANIMOTO 00 combined $e^+e^- \to \nu\overline{\nu}\gamma$ data from VENUS, TOPAZ, and AMY.

[25] AYALA 99 improves the limit of BARBIERI 88.

[26] BEACOM 99 obtain the limit using the shape, but not the absolute magnitude which is affected by oscillations, of the solar neutrino spectrum obtained by Superkamiokande (825 days). This μ_ν can be different from the reactor μ_ν in certain oscillation scenarios.

[27] RAFFELT 99 is an update of RAFFELT 90. This limit applies to all neutrino flavors which are light enough (< 5 keV) to be emitted from globular-cluster red giants. This limit pertains equally to electric dipole moments and magnetic transition moments, and it applies to both Dirac and Majorana neutrinos.

[28] RAFFELT 99 is essentially an update of BERNSTEIN 63, but is derived from the helioseismological limit on a new energy-loss channel of the Sun. This limit applies to all neutrino flavors which are light enough (<1 keV) to be emitted from the Sun. This limit pertains equally to electric dipole and magnetic transition moments, and it applies to both Dirac and Majorana neutrinos.

[29] ACCIARRI 97Q result applies to both direct and transition magnetic moments and for q^2=0.

[30] ELMFORS 97 calculate the rate of depolarization in a plasma for neutrinos with a magnetic moment and use the constraints from a big-bang nucleosynthesis on additional degrees of freedom.

[31] Applies to absolute value of magnetic moment.

[32] DERBIN 93 determine the cross section for 0.6–2.0 MeV electron energy as $(1.28 \pm 0.63) \times \sigma_{\rm weak}$. However, the (reactor on – reactor off)/(reactor off) is only $\sim 1/100$.

[33] COOPER-SARKAR 92 assume $f_{D_s}/f_\pi = 2$ and D_s, $\overline{D}_s$ production cross section = 2.6 μb to calculate ν flux.

[34] VIDYAKIN 92 limit is from a $e\overline{\nu}_e$ elastic scattering experiment. No experimental details are given except for the cross section from which this limit is derived. Signal/noise was 1/10. The limit uses $\sin^2\theta_W = 0.23$ as input.

[35] DORENBOSCH 91 corrects an incorrect statement in DORENBOSCH 89 that the ν magnetic moment is $< 1 \times 10^{-9}$ at the 95%CL. DORENBOSCH 89 measures both $\nu_\mu e$ and $\overline{\nu}e$ elastic scattering and assume $\mu(\nu) = \mu(\overline{\nu})$.

[36] KRAKAUER 90 experiment fully reported in ALLEN 93.

[37] RAFFELT 90 limit applies for a diagonal magnetic moment of a Dirac neutrino, or for a transition magnetic moment of a Majorana neutrino. In the latter case, the same analysis gives $< 1.4 \times 10^{-12}$. Limit at 95%CL obtained from δM_c.

[38] Significant dependence on details of stellar models.

[39] FUKUGITA 88 find magnetic dipole moments of any two neutrino species are bounded by $\mu < 10^{-16}$ $[10^{-9}\ G/B_0]$ where B_0 is the present-day intergalactic field strength.

[40] GROTCH 88 combined data from MAC, ASP, CELLO, and Mark J.

[41] For m_ν = 8–200 eV. NUSSINOV 87 examines transition magnetic moments for $\nu_\mu \to \nu_e$ and obtain $< 3 \times 10^{-15}$ for $m_\nu > 16$ eV and $< 6 \times 10^{-14}$ for $m_\nu > 4$ eV.

[42] We obtain above limit from SUTHERLAND 76 using their limit $f < 1/3$.

[43] KIM 74 is a theoretical analysis of $\overline{\nu}_\mu$ reaction data.

NEUTRINO CHARGE RADIUS SQUARED

We report limits on the so-called neutrino charge radius squared. While the straight-forward definition of a neutrino charge radius has been proven to be gauge-dependent and, hence, unphysical (LEE 77C), there have been recent attempts to define a physically observable neutrino charge radius (BERNABEU 00, BERNABEU 02). The issue is still controversial (FUJIKAWA 03, BERNABEU 03). A more general interpretation of the experimental results is that they are limits on certain nonstandard contributions to neutrino scattering.

VALUE (10^{-32} cm^2)	CL%	DOCUMENT ID		TECN	COMMENT
−2.1 to 3.3	90	[1] DENIZ	10	TEXO	Reactor $\overline{\nu}_e e$
• • • We do not use the following data for averages, fits, limits, etc. • • •					
−0.53 to 0.68	90	[2] HIRSCH	03		$\nu_\mu e$ scat.
−8.2 to 9.9	90	[3] HIRSCH	03		anomalous $e^+e^- \to \nu\overline{\nu}\gamma$
−2.97 to 4.14	90	[4] AUERBACH	01	LSND	$\nu_e e \to \nu_e e$
−0.6 to 0.6	90	VILAIN	95B	CHM2	$\nu_\mu e$ elastic scat.
0.9 ±2.7		ALLEN	93	CNTR	LAMPF $\nu e \to \nu e$
< 2.3	95	MOURAO	92	ASTR	HOME/KAM2 ν rates
< 7.3	90	[5] VIDYAKIN	92	CNTR	Reactor $\overline{\nu}e \to \overline{\nu}e$
1.1 ±2.3		ALLEN	91	CNTR	Repl. by ALLEN 93
−1.1 ±1.0		[6] AHRENS	90	CNTR	$\nu_\mu e$ elastic scat.
−0.3 ±1.5		[6] DORENBOS...	89	CHRM	$\nu_\mu e$ elastic scat.
		[7] GRIFOLS	89B	ASTR	SN 1987A

[1] DENIZ 10 observe reactor $\overline{\nu}_e e$ scattering with recoil kinetic energies 3–8 MeV using CsI(Tl) detectors. The observed rate and spectral shape are consistent with the Standard Model prediction, leading to the reported constraint on $\overline{\nu}_e$ charge radius.

[2] Based on analysis of CCFR 98 results. Limit is on $\langle r_V^2 \rangle + \langle r_A^2 \rangle$. The CHARM II and E734 at BNL results are reanalyzed, and weaker bounds on the charge radius squared

than previously published are obtained. The NuTeV result is discussed; when tentatively interpreted as ν_μ charge radius it implies $\langle r_V^2 \rangle + \langle r_A^2 \rangle = (4.20 \pm 1.64) \times 10^{-33}$ cm^2.

[3] Results of LEP-2 are interpreted as limits on the axial-vector charge radius squared of a Majorana ν_μ. Slightly weaker limits for both vector and axial-vector charge radius squared are obtained for the Dirac case, and somewhat weaker limits are obtained from the analysis of lower energy data (LEP-1.5 and TRISTAN).

[4] AUERBACH 01 measure $\nu_e e$ elastic scattering with LSND detector. The cross section agrees with the Standard Model expectation, including the charge and neutral current interference. The 90% CL applies to the range shown.

[5] VIDYAKIN 92 limit is from a $e\overline{\nu}$ elastic scattering experiment. No experimental details are given except for the cross section from which this limit is derived. Signal/noise was 1/10. The limit uses $\sin^2\theta_W = 0.23$ as input.

[6] Result is obtained from reanalysis given in ALLEN 91, followed by our reduction to obtain $1\,\sigma$ errors.

[7] GRIFOLS 89B sets a limit of $\langle r^2 \rangle < 0.2 \times 10^{-32}$ cm^2 for right-handed neutrinos.

REFERENCES FOR Neutrino Properties

AGOSTINI	17A	PR D96 091103	M. Agostini *et al.*	(Borexino Collab.)
VAGNOZZI	17	PR D96 123503	S. Vagnozzi *et al.*	
YECHE	17	JCAP 1706 047	C. Yeche *et al.*	
DELLA-VALLE	16	EPJ C76 24	F. Della Valle *et al.*	(PVLAS Collab.)
DIVALENTINO	16	PR D93 083527	E. Di Valentino *et al.*	
GIUSARMA	16	PR D94 083522	E. Guisarma *et al.*	
HUANG	16	EPJ C76 489	Q.-G. Huang, K. Wang, S. Wang	
ARCEO-DIAZ	15	ASP 70 1	S. Arceo-Diaz *et al.*	
PALANQUE-...	15A	JCAP 1511 011	N. Palanque-Delabrouille *et al.*	
ROSSI	15	PR D92 063505	G. Rossi *et al.*	
ADE	14	AA 571 A16	P.A.R. Ade *et al.*	(Planck Collab.)
BATTYE	14	PRL 112 051303	R.A. Battye, A. Moss	(MCHS, NOTT)
BEUTLER	14	MNRAS 444 3501	F. Beutler *et al.*	(BOSS Collab.)
CHEN	14A	PR D90 011301	J.-W. Chen *et al.*	(TEXONO Collab.)
CORSICO	14	JCAP 1408 054	A.H. Corsico	
COSTANZI	14	JCAP 1410 081	M. Costanzi *et al.*	(TRST, TRSTI)
GIUSARMA	14	PR D90 043507	E. Giusarma *et al.*	
HOU	14	APJ 782 74	Z. Hou *et al.*	
LEISTEDT	14	PRL 113 041301	B. Leistedt, H.V. Peiris, L. Verde	
MILLER-BER...	14B	AA 562 A123	M.M. Miller Bertolami	(MPIG, LAPL)
RIEMER-SOR...	14	PR D89 103505	S. Riemer-Sorensen, D. Parkinson, T.M. Davis	
STUDENIKIN	14	EPL 107 21001	A.I. Studenikin	
BEDA	13	PPNL 10 139	A.G. Beda *et al.*	(GEMMA Collab.)
VIAUX	13A	PRL 111 231301	N. Viaux *et al.*	
MORESCO	12	JCAP 1207 053	M. Moresco *et al.*	
XIA	12	JCAP 1206 010	J.-Q. Xia *et al.*	
ASEEV	11	PR D84 112003	V.N. Aseev *et al.*	
CECCHINI	11	ASP 34 486	S. Cecchini *et al.*	
SAITO	11	PR D83 043529	S. Saito, M. Takada, A. Taruya	
BEDA	10	PPNL 7 406	A.G. Beda *et al.*	(GEMMA Collab.)
DENIZ	10	PR D81 072001	M. Deniz *et al.*	(TEXONO Collab.)
HANNESTAD	10	JCAP 1008 001	S. Hannestad *et al.*	
PAGLIAROLI	10	ASP 33 287	G. Pagliaroli, F. Rossi-Torres, E. Vissani	(INFN+)
SEKIGUCHI	10	JCAP 1003 015	T. Sekiguchi *et al.*	
THOMAS	10	PRL 105 031301	S.A. Thomas, F.B. Abdalla, O. Lahav	(LOUC)
ICHIKI	09	PR D79 023520	K. Ichiki, M. Takada, T. Takahashi	
KOMATSU	09	APJS 180 330	E. Komatsu *et al.*	
KUZNETSOV	09	IJMP A24 5977	A.V. Kuznetsov, N.V. Mikheev, A.A. Okrugin	(YARO)
TERENO	09	AA 500 657	I. Tereno *et al.*	
VIKHLININ	09	APJ 692 1060	A. Vikhlinin *et al.*	
ARPESELLA	08A	PRL 101 091302	C. Arpesella *et al.*	(Borexino Collab.)
BERNARDIS	08	PR D78 083535	F. De Bernardis *et al.*	
BEDA	07	PAN 70 1873 Translated from YAF 70 1925.	A.G. Beda *et al.*	
FOGLI	07	PR D75 053001	G.L. Fogli *et al.*	
GNINENKO	07	PR D75 075014	S.N. Gninenko, N.V. Krasnikov, A. Rubbia	
KRISTIANSEN	07	PR D75 083510	J. Kristiansen, O. Elgaroy, H. Dahle	
MIRIZZI	07	PR D76 053007	A. Mirizzi, D. Montanino, P.D. Serpico	
SPERGEL	07	APJS 170 377	D.N. Spergel *et al.*	
WONG	07	PR D75 012001	H.T. Wong *et al.*	(TEXONO Collab.)
ZUNCKEL	07	JCAP 0708 004	C. Zunckel, P. Ferreira	
CIRELLI	06	JCAP 0612 013	M. Cirelli *et al.*	
FUKUGITA	06	PR D74 027302	M. Fukugita *et al.*	
GOOBAR	06	JCAP 0606 019	A. Goobar *et al.*	
HANNESTAD	06	JCAP 0611 016	S. Hannestad, G. Raffelt	
KRISTIANSEN	06	PR D74 123005	J. Kristiansen, O. Elgaroy, H. Eriksen	
SANCHEZ	06	MNRAS 366 189	A.G. Sanchez *et al.*	
SELJAK	06	JCAP 0610 014	U. Seljak, A. Slosar, P. McDonald	
DARAKTCH...	05	PL B615 153	Z. Daraktchieva *et al.*	(MUNU Collab.)
ICHIKAWA	05	PR D71 043001	K. Ichikawa, M. Fukugita, M. Kawasaki	(ICRR)
KRAUS	05	EPJ C40 447	Ch. Kraus *et al.*	
XIN	05	PR D72 012006	B. Xin *et al.*	(TEXONO Collab.)
AHARMIM	04	PR D70 093014	B. Aharmim *et al.*	(SNO Collab.)
BARGER	04	PL B595 55	V. Barger, D. Marfatia, A. Tregre	
CECCHINI	04	ASP 21 183	S. Cecchini *et al.*	(BGNA+)
CROTTY	04	PR D69 123007	P. Crotty, J. Lesgourgues, S. Pastor	
EGUCHI	04	PRL 92 071301	K. Eguchi *et al.*	(KamLAND Collab.)
GRIFOLS	04	PL B587 184	J.A. Grifols, E. Masso, S. Mohanty	(BARC, AHMED)
LIU	04	PRL 93 021802	D.W. Liu *et al.*	(Super-Kamiokande Collab.)
ARNABOLDI	03A	PRL 91 161802	C. Arnaboldi *et al.*	
BACK	03B	PL B563 35	H.O. Back *et al.*	(Borexino Collab.)
BANDYOPA...	03	PL B555 33	A. Bandyopadhyay, S. Choubey, S. Goswami	(SAHA+)
BERNABEU	03	hep-ph/0303202	J. Bernabeu, J. Papavassiliou, J. Vidal	
DARAKTCH...	03	PL B564 190	Z. Daraktchieva *et al.*	(MUNU Collab.)
FUJIKAWA	03	hep-ph/0303188	K. Fujikawa, R. Shrock	
HIRSCH	03	PR D67 033005	M. Hirsch, E. Nardi, D. Restrepo	
LI	03B	PRL 90 131802	H.B. Li *et al.*	(TEXONO Collab.)
SPERGEL	03	APJS 148 175	D.N. Spergel *et al.*	
BERNABEU Also	02	PRL 89 101802 PRL 89 229902 (errat.)	J. Bernabeu, J. Papavassiliou, J. Vidal J. Bernabeu, J. Papavassiliou, J. Vidal	
DERBIN	02B	JETPL 76 409 Translated from ZETFP 76 483.	A.V. Derbin, O.Ju. Smirnov	
GRIMUS	02	NP B648 376	W. Grimus *et al.*	
JOSHIPURA	02B	PR D66 113008	A.S. Joshipura, E. Masso, S. Mohanty	
LEWIS	02	PR D66 103511	A. Lewis, S. Bridle	
LOREDO	02	PR D65 063002	T.J. Loredo, D.Q. Lamb	
WANG	02	PR D65 123001	X. Wang, M. Tegmark, M. Zaldarriaga	
AUERBACH	01	PR D63 112001	L.B. Auerbach *et al.*	(LSND Collab.)
SCHWIENHO...	01	PL B513 23	R. Schwienhorst *et al.*	(DONUT Collab.)
ATHANAS	00	PR D61 052002	M. Athanas *et al.*	(CLEO Collab.)
BERNABEU	00	PR D62 113012	J. Bernabeu *et al.*	
FUKUGITA	00	PRL 84 1082	M. Fukugita, G.C. Liu, N. Sugiyama	
TANIMOTO	00	PL B478 1	N. Tanimoto *et al.*	
AYALA	99	PR D59 111901	A. Ayala, J.C. D'Olivo, M. Torres	
BEACOM	99	PRL 83 5222	J.F. Beacom, P. Vogel	
CROFT	99	PRL 83 1092	R.A.C. Croft, W. Hu, R. Dave	
DOLGOV	99	NP B548 385	A.D. Dolgov *et al.*	
LOBASHEV	99	PL B460 227	V.M. Lobashev *et al.*	
RAFFELT	99	PRPL 320 319	G.G. Raffelt	
WEINHEIMER	99	PL B460 219	Ch. Weinheimer *et al.*	
ACKERSTAFF	98T	EPJ C5 229	K. Ackerstaff *et al.*	(OPAL Collab.)
AMMAR	98	PL B431 209	R. Ammar *et al.*	(CLEO Collab.)
BARATE	98F	EPJ C2 395	R. Barate *et al.*	(ALEPH Collab.)
BILLER	98	PRL 80 2992	S.D. Biller *et al.*	(WHIPPLE Collab.)
FELDMAN	98	PR D57 3873	G.J. Feldman, R.D. Cousins	
LENZ	98	PL B416 50	S. Lenz *et al.*	
ABREU	97J	ZPHY C74 577	P. Abreu *et al.*	(DELPHI Collab.)
ACCIARRI	97Q	PL B412 201	M. Acciarri *et al.*	(L3 Collab.)
ANASTASSOV Also	97	PR D55 2559 PR D58 119903 (erratum)	A. Anastassov *et al.* A. Anastassov *et al.*	(CLEO Collab.) (CLEO Collab.)
ELMFORS	97	NP B503 3	P. Elmfors *et al.*	
ESCRIBANO	97	PL B395 369	R. Escribano, E. Masso	(BARC, PARIT)
FIELDS	97	ASP 6 169	B.D. Fields, K. Kainulainen, K.A. Olive	(NDAM+)
SWAIN	97	PR D55 1	J. Swain, L. Taylor	(NEAS)
ALEXANDER	96M	ZPHY C72 231	G. Alexander *et al.*	(OPAL Collab.)
ASSAMAGAN	96	PR D53 6065	K.A. Assamagan *et al.*	(PSI, ZURI, VILL+)
BAI	96	PR D53 20	J.Z. Bai *et al.*	(BES Collab.)
BOTTINO	96	PR D53 6361	A. Bottino *et al.*	
DOLGOV	96	PL B383 193	A.D. Dolgov, S. Pastor, J.W.F. Valle	(IFIC, VALE)
HANNESTAD	96	PRL 76 2848	S. Hannestad, J. Madsen	(AARH)
HANNESTAD	96B	PRL 77 5148 (erratum)	S. Hannestad, J. Madsen	(AARH)
HANNESTAD	96C	PR D54 7894	S. Hannestad, J. Madsen	(AARH)
SOBIE	96	ZPHY C70 383	R.J. Sobie, R.K. Keeler, I. Lawson	(VICT)
BELESEV	95	PL B350 263	A.I. Belesev *et al.*	(INRM, KIAE)
BUSKULIC	95H	PL B349 585	D. Buskulic *et al.*	(ALEPH Collab.)
CHING	95	IJMP A10 2841	C.R. Ching *et al.*	(CST, BEIJT, CIAE)
DOLGOV	95	PR D51 4129	A.D. Dolgov, K. Kainulainen, I.Z. Rothstein	(MICH+)
HIDDEMANN	95	JP G21 639	K.H. Hiddemann, H. Daniel, O. Schwentker	(MUNT)
KERNAN	95	NP B437 243	P.J. Kernan, L.M. Krauss	(CASE)
SIGL	95	PR D51 1499	G. Sigl, M.S. Turner	(FNAL, EFI)
STOEFFL	95	PRL 75 3237	W. Stoeffl, D.J. Decman	(LLNL)
VILAIN	95B	PL B345 115	P. Vilain *et al.*	(CHARM II Collab.)
ASSAMAGAN	94	PL B335 231	K.A. Assamagan *et al.*	(PSI, ZURI, VILL+)
BABU	94	PL B321 140	K.S. Babu, T.M. Gould, I.Z. Rothstein	(BART+)
DODELSON	94	PR D49 5068	S. Dodelson, G. Gyuk, M.S. Turner	(FNAL, CHIC+)
GOULD	94	PL B333 545	T.M. Gould, I.Z. Rothstein	(JHU, MICH)
JECKELMANN	94	PL B335 326	B. Jeckelmann, P.F.A. Goudsmit, H.J. Leisi	(WABRN+)
KAWASAKI	94	NP B419 105	M. Kawasaki *et al.*	(OSU)
PERES	94	PR D50 513	O.L.G. Peres, V. Pleitez, R. Zukanovich Funchal	
YASUMI	94	PL B334 229	S. Yasumi *et al.*	(KEK, TSUK, KYOT+)
ALLEN	93	PR D47 11	R.C. Allen *et al.*	(UCI, LANL, ANL+)
BALEST	93	PR D47 3671	R. Balest *et al.*	(CLEO Collab.)
CINABRO	93	PRL 70 3700	D. Cinabro *et al.*	(CLEO Collab.)
DERBIN	93	JETPL 57 768 Translated from ZETFP 57 755.	A.V. Derbin *et al.*	(PNPI)
DOLGOV	93	PRL 71 476	A.D. Dolgov, I.Z. Rothstein	(MICH)
ENQVIST	93	PL B301 376	K. Enqvist, H. Uibo	(NORD)
SUN	93	CJNP 15 261	H.C. Sun *et al.*	(CIAE, CST, BEIJT)
WEINHEIMER	93	PL B300 210	C. Weinheimer *et al.*	(MANZ)
ALBRECHT	92M	PL B292 221	H. Albrecht *et al.*	(ARGUS Collab.)
BLUDMAN	92	PR D45 4720	S.A. Bludman	(CFPA)
COOPER-...	92	PL B280 153	A.M. Cooper-Sarkar *et al.*	(BEBC WA66 Collab.)
DODELSON	92	PRL 68 2572	S. Dodelson, J.A. Frieman, M.S. Turner	(FNAL+)
HOLZSCHUH	92B	PL B287 381	E. Holzschuh, M. Fritschi, W. Kundig	(ZURI)
KAWANO	92	PL B275 487	L.H. Kawano *et al.*	(CIT, UCSD, LLL+)
MOURAO	92	PL B285 364	A.M. Mourao, J. Pulido, J.P. Ralston	(LISB, LISBT+)
PDG	92	PR D45 S1	K. Hikasa *et al.*	(KEK, LBL, BOST+)
VIDYAKIN	92	JETPL 55 206 Translated from ZETFP 55 212.	G.S. Vidyakin *et al.*	(KIAE)
ALLEN	91	PR D43 1	R.C. Allen *et al.*	(UCI, LANL, UMD)
DAVIDSON	91	PR D43 2314	S. Davidson, B.A. Campbell, D. Bailey	(ALBE+)
DESHPANDE	91	PR D43 943	N.G. Deshpande, K.V.L. Sarma	(OREG, TATA)
DORENBOS...	91	ZPHY C51 142 (erratum)	J. Dorenbosch *et al.*	(CHARM Collab.)
FULLER	91	PR D43 3136	G.M. Fuller, R.A. Malaney	(UCSD)
GRANEK	91	IJMP A6 2387	H. Granek, B.H.J. McKellar	(MELB)
KAWAKAMI	91	PL B256 105	H. Kawakami *et al.*	(INUS, TOHOK, TINT+)
KOLB	91	PRL 67 533	E.W. Kolb *et al.*	(FNAL, CHIC)
KRAKAUER	91	PR D44 6	D.A. Krakauer *et al.*	(LAMPF E225 Collab.)
LAM	91	PR D44 3345	W.P. Lam, K.W. Ng	(AST)
ROBERTSON	91	PRL 67 957	R.G.H. Robertson *et al.*	(LASL, LLL)
AHRENS	90	PR D41 3297	L.A. Ahrens *et al.*	(BNL, BROW, HIRO+)
AVIGNONE	90	PR D41 682	F.T. Avignone, J.I. Collar	(SCUC)
KRAKAUER	90	PL B252 177	D.A. Krakauer *et al.*	(LAMPF E225 Collab.)
RAFFELT	90	PRL 64 2856	G.G. Raffelt	(MPIM)
WALKER	90	PR D41 689	T.P. Walker	(HARV)
CHUPP	89	PRL 62 505	E.L. Chupp, W.T. Vestrand, C. Reppin	(UNH, MPIM)
DORENBOS...	89	ZPHY C41 567	J. Dorenbosch *et al.*	(CHARM Collab.)
GRIFOLS	89B	PR D40 3819	J.A. Grifols, E. Masso	(BARC)
KOLB	89	PRL 62 509	E.W. Kolb, M.S. Turner	(CHIC, FNAL)
LOREDO	89	ANYAS 571 601	T.J. Loredo, D.Q. Lamb	(CHIC)
RAFFELT	89	PR D39 2066	G.G. Raffelt	(PRIN, UCB)
RAFFELT	89B	APJ 336 61	G. Raffelt, D. Dearborn, J. Silk	(UCB, LLL)
ALBRECHT	88B	PL B202 149	H. Albrecht *et al.*	(ARGUS Collab.)
BARBIERI	88	PRL 61 27	R. Barbieri, R.N. Mohapatra	(PISA, UMD)
BORIS	88	PRL 61 245 (erratum)	S.D. Boris *et al.*	(ITEP, ASCI)
FUKUGITA	88	PRL 60 879	M. Fukugita *et al.*	(KYOTU, MPIM, UCB)
GROTCH	88	ZPHY C39 553	H. Grotch, R.W. Robinett	(PSU)
RAFFELT	88B	PR D37 549	G.G. Raffelt, D.S.P. Dearborn	(UCB, LLL)
SPERGEL	88	PL B200 366	D.N. Spergel, J.N. Bahcall	(IAS)
VONFEILIT...	88	PL B200 580	F. von Feilitzsch, L. Oberauer	(MUNT)
BARBIELLINI	87	NAT 329 21	G. Barbiellini, G. Cocconi	(CERN)
BORIS Also	87	PRL 58 2019 PRL 61 245 (erratum)	S.D. Boris *et al.* S.D. Boris *et al.*	(ITEP, ASCI) (ITEP, ASCI)
BORIS	87B	JETPL 45 333 Translated from ZETFP 45 267.	S.D. Boris *et al.*	(ITEP)
FUKUGITA	87	PR D36 3817	M. Fukugita, S. Yazaki	(KYOTU, TOKY)
NUSSINOV	87	PR D36 2278	S. Nussinov, Y. Rephaeli	(TELA)
OBERAUER	87	PL B198 113	L.F. Oberauer, F. von Feilitzsch, R.L. Mossbauer	
SPRINGER	87	PR A35 679	P.T. Springer *et al.*	(LLNL)
KETOV	86	JETPL 44 146 Translated from ZETFP 44 114.	S.N. Ketov *et al.*	(KIAE)
COWSIK	85	PL 151B 62	R. Cowsik	(TATA)
RAFFELT	85	PR D31 3002	G.G. Raffelt	(MPIM)
BINETRUY	84	PL 134B 174	P. Binetruy, G. Girardi, P. Salati	(LAPP)
FREESE	84	NP B233 167	K. Freese, D.N. Schramm	(CHIC, FNAL)
KYULDJIEV	84	NP B243 387	A.V. Kyuldjiev	(SOFI)
SCHRAMM	84	PL 141B 337	D.N. Schramm, G. Steigman	(FNAL, BART)
VOGEL	84	PR D30 1505	P. Vogel	
ANDERHUB	82	PL 114B 76	H.B. Anderhub *et al.*	(ETH, SIN)
OLIVE	82	PR D25 213	K.A. Olive, M.S. Turner	(CHIC, UCSB)
BERNSTEIN	81	PL 101B 39	J. Bernstein, G. Feinberg	(STEV, COLU)
FRANK	81	PR D24 2001	J.S. Frank *et al.*	(LASL, YALE, MIT+)
MORGAN	81	PL 102B 247	J.A. Morgan	(SUSS)
FUJIKAWA	80	PRL 45 963	K. Fujikawa, R. Shrock	(STON)
LUBIMOV	80	PL 94B 266	V.A. Lyubimov *et al.*	(ITEP)
STECKER	80	PRL 45 1460	F.W. Stecker	(NASA)
COWSIK	79	PR D19 2219	R. Cowsik	(TATA)
GOLDMAN	79	PR D19 2215	T. Goldman, G.J. Stephenson	(LASL)
BEG	78	PR D17 1395	M.A.B. Beg, W.J. Marciano, M. Ruderman	(ROCK+)
BLIETSCHAU	78	NP B133 205	J. Blietschau *et al.*	(Gargamelle Collab.)

FALK	78	PL 79B 511	S.W. Falk, D.N. Schramm	(CHIC)
BARNES	77	PRL 38 1049	V.E. Barnes *et al.*	(PURD, ANL)
COWSIK	77	PRL 39 784	R. Cowsik	(MPIM, TATA)
LEE	77C	PR D16 1444	B.W. Lee, R.E. Shrock	(STON)
VYSOTSKY	77	JETPL 26 188 Translated from ZETFP 26 200.	M.I. Vysotsky, A.D. Dolgov, Y.B. Zeldovich	(ITEP)
BELLOTTI	76	LNC 17 553	E. Bellotti *et al.*	(MILA)
SUTHERLAND	76	PR D13 2700	P. Sutherland *et al.*	(PENN, COLU, NYU)
SZALAY	76	AA 49 437	A.S. Szalay, G. Marx	(EOTV)
CLARK	74	PR D9 533	A.R. Clark *et al.*	(LBL)
KIM	74	PR D9 3050	J.E. Kim, V.S. Mathur, S. Okubo	(ROCH)
REINES	74	PRL 32 180	F. Reines, H.W. Sobel, H.S. Gurr	(UCI)
SZALAY	74	APAH 35 8	A.S. Szalay, G. Marx	(EOTV)
COWSIK	72	PRL 29 669	R. Cowsik, J. McClelland	(UCB)
MARX	72	Nu Conf. Budapest	G. Marx, A.S. Szalay	(EOTV)
GERSHTEIN	66	JETPL 4 120 Translated from ZETFP 4 189.	S.S. Gershtein, Y.B. Zeldovich	(KIAM)
BERNSTEIN	63	PR 132 1227	J. Bernstein, M. Ruderman, G. Feinberg	(NYU+)
COWAN	57	PR 107 528	C.L. Cowan, F. Reines	(LANL)

Number of Neutrino Types

The neutrinos referred to in this section are those of the Standard SU(2)×U(1) Electroweak Model possibly extended to allow nonzero neutrino masses. Light neutrinos are those with $m < m_Z/2$. The limits are on the number of neutrino mass eigenstates, including ν_1, ν_2, and ν_3.

See the related review(s):

Number of Light Neutrino Types from Collider Experiments

Number from e^+e^- Colliders

Number of Light ν Types

VALUE	DOCUMENT ID		TECN
2.9840±0.0082	[1] LEP-SLC	06	RVUE
• • • We do not use the following data for averages, fits, limits, etc. • • •			
3.00 ±0.05	[2] LEP	92	RVUE

[1] Combined fit from ALEPH, DELPHI, L3 and OPAL Experiments.
[2] Simultaneous fits to all measured cross section data from all four LEP experiments.

Number of Light ν Types from Direct Measurement of Invisible Z Width

In the following, the invisible Z width is obtained from studies of single-photon events from the reaction $e^+e^- \to \nu\overline{\nu}\gamma$. All are obtained from LEP runs in the $E_{\rm CM}^{ee}$ range 88–209 GeV.

VALUE	DOCUMENT ID		TECN	COMMENT
2.92±0.05 OUR AVERAGE Error includes scale factor of 1.2.				
2.84±0.10±0.14	ABDALLAH	05B	DLPH	$\sqrt{s}$ = 180–209 GeV
2.98±0.05±0.04	ACHARD	04E	L3	1990-2000 LEP runs
2.86±0.09	HEISTER	03C	ALEP	$\sqrt{s}$ = 189–209 GeV
2.69±0.13±0.11	ABBIENDI,G	00D	OPAL	1998 LEP run
2.89±0.32±0.19	ABREU	97J	DLPH	1993–1994 LEP runs
3.23±0.16±0.10	AKERS	95C	OPAL	1990–1992 LEP runs
2.68±0.20±0.20	BUSKULIC	93L	ALEP	1990–1991 LEP runs
• • • We do not use the following data for averages, fits, limits, etc. • • •				
2.84±0.15±0.14	ABREU	00Z	DLPH	1997–1998 LEP runs
3.01±0.08	ACCIARRI	99R	L3	1991–1998 LEP runs
3.1 ±0.6 ±0.1	ADAM	96C	DLPH	$\sqrt{s}$ = 130, 136 GeV

Limits from Astrophysics and Cosmology

Effective Number of Light ν Types

("Light" means < about 1 MeV). The quoted values correspond to $N_{\rm eff}$, where $N_{\rm eff}$ = 3.046 in the Standard Model with N_ν = 3. See also OLIVE 81. For a review of limits based on Nucleosynthesis, Supernovae, and also on terrestrial experiments, see DENEGRI 90. Also see "Big-Bang Nucleosynthesis" in this *Review*.

VALUE	CL%	DOCUMENT ID		TECN	COMMENT
• • • We do not use the following data for averages, fits, limits, etc. • • •					
2.3–3.2	95	[1] VERDE	17	COSM	
2.88±0.20	95	[2] ROSSI	15	COSM	
3.3 ±0.5	95	[3] ADE	14	COSM	Planck
$3.78^{+0.31}_{-0.30}$		[4] COSTANZI	14	COSM	
3.29±0.31		[5] HOU	14	COSM	
< 3.80	95	[6] LEISTEDT	14	COSM	
< 4.10	95	[7] MORESCO	12	COSM	
< 5.79	95	[8] XIA	12	COSM	
< 4.08	95	MANGANO	11	COSM	BBN
0.9–8.2		[9] ICHIKAWA	07	COSM	
3–7	95	[10] CIRELLI	06	COSM	
2.7–4.6	95	[11] HANNESTAD	06	COSM	
3.6–7.4	95	[10] SELJAK	06	COSM	
< 4.4		[12] CYBURT	05	COSM	
< 3.3		[13] BARGER	03C	COSM	
1.4–6.8		[14] CROTTY	03	COSM	
1.9–6.6		[14] PIERPAOLI	03	COSM	
2–4		LISI	99	COSM	BBN
< 4.3		OLIVE	99	COSM	BBN
< 4.9		COPI	97		Cosmology
< 3.6		HATA	97B		High D/H quasar abs.
< 4.0		OLIVE	97		BBN; high ^{4}He and ^{7}Li
< 4.7		CARDALL	96B	COSM	High D/H quasar abs.
< 3.9		FIELDS	96	COSM	BBN; high ^{4}He and ^{7}Li
< 4.5		KERNAN	96	COSM	High D/H quasar abs.
< 3.6		OLIVE	95		BBN; ≥ 3 massless ν
< 3.3		WALKER	91		Cosmology
< 3.4		OLIVE	90		Cosmology
< 4		YANG	84		Cosmology
< 4		YANG	79		Cosmology
< 7		STEIGMAN	77		Cosmology
		PEEBLES	71		Cosmology
<16	[15]	SHVARTSMAN	69		Cosmology
		HOYLE	64		Cosmology

[1] Uses Planck Data combined with an independent standard measure of distance to the sound horizon to set a limit on the total number of neutrinos. Only CMB and early-time information are used.
[2] ROSSI 15 sets limits on the number of neutrino types using BOSS Lyman alpha forest data combined with Planck CMB data and baryon acoustic oscillations.
[3] Fit to the number of neutrino degrees of freedom from Planck CMB data along with WMAP polarization, high L, and BAO data.
[4] Fit to the number of neutrinos degrees of freedom from Planck CMB data along with BAO, shear and cluster data.
[5] Fit based on the SPT-SZ survey combined with CMB, BAO, and H_0 data.
[6] Constrains the number of neutrino degrees of freedom (marginalizing over the total mass) from CMB, CMB lensing, BAO, and galaxy clustering data.
[7] Limit on the number of light neutrino types from observational Hubble parameter data with seven-year WMAP data, SPT, and the most recent estimate of H_0. Best fit is 3.45 ± 0.65.
[8] Limit on the number of light neutrino types from the CFHTLS combined with seven-year WMAP data and a prior on the Hubble parameter. Best fit is $4.17^{+1.62}_{-1.26}$. Limit is relaxed to $3.98^{+2.02}_{-1.20}$ when small scales affected by non-linearities are removed.
[9] Constrains the number of neutrino types from recent CMB and large scale structure data. No priors on other cosmological parameters are used.
[10] Constrains the number of neutrino types from recent CMB, large scale structure, Lyman-alpha forest, and SN1a data. The slight preference for $N_\nu > 3$ comes mostly from the Lyman-alpha forest data.
[11] Constrains the number of neutrino types from recent CMB and large scale structure data. See also HAMANN 07.
[12] Limit on the number of neutrino types based on ^{4}He and D/H abundance assuming a baryon density fixed to the WMAP data. Limit relaxes to 4.6 if D/H is not used or to 5.8 if only D/H and the CMB are used. See also CYBURT 01 and CYBURT 03.
[13] Limit on the number of neutrino types based on combination of WMAP data and big-bang nucleosynthesis. The limit from WMAP data alone is 8.3. See also KNELLER 01. $N_\nu \geq 3$ is assumed to compute the limit.
[14] 95% confidence level range on the number of neutrino flavors from WMAP data combined with other CMB measurements, the 2dfGRS data, and HST data.
[15] SHVARTSMAN 69 limit inferred from his equations.

Number Coupling with Less Than Full Weak Strength

VALUE	DOCUMENT ID		TECN
• • • We do not use the following data for averages, fits, limits, etc. • • •			
<20	[1] OLIVE	81C	COSM
<20	[1] STEIGMAN	79	COSM

[1] Limit varies with strength of coupling. See also WALKER 91.

REFERENCES FOR Limits on Number of Neutrino Types

VERDE	17	JCAP 1704 023	L. Verde *et al.*	
ROSSI	15	PR D92 063505	G. Rossi *et al.*	
ADE	14	AA 571 A16	P.A.R. Ade *et al.*	(Planck Collab.)
COSTANZI	14	JCAP 1410 081	M. Costanzi *et al.*	(TRST, TRSTI)
HOU	14	APJ 782 74	Z. Hou *et al.*	
LEISTEDT	14	PRL 113 041301	B. Leistedt, H.V. Peiris, L. Verde	
MORESCO	12	JCAP 1207 053	M. Moresco *et al.*	
XIA	12	JCAP 1206 010	J.-Q. Xia *et al.*	
MANGANO	11	PL B701 296	G. Mangano, P. Serpico	
HAMANN	07	JCAP 0708 021	J. Hamann *et al.*	
ICHIKAWA	07	JCAP 0705 007	K. Ichikawa, M. Kawasaki, F. Takahashi	
CIRELLI	06	JCAP 0612 013	M. Cirelli *et al.*	
HANNESTAD	06	JCAP 0611 016	S. Hannestad, G. Raffelt	
LEP-SLC	06	PRPL 427 257	ALEPH, DELPHI, L3, OPAL, SLD and working groups	
SELJAK	06	JCAP 0610 014	U. Seljak, A. Slosar, P. McDonald	
ABDALLAH	05B	EPJ C38 395	J. Abdallah *et al.*	(DELPHI Collab.)
CYBURT	05	ASP 23 313	R.H. Cyburt *et al.*	
ACHARD	04E	PL B587 16	P. Achard *et al.*	(L3 Collab.)
BARGER	03C	PL B566 8	V. Barger *et al.*	
CROTTY	03	PR D67 123005	P. Crotty, J. Lesgourgues, S. Pastor	
CYBURT	03	PL B567 227	R.H. Cyburt, B.D. Fields, K.A. Olive	
HEISTER	03C	EPJ C28 1	A. Heister *et al.*	(ALEPH Collab.)
PIERPAOLI	03	MNRAS 342 L63	E. Pierpaoli	
CYBURT	01	ASP 17 87	R.H. Cyburt, B.D. Fields, K.A. Olive	
KNELLER	01	PR D64 123506	J.P. Kneller *et al.*	
ABBIENDI,G	00D	EPJ C18 253	G. Abbiendi *et al.*	(OPAL Collab.)
ABREU	00Z	EPJ C17 53	P. Abreu *et al.*	(DELPHI Collab.)
ACCIARRI	99R	PL B470 268	M. Acciarri *et al.*	(L3 Collab.)
LISI	99	PR D59 123520	E. Lisi, S. Sarkar, F.L. Villante	
OLIVE	99	ASP 11 403	K.A. Olive, D. Thomas	
ABREU	97J	ZPHY C74 577	P. Abreu *et al.*	(DELPHI Collab.)
COPI	97	PR D55 3389	C.J. Copi, D.N. Schramm, M.S. Turner	(CHIC)
HATA	97B	PR D55 540	N. Hata *et al.*	(OSU, PENN)
OLIVE	97	ASP 7 27	K.A. Olive, D. Thomas	(MINN, FLOR)
ADAM	96C	PL B380 471	W. Adam *et al.*	(DELPHI Collab.)
CARDALL	96B	APJ 472 435	C.Y. Cardall, G.M. Fuller	(UCSD)
FIELDS	96	New Ast 1 77	B.D. Fields *et al.*	(NDAM, CERN, MINN+)
KERNAN	96	PR D54 3681	P.S. Kernan, S. Sarkar	(CASE, OXFTP)
AKERS	95C	ZPHY C65 47	R. Akers *et al.*	(OPAL Collab.)
OLIVE	95	PL B354 357	K.A. Olive, G. Steigman	(MINN, OSU)
BUSKULIC	93L	PL B313 520	D. Buskulic *et al.*	(ALEPH Collab.)
LEP	92	PL B276 247	LEP Collabs.	(LEP, ALEPH, DELPHI, L3, OPAL)
WALKER	91	APJ 376 51	T.P. Walker *et al.*	(HSCA, OSU, CHIC+)
DENEGRI	90	RMP 62 1	D. Denegri, B. Sadoulet, M. Spiro	(CERN, UCB+)
OLIVE	90	PL B236 454	K.A. Olive *et al.*	(MINN, CHIC, OSU+)
YANG	84	APJ 281 493	J. Yang *et al.*	(CHIC, BART)

Lepton Particle Listings

Number of Neutrino Types, Double-β Decay

OLIVE	81	APJ 246 557	K.A. Olive *et al.*	(CHIC, BART)
OLIVE	81C	NP B180 497	K.A. Olive, D.N. Schramm, G. Steigman	(EFI+)
STEIGMAN	79	PRL 43 239	G. Steigman, K.A. Olive, D.N. Schramm	(BART+)
YANG	79	APJ 227 697	J. Yang *et al.*	(CHIC, YALE, UVA)
STEIGMAN	77	PL 66B 202	G. Steigman, D.N. Schramm, J.E. Gunn	(YALE, CHIC+)
PEEBLES	71	Physical Cosmology Princeton Univ. Press (1971)	P.Z. Peebles	(PRIN)
SHVARTSMAN	69	JETPL 9 184 Translated from ZETFP 9 315.	V.F. Shvartsman	(MOSU)
HOYLE	64	NAT 203 1108	F. Hoyle, R.J. Tayler	(CAMB)

Double-β Decay

OMITTED FROM SUMMARY TABLE

See the related review(s):
Neutrinoless Double-β Decay

Half-life limits on the neutrino-less double-β decay

In most cases the transitions (Z,A) $\rightarrow$ (Z+2,A) + $2e^-$ to the 0^+ ground state of the final nucleus are listed. We also list transitions that decrease the nuclear charge ($2e^+$, e^+ CC and double EC) and transitions to an excited state of the final nucleus (0^+_i, 2^+, and 2^+_i). In the following Listings only the best or comparable limits for the half-lives of each transition are reported and only those with about $T_{1/2} > 10^{23}$ years that are relevant for particle physics.

$t_{1/2}(10^{23}$ yr)	CL%	ISOTOPE	TRANSITION	METHOD	DOCUMENT ID	
• • • We do not use the following data for averages, fits, limits, etc. • • •						
> 190	90	^{76}Ge		MAJORANA	[1] AALSETH	18
> 800	90	^{76}Ge		GERDA	[2] AGOSTINI	18
> 180	90	^{136}Xe		EXO-200	[3] ALBERT	18
> 150	90	^{130}Te		CUORE	[4] ALDUINO	18
> 530	90	^{76}Ge		GERDA	[5] AGOSTINI	17
> 1.1	90	^{134}Xe		EXO-200	[6] ALBERT	17C
> 1	90	^{116}Cd		NEMO-3	[7] ARNOLD	17
> 40	90	^{130}Te		CUORE(CINO)	[8] ALDUINO	16
> 260	90	^{136}Xe	g.s.$\rightarrow 2^+_1$	KamLAND-Zen	[9] ASAKURA	16
> 260	90	^{136}Xe	g.s.$\rightarrow 2^+_2$	KamLAND-Zen	[10] ASAKURA	16
> 240	90	^{136}Xe	g.s.$\rightarrow 0^+_1$	KamLAND-Zen	[11] ASAKURA	16
>1070	90	^{136}Xe		KamLAND-Zen	[12] GANDO	16
> 11	90	^{100}Mo		NEMO-3	[13] ARNOLD	15
> 110	90	^{136}Xe		EXO-200	[14] ALBERT	14B
> 9.4	90	^{130}Te	$0^+ \rightarrow 0^+_1$	CUORICINO	[15] ANDREOTTI	12
> 3.6	90	^{82}Se		NEMO-3	[16] BARABASH	11A
> 30	90	^{130}Te		CUORICINO	[17] ARNABOLDI	08
> 0.58	90	^{48}Ca		CaF_2 scint.	[18] UMEHARA	08
> 0.89	90	^{100}Mo	$0^+ \rightarrow 0^+_1$	NEMO-3	[19] ARNOLD	07
> 1.6	90	^{100}Mo	$0^+ \rightarrow 2^+$	NEMO-3	[20] ARNOLD	07
> 1	90	^{82}Se		NEMO-3	[21] ARNOLD	05A
> 1.1	90	^{128}Te		Cryog. det.	[22] ARNABOLDI	03
> 1.7	90	^{116}Cd		$^{116}CdWO_4$ scint.	[23] DANEVICH	03
> 157	90	^{76}Ge		Enriched HPGe	[24] AALSETH	02B
> 190	90	^{76}Ge		Enriched HPGe	[25] KLAPDOR-K...	01

[1] AALSETH 18 uses the MAJORANA Demonstrator to search for the $0\nu\ \beta\beta$ decay. The exposure is 9.95 kg·year. The median sensitivity is 2.1×10^{25} yr.

[2] AGOSTINI 18 uses the GERDA detector to search for the $0\nu\ \beta\beta$ decay. The exposure is 46.7 kg·year. The median sensitivity is 5.8×10^{25} yr. Supersedes AGOSTINI 17.

[3] ALBERT 18 uses the EXO-200 detector to search for the $0\nu\ \beta\beta$ decay. The exposure is 177.6 kg·year. The median sensitivity is 3.7×10^{25} years.

[4] ALDUINO 18 uses the CUORE detector to search for the $0\nu\ \beta\beta$ decay of ^{130}Te. The exposure is 86.3 kg·year of natural TeO_2 corresponding to 24.0 kg·year for ^{130}Te. The median sensitivity is 0.7×10^{25} yr. The limit is obtained combining the new data from CUORE with those of CUORE0 (9.8 kg·year of ^{130}Te) and Cuoricino (19.8 kg·year of ^{130}Te).

[5] AGOSTINI 17 result corresponds to data collected with GERDA phase 1 and first release of phase 2 for a total of 343 mol-yr exposure. Supersedes AGOSTINI 13A. The median sensitivity is 4.0 10^{25} yr.

[6] ALBERT 17C uses the EXO-200 detector that contains 19.098 ± 0.014% admixture of ^{134}Xe to search for the 0ν and $2\nu\ \beta\beta$ decay modes. The exposure is 29.6 kg·year. The median sensitivity is 1.9×10^{21} years.

[7] ARNOLD 17 use the NEMO-3 tracking calorimeter, containing 410 g of enriched ^{116}Cd exposed for 5.26 yr, to determine the half-life limit. Supersedes BARABASH 11A.

[8] ALDUINO 16 report result obtained with 9.8 kg y of data collected with the CUORE-0 bolometer, combined with data from the CUORICINO. Supersedes ALFONSO 15.

[9] ASAKURA 16 use the KamLAND-Zen liquid scintillator calorimeter (^{136}Xe 89.5 kg yr) to place a limit on the $0\nu\beta\beta$-decay into the first excited state of the daughter nuclide.

[10] ASAKURA 16 use the KamLAND-Zen liquid scintillator calorimeter (^{136}Xe 89.5 kg yr) to place a limit on the $0\nu\beta\beta$-decay into the second excited state of the daughter nuclide.

[11] ASAKURA 16 use the KamLAND-Zen liquid scintillator calorimeter (^{136}Xe 89.5 kg yr) to place a limit on the $0\nu\beta\beta$-decay into the third excited state of the daughter nuclide.

[12] GANDO 16 use the the KamLAND detector to search for the 0ν decay of ^{136}Xe. With a significant background reduction, the combination of results of the first (270.7 days) and the second phase (263.8 days) of the experiment leads to about six fold improvement over the previous limit. Supersedes GANDO 13A. The sensitivity is 5.6 10^{25} yr.

[13] ARNOLD 15 use the NEMO-3 tracking calorimeter with 34.3 kg yr exposure to determine the limit of $0\nu\beta\beta$-half life of ^{100}Mo. Supersedes ARNOLD 2005A and BARABASH 11A.

[14] ALBERT 14B use 100 kg yr of exposure of the EXO-200 tracking calorimeter to place a lower limit on the $0\nu\beta\beta$-half life of ^{136}Xe. Supersedes AUGER 12.

[15] ANDREOTTI 12 use high resolution TeO_2 bolometric calorimeter to search for the $0\nu\beta\beta$ decay of ^{130}Te leading to the excited 0^+_1 state at 1793.5 keV.

[16] BARABASH 11A use the NEMO-3 detector to measure $2\nu\beta\beta$ rates and place limits on $0\nu\beta\beta$ half lives for various nuclides. Supersedes ARNOLD 05A, ARNOLD 04, ARNOLD 98, and ELLIOTT 92.

[17] Supersedes ARNABOLDI 04. Bolometric TeO_2 detector array CUORICINO is used for high resolution search for $0\nu\beta\beta$ decay. The half-life limit is derived from 3.09 kg yr ^{130}Te exposure.

[18] UMEHARA 08 use CaF_2 scintillation calorimeter to search for double beta decay of ^{48}Ca. Limit is significantly more stringent than quoted sensitivity: 18×10^{21} years.

[19] Limit on 0ν-decay to the first excited 0^+_1-state of daughter nucleus using NEMO-3 tracking calorimeter. Supersedes DASSIE 95.

[20] Limit on 0ν-decay to the first excited 2^+-state of daughter nucleus using NEMO-3 tracking calorimeter.

[21] NEMO-3 tracking calorimeter is used in ARNOLD 05A to place limit on $0\nu\beta\beta$ half-life of ^{82}Se. Detector contains 0.93 kg of enriched ^{82}Se. Supersedes ARNOLD 04.

[22] Supersedes ALESSANDRELLO 00. Array of TeO_2 crystals in high resolution cryogenic calorimeter. Some enriched in ^{128}Te. Ground state to ground state decay.

[23] Limit on $0\nu\beta\beta$ decay of ^{116}Cd using enriched $CdWO_4$ scintillators. Supersedes DANEVICH 00.

[24] AALSETH 02B limit is based on 117 mol·yr of data using enriched Ge detectors. Background reduction by means of pulse shape analysis is applied to part of the data set. Reported limit is slightly less restrictive than that in KLAPDOR-KLEINGROTHAUS 01 However, it excludes part of the allowed half-life range reported in KLAPDOR-KLEINGROTHAUS 01B for the same nuclide. The analysis has been criticized in KLAPDOR-KLEINGROTHAUS 04B. The criticism was addressed and disputed in AALSETH 04.

[25] KLAPDOR-KLEINGROTHAUS 01 is a continuation of the work published in BAUDIS 99. Isotopically enriched Ge detectors are used in calorimetric measurement. The most stringent bound is derived from the data set in which pulse-shape analysis has been used to reduce background. Exposure time is 35.5 kg y. Supersedes BAUDIS 99 as most stringent result.

Half-life measurements of the two-neutrino double-β decay

The measured half-life values for the transitions (Z,A) $\rightarrow$ (Z+2,A) + $2e^-$ + $2\nu_e$ to the 0^+ ground state of the final nucleus are listed. We also list the transitions to an excited state of the final nucleus (0^+_i, etc.). We report only the measuremetnts with the smallest (or comparable) uncertainty for each transition.

$t_{1/2}(10^{21}$ yr)			ISOTOPE	TRANSITION	METHOD	DOCUMENT ID	
• • • We do not use the following data for averages, fits, limits, etc. • • •							
> 0.87			^{134}Xe		EXO-200	[1] ALBERT	17C
0.82	±0.02	±0.06	^{130}Te		CUORE-0	[2] ALDUINO	17
0.00690	±0.00015	±0.00037	^{100}Mo		CUPID	[3] ARMENGAUD	17
0.0274	±0.0004	±0.0018	^{116}Cd		NEMO-3	[4] ARNOLD	17
0.064	$^{+0.007}_{-0.006}$	$^{+0.012}_{-0.009}$	^{48}Ca		NEMO-3	[5] ARNOLD	16
0.00934	±0.00022	$^{+0.00062}_{-0.00060}$	^{150}Nd		NEMO-3	[6] ARNOLD	16A
1.926	±0.094		^{76}Ge		GERDA	[7] AGOSTINI	15A
0.00693	±0.00004		^{100}Mo		NEMO-3	[8] ARNOLD	15
2.165	±0.016	±0.059	^{136}Xe		EXO-200	[9] ALBERT	14
9.2	$^{+5.5}_{-2.6}$	±1.3	^{78}Kr		BAKSAN	[10] GAVRILYAK	13
2.38	±0.02	±0.14	^{136}Xe		KamLAND-Zen	[11] GANDO	12A
0.7	±0.09	±0.11	^{130}Te		NEMO-3	[12] ARNOLD	11
0.0235	±0.0014	±0.0016	^{96}Zr		NEMO-3	[13] ARGYRIADES	10
0.69	$^{+0.10}_{-0.08}$	±0.07	^{100}Mo	$0^+ \rightarrow 0^+_1$	Ge coinc.	[14] BELLI	10
0.57	$^{+0.13}_{-0.09}$	±0.08	^{100}Mo	$0^+ \rightarrow 0^+_1$	NEMO-3	[15] ARNOLD	07
0.096	±0.003	±0.010	^{82}Se		NEMO-3	[16] ARNOLD	05A
0.029	$^{+0.004}_{-0.003}$		^{116}Cd		$^{116}CdWO_4$ scint.	[17] DANEVICH	03

[1] ALBERT 17C uses the EXO-200 detector that contains 19.098 ± 0.014% admixture of ^{134}Xe to search for the $2\nu\ \beta\beta$ decay mode. The exposure is 29.6 kg·year. The median sensitivity is 1.2×10^{21} years.

[2] ALDUINO 17 use the CUORE-0 detector containing 10.8 kg of ^{130}Te in 52 crystals of TeO_2. The exposure was 9.3 kg yr of ^{130}Te. This is a more accurate rate determination than in ARNOLD 11 and BARABASH 11A.

[3] ARMENGAUD 17 use 185.9 ± 0.1 g crystal of $Li_2{}^{100}MoO_4$ to determine the ^{100}Mo $2\nu\ \beta\beta$ half-life. The exposure was of 1303 ± 26 hours only, using novel technique.

[4] ARNOLD 17 use the NEMO-3 tracking calorimeter, containing 410 grams of enriched ^{116}Cd exposed for 5.26 years, to determine the half-life value.

[5] ARNOLD 16 use the NEMO-3 detector and a source of 6.99 g of ^{48}Ca. The half-life is based on 36.7 g year exposure. It is consistent, although somewhat longer, than the previous determinations of the half-life. Supersedes BARABASH 11A.

[6] ARNOLD 16A use the NEMO-3 tracking calorimeter, containing 36.6 g of ^{150}Nd exposed for 1918.5 days, to determine the half-life. Supersedes ARGYRIADES 09.

[7] AGOSTINI 15A use 17.9 kg yr exposure of the GERDA calorimeter to derive an improved measurement of the $2\nu\beta\beta$ decay half life of ^{76}Ge.

[8] ARNOLD 15 use the NEMO-3 tracking calorimeter with 34.3 kg yr exposure to determine the $2\nu\beta\beta$-half life of ^{100}Mo. Supersedes ARNOLD 05A and ARNOLD 04.

[9] ALBERT 14 use the EXO-200 tracking detector for a re-measurement of the $2\nu\beta\beta$-half life of ^{136}Xe. A nuclear matrix element of 0.0218 ± 0.0003 MeV^{-1} is derived from this data. Supersedes ACKERMAN 11.

[10] GAVRILYAK 13 use a proportional counter filled with Kr gas to search for the 2ν2K decay of ^{78}Kr. Data with the enriched and depleted Kr were used to determine signal and background. A 2.5σ excess of events obtained with the enriched sample is interpreted as an indication for the presence of this decay.

[11] GANDO 12A use a modification of the existing KamLAND detector. The $\beta\beta$ decay source/detector is 13 tons of enriched ^{136}Xe-loaded scintillator contained in an inner balloon. The $2\nu\beta\beta$ decay rate is derived from the fit to the spectrum between 0.5 and 4.8 MeV. This result is in agreement with ACKERMAN 11.

[12] ARNOLD 11 use enriched ^{130}Te in the NEMO-3 detector to measure the 2ν $\beta\beta$ decay rate. This result is in agreement with, but more accurate than ARNABOLDI 03.

[13] ARGYRIADES 10 use 9.4 $\pm$ 0.2 g of ^{96}Zr in NEMO-3 detector and identify its $2\nu\beta\beta$ decay. The result is in agreement and supersedes ARNOLD 99.

[14] BELLI 10 use enriched ^{100}Mo with 4 HP Ge detectors to record the 590.8 and 539.5 keV γ rays from the decay of the 0^+_1 state in ^{100}Ru both in singles and coincidences. This result confirms the measurement of KIDD 09 and ARNOLD 07 and supersedes them.

[15] First exclusive measurement of 2ν-decay to the first excited 0^+_1-state of daughter nucleus. ARNOLD 07 use the NEMO-3 tracking calorimeter to detect all particles emitted in decay. Result agrees with the inclusive (0ν + 2ν) measurement of DEBRAECKELEER 01.

[16] ARNOLD 05A use the NEMO-3 tracking detector to determine the $2\nu\beta\beta$ half-life of ^{82}Se with high statistics and low background (389 days of data taking). Supersedes ARNOLD 04.

[17] Calorimetric measurement of $2\nu\beta\beta$ ground state decay of ^{116}Cd using enriched $CdWO_4$ scintillators. Agrees with EJIRI 95 and ARNOLD 96. Supersedes DANEVICH 00.

$\langle m_\nu \rangle$, The Effective Weighted Sum of Majorana Neutrino Masses Contributing to Neutrinoless Double-β Decay

$\langle m_\nu \rangle = |\Sigma U_{ei}^2 m_{\nu_i}|$, i = 1,2,3. It is assumed that ν_i are Majorana particles and that the transition is dominated by the known (light) neutrinos. Note that U_{ei}^2 and not $|U_{ei}|^2$ occur in the sum, and that consequently cancellations are possible. The experiments obtain the limits on $\langle m_\nu \rangle$ from the measured ones on $T_{1/2}$ using a range of nuclear matrix elements (NME), which is reflected in the spread of $\langle m_\nu \rangle$. Different experiments may choose different NME. All assume g_A = 1.27. In the following Listings, only the best or comparable limits for each isotope are reported. When not mentioned explicitly the transition is between ground states, but transitions between excited states are also reported.

VALUE (eV)	ISOTOPE	TRANSITION	METHOD	DOCUMENT ID	
• • • We do not use the following data for averages, fits, limits, etc. • • •					
< 0.24–0.52	^{76}Ge		MAJORANA Dem	[1] AALSETH	18
< 0.12–0.26	^{76}Ge		GERDA	[2] AGOSTINI	18
< 0.15–0.40	^{136}Xe		EXO-200	[3] ALBERT	18
< 0.11–0.52	^{130}Te		CUORE	[4] ALDUINO	18
< 0.15–0.33	^{76}Ge		GERDA	[5] AGOSTINI	17
< 1.4–2.5	^{116}Cd		NEMO-3	[6] ARNOLD	17
< 0.27–0.76	^{130}Te		CUORE(CINO)	[7] ALDUINO	16
< 1.6–5.3	^{150}Nd		NEMO-3	[8] ARNOLD	16A
< 0.061–0.165	^{136}Xe		KamLAND-Zen	[9] GANDO	16
< 0.33–0.62	^{100}Mo		NEMO-3	[10] ARNOLD	15
< 0.19–0.45	^{136}Xe		EXO-200	[11] ALBERT	14B
< 0.89–2.43	^{82}Se		NEMO-3	[12] BARABASH	11A
< 7.2–19.5	^{96}Zr		NEMO-3	[13] ARGYRIADES	10
< 3.5–22	^{48}Ca		CaF_2 scint.	[14] UMEHARA	08
< 0.2–1.1	^{130}Te		Cryog. det.	[15] ARNABOLDI	05
< 0.37–1.9	^{130}Te		Cryog. det.	[16] ARNABOLDI	04
< 1.5–1.7	^{116}Cd		$^{116}CdWO_4$ scint.	[17] DANEVICH	03
< 0.350	^{76}Ge		Enriched HPGe	[18] KLAPDOR-K...	01
<8.3	^{48}Ca		CaF_2 scint.	YOU	91

[1] AALSETH 18 uses the MAJORANA Demonstrator detector to establish this limit.

[2] AGOSTINI 18 uses the GERDA detector to establish this limit.

[3] ALBERT 18 uses the EXO-200 experiment to obtain this limit.

[4] ALDUINO 18 use the combined data of CUORE, CUORE0, and Cuoricino to obtain this limit.

[5] AGOSTINI 17 is based on 343 mol yr of data from GERDA phase 1 and phase 2 first part and the corresponding limit on $T_{1/2}$ using the different nuclear matrix elements mentioned by the authors. Supersedes AGOSTINI 13A.

[6] ARNOLD 17 utilize NEMO-3 data, taken with enriched ^{116}Cd to limit the effective Majorana neutrino mass. The reported range results from the use of different nuclear matrix elements. Supersedes BARABASH 11A.

[7] ALDUINO 16 place a limit on the effective Majorana neutrino mass using the combined data of the CUORE-0 and CUORICINO experiments. The range reflects the authors' evaluation of the variability of the nuclear matrix elements. Supersedes ALFONSO 15.

[8] ARNOLD 16A limit is derived from data taken with the NEMO-3 detector and ^{150}Nd. A range of nuclear matrix elements that include the effect of nuclear deformation have been used. Supersedes ARGYRIADES 09.

[9] GANDO 16 result is based on the 2016 KamLAND-Zen half-life limit. The stated range reflects different nuclear matrix elements, an unquenched g_A = 1.27 is used. Supersedes GANDO 13A.

[10] ARNOLD 15 use the NEMO-3 tracking calorimeter with 34.3 kg yr exposure to determine the neutrino mass limit based on the $0\nu\beta\beta$-half life of ^{100}Mo. The spread range reflects different nuclear matrix elements. Supersedes ARNOLD 14 and BARABASH 11A.

[11] ALBERT 14B is based on 100 kg yr of exposure of the EXO-200 tracking calorimeter. The mass range reflects the nuclear matrix element calculations. Supersedes AUGER 12.

[12] BARABASH 11A limit is based on NEMO-3 data for ^{82}Se. The reported range reflects different nuclear matrix elements. Supersedes ARNOLD 05A and ARNOLD 04.

[13] ARGYRIADES 10 use ^{96}Zr and the NEMO-3 tracking detector to obtain the reported mass limit. The range reflects the fluctuation of the nuclear matrix elements considered.

[14] Limit was obtained using CaF_2 scintillation calorimeter to search for double beta decay of ^{48}Ca. Reported range of limits reflects spread of QRPA and SM matrix element calculations used. Supersedes OGAWA 04.

[15] Supersedes ARNABOLDI 04. Reported range of limits due to use of different nuclear matrix element calculations.

[16] Supersedes ARNABOLDI 03. Reported range of limits due to use of different nuclear matrix element calculations.

[17] Limit for $\langle m_\nu \rangle$ is based on the nuclear matrix elements of STAUDT 90 and ARNOLD 96. Supersedes DANEVICH 00.

[18] KLAPDOR-KLEINGROTHAUS 01 uses the calculation by STAUDT 90. Using several other models in the literature could worsen the limit up to 1.2 eV. This is the most stringent experimental bound on m_ν. It supersedes BAUDIS 99B.

Limits on Lepton-Number Violating ($V+A$) Current Admixture

For reasons given in the discussion at the beginning of this section, we list only results from 1989 and later. $\langle \lambda \rangle = \lambda \sum U_{ej} V_{ej}$ and $\langle \eta \rangle = \eta \sum U_{ej} V_{ej}$, where the sum is over the number of neutrino generations. This sum vanishes for massless or unmixed neutrinos. In the following Listings, only best or comparable limits or lifetimes for each isotope are reported.

$\langle \lambda \rangle$ (10^{-6})	CL%	$\langle \eta \rangle$ (10^{-8})	CL%	ISOTOPE	METHOD	DOCUMENT ID	
• • • We do not use the following data for averages, fits, limits, etc. • • •							
< 0.9–1.3	90	< 0.5–0.8	90	^{100}Mo	NEMO-3	[1] ARNOLD	14
<120	90			^{100}Mo	$0^+ \rightarrow 2^+$	[2] ARNOLD	07
$0.692^{+0.058}_{-0.056}$	68	$0.305^{+0.026}_{-0.025}$	68	^{76}Ge	Enriched HPGe	[3] KLAPDOR-K...	06A
< 2.5	90			^{100}Mo	0ν, NEMO-3	[4] ARNOLD	05A
< 3.8	90			^{82}Se	0ν, NEMO-3	[5] ARNOLD	05A
< 1.5–2.0	90			^{100}Mo	0ν, NEMO-3	[6] ARNOLD	04
< 3.2–3.8	90			^{82}Se	0ν, NEMO-3	[7] ARNOLD	04
< 1.6–2.4	90	< 0.9–5.3	90	^{130}Te	Cryog. det.	[8] ARNABOLDI	03
< 2.2	90	<2.5	90	^{116}Cd	$^{116}CdWO_4$ scint.	[9] DANEVICH	03
< 3.2–4.7	90	< 2.4–2.7	90	^{100}Mo	ELEGANT V	[10] EJIRI	01
< 1.1	90	<0.64	90	^{76}Ge	Enriched HPGe	[11] GUENTHER	97
< 4.4	90	<2.3	90	^{136}Xe	TPC	[12] VUILLEUMIER	93
		<5.3		^{128}Te	Geochem	[13] BERNATOW...	92

[1] ARNOLD 14 is based on 34.7 kg yr of exposure of the NEMO-3 tracking calorimeter. The reported range limit on $\langle \lambda \rangle$ and $\langle \eta \rangle$ reflects the nuclear matrix element uncertainty in ^{100}Mo.

[2] ARNOLD 07 use NEMO-3 half life limit for 0ν-decay of ^{100}Mo to the first excited 2^+-state of daughter nucleus to limit the right-right handed admixture of weak currents $\langle \lambda \rangle$. This limit is not competitive when compared to the decay to the ground state.

[3] Re-analysis of data originally published in KLAPDOR-KLEINGROTHAUS 04A. Modified pulse shape analysis leads the authors to claim 6σ statistical evidence for observation of 0ν-decay. Authors use matrix element of MUTO 89 to determine $\langle \lambda \rangle$ and $\langle \eta \rangle$. Uncertainty of nuclear matrix element is not reflected in stated errors.

[4] ARNOLD 05A derive limit for $\langle \lambda \rangle$ based on ^{100}Mo data collected with NEMO-3 detector. No limit for $\langle \eta \rangle$ is given. Supersedes ARNOLD 04.

[5] ARNOLD 05A derive limit for $\langle \lambda \rangle$ based on ^{82}Se data collected with NEMO-3 detector. No limit for $\langle \eta \rangle$ is given. Supersedes ARNOLD 04.

[6] ARNOLD 04 use the matrix elements of SUHONEN 94 to obtain a limit for $\langle \lambda \rangle$, no limit for $\langle \eta \rangle$ is given. This limit is more stringent than the limit in EJIRI 01 for the same nucleus.

[7] ARNOLD 04 use the matrix elements of TOMODA 91 and SUHONEN 91 to obtain a limit for $\langle \lambda \rangle$, no limit for $\langle \eta \rangle$ is given.

[8] Supersedes ALESSANDRELLO 00. Cryogenic calorimeter search. Reported a range reflecting uncertainty in nuclear matrix element calculations.

[9] Limits for $\langle \lambda \rangle$ and $\langle \eta \rangle$ are based on nuclear matrix elements of STAUDT 90. Supersedes DANEVICH 00.

[10] The range of the reported $\langle \lambda \rangle$ and $\langle \eta \rangle$ values reflects the spread of the nuclear matrix elements. On axis value assuming $\langle m_\nu \rangle$=0 and $\langle \lambda \rangle$=$\langle \eta \rangle$=0, respectively.

[11] GUENTHER 97 limits use the matrix elements of STAUDT 90. Supersedes BALYSH 95 and BALYSH 92.

[12] VUILLEUMIER 93 uses the matrix elements of MUTO 89. Based on a half-life limit 2.6×10^{23} y at 90%CL.

[13] BERNATOWICZ 92 takes the measured geochemical decay width as a limit on the 0ν width, and uses the SUHONEN 91 coefficients to obtain the least restrictive limit on η. Further details of the experiment are given in BERNATOWICZ 93.

Double-β Decay REFERENCES

AALSETH	18	PRL 120 132502	C.E. Aalseth *et al.*	(MAJORANA Collab.)
AGOSTINI	18	PRL 120 132503	M. Agostini *et al.*	(GERDA Collab.)
ALBERT	18	PRL 120 072701	J. B. Albert *et al.*	(EXO-200 Collab.)
ALDUINO	18	PRL 120 132501	C. Alduino *et al.*	(CUORE Collab.)
AGOSTINI	17	NAT 544 47	M. Agostini *et al.*	(GERDA Collab.)
ALBERT	17C	PR D96 092001	J.B. Albert *et al.*	(EXO-200 Collab.)
ALDUINO	17	EPJ C77 13	C. Alduino *et al.*	(CUORE Collab.)
ARMENGAUD	17	EPJ C77 785	E. Armengaud *et al.*	(CUPID Collab.)
ARNOLD	17	PR D95 012007	R. Arnold *et al.*	(NEMO-3 Collab.)
ALDUINO	16	PR C93 045503	C. Alduino *et al.*	(CUORE Collab.)
ARNOLD	16	PR D93 112008	R. Arnold *et al.*	(NEMO-3 Collab.)
ARNOLD	16A	PR D94 072003	R. Arnold *et al.*	(NEMO-3 Collab.)
ASAKURA	16	NP A946 171	K. Asakura *et al.*	(KamLAND-Zen Collab.)
GANDO	16	PRL 117 082503	A. Gando *et al.*	(KamLAND-Zen Collab.)
AGOSTINI	15A	EPJ C75 416	M. Agostini *et al.*	(GERDA Collab.)
ALFONSO	15	PRL 115 102502	K. Alfonso *et al.*	(CUORE Collab.)
ARNOLD	15	PR D92 072011	R. Arnold *et al.*	(NEMO-3 Collab.)
ALBERT	14	PR C89 015502	J. Albert *et al.*	(EXO-200 Collab.)
ALBERT	14B	NAT 510 229	J.B. Albert *et al.*	(EXO-200 Collab.)
ARNOLD	14	PR D89 111101	R. Arnold *et al.*	(NEMO-3 Collab.)
AGOSTINI	13A	PRL 111 122503	M. Agostini *et al.*	(GERDA Collab.)
GANDO	13A	PRL 110 062502	A. Gando *et al.*	(KamLAND-Zen Collab.)
GAVRILYAK	13	PR C87 035501	Yu.M. Gavrilyuk *et al.*	
ANDREOTTI	12	PR C85 045503	E. Andreotti *et al.*	(CUORICINO Collab.)
AUGER	12	PRL 109 032505	M. Auger *et al.*	(EXO-200 Collab.)
GANDO	12A	PR C85 045504	A. Gando *et al.*	(KamLAND-Zen Collab.)
ACKERMAN	11	PRL 107 212501	N. Ackerman *et al.*	(EXO Collab.)
ARNOLD	11	PRL 107 062504	R. Arnold *et al.*	(NEMO-3 Collab.)
BARABASH	11A	PAN 74 312	A.S. Barabash *et al.*	(NEMO-3 Collab.)

Translated from YAF 74 330.

ARGYRIADES	10	NP A847 168	J. Argyriades *et al.*	(NEMO-3 Collab.)
BELLI	10	NP A846 143	P. Belli *et al.*	(DAMA-INR Collab.)
ARGYRIADES	09	PR C80 032501	J. Argyriades *et al.*	(NEMO-3 Collab.)
KIDD	09	NP A821 251	M. Kidd *et al.*	
ARNABOLDI	08	PR C78 035502	C. Arnaboldi *et al.*	(CUORICINO Collab.)
UMEHARA	08	PR C78 058501	S. Umehara *et al.*	
ARNOLD	07	NP A781 209	R. Arnold *et al.*	(NEMO-3 Collab.)
KLAPDOR-K...	06A	MPL A21 1547	H.V. Klapdor-Kleingrothaus, I.V. Krivosheina	
ARNABOLDI	05	PRL 95 142501	C. Arnaboldi *et al.*	(CUORICINO Collab.)
ARNOLD	05A	PRL 95 182302	R. Arnold *et al.*	(NEMO-3 Collab.)
AALSETH	04	PR D70 078302	C.E. Aalseth *et al.*	
ARNABOLDI	04	PL B584 260	C. Arnaboldi *et al.*	
ARNOLD	04	JETPL 80 377	R. Arnold *et al.*	(NEMO-3 Collab.)
		Translated from ZETFP 80 429.		
KLAPDOR-K...	04A	PL B586 198	H.V. Klapdor-Kleingrothaus *et al.*	
KLAPDOR-K...	04B	PR D70 078301	H.V. Klapdor-Kleingrothaus, A. Dietz, I.V. Krivosheina	
OGAWA	04	NP A730 215	I. Ogawa *et al.*	
ARNABOLDI	03	PL B557 167	C. Arnaboldi *et al.*	
DANEVICH	03	PR C68 035501	F.A. Danevich *et al.*	
AALSETH	02B	PR D65 092007	C.E. Aalseth *et al.*	(IGEX Collab.)
DEBRAECKEL...	01	PRL 86 3510	L. De Braeckeleer *et al.*	
EJIRI	01	PR C63 065501	H. Ejiri *et al.*	
KLAPDOR-K...	01	EPJ A12 147	H.V. Klapdor-Kleingrothaus *et al.*	
KLAPDOR-K...	01B	MPL A16 2409	H.V. Klapdor-Kleingrothaus *et al.*	
ALESSAND...	00	PL B486 13	A. Alessandrello *et al.*	
DANEVICH	00	PR C62 045501	F.A. Danevich *et al.*	
ARNOLD	99	NP A658 299	R. Arnold *et al.*	(NEMO Collab.)
BAUDIS	99	PR D59 022001	L. Baudis *et al.*	(Heidelberg-Moscow Collab.)
BAUDIS	99B	PRL 83 41	L. Baudis *et al.*	(Heidelberg-Moscow Collab.)
ARNOLD	98	NP A636 209	R. Arnold *et al.*	(NEMO-2 Collab.)
GUENTHER	97	PR D55 54	M. Gunther *et al.*	(Heidelberg-Moscow Collab.)
ARNOLD	96	ZPHY C72 239	R. Arnold *et al.*	(BCEN, CAEN, JINR+)
BALYSH	95	PL B356 450	A. Balysh *et al.*	(Heidelberg-Moscow Collab.)
DASSIE	95	PR D51 2090	D. Dassie *et al.*	(NEMO Collab.)
EJIRI	95	JPSJ 64 339	H. Ejiri *et al.*	(OSAK, KIEV)
SUHONEN	94	PR C49 3055	J. Suhonen, O. Civitarese	
BERNATOW...	93	PR C47 806	T. Bernatowicz *et al.*	(WUSL, TATA)
VUILLEUMIER	93	PR D48 1009	J.C. Vuilleumier *et al.*	(NEUC, CIT, VILL)
BALYSH	92	PL B283 32	A. Balysh *et al.*	(MPIH, KIAE, SASSO)
BERNATOW...	92	PRL 69 2341	T. Bernatowicz *et al.*	(WUSL, TATA)
ELLIOTT	92	PR C46 1535	S.R. Elliott *et al.*	(UCI)
SUHONEN	91	NP A535 509	J. Suhonen, S.B. Khadkikar, A. Faessler	(JYV+)
TOMODA	91	RPP 54 53	T. Tomoda	
YOU	91	PL B265 53	K. You *et al.*	(BHEP, CAST+)
STAUDT	90	EPL 13 31	A. Staudt, K. Muto, H.V. Klapdor-Kleingrothaus	
MUTO	89	ZPHY A334 187	K. Muto, E. Bender, H.V. Klapdor	(TINT, MPIH)

Neutrino Mixing

With the exception of the short-baseline anomalies such as LSND, current neutrino data can be described within the framework of a 3×3 mixing matrix between the flavor eigenstates ν_e, ν_μ, and ν_τ and the mass eigenstates ν_1, ν_2, and ν_3. (See Eq. (14.6) of the review "Neutrino Mass, Mixing, and Oscillations" by K. Nakamura and S.T. Petcov.) The Listings are divided into the following sections:

(A) Neutrino fluxes and event ratios: shows measurements which correspond to various oscillation tests for Accelerator, Reactor, Atmospheric, and Solar neutrino experiments. Typically ratios involve a measurement in a realm sensitive to oscillations compared to one for which no oscillation effect is expected.

(B) Three neutrino mixing parameters: shows measurements of $\sin^2(\theta_{12})$, $\sin^2(\theta_{23})$, Δm^2_{21}, Δm^2_{32}, $\sin^2(\theta_{13})$ and δ_{CP} which are all interpretations of data based on the three neutrino mixing scheme described in the review "Neutrino Mass, Mixing, and Oscillations." by K. Nakamura and S.T. Petcov. Many parameters have been calculated in the two-neutrino approximation.

(C) Other neutrino mixing results: shows measurements and limits for the probability of oscillation for experiments which might be relevant to the LSND oscillation claim. Included are experiments which are sensitive to $\nu_\mu \to \nu_e$, $\bar{\nu}_\mu \to \bar{\nu}_e$, eV sterile neutrinos, and CPT tests.

(A) Neutrino fluxes and event ratios

Events (observed/expected) from accelerator ν_μ experiments.

Some neutrino oscillation experiments compare the flux in two or more detectors. This is usually quoted as the ratio of the event rate in the far detector to the expected rate based on an extrapolation from the near detector in the absence of oscillations.

VALUE	DOCUMENT ID		TECN	COMMENT
• • • We do not use the following data for averages, fits, limits, etc. • • •				
1.01 ± 0.10	[1] ABE	14B	T2K	ν_e rate in T2K near detect.
0.71 ± 0.08	[2] AHN	06A	K2K	K2K to Super-K
0.64 ± 0.05	[3] MICHAEL	06	MINS	All charged current events
$0.71^{+0.08}_{-0.09}$	[4] ALIU	05	K2K	KEK to Super-K
$0.70^{+0.10}_{-0.11}$	[5] AHN	03	K2K	KEK to Super-K

[1] The rate of ν_e from μ decay was measured to be 0.68 ± 0.30 compared to the predicted flux. From K decay 1.10 ± 0.14 compared to the predicted flux.

[2] Based on the observation of 112 events when $158.1^{+9.2}_{-8.6}$ were expected without oscillations. Including not only the number of events but also the shape of the energy distribution, the evidence for oscillation is at the level of about 4.3 σ. Supersedes ALIU 05.

[3] This ratio is based on the observation of 215 events compared to an expectation of 336 ± 14 without oscillations. See also ADAMSON 08.

[4] This ratio is based on the observation of 107 events at the far detector 250 km away from KEK, and an expectation of 151^{+12}_{-10}.

[5] This ratio is based on the observation of 56 events with an expectation of $80.1^{+6.2}_{-5.4}$.

Events (observed/expected) from reactor $\overline{\nu}_e$ experiments.

The quoted values are the ratios of the measured reactor $\overline{\nu}_e$ event rate at the quoted distances, and the rate expected without oscillations. The expected rate is based on the experimental data for the most significant reactor fuels (^{235}U, ^{239}Pu, ^{241}Pu) and on calculations for ^{238}U.

A recent re-evaluation of the spectral conversion of electron to $\overline{\nu}_e$ in MUELLER 11 results in an upward shift of the reactor $\overline{\nu}_e$ spectrum by 3% and, thus, might require revisions to the ratios listed in this table.

VALUE	DOCUMENT ID		TECN	COMMENT
• • • We do not use the following data for averages, fits, limits, etc. • • •				
0.949 ± 0.0028	[1] AN	17A	DAYA	DayaBay, Ling Ao/Ao II reactors
	[2] AN	16	DAYA	DayaBay, Ling Ao/Ao II reactors
$0.944 \pm 0.007 \pm 0.003$	[3] AN	13	DAYA	DayaBay, Ling Ao/Ao II reactors
$0.944 \pm 0.016 \pm 0.040$	[4] ABE	12	DCHZ	Chooz reactors
$0.920 \pm 0.009 \pm 0.014$	[5] AHN	12	RENO	Yonggwang reactors
$0.940 \pm 0.011 \pm 0.004$	[6] AN	12	DAYA	DayaBay, LIng Ao/Ao II reactors
$1.08 \pm 0.21 \pm 0.16$	[7] DENIZ	10	TEXO	Kuo-Sheng reactor, 28 m
$0.658 \pm 0.044 \pm 0.047$	[8] ARAKI	05	KLND	Japanese react. $\sim$ 180 km
$0.611 \pm 0.085 \pm 0.041$	[9] EGUCHI	03	KLND	Japanese react. $\sim$ 180 km
$1.01 \pm 0.024 \pm 0.053$	[10] BOEHM	01		Palo Verde react. 0.75–0.89 km
$1.01 \pm 0.028 \pm 0.027$	[11] APOLLONIO	99	CHOZ	Chooz reactors 1 km
$0.987 \pm 0.006 \pm 0.037$	[12] GREENWOOD	96		Savannah River, 18.2 m
$0.988 \pm 0.004 \pm 0.05$	ACHKAR	95	CNTR	Bugey reactor, 15 m
$0.994 \pm 0.010 \pm 0.05$	ACHKAR	95	CNTR	Bugey reactor, 40 m
$0.915 \pm 0.132 \pm 0.05$	ACHKAR	95	CNTR	Bugey reactor, 95 m
$0.987 \pm 0.014 \pm 0.027$	[13] DECLAIS	94	CNTR	Bugey reactor, 15 m
$0.985 \pm 0.018 \pm 0.034$	KUVSHINN...	91	CNTR	Rovno reactor
$1.05 \pm 0.02 \pm 0.05$	VUILLEUMIER	82		Gösgen reactor
$0.955 \pm 0.035 \pm 0.110$	[14] KWON	81		$\overline{\nu}_e p \to e^+ n$
0.89 ± 0.15	[14] BOEHM	80		$\overline{\nu}_e p \to e^+ n$

[1] AN 17A use 1230 days of data of the Daya Bay experiment. The reported deficit is based on the ratio of the $\overline{\nu}_e$ signal observed by the far detectors versus the near detectors and correcting for differences in detector exposure. Supersedes AN 13.

[2] AN 16 use 217 days of data (338k events) to determine the neutrino flux ratio relative to the prediction of Mueller-Huber and ILL-Vogel models (see AN 16 for details). The reported flux ratios were corrected for θ_{13} oscillation effect. The flux measurement is consistent with results from previous short-baseline reactor experiments. The measured inverse beta decay yield is $(1.55 \pm 0.04) \times 10^{-18}$ cm^2/(GW day) or $\sigma_f = (5.92 \pm 0.14) \times 10^{-43}$ cm^2/fission. About 4σ excess of events was observed in the 4–6 MeV prompt energy region.

[3] AN 13 use six identical detectors, with three placed near the reactor cores (flux-weighted baselines of 470 and 576 m) and the remaining three at the far hall (at the flux averaged distance of 1648 m from all six reactor cores) to determine the mixing angle θ_{13} using the $\overline{\nu}_e$ observed interaction rate ratios. This rate-only analysis excludes the no-oscillation hypothesis at 7.7 standard deviations. The value of $\Delta m^2_{31} = 2.32 \times 10^{-3}$ eV^2 was assumed in the analysis. This is an improved result (2.5 times increase in statistics) compared to AN 12. Superseded by AN 17A.

[4] ABE 12 determine the $\overline{\nu}_e$ interaction rate in a single detector, located 1050 m from the cores of two reactors. The rate normalization is fixed by the results of the Bugey4 reactor experiment, thus avoiding any dependence on possible very short baseline oscillations.

[5] AHN 12 use two identical detectors, placed at flux weighted distances of 408.56 m and 1433.99m from six reactor cores, to determine the $\overline{\nu}_e$ interaction rate ratio.

[6] AN 12 use six identical detectors with three placed near the reactor cores (flux-weighted baselines of 470 m and 576 m) and the remaining three at the far hall (at the flux averaged distance of 1648 m from all six reactor cores) to determine the $\overline{\nu}_e$ interaction rate ratios. Superseded by AN 13.

[7] DENIZ 10 observe reactor $\overline{\nu}_e e$ scattering with recoil kinetic energies 3–8 MeV using CsI(Tl) detectors. The observed rate is consistent with the Standard Model prediction, leading to a constraint on $\sin^2\theta_W = 0.251 \pm 0.031(\text{stat}) \pm 0.024(\text{sys})$.

[8] Updated result of KamLAND, including the data used in EGUCHI 03. Note that the survival probabilities for different periods are not directly comparable because the effective baseline varies with power output of the reactor sources involved, and there were large variations in the reactor power production in Japan in 2003.

[9] EGUCHI 03 observe reactor neutrino disappearance at $\sim$ 180 km baseline to various Japanese nuclear power reactors.

[10] BOEHM 01 search for neutrino oscillations at 0.75 and 0.89 km distance from the Palo Verde reactors.

[11] APOLLONIO 99, APOLLONIO 98 search for neutrino oscillations at 1.1 km fixed distance from Chooz reactors. They use $\overline{\nu}_e p \rightarrow e^+ n$ in Gd-loaded scintillator target. APOLLONIO 99 supersedes APOLLONIO 98. See also APOLLONIO 03 for detailed description.

[12] GREENWOOD 96 search for neutrino oscillations at 18 m and 24 m from the reactor at Savannah River.

[13] DECLAIS 94 result based on integral measurement of neutrons only. Result is ratio of measured cross section to that expected in standard *V-A* theory. Replaced by ACHKAR 95.

[14] KWON 81 represents an analysis of a larger set of data from the same experiment as BOEHM 80.

Atmospheric neutrinos

Neutrinos and antineutrinos produced in the atmosphere induce μ-like and e-like events in underground detectors. The ratio of the numbers of the two kinds of events is defined as μ/e. It has the advantage that systematic effects, such as flux uncertainty, tend to cancel, for both experimental and theoretical values of the ratio. The "ratio of the ratios" of experimental to theoretical μ/e, $R(\mu/e)$, or that of experimental to theoretical μ/total, $R(\mu$/total) with total $= \mu+e$, is reported below. If the actual value is not unity, the value obtained in a given experiment may depend on the experimental conditions. In addition, the measured "up-down asymmetry" for μ ($N_{up}(\mu)/N_{down}(\mu)$) or e ($N_{up}(e)/N_{down}(e)$) is reported. The expected "up-down asymmetry" is nearly unity if there is no neutrino oscillation.

R(μ/e) = (Measured Ratio μ/e) / (Expected Ratio μ/e)

VALUE	DOCUMENT ID		TECN	COMMENT
• • • We do not use the following data for averages, fits, limits, etc. • • •				
$0.658 \pm 0.016 \pm 0.035$	[1] ASHIE	05	SKAM	sub-GeV
$0.702^{+0.032}_{-0.030} \pm 0.101$	[2] ASHIE	05	SKAM	multi-GeV
$0.69 \pm 0.10 \pm 0.06$	[3] SANCHEZ	03	SOU2	Calorimeter raw data
	[4] FUKUDA	96B	KAMI	Water Cherenkov
$1.00 \pm 0.15 \pm 0.08$	[5] DAUM	95	FREJ	Calorimeter
$0.60^{+0.06}_{-0.05} \pm 0.05$	[6] FUKUDA	94	KAMI	sub-GeV
$0.57^{+0.08}_{-0.07} \pm 0.07$	[7] FUKUDA	94	KAMI	multi-Gev
	[8] BECKER-SZ...	92B	IMB	Water Cherenkov

[1] ASHIE 05 results are based on an exposure of 92 kton yr during the complete Super-Kamiokande I running period. The analyzed data sample consists of fully-contained single-ring e-like events with 0.1 GeV/c $< p_e$ and μ-like events 0.2 GeV/c $< p_\mu$, both having a visible energy $<$ 1.33 GeV. These criteria match the definition used by FUKUDA 94.

[2] ASHIE 05 results are based on an exposure of 92 kton yr during the complete Super-Kamiokande I running period. The analyzed data sample consists of fully-contained single-ring events with visible energy $>$ 1.33 GeV and partially-contained events. All partially-contained events are classified as μ-like.

[3] SANCHEZ 03 result is based on an exposure of 5.9 kton yr, and updates ALLISON 99 result. The analyzed data sample consists of fully-contained e-flavor and μ-flavor events having lepton momentum $>$ 0.3 GeV/c.

[4] FUKUDA 96B studied neutron background in the atmospheric neutrino sample observed in the Kamiokande detector. No evidence for the background contamination was found.

[5] DAUM 95 results are based on an exposure of 2.0 kton yr which includes the data used by BERGER 90B. This ratio is for the contained and semicontained events. DAUM 95 also report $R(\mu/e) = 0.99 \pm 0.13 \pm 0.08$ for the total neutrino induced data sample which includes upward going stopping muons and horizontal muons in addition to the contained and semicontained events.

[6] FUKUDA 94 result is based on an exposure of 7.7 kton yr and updates the HIRATA 92 result. The analyzed data sample consists of fully-contained e-like events with 0.1 $< p_e <$ 1.33 GeV/c and fully-contained μ-like events with 0.2 $< p_\mu <$ 1.5 GeV/c.

[7] FUKUDA 94 analyzed the data sample consisting of fully contained events with visible energy $>$ 1.33 GeV and partially contained μ-like events.

[8] BECKER-SZENDY 92B reports the fraction of nonshowering events (mostly muons from atmospheric neutrinos) as $0.36 \pm 0.02 \pm 0.02$, as compared with expected fraction $0.51 \pm 0.01 \pm 0.05$. After cutting the energy range to the Kamiokande limits, BEIER 92 finds $R(\mu/e)$ very close to the Kamiokande value.

R(ν_μ) = (Measured Flux of ν_μ) / (Expected Flux of ν_μ)

VALUE	DOCUMENT ID		TECN	COMMENT
• • • We do not use the following data for averages, fits, limits, etc. • • •				
0.84 ± 0.12	[1] ADAMSON	06	MINS	MINOS atmospheric
$0.72 \pm 0.026 \pm 0.13$	[2] AMBROSIO	01	MCRO	upward through-going
$0.57 \pm 0.05 \pm 0.15$	[3] AMBROSIO	00	MCRO	upgoing partially contained
$0.71 \pm 0.05 \pm 0.19$	[4] AMBROSIO	00	MCRO	downgoing partially contained + upgoing stopping
$0.74 \pm 0.036 \pm 0.046$	[5] AMBROSIO	98	MCRO	Streamer tubes
	[6] CASPER	91	IMB	Water Cherenkov
	[7] AGLIETTA	89	NUSX	
0.95 ± 0.22	[8] BOLIEV	81		Baksan
0.62 ± 0.17	CROUCH	78		Case Western/UCI

[1] ADAMSON 06 uses a measurement of 107 total neutrinos compared to an expected rate of 127 $\pm$ 13 without oscillations.

[2] AMBROSIO 01 result is based on the upward through-going muon tracks with $E_\mu > 1$ GeV. The data came from three different detector configurations, but the statistics is largely dominated by the full detector run, from May 1994 to December 2000. The total live time, normalized to the full detector configuration, is 6.17 years. The first error is the statistical error, the second is the systematic error, dominated by the theoretical error in the predicted flux.

[3] AMBROSIO 00 result is based on the upgoing partially contained event sample. It came from 4.1 live years of data taking with the full detector, from April 1994 to February 1999. The average energy of atmospheric muon neutrinos corresponding to this sample is 4 GeV. The first error is statistical, the second is the systematic error, dominated by the 25% theoretical error in the rate (20% in the flux and 15% in the cross section, added in quadrature). Within statistics, the observed deficit is uniform over the zenith angle.

[4] AMBROSIO 00 result is based on the combined samples of downgoing partially contained events and upgoing stopping events. These two subsamples could not be distinguished due to the lack of timing information. The result came from 4.1 live years of data taking with the full detector, from April 1994 to February 1999. The average energy of atmospheric muon neutrinos corresponding to this sample is 4 GeV. The first error is statistical, the second is the systematic error, dominated by the 25% theoretical error in the rate (20% in the flux and 15% in the cross section, added in quadrature). Within statistics, the observed deficit is uniform over the zenith angle.

[5] AMBROSIO 98 result is for all nadir angles and updates AHLEN 95 result. The lower cutoff on the muon energy is 1 GeV. In addition to the statistical and systematic errors, there is a Monte Carlo flux error (theoretical error) of $\pm$0.13. With a neutrino oscillation hypothesis, the fit either to the flux or zenith distribution independently yields $\sin^2 2\theta$=1.0 and $\Delta(m^2) \sim$ a few times 10^{-3} eV^2. However, the fit to the observed zenith distribution gives a maximum probability for χ^2 of only 5% for the best oscillation hypothesis.

[6] CASPER 91 correlates showering/nonshowering signature of single-ring events with parent atmospheric-neutrino flavor. They find nonshowering ($\approx \nu_\mu$ induced) fraction is $0.41 \pm 0.03 \pm 0.02$, as compared with expected 0.51 ± 0.05 (syst).

[7] AGLIETTA 89 finds no evidence for any anomaly in the neutrino flux. They define ρ = (measured number of ν_e's)/(measured number of ν_μ's). They report ρ(measured)=ρ(expected) $= 0.96^{+0.32}_{-0.28}$.

[8] From this data BOLIEV 81 obtain the limit $\Delta(m^2) \leq 6 \times 10^{-3}$ eV^2 for maximal mixing, $\nu_\mu \not\rightarrow \nu_\mu$ type oscillation.

R(μ/total) = (Measured Ratio μ/total) / (Expected Ratio μ/total)

VALUE	DOCUMENT ID		TECN	COMMENT
• • • We do not use the following data for averages, fits, limits, etc. • • •				
$1.1^{+0.07}_{-0.12} \pm 0.11$	[1] CLARK	97	IMB	multi-GeV

[1] CLARK 97 obtained this result by an analysis of fully contained and partially contained events in the IMB water-Cherenkov detector with visible energy $>$ 0.95 GeV.

$N_{up}(\mu)/N_{down}(\mu)$

VALUE	DOCUMENT ID		TECN	COMMENT
• • • We do not use the following data for averages, fits, limits, etc. • • •				
0.71 ± 0.06	[1] ADAMSON	12B	MINS	contained-vertex muons
$0.551^{+0.035}_{-0.033} \pm 0.004$	[2] ASHIE	05	SKAM	multi-GeV

[1] ADAMSON 12B reports the atmospheric neutrino results obtained with MINOS far detector in 2,553 live days (an exposure of 37.9 kton-yr). This result is obtained with a sample of high resolution contained-vertex muons. The quoted error is statistical only.

[2] ASHIE 05 results are based on an exposure of 92 kton yr during the complete Super-Kamiokande I running period. The analyzed data sample consists of fully-contained single-ring μ-like events with visible energy $>$ 1.33 GeV and partially-contained events. All partially-contained events are classified as μ-like. Upward-going events are those with $-1 <$ cos(zenith angle) < -0.2 and downward-going events are those with 0.2$<$ cos(zenith angle) $<$1. The μ-like up-down ratio for the multi-GeV data deviates from 1 (the expectation for no atmospheric ν_μ oscillations) by more than 12 standard deviations.

$N_{up}(e)/N_{down}(e)$

VALUE	DOCUMENT ID		TECN	COMMENT
• • • We do not use the following data for averages, fits, limits, etc. • • •				
$0.961^{+0.086}_{-0.079} \pm 0.016$	[1] ASHIE	05	SKAM	multi-GeV

[1] ASHIE 05 results are based on an exposure of 92 kton yr during the complete Super-Kamiokande I running period. The analyzed data sample consists of fully-contained single-ring e-like events with visible energy $>$ 1.33 GeV. Upward-going events are those with $-1 <$ cos(zenith angle) < -0.2 and downward-going events are those with 0.2 $<$ cos(zenith angle) $<$ 1. The e-like up-down ratio for the multi-GeV data is consistent with 1 (the expectation for no atmospheric ν_e oscillations).

R(up/down; μ) = (Measured up/down; μ) / (Expected up/down; μ)

VALUE	DOCUMENT ID		TECN	COMMENT
• • • We do not use the following data for averages, fits, limits, etc. • • •				
$0.62 \pm 0.05 \pm 0.02$	[1] ADAMSON	12B	MINS	contained-vertex muons
$0.62^{+0.19}_{-0.14} \pm 0.02$	[2] ADAMSON	06	MINS	atmospheric ν with far detector

[1] ADAMSON 12B reports the atmospheric neutrino results obtained with MINOS far detector in 2,553 live days (an exposure of 37.9 kton-yr). This result is obtained with a sample of high resolution contained-vertex muons. The expected ratio is calculated with no neutrino oscillation.

[2] ADAMSON 06 result is obtained with the MINOS far detector with an exposure of 4.54 kton yr. The expected ratio is calculated with no neutrino oscillation.

N(μ^+)/N(μ^-)

VALUE	DOCUMENT ID		TECN	COMMENT
• • • We do not use the following data for averages, fits, limits, etc. • • •				
$0.46^{+0.05}_{-0.04}$	[1,2] ADAMSON	12B	MINS	contained-vertex muons
$0.63^{+0.09}_{-0.08}$	[1,3] ADAMSON	12B	MINS	ν-induced rock-muons

[1] ADAMSON 12B reports the atmospheric neutrino results obtained with MINOS far detector in 2,553 live days (an exposure of 37.9 kton-yr). The muon charge ratio N(μ^+)/N(μ^-) represents the $\overline{\nu}_\mu/\nu_\mu$ ratio.

[2] This result is obtained with a charge-separated sample of high resolution contained-vertex muons. The quoted error is statistical only.

[3] This result is obtained with a charge-separated sample of high resolution neutrino-induced rock-muons. The quoted error is statistical only.

$R(\mu^+/\mu^-)$ = (Measured $N(\mu^+)/N(\mu^-)$) / (Expected $N(\mu^+)/N(\mu^-)$)

VALUE	DOCUMENT ID		TECN	COMMENT
• • • We do not use the following data for averages, fits, limits, etc. • • •				
$0.93\pm0.09\pm0.09$	[1,2] ADAMSON	12B	MINS	contained-vertex muons
$1.29^{+0.19}_{-0.17}\pm0.16$	[1,3] ADAMSON	12B	MINS	ν-induced rock-muons
$1.03\pm0.08\pm0.08$	[1,4] ADAMSON	12B	MINS	contained
$1.39^{+0.35}_{-0.46}{}^{+0.08}_{-0.14}$	[5] ADAMSON	07	MINS	Upward and horizontal μ with far detector
$0.96^{+0.38}_{-0.27}\pm0.15$	[6] ADAMSON	06	MINS	atmospheric ν with far detector

[1] ADAMSON 12B reports the atmospheric neutrino results obtained with MINOS far detector in 2,553 live days (an exposure of 37.9 kton·yr). The muon charge ratio $N(\mu^+)/N(\mu^-)$ represents the $\overline{\nu}_\mu/\nu_\mu$ ratio. As far as the same oscillation parameters are used for νs and $\overline{\nu}$s, the expected $\overline{\nu}_\mu/\nu_\mu$ ratio is almost entirely independent of any input oscillations.
[2] This result is obtained with a charge-separated sample of high resolution contained-vertex muons.
[3] This result is obtained with a charge-separated sample of high resolution neutrino-induced rock-muons.
[4] The charge-separated samples of high resolution contained-vertex muons and neutrino-induced rock-muons are combined to obtain this result which is consistent with unity.
[5] ADAMSON 07 result is obtained with the MINOS far detector in 854.24 live days, based on neutrino-induced upward-going and horizontal muons. This result is consistent with CPT conservation.
[6] ADAMSON 06 result is obtained with the MINOS far detector with an exposure of 4.54 kton yr, based on contained events. The expected ratio is calculated by assuming the same oscillation parameters for neutrinos and antineutrinos.

Solar neutrinos

Solar neutrinos are produced by thermonuclear fusion reactions in the Sun. Radiochemical experiments measure particular combinations of fluxes from various neutrino-producing reactions, whereas water-Cherenkov experiments mainly measure a flux of neutrinos from decay of ^{8}B. Solar neutrino fluxes are composed of all active neutrino species, ν_e, ν_μ, and ν_τ. In addition, some other mechanisms may cause antineutrino components in solar neutrino fluxes. Each measurement method is sensitive to a particular component or a combination of components of solar neutrino fluxes. For details, see Section 13.4 of Reviews, Tables, and Plots.

ν_e Capture Rates from Radiochemical Experiments

1 SNU (Solar Neutrino Unit) = 10^{-36} captures per atom per second.

VALUE (SNU)	DOCUMENT ID		TECN	COMMENT
• • • We do not use the following data for averages, fits, limits, etc. • • •				
$73.4\ ^{+6.1}_{-6.0}\ ^{+3.7}_{-4.1}$	[1] KAETHER	10		GALX reanalysis
$67.6\ \pm4.0\ \pm3.2$	[2] KAETHER	10		GNO+GALX reanalysis combined
$65.4\ ^{+3.1}_{-3.0}\ ^{+2.6}_{-2.8}$	[3] ABDURASHI...	09	SAGE	^{71}Ga → ^{71}Ge
$62.9\ ^{+5.5}_{-5.3}\ \pm2.5$	[4] ALTMANN	05	GNO	^{71}Ga → ^{71}Ge
$69.3\ \pm4.1\ \pm3.6$	[5] ALTMANN	05	GNO	GNO + GALX combined
$77.5\ \pm6.2\ ^{+4.3}_{-4.7}$	[6] HAMPEL	99	GALX	^{71}Ga → ^{71}Ge
$2.56\pm0.16\pm0.16$	[7] CLEVELAND	98	HOME	^{37}Cl → ^{37}Ar

[1] KAETHER 10 reports the reanalysis results of a complete GALLEX data (GALLEX I+II+III+IV, reported in HAMPEL 99) based on the event selection with a new pulse shape analysis, which provides a better background reduction than the rise time analysis adopted in HAMPEL 99.
[2] Combined result of GALLEX I+II+III+IV reanalysis and GNO I+II+III (ALTMANN 05).
[3] ABDURASHITOV 09 reports a combined analysis of 168 extractions of the SAGE solar neutrino experiment during the period January 1990 through December 2007, and updates the ABDURASHITOV 02 result. The data are consistent with the assumption that the solar neutrino production rate is constant in time. Note that a $\sim$ 15% systematic uncertainty in the overall normalization may be added to the ABDURASHITOV 09 result, because calibration experiments for gallium solar neutrino measurements using intense ^{51}Cr (twice by GALLEX and once by SAGE) and ^{37}Ar (by SAGE) result in an average ratio of 0.87 $\pm$ 0.05 of the observed to calculated rates.
[4] ALTMANN 05 reports the complete result from the GNO solar neutrino experiment (GNO I+II+III), which is the successor project of GALLEX. Experimental technique of GNO is essentially the same as that of GALLEX. The run data cover the period 20 May 1998 through 9 April 2003.
[5] Combined result of GALLEX I+II+III+IV (HAMPEL 99) and GNO I+II+III.
[6] HAMPEL 99 report the combined result for GALLEX I+II+III+IV (65 runs in total), which update the HAMPEL 96 result. The GALLEX IV result (12 runs) is 118.4 $\pm$ 17.8 $\pm$ 6.6 SNU. (HAMPEL 99 discuss the consistency of partial results with the mean.) The GALLEX experimental program has been completed with these runs. The total run data cover the period 14 May 1991 through 23 January 1997. A total of 300 ^{71}Ge events were observed. Note that a $\sim$ 15% systematic uncertainty in the overall normalization may be added to the HAMPEL 99 result, because calibration experiments for gallium solar neutrino measurements using intense ^{51}Cr (twice by GALLEX and once by SAGE) and ^{37}Ar (by SAGE) result in an average ratio of 0.87 ± 0.05 of the observed to calculated rates.
[7] CLEVELAND 98 is a detailed report of the ^{37}Cl experiment at the Homestake Mine. The average solar neutrino-induced ^{37}Ar production rate from 108 runs between 1970 and 1994 updates the DAVIS 89 result.

ϕ_{ES} (^{8}B)

^{8}B solar-neutrino flux measured via νe elastic scattering. This process is sensitive to all active neutrino flavors, but with reduced sensitivity to ν_μ, ν_τ due to the cross-section difference, $\sigma(\nu_{\mu,\tau}\, e) \sim 0.16\sigma(\nu_e\, e)$. If the ^{8}B solar-neutrino flux involves nonelectron flavor active neutrinos, their contribution to the flux is $\sim$ 0.16 times of ν_e.

VALUE (10^6 cm^{-2}s^{-1})	DOCUMENT ID		TECN	COMMENT
• • • We do not use the following data for averages, fits, limits, etc. • • •				
$2.345\pm0.014\pm0.036$	[1] ABE	16C	SKAM	SK-I+II+III+IV average flux
$2.308\pm0.020^{+0.039}_{-0.040}$	[2] ABE	16C	SKAM	SK-IV average flux
$2.250^{+0.030}_{-0.029}\pm0.038$	[2] ABE	16C	SKAM	SK-IV day flux
$2.364\pm0.029\pm0.040$	[2] ABE	16C	SKAM	SK-IV night flux
$2.404\pm0.039\pm0.053$	[3] ABE	16C	SKAM	SK-III average flux
$2.41\ \pm0.05\ ^{+0.16}_{-0.15}$	[4] ABE	11	SKAM	SK-II average flux
$2.38\ \pm0.02\ \pm0.08$	[5] ABE	11	SKAM	SK-I average flux
$2.77\ \pm0.26\ \pm0.32$	[6] ABE	11B	KLND	average flux
$2.4\ \pm0.4\ \pm0.1$	[7] BELLINI	10A	BORX	average flux
$1.77\ ^{+0.24}_{-0.21}\ ^{+0.09}_{-0.10}$	[8] AHARMIM	08	SNO	Phase III
$2.38\ \pm0.05\ ^{+0.16}_{-0.15}$	[9] CRAVENS	08	SKAM	average flux
$2.35\ \pm0.02\ \pm0.08$	[10] HOSAKA	06	SKAM	average flux
$2.35\ \pm0.22\ \pm0.15$	[11] AHARMIM	05A	SNO	Salty D_2O; ^{8}B shape not constrained
$2.34\ \pm0.23\ ^{+0.15}_{-0.14}$	[11] AHARMIM	05A	SNO	Salty D_2O; ^{8}B shape constrained
$2.39\ ^{+0.24}_{-0.23}\ \pm0.12$	[12] AHMAD	02	SNO	average flux
$2.39\ \pm0.34\ ^{+0.16}_{-0.14}$	[13] AHMAD	01	SNO	average flux
$2.80\ \pm0.19\ \pm0.33$	[14] FUKUDA	96	KAMI	average flux
$2.70\ \pm0.27$	[14] FUKUDA	96	KAMI	day flux
$2.87\ ^{+0.27}_{-0.26}$	[14] FUKUDA	96	KAMI	night flux

[1] ABE 16C reports the combined results of the four phases of the Super-Kamiokande average flux measurements. Here the revised Super-Kamiokande-III result is used.
[2] ABE 16C reports the Super-Kamiokande-IV results for 1664 live days from September 2008 to February 2014. The analysis threshold is total electron energy of 4.0 MeV.
[3] ABE 16C revised the Super-Kamiokande-III average flux value reported in ABE 11. Super-Kamiokande-III results are for 548 live days from August 4, 2006 to August 18, 2008. The analysis threshold is 5.0 MeV, but the event sample in the 5.0–6.5 MeV total electron energy range has a total live time of 298 days.
[4] ABE 11 recalculated the Super-Kamiokande-II results using ^{8}B spectrum of WINTER 06A.
[5] ABE 11 recalculated the Super-Kamiokande-I results using ^{8}B spectrum of WINTER 06A.
[6] ABE 11B use a 123 kton·day exposure of the KamLAND liquid scintillation detector to measure the ^{8}B solar neutrino flux. They utilize $\nu - e$ elastic scattering above a reconstructed-energy threshold of 5.5 MeV, corresponding to 5 MeV electron recoil energy. 299 electron recoil candidate events are reported, of which 157 ± 23.6 are assigned to background.
[7] BELLINI 10A reports the Borexino result with 3 MeV energy threshold for scattered electrons. The data correspond to 345.3 live days with a target mass of 100 t, between July 15, 2007 and August 23, 2009.
[8] AHARMIM 08 reports the results from SNO Phase III measurement using an array of ^{3}He proportional counters to measure the rate of NC interactions in heavy water, over the period between November 27, 2004 and November 28, 2006, corresponding to 385.17 live days. A simultaneous fit was made for the number of NC events detected by the proportional counters and the numbers of NC, CC, and ES events detected by the PMTs, where the spectral distributions of the ES and CC events were not constrained to the ^{8}B shape.
[9] CRAVENS 08 reports the Super-Kamiokande-II results for 791 live days from December 2002 to October 2005. The photocathode coverage of the detector is 19% (reduced from 40% of that of Super-Kamiokande-I due to an accident in 2001). The analysis threshold for the average flux is 7 MeV.
[10] HOSAKA 06 reports the final results for 1496 live days with Super-Kamiokande-I between May 31, 1996 and July 15, 2001, and replace FUKUDA 02 results. The analysis threshold is 5 MeV except for the first 280 live days (6.5 MeV).
[11] AHARMIM 05A measurements were made with dissolved NaCl (0.195% by weight) in heavy water over the period between July 26, 2001 and August 28, 2003, corresponding to 391.4 live days, and update AHMED 04A. The *CC*, *ES*, and *NC* events were statistically separated. In one method, the ^{8}B energy spectrum was not constrained. In the other method, the constraint of an undistorted ^{8}B energy spectrum was added for comparison with AHMAD 02 results.
[12] AHMAD 02 reports the ^{8}B solar-neutrino flux measured via νe elastic scattering above the kinetic energy threshold of 5 MeV. The data correspond to 306.4 live days with SNO between November 2, 1999 and May 28, 2001, and updates AHMAD 01 results.
[13] AHMAD 01 reports the ^{8}B solar-neutrino flux measured via νe elastic scattering above the kinetic energy threshold of 6.75 MeV. The data correspond to 241 live days with SNO between November 2, 1999 and January 15, 2001.
[14] FUKUDA 96 results are for a total of 2079 live days with Kamiokande II and III from January 1987 through February 1995, covering the entire solar cycle 22, with threshold $E_e > 9.3$ MeV (first 449 days), > 7.5 MeV (middle 794 days), and > 7.0 MeV (last 836 days). These results update the HIRATA 90 result for the average ^{8}B solar-neutrino flux and HIRATA 91 result for the day-night variation in the ^{8}B solar-neutrino flux. The total data sample was also analyzed for short-term variations: within experimental errors, no strong correlation of the solar-neutrino flux with the sunspot numbers was found.

ϕ_{CC} (^{8}B)

^{8}B solar-neutrino flux measured with charged-current reaction which is sensitive exclusively to ν_e.

VALUE (10^6 cm^{-2}s^{-1})	DOCUMENT ID		TECN	COMMENT
• • • We do not use the following data for averages, fits, limits, etc. • • •				
$1.67^{+0.05}_{-0.04}{}^{+0.07}_{-0.08}$	[1] AHARMIM	08	SNO	Phase III
$1.68\pm0.06^{+0.08}_{-0.09}$	[2] AHARMIM	05A	SNO	Salty D_2O; ^{8}B shape not const.
$1.72\pm0.05\pm0.11$	[2] AHARMIM	05A	SNO	Salty D_2O; ^{8}B shape constrained
$1.76^{+0.06}_{-0.05}\pm0.09$	[3] AHMAD	02	SNO	average flux
$1.75\pm0.07^{+0.12}_{-0.11}\pm0.05$	[4] AHMAD	01	SNO	average flux

[1] AHARMIM 08 reports the results from SNO Phase III measurement using an array of ^{3}He proportional counters to measure the rate of NC interactions in heavy water, over the period between November 27, 2004 and November 28, 2006, corresponding to 385.17 live days. A simultaneous fit was made for the number of NC events detected by the proportional counters and the numbers of NC, CC, and ES events detected by the PMTs, where the spectral distributions of the ES and CC events were not constrained to the ^{8}B shape.

[2] AHARMIM 05A measurements were made with dissolved NaCl (0.195% by weight) in heavy water over the period between July 26, 2001 and August 28, 2003, corresponding to 391.4 live days, and update AHMED 04A. The *CC*, *ES*, and *NC* events were statistically separated. In one method, the ^{8}B energy spectrum was not constrained. In the other method, the constraint of an undistorted ^{8}B energy spectrum was added for comparison with AHMAD 02 results.

[3] AHMAD 02 reports the SNO result of the ^{8}B solar-neutrino flux measured with charged-current reaction on deuterium, $\nu_e d \rightarrow pp e^-$, above the kinetic energy threshold of 5 MeV. The data correspond to 306.4 live days with SNO between November 2, 1999 and May 28, 2001, and updates AHMAD 01 results. The complete description of the SNO Phase I data set is given in AHARMIM 07.

[4] AHMAD 01 reports the first SNO result of the ^{8}B solar-neutrino flux measured with the charged-current reaction on deuterium, $\nu_e d \rightarrow pp e^-$, above the kinetic energy threshold of 6.75 MeV. The data correspond to 241 live days with SNO between November 2, 1999 and January 15, 2001.

ϕ_{NC} (^{8}B)

^{8}B solar neutrino flux measured with neutral-current reaction, which is equally sensitive to ν_e, ν_μ, and ν_τ.

VALUE (10^6 cm^{-2}s^{-1})	DOCUMENT ID		TECN	COMMENT
• • • We do not use the following data for averages, fits, limits, etc. • • •				
$5.25\pm0.16^{+0.11}_{-0.13}$	[1] AHARMIM	13	SNO	All three phases combined
$5.140^{+0.160}_{-0.158}{}^{+0.132}_{-0.117}$	[2] AHARMIM	10	SNO	Phase I+II, low threshold
$5.54^{+0.33}_{-0.31}{}^{+0.36}_{-0.34}$	[3] AHARMIM	08	SNO	Phase III, prop. counter + PMT
$4.94\pm0.21^{+0.38}_{-0.34}$	[4] AHARMIM	05A	SNO	Salty D_2O; ^{8}B shape not const.
$4.81\pm0.19^{+0.28}_{-0.27}$	[4] AHARMIM	05A	SNO	Salty D_2O; ^{8}B shape constrained
$5.09^{+0.44}_{-0.43}{}^{+0.46}_{-0.43}$	[5] AHMAD	02	SNO	average flux; ^{8}B shape const.
$6.42\pm1.57^{+0.55}_{-0.58}$	[5] AHMAD	02	SNO	average flux; ^{8}B shape not const.

[1] AHARMIM 13 obtained this result from a combined analysis of the data from all three phases, SNO-I, II, and III. The measurement of the ^{8}B flux mostly comes from the NC signal, however, CC contribution is included in the fit.

[2] AHARMIM 10 reports this result from a joint analysis of SNO Phase I+II data with the "effective electron kinetic energy" threshold of 3.5 MeV. This result is obtained with a "binned-histogram unconstrained fit" where binned probability distribution functions of the neutrino signal observables were used without any model constraints on the shape of the neutrino spectrum.

[3] AHARMIM 08 reports the results from SNO Phase III measurement using an array of ^{3}He proportional counters to measure the rate of NC interactions in heavy water, over the period between November 27, 2004 and November 28, 2006, corresponding to 385.17 live days. A simultaneous fit was made for the number of NC events detected by the proportional counters and the numbers of NC, CC, and ES events detected by the PMTs, where the spectral distributions of the ES and CC events were not constrained to the ^{8}B shape.

[4] AHARMIM 05A measurements were made with dissolved NaCl (0.195% by weight) in heavy water over the period between July 26, 2001 and August 28, 2003, corresponding to 391.4 live days, and update AHMED 04A. The *CC*, *ES*, and *NC* events were statistically separated. In one method, the ^{8}B energy spectrum was not constrained. In the other method, the constraint of an undistorted ^{8}B energy spectrum was added for comparison with AHMAD 02 results.

[5] AHMAD 02 reports the first SNO result of the ^{8}B solar-neutrino flux measured with the neutral-current reaction on deuterium, $\nu_\ell d \rightarrow np\nu_\ell$, above the neutral-current reaction threshold of 2.2 MeV. The data correspond to 306.4 live days with SNO between November 2, 1999 and May 28, 2001. The complete description of the SNO Phase I data set is given in AHARMIM 07.

$\phi_{\nu_\mu+\nu_\tau}$ (^{8}B)

Nonelectron-flavor active neutrino component (ν_μ and ν_τ) in the ^{8}B solar-neutrino flux.

VALUE (10^6 cm^{-2}s^{-1})	DOCUMENT ID		TECN	COMMENT
• • • We do not use the following data for averages, fits, limits, etc. • • •				
$3.26\pm0.25^{+0.40}_{-0.35}$	[1] AHARMIM	05A	SNO	From ϕ_{NC}, ϕ_{CC}, and ϕ_{ES}; ^{8}B shape not const.
$3.09\pm0.22^{+0.30}_{-0.27}$	[1] AHARMIM	05A	SNO	From ϕ_{NC}, ϕ_{CC}, and ϕ_{ES}; ^{8}B shape constrained
$3.41\pm0.45^{+0.48}_{-0.45}$	[2] AHMAD	02	SNO	From ϕ_{NC}, ϕ_{CC}, and ϕ_{ES}
3.69 ± 1.13	[3] AHMAD	01		Derived from SNO+SuperKam, water Cherenkov

[1] AHARMIM 05A measurements were made with dissolved NaCl (0.195% by weight) in heavy water over the period between July 26, 2001 and August 28, 2003, corresponding to 391.4 live days, and update AHMED 04A. The *CC*, *ES*, and *NC* events were statistically separated. In one method, the ^{8}B energy spectrum was not constrained. In the other method, the constraint of an undistorted ^{8}B energy spectrum was added for comparison with AHMAD 02 results.

[2] AHMAD 02 deduced the nonelectron-flavor active neutrino component (ν_μ and ν_τ) in the ^{8}B solar-neutrino flux, by combining the charged-current result, the νe elastic-scattering result and the neutral-current result. The complete description of the SNO Phase I data set is given in AHARMIM 07.

[3] AHMAD 01 deduced the nonelectron-flavor active neutrino component (ν_μ and ν_τ) in the ^{8}B solar-neutrino flux, by combining the SNO charged-current result (AHMAD 01) and the Super-Kamiokande νe elastic-scattering result (FUKUDA 01).

Total Flux of Active ^{8}B Solar Neutrinos

Total flux of active neutrinos (ν_e, ν_μ, and ν_τ).

VALUE (10^6 cm^{-2}s^{-1})	DOCUMENT ID		TECN	COMMENT
• • • We do not use the following data for averages, fits, limits, etc. • • •				
$5.25\pm0.16^{+0.11}_{-0.13}$	[1] AHARMIM	13	SNO	All three phases combined
$5.046^{+0.159}_{-0.152}{}^{+0.107}_{-0.123}$	[2] AHARMIM	10	SNO	From ϕ_{NC} in Phase I+II, low threshold
$5.54^{+0.33}_{-0.31}{}^{+0.36}_{-0.34}$	[3] AHARMIM	08	SNO	ϕ_{NC} in Phase III
$4.94\pm0.21^{+0.38}_{-0.34}$	[4] AHARMIM	05A	SNO	From ϕ_{NC}; ^{8}B shape not const.
$4.81\pm0.19^{+0.28}_{-0.27}$	[4] AHARMIM	05A	SNO	From ϕ_{NC}; ^{8}B shape constrained
$5.09^{+0.44}_{-0.43}{}^{+0.46}_{-0.43}$	[5] AHMAD	02	SNO	Direct measurement from ϕ_{NC}
5.44 ± 0.99	[6] AHMAD	01		Derived from SNO+SuperKam, water Cherenkov

[1] AHARMIM 13 obtained this result from a combined analysis of the data from all three phases, SNO-I, II, and III. The measurement of the ^{8}B flux mostly comes from the NC signal, however, CC contribution is included in the fit.

[2] AHARMIM 10 reports this result from a joint analysis of SNO Phase I+II data with the "effective electron kinetic energy" threshold of 3.5 MeV. This result is obtained with the assumption of unitarity, which relates the NC, CC, and ES rates. The data were fit with the free parameters directly describing the total ^{8}B neutrino flux and the energy-dependent ν_e survival probability.

[3] AHARMIM 08 reports the results from SNO Phase III measurement using an array of ^{3}He proportional counters to measure the rate of NC interactions in heavy water, over the period between November 27, 2004 and November 28, 2006, corresponding to 385.17 live days. A simultaneous fit was made for the number of NC events detected by the proportional counters and the numbers of NC, CC, and ES events detected by the PMTs, where the spectral distributions of the ES and CC events were not constrained to the ^{8}B shape.

[4] AHARMIM 05A measurements were made with dissolved NaCl (0.195% by weight) in heavy water over the period between July 26, 2001 and August 28, 2003, corresponding to 391.4 live days, and update AHMED 04A. The CC, ES, and NC events were statistically separated. In one method, the ^{8}B energy spectrum was not constrained. In the other method, the constraint of an undistorted ^{8}B energy spectrum was added for comparison with AHMAD 02 results.

[5] AHMAD 02 determined the total flux of active ^{8}B solar neutrinos by directly measuring the neutral-current reaction, $\nu_\ell d \rightarrow np\nu_\ell$, which is equally sensitive to ν_e, ν_μ, and ν_τ. The complete description of the SNO Phase I data set is given in AHARMIM 07.

[6] AHMAD 01 deduced the total flux of active ^{8}B solar neutrinos by combining the SNO charged-current result (AHMAD 01) and the Super-Kamiokande νe elastic-scattering result (FUKUDA 01).

Day-Night Asymmetry (^{8}B)

$A = (\phi_{\text{night}} - \phi_{\text{day}}) / \phi_{\text{average}}$

VALUE	DOCUMENT ID		TECN	COMMENT
$0.033\pm0.010\pm0.005$	[1] ABE	16C	SKAM	SK combined; Based on ϕ_{ES}
• • • We do not use the following data for averages, fits, limits, etc. • • •				
$0.036\pm0.016\pm0.006$	[2] ABE	16C	SKAM	SK-IV; Based on ϕ_{ES}
$0.032\pm0.011\pm0.005$	[3] RENSHAW	14	SKAM	Based on ϕ_{ES}
$0.063\pm0.042\pm0.037$	[4] CRAVENS	08	SKAM	Based on ϕ_{ES}
$0.021\pm0.020^{+0.012}_{-0.013}$	[5] HOSAKA	06	SKAM	Based on ϕ_{ES}
$0.017\pm0.016^{+0.012}_{-0.013}$	[6] HOSAKA	06	SKAM	Fitted in the LMA region
$-0.056\pm0.074\pm0.053$	[7] AHARMIM	05A	SNO	From salty SNO ϕ_{CC}
$-0.037\pm0.063\pm0.032$	[7] AHARMIM	05A	SNO	From salty SNO ϕ_{CC}; const. of no ϕ_{NC} asymmetry
$0.14\pm0.063^{+0.015}_{-0.014}$	[8] AHMAD	02B	SNO	Derived from SNO ϕ_{CC}
$0.07\pm0.049^{+0.013}_{-0.012}$	[9] AHMAD	02B	SNO	Const. of no ϕ_{NC} asymmetry

[1] ABE 16C reports the combined day-night flux asymmetry results of the four phases of the Super-Kamiokande measurements. Amplitude fit method is used. See footnote to RENSHAW 14.

[2] ABE 16C reports the Super-Kamiokande-IV results for 1664 live days from September 2008 to February 2014. The analysis threshold for day-night flux asymmetry is recoil electron energy of 4.49 MeV (total electron energy of 5.0 MeV). Amplitude fit method is used. See footnote to RENSHAW 14.

[3] RENSHAW 14 obtains this result by using the "amplitude fit" introduced in SMY 04. The data from the Super-Kamiokande(SK)-I, -II, -III, and 1306 live days of the SK-IV measurements are used. The analysis threshold is recoil-electron kinetic energy of 4.5 MeV for SK-III, and SK-IV except for 250 live days in SK-III (6.0 MeV). The analysis threshold for SK-I and SK-II is the same as in the previous reports. (Note that in the previous SK solar-neutrino results, the analysis threshold is quoted as recoil-electron total energy.) This day-night asymmetry result is consistent with neutrino oscillations for 4×10^{-5} eV^2 $< \Delta m^2_{21} < 7 \times 10^{-5}$ eV^2 and large mixing values of θ_{12} at the 68% CL.

[4] CRAVENS 08 reports the Super-Kamiokande-II results for 791 live days from December 2002 to October 2005. The photocathode coverage of the detector is 19% (reduced from 40% of that of Super-Kamiokande-I due to an accident in 2001). The analysis threshold for the day and night fluxes is 7.5 MeV except for the first 159 live days (8.0 MeV).

[5] HOSAKA 06 reports the final results for 1496 live days with Super-Kamiokande-I between May 31, 1996 and July 15, 2001, and replace FUKUDA 02 results. The analysis threshold is 5 MeV except for the first 280 live days (6.5 MeV).

[6] This result with reduced statistical uncertainty is obtained by assuming two-neutrino oscillations within the LMA (large mixing angle) region and by fitting the time variation of the solar neutrino flux measured via ν_e elastic scattering to the variations expected from neutrino oscillations. For details, see SMY 04. There is an additional small systematic error of ± 0.0004 coming from uncertainty of oscillation parameters.

[7] AHARMIM 05A measurements were made with dissolved NaCl (0.195% by weight) in heavy water over the period between July 26, 2001 and August 28, 2003, with 176.5 days of the live time recorded during the day and 214.9 days during the night. This result is obtained with the spectral distribution of the CC events not constrained to the ^{8}B shape.

[8] AHMAD 02B results are based on the charged-current interactions recorded between November 2, 1999 and May 28, 2001, with the day and night live times of 128.5 and 177.9 days, respectively. The complete description of the SNO Phase I data set is given in AHARMIM 07.

[9] AHMAD 02B results are derived from the charged-current interactions, neutral-current interactions, and νe elastic scattering, with the total flux of active neutrinos constrained to have no asymmetry. The data were recorded between November 2, 1999 and May 28, 2001, with the day and night live times of 128.5 and 177.9 days, respectively. The complete description of the SNO Phase I data set is given in AHARMIM 07.

ϕ_{ES} (^{7}Be)

^{7}Be solar-neutrino flux measured via ν_e elastic scattering. This process is sensitive to all active neutrino flavors, but with reduced sensitivity to ν_μ, ν_τ due to the cross-section difference, $\sigma(\nu_{\mu,\tau}\, e) \sim 0.2\ \sigma(\nu_e\, e)$. If the ^{7}Be solar-neutrino flux involves nonelectron flavor active neutrinos, their contribution to the flux is ~ 0.2 times that of ν_e.

VALUE (10^9 cm^{-2} s^{-1})	DOCUMENT ID		TECN	COMMENT
• • • We do not use the following data for averages, fits, limits, etc. • • •				
3.26 ± 0.52	[1] GANDO	15	KLND	average flux
3.10 ± 0.15	[2] BELLINI	11A	BORX	average flux

[1] GANDO 15 uses 165.4 kton-day exposure of the KamLAND liquid scintillator detector to measure the 862 keV ^{7}Be solar neutrino flux via $\nu - e$ elastic scattering

[2] BELLINI 11A reports the ^{7}Be solar neutrino flux measured via $\nu - e$ elastic scattering. The data correspond to 740.7 live days between May 16, 2007 and May 8, 2010, and also correspond to 153.6 ton-year fiducial exposure. BELLINI 11A measured the 862 keV ^{7}Be solar neutrino flux, which is an 89.6% branch of the ^{7}Be solar neutrino flux, to be $(2.78 \pm 0.13) \times 10^9$ cm^{-2} s^{-1}. Supercedes ARPESELLA 08A.

ϕ_{ES} (pep)

pep solar-neutrino flux measured via ν_e elastic scattering. This process is sensitive to all active neutrino flavors, but with reduced sensitivity to ν_μ, ν_τ due to the cross section difference, $\sigma(\nu_{\mu,\tau}\, e) \sim 0.2\ \sigma(\nu_e e)$. If the pep solar-neutrino flux involves non-electron flavor active neutrinos, their contribution to the flux is ~ 0.2 times that of ν_e.

VALUE (10^8 cm^{-2}s^{-1})	DOCUMENT ID		TECN	COMMENT
• • • We do not use the following data for averages, fits, limits, etc. • • •				
1.0 ± 0.2	[1] BELLINI	12A	BORX	average flux

[1] BELLINI 12A reports 1.44 MeV pep solar-neutrino flux measured via ν_e elastic scattering. The data were collected between January 13, 2008 and May 9, 2010, corresponding to 20,4009 ton-day fiducial exposure. The listed flux value is calculated from the observed rate of pep solar neutrino interactions in Borexino ($3.1 \pm 0.6 \pm 0.3$ counts/(day·100 ton)) and the corresponding rate expected for no neutrino flavor oscillations (4.47 ± 0.05 counts/(day·100 ton)), using the SSM prediction for the pep solar neutrino flux of $(1.441 \pm 0.012) \times 10^8$ cm^{-2}s^{-1}.

ϕ_{ES} (CNO)

CNO solar-neutrino flux measured via ν_e elastic scattering. This process is sensitive to all active neutrino flavors, but with reduced sensitivity to ν_μ, ν_τ due to the cross section difference, $\sigma(\nu_{\mu,\tau}\, e) \sim 0.2\ \sigma(\nu_e\, e)$. If the CNO solar-neutrino flux involves non-electron flavor active neutrinos, their contribution to the flux is ~ 0.2 times that of ν_e.

VALUE (10^8 cm^{-2}s^{-1})	CL%	DOCUMENT ID		TECN	COMMENT
• • • We do not use the following data for averages, fits, limits, etc. • • •					
<7.7	90	[1] BELLINI	12A	BORX	MSW-LMA solution assumed

[1] BELLINI 12A reports an upper limit of the CNO solar neutrino flux measured via ν_e elastic scattering. The data were collected between January 13, 2008 and May 9, 2010, corresponding to 20,409 ton-day fiducial exposure.

$\phi_{ES}(pp)$

pp solar-neutrino flux measured via νe elastic scattering. This process is sensitive to all active neutrino flavors, but with reduced sensitivity to ν_μ, ν_τ due to the cross section difference, $\sigma(\nu_{\mu,\tau}\, e) \sim 0.3\ \sigma(\nu_e\, e)$. If the pp solar-neutrino flux involves nonelectron flavor active neutrinos, their contribution to the flux is ~ 0.3 times of ν_e.

VALUE (10^{10} cm^{-2} s^{-1})	DOCUMENT ID		TECN	COMMENT
• • • We do not use the following data for averages, fits, limits, etc. • • •				
4.4 ± 0.5	[1] BELLINI	14A	BORX	average flux

[1] BELLINI 14A reports pp solar-neutrino flux measured via νe elastic scattering. The data were collected between January 2012 and May 2013, corresponding to 408 days of data. The pp neutrino interaction rate in Borexino is measured to be $144 \pm 13 \pm 10$ counts/(day·100 ton) by fitting the measured energy spectrum of events in the 165–590 keV recoil electron kinetic energy window with the expected signal + background spectrum. The listed flux value $\phi_{ES}(pp)$ is calculated from the observed rate and the number of $(3.307 \pm 0.003) \times 10^{31}$ electrons for 100 tons of the Borexino scintillator, and the $\nu_e e$ integrated cross section over the pp neutrino spectrum, $\sigma(\nu_e e) = 11.38 \times 10^{-46}$ cm^2.

$\phi_{CC}(pp)$

pp solar-neutrino flux measured with charged-current reaction which is sensitive exclusively to ν_e.

VALUE (10^{10} cm^{-2} s^{-1})	DOCUMENT ID		TECN	COMMENT
• • • We do not use the following data for averages, fits, limits, etc. • • •				
3.38 ± 0.47	[1] ABDURASHI...	09	FIT	Fit existing solar-ν data

[1] ABDURASHITOV 09 reports the pp solar-neutrino flux derived from the Ga solar neutrino capture rate by subtracting contributions from ^{8}B, ^{7}Be, pep and CNO solar neutrino fluxes determined by other solar neutrino experiments as well as neutrino oscillation parameters determined from available world neutrino oscillation data.

ϕ_{ES} (hep)

hep solar-neutrino flux measured via νe elastic scattering. This process is sensitive to all active neutrino flavors, but with reduced sensitivity to ν_μ, ν_τ due to the cross-section difference, $\sigma(\nu_{\mu,\tau}\, e) \sim 0.16\sigma(\nu_e\, e)$. If the hep solar-neutrino flux involves nonelectron flavor active neutrinos, their contribution to the flux is ~ 0.16 times of ν_e.

VALUE (10^3 cm^{-2}s^{-1})	CL%	DOCUMENT ID		TECN	COMMENT
• • • We do not use the following data for averages, fits, limits, etc. • • •					
<73	90	[1] HOSAKA	06	SKAM	

[1] HOSAKA 06 result is obtained from the recoil electron energy window of 18–21 MeV, and updates FUKUDA 01 result.

$\phi_{\overline{\nu}_e}$ (^{8}B)

Searches are made for electron antineutrino flux from the Sun. Flux limits listed here are derived relative to the BS05(OP) Standard Solar Model ^{8}B solar neutrino flux (5.69×10^6 cm^{-2}s^{-1}), with an assumption that solar $\overline{\nu}_e$s follow an unoscillated ^{8}B neutrino spectrum.

VALUE (%)	CL%	DOCUMENT ID		TECN	COMMENT
• • • We do not use the following data for averages, fits, limits, etc. • • •					
<0.013	90	BELLINI	11	BORX	$E_{\overline{\nu}_e} > 1.8$ MeV
<1.9	90	[1] BALATA	06	CNTR	$1.8 < E_{\overline{\nu}_e} < 20.0$ MeV
<0.72	90	AHARMIM	04	SNO	$4.0 < E_{\overline{\nu}_e} < 14.8$ MeV
<0.022	90	EGUCHI	04	KLND	$8.3 < E_{\overline{\nu}_e} < 14.8$ MeV
<0.7	90	GANDO	03	SKAM	$8.0 < E_{\overline{\nu}_e} < 20.0$ MeV
<1.7	90	AGLIETTA	96	LSD	$7 < E_{\overline{\nu}_e} < 17$ MeV

[1] BALATA 06 obtained this result from the search for $\overline{\nu}_e$ interactions with Counting Test Facility (the prototype of the Borexino detector).

(B) Three-neutrino mixing parameters

See the related review(s):
Three-Neutrino Mixing Parameters

$\sin^2(\theta_{12})$

If an experiment reports $\sin^2(2\,\theta_{12})$ we convert the value to $\sin^2(\,\theta_{12})$.

VALUE	DOCUMENT ID		TECN	COMMENT
$\mathbf{0.307^{+0.013}_{-0.012}}$	[1] ABE	16C	FIT	KamLAND+global solar; 3ν
• • • We do not use the following data for averages, fits, limits, etc. • • •				
0.310 ± 0.014	[2] ABE	16C	FIT	SKAM+SNO; 3ν
$0.334^{+0.027}_{-0.023}$	[3] ABE	16C	FIT	SK-I+II+III+IV; 3ν
$0.327^{+0.026}_{-0.031}$	[4] ABE	16C	FIT	SK-IV; 3ν
0.323 ± 0.016	[5] FORERO	14	FIT	3ν
$0.304^{+0.013}_{-0.012}$	[6] GONZALEZ...	14	FIT	Either mass ordering; global fit
$0.299^{+0.014}_{-0.014}$	[7,8] AHARMIM	13	FIT	global solar: 2ν
$0.307^{+0.016}_{-0.013}$	[8,9] AHARMIM	13	FIT	global solar: 3ν
$0.304^{+0.022}_{-0.018}$	[8,10] AHARMIM	13	FIT	KamLAND + global solar: 3ν
$0.304^{+0.014}_{-0.013}$	[11] GANDO	13	FIT	KamLAND + global solar + SBL + accelerator: 3ν
$0.304^{+0.014}_{-0.013}$	[12] GANDO	13	FIT	KamLAND + global solar: 3ν

See key on page 885

$0.325^{+0.039}_{-0.039}$	[13] GANDO	13	FIT	KamLAND: 3ν	
$0.30^{+0.02}_{-0.01}$	[14] ABE	11	FIT	KamLAND + global solar: 2ν	
$0.30^{+0.02}_{-0.01}$	[15] ABE	11	FIT	global solar: 2ν	
$0.31^{+0.03}_{-0.02}$	[16] ABE	11	FIT	KamLAND + global solar: 3ν	
$0.31^{+0.03}_{-0.03}$	[17] ABE	11	FIT	global solar: 3ν	
$0.314^{+0.015}_{-0.012}$	[18] BELLINI	11A	FIT	KamLAND + global solar: 2ν	
$0.319^{+0.017}_{-0.015}$	[19] BELLINI	11A	FIT	global solar: 2ν	
$0.311^{+0.016}_{-0.016}$	[20] GANDO	11	FIT	KamLAND + solar: 3ν	
$0.304^{+0.046}_{-0.042}$	[21] GANDO	11	FIT	KamLAND: 3ν	
$0.314^{+0.018}_{-0.014}$	[22,23] AHARMIM	10	FIT	KamLAND + global solar: 2ν	
$0.314^{+0.017}_{-0.020}$	[22,24] AHARMIM	10	FIT	global solar: 2ν	
$0.319^{+0.019}_{-0.016}$	[22,25] AHARMIM	10	FIT	KamLAND + global solar: 3ν	
$0.319^{+0.023}_{-0.024}$	[22,26] AHARMIM	10	FIT	global solar: 3ν	
$0.36^{+0.05}_{-0.04}$	[27] ABE	08A	FIT	KamLAND	
0.32 ± 0.03	[28] ABE	08A	FIT	KamLAND + global fit	
0.32 ± 0.02	[29] AHARMIM	08	FIT	KamLAND + global solar	
$0.31^{+0.04}_{-0.04}$	[30] HOSAKA	06	FIT	KamLAND + global solar	
$0.31^{+0.04}_{-0.03}$	[31] HOSAKA	06	FIT	SKAM+SNO+KamLAND	
$0.31^{+0.03}_{-0.04}$	[32] HOSAKA	06	FIT	SKAM+SNO	
$0.31^{+0.02}_{-0.03}$	[33] AHARMIM	05A	FIT	KamLAND + global solar	
0.25–0.39	[34] AHARMIM	05A	FIT	global solar	
0.29 ± 0.03	[35] ARAKI	05	FIT	KamLAND + global solar	
$0.29^{+0.03}_{-0.02}$	[36] AHMED	04A	FIT	KamLAND + global solar	
0.23–0.37	[37] AHMED	04A	FIT	global solar	
$0.31^{+0.04}_{-0.04}$	[38] SMY	04	FIT	KamLAND + global solar	
$0.29^{+0.04}_{-0.04}$	[39] SMY	04	FIT	global solar	
$0.32^{+0.06}_{-0.05}$	[40] SMY	04	FIT	SKAM + SNO	
0.19–0.33	[41] AHMAD	02B	FIT	global solar	
0.19–0.39	[42] FUKUDA	02	FIT	global solar	

[1] ABE 16C obtained this result by a three-neutrino oscillation analysis, with a constraint of $\sin^2(\theta_{13}) = 0.0219 \pm 0.0014$ coming from reactor neutrino experiments, using all solar data and KamLAND data. *CPT* invariance is assumed.

[2] ABE 16C obtained this result by a three-neutrino oscillation analysis, with a constraint of $\sin^2(\theta_{13}) = 0.0219 \pm 0.0014$ coming from reactor neutrino experiments, using Super-Kamiokande (I+II+III+IV) and SNO data.

[3] ABE 16C obtained this result by a three-neutrino oscillation analysis, with a constraint of $\sin^2(\theta_{13}) = 0.0219 \pm 0.0014$ coming from reactor neutrino experiments, by combining the four phases of the Super-Kamiokande solar data.

[4] ABE 16C obtained this result by a three-neutrino oscillation analysis, with a constraint of $\sin^2(\theta_{13}) = 0.0219 \pm 0.0014$ coming from reactor neutrino experiments, using the Super-Kamiokande-IV data.

[5] FORERO 14 performs a global fit to neutrino oscillations using solar, reactor, long-baseline accelerator, and atmospheric neutrino data.

[6] GONZALEZ-GARCIA 14 result comes from a frequentist global fit. The corresponding Bayesian global fit to the same data results are reported in BERGSTROM 15 as $0.304^{+0.013}_{-0.012}$ for normal and $0.305^{+0.012}_{-0.013}$ for inverted mass ordering.

[7] AHARMIM 13 obtained this result by a two-neutrino oscillation analysis using global solar neutrino data.

[8] AHARMIM 13 global solar neutrino data include SNO's all-phases-combined analysis results on the total active ^{8}B neutrino flux and energy-dependent ν_e survival probability parameters, measurements of Cl (CLEVELAND 98), Ga (ABDURASHITOV 09 which contains combined analysis with GNO (ALTMANN 05 and Ph.D. thesis of F. Kaether)), and ^{7}Be (BELLINI 11A) rates, and ^{8}B solar-neutrino recoil electron measurements of SK-I (HOSAKA 06) zenith, SK-II (CRAVENS 08) and SK-III (ABE 11) day/night spectra, and Borexino (BELLINI 10A) spectra.

[9] AHARMIM 13 obtained this result by a three-neutrino oscillation analysis with the value of Δm^2_{32} fixed to 2.45×10^{-3} eV^2, using global solar neutrino data.

[10] AHARMIM 13 obtained this result by a three-neutrino oscillation analysis with the value of Δm^2_{32} fixed to 2.45×10^{-3} eV^2, using global solar neutrino and KamLAND (GANDO 11) data. CPT invariance is assumed.

[11] GANDO 13 obtained this result by a three-neutrino oscillation analysis using KamLAND, global solar neutrino, short-baseline (SBL) reactor, and accelerator data, assuming *CPT* invariance. Supersedes GANDO 11.

[12] GANDO 13 obtained this result by a three-neutrino oscillation analysis using KamLAND and global solar neutrino data, assuming CPT invariance. Supersedes GANDO 11.

[13] GANDO 13 obtained this result by a three-neutrino oscillation analysis using KamLAND data. Supersedes GANDO 11.

[14] ABE 11 obtained this result by a two-neutrino oscillation analysis using solar neutrino data including Super-Kamiokande, SNO, Borexino (ARPESELLA 08A), Homestake, GALLEX/GNO, SAGE, and KamLAND data. CPT invariance is assumed.

[15] ABE 11 obtained this result by a two-neutrino oscillation analysis using solar neutrino data including Super-Kamiokande, SNO, Borexino (ARPESELLA 08A), Homestake, GALLEX/GNO, and SAGE data.

[16] ABE 11 obtained this result by a three-neutrino oscillation analysis with the value of Δm^2_{32} fixed to 2.4×10^{-3} eV^2, using solar neutrino data including Super-Kamiokande, SNO, Borexino (ARPESELLA 08A), Homestake, GALLEX/GNO, SAGE, and KamLAND data. The normal neutrino mass ordering and CPT invariance are assumed.

[17] ABE 11 obtained this result by a three-neutrino oscillation analysis with the value of Δm^2_{32} fixed to 2.4×10^{-3} eV^2, using solar neutrino data including Super-Kamiokande, SNO, Borexino (ARPESELLA 08A), Homestake, and GALLEX/GNO data. The normal neutrino mass ordering is assumed.

[18] BELLINI 11A obtained this result by a two-neutrino oscillation analysis using KamLAND, Homestake, SAGE, Gallex, GNO, Kamiokande, Super-Kamiokande, SNO, and Borexino (BELLINI 11A) data and the SSM flux prediction in SERENELLI 11 (Astrophysical Journal **743** 24 (2011)) with the exception that the ^{8}B flux was left free. CPT invariance is assumed.

[19] BELLINI 11A obtained this result by a two-neutrino oscillation analysis using Homestake, SAGE, Gallex, GNO, Kamiokande, Super-Kamiokande, SNO, and Borexino (BELLINI 11A) data and the SSM flux prediction in SERENELLI 11 (Astrophysical Journal **743** 24 (2011)) with the exception that the ^{8}B flux was left free.

[20] GANDO 11 obtain this result with three-neutrino fit using the KamLAND + solar data. Superseded by GANDO 13.

[21] GANDO 11 obtain this result with three-neutrino fit using the KamLAND data only. Superseded by GANDO 13.

[22] AHARMIM 10 global solar neutrino data include SNO's low-energy-threshold analysis survival probability day/night curves, SNO Phase III integral rates (AHARMIM 08), Cl (CLEVELAND 98), SAGE (ABDURASHITOV 09), Gallex/GNO (HAMPEL 99, ALTMANN 05), Borexino (ARPESELLA 08A), SK-I zenith (HOSAKA 06), and SK-II day/night spectra (CRAVENS 08).

[23] AHARMIM 10 obtained this result by a two-neutrino oscillation analysis using global solar neutrino data and KamLAND data (ABE 08A). *CPT* invariance is assumed.

[24] AHARMIM 10 obtained this result by a two-neutrino oscillation analysis using global solar neutrino data.

[25] AHARMIM 10 obtained this result by a three-neutrino oscillation analysis with the value of Δm^2_{31} fixed to 2.3×10^{-3} eV^2, using global solar neutrino data and KamLAND data (ABE 08A). *CPT* invariance is assumed.

[26] AHARMIM 10 obtained this result by a three-neutrino oscillation analysis with the value of Δm^2_{31} fixed to 2.3×10^{-3} eV^2, using global solar neutrino data.

[27] ABE 08A obtained this result by a rate + shape + time combined geoneutrino and reactor two-neutrino fit for Δm^2_{21} and $\tan^2\theta_{12}$, using KamLAND data only. Superseded by GANDO 11.

[28] ABE 08A obtained this result by means of a two-neutrino fit using KamLAND, Homestake, SAGE, GALLEX, GNO, SK (zenith angle and E-spectrum), the SNO χ^2-map, and solar flux data. *CPT* invariance is assumed. Superseded by GANDO 11.

[29] The result given by AHARMIM 08 is $\theta = (34.4^{+1.3}_{-1.2})^\circ$. This result is obtained by a two-neutrino oscillation analysis using solar neutrino data including those of Borexino (ARPESELLA 08A) and Super-Kamiokande-I (HOSAKA 06), and KamLAND data (ABE 08A). *CPT* invariance is assumed.

[30] HOSAKA 06 obtained this result by a two-neutrino oscillation analysis using SK ν_e data, CC data from other solar neutrino experiments, and KamLAND data (ARAKI 05). *CPT* invariance is assumed.

[31] HOSAKA 06 obtained this result by a two-neutrino oscillation analysis using the data from Super-Kamiokande, SNO (AHMAD 02 and AHMAD 02B), and KamLAND (ARAKI 05) experiments. *CPT* invariance is assumed.

[32] HOSAKA 06 obtained this result by a two-neutrino oscillation analysis using the Super-Kamiokande and SNO (AHMAD 02 and AHMAD 02B) solar neutrino data.

[33] The result given by AHARMIM 05A is $\theta = (33.9 \pm 1.6)^\circ$. This result is obtained by a two-neutrino oscillation analysis using SNO pure deuteron and salt phase data, SK ν_e data, Cl and Ga CC data, and KamLAND data (ARAKI 05). *CPT* invariance is assumed. AHARMIM 05A also quotes $\theta = (33.9^{+2.4}_{-2.2})^\circ$ as the error enveloping the 68% CL two-dimensional region. This translates into $\sin^2 2\,\theta = 0.86^{+0.05}_{-0.06}$.

[34] AHARMIM 05A obtained this result by a two-neutrino oscillation analysis using the data from all solar neutrino experiments. The listed range of the parameter envelops the 95% CL two-dimensional region shown in figure 35a of AHARMIM 05A. AHARMIM 05A also quotes $\tan^2\theta = 0.45^{+0.09}_{-0.08}$ as the error enveloping the 68% CL two-dimensional region. This translates into $\sin^2 2\,\theta = 0.86^{+0.05}_{-0.07}$.

[35] ARAKI 05 obtained this result by a two-neutrino oscillation analysis using KamLAND and solar neutrino data. *CPT* invariance is assumed. The 1σ error shown here is translated from the number provided by the KamLAND collaboration, $\tan^2\theta = 0.40^{+0.07}_{-0.05}$. The corresponding number quoted in ARAKI 05 is $\tan^2\theta = 0.40^{+0.10}_{-0.07}$ ($\sin^2 2\,\theta = 0.82 \pm 0.07$), which envelops the 68% CL two-dimensional region.

[36] The result given by AHMED 04A is $\theta = (32.5^{+1.7}_{-1.6})^\circ$. This result is obtained by a two-neutrino oscillation analysis using solar neutrino and KamLAND data (EGUCHI 03). *CPT* invariance is assumed. AHMED 04A also quotes $\theta = (32.5^{+2.4}_{-2.3})^\circ$ as the error enveloping the 68% CL two-dimensional region. This translates into $\sin^2 2\,\theta = 0.82 \pm 0.06$.

[37] AHMED 04A obtained this result by a two-neutrino oscillation analysis using the data from all solar neutrino experiments. The listed range of the parameter envelops the 95% CL two-dimensional region shown in Fig. 5(a) of AHMED 04A. The best-fit point is $\Delta(m^2) = 6.5 \times 10^{-5}$ eV^2, $\tan^2\theta = 0.40$ ($\sin^2 2\,\theta = 0.82$).

[38] The result given by SMY 04 is $\tan^2\theta = 0.44 \pm 0.08$. This result is obtained by a two-neutrino oscillation analysis using solar neutrino and KamLAND data (IANNI 03). *CPT* invariance is assumed.

[39] SMY 04 obtained this result by a two-neutrino oscillation analysis using the data from all solar neutrino experiments. The 1σ errors are read from Fig. 6(a) of SMY 04.

[40] SMY 04 obtained this result by a two-neutrino oscillation analysis using the Super-Kamiokande and SNO (AHMAD 02 and AHMAD 02B) solar neutrino data. The 1σ errors are read from Fig. 6(a) of SMY 04.

[41] AHMAD 02B obtained this result by a two-neutrino oscillation analysis using the data from all solar neutrino experiments. The listed range of the parameter envelops the 95% CL two-dimensional region shown in Fig. 4(b) of AHMAD 02B. The best fit point is $\Delta(m^2) = 5.0 \times 10^{-5}$ eV^2 and $\tan\theta = 0.34$ ($\sin^2 2\,\theta = 0.76$).

[42] FUKUDA 02 obtained this result by a two-neutrino oscillation analysis using the data from all solar neutrino experiments. The listed range of the parameter envelops the 95% CL two-dimensional region shown in Fig. 4 of FUKUDA 02. The best fit point is $\Delta(m^2) = 6.9 \times 10^{-5}$ eV^2 and $\tan^2\theta = 0.38$ ($\sin^2 2\,\theta = 0.80$).

Δm^2_{21}

VALUE (10^{-5} eV^2)	DOCUMENT ID		TECN	COMMENT
7.53±0.18	[1] GANDO	13	FIT	KamLAND + global solar + SBL + accelerator: 3ν
• • • We do not use the following data for averages, fits, limits, etc. • • •				
$7.49^{+0.19}_{-0.18}$	[2] ABE	16C	FIT	KamLAND+global solar; 3ν
$4.8\ ^{+1.3}_{-0.6}$	[3] ABE	16C	FIT	SKAM+SNO; 3ν
$4.8\ ^{+1.5}_{-0.8}$	[4] ABE	16C	FIT	SK-I+II+III+IV; 3ν
$3.2\ ^{+2.8}_{-0.2}$	[5] ABE	16C	FIT	SK-IV; 3ν
$7.6\ ^{+0.19}_{-0.18}$	[6] FORERO	14	FIT	3ν
$7.50^{+0.19}_{-0.17}$	[7] GONZALEZ...	14	FIT	Either mass ordering; global fit
$5.13^{+1.29}_{-0.96}$	[8,9] AHARMIM	13	FIT	global solar: 2ν
$5.13^{+1.49}_{-0.98}$	[9,10] AHARMIM	13	FIT	global solar: 3ν
$7.46^{+0.20}_{-0.19}$	[9,11] AHARMIM	13	FIT	KamLAND + global solar: 3ν
$7.53^{+0.19}_{-0.18}$	[12] GANDO	13	FIT	KamLAND + global solar: 3ν
$7.54^{+0.19}_{-0.18}$	[13] GANDO	13	FIT	KamLAND: 3ν
7.6 ±0.2	[14] ABE	11	FIT	KamLAND + global solar: 2ν
$6.2\ ^{+1.1}_{-1.9}$	[15] ABE	11	FIT	global solar: 2ν
7.7 ±0.3	[16] ABE	11	FIT	KamLAND + global solar: 3ν
$6.0\ ^{+2.2}_{-2.5}$	[17] ABE	11	FIT	global solar: 3ν
$7.50^{+0.16}_{-0.24}$	[18] BELLINI	11A	FIT	KamLAND + global solar: 2ν
$5.2\ ^{+1.5}_{-0.9}$	[19] BELLINI	11A	FIT	global solar: 2ν
$7.50^{+0.19}_{-0.20}$	[20] GANDO	11	FIT	KamLAND + solar: 3ν
7.49±0.20	[21] GANDO	11	FIT	KamLAND: 3ν
$7.59^{+0.20}_{-0.21}$	[22,23] AHARMIM	10	FIT	KamLAND + global solar: 2ν
$5.89^{+2.13}_{-2.16}$	[22,24] AHARMIM	10	FIT	global solar: 2ν
7.59±0.21	[22,25] AHARMIM	10	FIT	KamLAND + global solar: 3ν
$6.31^{+2.49}_{-2.58}$	[22,26] AHARMIM	10	FIT	global solar: 3ν
$7.58^{+0.14}_{-0.13}\pm0.15$	[27] ABE	08A	FIT	KamLAND
7.59±0.21	[28] ABE	08A	FIT	KamLAND + global solar
$7.59^{+0.19}_{-0.21}$	[29] AHARMIM	08	FIT	KamLAND + global solar
8.0 ±0.3	[30] HOSAKA	06	FIT	KamLAND + global solar
8.0 ±0.3	[31] HOSAKA	06	FIT	SKAM+SNO+KamLAND
$6.3\ ^{+3.7}_{-1.5}$	[32] HOSAKA	06	FIT	SKAM+SNO
5–12	[33] HOSAKA	06	FIT	SKAM day/night in the LMA region
$8.0\ ^{+0.4}_{-0.3}$	[34] AHARMIM	05A	FIT	KamLAND + global solar LMA
3.3–14.4	[35] AHARMIM	05A	FIT	global solar
$7.9\ ^{+0.4}_{-0.3}$	[36] ARAKI	05	FIT	KamLAND + global solar
$7.1\ ^{+1.0}_{-0.3}$	[37] AHMED	04A	FIT	KamLAND + global solar
3.2–13.7	[38] AHMED	04A	FIT	global solar
$7.1\ ^{+0.6}_{-0.5}$	[39] SMY	04	FIT	KamLAND + global solar
$6.0\ ^{+1.7}_{-1.6}$	[40] SMY	04	FIT	global solar
$6.0\ ^{+2.5}_{-1.6}$	[41] SMY	04	FIT	SKAM + SNO
2.8–12.0	[42] AHMAD	02B	FIT	global solar
3.2–19.1	[43] FUKUDA	02	FIT	global solar

[1] GANDO 13 obtained this result by a three-neutrino oscillation analysis using KamLAND, global solar neutrino, short-baseline (SBL) reactor, and accelerator data, assuming CPT invariance. Supersedes GANDO 11.

[2] ABE 16C obtained this result by a three-neutrino oscillation analysis, with a constraint of $\sin^2(\theta_{13}) = 0.0219 \pm 0.0014$ coming from reactor neutrino experiments, using all solar data and KamLAND data. *CPT* invariance is assumed.

[3] ABE 16C obtained this result by a three-neutrino oscillation analysis, with a constraint of $\sin^2(\theta_{13}) = 0.0219 \pm 0.0014$ coming from reactor neutrino experiments, using Super-Kamiokande (I+II+III+IV) and SNO data.

[4] ABE 16C obtained this result by a three-neutrino oscillation analysis, with a constraint of $\sin^2(\theta_{13}) = 0.0219 \pm 0.0014$ coming from reactor neutrino experiments, by combining the four phases of the Super-Kamiokande solar data.

[5] ABE 16C obtained this result by a three-neutrino oscillation analysis, with a constraint of $\sin^2(\theta_{13}) = 0.0219 \pm 0.0014$ coming from reactor neutrino experiments, using the Super-Kamiokande-IV data.

[6] FORERO 14 performs a global fit to Δm^2_{21} using solar, reactor, long-baseline accelerator, and atmospheric neutrino data.

[7] GONZALEZ-GARCIA 14 result comes from a frequentist global fit. The corresponding Bayesian global fit to the same data results are reported in BERGSTROM 15 as $(7.50^{+0.19}_{-0.17}) \times 10^{-5}$ eV^2 for normal and $(7.50^{+0.18}_{-0.17}) \times 10^{-5}$ eV^2 for inverted mass ordering.

[8] AHARMIM 13 obtained this result by a two-neutrino oscillation analysis using global solar neutrino data.

[9] AHARMIM 13 global solar neutrino data include SNO's all-phases-combined analysis results on the total active ^{8}B neutrino flux and energy-dependent ν_e survival probability parameters, measurements of Cl (CLEVELAND 98), Ga (ABDURASHITOV 09 which contains combined analysis with GNO (ALTMANN 05 and Ph.D. thesis of F. Kaether)), and ^{7}Be (BELLINI 11A) rates, and ^{8}B solar-neutrino recoil electron measurements of SK-I (HOSAKA 06) zenith, SK-II (CRAVENS 08), and SK-III (ABE 11) day/night spectra, and Borexino (BELLINI 10A) spectra.

[10] AHARMIM 13 obtained this result by a three-neutrino oscillation analysis with the value of Δm^2_{31} fixed to 2.45×10^{-3} eV^2, using global solar neutrino data.

[11] AHARMIM 13 obtained this result by a three-neutrino oscillation analysis with the value of Δm^2_{31} fixed to 2.45×10^{-3} eV^2, using global solar neutrino and KamLAND data (GANDO 11). CPT invariance is assumed.

[12] GANDO 13 obtained this result by a three-neutrino oscillation analysis using KamLAND and global solar neutrino data, assuming CPT invariance. Supersedes GANDO 11.

[13] GANDO 13 obtained this result by a three-neutrino oscillation analysis using KamLAND data. Supersedes GANDO 11.

[14] ABE 11 obtained this result by a two-neutrino oscillation analysis using solar neutrino data including Super-Kamiokande, SNO, Borexino (ARPESELLA 08A), Homestake, GALLEX/GNO, SAGE, and KamLAND data. CPT invariance is assumed.

[15] ABE 11 obtained this result by a two-neutrino oscillation analysis using solar neutrino data including Super-Kamiokande, SNO, Borexino (ARPESELLA 08A), Homestake, GALLEX/GNO, and SAGE data.

[16] ABE 11 obtained this result by a three-neutrino oscillation analysis with the value of Δm^2_{32} fixed to 2.4×10^{-3} eV^2, using solar neutrino data including Super-Kamiokande, SNO, Borexino (ARPESELLA 08A), Homestake, GALLEX/GNO, SAGE, and KamLAND data. The normal neutrino mass ordering and CPT invariance are assumed.

[17] ABE 11 obtained this result by a three-neutrino oscillation analysis with the value of Δm^2_{32} fixed to 2.4×10^{-3} eV^2, using solar neutrino data including Super-Kamiokande, SNO, Borexino (ARPESELLA 08A), Homestake, and GALLEX/GNO data. The normal neutrino mass ordering is assumed.

[18] BELLINI 11A obtained this result by a two-neutrino oscillation analysis using KamLAND, Homestake, SAGE, Gallex, GNO, Kamiokande, Super-Kamiokande, SNO, and Borexino (BELLINI 11A) data and the SSM flux prediction in SERENELLI 11 (Astrophysical Journal **743** 24 (2011)) with the exception that the ^{8}B flux was left free. CPT invariance is assumed.

[19] BELLINI 11A obtained this result by a two-neutrino oscillation analysis using Homestake, SAGE, Gallex, GNO, Kamiokande, Super-Kamiokande, SNO, and Borexino (BELLINI 11A) data and the SSM flux prediction in SERENELLI 11 (Astrophysical Journal **743** 24 (2011)) with the exception that the ^{8}B flux was left free.

[20] GANDO 11 obtain this result with three-neutrino fit using the KamLAND + solar data. Superseded by GANDO 13.

[21] GANDO 11 obtain this result with three-neutrino fit using the KamLAND data only. Supersedes ABE 08A.

[22] AHARMIM 10 global solar neutrino data include SNO's low-energy-threshold analysis survival probability day/night curves, SNO Phase III integral rates (AHARMIM 08), Cl (CLEVELAND 98), SAGE (ABDURASHITOV 09), Gallex/GNO (HAMPEL 99, ALTMANN 05), Borexino (ARPESELLA 08A), SK-I zenith (HOSAKA 06), and SK-II day/night spectra (CRAVENS 08).

[23] AHARMIM 10 obtained this result by a two-neutrino oscillation analysis using global solar neutrino data and KamLAND data (ABE 08A). *CPT* invariance is assumed.

[24] AHARMIM 10 obtained this result by a two-neutrino oscillation analysis using global solar neutrino data.

[25] AHARMIM 10 obtained this result by a three-neutrino oscillation analysis with the value of Δm^2_{31} fixed to 2.3×10^{-3} eV^2, using global solar neutrino data and KamLAND data (ABE 08A). *CPT* invariance is assumed.

[26] AHARMIM 10 obtained this result by a three-neutrino oscillation analysis with the value of Δm^2_{31} fixed to 2.3×10^{-3} eV^2, using global solar neutrino data.

[27] ABE 08A obtained this result by a rate + shape + time combined geoneutrino and reactor two-neutrino fit for Δm^2_{21} and $\tan^2\theta_{12}$, using KamLAND data only. Superseded by GANDO 11.

[28] ABE 08A obtained this result by means of a two-neutrino fit using KamLAND, Homestake, SAGE, GALLEX, GNO, SK (zenith angle and E-spectrum), the SNO χ^2-map, and solar flux data. *CPT* invariance is assumed. Superseded by GANDO 11.

[29] AHARMIM 08 obtained this result by a two-neutrino oscillation analysis using all solar neutrino data including those of Borexino (ARPESELLA 08A) and Super-Kamiokande-I (HOSAKA 06), and KamLAND data (ABE 08A). *CPT* invariance is assumed.

[30] HOSAKA 06 obtained this result by a two-neutrino oscillation analysis using solar neutrino and KamLAND data (ARAKI 05). *CPT* invariance is assumed.

[31] HOSAKA 06 obtained this result by a two-neutrino oscillation analysis using the data from Super-Kamiokande, SNO (AHMAD 02 and AHMAD 02B), and KamLAND (ARAKI 05) experiments. *CPT* invariance is assumed.

[32] HOSAKA 06 obtained this result by a two-neutrino oscillation analysis using the Super-Kamiokande and SNO (AHMAD 02 and AHMAD 02B) solar neutrino data.

[33] HOSAKA 06 obtained this result from the consistency between the observed and expected day-night flux asymmetry amplitude. The listed 68% CL range is derived from the 1σ boundary of the amplitude fit to the data. Oscillation parameters are constrained to be in the LMA region. The mixing angle is fixed at $\tan^2\theta = 0.44$ because the fit depends only very weekly on it.

[34] AHARMIM 05A obtained this result by a two-neutrino oscillation analysis using solar neutrino and KamLAND data (ARAKI 05). *CPT* invariance is assumed. AHARMIM 05A also quotes $\Delta(m^2) = (8.0^{+0.6}_{-0.4}) \times 10^{-5}$ eV^2 as the error enveloping the 68% CL two-dimensional region.

[35] AHARMIM 05A obtained this result by a two-neutrino oscillation analysis using the data from all solar neutrino experiments. The listed range of the parameter envelops the 95% CL two-dimensional region shown in figure 35a of AHARMIM 05A. AHARMIM 05A also quotes $\Delta(m^2) = (6.5^{+4.4}_{-2.3}) \times 10^{-5}$ eV^2 as the error enveloping the 68% CL two-dimensional region.

[36] ARAKI 05 obtained this result by a two-neutrino oscillation analysis using KamLAND and solar neutrino data. *CPT* invariance is assumed. The 1σ error shown here is provided by the KamLAND collaboration. The error quoted in ARAKI 05, $\Delta(m^2) = (7.9^{+0.6}_{-0.5}) \times 10^{-5}$, envelops the 68% CL two-dimensional region.

[37] AHMED 04A obtained this result by a two-neutrino oscillation analysis using solar neutrino and KamLAND data (EGUCHI 03). *CPT* invariance is assumed. AHMED 04A also quotes $\Delta(m^2) = (7.1^{+1.2}_{-0.6}) \times 10^{-5}$ eV^2 as the error enveloping the 68% CL two-dimensional region.

[38] AHMED 04A obtained this result by a two-neutrino oscillation analysis using the data from all solar neutrino experiments. The listed range of the parameter envelops the 95% CL two-dimensional region shown in Fig. 5(a) of AHMED 04A. The best-fit point is $\Delta(m^2) = 6.5 \times 10^{-5}$ eV^2, $\tan^2\theta = 0.40$ ($\sin^2 2\,\theta = 0.82$).

[39] SMY 04 obtained this result by a two-neutrino oscillation analysis using solar neutrino and KamLAND data (IANNI 03). *CPT* invariance is assumed.

[40] SMY 04 obtained this result by a two-neutrino oscillation analysis using the data from all solar neutrino experiments. The 1σ errors are read from Fig. 6(a) of SMY 04.

[41] SMY 04 obtained this result by a two-neutrino oscillation analysis using the Super-Kamiokande and SNO (AHMAD 02 and AHMAD 02B) solar neutrino data. The 1σ errors are read from Fig. 6(a) of SMY 04.

[42] AHMAD 02B obtained this result by a two-neutrino oscillation analysis using the data from all solar neutrino experiments. The listed range of the parameter envelops the 95% CL two-dimensional region shown in Fig. 4(b) of AHMAD 02B. The best fit point is $\Delta(m^2) = 5.0 \times 10^{-5}$ eV^2 and $\tan\theta = 0.34$ ($\sin^2 2\,\theta = 0.76$).

[43] FUKUDA 02 obtained this result by a two-neutrino oscillation analysis using the data from all solar neutrino experiments. The listed range of the parameter envelops the 95% CL two-dimensional region shown in Fig. 4 of FUKUDA 02. The best fit point is $\Delta(m^2) = 6.9 \times 10^{-5}$ eV^2 and $\tan^2\theta = 0.38$ ($\sin^2 2\,\theta = 0.80$).

$\sin^2(\theta_{23})$

The reported limits below correspond to the projection onto the $\sin^2(\theta_{23})$ axis of the 90% CL contours in the $\sin^2(\theta_{23}) - \Delta m^2_{32}$ plane presented by the authors. Unless otherwise specified, the limits are 90% CL and the reported uncertainties are 68% CL.

If an experiment reports $\sin^2(2\,\theta_{23})$ we convert the value to $\sin^2(\,\theta_{23})$.

VALUE	DOCUMENT ID		TECN	COMMENT
$0.421^{+0.033}_{-0.025}$ OUR FIT	Error includes scale factor of 1.3. Inverted ordering, quadrant I			
$0.592^{+0.023}_{-0.030}$ OUR FIT	Error includes scale factor of 1.1. Inverted ordering, quadrant II			
$0.417^{+0.025}_{-0.028}$ OUR FIT	Error includes scale factor of 1.2. Normal ordering, quadrant I			
$0.597^{+0.024}_{-0.030}$ OUR FIT	Error includes scale factor of 1.2. Normal ordering, quadrant II			
$0.55\ ^{+0.05}_{-0.09}$	[1] ABE	17F	T2K	normal mass ordering
$0.55\ ^{+0.05}_{-0.08}$	[1] ABE	17F	T2K	inverted mass ordering
$0.404^{+0.022}_{-0.030}$	ADAMSON	17A	NOVA	normal mass ordering; first quadrant
$0.624^{+0.022}_{-0.030}$	ADAMSON	17A	NOVA	normal mass ordering; second quadrant
$0.398^{+0.030}_{-0.022}$	ADAMSON	17A	NOVA	inverted mass ordering; first quadrant
$0.618^{+0.022}_{-0.030}$	ADAMSON	17A	NOVA	inverted mass ordering; second quadrant
$0.53\ ^{+0.09}_{-0.12}$	[2] AARTSEN	15A	ICCB	3ν osc; normal mass ordering
$0.51\ ^{+0.09}_{-0.11}$	[2] AARTSEN	15A	ICCB	3ν osc; inverted mass ordering
$0.41\ ^{+0.23}_{-0.06}$	[3] ADAMSON	14	MINS	3ν osc., normal mass ordering
$0.41\ ^{+0.26}_{-0.07}$	[3] ADAMSON	14	MINS	3ν osc.; inverted mass ordering
• • • We do not use the following data for averages, fits, limits, etc. • • •				
$0.532^{+0.061}_{-0.087}$	[1] ABE	17A	T2K	normal mass ordering
$0.534^{+0.061}_{-0.087}$	[1] ABE	17A	T2K	inverted mass ordering
$0.51\ ^{+0.08}_{-0.07}$	ABE	17C	T2K	normal mass ordering with neutrinos
$0.42\ ^{+0.25}_{-0.07}$	ABE	17C	T2K	normal mass ordering with antineutrinos
$0.52\ ^{+0.075}_{-0.09}$	ABE	17C	T2K	normal mass ordering with neutrinos and antineutrinos
$0.45\ ^{+0.19}_{-0.07}$	[4] ABE	16D	T2K	3ν osc; normal mass ordering; $\overline{\nu}$ beam
0.38 to 0.65	[5] ADAMSON	16A	NOVA	normal mass ordering
0.37 to 0.64	[5] ADAMSON	16A	NOVA	inverted mass ordering
$0.514^{+0.055}_{-0.056}$	[6] ABE	14	T2K	3ν osc.; normal mass ordering
0.511 ± 0.055	[6] ABE	14	T2K	3ν osc.; inverted mass ordering
$0.567^{+0.032}_{-0.128}$	[7] FORERO	14	FIT	Normal mass ordering
$0.573^{+0.025}_{-0.043}$	[7] FORERO	14	FIT	Inverted mass ordering
$0.452^{+0.052}_{-0.028}$	[8] GONZALEZ...	14	FIT	Normal mass ordering; global fit
$0.579^{+0.025}_{-0.037}$	[8] GONZALEZ...	14	FIT	Inverted mass ordering; global fit
0.24 to 0.76	[9] AARTSEN	13B	ICCB	DeepCore, 2ν oscillation
0.514 ± 0.082	[10] ABE	13G	T2K	3ν osc.; normal mass ordering
$0.388^{+0.051}_{-0.053}$	[11] ADAMSON	13B	MINS	Beam + Atmospheric; identical ν & $\overline{\nu}$
0.3 to 0.7	[12] ABE	12A	T2K	off-axis beam
0.28 to 0.72	[13] ADAMSON	12	MINS	$\overline{\nu}$ beam
0.25 to 0.75	[14,15] ADAMSON	12B	MINS	MINOS atmospheric
0.27 to 0.73	[14,16] ADAMSON	12B	MINS	MINOS pure atmospheric ν
0.21 to 0.79	[14,16] ADAMSON	12B	MINS	MINOS pure atmospheric $\overline{\nu}$
0.15 to 0.85	[17] ADRIAN-MAR...	12	ANTR	atmospheric ν with deep see telescope
0.39 to 0.61	[18] ABE	11C	SKAM	Super-Kamiokande
0.34 to 0.66	ADAMSON	11	MINS	2ν osc.; maximal mixing
$0.31\ ^{+0.10}_{-0.07}$	[19] ADAMSON	11B	MINS	$\overline{\nu}$ beam
0.41 to 0.59	[20] WENDELL	10	SKAM	3ν osc. with solar terms; θ_{13}=0
0.39 to 0.61	[21] WENDELL	10	SKAM	3ν osc.; normal mass ordering
0.37 to 0.63	[22] WENDELL	10	SKAM	3ν osc.; inverted mass ordering
0.31 to 0.69	ADAMSON	08A	MINS	MINOS
0.05 to 0.95	[23] ADAMSON	06	MINS	atmospheric ν with far detector
0.18 to 0.82	[24] AHN	06A	K2K	KEK to Super-K
0.23 to 0.77	[25] MICHAEL	06	MINS	MINOS
0.18 to 0.82	[26] ALIU	05	K2K	KEK to Super-K
0.18 to 0.82	[27] ALLISON	05	SOU2	
0.36 to 0.64	[28] ASHIE	05	SKAM	Super-Kamiokande
0.28 to 0.72	[29] AMBROSIO	04	MCRO	MACRO
0.34 to 0.66	[30] ASHIE	04	SKAM	L/E distribution
0.08 to 0.92	[31] AHN	03	K2K	KEK to Super-K
0.13 to 0.87	[32] AMBROSIO	03	MCRO	MACRO
0.26 to 0.74	[33] AMBROSIO	03	MCRO	MACRO
0.15 to 0.85	[34] SANCHEZ	03	SOU2	Soudan-2 Atmospheric
0.28 to 0.72	[35] AMBROSIO	01	MCRO	upward μ
0.29 to 0.71	[36] AMBROSIO	01	MCRO	upward μ
0.13 to 0.87	[37] FUKUDA	99C	SKAM	upward μ
0.23 to 0.77	[38] FUKUDA	99D	SKAM	upward μ
0.08 to 0.92	[39] FUKUDA	99D	SKAM	stop μ / through
0.29 to 0.71	[40] FUKUDA	98C	SKAM	Super-Kamiokande
0.08 to 0.92	[41] HATAKEYAMA	98	KAMI	Kamiokande
0.24 to 0.76	[42] HATAKEYAMA	98	KAMI	Kamiokande
0.20 to 0.80	[43] FUKUDA	94	KAMI	Kamiokande

[1] Errors are from the projections of the 68% contour on 2D plot of Δm^2 versus $\sin^2(\theta_{23})$. ABE 17F supersedes ABE 17A.

[2] AARTSEN 15A obtains this result by a three-neutrino oscillation analysis using 10–100 GeV muon neutrino sample from a total of 953 days of measurement with the low-energy subdetector DeepCore of the IceCube neutrino telescope.

[3] ADAMSON 14 uses a complete set of accelerator and atmospheric data. The analysis combines the ν_μ disappearance and ν_e appearance data using three-neutrino oscillation fit. The fit results are obtained for normal and inverted mass ordering assumptions. The best fit is for lower θ_{23} quadrant and inverted mass ordering.

[4] ABE 16D reports oscillation results using $\overline{\nu}_\mu$ disappearance in an off-axis beam.

[5] ADAMSON 16A obtains $\sin^2(\theta_{23})$ in the 68% C.L. range [0.38, 0.65] ([0.37, 0.64]), with two statistically degenerate best-fit values of 0.44 and 0.59 (0.44 and 0.59) for normal (inverted) mass ordering. Superseded by ADAMSON 17A.

[6] ABE 14 results are based on ν_μ disappearance using three-neutrino oscillation fit. The confidence intervals are derived from one dimensional profiled likelihoods. Superseded by ABE 17A.

[7] FORERO 14 performs a global fit to neutrino oscillations using solar, reactor, long-baseline accelerator, and atmospheric neutrino data.

[8] GONZALEZ-GARCIA 14 result comes from a frequentist global fit. The corresponding Bayesian global fit to the same data results are reported in BERGSTROM 15 as 68% CL intervals of 0.433–0.496 or 0.530–0.594 for normal and 0.514–0.612 for inverted mass ordering.

[9] AARTSEN 13B obtained this result by a two-neutrino oscillation analysis using 20–100 GeV muon neutrino sample from a total of 318.9 days of live-time measurement with the low-energy subdetector DeepCore of the IceCube neutrino telescope.

[10] The best fit value is $\sin^2(\theta_{23}) = 0.514 \pm 0.082$. Superseded by ABE 14.

[11] ADAMSON 13B obtained this result from ν_μ and $\overline{\nu}_\mu$ disappearance using ν_μ (10.71×10^{20} POT) and $\overline{\nu}_\mu$ (3.36×10^{20} POT) beams, and atmospheric (37.88kton-years) data from MINOS The fit assumed two-flavor neutrino hypothesis and identical ν_μ and $\overline{\nu}_\mu$ oscillation parameters. Superseded by ADAMSON 14.

[12] ABE 12A obtained this result by a two-neutrino oscillation analysis. The best-fit point is $\sin^2(2\theta_{23}) = 0.98$.

[13] ADAMSON 12 is a two-neutrino oscillation analysis using antineutrinos. The best fit value is $\sin^2(2\theta_{23}) = 0.95^{+0.10}_{-0.11} \pm 0.01$.

[14] ADAMSON 12B obtained this result by a two-neutrino oscillation analysis of the L/E distribution using 37.9 kton-yr atmospheric neutrino data with the MINOS far detector.

[15] The best fit point is $\Delta m^2 = 0.0019$ eV^2 and $\sin^2 2\theta = 0.99$. The 90% single-parameter confidence interval at the best fit point is $\sin^2 2\theta > 0.86$.

[16] The data are separated into pure samples of νs and $\overline{\nu}$s, and separate oscillation parameters for νs and $\overline{\nu}$s are fit to the data. The best fit point is (Δm^2, $\sin^2 2\theta$) = (0.0022 eV^2, 0.99) and ($\Delta\overline{m}^2$, $\sin^2 2\overline{\theta}$) = (0.0016 eV^2, 1.00). The quoted result is taken from the 90% C.L. contour in the (Δm^2, $\sin^2 2\theta$) plane obtained by minimizing the four parameter log-likelihood function with respect to the other oscillation parameters.

[17] ADRIAN-MARTINEZ 12 measured the oscillation parameters of atmospheric neutrinos with the ANTARES deep sea neutrino telescope using the data taken from 2007 to 2010 (863 days of total live time).

[18] ABE 11C obtained this result by a two-neutrino oscillation analysis using the Super-Kamiokande-I+II+III atmospheric neutrino data. ABE 11C also reported results under a two-neutrino disappearance model with separate mixing parameters between ν and $\overline{\nu}$, and obtained $\sin^2 2\theta > 0.93$ for ν and $\sin^2 2\theta > 0.83$ for $\overline{\nu}$ at 90% C.L.

[19] ADAMSON 11B obtained this result by a two-neutrino oscillation analysis of antineutrinos in an antineutrino enhanced beam with 1.71×10^{20} protons on target. This results is consistent with the neutrino measurements of ADAMSON 11 at 2% C.L.

[20] WENDELL 10 obtained this result ($\sin^2\theta_{23} = 0.407$–$0.583$) by a three-neutrino oscillation analysis using the Super-Kamiokande-I+II+III atmospheric neutrino data, assuming $\theta_{13} = 0$ but including the solar oscillation parameters Δm^2_{21} and $\sin^2\theta_{12}$ in the fit.

[21] WENDELL 10 obtained this result ($\sin^2\theta_{23} = 0.43$–0.61) by a three-neutrino oscillation analysis with one mass scale dominance ($\Delta m^2_{21} = 0$) using the Super-Kamiokande-I+II+III atmospheric neutrino data, and updates the HOSAKA 06A result.

[22] WENDELL 10 obtained this result ($\sin^2\theta_{23} = 0.44$–0.63) by a three-neutrino oscillation analysis with one mass scale dominance ($\Delta m^2_{21} = 0$) using the Super-Kamiokande-I+II+III atmospheric neutrino data, and updates the HOSAKA 06A result.

[23] ADAMSON 06 obtained this result by a two-neutrino oscillation analysis of the L/E distribution using 4.54 kton yr atmospheric neutrino data with the MINOS far detector.

[24] Supercedes ALIU 05.

[25] MICHAEL 06 best fit is for maximal mixing. See also ADAMSON 08.

[26] The best fit is for maximal mixing.

[27] ALLISON 05 result is based upon atmospheric neutrino interactions including upward-stopping muons, with an exposure of 5.9 kton yr. From a two-flavor oscillation analysis the best-fit point is $\Delta m^2 = 0.0017$ eV^2 and $\sin^2(2\theta) = 0.97$.

[28] ASHIE 05 obtained this result by a two-neutrino oscillation analysis using 92 kton yr atmospheric neutrino data from the complete Super-Kamiokande I running period.

[29] AMBROSIO 04 obtained this result, without using the absolute normalization of the neutrino flux, by combining the angular distribution of upward through-going muon tracks with $E_\mu > 1$ GeV, N_{low} and N_{high}, and the numbers of InDown + UpStop and InUp events. Here, N_{low} and N_{high} are the number of events with reconstructed neutrino energies < 30 GeV and > 130 GeV, respectively. InDown and InUp represent events with downward and upward-going tracks starting inside the detector due to neutrino interactions, while UpStop represents entering upward-going tracks which stop in the detector. The best fit is for maximal mixing.

[30] ASHIE 04 obtained this result from the L(flight length)/E(estimated neutrino energy) distribution of ν_μ disappearance probability, using the Super-Kamiokande-I 1489 live-day atmospheric neutrino data.

[31] There are several islands of allowed region from this K2K analysis, extending to high values of Δm^2. We only include the one that overlaps atmospheric neutrino analyses. The best fit is for maximal mixing.

[32] AMBROSIO 03 obtained this result on the basis of the ratio $R = N_{low}/N_{high}$, where N_{low} and N_{high} are the number of upward through-going muon events with reconstructed neutrino energy < 30 GeV and > 130 GeV, respectively. The data came from the full detector run started in 1994. The method of FELDMAN 98 is used to obtain the limits.

[33] AMBROSIO 03 obtained this result by using the ratio R and the angular distribution of the upward through-going muons. R is given in the previous note and the angular distribution is reported in AMBROSIO 01. The method of FELDMAN 98 is used to obtain the limits. The best fit is to maximal mixing.

[34] SANCHEZ 03 is based on an exposure of 5.9 kton yr. The result is obtained using a likelihood analysis of the neutrino L/E distribution for a selection μ flavor sample while the e-flavor sample provides flux normalization. The method of FELDMAN 98 is used to obtain the allowed region. The best fit is $\sin^2(2\theta) = 0.97$.

[35] AMBROSIO 01 result is based on the angular distribution of upward through-going muon tracks with $E_\mu > 1$ GeV. The data came from three different detector configurations, but the statistics is largely dominated by the full detector run, from May 1994 to December 2000. The total live time, normalized to the full detector configuration is 6.17 years. The best fit is obtained outside the physical region. The method of FELDMAN 98 is used to obtain the limits. The best fit is for maximal mixing.

[36] AMBROSIO 01 result is based on the angular distribution and normalization of upward through-going muon tracks with $E_\mu > 1$ GeV. See the previous footnote.

[37] FUKUDA 99C obtained this result from a total of 537 live days of upward through-going muon data in Super-Kamiokande between April 1996 to January 1998. With a threshold of $E_\mu > 1.6$ GeV, the observed flux is $(1.74 \pm 0.07 \pm 0.02) \times 10^{-13}$ cm^{-2}s^{-1}sr^{-1}. The best fit is $\sin^2(2\theta) = 0.95$.

[38] FUKUDA 99D obtained this result from a simultaneous fitting to zenith angle distributions of upward-stopping and through-going muons. The flux of upward-stopping muons of minimum energy of 1.6 GeV measured between April 1996 and January 1998 is $(0.39 \pm 0.04 \pm 0.02) \times 10^{-13}$ cm^{-2}s^{-1}sr^{-1}. This is compared to the expected flux of $(0.73 \pm 0.16$ (theoretical error)$) \times 10^{-13}$ cm^{-2}s^{-1}sr^{-1}. The best fit is to maximal mixing.

[39] FUKUDA 99D obtained this result from the zenith dependence of the upward-stopping/through-going flux ratio. The best fit is to maximal mixing.

[40] FUKUDA 98C obtained this result by an analysis of 33.0 kton yr atmospheric neutrino data. The best fit is for maximal mixing.

[41] HATAKEYAMA 98 obtained this result from a total of 2456 live days of upward-going muon data in Kamiokande between December 1985 and May 1995. With a threshold of $E_\mu > 1.6$ GeV, the observed flux of upward through-going muons is $(1.94 \pm 0.10^{+0.07}_{-0.06}) \times 10^{-13}$ cm^{-2}s^{-1}sr^{-1}. This is compared to the expected flux of $(2.46 \pm 0.54$ (theoretical error)$) \times 10^{-13}$ cm^{-2}s^{-1}sr^{-1}. The best fit is for maximal mixing.

[42] HATAKEYAMA 98 obtained this result from a combined analysis of Kamiokande contained events (FUKUDA 94) and upward going muon events. The best fit is $\sin^2(2\theta) = 0.95$.

[43] FUKUDA 94 obtained the result by a combined analysis of sub- and multi-GeV atmospheric neutrino events in Kamiokande. The best fit is for maximal mixing.

Δm^2_{32}

The sign of Δm^2_{32} is not known at this time. If given, values are shown separately for the normal and inverted mass ordering. Unless otherwise specified, the ranges below correspond to the projection onto the Δm^2_{32} axis of the 90% CL contours in the $\sin^2(2\theta_{23}) - \Delta m^2_{32}$ plane presented by the authors. If uncertainties are reported with the value, they correspond to one standard deviation uncertainty.

VALUE (10^{-3} eV^2)	DOCUMENT ID		TECN	COMMENT
-2.56 ± 0.04 OUR FIT	Assuming inverted mass hierarchy			
2.51 ± 0.05 OUR FIT	Error includes scale factor of 1.1. Assuming normal mass hierarchy			
2.54 ± 0.08	[1] ABE	17F	T2K	Normal mass ordering with neutrinos and antineutrinos
-2.51 ± 0.08	[1] ABE	17F	T2K	Inverted mass ordering with neutrinos and antineutrinos
2.67 ± 0.11	ADAMSON	17A	NOVA	3ν osc; normal mass ordering
-2.72 ± 0.11	ADAMSON	17A	NOVA	3ν osc; inverted mass ordering
$2.45 \pm 0.06 \pm 0.06$	[2] AN	17A	DAYA	3ν osc; normal mass ordering
$-2.56 \pm 0.06 \pm 0.06$	[2] AN	17A	DAYA	3ν osc; inverted mass ordering
$2.56 \, ^{+0.21}_{-0.23} \, ^{+0.12}_{-0.13}$	[3] CHOI	16	RENO	3ν osc; normal mass ordering
$-2.69 \, ^{+0.23}_{-0.21} \, ^{+0.13}_{-0.12}$	[3] CHOI	16	RENO	3ν osc; inverted mass ordering
$2.72 \, ^{+0.19}_{-0.20}$	[4] AARTSEN	15A	ICCB	3ν osc; normal mass ordering
$-2.73 \, ^{+0.21}_{-0.18}$	[4] AARTSEN	15A	ICCB	3ν osc; inverted mass ordering
2.37 ± 0.09	[5] ADAMSON	14	MINS	3ν osc., accel., atmospheric; normal mass ordering
$-2.41 \, ^{+0.09}_{-0.12}$	[5] ADAMSON	14	MINS	3ν osc., accel., atmsopheric; inverted mass ordering
• • • We do not use the following data for averages, fits, limits, etc. • • •				
$2.53 \, ^{+0.15}_{-0.13}$	ABE	17C	T2K	normal mass ordering with neutrinos
$2.55 \, ^{+0.33}_{-0.27}$	ABE	17C	T2K	normal mass ordering with antineutrinos
$2.55 \, ^{+0.08}_{-0.08}$	ABE	17C	T2K	Normal mass ordering with neutrinos and antineutrinos
$-2.63 \, ^{+0.08}_{-0.08}$	ABE	17C	T2K	Inverted mass ordering with neutrinos and antineutrinos
$2.51 \, ^{+0.29}_{-0.25}$	[6] ABE	16D	T2K	3ν osc.; normal mass ordering; $\overline{\nu}$ beam
$2.52 \, ^{+0.20}_{-0.18}$	[7] ADAMSON	16A	NOVA	3ν osc; normal mass ordering
-2.56 ± 0.19	[7] ADAMSON	16A	NOVA	3ν osc; inverted mass ordering
2.0–5.0	[8] AGAFONOVA	15A	OPER	90% CL, 5 events
2.37 ± 0.11	[9] AN	15	DAYA	3ν osc.; normal mass ordering
-2.47 ± 0.11	[9] AN	15	DAYA	3ν osc.; inverted mass ordering
2.51 ± 0.10	[10] ABE	14	T2K	3ν osc.; normal mass ordering
-2.56 ± 0.10	[10] ABE	14	T2K	3ν osc.; inverted mass ordering
$2.54 \, ^{+0.19}_{-0.20}$	[11] AN	14	DAYA	3ν osc.; normal mass ordering
$-2.64 \, ^{+0.20}_{-0.19}$	[11] AN	14	DAYA	3ν osc.; inverted mass ordering
$2.48 \, ^{+0.05}_{-0.07}$	[12] FORERO	14	FIT	3ν; normal mass ordering
$-2.38 \, ^{+0.06}_{-0.05}$	[12] FORERO	14	FIT	3ν; inverted mass ordering
2.457 ± 0.047	[13,14] GONZALEZ...	14	FIT	Normal mass ordering; global fit
$-2.449 \, ^{+0.047}_{-0.048}$	[13] GONZALEZ...	14	FIT	Inverted mass ordering; global fit
$2.3 \, ^{+0.6}_{-0.5}$	[15] AARTSEN	13B	ICCB	DeepCore, 2ν oscillation
$2.44 \, ^{+0.17}_{-0.15}$	[16] ABE	13G	T2K	3ν osc.; normal mass ordering
$2.41 \, ^{+0.09}_{-0.10}$	[17] ADAMSON	13B	MINS	2ν osc.; beam + atmospheric; identical ν & $\overline{\nu}$
2.2–3.1	[18] ABE	12A	T2K	off-axis beam
$2.62 \, ^{+0.31}_{-0.28} \pm 0.09$	[19] ADAMSON	12	MINS	$\overline{\nu}$ beam
1.35–2.55	[20,21] ADAMSON	12B	MINS	MINOS atmospheric
1.4–5.6	[20,22] ADAMSON	12B	MINS	MINOS pure atmospheric ν
0.9–2.5	[20,22] ADAMSON	12B	MINS	MINOS pure atmospheric $\overline{\nu}$
1.8–5.0	[23] ADRIAN-MAR...	12	ANTR	atm. ν with deep see telescope
1.3–4.0	[24] ABE	11C	SKAM	atmospheric $\overline{\nu}$
$2.32 \, ^{+0.12}_{-0.08}$	ADAMSON	11	MINS	2ν oscillation; maximal mixing
$3.36 \, ^{+0.46}_{-0.40}$	[25] ADAMSON	11B	MINS	$\overline{\nu}$ beam
< 3.37	[26] ADAMSON	11C	MINS	MINOS
1.9–2.6	[27] WENDELL	10	SKAM	3ν osc.; normal mass ordering
-1.7– -2.7	[27] WENDELL	10	SKAM	3ν osc.; inverted mass ordering
2.43 ± 0.13	ADAMSON	08A	MINS	MINOS
0.07–50	[28] ADAMSON	06	MINS	atmospheric ν with far detector
1.9–4.0	[29,30] AHN	06A	K2K	KEK to Super-K
2.2–3.8	[31] MICHAEL	06	MINS	MINOS
1.9–3.6	[29] ALIU	05	K2K	KEK to Super-K
0.3–12	[32] ALLISON	05	SOU2	
1.5–3.4	[33] ASHIE	05	SKAM	atmospheric neutrino
0.6–8.0	[34] AMBROSIO	04	MCRO	MACRO
1.9 to 3.0	[35] ASHIE	04	SKAM	L/E distribution
1.5–3.9	[36] AHN	03	K2K	KEK to Super-K
0.25–9.0	[37] AMBROSIO	03	MCRO	MACRO
0.6–7.0	[38] AMBROSIO	03	MCRO	MACRO
0.15–15	[39] SANCHEZ	03	SOU2	Soudan-2 Atmospheric
0.6–15	[40] AMBROSIO	01	MCRO	upward μ
1.0–6.0	[41] AMBROSIO	01	MCRO	upward μ
1.0–50	[42] FUKUDA	99C	SKAM	upward μ
1.5–15.0	[43] FUKUDA	99D	SKAM	upward μ
0.7–18	[44] FUKUDA	99D	SKAM	stop μ / through
0.5–6.0	[45] FUKUDA	98C	SKAM	Super-Kamiokande
0.55–50	[46] HATAKEYAMA	98	KAMI	Kamiokande
4–23	[47] HATAKEYAMA	98	KAMI	Kamiokande
5–25	[48] FUKUDA	94	KAMI	Kamiokande

[1] Supersedes ABE 17C.

[2] AN 17A report results from combined rate and spectral shape analysis of 1230 days of data taken with the Daya Bay reactor experiment. The data set contains more than 2.5×10^6 inverse beta-decay events with neutron capture on Gd. The fit to the data gives $\Delta^2_{ee} = (2.50 \pm 0.06 \pm 0.06) \times 10^{-3}$ eV. Supersedes AN 15.

[3] CHOI 16 reports result of the RENO experiment from a rate and shape analysis of 500 days of data. A simultaneous fit to θ_{13} and Δm^2_{ee} yields $\Delta m^2_{ee} = (2.62^{+0.21}_{-0.23}{}^{+0.12}_{-0.13}) \times 10^{-3}$ eV. We convert the results to Δm^2_{32} using PDG 14 values of $\sin^2(\theta_{12})$ and Δm^2_{21}.

[4] AARTSEN 15A obtains this result by a three-neutrino oscillation analysis using 10–100 GeV muon neutrino sample from a total of 953 days of measurements with the low-energy subdetector DeepCore of the IceCube neutrino telescope.

[5] ADAMSON 14 uses a complete set of accelerator and atmospheric data. The analysis combines The analysis combines the ν_μ disappearance and ν_e appearance data using three-neutrino oscillation fit. The fit results are obtained for normal and inverted mass ordering assumptions.

[6] ABE 16D reports oscillation results using $\overline{\nu}_\mu$ disappearance in an off-axis beam.

[7] Superseded by ADAMSON 17A.

[8] AGAFONOVA 15A result is based on 5 $\nu_\mu \rightarrow \nu_\tau$ appearance candidates with an expected background of 0.25 ± 0.05 events. The best fit is for Δm^2_{32}=3.3 × 10^{-3} eV^2.

[9] AN 15 uses all eight identical detectors, with four placed near the reactor cores and the remaining four at the far hall to determine prompt energy spectra. The results correspond to the exposure of 6.9×10^5 GW$_{th}$-ton-days. They derive $\Delta m^2_{ee} = (2.42 \pm 0.11) \times 10^{-3}$ eV^2. Assuming the normal (inverted) ordering, the fitted $\Delta m^2_{32} = (2.37 \pm 0.11) \times 10^{-3}$ ($(2.47 \pm 0.11) \times 10^{-3}$) eV^2. Superseded by AN 17A.

[10] ABE 14 results are based on ν_μ disappearance using three-neutrino oscillation fit. The confidence intervals are derived from one dimensional profiled likelihoods. In ABE 14 the inverted mass ordering result is reported as $\Delta m^2_{13} = (2.48 \pm 0.10) \times 10^{-3}$ eV^2 which we converted to Δm^2_{32} by adding PDG 14 value of $\Delta m^2_{21} = (7.53 \pm 0.18) \times 10^{-5}$ eV^2. Superseded by ABE 17C.

[11] AN 14 uses six identical detectors, with three placed near the reactor cores (flux-weighted baselines of 512 and 561 m) and the remaining three at the far hall (at the flux averaged distance of 1579 m from all six reactor cores) to determine prompt energy spectra and derive $\Delta m^2_{ee} = (2.59^{+0.19}_{-0.20}) \times 10^{-3}$ eV^2. Assuming the normal (inverted) ordering, the fitted $\Delta m^2_{32} = (2.54^{+0.19}_{-0.20}) \times 10^{-3}$ ($(2.64^{+0.19}_{-0.20}) \times 10^{-3}$) eV^2. Superseded by AN 15.

[12] FORERO 14 performs a global fit to Δm^2_{31} using solar, reactor, long-baseline accelerator, and atmospheric neutrino data.

[13] GONZALEZ-GARCIA 14 result comes from a frequentist global fit. The corresponding Bayesian global fit to the same data results are reported in BERGSTROM 15 as $(2.460 \pm 0.046) \times 10^{-3}$ eV^2 for normal and $(2.445^{+0.047}_{-0.045}) \times 10^{-3}$ eV^2 for inverted mass ordering.

[14] The value for normal mass ordering is actually a measurement of Δm^2_{31} which differs from Δm^2_{32} by a much smaller value of Δm^2_{12}.

[15] AARTSEN 13B obtained this result by a two-neutrino oscillation analysis using 20–100 GeV muon neutrino sample from a total of 318.9 days of live-time measurement with the low-energy subdetector DeepCore of the IceCube neutrino telescope.

[16] Based on the observation of 58 ν_μ events with 205 ± 17(syst) expected in the absence of neutrino oscillations. Superseded by ABE 14.

[17] ADAMSON 13B obtained this result from ν_μ and $\overline{\nu}_\mu$ disappearance using ν_μ (10.71×10^{20} POT) and $\overline{\nu}_\mu$ (3.36×10^{20} POT) beams, and atmospheric (37.88 kton-years) data from MINOS. The fit assumed two-flavor neutrino hypothesis and identical ν_μ and $\overline{\nu}_\mu$ oscillation parameters.

[18] ABE 12A obtained this result by a two-neutrino oscillation analysis. The best-fit point is $\Delta m^2_{32} = 2.65 \times 10^{-3}$ eV^2.

[19] ADAMSON 12 is a two-neutrino oscillation analysis using antineutrinos.

[20] ADAMSON 12B obtained this result by a two-neutrino oscillation analysis of the L/E distribution using 37.9 kton-yr atmospheric neutrino data with the MINOS far detector.

[21] The 90% single-parameter confidence interval at the best fit point is $\Delta m^2 = 0.0019 \pm 0.0004$ eV^2.

[22] The data are separated into pure samples of νs and $\overline{\nu}$s, and separate oscillation parameters for νs and $\overline{\nu}$s are fit to the data. The best fit point is (Δm^2, $\sin^2 2\theta$) = (0.0022 eV^2, 0.99) and ($\Delta\overline{m}^2$, $\sin^2 2\overline{\theta}$) = (0.0016 eV^2, 1.00). The quoted result is taken from the 90% C.L. contour in the (Δm^2, $\sin^2 2\theta$) plane obtained by minimizing the four parameter log-likelihood function with respect to the other oscillation parameters.

[23] ADRIAN-MARTINEZ 12 measured the oscillation parameters of atmospheric neutrinos with the ANTARES deep sea neutrino telescope using the data taken from 2007 to 2010 (863 days of total live time).

[24] ABE 11C obtained this result by a two-neutrino oscillation analysis with separate mixing parameters between neutrinos and antineutrinos, using the Super-Kamiokande-I+II+III atmospheric neutrino data. The corresponding 90% CL neutrino oscillation parameter range obtained from this analysis is $\Delta m^2 = 1.7$–3.0×10^{-3} eV^2.

[25] ADAMSON 11B obtained this result by a two-neutrino oscillation analysis of antineutrinos in an antineutrino enhanced beam with 1.71×10^{20} protons on target. This results is consistent with the neutrino measurements of ADAMSON 11 at 2% C.L.

[26] ADAMSON 11C obtains this result based on a study of antineutrinos in a neutrino beam and assumes maximal mixing in the two-flavor approximation.

[27] WENDELL 10 obtained this result by a three-neutrino oscillation analysis with one mass scale dominance ($\Delta m^2_{21} = 0$) using the Super-Kamiokande-I+II+III atmospheric neutrino data, and updates the HOSAKA 06A result.

[28] ADAMSON 06 obtained this result by a two-neutrino oscillation analysis of the L/E distribution using 4.54 kton yr atmospheric neutrino data with the MINOS far detector.

[29] The best fit in the physical region is for $\Delta m^2 = 2.8 \times 10^{-3}$ eV^2.

[30] Supercedes ALIU 05.

[31] MICHAEL 06 best fit is 2.74×10^{-3} eV^2. See also ADAMSON 08.

[32] ALLISON 05 result is based on an atmospheric neutrino observation with an exposure of 5.9 kton yr. From a two-flavor oscillation analysis the best-fit point is $\Delta m^2 = 0.0017$ eV^2 and $\sin^2 2\,\theta = 0.97$.

[33] ASHIE 05 obtained this result by a two-neutrino oscillation analysis using 92 kton yr atmospheric neutrino data from the complete Super-Kamiokande I running period. The best fit is for $\Delta m^2 = 2.1 \times 10^{-3}$ eV^2.

[34] AMBROSIO 04 obtained this result, without using the absolute normalization of the neutrino flux, by combining the angular distribution of upward through-going muon tracks with $E_\mu > 1$ GeV, N_{low} and N_{high}, and the numbers of InDown + UpStop and InUp events. Here, N_{low} and N_{high} are the number of events with reconstructed neutrino energies < 30 GeV and > 130 GeV, respectively. InDown and InUp represent events with downward and upward-going tracks starting inside the detector due to neutrino interactions, while UpStop represents entering upward-going tracks which stop in the detector. The best fit is for $\Delta m^2 = 2.3 \times 10^{-3}$ eV^2.

[35] ASHIE 04 obtained this result from the L(flight length)/E(estimated neutrino energy) distribution of ν_μ disappearance probability, using the Super-Kamiokande-I 1489 live-day atmospheric neutrino data. The best fit is for $\Delta m^2 = 2.4 \times 10^{-3}$ eV^2.

[36] There are several islands of allowed region from this K2K analysis, extending to high values of Δm^2. We only include the one that overlaps atmospheric neutrino analyses. The best fit is for $\Delta m^2 = 2.8 \times 10^{-3}$ eV^2.

[37] AMBROSIO 03 obtained this result on the basis of the ratio R = N_{low}/N_{high}, where N_{low} and N_{high} are the number of upward through-going muon events with reconstructed neutrino energy < 30 GeV and > 130 GeV, respectively. The data came from the full detector run started in 1994. The method of FELDMAN 98 is used to obtain the limits. The best fit is for $\Delta m^2 = 2.5 \times 10^{-3}$ eV^2.

[38] AMBROSIO 03 obtained this result by using the ratio R and the angular distribution of the upward through-going muons. R is given in the previous note and the angular distribution is reported in AMBROSIO 01. The method of FELDMAN 98 is used to obtain the limits. The best fit is for $\Delta m^2 = 2.5 \times 10^{-3}$ eV^2.

[39] SANCHEZ 03 is based on an exposure of 5.9 kton yr. The result is obtained using a likelihood analysis of the neutrino L/E distribution for a selection μ flavor sample while the e-flavor sample provides flux normalization. The method of FELDMAN 98 is used to obtain the allowed region. The best fit is for $\Delta m^2 = 5.2 \times 10^{-3}$ eV^2.

[40] AMBROSIO 01 result is based on the angular distribution of upward through-going muon tracks with $E_\mu > 1$ GeV. The data came from three different detector configurations, but the statistics is largely dominated by the full detector run, from May 1994 to December 2000. The total live time, normalized to the full detector configuration is 6.17 years. The best fit is obtained outside the physical region. The method of FELDMAN 98 is used to obtain the limits.

[41] AMBROSIO 01 result is based on the angular distribution and normalization of upward through-going muon tracks with $E_\mu > 1$ GeV. See the previous footnote.

[42] FUKUDA 99C obtained this result from a total of 537 live days of upward through-going muon data in Super-Kamiokande between April 1996 to January 1998. With a threshold of $E_\mu > 1.6$ GeV, the observed flux is $(1.74 \pm 0.07 \pm 0.02) \times 10^{-13}$ cm^{-2}s^{-1}sr^{-1}. The best fit is for $\Delta m^2 = 5.9 \times 10^{-3}$ eV^2.

[43] FUKUDA 99D obtained this result from a simultaneous fitting to zenith angle distributions of upward-stopping and through-going muons. The flux of upward-stopping muons of minimum energy of 1.6 GeV measured between April 1996 and January 1998 is $(0.39 \pm 0.04 \pm 0.02) \times 10^{-13}$ cm^{-2}s^{-1}sr^{-1}. This is compared to the expected flux of $(0.73 \pm 0.16$ (theoretical error)$) \times 10^{-13}$ cm^{-2}s^{-1}sr^{-1}. The best fit is for $\Delta m^2 = 3.9 \times 10^{-3}$ eV^2.

[44] FUKUDA 99D obtained this result from the zenith dependence of the upward-stopping/through-going flux ratio. The best fit is for $\Delta m^2 = 3.1 \times 10^{-3}$ eV^2.

[45] FUKUDA 98C obtained this result by an analysis of 33.0 kton yr atmospheric neutrino data. The best fit is for $\Delta m^2 = 2.2 \times 10^{-3}$ eV^2.

[46] HATAKEYAMA 98 obtained this result from a total of 2456 live days of upward-going muon data in Kamiokande between December 1985 and May 1995. With a threshold of $E_\mu > 1.6$ GeV, the observed flux of upward through-going muons is $(1.94 \pm 0.10^{+0.07}_{-0.06}) \times 10^{-13}$ cm^{-2}s^{-1}sr^{-1}. This is compared to the expected flux of $(2.46 \pm 0.54$ (theoretical error)$) \times 10^{-13}$ cm^{-2}s^{-1}sr^{-1}. The best fit is for $\Delta m^2 = 2.2 \times 10^{-3}$ eV^2.

[47] HATAKEYAMA 98 obtained this result from a combined analysis of Kamiokande contained events (FUKUDA 94) and upward going muon events. The best fit is for $\Delta m^2 = 13 \times 10^{-3}$ eV^2.

[48] FUKUDA 94 obtained the result by a combined analysis of sub- and multi-GeV atmospheric neutrino events in Kamiokande. The best fit is for $\Delta m^2 = 16 \times 10^{-3}$ eV^2.

$\sin^2(\theta_{13})$

At present time direct measurements of $\sin^2(\theta_{13})$ are derived from the reactor $\overline{\nu}_e$ disappearance at distances corresponding to the Δm^2_{32} value, i.e. L ∼ 1km. Alternatively, limits can also be obtained from the analysis of the solar neutrino data and accelerator-based $\nu_\mu \rightarrow \nu_e$ experiments.

If an experiment reports $\sin^2(2\,\theta_{13})$ we convert the value to $\sin^2(\theta_{13})$.

VALUE (units 10^{-2})	CL%	DOCUMENT ID		TECN	COMMENT
2.12 ± 0.08 OUR AVERAGE					
2.149 ± 0.071 ± 0.050		[1] AN	17A	DAYA	DayaBay, LingAo/Ao II reactors
$2.25\ ^{+\ 0.87}_{-\ 0.86}$		[2] ABE	16B	DCHZ	Chooz reactors
1.81 ± 0.29		[3] AN	16A	DAYA	DayaBay, Ling Ao/Ao II reactors
2.09 ± 0.23 ± 0.16		[4] CHOI	16	RENO	Yonggwang reactors
• • • We do not use the following data for averages, fits, limits, etc. • • •					
2.7 ± 0.7		[5] ABE	17F	T2K	Normal mass ordering, T2K only
2.15 ± 0.13		[6] AN	15	DAYA	DayaBay, Ling Ao/Ao II reactors
$2.6\ ^{+\ 1.2}_{-\ 1.1}$		[7] ABE	14A	DCHZ	Chooz reactors
$3.0\ ^{+\ 1.3}_{-\ 1.0}$		[8] ABE	14C	T2K	Inverted mass ordering
$3.6\ ^{+\ 1.0}_{-\ 0.9}$		[8] ABE	14C	T2K	Normal mass ordering
$2.3\ ^{+\ 0.9}_{-\ 0.8}$		[9] ABE	14H	DCHZ	Chooz reactors
2.3 ± 0.2		[10] AN	14	DAYA	DayaBay, Ling Ao/Ao II reactors
2.12 ± 0.47		[11] AN	14B	DAYA	DayaBay, Ling Ao/Ao II reactors
2.34 ± 0.20		[12] FORERO	14	FIT	Normal mass ordering
2.40 ± 0.19		[12] FORERO	14	FIT	Inverted mass ordering

2.18	± 0.10			[13] GONZALEZ...	14	FIT	Normal mass ordering; global fit
2.19	$^{+0.11}_{-0.10}$			[13] GONZALEZ...	14	FIT	Inverted mass ordering; global fit
2.5	± 0.9	±0.9		[14] ABE	13C	DCHZ	Chooz reactors
2.3	$^{+1.3}_{-1.0}$			[15] ABE	13E	T2K	Normal mass ordering
2.8	$^{+1.6}_{-1.2}$			[15] ABE	13E	T2K	Inverted mass ordering
1.6	$^{+1.3}_{-0.9}$			[16] ADAMSON	13A	MINS	Normal mass ordering
3.0	$^{+1.8}_{-1.6}$			[16] ADAMSON	13A	MINS	Inverted mass ordering
<13			90	AGAFONOVA	13	OPER	OPERA: 3ν
< 3.6			95	[17] AHARMIM	13	FIT	global solar: 3ν
2.3	± 0.3	±0.1		[18] AN	13	DAYA	DayaBay, LIng Ao/Ao II reactors
2.2	± 1.1	±0.8		[19] ABE	12	DCHZ	Chooz reactors
2.8	± 0.8	±0.7		[20] ABE	12B	DCHZ	Chooz reactors
2.9	± 0.3	±0.5		[21] AHN	12	RENO	Yonggwang reactors
2.4	± 0.4	±0.1		[22] AN	12	DAYA	DayaBay, LIng Ao/Ao II reactors
2.5	$^{+1.8}_{-1.6}$			[23] ABE	11	FIT	KamLAND + global solar
< 6.1			95	[24] ABE	11	FIT	Global solar
1.3	to 5.6		68	[25] ABE	11A	T2K	Normal mass ordering
1.5	to 5.6		68	[26] ABE	11A	T2K	Inverted mass ordering
0.3	to 2.3		68	[27] ADAMSON	11D	MINS	Normal mass ordering
0.8	to 3.9		68	[28] ADAMSON	11D	MINS	Inverted mass ordering
8	± 3			[29] FOGLI	11	FIT	Global neutrino data
7.8	± 6.2			[30] GANDO	11	FIT	KamLAND + solar: 3ν
12.4	±13.3			[31] GANDO	11	FIT	KamLAND: 3ν
3	$^{+9}_{-7}$		90	[32] ADAMSON	10A	MINS	Normal mass ordering
6	$^{+14}_{-6}$		90	[33] ADAMSON	10A	MINS	Inverted mass ordering
8	$^{+8}_{-7}$			[34,35] AHARMIM	10	FIT	KamLAND + global solar: 3ν
< 30			95	[34,36] AHARMIM	10	FIT	global solar: 3ν
< 15			90	[37] WENDELL	10	SKAM	3ν osc.; normal m ordering
< 33			90	[37] WENDELL	10	SKAM	3ν osc.; inverted m ordering
11	$^{+11}_{-8}$			[38] ADAMSON	09	MINS	Normal mass ordering
18	$^{+15}_{-11}$			[39] ADAMSON	09	MINS	Inverted mass ordering
6	± 4			[40] FOGLI	08	FIT	Global neutrino data
8	± 7			[41] FOGLI	08	FIT	Solar + KamLAND data
5	± 5			[42] FOGLI	08	FIT	Atmospheric + LBL + CHOOZ
< 36			90	[43] YAMAMOTO	06	K2K	Accelerator experiment
< 48			90	[44] AHN	04	K2K	Accelerator experiment
< 36			90	[45] BOEHM	01		Palo Verde react.
< 45			90	[46] BOEHM	00		Palo Verde react.
< 15			90	[47] APOLLONIO	99	CHOZ	Reactor Experiment

[1] AN 17A report results from combined rate and spectral shape analysis of 1230 days of data taken with the Daya Bay reactor experiment. The data set contains more than 2.5×10^6 inverse beta-decay events with neutron capture on Gd. A simultaneous fit to θ_{13} and Δm^2_{ee} is performed. Supersedes AN 15.

[2] ABE 16B uses 455.57 live days of data from a detector 1050 m away from two reactor cores of the Chooz nuclear power station, to determine the mixing parameter $\sin^2(2\theta_{13})$. This analysis uses 7.15 reactor-off days for constraining backgrounds. A rate and shape analysis is performed on combined neutron captures on H and Gd. Supersedes ABE 14H and ABE 13C.

[3] AN 16A uses data from the eight antineutrino detectors (404 days) and six antineutrino detectors (217 days) runs to determine the mixing parameter $\sin^2(2\theta_{13})$ using the neutron capture on H only. Supersedes AN 14B.

[4] CHOI 16 reports results of the RENO experiment using about 500 days of data, performing a rate and shape analysis. Compared to AHN 12, a significant reduction of the systematic uncertainties is reported. A 3% excess of events near 5 MeV of the prompt energy is observed. Supersedes AHN 12.

[5] Using T2K data only. For inverted mass ordering, all values of θ_{13} are ruled out at 68% CL.

[6] AN 15 uses all eight identical detectors, with four placed near the reactor cores and the remaining four at the far hall to determine the mixing angle θ_{13} using the $\overline{\nu}_e$ observed interaction rates with neutron capture on Gd and energy spectra. The result corresponds to the exposure of 6.9×10^5 GW_{th}-ton-days. Superseded by AN 17A.

[7] ABE 14A uses 467.9 live days of one detector, 1050 m away from two reactor cores of the Chooz nuclear power station, to determine the mixing parameter $\sin^2(2\ \theta_{13})$. The Bugey4 data (DECLAIS 94) is used to constrain the neutrino flux. The data set includes 7.24 reactor-off days. A "rate-modulation" analysis is performed. Supercedes ABE 12B.

[8] ABE 14C result is for ν_e appearance and assumes $\Delta m^2_{32} = 2.4 \times 10^{-3}$ eV^2, $\sin^2(\ \theta_{23}) = 0.5$, and $\delta = 0$.

[9] ABE 14H uses 467.9 live days of one detector, 1050 m away from two reactor cores of the Chooz nuclear power station, to determine the mixing parameter $\sin^2(2\ \theta_{13})$. The Bugey4 data (DECLAIS 94) is used to constrain the neutrino flux. The data set includes 7.24 reactor-off days. A rate and shape analysis is performed. Superceded by ABE 16B.

[10] AN 14 uses six identical detectors, with three placed near the reactor cores (flux-weighted baselines of 512 and 561 m) and the remaining three at the far hall (at the flux averaged distance of 1579 m from all six reactor cores) to determine the mixing angle θ_{13} using the $\overline{\nu}_e$ observed interaction rates with neutron capture on Gd and energy spectra. Supersedes AN 13 and superseded by AN 15.

[11] AN 14B uses six identical anti-neutrino detectors with flux-weighted baselines of ~ 500 m and ~ 1.6 km to six power reactors. This rate analysis uses a 217-day data set and neutron capture on protons (not Gd) only. $\Delta m^2_{31} = 2.32 \times 10^{-3}$ eV^2 is assumed. Superseded by AN 16A.

[12] FORERO 14 performs a global fit to neutrino oscillations using solar, reactor, long-baseline accelerator, and atmospheric neutrino data.

[13] GONZALEZ-GARCIA 14 result comes from a frequentist global fit. The corresponding Bayesian global fit to the same data results are reported in BERGSTROM 15 as $(2.18^{+0.10}_{-0.11}) \times 10^{-2}$ eV^2 for normal and $(2.19^{+0.12}_{-0.10}) \times 10^{-2}$ eV^2 for inverted mass ordering.

[14] ABE 13C uses delayed neutron capture on hydrogen instead of on Gd used previously. The physical volume is thus three times larger. The fit is based on the rate and shape analysis as in ABE 12B. The Bugey4 data (DECLAIS 94) is used to constrain the neutrino flux. Superseded by ABE 16B.

[15] ABE 13E assumes maximal θ_{23} mixing and CP phase $\delta = 0$.

[16] ADAMSON 13A results obtained from ν_e appearance, assuming $\delta = 0$, and $\sin^2(2\ \theta_{23}) = 0.957$.

[17] AHARMIM 13 obtained this result by a three-neutrino oscillation analysis with the value of Δm^2_{32} fixed to 2.45×10^{-3} eV^2, using global solar neutrino data. AHARMIM 13 global solar neutrino data include SNO's all-phases-combined analysis results on the total active ^{8}B neutrino flux and energy-dependent ν_e survival probability parameters, measurements of Cl (CLEVELAND 98), Ga (ABDURASHITOV 09 which contains combined analysis with GNO (ALTMANN 05 and Ph.D. thesis of F. Kaether)), and ^{7}Be (BELLINI 11A) rates, and ^{8}B solar-neutrino recoil electron measurements of SK-I (HOSAKA 06) zenith, SK-II (CRAVENS 08) and SK-III (ABE 11) day/night spectra, and Borexino (BELLINI 10A) spectra. AHARMIM 13 also reported a result combining global solar and KamLAND data, which is $\sin^2(2\ \theta_{13}) = (9.1^{+2.9}_{-3.1}) \times 10^{-2}$.

[18] AN 13 uses six identical detectors, with three placed near the reactor cores (flux-weighted baselines of 498 and 555 m) and the remaining three at the far hall (at the flux averaged distance of 1628 m from all six reactor cores) to determine the $\overline{\nu}_e$ interaction rate ratios. Superseded by AN 14.

[19] ABE 12 determines the $\overline{\nu}_e$ interaction rate in a single detector, located 1050 m from the cores of two reactors. A rate and shape analysis is performed. The rate normalization is fixed by the results of the Bugey4 reactor experiment, thus avoiding any dependence on possible very short baseline oscillations. The value of $\Delta m^2_{31} = 2.4 \times 10^{-3}$ eV^2 is used in the analysis. Superseded by ABE 12B.

[20] ABE 12B determines the neutrino mixing angle θ_{13} using a single detector, located 1050 m from the cores of two reactors. This result is based on a spectral shape and rate analysis. The Bugey4 data (DECLAIS 94) is used to constrain the neutrino flux. Superseded by ABE 14A.

[21] AHN 12 uses two identical detectors, placed at flux weighted distances of 408.56 m and 1433.99 m from six reactor cores, to determine the mixing angle θ_{13}. This rate-only analysis excludes the no-oscillation hypothesis at 4.9 standard deviations. The value of $\Delta m^2_{31} = (2.32^{+0.12}_{-0.08}) \times 10^{-3}$ eV^2 was assumed in the analysis. Superseded by CHOI 16.

[22] AN 12 uses six identical detectors with three placed near the reactor cores (flux-weighted baselines of 470 m and 576 m) and the remaining three at the far hall (at the flux averaged distance of 1648 m from all six reactor cores) to determine the mixing angle θ_{13} using the $\overline{\nu}_e$ observed interaction rate ratios. This rate-only analysis excludes the no-oscillation hypothesis at 5.2 standard deviations. The value of $\Delta m^2_{31} = (2.32^{+0.12}_{-0.08}) \times 10^{-3}$ eV^2 was assumed in the analysis. Superseded by AN 13.

[23] ABE 11 obtained this result by a three-neutrino oscillation analysis with the value of Δm^2_{32} fixed to 2.4×10^{-3} eV^2, using solar neutrino data including Super-Kamiokande, SNO, Borexino (ARPESELLA 08A), Homestake, GALLEX/GNO, SAGE, and KamLAND data. This result implies an upper bound of $\sin^2\theta_{13} < 0.059$ (95% CL) or $\sin^2 2\theta_{13} < 0.22$ (95% CL). The normal neutrino mass ordering and CPT invariance are assumed.

[24] ABE 11 obtained this result by a three-neutrino oscillation analysis with the value of Δm^2_{32} fixed to 2.4×10^{-3} eV^2, using solar neutrino data including Super-Kamiokande, SNO, Borexino (ARPESELLA 08A), Homestake, and GALLEX/GNO data. The normal neutrino mass ordering is assumed.

[25] The quoted limit is for $\Delta m^2_{32} = 2.4 \times 10^{-3}$ eV^2, $\theta_{23} = \pi/2$, $\delta = 0$, and the normal mass ordering. For other values of δ, the 68% region spans from 0.03 to 0.25, and the 90% region from 0.02 to 0.32.

[26] The quoted limit is for $\Delta m^2_{32} = 2.4 \times 10^{-3}$ eV^2, $\theta_{23} = \pi/2$, $\delta = 0$, and the inverted mass ordering. For other values of δ, the 68% region spans from 0.04 to 0.30, and the 90% region from 0.02 to 0.39.

[27] The quoted limit is for $\Delta m^2_{32} = 2.32 \times 10^{-3}$ eV^2, $\theta_{23} = \pi/2$, $\delta = 0$, and the normal mass ordering. For other values of δ, the 68% region spans from 0.02 to 0.12, and the 90% region from 0 to 0.16.

[28] The quoted limit is for $\Delta m^2_{32} = 2.32 \times 10^{-3}$ eV^2, $\theta_{23} = \pi/2$, $\delta = 0$, and the inverted mass ordering. For other values of δ, the 68% region spans from 0.02 to 0.16, and the 90% region from 0 to 0.21.

[29] FOGLI 11 obtained this result from an analysis using the atmospheric, accelerator long baseline, CHOOZ, solar, and KamLAND data. Recently, MUELLER 11 suggested an average increase of about 3.5% in normalization of the reactor $\overline{\nu}_e$ fluxess, and using these fluxes, the fitted result becomes 0.10 ± 0.03.

[30] GANDO 11 report $\sin^2\theta_{13} = 0.020 \pm 0.016$. This result was obtained with three-neutrino fit using the KamLAND + solar data.

[31] GANDO 11 report $\sin^2\theta_{13} = 0.032 \pm 0.037$. This result was obtained with three-neutrino fit using the KamLAND data only.

[32] This result corresponds to the limit of <0.12 at 90% CL for $\Delta m^2_{32} = 2.43 \times 10^{-3}$ eV^2, $\theta_{23} = \pi/2$, and $\delta = 0$. For other values of δ, the 90% CL region spans from 0 to 0.16.

[33] This result corresponds to the limit of <0.20 at 90% CL for $\Delta m^2_{32} = 2.43 \times 10^{-3}$ eV^2, $\theta_{23} = \pi/2$, and $\delta = 0$. For other values of δ, the 90% CL region spans from 0 to 0.21.

[34] AHARMIM 10 global solar neutrino data include SNO's low-energy-threshold analysis survival probability day/night curves, SNO Phase III integral rates (AHARMIM 08), Cl (CLEVELAND 98), SAGE (ABDURASHITOV 09), Gallex/GNO (HAMPEL 99, ALTMANN 05), Borexino (ARPESELLA 08A), SK-I zenith (HOSAKA 06), and SK-II day/night spectra (CRAVENS 08).

[35] AHARMIM 10 obtained this result by a three-neutrino oscillation analysis with the value of Δm^2_{31} fixed to 2.3×10^{-3} eV^2, using global solar neutrino data and KamLAND data

(ABE 08A). *CPT* invariance is assumed. This result implies an upper bound of $\sin^2\theta_{13} < 0.057$ (95% CL) or $\sin^2 2\theta_{13} < 0.22$ (95% CL).

[36] AHARMIM 10 obtained this result by a three-neutrino oscillation analysis with the value of Δm^2_{31} fixed to 2.3×10^{-3} eV^2, using global solar neutrino data.

[37] WENDELL 10 obtained this result by a three-neutrino oscillation analysis with one mass scale dominance ($\Delta m^2_{21} = 0$) using the Super-Kamiokande-I+II+III atmospheric neutrino data, and updates the HOSAKA 06A result.

[38] The quoted limit is for $\Delta m^2_{32} = 2.43\times10^{-3}$ eV^2, $\theta_{23} = \pi/2$, and $\delta = 0$. For other values of δ, the 68% CL region spans from 0.02 to 0.26.

[39] The quoted limit is for $\Delta m^2_{32} = 2.43\times10^{-3}$ eV^2, $\theta_{23} = \pi/2$, and $\delta = 0$. For other values of δ, the 68% CL region spans from 0.04 to 0.34.

[40] FOGLI 08 obtained this result from a global analysis of all neutrino oscillation data, that is, solar + KamLAND + atmospheric + accelerator long baseline + CHOOZ.

[41] FOGLI 08 obtained this result from an analysis using the solar and KamLAND neutrino oscillation data.

[42] FOGLI 08 obtained this result from an analysis using the atmospheric, accelerator long baseline, and CHOOZ neutrino oscillation data.

[43] YAMAMOTO 06 searched for $\nu_\mu \to \nu_e$ appearance. Assumes $2\sin^2(2\theta_{\mu e}) = \sin^2(2\theta_{13})$. The quoted limit is for $\Delta m^2_{32} = 1.9\times10^{-3}$ eV^2. That value of Δm^2_{32} is the one-σ low value for AHN 06A. For the AHN 06A best fit value of 2.8×10^{-3} eV^2, the $\sin^2(2\theta_{13})$ limit is < 0.26. Supersedes AHN 04.

[44] AHN 04 searched for $\nu_\mu \to \nu_e$ appearance. Assuming $2\sin^2(2\,\theta_{\mu_e}) = \sin^2(2\,\theta_{13})$, a limit on $\sin^2(2\,\theta_{\mu_e})$ is converted to a limit on $\sin^2(2\,\theta_{13})$.The quoted limit is for $\Delta m^2_{32} = 1.9\times10^{-3}$ eV^2. That value of Δm^2_{32} is the one-σ low value for ALIU 05. For the ALIU 05 best fit value of 2.8×10^{-3} eV^2, the $\sin^2(2\,\theta_{13})$ limit is < 0.30.

[45] The quoted limit is for $\Delta m^2_{32} = 1.9\times10^{-3}$ eV^2. That value of Δm^2_{32} is the 1-σ low value for ALIU 05. For the ALIU 05 best fit value of 2.8×10^{-3} eV^2, the $\sin^2 2\,\theta_{13}$ limit is < 0.19. In this range, the θ_{13} limit is larger for lower values of Δm^2_{32}, and smaller for higher values of Δm^2_{32}.

[46] The quoted limit is for $\Delta m^2_{32} = 1.9\times10^{-3}$ eV^2. That value of Δm^2_{32} is the 1-σ low value for ALIU 05. For the ALIU 05 best fit value of 2.8×10^{-3} eV^2, the $\sin^2 2\,\theta_{13}$ limit is < 0.23.

[47] The quoted limit is for $\Delta m^2_{32} = 2.43\times10^{-3}$ eV^2. That value of Δm^2_{32} is the central value for ADAMSON 08. For the ADAMSON 08 1-σ low value of 2.30×10^{-3} eV^2, the $\sin^2 2\,\theta_{13}$ limit is < 0.16. See also APOLLONIO 03 for a detailed description of the experiment.

CP violating phase

δ, *CP* violating phase

Measurements of δ come from atmospheric and accelarator experiments looking at ν_e appearance. We encode values between 0 and 2π, though it is equivalent to use $-\pi$ to π.

VALUE (π rad)	CL%	DOCUMENT ID		TECN	COMMENT
• • • We do not use the following data for averages, fits, limits, etc. • • •					
$1.45^{+0.27}_{-0.26}$		ABE	17F	T2K	Normal mass ordering
$1.54^{+0.22}_{-0.23}$		ABE	17F	T2K	Inverted mass ordering
$1.50^{+0.53}_{-0.57}$		[1] ADAMSON	17B	NOVA	Inverted mass ordering for angle second quadrant
$0.74^{+0.57}_{-0.93}$		[1] ADAMSON	17B	NOVA	Normal mass ordering for angle second quadrant
$1.48^{+0.69}_{-0.58}$		[1] ADAMSON	17B	NOVA	Normal mass ordering for angle first quadrant
0.0 to 0.1, 0.5 to 2.0	90	[1,2] ADAMSON	16	NOVA	Inverted mass ordering
0.0 to 2.0	90	[2] ADAMSON	16	NOVA	Normal mass ordering
0 to 0.15, 0.83 to 2	90	ABE	15D	T2K	Normal mass ordering
1.09 to 1.92	90	ABE	15D	T2K	Inverted mass ordering
0.05 to 1.2	90	[3] ADAMSON	14	MINS	Normal mass ordering
$1.34^{+0.64}_{-0.38}$		FORERO	14	FIT	Normal mass ordering
$1.48^{+0.34}_{-0.32}$		FORERO	14	FIT	Inverted mass ordering
$1.70^{+0.22}_{-0.39}$		[4] GONZALEZ...	14	FIT	Normal mass ordering; global fit
$1.41^{+0.35}_{-0.34}$		[4] GONZALEZ...	14	FIT	Inverted mass ordering; global fit
0 to 1.5 or 1.9 to 2	90	[5] ADAMSON	13A	MINS	Normal mass ordering

[1] Errors are projections of 68% C.L. curve of δ_{CP} vs. $\sin^2\theta_{23}$.

[2] ADAMSON 16 result is based on a data sample with 2.74×10^{20} protons on target. The likelihood-based analysis observed 6 ν_e events with an expected background of 0.99 ± 0.11 events.

[3] ADAMSON 14 result is based on three-flavor formalism and $\theta_{23} > \pi/4$. Likelihood as a function of δ is also shown for the other three combinations of hierarchy and θ_{23} quadrant; all values of δ are allowed at 90% C.L.

[4] GONZALEZ-GARCIA 14 result comes from a frequentist global fit. The corresponding Bayesian global fit to the same data results are reported in BERGSTROM 15 as 68% CL intervals of 1.24–1.94 for normal and 1.15–1.77 for inverted mass ordering.

[5] ADAMSON 13A result is based on ν_e appearance in MINOS and the calculated $\sin^2(2\theta_{23}) = 0.957$,$\theta_{23} > \pi/4$, and normal mass hierarchy. Likelihood as a function ofδ is also shown for the other three combinations of hierarchy and θ_{23}quadrant; all values of δ are allowed at 90% C.L.

(C) Other neutrino mixing results

The LSND collaboration reported in AGUILAR 01 a signal which is consistent with $\overline{\nu}_\mu \to \overline{\nu}_e$ oscillations. In a three neutrino framework, this would be a measurement of θ_{12} and Δm^2_{21}. This does not appear to be consistent with most of the other neutrino data. The MiniBooNE experiment, reported in AGUILAR-AREVALO 07, does a two-neutrino analysis which, assuming *CP* conservation, rules out AGUILAR 01. However, the MiniBooNE antineutrino data reported in AGUILAR-AREVALO 13A are consistent with the signal reported in AGUILAR 01. The following listings include results which might be relevant towards understanding these observations. They include searches for $\nu_\mu \to \nu_e$, $\overline{\nu}_\mu \to \overline{\nu}_e$, sterile neutrino oscillations, and *CPT* violation.

$\Delta(m^2)$ for $\sin^2(2\theta) = 1$ ($\nu_\mu \to \nu_e$)

VALUE (eV^2)	CL%	DOCUMENT ID		TECN	COMMENT
• • • We do not use the following data for averages, fits, limits, etc. • • •					
0.015 to 0.050	90	[1] AGUILAR-AR...	13A	MBNE	MiniBooNE
<0.34	90	[2] MAHN	12	MBNE	MiniBooNE/SciBooNE
<0.034	90	AGUILAR-AR...	07	MBNE	MiniBooNE
<0.0008	90	AHN	04	K2K	Water Cherenkov
<0.4	90	ASTIER	03	NOMD	CERN SPS
<2.4	90	AVVAKUMOV	02	NTEV	NUTEV FNAL
		[3] AGUILAR	01	LSND	$\nu\mu \to \nu_e$ osc.prob.
0.03 to 0.3	95	[4] ATHANASSO...	98	LSND	$\nu_\mu \to \nu_e$
<2.3	90	[5] LOVERRE	96		CHARM/CDHS
<0.9	90	VILAIN	94C	CHM2	CERN SPS
<0.09	90	ANGELINI	86	HLBC	BEBC CERN PS

[1] Based on $\nu_\mu \to \nu_e$ appearance of 162.0 ± 47.8 events; marginally compatible with two neutrino oscillations. The best fit value is $\Delta m^2 = 3.14$ eV^2.

[2] MAHN 12 is a combined spectral fit of MiniBooNE and SciBooNE neutrino data with the range of Δm^2 up to 25 eV^2. The best limit is 0.04 at 7 eV^2.

[3] AGUILAR 01 is the final analysis of the LSND full data set. Search is made for the $\nu_\mu \to \nu_e$ oscillations using ν_μ from π^+ decay in flight by observing beam-on electron events from $\nu_e C \to e^- X$. Present analysis results in $8.1\pm12.2\pm1.7$ excess events in the $60<E_e<200$ MeV energy range, corresponding to oscillation probability of $0.10\pm0.16\pm0.04$%. This is consistent, though less significant, with the previous result of ATHANASSOPOULOS 98, which it supersedes. The present analysis uses selection criteria developed for the decay at rest region, and is less effective in removing the background above 60 MeV than ATHANASSOPOULOS 98.

[4] ATHANASSOPOULOS 98 is a search for the $\nu_\mu \to \nu_e$ oscillations using ν_μ from π^+ decay in flight. The 40 observed beam-on electron events are consistent with $\nu_e C \to e^- X$; the expected background is 21.9 ± 2.1. Authors interpret this excess as evidence for an oscillation signal corresponding to oscillations with probability $(0.26\pm0.10\pm0.05)$%. Although the significance is only $2.3\,\sigma$, this measurement is an important and consistent cross check of ATHANASSOPOULOS 96 who reported evidence for $\overline{\nu}_\mu \to \overline{\nu}_e$ oscillations from μ^+ decay at rest. See also ATHANASSOPOULOS 98B.

[5] LOVERRE 96 uses the charged-current to neutral-current ratio from the combined CHARM (ALLABY 86) and CDHS (ABRAMOWICZ 86) data from 1986.

$\sin^2(2\theta)$ for "Large" $\Delta(m^2)$ ($\nu_\mu \to \nu_e$)

VALUE (units 10^{-3})	CL%	DOCUMENT ID		TECN	COMMENT
• • • We do not use the following data for averages, fits, limits, etc. • • •					
< 7.2	90	AGAFONOVA	13	OPER	$\Delta(m^2) > 0.1$ eV^2
0.8 to 3	90	[1] AGUILAR-AR...	13A	MBNE	MiniBooNE
< 11	90	[2] ANTONELLO	13	ICAR	$\nu_\mu \to \nu_e$
< 6.8	90	[3] ANTONELLO	13A	ICAR	$\nu_\mu \to \nu_e$
<100	90	[4] MAHN	12	MBNE	MiniBooNE/SciBooNE
< 1.8	90	[5] AGUILAR-AR...	07	MBNE	MiniBooNE
<110	90	[6] AHN	04	K2K	Water Cherenkov
< 1.4	90	ASTIER	03	NOMD	CERN SPS
< 1.6	90	AVVAKUMOV	02	NTEV	NUTEV FNAL
		[7] AGUILAR	01	LSND	$\nu_\mu \to \nu_e$ osc.prob.
0.5 to 30	95	[8] ATHANASSO...	98	LSND	$\nu_\mu \to \nu_e$
< 3.0	90	[9] LOVERRE	96		CHARM/CDHS
< 9.4	90	VILAIN	94C	CHM2	CERN SPS
< 5.6	90	[10] VILAIN	94C	CHM2	CERN SPS

[1] Based on $\nu_\mu \to \nu_e$ appearance of 162.0 ± 47.8 events; marginally compatible with two neutrino oscillations. The best fit value is $\sin^2 2\theta = 0.002$.

[2] ANTONELLO 13 use the ICARUS T600 detector at LNGS and ~ 20 GeV beam of ν_μ from CERN 730 km away to search for an excess of ν_e events. Two events are found with 3.7 ± 0.6 expected from conventional sources. This result excludes some parts of the parameter space expected by LSND. Superseded by ANTONELLO 13A.

[3] Based on four events with a background of 6.4 ± 0.9 from conventional sources with an average energy of 20 GeV and 730 km from the source of ν_μ.

[4] MAHN 12 is a combined fit of MiniBooNE and SciBooNE neutrino data.

[5] The limit is $\sin^2 2\theta < 0.9\times10^{-3}$ at $\Delta m^2 = 2$ eV^2. That value of Δm^2 corresponds to the smallest mixing angle consistent with the reported signal from LSND in AGUILAR 01.

[6] The limit becomes $\sin^2 2\theta < 0.15$ at $\Delta m^2 = 2.8\times10^{-3}$ eV^2, the bets-fit value of the ν_μ disappearance analysis in K2K.

[7] AGUILAR 01 is the final analysis of the LSND full data set of the search for the $\nu_\mu \to \nu_e$ oscillations. See footnote in preceding table for further details.

[8] ATHANASSOPOULOS 98 report $(0.26\pm0.10\pm0.05)$% for the oscillation probability; the value of $\sin^2 2\theta$ for large Δm^2 is deduced from this probability. See footnote in preceding table for further details, and see the paper for a plot showing allowed regions.

If effect is due to oscillation, it is most likely to be intermediate $\sin^2 2\theta$ and Δm^2. See also ATHANASSOPOULOS 98B.

[9] LOVERRE 96 uses the charged-current to neutral-current ratio from the combined CHARM (ALLABY 86) and CDHS (ABRAMOWICZ 86) data from 1986.

[10] VILAIN 94C limit derived by combining the ν_μ and $\overline{\nu}_\mu$ data assuming *CP* conservation.

$\Delta(m^2)$ for $\sin^2(2\theta) = 1$ $(\overline{\nu}_\mu \to \overline{\nu}_e)$

VALUE (eV^2)	CL%	DOCUMENT ID		TECN	COMMENT
• • • We do not use the following data for averages, fits, limits, etc. • • •					
0.023 to 0.060	90	[1] AGUILAR-AR...	13A	MBNE	MiniBooNE
<0.16	90	[2] CHENG	12	MBNE	MiniBooNE/SciBooNE
0.03–0.09	90	[3] AGUILAR-AR...	10	MBNE	$E_\nu > 475$ MeV
0.03–0.07	90	[4] AGUILAR-AR...	10	MBNE	$E_\nu > 200$ MeV
<0.06	90	AGUILAR-AR...	09B	MBNE	MiniBooNE
<0.055	90	[5] ARMBRUSTER	02	KAR2	Liquid Sci. calor.
<2.6	90	AVVAKUMOV	02	NTEV	NUTEV FNAL
0.03–0.05		[6] AGUILAR	01	LSND	LAMPF
0.05–0.08	90	[7] ATHANASSO...	96	LSND	LAMPF
0.048–0.090	80	[8] ATHANASSO...	95		
<0.07	90	[9] HILL	95		
<0.9	90	VILAIN	94C	CHM2	CERN SPS
<0.14	90	[10] FREEDMAN	93	CNTR	LAMPF

[1] Based on $\overline{\nu}_\mu \to \overline{\nu}_e$ appearance of 78.4 ± 28.5 events. The best fit values are $\Delta m^2 = 0.043$ eV^2 and $\sin^2 2\theta = 0.88$.

[2] CHENG 12 is a combined fit of MiniBooNE and SciBooNE antineutrino data.

[3] This value is for a two neutrino oscillation analysis for excess antineutrino events with $E_\nu > 475$ MeV. The best fit is at 0.07. The allowed region is consistent with LSND reported by AGUILAR 01. Supercedes AGUILAR-AREVALO 09B.

[4] This value is for a two neutrino oscillation analysis for excess antineutrino events with $E_\nu > 200$ MeV with subtraction of the expected 12 events low energy excess seen in the neutrino component of the beam. The best fit value is 0.007 for $\Delta(m^2) = 4.4$ eV^2.

[5] ARMBRUSTER 02 is the final analysis of the KARMEN 2 data for 17.7 m distance from the ISIS stopped pion and muon neutrino source. It is a search for $\overline{\nu}_e$, detected by the inverse β-decay reaction on protons and ^{12}C. 15 candidate events are observed, and 15.8 ± 0.5 background events are expected, hence no oscillation signal is detected. The results exclude large regions of the parameter area favored by the LSND experiment.

[6] AGUILAR 01 is the final analysis of the LSND full data set. It is a search for $\overline{\nu}_e$ 30 m from LAMPF beam stop. Neutrinos originate mainly for π^+ decay at rest. $\overline{\nu}_e$ are detected through $\overline{\nu}_e p \to e^+ n$ ($20 < E_{e^+} < 60$ MeV) in delayed coincidence with $np \to d\gamma$. Authors observe 87.9 ± 22.4 ± 6.0 total excess events. The observation is attributed to $\overline{\nu}_\mu \to \overline{\nu}_e$ oscillations with the oscillation probability of 0.264 ± 0.067 ± 0.045%, consistent with the previously published result. Taking into account all constraints, the most favored allowed region of oscillation parameters is a band of $\Delta(m^2)$ from 0.2–2.0 eV^2. Supersedes ATHANASSOPOULOS 95, ATHANASSOPOULOS 96, and ATHANASSOPOULOS 98.

[7] ATHANASSOPOULOS 96 is a search for $\overline{\nu}_e$ 30 m from LAMPF beam stop. Neutrinos originate mainly from π^+ decay at rest. $\overline{\nu}_e$ could come from either $\overline{\nu}_\mu \to \overline{\nu}_e$ or $\nu_e \to \overline{\nu}_e$; our entry assumes the first interpretation. They are detected through $\overline{\nu}_e p \to e^+ n$ (20 MeV $< E_{e^+} <$ 60 MeV) in delayed coincidence with $np \to d\gamma$. Authors observe 51 ± 20 ± 8 total excess events over an estimated background 12.5 ± 2.9. ATHANASSOPOULOS 96B is a shorter version of this paper.

[8] ATHANASSOPOULOS 95 error corresponds to the 1.6σ band in the plot. The expected background is 2.7 ± 0.4 events. Corresponds to an oscillation probability of $(0.34^{+0.20}_{-0.18} \pm 0.07)$%. For a different interpretation, see HILL 95. Replaced by ATHANASSOPOULOS 96.

[9] HILL 95 is a report by one member of the LSND Collaboration, reporting a different conclusion from the analysis of the data of this experiment (see ATHANASSOPOULOS 95). Contrary to the rest of the LSND Collaboration, Hill finds no evidence for the neutrino oscillation $\overline{\nu}_\mu \to \overline{\nu}_e$ and obtains only upper limits.

[10] FREEDMAN 93 is a search at LAMPF for $\overline{\nu}_e$ generated from any of the three neutrino types ν_μ, $\overline{\nu}_\mu$, and ν_e which come from the beam stop. The $\overline{\nu}_e$'s would be detected by the reaction $\overline{\nu}_e p \to e^+ n$. FREEDMAN 93 replaces DURKIN 88.

$\sin^2(2\theta)$ for "Large" $\Delta(m^2)$ $(\overline{\nu}_\mu \to \overline{\nu}_e)$

VALUE (units 10^{-3})	CL%	DOCUMENT ID		TECN	COMMENT
• • • We do not use the following data for averages, fits, limits, etc. • • •					
<640	90	[1] ANTONELLO	13A	ICAR	$\overline{\nu}_e$ appearance
<150	90	[2] CHENG	12	MBNE	MiniBooNE/SciBooNE
0.4–9.0	99	[3] AGUILAR-AR...	10	MBNE	$E_\nu > 475$ MeV
0.4–9.0	99	[4] AGUILAR-AR...	10	MBNE	$E_\nu > 200$ MeV
< 3.3	90	[5] AGUILAR-AR...	09B	MBNE	MiniBooNE
< 1.7	90	[6] ARMBRUSTER	02	KAR2	Liquid Sci. calor.
< 1.1	90	AVVAKUMOV	02	NTEV	NUTEV FNAL
5.3±1.3±9.0		[7] AGUILAR	01	LSND	LAMPF
6.2±2.4±1.0		[8] ATHANASSO...	96	LSND	LAMPF
3–12	80	[9] ATHANASSO...	95		
< 6	90	[10] HILL	95		

[1] ANTONELLO 13A obtained the limit by assuming $\overline{\nu}_\mu \to \overline{\nu}_e$ oscillation from the ∼ 2% of $\overline{\nu}_\mu$ evnets contamination in the CNGS beam.

[2] CHENG 12 is a combined fit of MiniBooNE and SciBooNE antineutrino data.

[3] This value is for a two neutrino oscillation analysis for excess antineutrino events with $E_\nu > 475$ MeV. At 90% CL there is no solution at high $\Delta(m^2)$. The best fit is at maximal mixing. The allowed region is consistent with LSND reported by AGUILAR 01. Supercedes AGUILAR-AREVALO 09B.

[4] This value is for a two neutrino oscillation analysis for excess antineutrino events with $E_\nu > 200$ MeV with subtraction of the expected 12 events low energy excess seen in the neutrino component of the beam. At 90% CL there is no solution at high $\Delta(m^2)$. The best fit value is 0.007 for $\Delta(m^2) = 4.4$ eV^2.

[5] This result is inconclusive with respect to small amplitude mixing suggested by LSND.

[6] ARMBRUSTER 02 is the final analysis of the KARMEN 2 data. See footnote in the preceding table for further details, and the paper for the exclusion plot.

[7] AGUILAR 01 is the final analysis of the LSND full data set. The deduced oscillation probability is 0.264 ± 0.067 ± 0.045%; the value of $\sin^2 2\theta$ for large $\Delta(m^2)$ is twice this probability (although these values are excluded by other constraints). See footnote in preceding table for further details, and the paper for a plot showing allowed regions. Supersedes ATHANASSOPOULOS 95, ATHANASSOPOULOS 96, and ATHANASSOPOULOS 98.

[8] ATHANASSOPOULOS 96 reports (0.31 ± 0.12 ± 0.05)% for the oscillation probability; the value of $\sin^2 2\theta$ for large $\Delta(m^2)$ should be twice this probability. See footnote in preceding table for further details, and see the paper for a plot showing allowed regions.

[9] ATHANASSOPOULOS 95 error corresponds to the 1.6σ band in the plot. The expected background is 2.7 ± 0.4 events. Corresponds to an oscillation probability of $(0.34^{+0.20}_{-0.18} \pm 0.07)$%. For a different interpretation, see HILL 95. Replaced by ATHANASSOPOULOS 96.

[10] HILL 95 is a report by one member of the LSND Collaboration, reporting a different conclusion from the analysis of the data of this experiment (see ATHANASSOPOULOS 95). Contrary to the rest of the LSND Collaboration, Hill finds no evidence for the neutrino oscillation $\overline{\nu}_\mu \to \overline{\nu}_e$ and obtains only upper limits.

$\Delta(m^2)$ for $\sin^2(2\theta) = 1$ $(\nu_\mu(\overline{\nu}_\mu) \to \nu_e(\overline{\nu}_e))$

VALUE (eV^2)	CL%	DOCUMENT ID		TECN	COMMENT
<0.075	90	BORODOV...	92	CNTR	BNL E776
• • • We do not use the following data for averages, fits, limits, etc. • • •					
<1.6	90	[1] ROMOSAN	97	CCFR	FNAL

[1] ROMOSAN 97 uses wideband beam with a 0.5 km decay region.

$\sin^2(2\theta)$ for "Large" $\Delta(m^2)$ $(\nu_\mu(\overline{\nu}_\mu) \to \nu_e(\overline{\nu}_e))$

VALUE (units 10^{-3})	CL%	DOCUMENT ID		TECN	COMMENT
<1.8	90	[1] ROMOSAN	97	CCFR	FNAL
• • • We do not use the following data for averages, fits, limits, etc. • • •					
<3.8	90	[2] MCFARLAND	95	CCFR	FNAL
<3	90	BORODOV...	92	CNTR	BNL E776

[1] ROMOSAN 97 uses wideband beam with a 0.5 km decay region.

[2] MCFARLAND 95 state that "This result is the most stringent to date for $250 < \Delta(m^2) < 450$ eV^2 and also excludes at 90%CL much of the high $\Delta(m^2)$ region favored by the recent LSND observation." See ATHANASSOPOULOS 95 and ATHANASSOPOULOS 96.

$\Delta(m^2)$ for $\sin^2(2\theta) = 1$ $(\overline{\nu}_e \not\to \overline{\nu}_e)$

VALUE (eV^2)	CL%	DOCUMENT ID		TECN	COMMENT
• • • We do not use the following data for averages, fits, limits, etc. • • •					
<0.01	90	[1] ACHKAR	95	CNTR	Bugey reactor

[1] ACHKAR 95 bound is for L=15, 40, and 95 m.

$\sin^2(2\theta)$ for "Large" $\Delta(m^2)$ $(\overline{\nu}_e \not\to \overline{\nu}_e)$

VALUE	CL%	DOCUMENT ID		TECN	COMMENT
• • • We do not use the following data for averages, fits, limits, etc. • • •					
<0.02	90	[1] ACHKAR	95	CNTR	For $\Delta(m^2) = 0.6$ eV^2

[1] ACHKAR 95 bound is from data for L=15, 40, and 95 m distance from the Bugey reactor.

Sterile neutrino limits

$\Delta(m^2)$ for $\sin^2(2\theta) = 1$ $(\nu_\mu \to \nu_s)$

ν_s means ν_τ or any sterile (noninteracting) ν.

VALUE (10^{-5} eV^2)	CL%	DOCUMENT ID		TECN	COMMENT
• • • We do not use the following data for averages, fits, limits, etc. • • •					
<3000 (or <550)	90	[1] OYAMA	89	KAMI	Water Cherenkov
< 4.2 or > 54.	90	BIONTA	88	IMB	Flux has ν_μ, $\overline{\nu}_\mu$, ν_e, and $\overline{\nu}_e$

[1] OYAMA 89 gives a range of limits, depending on assumptions in their analysis. They argue that the region $\Delta(m^2) = (100–1000) \times 10^{-5}$ eV^2 is not ruled out by any data for large mixing.

Search for ν_μ or $\nu_e \to \nu_s$

VALUE	CL%	DOCUMENT ID		TECN	COMMENT
• • • We do not use the following data for averages, fits, limits, etc. • • •					
<0.4	90	[1] AARTSEN	17B	ICCB	IceCube-DeepCore
$<8 \times 10^{-3}$	95	[2] ABDURASHI...	17		T β decay
$<1 \times 10^{-2}$	90	[3] KO	17	NEOS	
$<2 \times 10^{-2}$	90	[4] AARTSEN	16	ICCB	IceCube
$<4.5 \times 10^{-4}$	95	[5] ADAMSON	16B		MINOS, DayaBay
$<8.6 \times 10^{-2}$	95	[6] ADAMSON	16C	MINS	
$<1.1 \times 10^{-2}$	95	[7] AN	16B	DAYA	
		[8] AMBROSIO	01	MCRO	matter effects
		[9] FUKUDA	00	SKAM	neutral currents + matter effects

[1] AARTSEN 17B uses three years of upward-going atmospheric neutrino data in the energy range of 10-60 GeV to constrain their disappearance into light sterile neutrinos. The reported limit $\sin^2\theta_{24} < 0.11$ at 90% C.L. is for $\Delta m^2_{41} = 1.0$ eV^2. We convert the result to $\sin^2 2\theta_{24}$ for the listing. AARTSEN 17B also reports $\cos^2\theta_{24} \cdot \sin^2\theta_{34} < 0.15$ at 90% C.L. for $\Delta m^2_{41} = 1.0$ eV^2.

[2] ABDURASHITOV 17 use the Troitsk nu-mass experiment to search for sterile neutrinos with mass 0.1 - 2 keV. We convert the reported limit from U_{e4}^2 <0.002 to $\sin^2 2\theta_{14}$ <0.008 assume $U_{e4} \sim \sin\theta_{14}$. The stated limit corresponds to the smallest U_{e4}^2. The exclusion curve begins at U_{e4}^2 of 0.02 for $m_4 = 0.1$ keV.

[3] KO 17 reports on short baseline reactor oscillation search ($\overline{\nu}_e \rightarrow \overline{\nu}_s$), motivated be the so-called "reactor antineutrino anomaly". The experiment is conducted at 23.7 m from the core of unit 5 of the Hanbit Nuclear Power Complex in Korea. the reported limited on $\sin^2(2\theta_{41})$ for sterile neutrinos was determined using the reactor antineutrino spectrum determined by the Daya Bay experiment for Δm_{14}^2 around 0.55 eV^2 where the sensitivity is maximal. A fraction of the parameter space derived from the "reactor antineutrino anomaly" is excluded by this work. Compared to reactor models an event excess is observed at about 5 MeV, in agreement with other experiments.

[4] AARTSEN 16 use one year of upward-going atmospheric muon neutrino data in the energy range of 320 GeV to 20 TeV to constrain their disappearance into light sterile neutrinos. Sterile neutrinos are expected to produce distinctive zenith distribution for these energies for $0.01 \leq \Delta m^2 \leq 10$ eV^2. The stated limit is for $\sin^2 2\theta_{24}$ at Δm^2 around 0.3 eV^2.

[5] ADAMSON 16B combine the results of AN 16B, ADAMSON 16C, and Bugey-3 reactor experiments to constrain ν_μ to ν_e mixing through oscillations into light sterile neutrinos. The stated limit for $\sin^2 2\theta_{\mu e}$ is at $|\Delta m_{41}^2| = 1.2$ eV^2.

[6] ADAMSON 16C use the NuMI beam and exposure of 10.56×10^{20} protons on target to search for the oscillation of ν_μ dominated beam into light sterile neutrinos with detectors at 1.04 and 735 km. The reported limit $\sin^2(\theta_{24}) < 0.022$ at 95% C.L. is for $|\Delta m_{41}^2| = 0.5$ eV^2. We convert the result to $\sin^2(2\theta_{24})$ for the listing.

[7] AN 16B utilize 621 days of data to place limits on the $\overline{\nu}_e$ disappearance into a light sterile neutrino. The stated limit corresponds to the smallest $\sin^2(2\theta_{14})$ at $|\Delta m_{41}^2| \sim 3 \times 10^{-2}$ eV^2 (obtained from Figure 3 in AN 16B). The exclusion curve begins at $|\Delta m_{41}^2| \sim 1.5 \times 10^{-4}$ eV^2 and extends to ~ 0.25 eV^2. The analysis assumes $\sin^2(2\theta_{12}) = 0.846 \pm 0.021$, $\Delta m_{21}^2 = (7.53 \pm 0.18) \times 10^{-5}$ eV^2, and $|\Delta m_{32}^2| = (2.44 \pm 0.06) \times 10^{-3}$ eV^2.

[8] AMBROSIO 01 tested the pure 2-flavor $\nu_\mu \rightarrow \nu_s$ hypothesis using matter effects which change the shape of the zenith-angle distribution of upward through-going muons. With maximum mixing and Δm^2 around 0.0024 eV^2, the $\nu_\mu \rightarrow \nu_s$ oscillation isdisfavored with 99% confidence level with respect to the $\nu_\mu \rightarrow \nu_\tau$ hypothesis.

[9] FUKUDA 00 tested the pure 2-flavor $\nu_\mu \rightarrow \nu_s$ hypothesis using three complementary atmospheric-neutrino data samples. With this hypothesis, zenith-angle distributions are expected to show characteristic behavior due to neutral currents and matter effects. In the Δm^2 and $\sin^2 2\theta$ region preferred by the Super-Kamiokande data, the $\nu_\mu \rightarrow \nu_s$ hypothesis isrejected at the 99% confidence level, while the $\nu_\mu \rightarrow \nu_\tau$ hypothesis consistently fits all of the data sample.

CPT tests

$\langle \Delta m_{21}^2 - \Delta \overline{m}_{21}^2 \rangle$

VALUE (10^{-4} eV^2)	CL%	DOCUMENT ID		TECN	COMMENT
• • • We do not use the following data for averages, fits, limits, etc. • • •					
<1.1	99.7	[1] DEGOUVEA	05	FIT	solar vs. reactor

[1] DEGOUVEA 05 obtained this bound at the 3σ CL from the KamLAND (ARAKI 05) and solar neutrino data.

$\langle \Delta m_{32}^2 - \Delta \overline{m}_{32}^2 \rangle$

VALUE (10^{-3} eV^2)	CL%	DOCUMENT ID		TECN	COMMENT
• • • We do not use the following data for averages, fits, limits, etc. • • •					
$0.6^{+2.4}_{-0.8}$	90	[1] ADAMSON	12B	MINS	MINOS atmospheric

[1] The quoted result is the single-parameter 90% C.L. interval determined from the 90% C.L. contour in the (Δm^2, $\Delta \overline{m}^2$) plane, which is obtained by minimizing the four parameter log-likelihood function with respect to the other oscillation parameters.

REFERENCES FOR Neutrino Mixing

AARTSEN	17B	PR D95 112002	M.G. Aartsen *et al.*	(IceCube Collab.)
ABDURASHI...	17	JETPL 105 753	J.N. Abdurashitov *et al.*	(Troitsk nu-mass Collab.)
ABE	17A	PRL 118 151801	K. Abe *et al.*	(T2K Collab.)
ABE	17C	PR D96 011102	K. Abe *et al.*	(T2K Collab.)
ABE	17F	PR D96 092006	K. Abe *et al.*	(T2K Collab.)
ADAMSON	17A	PRL 118 151802	P. Adamson *et al.*	(NOvA Collab.)
ADAMSON	17B	PRL 118 231801	P. Adamson *et al.*	(NOvA Collab.)
AN	17A	PR D95 072006	F.P. An *et al.*	(Daya Bay Collab.)
KO	17	PRL 118 121802	Y.J. Ko *et al.*	(NEOS Collab.)
AARTSEN	16	PRL 117 071801	M.G. Aartsen *et al.*	(IceCube Collab.)
ABE	16B	JHEP 1601 163	Y. Abe *et al.*	(Double Chooz Collab.)
ABE	16C	PR D94 052010	K. Abe *et al.*	(Super-Kamiokande Collab.)
ABE	16D	PRL 116 181801	K. Abe *et al.*	(T2K Collab.)
ADAMSON	16	PRL 116 151806	P. Adamson *et al.*	(NOvA Collab.)
ADAMSON	16A	PR D93 051104	P. Adamson *et al.*	(NOvA Collab.)
ADAMSON	16B	PRL 117 151801	P. Adamson *et al.*	(Daya Bay and MINOS Collab.)
ADAMSON	16C	PRL 117 151803	P. Adamson *et al.*	(MINOS Collab.)
AN	16	PRL 116 061801	F.P. An *et al.*	(Daya Bay Collab.)
AN	16A	PR D93 072011	F.P. An *et al.*	(Daya Bay Collab.)
AN	16B	PRL 117 151802	F.P. An *et al.*	(Daya Bay Collab.)
CHOI	16	PRL 116 211801	J.H. Choi *et al.*	(RENO Collab.)
AARTSEN	15A	PR D91 072004	M.G. Aartsen	(IceCube Collab.)
ABE	15D	PR D91 072010	K. Abe *et al.*	(T2K Collab.)
AGAFONOVA	15A	PRL 115 121802	N. Agafonova *et al.*	(OPERA Collab.)
AN	15	PRL 115 111802	F.P. An *et al.*	(Daya Bay Collab.)
BERGSTROM	15	JHEP 1509 200	J. Bergstrom *et al.*	(BARC, STON, MADU+)
GANDO	15	PR C92 055808	A. Gando *et al.*	(KamLAND Collab.)
ABE	14	PRL 112 181801	K. Abe *et al.*	(T2K Collab.)
Also		PR D91 072010	K. Abe *et al.*	(T2K Collab.)
ABE	14A	PL B735 51	Y. Abe *et al.*	(Double Chooz Collab.)
ABE	14B	PR D89 092003	K. Abe *et al.*	(T2K Collab.)
ABE	14C	PRL 112 061802	K. Abe *et al.*	(T2K Collab.)
ABE	14H	JHEP 1410 086	Y. Abe *et al.*	(Double Chooz Collab.)
Also		JHEP 1502 074 (errat.)	Y. Abe *et al.*	(Double Chooz Collab.)
ADAMSON	14	PRL 112 191801	P. Adamson *et al.*	(MINOS Collab.)
AN	14	PRL 112 061801	F.P. An *et al.*	(Daya Bay Collab.)
AN	14B	PR D90 071101	F.P. An *et al.*	(Daya Bay Collab.)
BELLINI	14A	NAT 512 383	G. Bellini *et al.*	(Borexino Collab.)
FORERO	14	PR D90 093006	D.V. Forero, M. Tortola, J.W.F. Valle	
GONZALEZ...	14	JHEP 1411 052	M.C. Gonzalez-Garcia, M. Maltoni, T. Schwetz	
PDG	14	CP C38 070001	K. Olive *et al.*	(PDG Collab.)
RENSHAW	14	PRL 112 091805	A. Renshaw *et al.*	(Super-Kamiokande Collab.)
AARTSEN	13B	PRL 111 081801	M.G. Aartsen *et al.*	(IceCube Collab.)
ABE	13C	PL B723 66	Y. Abe *et al.*	(Double Chooz Collab.)
ABE	13E	PR D88 032002	K. Abe *et al.*	(T2K Collab.)
ABE	13G	PRL 111 211803	K. Abe *et al.*	(T2K Collab.)
ADAMSON	13A	PRL 110 171801	P. Adamson *et al.*	(MINOS Collab.)
ADAMSON	13B	PRL 110 251801	P. Adamson *et al.*	(MINOS Collab.)
AGAFONOVA	13	JHEP 1307 004	N. Agafonova *et al.*	(OPERA Collab.)
AGUILAR-AR...	13A	PRL 110 161801	A.A. Aguilar-Arevalo *et al.*	(MiniBooNE Collab.)
AHARMIM	13	PR C88 025501	B. Aharmim *et al.*	(SNO Collab.)
AN	13	CP C37 011001	F.P. An *et al.*	(Daya Bay Collab.)
ANTONELLO	13	EPJ C73 2345	M. Antonello *et al.*	(ICARUS Collab.)
ANTONELLO	13A	EPJ C73 2599	M. Antonello *et al.*	(ICARUS Collab.)
GANDO	13	PR D88 033001	A. Gando *et al.*	(KamLAND Collab.)
ABE	12	PRL 108 131801	Y. Abe *et al.*	(Double Chooz Collab.)
ABE	12A	PR D85 031103	K. Abe *et al.*	(T2K Collab.)
ABE	12B	PR D86 052008	Y. Abe *et al.*	(Double Chooz Collab.)
ADAMSON	12	PRL 108 191801	P. Adamson *et al.*	(MINOS Collab.)
ADAMSON	12B	PR D86 052007	P. Adamson *et al.*	(MINOS Collab.)
ADRIAN-MAR...	12	PL B714 224	S. Adrian-Martinez *et al.*	(ANTARES Collab.)
AHN	12	PRL 108 191802	J.K. Ahn *et al.*	(RENO Collab.)
AN	12	PRL 108 171803	F.P. An *et al.*	(Daya Bay Collab.)
BELLINI	12A	PRL 108 051302	G. Bellini *et al.*	(Borexino Collab.)
CHENG	12	PR D86 052009	G. Cheng *et al.*	(MiniBooNE/SciBooNE Collab.)
MAHN	12	PR D85 032007	K.B.M. Mahn *et al.*	(MiniBooNE/SciBooNE Collab.)
ABE	11	PR D83 052010	K. Abe *et al.*	(Super-Kamiokande Collab.)
ABE	11A	PRL 107 041801	K. Abe *et al.*	(T2K Collab.)
ABE	11B	PR C84 035804	S. Abe *et al.*	(KamLAND Collab.)
ABE	11C	PRL 107 241801	K. Abe *et al.*	(Super-Kamiokande Collab.)
ADAMSON	11	PRL 106 181801	P. Adamson *et al.*	(MINOS Collab.)
ADAMSON	11B	PRL 107 021801	P. Adamson *et al.*	(MINOS Collab.)
ADAMSON	11C	PR D84 071103	P. Adamson *et al.*	(MINOS Collab.)
ADAMSON	11D	PRL 107 181802	P. Adamson *et al.*	(MINOS Collab.)
BELLINI	11	PL B696 191	G. Bellini *et al.*	(Borexino Collab.)
BELLINI	11A	PRL 107 141302	G. Bellini *et al.*	(Borexino Collab.)
FOGLI	11	PR D84 053007	G.L. Fogli *et al.*	
GANDO	11	PR D83 052002	A. Gando *et al.*	(KamLAND Collab.)
MUELLER	11	PR C83 054615	Th.A Mueller *et al.*	
SERENELLI	11	APJ 743 24	A.M. Serenelli, W.C. Haxton, C. Pena-Garay	
ADAMSON	10A	PR D82 051102	P. Adamson *et al.*	(MINOS Collab.)
AGUILAR-AR...	10	PRL 105 181801	A.A. Aguillar-Arevalo *et al.*	(MiniBooNE Collab.)
AHARMIM	10	PR C81 055504	B. Aharmim *et al.*	(SNO Collab.)
BELLINI	10A	PR D82 033006	G. Bellini *et al.*	(Borexino Collab.)
DENIZ	10	PR D81 072001	M. Deniz *et al.*	(TEXONO Collab.)
KAETHER	10	PL B685 47	F. Kaether *et al.*	
WENDELL	10	PR D81 092004	R. Wendell *et al.*	(Super-Kamiokande Collab.)
ABDURASHI...	09	PR C80 015807	J.N. Abdurashitov *et al.*	(SAGE Collab.)
ADAMSON	09	PRL 103 261802	P. Adamson *et al.*	(MINOS Collab.)
AGUILAR-AR...	09B	PRL 103 111801	A.A. Aguilar-Arevalo *et al.*	(MiniBooNE Collab.)
ABE	08A	PRL 100 221803	S. Abe *et al.*	(KamLAND Collab.)
Also		PRL 101 119904E	S. Abe *et al.*	(KamLAND Collab.)
ADAMSON	08	PR D77 072002	P. Adamson *et al.*	(MINOS Collab.)
ADAMSON	08A	PRL 101 131802	P. Adamson *et al.*	(MINOS Collab.)
AHARMIM	08	PRL 101 111301	B. Aharmim *et al.*	(SNO Collab.)
Also		PR C87 015502	B. Aharmim *et al.*	(SNO Collab.)
ARPESELLA	08A	PRL 101 091302	C. Arpesella *et al.*	(Borexino Collab.)
CRAVENS	08	PR D78 032002	J.P. Cravens *et al.*	(Super-Kamiokande Collab.)
FOGLI	08	PRL 101 141801	G.L. Fogli	
ADAMSON	07	PR D75 092003	P. Adamson *et al.*	(MINOS Collab.)
AGUILAR-AR...	07	PRL 98 231801	A.A. Aguilar-Arevalo *et al.*	(MiniBooNE Collab.)
AHARMIM	07	PR C75 045502	B. Aharmim *et al.*	(SNO Collab.)
ADAMSON	06	PR D73 072002	P. Adamson *et al.*	(MINOS Collab.)
AHN	06A	PR D74 072003	M.H. Ahn *et al.*	(K2K Collab.)
BALATA	06	EPJ C47 21	M. Balata *et al.*	(Borexino Collab.)
HOSAKA	06	PR D73 112001	J. Hosaka *et al.*	(Super-Kamiokande Collab.)
HOSAKA	06A	PR D74 032002	J. Hosaka *et al.*	(Super-Kamiokande Collab.)
MICHAEL	06	PRL 97 191801	D. Michael *et al.*	(MINOS Collab.)
WINTER	06A	PR C73 025503	W.T. Winter *et al.*	
YAMAMOTO	06	PRL 96 181801	S. Yamamoto *et al.*	(K2K Collab.)
AHARMIM	05A	PR C72 055502	B. Aharmim *et al.*	(SNO Collab.)
ALIU	05	PRL 94 081802	E. Aliu *et al.*	(K2K Collab.)
ALLISON	05	PR D72 052005	W.W.M. Allison *et al.*	(SOUDAN-2 Collab.)
ALTMANN	05	PL B616 174	M. Altmann *et al.*	(GNO Collab.)
ARAKI	05	PRL 94 081801	T. Araki *et al.*	(KamLAND Collab.)
ASHIE	05	PR D71 112005	Y. Ashie *et al.*	(Super-Kamiokande Collab.)
DEGOUVEA	05	PR D71 093002	A. de Gouvea, C. Pena-Garay	
AHARMIM	04	PR D70 093014	B. Aharmim *et al.*	(SNO Collab.)
AHMED	04A	PRL 92 181301	S.N. Ahmed *et al.*	(SNO Collab.)
AHN	04	PRL 93 051801	M.H. Ahn *et al.*	(K2K Collab.)
AMBROSIO	04	EPJ C36 323	M. Ambrosio *et al.*	(MACRO Collab.)
ASHIE	04	PRL 93 101801	Y. Ashie *et al.*	(Super-Kamiokande Collab.)
EGUCHI	04	PRL 92 071301	K. Eguchi *et al.*	(KamLAND Collab.)
SMY	04	PR D69 011104	M.B. Smy *et al.*	(Super-Kamiokande Collab.)
AHN	03	PRL 90 041801	M.H. Ahn *et al.*	(K2K Collab.)
AMBROSIO	03	PL B566 35	M. Ambrosio *et al.*	(MACRO Collab.)
APOLLONIO	03	EPJ C27 331	M. Apollonio *et al.*	(CHOOZ Collab.)
ASTIER	03	PL B570 19	P. Astier *et al.*	(NOMAD Collab.)
EGUCHI	03	PRL 90 021802	K. Eguchi *et al.*	(KamLAND Collab.)
GANDO	03	PRL 90 171302	Y. Gando *et al.*	(Super-Kamiokande Collab.)
IANNI	03	JP G29 2107	A. Ianni	(INFN Gran Sasso)
SANCHEZ	03	PR D68 113004	M. Sanchez *et al.*	(Soudan 2 Collab.)
ABDURASHI...	02	JETP 95 181	J.N. Abdurashitov *et al.*	(SAGE Collab.)
		Translated from ZETF 122 211.		
AHMAD	02	PRL 89 011301	Q.R. Ahmad *et al.*	(SNO Collab.)
AHMAD	02B	PRL 89 011302	Q.R. Ahmad *et al.*	(SNO Collab.)
ARMBRUSTER	02	PR D65 112001	B. Armbruster *et al.*	(KARMEN 2 Collab.)
AVVAKUMOV	02	PRL 89 011804	S. Avvakumov *et al.*	(NuTeV Collab.)
FUKUDA	02	PL B539 179	S. Fukuda *et al.*	(Super-Kamiokande Collab.)
AGUILAR	01	PR D64 112007	A. Aguilar *et al.*	(LSND Collab.)
AHMAD	01	PRL 87 071301	Q.R. Ahmad *et al.*	(SNO Collab.)
AMBROSIO	01	PL B517 59	M. Ambrosio *et al.*	(MACRO Collab.)
BOEHM	01	PR D64 112001	F. Boehm *et al.*	
FUKUDA	01	PRL 86 5651	S. Fukuda *et al.*	(Super-Kamiokande Collab.)
AMBROSIO	00	PL B478 5	M. Ambrosio *et al.*	(MACRO Collab.)
BOEHM	00	PRL 84 3764	F. Boehm *et al.*	
FUKUDA	00	PRL 85 3999	S. Fukuda *et al.*	(Super-Kamiokande Collab.)
ALLISON	99	PL B449 137	W.W.M. Allison *et al.*	(Soudan 2 Collab.)
APOLLONIO	99	PL B466 415	M. Apollonio *et al.*	(CHOOZ Collab.)
Also		PL B472 434 (errat.)	M. Apollonio *et al.*	(CHOOZ Collab.)
FUKUDA	99C	PRL 82 2644	Y. Fukuda *et al.*	(Super-Kamiokande Collab.)
FUKUDA	99D	PL B467 185	Y. Fukuda *et al.*	(Super-Kamiokande Collab.)
HAMPEL	99	PL B447 127	W. Hampel *et al.*	(GALLEX Collab.)
AMBROSIO	98	PL B434 451	M. Ambrosio *et al.*	(MACRO Collab.)

APOLLONIO	98	PL B420 397	M. Apollonio *et al.*	(CHOOZ Collab.)
ATHANASSO...	98	PRL 81 1774	C. Athanassopoulos *et al.*	(LSND Collab.)
ATHANASSO...	98B	PR C58 2489	C. Athanassopoulos *et al.*	(LSND Collab.)
CLEVELAND	98	APJ 496 505	B.T. Cleveland *et al.*	(Homestake Collab.)
FELDMAN	98	PR D57 3873	G.J. Feldman, R.D. Cousins	
FUKUDA	98C	PRL 81 1562	Y. Fukuda *et al.*	(Super-Kamiokande Collab.)
HATAKEYAMA	98	PRL 81 2016	S. Hatakeyama *et al.*	(Kamiokande Collab.)
CLARK	97	PRL 79 345	R. Clark *et al.*	(IMB Collab.)
ROMOSAN	97	PRL 78 2912	A. Romosan *et al.*	(CCFR Collab.)
AGLIETTA	96	JETPL 63 791	M. Aglietta *et al.*	(LSD Collab.)
		Translated from ZETFP 63 753.		
ATHANASSO...	96	PR C54 2685	C. Athanassopoulos *et al.*	(LSND Collab.)
ATHANASSO...	96B	PRL 77 3082	C. Athanassopoulos *et al.*	(LSND Collab.)
FUKUDA	96	PRL 77 1683	Y. Fukuda *et al.*	(Kamiokande Collab.)
FUKUDA	96B	PL B388 397	Y. Fukuda *et al.*	(Kamiokande Collab.)
GREENWOOD	96	PR D53 6054	Z.D. Greenwood *et al.*	(UCI, SVR, SCUC)
HAMPEL	96	PL B388 384	W. Hampel *et al.*	(GALLEX Collab.)
LOVERRE	96	PL B370 156	P.F. Loverre	
ACHKAR	95	NP B434 503	B. Achkar *et al.*	(SING, SACLD, CPPM, CDEF+)
AHLEN	95	PL B357 481	S.P. Ahlen *et al.*	(MACRO Collab.)
ATHANASSO...	95	PRL 75 2650	C. Athanassopoulos *et al.*	(LSND Collab.)
DAUM	95	ZPHY C66 417	K. Daum *et al.*	(FREJUS Collab.)
HILL	95	PRL 75 2654	J.E. Hill	(PENN)
MCFARLAND	95	PRL 75 3993	K.S. McFarland *et al.*	(CCFR Collab.)
DECLAIS	94	PL B338 383	Y. Declais *et al.*	
FUKUDA	94	PL B335 237	Y. Fukuda *et al.*	(Kamiokande Collab.)
VILAIN	94C	ZPHY C64 539	P. Vilain *et al.*	(CHARM II Collab.)
FREEDMAN	93	PR D47 811	S.J. Freedman *et al.*	(LAMPF E645 Collab.)
BECKER-SZ...	92B	PR D46 3720	R.A. Becker-Szendy *et al.*	(IMB Collab.)
BEIER	92	PL B283 446	E.W. Beier *et al.*	(KAM2 Collab.)
Also		PTRSL A346 63	E.W. Beier, E.D. Frank	(PENN)
BORODOV...	92	PRL 68 274	L. Borodovsky *et al.*	(COLU, JHU, ILL)
HIRATA	92	PL B280 146	K.S. Hirata *et al.*	(Kamiokande II Collab.)
CASPER	91	PRL 66 2561	D. Casper *et al.*	(IMB Collab.)
HIRATA	91	PRL 66 9	K.S. Hirata *et al.*	(Kamiokande II Collab.)
KUVSHINN...	91	JETPL 54 253	A.A. Kuvshinnikov *et al.*	(KIAE)
BERGER	90B	PL B245 305	C. Berger *et al.*	(FREJUS Collab.)
HIRATA	90	PRL 65 1297	K.S. Hirata *et al.*	(Kamiokande II Collab.)
AGLIETTA	89	EPL 8 611	M. Aglietta *et al.*	(FREJUS Collab.)
DAVIS	89	ARNPS 39 467	R. Davis, A.K. Mann, L. Wolfenstein	(BNL, PENN+)
OYAMA	89	PR D39 1481	Y. Oyama *et al.*	(Kamiokande II Collab.)
BIONTA	88	PR D38 768	R.M. Bionta *et al.*	(IMB Collab.)
DURKIN	88	PRL 61 1811	L.S. Durkin *et al.*	(OSU, ANL, CIT+)
ABRAMOWICZ	86	PRL 57 298	H. Abramowicz *et al.*	(CDHS Collab.)
ALLABY	86	PL B177 446	J.V. Allaby *et al.*	(CHARM Collab.)
ANGELINI	86	PL B179 307	C. Angelini *et al.*	(PISA, ATHU, PADO+)
VUILLEUMIER	82	PL 114B 298	J.L. Vuilleumier *et al.*	(CIT, SIN, MUNI)
BOLIEV	81	SJNP 34 787	M.M. Boliev *et al.*	(INRM)
		Translated from YAF 34 1418.		
KWON	81	PR D24 1097	H. Kwon *et al.*	(CIT, ISNG, MUNI)
BOEHM	80	PL 97B 310	F. Boehm *et al.*	(ILLG, CIT, ISNG, MUNI)
CROUCH	78	PR D18 2239	M.F. Crouch *et al.*	(CASE, UCI, WITW)

Heavy Neutral Leptons, Searches for

(A) Heavy Neutral Leptons

Stable Neutral Heavy Lepton MASS LIMITS

Note that LEP results in combination with REUSSER 91 exclude a fourth stable neutrino with $m <$ 2400 GeV.

VALUE (GeV)	CL%	DOCUMENT ID		TECN	COMMENT
>45.0	95	ABREU	92B	DLPH	Dirac
>39.5	95	ABREU	92B	DLPH	Majorana
>44.1	95	ALEXANDER	91F	OPAL	Dirac
>37.2	95	ALEXANDER	91F	OPAL	Majorana
none 3–100	90	SATO	91	KAM2	Kamiokande II
>42.8	95	[1] ADEVA	90S	L3	Dirac
>34.8	95	[1] ADEVA	90S	L3	Majorana
>42.7	95	DECAMP	90F	ALEP	Dirac

[1] ADEVA 90S limits for the heavy neutrino apply if the mixing with the charged leptons satisfies $|U_{1j}|^2 + |U_{2j}|^2 + |U_{3j}|^2 > 6.2\times10^{-8}$ at $m_{L^0} = 20$ GeV and $> 5.1\times10^{-10}$ for $m_{L^0} = 40$ GeV.

Heavy Neutral Lepton MASS LIMITS

Limits apply only to heavy lepton type given in comment at right of data Listings.

See the "Quark and Lepton Compositeness, Searches for" Listings for limits on radiatively decaying excited neutral leptons, *i.e.* $\nu^* \to \nu\gamma$.

VALUE (GeV)	CL%	DOCUMENT ID		TECN	COMMENT
>101.3	95	ACHARD	01B	L3	Dirac coupling to e
>101.5	95	ACHARD	01B	L3	Dirac coupling to μ
> 90.3	95	ACHARD	01B	L3	Dirac coupling to τ
> 89.5	95	ACHARD	01B	L3	Majorana coupling to e
> 90.7	95	ACHARD	01B	L3	Majorana coupling to μ
> 80.5	95	ACHARD	01B	L3	Majorana coupling to τ
• • • We do not use the following data for averages, fits, limits, etc. • • •					
> 76.0	95	ABBIENDI	00I	OPAL	Majorana, coupling to e
> 88.0	95	ABBIENDI	00I	OPAL	Dirac, coupling to e
> 76.0	95	ABBIENDI	00I	OPAL	Majorana, coupling to μ
> 88.1	95	ABBIENDI	00I	OPAL	Dirac, coupling to μ
> 53.8	95	ABBIENDI	00I	OPAL	Majorana, coupling to τ
> 71.1	95	ABBIENDI	00I	OPAL	Dirac, coupling to τ
> 76.5	95	ABREU	99O	DLPH	Dirac coupling to e
> 79.5	95	ABREU	99O	DLPH	Dirac coupling to μ
> 60.5	95	ABREU	99O	DLPH	Dirac coupling to τ
> 63	95	[2,3] BUSKULIC	96S	ALEP	Dirac
> 54.3	95	[2,4] BUSKULIC	96S	ALEP	Majorana

[2] BUSKULIC 96S requires the decay length of the heavy lepton to be < 1 cm, limiting the square of the mixing angle $|U_{\ell j}|^2$ to 10^{-10}.

[3] BUSKULIC 96S limit for mixing with τ. Mass is > 63.6 GeV for mixing with e or μ.

[4] BUSKULIC 96S limit for mixing with τ. Mass is > 55.2 GeV for mixing with e or μ.

Astrophysical Limits on Neutrino MASS for $m_\nu > 1$ GeV

VALUE (GeV)	CL%	DOCUMENT ID		TECN	COMMENT
• • • We do not use the following data for averages, fits, limits, etc. • • •					
none 60–115		[5] FARGION	95	ASTR	Dirac
none 9.2–2000		[6] GARCIA	95	COSM	Nucleosynthesis
none 26–4700		[6] BECK	94	COSM	Dirac
none 6 – hundreds		[7,8] MORI	92B	KAM2	Dirac neutrino
none 24 – hundreds		[7,8] MORI	92B	KAM2	Majorana neutrino
none 10–2400	90	[9] REUSSER	91	CNTR	HPGe search
none 3–100	90	SATO	91	KAM2	Kamiokande II
		[10] ENQVIST	89	COSM	
none 12–1400		[6] CALDWELL	88	COSM	Dirac ν
none 4–16	90	[6,7] OLIVE	88	COSM	Dirac ν
none 4–35	90	OLIVE	88	COSM	Majorana ν
>4.2 to 4.7		SREDNICKI	88	COSM	Dirac ν
>5.3 to 7.4		SREDNICKI	88	COSM	Majorana ν
none 20–1000	95	[6] AHLEN	87	COSM	Dirac ν
>4.1		GRIEST	87	COSM	Dirac ν

[5] FARGION 95 bound is sensitive to assumed ν concentration in the Galaxy. See also KONOPLICH 94.

[6] These results assume that neutrinos make up dark matter in the galactic halo.

[7] Limits based on annihilations in the sun and are due to an absence of high energy neutrinos detected in underground experiments.

[8] MORI 92B results assume that neutrinos make up dark matter in the galactic halo. Limits based on annihilations in earth are also given.

[9] REUSSER 91 uses existing $\beta\beta$ detector (see FISHER 89) to search for CDM Dirac neutrinos.

[10] ENQVIST 89 argue that there is no cosmological upper bound on heavy neutrinos.

(B) Other Bounds from Nuclear and Particle Decays

Limits on $|U_{ex}|^2$ as Function of m_{ν_x}

Peak and kink search tests

Limits on $|U_{ex}|^2$ as function of m_{ν_j}

VALUE	CL%	DOCUMENT ID		TECN	COMMENT
<1 $\times 10^{-7}$	90	[11] BRITTON	92B	CNTR	50 MeV $< m_{\nu_x} <$ 130 MeV
• • • We do not use the following data for averages, fits, limits, etc. • • •					
$<5 \times 10^{-6}$	90	DELEENER-...	91		m_{ν_x}=20 MeV
$<5 \times 10^{-7}$	90	DELEENER-...	91		m_{ν_x}=40 MeV
$<3 \times 10^{-7}$	90	DELEENER-...	91		m_{ν_x}=60 MeV
$<1 \times 10^{-6}$	90	DELEENER-...	91		m_{ν_x}=80 MeV
$<1 \times 10^{-6}$	90	DELEENER-...	91		m_{ν_x}=100 MeV
$<5 \times 10^{-7}$	90	AZUELOS	86	CNTR	m_{ν_x}=60 MeV
$<2 \times 10^{-7}$	90	AZUELOS	86	CNTR	m_{ν_x}=80 MeV
$<3 \times 10^{-7}$	90	AZUELOS	86	CNTR	m_{ν_x}=100 MeV
$<1 \times 10^{-6}$	90	AZUELOS	86	CNTR	m_{ν_x}=120 MeV
$<2 \times 10^{-7}$	90	AZUELOS	86	CNTR	m_{ν_x}=130 MeV
$<1 \times 10^{-4}$	90	[12] BRYMAN	83B	CNTR	m_{ν_x}=5 MeV
$<1.5 \times 10^{-6}$	90	BRYMAN	83B	CNTR	m_{ν_x}=53 MeV
$<1 \times 10^{-5}$	90	BRYMAN	83B	CNTR	m_{ν_x}=70 MeV
$<1 \times 10^{-4}$	90	BRYMAN	83B	CNTR	m_{ν_x}=130 MeV
$<1 \times 10^{-4}$	68	[13] SHROCK	81	THEO	m_{ν_x}=10 MeV
$<5 \times 10^{-6}$	68	[13] SHROCK	81	THEO	m_{ν_x}=60 MeV
$<1 \times 10^{-5}$	68	[14] SHROCK	80	THEO	m_{ν_x}=80 MeV
$<3 \times 10^{-6}$	68	[14] SHROCK	80	THEO	m_{ν_x}=160 MeV

[11] BRITTON 92B is from a search for additional peaks in the e^+ spectrum from $\pi^+ \to e^+\nu_e$ decay at TRIUMF. See also BRITTON 92.

[12] BRYMAN 83B obtain upper limits from both direct peak search and analysis of $B(\pi \to e\nu)/B(\pi \to \mu\nu)$. Latter limits are not listed, except for this entry (i.e. — we list the most stringent limits for given mass).

[13] Analysis of $(\pi^+ \to e^+\nu_e)/(\pi^+ \to \mu^+\nu_\mu)$ and $(K^+ \to e^+\nu_e)/(K^+ \to \mu^+\nu_\mu)$ decay ratios.

[14] Analysis of $(K^+ \to e^+\nu_e)$ spectrum.

Kink search in nuclear β decay

High-sensitivity follow-up experiments show that indications for a neutrino with mass 17 keV (Simpson, Hime, and others) were not valid. Accordingly, we no longer list the experiments by these authors and some others which made positive claims of 17 keV neutrino emission. Complete listings are given in the 1994 edition (Physical Review **D50** 1173 (1994)) and in the 1998 edition (The European Physical Journal **C3** 1 (1998)). We list below only the best limits on $|U_{ex}|^2$ for each m_{ν_x}. See WIETFELDT 96 for a comprehensive review.

VALUE (units 10^{-3})	CL%	m_{ν_j} (keV)	ISOTOPE	METHOD	DOCUMENT ID	
• • • We do not use the following data for averages, fits, limits, etc. • • •						
< 4–20	90	700–3500	^{38m}K	Trap	[15] TRINCZEK	03
< 9–116	95	1–0.1	^{187}Re	cryog.	[16] GALEAZZI	01
< 1	95	10–90	^{35}S	Mag spect	[17] HOLZSCHUH	00
< 4	95	14–17	^{241}Pu	Electrostatic spec	[18] DRAGOUN	99
< 1	95	4–30	^{63}Ni	Mag spect	[19] HOLZSCHUH	99
< 10–40	90	370–640	^{37}Ar	EC ion recoil	[20] HINDI	98
< 10	95	1	^{3}H	SPEC	[21] HIDDEMANN	95
< 6	95	2	^{3}H	SPEC	[21] HIDDEMANN	95
< 2	95	3	^{3}H	SPEC	[21] HIDDEMANN	95
< 0.7	99	16.3–16.6	^{3}H	Prop chamber	[22] KALBFLEISCH	93
< 2	95	13–40	^{35}S	Si(Li)	[23] MORTARA	93
< 0.73	95	17	^{63}Ni	Mag spect	OHSHIMA	93
< 1.0	95	10–24	^{63}Ni	Mag spect	KAWAKAMI	92
< 0.9–2.5	90	1200–6800	^{20}F	beta spectrum	[24] DEUTSCH	90
< 8	90	80	^{35}S	Mag spect	[25] APALIKOV	85
< 1.5	90	60	^{35}S	Mag spect	APALIKOV	85
< 3.0	90	5–50		Mag spect	MARKEY	85
< 0.62	90	48	^{35}S	Si(Li)	OHI	85
< 0.90	90	30	^{35}S	Si(Li)	OHI	85
< 4	90	140	^{64}Cu	Mag spect	[26] SCHRECK...	83
< 8	90	440	^{64}Cu	Mag spect	[26] SCHRECK...	83
<100	90	0.1–3000		THEO	[27] SHROCK	80
< 0.1	68	80		THEO	[28] SHROCK	80

[15] TRINCZEK 03 is a search for admixture of heavy neutrino to ν_e, in contrast to $\overline{\nu}_e$ used in many other searches. Full kinematic reconstruction of the neutrino momentum by use of a magneto optical trap.

[16] GALEAZZI 01 use an cryogenic microcalorimeter to search for mass 50–1000 eV neutrino admixtures using the ^{187}Re beta spectrum with 2.4 keV endpoint. They derive limits for the admixture of heavy neutrinos, ranging from 9×10^{-3} for mass 1 keV to 0.116 for mass 100 eV. This is a significant improvement with respect to HIDDEMANN 95, especially for masses below $\sim$ 500 MeV, where the limit is about a factor of $\sim$ 2 higher.

[17] HOLZSCHUH 00 use an iron-free β spectrometer to measure the ^{35}S β decay spectrum. An analysis of the spectrum in the energy range 56–173 keV is used to derive limits for the admixture of heavy neutrinos. This extends the range of neutrino masses explored in HOLZSCHUH 99.

[18] DRAGOUN 99 analyze the β decay spectrum of ^{241}Pu in the energy range 0.2–9.2 keV to derive limits for the admixture of heavy neutrinos. It is not competitive with HOLZSCHUH 99.

[19] HOLZSCHUH 99 use an iron-free β spectrometer to measure the ^{63}Ni β decay spectrum. An analysis of the spectrum in the energy rage 33–67.8 keV is used to derive limits for the admixture of heavy neutrinos.

[20] HINDI 98 obtain a limit on heavy neutrino admixture from EC decay of ^{37}Ar by measuring the time-of-flight distribution of the recoiling ions in coincidence with x-rays or Auger electrons. The authors report upper limit for $|U_{ex}|^2$ of $\approx$ 3% for m_{ν_x}=500 keV, 1% for m_{ν_x}=550 keV, 2% for m_{ν_x}=600 keV, and 4% for m_X=650 keV. Their reported limits for $m_{\nu_x} \leq$ 450 keV are inferior to the limits of SCHRECKENBACH 83.

[21] In the beta spectrum from tritium β decay nonvanishing or mixed $m_{\overline{\nu}_1}$ state in the mass region 0.01–4 keV. For m_{ν_x} <1 keV, their upper limit on $|U_{ex}|^2$ becomes less

[22] KALBFLEISCH 93 extends the 17 keV neutrino search of BAHRAN 92, using an improved proportional chamber to which a small amount of ^{3}H is added. Systematics are significantly reduced, allowing for an improved upper limit. The authors give a 99% confidence limit on $|U_{ex}|^2$ as a function of m_{ν_x} in the range from 13.5 keV to 17.5 keV. See also the related papers BAHRAN 93, BAHRAN 93B, and BAHRAN 95 on theoretical aspects of beta spectra and fitting methods for heavy neutrinos.

[23] MORTARA 93 limit is from study using a high-resolution solid-state detector with a superconducting solenoid. The authors note that "The sensitivity to neutrino mass is verified by measurement with a mixed source of ^{35}S and ^{14}C, which artificially produces a distortion in the beta spectrum similar to that expected from the massive neutrino."

[24] DEUTSCH 90 search for emission of heavy $\overline{\nu}_e$ in super-allowed beta decay of ^{20}F by spectral analysis of the electrons.

[25] This limit was taken from the figure 3 of APALIKOV 85; the text gives a more restrictive limit of 1.7×10^{-3} at CL = 90%.

[26] SCHRECKENBACH 83 is a combined measurement of the β^+ and β^- spectrum.

[27] SHROCK 80 was a retroactive analysis of data on several superallowed β decays to search for kinks in the Kurie plot.

[28] Application of test to search for kinks in β decay Kurie plots.

Searches for Decays of Massive ν

Limits on $|U_{ex}|^2$ as function of m_{ν_x}

VALUE	CL%	DOCUMENT ID		TECN	COMMENT
• • • We do not use the following data for averages, fits, limits, etc. • • •					
$<1.6 \times 10^{-4}$	90	[29] BACK	03A	CNTR	m_{ν_x} = 4 MeV
$<4.5 \times 10^{-5}$	90	[29] BACK	03A	CNTR	m_{ν_x} = 7 MeV
$<3.8 \times 10^{-5}$	90	[29] BACK	03A	CNTR	m_{ν_x} = 10 MeV
$<1.5 \times 10^{-3}$	95	ACHARD	01	L3	m_{ν_x}=80 GeV
$<2 \times 10^{-2}$	95	ACHARD	01	L3	m_{ν_x}=175 GeV
<0.3	95	ACHARD	01	L3	m_{ν_x}=200 GeV
$<4 \times 10^{-3}$	95	ACCIARRI	99K	L3	m_{ν_x}=80 GeV
$<5 \times 10^{-2}$	95	ACCIARRI	99K	L3	m_{ν_x}= 175 GeV
$<2 \times 10^{-5}$	95	[30] ABREU	97I	DLPH	m_{ν_x}=6 GeV
$<3 \times 10^{-5}$	95	[30] ABREU	97I	DLPH	m_{ν_x}=50 GeV
$<1.8 \times 10^{-3}$	90	[31] HAGNER	95	MWPC	m_{ν_h} = 1.5 MeV
$<2.5 \times 10^{-4}$	90	[31] HAGNER	95	MWPC	m_{ν_h} = 4 MeV
$<4.2 \times 10^{-3}$	90	[31] HAGNER	95	MWPC	m_{ν_h} = 9 MeV
$<1 \times 10^{-5}$	90	[32] BARANOV	93		m_{ν_x}=100 MeV
$<1 \times 10^{-6}$	90	[32] BARANOV	93		m_{ν_x}= 200 MeV
$<3 \times 10^{-7}$	90	[32] BARANOV	93		m_{ν_x}= 300 MeV
$<2 \times 10^{-7}$	90	[32] BARANOV	93		m_{ν_x}=400 MeV
$<6.2 \times 10^{-8}$	95	ADEVA	90S	L3	m_{ν_x}=20 GeV
$<5.1 \times 10^{-10}$	95	ADEVA	90S	L3	m_{ν_x}=40 GeV
all values ruled out	95	[33] BURCHAT	90	MRK2	m_{ν_x} < 19.6 GeV
$<1 \times 10^{-10}$	95	[33] BURCHAT	90	MRK2	m_{ν_x}= 22 GeV
$<1 \times 10^{-11}$	95	[33] BURCHAT	90	MRK2	m_{ν_x}= 41 GeV
all values ruled out	95	DECAMP	90F	ALEP	m_{ν_x}= 25.0–42.7 GeV
$<1 \times 10^{-13}$	95	DECAMP	90F	ALEP	m_{ν_x}= 42.7–45.7 GeV
$<5 \times 10^{-3}$	90	AKERLOF	88	HRS	m_{ν_x}=1.8 GeV
$<2 \times 10^{-5}$	90	AKERLOF	88	HRS	m_{ν_x}=4 GeV
$<3 \times 10^{-6}$	90	AKERLOF	88	HRS	m_{ν_x}=6 GeV
$<1.2 \times 10^{-7}$	90	BERNARDI	88	CNTR	m_{ν_x}=100 MeV
$<1 \times 10^{-8}$	90	BERNARDI	88	CNTR	m_{ν_x}=200 MeV
$<2.4 \times 10^{-9}$	90	BERNARDI	88	CNTR	m_{ν_x}=300 MeV
$<2.1 \times 10^{-9}$	90	BERNARDI	88	CNTR	m_{ν_x}=400 MeV
$<2 \times 10^{-2}$	68	[34] OBERAUER	87		m_{ν_x}=1.5 MeV
$<8 \times 10^{-4}$	68	[34] OBERAUER	87		m_{ν_x}=4.0 MeV
$<8 \times 10^{-3}$	90	BADIER	86	CNTR	m_{ν_x}=400 MeV
$<8 \times 10^{-5}$	90	BADIER	86	CNTR	m_{ν_x}=1.7 GeV
$<8 \times 10^{-8}$	90	BERNARDI	86	CNTR	m_{ν_x}=100 MeV
$<4 \times 10^{-8}$	90	BERNARDI	86	CNTR	m_{ν_x}=200 MeV
$<6 \times 10^{-9}$	90	BERNARDI	86	CNTR	m_{ν_x}=400 MeV
$<3 \times 10^{-5}$	90	DORENBOS...	86	CNTR	m_{ν_x}=150 MeV
$<1 \times 10^{-6}$	90	DORENBOS...	86	CNTR	m_{ν_x}=500 MeV
$<1 \times 10^{-7}$	90	DORENBOS...	86	CNTR	m_{ν_x}=1.6 GeV
$<7 \times 10^{-7}$	90	[35] COOPER-...	85	HLBC	m_{ν_x}=0.4 GeV
$<8 \times 10^{-8}$	90	[35] COOPER-...	85	HLBC	m_{ν_x}=1.5 GeV
$<1 \times 10^{-2}$	90	[36] BERGSMA	83B	CNTR	m_{ν_x}=10 MeV
$<1 \times 10^{-5}$	90	[36] BERGSMA	83B	CNTR	m_{ν_x}=110 MeV
$<6 \times 10^{-7}$	90	[36] BERGSMA	83B	CNTR	m_{ν_x}=410 MeV
$<1 \times 10^{-5}$	90	GRONAU	83		m_{ν_x}=160 MeV
$<1 \times 10^{-6}$	90	GRONAU	83		m_{ν_x}=480 MeV

[29] BACK 03A searched for heavy neutrinos emitted from ^{8}B decay in the Sun using the decay $\nu_h \rightarrow \nu_e e^+ e^-$ in the Counting Test Facility (the prototype of the Borexino detector) and obtained limits on heavy neutrino admixture for the ν_h mass range 1.1–12 MeV.

[30] ABREU 97I long-lived ν_X analysis. Short-lived analysis extends limit to lower masses with decreasing sensitivity except at 3.5 GeV, where the limit is the same as at 6 GeV.

[31] HAGNER 95 obtain limits on heavy neutrino admixture from the decay $\nu_h \rightarrow \nu_e e^+ e^-$ at a nuclear reactor for the ν_h mass range 2–9 MeV.

[32] BARANOV 93 is a search for neutrino decays into $e^+ e^- \nu_e$ using a beam dump experiment at the 70 GeV Serpukhov proton synchrotron. The limits are not as good as those achieved earlier by BERGSMA 83 and BERNARDI 86, BERNARDI 88.

[33] BURCHAT 90 includes the analyses reported in JUNG 90, ABRAMS 89C, and WENDT 87.

[34] OBERAUER 87 bounds from search for $\nu \rightarrow \nu' e e$ decay mode using reactor (anti)neutrinos.

[35] COOPER-SARKAR 85 also give limits based on model-dependent assumptions for ν_τ flux. We do not list these. Note that for this bound to be nontrivial, x is not equal to 3, i.e. ν_X cannot be the dominant mass eigenstate in ν_τ since m_{ν_3} <70 MeV (ALBRECHT 85I). Also, of course, x is not equal to 1 or 2, so a fourth generation would be required for this bound to be nontrivial.

[36] BERGSMA 83B also quote limits on $|U_{e3}|^2$ where the index 3 refers to the mass eigenstate dominantly coupled to the τ. Those limits were based on assumptions about the D_s mass and $D_s \rightarrow \tau \nu_\tau$ branching ratio which are no longer valid. See COOPER-SARKAR 85.

Limits on Coupling of μ to ν_x as Function of m_{ν_x}

Peak search test

Limits on B(π (or K) $\rightarrow \mu \nu_x$).

VALUE	CL%	DOCUMENT ID		TECN	COMMENT
• • • We do not use the following data for averages, fits, limits, etc. • • •					
		[37] ASTIER	02	NOMD	$\pi \rightarrow \mu X$ for m_X=33.9 MeV
$<6.0 \times 10^{-10}$	95	[38] DAUM	00	CNTR	$\pi \rightarrow \mu X$ for m_X=33.9 MeV
		[39] FORMAGGIO	00	CNTR	$\pi \rightarrow \mu X$ for m_X=33.9 MeV
<0.22	90	[40] ASSAMAGAN	98	SILI	m_{ν_x}= 0.53 MeV
<0.029	90	[40] ASSAMAGAN	98	SILI	m_{ν_x}= 0.75 MeV
<0.016	90	[40] ASSAMAGAN	98	SILI	m_{ν_x}= 1.0 MeV
$< 4–6 \times 10^{-5}$		[41] BRYMAN	96	CNTR	m_{ν_x}= 30–33.91 MeV
$\sim 1 \times 10^{-16}$		[42] ARMBRUSTER	95	KARM	m_{ν_x} = 33.9 MeV

Lepton Particle Listings

Heavy Neutral Leptons, Searches for

<4	$\times 10^{-7}$	95	[43] BILGER	95	LEPS	$m_{\overline{\nu}_x}$ = 33.9 MeV
<7	$\times 10^{-8}$	95	[43] BILGER	95	LEPS	m_{ν_x} = 33.9 MeV
<2.6	$\times 10^{-8}$	95	[43] DAUM	95B	TOF	m_{ν_x} = 33.9 MeV
<2	$\times 10^{-2}$	90	DAUM	87		m_{ν_x}=1 MeV
<1	$\times 10^{-3}$	90	DAUM	87		m_{ν_x}=2 MeV
<6	$\times 10^{-5}$	90	DAUM	87		3 MeV < m_{ν_x} < 19.5 MeV
<3	$\times 10^{-2}$	90	[44] MINEHART	84		m_{ν_x}=2 MeV
<1	$\times 10^{-3}$	90	[44] MINEHART	84		m_{ν_x}=4 MeV
<3	$\times 10^{-4}$	90	[44] MINEHART	84		m_{ν_x}=10 GeV
<5	$\times 10^{-6}$	90	[45] HAYANO	82		m_{ν_x}=330 MeV
<1	$\times 10^{-4}$	90	[45] HAYANO	82		m_{ν_x}=70 MeV
<9	$\times 10^{-7}$	90	[45] HAYANO	82		m_{ν_x}=250 MeV
<1	$\times 10^{-1}$	90	[44] ABELA	81		m_{ν_x}=4 MeV
<7	$\times 10^{-5}$	90	[44] ABELA	81		m_{ν_x}=10.5 MeV
<2	$\times 10^{-4}$	90	[44] ABELA	81		m_{ν_x}=11.5 MeV
<2	$\times 10^{-5}$	90	[44] ABELA	81		m_{ν_x}=16–30 MeV

[37] ASTIER 02 search for anomalous pion decay into a 33.9 MeV neutral particle. No evidence was found and the sensitivity to the branching ratio $B(\pi \rightarrow \mu X)\cdot B(X \rightarrow \nu e^+ e^-)$ is as low as 3.7×10^{-15}, depending on the X lifetime.

[38] DAUM 00 search for anomalous pion decay into a 33.9 MeV neutral particle that might be responsible for the time-distribution anomaly observed by the KARMEN Collaboration.

[39] FORMAGGIO 00 search for anomalous pion decay into a 33.9 MeV neutral particle Q^0 that might be responsible for the time-distribution anomaly observed by the KARMEN Collaboration. In the E815 (NuTeV) experiment at Fermilab no evidence was found, with sensitivity for the pion branching ratio $B(\pi \rightarrow \mu Q^0)\cdot B(Q^0 \rightarrow$ visible) as low as 10^{-13}.

[40] ASSAMAGAN 98 obtain a limit on heavy neutrino admixture from π^+ decay essentially at rest, by measuring with good resolution the momentum distribution of the muons. However, the search uses an ad hoc shape correction. The authors report upper limit for $|U_{\mu x}|^2$ of 0.22 for m_ν = 0.53 MeV, 0.029 for m_ν = 0.75 MeV, and 0.016 for m_ν = 1.0 MeV at 90%CL.

[41] BRYMAN 96 search for massive unconventional neutrinos of mass m_{ν_x} in π^+ decay.

[42] ARMBRUSTER 95 study the reactions $^{12}C(\nu_e,e^-)\,^{12}N$ and $^{12}C(\nu,\nu')\,^{12}C^*$ induced by neutrinos from π^+ and μ^+ decay at the ISIS neutron spallation source at the Rutherford-Appleton laboratory. An anomaly in the time distribution can be interpreted as the decay $\pi^+ \rightarrow \mu^+ \nu_x$, where ν_x is a neutral weakly interacting particle with mass $\approx$ 33.9 MeV and spin 1/2. The lower limit to the branching ratio is a function of the lifetime of the new massive neutral particle, and reaches a minimum of a few $\times 10^{-16}$ for $\tau_x \sim 5$ s.

[43] From experiments of π^+ and π^- decay in flight at PSI, to check the claim of the KARMEN Collaboration quoted above (ARMBRUSTER 95).

[44] $\pi^+ \rightarrow \mu^+ \nu_\mu$ peak search experiment.

[45] $K^+ \rightarrow \mu^+ \nu_\mu$ peak search experiment.

Peak search test

Limits on $|U_{\mu x}|^2$ as function of m_{ν_x}

VALUE	CL%	DOCUMENT ID		TECN	COMMENT
• • • We do not use the following data for averages, fits, limits, etc. • • •					
$< 1–10 \times 10^{-4}$		[46] BRYMAN	96	CNTR	m_{ν_x} = 30–33.91 MeV
$<2 \times 10^{-5}$	95	[47] ASANO	81		m_{ν_x}=70 MeV
$<3 \times 10^{-6}$	95	[47] ASANO	81		m_{ν_x}=210 MeV
$<3 \times 10^{-6}$	95	[47] ASANO	81		m_{ν_x}=230 MeV
$<6 \times 10^{-6}$	95	[48] ASANO	81		m_{ν_x}=240 MeV
$<5 \times 10^{-7}$	95	[48] ASANO	81		m_{ν_x}=280 MeV
$<6 \times 10^{-6}$	95	[48] ASANO	81		m_{ν_x}=300 MeV
$<1 \times 10^{-2}$	95	CALAPRICE	81		m_{ν_x}=7 MeV
$<3 \times 10^{-3}$	95	[49] CALAPRICE	81		m_{ν_x}=33 MeV
$<1 \times 10^{-4}$	68	[50] SHROCK	81	THEO	m_{ν_x}=13 MeV
$<3 \times 10^{-5}$	68	[50] SHROCK	81	THEO	m_{ν_x}=33 MeV
$<6 \times 10^{-3}$	68	[51] SHROCK	81	THEO	m_{ν_x}=80 MeV
$<5 \times 10^{-3}$	68	[51] SHROCK	81	THEO	m_{ν_x}=120 MeV

[46] BRYMAN 96 search for massive unconventional neutrinos of mass m_{ν_x} in π^+ decay. They interpret the result as an upper limit for the admixture of a heavy sterile or otherwise

[47] $K^+ \rightarrow \mu^+ \nu_\mu$ peak search experiment.

[48] Analysis of experiment on $K^+ \rightarrow \mu^+ \nu_\mu \nu_x \overline{\nu}_x$ decay.

[49] $\pi^+ \rightarrow \mu^+ \nu_\mu$ peak search experiment.

[50] Analysis of magnetic spectrometer experiment, bubble chamber experiment, and emulsion experiment on $\pi^+ \rightarrow \mu^+ \nu_\mu$ decay.

[51] Analysis of magnetic spectrometer experiment on $K \rightarrow \mu, \nu_\mu$ decay.

Peak Search in Muon Capture

Limits on $|U_{\mu x}|^2$ as function of m_{ν_x}

VALUE	DOCUMENT ID		COMMENT
• • • We do not use the following data for averages, fits, limits, etc. • • •			
$<1 \times 10^{-1}$	DEUTSCH	83	m_{ν_x}=45 MeV
$<7 \times 10^{-3}$	DEUTSCH	83	m_{ν_x}=70 MeV
$<1 \times 10^{-1}$	DEUTSCH	83	m_{ν_x}=85 MeV

Searches for Decays of Massive ν

Limits on $|U_{\mu x}|^2$ as function of m_{ν_x}

VALUE	CL%	DOCUMENT ID		TECN	COMMENT
• • • We do not use the following data for averages, fits, limits, etc. • • •					
<5 $\times 10^{-7}$	90	[52] VAITAITIS	99	CCFR	m_{ν_x}=0.28 GeV
<8 $\times 10^{-8}$	90	[52] VAITAITIS	99	CCFR	m_{ν_x}=0.37 GeV
<5 $\times 10^{-7}$	90	[52] VAITAITIS	99	CCFR	m_{ν_x}= 0.50 GeV
<6 $\times 10^{-8}$	90	[52] VAITAITIS	99	CCFR	m_{ν_x}= 1.50 GeV
<2 $\times 10^{-5}$	95	[53] ABREU	97I	DLPH	m_{ν_x}=6 GeV
<3 $\times 10^{-5}$	95	[53] ABREU	97I	DLPH	m_{ν_x}=50 GeV
<3 $\times 10^{-6}$	90	GALLAS	95	CNTR	m_{ν_x} = 1 GeV
<3 $\times 10^{-5}$	90	[54] VILAIN	95C	CHM2	m_{ν_x} = 2 GeV
<6.2 $\times 10^{-8}$	95	ADEVA	90S	L3	m_{ν_x}=20 GeV
<5.1 $\times 10^{-10}$	95	ADEVA	90S	L3	m_{ν_x}=40 GeV
all values ruled out	95	[55] BURCHAT	90	MRK2	m_{ν_x} < 19.6 GeV
<1 $\times 10^{-10}$	95	[55] BURCHAT	90	MRK2	m_{ν_x} = 22 GeV
<1 $\times 10^{-11}$	95	[55] BURCHAT	90	MRK2	m_{ν_x} = 41 GeV
all values ruled out	95	DECAMP	90F	ALEP	m_{ν_x} = 25.0–42.7 GeV
<1 $\times 10^{-13}$	95	DECAMP	90F	ALEP	m_{ν_x}= 42.7–45.7 GeV
<5 $\times 10^{-3}$	90	AKERLOF	88	HRS	m_{ν_x}=1.8 GeV
<2 $\times 10^{-5}$	90	AKERLOF	88	HRS	m_{ν_x}=4 GeV
<3 $\times 10^{-6}$	90	AKERLOF	88	HRS	m_{ν_x}=6 GeV
<1 $\times 10^{-7}$	90	BERNARDI	88	CNTR	m_{ν_x}=200 MeV
<3 $\times 10^{-9}$	90	BERNARDI	88	CNTR	m_{ν_x}=300 MeV
<4 $\times 10^{-4}$	90	[56] MISHRA	87	CNTR	m_{ν_x}=1.5 GeV
<4 $\times 10^{-3}$	90	[56] MISHRA	87	CNTR	m_{ν_x}=2.5 GeV
<0.9 $\times 10^{-2}$	90	[56] MISHRA	87	CNTR	m_{ν_x}=5 GeV
<0.1	90	[56] MISHRA	87	CNTR	m_{ν_x}=10 GeV
<8 $\times 10^{-4}$	90	BADIER	86	CNTR	m_{ν_x}=600 MeV
<1.2 $\times 10^{-5}$	90	BADIER	86	CNTR	m_{ν_x}=1.7 GeV
<3 $\times 10^{-8}$	90	BERNARDI	86	CNTR	m_{ν_x}=200 MeV
<6 $\times 10^{-9}$	90	BERNARDI	86	CNTR	m_{ν_x}=350 MeV
<1 $\times 10^{-6}$	90	DORENBOS...	86	CNTR	m_{ν_x}=500 MeV
<1 $\times 10^{-7}$	90	DORENBOS...	86	CNTR	m_{ν_x}=1600 MeV
<0.8 $\times 10^{-5}$	90	[57] COOPER-...	85	HLBC	m_{ν_x}=0.4 GeV
<1.0 $\times 10^{-7}$	90	[57] COOPER-...	85	HLBC	m_{ν_x}=1.5 GeV

[52] VAITAITIS 99 search for $L^0_\mu \rightarrow \mu X$. See paper for rather complicated limit as function of m_{ν_x}.

[53] ABREU 97I long-lived ν_x analysis. Short-lived analysis extends limit to lower masses with decreasing sensitivity except at 3.5 GeV, where the limit is the same as at 6 GeV.

[54] VILAIN 95C is a search for the decays of heavy isosinglet neutrinos produced by neutral current neutrino interactions. Limits were quoted for masses in the range from 0.3 to 24 GeV. The best limit is listed above.

[55] BURCHAT 90 includes the analyses reported in JUNG 90, ABRAMS 89C, and WENDT 87.

[56] See also limits on $|U_{3x}|$ from WENDT 87.

[57] COOPER-SARKAR 85 also give limits based on model-dependent assumptions for ν_τ flux. We do not list these. Note that for this bound to be nontrivial, x is not equal to 3, i.e. ν_x cannot be the dominant mass eigenstate in ν_τ since m_{ν_3} <70 MeV (ALBRECHT 85I). Also, of course, x is not equal to 1 or 2, so a fourth generation would be required for this bound to be nontrivial.

Limits on $|U_{\tau x}|^2$ as a Function of m_{ν_x}

VALUE	CL%	DOCUMENT ID		TECN	COMMENT
• • • We do not use the following data for averages, fits, limits, etc. • • •					
<1 $\times 10^{-2}$	90	[58] ORLOFF	02	CHRM	m_{ν_x}=45 MeV
<1.4 $\times 10^{-4}$	90	[58] ORLOFF	02	CHRM	m_{ν_x}=180 MeV
<0.025	90	ASTIER	01		m_{ν_x}=45 MeV
<0.002	90	ASTIER	01		m_{ν_x}=140 MeV
<2 $\times 10^{-5}$	95	[59] ABREU	97I	DLPH	m_{ν_x}=6 GeV
<3 $\times 10^{-5}$	95	[59] ABREU	97I	DLPH	m_{ν_x}=50 GeV
<6.2 $\times 10^{-8}$	95	ADEVA	90S	L3	m_{ν_x}=20 GeV
<5.1 $\times 10^{-10}$	95	ADEVA	90S	L3	m_{ν_x}=40 GeV
all values ruled out	95	[60] BURCHAT	90	MRK2	m_{ν_x} < 19.6 GeV
<1 $\times 10^{-10}$	95	[60] BURCHAT	90	MRK2	m_{ν_x} = 22 GeV
<1 $\times 10^{-11}$	95	[60] BURCHAT	90	MRK2	m_{ν_x} = 41 GeV
all values ruled out	95	DECAMP	90F	ALEP	m_{ν_x} = 25.0–42.7 GeV
<1 $\times 10^{-13}$	95	DECAMP	90F	ALEP	m_{ν_x}= 42.7–45.7 GeV
<5 $\times 10^{-2}$	80	AKERLOF	88	HRS	m_{ν_x}=2.5 GeV
<9 $\times 10^{-5}$	80	AKERLOF	88	HRS	m_{ν_x}=4.5 GeV

[58] ORLOFF 02 use the negative result of a search for neutral particles decaying into two electrons performed by CHARM to get these limits for a mostly isosinglet heavy neutrino.

[59] ABREU 97I long-lived ν_x analysis. Short-lived analysis extends limit to lower masses with decreasing sensitivity.

[60] BURCHAT 90 includes the analyses reported in JUNG 90, ABRAMS 89C, and WENDT 87.

Limits on $|U_{ax}|^2$

Where $a = e$, μ from ρ parameter in μ decay.

VALUE	CL%	DOCUMENT ID		TECN	COMMENT
• • • We do not use the following data for averages, fits, limits, etc. • • •					
$<1 \times 10^{-2}$	68	SHROCK	81B	THEO	m_{ν_x}=10 GeV
$<2 \times 10^{-3}$	68	SHROCK	81B	THEO	m_{ν_x}=40 MeV
$<4 \times 10^{-2}$	68	SHROCK	81B	THEO	m_{ν_x}=70 MeV

Limits on $|U_{1j} \times U_{2j}|$ as Function of m_{ν_j}

VALUE	CL%	DOCUMENT ID		TECN	COMMENT
• • • We do not use the following data for averages, fits, limits, etc. • • •					
$<3 \times 10^{-5}$	90	[61] BARANOV	93		m_{ν_j}= 80 MeV
$<3 \times 10^{-6}$	90	[61] BARANOV	93		m_{ν_j}= 160 MeV
$<6 \times 10^{-7}$	90	[61] BARANOV	93		m_{ν_j}= 240 MeV
$<2 \times 10^{-7}$	90	[61] BARANOV	93		m_{ν_j}= 320 MeV
$<9 \times 10^{-5}$	90	BERNARDI	86	CNTR	m_{ν_j}=25 MeV
$<3.6 \times 10^{-7}$	90	BERNARDI	86	CNTR	m_{ν_j}=100 MeV
$<3 \times 10^{-8}$	90	BERNARDI	86	CNTR	m_{ν_j}=200 MeV
$<6 \times 10^{-9}$	90	BERNARDI	86	CNTR	m_{ν_j}=350 MeV
$<1 \times 10^{-2}$	90	BERGSMA	83B	CNTR	m_{ν_j}=10 MeV
$<1 \times 10^{-5}$	90	BERGSMA	83B	CNTR	m_{ν_j}=140 MeV
$<7 \times 10^{-7}$	90	BERGSMA	83B	CNTR	m_{ν_j}=370 MeV

[61] BARANOV 93 is a search for neutrino decays into $e^+ e^- \nu_e$ using a beam dump experiment at the 70 GeV Serpukhov proton synchrotron.

REFERENCES FOR Heavy Neutral Leptons, Searches for

BACK	03A	JETPL 78 261	H.O. Back *et al.*	(Borexino Collab.)
		Translated from ZETFP 78 707.		
TRINCZEK	03	PRL 90 012501	M. Trinczek *et al.*	
ASTIER	02	PL B527 23	P. Astier *et al.*	(NOMAD Collab.)
ORLOFF	02	PL B550 8	J. Orloff *et al.*	
ACHARD	01	PL B517 67	P. Achard *et al.*	(L3 Collab.)
ACHARD	01B	PL B517 75	P. Achard *et al.*	(L3 Collab.)
ASTIER	01	PL B506 27	P. Astier *et al.*	(NOMAD Collab.)
GALEAZZI	01	PRL 86 1978	M. Galeazzi *et al.*	
ABBIENDI	00I	EPJ C14 73	G. Abbiendi *et al.*	(OPAL Collab.)
DAUM	00	PRL 85 1815	M. Daum *et al.*	
FORMAGGIO	00	PRL 84 4043	J.A. Formaggio *et al.*	
HOLZSCHUH	00	PL B482 1	E. Holzschuh *et al.*	
ABREU	99O	EPJ C8 41	P. Abreu *et al.*	(DELPHI Collab.)
ACCIARRI	99K	PL B461 397	M. Acciarri *et al.*	(L3 Collab.)
DRAGOUN	99	JP G25 1839	O. Dragoun *et al.*	
HOLZSCHUH	99	PL B451 247	E. Holzschuh *et al.*	
VAITAITIS	99	PRL 83 4943	A. Vaitaitis *et al.*	(CCFR Collab.)
ASSAMAGAN	98	PL B434 158	K. Assamagan *et al.*	
HINDI	98	PR C58 2512	M.M. Hindi *et al.*	
PDG	98	EPJ C3 1	C. Caso *et al.*	(PDG Collab.)
ABREU	97I	ZPHY C74 57	P. Abreu *et al.*	(DELPHI Collab.)
Also		ZPHY C75 580 (erratum)	P. Abreu *et al.*	(DELPHI Collab.)
BRYMAN	96	PR D53 558	D.A. Bryman, T. Numao	(TRIU)
BUSKULIC	96S	PL B384 439	D. Buskulic *et al.*	(ALEPH Collab.)
WIETFELDT	96	PRPL 273 149	F.E. Wietfeldt, E.B. Norman	(LBL)
ARMBRUSTER	95	PL B348 19	B. Armbruster *et al.*	(KARMEN Collab.)
BAHRAN	95	PL B354 481	M.Y. Bahran, G.R. Kalbfleisch	(OKLA)
BILGER	95	PL B363 41	R. Bilger *et al.*	(TUBIN, KARLE, PSI)
DAUM	95B	PL B361 179	M. Daum *et al.*	(PSI, UVA)
FARGION	95	PR D52 1828	D. Fargion *et al.*	(ROMA, KIAM, MPEI)
GALLAS	95	PR D52 6	E. Gallas *et al.*	(MSU, FNAL, MIT, FLOR)
GARCIA	95	PR D51 1458	E. Garcia *et al.*	(ZARA, SCUC, PNL)
HAGNER	95	PR D52 1343	C. Hagner *et al.*	(MUNT, LAPP, CPPM)
HIDDEMANN	95	JP G21 639	K.H. Hiddemann, H. Daniel, O. Schwentker	(MUNT)
VILAIN	95C	PL B351 387	P. Vilain *et al.*	(CHARM II Collab.)
Also		PL B343 453	P. Vilain *et al.*	(CHARM II Collab.)
BECK	94	PL B336 141	M. Beck *et al.*	(MPIH, KIAE, SASSO)
KONOPLICH	94	PAN 57 425	R.V. Konoplich, M.Y. Khlopov	(MPEI)
PDG	94	PR D50 1173	L. Montanet *et al.*	(CERN, LBL, BOST+)
BAHRAN	93	PR D47 754	M. Bahran, G.R. Kalbfleisch	(OKLA)
BAHRAN	93B	PR D47 759	M. Bahran, G.R. Kalbfleisch	(OKLA)
BARANOV	93	PL B302 336	S.A. Baranov *et al.*	(JINR, SERP, BUDA)
KALBFLEISCH	93	PL B303 355	G.R. Kalbfleisch, M.Y. Bahran	(OKLA)
MORTARA	93	PRL 70 394	J.L. Mortara *et al.*	(ANL, LBL, UCB)
OHSHIMA	93	PR D47 4840	T. Ohshima *et al.*	(KEK, TUAT, RIKEN+)
ABREU	92B	PL B274 230	P. Abreu *et al.*	(DELPHI Collab.)
BAHRAN	92	PL B291 336	M.Y. Bahran, G.R. Kalbfleisch	(OKLA)
BRITTON	92	PRL 68 3000	D.I. Britton *et al.*	(TRIU, CARL)
Also		PR D49 28	D.I. Britton *et al.*	(TRIU, CARL)
BRITTON	92B	PR D46 885	D.I. Britton *et al.*	(TRIU, CARL)
KAWAKAMI	92	PL B287 45	H. Kawakami *et al.*	(INUS, KEK, SCUC+)
MORI	92B	PL B289 463	M. Mori *et al.*	(KAM2 Collab.)
ALEXANDER	91F	ZPHY C52 175	G. Alexander *et al.*	(OPAL Collab.)
DELEENER-...	91	PR D43 3611	N. de Leener-Rosier *et al.*	(LOUV, ZURI+)
REUSSER	91	PL B255 143	D. Reusser *et al.*	(NEUC, CIT, PSI)
SATO	91	PR D44 2220	N. Sato *et al.*	(Kamiokande Collab.)
ADEVA	90S	PL B251 321	B. Adeva *et al.*	(L3 Collab.)
BURCHAT	90	PR D41 3542	P.R. Burchat *et al.*	(Mark II Collab.)
DECAMP	90F	PL B236 511	D. Decamp *et al.*	(ALEPH Collab.)
DEUTSCH	90	NP A518 149	J. Deutsch, M. Lebrun, R. Prieels	
JUNG	90	PRL 64 1091	C. Jung *et al.*	(Mark II Collab.)
ABRAMS	89C	PRL 63 2447	G.S. Abrams *et al.*	(Mark II Collab.)
ENQVIST	89	NP B317 647	K. Enqvist, K. Kainulainen, J. Maalampi	(HELS)
FISHER	89	PL B218 257	P.H. Fisher *et al.*	(CIT, NEUC, PSI)
AKERLOF	88	PR D37 577	C.W. Akerlof *et al.*	(HRS Collab.)
BERNARDI	88	PL B203 332	G. Bernardi *et al.*	(PARIN, CERN, INFN+)
CALDWELL	88	PRL 61 510	D.O. Caldwell *et al.*	(UCSB, UCB, LBL)
OLIVE	88	PL B205 553	K.A. Olive, M. Srednicki	(MINN, UCSB)
SREDNICKI	88	NP B310 693	M. Srednicki, R. Watkins, K.A. Olive	(MINN, UCSB)
AHLEN	87	PL B195 603	S.P. Ahlen *et al.*	(BOST, SCUC, HARV+)
DAUM	87	PR D36 2624	M. Daum *et al.*	(SIN, UVA)
GRIEST	87	NP B283 681	K. Griest, D. Seckel	(UCSC, CERN)
Also		NP B296 1034 (erratum)	K. Griest, D. Seckel	(UCSC, CERN)
MISHRA	87	PRL 59 1397	S.R. Mishra *et al.*	(COLU, CIT, FNAL+)
OBERAUER	87	PL B198 113	L.F. Oberauer, F. von Feilitzsch, R.L. Mossbauer	
WENDT	87	PRL 58 1810	C. Wendt *et al.*	(Mark II Collab.)
AZUELOS	86	PRL 56 2241	G. Azuelos *et al.*	(TRIU, CNRC)
BADIER	86	ZPHY C31 21	J. Badier *et al.*	(NA3 Collab.)
BERNARDI	86	PL 166B 479	G. Bernardi *et al.*	(CURIN, INFN, CDEF+)
DORENBOS...	86	PL 166B 473	J. Dorenbosch *et al.*	(CHARM Collab.)
ALBRECHT	85I	PL 163B 404	H. Albrecht *et al.*	(ARGUS Collab.)
APALIKOV	85	JETPL 42 289	A.M. Apalikov *et al.*	(ITEP)
		Translated from ZETFP 42 233.		
COOPER-...	85	PL 160B 207	A.M. Cooper-Sarkar *et al.*	(CERN, LOIC+)
MARKEY	85	PR C32 2215	J. Markey, F. Boehm	(CIT)
OHI	85	PL 160B 322	T. Ohi *et al.*	(TOKY, INUS, KEK)
MINEHART	84	PRL 52 804	R.C. Minehart *et al.*	(UVA, SIN)
BERGSMA	83	PL 122B 465	F. Bergsma *et al.*	(CHARM Collab.)
BERGSMA	83B	PL 128B 361	F. Bergsma *et al.*	(CHARM Collab.)
BRYMAN	83B	PRL 50 1546	D.A. Bryman *et al.*	(TRIU, CNRC)
DEUTSCH	83	PR D27 1644	J.P. Deutsch, M. Lebrun, R. Prieels	(LOUV)
GRONAU	83	PR D28 2762	M. Gronau	(HAIF)
SCHRECK...	83	PL 129B 265	K. Schreckenbach *et al.*	(ISNG, ILLG)
HAYANO	82	PRL 49 1305	R.S. Hayano *et al.*	(TOKY, KEK, TSUK)
ABELA	81	PL 105B 263	R. Abela *et al.*	(SIN)
ASANO	81	PL 104B 84	Y. Asano *et al.*	(KEK, TOKY, INUS, OSAK)
CALAPRICE	81	PL 106B 175	F.P. Calaprice *et al.*	(PRIN, IND)
SHROCK	81	PR D24 1232	R.E. Shrock	(STON)
SHROCK	81B	PR D24 1275	R.E. Shrock	(STON)
SHROCK	80	PL 96B 159	R.E. Shrock	(STON)

QUARKS

Related Reviews in Volume 1

QUARKS

See the related review(s):

Quark Masses

u

$I(J^P) = \frac{1}{2}(\frac{1}{2}^+)$

Mass $m = 2.2^{+0.5}_{-0.4}$ MeV Charge $= \frac{2}{3}\ e$ $I_z = +\frac{1}{2}$

$m_u/m_d = 0.48^{+0.07}_{-0.08}$

d

$I(J^P) = \frac{1}{2}(\frac{1}{2}^+)$

Mass $m = 4.7^{+0.5}_{-0.3}$ MeV Charge $= -\frac{1}{3}\ e$ $I_z = -\frac{1}{2}$

$m_s/m_d = 17$–22

$\overline{m} = (m_u + m_d)/2 = 3.5^{+0.5}_{-0.2}$ MeV

s

$I(J^P) = 0(\frac{1}{2}^+)$

Mass $m = 95^{+9}_{-3}$ MeV Charge $= -\frac{1}{3}\ e$ Strangeness $= -1$

$(m_s - (m_u + m_d)/2)/(m_d - m_u) = 27.3 \pm 0.7$

Light Quarks (u, d, s)

OMITTED FROM SUMMARY TABLE

u-QUARK MASS

The u-, d-, and s-quark masses are estimates of so-called "current-quark masses," in a mass- independent subtraction scheme such as $\overline{\text{MS}}$. The ratios m_u/m_d and m_s/m_d are extracted from pion and kaon masses using chiral symmetry. The estimates of d and u masses are not without controversy and remain under active investigation. Within the literature there are even suggestions that the u quark could be essentially massless. The s-quark mass is estimated from SU(3) splittings in hadron masses.

We have normalized the $\overline{\text{MS}}$ masses at a renormalization scale of $\mu = 2$ GeV. Results quoted in the literature at $\mu = 1$ GeV have been rescaled by dividing by 1.35. The values of "Our Evaluation" were determined in part via Figures 1 and 2.

$\overline{\text{MS}}$ MASS (MeV)		DOCUMENT ID		TECN
2.2 $^{+0.5}_{-0.4}$	**OUR EVALUATION**	See the ideogram below.		
$2.27 \pm 0.06 \pm 0.06$	[1]	FODOR	16	LATT
2.36 ± 0.24	[2]	CARRASCO	14	LATT
$2.57 \pm 0.26 \pm 0.07$	[3]	AOKI	12	LATT
$2.15 \pm 0.03 \pm 0.10$	[4]	DURR	11	LATT
1.9 ± 0.2	[5]	BAZAVOV	10	LATT
$2.24 \pm 0.10 \pm 0.34$	[6]	BLUM	10	LATT
2.01 ± 0.14	[7]	MCNEILE	10	LATT
2.9 ± 0.2	[8]	DOMINGUEZ	09	THEO
• • • We do not use the following data for averages, fits, limits, etc. • • •				
2.01 ± 0.14	[7]	DAVIES	10	LATT
2.9 ± 0.8	[9]	DEANDREA	08	THEO
3.02 ± 0.33	[10]	BLUM	07	LATT
2.7 ± 0.4	[11]	JAMIN	06	THEO
1.9 ± 0.2	[12]	MASON	06	LATT
2.8 ± 0.2	[13]	NARISON	06	THEO
1.7 ± 0.3	[14]	AUBIN	04A	LATT

[1] FODOR 16 is a lattice simulation with $N_f = 2 + 1$ dynamical flavors and includes partially quenched QED effects.

[2] CARRASCO 14 is a lattice QCD computation of light quark masses using $2 + 1 + 1$ dynamical quarks, with $m_u = m_d \neq m_s \neq m_c$. The u and d quark masses are obtained separately by using the K meson mass splittings and lattice results for the electromagnetic contributions.

[3] AOKI 12 is a lattice computation using $1 + 1 + 1$ dynamical quark flavors.

[4] DURR 11 determine quark mass from a lattice computation of the meson spectrum using $N_f = 2 + 1$ dynamical flavors. The lattice simulations were done at the physical quark mass, so that extrapolation in the quark mass was not needed. The individual m_u, m_d values are obtained using the lattice determination of the average mass m_{ud} and of the ratio m_s/m_{ud} and the value of $Q = (m_s^2 - m_{ud}^2)\ /\ (m_d^2 - m_u^2)$ as determined from $\eta \to 3\pi$ decays.

[5] BAZAVOV 10 is a lattice computation using 2+1 dynamical quark flavors.

[6] BLUM 10 determines light quark masses using a QCD plus QED lattice computation of the electromagnetic mass splittings of the low-lying hadrons. The lattice simulations use 2+1 dynamical quark flavors.

[7] DAVIES 10 and MCNEILE 10 determine $\overline{m}_c(\mu)/\overline{m}_s(\mu) = 11.85 \pm 0.16$ using a lattice computation with $N_f = 2 + 1$ dynamical fermions of the pseudoscalar meson masses. Mass m_u is obtained from this using the value of m_c from ALLISON 08 or MCNEILE 10 and the BAZAVOV 10 values for the light quark mass ratios, $m_s/\overline{m}$ and m_u/m_d.

[8] DOMINGUEZ 09 use QCD finite energy sum rules for the two-point function of the divergence of the axial vector current computed to order α_s^4.

[9] DEANDREA 08 determine $m_u - m_d$ from $\eta \to 3\pi^0$, and combine with the PDG 06 lattice average value of $m_u + m_d = 7.6 \pm 1.6$ to determine m_u and m_d.

[10] BLUM 07 determine quark masses from the pseudoscalar meson masses using a QED plus QCD lattice computation with two dynamical quark flavors.

[11] JAMIN 06 determine $m_u(2\ \text{GeV})$ by combining the value of m_s obtained from the spectral function for the scalar $K\pi$ form factor with other determinations of the quark mass ratios.

[12] MASON 06 extract light quark masses from a lattice simulation using staggered fermions with an improved action, and three dynamical light quark flavors with degenerate u and d quarks. Perturbative corrections were included at NNLO order. The quark masses m_u and m_d were determined from their $(m_u + m_d)/2$ measurement and AUBIN 04A m_u/m_d value.

[13] NARISON 06 uses sum rules for $e^+e^- \to$ hadrons to order α_s^3 to determine m_s combined with other determinations of the quark mass ratios.

[14] AUBIN 04A employ a partially quenched lattice calculation of the pseudoscalar meson masses.

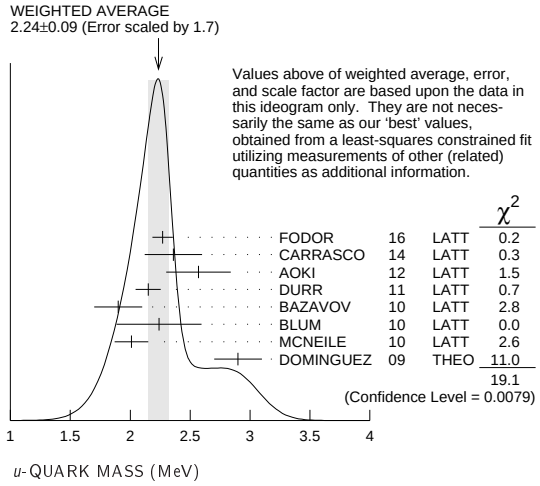

d-QUARK MASS

See the comment for the u quark above.

We have normalized the $\overline{\text{MS}}$ masses at a renormalization scale of $\mu = 2$ GeV. Results quoted in the literature at $\mu = 1$ GeV have been rescaled by dividing by 1.35. The values of "Our Evaluation" were determined in part via Figures 1 and 2.

$\overline{\text{MS}}$ MASS (MeV)		DOCUMENT ID		TECN
4.7 $^{+0.5}_{-0.3}$	**OUR EVALUATION**	See the ideogram below.		
$4.67 \pm 0.06 \pm 0.06$	[1]	FODOR	16	LATT
5.03 ± 0.26	[2]	CARRASCO	14	LATT
$3.68 \pm 0.29 \pm 0.10$	[3]	AOKI	12	LATT
$4.79 \pm 0.07 \pm 0.12$	[4]	DURR	11	LATT
4.6 ± 0.3	[5]	BAZAVOV	10	LATT
$4.65 \pm 0.15 \pm 0.32$	[6]	BLUM	10	LATT
4.77 ± 0.15	[7]	MCNEILE	10	LATT
5.3 ± 0.4	[8]	DOMINGUEZ	09	THEO
• • • We do not use the following data for averages, fits, limits, etc. • • •				
4.79 ± 0.16	[7]	DAVIES	10	LATT
4.7 ± 0.8	[9]	DEANDREA	08	THEO
5.49 ± 0.39	[10]	BLUM	07	LATT
4.8 ± 0.5	[11]	JAMIN	06	THEO
4.4 ± 0.3	[12]	MASON	06	LATT
5.1 ± 0.4	[13]	NARISON	06	THEO
3.9 ± 0.5	[14]	AUBIN	04A	LATT

[1] FODOR 16 is a lattice simulation with $N_f = 2 + 1$ dynamical flavors and includes partially quenched QED effects.

[2] CARRASCO 14 is a lattice QCD computation of light quark masses using $2 + 1 + 1$ dynamical quarks, with $m_u = m_d \neq m_s \neq m_c$. The u and d quark masses are obtained separately by using the K meson mass splittings and lattice results for the electromagnetic contributions.

[3] AOKI 12 is a lattice computation using $1 + 1 + 1$ dynamical quark flavors.

[4] DURR 11 determine quark mass from a lattice computation of the meson spectrum using $N_f = 2 + 1$ dynamical flavors. The lattice simulations were done at the physical quark mass, so that extrapolation in the quark mass was not needed. The individual m_u, m_d values are obtained using the lattice determination of the average mass m_{ud} and of the ratio m_s/m_{ud} and the value of $Q = (m_s^2 - m_{ud}^2)\ /\ (m_d^2 - m_u^2)$ as determined from $\eta \to 3\pi$ decays.

[5] BAZAVOV 10 is a lattice computation using 2+1 dynamical quark flavors.

[6] BLUM 10 determines light quark masses using a QCD plus QED lattice computation of the electromagnetic mass splittings of the low-lying hadrons. The lattice simulations use 2+1 dynamical quark flavors.
[7] DAVIES 10 and MCNEILE 10 determine $\overline{m}_c(\mu)/\overline{m}_s(\mu) = 11.85 \pm 0.16$ using a lattice computation with $N_f = 2 + 1$ dynamical fermions of the pseudoscalar meson masses. Mass m_d is obtained from this using the value of m_c from ALLISON 08 or MCNEILE 10 and the BAZAVOV 10 values for the light quark mass ratios, $m_s/\overline{m}$ and m_u/m_d.
[8] DOMINGUEZ 09 use QCD finite energy sum rules for the two-point function of the divergence of the axial vector current computed to order α_s^4.
[9] DEANDREA 08 determine $m_u - m_d$ from $\eta \to 3\pi^0$, and combine with the PDG 06 lattice average value of $m_u + m_d = 7.6 \pm 1.6$ to determine m_u and m_d.
[10] BLUM 07 determine quark masses from the pseudoscalar meson masses using a QED plus QCD lattice computation with two dynamical quark flavors.
[11] JAMIN 06 determine m_d(2 GeV) by combining the value of m_s obtained from the spectral function for the scalar $K\pi$ form factor with other determinations of the quark mass ratios.
[12] MASON 06 extract light quark masses from a lattice simulation using staggered fermions with an improved action, and three dynamical light quark flavors with degenerate u and d quarks. Perturbative corrections were included at NNLO order. The quark masses m_u and m_d were determined from their $(m_u+m_d)/2$ measurement and AUBIN 04A m_u/m_d value.
[13] NARISON 06 uses sum rules for $e^+e^- \to$ hadrons to order α_s^3 to determine m_s combined with other determinations of the quark mass ratios.
[14] AUBIN 04A perform three flavor dynamical lattice calculation of pseudoscalar meson masses, with continuum estimate of electromagnetic effects in the kaon masses, and one-loop perturbative renormalization constant.

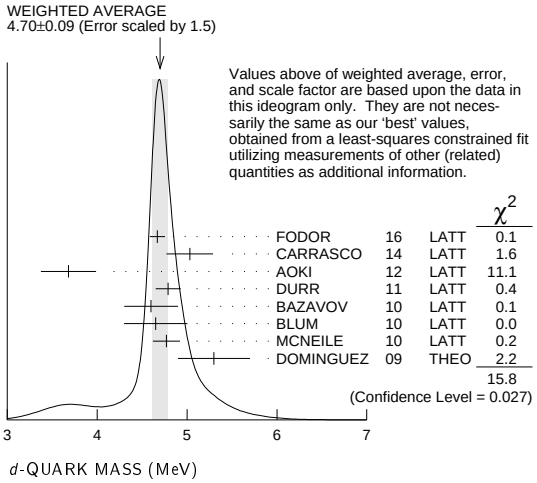

$\overline{m} = (m_u+m_d)/2$

See the comments for the u quark above.

We have normalized the $\overline{\text{MS}}$ masses at a renormalization scale of $\mu = 2$ GeV. Results quoted in the literature at $\mu = 1$ GeV have been rescaled by dividing by 1.35. The values of "Our Evaluation" were determined in part via Figures 1 and 2.

$\overline{\text{MS}}$ MASS (MeV)		DOCUMENT ID		TECN
3.5	$^{+0.5}_{-0.2}$ **OUR EVALUATION**	See the ideogram below.		
4.7	$^{+0.8}_{-0.7}$	[1] YUAN	17	THEO
3.70	±0.17	[2] CARRASCO	14	LATT
3.45	±0.12	[3] ARTHUR	13	LATT
3.59	±0.21	[4] AOKI	11A	LATT
3.469	±0.047±0.048	[5] DURR	11	LATT
3.6	±0.2	[6] BLOSSIER	10	LATT
3.39	±0.06	[7] MCNEILE	10	LATT
4.1	±0.2	[8] DOMINGUEZ	09	THEO
3.72	±0.41	[9] ALLTON	08	LATT
3.55	$^{+0.65}_{-0.28}$	[10] ISHIKAWA	08	LATT
4.25	±0.35	[11] BLUM	07	LATT
• • • We do not use the following data for averages, fits, limits, etc. • • •				
3.40	±0.07	[7] DAVIES	10	LATT
3.85	±0.12 ±0.4	[12] BLOSSIER	08	LATT
≥ 4.85	±0.20	[13] DOMINGUEZ...	08B	THEO
4.026	±0.048	[14] NAKAMURA	08	LATT
4.08	±0.25 ±0.42	[15] GOCKELER	06	LATT
4.7	±0.2 ±0.3	[16] GOCKELER	06A	LATT
3.2	±0.3	[17] MASON	06	LATT
3.95	±0.3	[18] NARISON	06	THEO
2.8	±0.3	[19] AUBIN	04	LATT
4.29	±0.14 ±0.65	[20] AOKI	03	LATT
3.223	±0.3	[21] AOKI	03B	LATT
4.4	±0.1 ±0.4	[22] BECIREVIC	03	LATT
4.1	±0.3 ±1.0	[23] CHIU	03	LATT

[1] YUAN 17 determine $\overline{m}$ using QCD sum rules in the isospin I=0 scalar channel. At the end of the "Numerical Results" section of YUAN 17 the authors discuss the significance of their larger value of the light quark mass compared to previous determinations.
[2] CARRASCO 14 is a lattice QCD computation of light quark masses using $2 + 1 + 1$ dynamical quarks, with $m_u = m_d \neq m_s \neq m_c$. The u and d quark masses are obtained separately by using the K meson mass splittings and lattice results for the electromagnetic contributions.
[3] ARTHUR 13 is a lattice computation using 2+1 dynamical domain wall fermions. Masses at $\mu = 3$ GeV have been converted to $\mu = 2$ GeV using conversion factors given in their paper.
[4] AOKI 11A determine quark masses from a lattice computation of the hadron spectrum using $N_f = 2 + 1$ dynamical flavors of domain wall fermions.
[5] DURR 11 determine quark mass from a lattice computation of the meson spectrum using $N_f = 2 + 1$ dynamical flavors. The lattice simulations were done at the physical quark mass, so that extrapolation in the quark mass was not needed.
[6] BLOSSIER 10 determines quark masses from a computation of the hadron spectrum using N_f=2 dynamical twisted-mass Wilson fermions.
[7] DAVIES 10 and MCNEILE 10 determine $\overline{m}_c(\mu)/\overline{m}_s(\mu) = 11.85 \pm 0.16$ using a lattice computation with $N_f = 2 + 1$ dynamical fermions of the pseudoscalar meson masses. Mass $\overline{m}$ is obtained from this using the value of m_c from ALLISON 08 or MCNEILE 10 and the BAZAVOV 10 values for the light quark mass ratio, $m_s/\overline{m}$.
[8] DOMINGUEZ 09 use QCD finite energy sum rules for the two-point function of the divergence of the axial vector current computed to order α_s^4.
[9] ALLTON 08 use a lattice computation of the π, K, and Ω masses with 2+1 dynamical flavors of domain wall quarks, and non-perturbative renormalization.
[10] ISHIKAWA 08 use a lattice computation of the light meson spectrum with 2+1 dynamical flavors of $\mathcal{O}(a)$ improved Wilson quarks, and one-loop perturbative renormalization.
[11] BLUM 07 determine quark masses from the pseudoscalar meson masses using a QED plus QCD lattice computation with two dynamical quark flavors.
[12] BLOSSIER 08 use a lattice computation of pseudoscalar meson masses and decay constants with 2 dynamical flavors and non-perturbative renormalization.
[13] DOMINGUEZ-CLARIMON 08B obtain an inequality from sum rules for the scalar two-point correlator.
[14] NAKAMURA 08 do a lattice computation using quenched domain wall fermions and non-perturbative renormalization.
[15] GOCKELER 06 use an unquenched lattice computation of the axial Ward Identity with $N_f = 2$ dynamical light quark flavors, and non-perturbative renormalization, to obtain $\overline{m}$(2 GeV) = 4.08 ± 0.25 ± 0.19 ± 0.23 MeV, where the first error is statistical, the second and third are systematic due to the fit range and force scale uncertainties, respectively. We have combined the systematic errors linearly.
[16] GOCKELER 06A use an unquenched lattice computation of the pseudoscalar meson masses with $N_f = 2$ dynamical light quark flavors, and non-perturbative renormalization.
[17] MASON 06 extract light quark masses from a lattice simulation using staggered fermions with an improved action, and three dynamical light quark flavors with degenerate u and d quarks. Perturbative corrections were included at NNLO order.
[18] NARISON 06 uses sum rules for $e^+e^- \to$ hadrons to order α_s^3 to determine m_s combined with other determinations of the quark mass ratios.
[19] AUBIN 04 perform three flavor dynamical lattice calculation of pseudoscalar meson masses, with one-loop perturbative renormalization constant.
[20] AOKI 03 uses quenched lattice simulation of the meson and baryon masses with degenerate light quarks. The extrapolations are done using quenched chiral perturbation theory.
[21] The errors given in AOKI 03B were $^{+0.046}_{-0.069}$. We changed them to ±0.3 for calculating the overall best values. AOKI 03B uses lattice simulation of the meson and baryon masses with two dynamical light quarks. Simulations are performed using the $\mathcal{O}(a)$ improved Wilson action.
[22] BECIREVIC 03 perform quenched lattice computation using the vector and axial Ward identities. Uses $\mathcal{O}(a)$ improved Wilson action and nonperturbative renormalization.
[23] CHIU 03 determines quark masses from the pion and kaon masses using a lattice simulation with a chiral fermion action in quenched approximation.

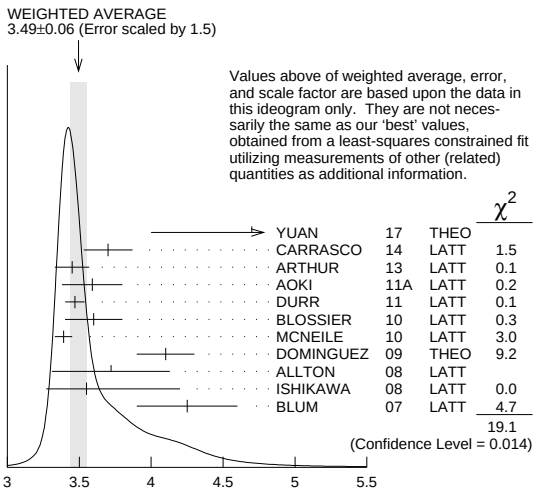

m_u/m_d MASS RATIO

VALUE		DOCUMENT ID		TECN	COMMENT
0.48	$^{+0.07}_{-0.08}$ **OUR EVALUATION**	See the ideogram below.			
0.485	$\pm 0.011 \pm 0.016$	[1] FODOR	16	LATT	
0.4482	$^{+0.0173}_{-0.0206}$	[2] BASAK	15	LATT	
0.470	± 0.056	[3] CARRASCO	14	LATT	
0.698	± 0.051	[4] AOKI	12	LATT	
0.42	$\pm 0.01 \pm 0.04$	[5] BAZAVOV	10	LATT	
0.4818	$\pm 0.0096 \pm 0.0860$	[6] BLUM	10	LATT	
0.550	± 0.031	[7] BLUM	07	LATT	
• • • We do not use the following data for averages, fits, limits, etc. • • •					
0.43	± 0.08	[8] AUBIN	04A	LATT	
0.410	± 0.036	[9] NELSON	03	LATT	
0.553	± 0.043	[10] LEUTWYLER	96	THEO	Compilation

[1] FODOR 16 is a lattice simulation with $N_f = 2 + 1$ dynamical flavors and includes partially quenched QED effects.

[2] BASAK 15 is a lattice computation using 2+1 dynamical quark flavors.

[3] CARRASCO 14 is a lattice QCD computation of light quark masses using $2 + 1 + 1$ dynamical quarks, with $m_u = m_d \neq m_s \neq m_c$. The u and d quark masses are obtained separately by using the K meson mass splittings and lattice results for the electromagnetic contributions.

[4] AOKI 12 is a lattice computation using $1 + 1 + 1$ dynamical quark flavors.

[5] BAZAVOV 10 is a lattice computation using 2+1 dynamical quark flavors.

[6] BLUM 10 is a lattice computation using 2+1 dynamical quark flavors.

[7] BLUM 07 determine quark masses from the pseudoscalar meson masses using a QED plus QCD lattice computation with two dynamical quark flavors.

[8] AUBIN 04A perform three flavor dynamical lattice calculation of pseudoscalar meson masses, with continuum estimate of electromagnetic effects in the kaon masses.

[9] NELSON 03 computes coefficients in the order p^4 chiral Lagrangian using a lattice calculation with three dynamical flavors. The ratio m_u/m_d is obtained by combining this with the chiral perturbation theory computation of the meson masses to order p^4.

[10] LEUTWYLER 96 uses a combined fit to $\eta \to 3\pi$ and $\psi' \to J/\psi\,(\pi,\eta)$ decay rates, and the electromagnetic mass differences of the π and K.

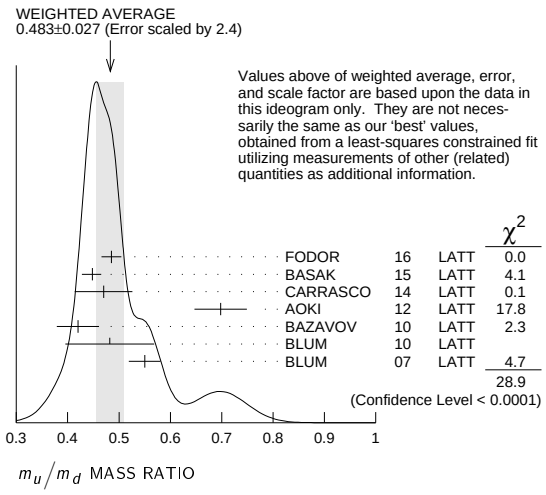

s-QUARK MASS

See the comment for the u quark above.

We have normalized the $\overline{\text{MS}}$ masses at a renormalization scale of $\mu = 2$ GeV. Results quoted in the literature at $\mu = 1$ GeV have been rescaled by dividing by 1.35.

$\overline{\text{MS}}$ MASS (MeV)		DOCUMENT ID		TECN
95	$^{+9}_{-3}$ **OUR EVALUATION**	See the ideogram below.		
87.6	± 6.0	[1] ANANTHANA..16		THEO
93.6	± 0.8	[2] CHAKRABOR..15		LATT
99.6	± 4.3	[3] CARRASCO	14	LATT
94.4	± 2.3	[4] ARTHUR	13	LATT
94	± 9	[5] BODENSTEIN	13	THEO
102	$\pm 3 \pm 1$	[6] FRITZSCH	12	LATT
96.2	± 2.7	[7] AOKI	11A	LATT
95.5	$\pm 1.1 \pm 1.5$	[8] DURR	11	LATT
95	± 6	[9] BLOSSIER	10	LATT
97.6	$\pm 2.9 \pm 5.5$	[10] BLUM	10	LATT
107.3	± 11.7	[11] ALLTON	08	LATT
102	± 8	[12] DOMINGUEZ	08A	THEO
90.1	$^{+17.2}_{-6.1}$	[13] ISHIKAWA	08	LATT
92.4	± 1.5	[14] DAVIES	10	LATT
92.2	± 1.3	[14] MCNEILE	10	LATT
105	$\pm 3 \pm 9$	[15] BLOSSIER	08	LATT
105.6	± 1.2	[16] NAKAMURA	08	LATT
119.5	± 9.3	[17] BLUM	07	LATT
105	$\pm 6 \pm 7$	[18] CHETYRKIN	06	THEO
111	$\pm 6 \pm 10$	[19] GOCKELER	06	LATT
119	$\pm 5 \pm 8$	[20] GOCKELER	06A	LATT
92	± 9	[21] JAMIN	06	THEO
87	± 6	[22] MASON	06	LATT
104	± 15	[23] NARISON	06	THEO
$\geq 71 \pm 4$,	$\leq 151 \pm 14$	[24] NARISON	06	THEO
96	$^{+5}_{-3}$ $^{+16}_{-18}$	[25] BAIKOV	05	THEO
81	± 22	[26] GAMIZ	05	THEO
125	± 28	[27] GORBUNOV	05	THEO
93	± 32	[28] NARISON	05	THEO
76	± 8	[29] AUBIN	04	LATT
116	$\pm 6 \pm 0.65$	[30] AOKI	03	LATT
84.5	$^{+12}_{-1.7}$	[31] AOKI	03B	LATT
106	$\pm 2 \pm 8$	[32] BECIREVIC	03	LATT
92	$\pm 9 \pm 16$	[33] CHIU	03	LATT
117	± 17	[34] GAMIZ	03	THEO
103	± 17	[35] GAMIZ	03	THEO

[1] ANANTHANARAYAN 16 determine $\overline{m}_s(2\text{ GeV}) = 106.70 \pm 9.36$ MeV and 74.47 ± 7.77 MeV from fits to ALEPH and OPAL τ decay data, respectively. We have used the weighted average of the two.

[2] CHAKRABORTY 15 is a lattice QCD computation that determines m_c and m_c/m_s using pseudoscalar mesons masses tuned on gluon field configurations with 2+1+1 dynamical flavors of HISQ quarks with u/d masses down to the physical value.

[3] CARRASCO 14 is a lattice QCD computation of light quark masses using $2 + 1 + 1$ dynamical quarks, with $m_u = m_d \neq m_s \neq m_c$. The u and d quark masses are obtained separately by using the K meson mass splittings and lattice results for the electromagnetic contributions.

[4] ARTHUR 13 is a lattice computation using 2+1 dynamical domain wall fermions. Masses at $\mu = 3$ GeV have been converted to $\mu = 2$ GeV using conversion factors given in their paper.

[5] BODENSTEIN 13 determines m_s from QCD finite energy sum rules, and the perturbative computation of the pseudoscalar correlator to five-loop order.

[6] FRITZSCH 12 determine m_s using a lattice computation with $N_f = 2$ dynamical flavors.

[7] AOKI 11A determine quark masses from a lattice computation of the hadron spectrum using $N_f = 2 + 1$ dynamical flavors of domain wall fermions.

[8] DURR 11 determine quark mass from a lattice computation of the meson spectrum using $N_f = 2 + 1$ dynamical flavors. The lattice simulations were done at the physical quark mass, so that extrapolation in the quark mass was not needed.

[9] BLOSSIER 10 determines quark masses from a computation of the hadron spectrum using N_f=2 dynamical twisted-mass Wilson fermions.

[10] BLUM 10 determines light quark masses using a QCD plus QED lattice computation of the electromagnetic mass splittings of the low-lying hadrons. The lattice simulations use 2+1 dynamical quark flavors.

[11] ALLTON 08 use a lattice computation of the π, K, and Ω masses with 2+1 dynamical flavors of domain wall quarks, and non-perturbative renormalization.

[12] DOMINGUEZ 08A make determination from QCD finite energy sum rules for the pseudoscalar two-point function computed to order α_s^4.

[13] ISHIKAWA 08 use a lattice computation of the light meson spectrum with 2+1 dynamical flavors of $\mathcal{O}(a)$ improved Wilson quarks, and one-loop perturbative renormalization.

[14] DAVIES 10 and MCNEILE 10 determine $\overline{m}_c(\mu)/\overline{m}_s(\mu) = 11.85 \pm 0.16$ using a lattice computation with $N_f = 2 + 1$ dynamical fermions of the pseudoscalar meson masses. Mass m_s is obtained from this using the value of m_c from ALLISON 08 or MCNEILE 10.

[15] BLOSSIER 08 use a lattice computation of pseudoscalar meson masses and decay constants with 2 dynamical flavors and non-perturbative renormalization.

[16] NAKAMURA 08 do a lattice computation using quenched domain wall fermions and non-perturbative renormalization.

[17] BLUM 07 determine quark masses from the pseudoscalar meson masses using a QED plus QCD lattice computation with two dynamical quark flavors.

[18] CHETYRKIN 06 use QCD sum rules in the pseudoscalar channel to order α_s^4.

[19] GOCKELER 06 use an unquenched lattice computation of the axial Ward Identity with $N_f = 2$ dynamical light quark flavors, and non-perturbative renormalization, to obtain $\overline{m}_s(2\text{ GeV}) = 111 \pm 6 \pm 4 \pm 6$ MeV, where the first error is statistical, the second and third are systematic due to the fit range and force scale uncertainties, respectively. We have combined the systematic errors linearly.

[20] GOCKELER 06A use an unquenched lattice computation of the pseudoscalar meson masses with $N_f = 2$ dynamical light quark flavors, and non-perturbative renormalization.

[21] JAMIN 06 determine $\overline{m}_s(2\text{ GeV})$ from the spectral function for the scalar $K\pi$ form factor.

[22] MASON 06 extract light quark masses from a lattice simulation using staggered fermions with an improved action, and three dynamical light quark flavors with degenerate u and d quarks. Perturbative corrections were included at NNLO order.

[23] NARISON 06 uses sum rules for $e^+e^- \to$ hadrons to order α_s^3.

[24] NARISON 06 obtains the quoted range from positivity of the spectral functions.

[25] BAIKOV 05 determines $\overline{m}_s(M_\tau) = 100^{+5}_{-3}{}^{+17}_{-19}$ from sum rules using the strange spectral function in τ decay. The computations were done to order α_s^3, with an estimate of the α_s^4 terms. We have converted the result to $\mu = 2$ GeV.

[26] GAMIZ 05 determines $\overline{m}_s(2\text{ GeV})$ from sum rules using the strange spectral function in τ decay. The computations were done to order α_s^2, with an estimate of the α_s^3 terms.

[27] GORBUNOV 05 use hadronic tau decays to N3LO, including power corrections.

[28] NARISON 05 determines $\overline{m}_s(2\text{ GeV})$ from sum rules using the strange spectral function in τ decay. The computations were done to order α_s^3.

[29] AUBIN 04 perform three flavor dynamical lattice calculation of pseudoscalar meson masses, with one-loop perturbative renormalization constant.
[30] AOKI 03 uses quenched lattice simulation of the meson and baryon masses with degenerate light quarks. The extrapolations are done using quenched chiral perturbation theory. Determines m_s=113.8 ± 2.3 $^{+5.8}_{-2.9}$ using K mass as input and m_s=142.3 ± 5.8 $^{+22}_{-0}$ using ϕ mass as input. We have performed a weighted average of these values.
[31] AOKI 03B uses lattice simulation of the meson and baryon masses with two dynamical light quarks. Simulations are performed using the $\mathcal{O}(a)$ improved Wilson action.
[32] BECIREVIC 03 perform quenched lattice computation using the vector and axial Ward identities. Uses $\mathcal{O}(a)$ improved Wilson action and nonperturbative renormalization. They also quote $\overline{m}/m_s$=24.3 ± 0.2 ± 0.6.
[33] CHIU 03 determines quark masses from the pion and kaon masses using a lattice simulation with a chiral fermion action in quenched approximation.
[34] GAMIZ 03 determines m_s from SU(3) breaking in the τ hadronic width. The value of V_{us} is chosen to satisfy CKM unitarity.
[35] GAMIZ 03 determines m_s from SU(3) breaking in the τ hadronic width. The value of V_{us} is taken from the PDG.

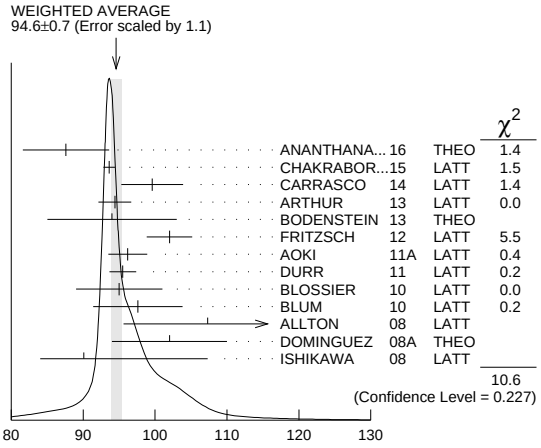

OTHER LIGHT QUARK MASS RATIOS

m_s/m_d MASS RATIO

VALUE		DOCUMENT ID		TECN	COMMENT
17–22 OUR EVALUATION					
• • • We do not use the following data for averages, fits, limits, etc. • • •					
20.0	[1]	GAO	97	THEO	
18.9±0.8	[2]	LEUTWYLER	96	THEO	Compilation
21	[3]	DONOGHUE	92	THEO	
18	[4]	GERARD	90	THEO	
18 to 23	[5]	LEUTWYLER	90B	THEO	

[1] GAO 97 uses electromagnetic mass splittings of light mesons.
[2] LEUTWYLER 96 uses a combined fit to $\eta \to 3\pi$ and $\psi' \to J/\psi\,(\pi,\eta)$ decay rates, and the electromagnetic mass differences of the π and K.
[3] DONOGHUE 92 result is from a combined analysis of meson masses, $\eta \to 3\pi$ using second-order chiral perturbation theory including nonanalytic terms, and $(\psi(2S) \to J/\psi(1S)\,\pi)/(\psi(2S) \to J/\psi(1S)\,\eta)$.
[4] GERARD 90 uses large N and η-η' mixing.
[5] LEUTWYLER 90B determines quark mass ratios using second-order chiral perturbation theory for the meson and baryon masses, including nonanalytic corrections. Also uses Weinberg sum rules to determine L_7.

$m_s/\overline{m}$ MASS RATIO

$\overline{m} \equiv (m_u + m_d)/2$

VALUE		DOCUMENT ID		TECN
27.3 ±0.7 OUR EVALUATION	See the ideogram below.			
27.35±0.05 $^{+0.10}_{-0.07}$	[1]	BAZAVOV	14A	LATT
26.66±0.32	[2]	CARRASCO	14	LATT
27.36±0.54	[3]	ARTHUR	13	LATT
26.8 ±1.4	[4]	AOKI	11A	LATT
27.53±0.20±0.08	[5]	DURR	11	LATT
27.3 ±0.9	[6]	BLOSSIER	10	LATT
28.8 ±1.65	[7]	ALLTON	08	LATT
27.3 ±0.3 ±1.2	[8]	BLOSSIER	08	LATT
23.5 ±1.5	[9]	OLLER	07A	THEO
• • • We do not use the following data for averages, fits, limits, etc. • • •				
27.4 ±0.4	[10]	AUBIN	04	LATT

[1] BAZAVOV 14A is a lattice computation using 4 dynamical flavors of HISQ fermions.
[2] CARRASCO 14 is a lattice QCD computation of light quark masses using $2+1+1$ dynamical quarks, with $m_u = m_d \neq m_s \neq m_c$. The u and d quark masses are obtained separately by using the K meson mass splittings and lattice results for the electromagnetic contributions.
[3] ARTHUR 13 is a lattice computation using 2+1 dynamical domain wall fermions.
[4] AOKI 11A determine quark masses from a lattice computation of the hadron spectrum using $N_f = 2+1$ dynamical flavors of domain wall fermions.
[5] DURR 11 determine quark mass from a lattice computation of the meson spectrum using $N_f = 2+1$ dynamical flavors. The lattice simulations were done at the physical quark mass, so that extrapolation in the quark mass was not needed.
[6] BLOSSIER 10 determines quark masses from a computation of the hadron spectrum using N_f=2 dynamical twisted-mass Wilson fermions.
[7] ALLTON 08 use a lattice computation of the π, K, and Ω masses with 2+1 dynamical flavors of domain wall quarks, and non-perturbative renormalization.
[8] BLOSSIER 08 use a lattice computation of pseudoscalar meson masses and decay constants with 2 dynamical flavors and non-perturbative renormalization.
[9] OLLER 07A use unitarized chiral perturbation theory to order p^4.
[10] Three flavor dynamical lattice calculation of pseudoscalar meson masses.

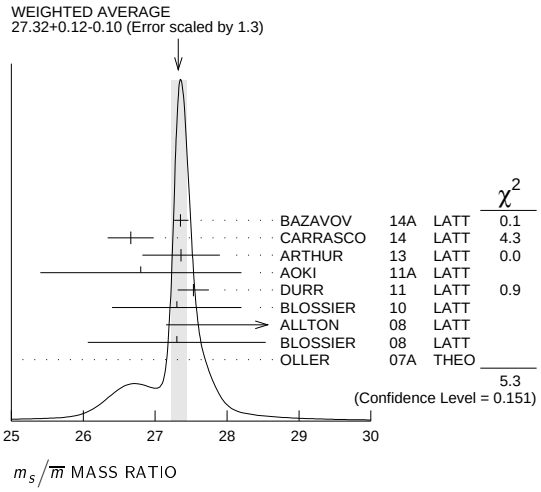

Q MASS RATIO

$Q \equiv \sqrt{(m^2{}_s - \overline{m}^2)/(m^2{}_d - m^2{}_u)}$; $\overline{m} \equiv (m_u + m_d)/2$

VALUE		DOCUMENT ID		TECN
• • • We do not use the following data for averages, fits, limits, etc. • • •				
22.0±0.7	[1]	COLANGELO	17	
21.6±1.1	[2]	GUO	17	THEO
23.4±0.4±0.5	[3]	FODOR	16	LATT
21.4±0.4	[4]	GUO	15F	THEO
22.8±0.4	[5]	MARTEMYA...	05	THEO
22.7±0.8	[6]	ANISOVICH	96	THEO

[1] COLANGELO 17 obtain Q from a dispersive analysis of KLOE collaboration data on $\eta \to \pi^+\pi^-\pi^0$ decays and chiral perturbation theory input.
[2] GUO 17 determine Q from a dispersive model fit to KLOE and WASA-at-COSY data on $\eta \to \pi^+\pi^-\pi^0$ decay and matching to chiral perturbation theory .
[3] FODOR 16 is a lattice simulation with $N_f = 2+1$ dynamical flavors and includes partially quenched QED effects.
[4] GUO 15F determine Q from a Khuri-Treiman analysis of $\eta \to 3\pi$ decays.
[5] MARTEMYANOV 05 determine Q from $\eta \to 3\pi$ decay.
[6] ANISOVICH 96 find Q from $\eta \to \pi^+\pi^-\pi^0$ decay using dispersion relations and chiral perturbation theory.

LIGHT QUARKS (u, d, s) REFERENCES

COLANGELO	17	PRL 118 022001	G. Colangelo *et al.*	(BERN, IND, JLAB)
GUO	17	PL B771 497	P. Guo *et al.*	
YUAN	17	PR D96 014034	J.-M. Yuan *et al.*	
ANANTHANA...	16	PR D94 116014	B. Ananthanarayan, D. Das	(BANG, AHMED)
FODOR	16	PRL 117 082001	Z. Fodor *et al.*	(BMW Collab.)
BASAK	15	JPCS 640 012052	S. Basak *et al.*	(MILC Collab.)
CHAKRABOR...	15	PR D91 054508	B. Chakraborty *et al.*	(HPQCD Collab.)
GUO	15F	PR D92 054016	P. Guo *et al.*	
BAZAVOV	14A	PR D90 074509	A. Bazavov *et al.*	(Fermi-LAT and MILC Collabs.)
CARRASCO	14	NP B887 19	N. Carrasco *et al.*	(European Twisted Mass Collab.)
ARTHUR	13	PR D87 094514	R. Arthur *et al.*	(RBC and UKQCD Collabs.)
BODENSTEIN	13	JHEP 1307 138	S. Bodenstein, C.A. Dominguez, K. Schilcher	(MANZ+)
AOKI	12	PR D86 034507	S. Aoki *et al.*	(PACS-CS Collab.)
FRITZSCH	12	NP B865 397	P. Fritzsch *et al.*	(ALPHA Collab.)
AOKI	11A	PR D83 074508	Y. Aoki *et al.*	(RBC-UKQCD Collab.)
DURR	11	PL B701 265	S. Durr *et al.*	(BMW Collab.)
BAZAVOV	10	RMP 82 1349	A. Bazavov *et al.*	(MILC Collab.)
BLOSSIER	10	PR D82 114513	B. Blossier *et al.*	(ETM Collab.)
BLUM	10	PR D82 094508	T. Blum *et al.*	
DAVIES	10	PRL 104 132003	C.T.H. Davies *et al.*	(HPQCD Collab.)
MCNEILE	10	PR D82 034512	C. McNeile *et al.*	(HPQCD Collab.)
DOMINGUEZ	09	PR D79 014009	C.A. Dominguez *et al.*	
ALLISON	08	PR D78 054513	I. Allison *et al.*	(HPQCD Collab.)
ALLTON	08	PR D78 114509	C. Allton *et al.*	(RBC and UKQCD Collabs.)
BLOSSIER	08	JHEP 0804 020	B. Blossier *et al.*	(ETM Collab.)
DEANDREA	08	PR D78 034032	A. Deandrea, A. Nehme, P. Talavera	
DOMINGUEZ	08A	JHEP 0805 020	C.A. Dominguez *et al.*	
DOMINGUEZ...	08B	PL B660 49	A. Dominguez-Clarimon, E. de Rafael, J. Taron	
ISHIKAWA	08	PR D78 011502	T. Ishikawa *et al.*	(CP-PACS and JLQCD Collabs.)
NAKAMURA	08	PR D78 034502	Y. Nakamura *et al.*	(CP-PACS Collab.)
BLUM	07	PR D76 114508	T. Blum *et al.*	(RBC Collab.)
OLLER	07A	EPJ A34 371	J.A. Oller, L. Roca	
CHETYRKIN	06	EPJ C46 721	K.G. Chetyrkin, A. Khodjamirian	
GOCKELER	06	PR D73 054508	M. Gockeler *et al.*	(QCDSF, UKQCD Collabs)
GOCKELER	06A	PL B639 307	M. Gockeler *et al.*	(QCDSF, UKQCD Collabs)

JAMIN	06	PR D74 074009	M. Jamin, J.A. Oller, A. Pich	
MASON	06	PR D73 114501	Q. Mason *et al.*	(HPQCD Collab.)
NARISON	06	PR D74 034013	S. Narison	
PDG	06	JP G33 1	W.-M. Yao *et al.*	(PDG Collab.)
BAIKOV	05	PRL 95 012003	P.A. Baikov, K.G. Chetyrkin, J.H. Kuhn	
GAMIZ	05	PRL 94 011803	E. Gamiz *et al.*	
GORBUNOV	05	PR D71 013002	D.S. Gorbunov, A.A. Pivovarov	
MARTEMYA...	05	PR D71 017501	B.V. Martemyanov, V.S. Sopov	
NARISON	05	PL B626 101	S. Narison	
AUBIN	04	PR D70 031504	C. Aubin *et al.*	(HPQCD, MILC, UKQCD Collabs.)
AUBIN	04A	PR D70 114501	C. Aubin *et al.*	(MILC Collab.)
AOKI	03	PR D67 034503	S. Aoki *et al.*	(CP-PACS Collab.)
AOKI	03B	PR D68 054502	S. Aoki *et al.*	(CP-PACS Collab.)
BECIREVIC	03	PL B558 69	D. Becirevic, V. Lubicz, C. Tarantino	
CHIU	03	NP B673 217	T.-W. Chiu, T.-H. Hsieh	
GAMIZ	03	JHEP 0301 060	E. Gamiz *et al.*	
NELSON	03	PRL 90 021601	D. Nelson, G.T. Fleming, G.W. Kilcup	
GAO	97	PR D56 4115	D.-N. Gao, B.A. Li, M.-L. Yan	
ANISOVICH	96	PL B375 335	A.V. Anisovich, H. Leutwyler	
LEUTWYLER	96	PL B378 313	H. Leutwyler	
DONOGHUE	92	PRL 69 3444	J.F. Donoghue, B.R. Holstein, D. Wyler	(MASA+)
GERARD	90	MPL A5 391	J.M. Gerard	(MPIM)
LEUTWYLER	90B	NP B337 108	H. Leutwyler	(BERN)

c

$I(J^P) = 0(\frac{1}{2}^+)$

Charge $= \frac{2}{3}\,e$ Charm $= +1$

c-QUARK MASS

The c-quark mass corresponds to the "running" mass m_c ($\mu = m_c$) in the $\overline{\text{MS}}$ scheme. We have converted masses in other schemes to the $\overline{\text{MS}}$ scheme using two-loop QCD perturbation theory with $\alpha_s(\mu{=}m_c) = 0.38 \pm 0.03$. The value $1.275^{+0.025}_{-0.035}$ GeV for the $\overline{\text{MS}}$ mass corresponds to 1.67 ± 0.07 GeV for the pole mass (see the "Note on Quark Masses").

$\overline{\text{MS}}$ MASS (GeV)			DOCUMENT ID		TECN
1.275	$^{+0.025}_{-0.035}$	**OUR EVALUATION**	See the ideogram below.		
1.279	± 0.008		[1] CHETYRKIN	17	THEO
1.335	± 0.043	$^{+0.040}_{-0.011}$	[2] BERTONE	16	THEO
1.246	± 0.023		[3] KIYO	16	THEO
1.2715	± 0.0095		[4] CHAKRABOR...	15	LATT
1.288	± 0.020		[5] DEHNADI	15	THEO
1.348	± 0.046		[6] CARRASCO	14	LATT
1.26	± 0.05	± 0.04	[7] ABRAMOWICZ	13C	COMB
1.24	± 0.03	$^{+0.03}_{-0.07}$	[8] ALEKHIN	13	THEO
1.282	± 0.011	± 0.022	[9] DEHNADI	13	THEO
1.286	± 0.066		[10] NARISON	13	THEO
1.159	± 0.075		[11] SAMOYLOV	13	NOMD
1.36	± 0.04	± 0.10	[12] ALEKHIN	12	THEO
1.261	± 0.016		[13] NARISON	12A	THEO
1.278	± 0.009		[14] BODENSTEIN	11	THEO
1.28	$^{+0.07}_{-0.06}$		[15] LASCHKA	11	THEO
1.196	± 0.059	± 0.050	[16] AUBERT	10A	BABR
1.28	± 0.04		[17] BLOSSIER	10	LATT
1.25	± 0.04		[18] SIGNER	09	THEO
• • • We do not use the following data for averages, fits, limits, etc. • • •					
1.01	± 0.09	± 0.03	[19] ALEKHIN	11	THEO
1.299	± 0.026		[20] BODENSTEIN	10	THEO
1.273	± 0.006		[21] MCNEILE	10	LATT
1.261	± 0.018		[22] NARISON	10	THEO
1.279	± 0.013		[23] CHETYRKIN	09	THEO
1.268	± 0.009		[24] ALLISON	08	LATT
1.286	± 0.013		[25] KUHN	07	THEO
1.295	± 0.015		[26] BOUGHEZAL	06	THEO
1.24	± 0.09		[27] BUCHMUEL...	06	THEO
1.224	± 0.017	± 0.054	[28] HOANG	06	THEO
1.33	± 0.10		[29] AUBERT	04X	THEO
1.29	± 0.07		[30] HOANG	04	THEO
1.319	± 0.028		[31] DEDIVITIIS	03	LATT
1.19	± 0.11		[32] EIDEMULLER	03	THEO
1.289	± 0.043		[33] ERLER	03	THEO
1.26	± 0.02		[34] ZYABLYUK	03	THEO

[1] CHETYRKIN 17 determine $\overline{m}_c(\mu = 3\ \text{GeV}) = 0.993 \pm 0.008$ GeV and $\overline{m}_c(\overline{m}_c)$ from a four-loop sum-rule computation of the cross-section for $e^+e^- \to$ hadrons in the charm threshold region.

[2] BERTONE 16 determine $\overline{m}_c(\overline{m}_c)$ from HERA deep inelastic scattering data using the FONLL scheme. Also determine $\overline{m}_c(\overline{m}_c){=}1.318 \pm 0.054^{+0.490}_{-0.022}$ using the fixed flavor number scheme.

[3] KIYO 16 determine $\overline{m}_c(\overline{m}_c)$ from the $J/\psi(1S)$ mass at order α_s^3 (N3LO).

[4] CHAKRABORTY 15 is a lattice QCD computation using 2+1+1 dynamical flavors. Moments of pseudoscalar current-current correlators are matched to α_s^3-accurate QCD perturbation theory with the η_c meson mass tuned to experiment.

[5] DEHNADI 15 determine $\overline{m}_c(\overline{m}_c)$ using sum rules for $e^+e^- \to$ hadrons at order α_s^3 (N3LO), and fitting to both experimental data and lattice results.

[6] CARRASCO 14 is a lattice QCD computation of light quark masses using $2 + 1 + 1$ dynamical quarks, with $m_u = m_d \neq m_s \neq m_c$. The u and d quark masses are obtained separately by using the K meson mass splittings and lattice results for the electromagnetic contributions.

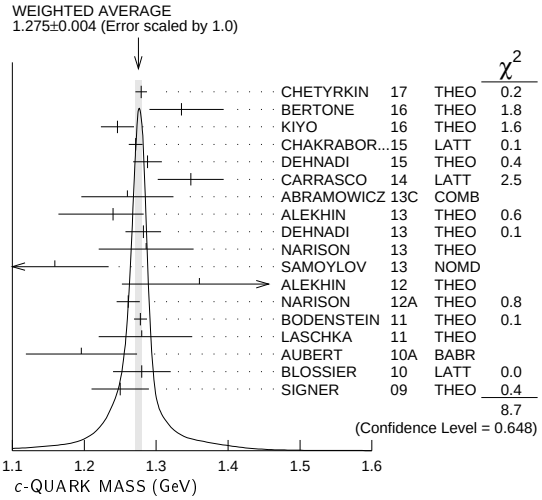

[7] ABRAMOWICZ 13C determines m_c from charm production in deep inelastic ep scattering, using the QCD prediction at NLO order. The uncertainties from model and parameterization assumptions, and the value of α_s, of ± 0.03, ± 0.02, and ± 0.02 respectively, have been combined in quadrature.

[8] ALEKHIN 13 determines m_c from charm production in deep inelastic scattering at HERA using approximate NNLO QCD.

[9] DEHNADI 13 determines m_c using QCD sum rules for the charmonium spectrum and charm continuum to order α_s^3 (N3LO). The statistical and systematic experimental errors of ± 0.006 and ± 0.009 have been combined in quadrature. The theoretical uncertainties ± 0.019 from truncation of the perturbation series, ± 0.010 from α_s, and ± 0.002 from the gluon condensate have been combined in quadrature.

[10] NARISON 13 determines m_c using QCD spectral sum rules to order α_s^2 (NNLO) and including condensates up to dimension 6.

[11] SAMOYLOV 13 determines m_c from a study of charm dimuon production in neutrino-iron scattering using the NLO QCD result for the charm quark production cross section.

[12] ALEKHIN 12 determines m_c from heavy quark production in deep inelastic scattering at HERA using approximate NNLO QCD.

[13] NARISON 12A determines m_c using sum rules for the vector current correlator to order α_s^3, including the effect of gluon condensates up to dimension eight.

[14] BODENSTEIN 11 determine $\overline{m}_c(3\ \text{GeV}) = 0.987 \pm 0.009$ GeV and $\overline{m}_c(\overline{m}_c) = 1.278 \pm 0.009$ GeV using QCD sum rules for the charm quark vector current correlator.

[15] LASCHKA 11 determine the c mass from the charmonium spectrum. The theoretical computation uses the heavy $Q\overline{Q}$ potential to order $1/m_Q$ obtained by matching the short-distance perturbative result onto lattice QCD result at larger scales.

[16] AUBERT 10A determine the b- and c-quark masses from a fit to the inclusive decay spectra in semileptonic B decays in the kinetic scheme (and convert it to the $\overline{\text{MS}}$ scheme).

[17] BLOSSIER 10 determines quark masses from a computation of the hadron spectrum using $N_f{=}2$ dynamical twisted-mass Wilson fermions.

[18] SIGNER 09 determines the c-quark mass using non-relativistic sum rules to analyze the $e^+e^- \to c\overline{c}$ cross-section near threshold. Also determine the PS mass $m_{PS}(\mu_F{=}\ 0.7\ \text{GeV}) = 1.50 \pm 0.04$ GeV.

[19] ALEKHIN 11 determines m_c from heavy quark production in deep inelastic scattering using fixed target and HERA data, and approximate NNLO QCD.

[20] BODENSTEIN 10 determines $\overline{m}_c(3\ \text{GeV}) = 1.008 \pm 0.026$ GeV using finite energy sum rules for the vector current correlator. The authors have converted this to $\overline{m}_c(\overline{m}_c)$ using $\alpha_s(M_Z) = 0.1189 \pm 0.0020$.

[21] MCNEILE 10 determines m_c by comparing the order α_s^3 perturbative results for the pseudo-scalar current to lattice simulations with $N_f = 2{+}1$ sea-quarks by the HPQCD collaboration.

[22] NARISON 10 determines m_c from ratios of moments of vector current correlators computed to order α_s^3 and including the dimension-six gluon condensate.

[23] CHETYRKIN 09 determine m_c and m_b from the $e^+e^- \to Q\overline{Q}$ cross-section and sum rules, using an order α_s^3 computation of the heavy quark vacuum polarization. They also determine $m_c(3\ \text{GeV}) = 0.986 \pm 0.013$GeV.

[24] ALLISON 08 determine m_c by comparing four-loop perturbative results for the pseudo-scalar current correlator to lattice simulations by the HPQCD collaboration. The result has been updated in MCNEILE 10.

[25] KUHN 07 determine $\overline{m}_c(\mu = 3\ \text{GeV}) = 0.986 \pm 0.013$ GeV and $\overline{m}_c(\overline{m}_c)$ from a four-loop sum-rule computation of the cross-section for $e^+e^- \to$ hadrons in the charm threshold region.

[26] BOUGHEZAL 06 result comes from the first moment of the hadronic production cross-section to order α_s^3.

[27] BUCHMUELLER 06 determine m_b and m_c by a global fit to inclusive B decay spectra.
[28] HOANG 06 determines $\overline{m}_c(\overline{m}_c)$ from a global fit to inclusive B decay data. The B decay distributions were computed to order $\alpha_s^2\beta_0$, and the conversion between different m_c mass schemes to order α_s^3.
[29] AUBERT 04X obtain m_c from a fit to the hadron mass and lepton energy distributions in semileptonic B decay. The paper quotes values in the kinetic scheme. The $\overline{\rm MS}$ value has been provided by the BABAR collaboration.
[30] HOANG 04 determines $\overline{m}_c(\overline{m}_c)$ from moments at order α_s^2 of the charm production cross-section in e^+e^- annihilation.
[31] DEDIVITIIS 03 use a quenched lattice computation of heavy-heavy and heavy-light meson masses.
[32] EIDEMULLER 03 determines m_b and m_c using QCD sum rules.
[33] ERLER 03 determines m_b and m_c using QCD sum rules. Includes recent BES data.
[34] ZYABLYUK 03 determines m_c by using QCD sum rules in the pseudoscalar channel and comparing with the η_c mass.

m_c/m_s MASS RATIO

VALUE	DOCUMENT ID		TECN
11.72 ±0.25 OUR EVALUATION	See the ideogram below.		
11.652±0.065	[1] CHAKRABOR...	15	LATT
$11.747\pm0.019^{+0.059}_{-0.043}$	[2] BAZAVOV	14A	LATT
11.62 ±0.16	[3] CARRASCO	14	LATT
11.27 ±0.30 ±0.26	[4] DURR	12	LATT
12.0 ±0.3	[5] BLOSSIER	10	LATT
11.85 ±0.16	[6] DAVIES	10	LATT

[1] CHAKRABORTY 15 is a lattice QCD computation on gluon field configurations with 2+1+1 dynamical flavors of HISQ quarks with u/d masses down to the physical value. m_c and m_s are tuned from pseudoscalar meson masses.
[2] BAZAVOV 14A is a lattice computation using 4 dynamical flavors of HISQ fermions.
[3] CARRASCO 14 is a lattice QCD computation of light quark masses using $2+1+1$ dynamical quarks, with $m_u = m_d \neq m_s \neq m_c$. The u and d quark masses are obtained separately by using the K meson mass splittings and lattice results for the electromagnetic contributions.
[4] DURR 12 determine m_c/m_s using a lattice computation with $N_f = 2$ dynamical fermions. The result is combined with other determinations of m_c to obtain $m_s(2\ \text{GeV}) = 97.0 \pm 2.6 \pm 2.5$ MeV.
[5] BLOSSIER 10 determine m_c/m_s from a computation of the hadron spectrum using $N_f = 2$ dynamical twisted-mass Wilson fermions.
[6] DAVIES 10 determine m_c/m_s from meson masses calculated on gluon fields including u, d, and s sea quarks with lattice spacing down to 0.045 fm. The Highly Improved Staggered quark formalism is used for the valence quarks.

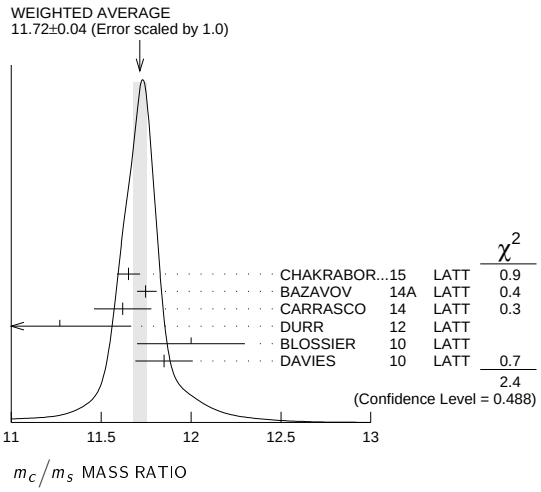

m_b/m_c MASS RATIO

VALUE	DOCUMENT ID		TECN
4.528±0.054	[1] CHAKRABOR...	15	LATT

[1] CHAKRABORTY 15 is a lattice computation using 4 dynamical quark flavors.

$m_b - m_c$ QUARK MASS DIFFERENCE

VALUE (GeV)	DOCUMENT ID		TECN
3.45 ±0.05 OUR EVALUATION			
• • • We do not use the following data for averages, fits, limits, etc. • • •			
3.472±0.032	[1] AUBERT	10A	BABR
3.42 ±0.06	[2] ABDALLAH	06B	DLPH
3.44 ±0.03	[3] AUBERT	04X	BABR
3.41 ±0.01	[3] BAUER	04	THEO

[1] AUBERT 10A determine the b- and c-quark masses from a fit to the inclusive decay spectra in semileptonic B decays in the kinetic scheme.
[2] ABDALLAH 06B determine $m_b - m_c$ from moments of the hadron invariant mass and lepton energy spectra in semileptonic inclusive B decays.
[3] Determine $m_b - m_c$ from a global fit to inclusive B decay spectra.

c-QUARK REFERENCES

CHETYRKIN	17	PR D96 116007	K.G. Chetyrkin *et al.*
BERTONE	16	JHEP 1608 050	V. Bertone *et al.* (xFitter Developers)
KIYO	16	PL B752 122	Y. Kiyo, G. Mishima, Y. Sumino
CHAKRABOR...	15	PR D91 054508	B. Chakraborty *et al.* (HPQCD Collab.)
DEHNADI	15	JHEP 1508 155	B. Dehnadi, A.H. Hoang, V. Mateu
BAZAVOV	14A	PR D90 074509	A. Bazavov *et al.* (Fermi-LAT and MILC Collabs.)
CARRASCO	14	NP B887 19	N. Carrasco *et al.* (European Twisted Mass Collab.)
ABRAMOWICZ	13C	EPJ C73 2311	H. Abramowicz *et al.* (H1 and Zeus Collabs.)
ALEKHIN	13	PL B720 172	S. Alekhin *et al.* (SERP, DESYZ, WUPP+)
DEHNADI	13	JHEP 1309 103	B. Dehnadi *et al.* (SHRZ, VIEN, MPIM+)
NARISON	13	PL B718 1321	S. Narison (MONP)
SAMOYLOV	13	NP B876 339	O. Samoylov *et al.* (NOMAD Collab.)
ALEKHIN	12	PL B718 550	S. Alekhin *et al.* (SERP, WUPP, DESY+)
DURR	12	PRL 108 122003	S. Durr, G. Koutsou (WUPP, JULI, CYPR)
NARISON	12A	PL B706 412	S. Narison (MONP)
ALEKHIN	11	PL B699 345	S. Alekhin, S. Moch (DESY, SERP)
BODENSTEIN	11	PR D83 074014	S. Bodenstein *et al.*
LASCHKA	11	PR D83 094002	A. Laschka, N. Kaiser, W. Weise
AUBERT	10A	PR D81 032003	B. Aubert *et al.* (BABAR Collab.)
BLOSSIER	10	PR D82 114513	B. Blossier *et al.* (ETM Collab.)
BODENSTEIN	10	PR D82 114013	S. Bodenstein *et al.*
DAVIES	10	PRL 104 132003	C.T.H. Davies *et al.* (HPQCD Collab.)
MCNEILE	10	PR D82 034512	C. McNeile *et al.* (HPQCD Collab.)
NARISON	10	PL B693 559	S. Narison (MONP)
Also		PL B705 544 (errat.)	S. Narison (MONP)
CHETYRKIN	09	PR D80 074010	K.G. Chetyrkin *et al.* (KARL, BNL)
SIGNER	09	PL B672 333	A. Signer (DURH)
ALLISON	08	PR D78 054513	I. Allison *et al.* (HPQCD Collab.)
KUHN	07	NP B778 192	J.H. Kuhn, M. Steinhauser, C. Sturm
ABDALLAH	06B	EPJ C45 35	J. Abdallah *et al.* (DELPHI Collab.)
BOUGHEZAL	06	PR D74 074006	R. Boughezal, M. Czakon, T. Schutzmeier
BUCHMUEL...	06	PR D73 073008	O.L. Buchmueller, H.U. Flacher (RHBL)
HOANG	06	PL B633 526	A.H. Hoang, A.V. Manohar
AUBERT	04X	PRL 93 011803	B. Aubert *et al.* (BABAR Collab.)
BAUER	04	PR D70 094017	C. Bauer *et al.*
HOANG	04	PL B594 127	A.H. Hoang, M. Jamin
DEDIVITIIS	03	NP B675 309	G.M. de Divitiis *et al.*
EIDEMULLER	03	PR D67 113002	M. Eidemuller
ERLER	03	PL B558 125	J. Erler, M. Luo
ZYABLYUK	03	JHEP 0301 081	K.N. Zyablyuk (ITEP)

b

$I(J^P) = 0(\frac{1}{2}^+)$

Charge $= -\frac{1}{3}\ e$ Bottom $= -1$

b-QUARK MASS

b-quark mass corresponds to the "running mass" $\overline{m}_b(\mu = \overline{m}_b)$ in the $\overline{\rm MS}$ scheme. We have converted masses in other schemes to the $\overline{\rm MS}$ mass using two-loop QCD perturbation theory with $\alpha_s(\mu = \overline{m}_b) = 0.223 \pm 0.008$. The value $4.18^{+0.04}_{-0.03}$ GeV for the $\overline{\rm MS}$ mass corresponds to 4.78 ± 0.06 GeV for the pole mass, using the two-loop conversion formula. A discussion of masses in different schemes can be found in the "Note on Quark Masses."

$\overline{\rm MS}$ MASS (GeV)	DOCUMENT ID		TECN
$4.18\ ^{+0.04}_{-0.03}$ OUR EVALUATION	of $\overline{\rm MS}$ Mass. See the ideogram below.		
4.197±0.022	[1] KIYO	16	THEO
4.183±0.037	[2] ALBERTI	15	THEO
$4.203^{+0.016}_{-0.034}$	[3] BENEKE	15	THEO
4.176±0.023	[4] DEHNADI	15	THEO
4.07 ±0.17	[5] ABRAMOWICZ	14A	ZEUS
4.201±0.043	[6] AYALA	14A	THEO
4.21 ±0.11	[7] BERNARDONI	14	LATT
4.169±0.002±0.008	[8] PENIN	14	THEO
4.166±0.043	[9] LEE	13O	LATT
4.247±0.034	[10] LUCHA	13	THEO
4.236±0.069	[11] NARISON	13	THEO
4.213±0.059	[12] NARISON	13A	THEO
4.171±0.009	[13] BODENSTEIN	12	THEO
4.29 ±0.14	[14] DIMOPOUL...	12	LATT
4.235±0.003±0.055	[15] HOANG	12	THEO
4.177±0.011	[16] NARISON	12	THEO
$4.18\ ^{+0.05}_{-0.04}$	[17] LASCHKA	11	THEO
4.186±0.044±0.015	[18] AUBERT	10A	BABR
4.164±0.023	[19] MCNEILE	10	LATT
4.163±0.016	[20] CHETYRKIN	09	THEO
4.243±0.049	[21] SCHWANDA	08	BELL
• • • We do not use the following data for averages, fits, limits, etc. • • •			
4.212±0.032	[22] NARISON	12	THEO
4.171±0.014	[23] NARISON	12A	THEO
4.173±0.010	[24] NARISON	10	THEO
5.26 ±1.2	[25] ABDALLAH	08D	DLPH
4.42 ±0.06 ±0.08	[26] GUAZZINI	08	LATT
4.347±0.048±0.08	[27] DELLA-MOR...	07	LATT
4.164±0.025	[28] KUHN	07	THEO
4.19 ±0.40	[29] ABDALLAH	06D	DLPH
4.205±0.058	[30] BOUGHEZAL	06	THEO
4.20 ±0.04	[31] BUCHMUEL...	06	THEO
4.19 ±0.06	[32] PINEDA	06	THEO
4.4 ±0.3	[33] GRAY	05	LATT
4.22 ±0.06	[34] AUBERT	04X	THEO

4.17 ±0.03	[35] BAUER	04	THEO
4.22 ±0.11	[36] HOANG	04	THEO
4.25 ±0.11	[37] MCNEILE	04	LATT
4.22 ±0.09	[38] BAUER	03	THEO
4.19 ±0.05	[39] BORDES	03	THEO
4.20 ±0.09	[40] CORCELLA	03	THEO
4.33 ±0.10	[41] DEDIVITIIS	03	LATT
4.24 ±0.10	[42] EIDEMULLER	03	THEO
4.207±0.03	[43] ERLER	03	THEO
4.33 ±0.06 ±0.10	[44] MAHMOOD	03	CLEO
4.190±0.032	[45] BRAMBILLA	02	THEO
4.346±0.070	[46] PENIN	02	THEO

[1] KIYO 16 determine $\overline{m}_b(\overline{m}_b)$ from the $\Upsilon(1S)$ mass at order α_s^3 (N3LO).

[2] ALBERTI 15 determine $\overline{m}_b(\overline{m}_b)$ from fits to inclusive $B \to X_c e \overline{\nu}$ decay. They also find $m_b^{\rm kin}(1\ {\rm GeV}) = 4.553 \pm 0.020$ GeV.

[3] BENEKE 15 determine $\overline{m}_b(\overline{m}_b)$ using sum rules for $e^+e^- \to$ hadrons at order N3LO including finite m_c effects. They find $m_b^{\rm PS}(2\ {\rm GeV}) = 4.532^{+0.013}_{-0.039}$ GeV, and $\overline{m}_b(\overline{m}_b) = 4.193^{+0.022}_{-0.035}$ GeV. The value quoted is obtained using the four-loop conversion given in BENEKE 16.

[4] DEHNADI 15 determine $\overline{m}_b(\overline{m}_b)$ using sum rules for $e^+e^- \to$ hadrons at order α_s^3 (N3LO), and fitting to both experimental data and lattice results.

[5] ABRAMOWICZ 14A determine $\overline{m}_b(\overline{m}_b) = 4.07 \pm 0.14^{+0.01}_{-0.07}{}^{+0.05}_{-0.00}{}^{+0.08}_{-0.05}$ from the production of b quarks in ep collisions at HERA. The errors due to fitting, modeling, PDF parameterization, and theoretical QCD uncertainties due to the values of α_s, m_c, and the renormalization scale μ have been combined in quadrature.

[6] AYALA 14A determine $\overline{m}_b(\overline{m}_b)$ from the $\Upsilon(1S)$ mass computed to N3LO order in perturbation theory using a renormalon subtracted scheme.

[7] BERNARDONI 14 determine m_b from $N_f = 2$ lattice calculations using heavy quark effective theory non-perturbatively renormalized and matched to QCD at $1/m$ order.

[8] PENIN 14 determine $\overline{m}_b(\overline{m}_b) = 4.169 \pm 0.008 \pm 0.002 \pm 0.002$ using an estimate of the order α_s^3 b-quark vacuum polarization function in the threshold region, including finite m_c effects. The errors of ± 0.008 from theoretical uncertainties, and ± 0.002 from α_s have been combined in quadrature.

[9] LEE 13O determines m_b using lattice calculations of the Υ and B_s binding energies in NRQCD, including three light dynamical quark flavors. The quark mass shift in NRQCD is determined to order α_s^2, with partial α_s^3 contributions.

[10] LUCHA 13 determines m_b from QCD sum rules for heavy-light currents using the lattice value for f_B of 191.5 ± 7.3 GeV.

[11] NARISON 13 determines m_b using QCD spectral sum rules to order α_s^2 (NNLO) and including condensates up to dimension 6.

[12] NARISON 13A determines m_b using HQET sum rules to order α_s^2 (NNLO) and the B meson mass and decay constant.

[13] BODENSTEIN 12 determine m_b using sum rules for the vector current correlator and the $e^+e^- \to Q\overline{Q}$ total cross-section.

[14] DIMOPOULOS 12 determine quark masses from a lattice computation using $N_f = 2$ dynamical flavors of twisted mass fermions.

[15] HOANG 12 determine m_b using non-relativistic sum rules for the Υ system at order α_s^2 (NNLO) with renormalization group improvement.

[16] Determines m_b to order α_s^3 (N3LO), including the effect of gluon condensates up to dimension eight combining the methods of NARISON 12 and NARISON 12A.

[17] LASCHKA 11 determine the b mass from the charmonium spectrum. The theoretical computation uses the heavy $Q\overline{Q}$ potential to order $1/m_Q$ obtained by matching the short-distance perturbative result onto lattice QCD result at larger scales.

[18] AUBERT 10A determine the b- and c-quark masses from a fit to the inclusive decay spectra in semileptonic B decays in the kinetic scheme (and convert it to the $\overline{\rm MS}$ scheme).

[19] MCNEILE 10 determines m_b by comparing order α_s^3 (N3LO) perturbative results for the pseudo-scalar current to lattice simulations with $N_f = 2{+}1$ sea-quarks by the HPQCD collaboration.

[20] CHETYRKIN 09 determine m_c and m_b from the $e^+e^- \to Q\overline{Q}$ cross-section and sum rules, using an order α_s^3 (N3LO) computation of the heavy quark vacuum polarization.

[21] SCHWANDA 08 measure moments of the inclusive photon spectrum in $B \to X_s\gamma$ decay to determine m_b^{1S}. We have converted this to $\overline{\rm MS}$ scheme.

[22] NARISON 12 determines m_b using exponential sum rules for the vector current correlator to order α_s^3, including the effect of gluon condensates up to dimension eight.

[23] NARISON 12A determines m_b using sum rules for the vector current correlator to order α_s^3, including the effect of gluon condensates up to dimension eight.

[24] NARISON 10 determines m_b from ratios of moments of vector current correlators computed to order α_s^3 and including the dimension-six gluon condensate. These values are taken from the erratum to that reference.

[25] ABDALLAH 08D determine $\overline{m}_b(M_Z) = 3.76 \pm 1.0$ GeV from a leading order study of four-jet rates at LEP.

[26] GUAZZINI 08 determine $\overline{m}_b(\overline{m}_b)$ from a quenched lattice simulation of heavy meson masses. The ±0.08 is an estimate of the quenching error.

[27] DELLA-MORTE 07 determine $\overline{m}_b(\overline{m}_b)$ from a computation of the spin-averaged B meson mass using quenched lattice HQET at order $1/m$. The ±0.08 is an estimate of the quenching error.

[28] KUHN 07 determine $\overline{m}_b(\mu = 10\ {\rm GeV}) = 3.609 \pm 0.025$ GeV and $\overline{m}_b(\overline{m}_b)$ from a four-loop sum-rule computation of the cross-section for $e^+e^- \to$ hadrons in the bottom threshold region.

[29] ABDALLAH 06D determine $m_b(M_Z) = 2.85 \pm 0.32$ GeV from Z-decay three-jet events containing a b-quark.

[30] BOUGHEZAL 06 $\overline{\rm MS}$ scheme result comes from the first moment of the hadronic production cross-section to order α_s^3.

[31] BUCHMUELLER 06 determine m_b and m_c by a global fit to inclusive B decay spectra.

[32] PINEDA 06 $\overline{\rm MS}$ scheme result comes from a partial NNLL evaluation (complete at order α_s^2 (NNLO)) of sum rules of the bottom production cross-section in e^+e^- annihilation.

[33] GRAY 05 determines $\overline{m}_b(\overline{m}_b)$ from a lattice computation of the Υ spectrum. The simulations have 2+1 dynamical light flavors. The b quark is implemented using NRQCD.

[34] AUBERT 04X obtain m_b from a fit to the hadron mass and lepton energy distributions in semileptonic B decay. The paper quotes values in the kinetic scheme. The $\overline{\rm MS}$ value has been provided by the BABAR collaboration.

[35] BAUER 04 determine m_b, m_c and $m_b - m_c$ by a global fit to inclusive B decay spectra.

[36] HOANG 04 determines $\overline{m}_b(\overline{m}_b)$ from moments at order α_s^2 of the bottom production cross-section in e^+e^- annihilation.

[37] MCNEILE 04 use lattice QCD with dynamical light quarks and a static heavy quark to compute the masses of heavy-light mesons.

[38] BAUER 03 determine the b quark mass by a global fit to B decay observables. The experimental data includes lepton energy and hadron invariant mass moments in semileptonic $B \to X_c \ell\nu_\ell$ decay, and the inclusive photon spectrum in $B \to X_s\gamma$ decay. The theoretical expressions used are of order $1/m^3$, and $\alpha_s^2\beta_0$.

[39] BORDES 03 determines m_b using QCD finite energy sum rules to order α_s^2.

[40] CORCELLA 03 determines $\overline{m}_b$ using sum rules computed to order α_s^2. Includes charm quark mass effects.

[41] DEDIVITIIS 03 use a quenched lattice computation of heavy-heavy and heavy-light meson masses.

[42] EIDEMULLER 03 determines $\overline{m}_b$ and $\overline{m}_c$ using QCD sum rules.

[43] ERLER 03 determines $\overline{m}_b$ and $\overline{m}_c$ using QCD sum rules. Includes recent BES data.

[44] MAHMOOD 03 determines m_b^{1S} by a fit to the lepton energy moments in $B \to X_c \ell\nu_\ell$ decay. The theoretical expressions used are of order $1/m^3$ and $\alpha_s^2\beta_0$. We have converted their result to the $\overline{\rm MS}$ scheme.

[45] BRAMBILLA 02 determine $\overline{m}_b(\overline{m}_b)$ from a computation of the $\Upsilon(1S)$ mass to order α_s^4, including finite m_c corrections.

[46] PENIN 02 determines $\overline{m}_b$ from the spectrum of the Υ system.

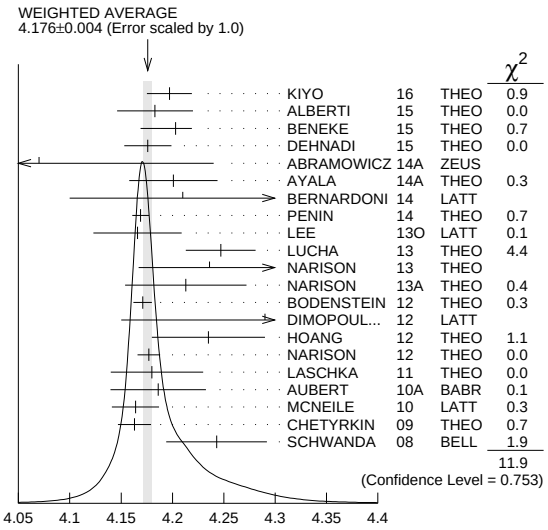

b-QUARK REFERENCES

BENEKE	16	PoS RADCOR2015 035	M. Beneke *et al.*	
KIYO	16	PL B752 122	Y. Kiyo, G. Mishima, Y. Sumino	
ALBERTI	15	PRL 114 061802	A. Alberti *et al.*	
BENEKE	15	NP B891 42	M. Beneke *et al.*	
DEHNADI	15	JHEP 1508 155	B. Dehnadi, A.H. Hoang, V. Mateu	
ABRAMOWICZ	14A	JHEP 1409 127	H. Abramowicz *et al.*	(ZEUS Collab.)
AYALA	14A	JHEP 1409 045	C. Ayala, G. Cvetic, A. Pineda	
BERNARDONI	14	PL B730 171	F. Bernardoni *et al.*	(ALPHA Collab.)
PENIN	14	JHEP 1404 120	A.A. Penin, N. Zerf	
LEE	13O	PR D87 074018	A.J. Lee *et al.*	(HPQCD Collab.)
LUCHA	13	PR D88 056011	W. Lucha, D. Melikhov, S. Simula	(VIEN, MOSU+)
NARISON	13	PL B718 1321	S. Narison	(MONP)
NARISON	13A	PL B721 269	S. Narison	(MONP)
BODENSTEIN	12	PR D85 034003	S. Bodenstein *et al.*	(CAPE, VALE, MANZ+)
DIMOPOUL...	12	JHEP 1201 046	P. Dimopoulos *et al.*	(ETM Collab.)
HOANG	12	JHEP 1210 188	A.H. Hoang, P. Ruiz-Femenia, M. Stahlhofen	(WIEN+)
NARISON	12	PL B707 259	S. Narison	(MONP)
NARISON	12A	PL B706 412	S. Narison	(MONP)
LASCHKA	11	PR D83 094002	A. Laschka, N. Kaiser, W. Weise	
AUBERT	10A	PR D81 032003	B. Aubert *et al.*	(BABAR Collab.)
MCNEILE	10	PR D82 034512	C. McNeile *et al.*	(HPQCD Collab.)
NARISON	10	PL B693 559	S. Narison	(MONP)
Also		PL B705 544 (errat.)	S. Narison	(MONP)
CHETYRKIN	09	PR D80 074010	K.G. Chetyrkin *et al.*	(KARL, BNL)
ABDALLAH	08D	EPJ C55 525	J. Abdallah *et al.*	(DELPHI Collab.)
GUAZZINI	08	JHEP 0801 076	D. Guazzini, R. Sommer, N. Tantalo	
SCHWANDA	08	PR D78 032016	C. Schwanda *et al.*	(BELLE Collab.)
DELLA-MOR...	07	JHEP 0701 007	M. Della Morte *et al.*	
KUHN	07	NP B778 192	J.H. Kuhn, M. Steinhauser, C. Sturm	
ABDALLAH	06D	EPJ C46 569	J. Abdallah *et al.*	(DELPHI Collab.)
BOUGHEZAL	06	PR D74 074006	R. Boughezal, M. Czakon, T. Schutzmeier	
BUCHMUEL...	06	PR D73 073008	O.L. Buchmueller, H.U. Flacher	(RHBL)
PINEDA	06	PR D73 111501	A. Pineda, A. Signer	
GRAY	05	PR D72 094507	A. Gray *et al.*	(HPQCD, UKQCD Collab.)
AUBERT	04X	PRL 93 011803	B. Aubert *et al.*	(BABAR Collab.)
BAUER	04	PR D70 094017	C. Bauer *et al.*	
HOANG	04	PL B594 127	A.H. Hoang, M. Jamin	
MCNEILE	04	PL B600 77	C. McNeile, C. Michael, G. Thompson	(UKQCD Collab.)
BAUER	03	PR D67 054012	C.W. Bauer *et al.*	

Quark Particle Listings

b, t

BORDES	03	PL B562 81	J. Bordes, J. Penarrocha, K. Schilcher	
CORCELLA	03	PL B554 133	G. Corcella, A.H. Hoang	
DEDIVITIIS	03	NP B675 309	G.M. de Divitiis *et al.*	
EIDEMULLER	03	PR D67 113002	M. Eidemuller	
ERLER	03	PL B558 125	J. Erler, M. Luo	
MAHMOOD	03	PR D67 072001	A.H. Mahmood *et al.*	(CLEO Collab.)
BRAMBILLA	02	PR D65 034001	N. Brambilla, Y. Sumino, A. Vairo	
PENIN	02	PL B538 335	A. Penin, M. Steinhauser	

t

$I(J^P) = 0(\frac{1}{2}^+)$

Charge $= \frac{2}{3}$ e Top $= +1$

See the related review(s):
Top Quark

t-QUARK MASS

We first list the direct measurements of the top quark mass which employ the event kinematics and then list the measurements which extract a top quark mass from the measured $t\bar{t}$ cross-section using theory calculations. A discussion of the definition of the top quark mass in these measurements can be found in the review "The Top Quark."

For earlier search limits see PDG 96, Physical Review **D54** 1 (1996). We no longer include a compilation of indirect top mass determinations from Standard Model Electroweak fits in the Listings (our last compilation can be found in the Listings of the 2007 partial update). For a discussion of current results see the reviews "The Top Quark" and "Electroweak Model and Constraints on New Physics."

t-Quark Mass (Direct Measurements)

The following measurements extract a t-quark mass from the kinematics of $t\bar{t}$ events. They are sensitive to the top quark mass used in the MC generator that is usually interpreted as the pole mass, but the theoretical uncertainty in this interpretation is hard to quantify. See the review "The Top Quark" and references therein for more information.

OUR AVERAGE of 173.0 ± 0.4 GeV is an average of top mass measurements from LHC and Tevatron Runs. The latest Tevatron average, 174.30 ± 0.35 ± 0.54 GeV, was provided by the Tevatron Electroweak Working Group (TEVEWWG).

VALUE (GeV)		*DOCUMENT ID*		*TECN*	*COMMENT*
173.0 ± 0.4 OUR AVERAGE		Error includes scale factor of 1.3. See the ideogram below.			
172.95 ± 0.77 $^{+0.97}_{-0.93}$	[1]	SIRUNYAN	17L	CMS	t-channel single top production
172.84 ± 0.34 ± 0.61	[2]	AABOUD	16T	ATLS	combination of ATLAS
172.44 ± 0.13 ± 0.47	[3]	KHACHATRY...	16AK	CMS	combination of CMS
174.30 ± 0.35 ± 0.54	[4]	TEVEWWG	16	TEVA	Tevatron combination
• • • We do not use the following data for averages, fits, limits, etc. • • •					
173.72 ± 0.55 ± 1.01	[5]	AABOUD	17AH	ATLS	≥ 5 jets (2b)
174.95 ± 0.40 ± 0.64	[6]	ABAZOV	17B	D0	ℓ + jets and dilepton channels
170.8 ± 9.0	[7]	SIRUNYAN	17N	CMS	jet mass in highly-boosted $t\bar{t}$ events
172.22 ± 0.18 $^{+0.89}_{-0.93}$	[8]	SIRUNYAN	17O	CMS	Dilepton channel
172.99 ± 0.41 ± 0.74	[9]	AABOUD	16T	ATLS	dilepton channel
173.32 ± 1.36 ± 0.85	[10]	ABAZOV	16	D0	$\ell\ell + \not{E}_T +$ ≥ 2j (≥ 2b)
173.93 ± 1.61 ± 0.88	[11]	ABAZOV	16D	D0	$\ell\ell + \not{E}_T +$ ≥ 2j (≥ 2b)
172.35 ± 0.16 ± 0.48	[12,13]	KHACHATRY...	16AK	CMS	ℓ + ≥ 4j (2b)
172.32 ± 0.25 ± 0.59	[12,13]	KHACHATRY...	16AK	CMS	≥ 6 jets (2b)
172.82 ± 0.19 ± 1.22	[12,14]	KHACHATRY...	16AK	CMS	$(ee/\mu\mu)+\not{E}_T+$ ≥ 2b,$e\mu+$ ≥ 2b
173.68 ± 0.20 $^{+1.58}_{-0.97}$	[15]	KHACHATRY...	16AL	CMS	semi- + di-leptonic channels
173.5 ± 3.0 ± 0.9	[16]	KHACHATRY...	16CB	CMS	$t \to (W \to \ell\nu)(b \to J/\psi X \to \mu^+\mu^- X)$
175.1 ± 1.4 ± 1.2	[17]	AAD	15AW	ATLS	small $\not{E}_T$, ≥ 6 jets (2b-tag)
172.99 ± 0.48 ± 0.78	[18]	AAD	15BF	ATLS	ℓ + jets and dilepton
171.5 ± 1.9 ± 2.5	[19]	AALTONEN	15D	CDF	$\ell\ell + \not{E}_T +$ ≥ 2j
175.07 ± 1.19 $^{+1.55}_{-1.58}$	[20]	AALTONEN	14N	CDF	small $\not{E}_T$, 6–8 jets (≥ 1b-tag)
174.98 ± 0.58 ± 0.49	[21]	ABAZOV	14C	D0	$\ell + \not{E}_T$ + 4 jets (≥ 1 b-tag)
173.49 ± 0.69 ± 1.21	[22]	CHATRCHYAN	14C	CMS	≥ 6 jets (≥ 2 b-tag)
173.93 ± 1.64 ± 0.87	[23]	AALTONEN	13H	CDF	$\not{E}_T$ + ≥ 4 jets (≥ 1 b)
173.9 ± 0.9 $^{+1.7}_{-2.1}$	[24]	CHATRCHYAN	13S	CMS	$\ell\ell$+$\not{E}_T$+ ≥ 2b-tag (MT2$_{(T)}$)
174.5 ± 0.6 ± 2.3	[25]	AAD	12I	ATLS	ℓ+$\not{E}_T$+ ≥ 4 jets (≥ 1 b), MT
172.85 ± 0.71 ± 0.85	[26]	AALTONEN	12AI	CDF	ℓ+$\not{E}_T$+ ≥ 4j (0,1,2b) template
172.7 ± 9.3 ± 3.7	[27]	AALTONEN	12AL	CDF	$\tau_h + \not{E}_T$ +4j (≥ 1b)
173.18 ± 0.56 ± 0.75	[28]	AALTONEN	12AP	TEVA	CDF, D0 combination
172.5 ± 1.4 ± 1.5	[29]	AALTONEN	12G	CDF	6–8 jets with ≥ 1 b
173.7 ± 2.8 ± 1.5	[30]	ABAZOV	12AB	D0	$\ell\ell + \not{E}_T +$ ≥ 2 j (νWT)
173.9 ± 1.9 ± 1.6	[31]	ABAZOV	12AB	D0	$\ell\ell$+$\not{E}_T$+ ≥ 2j (νWT+MWT)
172.5 ± 0.4 ± 1.5	[32]	CHATRCHYAN	12BA	CMS	$\ell\ell$+$\not{E}_T$+ ≥ 2j (≥ 1b), AMWT
173.49 ± 0.43 ± 0.98	[33]	CHATRCHYAN	12BP	CMS	ℓ+$\not{E}_T$+ ≥ 4j (≥ 2b)
172.4 ± 1.4 ± 1.3	[34]	AALTONEN	11AC	CDF	$\ell + \not{E}_T$ + 4 jets (≥ 1 b-tag)
172.3 ± 2.4 ± 1.0	[35]	AALTONEN	11AK	CDF	Repl. by AALTONEN 13H
172.1 ± 1.1 ± 0.9	[36]	AALTONEN	11E	CDF	ℓ + jets and dilepton
176.9 ± 8.0 ± 2.7	[37]	AALTONEN	11T	CDF	$\ell + \not{E}_T$ + 4 jets (≥ 1 b-tag), $p_T(\ell)$ shape
174.94 ± 0.83 ± 1.24	[38]	ABAZOV	11P	D0	$\ell + \not{E}_T$ + 4 jets (≥ 1 b-tag)
174.0 ± 1.8 ± 2.4	[39]	ABAZOV	11R	D0	dilepton + $\not{E}_T$ + ≥ 2 jets
175.5 ± 4.6 ± 4.6	[40]	CHATRCHYAN	11F	CMS	dilepton + $\not{E}_T$ + jets
173.0 ± 0.9 ± 0.9	[41]	AALTONEN	10AE	CDF	$\ell + \not{E}_T$ + 4 jets (≥ 1 b-tag), ME method
169.3 ± 2.7 ± 3.2	[42]	AALTONEN	10C	CDF	dilepton + b-tag (MT2+NWA)
170.7 ± 6.3 ± 2.6	[43]	AALTONEN	10D	CDF	$\ell + \not{E}_T$ + 4 jets (b-tag)
174.8 ± 2.4 $^{+1.2}_{-1.0}$	[44]	AALTONEN	10E	CDF	≥ 6 jets, vtx b-tag
180.5 ±12.0 ± 3.6	[45]	AALTONEN	09AK	CDF	$\ell + \not{E}_T$ + jets (soft μ b-tag)
172.7 ± 1.8 ± 1.2	[46]	AALTONEN	09J	CDF	$\ell + \not{E}_T$ + 4 jets (b-tag)
171.1 ± 3.7 ± 2.1	[47]	AALTONEN	09K	CDF	6 jets, vtx b-tag
171.9 ± 1.7 ± 1.1	[48]	AALTONEN	09L	CDF	ℓ + jets, $\ell\ell$ + jets
171.2 ± 2.7 ± 2.9	[49]	AALTONEN	09O	CDF	dilepton
165.5 $^{+3.4}_{-3.3}$ ± 3.1	[50]	AALTONEN	09X	CDF	$\ell\ell + \not{E}_T$ ($\nu\phi$ weighting)
174.7 ± 4.4 ± 2.0	[51]	ABAZOV	09AH	D0	dilepton + b-tag (νWT+MWT)
170.7 $^{+4.2}_{-3.9}$ ± 3.5	[52,53]	AALTONEN	08C	CDF	dilepton, $\sigma_{t\bar{t}}$ constrained
171.5 ± 1.8 ± 1.1	[54]	ABAZOV	08AH	D0	$\ell + \not{E}_T$ + 4 jets
177.1 ± 4.9 ± 4.7	[55,56]	AALTONEN	07	CDF	6 jets with ≥ 1 b vtx
172.3 $^{+10.8}_{-9.6}$ ±10.8	[57]	AALTONEN	07B	CDF	≥ 4 jets (b-tag)
174.0 ± 2.2 ± 4.8	[58]	AALTONEN	07D	CDF	≥ 6 jets, vtx b-tag
170.8 ± 2.2 ± 1.4	[59,60]	AALTONEN	07I	CDF	lepton + jets (b-tag)
173.7 ± 4.4 $^{+2.1}_{-2.0}$	[56,61]	ABAZOV	07F	D0	lepton + jets
176.2 ± 9.2 ± 3.9	[62]	ABAZOV	07W	D0	dilepton (MWT)
179.5 ± 7.4 ± 5.6	[62]	ABAZOV	07W	D0	dilepton (νWT)
164.5 ± 3.9 ± 3.9	[60,63]	ABULENCIA	07D	CDF	dilepton
180.7 $^{+15.5}_{-13.4}$ ± 8.6	[64]	ABULENCIA	07J	CDF	lepton + jets
170.3 $^{+4.1}_{-4.5}$ $^{+1.2}_{-1.8}$	[60,65]	ABAZOV	06U	D0	lepton + jets (b-tag)
173.2 $^{+2.6}_{-2.4}$ ± 3.2	[66,67]	ABULENCIA	06D	CDF	lepton + jets
173.5 $^{+3.7}_{-3.6}$ ± 1.3	[53,66]	ABULENCIA	06D	CDF	lepton + jets
165.2 ± 6.1 ± 3.4	[60,68]	ABULENCIA	06G	CDF	dilepton
170.1 ± 6.0 ± 4.1	[53,69]	ABULENCIA	06V	CDF	dilepton
178.5 ±13.7 ± 7.7	[70,71]	ABAZOV	05	D0	6 or more jets
180.1 ± 3.6 ± 3.9	[72,73]	ABAZOV	04G	D0	lepton + jets
176.1 ± 5.1 ± 5.3	[74]	AFFOLDER	01	CDF	lepton + jets
176.1 ± 6.6	[75]	AFFOLDER	01	CDF	dilepton, lepton+jets, all-jets
172.1 ± 5.2 ± 4.9	[76]	ABBOTT	99G	D0	di-lepton, lepton+jets
176.0 ± 6.5	[77,78]	ABE	99B	CDF	dilepton, lepton+jets, all-jets
167.4 ±10.3 ± 4.8	[78,79]	ABE	99B	CDF	dilepton
168.4 ±12.3 ± 3.6	[73]	ABBOTT	98D	D0	dilepton
173.3 ± 5.6 ± 5.5	[73,80]	ABBOTT	98F	D0	lepton + jets
175.9 ± 4.8 ± 5.3	[79,81]	ABE	98E	CDF	lepton + jets
161 ±17 ±10	[79]	ABE	98F	CDF	dilepton
172.1 ± 5.2 ± 4.9	[82]	BHAT	98B	RVUE	dilepton and lepton+jets
173.8 ± 5.0	[83]	BHAT	98B	RVUE	dilepton, lepton+jets, all-jets
173.3 ± 5.6 ± 6.2	[73]	ABACHI	97E	D0	lepton + jets
186 ±10 ± 5.7	[79,84]	ABE	97R	CDF	6 or more jets
199 $^{+19}_{-21}$ ±22		ABACHI	95	D0	lepton + jets
176 ± 8 ±10		ABE	95F	CDF	lepton + b-jet
174 ±10 $^{+13}_{-12}$		ABE	94E	CDF	lepton + b-jet

[1] SIRUNYAN 17L based on 19.7 fb^{-1} of pp data at $\sqrt{s} = 8$ TeV. m_t is reconstructed from a fit to the invariant mass distribution of $\mu\nu b$, where p_T^{miss} and W mass constraint are used to reconstruct ν momentum. The number of events for various contributions, except for the t-channel single top one, are fixed to the values extracted from simulation.

[2] AABOUD 16T is an ATLAS combination of 8 TeV top-quark mass in the dilepton channel with previous measurements from $\sqrt{s} = 7$ TeV data in the dilepton and lepton + jets channels.

[3] KHACHATRYAN 16AK based on 19.7 fb^{-1} of pp data at $\sqrt{s} = 8$ TeV. Combination of the three top mass measurements in KHACHATRYAN 16AK and with the CMS results at $\sqrt{s} = 7$ TeV.

[4] TEVEWWG 16 is the latest Tevatron average (July 2016) provided by the Tevatron Electroweak Working Group. It takes correlated uncertainties into account and has a χ^2 of 10.8 for 11 degrees of freedom.

[5] AABOUD 17AH based on 20.2 fb^{-1} of pp data at $\sqrt{s} = 8$ TeV. Uses template fits to the ratio of the masses of three-jets (from t candidate) and dijets (from W candidate), to suppress jet energy scale uncertainty. Large QCD background is modelled using a data-driven method.

[6] ABAZOV 17B is a combination of measurements of the top quark mass by D0 in the lepton+jets and dilepton channels, using all data collected in Run I (1992–1996) at $\sqrt{s}$ = 1.8 TeV and Run II (2001–2011) at $\sqrt{s} = 1.96$ TeV of the Tevatron, corresponding to integrated luminosities of 0.1 fb^{-1} and 9.7 fb^{-1}, respectively.

[7] SIRUNYAN 17N based on 19.7 fb^{-1} of pp data at $\sqrt{s} = 8$ TeV. The fully hadronic decay of a highly-boosted t is reconstructed in the ℓ+jets channel and unfolded at the particle level. The sensitivity of the peak position of the m_{jet} distribution is used to test quality of the modelling by the simulation.

[8] SIRUNYAN 17O based on 19.7 fb^{-1} of pp data at $\sqrt{s} = 8$ TeV. Analysis is based on the kinematical observables $M(b\ell)$, M_{T2} and $M(b\ell\nu)$. A fit is performed to determine m_t and an overall jet energy scale factor simultaneously.

[9] AABOUD 16T based on 20.2 fb^{-1} of pp data at $\sqrt{s} = 8$ TeV. The analysis is refined using the p_T and invariant mass distributions of ℓ+b-jet system. A combination with measurements from $\sqrt{s} = 7$ TeV data in the dilepton and lepton+jets channels gives 172.84 ± 0.34 ± 0.61 GeV.

[10] ABAZOV 16 based on 9.7 fb^{-1} of data in $p\bar{p}$ collisions at $\sqrt{s} = 1.96$ TeV. Employs improved fit to minimize statistical errors and improved jet energy calibration, using lepton

+ jets mode, which reduces error of jet energy scale. Based on previous determination in ABAZOV 12AB with increased integrated luminosity and improved fit and calibrations.

[11] ABAZOV 16D based on 9.7 fb^{-1} of data in $p\overline{p}$ collisions at $\sqrt{s}$ = 1.96 TeV, using the matrix element technique. Based on previous determination in ABAZOV 11R with increased integrated luminosity. There is a strong correlation with the determination in ABAZOV 16. (See ABAZOV 17B.)

[12] KHACHATRYAN 16AK based on 19.7 fb^{-1} of pp data at $\sqrt{s}$ = 8 TeV. Combination of the three top mass measurements in KHACHATRYAN 16AK and with the CMS results at $\sqrt{s}$ = 7 TeV gives 172.44 ± 0.13 ± 0.47 GeV.

[13] The top mass and jet energy scale factor are determined by a fit.

[14] Uses the analytical matrix weighting technique method.

[15] KHACHATRYAN 16AL based on 19.7 fb^{-1} in pp collisions at $\sqrt{s}$ = 8 TeV. Determined from the invariant mass distribution of leptons and reconstructed secondary vertices from b decays using only charged particles. The uncertainty is dominated by modeling of b fragmentation and top p_T distribution.

[16] KHACHATRYAN 16CB based on 666 candidate reconstructed events corresponding to 19.7 fb^{-1} of pp data at $\sqrt{s}$ = 8 TeV. The measurement exploits correlation of m_t with M($J/\psi\ell$) in the same top quark decay, using a high-purity event sample. A study on modeling of b-quark fragmentation is given in Sec.3.3.

[17] AAD 15AW based on 4.6 fb^{-1} of pp data at $\sqrt{s}$ = 7 TeV. Uses template fits to the ratio of the masses of three-jets (from t candidate) and dijets (from W candidate). Large background from multijet production is modeled with data-driven methods.

[18] AAD 15BF based on 4.6 fb^{-1} in pp collisions at $\sqrt{s}$ = 7 TeV. Using a three-dimensional template likelihood technique the lepton plus jets ($\geq$ 1b-tagged) channel gives 172.33 ± 0.75 ± 1.02 GeV, while exploiting a one dimensional template method using $m_{\ell b}$ the dilepton channel (1 or 2b-tags) gives 173.79 ± 0.54 ± 1.30 GeV. The results are combined.

[19] AALTONEN 15D based on 9.1 fb^{-1} of $p\overline{p}$ data at $\sqrt{s}$ = 1.96 TeV. Uses a template technique to fit a distribution of a variable defined by a linear combination of variables sensitive and insensitive to jet energy scale to optimize reduction of systematic errors. b-tagged and non-b-tagged events are separately analyzed and combined.

[20] Based on 9.3 fb^{-1} of $p\overline{p}$ data at $\sqrt{s}$ = 1.96 TeV. Multivariate algorithm is used to discriminate signal from backgrounds, and templates are used to measure m_t.

[21] Based on 9.7 fb^{-1} of $p\overline{p}$ data at $\sqrt{s}$ = 1.96 TeV. A matrix element method is used to calculate the probability of an event to be signal or background, and the overall jet energy scale is constrained *in situ* by m_W. See ABAZOV 15G for further details.

[22] Based on 3.54 fb^{-1} of pp data at $\sqrt{s}$ = 7 TeV. The mass is reconstructed for each event employing a kinematic fit of the jets to a ttbar hypothesis. The combination with the pervious CMS measurements in the dilepton and the lepton+jets channels gives 173.54 ± 0.33 ± 0.96 GeV.

[23] Based on 8.7 fb^{-1} in $p\overline{p}$ collisions at $\sqrt{s}$ = 1.96 TeV. Events with an identified charged lepton or small $\not\!\!E_T$ are rejected from the event sample, so that the measurement is statistically independent from those in the ℓ + jets and all hadronic channels while being sensitive to those events with a τ lepton in the final state.

[24] Based on 5.0 fb^{-1} of pp data at $\sqrt{s}$ = 7 TeV. CHATRCHYAN 13S studied events with di-lepton + $\not\!\!E_T$ + $\geq$ 2 b-jets, and looked for kinematical endpoints of MT2, MT2$_T$, and subsystem variables.

[25] AAD 12I based on 1.04 fb^{-1} of pp data at $\sqrt{s}$ = 7 TeV. Uses 2d-template analysis (MT) with m_t and jet energy scale factor (JSF) from m_W mass fit.

[26] Based on 8.7 fb^{-1} of data in $p\overline{p}$ collisions at 1.96 TeV. The JES is calibrated by using the dijet mass from the W boson decay.

[27] Use the ME method based on 2.2 fb^{-1} of data in $p\overline{p}$ collisions at 1.96 TeV.

[28] Combination based on up to 5.8 fb^{-1} of data in $p\overline{p}$ collisions at 1.96 TeV.

[29] Based on 5.8 fb^{-1} of data in $p\overline{p}$ collisions at 1.96 TeV the quoted value is m_t = 172.5 ± 1.4(stat)±1.0(JES)±1.1(syst) GeV. The measurement is performed with a liklihood fit technique which simultaneously determines m_t and JES (Jet Energy Scale).

[30] Based on 4.3 fb^{-1} of data in p-pbar collisions at 1.96 TeV. The measurement reduces the JES uncertainty by using the single lepton channel study of ABAZOV 11P.

[31] Combination with the result in 1 fb^{-1} of preceding data reported in ABAZOV 09AH as well as the MWT result of ABAZOV 11R with a statistical correlation of 60%.

[32] Based on 5.0 fb^{-1} of pp data at $\sqrt{s}$ = 7 TeV. Uses an analytical matrix weighting technique (AMWT) and full kinematic analysis (KIN).

[33] Based on 5.0 fb^{-1} of pp data at $\sqrt{s}$ = 7 TeV. The first error is statistical and JES combined, and the second is systematic. Ideogram method is used to obtain 2D liklihood for the kinematical fit with two parameters mtop and JES.

[34] Based on 3.2 fb^{-1} in $p\overline{p}$ collisions at $\sqrt{s}$ = 1.96 TeV. The first error is from statistics and JES combined, and the latter is from the other systematic uncertainties. The result is obtained using an unbinned maximum likelihood method where the top quark mass and the JES are measured simultaneously, with Δ_{JES} = 0.3 ± 0.3(stat).

[35] Based on 5.7 fb^{-1} in $p\overline{p}$ collisions at $\sqrt{s}$ = 1.96 TeV. Events with an identified charged lepton or small $\not\!\!E_T$ are rejected from the event sample, so that the measurement is statistically independent from those in the ℓ + jets and all hadronic channels while being sensitive to those events with a τ lepton in the final state. Supersedes AALTONEN 07B.

[36] AALTONEN 11E based on 5.6 fb^{-1} in $p\overline{p}$ collisions at $\sqrt{s}$ = 1.96 TeV. Employs a multi-dimensional template likelihood technique where the lepton plus jets (one or two b-tags) channel gives 172.2 ± 1.2 ± 0.9 GeV while the dilepton channel yields 170.3 ± 2.0 ± 3.1 GeV. The results are combined. OUR EVALUATION includes the measurement in the dilepton channel only.

[37] Uses a likelihood fit of the lepton p_T distribution based on 2.7 fb^{-1} in $p\overline{p}$ collisions at $\sqrt{s}$ = 1.96 TeV.

[38] Based on 3.6 fb^{-1} in $p\overline{p}$ collisions at $\sqrt{s}$ = 1.96 TeV. ABAZOV 11P reports 174.94 ± 0.83±0.78±0.96 GeV, where the first uncertainty is from statistics, the second from JES, and the last from other systematic uncertainties. We combine the JES and systematic uncertainties. A matrix-element method is used where the JES uncertainty is constrained by the W mass. ABAZOV 11P describes a measurement based on 2.6 fb^{-1} that is combined with ABAZOV 08AH, which employs an independent 1 fb^{-1} of data.

[39] Based on a matrix-element method which employs 5.4 fb^{-1} in $p\overline{p}$ collisions at $\sqrt{s}$ = 1.96 TeV. Superseded by ABAZOV 12AB.

[40] Based on 36 pb^{-1} of pp collisions at $\sqrt{s}$ = 7 TeV. A Kinematic Method using b-tagging and an analytical Matrix Weighting Technique give consistent results and are combined. Superseded by CHATRCHYAN 12BA.

[41] Based on 5.6 fb^{-1} in $p\overline{p}$ collisions at $\sqrt{s}$ = 1.96 TeV. The likelihood calculated using a matrix element method gives m_t = 173.0 ± 0.7(stat)±0.6(JES)±0.9(syst) GeV, for a total uncertainty of 1.2 GeV.

[42] Based on 3.4 fb^{-1} of $p\overline{p}$ collisions at $\sqrt{s}$ = 1.96 TeV. The result is obtained by combining the MT2 variable method and the NWA (Neutrino Weighting Algorithm). The MT2 method alone gives $m_t = 168.0^{+4.8}_{-4.0}$(stat)±2.9(syst) GeV with smaller systematic error due to small JES uncertainty.

[43] Based on 1.9 fb^{-1} in $p\overline{p}$ collisions at $\sqrt{s}$ = 1.96 TeV. The result is from the measurement using the transverse decay length of b-hadrons and that using the transverse momentum of the W decay muons, which are both insensitive to the JES (jet energy scale) uncertainty. OUR EVALUATION uses only the measurement exploiting the decay length significance which yields $166.9^{+9.5}_{-8.5}$(stat)±2.9 (syst) GeV. The measurement that uses the lepton transverse momentum is excluded from the average because of a statistical correlation with other samples.

[44] Based on 2.9 fb^{-1} of $p\overline{p}$ collisions at $\sqrt{s}$ = 1.96 TeV. The first error is from statistics and JES uncertainty, and the latter is from the other systematics. Neural-network-based kinematical selection of 6 highest E_T jets with a vtx b-tag is used to distinguish signal from background. Superseded by AALTONEN 12G.

[45] Based on 2 fb^{-1} of data at $\sqrt{s}$ = 1.96 TeV. The top mass is obtained from the measurement of the invariant mass of the lepton (e or μ) from W decays and the soft μ in b-jet. The result is insensitive to jet energy scaling.

[46] Based on 1.9 fb^{-1} of data at $\sqrt{s}$ = 1.96 TeV. The first error is from statistics and jet energy scale uncertainty, and the latter is from the other systematics. Matrix element method with effective propagators.

[47] Based on 943 pb^{-1} of data at $\sqrt{s}$ = 1.96 TeV. The first error is from statistical and jet-energy-scale uncertainties, and the latter is from other systematics. AALTONEN 09K selected 6 jet events with one or more vertex b-tags and used the tree-level matrix element to construct template models of signal and background.

[48] Based on 1.9 fb^{-1} of data at $\sqrt{s}$ = 1.96 TeV. The first error is from statistical and jet-energy-scale (JES) uncertainties, and the second is from other systematics. Events with lepton + jets and those with dilepton + jets were simultaneously fit to constrain m_t and JES. Lepton + jets data only give m_t = 171.8 ± 2.2 GeV, and dilepton data only give $m_t = 171.2^{+5.3}_{-5.1}$ GeV.

[49] Based on 2 fb^{-1} of data at $\sqrt{s}$ = 1.96 TeV. Matrix Element method. Optimal selection criteria for candidate events with two high p_T leptons, high $\not\!\!E_T$, and two or more jets with and without b-tag are obtained by neural network with neuroevolution technique to minimize the statistical error of m_t.

[50] Based on 2.9 fb^{-1} of data at $\sqrt{s}$ = 1.96 TeV. Mass m_t is estimated from the likelihood for the eight-fold kinematical solutions in the plane of the azimuthal angles of the two neutrino momenta.

[51] Based on 1 fb^{-1} of data at $\sqrt{s}$ = 1.96 TeV. Events with two identified leptons, and those with one lepton plus one isolated track and a b-tag were used to constrain m_t. The result is a combination of the νWT (ν Weighting Technique) result of 176.2 ± 4.8 ± 2.1 GeV and the MWT (Matrix-element Weighting Technique) result of 173.2 ± 4.9 ± 2.0 GeV.

[52] Reports measurement of $170.7^{+4.2}_{-3.9}$ ± 2.6 ± 2.4 GeV based on 1.2 fb^{-1} of data at $\sqrt{s}$ = 1.96 TeV. The last error is due to the theoretical uncertainty on $\sigma_{t\overline{t}}$. Without the cross-section constraint a top mass of $169.7^{+5.2}_{-4.9}$ ± 3.1 GeV is obtained.

[53] Template method.

[54] Result is based on 1 fb^{-1} of data at $\sqrt{s}$ = 1.96 TeV. The first error is from statistics and jet energy scale uncertainty, and the latter is from the other systematics.

[55] Based on 310 pb^{-1} of data at $\sqrt{s}$ = 1.96 TeV.

[56] Ideogram method.

[57] Based on 311 pb^{-1} of data at $\sqrt{s}$ = 1.96 TeV. Events with 4 or more jets with $E_T >$ 15 GeV, significant missing E_T, and secondary vertex b-tag are used in the fit. About 44% of the signal acceptance is from $\tau\nu$ + 4 jets. Events with identified e or μ are vetoed to provide a statistically independent measurement.

[58] Based on 1.02 fb^{-1} of data at $\sqrt{s}$ = 1.96 TeV. Superseded by AALTONEN 12G.

[59] Based on 955 pb^{-1} of data $\sqrt{s}$ = 1.96 TeV. m_t and JES (Jet Energy Scale) are fitted simultaneously, and the first error contains the JES contribution of 1.5 GeV.

[60] Matrix element method.

[61] Based on 425 pb^{-1} of data at $\sqrt{s}$ = 1.96 TeV. The first error is a combination of statistics and JES (Jet Energy Scale) uncertainty, which has been measured simultaneously to give JES = 0.989 ± 0.029(stat).

[62] Based on 370 pb^{-1} of data at $\sqrt{s}$ = 1.96 TeV. Combined result of MWT (Matrix-element Weighting Technique) and νWT (ν Weighting Technique) analyses is 178.1 ± 6.7 ± 4.8 GeV.

[63] Based on 1.0 fb^{-1} of data at $\sqrt{s}$ = 1.96 TeV. ABULENCIA 07D improves the matrix element description by including the effects of initial-state radiation.

[64] Based on 695 pb^{-1} of data at $\sqrt{s}$ = 1.96 TeV. The transverse decay length of the b hadron is used to determine m_t, and the result is free from the JES (jet energy scale) uncertainty.

[65] Based on $\sim$ 400 pb^{-1} of data at $\sqrt{s}$ = 1.96 TeV. The first error includes statistical and systematic jet energy scale uncertainties, the second error is from the other systematics. The result is obtained with the b-tagging information. The result without b-tagging is $169.2^{+5.0+1.5}_{-7.4-1.4}$ GeV. Superseded by ABAZOV 08AH.

[66] Based on 318 pb^{-1} of data at $\sqrt{s}$ = 1.96 TeV.

[67] Dynamical likelihood method.

[68] Based on 340 pb^{-1} of data at $\sqrt{s}$ = 1.96 TeV.

[69] Based on 360 pb^{-1} of data at $\sqrt{s}$ = 1.96 TeV.

[70] Based on 110.2 ± 5.8 pb^{-1} at $\sqrt{s}$ = 1.8 TeV.

[71] Based on the all hadronic decays of $t\overline{t}$ pairs. Single b-quark tagging via the decay chain $b \to c \to \mu$ was used to select signal enriched multijet events. The result was obtained by the maximum likelihood method after bias correction.

[72] Obtained by re-analysis of the lepton + jets candidate events that led to ABBOTT 98F. It is based upon the maximum likelihood method which makes use of the leading order matrix elements.

[73] Based on 125 ± 7 pb^{-1} of data at $\sqrt{s}$ = 1.8 TeV.

[74] Based on $\sim$ 106 pb^{-1} of data at $\sqrt{s}$= 1.8 TeV.

[75] Obtained by combining the measurements in the lepton + jets [AFFOLDER 01], all-jets [ABE 97R, ABE 99B], and dilepton [ABE 99B] decay topologies.

[76] Obtained by combining the D0 result m_t (GeV) = 168.4 ± 12.3 ± 3.6 from 6 di-lepton events (see also ABBOTT 98D) and m_t (GeV) = 173.3 ± 5.6 ± 5.5 from lepton+jet events (ABBOTT 98F).

[77] Obtained by combining the CDF results of m_t (GeV)=167.4 ± 10.3 ± 4.8 from 8 dilepton events, m_t (GeV)=175.9 ± 4.8 ± 5.3 from lepton+jet events (ABE 98E), and m_t (GeV)=186.0 ± 10.0 ± 5.7 from all-jet events (ABE 97R). The systematic errors in the latter two measurements are changed in this paper.
[78] See AFFOLDER 01 for details of systematic error re-evaluation.
[79] Based on 109 ± 7 pb^{-1} of data at $\sqrt{s}$ = 1.8 TeV.
[80] See ABAZOV 04G.
[81] The updated systematic error is listed. See AFFOLDER 01, appendix C.
[82] Obtained by combining the DØ results of m_t(GeV)=168.4 ± 12.3 ± 3.6 from 6 dilepton events and m_t(GeV)=173.3 ± 5.6 ± 5.5 from 77 lepton+jet events.
[83] Obtained by combining the DØ results from dilepton and lepton+jet events, and the CDF results (ABE 99B) from dilepton, lepton+jet events, and all-jet events.
[84] Based on the first observation of all hadronic decays of $t\bar{t}$ pairs. Single b-quark tagging with jet-shape variable constraints was used to select signal enriched multi-jet events. The updated systematic error is listed. See AFFOLDER 01, appendix C.

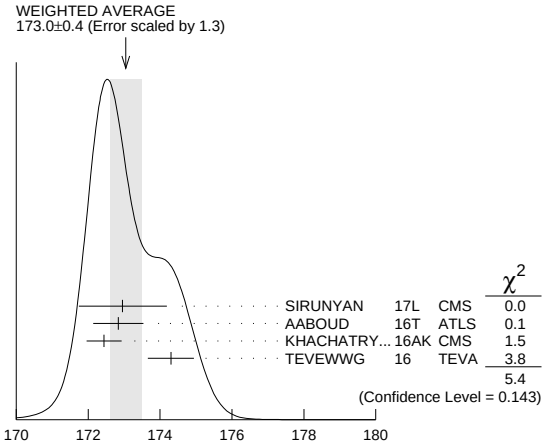

t-Quark Mass (Direct Measurements) (GeV)

t-Quark Mass from Cross-Section Measurements

The top quark $\overline{\text{MS}}$ or pole mass can be extracted from a measurement of $\sigma(t\bar{t})$ by using theory calculations. We quote below the $\overline{\text{MS}}$ mass. See the review "The Top Quark" and references therein for more information.

VALUE (GeV)	DOCUMENT ID		TECN	COMMENT
$160.0^{+4.8}_{-4.3}$	[1] ABAZOV	11S	D0	$\sigma(t\bar{t})$ + theory
• • • We do not use the following data for averages, fits, limits, etc. • • •				
	[2] ABAZOV	09AG	D0	cross sects, theory + exp
	[3] ABAZOV	09R	D0	cross sects, theory + exp

[1] Based on 5.3 fb^{-1} in $p\bar{p}$ collisions at $\sqrt{s}$ = 1.96 TeV. ABAZOV 11S uses the measured $t\bar{t}$ production cross section of $8.13^{+1.02}_{-0.90}$ pb [ABAZOV 11E] in the lepton plus jets channel to obtain the top quark $\overline{\text{MS}}$ mass by using an approximate NNLO computation (MOCH 08, LANGENFELD 09). The corresponding top quark pole mass is $167.5^{+5.4}_{-4.9}$ GeV. A different theory calculation (AHRENS 10, AHRENS 10A) is also used and yields $m_t^{\overline{\text{MS}}} = 154.5^{+5.0}_{-4.3}$ GeV.
[2] Based on 1 fb^{-1} of data at $\sqrt{s}$ = 1.96 TeV. Uses the ℓ + jets, $\ell\ell$, and $\ell\tau$ + jets channels. ABAZOV 09AG extract the pole mass of the top quark using two different calculations that yield $169.1^{+5.9}_{-5.2}$ GeV (MOCH 08, LANGENFELD 09) and $168.2^{+5.9}_{-5.4}$ GeV (KIDONAKIS 08).
[3] Based on 1 fb^{-1} of data at $\sqrt{s}$ = 1.96 TeV. Uses the $\ell\ell$ and $\ell\tau$ + jets channels. ABAZOV 09R extract the pole mass of the top quark using two different calculations that yield $173.3^{+9.8}_{-8.6}$ GeV (MOCH 08, LANGENFELD 09) and $171.5^{+9.9}_{-8.8}$ GeV (CACCIARI 08).

t-Quark Pole Mass from Cross-Section Measurements

VALUE (GeV)	DOCUMENT ID		TECN	COMMENT
173.1±0.9 OUR AVERAGE				
173.2±0.9±0.8±1.2	[1] AABOUD	17BC	ATLS	$e+\mu+\geq 1b$ jets
170.6±2.7	[2] SIRUNYAN	17W	CMS	$\ell+\geq$ 1j
$172.8\pm1.1^{+3.3}_{-3.1}$	[3] ABAZOV	16F	D0	$\ell\ell$, ℓ+jets channels
$173.8^{+1.7}_{-1.8}$	[4] KHACHATRY...	16AW	CMS	$e+\mu+\not{E}_T+\geq$0j
$173.7^{+2.3}_{-2.1}$	[5] AAD	15BW	ATLS	$\ell+\not{E}_T+\geq$5j (2b-tag)
$172.9^{+2.5}_{-2.6}$	[6] AAD	14AY	ATLS	pp at $\sqrt{s}$ = 7, 8 TeV
• • • We do not use the following data for averages, fits, limits, etc. • • •				
$176.7^{+3.0}_{-2.8}$	[7] CHATRCHYAN	14	CMS	pp at $\sqrt{s}$ = 7 TeV

[1] AABOUD 17BC based on 20.2 fb^{-1} of pp data at $\sqrt{s}$ = 8 TeV. The pole mass is extracted from a fit of NLO predictions to eight single lepton and dilepton differential distributions, while simultaneously constraining uncertainties due to PDFs and QCD scales. The three reported uncertainties come from statistics, experimental systematics, and theoretical sources.
[2] SIRUNYAN 17W based on 2.2 fb^{-1} of pp data at $\sqrt{s}$ = 13 TeV. Events are categorized according to the jet multiplicity and the number of b-tagged jets. The pole mass is obtained from the inclusive cross section measurement and the NNLO prediction.
[3] ABAZOV 16F based on 9.7 fb^{-1} of data in $p\bar{p}$ collisions at $\sqrt{s}$ = 1.96 TeV. The result is obtained from the inclusive cross section measurement and the NNLO+NNLL prediction.
[4] KHACHATRYAN 16AW based on 5.0 fb^{-1} of pp collisions at 7 TeV and 19.7 fb^{-1} at 8 TeV. The 7 TeV data include those used in CHATRCHYAN 14. The result is obtained from the inclusive cross sections.
[5] AAD 15BW based on 4.6 fb^{-1} of pp data at $\sqrt{s}$ = 7 TeV. Uses normalized differential cross section for $t\bar{t}$ + 1 jet as a function of the inverse of the invariant mass of the $t\bar{t}$ + 1 jet system. The measured cross section is corrected to the parton level. Then a fit to the data using NLO + parton shower prediction is performed.
[6] AAD 14AY used $\sigma(t\bar{t})$ for $e\mu$ events. The result is a combination of the measurements m_t = 171.4 ± 2.6 GeV based on 4.6 fb^{-1} of data at 7 TeV and m_t = 174.1 ± 2.6 GeV based on 20.3 fb^{-1} of data at 8 TeV.
[7] CHATRCHYAN 14 used $\sigma(t\bar{t})$ from pp collisions at $\sqrt{s}$ = 7 TeV measured in CHATRCHYAN 12AX to obtain m_t(pole) for $\alpha_s(m_Z)$ = 0.1184 ± 0.0007. The errors have been corrected in KHACHATRYAN 14K.

$m_t - m_{\bar{t}}$

Test of CPT conservation. OUR AVERAGE assumes that the systematic uncertainties are uncorrelated.

VALUE (GeV)	DOCUMENT ID		TECN	COMMENT
−0.16±0.19 OUR AVERAGE				
−0.15±0.19±0.09	[1] CHATRCHYAN	17	CMS	$\ell+\not{E}_T+\geq$4j ($\geq$1b j)
0.67±0.61±0.41	[2] AAD	14	ATLS	$\ell+\not{E}_T+\geq$4j ($\geq$2 b-tags)
−1.95±1.11±0.59	[3] AALTONEN	13E	CDF	$\ell+\not{E}_T+\geq$4j (0,1,2 b-tags)
−0.44±0.46±0.27	[4] CHATRCHYAN	12Y	CMS	$\ell+\not{E}_T+\geq$4j
0.8 ±1.8 ±0.5	[5] ABAZOV	11T	D0	$\ell+\not{E}_T+$ 4 jets ($\geq$1 b-tag)
• • • We do not use the following data for averages, fits, limits, etc. • • •				
−3.3 ±1.4 ±1.0	[6] AALTONEN	11K	CDF	Repl. by AALTONEN 13E
3.8 ±3.4 ±1.2	[7] ABAZOV	09AA	D0	$\ell+\not{E}_T+$ 4 jets ($\geq$1 b-tag)

[1] CHATRCHYAN 17 based on 19.6 fb^{-1} of pp data at $\sqrt{s}$ = 8 TeV and an average top mass of 172.84 ± 0.10 (stat) GeV is obtained.
[2] Based on 4.7 fb^{-1} of pp data at $\sqrt{s}$ = 7 TeV and an average top mass of 172.5 GeV/c^2.
[3] Based on 8.7 fb^{-1} of $p\bar{p}$ collisions at $\sqrt{s}$ = 1.96 TeV and an average top mass of 172.5 GeV/c^2.
[4] Based on 4.96 fb^{-1} of pp data at $\sqrt{s}$ = 7 TeV. Based on the fitted m_t for ℓ^+ and ℓ^- events using the Ideogram method.
[5] Based on a matrix-element method which employs 3.6 fb^{-1} in $p\bar{p}$ collisions at $\sqrt{s}$ = 1.96 TeV.
[6] Based on a template likelihood technique which employs 5.6 fb^{-1} in $p\bar{p}$ collisions at $\sqrt{s}$ = 1.96 TeV.
[7] Based on 1 fb^{-1} of data in $p\bar{p}$ collisions at $\sqrt{s}$ = 1.96 TeV.

t-quark DECAY WIDTH

VALUE (GeV)	CL%	DOCUMENT ID		TECN	COMMENT
$1.41^{+0.19}_{-0.15}$ OUR AVERAGE Error includes scale factor of 1.4.					
$1.36\pm0.02^{+0.14}_{-0.11}$		[1] KHACHATRY...	14E	CMS	$\ell\ell$+$\not{E}_T$+2-4jets (0-2b-tag)
$2.00^{+0.47}_{-0.43}$		[2] ABAZOV	12T	D0	$\Gamma(t\to bW)/\Gamma(t\to bW)$
• • • We do not use the following data for averages, fits, limits, etc. • • •					
< 6.38	95	[3] AALTONEN	13Z	CDF	ℓ+$\not{E}_T$+ $\geq$ 4j ($\geq$ 0 b), direct
$1.99^{+0.69}_{-0.55}$		[4] ABAZOV	11B	D0	Repl. by ABAZOV 12T
> 1.21	95	[4] ABAZOV	11B	D0	$\Gamma(t\to Wb)$
< 7.6	95	[5] AALTONEN	10AC	CDF	ℓ + jets, direct
<13.1	95	[6] AALTONEN	09M	CDF	m_t(rec) distribution

[1] Based on 19.7 fb^{-1} of pp data at $\sqrt{s}$ = 8 TeV. The result is obtained by combining the measurement of $R=\Gamma(t\to Wb)/\Gamma(t\to Wq\ (q$=$b,s,d))$ and a previous CMS measurement of the t-channel single top production cross section of CHATRCHYAN 12BQ, by using the theoretical calculation of $\Gamma(t\to Wb)$ for m_t = 172.5 GeV.
[2] Based on 5.4 fb^{-1} of data in $p\bar{p}$ collisions at 1.96 TeV. $\Gamma(t\to bW) = 1.87^{+0.44}_{-0.40}$ GeV is obtained from the observed t-channel single top quark production cross section, whereas $B(t\to bW) = 0.90\pm0.04$ is used assuming $\sum_q B(t\to qW) = 1$. The result is valid for m_t = 172.5 GeV. See the paper for the values for m_t = 170 or 175 GeV.
[3] Based on 8.7 fb^{-1} of data. The two sided 68% CL interval is 1.10 GeV < Γ_t < 4.05 GeV for m_t = 172.5 GeV.
[4] Based on 2.3 fb^{-1} in $p\bar{p}$ collisions at $\sqrt{s}$ = 1.96 TeV. ABAZOV 11B extracted Γ_t from the partial width $\Gamma(t\to Wb) = 1.92^{+0.58}_{-0.51}$ GeV measured using the t-channel single top production cross section, and the branching fraction $\text{br}t\to Wb = 0.962^{+0.068}_{-0.066}(\text{stat})^{+0.064}_{-0.052}(\text{syst})$. The $\Gamma(t\to Wb)$ measurement gives the 95% CL lowerbound of $\Gamma(t\to Wb)$ and hence that of Γ_t.
[5] Results are based on 4.3 fb^{-1} of data in $p\bar{p}$ collisions at $\sqrt{s}$ = 1.96 TeV. The top quark mass and the hadronically decaying W boson mass are reconstructed for each candidate events and compared with templates of different top quark width. The two sided 68% CL interval is 0.3 GeV< Γ_t < 4.4 GeV for m_t = 172.5 GeV.
[6] Based on 955 pb^{-1} of $p\bar{p}$ collision data at $\sqrt{s}$ = 1.96 TeV. AALTONEN 09M selected $t\bar{t}$ candidate events for the $\ell+\not{E}_T$ + jets channel with one or two b-tags, and examine the decay width dependence of the reconstructed m_t distribution. The result is for m_t =175 GeV, whereas the upper limit is lower for smaller m_t.

t DECAY MODES

	Mode		Fraction (Γ_i/Γ)		Confidence level
Γ_1	$t \to W\,q\,(q = b, s, d)$				
Γ_2	$t \to W\,b$				
Γ_3	$t \to e\,\nu_e\,b$		(13.3 ± 0.6) %		
Γ_4	$t \to \mu\,\nu_\mu\,b$		(13.4 ± 0.6) %		
Γ_5	$t \to \tau\,\nu_\tau\,b$		(7.1 ± 0.6) %		
Γ_6	$t \to q\,\overline{q}\,b$		(66.5 ± 1.4) %		
Γ_7	$t \to \gamma\,q\,(q{=}u,c)$		[a]		
	$\Delta T = 1$ weak neutral current ($T1$) modes				
Γ_8	$t \to Z\,q\,(q{=}u,c)$	$T1$	[b] < 5	$\times 10^{-4}$	95%
Γ_9	$t \to H\,u$	$T1$	< 2.4	$\times 10^{-3}$	95%
Γ_{10}	$t \to H\,c$	$T1$	< 2.2	$\times 10^{-3}$	95%
Γ_{11}	$t \to \ell^+\,\overline{q\,q'}\,(q{=}d,s,b;\ q'{=}u,c)$	$T1$	< 1.6	$\times 10^{-3}$	95%

[a] This limit is for $\Gamma(t \to \gamma q)/\Gamma(t \to W b)$.

[b] This limit is for $\Gamma(t \to Z q)/\Gamma(t \to W b)$.

t BRANCHING RATIOS

$\Gamma(Wb)/\Gamma(Wq(q=b,s,d))$ Γ_2/Γ_1

OUR AVERAGE assumes that the systematic uncertainties are uncorrelated.

VALUE	DOCUMENT ID		TECN	COMMENT
0.957±0.034 OUR AVERAGE	Error includes scale factor of 1.5. See the ideogram below.			
0.87 ±0.07	[1] AALTONEN	14G	CDF	$\ell\ell$+$\not\!\!E_T$+ ≥2j (0,1,2 b-tag)
1.014±0.003±0.032	[2] KHACHATRY...	14E	CMS	$\ell\ell$+$\not\!\!E_T$ + 2,3,4j (0–2b-tag)
0.94 ±0.09	[3] AALTONEN	13G	CDF	ℓ+$\not\!\!E_T$+ ≥ 3jets (≥ 1b-tag)
0.90 ±0.04	[4] ABAZOV	11X	D0	
• • • We do not use the following data for averages, fits, limits, etc. • • •				
0.97 $^{+0.09}_{-0.08}$	[5] ABAZOV	08M	D0	ℓ + n jets with 0,1,2 b-tag
1.03 $^{+0.19}_{-0.17}$	[6] ABAZOV	06K	D0	
1.12 $^{+0.21}_{-0.19}$ $^{+0.17}_{-0.13}$	[7] ACOSTA	05A	CDF	Repl. by AALTONEN 13G
0.94 $^{+0.26}_{-0.21}$ $^{+0.17}_{-0.12}$	[8] AFFOLDER	01C	CDF	

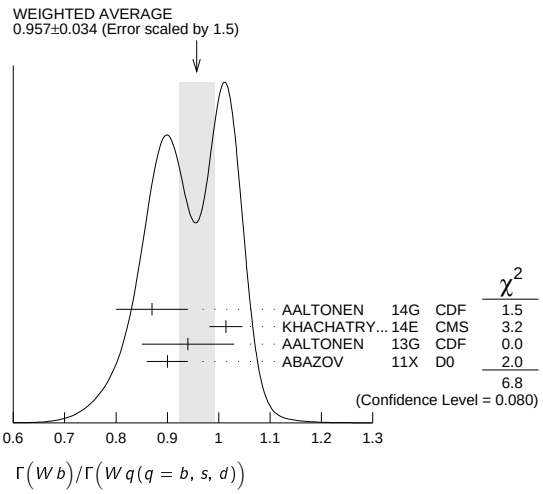

[1] Based on 8.7 fb^{-1} of data. This measurement gives $|V_{tb}| = 0.93 \pm 0.04$ and $|V_{tb}| > 0.85$ (95% CL) in the SM.

[2] Based on 19.7 fb^{-1} of pp data at $\sqrt{s} = 8$ TeV. The result is obtained by counting the number of b jets per $t\overline{t}$ signal events in the dilepton channel. The $t\overline{t}$ production cross section is measured to be $\sigma(t\overline{t}) = 238 \pm 1 \pm 15$ pb, in good agreement with the SM prediction and the latest CMS measurement of CHATRCHYAN 14F. The measurement gives $R > 0.995$ (95% CL), or $|V_{tb}| > 0.975$ (95% CL) in the SM, requiring $R \leq 1$.

[3] Based on 8.7 fb^{-1} of $p\overline{p}$ collisions at $\sqrt{s} = 1.96$ TeV. Measure the fraction of $t \to Wb$ decays simultaneously with the $t\overline{t}$ cross section. The correlation coefficient between those two measurements is -0.434. Assume unitarity of the 3×3 CKM matrix and set $|V_{tb}| > 0.89$ at 95% CL.

[4] Based on 5.4 fb^{-1} of data. The error is statistical and systematic combined. The result is a combination of 0.95 ± 0.07 from ℓ + jets channel and 0.86 ± 0.05 from $\ell\ell$ channel. $|V^{tb}| = 0.95 \pm 0.02$ follows from the result by assuming unitarity of the 3x3 CKM matrix.

[5] Result is based on 0.9 fb^{-1} of data. The 95% CL lower bound R > 0.79 gives $|V_{tb}| > 0.89$ (95% CL).

[6] ABAZOV 06K result is from the analysis of $t\overline{t} \to \ell\nu$ + ≥ 3 jets with 230 pb^{-1} of data at $\sqrt{s} = 1.96$ TeV. It gives R > 0.61 and $|V_{tb}| > 0.78$ at 95% CL. Superseded by ABAZOV 08M.

[7] ACOSTA 05A result is from the analysis of lepton + jets and di-lepton + jets final states of $t\overline{t}$ candidate events with ∼ 162 pb^{-1} of data at $\sqrt{s} = 1.96$ TeV. The first error is statistical and the second systematic. It gives R > 0.61, or $|V_{tb}| > 0.78$ at 95% CL.

[8] AFFOLDER 01C measures the top-quark decay width ratio $R = \Gamma(Wb)/\Gamma(Wq)$, where q is a d, s, or b quark, by using the number of events with multiple b tags. The first error is statistical and the second systematic. A numerical integration of the likelihood function gives $R > 0.61$ (0.56) at 90% (95%) CL. By assuming three generation unitarity, $|V_{tb}| = 0.97^{+0.16}_{-0.12}$ or $|V_{tb}| > 0.78$ (0.75) at 90% (95%) CL is obtained. The result is based on 109 pb^{-1} of data at $\sqrt{s} = 1.8$ TeV.

$\Gamma(e\nu_e b)/\Gamma_{\rm total}$ Γ_3/Γ

VALUE	DOCUMENT ID		TECN	COMMENT
0.133±0.004±0.005	[1] AAD	15CC	ATLS	ℓ+jets, $\ell\ell$+jets, $\ell\tau_h$+jets

[1] AAD 15CC based on 4.6 fb^{-1} of pp data at $\sqrt{s} = 7$ TeV. It is assumed that the top branching ratios to leptons and jets add up to one and that only SM processes contribute to the background. The event selection criteria are optimized for the $\ell\tau_h$ + jets channel.

$\Gamma(\mu\nu_\mu b)/\Gamma_{\rm total}$ Γ_4/Γ

VALUE	DOCUMENT ID		TECN	COMMENT
0.134±0.003±0.005	[1] AAD	15CC	ATLS	ℓ+jets, $\ell\ell$+jets, $\ell\tau_h$+jets

[1] AAD 15CC based on 4.6 fb^{-1} of pp data at $\sqrt{s} = 7$ TeV. It is assumed that the top branching ratios to leptons and jets add up to one and that only SM processes contribute to the background. The event selection criteria are optimized for the $\ell\tau_h$ + jets channel.

$\Gamma(\tau\nu_\tau b)/\Gamma_{\rm total}$ Γ_5/Γ

VALUE	DOCUMENT ID		TECN	COMMENT
0.071±0.006 OUR AVERAGE				
0.070±0.003±0.005	[1] AAD	15CC	ATLS	ℓ+jets, $\ell\ell$+jets, $\ell\tau_h$+jets
0.096±0.028	[2] AALTONEN	14A	CDF	ℓ+τ_h+ ≥ 2jets (≥ 1b-tag)
• • • We do not use the following data for averages, fits, limits, etc. • • •				
	[3] ABULENCIA	06R	CDF	$\ell\tau$ + jets
	[4] ABE	97V	CDF	$\ell\tau$ + jets

[1] AAD 15CC based on 4.6 fb^{-1} of pp data at $\sqrt{s} = 7$ TeV. It is assumed that the top branching ratios to leptons and jets add up to one and that only SM processes contribute to the background. The event selection criteria are optimized for the $\ell\tau_h$ + jets channel.

[2] Based on 9 fb^{-1} of data. The measurement is in the channel $t\overline{t} \to (b\ell\nu)(b\tau\nu)$, where τ decays into hadrons (τ_h), and ℓ (e or μ) include ℓ from τ decays (τ_ℓ). The result is consistent with lepton universality.

[3] ABULENCIA 06R looked for $t\overline{t} \to (\ell\nu_\ell)\,(\tau\nu_\tau)\,b\overline{b}$ events in 194 pb^{-1} of $p\overline{p}$ collisions at $\sqrt{s} = 1.96$ TeV. 2 events are found where 1.00 ± 0.17 signal and 1.29 ± 0.25 background events are expected, giving a 95% CL upper bound for the partial width ratio $\Gamma(t \to \tau\nu q)\ /\ \Gamma_{SM}(t \to \tau\nu q) < 5.2$.

[4] ABE 97V searched for $t\overline{t} \to (\ell\nu_\ell)\,(\tau\nu_\tau)\,b\overline{b}$ events in 109 pb^{-1} of $p\overline{p}$ collisions at $\sqrt{s} = 1.8$ TeV. They observed 4 candidate events where one expects ∼ 1 signal and ∼ 2 background events. Three of the four observed events have jets identified as b candidates.

$\Gamma(q\overline{q}b)/\Gamma_{\rm total}$ Γ_6/Γ

VALUE	DOCUMENT ID		TECN	COMMENT
0.665±0.004±0.013	[1] AAD	15CC	ATLS	ℓ+jets, $\ell\ell$+jets, $\ell\tau_h$+jets

[1] AAD 15CC based on 4.6 fb^{-1} of pp data at $\sqrt{s} = 7$ TeV. Branching ratio of top quark into b and jets. It is assumed that the top branching ratios to leptons and jets add up to one and that only SM processes contribute to the background. The event selection criteria are optimized for the $\ell\tau_h$ + jets channel.

$\Gamma(\gamma q(q{=}u,c))/\Gamma_{\rm total}$ Γ_7/Γ

VALUE	CL%	DOCUMENT ID		TECN	COMMENT
<1.3 $\times 10^{-4}$	95	[1] KHACHATRY...16AS		CMS	B($t \to \gamma u$)
<1.7 $\times 10^{-3}$	95	[1] KHACHATRY...16AS		CMS	B($t \to \gamma c$)
<5.9 $\times 10^{-3}$	95	[2] CHEKANOV	03	ZEUS	B($t \to \gamma u$)
• • • We do not use the following data for averages, fits, limits, etc. • • •					
<0.0064	95	[3] AARON	09A	H1	$t \to \gamma u$
<0.0465	95	[4] ABDALLAH	04C	DLPH	B(γc or γu)
<0.0132	95	[5] AKTAS	04	H1	B($t \to \gamma u$)
<0.041	95	[6] ACHARD	02J	L3	B($t \to \gamma c$ or γu)
<0.032	95	[7] ABE	98G	CDF	$t\overline{t} \to (Wb)\,(\gamma c$ or $\gamma u)$

[1] KHACHATRYAN 16AS based on 19.8 fb^{-1} of data in pp collisions at $\sqrt{s} = 8$ TeV. FCNC through single top production in association with a photon is searched for in the mode $\mu + \gamma + \not\!\!E_T$ + ≥ 1j (0,1b). Bounds on the anomalous FCNC couplings are given by $\kappa_{tu\gamma} < 0.025$ and $\kappa_{tc\gamma} < 0.091$.

[2] CHEKANOV 03 looked for single top production via FCNC in the reaction $e^\pm p \to e^\pm$ (t or $\overline{t}$) X in 130.1 pb^{-1} of data at $\sqrt{s}$=300–318 GeV. No evidence for top production and its decay into bW was found. The result is obtained for m_t=175 GeV when B(γc)=B(Zq)=0, where q is a u or c quark. Bounds on the effective t-u-γ and t-u-Z couplings are found in their Fig. 4. The conversion to the constraint listed is from private communication, E. Gallo, January 2004.

[3] AARON 09A looked for single top production via FCNC in $e^\pm p$ collisions at HERA with 474 pb^{-1}. The upper bound of the cross section gives the bound on the FCNC coupling $\kappa_{tu\gamma}/\Lambda < 1.03$ TeV^{-1}, which corresponds to the result for $m_t = 175$ GeV.

[4] ABDALLAH 04C looked for single top production via FCNC in the reaction $e^+e^- \to \overline{t}c$ or $\overline{t}u$ in 541 pb^{-1} of data at $\sqrt{s}$=189–208 GeV. No deviation from the SM is found, which leads to the bound on B($t \to \gamma q$), where q is a u or a c quark, for m_t = 175 GeV when B($t \to Zq$)=0 is assumed. The conversion to the listed bound is from private communication, O. Yushchenko, April 2005. The bounds on the effective t-q-γ and t-q-Z couplings are given in their Fig. 7 and Table 4, for m_t = 170–180 GeV, where most conservative bounds are found by choosing the chiral couplings to maximize the negative interference between the virtual γ and Z exchange amplitudes.

[5] AKTAS 04 looked for single top production via FCNC in $e^\pm$ collisions at HERA with 118.3 pb^{-1}, and found 5 events in the e or μ channels. By assuming that they are due to statistical fluctuation, the upper bound on the $tu\gamma$ coupling $\kappa_{tu\gamma} < 0.27$ (95% CL) is obtained. The conversion to the partial width limit, when B(γc) = B(Zu) = B(Zc) = 0, is from private communication, E. Perez, May 2005.

[6] ACHARD 02J looked for single top production via FCNC in the reaction $e^+e^- \to \bar{t}c$ or $\bar{t}u$ in 634 pb^{-1} of data at $\sqrt{s}$= 189–209 GeV. No deviation from the SM is found, which leads to a bound on the top-quark decay branching fraction B(Zq), where q is a u or c quark. The bound assumes B(Zq)=0 and is for m_t= 175 GeV; bounds for m_t=170 GeV and 180 GeV and B(Zq) $\neq$ 0 are given in Fig. 5 and Table 7.

[7] ABE 98G looked for $t\bar{t}$ events where one t decays into $q\gamma$ while the other decays into bW. The quoted bound is for $\Gamma(\gamma q)/\Gamma(Wb)$.

$\Gamma(Zq(q=u,c))/\Gamma_{total}$ Γ_8/Γ

Test for ΔT=1 weak neutral current. Allowed by higher-order electroweak interaction.

VALUE (units 10^{-3})	CL%	DOCUMENT ID		TECN	COMMENT
< 0.22	95	[1] SIRUNYAN	17E	CMS	$t \to Zu$
< 0.49	95	[1] SIRUNYAN	17E	CMS	$t \to Zc$
< 0.7	95	[2] AAD	16D	ATLS	$t \to Zq$ ($q = u, c$)
< 0.5	95	[3] CHATRCHYAN	14S	CMS	$t \to Zq$ ($q = u, c$)
• • • We do not use the following data for averages, fits, limits, etc. • • •					
< 0.6	95	[4] CHATRCHYAN	14S	CMS	$t \to Zq$ ($q = u, c$)
< 2.1	95	[5] CHATRCHYAN	13F	CMS	$t \to Zq$ ($q = u, c$)
< 7.3	95	[6] AAD	12BT	ATLS	$t\bar{t} \to \ell^+\ell^-\ell'^{\pm} + \not{E}_T$ + jets
<32	95	[7] ABAZOV	11M	D0	$t \to Zq$ ($q = u, c$)
<83	95	[8] AALTONEN	09AL	CDF	$t \to Zq$ (q=c)
<37	95	[9] AALTONEN	08AD	CDF	$t \to Zq$ ($q = u, c$)
$< 1.59 \times 10^2$	95	[10] ABDALLAH	04C	DLPH	$e^+e^- \to \bar{t}c$ or $\bar{t}u$
$< 1.37 \times 10^2$	95	[11] ACHARD	02J	L3	$e^+e^- \to \bar{t}c$ or $\bar{t}u$
$< 1.4 \times 10^2$	95	[12] HEISTER	02Q	ALEP	$e^+e^- \to \bar{t}c$ or $\bar{t}u$
$< 1.37 \times 10^2$	95	[13] ABBIENDI	01T	OPAL	$e^+e^- \to \bar{t}c$ or $\bar{t}u$
$< 1.7 \times 10^2$	95	[14] BARATE	00S	ALEP	$e^+e^- \to \bar{t}c$ or $\bar{t}u$
$< 3.3 \times 10^2$	95	[15] ABE	98G	CDF	$t\bar{t} \to (Wb)(Zc$ or $Zu)$

[1] SIRUNYAN 17E based on 19.7 fb^{-1} of pp data at $\sqrt{s}$ = 8 TeV. The final states $t\bar{t} \to \ell^+\ell^-\ell'^{\pm}\nu$ + jets ($\ell, \ell' = e, \mu$) are investigated and the cross section $\sigma(pp \to tZq \to \ell\nu b\ell^+\ell^- q) = 10^{+8}_{-7}$ fb is measured, giving no sign of FCNC decays of the top quark.

[2] AAD 16D based on 20.3 fb^{-1} of pp data at $\sqrt{s}$ = 8 TeV. The FCNC decay is searched for in $t\bar{t}$ events in the final state $(bW)(qZ)$ when both W and Z decay leptonically, giving 3 charged leptons.

[3] CHATRCHYAN 14S combined search limit from this and CHATRCHYAN 13F data.

[4] Based on 19.7 fb^{-1} of pp data at $\sqrt{s}$ = 8 TeV. The flavor changing decay is searched for in $t\bar{t}$ events in the final state $(bW)(qZ)$ when both W and Z decay leptoically, giving 3 charged leptons.

[5] Based on 5.0 fb^{-1} of pp data at $\sqrt{s}$ = 7 TeV. Search for FCNC decays of the top quark in $t\bar{t} \to \ell^+\ell^-\ell'^{\pm}\nu$ + jets ($\ell, \ell' = e, \mu$) final states found no excess of signal events.

[6] Based on 2.1 fb^{-1} of pp data at $\sqrt{s}$ = 7 TeV.

[7] Based on 4.1 fb^{-1} of data. ABAZOV 11M searched for FCNC decays of the top quark in $t\bar{t} \to \ell^+\ell^-\ell'^{\pm}\nu$ + jets ($\ell, \ell' = e, \mu$) final states, and absence of the signal gives the bound.

[8] Based on $p\bar{p}$ data of 1.52 fb^{-1}. AALTONEN 09AL compared $t\bar{t} \to WbWb \to \ell\nu bjjb$ and $t\bar{t} \to ZcWb \to \ell\ell cjjb$ decay chains, and absence of the latter signal gives the bound. The result is for 100% longitudinally polarized Z boson and the theoretical $t\bar{t}$ production cross section The results for different Z polarizations and those without the cross section assumption are given in their Table XII.

[9] Result is based on 1.9 fb^{-1} of data at $\sqrt{s}$ = 1.96 TeV. $t\bar{t} \to WbZq$ or $ZqZq$ processes have been looked for in Z + $\geq$ 4 jet events with and without b-tag. No signal leads to the bound B($t \to Zq$) < 0.037 (0.041) for m_t = 175 (170) GeV.

[10] ABDALLAH 04C looked for single top production via FCNC in the reaction $e^+e^- \to \bar{t}c$ or $\bar{t}u$ in 541 pb^{-1} of data at $\sqrt{s}$=189–208 GeV. No deviation from the SM is found, which leads to the bound on B($t \to Zq$), where q is a u or a c quark, for m_t = 175 GeV when B($t \to \gamma q$)=0 is assumed. The conversion to the listed bound is from private communication, O. Yushchenko, April 2005. The bounds on the effective t-q-γ and t-q-Z couplings are given in their Fig. 7 and Table 4, for m_t = 170–180 GeV, where most conservative bounds are found by choosing the chiral couplings to maximize the negative interference between the virtual γ and Z exchange amplitudes.

[11] ACHARD 02J looked for single top production via FCNC in the reaction $e^+e^- \to \bar{t}c$ or $\bar{t}u$ in 634 pb^{-1} of data at $\sqrt{s}$= 189–209 GeV. No deviation from the SM is found, which leads to a bound on the top-quark decay branching fraction B(Zq), where q is a u or c quark. The bound assumes B(γq)=0 and is for m_t= 175 GeV; bounds for m_t=170 GeV and 180 GeV and B(γq) $\neq$0 are given in Fig. 5 and Table 7. Table 6 gives constraints on t-c-e-e four-fermi contact interactions.

[12] HEISTER 02Q looked for single top production via FCNC in the reaction $e^+e^- \to \bar{t}c$ or $\bar{t}u$ in 214 pb^{-1} of data at $\sqrt{s}$= 204–209 GeV. No deviation from the SM is found, which leads to a bound on the branching fraction B(Zq), where q is a u or c quark. The bound assumes B(γq)=0 and is for m_t= 174 GeV. Bounds on the effective t- (c or u)-γ and t- (c or u)- Z couplings are given in their Fig. 2.

[13] ABBIENDI 01T looked for single top production via FCNC in the reaction $e^+e^- \to \bar{t}c$ or $\bar{t}u$ in 600 pb^{-1} of data at $\sqrt{s}$= 189–209 GeV. No deviation from the SM is found, which leads to bounds on the branching fractions B(Zq) and B(γq), where q is a u or c quark. The result is obtained for m_t= 174 GeV. The upper bound becomes 9.7% (20.6%) for m_t= 169 (179) GeV. Bounds on the effective t- (c or u)-γ and t- (c or u)-Z couplings are given in their Fig. 4.

[14] BARATE 00S looked for single top production via FCNC in the reaction $e^+e^- \to \bar{t}c$ or $\bar{t}u$ in 411 pb^{-1} of data at c.m. energies between 189 and 202 GeV. No deviation from the SM is found, which leads to a bound on the branching fraction. The bound assumes B(γq)=0. Bounds on the effective t- (c or u)-γ and t- (c or u)-Z couplings are given in their Fig. 4.

[15] ABE 98G looked for $t\bar{t}$ events where one t decays into three jets and the other decays into qZ with $Z \to \ell\ell$. The quoted bound is for $\Gamma(Zq)/\Gamma(Wb)$.

$\Gamma(Hu)/\Gamma_{total}$ Γ_9/Γ

VALUE (units 10^{-3})	CL%	DOCUMENT ID		TECN	COMMENT
<2.4	95	[1] AABOUD	17AV	ATLS	$t \to Hu$ ($H \to \gamma\gamma$)
<5.5	95	[2] KHACHATRY...17I		CMS	$t \to Hu$ ($H \to WW$, ZZ, $\tau\tau$, $\gamma\gamma$, $b\bar{b}$)
<6.1	95	[3] AAD	15CO	ATLS	$t \to Hu$ ($H \to b\bar{b}$)
• • • We do not use the following data for averages, fits, limits, etc. • • •					
<7.9	95	[4] AAD	14AA	ATLS	$t \to Hq$ (q=u,c; $H \to \gamma\gamma$)

[1] AABOUD 17AV based on 36.1 fb^{-1} at $\sqrt{s}$ = 13 TeV of pp data. Search for $t\bar{t}$ events, where the other top quark decays hadronically or semi-leptonically.

[2] KHACHATRYAN 17I based on 19.7 fb^{-1} of pp data at $\sqrt{s}$ = 8 TeV, using the topologies $t\bar{t} \to Hq$+Wb, where q=u, c.

[3] AAD 15CO based on 20.3 fb^{-1} at $\sqrt{s}$ = 8 TeV of pp data. Searches for $t\bar{t}$ events, where the other top quark decays semi-leptonically. Exploits high multiplicity of b-jets and uses a likelihood discriminant. Combining with other ATLAS searches for different Higgs decay modes, B($t \to Hc$) < 0.46% and B($t \to Hu$) < 0.45% are obtained.

[4] AAD 14AA based on 4.7 fb^{-1} at $\sqrt{s}$ = 7 TeV and 20.3 fb^{-1} at $\sqrt{s}$ = 8 TeV of pp data. The upper-bound is for the sum of Br($t \to Hc$) and Br($t \to Hu$). Search for $t\bar{t}$ events, where the other top quark decays hadronically or semi-leptonically. The upper bound constrains the H-t-c Yukawa couplings $\sqrt{|Y^H_{tc_L}|^2 + |Y^H_{tc_R}|^2} < 0.17$ (95% CL).

$\Gamma(Hc)/\Gamma_{total}$ Γ_{10}/Γ

VALUE (units 10^{-3})	CL%	DOCUMENT ID		TECN	COMMENT
< 2.2	95	[1] AABOUD	17AV	ATLS	$t \to Hc$ ($H \to \gamma\gamma$)
< 4	95	[2] KHACHATRY...17I		CMS	$t \to Hc$ ($H \to WW$, ZZ, $\tau\tau$, $\gamma\gamma$, $b\bar{b}$)
< 5.6	95	[3] AAD	15CO	ATLS	$t \to Hc$ ($H \to b\bar{b}$)
• • • We do not use the following data for averages, fits, limits, etc. • • •					
< 7.9	95	[4] AAD	14AA	ATLS	$t \to Hq$ (q=u,c; $H \to \gamma\gamma$)
<13	95	[5] CHATRCHYAN	14R	CMS	$t \to Hc$ ($H \to \geq 2\ \ell$)
< 5.6	95	[6] KHACHATRY...14Q		CMS	$t \to Hc$ ($H \to \gamma\gamma$ or leptons)

[1] AABOUD 17AV based on 36.1 fb^{-1} at $\sqrt{s}$ = 13 TeV of pp data. Search for $t\bar{t}$ events, where the other top quark decays hadronically or semi-leptonically. The upper bound on the H-t-c Yukawa couplings is 0.090 (95% CL).

[2] KHACHATRYAN 17I based on 19.7 fb^{-1} of pp data at $\sqrt{s}$ = 8 TeV, using the topologies $t\bar{t} \to Hq$+Wb, where q=u, c.

[3] AAD 15CO based on 20.3 fb^{-1} at $\sqrt{s}$ = 8 TeV of pp data. Searches for $t\bar{t}$ events, where the other top quark decays semi-leptonically. Exploits high multiplicity of b-jets and uses a likelihood discriminant. Combining with other ATLAS searches for different Higgs decay modes, B($t \to Hc$) < 0.46% and B($t \to Hu$) < 0.45% are obtained.

[4] AAD 14AA based on 4.7 fb^{-1} at $\sqrt{s}$ = 7 TeV and 20.3 fb^{-1} at $\sqrt{s}$ = 8 TeV of pp data. The upper-bound is for the sum of Br($t \to Hc$) and Br($t \to Hu$). Search for $t\bar{t}$ events, where the other top quark decays hadronically or semi-leptonically. The upper bound constrains the H-t-c Yukawa couplings $\sqrt{|Y^H_{tc_L}|^2 + |Y^H_{tc_R}|^2} < 0.17$ (95% CL).

[5] Based on 19.5 fb^{-1} of pp data at $\sqrt{s}$ = 8 TeV. Search for final states with 3 or more isolated high E_T charged leptons ($\ell = e, \mu$) bounds the $t \to Hc$ decay in $t\bar{t}$ events when H decays contain a pair of leptons. The upper bound constrains the H-t-c Yukawa couplings $\sqrt{|Y^H_{tc_L}|^2 + |Y^H_{tc_R}|^2} < 0.21$ (95% CL).

[6] KHACHATRYAN 14Q based on 19.5 fb^{-1} at $\sqrt{s}$ = 8 TeV of pp data. Search for final states with $\geq$ 3 isolated charged leptons or with a photon pair accompanied by $\geq$ 1 lepton(s).

$\Gamma(\ell^+\overline{qq'}\ (q$=$d,s,b; q'$=$u,c))/\Gamma_{total}$ Γ_{11}/Γ

VALUE	CL%	DOCUMENT ID	TECN	COMMENT
<1.6 × 10^{-3}	95	[1] CHATRCHYAN 14O	CMS	μ + dijets
• • • We do not use the following data for averages, fits, limits, etc. • • •				
<1.7 × 10^{-3}	95	[1] CHATRCHYAN 14O	CMS	e + dijets

[1] Based on 19.5 fb^{-1} of pp data at $\sqrt{s}$ = 8 TeV. Baryon number violating decays of the top quark are searched for in $t\bar{t}$ production events where one of the pair decays into hadronic three jets.

t-quark EW Couplings

W helicity fractions in top decays. F_0 is the fraction of longitudinal and F_+ the fraction of right-handed W bosons. F_{V+A} is the fraction of V+A current in top decays. The effective Lagrangian (cited by ABAZOV 08AI) has terms f_1^L and f_1^R for $V-A$ and $V+A$ couplings, f_2^L and f_2^R for tensor couplings with b_R and b_L respectively.

F_0

VALUE	DOCUMENT ID		TECN	COMMENT
0.687±0.018 OUR AVERAGE				
0.70 ±0.05	[1] AABOUD	17BB	ATLS	$F_0 = 1 - f_1$
0.681±0.012±0.023	[2] KHACHATRY...16BU		CMS	$F_0 = B(t \to W_0 b)$
0.726±0.066±0.067	[3] AALTONEN	13D	CDF	$F_0 = B(t \to W_0 b)$
0.682±0.030±0.033	[4] CHATRCHYAN	13BH	CMS	$F_0 = B(t \to W_0 b)$
0.67 ±0.07	[5] AAD	12BG	ATLS	$F_0 = B(t \to W_0 b)$
0.722±0.062±0.052	[6] AALTONEN	12Z	TEVA	$F_0 = B(t \to W_0 b)$
0.669±0.078±0.065	[7] ABAZOV	11C	D0	$F_0 = B(t \to W_0 b)$
0.91 ±0.37 ±0.13	[8] AFFOLDER	00B	CDF	$F_0 = B(t \to W_0 b)$

• • • We do not use the following data for averages, fits, limits, etc. • • •

0.70 ±0.07 ±0.04	[9] AALTONEN	10Q	CDF	Repl. by AALTONEN 12Z	
0.62 ±0.10 ±0.05	[10] AALTONEN	09Q	CDF	Repl. by AALTONEN 10Q	
0.425±0.166±0.102	[11] ABAZOV	08B	D0	Repl. by ABAZOV 11C	
$0.85\ ^{+0.15}_{-0.22}\ \pm0.06$	[12] ABULENCIA	07I	CDF	$F_0 = B(t \to W_0 b)$	
$0.74\ ^{+0.22}_{-0.34}$	[13] ABULENCIA	06U	CDF	$F_0 = B(t \to W_0 b)$	
0.56 ±0.31	[14] ABAZOV	05G	D0	$F_0 = B(t \to W_0 b)$	

[1] AABOUD 17BB based on 20.2 fb^{-1} of pp data at $\sqrt{s}$ = 8 TeV. Triple-differential decay rate of top quark in the t-channel single-top production is used to simultaneously determine five generalized Wtb couplings as well as the top polarization. No assumption is made for the other couplings. See this paper for constraints on other couplings not included here. The paper reported f_1, and we converted it to F_0.

[2] KHACHATRYAN 16BU based on 19.8 fb^{-1} of pp data at $\sqrt{s}$ = 8 TeV using $t\bar{t}$ events with ℓ + $\not{E}_T$ + ≥ 4 jets(≥ 2 b). The errors of F_0 and F_- are correlated with a correlation coefficient $\rho(F_0, F_-) = -0.87$. The result is consistent with the NNLO SM prediction of 0.687 ± 0.005 for m_t = 172.8 ± 1.3 GeV.

[3] Based on 8.7 fb^{-1} of data in $p\bar{p}$ collisions at $\sqrt{s}$ = 1.96 TeV using $t\bar{t}$ events with ℓ + $\not{E}_T$ + ≥ 4 jets(≥ 1 b), and under the constraint $F_0 + F_+ + F_- = 1$. The statstical errors of F_0 and F_+ are correlated with correlation coefficient $\rho(F_0,F_+) = -0.69$.

[4] Based on 5.0 fb^{-1} of pp data at $\sqrt{s}$ = 7 TeV. CHATRCHYAN 13BH studied tt events with large $\not{E}_T$ and ℓ + ≥ 4 jets using a constrained kinematic fit.

[5] Based on 1.04 fb^{-1} of pp data at $\sqrt{s}$ = 7 TeV. AAD 12BG studied tt events with large $\not{E}_T$ and either ℓ + ≥ 4j or $\ell\ell$ + ≥ 2j. The uncertainties are not independent, $\rho(F_0,F_-) = -0.96$.

[6] Based on 2.7 and 5.1 fb^{-1} of CDF data in ℓ + jets and dilepton channels, and 5.4 fb^{-1} of D0 data in ℓ + jets and dilepton channels. F_0 = 0.682 ± 0.035 ± 0.046 if F_+ = 0.0017(1), while F_+ = −0.015 ± 0.018 ± 0.030 if F_0 = 0.688(4), where the assumed fixed values are the SM prediction for m_t = 173.3 ± 1.1 GeV and m_W = 80.399 ± 0.023 GeV.

[7] Results are based on 5.4 fb^{-1} of data in $p\bar{p}$ collisions at 1.96 TeV, including those of ABAZOV 08B. Under the SM constraint of f_0 = 0.698 (for m_t = 173.3 GeV, m_W = 80.399 GeV), f_+ = 0.010 ± 0.022 ± 0.030 is obtained.

[8] AFFOLDER 00B studied the angular distribution of leptonic decays of W bosons in $t \to Wb$ events. The ratio F_0 is the fraction of the helicity zero (longitudinal) W bosons in the decaying top quark rest frame. $B(t \to W_+ b)$ is the fraction of positive helicity (right-handed) positive charge W bosons in the top quark decays. It is obtained by assuming the Standard Model value of F_0.

[9] Results are based on 2.7 fb^{-1} of data in $p\bar{p}$ collisions at $\sqrt{s}$ = 1.96 TeV. F_0 result is obtained by assuming $F_+ = 0$, while F_+ result is obtained for F_0 = 0.70, the SM value. Model independent fits for the two fractions give F_0 = 0.88 ± 0.11 ± 0.06 and F_+ = −0.15 ± 0.07 ± 0.06 with correlation coefficient of −0.59. The results are for m_t = 175 GeV.

[10] Results are based on 1.9 fb^{-1} of data in $p\bar{p}$ collisions at $\sqrt{s}$ = 1.96 TeV. F_0 result is obtained assuming $F_+ = 0$, while F_+ result is obtained for F_0 = 0.70, the SM values. Model independent fits for the two fractions give F_0 = 0.66 ± 0.16 ± 0.05 and F_+ = −0.03 ± 0.06 ± 0.03.

[11] Based on 1 fb^{-1} at $\sqrt{s}$ = 1.96 TeV.

[12] Based on 318 pb^{-1} of data at $\sqrt{s}$ = 1.96 TeV.

[13] Based on 200 pb^{-1} of data at $\sqrt{s}$ = 1.96 TeV. $t \to Wb \to \ell\nu b$ (ℓ = e or μ). The errors are stat + syst.

[14] ABAZOV 05G studied the angular distribution of leptonic decays of W bosons in $t\bar{t}$ candidate events with lepton + jets final states, and obtained the fraction of longitudinally polarized W under the constraint of no right-handed current, $F_+ = 0$. Based on 125 pb^{-1} of data at $\sqrt{s}$ = 1.8 TeV.

F_-

VALUE	CL%	DOCUMENT ID		TECN	COMMENT
0.320±0.013 OUR AVERAGE					
> 0.264 ± 0.044	95	[1] AABOUD	17BB	ATLS	$F_- = f_1(1 - f_1^+)$
0.323±0.008±0.014		[2] KHACHATRY...	16BU	CMS	$F_- = B(t \to W_- b)$
0.310±0.022±0.022		[3] CHATRCHYAN	13BH	CMS	$F_- = B(t \to W_- b)$
0.32 ±0.04		[4] AAD	12BG	ATLS	$F_- = B(t \to W_- b)$

[1] AABOUD 17BB based on 20.2 fb^{-1} of pp data at $\sqrt{s}$ = 8 TeV. Triple-differential decay rate of top quark in the t-channel single-top production is used to simultaneously determine five generalized Wtb couplings as well as the top polarization. No assumption is made for the other couplings. The authors reported $f_1 = 0.30 \pm 0.05$ and $f_1^+ < 0.120$ which we converted to $F_- = f_1(1 - f_1^+)$. See this paper for constraints on other couplings not included here.

[2] KHACHATRYAN 16BU based on 19.8 fb^{-1} of pp data at $\sqrt{s}$ = 8 TeV using $t\bar{t}$ events with ℓ + $\not{E}_T$ + ≥ 4 jets(≥ 2 b). The errors of F_0 and F_- are correlated with a correlation coefficient $\rho(F_0, F_-) = -0.87$. The result is consistent with the NNLO SM prediction of 0.311 ± 0.005 for m_t = 172.8 ± 1.3 GeV.

[3] Based on 5.0 fb^{-1} of pp data at $\sqrt{s}$ = 7 TeV. CHATRCHYAN 13BH studied tt events with large $\not{E}_T$ and ℓ + ≥ 4 jets using a constrained kinematic fit.

[4] Based on 1.04 fb^{-1} of pp data at $\sqrt{s}$ = 7 TeV. AAD 12BG studied tt events with large $\not{E}_T$ and either ℓ + ≥ 4j or $\ell\ell$ + ≥ 2j. The uncertainties are not independent, $\rho(F_0,F_-) = -0.96$.

F_+

VALUE	CL%	DOCUMENT ID		TECN	COMMENT
0.002±0.011 OUR AVERAGE					
< 0.036 ± 0.006	95	[1] AABOUD	17BB	ATLS	$F_+ = f_1\ f_1^+$
−0.004±0.005±0.014		[2] KHACHATRY...	16BU	CMS	$F_+ = B(t \to W_+ b)$
−0.045±0.044±0.058		[3] AALTONEN	13D	CDF	$F_+ = B(t \to W_+ b)$
0.008±0.012±0.014		[4] CHATRCHYAN	13BH	CMS	$F_+ = B(t \to W_+ b)$
0.01 ±0.05		[5] AAD	12BG	ATLS	$F_+ = B(t \to W_+ b)$
0.023±0.041±0.034		[6] ABAZOV	11C	D0	$F_+ = B(t \to W_+ b)$
0.11 ±0.15		[7] AFFOLDER	00B	CDF	$F_+ = B(t \to W_+ b)$

• • • We do not use the following data for averages, fits, limits, etc. • • •

−0.033±0.034±0.031	[8] AALTONEN	12Z	TEVA	$F_+ = B(t \to W_+ b)$	
−0.01 ±0.02 ±0.05	[9] AALTONEN	10Q	CDF	Repl. by AALTONEN 13D	
−0.04 ±0.04 ±0.03	[10] AALTONEN	09Q	CDF	Repl. by AALTONEN 10Q	
0.119±0.090±0.053	[11] ABAZOV	08B	D0	Repl. by ABAZOV 11C	
0.056±0.080±0.057	[12] ABAZOV	07D	D0	$F_+ = B(t \to W_+ b)$	
$0.05\ ^{+0.11}_{-0.05}\ \pm0.03$	[13] ABULENCIA	07I	CDF	$F_+ = B(t \to W_+ b)$	
< 0.26	95 [13] ABULENCIA	07I	CDF	$F_+ = B(t \to W_+ b)$	
< 0.27	95 [14] ABULENCIA	06U	CDF	$F_+ = B(t \to W_+ b)$	
0.00 ±0.13 ±0.07	[15] ABAZOV	05L	D0	$F_+ = B(t \to W_+ b)$	
< 0.25	95 [15] ABAZOV	05L	D0	$F_+ = B(t \to W_+ b)$	
< 0.24	95 [16] ACOSTA	05D	CDF	$F_+ = B(t \to W_+ b)$	

[1] AABOUD 17BB based on 20.2 fb^{-1} of pp data at $\sqrt{s}$ = 8 TeV. Triple-differential decay rate of top quark in the t-channel single-top production is used to simultaneously determine five generalized Wtb couplings as well as the top polarization. No assumption is made for the other couplings. The authors reported $f_1 = 0.30 \pm 0.05$ and $f_1^+ < 0.120$ which we converted to $F_+ = f_1\ f_1^+$. See this paper for constraints on other couplings not included here.

[2] KHACHATRYAN 16BU based on 19.8 fb^{-1} of pp data at $\sqrt{s}$ = 8 TeV using $t\bar{t}$ events with ℓ + $\not{E}_T$ + ≥ 4 jets(≥ 2 b). The result is consistent with the NNLO SM prediction of 0.0017 ± 0.0001 for m_t = 172.8 ± 1.3 GeV.

[3] Based on 8.7 fb^{-1} of data in $p\bar{p}$ collisions at $\sqrt{s}$ = 1.96 TeV using $t\bar{t}$ events with ℓ + $\not{E}_T$ + ≥ 4 jets(≥ 1 b), and under the constraint $F_0 + F_+ + F_- = 1$. The statstical errors of F_0 and F_+ are correlated with correlation coefficient $\rho(F_0,F_+) = -0.69$.

[4] Based on 5.0 fb^{-1} of pp data at $\sqrt{s}$ = 7 TeV. CHATRCHYAN 13BH studied tt events with large $\not{E}_T$ and ℓ + ≥ 4 jets using a constrained kinematic fit.

[5] Based on 1.04 fb^{-1} of pp data at $\sqrt{s}$ = 7 TeV. AAD 12BG studied tt events with large $\not{E}_T$ and either ℓ + ≥ 4j or $\ell\ell$ + ≥ 2j.

[6] Results are based on 5.4 fb^{-1} of data in $p\bar{p}$ collisions at 1.96 TeV, including those of ABAZOV 08B. Under the SM constraint of f_0 = 0.698 (for m_t = 173.3 GeV, m_W = 80.399 GeV), f_+ = 0.010 ± 0.022 ± 0.030 is obtained.

[7] AFFOLDER 00B studied the angular distribution of leptonic decays of W bosons in $t \to Wb$ events. The ratio F_0 is the fraction of the helicity zero (longitudinal) W bosons in the decaying top quark rest frame. $B(t \to W_+ b)$ is the fraction of positive helicity (right-handed) positive charge W bosons in the top quark decays. It is obtained by assuming the Standard Model value of F_0.

[8] Based on 2.7 and 5.1 fb^{-1} of CDF data in ℓ + jets and dilepton channels, and 5.4 fb^{-1} of D0 data in ℓ + jets and dilepton channels. F_0 = 0.682 ± 0.035 ± 0.046 if F_+ = 0.0017(1), while F_+ = −0.015 ± 0.018 ± 0.030 if F_0 = 0.688(4), where the assumed fixed values are the SM prediction for m_t = 173.3 ± 1.1 GeV and m_W = 80.399 ± 0.023 GeV.

[9] Results are based on 2.7 fb^{-1} of data in $p\bar{p}$ collisions at $\sqrt{s}$ = 1.96 TeV. F_0 result is obtained by assuming $F_+ = 0$, while F_+ result is obtained for F_0 = 0.70, the SM value. Model independent fits for the two fractions give F_0 = 0.88 ± 0.11 ± 0.06 and F_+ = −0.15 ± 0.07 ± 0.06 with correlation coefficient of −0.59. The results are for m_t = 175 GeV.

[10] Results are based on 1.9 fb^{-1} of data in $p\bar{p}$ collisions at $\sqrt{s}$ = 1.96 TeV. F_0 result is obtained assuming $F_+ = 0$, while F_+ result is obtained for F_0 = 0.70, the SM values. Model independent fits for the two fractions give F_0 = 0.66 ± 0.16 ± 0.05 and F_+ = −0.03 ± 0.06 ± 0.03.

[11] Based on 1 fb^{-1} at $\sqrt{s}$ = 1.96 TeV.

[12] Based on 370 pb^{-1} of data at $\sqrt{s}$ = 1.96 TeV, using the ℓ + jets and dilepton decay channels. The result assumes F_0 = 0.70, and it gives $F_+ < 0.23$ at 95% CL.

[13] Based on 318 pb^{-1} of data at $\sqrt{s}$ = 1.96 TeV.

[14] Based on 200 pb^{-1} of data at $\sqrt{s}$ = 1.96 TeV. $t \to Wb \to \ell\nu b$ (ℓ = e or μ). The errors are stat + syst.

[15] ABAZOV 05L studied the angular distribution of leptonic decays of W bosons in $t\bar{t}$ events, where one of the W's from t or $\bar{t}$ decays into e or μ and the other decays hadronically. The fraction of the "+" helicity W boson is obtained by assuming F_0 = 0.7, which is the generic prediction for any linear combination of V and A currents. Based on 230 ± 15 pb^{-1} of data at $\sqrt{s}$ = 1.96 TeV.

[16] ACOSTA 05D measures the $m^2_{\ell+b}$ distribution in $t\bar{t}$ production events where one or both W's decay leptonically to ℓ = e or μ, and finds a bound on the V+A coupling of the tbW vertex. By assuming the SM value of the longitudinal W fraction $F_0 = B(t \to W_0 b) = 0.70$, the bound on F_+ is obtained. If the results are combined with those of AFFOLDER 00B, the bounds become $F_{V+A} < 0.61$ (95% CL) and $F_+ < 0.18$ (95 %CL), respectively. Based on 109 ± 7 pb^{-1} of data at $\sqrt{s}$ = 1.8 TeV (run I).

F_{V+A}

VALUE	CL%	DOCUMENT ID		TECN	COMMENT
< 0.29	95	[1] ABULENCIA	07G	CDF	$F_{V+A} = B(t \to W b_R)$
• • • We do not use the following data for averages, fits, limits, etc. • • •					
−0.06±0.22±0.12		[1] ABULENCIA	07G	CDF	$F_{V+A} = B(t \to W b_R)$
< 0.80	95	[2] ACOSTA	05D	CDF	$F_{V+A} = B(t \to W b_R)$

[1] Based on 700 pb^{-1} of data at $\sqrt{s}$ = 1.96 TeV.

[2] ACOSTA 05D measures the $m^2_{\ell+b}$ distribution in $t\bar{t}$ production events where one or both W's decay leptonically to ℓ = e or μ, and finds a bound on the V+A coupling of the tbW vertex. By assuming the SM value of the longitudinal W fraction $F_0 = B(t \to W_0 b) = 0.70$, the bound on F_+ is obtained. If the results are combined with those of AFFOLDER 00B, the bounds become $F_{V+A} < 0.61$ (95% CL) and $F_+ < 0.18$ (95 %CL), respectively. Based on 109 ± 7 pb^{-1} of data at $\sqrt{s}$ = 1.8 TeV (run I).

f_1^R

VALUE	CL%	DOCUMENT ID		TECN	COMMENT
• • • We do not use the following data for averages, fits, limits, etc. • • •					
$\lvert f_1^R/f_2^L\rvert < 0.37$	95	[1] AABOUD	17BB	ATLS	t-channel single top
$\lvert f_1^R\rvert < 0.16$	95	[2] KHACHATRY...	17G	CMS	t-channel single-t prod.
$-0.20 < \mathrm{Re}(V_{tb}\, f_1^R) < 0.23$	95	[3] AAD	12BG	ATLS	Constr. on Wtb vtx
$(V_{tb}\, f_1^R)^2 < 0.93$	95	[4] ABAZOV	12E	D0	Single-top
$\lvert f_1^R\rvert^2 < 0.30$	95	[5] ABAZOV	12I	D0	single-t + W helicity
$\lvert f_1^R\rvert^2 < 1.01$	95	[6] ABAZOV	09J	D0	$\lvert f_1^L\rvert = 1$, $\lvert f_2^L\rvert = \lvert f_2^R\rvert = 0$
$\lvert f_1^R\rvert^2 < 2.5$	95	[7] ABAZOV	08AI	D0	$\lvert f_1^L\rvert^2 = 1.8^{+1.0}_{-1.3}$

[1] AABOUD 17BB based on 20.2 fb^{-1} of pp data at $\sqrt{s} = 8$ TeV. Triple-differential decay rate of top quark is used to simultaneously determine five generalized Wtb couplings as well as the top polarization. No assumption is made for the other couplings. See this paper for constraints on other couplings not included here.

[2] KHACHATRYAN 17G based on 5.0 and 19.7 fb^{-1} of pp data at $\sqrt{s} = 7$ and 8 TeV, respectively. A Bayesian neural network technique is used to discriminate between signal and backgrounds. This is a 95% CL exclusion limit obtained by a three-dimensional fit with simultaneous variation of (f_1^L, f_1^R, f_2^R).

[3] Based on 1.04 fb^{-1} of pp data at $\sqrt{s} = 7$ TeV. AAD 12BG studied tt events with large $\not{E}_T$ and either $\ell + \geq 4$j or $\ell\ell + \geq 2$j.

[4] Based on 5.4 fb^{-1} of data. For each value of the form factor quoted the other two are assumed to have their SM value. Their Fig. 4 shows two-dimensional posterior probability density distributions for the anomalous couplings.

[5] Based on 5.4 fb^{-1} of data in $p\overline{p}$ collisions at 1.96 TeV. Results are obtained by combining the limits from the W helicity measurements and those from the single top quark production.

[6] Based on 1 fb^{-1} of data at $p\overline{p}$ collisions $\sqrt{s} = 1.96$ TeV. Combined result of the W helicity measurement in $t\overline{t}$ events (ABAZOV 08B) and the search for anomalous tbW couplings in the single top production (ABAZOV 08AI). Constraints when f_1^L and one of the anomalous couplings are simultaneously allowed to vary are given in their Fig. 1 and Table 1.

[7] Result is based on 0.9 fb^{-1} of data at $\sqrt{s} = 1.96$ TeV. Single top quark production events are used to measure the Lorentz structure of the tbW coupling. The upper bounds on the non-standard couplings are obtained when only one non-standard coupling is allowed to be present together with the SM one, $f_1^L = V_{tb}^*$.

f_2^L

VALUE	CL%	DOCUMENT ID		TECN	COMMENT
• • • We do not use the following data for averages, fits, limits, etc. • • •					
$\lvert f_2^L/f_1^L\rvert < 0.29$	95	[1] AABOUD	17BB	ATLS	t-channel single top
$\lvert f_2^L\rvert < 0.057$	95	[2] KHACHATRY...	17G	CMS	t-channel single-t prod.
$-0.14 < \mathrm{Re}(f_2^L) < 0.11$	95	[3] AAD	12BG	ATLS	Constr. on Wtb vtx
$(V_{tb}\, f_2^L)^2 < 0.13$	95	[4] ABAZOV	12E	D0	Single-top
$\lvert f_2^L\rvert^2 < 0.05$	95	[5] ABAZOV	12I	D0	single-t + W helicity
$\lvert f_2^L\rvert^2 < 0.28$	95	[6] ABAZOV	09J	D0	$\lvert f_1^L\rvert = 1$, $\lvert f_1^R\rvert = \lvert f_2^R\rvert = 0$
$\lvert f_2^L\rvert^2 < 0.5$	95	[7] ABAZOV	08AI	D0	$\lvert f_1^L\rvert^2 = 1.4^{+0.6}_{-0.5}$

[1] AABOUD 17BB based on 20.2 fb^{-1} of pp data at $\sqrt{s} = 8$ TeV. Triple-differential decay rate of top quark is used to simultaneously determine five generalized Wtb couplings as well as the top polarization. No assumption is made for the other couplings. See this paper for constraints on other couplings not included here.

[2] KHACHATRYAN 17G based on 5.0 and 19.7 fb^{-1} of pp data at $\sqrt{s} = 7$ and 8 TeV, respectively. A Bayesian neural network technique is used to discriminate between signal and backgrounds. This is a 95% CL exclusion limit obtained by a three-dimensional fit with simultaneous variation of (f_1^L, f_2^L, f_2^R).

[3] Based on 1.04 fb^{-1} of pp data at $\sqrt{s} = 7$ TeV. AAD 12BG studied tt events with large $\not{E}_T$ and either $\ell + \geq 4$j or $\ell\ell + \geq 2$j.

[4] Based on 5.4 fb^{-1} of data. For each value of the form factor quoted the other two are assumed to have their SM value. Their Fig. 4 shows two-dimensional posterior probability density distributions for the anomalous couplings.

[5] Based on 5.4 fb^{-1} of data in $p\overline{p}$ collisions at 1.96 TeV. Results are obtained by combining the limits from the W helicity measurements and those from the single top quark production.

[6] Based on 1 fb^{-1} of data at $p\overline{p}$ collisions $\sqrt{s} = 1.96$ TeV. Combined result of the W helicity measurement in $t\overline{t}$ events (ABAZOV 08B) and the search for anomalous tbW couplings in the single top production (ABAZOV 08AI). Constraints when f_1^L and one of the anomalous couplings are simultaneously allowed to vary are given in their Fig. 1 and Table 1.

[7] Result is based on 0.9 fb^{-1} of data at $\sqrt{s} = 1.96$ TeV. Single top quark production events are used to measure the Lorentz structure of the tbW coupling. The upper bounds on the non-standard couplings are obtained when only one non-standard coupling is allowed to be present together with the SM one, $f_1^L = V_{tb}^*$.

f_2^R

VALUE	CL%	DOCUMENT ID		TECN	COMMENT
• • • We do not use the following data for averages, fits, limits, etc. • • •					
$-0.12 < \mathrm{Re}(f_2^R/f_1^L) < 0.17$	95	[1] AABOUD	17BB	ATLS	t-channel single top
$-0.07 < \mathrm{Im}(f_2^R/f_1^L) < 0.06$	95	[1] AABOUD	17BB	ATLS	t-channel single top
$-0.18 < \mathrm{Im}(f_2^R) < 0.06$	95	[2] AABOUD	17I	ATLS	t-channel single top
$-0.049 < f_2^R < 0.048$	95	[3] KHACHATRY...	17G	CMS	t-channel single top
$-0.36 < \mathrm{Re}(f_2^R/f_1^L) < 0.10$	95	[4] AAD	16AK	ATLS	Single-top
$-0.17 < \mathrm{Im}(f_2^R/f_1^L) < 0.23$	95	[4] AAD	16AK	ATLS	Single-top
$-0.08 < \mathrm{Re}(f_2^R) < 0.04$	95	[5] AAD	12BG	ATLS	Constr. on Wtb vtx
$(V_{tb}\, f_2^R)^2 < 0.06$	95	[6] ABAZOV	12E	D0	Single-top
$\lvert f_2^R\rvert^2 < 0.12$	95	[7] ABAZOV	12I	D0	single-t + W helicity
$\lvert f_2^R\rvert^2 < 0.23$	95	[8] ABAZOV	09J	D0	$\lvert f_1^L\rvert = 1$, $\lvert f_1^R\rvert = \lvert f_2^L\rvert = 0$
$\lvert f_2^R\rvert^2 < 0.3$	95	[9] ABAZOV	08AI	D0	$\lvert f_1^L\rvert^2 = 1.4^{+0.9}_{-0.8}$

[1] AABOUD 17BB based on 20.2 fb^{-1} of pp data at $\sqrt{s} = 8$ TeV. Triple-differential decay rate of top quark is used to simultaneously determine five generalized Wtb couplings as well as the top polarization. No assumption is made for the other couplings. See this paper for constraints on other couplings not included here.

[2] AABOUD 17I based on 20.2 fb^{-1} of pp data at $\sqrt{s} = 8$ TeV. A cut-based analysis is used to discriminate between signal and backgrounds. All anomalous couplings other than $\mathrm{Im}(f_2^R)$ are assumed to be zero. See this paper for a number of other asymmetries and measurements that are not included here.

[3] KHACHATRYAN 17G based on 5.0 and 19.7 fb^{-1} of pp data at $\sqrt{s} = 7$ and 8 TeV, respectively. A Bayesian neural network technique is used to discriminate between signal and backgrounds. This is a 95% CL exclusion limit obtained by a three-dimensional fit with simultaneous variation of (f_1^L, f_2^L, f_2^R).

[4] AAD 16AK based on 4.6 fb^{-1} of pp data at $\sqrt{s} = 7$ TeV. The results are obtained from an analysis of angular distributions of the decay products of single top quarks, assuming $f_1^R = f_2^L = 0$. The fraction of decays containing transversely polarized W is measured to be $F_+ + F_- = 0.37 \pm 0.07$.

[5] Based on 1.04 fb^{-1} of pp data at $\sqrt{s} = 7$ TeV. AAD 12BG studied tt events with large $\not{E}_T$ and either $\ell + \geq 4$j or $\ell\ell + \geq 2$j.

[6] Based on 5.4 fb^{-1} of data. For each value of the form factor quoted the other two are assumed to have their SM value. Their Fig. 4 shows two-dimensional posterior probability density distributions for the anomalous couplings.

[7] Based on 5.4 fb^{-1} of data in $p\overline{p}$ collisions at 1.96 TeV. Results are obtained by combining the limits from the W helicity measurements and those from the single top quark production.

[8] Based on 1 fb^{-1} of data at $p\overline{p}$ collisions $\sqrt{s} = 1.96$ TeV. Combined result of the W helicity measurement in $t\overline{t}$ events (ABAZOV 08B) and the search for anomalous tbW couplings in the single top production (ABAZOV 08AI). Constraints when f_1^L and one of the anomalous couplings are simultaneously allowed to vary are given in their Fig. 1 and Table 1.

[9] Result is based on 0.9 fb^{-1} of data at $\sqrt{s} = 1.96$ TeV. Single top quark production events are used to measure the Lorentz structure of the tbW coupling. The upper bounds on the non-standard couplings are obtained when only one non-standard coupling is allowed to be present together with the SM one, $f_1^L = V_{tb}^*$.

Chromo-magnetic dipole moment $\mu_t = g_s\hat{\mu}_t/m_t$

VALUE	CL%	DOCUMENT ID		TECN	COMMENT
• • • We do not use the following data for averages, fits, limits, etc. • • •					
$-0.053 < \mathrm{Re}(\hat{\mu}_t) < 0.026$	95	[1] KHACHATRY...	16AI	CMS	$\ell\ell + \geq 2$j ($\geq 1b$)

[1] KHACHATRYAN 16AI based on 19.5 fb^{-1} of pp data at $\sqrt{s} = 8$ TeV, using lepton angular distributions as a function of the $t\overline{t}$-system kinematical variables.

Chromo-electric dipole moment $d_t = g_s\hat{d}_t/m_t$

VALUE	CL%	DOCUMENT ID		TECN	COMMENT
• • • We do not use the following data for averages, fits, limits, etc. • • •					
$-0.068 < \mathrm{Im}(\hat{d}_t) < 0.067$	95	[1] KHACHATRY...	16AI	CMS	$\ell\ell + \geq 2$j ($\geq 1b$)

[1] KHACHATRYAN 16AI based on 19.5 fb^{-1} of pp data at $\sqrt{s} = 8$ TeV, using lepton angular distributions as a function of the $t\overline{t}$-system kinematical variables.

Spin Correlation in $t\overline{t}$ Production in $p\overline{p}$ Collisions

C is the correlation strength parameter, f is the ratio of events with correlated t and $\overline{t}$ spins (SM prediction: f = 1), and κ is the spin correlation coefficient. See "The Top Quark" review for more information.

VALUE	DOCUMENT ID		TECN	COMMENT
• • • We do not use the following data for averages, fits, limits, etc. • • •				
0.89 ± 0.22	[1] ABAZOV	16A	D0	f ($\ell\ell + \geq 2$ jets, $\ell + \geq 4$ jets)
0.85 ± 0.29	[2] ABAZOV	12B	D0	f ($\ell\ell + \geq 2$ jets, $\ell + \geq 4$ jets)
$1.15^{+0.42}_{-0.43}$	[3] ABAZOV	12B	D0	f ($\ell + \not{E}_T + \geq 4$ jets)
$0.60^{+0.50}_{-0.16}$	[4] AALTONEN	11AR	CDF	κ ($\ell + \not{E}_T + \geq 4$ jets)
$0.74^{+0.40}_{-0.41}$	[5] ABAZOV	11AE	D0	f ($\ell\ell + \not{E}_T + \geq 2$ jets)
0.10 ± 0.45	[6] ABAZOV	11AF	D0	C ($\ell\ell + \not{E}_T + \geq 2$ jets)

[1] ABAZOV 16A based on 9.7 fb^{-1} of data. A matrix element method is used. It corresponds to evidence of spin correlation at 4.2σ and is in agreement with the NLO SM prediction $0.80^{+0.01}_{-0.02}$.

[2] This is a combination of the lepton + jets analysis presented in ABAZOV 12B and the dilepton measurement of ABAZOV 11AE. It provides a 3.1 σ evidence for the $t\overline{t}$ spin correlation.

[3] Based on 5.3 fb^{-1} of data. The error is statistical and systematic combined. A matrix element method is used.

[4] Based on 4.3 fb^{-1} of data. The measurement is based on the angular study of the top quark decay products in the helicity basis.The theory prediction is $\kappa \approx 0.40$.

[5] Based on 5.4 fb^{-1} of data using a matrix element method. The error is statistical and systematic combined. The no-correlation hypothesis is excluded at the 97.7% CL.

[6] Based on 5.4 fb^{-1} of data. The error is statistical and systematic combined. The NLO QCD prediction is C = 0.78 ± 0.03. The neutrino weighting method is used for reconstruction of kinematics.

Spin Correlation in $t\overline{t}$ Production in pp Collisions

Spin correlation, f_{SM}, measures the strength of the correlation between the spins of the pair produced $t\overline{t}$. f_{SM} =1 for the SM, while f_{SM} =0 for no spin correlation.

VALUE	DOCUMENT ID		TECN	COMMENT
• • • We do not use the following data for averages, fits, limits, etc. • • •				
$1.12^{+0.12}_{-0.15}$	[1] KHACHATRY...	16AI	CMS	$\ell\ell + \geq 2$j ($\geq 1b$)
$0.72 \pm 0.08^{+0.15}_{-0.13}$	[2] KHACHATRY...	16X	CMS	$\mu + 4,5$j
$1.20 \pm 0.05 \pm 0.13$	[3] AAD	15J	ATLS	$\Delta\phi(\ell\ell)$ in $\ell\ell + \geq 2$j($\geq 1b$)
$1.19 \pm 0.09 \pm 0.18$	[4] AAD	14BB	ATLS	$\Delta\phi(\ell\ell)$ in $\ell\ell + \geq 2$j events

1.12±0.11±0.22	[4] AAD	14BB	ATLS	$\Delta\phi(\ell j)$ in $\ell +\ \geq 4$j events
0.87±0.11±0.14	[4,5] AAD	14BB	ATLS	S-ratio in $\ell\ell +\ \geq 2$j events
0.75±0.19±0.23	[4,6] AAD	14BB	ATLS	$\cos\theta(\ell^+)\cos\theta(\ell^-)$ in $\ell\ell +\ \geq 2$j events
0.83±0.14±0.18	[4,7] AAD	14BB	ATLS	$\cos\theta(\ell^+)\cos\theta(\ell^-)$ in $\ell\ell +\ \geq 2$j events

[1] KHACHATRYAN 16AI based on 19.5 fb^{-1} of pp data at $\sqrt{s}$ = 8 TeV, using lepton angular distributions as a function of the $t\bar{t}$-system kinematical variables.

[2] KHACHATRYAN 16X based on 19.7 fb^{-1} of pp data at $\sqrt{s}$ = 8 TeV. Uses a template fit method. Spin correlation strength in the helicity basis is given by $A_{\rm hel}$ = 0.23 ± $0.03^{+0.05}_{-0.04}$.

[3] AAD 15J based on 20.3 fb^{-1} of pp data at $\sqrt{s}$ = 8 TeV. Uses a fit including a linear superposition of $\Delta\phi$ distribution from the SM NLO simulation with coefficient f_{SM} and from $t\bar{t}$ simulation without spin correlation with coefficient $(1 - f_{SM})$.

[4] Based on 4.6 fb^{-1} of pp data at $\sqrt{s}$ =7 TeV. The results are for m_t = 172.5 GeV.

[5] The S-ratio is defined as the SM spin correlation in the like-helicity gluon-gluon collisions normalized to the no spin correlation case; see eq.(6) for the LO expression.

[6] The polar angle correlation along the helicity axis.

[7] The polar angle correlation along the direction which maximizes the correlation.

t-quark FCNC Couplings κ^{utg}/Λ and κ^{ctg}/Λ

VALUE (TeV^{-1})	CL%	DOCUMENT ID		TECN	COMMENT
• • • We do not use the following data for averages, fits, limits, etc. • • •					
<0.0041	95	[1] KHACHATRY...17G		CMS	$\lvert\kappa^{tug}\rvert/\Lambda$
<0.018	95	[1] KHACHATRY...17G		CMS	$\lvert\kappa^{tcg}\rvert/\Lambda$
<0.0058	95	[2] AAD	16AS	ATLS	κ^{tug}/Λ
<0.013	95	[2] AAD	16AS	ATLS	κ^{tcg}/Λ
<0.0069	95	[3] AAD	12BP	ATLS	t^{tug}/Λ (t^{tcg} = 0)
<0.016	95	[3] AAD	12BP	ATLS	t^{tcg}/Λ (t^{tug} = 0)
<0.013	95	[4] ABAZOV	10K	D0	κ^{tug}/Λ
<0.057	95	[4] ABAZOV	10K	D0	κ^{tcg}/Λ
<0.018	95	[5] AALTONEN	09N	CDF	κ^{tug}/Λ (κ^{tcg} = 0)
<0.069	95	[5] AALTONEN	09N	CDF	κ^{tcg}/Λ (κ^{tug} = 0)
<0.037	95	[6] ABAZOV	07V	D0	κ^{utg}/Λ
<0.15	95	[6] ABAZOV	07V	D0	κ^{ctg}/Λ

[1] KHACHATRYAN 17G based on 5.0 and 19.7 fb^{-1} of pp data at $\sqrt{s}$ = 7 and 8 TeV, respectively. t-channel single top production is used. The result corresponds to $B(t \to ug) < 2.0\times10^{-5}$ or $B(t \to cg) < 4.1\times10^{-4}$.

[2] AAD 16AS based on 20.3 fb^{-1} of pp data at $\sqrt{s}$ = 8 TeV. The results are obtained from the 95% CL upper limit on the single top-quark production $\sigma(qg \to t)\cdot B(t \to bW) < 3.4$ pb, $B(t \to ug) < 4.0\times10^{-5}$ and $B(t \to cg) < 20\times10^{-5}$.

[3] Based on 2.05 fb^{-1} of pp data at $\sqrt{s}$ = 7 TeV. The results are obtained from the 95% CL upper limit on the single top-quark production $\sigma(qg \to t)\cdot B(t \to bW) < 3.9$ pb, for q=u or q=c, $B(t \to ug) < 5.7\times10^{-5}$ and $B(t \to ug) < 2.7\times10^{-4}$.

[4] Based on 2.3 fb^{-1} of data in $p\overline{p}$ collisions at $\sqrt{s}$ = 1.96 TeV. Upper limit of single top quark production cross section 0.20 pb and 0.27 pb via FCNC t-u-g and t-c-g couplings, respectively, lead to the bounds without assuming the absence of the other coupling. $B(t \to u + g) < 2.0\times10^{-4}$ and $B(t \to c + g) < 3.9\times10^{-3}$ follow.

[5] Based on 2.2 fb^{-1} of data in $p\overline{p}$ collisions at $\sqrt{s}$ = 1.96 TeV. Upper limit of single top quark production cross section $\sigma(u(c) + g \to t) < 1.8$ pb (95% CL) via FCNC t-u-g and t-c-g couplings lead to the bounds. $B(t \to u + g) < 3.9\times10^{-4}$ and $B(t \to c + g) < 5.7\times10^{-3}$ follow.

[6] Result is based on 230 pb^{-1} of data at $\sqrt{s}$ = 1.96 TeV. Absence of single top quark production events via FCNC t-u-g and t-c-g couplings lead to the upper bounds on the dimensioned couplings, κ^{utg}/Λ and κ^{ctg}/Λ, respectively.

$\sigma(Ht\overline{t})$ /$\sigma(Ht\overline{t})_{SM}$

VALUE	CL%	DOCUMENT ID		TECN	COMMENT
• • • We do not use the following data for averages, fits, limits, etc. • • •					
<6.7	95	[1] AAD	15	ATLS	$Ht\bar{t}$; $H \to \gamma\gamma$
2.8±1.0		[2] KHACHATRY...14H		CMS	$H \to b\overline{b}$, $\tau_h\tau_h$, $\gamma\gamma$, WW/ZZ(leptons)

[1] Based on 4.5 fb^{-1} of data at 7 TeV and 20.3 fb^{-1} at 8 TeV. The result is for m_H = 125.4 GeV. The measurement constrains the top quark Yukawa coupling strength parameter $\kappa_t = Y_t/Y_t^{SM}$ to be $-1.3 < \kappa_t < 8.0$ (95% CL).

[2] Based on 5.1 fb^{-1} of pp data at 7 TeV and 19.7 fb^{-1} at 8 TeV. The results are obtained by assuming the SM decay branching fractions for the Higgs boson of mass 125.6 GeV. The signal strength for individual Higgs decay channels are given in Fig. 13, and the preferred region in the (κ_V, κ_f) space is given in Fig. 14.

Single t-Quark Production Cross Section in $p\overline{p}$ Collisions at $\sqrt{s}$ = 1.8 TeV

Direct probe of the tbW coupling and possible new physics at $\sqrt{s}$ = 1.8 TeV.

VALUE (pb)	CL%	DOCUMENT ID		TECN	COMMENT
• • • We do not use the following data for averages, fits, limits, etc. • • •					
<24	95	[1] ACOSTA	04H	CDF	$p\overline{p} \to tb + X$, $tqb + X$
<18	95	[2] ACOSTA	02	CDF	$p\overline{p} \to tb + X$
<13	95	[3] ACOSTA	02	CDF	$p\overline{p} \to tqb + X$

[1] ACOSTA 04H bounds single top-quark production from the s-channel W-exchange process, $q'\overline{q} \to t\overline{b}$, and the t-channel W-exchange process, $q'g \to qt\overline{b}$. Based on ∼ 106 pb^{-1} of data.

[2] ACOSTA 02 bounds the cross section for single top-quark production via the s-channel W-exchange process, $q'\overline{q} \to t\overline{b}$. Based on ∼ 106 pb^{-1} of data.

[3] ACOSTA 02 bounds the cross section for single top-quark production via the t-channel W-exchange process, $q'g \to qt\overline{b}$. Based on ∼ 106 pb^{-1} of data.

Single t-Quark Production Cross Section in $p\overline{p}$ Collisions at $\sqrt{s}$ = 1.96 TeV

Direct probes of the tbW coupling and possible new physics at $\sqrt{s}$ = 1.96 TeV.
OUR AVERAGE assumes that the systematic uncertainties are uncorrelated.

VALUE (pb)	CL%	DOCUMENT ID		TECN	COMMENT
• • • We do not use the following data for averages, fits, limits, etc. • • •					
$3.53^{+1.25}_{-1.16}$		[1] AALTONEN	16	CDF	$s-+t$-channels (0ℓ+$\not\!\!E_T$ + 2,3j (≥ 1b-tag))
$2.25^{+0.29}_{-0.31}$		[2] AALTONEN	15H	TEVA	t-channel
$3.30^{+0.52}_{-0.40}$		[2,3] AALTONEN	15H	TEVA	$s-+$ t-channels
$1.12^{+0.61}_{-0.57}$		[4] AALTONEN	14K	CDF	s-channel (0ℓ+$\not\!\!E_T$+2,3j (≥ 1b-tag))
$1.41^{+0.44}_{-0.42}$		[5] AALTONEN	14L	CDF	s-channel (ℓ+$\not\!\!E_T$+2j (≥ 1b-tag))
$1.29^{+0.26}_{-0.24}$		[6] AALTONEN	14M	TEVA	s-channel (CDF + D0)
$3.04^{+0.57}_{-0.53}$		[7] AALTONEN	14O	CDF	$s + t + Wt$ ($\ell + \not\!\!E_T$ + 2 or 3 jets (≥ 1b-tag))
$1.10^{+0.33}_{-0.31}$		[8] ABAZOV	13O	D0	s-channel
$3.07^{+0.54}_{-0.49}$		[8] ABAZOV	13O	D0	t-channel
$4.11^{+0.60}_{-0.55}$		[8] ABAZOV	13O	D0	$s-+$ t-channels
0.98±0.63		[9] ABAZOV	11AA	D0	s-channel
2.90±0.59		[9] ABAZOV	11AA	D0	t-channel
$3.43^{+0.73}_{-0.74}$		[10] ABAZOV	11AD	D0	$s-+t$-channels
$1.8\ ^{+0.7}_{-0.5}$		[11] AALTONEN	10AB	CDF	s-channel
0.8 ±0.4		[11] AALTONEN	10AB	CDF	t-channel
$4.9\ ^{+2.5}_{-2.2}$		[12] AALTONEN	10U	CDF	$\not\!\!E_T$ + jets decay
$3.14^{+0.94}_{-0.80}$		[13] ABAZOV	10	D0	t-channel
1.05±0.81		[13] ABAZOV	10	D0	s-channel
< 7.3	95	[14] ABAZOV	10J	D0	τ + jets decay
$2.3\ ^{+0.6}_{-0.5}$		[15] AALTONEN	09AT	CDF	$s-+t$-channel
3.94±0.88		[16] ABAZOV	09Z	D0	$s-+t$-channel
$2.2\ ^{+0.7}_{-0.6}$		[17] AALTONEN	08AH	CDF	$s-+t$-channel
4.7 ±1.3		[18] ABAZOV	08I	D0	$s-+t$-channel
4.9 ±1.4		[19] ABAZOV	07H	D0	$s-+t$-channel
< 6.4	95	[20] ABAZOV	05P	D0	$p\overline{p} \to tb + X$
< 5.0	95	[20] ABAZOV	05P	D0	$p\overline{p} \to tqb + X$
<10.1	95	[21] ACOSTA	05N	CDF	$p\overline{p} \to tqb + X$
<13.6	95	[21] ACOSTA	05N	CDF	$p\overline{p} \to tb + X$
<17.8	95	[21] ACOSTA	05N	CDF	$p\overline{p} \to tb + X$, $tqb + X$

[1] AALTONEN 16 based on 9.5 fb^{-1} of data. This includes, as a part, the result of AALTONEN 14K. Combination of this result with that of AALTONEN 14O gives a $s + t$ cross section of $3.02^{+0.49}_{-0.48}$ pb and $|V_{tb}| > 0.84$ (95% CL).

[2] AALTONEN 15H based on 9.7 fb^{-1} of data per experiment. The result is for m_t = 172.5 GeV, and is a combination of the CDF measurements (AALTONEN 16) and the D0 measurements (ABAZOV 13O) on the t-channel single t-quark production cross section. The result is consistent with the NLO+NNLL SM prediction and gives $|V_{tb}| = 1.02^{+0.06}_{-0.05}$ and $|V_{tb}| > 0.92$ (95% CL).

[3] AALTONEN 15H is a combined measurement of s-channel single top cross section by CDF + D0. AALTONEN 14M is not included.

[4] Based on 9.45 fb^{-1} of data, using neural networks to separate signal from backgrounds. The result is for m_t = 172.5 GeV. Combination of this result with the CDF measurement in the 1 lepton channel AALTONEN 14L gives $1.36^{+0.37}_{-0.32}$ pb, consistent with the SM prediction, and is 4.2 sigma away from the background only hypothesis.

[5] Based on 9.4 fb^{-1} of data, using neural networks to separate signal from backgrounds. The result is for m_t = 172.5 GeV. The result is 3.8 sigma away from the background only hypothesis.

[6] Based on 9.7 fb^{-1} of data per experiment. The result is for m_t = 172.5 GeV, and is a combination of the CDF measurements AALTONEN 14L, AALTONEN 14K and the D0 measurement ABAZOV 13O on the s-channel single t-quark production cross section. The result is consistent with the SM prediction of 1.05 ± 0.06 pb and the significance of the observation is of 6.3 standard deviations.

[7] Based on 7.5 fb^{-1} of data. Neural network is used to discriminate signals (s-, t- and Wt-channel single top production) from backgrounds. The result is consistent with the SM prediction, and gives $|V_{tb}| = 0.95 \pm 0.09$(stat + syst)± 0.05(theory) and $|V_{tb}| > 0.78$ (95% CL). The result is for m_t = 172.5 GeV.

[8] Based on 9.7 fb^{-1} of data. Events with $\ell + \not\!\!E_T$ + 2 or 3 jets (1 or 2 b-tag) are analysed, assuming m_t = 172.5 GeV. The combined s- + t-channel cross section gives $|V_{tb}\ f_1^L| = 1.12^{+0.09}_{-0.08}$, or $|V_{tb}| > 0.92$ at 95% CL for $f_1^L = 1$ and a flat prior within $0 \leq |V_{tb}|^2 \leq 1$.

[9] Based on 5.4 fb^{-1} of data. The error is statistical + systematic combined. The results are for m_t = 172.5 GeV. Results for other m_t values are given in Table 2 of ABAZOV 11AA.

[10] Based on 5.4 fb^{-1} of data and for m_t = 172.5 GeV. The error is statistical + systematic combined. Results for other m_t values are given in Table III of ABAZOV 11AD. The result is obtained by assuming the SM ratio between tb (s-channel) and tqb (t-channel) productions, and gives $|V_{tb}\ f_1^L| = 1.02^{+0.10}_{-0.11}$, or $|V_{tb}| > 0.79$ at 95% CL for a flat prior within $0 < |V_{tb}|^2 < 1$.

[11] Based on 3.2 fb^{-1} of data. For combined $s-+t$-channel result see AALTONEN 09AT.

[12] Result is based on 2.1 fb^{-1} of data. Events with large missing E_T and jets with at least one b-jet without identified electron or muon are selected. Result is obtained when observed 2.1 σ excess over the background originates from the signal for $m_t = 175$ GeV, giving $|V_{tb}| = 1.24^{+0.34}_{-0.29} \pm 0.07$(theory).

[13] Result is based on 2.3 fb^{-1} of data. Events with isolated $\ell + \not{E}_T + 2$,3, 4 jets with one or two b-tags are selected. The analysis assumes $m_t = 170$ GeV.

[14] Result is based on 4.8 fb^{-1} of data. Events with an isolated reconstructed tau lepton, missing E_T + 2, 3 jets with one or two b-tags are selected. When combined with ABAZOV 09Z result for $e + \mu$ channels, the s- and t-channels combined cross section is $3.84^{+0.89}_{-0.83}$ pb.

[15] Based on 3.2 fb^{-1} of data. Events with isolated $\ell + \not{E}_T$ + jets with at least one b-tag are analyzed and s- and t-channel single top events are selected by using the likelihood function, matrix element, neural-network, boosted decision tree, likelihood function optimized for s-channel process, and neural-networked based analysis of events with $\not{E}_T$ that has sensitivity for $W \to \tau\nu$ decays. The result is for $m_t = 175$ GeV, and the mean value decreases by 0.02 pb/GeV for smaller m_t. The signal has 5.0 sigma significance. The result gives $|V_{tb}| = 0.91 \pm 0.11$ (stat+syst) ± 0.07 (theory), or $|V_{tb}| > 0.71$ at 95% CL.

[16] Based on 2.3 fb^{-1} of data. Events with isolated $\ell + \not{E}_T + \geq 2$ jets with 1 or 2 b-tags are analyzed and s- and t-channel single top events are selected by using boosted decision tree, Bayesian neural networks and the matrix element method. The signal has 5.0 sigma significance. The result gives $|V_{tb}| = 1.07 \pm 0.12$, or $|V_{tb}| > 0.78$ at 95% CL. The analysis assumes $m_t = 170$ GeV.

[17] Result is based on 2.2 fb^{-1} of data. Events with isolated $\ell + \not{E}_T + 2$, 3 jets with at least one b-tag are selected, and s- and t-channel single top events are selected by using likelihood, matrix element, and neural network discriminants. The result can be interpreted as $|V_{tb}| = 0.88^{+0.13}_{-0.12}$(stat + syst) ± 0.07(theory), and $|V_{tb}| > 0.66$ (95% CL) under the $|V_{tb}| < 1$ constraint.

[18] Result is based on 0.9 fb^{-1} of data. Events with isolated $\ell + \not{E}_T + 2$, 3, 4 jets with one or two b-vertex-tag are selected, and contributions from W + jets, $t\bar{t}$, s- and t-channel single top events are identified by using boosted decision trees, Bayesian neural networks, and matrix element analysis. The result can be interpreted as the measurement of the CKM matrix element $|V_{tb}| = 1.31^{+0.25}_{-0.21}$, or $|V_{tb}| > 0.68$ (95% CL) under the $|V_{tb}| < 1$ constraint.

[19] Result is based on 0.9 fb^{-1} of data. This result constrains V_{tb} to $0.68 < |V_{tb}| \leq 1$ at 95% CL.

[20] ABAZOV 05P bounds single top-quark production from either the s-channel W-exchange process, $q'\overline{q} \to t\overline{b}$, or the t-channel W-exchange process, $q'g \to q\,t\overline{b}$, based on ~ 230 pb^{-1} of data.

[21] ACOSTA 05N bounds single top-quark production from the t-channel W-exchange process ($q'g \to q\,t\overline{b}$), the s-channel W-exchange process ($q'\overline{q} \to t\overline{b}$), and from the combined cross section of t- and s-channel. Based on $\sim$ 162 pb^{-1} of data.

t-channel Single t Production Cross Section in pp Collisions at $\sqrt{s} = 7$ TeV

Direct probe of the tbW coupling and possible new physics at $\sqrt{s} = 7$ TeV.

VALUE (pb)	DOCUMENT ID		TECN	COMMENT
• • • We do not use the following data for averages, fits, limits, etc. • • •				
68 ± 2 ± 8	[1] AAD	14BI	ATLS	$\ell + \not{E}_T$ + 2j or 3j
83 ± 4 $^{+20}_{-19}$	[2] AAD	12CH	ATLS	t-channel $\ell + \not{E}_T$+ (2,3)j (1b)
67.2 ± 6.1	[3] CHATRCHYAN	12BQ	CMS	t-channel $\ell + \not{E}_T$+ $\geq$ 2j (1b)
83.6 ± 29.8 ± 3.3	[4] CHATRCHYAN	11R	CMS	t-channel

[1] Based on 4.59 fb^{-1} of data, using neural networks for signal and background separation. $\sigma(tq) = 46 \pm 1 \pm 6$ pb and $\sigma(\bar{t}q) = 23 \pm 1 \pm 3$ pb are separately measured, as well as their ratio $R = \sigma(tq)/\sigma(\bar{t}q) = 2.04 \pm 0.13 \pm 0.12$. The results are for $m_t = 172.5$ GeV, and those for other m_t values are given by eq.(4) and Table IV. The measurements give $|V_{tb}| = 1.02 \pm 0.07$ or $|V_{tb}| > 0.88$ (95% CL).

[2] Based on 1.04 fb^{-1} of data. The result gives $|V_{tb}| = 1.13^{+0.14}_{-0.13}$ from the ratio σ(exp)/σ(th), where σ(th) is the SM prediction for $|V_{tb}| = 1$. The 95% CL lower bound of $|V_{tb}| > 0.75$ is found if $|V_{tb}| < 1$ is assumed. $\sigma(t) = 59^{+18}_{-16}$ pb and $\sigma(\bar{t}) = 33^{+13}_{-12}$ pb are found for the separate single t and $\bar{t}$ production cross sections, respectively. The results assume $m_t = 172.5$ GeV for the acceptance.

[3] Based on 1.17 fb^{-1} of data for $\ell = \mu$, 1.56 fb^{-1} of data for $\ell = e$ at 7 TeV collected during 2011. The result gives $|V_{tb}| = 1.020 \pm 0.046$(meas) ± 0.017(th). The 95% CL lower bound of $|V_{tb}| > 0.92$ is found if $|V_{tb}| < 1$ is assumed. The results assume m_t = 172.5 GeV for the acceptance.

[4] Based on 36 pb^{-1} of data. The first error is statistical + systematic combined, the second is luminosity. The result gives $|V_{tb}| = 1.114 \pm 0.22$(exp) ± 0.02(th) from the ratio σ(exp)/σ(th), where σ(th) is the SM prediction for $|V_{tb}| = 1$. The 95% CL lower bound of $|V_{tb}| > 0.62$ (0.68) is found from the 2D (BDT) analysis under the constraint $0 < |V_{tb}|^2 < 1$.

t-channel Single t Production Cross Section in pp Collisions at $\sqrt{s} = 8$ TeV

VALUE (pb)	DOCUMENT ID		TECN	COMMENT
• • • We do not use the following data for averages, fits, limits, etc. • • •				
89.6 $^{+7.1}_{-6.3}$	[1] AABOUD	17T	ATLS	ℓ+$\not{E}_T$+2 j (1b j)
83.6 ± 2.3 ± 7.4	[2] KHACHATRY...14F		CMS	ℓ+$\not{E}_T$+ $\geq$ 2 j (1,2 b, 1 forward j)

[1] AABOUD 17T based on 20.2 fb^{-1} of data. A maximum-likelihood fit to neural-network discriminant distributions is used to separate signal and background events. Individual cross sections are measured as $\sigma(tq) = 56.7^{+4.3}_{-3.8}$ pb and $\sigma(\bar{t}q) = 32.9^{+3.0}_{-2.7}$ pb, while their ratio is given by $\sigma(tq)/\sigma(\bar{t}q) = 1.72 \pm 0.09$. A lower limit $|V_{tb}| > 0.92$ (95% CL) is obtained. Measured total and differential cross sections are described well by the SM.

[2] Based on 19.7 fb^{-1} of data. The t and $\bar{t}$ production cross sections are measured separately as $\sigma_{t-ch.}(t) = 53.8 \pm 1.5 \pm 4.4$ pb and $\sigma_{t-ch.}(\bar{t}) = 27.6 \pm 1.3 \pm 3.7$ pb, respectively, as well as their ratio $R_{t-ch} = \sigma_{t-ch.}(t)/\sigma_{t-ch.}(\bar{t}) = 1.95 \pm 0.10 \pm 0.19$, in agreement with the SM predictions. Combination with a previous CMS result at $\sqrt{s}$ = 7 TeV [CHATRCHYAN 12BQ] gives $|V_{tb}| = 0.998 \pm 0.038 \pm 0.016$. Also obtained is the ratio $R_{8/7} = \sigma_{t-ch.}(8\text{TeV})/\sigma_{t-ch.}(7\text{TeV}) = 1.24 \pm 0.08 \pm 0.12$.

s-channel Single t Production Cross Section in pp Collisions at $\sqrt{s} = 8$ TeV

VALUE (pb)	DOCUMENT ID		TECN	COMMENT
• • • We do not use the following data for averages, fits, limits, etc. • • •				
4.8 ± 0.8 $^{+1.6}_{-1.3}$	[1] AAD	16U	ATLS	$\ell + \not{E}_T + 2b$
13.4 ± 7.3	[2] KHACHATRY...16AZ		CMS	$\ell + \not{E}_T + 2b$
5.0 ± 4.3	[3] AAD	15A	ATLS	$\ell + \not{E}_T + 2b$

[1] AAD 16U based on 20.3 fb^{-1} of data, using a maximum-likelihood fit of a matrix element method discriminant. The same data set as in AAD 15A is used. The result corresponds to an observed significance of 3.2σ.

[2] KHACHATRYAN 16AZ based on 19.7 fb^{-1} of data, using a multivariate analysis to separate signal and backgrounds. The same method is applied to 5.1 fb^{-1} of data at $\sqrt{s} = 7$ TeV, giving 7.1 ± 8.1 pb. Combining both measurements, the observed significance is 2.5σ. A best fit value of 2.0 ± 0.9 is obtained for the combined ratio of the measured values and SM expectations.

[3] AAD 15A based on 20.3 fb^{-1} of data, using a multivariate analysis to separate signal and backgrounds. The 95% CL upper bound of the cross section is 14.6 pb. The results are consistent with the SM prediction of 5.61 ± 0.22 pb at approximate NNLO.

t-channel Single t Production Cross Section in pp Collisions at $\sqrt{s} = 13$ TeV

VALUE (pb)	DOCUMENT ID		TECN	COMMENT
• • • We do not use the following data for averages, fits, limits, etc. • • •				
156 ± 5 ± 27 ± 3	[1] AABOUD	17H	ATLS	$\sigma(tq)$, ℓ+$\not{E}_T$+2 j (1b, 1 forward j)
91 ± 4 ± 18 ± 2	[1] AABOUD	17H	ATLS	$\sigma(\bar{t}q)$, ℓ+$\not{E}_T$+2 j (1b, 1 forward j)
154 ± 8 ± 9 ± 19 ± 4	[2] SIRUNYAN	17AA	CMS	$\sigma(tq)$, μ+ $\geq$ 2 j (1b)
85 ± 10 ± 4 ± 11 ± 2	[2] SIRUNYAN	17AA	CMS	$\sigma(\bar{t}q)$, μ+ $\geq$ 2 j (1b)

[1] AABOUD 17H based on 3.2 fb^{-1} of data. A maximum-likelihood fit to neural-network discriminant distributions is used to separate signal and background events. The third error is for luminosity. The cross section ratio is measured to be $\sigma(tq)/\sigma(\bar{t}q) = 1.72 \pm 0.09 \pm 0.18$. A lower limit $|V_{tb}| > 0.84$ (95% CL) is obtained. All results are in agreement with the SM.

[2] SIRUNYAN 17AA based on 2.2 fb^{-1} of data. A multivariate discriminator is used to separate signal and background events. The four errors are from statitics, experimental systematics, theory, and luminosity. The cross section ratio is measured to be $\sigma(tq)/\sigma(\bar{t}q) = 1.81 \pm 0.18 \pm 0.15$. CKM matrix element is obtained as $|V_{tb}| = 1.05 \pm 0.07$(exp) ± 0.02(theo). All results are in agreement with the SM.

Wt Production Cross Section in pp Collisions at $\sqrt{s} = 7$ TeV

VALUE (pb)	DOCUMENT ID		TECN	COMMENT
• • • We do not use the following data for averages, fits, limits, etc. • • •				
16 $^{+5}_{-4}$	[1] CHATRCHYAN	13C	CMS	$t+W$ channel, 2ℓ+$\not{E}_T$+1b

[1] Based on 4.9 fb^{-1} of data. The result gives $V_{tb} = 1.01^{+0.16}_{-0.13}$(exp) $^{+0.03}_{-0.04}$(th). $V_{tb} > 0.79$ (95% CL) if $V_{tb} < 1$ is assumed. The results assume $m_t = 172.5$ GeV for the acceptance.

Wt Production Cross Section in pp Collisions at $\sqrt{s} = 8$ TeV

VALUE (pb)	DOCUMENT ID		TECN	COMMENT
• • • We do not use the following data for averages, fits, limits, etc. • • •				
23.0 ± 1.3 $^{+3.2}_{-3.5}$ ± 1.1	[1] AAD	16B	ATLS	2ℓ+$\not{E}_T$+1b
23.4 ± 5.4	[2] CHATRCHYAN	14AC	CMS	$t+W$ channel, 2ℓ+$\not{E}_T$+1b

[1] AAD 16B based on 20.3 fb^{-1} of data. The result gives $|V_{tb}| = 1.01 \pm 0.10$ and $|V_{tb}| > 0.80$ (95% CL) without assuming unitarity of the CKM matrix. The results assume m_t = 172.5 GeV for the acceptance.

[2] Based on 12.2 fb^{-1} of data. Events with two oppositely charged leptons, large $\not{E}_T$ and a b-tagged jet are selected, and a multivariate analysis is used to separate the signal from the backgrounds. The result is consistent with the SM prediction of 22.2 ± 0.6(scale) ± 1.4(PDF) pb at approximate NNLO.

Wt Production Cross Section in pp Collisions at $\sqrt{s} = 13$ TeV

VALUE (pb)	DOCUMENT ID		TECN	COMMENT
• • • We do not use the following data for averages, fits, limits, etc. • • •				
94 ± 10 $^{+28}_{-22}$ ± 2	[1] AABOUD	18H	ATLS	$\ell^+\ell^-$ + $\geq$ 1j

[1] AABOUD 18H based on 3.2 fb^{-1} of data. The last error is from luminosity. A multivariate analysis is used to separate the signal from the backgrounds. The result is consistent with the NLO+NNLL SM prediction of 71.7 ± 1.8(scale) ± 3.4(PDF) pb.

Single t-Quark Production Cross Section in ep Collisions

VALUE (pb)	CL%	DOCUMENT ID		TECN	COMMENT
• • • We do not use the following data for averages, fits, limits, etc. • • •					
<0.25	95	[1] AARON	09A	H1	$e^\pm p \to e^\pm tX$
<0.55	95	[2] AKTAS	04	H1	$e^\pm p \to e^\pm tX$
<0.225	95	[3] CHEKANOV	03	ZEUS	$e^\pm p \to e^\pm tX$

[1] AARON 09A looked for single top production via FCNC in $e^\pm p$ collisions at HERA with 474 pb^{-1} of data at $\sqrt{s}$ = 301–319 GeV. The result supersedes that of AKTAS 04.

[2] AKTAS 04 looked for single top production via FCNC in $e^\pm$ collisions at HERA with 118.3 pb^{-1}, and found 5 events in the e or μ channels while 1.31 ± 0.22 events are expected from the Standard Model background. No excess was found for the hadronic channel. The observed cross section of $\sigma(ep \to etX) = 0.29^{+0.15}_{-0.14}$ pb at $\sqrt{s}$ = 319 GeV gives the quoted upper bound if the observed events are due to statistical fluctuation.

[3] CHEKANOV 03 looked in 130.1 pb^{-1} of data at $\sqrt{s} = 301$ and 318 GeV. The limit is for $\sqrt{s} = 318$ GeV and assumes $m_t = 175$ GeV.

$t\bar{t}$ Production Cross Section in $p\bar{p}$ Collisions at $\sqrt{s} = 1.8$ TeV

Only the final combined $t\bar{t}$ production cross sections obtained from Tevatron Run I by the CDF and D0 experiments are quoted below.

VALUE (pb)	DOCUMENT ID		TECN	COMMENT
• • • We do not use the following data for averages, fits, limits, etc. • • •				
$5.69 \pm 1.21 \pm 1.04$	[1] ABAZOV	03A	D0	Combined Run I data
$6.5\ ^{+1.7}_{-1.4}$	[2] AFFOLDER	01A	CDF	Combined Run I data

[1] Combined result from 110 pb^{-1} of Tevatron Run I data. Assume $m_t = 172.1$ GeV.

[2] Combined result from 105 pb^{-1} of Tevatron Run I data. Assume $m_t = 175$ GeV.

$t\bar{t}$ Production Cross Section in $p\bar{p}$ Collisions at $\sqrt{s} = 1.96$ TeV

Unless otherwise noted the first quoted error is from statistics, the second from systematic uncertainties, and the third from luminosity. If only two errors are quoted the luminosity is included in the systematic uncertainties.

VALUE (pb)	DOCUMENT ID		TECN	COMMENT
• • • We do not use the following data for averages, fits, limits, etc. • • •				
$7.26 \pm 0.13\ ^{+0.57}_{-0.50}$	[1] ABAZOV	16F	D0	$\ell\ell$, ℓ+jets channels
8.1 ± 2.1	[2] AALTONEN	14A	CDF	$\ell + \tau_h + \geq$ 2jets ($\geq 1b$-tag)
$7.60 \pm 0.20 \pm 0.29 \pm 0.21$	[3] AALTONEN	14H	TEVA	$\ell\ell$, ℓ+jets, all-jets channels
$8.0 \pm 0.7 \pm 0.6 \pm 0.5$	[4] ABAZOV	14K	D0	$\ell + \not\!\!E_T + \geq 4$ jets ($\geq 1b$-tag)
7.09 ± 0.84	[5] AALTONEN	13AB	CDF	$\ell\ell + \not\!\!E_T + \geq 2$ jets
7.5 ± 1.0	[6] AALTONEN	13G	CDF	$\ell + \not\!\!E_T + \geq$ 3jets ($\geq 1b$-tag)
$8.8 \pm 3.3 \pm 2.2$	[7] AALTONEN	12AL	CDF	$\tau_h + \not\!\!E_T$ +4j ($\geq 1b$)
$8.5 \pm 0.6 \pm 0.7$	[8] AALTONEN	11D	CDF	$\ell + \not\!\!E_T$ + jets ($\geq 1b$-tag)
$7.64 \pm 0.57 \pm 0.45$	[9] AALTONEN	11W	CDF	$\ell + \not\!\!E_T$ + jets ($\geq 1b$-tag)
$7.99 \pm 0.55 \pm 0.76 \pm 0.46$	[10] AALTONEN	11Y	CDF	$\not\!\!E_T + \geq$ 4jets (0,1,2 b-tag)
$7.78\ ^{+0.77}_{-0.64}$	[11] ABAZOV	11E	D0	$\ell + \not\!\!E_T + \geq 2$ jets
$7.56\ ^{+0.63}_{-0.56}$	[12] ABAZOV	11Z	D0	Combination
$6.27 \pm 0.73 \pm 0.63 \pm 0.39$	[13] AALTONEN	10AA	CDF	Repl. by AALTONEN 13AB
$7.2 \pm 0.5 \pm 1.0 \pm 0.4$	[14] AALTONEN	10E	CDF	≥ 6 jets, vtx b-tag
$7.8 \pm 2.4 \pm 1.6 \pm 0.5$	[15] AALTONEN	10V	CDF	$\ell + \geq 3$ jets, soft-e b-tag
7.70 ± 0.52	[16] AALTONEN	10W	CDF	$\ell + \not\!\!E_T + \geq 3$ jets + b-tag, norm. to $\sigma(Z \to \ell\ell)_{TH}$
6.9 ± 2.0	[17] ABAZOV	10I	D0	≥ 6 jets with 2 b-tags
$6.9 \pm 1.2\ ^{+0.8}_{-0.7} \pm 0.4$	[18] ABAZOV	10Q	D0	τ_h + jets
$9.6 \pm 1.2\ ^{+0.6}_{-0.5} \pm 0.6$	[19] AALTONEN	09AD	CDF	$\ell\ell + \not\!\!E_T$ / vtx b-tag
$9.1 \pm 1.1\ ^{+1.0}_{-0.9} \pm 0.6$	[20] AALTONEN	09H	CDF	$\ell + \geq 3$ jets+$\not\!\!E_T$/soft μ b-tag
$8.18\ ^{+0.98}_{-0.87}$	[21] ABAZOV	09AG	D0	ℓ + jets, $\ell\ell$ and $\ell\tau$ + jets
$7.5 \pm 1.0\ ^{+0.7}_{-0.6}\ ^{+0.6}_{-0.5}$	[22] ABAZOV	09R	D0	$\ell\ell$ and $\ell\tau$ + jets
$8.18\ ^{+0.90}_{-0.84} \pm 0.50$	[23] ABAZOV	08M	D0	ℓ + n jets with 0,1,2 b-tag
7.62 ± 0.85	[24] ABAZOV	08N	D0	ℓ + n jets + b-tag or kinematics
$8.5\ ^{+2.7}_{-2.2}$	[25] ABULENCIA	08	CDF	$\ell^+\ell^-$ ($\ell = e, \mu$)
$8.3 \pm 1.0\ ^{+2.0}_{-1.5} \pm 0.5$	[26] AALTONEN	07D	CDF	≥ 6 jets, vtx b-tag
$7.4 \pm 1.4 \pm 1.0$	[27] ABAZOV	07O	D0	$\ell\ell$ + jets, vtx b-tag
$4.5\ ^{+2.0}_{-1.9}\ ^{+1.4}_{-1.1} \pm 0.3$	[28] ABAZOV	07P	D0	≥ 6 jets, vtx b-tag
$6.4\ ^{+1.3}_{-1.2} \pm 0.7 \pm 0.4$	[29] ABAZOV	07R	D0	$\ell + \geq 4$ jets
$6.6 \pm 0.9 \pm 0.4$	[30] ABAZOV	06X	D0	ℓ + jets, vtx b-tag
$8.7 \pm 0.9\ ^{+1.1}_{-0.9}$	[31] ABULENCIA	06Z	CDF	ℓ + jets, vtx b-tag
$5.8 \pm 1.2\ ^{+0.9}_{-0.7}$	[32] ABULENCIA,A	06C	CDF	missing E_T + jets, vtx b-tag
$7.5 \pm 2.1\ ^{+3.3}_{-2.2}\ ^{+0.5}_{-0.4}$	[33] ABULENCIA,A	06E	CDF	6–8 jets, b-tag
$8.9 \pm 1.0\ ^{+1.1}_{-1.0}$	[34] ABULENCIA,A	06F	CDF	$\ell \geq 3$ jets, b-tag
$8.6\ ^{+1.6}_{-1.5} \pm 0.6$	[35] ABAZOV	05Q	D0	ℓ + n jets
$8.6^{+3.2}_{-2.7} \pm 1.1 \pm 0.6$	[36] ABAZOV	05R	D0	di-lepton + n jets
$6.7\ ^{+1.4}_{-1.3}\ ^{+1.6}_{-1.1} \pm 0.4$	[37] ABAZOV	05X	D0	ℓ + jets / kinematics
$5.3 \pm 3.3\ ^{+1.3}_{-1.0}$	[38] ACOSTA	05S	CDF	ℓ + jets / soft μ b-tag
$6.6 \pm 1.1 \pm 1.5$	[39] ACOSTA	05T	CDF	ℓ + jets / kinematics
$6.0\ ^{+1.5}_{-1.6}\ ^{+1.2}_{-1.3}$	[40] ACOSTA	05U	CDF	ℓ + jets/kinematics + vtx b-tag
$5.6\ ^{+1.2}_{-1.1}\ ^{+0.9}_{-0.6}$	[41] ACOSTA	05V	CDF	ℓ + n jets
$7.0\ ^{+2.4}_{-2.1}\ ^{+1.6}_{-1.1} \pm 0.4$	[42] ACOSTA	04I	CDF	di-lepton + jets + missing ET

[1] ABAZOV 16F based on 9.7 fb^{-1} of data. The result is for $m_t = 172.5$ GeV, and the m_t dependence is shown in Table V and Fig. 9. The result agrees with the NNLO+NNLL SM prediction of $7.35\ ^{+0.23}_{-0.27}$ pb.

[2] Based on 9 fb^{-1} of data. The measurement is in the channel $t\bar{t} \to (b\ell\nu)(b\tau\nu)$, where τ decays into hadrons (τ_h), and ℓ (e or μ) include ℓ from τ decays (τ_ℓ). The result is for $m_t = 173$ GeV.

[3] Based on 8.8 fb^{-1} of data. Combination of CDF and D0 measurements given, respectively, by $\sigma(t\bar{t}$; CDF) $= 7.63 \pm 0.31 \pm 0.36 \pm 0.16$ pb, $\sigma(t\bar{t}$; D0) $= 7.56 \pm 0.20 \pm 0.32 \pm 0.46$ pb. All the results are for $m_t = 172.5$ GeV. The m_t dependence of the mean value is parametrized in eq. (1) and shown in Fig. 2.

[4] Based on 9.7 fb^{-1} of data. Differential cross sections with respect to m_{tt}, $|y(\text{top})|$, $E_T(\text{top})$ are shown in Figs. 9, 10, 11, respectively, and are compared to the predictions of MC models.

[5] Based on 8.8 fb^{-1} of $p\bar{p}$ collisions at $\sqrt{s} = 1.96$ TeV.

[6] Based on 8.7 fb^{-1} of $p\bar{p}$ collisions at $\sqrt{s} = 1.96$ TeV. Measure the $t\bar{t}$ cross section simultaneously with the fraction of $t \to Wb$ decays. The correlation coefficient between those two measurements is -0.434. Assume unitarity of the 3×3 CKM matrix and set $|V_{tb}| > 0.89$ at 95% CL.

[7] Based on 2.2 fb^{-1} of data in $p\bar{p}$ collisions at 1.96 TeV. The result assumes the acceptance for $m_t = 172.5$ GeV.

[8] Based on 1.12 fb^{-1} and assumes $m_t = 175$ GeV, where the cross section changes by ± 0.1 pb for every ∓ 1 GeV shift in m_t. AALTONEN 11D fits simultaneously the $t\bar{t}$ production cross section and the b-tagging efficiency and find improvements in both measurements.

[9] Based on 2.7 fb^{-1}. The first error is from statistics and systematics, the second is from luminosity. The result is for $m_t = 175$ GeV. AALTONEN 11W fits simultaneously a jet flavor discriminator between b-, c-, and light-quarks, and find significant reduction in the systematic error.

[10] Based on 2.2 fb^{-1}. The result is for $m_t = 172.5$ GeV. AALTONEN 11Y selects multi-jet events with large $\not\!\!E_T$, and vetoes identified electrons and muons.

[11] Based on 5.3 fb^{-1}. The error is statistical + systematic + luminosity combined. The result is for $m_t = 172.5$ GeV. The results for other m_t values are given in Table XII and eq.(10) of ABAZOV 11E.

[12] Combination of a dilepton measurement presented in ABAZOV 11Z (based on 5.4 fb^{-1}), which yields $7.36\ ^{+0.90}_{-0.79}$ (stat+syst) pb, and the lepton + jets measurement of ABAZOV 11E. The result is for $m_t = 172.5$ GeV. The results for other m_t values is given by eq.(5) of ABAZOV 11A.

[13] Based on 2.8 fb^{-1}. The result is for $m_t = 175$ GeV.

[14] Based on 2.9 fb^{-1}. Result is obtained from the fraction of signal events in the top quark mass measurement in the all hadronic decay channel.

[15] Based on 1.7 fb^{-1}. The result is for $m_t = 175$ GeV. AALTONEN 10V uses soft electrons from b-hadron decays to suppress W+jets background events.

[16] Based on 4.6 fb^{-1}. The result is for $m_t = 172.5$ GeV. The ratio $\sigma(t\bar{t} \to \ell$+jets) / $\sigma(Z/\gamma^* \to \ell\ell)$ is measured and then multiplied by the theoretical $Z/\gamma^* \to \ell\ell$ cross section of $\sigma(Z/\gamma^* \to \ell\ell) = 251.3 \pm 5.0$ pb, which is free from the luminosity error.

[17] Based on 1 fb^{-1}. The result is for $m_t = 175$ GeV. 7.9 ± 2.3 pb is found for $m_t = 170$ GeV. ABAZOV 10I uses a likelihood discriminant to separate signal from background, where the background model was created from lower jet-multiplicity data.

[18] Based on 1 fb^{-1}. The result is for $m_t = 170$ GeV. For $m_t = 175$ GeV, the result is $6.3\ ^{+1.2}_{-1.1}$(stat)± 0.7(syst)± 0.4(lumi) pb. Cross section of $t\bar{t}$ production has been measured in the $t\bar{t} \to \tau_h +$ jets topology, where τ_h denotes hadronically decaying τ leptons. The result for the cross section times the branching ratio is $\sigma(t\bar{t}) \cdot$ B($t\bar{t} \to \tau_h +$ jets) $= 0.60^{+0.23}_{-0.22}{}^{+0.15}_{-0.14} \pm 0.04$ pb for $m_t = 170$ GeV.

[19] Based on 1.1 fb^{-1}. The result is for B($W \to \ell\nu$) = 10.8% and $m_t = 175$ GeV; the mean value is 9.8 for $m_t = 172.5$ GeV and 10.1 for $m_t = 170$ GeV. AALTONEN 09AD used high p_T e or μ with an isolated track to select $t\bar{t}$ decays into dileptons including $\ell = \tau$. The result is based on the candidate event samples with and without vertex b-tag.

[20] Based on 2 fb^{-1}. The result is for $m_t = 175$ GeV; the mean value is 3% higher for $m_t = 170$ GeV and 4% lower for $m_t = 180$ GeV.

[21] Result is based on 1 fb^{-1} of data. The result is for $m_t = 170$ GeV, and the mean value decreases with increasing m_t; see their Fig. 2. The result is obtained after combining ℓ + jets, $\ell\ell$, and $\ell\tau$ final states, and the ratios of the extracted cross sections are $R^{\ell\ell/\ell j} = 0.86^{+0.19}_{-0.17}$ and $R^{\ell\tau/\ell\ell-\ell j} = 0.97^{+0.32}_{-0.29}$, consistent with the SM expectation of R = 1. This leads to the upper bound of B($t \to bH^+$) as a function of m_{H^+}. Results are shown in their Fig. 1 for B($H^+ \to \tau\nu$) = 1 and B($H^+ \to c\bar{s}$) = 1 cases. Comparison of the m_t dependence of the extracted cross section and a partial NNLO prediction gives $m_t = 169.1^{+5.9}_{-5.2}$ GeV.

[22] Result is based on 1 fb^{-1} of data. The result is for $m_t = 170$ GeV, and the mean value changes by -0.07 [m_t(GeV)-170] pb near the reference m_t value. Comparison of the m_t dependence of the extracted cross section and a partial NNLO QCD prediction gives $m_t = 171.5^{+9.9}_{-8.8}$ GeV. The $\ell\tau$ channel alone gives $7.6^{+4.9}_{-4.3}{}^{+3.5}_{-3.4}{}^{+1.4}_{-0.9}$ pb and the $\ell\ell$ channel gives $7.5^{+1.2}_{-1.1}{}^{+0.7}_{-0.6}{}^{+0.7}_{-0.5}$ pb.

[23] Result is based on 0.9 fb^{-1} of data. The first error is from stat + syst, while the latter error is from luminosity. The result is for m_t=175 GeV, and the mean value changes by -0.09 pb·[m_t(GeV)-175].

[24] Result is based on 0.9 fb^{-1} of data. The cross section is obtained from the $\ell + \geq 3$jet event rates with 1 or 2 b-tag, and also from the kinematical likelihood analysis of the $\ell +$ 3, 4 jet events. The result is for m_t= 172.6 GeV, and its m_t dependence shown in Fig. 3 leads to the constraint $m_t = 170 \pm 7$ GeV when compared to the SM prediction.

[25] Result is based on 360 pb^{-1} of data. Events with high p_T oppositely charged dileptons $\ell^+\ell^-$ ($\ell = e, \mu$) are used to obtain cross sections for $t\bar{t}$, W^+W^-, and $Z \to \tau^+\tau^-$ production processes simultaneously. The other cross sections are given in Table IV.

[26] Based on 1.02 fb^{-1} of data. Result is for $m_t = 175$ GeV. Secondary vertex b-tag and neural network selections are used to achieve a signal-to-background ratio of about 1/2.

[27] Based on 425 pb^{-1} of data. Result is for $m_t = 175$ GeV. For $m_t = 170.9$ GeV, 7.8 ± 1.8(stat + syst) pb is obtained.

[28] Based on 405 ± 25 pb^{-1} of data. Result is for $m_t = 175$ GeV. The last error is for luminosity. Secondary vertex b-tag and neural network are used to separate the signal events from the background.

[29] Based on 425 pb^{-1} of data. Assumes $m_t = 175$ GeV.

[30] Based on $\sim$ 425 pb^{-1}. Assuming $m_t = 175$ GeV. The first error is combined statistical and systematic, the second one is luminosity.

[31] Based on $\sim$ 318 pb^{-1}. Assuming $m_t = 178$ GeV. The cross section changes by ± 0.08 pb for each $\mp$ GeV change in the assumed m_t. Result is for at least one b-tag. For at least two b-tagged jets, $t\bar{t}$ signal of significance greater than 5σ is found, and the cross section is $10.1\ ^{+1.6}_{-1.4}{}^{+2.0}_{-1.3}$ pb for $m_t = 178$ GeV.

[32] Based on ~ 311 pb^{-1}. Assuming $m_t = 178$ GeV. For $m_t = 175$ GeV, the result is $6.0 \pm 1.2^{+0.9}_{-0.7}$. This is the first CDF measurement without lepton identification, and hence it has sensitivity to the $W \to \tau\nu$ mode.

[33] ABULENCIA,A 06E measures the $t\bar{t}$ production cross section in the all hadronic decay mode by selecting events with 6 to 8 jets and at least one b-jet. S/B = 1/5 has been achieved. Based on 311 pb^{-1}. Assuming $m_t = 178$ GeV.

[34] Based on ~ 318 pb^{-1}. Assuming $m_t = 178$ GeV. Result is for at least one b-tag. For at least two b-tagged jets, the cross section is $11.1^{+2.3}_{-1.9}{}^{+2.5}_{-1.9}$ pb.

[35] ABAZOV 05Q measures the top-quark pair production cross section with ~ 230 pb^{-1} of data, based on the analysis of W plus n-jet events where W decays into e or μ plus neutrino, and at least one of the jets is b-jet like. The first error is statistical and systematic, and the second accounts for the luminosity uncertainty. The result assumes $m_t = 175$ GeV; the mean value changes by $(175 - m_t(\text{GeV})) \times 0.06$ pb in the mass range 160 to 190 GeV.

[36] ABAZOV 05R measures the top-quark pair production cross section with 224–243 pb^{-1} of data, based on the analysis of events with two charged leptons in the final state. The result assumes $m_t = 175$ GeV; the mean value changes by $(175 - m_t(\text{GeV})) \times 0.08$ pb in the mass range 160 to 190 GeV.

[37] Based on 230 pb^{-1}. Assuming $m_t = 175$ GeV.

[38] Based on 194 pb^{-1}. Assuming $m_t = 175$ GeV.

[39] Based on 194 ± 11 pb^{-1}. Assuming $m_t = 175$ GeV.

[40] Based on 162 ± 10 pb^{-1}. Assuming $m_t = 175$ GeV.

[41] ACOSTA 05V measures the top-quark pair production cross section with ~ 162 pb^{-1} data, based on the analysis of W plus n-jet events where W decays into e or μ plus neutrino, and at least one of the jets is b-jet like. Assumes $m_t = 175$ GeV.

[42] ACOSTA 04I measures the top-quark pair production cross section with 197 ± 12 pb^{-1} data, based on the analysis of events with two charged leptons in the final state. Assumes $m_t = 175$ GeV.

Ratio of the Production Cross Sections of $t\bar{t}\gamma$ to $t\bar{t}$ at $\sqrt{s} = 1.96$ TeV

VALUE	DOCUMENT ID		TECN	COMMENT
• • • We do not use the following data for averages, fits, limits, etc. • • •				
0.024 ± 0.009	[1] AALTONEN	11Z	CDF	$E_T(\gamma) > 10$ GeV, $\lvert\eta(\gamma)\rvert < 1.0$

[1] Based on 6.0 fb^{-1} of data. The error is statistical and systematic combined. Events with lepton + $\not{E}_T$ + ≥ 3 jets($\geq 1b$) with and without central, high E_T photon are measured. The result is consistent with the SM prediction of 0.024 ± 0.005. The absolute production cross section is measured to be 0.18 ± 0.08 fb. The statistical significance is 3.0 standard deviations.

tt Production Cross Section in pp Collisions at $\sqrt{s} = 7$ TeV

VALUE (pb)	CL%	DOCUMENT ID		TECN	COMMENT
• • • We do not use the following data for averages, fits, limits, etc. • • •					
<1.7	95	[1] AAD	12BE	ATLS	$\ell^+\ell^+ + \not{E}_T + \geq 2$j + HT

[1] Based on 1.04 fb^{-1} of pp data at $\sqrt{s} = 7$ TeV. The upper bounds are the same for LL, LR and RR chiral components of the two top quarks.

$t\bar{t}$ Production Cross Section in pp Collisions at $\sqrt{s} = 7$ TeV

Unless otherwise noted the first quoted error is from statistics, the second from systematic uncertainties, and the third from luminosity. If only two errors are quoted the luminosity is included in the systematic uncertainties.

VALUE (pb)	DOCUMENT ID		TECN	COMMENT
• • • We do not use the following data for averages, fits, limits, etc. • • •				
$161.7 \pm 6.0 \pm 12.0 \pm 3.6$	[1] KHACHATRY...17B		CMS	$\ell + \not{E}_T + \geq 4$j ($\geq 1b$)
$173.6 \pm 2.1^{+4.5}_{-4.0} \pm 3.8$	[2] KHACHATRY...16AW		CMS	$e + \mu + \not{E}_T + \geq 0$j
$181.2 \pm 2.8^{+10.8}_{-10.6}$	[3] AAD	15BO	ATLS	$e + \mu + \not{E}_T + \geq 0$j
$178 \pm 3 \pm 16 \pm 3$	[4] AAD	15CC	ATLS	ℓ+jets, $\ell\ell$+jets, $\ell\tau_h$+jets
	[5] AAIJ	15R	LHCB	$\mu + \geq 1$j(b-tag) forward region
$182.9 \pm 3.1 \pm 6.4$	[6] AAD	14AY	ATLS	$e + \mu + 1$ or $2b$ jets
$194 \pm 18 \pm 46$	[7] AAD	13X	ATLS	$\tau_h + \not{E}_T + \geq 5$j ($\geq 2b$)
$139 \pm 10 \pm 26$	[8] CHATRCHYAN	13AY	CMS	≥ 6 jets with 2 b-tags
$158.1 \pm 2.1 \pm 10.8$	[9] CHATRCHYAN	13BB	CMS	$\ell + \not{E}_T +$ jets(≥ 1 b-tag)
$152 \pm 12 \pm 32$	[10] CHATRCHYAN	13BE	CMS	$\tau_h + \not{E}_T + \geq 4$ jets (≥ 1 b)
$177 \pm 20 \pm 14 \pm 7$	[11] AAD	12B	ATLS	Repl. by AAD 12BF
$176 \pm 5 \pm 14 \pm 8$	[12] AAD	12BF	ATLS	$\ell\ell + \not{E}_T + \geq 2$j
$187 \pm 11 \pm 18 \pm 6$	[13] AAD	12BO	ATLS	$\ell + \not{E}_T + \geq 3$j with b-tag
$186 \pm 13 \pm 20 \pm 7$	[14] AAD	12CG	ATLS	$\ell + \tau_h + \not{E}_T + \geq 2$j ($\geq 1b$)
$143 \pm 14 \pm 22 \pm 3$	[15] CHATRCHYAN	12AC	CMS	$\ell + \tau_h + \not{E}_T + \geq 2$j ($\geq 1b$)
$161.9 \pm 2.5^{+5.1}_{-5.0} \pm 3.6$	[16] CHATRCHYAN	12AX	CMS	$\ell\ell + \not{E}_T + \geq 2b$
$145 \pm 31 \pm 42$	[17] AAD	11A	ATLS	$\ell + \not{E}_T + \geq 4$j, $\ell\ell + \not{E}_T + \geq 2$j
$173 \pm 39 \pm 7$	[18] CHATRCHYAN	11AA	CMS	$\ell + \not{E}_T + \geq 3$ jets
$168 \pm 18 \pm 14 \pm 7$	[19] CHATRCHYAN	11F	CMS	$\ell\ell + \not{E}_T +$ jets
$154 \pm 17 \pm 6$	[20] CHATRCHYAN	11Z	CMS	Combination
$194 \pm 72 \pm 24 \pm 21$	[21] KHACHATRY...11A		CMS	$\ell\ell + \not{E}_T + \geq 2$ jets

[1] KHACHATRYAN 17B based on 5.0 fb^{-1} of data, using a binned likelihood fit of templates to the data. Also the ratio $\sigma(t\bar{t}; 8\text{ TeV})/\sigma(t\bar{t}; 7\text{ TeV}) = 1.43 \pm 0.04 \pm 0.07 \pm 0.05$ is reported. The results are in agreement with NNLO SM predictions.

[2] KHACHATRYAN 16AW based on 5.0 fb^{-1} of data, using a binned likelihood fit to differential distributions of b-tagged and non-b-tagged jets. The result is in good agreement with NNLO SM predictions.

[3] Based on 4.6 fb^{-1} of data. Uses a template fit to distributions of $\not{E}_T$ and jet multiplicities to measure simultaneously $t\bar{t}$, WW, and $Z/\gamma^* \to \tau\tau$ cross sections, assuming $m_t = 172.5$ GeV.

[4] AAD 15CC based on 4.6 fb^{-1} of data. The event selection criteria are optimized for the $\ell\tau_h$ + jets channel. Using only this channel $183 \pm 9 \pm 23 \pm 3$ pb is derived for the cross section.

[5] AAIJ 15R, based on 1.0 fb^{-1} of data, reports $0.239 \pm 0.053 \pm 0.033 \pm 0.024$ pb cross section for the forward fiducial region $p_T(\mu) > 25$ GeV, $2.0 < \eta(\mu) < 4.5$, 50 GeV $< p_T(b) < 100$ GeV, $2.2 < \eta(b) < 4.2$, $\Delta R(\mu,b) > 0.5$, and $p_T(\mu+b) > 20$ GeV. The three errors are from statistics, systematics, and theory. The result agrees with the SM NLO prediction.

[6] AAD 14AY reports $182.9 \pm 3.1 \pm 4.2 \pm 3.6 \pm 3.3$ pb value based on 4.6 fb^{-1} of data. The four errors are from statistics, systematic, luminosity, and the 0.66% beam energy uncertainty. We have combined the systematic uncertainties in quadrature. The result is for $m_t = 172.5$GeV; for other m_t, $\sigma(m_t) = \sigma(172.5\text{GeV}) \times [1 - 0.0028 \times (m_t - 172.5\text{GeV})]$. The result is consistent with the SM prediction at NNLO.

[7] Based on 1.67 fb^{-1} of data. The result uses the acceptance for $m_t = 172.5$ GeV.

[8] Based on 3.54 fb^{-1} of data.

[9] Based on 2.3 fb^{-1} of data.

[10] Based on 3.9 fb^{-1} of data.

[11] Based on 35 pb^{-1} of data for an assumed top quark mass of $m_t = 172.5$ GeV.

[12] Based on 0.70 fb^{-1} of data. The 3 errors are from statistics, systematics, and luminosity. The result uses the acceptance for $m_t = 172.5$ GeV.

[13] Based on 35 pb^{-1} of data. The 3 errors are from statistics, systematics, and luminosity. The result uses the acceptance for $m_t = 172.5$ GeV and $173 \pm 17^{+18}_{-16} \pm 6$ pb is found without the b-tag.

[14] Based on 2.05 fb^{-1} of data. The hadronic τ candidates are selected using a BDT technique. The 3 errors are from statistics, systematics, and luminosity. The result uses the acceptance for $m_t = 172.5$ GeV.

[15] Based on 2.0 fb^{-1} and 2.2 fb^{-1} of data for $\ell = e$ and $\ell = \mu$, respectively. The 3 errors are from statistics, systematics, and luminosity. The result uses the acceptance for $m_t = 172.5$ GeV.

[16] Based on 2.3 fb^{-1} of data. The 3 errors are from statistics, systematics, and luminosity. The result uses the profile likelihood-ratio (PLB) method and an assumed m_t of 172.5 GeV.

[17] Based on 2.9 pb^{-1} of data. The result for single lepton channels is $142 \pm 34^{+50}_{-31}$ pb, while for the dilepton channels is $151^{+78}_{-62}{}^{+37}_{-24}$ pb.

[18] Result is based on 36 pb^{-1} of data. The first uncertainty corresponds to the statistical and systematic uncertainties, and the second corresponds to the luminosity.

[19] Based on 36 pb^{-1} of data. The ratio of $t\bar{t}$ and Z/γ^* cross sections is measured as $\sigma(pp \to t\bar{t})/\sigma(pp \to Z/\gamma^* \to e^+e^-/\mu^+\mu^-) = 0.175 \pm 0.018(\text{stat}) \pm 0.015(\text{syst})$ for $60 < m_{\ell\ell} < 120$ GeV, for which they use an NNLO prediction for the denominator cross section of 972 ± 42 pb.

[20] Result is based on 36 pb^{-1} of data. The first error is from statistical and systematic uncertainties, and the second from luminosity. This is a combination of a measurement in the dilepton channel (CHATRCHYAN 11F) and the measurement in the ℓ + jets channel (CHATRCHYAN 11Z) which yields $150 \pm 9 \pm 17 \pm 6$ pb.

[21] Result is based on 3.1 ± 0.3 pb^{-1} of data.

$t\bar{t}$ Production Cross Section in pp Collisions at $\sqrt{s} = 8$ TeV

Unless otherwise noted the first quoted error is from statistics, the second from systematic uncertainties, and the third from luminosity. If only two errors are quoted the luminosity is included in the systematic uncertainties.

VALUE (pb)	DOCUMENT ID		TECN	COMMENT
• • • We do not use the following data for averages, fits, limits, etc. • • •				
$239 \pm 4 \pm 28 \pm 5$	[1] AABOUD	17Z	ATLS	$\tau_h + \not{E}_T + \geq 2$j ($\geq 2b$)
$228.5 \pm 3.8 \pm 13.7 \pm 6.0$	[2] KHACHATRY...17B		CMS	$\ell + \not{E}_T + \geq 4$j ($\geq 1b$)
$242.9 \pm 1.7 \pm 8.6$	[3] AAD	16BK	ATLS	$e + \mu + 1$ or $2b$ jets
$244.9 \pm 1.4^{+6.3}_{-5.5} \pm 6.4$	[4] KHACHATRY...16AW		CMS	$e + \mu + \not{E}_T + \geq 0$j
$275.6 \pm 6.1 \pm 37.8 \pm 7.2$	[5] KHACHATRY...16BC		CMS	≥ 6j ($\geq 2b$)
$260 \pm 1 \pm 24$	[6] AAD	15BP	ATLS	$\ell + \not{E}_T + \geq 3$j ($\geq 1b$)
	[7] AAIJ	15R	LHCB	$\mu + \geq 1$j(b-tag) forward region
$242.4 \pm 1.7 \pm 10.2$	[8] AAD	14AY	ATLS	$e + \mu + 1$ or $2b$ jets
$239 \pm 2 \pm 11 \pm 6$	[9] CHATRCHYAN	14F	CMS	$\ell\ell + \not{E}_T + \geq 2$j (≥ 1 b-tag)
$257 \pm 3 \pm 24 \pm 7$	[10] KHACHATRY...14S		CMS	$\ell + \tau_h + \not{E}_T + \geq 2$j ($\geq 1b$)

[1] AABOUD 17Z based on 20.2 fb^{-1} of data, using the mode $t\bar{t} \to \tau\nu q'\overline{q}b\overline{b}$ with τ decaying hadronically. Single prong and 3 prong decays of τ are separately analyzed. The result is consistent with the SM. The third quoted uncertainty is due to luminosity.

[2] KHACHATRYAN 17B based on 19.6 fb^{-1} of data, using a binned likelihood fit of templates to the data. Also the ratio $\sigma(t\bar{t}; 8\text{ TeV})/\sigma(t\bar{t}; 7\text{ TeV}) = 1.43 \pm 0.04 \pm 0.07 \pm 0.05$ is reported. The results are in agreement with NNLO SM predictions.

[3] AAD 16BK is an update of the value from AAD 14AY using the improved luminosity calibration. The value $242.9 \pm 1.7 \pm 5.5 \pm 5.1 \pm 4.2$ pb is reported, where we have combined the systematic uncertainties in quadrature. Also the ratio $\sigma(t\bar{t};\ 8\text{TeV})/\sigma(t\bar{t};\ 7\text{TeV}) = 1.328 \pm 0.024 \pm 0.015 \pm 0.038 \pm 0.001$ has been updated. The former result is consistent with the SM predictions at NNLO, while the latter result is 2.1 σ below the expectation.

[4] KHACHATRYAN 16AW based on 19.7 fb^{-1} of data, using a binned likelihood fit to differential distributions of b-tagged and non-b-tagged jets. The result is in good agreement with NNLO SM predictions.

[5] KHACHATRYAN 16BC based on 18.4 fb^{-1} of data. The last uncertainty is due to luminosity. Cuts on kinematical fit probability and $\Delta R(b,b)$ are imposed. The major QCD background is determined from the data. The result is for $m_t = 172.5$ GeV and in agreement with the SM prediction. The top quark p_T spectra, also measured, are significantly softer than theoretical predictions.

[6] AAD 15BP based on 20.3 fb^{-1} of data. The result is for $m_t = 172.5$ GeV and in agreement with the SM prediction 253^{+13}_{-15} pb at NNLO+NNLL.

[7] AAIJ 15R, based on 2.0 fb^{-1} of data, reports $0.289 \pm 0.043 \pm 0.040 \pm 0.029$ pb cross section for the forward fiducial region $p_T(\mu) > 25$ GeV, $2.0 < \eta(\mu) < 4.5$, 50 GeV $< p_T(b) < 100$ GeV, $2.2 < \eta(b) < 4.2$, $\Delta R(\mu,b) > 0.5$, and $p_T(\mu+b) > 20$ GeV. The three errors are from statistics, systematics, and theory. The result agrees with the SM NLO prediction.

[8] AAD 14AY reports 242.4 ± 1.7 ± 5.5 ± 7.5 ± 4.2 pb value based on 20.3 fb^{-1} of data. The four errors are from statistics, systematic, luminosity, and the 0.66% beam energy uncertainty. We have combined the systematic uncertainties in quadrature. The result is for m_t = 172.5GeV; for other m_t, $\sigma(m_t) = \sigma(172.5\text{GeV}) \times [1 - 0.0028 \times (m_t - 172.5\text{GeV})]$. Also measured is the ratio $\sigma(t\bar{t}; 8\text{TeV})/\sigma(t\bar{t}; 7\text{TeV}) = 1.326 \pm 0.024 \pm 0.015 \pm 0.049 \pm 0.001$. The results are consistent with the SM predictions at NNLO.

[9] Based on 5.3 fb^{-1} of data. The result is for m_t = 172.5 GeV, and a parametrization is given in eq.(6.1) for the mean value at other m_t values. The result is in agreement with the SM prediction $252.9^{+6.4}_{-8.6}$ pb at NNLO.

[10] Based on 19.6 fb^{-1} of data. The measurement is in the channel $t\bar{t} \to (b\ell\nu)(b\tau\nu)$, where τ decays into hadrons (τ_h). The result is for m_t = 172.5 GeV. For m_t = 173.3 GeV, the cross section is lower by 3.1 pb.

$t\bar{t}$ Production Cross Section in pp Collisions at $\sqrt{s}$ = 13 TeV

VALUE (pb)	DOCUMENT ID		TECN	COMMENT
• • • We do not use the following data for averages, fits, limits, etc. • • •				
815 ± 9 ± 38 ± 19	[1] KHACHATRY...17N		CMS	$e\mu$ + ≥2j (≥1b j)
888 ± 2^{+26}_{-28} ± 20	[2] SIRUNYAN	17W	CMS	ℓ + ≥1j
818 ± 8 ± 35	[3] AABOUD	16R	ATLS	$e + \mu$ + 1 or 2b jets
746 ± 58 ± 53 ± 36	[4] KHACHATRY...16J		CMS	$e + \mu$ + ≥2j

[1] KHACHATRYAN 17N based on 2.2 fb^{-1} of data. The last quoted uncertainty is due to the beam luminosity. This measurement supersedes that of KHACHATRYAN 16J.

[2] SIRUNYAN 17W based on 2.2 fb^{-1} of pp data at $\sqrt{s}$ = 13 TeV. Events are categorized according to the jet multiplicity and the number of b-tagged jets. A likelihood fit is performed to the event distributions to compare to the NNLO+NNLL prediction.

[3] AABOUD 16R reported value 818 ± 8 ± 27 ± 19 ± 12 pb based on 3.2 fb^{-1} of data. The four errors are from statistics, systematic, luminosity, and beam energy. We have combined the systematic uncertainties in quadrature. The result is in agreement with the SM prediction 832^{+40}_{-46} pb at NNLO+NNLL for m_t = 172.5 GeV .

[4] KHACHATRYAN 16J based on 43 pb^{-1} of data. The last uncertainty is due to luminosity. The result is for m_t = 172.5 GeV and in agreement with the SM prediction 832^{+40}_{-46} pb at NNLO+NNLL.

$t\bar{t}\,t\bar{t}$ Production Cross Section in pp Collisions at $\sqrt{s}$ = 8 TeV

VALUE (fb)	CL%	DOCUMENT ID		TECN	COMMENT
• • • We do not use the following data for averages, fits, limits, etc. • • •					
<23	95	[1] AAD	15AR	ATLS	$\ell + \not{E}_T$ + ≥5j (≥2 b)
<70	95	[2] AAD	15BY	ATLS	≥2$\ell + \not{E}_T$ + ≥2j (≥1 b)
<32	95	[3] KHACHATRY...14R		CMS	$\ell + \not{E}_T$ + ≥6j (≥2 b)

[1] AAD 15AR based on 20.3 fb^{-1} of data. A fit to H_T distributions in multi-channels classified by the number of jets and of b-tagged jets is performed.

[2] AAD 15BY based on 20.3 fb^{-1} of data. A same-sign lepton pair is required. An excess over the SM prediction reaches 2.5σ for hypotheses involving heavy resonances decaying into $t\bar{t}\,t\bar{t}$.

[3] Based on 19.6 fb^{-1} of data, using a multivariate analysis to separate signal from backgrounds. About $\sigma(t\bar{t}\,t\bar{t}) = 1$ fb is expected in the SM.

$t\bar{t}\,t\bar{t}$ Production Cross Section in pp Collisions at $\sqrt{s}$ = 13 TeV

VALUE (fb)	CL%	DOCUMENT ID		TECN	COMMENT
• • • We do not use the following data for averages, fits, limits, etc. • • •					
<94	95	[1] SIRUNYAN	17AB	CMS	ℓ+jets, $\ell^+\ell^-$+jets channels

[1] SIRUNYAN 17AB based on 2.6 fb^{-1} of data. A multivariate analysis is used to discriminate between $t\bar{t}\,t\bar{t}$ signal and $t\bar{t}$ background. A combination with a previous search (CMS, KHACHATRYAN 16BJ) in the same-sign dilepton channel gives an upper limit of 69 fb (95% CL), corresponding to 7.4·(SM prediction).

$t\bar{t}W$ Production Cross Section in pp Collisions at $\sqrt{s}$ = 8 TeV

VALUE (fb)	DOCUMENT ID		TECN	COMMENT
• • • We do not use the following data for averages, fits, limits, etc. • • •				
170^{+90}_{-80} ± 70	[1] KHACHATRY...14N		CMS	$t\bar{t}W \to$ same sign dilepton + $\not{E}_T$ + jets

[1] Based on 19.5 fb^{-1} of data. The result is consistent with the SM prediction of $\sigma(t\bar{t}W) = 206^{+21}_{-23}$ fb.

$t\bar{t}Z$ Production Cross Section in pp Collisions at $\sqrt{s}$ = 8 TeV

VALUE (fb)	DOCUMENT ID		TECN	COMMENT
• • • We do not use the following data for averages, fits, limits, etc. • • •				
$200^{+80}_{-70}{}^{+40}_{-30}$	[1] KHACHATRY...14N		CMS	$t\bar{t}Z \to 3,4\ \ell + \not{E}_T$ + jets

[1] Based on 19.5 fb^{-1} of data. The result is consistent with the SM prediction of $\sigma(t\bar{t}Z) = 197^{+22}_{-25}$ fb.

f(Q_0): $t\bar{t}$ Fraction of Events with a Veto on Additional Central Jet Activity in pp Collisions at $\sqrt{s}$ = 7 TeV

Q_0 denotes the threshold of the additional jet p_T.

VALUE (%)	DOCUMENT ID		TECN	COMMENT
• • • We do not use the following data for averages, fits, limits, etc. • • •				
80.0 ± 1.1 ± 1.6	[1] CHATRCHYAN 14AE		CMS	Q_0 = 75 GeV ($\|y\|$ <2.4)
92.0 ± 0.7 ± 0.8	[1] CHATRCHYAN 14AE		CMS	Q_0= 150 GeV ($\|y\|$ <2.4)
98.0 ± 0.3 ± 0.3	[1] CHATRCHYAN 14AE		CMS	Q_0= 300 GeV ($\|y\|$ <2.4)
56.4 ± 1.3 $^{+2.6}_{-2.8}$	[2] AAD	12BL	ATLS	Q_0 = 25 GeV ($\|y\|$ <2.1)
84.7 ± 0.9 ± 1.0	[2] AAD	12BL	ATLS	Q_0 = 75 GeV ($\|y\|$ <2.1)
95.2 $^{+0.5}_{-0.6}$ ± 0.4	[2] AAD	12BL	ATLS	Q_0= 150 GeV ($\|y\|$ <2.1)

[1] CHATRCHYAN 15 based on 5.0 fb^{-1} of data. The $t\bar{t}$ events are selected in the dilepton and lepton + jets decay channels. For other values of Q_0 see Table 5.

[2] Based on 2.05 fb^{-1} of data. The $t\bar{t}$ events are selected in the dilepton decay channel with two identified b-jets.

Fraction of $t\bar{t}$ + multi-jet Events in pp Collisions at $\sqrt{s}$ = 7 TeV

VALUE	DOCUMENT ID		TECN	COMMENT
• • • We do not use the following data for averages, fits, limits, etc. • • •				
	[1] AAD	15D	ATLS	$\ell + \not{E}_T$ + nj (n=3 to 8)
0.332 ± 0.090	[2] CHATRCHYAN	14AE	CMS	$t\bar{t}(\ell\ell)$ + 0 jet (E_T > 30GeV)
0.436 ± 0.098	[2] CHATRCHYAN	14AE	CMS	$t\bar{t}(\ell\ell)$ + 1 jet (E_T > 30GeV)
0.232 ± 0.125	[2] CHATRCHYAN	14AE	CMS	$t\bar{t}(\ell\ell)$ + ≥2 jet (E_T > 30GeV)

[1] Based on 4.6 fb^{-1} of data. Fiducial $t\bar{t}$ production cross section is presented as a function of the jet multiplicity for up to eight jets with the jet p_T threshold of 25, 40, 60, and 80 GeV, and as a function of jet p_T up to the 5th jet. MC models can be discriminated by using data for high jet multiplicity and by p_T distributions of the leading and 5th jet.

[2] Based on 5.0 fb^{-1} of data. Events with two oppositely charged leptons, large $\not{E}_T$ and jets with at least 1 b-tag are used to measure the fraction of $t\bar{t}$ plus additional jets. The gap fraction (n=0 jet rate) as a function of the jet p_T and that of H_T, the scalar sum of the p_T's of additional jets, is shown in Fig. 8.

$t\bar{t}$ Charge Asymmetry (A_C) in pp Collisions at $\sqrt{s}$ = 7 TeV

A_C = (N(Δ|y| >0) − N(Δ|y| <0)) / (N(Δ|y| >0) + N(Δ|y| <0)) where Δ|y| = $|y_t| - |y_{\bar{t}}|$ is the difference between the absolute values of the top and antitop rapidities and N is the number of events with Δ|y| positive or negative.

VALUE (%)	DOCUMENT ID		TECN	COMMENT
• • • We do not use the following data for averages, fits, limits, etc. • • •				
2.1 ± 2.5 ± 1.7	[1] AAD	15AJ	ATLS	$\ell\ell + \not{E}_T$ + ≥2j
0.6 ± 1.0	[2] AAD	14I	ATLS	$\ell + \not{E}_T$ + ≥4j (≥1b)
−1.0 ± 1.7 ± 0.8	[3] CHATRCHYAN	14D	CMS	$\ell\ell + \not{E}_T$ + ≥2j (≥1b)
−1.9 ± 2.8 ± 2.4	[4] AAD	12BK	ATLS	$\ell + \not{E}_T$ + ≥4j (≥1b)
0.4 ± 1.0 ± 1.1	[5] CHATRCHYAN	12BB	CMS	$\ell + \not{E}_T$ + ≥4j (≥1b)
−1.3 ± 2.8 $^{+2.9}_{-3.1}$	[6] CHATRCHYAN	12BS	CMS	$\ell + \not{E}_T$ + ≥4j (≥1b)

[1] AAD 15AJ based on 4.6 fb^{-1} of data. After kinematic reconstruction the top quark momenta are corrected for detector resolution and acceptance effects by unfolding, using parton level information of the MC generators. The lepton charge asymmetry is measured as $A_C^{\ell} = 0.024 \pm 0.015 \pm 0.009$. All the measurements are consistent with the SM predictions.

[2] Based on 4.7 fb^{-1} of data. The result is consistent with the SM prediction of A_C = 0.0123 ± 0.0005. The asymmetry is 0.011 ± 0.018 if restricted to those events where $\beta_Z(t\bar{t}) > 0.6$, which is also consistent with the SM prediction of $0.020^{+0.006}_{-0.007}$.

[3] Based on 5.0 fb^{-1} of data. The lepton charge asymmetry is measured as $A_C^{\ell} = 0.009 \pm 0.0010 \pm 0.006$. A_C^{ℓ} dependences on $m_{t\bar{t}}$, $|y(t\bar{t})|$, and $p_T(t\bar{t})$ are given in Fig. 5. All measurements are consistent with the SM predictions.

[4] Based on 1.04 fb^{-1} of data. The result is consistent with A_C = 0.006 ± 0.002 (MC at NLO). No significant dependence of A_C on $m_{t\bar{t}}$ is observed.

[5] Based on 5.0 fb^{-1} of data at 7 TeV.

[6] Based on 1.09 fb^{-1} of data. The result is consistent with the SM predictions.

$t\bar{t}$ Charge Asymmetry (A_C) in pp Collisions at $\sqrt{s}$ = 8 TeV

VALUE (%)	DOCUMENT ID		TECN	COMMENT
• • • We do not use the following data for averages, fits, limits, etc. • • •				
2.1 ± 1.6	[1] AAD	16AE	ATLS	$\ell\ell + \not{E}_T$ + ≥2j
0.9 ± 0.5	[2] AAD	16AZ	ATLS	$\ell + \not{E}_T$ + ≥4j
4.2 ± 3.2	[3] AAD	16T	ATLS	$m_{t\bar{t}}$ >0.75 TeV, $\|\|y_t\| - \|y_{\bar{t}}\|\|$ <2, $\ell + \not{E}_T$ + jets
1.1 ± 1.1 ± 0.7	[4] KHACHATRY...16AD		CMS	$\ell\ell + \not{E}_T$ + ≥2j (≥1b)
0.33 ± 0.26 ± 0.33	[5] KHACHATRY...16AH		CMS	$\ell + \not{E}_T$ + ≥4j (≥1b)
0.10 ± 0.68 ± 0.37	[6] KHACHATRY...16T		CMS	$\ell + \not{E}_T$ + ≥4j (≥1b)

[1] AAD 16AE is based on 20.3 fb^{-1} of data. After kinematic reconstruction, the top quark momenta are corrected for detector resolution and acceptance effects by unfolding, using parton level information of the MC generators. The lepton charge asymmetry is measured as $A_C^{\ell\ell} = 0.008 \pm 0.006$. All the measurements are consistent with the SM predictions.

[2] AAD 16AZ based on 20.3 fb^{-1} of data. All the differential and inclusive measurements are statistically limited and consistent with the SM predictions.

[3] AAD 16T based on 20.3 fb^{-1} of data. Uses reconstruction techniques for the decay topology of highly boosted top quarks. The observed asymmetry is transformed by unfolding to a parton-level result in the shown fiducial region. The result is consistent with the NLO SM prediction.

[4] KHACHATRYAN 16AD based on 19.5 fb^{-1} of data. The lepton charge asymmetry is measured as $A_C^{\ell\ell} = 0.003 \pm 0.006 \pm 0.003$. All the measurements are consistent with the SM predictions.

[5] KHACHATRYAN 16AH based on 19.6 fb^{-1} of data. The same data set as in KHACHATRYAN 16T is used. A template technique is used, which is sensitive to the charge anti-symmetric component of the $t\bar{t}$ rapidity distributions and statistically advantageous. The result is consistent with the SM predictions.

[6] KHACHATRYAN 16T based on 19.7 fb^{-1} of data. The same data set as in KHACHATRYAN 16AH is used. After kinematic reconstruction the top quark momenta are corrected for detector resolution and acceptance effects by unfolding, using parton level information of the MC generators. All the measurements are consistent with the SM predictions.

Quark Particle Listings

t

t-quark Polarization in $t\bar{t}$ Events in $p\bar{p}$ Collisions at $\sqrt{s} = 1.96$ TeV

VALUE		DOCUMENT ID		TECN	COMMENT
• • • We do not use the following data for averages, fits, limits, etc. • • •					
0.070 ± 0.055	[1]	ABAZOV	17	D0	ℓ+$\not\!\!E_T$+ $\geq$ 3j($\geq$ 1b)
-0.102 ± 0.061	[2]	ABAZOV	17	D0	ℓ+$\not\!\!E_T$+ $\geq$ 3j($\geq$ 1b)
0.040 ± 0.035	[3]	ABAZOV	17	D0	ℓ+$\not\!\!E_T$+ $\geq$ 3j($\geq$ 1b)
$0.113 \pm 0.091 \pm 0.019$	[4]	ABAZOV	15K	D0	A_{FB}^{ℓ} in $\ell\ell$+$\not\!\!E_T$+ $\geq$ 2j($\geq$ 1b)

[1] ABAZOV 17 based on 9.7 fb^{-1} of data. The value is top quark polarization times spin analyzing power in the beam basis. Combination with the result of ABAZOV 15K yields 0.081 ± 0.048. This result together with the helicity polarization is shown in a 2-dimensional plot in Fig.4. These results are consistent with the SM prediction.

[2] ABAZOV 17 based on 9.7 fb^{-1} of data. The value is top quark polarization times spin analyzing power in the helicity basis. The result is consistent with the SM prediction. This result together with the beam polarization is shown in a 2-dimensional plot in Fig.4.

[3] ABAZOV 17 based on 9.7 fb^{-1} of data. The value is top quark polarization times spin analyzing power in the transverse basis. The result is consistent with the SM prediction.

[4] ABAZOV 15K based on 9.7 fb^{-1} of data. The value is top quark polarization times spin analyzing power in the beam basis. The result is consistent with the SM prediction of -0.0019 ± 0.0005.

t-quark Polarization in $t\bar{t}$ Events in pp Collisions at $\sqrt{s} = 7$ TeV

The double differential distribution in polar angles, θ_1 (θ_2) of the decay particle of the top (anti-top) decay products, is parametrized as $(1/\sigma)d\sigma/(d\cos\theta_1\ d\cos\theta_2) = (1/4)\ (\ 1 + A_t\ \cos\theta_1 + A_{\bar{t}}\ \cos\theta_2 - C\ \cos\theta_1\ \cos\theta_2\ )$. The charged lepton is used to tag t or $\bar{t}$. The coefficient A_t and $A_{\bar{t}}$ measure the average helicity of t and $\bar{t}$, respectively. $A_{CPC} = A_t = A_{\bar{t}}$ assumes CP conservation, whereas $A_{CPV} = A_t = -A_{\bar{t}}$ corresponds to maximal CP violation.

VALUE	DOCUMENT ID		TECN	COMMENT
• • • We do not use the following data for averages, fits, limits, etc. • • •				
$-0.035 \pm 0.014 \pm 0.037$	[1] AAD		13BE	ATLS A_{CPC}
$0.020 \pm 0.016 {}^{+0.013}_{-0.017}$	[1] AAD		13BE	ATLS A_{CPV}

[1] Based on 4.7 fb^{-1} of data using the final states containing one or two isolated electrons or muons and jets with at least one b-tag.

t-quark Polarization in $t\bar{t}$ Events in pp Collisions at $\sqrt{s} = 8$ TeV

A_t, $A_{\bar{t}}$, A_{CPC}, A_{CPV}, and A_C are defined in header texts in the subsections, just above.

VALUE	DOCUMENT ID		TECN	COMMENT
• • • We do not use the following data for averages, fits, limits, etc. • • •				
$-0.044 \pm 0.038 \pm 0.027$	[1] AABOUD	17G	ATLS	A_t
$-0.064 \pm 0.040 \pm 0.027$	[1] AABOUD	17G	ATLS	$A_{\bar{t}}$
$0.296 \pm 0.093 \pm 0.037$	[1] AABOUD	17G	ATLS	A_C
-0.022 ± 0.058	[2] KHACHATRY...16AI		CMS	A_{CPC}
0.000 ± 0.016	[2] KHACHATRY...16AI		CMS	A_{CPV}

[1] AABOUD 17G based on 20.2 fb^{-1} of pp data, using events with two leptons and two or more jets with at least one b-tag. Determined from measurements of 15 top quark spin observables. The second error corresponds to a variation of m_t about 172.5 GeV by 0.7 GeV. The values are consistent with the NLO SM predictions.

[2] KHACHATRYAN 16AI based on 19.5 fb^{-1} of pp data at $\sqrt{s} = 8$ TeV, using events with two leptons and two or more jets with at least one b-tag. Determined from the lepton angular distributions as a function of the $t\bar{t}$-system kinematical variables.

t-quark Polarization in Single Top Events in pp Collisions at $\sqrt{s} = 8$ TeV

VALUE	CL%	DOCUMENT ID		TECN	COMMENT
• • • We do not use the following data for averages, fits, limits, etc. • • •					
>0.72	95	[1] AABOUD	17BB	ATLS	$\alpha_\ell P$; t-channel
$0.97 \pm 0.05 \pm 0.11$		[2] AABOUD	17I	ATLS	$\alpha_\ell P$; t-channel
$0.25 \pm 0.08 \pm 0.14$		[3] AABOUD	17I	ATLS	$(F_+ + F_-)P$; t-channel
$0.26 \pm 0.03 \pm 0.10$		[4] KHACHATRY...16BO		CMS	$(\alpha_\mu P)/2$; t-channel

[1] AABOUD 17BB based on 20.2 fb^{-1} of pp data. Triple-differential decay rate of top quark is used to simultaneously determine five generalized Wtb couplings as well as the top polarization. α_ℓ denotes the spin analyzing power of charged lepton, and the spin axis of the top polarization P is taken along the spectator-quark momentum in the top rest frame. The value is compatible with the SM prediction of about 0.9.

[2] AABOUD 17I based on 20.2 fb^{-1} of pp data. A cut-based analysis is used to discriminate between signal and backgrounds. α_ℓ denotes the spin analyzing power of charged lepton, and the spin axis of the top polarization P is taken along the spectator-quark momentum in the top rest frame. See this paper for a number of other asymmetries and measurements that are not included here.

[3] AABOUD 17I based on 20.2 fb^{-1} of pp data. A cut-based analysis is used to discriminate between signal and backgrounds. $F_\pm$ denotes W helicity fraction, and the spin axis of the top polarization P is taken along the spectator-quark momentum in the top rest frame. See this paper for a number of other asymmetries and measurements that are not included here.

[4] KHACHATRYAN 16BO based on 19.7 fb^{-1} of data. A high-purity sample with a muon is selected by a multivariate analysis. The value is the top spin asymmetry, given by one half of the spin analyzing power α_μ (=1 at LO of SM) times the top polarization, P, where the spin axis is defined as the direction of the untagged jet in the top rest frame. The value is compatible with the SM prediction of 0.44 with a 2.0σ deviation.

$gg \rightarrow t\bar{t}$ Fraction in $p\bar{p}$ Collisions at $\sqrt{s} = 1.96$ TeV

VALUE	CL%	DOCUMENT ID		TECN	COMMENT
• • • We do not use the following data for averages, fits, limits, etc. • • •					
<0.33	68	[1] AALTONEN	09F	CDF	$t\bar{t}$ correlations
$0.07 \pm 0.14 \pm 0.07$		[2] AALTONEN	08AG	CDF	low p_T number of tracks

[1] Based on 955 pb^{-1}. AALTONEN 09F used differences in the $t\bar{t}$ production angular distribution and polarization correlation to descriminate between $gg \rightarrow t\bar{t}$ and $q\bar{q} \rightarrow t\bar{t}$ subprocesses. The combination with the result of AALTONEN 08AG gives $0.07 {}^{+0.15}_{-0.07}$.

[2] Result is based on 0.96 fb^{-1} of data. The contribution of the subprocesses $gg \rightarrow t\bar{t}$ and $q\bar{q} \rightarrow t\bar{t}$ is distinguished by using the difference between quark and gluon initiated jets in the number of small p_T (0.3 GeV $< p_T <$ 3 GeV) charged particles in the central region ($|\eta| < 1.1$).

A_{FB} of $t\bar{t}$ in $p\bar{p}$ Collisions at $\sqrt{s} = 1.96$ TeV

A_{FB} = Forward-backward asymmetry.

VALUE (%)		DOCUMENT ID		TECN	COMMENT
• • • We do not use the following data for averages, fits, limits, etc. • • •					
$12.8 \pm 2.1 \pm 1.4$	[1]	AALTONEN	18	TEVA	CDF, D0 combination
$17.5 \pm 5.6 \pm 3.1$	[2]	ABAZOV	15K	D0	A_{FB}^{ℓ} in $\ell\ell$+$\not\!\!E_T$+ $\geq$ 2j($\geq$ 1b)
7.2 ± 6.0	[3]	AALTONEN	14F	CDF	A_{FB}^{ℓ} in dilepton channel ($\ell\ell$+$\not\!\!E_T$+ $\geq$ 2j)
7.6 ± 8.2	[3]	AALTONEN	14F	CDF	$A_{FB}^{\ell\ell}$ in dilepton channel ($\ell\ell$+$\not\!\!E_T$+ $\geq$ 2j)
$4.2 \pm 2.3 {}^{+1.7}_{-2.0}$	[4]	ABAZOV	14G	D0	A_{FB}^{ℓ} (ℓ + $\not\!\!E_T$+ $\geq$ 3j (0,1 $\geq$ 2b))
10.6 ± 3.0	[5]	ABAZOV	14H	D0	A_{FB} (ℓ + $\not\!\!E_T$ + $\geq$ 3j ($\geq$ 1b))
20.1 ± 6.7	[6]	AALTONEN	13AD	CDF	a_1/a_0 in ℓ+$\not\!\!E_T$+ $\geq$ 4j ($\geq$ 1b)
-0.2 ± 3.1	[6]	AALTONEN	13AD	CDF	a_3,a_5,a_7 in ℓ+$\not\!\!E_T$+ $\geq$ 4j ($\geq$ 1b)
16.4 ± 4.7	[7]	AALTONEN	13S	CDF	ℓ + $\not\!\!E_T$ + $\geq$ 4 jets($\geq$ 1b-tag)
$9.4 {}^{+3.2}_{-2.9}$	[8]	AALTONEN	13X	CDF	ℓ + $\not\!\!E_T$ + $\geq$ 4 jets ($\geq$ 1 b-tag)
11.8 ± 3.2	[9]	ABAZOV	13A	D0	$\ell\ell$ & ℓ+ jets comb.
-11.6 ± 15.3	[10]	AALTONEN	11F	CDF	$m_{t\bar{t}} <$ 450 GeV
47.5 ± 11.4	[10]	AALTONEN	11F	CDF	$m_{t\bar{t}} >$ 450 GeV
19.6 ± 6.5	[11]	ABAZOV	11AH	D0	ℓ + $\not\!\!E_T$ + $\geq$ 4 jets($\geq$ 1b-tag)
17 $\pm$ 8	[12]	AALTONEN	08AB	CDF	$p\bar{p}$ frame
24 $\pm$14	[12]	AALTONEN	08AB	CDF	$t\bar{t}$ frame
12 $\pm$ 8 $\pm$1	[13]	ABAZOV	08L	D0	ℓ + $\not\!\!E_T$ + $\geq$ 4 jets

[1] AALTONEN 18 based on 9–10 fb^{-1} of $p\bar{p}$ data at $\sqrt{s} = 1.96$ TeV. The value is the asymmetry in the number of reconstructed $t\bar{t}$ events with rapidity $y_t > y_{\bar{t}}$ and those with $y_t < y_{\bar{t}}$. The combined fits to CDF and D0 single lepton and $\ell\ell$ asymmetries give $A_{FB}^{\ell} = 0.073 \pm 0.016 \pm 0.012$ and $A_{FB}^{\ell\ell} = 0.108 \pm 0.043 \pm 0.016$, respectively. The results are consistent with the SM predictions.

[2] ABAZOV 15K based on 9.7 fb^{-1} of data. The result is consistent with the SM predictions. By combining with the previous D0 measurement in the ℓ + jet channel ABAZOV 14H, $A_{FB}^{\ell} = 0.118 \pm 0.025 \pm 0.013$ is obtained.

[3] AALTONEN 14F based on 9.1 fb^{-1} of data. A_{FB}^{ℓ} and $A_{FB}^{\ell\ell}$ denote, respectively, the asymmetries $(N(x{>}0) - N(x{<}0))/N_{tot}$ for $x{=}q_\ell\eta_\ell$ (q_ℓ is the charge of ℓ) and $x{=}\eta_{\ell^+} - \eta_{\ell^-}$. Both results are consistent with the SM predictions. By combining with the previous CDF measurement in the ℓ+jet channel AALTONEN 13X, $A_{FB}^{\ell} = 0.098 {}^{+0.028}_{-0.026}$ is obtained. The combined result is about two sigma larger than the SM prediction of $A_{FB}^{\ell} = 0.038 \pm 0.003$.

[4] Based on 9.7 fb^{-1} of $p\bar{p}$ data at $\sqrt{s} = 1.96$ TeV. The asymmetry is corrected for the production level for events with $|y_l| < 1.5$. Asymmetry as functions of $E_T(\ell)$ and $|y_l|$ are given in Figs. 7 and 8, respectively. Combination with the asymmetry measured in the dilepton channel [ABAZOV 13P] gives $A_{FB}^{\ell} = 4.2 \pm 2.0 \pm 1.4$ %, in agreement with the SM prediction of 2.0%.

[5] Based on 9.7 fb^{-1} of data of $p\bar{p}$ data at $\sqrt{s}$=1.96 TeV. The measured asymmetry is in agreement with the SM predictions of 8.8 ± 0.9 % [BERNREUTHER 12], which includes the EW effects. The dependences of the asymmetry on $|y(t) - y(\bar{t})|$ and $m_{t\bar{t}}$ are shown in Figs. 9 and 10, respectively.

[6] Based on 9.4 fb^{-1} of data. Reported A_{FB} values come from the determination of a_i coefficients of $d\sigma/d(\cos\theta_t) = \Sigma_i\ a_i P_i(\cos(\theta_t))$ measurement. The result of $a_1/a_0 = (40 \pm 12)$% seems higher than the NLO SM prediction of $(15 {}^{+7}_{-3})$%.

[7] Based on 9.4 fb^{-1} of data. The quoted result is the asymmetry at the parton level.

[8] Based on 9.4 fb^{-1} of data. The observed asymmetry is to be compared with the SM prediction of $A_{FB}^{\ell} = 0.038 \pm 0.003$.

[9] Based on 5.4 fb^{-1} of data. ABAZOV 13A studied the dilepton channel of the $t\bar{t}$ events and measured the leptonic forward-backward asymmetry to be $A_{FB}^{\ell} = 5.8 \pm 5.1 \pm 1.3$%, which is consistent with the SM (QCD+EW) prediction of 4.7 ± 0.1%. The result is obtained after combining the measurement (15.2 ± 4.0%) in the ℓ + jets channel ABAZOV 11AH. The top quark helicity is measured by using the neutrino weighting method to be consistent with zero in both dilepton and ℓ + jets channels.

[10] Based on 5.3 fb^{-1} of data. The error is statistical and systematic combined. Events with lepton + $\not\!\!E_T$ + $\geq$ 4jets($\geq$ 1b) are used. AALTONEN 11F also measures the asymmetry as a function of the rapidity difference $|y_t - y_{\bar{t}}|$. The NLO QCD predictions [MCFM] are (4.0 ± 0.6)% and (8.8 ± 1.3)% for $m_{t\bar{t}} <$ 450 and $>$ 450 GeV, respectively.

[11] Based on 5.4 fb^{-1} of data. The error is statistical and systematic combined. The quoted asymmetry is obtained after unfolding to be compared with the MC@NLO prediction of (5.0 ± 0.1)%. No significant difference between the $m_{t\bar{t}} <$ 450 and $>$ 450 GeV data samples is found. A corrected asymmetry based on the lepton from a top quark decay of (15.2 ± 4.0)% is measured to be compared to the MC@NLO prediction of (2.1 ± 0.1)%.

[12] Result is based on 1.9 fb^{-1} of data. The FB asymmetry in the $t\bar{t}$ events has been measured in the ℓ + jets mode, where the lepton charge is used as the flavor tag. The asymmetry in the $p\bar{p}$ frame is defined in terms of $\cos(\theta)$ of hadronically decaying t-quark momentum, whereas that in the $t\bar{t}$ frame is defined in terms of the t and $\bar{t}$ rapidity difference. The results are consistent ($\leq$ 2 σ) with the SM predictions.

[13] Result is based on 0.9 fb^{-1} of data. The asymmetry in the number of $t\bar{t}$ events with $y_t > y_{\bar{t}}$ and those with $y_t < y_{\bar{t}}$ has been measured in the lepton + jets final state. The observed value is consistent with the SM prediction of 0.8% by MC@NLO, and an upper bound on the $Z' \rightarrow t\bar{t}$ contribution for the SM Z-like couplings is given in in Fig. 2 for 350 GeV $< m_{Z'} <$ 1 TeV.

t-Quark Electric Charge

VALUE	DOCUMENT ID		TECN	COMMENT
0.64±0.02±0.08	[1] AAD	13AY	ATLS	ℓ+$\not{E}_T$+ $\geq$ 4 jets ($\geq$ 1 b)
• • • We do not use the following data for averages, fits, limits, etc. • • •				
	[2] ABAZOV	14D	D0	ℓ+$\not{E}_T$+ $\geq$ 4 jets ($\geq$ 2 b)
	[3] AALTONEN	13J	CDF	$p\overline{p}$ at 1.96 TeV
	[4] AALTONEN	10S	CDF	Repl. by AALTONEN 13J
	[5] ABAZOV	07C	D0	fraction of $\vert q\vert$=4e/3 pair

[1] AAD 13AY result is based on 2.05 fb^{-1} of pp data at $\sqrt{s}$ = 7 TeV, the result is obtained by reconstructing $t\overline{t}$ events in the lepton + jets final state, where b-jet charges are tagged by the jet-charge algorithm. This measurement excludes the charge $-4/3$ assignment to the top quark at more than 8 standard deviations.

[2] ABAZOV 14D result is based on 5.3 fb^{-1} of $p\overline{p}$ data at $\sqrt{s}$=1.96 TeV. The electric charge of $b+W$ system in $t\overline{t}$ candidate events is measured from the charges of the leptons from W decay and in b jets. Under the assumption that the $b+W$ system consists of the sum of the top quark and the charge $-4/3$ quark b'(-4/3) of the same mass, the top quark fraction is found to be f = 0.88 ± 0.13 (stat) ±0.11 (syst), or the upper bound for the b'(-4/3) contamination of $1-f$ < 0.46 (95% CL).

[3] AALTONEN 13J excludes the charge $-4/3$ assignment to the top quark at 99% CL, using 5.6 fb^{-1} of data in $p\overline{p}$ collisions at $\sqrt{s}$ = 1.96 TeV. Result is obtained by reconstructing $t\overline{t}$ events in the lepton + jets final state, where b-jet charges are tagged by the jet-charge algorithm.

[4] AALTONEN 10S excludes the charge $-4/3$ assignment for the top quark [CHANG 99] at 95%CL, using 2.7 fb^{-1} of data in $p\overline{p}$ collisions at $\sqrt{s}$ = 1.96 TeV. Result is obtained by reconstructing $t\overline{t}$ events in the lepton + jets final state, where b-jet charges are tagged by the SLT (soft lepton tag) algorithm.

[5] ABAZOV 07C reports an upper limit ρ < 0.80 (90% CL) on the fraction ρ of exotic quark pairs $Q\overline{Q}$ with electric charge $\vert q\vert$ = 4e/3 in $t\overline{t}$ candidate events with high p_T lepton, missing E_T and $\geq$ 4 jets. The result is obtained by measuring the fraction of events in which the quark pair decays into W^-+b and $W^++\overline{b}$, where b and $\overline{b}$ jets are discriminated by using the charge and momenta of tracks within the jet cones. The maximum CL at which the model of CHANG 99 can be excluded is 92%. Based on 370 pb^{-1} of data at $\sqrt{s}$ = 1.96 TeV.

t-Quark REFERENCES

AABOUD	18H	JHEP 1801 063	M. Aaboud *et al.*	(ATLAS Collab.)
AALTONEN	18	PRL 120 042001	T. Aaltonen *et al.*	(CDF and D0 Collabs.)
AABOUD	17AH	JHEP 1709 118	M. Aaboud *et al.*	(ATLAS Collab.)
AABOUD	17AV	JHEP 1710 129	M. Aaboud *et al.*	(ATLAS Collab.)
AABOUD	17BB	JHEP 1712 017	M. Aaboud *et al.*	(ATLAS Collab.)
AABOUD	17BC	EPJ C77 804	M. Aaboud *et al.*	(ATLAS Collab.)
AABOUD	17G	JHEP 1703 113	M. Aaboud *et al.*	(ATLAS Collab.)
AABOUD	17H	JHEP 1704 086	M. Aaboud *et al.*	(ATLAS Collab.)
AABOUD	17I	JHEP 1704 124	M. Aaboud *et al.*	(ATLAS Collab.)
AABOUD	17T	EPJ C77 531	M. Aaboud *et al.*	(ATLAS Collab.)
AABOUD	17Z	PR D95 072003	M. Aaboud *et al.*	(ATLAS Collab.)
ABAZOV	17	PR D95 011101	V.M. Abazov *et al.*	(D0 Collab.)
ABAZOV	17B	PR D95 112004	V.M. Abazov *et al.*	(D0 Collab.)
CHATRCHYAN	17	PL B770 50	S. Chatrchyan *et al.*	(CMS Collab.)
KHACHATRY...	17B	EPJ C77 15	V. Khachatryan *et al.*	(CMS Collab.)
KHACHATRY...	17G	JHEP 1702 028	V. Khachatryan *et al.*	(CMS Collab.)
KHACHATRY...	17I	JHEP 1702 079	V. Khachatryan *et al.*	(CMS Collab.)
KHACHATRY...	17N	EPJ C77 172	V. Khachatryan *et al.*	(CMS Collab.)
SIRUNYAN	17AA	PL B772 752	A.M. Sirunyan *et al.*	(CMS Collab.)
SIRUNYAN	17AB	PL B772 336	A.M. Sirunyan *et al.*	(CMS Collab.)
SIRUNYAN	17E	JHEP 1707 003	A.M. Sirunyan *et al.*	(CMS Collab.)
SIRUNYAN	17L	EPJ C77 354	A.M. Sirunyan *et al.*	(CMS Collab.)
SIRUNYAN	17N	EPJ C77 467	A.M. Sirunyan *et al.*	(CMS Collab.)
SIRUNYAN	17O	PR D96 032002	A.M. Sirunyan *et al.*	(CMS Collab.)
SIRUNYAN	17W	JHEP 1709 051	A.M. Sirunyan *et al.*	(CMS Collab.)
AABOUD	16R	PL B761 136	M. Aaboud *et al.*	(ATLAS Collab.)
AABOUD	16T	PL B761 350	M. Aaboud *et al.*	(ATLAS Collab.)
AAD	16AE	PR D94 032006	G. Aad *et al.*	(ATLAS Collab.)
AAD	16AK	JHEP 1604 023	G. Aad *et al.*	(ATLAS Collab.)
AAD	16AS	EPJ C76 55	G. Aad *et al.*	(ATLAS Collab.)
AAD	16AZ	EPJ C76 87	G. Aad *et al.*	(ATLAS Collab.)
AAD	16B	JHEP 1601 064	G. Aad *et al.*	(ATLAS Collab.)
AAD	16BK	EPJ C76 642	G. Aad *et al.*	(ATLAS Collab.)
AAD	16D	EPJ C76 12	G. Aad *et al.*	(ATLAS Collab.)
AAD	16T	PL B756 52	G. Aad *et al.*	(ATLAS Collab.)
AAD	16U	PL B756 228	G. Aad *et al.*	(ATLAS Collab.)
AALTONEN	16	PR D93 032011	T. Aaltonen *et al.*	(CDF Collab.)
ABAZOV	16	PL B752 18	V.M. Abazov *et al.*	(D0 Collab.)
ABAZOV	16A	PL B757 199	V.M. Abazov *et al.*	(D0 Collab.)
ABAZOV	16D	PR D94 032004	V.M. Abazov *et al.*	(D0 Collab.)
ABAZOV	16F	PR D94 092004	V.M. Abazov *et al.*	(D0 Collab.)
KHACHATRY...	16AD	PL B760 365	V. Khachatryan *et al.*	(CMS Collab.)
KHACHATRY...	16AH	PR D93 034014	V. Khachatryan *et al.*	(CMS Collab.)
KHACHATRY...	16AI	PR D93 052007	V. Khachatryan *et al.*	(CMS Collab.)
KHACHATRY...	16AK	PR D93 072004	V. Khachatryan *et al.*	(CMS Collab.)
KHACHATRY...	16AL	PR D93 092006	V. Khachatryan *et al.*	(CMS Collab.)
KHACHATRY...	16AS	JHEP 1604 035	V. Khachatryan *et al.*	(CMS Collab.)
KHACHATRY...	16AW	JHEP 1608 029	V. Khachatryan *et al.*	(CMS Collab.)
KHACHATRY...	16AZ	JHEP 1609 027	V. Khachatryan *et al.*	(CMS Collab.)
KHACHATRY...	16BC	EPJ C76 128	V. Khachatryan *et al.*	(CMS Collab.)
KHACHATRY...	16BJ	EPJ C76 439	V. Khachatryan *et al.*	(CMS Collab.)
KHACHATRY...	16BO	JHEP 1604 073	V. Khachatryan *et al.*	(CMS Collab.)
KHACHATRY...	16BU	PL B762 512	V. Khachatryan *et al.*	(CMS Collab.)
KHACHATRY...	16CB	JHEP 1612 123	V. Khachatryan *et al.*	(CMS Collab.)
KHACHATRY...	16J	PRL 116 052002	V. Khachatryan *et al.*	(CMS Collab.)
KHACHATRY...	16T	PL B757 154	V. Khachatryan *et al.*	(CMS Collab.)
KHACHATRY...	16X	PL B758 321	V. Khachatryan *et al.*	(CMS Collab.)
TEVEWWG	16	arXiv:1608.01881	Tevatron Electroweak Working Group	
AAD	15	PL B740 222	G. Aad *et al.*	(ATLAS Collab.)
AAD	15A	PL B740 118	G. Aad *et al.*	(ATLAS Collab.)
AAD	15AJ	JHEP 1505 061	G. Aad *et al.*	(ATLAS Collab.)
AAD	15AR	JHEP 1508 105	G. Aad *et al.*	(ATLAS Collab.)
AAD	15AW	EPJ C75 158	G. Aad *et al.*	(ATLAS Collab.)
AAD	15BF	EPJ C75 330	G. Aad *et al.*	(ATLAS Collab.)
AAD	15BO	PR D91 052005	G. Aad *et al.*	(ATLAS Collab.)
AAD	15BP	PR D91 112013	G. Aad *et al.*	(ATLAS Collab.)
AAD	15BW	JHEP 1510 121	G. Aad *et al.*	(ATLAS Collab.)
AAD	15BY	JHEP 1510 150	G. Aad *et al.*	(ATLAS Collab.)
AAD	15CC	PR D92 072005	G. Aad *et al.*	(ATLAS Collab.)
AAD	15CO	JHEP 1512 061	G. Aad *et al.*	(ATLAS Collab.)
AAD	15D	JHEP 1501 020	G. Aad *et al.*	(ATLAS Collab.)
AAD	15J	PRL 114 142001	G. Aad *et al.*	(ATLAS Collab.)
AAIJ	15R	PRL 115 112001	R. Aaij *et al.*	(LHCb Collab.)
AALTONEN	15D	PR D92 032003	T. Aaltonen *et al.*	(CDF Collab.)
AALTONEN	15H	PRL 115 152003	T. Aaltonen *et al.*	(CDF, D0 Collab.)
ABAZOV	15G	PR D91 112003	V.M. Abazov *et al.*	(D0 Collab.)
ABAZOV	15K	PR D92 052007	V.M. Abazov *et al.*	(D0 Collab.)
CHATRCHYAN	15	EPJ C75 216 (errat.)	S. Chatrchyan *et al.*	(CMS Collab.)
AAD	14	PL B728 363	G. Aad *et al.*	(ATLAS Collab.)
AAD	14AA	JHEP 1406 008	G. Aad *et al.*	(ATLAS Collab.)
AAD	14AY	EPJ C74 3109	G. Aad *et al.*	(ATLAS Collab.)
AAD	14BB	PR D90 112016	G. Aad *et al.*	(ATLAS Collab.)
AAD	14BI	PR D90 112006	G. Aad *et al.*	(ATLAS Collab.)
AAD	14I	JHEP 1402 107	G. Aad *et al.*	(ATLAS Collab.)
AALTONEN	14A	PR D89 091101	T. Aaltonen *et al.*	(CDF Collab.)
AALTONEN	14F	PRL 113 042001	T. Aaltonen *et al.*	(CDF Collab.)
Also		PRL 117 199901 (errat.)	T. Aaltonen *et al.*	(CDF Collab.)
AALTONEN	14G	PRL 112 221801	T. Aaltonen *et al.*	(CDF Collab.)
AALTONEN	14H	PR D89 072001	T. Aaltonen *et al.*	(CDF, D0 Collab.)
AALTONEN	14K	PRL 112 231805	T. Aaltonen *et al.*	(CDF Collab.)
AALTONEN	14L	PRL 112 231804	T. Aaltonen *et al.*	(CDF Collab.)
AALTONEN	14M	PRL 112 231803	T. Aaltonen *et al.*	(CDF, D0 Collab.)
AALTONEN	14N	PR D90 091101	T. Aaltonen *et al.*	(CDF Collab.)
AALTONEN	14O	PRL 113 261804	T. Aaltonen *et al.*	(CDF Collab.)
ABAZOV	14C	PRL 113 032002	V.M. Abazov *et al.*	(D0 Collab.)
Also		PR D91 112003	V.M. Abazov *et al.*	(D0 Collab.)
ABAZOV	14D	PR D90 051101	V.M. Abazov *et al.*	(D0 Collab.)
ABAZOV	14G	PR D90 072001	V.M. Abazov *et al.*	(D0 Collab.)
ABAZOV	14H	PR D90 072011	V.M. Abazov *et al.*	(D0 Collab.)
ABAZOV	14K	PR D90 092006	V.M. Abazov *et al.*	(D0 Collab.)
CHATRCHYAN	14	PL B728 496	S. Chatrchyan *et al.*	(CMS Collab.)
CHATRCHYAN	14AC	PRL 112 231802	S. Chatrchyan *et al.*	(CMS Collab.)
CHATRCHYAN	14AE	EPJ C74 3014	S. Chatrchyan *et al.*	(CMS Collab.)
Also		EPJ C75 216 (errat.)	S. Chatrchyan *et al.*	(CMS Collab.)
CHATRCHYAN	14C	EPJ C74 2758	S. Chatrchyan *et al.*	(CMS Collab.)
CHATRCHYAN	14D	JHEP 1404 191	S. Chatrchyan *et al.*	(CMS Collab.)
CHATRCHYAN	14F	JHEP 1402 024	S. Chatrchyan *et al.*	(CMS Collab.)
CHATRCHYAN	14O	PL B731 173	S. Chatrchyan *et al.*	(CMS Collab.)
CHATRCHYAN	14R	PR D90 032006	S. Chatrchyan *et al.*	(CMS Collab.)
CHATRCHYAN	14S	PRL 112 171802	S. Chatrchyan *et al.*	(CMS Collab.)
KHACHATRY...	14E	PL B736 33	V. Khachartryan *et al.*	(CMS Collab.)
KHACHATRY...	14F	JHEP 1406 090	V. Khachartryan *et al.*	(CMS Collab.)
KHACHATRY...	14H	JHEP 1409 087	V. Khachartryan *et al.*	(CMS Collab.)
KHACHATRY...	14K	PL B738 526 (errat.)	S. Chatrchyan *et al.*	(CMS Collab.)
KHACHATRY...	14N	EPJ C74 3060	V. Khachartryan *et al.*	(CMS Collab.)
KHACHATRY...	14Q	PR D90 112013	V. Khachatryan *et al.*	(CMS Collab.)
KHACHATRY...	14R	JHEP 1411 154	V. Khachartryan *et al.*	(CMS Collab.)
KHACHATRY...	14S	PL B739 23	V. Khachartryan *et al.*	(CMS Collab.)
AAD	13AY	JHEP 1311 031	G. Aad *et al.*	(ATLAS Collab.)
AAD	13BE	PRL 111 232002	G. Aad *et al.*	(ATLAS Collab.)
AAD	13X	EPJ C73 2328	G. Aad *et al.*	(ATLAS Collab.)
AALTONEN	13AB	PR D88 091103	T. Aaltonen *et al.*	(CDF Collab.)
AALTONEN	13AD	PRL 111 182002	T. Aaltonen *et al.*	(CDF Collab.)
AALTONEN	13D	PR D87 031104	T. Aaltonen *et al.*	(CDF Collab.)
AALTONEN	13E	PR D87 052013	T. Aaltonen *et al.*	(CDF Collab.)
AALTONEN	13G	PR D87 111101	T. Aaltonen *et al.*	(CDF Collab.)
AALTONEN	13H	PR D88 011101	T. Aaltonen *et al.*	(CDF Collab.)
AALTONEN	13J	PR D88 032003	T. Aaltonen *et al.*	(CDF Collab.)
AALTONEN	13S	PR D87 092002	T. Aaltonen *et al.*	(CDF Collab.)
AALTONEN	13X	PR D88 072003	T. Aaltonen *et al.*	(CDF Collab.)
AALTONEN	13Z	PRL 111 202001	T. Aaltonen *et al.*	(CDF Collab.)
ABAZOV	13A	PR D87 011103	V.M. Abazov *et al.*	(D0 Collab.)
ABAZOV	13O	PL B726 656	V.M. Abazov *et al.*	(D0 Collab.)
ABAZOV	13P	PR D88 112002	V.M. Abazov *et al.*	(D0 Collab.)
CHATRCHYAN	13AY	JHEP 1305 065	S. Chatrchyan *et al.*	(CMS Collab.)
CHATRCHYAN	13BB	PL B720 83	S. Chatrchyan *et al.*	(CMS Collab.)
CHATRCHYAN	13BE	EPJ C73 2386	S. Chatrchyan *et al.*	(CMS Collab.)
CHATRCHYAN	13BH	JHEP 1310 167	S. Chatrchyan *et al.*	(CMS Collab.)
CHATRCHYAN	13C	PRL 110 022003	S. Chatrchyan *et al.*	(CMS Collab.)
CHATRCHYAN	13F	PL B718 1252	S. Chatrchyan *et al.*	(CMS Collab.)
CHATRCHYAN	13S	EPJ C73 2494	S. Chatrchyan *et al.*	(CMS Collab.)
AAD	12B	PL B707 459	G. Aad *et al.*	(ATLAS Collab.)
AAD	12BE	JHEP 1204 069	G. Aad *et al.*	(ATLAS Collab.)
AAD	12BF	JHEP 1205 059	G. Aad *et al.*	(ATLAS Collab.)
AAD	12BG	JHEP 1206 088	G. Aad *et al.*	(ATLAS Collab.)
AAD	12BK	EPJ C72 2039	G. Aad *et al.*	(ATLAS Collab.)
AAD	12BL	EPJ C72 2043	G. Aad *et al.*	(ATLAS Collab.)
AAD	12BO	PL B711 244	G. Aad *et al.*	(ATLAS Collab.)
AAD	12BP	PL B712 351	G. Aad *et al.*	(ATLAS Collab.)
AAD	12BT	JHEP 1209 139	G. Aad *et al.*	(ATLAS Collab.)
AAD	12CG	PL B717 89	G. Aad *et al.*	(ATLAS Collab.)
AAD	12CH	PL B717 330	G. Aad *et al.*	(ATLAS Collab.)
AAD	12I	EPJ C72 2046	G. Aad *et al.*	(ATLAS Collab.)
AALTONEN	12AI	PRL 109 152003	T. Aaltonen *et al.*	(CDF Collab.)
AALTONEN	12AL	PRL 109 192001	T. Aaltonen *et al.*	(CDF Collab.)
AALTONEN	12AP	PR D86 092003	T. Aaltonen *et al.*	(CDF, D0 Collab.)
AALTONEN	12G	PL B714 24	T. Aaltonen *et al.*	(CDF Collab.)
AALTONEN	12Z	PR D85 071106	T. Aaltonen *et al.*	(CDF, D0 Collab.)
ABAZOV	12AB	PR D86 051103	V.M. Abazov *et al.*	(D0 Collab.)
ABAZOV	12B	PRL 108 032004	V.M. Abazov *et al.*	(D0 Collab.)
ABAZOV	12E	PL B708 21	V.M. Abazov *et al.*	(D0 Collab.)
ABAZOV	12I	PL B713 165	V.M. Abazov *et al.*	(D0 Collab.)
ABAZOV	12T	PR D85 091104	V.M. Abazov *et al.*	(D0 Collab.)
BERNREUTH...	12	PR D86 034026	W. Bernreuther, Z.-G. Si	(AACH, SHDN)
CHATRCHYAN	12AC	PR D85 112007	S. Chatrchyan *et al.*	(CMS Collab.)
CHATRCHYAN	12AX	JHEP 1211 067	S. Chatrchyan *et al.*	(CMS Collab.)
CHATRCHYAN	12BA	EPJ C72 2202	S. Chatrchyan *et al.*	(CMS Collab.)
CHATRCHYAN	12BB	PL B717 129	S. Chatrchyan *et al.*	(CMS Collab.)
CHATRCHYAN	12BP	JHEP 1212 105	S. Chatrchyan *et al.*	(CMS Collab.)
CHATRCHYAN	12BQ	JHEP 1212 035	S. Chatrchyan *et al.*	(CMS Collab.)
CHATRCHYAN	12BS	PL B709 28	S. Chatrchyan *et al.*	(CMS Collab.)
CHATRCHYAN	12Y	JHEP 1206 109	S. Chatrchyan *et al.*	(CMS Collab.)
AAD	11A	EPJ C71 1577	G. Aad *et al.*	(ATLAS Collab.)
AALTONEN	11AC	PR D84 071105	T. Aaltonen *et al.*	(CDF Collab.)
AALTONEN	11AK	PRL 107 232002	T. Aaltonen *et al.*	(CDF Collab.)
AALTONEN	11AR	PR D83 031104	T. Aaltonen *et al.*	(CDF Collab.)
AALTONEN	11D	PR D83 071102	T. Aaltonen *et al.*	(CDF Collab.)
AALTONEN	11E	PR D83 111101	T. Aaltonen *et al.*	(CDF Collab.)
AALTONEN	11F	PR D83 112003	T. Aaltonen *et al.*	(CDF Collab.)
AALTONEN	11K	PRL 106 152001	T. Aaltonen *et al.*	(CDF Collab.)
AALTONEN	11T	PL B698 371	T. Aaltonen *et al.*	(CDF Collab.)
AALTONEN	11W	PR D84 031101	T. Aaltonen *et al.*	(CDF Collab.)
AALTONEN	11Y	PR D84 032003	T. Aaltonen *et al.*	(CDF Collab.)
AALTONEN	11Z	PR D84 031104	T. Aaltonen *et al.*	(CDF Collab.)
ABAZOV	11A	PL B695 88	V.M. Abazov *et al.*	(D0 Collab.)
ABAZOV	11AA	PL B705 313	V.M. Abazov *et al.*	(D0 Collab.)
ABAZOV	11AD	PR D84 112001	V.M. Abazov *et al.*	(D0 Collab.)
ABAZOV	11AE	PRL 107 032001	V.M. Abazov *et al.*	(D0 Collab.)
ABAZOV	11AF	PL B702 16	V.M. Abazov *et al.*	(D0 Collab.)
ABAZOV	11AH	PR D84 112005	V.M. Abazov *et al.*	(D0 Collab.)
ABAZOV	11B	PRL 106 022001	V.M. Abazov *et al.*	(D0 Collab.)
ABAZOV	11C	PR D83 032009	V.M. Abazov *et al.*	(D0 Collab.)
ABAZOV	11E	PR D84 012008	V.M. Abazov *et al.*	(D0 Collab.)
ABAZOV	11M	PL B701 313	V.M. Abazov *et al.*	(D0 Collab.)

Quark Particle Listings

t, b' (Fourth Generation) Quark

ABAZOV 11P PR D84 032004 V.M. Abazov *et al.* (D0 Collab.)
ABAZOV 11R PRL 107 082004 V.M. Abazov *et al.* (D0 Collab.)
ABAZOV 11S PL B703 422 V.M. Abazov *et al.* (D0 Collab.)
ABAZOV 11T PR D84 052005 V.M. Abazov *et al.* (D0 Collab.)
ABAZOV 11X PRL 107 121802 V.M. Abazov *et al.* (D0 Collab.)
ABAZOV 11Z PL B704 403 V.M. Abazov *et al.* (D0 Collab.)
CHATRCHYAN 11AA EPJ C71 1721 S. Chatrchyan *et al.* (CMS Collab.)
CHATRCHYAN 11F JHEP 1107 049 S. Chatrchyan *et al.* (CMS Collab.)
CHATRCHYAN 11R PRL 107 091802 S. Chatrchyan *et al.* (CMS Collab.)
CHATRCHYAN 11Z PR D84 092004 S. Chatrchyan *et al.* (CMS Collab.)
KHACHATRY... 11A PL B695 424 V. Khachatryan *et al.* (CMS Collab.)
AALTONEN 10AA PR D82 052002 T. Aaltonen *et al.* (CDF Collab.)
AALTONEN 10AB PR D82 112005 T. Aaltonen *et al.* (CDF Collab.)
AALTONEN 10AC PRL 105 232003 T. Aaltonen *et al.* (CDF Collab.)
AALTONEN 10AE PRL 105 252001 T. Aaltonen *et al.* (CDF Collab.)
AALTONEN 10C PR D81 031102 T. Aaltonen *et al.* (CDF Collab.)
AALTONEN 10D PR D81 032002 T. Aaltonen *et al.* (CDF Collab.)
AALTONEN 10E PR D81 052011 T. Aaltonen *et al.* (CDF Collab.)
AALTONEN 10Q PRL 105 042002 T. Aaltonen *et al.* (CDF Collab.)
AALTONEN 10S PRL 105 101801 T. Aaltonen *et al.* (CDF Collab.)
AALTONEN 10U PR D81 072003 T. Aaltonen *et al.* (CDF Collab.)
AALTONEN 10V PR D81 092002 T. Aaltonen *et al.* (CDF Collab.)
AALTONEN 10W PRL 105 012001 T. Aaltonen *et al.* (CDF Collab.)
ABAZOV 10 PL B682 363 V.M. Abazov *et al.* (D0 Collab.)
ABAZOV 10I PR D82 032002 V.M. Abazov *et al.* (D0 Collab.)
ABAZOV 10J PL B690 5 V.M. Abazov *et al.* (D0 Collab.)
ABAZOV 10K PL B693 81 V.M. Abazov *et al.* (D0 Collab.)
ABAZOV 10Q PR D82 071102 V.M. Abazov *et al.* (D0 Collab.)
AHRENS 10 JHEP 1009 097 V. Ahrens *et al.* (MANZ, HEIDH)
AHRENS 10A NPBPS 205-206 48 V. Ahrens *et al.* (MANZ, HEIDH)
AALTONEN 09AD PR D79 112007 T. Aaltonen *et al.* (CDF Collab.)
AALTONEN 09AK PR D80 051104 T. Aaltonen *et al.* (CDF Collab.)
AALTONEN 09AL PR D80 052001 T. Aaltonen *et al.* (CDF Collab.)
AALTONEN 09AT PRL 103 092002 T. Aaltonen *et al.* (CDF Collab.)
AALTONEN 09F PR D79 031101 T. Aaltonen *et al.* (CDF Collab.)
AALTONEN 09H PR D79 052007 T. Aaltonen *et al.* (CDF Collab.)
AALTONEN 09J PR D79 072001 T. Aaltonen *et al.* (CDF Collab.)
AALTONEN 09K PR D79 072010 T. Aaltonen *et al.* (CDF Collab.)
AALTONEN 09L PR D79 092005 T. Aaltonen *et al.* (CDF Collab.)
AALTONEN 09M PRL 102 042001 T. Aaltonen *et al.* (CDF Collab.)
AALTONEN 09N PRL 102 151801 T. Aaltonen *et al.* (CDF Collab.)
AALTONEN 09O PRL 102 152001 T. Aaltonen *et al.* (CDF Collab.)
AALTONEN 09Q PL B674 160 T. Aaltonen *et al.* (CDF Collab.)
AALTONEN 09X PR D79 072005 T. Aaltonen *et al.* (CDF Collab.)
AARON 09A PL B678 450 F.D. Aaron *et al.* (H1 Collab.)
ABAZOV 09AA PRL 103 132001 V.M. Abazov *et al.* (D0 Collab.)
ABAZOV 09AG PR D80 071102 V.M. Abazov *et al.* (D0 Collab.)
ABAZOV 09AH PR D80 092006 V.M. Abazov *et al.* (D0 Collab.)
ABAZOV 09J PRL 102 092002 V.M. Abazov *et al.* (D0 Collab.)
ABAZOV 09R PL B679 177 V.M. Abazov *et al.* (D0 Collab.)
ABAZOV 09Z PRL 103 092001 V.M. Abazov *et al.* (D0 Collab.)
LANGENFELD 09 PR D80 054009 U. Langenfeld, S. Moch, P. Uwer
AALTONEN 08AB PRL 101 202001 T. Aaltonen *et al.* (CDF Collab.)
AALTONEN 08AD PRL 101 192002 T. Aaltonen *et al.* (CDF Collab.)
AALTONEN 08AG PR D78 111101 T. Aaltonen *et al.* (CDF Collab.)
AALTONEN 08AH PRL 101 252001 T. Aaltonen *et al.* (CDF Collab.)
AALTONEN 08C PRL 100 062005 T. Aaltonen *et al.* (CDF Collab.)
ABAZOV 08AH PRL 101 182001 V.M. Abazov *et al.* (D0 Collab.)
ABAZOV 08AI PRL 101 221801 V.M. Abazov *et al.* (D0 Collab.)
ABAZOV 08B PRL 100 062004 V.M. Abazov *et al.* (D0 Collab.)
ABAZOV 08I PR D78 012005 V.M. Abazov *et al.* (D0 Collab.)
ABAZOV 08L PRL 100 142002 V.M. Abazov *et al.* (D0 Collab.)
ABAZOV 08M PRL 100 192003 V.M. Abazov *et al.* (D0 Collab.)
ABAZOV 08N PRL 100 192004 V.M. Abazov *et al.* (D0 Collab.)
ABULENCIA 08 PR D78 012003 A. Abulencia *et al.* (CDF Collab.)
CACCIARI 08 JHEP 0809 127 M. Cacciari *et al.*
KIDONAKIS 08 PR D78 074005 N. Kidonakis, R. Vogt
MOCH 08 PR D78 034003 S. Moch, P. Uwer (BERL, KARLE)
AALTONEN 07 PRL 98 142001 T. Aaltonen *et al.* (CDF Collab.)
AALTONEN 07B PR D75 111103 T. Aaltonen *et al.* (CDF Collab.)
AALTONEN 07D PR D76 072009 T. Aaltonen *et al.* (CDF Collab.)
AALTONEN 07I PRL 99 182002 T. Aaltonen *et al.* (CDF Collab.)
ABAZOV 07C PRL 98 041801 V.M. Abazov *et al.* (D0 Collab.)
ABAZOV 07D PR D75 031102 V.M. Abazov *et al.* (D0 Collab.)
ABAZOV 07F PR D75 092001 V.M. Abazov *et al.* (D0 Collab.)
ABAZOV 07H PRL 98 181802 V.M. Abazov *et al.* (D0 Collab.)
ABAZOV 07O PR D76 052006 V.M. Abazov *et al.* (D0 Collab.)
ABAZOV 07P PR D76 072007 V.M. Abazov *et al.* (D0 Collab.)
ABAZOV 07R PR D76 092007 V.M. Abazov *et al.* (D0 Collab.)
ABAZOV 07V PRL 99 191802 V.M. Abazov *et al.* (D0 Collab.)
ABAZOV 07W PL B655 7 V.M. Abazov *et al.* (D0 Collab.)
ABULENCIA 07D PR D75 031105 A. Abulencia *et al.* (CDF Collab.)
ABULENCIA 07G PRL 98 072001 A. Abulencia *et al.* (CDF Collab.)
ABULENCIA 07I PR D75 052001 A. Abulencia *et al.* (CDF Collab.)
ABULENCIA 07J PR D75 071102 A. Abulencia *et al.* (CDF Collab.)
ABAZOV 06K PL B639 616 V.M. Abazov *et al.* (D0 Collab.)
ABAZOV 06U PR D74 092005 V.M. Abazov *et al.* (D0 Collab.)
ABAZOV 06X PR D74 112004 V.M. Abazov *et al.* (D0 Collab.)
ABULENCIA 06D PRL 96 022004 A. Abulencia *et al.* (CDF Collab.)
Also PR D73 032003 A. Abulencia *et al.* (CDF Collab.)
Also PR D73 092002 A. Abulencia *et al.* (CDF Collab.)
ABULENCIA 06G PRL 96 152002 A. Abulencia *et al.* (CDF Collab.)
Also PR D74 032009 A. Abulencia *et al.* (CDF Collab.)
ABULENCIA 06R PL B639 172 A. Abulencia *et al.* (CDF Collab.)
ABULENCIA 06U PR D73 111103 A. Abulencia *et al.* (CDF Collab.)
ABULENCIA 06V PR D73 112006 A. Abulencia *et al.* (CDF Collab.)
ABULENCIA 06Z PRL 97 082004 A. Abulencia *et al.* (CDF Collab.)
ABULENCIA,A 06C PRL 96 202002 A. Abulencia *et al.* (CDF Collab.)
ABULENCIA,A 06E PR D74 072005 A. Abulencia *et al.* (CDF Collab.)
ABULENCIA,A 06F PR D74 072006 A. Abulencia *et al.* (CDF Collab.)
ABAZOV 05 PL B606 25 V.M. Abazov *et al.* (D0 Collab.)
ABAZOV 05G PL B617 1 V.M. Abazov *et al.* (D0 Collab.)
ABAZOV 05L PR D72 011104 V.M. Abazov *et al.* (D0 Collab.)
ABAZOV 05P PL B622 265 V.M. Abazov *et al.* (D0 Collab.)
Also PL B517 282 V.M. Abazov *et al.* (D0 Collab.)
Also PR D63 031101 B. Abbott *et al.* (D0 Collab.)
Also PR D75 092007 V.M. Abazov *et al.* (D0 Collab.)
ABAZOV 05Q PL B626 35 V.M. Abazov *et al.* (D0 Collab.)
ABAZOV 05R PL B626 55 V.M. Abazov *et al.* (D0 Collab.)
ABAZOV 05X PL B626 45 V.M. Abazov *et al.* (D0 Collab.)
ACOSTA 05A PRL 95 102002 D. Acosta *et al.* (CDF Collab.)
ACOSTA 05D PR D71 031101 D. Acosta *et al.* (CDF Collab.)
ACOSTA 05N PR D71 012005 D. Acosta *et al.* (CDF Collab.)
ACOSTA 05S PR D72 032002 D. Acosta *et al.* (CDF Collab.)
ACOSTA 05T PR D72 052003 D. Acosta *et al.* (CDF Collab.)
ACOSTA 05U PR D71 072005 D. Acosta *et al.* (CDF Collab.)
ACOSTA 05V PR D71 052003 D. Acosta *et al.* (CDF Collab.)
ABAZOV 04G NAT 429 638 V.M. Abazov *et al.* (D0 Collab.)
ABDALLAH 04C PL B590 21 J. Abdallah *et al.* (DELPHI Collab.)
ACOSTA 04H PR D69 052003 D. Acosta *et al.* (CDF Collab.)
ACOSTA 04I PRL 93 142001 D. Acosta *et al.* (CDF Collab.)
AKTAS 04 EPJ C33 9 A. Aktas *et al.* (H1 Collab.)
ABAZOV 03A PR D67 012004 V.M. Abazov *et al.* (D0 Collab.)
CHEKANOV 03 PL B559 153 S. Chekanov *et al.* (ZEUS Collab.)
ACHARD 02J PL B549 290 P. Achard *et al.* (L3 Collab.)
ACOSTA 02 PR D65 091102 D. Acosta *et al.* (CDF Collab.)
HEISTER 02Q PL B543 173 A. Heister *et al.* (ALEPH Collab.)
ABBIENDI 01T PL B521 181 G. Abbiendi *et al.* (OPAL Collab.)
AFFOLDER 01 PR D63 032003 T. Affolder *et al.* (CDF Collab.)
AFFOLDER 01A PR D64 032002 T. Affolder *et al.* (CDF Collab.)
AFFOLDER 01C PRL 86 3233 T. Affolder *et al.* (CDF Collab.)
AFFOLDER 00B PRL 84 216 T. Affolder *et al.* (CDF Collab.)
BARATE 00S PL B494 33 S. Barate *et al.* (ALEPH Collab.)
ABBOTT 99G PR D60 052001 B. Abbott *et al.* (D0 Collab.)
ABE 99B PRL 82 271 F. Abe *et al.* (CDF Collab.)
Also PRL 82 2808 (erratum) F. Abe *et al.* (CDF Collab.)
CHANG 99 PR D59 091503 D. Chang, W. Chang, E. Ma
ABBOTT 98D PRL 80 2063 B. Abbott *et al.* (D0 Collab.)
ABBOTT 98F PR D58 052001 B. Abbott *et al.* (D0 Collab.)
ABE 98E PRL 80 2767 F. Abe *et al.* (CDF Collab.)
ABE 98F PRL 80 2779 F. Abe *et al.* (CDF Collab.)
ABE 98G PRL 80 2525 F. Abe *et al.* (CDF Collab.)
BHAT 98B IJMP A13 5113 P.C. Bhat, H.B. Prosper, S.S. Snyder
ABACHI 97E PRL 79 1197 S. Abachi *et al.* (D0 Collab.)
ABE 97R PRL 79 1992 F. Abe *et al.* (CDF Collab.)
ABE 97V PRL 79 3585 F. Abe *et al.* (CDF Collab.)
PDG 96 PR D54 1 R. M. Barnett *et al.* (PDG Collab.)
ABACHI 95 PRL 74 2632 S. Abachi *et al.* (D0 Collab.)
ABE 95F PRL 74 2626 F. Abe *et al.* (CDF Collab.)
ABE 94E PR D50 2966 F. Abe *et al.* (CDF Collab.)
Also PRL 73 225 F. Abe *et al.* (CDF Collab.)

b' (4^{th} Generation) Quark, Searches for

$b'(-1/3)$-quark/hadron mass limits in $p\overline{p}$ and pp collisions

VALUE (GeV)	CL%	DOCUMENT ID		TECN	COMMENT
>730	95	[1] SIRUNYAN	17AU	CMS	
>880	95	[2] KHACHATRY...	16AN	CMS	B($b' \to Wt$) = 1
>620	95	[3] AAD	15BY	ATLS	Wt, Zb, hb modes
>730	95	[4] AAD	15BY	ATLS	B($b' \to Wt$) = 1
>810	95	[5] AAD	15Z	ATLS	
>755	95	[6] AAD	14AZ	ATLS	
>675	95	[7] CHATRCHYAN	13I	CMS	B($b' \to Wt$) = 1
>190	95	[8] ABAZOV	08X	D0	$c\tau$= 200mm
>190	95	[9] ACOSTA	03	CDF	quasi-stable b'

• • • We do not use the following data for averages, fits, limits, etc. • • •

<350, 580–635, >700	95	[10] AAD	15AR	ATLS	B($b' \to Hb$) = 1
>690	95	[11] AAD	15CN	ATLS	B($b' \to Wq$) = 1 (q=u)
>480	95	[12] AAD	12AT	ATLS	B($b' \to Wt$) = 1
>400	95	[13] AAD	12AU	ATLS	B($b' \to Zb$) = 1
>350	95	[14] AAD	12BC	ATLS	B($b' \to Wq$) = 1 (q=u,c)
>450	95	[15] AAD	12BE	ATLS	B($b' \to Wt$) = 1
>685	95	[16] CHATRCHYAN	12BH	CMS	$m_{t'} = m_{b'}$
>611	95	[17] CHATRCHYAN	12X	CMS	B($b' \to Wt$) = 1
>372	95	[18] AALTONEN	11J	CDF	$b' \to Wt$
>361	95	[19] CHATRCHYAN	11L	CMS	Repl. by CHATRCHYAN 12X
>338	95	[20] AALTONEN	10H	CDF	$b' \to Wt$
> 380–430	95	[21] FLACCO	10	RVUE	$m_{b'} > m_{t'}$
>268	95	[22,23] AALTONEN	07C	CDF	B($b' \to Zb$) = 1
>199	95	[24] AFFOLDER	00	CDF	NC: $b' \to Zb$
>148	95	[25] ABE	98N	CDF	NC: $b' \to Zb$ + vertex
> 96	95	[26] ABACHI	97D	D0	NC: $b' \to b\gamma$
>128	95	[27] ABACHI	95F	D0	$\ell\ell$ + jets, ℓ + jets
> 75	95	[28] MUKHOPAD...	93	RVUE	NC: $b' \to b\ell\ell$
> 85	95	[29] ABE	92	CDF	CC: $\ell\ell$
> 72	95	[30] ABE	90B	CDF	CC: e + μ
> 54	95	[31] AKESSON	90	UA2	CC: e + jets + $\not\!\!E_T$
> 43	95	[32] ALBAJAR	90B	UA1	CC: μ + jets
> 34	95	[33] ALBAJAR	88	UA1	CC: e or μ + jets

[1] SIRUNYAN 17AU based on 2.3–2.6 fb^{-1} of pp data at $\sqrt{s}$ = 13 TeV. Limit on pair-produced singlet vector-like b' using one lepton and several jets. The mass bound is given for a b' transforming as a singlet under the electroweak symmetry group, assumed to decay through W, Z or Higgs boson (which decays to jets) and to a third generation quark.

[2] KHACHATRYAN 16AN based on 19.7 fb^{-1} of pp data at $\sqrt{s}$ = 8 TeV. Limit on pair-produced vector-like b' using 1, 2, and >2 leptons as well as fully hadronic final states. Other limits depending on the branching fractions to tW, bZ, and bH are given in Table IX.

[3] AAD 15BY based on 20.3 fb^{-1} of pp data at $\sqrt{s}$ = 8 TeV. Limit on pair-produced vector-like b' assuming the branching fractions to W, Z, and h modes of the singlet model. Used events containing $\geq 2\ell + \not\!\!E_T + \geq 2$j (≥ 1 b) and including a same-sign lepton pair.

[4] AAD 15BY based on 20.3 fb^{-1} of pp data at $\sqrt{s}$ = 8 TeV. Limit on pair-produced chiral b'-quark. Used events containing $\geq 2\ell + \not\!\!E_T + \geq 2$j (≥ 1 b) and including a same-sign lepton pair.

[5] AAD 15Z based on 20.3 fb^{-1} of pp data at $\sqrt{s}$ = 8 TeV. Used events with $\ell + \not\!\!E_T + \geq 6$j (≥ 1 b) and at least one pair of jets from weak boson decay, primarily designed to select the signature $b'\overline{b}' \to WWt\overline{t} \to WWWWb\overline{b}$. This is a limit on pair-produced vector-like b'. The lower mass limit is 640 GeV for a vector-like singlet b'.

[6] Based on 20.3 fb^{-1} of pp data at $\sqrt{s}$ = 8 TeV. No significant excess over SM expectation is found in the search for pair production or single production of b' in the events with

dilepton from a high p_T Z and additional jets ($\geq$ 1 b-tag). If instead of B($b' \rightarrow Wt$) = 1 an electroweak singlet with B($b' \rightarrow Wt$) $\sim$ 0.45 is assumed, the limit reduces to 685 GeV.

[7] Based on 5.0 fb^{-1} of pp data at $\sqrt{s}$ = 7 TeV. CHATRCHYAN 13I looked for events with one isolated electron or muon, large $\not{E}_T$, and at least four jets with large transverse momenta, where one jet is likely to originate from the decay of a bottom quark.

[8] Result is based on 1.1 fb^{-1} of data. No signal is found for the search of long-lived particles which decay into final states with two electrons or photons, and upper bound on the cross section times branching fraction is obtained for 2 $<$ cτ $<$ 7000 mm; see Fig. 3. 95% CL excluded region of b' lifetime and mass is shown in Fig. 4.

[9] ACOSTA 03 looked for long-lived fourth generation quarks in the data sample of 90 pb^{-1} of $\sqrt{s}$=1.8 TeV $p\overline{p}$ collisions by using the muon-like penetration and anomalously high ionization energy loss signature. The corresponding lower mass bound for the charge (2/3)e quark (t') is 220 GeV. The t' bound is higher than the b' bound because t' is more likely to produce charged hadrons than b'. The 95% CL upper bounds for the production cross sections are given in their Fig. 3.

[10] AAD 15AR based on 20.3 fb^{-1} of pp data at $\sqrt{s}$ = 8 TeV. Used lepton-plus-jets final state. See Fig. 24 for mass limits in the plane of B($b' \rightarrow Wt$) vs. B($b' \rightarrow Hb$) from $b'\overline{b}' \rightarrow Hb + X$ searches.

[11] AAD 15CN based on 20.3 fb^{-1} of pp data at $\sqrt{s}$ = 8 TeV. Limit on pair-production of chiral b'-quark. Used events with $\ell + \not{E}_T + \geq$4j (non-b-tagged). Limits on a heavy vector-like quark, which decays into Wq, Zq, hq, are presented in the plane B($Q \rightarrow Wq$) vs. B($Q \rightarrow hq$) in Fig. 12.

[12] Based on 1.04 fb^{-1} of pp data at $\sqrt{s}$ = 7 TeV. No signal is found for the search of heavy quark pair production that decay into W and a t quark in the events with a high p_T isolated lepton, large $\not{E}_T$, and at least 6 jets in which one, two or more dijets are from W.

[13] Based on 2.0 fb^{-1} of pp data at $\sqrt{s}$ = 7 TeV. No $b' \rightarrow Zb$ invariant mass peak is found in the search of heavy quark pair production that decay into Z and a b quark in events with $Z \rightarrow e^+e^-$ and at least one b-jet. The lower mass limit is 358 GeV for a vector-like singlet b' mixing solely with the third SM generation.

[14] Based on 1.04 fb^{-1} of pp data at $\sqrt{s}$ = 7 TeV. No signal is found for the search of heavy quark pair production that decay into W and a quark in the events with dileptons, large $\not{E}_T$, and $\geq$ 2 jets.

[15] Based on 1.04 fb^{-1} of pp data at $\sqrt{s}$ = 7 TeV. AAD 12BE looked for events with two isolated like-sign leptons and at least 2 jets, large $\not{E}_T$ and H_T $>$ 350 GeV.

[16] Based on 5 fb^{-1} of pp data at $\sqrt{s}$ = 7 TeV. CHATRCHYAN 12BH searched for QCD and EW production of single and pair of degenerate 4'th generation quarks that decay to bW or tW. Absence of signal in events with one lepton, same-sign dileptons or tri-leptons gives the bound. With a mass difference of 25 GeV/c^2 between $m_{t'}$ and $m_{b'}$, the corresponding limit shifts by about $\pm$20 GeV/c^2.

[17] Based on 4.9 fb^{-1} of pp data at $\sqrt{s}$ = 7 TeV. CHATRCHYAN 12X looked for events with trileptons or same-sign dileptons and at least one b jet.

[18] Based on 4.8 fb^{-1} of data in $p\overline{p}$ collisions at 1.96 TeV. AALTONEN 11J looked for events with $\ell + \not{E}_T + \geq$5j ($\geq$ 1 b or c). No signal is observed and the bound $\sigma(b'\overline{b}')$ $<$ 30 fb for $m_{b'}$ $>$ 375 GeV is found for B($b' \rightarrow Wt$) = 1.

[19] Based on 34 pb^{-1} of data in pp collisions at 7 TeV. CHATRCHYAN 11L looked for multi-jet events with trileptons or same-sign dileptons. No excess above the SM background excludes $m_{b'}$ between 255 and 361 GeV at 95% CL for B($b' \rightarrow Wt$) = 1.

[20] Based on 2.7 fb^{-1} of data in $p\overline{p}$ collisions at $\sqrt{s}$ = 1.96 TeV. AALTONEN 10H looked for pair production of heavy quarks which decay into tW^- or tW^+, in events with same sign dileptons (e or μ), several jets and large missing E_T. The result is obtained for b' which decays into tW^-. For the charge 5/3 quark ($T_{5/3}$) which decays into tW^+, $m_{T_{5/3}}$ $>$ 365 GeV (95% CL) is found when it has the charge $-1/3$ partner B of the same mass.

[21] FLACCO 10 result is obtained from AALTONEN 10H result of $m_{b'}$ $>$ 338 GeV, by relaxing the condition B($b' \rightarrow Wt$) = 100% when $m_{b'} > m_{t'}$.

[22] Result is based on 1.06 fb^{-1} of data. No excess from the SM Z+jet events is found when Z decays into ee or $\mu\mu$. The $m_{b'}$ bound is found by comparing the resulting upper bound on $\sigma(b'\overline{b}')$ [1-(1-B($b' \rightarrow Zb$))^2] and the LO estimate of the b' pair production cross section shown in Fig. 38 of the article.

[23] HUANG 08 reexamined the b' mass lower bound of 268 GeV obtained in AALTONEN 07C that assumes B($b' \rightarrow Zb$) = 1, which does not hold for $m_{b'}$ $>$ 255 GeV. The lower mass bound is given in the plane of $\sin^2(\theta_{tb'})$ and $m_{b'}$.

[24] AFFOLDER 00 looked for b' that decays in to b+Z. The signal searched for is $bbZZ$ events where one Z decays into e^+e^- or $\mu^+\mu^-$ and the other Z decays hadronically. The bound assumes B($b' \rightarrow Zb$)= 100%. Between 100 GeV and 199 GeV, the 95%CL upper bound on $\sigma(b' \rightarrow \overline{b}') \times$B^2($b' \rightarrow Zb$) is also given (see their Fig. 2).

[25] ABE 98N looked for $Z \rightarrow e^+e^-$ decays with displaced vertices. Quoted limit assumes B($b' \rightarrow Zb$)=1 and $c\tau_{b'}$=1 cm. The limit is lower than m_Z+m_b ($\sim$ 96 GeV) if $c\tau$ $>$ 22 cm or $c\tau$ $<$ 0.009 cm. See their Fig. 4.

[26] ABACHI 97D searched for b' that decays mainly via FCNC. They obtained 95%CL upper bounds on B($b'\overline{b}' \rightarrow \gamma$+ 3 jets) and B($b'\overline{b}' \rightarrow 2\gamma$+ 2 jets), which can be interpreted as the lower mass bound $m_{b'} > m_Z + m_b$.

[27] ABACHI 95F bound on the top-quark also applies to b' and t' quarks that decay predominantly into W. See FROGGATT 97.

[28] MUKHOPADHYAYA 93 analyze CDF dilepton data of ABE 92G in terms of a new quark decaying via flavor-changing neutral current. The above limit assumes B($b' \rightarrow b\ell^+\ell^-$)=1%. For an exotic quark decaying only via virtual Z [B($b\ell^+\ell^-$) = 3%], the limit is 85 GeV.

[29] ABE 92 dilepton analysis limit of $>$85 GeV at CL=95% also applies to b' quarks, as discussed in ABE 90B.

[30] ABE 90B exclude the region 28–72 GeV.

[31] AKESSON 90 searched for events having an electron with p_T $>$ 12 GeV, missing momentum $>$ 15 GeV, and a jet with E_T $>$ 10 GeV, $|\eta|$ $<$ 2.2, and excluded $m_{b'}$ between 30 and 69 GeV.

[32] For the reduction of the limit due to non-charged-current decay modes, see Fig. 19 of ALBAJAR 90B.

[33] ALBAJAR 88 study events at E_{cm} = 546 and 630 GeV with a muon or isolated electron, accompanied by one or more jets and find agreement with Monte Carlo predictions for the production of charm and bottom, without the need for a new quark. The lower mass limit is obtained by using a conservative estimate for the $b'\overline{b}'$ production cross section and by assuming that it cannot be produced in W decays. The value quoted here is revised using the full $O(\alpha_s^3)$ cross section of ALTARELLI 88.

b'(−1/3) mass limits from single production in $p\overline{p}$ and pp collisions

VALUE (GeV)	CL%	DOCUMENT ID		TECN	COMMENT
$>$1500	95	[1] AAD	16AH	ATLS	$gb \rightarrow b' \rightarrow tW$, B($b' \rightarrow tW$)=1
$>$1390	95	[2] KHACHATRY...	16I	CMS	$gb \rightarrow b' \rightarrow tW$, B($b' \rightarrow tW$)=1
$>$1430	95	[3] KHACHATRY...	16I	CMS	$gb \rightarrow b' \rightarrow tW$, B($b' \rightarrow tW$)=1
$>$1530	95	[4] KHACHATRY...	16I	CMS	$gb \rightarrow b' \rightarrow tW$, B($b' \rightarrow tW$)=1
$>$ 693	95	[5] ABAZOV	11F	D0	$qu \rightarrow q'b' \rightarrow q'(Wu)$ $\tilde{\kappa}_{ub'}$=1, B($b' \rightarrow Wu$)=1
$>$ 430	95	[5] ABAZOV	11F	D0	$qd \rightarrow qb' \rightarrow q(Zd)$ $\tilde{\kappa}_{db'}$=$\sqrt{2}$, B($b' \rightarrow Zd$)=1

[1] AAD 16AH based on 20.3 fb^{-1} of data in pp collisions at 8 TeV. No significant excess over SM expectation is found in the search for a vector-like b' in the single-lepton and dilepton channels (ℓ or $\ell\ell$) + 1,2,3 j ($\geq$ 1b). The model assumes that the b' has the excited quark couplings.

[2] Based on 19.7 fb^{-1} of data in pp collisions at 8 TeV. Limit on left-handed b' assuming 100% decay to tW and using all-hadronic, lepton + jets, and dilepton final states.

[3] Based on 19.7 fb^{-1} of data in pp collisions at 8 TeV. Limit on right-handed b' assuming 100% decay to tW and using all-hadronic, lepton + jets, and dilepton final states.

[4] Based on 19.7 fb^{-1} of data in pp collisions at 8 TeV. Limit on vector-like b' assuming 100% decay to tW and using all-hadronic, lepton+jets, and dilepton final states.

[5] Based on 5.4 fb^{-1} of data in ppbar collisions at 1.96 TeV. ABAZOV 11F looked for single production of b' via the W or Z coupling to the first generation up or down quarks, respectively. Model independent cross section limits for the single production processes $p\overline{p} \rightarrow b'q \rightarrow Wuq$, and $p\overline{p} \rightarrow b'q \rightarrow Zdq$ are given in Figs. 3 and 4, respectively, and the mass limits are obtained for the model of ATRE 09 with degenerate bi-doublets of vector-like quarks.

MASS LIMITS for b' (4th Generation) Quark or Hadron in e^+e^- Collisions

Search for hadrons containing a fourth-generation $-1/3$ quark denoted b'.

The last column specifies the assumption for the decay mode (CC denotes the conventional charged-current decay) and the event signature which is looked for.

VALUE (GeV)	CL%	DOCUMENT ID		TECN	COMMENT
$>$46.0	95	[1] DECAMP	90F	ALEP	any decay
• • • We do not use the following data for averages, fits, limits, etc. • • •					
none 96–103	95	[2] ABDALLAH	07	DLPH	$b' \rightarrow bZ$, cW
		[3] ADRIANI	93G	L3	Quarkonium
$>$44.7	95	ADRIANI	93M	L3	$\Gamma(Z)$
$>$45	95	ABREU	91F	DLPH	$\Gamma(Z)$
none 19.4–28.2	95	ABE	90D	VNS	Any decay; event shape
$>$45.0	95	ABREU	90D	DLPH	B(CC) = 1; event shape
$>$44.5	95	[4] ABREU	90D	DLPH	$b' \rightarrow cH^-$, $H^- \rightarrow \overline{c}s$, $\tau^-\nu$
$>$40.5	95	[5] ABREU	90D	DLPH	$\Gamma(Z \rightarrow$ hadrons)
$>$28.3	95	ADACHI	90	TOPZ	B(FCNC)=100%; isol. γ or 4 jets
$>$41.4	95	[6] AKRAWY	90B	OPAL	Any decay; acoplanarity
$>$45.2	95	[6] AKRAWY	90B	OPAL	B(CC) = 1; acoplanarity
$>$46	95	[7] AKRAWY	90J	OPAL	$b' \rightarrow \gamma$ + any
$>$27.5	95	[8] ABE	89E	VNS	B(CC) =1; μ, e
none 11.4–27.3	95	[9] ABE	89G	VNS	B($b' \rightarrow b\gamma$) $>$ 10%; isolated γ
$>$44.7	95	[10] ABRAMS	89C	MRK2	B(CC)= 100%; isol. track
$>$42.7	95	[10] ABRAMS	89C	MRK2	B(bg)= 100%; event shape
$>$42.0	95	[10] ABRAMS	89C	MRK2	Any decay; event shape
$>$28.4	95	[11,12] ADACHI	89C	TOPZ	B(CC) =1; μ
$>$28.8	95	[13] ENO	89	AMY	B(CC) $\gtrsim$ 90%; μ, e
$>$27.2	95	[13,14] ENO	89	AMY	any decay; event shape
$>$29.0	95	[13] ENO	89	AMY	B($b' \rightarrow bg$) $\gtrsim$ 85%; event shape
$>$24.4	95	[15] IGARASHI	88	AMY	μ,e
$>$23.8	95	[16] SAGAWA	88	AMY	event shape
$>$22.7	95	[17] ADEVA	86	MRKJ	μ
$>$21		[18] ALTHOFF	84C	TASS	R, event shape
$>$19		[19] ALTHOFF	84I	TASS	Aplanarity

[1] DECAMP 90F looked for isolated charged particles, for isolated photons, and for four-jet final states. The modes $b' \rightarrow bg$ for B($b' \rightarrow bg$) $>$ 65% $b' \rightarrow b\gamma$ for B($b' \rightarrow b\gamma$) $>$ 5% are excluded. Charged Higgs decay were not discussed.

[2] ABDALLAH 07 searched for b' pair production at E_{cm}=196–209 GeV, with 420 pb^{-1}. No signal leads to the 95% CL upper limits on B($b' \rightarrow bZ$) and B($b' \rightarrow cW$) for $m_{b'}$ = 96 to 103 GeV.

[3] ADRIANI 93G search for vector quarkonium states near Z and give limit on quarkonium-Z mixing parameter $\delta m^2 < (10–30)$ GeV^2 (95%CL) for the mass 88–94.5 GeV. Using Richardson potential, a 1S ($b'\overline{b}'$) state is excluded for the mass range 87.7–94.7 GeV. This range depends on the potential choice.

[4] ABREU 90D assumed $m_{H^-} < m_{b'} - 3$ GeV.

[5] Superseded by ABREU 91F.

[6] AKRAWY 90B search was restricted to data near the Z peak at $E_{cm} = 91.26$ GeV at LEP. The excluded region is between 23.6 and 41.4 GeV if no H^+ decays exist. For charged Higgs decays the excluded regions are between ($m_{H^+} + 1.5$ GeV) and 45.5 GeV.

[7] AKRAWY 90J search for isolated photons in hadronic Z decay and derive $B(Z \to b'\overline{b}')\cdot B(b' \to \gamma X)/B(Z \to \text{hadrons}) < 2.2 \times 10^{-3}$. Mass limit assumes $B(b' \to \gamma X) > 10\%$.

[8] ABE 89E search at $E_{cm} = 56–57$ GeV at TRISTAN for multihadron events with a spherical shape (using thrust and acoplanarity) or containing isolated leptons.

[9] ABE 89G search was at $E_{cm} = 55–60.8$ GeV at TRISTAN.

[10] If the photonic decay mode is large ($B(b' \to b\gamma) > 25\%$), the ABRAMS 89C limit is 45.4 GeV. The limit for for Higgs decay ($b' \to c H^-$, $H^- \to \overline{c}s$) is 45.2 GeV.

[11] ADACHI 89C search was at $E_{cm} = 56.5–60.8$ GeV at TRISTAN using multi-hadron events accompanying muons.

[12] ADACHI 89C also gives limits for any mixture of CC and bg decays.

[13] ENO 89 search at $E_{cm} = 50–60.8$ at TRISTAN.

[14] ENO 89 considers arbitrary mixture of the charged current, bg, and $b\gamma$ decays.

[15] IGARASHI 88 searches for leptons in low-thrust events and gives $\Delta R(b') < 0.26$ (95% CL) assuming charged current decay, which translates to $m_{b'} > 24.4$ GeV.

[16] SAGAWA 88 set limit $\sigma(\text{top}) < 6.1$ pb at CL=95% for top-flavored hadron production from event shape analyses at $E_{cm} = 52$ GeV. By using the quark parton model cross-section formula near threshold, the above limit leads to lower mass bounds of 23.8 GeV for charge $-1/3$ quarks.

[17] ADEVA 86 give 95%CL upper bound on an excess of the normalized cross section, ΔR, as a function of the minimum c.m. energy (see their figure 3). Production of a pair of 1/3 charge quarks is excluded up to $E_{cm} = 45.4$ GeV.

[18] ALTHOFF 84C narrow state search sets limit $\Gamma(e^+e^-)B(\text{hadrons}) < 2.4$ keV CL = 95% and heavy charge 1/3 quark pair production $m > 21$ GeV, CL = 95%.

[19] ALTHOFF 84I exclude heavy quark pair production for $7 < m < 19$ GeV (1/3 charge) using aplanarity distributions (CL = 95%).

REFERENCES FOR Searches for (Fourth Generation) b' Quark

SIRUNYAN	17AU	JHEP 1711 085	A.M. Sirunyan *et al.*	(CMS Collab.)
AAD	16AH	JHEP 1602 110	G. Aad *et al.*	(ATLAS Collab.)
KHACHATRY...	16AN	PR D93 112009	V. Khachatryan *et al.*	(CMS Collab.)
KHACHATRY...	16I	JHEP 1601 166	V. Khachatryan *et al.*	(CMS Collab.)
AAD	15AR	JHEP 1508 105	G. Aad *et al.*	(ATLAS Collab.)
AAD	15BY	JHEP 1510 150	G. Aad *et al.*	(ATLAS Collab.)
AAD	15CN	PR D92 112007	G. Aad *et al.*	(ATLAS Collab.)
AAD	15Z	PR D91 112011	G. Aad *et al.*	(ATLAS Collab.)
AAD	14AZ	JHEP 1411 104	G. Aad *et al.*	(ATLAS Collab.)
CHATRCHYAN	13I	JHEP 1301 154	S. Chatrchyan *et al.*	(CMS Collab.)
AAD	12AT	PRL 109 032001	G. Aad *et al.*	(ATLAS Collab.)
AAD	12AU	PRL 109 071801	G. Aad *et al.*	(ATLAS Collab.)
AAD	12BC	PR D86 012007	G. Aad *et al.*	(ATLAS Collab.)
AAD	12BE	JHEP 1204 069	G. Aad *et al.*	(ATLAS Collab.)
CHATRCHYAN	12BH	PR D86 112003	S. Chatrchyan *et al.*	(CMS Collab.)
CHATRCHYAN	12X	JHEP 1205 123	S. Chatrchyan *et al.*	(CMS Collab.)
AALTONEN	11J	PRL 106 141803	T. Aaltonen *et al.*	(CDF Collab.)
ABAZOV	11F	PRL 106 081801	V.M. Abazov *et al.*	(D0 Collab.)
CHATRCHYAN	11L	PL B701 204	S. Chatrchyan *et al.*	(CMS Collab.)
AALTONEN	10H	PRL 104 091801	T. Aaltonen *et al.*	(CDF Collab.)
FLACCO	10	PRL 105 111801	C.J. Flacco *et al.*	(UCI, HAIF)
ATRE	09	PR D79 054018	A. Atre *et al.*	
ABAZOV	08X	PRL 101 111802	V.M. Abazov *et al.*	(D0 Collab.)
HUANG	08	PR D77 037302	P.Q. Hung, M. Sher	(UVA, WILL)
AALTONEN	07C	PR D76 072006	T. Aaltonen *et al.*	(CDF Collab.)
ABDALLAH	07	EPJ C50 507	J. Abdallah *et al.*	(DELPHI Collab.)
ACOSTA	03	PRL 90 131801	D. Acosta *et al.*	(CDF Collab.)
AFFOLDER	00	PRL 84 835	A. Affolder *et al.*	(CDF Collab.)
ABE	98N	PR D58 051102	F. Abe *et al.*	(CDF Collab.)
ABACHI	97D	PRL 78 3818	S. Abachi *et al.*	(D0 Collab.)
FROGGATT	97	ZPHY C73 333	C.D. Froggatt, D.J. Smith, H.B. Nielsen	(GLAS+)
ABACHI	95F	PR D52 4877	S. Abachi *et al.*	(D0 Collab.)
ADRIANI	93G	PL B313 326	O. Adriani *et al.*	(L3 Collab.)
ADRIANI	93M	PRPL 236 1	O. Adriani *et al.*	(L3 Collab.)
MUKHOPAD...	93	PR D48 2105	B. Mukhopadhyaya, D.P. Roy	(TATA)
ABE	92	PRL 68 447	F. Abe *et al.*	(CDF Collab.)
Also		PR D45 3921	F. Abe *et al.*	(CDF Collab.)
ABE	92G	PR D45 3921	F. Abe *et al.*	(CDF Collab.)
ABREU	91F	NP B367 511	P. Abreu *et al.*	(DELPHI Collab.)
ABE	90B	PRL 64 147	F. Abe *et al.*	(CDF Collab.)
ABE	90D	PL B234 382	K. Abe *et al.*	(VENUS Collab.)
ABREU	90D	PL B242 536	P. Abreu *et al.*	(DELPHI Collab.)
ADACHI	90	PL B234 197	I. Adachi *et al.*	(TOPAZ Collab.)
AKESSON	90	ZPHY C46 179	T. Akesson *et al.*	(UA2 Collab.)
AKRAWY	90B	PL B236 364	M.Z. Akrawy *et al.*	(OPAL Collab.)
AKRAWY	90J	PL B246 285	M.Z. Akrawy *et al.*	(OPAL Collab.)
ALBAJAR	90B	ZPHY C48 1	C. Albajar *et al.*	(UA1 Collab.)
DECAMP	90F	PL B236 511	D. Decamp *et al.*	(ALEPH Collab.)
ABE	89E	PR D39 3524	K. Abe *et al.*	(VENUS Collab.)
ABE	89G	PRL 63 1776	K. Abe *et al.*	(VENUS Collab.)
ABRAMS	89C	PRL 63 2447	G.S. Abrams *et al.*	(Mark II Collab.)
ADACHI	89C	PL B229 427	I. Adachi *et al.*	(TOPAZ Collab.)
ENO	89	PRL 63 1910	S. Eno *et al.*	(AMY Collab.)
ALBAJAR	88	ZPHY C37 505	C. Albajar *et al.*	(UA1 Collab.)
ALTARELLI	88	NP B308 724	G. Altarelli *et al.*	(CERN, ROMA, ETH)
IGARASHI	88	PRL 60 2359	S. Igarashi *et al.*	(AMY Collab.)
SAGAWA	88	PRL 60 93	H. Sagawa *et al.*	(AMY Collab.)
ADEVA	86	PR D34 681	B. Adeva *et al.*	(Mark-J Collab.)
ALTHOFF	84C	PL 138B 441	M. Althoff *et al.*	(TASSO Collab.)
ALTHOFF	84I	ZPHY C22 307	M. Althoff *et al.*	(TASSO Collab.)

t' (4^{th} Generation) Quark, Searches for

$t'(2/3)$-quark/hadron mass limits in $p\overline{p}$ and pp collisions

VALUE (GeV)	CL%	DOCUMENT ID		TECN	COMMENT
>1160 (CL = 95%) OUR LIMIT					
>1160	95	[1] AABOUD	17L	ATLS	$B(t' \to Zt) = 1$
> 860	95	[2] SIRUNYAN	17AU	CMS	
> 770	95	[3] AAD	15AR	ATLS	$B(t' \to Wb) = 1$
> 590	95	[4] AAD	15BY	ATLS	Wb, Zt, ht modes
> 745	95	[5] KHACHATRY...	15AI	CMS	$B(t' \to ht) = 1$
> 735	95	[6] AAD	14AZ	ATLS	$B(b' \to Wt) = 1$
> 700	95	[7] CHATRCHYAN	14A	CMS	$B(t' \to Wb) = 1$
> 706	95	[7] CHATRCHYAN	14A	CMS	$B(t' \to Zt) = 1$
> 782	95	[7] CHATRCHYAN	14A	CMS	$B(t' \to ht) = 1$
> 350	95	[8] AAD	12BC	ATLS	$B(t' \to Wq)$=1 (q=d,s,b)
> 420	95	[9] AAD	12C	ATLS	$t' \to Xt$ ($m_X < 140$ GeV)
> 685	95	[10] CHATRCHYAN	12BH	CMS	$m_{b'} = m_{t'}$
> 557	95	[11] CHATRCHYAN	12P	CMS	$t'\overline{t}' \to W^+ b\, W^- \overline{b} \to b\ell^+\nu\overline{b}\ell^-\overline{\nu}$
• • • We do not use the following data for averages, fits, limits, etc. • • •					
> 656	95	[12] AAD	13F	ATLS	$B(t' \to Wb) = 1$
> 625	95	[13] CHATRCHYAN	13I	CMS	$B(t' \to Zt) = 1$
> 404	95	[14] AAD	12AR	ATLS	$B(t' \to Wb) = 1$
> 570	95	[15] CHATRCHYAN	12BC	CMS	$t'\overline{t}' \to W^+ b\, W^- \overline{b}$
> 400	95	[16] AALTONEN	11AH	CDF	$t' \to Xt$ ($m_X < 70$ GeV)
> 358	95	[17] AALTONEN	11AL	CDF	$t' \to Wb$
> 340	95	[17] AALTONEN	11AL	CDF	$t' \to Wq$ (q=d,s,b)
> 360	95	[18] AALTONEN	11O	CDF	$t' \to Xt$ ($m_X < 100$ GeV)
> 285	95	[19] ABAZOV	11Q	D0	$t' \to Wq$ (q=d,s,b)
> 256	95	[20,21] AALTONEN	08H	CDF	$t' \to Wq$

[1] AABOUD 17L based on 36.1 fb^{-1} of pp data at $\sqrt{s} = 13$ TeV. No signal is found in the search for heavy quark pair production that decay into Zt followed by $Z \to \nu\nu$ in the events with one lepton, large $\not{E}_T$, and ≥ 4 jets. The lower mass limit 0.87 (1.05) TeV is obtained for the singlet (doublet) model with other possible decay modes.

[2] SIRUNYAN 17AU based on 2.3-2.6 fb^{-1} of pp data at $\sqrt{s} = 13$ TeV. Limit on pair-produced singlet vector-like t' using one lepton and several jets. The mass bound is given for a t' transforming as a singlet under the electroweak symmetry group, assumed to decay through W, Z or Higgs boson (which decays to jets) and to a third generation quark. For a doublet, the limit is >830 GeV. Other limits are also given in the paper.

[3] AAD 15AR based on 20.3 fb^{-1} of pp data at $\sqrt{s} = 8$ TeV. Used lepton-plus-jets final state. See Fig. 20 for mass limits in the plane of $B(t' \to Ht)$ vs. $B(t' \to Wb)$ from a combination of $t'\overline{t}' \to Wb + X$ and $t'\overline{t}' \to Ht + X$ searches. Any branching ratio scenario is excluded for mass below 715 GeV.

[4] AAD 15BY based on 20.3 fb^{-1} of pp data at $\sqrt{s} = 8$ TeV. Limit on pair-produced vector-like t' assuming the branching fractions to W, Z, and h modes of the singlet model. Used events containing $\geq 2\ell + \not{E}_T + \geq 2j$ (≥ 1 b) and including a same-sign lepton pair.

[5] KHACHATRYAN 15AI based on 19.7 fb^{-1} of pp data at $\sqrt{s} = 8$ TeV. The search exploits all-hadronic final states by tagging boosted Higgs boson using jet substructure and b-tagging.

[6] Based on 20.3 fb^{-1} of pp data at $\sqrt{s} = 8$ TeV. No significant excess over SM expectation is found in the search for pair production or single production of t' in the events with dilepton from a high p_T Z and additional jets (≥ 1 b-tag). If instead of $B(b' \to Wt) = 1$ an electroweak singlet with $B(b' \to Wt) \sim 0.45$ is assumed, the limit reduces to 685 GeV.

[7] Based on 19.5 fb^{-1} of pp data at $\sqrt{s} = 8$TeV. The t' quark is pair produced and is assumed to decay into three different final states of bW, tZ, and th. The search is carried out using events with at least one isolated lepton.

[8] Based on 1.04 fb^{-1} of pp data at $\sqrt{s} = 7$ TeV. No signal is found for the search of heavy quark pair production that decay into W and a quark in the events with dileptons, large $\not{E}_T$, and ≥ 2 jets.

[9] Based on 1.04 fb^{-1} of data in pp collisions at 7 TeV. AAD 12C looked for $t'\overline{t}'$ production followed by t' decaying into a top quark and X, an invisible particle, in a final state with an isolated high-P_T lepton, four or more jets, and a large missing transverse energy. No excess over the SM $t\overline{t}$ production gives the upper limit on $t'\overline{t}'$ production cross section as a function of $m_{t'}$ and m_X. The result is obtained for $B(t' \to Wt) = 1$.

[10] Based on 5 fb^{-1} of pp data at $\sqrt{s} = 7$ TeV. CHATRCHYAN 12BH searched for QCD and EW production of single and pair of degenerate 4'th generation quarks that decay to Wb or Wt. Absence of signal in events with one lepton, same-sign dileptons or tri-leptons gives the bound. With a mass difference of 25 GeV/c^2 between $m_{t'}$ and $m_{b'}$, the corresponding limit shifts by about ± 20 GeV/c^2.

[11] Based on 5.0 fb^{-1} of pp data at $\sqrt{s} = 7$ TeV. CHATRCHYAN 12P looked for $t'\overline{t}'$ production events with two isolated high p_T leptons, large $\not{E}_T$, and 2 high p_T jets with b-tag. The absence of signal above the SM background gives the limit for $B(t' \to Wb) = 1$.

[12] Based on 4.7 fb^{-1} of pp data at $\sqrt{s} = 7$ TeV. No signal is found for the search of heavy quark pair production that decay into W and a b quark in the events with a high p_T isolated lepton, large $\not{E}_T$ and at least 3 jets (≥ 1 b-tag). Vector-like quark of charge 2/3 with $400 < m_{t'} < 550$ GeV and $B(t' \to Wb) > 0.63$ is excluded at 95% CL.

[13] Based on 5.0 fb^{-1} of pp data at $\sqrt{s} = 7$ TeV. CHATRCHYAN 13I looked for events with one isolated electron or muon, large $\not{E}_T$, and at least four jets with large transverse momenta, where one jet is likely to originate from the decay of a bottom quark.

[14] Based on 1.04 fb^{-1} of pp data at $\sqrt{s} = 7$ TeV. No signal is found in the search for pair produced heavy quarks that decay into W boson and a b quark in the events with a high p_T isolated lepton, large $\not{E}_T$ and at least 3 jets (≥ 1 b-tag).

[15] Based on 5.0 fb^{-1} of pp data at $\sqrt{s}$ = 7 TeV. CHATRCHYAN 12BC looked for $t'\overline{t}'$ production events with a single isolated high p_T lepton, large $\not{E}_T$ and at least 4 high p_T jets with a b-tag. The absence of signal above the SM background gives the limit for B($t' \rightarrow Wb$) = 1.

[16] Based on 5.7 fb^{-1} of data in $p\overline{p}$ collisions at 1.96 TeV. AALTONEN 11AH looked for $t'\overline{t}'$ production followed by t' decaying into a top quark and X, an invisible particle, in the all hadronic decay mode of $t\overline{t}$. No excess over the SM $t\overline{t}$ production gives the upper limit on $t'\overline{t}'$ production cross section as a function of $m_{t'}$ and m_X. The result is obtained for B($t' \rightarrow X\,t$) = 1.

[17] Based on 5.6 fb^{-1} of data in ppbar collisions at 1.96 TeV. AALTONEN 11AL looked for $\ell + \geq$ 4j events and set upper limits on $\sigma(t'\overline{t}')$ as functions of $m_{t'}$.

[18] Based on 4.8 fb^{-1} of data in $p\overline{p}$ collisions at 1.96 TeV. AALTONEN 11O looked for $t'\overline{t}'$ production signal when t' decays into a top quark and X, an invisible particle, in $\ell + \not{E}_T$ + jets channel. No excess over the SM $t\overline{t}$ production gives the upper limit on $t'\overline{t}'$ production cross section as a function of $m_{t'}$ and m_X. The result is obtained for B($t' \rightarrow X\,t$) = 1.

[19] Based on 5.3 fb^{-1} of data in $p\overline{p}$ collisions at 1.96 TeV. ABAZOV 11Q looked for $\ell + \not{E}_T + \geq$ 4j events and set upper limits on $\sigma(t'\overline{t}')$ as functions of $m_{t'}$.

[20] Searches for pair production of a new heavy top-like quark t' decaying to a W boson and another quark by fitting the observed spectrum of total transverse energy and reconstructed t' mass in the lepton + jets events.

[21] HUANG 08 reexamined the t' mass lower bound of 256 GeV obtained in AALTONEN 08H that assumes B($b' \rightarrow qZ$) = 1 for $q = u, c$ which does not hold when $m_{b'} < m_{t'} - m_W$ or the mixing $\sin^2(\theta_{bt'})$ is so tiny that the decay occurs outside of the vertex detector. Fig. 1 gives that lower bound on $m_{t'}$ in the plane of $\sin^2(\theta_{bt'})$ and $m_{b'}$.

$t'(5/3)$-quark/hadron mass limits in $p\overline{p}$ and pp collisions

VALUE (GeV)	CL%	DOCUMENT ID		TECN	COMMENT
>1020	95	[1] SIRUNYAN	17J	CMS	$t'_R(5/3) \rightarrow t\,W^+$
> 990	95	[1] SIRUNYAN	17J	CMS	$t'_L(5/3) \rightarrow t\,W^+$
> 750	95	[2] AAD	15BY	ATLS	$t'(5/3) \rightarrow t\,W^+$
> 840	95	[3] AAD	15Z	ATLS	$t'(5/3) \rightarrow t\,W^+$
> 800	95	[4] CHATRCHYAN	14T	CMS	$t'(5/3) \rightarrow t\,W^+$

[1] SIRUNYAN 17J based on 2.3 fb^{-1} of pp data at $\sqrt{s}$ = 13 TeV. Signals are searched in the final states of t' pair production, with same-sign leptons (which come from a t' decay) or a single lepton (which comes from a W out of 4Ws), along with jets, and no excess over the SM expectation is found.

[2] AAD 15BY based on 20.3 fb^{-1} of pp data at $\sqrt{s}$ = 8 TeV. Limit on $t'(5/3)$ in pair and single production assuming its coupling to Wt is equal to one. Used events containing $\geq 2\ell + \not{E}_T + \geq 2j$ (≥ 1 b) and including a same-sign lepton pair.

[3] AAD 15Z based on 20.3 fb^{-1} of pp data at $\sqrt{s}$ = 8 TeV. Used events with $\ell + \not{E}_T + \geq 6j$ (≥ 1 b) and at least one pair of jets from weak boson decay, sensitive to the final state $b\overline{b}W^+W^-W^+W^-$.

[4] CHATRCHYAN 14T based on 19.5 fb^{-1} of pp data at $\sqrt{s}$ = 8 TeV. Non-observation of anomaly in H_T distribution in the same-sign dilepton events leads to the limit when pair produced $t'(5/3)$ quark decays exclusively into t and W^+, resulting in the final state with $b\overline{b}W^+W^-W^+W^-$.

$t'(2/3)$ mass limits from single production in $p\overline{p}$ and pp collisions

VALUE (GeV)	CL%	DOCUMENT ID		TECN	COMMENT
>950	95	[1] AAD	16AV	ATLS	$qg \rightarrow q't'b$, B($t' \rightarrow Wb$)=0.5
>403	95	[2] ABAZOV	11F	D0	$qd \rightarrow q't' \rightarrow q'(Wd)$ $\tilde{\kappa}_{dt'}$=1, B($t' \rightarrow Wd$)=1
>551	95	[2] ABAZOV	11F	D0	$qu \rightarrow qt' \rightarrow q(Zu)$ $\tilde{\kappa}_{ut'}=\sqrt{2}$, B($t' \rightarrow Zu$)=1

[1] AAD 16AV based on 20.3 fb^{-1} of pp data at $\sqrt{s}$ = 8 TeV. No significant excess over SM expectation is found in the search for a fully reconstructed vector-like t' in the mode $\ell + \not{E}_T + \geq 2j$ ($\geq 1b$). A veto on massive large-radius jets is used to reject the $t\overline{t}$ background.

[2] Based on 5.4 fb^{-1} of data in ppbar collisions at 1.96 TeV. ABAZOV 11F looked for single production of t' via the Z or E coupling to the first generation up or down quarks, respectively. Model independent cross section limits for the single production processes $p\overline{p} \rightarrow t'q \rightarrow (Wd)q$, and $p\overline{p} \rightarrow t'q \rightarrow (Zd)q$ are given in Figs. 3 and 4, respectively, and the mass limits are obtained for the model of ATRE 09 with degenerate bi-doublets of vector-like quarks.

REFERENCES FOR Searches for (Fourth Generation) t' Quark

AABOUD	17L	JHEP 1708 052	M. Aaboud *et al.*	(ATLAS Collab.)
SIRUNYAN	17AU	JHEP 1711 085	A.M. Sirunyan *et al.*	(CMS Collab.)
SIRUNYAN	17J	JHEP 1708 073	A.M. Sirunyan *et al.*	(CMS Collab.)
AAD	16AV	EPJ C76 442	G. Aad *et al.*	(ATLAS Collab.)
AAD	15AR	JHEP 1508 105	G. Aad *et al.*	(ATLAS Collab.)
AAD	15BY	JHEP 1510 150	G. Aad *et al.*	(ATLAS Collab.)
AAD	15Z	PR D91 112011	G. Aad *et al.*	(ATLAS Collab.)
KHACHATRY...	15AI	JHEP 1506 080	V. Khachatryan *et al.*	(CMS Collab.)
AAD	14AZ	JHEP 1411 104	G. Aad *et al.*	(ATLAS Collab.)
CHATRCHYAN	14A	PL B729 149	S. Chatrchyan *et al.*	(CMS Collab.)
CHATRCHYAN	14T	PRL 112 171801	S. Chatrchyan *et al.*	(CMS Collab.)
AAD	13F	PL B718 1284	G. Aad *et al.*	(ATLAS Collab.)
CHATRCHYAN	13I	JHEP 1301 154	S. Chatrchyan *et al.*	(CMS Collab.)
AAD	12AR	PRL 108 261802	G. Aad *et al.*	(ATLAS Collab.)
AAD	12BC	PR D86 012007	G. Aad *et al.*	(ATLAS Collab.)
AAD	12C	PRL 108 041805	G. Aad *et al.*	(ATLAS Collab.)
CHATRCHYAN	12BC	PL B718 307	S. Chatrchyan *et al.*	(CMS Collab.)
CHATRCHYAN	12BH	PR D86 112003	S. Chatrchyan *et al.*	(CMS Collab.)
CHATRCHYAN	12P	PL B716 103	S. Chatrchyan *et al.*	(CMS Collab.)
AALTONEN	11AH	PRL 107 191803	T. Aaltonen *et al.*	(CDF Collab.)
AALTONEN	11AL	PRL 107 261801	T. Aaltonen *et al.*	(CDF Collab.)
AALTONEN	11O	PRL 106 191801	T. Aaltonen *et al.*	(CDF Collab.)
ABAZOV	11F	PRL 106 081801	V.M. Abazov *et al.*	(D0 Collab.)
ABAZOV	11Q	PRL 107 082001	V.M. Abazov *et al.*	(D0 Collab.)
ATRE	09	PR D79 054018	A. Atre *et al.*	
AALTONEN	08H	PRL 100 161803	T. Aaltonen *et al.*	(CDF Collab.)
HUANG	08	PR D77 037302	P.Q. Hung, M. Sher	(UVA, WILL)

Free Quark Searches

FREE QUARK SEARCHES

The basis for much of the theory of particle scattering and hadron spectroscopy is the construction of the hadrons from a set of fractionally charged constituents (quarks). A central but unproven hypothesis of this theory, Quantum Chromodynamics, is that quarks cannot be observed as free particles but are confined to mesons and baryons.

Experiments show that it is at best difficult to "unglue" quarks. Accelerator searches at increasing energies have produced no evidence for free quarks, while only a few cosmic-ray and matter searches have produced uncorroborated events.

This compilation is only a guide to the literature, since the quoted experimental limits are often only indicative. Reviews can be found in Refs. 1–4.

References

1. M.L. Perl, E.R. Lee, and D. Lomba, Mod. Phys. Lett. **A19**, 2595 (2004).
2. P.F. Smith, Ann. Rev. Nucl. and Part. Sci. **39**, 73 (1989).
3. L. Lyons, Phys. Reports **129**, 225 (1985).
4. M. Marinelli and G. Morpurgo, Phys. Reports **85**, 161 (1982).

Quark Production Cross Section — Accelerator Searches

X-SECT (cm^2)	CHG (e/3)	MASS (GeV)	ENERGY (GeV)	BEAM	EVTS		DOCUMENT ID		TECN
<1.7-2.3E−39	±2	100–600	7000	pp	0	[1]	CHATRCHYAN	13AR	CMS
<14-5.4E−39	±1	100–600	7000	pp	0	[1]	CHATRCHYAN	13AR	CMS
<1.3E−36	±2	45–84	130–172	e^+e^-	0		ABREU	97D	DLPH
<2.E−35	+2	250	1800	$p\overline{p}$	0	[2]	ABE	92J	CDF
<1.E−35	+4	250	1800	$p\overline{p}$	0	[2]	ABE	92J	CDF
<3.8E−28			14.5A	[28]Si–Pb	0	[3]	HE	91	PLAS
<3.2E−28			14.5A	[28]Si–Cu	0	[3]	HE	91	PLAS
<1.E−40	±1,2	<10		$p,\nu,\overline{\nu}$	0		BERGSMA	84B	CHRM
<1.E−36	±1,2	<9	200	μ	0		AUBERT	83C	SPEC
<2.E−10	±2,4	1–3	200	p	0	[4]	BUSSIERE	80	CNTR
<5.E−38	+1,2	>5	300	p	0	[5,6]	STEVENSON	79	CNTR
<1.E−33	±1	<20	52	pp	0		BASILE	78	SPEC
<9.E−39	±1,2	<6	400	p	0	[5]	ANTREASYAN	77	SPEC
<8.E−35	+1,2	<20	52	pp	0	[7]	FABJAN	75	CNTR
<5.E−38	−1,2	4–9	200	p	0		NASH	74	CNTR
<1.E−32	+2,4	4–24	52	pp	0		ALPER	73	SPEC
<5.E−31	+1,2,4	<12	300	p	0		LEIPUNER	73	CNTR
<6.E−34	±1,2	<13	52	pp	0		BOTT	72	CNTR
<1.E−36	−4	4	70	p	0		ANTIPOV	71	CNTR
<1.E−35	±1,2	2	28	p	0	[8]	ALLABY	69B	CNTR
<4.E−37	−2	<5	70	p	0	[4]	ANTIPOV	69	CNTR
<3.E−37	−1,2	2–5	70	p	0	[8]	ANTIPOV	69B	CNTR
<1.E−35	+1,2	<7	30	p	0		DORFAN	65	CNTR
<2.E−35	−2	< 2.5–5	30	p	0	[9]	FRANZINI	65B	CNTR
<5.E−35	+1,2	<2.2	21	p	0		BINGHAM	64	HLBC
<1.E−32	+1,2	<4.0	28	p	0		BLUM	64	HBC
<1.E−35	+1,2	<2.5	31	p	0	[9]	HAGOPIAN	64	HBC
<1.E−34	+1	<2	28	p	0		LEIPUNER	64	CNTR
<1.E−33	+1,2	<2.4	24	p	0		MORRISON	64	HBC

[1] CHATRCHYAN 13AR limits assume pair-produced long-lived spin-1/2 particles neutral under SU(3)$_C$ and SU(2)$_L$.

[2] ABE 92J flux limits decrease as the mass increases from 50 to 500 GeV.

[3] HE 91 limits are for charges of the form $N\pm1/3$ from 23/3 to 38/3.

[4] Hadronic or leptonic quarks.

[5] Cross section cm^2/GeV^2.

[6] 3×10^{-5} <lifetime < 1×10^{-3} s.

[7] Includes BOTT 72 results.

[8] Assumes isotropic cm production.

[9] Cross section inferred from flux.

Quark Particle Listings

Free Quark Searches

Quark Differential Production Cross Section — Accelerator Searches

X-SECT ($cm^2 sr^{-1} GeV^{-1}$)	CHG $e/3$	MASS (GeV)	ENERGY (GeV)	BEAM	EVTS	DOCUMENT ID		TECN
<4.E−36	−2,4	1.5–6	70	p	0	BALDIN	76	CNTR
<2.E−33	±4	5–20	52	pp	0	ALBROW	75	SPEC
<5.E−34	<7	7–15	44	pp	0	JOVANOV...	75	CNTR
<5.E−35			20	γ	0	[1] GALIK	74	CNTR
<9.E−35	−1,2		200	p	0	NASH	74	CNTR
<4.E−36	−4	2.3–2.7	70	p	0	ANTIPOV	71	CNTR
<3.E−35	±1,2	<2.7	27	p	0	ALLABY	69B	CNTR
<7.E−38	−1,2	<2.5	70	p	0	ANTIPOV	69B	CNTR

[1] Cross section in cm^2/sr/equivalent quanta.

Quark Flux — Accelerator Searches

The definition of FLUX depends on the experiment

(a) is the ratio of measured free quarks to predicted free quarks if there is no "confinement."
(b) is the probability of fractional charge on nuclear fragments. Energy is in GeV/nucleon.
(c) is the 90%CL upper limit on fractionally-charged particles produced per interaction.
(d) is quarks per collision.
(e) is inclusive quark-production cross-section ratio to $\sigma(e^+e^- \to \mu^+\mu^-)$.
(f) is quark flux per charged particle.
(g) is the flux per ν-event.
(h) is quark yield per π^- yield.
(i) is 2-body exclusive quark-production cross-section ratio to $\sigma(e^+e^- \to \mu^+\mu^-)$.

FLUX		CHG ($e/3$)	MASS (GeV)	ENRGY (GeV)	BEAM	EVTS	DOCUMENT ID		TECN
<1.6E−3	b	see note		200	^{32}S–Pb	0	[1] HUENTRUP	96	PLAS
<6.2E−4	b	see note		10.6	^{32}S–Pb	0	[1] HUENTRUP	96	PLAS
<0.94E−4	e	±2	2–30	88–94	e^+e^-	0	AKERS	95R	OPAL
<1.7E−4	e	±2	30–40	88–94	e^+e^-	0	AKERS	95R	OPAL
<3.6E−4	e	±4	5–30	88–94	e^+e^-	0	AKERS	95R	OPAL
<1.9E−4	e	±4	30–45	88–94	e^+e^-	0	AKERS	95R	OPAL
<2.E−3	e	+1	5–40	88–94	e^+e^-	0	[2] BUSKULIC	93C	ALEP
<6.E−4	e	+2	5–30	88–94	e^+e^-	0	[2] BUSKULIC	93C	ALEP
<1.2E−3	e	+4	15–40	88–94	e^+e^-	0	[2] BUSKULIC	93C	ALEP
<3.6E−4	i	+4	5.0–10.2	88–94	e^+e^-	0	BUSKULIC	93C	ALEP
<3.6E−4	i	+4	16.5–26.0	88–94	e^+e^-	0	BUSKULIC	93C	ALEP
<6.9E−4	i	+4	26.0–33.3	88–94	e^+e^-	0	BUSKULIC	93C	ALEP
<9.1E−4	i	+4	33.3–38.6	88–94	e^+e^-	0	BUSKULIC	93C	ALEP
<1.1E−3	i	+4	38.6–44.9	88–94	e^+e^-	0	BUSKULIC	93C	ALEP
<1.6E−4	b	see note		see note		0	[3] CECCHINI	93	PLAS
	b	4,5,7,8		2.1A	^{16}O	0,2,0,6	[4] GHOSH	92	EMUL
<6.4E−5	g	1			$\nu,\overline{\nu}$	1	[5] BASILE	91	CNTR
<3.7E−5	g	2			$\nu,\overline{\nu}$	0	[5] BASILE	91	CNTR
<3.9E−5	g	1			$\nu,\overline{\nu}$	1	[6] BASILE	91	CNTR
<2.8E−5	g	2			$\nu,\overline{\nu}$	0	[6] BASILE	91	CNTR
<1.9E−4	c			14.5A	^{28}Si–Pb	0	[7] HE	91	PLAS
<3.9E−4	c			14.5A	^{28}Si–Cu	0	[7] HE	91	PLAS
<1.E−9	c	±1,2,4		14.5A	^{16}O–Ar	0	MATIS	91	MDRP
<5.1E−10	c	±1,2,4		14.5A	^{16}O–Hg	0	MATIS	91	MDRP
<8.1E−9	c	±1,2,4		14.5A	Si–Hg	0	MATIS	91	MDRP
<1.7E−6	c	±1,2,4		60A	^{16}O–Hg	0	MATIS	91	MDRP
<3.5E−7	c	±1,2,4		200A	^{16}O–Hg	0	MATIS	91	MDRP
<1.3E−6	c	±1,2,4		200A	S–Hg	0	MATIS	91	MDRP
<5E−2	e	2	19–27	52–60	e^+e^-	0	ADACHI	90C	TOPZ
<5E−2	e	4	<24	52–60	e^+e^-	0	ADACHI	90C	TOPZ
<1.E−4	e	+2	<3.5	10	e^+e^-	0	BOWCOCK	89B	CLEO
<1.E−6	d	±1,2		60	^{16}O–Hg	0	CALLOWAY	89	MDRP
<3.5E−7	d	±1,2		200	^{16}O–Hg	0	CALLOWAY	89	MDRP
<1.3E−6	d	±1,2		200	S–Hg	0	CALLOWAY	89	MDRP
<1.2E−10	d	±1	1	800	p–Hg	0	MATIS	89	MDRP
<1.1E−10	d	±2	1	800	p–Hg	0	MATIS	89	MDRP
<1.2E−10	d	±1	1	800	p–N_2	0	MATIS	89	MDRP
<7.7E−11	d	±2	1	800	p–N_2	0	MATIS	89	MDRP
<6.E−9	h	−5	0.9–2.3	12	p	0	NAKAMURA	89	SPEC
<5.E−5	g	1,2	<0.5		$\nu,\overline{\nu}d$	0	ALLASIA	88	BEBC
<3.E−4	b	See note		14.5	^{16}O–Pb	0	[8] HOFFMANN	88	PLAS
<2.E−4	b	See note		200	^{16}O–Pb	0	[9] HOFFMANN	88	PLAS
<8E−5	b	19,20,22,23		200A			GERBIER	87	PLAS
<2.E−4	a	±1,2	<300	320	$\overline{p}p$	0	LYONS	87	MLEV
<1.E−9	c	±1,2,4,5		14.5	^{16}O–Hg	0	SHAW	87	MDRP
<3.E−3	d	−1,2,3,4,6	<5	2	Si–Si	0	[10] ABACHI	86C	CNTR
<1.E−4	e	±1,2,4	<4	10	e^+e^-	0	ALBRECHT	85G	ARG
<6.E−5	b	±1,2	1	540	$p\overline{p}$	0	BANNER	85	UA2
<5.E−3	e	−4	1–8	29	e^+e^-	0	AIHARA	84	TPC
<1.E−2	e	±1,2	1–13	29	e^+e^-	0	AIHARA	84B	TPC
<2.E−4	b	±1		72	^{40}Ar	0	[11] BARWICK	84	CNTR
<1.E−4	e	±2	<0.4	1.4	e^+e^-	0	BONDAR	84	OLYA
<5.E−1	e	±1,2	<13	29	e^+e^-	0	GURYN	84	CNTR
<3.E−3	b	±1,2	<2	540	$p\overline{p}$	0	BANNER	83	CNTR
<1.E−4	b	±1,2		106	^{56}Fe	0	LINDGREN	83	CNTR
<3.E−3	b	$>\lvert\pm 0.1\rvert$		74	^{40}Ar	0	[11] PRICE	83	PLAS
<1.E−2	e	±1,2	<14	29	e^+e^-	0	MARINI	82B	CNTR
<8.E−2	e	±1,2	<12	29	e^+e^-	0	ROSS	82	CNTR
<3.E−4	e	±2	1.8–2	7	e^+e^-	0	WEISS	81	MRK2
<5.E−2	e	+1,2,4,5	2–12	27	e^+e^-	0	BARTEL	80	JADE
<2.E−5	g	1,2			ν	0	[5,6] BASILE	80	CNTR
<3.E−10	f	±2,4	1–3	200	p	0	[12] BOZZOLI	79	CNTR
<6.E−11	f	±1	<21	52	pp	0	BASILE	78	SPEC
<5.E−3	g				ν_μ	0	BASILE	78B	CNTR
<2.E−9	f	±1	<26	62	pp	0	BASILE	77	SPEC
<7.E−10	f	+1,2	<20	52	p	0	[13] FABJAN	75	CNTR
		+1,2	>4.5		γ	0	[5,6] GALIK	74	CNTR
		+1,2	>1.5	12	e^-	0	[5,6] BELLAMY	68	CNTR
		+1,2	>0.9		γ	0	[6] BATHOW	67	CNTR
		+1,2	>0.9	6	γ	0	[6] FOSS	67	CNTR

[1] HUENTRUP 96 quote 95% CL limits for production of fragments with charge differing by as much as ±1/3 (in units of e) for charge $6 \le Z \le 10$.
[2] BUSKULIC 93C limits for inclusive quark production are more conservative if the ALEPH hadronic fragmentation function is assumed.
[3] CECCHINI 93 limit at 90%CL for $23/3 \le Z \le 40/3$, for 16A GeV O, 14.5A Si, and 200A S incident on Cu target. Other limits are 2.3×10^{-4} for $17/3 \le Z \le 20/3$ and 1.2×10^{-4} for $20/3 \le Z \le 23/3$.
[4] GHOSH 92 reports measurement of spallation fragment charge based on ionization in emulsion. Out of 650 measured tracks, 2 were consistent with charge $5e/3$, and 4 with $7e/3$.
[5] Hadronic quark.
[6] Leptonic quark.
[7] HE 91 limits are for charges of the form $N \pm 1/3$ from 23/3 to 38/3, and correspond to cross-section limits of 380μb (Pb) and 320μb (Cu).
[8] The limits apply to projectile fragment charges of 17, 19, 20, 22, 23 in units of $e/3$.
[9] The limits apply to projectile fragment charges of 16, 17, 19, 20, 22, 23 in units of $e/3$.
[10] Flux limits and mass range depend on charge.
[11] Bound to nuclei.
[12] Quark lifetimes $> 1 \times 10^{-8}$ s.
[13] One candidate m <0.17 GeV.

Quark Flux — Cosmic Ray Searches

Shielding values followed with an asterisk indicate altitude in km. Shielding values not followed with an asterisk indicate sea level in kg/cm^2.

FLUX ($cm^{-2} sr^{-1} s^{-1}$)	CHG ($e/3$)	MASS (GeV)	SHIELDING	DOCUMENT ID		TECN
< 1.E−8	±1/6–1/10			[1] AGNESE	15	CDMS
< 9.2E−15	±1		3800	[2] AMBROSIO	00C	MCRO
<2.1E−15	±1			MORI	91	KAM2
<2.3E−15	±2			MORI	91	KAM2
<2.E−10	±1,2		0.3	WADA	88	CNTR
	±4		0.3	[3] WADA	88	CNTR
	±4		0.3	[4] WADA	86	CNTR
<1.E−12	±2,3/2		−70.	[5] KAWAGOE	84B	PLAS
<9.E−10	±1,2		0.3	WADA	84B	CNTR
<4.E−9	±4		0.3	WADA	84B	CNTR
<2.E−12	±1,2,3		−0.3 *	MASHIMO	83	CNTR
<3.E−10	±1,2		0.3	MARINI	82	CNTR
<2.E−11	±1,2			MASHIMO	82	CNTR
<8.E−10	±1,2		0.3	[5] NAPOLITANO	82	CNTR
				[6] YOCK	78	CNTR
<1.E−9				[7] BRIATORE	76	ELEC
<2.E−11	+1			[8] HAZEN	75	CC
<2.E−10	+1,2			KRISOR	75	CNTR
<1.E−7	+1,2			[8,9] CLARK	74B	CC
<3.E−10	+1	>20		KIFUNE	74	CNTR
<8.E−11	+1			[8] ASHTON	73	CNTR
<2.E−8	+1,2			HICKS	73B	CNTR
<5.E−10	+4		2.8 *	BEAUCHAMP	72	CNTR
<1.E−10	+1,2			[8] BOHM	72B	CNTR
<1.E−10	+1,2		2.8 *	COX	72	ELEC
<3.E−10	+2			CROUCH	72	CNTR
<3.E−8			7	[7] DARDO	72	CNTR
<4.E−9	+1			[8] EVANS	72	CC
<2.E−9		>10		[7] TONWAR	72	CNTR
<2.E−10	+1		2.8 *	CHIN	71	CNTR
<3.E−10	+1,2			[8] CLARK	71B	CC
<1.E−10	+1,2			[8] HAZEN	71	CC
<5.E−10	+1,2		3.5 *	BOSIA	70	CNTR
	+1,2	<6.5		[8] CHU	70	HLBC
<2.E−9	+1			FAISSNER	70B	CNTR
<2.E−10	+1,2		0.8 *	KRIDER	70	CNTR
<5.E−11	+2			CAIRNS	69	CC
<8.E−10	+1,2	<10		FUKUSHIMA	69	CNTR
	+2			[8,10] MCCUSKER	69	CC
<1.E−10		>5	1.7,3.6	[7] BJORNBOE	68	CNTR
<1.E−8	±1,2,4		6.3,.2 *	[5] BRIATORE	68	CNTR
<3.E−8		>2		FRANZINI	68	CNTR
<9.E−11	±1,2			GARMIRE	68	CNTR

<4.E−10	±1			HANAYAMA	68	CNTR
<3.E−8		>15		KASHA	68	OSPK
<2.E−10	+2			KASHA	68B	CNTR
<2.E−10	+4			KASHA	68C	CNTR
<2.E−10	+2		6	BARTON	67	CNTR
<2.E−7	+4		0.008,0.5 *	BUHLER	67	CNTR
<5.E−10	1,2		0.008,0.5 *	BUHLER	67B	CNTR
<4.E−10	+1,2			GOMEZ	67	CNTR
<2.E−9	+2			KASHA	67	CNTR
<2.E−10	+2		220	BARTON	66	CNTR
<2.E−9	+1,2		0.5 *	BUHLER	66	CNTR
<3.E−9	+1,2			KASHA	66	CNTR
<2.E−9	+1,2			LAMB	66	CNTR
<2.E−8	+1,2	>7	2.8 *	DELISE	65	CNTR
<5.E−8	+2	>2.5	0.5 *	MASSAM	65	CNTR
<2.E−8	+1		2.5 *	BOWEN	64	CNTR
<2.E−7	+1		0.8	SUNYAR	64	CNTR

[1] See AGNESE 15 Fig.6 for limits on vertical density as function of charge extending to $|q|/e < 1/10$.

[2] AMBROSIO 00C limit is below 11×10^{-15} for $0.25 < q/e < 0.5$, and is changing rapidly near q/e=2/3, where it is 2×10^{-14}.

[3] Distribution in celestial sphere was described as anisotropic.

[4] With telescope axis at zenith angle 40° to the south.

[5] Leptonic quarks.

[6] Lifetime $> 10^{-8}$ s; charge ±0.70, 0.68, 0.42; and mass >4.4, 4.8, and 20 GeV, respectively.

[7] Time delayed air shower search.

[8] Prompt air shower search.

[9] Also $e/4$ and $e/6$ charges.

[10] No events in subsequent experiments.

Quark Density — Matter Searches

QUARKS/ NUCLEON	CHG (e/3)	MASS (GeV)	MATERIAL/METHOD	EVTS	DOCUMENT ID	
<1.17E−22			silicone oil drops	0	[1] LEE	02
<4.71E−22			silicone oil drops	1	[2] HALYO	00
<4.7E−21	±1,2		silicone oil drops	0	MAR	96
<8.E−22	+2		Si/infrared photoionization	0	PERERA	93
<5.E−27	±1,2		sea water/levitation	0	HOMER	92
<4.E−20	±1,2		meteorites/mag. levitation	0	JONES	89
<1.E−19	±1,2		various/spectrometer	0	MILNER	87
<5.E−22	±1,2		W/levitation	0	SMITH	87
<3.E−20	+1,2		org liq/droplet tower	0	VANPOLEN	87
<6.E−20	−1,2		org liq/droplet tower	0	VANPOLEN	87
<3.E−21	±1		Hg drops-untreated	0	SAVAGE	86
<3.E−22	±1,2		levitated niobium	0	SMITH	86
<2.E−26	±1,2		^{4}He/levitation	0	SMITH	86B
<2.E−20	>±1	0.2–250	niobium+tungs/ion	0	MILNER	85
<1.E−21	±1		levitated niobium	0	SMITH	85
	+1,2	<100	niobium/mass spec	0	KUTSCHERA	84
<5.E−22			levitated steel	0	MARINELLI	84
<9.E−20	± <13		water/oil drop	0	JOYCE	83
<2.E−21	> | ± 1/2|		levitated steel	0	LIEBOWITZ	83
<1.E−19	±1,2		photo ion spec	0	VANDESTEEG	83
<2.E−20			mercury/oil drop	0	[3] HODGES	81
1.E−20	+1		levitated niobium	4	[4] LARUE	81
1.E−20	−1		levitated niobium	4	[4] LARUE	81
<1.E−21			levitated steel	0	MARINELLI	80B
<6.E−16			helium/mass spec	0	BOYD	79
1.E−20	+1		levitated niobium	2	[4] LARUE	79
<4.E−28			earth+/ion beam	0	OGOROD...	79
<5.E−15	+1		tungs./mass spec	0	BOYD	78
<5.E−16	+3	<1.7	hydrogen/mass spec	0	BOYD	78B
<1.E−21	±2,4		water/ion beam	0	LUND	78
<6.E−15	>1/2		levitated tungsten	0	PUTT	78
<1.E−22			metals/mass spec	0	SCHIFFER	78
<5.E−15			levitated tungsten ox	0	BLAND	77
<3.E−21			levitated iron	0	GALLINARO	77
2.E−21	−1		levitated niobium	1	[4] LARUE	77
4.E−21	+1		levitated niobium	2	[4] LARUE	77
<1.E−13	+3	<7.7	hydrogen/mass spec	0	MULLER	77
<5.E−27			water+/ion beam	0	OGOROD...	77
<1.E−21			lunar+/ion spec	0	STEVENS	76
<1.E−15	+1	<60	oxygen+/ion spec	0	ELBERT	70
<5.E−19			levitated graphite	0	MORPURGO	70
<5.E−23			water+/atom beam	0	COOK	69
<1.E−17	±1,2		levitated graphite	0	BRAGINSK	68
<1.E−17			water+/uv spec	0	RANK	68
<3.E−19	±1		levitated iron	0	STOVER	67
<1.E−10			sun/uv spec	0	[5] BENNETT	66
<1.E−17	+1,2		meteorites+/ion beam	0	CHUPKA	66
<1.E−16	±1		levitated graphite	0	GALLINARO	66
<1.E−22			argon/electrometer	0	HILLAS	59
	−2		levitated oil	0	MILLIKAN	10

[1] 95% CL limit for fractional charge particles with $0.18e \leq |Q_{residual}| \leq 0.82e$ in total of 70.1 mg of silicone oil.

[2] 95% CL limit for particles with fractional charge $|Q_{residual}| > 0.16e$ in total of 17.4 mg of silicone oil.

[3] Also set limits for $Q = \pm e/6$.

[4] Note that in PHILLIPS 88 these authors report a subtle magnetic effect which could account for the apparent fractional charges.

[5] Limit inferred by JONES 77B.

REFERENCES FOR Free Quark Searches

AGNESE	15	PRL 114 111302	R. Agnese *et al.*	(CDMS Collab.)
CHATRCHYAN	13AR	PR D87 092008	S. Chatrchyan *et al.*	(CMS Collab.)
LEE	02	PR D66 012002	I.T. Lee *et al.*	
AMBROSIO	00C	PR D62 052003	M. Ambrosio *et al.*	(MACRO Collab.)
HALYO	00	PRL 84 2576	V. Halyo *et al.*	
ABREU	97D	PL B396 315	P. Abreu *et al.*	(DELPHI Collab.)
HUENTRUP	96	PR C53 358	G. Huentrup *et al.*	(SIEG)
MAR	96	PR D53 6017	N.M. Mar *et al.*	(SLAC, SCHAF, LANL, UCI)
AKERS	95R	ZPHY C67 203	R. Akers *et al.*	(OPAL Collab.)
BUSKULIC	93C	PL B303 198	D. Buskulic *et al.*	(ALEPH Collab.)
CECCHINI	93	ASP 1 369	S. Cecchini *et al.*	
PERERA	93	PRL 70 1053	A.G.U. Perera *et al.*	(PITT)
ABE	92J	PR D46 1889	F. Abe *et al.*	(CDF Collab.)
GHOSH	92	NC 105A 99	D. Ghosh *et al.*	(JADA, BANGB)
HOMER	92	ZPHY C55 549	G.J. Homer *et al.*	(RAL, SHMP, LOQM)
BASILE	91	NC 104A 405	M. Basile *et al.*	(BGNA, INFN, CERN, PLRM+)
HE	91	PR C44 1672	Y.B. He, P.B. Price	(UCB)
MATIS	91	NP A525 513	H.S. Matis *et al.*	(LBL, SFSU, UCI+)
MORI	91	PR D43 2843	M. Mori *et al.*	(Kamiokande II Collab.)
ADACHI	90C	PL B244 352	I. Adachi *et al.*	(TOPAZ Collab.)
BOWCOCK	89B	PR D40 263	T.J.V. Bowcock *et al.*	(CLEO Collab.)
CALLOWAY	89	PL B232 549	D. Calloway *et al.*	(SFSU, UCI, LBL+)
JONES	89	ZPHY C43 349	W.G. Jones *et al.*	(LOIC, RAL)
MATIS	89	PR D39 1851	H.S. Matis *et al.*	(LBL, SFSU, UCI+)
NAKAMURA	89	PR D39 1261	T.T. Nakamura *et al.*	(KYOT, TMTC)
ALLASIA	88	PR D37 219	D. Allasia *et al.*	(WA25 Collab.)
HOFFMANN	88	PL B200 583	A. Hofmann *et al.*	(SIEG, USF)
PHILLIPS	88	NIM A264 125	J.D. Phillips, W.M. Fairbank, J. Navarro	(STAN)
WADA	88	NC 11C 229	T. Wada, Y. Yamashita, I. Yamamoto	(OKAY)
GERBIER	87	PRL 59 2535	G. Gerbier *et al.*	(UCB, CERN)
LYONS	87	ZPHY C36 363	L. Lyons *et al.*	(OXF, RAL, LOIC)
MILNER	87	PR D36 37	R.E. Milner *et al.*	(CIT)
SHAW	87	PR D36 3533	G.L. Shaw *et al.*	(UCI, LBL, LANL, SFSU)
SMITH	87	PL B197 447	P.F. Smith *et al.*	(RAL, LOIC)
VANPOLEN	87	PR D36 1983	J. van Polen, R.T. Hagstrom, G. Hirsch	(ANL+)
ABACHI	86C	PR D33 2733	S. Abachi *et al.*	(UCLA, LBL, UCD)
SAVAGE	86	PL 167B 481	M.L. Savage *et al.*	(SFSU)
SMITH	86	PL B171 129	P.F. Smith *et al.*	(RAL, LOIC)
SMITH	86B	PL B181 407	P.F. Smith *et al.*	(RAL, LOIC)
WADA	86	NC 9C 358	T. Wada	(OKAY)
ALBRECHT	85G	PL 156B 134	H. Albrecht *et al.*	(ARGUS Collab.)
BANNER	85	PL 156B 129	M. Banner *et al.*	(UA2 Collab.)
MILNER	85	PRL 54 1472	R.E. Milner *et al.*	(CIT)
SMITH	85	PL 153B 188	P.F. Smith *et al.*	(RAL, LOIC)
AIHARA	84	PRL 52 168	H. Aihara *et al.*	(TPC Collab.)
AIHARA	84B	PRL 52 2332	H. Aihara *et al.*	(TPC Collab.)
BARWICK	84	PR D30 691	S.W. Barwick, J.A. Musser, J.D. Stevenson	(UCB)
BERGSMA	84B	ZPHY C24 217	F. Bergsma *et al.*	(CHARM Collab.)
BONDAR	84	JETPL 40 1265	A.E. Bondar *et al.*	(NOVO)
		Translated from ZETFP 40 440.		
GURYN	84	PL 139B 313	W. Guryn *et al.*	(FRAS, LBL, NWES, STAN+)
KAWAGOE	84B	LNC 41 604	K. Kawagoe *et al.*	(TOKY)
KUTSCHERA	84	PR D29 791	W. Kutschera *et al.*	(ANL, FNAL)
MARINELLI	84	PL 137B 439	M. Marinelli, G. Morpurgo	(GENO)
WADA	84B	LNC 40 329	T. Wada, Y. Yamashita, I. Yamamoto	(OKAY)
AUBERT	83C	PL 133B 461	J.J. Aubert *et al.*	(EMC Collab.)
BANNER	83	PL 121B 187	M. Banner *et al.*	(UA2 Collab.)
JOYCE	83	PRL 51 731	D.C. Joyce *et al.*	(SFSU)
LIEBOWITZ	83	PRL 50 1640	D. Liebowitz, M. Binder, K.O.H. Ziock	(UVA)
LINDGREN	83	PRL 51 1621	M.A. Lindgren *et al.*	(SFSU, UCR, UCI+)
MASHIMO	83	PL 128B 327	T. Mashimo *et al.*	(ICEPP)
PRICE	83	PRL 50 566	P.B. Price *et al.*	(UCB)
VANDESTEEG	83	PRL 50 1234	M.J.H. van de Steeg, H.W.H.M. Jongbloets, P. Wyder	
MARINI	82	PR D26 1777	A. Marini *et al.*	(FRAS, LBL, NWES, STAN+)
MARINI	82B	PRL 48 1649	A. Marini *et al.*	(FRAS, LBL, NWES, STAN+)
MASHIMO	82	JPSJ 51 3067	T. Mashimo, K. Kawagoe, M. Koshiba	(INUS)
NAPOLITANO	82	PR D25 2837	J. Napolitano *et al.*	(STAN, FRAS, LBL+)
ROSS	82	PL 118B 199	M.C. Ross *et al.*	(FRAS, LBL, NWES, STAN+)
HODGES	81	PRL 47 1651	C.L. Hodges *et al.*	(UCR, SFSU)
LARUE	81	PRL 46 967	G.S. Larue, J.D. Phillips, W.M. Fairbank	(STAN)
WEISS	81	PL 101B 439	J.M. Weiss *et al.*	(SLAC, LBL, UCB)
BARTEL	80	ZPHY C6 295	W. Bartel *et al.*	(JADE Collab.)
BASILE	80	LNC 29 251	M. Basile *et al.*	(BGNA, CERN, FRAS, ROMA+)
BUSSIERE	80	NP B174 1	A. Bussiere *et al.*	(BGNA, SACL, LAPP)
MARINELLI	80B	PL 94B 433	M. Marinelli, G. Morpurgo	(GENO)
Also		PL 94B 427	M. Marinelli, G. Morpurgo	(GENO)
BOYD	79	PRL 43 1288	R.N. Boyd *et al.*	(OSU)
BOZZOLI	79	NP B159 363	W. Bozzoli *et al.*	(BGNA, LAPP, SACL+)
LARUE	79	PRL 42 142	G.S. Larue, W.M. Fairbank, J.D. Phillips	(STAN)
Also		PRL 42 1019	G.S. Larue, W.M. Fairbank, J.D. Phillips	
OGOROD...	79	JETP 49 953	D.D. Ogorodnikov, I.M. Samoilov, A.M. Solntsev	
		Translated from ZETF 76 1881.		
STEVENSON	79	PR D20 82	M.L. Stevenson	(LBL)
BASILE	78	NC 45A 171	M. Basile *et al.*	(CERN, BGNA)
BASILE	78B	NC 45A 281	M. Basile *et al.*	(CERN, BGNA)
BOYD	78	PRL 40 216	R.N. Boyd *et al.*	(ROCH)
BOYD	78B	PL 72B 484	R.N. Boyd *et al.*	(ROCH)
LUND	78	RA 25 75	T. Lund, R. Brandt, Y. Fares	(MARB)
PUTT	78	PR D17 1466	G.D. Putt, P.C.M. Yock	(AUCK)
SCHIFFER	78	PR D17 2241	J.P. Schiffer *et al.*	(CHIC, ANL)
YOCK	78	PR D18 641	P.C.M. Yock	(AUCK)
ANTREASYAN	77	PRL 39 513	D. Antreasyan *et al.*	(EFI, PRIN)
BASILE	77	NC 40A 41	M. Basile *et al.*	(CERN, BGNA)
BLAND	77	PRL 39 369	R.W. Bland *et al.*	(SFSU)
GALLINARO	77	PRL 38 1255	G. Gallinaro, M. Marinelli, G. Morpurgo	(GENO)
JONES	77B	RMP 49 717	L.W. Jones	
LARUE	77	PRL 38 1011	G.S. Larue, W.M. Fairbank, A.F. Hebard	(STAN)
MULLER	77	SCI 196 521	R.A. Muller *et al.*	(LBL)
OGOROD...	77	JETP 45 857	D.D. Ogorodnikov, I.M. Samoilov, A.M. Solntsev	
		Translated from ZETF 72 1633.		
BALDIN	76	SJNP 22 264	B.Y. Baldin *et al.*	(JINR)
		Translated from YAF 22 512.		
BRIATORE	76	NC 31A 553	L. Briatore *et al.*	(LCGT, FRAS, FREIB)
STEVENS	76	PR D14 716	C.M. Stevens, J.P. Schiffer, W. Chupka	(ANL)
ALBROW	75	NP B97 189	M.G. Albrow *et al.*	(CERN, DARE, FOM+)
FABJAN	75	NP B101 349	C.W. Fabjan *et al.*	(CERN, MPIM)
HAZEN	75	NP B95 189	W.E. Hazen *et al.*	(MICH, LEED)
JOVANOV...	75	PL 56B 105	J.V. Jovanovich *et al.*	(MANI, AACH, CERN+)
KRISOR	75	NC 27A 132	K. Krisor	(AACH3)
CLARK	74B	PR D10 2721	A.F. Clark *et al.*	(LLL)

Quark Particle Listings

Free Quark Searches

GALIK 74 PR D9 1856 R.S. Galik *et al.* (SLAC, FNAL)
KIFUNE 74 JPSJ 36 629 T. Kifune *et al.* (TOKY, KEK)
NASH 74 PRL 32 858 T. Nash *et al.* (FNAL, CORN, NYU)
ALPER 73 PL 46B 265 B. Alper *et al.* (CERN, LIVP, LUND, BOHR+)
ASHTON 73 JP A6 577 F. Ashton *et al.* (DURH)
HICKS 73B NC 14A 65 R.B. Hicks, R.W. Flint, S. Standil (MANI)
LEIPUNER 73 PRL 31 1226 L.B. Leipuner *et al.* (BNL, YALE)
BEAUCHAMP 72 PR D6 1211 W.T. Beauchamp *et al.* (ARIZ)
BOHM 72B PRL 28 326 A. Bohm *et al.* (AACH)
BOTT 72 PL 40B 693 M. Bott-Bodenhausen *et al.* (CERN, MPIM)
COX 72 PR D6 1203 A.J. Cox *et al.* (ARIZ)
CROUCH 72 PR D5 2667 M.F. Crouch, K. Mori, G.R. Smith (CASE)
DARDO 72 NC 9A 319 M. Dardo *et al.* (TORI)
EVANS 72 PRSE A70 143 G.R. Evans *et al.* (EDIN, LEED)
TONWAR 72 JP A5 569 S.C. Tonwar, S. Naranan, B.V. Sreekantan (TATA)
ANTIPOV 71 NP B29 374 Y.M. Antipov *et al.* (SERP)
CHIN 71 NC 2A 419 S. Chin *et al.* (OSAK)
CLARK 71B PRL 27 51 A.F. Clark *et al.* (LLL, LBL)
HAZEN 71 PRL 26 582 W.E. Hazen (MICH)
BOSIA 70 NC 66A 167 G.F. Bosia, L. Briatore (TORI)
CHU 70 PRL 24 917 W.T. Chu *et al.* (OSU, ROSE, KANS)
Also PRL 25 550 W.W.M. Allison *et al.* (ANL)
ELBERT 70 NP B20 217 J.W. Elbert *et al.* (WISC)
FAISSNER 70B PRL 24 1357 H. Faissner *et al.* (AACH3)
KRIDER 70 PR D1 835 E.P. Krider, T. Bowen, R.M. Kalbach (ARIZ)
MORPURGO 70 NIM 79 95 G. Morpurgo, G. Gallinaro, G. Palmieri (GENO)
ALLABY 69B NC 64A 75 J.V. Allaby *et al.* (CERN)
ANTIPOV 69 PL 29B 245 Y.M. Antipov *et al.* (SERP)
ANTIPOV 69B PL 30B 576 Y.M. Antipov *et al.* (SERP)
CAIRNS 69 PR 186 1394 I. Cairns *et al.* (SYDN)
COOK 69 PR 188 2092 D.D. Cook *et al.* (ILL)
FUKUSHIMA 69 PR 178 2058 Y. Fukushima *et al.* (TOKY)
MCCUSKER 69 PRL 23 658 C.B.A. McCusker, I. Cairns (SYDN)
BELLAMY 68 PR 166 1391 E.H. Bellamy *et al.* (STAN, SLAC)
BJORNBOE 68 NC B53 241 J. Bjornboe *et al.* (BOHR, TATA, BERN+)
BRAGINSK 68 JETP 27 51 V.B. Braginsky *et al.* (MOSU)
Translated from ZETF 54 91.
BRIATORE 68 NC 57A 850 L. Briatore *et al.* (TORI, CERN, BGNA)
FRANZINI 68 PRL 21 1013 P. Franzini, S. Shulman (COLU)
GARMIRE 68 PR 166 1280 G. Garmire, C. Leong, V. Sreekantan (MIT)
HANAYAMA 68 CJP 46 S734 Y. Hanayama *et al.* (OSAK)
KASHA 68 PR 172 1297 H. Kasha, R.J. Stefanski (BNL, YALE)
KASHA 68B PRL 20 217 H. Kasha *et al.* (BNL, YALE)
KASHA 68C CJP 46 S730 H. Kasha *et al.* (BNL, YALE)
RANK 68 PR 176 1635 D. Rank (MICH)
BARTON 67 PRSL 90 87 J.C. Barton (NPOL)
BATHOW 67 PL 25B 163 G. Bathow *et al.* (DESY)
BUHLER 67 NC 49A 209 A. Buhler-Broglin *et al.* (CERN, BGNA)
BUHLER 67B NC 51A 837 A. Buhler-Broglin *et al.* (CERN, BGNA+)
FOSS 67 PL 25B 166 J. Foss *et al.* (MIT)
GOMEZ 67 PRL 18 1022 R. Gomez *et al.* (CIT)
KASHA 67 PR 154 1263 H. Kasha *et al.* (BNL, YALE)
STOVER 67 PR 164 1599 R.W. Stover, T.I. Moran, J.W. Trischka (SYRA)
BARTON 66 PL 21 360 J.C. Barton, C.T. Stockel (NPOL)
BENNETT 66 PRL 17 1196 W.R. Bennett (YALE)
BUHLER 66 NC 45A 520 A. Buhler-Broglin *et al.* (CERN, BGNA+)
CHUPKA 66 PRL 17 60 W.A. Chupka, J.P. Schiffer, C.M. Stevens (ANL)
GALLINARO 66 PL 23 609 G. Gallinaro, G. Morpurgo (GENO)
KASHA 66 PR 150 1140 H. Kasha, L.B. Leipuner, R.K. Adair (BNL, YALE)
LAMB 66 PRL 17 1068 R.C. Lamb *et al.* (ANL)
DELISE 65 PR 140 B458 D.A. de Lise, T. Bowen (ARIZ)
DORFAN 65 PRL 14 999 D.E. Dorfan *et al.* (COLU)
FRANZINI 65B PRL 14 196 P. Franzini *et al.* (BNL, COLU)
MASSAM 65 NC 40A 589 T. Massam, T. Muller, A. Zichichi (CERN)
BINGHAM 64 PL 9 201 H.H. Bingham *et al.* (CERN, EPOL)
BLUM 64 PRL 13 353A W. Blum *et al.* (CERN)
BOWEN 64 PRL 13 728 T. Bowen *et al.* (ARIZ)
HAGOPIAN 64 PRL 13 280 V. Hagopian *et al.* (PENN, BNL)
LEIPUNER 64 PRL 12 423 L.B. Leipuner *et al.* (BNL, YALE)
MORRISON 64 PL 9 199 D.R.O. Morrison (CERN)
SUNYAR 64 PR 136 B1157 A.W. Sunyar, A.Z. Schwarzschild, P.I. Connors (BNL)
HILLAS 59 NAT 184 B92 A.M. Hillas, T.E. Cranshaw (AERE)
MILLIKAN 10 Phil Mag 19 209 R.A. Millikan (CHIC)

OTHER RELATED PAPERS

LYONS 85 PRPL C129 225 L. Lyons (OXF)
Review
MARINELLI 82 PRPL 85 161 M. Marinelli, G. Morpurgo (GENO)
Review

• Indicates the particle is in the Meson Summary Table

(continued on the next page)

CHARMED, STRANGE MESONS ($C = S = \pm 1$)

BOTTOM MESONS ($B = \pm 1$)

BOTTOM, STRANGE MESONS ($B = \pm 1$, $S = \mp 1$)

BOTTOM, CHARMED MESONS ($B = C = \pm 1$)

***c*$\overline{c}$ MESONS**

***b*$\overline{b}$ MESONS**

• Indicates the particle is in the Meson Summary Table

Related Reviews in Volume 1

(Continued on next page.)

LIGHT UNFLAVORED MESONS ($S = C = B = 0$)

For $I = 1$ (π, b, ρ, a): $u\overline{d}$, $(u\overline{u}-d\overline{d})/\sqrt{2}$, $d\overline{u}$;
for $I = 0$ (η, η', h, h', ω, ϕ, f, f'): $c_1(u\overline{u} + d\overline{d}) + c_2(s\overline{s})$

$\pi^{\pm}$

$I^G(J^P) = 1^-(0^-)$

We have omitted some results that have been superseded by later experiments. The omitted results may be found in our 1988 edition Physics Letters **B204** 1 (1988).

$\pi^{\pm}$ MASS

The most accurate charged pion mass measurements are based upon x-ray wavelength measurements for transitions in π^--mesonic atoms. The observed line is the blend of three components, corresponding to different K-shell occupancies. JECKELMANN 94 revisits the occupancy question, with the conclusion that two sets of occupancy ratios, resulting in two different pion masses (Solutions A and B), are equally probable. We choose the higher Solution B since only this solution is consistent with a positive mass-squared for the muon neutrino, given the precise muon momentum measurements now available (DAUM 91, ASSAMAGAN 94, and ASSAMAGAN 96) for the decay of pions at rest. Earlier mass determinations with pi-mesonic atoms may have used incorrect K-shell screening corrections.

Measurements with an error of > 0.005 MeV have been omitted from this Listing.

VALUE (MeV)		DOCUMENT ID		TECN	CHG	COMMENT
139.57061±0.00024 OUR FIT	Error includes scale factor of 1.6.					
139.57061±0.00023 OUR AVERAGE	Error includes scale factor of 1.5. See the ideogram below.					
139.57077±0.00018	[1] TRASSINELLI	16	CNTR			X-ray transitions in pionic N2
139.57071±0.00053	[2] LENZ	98	CNTR	–		pionic N2-atoms gas target
139.56995±0.00035	[3] JECKELMANN	94	CNTR	–		π^- atom, Soln. B
• • • We do not use the following data for averages, fits, limits, etc. • • •						
139.57022±0.00014	[4] ASSAMAGAN	96	SPEC	+		$\pi^+ \to \mu^+\nu_\mu$
139.56782±0.00037	[5] JECKELMANN	94	CNTR	–		π^- atom, Soln. A
139.56996±0.00067	[6] DAUM	91	SPEC	+		$\pi^+ \to \mu^+\nu$
139.56752±0.00037	[7] JECKELMANN	86B	CNTR	–		Mesonic atoms
139.5704 ±0.0011	[6] ABELA	84	SPEC	+		See DAUM 91
139.5664 ±0.0009	[8] LU	80	CNTR	–		Mesonic atoms
139.5686 ±0.0020	CARTER	76	CNTR	–		Mesonic atoms
139.5660 ±0.0024	[8,9] MARUSHEN...	76	CNTR	–		Mesonic atoms

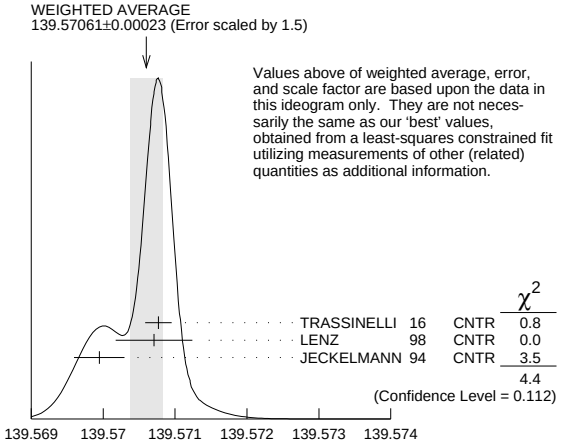

[1] TRASSINELLI 16 use the muonic oxygen line for online energy calibration of the pionic line.

[2] LENZ 98 result does not suffer K-electron configuration uncertainties as does JECKELMANN 94.

[3] JECKELMANN 94 Solution B (dominant 2-electron K-shell occupancy), chosen for consistency with positive $m^2_{\nu_\mu}$.

[4] ASSAMAGAN 96 measures the μ^+ momentum p_μ in $\pi^+ \to \mu^+\nu_\mu$ decay at rest to be 29.79200 ± 0.00011 MeV/c. Combined with the μ^+ mass and the assumption $m_{\nu_\mu} = 0$, this gives the π^+ mass above; if $m_{\nu_\mu} > 0$, m_{π^+} given above is a lower limit. Combined instead with m_μ and (assuming CPT) the π^- mass of JECKELMANN 94, p_μ gives an upper limit on m_{ν_μ} (see the ν_μ).

[5] JECKELMANN 94 Solution A (small 2-electron K-shell occupancy) in combination with either the DAUM 91 or ASSAMAGAN 94 pion decay muon momentum measurement yields a significantly negative $m^2_{\nu_\mu}$. It is accordingly not used in our fits.

[6] The DAUM 91 value includes the ABELA 84 result. The value is based on a measurement of the μ^+ momentum for π^+ decay at rest, $p_\mu = 29.79179 \pm 0.00053$ MeV, uses $m_\mu = 105.658389 \pm 0.000034$ MeV, and assumes that $m_{\nu_\mu} = 0$. The last assumption means that in fact the value is a lower limit.

[7] JECKELMANN 86B gives $m_\pi/m_e = 273.12677(71)$. We use $m_e = 0.51099906(15)$ MeV from COHEN 87. The authors note that two solutions for the probability distribution of K-shell occupancy fit equally well, and use other data to choose the lower of the two possible $\pi^\pm$ masses.

[8] These values are scaled with a new wavelength-energy conversion factor $V\lambda = 1.23984244(37) \times 10^{-6}$ eV m from COHEN 87. The LU 80 screening correction relies upon a theoretical calculation of inner-shell refilling rates.

[9] This MARUSHENKO 76 value used at the authors' request to use the accepted set of calibration γ energies. Error increased from 0.0017 MeV to include QED calculation error of 0.0017 MeV (12 ppm).

$m_{\pi^+} - m_{\mu^+}$

Measurements with an error > 0.05 MeV have been omitted from this Listing.

VALUE (MeV)	EVTS	DOCUMENT ID		TECN	CHG	COMMENT
• • • We do not use the following data for averages, fits, limits, etc. • • •						
33.91157±0.00067		[1] DAUM	91	SPEC	+	$\pi^+ \to \mu^+\nu$
33.9111 ±0.0011		ABELA	84	SPEC		See DAUM 91
33.925 ±0.025		BOOTH	70	CNTR	+	Magnetic spect.
33.881 ±0.035	145	HYMAN	67	HEBC	+	K^- He

[1] The DAUM 91 value assumes that $m_{\nu_\mu} = 0$ and uses our $m_\mu = 105.658389 \pm 0.000034$ MeV.

$(m_{\pi^+} - m_{\pi^-}) / m_{\text{average}}$

A test of CPT invariance.

VALUE (units 10^{-4})	DOCUMENT ID		TECN
2±5	AYRES	71	CNTR

$\pi^{\pm}$ MEAN LIFE

Measurements with an error $> 0.02 \times 10^{-8}$ s have been omitted.

VALUE (10^{-8} s)	DOCUMENT ID		TECN	CHG	COMMENT
2.6033 ±0.0005 OUR AVERAGE	Error includes scale factor of 1.2.				
2.60361±0.00052	[1] KOPTEV	95	SPEC	+	Surface μ^+'s
2.60231±0.00050±0.00084	NUMAO	95	SPEC	+	Surface μ^+'s
2.609 ±0.008	DUNAITSEV	73	CNTR	+	
2.602 ±0.004	AYRES	71	CNTR	±	
2.604 ±0.005	NORDBERG	67	CNTR	+	
2.602 ±0.004	ECKHAUSE	65	CNTR	+	
• • • We do not use the following data for averages, fits, limits, etc. • • •					
2.640 ±0.008	[2] KINSEY	66	CNTR	+	

[1] KOPTEV 95 combines the statistical and systematic errors; the statistical error dominates.

[2] Systematic errors in the calibration of this experiment are discussed by NORDBERG 67.

$(\tau_{\pi^+} - \tau_{\pi^-}) / \tau_{\text{average}}$

A test of CPT invariance.

VALUE (units 10^{-4})	DOCUMENT ID		TECN
5.5± 7.1	AYRES	71	CNTR
• • • We do not use the following data for averages, fits, limits, etc. • • •			
−14 ±29	PETRUKHIN	68	CNTR
40 ±70	BARDON	66	CNTR
23 ±40	[1] LOBKOWICZ	66	CNTR

[1] This is the most conservative value given by LOBKOWICZ 66.

π ELECTRIC POLARIZABILITY α_π

See HOLSTEIN 14 for a general review on hadron polarizability.

VALUE (10^{-4} fm^3)	EVTS	DOCUMENT ID		TECN	COMMENT
2.0±0.6±0.7	63k	[1] ADOLPH	15A	SPEC	$\pi^-\gamma \to \pi^-\gamma$ Compton scatt.

[1] Value is derived assuming $\alpha_\pi = -\beta_\pi$.

π^+ DECAY MODES

π^- modes are charge conjugates of the modes below.

For decay limits to particles which are not established, see the section on Searches for Axions and Other Very Light Bosons.

Meson Particle Listings

$\pi^{\pm}$

	Mode		Fraction (Γ_i/Γ)		Confidence level
Γ_1	$\mu^+\nu_\mu$	[a]	(99.98770 ± 0.00004) %		
Γ_2	$\mu^+\nu_\mu\gamma$	[b]	(2.00 ± 0.25) × 10^{-4}		
Γ_3	$e^+\nu_e$	[a]	(1.230 ± 0.004) × 10^{-4}		
Γ_4	$e^+\nu_e\gamma$	[b]	(7.39 ± 0.05) × 10^{-7}		
Γ_5	$e^+\nu_e\pi^0$		(1.036 ± 0.006) × 10^{-8}		
Γ_6	$e^+\nu_e e^+e^-$		(3.2 ± 0.5) × 10^{-9}		
Γ_7	$e^+\nu_e\nu\overline{\nu}$		< 5	× 10^{-6}	90%
	Lepton Family number (*LF*) or Lepton number (*L*) violating modes				
Γ_8	$\mu^+\overline{\nu}_e$	*L*	[c] < 1.5	× 10^{-3}	90%
Γ_9	$\mu^+\nu_e$	*LF*	[c] < 8.0	× 10^{-3}	90%
Γ_{10}	$\mu^-e^+e^+\nu$	*LF*	< 1.6	× 10^{-6}	90%

[a] Measurements of $\Gamma(e^+\nu_e)/\Gamma(\mu^+\nu_\mu)$ always include decays with γ's, and measurements of $\Gamma(e^+\nu_e\gamma)$ and $\Gamma(\mu^+\nu_\mu\gamma)$ never include low-energy γ's. Therefore, since no clean separation is possible, we consider the modes with γ's to be subreactions of the modes without them, and let $[\Gamma(e^+\nu_e) + \Gamma(\mu^+\nu_\mu)]/\Gamma_{\rm total} = 100\%$.

[b] See the Particle Listings below for the energy limits used in this measurement; low-energy γ's are not included.

[c] Derived from an analysis of neutrino-oscillation experiments.

π^+ BRANCHING RATIOS

$\Gamma(e^+\nu_e)/\Gamma_{\rm total}$ Γ_3/Γ

See note [a] in the list of π^+ decay modes just above, and see also the next block of data. See also the note on "Decay Constants of Charged Pseudoscalar Mesons" in the D_s^+ Listings.

VALUE (units 10^{-4})	DOCUMENT ID
1.230±0.004 OUR EVALUATION	

$[\Gamma(e^+\nu_e) + \Gamma(e^+\nu_e\gamma)]/[\Gamma(\mu^+\nu_\mu) + \Gamma(\mu^+\nu_\mu\gamma)]$ $(\Gamma_3+\Gamma_4)/(\Gamma_1+\Gamma_2)$

See note [a] in the list of π^+ decay modes above. See NUMAO 92 for a discussion of e-μ universality. See also the note on "Decay Constants of Charged Pseudoscalar Mesons" in the D_s^+ Listings.

VALUE (units 10^{-4})	EVTS	DOCUMENT ID		TECN	CHG	COMMENT
1.2327±0.0023 OUR AVERAGE						
1.2344 ± 0.0023 ± 0.0019	400k	AGUILAR-AR...15		CNTR	+	Stopping π^+
1.2346 ± 0.0035 ± 0.0036	120k	CZAPEK	93	CALO		Stopping π^+
1.2265 ± 0.0034 ± 0.0044	190k	BRITTON	92	CNTR		Stopping π^+
1.218 ± 0.014	32k	BRYMAN	86	CNTR		Stopping π^+
• • • We do not use the following data for averages, fits, limits, etc. • • •						
1.273 ± 0.028	11k	[1] DICAPUA	64	CNTR		
1.21 ± 0.07		ANDERSON	60	SPEC		

[1] DICAPUA 64 has been updated using the current mean life.

$\Gamma(\mu^+\nu_\mu\gamma)/\Gamma_{\rm total}$ Γ_2/Γ

Note that measurements here do not cover the full kinematic range.

VALUE (units 10^{-4})	EVTS	DOCUMENT ID		TECN	CHG	COMMENT
2.0 ±0.24±0.08		[1] BRESSI	98	CALO	+	Stopping π^+
• • • We do not use the following data for averages, fits, limits, etc. • • •						
1.24±0.25	26	CASTAGNOLI	58	EMUL		KE_μ < 3.38 MeV

[1] BRESSI 98 result is given for $E_\gamma > 1$ MeV only. Result agrees with QED expectation, 2.283×10^{-4} and does not confirm discrepancy of earlier experiment CASTAGNOLI 58.

$\Gamma(e^+\nu_e\gamma)/\Gamma_{\rm total}$ Γ_4/Γ

The very different values reflect the very different kinematic ranges covered (bigger range, bigger value). And none of them covers the whole kinematic range.

VALUE (units 10^{-8})	EVTS	DOCUMENT ID		TECN	COMMENT
73.86±0.54	65k	[1] BYCHKOV	09	PIBE	$e^+\nu\gamma$ at rest
• • • We do not use the following data for averages, fits, limits, etc. • • •					
16.1 ±2.3		[2] BOLOTOV	90B	SPEC	17 GeV $\pi^- \to e^-\overline{\nu}_e\gamma$
5.6 ±0.7	226	[3] STETZ	78	SPEC	$P_e > 56$ MeV/c
3.0	143	DEPOMMIER	63B	CNTR	$(KE)_{e^+\gamma} > 48$ MeV

[1] This BYCHKOV 09 value is for $E_\gamma > 10$ MeV and $\Theta_{e^+\gamma} > 40^\circ$.

[2] BOLOTOV 90B is for $E_\gamma > 21$ MeV, $E_e > 70 - 0.8\,E_\gamma$.

[3] STETZ 78 is for an $e^-\gamma$ opening angle $> 132^\circ$. Obtains 3.7 when using same cutoffs as DEPOMMIER 63B.

$\Gamma(e^+\nu_e\pi^0)/\Gamma_{\rm total}$ Γ_5/Γ

VALUE (units 10^{-8})	EVTS	DOCUMENT ID		TECN	CHG	COMMENT
1.036±0.006 OUR AVERAGE						
1.036±0.006	64k	[1,2] POCANIC	04	PIBE	+	π decay at rest
1.026±0.039	1224	[3] MCFARLANE	85	CNTR	+	Decay in flight
1.00 $^{+0.08}_{-0.10}$	332	DEPOMMIER	68	CNTR	+	
1.07 ±0.21	38	[4] BACASTOW	65	OSPK	+	
1.10 ±0.26		[4] BERTRAM	65	OSPK	+	
1.1 ±0.2	43	[4] DUNAITSEV	65	CNTR	+	
0.97 ±0.20	36	[4] BARTLETT	64	OSPK	+	
• • • We do not use the following data for averages, fits, limits, etc. • • •						
1.15 ±0.22	52	[4] DEPOMMIER	63	CNTR	+	See DEPOMMIER 68

[1] POCANIC 04 normalizes to $e^+\nu_e$ decays, using the PDG 2004 value $B(\pi^+ \to e^+\nu_e) = (1.230 \pm 0.004) \times 10^{-4}$. We add their statistical (0.004×10^{-8}), systematic (0.004×10^{-8}) and systematic error due to the uncertainty of $B(\pi^+ \to e^+\nu_e)$ (0.003×10^{-8}) in quadrature.

[2] This result can be used to calculate V_{ud} from pion beta decay: $V_{ud}^{PIBETA} = 0.9728 \pm 0.0030$.

[3] MCFARLANE 85 combines a measured rate (0.394 ± 0.015)/s with 1982 PDG mean life.

[4] DEPOMMIER 68 says the result of DEPOMMIER 63 is at least 10% too large because of a systematic error in the π^0 detection efficiency, and that this may be true of all the previous measurements (also V. Soergel, private communication, 1972).

$\Gamma(e^+\nu_e e^+e^-)/\Gamma(\mu^+\nu_\mu)$ Γ_6/Γ_1

VALUE (units 10^{-9})	CL%	EVTS	DOCUMENT ID		TECN	COMMENT
3.2 ±0.5 ±0.2		98	EGLI	89	SPEC	Uses $R_{\rm PCAC}$ = 0.068 ± 0.004
• • • We do not use the following data for averages, fits, limits, etc. • • •						
0.46±0.16±0.07		7	[1] BARANOV	92	SPEC	Stopped π^+
< 4.8	90		KORENCHE...	76B	SPEC	
<34	90		KORENCHE...	71	OSPK	

[1] This measurement by BARANOV 92 is of the structure-dependent part of the decay. The value depends on values assumed for ratios of form factors.

$\Gamma(e^+\nu_e\nu\overline{\nu})/\Gamma_{\rm total}$ Γ_7/Γ

VALUE (units 10^{-6})	CL%	DOCUMENT ID		TECN
<5	90	PICCIOTTO	88	SPEC

$\Gamma(\mu^+\overline{\nu}_e)/\Gamma_{\rm total}$ Γ_8/Γ

Forbidden by total lepton number conservation. See the note on "Decay Constants of Charged Pseudoscalar Mesons" in the D_s^+ Listings.

VALUE (units 10^{-3})	CL%	DOCUMENT ID		TECN	COMMENT
<1.5	90	[1] COOPER	82	HLBC	Wideband ν beam

[1] COOPER 82 limit on $\overline{\nu}_e$ observation is here interpreted as a limit on lepton number violation.

$\Gamma(\mu^+\nu_e)/\Gamma_{\rm total}$ Γ_9/Γ

Forbidden by lepton family number conservation.

VALUE (units 10^{-3})	CL%	DOCUMENT ID		TECN	COMMENT
<8.0	90	[1] COOPER	82	HLBC	Wideband ν beam

[1] COOPER 82 limit on ν_e observation is here interpreted as a limit on lepton family number violation.

$\Gamma(\mu^-e^+e^+\nu)/\Gamma_{\rm total}$ Γ_{10}/Γ

Forbidden by lepton family number conservation.

VALUE (units 10^{-6})	CL%	DOCUMENT ID		TECN	CHG
<1.6	90	BARANOV	91B	SPEC	+
• • • We do not use the following data for averages, fits, limits, etc. • • •					
<7.7	90	KORENCHE...	87	SPEC	+

π^+ — POLARIZATION OF EMITTED μ^+

$\pi^+ \to \mu^+\nu$

Tests the Lorentz structure of leptonic charged weak interactions.

VALUE	CL%	DOCUMENT ID		TECN	CHG	COMMENT
• • • We do not use the following data for averages, fits, limits, etc. • • •						
<(−0.9959)	90	[1] FETSCHER	84	RVUE	+	
−0.99±0.16		[2] ABELA	83	SPEC	−	μ X-rays

[1] FETSCHER 84 uses only the measurement of CARR 83.

[2] Sign of measurement reversed in ABELA 83 to compare with μ^+ measurements.

See the related review(s):
Form Factors for Radiative Pion and Kaon Decays

$\pi^{\pm}$ FORM FACTORS

F_V, VECTOR FORM FACTOR

VALUE	EVTS	DOCUMENT ID		TECN	COMMENT
0.0254±0.0017 OUR AVERAGE					
0.0258±0.0017	65k	[1] BYCHKOV	09	PIBE	$e^+\nu\gamma$ at rest
0.014 ±0.009		[2] BOLOTOV	90B	SPEC	17 GeV $\pi^- \to e^-\overline{\nu}_e\gamma$
0.023 $^{+0.015}_{-0.013}$	98	EGLI	89	SPEC	$\pi^+ \to e^+\nu_e e^+e^-$

[1] The BYCHKOV 09 F_A and F_V results are highly (anti-)correlated: $F_A + 1.0286\,F_V = 0.03853 \pm 0.00014$.

[2] BOLOTOV 90B only determines the absolute value.

F_A, AXIAL-VECTOR FORM FACTOR

VALUE	EVTS	DOCUMENT ID		TECN	COMMENT
0.0119±0.0001	65k	[1,2] BYCHKOV	09	PIBE	$e^+\nu\gamma$ at rest

• • • We do not use the following data for averages, fits, limits, etc. • • •

0.0115 ± 0.0004	41k	[1,3]	FRLEZ	04	PIBE	$\pi^+ \to e^+ \nu\gamma$ at rest
0.0106 ± 0.0060		[1,4]	BOLOTOV	90B	SPEC	17 GeV $\pi^- \to e^- \overline{\nu}_e \gamma$
$0.021\ ^{+0.011}_{-0.013}$	98		EGLI	89	SPEC	$\pi^+ \to e^+ \nu_e e^+ e^-$
0.0135 ± 0.0016		[1,4]	BAY	86	SPEC	$\pi^+ \to e^+ \nu\gamma$
0.006 ± 0.003		[1,4]	PIILONEN	86	SPEC	$\pi^+ \to e^+ \nu\gamma$
0.011 ± 0.003		[1,4,5]	STETZ	78	SPEC	$\pi^+ \to e^+ \nu\gamma$

[1] These values come from fixing the vector form factor at the CVC prediction, $F_V = 0.0259 \pm 0.0005$.

[2] When F_V is released, the BYCHKOV 09 F_A is 0.0117 ± 0.0017, and F_A and F_V results are highly (anti-)correlated: $F_A + 1.0286\, F_V = 0.03853 \pm 0.00014$.

[3] The sign of $\gamma = F_A / F_V$ is determined to be positive.

[4] Only the absolute value of F_A is determined.

[5] The result of STETZ 78 has a two-fold ambiguity. We take the solution compatible with later determinations.

VECTOR FORM FACTOR SLOPE PARAMETER *a*

This is a in $F_V(q^2) = F_V(0)\,(1 + a\,q^2)$

VALUE	EVTS	DOCUMENT ID		TECN	COMMENT
0.10±0.06	65k	BYCHKOV	09	PIBE	$e^+ \nu\gamma$ at rest

R, SECOND AXIAL-VECTOR FORM FACTOR

VALUE	EVTS	DOCUMENT ID		TECN	COMMENT
$\mathbf{0.059\ ^{+0.009}_{-0.008}}$	98	EGLI	89	SPEC	$\pi^+ \to e^+ \nu_e e^+ e^-$

$\pi^{\pm}$ CHARGE RADIUS

VALUE (fm)	DOCUMENT ID		TECN	COMMENT
0.672±0.008 OUR AVERAGE	Error includes scale factor of 1.7. See the ideogram below.			
$0.65 \pm 0.05 \pm 0.06$	ESCHRICH	01	CNTR	$\pi e \to \pi e$
0.740 ± 0.031	LIESENFELD	99	CNTR	$ep \to e\pi^+ n$
0.663 ± 0.006	AMENDOLIA	86	CNTR	$\pi e \to \pi e$
0.663 ± 0.023	DALLY	82	CNTR	$\pi e \to \pi e$
$0.711 \pm 0.009 \pm 0.016$	BEBEK	78	CNTR	$eN \to e\pi N$
$0.678 \pm 0.004 \pm 0.008$	QUENZER	78	CNTR	$e^+ e^- \to \pi^+ \pi^-$
• • • We do not use the following data for averages, fits, limits, etc. • • •				
0.657 ± 0.003	[1] ANANTHANA..17		FIT	Fit existing data
0.661 ± 0.012	[2] BIJNENS	98	CNTR	χPT extraction
0.660 ± 0.024	AMENDOLIA	84	CNTR	$\pi e \to \pi e$
$0.78\ ^{+0.09}_{-0.10}$	ADYLOV	77	CNTR	$\pi e \to \pi e$
$0.74\ ^{+0.11}_{-0.13}$	BARDIN	77	CNTR	$ep \to e\pi^+ n$
0.56 ± 0.04	DALLY	77	CNTR	$\pi e \to \pi e$

[1] ANANTHANARAYAN 17 fit existing F_V data, using a mixed phase-modulus dispersive representation.

[2] BIJNENS 98 fits existing data.

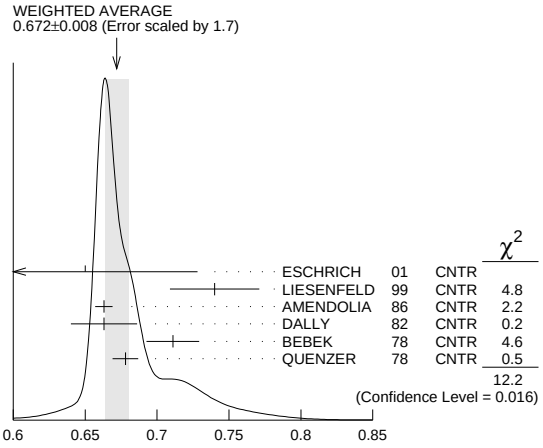

$\pi^{\pm}$ REFERENCES

We have omitted some papers that have been superseded by later experiments. The omitted papers may be found in our 1988 edition Physics Letters **B204** 1 (1988).

ANANTHANA...	17	PRL 119 132002	B. Ananthanarayan *et al.*	
TRASSINELLI	16	PL B759 583	M. Trassinelli *et al.*	
ADOLPH	15A	PRL 114 062002	C. Adolph *et al.*	(COMPASS Collab.)
AGUILAR-AR...	15	PRL 115 071801	A.A. Aguilar-Arevalo *et al.*	(PIENu Collab.)
HOLSTEIN	14	ARNPS 64 51	B. Holstein, S. Scherer	(MASA, MANZ)
BYCHKOV	09	PRL 103 051802	M. Bychkov *et al.*	(PSI PIBETA Collab.)
FRLEZ	04	PRL 93 181804	E. Frlez *et al.*	(PSI PIBETA Collab.)
POCANIC	04	PRL 93 181803	D. Pocanic *et al.*	(PSI PIBETA Collab.)
ESCHRICH	01	PL B522 233	I. Eschrich *et al.*	(FNAL SELEX Collab.)
LIESENFELD	99	PL B468 20	A. Liesenfeld *et al.*	
BIJNENS	98	JHEP 9805 014	J. Bijnens *et al.*	
BRESSI	98	NP B513 555	G. Bressi *et al.*	
LENZ	98	PL B416 50	S. Lenz *et al.*	
ASSAMAGAN	96	PR D53 6065	K.A. Assamagan *et al.*	(PSI, ZURI, VILL+)
KOPTEV	95	JETPL 61 877	V.P. Koptev *et al.*	(PNPI)
		Translated from ZETFP 61 865.		
NUMAO	95	PR D52 4855	T. Numao *et al.*	(TRIU, BRCO)
ASSAMAGAN	94	PL B335 231	K.A. Assamagan *et al.*	(PSI, ZURI, VILL+)
JECKELMANN	94	PL B335 326	B. Jeckelmann, P.F.A. Goudsmit, H.J. Leisi	(WABRN+)
CZAPEK	93	PRL 70 17	G. Czapek *et al.*	(BERN, VILL)
BARANOV	92	SJNP 55 1644	V.A. Baranov *et al.*	(JINR)
		Translated from YAF 55 2940.		
BRITTON	92	PRL 68 3000	D.I. Britton *et al.*	(TRIU, CARL)
Also		PR D49 28	D.I. Britton *et al.*	(TRIU, CARL)
NUMAO	92	MPL A7 3357	T. Numao	(TRIU)
BARANOV	91B	SJNP 54 790	V.A. Baranov *et al.*	(JINR)
		Translated from YAF 54 1298.		
DAUM	91	PL B265 425	M. Daum *et al.*	(VILL)
BOLOTOV	90B	PL B243 308	V.N. Bolotov *et al.*	(INRM)
EGLI	89	PL B222 533	S. Egli *et al.*	(SINDRUM Collab.)
Also		PL B175 97	S. Egli *et al.*	(AACH3, ETH, SIN, ZURI)
PDG	88	PL B204 1	G.P. Yost *et al.*	(LBL+)
PICCIOTTO	88	PR D37 1131	C.E. Picciotto *et al.*	(TRIU, CNRC)
COHEN	87	RMP 59 1121	E.R. Cohen, B.N. Taylor	(RISC, NBS)
KORENCHE...	87	SJNP 46 192	S.M. Korenchenko *et al.*	(JINR)
		Translated from YAF 46 313.		
AMENDOLIA	86	NP B277 168	S.R. Amendolia *et al.*	(CERN NA7 Collab.)
BAY	86	PL B174 445	A. Bay *et al.*	(LAUS, ZURI)
BRYMAN	86	PR D33 1211	D.A. Bryman *et al.*	(TRIU, CNRC)
Also		PRL 50 7	D.A. Bryman *et al.*	(TRIU, CNRC)
JECKELMANN	86B	NP A457 709	B. Jeckelmann *et al.*	(ETH, FRIB)
Also		PRL 56 1444	B. Jeckelmann *et al.*	(ETH, FRIB)
PIILONEN	86	PRL 57 1402	L.E. Piilonen *et al.*	(LANL, TEMP, CHIC)
MCFARLANE	85	PR D32 547	W.K. McFarlane *et al.*	(TEMP, LANL)
ABELA	84	PL 146B 431	R. Abela *et al.*	(SIN)
Also		PL 74B 126	M. Daum *et al.*	(SIN)
Also		PR D20 2692	M. Daum *et al.*	(SIN)
AMENDOLIA	84	PL 146B 116	S.R. Amendolia *et al.*	(CERN NA7 Collab.)
FETSCHER	84	PL 140B 117	W. Fetscher	(ETH)
ABELA	83	NP A395 413	R. Abela *et al.*	(BASL, KARLK, KARLE)
CARR	83	PRL 51 627	J. Carr *et al.*	(LBL, NWES, TRIU)
COOPER	82	PL 112B 97	A.M. Cooper *et al.*	(RL)
DALLY	82	PRL 48 375	E.B. Dally *et al.*	
LU	80	PRL 45 1066	D.C. Lu *et al.*	(YALE, COLU, JHU)
BEBEK	78	PR D17 1693	C.J. Bebek *et al.*	
QUENZER	78	PL 76B 512	A. Quenzer *et al.*	(LALO)
STETZ	78	NP B138 285	A.W. Stetz *et al.*	(LBL, UCLA)
ADYLOV	77	NP B128 461	G.T. Adylov *et al.*	
BARDIN	77	NP B120 45	G. Bardin *et al.*	
DALLY	77	PRL 39 1176	E.B. Dally *et al.*	
CARTER	76	PRL 37 1380	A.L. Carter *et al.*	(CARL, CNRC, CHIC+)
KORENCHE...	76B	JETP 44 35	S.M. Korenchenko *et al.*	(JINR)
		Translated from ZETF 71 69.		
MARUSHEN...	76	JETPL 23 72	V.I. Marushenko *et al.*	(PNPI)
		Translated from ZETFP 23 80.		
Also		Private Comm.	R.E. Shafer	(FNAL)
Also		Private Comm.	A. Smirnov	(PNPI)
DUNAITSEV	73	SJNP 16 292	A.F. Dunaitsev *et al.*	(SERP)
		Translated from YAF 16 524.		
AYRES	71	PR D3 1051	D.S. Ayres *et al.*	(LRL, UCSB)
Also		PR 157 1288	D.S. Ayres *et al.*	(LRL)
Also		PRL 21 261	D.S. Ayres *et al.*	(LRL, UCSB)
Also		Thesis UCRL 18369	D.S. Ayres	(LRL)
Also		PRL 23 1267	A.J. Greenberg *et al.*	(LRL, UCSB)
KORENCHE...	71	SJNP 13 189	S.M. Korenchenko *et al.*	(JINR)
		Translated from YAF 13 339.		
BOOTH	70	PL 32B 723	P.S.L. Booth *et al.*	(LIVP)
DEPOMMIER	68	NP B4 189	P. Depommier *et al.*	(CERN)
PETRUKHIN	68	JINR P1 3862	V.I. Petrukhin *et al.*	(JINR)
HYMAN	67	PL 25B 376	L.G. Hyman *et al.*	(ANL, CMU, NWES)
NORDBERG	67	PL 24B 594	M.E. Nordberg, F. Lobkowicz, R.L. Burman	(ROCH)
BARDON	66	PRL 16 775	M. Bardon *et al.*	(COLU)
KINSEY	66	PR 144 1132	K.F. Kinsey, F. Lobkowicz, M.E. Nordberg	(ROCH)
LOBKOWICZ	66	PRL 17 548	F. Lobkowicz *et al.*	(ROCH, BNL)
BACASTOW	65	PR 139 B407	R.B. Bacastow *et al.*	(LRL, SLAC)
BERTRAM	65	PR 139 B617	W.K. Bertram *et al.*	(MICH, CMU)
DUNAITSEV	65	JETP 20 58	A.F. Dunaitsev *et al.*	(JINR)
		Translated from ZETF 47 84.		
ECKHAUSE	65	PL 19 348	M. Eckhause *et al.*	(WILL)
BARTLETT	64	PR 136 B1452	D. Bartlett *et al.*	(COLU)
DICAPUA	64	PR 133 B1333	M. di Capua *et al.*	(COLU)
Also		Private Comm.	L. Pondrom	(WISC)
DEPOMMIER	63	PL 5 61	P. Depommier *et al.*	(CERN)
DEPOMMIER	63B	PL 7 285	P. Depommier *et al.*	(CERN)
ANDERSON	60	PR 119 2050	H.L. Anderson *et al.*	(EFI)
CASTAGNOLI	58	PR 112 1779	C. Castagnoli, M. Muchnik	(ROMA)

π^0

$I^G(J^{PC}) = 1^-(0^{-+})$

We have omitted some results that have been superseded by later experiments. The omitted results may be found in our 1988 edition Physics Letters **B204** 1 (1988).

π^0 MASS

The value is calculated from $m_{\pi^\pm}$ and $(m_{\pi^\pm} - m_{\pi^0})$. See also the notes under the $\pi^\pm$ Mass Listings.

VALUE (MeV)	DOCUMENT ID	
134.9770±0.0005 OUR FIT	Error includes scale factor of 1.1.	

$m_{\pi^\pm} - m_{\pi^0}$

Measurements with an error > 0.01 MeV have been omitted.

VALUE (MeV)	DOCUMENT ID		TECN	COMMENT
4.5936 ±0.0005 OUR FIT				
4.5936 ±0.0005 OUR AVERAGE				
4.59364 ± 0.00048	CRAWFORD	91	CNTR	$\pi^- p \to \pi^0 n$, n TOF
4.5930 ± 0.0013	CRAWFORD	86	CNTR	$\pi^- p \to \pi^0 n$, n TOF

Meson Particle Listings

π^0

• • • We do not use the following data for averages, fits, limits, etc. • • •

4.59366±0.00048	CRAWFORD	88B	CNTR	See CRAWFORD 91
4.6034 ±0.0052	VASILEVSKY	66	CNTR	
4.6056 ±0.0055	CZIRR	63	CNTR	

π^0 MEAN LIFE

Most experiments measure the π^0 width which we convert to a lifetime. ATHERTON 85 is the only direct measurement of the π^0 lifetime. Our average based only on indirect measurement yields $(8.30 \pm 0.19) \times 10^{-17}$ s. The two Primakoff measurements from 1970 have been excluded from our average because they suffered model-related systematics unknown at the time. More information on the π^0 lifetime can be found in BERNSTEIN 13.

VALUE (10^{-17} s)	EVTS	DOCUMENT ID		TECN	COMMENT
8.52±0.18 OUR AVERAGE		Error includes scale factor of 1.2.			
8.32±0.15±0.18		[1] LARIN	11	PRMX	Primakoff effect
8.5 ±1.1		[2] BYCHKOV	09	PIBE	$\pi^+ \to e^+ \nu\gamma$ at rest
8.4 ±0.5 ±0.5	1182	[3] WILLIAMS	88	CBAL	$e^+e^- \to e^+e^-\pi^0$
8.97±0.22±0.17		ATHERTON	85	CNTR	Direct measurement
8.2 ±0.4		[4] BROWMAN	74	CNTR	Primakoff effect
• • • We do not use the following data for averages, fits, limits, etc. • • •					
5.6 ±0.6		BELLETTINI	70	CNTR	Primakoff effect
9 ±0.68		KRYSHKIN	70	CNTR	Primakoff effect
7.3 ±1.1		BELLETTINI	65B	CNTR	Primakoff effect

[1] LARIN 11 reported $\Gamma(\pi^0 \to \gamma\gamma) = 7.82 \pm 0.14 \pm 0.17$ eV which we converted to mean life $\tau = \hbar/\Gamma(\text{total})$.
[2] BYCHKOV 09 obtains this using the conserved-vector-current relation between the vector form factor F_V and the π^0 lifetime.
[3] WILLIAMS 88 gives $\Gamma(\gamma\gamma) = 7.7 \pm 0.5 \pm 0.5$ eV. We give here $\tau = \hbar/\Gamma(\text{total})$.
[4] BROWMAN 74 gives a π^0 width $\Gamma = 8.02 \pm 0.42$ eV. The mean life is $\hbar/\Gamma$.

π^0 DECAY MODES

For decay limits to particles which are not established, see the appropriate Search sections (A^0 (axion) and Other Light Boson (X^0) Searches, etc.).

	Mode	Fraction (Γ_i/Γ)	Scale factor/ Confidence level
Γ_1	2γ	(98.823±0.034) %	S=1.5
Γ_2	$e^+e^-\gamma$	(1.174±0.035) %	S=1.5
Γ_3	γpositronium	(1.82 ±0.29) $\times 10^{-9}$	
Γ_4	$e^+e^+e^-e^-$	(3.34 ±0.16) $\times 10^{-5}$	
Γ_5	e^+e^-	(6.46 ±0.33) $\times 10^{-8}$	
Γ_6	4γ	$< 2 \times 10^{-8}$	CL=90%
Γ_7	$\nu\overline{\nu}$	[a] $< 2.7 \times 10^{-7}$	CL=90%
Γ_8	$\nu_e\overline{\nu}_e$	$< 1.7 \times 10^{-6}$	CL=90%
Γ_9	$\nu_\mu\overline{\nu}_\mu$	$< 1.6 \times 10^{-6}$	CL=90%
Γ_{10}	$\nu_\tau\overline{\nu}_\tau$	$< 2.1 \times 10^{-6}$	CL=90%
Γ_{11}	$\gamma\nu\overline{\nu}$	$< 6 \times 10^{-4}$	CL=90%
	Charge conjugation (C) or Lepton Family number (LF) violating modes		
Γ_{12}	3γ	C $< 3.1 \times 10^{-8}$	CL=90%
Γ_{13}	μ^+e^-	LF $< 3.8 \times 10^{-10}$	CL=90%
Γ_{14}	μ^-e^+	LF $< 3.4 \times 10^{-9}$	CL=90%
Γ_{15}	$\mu^+e^- + \mu^-e^+$	LF $< 3.6 \times 10^{-10}$	CL=90%

[a] Astrophysical and cosmological arguments give limits of order 10^{-13}; see the Particle Listings below.

CONSTRAINED FIT INFORMATION

An overall fit to 2 branching ratios uses 6 measurements and one constraint to determine 3 parameters. The overall fit has a $\chi^2 = 4.6$ for 4 degrees of freedom.

The following *off-diagonal* array elements are the correlation coefficients $\langle \delta x_i \delta x_j \rangle / (\delta x_i \cdot \delta x_j)$, in percent, from the fit to the branching fractions, $x_i \equiv \Gamma_i/\Gamma_{\text{total}}$. The fit constrains the x_i whose labels appear in this array to sum to one.

x_2	−100	
x_4	0	−1
	x_1	x_2

π^0 BRANCHING RATIOS

$\Gamma(e^+e^-\gamma)/\Gamma(2\gamma)$ Γ_2/Γ_1

VALUE (%)	EVTS	DOCUMENT ID		TECN	COMMENT
1.188±0.035 OUR FIT		Error includes scale factor of 1.5.			
1.188±0.034 OUR AVERAGE		Error includes scale factor of 1.4. See the ideogram below.			
1.140±0.024±0.033	12.5k	[1] BEDDALL	08	ALEP	$e^+e^- \to Z \to$ hadrons
1.25 ±0.04		SCHARDT	81	SPEC	$\pi^- p \to n\pi^0$
1.166±0.047	3071	[2] SAMIOS	61	HBC	$\pi^- p \to n\pi^0$
1.17 ±0.15	27	BUDAGOV	60	HBC	
• • • We do not use the following data for averages, fits, limits, etc. • • •					
1.196		JOSEPH	60	THEO	QED calculation

[1] This BEDDALL 08 value is obtained from ALEPH archived data.
[2] SAMIOS 61 value uses a Panofsky ratio = 1.62.

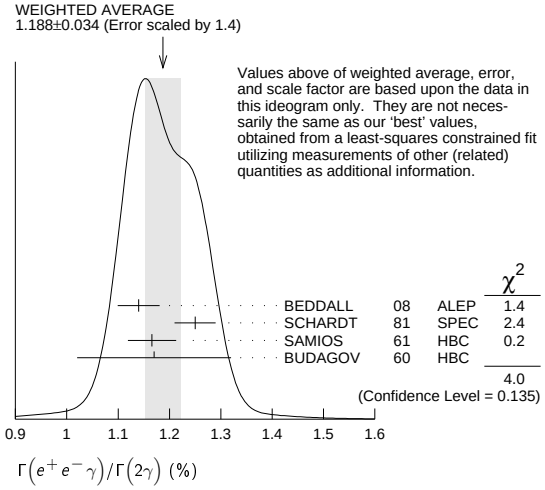

$\Gamma(\gamma\text{positronium})/\Gamma(2\gamma)$ Γ_3/Γ_1

VALUE (units 10^{-9})	EVTS	DOCUMENT ID		TECN	COMMENT
1.84±0.29	277	AFANASYEV	90	CNTR	pC 70 GeV

$\Gamma(e^+e^+e^-e^-)/\Gamma(2\gamma)$ Γ_4/Γ_1

VALUE (units 10^{-5})	EVTS	DOCUMENT ID		TECN	COMMENT
3.38±0.16 OUR FIT					
3.38±0.16 OUR AVERAGE					
3.46±0.19	30.5k	[1] ABOUZAID	08D	KTEV	$K_L^0 \to \pi^0\pi^0\pi^0_{DD}$
3.18±0.30	146	[2] SAMIOS	62B	HBC	

[1] This ABOUZAID 08D value includes all radiative final states. The error includes both statistical and systematic errors. The correlation between the Dalitz-pair planes gives a direct measurement of the π^0 parity. The $\pi^0 2\gamma^*$ form factor is measured and limits are placed on a scalar contribution to the decay.
[2] SAMIOS 62B value uses a Panofsky ratio = 1.62.

$\Gamma(e^+e^-)/\Gamma_{\text{total}}$ Γ_5/Γ

Experimental results are listed; branching ratios corrected for radiative effects are given in the footnotes. BERMAN 60 found $B(\pi^0 \to e^+e^-) \geq 4.69 \times 10^{-8}$ via an exact QED calculation.

VALUE (units 10^{-8})	EVTS	DOCUMENT ID		TECN	CHG	COMMENT
6.46±0.33 OUR AVERAGE						
6.44±0.25±0.22	794	[1] ABOUZAID	07	KTEV		$K_L^0 \to 3\pi^0$ in flight
6.9 ±2.3 ±0.6	21	[2] DESHPANDE	93	SPEC		$K^+ \to \pi^+\pi^0$
7.6 $^{+2.9}_{-2.8}$ ±0.5	8	[3] MCFARLAND	93	SPEC		$K_L^0 \to 3\pi^0$ in flight
• • • We do not use the following data for averages, fits, limits, etc. • • •						
6.09±0.40±0.24	275	[4] ALAVI-HARATI	99C	SPEC	0	Repl. by ABOUZAID 07

[1] ABOUZAID 07 result is for $m_{e^+e^-}/m_{\pi^0} > 0.95$. With radiative corrections the result becomes $(7.48 \pm 0.29 \pm 0.25) \times 10^{-8}$.
[2] The DESHPANDE 93 result with bremsstrahlung radiative corrections is $(8.0 \pm 2.6 \pm 0.6) \times 10^{-8}$.
[3] The MCFARLAND 93 result is for $B[\pi^0 \to e^+e^-, (m_{e^+e^-}/m_{\pi^0})^2 > 0.95]$. With radiative corrections it becomes $(8.8^{+4.5}_{-3.2} \pm 0.6) \times 10^{-8}$.
[4] ALAVI-HARATI 99C quote result for $B[\pi^0 \to e^+e^-, (m_{e^+e^-}/m_{\pi^0})^2 > 0.95]$ to minimize radiative contributions from $\pi^0 \to e^+e^-\gamma$. After radiative corrections they obtain $(7.04 \pm 0.46 \pm 0.28) \times 10^{-8}$.

$\Gamma(e^+e^-)/\Gamma(2\gamma)$ Γ_5/Γ_1

VALUE (units 10^{-7})	CL%	EVTS	DOCUMENT ID		TECN	COMMENT
• • • We do not use the following data for averages, fits, limits, etc. • • •						
<1.3	90		NIEBUHR	89	SPEC	$\pi^- p \to \pi^0 n$ at rest
<5.3	90		ZEPHAT	87	SPEC	$\pi^- p \to \pi^0 n$ 0.3 GeV/c

$1.7 \pm 0.6 \pm 0.3$		59	FRANK	83	SPEC	$\pi^- p \to n\pi^0$
1.8 ± 0.6		58	MISCHKE	82	SPEC	See FRANK 83
$2.23^{+2.40}_{-1.10}$	90	8	FISCHER	78B	SPRK	$K^+ \to \pi^+\pi^0$

$\Gamma(4\gamma)/\Gamma_{total}$ Γ_6/Γ

VALUE (units 10^{-8})	CL%	EVTS	DOCUMENT ID		TECN	COMMENT
< 2	90		MCDONOUGH	88	CBOX	$\pi^- p$ at rest
• • • We do not use the following data for averages, fits, limits, etc. • • •						
<160	90		BOLOTOV	86C	CALO	
<440	90	0	AUERBACH	80	CNTR	

$\Gamma(\nu\overline{\nu})/\Gamma_{total}$ Γ_7/Γ

The astrophysical and cosmological limits are many orders of magnitude lower, but we use the best laboratory limit for the Summary Tables.

VALUE (units 10^{-6})	CL%	EVTS	DOCUMENT ID		TECN	COMMENT
< 0.27	90		[1] ARTAMONOV	05A	B949	$K^+ \to \pi^+\pi^0$
• • • We do not use the following data for averages, fits, limits, etc. • • •						
< 0.83	90		[1] ATIYA	91	B787	$K^+ \to \pi^+\nu\nu'$
$< 2.9 \times 10^{-7}$			[2] LAM	91		Cosmological limit
$< 3.2 \times 10^{-7}$			[3] NATALE	91		SN 1987A
< 6.5	90		DORENBOS...	88	CHRM	Beam dump, prompt ν
<24	90	0	[1] HERCZEG	81	RVUE	$K^+ \to \pi^+\nu\nu'$

[1] This limit applies to all possible $\nu\nu'$ states as well as to other massless, weakly interacting states.

[2] LAM 91 considers the production of right-handed neutrinos produced from the cosmic thermal background at the temperature of about the pion mass through the reaction $\gamma\gamma \to \pi^0 \to \nu\overline{\nu}$.

[3] NATALE 91 considers the excess energy-loss rate from SN 1987A if the process $\gamma\gamma \to \pi^0 \to \nu\overline{\nu}$ occurs, permitted if the neutrinos have a right-handed component. As pointed out in LAM 91 (and confirmed by Natale), there is a factor 4 error in the NATALE 91 published result (0.8×10^{-7}).

$\Gamma(\nu_e\overline{\nu}_e)/\Gamma_{total}$ Γ_8/Γ

VALUE (units 10^{-6})	CL%	DOCUMENT ID		TECN	COMMENT
<1.7	90	DORENBOS...	88	CHRM	Beam dump, prompt ν
• • • We do not use the following data for averages, fits, limits, etc. • • •					
<3.1	90	[1] HOFFMAN	88	RVUE	Beam dump, prompt ν

[1] HOFFMAN 88 analyzes data from a 400-GeV BEBC beam-dump experiment.

$\Gamma(\nu_\mu\overline{\nu}_\mu)/\Gamma_{total}$ Γ_9/Γ

VALUE (units 10^{-6})	CL%	EVTS	DOCUMENT ID		TECN	COMMENT
<1.6	90	8.7	AUERBACH	04	LSND	800 MeV p on Cu
<3.1	90		[1] HOFFMAN	88	RVUE	Beam dump, prompt ν
• • • We do not use the following data for averages, fits, limits, etc. • • •						
<7.8	90		DORENBOS...	88	CHRM	Beam dump, prompt ν

[1] HOFFMAN 88 analyzes data from a 400-GeV BEBC beam-dump experiment.

$\Gamma(\nu_\tau\overline{\nu}_\tau)/\Gamma_{total}$ Γ_{10}/Γ

VALUE (units 10^{-6})	CL%	DOCUMENT ID		TECN	COMMENT
<2.1	90	[1] HOFFMAN	88	RVUE	Beam dump, prompt ν
• • • We do not use the following data for averages, fits, limits, etc. • • •					
<4.1	90	DORENBOS...	88	CHRM	Beam dump, prompt ν

[1] HOFFMAN 88 analyzes data from a 400-GeV BEBC beam-dump experiment.

$\Gamma(\gamma\nu\overline{\nu})/\Gamma_{total}$ Γ_{11}/Γ

Standard Model prediction is 6×10^{-18}.

VALUE	CL%	DOCUMENT ID		TECN	COMMENT
$< 6 \times 10^{-4}$	90	ATIYA	92	CNTR	$K^+ \to \gamma\nu\overline{\nu}\pi^+$

$\Gamma(3\gamma)/\Gamma_{total}$ Γ_{12}/Γ

Forbidden by C invariance.

VALUE (units 10^{-8})	CL%	EVTS	DOCUMENT ID		TECN	COMMENT
< 3.1	90		MCDONOUGH	88	CBOX	$\pi^- p$ at rest
• • • We do not use the following data for averages, fits, limits, etc. • • •						
< 38	90	0	HIGHLAND	80	CNTR	
<150	90	0	AUERBACH	78	CNTR	
<490	90	0	[1] DUCLOS	65	CNTR	
<490	90		[1] KUTIN	65	CNTR	

[1] These experiments give $B(3\gamma/2\gamma) < 5.0 \times 10^{-6}$.

$\Gamma(\mu^+ e^-)/\Gamma_{total}$ Γ_{13}/Γ

Forbidden by lepton family number conservation.

VALUE (units 10^{-9})	CL%	EVTS	DOCUMENT ID		TECN	COMMENT
< 0.38	90	0	APPEL	00	SPEC	$K^+ \to \pi^+\mu^+e^-$
• • • We do not use the following data for averages, fits, limits, etc. • • •						
<16	90		LEE	90	SPEC	$K^+ \to \pi^+\mu^+e^-$
<78	90		CAMPAGNARI	88	SPEC	See LEE 90

$\Gamma(\mu^- e^+)/\Gamma_{total}$ Γ_{14}/Γ

Forbidden by lepton family number conservation.

VALUE (units 10^{-9})	CL%	EVTS	DOCUMENT ID		TECN	COMMENT
<3.4	90	0	APPEL	00B	B865	$K^+ \to \pi^+ e^+ \mu^-$

$[\Gamma(\mu^+ e^-) + \Gamma(\mu^- e^+)]/\Gamma_{total}$ Γ_{15}/Γ

Forbidden by lepton family number conservation.

VALUE (units 10^{-9})	CL%	DOCUMENT ID		TECN	COMMENT
< 0.36	90	ABOUZAID	08C	KTEV	$K_L^0 \to 2\pi^0\mu^\pm e^\mp$
• • • We do not use the following data for averages, fits, limits, etc. • • •					
< 17.2	90	KROLAK	94	E799	In $K_L^0 \to 3\pi^0$
<140		HERCZEG	84	RVUE	$K^+ \to \pi^+\mu e$
$< 2 \times 10^{-6}$		HERCZEG	84	THEO	$\mu^- \to e^-$ conversion
< 70	90	BRYMAN	82	RVUE	$K^+ \to \pi^+\mu e$

π^0 ELECTROMAGNETIC FORM FACTOR

The amplitude for the process $\pi^0 \to e^+e^-\gamma$ contains a form factor $F(x)$ at the $\pi^0\gamma\gamma$ vertex, where $x = [m_{e^+e^-}/m_{\pi^0}]^2$. The parameter a in the linear expansion $F(x) = 1 + ax$ is listed below.

All the measurements except that of BEHREND 91 are in the time-like region of momentum transfer.

LINEAR COEFFICIENT OF π^0 ELECTROMAGNETIC FORM FACTOR

VALUE (10^{-2})	EVTS	DOCUMENT ID		TECN	COMMENT
3.35 ± 0.31 OUR AVERAGE					
$3.68 \pm 0.51 \pm 0.25$	1.1M	LAZZERONI	17	SPEC	$K^\pm \to \pi^0\pi^\pm$; $\pi^0 \to e^+e^-\gamma$
$2.6 \pm 2.4 \pm 4.8$	7.5k	FARZANPAY	92	SPEC	$\pi^- p \to \pi^0 n$ at rest
$2.5 \pm 1.4 \pm 2.6$	54k	MEIJERDREES	92B	SPEC	$\pi^- p \to \pi^0 n$ at rest
$3.26 \pm 0.26 \pm 0.26$	127	[1] BEHREND	91	CELL	$e^+e^- \to e^+e^-\pi^0$
$-11 \pm 3 \pm 8$	32k	FONVIEILLE	89	SPEC	Radiation corr.
• • • We do not use the following data for averages, fits, limits, etc. • • •					
$12 \pm {}^{5}_{4}$		[2] TUPPER	83	THEO	FISCHER 78 data
10 ± 3	31k	[3] FISCHER	78	SPEC	Radiation corr.
1 ± 11	2.2k	DEVONS	69	OSPK	No radiation corr.
-15 ± 10	7.6k	KOBRAK	61	HBC	No radiation corr.
-24 ± 16	3.0k	SAMIOS	61	HBC	No radiation corr.

[1] BEHREND 91 estimates that their systematic error is of the same order of magnitude as their statistical error, and so we have included a systematic error of this magnitude. The value of a is obtained by extrapolation from the region of large space-like momentum transfer assuming vector dominance.

[2] TUPPER 83 is a theoretical analysis of FISCHER 78 including 2-photon exchange in the corrections.

[3] The FISCHER 78 error is statistical only. The result without radiation corrections is $+0.05 \pm 0.03$.

π^0 REFERENCES

We have omitted some papers that have been superseded by later experiments. The omitted papers may be found in our 1988 edition Physics Letters **B204** 1 (1988).

LAZZERONI	17	PL B768 38	C. Lazzeroni *et al.*	(NA62 Collab.)
BERNSTEIN	13	RMP 85 49	A. M. Bernstein, B. R. Holstein	(AMHT, MIT)
LARIN	11	PRL 106 162303	I. Larin *et al.*	(PrimEx Collab.)
BYCHKOV	09	PRL 103 051802	M. Bychkov *et al.*	(PSI PIBETA Collab.)
ABOUZAID	08C	PRL 100 131803	E. Abouzaid *et al.*	(FNAL KTeV Collab.)
ABOUZAID	08D	PRL 100 182001	E. Abouzaid *et al.*	(FNAL KTeV Collab.)
BEDDALL	08	EPJ C54 365	A. Beddall, A. Beddall	(UGAZ)
ABOUZAID	07	PR D75 012004	E. Abouzaid *et al.*	(KTeV Collab.)
ARTAMONOV	05A	PR D72 091102	A.V. Artamonov *et al.*	(BNL E949 Collab.)
AUERBACH	04	PRL 92 091801	L.B. Auerbach *et al.*	(LSND Collab.)
APPEL	00	PRL 85 2450	R. Appel *et al.*	(BNL 865 Collab.)
Also		Thesis, Yale Univ.	D.R. Bergman	
Also		Thesis, Univ. Zurich	S. Pislak	
APPEL	00B	PRL 85 2877	R. Appel *et al.*	(BNL 865 Collab.)
ALAVI-HARATI	99C	PRL 83 922	A. Alavi-Harati *et al.*	(FNAL KTeV Collab.)
KROLAK	94	PL B320 407	P. Krolak *et al.*	(EFI, UCLA, COLO, ELMT+)
DESHPANDE	93	PRL 71 27	A. Deshpande *et al.*	(BNL E851 Collab.)
MCFARLAND	93	PRL 71 31	K.S. McFarland *et al.*	(EFI, UCLA, COLQ+)
ATIYA	92	PRL 69 733	M.S. Atiya *et al.*	(BNL, LANL, PRIN+)
FARZANPAY	92	PL B278 413	F. Farzanpay *et al.*	(ORST, TRIU, BRCO+)
MEIJERDREES	92B	PR D45 1439	R. Meijer Drees *et al.*	(PSI SINDRUM-I Collab.)
ATIYA	91	PRL 66 2189	M.S. Atiya *et al.*	(BNL, LANL, PRIN+)
BEHREND	91	ZPHY C49 401	H.J. Behrend *et al.*	(CELLO Collab.)
CRAWFORD	91	PR D43 46	J.F. Crawford *et al.*	(VILL, UVA)
LAM	91	PR D44 3345	W.P. Lam, K.W. Ng	(AST)
NATALE	91	PL B258 227	A.A. Natale	(SPIFT)
AFANASYEV	90	PL B236 116	L.G. Afanasyev *et al.*	(JINR, MOSU, SERP)
Also		SJNP 51 664	L.G. Afanasyev *et al.*	(JINR)
		Translated from YAF 51 1040.		
LEE	90	PRL 64 165	A.M. Lee *et al.*	(BNL, FNAL, VILL, WASH+)
FONVIEILLE	89	PL B233 65	H. Fonvieille *et al.*	(CLER, LYON, SACL)
NIEBUHR	89	PR D40 2796	C. Niebuhr *et al.*	(SINDRUM Collab.)
CAMPAGNARI	88	PRL 61 2062	C. Campagnari *et al.*	(BNL, FNAL, PSI+)
CRAWFORD	88B	PL B213 391	J.F. Crawford *et al.*	(PSI, UVA)
DORENBOS...	88	ZPHY C40 497	J. Dorenbosch *et al.*	(CHARM Collab.)
HOFFMAN	88	PL B208 149	C.M. Hoffman	(LANL)
MCDONOUGH	88	PR D38 2121	J.M. McDonough *et al.*	(TEMP, LANL, CHIC)
PDG	88	PL B204 1	G.P. Yost *et al.*	(LBL+)
WILLIAMS	88	PR D38 1365	D.A. Williams *et al.*	(Crystal Ball Collab.)
ZEPHAT	87	JP G13 1375	A.G. Zephat *et al.*	(OMICRON Collab.)
BOLOTOV	86C	JETPL 43 520	V.N. Bolotov *et al.*	(INRM)
		Translated from ZETFP 43 405.		
CRAWFORD	86	PRL 56 1043	J.F. Crawford *et al.*	(SIN, UVA)
ATHERTON	85	PL 158B 81	H.W. Atherton *et al.*	(CERN, ISU, LUND+)
HERCZEG	84	PR D29 1954	P. Herczeg, C.M. Hoffman	(LANL)
FRANK	83	PR D28 423	J.S. Frank *et al.*	(LANL, ARZS)
TUPPER	83	PR D28 2905	G.B. Tupper, T.R. Grose, M.A. Samuel	(OKSU)
BRYMAN	82	PR D26 2538	D.A. Bryman	(TRIU)
MISCHKE	82	PRL 48 1153	R.E. Mischke *et al.*	(LANL, ARZS)
HERCZEG	81	PL 100B 347	P. Herczeg, C.M. Hoffman	(LANL)
SCHARDT	81	PR D23 639	M.A. Schardt *et al.*	(ARZS, LANL)

AUERBACH	80	PL 90B 317	L.B. Auerbach *et al.*	(TEMP, LASL)
HIGHLAND	80	PRL 44 628	V.L. Highland *et al.*	(TEMP, LASL)
AUERBACH	78	PRL 41 275	L.B. Auerbach *et al.*	(TEMP, LASL)
FISCHER	78	PL 73B 359	J. Fischer *et al.*	(GEVA, SACL)
FISCHER	78B	PL 73B 364	J. Fischer *et al.*	(GEVA, SACL)
BROWMAN	74	PRL 33 1400	A. Browman *et al.*	(CORN, BING)
BELLETTINI	70	NC 66A 243	G. Bellettini *et al.*	(PISA, BONN)
KRYSHKIN	70	JETP 30 1037	V.I. Kryshkin, A.G. Sterligov, Y.P. Usov	(TMSK)
		Translated from ZETF 57 1917.		
DEVONS	69	PR 184 1356	S. Devons *et al.*	(COLU, ROMA)
VASILEVSKY	66	PL 23 281	I.M. Vasilevsky *et al.*	(JINR)
BELLETTINI	65B	NC 40A 1139	G. Bellettini *et al.*	(PISA, FIRZ)
DUCLOS	65	PL 19 253	J. Duclos *et al.*	(CERN, HEID)
KUTIN	65	JETPL 2 243	V.M. Kutjin, V.I. Petrukhin, Y.D. Prokoshkin	(JINR)
		Translated from ZETFP 2 387.		
CZIRR	63	PR 130 341	J.B. Czirr	(LRL)
SAMIOS	62B	PR 126 1844	N.P. Samios *et al.*	(COLU, BNL)
KOBRAK	61	NC 20 1115	H. Kobrak	(EFI)
SAMIOS	61	PR 121 275	N.P. Samios	(COLU, BNL)
BERMAN	60	NC 18 1192	S. Berman, D. Geffen	
BUDAGOV	60	JETP 11 755	Y.A. Budagov *et al.*	(JINR)
		Translated from ZETF 38 1047.		
JOSEPH	60	NC 16 997	D.W. Joseph	(EFI)

η

$I^G(J^{PC}) = 0^+(0^{-+})$

We have omitted some results that have been superseded by later experiments. The omitted results may be found in our 1988 edition Physics Letters **B204** (1988).

η MASS

Recent measurements resolve the obvious inconsistency in previous η mass measurements in favor of the higher value first reported by NA48 (LAI 02). We use only precise measurements consistent with this higher mass value for our η mass average.

VALUE (MeV)	*EVTS*	*DOCUMENT ID*		*TECN*	*COMMENT*
547.862±0.017 OUR AVERAGE					
547.865±0.031±0.062		NIKOLAEV	14	CRYB	$\gamma p \to p\eta$
547.873±0.005±0.027	1M	GOSLAWSKI	12	SPEC	$dp \to {}^3\mathrm{He}\,\eta$
547.874±0.007±0.029		AMBROSINO	07B	KLOE	$e^+e^- \to \phi \to \eta\gamma$
547.785±0.017±0.057	16k	MILLER	07	CLEO	$\psi(2S) \to J/\psi\eta$
547.843±0.030±0.041	1134	LAI	02	NA48	$\eta \to 3\pi^0$
• • • We do not use the following data for averages, fits, limits, etc. • • •					
547.311±0.028±0.032		[1] ABDEL-BARY	05	SPEC	$dp \to {}^3\mathrm{He}\,\eta$
547.12 ±0.06 ±0.25		KRUSCHE	95D	SPEC	$\gamma p \to \eta p$, threshold
547.30 ±0.15		PLOUIN	92	SPEC	$dp \to {}^3\mathrm{He}\,\eta$
547.45 ±0.25		DUANE	74	SPEC	$\pi^- p \to n$ neutrals
548.2 ±0.65		FOSTER	65C	HBC	
549.0 ±0.7	148	FOELSCHE	64	HBC	
548.0 ±1.0	91	ALFF-...	62	HBC	
549.0 ±1.2	53	BASTIEN	62	HBC	

[1] ABDEL-BARY 05 disagrees significantly with recent measurements of similar or better precision. See comment in the header.

η WIDTH

This is the partial decay rate $\Gamma(\eta \to \gamma\gamma)$ divided by the fitted branching fraction for that mode. See the note at the start of the $\Gamma(2\gamma)$ data block, next below.

VALUE (keV)	*DOCUMENT ID*
1.31±0.05 OUR FIT	

η DECAY MODES

	Mode	Fraction (Γ_i/Γ)		Scale factor / Confidence level
	Neutral modes			
Γ_1	neutral modes	(72.12±0.34) %		S=1.2
Γ_2	2γ	(39.41±0.20) %		S=1.1
Γ_3	$3\pi^0$	(32.68±0.23) %		S=1.1
Γ_4	$\pi^0 2\gamma$	(2.56±0.22)	$\times 10^{-4}$	
Γ_5	$2\pi^0 2\gamma$	< 1.2	$\times 10^{-3}$	CL=90%
Γ_6	4γ	< 2.8	$\times 10^{-4}$	CL=90%
Γ_7	invisible	< 1.0	$\times 10^{-4}$	CL=90%
	Charged modes			
Γ_8	charged modes	(28.10±0.34) %		S=1.2
Γ_9	$\pi^+\pi^-\pi^0$	(22.92±0.28) %		S=1.2
Γ_{10}	$\pi^+\pi^-\gamma$	(4.22±0.08) %		S=1.1
Γ_{11}	$e^+e^-\gamma$	(6.9 ±0.4)	$\times 10^{-3}$	S=1.3
Γ_{12}	$\mu^+\mu^-\gamma$	(3.1 ±0.4)	$\times 10^{-4}$	
Γ_{13}	e^+e^-	< 2.3	$\times 10^{-6}$	CL=90%
Γ_{14}	$\mu^+\mu^-$	(5.8 ±0.8)	$\times 10^{-6}$	
Γ_{15}	$2e^+2e^-$	(2.40±0.22)	$\times 10^{-5}$	
Γ_{16}	$\pi^+\pi^-e^+e^-(\gamma)$	(2.68±0.11)	$\times 10^{-4}$	
Γ_{17}	$e^+e^-\mu^+\mu^-$	< 1.6	$\times 10^{-4}$	CL=90%
Γ_{18}	$2\mu^+2\mu^-$	< 3.6	$\times 10^{-4}$	CL=90%
Γ_{19}	$\mu^+\mu^-\pi^+\pi^-$	< 3.6	$\times 10^{-4}$	CL=90%
Γ_{20}	$\pi^+e^-\overline{\nu}_e$ + c.c.	< 1.7	$\times 10^{-4}$	CL=90%
Γ_{21}	$\pi^+\pi^-2\gamma$	< 2.1	$\times 10^{-3}$	
Γ_{22}	$\pi^+\pi^-\pi^0\gamma$	< 5	$\times 10^{-4}$	CL=90%
Γ_{23}	$\pi^0\mu^+\mu^-\gamma$	< 3	$\times 10^{-6}$	CL=90%
	Charge conjugation (C), Parity (P), Charge conjugation × Parity (CP), or Lepton Family number (LF) violating modes			
Γ_{24}	$\pi^0\gamma$	C	< 9	$\times 10^{-5}$ CL=90%
Γ_{25}	$\pi^+\pi^-$	P,CP	< 1.3	$\times 10^{-5}$ CL=90%
Γ_{26}	$2\pi^0$	P,CP	< 3.5	$\times 10^{-4}$ CL=90%
Γ_{27}	$2\pi^0\gamma$	C	< 5	$\times 10^{-4}$ CL=90%
Γ_{28}	$3\pi^0\gamma$	C	< 6	$\times 10^{-5}$ CL=90%
Γ_{29}	3γ	C	< 1.6	$\times 10^{-5}$ CL=90%
Γ_{30}	$4\pi^0$	P,CP	< 6.9	$\times 10^{-7}$ CL=90%
Γ_{31}	$\pi^0e^+e^-$	C	[a] < 4	$\times 10^{-5}$ CL=90%
Γ_{32}	$\pi^0\mu^+\mu^-$	C	[a] < 5	$\times 10^{-6}$ CL=90%
Γ_{33}	$\mu^+e^- + \mu^-e^+$	LF	< 6	$\times 10^{-6}$ CL=90%

[a] C parity forbids this to occur as a single-photon process.

CONSTRAINED FIT INFORMATION

An overall fit to 2 decay rate and 19 branching ratios uses 50 measurements and one constraint to determine 9 parameters. The overall fit has a $\chi^2 = 43.8$ for 42 degrees of freedom.

The following *off-diagonal* array elements are the correlation coefficients $\langle \delta x_i \delta x_j \rangle / (\delta x_i \cdot \delta x_j)$, in percent, from the fit to the branching fractions, $x_i \equiv \Gamma_i/\Gamma_{\mathrm{total}}$. The fit constrains the x_i whose labels appear in this array to sum to one.

	x_2	x_3	x_4	x_9	x_{10}	x_{11}	x_{12}	x_{16}
x_3	24							
x_4	4	1						
x_9	−73	−80	−4					
x_{10}	−56	−60	−3	61				
x_{11}	−5	−5	0	−6	−4			
x_{12}	−1	0	0	−1	0	0		
x_{16}	0	0	0	0	0	0	0	
Γ	−14	−3	−32	11	8	1	0	0

	Mode	Rate (keV)		Scale factor
Γ_2	2γ	0.515 ±0.018		
Γ_3	$3\pi^0$	0.427 ±0.015		
Γ_4	$\pi^0 2\gamma$	(3.34 ±0.28)	$\times 10^{-4}$	
Γ_9	$\pi^+\pi^-\pi^0$	0.299 ±0.011		
Γ_{10}	$\pi^+\pi^-\gamma$	0.0551±0.0022		
Γ_{11}	$e^+e^-\gamma$	0.0090±0.0006		1.2
Γ_{12}	$\mu^+\mu^-\gamma$	(4.1 ±0.5)	$\times 10^{-4}$	
Γ_{16}	$\pi^+\pi^-e^+e^-(\gamma)$	(3.50 ±0.19)	$\times 10^{-4}$	

η DECAY RATES

$\Gamma(2\gamma)$ Γ_2

See the table immediately above giving the fitted decay rates. Following the advice of NEFKENS 02, we have removed the Primakoff-effect measurement from the average. See also the "Note on the Decay Width $\Gamma(\eta \to \gamma\gamma)$," in our 1994 edition, Phys. Rev. **D50**, 1 August 1994, Part I, p. 1451, for a discussion of the various measurements.

VALUE (keV)	*EVTS*	*DOCUMENT ID*		*TECN*	*COMMENT*
0.515±0.018 OUR FIT					
0.516±0.018 OUR AVERAGE					
0.520±0.020±0.013		BABUSCI	13A	KLOE	$e^+e^- \to e^+e^-\eta$
0.51 ±0.12 ±0.05	36	BARU	90	MD1	$e^+e^- \to e^+e^-\eta$
0.490±0.010±0.048	2287	ROE	90	ASP	$e^+e^- \to e^+e^-\eta$
0.514±0.017±0.035	1295	WILLIAMS	88	CBAL	$e^+e^- \to e^+e^-\eta$
0.53 ±0.04 ±0.04		BARTEL	85E	JADE	$e^+e^- \to e^+e^-\eta$
• • • We do not use the following data for averages, fits, limits, etc. • • •					
0.476±0.062		[1] RODRIGUES	08	CNTR	Reanalysis
0.64 ±0.14 ±0.13		AIHARA	86	TPC	$e^+e^- \to e^+e^-\eta$
0.56 ±0.16	56	WEINSTEIN	83	CBAL	$e^+e^- \to e^+e^-\eta$
0.324±0.046		BROWMAN	74B	CNTR	Primakoff effect
1.00 ±0.22		[2] BEMPORAD	67	CNTR	Primakoff effect

[1] RODRIGUES 08 uses a more sophisticated calculation for the inelastic background due to incoherent photoproduction to reanalyze the η photoproduction data on Be and Cu at 9 GeV from BROWMAN 74B. This brings the value of $\Gamma(\eta \to 2\gamma)$ in line with direct measurements of the width. The error here is only statistical.

[2] BEMPORAD 67 gives $\Gamma(2\gamma) = 1.21 \pm 0.26$ keV assuming $\Gamma(2\gamma)/\Gamma(\text{total}) = 0.314$. Bemporad private communication gives $\Gamma(2\gamma)^2/\Gamma(\text{total}) = 0.380 \pm 0.083$. We evaluate this using $\Gamma(2\gamma)/\Gamma(\text{total}) = 0.38 \pm 0.01$. Not included in average because the uncertainty resulting from the separation of the coulomb and nuclear amplitudes has apparently been underestimated.

$\Gamma(\pi^0 2\gamma)$ Γ_4

VALUE (eV)	EVTS	DOCUMENT ID		TECN	COMMENT
0.334±0.028 OUR FIT					
0.33 ±0.03	1200	NEFKENS	14	CRYB	$\gamma p \to \eta p$

η BRANCHING RATIOS

Neutral modes

$\Gamma(\text{neutral modes})/\Gamma_{\text{total}}$ $\Gamma_1/\Gamma = (\Gamma_2+\Gamma_3+\Gamma_4)/\Gamma$

VALUE	EVTS	DOCUMENT ID		TECN	COMMENT
0.7212±0.0034 OUR FIT Error includes scale factor of 1.2.					
0.705 ±0.008	16k	BASILE	71D	CNTR	MM spectrometer
• • • We do not use the following data for averages, fits, limits, etc. • • •					
0.79 ±0.08		BUNIATOV	67	OSPK	

$\Gamma(2\gamma)/\Gamma_{\text{total}}$ Γ_2/Γ

VALUE (units 10^{-2})	EVTS	DOCUMENT ID		TECN	COMMENT
39.41±0.20 OUR FIT Error includes scale factor of 1.1.					
39.49±0.17±0.30	65k	ABEGG	96	SPEC	$pd \to {}^3\text{He}\eta$
• • • We do not use the following data for averages, fits, limits, etc. • • •					
38.45±0.40±0.36	14k	[1] LOPEZ	07	CLEO	$\psi(2S) \to J/\psi\eta$

[1] Not independent of other results listed for LOPEZ 07. Assuming decays of $\eta \to \gamma\gamma$, $3\pi^0$, $\pi^+\pi^-\pi^0$, $\pi^+\pi^-\gamma$, and $e^+e^-\gamma$ account for all η decays within a contribution of 0.3% to the systematic error.

$\Gamma(2\gamma)/\Gamma(\text{neutral modes})$ $\Gamma_2/\Gamma_1 = \Gamma_2/(\Gamma_2+\Gamma_3+\Gamma_4)$

VALUE	EVTS	DOCUMENT ID		TECN	COMMENT
0.5465±0.0019 OUR FIT					
0.548 ±0.023 OUR AVERAGE Error includes scale factor of 1.5.					
0.535 ±0.018		BUTTRAM	70	OSPK	
0.59 ±0.033		BUNIATOV	67	OSPK	
• • • We do not use the following data for averages, fits, limits, etc. • • •					
0.52 ±0.09	88	ABROSIMOV	80	HLBC	
0.60 ±0.14	113	KENDALL	74	OSPK	
0.57 ±0.09		STRUGALSKI	71	HLBC	
0.579 ±0.052		FELDMAN	67	OSPK	
0.416 ±0.044		DIGIUGNO	66	CNTR	Error doubled
0.44 ±0.07		GRUNHAUS	66	OSPK	
0.39 ±0.06		[1] JONES	66	CNTR	

[1] This result from combining cross sections from two different experiments.

$\Gamma(3\pi^0)/\Gamma_{\text{total}}$ Γ_3/Γ

VALUE (units 10^{-2})	EVTS	DOCUMENT ID		TECN	COMMENT
32.68±0.23 OUR FIT Error includes scale factor of 1.1.					
• • • We do not use the following data for averages, fits, limits, etc. • • •					
34.03±0.56±0.49	1821	[1] LOPEZ	07	CLEO	$\psi(2S) \to J/\psi\eta$

[1] Not independent of other results listed for LOPEZ 07. Assuming decays of $\eta \to \gamma\gamma$, $3\pi^0$, $\pi^+\pi^-\pi^0$, $\pi^+\pi^-\gamma$, and $e^+e^-\gamma$ account for all η decays within a contribution of 0.3% to the systematic error.

$\Gamma(3\pi^0)/\Gamma(\text{neutral modes})$ $\Gamma_3/\Gamma_1 = \Gamma_3/(\Gamma_2+\Gamma_3+\Gamma_4)$

VALUE	EVTS	DOCUMENT ID		TECN	COMMENT
0.4531±0.0019 OUR FIT					
0.439 ±0.024		BUTTRAM	70	OSPK	
• • • We do not use the following data for averages, fits, limits, etc. • • •					
0.44 ±0.08	75	ABROSIMOV	80	HLBC	
0.32 ±0.09		STRUGALSKI	71	HLBC	
0.41 ±0.033		BUNIATOV	67	OSPK	Not indep. of $\Gamma(2\gamma)/\Gamma(\text{neutral modes})$
0.177 ±0.035		FELDMAN	67	OSPK	
0.209 ±0.054		DIGIUGNO	66	CNTR	Error doubled
0.29 ±0.10		GRUNHAUS	66	OSPK	

$\Gamma(3\pi^0)/\Gamma(2\gamma)$ Γ_3/Γ_2

VALUE	EVTS	DOCUMENT ID		TECN	COMMENT
0.829±0.006 OUR FIT					
0.829±0.007 OUR AVERAGE					
0.884±0.022±0.019	1821	LOPEZ	07	CLEO	$\psi(2S) \to J/\psi\eta$
0.817±0.012±0.032	17.4k	[1] AKHMETSHIN	05	CMD2	$e^+e^- \to \phi \to \eta\gamma$
0.826±0.024		ACHASOV	00D	SND	$e^+e^- \to \phi \to \eta\gamma$
0.832±0.005±0.012		KRUSCHE	95D	SPEC	$\gamma p \to \eta p$, threshold
0.841±0.034		AMSLER	93	CBAR	$\bar{p}p \to \pi^+\pi^-\eta$ at rest
0.822±0.009		ALDE	84	GAM2	
• • • We do not use the following data for averages, fits, limits, etc. • • •					
0.796±0.016±0.016		ACHASOV	00	SND	See ACHASOV 00D
0.91 ±0.14		COX	70B	HBC	
0.75 ±0.09		DEVONS	70	OSPK	
0.88 ±0.16		BALTAY	67D	DBC	
1.1 ±0.2		CENCE	67	OSPK	
1.25 ±0.39		BACCI	63	CNTR	Inverse BR reported

[1] Uses result from AKHMETSHIN 01B.

$\Gamma(\pi^0 2\gamma)/\Gamma_{\text{total}}$ Γ_4/Γ

Early results are summarized in the review by LANDSBERG 85.

VALUE (units 10^{-4})	CL%	EVTS	DOCUMENT ID		TECN	COMMENT
2.56±0.22 OUR FIT						
2.21±0.24±0.47		≈ 500	[1] PRAKHOV	08	CRYB	$\pi^- p \to \eta n \approx$ threshold
• • • We do not use the following data for averages, fits, limits, etc. • • •						
3.5 ±0.7 ±0.6		1.6k	[2,3] PRAKHOV	05	CRYB	See PRAKHOV 08
<8.4	90	7	ACHASOV	01D	SND	$e^+e^- \to \phi \to \eta\gamma$
<30	90	0	DAVYDOV	81	GAM2	$\pi^- p \to \eta n$

[1] PRAKHOV 08 is a reanalysis of the data of PRAKHOV 05, using for the first time the invariant-mass spectrum of the two photons.

[2] Normalized using $\Gamma(\eta \to 2\gamma)/\Gamma = 0.3943 \pm 0.0026$.

[3] This measurement and the independent analysis of the same data by KNECHT 04 both imply a lower value of $\Gamma(\pi^0 2\gamma)$ than the one obtained by ALDE 84 from $\Gamma(\pi^0 2\gamma)/\Gamma(2\gamma)$.

$\Gamma(\pi^0 2\gamma)/\Gamma(2\gamma)$ Γ_4/Γ_2

VALUE (units 10^{-3})	EVTS	DOCUMENT ID		TECN	CHG	COMMENT
0.65±0.06 OUR FIT						
1.8 ±0.4		ALDE	84	GAM2	0	
• • • We do not use the following data for averages, fits, limits, etc. • • •						
2.5 ±0.6	70	BINON	82	GAM2		See ALDE 84

$\Gamma(\pi^0 2\gamma)/\Gamma(3\pi^0)$ Γ_4/Γ_3

VALUE (units 10^{-4})	DOCUMENT ID		TECN	COMMENT
7.8±0.7 OUR FIT				
• • • We do not use the following data for averages, fits, limits, etc. • • •				
8.3±2.8±1.4	[1] KNECHT	04	CRYB	$\pi^- p \to n\eta$

[1] Independent analysis of same data as PRAKHOV 05.

$\Gamma(2\pi^0 2\gamma)/\Gamma_{\text{total}}$ Γ_5/Γ

VALUE	CL%	DOCUMENT ID		TECN	COMMENT
<1.2 × 10⁻³	90	[1] NEFKENS	05A	CRYB	p(720 MeV/c) $\pi^- \to n\eta$
• • • We do not use the following data for averages, fits, limits, etc. • • •					
<4.0 × 10⁻³	90	BLIK	07	GAM4	$\pi^- p \to \eta n$

[1] Measurement is done in limited $\gamma\gamma$ energy range.

$\Gamma(4\gamma)/\Gamma_{\text{total}}$ Γ_6/Γ

VALUE	CL%	DOCUMENT ID		TECN	COMMENT
<2.8 × 10⁻⁴	90	BLIK	07	GAM4	$\pi^- p \to \eta n$

$\Gamma(\text{invisible})/\Gamma(2\gamma)$ Γ_7/Γ_2

VALUE	CL%	DOCUMENT ID		TECN	COMMENT
<2.6 × 10⁻⁴	90	[1] ABLIKIM	13	BES3	$J/\psi \to \phi\eta$
• • • We do not use the following data for averages, fits, limits, etc. • • •					
<1.65 × 10⁻³	90	[2] ABLIKIM	06Q	BES2	$J/\psi \to \phi\eta$

[1] Based on 225M J/ψ decays.

[2] Based on 58M J/ψ decays.

Charged modes

$\Gamma(\pi^+\pi^-\pi^0)/\Gamma_{\text{total}}$ Γ_9/Γ

VALUE (units 10^{-2})	EVTS	DOCUMENT ID		TECN	COMMENT
22.92±0.28 OUR FIT Error includes scale factor of 1.2.					
• • • We do not use the following data for averages, fits, limits, etc. • • •					
22.60±0.35±0.29	3915	[1] LOPEZ	07	CLEO	$\psi(2S) \to J/\psi\eta$

[1] Not independent of other results listed for LOPEZ 07. Assuming decays of $\eta \to \gamma\gamma$, $3\pi^0$, $\pi^+\pi^-\pi^0$, $\pi^+\pi^-\gamma$, and $e^+e^-\gamma$ account for all η decays within a contribution of 0.3% to the systematic error.

$\Gamma(\text{neutral modes})/\Gamma(\pi^+\pi^-\pi^0)$ $\Gamma_1/\Gamma_9 = (\Gamma_2+\Gamma_3+\Gamma_4)/\Gamma_9$

VALUE	EVTS	DOCUMENT ID		TECN
3.15±0.05 OUR FIT Error includes scale factor of 1.2.				
3.26±0.30 OUR AVERAGE				
2.54±1.89	74	KENDALL	74	OSPK
3.4 ±1.1	29	AGUILAR-...	72B	HBC
2.83±0.80	70	[1] BLOODWO...	72B	HBC
3.6 ±0.6	244	FLATTE	67B	HBC
2.89±0.56		ALFF-...	66	HBC
3.6 ±0.8	50	KRAEMER	64	DBC
3.8 ±1.1		PAULI	64	DBC

[1] Error increased from published value 0.5 by Bloodworth (private communication).

$\Gamma(2\gamma)/\Gamma(\pi^+\pi^-\pi^0)$ Γ_2/Γ_9

VALUE	EVTS	DOCUMENT ID		TECN	COMMENT
1.720±0.028 OUR FIT Error includes scale factor of 1.2.					
1.70 ±0.04 OUR AVERAGE					
1.704±0.032±0.026	3915	[1] LOPEZ	07	CLEO	$\psi(2S) \to J/\psi\eta$
1.61 ±0.14		ABLIKIM	06E	BES2	$e^+e^- \to J/\psi \to \eta\gamma$
1.78 ±0.10 ±0.13	1077	AMSLER	95	CBAR	$\bar{p}p \to \pi^+\pi^-\eta$ at rest

1.72 ±0.25	401	BAGLIN	69	HLBC	
1.61 ±0.39		FOSTER	65	HBC	

[1] LOPEZ 07 reports $\Gamma(\eta \to \pi^+\pi^-\pi^0) / \Gamma(\eta \to 2\gamma) = \Gamma_9/\Gamma_2 = 0.587 \pm 0.011 \pm 0.009$.

$\Gamma(3\pi^0)/\Gamma(\pi^+\pi^-\pi^0)$ Γ_3/Γ_9

VALUE	EVTS	DOCUMENT ID		TECN	COMMENT
1.426±0.026 OUR FIT Error includes scale factor of 1.2.					
1.48 ±0.05 OUR AVERAGE					
1.46 ±0.03 ±0.09		ACHASOV	06A	SND	$e^+e^- \to \eta\gamma$
1.52 ±0.04 ±0.08	23k	[1] AKHMETSHIN	01B	CMD2	$e^+e^- \to \phi \to \eta\gamma$
1.44 ±0.09 ±0.10	1627	AMSLER	95	CBAR	$\overline{p}p \to \pi^+\pi^-\eta$ at rest
1.50 $^{+0.15}_{-0.29}$	199	BAGLIN	69	HLBC	
1.47 $^{+0.20}_{-0.17}$		BULLOCK	68	HLBC	
• • • We do not use the following data for averages, fits, limits, etc. • • •					
1.3 ±0.4		BAGLIN	67B	HLBC	
0.90 ±0.24		FOSTER	65	HBC	
2.0 ±1.0		FOELSCHE	64	HBC	
0.83 ±0.32		CRAWFORD	63	HBC	

[1] AKHMETSHIN 01B uses results from AKHMETSHIN 99F.

$\Gamma(\pi^+\pi^-\pi^0)/[\Gamma(2\gamma)+\Gamma(3\pi^0)]$ $\Gamma_9/(\Gamma_2+\Gamma_3)$

VALUE	DOCUMENT ID		TECN	COMMENT
0.318 ±0.005 OUR FIT Error includes scale factor of 1.2.				
0.304 ±0.012	ACHASOV	00D	SND	$e^+e^- \to \phi \to \eta\gamma$
• • • We do not use the following data for averages, fits, limits, etc. • • •				
0.3141±0.0081±0.0058	ACHASOV	00B	SND	See ACHASOV 00D

$\Gamma(\pi^+\pi^-\gamma)/\Gamma_{\text{total}}$ Γ_{10}/Γ

VALUE (units 10^{-2})	EVTS	DOCUMENT ID		TECN	COMMENT
4.22±0.08 OUR FIT Error includes scale factor of 1.1.					
• • • We do not use the following data for averages, fits, limits, etc. • • •					
3.96±0.14±0.14	859	[1] LOPEZ	07	CLEO	$\psi(2S) \to J/\psi\eta$

[1] Not independent of other results listed for LOPEZ 07. Assuming decays of $\eta \to \gamma\gamma$, $3\pi^0$, $\pi^+\pi^-\pi^0$, $\pi^+\pi^-\gamma$, and $e^+e^-\gamma$ account for all η decays within a contribution of 0.3% to the systematic error.

$\Gamma(\pi^+\pi^-\gamma)/\Gamma(\pi^+\pi^-\pi^0)$ Γ_{10}/Γ_9

VALUE	EVTS	DOCUMENT ID		TECN	COMMENT
0.1842±0.0027 OUR FIT					
0.1847±0.0030 OUR AVERAGE Error includes scale factor of 1.1.					
0.1856±0.0005±0.0028	200k	BABUSCI	13	KLOE	$e^+e^- \to \phi \to \eta\gamma$
0.175 ±0.007 ±0.006	859	LOPEZ	07	CLEO	$\psi(2S) \to J/\psi\eta$
• • • We do not use the following data for averages, fits, limits, etc. • • •					
0.209 ±0.004	18k	THALER	73	ASPK	
0.201 ±0.006	7250	GORMLEY	70	ASPK	
0.28 ±0.04		BALTAY	67B	DBC	
0.25 ±0.035		LITCHFIELD	67	DBC	
0.30 ±0.06		CRAWFORD	66	HBC	
0.196 ±0.041		FOSTER	65C	HBC	

$\Gamma(e^+e^-\gamma)/\Gamma_{\text{total}}$ Γ_{11}/Γ

VALUE (units 10^{-3})	EVTS	DOCUMENT ID		TECN	COMMENT
6.9 ±0.4 OUR FIT Error includes scale factor of 1.3.					
6.7 ±0.5 OUR AVERAGE Error includes scale factor of 1.2.					
6.6 ±0.4 ±0.4	1345	BERGHAUSER	11	SPEC	$\gamma p \to p\eta$
7.8 ±0.5 ±0.8	435 ± 31	BERLOWSKI	08	WASA	$pd \to {}^3\text{He}\,\eta$
5.15±0.62±0.74	283	ACHASOV	01B	SND	$e^+e^- \to \phi \to \eta\gamma$
7.10±0.64±0.46	323	AKHMETSHIN	01	CMD2	$e^+e^- \to \phi \to \eta\gamma$
• • • We do not use the following data for averages, fits, limits, etc. • • •					
9.4 ±0.7 ±0.5	172	[1] LOPEZ	07	CLEO	$\psi(2S) \to J/\psi\eta$

[1] Not independent of other results listed for LOPEZ 07. Assuming decays of $\eta \to \gamma\gamma$, $3\pi^0$, $\pi^+\pi^-\pi^0$, $\pi^+\pi^-\gamma$, and $e^+e^-\gamma$ account for all η decays within a contribution of 0.3% to the systematic error.

$\Gamma(e^+e^-\gamma)/\Gamma(\pi^+\pi^-\gamma)$ Γ_{11}/Γ_{10}

VALUE	EVTS	DOCUMENT ID		TECN	COMMENT
0.163±0.011 OUR FIT Error includes scale factor of 1.2.					
0.237±0.021±0.015	172	LOPEZ	07	CLEO	$\psi(2S) \to J/\psi\eta$

$\Gamma(e^+e^-\gamma)/\Gamma(\pi^+\pi^-\pi^0)$ Γ_{11}/Γ_9

VALUE (units 10^{-2})	EVTS	DOCUMENT ID		TECN	COMMENT
3.00±0.19 OUR FIT Error includes scale factor of 1.3.					
2.1 ±0.5	80	JANE	75B	OSPK	See the erratum

$\Gamma(\text{neutral modes})/[\Gamma(\pi^+\pi^-\pi^0)+\Gamma(\pi^+\pi^-\gamma)+\Gamma(e^+e^-\gamma)]$ $\Gamma_1/(\Gamma_9+\Gamma_{10}+\Gamma_{11}) = (\Gamma_2+\Gamma_3+\Gamma_4)/(\Gamma_9+\Gamma_{10}+\Gamma_{11})$

VALUE	EVTS	DOCUMENT ID		TECN
2.59±0.04 OUR FIT Error includes scale factor of 1.2.				
2.64±0.23		BALTAY	67B	DBC
• • • We do not use the following data for averages, fits, limits, etc. • • •				
4.5 ±1.0	280	[1] JAMES	66	HBC
3.20±1.26	53	[1] BASTIEN	62	HBC
2.5 ±1.0	10	[1] PICKUP	62	HBC

[1] These experiments are not used in the averages as they do not separate clearly $\eta \to \pi^+\pi^-\pi^0$ and $\eta \to \pi^+\pi^-\gamma$ from each other. The reported values thus probably contain some unknown fraction of $\eta \to \pi^+\pi^-\gamma$.

$\Gamma(2\gamma)/[\Gamma(\pi^+\pi^-\pi^0)+\Gamma(\pi^+\pi^-\gamma)+\Gamma(e^+e^-\gamma)]$ $\Gamma_2/(\Gamma_9+\Gamma_{10}+\Gamma_{11})$

VALUE	EVTS	DOCUMENT ID		TECN
1.417±0.023 OUR FIT Error includes scale factor of 1.2.				
1.1 ±0.4 OUR AVERAGE				
1.51 ±0.93	75	KENDALL	74	OSPK
0.99 ±0.48		CRAWFORD	63	HBC

$\Gamma(\mu^+\mu^-\gamma)/\Gamma_{\text{total}}$ Γ_{12}/Γ

VALUE (units 10^{-4})	EVTS	DOCUMENT ID		TECN	COMMENT
3.1±0.4 OUR FIT					
3.1±0.4	600	DZHELYADIN	80	SPEC	$\pi^- p \to \eta n$
• • • We do not use the following data for averages, fits, limits, etc. • • •					
1.5±0.75	100	BUSHNIN	78	SPEC	See DZHELYADIN 80

$\Gamma(e^+e^-)/\Gamma_{\text{total}}$ Γ_{13}/Γ

VALUE	CL%	DOCUMENT ID		TECN	COMMENT
<2.3 ×10^{-6}	90	AGAKISHIEV	14		$pp \to \eta + X$
• • • We do not use the following data for averages, fits, limits, etc. • • •					
<5.6 ×10^{-6}	90	[1] AGAKISHIEV	12A	SPEC	$pp \to \eta + X$
<2.7 ×10^{-5}	90	BERLOWSKI	08	WASA	$pd \to {}^3\text{He}\,\eta$
<0.77 ×10^{-4}	90	BROWDER	97B	CLE2	$e^+e^- \simeq 10.5$ GeV
<2 ×10^{-4}	90	WHITE	96	SPEC	$pd \to \eta {}^3\text{He}$
<3 ×10^{-4}	90	DAVIES	74	RVUE	Uses ESTEN 67

[1] AGAKISHIEV 12A uses a data sample of 3.5 GeV proton beam collisions on liquid hydrogen target collected by the HADES detector.

$\Gamma(\mu^+\mu^-)/\Gamma_{\text{total}}$ Γ_{14}/Γ

VALUE (units 10^{-6})	CL%	EVTS	DOCUMENT ID		TECN	COMMENT
5.8±0.8 OUR AVERAGE						
5.7±0.7±0.5		114	ABEGG	94	SPEC	$pd \to \eta {}^3\text{He}$
6.5±2.1		27	DZHELYADIN	80B	SPEC	$\pi^- p \to \eta n$
• • • We do not use the following data for averages, fits, limits, etc. • • •						
5.6 $^{+0.6}_{-0.7}$ ±0.5		100	KESSLER	93	SPEC	See ABEGG 94
< 20	95	0	WEHMANN	68	OSPK	

$\Gamma(\mu^+\mu^-)/\Gamma(2\gamma)$ Γ_{14}/Γ_2

VALUE (units 10^{-5})	DOCUMENT ID		TECN
• • • We do not use the following data for averages, fits, limits, etc. • • •			
5.9±2.2	HYAMS	69	OSPK

$\Gamma(2e^+2e^-)/\Gamma_{\text{total}}$ Γ_{15}/Γ

VALUE (units 10^{-5})	CL%	EVTS	DOCUMENT ID		TECN	COMMENT
2.4±0.2±0.1		362	[1] AMBROSINO	11B	KLOE	$e^+e^- \to \phi \to \eta\gamma$
• • • We do not use the following data for averages, fits, limits, etc. • • •						
<9.7	90		BERLOWSKI	08	WASA	$pd \to {}^3\text{He}\,\eta$
<6.9	90		AKHMETSHIN	01	CMD2	$e^+e^- \to \phi \to \eta\gamma$

[1] This measurement is fully inclusive (includes "$2e^+2e^-\gamma$" channel).

$\Gamma(\pi^+\pi^-e^+e^-(\gamma))/\Gamma_{\text{total}}$ Γ_{16}/Γ

VALUE (units 10^{-4})	EVTS	DOCUMENT ID		TECN	COMMENT
2.68±0.11 OUR FIT					
2.68±0.09±0.07	1555 ±52	[1] AMBROSINO	09B	KLOE	$e^+e^- \to \phi \to \eta\gamma$
• • • We do not use the following data for averages, fits, limits, etc. • • •					
4.3 $^{+2.0}_{-1.6}$ ±0.4	16	BERLOWSKI	08	WASA	$pd \to {}^3\text{He}\,\eta$
4.3 ±1.3 ±0.4	16	BARGHOLTZ	07	CNTR	See BERLOWSKI 08
3.7 $^{+2.5}_{-1.8}$ ±0.3	4	AKHMETSHIN	01	CMD2	$e^+e^- \to \phi \to \eta\gamma$

[1] This AMBROSINO 09B value includes radiative events.

$\Gamma(e^+e^-\mu^+\mu^-)/\Gamma_{\text{total}}$ Γ_{17}/Γ

VALUE	CL%	DOCUMENT ID		TECN	COMMENT
<1.6 × 10^{-4}	90	BERLOWSKI	08	WASA	$pd \to {}^3\text{He}\,\eta$

$\Gamma(2\mu^+2\mu^-)/\Gamma_{\text{total}}$ Γ_{18}/Γ

VALUE	CL%	DOCUMENT ID		TECN	COMMENT
<3.6 × 10^{-4}	90	BERLOWSKI	08	WASA	$pd \to {}^3\text{He}\,\eta$

$\Gamma(\mu^+\mu^-\pi^+\pi^-)/\Gamma_{\text{total}}$ Γ_{19}/Γ

VALUE	CL%	DOCUMENT ID		TECN	COMMENT
<3.6 × 10^{-4}	90	BERLOWSKI	08	WASA	$pd \to {}^3\text{He}\,\eta$

$\Gamma(\pi^+ e^- \overline{\nu}_e + \text{c.c.})/\Gamma(\pi^+\pi^-\pi^0)$ Γ_{20}/Γ_9

VALUE	CL%	DOCUMENT ID		TECN	COMMENT
$<7.3\times10^{-4}$	90	ABLIKIM	13G	BES3	$J/\psi \to \phi\eta$

$\Gamma(\pi^+\pi^-2\gamma)/\Gamma(\pi^+\pi^-\pi^0)$ Γ_{21}/Γ_9

VALUE	CL%	DOCUMENT ID		TECN
$< 9\times10^{-3}$		PRICE	67	HBC
• • • We do not use the following data for averages, fits, limits, etc. • • •				
$<16\times10^{-3}$	95	BALTAY	67B	DBC

$\Gamma(\pi^+\pi^-\pi^0\gamma)/\Gamma(\pi^+\pi^-\pi^0)$ Γ_{22}/Γ_9

VALUE	CL%	EVTS	DOCUMENT ID		TECN
$<0.24\times10^{-2}$	90	0	THALER	73	ASPK
• • • We do not use the following data for averages, fits, limits, etc. • • •					
$<1.7\times10^{-2}$	90		ARNOLD	68	HLBC
$<1.6\times10^{-2}$	95		BALTAY	67B	DBC
$<7.0\times10^{-2}$			FLATTE	67	HBC
$<0.9\times10^{-2}$			PRICE	67	HBC

$\Gamma(\pi^0\mu^+\mu^-\gamma)/\Gamma_{\text{total}}$ Γ_{23}/Γ

VALUE	CL%	DOCUMENT ID		TECN	COMMENT
$<3\times10^{-6}$	90	DZHELYADIN	81	SPEC	$\pi^- p \to \eta n$

Forbidden modes

$\Gamma(\pi^0\gamma)/\Gamma_{\text{total}}$ Γ_{24}/Γ

Forbidden by angular momentum conservation.

VALUE	CL%	DOCUMENT ID		TECN	COMMENT
$<9\times10^{-5}$	90	NEFKENS	05A	CRYB	p(720 MeV/c) $\pi^- \to n\eta$

$\Gamma(\pi^+\pi^-)/\Gamma_{\text{total}}$ Γ_{25}/Γ

Forbidden by P and CP invariance.

VALUE	CL%	EVTS	DOCUMENT ID		TECN	COMMENT
$< 1.3\times10^{-5}$	90	16M	AMBROSINO	05A	KLOE	$e^+e^- \to \phi \to \eta\gamma$
• • • We do not use the following data for averages, fits, limits, etc. • • •						
$< 1.6\times10^{-5}$	90	25M	AAIJ	17D	LHCB	in $D \to \pi\pi\pi$ decays
$< 3.9\times10^{-4}$	90	225M	ABLIKIM	11G	BES3	$e^+e^- \to J/\psi \to \eta\gamma$
$< 3.3\times10^{-4}$	90		AKHMETSHIN	99B	CMD2	$e^+e^- \to \phi \to \eta\gamma$
$< 9\times10^{-4}$	90		AKHMETSHIN	97C	CMD2	See AKHMETSHIN 99B
$<15\times10^{-4}$		0	THALER	73	ASPK	

$\Gamma(2\pi^0)/\Gamma_{\text{total}}$ Γ_{26}/Γ

Forbidden by P and CP invariance.

VALUE	CL%	EVTS	DOCUMENT ID		TECN	COMMENT
$<3.5\times10^{-4}$	90		BLIK	07	GAM4	$\pi^- p \to \eta n$
• • • We do not use the following data for averages, fits, limits, etc. • • •						
$<6.9\times10^{-4}$	90	225M	ABLIKIM	11G	BES3	$e^+e^- \to J/\psi \to \eta\gamma$
$<4.3\times10^{-4}$	90		AKHMETSHIN	99C	CMD2	$e^+e^- \to \phi \to \eta\gamma$
$<6\times10^{-4}$	90		[1] ACHASOV	98	SND	$e^+e^- \to \phi \to \eta\gamma$

[1] ACHASOV 98 observes one event in a $\pm3\sigma$ region around the η mass, while a Monte Carlo calculation gives 10 ± 5 events. The limit here is the Poisson upper limit for one observed event and no background.

$\Gamma(2\pi^0\gamma)/\Gamma_{\text{total}}$ Γ_{27}/Γ

Forbidden by C invariance.

VALUE	CL%	DOCUMENT ID		TECN	CHG	COMMENT
$< 5\times10^{-4}$	90	NEFKENS	05	CRYB	0	p(720 MeV/c) $\pi^- \to n\eta$
• • • We do not use the following data for averages, fits, limits, etc. • • •						
$<17\times10^{-4}$	90	BLIK	07	GAM4		$\pi^- p \to \eta n$

$\Gamma(3\pi^0\gamma)/\Gamma_{\text{total}}$ Γ_{28}/Γ

Forbidden by C invariance.

VALUE	CL%	DOCUMENT ID		TECN	CHG	COMMENT
$< 6\times10^{-5}$	90	NEFKENS	05	CRYB	0	p(720 MeV/c) $\pi^- \to n\eta$
• • • We do not use the following data for averages, fits, limits, etc. • • •						
$<24\times10^{-5}$	90	BLIK	07	GAM4		$\pi^- p \to \eta n$

$\Gamma(3\gamma)/\Gamma_{\text{total}}$ Γ_{29}/Γ

Forbidden by C invariance.

VALUE	CL%	DOCUMENT ID		TECN	COMMENT
• • • We do not use the following data for averages, fits, limits, etc. • • •					
$<16\times10^{-5}$	90	BLIK	07	GAM4	$\pi^- p \to \eta n$
$< 4\times10^{-5}$	90	NEFKENS	05A	CRYB	p(720 MeV/c) $\pi^- \to n\eta$

$\Gamma(3\gamma)/\Gamma(2\gamma)$ Γ_{29}/Γ_2

VALUE	CL%	DOCUMENT ID		TECN	CHG
$<1.2\times10^{-3}$	95	ALDE	84	GAM2	0

$\Gamma(3\gamma)/\Gamma(3\pi^0)$ Γ_{29}/Γ_3

VALUE	CL%	DOCUMENT ID		TECN	COMMENT
$<4.9\times10^{-5}$	90	ALOISIO	04	KLOE	$\phi \to \eta\gamma$

$\Gamma(4\pi^0)/\Gamma_{\text{total}}$ Γ_{30}/Γ

Forbidden by P and CP invariance.

VALUE	CL%	DOCUMENT ID		TECN	COMMENT
$< 6.9\times10^{-7}$	90	PRAKHOV	00	CRYB	$\pi^- p \to n\eta$, 720 MeV/c
• • • We do not use the following data for averages, fits, limits, etc. • • •					
$<200\times10^{-7}$	90	BLIK	07	GAM4	$\pi^- p \to \eta n$

$\Gamma(\pi^0 e^+ e^-)/\Gamma_{\text{total}}$ Γ_{31}/Γ

C parity forbids this to occur as a single-photon process.

VALUE	CL%	DOCUMENT ID		TECN
• • • We do not use the following data for averages, fits, limits, etc. • • •				
$< 1.6\times10^{-4}$	90	MARTYNOV	76	HLBC
$< 8.4\times10^{-4}$	90	BAZIN	68	DBC
$<70\times10^{-4}$		RITTENBERG	65	HBC

$\Gamma(\pi^0 e^+ e^-)/\Gamma(\pi^+\pi^-\pi^0)$ Γ_{31}/Γ_9

C parity forbids this to occur as a single-photon process.

VALUE	CL%	EVTS	DOCUMENT ID		TECN
$< 1.9\times10^{-4}$	90		JANE	75	OSPK
• • • We do not use the following data for averages, fits, limits, etc. • • •					
$< 42\times10^{-4}$	90		BAGLIN	67	HLBC
$< 16\times10^{-4}$	90	0	BILLING	67	HLBC
$< 77\times10^{-4}$		0	FOSTER	65B	HBC
$<110\times10^{-4}$			PRICE	65	HBC

$\Gamma(\pi^0\mu^+\mu^-)/\Gamma_{\text{total}}$ Γ_{32}/Γ

C parity forbids this to occur as a single-photon process.

VALUE	CL%	DOCUMENT ID		TECN	COMMENT
$< 5\times10^{-6}$	90	DZHELYADIN	81	SPEC	$\pi^- p \to \eta n$
• • • We do not use the following data for averages, fits, limits, etc. • • •					
$<500\times10^{-6}$		WEHMANN	68	OSPK	

$[\Gamma(\mu^+ e^-) + \Gamma(\mu^- e^+)]/\Gamma_{\text{total}}$ Γ_{33}/Γ

Forbidden by lepton family number conservation.

VALUE	CL%	DOCUMENT ID		TECN	COMMENT
$<6\times10^{-6}$	90	WHITE	96	SPEC	$pd \to \eta\,{}^3\text{He}$

η C-NONCONSERVING DECAY PARAMETERS

$\pi^+\pi^-\pi^0$ LEFT-RIGHT ASYMMETRY PARAMETER

Measurements with an error $> 1.0\times10^{-2}$ have been omitted.

VALUE (units 10^{-2})	EVTS	DOCUMENT ID		TECN
$0.09^{+0.11}_{-0.12}$ OUR AVERAGE				
$+0.09\pm0.10^{+0.09}_{-0.14}$	1.34M	AMBROSINO	08D	KLOE
0.28 ± 0.26	165k	JANE	74	OSPK
-0.05 ± 0.22	220k	LAYTER	72	ASPK
• • • We do not use the following data for averages, fits, limits, etc. • • •				
$1.5\ \pm0.5$	37k	[1] GORMLEY	68C	ASPK

[1] The GORMLEY 68C asymmetry is probably due to unmeasured ($\mathbf{E}\times\mathbf{B}$) spark chamber effects. New experiments with ($\mathbf{E}\times\mathbf{B}$) controls don't observe an asymmetry.

$\pi^+\pi^-\pi^0$ SEXTANT ASYMMETRY PARAMETER

Measurements with an error $> 2.0\times10^{-2}$ have been omitted.

VALUE (units 10^{-2})	EVTS	DOCUMENT ID		TECN
$0.12^{+0.10}_{-0.11}$ OUR AVERAGE				
$+0.08\pm0.10^{+0.08}_{-0.13}$	1.34M	AMBROSINO	08D	KLOE
0.20 ± 0.25	165k	JANE	74	OSPK
0.10 ± 0.22	220k	LAYTER	72	ASPK
$0.5\ \pm0.5$	37k	GORMLEY	68C	WIRE

$\pi^+\pi^-\pi^0$ QUADRANT ASYMMETRY PARAMETER

VALUE (units 10^{-2})	EVTS	DOCUMENT ID		TECN
-0.09 ± 0.09 OUR AVERAGE				
$-0.05\pm0.10^{+0.03}_{-0.05}$	1.34M	AMBROSINO	08D	KLOE
-0.30 ± 0.25	165k	JANE	74	OSPK
-0.07 ± 0.22	220k	LAYTER	72	ASPK

$\pi^+\pi^-\gamma$ LEFT-RIGHT ASYMMETRY PARAMETER

Measurements with an error $> 2.0\times10^{-2}$ have been omitted.

VALUE (units 10^{-2})	EVTS	DOCUMENT ID		TECN
$0.9\ \pm0.4$ OUR AVERAGE				
$1.2\ \pm0.6$	35k	JANE	74B	OSPK
$0.5\ \pm0.6$	36k	THALER	72	ASPK
1.22 ± 1.56	7257	GORMLEY	70	ASPK

$\pi^+\pi^-\gamma$ PARAMETER β (D-wave)

Sensitive to a D-wave contribution: $dN/d\cos\theta = \sin^2\theta\ (1 + \beta\ \cos^2\theta)$.

VALUE	EVTS	DOCUMENT ID		TECN
$-0.02\ \pm0.07$ OUR AVERAGE Error includes scale factor of 1.3.				
$0.11\ \pm0.11$	35k	JANE	74B	OSPK
-0.060 ± 0.065	7250	GORMLEY	70	WIRE

• • • We do not use the following data for averages, fits, limits, etc. • • •

0.12 ±0.06	[1] THALER	72	ASPK	

[1] The authors don't believe this indicates D-wave because the dependence of β on the γ energy is inconsistent with the theoretical prediction. A $\cos^2\theta$ dependence can also come from P- and F-wave interference.

η CP-NONCONSERVING DECAY PARAMETER

$\pi^+\pi^-e^+e^-$ DECAY-PLANE ASYMMETRY PARAMETER A_ϕ

In the η rest frame, the total momentum of the e^+e^- pair is equal and opposite to that of the $\pi^+\pi^-$ pair. Let $\hat{z}$ be the unit vector along the momentum of the e^+e^- pair; let $\hat{n}_{ee}$ and $\hat{n}_{\pi\pi}$ be the unit vectors normal to the e^+e^- and $\pi^+\pi^-$ planes; and let ϕ be the angle between the two normals. Then

$$\sin\phi\,\cos\phi = [(\hat{n}_{ee}\times\hat{n}_{\pi\pi})\cdot\hat{z}]\,(\hat{n}_{ee}\cdot\hat{n}_{\pi\pi})\ ,$$

and

$$A_\phi \equiv \frac{N_{\sin\phi\cos\phi>0} - N_{\sin\phi\cos\phi<0}}{N_{\sin\phi\cos\phi>0} + N_{\sin\phi\cos\phi<0}}\ .$$

VALUE (units 10^{-2})	EVTS	DOCUMENT ID		TECN	COMMENT
−0.6±2.5±1.8	1555 ±52	AMBROSINO	09B	KLOE	$e^+e^-\to\phi\to\eta\gamma$

ENERGY DEPENDENCE OF $\eta\to 3\pi$ DALITZ PLOTS

PARAMETERS FOR $\eta\to\pi^+\pi^-\pi^0$

See the "Note on η Decay Parameters," page 1454, in our 1994 edition (Physical Review **D50** 1173 (1994)). The following experiments fit to one or more of the coefficients a, b, c, d, e, f or g for $|\text{matrix element}|^2 = 1 + ay + by^2 + cx + dx^2 + exy + fy^3 + gx^2y$.

VALUE	EVTS	DOCUMENT ID		TECN	COMMENT
• • • We do not use the following data for averages, fits, limits, etc. • • •					
4.7M		[1] ANASTASI	16A	KLOE	$e^+e^-\to\phi\to\eta\gamma$
79k		ABLIKIM	15G	BES3	$e^+e^-\to J/\psi\to\gamma\eta$
174k		ADLARSON	14A	WASA	$pd\to\eta\,{}^3$He
1.34M		AMBROSINO	08D	KLOE	
3230		[2] ABELE	98D	CBAR	$\overline{p}p\to\pi^0\pi^0\eta$ at rest
1077		[3] AMSLER	95	CBAR	$\overline{p}p\to\pi^+\pi^-\eta$ at rest
81k		LAYTER	73	ASPK	
220k		LAYTER	72	ASPK	
1138		CARPENTER	70	HBC	
349		DANBURG	70	DBC	
7250		GORMLEY	70	WIRE	
526		BAGLIN	69	HLBC	
7170		CNOPS	68	OSPK	
37k		GORMLEY	68C	WIRE	
1300		CLPWY	66	HBC	
705		LARRIBE	66	HBC	

[1] ANASTASI 16A measure the Dalitz parameters a, b, d, f, and g. This is the first measurement of g.
[2] ABELE 98D obtains $a=-1.22\pm0.07$ and $b=0.22\pm0.11$ when c (or d) is fixed at 0.06.
[3] AMSLER 95 fits to $(1+ay+by^2)$ and obtains $a=-0.94\pm0.15$ and $b=0.11\pm0.27$.

α PARAMETER FOR $\eta\to 3\pi^0$

See the "Note on η Decay Parameters" in our 1994 edition, Phys. Rev. **D50**, 1 August 1994, Part I, p. 1454. The value here is of α in $|\text{matrix element}|^2 = 1 + 2\alpha z$.

VALUE	EVTS	DOCUMENT ID		TECN	COMMENT
−0.0318±0.0015 OUR AVERAGE					
$-0.055\ \pm0.014\ \pm0.004$	33k	ABLIKIM	15G	BES3	$e^+e^-\to J/\psi\to\gamma\eta$
$-0.0301\pm0.0035\ ^{+0.0022}_{-0.0035}$	512k	AMBROSINO	10A	KLOE	$e^+e^-\to\phi\to\eta\gamma$
$-0.027\ \pm0.008\ \pm0.005$	120k	[1] ADOLPH	09	WASA	$pp\to pp\eta$
$-0.0322\pm0.0012\pm0.0022$	3M	[2] PRAKHOV	09	CRYB	$\gamma p\to p\eta$
$-0.032\ \pm0.002\ \pm0.002$	1.8M	[2] UNVERZAGT	09	CRYB	$\gamma p\to p\eta$
$-0.026\ \pm0.010\ \pm0.010$	75k	BASHKANOV	07	WASA	$pp\to pp\eta$
$-0.010\ \pm0.021\ \pm0.010$	12k	ACHASOV	01C	SND	$e^+e^-\to\phi\to\eta\gamma$
$-0.031\ \pm0.004$	1M	TIPPENS	01	CRYB	$\pi^-p\to n\eta$, 720 MeV
$-0.052\ \pm0.017\ \pm0.010$	98k	ABELE	98C	CBAR	$\overline{p}p\to 5\pi^0$
$-0.022\ \pm0.023$	50k	ALDE	84	GAM2	
• • • We do not use the following data for averages, fits, limits, etc. • • •					
$-0.038\ \pm0.003\ ^{+0.012}_{-0.008}$	1.34M	[3] AMBROSINO	08D	KLOE	
$-0.32\ \pm0.37$	192	BAGLIN	70	HLBC	

[1] This ADOLPH 09 result is independent of the BASHKANOV 07 result.
[2] The PRAKHOV 09 and UNVERZAGT 09 results are independent.
[3] This AMBROSINO 08D value is an indirect result using $\eta\to\pi^+\pi^0\pi^-$ events and a rescattering matrix that mixes isospin decay amplitudes.

PARAMETER Λ IN $\eta\to\ell^+\ell^-\gamma$ DECAY

In the pole approximation the electromagnetic transition form factor for a resonance of mass M is given by the expression:

$$|F|^2 = (1 - M^2_{\ell\ell}/\Lambda^2)^{-2},$$

where for the parameter Λ vector dominance predicts $\Lambda\approx 0.770$ GeV.

VALUE (GeV/c^2)	EVTS	DOCUMENT ID		TECN	COMMENT
0.716 ±0.011 OUR AVERAGE					
0.712 ±0.020		[1] ADLARSON	17B	A2MM	$\gamma p\to\eta p$
$0.7191\pm0.0125\pm0.0093$		[2] ARNALDI	16	NA60	400 GeV p-A collisions
0.716 ±0.031 ±0.009		[3] ARNALDI	09	NA60	158A In−In collisions
0.72 ±0.09	600	DZHELYADIN	80	SPEC	$\pi^-p\to\eta n$, $\eta\to\gamma\mu^+\mu^-$

[1] ADLARSON 17B reports $\Lambda^{-2}(\eta\to\gamma e^+e^-) = 1.97\pm0.11$ (GeV/c^2)$^{-2}$ which we converted to the quoted Λ value and uncertainty (total=statistical plus systematic).
[2] ARNALDI 16 reports $\Lambda^{-2}(\eta\to\gamma\mu^+\mu^-) = 1.934\pm0.067\pm0.050$ (GeV/c^2)$^{-2}$ which we converted to the quoted Λ value.
[3] ARNALDI 09 reports $\Lambda^{-2}(\eta\to\gamma\mu^+\mu^-) = 1.95\pm0.17\pm0.05$ (GeV/c^2)$^{-2}$ which we converted to the quoted Λ value.

η REFERENCES

AAIJ	17D	PL B764 233	R. Aaij *et al.*	(LHCb Collab.)
ADLARSON	17B	PR C95 035208	P. Adlarson *et al.*	(A2 Collab. at MAMI)
ANASTASI	16A	JHEP 1605 019	A. Anastasi *et al.*	(KLOE-2 Collab.)
ARNALDI	16	PL B757 437	R. Arnaldi *et al.*	(NA60 Collab.)
ABLIKIM	15G	PR D92 012014	M. Ablikim *et al.*	(BES III Collab.)
ADLARSON	14A	PR C90 045207	P. Adlarson *et al.*	(WASA-at-COSY Collab.)
AGAKISHIEV	14	PL B731 265	G. Agakishiev *et al.*	(HADES Collab.)
NEFKENS	14	PR C90 025206	B.M.K. Nefkens *et al.*	(A2 Collab. at MAMI)
NIKOLAEV	14	EPJ A50 58	A. Nikolaev *et al.*	(MAMI-B, MAINZ, BONN)
ABLIKIM	13	PR D87 012009	M. Ablikim *et al.*	(BES III Collab.)
ABLIKIM	13G	PR D87 032006	M. Ablikim *et al.*	(BES III Collab.)
BABUSCI	13	PL B718 910	D. Babusci *et al.*	(KLOE/KLOE-2 Collab.)
BABUSCI	13A	JHEP 1301 119	D. Babusci *et al.*	(KLOE-2 Collab.)
AGAKISHIEV	12A	EPJ A48 64	G. Agakishiev *et al.*	(HADES Collab.)
GOSLAWSKI	12	PR D85 112011	P. Goslawski *et al.*	(COSY-ANKE Collab.)
ABLIKIM	11G	PR D84 032006	M. Ablikim *et al.*	(BES III Collab.)
AMBROSINO	11B	PL B702 324	F. Ambrosino *et al.*	(KLOE Collab.)
BERGHAUSER	11	PL B701 562	H. Berghauser *et al.*	(GIES, UCLA, GUTE)
AMBROSINO	10A	PL B694 16	F. Ambrosino *et al.*	(KLOE Collab.)
ADOLPH	09	PL B677 24	C. Adolph *et al.*	(WASA-at-COSY Collab.)
AMBROSINO	09B	PL B675 283	F. Ambrosino *et al.*	(KLOE Collab.)
ARNALDI	09	PL B677 260	R. Arnaldi *et al.*	(NA60 Collab.)
PRAKHOV	09	PR C79 035204	S. Prakhov *et al.*	(MAMI-C Crystal Ball Collab.)
UNVERZAGT	09	EPJ A39 169	M. Unverzagt *et al.*	(MAMI-B Crystal Ball Collab.)
AMBROSINO	08D	JHEP 0805 006	F. Ambrosino *et al.*	(DAPHNE KLOE Collab.)
BERLOWSKI	08	PR D77 032004	M. Berlowski *et al.*	(CELSIUS/WASA Collab.)
PRAKHOV	08	PR C78 015206	S. Prakhov *et al.*	(BNL Crystal Ball Collab.)
RODRIGUES	08	PRL 101 012301	T.E. Rodrigues *et al.*	(USP, FESP, UNESP+)
AMBROSINO	07B	JHEP 0712 073	F. Ambrosino *et al.*	(KLOE Collab.)
BARGHOLTZ	07	PL B644 299	Chr. Bargholtz *et al.*	(CELSIUS/WASA Collab.)
BASHKANOV	07	PR C76 048201	M. Bashkanov *et al.*	(CELSIUS/WASA Collab.)
BLIK	07	PAN 70 693 Translated from YAF 70 724.	A.M. Blik *et al.*	(GAMS Collab.)
LOPEZ	07	PRL 99 122001	A. Lopez *et al.*	(CLEO Collab.)
MILLER	07	PRL 99 122002	D.H. Miller *et al.*	(CLEO Collab.)
ABLIKIM	06E	PR D73 052008	M. Ablikim *et al.*	(BES Collab.)
ABLIKIM	06Q	PRL 97 202002	M. Ablikim *et al.*	(BES Collab.)
ACHASOV	06A	PR D74 014016	M.N. Achasov *et al.*	(SND Collab.)
ABDEL-BARY	05	PL B619 281	M. Abdel-Bary *et al.*	(GEM Collab.)
AKHMETSHIN	05	PL B605 26	R.R. Akhmetshin *et al.*	(Novosibirsk CMD-2 Collab.)
AMBROSINO	05A	PL B606 276	F. Ambrosino *et al.*	(KLOE Collab.)
NEFKENS	05	PRL 94 041601	B.M.K. Nefkens *et al.*	(BNL Crystal Ball Collab.)
NEFKENS	05A	PR C72 035212	B.M.K. Nefkens *et al.*	(BNL Crystal Ball Collab.)
PRAKHOV	05	PR C72 025201	S. Prakhov *et al.*	(BNL Crystal Ball Collab.)
ALOISIO	04	PL B591 49	A. Aloisio *et al.*	(KLOE Collab.)
KNECHT	04	PL B589 14	N. Knecht *et al.*	
LAI	02	PL B533 196	A. Lai *et al.*	(CERN NA48 Collab.)
NEFKENS	02	PS T99 114	B.M.K. Nefkens, J.W. Price	(UCLA)
ACHASOV	01B	PL B504 275	M.N. Achasov *et al.*	(Novosibirsk SND Collab.)
ACHASOV	01C	JETPL 73 451 Translated from ZETFP 73 511.	M.N. Achasov *et al.*	(Novosibirsk SND Collab.)
ACHASOV	01D	NP B600 3	M.N. Achasov *et al.*	(Novosibirsk SND Collab.)
AKHMETSHIN	01	PL B501 191	R.R. Akhmetshin *et al.*	(Novosibirsk CMD-2 Collab.)
AKHMETSHIN	01B	PL B509 217	R.R. Akhmetshin *et al.*	(Novosibirsk CMD-2 Collab.)
TIPPENS	01	PRL 87 192001	W.B. Tippens *et al.*	(BNL Crystal Ball Collab.)
ACHASOV	00	EPJ C12 25	M.N. Achasov *et al.*	(Novosibirsk SND Collab.)
ACHASOV	00B	JETP 90 17 Translated from ZETF 117 22.	M.N. Achasov *et al.*	(Novosibirsk SND Collab.)
ACHASOV	00D	JETPL 72 282 Translated from ZETFP 72 411.	M.N. Achasov *et al.*	(Novosibirsk SND Collab.)
PRAKHOV	00	PRL 84 4802	S. Prakhov *et al.*	(BNL Crystal Ball Collab.)
AKHMETSHIN	99B	PL B462 371	R.R. Akhmetshin *et al.*	(Novosibirsk CMD-2 Collab.)
AKHMETSHIN	99C	PL B462 380	R.R. Akhmetshin *et al.*	(Novosibirsk CMD-2 Collab.)
AKHMETSHIN	99F	PL B460 242	R.R. Akhmetshin *et al.*	(Novosibirsk CMD-2 Collab.)
ABELE	98C	PL B417 193	A. Abele *et al.*	(Crystal Barrel Collab.)
ABELE	98D	PL B417 197	A. Abele *et al.*	(Crystal Barrel Collab.)
ACHASOV	98	PL B425 388	M.N. Achasov *et al.*	(Novosibirsk SND Collab.)
AKHMETSHIN	97C	PL B415 452	R.R. Akhmetshin *et al.*	(Novosibirsk CMD-2 Collab.)
BROWDER	97B	PR D56 5359	T.E. Browder *et al.*	(CLEO Collab.)
ABEGG	96	PR D53 11	R. Abegg *et al.*	(Saturne SPES2 Collab.)
WHITE	96	PR D53 6658	D.B. White *et al.*	(Saturne SPES2 Collab.)
AMSLER	95	PL B346 203	C. Amsler *et al.*	(Crystal Barrel Collab.)
KRUSCHE	95D	ZPHY A351 237	B. Krusche *et al.*	(TAPS + A2 Collab.)
ABEGG	94	PR D50 92	R. Abegg *et al.*	(Saturne SPES2 Collab.)
PDG	94	PR D50 1173	L. Montanet *et al.*	(CERN, LBL, BOST+)
AMSLER	93	ZPHY C58 175	C. Amsler *et al.*	(Crystal Barrel Collab.)
KESSLER	93	PRL 70 892	R.S. Kessler *et al.*	(Saturne SPES2 Collab.)
PLOUIN	92	PL B276 526	F. Plouin *et al.*	(Saturne SPES4 Collab.)
BARU	90	ZPHY C48 581	S.E. Baru *et al.*	(MD-1 Collab.)
ROE	90	PR D41 17	N.A. Roe *et al.*	(ASP Collab.)
WILLIAMS	88	PR D38 1365	D.A. Williams *et al.*	(Crystal Ball Collab.)
AIHARA	86	PR D33 844	H. Aihara *et al.*	(TPC-2γ Collab.)
BARTEL	85E	PL 160B 421	W. Bartel *et al.*	(JADE Collab.)
LANDSBERG	85	PRPL 128 301	L.G. Landsberg	(SERP)
ALDE	84	ZPHY C25 225	D.M. Alde *et al.*	(SERP, BELG, LAPP)
Also		SJNP 40 918 Translated from YAF 40 1447.	D.M. Alde *et al.*	(SERP, BELG, LAPP)
WEINSTEIN	83	PR D28 2896	A.J. Weinstein *et al.*	(Crystal Ball Collab.)
BINON	82	SJNP 36 391 Translated from YAF 36 670.	F.G. Binon *et al.*	(SERP, BELG, LAPP+)
Also		NC 71A 497	F.G. Binon *et al.*	(SERP, BELG, LAPP+)
DAVYDOV	81	LNC 32 45	V.A. Davydov *et al.*	(SERP, BELG, LAPP+)
Also		SJNP 33 825 Translated from YAF 33 1534.	V.A. Davydov *et al.*	(SERP, BELG, LAPP+)
DZHELYADIN	81	PL 105B 239	R.I. Dzhelyadin *et al.*	(SERP)
Also		SJNP 33 822 Translated from YAF 33 1529.	R.I. Dzhelyadin *et al.*	(SERP)
ABROSIMOV	80	SJNP 31 195 Translated from YAF 31 371.	A.T. Abrosimov *et al.*	(JINR)
DZHELYADIN	80	PL 94B 548	R.I. Dzhelyadin *et al.*	(SERP)
Also		SJNP 32 516 Translated from YAF 32 998.	R.I. Dzhelyadin *et al.*	(SERP)
DZHELYADIN	80B	PL 97B 471	R.I. Dzhelyadin *et al.*	(SERP)
Also		SJNP 32 518 Translated from YAF 32 1002.	R.I. Dzhelyadin *et al.*	(SERP)

BUSHNIN	78	PL 79B 147	Y.B. Bushnin *et al.*	(SERP)
Also		SJNP 28 775	Y.B. Bushnin *et al.*	(SERP)
		Translated from YAF 28 1507.		
MARTYNOV	76	SJNP 23 48	A.S. Martynov *et al.*	(JINR)
		Translated from YAF 23 93.		
JANE	75	PL 59B 99	M.R. Jane *et al.*	(RHEL, LOWC)
JANE	75B	PL 59B 103	M.R. Jane *et al.*	(RHEL, LOWC)
Also		PL 73B 503	M.R. Jane	
		Erratum in private communication.		
BROWMAN	74B	PRL 32 1067	A. Browman *et al.*	(CORN, BING)
DAVIES	74	NC 24A 324	J.D. Davies, J.G. Guy, R.K.P. Zia	(BIRM, RHEL+)
DUANE	74	PRL 32 425	A. Duane *et al.*	(LOIC, SHMP)
JANE	74	PL 48B 260	M.R. Jane *et al.*	(RHEL, LOWC, SUSS)
JANE	74B	PL 48B 265	M.R. Jane *et al.*	(RHEL, LOWC, SUSS)
KENDALL	74	NC 21A 387	B.N. Kendall *et al.*	(BROW, BARI, MIT)
LAYTER	73	PR D7 2565	J.G. Layter *et al.*	(COLU)
THALER	73	PR D7 2569	J.J. Thaler *et al.*	(COLU)
AGUILAR-...	72B	PR D6 29	M. Aguilar-Benitez *et al.*	(BNL)
BLOODWO...	72B	NP B39 525	I.J. Bloodworth *et al.*	(TNTO)
LAYTER	72	PRL 29 316	J.G. Layter *et al.*	(COLU)
THALER	72	PRL 29 313	J.J. Thaler *et al.*	(COLU)
BASILE	71D	NC 3A 796	M. Basile *et al.*	(CERN, BGNA, STRB)
STRUGALSKI	71	NP B27 429	Z.S. Strugalski *et al.*	(JINR)
BAGLIN	70	NP B22 66	C. Baglin *et al.*	(EPOL, MADR, STRB)
BUTTRAM	70	PRL 25 1358	M.T. Buttram, M.N. Kreisler, R.E. Mischke	(PRIN)
CARPENTER	70	PR D1 1303	D.W. Carpenter *et al.*	(DUKE)
COX	70B	PRL 24 534	B. Cox, L. Fortney, J.P. Golson	(DUKE)
DANBURG	70	PR D2 2564	J.S. Danburg *et al.*	(LRL)
DEVONS	70	PR D1 1936	S. Devons *et al.*	(COLU, SYRA)
GORMLEY	70	PR D2 501	M. Gormley *et al.*	(COLU, BNL)
Also		Thesis Nevis 181	M. Gormley	(COLU)
BAGLIN	69	PL 29B 445	C. Baglin *et al.*	(EPOL, UCB, MADR, STRB)
Also		NP B22 66	C. Baglin *et al.*	(EPOL, MADR, STRB)
HYAMS	69	PL 29B 128	B.D. Hyams *et al.*	(CERN, MPIM)
ARNOLD	68	PL 27B 466	R.G. Arnold *et al.*	(STRB, MADR, EPOL+)
BAZIN	68	PRL 20 895	M.J. Bazin *et al.*	(PRIN, QUKI)
BULLOCK	68	PL 27B 402	F.W. Bullock *et al.*	(LOUC)
CNOPS	68	PRL 21 1609	A.M. Cnops *et al.*	(BNL, ORNL, UCND+)
GORMLEY	68C	PRL 21 402	M. Gormley *et al.*	(COLU, BNL)
WEHMANN	68	PRL 20 748	A.W. Wehmann *et al.*	(HARV, CASE, SLAC+)
BAGLIN	67	PL 24B 637	C. Baglin *et al.*	(EPOL, UCB)
BAGLIN	67B	BAPS 12 567	C. Baglin *et al.*	(EPOL, UCB)
BALTAY	67B	PRL 19 1498	C. Baltay *et al.*	(COLU, STON)
BALTAY	67D	PRL 19 1495	C. Baltay *et al.*	(COLU, BRAN)
BEMPORAD	67	PL 25B 380	C. Bemporad *et al.*	(PISA, BONN)
Also		Private Comm.	I. Ion	
BILLING	67	PL 25B 435	K.D. Billing *et al.*	(LOUC, OXF)
BUNIATOV	67	PL 25B 560	S.A. Bunyatov *et al.*	(CERN, KARL)
CENCE	67	PRL 19 1393	R.J. Cence *et al.*	(HAWA, LRL)
ESTEN	67	PL 24B 115	M.J. Esten *et al.*	(LOUC, OXF)
FELDMAN	67	PRL 18 868	M. Feldman *et al.*	(PENN)
FLATTE	67	PRL 18 976	S.M. Flatte	(LRL)
FLATTE	67B	PR 163 1441	S.M. Flatte, C.G. Wohl	(LRL)
LITCHFIELD	67	PL 24B 486	P.J. Litchfield *et al.*	(RHEL, SACL)
PRICE	67	PRL 18 1207	L.R. Price, F.S. Crawford	(LRL)
ALFF-...	66	PR 145 1072	C. Alff-Steinberger *et al.*	(COLU, RUTG)
CLPWY	66	PR 149 1044	C. Baltay	(SCUC, LRL, PURD, WISC, YALE)
CRAWFORD	66	PRL 16 333	F.S. Crawford, L.R. Price	(LRL)
DIGIUGNO	66	PRL 16 767	G. di Giugno *et al.*	(NAPL, TRST, FRAS)
GRUNHAUS	66	Thesis	J. Grunhaus	(COLU)
JAMES	66	PR 142 896	F.E. James, H.L. Kraybill	(YALE, BNL)
JONES	66	PL 23 597	W.G. Jones *et al.*	(LOIC, RHEL)
LARRIBE	66	PL 23 600	A. Larribe *et al.*	(SACL, RHEL)
FOSTER	65	PR 138 B652	M. Foster *et al.*	(WISC, PURD)
FOSTER	65B	Athens Conf.	M. Foster, M. Good, M. Meer	(WISC)
FOSTER	65C	Thesis	M. Foster	(WISC)
PRICE	65	PRL 15 123	L.R. Price, F.S. Crawford	(LRL)
RITTENBERG	65	PRL 15 556	A. Rittenberg, G.R. Kalbfleisch	(LRL, BNL)
FOELSCHE	64	PR 134 B1138	H.W.J. Foelsche, H.L. Kraybill	(YALE)
KRAEMER	64	PR 136 B496	R.W. Kraemer *et al.*	(JHU, NWES, WOOD)
PAULI	64	PL 13 351	E. Pauli, A. Muller	(SACL)
BACCI	63	PRL 11 37	C. Bacci *et al.*	(ROMA, FRAS)
CRAWFORD	63	PRL 10 546	F.S.Jr. Crawford, L.J. Lloyd, E.C. Fowler	(LRL+)
Also		PRL 16 907	F.S. Crawford, L.J. Lloyd, E.C. Fowler	(LRL+)
ALFF-...	62	PRL 9 322	C. Alff-Steinberger *et al.*	(COLU, RUTG)
BASTIEN	62	PRL 8 114	P.L. Bastien *et al.*	(LRL)
PICKUP	62	PRL 8 329	E. Pickup, D.K. Robinson, E.O. Salant	(CNRC+)

$f_0(500)$

$I^G(J^{PC}) = 0^+(0^{++})$

also known as σ; was $f_0(600)$

See the related review(s):

Scalar Mesons below 2 GeV

$f_0(500)$ T-MATRIX POLE $\sqrt{s}$

Note that $\Gamma \approx 2\ \mathrm{Im}(\sqrt{s_{\mathrm{pole}}})$.

VALUE (MeV)	DOCUMENT ID		TECN	COMMENT
(400–550)−*i*(200–350) OUR ESTIMATE				
• • • We do not use the following data for averages, fits, limits, etc. • • •				
$(512 \pm 15) - i(188 \pm 12)$	[1] ABLIKIM	17	BES3	$J/\psi \to \gamma 3\pi$
$(440 \pm 10) - i(238 \pm 10)$	[2] ALBALADEJO	12	RVUE	Compilation
$(445 \pm 25) - i(278^{+22}_{-18})$	[3,4] GARCIA-MAR..	11	RVUE	Compilation
$(457^{+14}_{-13}) - i(279^{+11}_{-7})$	[3,5] GARCIA-MAR..	11	RVUE	Compilation
$(442^{+5}_{-8}) - i(274^{+6}_{-5})$	[6] MOUSSALLAM	11	RVUE	Compilation
$(452 \pm 13) - i(259 \pm 16)$	[7] MENNESSIER	10	RVUE	Compilation
$(448 \pm 43) - i(266 \pm 43)$	[8] MENNESSIER	10	RVUE	Compilation
$(455 \pm 6^{+31}_{-13}) - i(278 \pm 6^{+34}_{-43})$	[9] CAPRINI	08	RVUE	Compilation
$(463 \pm 6^{+31}_{-17}) - i(259 \pm 6^{+33}_{-34})$	[10] CAPRINI	08	RVUE	Compilation
$(552^{+84}_{-106}) - i(232^{+81}_{-72})$	[11] ABLIKIM	07A	BES2	$\psi(2S) \to \pi^+\pi^- J/\psi$
$(466 \pm 18) - i(223 \pm 28)$	[12] BONVICINI	07	CLEO	$D^+ \to \pi^-\pi^+\pi^+$
$(472 \pm 30) - i(271 \pm 30)$	[13] BUGG	07A	RVUE	Compilation
$(484 \pm 17) - i(255 \pm 10)$	GARCIA-MAR..	07	RVUE	Compilation
$(430) - i(325)$	[14] ANISOVICH	06	RVUE	Compilation
$(441^{+16}_{-8}) - i(272^{+9}_{-12.5})$	[15] CAPRINI	06	RVUE	$\pi\pi \to \pi\pi$
$(470 \pm 50) - i(285 \pm 25)$	[16] ZHOU	05	RVUE	
$(541 \pm 39) - i(252 \pm 42)$	[17] ABLIKIM	04A	BES2	$J/\psi \to \omega\pi^+\pi^-$
$(528 \pm 32) - i(207 \pm 23)$	[18] GALLEGOS	04	RVUE	Compilation
$(440 \pm 8) - i(212 \pm 15)$	[19] PELAEZ	04A	RVUE	$\pi\pi \to \pi\pi$
$(533 \pm 25) - i(249 \pm 25)$	[20] BUGG	03	RVUE	
$517 - i240$	BLACK	01	RVUE	$\pi^0\pi^0 \to \pi^0\pi^0$
$(470 \pm 30) - i(295 \pm 20)$	[15] COLANGELO	01	RVUE	$\pi\pi \to \pi\pi$
$(535^{+48}_{-36}) - i(155^{+76}_{-53})$	[21] ISHIDA	01		$\Upsilon(3S) \to \Upsilon\pi\pi$
$610 \pm 14 - i620 \pm 26$	[22] SUROVTSEV	01	RVUE	$\pi\pi \to \pi\pi, K\overline{K}$
$(540^{+36}_{-29}) - i(193^{+32}_{-40})$	ISHIDA	00B		$p\overline{p} \to \pi^0\pi^0\pi^0$
$445 - i235$	HANNAH	99	RVUE	π scalar form factor
$(523 \pm 12) - i(259 \pm 7)$	KAMINSKI	99	RVUE	$\pi\pi \to \pi\pi, K\overline{K}, \sigma\sigma$
$442 - i\ 227$	OLLER	99	RVUE	$\pi\pi \to \pi\pi, K\overline{K}$
$469 - i203$	OLLER	99B	RVUE	$\pi\pi \to \pi\pi, K\overline{K}$
$445 - i221$	OLLER	99C	RVUE	$\pi\pi \to \pi\pi, K\overline{K}, \eta\eta$
$(1530^{+90}_{-250}) - i(560 \pm 40)$	ANISOVICH	98B	RVUE	Compilation
$420 - i\ 212$	LOCHER	98	RVUE	$\pi\pi \to \pi\pi\ ,\ K\overline{K}$
$440 - i245$	[23] DOBADO	97	RVUE	Compilation
$(602 \pm 26) - i(196 \pm 27)$	[24] ISHIDA	97		$\pi\pi \to \pi\pi$
$(537 \pm 20) - i(250 \pm 17)$	[25] KAMINSKI	97B	RVUE	$\pi\pi \to \pi\pi, K\overline{K}, 4\pi$
$470 - i250$	[26,27] TORNQVIST	96	RVUE	$\pi\pi \to \pi\pi, K\overline{K}, K\pi, \eta\pi$
$387 - i305$	[27,28] JANSSEN	95	RVUE	$\pi\pi \to \pi\pi, K\overline{K}$
$420 - i370$	[29] ACHASOV	94	RVUE	$\pi\pi \to \pi\pi$
$(506 \pm 10) - i(247 \pm 3)$	KAMINSKI	94	RVUE	$\pi\pi \to \pi\pi, K\overline{K}$
$370 - i356$	[30] ZOU	94B	RVUE	$\pi\pi \to \pi\pi, K\overline{K}$
$408 - i342$	[27,30] ZOU	93	RVUE	$\pi\pi \to \pi\pi, K\overline{K}$
$470 - i208$	[31] VANBEVEREN	86	RVUE	$\pi\pi \to \pi\pi, K\overline{K}, \eta\eta,$ ...
$(750 \pm 50) - i(450 \pm 50)$	[32] ESTABROOKS	79	RVUE	$\pi\pi \to \pi\pi, K\overline{K}$
$(660 \pm 100) - i(320 \pm 70)$	PROTOPOP...	73	HBC	$\pi\pi \to \pi\pi, K\overline{K}$
$650 - i370$	[33] BASDEVANT	72	RVUE	$\pi\pi \to \pi\pi$

[1] S-matrix pole; 8595 events.

[2] Applying the chiral unitary approach at NLO to the K_{e4} data of BATLEY 10 and $\pi N \to \pi\pi N$ data of HYAMS 73, GRAYER 74, and PROTOPOPESCU 73.

[3] Uses the K_{e4} data of BATLEY 10C and the $\pi N \to \pi\pi N$ data of HYAMS 73, GRAYER 74, and PROTOPOPESCU 73.

[4] Analytic continuation using Roy equations.

[5] Analytic continuation using GKPY equations.

[6] Using Roy equations.

[7] Average of three variants of the analytic K-matrix model. Uses the K_{e4} data of BATLEY 08A and the $\pi N \to \pi\pi N$ data of HYAMS 73 and GRAYER 74.

[8] Average of the analyses of three data sets in the K-matrix model. Uses the data of BATLEY 08A, HYAMS 73, and GRAYER 74, partially of COHEN 80 or ETKIN 82B.

[9] From the K_{e4} data of BATLEY 08A and $\pi N \to \pi\pi N$ data of HYAMS 73.

[10] From the K_{e4} data of BATLEY 08A and $\pi N \to \pi\pi N$ data of PROTOPOPESCU 73, GRAYER 74, and ESTABROOKS 74.

[11] From a mean of three different $f_0(500)$ parametrizations. Uses 40k events.

[12] From an isobar model using 2.6k events.

[13] Reanalysis of ABLIKIM 04A, PISLAK 01, and HYAMS 73 data.

[14] Using the N/D method.

[15] From the solution of the Roy equation (ROY 71) for the isoscalar S-wave and using a phase-shift analysis of HYAMS 73 and PROTOPOPESCU 73 data.

[16] Reanalysis of the data from PROTOPOPESCU 73, ESTABROOKS 74, GRAYER 74, ROSSELET 77, PISLAK 03, and AKHMETSHIN 04.

[17] From a mean of six different analyses and $f_0(500)$ parameterizations.

[18] Using data on $\psi(2S) \to J/\psi\pi\pi$ from BAI 00E and on $\Upsilon(\mathrm{nS}) \to \Upsilon(\mathrm{mS})\pi\pi$ from BUTLER 94B and ALEXANDER 98.

[19] Reanalysis of data from PROTOPOPESCU 73, ESTABROOKS 74, GRAYER 74, and COHEN 80 in the unitarized ChPT model.

[20] From a combined analysis of HYAMS 73, AUGUSTIN 89, AITALA 01B, and PISLAK 01.

[21] A similar analysis (KOMADA 01) finds $(580^{+79}_{-30}) - i(190^{+107}_{-49})$ MeV.

[22] Coupled channel reanalysis of BATON 70, BENSINGER 71, BAILLON 72, HYAMS 73, HYAMS 75, ROSSELET 77, COHEN 80, and ETKIN 82B using the uniformizing variable.

[23] Using the inverse amplitude method and data of ESTABROOKS 73, GRAYER 74, and PROTOPOPESCU 73.

[24] Reanalysis of data from HYAMS 73, GRAYER 74, SRINIVASAN 75, and ROSSELET 77 using the interfering amplitude method.

[25] Average and spread of 4 variants ("up" and "down") of KAMINSKI 97B 3-channel model.

[26] Uses data from BEIER 72B, OCHS 73, HYAMS 73, GRAYER 74, ROSSELET 77, CASON 83, ASTON 88, and ARMSTRONG 91B. Coupled channel analysis with flavor symmetry and all light two-pseudoscalars systems.

[27] Demonstrates explicitly that $f_0(500)$ and $f_0(1370)$ are two different poles.

[28] Analysis of data from FALVARD 88.

[29] Analysis of data from OCHS 73, ESTABROOKS 75, ROSSELET 77, and MUKHIN 80.

[30] Analysis of data from OCHS 73, GRAYER 74, and ROSSELET 77.

[31] Coupled-channel analysis using data from PROTOPOPESCU 73, HYAMS 73, HYAMS 75, GRAYER 74, ESTABROOKS 74, ESTABROOKS 75, FROGGATT 77, CORDEN 79, BISWAS 81.

[32] Analysis of data from APEL 72C, GRAYER 74, CASON 76, PAWLICKI 77. Includes spread and errors of 4 solutions.

[33] Analysis of data from BATON 70, BENSINGER 71, COLTON 71, BAILLON 72,PROTOPOPESCU 73, and WALKER 67.

$f_0(500)$ BREIT-WIGNER MASS OR K-MATRIX POLE PARAMETERS

VALUE (MeV)	DOCUMENT ID	TECN	COMMENT
(400–550) OUR ESTIMATE			

Meson Particle Listings

$f_0(500)$

• • • We do not use the following data for averages, fits, limits, etc. • • •

513 ± 32	[34] MURAMATSU	02	CLEO	$e^+e^- \approx 10$ GeV	
$478^{+24}_{-23} \pm 17$	AITALA	01B	E791	$D^+ \to \pi^-\pi^+\pi^+$	
563^{+58}_{-29}	[35] ISHIDA	01		$\Upsilon(3S) \to \Upsilon\pi\pi$	
555	[36] ASNER	00	CLE2	$\tau^- \to \pi^-\pi^0\pi^0\nu_\tau$	
540 ± 36	ISHIDA	00B		$p\overline{p} \to \pi^0\pi^0\pi^0$	
750 ± 4	ALEKSEEV	99	SPEC	$1.78\ \pi^-\ p_{\rm polar} \to \pi^-\pi^+ n$	
744 ± 5	ALEKSEEV	98	SPEC	$1.78\ \pi^-\ p_{\rm polar} \to \pi^-\pi^+ n$	
759 ± 5	[37] TROYAN	98		$5.2\ np \to np\pi^+\pi^-$	
780 ± 30	ALDE	97	GAM2	$450\ pp \to pp\pi^0\pi^0$	
585 ± 20	[38] ISHIDA	97		$\pi\pi \to \pi\pi$	
761 ± 12	[39] SVEC	96	RVUE	6–$17\ \pi N_{\rm polar} \to \pi^+\pi^- N$	
~ 860	[40,41] TORNQVIST	96	RVUE	$\pi\pi \to \pi\pi, K\overline{K}, K\pi, \eta\pi$	
1165 ± 50	[42,43] ANISOVICH	95	RVUE	$\pi^- p \to \pi^0\pi^0 n$, $\overline{p}p \to \pi^0\pi^0\pi^0, \pi^0\pi^0\eta, \pi^0\eta\eta$	
~ 1000	[44] ACHASOV	94	RVUE	$\pi\pi \to \pi\pi$	
414 ± 20	[39] AUGUSTIN	89	DM2		

[34] Statistical uncertainty only.
[35] A similar analysis (KOMADA 01) finds 526^{+48}_{-37} MeV.
[36] From the best fit of the Dalitz plot.
[37] 6σ effect, no PWA.
[38] Reanalysis of data from HYAMS 73, GRAYER 74, SRINIVASAN 75, and ROSSELET 77 using the interfering amplitude method.
[39] Breit-Wigner fit to S-wave intensity measured in $\pi N \to \pi^-\pi^+ N$ on polarized targets. The fit does not include $f_0(980)$.
[40] Uses data from ASTON 88, OCHS 73, HYAMS 73, ARMSTRONG 91B, GRAYER 74, CASON 83, ROSSELET 77, and BEIER 72B. Coupled channel analysis with flavor symmetry and all light two-pseudoscalars systems.
[41] Also observed by ASNER 00 in $\tau^- \to \pi^-\pi^0\pi^0\nu_\tau$ decays.
[42] Uses $\pi^0\pi^0$ data from ANISOVICH 94, AMSLER 94D, and ALDE 95B, $\pi^+\pi^-$ data from OCHS 73, GRAYER 74 and ROSSELET 77, and $\eta\eta$ data from ANISOVICH 94.
[43] The pole is on Sheet III. Demonstrates explicitly that $f_0(500)$ and $f_0(1370)$ are two different poles.
[44] Analysis of data from OCHS 73, ESTABROOKS 75, ROSSELET 77, and MUKHIN 80.

$f_0(500)$ BREIT-WIGNER WIDTH

VALUE (MeV)	DOCUMENT ID		TECN	COMMENT
(400–700) OUR ESTIMATE				
• • • We do not use the following data for averages, fits, limits, etc. • • •				
335 ± 67	[45] MURAMATSU	02	CLEO	$e^+e^- \approx 10$ GeV
$324^{+42}_{-40} \pm 21$	AITALA	01B	E791	$D^+ \to \pi^-\pi^+\pi^+$
372^{+229}_{-95}	[46] ISHIDA	01		$\Upsilon(3S) \to \Upsilon\pi\pi$
540	[47] ASNER	00	CLE2	$\tau^- \to \pi^-\pi^0\pi^0\nu_\tau$
372 ± 80	ISHIDA	00B		$p\overline{p} \to \pi^0\pi^0\pi^0$
119 ± 13	ALEKSEEV	99	SPEC	$1.78\ \pi^-\ p_{\rm polar} \to \pi^-\pi^+ n$
77 ± 22	ALEKSEEV	98	SPEC	$1.78\ \pi^-\ p_{\rm polar} \to \pi^-\pi^+ n$
35 ± 12	[48] TROYAN	98		$5.2\ np \to np\pi^+\pi^-$
780 ± 60	ALDE	97	GAM2	$450\ pp \to pp\pi^0\pi^0$
385 ± 70	[49] ISHIDA	97		$\pi\pi \to \pi\pi$
290 ± 54	[50] SVEC	96	RVUE	6–$17\ \pi N_{\rm polar} \to \pi^+\pi^- N$
~ 880	[51,52] TORNQVIST	96	RVUE	$\pi\pi \to \pi\pi, K\overline{K}, K\pi, \eta\pi$
460 ± 40	[53,54] ANISOVICH	95	RVUE	$\pi^- p \to \pi^0\pi^0 n$, $\overline{p}p \to \pi^0\pi^0\pi^0, \pi^0\pi^0\eta, \pi^0\eta\eta$
~ 3200	[55] ACHASOV	94	RVUE	$\pi\pi \to \pi\pi$
494 ± 58	[50] AUGUSTIN	89	DM2	

[45] Statistical uncertainty only.
[46] A similar analysis (KOMADA 01) finds 301^{+145}_{-100} MeV.
[47] From the best fit of the Dalitz plot.
[48] 6σ effect, no PWA.
[49] Reanalysis of data from HYAMS 73, GRAYER 74, SRINIVASAN 75, and ROSSELET 77 using the interfering amplitude method.
[50] Breit-Wigner fit to S-wave intensity measured in $\pi N \to \pi^-\pi^+ N$ on polarized targets. The fit does not include $f_0(980)$.
[51] Uses data from ASTON 88, OCHS 73, HYAMS 73, ARMSTRONG 91B, GRAYER 74, CASON 83, ROSSELET 77, and BEIER 72B. Coupled channel analysis with flavor symmetry and all light two-pseudoscalars systems.
[52] Also observed by ASNER 00 in $\tau^- \to \pi^-\pi^0\pi^0\nu_\tau$ decays.
[53] Uses $\pi^0\pi^0$ data from ANISOVICH 94, AMSLER 94D, and ALDE 95B, $\pi^+\pi^-$ data from OCHS 73, GRAYER 74 and ROSSELET 77, and $\eta\eta$ data from ANISOVICH 94.
[54] The pole is on Sheet III. Demonstrates explicitly that $f_0(500)$ and $f_0(1370)$ are two different poles.
[55] Analysis of data from OCHS 73, ESTABROOKS 75, ROSSELET 77, and MUKHIN 80.

$f_0(500)$ DECAY MODES

	Mode	Fraction (Γ_i/Γ)
Γ_1	$\pi\pi$	dominant
Γ_2	$\gamma\gamma$	seen

$f_0(500)$ PARTIAL WIDTHS

$\Gamma(\gamma\gamma)$ **Γ_2**

VALUE (keV)	DOCUMENT ID		TECN	COMMENT
• • • We do not use the following data for averages, fits, limits, etc. • • •				
2.05 ± 0.21	[56] DAI	14A	RVUE	Compilation
1.7 ± 0.4	[57] HOFERICHTER	11	RVUE	Compilation
3.08 ± 0.82	[58] MENNESSIER	11	RVUE	Compilation
$2.08 \pm 0.2\ ^{+0.07}_{-0.04}$	[59] MOUSSALLAM	11	RVUE	Compilation
2.08	[60] MAO	09	RVUE	Compilation
1.2 ± 0.4	[61] BERNABEU	08	RVUE	
3.9 ± 0.6	[58] MENNESSIER	08	RVUE	$\gamma\gamma \to \pi^+\pi^-, \pi^0\pi^0$
1.8 ± 0.4	[62] OLLER	08	RVUE	Compilation
1.68 ± 0.15	[62,63] OLLER	08A	RVUE	Compilation
3.1 ± 0.5	[64,65] PENNINGTON	08	RVUE	Compilation
2.4 ± 0.4	[65,66] PENNINGTON	08	RVUE	Compilation
4.1 ± 0.3	[67] PENNINGTON	06	RVUE	$\gamma\gamma \to \pi^0\pi^0$
3.8 ± 1.5	[68,69] BOGLIONE	99	RVUE	$\gamma\gamma \to \pi^+\pi^-, \pi^0\pi^0$
5.4 ± 2.3	[68] MORGAN	90	RVUE	$\gamma\gamma \to \pi^+\pi^-, \pi^0\pi^0$
10 ± 6	COURAU	86	DM1	$e^+e^- \to \pi^+\pi^- e^+e^-$

[56] Using dispersive analysis with phases from GARCIA-MARTIN 11A and BUETTIKER 04 as input.
[57] Using Roy-Steiner equations with $\pi\pi$ phase shifts from an update of COLANGELO 01 and from GARCIA-MARTIN 11A.
[58] Using an analytic K-matrix model.
[59] Using dispersion integral with phase input from Roy equations and data from MARSISKE 90, BOYER 90, BEHREND 92, UEHARA 08A, and MORI 07.
[60] Used dispersion theory. The value quoted used the $f_0(500)$ pole position of $457 - i276$ MeV.
[61] Using p, n polarizabilities from PDG 06 and fitting to $\pi\pi$ phase motion from GARCIA-MARTIN 07 and σ-poles from GARCIA-MARTIN 07 and CAPRINI 06.
[62] Using twice-subtracted dispersion integrals.
[63] Supersedes OLLER 08.
[64] Solution A (preferred solution based on χ^2-analysis).
[65] Dispersion theory based amplitude analysis of BOYER 90, MARSISKE 90, BEHREND 92, and MORI 07.
[66] Solution B (worse than solution A; still acceptable when systematic uncertainties are included).
[67] Using unitarity and the σ pole position from CAPRINI 06.
[68] This width could equally well be assigned to the $f_0(1370)$. The authors analyse data from BOYER 90 and MARSISKE 90 and report strong correlation with $\gamma\gamma$ width of $f_2(1270)$.
[69] Supersedes MORGAN 90.

$f_0(500)$ REFERENCES

ABLIKIM	17	PRL 118 012001	M. Ablikim *et al.*	(BES III Collab.)
DAI	14A	PR D90 036004	L.-Y. Dai, M.R. Pennington	(CEBAF)
ALBALADEJO	12	PR D86 034003	M. Albaladejo, J.A. Oller	(MURC)
GARCIA-MAR...	11	PRL 107 072001	R. Garcia-Martin *et al.*	(MADR, CRAC)
GARCIA-MAR...	11A	PR D83 074004	R. Garcia-Martin *et al.*	(MADR, CRAC)
HOFERICHTER	11	EPJ C71 1743	M. Hoferichter, D.R. Phillips, C. Schat	(BONN+)
MENNESSIER	11	PL B696 40	G. Mennessier, S. Narison, X.-G. Wang	
MOUSSALLAM	11	EPJ C71 1814	B. Moussallam	
BATLEY	10	PL B686 101	J.R. Batley *et al.*	(CERN NA48/2 Collab.)
BATLEY	10C	EPJ C70 635	J.R. Batley *et al.*	(CERN NA48/2 Collab.)
MENNESSIER	10	PL B688 59	G. Mennessier, S. Narison, X.-G. Wang	
MAO	09	PR D79 116008	Y. Mao *et al.*	
BATLEY	08A	EPJ C54 411	J.R. Batley *et al.*	(CERN NA48/2 Collab.)
BERNABEU	08	PRL 100 241804	J. Bernabeu, J. Prades	(IFIC, GRAN)
CAPRINI	08	PR D77 114019	I. Caprini	
MENNESSIER	08	PL B665 205	G. Mennessier, S. Narison, W. Ochs	
OLLER	08	PL B659 201	J.A. Oller, L. Roca, C. Schat	(MURC, UBA)
OLLER	08A	EPJ A37 15	J.A. Oller, L. Roca	(MURC)
PENNINGTON	08	EPJ C56 1	M.R. Pennington *et al.*	
UEHARA	08A	PR D78 052004	S. Uehara *et al.*	(BELLE Collab.)
ABLIKIM	07A	PL B645 19	M. Ablikim *et al.*	(BES Collab.)
BONVICINI	07	PR D76 012001	G. Bonvicini *et al.*	(CLEO Collab.)
BUGG	07A	JP G34 151	D.V. Bugg *et al.*	
GARCIA-MAR...	07	PR D76 074034	R. Garcia-Martin, J.R. Pelaez, F.J. Yndurain	
MORI	07	PR D75 051101	T. Mori *et al.*	(BELLE Collab.)
ANISOVICH	06	IJMP A21 3615	V.V. Anisovich	
CAPRINI	06	PRL 96 132001	I. Caprini, G. Colangelo, H. Leutwyler	(BCIP+)
PDG	06	JP G33 1	W.-M. Yao *et al.*	(PDG Collab.)
PENNINGTON	06	PRL 97 011601	M.R. Pennington	
ZHOU	05	JHEP 0502 043	Z.Y. Zhou *et al.*	
ABLIKIM	04A	PL B598 149	M. Ablikim *et al.*	(BES Collab.)
AKHMETSHIN	04	PL B578 285	R.R. Akhmetshin *et al.*	(Novosibirsk CMD-2 Collab.)
BUETTIKER	04	EPJ C33 409	P. Buettiker, S. Descotes-Genon, B. Moussallam	
GALLEGOS	04	PR D69 074033	A. Gallegos *et al.*	
PELAEZ	04A	MPL A19 2879	J.R. Pelaez	
BUGG	03	PL B572 1	D.V. Bugg	
PISLAK	03	PR D67 072004	S. Pislak *et al.*	(BNL E865 Collab.)
Also		PR D81 119903E	S. Pislak *et al.*	(BNL E865 Collab.)
MURAMATSU	02	PRL 89 251802	H. Muramatsu *et al.*	(CLEO Collab.)
Also		PRL 90 059901 (errat.)	H. Muramatsu *et al.*	(CLEO Collab.)
AITALA	01B	PRL 86 770	E.M. Aitala *et al.*	(FNAL E791 Collab.)
BLACK	01	PR D64 014031	D. Black *et al.*	
COLANGELO	01	NP B603 125	G. Colangelo, J. Gasser, H. Leytwyler	
ISHIDA	01	PL B518 47	M. Ishida *et al.*	
KOMADA	01	PL B508 31	T. Komada *et al.*	
PISLAK	01	PRL 87 221801	S. Pislak *et al.*	(BNL E865 Collab.)
Also		PR D67 072004	S. Pislak *et al.*	(BNL E865 Collab.)
Also		PRL 105 019901E	S. Pislak *et al.*	(BNL E865 Collab.)
SUROVTSEV	01	PR D63 054024	Y.S. Surovtsev, D. Krupa, M. Nagy	
ASNER	00	PR D61 012002	D.M. Asner *et al.*	(CLEO Collab.)
BAI	00E	PR D62 032002	J. Bai *et al.*	(BES Collab.)
ISHIDA	00B	PTP 104 203	M. Ishida *et al.*	
ALEKSEEV	99	NP B541 3	I.G. Alekseev *et al.*	
BOGLIONE	99	EPJ C9 11	M. Boglione, M.R. Pennington	
HANNAH	99	PR D60 017502	T. Hannah	
KAMINSKI	99	EPJ C9 141	R. Kaminski, L. Lesniak, B. Loiseau	(CRAC, PARIN)
OLLER	99	PR D60 099906 (erratum)	J.A. Oller *et al.*	
OLLER	99B	NP A652 407 (erratum)	J.A. Oller, E. Oset	
OLLER	99C	PR D60 074023	J.A. Oller, E. Oset	

ALEKSEEV 98 PAN 61 174 I.G. Alekseev *et al.*
ALEXANDER 98 PR D58 052004 J.P. Alexander *et al.* (CLEO Collab.)
ANISOVICH 98B SPU 41 419 V.V. Anisovich *et al.*
Translated from UFN 168 481.
LOCHER 98 EPJ C4 317 M.P. Locher *et al.* (PSI)
TROYAN 98 JINRRC 5-91 33 Yu. Troyan *et al.*
ALDE 97 PL B397 350 D.M. Alde *et al.* (GAMS Collab.)
DOBADO 97 PR D56 3057 A. Dobado, J.R. Pelaez
ISHIDA 97 PTP 98 1005 S. Ishida *et al.* (TOKY, MIYA, KEK)
KAMINSKI 97B PL B413 130 R. Kaminski, L. Lesniak, B. Loiseau (CRAC, IPN)
Also PTP 95 745 S. Ishida *et al.* (TOKY, MIYA, KEK)
SVEC 96 PR D53 2343 M. Svec (MCGI)
TORNQVIST 96 PRL 76 1575 N.A. Tornqvist, M. Roos (HELS)
ALDE 95B ZPHY C66 375 D.M. Alde *et al.* (GAMS Collab.)
ANISOVICH 95 PL B355 363 V.V. Anisovich *et al.* (PNPI, SERP)
JANSSEN 95 PR D52 2690 G. Janssen *et al.* (STON, ADLD, JULI)
ACHASOV 94 PR D49 5779 N.N. Achasov, G.N. Shestakov (NOVM)
AMSLER 94D PL B333 277 C. Amsler *et al.* (Crystal Barrel Collab.)
ANISOVICH 94 PL B323 233 V.V. Anisovich *et al.* (Crystal Barrel Collab.)
BUTLER 94B PR D49 40 F. Butler *et al.* (CLEO Collab.)
KAMINSKI 94 PR D50 3145 R. Kaminski, L. Lesniak, J.P. Maillet (CRAC+)
ZOU 94B PR D50 591 B.S. Zou, D.V. Bugg (LOQM)
ZOU 93 PR D48 3948 B.S. Zou, D.V. Bugg (LOQM)
BEHREND 92 ZPHY C56 381 H.J. Behrend (CELLO Collab.)
ARMSTRONG 91B ZPHY C52 389 T.A. Armstrong *et al.* (ATHU, BARI, BIRM+)
BOYER 90 PR D42 1350 J. Boyer *et al.* (Mark II Collab.)
MARSISKE 90 PR D41 3324 H. Marsiske *et al.* (Crystal Ball Collab.)
MORGAN 90 ZPHY C48 623 D. Morgan, M.R. Pennington (RAL, DURH)
AUGUSTIN 89 NP B320 1 J.E. Augustin, G. Cosme (DM2 Collab.)
ASTON 88 NP B296 493 D. Aston *et al.* (SLAC, NAGO, CINC, INUS)
FALVARD 88 PR D38 2706 A. Falvard *et al.* (CLER, FRAS, LALO+)
COURAU 86 NP B271 1 A. Courau *et al.* (CLER, LALO)
VANBEVEREN 86 ZPHY C30 615 E. van Beveren *et al.* (NIJM, BIEL)
CASON 83 PR D28 1586 N.M. Cason *et al.* (NDAM, ANL)
ETKIN 82B PR D25 1786 A. Etkin *et al.* (BNL, CUNY, TUFTS, VAND)
BISWAS 81 PRL 47 1378 N.N. Biswas *et al.* (NDAM, ANL)
COHEN 80 PR D22 2595 D. Cohen *et al.* (ANL) IJP
MUKHIN 80 JETPL 32 601 K.N. Mukhin *et al.* (KIAE)
Translated from ZETFP 32 616.
CORDEN 79 NP B157 250 M.J. Corden *et al.* (BIRM, RHEL, TELA+) JP
ESTABROOKS 79 PR D19 2678 P. Estabrooks (CARL)
FROGGATT 77 NP B129 89 C.D. Froggatt, J.L. Petersen (GLAS, NORD)
PAWLICKI 77 PR D15 3196 A.J. Pawlicki *et al.* (ANL) IJ
ROSSELET 77 PR D15 574 L. Rosselet *et al.* (GEVA, SACL)
CASON 76 PRL 36 1485 N.M. Cason *et al.* (NDAM, ANL) IJ
ESTABROOKS 75 NP B95 322 P.G. Estabrooks, A.D. Martin (DURH)
HYAMS 75 NP B100 205 B.D. Hyams *et al.* (CERN, MPIM)
SRINIVASAN 75 PR D12 681 V. Srinivasan *et al.* (NDAM, ANL)
ESTABROOKS 74 NP B79 301 P.G. Estabrooks, A.D. Martin (DURH)
GRAYER 74 NP B75 189 G. Grayer *et al.* (CERN, MPIM)
ESTABROOKS 73 Tallahassee P.G. Estabrooks *et al.* (CERN, MPIM)
HYAMS 73 NP B64 134 B.D. Hyams *et al.* (CERN, MPIM)
OCHS 73 Thesis W. Ochs (MPIM, MUNI)
PROTOPOP... 73 PR D7 1279 S.D. Protopopescu *et al.* (LBL)
APEL 72C PL 41B 542 W.D. Apel *et al.* (KARLK, KARLE, PISA)
BAILLON 72 PL 38B 555 P.H. Baillon *et al.* (SLAC)
BASDEVANT 72 PL 41B 178 J.L. Basdevant, C.D. Froggatt, J.L. Petersen (CERN)
BEIER 72B PRL 29 511 E.W. Beier *et al.* (PENN)
BENSINGER 71 PL 36B 134 J.R. Bensinger *et al.* (WISC)
COLTON 71 PR D3 2028 E.P. Colton *et al.* (LBL, FNAL, UCLA+)
ROY 71 PL 36B 353 S.M. Roy
BATON 70 PL 33B 528 J.P. Baton, G. Laurens, J. Reignier (SACL)
WALKER 67 RMP 39 695 W.D. Walker (WISC)

$\rho(770)$

$I^G(J^{PC}) = 1^+(1^{--})$

See the related review(s):
$\rho(770)$

$\rho(770)$ MASS

We no longer list *S*-wave Breit-Wigner fits, or data with high combinatorial background.

NEUTRAL ONLY, e^+e^-

VALUE (MeV)	EVTS	DOCUMENT ID		TECN	COMMENT
775.26±0.25 OUR AVERAGE					
775.02±0.35		[1] LEES	12G	BABR	$e^+e^- \to \pi^+\pi^-\gamma$
775.97±0.46±0.70	900k	[2] AKHMETSHIN	07		$e^+e^- \to \pi^+\pi^-$
774.6 ±0.4 ±0.5	800k	[3,4] ACHASOV	06	SND	$e^+e^- \to \pi^+\pi^-$
775.65±0.64±0.50	114k	[5,6] AKHMETSHIN	04	CMD2	$e^+e^- \to \pi^+\pi^-$
775.9 ±0.5 ±0.5	1.98M	[7] ALOISIO	03	KLOE	1.02 $e^+e^- \to \pi^+\pi^-\pi^0$
775.8 ±0.9 ±2.0	500k	[7] ACHASOV	02	SND	1.02 $e^+e^- \to \pi^+\pi^-\pi^0$
775.9 ±1.1		[8] BARKOV	85	OLYA	$e^+e^- \to \pi^+\pi^-$
• • • We do not use the following data for averages, fits, limits, etc. • • •					
763.49±0.53		[9] BARTOS	17	RVUE	$e^+e^- \to \pi^+\pi^-$
758.23±0.46		[10] BARTOS	17A	RVUE	$e^+e^- \to \pi^+\pi^-$
775.8 ±0.5 ±0.3	1.98M	[11] ALOISIO	03	KLOE	1.02 $e^+e^- \to \pi^+\pi^-\pi^0$
775.9 ±0.6 ±0.5	1.98M	[12] ALOISIO	03	KLOE	1.02 $e^+e^- \to \pi^+\pi^-\pi^0$
775.0 ±0.6 ±1.1	500k	[13] ACHASOV	02	SND	1.02 $e^+e^- \to \pi^+\pi^-\pi^0$
775.1 ±0.7 ±5.3		[14] BENAYOUN	98	RVUE	$e^+e^- \to \pi^+\pi^-$, $\mu^+\mu^-$
770.5 ±1.9 ±5.1		[15] GARDNER	98	RVUE	0.28–0.92 $e^+e^- \to \pi^+\pi^-$
764.1 ±0.7		[16] O'CONNELL	97	RVUE	$e^+e^- \to \pi^+\pi^-$
757.5 ±1.5		[17] BERNICHA	94	RVUE	$e^+e^- \to \pi^+\pi^-$
768 ±1		[18] GESHKEN...	89	RVUE	$e^+e^- \to \pi^+\pi^-$

CHARGED ONLY, τ DECAYS and e^+e^-

VALUE (MeV)	EVTS	DOCUMENT ID		TECN	CHG	COMMENT
775.11±0.34 OUR AVERAGE						
774.6 ±0.2 ±0.5	5.4M	[19,20] FUJIKAWA	08	BELL	±	$\tau^- \to \pi^-\pi^0\nu_\tau$
775.5 ±0.7		[20,21] SCHAEL	05C	ALEP		$\tau^- \to \pi^-\pi^0\nu_\tau$
775.5 ±0.5 ±0.4	1.98M	[7] ALOISIO	03	KLOE		1.02 $e^+e^- \to \pi^+\pi^-\pi^0$
775.1 ±1.1 ±0.5	87k	[22,23] ANDERSON	00A	CLE2		$\tau^- \to \pi^-\pi^0\nu_\tau$
• • • We do not use the following data for averages, fits, limits, etc. • • •						
761.60±0.95		[24] BARTOS	17A	RVUE		$\tau^- \to \pi^-\pi^0\nu_\tau$
774.8 ±0.6 ±0.4	1.98M	[12] ALOISIO	03	KLOE	−	1.02 $e^+e^- \to \pi^+\pi^-\pi^0$
776.3 ±0.6 ±0.7	1.98M	[12] ALOISIO	03	KLOE	+	1.02 $e^+e^- \to \pi^+\pi^-\pi^0$
773.9 ±2.0 $^{+0.3}_{-1.0}$		[25] SANZ-CILLERO	03	RVUE		$\tau^- \to \pi^-\pi^0\nu_\tau$
774.5 ±0.7 ±1.5	500k	[7] ACHASOV	02	SND	±	1.02 $e^+e^- \to \pi^+\pi^-\pi^0$
775.1 ±0.5		[26] PICH	01	RVUE		$\tau^- \to \pi^-\pi^0\nu_\tau$

MIXED CHARGES, OTHER REACTIONS

VALUE (MeV)	EVTS	DOCUMENT ID		TECN	CHG	COMMENT
763.0±0.3±1.2	600k	[27] ABELE	99E	CBAR	0±	0.0 $\overline{p}p \to \pi^+\pi^-\pi^0$

CHARGED ONLY, HADROPRODUCED

VALUE (MeV)	EVTS	DOCUMENT ID		TECN	CHG	COMMENT
766.5±1.1 OUR AVERAGE						
763.7±3.2		ABELE	97	CBAR		$\overline{p}n \to \pi^-\pi^0\pi^0$
768 ±9		AGUILAR-...	91	EHS		400 pp
767 ±3	2935	[28] CAPRARO	87	SPEC	−	200 π^-Cu $\to \pi^-\pi^0$Cu
761 ±5	967	[28] CAPRARO	87	SPEC	−	200 π^-Pb $\to \pi^-\pi^0$Pb
771 ±4		HUSTON	86	SPEC	+	202 π^+A $\to \pi^+\pi^0$A
766 ±7	6500	[29] BYERLY	73	OSPK	−	5 π^-p
766.8±1.5	9650	[30] PISUT	68	RVUE	−	1.7–3.2 π^-p, $t<10$
767 ±6	900	[28] EISNER	67	HBC	−	4.2 π^-p, $t<10$

NEUTRAL ONLY, PHOTOPRODUCED

VALUE (MeV)	EVTS	DOCUMENT ID		TECN	COMMENT
769.0± 1.0 OUR AVERAGE					
771 ± 2 $^{+2}_{-1}$	63.5k	[31] ABRAMOWICZ	12	ZEUS	$ep \to e\pi^+\pi^-p$
770 ± 2 ±1	79k	[32] BREITWEG	98B	ZEUS	50–100 γp
767.6± 2.7		BARTALUCCI	78	CNTR	$\gamma p \to e^+e^-p$
775 ± 5		GLADDING	73	CNTR	2.9–4.7 γp
767 ± 4	1930	BALLAM	72	HBC	2.8 γp
770 ± 4	2430	BALLAM	72	HBC	4.7 γp
765 ±10		ALVENSLEB...	70	CNTR	γA, $t<0.01$
767.7± 1.9	140k	BIGGS	70	CNTR	$<4.1\ \gamma$C $\to \pi^+\pi^-$C
765 ± 5	4000	ASBURY	67B	CNTR	γ + Pb
• • • We do not use the following data for averages, fits, limits, etc. • • •					
771 ± 2	79k	[33] BREITWEG	98B	ZEUS	50–100 γp

NEUTRAL ONLY, OTHER REACTIONS

VALUE (MeV)	EVTS	DOCUMENT ID		TECN	CHG	COMMENT
769.0±0.9 OUR AVERAGE		Error includes scale factor of 1.4. See the ideogram below.				
765 ±6		BERTIN	97C	OBLX		0.0 $\overline{p}p \to \pi^+\pi^-\pi^0$
773 ±1.6		WEIDENAUER	93	ASTE		$\overline{p}p \to \pi^+\pi^-\omega$
762.6±2.6		AGUILAR-...	91	EHS		400 pp
770 ±2		[34] HEYN	81	RVUE		Pion form factor
768 ±4		[35,36] BOHACIK	80	RVUE	0	
769 ±3		[29] WICKLUND	78	ASPK	0	3,4,6 $\pi^\pm N$
768 ±1	76000	DEUTSCH...	76	HBC	0	16 π^+p
767 ±4	4100	ENGLER	74	DBC	0	6 $\pi^+n \to \pi^+\pi^-p$
775 ±4	32000	[35] PROTOPOP...	73	HBC	0	7.1 π^+p, $t<0.4$
764 ±3	6800	RATCLIFF	72	ASPK	0	15 π^-p, $t<0.3$
774 ±3	1700	REYNOLDS	69	HBC	0	2.26 π^-p
769.2±1.5	13300	[37] PISUT	68	RVUE	0	1.7–3.2 π^-p, $t<10$
• • • We do not use the following data for averages, fits, limits, etc. • • •						
773.5±2.5		[38] COLANGELO	01	RVUE		$\pi\pi \to \pi\pi$
762.3±0.5±1.2	600k	[39] ABELE	99E	CBAR	0	0.0 $\overline{p}p \to \pi^+\pi^-\pi^0$
777 ±2	4943	[40] ADAMS	97	E665		470 $\mu p \to \mu XB$
770 ±2		[41] BOGOLYUB...	97	MIRA		32 $\overline{p}p \to \pi^+\pi^-$X
768 ±8		[41] BOGOLYUB...	97	MIRA		32 $pp \to \pi^+\pi^-$X
761.1±2.9		DUBNICKA	89	RVUE		π form factor
777.4±2.0		[42] CHABAUD	83	ASPK	0	17 π^-p polarized
769.5±0.7		[35,36] LANG	79	RVUE	0	
770 ±9		[36] ESTABROOKS	74	RVUE	0	17 $\pi^-p \to \pi^+\pi^-n$
773.5±1.7	11200	[28] JACOBS	72	HBC	0	2.8 π^-p
775 ±3	2250	HYAMS	68	OSPK	0	11.2 π^-p

[1] Using the GOUNARIS 68 parametrization with the complex phase of the ρ–ω interference and leaving the masses and widths of the $\rho(1450)$, $\rho(1700)$, and $\rho(2150)$ resonances as free parameters of the fit.
[2] A combined fit of AKHMETSHIN 07, AULCHENKO 06, and AULCHENKO 05.
[3] Supersedes ACHASOV 05A.
[4] A fit of the SND data from 400 to 1000 MeV using parameters of the $\rho(1450)$ and $\rho(1700)$ from a fit of the data of BARKOV 85, BISELLO 89 and ANDERSON 00A.
[5] Using the GOUNARIS 68 parametrization with the complex phase of the ρ–ω interference.
[6] Update of AKHMETSHIN 02.
[7] Assuming $m_{\rho^+} = m_{\rho^-}$, $\Gamma_{\rho^+} = \Gamma_{\rho^-}$.
[8] From the GOUNARIS 68 parametrization of the pion form factor.
[9] Applies the Unitary & Analytic Model of the pion electromagnetic form factor of DUBNICKA 10 to analyze the data of LEES 12G and ABLIKIM 16C.

Meson Particle Listings

$\rho(770)$

[10] Applies the Unitary & Analytic Model of the pion electromagnetic form factor of DUBNICKA 10 to analyze the data of ACHASOV 06, AKHMETSHIN 07, AUBERT 09AS, and AMBROSINO 11A.
[11] Assuming $m_{\rho^+} = m_{\rho^-} = m_{\rho^0}$, $\Gamma_{\rho^+} = \Gamma_{\rho^-} = \Gamma_{\rho^0}$.
[12] Without limitations on masses and widths.
[13] Assuming $m_{\rho^0} = m_{\rho^\pm}$, $g_{\rho^0\pi\pi} = g_{\rho^\pm\pi\pi}$.
[14] Using the data of BARKOV 85 in the hidden local symmetry model.
[15] From the fit to $e^+e^- \to \pi^+\pi^-$ data from the compilations of HEYN 81 and BARKOV 85, including the GOUNARIS 68 parametrization of the pion form factor.
[16] A fit of BARKOV 85 data assuming the direct $\omega\pi\pi$ coupling.
[17] Applying the S-matrix formalism to the BARKOV 85 data.
[18] Includes BARKOV 85 data. Model-dependent width definition.
[19] $|F_\pi(0)|^2$ fixed to 1.
[20] From the GOUNARIS 68 parametrization of the pion form factor.
[21] The error combines statistical and systematic uncertainties. Supersedes BARATE 97M.
[22] $\rho(1700)$ mass and width fixed at 1700 MeV and 235 MeV respectively.
[23] From the GOUNARIS 68 parametrization of the pion form factor. The second error is a model error taking into account different parametrizations of the pion form factor.
[24] Applies the Unitary & Analytic Model of the pion electromagnetic form factor of DUBNICKA 10 to analyze the data of FUJIKAWA 08.
[25] Using the data of BARATE 97M and the effective chiral Lagrangian.
[26] From a fit of the model-independent parameterization of the pion form factor to the data of BARATE 97M.
[27] Assuming the equality of ρ^+ and ρ^- masses and widths.
[28] Mass errors enlarged by us to $\Gamma/\sqrt{N}$; see the note with the $K^*(892)$ mass.
[29] Phase shift analysis. Systematic errors added corresponding to spread of different fits.
[30] From fit of 3-parameter relativistic P-wave Breit-Wigner to total mass distribution. Includes BATON 68, MILLER 67B, ALFF-STEINBERGER 66, HAGOPIAN 66, HAGOPIAN 66B, JACOBS 66B, JAMES 66, WEST 66, BLIEDEN 65 and CARMONY 64.
[31] Using the KUHN 90 parametrization of the pion form factor, neglecting ρ–ω interference.
[32] From the parametrization according to SOEDING 66.
[33] From the parametrization according to ROSS 66.
[34] HEYN 81 includes all spacelike and timelike F_π values until 1978.
[35] From pole extrapolation.
[36] From phase shift analysis of GRAYER 74 data.
[37] Includes MALAMUD 69, ARMENISE 68, BACON 67, HUWE 67, MILLER 67B, ALFF-STEINBERGER 66, HAGOPIAN 66, HAGOPIAN 66B, JACOBS 66B, JAMES 66, WEST 66, GOLDHABER 64, ABOLINS 63.
[38] Breit-Wigner mass from a phase-shift analysis of HYAMS 73 and PROTOPOPESCU 73 data.
[39] Using relativistic Breit-Wigner and taking into account ρ-ω interference.
[40] Systematic errors not evaluated.
[41] Systematic effects not studied.
[42] From fit of 3-parameter relativistic Breit-Wigner to helicity-zero part of P-wave intensity. CHABAUD 83 includes data of GRAYER 74.

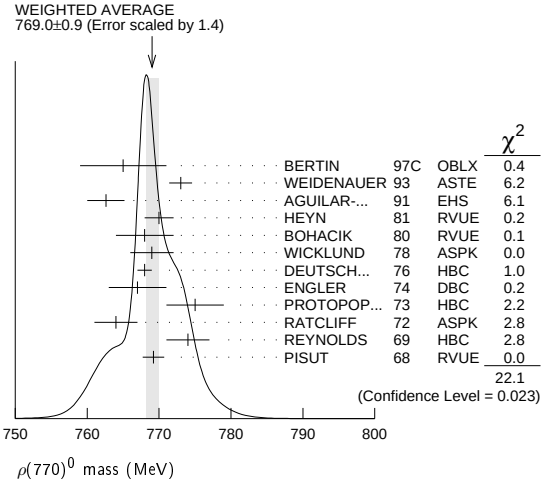

$m_{\rho(770)^0} - m_{\rho(770)^\pm}$

VALUE (MeV)	EVTS	DOCUMENT ID		TECN	CHG	COMMENT
−0.7 ±0.8 OUR AVERAGE		Error includes scale factor of 1.5. See the ideogram below.				
−2.4 ±0.8		[1] SCHAEL	05C	ALEP		$\tau^- \to \pi^-\pi^0\nu_\tau$
0.4 ±0.7 ±0.6	1.98M	[2] ALOISIO	03	KLOE		1.02 $e^+e^- \to \pi^+\pi^-\pi^0$
1.3 ±1.1 ±2.0	500k	[2] ACHASOV	02	SND		1.02 $e^+e^- \to \pi^+\pi^-\pi^0$
1.6 ±0.6 ±1.7	600k	ABELE	99E	CBAR	±0	0.0 $\overline{p}p \to \pi^+\pi^-\pi^0$
−4 ±4	3000	[3] REYNOLDS	69	HBC	−0	2.26 $\pi^- p$
−5 ±5	3600	[3] FOSTER	68	HBC	±0	0.0 $\overline{p}p$
2.4 ±2.1	22950	[4] PISUT	68	RVUE		$\pi N \to \rho N$
• • • We do not use the following data for averages, fits, limits, etc. • • •						
−3.37±1.06		[5] BARTOS	17A	RVUE		$e^+e^- \to \pi^+\pi^-$, $\tau^- \to \pi^-\pi^0\nu_\tau$

[1] From the combined fit of the τ^- data from ANDERSON 00A and SCHAEL 05C and e^+e^- data from the compilation of BARKOV 85, AKHMETSHIN 04, and ALOISIO 05. Supersedes BARATE 97M.
[2] Assuming $m_{\rho^+} = m_{\rho^-}$, $\Gamma_{\rho^+} = \Gamma_{\rho^-}$.
[3] From quoted masses of charged and neutral modes.
[4] Includes MALAMUD 69, ARMENISE 68, BATON 68, BACON 67, HUWE 67, MILLER 67B, ALFF-STEINBERGER 66, HAGOPIAN 66, HAGOPIAN 66B, JACOBS 66B, JAMES 66, WEST 66, BLIEDEN 65, CARMONY 64, GOLDHABER 64, ABOLINS 63.
[5] Applies the Unitary & Analytic Model of the pion electromagnetic form factor of DUBNICKA 10 to analyze the data of ACHASOV 06, AKHMETSHIN 07, AUBERT 09AS, AMBROSINO 11A, and FUJIKAWA 08.

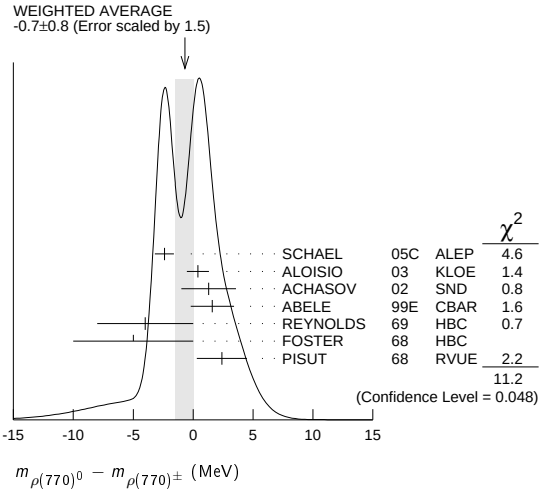

$m_{\rho(770)^+} - m_{\rho(770)^-}$

VALUE (MeV)	EVTS	DOCUMENT ID		TECN	COMMENT
• • • We do not use the following data for averages, fits, limits, etc. • • •					
1.5±0.8±0.7	1.98M	[1] ALOISIO	03	KLOE	1.02 $e^+e^- \to \pi^+\pi^-\pi^0$

[1] Without limitations on masses and widths.

$\rho(770)$ RANGE PARAMETER

The range parameter R enters an energy-dependent correction to the width, of the form $(1 + q_r^2\,R^2)\,/\,(1 + q^2\,R^2)$, where q is the momentum of one of the pions in the $\pi\pi$ rest system. At resonance, $q = q_r$.

VALUE (GeV^{-1})	DOCUMENT ID		TECN	CHG	COMMENT
$5.3^{+0.9}_{-0.7}$	CHABAUD	83	ASPK	0	17 $\pi^- p$ polarized

$\rho(770)$ WIDTH

We no longer list S-wave Breit-Wigner fits, or data with high combinatorial background.

NEUTRAL ONLY, e^+e^-

VALUE (MeV)	EVTS	DOCUMENT ID		TECN	CHG	COMMENT
147.8 ±0.9 OUR AVERAGE		Error includes scale factor of 2.0. See the ideogram below.				
149.59±0.67		[1] LEES	12G	BABR		$e^+e^- \to \pi^+\pi^-\gamma$
145.98±0.75±0.50	900k	[2] AKHMETSHIN	07			$e^+e^- \to \pi^+\pi^-$
146.1 ±0.8 ±1.5	800k	[3,4] ACHASOV	06	SND		$e^+e^- \to \pi^+\pi^-$
143.85±1.33±0.80	114k	[5,6] AKHMETSHIN	04	CMD2		$e^+e^- \to \pi^+\pi^-$
147.3 ±1.5 ±0.7	1.98M	[7] ALOISIO	03	KLOE		1.02 $e^+e^- \to \pi^+\pi^-\pi^0$
151.1 ±2.6 ±3.0	500k	[7] ACHASOV	02	SND	0	1.02 $e^+e^- \to \pi^+\pi^-\pi^0$
150.5 ±3.0		[8] BARKOV	85	OLYA	0	$e^+e^- \to \pi^+\pi^-$
• • • We do not use the following data for averages, fits, limits, etc. • • •						
144.06±0.85		[9] BARTOS	17	RVUE		$e^+e^- \to \pi^+\pi^-$
144.56±0.80		[10] BARTOS	17A	RVUE		$e^+e^- \to \pi^+\pi^-$
143.9 ±1.3 ±1.1	1.98M	[11] ALOISIO	03	KLOE		1.02 $e^+e^- \to \pi^+\pi^-\pi^0$
147.4 ±1.5 ±0.7	1.98M	[12] ALOISIO	03	KLOE		1.02 $e^+e^- \to \pi^+\pi^-\pi^0$
149.8 ±2.2 ±2.0	500k	[13] ACHASOV	02	SND		1.02 $e^+e^- \to \pi^+\pi^-\pi^0$
147.9 ±1.5 ±7.5		[14] BENAYOUN	98	RVUE		$e^+e^- \to \pi^+\pi^-$, $\mu^+\mu^-$
153.5 ±1.3 ±4.6		[15] GARDNER	98	RVUE		0.28–0.92 $e^+e^- \to \pi^+\pi^-$
145.0 ±1.7		[16] O'CONNELL	97	RVUE		$e^+e^- \to \pi^+\pi^-$
142.5 ±3.5		[17] BERNICHA	94	RVUE		$e^+e^- \to \pi^+\pi^-$
138 ±1		[18] GESHKEN...	89	RVUE		$e^+e^- \to \pi^+\pi^-$

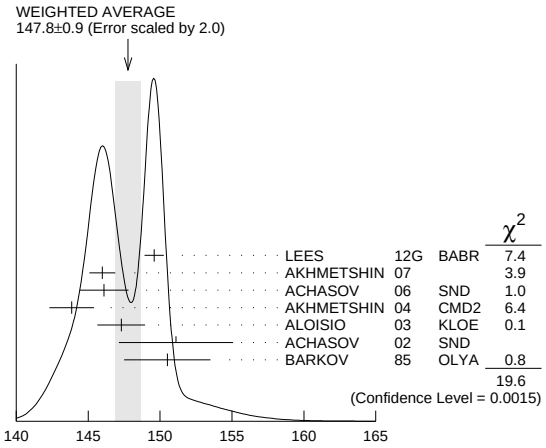

CHARGED ONLY, τ DECAYS and e^+e^-

VALUE (MeV)	EVTS	DOCUMENT ID		TECN	CHG	COMMENT
149.1 ±0.8 OUR FIT						
149.1 ±0.8 OUR AVERAGE						
148.1 ±0.4 ±1.7	5.4M	[19,20] FUJIKAWA	08	BELL	±	$\tau^- \to \pi^-\pi^0\nu_\tau$
149.0 ±1.2		[20,21] SCHAEL	05C	ALEP		$\tau^- \to \pi^-\pi^0\nu_\tau$
149.9 ±2.3 ±2.0	500k	[7] ACHASOV	02	SND	±	1.02 $e^+e^- \to \pi^+\pi^-\pi^0$
150.4 ±1.4 ±1.4	87k	[22,23] ANDERSON	00A	CLE2		$\tau^- \to \pi^-\pi^0\nu_\tau$
• • • We do not use the following data for averages, fits, limits, etc. • • •						
139.90±0.46		[24] BARTOS	17A	RVUE		$\tau^- \to \pi^-\pi^0\nu_\tau$
143.7 ±1.3 ±1.2	1.98M	[7] ALOISIO	03	KLOE	±	1.02 $e^+e^- \to \pi^+\pi^-\pi^0$
142.9 ±1.3 ±1.4	1.98M	[12] ALOISIO	03	KLOE	−	1.02 $e^+e^- \to \pi^+\pi^-\pi^0$
144.7 ±1.4 ±1.2	1.98M	[12] ALOISIO	03	KLOE	+	1.02 $e^+e^- \to \pi^+\pi^-\pi^0$
150.2 ±2.0 $^{+0.7}_{-1.6}$		[25] SANZ-CILLERO	03	RVUE		$\tau^- \to \pi^-\pi^0\nu_\tau$
150.9 ±2.2 ±2.0	500k	[13] ACHASOV	02	SND		1.02 $e^+e^- \to \pi^+\pi^-\pi^0$

MIXED CHARGES, OTHER REACTIONS

VALUE (MeV)	EVTS	DOCUMENT ID		TECN	CHG	COMMENT
149.5±1.3	600k	[26] ABELE	99E	CBAR	0±	0.0 $\overline{p}p \to \pi^+\pi^-\pi^0$

CHARGED ONLY, HADROPRODUCED

VALUE (MeV)	EVTS	DOCUMENT ID		TECN	CHG	COMMENT
150.2± 2.4 OUR FIT						
150.2± 2.4 OUR AVERAGE						
152.8± 4.3		ABELE	97	CBAR		$\overline{p}n \to \pi^-\pi^0\pi^0$
155 ±11	2.9k	[27] CAPRARO	87	SPEC	−	200 π^-Cu $\to \pi^-\pi^0$Cu
154 ±20	967	[27] CAPRARO	87	SPEC	−	200 π^-Pb $\to \pi^-\pi^0$Pb
150 ± 5		HUSTON	86	SPEC	+	202 π^+A $\to \pi^+\pi^0$A
146 ±12	6.5k	[28] BYERLY	73	OSPK	−	5 π^-p
148.2± 4.1	9.6k	[29] PISUT	68	RVUE	−	1.7–3.2 π^-p, $t<10$
146 ±13	900	EISNER	67	HBC	−	4.2 π^-p, $t<10$
• • • We do not use the following data for averages, fits, limits, etc. • • •						
137.0± 0.4		[30] ABLIKIM	17	BES3		$J/\psi \to \gamma 3\pi$

NEUTRAL ONLY, PHOTOPRODUCED

VALUE (MeV)	EVTS	DOCUMENT ID		TECN	COMMENT
151.7± 2.6 OUR AVERAGE					
155 ± 5 ± 2	63.5k	[31] ABRAMOWICZ	12	ZEUS	$ep \to e\pi^+\pi^-p$
146 ± 3 ±13	79k	[32] BREITWEG	98B	ZEUS	50–100 γp
150.9± 3.0		BARTALUCCI	78	CNTR	$\gamma p \to e^+e^-p$
• • • We do not use the following data for averages, fits, limits, etc. • • •					
138 ± 3	79k	[33] BREITWEG	98B	ZEUS	50–100 γp
147 ±11		GLADDING	73	CNTR	2.9–4.7 γp
155 ±12	2430	BALLAM	72	HBC	4.7 γp
145 ±13	1930	BALLAM	72	HBC	2.8 γp
140 ± 5		ALVENSLEB...	70	CNTR	γA, $t<0.01$
146.1± 2.9	140k	BIGGS	70	CNTR	$<4.1\ \gamma$C $\to \pi^+\pi^-$C
160 ±10		LANZEROTTI	68	CNTR	γp
130 ± 5	4000	ASBURY	67B	CNTR	γ + Pb

NEUTRAL ONLY, OTHER REACTIONS

VALUE (MeV)	EVTS	DOCUMENT ID		TECN	CHG	COMMENT
150.9± 1.7 OUR AVERAGE		Error includes scale factor of 1.1.				
122 ±20		BERTIN	97C	OBLX		0.0 $\overline{p}p \to \pi^+\pi^-\pi^0$
145.7± 5.3		WEIDENAUER	93	ASTE		$\overline{p}p \to \pi^+\pi^-\omega$
144.9± 3.7		DUBNICKA	89	RVUE		π form factor
148 ± 6		[34,35] BOHACIK	80	RVUE	0	
152 ± 9		[28] WICKLUND	78	ASPK	0	3,4,6 $\pi^\pm p\,N$
154 ± 2	76000	DEUTSCH...	76	HBC	0	16 π^+p
157 ± 8	6800	RATCLIFF	72	ASPK	0	15 π^-p, $t<0.3$
143 ± 8	1700	REYNOLDS	69	HBC	0	2.26 π^-p
• • • We do not use the following data for averages, fits, limits, etc. • • •						
147.0± 2.5	600k	[36] ABELE	99E	CBAR	0	0.0 $\overline{p}p \to \pi^+\pi^-\pi^0$
146 ± 3	4943	[37] ADAMS	97	E665		470 $\mu p \to \mu XB$
160.0 $^{+4.1}_{-4.0}$		[38] CHABAUD	83	ASPK	0	17 π^-p polarized
155 ± 1		[39] HEYN	81	RVUE	0	π form factor
148.0± 1.3		[34,35] LANG	79	RVUE	0	
146 ±14	4100	ENGLER	74	DBC	0	6 $\pi^+n \to \pi^+\pi^-p$
143 ±13		[35] ESTABROOKS	74	RVUE	0	17 $\pi^-p \to \pi^+\pi^-n$
160 ±10	32000	[34] PROTOPOP...	73	HBC	0	7.1 π^+p, $t<0.4$
145 ±12	2250	[27] HYAMS	68	OSPK	0	11.2 π^-p
163 ±15	13300	[40] PISUT	68	RVUE	0	1.7–3.2 π^-p, $t<10$

[1] Using the GOUNARIS 68 parametrization with the complex phase of the $\rho-\omega$ interference and leaving the masses and widths of the $\rho(1450)$, $\rho(1700)$, and $\rho(2150)$ resonances as free parameters of the fit.
[2] A combined fit of AKHMETSHIN 07, AULCHENKO 06, and AULCHENKO 05.
[3] Supersedes ACHASOV 05A.
[4] A fit of the SND data from 400 to 1000 MeV using parameters of the $\rho(1450)$ and $\rho(1700)$ from a fit of the data of BARKOV 85, BISELLO 89 and ANDERSON 00A.
[5] Using the GOUNARIS 68 parametrization with the complex phase of the $\rho-\omega$ interference.
[6] From a fit in the energy range 0.61 to 0.96 GeV. Update of AKHMETSHIN 02.
[7] Assuming $m_{\rho^+} = m_{\rho^-}$, $\Gamma_{\rho^+} = \Gamma_{\rho^-}$.
[8] From the GOUNARIS 68 parametrization of the pion form factor.
[9] Applies the Unitary & Analytic Model of the pion electromagnetic form factor of DUBNICKA 10 to analyze the data of LEES 12G and ABLIKIM 16C.
[10] Applies the Unitary & Analytic Model of the pion electromagnetic form factor of DUBNICKA 10 to analyze the data of ACHASOV 06, AKHMETSHIN 07, AUBERT 09AS, and AMBROSINO 11A.
[11] Assuming $m_{\rho^+} = m_{\rho^-} = m_{\rho^0}$, $\Gamma_{\rho^+} = \Gamma_{\rho^-} = \Gamma_{\rho^0}$.
[12] Without limitations on masses and widths.
[13] Assuming $m_{\rho^0} = m_{\rho^\pm}$, $g_{\rho^0\pi\pi} = g_{\rho^\pm\pi\pi}$.
[14] Using the data of BARKOV 85 in the hidden local symmetry model.
[15] From the fit to $e^+e^- \to \pi^+\pi^-$ data from the compilations of HEYN 81 and BARKOV 85, including the GOUNARIS 68 parametrization of the pion form factor.
[16] A fit of BARKOV 85 data assuming the direct $\omega\pi\pi$ coupling.
[17] Applying the S-matrix formalism to the BARKOV 85 data.
[18] Includes BARKOV 85 data. Model-dependent width definition.
[19] $|F_\pi(0)|^2$ fixed to 1.
[20] From the GOUNARIS 68 parametrization of the pion form factor.
[21] The error combines statistical and systematic uncertainties. Supersedes BARATE 97M.
[22] $\rho(1700)$ mass and width fixed at 1700 MeV and 235 MeV respectively.
[23] From the GOUNARIS 68 parametrization of the pion form factor. The second error is a model error taking into account different parametrizations of the pion form factor.
[24] Applies the Unitary & Analytic Model of the pion electromagnetic form factor of DUBNICKA 10 to analyze the data of FUJIKAWA 08.
[25] Using the data of BARATE 97M and the effective chiral Lagrangian.
[26] Assuming the equality of ρ^+ and ρ^- masses and widths.
[27] Width errors enlarged by us to $4\Gamma/\sqrt{N}$; see the note with the $K^*(892)$ mass.
[28] Phase shift analysis. Systematic errors added corresponding to spread of different fits.
[29] From fit of 3-parameter relativistic P-wave Breit-Wigner to total mass distribution. Includes BATON 68, MILLER 67B, ALFF-STEINBERGER 66, HAGOPIAN 66, HAGOPIAN 66B, JACOBS 66B, JAMES 66, WEST 66, BLIEDEN 65 and CARMONY 64.
[30] S-matrix pole at a fixed ρ meson mass of 775.49 MeV.
[31] Using the KUHN 90 parametrization of the pion form factor, neglecting $\rho-\omega$ interference.
[32] From the parametrization according to SOEDING 66.
[33] From the parametrization according to ROSS 66.
[34] From pole extrapolation.
[35] From phase shift analysis of GRAYER 74 data.
[36] Using relativistic Breit-Wigner and taking into account $\rho-\omega$ interference.
[37] Systematic errors not evaluated.
[38] From fit of 3-parameter relativistic Breit-Wigner to helicity-zero part of P-wave intensity. CHABAUD 83 includes data of GRAYER 74.
[39] HEYN 81 includes all spacelike and timelike F_π values until 1978.
[40] Includes MALAMUD 69, ARMENISE 68, BACON 67, HUWE 67, MILLER 67B, ALFF-STEINBERGER 66, HAGOPIAN 66, HAGOPIAN 66B, JACOBS 66B, JAMES 66, WEST 66, GOLDHABER 64, ABOLINS 63.

$\Gamma_{\rho(770)^0} - \Gamma_{\rho(770)^\pm}$

VALUE (MeV)	EVTS	DOCUMENT ID		TECN	COMMENT
0.3 ±1.3 OUR AVERAGE		Error includes scale factor of 1.4.			
−0.2 ±1.0		[1] SCHAEL	05C	ALEP	$\tau^- \to \pi^-\pi^0\nu_\tau$
3.6 ±1.8 ±1.7	1.98M	[2] ALOISIO	03	KLOE	1.02 $e^+e^- \to \pi^+\pi^-\pi^0$
• • • We do not use the following data for averages, fits, limits, etc. • • •					
4.66±0.85		[3] BARTOS	17A	RVUE	$e^+e^- \to \pi^+\pi^-$, $\tau^- \to \pi^-\pi^0\nu_\tau$

$\Gamma_{\rho(770)^+} - \Gamma_{\rho(770)^-}$

VALUE	EVTS	DOCUMENT ID		TECN	COMMENT
1.8±2.0±0.5	1.98M	[4] ALOISIO	03	KLOE	1.02 $e^+e^- \to \pi^+\pi^-\pi^0$

[1] From the combined fit of the τ^- data from ANDERSON 00A and SCHAEL 05C and e^+e^- data from the compilation of BARKOV 85, AKHMETSHIN 04, and ALOISIO 05. Supersedes BARATE 97M.
[2] Assuming $m_{\rho^+} = m_{\rho^-}$, $\Gamma_{\rho^+} = \Gamma_{\rho^-}$.
[3] Applies the Unitary & Analytic Model of the pion electromagnetic form factor of DUBNICKA 10 to analyze the data of ACHASOV 06, AKHMETSHIN 07, AUBERT 09AS, AMBROSINO 11A, and FUJIKAWA 08.

[4] Without limitations on masses and widths.

$\rho(770)$ DECAY MODES

	Mode	Fraction (Γ_i/Γ)	Scale factor / Confidence level
Γ_1	$\pi\pi$	$\sim$ 100 %	
	$\rho(770)^\pm$ decays		
Γ_2	$\pi^\pm\pi^0$	$\sim$ 100 %	
Γ_3	$\pi^\pm\gamma$	(4.5 $\pm$0.5) $\times 10^{-4}$	S=2.2
Γ_4	$\pi^\pm\eta$	$<$ 6 $\times 10^{-3}$	CL=84%
Γ_5	$\pi^\pm\pi^+\pi^-\pi^0$	$<$ 2.0 $\times 10^{-3}$	CL=84%
	$\rho(770)^0$ decays		
Γ_6	$\pi^+\pi^-$	$\sim$ 100 %	
Γ_7	$\pi^+\pi^-\gamma$	(9.9 $\pm$1.6) $\times 10^{-3}$	
Γ_8	$\pi^0\gamma$	(4.7 $\pm$0.6) $\times 10^{-4}$	S=1.4
Γ_9	$\eta\gamma$	(3.00$\pm$0.21) $\times 10^{-4}$	
Γ_{10}	$\pi^0\pi^0\gamma$	(4.5 $\pm$0.8) $\times 10^{-5}$	
Γ_{11}	$\mu^+\mu^-$	[a] (4.55$\pm$0.28) $\times 10^{-5}$	
Γ_{12}	e^+e^-	[a] (4.72$\pm$0.05) $\times 10^{-5}$	
Γ_{13}	$\pi^+\pi^-\pi^0$	($1.01^{+0.54}_{-0.36}\pm0.34$) $\times 10^{-4}$	
Γ_{14}	$\pi^+\pi^-\pi^+\pi^-$	(1.8 $\pm$0.9) $\times 10^{-5}$	
Γ_{15}	$\pi^+\pi^-\pi^0\pi^0$	(1.6 $\pm$0.8) $\times 10^{-5}$	
Γ_{16}	$\pi^0 e^+e^-$	$<$ 1.2 $\times 10^{-5}$	CL=90%
Γ_{17}	ηe^+e^-		

[a] The $\omega\rho$ interference is then due to $\omega\rho$ mixing only, and is expected to be small. If $e\mu$ universality holds, $\Gamma(\rho^0 \to \mu^+\mu^-) = \Gamma(\rho^0 \to e^+e^-) \times 0.99785$.

CONSTRAINED FIT INFORMATION

An overall fit to the total width and a partial width uses 10 measurements and one constraint to determine 3 parameters. The overall fit has a $\chi^2 = 10.7$ for 8 degrees of freedom.

The following *off-diagonal* array elements are the correlation coefficients $\langle \delta p_i \delta p_j \rangle / (\delta p_i \cdot \delta p_j)$, in percent, from the fit to parameters p_i, including the branching fractions, $x_i \equiv \Gamma_i/\Gamma_{total}$. The fit constrains the x_i whose labels appear in this array to sum to one.

x_3	-100	
Γ	15	-15
	x_2	x_3

	Mode	Rate (MeV)	Scale factor
Γ_2	$\pi^\pm\pi^0$	150.2 $\pm$2.4	
Γ_3	$\pi^\pm\gamma$	0.068$\pm$0.007	2.3

CONSTRAINED FIT INFORMATION

An overall fit to the total width, a partial width, and 7 branching ratios uses 22 measurements and one constraint to determine 9 parameters. The overall fit has a $\chi^2 = 9.5$ for 14 degrees of freedom.

The following *off-diagonal* array elements are the correlation coefficients $\langle \delta p_i \delta p_j \rangle / (\delta p_i \cdot \delta p_j)$, in percent, from the fit to parameters p_i, including the branching fractions, $x_i \equiv \Gamma_i/\Gamma_{total}$. The fit constrains the x_i whose labels appear in this array to sum to one.

x_7	-100							
x_8	-4	0						
x_9	-1	0	1					
x_{10}	-1	0	0	0				
x_{11}	2	-3	0	0	0			
x_{12}	0	0	-8	-9	0	0		
x_{14}	-1	0	0	0	0	0	0	
Γ	0	0	4	5	0	0	-54	0
	x_6	x_7	x_8	x_9	x_{10}	x_{11}	x_{12}	x_{14}

	Mode	Rate (MeV)	Scale factor
Γ_6	$\pi^+\pi^-$	147.5 $\pm$0.9	
Γ_7	$\pi^+\pi^-\gamma$	1.48 $\pm$0.24	
Γ_8	$\pi^0\gamma$	0.070 $\pm$0.009	1.4
Γ_9	$\eta\gamma$	0.0447 $\pm$0.0032	
Γ_{10}	$\pi^0\pi^0\gamma$	0.0066 $\pm$0.0012	
Γ_{11}	$\mu^+\mu^-$	[a] 0.0068 $\pm$0.0004	
Γ_{12}	e^+e^-	[a] 0.00704$\pm$0.00006	
Γ_{14}	$\pi^+\pi^-\pi^+\pi^-$	0.0027 $\pm$0.0014	

$\rho(770)$ PARTIAL WIDTHS

$\Gamma(\pi^\pm\gamma)$ Γ_3

VALUE (keV)	DOCUMENT ID		TECN	CHG	COMMENT
68 $\pm$7 OUR FIT Error includes scale factor of 2.3.					
68 $\pm$7 OUR AVERAGE Error includes scale factor of 2.2. See the ideogram below.					
81 $\pm$4 $\pm$4	CAPRARO	87	SPEC	$-$	200 π^-A $\to$ $\pi^-\pi^0$A
59.8$\pm$4.0	HUSTON	86	SPEC	+	202 π^+A $\to$ $\pi^+\pi^0$A
71 $\pm$7	JENSEN	83	SPEC	$-$	156–260 π^-A $\to$ $\pi^-\pi^0$A

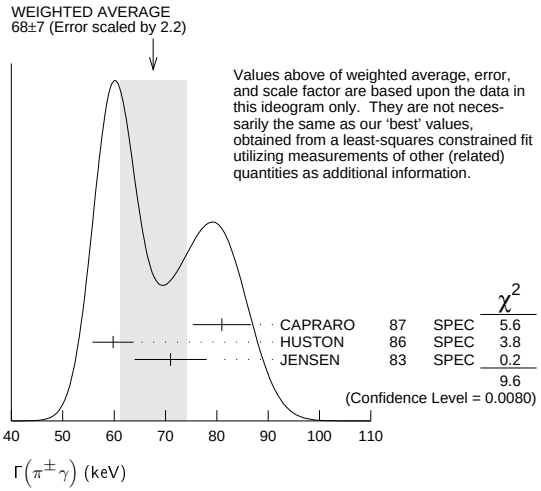

$\Gamma(e^+e^-)$ Γ_{12}

VALUE (keV)	EVTS	DOCUMENT ID		TECN	COMMENT
7.04 $\pm$0.06 OUR FIT					
7.04 $\pm$0.06 OUR AVERAGE					
7.048$\pm$0.057$\pm$0.050	900k	[1] AKHMETSHIN	07		$e^+e^- \to \pi^+\pi^-$
7.06 $\pm$0.11 $\pm$0.05	114k	[2,3] AKHMETSHIN	04	CMD2	$e^+e^- \to \pi^+\pi^-$
6.77 $\pm$0.10 $\pm$0.30		BARKOV	85	OLYA	$e^+e^- \to \pi^+\pi^-$
• • • We do not use the following data for averages, fits, limits, etc. • • •					
7.12 $\pm$0.02 $\pm$0.11	800k	[4] ACHASOV	06	SND	$e^+e^- \to \pi^+\pi^-$
6.3 $\pm$0.1		[5] BENAYOUN	98	RVUE	$e^+e^- \to \pi^+\pi^-$, $\mu^+\mu^-$

$\Gamma(\pi^0\gamma)$ Γ_8

VALUE (keV)	EVTS	DOCUMENT ID		TECN	COMMENT
• • • We do not use the following data for averages, fits, limits, etc. • • •					
77$\pm$17$\pm$11	36500	[6] ACHASOV	03	SND	0.60–0.97 $e^+e^- \to \pi^0\gamma$
121$\pm$31		DOLINSKY	89	ND	$e^+e^- \to \pi^0\gamma$

$\Gamma(\eta\gamma)$ Γ_9

VALUE (keV)	DOCUMENT ID		TECN	COMMENT
• • • We do not use the following data for averages, fits, limits, etc. • • •				
62$\pm$17	[7] DOLINSKY	89	ND	$e^+e^- \to \eta\gamma$

$\Gamma(\pi^+\pi^-\pi^+\pi^-)$ Γ_{14}

VALUE (keV)	EVTS	DOCUMENT ID		TECN	COMMENT
• • • We do not use the following data for averages, fits, limits, etc. • • •					
2.8$\pm$1.4$\pm$0.5	153	AKHMETSHIN	00	CMD2	0.6–0.97 $e^+e^- \to \pi^+\pi^-\pi^+\pi^-$

[1] A combined fit of AKHMETSHIN 07, AULCHENKO 06, and AULCHENKO 05.
[2] Using the GOUNARIS 68 parametrization with the complex phase of the ρ-ω interference.
[3] From a fit in the energy range 0.61 to 0.96 GeV. Update of AKHMETSHIN 02.
[4] Supersedes ACHASOV 05A.
[5] Using the data of BARKOV 85 in the hidden local symmetry model.
[6] Using Γ_{total}= 147.9 $\pm$ 1.3 MeV and B($\rho \to \pi^0\gamma$) from ACHASOV 03.
[7] Solution corresponding to constructive ω-ρ interference.

$\rho(770)$ $\Gamma(e^+e^-)\Gamma(i)/\Gamma^2(total)$

$\Gamma(e^+e^-)/\Gamma_{total} \times \Gamma(\pi^+\pi^-)/\Gamma_{total}$ $\Gamma_{12}/\Gamma \times \Gamma_6/\Gamma$

VALUE (units 10^{-5})	EVTS	DOCUMENT ID		TECN	COMMENT
4.876$\pm$0.023$\pm$0.064	800k	[1,2] ACHASOV	06	SND	$e^+e^- \to \pi^+\pi^-$
• • • We do not use the following data for averages, fits, limits, etc. • • •					
4.72 $\pm$0.02		[3] BENAYOUN	10	RVUE	0.4–1.05 e^+e^-

[1] Supersedes ACHASOV 05A.
[2] A fit of the SND data from 400 to 1000 MeV using parameters of the $\rho(1450)$ and $\rho(1700)$ from a fit of the data of BARKOV 85, BISELLO 89 and ANDERSON 00A.
[3] A simultaneous fit of $e^+e^- \to \pi^+\pi^-$, $\pi^+\pi^-\pi^0$, $\pi^0\gamma$, $\eta\gamma$ data.

$\Gamma(e^+e^-)/\Gamma_{total} \times \Gamma(\eta\gamma)/\Gamma_{total}$ $\Gamma_{12}/\Gamma \times \Gamma_9/\Gamma$

VALUE (units 10^{-8})	EVTS	DOCUMENT ID		TECN	COMMENT
1.42±0.10 OUR FIT					
1.45±0.12 OUR AVERAGE					
1.32±0.14±0.08	33k	[1] ACHASOV	07B	SND	0.6–1.38 $e^+e^- \to \eta\gamma$
1.50±0.65±0.09	17.4k	[2] AKHMETSHIN	05	CMD2	0.60-1.38 $e^+e^- \to \eta\gamma$
1.61±0.20±0.11	23k	[3,4] AKHMETSHIN	01B	CMD2	$e^+e^- \to \eta\gamma$
1.85±0.49		[5] DOLINSKY	89	ND	$e^+e^- \to \eta\gamma$
• • • We do not use the following data for averages, fits, limits, etc. • • •					
1.05±0.02		[6] BENAYOUN	10	RVUE	0.4–1.05 e^+e^-

[1] From a combined fit of $\sigma(e^+e^- \to \eta\gamma)$ with $\eta \to 3\pi^0$ and $\eta \to \pi^+\pi^-\pi^0$, and fixing $B(\eta \to 3\pi^0) / B(\eta \to \pi^+\pi^-\pi^0) = 1.44 \pm 0.04$. Recalculated by us from the cross section at the peak. Supersedes ACHASOV 00D and ACHASOV 06A.
[2] From the $\eta \to 2\gamma$ decay and using $B(\eta \to \gamma\gamma) = 39.43 \pm 0.26\%$.
[3] From the $\eta \to 3\pi^0$ decay and using $B(\eta \to 3\pi^0) = (32.24 \pm 0.29) \times 10^{-2}$.
[4] The combined fit from 600 to 1380 MeV taking into account $\rho(770)$, $\omega(782)$, $\phi(1020)$, and $\rho(1450)$ (mass and width fixed at 1450 MeV and 310 MeV respectively).
[5] Recalculated by us from the cross section in the peak.
[6] A simultaneous fit of $e^+e^- \to \pi^+\pi^-$, $\pi^+\pi^-\pi^0$, $\pi^0\gamma$, $\eta\gamma$ data.

$\Gamma(e^+e^-)/\Gamma_{total} \times \Gamma(\pi^0\gamma)/\Gamma_{total}$ $\Gamma_{12}/\Gamma \times \Gamma_8/\Gamma$

VALUE (units 10^{-8})	EVTS	DOCUMENT ID		TECN	COMMENT
2.22 ±0.29 OUR FIT Error includes scale factor of 1.4.					
2.22 ±0.26 OUR AVERAGE Error includes scale factor of 1.3. See the ideogram below.					
1.98 ±0.22 ±0.10		[1] ACHASOV	16A	SND	0.60-1.38 $e^+e^- \to \pi^0\gamma$
2.90 $^{+0.60}_{-0.55}$ ±0.18	18k	AKHMETSHIN	05	CMD2	0.60-1.38 $e^+e^- \to \pi^0\gamma$
2.37 ±0.53 ±0.33	36k	[2] ACHASOV	03	SND	0.60–0.97 $e^+e^- \to \pi^0\gamma$
3.61 ±0.74 ±0.49	10k	[3] DOLINSKY	89	ND	$e^+e^- \to \pi^0\gamma$
• • • We do not use the following data for averages, fits, limits, etc. • • •					
1.875±0.026		[4] BENAYOUN	10	RVUE	0.4–1.05 e^+e^-

[1] From the VMD model with the prho(770), $\omega(782)$, $\phi(1020)$ resonances, and an additional resonance describing the total contribution of the $\rho(1450)$ and $\omega(1420)$ states. Supersedes ACHASOV 03.
[2] Using $\sigma_{\phi \to \pi^0\gamma}$ from ACHASOV 00 and $m_\rho = 775.97$ MeV in the model with the energy-independent phase of ρ-ω interference equal to $(-10.2 \pm 7.0)^\circ$.
[3] Recalculated by us from the cross section in the peak.
[4] A simultaneous fit of $e^+e^- \to \pi^+\pi^-$, $\pi^+\pi^-\pi^0$, $\pi^0\gamma$, $\eta\gamma$ data.

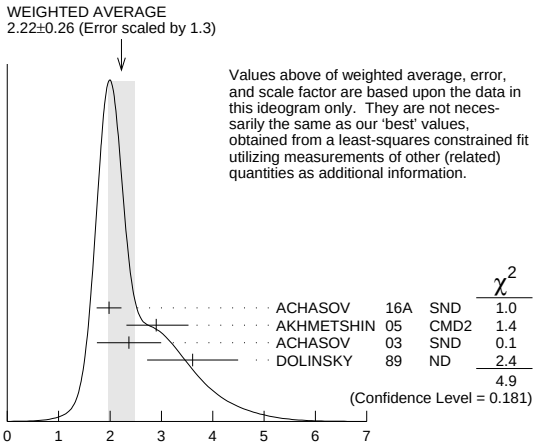

$\Gamma(e^+e^-)/\Gamma_{total} \times \Gamma(\pi^+\pi^-\pi^0)/\Gamma_{total}$ $\Gamma_{12}/\Gamma \times \Gamma_{13}/\Gamma$

VALUE (units 10^{-9})	EVTS	DOCUMENT ID		TECN	COMMENT
• • • We do not use the following data for averages, fits, limits, etc. • • •					
0.903±0.076		[1] BENAYOUN	10	RVUE	0.4–1.05 e^+e^-
4.58 $^{+2.46}_{-1.64}$ ±1.56	1.2M	[2] ACHASOV	03D	RVUE	0.44–2.00 $e^+e^- \to \pi^+\pi^-\pi^0$

[1] A simultaneous fit of $e^+e^- \to \pi^+\pi^-$, $\pi^+\pi^-\pi^0$, $\pi^0\gamma$, $\eta\gamma$ data.
[2] Statistical significance is less than 3σ.

$\rho(770)$ BRANCHING RATIOS

$\Gamma(\pi^\pm\eta)/\Gamma(\pi\pi)$ Γ_4/Γ_1

VALUE (units 10^{-4})	CL%	DOCUMENT ID		TECN	CHG	COMMENT
<60	84	FERBEL	66	HBC	±	$\pi^\pm p$ above 2.5

$\Gamma(\pi^\pm\pi^+\pi^-\pi^0)/\Gamma(\pi\pi)$ Γ_5/Γ_1

VALUE (units 10^{-4})	CL%	DOCUMENT ID		TECN	CHG	COMMENT
<20	84	FERBEL	66	HBC	±	$\pi^\pm p$ above 2.5
• • • We do not use the following data for averages, fits, limits, etc. • • •						
35±40		JAMES	66	HBC	+	2.1 $\pi^+ p$

$\Gamma(\mu^+\mu^-)/\Gamma(\pi^+\pi^-)$ Γ_{11}/Γ_6

VALUE (units 10^{-5})	DOCUMENT ID		TECN	COMMENT
4.60±0.28 OUR FIT				
4.6 ±0.2 ±0.2	ANTIPOV	89	SIGM	π^- Cu → $\mu^+\mu^-\pi^-$ Cu
• • • We do not use the following data for averages, fits, limits, etc. • • •				
8.2 $^{+1.6}_{-3.6}$	[1] ROTHWELL	69	CNTR	Photoproduction
5.6 ±1.5	[2] WEHMANN	69	OSPK	12 π^- C, Fe
9.7 $^{+3.1}_{-3.3}$	[3] HYAMS	67	OSPK	11 π^- Li, H

$\Gamma(e^+e^-)/\Gamma(\pi\pi)$ Γ_{12}/Γ_1

VALUE (units 10^{-4})	DOCUMENT ID		TECN	COMMENT
• • • We do not use the following data for averages, fits, limits, etc. • • •				
0.40±0.05	[4] BENAKSAS	72	OSPK	$e^+e^- \to \pi^+\pi^-$

$\Gamma(\eta\gamma)/\Gamma_{total}$ Γ_9/Γ

VALUE (units 10^{-4})	EVTS	DOCUMENT ID		TECN	CHG	COMMENT
3.00±0.21 OUR FIT						
2.90±0.32 OUR AVERAGE						
2.79±0.34±0.03	33k	[5] ACHASOV	07B	SND		0.6–1.38 $e^+e^- \to \eta\gamma$
3.6 ±0.9		[6] ANDREWS	77	CNTR	0	6.7–10 γCu
• • • We do not use the following data for averages, fits, limits, etc. • • •						
3.21±1.39±0.20	17.4k	[7,8] AKHMETSHIN	05	CMD2		0.60-1.38 $e^+e^- \to \eta\gamma$
3.39±0.42±0.23		[6,9,10] AKHMETSHIN	01B	CMD2		$e^+e^- \to \eta\gamma$
1.9 $^{+0.6}_{-0.8}$		[11] BENAYOUN	96	RVUE		0.54–1.04 $e^+e^- \to \eta\gamma$
4.0 ±1.1		[6,8] DOLINSKY	89	ND		$e^+e^- \to \eta\gamma$

$\Gamma(\pi^+\pi^-\pi^+\pi^-)/\Gamma_{total}$ Γ_{14}/Γ

VALUE (units 10^{-5})	CL%	EVTS	DOCUMENT ID		TECN	COMMENT
1.8±0.9 OUR FIT						
1.8±0.9±0.3		153	AKHMETSHIN	00	CMD2	0.6–0.97 $e^+e^- \to \pi^+\pi^-\pi^+\pi^-$
• • • We do not use the following data for averages, fits, limits, etc. • • •						
<20	90		KURDADZE	88	OLYA	$e^+e^- \to \pi^+\pi^-\pi^+\pi^-$

$\Gamma(\pi^+\pi^-\pi^+\pi^-)/\Gamma(\pi\pi)$ Γ_{14}/Γ_1

VALUE (units 10^{-4})	CL%	DOCUMENT ID		TECN	CHG	COMMENT
• • • We do not use the following data for averages, fits, limits, etc. • • •						
<15	90	ERBE	69	HBC	0	2.5–5.8 γp
<20		CHUNG	68	HBC	0	3.2,4.2 $\pi^- p$
<20	90	HUSON	68	HLBC	0	16.0 $\pi^- p$
<80		JAMES	66	HBC	0	2.1 $\pi^+ p$

$\Gamma(\pi^+\pi^-\pi^0)/\Gamma_{total}$ Γ_{13}/Γ

VALUE (units 10^{-4})	CL%	EVTS	DOCUMENT ID		TECN	COMMENT
• • • We do not use the following data for averages, fits, limits, etc. • • •						
1.01 $^{+0.54}_{-0.36}$ ±0.34		1.2M	[12] ACHASOV	03D	RVUE	0.44–2.00 $e^+e^- \to \pi^+\pi^-\pi^0$
<1.2	90		VASSERMAN	88B	ND	$e^+e^- \to \pi^+\pi^-\pi^0$

$\Gamma(\pi^+\pi^-\pi^0)/\Gamma(\pi\pi)$ Γ_{13}/Γ_1

VALUE	CL%	DOCUMENT ID		TECN	CHG	COMMENT
• • • We do not use the following data for averages, fits, limits, etc. • • •						
~ 0.01		BRAMON	86	RVUE	0	$J/\psi \to \omega\pi^0$
<0.01	84	[13] ABRAMS	71	HBC	0	3.7 $\pi^+ p$

$\Gamma(\pi^+\pi^-\pi^0\pi^0)/\Gamma_{total}$ Γ_{15}/Γ

VALUE (units 10^{-5})	CL%	DOCUMENT ID		TECN	COMMENT
1.60±0.74±0.18		[14] ACHASOV	09A	SND	$e^+e^- \to \pi^+\pi^-\pi^0\pi^0$
• • • We do not use the following data for averages, fits, limits, etc. • • •					
< 4	90	AULCHENKO	87C	ND	$e^+e^- \to \pi^+\pi^-\pi^0\pi^0$
<20	90	KURDADZE	86	OLYA	$e^+e^- \to \pi^+\pi^-\pi^0\pi^0$

$\Gamma(\pi^+\pi^-\gamma)/\Gamma_{total}$ Γ_7/Γ

VALUE	CL%	DOCUMENT ID		TECN	COMMENT
0.0099±0.0016 OUR FIT					
0.0099±0.0016		[15] DOLINSKY	91	ND	$e^+e^- \to \pi^+\pi^-\gamma$
• • • We do not use the following data for averages, fits, limits, etc. • • •					
0.0111±0.0014		[16] VASSERMAN	88	ND	$e^+e^- \to \pi^+\pi^-\gamma$
<0.005	90	[17] VASSERMAN	88	ND	$e^+e^- \to \pi^+\pi^-\gamma$

Meson Particle Listings

$\rho(770)$

$\Gamma(\pi^0\gamma)/\Gamma_{total}$ Γ_8/Γ

VALUE (units 10^{-4})	EVTS	DOCUMENT ID		TECN	COMMENT
• • • We do not use the following data for averages, fits, limits, etc. • • •					
4.20 ± 0.52		[18] ACHASOV	16A	SND	0.60–1.38 $e^+e^- \to \pi^0\gamma$
$6.21^{+1.28}_{-1.18}\pm0.39$	18k	[19,20] AKHMETSHIN	05	CMD2	0.60–1.38 $e^+e^- \to \pi^0\gamma$
$5.22\pm1.17\pm0.75$	36k	[20,21] ACHASOV	03	SND	0.60–0.97 $e^+e^- \to \pi^0\gamma$
$6.8\ \pm1.7$		[22] BENAYOUN	96	RVUE	0.54–1.04 $e^+e^- \to \pi^0\gamma$
$7.9\ \pm2.0$		[20] DOLINSKY	89	ND	$e^+e^- \to \pi^0\gamma$

$\Gamma(\pi^0 e^+ e^-)/\Gamma_{total}$ Γ_{16}/Γ

VALUE (units 10^{-5})	CL%	DOCUMENT ID		TECN	COMMENT
<1.2	90	ACHASOV	08	SND	0.36–0.97 $e^+e^- \to \pi^0 e^+e^-$
• • • We do not use the following data for averages, fits, limits, etc. • • •					
<1.6		AKHMETSHIN	05A	CMD2	0.72-0.84 e^+e^-

$\Gamma(\eta e^+ e^-)/\Gamma_{total}$ Γ_{17}/Γ

VALUE (units 10^{-5})	DOCUMENT ID		TECN	COMMENT
• • • We do not use the following data for averages, fits, limits, etc. • • •				
<0.7	AKHMETSHIN	05A	CMD2	0.72-0.84 e^+e^-

$\Gamma(\pi^0\pi^0\gamma)/\Gamma_{total}$ Γ_{10}/Γ

VALUE (units 10^{-5})	EVTS	DOCUMENT ID		TECN	COMMENT
4.5 ± 0.8 OUR FIT					
$4.5^{+0.9}_{-0.8}$ OUR AVERAGE					
$5.2^{+1.5}_{-1.3}\pm0.6$	190	[23] AKHMETSHIN	04B	CMD2	0.6–0.97 $e^+e^- \to \pi^0\pi^0\gamma$
$4.1^{+1.0}_{-0.9}\pm0.3$	295	[24] ACHASOV	02F	SND	0.36–0.97 $e^+e^- \to \pi^0\pi^0\gamma$
• • • We do not use the following data for averages, fits, limits, etc. • • •					
$4.8^{+3.4}_{-1.8}\pm0.5$	63	[25] ACHASOV	00G	SND	$e^+e^- \to \pi^0\pi^0\gamma$

[1] Possibly large ρ-ω interference leads us to increase the minus error.
[2] Result contains 11 ± 11% correction using SU(3) for central value. The error on the correction takes account of possible ρ-ω interference and the upper limit agrees with the upper limit of $\omega \to \mu^+\mu^-$ from this experiment.
[3] HYAMS 67's mass resolution is 20 MeV. The ω region was excluded.
[4] The ρ' contribution is not taken into account.
[5] ACHASOV 07B reports $[\Gamma(\rho(770) \to \eta\gamma)/\Gamma_{total}] \times [B(\rho(770) \to e^+e^-)] = (1.32 \pm 0.14 \pm 0.08) \times 10^{-8}$ which we divide by our best value $B(\rho(770) \to e^+e^-) = (4.72 \pm 0.05) \times 10^{-5}$. Our first error is their experiment's error and our second error is the systematic error from using our best value. Supersedes ACHASOV 00D and ACHASOV 06A.
[6] Solution corresponding to constructive ω-ρ interference.
[7] Using $B(\rho \to e^+e^-) = (4.67 \pm 0.09) \times 10^{-5}$ and $B(\eta \to \gamma\gamma) = 39.43 \pm 0.26\%$.
[8] Not independent of the corresponding $\Gamma(e^+e^-) \times \Gamma(\eta\gamma)/\Gamma^2_{total}$.
[9] The combined fit from 600 to 1380 MeV taking into account $\rho(770)$, $\omega(782)$, $\phi(1020)$, and $\rho(1450)$ (mass and width fixed at 1450 MeV and 310 MeV respectively).
[10] Using $B(\rho \to e^+e^-) = (4.75 \pm 0.10) \times 10^{-5}$ from AKHMETSHIN 02 and $B(\eta \to 3\pi^0) = (32.24 \pm 0.29) \times 10^{-2}$.
[11] Reanalysis of DRUZHININ 84, DOLINSKY 89, and DOLINSKY 91 taking into account a triangle anomaly contribution. Constructive ρ-ω interference solution.
[12] Statistical significance is less than 3σ.
[13] Model dependent, assumes $I = 1$, 2, or 3 for the 3π system.
[14] Assuming no interference between the ρ and ω contributions.
[15] Bremsstrahlung from a decay pion and for photon energy above 50 MeV.
[16] Superseded by DOLINSKY 91.
[17] Structure radiation due to quark rearrangement in the decay.
[18] Using $B(\rho \to e^+e^-)$ from PDG 15. Supersedes ACHASOV 03.
[19] Using $B(\rho \to e^+e^-) = (4.67 \pm 0.09) \times 10^{-5}$.
[20] Not independent of the corresponding $\Gamma(e^+e^-) \times \Gamma(\pi^0\gamma)/\Gamma^2_{total}$.
[21] Using $B(\rho \to e^+e^-) = (4.54 \pm 0.10) \times 10^{-5}$.
[22] Reanalysis of DRUZHININ 84, DOLINSKY 89, and DOLINSKY 91 taking into account a triangle anomaly contribution.
[23] This branching ratio includes the conventional VMD mechanism $\rho \to \omega\pi^0$, $\omega \to \pi^0\gamma$, and the new decay mode $\rho \to f_0(500)\gamma$, $f_0(500) \to \pi^0\pi^0$ with a branching ratio $(2.0^{+1.1}_{-0.9} \pm 0.3) \times 10^{-5}$ differing from zero by 2.0 standard deviations.
[24] This branching ratio includes the conventional VMD mechanism $\rho \to \omega\pi^0$, $\omega \to \pi^0\gamma$ and the new decay mode $\rho \to f_0(500)\gamma$, $f_0(500) \to \pi^0\pi^0$ with a branching ratio $(1.9^{+0.9}_{-0.8} \pm 0.4) \times 10^{-5}$ differing from zero by 2.4 standard deviations. Supersedes ACHASOV 00G.
[25] Superseded by ACHASOV 02F.

$\rho(770)$ REFERENCES

ABLIKIM	17	PRL 118 012001	M. Ablikim *et al.*	(BES III Collab.)
BARTOS	17	PR D96 113004	E. Bartos *et al.*	
BARTOS	17A	IJMP A32 1750154	E. Bartos *et al.*	
ABLIKIM	16C	PL B753 629	M. Ablikim *et al.*	(BES III Collab.)
ACHASOV	16A	PR D93 092001	M.N. Achasov *et al.*	(SND Collab.)
PDG	15	RPP 2015 at pdg.lbl.gov		(PDG Collab.)
ABRAMOWICZ	12	EPJ C72 1869	H. Abramowicz *et al.*	(ZEUS Collab.)
LEES	12G	PR D86 032013	J.P. Lees *et al.*	(BABAR Collab.)
AMBROSINO	11A	PL B700 102	F. Ambrosino *et al.*	(KLOE Collab.)
BENAYOUN	10	EPJ C65 211	M. Benayoun *et al.*	
DUBNICKA	10	APS 60 1	S. Dubnicka, A.Z. Dubnickova	
ACHASOV	09A	JETP 109 379	M.N. Achasov *et al.*	(SND Collab.)
		Translated from ZETF 136 442.		
AUBERT	09AS	PRL 103 231801	B. Aubert *et al.*	(BABAR Collab.)
ACHASOV	08	JETP 107 61	M.N. Achasov *et al.*	(SND Collab.)
		Translated from ZETF 134 80.		
FUJIKAWA	08	PR D78 072006	M. Fujikawa *et al.*	(BELLE Collab.)
ACHASOV	07B	PR D76 077101	M.N. Achasov *et al.*	(SND Collab.)
AKHMETSHIN	07	PL B648 28	R.R. Akhmetshin *et al.*	(Novosibirsk CMD-2 Collab.)
ACHASOV	06	JETP 103 380	M.N. Achasov *et al.*	(Novosibirsk SND Collab.)
		Translated from ZETF 130 437.		
ACHASOV	06A	PR D74 014016	M.N. Achasov *et al.*	(SND Collab.)
AULCHENKO	06	JETPL 84 413	V.M. Aulchenko *et al.*	(Novosibirsk CMD-2 Collab.)
		Translated from ZETFP 84 491.		
ACHASOV	05A	JETP 101 1053	M.N. Achasov *et al.*	(Novosibirsk SND Collab.)
		Translated from ZETF 128 1201.		
AKHMETSHIN	05	PL B605 26	R.R. Akhmetshin *et al.*	(Novosibirsk CMD-2 Collab.)
AKHMETSHIN	05A	PL B613 29	R.R. Akhmetshin *et al.*	(Novosibirsk CMD-2 Collab.)
ALOISIO	05	PL B606 12	A. Aloisio *et al.*	(KLOE Collab.)
AULCHENKO	05	JETPL 82 743	V.M. Aulchenko *et al.*	(Novosibirsk CMD-2 Collab.)
		Translated from ZETFP 82 841.		
SCHAEL	05C	PRPL 421 191	S. Schael *et al.*	(ALEPH Collab.)
AKHMETSHIN	04	PL B578 285	R.R. Akhmetshin *et al.*	(Novosibirsk CMD-2 Collab.)
AKHMETSHIN	04B	PL B580 119	R.R. Akhmetshin *et al.*	(Novosibirsk CMD-2 Collab.)
ACHASOV	03	PL B559 171	M.N. Achasov *et al.*	(Novosibirsk SND Collab.)
ACHASOV	03D	PR D68 052006	M.N. Achasov *et al.*	(Novosibirsk SND Collab.)
ALOISIO	03	PL B561 55	A. Aloisio *et al.*	(KLOE Collab.)
SANZ-CILLERO	03	EPJ C27 587	J.J. Sanz-Cillero, A. Pich	
ACHASOV	02	PR D65 032002	M.N. Achasov *et al.*	(Novosibirsk SND Collab.)
ACHASOV	02F	PL B537 201	M.N. Achasov *et al.*	(Novosibirsk SND Collab.)
AKHMETSHIN	02	PL B527 161	R.R. Akhmetshin *et al.*	(Novosibirsk CMD-2 Collab.)
AKHMETSHIN	01B	PL B509 217	R.R. Akhmetshin *et al.*	(Novosibirsk CMD-2 Collab.)
COLANGELO	01	NP B603 125	G. Colangelo, J. Gasser, H. Leytwyler	
PICH	01	PR D63 093005	A. Pich, J. Portoles	
ACHASOV	00	EPJ C12 25	M.N. Achasov *et al.*	(Novosibirsk SND Collab.)
ACHASOV	00D	JETPL 72 282	M.N. Achasov *et al.*	(Novosibirsk SND Collab.)
		Translated from ZETFP 72 411.		
ACHASOV	00G	JETPL 71 355	M.N. Achasov *et al.*	(Novosibirsk SND Collab.)
		Translated from ZETFP 71 519.		
AKHMETSHIN	00	PL B475 190	R.R. Akhmetshin *et al.*	(Novosibirsk CMD-2 Collab.)
ANDERSON	00A	PR D61 112002	S. Anderson *et al.*	(CLEO Collab.)
ABELE	99E	PL B469 270	A. Abele *et al.*	(Crystal Barrel Collab.)
BENAYOUN	98	EPJ C2 269	M. Benayoun *et al.*	(IPNP, NOVO, ADLD+)
BREITWEG	98B	EPJ C2 247	J. Breitweg *et al.*	(ZEUS Collab.)
GARDNER	98	PR D57 2716	S. Gardner, H.B. O'Connell	
Also		PR D62 019903 (errat.)	S. Gardner, H.B. O'Connell	
ABELE	97	PL B391 191	A. Abele *et al.*	(Crystal Barrel Collab.)
ADAMS	97	ZPHY C74 237	M.R. Adams *et al.*	(E665 Collab.)
BARATE	97M	ZPHY C76 15	R. Barate *et al.*	(ALEPH Collab.)
BERTIN	97C	PL B408 476	A. Bertin *et al.*	(OBELIX Collab.)
BOGOLYUB...	97	PAN 60 46	M.Y. Bogolyubsky *et al.*	(MOSU, SERP)
		Translated from YAF 60 53.		
O'CONNELL	97	NP A623 559	H.B. O'Connell *et al.*	(ADLD)
BENAYOUN	96	ZPHY C72 221	M. Benayoun *et al.*	(IPNP, NOVO)
BERNICHA	94	PR D50 4454	A. Bernicha, G. Lopez Castro, J. Pestieau	(LOUV+)
WEIDENAUER	93	ZPHY C59 387	P. Weidenauer *et al.*	(ASTERIX Collab.)
AGUILAR-...	91	ZPHY C50 405	M. Aguilar-Benitez *et al.*	(LEBC-EHS Collab.)
DOLINSKY	91	PRPL 202 99	S.I. Dolinsky *et al.*	(NOVO)
KUHN	90	ZPHY C48 445	J.H. Kuhn *et al.*	(MPIM)
ANTIPOV	89	ZPHY C42 185	Y.M. Antipov *et al.*	(SERP, JINR, BGNA+)
BISELLO	89	PL B220 321	D. Bisello *et al.*	(DM2 Collab.)
DOLINSKY	89	ZPHY C42 511	S.I. Dolinsky *et al.*	(NOVO)
DUBNICKA	89	JP G15 1349	S. Dubnicka *et al.*	(JINR, SLOV)
GESHKEN...	89	ZPHY C45 351	B.V. Geshkenbein	(ITEP)
KURDADZE	88	JETPL 47 512	L.M. Kurdadze *et al.*	(NOVO)
		Translated from ZETFP 47 432.		
VASSERMAN	88	SJNP 47 1035	I.B. Vasserman *et al.*	(NOVO)
		Translated from YAF 47 1635.		
VASSERMAN	88B	SJNP 48 480	I.B. Vasserman *et al.*	(NOVO)
		Translated from YAF 48 753.		
AULCHENKO	87C	IYF 87-90 Preprint	V.M. Aulchenko *et al.*	(NOVO)
CAPRARO	87	NP B288 659	L. Capraro *et al.*	(CLER, FRAS, MILA+)
BRAMON	86	PL B173 97	A. Bramon, J. Casulleras	(BARC)
HUSTON	86	PR D33 3199	J. Huston *et al.*	(ROCH, FNAL, MINN)
KURDADZE	86	JETPL 43 643	L.M. Kurdadze *et al.*	(NOVO)
		Translated from ZETFP 43 497.		
BARKOV	85	NP B256 365	L.M. Barkov *et al.*	(NOVO)
DRUZHININ	84	PL 144B 136	V.P. Druzhinin *et al.*	(NOVO)
CHABAUD	83	NP B223 1	V. Chabaud *et al.*	(CERN, CRAC, MPIM)
JENSEN	83	PR D27 26	T. Jensen *et al.*	(ROCH, FNAL, MINN)
HEYN	81	ZPHY C7 169	M.F. Heyn, C.B. Lang	(GRAZ)
BOHACIK	80	PR D21 1342	J. Bohacik, H. Kuhnelt	(SLOV, WIEN)
LANG	79	PR D19 956	C.B. Lang, A. Mas-Parareda	(GRAZ)
BARTALUCCI	78	NC 44A 587	S. Bartalucci *et al.*	(DESY, FRAS)
WICKLUND	78	PR D17 1197	A.B. Wicklund *et al.*	(ANL)
ANDREWS	77	PRL 38 198	D.E. Andrews *et al.*	(ROCH)
DEUTSCH...	76	NP B103 426	M. Deutschmann *et al.*	(AACH3, BERL, BONN+)
ENGLER	74	PR D10 2070	A. Engler *et al.*	(CMU, CASE)
ESTABROOKS	74	NP B79 301	P.G. Estabrooks, A.D. Martin	(DURH)
GRAYER	74	NP B75 189	G. Grayer *et al.*	(CERN, MPIM)
BYERLY	73	PR D7 637	W.L. Byerly *et al.*	(MICH)
GLADDING	73	PR D8 3721	G.E. Gladding *et al.*	(HARV)
HYAMS	73	NP B64 134	B.D. Hyams *et al.*	(CERN, MPIM)
PROTOPOP...	73	PR D7 1279	S.D. Protopopescu *et al.*	(LBL)
BALLAM	72	PR D5 545	J. Ballam *et al.*	(SLAC, LBL, TUFTS)
BENAKSAS	72	PL 39B 289	D. Benaksas *et al.*	(ORSAY)
JACOBS	72	PR D6 1291	L.D. Jacobs	(SACL)
RATCLIFF	72	PL 38B 345	B.N. Ratcliff *et al.*	(SLAC)
ABRAMS	71	PR D4 653	G.S. Abrams *et al.*	(LBL)
ALVENSLEB...	70	PRL 24 786	H. Alvensleben *et al.*	(DESY)
BIGGS	70	PRL 24 1197	P.J. Biggs *et al.*	(DARE)
ERBE	69	PR 188 2060	R. Erbe *et al.*	(German Bubble Chamber Collab.)
MALAMUD	69	Argonne Conf. 93	E.I. Malamud, P.E. Schlein	(UCLA)
REYNOLDS	69	PR 184 1424	B.G. Reynolds *et al.*	(FSU)
ROTHWELL	69	PRL 23 1521	P.L. Rothwell *et al.*	(NEAS)
WEHMANN	69	PR 178 2095	A.A. Wehmann *et al.*	(HARV, CASE, SLAC+)
ARMENISE	68	NC 54A 999	N. Armenise *et al.*	(BARI, BGNA, FIRZ+)
BATON	68	PR 176 1574	J.P. Baton, G. Laurens	(SACL)
CHUNG	68	PR 165 1491	S.U. Chung *et al.*	(LRL)
FOSTER	68	NP B6 107	M. Foster *et al.*	(CERN, CDEF)
GOUNARIS	68	PRL 21 244	G.J. Gounaris, J.J. Sakurai	
HUSON	68	PL 28B 208	R. Huson *et al.*	(ORSAY, MILA, UCLA)
HYAMS	68	NP B7 1	B.D. Hyams *et al.*	(CERN, MPIM)
LANZEROTTI	68	PR 166 1365	L.J. Lanzerotti *et al.*	(HARV)
PISUT	68	NP B6 325	J. Pisut, M. Roos	(CERN)
ASBURY	67B	PRL 19 865	J.G. Asbury *et al.*	(DESY, COLU)
BACON	67	PR 157 1263	T.C. Bacon *et al.*	(BNL)
EISNER	67	PR 164 1699	R.L. Eisner *et al.*	(PURD)
HUWE	67	PL 24B 252	D.O. Huwe *et al.*	(COLU)
HYAMS	67	PL 24B 634	B.D. Hyams *et al.*	(CERN, MPIM)
MILLER	67B	PR 153 1423	D.H. Miller *et al.*	(PURD)
ALFF-...	66	PR 145 1072	C. Alff-Steinberger *et al.*	(COLU, RUTG)
FERBEL	66	PL 21 111	T. Ferbel	(ROCH)
HAGOPIAN	66	PR 145 1128	V. Hagopian *et al.*	(PENN, SACL)
HAGOPIAN	66B	PR 152 1183	V. Hagopian, Y.L. Pan	(PENN, LRL)

JACOBS	66B	UCRL 16877	L.D. Jacobs	(LRL)
JAMES	66	PR 142 896	F.E. James, H.L. Kraybill	(YALE, BNL)
ROSS	66	PR 149 1172	M. Ross, L. Stodolsky	
SOEDING	66	PL B19 702	P. Soeding	
WEST	66	PR 149 1089	E. West *et al.*	(WISC)
BLIEDEN	65	PL 19 444	H.R. Blieden *et al.*	(CERN MMS Collab.)
CARMONY	64	PRL 12 254	D.D. Carmony *et al.*	(UCB)
GOLDHABER	64	PRL 12 336	G. Goldhaber *et al.*	(LRL, UCB)
ABOLINS	63	PRL 11 381	M.A. Abolins *et al.*	(UCSD)

$\omega(782)$

$I^G(J^{PC}) = 0^-(1^{--})$

$\omega(782)$ MASS

VALUE (MeV)	EVTS	DOCUMENT ID		TECN	COMMENT
782.65±0.12 OUR AVERAGE		Error includes scale factor of 1.9.			See the ideogram below.
783.20±0.13±0.16	18680	AKHMETSHIN	05	CMD2	0.60-1.38 $e^+e^- \to \pi^0\gamma$
782.68±0.09±0.04	11200	[1] AKHMETSHIN	04	CMD2	$e^+e^- \to \pi^+\pi^-\pi^0$
782.79±0.08±0.09	1.2M	[2] ACHASOV	03D	RVUE	0.44–2.00 $e^+e^- \to \pi^+\pi^-\pi^0$
782.7 ±0.1 ±1.5	19500	WURZINGER	95	SPEC	1.33 $pd \to {}^3\mathrm{He}\omega$
781.96±0.17±0.80	11k	[3] AMSLER	94C	CBAR	0.0 $\overline{p}p \to \omega\eta\pi^0$
782.08±0.36±0.82	3463	[4] AMSLER	94C	CBAR	0.0 $\overline{p}p \to \omega\eta\pi^0$
781.96±0.13±0.17	15k	AMSLER	93B	CBAR	0.0 $\overline{p}p \to \omega\pi^0\pi^0$
782.4 ±0.2	270k	WEIDENAUER	93	ASTE	$\overline{p}p \to 2\pi^+2\pi^-\pi^0$
782.2 ±0.4	1488	KURDADZE	83B	OLYA	$e^+e^- \to \pi^+\pi^-\pi^0$
782.4 ±0.5	7000	[5] KEYNE	76	CNTR	$\pi^-p \to \omega n$
• • • We do not use the following data for averages, fits, limits, etc. • • •					
781.91±0.24		[6] LEES	12G	BABR	$e^+e^- \to \pi^+\pi^-\gamma$
781.78±0.10		[7] BARKOV	87	CMD	$e^+e^- \to \pi^+\pi^-\pi^0$
783.3 ±0.4	433	CORDIER	80	DM1	$e^+e^- \to \pi^+\pi^-\pi^0$
782.5 ±0.8	33260	ROOS	80	RVUE	0.0–3.6 $\overline{p}p$
782.6 ±0.8	3000	BENKHEIRI	79	OMEG	9–12 $\pi^\pm p$
781.8 ±0.6	1430	COOPER	78B	HBC	0.7–0.8 $\overline{p}p \to 5\pi$
782.7 ±0.9	535	VANAPEL...	78	HBC	7.2 $\overline{p}p \to \overline{p}p\omega$
783.5 ±0.8	2100	GESSAROLI	77	HBC	11 $\pi^-p \to \omega n$
782.5 ±0.8	418	AGUILAR-...	72B	HBC	3.9,4.6 K^-p
783.4 ±1.0	248	BIZZARRI	71	HBC	0.0 $p\overline{p} \to K^+K^-\omega$
781.0 ±0.6	510	BIZZARRI	71	HBC	0.0 $p\overline{p} \to K_1K_1\omega$
783.7 ±1.0	3583	[8] COYNE	71	HBC	3.7 $\pi^+p \to p\pi^+\pi^+\pi^-\pi^0$
784.1 ±1.2	750	ABRAMOVI...	70	HBC	3.9 π^-p
783.2 ±1.6		[9] BIGGS	70B	CNTR	$<4.1\ \gamma C \to \pi^+\pi^-C$
782.4 ±0.5	2400	BIZZARRI	69	HBC	0.0 $\overline{p}p$

[1] Update of AKHMETSHIN 00C.
[2] From the combined fit of ANTONELLI 92, ACHASOV 01E, ACHASOV 02E, and ACHASOV 03D data on the $\pi^+\pi^-\pi^0$ and ANTONELLI 92 on the $\omega\pi^+\pi^-$ final states. Supersedes ACHASOV 99E and ACHASOV 02E.
[3] From the $\eta \to \gamma\gamma$ decay.
[4] From the $\eta \to 3\pi^0$ decay.
[5] Observed by threshold-crossing technique. Mass resolution = 4.8 MeV FWHM.
[6] From the $\rho-\omega$ interference in the $\pi^+\pi^-$ mass spectrum using the Breit-Wigner for the ω and leaving its mass and width as free parameters of the fit.
[7] Systematic uncertainties underestimated.
[8] From best-resolution sample of COYNE 71.
[9] From ω-ρ interference in the $\pi^+\pi^-$ mass spectrum assuming ω width 12.6 MeV.

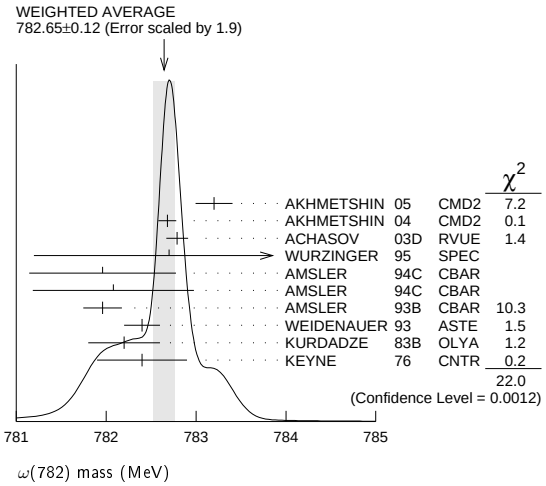

$\omega(782)$ WIDTH

VALUE (MeV)	EVTS	DOCUMENT ID		TECN	COMMENT
8.49±0.08 OUR AVERAGE					
8.68±0.23±0.10	11200	[1] AKHMETSHIN	04	CMD2	$e^+e^- \to \pi^+\pi^-\pi^0$
8.68±0.04±0.15	1.2M	[2] ACHASOV	03D	RVUE	0.44–2.00 $e^+e^- \to \pi^+\pi^-\pi^0$
8.2 ±0.3	19500	WURZINGER	95	SPEC	1.33 $pd \to {}^3\mathrm{He}\omega$
8.4 ±0.1		[3] AULCHENKO	87	ND	$e^+e^- \to \pi^+\pi^-\pi^0$
8.30±0.40		BARKOV	87	CMD	$e^+e^- \to \pi^+\pi^-\pi^0$
9.8 ±0.9	1488	KURDADZE	83B	OLYA	$e^+e^- \to \pi^+\pi^-\pi^0$
9.0 ±0.8	433	CORDIER	80	DM1	$e^+e^- \to \pi^+\pi^-\pi^0$
9.1 ±0.8	451	BENAKSAS	72B	OSPK	$e^+e^- \to \pi^+\pi^-\pi^0$
• • • We do not use the following data for averages, fits, limits, etc. • • •					
8.13±0.45		[4] LEES	12G	BABR	$e^+e^- \to \pi^+\pi^-\gamma$
12 ±2	1430	COOPER	78B	HBC	0.7–0.8 $\overline{p}p \to 5\pi$
9.4 ±2.5	2100	GESSAROLI	77	HBC	11 $\pi^-p \to \omega n$
10.22±0.43	20000	[5] KEYNE	76	CNTR	$\pi^-p \to \omega n$
13.3 ±2	418	AGUILAR-...	72B	HBC	3.9,4.6 K^-p
10.5 ±1.5		BORENSTEIN	72	HBC	2.18 K^-p
7.70±0.9 ±1.15	940	BROWN	72	MMS	2.5 $\pi^-p \to n\mathrm{MM}$
10.3 ±1.4	510	BIZZARRI	71	HBC	0.0 $p\overline{p} \to K_1K_1\omega$
12.8 ±3.0	248	BIZZARRI	71	HBC	0.0 $p\overline{p} \to K^+K^-\omega$
9.5 ±1.0	3583	COYNE	71	HBC	3.7 $\pi^+p \to p\pi^+\pi^+\pi^-\pi^0$

[1] Update of AKHMETSHIN 00C.
[2] From the combined fit of ANTONELLI 92, ACHASOV 01E, ACHASOV 02E, and ACHASOV 03D data on the $\pi^+\pi^-\pi^0$ and ANTONELLI 92 on the $\omega\pi^+\pi^-$ final states. Supersedes ACHASOV 99E and ACHASOV 02E.
[3] Relativistic Breit-Wigner includes radiative corrections.
[4] From the $\rho-\omega$ interference in the $\pi^+\pi^-$ mass spectrum using the Breit-Wigner for the ω and leaving its mass and width as free parameters of the fit.
[5] Observed by threshold-crossing technique. Mass resolution = 4.8 MeV FWHM.

$\omega(782)$ DECAY MODES

	Mode	Fraction (Γ_i/Γ)	Scale factor/ Confidence level
Γ_1	$\pi^+\pi^-\pi^0$	(89.2 ±0.7) %	
Γ_2	$\pi^0\gamma$	(8.40±0.22) %	S=1.8
Γ_3	$\pi^+\pi^-$	($1.53^{+0.11}_{-0.13}$) %	S=1.2
Γ_4	neutrals (excluding $\pi^0\gamma$)	($7\ ^{+7}_{-4}$) $\times 10^{-3}$	S=1.1
Γ_5	$\eta\gamma$	(4.5 ±0.4) $\times 10^{-4}$	S=1.1
Γ_6	$\pi^0e^+e^-$	(7.7 ±0.6) $\times 10^{-4}$	
Γ_7	$\pi^0\mu^+\mu^-$	(1.34±0.18) $\times 10^{-4}$	S=1.5
Γ_8	ηe^+e^-		
Γ_9	e^+e^-	(7.36±0.15) $\times 10^{-5}$	S=1.5
Γ_{10}	$\pi^+\pi^-\pi^0\pi^0$	< 2 $\times 10^{-4}$	CL=90%
Γ_{11}	$\pi^+\pi^-\gamma$	< 3.6 $\times 10^{-3}$	CL=95%
Γ_{12}	$\pi^+\pi^-\pi^+\pi^-$	< 1 $\times 10^{-3}$	CL=90%
Γ_{13}	$\pi^0\pi^0\gamma$	(6.7 ±1.1) $\times 10^{-5}$	
Γ_{14}	$\eta\pi^0\gamma$	< 3.3 $\times 10^{-5}$	CL=90%
Γ_{15}	$\mu^+\mu^-$	(7.4 ±1.8) $\times 10^{-5}$	
Γ_{16}	3γ	< 1.9 $\times 10^{-4}$	CL=95%
	Charge conjugation (C) violating modes		
Γ_{17}	$\eta\pi^0$ C	< 2.2 $\times 10^{-4}$	CL=90%
Γ_{18}	$2\pi^0$ C	< 2.2 $\times 10^{-4}$	CL=90%
Γ_{19}	$3\pi^0$ C	< 2.3 $\times 10^{-4}$	CL=90%

CONSTRAINED FIT INFORMATION

An overall fit to 15 branching ratios uses 54 measurements and one constraint to determine 10 parameters. The overall fit has a $\chi^2 = 57.0$ for 45 degrees of freedom.

The following *off-diagonal* array elements are the correlation coefficients $\langle \delta x_i \delta x_j \rangle / (\delta x_i \cdot \delta x_j)$, in percent, from the fit to the branching fractions, $x_i \equiv \Gamma_i/\Gamma_{\mathrm{total}}$. The fit constrains the x_i whose labels appear in this array to sum to one.

	x_1	x_2	x_3	x_4	x_5	x_6	x_7	x_9	x_{13}
x_2	29								
x_3	−18	−5							
x_4	−94	−55	1						
x_5	7	16	−1	−12					
x_6	−1	0	0	0	0				
x_7	0	0	0	0	0	0			
x_9	−36	−70	6	52	−22	0	0		
x_{13}	1	3	0	−2	0	0	0	−2	
x_{15}	0	0	0	0	0	0	0	0	0

$\omega(782)$ PARTIAL WIDTHS

$\Gamma(\pi^0\gamma)$ Γ_2

VALUE (keV)	EVTS	DOCUMENT ID		TECN	COMMENT
• • • We do not use the following data for averages, fits, limits, etc. • • •					
880±50	7815	[1] ACHASOV	13	SND	1.05–2.00 $e^+e^- \to \pi^0\pi^0\gamma$
788±12±27	36500	[2] ACHASOV	03	SND	0.60–0.97 $e^+e^- \to \pi^0\gamma$
764±51	10625	DOLINSKY	89	ND	$e^+e^- \to \pi^0\gamma$

[1] Systematic uncertainty not estimated.
[2] Using Γ_ω = 8.44 ± 0.09 MeV and B($\omega \to \pi^0\gamma$) from ACHASOV 03.

$\Gamma(\eta\gamma)$ Γ_5

VALUE (keV)	DOCUMENT ID		TECN	COMMENT
• • • We do not use the following data for averages, fits, limits, etc. • • •				
6.1±2.5	[1] DOLINSKY	89	ND	$e^+e^- \to \eta\gamma$

[1] Using Γ_ω = 8.4 ± 0.1 MeV and B($\omega \to \eta\gamma$) from DOLINSKY 89.

$\Gamma(e^+e^-)$ Γ_9

VALUE (keV)	EVTS	DOCUMENT ID		TECN	COMMENT
0.60 ±0.02 OUR EVALUATION					
• • • We do not use the following data for averages, fits, limits, etc. • • •					
0.591±0.015	11200	[1,2] AKHMETSHIN	04	CMD2	$e^+e^- \to \pi^+\pi^-\pi^0$
0.653±0.003±0.021	1.2M	[3] ACHASOV	03D	RVUE	0.44–2.00 $e^+e^- \to \pi^+\pi^-\pi^0$
0.600±0.031	10625	DOLINSKY	89	ND	$e^+e^- \to \pi^0\gamma$

[1] Using B($\omega \to \pi^+\pi^-\pi^0$) = 0.891 ± 0.007 and Γ_{total} = 8.44 ± 0.09 MeV.
[2] Update of AKHMETSHIN 00C.
[3] Using ACHASOV 03, ACHASOV 03D and B($\omega \to \pi^+\pi^-$) = (1.70 ± 0.28)%.

$\omega(782)$ $\Gamma(e^+e^-)\Gamma(i)/\Gamma^2(total)$

$\Gamma(e^+e^-)/\Gamma_{total} \times \Gamma(\pi^+\pi^-\pi^0)/\Gamma_{total}$ $\Gamma_9/\Gamma \times \Gamma_1/\Gamma$

VALUE (units 10^{-5})	EVTS	DOCUMENT ID		TECN	COMMENT
6.56±0.12 OUR FIT Error includes scale factor of 1.6.					
6.38±0.10 OUR AVERAGE Error includes scale factor of 1.1.					
6.24±0.11±0.08	11.2k	[1] AKHMETSHIN	04	CMD2	$e^+e^- \to \pi^+\pi^-\pi^0$
6.70±0.06±0.27		AUBERT,B	04N	BABR	10.6 $e^+e^- \to \pi^+\pi^-\pi^0\gamma$
6.74±0.04±0.24	1.2M	[2,3] ACHASOV	03D	RVUE	0.44–2.00 $e^+e^- \to \pi^+\pi^-\pi^0$
6.37±0.35		[2] DOLINSKY	89	ND	$e^+e^- \to \pi^+\pi^-\pi^0$
6.45±0.24		[2] BARKOV	87	CMD	$e^+e^- \to \pi^+\pi^-\pi^0$
5.79±0.42	1488	[2] KURDADZE	83B	OLYA	$e^+e^- \to \pi^+\pi^-\pi^0$
5.89±0.54	433	[2] CORDIER	80	DM1	$e^+e^- \to \pi^+\pi^-\pi^0$
7.54±0.84	451	[2] BENAKSAS	72B	OSPK	$e^+e^- \to \pi^+\pi^-\pi^0$
• • • We do not use the following data for averages, fits, limits, etc. • • •					
6.20±0.13		[4] BENAYOUN	10	RVUE	0.4–1.05 e^+e^-

[1] Update of AKHMETSHIN 00C.
[2] Recalculated by us from the cross section in the peak.
[3] From the combined fit of ANTONELLI 92, ACHASOV 01E, ACHASOV 02E, and ACHASOV 03D data on the $\pi^+\pi^-\pi^0$ and ANTONELLI 92 on the $\omega\pi^+\pi^-$ final states. Supersedes ACHASOV 99E and ACHASOV 02E.
[4] A simultaneous fit of $e^+e^- \to \pi^+\pi^-$, $\pi^+\pi^-\pi^0$, $\pi^0\gamma$, $\eta\gamma$ data.

$\Gamma(e^+e^-)/\Gamma_{total} \times \Gamma(\pi^0\gamma)/\Gamma_{total}$ $\Gamma_9/\Gamma \times \Gamma_2/\Gamma$

VALUE (units 10^{-6})	EVTS	DOCUMENT ID		TECN	COMMENT
6.18 ±0.11 OUR FIT Error includes scale factor of 1.6.					
6.37 ±0.09 OUR AVERAGE					
6.336±0.056±0.089		[1] ACHASOV	16A	SND	0.60–1.38 $e^+e^- \to \pi^0\gamma$
6.47 ±0.14 ±0.39	18k	AKHMETSHIN	05	CMD2	0.60–1.38 $e^+e^- \to \pi^0\gamma$
6.50 ±0.11 ±0.20	36k	[2] ACHASOV	03	SND	0.60–0.97 $e^+e^- \to \pi^0\gamma$
6.34 ±0.21 ±0.21	10k	[3] DOLINSKY	89	ND	$e^+e^- \to \pi^0\gamma$
• • • We do not use the following data for averages, fits, limits, etc. • • •					
6.80 ±0.13		[4] BENAYOUN	10	RVUE	0.4–1.05 e^+e^-

[1] From the VMD model with the interfering $\rho(770)$, $\omega(782)$, $\phi(1020)$, and an additional resonance describing the total contribution of the $\rho(1450)$ and $\omega(1420)$ states. Supersedes ACHASOV 03.
[2] Using $\sigma_{\phi \to \pi^0\gamma}$ from ACHASOV 00 and m_ω= 782.57 MeV in the model with the energy-independent phase of ρ-ω interference equal to $(-10.2 \pm 7.0)^\circ$.
[3] Recalculated by us from the cross section in the peak.
[4] A simultaneous fit of $e^+e^- \to \pi^+\pi^-$, $\pi^+\pi^-\pi^0$, $\pi^0\gamma$, $\eta\gamma$ data.

$\Gamma(e^+e^-)/\Gamma_{total} \times \Gamma(\pi^+\pi^-)/\Gamma_{total}$ $\Gamma_9/\Gamma \times \Gamma_3/\Gamma$

VALUE (units 10^{-6})	EVTS	DOCUMENT ID		TECN	COMMENT
1.225±0.058±0.041	800k	[1] ACHASOV	06	SND	$e^+e^- \to \pi^+\pi^-$
• • • We do not use the following data for averages, fits, limits, etc. • • •					
1.166±0.036		[2] BENAYOUN	13	RVUE	0.4–1.05 e^+e^-
1.05 ±0.08		[3] DAVIER	13	RVUE	$e^+e^- \to \pi^+\pi^-(\gamma)$

[1] Supersedes ACHASOV 05A.
[2] A simultaneous fit to $e^+e^- \to \pi^+\pi^-$, $\pi^+\pi^-\pi^0$, $\pi^0\gamma$, $\eta\gamma$, $K\overline{K}$, and $\tau^- \to \pi^-\pi^0\nu_\tau$ data. Supersedes BENAYOUN 10.
[3] From $e^+e^- \to \pi^+\pi^-(\gamma)$ data of LEES 12G.

$\Gamma(e^+e^-)/\Gamma_{total} \times \Gamma(\eta\gamma)/\Gamma_{total}$ $\Gamma_9/\Gamma \times \Gamma_5/\Gamma$

VALUE (units 10^{-8})	EVTS	DOCUMENT ID		TECN	COMMENT
3.32±0.28 OUR FIT Error includes scale factor of 1.1.					
3.18±0.28 OUR AVERAGE					
3.10±0.31±0.11	33k	[1] ACHASOV	07B	SND	0.6–1.38 $e^+e^- \to \eta\gamma$
$3.17^{+1.85}_{-1.31}$±0.21	17.4k	[2] AKHMETSHIN	05	CMD2	0.60–1.38 $e^+e^- \to \eta\gamma$
3.41±0.52±0.21	23k	[3,4] AKHMETSHIN	01B	CMD2	$e^+e^- \to \eta\gamma$
• • • We do not use the following data for averages, fits, limits, etc. • • •					
4.50±0.10		[5] BENAYOUN	10	RVUE	0.4–1.05 e^+e^-

[1] From a combined fit of $\sigma(e^+e^- \to \eta\gamma)$ with $\eta \to 3\pi^0$ and $\eta \to \pi^+\pi^-\pi^0$, and fixing B($\eta \to 3\pi^0$) / B($\eta \to \pi^+\pi^-\pi^0$) = 1.44 ± 0.04. Recalculated by us from the cross section at the peak. Supersedes ACHASOV 00D and ACHASOV 06A.
[2] From the $\eta \to 2\gamma$ decay and using B($\eta \to \gamma\gamma$)= 39.43 ± 0.26%.
[3] From the $\eta \to 3\pi^0$ decay and using B($\eta \to 3\pi^0$)= (32.24 ± 0.29) × 10^{-2}.
[4] The combined fit from 600 to 1380 MeV taking into account $\rho(770)$, $\omega(782)$, $\phi(1020)$, and $\rho(1450)$ (mass and width fixed at 1450 MeV and 310 MeV respectively).
[5] A simultaneous fit of $e^+e^- \to \pi^+\pi^-$, $\pi^+\pi^-\pi^0$, $\pi^0\gamma$, $\eta\gamma$ data.

$\Gamma(e^+e^-)/\Gamma_{total} \times \Gamma(\mu^+\mu^-)/\Gamma_{total}$ $\Gamma_9/\Gamma \times \Gamma_{15}/\Gamma$

VALUE (units 10^{-9})	EVTS	DOCUMENT ID		TECN	COMMENT
4.3±1.8±2.2	4.5 M	[1] ANASTASI	17	KLOE	$e^+e^- \to \mu^+\mu^-\gamma$

[1] From a fit of the real part of the vacuum polarization by a sum of the leptonic and hadronic contributions, where the hadronic contribution is parametrized as a sum of Breit-Wigner resonances $\omega(782)$, $\phi(1020)$ and using a GOUNARIS 68 parametrization for the $\rho(770)$, and a non-resonant term.

$\omega(782)$ BRANCHING RATIOS

$\Gamma(\pi^+\pi^-\pi^0)/\Gamma_{total}$ Γ_1/Γ

NIECKNIG 12 describes final-state interactions between the three pions in a dispersive framework using data on the $\pi\pi$ P-wave scattering phase shift.

VALUE	EVTS	DOCUMENT ID		TECN	COMMENT
• • • We do not use the following data for averages, fits, limits, etc. • • •					
0.9024±0.0019		[1] AMBROSINO	08G	KLOE	1.0–1.03 $e^+e^- \to \pi^+\pi^-2\pi^0$, $2\pi^0\gamma$
0.8965±0.0016±0.0048	1.2M	[2,3] ACHASOV	03D	RVUE	0.44–2.00 $e^+e^- \to \pi^+\pi^-\pi^0$
0.880 ±0.020 ±0.032	11200	[3,4] AKHMETSHIN	00C	CMD2	$e^+e^- \to \pi^+\pi^-\pi^0$
0.8942±0.0062		[3] DOLINSKY	89	ND	$e^+e^- \to \pi^+\pi^-\pi^0$

[1] Not independent of $\Gamma(\pi^0\gamma)$ / $\Gamma(\pi^+\pi^-\pi^0)$ from AMBROSINO 08G.
[2] Using ACHASOV 03, ACHASOV 03D and B($\omega \to \pi^+\pi^-$) = (1.70 ± 0.28)%.
[3] Not independent of the corresponding $\Gamma(e^+e^-) \times \Gamma(\pi^+\pi^-\pi^0)/\Gamma^2_{total}$.
[4] Using $\Gamma(e^+e^-)$=0.60 ± 0.02 keV.

$\Gamma(\pi^0\gamma)/\Gamma_{total}$ Γ_2/Γ

VALUE (units 10^{-2})	EVTS	DOCUMENT ID		TECN	COMMENT
• • • We do not use the following data for averages, fits, limits, etc. • • •					
8.88±0.18		[1] ACHASOV	16A	SND	0.60–1.38 $e^+e^- \to \pi^0\gamma$
8.09±0.14		[2] AMBROSINO	08G	KLOE	$e^+e^- \to \pi^+\pi^-2\pi^0$, $2\pi^0\gamma$
9.06±0.20±0.57	18k	[3,4] AKHMETSHIN	05	CMD2	0.60–1.38 $e^+e^- \to \pi^0\gamma$
9.34±0.15±0.31	36k	[4] ACHASOV	03	SND	0.60–0.97 $e^+e^- \to \pi^0\gamma$
8.65±0.16±0.42	1.2M	[5,6] ACHASOV	03D	RVUE	0.44–2.00 $e^+e^- \to \pi^+\pi^-\pi^0$
8.39±0.24	9k	[7] BENAYOUN	96	RVUE	$e^+e^- \to \pi^0\gamma$
8.88±0.62	10k	[4] DOLINSKY	89	ND	$e^+e^- \to \pi^0\gamma$

[1] Using B($\omega \to e^+e^-$) from PDG 15. Supersedes ACHASOV 03.
[2] Not independent of $\Gamma(\pi^0\gamma)$ / $\Gamma(\pi^+\pi^-\pi^0)$ from AMBROSINO 08G.
[3] Using B($\omega \to e^+e^-$)= (7.14 ± 0.13) × 10^{-5}.
[4] Not independent of the corresponding $\Gamma(e^+e^-) \times \Gamma(\pi^0\gamma)/\Gamma^2_{total}$.
[5] Using ACHASOV 03, ACHASOV 03D and B($\omega \to \pi^+\pi^-$) = (1.70 ± 0.28)%.
[6] Not independent of the corresponding $\Gamma(e^+e^-) \times \Gamma(\pi^+\pi^-\pi^0)/\Gamma^2_{total}$.
[7] Reanalysis of DRUZHININ 84, DOLINSKY 89, DOLINSKY 91 taking into account the triangle anomaly contributions.

$\Gamma(\pi^0\gamma)/\Gamma(\pi^+\pi^-\pi^0)$ Γ_2/Γ_1

VALUE (units 10^{-2})	DOCUMENT ID		TECN	COMMENT
9.41±0.23 OUR FIT Error includes scale factor of 2.0.				
9.05±0.27 OUR AVERAGE Error includes scale factor of 1.8.				
8.97±0.16	AMBROSINO	08G	KLOE	$e^+e^- \to \pi^+\pi^-2\pi^0$, $2\pi^0\gamma$
9.94±0.36±0.38	[1] AULCHENKO	00A	SND	$e^+e^- \to \pi^+\pi^-2\pi^0$, $2\pi^0\gamma$
8.4 ±1.3	KEYNE	76	CNTR	$\pi^-p \to \omega n$
10.9 ±2.5	BENAKSAS	72C	OSPK	$e^+e^- \to \pi^0\gamma$
8.1 ±2.0	BALDIN	71	HLBC	2.9 π^+p
13 ±4	JACQUET	69B	HLBC	2.05 $\pi^+p \to \pi^+p\omega$
• • • We do not use the following data for averages, fits, limits, etc. • • •				
9.7 ±0.2 ±0.5	[2,3] ACHASOV	03D	RVUE	0.44–2.00 $e^+e^- \to \pi^+\pi^-\pi^0$
9.9 ±0.7	[2] DOLINSKY	89	ND	$e^+e^- \to \pi^0\gamma$

[1] From $\sigma^{\omega\pi^0}_0 \to \pi^0\pi^0\gamma(m_\phi)/\sigma^{\omega\pi^0}_0 \to \pi^+\pi^-\pi^0\pi^0(m_\phi)$ with a phase-space correction factor of 1/1.023.
[2] Not independent of the corresponding $\Gamma(e^+e^-) \times \Gamma(\pi^0\gamma)/\Gamma^2_{total}$.
[3] Using ACHASOV 03. Based on 1.2M events.

$\Gamma(\pi^+\pi^-)/\Gamma_{total}$ Γ_3/Γ

See also $\Gamma(\pi^+\pi^-)/\Gamma(\pi^+\pi^-\pi^0)$.

VALUE (units 10^{-2})	EVTS	DOCUMENT ID		TECN	COMMENT
$1.53^{+0.11}_{-0.13}$ OUR FIT		Error includes scale factor of 1.2.			
1.49±0.13 OUR AVERAGE		Error includes scale factor of 1.3. See the ideogram below.			
1.46±0.12±0.02	900k	[1] AKHMETSHIN	07		$e^+e^- \to \pi^+\pi^-$
1.30±0.24±0.05	11.2k	[2] AKHMETSHIN	04	CMD2	$e^+e^- \to \pi^+\pi^-$
$2.38^{+1.77}_{-0.90}$±0.18	5.4k	[3] ACHASOV	02E	SND	1.1–1.38 $e^+e^- \to \pi^+\pi^-\pi^0$
2.3 ±0.5		BARKOV	85	OLYA	$e^+e^- \to \pi^+\pi^-$
$1.6^{+0.9}_{-0.7}$		QUENZER	78	DM1	$e^+e^- \to \pi^+\pi^-$
3.6 ±1.9		BENAKSAS	72	OSPK	$e^+e^- \to \pi^+\pi^-$
• • • We do not use the following data for averages, fits, limits, etc. • • •					
1.75±0.11	4.5M	[4] ACHASOV	05A	SND	$e^+e^- \to \pi^+\pi^-$
2.01±0.29		[5] BENAYOUN	03	RVUE	$e^+e^- \to \pi^+\pi^-$
1.9 ±0.3		[6] GARDNER	99	RVUE	$e^+e^- \to \pi^+\pi^-$
2.3 ±0.4		[7] BENAYOUN	98	RVUE	$e^+e^- \to \pi^+\pi^-, \mu^+\mu^-$
1.0 ±0.11		[8] WICKLUND	78	ASPK	3,4,6 $\pi^\pm N$
1.22±0.30		ALVENSLEB...	71C	CNTR	Photoproduction
$1.3^{+1.2}_{-0.9}$		MOFFEIT	71	HBC	2.8,4.7 γp
$0.80^{+0.28}_{-0.20}$		[9] BIGGS	70B	CNTR	4.2 γC $\to \pi^+\pi^-$ C

[1] A combined fit of AKHMETSHIN 07, AULCHENKO 06, and AULCHENKO 05.
[2] Update of AKHMETSHIN 02.
[3] From the $m_{\pi^+\pi^-}$ spectrum taking into account the interference of the $\rho\pi$ and $\omega\pi$ amplitudes.
[4] Using $\Gamma(\omega \to e^+e^-)$ from the 2004 Edition of this Review (PDG 04).
[5] Using the data of AKHMETSHIN 02 in the hidden local symmetry model.
[6] Using the data of BARKOV 85.
[7] Using the data of BARKOV 85 in the hidden local symmetry model.
[8] From a model-dependent analysis assuming complete coherence.
[9] Re-evaluated under $\Gamma(\pi^+\pi^-)/\Gamma(\pi^+\pi^-\pi^0)$ by BEHREND 71 using more accurate $\omega \to \rho$ photoproduction cross-section ratio.

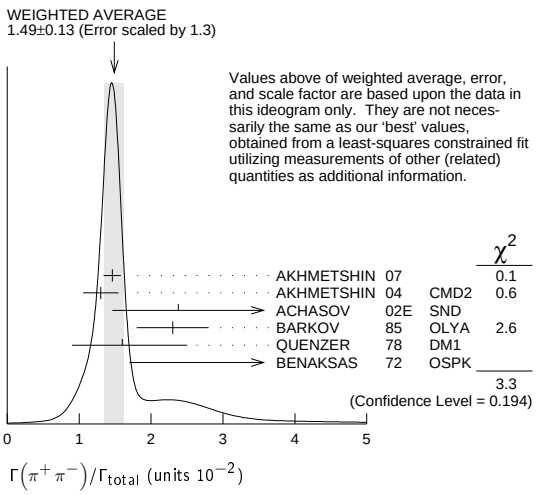

$\Gamma(\pi^+\pi^-)/\Gamma(\pi^+\pi^-\pi^0)$ Γ_3/Γ_1

See also $\Gamma(\pi^+\pi^-)/\Gamma_{total}$.

VALUE	DOCUMENT ID		TECN	COMMENT
0.0172±0.0014 OUR FIT	Error includes scale factor of 1.2.			
0.026 ±0.005 OUR AVERAGE				
$0.021^{+0.028}_{-0.009}$	[1,2] RATCLIFF	72	ASPK	15 $\pi^- p \to n2\pi$
0.028 ±0.006	[1] BEHREND	71	ASPK	Photoproduction
$0.022^{+0.009}_{-0.01}$	[3] ROOS	70	RVUE	

[1] The fitted width of these data is 160 MeV in agreement with present average, thus the ω contribution is overestimated. Assuming ρ width 145 MeV.
[2] Significant interference effect observed. NB of $\omega \to 3\pi$ comes from an extrapolation.
[3] ROOS 70 combines ABRAMOVICH 70 and BIZZARRI 70.

$\Gamma(\pi^+\pi^-)/\Gamma(\pi^0\gamma)$ Γ_3/Γ_2

VALUE	EVTS	DOCUMENT ID		TECN	COMMENT
0.20±0.04	1.98M	[1] ALOISIO	03	KLOE	1.02 $e^+e^- \to \pi^+\pi^-\pi^0$

[1] Using the data of ALOISIO 02D.

$\Gamma(\text{neutrals})/\Gamma_{total}$ $(\Gamma_2+\Gamma_4)/\Gamma$

VALUE	EVTS	DOCUMENT ID		TECN	COMMENT
0.091±0.006 OUR FIT					
0.081±0.011 OUR AVERAGE					
0.075±0.025		BIZZARRI	71	HBC	0.0 $p\overline{p}$
0.079±0.019		DEINET	69B	OSPK	1.5 $\pi^- p$
0.084±0.015		BOLLINI	68C	CNTR	2.1 $\pi^- p$
• • • We do not use the following data for averages, fits, limits, etc. • • •					
0.073±0.018	42	BASILE	72B	CNTR	1.67 $\pi^- p$

$\Gamma(\text{neutrals})/\Gamma(\pi^+\pi^-\pi^0)$ $(\Gamma_2+\Gamma_4)/\Gamma_1$

VALUE	EVTS	DOCUMENT ID		TECN	COMMENT
0.102±0.008 OUR FIT					
$0.103^{+0.011}_{-0.010}$ OUR AVERAGE					
0.15 ±0.04	46	AGUILAR-...	72B	HBC	3.9,4.6 $K^- p$
0.10 ±0.03	19	BARASH	67B	HBC	0.0 $\overline{p}p$
0.134±0.026	850	DIGIUGNO	66B	CNTR	1.4 $\pi^- p$
0.097±0.016	348	FLATTE	66	HBC	1.4 – 1.7 $K^- p \to \Lambda$MM
$0.06^{+0.05}_{-0.02}$		JAMES	66	HBC	2.1 $\pi^+ p$
0.08 ±0.03	35	KRAEMER	64	DBC	1.2 $\pi^+ d$
• • • We do not use the following data for averages, fits, limits, etc. • • •					
0.11 ±0.02	20	BUSCHBECK	63	HBC	1.5 $K^- p$

$\Gamma(\pi^0\gamma)/\Gamma(\text{neutrals})$ $\Gamma_2/(\Gamma_2+\Gamma_4)$

VALUE	CL%	DOCUMENT ID		TECN	COMMENT
• • • We do not use the following data for averages, fits, limits, etc. • • •					
0.78±0.07		[1] DAKIN	72	OSPK	1.4 $\pi^- p \to n$MM
>0.81	90	DEINET	69B	OSPK	

[1] Error statistical only. Authors obtain good fit also assuming $\pi^0\gamma$ as the only neutral decay.

$\Gamma(\text{neutrals})/\Gamma(\text{charged particles})$ $(\Gamma_2+\Gamma_4)/(\Gamma_1+\Gamma_3)$

VALUE	DOCUMENT ID		TECN	COMMENT
0.100±0.008 OUR FIT				
0.124±0.021	FELDMAN	67C	OSPK	1.2 $\pi^- p$

$\Gamma(\eta\gamma)/\Gamma_{total}$ Γ_5/Γ

VALUE (units 10^{-4})	EVTS	DOCUMENT ID		TECN	COMMENT
4.5 ±0.4 OUR FIT	Error includes scale factor of 1.1.				
6.3 ±1.3 OUR AVERAGE	Error includes scale factor of 1.2.				
6.6 ±1.7		[1] ABELE	97E	CBAR	0.0 $\overline{p}p \to 5\gamma$
8.3 ±2.1		ALDE	93	GAM2	38 $\pi^- p \to \omega n$
$3.0^{+2.5}_{-1.8}$		[2] ANDREWS	77	CNTR	6.7–10 γCu
• • • We do not use the following data for averages, fits, limits, etc. • • •					
4.2 ±0.4 ±0.1	33k	[3] ACHASOV	07B	SND	0.6–1.38 $e^+e^- \to \eta\gamma$
$4.44^{+2.59}_{-1.83}$±0.28	17.4k	[4,5] AKHMETSHIN	05	CMD2	0.60-1.38 $e^+e^- \to \eta\gamma$
5.10±0.72±0.34	23k	[6] AKHMETSHIN	01B	CMD2	$e^+e^- \to \eta\gamma$
0.7 to 5.5		[7] CASE	00	CBAR	0.0 $p\overline{p} \to \eta\eta\gamma$
$6.56^{+2.41}_{-2.55}$	3525	[2,8] BENAYOUN	96	RVUE	$e^+e^- \to \eta\gamma$
7.3 ±2.9		[2,4] DOLINSKY	89	ND	$e^+e^- \to \eta\gamma$

[1] No flat $\eta\eta\gamma$ background assumed.
[2] Solution corresponding to constructive ω-ρ interference.
[3] ACHASOV 07B reports $[\Gamma(\omega(782) \to \eta\gamma)/\Gamma_{total}] \times [B(\omega(782) \to e^+e^-)] = (3.10 \pm 0.31 \pm 0.11) \times 10^{-8}$ which we divide by our best value $B(\omega(782) \to e^+e^-) = (7.36 \pm 0.15) \times 10^{-5}$. Our first error is their experiment's error and our second error is the systematic error from using our best value. Supersedes ACHASOV 00D and ACHASOV 06A.
[4] Not independent of the corresponding $\Gamma(e^+e^-) \times \Gamma(\eta\gamma)/\Gamma^2_{total}$.
[5] Using $B(\omega \to e^+e^-) = (7.14 \pm 0.13) \times 10^{-5}$ and $B(\eta \to \gamma\gamma) = 39.43 \pm 0.26\%$.
[6] Using $B(\omega \to e^+e^-) = (7.07 \pm 0.19) \times 10^{-5}$ and using $B(\eta \to 3\pi^0) = (32.24 \pm 0.29) \times 10^{-2}$. Solution corresponding to constructive ω-ρ interference. The combined fit from 600 to 1380 MeV taking into account $\rho(770)$, $\omega(782)$, $\phi(1020)$, and $\rho(1450)$ (mass and width fixed at 1450 MeV and 310 MeV respectively). Not independent of the corresponding $\Gamma(e^+e^-) \times \Gamma(\eta\gamma)/\Gamma^2_{total}$.
[7] Depending on the degree of coherence with the flat $\eta\eta\gamma$ background and using $B(\omega \to \pi^0\gamma) = (8.5 \pm 0.5) \times 10^{-2}$.
[8] Reanalysis of DRUZHININ 84, DOLINSKY 89, DOLINSKY 91 taking into account the triangle anomaly contributions.

$\Gamma(\eta\gamma)/\Gamma(\pi^0\gamma)$ Γ_5/Γ_2

VALUE	DOCUMENT ID		TECN	COMMENT
• • • We do not use the following data for averages, fits, limits, etc. • • •				
0.0098±0.0024	[1] ALDE	93	GAM2	38 $\pi^- p \to \omega n$
0.0082±0.0033	[2] DOLINSKY	89	ND	$e^+e^- \to \eta\gamma$
0.010 ±0.045	APEL	72B	OSPK	4–8 $\pi^- p \to n3\gamma$

[1] Model independent determination.
[2] Solution corresponding to constructive ω-ρ interference.

Meson Particle Listings

$\omega(782)$

$\Gamma(\pi^0 e^+ e^-)/\Gamma_{total}$ Γ_6/Γ

VALUE (units 10^{-4})	EVTS	DOCUMENT ID		TECN	COMMENT
7.7 ±0.6 OUR FIT					
7.7 ±0.6 OUR AVERAGE					
7.61±0.53±0.64		ACHASOV	08	SND	0.36–0.97 $e^+e^- \to \pi^0 e^+ e^-$
8.19±0.71±0.62		AKHMETSHIN	05A	CMD2	0.72–0.84 e^+e^-
5.9 ±1.9	43	DOLINSKY	88	ND	$e^+e^- \to \pi^0 e^+ e^-$

$\Gamma(\pi^0 \mu^+ \mu^-)/\Gamma_{total}$ Γ_7/Γ

VALUE (units 10^{-4})	EVTS	DOCUMENT ID		TECN	COMMENT
1.34±0.18 OUR FIT Error includes scale factor of 1.5.					
1.34±0.19 OUR AVERAGE Error includes scale factor of 1.5. See the ideogram below.					
1.41±0.09±0.15		ARNALDI	16	NA60	400 GeV (p-A) collisions
1.72±0.25±0.14	3k	ARNALDI	09	NA60	158A In–In collisions
0.96±0.23		DZHELYADIN	81B	CNTR	25–33 $\pi^- p \to \omega n$

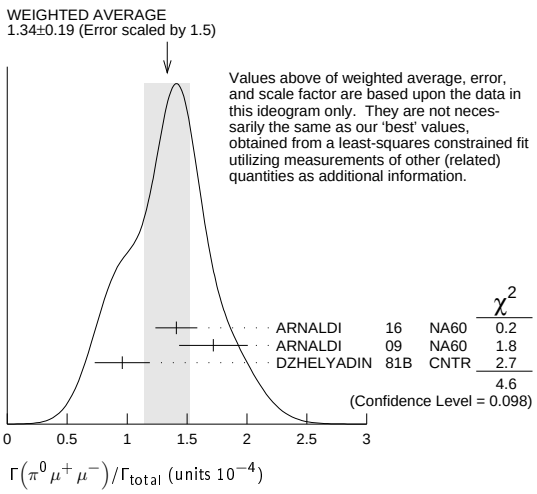

$\Gamma(\eta e^+ e^-)/\Gamma_{total}$ Γ_8/Γ

VALUE (units 10^{-5})	DOCUMENT ID		TECN	COMMENT
• • • We do not use the following data for averages, fits, limits, etc. • • •				
<1.1	AKHMETSHIN	05A	CMD2	0.72-0.84 e^+e^-

$\Gamma(e^+ e^-)/\Gamma_{total}$ Γ_9/Γ

VALUE (units 10^{-4})	EVTS	DOCUMENT ID		TECN	COMMENT
0.736±0.015 OUR FIT Error includes scale factor of 1.5.					
• • • We do not use the following data for averages, fits, limits, etc. • • •					
0.700±0.016	11200	[1,2] AKHMETSHIN	04	CMD2	$e^+e^- \to \pi^+\pi^-\pi^0$
0.752±0.004±0.024	1.2M	[2,3] ACHASOV	03D	RVUE	0.44–2.00 $e^+e^- \to \pi^+\pi^-\pi^0$
0.714±0.036		[2] DOLINSKY	89	ND	$e^+e^- \to \pi^+\pi^-\pi^0$
0.72 ±0.03		[2] BARKOV	87	CMD	$e^+e^- \to \pi^+\pi^-\pi^0$
0.64 ±0.04	1488	[2] KURDADZE	83B	OLYA	$e^+e^- \to \pi^+\pi^-\pi^0$
0.675±0.069	433	[2] CORDIER	80	DM1	$e^+e^- \to \pi^+\pi^-\pi^0$
0.83 ±0.10	451	[2] BENAKSAS	72B	OSPK	$e^+e^- \to \pi^+\pi^-\pi^0$
0.77 ±0.06		[4] AUGUSTIN	69D	OSPK	$e^+e^- \to \pi^+\pi^-\pi^0$
0.65 ±0.13	33	[5] ASTVACAT...	68	OSPK	Assume SU(3)+mixing

[1] Using B($\omega \to \pi^+\pi^-\pi^0$) = 0.891 ± 0.007. Update of AKHMETSHIN 00C.
[2] Not independent of the corresponding $\Gamma(e^+e^-) \times \Gamma(\pi^+\pi^-\pi^0)/\Gamma^2_{total}$.
[3] Using ACHASOV 03, ACHASOV 03D and B($\omega \to \pi^+\pi^-$) = (1.70 ± 0.28)%.
[4] Rescaled by us to correspond to ω width 8.4 MeV. Systematic errors underestimated.
[5] Not resolved from ρ decay. Error statistical only.

$\Gamma(\pi^+\pi^-\pi^0\pi^0)/\Gamma_{total}$ Γ_{10}/Γ

VALUE (units 10^{-4})	CL%	DOCUMENT ID		TECN	COMMENT
< 2	90	ACHASOV	09A	SND	$e^+e^- \to \pi^+\pi^-\pi^0\pi^0$
• • • We do not use the following data for averages, fits, limits, etc. • • •					
<200	90	KURDADZE	86	OLYA	$e^+e^- \to \pi^+\pi^-\pi^0\pi^0$

$\Gamma(\pi^+\pi^-\gamma)/\Gamma_{total}$ Γ_{11}/Γ

VALUE	CL%	DOCUMENT ID		TECN	COMMENT
<0.0036	95	WEIDENAUER	90	ASTE	$p\overline{p} \to \pi^+\pi^-\pi^+\pi^-\gamma$
• • • We do not use the following data for averages, fits, limits, etc. • • •					
<0.004	95	BITYUKOV	88B	SPEC	32 $\pi^- p \to \pi^+\pi^-\gamma X$

$\Gamma(\pi^+\pi^-\gamma)/\Gamma(\pi^+\pi^-\pi^0)$ Γ_{11}/Γ_1

VALUE	CL%	DOCUMENT ID		TECN	COMMENT
• • • We do not use the following data for averages, fits, limits, etc. • • •					
<0.066	90	KALBFLEISCH	75	HBC	2.18 $K^- p \to \Lambda\pi^+\pi^-\gamma$
<0.05	90	FLATTE	66	HBC	1.2 – 1.7 $K^- p \to \Lambda\pi^+\pi^-\gamma$

$\Gamma(\pi^+\pi^-\pi^+\pi^-)/\Gamma_{total}$ Γ_{12}/Γ

VALUE	CL%	DOCUMENT ID		TECN	COMMENT
<1 × 10^{-3}	90	KURDADZE	88	OLYA	$e^+e^- \to \pi^+\pi^-\pi^+\pi^-$

$\Gamma(\pi^0\pi^0\gamma)/\Gamma_{total}$ Γ_{13}/Γ

VALUE (units 10^{-5})	EVTS	DOCUMENT ID		TECN	COMMENT
6.7±1.1 OUR FIT					
6.5±1.2 OUR AVERAGE					
$6.4^{+2.4}_{-2.0}\pm0.8$	190	[1] AKHMETSHIN	04B	CMD2	0.6–0.97 $e^+e^- \to \pi^0\pi^0\gamma$
$6.6^{+1.4}_{-1.3}\pm0.6$	295	ACHASOV	02F	SND	0.36–0.97 $e^+e^- \to \pi^0\pi^0\gamma$
• • • We do not use the following data for averages, fits, limits, etc. • • •					
$11.8^{+2.1}_{-1.9}\pm1.4$	190	[2] AKHMETSHIN	04B	CMD2	0.6–0.97 $e^+e^- \to \pi^0\pi^0\gamma$
7.8±2.7±2.0	63	[1,3] ACHASOV	00G	SND	$e^+e^- \to \pi^0\pi^0\gamma$
12.7±2.3±2.5	63	[2,3] ACHASOV	00G	SND	$e^+e^- \to \pi^0\pi^0\gamma$

[1] In the model assuming the $\rho \to \pi^0\pi^0\gamma$ decay via the $\omega\pi$ and $f_0(500)\gamma$ mechanisms.
[2] In the model assuming the $\rho \to \pi^0\pi^0\gamma$ decay via the $\omega\pi$ mechanism only.
[3] Superseded by ACHASOV 02F.

$\Gamma(\pi^0\pi^0\gamma)/\Gamma(\pi^+\pi^-\pi^0)$ Γ_{13}/Γ_1

VALUE	CL%	DOCUMENT ID		TECN	COMMENT
<0.00045	90	DOLINSKY	89	ND	$e^+e^- \to \pi^0\pi^0\gamma$
• • • We do not use the following data for averages, fits, limits, etc. • • •					
<0.08	95	JACQUET	69B	HLBC	2.05 $\pi^+ p \to \pi^+ p\omega$

$\Gamma(\pi^0\pi^0\gamma)/\Gamma(\pi^0\gamma)$ Γ_{13}/Γ_2

VALUE (units 10^{-4})	CL%	EVTS	DOCUMENT ID		TECN	COMMENT
7.9±1.3 OUR FIT						
8.5±2.9		40 ± 14	ALDE	94B	GAM2	38$\pi^- p \to \pi^0\pi^0\gamma n$
• • • We do not use the following data for averages, fits, limits, etc. • • •						
< 50	90		DOLINSKY	89	ND	$e^+e^- \to \pi^0\pi^0\gamma$
<1800	95		KEYNE	76	CNTR	$\pi^- p \to \omega n$
<1500	90		BENAKSAS	72C	OSPK	e^+e^-
<1400			BALDIN	71	HLBC	2.9 $\pi^+ p$
<1000	90		BARMIN	64	HLBC	1.3–2.8 $\pi^- p$

$\Gamma(\pi^0\pi^0\gamma)/\Gamma(\text{neutrals})$ $\Gamma_{13}/(\Gamma_2+\Gamma_4)$

VALUE	CL%	DOCUMENT ID		TECN	COMMENT
• • • We do not use the following data for averages, fits, limits, etc. • • •					
0.22±0.07		[1] DAKIN	72	OSPK	1.4 $\pi^- p \to n$MM
<0.19	90	DEINET	69B	OSPK	

[1] See $\Gamma(\pi^0\gamma)/\Gamma(\text{neutrals})$.

$\Gamma(\eta\pi^0\gamma)/\Gamma_{total}$ Γ_{14}/Γ

VALUE (units 10^{-5})	CL%	DOCUMENT ID		TECN	COMMENT
<3.3	90	AKHMETSHIN	04B	CMD2	0.6–0.97 $e^+e^- \to \eta\pi^0\gamma$

$\Gamma(\mu^+\mu^-)/\Gamma_{total}$ Γ_{15}/Γ

VALUE (units 10^{-5})	EVTS	DOCUMENT ID		TECN	COMMENT
7.4±1.8 OUR FIT					
7.4±1.8 OUR AVERAGE					
6.6±1.4±1.7	4.5M	[1] ANASTASI	17	KLOE	$e^+e^- \to \mu^+\mu^-\gamma$
9.0±2.9±1.1	18	HEISTER	02C	ALEP	$Z \to \mu^+\mu^- + X$

[1] Assuming lepton universality in the decay $\omega \to \ell^+\ell^-$ and correcting for different phase space between electron and muon final states.

$\Gamma(\mu^+\mu^-)/\Gamma(\pi^+\pi^-\pi^0)$ Γ_{15}/Γ_1

VALUE (units 10^{-3})	CL%	DOCUMENT ID		TECN	COMMENT
<0.2	90	WILSON	69	OSPK	12 π^-C → Fe
• • • We do not use the following data for averages, fits, limits, etc. • • •					
<1.7	74	FLATTE	66	HBC	1.2 – 1.7 $K^- p \to \Lambda\mu^+\mu^-$
<1.2		BARBARO-...	65	HBC	2.7 $K^- p$

$\Gamma(\pi^0\mu^+\mu^-)/\Gamma(\mu^+\mu^-)$ Γ_7/Γ_{15}

VALUE	EVTS	DOCUMENT ID		TECN	COMMENT
• • • We do not use the following data for averages, fits, limits, etc. • • •					
1.2±0.6	30	[1] DZHELYADIN	79	CNTR	25–33 $\pi^- p$

[1] Superseded by DZHELYADIN 81B result above.

$\Gamma(3\gamma)/\Gamma_{total}$ Γ_{16}/Γ

VALUE (units 10^{-4})	CL%	DOCUMENT ID		TECN	COMMENT
<1.9	95	[1] ABELE	97E	CBAR	0.0 $\overline{p}p \to 5\gamma$
• • • We do not use the following data for averages, fits, limits, etc. • • •					
<2	90	[1] PROKOSHKIN	95	GAM2	38 $\pi^- p \to 3\gamma n$

[1] From direct 3γ decay search.

$\Gamma(\eta\pi^0)/\Gamma_{total}$ Γ_{17}/Γ

Violates C conservation.

VALUE	CL%	DOCUMENT ID		TECN	COMMENT
• • • We do not use the following data for averages, fits, limits, etc. • • •					
<0.001	90	ALDE	94B	GAM2	$38\pi^- p \to \eta\pi^0 n$

$[\Gamma(\eta\gamma)+\Gamma(\eta\pi^0)]/\Gamma(\pi^+\pi^-\pi^0)$ $(\Gamma_5+\Gamma_{17})/\Gamma_1$

VALUE	CL%	DOCUMENT ID		TECN	COMMENT
<0.016	90	[1] FLATTE	66	HBC	$1.2-1.7\ K^- p \to \Lambda\pi^+\pi^-$ MM
• • • We do not use the following data for averages, fits, limits, etc. • • •					
<0.045	95	JACQUET	69B	HLBC	$2.05\ \pi^+ p \to \pi^+ p\omega$

[1] Restated by us using B($\eta \to$ charged modes) = 29.2%.

$\Gamma(\eta\pi^0)/\Gamma(\pi^0\gamma)$ Γ_{17}/Γ_2

Violates C conservation.

VALUE (units 10^{-3})	CL%	DOCUMENT ID		TECN	COMMENT
<2.6	90	[1] STAROSTIN	09	CRYM	$\gamma p \to \eta\pi^0 p$

[1] STAROSTIN 09 reports $[\Gamma(\omega(782) \to \eta\pi^0)/\Gamma(\omega(782) \to \pi^0\gamma)] \times [B(\eta \to 2\gamma)] < 1.01\times10^{-3}$ which we divide by our best value $B(\eta \to 2\gamma) = 39.41\times10^{-2}$.

$\Gamma(2\pi^0)/\Gamma(\pi^0\gamma)$ Γ_{18}/Γ_2

Violates C conservation and Bose-Einstein statistics.

VALUE (units 10^{-3})	CL%	DOCUMENT ID		TECN	COMMENT
<2.59	90	STAROSTIN	09	CRYM	$\gamma p \to 2\pi^0 p$

$\Gamma(3\pi^0)/\Gamma_{total}$ Γ_{19}/Γ

Violates C conservation.

VALUE	CL%	DOCUMENT ID		TECN	COMMENT
• • • We do not use the following data for averages, fits, limits, etc. • • •					
$<3\times10^{-4}$	90	PROKOSHKIN	95	GAM2	$38\ \pi^- p \to 3\pi^0 n$

$\Gamma(3\pi^0)/\Gamma(\pi^0\gamma)$ Γ_{19}/Γ_2

Violates C conservation.

VALUE (units 10^{-3})	CL%	DOCUMENT ID		TECN	COMMENT
<2.72	90	STAROSTIN	09	CRYM	$\gamma p \to 3\pi^0 p$

$\Gamma(3\pi^0)/\Gamma(\pi^+\pi^-\pi^0)$ Γ_{19}/Γ_1

Violates C conservation.

VALUE	CL%	DOCUMENT ID		TECN	COMMENT
• • • We do not use the following data for averages, fits, limits, etc. • • •					
<0.009	90	BARBERIS	01		$450\ pp \to p_f 3\pi^0 p_s$

PARAMETER Λ IN $\omega \to \pi^0\ell^+\ell^-$ DECAY

In the pole approximation the electromagnetic transition form factor for a resonance of mass M is given by the expression:

$$|F|^2 = (1 - M^2/\Lambda^2)^{-2},$$

where for the parameter Λ vector dominance predicts $\Lambda = M_\rho \approx 0.770$ GeV. The ARNALDI 09 measurement is in obvious conflict with this expectation. Note that for $\eta \to \gamma\mu^+\mu^-$ decay ARNALDI 09 and DZHELYADIN 80 obtain the value of Λ consistent with vector dominance.

PARAMETER Λ IN $\omega \to \pi^0\mu^+\mu^-$ DECAY

VALUE (GeV)	EVTS	DOCUMENT ID		TECN	COMMENT
0.670 ±0.006 OUR AVERAGE					
$0.6707\pm0.0039\pm0.0056$		[1] ARNALDI	16	NA60	400 GeV (p-A) collisions
$0.668\ \pm0.009\ \pm0.003$	3k	[2] ARNALDI	09	NA60	158A In−In collisions
• • • We do not use the following data for averages, fits, limits, etc. • • •					
$0.65\ \ \pm0.03$		DZHELYADIN	81B	CNTR	$25-33\ \pi^- p \to \omega n$

[1] ARNALDI 16 reports $\Lambda^{-2}(\omega) = 2.223 \pm 0.026 \pm 0.037$ GeV^{-2} which we converted to the quoted Λ value.

[2] ARNALDI 09 reports $\Lambda^{-2}(\omega) = 2.24 \pm 0.06 \pm 0.02$ GeV^{-2} which we converted to the quoted Λ value.

PARAMETER Λ IN $\omega \to \pi^0 e^+ e^-$ DECAY

VALUE (GeV)	EVTS	DOCUMENT ID		TECN	COMMENT
0.709±0.037	1.1k	[1] ADLARSON	17B	A2MM	$\gamma p \to \omega p$

[1] ADLARSON 17B reports $\Lambda^{-2}(\omega\pi^0) = 1.99 \pm 0.21$ GeV^{-2} that we converted to the quoted Λ value.

ENERGY DEPENDENCE OF $\omega \to \pi^+\pi^-\pi^0$ DALITZ PLOT

The following experiments fit to one or more of the coefficients α, β, γ for |matrix element|$^2 \propto P\ (1 + 2\alpha\ Z + 2\beta\ Z^{3/2} \sin(3\phi) + 2\gamma Z^2 + O(Z^{5/2}))$ where P is the P-wave phase-space factor and Z, ϕ are kinematical variables as defined in ADLARSON 17.

VALUE	EVTS	DOCUMENT ID		TECN	COMMENT
0.147±0.036	44k	ADLARSON	17	WASA	α in $pd \to {}^3\mathrm{He}\ \omega$, $pp \to pp\omega$

$\omega(782)$ REFERENCES

ADLARSON	17	PL B770 418	P. Adlarson *et al.*	(WASA-at-COSY Collab.)
ADLARSON	17B	PR C95 035208	P. Adlarson *et al.*	(A2 Collab. at MAMI)
ANASTASI	17	PL B767 485	A. Anastasi *et al.*	(KLOE-2 Collab.)
ACHASOV	16A	PR D93 092001	M.N. Achasov *et al.*	(SND Collab.)
ARNALDI	16	PL B757 437	R. Arnaldi *et al.*	(NA60 Collab.)
PDG	15	RPP 2015 at pdg.lbl.gov		(PDG Collab.)
ACHASOV	13	PR D88 054013	M.N. Achasov *et al.*	(SND Collab.)
BENAYOUN	13	EPJ C73 2453	M. Benayoun, P. David, L. DelBuono	(PARIN, BERLIN+)
DAVIER	13	EPJ C73 2597	M. Davier *et al.*	
LEES	12G	PR D86 032013	J.P. Lees *et al.*	(BABAR Collab.)
NIECKNIG	12	EPJ C72 2014	F. Niecknig, B. Kubis, S.P. Schneider	(BONN)
BENAYOUN	10	EPJ C65 211	M. Benayoun *et al.*	
ACHASOV	09A	JETP 109 379	M.N. Achasov *et al.*	(SND Collab.)
		Translated from ZETF 136 442.		
ARNALDI	09	PL B677 260	R. Arnaldi *et al.*	(NA60 Collab.)
STAROSTIN	09	PR C79 065201	A. Starostin *et al.*	(Crystal Ball Collab. at MAMI)
ACHASOV	08	JETP 107 61	M.N. Achasov *et al.*	(SND Collab.)
		Translated from ZETF 134 80.		
AMBROSINO	08G	PL B669 223	F. Ambrosino *et al.*	(KLOE Collab.)
ACHASOV	07B	PR D76 077101	M.N. Achasov *et al.*	(SND Collab.)
AKHMETSHIN	07	PL B648 28	R.R. Akhmetshin *et al.*	(Novosibirsk CMD-2 Collab.)
ACHASOV	06	JETP 103 380	M.N. Achasov *et al.*	(Novosibirsk SND Collab.)
		Translated from ZETF 130 437.		
ACHASOV	06A	PR D74 014016	M.N. Achasov *et al.*	(SND Collab.)
AULCHENKO	06	JETPL 84 413	V.M. Aulchenko *et al.*	(Novosibirsk CMD-2 Collab.)
		Translated from ZETFP 84 491.		
ACHASOV	05A	JETP 101 1053	M.N. Achasov *et al.*	(Novosibirsk SND Collab.)
		Translated from ZETF 128 1201.		
AKHMETSHIN	05	PL B605 26	R.R. Akhmetshin *et al.*	(Novosibirsk CMD-2 Collab.)
AKHMETSHIN	05A	PL B613 29	R.R. Akhmetshin *et al.*	(Novosibirsk CMD-2 Collab.)
AULCHENKO	05	JETPL 82 743	V.M. Aulchenko *et al.*	(Novosibirsk CMD-2 Collab.)
		Translated from ZETFP 82 841.		
AKHMETSHIN	04	PL B578 285	R.R. Akhmetshin *et al.*	(Novosibirsk CMD-2 Collab.)
AKHMETSHIN	04B	PL B580 119	R.R. Akhmetshin *et al.*	(Novosibirsk CMD-2 Collab.)
AUBERT,B	04N	PR D70 072004	B. Aubert *et al.*	(BABAR Collab.)
PDG	04	PL B592 1	S. Eidelman *et al.*	(PDG Collab.)
ACHASOV	03	PL B559 171	M.N. Achasov *et al.*	(Novosibirsk SND Collab.)
ACHASOV	03D	PR D68 052006	M.N. Achasov *et al.*	(Novosibirsk SND Collab.)
ALOISIO	03	PL B561 55	A. Aloisio *et al.*	(KLOE Collab.)
BENAYOUN	03	EPJ C29 397	M. Benayoun *et al.*	
ACHASOV	02E	PR D66 032001	M.N. Achasov *et al.*	(Novosibirsk SND Collab.)
ACHASOV	02F	PL B537 201	M.N. Achasov *et al.*	(Novosibirsk SND Collab.)
AKHMETSHIN	02	PL B527 161	R.R. Akhmetshin *et al.*	(Novosibirsk CMD-2 Collab.)
ALOISIO	02D	PL B537 21	A. Aloisio *et al.*	(KLOE Collab.)
HEISTER	02C	PL B528 19	A. Heister *et al.*	(ALEPH Collab.)
ACHASOV	01E	PR D63 072002	M.N. Achasov *et al.*	(Novosibirsk SND Collab.)
AKHMETSHIN	01B	PL B509 217	R.R. Akhmetshin *et al.*	(Novosibirsk CMD-2 Collab.)
BARBERIS	01	PL B507 14	D. Barberis *et al.*	
ACHASOV	00	EPJ C12 25	M.N. Achasov *et al.*	(Novosibirsk SND Collab.)
ACHASOV	00D	JETPL 72 282	M.N. Achasov *et al.*	(Novosibirsk SND Collab.)
		Translated from ZETFP 72 411.		
ACHASOV	00G	JETPL 71 355	M.N. Achasov *et al.*	(Novosibirsk SND Collab.)
		Translated from ZETFP 71 519.		
AKHMETSHIN	00C	PL B476 33	R.R. Akhmetshin *et al.*	(Novosibirsk CMD-2 Collab.)
AULCHENKO	00A	JETP 90 927	V.M. Aulchenko *et al.*	(Novosibirsk SND Collab.)
		Translated from ZETF 117 1067.		
CASE	00	PR D61 032002	T. Case *et al.*	(Crystal Barrel Collab.)
ACHASOV	99E	PL B462 365	M.N. Achasov *et al.*	(Novosibirsk SND Collab.)
GARDNER	99	PR D59 076002	S. Gardner, H.B. O'Connell	
BENAYOUN	98	EPJ C2 269	M. Benayoun *et al.*	(IPNP, NOVO, ADLD+)
ABELE	97E	PL B411 361	A. Abele *et al.*	(Crystal Barrel Collab.)
BENAYOUN	96	ZPHY C72 221	M. Benayoun *et al.*	(IPNP, NOVO)
PROKOSHKIN	95	PD 40 273	Y.D. Prokoshkin, V.D. Samoilenko	(SERP)
		Translated from DANS 342 610.		
WURZINGER	95	PR C51 443	R. Wurzinger *et al.*	(BONN, ORSAY, SACL+)
ALDE	94B	PL B340 122	D.M. Alde *et al.*	(SERP, BELG, LANL, LAPP+)
AMSLER	94C	PL B327 425	C. Amsler *et al.*	(Crystal Barrel Collab.)
ALDE	93	PAN 56 1229	D.M. Alde *et al.*	(SERP, LAPP, LANL, BELG+)
		Translated from YAF 56 137.		
Also		ZPHY C61 35	D.M. Alde *et al.*	(SERP, LAPP, LANL, BELG+)
AMSLER	93B	PL B311 362	C. Amsler *et al.*	(Crystal Barrel Collab.)
WEIDENAUER	93	ZPHY C59 387	P. Weidenauer *et al.*	(ASTERIX Collab.)
ANTONELLI	92	ZPHY C56 15	A. Antonelli *et al.*	(DM2 Collab.)
DOLINSKY	91	PRPL 202 99	S.I. Dolinsky *et al.*	(NOVO)
WEIDENAUER	90	ZPHY C47 353	P. Weidenauer *et al.*	(ASTERIX Collab.)
DOLINSKY	89	ZPHY C42 511	S.I. Dolinsky *et al.*	(NOVO)
BITYUKOV	88B	SJNP 47 800	S.I. Bityukov *et al.*	(SERP)
		Translated from YAF 47 1258.		
DOLINSKY	88	SJNP 48 277	S.I. Dolinsky *et al.*	(NOVO)
		Translated from YAF 48 442.		
KURDADZE	88	JETPL 47 512	L.M. Kurdadze *et al.*	(NOVO)
		Translated from ZETFP 47 432.		
AULCHENKO	87	PL B186 432	V.M. Aulchenko *et al.*	(NOVO)
BARKOV	87	JETPL 46 164	L.M. Barkov *et al.*	(NOVO)
		Translated from ZETFP 46 132.		
KURDADZE	86	JETPL 43 643	L.M. Kurdadze *et al.*	(NOVO)
		Translated from ZETFP 43 497.		
BARKOV	85	NP B256 365	L.M. Barkov *et al.*	(NOVO)
DRUZHININ	84	PL 144B 136	V.P. Druzhinin *et al.*	(NOVO)
KURDADZE	83B	JETPL 36 274	A.M. Kurdadze *et al.*	(NOVO)
		Translated from ZETFP 36 221.		
DZHELYADIN	81B	PL 102B 296	R.I. Dzhelyadin *et al.*	(SERP)
CORDIER	80	NP B172 13	A. Cordier *et al.*	(LALO)
DZHELYADIN	80	PL 94B 548	R.I. Dzhelyadin *et al.*	(SERP)
ROOS	80	LNC 27 321	M. Roos, A. Pellinen	(HELS)
BENKHEIRI	79	NP B150 268	P. Benkheiri *et al.*	(EPOL, CERN, CDEF+)
DZHELYADIN	79	PL 84B 143	R.I. Dzhelyadin *et al.*	(SERP)
COOPER	78B	NP B146 1	A.M. Cooper *et al.*	(TATA, CERN, CDEF+)
QUENZER	78	PL 76B 512	A. Quenzer *et al.*	(LALO)
VANAPEL...	78	NP B133 245	G.W. van Apeldoorn *et al.*	(ZEEM)
WICKLUND	78	PR D17 1197	A.B. Wicklund *et al.*	(ANL)
ANDREWS	77	PRL 38 198	D.E. Andrews *et al.*	(ROCH)
GESSAROLI	77	NP B126 382	R. Gessaroli *et al.*	(BGNA, FIRZ, GENO+)
KEYNE	76	PR D14 28	J. Keyne *et al.*	(LOIC, SHMP)
Also		PR D8 2789	D.M. Binnie *et al.*	(LOIC, SHMP)
KALBFLEISCH	75	PR D11 987	G.R. Kalbfleisch, R.C. Strand, J.W. Chapman	(BNL+)
AGUILAR-...	72B	PR D6 29	M. Aguilar-Benitez *et al.*	(BNL)
APEL	72B	PL 41B 234	W.D. Apel *et al.*	(KARLK, KARLE, PISA)
BASILE	72B	Phil. Conf. 153	M. Basile *et al.*	(CERN)
BENAKSAS	72	PL 39B 289	D. Benaksas *et al.*	(ORSAY)
BENAKSAS	72B	PL 42B 507	D. Benaksas *et al.*	(ORSAY)
BENAKSAS	72C	PL 42B 511	D. Benaksas *et al.*	(ORSAY)
BORENSTEIN	72	PR D5 1559	S.R. Borenstein *et al.*	(BNL, MICH)
BROWN	72	PL 42B 117	R.M. Brown *et al.*	(ILL, ILLC)
DAKIN	72	PR D6 2321	J.T. Dakin *et al.*	(PRIN)
RATCLIFF	72	PL 38B 345	B.N. Ratcliff *et al.*	(SLAC)
ALVENSLEB...	71C	PRL 27 888	H. Alvensleben *et al.*	(DESY)
BALDIN	71	SJNP 13 758	A.B. Baldin *et al.*	(ITEP)
		Translated from YAF 13 1318.		
BEHREND	71	PRL 27 61	H.J. Behrend *et al.*	(ROCH, CORN, FNAL)
BIZZARRI	71	NP B27 140	R. Bizzarri *et al.*	(CERN, CDEF)
COYNE	71	NP B32 333	D.G. Coyne *et al.*	(LRL)
MOFFEIT	71	NP B29 349	K.C. Moffeit *et al.*	(LRL, UCB, SLAC+)
ABRAMOVI...	70	NP B20 209	M. Abramovich *et al.*	(CERN)
BIGGS	70B	PRL 24 1201	P.J. Biggs *et al.*	(DARE)
BIZZARRI	70	PRL 25 1385	R. Bizzarri *et al.*	(ROMA, SYRA)
ROOS	70	DNPL/R7 173	M. Roos	(CERN)
		Proc. Daresbury Study Weekend No. 1.		

AUGUSTIN	69D	PL 28B 513	J.E. Augustin *et al.*	(ORSAY)
BIZZARRI	69	NP B14 169	R. Bizzarri *et al.*	(CERN, CDEF)
DEINET	69B	PL 30B 426	W. Deinet *et al.*	(KARL, CERN)
JACQUET	69B	NC 63A 743	F. Jacquet *et al.*	(EPOL, BERG)
WILSON	69	Private Comm.	R. Wilson	(HARV)
Also		PR 178 2095	A.A. Wehmann *et al.*	(HARV, CASE, SLAC+)
ASTVACAT...	68	PL 27B 45	R.G. Astvatsaturov *et al.*	(JINR, MOSU)
BOLLINI	68C	NC 56A 531	D. Bollini *et al.*	(CERN, BGNA, STRB)
GOUNARIS	68	PRL 21 244	G.J. Gounaris, J.J. Sakurai	
BARASH	67B	PR 156 1399	N. Barash *et al.*	(COLU)
FELDMAN	67C	PR 159 1219	M. Feldman *et al.*	(PENN)
DIGIUGNO	66B	NC 44A 1272	G. Di Giugno *et al.*	(NAPL, FRAS, TRST)
FLATTE	66	PR 145 1050	S.M. Flatte *et al.*	(LRL)
JAMES	66	PR 142 896	F.E. James, H.L. Kraybill	(YALE, BNL)
BARBARO-...	65	PRL 14 279	A. Barbaro-Galtieri, R.D. Tripp	(LRL)
BARMIN	64	JETP 18 1289	V.V. Barmin *et al.*	(ITEP)
		Translated from ZETF 45 1879.		
KRAEMER	64	PR 136 B496	R.W. Kraemer *et al.*	(JHU, NWES, WOOD)
BUSCHBECK	63	Siena Conf. 1 166	B. Buschbeck *et al.*	(VIEN, CERN, ANIK)

$\eta'(958)$

$I^G(J^{PC}) = 0^+(0^{-+})$

$\eta'(958)$ MASS

VALUE (MeV)	EVTS	DOCUMENT ID		TECN	COMMENT
957.78 ±0.06 OUR AVERAGE					
957.793±0.054±0.036	3.9k	LIBBY	08	CLEO	$J/\psi \to \gamma\eta'$
957.9 ±0.2 ±0.6	4800	WURZINGER	96	SPEC	1.68 $pd \to {}^3\mathrm{He}\eta'$
957.46 ±0.33		DUANE	74	MMS	$\pi^- p \to n$MM
958.2 ±0.5	1414	DANBURG	73	HBC	2.2 $K^- p \to \Lambda\eta'$
958 ±1	400	JACOBS	73	HBC	2.9 $K^- p \to \Lambda\eta'$
956.1 ±1.1	3415	[1] BASILE	71	CNTR	1.6 $\pi^- p \to n\eta'$
• • • We do not use the following data for averages, fits, limits, etc. • • •					
957.5 ±0.2		BAI	04J	BES2	$J/\psi \to \gamma\gamma\pi^+\pi^-$
959 ±1	630	[2] BELADIDZE	92C	VES	36 π^-Be $\to \pi^-\eta'\eta$Be
958 ±1	340	[2] ARMSTRONG	91B	OMEG	300 $pp \to pp\eta\pi^+\pi^-$
958.2 ±0.4	622	[2] AUGUSTIN	90	DM2	$J/\psi \to \gamma\eta\pi^+\pi^-$
957.8 ±0.2	2420	[2] AUGUSTIN	90	DM2	$J/\psi \to \gamma\gamma\pi^+\pi^-$
956.3 ±1.0	143	[2] GIDAL	87	MRK2	$e^+e^- \to e^+e^-\eta\pi^+\pi^-$
957.4 ±1.4	535	[3] BASILE	71	CNTR	1.6 $\pi^- p \to n\eta'$
957 ±1		RITTENBERG	69	HBC	1.7–2.7 $K^- p$

[1] Using all η' decays.
[2] Systematic uncertainty not estimated.
[3] Using η' decays into neutrals. Not independent of the other listed BASILE 71 η' mass measurement.

$\eta'(958)$ WIDTH

VALUE (MeV)	EVTS	DOCUMENT ID		TECN	CHG	COMMENT
0.196±0.009 OUR FIT						
0.230±0.021 OUR AVERAGE						
0.226±0.017±0.014	2300	CZERWINSKI	10	MMS		$pp \to pp\eta'$
0.40 ±0.22	4800	WURZINGER	96	SPEC		1.68 $pd \to {}^3\mathrm{He}\eta'$
0.28 ±0.10	1000	BINNIE	79	MMS	0	$\pi^- p \to n$MM
• • • We do not use the following data for averages, fits, limits, etc. • • •						
0.20 ±0.04		BAI	04J	BES2		$J/\psi \to \gamma\gamma\pi^+\pi^-$

$\eta'(958)$ DECAY MODES

	Mode	Fraction (Γ_i/Γ)	Confidence level
Γ_1	$\pi^+\pi^-\eta$	(42.6 ±0.7) %	
Γ_2	$\rho^0\gamma$(including non-resonant $\pi^+\pi^-\gamma$)	(28.9 ±0.5) %	
Γ_3	$\pi^0\pi^0\eta$	(22.8 ±0.8) %	
Γ_4	$\omega\gamma$	(2.62±0.13) %	
Γ_5	ωe^+e^-	(2.0 ±0.4) $\times 10^{-4}$	
Γ_6	$\gamma\gamma$	(2.22±0.08) %	
Γ_7	$3\pi^0$	(2.54±0.18) $\times 10^{-3}$	
Γ_8	$\mu^+\mu^-\gamma$	(1.09±0.27) $\times 10^{-4}$	
Γ_9	$\pi^+\pi^-\mu^+\mu^-$	< 2.9 $\times 10^{-5}$	90%
Γ_{10}	$\pi^+\pi^-\pi^0$	(3.61±0.17) $\times 10^{-3}$	
Γ_{11}	$(\pi^+\pi^-\pi^0)$ S-wave	(3.8 ±0.5) $\times 10^{-3}$	
Γ_{12}	$\pi^\mp\rho^\pm$	(7.4 ±2.3) $\times 10^{-4}$	
Γ_{13}	$\pi^0\rho^0$	< 4 %	90%
Γ_{14}	$2(\pi^+\pi^-)$	(8.6 ±0.9) $\times 10^{-5}$	
Γ_{15}	$\pi^+\pi^-2\pi^0$	(1.8 ±0.4) $\times 10^{-4}$	
Γ_{16}	$2(\pi^+\pi^-)$ neutrals	< 1 %	95%
Γ_{17}	$2(\pi^+\pi^-)\pi^0$	< 1.8 $\times 10^{-3}$	90%
Γ_{18}	$2(\pi^+\pi^-)2\pi^0$	< 1 %	95%
Γ_{19}	$3(\pi^+\pi^-)$	< 3.1 $\times 10^{-5}$	90%
Γ_{20}	$K^\pm\pi^\mp$	< 4 $\times 10^{-5}$	90%
Γ_{21}	$\pi^+\pi^-e^+e^-$	(2.4 $^{+1.3}_{-1.0}$) $\times 10^{-3}$	
Γ_{22}	$\pi^+e^-\nu_e$ + c.c.	< 2.1 $\times 10^{-4}$	90%
Γ_{23}	γe^+e^-	(4.73±0.30) $\times 10^{-4}$	
Γ_{24}	$\pi^0\gamma\gamma$	(3.20±0.24) $\times 10^{-3}$	
Γ_{25}	$\pi^0\gamma\gamma$(non resonant)	(6.2 ±0.9) $\times 10^{-4}$	
Γ_{26}	$4\pi^0$	< 3.2 $\times 10^{-4}$	90%
Γ_{27}	e^+e^-	< 5.6 $\times 10^{-9}$	90%
Γ_{28}	invisible	< 5 $\times 10^{-4}$	90%

Charge conjugation (C), Parity (P), Lepton family number (LF) violating modes

Γ_{29}	$\pi^+\pi^-$	P,CP	< 1.8	$\times 10^{-5}$	90%
Γ_{30}	$\pi^0\pi^0$	P,CP	< 5	$\times 10^{-4}$	90%
Γ_{31}	$\pi^0e^+e^-$	C	[a] < 1.4	$\times 10^{-3}$	90%
Γ_{32}	ηe^+e^-	C	[a] < 2.4	$\times 10^{-3}$	90%
Γ_{33}	3γ	C	< 1.1	$\times 10^{-4}$	90%
Γ_{34}	$\mu^+\mu^-\pi^0$	C	[a] < 6.0	$\times 10^{-5}$	90%
Γ_{35}	$\mu^+\mu^-\eta$	C	[a] < 1.5	$\times 10^{-5}$	90%
Γ_{36}	$e\mu$	LF	< 4.7	$\times 10^{-4}$	90%

[a] C parity forbids this to occur as a single-photon process.

CONSTRAINED FIT INFORMATION

An overall fit to the total width, a partial width, 2 combinations of partial widths obtained from integrated cross section, and 16 branching ratios uses 46 measurements and one constraint to determine 9 parameters. The overall fit has a $\chi^2 = 62.7$ for 38 degrees of freedom.

The following *off-diagonal* array elements are the correlation coefficients $\langle \delta p_i \delta p_j \rangle / (\delta p_i \cdot \delta p_j)$, in percent, from the fit to parameters p_i, including the branching fractions, $x_i \equiv \Gamma_i/\Gamma_{\text{total}}$. The fit constrains the x_i whose labels appear in this array to sum to one.

	x_1	x_2	x_3	x_4	x_6	x_7	x_{10}	x_{21}
x_2	−3							
x_3	−76	−58						
x_4	−10	−13	1					
x_6	−27	−24	29	−1				
x_7	−23	−18	28	0	8			
x_{10}	0	−1	−1	0	−1	0		
x_{21}	−5	−6	−5	−1	−3	−2	0	
Γ	24	4	−17	3	−71	−4	1	3

	Mode	Rate (MeV)
Γ_1	$\pi^+\pi^-\eta$	0.084 ±0.004
Γ_2	$\rho^0\gamma$(including non-resonant $\pi^+\pi^-\gamma$)	0.0567 ±0.0027
Γ_3	$\pi^0\pi^0\eta$	0.0448 ±0.0023
Γ_4	$\omega\gamma$	0.00514±0.00035
Γ_6	$\gamma\gamma$	0.00436±0.00013
Γ_7	$3\pi^0$	(5.0 ±0.4) $\times 10^{-4}$
Γ_{10}	$\pi^+\pi^-\pi^0$	(7.1 ±0.5) $\times 10^{-4}$
Γ_{21}	$\pi^+\pi^-e^+e^-$	(4.6 $^{+2.5}_{-1.9}$) $\times 10^{-4}$

$\eta'(958)$ PARTIAL WIDTHS

$\Gamma(\gamma\gamma)$ Γ_6

VALUE (keV)	EVTS	DOCUMENT ID		TECN	COMMENT
4.36±0.14 OUR FIT					
4.28±0.19 OUR AVERAGE					
4.17±0.10±0.27	2000	[1] ACCIARRI	98Q	L3	$e^+e^- \to e^+e^-\pi^+\pi^-\gamma$
4.53±0.29±0.51	266	KARCH	92	CBAL	$e^+e^- \to e^+e^-\eta\pi^0\pi^0$
3.61±0.13±0.48		[2] BEHREND	91	CELL	$e^+e^- \to e^+e^-\eta'(958)$
4.6 ±1.1 ±0.6	23	BARU	90	MD1	$e^+e^- \to e^+e^-\pi^+\pi^-\gamma$
4.57±0.25±0.44		BUTLER	90	MRK2	$e^+e^- \to e^+e^-\eta'(958)$
5.08±0.24±0.71	547	[3] ROE	90	ASP	$e^+e^- \to e^+e^-2\gamma$
3.8 ±0.7 ±0.6	34	AIHARA	88C	TPC	$e^+e^- \to e^+e^-\eta\pi^+\pi^-$
4.9 ±0.5 ±0.5	136	[4] WILLIAMS	88	CBAL	$e^+e^- \to e^+e^-2\gamma$
• • • We do not use the following data for averages, fits, limits, etc. • • •					
4.7 ±0.6 ±0.9	143	[5] GIDAL	87	MRK2	$e^+e^- \to e^+e^-\eta\pi^+\pi^-$
4.0 ±0.9		[6] BARTEL	85E	JADE	$e^+e^- \to e^+e^-2\gamma$

[1] No non-resonant $\pi^+\pi^-$ contribution found.
[2] Reevaluated by us using $B(\eta' \to \rho(770)\gamma) = (30.2 \pm 1.3)\%$.
[3] Reevaluated by us using $B(\eta' \to \gamma\gamma) = (2.11 \pm 0.13)\%$.
[4] Reevaluated by us using $B(\eta' \to \gamma\gamma) = (2.11 \pm 0.13)\%$.
[5] Superseded by BUTLER 90.
[6] Systematic error not evaluated.

$\Gamma(e^+e^-)$ Γ_{27}

VALUE (eV)	CL%	DOCUMENT ID		TECN	COMMENT
$<1.1\times10^{-3}$	90	[1,2] ACHASOV	15	SND	0.958 $e^+e^-\to\pi\pi\eta$
• • • We do not use the following data for averages, fits, limits, etc. • • •					
$<2.0\times10^{-3}$	90	[2] ACHASOV	15	SND	0.958 $e^+e^-\to\pi\pi\eta$
$<2.4\times10^{-3}$	90	[2] AKHMETSHIN	15	CMD3	0.958 $e^+e^-\to\pi^+\pi^-\eta$

[1] Combining data of ACHASOV 15 and AKHMETSHIN 15.
[2] Using η and η' branching fractions from PDG 14.

$\eta'(958)$ Γ(i)$\Gamma(\gamma\gamma)/\Gamma$(total)

This combination of a partial width with the partial width into $\gamma\gamma$ and with the total width is obtained from the integrated cross section into channel(i) in the $\gamma\gamma$ annihilation.

$\Gamma(\gamma\gamma)\times\Gamma(\rho^0\gamma(\text{including non-resonant}\,\pi^+\pi^-\gamma))/\Gamma_{\text{total}}$ $\Gamma_6\Gamma_2/\Gamma$

VALUE (keV)	EVTS	DOCUMENT ID		TECN	COMMENT
1.26±0.04 OUR FIT					
1.26±0.07 OUR AVERAGE		Error includes scale factor of 1.2.			
1.09±0.04±0.13		BEHREND	91	CELL	$e^+e^-\to e^+e^-\rho(770)^0\gamma$
1.35±0.09±0.21		AIHARA	87	TPC	$e^+e^-\to e^+e^-\rho\gamma$
1.13±0.04±0.13	867	ALBRECHT	87B	ARG	$e^+e^-\to e^+e^-\rho\gamma$
1.53±0.09±0.21		ALTHOFF	84E	TASS	$e^+e^-\to e^+e^-\rho\gamma$
1.14±0.08±0.11	243	BERGER	84B	PLUT	$e^+e^-\to e^+e^-\rho\gamma$
1.73±0.34±0.35	95	JENNI	83	MRK2	$e^+e^-\to e^+e^-\rho\gamma$
1.49±0.13±0.027	213	BARTEL	82B	JADE	$e^+e^-\to e^+e^-\rho\gamma$
• • • We do not use the following data for averages, fits, limits, etc. • • •					
1.85±0.31±0.24	43	BEHREND	82C	CELL	$e^+e^-\to e^+e^-\rho\gamma$

$\Gamma(\gamma\gamma)\times\Gamma(\pi^0\pi^0\eta)/\Gamma_{\text{total}}$ $\Gamma_6\Gamma_3/\Gamma$

VALUE (keV)	DOCUMENT ID		TECN	COMMENT
1.00±0.05 OUR FIT				
0.92±0.06±0.11	[1] KARCH	92	CBAL	$e^+e^-\to e^+e^-\eta\pi^0\pi^0$
• • • We do not use the following data for averages, fits, limits, etc. • • •				
0.95±0.05±0.08	[2] KARCH	90	CBAL	$e^+e^-\to e^+e^-\eta\pi^0\pi^0$
1.00±0.08±0.10	[2,3] ANTREASYAN	87	CBAL	$e^+e^-\to e^+e^-\eta\pi^0\pi^0$

[1] Reevaluated by us using $B(\eta\to\gamma\gamma)=(39.21\pm0.34)\%$. Supersedes ANTREASYAN 87 and KARCH 90.
[2] Superseded by KARCH 92.
[3] Using BR($\eta\to 2\gamma$)=(38.9 ± 0.5)%.

$\eta'(958)$ Γ(i)$\Gamma(e^+e^-)/\Gamma$(total)

$\Gamma(\pi^+\pi^-\eta)\times\Gamma(e^+e^-)/\Gamma_{\text{total}}$ $\Gamma_1\Gamma_{27}/\Gamma$

VALUE (10^{-3} eV)	CL%	DOCUMENT ID		TECN	COMMENT
<1.0	90	[1] AKHMETSHIN	15	CMD3	0.958 $e^+e^-\to\pi^+\pi^-\eta$

[1] AKHMETSHIN 15 reports $[\Gamma(\eta'(958)\to\pi^+\pi^-\eta)\times\Gamma(\eta'(958)\to e^+e^-)/\Gamma_{\text{total}}]\times[B(\eta\to 2\gamma)]<4.1\times10^{-4}$ eV which we divide by our best value $B(\eta\to 2\gamma)=39.41\times10^{-2}$.

$\eta'(958)$ BRANCHING RATIOS

$\Gamma(\pi^+\pi^-\eta)/\Gamma_{\text{total}}$ Γ_1/Γ

VALUE	EVTS	DOCUMENT ID		TECN	COMMENT
0.426±0.007 OUR FIT					
• • • We do not use the following data for averages, fits, limits, etc. • • •					
0.424±0.011±0.004	1.2k	[1] PEDLAR	09	CLEO	$J/\psi\to\gamma\eta'$

[1] Not independent of other η' branching fractions and ratios in PEDLAR 09.

$\Gamma(\pi^+\pi^-\eta(\text{charged decay}))/\Gamma_{\text{total}}$ $0.2810\Gamma_1/\Gamma$

VALUE	EVTS	DOCUMENT ID		TECN	COMMENT
0.1196±0.0019 OUR FIT					
• • • We do not use the following data for averages, fits, limits, etc. • • •					
0.123 ±0.014	107	RITTENBERG	69	HBC	1.7–2.7 K^-p
0.10 ±0.04	10	LONDON	66	HBC	2.24 $K^-p\to\Lambda 2\pi^+2\pi^-\pi^0$
0.07 ±0.04	7	BADIER	65B	HBC	3 K^-p

$\Gamma(\pi^+\pi^-\eta(\text{neutral decay}))/\Gamma_{\text{total}}$ $0.7212\Gamma_1/\Gamma$

VALUE	EVTS	DOCUMENT ID		TECN	COMMENT
0.307±0.005 OUR FIT					
• • • We do not use the following data for averages, fits, limits, etc. • • •					
0.314±0.026	281	RITTENBERG	69	HBC	1.7–2.7 K^-p

$\Gamma(\rho^0\gamma(\text{including non-resonant}\,\pi^+\pi^-\gamma))/\Gamma_{\text{total}}$ Γ_2/Γ

VALUE	EVTS	DOCUMENT ID		TECN	COMMENT
0.289±0.005 OUR FIT					
• • • We do not use the following data for averages, fits, limits, etc. • • •					
0.287±0.007±0.004	0.2k	[1] PEDLAR	09	CLEO	$J/\psi\to\gamma\eta'$
0.329±0.033	298	RITTENBERG	69	HBC	1.7–2.7 K^-p
0.2 ±0.1	20	LONDON	66	HBC	2.24 $K^-p\to\Lambda\pi^+\pi^-\gamma$
0.34 ±0.09	35	BADIER	65B	HBC	3 K^-p

[1] Not independent of other η' branching fractions and ratios in PEDLAR 09.

$\Gamma(\rho^0\gamma(\text{including non-resonant}\,\pi^+\pi^-\gamma))/\Gamma(\pi^+\pi^-\eta)$ Γ_2/Γ_1

VALUE	DOCUMENT ID		TECN	COMMENT
0.679±0.017 OUR FIT				
0.683±0.020 OUR AVERAGE				
0.677±0.024±0.011	PEDLAR	09	CLE3	$J/\psi\to\eta'\gamma$
0.69 ±0.03	ABLIKIM	06E	BES2	$J/\psi\to\eta'\gamma$

$\Gamma(\rho^0\gamma(\text{including non-resonant}\,\pi^+\pi^-\gamma))/\Gamma(\pi^+\pi^-\eta(\text{neutral decay}))$ $\Gamma_2/0.714\Gamma_1$

VALUE	EVTS	DOCUMENT ID		TECN	COMMENT
0.951±0.024 OUR FIT					
0.97 ±0.09 OUR AVERAGE					
0.70 ±0.22		AMSLER	04B	CBAR	0 $\bar{p}p\to\pi^+\pi^-\eta$
1.07 ±0.17		BELADIDZE	92C	VES	36 π^-Be $\to\pi^-\eta'\eta$Be
0.92 ±0.14	473	DANBURG	73	HBC	2.2 $K^-p\to\Lambda X^0$
1.11 ±0.18	192	JACOBS	73	HBC	2.9 $K^-p\to\Lambda X^0$

$\Gamma(\pi^0\pi^0\eta)/\Gamma_{\text{total}}$ Γ_3/Γ

VALUE	EVTS	DOCUMENT ID		TECN	COMMENT
0.228±0.008 OUR FIT					
• • • We do not use the following data for averages, fits, limits, etc. • • •					
0.235±0.013±0.004	3.2k	[1] PEDLAR	09	CLEO	$J/\psi\to\gamma\eta'$

[1] Not independent of other η' branching fractions and ratios in PEDLAR 09.

$\Gamma(\pi^0\pi^0\eta(3\pi^0\text{ decay}))/\Gamma_{\text{total}}$ $0.321\Gamma_3/\Gamma$

VALUE	EVTS	DOCUMENT ID		TECN	COMMENT
0.0733±0.0026 OUR FIT					
• • • We do not use the following data for averages, fits, limits, etc. • • •					
0.11 ±0.06	4	BENSINGER	70	DBC	2.2 π^+d

$\Gamma(\pi^0\pi^0\eta)/\Gamma(\pi^+\pi^-\eta)$ Γ_3/Γ_1

VALUE	DOCUMENT ID		TECN	COMMENT
0.536±0.026 OUR FIT				
0.555±0.043±0.013	PEDLAR	09	CLE3	$J/\psi\to\eta'\gamma$

$\Gamma(\rho^0\gamma(\text{including non-resonant}\,\pi^+\pi^-\gamma))/\Gamma(\pi\pi\eta)$ $\Gamma_2/(\Gamma_1+\Gamma_3)$

VALUE	DOCUMENT ID		TECN	COMMENT
0.442±0.012 OUR FIT				
0.43 ±0.02 ±0.02	BARBERIS	98C	OMEG	450 $pp\to p_f\eta' p_s$
• • • We do not use the following data for averages, fits, limits, etc. • • •				
0.31 ±0.15	DAVIS	68	HBC	5.5 K^-p

$\Gamma(\omega\gamma)/\Gamma_{\text{total}}$ Γ_4/Γ

VALUE (units 10^{-2})	EVTS	DOCUMENT ID		TECN	COMMENT
2.62±0.13 OUR FIT					
2.55±0.03±0.16	33.2k	[1] ABLIKIM	15AD	BES3	$J/\psi\to\eta'\gamma$
• • • We do not use the following data for averages, fits, limits, etc. • • •					
2.34±0.30±0.04	70	[2] PEDLAR	09	CLEO	$J/\psi\to\gamma\eta'$

[1] Using $B(J/\psi\to\eta'\gamma)=(5.15\pm0.16)\times10^{-3}$ and $B(\omega\to\pi^+\pi^-\pi^0)=(89.2\pm0.7)\%$.
[2] Not independent of other η' branching fractions and ratios in PEDLAR 09.

$\Gamma(\omega\gamma)/\Gamma(\pi^+\pi^-\eta)$ Γ_4/Γ_1

VALUE	EVTS	DOCUMENT ID		TECN	COMMENT
0.0615±0.0033 OUR FIT					
0.055 ±0.007 ±0.001		PEDLAR	09	CLE3	$J/\psi\to\eta'\gamma$
• • • We do not use the following data for averages, fits, limits, etc. • • •					
0.068 ±0.013	68	ZANFINO	77	ASPK	8.4 π^-p

$\Gamma(\omega\gamma)/\Gamma(\pi^0\pi^0\eta)$ Γ_4/Γ_3

VALUE	DOCUMENT ID		TECN	COMMENT
0.115±0.007 OUR FIT				
0.147±0.016	ALDE	87B	GAM2	38 $\pi^-p\to n4\gamma$

$\Gamma(\omega e^+e^-)/\Gamma(\omega\gamma)$ Γ_5/Γ_4

VALUE (units 10^{-3})	DOCUMENT ID		TECN	COMMENT
• • • We do not use the following data for averages, fits, limits, etc. • • •				
7.71±1.34±0.54	[1] ABLIKIM	15AD	BES3	$J/\psi\to\eta'\gamma$

[1] Obtained from other ABLIKIM 15AD meausurements with common systematics taken into account.

$\Gamma(\omega e^+e^-)/\Gamma_{\text{total}}$ Γ_5/Γ

VALUE (units 10^{-4})	EVTS	DOCUMENT ID		TECN	COMMENT
1.97±0.34±0.17	66	[1] ABLIKIM	15AD	BES3	$J/\psi\to\eta'\gamma$

[1] Using $B(J/\psi\to\eta'\gamma)=(5.15\pm0.16)\times10^{-3}$ and $B(\omega\to\pi^+\pi^-\pi^0)=(89.2\pm0.7)\%$.

$\Gamma(\rho^0\gamma(\text{including non-resonant}\,\pi^+\pi^-\gamma))/[\Gamma(\pi^+\pi^-\eta)+\Gamma(\pi^0\pi^0\eta)+\Gamma(\omega\gamma)]$ $\Gamma_2/(\Gamma_1+\Gamma_3+\Gamma_4)$

VALUE	DOCUMENT ID		TECN	COMMENT
0.425±0.011 OUR FIT				
• • • We do not use the following data for averages, fits, limits, etc. • • •				
0.25 ±0.14	DAUBER	64	HBC	1.95 K^-p

Meson Particle Listings

$\eta'(958)$

$[\Gamma(\pi^0\pi^0\eta(\text{charged decay})) + \Gamma(\omega(\text{charged decay})\gamma)]/\Gamma_{\text{total}}$ $(0.286\Gamma_3+0.89\Gamma_4)/\Gamma$

VALUE	EVTS	DOCUMENT ID		TECN	COMMENT
0.0886±0.0026 OUR FIT					
• • • We do not use the following data for averages, fits, limits, etc. • • •					
0.045 ±0.029	42	RITTENBERG	69	HBC	1.7–2.7 K^-p

$\Gamma(\pi^+\pi^-\text{neutrals})/\Gamma_{\text{total}}$ $(0.714\Gamma_1+0.286\Gamma_3+0.89\Gamma_4)/\Gamma$

VALUE	EVTS	DOCUMENT ID		TECN	COMMENT
0.3926±0.0035 OUR FIT					
• • • We do not use the following data for averages, fits, limits, etc. • • •					
0.4 ±0.1	39	LONDON	66	HBC	2.24 $K^-p \to \Lambda\pi^+\pi^-$ neutrals
0.35 ±0.06	33	BADIER	65B	HBC	3 K^-p

$\Gamma(\gamma\gamma)/\Gamma_{\text{total}}$ Γ_6/Γ

VALUE (units 10^{-2})	EVTS	DOCUMENT ID		TECN	COMMENT
2.22±0.08 OUR FIT					
2.00±0.15 OUR AVERAGE					
$1.98^{+0.31}_{-0.27}\pm0.07$	114	[1] WICHT	08	BELL	$B^\pm \to K^\pm\gamma\gamma$
2.00±0.18		[2] STANTON	80	SPEC	8.45 $\pi^-p \to n\pi^+\pi^-2\gamma$
• • • We do not use the following data for averages, fits, limits, etc. • • •					
2.25±0.16±0.03	0.3k	[3] PEDLAR	09	CLEO	$J/\psi \to \gamma\eta'$
1.8 ±0.2	6000	[4] APEL	79	NICE	15–40 $\pi^-p \to n2\gamma$
2.5 ±0.7		DUANE	74	MMS	$\pi^-p \to n$MM
1.71±0.33	68	DALPIAZ	72	CNTR	1.6 $\pi^-p \to nX^0$
$2.0\ ^{+0.8}_{-0.6}$	31	HARVEY	71	OSPK	3.65 $\pi^-p \to nX^0$

[1] WICHT 08 reports $[\Gamma(\eta'(958) \to \gamma\gamma)/\Gamma_{\text{total}}] \times [B(B^+ \to \eta' K^+)] = (1.40^{+0.16}_{-0.15}{}^{+0.15}_{-0.12}) \times 10^{-6}$ which we divide by our best value $B(B^+ \to \eta' K^+) = (7.06 \pm 0.25) \times 10^{-5}$. Our first error is their experiment's error and our second error is the systematic error from using our best value.
[2] Includes APEL 79 result.
[3] Not independent of other η' branching fractions and ratios in PEDLAR 09.
[4] Data is included in STANTON 80 evaluation.

$\Gamma(\gamma\gamma)/\Gamma(\pi^+\pi^-\eta)$ Γ_6/Γ_1

VALUE	DOCUMENT ID		TECN	COMMENT
0.0522±0.0022 OUR FIT				
0.053 ±0.004 ±0.001	PEDLAR	09	CLE3	$J/\psi \to \eta'\gamma$

$\Gamma(\gamma\gamma)/\Gamma(\rho^0\gamma(\text{including non-resonant } \pi^+\pi^-\gamma))$ Γ_6/Γ_2

VALUE	DOCUMENT ID		TECN	COMMENT
0.0768±0.0033 OUR FIT				
0.080 ±0.008	ABLIKIM	06E	BES2	$J/\psi \to \eta'\gamma$

$\Gamma(\gamma\gamma)/\Gamma(\pi^0\pi^0\eta)$ Γ_6/Γ_3

VALUE	DOCUMENT ID		TECN	COMMENT
0.097±0.004 OUR FIT				
0.105±0.010 OUR AVERAGE Error includes scale factor of 1.9.				
0.091±0.009	AMSLER	93	CBAR	0.0 $\bar{p}p$
0.112±0.002±0.006	ALDE	87B	GAM2	38 $\pi^-p \to n2\gamma$

$\Gamma(\gamma\gamma)/\Gamma(\pi^0\pi^0\eta(\text{neutral decay}))$ $\Gamma_6/0.714\Gamma_3$

VALUE	EVTS	DOCUMENT ID		TECN	COMMENT
0.136±0.006 OUR FIT					
• • • We do not use the following data for averages, fits, limits, etc. • • •					
0.188±0.058	16	APEL	72	OSPK	3.8 $\pi^-p \to nX^0$

$\Gamma(\text{neutrals})/\Gamma_{\text{total}}$ $(0.714\Gamma_3+0.09\Gamma_4+\Gamma_6)/\Gamma$

VALUE	EVTS	DOCUMENT ID		TECN	COMMENT
0.188±0.006 OUR FIT					
• • • We do not use the following data for averages, fits, limits, etc. • • •					
0.185±0.022	535	BASILE	71	CNTR	1.6 $\pi^-p \to nX^0$
0.189±0.026	123	RITTENBERG	69	HBC	1.7–2.7 K^-p

$\Gamma(3\pi^0)/\Gamma_{\text{total}}$ Γ_7/Γ

VALUE (units 10^{-3})	EVTS	DOCUMENT ID		TECN	COMMENT
2.54 ±0.18 OUR FIT					
3.57 ±0.26 OUR AVERAGE					
3.522±0.082±0.254	2015	ABLIKIM	17	BES3	$J/\psi \to \gamma(3\pi^0)$
4.79 ±0.59 ±1.14	183	[1] ABLIKIM	15P	BES3	$J/\psi \to K^+K^-3\pi$
• • • We do not use the following data for averages, fits, limits, etc. • • •					
3.56 ±0.22 ±0.34	309	[2] ABLIKIM	12E	BES3	$J/\psi \to \gamma(3\pi^0)$

[1] We have added all systematic uncertainties in quadrature to a single value.
[2] Superseded by ABLIKIM 17.

$\Gamma(3\pi^0)/\Gamma(\pi^0\pi^0\eta)$ Γ_7/Γ_3

VALUE (units 10^{-4})	EVTS	DOCUMENT ID		TECN	COMMENT
111± 8 OUR FIT					
78±10 OUR AVERAGE					
86±19	235	BLIK	08	GAMS	32 $\pi^-p \to \eta' n$
74±15		ALDE	87B	GAM2	38 $\pi^-p \to n6\gamma$
75±18		BINON	84	GAM2	30–40 $\pi^-p \to n6\gamma$

$\Gamma(\mu^+\mu^-\gamma)/\Gamma(\gamma\gamma)$ Γ_8/Γ_6

VALUE (units 10^{-3})	EVTS	DOCUMENT ID		TECN	COMMENT
4.9±1.2	33	VIKTOROV	80	CNTR	25,33 $\pi^-p \to 2\mu\gamma$

$\Gamma(\pi^+\pi^-\mu^+\mu^-)/\Gamma_{\text{total}}$ Γ_9/Γ

VALUE (units 10^{-4})	CL%	DOCUMENT ID		TECN	COMMENT
• • • We do not use the following data for averages, fits, limits, etc. • • •					
<0.29	90	[1] ABLIKIM	13O	BES3	$J/\psi \to \gamma\eta'$
<2.4	90	[2] NAIK	09	CLEO	$J/\psi \to \gamma\eta'$

[1] Using $\Gamma_2/\Gamma = (29.3 \pm 0.6)\%$ from PDG 12.
[2] Not independent of measured value of Γ_9/Γ_1 from NAIK 09.

$\Gamma(\pi^+\pi^-\mu^+\mu^-)/\Gamma(\pi^+\pi^-\eta)$ Γ_9/Γ_1

VALUE (units 10^{-3})	CL%	DOCUMENT ID		TECN	COMMENT
<0.5	90	[1] NAIK	09	CLEO	$J/\psi \to \gamma\eta'$

[1] NAIK 09 reports $[\Gamma(\eta'(958) \to \pi^+\pi^-\mu^+\mu^-)/\Gamma(\eta'(958) \to \pi^+\pi^-\eta)]$ / $[B(\eta \to 2\gamma)] < 1.3 \times 10^{-3}$ which we multiply by our best value $B(\eta \to 2\gamma) = 39.41 \times 10^{-2}$.

$\Gamma(\pi^+\pi^-\mu^+\mu^-)/\Gamma(\rho^0\gamma(\text{including non-resonant } \pi^+\pi^-\gamma))$ Γ_9/Γ_2

VALUE (units 10^{-4})	CL%	DOCUMENT ID		TECN	COMMENT
<1.0	90	ABLIKIM	13O	BES3	$J/\psi \to \gamma\eta'$

$\Gamma(\pi^+\pi^-\pi^0)/\Gamma_{\text{total}}$ Γ_{10}/Γ

VALUE (units 10^{-3})	EVTS	DOCUMENT ID		TECN	COMMENT
3.61 ±0.18 OUR FIT					
3.61 ±0.18 OUR AVERAGE					
3.591±0.054±0.174	6067	ABLIKIM	17	BES3	$J/\psi \to \gamma(\pi^+\pi^-\pi^0)$
4.28 ±0.49 ±1.11	78	[1] ABLIKIM	15P	BES3	$J/\psi \to K^+K^-3\pi$
$3.7\ ^{+1.1}_{-0.9}$ ±0.4		[2] NAIK	09	CLEO	$J/\psi \to \gamma\eta'$
• • • We do not use the following data for averages, fits, limits, etc. • • •					
3.83 ±0.15 ±0.39	1014	[3] ABLIKIM	12E	BES3	$J/\psi \to \gamma(\pi^+\pi^-\pi^0)$

[1] We have added all systematic uncertainties in quadrature to a single value.
[2] Not independent of measured value of Γ_{10}/Γ_1 from NAIK 09.
[3] Superseded by ABLIKIM 17.

$\Gamma((\pi^+\pi^-\pi^0)\ S\text{-wave})/\Gamma_{\text{total}}$ Γ_{11}/Γ

VALUE (units 10^{-4})	EVTS	DOCUMENT ID		TECN	COMMENT
37.63±0.77±5.00	6580	[1] ABLIKIM	17	BES3	$J/\psi \to \gamma(\pi^+\pi^-\pi^0)$

[1] We have added all systematic uncertainties in quadrature .

$\Gamma(\pi^\mp\rho^\pm)/\Gamma_{\text{total}}$ Γ_{12}/Γ

VALUE (units 10^{-4})	EVTS	DOCUMENT ID		TECN	COMMENT
7.44±0.60±2.23	1231	[1] ABLIKIM	17	BES3	$J/\psi \to \gamma(\pi^\mp\rho^\pm)$

[1] We have added all systematic uncertainties in quadrature .

$\Gamma(\pi^+\pi^-\pi^0)/\Gamma(\pi^+\pi^-\eta)$ Γ_{10}/Γ_1

VALUE (units 10^{-3})	EVTS	DOCUMENT ID		TECN	COMMENT
8.5 ±0.4 OUR FIT					
$8.28^{+2.49}_{-2.12}\pm0.04$	20	[1] NAIK	09	CLEO	$J/\psi \to \gamma\eta'$

[1] NAIK 09 reports $[\Gamma(\eta'(958) \to \pi^+\pi^-\pi^0)/\Gamma(\eta'(958) \to \pi^+\pi^-\eta)]$ / $[B(\eta \to 2\gamma)] = (21^{+6}_{-5} \pm 2) \times 10^{-3}$ which we multiply by our best value $B(\eta \to 2\gamma) = (39.41 \pm 0.20) \times 10^{-2}$. Our first error is their experiment's error and our second error is the systematic error from using our best value.

$\Gamma(\pi^0\rho^0)/\Gamma_{\text{total}}$ Γ_{13}/Γ

VALUE	CL%	DOCUMENT ID		TECN	COMMENT
<0.04	90	RITTENBERG	65	HBC	2.7 K^-p

$\Gamma(2(\pi^+\pi^-))/\Gamma_{\text{total}}$ Γ_{14}/Γ

VALUE (units 10^{-5})	CL%	EVTS	DOCUMENT ID		TECN	COMMENT
8.6±0.9±0.3		199	[1] ABLIKIM	14M	BES3	$J/\psi \to \gamma\eta'$
• • • We do not use the following data for averages, fits, limits, etc. • • •						
< 24	90		[2] NAIK	09	CLEO	$J/\psi \to \gamma\eta'$
<1000	90		RITTENBERG	69	HBC	1.7–2.7 K^-p

[1] ABLIKIM 14M reports $[\Gamma(\eta'(958) \to 2(\pi^+\pi^-))/\Gamma_{\text{total}}] \times [B(J/\psi(1S) \to \gamma\eta'(958))] = (4.40 \pm 0.35 \pm 0.30) \times 10^{-7}$ which we divide by our best value $B(J/\psi(1S) \to \gamma\eta'(958)) = (5.13 \pm 0.17) \times 10^{-3}$. Our first error is their experiment's error and our second error is the systematic error from using our best value.
[2] Not independent of measured value of Γ_{14}/Γ_1 from NAIK 09.

$\Gamma(2(\pi^+\pi^-))/\Gamma(\pi^+\pi^-\eta)$ Γ_{14}/Γ_1

VALUE (units 10^{-3})	CL%	DOCUMENT ID		TECN	COMMENT
<0.6	90	[1] NAIK	09	CLEO	$J/\psi \to \gamma\eta'$

[1] NAIK 09 reports $[\Gamma(\eta'(958) \to 2(\pi^+\pi^-))/\Gamma(\eta'(958) \to \pi^+\pi^-\eta)]$ / $[B(\eta \to 2\gamma)] < 1.4 \times 10^{-3}$ which we multiply by our best value $B(\eta \to 2\gamma) = 39.41 \times 10^{-2}$.

$\Gamma(\pi^+\pi^-2\pi^0)/\Gamma_{total}$ Γ_{15}/Γ

VALUE (units 10^{-4})	CL%	EVTS	DOCUMENT ID		TECN	COMMENT
1.8±0.4±0.1		84	[1] ABLIKIM	14M	BES3	$J/\psi \to \gamma\eta'$
• • • We do not use the following data for averages, fits, limits, etc. • • •						
<27	90		[2] NAIK	09	CLEO	$J/\psi \to \gamma\eta'$

[1] ABLIKIM 14M reports $[\Gamma(\eta'(958) \to \pi^+\pi^-2\pi^0)/\Gamma_{total}] \times [B(J/\psi(1S) \to \gamma\eta'(958))] = (9.38\pm1.79\pm0.89)\times10^{-7}$ which we divide by our best value $B(J/\psi(1S) \to \gamma\eta'(958)) = (5.13\pm0.17)\times10^{-3}$. Our first error is their experiment's error and our second error is the systematic error from using our best value.
[2] Not independent of measured value of Γ_{15}/Γ_1 from NAIK 09.

$\Gamma(\pi^+\pi^-2\pi^0)/\Gamma(\pi^+\pi^-\eta)$ Γ_{15}/Γ_1

VALUE (units 10^{-3})	CL%	DOCUMENT ID		TECN	COMMENT
<6	90	[1] NAIK	09	CLEO	$J/\psi \to \gamma\eta'$

[1] NAIK 09 reports $[\Gamma(\eta'(958) \to \pi^+\pi^-2\pi^0)/\Gamma(\eta'(958) \to \pi^+\pi^-\eta)] / [B(\eta \to 2\gamma)] < 15\times10^{-3}$ which we multiply by our best value $B(\eta \to 2\gamma) = 39.41\times10^{-2}$.

$\Gamma(2(\pi^+\pi^-)$ neutrals$)/\Gamma_{total}$ Γ_{16}/Γ

VALUE	CL%	DOCUMENT ID		TECN	COMMENT
<0.01	95	DANBURG	73	HBC	2.2 $K^-p \to \Lambda X^0$
• • • We do not use the following data for averages, fits, limits, etc. • • •					
<0.01	90	RITTENBERG	69	HBC	1.7–2.7 K^-p

$\Gamma(2(\pi^+\pi^-)\pi^0)/\Gamma_{total}$ Γ_{17}/Γ

VALUE	CL%	DOCUMENT ID		TECN	COMMENT
• • • We do not use the following data for averages, fits, limits, etc. • • •					
<0.002	90	[1] NAIK	09	CLEO	$J/\psi \to \gamma\eta'$
<0.01	90	RITTENBERG	69	HBC	1.7–2.7 K^-p

[1] Not independent of measured value of Γ_{17}/Γ_1 from NAIK 09.

$\Gamma(2(\pi^+\pi^-)\pi^0)/\Gamma(\pi^+\pi^-\eta)$ Γ_{17}/Γ_1

VALUE (units 10^{-3})	CL%	DOCUMENT ID		TECN	COMMENT
<4	90	[1] NAIK	09	CLEO	$J/\psi \to \gamma\eta'$

[1] NAIK 09 reports $[\Gamma(\eta'(958) \to 2(\pi^+\pi^-)\pi^0)/\Gamma(\eta'(958) \to \pi^+\pi^-\eta)] / [B(\eta \to 2\gamma)] < 11\times10^{-3}$ which we multiply by our best value $B(\eta \to 2\gamma) = 39.41\times10^{-2}$.

$\Gamma(2(\pi^+\pi^-)2\pi^0)/\Gamma_{total}$ Γ_{18}/Γ

VALUE	CL%	DOCUMENT ID		TECN	COMMENT
<0.01	95	KALBFLEISCH	64B	HBC	$K^-p \to \Lambda 2(\pi^+\pi^-)$+MM
• • • We do not use the following data for averages, fits, limits, etc. • • •					
<0.01	90	LONDON	66	HBC	Compilation

$\Gamma(3(\pi^+\pi^-))/\Gamma_{total}$ Γ_{19}/Γ

VALUE (units 10^{-5})	CL%	DOCUMENT ID		TECN	COMMENT
< 3.1	90	[1] ABLIKIM	13U	BES3	$J/\psi \to \gamma 3(\pi^+\pi^-)$
• • • We do not use the following data for averages, fits, limits, etc. • • •					
< 53	90	[2] NAIK	09	CLEO	$J/\psi \to \gamma\eta'$
<500	95	KALBFLEISCH	64B	HBC	$K^-p \to \Lambda 2(\pi^+\pi^-)$

[1] Using $B(J/\psi \to \gamma\eta'(958)) = (5.16\pm0.15)\times10^{-3}$.
[2] Not independent of measured value of Γ_{19}/Γ_1 from NAIK 09.

$\Gamma(3(\pi^+\pi^-))/\Gamma(\pi^+\pi^-\eta)$ Γ_{19}/Γ_1

VALUE (units 10^{-3})	CL%	DOCUMENT ID		TECN	COMMENT
<1.2	90	[1] NAIK	09	CLEO	$J/\psi \to \gamma\eta'$

[1] NAIK 09 reports $[\Gamma(\eta'(958) \to 3(\pi^+\pi^-))/\Gamma(\eta'(958) \to \pi^+\pi^-\eta)] / [B(\eta \to 2\gamma)] < 3.0\times10^{-3}$ which we multiply by our best value $B(\eta \to 2\gamma) = 39.41\times10^{-2}$.

$\Gamma(K^\pm\pi^\mp)/\Gamma(\rho^0\gamma$(including non-resonant $\pi^+\pi^-\gamma))$ Γ_{20}/Γ_2

VALUE	CL%	DOCUMENT ID		TECN	COMMENT
<1.3 × 10^{-4}	90	ABLIKIM	16M	BES3	$e^+e^- \to J/\psi \to$ hadrons

$\Gamma(\pi^+\pi^-e^+e^-)/\Gamma_{total}$ Γ_{21}/Γ

VALUE (units 10^{-3})	CL%	EVTS	DOCUMENT ID		TECN	COMMENT
2.4 $^{+1.3}_{-1.0}$ OUR FIT						
• • • We do not use the following data for averages, fits, limits, etc. • • •						
2.11±0.12±0.14		429	[1] ABLIKIM	13O	BES3	$J/\psi \to \gamma\eta'$
2.5 $^{+1.2}_{-0.9}$ ±0.5			[2] NAIK	09	CLEO	$J/\psi \to \gamma\eta'$
<6	90		RITTENBERG	65	HBC	2.7 K^-p

[1] Using $\Gamma_2/\Gamma = (29.3\pm0.6)\%$ from PDG 12.
[2] Not independent of measured value of Γ_{21}/Γ_1 from NAIK 09.

$\Gamma(\pi^+\pi^-e^+e^-)/\Gamma(\pi^+\pi^-\eta)$ Γ_{21}/Γ_1

VALUE (units 10^{-3})	EVTS	DOCUMENT ID		TECN	COMMENT
5.5 $^{+3.0}_{-2.2}$ OUR FIT					
5.52$^{+3.00}_{-2.30}$±0.03	8	[1] NAIK	09	CLEO	$J/\psi \to \gamma\eta'$

[1] NAIK 09 reports $[\Gamma(\eta'(958) \to \pi^+\pi^-e^+e^-)/\Gamma(\eta'(958) \to \pi^+\pi^-\eta)] / [B(\eta \to 2\gamma)] = (14^{+7}_{-5} \pm 3)\times10^{-3}$ which we multiply by our best value $B(\eta \to 2\gamma) = (39.41\pm0.20)\times10^{-2}$. Our first error is their experiment's error and our second error is the systematic error from using our best value.

$\Gamma(\pi^+\pi^-e^+e^-)/\Gamma(\rho^0\gamma$(including non-resonant $\pi^+\pi^-\gamma))$ Γ_{21}/Γ_2

VALUE (units 10^{-3})	EVTS	DOCUMENT ID		TECN	COMMENT
7.2±0.4±0.5	429	ABLIKIM	13O	BES3	$J/\psi \to \gamma\eta'$

$\Gamma(\pi^+e^-\nu_e$ + c.c.$)/\Gamma(\pi^+\pi^-\eta)$ Γ_{22}/Γ_1

VALUE (units 10^{-4})	CL%	DOCUMENT ID		TECN	COMMENT
<5.0	90	ABLIKIM	13G	BES3	$J/\psi \to \phi\eta'$

$\Gamma(\gamma e^+e^-)/\Gamma_{total}$ Γ_{23}/Γ

VALUE (units 10^{-3})	CL%	DOCUMENT ID		TECN	COMMENT
• • • We do not use the following data for averages, fits, limits, etc. • • •					
<0.9	90	BRIERE	00	CLEO	10.6 e^+e^-

$\Gamma(\gamma e^+e^-)/\Gamma(\gamma\gamma)$ Γ_{23}/Γ_6

VALUE (units 10^{-2})	EVTS	DOCUMENT ID		TECN	COMMENT
2.13±0.09±0.07	864	ABLIKIM	15O	BES3	$J/\psi \to \gamma e^+e^-$

$\Gamma(\pi^0\gamma\gamma)/\Gamma_{total}$ Γ_{24}/Γ

VALUE (units 10^{-3})	EVTS	DOCUMENT ID		TECN	COMMENT
3.20±0.07±0.23	3.4k	ABLIKIM	17T	BES3	$J/\psi \to \gamma\eta'$

$\Gamma(\pi^0\gamma\gamma$(non resonant$))/\Gamma_{total}$ Γ_{25}/Γ

VALUE (units 10^{-4})	EVTS	DOCUMENT ID		TECN	COMMENT
6.16±0.64±0.67	655	ABLIKIM	17T	BES3	$J/\psi \to \gamma\eta'$

$\Gamma(\pi^0\gamma\gamma)/\Gamma(\pi^0\pi^0\eta)$ Γ_{24}/Γ_3

VALUE (units 10^{-4})	CL%	DOCUMENT ID		TECN	COMMENT
<37	90	ALDE	87B	GAM2	38 $\pi^-p \to n4\gamma$

$\Gamma(4\pi^0)/\Gamma_{total}$ Γ_{26}/Γ

VALUE	CL%	DOCUMENT ID		TECN	COMMENT
<3.2 × 10^{-4}	90	DONSKOV	14	GAM4	32.5 $\pi^-p \to \eta' n$

$\Gamma(4\pi^0)/\Gamma(\pi^0\pi^0\eta)$ Γ_{26}/Γ_3

VALUE (units 10^{-4})	CL%	DOCUMENT ID		TECN	COMMENT
• • • We do not use the following data for averages, fits, limits, etc. • • •					
<23	90	ALDE	87B	GAM2	38 $\pi^-p \to n8\gamma$

$\Gamma(e^+e^-)/\Gamma_{total}$ Γ_{27}/Γ

VALUE	CL%	DOCUMENT ID		TECN	COMMENT
< 5.6 × 10^{-9}	90	[1] ACHASOV	15	SND	0.958 $e^+e^- \to \pi\pi\eta$
• • • We do not use the following data for averages, fits, limits, etc. • • •					
<12 × 10^{-9}	90	[2] AKHMETSHIN	15	CMD3	0.958 $e^+e^- \to \pi^+\pi^-\eta$
< 2.1 × 10^{-7}	90	VOROBYEV	88	ND	$e^+e^- \to \pi^+\pi^-\eta$

[1] Combining data of ACHASOV 15 and AKHMETSHIN 15 and using $\Gamma(\eta') = 0.198\pm0.009$ MeV.
[2] Using $\Gamma_{\eta'(958)} = 198\pm9$ keV, $B(\eta'(958) \to \pi^+\pi^-\eta) = (42.9\pm0.7)\%$, and $B(\eta \to \gamma\gamma) = (39.41\pm0.20)\%$.

Γ(invisible$)/\Gamma_{total}$ Γ_{28}/Γ

VALUE (units 10^{-4})	CL%	DOCUMENT ID		TECN	COMMENT
• • • We do not use the following data for averages, fits, limits, etc. • • •					
<9.5	90	[1] NAIK	09	CLEO	$J/\psi \to \gamma\eta'$

[1] Not independent of measured value of Γ_{28}/Γ_1 from NAIK 09.

Γ(invisible$)/\Gamma(\gamma\gamma)$ Γ_{28}/Γ_6

VALUE (units 10^{-2})	CL%	DOCUMENT ID		TECN	COMMENT
<2.4	90	ABLIKIM	13	BES3	$J/\psi \to \phi\eta'$
• • • We do not use the following data for averages, fits, limits, etc. • • •					
<6.69	90	ABLIKIM	06Q	BES	$J/\psi \to \phi\eta'$

Γ(invisible$)/\Gamma(\pi^+\pi^-\eta)$ Γ_{28}/Γ_1

VALUE (units 10^{-3})	CL%	DOCUMENT ID		TECN	COMMENT
• • • We do not use the following data for averages, fits, limits, etc. • • •					
<2.1	90	[1] NAIK	09	CLEO	$J/\psi \to \gamma\eta'$

[1] NAIK 09 reports $[\Gamma(\eta'(958) \to$ invisible$)/\Gamma(\eta'(958) \to \pi^+\pi^-\eta)] / [B(\eta \to 2\gamma)] < 5.4\times10^{-3}$ which we multiply by our best value $B(\eta \to 2\gamma) = 39.41\times10^{-2}$.

$\Gamma(\pi^+\pi^-)/\Gamma_{total}$ Γ_{29}/Γ

VALUE (units 10^{-4})	CL%	DOCUMENT ID		TECN	COMMENT
< 0.18	90	[1] AAIJ	17D	LHCB	$D^+_{(s)} \to \pi^+\pi^-\pi^+$

• • • We do not use the following data for averages, fits, limits, etc. • • •

< 0.6	90	[2] ABLIKIM	11G	BES3	$J/\psi \to \gamma\pi^+\pi^-$	
< 29	90	[3] MORI	07A	BELL	$\gamma\gamma \to \pi^+\pi^-$	
< 3.3	90	[4] MORI	07A	BELL	$\gamma\gamma \to \pi^+\pi^-$	
<800	95	DANBURG	73	HBC	2.2 $K^- p \to \Lambda X^0$	
<200	90	RITTENBERG	69	HBC	1.7–2.7 $K^- p$	

[1] Using branching fractions of $D_{(s)}^+$ decays from PDG 15.
[2] ABLIKIM 11G reports $[\Gamma(\eta'(958) \to \pi^+\pi^-)/\Gamma_{\rm total}] \times [B(J/\psi(1S) \to \gamma\eta'(958))] < 2.84\times10^{-7}$ which we divide by our best value $B(J/\psi(1S) \to \gamma\eta'(958)) = 5.13\times10^{-3}$.
[3] Taking into account interference with the $\gamma\gamma \to \pi^+\pi^-$ continuum.
[4] Without interference with the $\gamma\gamma \to \pi^+\pi^-$ continuum.

$\Gamma(\pi^0\pi^0)/\Gamma_{\rm total}$ Γ_{30}/Γ

VALUE	CL%	DOCUMENT ID		TECN	COMMENT
<5 × 10⁻⁴	90	[1] ABLIKIM	11G	BES3	$J/\psi \to \gamma\pi^0\pi^0$

[1] ABLIKIM 11G reports $[\Gamma(\eta'(958) \to \pi^+\pi^-)/\Gamma_{\rm total}] \times [B(J/\psi(1S) \to \gamma\eta'(958))] < 2.84\times10^{-7}$ which we divide by our best value $B(J/\psi(1S) \to \gamma\eta'(958)) = 5.13\times10^{-3}$.

$\Gamma(\pi^0\pi^0)/\Gamma(\pi^0\pi^0\eta)$ Γ_{30}/Γ_3

VALUE (units 10^{-4})	CL%	DOCUMENT ID		TECN	COMMENT
<45	90	ALDE	87B	GAM2	38 $\pi^- p \to n4\gamma$

$\Gamma(\pi^0 e^+ e^-)/\Gamma_{\rm total}$ Γ_{31}/Γ

VALUE (units 10^{-3})	CL%	DOCUMENT ID		TECN	COMMENT
< 1.4	90	BRIERE	00	CLEO	10.6 e^+e^-

• • • We do not use the following data for averages, fits, limits, etc. • • •

<13	90	RITTENBERG	65	HBC	2.7 $K^- p$	

$\Gamma(\eta e^+ e^-)/\Gamma_{\rm total}$ Γ_{32}/Γ

VALUE (units 10^{-3})	CL%	DOCUMENT ID		TECN	COMMENT
< 2.4	90	BRIERE	00	CLEO	10.6 e^+e^-

• • • We do not use the following data for averages, fits, limits, etc. • • •

<11	90	RITTENBERG	65	HBC	2.7 $K^- p$	

$\Gamma(3\gamma)/\Gamma(\pi^0\pi^0\eta)$ Γ_{33}/Γ_3

VALUE (units 10^{-4})	CL%	DOCUMENT ID		TECN	COMMENT
<4.6	90	ALDE	87B	GAM2	38 $\pi^- p \to n3\gamma$

$\Gamma(\mu^+\mu^-\pi^0)/\Gamma_{\rm total}$ Γ_{34}/Γ

VALUE (units 10^{-5})	CL%	DOCUMENT ID		TECN	COMMENT
<6.0	90	DZHELYADIN	81	CNTR	30 $\pi^- p \to \eta' n$

$\Gamma(\mu^+\mu^-\eta)/\Gamma_{\rm total}$ Γ_{35}/Γ

VALUE (units 10^{-5})	CL%	DOCUMENT ID		TECN	COMMENT
<1.5	90	DZHELYADIN	81	CNTR	30 $\pi^- p \to \eta' n$

$\Gamma(e\mu)/\Gamma_{\rm total}$ Γ_{36}/Γ

VALUE (units 10^{-4})	CL%	DOCUMENT ID		TECN	COMMENT
<4.7	90	BRIERE	00	CLEO	10.6 e^+e^-

$\eta'(958) \to \eta\pi\pi$ DECAY PARAMETERS

$$|\text{MATRIX ELEMENT}|^2 = |1 + \alpha Y|^2 + CX + DX^2$$

X and Y are Dalitz variables; α is complex and C, and D are real-valued. Parameters C and D are not necessarily equal to c and d, respectively, in the generalized parameterization following this one. May be different for $\eta'(958) \to \eta\pi^+\pi^-$ and $\eta'(958) \to \eta\pi^0\pi^0$ decays. Because of different initial assumptions and strong correlations of the parameters we do not average the parameters in the section below.

Re(α) decay parameter

VALUE	EVTS	DOCUMENT ID		TECN	COMMENT
• • • We do not use the following data for averages, fits, limits, etc. • • •					
$-0.034\pm0.002\pm0.002$	351k	ABLIKIM	18	BES3	$\eta' \to \eta\pi^+\pi^-$
$-0.054\pm0.004\pm0.001$	56k	ABLIKIM	18	BES3	$\eta' \to \eta\pi^0\pi^0$
$-0.033\pm0.005\pm0.003$	44k	[1] ABLIKIM	11	BES3	$J/\psi \to \gamma\eta\pi^+\pi^-$
$-0.072\pm0.012\pm0.006$	7k	[2] AMELIN	05A	VES	28 $\pi^- A \to \eta\pi^+\pi^-\pi^- A^*$
$-0.021\pm0.018\pm0.017$	6.7k	[3] BRIERE	00	CLEO	10.6 $e^+e^- \to \eta\pi^+\pi^- X$
$-0.058\pm0.013\pm0.003$	5.4k	[4] ALDE	86	GAM2	38 $\pi^- p \to n\eta\pi^0\pi^0$
$-0.08\ \pm0.03$		[4,5] KALBFLEISCH	74	RVUE	$\eta' \to \eta\pi^+\pi^-$

[1] See ABLIKIM 11 for the full correlation matrix.
[2] Superseded by DOROFEEV 07, which found this parameterization unacceptable. See below.
[3] Assuming $\mathrm{Im}(\alpha) = 0$, $C = 0$, and $D = 0$.
[4] Assuming $C = 0$.
[5] From the data of DAUBER 64, RITTENBERG 69, AGUILAR-BENITEZ 72B, JACOBS 73, and DANBURG 73.

Im(α) decay parameter

VALUE	EVTS	DOCUMENT ID		TECN	COMMENT
• • • We do not use the following data for averages, fits, limits, etc. • • •					
$0.000\pm0.019\pm0.001$	351k	ABLIKIM	18	BES3	$\eta' \to \eta\pi^+\pi^-$
$0.000\pm0.038\pm0.002$	56k	ABLIKIM	18	BES3	$\eta' \to \eta\pi^0\pi^0$
$0.000\pm0.049\pm0.001$	44k	[1] ABLIKIM	11	BES3	$J/\psi \to \gamma\eta\pi^+\pi^-$
$0.0\ \ \pm0.1\ \ \pm0.0$	7k	[2] AMELIN	05A	VES	28 $\pi^- A \to \eta\pi^+\pi^-\pi^- A^*$
$-0.00\ \pm0.13\ \pm0.00$	5.4k	[3] ALDE	86	GAM2	38 $\pi^- p \to n\eta\pi^0\pi^0$
$0.0\ \ \pm0.3$		[3,4] KALBFLEISCH	74	RVUE	$\eta' \to \eta\pi^+\pi^-$

[1] See ABLIKIM 11 for the full correlation matrix.
[2] Superseded by DOROFEEV 07, which found this parameterization unacceptable. See below.
[3] Assuming $C = 0$.
[4] From the data of DAUBER 64, RITTENBERG 69, AGUILAR-BENITEZ 72B, JACOBS 73, and DANBURG 73.

C decay parameter

VALUE	EVTS	DOCUMENT ID		TECN	COMMENT
• • • We do not use the following data for averages, fits, limits, etc. • • •					
$0.0027\pm0.0024\pm0.0015$	351k	ABLIKIM	18	BES3	$\eta' \to \eta\pi^+\pi^-$
$0.018\ \pm0.009\ \pm0.003$	44k	[1] ABLIKIM	11	BES3	$J/\psi \to \gamma\eta\pi^+\pi^-$
$0.020\ \pm0.018\ \pm0.004$	7k	[2] AMELIN	05A	VES	28 $\pi^- A \to \eta\pi^+\pi^-\pi^- A^*$

[1] See ABLIKIM 11 for the full correlation matrix.
[2] Superseded by DOROFEEV 07, which found this parameterization unacceptable. See below.

D decay parameter

VALUE	EVTS	DOCUMENT ID		TECN	COMMENT
• • • We do not use the following data for averages, fits, limits, etc. • • •					
$-0.053\pm0.004\pm0.004$	351k	ABLIKIM	18	BES3	$\eta' \to \eta\pi^+\pi^-$
$-0.061\pm0.009\pm0.005$	56k	ABLIKIM	18	BES3	$\eta' \to \eta\pi^0\pi^0$
$-0.059\pm0.012\pm0.004$	44k	[1] ABLIKIM	11	BES3	$J/\psi \to \gamma\eta\pi^+\pi^-$
$-0.066\pm0.030\pm0.015$	7k	[2] AMELIN	05A	VES	28 $\pi^- A \to \eta\pi^+\pi^-\pi^- A^*$
$0.00\ \pm0.03\ \pm0.00$	5.4k	[3] ALDE	86	GAM2	38 $\pi^- p \to n\eta\pi^0\pi^0$
0		[3,4] KALBFLEISCH	74	RVUE	$\eta' \to \eta\pi^+\pi^-$

[1] See ABLIKIM 11 for the full correlation matrix.
[2] Superseded by DOROFEEV 07, which found this parameterization unacceptable. See below.
[3] Assuming $C = 0$.
[4] From the data of DAUBER 64, RITTENBERG 69, AGUILAR-BENITEZ 72B, JACOBS 73, and DANBURG 73.

$\eta'(958) \to \eta\pi\pi$ DECAY PARAMETERS

$$|\text{MATRIX ELEMENT}|^2 \propto 1 + aY + bY^2 + cX + dX^2$$

X and Y are Dalitz variables and a, b, c, and d are real-valued parameters. May be different for $\eta'(958) \to \eta\pi^+\pi^-$ and $\eta'(958) \to \eta\pi^0\pi^0$ decays. We do not average measurements in the section below because parameter values from each experiment are strongly correlated.

a decay parameter

VALUE	EVTS	DOCUMENT ID		TECN	COMMENT
• • • We do not use the following data for averages, fits, limits, etc. • • •					
$-0.056\pm0.004\pm0.002$	351k	ABLIKIM	18	BES3	$\eta' \to \eta\pi^+\pi^-$
$-0.087\pm0.009\pm0.006$	56k	ABLIKIM	18	BES3	$\eta' \to \eta\pi^0\pi^0$
$-0.047\pm0.011\pm0.003$	44k	[1] ABLIKIM	11	BES3	$J/\psi \to \gamma\eta\pi^+\pi^-$
$-0.066\pm0.016\pm0.003$	15k	[2] BLIK	09	GAM4	32.5 $\pi^- p \to \eta' n$
$-0.127\pm0.016\pm0.008$	20k	[3] DOROFEEV	07	VES	27 $\pi^- p \to \eta' n$, $\pi^- A \to \eta'\pi^- A^*$

[1] See ABLIKIM 11 for the full correlation matrix.
[2] From $\eta' \to \eta\pi^0\pi^0$ decay.
[3] From $\eta' \to \eta\pi^+\pi^-$ decay.

b decay parameter

VALUE	EVTS	DOCUMENT ID		TECN	COMMENT
• • • We do not use the following data for averages, fits, limits, etc. • • •					
$-0.049\pm0.006\pm0.006$	351k	ABLIKIM	18	BES3	$\eta' \to \eta\pi^+\pi^-$
$-0.073\pm0.014\pm0.005$	56k	ABLIKIM	18	BES3	$\eta' \to \eta\pi^0\pi^0$
$-0.069\pm0.019\pm0.009$	44k	[1] ABLIKIM	11	BES3	$J/\psi \to \gamma\eta\pi^+\pi^-$
$-0.063\pm0.028\pm0.004$	15k	[2] BLIK	09	GAM4	32.5 $\pi^- p \to \eta' n$
$-0.106\pm0.028\pm0.014$	20k	[3] DOROFEEV	07	VES	27 $\pi^- p \to \eta' n$, $\pi^- A \to \eta'\pi^- A^*$

[1] See ABLIKIM 11 for the full correlation matrix.
[2] From $\eta' \to \eta\pi^0\pi^0$ decay.
[3] From $\eta' \to \eta\pi^+\pi^-$ decay.

c decay parameter

VALUE	EVTS	DOCUMENT ID		TECN	COMMENT
• • • We do not use the following data for averages, fits, limits, etc. • • •					
$0.0027\pm0.0024\pm0.0018$	351k	ABLIKIM	18	BES3	$\eta' \to \eta\pi^+\pi^-$
$0.019\ \pm0.011\ \pm0.003$	44k	[1] ABLIKIM	11	BES3	$J/\psi \to \gamma\eta\pi^+\pi^-$

$-0.107 \pm 0.096 \pm 0.003$	15k	[2] BLIK	09	GAM4	32.5	$\pi^- p \to \eta' n$
$0.015 \pm 0.011 \pm 0.014$	20k	[3] DOROFEEV	07	VES	27	$\pi^- p \to \eta' n$, $\pi^- A \to \eta' \pi^- A^*$

[1] See ABLIKIM 11 for the full correlation matrix.
[2] From $\eta' \to \eta\pi^0\pi^0$ decay.
[3] From $\eta' \to \eta\pi^+\pi^-$ decay.

d decay parameter

VALUE	EVTS	DOCUMENT ID		TECN	COMMENT
• • • We do not use the following data for averages, fits, limits, etc. • • •					
$-0.063 \pm 0.004 \pm 0.003$	351k	ABLIKIM	18	BES3	$\eta' \to \eta\pi^+\pi^-$
$-0.074 \pm 0.009 \pm 0.004$	56k	ABLIKIM	18	BES3	$\eta' \to \eta\pi^0\pi^0$
$-0.073 \pm 0.012 \pm 0.003$	44k	[1] ABLIKIM	11	BES3	$J/\psi \to \gamma\eta\pi^+\pi^-$
$0.018 \pm 0.078 \pm 0.006$	15k	[2] BLIK	09	GAM4	32.5 $\pi^- p \to \eta' n$
$-0.082 \pm 0.017 \pm 0.008$	20k	[3] DOROFEEV	07	VES	27 $\pi^- p \to \eta' n$, $\pi^- A \to \eta' \pi^- A^*$

[1] See ABLIKIM 11 for the full correlation matrix.
[2] From $\eta' \to \eta\pi^0\pi^0$ decay. If $c \equiv 0$ from Bose-Einstein symmetry, $d = -0.067 \pm 0.020 \pm 0.003$.
[3] From $\eta' \to \eta\pi^+\pi^-$ decay.

$\eta'(958)$ β PARAMETER
$|\text{MATRIX ELEMENT}|^2 = (1 + 2\beta Z)$

See the "Note on η Decay Parameters" in our 1994 edition Physical Review **D50** 1173 (1994), p. 1454.

β decay parameter

VALUE	EVTS	DOCUMENT ID		TECN	COMMENT
-0.61 ± 0.08 OUR AVERAGE		Error includes scale factor of 1.2.			
$-0.640 \pm 0.046 \pm 0.047$	1.8k	ABLIKIM	15G	BES3	$J/\psi \to \gamma(\pi^0\pi^0\pi^0)$
-0.59 ± 0.18	235	BLIK	08	GAMS	32 $\pi^- p \to \eta' n$
-0.1 ± 0.3		ALDE	87B	GAM2	38 $\pi^- p \to n 3\pi^0$

$\eta'(958)$ C-NONCONSERVING DECAY PARAMETER

See the note on η decay parameters in the Stable Particle Particle Listings for definition of this parameter.

DECAY ASYMMETRY PARAMETER FOR $\pi^+\pi^-\gamma$

VALUE	EVTS	DOCUMENT ID		TECN	COMMENT
-0.03 ± 0.04 OUR AVERAGE					
-0.019 ± 0.056		AIHARA	87	TPC	$2\gamma \to \pi^+\pi^-\gamma$
-0.069 ± 0.078	295	GRIGORIAN	75	STRC	2.1 $\pi^- p$
0.00 ± 0.10	103	KALBFLEISCH	75	HBC	2.18 $K^- p \to \Lambda\pi^+\pi^-\gamma$
• • • We do not use the following data for averages, fits, limits, etc. • • •					
0.07 ± 0.08	152	RITTENBERG	65	HBC	2.1–2.7 $K^- p$

$\eta'(958) \to \gamma\ell^+\ell^-$ TRANSITION FORM FACTOR SLOPE

Related to the effective virtual meson mass Λ, via slope $\approx \Lambda^{-2}$. See e.g. LANDSBERG 85, eq. (3.8), for a detailed definition.

VALUE (GeV^{-2})	EVTS	DOCUMENT ID		TECN	COMMENT
1.62±0.17 OUR AVERAGE					
$1.60 \pm 0.17 \pm 0.08$	864	[1] ABLIKIM	15O	BES3	$J/\psi \to \gamma e^+ e^-$
1.7 ± 0.4	33	[1] VIKTOROV	80		25,33 $\pi^- p \to 2\mu\gamma$

[1] In the single-pole Ansatz where slope $= 1/(\Lambda^2 + \gamma^2)$ with Λ, γ being a Breit-Wigner mass, width for the effective contributing vector meson.

$\eta'(958)$ REFERENCES

ABLIKIM	18	PR D97 012003	M. Ablikim *et al.*	(BES III Collab.)
AAIJ	17D	PL B764 233	R. Aaij *et al.*	(LHCb Collab.)
ABLIKIM	17	PRL 118 012001	M. Ablikim *et al.*	(BES III Collab.)
ABLIKIM	17T	PR D96 012005	M. Ablikim *et al.*	(BES III Collab.)
ABLIKIM	16M	PR D93 072008	M. Ablikim *et al.*	(BES III Collab.)
ABLIKIM	15AD	PR D92 051101	M. Ablikim *et al.*	(BES III Collab.)
ABLIKIM	15G	PR D92 012014	M. Ablikim *et al.*	(BES III Collab.)
ABLIKIM	15O	PR D92 012001	M. Ablikim *et al.*	(BES III Collab.)
ABLIKIM	15P	PR D92 012007	M. Ablikim *et al.*	(BES III Collab.)
ACHASOV	15	PR D91 092010	M.N. Achasov *et al.*	(SND Collab.)
AKHMETSHIN	15	PL B740 273	R.R. Akhmetshin *et al.*	(CMD-3 Collab.)
PDG	15	RPP 2015 at pdg.lbl.gov		(PDG Collab.)
ABLIKIM	14M	PRL 112 251801	M. Ablikim *et al.*	(BES III Collab.)
DONSKOV	14	MPL A29 1450213	S. Donskov *et al.*	(GAMS-4π Collab.)
PDG	14	CP C38 070001	K. Olive *et al.*	(PDG Collab.)
ABLIKIM	13	PR D87 012009	M. Ablikim *et al.*	(BES III Collab.)
ABLIKIM	13G	PR D87 032006	M. Ablikim *et al.*	(BES III Collab.)
ABLIKIM	13O	PR D87 092011	M. Ablikim *et al.*	(BES III Collab.)
ABLIKIM	13U	PR D88 091502	M. Ablikim *et al.*	(BES III Collab.)
ABLIKIM	12E	PRL 108 182001	M. Ablikim *et al.*	(BES III Collab.)
PDG	12	PR D86 010001	J. Beringer *et al.*	(PDG Collab.)
ABLIKIM	11	PR D83 012003	M. Ablikim *et al.*	(BES III Collab.)
ABLIKIM	11G	PR D84 032006	M. Ablikim *et al.*	(BES III Collab.)
CZERWINSKI	10	PRL 105 122001	E. Czerwinski *et al.*	(COSY-11 Collab.)
BLIK	09	PAN 72 231 Translated from YAF 72 258.	A.M. Blik *et al.*	(IHEP (Protvino))
NAIK	09	PRL 102 061801	P. Naik *et al.*	(CLEO Collab.)
PEDLAR	09	PR D79 111101	T.K. Pedlar *et al.*	(CLEO Collab.)
BLIK	08	PAN 71 2124 Translated from YAF 71 2161.	A. Blik *et al.*	(GAMS-4π Collab.)
LIBBY	08	PRL 101 182002	J. Libby *et al.*	(CLEO Collab.)
WICHT	08	PL B662 323	J. Wicht *et al.*	(BELLE Collab.)
DOROFEEV	07	PL B651 22	V. Dorofeev *et al.*	(VES Collab.)
MORI	07A	JPSJ 76 074102	T. Mori *et al.*	(BELLE Collab.)
ABLIKIM	06E	PR D73 052008	M. Ablikim *et al.*	(BES Collab.)
ABLIKIM	06Q	PRL 97 202002	M. Ablikim *et al.*	(BES Collab.)
AMELIN	05A	PAN 68 372 Translated from YAF 68 401.	D.V. Amelin *et al.*	(VES Collab.)
AMSLER	04B	EPJ C33 23	C. Amsler *et al.*	(Crystal Barrel Collab.)
BAI	04J	PL B594 47	J.Z. Bai *et al.*	(BES Collab.)
BRIERE	00	PRL 84 26	R. Briere *et al.*	(CLEO Collab.)
ACCIARRI	98Q	PL B418 399	M. Acciarri *et al.*	(L3 Collab.)
BARBERIS	98C	PL B440 225	D. Barberis *et al.*	(WA 102 Collab.)
WURZINGER	96	PL B374 283	R. Wurzinger *et al.*	(BONN, ORSAY, SACL+)
PDG	94	PR D50 1173	L. Montanet *et al.*	(CERN, LBL, BOST+)
AMSLER	93	ZPHY C58 175	C. Amsler *et al.*	(Crystal Barrel Collab.)
BELADIDZE	92C	SJNP 55 1535 Translated from YAF 55 2748.	G.M. Beladidze, S.I. Bityukov, G.V. Borisov	(SERP+)
KARCH	92	ZPHY C54 33	K. Karch *et al.*	(Crystal Ball Collab.)
ARMSTRONG	91B	ZPHY C52 389	T.A. Armstrong *et al.*	(ATHU, BARI, BIRM+)
BEHREND	91	ZPHY C49 401	H.J. Behrend *et al.*	(CELLO Collab.)
AUGUSTIN	90	PR D42 10	J.E. Augustin *et al.*	(DM2 Collab.)
BARU	90	ZPHY C48 581	S.E. Baru *et al.*	(MD-1 Collab.)
BUTLER	90	PR D42 1368	F. Butler *et al.*	(Mark II Collab.)
KARCH	90	PL B249 353	K. Karch *et al.*	(Crystal Ball Collab.)
ROE	90	PR D41 17	N.A. Roe *et al.*	(ASP Collab.)
AIHARA	88C	PR D38 1	H. Aihara *et al.*	(TPC-2γ Collab.)
VOROBYEV	88	SJNP 48 273 Translated from YAF 48 436.	P.V. Vorobiev *et al.*	(NOVO)
WILLIAMS	88	PR D38 1365	D.A. Williams *et al.*	(Crystal Ball Collab.)
AIHARA	87	PR D35 2650	H. Aihara *et al.*	(TPC-2γ Collab.) JP
ALBRECHT	87B	PL B199 457	H. Albrecht *et al.*	(ARGUS Collab.)
ALDE	87B	ZPHY C36 603	D.M. Alde *et al.*	(LANL, BELG, SERP, LAPP)
ANTREASYAN	87	PR D36 2633	D. Antreasyan *et al.*	(Crystal Ball Collab.)
GIDAL	87	PRL 59 2012	G. Gidal *et al.*	(LBL, SLAC, HARV)
ALDE	86	PL B177 115	D.M. Alde *et al.*	(SERP, BELG, LANL, LAPP)
BARTEL	85E	PL 160B 421	W. Bartel *et al.*	(JADE Collab.)
LANDSBERG	85	PRPL 128 301	L.G. Landsberg	(SERP)
ALTHOFF	84E	PL 147B 487	M. Althoff *et al.*	(TASSO Collab.)
BERGER	84B	PL 142B 125	C. Berger	(PLUTO Collab.)
BINON	84	PL 140B 264	F.G. Binon *et al.*	(SERP, BELG, LAPP+)
JENNI	83	PR D27 1031	P. Jenni *et al.*	(SLAC, LBL)
BARTEL	82B	PL 113B 190	W. Bartel *et al.*	(JADE Collab.)
BEHREND	82C	PL 114B 378	H.J. Behrend *et al.*	(CELLO Collab.)
Also		PL 125B 518 (erratum)	H.J. Behrend *et al.*	(CELLO Collab.)
DZHELYADIN	81	PL 105B 239	R.I. Dzhelyadin *et al.*	(SERP)
STANTON	80	PL B92 353	N.R. Stanton *et al.*	(OSU, CARL, MCGI+)
VIKTOROV	80	SJNP 32 520 Translated from YAF 32 1005.	V.A. Viktorov *et al.*	(SERP)
APEL	79	PL 83B 131	W.D. Apel, K.H. Augenstein, E. Bertolucci	(KARLK+)
BINNIE	79	PL 83B 141	D.M. Binnie *et al.*	(LOIC)
ZANFINO	77	PRL 38 930	C. Zanfino *et al.*	(CARL, MCGI, OHIO+)
GRIGORIAN	75	NP B91 232	A. Grigorian *et al.*	(+)
KALBFLEISCH	75	PR D11 987	G.R. Kalbfleisch, R.C. Strand, J.W. Chapman	(BNL+)
DUANE	74	PRL 32 425	A. Duane *et al.*	(LOIC, SHMP)
KALBFLEISCH	74	PR D10 916	G.R. Kalbfleisch	(BNL)
DANBURG	73	PR D8 3744	J.S. Danburg *et al.*	(BNL, MICH) JP
JACOBS	73	PR D8 18	S.M. Jacobs *et al.*	(BRAN, UMD, SYRA+) JP
AGUILAR-...	72B	PR D6 29	M. Aguilar-Benitez *et al.*	(BNL)
APEL	72	PL 40B 680	W.D. Apel *et al.*	(KARLK, KARLE, PISA)
DALPIAZ	72	PL 42B 377	P.F. Dalpiaz *et al.*	(CERN)
BASILE	71	NC 3A 371	M. Basile *et al.*	(CERN, BGNA, STRB)
HARVEY	71	PRL 27 885	E.H. Harvey *et al.*	(MINN, MICH)
BENSINGER	70	PL 33B 505	J.R. Bensinger *et al.*	(WISC)
RITTENBERG	69	Thesis UCRL 18863	A. Rittenberg	(LRL) I
DAVIS	68	PL 27B 532	R. Davis *et al.*	(NWES, ANL)
LONDON	66	PR 143 1034	G.W. London *et al.*	(BNL, SYRA) IJP
BADIER	65B	PL 17 337	J. Badier *et al.*	(EPOL, SACL, AMST)
RITTENBERG	65	PRL 15 556	A. Rittenberg, G.R. Kalbfleisch	(LRL, BNL)
DAUBER	64	PRL 13 449	P.M. Dauber *et al.*	(UCLA) JP
KALBFLEISCH	64B	PRL 13 349	G.R. Kalbfleisch, O.I. Dahl, A. Rittenberg	(LRL) JP

$f_0(980)$

$I^G(J^{PC}) = 0^+(0^{++})$

See also the minireview on scalar mesons under $f_0(500)$. (See the index for the page number.)

$f_0(980)$ MASS

VALUE (MeV)	EVTS	DOCUMENT ID		TECN	COMMENT
990 ±20 OUR ESTIMATE					
• • • We do not use the following data for averages, fits, limits, etc. • • •					
989.4 ± 1.3	424	ABLIKIM	15P	BES3	$J/\psi \to K^+K^-3\pi$
989.9 ± 0.4	706	ABLIKIM	12E	BES3	$J/\psi \to \gamma 3\pi$
$1003\ ^{+5}_{-27}$		[1,2] GARCIA-MAR..11		RVUE	Compilation
996 ± 7		[1,3] GARCIA-MAR..11		RVUE	Compilation
$996\ ^{+4}_{-14}$		[4] MOUSSALLAM11		RVUE	Compilation
981 ± 43		[5] MENNESSIER 10		RVUE	Compilation
$1030\ ^{+30}_{-10}$		[6] ANISOVICH	09	RVUE	0.0 $\overline{p}p$, πN
$977\ ^{+11}_{-9} \pm 1$	44	[7] ECKLUND	09	CLEO	4.17 $e^+e^- \to D_s^- D_s^{*+}$ + c.c.
$982.2 \pm 1.0\ ^{+8.1}_{-8.0}$		[8] UEHARA	08A	BELL	10.6 $e^+e^- \to e^+e^-\pi^0\pi^0$
$976.8 \pm 0.3\ ^{+10.1}_{-0.6}$	64k	[9] AMBROSINO	07	KLOE	1.02 $e^+e^- \to \pi^0\pi^0\gamma$
$984.7 \pm 0.4\ ^{+2.4}_{-3.7}$	64k	[10] AMBROSINO	07	KLOE	1.02 $e^+e^- \to \pi^0\pi^0\gamma$
973 ± 3	262 ± 30	[11] AUBERT	07AK	BABR	10.6 $e^+e^- \to \phi\pi^+\pi^-\gamma$
970 ± 7	54 ± 9	[11] AUBERT	07AK	BABR	10.6 $e^+e^- \to \phi\pi^0\pi^0\gamma$
953 ± 20	2.6k	[12] BONVICINI	07	CLEO	$D^+ \to \pi^-\pi^+\pi^+$
$985.6\ ^{+1.2}_{-1.5} \pm 1.1 - 1.6$		[13] MORI	07	BELL	10.6 $e^+e^- \to e^+e^-\pi^+\pi^-$
$983.0 \pm 0.6\ ^{+4.0}_{-3.0}$		[14] AMBROSINO	06B	KLOE	1.02 $e^+e^- \to \pi^+\pi^-\gamma$

Meson Particle Listings

$f_0(980)$

977.3± 0.9$^{+\ 3.7}_{-\ 4.3$		[15] AMBROSINO	06B	KLOE	1.02 $e^+e^- \to \pi^+\pi^-\gamma$
950 ± 9	4286	[16] GARMASH	06	BELL	$B^+ \to K^+\pi^+\pi^-$
965 ±10		[17] ABLIKIM	05	BES2	$J/\psi \to \phi\pi^+\pi^-$, ϕK^+K^-
1031 ± 8		[18] ANISOVICH	03	RVUE	
1037 ±31		TIKHOMIROV	03	SPEC	40.0 $\pi^-C \to K^0_S K^0_S K^0_L X$
973 ± 1	2438	[19] ALOISIO	02D	KLOE	$e^+e^- \to \pi^0\pi^0\gamma$
977 ± 3 ± 2	848	[20] AITALA	01A	E791	$D^+_s \to \pi^-\pi^+\pi^+$
969.8± 4.5	419	[21] ACHASOV	00H	SND	$e^+e^- \to \pi^0\pi^0\gamma$
985 $^{+16}_{-12}$	419	[22,23] ACHASOV	00H	SND	$e^+e^- \to \pi^0\pi^0\gamma$
976 ± 5 ± 6		[24] AKHMETSHIN	99B	CMD2	$e^+e^- \to \pi^+\pi^-\gamma$
977 ± 3 ± 6	268	[24] AKHMETSHIN	99C	CMD2	$e^+e^- \to \pi^0\pi^0\gamma$
975 ± 4 ± 6		[25] AKHMETSHIN	99C	CMD2	$e^+e^- \to \pi^0\pi^0\gamma$
975 ± 4 ± 6		[26] AKHMETSHIN	99C	CMD2	$e^+e^- \to \pi^+\pi^-\gamma$, $\pi^0\pi^0\gamma$
985 ±10		BARBERIS	99	OMEG	450 $pp \to p_s p_f K^+K^-$
982 ± 3		BARBERIS	99B	OMEG	450 $pp \to p_s p_f \pi^+\pi^-$
982 ± 3		BARBERIS	99C	OMEG	450 $pp \to p_s p_f \pi^0\pi^0$
987 ± 6 ± 6		[27] BARBERIS	99D	OMEG	450 $pp \to K^+K^-$, $\pi^+\pi^-$
989 ±15		BELLAZZINI	99	GAM4	450 $pp \to pp\pi^0\pi^0$
991 ± 3		[28] KAMINSKI	99	RVUE	$\pi\pi \to \pi\pi$, $K\overline{K}$, $\sigma\sigma$
~ 980		[28] OLLER	99	RVUE	$\pi\pi \to \pi\pi$, $K\overline{K}$
~ 993.5		OLLER	99B	RVUE	$\pi\pi \to \pi\pi$, $K\overline{K}$
~ 987		[28] OLLER	99C	RVUE	$\pi\pi \to \pi\pi$, $K\overline{K}$, $\eta\eta$
957 ± 6		[29] ACKERSTAFF	98Q	OPAL	$Z \to f_0 X$
960 ±10		ALDE	98	GAM4	
1015 ±15		[28] ANISOVICH	98B	RVUE	Compilation
1008		[30] LOCHER	98	RVUE	$\pi\pi \to \pi\pi$, $K\overline{K}$
955 ±10		[29] ALDE	97	GAM2	450 $pp \to pp\pi^0\pi^0$
994 ± 9		[31] BERTIN	97C	OBLX	0.0 $\overline{p}p \to \pi^+\pi^-\pi^0$
993.2± 6.5± 6.9		[32] ISHIDA	96	RVUE	$\pi\pi \to \pi\pi$, $K\overline{K}$
1006		TORNQVIST	96	RVUE	$\pi\pi \to \pi\pi$, $K\overline{K}$, $K\pi$, $\eta\pi$
997 ± 5	3k	[33] ALDE	95B	GAM2	38 $\pi^-p \to \pi^0\pi^0 n$
960 ±10	10k	[34] ALDE	95B	GAM2	38 $\pi^-p \to \pi^0\pi^0 n$
994 ± 5		AMSLER	95B	CBAR	0.0 $\overline{p}p \to 3\pi^0$
~ 996		[35] AMSLER	95D	CBAR	0.0 $\overline{p}p \to \pi^0\pi^0\pi^0$, $\pi^0\eta\eta$, $\pi^0\pi^0\eta$
987 ± 6		[36] ANISOVICH	95	RVUE	
1015		JANSSEN	95	RVUE	$\pi\pi \to \pi\pi$, $K\overline{K}$
983		[37] BUGG	94	RVUE	$\overline{p}p \to \eta 2\pi^0$
973 ± 2		[38] KAMINSKI	94	RVUE	$\pi\pi \to \pi\pi$, $K\overline{K}$
988		[39] ZOU	94B	RVUE	
988 ±10		[40] MORGAN	93	RVUE	$\pi\pi(K\overline{K}) \to \pi\pi(K\overline{K})$, $J/\psi \to \phi\pi\pi(K\overline{K})$, $D_s \to \pi(\pi\pi)$
971.1± 4.0		[29] AGUILAR-...	91	EHS	400 pp
979 ± 4		[41] ARMSTRONG	91	OMEG	300 $pp \to pp\pi\pi$, $pp K\overline{K}$
956 ±12		BREAKSTONE	90	SFM	$pp \to pp\pi^+\pi^-$
959.4± 6.5		[29] AUGUSTIN	89	DM2	$J/\psi \to \omega\pi^+\pi^-$
978 ± 9		[29] ABACHI	86B	HRS	$e^+e^- \to \pi^+\pi^- X$
985.0$^{+\ 9.0}_{-39.0}$		ETKIN	82B	MPS	23 $\pi^-p \to n2K^0_S$
974 ± 4		[41] GIDAL	81	MRK2	$J/\psi \to \pi^+\pi^- X$
975		[42] ACHASOV	80	RVUE	
986 ±10		[41] AGUILAR-...	78	HBC	0.7 $\overline{p}p \to K^0_S K^0_S$
969 ± 5		[41] LEEPER	77	ASPK	2–2.4 $\pi^-p \to \pi^+\pi^-n$, K^+K^-n
987 ± 7		[41] BINNIE	73	CNTR	$\pi^-p \to n$MM
1012 ± 6		[43] GRAYER	73	ASPK	17 $\pi^-p \to \pi^+\pi^-n$
1007 ±20		[43] HYAMS	73	ASPK	17 $\pi^-p \to \pi^+\pi^-n$
997 ± 6		[43] PROTOPOP...	73	HBC	7 $\pi^+p \to \pi^+p\pi^+\pi^-$

[1] Quoted number refers to real part of pole position.

[2] Analytic continuation using Roy equations. Uses the K_{e4} data of BATLEY 10C and the $\pi N \to \pi\pi N$ data of HYAMS 73, GRAYER 74, and PROTOPOPESCU 73.

[3] Analytic continuation using GKPY equations. Uses the K_{e4} data of BATLEY 10C and the $\pi N \to \pi\pi N$ data of HYAMS 73, GRAYER 74, and PROTOPOPESCU 73.

[4] Pole position. Used Roy equations.

[5] Average of the analyses of three data sets in the K-matrix model. Uses the data of BATLEY 08A, HYAMS 73, and GRAYER 74, partially of COHEN 80 or ETKIN 82B.

[6] On sheet II in a 2-pole solution. The other pole is found on sheet III at (850−100i) MeV

[7] Using a relativistic Breit-Wigner function and taking into account the finite D_s mass.

[8] Breit-Wigner mass. Using finite width corrections according to FLATTE 76 and ACHASOV 05, and the ratio $g_{f_0 K K}/g_{f_0 \pi\pi} = 0$.

[9] In the kaon-loop fit.

[10] In the no-structure fit.

[11] Systematic errors not estimated.

[12] FLATTE 76 parameterization. $g_{f_0 \pi\pi} = 329 \pm 96$ MeV/c^2 assuming $g_{f_0 K\overline{K}}/g_{f_0 \pi\pi}$=2.

[13] Breit-Wigner mass. Using finite width corrections according to FLATTE 76 and ACHASOV 05, and the ratio $g_{f_0 K K}/g_{f_0 \pi\pi} = 4.21 \pm 0.25 \pm 0.21$ from ABLIKIM 05.

[14] In the kaon-loop fit following formalism of ACHASOV 89.

[15] In the no-structure fit assuming a direct coupling of ϕ to $f_0\gamma$.

[16] FLATTE 76 parameterization. Supersedes GARMASH 05.

[17] FLATTE 76 parameterization, $g_{f_0 K\overline{K}}/g_{f_0 \pi\pi} = 4.21 \pm 0.25 \pm 0.21$.

[18] K-matrix pole from combined analysis of $\pi^-p \to \pi^0\pi^0 n$, $\pi^-p \to K\overline{K}n$, $\pi^+\pi^- \to \pi^+\pi^-$, $\overline{p}p \to \pi^0\pi^0\pi^0$, $\pi^0\eta\eta$, $\pi^0\pi^0\eta$, $\pi^+\pi^-\pi^0$, $K^+K^-\pi^0$, $K^0_S K^0_S\pi^0$, $K^+K^0_S\pi^-$ at rest, $\overline{p}n \to \pi^-\pi^-\pi^+$, $K^0_S K^-\pi^0$, $K^0_S K^0_S\pi^-$ at rest.

[19] From the negative interference with the $f_0(500)$ meson of AITALA 01B using the ACHASOV 89 parameterization for the $f_0(980)$, a Breit-Wigner for the $f_0(500)$, and ACHASOV 01F for the $\rho\pi$ contribution.

[20] Coupled-channel Breit-Wigner, couplings g_π=0.09±0.01±0.01, g_K=0.02±0.04±0.03.

[21] Supersedes ACHASOV 98I. Using the model of ACHASOV 89.

[22] Supersedes ACHASOV 98I.

[23] In the "narrow resonance" approximation.

[24] Assuming $\Gamma(f_0)$= 40 MeV.

[25] From a narrow pole fit taking into account $f_0(980)$ and $f_0(1200)$ intermediate mechanisms.

[26] From the combined fit of the photon spectra in the reactions $e^+e^- \to \pi^+\pi^-\gamma$, $\pi^0\pi^0\gamma$.

[27] Supersedes BARBERIS 99 and BARBERIS 99B

[28] T-matrix pole.

[29] From invariant mass fit.

[30] On sheet II in a 2 pole solution. The other pole is found on sheet III at (1039−93i) MeV.

[31] On sheet II in a 2 pole solution. The other pole is found on sheet III at (963-29i) MeV.

[32] Reanalysis of data from HYAMS 73, GRAYER 74, SRINIVASAN 75, and ROSSELET 77 using the interfering amplitude method.

[33] At high $|t|$.

[34] At low $|t|$.

[35] On sheet II in a 4-pole solution, the other poles are found on sheet III at (953−55i) MeV and on sheet IV at (938−35i) MeV.

[36] Combined fit of ALDE 95B, ANISOVICH 94, AMSLER 94D.

[37] On sheet II in a 2 pole solution. The other pole is found on sheet III at (996−103i) MeV.

[38] From sheet II pole position.

[39] On sheet II in a 2 pole solution. The other pole is found on sheet III at (797−185i) MeV and can be interpreted as a shadow pole.

[40] On sheet II in a 2 pole solution. The other pole is found on sheet III at (978−28i) MeV.

[41] From coupled channel analysis.

[42] Coupled channel analysis with finite width corrections.

[43] Included in AGUILAR-BENITEZ 78 fit.

$f_0(980)$ WIDTH

Width determination very model dependent. Peak width in $\pi\pi$ is about 50 MeV, but decay width can be much larger.

VALUE (MeV)	EVTS	DOCUMENT ID		TECN	COMMENT
10 to 100 OUR ESTIMATE					
• • • We do not use the following data for averages, fits, limits, etc. • • •					
15.3± 4.7	424	ABLIKIM	15P	BES3	$J/\psi \to K^+K^-3\pi$
9.5± 1.1	706	ABLIKIM	12E	BES3	$J/\psi \to \gamma 3\pi$
42 $^{+\ 20}_{-\ 16}$		[1,2] GARCIA-MAR...	11	RVUE	Compilation
50 $^{+\ 20}_{-\ 12}$		[2,3] GARCIA-MAR...	11	RVUE	Compilation
48 $^{+\ 22}_{-\ 6}$		[4] MOUSSALLAM	11	RVUE	Compilation
36 ± 22		[5] MENNESSIER	10	RVUE	Compilation
70 $^{+\ 20}_{-\ 32}$		[6] ANISOVICH	09	RVUE	0.0 $\overline{p}p$, πN
91 $^{+\ 30}_{-\ 22}$ ± 3	44	[7] ECKLUND	09	CLEO	4.17 $e^+e^- \to D^-_s D^{*+}_s$ + c.c.
66.9± 2.2$^{+17.6}_{-12.5}$		[8] UEHARA	08A	BELL	10.6 $e^+e^- \to e^+e^-\pi^0\pi^0$
65 ± 13	262 ± 30	[9] AUBERT	07AK	BABR	10.6 $e^+e^- \to \phi\pi^+\pi^-\gamma$
81 ± 21	54 ± 9	[9] AUBERT	07AK	BABR	10.6 $e^+e^- \to \phi\pi^0\pi^0\gamma$
51.3$^{+\ 20.8+13.2}_{-\ 17.7-\ 3.8}$		[10] MORI	07	BELL	10.6 $e^+e^- \to e^+e^-\pi^+\pi^-$
61 ± 9 $^{+14}_{-\ 8}$	2584	[11] GARMASH	05	BELL	$B^+ \to K^+\pi^+\pi^-$
64 ± 16		[12] ANISOVICH	03	RVUE	
121 ± 23		TIKHOMIROV	03	SPEC	40.0 $\pi^-C \to K^0_S K^0_S K^0_L X$
~ 70		[13] BRAMON	02	RVUE	1.02 $e^+e^- \to \pi^0\pi^0\gamma$
44 ± 2 ± 2	848	[14] AITALA	01A	E791	$D^+_s \to \pi^-\pi^+\pi^+$
201 ± 28	419	[15] ACHASOV	00H	SND	$e^+e^- \to \pi^0\pi^0\gamma$
122 ± 13	419	[16,17] ACHASOV	00H	SND	$e^+e^- \to \pi^0\pi^0\gamma$
56 ± 20		[18] AKHMETSHIN	99C	CMD2	$e^+e^- \to \pi^0\pi^0\gamma$
65 ± 20		BARBERIS	99	OMEG	450 $pp \to p_s p_f K^+K^-$
80 ± 10		BARBERIS	99B	OMEG	450 $pp \to p_s p_f \pi^+\pi^-$
80 ± 10		BARBERIS	99C	OMEG	450 $pp \to p_s p_f \pi^0\pi^0$
48 ± 12 ± 8		[19] BARBERIS	99D	OMEG	450 $pp \to K^+K^-$, $\pi^+\pi^-$
65 ± 25		BELLAZZINI	99	GAM4	450 $pp \to pp\pi^0\pi^0$
71 ± 14		[20] KAMINSKI	99	RVUE	$\pi\pi \to \pi\pi$, $K\overline{K}$, $\sigma\sigma$

~ 28			[20] OLLER	99	RVUE	$\pi\pi \to \pi\pi$, $K\overline{K}$
~ 25			OLLER	99B	RVUE	$\pi\pi \to \pi\pi$, $K\overline{K}$
~ 14			[20] OLLER	99C	RVUE	$\pi\pi \to \pi\pi$, $K\overline{K}$, $\eta\eta$
70	± 20		ALDE	98	GAM4	
86	± 16		[20] ANISOVICH	98B	RVUE	Compilation
54			[21] LOCHER	98	RVUE	$\pi\pi \to \pi\pi$, $K\overline{K}$
69	± 15		[22] ALDE	97	GAM2	450 $pp \to pp\pi^0\pi^0$
38	± 20		[23] BERTIN	97C	OBLX	0.0 $\overline{p}p \to \pi^+\pi^-\pi^0$
~ 100			[24] ISHIDA	96	RVUE	$\pi\pi \to \pi\pi$, $K\overline{K}$
34			TORNQVIST	96	RVUE	$\pi\pi \to \pi\pi$, $K\overline{K}$, $K\pi$, $\eta\pi$
48	± 10	3k	[25] ALDE	95B	GAM2	38 $\pi^- p \to \pi^0\pi^0 n$
95	± 20	10k	[26] ALDE	95B	GAM2	38 $\pi^- p \to \pi^0\pi^0 n$
26	± 10		AMSLER	95B	CBAR	0.0 $\overline{p}p \to 3\pi^0$
~ 112			[27] AMSLER	95D	CBAR	0.0 $\overline{p}p \to \pi^0\pi^0\pi^0$, $\pi^0\eta\eta$, $\pi^0\pi^0\eta$
80	± 12		[28] ANISOVICH	95	RVUE	
30			JANSSEN	95	RVUE	$\pi\pi \to \pi\pi$, $K\overline{K}$
74			[29] BUGG	94	RVUE	$\overline{p}p \to \eta 2\pi^0$
29	± 2		[30] KAMINSKI	94	RVUE	$\pi\pi \to \pi\pi$, $K\overline{K}$
46			[31] ZOU	94B	RVUE	
48	± 12		[32] MORGAN	93	RVUE	$\pi\pi(K\overline{K}) \to \pi\pi(K\overline{K})$, $J/\psi \to \phi\pi\pi(K\overline{K})$, $D_s \to \pi(\pi\pi)$
37.4	± 10.6		[22] AGUILAR-...	91	EHS	400 pp
72	± 8		[33] ARMSTRONG	91	OMEG	300 $pp \to pp\pi\pi$, $pp K\overline{K}$
110	± 30		BREAKSTONE	90	SFM	$pp \to pp\pi^+\pi^-$
29	± 13		[22] ABACHI	86B	HRS	$e^+e^- \to \pi^+\pi^-$X
120	±281 ±20		ETKIN	82B	MPS	23 $\pi^- p \to n2K^0_S$
28	± 10		[33] GIDAL	81	MRK2	$J/\psi \to \pi^+\pi^-$X
70	to 300		[34] ACHASOV	80	RVUE	
100	± 80		[35] AGUILAR-...	78	HBC	0.7 $\overline{p}p \to K^0_S K^0_S$
30	± 8		[33] LEEPER	77	ASPK	2–2.4 $\pi^- p \to \pi^+\pi^- n$, $K^+K^- n$
48	± 14		[33] BINNIE	73	CNTR	$\pi^- p \to n$MM
32	± 10		[36] GRAYER	73	ASPK	17 $\pi^- p \to \pi^+\pi^- n$
30	± 10		[36] HYAMS	73	ASPK	17 $\pi^- p \to \pi^+\pi^- n$
54	± 16		[36] PROTOPOP...	73	HBC	7 $\pi^+ p \to \pi^+ p\pi^+\pi^-$

[1] Analytic continuation using Roy equations. Uses the K_{e4} data of BATLEY 10C and the $\pi N \to \pi\pi N$ data of HYAMS 73, GRAYER 74, and PROTOPOPESCU 73.
[2] Quoted number refers to twice imaginary part of pole position.
[3] Analytic continuation using GKPY equations. Uses the K_{e4} data of BATLEY 10C and the $\pi N \to \pi\pi N$ data of HYAMS 73, GRAYER 74, and PROTOPOPESCU 73.
[4] Pole position. Used Roy equations.
[5] Average of the analyses of three data sets in the K-matrix model. Uses the data of BATLEY 08A, HYAMS 73, and GRAYER 74, partially of COHEN 80 or ETKIN 82B.
[6] On sheet II in a 2-pole solution. The other pole is found on sheet III at (850−100i) MeV
[7] Using a relativistic Breit-Wigner function and taking into account the finite D_s mass.
[8] Breit-Wigner $\pi\pi$ width. Using finite width corrections according to FLATTE 76 and ACHASOV 05, and the ratio $g_{f_0 KK}/g_{f_0\pi\pi} = 0$.
[9] Systematic errors not estimated.
[10] Breit-Wigner $\pi\pi$ width. Using finite width corrections according to FLATTE 76 and ACHASOV 05, and the ratio $g_{f_0 KK}/g_{f_0\pi\pi} = 4.21 \pm 0.25 \pm 0.21$ from ABLIKIM 05.
[11] Breit-Wigner, solution 1, PWA ambiguous.
[12] K-matrix pole from combined analysis of $\pi^- p \to \pi^0\pi^0 n$, $\pi^- p \to K\overline{K} n$, $\pi^+\pi^- \to \pi^+\pi^-$, $\overline{p}p \to \pi^0\pi^0\pi^0$, $\pi^0\eta\eta$, $\pi^0\pi^0\eta$, $\pi^+\pi^-\pi^0$, $K^+K^-\pi^0$, $K^0_S K^0_S\pi^0$, $K^+K^0_S\pi^-$ at rest, $\overline{p}n \to \pi^-\pi^-\pi^+$, $K^0_S K^-\pi^0$, $K^0_S K^0_S\pi^-$ at rest.
[13] Using the data of AKHMETSHIN 99C, ACHASOV 00H, and ALOISIO 02D.
[14] Breit-Wigner width.
[15] Supersedes ACHASOV 98I. Using the model of ACHASOV 89.
[16] Supersedes ACHASOV 98I.
[17] In the "narrow resonance" approximation.
[18] From the combined fit of the photon spectra in the reactions $e^+e^- \to \pi^+\pi^-\gamma$, $\pi^0\pi^0\gamma$.
[19] Supersedes BARBERIS 99 and BARBERIS 99B
[20] T-matrix pole.
[21] On sheet II in a 2 pole solution. The other pole is found on sheet III at (1039−93i) MeV.
[22] From invariant mass fit.
[23] On sheet II in a 2 pole solution. The other pole is found on sheet III at (963-29i) MeV.
[24] Reanalysis of data from HYAMS 73, GRAYER 74, SRINIVASAN 75, and ROSSELET 77 using the interfering amplitude method.
[25] At high $|t|$.
[26] At low $|t|$.
[27] On sheet II in a 4-pole solution, the other poles are found on sheet III at (953−55i) MeV and on sheet IV at (938−35i) MeV.
[28] Combined fit of ALDE 95B, ANISOVICH 94,
[29] On sheet II in a 2 pole solution. The other pole is found on sheet III at (996−103i) MeV.
[30] From sheet II pole position.
[31] On sheet II in a 2 pole solution. The other pole is found on sheet III at (797−185i) MeV and can be interpreted as a shadow pole.
[32] On sheet II in a 2 pole solution. The other pole is found on sheet III at (978−28i) MeV.
[33] From coupled channel analysis.
[34] Coupled channel analysis with finite width corrections.
[35] From coupled channel fit to the HYAMS 73 and PROTOPOPESCU 73 data. With a simultaneous fit to the $\pi\pi$ phase-shifts, inelasticity and to the $K^0_S K^0_S$ invariant mass.
[36] Included in AGUILAR-BENITEZ 78 fit.

$f_0(980)$ DECAY MODES

	Mode	Fraction (Γ_i/Γ)
Γ_1	$\pi\pi$	dominant
Γ_2	$K\overline{K}$	seen
Γ_3	$\gamma\gamma$	seen
Γ_4	e^+e^-	

$f_0(980)$ PARTIAL WIDTHS

$\Gamma(\gamma\gamma)$ Γ_3

VALUE (keV)	DOCUMENT ID		TECN	COMMENT
0.31 $^{+0.05}_{-0.04}$ OUR AVERAGE				
0.32 ±0.05	[1] DAI	14A	RVUE	Compilation
0.286±0.017$^{+0.211}_{-0.070}$	[2] UEHARA	08A	BELL	10.6 $e^+e^- \to e^+e^-\pi^0\pi^0$
0.205$^{+0.095}_{-0.083}$ $^{+0.147}_{-0.117}$	[3] MORI	07	BELL	10.6 $e^+e^- \to e^+e^-\pi^+\pi^-$
0.42 ±0.06 ±0.18	[4] OEST	90	JADE	$e^+e^- \to e^+e^-\pi^0\pi^0$
• • • We do not use the following data for averages, fits, limits, etc. • • •				
0.16 ±0.01	[5] MENNESSIER	11	RVUE	
0.29 ±0.21 $^{+0.02}_{-0.07}$	[6] MOUSSALLAM	11	RVUE	Compilation
0.42	[7,8] PENNINGTON	08	RVUE	Compilation
0.10	[8,9] PENNINGTON	08	RVUE	Compilation
0.28 $^{+0.09}_{-0.13}$	[10] BOGLIONE	99	RVUE	$\gamma\gamma \to \pi^+\pi^-$, $\pi^0\pi^0$
0.29 ±0.07 ±0.12	[11,12] BOYER	90	MRK2	$e^+e^- \to e^+e^-\pi^+\pi^-$
0.31 ±0.14 ±0.09	[11,12] MARSISKE	90	CBAL	$e^+e^- \to e^+e^-\pi^0\pi^0$
0.63 ±0.14	[13] MORGAN	90	RVUE	$\gamma\gamma \to \pi^+\pi^-$, $\pi^0\pi^0$

[1] Using dispersive analysis with phases from GARCIA-MARTIN 11A and BUETTIKER 04 as input.
[2] Using finite width corrections according to FLATTE 76 and ACHASOV 05, and the ratio $g_{f_0 KK}/g_{f_0\pi\pi} = 0$.
[3] Using finite width corrections according to FLATTE 76 and ACHASOV 05, and the ratio $g_{f_0 KK}/g_{f_0\pi\pi} = 4.21 \pm 0.25 \pm 0.21$ from ABLIKIM 05.
[4] OEST 90 quote systematic errors $^{+0.08}_{-0.18}$. We use ±0.18. Observed 60 events.
[5] Uses an analytic K-matrix model. Compilation.
[6] Using dispersion integral with phase input from Roy equations and data from MARSISKE 90, BOYER 90, BEHREND 92, UEHARA 08A, and MORI 07.
[7] Solution A (preferred solution based on χ^2-analysis).
[8] Dispersion theory based amplitude analysis of BOYER 90, MARSISKE 90, BEHREND 92, and MORI 07.
[9] Solution B (worse than solution A; still acceptable when systematic uncertainties are included).
[10] Supersedes MORGAN 90.
[11] From analysis allowing arbitrary background unconstrained by unitarity.
[12] Data included in MORGAN 90, BOGLIONE 99 analyses.
[13] From amplitude analysis of BOYER 90 and MARSISKE 90, data corresponds to resonance parameters m = 989 MeV, Γ = 61 MeV.

$\Gamma(e^+e^-)$ Γ_4

VALUE (eV)	CL%	DOCUMENT ID		TECN	COMMENT
<8.4	90	VOROBYEV	88	ND	$e^+e^- \to \pi^0\pi^0$

$f_0(980)$ BRANCHING RATIOS

$\Gamma(\pi\pi)/[\Gamma(\pi\pi)+\Gamma(K\overline{K})]$ $\Gamma_1/(\Gamma_1+\Gamma_2)$

VALUE	EVTS	DOCUMENT ID		TECN	COMMENT
• • • We do not use the following data for averages, fits, limits, etc. • • •					
0.52±0.12	9.9k	[1] AUBERT	06O	BABR	$B^\pm \to K^\pm\pi^\pm\pi^\mp$
0.75$^{+0.11}_{-0.13}$		[2] ABLIKIM	05Q	BES2	$\chi_{c0} \to 2\pi^+2\pi^-$, $\pi^+\pi^- K^+K^-$
0.84±0.02		[3] ANISOVICH	02D	SPEC	Combined fit
~ 0.68		OLLER	99B	RVUE	$\pi\pi \to \pi\pi$, $K\overline{K}$
0.67±0.09		[4] LOVERRE	80	HBC	4 $\pi^- p \to n2K^0_S$
0.81$^{+0.09}_{-0.04}$		[4] CASON	78	STRC	7 $\pi^- p \to n2K^0_S$
0.78±0.03		[4] WETZEL	76	OSPK	8.9 $\pi^- p \to n2K^0_S$

[1] Recalculated by us using $\Gamma(K^+K^-)$ / $\Gamma(\pi^+\pi^-) = 0.69 \pm 0.32$ from AUBERT 06O and isospin relations.
[2] Using data from ABLIKIM 04G.
[3] From a combined K-matrix analysis of Crystal Barrel (0. $p\overline{p} \to \pi^0\pi^0\pi^0$, $\pi^0\eta\eta$, $\pi^0\pi^0\eta$), GAMS ($\pi p \to \pi^0\pi^0 n$, $\eta\eta n$, $\eta\eta' n$), and BNL ($\pi p \to K\overline{K} n$) data.
[4] Measure $\pi\pi$ elasticity assuming two resonances coupled to the $\pi\pi$ and $K\overline{K}$ channels only.

Meson Particle Listings

$f_0(980)$, $a_0(980)$

$f_0(980)$ REFERENCES

ABLIKIM	15P	PR D92 012007	M. Ablikim *et al.*	(BES III Collab.)
DAI	14A	PR D90 036004	L.-Y. Dai, M.R. Pennington	(CEBAF)
ABLIKIM	12E	PRL 108 182001	M. Ablikim *et al.*	(BES III Collab.)
GARCIA-MAR...	11	PRL 107 072001	R. Garcia-Martin *et al.*	(MADR, CRAC)
GARCIA-MAR...	11A	PR D83 074004	R. Garcia-Martin *et al.*	(MADR, CRAC)
MENNESSIER	11	PL B696 40	G. Mennessier, S. Narison, X.-G. Wang	
MOUSSALLAM	11	EPJ C71 1814	B. Moussallam	
BATLEY	10C	EPJ C70 635	J.R. Batley *et al.*	(CERN NA48/2 Collab.)
MENNESSIER	10	PL B688 59	G. Mennessier, S. Narison, X.-G. Wang	
ANISOVICH	09	IJMP A24 2481	V.V. Anisovich, A.V. Sarantsev	
ECKLUND	09	PR D80 052009	K.M. Ecklund *et al.*	(CLEO Collab.)
BATLEY	08A	EPJ C54 411	J.R. Batley *et al.*	(CERN NA48/2 Collab.)
PENNINGTON	08	EPJ C56 1	M.R. Pennington *et al.*	
UEHARA	08A	PR D78 052004	S. Uehara *et al.*	(BELLE Collab.)
AMBROSINO	07	EPJ C49 473	F. Ambrosino *et al.*	(KLOE Collab.)
AUBERT	07AK	PR D76 012008	B. Aubert *et al.*	(BABAR Collab.)
BONVICINI	07	PR D76 012001	G. Bonvicini *et al.*	(CLEO Collab.)
MORI	07	PR D75 051101	T. Mori *et al.*	(BELLE Collab.)
AMBROSINO	06B	PL B634 148	F. Ambrosino *et al.*	(KLOE Collab.)
AUBERT	06O	PR D74 032003	B. Aubert *et al.*	(BABAR Collab.)
GARMASH	06	PRL 96 251803	A. Garmash *et al.*	(BELLE Collab.)
ABLIKIM	05	PL B607 243	M. Ablikim *et al.*	(BES Collab.)
ABLIKIM	05Q	PR D72 092002	M. Ablikim *et al.*	(BES Collab.)
ACHASOV	05	PR D72 013006	N.N. Achasov, G.N. Shestakov	
GARMASH	05	PR D71 092003	A. Garmash *et al.*	(BELLE Collab.)
ABLIKIM	04G	PR D70 092002	M. Ablikim *et al.*	(BES Collab.)
BUETTIKER	04	EPJ C33 409	P. Buettiker, S. Descotes-Genon, B. Moussallam	
ANISOVICH	03	EPJ A16 229	V.V. Anisovich *et al.*	
TIKHOMIROV	03	PAN 66 828	G.D. Tikhomirov *et al.*	
		Translated from YAF 66 860.		
ALOISIO	02D	PL B537 21	A. Aloisio *et al.*	(KLOE Collab.)
ANISOVICH	02D	PAN 65 1545	V.V. Anisovich *et al.*	
		Translated from YAF 65 1583.		
BRAMON	02	EPJ C26 253	A. Bramon *et al.*	
ACHASOV	01F	PR D63 094007	N.N. Achasov, V.V. Gubin	(Novosibirsk SND Collab.)
AITALA	01A	PRL 86 765	E.M. Aitala *et al.*	(FNAL E791 Collab.)
AITALA	01B	PRL 86 770	E.M. Aitala *et al.*	(FNAL E791 Collab.)
ACHASOV	00H	PL B485 349	M.N. Achasov *et al.*	(Novosibirsk SND Collab.)
AKHMETSHIN	99B	PL B462 371	R.R. Akhmetshin *et al.*	(Novosibirsk CMD-2 Collab.)
AKHMETSHIN	99C	PL B462 380	R.R. Akhmetshin *et al.*	(Novosibirsk CMD-2 Collab.)
BARBERIS	99	PL B453 305	D. Barberis *et al.*	(Omega Expt.)
BARBERIS	99B	PL B453 316	D. Barberis *et al.*	(Omega Expt.)
BARBERIS	99C	PL B453 325	D. Barberis *et al.*	(Omega Expt.)
BARBERIS	99D	PL B462 462	D. Barberis *et al.*	(Omega Expt.)
BELLAZZINI	99	PL B467 296	R. Bellazzini *et al.*	
BOGLIONE	99	EPJ C9 11	M. Boglione, M.R. Pennington	
KAMINSKI	99	EPJ C9 141	R. Kaminski, L. Lesniak, B. Loiseau	(CRAC, PARIN)
OLLER	99	PR D60 099906 (erratum)	J.A. Oller *et al.*	
OLLER	99B	NP A652 407 (erratum)	J.A. Oller, E. Oset	
OLLER	99C	PR D60 074023	J.A. Oller, E. Oset	
ACHASOV	98I	PL B440 442	M.N. Achasov *et al.*	
ACKERSTAFF	98Q	EPJ C4 19	K. Ackerstaff *et al.*	(OPAL Collab.)
ALDE	98	EPJ A3 361	D. Alde *et al.*	(GAM4 Collab.)
Also		PAN 62 405	D. Alde *et al.*	(GAMS Collab.)
		Translated from YAF 62 446.		
ANISOVICH	98B	SPU 41 419	V.V. Anisovich *et al.*	
		Translated from UFN 168 481.		
LOCHER	98	EPJ C4 317	M.P. Locher *et al.*	(PSI)
ALDE	97	PL B397 350	D.M. Alde *et al.*	(GAMS Collab.)
BERTIN	97C	PL B408 476	A. Bertin *et al.*	(OBELIX Collab.)
ISHIDA	96	PTP 95 745	S. Ishida *et al.*	(TOKY, MIYA, KEK)
TORNQVIST	96	PRL 76 1575	N.A. Tornqvist, M. Roos	(HELS)
ALDE	95B	ZPHY C66 375	D.M. Alde *et al.*	(GAMS Collab.)
AMSLER	95B	PL B342 433	C. Amsler *et al.*	(Crystal Barrel Collab.)
AMSLER	95D	PL B355 425	C. Amsler *et al.*	(Crystal Barrel Collab.)
ANISOVICH	95	PL B355 363	V.V. Anisovich *et al.*	(PNPI, SERP)
JANSSEN	95	PR D52 2690	G. Janssen *et al.*	(STON, ADLD, JULI)
AMSLER	94D	PL B333 277	C. Amsler *et al.*	(Crystal Barrel Collab.)
ANISOVICH	94	PL B323 233	V.V. Anisovich *et al.*	(Crystal Barrel Collab.)
BUGG	94	PR D50 4412	D.V. Bugg *et al.*	(LOQM)
KAMINSKI	94	PR D50 3145	R. Kaminski, L. Lesniak, J.P. Maillet	(CRAC+)
ZOU	94B	PR D50 591	B.S. Zou, D.V. Bugg	(LOQM)
MORGAN	93	PR D48 1185	D. Morgan, M.R. Pennington	(RAL, DURH)
BEHREND	92	ZPHY C56 381	H.J. Behrend	(CELLO Collab.)
AGUILAR-...	91	ZPHY C50 405	M. Aguilar-Benitez *et al.*	(LEBC-EHS Collab.)
ARMSTRONG	91	ZPHY C51 351	T.A. Armstrong *et al.*	(ATHU, BARI, BIRM+)
BOYER	90	PR D42 1350	J. Boyer *et al.*	(Mark II Collab.)
BREAKSTONE	90	ZPHY C48 569	A.M. Breakstone *et al.*	(ISU, BGNA, CERN+)
MARSISKE	90	PR D41 3324	H. Marsiske *et al.*	(Crystal Ball Collab.)
MORGAN	90	ZPHY C48 623	D. Morgan, M.R. Pennington	(RAL, DURH)
OEST	90	ZPHY C47 343	T. Oest *et al.*	(JADE Collab.)
ACHASOV	89	NP B315 465	N.N. Achasov, V.N. Ivanchenko	
AUGUSTIN	89	NP B320 1	J.E. Augustin, G. Cosme	(DM2 Collab.)
VOROBYEV	88	SJNP 48 273	P.V. Vorobiev *et al.*	(NOVO)
		Translated from YAF 48 436.		
ABACHI	86B	PRL 57 1990	S. Abachi *et al.*	(PURD, ANL, IND, MICH+)
ETKIN	82B	PR D25 1786	A. Etkin *et al.*	(BNL, CUNY, TUFTS, VAND)
GIDAL	81	PL 107B 153	G. Gidal *et al.*	(SLAC, LBL)
ACHASOV	80	SJNP 32 566	N.N. Achasov, S.A. Devyanin, G.N. Shestakov	(NOVM)
		Translated from YAF 32 1098.		
COHEN	80	PR D22 2595	D. Cohen *et al.*	(ANL) IJP
LOVERRE	80	ZPHY C6 187	P.F. Loverre *et al.*	(CERN, CDEF, MADR+) IJP
AGUILAR-...	78	NP B140 73	M. Aguilar-Benitez *et al.*	(MADR, BOMB+)
CASON	78	PRL 41 271	N.M. Cason *et al.*	(NDAM, ANL)
LEEPER	77	PR D16 2054	R.J. Leeper *et al.*	(ISU)
ROSSELET	77	PR D15 574	L. Rosselet *et al.*	(GEVA, SACL)
FLATTE	76	PL 63B 224	S.M. Flatte	(CERN)
WETZEL	76	NP B115 208	W. Wetzel *et al.*	(ETH, CERN, LOIC)
SRINIVASAN	75	PR D12 681	V. Srinivasan *et al.*	(NDAM, ANL)
GRAYER	74	NP B75 189	G. Grayer *et al.*	(CERN, MPIM)
BINNIE	73	PRL 31 1534	D.M. Binnie *et al.*	(LOIC, SHMP)
GRAYER	73	Tallahassee	G. Grayer *et al.*	(CERN, MPIM)
HYAMS	73	NP B64 134	B.D. Hyams *et al.*	(CERN, MPIM)
PROTOPOP...	73	PR D7 1279	S.D. Protopopescu *et al.*	(LBL)

$a_0(980)$

$I^G(J^{PC}) = 1^-(0^{++})$

See our minireview on scalar mesons under $f_0(500)$. (See the index for the page number.)

$a_0(980)$ MASS

VALUE (MeV)	DOCUMENT ID
980±20 OUR ESTIMATE	Mass determination very model dependent

$\eta\pi$ FINAL STATE ONLY

VALUE (MeV)	EVTS	DOCUMENT ID		TECN	CHG	COMMENT
• • • We do not use the following data for averages, fits, limits, etc. • • •						
982.5 ± 1.6 ±1.1	16.9k	[1] AMBROSINO	09F	KLOE		$1.02\ e^+e^- \to \eta\pi^0\gamma$
986 ± 4		ANISOVICH	09	RVUE		$0.0\ \overline{p}p,\ \pi N$
982.3 $^{+\ 0.6}_{-\ 0.7}$ $^{+3.1}_{-4.7}$		[2] UEHARA	09A	BELL		$\gamma\gamma \to \pi^0\eta$
987.4 ± 1.0 ±3.0		[3,4] BUGG	08A	RVUE	0	$\overline{p}p \to \pi^0\pi^0\eta$
989.1 ± 1.0 ±3.0		[4,5] BUGG	08A	RVUE	0	$\overline{p}p \to \pi^0\pi^0\eta$
985 ± 4 ±6	318	ACHARD	02B	L3		183–209 $e^+e^- \to e^+e^-\eta\pi^+\pi^-$
995 $^{+52}_{-10}$	36	[6] ACHASOV	00F	SND		$e^+e^- \to \eta\pi^0\gamma$
994 $^{+33}_{-\ 8}$	36	[7] ACHASOV	00F	SND		$e^+e^- \to \eta\pi^0\gamma$
975 ± 7		BARBERIS	00H			$450\ pp \to p_f\eta\pi^0 p_s$
988 ± 8		BARBERIS	00H			$450\ pp \to \Delta_f^{++}\eta\pi^- p_s$
~ 1055		[8] OLLER	99	RVUE		$\eta\pi,\ K\overline{K}$
~ 1009.2		[8] OLLER	99B	RVUE		$\pi\pi \to \pi\pi,\ K\overline{K}$
993.1 ± 2.1		[9] TEIGE	99	B852		$18.3\ \pi^- p \to \eta\pi^+\pi^- n$
988 ± 6		[8] ANISOVICH	98B	RVUE		Compilation
987		TORNQVIST	96	RVUE		$\pi\pi \to \pi\pi,\ K\overline{K},\ K\pi,\ \eta\pi$
991		JANSSEN	95	RVUE		$\eta\pi \to \eta\pi,\ K\overline{K},\ K\pi,\ \eta\pi$
984.45 ± 1.23 ± 0.34		AMSLER	94C	CBAR		$0.0\ \overline{p}p \to \omega\eta\pi^0$
982 ± 2		[10] AMSLER	92	CBAR		$0.0\ \overline{p}p \to \eta\eta\pi^0$
984 ± 4	1040	[10] ARMSTRONG	91B	OMEG ±		$300\ pp \to pp\eta\pi^+\pi^-$
976 ± 6		ATKINSON	84E	OMEG ±		25–55 $\gamma p \to \eta\pi n$
986 ± 3	500	[11] EVANGELIS...	81	OMEG ±		$12\ \pi^- p \to \eta\pi^+\pi^-\pi^- p$
990 ± 7	145	[11] GURTU	79	HBC ±		$4.2\ K^- p \to \Lambda\eta 2\pi$
980 ±11	47	CONFORTO	78	OSPK −		$4.5\ \pi^- p \to pX^-$
978 ±16	50	CORDEN	78	OMEG ±		12–15 $\pi^- p \to n\eta 2\pi$
977 ± 7		GRASSLER	77	HBC −		$16\ \pi^\mp p \to p\eta 3\pi$
989 ± 4	70	WELLS	75	HBC −		3.1–6 $K^- p \to \Lambda\eta 2\pi$
972 ±10	150	DEFOIX	72	HBC ±		$0.7\ \overline{p}p \to 7\pi$
970 ±15	20	BARNES	69C	HBC −		4–5 $K^- p \to \Lambda\eta 2\pi$
980 ±10		CAMPBELL	69	DBC ±		$2.7\ \pi^+ d$
980 ±10	15	MILLER	69B	HBC −		$4.5\ K^- N \to \eta\pi\Lambda$
980 ±10	30	AMMAR	68	HBC ±		$5.5\ K^- p \to \Lambda\eta 2\pi$

[1] Using the model of ACHASOV 89 and ACHASOV 03B.
[2] From a fit with the S-wave amplitude including two interfering Breit-Wigners plus a background term.
[3] Parameterizes couplings to $\overline{K}K$, $\pi\eta$, and $\pi\eta'$.
[4] Using AMSLER 94D and ABELE 98.
[5] From the T-matrix pole on sheet II.
[6] Using the model of ACHASOV 89. Supersedes ACHASOV 98B.
[7] Using the model of JAFFE 77. Supersedes ACHASOV 98B.
[8] T-matrix pole.
[9] Breit-Wigner fit, average between $a_0^\pm$ and a_0^0. The fit favors a slightly heavier $a_0^\pm$.
[10] From a single Breit-Wigner fit.
[11] From $f_1(1285)$ decay.

$K\overline{K}$ ONLY

VALUE (MeV)	EVTS	DOCUMENT ID		TECN	CHG	COMMENT
925 ± 5 ±8	190k	[1] AAIJ	16N	LHCB		$D^0 \to K_S^0 K^\pm\pi^\mp$
• • • We do not use the following data for averages, fits, limits, etc. • • •						
~ 1053		[2] OLLER	99C	RVUE		$\pi\pi \to \pi\pi,\ K\overline{K}$
982 ± 3		[3] ABELE	98	CBAR		$0.0\ \overline{p}p \to K_L^0 K^\pm\pi^\mp$
975 ±15		BERTIN	98B	OBLX ±		$0.0\ \overline{p}p \to K^\pm K_S\pi^\mp$
976 ± 6	316	DEBILLY	80	HBC ±		1.2–2 $\overline{p}p \to f_1(1285)\omega$
1016 ±10	100	[4] ASTIER	67	HBC ±		$0.0\ \overline{p}p$
1003.3 ± 7.0	143	[5] ROSENFELD	65	RVUE ±		

[1] Using a two-channel resonance parametrization with couplings fixed to ABELE 98.
[2] T-matrix pole.
[3] T-matrix pole on sheet II, the pole on sheet III is at 1006-i49 MeV.
[4] ASTIER 67 includes data of BARLOW 67, CONFORTO 67, ARMENTEROS 65.
[5] Plus systematic errors.

$a_0(980)$ WIDTH

VALUE (MeV)	EVTS	DOCUMENT ID		TECN	CHG	COMMENT
50 to 100 OUR ESTIMATE		Width determination very model dependent. Peak width in $\eta\pi$ is about 60 MeV, but decay width can be much larger.				
• • • We do not use the following data for averages, fits, limits, etc. • • •						
75.6 ± 1.6 $^{+17.4}_{-10.0}$		[1] UEHARA	09A	BELL		$\gamma\gamma \to \pi^0\eta$
80.2 ± 3.8 ± 5.4		[2] BUGG	08A	RVUE	0	$\overline{p}p \to \pi^0\pi^0\eta$

50	±13 ± 4	318	ACHARD	02B	L3	183–209 $e^+e^- \to e^+e^-\eta\pi^+\pi^-$
72	±16		BARBERIS	00H		450 $pp \to p_f\eta\pi^0 p_s$
61	±19		BARBERIS	00H		450 $pp \to \Delta_f^{++}\eta\pi^- p_s$
~ 42			[3] OLLER	99	RVUE	$\eta\pi$, $K\overline{K}$
~ 112			[3] OLLER	99B	RVUE	$\pi\pi \to \eta\pi$, $K\overline{K}$
71	± 7		TEIGE	99	B852	18.3 $\pi^- p \to \eta\pi^+\pi^- n$
92	±20		[3] ANISOVICH	98B	RVUE	Compilation
65	±10		[4] BERTIN	98B	OBLX ±	0.0 $\overline{p}p \to K^\pm K_S\pi^\mp$
~ 100			TORNQVIST	96	RVUE	$\pi\pi \to \pi\pi$, $K\overline{K}$, $K\pi$, $\eta\pi$
202			JANSSEN	95	RVUE	$\eta\pi \to \eta\pi$, $K\overline{K}$, $K\pi$, $\eta\pi$
54.12	± 0.34 ± 0.12		AMSLER	94C	CBAR	0.0 $\overline{p}p \to \omega\eta\pi^0$
54	±10		[5] AMSLER	92	CBAR	0.0 $\overline{p}p \to \eta\eta\pi^0$
95	±14	1040	[5] ARMSTRONG	91B	OMEG ±	300 $pp \to pp\eta\pi^+\pi^-$
62	±15	500	[6] EVANGELIS...	81	OMEG ±	12 $\pi^- p \to \eta\pi^+\pi^-\pi^- p$
60	±20	145	[6] GURTU	79	HBC ±	4.2 $K^- p \to \Lambda\eta 2\pi$
60	$^{+50}_{-30}$	47	CONFORTO	78	OSPK −	4.5 $\pi^- p \to pX^-$
86.0	$^{+60.0}_{-50.0}$	50	CORDEN	78	OMEG ±	12–15 $\pi^- p \to n\eta 2\pi$
44	±22		GRASSLER	77	HBC −	16 $\pi^\mp p \to p\eta 3\pi$
80	to 300		[7] FLATTE	76	RVUE −	4.2 $K^- p \to \Lambda\eta 2\pi$
16.0	$^{+25.0}_{-16.0}$	70	WELLS	75	HBC −	3.1–6 $K^- p \to \Lambda\eta 2\pi$
30	± 5	150	DEFOIX	72	HBC ±	0.7 $\overline{p}p \to 7\pi$
40	±15		CAMPBELL	69	DBC ±	2.7 $\pi^+ d$
60	±30	15	MILLER	69B	HBC −	4.5 $K^- N \to \eta\pi\Lambda$
80	±30	30	AMMAR	68	HBC ±	5.5 $K^- p \to \Lambda\eta 2\pi$

[1] From a fit with the S-wave amplitude including two interfering Breit-Wigners plus a background term.
[2] From the T-matrix pole on sheet II, using AMSLER 94D and ABELE 98.
[3] T-matrix pole.
[4] The $\eta\pi$ width.
[5] From a single Breit-Wigner fit.
[6] From $f_1(1285)$ decay.
[7] Using a two-channel resonance parametrization of GAY 76B data.

$K\overline{K}$ ONLY

VALUE (MeV)	EVTS	DOCUMENT ID		TECN	CHG	COMMENT
92± 8		[1] ABELE	98	CBAR		0.0 $\overline{p}p \to K^0_L K^\pm\pi^\mp$
• • • We do not use the following data for averages, fits, limits, etc. • • •						
~ 24		[2] OLLER	99C	RVUE		$\pi\pi \to \pi\pi$, $K\overline{K}$
~ 25	100	[3] ASTIER	67	HBC	±	
57±13	143	[4] ROSENFELD	65	RVUE	±	

[1] T-matrix pole on sheet II, the pole on sheet III is at 1006-i49 MeV.
[2] T-matrix pole.
[3] ASTIER 67 includes data of BARLOW 67, CONFORTO 67, ARMENTEROS 65.
[4] Plus systematic errors.

$a_0(980)$ DECAY MODES

	Mode	Fraction (Γ_i/Γ)
Γ_1	$\eta\pi$	dominant
Γ_2	$K\overline{K}$	seen
Γ_3	$\rho\pi$	
Γ_4	$\gamma\gamma$	seen
Γ_5	e^+e^-	

$a_0(980)$ PARTIAL WIDTHS

$\Gamma(\gamma\gamma)$ Γ_4

VALUE (keV)	DOCUMENT ID		TECN
• • • We do not use the following data for averages, fits, limits, etc. • • •			
0.30±0.10	[1] AMSLER	98	RVUE

[1] Using $\Gamma_{\gamma\gamma}B(a0(980) \to \eta\pi) = 0.24 \pm 0.08$ keV.

$a_0(980)$ Γ(i)$\Gamma(\gamma\gamma)/\Gamma$(total)

$\Gamma(\eta\pi) \times \Gamma(\gamma\gamma)/\Gamma_{\text{total}}$ $\Gamma_1\Gamma_4/\Gamma$

VALUE (keV)	EVTS	DOCUMENT ID		TECN	COMMENT
0.21 $^{+0.08}_{-0.04}$ OUR AVERAGE					
$0.128^{+0.003+0.502}_{-0.002-0.043}$		[1] UEHARA	09A	BELL	$\gamma\gamma \to \pi^0\eta$
0.28 ±0.04 ±0.10	44	OEST	90	JADE	$e^+e^- \to e^+e^-\pi^0\eta$
0.19 ±0.07 $^{+0.10}_{-0.07}$		ANTREASYAN	86	CBAL	$e^+e^- \to e^+e^-\pi^0\eta$

[1] From a fit with the S-wave amplitude including two interfering Breit-Wigners plus a background term.

$\Gamma(\eta\pi) \times \Gamma(e^+e^-)/\Gamma_{\text{total}}$ $\Gamma_1\Gamma_5/\Gamma$

VALUE (eV)	CL%	DOCUMENT ID		TECN	COMMENT
<1.5	90	VOROBYEV	88	ND	$e^+e^- \to \pi^0\eta$

$a_0(980)$ BRANCHING RATIOS

$\Gamma(K\overline{K})/\Gamma(\eta\pi)$ Γ_2/Γ_1

VALUE	DOCUMENT ID		TECN	CHG	COMMENT
0.183±0.024 OUR AVERAGE Error includes scale factor of 1.2.					
0.57 ±0.16	[1] BARGIOTTI	03	OBLX		$\overline{p}p$
0.23 ±0.05	[2] ABELE	98	CBAR		0.0 $\overline{p}p \to K^0_L K^\pm\pi^\mp$
0.166±0.01 ±0.02	[3] BARBERIS	98C	OMEG		450 $pp \to p_f f_1(1285) p_s$
• • • We do not use the following data for averages, fits, limits, etc. • • •					
1.20 ±0.15	[4] ANISOVICH	09	RVUE		0.0 $\overline{p}p$, πN
1.05 ±0.07 ±0.05	[5] BUGG	08A	RVUE	0	$\overline{p}p \to \pi^0\pi^0\eta$
~ 0.60	OLLER	99B	RVUE		$\pi\pi \to \eta\pi$, $K\overline{K}$
0.7 ±0.3	[3] CORDEN	78	OMEG		12–15 $\pi^- p \to n\eta 2\pi$
0.25 ±0.08	[3] DEFOIX	72	HBC	±	0.7 $\overline{p} \to 7\pi$

$\Gamma(\rho\pi)/\Gamma(\eta\pi)$ Γ_3/Γ_1

$\rho\pi$ forbidden.

VALUE	CL%	DOCUMENT ID		TECN	CHG	COMMENT
• • • We do not use the following data for averages, fits, limits, etc. • • •						
<0.25	70	AMMAR	70	HBC	±	4.1,5.5 $K^- p \to \Lambda\eta 2\pi$

[1] Coupled channel analysis of $\pi^+\pi^-\pi^0$, $K^+K^-\pi^0$, and $K^\pm K^0_S\pi^\mp$.
[2] Using $\pi^0\pi^0\eta$ from AMSLER 94D.
[3] From the decay of $f_1(1285)$.
[4] This is a ratio of couplings.
[5] A ratio of couplings, using AMSLER 94D and ABELE 98. Supersedes BUGG 94.

$a_0(980)$ REFERENCES

AAIJ	16N	PR D93 052018	R. Aaij *et al.*	(LHCb Collab.)
AMBROSINO	09F	PL B681 5	F. Ambrosino *et al.*	(KLOE Collab.)
ANISOVICH	09	IJMP A24 2481	V.V. Anisovich, A.V. Sarantsev	
UEHARA	09A	PR D80 032001	S. Uehara *et al.*	(BELLE Collab.)
BUGG	08A	PR D78 074023	D.V. Bugg	(LOQM)
ACHASOV	03B	PR D68 014006	N.N. Achsaov, A.V. Kiselev	
BARGIOTTI	03	EPJ C26 371	M. Bargiotti *et al.*	(OBELIX Collab.)
ACHARD	02B	PL B526 269	P. Achard *et al.*	(L3 Collab.)
ACHASOV	00F	PL B479 53	M.N. Achasov *et al.*	(Novosibirsk SND Collab.)
BARBERIS	00H	PL B488 225	D. Barberis *et al.*	(WA 102 Collab.)
OLLER	99	PR D60 099906 (erratum)	J.A. Oller *et al.*	
OLLER	99B	NP A652 407 (erratum)	J.A. Oller, E. Oset	
OLLER	99C	PR D60 074023	J.A. Oller, E. Oset	
TEIGE	99	PR D59 012001	S. Teige *et al.*	(BNL E852 Collab.)
ABELE	98	PR D57 3860	A. Abele *et al.*	(Crystal Barrel Collab.)
ACHASOV	98B	PL B438 441	M.N. Achasov *et al.*	(Novosibirsk SND Collab.)
AMSLER	98	RMP 70 1293	C. Amsler	
ANISOVICH	98B	SPU 41 419	V.V. Anisovich *et al.*	
		Translated from UFN 168 481.		
BARBERIS	98C	PL B440 225	D. Barberis *et al.*	(WA 102 Collab.)
BERTIN	98B	PL B434 180	A. Bertin *et al.*	(OBELIX Collab.)
TORNQVIST	96	PRL 76 1575	N.A. Tornqvist, M. Roos	(HELS)
JANSSEN	95	PR D52 2690	G. Janssen *et al.*	(STON, ADLD, JULI)
AMSLER	94C	PL B327 425	C. Amsler *et al.*	(Crystal Barrel Collab.)
AMSLER	94D	PL B333 277	C. Amsler *et al.*	(Crystal Barrel Collab.)
BUGG	94	PR D50 4412	D.V. Bugg *et al.*	(LOQM)
AMSLER	92	PL B291 347	C. Amsler *et al.*	(Crystal Barrel Collab.)
ARMSTRONG	91B	ZPHY C52 389	T.A. Armstrong *et al.*	(ATHU, BARI, BIRM+)
OEST	90	ZPHY C47 343	T. Oest *et al.*	(JADE Collab.)
ACHASOV	89	NP B315 465	N.N. Achasov, V.N. Ivanchenko	
VOROBYEV	88	SJNP 48 273	P.V. Vorobiev *et al.*	(NOVO)
		Translated from YAF 48 436.		
ANTREASYAN	86	PR D33 1847	D. Antreasyan *et al.*	(Crystal Ball Collab.)
ATKINSON	84E	PL 138B 459	M. Atkinson *et al.*	(BONN, CERN, GLAS+)
EVANGELIS...	81	NP B178 197	C. Evangelista *et al.*	(BARI, BONN, CERN+)
DEBILLY	80	NP B176 1	L. de Billy *et al.*	(CURIN, LAUS, NEUC+)
GURTU	79	NP B151 181	A. Gurtu *et al.*	(CERN, ZEEM, NIJM, OXF)
CONFORTO	78	LNC 23 419	B. Conforto *et al.*	(RHEL, TNTO, CHIC+)
CORDEN	78	NP B144 253	M.J. Corden *et al.*	(BIRM, RHEL, TELA+)
GRASSLER	77	NP B121 189	H. Grassler *et al.*	(AACH3, BERL, BONN+)
JAFFE	77	PR D15 267,281	R. Jaffe	(MIT)
FLATTE	76	PL 63B 224	S.M. Flatte	(CERN)
GAY	76B	PL 63B 220	J.B. Gay *et al.*	(CERN, AMST, NIJM) JP
WELLS	75	NP B101 333	J. Wells *et al.*	(OXF)
DEFOIX	72	NP B44 125	C. Defoix *et al.*	(CDEF, CERN)
AMMAR	70	PR D2 430	R. Ammar *et al.*	(KANS, NWES, ANL, WISC)
BARNES	69C	PRL 23 610	V.E. Barnes *et al.*	(BNL, SYRA)
CAMPBELL	69	PRL 22 1204	J.H. Campbell *et al.*	(PURD)
MILLER	69B	PL 29B 255	D.H. Miller *et al.*	(PURD)
Also		PR 188 2011	W.L. Yen *et al.*	(PURD)
AMMAR	68	PRL 21 1832	R. Ammar *et al.*	(NWES, ANL)
ASTIER	67	PL 25B 294	A. Astier *et al.*	(CDEF, CERN, IRAD)
		Includes data of BARLOW 67, CONFORTO 67, and ARMENTEROS 65.		
BARLOW	67	NC 50A 701	J. Barlow *et al.*	(CERN, CDEF, IRAD, LIVP)
CONFORTO	67	NP B3 469	G. Conforto *et al.*	(CERN, CDEF, IPNP+)
ARMENTEROS	65	PL 17 344	R. Armenteros *et al.*	(CERN, CDEF)
ROSENFELD	65	Oxford Conf. 58	A.H. Rosenfeld	(LRL)

$\phi(1020)$

$I^G(J^{PC}) = 0^-(1^{--})$

$\phi(1020)$ MASS

VALUE (MeV)	EVTS	DOCUMENT ID		TECN	COMMENT
1019.461±0.016 OUR AVERAGE					
1019.463±0.061	2.3M	[1] KOZYREV	18	CMD3	$e^+e^- \to K^+K^-$, $K^0_S K^0_L$
1019.462±0.042±0.056	28k	[2] LEES	14H	BABR	$e^+e^- \to K^0_S K^0_L\gamma$

Meson Particle Listings

$\phi(1020)$

1019.51	±0.02	±0.05		[3] LEES	13Q	BABR	$e^+e^- \to K^+K^-\gamma$
1019.30	±0.02	±0.10	105k	AKHMETSHIN	06	CMD2	0.98–1.06 $e^+e^- \to \pi^+\pi^-\pi^0$
1019.52	±0.05	±0.05	17.4k	AKHMETSHIN	05	CMD2	0.60–1.38 $e^+e^- \to \eta\gamma$
1019.483	±0.011	±0.025	272k	[4] AKHMETSHIN	04	CMD2	$e^+e^- \to K_L^0 K_S^0$
1019.42	±0.05		1900k	[5] ACHASOV	01E	SND	$e^+e^- \to K^+K^-$, $K_S K_L$, $\pi^+\pi^-\pi^0$
1019.40	±0.04	±0.05	23k	AKHMETSHIN	01B	CMD2	$e^+e^- \to \eta\gamma$
1019.36	±0.12			[6] ACHASOV	00B	SND	$e^+e^- \to \eta\gamma$
1019.38	±0.07	±0.08	2200	[7] AKHMETSHIN	99F	CMD2	$e^+e^- \to \pi^+\pi^- \geq 2\gamma$
1019.51	±0.07	±0.10	11169	AKHMETSHIN	98	CMD2	$e^+e^- \to \pi^+\pi^-\pi^0$
1019.5	±0.4			BARBERIS	98	OMEG	450 $pp \to pp2K^+2K^-$
1019.42	±0.06		55600	AKHMETSHIN	95	CMD2	$e^+e^- \to$ hadrons
1019.7	±0.3		2012	DAVENPORT	86	MPSF	400 $pA \to 4KX$
1019.7	±0.1	±0.1	5079	ALBRECHT	85D	ARG	10 $e^+e^- \to K^+K^-X$
1019.3	±0.1		1500	ARENTON	82	AEMS	11.8 polar. $pp \to KK$
1019.67	±0.17		25080	[8] PELLINEN	82	RVUE	
1019.52	±0.13		3681	BUKIN	78C	OLYA	$e^+e^- \to$ hadrons

• • • We do not use the following data for averages, fits, limits, etc. • • •

1019.469	±0.061		1.7M	KOZYREV	18	CMD3	$e^+e^- \to K^+K^-$
1019.457	±0.061		610k	KOZYREV	16	CMD3	$e^+e^- \to K_S^0 K_L^0$
1019.48	±0.01			LEES	13F	BABR	$D^+ \to K^+K^-\pi^+$
1019.441	±0.008	±0.080	542k	[9] AKHMETSHIN	08	CMD2	1.02 $e^+e^- \to K^+K^-$
1019.63	±0.07		12540	[10] AUBERT,B	05J	BABR	$D^0 \to \overline{K}^0 K^+K^-$
1019.8	±0.7			ARMSTRONG	86	OMEG	85 $\pi^+/pp \to \pi^+/p4Kp$
1020.1	±0.11		5526	[10] ATKINSON	86	OMEG	20–70 γp
1019.7	±1.0			BEBEK	86	CLEO	$e^+e^- \to \Upsilon(4S)$
1019.411	±0.008		642k	[11] DIJKSTRA	86	SPEC	100–200 $\pi^\pm$, $\overline{p}$, p, $K^\pm$, on Be
1020.9	±0.2			[10] FRAME	86	OMEG	13 $K^+p \to \phi K^+p$
1021.0	±0.2			[10] ARMSTRONG	83B	OMEG	18.5 $K^-p \to K^-K^+\Lambda$
1020.0	±0.5			[10] ARMSTRONG	83B	OMEG	18.5 $K^-p \to K^-K^+\Lambda$
1019.7	±0.3			[10] BARATE	83	GOLI	190 π^-Be $\to 2\mu X$
1019.8	±0.2	±0.5	766	IVANOV	81	OLYA	1–1.4 $e^+e^- \to K^+K^-$
1019.4	±0.5		337	COOPER	78B	HBC	0.7–0.8 $\overline{p}p \to K_S^0 K_L^0 \pi^+\pi^-$
1020	±1		383	[10] BALDI	77	CNTR	10 $\pi^-p \to \pi^-\phi p$
1018.9	±0.6		800	COHEN	77	ASPK	6 $\pi^\pm N \to K^+K^-N$
1019.7	±0.5		454	KALBFLEISCH	76	HBC	2.18 $K^-p \to \Lambda K\overline{K}$
1019.4	±0.8		984	BESCH	74	CNTR	2 $\gamma p \to pK^+K^-$
1020.3	±0.4		100	BALLAM	73	HBC	2.8–9.3 γp
1019.4	±0.7			BINNIE	73B	CNTR	$\pi^-p \to \phi n$
1019.6	±0.5		120	[12] AGUILAR-...	72B	HBC	3.9,4.6 $K^-p \to \Lambda K^+K^-$
1019.9	±0.5		100	[12] AGUILAR-...	72B	HBC	3.9,4.6 $K^-p \to K^-pK^+K^-$
1020.4	±0.5		131	COLLEY	72	HBC	10 $K^+p \to K^+p\phi$
1019.9	±0.3		410	STOTTLE...	71	HBC	2.9 $K^-p \to \Sigma/\Lambda K\overline{K}$

[1] Average of KOZYREV 16 and KOZYREV 18 values taking into account the correlated uncertainties. Supersedes individual KOZYREV 16 and KOZYREV 18 results.
[2] Using a vector meson dominance model with contribution from $\phi(1020)$ and higher mass excitations of $\rho(770)$, $\omega(782)$, and $\phi(1020)$.
[3] Using a phenomenological model based on KUHN 90 with a sum of Breit-Wigner resonances for $\rho(770)$, $\omega(782)$, $\phi(1020)$ and their higher mass excitations.
[4] Update of AKHMETSHIN 99D
[5] From the combined fit assuming that the total $\phi(1020)$ production cross section is saturated by those of K^+K^-, $K_S K_L$, $\pi^+\pi^-\pi^0$, and $\eta\gamma$ decays modes and using ACHASOV 00B for the $\eta\gamma$ decay mode.
[6] Using a total width of 4.43 ± 0.05 MeV. Systematic uncertainty included.
[7] Using a total width of 4.43 ± 0.05 MeV.
[8] PELLINEN 82 review includes AKERLOF 77, DAUM 81, BALDI 77, AYRES 74, DEGROOT 74.
[9] Strongly correlated with AKHMETSHIN 04.
[10] Systematic errors not evaluated.
[11] Weighted and scaled average of 12 measurements of DIJKSTRA 86.
[12] Mass errors enlarged by us to $\Gamma/\sqrt{N}$; see the note with the $K^*(892)$ mass.

$\phi(1020)$ WIDTH

VALUE (MeV)	EVTS	DOCUMENT ID		TECN	COMMENT
4.249±0.013 OUR AVERAGE		Error includes scale factor of 1.1.			
4.245±0.013	2.3M	[1] KOZYREV	18	CMD3	$e^+e^- \to K^+K^-$, $K_S^0 K_L^0$
4.205±0.103±0.067	28k	[2] LEES	14H	BABR	$e^+e^- \to K_S^0 K_L^0\gamma$
4.29 ±0.04 ±0.07		[3] LEES	13Q	BABR	$e^+e^- \to K^+K^-\gamma$
4.30 ±0.06 ±0.17	105k	AKHMETSHIN	06	CMD2	0.98–1.06 $e^+e^- \to \pi^+\pi^-\pi^0$
4.280±0.033±0.025	272k	[4] AKHMETSHIN	04	CMD2	$e^+e^- \to K_L^0 K_S^0$
4.21 ±0.04	1900k	[5] ACHASOV	01E	SND	$e^+e^- \to K^+K^-$, $K_S K_L$, $\pi^+\pi^-\pi^0$
4.44 ±0.09	55600	AKHMETSHIN	95	CMD2	$e^+e^- \to$ hadrons
4.5 ±0.7	1500	ARENTON	82	AEMS	11.8 polar. $pp \to KK$
4.2 ±0.6	766	[6] IVANOV	81	OLYA	1–1.4 $e^+e^- \to K^+K^-$
4.3 ±0.6		[6] CORDIER	80	DM1	$e^+e^- \to \pi^+\pi^-\pi^0$
4.36 ±0.29	3681	[6] BUKIN	78C	OLYA	$e^+e^- \to$ hadrons
4.4 ±0.6	984	[6] BESCH	74	CNTR	2 $\gamma p \to pK^+K^-$
4.67 ±0.72	681	[6] BALAKIN	71	OSPK	$e^+e^- \to$ hadrons
4.09 ±0.29		BIZOT	70	OSPK	$e^+e^- \to$ hadrons

• • • We do not use the following data for averages, fits, limits, etc. • • •

4.249±0.015	1.7M	KOZYREV	18	CMD3	$e^+e^- \to K^+K^-$
4.240±0.017	610k	KOZYREV	16	CMD3	$e^+e^- \to K_S^0 K_L^0$
4.37 ±0.02		LEES	13F	BABR	$D^+ \to K^+K^-\pi^+$
4.24 ±0.02 ±0.03	542k	[7] AKHMETSHIN	08	CMD2	1.02 $e^+e^- \to K^+K^-$
4.28 ±0.13	12540	[8] AUBERT,B	05J	BABR	$D^0 \to \overline{K}^0 K^+K^-$
4.45 ±0.06	271k	DIJKSTRA	86	SPEC	100 π^-Be
3.6 ±0.8	337	[6] COOPER	78B	HBC	0.7–0.8 $\overline{p}p \to K_S^0 K_L^0 \pi^+\pi^-$
4.5 ±0.50	1300	[6,8] AKERLOF	77	SPEC	400 $pA \to K^+K^-X$
4.5 ±0.8	500	[6,8] AYRES	74	ASPK	3–6 $\pi^-p \to K^+K^-n$, $K^-p \to K^+K^-\Lambda/\Sigma^0$
3.81 ±0.37		COSME	74B	OSPK	$e^+e^- \to K_L^0 K_S^0$
3.8 ±0.7	454	[6] BORENSTEIN	72	HBC	2.18 $K^-p \to K\overline{K}n$

[1] Average of KOZYREV 16 and KOZYREV 18 values taking into account the correlated uncertainties. Supersedes individual KOZYREV 16 and KOZYREV 18 results.
[2] Using a vector meson dominance model with contribution from $\phi(1020)$ and higher mass excitations of $\rho(770)$, $\omega(782)$, and $\phi(1020)$.
[3] Using a phenomenological model based on KUHN 90 with a sum of Breit-Wigner resonances for $\rho(770)$, $\omega(782)$, $\phi(1020)$ and their higher mass excitations.
[4] Update of AKHMETSHIN 99D
[5] From the combined fit assuming that the total $\phi(1020)$ production cross section is saturated by those of K^+K^-, $K_S K_L$, $\pi^+\pi^-\pi^0$, and $\eta\gamma$ decays modes and using ACHASOV 00B for the $\eta\gamma$ decay mode.
[6] Width errors enlarged by us to $4\Gamma/\sqrt{N}$; see the note with the $K^*(892)$ mass.
[7] Strongly correlated with AKHMETSHIN 04.
[8] Systematic errors not evaluated.

$\phi(1020)$ DECAY MODES

	Mode	Fraction (Γ_i/Γ)	Scale factor/ Confidence level
Γ_1	K^+K^-	(49.2 ±0.5) %	S=1.3
Γ_2	$K_L^0 K_S^0$	(34.0 ±0.4) %	S=1.3
Γ_3	$\rho\pi$ + $\pi^+\pi^-\pi^0$	(15.24 ±0.33) %	S=1.2
Γ_4	$\rho\pi$		
Γ_5	$\pi^+\pi^-\pi^0$		
Γ_6	$\eta\gamma$	(1.303±0.025) %	S=1.2
Γ_7	$\pi^0\gamma$	(1.30 ±0.05) $\times 10^{-3}$	
Γ_8	$\ell^+\ell^-$	—	
Γ_9	e^+e^-	(2.973±0.034) $\times 10^{-4}$	S=1.3
Γ_{10}	$\mu^+\mu^-$	(2.86 ±0.19) $\times 10^{-4}$	
Γ_{11}	ηe^+e^-	(1.08 ±0.04) $\times 10^{-4}$	
Γ_{12}	$\pi^+\pi^-$	(7.3 ±1.3) $\times 10^{-5}$	
Γ_{13}	$\omega\pi^0$	(4.7 ±0.5) $\times 10^{-5}$	
Γ_{14}	$\omega\gamma$	< 5 %	CL=84%
Γ_{15}	$\rho\gamma$	< 1.2 $\times 10^{-5}$	CL=90%
Γ_{16}	$\pi^+\pi^-\gamma$	(4.1 ±1.3) $\times 10^{-5}$	
Γ_{17}	$f_0(980)\gamma$	(3.22 ±0.19) $\times 10^{-4}$	S=1.1
Γ_{18}	$\pi^0\pi^0\gamma$	(1.12 ±0.06) $\times 10^{-4}$	
Γ_{19}	$\pi^+\pi^-\pi^+\pi^-$	(3.9 $^{+2.8}_{-2.2}$) $\times 10^{-6}$	
Γ_{20}	$\pi^+\pi^+\pi^-\pi^-\pi^0$	< 4.6 $\times 10^{-6}$	CL=90%
Γ_{21}	$\pi^0 e^+e^-$	(1.33 $^{+0.07}_{-0.10}$) $\times 10^{-5}$	
Γ_{22}	$\pi^0\eta\gamma$	(7.27 ±0.30) $\times 10^{-5}$	S=1.5
Γ_{23}	$a_0(980)\gamma$	(7.6 ±0.6) $\times 10^{-5}$	
Γ_{24}	$K^0\overline{K}^0\gamma$	< 1.9 $\times 10^{-8}$	CL=90%
Γ_{25}	$\eta'(958)\gamma$	(6.22 ±0.21) $\times 10^{-5}$	
Γ_{26}	$\eta\pi^0\pi^0\gamma$	< 2 $\times 10^{-5}$	CL=90%
Γ_{27}	$\mu^+\mu^-\gamma$	(1.4 ±0.5) $\times 10^{-5}$	
Γ_{28}	$\rho\gamma\gamma$	< 1.2 $\times 10^{-4}$	CL=90%
Γ_{29}	$\eta\pi^+\pi^-$	< 1.8 $\times 10^{-5}$	CL=90%
Γ_{30}	$\eta\mu^+\mu^-$	< 9.4 $\times 10^{-6}$	CL=90%
Γ_{31}	$\eta U \to \eta e^+e^-$	< 1 $\times 10^{-6}$	CL=90%

Lepton Family number (LF) violating modes

Γ_{32}	$e^\pm\mu^\mp$	LF	< 2 $\times 10^{-6}$	CL=90%

CONSTRAINED FIT INFORMATION

An overall fit to 30 branching ratios uses 82 measurements and one constraint to determine 14 parameters. The overall fit has a $\chi^2 = 63.7$ for 69 degrees of freedom.

The following *off-diagonal* array elements are the correlation coefficients $\langle \delta x_i \delta x_j \rangle / (\delta x_i \cdot \delta x_j)$, in percent, from the fit to the branching fractions, $x_i \equiv \Gamma_i/\Gamma_{total}$. The fit constrains the x_i whose labels appear in this array to sum to one.

x_2	−78									
x_3	−59	−4								
x_6	−23	19	6							
x_7	−15	14	4	10						
x_9	54	−52	−17	−38	−27					
x_{10}	−7	7	2	5	3	−13				
x_{12}	−3	3	1	2	2	−6	1			
x_{13}	−5	4	1	3	2	−8	1	1		
x_{17}	0	0	0	0	0	0	0	0	0	
x_{18}	−11	10	3	19	5	−20	2	1	2	0
x_{19}	−1	1	0	1	0	−2	0	0	0	0
x_{23}	0	0	0	0	0	0	0	0	0	0
x_{25}	−8	6	2	33	3	−12	2	1	1	0
	x_1	x_2	x_3	x_6	x_7	x_9	x_{10}	x_{12}	x_{13}	x_{17}

x_{19}	0		
x_{23}	0	0	
x_{25}	6	0	0
	x_{18}	x_{19}	x_{23}

$\phi(1020)$ PARTIAL WIDTHS

$\Gamma(\eta\gamma)$ Γ_6

VALUE (keV)	DOCUMENT ID		TECN	COMMENT
• • • We do not use the following data for averages, fits, limits, etc. • • •				
58.9 ± 0.5 ± 2.4	ACHASOV	00	SND	$e^+e^- \to \eta\gamma$

$\Gamma(\pi^0\gamma)$ Γ_7

VALUE (keV)	DOCUMENT ID		TECN	COMMENT
• • • We do not use the following data for averages, fits, limits, etc. • • •				
$5.40 \pm 0.16 ^{+0.43}_{-0.40}$	ACHASOV	00	SND	$e^+e^- \to \pi^0\gamma$

$\Gamma(\ell^+\ell^-)$ Γ_8

VALUE (keV)	DOCUMENT ID		TECN	COMMENT
• • • We do not use the following data for averages, fits, limits, etc. • • •				
1.320 ± 0.017 ± 0.015	[1] AMBROSINO	05	KLOE	1.02 $e^+e^- \to \mu^+\mu^-$

[1] Weighted average of Γ_{ee} and $\sqrt{\Gamma_{ee}\Gamma_{\mu\mu}}$ from AMBROSINO 05 assuming lepton universality.

$\Gamma(e^+e^-)$ Γ_9

VALUE (keV)	DOCUMENT ID		TECN	COMMENT
1.27 ± 0.04 OUR EVALUATION				
1.251 ± 0.021 OUR AVERAGE Error includes scale factor of 1.1.				
1.235 ± 0.006 ± 0.022	[1] AKHMETSHIN	11	CMD2	1.02 $e^+e^- \to \phi$
1.32 ± 0.05 ± 0.03	[2] AMBROSINO	05	KLOE	1.02 $e^+e^- \to e^+e^-$
1.28 ± 0.05	AKHMETSHIN	95	CMD2	1.02 $e^+e^- \to \phi$

[1] Combined analysis of the CMD-2 data on $\phi \to K^+K^-$, $K^0_S K^0_L$, $\pi^+\pi^-\pi^0$, $\eta\gamma$ assuming that the sum of their branching fractions is 0.99741 ± 0.00007.

[2] From forward-backward asymmetry and using $\Gamma_{total} = 4.26 \pm 0.05$ MeV from the 2004 edition of this Review.

$(\Gamma(e^+e^-) \times \Gamma(\mu^+\mu^-))^{1/2}$ $(\Gamma_9\Gamma_{10})^{1/2}$

VALUE (keV)	DOCUMENT ID		TECN	COMMENT
1.320 ± 0.018 ± 0.017	AMBROSINO	05	KLOE	1.02 $e^+e^- \to \mu^+\mu^-$

$\phi(1020)\ \Gamma(i)\Gamma(e^+e^-)/\Gamma(total)$

$\Gamma(K^+K^-) \times \Gamma(e^+e^-)/\Gamma_{total}$ $\Gamma_1\Gamma_9/\Gamma$

VALUE (keV)	EVTS	DOCUMENT ID		TECN	COMMENT
0.6340 ± 0.0070 ± 0.0039		[1] LEES	13Q	BABR	$e^+e^- \to K^+K^-\gamma$
• • • We do not use the following data for averages, fits, limits, etc. • • •					
0.669 ± 0.001 ± 0.023	1.7M	KOZYREV	18	CMD3	$e^+e^- \to K^+K^-$

[1] Using a phenomenological model based on KUHN 90 with a sum of Breit-Wigner resonances for $\rho(770)$, $\omega(782)$, $\phi(1020)$ and their higher mass excitations. The first error combines statistical and systematic uncertainties. The second one is due to the parametrization of the charged kaon form factor and mass calibration.

$\Gamma(K^0_L K^0_S) \times \Gamma(e^+e^-)/\Gamma_{total}$ $\Gamma_2\Gamma_9/\Gamma$

VALUE (keV)	EVTS	DOCUMENT ID		TECN	COMMENT
0.4200 ± 0.0033 ± 0.0123	28k	[1] LEES	14H	BABR	$e^+e^- \to K^0_S K^0_L\gamma$

[1] Using a vector meson dominance model with contribution from $\phi(1020)$ and higher mass excitations of $\rho(770)$, $\omega(782)$, and $\phi(1020)$.

$\phi(1020)\ \Gamma(i)\Gamma(e^+e^-)/\Gamma^2(total)$

$\Gamma(K^+K^-)/\Gamma_{total} \times \Gamma(e^+e^-)/\Gamma_{total}$ $\Gamma_1/\Gamma \times \Gamma_9/\Gamma$

VALUE (units 10^{-5})	EVTS	DOCUMENT ID		TECN	COMMENT
14.63 ± 0.29 OUR FIT Error includes scale factor of 1.5.					
14.6 ± 0.5 OUR AVERAGE Error includes scale factor of 1.8. See the ideogram below.					
15.789 ± 0.541	1.7M	KOZYREV	18	CMD3	$e^+e^- \to K^+K^-$
14.27 ± 0.05 ± 0.31	542k	AKHMETSHIN	08	CMD2	1.02 $e^+e^- \to K^+K^-$
13.93 ± 0.14 ± 0.99	1000k	[1] ACHASOV	01E	SND	$e^+e^- \to K^+K^-$, $K_S K_L$, $\pi^+\pi^-\pi^0$

[1] From the combined fit assuming that the total $\phi(1020)$ production cross section is saturated by those of K^+K^-, $K_S K_L$, $\pi^+\pi^-\pi^0$, and $\eta\gamma$ decays modes and using ACHASOV 00B for the $\eta\gamma$ decay mode.

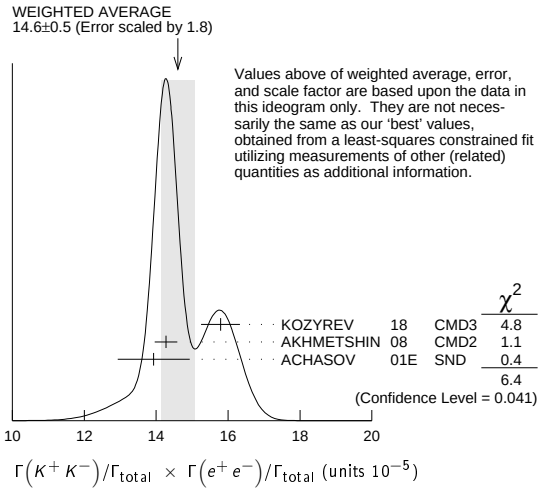

$\Gamma(K^0_L K^0_S)/\Gamma_{total} \times \Gamma(e^+e^-)/\Gamma_{total}$ $\Gamma_2/\Gamma \times \Gamma_9/\Gamma$

VALUE (units 10^{-5})	EVTS	DOCUMENT ID		TECN	COMMENT
10.10 ± 0.12 OUR FIT Error includes scale factor of 1.1.					
10.07 ± 0.13 OUR AVERAGE					
10.078 ± 0.223	610k	[1] KOZYREV	16	CMD3	$e^+e^- \to K^0_S K^0_L$
10.01 ± 0.04 ± 0.17	272k	[2] AKHMETSHIN	04	CMD2	$e^+e^- \to K^0_L K^0_S$
10.27 ± 0.07 ± 0.34	500k	[3] ACHASOV	01E	SND	$e^+e^- \to K^+K^-$, $K_S K_L$, $\pi^+\pi^-\pi^0$

[1] KOZYREV 16 also reports $\Gamma(e^+e^-)\ B(\phi \to K^0_S K^0_L) = (0.428 \pm 0.001 \pm 0.009)$ keV.

[2] Update of AKHMETSHIN 99D

[3] From the combined fit assuming that the total $\phi(1020)$ production cross section is saturated by those of K^+K^-, $K_S K_L$, $\pi^+\pi^-\pi^0$, and $\eta\gamma$ decays modes and using ACHASOV 00B for the $\eta\gamma$ decay mode.

$[\Gamma(\rho\pi) + \Gamma(\pi^+\pi^-\pi^0)]/\Gamma_{total} \times \Gamma(e^+e^-)/\Gamma_{total}$ $\Gamma_3/\Gamma \times \Gamma_9/\Gamma$

VALUE (units 10^{-5})	EVTS	DOCUMENT ID		TECN	COMMENT
4.53 ± 0.10 OUR FIT Error includes scale factor of 1.1.					
4.46 ± 0.12 OUR AVERAGE					
4.51 ± 0.16 ± 0.11	105k	AKHMETSHIN	06	CMD2	0.98–1.06 $e^+e^- \to \pi^+\pi^-\pi^0$
4.30 ± 0.08 ± 0.21		AUBERT,B	04N	BABR	10.6 $e^+e^- \to \pi^+\pi^-\pi^0\gamma$
4.665 ± 0.042 ± 0.261	400k	[1] ACHASOV	01E	SND	$e^+e^- \to K^+K^-$, $K_S K_L$, $\pi^+\pi^-\pi^0$
4.35 ± 0.27 ± 0.08	11169	[2] AKHMETSHIN	98	CMD2	$e^+e^- \to \pi^+\pi^-\pi^0$
• • • We do not use the following data for averages, fits, limits, etc. • • •					
4.38 ± 0.12		BENAYOUN	10	RVUE	0.4–1.05 e^+e^-

[1] From the combined fit assuming that the total $\phi(1020)$ production cross section is saturated by those of K^+K^-, $K_S K_L$, $\pi^+\pi^-\pi^0$, and $\eta\gamma$ decays modes and using ACHASOV 00B for the $\eta\gamma$ decay mode.

[2] Recalculated by us from the cross section in the peak.

$\Gamma(\eta\gamma)/\Gamma_{total} \times \Gamma(e^+e^-)/\Gamma_{total}$ $\Gamma_6/\Gamma \times \Gamma_9/\Gamma$

VALUE (units 10^{-6})	EVTS	DOCUMENT ID		TECN	COMMENT
3.87 ± 0.07 OUR FIT Error includes scale factor of 1.2.					
3.93 ± 0.09 OUR AVERAGE Error includes scale factor of 1.3. See the ideogram below.					
4.050 ± 0.067 ± 0.118	33k	[1] ACHASOV	07B	SND	0.6–1.38 $e^+e^- \to \eta\gamma$
$4.093 ^{+0.040}_{-0.043} \pm 0.247$	17.4k	[2] AKHMETSHIN	05	CMD2	0.60–1.38 $e^+e^- \to \eta\gamma$

3.850±0.041±0.159	23k	[3,4] AKHMETSHIN	01B	CMD2	$e^+e^- \to \eta\gamma$	
4.00 ±0.04 ±0.11		[5] ACHASOV	00	SND	$e^+e^- \to \eta\gamma$	
3.53 ±0.08 ±0.17	2200	[6,7] AKHMETSHIN	99F	CMD2	$e^+e^- \to \eta\gamma$	

• • • We do not use the following data for averages, fits, limits, etc. • • •

4.19 ±0.06	[8] BENAYOUN	10	RVUE	0.4–1.05	e^+e^-

[1] From a combined fit of $\sigma(e^+e^- \to \eta\gamma)$ with $\eta \to 3\pi^0$ and $\eta \to \pi^+\pi^-\pi^0$, and fixing $B(\eta \to 3\pi^0) / B(\eta \to \pi^+\pi^-\pi^0) = 1.44 \pm 0.04$. Recalculated by us from the cross section at the peak. Supersedes ACHASOV 00D and ACHASOV 06A.
[2] From the $\eta \to 2\gamma$ decay and using $B(\eta \to \gamma\gamma) = 39.43 \pm 0.26\%$.
[3] From the $\eta \to 3\pi^0$ decay and using $B(\eta \to 3\pi^0) = (32.24 \pm 0.29) \times 10^{-2}$.
[4] The combined fit from 600 to 1380 MeV taking into account $\rho(770)$, $\omega(782)$, $\phi(1020)$, and $\rho(1450)$ (mass and width fixed at 1450 MeV and 310 MeV respectively).
[5] From the $\eta \to 2\gamma$ decay and using $B(\eta \to 2\gamma) = (39.21 \pm 0.34) \times 10^{-2}$.
[6] Recalculated by the authors from the cross section in the peak.
[7] From the $\eta \to \pi^+\pi^-\pi^0$ decay and using $B(\eta \to \pi^+\pi^-\pi^0) = (23.1 \pm 0.5) \times 10^{-2}$.
[8] A simultaneous fit of $e^+e^- \to \pi^+\pi^-$, $\pi^+\pi^-\pi^0$, $\pi^0\gamma$, $\eta\gamma$ data.

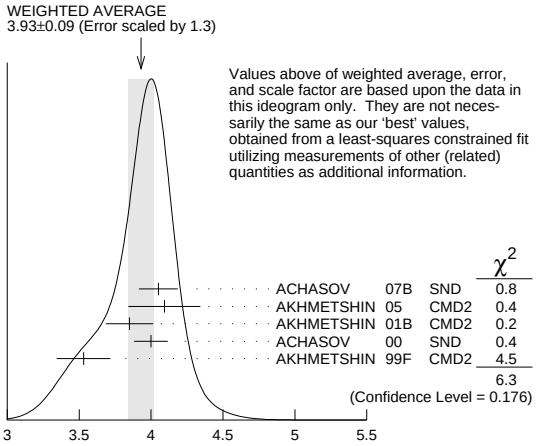

$\Gamma(\eta\gamma)/\Gamma_{total} \times \Gamma(e^+e^-)/\Gamma_{total}$ — $\Gamma_6/\Gamma \times \Gamma_9/\Gamma$

$\Gamma(\pi^0\gamma)/\Gamma_{total} \times \Gamma(e^+e^-)/\Gamma_{total}$ — $\Gamma_7/\Gamma \times \Gamma_9/\Gamma$

VALUE (units 10^{-7})	EVTS	DOCUMENT ID		TECN	COMMENT
3.88±0.14 OUR FIT					
3.87±0.15 OUR AVERAGE					
4.04±0.09±0.19		[1] ACHASOV	16A	SND	0.60–1.38 $e^+e^- \to \pi^0\gamma$
3.75±0.11±0.29	18k	AKHMETSHIN	05	CMD2	0.60–1.38 $e^+e^- \to \pi^0\gamma$
$3.67 \pm 0.10^{+0.27}_{-0.25}$		[2] ACHASOV	00	SND	$e^+e^- \to \pi^0\gamma$

• • • We do not use the following data for averages, fits, limits, etc. • • •

4.29±0.11	[3] BENAYOUN	10	RVUE	0.4–1.05	e^+e^-

[1] From the VMD model with the interfering $\rho(770)$, $\omega(782)$, $\phi(1020)$ resonances, and an additional resonance describing the total contribution of the $\rho(1450)$ and $\omega(1420)$ states. Supersedes ACHASOV 00.
[2] From the $\pi^0 \to 2\gamma$ decay and using $B(\pi^0 \to 2\gamma) = (98.798 \pm 0.032) \times 10^{-2}$.
[3] A simultaneous fit of $e^+e^- \to \pi^+\pi^-$, $\pi^+\pi^-\pi^0$, $\pi^0\gamma$, $\eta\gamma$ data.

$\Gamma(\mu^+\mu^-)/\Gamma_{total} \times \Gamma(e^+e^-)/\Gamma_{total}$ — $\Gamma_{10}/\Gamma \times \Gamma_9/\Gamma$

VALUE (units 10^{-8})	DOCUMENT ID		TECN	COMMENT
$\mathbf{8.5\ ^{+0.5}_{-0.6}}$ **OUR FIT**				
8.8 ±0.9 OUR AVERAGE	Error includes scale factor of 1.5. See the ideogram below.			
8.36±0.59±0.37	ACHASOV	01G	SND	$e^+e^- \to \mu^+\mu^-$
9.9 ±1.4 ±0.9	[1] ACHASOV	99C	SND	$e^+e^- \to \mu^+\mu^-$
14.4 ±3.0	[2] VASSERMAN	81	OLYA	$e^+e^- \to \mu^+\mu^-$
8.6 ±5.9	[2] AUGUSTIN	73	OSPK	$e^+e^- \to \mu^+\mu^-$

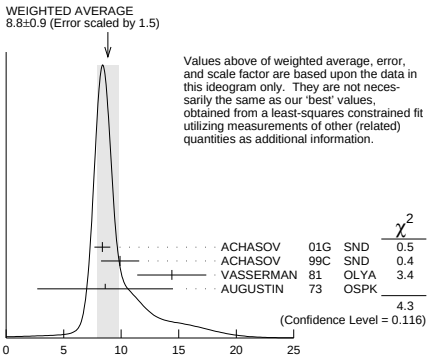

$\Gamma(\mu^+\mu^-)/\Gamma_{total} \times \Gamma(e^+e^-)/\Gamma_{total}$ — $\Gamma_{10}/\Gamma \times \Gamma_9/\Gamma$

[1] Recalculated by the authors from the cross section in the peak.
[2] Recalculated by us from the cross section in the peak.

$\Gamma(\pi^+\pi^-)/\Gamma_{total} \times \Gamma(e^+e^-)/\Gamma_{total}$ — $\Gamma_{12}/\Gamma \times \Gamma_9/\Gamma$

VALUE (units 10^{-8})	DOCUMENT ID		TECN	COMMENT
2.2 ±0.4 OUR FIT				
2.2 ±0.4 OUR AVERAGE				
2.1 ±0.3 ±0.3	[1] ACHASOV	00C	SND	$e^+e^- \to \pi^+\pi^-$
$1.95^{+1.15}_{-0.87}$	[2] GOLUBEV	86	ND	$e^+e^- \to \pi^+\pi^-$
$6.01^{+3.19}_{-2.51}$	[2] VASSERMAN	81	OLYA	$e^+e^- \to \pi^+\pi^-$

• • • We do not use the following data for averages, fits, limits, etc. • • •

3.31±0.99	[3] BENAYOUN	13	RVUE	0.4–1.05	e^+e^-

[1] Recalculated by the authors from the cross section in the peak.
[2] Recalculated by us from the cross section in the peak.
[3] A simultaneous fit to $e^+e^- \to \pi^+\pi^-$, $\pi^+\pi^-\pi^0$, $\pi^0\gamma$, $\eta\gamma$, $K\overline{K}$, and $\tau^- \to \pi^-\pi^0\nu_\tau$ data.

$\Gamma(\omega\pi^0)/\Gamma_{total} \times \Gamma(e^+e^-)/\Gamma_{total}$ — $\Gamma_{13}/\Gamma \times \Gamma_9/\Gamma$

VALUE (units 10^{-8})	DOCUMENT ID		TECN	COMMENT
1.40±0.15 OUR FIT				
1.37±0.17±0.01	[1,2] AMBROSINO	08G	KLOE	$e^+e^- \to \pi^+\pi^-2\pi^0$, $2\pi^0\gamma$

[1] Recalculated by the authors from the cross section at the peak.
[2] AMBROSINO 08G reports $[\Gamma(\phi(1020) \to \omega\pi^0)/\Gamma_{total} \times \Gamma(\phi(1020) \to e^+e^-)/\Gamma_{total}] \times [B(\omega(782) \to \pi^+\pi^-\pi^0)] = (1.22 \pm 0.13 \pm 0.08) \times 10^{-8}$ which we divide by our best value $B(\omega(782) \to \pi^+\pi^-\pi^0) = (89.2 \pm 0.7) \times 10^{-2}$. Our first error is their experiment's error and our second error is the systematic error from using our best value.

$\Gamma(\pi^0\pi^0\gamma)/\Gamma_{total} \times \Gamma(e^+e^-)/\Gamma_{total}$ — $\Gamma_{18}/\Gamma \times \Gamma_9/\Gamma$

VALUE (units 10^{-8})	DOCUMENT ID		TECN	COMMENT
3.34±0.17 OUR FIT				
$\mathbf{3.33^{+0.04}_{-0.09}\ ^{+0.19}_{-0.20}}$	[1] AMBROSINO	07	KLOE	$e^+e^- \to \pi^0\pi^0\gamma$

[1] Calculated by the authors from the cross section at the peak.

$\Gamma(\pi^+\pi^-\pi^+\pi^-)/\Gamma_{total} \times \Gamma(e^+e^-)/\Gamma_{total}$ — $\Gamma_{19}/\Gamma \times \Gamma_9/\Gamma$

VALUE (units 10^{-9})	EVTS	DOCUMENT ID		TECN	COMMENT
$\mathbf{1.2\ ^{+0.8}_{-0.7}}$ **OUR FIT**					
1.17±0.52±0.64	3285	[1] AKHMETSHIN	00E	CMD2	$e^+e^- \to \pi^+\pi^-\pi^+\pi^-$

[1] Recalculated by the authors from the cross section in the peak.

$\phi(1020)$ BRANCHING RATIOS

$\Gamma(K^+K^-)/\Gamma_{total}$ — Γ_1/Γ

VALUE	EVTS	DOCUMENT ID		TECN	COMMENT
0.492±0.005 OUR FIT	Error includes scale factor of 1.3.				
0.493±0.010 OUR AVERAGE					
0.492±0.012	2913	AKHMETSHIN	95	CMD2	$e^+e^- \to K^+K^-$
0.44 ±0.05	321	KALBFLEISCH	76	HBC	2.18 $K^-p \to \Lambda K^+K^-$
0.49 ±0.06	270	DEGROOT	74	HBC	4.2 $K^-p \to \Lambda\phi$
0.540±0.034	565	BALAKIN	71	OSPK	$e^+e^- \to K^+K^-$
0.48 ±0.04	252	LINDSEY	66	HBC	2.1–2.7 $K^-p \to \Lambda K^+K^-$

• • • We do not use the following data for averages, fits, limits, etc. • • •

0.493±0.003±0.007		[1] AKHMETSHIN	11	CMD2	1.02	$e^+e^- \to K^+K^-$
0.476±0.017	1000k	[2] ACHASOV	01E	SND	$e^+e^- \to K^+K^-$, K_SK_L, $\pi^+\pi^-\pi^0$	

[1] Combined analysis of the CMD-2 data on $\phi \to K^+K^-$, $K^0_SK^0_L$, $\pi^+\pi^-\pi^0$, $\eta\gamma$ assuming that the sum of their branching fractions is 0.99741 ± 0.00007.
[2] Using $B(\phi \to e^+e^-) = (2.93 \pm 0.14) \times 10^{-4}$.

$\Gamma(K^0_LK^0_S)/\Gamma_{total}$ — Γ_2/Γ

VALUE	EVTS	DOCUMENT ID		TECN	COMMENT
0.340±0.004 OUR FIT	Error includes scale factor of 1.3.				
0.331±0.009 OUR AVERAGE					
0.335±0.010	40644	AKHMETSHIN	95	CMD2	$e^+e^- \to K^0_LK^0_S$
0.326±0.035		DOLINSKY	91	ND	$e^+e^- \to K^0_LK^0_S$
0.310±0.024		DRUZHININ	84	ND	$e^+e^- \to K^0_LK^0_S$

• • • We do not use the following data for averages, fits, limits, etc. • • •

0.336±0.002±0.006		[1] AKHMETSHIN	11	CMD2	1.02	$e^+e^- \to K^0_SK^0_L$
0.351±0.013	500k	[2] ACHASOV	01E	SND	$e^+e^- \to K^+K^-$, K_SK_L, $\pi^+\pi^-\pi^0$	
0.27 ±0.03	133	KALBFLEISCH	76	HBC	2.18 $K^-p \to \Lambda K^0_LK^0_S$	
0.257±0.030	95	[3] BALAKIN	71	OSPK	$e^+e^- \to K^0_LK^0_S$	
0.40 ±0.04	167	LINDSEY	66	HBC	2.1–2.7 $K^-p \to \Lambda K^0_LK^0_S$	

[1] Combined analysis of the CMD-2 data on $\phi \to K^+K^-$, $K^0_SK^0_L$, $\pi^+\pi^-\pi^0$, $\eta\gamma$ assuming that the sum of their branching fractions is 0.99741 ± 0.00007.
[2] Using $B(\phi \to e^+e^-) = (2.93 \pm 0.14) \times 10^{-4}$.
[3] Balakin error increased by Paul.

$\Gamma(K_L^0 K_S^0)/\Gamma(K^+K^-)$ Γ_2/Γ_1

VALUE	EVTS	DOCUMENT ID		TECN	COMMENT
0.690±0.015 OUR FIT	Error includes scale factor of 1.3.				
0.740±0.031 OUR AVERAGE					
0.70 ±0.06	2732	BUKIN	78C	OLYA	$e^+e^- \to K_L^0 K_S^0$
0.82 ±0.08		LOSTY	78	HBC	4.2 $K^-p \to \phi$hyperon
0.71 ±0.05		LAVEN	77	HBC	10 $K^-p \to K^+K^-\Lambda$
0.71 ±0.08		LYONS	77	HBC	3–4 $K^-p \to \Lambda\phi$
0.89 ±0.10	144	AGUILAR-...	72B	HBC	3.9,4.6 K^-p
• • • We do not use the following data for averages, fits, limits, etc. • • •					
0.638±0.022	2.3M	[1] KOZYREV	18	CMD3	$e^+e^- \to K_L^0 K_S^0$, K^+K^-
0.68 ±0.03		[2] AKHMETSHIN	95	CMD2	$e^+e^- \to K_L^0 K_S^0$, K^+K^-

[1] The prediction taking into account phase-space difference, radiative corrections, isospin breaking, and the Sommerfeld-Gamow-Sakharov factor gives 0.630.

[2] Theoretical analysis of BRAMON 00 taking into account phase-space difference, electromagnetic radiative corrections, as well as isospin breaking, predicts 0.62. FLOREZ-BAEZ 08 predicts 0.63 considering also structure-dependent radiative corrections. FISCHBACH 02 calculates additional corrections caused by the close threshold and predicts 0.68. See also BENAYOUN 01 and DUBYNSKIY 07. BENAYOUN 12 obtains 0.71±0.01 in the HLS model.

$\Gamma(K_L^0 K_S^0)/\Gamma(K\overline{K})$ $\Gamma_2/(\Gamma_1+\Gamma_2)$

VALUE	EVTS	DOCUMENT ID		TECN	COMMENT
0.408±0.005 OUR FIT	Error includes scale factor of 1.3.				
0.45 ±0.04 OUR AVERAGE					
0.44 ±0.07		[1] LONDON	66	HBC	2.24 $K^-p \to \Lambda K\overline{K}$
0.48 ±0.07	52	BADIER	65B	HBC	3 K^-p
0.40 ±0.10	34	SCHLEIN	63	HBC	1.95 $K^-p \to \Lambda K\overline{K}$

[1] This is probably not affected by their controversial background subtraction; the value is from their numbers of $K_1 K_2$ vs K^+K^- events.

$[\Gamma(\rho\pi)+\Gamma(\pi^+\pi^-\pi^0)]/\Gamma_{\text{total}}$ Γ_3/Γ

VALUE	EVTS	DOCUMENT ID		TECN	COMMENT
0.1524±0.0033 OUR FIT	Error includes scale factor of 1.2.				
0.151 ±0.009 OUR AVERAGE	Error includes scale factor of 1.7.				
0.161 ±0.008	11761	AKHMETSHIN	95	CMD2	$e^+e^- \to \pi^+\pi^-\pi^0$
0.143 ±0.007		DOLINSKY	91	ND	$e^+e^- \to \pi^+\pi^-\pi^0$
• • • We do not use the following data for averages, fits, limits, etc. • • •					
0.155 ±0.002 ±0.005		[1] AKHMETSHIN	11	CMD2	1.02 $e^+e^- \to \pi^+\pi^-\pi^0$
0.159 ±0.008	400k	[2] ACHASOV	01E	SND	$e^+e^- \to K^+K^-$, $K_S K_L$, $\pi^+\pi^-\pi^0$
0.145 ±0.009 ±0.003	11169	[3] AKHMETSHIN	98	CMD2	$e^+e^- \to \pi^+\pi^-\pi^0$
0.139 ±0.007		[4] PARROUR	76B	OSPK	e^+e^-

[1] Combined analysis of the CMD-2 data on $\phi \to K^+K^-$, $K_S^0 K_L^0$, $\pi^+\pi^-\pi^0$, $\eta\gamma$ assuming that the sum of their branching fractions is 0.99741 ± 0.00007.

[2] Using B($\phi \to e^+e^-$)= (2.93 ± 0.14) × 10^{-4}.

[3] Using B($\phi \to e^+e^-$)=(2.99 ± 0.08) × 10^{-4}.

[4] Using $\Gamma(\phi)$= 4.1 MeV. If interference between the $\rho\pi$ and 3π modes is neglected, the fraction of the $\rho\pi$ is more than 80% at the 90% confidence level.

$[\Gamma(\rho\pi)+\Gamma(\pi^+\pi^-\pi^0)]/\Gamma(K^+K^-)$ Γ_3/Γ_1

VALUE	EVTS	DOCUMENT ID		TECN	COMMENT
0.310±0.009 OUR FIT	Error includes scale factor of 1.2.				
0.28 ±0.09	34	AGUILAR-...	72B	HBC	3.9,4.6 K^-p

$[\Gamma(\rho\pi)+\Gamma(\pi^+\pi^-\pi^0)]/\Gamma(K\overline{K})$ $\Gamma_3/(\Gamma_1+\Gamma_2)$

VALUE	DOCUMENT ID		TECN	COMMENT
0.183±0.005 OUR FIT	Error includes scale factor of 1.2.			
0.24 ±0.04 OUR AVERAGE				
0.237±0.039	CERRADA	77B	HBC	4.2 $K^-p \to \Lambda 3\pi$
0.30 ±0.15	LONDON	66	HBC	2.24 $K^-p \to \Lambda\pi^+\pi^-\pi^0$

$[\Gamma(\rho\pi)+\Gamma(\pi^+\pi^-\pi^0)]/\Gamma(K_L^0 K_S^0)$ Γ_3/Γ_2

VALUE	EVTS	DOCUMENT ID		TECN	COMMENT
0.448±0.011 OUR FIT	Error includes scale factor of 1.1.				
0.51 ±0.05 OUR AVERAGE					
0.56 ±0.07	3681	BUKIN	78C	OLYA	$e^+e^- \to K_L^0 K_S^0$, $\pi^+\pi^-\pi^0$
0.47 ±0.06	516	COSME	74	OSPK	$e^+e^- \to \pi^+\pi^-\pi^0$

$\Gamma(\pi^+\pi^-\pi^0)/\Gamma_{\text{total}}$ Γ_5/Γ

VALUE	CL%	EVTS	DOCUMENT ID		TECN	COMMENT
• • • We do not use the following data for averages, fits, limits, etc. • • •						
≃ 0.0087		1.98M	[1,2] ALOISIO	03	KLOE	1.02 $e^+e^- \to \pi^+\pi^-\pi^0$
<0.0006	90		[3] ACHASOV	02	SND	1.02 $e^+e^- \to \pi^+\pi^-\pi^0$
<0.23	90		[3] CORDIER	80	DM1	$e^+e^- \to \pi^+\pi^-\pi^0$
<0.20	90		[3] PARROUR	76B	OSPK	$e^+e^- \to \pi^+\pi^-\pi^0$

[1] From a fit without limitations on charged and neutral ρ masses and widths.

[2] Adding the direct and $\omega\pi$ contributions and considering the interference between the $\rho\pi$ and $\pi^+\pi^-\pi^0$.

[3] Neglecting the interference between the $\rho\pi$ and $\pi^+\pi^-\pi^0$.

$\Gamma(\eta\gamma)/\Gamma_{\text{total}}$ Γ_6/Γ

VALUE (units 10^{-2})	EVTS	DOCUMENT ID		TECN	COMMENT
1.303±0.025 OUR FIT	Error includes scale factor of 1.2.				
1.26 ±0.04 OUR AVERAGE					
1.246±0.025±0.057	10k	[1] ACHASOV	98F	SND	$e^+e^- \to 7\gamma$
1.18 ±0.11	279	[2] AKHMETSHIN	95	CMD2	$e^+e^- \to \pi^+\pi^-3\gamma$
1.30 ±0.06		[3] DRUZHININ	84	ND	$e^+e^- \to 3\gamma$
1.4 ±0.2		[4] DRUZHININ	84	ND	$e^+e^- \to 6\gamma$
0.88 ±0.20	290	KURDADZE	83C	OLYA	$e^+e^- \to 3\gamma$
1.35 ±0.29		ANDREWS	77	CNTR	6.7–10 γCu
1.5 ±0.4	54	[3] COSME	76	OSPK	e^+e^-
• • • We do not use the following data for averages, fits, limits, etc. • • •					
1.38 ±0.02 ±0.02		[5] AKHMETSHIN	11	CMD2	1.02 $e^+e^- \to \eta\gamma$
1.36 ±0.05 ±0.02	33k	[6] ACHASOV	07B	SND	0.6–1.38 $e^+e^- \to \eta\gamma$
1.373±0.014±0.085	17.4k	[7,8] AKHMETSHIN	05	CMD2	0.60–1.38 $e^+e^- \to \eta\gamma$
1.287±0.013±0.063		[9,10] AKHMETSHIN	01B	CMD2	$e^+e^- \to \eta\gamma$
1.338±0.012±0.052		[11] ACHASOV	00	SND	$e^+e^- \to \eta\gamma$
1.18 ±0.03 ±0.06	2200	[12] AKHMETSHIN	99F	CMD2	$e^+e^- \to \eta\gamma$
1.21 ±0.07		[13] BENAYOUN	96	RVUE	0.54-1.04 $e^+e^- \to \eta\gamma$

[1] Using B($\phi \to e^+e^-$) = (2.99 ± 0.08) × 10^{-4} and B($\eta \to 3\pi^0$)= (32.2 ± 0.4) × 10^{-2}.

[2] From $\pi^+\pi^-\pi^0$ decay mode of η.

[3] From 2γ decay mode of η.

[4] From $3\pi^0$ decay mode of η.

[5] Combined analysis of the CMD-2 data on $\phi \to K^+K^-$, $K_S^0 K_L^0$, $\pi^+\pi^-\pi^0$, $\eta\gamma$ assuming that the sum of their branching fractions is 0.99741 ± 0.00007.

[6] ACHASOV 07B reports [$\Gamma(\phi(1020) \to \eta\gamma)/\Gamma_{\text{total}}$] × [B($\phi(1020) \to e^+e^-$)] = (4.050 ± 0.067 ± 0.118) × 10^{-6} which we divide by our best value B($\phi(1020) \to e^+e^-$) = (2.973 ± 0.034) × 10^{-4}. Our first error is their experiment's error and our second error is the systematic error from using our best value. Supersedes ACHASOV 00D and ACHASOV 06A.

[7] Using B($\phi \to e^+e^-$) = (2.98 ± 0.04) × 10^{-4} and B($\eta \to \gamma\gamma$) = 39.43 ± 0.26%.

[8] Not independent of the corresponding $\Gamma(e^+e^-) \times \Gamma(\eta\gamma)/\Gamma^2_{\text{total}}$.

[9] Using B($\phi \to e^+e^-$) = (2.99±0.08) × 10^{-4} and B($\eta \to 3\pi^0$)=(32.24±0.29) × 10^{-2}.

[10] The combined fit from 600 to 1380 MeV taking into account $\rho(770)$, $\omega(782)$, $\phi(1020)$, and $\rho(1450)$ (mass and width fixed at 1450 MeV and 310 MeV respectively).

[11] From the $\eta \to 2\gamma$ decay and using B($\phi \to e^+e^-$) =(2.99 ± 0.08) × 10^{-4}.

[12] From $\pi^+\pi^-\pi^0$ decay mode of η and using B($\phi \to e^+e^-$)= (2.99 ± 0.08) × 10^{-4}.

[13] Reanalysis of DRUZHININ 84, DOLINSKY 89, and DOLINSKY 91 taking into account a triangle anomaly contribution.

$\Gamma(\pi^0\gamma)/\Gamma_{\text{total}}$ Γ_7/Γ

VALUE (units 10^{-3})	EVTS	DOCUMENT ID		TECN	COMMENT
1.30 ±0.05 OUR FIT					
1.31 ±0.13 OUR AVERAGE					
1.30 ±0.13		DRUZHININ	84	ND	$e^+e^- \to 3\gamma$
1.4 ±0.5	32	COSME	76	OSPK	e^+e^-
• • • We do not use the following data for averages, fits, limits, etc. • • •					
1.367±0.072		[1] ACHASOV	16A	SND	0.60–1.38 $e^+e^- \to \pi^0\gamma$
1.258±0.037±0.077	18k	[2,3] AKHMETSHIN	05	CMD2	0.60–1.38 $e^+e^- \to \pi^0\gamma$
$1.226\pm0.036^{+0.096}_{-0.089}$		[4] ACHASOV	00	SND	$e^+e^- \to \pi^0\gamma$
1.26 ±0.17		[5] BENAYOUN	96	RVUE	0.54-1.04 $e^+e^- \to \pi^0\gamma$

[1] Using B($\phi \to e^+e^-$) from PDG 15. Supersedes ACHASOV 00.

[2] Using B($\phi \to e^+e^-$) = (2.98 ± 0.04) × 10^{-4}.

[3] Not independent of the corresponding $\Gamma(e^+e^-) \times \Gamma(\pi^0\gamma)/\Gamma^2_{\text{total}}$.

[4] From the $\pi^0 \to 2\gamma$ decay and using B($\phi \to e^+e^-$) = (2.99 ± 0.08) × 10^{-4}.

[5] Reanalysis of DRUZHININ 84, DOLINSKY 89, and DOLINSKY 91 taking into account a triangle anomaly contribution.

$\Gamma(\eta\gamma)/\Gamma(\pi^0\gamma)$ Γ_6/Γ_7

VALUE	DOCUMENT ID		TECN	COMMENT
• • • We do not use the following data for averages, fits, limits, etc. • • •				
$10.9\pm0.3^{+0.7}_{-0.8}$	ACHASOV	00	SND	$e^+e^- \to \eta\gamma, \pi^0\gamma$

$\Gamma(e^+e^-)/\Gamma_{\text{total}}$ Γ_9/Γ

VALUE (units 10^{-4})	EVTS	DOCUMENT ID		TECN	COMMENT
2.973±0.034 OUR FIT	Error includes scale factor of 1.3.				
2.98 ±0.07 OUR AVERAGE	Error includes scale factor of 1.1.				
2.93 ±0.14	1900k	[1] ACHASOV	01E	SND	$e^+e^- \to K^+K^-$, $K_S K_L$, $\pi^+\pi^-\pi^0$
2.88 ±0.09	55600	AKHMETSHIN	95	CMD2	$e^+e^- \to$ hadrons
3.00 ±0.21	3681	BUKIN	78C	OLYA	$e^+e^- \to$ hadrons
3.10 ±0.14		[2] PARROUR	76	OSPK	e^+e^-
3.3 ±0.3		COSME	74	OSPK	$e^+e^- \to$ hadrons
2.81 ±0.25	681	BALAKIN	71	OSPK	$e^+e^- \to$ hadrons
3.50 ±0.27		CHATELUS	71	OSPK	e^+e^-

[1] From the combined fit assuming that the total $\phi(1020)$ production cross section is saturated by those of K^+K^-, $K_S K_L$, $\pi^+\pi^-\pi^0$, and $\eta\gamma$ decays modes and using ACHASOV 00B for the $\eta\gamma$ decay mode.

[2] Using total width 4.2 MeV. They detect 3π mode and observe significant interference with ω tail. This is accounted for in the result quoted above.

Meson Particle Listings

$\phi(1020)$

$\Gamma(\mu^+\mu^-)/\Gamma_{total}$ Γ_{10}/Γ

VALUE (units 10^{-4})	DOCUMENT ID		TECN	COMMENT
2.86±0.19 OUR FIT				
2.5 ±0.4 OUR AVERAGE				
2.69±0.46	[1] HAYES	71	CNTR	8.3,9.8 $\gamma C \rightarrow \mu^+\mu^- X$
2.17±0.60	[1] EARLES	70	CNTR	6.0 $\gamma C \rightarrow \mu^+\mu^- X$
• • • We do not use the following data for averages, fits, limits, etc. • • •				
2.87±0.20±0.14	[2] ACHASOV	01G	SND	$e^+e^- \rightarrow \mu^+\mu^-$
3.30±0.45±0.32	[3] ACHASOV	99C	SND	$e^+e^- \rightarrow \mu^+\mu^-$
4.83±1.02	[4] VASSERMAN	81	OLYA	$e^+e^- \rightarrow \mu^+\mu^-$
2.87±1.98	[4] AUGUSTIN	73	OSPK	$e^+e^- \rightarrow \mu^+\mu^-$

[1] Neglecting interference between resonance and continuum.
[2] Using $B(\phi \rightarrow e^+e^-) = (2.91 \pm 0.07) \times 10^{-4}$.
[3] Using $B(\phi \rightarrow e^+e^-) = (2.99 \pm 0.08) \times 10^{-4}$.
[4] Recalculated by us using $B(\phi \rightarrow e^+e^-) = (2.99 \pm 0.08) \times 10^{-4}$.

$\Gamma(\eta e^+e^-)/\Gamma_{total}$ Γ_{11}/Γ

VALUE (units 10^{-4})	EVTS	DOCUMENT ID		TECN	COMMENT
1.08 ±0.04 OUR AVERAGE					
1.075±0.007±0.038	30k	[1] BABUSCI	15	KLOE	$1.02\ e^+e^- \rightarrow \eta e^+e^-$
1.19 ±0.19 ±0.12	213	[2] ACHASOV	01B	SND	$e^+e^- \rightarrow \eta e^+e^-$
1.14 ±0.10 ±0.06	355	[3] AKHMETSHIN	01	CMD2	$e^+e^- \rightarrow \eta e^+e^-$
• • • We do not use the following data for averages, fits, limits, etc. • • •					
1.13 ±0.14 ±0.07	183	[4] AKHMETSHIN	01	CMD2	$e^+e^- \rightarrow \eta e^+e^-$
1.21 ±0.14 ±0.09	130	[5] AKHMETSHIN	01	CMD2	$e^+e^- \rightarrow \eta e^+e^-$
1.04 ±0.20 ±0.08	42	[6] AKHMETSHIN	01	CMD2	$e^+e^- \rightarrow \eta e^+e^-$
$1.3\ ^{+0.8}_{-0.6}$	7	GOLUBEV	85	ND	$e^+e^- \rightarrow \eta e^+e^-$

[1] Using $B(\eta \rightarrow 3\pi^0) = (32.57 \pm 0.23)\%$ from PDG 12.
[2] Using $B(\eta \rightarrow \gamma\gamma) = (39.25 \pm 0.32)\%$, $B(\phi \rightarrow \eta\gamma) = (1.26 \pm 0.06)\%$, and $B(\phi \rightarrow e^+e^-) = (3.00 \pm 0.06) \times 10^{-4}$.
[3] The average of the branching ratios separately obtained from the $\eta \rightarrow \gamma\gamma$, $3\pi^0$, $\pi^+\pi^-\pi^0$ decays.
[4] From $\eta \rightarrow \gamma\gamma$ decays and using $B(\eta \rightarrow \gamma\gamma) = (39.33 \pm 0.25) \times 10^{-2}$, $B(\eta \rightarrow \pi^+\pi^-\gamma) = (4.75 \pm 11) \times 10^{-2}$, and $B(\phi \rightarrow \eta\gamma) = (1.297 \pm 0.033) \times 10^{-2}$.
[5] From $\eta \rightarrow 3\pi^0$ decays and using $B(\pi^0 \rightarrow \gamma\gamma) = (98.798 \pm 0.033) \times 10^{-2}$, $B(\eta \rightarrow 3\pi^0) = (32.24 \pm 0.29) \times 10^{-2}$, $B(\eta \rightarrow \pi^+\pi^-\gamma) = (4.75 \pm 0.11) \times 10^{-2}$, and $B(\phi \rightarrow \eta\gamma) = (1.297 \pm 0.033) \times 10^{-2}$.
[6] From $\eta \rightarrow \pi^+\pi^-\pi^0$ decays and using $B(\pi^0 \rightarrow \gamma\gamma) = (98.798 \pm 0.033) \times 10^{-2}$, $B(\pi^0 \rightarrow e^+e^-\gamma) = (1.198 \pm 0.032) \times 10^{-2}$, $B(\eta \rightarrow \pi^+\pi^-\pi^0) = (23.0 \pm 0.4) \times 10^{-2}$, $B(\phi \rightarrow \pi^+\pi^-\pi^0) = (15.5 \pm 0.6) \times 10^{-2}$, and $B(\phi \rightarrow \eta\gamma) = (1.297 \pm 0.033) \times 10^{-2}$.

$\Gamma(\pi^+\pi^-)/\Gamma_{total}$ Γ_{12}/Γ

VALUE (units 10^{-4})	CL%	DOCUMENT ID		TECN	COMMENT
• • • We do not use the following data for averages, fits, limits, etc. • • •					
0.71±0.11±0.09		[1] ACHASOV	00C	SND	$e^+e^- \rightarrow \pi^+\pi^-$
$0.65\ ^{+0.38}_{-0.29}$		[1] GOLUBEV	86	ND	$e^+e^- \rightarrow \pi^+\pi^-$
$2.01\ ^{+1.07}_{-0.84}$		[1] VASSERMAN	81	OLYA	$e^+e^- \rightarrow \pi^+\pi^-$
<6.6	95	BUKIN	78B	OLYA	$e^+e^- \rightarrow \pi^+\pi^-$
<2.7	95	ALVENSLEB...	72	CNTR	$6.7\ \gamma C \rightarrow C\pi^+\pi^-$

[1] Using $B(\phi \rightarrow e^+e^-) = (2.99 \pm 0.08) \times 10^{-4}$.

$\Gamma(\omega\pi^0)/\Gamma_{total}$ Γ_{13}/Γ

VALUE (units 10^{-5})	DOCUMENT ID		TECN	COMMENT
4.7±0.5 OUR FIT				
$\mathbf{5.2\ ^{+1.3}_{-1.1}}$	[1,2] AULCHENKO	00A	SND	$e^+e^- \rightarrow \pi^+\pi^-\pi^0\pi^0$
• • • We do not use the following data for averages, fits, limits, etc. • • •				
4.4±0.6	[3] AMBROSINO	08G	KLOE	$e^+e^- \rightarrow \pi^+\pi^-2\pi^0$, $2\pi^0\gamma$
~5.4	[4] ACHASOV	00E	SND	$e^+e^- \rightarrow \pi^0\pi^0\gamma$
$5.5\ ^{+1.6}_{-1.4}$±0.3	[2,5] AULCHENKO	00A	SND	$e^+e^- \rightarrow \pi^+\pi^-\pi^0\pi^0$
$4.8\ ^{+1.9}_{-1.7}$±0.8	[4] ACHASOV	99	SND	$e^+e^- \rightarrow \pi^+\pi^-\pi^0\pi^0$

[1] Using the 1996 and 1998 data.
[2] (2.3 ± 0.3)% correction for other decay modes of the $\omega(782)$ applied.
[3] Not independent of the corresponding $\Gamma(\omega\pi^0) \times \Gamma(e^+e^-) / \Gamma^2(\text{total})$.
[4] Using the 1996 data.
[5] Using the 1998 data.

$\Gamma(\omega\gamma)/\Gamma_{total}$ Γ_{14}/Γ

VALUE	CL%	DOCUMENT ID		TECN	COMMENT
<0.05	84	LINDSEY	66	HBC	2.1–2.7 $K^-p \rightarrow \Lambda\pi^+\pi^-$ neutrals

$\Gamma(\rho\gamma)/\Gamma_{total}$ Γ_{15}/Γ

VALUE (units 10^{-4})	CL%	DOCUMENT ID		TECN	COMMENT
< 0.12	90	[1] AKHMETSHIN	99B	CMD2	$e^+e^- \rightarrow \pi^+\pi^-\gamma$
• • • We do not use the following data for averages, fits, limits, etc. • • •					
< 7	90	AKHMETSHIN	97C	CMD2	$e^+e^- \rightarrow \pi^+\pi^-\gamma$
<200	84	LINDSEY	66	HBC	2.1–2.7 $K^-p \rightarrow \Lambda\pi^+\pi^-$ neutrals

[1] Supersedes AKHMETSHIN 97C.

$\Gamma(\pi^+\pi^-\gamma)/\Gamma_{total}$ Γ_{16}/Γ

VALUE (units 10^{-4})	CL%	EVTS	DOCUMENT ID		TECN	COMMENT
0.41±0.12±0.04		30175	[1] AKHMETSHIN	99B	CMD2	$e^+e^- \rightarrow \pi^+\pi^-\gamma$
• • • We do not use the following data for averages, fits, limits, etc. • • •						
< 0.3	90		[2] AKHMETSHIN	97C	CMD2	$e^+e^- \rightarrow \pi^+\pi^-\gamma$
<600	90		KALBFLEISCH	75	HBC	2.18 $K^-p \rightarrow \Lambda\pi^+\pi^-\gamma$
< 70	90		COSME	74	OSPK	$e^+e^- \rightarrow \pi^+\pi^-\gamma$
<400	90		LINDSEY	65	HBC	2.1–2.7 $K^-p \rightarrow \Lambda\pi^+\pi^-$ neutrals

[1] For $E_\gamma > 20$ MeV and assuming that $B(\phi(1020) \rightarrow f_0(980)\gamma)$ is negligible. Supersedes AKHMETSHIN 97C.
[2] For $E_\gamma > 20$ MeV and assuming that $B(\phi(1020) \rightarrow f_0(980)\gamma)$ is negligible.

$\Gamma(f_0(980)\gamma)/\Gamma_{total}$ Γ_{17}/Γ

VALUE (units 10^{-4})	CL%	EVTS	DOCUMENT ID		TECN	COMMENT
3.22±0.19 OUR FIT Error includes scale factor of 1.1.						
3.21±0.19 OUR AVERAGE						
$3.21\ ^{+0.03}_{-0.09}$±0.18			[1] AMBROSINO	07	KLOE	$e^+e^- \rightarrow \pi^0\pi^0\gamma$
2.90±0.21±1.54			[2] AKHMETSHIN	99C	CMD2	$e^+e^- \rightarrow \pi^+\pi^-\gamma$, $\pi^0\pi^0\gamma$
• • • We do not use the following data for averages, fits, limits, etc. • • •						
4.47±0.21		2438	[3] ALOISIO	02D	KLOE	$e^+e^- \rightarrow \pi^0\pi^0\gamma$
3.5 ±0.3 $^{+1.3}_{-0.5}$		419	[4,5] ACHASOV	00H	SND	$e^+e^- \rightarrow \pi^0\pi^0\gamma$
1.93±0.46±0.50		27188	[6] AKHMETSHIN	99B	CMD2	$e^+e^- \rightarrow \pi^+\pi^-\gamma$
3.05±0.25±0.72		268	[7] AKHMETSHIN	99C	CMD2	$e^+e^- \rightarrow \pi^0\pi^0\gamma$
1.5 ±0.5		268	[8] AKHMETSHIN	99C	CMD2	$e^+e^- \rightarrow \pi^0\pi^0\gamma$
3.42±0.30±0.36		164	[4] ACHASOV	98I	SND	$e^+e^- \rightarrow 5\gamma$
< 1	90		[9] AKHMETSHIN	97C	CMD2	$e^+e^- \rightarrow \pi^+\pi^-\gamma$
< 7	90		[10] AKHMETSHIN	97C	CMD2	$e^+e^- \rightarrow \pi^+\pi^-\gamma$
< 20	90		DRUZHININ	87	ND	$e^+e^- \rightarrow \pi^0\pi^0\gamma$

[1] Obtained by the authors taking into account the $\pi^+\pi^-$ decay mode. Includes a component due to $\pi\pi$ production via the $f_0(500)$ meson. Supersedes ALOISIO 02D.
[2] From the combined fit of the photon spectra in the reactions $e^+e^- \rightarrow \pi^+\pi^-\gamma$, $\pi^0\pi^0\gamma$.
[3] From the negative interference with the $f_0(500)$ meson of AITALA 01B using the ACHASOV 89 parameterization for the $f_0(980)$, a Breit-Wigner for the $f_0(500)$, and ACHASOV 01F for the $\rho\pi$ contribution. Superseded by AMBROSINO 07.
[4] Assuming that the $\pi^0\pi^0\gamma$ final state is completely determined by the $f_0\gamma$ mechanism, neglecting the decay $B(\phi \rightarrow K\overline{K}\gamma)$ and using $B(f_0 \rightarrow \pi^+\pi^-) = 2B(f_0 \rightarrow \pi^0\pi^0)$.
[5] Using the value $B(\phi \rightarrow \eta\gamma) = (1.338 \pm 0.053) \times 10^{-2}$.
[6] For $E_\gamma > 20$ MeV. Supersedes AKHMETSHIN 97C.
[7] Neglecting other intermediate mechanisms ($\rho\pi$, $\sigma\gamma$).
[8] A narrow pole fit taking into account $f_0(980)$ and $f_0(1200)$ intermediate mechanisms.
[9] For destructive interference with the Bremsstrahlung process
[10] For constructive interference with the Bremsstrahlung process

$\Gamma(f_0(980)\gamma)/\Gamma(\eta\gamma)$ Γ_{17}/Γ_6

VALUE (units 10^{-2})	EVTS	DOCUMENT ID		TECN	COMMENT
$\mathbf{2.47\ ^{+0.15}_{-0.16}}$ **OUR FIT** Error includes scale factor of 1.1.					
2.6 ±0.2 $^{+0.8}_{-0.3}$	419	[1] ACHASOV	00H	SND	$e^+e^- \rightarrow \pi^0\pi^0\gamma$

[1] Assuming that the $\pi^0\pi^0\gamma$ final state is completely determined by the $f_0\gamma$ mechanism, neglecting the decay $B(\phi \rightarrow K\overline{K}\gamma)$ and using $B(f_0 \rightarrow \pi^+\pi^-) = 2B(f_0 \rightarrow \pi^0\pi^0)$.

$\Gamma(\pi^0\pi^0\gamma)/\Gamma_{total}$ Γ_{18}/Γ

VALUE (units 10^{-4})	CL%	EVTS	DOCUMENT ID		TECN	COMMENT
1.07 ±0.06 OUR AVERAGE						
1.07 $^{+0.01}_{-0.03}$ $^{+0.06}_{-0.06}$			[1] AMBROSINO	07	KLOE	$e^+e^- \rightarrow \pi^0\pi^0\gamma$
1.08 ±0.17 ±0.09		268	AKHMETSHIN	99C	CMD2	$e^+e^- \rightarrow \pi^0\pi^0\gamma$
• • • We do not use the following data for averages, fits, limits, etc. • • •						
1.09 ±0.03 ±0.05		2438	ALOISIO	02D	KLOE	$e^+e^- \rightarrow \pi^0\pi^0\gamma$
1.158±0.093±0.052		419	[2,3] ACHASOV	00H	SND	$e^+e^- \rightarrow \pi^0\pi^0\gamma$
<10	90		DRUZHININ	87	ND	$e^+e^- \rightarrow 5\gamma$

[1] Supersedes ALOISIO 02D.
[2] Using the value $B(\phi \rightarrow \eta\gamma) = (1.338 \pm 0.053) \times 10^{-2}$.
[3] Supersedes ACHASOV 98I. Excluding $\omega\pi^0$.

$\Gamma(\pi^0\pi^0\gamma)/\Gamma(\eta\gamma)$ Γ_{18}/Γ_6

VALUE (units 10^{-2})	EVTS	DOCUMENT ID		TECN	COMMENT
0.86 ±0.04 OUR FIT					
0.865±0.070±0.017	419	[1] ACHASOV	00H	SND	$e^+e^- \rightarrow \pi^0\pi^0\gamma$
• • • We do not use the following data for averages, fits, limits, etc. • • •					
0.90 ±0.08 ±0.07	164	ACHASOV	98I	SND	$e^+e^- \rightarrow 5\gamma$

[1] Supersedes ACHASOV 98I. Excluding $\omega\pi^0$.

$\Gamma(\pi^+\pi^-\pi^+\pi^-)/\Gamma_{total}$ Γ_{19}/Γ

VALUE (units 10^{-6})	CL%	EVTS	DOCUMENT ID		TECN	COMMENT
6.5 ±2.7 ±1.6		6.8k	[1] AKHMETSHIN	17	CMD3	$e^+e^- \rightarrow \pi^+\pi^-\pi^+\pi^-$

• • • We do not use the following data for averages, fits, limits, etc. • • •

3.93±1.74±2.14	3.3k	AKHMETSHIN	00E	CMD2	$e^+e^- \to \pi^+\pi^-\pi^+\pi^-$	
< 870	90	CORDIER	79	WIRE	$e^+e^- \to \pi^+\pi^-\pi^+\pi^-$	

[1] Using the cross section at the ϕ meson peak $\sigma(\phi) = 4172 \pm 42$ nb, the nonresonant cross section $\sigma(0) = 1.263 \pm 0.027$ nb and Re(Z) = 0.146 ± 0.030, Im(Z) = −0.002 ± 0.024 for the complex amplitude of the $\phi \to \pi^+\pi^-\pi^+\pi^-$ transition.

$\Gamma(\pi^+\pi^+\pi^-\pi^-\pi^0)/\Gamma_{\text{total}}$ Γ_{20}/Γ

VALUE (units 10^{-6})	CL%	DOCUMENT ID		TECN	COMMENT
< 4.6	90	AKHMETSHIN	00E	CMD2	$e^+e^- \to \pi^+\pi^-\pi^+\pi^-\pi^0$

• • • We do not use the following data for averages, fits, limits, etc. • • •

<150	95	BARKOV	88	CMD	$e^+e^- \to \pi^+\pi^-\pi^+\pi^-\pi^0$	

$\Gamma(\pi^0 e^+ e^-)/\Gamma_{\text{total}}$ Γ_{21}/Γ

VALUE (units 10^{-5})	CL%	EVTS	DOCUMENT ID		TECN	COMMENT
$1.33^{+0.07}_{-0.10}$ OUR AVERAGE						
$1.35 \pm 0.05^{+0.05}_{-0.10}$		9.5k	[1] ANASTASI	16B	KLOE	$e^+e^- \to \pi^0 e^+ e^-$
1.01±0.28±0.29		52	[2] ACHASOV	02D	SND	$e^+e^- \to \pi^0 e^+ e^-$
1.22±0.34±0.21		46	[3] AKHMETSHIN	01C	CMD2	$e^+e^- \to \pi^0 e^+ e^-$

• • • We do not use the following data for averages, fits, limits, etc. • • •

<12	90	DOLINSKY	88	ND	$e^+e^- \to \pi^0 e^+ e^-$	

[1] Using B($\pi^0 \to \gamma\gamma$) from the 2014 Edition of this Review (PDG 14).
[2] Using various branching ratios from the 2000 Edition of this Review (PDG 00).
[3] Using B($\pi^0 \to \gamma\gamma$) = 0.98798 ± 0.00032, B($\phi \to \eta\gamma$) = (1.297 ± 0.033) × 10^{-2}, and B($\eta \to \pi^+\pi^-\gamma$) = (4.75 ± 0.11) × 10^{-2}.

$\Gamma(\pi^0\eta\gamma)/\Gamma_{\text{total}}$ Γ_{22}/Γ

VALUE (units 10^{-5})	CL%	EVTS	DOCUMENT ID		TECN	COMMENT
7.27±0.30 OUR AVERAGE Error includes scale factor of 1.5. See the ideogram below.						
7.06±0.22		16.9k	[1] AMBROSINO	09F	KLOE	1.02 $e^+e^- \to \eta\pi^0\gamma$
8.51±0.51±0.57		607	[2] ALOISIO	02C	KLOE	$e^+e^- \to \eta\pi^0\gamma$
7.96±0.60±0.40		197	[3] ALOISIO	02C	KLOE	$e^+e^- \to \eta\pi^0\gamma$
8.8 ±1.4 ±0.9		36	[4] ACHASOV	00F	SND	$e^+e^- \to \eta\pi^0\gamma$
9.0 ±2.4 ±1.0		80	AKHMETSHIN	99C	CMD2	$e^+e^- \to \eta\pi^0\gamma$

• • • We do not use the following data for averages, fits, limits, etc. • • •

7.01±0.10±0.20	13.3k	[2,5] AMBROSINO	09F	KLOE	1.02 $e^+e^- \to \eta\pi^0\gamma$	
7.12±0.13±0.22	3.6k	[3,6] AMBROSINO	09F	KLOE	1.02 $e^+e^- \to \eta\pi^0\gamma$	
8.3 ±2.3 ±1.2	20	ACHASOV	98B	SND	$e^+e^- \to 5\gamma$	
<250	90	DOLINSKY	91	ND	$e^+e^- \to \pi^0\eta\gamma$	

[1] Combined results of $\eta \to \gamma\gamma$ and $\eta \to \pi^+\pi^-\pi^0$ decay modes measurements.
[2] From the decay mode $\eta \to \gamma\gamma$.
[3] From the decay mode $\eta \to \pi^+\pi^-\pi^0$.
[4] Supersedes ACHASOV 98B.
[5] Using B($\phi \to \eta\gamma$) = (1.304 ± 0.025)%, B($\eta \to 3\pi^0$) = (32.56 ± 0.23)%, and B($\eta \to \gamma\gamma$) = (39.31 ± 0.20)%.
[6] Using B($\phi \to \eta\gamma$) = (1.304 ± 0.025)%, B($\eta \to 3\pi^0$) = (32.56 ± 0.23)%, and B($\eta \to \pi^+\pi^-\pi^0$) = (22.73 ± 0.28)%.

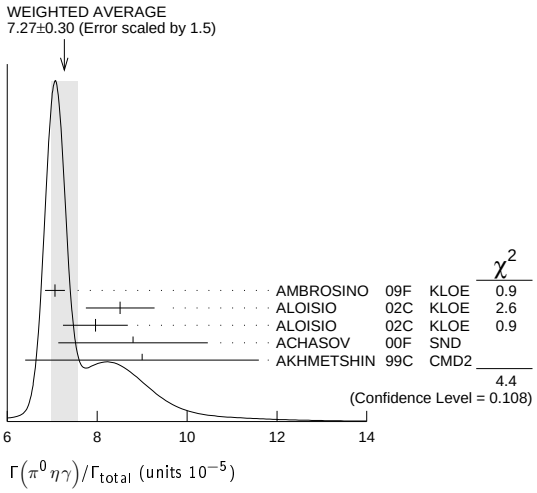

$\Gamma(a_0(980)\gamma)/\Gamma_{\text{total}}$ Γ_{23}/Γ

VALUE (units 10^{-5})	CL%	EVTS	DOCUMENT ID		TECN	COMMENT
7.6±0.6 OUR FIT						
7.6±0.6 OUR AVERAGE						
7.4±0.7			[1] ALOISIO	02C	KLOE	$e^+e^- \to \eta\pi^0\gamma$
8.8±1.7		36	[2] ACHASOV	00F	SND	$e^+e^- \to \eta\pi^0\gamma$

• • • We do not use the following data for averages, fits, limits, etc. • • •

11 ±2		[3] GOKALP	02	RVUE	$e^+e^- \to \eta\pi^0\gamma$	
<500	90	DOLINSKY	91	ND	$e^+e^- \to \pi^0\eta\gamma$	

[1] Using $M_{a_0(980)}$=984.8 MeV and assuming $a_0(980)\gamma$ dominance.
[2] Assuming $a_0(980)\gamma$ dominance in the $\eta\pi^0\gamma$ final state.
[3] Using data of ACHASOV 00F.

$\Gamma(f_0(980)\gamma)/\Gamma(a_0(980)\gamma)$ Γ_{17}/Γ_{23}

VALUE	DOCUMENT ID		TECN	COMMENT
6.1±0.6	[1] ALOISIO	02C	KLOE	$e^+e^- \to \eta\pi^0\gamma$

[1] Using results of ALOISIO 02D and assuming that $f_0(980)$ decays into $\pi\pi$ only and $a_0(980)$ into $\eta\pi$ only.

$\Gamma(K^0\overline{K}{}^0\gamma)/\Gamma_{\text{total}}$ Γ_{24}/Γ

VALUE	CL%	DOCUMENT ID		TECN	COMMENT
$<1.9 \times 10^{-8}$	90	AMBROSINO	09C	KLOE	$e^+e^- \to K^0_S K^0_S\gamma$

$\Gamma(\eta'(958)\gamma)/\Gamma_{\text{total}}$ Γ_{25}/Γ

VALUE (units 10^{-5})	CL%	EVTS	DOCUMENT ID		TECN	COMMENT
6.22±0.21 OUR FIT						
6.22±0.30 OUR AVERAGE						
6.22±0.27±0.12		3407	[1] AMBROSINO	07A	KLOE	1.02 $e^+e^- \to \pi^+\pi^-7\gamma$
$6.7\ ^{+2.8}_{-2.4}$ ±0.8		12	[2] AULCHENKO	03B	SND	$e^+e^- \to \eta'\gamma$

• • • We do not use the following data for averages, fits, limits, etc. • • •

$6.7\ ^{+5.0}_{-4.2}$ ±1.5		7	AULCHENKO	03B	SND	$e^+e^- \to 7\gamma$
6.10±0.61±0.43		120	[3] ALOISIO	02E	KLOE	1.02 $e^+e^- \to \pi^+\pi^-3\gamma$
$8.2\ ^{+2.1}_{-1.9}$ ±1.1		21	[4] AKHMETSHIN	00B	CMD2	$e^+e^- \to \pi^+\pi^-3\gamma$
$4.9\ ^{+2.2}_{-1.8}$ ±0.6		9	[5] AKHMETSHIN	00F	CMD2	$e^+e^- \to \pi^+\pi^-\pi^+\pi^- \geq 2\gamma$
6.4 ±1.6		30	[6] AKHMETSHIN	00F	CMD2	$e^+e^- \to \eta'(958)\gamma$
$6.7\ ^{+3.4}_{-2.9}$ ±1.0		5	[7] AULCHENKO	99	SND	$e^+e^- \to \pi^+\pi^-3\gamma$
<11	90		AULCHENKO	98	SND	$e^+e^- \to 7\gamma$
$12\ ^{+7}_{-5}$ ±2		6	[4] AKHMETSHIN	97B	CMD2	$e^+e^- \to \pi^+\pi^-3\gamma$
<41	90		DRUZHININ	87	ND	$e^+e^- \to \gamma\eta\pi^+\pi^-$

[1] AMBROSINO 07A reports [$\Gamma(\phi(1020) \to \eta'(958)\gamma)/\Gamma_{\text{total}}$] / [B($\phi(1020) \to \eta\gamma$)] = (4.77 ± 0.09 ± 0.19) × 10^{-3} which we multiply by our best value B($\phi(1020) \to \eta\gamma$) = (1.303 ± 0.025) × 10^{-2}. Our first error is their experiment's error and our second error is the systematic error from using our best value.
[2] Averaging AULCHENKO 03B with AULCHENKO 99.
[3] Using B($\phi \to \eta\gamma$)= (1.297 ± 0.033)%.
[4] Using the value B($\phi \to \eta\gamma$) = (1.26 ± 0.06) × 10^{-2}.
[5] Using B($\phi \to K^0_L K^0_S$) = (33.8 ± 0.6)%.
[6] Averaging AKHMETSHIN 00B with AKHMETSHIN 00F.
[7] Using the value B($\eta' \to \eta\pi^+\pi^-$)= (43.7 ± 1.5) × 10^{-2} and B($\eta \to \gamma\gamma$)= (39.25 ± 0.31) × 10^{-2}.

$\Gamma(\eta'(958)\gamma)/\Gamma(K^0_L K^0_S)$ Γ_{25}/Γ_2

VALUE (units 10^{-4})	EVTS	DOCUMENT ID		TECN	COMMENT
1.83±0.06 OUR FIT					
$1.46^{+0.64}_{-0.54}$ ±0.18	9	[1] AKHMETSHIN	00F	CMD2	$e^+e^- \to \pi^+\pi^-\pi^+\pi^- \geq 2\gamma$

[1] Using various branching ratios of K^0_S, K^0_L, η, η' from the 2000 edition (The European Physical Journal **C15** 1 (2000)) of this Review.

$\Gamma(\eta'(958)\gamma)/\Gamma(\eta\gamma)$ Γ_{25}/Γ_6

VALUE (units 10^{-3})	EVTS	DOCUMENT ID		TECN	COMMENT
4.77±0.15 OUR FIT					
4.78±0.20 OUR AVERAGE					
4.77±0.09±0.19	3407	AMBROSINO	07A	KLOE	1.02 $e^+e^- \to \pi^+\pi^-7\gamma$
4.70±0.47±0.31	120	[1] ALOISIO	02E	KLOE	1.02 $e^+e^- \to \pi^+\pi^-3\gamma$
$6.5\ ^{+1.7}_{-1.5}$ ±0.8	21	AKHMETSHIN	00B	CMD2	$e^+e^- \to \pi^+\pi^-3\gamma$

• • • We do not use the following data for averages, fits, limits, etc. • • •

$9.5\ ^{+5.2}_{-4.0}$ ±1.4	6	[2] AKHMETSHIN	97B	CMD2	$e^+e^- \to \pi^+\pi^-3\gamma$	

[1] From the decay mode $\eta' \to \eta\pi^+\pi^-$, $\eta \to \gamma\gamma$.
[2] Superseded by AKHMETSHIN 00B.

$\Gamma(\eta\pi^0\pi^0\gamma)/\Gamma_{\text{total}}$ Γ_{26}/Γ

VALUE (units 10^{-5})	CL%	DOCUMENT ID		TECN	COMMENT
<2	90	AULCHENKO	98	SND	$e^+e^- \to 7\gamma$

$\Gamma(\mu^+\mu^-\gamma)/\Gamma_{\text{total}}$ Γ_{27}/Γ

VALUE (units 10^{-5})	EVTS	DOCUMENT ID		TECN	COMMENT
1.43±0.45±0.14	27188	[1] AKHMETSHIN	99B	CMD2	$e^+e^- \to \mu^+\mu^-\gamma$

• • • We do not use the following data for averages, fits, limits, etc. • • •

2.3 ±1.0	824 ± 33	[2] AKHMETSHIN	97C	CMD2	$e^+e^- \to \mu^+\mu^-\gamma$	

[1] For $E_\gamma > 20$ MeV. Supersedes AKHMETSHIN 97C.
[2] For $E_\gamma > 20$ MeV.

$\Gamma(\rho\gamma\gamma)/\Gamma_{total}$ Γ_{28}/Γ

VALUE (units 10^{-4})	CL%	DOCUMENT ID	TECN	COMMENT
<1.2	90	AULCHENKO 08	CMD2	$\phi \to \pi^+\pi^-\gamma\gamma$
• • • We do not use the following data for averages, fits, limits, etc. • • •				
<5	90	AKHMETSHIN 98	CMD2	$e^+e^- \to \pi^+\pi^-\gamma\gamma$

$\Gamma(\eta\pi^+\pi^-)/\Gamma_{total}$ Γ_{29}/Γ

VALUE (units 10^{-5})	CL%	DOCUMENT ID	TECN	COMMENT
< 1.8	90	AKHMETSHIN 00E	CMD2	$e^+e^- \to \pi^+\pi^-\pi^+\pi^-\pi^0$
• • • We do not use the following data for averages, fits, limits, etc. • • •				
< 6.1	90	AULCHENKO 08	CMD2	$\phi \to \eta\pi^+\pi^-$
<30	90	AKHMETSHIN 98	CMD2	$e^+e^- \to \pi^+\pi^-\gamma\gamma$

$\Gamma(\eta\mu^+\mu^-)/\Gamma_{total}$ Γ_{30}/Γ

VALUE (units 10^{-6})	CL%	DOCUMENT ID	TECN	COMMENT
<9.4	90	AKHMETSHIN 01	CMD2	$e^+e^- \to \eta e^+e^-$

$\Gamma(\eta U \to \eta e^+e^-)/\Gamma_{total}$ Γ_{31}/Γ

VALUE	CL%	DOCUMENT ID	TECN	COMMENT
$<1\times10^{-6}$	90	[1] BABUSCI 13B	KLOE	$1.02\ e^+e^- \to \eta e^+e^-$

[1] For a narrow vector U with mass between 5 and 470 MeV, from the combined analysis of $\eta \to \pi^+\pi^-\pi^0$ and $\eta \to \pi^0\pi^0\pi^0$ from ARCHILLI 12. Measured 90% CL limits as a function of m_U range from 2.2×10^{-8} to 10^{-6}.

Lepton Family number (LF) violating modes

$\Gamma(e^\pm\mu^\mp)/\Gamma_{total}$ Γ_{32}/Γ

VALUE	CL%	DOCUMENT ID	TECN	COMMENT
$<2\times10^{-6}$	90	ACHASOV 10A	SND	$e^+e^- \to e^\pm\mu^\mp$

$\pi^+\pi^-\pi^0$ / $\rho\pi$ AMPLITUDE RATIO a_1 IN DECAY OF $\phi \to \pi^+\pi^-\pi^0$

NIECKNIG 12 describes final-state interactions between the three pions in a dispersive framework using data on the $\pi\pi$ P-wave scattering phase shift.

VALUE (units 10^{-2})	CL%	EVTS	DOCUMENT ID	TECN	COMMENT
9.1±1.2 OUR AVERAGE					
10.1±4.4±1.7		80k	[1] AKHMETSHIN 06	CMD2	1.017–1.021 $e^+e^- \to \pi^+\pi^-\pi^0$
9.0±1.1±0.6		1.98M	[2,3] ALOISIO 03	KLOE	$1.02\ e^+e^- \to \pi^+\pi^-\pi^0$
• • • We do not use the following data for averages, fits, limits, etc. • • •					
$-6 < a_1 < 6$		500k	[3] ACHASOV 02	SND	$e^+e^- \to \pi^+\pi^-\pi^0$
$-16 < a_1 < 11$	90	9.8k	[1,4] AKHMETSHIN 98	CMD2	$e^+e^- \to \pi^+\pi^-\gamma\gamma$

[1] Dalitz plot analysis taking into account interference between the contact and $\rho\pi$ amplitudes.
[2] From a fit without limitations on charged and neutral ρ masses and widths.
[3] Recalculated by us to match the notations of AKHMETSHIN 98.
[4] Assuming zero phase for the contact term.

PARAMETER β IN $\phi \to P e^+e^-$ DECAYS

In the one-pole approximation the electromagnetic transition form factor for $\phi \to P e^+e^-$ ($P = \pi,\eta$) is given as a function of the e^+e^- invariant mass squared, q^2, by the expression:

$$|F(q^2)|^2 = (1 - q^2/\Lambda^2)^{-2},$$

where vector meson dominance predicts parameter $\Lambda \approx 0.770$ GeV ($\Lambda^{-2} \approx 1.687$ GeV^{-2}). The slope of this form factor, $\beta = dF/dq^2(q^2{=}0)$, equals Λ^{-2} in this approximation.

The measurements below obtain β in the one-pole approximation.

PARAMETER β IN $\phi \to \pi^0 e^+e^-$ DECAY

VALUE (GeV^{-2})	EVTS	DOCUMENT ID	TECN	COMMENT
2.02±0.11	9.5k	[1] ANASTASI 16B	KLOE	$1.02\ e^+e^- \to \pi^0 e^+e^-$

[1] The error combines statistical and systematic uncertainties.

PARAMETER β IN $\phi \to \eta e^+e^-$ DECAY

VALUE (GeV^{-2})	EVTS	DOCUMENT ID	TECN	COMMENT
1.29±0.13 OUR AVERAGE				
$1.28\pm0.10^{+0.09}_{-0.08}$	30k	BABUSCI 15	KLOE	$1.02\ e^+e^- \to \eta e^+e^-$
3.8 ±1.8	213	[1] ACHASOV 01B	SND	$1.02\ e^+e^- \to \eta e^+e^-$

[1] The uncertainty is statistical only. The systematic one is negligible, in comparison.

$\phi(1020)$ REFERENCES

KOZYREV	18	PL B779 64	E.A. Kozyrev *et al.*	(CMD3 Collab.)
AKHMETSHIN	17	PL B768 345	R.R. Akhmetshin *et al.*	(CMD-3 Collab.)
ACHASOV	16A	PR D93 092001	M.N. Achasov *et al.*	(SND Collab.)
ANASTASI	16B	PL B757 362	A. Anastasi *et al.*	(KLOE-2 Collab.)
KOZYREV	16	PL B760 314	E.A. Kozyrev *et al.*	(CMD3 Collab.)
BABUSCI	15	PL B742 1	D. Babusci *et al.*	(KLOE-2 Collab.)
PDG	15	RPP 2015 at pdg.lbl.gov		(PDG Collab.)
LEES	14H	PR D89 092002	J.P. Lees *et al.*	(BABAR Collab)
PDG	14	CP C38 070001	K. Olive *et al.*	(PDG Collab.)
BABUSCI	13B	PL B720 111	D. Babusci *et al.*	(KLOE-2 Collab.)
BENAYOUN	13	EPJ C73 2453	M. Benayoun, P. David, L. DelBuono	(PARIN, BERLIN+)
LEES	13F	PR D87 052010	J.P. Lees *et al.*	(BABAR Collab.)
LEES	13Q	PR D88 032013	J.P. Lees *et al.*	(BABAR Collab.)
ARCHILLI	12	PL B706 251	F. Archilli *et al.*	(KLOE-2 Collab.)
BENAYOUN	12	EPJ C72 1848	M. Benayoun *et al.*	
NIECKNIG	12	EPJ C72 2014	F. Niecknig, B. Kubis, S.P. Schneider	(BONN)
PDG	12	PR D86 010001	J. Beringer *et al.*	(PDG Collab.)
AKHMETSHIN	11	PL B695 412	R.R. Akhmetshin *et al.*	(CMD2 Collab.)
ACHASOV	10A	PR D81 057102	M.N. Achasov *et al.*	(Novosibirsk SND Collab.)
BENAYOUN	10	EPJ C65 211	M. Benayoun *et al.*	
AMBROSINO	09C	PL B679 10	F. Ambrosino *et al.*	(KLOE Collab.)
AMBROSINO	09F	PL B681 5	F. Ambrosino *et al.*	(KLOE Collab.)
AKHMETSHIN	08	PL B669 217	R.R. Akhmetshin *et al.*	(CMD-2 Collab.)
AMBROSINO	08G	PL B669 223	F. Ambrosino *et al.*	(KLOE Collab.)
AULCHENKO	08	JETPL 88 85 Translated from ZETFP 88 93.	V. Aulchenko *et al.*	(CMD-2 Collab.)
FLOREZ-BAEZ	08	PR D78 077301	F.V. Florez-Baez, G. Lopez Castro	
ACHASOV	07B	PR D76 077101	M.N. Achasov *et al.*	(SND Collab.)
AMBROSINO	07	EPJ C49 473	F. Ambrosino *et al.*	(KLOE Collab.)
AMBROSINO	07A	PL B648 267	F. Ambrosino *et al.*	(KLOE Collab.)
DUBYNSKIY	07	PR D75 113001	S. Dubynskiy *et al.*	
ACHASOV	06A	PR D74 014016	M.N. Achasov *et al.*	(SND Collab.)
AKHMETSHIN	06	PL B642 203	R.R. Akhmetshin *et al.*	(CMD-2 Collab.)
AKHMETSHIN	05	PL B605 26	R.R. Akhmetshin *et al.*	(Novosibirsk CMD-2 Collab.)
AMBROSINO	05	PL B608 199	F. Ambrosino *et al.*	(KLOE Collab.)
AUBERT,B	05J	PR D72 052008	B. Aubert *et al.*	(BABAR Collab.)
AKHMETSHIN	04	PL B578 285	R.R. Akhmetshin *et al.*	(Novosibirsk CMD-2 Collab.)
AUBERT,B	04N	PR D70 072004	B. Aubert *et al.*	(BABAR Collab.)
ALOISIO	03	PL B561 55	A. Aloisio *et al.*	(KLOE Collab.)
AULCHENKO	03B	JETP 97 24 Translated from ZETF 124 28.	V.M. Aulchenko *et al.*	(Novosibirsk SND Collab.)
ACHASOV	02	PR D65 032002	M.N. Achasov *et al.*	(Novosibirsk SND Collab.)
ACHASOV	02D	JETPL 75 449 Translated from ZETFP 75 539.	M.N. Achasov *et al.*	(Novosibirsk SND Collab.)
ALOISIO	02C	PL B536 209	A. Aloisio *et al.*	(KLOE Collab.)
ALOISIO	02D	PL B537 21	A. Aloisio *et al.*	(KLOE Collab.)
ALOISIO	02E	PL B541 45	A. Aloisio *et al.*	(KLOE Collab.)
FISCHBACH	02	PL B526 355	E. Fischbach, A.W. Overhauser, B. Woodahl	
GOKALP	02	JP G28 2783	A. Gokalp *et al.*	
ACHASOV	01B	PL B504 275	M.N. Achasov *et al.*	(Novosibirsk SND Collab.)
ACHASOV	01E	PR D63 072002	M.N. Achasov *et al.*	(Novosibirsk SND Collab.)
ACHASOV	01F	PR D63 094007	N.N. Achasov, V.V. Gubin	(Novosibirsk SND Collab.)
ACHASOV	01G	PRL 86 1698	M.N. Achasov *et al.*	(Novosibirsk SND Collab.)
AITALA	01B	PRL 86 770	E.M. Aitala *et al.*	(FNAL E791 Collab.)
AKHMETSHIN	01	PL B501 191	R.R. Akhmetshin *et al.*	(Novosibirsk CMD-2 Collab.)
AKHMETSHIN	01B	PL B509 217	R.R. Akhmetshin *et al.*	(Novosibirsk CMD-2 Collab.)
AKHMETSHIN	01C	PL B503 237	R.R. Akhmetshin *et al.*	(Novosibirsk CMD-2 Collab.)
BENAYOUN	01	EPJ C22 503	M. Benayoun, H.B. O'Connell	
ACHASOV	00	EPJ C12 25	M.N. Achasov *et al.*	(Novosibirsk SND Collab.)
ACHASOV	00B	JETP 90 17 Translated from ZETF 117 22.	M.N. Achasov *et al.*	(Novosibirsk SND Collab.)
ACHASOV	00C	PL B474 188	M.N. Achasov *et al.*	(Novosibirsk SND Collab.)
ACHASOV	00D	JETPL 72 282 Translated from ZETFP 72 411.	M.N. Achasov *et al.*	(Novosibirsk SND Collab.)
ACHASOV	00E	NP B569 158	M.N. Achasov *et al.*	(Novosibirsk SND Collab.)
ACHASOV	00F	PL B479 53	M.N. Achasov *et al.*	(Novosibirsk SND Collab.)
ACHASOV	00H	PL B485 349	M.N. Achasov *et al.*	(Novosibirsk SND Collab.)
AKHMETSHIN	00B	PL B473 337	R.R. Akhmetshin *et al.*	(Novosibirsk CMD-2 Collab.)
AKHMETSHIN	00E	PL B491 81	R.R. Akhmetshin *et al.*	(Novosibirsk CMD-2 Collab.)
AKHMETSHIN	00F	PL B494 26	R.R. Akhmetshin *et al.*	(Novosibirsk CMD-2 Collab.)
AULCHENKO	00A	JETP 90 927 Translated from ZETF 117 1067.	V.M. Aulchenko *et al.*	(Novosibirsk SND Collab.)
BRAMON	00	PL B486 406	A. Bramon *et al.*	
PDG	00	EPJ C15 1	D.E. Groom *et al.*	(PDG Collab.)
ACHASOV	99	PL B449 122	M.N. Achasov *et al.*	
ACHASOV	99C	PL B456 304	M.N. Achasov *et al.*	
AKHMETSHIN	99B	PL B462 371	R.R. Akhmetshin *et al.*	(Novosibirsk CMD-2 Collab.)
AKHMETSHIN	99C	PL B462 380	R.R. Akhmetshin *et al.*	(Novosibirsk CMD-2 Collab.)
AKHMETSHIN	99D	PL B466 385	R.R. Akhmetshin *et al.*	
Also		PL B508 217 (errat.)	R.R. Akhmetshin *et al.*	(Novosibirsk CMD-2 Collab.)
AKHMETSHIN	99F	PL B460 242	R.R. Akhmetshin *et al.*	(Novosibirsk CMD-2 Collab.)
AULCHENKO	99	JETPL 69 97 Translated from ZETFP 69 87.	V.M. Aulchenko *et al.*	
ACHASOV	98B	PL B438 441	M.N. Achasov *et al.*	(Novosibirsk SND Collab.)
ACHASOV	98F	JETPL 68 573	M.N. Achasov *et al.*	(Novosibirsk SND Collab.)
ACHASOV	98I	PL B440 442	M.N. Achasov *et al.*	
AKHMETSHIN	98	PL B434 426	R.R. Akhmetshin *et al.*	(CMD-2 Collab.)
AULCHENKO	98	PL B436 199	V.M. Aulchenko *et al.*	(Novosibirsk SND Collab.)
BARBERIS	98	PL B432 436	D. Barberis *et al.*	(Omega Expt.)
AKHMETSHIN	97B	PL B415 445	R.R. Akhmetshin *et al.*	(NOVO, BOST, PITT+)
AKHMETSHIN	97C	PL B415 452	R.R. Akhmetshin *et al.*	(Novosibirsk CMD-2 Collab.)
BENAYOUN	96	ZPHY C72 221	M. Benayoun *et al.*	(IPNP, NOVO)
AKHMETSHIN	95	PL B364 199	R.R. Akhmetshin *et al.*	(Novosibirsk CMD-2 Collab.)
DOLINSKY	91	PRPL 202 99	S.I. Dolinsky *et al.*	(NOVO)
KUHN	90	ZPHY C48 445	J.H. Kuhn *et al.*	(MPIM)
ACHASOV	89	NP B315 465	N.N. Achasov, V.N. Ivanchenko	
DOLINSKY	89	ZPHY C42 511	S.I. Dolinsky *et al.*	(NOVO)
BARKOV	88	SJNP 47 248 Translated from YAF 47 393.	L.M. Barkov *et al.*	(NOVO)
DOLINSKY	88	SJNP 48 277 Translated from YAF 48 442.	S.I. Dolinsky *et al.*	(NOVO)
DRUZHININ	87	ZPHY C37 1	V.P. Druzhinin *et al.*	(NOVO)
ARMSTRONG	86	PL 166B 245	T.A. Armstrong *et al.*	(ATHU, BARI, BIRM+)
ATKINSON	86	ZPHY C30 521	M. Atkinson *et al.*	(BONN, CERN, GLAS+)
BEBEK	86	PRL 56 1893	C. Bebek *et al.*	(CLEO Collab.)
DAVENPORT	86	PR D33 2519	T.F. Davenport	(TUFTS, ARIZ, FNAL, FSU, NDAM+)
DIJKSTRA	86	ZPHY C31 375	H. Dijkstra *et al.*	(ANIK, BRIS, CERN+)
FRAME	86	NP B276 667	D. Frame *et al.*	(GLAS)
GOLUBEV	86	SJNP 44 409 Translated from YAF 44 633.	V.B. Golubev *et al.*	(NOVO)
ALBRECHT	85D	PL 153B 343	H. Albrecht *et al.*	(ARGUS Collab.)
GOLUBEV	85	SJNP 41 756 Translated from YAF 41 1183.	V.B. Golubev *et al.*	(NOVO)
DRUZHININ	84	PL 144B 136	V.P. Druzhinin *et al.*	(NOVO)
ARMSTRONG	83B	NP B224 193	T.A. Armstrong *et al.*	(BARI, BIRM, CERN+)
BARATE	83	PL 121B 449	R. Barate *et al.*	(SACL, LOIC, SHMP, IND)
KURDADZE	83C	JETPL 38 366 Translated from ZETFP 38 306.	L.M. Kurdadze *et al.*	(NOVO)
ARENTON	82	PR D25 2241	M.W. Arenton *et al.*	(ANL, ILL)
PELLINEN	82	PS 25 599	A. Pellinen, M. Roos	(HELS)
DAUM	81	PL 100B 439	C. Daum *et al.*	(AMST, BRIS, CERN, CRAC+)
IVANOV	81	PL 107B 297	P.M. Ivanov *et al.*	(NOVO)
Also		Private Comm.	S.I. Eidelman	(NOVO)
VASSERMAN	81	PL 99B 62	I.B. Vasserman *et al.*	(NOVO)
Also		SJNP 35 240 Translated from YAF 35 352.	L.M. Kurdadze *et al.*	
CORDIER	80	NP B172 13	A. Cordier *et al.*	(LALO)

CORDIER	79	PL 81B 389	A. Cordier *et al.*	(LALO)
BUKIN	78B	SJNP 27 521	A.D. Bukin *et al.*	(NOVO)
		Translated from YAF 27 985.		
BUKIN	78C	SJNP 27 516	A.D. Bukin *et al.*	(NOVO)
		Translated from YAF 27 976.		
COOPER	78B	NP B146 1	A.M. Cooper *et al.*	(TATA, CERN, CDEF+)
LOSTY	78	NP B133 38	M.J. Losty *et al.*	(CERN, AMST, NIJM+)
AKERLOF	77	PRL 39 861	C.W. Akerlof *et al.*	(FNAL, MICH, PURD)
ANDREWS	77	PRL 38 198	D.E. Andrews *et al.*	(ROCH)
BALDI	77	PL 68B 381	R. Baldi *et al.*	(GEVA)
CERRADA	77B	NP B126 241	M. Cerrada *et al.*	(AMST, CERN, NIJM+)
COHEN	77	PRL 38 269	D. Cohen *et al.*	(ANL)
LAVEN	77	NP B127 43	H. Laven *et al.*	(AACH3, BERL, CERN, LOIC+)
LYONS	77	NP B125 207	L. Lyons, A.M. Cooper, A.G. Clark	(OXF)
COSME	76	PL 63B 352	G. Cosme *et al.*	(ORSAY)
KALBFLEISCH	76	PR D13 22	G.R. Kalbfleisch, R.C. Strand, J.W. Chapman	(BNL+)
PARROUR	76	PL 63B 357	G. Parrour *et al.*	(ORSAY)
PARROUR	76B	PL 63B 362	G. Parrour *et al.*	(ORSAY)
KALBFLEISCH	75	PR D11 987	G.R. Kalbfleisch, R.C. Strand, J.W. Chapman	(BNL+)
AYRES	74	PRL 32 1463	D.S. Ayres *et al.*	(ANL)
BESCH	74	NP B70 257	H.J. Besch *et al.*	(BONN)
COSME	74	PL 48B 155	G. Cosme *et al.*	(ORSAY)
COSME	74B	PL 48B 159	G. Cosme *et al.*	(ORSAY)
DEGROOT	74	NP B74 77	A.J. de Groot *et al.*	(AMST, NIJM)
AUGUSTIN	73	PRL 30 462	J.E. Augustin *et al.*	(ORSAY)
BALLAM	73	PR D7 3150	J. Ballam *et al.*	(SLAC, LBL)
BINNIE	73B	PR D8 2789	D.M. Binnie *et al.*	(LOIC, SHMP)
AGUILAR-...	72B	PR D6 29	M. Aguilar-Benitez *et al.*	(BNL)
ALVENSLEB...	72	PRL 28 66	H. Alvensleben *et al.*	(MIT, DESY)
BORENSTEIN	72	PR D5 1559	S.R. Borenstein *et al.*	(BNL, MICH)
COLLEY	72	NP B50 1	D.C. Colley *et al.*	(BIRM, GLAS)
BALAKIN	71	PL 34B 328	V.E. Balakin *et al.*	(NOVO)
CHATELUS	71	Thesis LAL 1247	Y. Chatelus	(STRB)
Also		PL 32B 416	J.C. Bizot *et al.*	(ORSAY)
HAYES	71	PR D4 899	S. Hayes *et al.*	(CORN)
STOTTLE...	71	Thesis ORO 2504 170	A.R. Stottlemyer	(UMD)
BIZOT	70	PL 32B 416	J.C. Bizot *et al.*	(ORSAY)
Also		Liverpool Sym. 69	J.P. Perez-y-Jorba	
EARLES	70	PRL 25 1312	D.R. Earles *et al.*	(NEAS)
LINDSEY	66	PR 147 913	J.S. Lindsey, G. Smith	(LRL)
LONDON	66	PR 143 1034	G.W. London *et al.*	(BNL, SYRA) IGJPC
BADIER	65B	PL 17 337	J. Badier *et al.*	(EPOL, SACL, AMST)
LINDSEY	65	PRL 15 221	J.S. Lindsey, G.A. Smith	(LRL)
LINDSEY 65 data included in LINDSEY 66.				
SCHLEIN	63	PRL 10 368	P.E. Schlein *et al.*	(UCLA) IGJP

$h_1(1170)$

$I^G(J^{PC}) = 0^-(1^{+-})$

$h_1(1170)$ MASS

VALUE (MeV)	DOCUMENT ID		TECN	CHG	COMMENT
1170±20 OUR ESTIMATE					
• • • We do not use the following data for averages, fits, limits, etc. • • •					
1168± 4	ANDO	92	SPEC		8 $\pi^- p \rightarrow \pi^+\pi^-\pi^0 n$
1166± 5±3	[1] ANDO	92	SPEC		8 $\pi^- p \rightarrow \pi^+\pi^-\pi^0 n$
1190±60	[2] DANKOWY...	81	SPEC	0	8 $\pi p \rightarrow 3\pi n$

[1] Average and spread of values using 2 variants of the model of BOWLER 75.
[2] Uses the model of BOWLER 75.

$h_1(1170)$ WIDTH

VALUE (MeV)	DOCUMENT ID		TECN	CHG	COMMENT
360±40 OUR ESTIMATE					
• • • We do not use the following data for averages, fits, limits, etc. • • •					
345± 6	ANDO	92	SPEC		8 $\pi^- p \rightarrow \pi^+\pi^-\pi^0 n$
375± 6±34	[3] ANDO	92	SPEC		8 $\pi^- p \rightarrow \pi^+\pi^-\pi^0 n$
320±50	[4] DANKOWY...	81	SPEC	0	8 $\pi p \rightarrow 3\pi n$

[3] Average and spread of values using 2 variants of the model of BOWLER 75.
[4] Uses the model of BOWLER 75.

$h_1(1170)$ DECAY MODES

	Mode	Fraction (Γ_i/Γ)
Γ_1	$\rho\pi$	seen

$h_1(1170)$ BRANCHING RATIOS

$\Gamma(\rho\pi)/\Gamma_{total}$ **Γ_1/Γ**

VALUE	DOCUMENT ID		TECN	COMMENT
• • • We do not use the following data for averages, fits, limits, etc. • • •				
seen	ANDO	92	SPEC	8 $\pi^- p \rightarrow \pi^+\pi^-\pi^0 n$
seen	ATKINSON	84	OMEG	20–70 $\gamma p \rightarrow \pi^+\pi^-\pi^0 p$
seen	DANKOWY...	81	SPEC	8 $\pi p \rightarrow 3\pi n$

$h_1(1170)$ REFERENCES

ANDO	92	PL B291 496	A. Ando *et al.*	(KEK, KYOT, NIRS, SAGA+)
ATKINSON	84	NP B231 15	M. Atkinson *et al.*	(BONN, CERN, GLAS+)
DANKOWY...	81	PRL 46 580	J.A. Dankowych *et al.*	(TNTO, BNL, CARL+)
BOWLER	75	NP B97 227	M.G. Bowler *et al.*	(OXFTP, DARE)

$b_1(1235)$

$I^G(J^{PC}) = 1^+(1^{+-})$

$b_1(1235)$ MASS

VALUE (MeV)	EVTS	DOCUMENT ID		TECN	CHG	COMMENT
1229.5± 3.2 OUR AVERAGE		Error includes scale factor of 1.6. See the ideogram below.				
1225 ± 5		WEIDENAUER	93	ASTE		$\overline{p}p \rightarrow 2\pi^+2\pi^-\pi^0$
1235 ±15		ALDE	92C	GAM2		38,100 $\pi^- p \rightarrow \omega\pi^0 n$
1236 ±16		FUKUI	91	SPEC		8.95 $\pi^- p \rightarrow \omega\pi^0 n$
1222 ± 6		ATKINSON	84E	OMEG	±	25–55 $\gamma p \rightarrow \omega\pi X$
1237 ± 7		ATKINSON	84E	OMEG	0	25–55 $\gamma p \rightarrow \omega\pi X$
1239 ± 5		EVANGELIS...	81	OMEG	−	12 $\pi^- p \rightarrow \omega\pi p$
1251 ± 8	450	GESSAROLI	77	HBC	−	11 $\pi^- p \rightarrow \pi^-\omega p$
1245 ±11	890	FLATTE	76C	HBC	−	4.2 $K^- p \rightarrow \pi^-\omega\Sigma^+$
1222 ± 4	1400	CHALOUPKA	74	HBC	−	3.9 $\pi^- p$
1220 ± 7	600	KARSHON	74B	HBC	+	4.9 $\pi^+ p$
• • • We do not use the following data for averages, fits, limits, etc. • • •						
1190 ±10		AUGUSTIN	89	DM2	±	$e^+e^- \rightarrow 5\pi$
1213 ± 5		ATKINSON	84C	OMEG	0	20–70 γp
1271 ±11		COLLICK	84	SPEC	+	200 $\pi^+ Z \rightarrow Z\pi\omega$

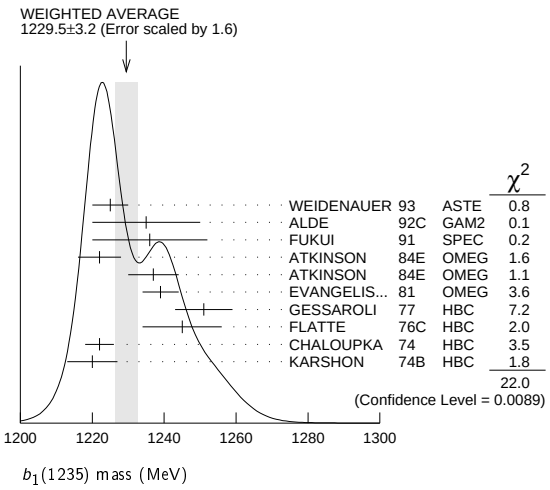

$b_1(1235)$ WIDTH

VALUE (MeV)	EVTS	DOCUMENT ID		TECN	CHG	COMMENT
142± 9 OUR AVERAGE		Error includes scale factor of 1.2.				
113±12		WEIDENAUER	93	ASTE		$\overline{p}p \rightarrow 2\pi^+2\pi^-\pi^0$
160±30		ALDE	92C	GAM2		38,100 $\pi^- p \rightarrow \omega\pi^0 n$
151±31		FUKUI	91	SPEC		8.95 $\pi^- p \rightarrow \omega\pi^0 n$
170±15		EVANGELIS...	81	OMEG	−	12 $\pi^- p \rightarrow \omega\pi p$
170±50	225	BALTAY	78B	HBC	+	15 $\pi^+ p \rightarrow p4\pi$
155±32	450	GESSAROLI	77	HBC	−	11 $\pi^- p \rightarrow \pi^-\omega p$
182±45	890	FLATTE	76C	HBC	−	4.2 $K^- p \rightarrow \pi^-\omega\Sigma^+$
135±20	1400	CHALOUPKA	74	HBC	−	3.9 $\pi^- p$
156±22	600	KARSHON	74B	HBC	+	4.9 $\pi^+ p$
• • • We do not use the following data for averages, fits, limits, etc. • • •						
210±19		AUGUSTIN	89	DM2	±	$e^+e^- \rightarrow 5\pi$
231±14		ATKINSON	84C	OMEG	0	20–70 γp
232±29		COLLICK	84	SPEC	+	200 $\pi^+ Z \rightarrow Z\pi\omega$

$b_1(1235)$ DECAY MODES

	Mode	Fraction (Γ_i/Γ)		Confidence level
Γ_1	$\omega\pi$ [D/S amplitude ratio = 0.277 ± 0.027]	dominant		
Γ_2	$\pi^\pm\gamma$	$(1.6\pm0.4)\times10^{-3}$		
Γ_3	$\eta\rho$	seen		
Γ_4	$\pi^+\pi^+\pi^-\pi^0$	< 50	%	84%
Γ_5	$K^*(892)^\pm K^\mp$	seen		
Γ_6	$(K\overline{K})^\pm\pi^0$	< 8	%	90%
Γ_7	$K^0_S K^0_L \pi^\pm$	< 6	%	90%
Γ_8	$K^0_S K^0_S \pi^\pm$	< 2	%	90%
Γ_9	$\phi\pi$	< 1.5	%	84%

$b_1(1235)$ PARTIAL WIDTHS

$\Gamma(\pi^\pm\gamma)$ **Γ_2**

VALUE (keV)	DOCUMENT ID		TECN	CHG	COMMENT
230±60	COLLICK	84	SPEC	+	200 π^+Z → Z$\pi\omega$

$b_1(1235)$ D-wave/S-wave AMPLITUDE RATIO IN DECAY OF $b_1(1235) \to \omega\pi$

VALUE	EVTS	DOCUMENT ID		TECN	CHG	COMMENT
0.277±0.027 OUR AVERAGE		Error includes scale factor of 2.4. See the ideogram below.				
0.269±0.009±0.010		NOZAR	02	MPS	−	18 $\pi^- p \to \omega\pi^- p$
0.23 ±0.03		AMSLER	94C	CBAR		0.0 $\overline{p}p \to \omega\eta\pi^0$
0.45 ±0.04		AMSLER	93B	CBAR		0.0 $\overline{p}p \to \omega\pi^0\pi^0$
0.235±0.047		ATKINSON	84C	OMEG		20–70 γp
0.4 $^{+0.1}_{-0.1}$		GESSAROLI	77	HBC	−	11 $\pi^- p \to \pi^-\omega p$
0.21 ±0.08		CHUNG	75B	HBC	+	7.1 $\pi^+ p$
0.3 ±0.1		CHALOUPKA	74	HBC	−	3.9–7.5 $\pi^- p$
0.35 ±0.25	600	KARSHON	74B	HBC	+	4.9 $\pi^+ p$

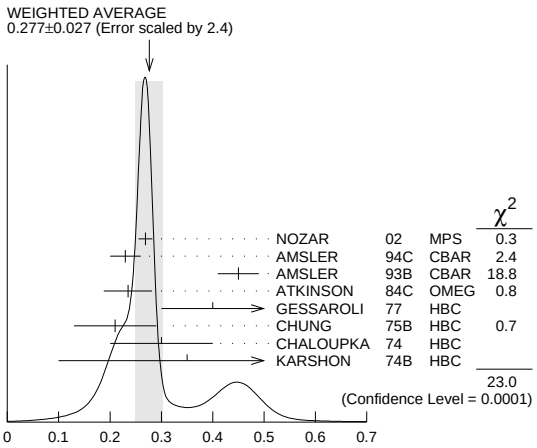

$b_1(1235)$ D-wave/S-wave amplitude ratio in decay of $b_1(1235) \to \omega\pi$

$b_1(1235)$ D-wave/S-wave AMPLITUDE PHASE DIFFERENCE IN DECAY OF $b_1(1235) \to \omega\pi$

VALUE (°)	DOCUMENT ID		TECN	CHG	COMMENT
10.5±2.4±3.9	NOZAR	02	MPS	−	18 $\pi^- p \to \omega\pi^- p$

$b_1(1235)$ BRANCHING RATIOS

$\Gamma(\eta\rho)/\Gamma(\omega\pi)$ **Γ_3/Γ_1**

VALUE	DOCUMENT ID		TECN	COMMENT
<0.10	ATKINSON	84D	OMEG	20–70 γp

$\Gamma(\pi^+\pi^+\pi^-\pi^0)/\Gamma(\omega\pi)$ **Γ_4/Γ_1**

VALUE	DOCUMENT ID		TECN	CHG	COMMENT
<0.5	ABOLINS	63	HBC	+	3.5 $\pi^+ p$

$\Gamma(K^*(892)^\pm K^\mp)/\Gamma_{\text{total}}$ **Γ_5/Γ**

VALUE	DOCUMENT ID		TECN	COMMENT
seen	[1] ABLIKIM	10E	BES2	$J/\psi \to K^\pm K^0_S \pi^\mp \pi^0$

[1] From a fit including ten additional resonances and energy-independent Breit-Wigner width.

$\Gamma((K\overline{K})^\pm\pi^0)/\Gamma(\omega\pi)$ **Γ_6/Γ_1**

VALUE	CL%	DOCUMENT ID		TECN	CHG	COMMENT
<0.08	90	BALTAY	67	HBC	±	0.0 $\overline{p}p$

$\Gamma(K^0_S K^0_L \pi^\pm)/\Gamma(\omega\pi)$ **Γ_7/Γ_1**

VALUE	CL%	DOCUMENT ID		TECN	CHG	COMMENT
<0.06	90	BALTAY	67	HBC	±	0.0 $\overline{p}p$

$\Gamma(K^0_S K^0_S \pi^\pm)/\Gamma(\omega\pi)$ **Γ_8/Γ_1**

VALUE	CL%	DOCUMENT ID		TECN	CHG	COMMENT
<0.02	90	BALTAY	67	HBC	±	0.0 $\overline{p}p$

$\Gamma(\phi\pi)/\Gamma(\omega\pi)$ **Γ_9/Γ_1**

VALUE	CL%	DOCUMENT ID		TECN	CHG	COMMENT
<0.004	95	VIKTOROV	96	SPEC	0	32.5 $\pi^- p \to K^+ K^- \pi^0 n$

• • • We do not use the following data for averages, fits, limits, etc. • • •

<0.04	95	BIZZARRI	69	HBC	± 0.0 $\overline{p}p$
<0.015		DAHL	67	HBC	1.6–4.2 $\pi^- p$

$b_1(1235)$ REFERENCES

ABLIKIM	10E	PL B693 88	M. Ablikim *et al.*	(BES II Collab.)
NOZAR	02	PL B541 35	M. Nozar *et al.*	
VIKTOROV	96	PAN 59 1184 Translated from YAF 59 1239.	V.A. Viktorov *et al.*	(SERP)
AMSLER	94C	PL B327 425	C. Amsler *et al.*	(Crystal Barrel Collab.)
AMSLER	93B	PL B311 362	C. Amsler *et al.*	(Crystal Barrel Collab.)
WEIDENAUER	93	ZPHY C59 387	P. Weidenauer *et al.*	(ASTERIX Collab.)
ALDE	92C	ZPHY C54 553	D.M. Alde *et al.*	(BELG, SERP, KEK, LANL+)
FUKUI	91	PL B257 241	S. Fukui *et al.*	(SUGI, NAGO, KEK, KYOT+)
AUGUSTIN	89	NP B320 1	J.E. Augustin, G. Cosme	(DM2 Collab.)
ATKINSON	84C	NP B243 1	M. Atkinson *et al.*	(BONN, CERN, GLAS+) JP
ATKINSON	84D	NP B242 269	M. Atkinson *et al.*	(BONN, CERN, GLAS+)
ATKINSON	84E	PL 138B 459	M. Atkinson *et al.*	(BONN, CERN, GLAS+)
COLLICK	84	PRL 53 2374	B. Collick *et al.*	(MINN, ROCH, FNAL)
EVANGELIS...	81	NP B178 197	C. Evangelista *et al.*	(BARI, BONN, CERN+)
BALTAY	78B	PR D17 62	C. Baltay *et al.*	(COLU, BING)
GESSAROLI	77	NP B126 382	R. Gessaroli *et al.*	(BGNA, FIRZ, GENO+) JP
FLATTE	76C	PL 64B 225	S.M. Flatte *et al.*	(CERN, AMST, NIJM+) JP
CHUNG	75B	PR D11 2426	S.U. Chung *et al.*	(BNL, LBL, UCSC) JP
CHALOUPKA	74	PL 51B 407	V. Chaloupka *et al.*	(CERN) JP
KARSHON	74B	PR D10 3608	U. Karshon *et al.*	(REHO) JP
BIZZARRI	69	NP B14 169	R. Bizzarri *et al.*	(CERN, CDEF)
BALTAY	67	PRL 18 93	C. Baltay *et al.*	(COLU)
DAHL	67	PR 163 1377	O.I. Dahl *et al.*	(LRL)
ABOLINS	63	PRL 11 381	M.A. Abolins *et al.*	(UCSD)

$a_1(1260)$ $I^G(J^{PC}) = 1^-(1^{++})$

See also our review under the $a_1(1260)$ in PDG 06, Journal of Physics **G33** 1 (2006).

$a_1(1260)$ MASS

VALUE (MeV)	EVTS	DOCUMENT ID		TECN	COMMENT
1230±40 OUR ESTIMATE					
1245 $^{+10}_{-16}$ OUR AVERAGE		Error includes scale factor of 1.1.			
1225± 9±20		DARGENT	17	RVUE	$D^0 \to \pi^-\pi^+\pi^-\pi^+$
1255± 6 $^{+7}_{-17}$	420k	ALEKSEEV	10	COMP	190 $\pi^- Pb \to \pi^-\pi^-\pi^+ Pb'$

• • • We do not use the following data for averages, fits, limits, etc. • • •

1243±12±20		[1] AUBERT	07AU	BABR	10.6 $e^+e^- \to \rho^0\rho^\pm\pi^\mp\gamma$
1230–1270	6360	[2] LINK	07A	FOCS	$D^0 \to \pi^-\pi^+\pi^-\pi^+$
1203± 3		[3] GOMEZ-DUM..	04	RVUE	$\tau^+ \to \pi^+\pi^+\pi^-\nu_\tau$
1330±24	90k	SALVINI	04	OBLX	$\overline{p}p \to 2\pi^+2\pi^-$
1331±10± 3	37k	[4] ASNER	00	CLE2	10.6 $e^+e^- \to \tau^+\tau^-$, $\tau^- \to \pi^-\pi^0\pi^0\nu_\tau$
1255± 7± 6	5904	[5] ABREU	98G	DLPH	e^+e^-
1207± 5± 8	5904	[6] ABREU	98G	DLPH	e^+e^-
1196± 4± 5	5904	[7,8] ABREU	98G	DLPH	e^+e^-
1240±10		BARBERIS	98B		450 $pp \to p_f\pi^+\pi^-\pi^0 p_s$
1262± 9± 7		[5,9] ACKERSTAFF	97R	OPAL	E^{ee}_{cm}= 88–94, $\tau \to 3\pi\nu$
1210± 7± 2		[6,9] ACKERSTAFF	97R	OPAL	E^{ee}_{cm}= 88–94, $\tau \to 3\pi\nu$
1211± 7 $^{+50}_{-0}$		[6] ALBRECHT	93C	ARG	$\tau^+ \to \pi^+\pi^+\pi^-\nu$
1121± 8		[10] ANDO	92	SPEC	8 $\pi^- p \to \pi^+\pi^-\pi^0 n$
1242±37		[11] IVANOV	91	RVUE	$\tau \to \pi^+\pi^+\pi^-\nu$
1260±14		[12] IVANOV	91	RVUE	$\tau \to \pi^+\pi^+\pi^-\nu$
1250± 9		[13] IVANOV	91	RVUE	$\tau \to \pi^+\pi^+\pi^-\nu$
1208±15		ARMSTRONG	90	OMEG	300.0$pp \to pp\pi^+\pi^-\pi^0$
1220±15		[14] ISGUR	89	RVUE	$\tau^+ \to \pi^+\pi^+\pi^-\nu$
1260±25		[15] BOWLER	88	RVUE	
1166±18±11		BAND	87	MAC	$\tau^+ \to \pi^+\pi^+\pi^-\nu$
1164±41±23		BAND	87	MAC	$\tau^+ \to \pi^+\pi^0\pi^0\nu$
1250±40		[14] TORNQVIST	87	RVUE	
1046±11		ALBRECHT	86B	ARG	$\tau^+ \to \pi^+\pi^+\pi^-\nu$
1056±20±15		RUCKSTUHL	86	DLCO	$\tau^+ \to \pi^+\pi^+\pi^-\nu$
1194±14±10		SCHMIDKE	86	MRK2	$\tau^+ \to \pi^+\pi^+\pi^-\nu$
1255±23		BELLINI	85	SPEC	40 $\pi^- A \to \pi^-\pi^+\pi^- A$
1240±80		[16] DANKOWY...	81	SPEC	8.45 $\pi^- p \to n3\pi$
1280±30		[16] DAUM	81B	CNTR	63,94 $\pi^- p \to p3\pi$
1041±13		[17] GAVILLET	77	HBC	4.2 $K^- p \to \Sigma 3\pi$

[1] The $\rho^\pm\pi^\mp$ state can be also due to the $\pi(1300)$.
[2] Using the Breit-Wigner parameterization; strong correlation between mass and width.
[3] Using the data of BARATE 98R.
[4] From a fit to the 3π mass spectrum including the $K\overline{K}^*(892)$ threshold.
[5] Uses the model of KUHN 90.
[6] Uses the model of ISGUR 89.
[7] Includes the effect of a possible a_1' state.
[8] Uses the model of FEINDT 90.
[9] Supersedes AKERS 95P.
[10] Average and spread of values using 2 variants of the model of BOWLER 75.
[11] Reanalysis of RUCKSTUHL 86.
[12] Reanalysis of SCHMIDKE 86.

[13] Reanalysis of ALBRECHT 86B.
[14] From a combined reanalysis of ALBRECHT 86B, SCHMIDKE 86, and RUCKSTUHL 86.
[15] From a combined reanalysis of ALBRECHT 86B and DAUM 81B.
[16] Uses the model of BOWLER 75.
[17] Produced in K^- backward scattering.

$a_1(1260)$ WIDTH

VALUE (MeV)	EVTS	DOCUMENT ID		TECN	COMMENT
250 to 600 OUR ESTIMATE					
389± 29 OUR AVERAGE	Error includes scale factor of 1.3.				
430± 24± 31		DARGENT	17	RVUE	$D^0 \to \pi^-\pi^+\pi^-\pi^+$
367± 9^{+28}_{-25}	420k	ALEKSEEV	10	COMP	190 $\pi^- Pb \to \pi^-\pi^-\pi^+ Pb'$
• • • We do not use the following data for averages, fits, limits, etc. • • •					
410± 31± 30		[18] AUBERT	07AU	BABR	10.6 $e^+e^- \to \rho^0\rho^\pm\pi^\mp\gamma$
520–680	6360	[19] LINK	07A	FOCS	$D^0 \to \pi^-\pi^+\pi^-\pi^+$
480± 20		[20] GOMEZ-DUM..	04	RVUE	$\tau^+ \to \pi^+\pi^+\pi^-\nu_\tau$
580± 41	90k	SALVINI	04	OBLX	$\bar{p}p \to 2\pi^+2\pi^-$
460± 85	205	[21] DRUTSKOY	02	BELL	$B \to D^{(*)} K^- K^{*0}$
814± 36± 13	37k	[22] ASNER	00	CLE2	10.6 $e^+e^- \to \tau^+\tau^-$, $\tau^- \to \pi^-\pi^0\pi^0\nu_\tau$
450± 50	22k	[23] AKHMETSHIN	99E	CMD2	1.05–1.38 $e^+e^- \to \pi^+\pi^-\pi^0\pi^0$
570± 10		[24] BONDAR	99	RVUE	$e^+e^- \to 4\pi$, $\tau \to 3\pi\nu_\tau$
587± 27± 21	5904	[25] ABREU	98G	DLPH	e^+e^-
478± 3± 15	5904	[26] ABREU	98G	DLPH	e^+e^-
425± 14± 8	5904	[27,28] ABREU	98G	DLPH	e^+e^-
400± 35		BARBERIS	98B		450 $pp \to p_f\pi^+\pi^-\pi^0 p_s$
621± 32± 58		[25,29] ACKERSTAFF	97R	OPAL	E^{ee}_{cm} = 88–94, $\tau \to 3\pi\nu$
457± 15± 17		[26,29] ACKERSTAFF	97R	OPAL	E^{ee}_{cm} = 88–94, $\tau \to 3\pi\nu$
446± 21$^{+140}_{-0}$		[26] ALBRECHT	93C	ARG	$\tau^+ \to \pi^+\pi^+\pi^-\nu$
239± 11		ANDO	92	SPEC	8 $\pi^- p \to \pi^+\pi^-\pi^0 n$
266± 13± 4		[30] ANDO	92	SPEC	8 $\pi^- p \to \pi^+\pi^-\pi^0 n$
465$^{+228}_{-143}$		[31] IVANOV	91	RVUE	$\tau \to \pi^+\pi^+\pi^-\nu$
298$^{+40}_{-34}$		[32] IVANOV	91	RVUE	$\tau \to \pi^+\pi^+\pi^-\nu$
488± 32		[33] IVANOV	91	RVUE	$\tau \to \pi^+\pi^+\pi^-\nu$
430± 50		ARMSTRONG	90	OMEG	300.0 $pp \to pp\pi^+\pi^-\pi^0$
420± 40		[34] ISGUR	89	RVUE	$\tau^+ \to \pi^+\pi^+\pi^-\nu$
396± 43		[35] BOWLER	88	RVUE	
405± 75± 25		BAND	87	MAC	$\tau^+ \to \pi^+\pi^+\pi^-\nu$
419±108± 57		BAND	87	MAC	$\tau^+ \to \pi^+\pi^0\pi^0\nu$
521± 27		ALBRECHT	86B	ARG	$\tau^+ \to \pi^+\pi^+\pi^-\nu$
476$^{+132}_{-120}$± 54		RUCKSTUHL	86	DLCO	$\tau^+ \to \pi^+\pi^+\pi^-\nu$
462± 56± 30		SCHMIDKE	86	MRK2	$\tau^+ \to \pi^+\pi^+\pi^-\nu$
292± 40		BELLINI	85	SPEC	40 $\pi^- A \to \pi^-\pi^+\pi^- A$
380±100		[36] DANKOWY...	81	SPEC	8.45 $\pi^- p \to n3\pi$
300± 50		[36] DAUM	81B	CNTR	63,94 $\pi^- p \to p3\pi$
230± 50		[37] GAVILLET	77	HBC	4.2 $K^- p \to \Sigma 3\pi$

[18] The $\rho^\pm\pi^\mp$ state can be also due to the $\pi(1300)$.
[19] Using the Breit-Wigner parameterization; strong correlation between mass and width.
[20] Using the data of BARATE 98R.
[21] From a fit of the $K^- K^{*0}$ distribution assuming m_{a_1} = 1230 MeV and purely resonant production of the $K^- K^{*0}$ system.
[22] From a fit to the 3π mass spectrum including the $K\overline{K}^*(892)$ threshold.
[23] Using the $a_1(1260)$ mass of 1230 MeV.
[24] From AKHMETSHIN 99E and ASNER 00 data using the $a_1(1260)$ mass of 1230 MeV.
[25] Uses the model of KUHN 90.
[26] Uses the model of ISGUR 89.
[27] Includes the effect of a possible a_1' state.
[28] Uses the model of FEINDT 90.
[29] Supersedes AKERS 95P.
[30] Average and spread of values using 2 variants of the model of BOWLER 75.
[31] Reanalysis of RUCKSTUHL 86.
[32] Reanalysis of SCHMIDKE 86.
[33] Reanalysis of ALBRECHT 86B.
[34] From a combined reanalysis of ALBRECHT 86B, SCHMIDKE 86, and RUCKSTUHL 86.
[35] From a combined reanalysis of ALBRECHT 86B and DAUM 81B.
[36] Uses the model of BOWLER 75.
[37] Produced in K^- backward scattering.

$a_1(1260)$ DECAY MODES

	Mode	Fraction (Γ_i/Γ)
Γ_1	$\pi^+\pi^-\pi^0$	
Γ_2	$\pi^0\pi^0\pi^0$	
Γ_3	$(\rho\pi)_{S-\text{wave}}$	seen
Γ_4	$(\rho\pi)_{D-\text{wave}}$	seen
Γ_5	$(\rho(1450)\pi)_{S-\text{wave}}$	seen
Γ_6	$(\rho(1450)\pi)_{D-\text{wave}}$	seen
Γ_7	$\sigma\pi$	seen
Γ_8	$f_0(980)\pi$	not seen
Γ_9	$f_0(1370)\pi$	seen
Γ_{10}	$f_2(1270)\pi$	seen
Γ_{11}	$K\overline{K}^*(892)$ + c.c.	seen
Γ_{12}	$\pi\gamma$	seen

$a_1(1260)$ PARTIAL WIDTHS

$\Gamma(\pi\gamma)$ Γ_{12}

VALUE (keV)	DOCUMENT ID		TECN	COMMENT
640±246	ZIELINSKI	84C	SPEC	200 π^+ Z $\to$ Z3π

D-wave/S-wave AMPLITUDE RATIO IN DECAY OF $a_1(1260) \to \rho\pi$

VALUE	DOCUMENT ID		TECN	COMMENT
−0.062±0.020 OUR AVERAGE	Error includes scale factor of 2.3. See the ideogram below.			
−0.043±0.009±0.005	LINK	07A	FOCS	$D^0 \to \pi^-\pi^+\pi^-\pi^+$
−0.14 ±0.04 ±0.07	[38] CHUNG	02	B852	18.3 $\pi^- p \to \pi^+\pi^-\pi^- p$
−0.10 ±0.02 ±0.02	[39,40] ACKERSTAFF	97R	OPAL	E^{ee}_{cm} = 88–94, $\tau \to 3\pi\nu$
−0.11 ±0.02	[39] ALBRECHT	93C	ARG	$\tau^+ \to \pi^+\pi^+\pi^-\nu$

[38] Deck-type background not subtracted.
[39] Uses the model of ISGUR 89.
[40] Supersedes AKERS 95P.

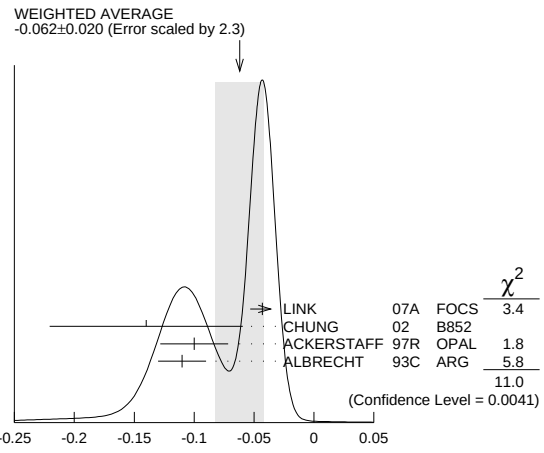

D-wave/S-wave AMPLITUDE RATIO IN DECAY OF $a_1(1260) \to \rho\pi$

$a_1(1260)$ BRANCHING RATIOS

$\Gamma((\rho\pi)_{S-\text{wave}})/\Gamma_{\text{total}}$ Γ_3/Γ

VALUE (units 10^{-2})	EVTS	DOCUMENT ID		TECN	COMMENT
• • • We do not use the following data for averages, fits, limits, etc. • • •					
60.19	37k	[41] ASNER	00	CLE2	10.6 $e^+e^- \to \tau^+\tau^-$, $\tau^- \to \pi^-\pi^0\pi^0\nu_\tau$

$\Gamma((\rho\pi)_{D-\text{wave}})/\Gamma_{\text{total}}$ Γ_4/Γ

VALUE (units 10^{-2})	EVTS	DOCUMENT ID		TECN	COMMENT
• • • We do not use the following data for averages, fits, limits, etc. • • •					
1.30±0.60±0.22	37k	[41] ASNER	00	CLE2	10.6 $e^+e^- \to \tau^+\tau^-$, $\tau^- \to \pi^-\pi^0\pi^0\nu_\tau$

$\Gamma((\rho(1450)\pi)_{S-\text{wave}})/\Gamma_{\text{total}}$ Γ_5/Γ

VALUE (units 10^{-2})	EVTS	DOCUMENT ID		TECN	COMMENT
• • • We do not use the following data for averages, fits, limits, etc. • • •					
0.56±0.84±0.32	37k	[41,42] ASNER	00	CLE2	10.6 $e^+e^- \to \tau^+\tau^-$, $\tau^- \to \pi^-\pi^0\pi^0\nu_\tau$

$\Gamma((\rho(1450)\pi)_{D-\text{wave}})/\Gamma_{\text{total}}$ Γ_6/Γ

VALUE (units 10^{-2})	EVTS	DOCUMENT ID		TECN	COMMENT
• • • We do not use the following data for averages, fits, limits, etc. • • •					
2.04±1.20±0.28	37k	[41,42] ASNER	00	CLE2	10.6 $e^+e^- \to \tau^+\tau^-$, $\tau^- \to \pi^-\pi^0\pi^0\nu_\tau$

$\Gamma(\sigma\pi)/\Gamma_{\text{total}}$ Γ_7/Γ

VALUE (units 10^{-2})	EVTS	DOCUMENT ID		TECN	COMMENT
• • • We do not use the following data for averages, fits, limits, etc. • • •					
seen		CHUNG	02	B852	18.3 $\pi^- p \to \pi^+\pi^-\pi^- p$
18.76±4.29±1.48	37k	[41,43] ASNER	00	CLE2	10.6 $e^+e^- \to \tau^+\tau^-$, $\tau^- \to \pi^-\pi^0\pi^0\nu_\tau$

Meson Particle Listings

$a_1(1260)$, $f_2(1270)$

$\Gamma(f_0(980)\pi)/\Gamma_{total}$ Γ_8/Γ

VALUE (units 10^{-2})	EVTS	DOCUMENT ID		TECN	COMMENT
• • • We do not use the following data for averages, fits, limits, etc. • • •					
not seen	37k	ASNER	00	CLE2	10.6 $e^+e^- \to \tau^+\tau^-$, $\tau^- \to \pi^-\pi^0\pi^0\nu_\tau$

$\Gamma(f_0(1370)\pi)/\Gamma_{total}$ Γ_9/Γ

VALUE (units 10^{-2})	EVTS	DOCUMENT ID		TECN	COMMENT
• • • We do not use the following data for averages, fits, limits, etc. • • •					
$7.40\pm2.71\pm1.26$	37k	[41,44] ASNER	00	CLE2	10.6 $e^+e^- \to \tau^+\tau^-$, $\tau^- \to \pi^-\pi^0\pi^0\nu_\tau$

$\Gamma(f_2(1270)\pi)/\Gamma_{total}$ Γ_{10}/Γ

VALUE (units 10^{-2})	EVTS	DOCUMENT ID		TECN	COMMENT
• • • We do not use the following data for averages, fits, limits, etc. • • •					
$1.19\pm0.49\pm0.17$	37k	[41,45] ASNER	00	CLE2	10.6 $e^+e^- \to \tau^+\tau^-$, $\tau^- \to \pi^-\pi^0\pi^0\nu_\tau$

$\Gamma(K\overline{K}^*(892)+\text{c.c.})/\Gamma_{total}$ Γ_{11}/Γ

VALUE (units 10^{-2})	EVTS	DOCUMENT ID		TECN	COMMENT
• • • We do not use the following data for averages, fits, limits, etc. • • •					
2.2 ± 0.5	2255	[46] COAN	04	CLEO	$\tau^- \to K^-\pi^-K^+\nu_\tau$
8 to 15	205	[47] DRUTSKOY	02	BELL	$B \to D^{(*)}K^-K^{*0}$
$3.3\pm0.5\pm0.1$	37k	[48] ASNER	00	CLE2	10.6 $e^+e^- \to \tau^+\tau^-$, $\tau^- \to \pi^-\pi^0\pi^0\nu_\tau$
2.6 ± 0.3		[49] BARATE	99R	ALEP	$\tau \to K\overline{K}\pi\nu_\tau$

$\Gamma(\sigma\pi)/\Gamma((\rho\pi)_{S-wave})$ Γ_7/Γ_3

VALUE	EVTS	DOCUMENT ID		TECN	COMMENT
• • • We do not use the following data for averages, fits, limits, etc. • • •					
$0.06\ \pm0.05$	90k	SALVINI	04	OBLX	$\overline{p}p \to 2\pi^+2\pi^-$
~ 0.3	28k	AKHMETSHIN	99E	CMD2	1.05–1.38 $e^+e^- \to \pi^+\pi^-\pi^+\pi^-$
0.003 ± 0.003		[50] LONGACRE	82	RVUE	

$\Gamma(\pi^0\pi^0\pi^0)/\Gamma(\pi^+\pi^-\pi^0)$ Γ_2/Γ_1

VALUE	CL%	DOCUMENT ID		COMMENT
• • • We do not use the following data for averages, fits, limits, etc. • • •				
<0.008	90	[51] BARBERIS	01	450 $pp \to p_f 3\pi^0 p_s$

[41] From a fit to the Dalitz plot.
[42] Assuming for $\rho(1450)$ mass and width of 1370 and 386 MeV respectively.
[43] Assuming for σ mass and width of 860 and 880 MeV respectively.
[44] Assuming for $f_0(1370)$ mass and width of 1186 and 350 MeV respectively.
[45] Assuming for $f_2(1270)$ mass and width of 1275 and 185 MeV respectively.
[46] Using structure functions from KUHN 92 and DECKER 93A and B($\tau^- \to K^-\pi^-K^+\nu_\tau$) = (0.155 ± 0.006 ± 0.009)% from BRIERE 03.
[47] From a comparison to ALAM 94 assuming purely resonant production of the K^-K^{*0} system.
[48] From a fit to the 3π mass spectrum including the $K\overline{K}^*(892)$ threshold.
[49] Assuming $a_1(1260)$ dominance and taking B($\tau \to a_1(1260)\nu_\tau$) from BUSKULIC 96.
[50] Uses multichannel Aitchison-Bowler model (BOWLER 75). Uses data from GAVILLET 77, DAUM 80, and DANKOWYCH 81.
[51] Inconsistent with observations of $\sigma\pi$, $f_0(1370)\pi$, and $f_2(1270)\pi$ decay modes.

$a_1(1260)$ REFERENCES

DARGENT	17	JHEP 1705 143	P. dArgent *et al.*	(HEID, BRIS)
ALEKSEEV	10	PRL 104 241803	M.G. Alekseev *et al.*	(COMPASS Collab.)
AUBERT	07AU	PR D76 092005	B. Aubert *et al.*	(BABAR Collab.)
LINK	07A	PR D75 052003	J.M. Link *et al.*	(FNAL FOCUS Collab.)
PDG	06	JP G33 1	W.-M. Yao *et al.*	(PDG Collab.)
COAN	04	PRL 92 232001	T.E. Coan *et al.*	(CLEO Collab.)
GOMEZ-DUM...	04	PR D69 073002	D. Gomez Dumm, A. Pich, J. Portoles	
SALVINI	04	EPJ C35 21	P. Salvini *et al.*	(OBELIX Collab.)
BRIERE	03	PRL 90 181802	R. A. Briere *et al.*	(CLEO Collab.)
CHUNG	02	PR D65 072001	S.U. Chung *et al.*	(BNL E852 Collab.)
DRUTSKOY	02	PL B542 171	A. Drutskoy *et al.*	(BELLE Collab.)
BARBERIS	01	PL B507 14	D. Barberis *et al.*	
ASNER	00	PR D61 012002	D.M. Asner *et al.*	(CLEO Collab.)
AKHMETSHIN	99E	PL B466 392	R.R. Akhmetshin *et al.*	(Novosibirsk CMD-2 Collab.)
BARATE	99R	EPJ C11 599	R. Barate *et al.*	(ALEPH Collab.)
BONDAR	99	PL B466 403	A.E. Bondar *et al.*	(Novosibirsk CMD-2 Collab.)
ABREU	98G	PL B426 411	P. Abreu *et al.*	(DELPHI Collab.)
BARATE	98R	EPJ C4 409	R. Barate *et al.*	(ALEPH Collab.)
BARBERIS	98B	PL B422 399	D. Barberis *et al.*	(WA 102 Collab.)
ACKERSTAFF	97R	ZPHY C75 593	K. Ackerstaff *et al.*	(OPAL Collab.)
BUSKULIC	96	ZPHY C70 579	D. Buskulic *et al.*	(ALEPH Collab.)
AKERS	95P	ZPHY C67 45	R. Akers *et al.*	(OPAL Collab.)
ALAM	94	PR D50 43	M.S. Alam *et al.*	(CLEO Collab.)
ALBRECHT	93C	ZPHY C58 61	H. Albrecht *et al.*	(ARGUS Collab.)
DECKER	93A	ZPHY C58 445	R. Decker *et al.*	
ANDO	92	PL B291 496	A. Ando *et al.*	(KEK, KYOT, NIRS, SAGA+)
KUHN	92	ZPHY C56 661	J.H. Kuhn, E. Mirkes	
IVANOV	91	ZPHY C49 563	Y.P. Ivanov, A.A. Osipov, M.K. Volkov	(JINR)
ARMSTRONG	90	ZPHY C48 213	T.A. Armstrong, M. Benayoun, W. Beusch	(WA76 Coll.)
FEINDT	90	ZPHY C48 681	M. Feindt	(HAMB)
KUHN	90	ZPHY C48 445	J.H. Kuhn *et al.*	(MPIM)
ISGUR	89	PR D39 1357	N. Isgur, C. Morningstar, C. Reader	(TNTO)
BOWLER	88	PL B209 99	M.G. Bowler	(OXF)
BAND	87	PL B198 297	H.R. Band *et al.*	(MAC Collab.)
TORNQVIST	87	ZPHY C36 695	N.A. Tornqvist	(HELS)
ALBRECHT	86B	ZPHY C33 7	H. Albrecht *et al.*	(ARGUS Collab.)
RUCKSTUHL	86	PRL 56 2132	W. Ruckstuhl *et al.*	(DELCO Collab.)
SCHMIDKE	86	PRL 57 527	W.B. Schmidke *et al.*	(Mark II Collab.)
BELLINI	85	SJNP 41 781 Translated from YAF 41 1223.	D. Bellini *et al.*	
ZIELINSKI	84C	PRL 52 1195	M. Zielinski *et al.*	(ROCH, MINN, FNAL)
LONGACRE	82	PR D26 82	R.S. Longacre	(BNL)
DANKOWY...	81	PRL 46 580	J.A. Dankowych *et al.*	(TNTO, BNL, CARL+)
DAUM	81B	NP B182 269	C. Daum *et al.*	(AMST, CERN, CRAC, MPIM+)
DAUM	80	PL 89B 281	C. Daum *et al.*	(AMST, CERN, CRAC, MPIM+) JP
GAVILLET	77	PL 69B 119	P. Gavillet *et al.*	(AMST, CERN, NIJM+) JP
BOWLER	75	NP B97 227	M.G. Bowler *et al.*	(OXFTP, DARE)

$f_2(1270)$ $I^G(J^{PC}) = 0^+(2^{++})$

$f_2(1270)$ MASS

VALUE (MeV)	EVTS	DOCUMENT ID		TECN	COMMENT
1275.5± 0.8 OUR AVERAGE					
$1275.8\pm1.0\pm0.4$		[1] BOGOLYUB...	13	SPEC	$7\pi^+(K^+,p)A \to n\gamma + X$
$1262\ ^{+1}_{-2}\ \pm8$		ABLIKIM	06V	BES2	$e^+e^- \to J/\psi \to \gamma\pi^+\pi^-$
$1275\ \pm15$		ABLIKIM	05	BES2	$J/\psi \to \phi\pi^+\pi^-$
$1283\ \pm5$		ALDE	98	GAM4	100 $\pi^-p \to \pi^0\pi^0n$
$1278\ \pm5$		[2] BERTIN	97C	OBLX	0.0 $\overline{p}p \to \pi^+\pi^-\pi^0$
$1272\ \pm8$	200k	PROKOSHKIN	94	GAM2	38 $\pi^-p \to \pi^0\pi^0n$
1269.7 ± 5.2	5730	AUGUSTIN	89	DM2	$e^+e^- \to 5\pi$
$1283\ \pm8$	400	[3] ALDE	87	GAM4	100 $\pi^-p \to 4\pi^0n$
$1274\ \pm5$		[3] AUGUSTIN	87	DM2	$J/\psi \to \gamma\pi^+\pi^-$
$1283\ \pm6$		[4] LONGACRE	86	MPS	22 $\pi^-p \to n2K^0_S$
$1276\ \pm7$		COURAU	84	DLCO	$e^+e^- \to e^+e^-\pi^+\pi^-$
1273.3 ± 2.3		[5] CHABAUD	83	ASPK	17 π^-p polarized
$1280\ \pm4$		[6] CASON	82	STRC	8 $\pi^+p \to \Delta^{++}\pi^0\pi^0$
$1281\ \pm7$	11600	GIDAL	81	MRK2	J/ψ decay
$1282\ \pm5$		[7] CORDEN	79	OMEG	12–15 $\pi^-p \to n2\pi$
$1269\ \pm4$	10k	APEL	75	NICE	40 $\pi^-p \to n2\pi^0$
$1272\ \pm4$	4600	ENGLER	74	DBC	6 $\pi^+n \to \pi^+\pi^-p$
$1277\ \pm4$	5300	FLATTE	71	HBC	7.0 π^+p
$1273\ \pm8$		[3] STUNTEBECK	70	HBC	8 π^-p, 5.4 π^+d
$1265\ \pm8$		BOESEBECK	68	HBC	8 π^+p
• • • We do not use the following data for averages, fits, limits, etc. • • •					
$1259\ \pm4\ \pm4$	1.7k	[8,9] DOBBS	15		$J/\psi \to \gamma\pi^+\pi^-$
$1267\ \pm4\ \pm3$	1.5k	[8,9] DOBBS	15		$\psi(2S) \to \gamma\pi^+\pi^-$
$1270\ \pm8$		[10] ANISOVICH	09	RVUE	0.0 $\overline{p}p$, πN
$1277\ \pm6$	870	[11] SCHEGELSKY	06A	RVUE	$\gamma\gamma \to K^0_SK^0_S$
$1251\ \pm10$		TIKHOMIROV	03	SPEC	40.0 $\pi^-C \to K^0_SK^0_SK^0_LX$
$1260\ \pm10$		[12] ALDE	97	GAM2	450 $pp \to pp\pi^0\pi^0$
$1278\ \pm6$		[12] GRYGOREV	96	SPEC	40 $\pi^-N \to K^0_SK^0_SX$
$1262\ \pm11$		AGUILAR-...	91	EHS	400 pp
$1275\ \pm10$		AKER	91	CBAR	0.0 $\overline{p}p \to 3\pi^0$
$1220\ \pm10$		BREAKSTONE	90	SFM	$pp \to pp\pi^+\pi^-$
$1288\ \pm12$		ABACHI	86B	HRS	$e^+e^- \to \pi^+\pi^-X$
$1284\ \pm30$	3k	BINON	83	GAM2	38 $\pi^-p \to n2\eta$
$1280\ \pm20$	3k	APEL	82	CNTR	25 $\pi^-p \to n2\pi^0$
$1284\ \pm10$	16000	DEUTSCH...	76	HBC	16 π^+p
$1258\ \pm10$	600	TAKAHASHI	72	HBC	8 $\pi^-p \to n2\pi$
$1275\ \pm13$		ARMENISE	70	HBC	9 $\pi^+n \to p\pi^+\pi^-$
$1261\ \pm5$	1960	[3] ARMENISE	68	DBC	5.1 $\pi^+n \to p\pi^+$ MM$^-$
$1270\ \pm10$	360	[3] ARMENISE	68	DBC	5.1 $\pi^+n \to p\pi^0$ MM
$1268\ \pm6$		[13] JOHNSON	68	HBC	3.7–4.2 π^-p

[1] Averaged over six nuclear targets, no statistically significant dependence on target nucleus observed.
[2] T-matrix pole.
[3] Mass errors enlarged by us to $\Gamma/\sqrt{N}$; see the note with the $K^*(892)$ mass.
[4] From a partial-wave analysis of data using a K-matrix formalism with 5 poles.
[5] From an energy-independent partial-wave analysis.
[6] From an amplitude analysis of the reaction $\pi^+\pi^- \to 2\pi^0$.
[7] From an amplitude analysis of $\pi^+\pi^- \to \pi^+\pi^-$ scattering data.
[8] Using CLEO-c data but not authored by the CLEO Collaboration.
[9] From a fit to a Breit-Wigner line shape with fixed $\Gamma = 185$ MeV.
[10] 4-poles, 5-channel K matrix fit.
[11] From analysis of L3 data at 91 and 183–209 GeV.
[12] Systematic uncertainties not estimated.
[13] JOHNSON 68 includes BONDAR 63, LEE 64, DERADO 65, EISNER 67.

$f_2(1270)$ WIDTH

VALUE (MeV)	EVTS	DOCUMENT ID		TECN	COMMENT
$186.7^{+2.2}_{-2.5}$ OUR FIT Error includes scale factor of 1.4.					
$185.9^{+2.8}_{-2.1}$ OUR AVERAGE Error includes scale factor of 1.6. See the ideogram below.					
$190.3\pm1.9\pm1.8$		[1] BOGOLYUB...	13	SPEC	$7\pi^+(K^+,p)A \to n\gamma + X$
$175\ ^{+6}_{-4}\ \pm10$		ABLIKIM	06V	BES2	$e^+e^- \to J/\psi \to \gamma\pi^+\pi^-$
$190\ \pm20$		ABLIKIM	05	BES2	$J/\psi \to \phi\pi^+\pi^-$

See key on page 885

171	±10			ALDE	98	GAM4	100 $\pi^- p \to \pi^0\pi^0 n$
204	±20		[2]	BERTIN	97C	OBLX	0.0 $\overline{p}p \to \pi^+\pi^-\pi^0$
192	± 5	200k		PROKOSHKIN	94	GAM2	38 $\pi^- p \to \pi^0\pi^0 n$
180	±24			AGUILAR-...	91	EHS	400 pp
169	± 9	5730	[3]	AUGUSTIN	89	DM2	$e^+e^- \to 5\pi$
150	±30	400	[3]	ALDE	87	GAM4	100 $\pi^- p \to 4\pi^0 n$
186	$^{+\ 9}_{-\ 2}$		[4]	LONGACRE	86	MPS	22 $\pi^- p \to n 2K^0_S$
179.2	$^{+\ 6.9}_{-\ 6.6}$		[5]	CHABAUD	83	ASPK	17 $\pi^- p$ polarized
160	±11			DENNEY	83	LASS	10 $\pi^+ N$
196	±10	3k		APEL	82	CNTR	25 $\pi^- p \to n 2\pi^0$
152	± 9		[6]	CASON	82	STRC	8 $\pi^+ p \to \Delta^{++}\pi^0\pi^0$
186	±27	11600		GIDAL	81	MRK2	J/ψ decay
216	±13		[7]	CORDEN	79	OMEG	12–15 $\pi^- p \to n 2\pi$
190	±10	10k		APEL	75	NICE	40 $\pi^- p \to n 2\pi^0$
192	±16	4600		ENGLER	74	DBC	6 $\pi^+ n \to \pi^+\pi^- p$
183	±15	5300		FLATTE	71	HBC	7 $\pi^+ p \to \Delta^{++} f_2$
196	±30		[3]	STUNTEBECK	70	HBC	8 $\pi^- p$, 5.4 $\pi^+ d$
216	±20	1960	[3]	ARMENISE	68	DBC	5.1 $\pi^+ n \to p\pi^+$ MM$^-$
128	±27		[3]	BOESEBECK	68	HBC	8 $\pi^+ p$
176	±21		[3,8]	JOHNSON	68	HBC	3.7–4.2 $\pi^- p$
• • • We do not use the following data for averages, fits, limits, etc. • • •							
194	±36		[9]	ANISOVICH	09	RVUE	0.0 $\overline{p}p$, πN
195	±15	870	[10]	SCHEGELSKY	06A	RVUE	$\gamma\gamma \to K^0_S K^0_S$
121	±26			TIKHOMIROV	03	SPEC	40.0 π^- C $\to K^0_S K^0_S K^0_L$ X
187	±20		[11]	ALDE	97	GAM2	450 $pp \to pp\pi^0\pi^0$
184	±10		[11]	GRYGOREV	96	SPEC	40 $\pi^- N \to K^0_S K^0_S$ X
200	±10			AKER	91	CBAR	0.0 $\overline{p}p \to 3\pi^0$
240	±40	3k		BINON	83	GAM2	38 $\pi^- p \to n 2\eta$
187	±30	650	[3]	ANTIPOV	77	CIBS	25 $\pi^- p \to p 3\pi$
225	±38	16000		DEUTSCH...	76	HBC	16 $\pi^+ p$
166	±28	600	[3]	TAKAHASHI	72	HBC	8 $\pi^- p \to n 2\pi$
173	±53		[3]	ARMENISE	70	HBC	9 $\pi^+ n \to p\pi^+\pi^-$

[1] Averaged over six nuclear targets, no statistically significant dependence on target nucleus observed.
[2] T-matrix pole.
[3] Width errors enlarged by us to $4\Gamma/\sqrt{N}$; see the note with the $K^*(892)$ mass.
[4] From a partial-wave analysis of data using a K-matrix formalism with 5 poles.
[5] From an energy-independent partial-wave analysis.
[6] From an amplitude analysis of the reaction $\pi^+\pi^- \to 2\pi^0$.
[7] From an amplitude analysis of $\pi^+\pi^- \to \pi^+\pi^-$ scattering data.
[8] JOHNSON 68 includes BONDAR 63, LEE 64, DERADO 65, EISNER 67.
[9] 4-poles, 5-channel K matrix fit.
[10] From analysis of L3 data at 91 and 183–209 GeV.
[11] Systematic uncertainties not estimated.

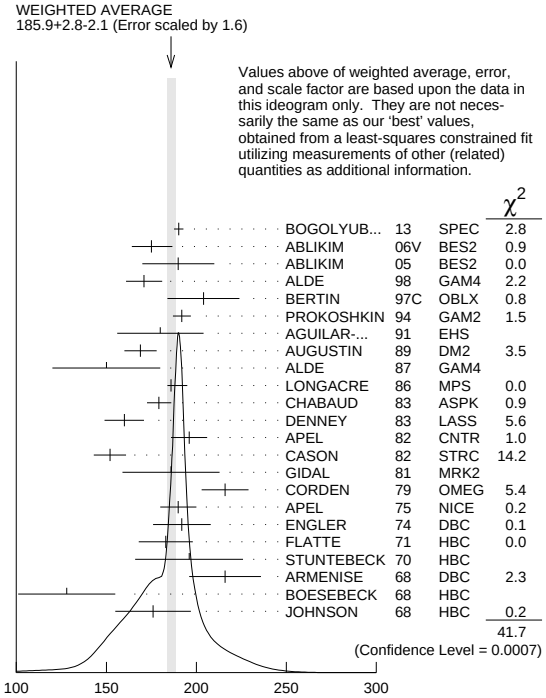

$f_2(1270)$ DECAY MODES

	Mode	Fraction (Γ_i/Γ)	Scale factor/ Confidence level
Γ_1	$\pi\pi$	(84.2 $^{+2.9}_{-0.9}$) %	S=1.1
Γ_2	$\pi^+\pi^- 2\pi^0$	(7.7 $^{+1.1}_{-3.2}$) %	S=1.2
Γ_3	$K\overline{K}$	(4.6 $^{+0.5}_{-0.4}$) %	S=2.7
Γ_4	$2\pi^+ 2\pi^-$	(2.8 ±0.4) %	S=1.2
Γ_5	$\eta\eta$	(4.0 ±0.8) $\times 10^{-3}$	S=2.1
Γ_6	$4\pi^0$	(3.0 ±1.0) $\times 10^{-3}$	
Γ_7	$\gamma\gamma$	(1.42±0.24) $\times 10^{-5}$	S=1.4
Γ_8	$\eta\pi\pi$	< 8 $\times 10^{-3}$	CL=95%
Γ_9	$K^0 K^-\pi^+$ + c.c.	< 3.4 $\times 10^{-3}$	CL=95%
Γ_{10}	$e^+ e^-$	< 6 $\times 10^{-10}$	CL=90%

CONSTRAINED FIT INFORMATION

An overall fit to the total width, 4 partial widths, a combination of partial widths obtained from integrated cross sections, and 6 branching ratios uses 45 measurements and one constraint to determine 8 parameters. The overall fit has a $\chi^2 = 83.0$ for 38 degrees of freedom.

The following *off-diagonal* array elements are the correlation coefficients $\langle \delta p_i \delta p_j \rangle / (\delta p_i \cdot \delta p_j)$, in percent, from the fit to parameters p_i, including the branching fractions, $x_i \equiv \Gamma_i/\Gamma_{\text{total}}$. The fit constrains the x_i whose labels appear in this array to sum to one.

	x_1	x_2	x_3	x_4	x_5	x_6	x_7
x_2	−90						
x_3	10	−39					
x_4	10	−38	1				
x_5	1	−6	0	0			
x_6	0	−7	0	0	0		
x_7	3	1	−15	0	0	0	
Γ	−71	65	−10	−7	−1	0	−6

	Mode	Rate (MeV)	Scale factor
Γ_1	$\pi\pi$	157.2 $^{+4.0}_{-1.1}$	
Γ_2	$\pi^+\pi^- 2\pi^0$	14.4 $^{+2.1}_{-6.0}$	1.2
Γ_3	$K\overline{K}$	8.5 ±0.8	2.8
Γ_4	$2\pi^+ 2\pi^-$	5.2 ±0.7	1.2
Γ_5	$\eta\eta$	0.75 ±0.14	2.1
Γ_6	$4\pi^0$	0.56 ±0.19	
Γ_7	$\gamma\gamma$	0.0026±0.0005	1.4

$f_2(1270)$ PARTIAL WIDTHS

$\Gamma(\pi\pi)$ Γ_1

VALUE (MeV)	EVTS	DOCUMENT ID		TECN	COMMENT
157.2 $^{+4.0}_{-1.1}$ OUR FIT					
157.0 $^{+6.0}_{-1.0}$		[1] LONGACRE	86	MPS	22 $\pi^- p \to n 2K^0_S$
• • • We do not use the following data for averages, fits, limits, etc. • • •					
152 ±8	870	[2] SCHEGELSKY	06A	RVUE	$\gamma\gamma \to K^0_S K^0_S$

$\Gamma(K\overline{K})$ Γ_3

VALUE (MeV)	EVTS	DOCUMENT ID		TECN	COMMENT
8.5 ±0.8 OUR FIT Error includes scale factor of 2.8.					
9.0 $^{+0.7}_{-0.3}$		[1] LONGACRE	86	MPS	22 $\pi^- p \to n 2K^0_S$
• • • We do not use the following data for averages, fits, limits, etc. • • •					
7.5 ±2.0	870	[2] SCHEGELSKY	06A	RVUE	$\gamma\gamma \to K^0_S K^0_S$

$\Gamma(\eta\eta)$ Γ_5

VALUE (MeV)	EVTS	DOCUMENT ID		TECN	COMMENT
0.75 ±0.14 OUR FIT Error includes scale factor of 2.1.					
1.0 ±0.1		[1] LONGACRE	86	MPS	22 $\pi^- p \to n 2K^0_S$
• • • We do not use the following data for averages, fits, limits, etc. • • •					
1.8 ±0.4	870	[2] SCHEGELSKY	06A	RVUE	$\gamma\gamma \to K^0_S K^0_S$

$\Gamma(\gamma\gamma)$ Γ_7

The value of this width depends on the theoretical model used. Unitary approaches with scalars typically (with exception of PENNINGTON 08) give values clustering

around 2.6 keV; without an S-wave contribution, values are systematically higher (typically around 3 keV).

VALUE (keV)	EVTS	DOCUMENT ID		TECN	COMMENT
2.6 ±0.5 OUR FIT		Error includes scale factor of 1.4.			
2.93±0.40		[3] DAI	14A	RVUE	Compilation
• • • We do not use the following data for averages, fits, limits, etc. • • •					
3.14±0.20		[4,5] PENNINGTON	08	RVUE	Compilation
3.82±0.30		[5,6] PENNINGTON	08	RVUE	Compilation
2.55±0.15	870	[2] SCHEGELSKY	06A	RVUE	$\gamma\gamma \to K^0_S K^0_S$
2.84±0.35		BOGLIONE	99	RVUE	$\gamma\gamma \to \pi^+\pi^-, \pi^0\pi^0$
2.93±0.23±0.32		[7] YABUKI	95	VNS	
$2.58\pm0.13^{+0.36}_{-0.27}$		[8] BEHREND	92	CELL	$e^+e^- \to e^+e^-\pi^+\pi^-$
3.10±0.35±0.35		[9] BLINOV	92	MD1	$e^+e^- \to e^+e^-\pi^+\pi^-$
2.27±0.47±0.11		ADACHI	90D	TOPZ	$e^+e^- \to e^+e^-\pi^+\pi^-$
3.15±0.04±0.39		BOYER	90	MRK2	$e^+e^- \to e^+e^-\pi^+\pi^-$
$3.19\pm0.16^{+0.29}_{-0.28}$		MARSISKE	90	CBAL	$e^+e^- \to e^+e^-\pi^0\pi^0$
2.35±0.65		[10] MORGAN	90	RVUE	$\gamma\gamma \to \pi^+\pi^-, \pi^0\pi^0$
$3.19\pm0.09^{+0.22}_{-0.38}$	2177	OEST	90	JADE	$e^+e^- \to e^+e^-\pi^0\pi^0$
3.2 ±0.1 ±0.4		[11] AIHARA	86B	TPC	$e^+e^- \to e^+e^-\pi^+\pi^-$
2.5 ±0.1 ±0.5		BEHREND	84B	CELL	$e^+e^- \to e^+e^-\pi^+\pi^-$
2.85±0.25±0.5		[12] BERGER	84	PLUT	$e^+e^- \to e^+e^-2\pi$
2.70±0.05±0.20		COURAU	84	DLCO	$e^+e^- \to e^+e^-\pi^+\pi^-$
2.52±0.13±0.38		[13] SMITH	84C	MRK2	$e^+e^- \to e^+e^-\pi^+\pi^-$
2.7 ±0.2 ±0.6		EDWARDS	82F	CBAL	$e^+e^- \to e^+e^-2\pi^0$
$2.9\ ^{+0.6}_{-0.4}$ ±0.6		[14] EDWARDS	82F	CBAL	$e^+e^- \to e^+e^-2\pi^0$
3.2 ±0.2 ±0.6		BRANDELIK	81B	TASS	$e^+e^- \to e^+e^-\pi^+\pi^-$
3.6 ±0.3 ±0.5		ROUSSARIE	81	MRK2	$e^+e^- \to e^+e^-\pi^+\pi^-$
2.3 ±0.8		[15] BERGER	80B	PLUT	e^+e^-

$\Gamma(e^+e^-)$ Γ_{10}

VALUE (eV)	CL%	DOCUMENT ID		TECN	COMMENT
<0.11	90	ACHASOV	00K	SND	$e^+e^- \to \pi^0\pi^0$
• • • We do not use the following data for averages, fits, limits, etc. • • •					
<1.7	90	VOROBYEV	88	ND	$e^+e^- \to \pi^0\pi^0$

[1] From a partial-wave analysis of data using a K-matrix formalism with 5 poles.
[2] From analysis of L3 data at 91 and 183–209 GeV and using SU(3) relations.
[3] Based on a K-matrix analysis of BELLE data from MORI 07, UEHARA 08A, UEHARA 09 and UEHARA 13. The width is derived for the pole on the third sheet which is closest to the physical axis. Supersedes PENNINGTON 08.
[4] Solution A (preferred solution based on χ^2-analysis).
[5] Dispersion theory based amplitude analysis of BOYER 90, MARSISKE 90, BEHREND 92, and MORI 07.
[6] Solution B (worse than solution A; still acceptable when systematic uncertainties are included).
[7] With a narrow scalar state around 1220 MeV.
[8] Using a unitarized model with a 300 - 500 keV wide scalar at 1100 MeV.
[9] Using the unitarized model of LYTH 85.
[10] Error includes spread of different solutions. Data of MARK2 and CRYSTAL BALL used in the analysis. Authors report strong correlations with $\gamma\gamma$ width of $f_0(1370)$: $\Gamma(f_2) + 1/4\ \Gamma(f^0) = 3.6 \pm 0.3$ KeV.
[11] Radiative corrections modify the partial widths; for instance the COURAU 84 value becomes 2.66 ± 0.21 in the calculation of LANDRO 86.
[12] Using the MENNESSIER 83 model.
[13] Superseded by BOYER 90.
[14] If helicity = 2 assumption is not made.
[15] Using mass, width and B($f_2(1270) \to 2\pi$) from PDG 78.

$f_2(1270)$ Γ(i)$\Gamma(\gamma\gamma)/\Gamma$(total)

$\Gamma(K\overline{K}) \times \Gamma(\gamma\gamma)/\Gamma_{\text{total}}$ $\Gamma_3\Gamma_7/\Gamma$

VALUE (keV)	DOCUMENT ID		TECN	COMMENT
0.121±0.020 OUR FIT	Error includes scale factor of 1.3.			
0.091±0.007±0.027	[1] ALBRECHT	90G	ARG	$e^+e^- \to e^+e^-K^+K^-$
• • • We do not use the following data for averages, fits, limits, etc. • • •				
0.104±0.007±0.072	[2] ALBRECHT	90G	ARG	$e^+e^- \to e^+e^-K^+K^-$

[1] Using an incoherent background.
[2] Using a coherent background.

$\Gamma(\eta\eta) \times \Gamma(\gamma\gamma)/\Gamma_{\text{total}}$ $\Gamma_5\Gamma_7/\Gamma$

VALUE (eV)	DOCUMENT ID		TECN	COMMENT
$\mathbf{11.5\ ^{+1.8}_{-2.0}\ ^{+4.5}_{-3.7}}$	[1] UEHARA	10A	BELL	10.6 $e^+e^- \to e^+e^-\eta\eta$

[1] Including interference with the $f_2'(1525)$ (parameters fixed to the values from the 2008 edition of this review, PDG 08) and $f_0(Y)$.

Helicity-0/Helicity-2 RATIO IN $\gamma\gamma \to f_2(1270) \to \pi\pi$

VALUE (units 10^{-2})	DOCUMENT ID		TECN	COMMENT
$\mathbf{3.7\pm0.3\ ^{+15.9}_{-2.9}}$	UEHARA	08A	BELL	10.6 $e^+e^- \to e^+e^-\pi^0\pi^0$
• • • We do not use the following data for averages, fits, limits, etc. • • •				
9.5±1.8	[1] DAI	14A	RVUE	Compilation
13	[2,3] PENNINGTON	08	RVUE	Compilation
26	[3,4] PENNINGTON	08	RVUE	Compilation

[1] Based on a K-matrix analysis of BELLE data from MORI 07, UEHARA 08A, UEHARA 09 and UEHARA 13. The width is derived for the pole on the third sheet which is closest to the physical axis.
[2] Solution A (preferred solution based on χ^2-analysis).
[3] Dispersion theory based amplitude analysis of BOYER 90, MARSISKE 90, BEHREND 92, and MORI 07.
[4] Solution B (worse than solution A; still acceptable when systematic uncertainties are included).

$f_2(1270)$ BRANCHING RATIOS

$\Gamma(\pi\pi)/\Gamma_{\text{total}}$ Γ_1/Γ

VALUE	EVTS	DOCUMENT ID		TECN	COMMENT
$\mathbf{0.842\ ^{+0.029}_{-0.009}}$ **OUR FIT**	Error includes scale factor of 1.1.				
0.837±0.020 OUR AVERAGE					
0.849±0.025		CHABAUD	83	ASPK	17 π^-p polarized
0.85 ±0.05	250	BEAUPRE	71	HBC	8 $\pi^+p \to \Delta^{++}f_2$
0.8 ±0.04	600	OH	70	HBC	1.26 $\pi^-p \to \pi^+\pi^-n$

$\Gamma(\pi^+\pi^-2\pi^0)/\Gamma(\pi\pi)$ Γ_2/Γ_1

Should be twice $\Gamma(2\pi^+2\pi^-)/\Gamma(\pi\pi)$ if decay is $\rho\rho$. (See ASCOLI 68D.)

VALUE	EVTS	DOCUMENT ID		TECN	COMMENT
$\mathbf{0.091\ ^{+0.014}_{-0.040}}$ **OUR FIT**	Error includes scale factor of 1.2.				
0.15 ±0.06	600	EISENBERG	74	HBC	4.9 $\pi^+p \to \Delta^{++}f_2$
• • • We do not use the following data for averages, fits, limits, etc. • • •					
0.07		EMMS	75D	DBC	4 $\pi^+n \to pf_2$

$\Gamma(K\overline{K})/\Gamma(\pi\pi)$ Γ_3/Γ_1

We average only experiments which either take into account $f_2(1270)$-$a_2(1320)$ interference explicitly or demonstrate that $a_2(1320)$ production is negligible.

VALUE	EVTS	DOCUMENT ID		TECN	COMMENT
$\mathbf{0.054\ ^{+0.005}_{-0.006}}$ **OUR FIT**	Error includes scale factor of 2.7.				
$\mathbf{0.041\ ^{+0.004}_{-0.005}}$ **OUR AVERAGE**					
0.045±0.01		[1] BARGIOTTI	03	OBLX	$\overline{p}p$
$0.037\ ^{+0.008}_{-0.021}$		ETKIN	82B	MPS	23 $\pi^-p \to n2K^0_S$
0.045±0.009		CHABAUD	81	ASPK	17 π^-p polarized
0.039±0.008		LOVERRE	80	HBC	4 $\pi^-p \to K\overline{K}N$
• • • We do not use the following data for averages, fits, limits, etc. • • •					
0.052±0.025		ABLIKIM	04E	BES2	$J/\psi \to \omega K^+K^-$
0.036±0.005		[2] COSTA	80	OMEG	1–2.2 $\pi^-p \to K^+K^-n$
0.030±0.005		[3] MARTIN	79	RVUE	
0.027±0.009		[4] POLYCHRO...	79	STRC	7 $\pi^-p \to n2K^0_S$
0.025±0.015		EMMS	75D	DBC	4 $\pi^+n \to pf_2$
0.031±0.012	20	ADERHOLZ	69	HBC	8 $\pi^+p \to K^+K^-\pi^+p$

$\Gamma(2\pi^+2\pi^-)/\Gamma(\pi\pi)$ Γ_4/Γ_1

VALUE	EVTS	DOCUMENT ID		TECN	COMMENT
0.033±0.005 OUR FIT	Error includes scale factor of 1.2.				
0.033±0.004 OUR AVERAGE	Error includes scale factor of 1.1.				
0.024±0.006	160	EMMS	75D	DBC	4 $\pi^+n \to pf_2$
0.051±0.025	70	EISENBERG	74	HBC	4.9 $\pi^+p \to \Delta^{++}f_2$
$0.043\ ^{+0.007}_{-0.011}$	285	LOUIE	74	HBC	3.9 $\pi^-p \to nf_2$
0.037±0.007	154	ANDERSON	73	DBC	6 $\pi^+n \to pf_2$
0.047±0.013		OH	70	HBC	1.26 $\pi^-p \to \pi^+\pi^-n$

$\Gamma(\eta\eta)/\Gamma_{\text{total}}$ Γ_5/Γ

VALUE (units 10^{-3})	DOCUMENT ID		TECN	COMMENT
4.0±0.8 OUR FIT	Error includes scale factor of 2.1.			
2.9±0.5 OUR AVERAGE				
2.7±0.7	BINON	05	GAMS	33 $\pi^-p \to \eta\eta n$
2.8±0.7	ALDE	86D	GAM4	100 $\pi^-p \to 2\eta n$
5.2±1.7	BINON	83	GAM2	38 $\pi^-p \to 2\eta n$

$\Gamma(\eta\eta)/\Gamma(\pi\pi)$ Γ_5/Γ_1

VALUE	CL%	DOCUMENT ID		TECN	COMMENT
0.003±0.001		BARBERIS	00E		450 $pp \to p_f\eta\eta p_s$
• • • We do not use the following data for averages, fits, limits, etc. • • •					
<0.05	95	EDWARDS	82F	CBAL	$e^+e^- \to e^+e^-2\eta$
<0.016	95	EMMS	75D	DBC	4 $\pi^+n \to pf_2$
<0.09	95	EISENBERG	74	HBC	4.9 $\pi^+p \to \Delta^{++}f_2$

$\Gamma(4\pi^0)/\Gamma_{\text{total}}$ Γ_6/Γ

VALUE	EVTS	DOCUMENT ID		TECN	COMMENT
0.0030±0.0010 OUR FIT					
0.003 ±0.001	400 ± 50	ALDE	87	GAM4	100 $\pi^-p \to 4\pi^0n$

$\Gamma(\gamma\gamma)/\Gamma_{total}$ Γ_7/Γ

VALUE (units 10^{-5})	DOCUMENT ID		TECN	COMMENT
• • • We do not use the following data for averages, fits, limits, etc. • • •				
$1.57\pm0.01^{+1.39}_{-0.14}$	UEHARA	08A	BELL	10.6 $e^+e^-\to e^+e^-\pi^0\pi^0$

$\Gamma(\eta\pi\pi)/\Gamma(\pi\pi)$ Γ_8/Γ_1

VALUE	CL%	DOCUMENT ID		TECN	COMMENT
<0.010	95	EMMS	75D	DBC	4 $\pi^+ n \to p f_2$

$\Gamma(K^0K^-\pi^+ + \text{c.c.})/\Gamma(\pi\pi)$ Γ_9/Γ_1

VALUE	CL%	DOCUMENT ID		TECN	COMMENT
<0.004	95	EMMS	75D	DBC	4 $\pi^+ n \to p f_2$

$\Gamma(e^+e^-)/\Gamma_{total}$ Γ_{10}/Γ

VALUE (units 10^{-10})	CL%	DOCUMENT ID		TECN	COMMENT
<6	90	ACHASOV	00K	SND	$e^+e^-\to\pi^0\pi^0$

[1] Coupled channel analysis of $\pi^+\pi^-\pi^0$, $K^+K^-\pi^0$, and $K^\pm K^0_S\pi^\mp$.

[2] Re-evaluated by CHABAUD 83.

[3] Includes PAWLICKI 77 data.

[4] Takes into account the $f_2(1270)$-$f'_2(1525)$ interference.

$f_2(1270)$ REFERENCES

DOBBS	15	PR D91 052006	S. Dobbs *et al.*	(NWES)
DAI	14A	PR D90 036004	L.-Y. Dai, M.R. Pennington	(CEBAF)
BOGOLYUB...	13	PAN 76 1324	M.Yu. Bogolyubsky *et al.*	(HYPERON-M Collab.)
		Translated from YAF 76 1389.		
UEHARA	13	PTEP 2013 123C01	S. Uehara *et al.*	(BELLE Collab.)
UEHARA	10A	PR D82 114031	S. Uehara *et al.*	(BELLE Collab.)
ANISOVICH	09	IJMP A24 2481	V.V. Anisovich, A.V. Sarantsev	
UEHARA	09	PR D79 052009	S. Uehara *et al.*	(BELLE Collab.)
PDG	08	PL B667 1	C. Amsler *et al.*	(PDG Collab.)
PENNINGTON	08	EPJ C56 1	M.R. Pennington *et al.*	
UEHARA	08A	PR D78 052004	S. Uehara *et al.*	(BELLE Collab.)
MORI	07	PR D75 051101	T. Mori *et al.*	(BELLE Collab.)
ABLIKIM	06V	PL B642 441	M. Ablikim *et al.*	(BES Collab.)
SCHEGELSKY	06A	EPJ A27 207	V.A. Schegelsky *et al.*	
ABLIKIM	05	PL B607 243	M. Ablikim *et al.*	(BES Collab.)
BINON	05	PAN 68 960	F. Binon *et al.*	
		Translated from YAF 68 998.		
ABLIKIM	04E	PL B603 138	M. Ablikim *et al.*	(BES Collab.)
BARGIOTTI	03	EPJ C26 371	M. Bargiotti *et al.*	(OBELIX Collab.)
TIKHOMIROV	03	PAN 66 828	G.D. Tikhomirov *et al.*	
		Translated from YAF 66 860.		
ACHASOV	00K	PL B492 8	M.N. Achasov *et al.*	(Novosibirsk SND Collab.)
BARBERIS	00E	PL B479 59	D. Barberis *et al.*	(WA 102 Collab.)
BOGLIONE	99	EPJ C9 11	M. Boglione, M.R. Pennington	
ALDE	98	EPJ A3 361	D. Alde *et al.*	(GAM4 Collab.)
Also		PAN 62 405	D. Alde *et al.*	(GAMS Collab.)
		Translated from YAF 62 446.		
ALDE	97	PL B397 350	D.M. Alde *et al.*	(GAMS Collab.)
BERTIN	97C	PL B408 476	A. Bertin *et al.*	(OBELIX Collab.)
GRYGOREV	96	PAN 59 2105	V.K. Grigoriev, O.N. Baloshin, B.P. Barkov	(ITEP)
		Translated from YAF 59 2187.		
YABUKI	95	JPSJ 64 435	F. Yabuki *et al.*	(VENUS Collab.)
PROKOSHKIN	94	PD 39 420	Y.D. Prokoshkin, A.A. Kondashov	(SERP)
		Translated from DANS 336 613.		
BEHREND	92	ZPHY C56 381	H.J. Behrend	(CELLO Collab.)
BLINOV	92	ZPHY C53 33	A.E. Blinov *et al.*	(NOVO)
AGUILAR-...	91	ZPHY C50 405	M. Aguilar-Benitez *et al.*	(LEBC-EHS Collab.)
AKER	91	PL B260 249	E. Aker *et al.*	(Crystal Barrel Collab.)
ADACHI	90D	PL B234 185	I. Adachi *et al.*	(TOPAZ Collab.)
ALBRECHT	90G	ZPHY C48 183	H. Albrecht *et al.*	(ARGUS Collab.)
BOYER	90	PR D42 1350	J. Boyer *et al.*	(Mark II Collab.)
BREAKSTONE	90	ZPHY C48 569	A.M. Breakstone *et al.*	(ISU, BGNA, CERN+)
MARSISKE	90	PR D41 3324	H. Marsiske *et al.*	(Crystal Ball Collab.)
MORGAN	90	ZPHY C48 623	D. Morgan, M.R. Pennington	(RAL, DURH)
OEST	90	ZPHY C47 343	T. Oest *et al.*	(JADE Collab.)
AUGUSTIN	89	NP B320 1	J.E. Augustin, G. Cosme	(DM2 Collab.)
VOROBYEV	88	SJNP 48 273	P.V. Vorobiev *et al.*	(NOVO)
		Translated from YAF 48 436.		
ALDE	87	PL B198 286	D.M. Alde *et al.*	(LANL, BRUX, SERP, LAPP)
AUGUSTIN	87	ZPHY C36 369	J.E. Augustin *et al.*	(LALO, CLER, FRAS+)
ABACHI	86B	PRL 57 1990	S. Abachi *et al.*	(PURD, ANL, IND, MICH+)
AIHARA	86B	PRL 57 404	H. Aihara *et al.*	(TPC-2γ Collab.)
ALDE	86D	NP B269 485	D.M. Alde *et al.*	(BELG, LAPP, SERP, CERN+)
LANDRO	86	PL B172 445	M. Landro, K.J. Mork, H.A. Olsen	(UTRO)
LONGACRE	86	PL B177 223	R.S. Longacre *et al.*	(BNL, BRAN, CUNY+)
LYTH	85	JP G11 459	D.H. Lyth	
BEHREND	84B	ZPHY C23 223	H.J. Behrend *et al.*	(CELLO Collab.)
BERGER	84	ZPHY C26 199	C. Berger *et al.*	(PLUTO Collab.)
COURAU	84	PL 147B 227	A. Courau *et al.*	(CIT, SLAC)
SMITH	84C	PR D30 851	J.R. Smith *et al.*	(SLAC, LBL, HARV)
BINON	83	NC 78A 313	F.G. Binon *et al.*	(BELG, LAPP, SERP+)
Also		SJNP 38 561	F.G. Binon *et al.*	(BELG, LAPP, SERP+)
		Translated from YAF 38 934.		
CHABAUD	83	NP B223 1	V. Chabaud *et al.*	(CERN, CRAC, MPIM)
DENNEY	83	PR D28 2726	D.L. Denney *et al.*	(IOWA, MICH)
MENNESSIER	83	ZPHY C16 241	G. Mennessier	(MONP)
APEL	82	NP B201 197	W.D. Apel *et al.*	(KARLK, KARLE, PISA, SERP+)
CASON	82	PRL 48 1316	N.M. Cason *et al.*	(NDAM, ANL)
EDWARDS	82F	PL 110B 82	C. Edwards *et al.*	(CIT, HARV, PRIN+)
ETKIN	82B	PR D25 1786	A. Etkin *et al.*	(BNL, CUNY, TUFTS, VAND)
BRANDELIK	81B	ZPHY C10 117	R. Brandelik *et al.*	(TASSO Collab.)
CHABAUD	81	APP B12 575	V. Chabaud *et al.*	(CERN, CRAC, MPIM)
GIDAL	81	PL 107B 153	G. Gidal *et al.*	(SLAC, LBL)
ROUSSARIE	81	PL 105B 304	A. Roussarie *et al.*	(SLAC, LBL)
BERGER	80B	PL 94B 254	C. Berger *et al.*	(PLUTO Collab.)
COSTA	80	NP B175 402	G. Costa *et al.*	(BARI, BONN, CERN, GLAS+)
LOVERRE	80	ZPHY C6 187	P.F. Loverre *et al.*	(CERN, CDEF, MADR+)
CORDEN	79	NP B157 250	M.J. Corden *et al.*	(BIRM, RHEL, TELA+)
MARTIN	79	NP B158 520	A.D. Martin, E.N. Ozmutlu	(DURH)
POLYCHRO...	79	PR D19 1317	V.A. Polychronakos *et al.*	(NDAM, ANL)
PDG	78	PL 75B 1	C. Bricman *et al.*	
ANTIPOV	77	NP B119 45	Y.M. Antipov *et al.*	(SERP, GEVA)
PAWLICKI	77	PR D15 3196	A.J. Pawlicki *et al.*	(ANL)
DEUTSCH...	76	NP B103 426	M. Deutschmann *et al.*	(AACH3, BERL, BONN+)
APEL	75	PL 57B 398	W.D. Apel *et al.*	(KARLK, KARLE, PISA, SERP+)
EMMS	75D	NP B96 155	M.J. Emms *et al.*	(BIRM, DURH, RHEL)
EISENBERG	74	PL 52B 239	Y. Eisenberg *et al.*	(REHO)
ENGLER	74	PR D10 2070	A. Engler *et al.*	(CMU, CASE)
LOUIE	74	PL 48B 385	J. Louie *et al.*	(SACL, CERN)
ANDERSON	73	PRL 31 562	J.C. Anderson *et al.*	(CMU, CASE)
TAKAHASHI	72	PR D6 1266	K. Takahashi *et al.*	(TOHOK, PENN, NDAM+)
BEAUPRE	71	NP B28 77	J.V. Beaupre *et al.*	(AACH, BERL, CERN)
FLATTE	71	PL 34B 551	S.M. Flatte *et al.*	(LBL)
ARMENISE	70	LNC 4 199	N. Armenise *et al.*	(BARI, BGNA, FIRZ)
OH	70	PR D1 2494	B.Y. Oh *et al.*	(WISC, TNTO) JP
STUNTEBECK	70	PL 32B 391	P.H. Stuntebeck *et al.*	(NDAM)
ADERHOLZ	69	NP B11 259	M. Aderholz *et al.*	(AACH3, BERL, CERN+)
ARMENISE	68	NC 54A 999	N. Armenise *et al.*	(BARI, BGNA, FIRZ+)
ASCOLI	68D	PRL 21 1712	G. Ascoli *et al.*	(ILL)
BOESEBECK	68	NP B4 501	K. Boesebeck *et al.*	(AACH, BERL, CERN)
JOHNSON	68	PR 176 1651	P.B. Johnson *et al.*	(NDAM, PURD, SLAC)
EISNER	67	PR 164 1699	R.L. Eisner *et al.*	(PURD)
DERADO	65	PRL 14 872	I. Derado *et al.*	(NDAM)
LEE	64	PRL 12 342	Y.Y. Lee *et al.*	(MICH)
BONDAR	63	PL 5 153	L. Bondar *et al.*	(AACH, BIRM, BONN, DESY+)

$f_1(1285)$ $I^G(J^{PC}) = 0^+(1^{++})$

$f_1(1285)$ MASS

VALUE (MeV)	EVTS	DOCUMENT ID		TECN	COMMENT
1281.9 ± 0.5 OUR AVERAGE		Error includes scale factor of 1.8. See the ideogram below.			
1281.0 ± 0.8		DICKSON	16	CLAS	2.55 $\gamma p \to \eta\pi^+\pi^- p$
1287.4 ± 3.0	87	ABLIKIM	15P	BES3	$J/\psi \to K^+K^-3\pi$
1281.16± 0.39± 0.45	[1]	LEES	12X	BABR	$\tau^- \to \pi^- f_1(1285)\nu_\tau$
1285.1 ± 1.0 $^{+1.6}_{-0.3}$	[2]	ABLIKIM	11J	BES3	$J/\psi \to \omega(\eta\pi^+\pi^-)$
1281 ± 2 ± 1		AUBERT	07AU	BABR	10.6 $e^+e^- \to f_1(1285)\pi^+\pi^-\gamma$
1276.1 ± 8.1 ± 8.0	203	BAI	04J	BES2	$J/\psi \to \gamma\gamma\pi^+\pi^-$
1274 ± 6	237	ABDALLAH	03H	DLPH	91.2 $e^+e^- \to K^0_S K^\pm\pi^\mp + X$
1280 ± 4		ACCIARRI	01G	L3	
1288 ± 4 ± 5	20k	ADAMS	01B	B852	18 GeV $\pi^- p \to K^+K^-\pi^0 n$
1284 ± 6	1400	ALDE	97B	GAM4	100 $\pi^- p \to \eta\pi^0\pi^0 n$
1281 ± 1		BARBERIS	97B	OMEG	450 $pp \to pp2(\pi^+\pi^-)$
1281 ± 1		BARBERIS	97C	OMEG	450 $pp \to pp K^0_S K^\pm\pi^\mp$
1280 ± 2	[3]	ANTINORI	95	OMEG	300,450 $pp \to pp2(\pi^+\pi^-)$
1282.2 ± 1.5		LEE	94	MPS2	18 $\pi^- p \to K^+\overline{K}^0 2\pi^- p$
1279 ± 5		FUKUI	91C	SPEC	8.95 $\pi^- p \to \eta\pi^+\pi^- n$
1278 ± 2	140	ARMSTRONG	89	OMEG	300 $pp \to K\overline{K}\pi pp$
1278 ± 2		ARMSTRONG	89G	OMEG	85 $\pi^+ p \to 4\pi\pi p$, $pp \to 4\pi pp$
1280.1 ± 2.1	60	RATH	89	MPS	21.4 $\pi^- p \to K^0_S K^0_S \pi^0 n$
1285 ± 1	4750	[4] BIRMAN	88	MPS	8 $\pi^- p \to K^+\overline{K}^0\pi^- n$
1280 ± 1	504	BITYUKOV	88	SPEC	32.5 $\pi^- p \to K^+K^-\pi^0 n$
1280 ± 4		ANDO	86	SPEC	8 $\pi^- p \to \eta\pi^+\pi^- n$
1277 ± 2	420	REEVES	86	SPEC	6.6 $p\overline{p} \to K K\pi X$
1285 ± 2		CHUNG	85	SPEC	8 $\pi^- p \to N K\overline{K}\pi$
1279 ± 2	604	ARMSTRONG	84	OMEG	85 $\pi^+ p \to K\overline{K}\pi\pi p$, $pp \to K\overline{K}\pi pp$
1286 ± 1		CHAUVAT	84	SPEC	ISR 31.5 pp
1278 ± 4		EVANGELIS...	81	OMEG	12 $\pi^- p \to \eta\pi^+\pi^-\pi^- p$
1283 ± 3	103	DIONISI	80	HBC	4 $\pi^- p \to K\overline{K}\pi n$
1282 ± 2	320	NACASCH	78	HBC	0.7,0.76 $\overline{p}p \to K\overline{K}3\pi$
1279 ± 5	210	GRASSLER	77	HBC	16 $\pi^\mp p$
1286 ± 3	180	DUBOC	72	HBC	1.2 $\overline{p}p \to 2K4\pi$
1283 ± 5		DAHL	67	HBC	1.6–4.2 $\pi^- p$
• • • We do not use the following data for averages, fits, limits, etc. • • •					
1284.2 ± 2.2		[5] AAIJ	14Y	LHCB	$\overline{B}^0_{(s)} \to J/\psi 2(\pi^+\pi^-)$
1281.9 ± 0.5		[5] SOSA	99	SPEC	$pp \to p_{slow}(K^0_S K^+\pi^-) p_{fast}$
1282.8 ± 0.6		[5] SOSA	99	SPEC	$pp \to p_{slow}(K^0_S K^-\pi^+) p_{fast}$
1270 ±10		AMELIN	95	VES	37 $\pi^- N \to \pi^-\pi^+\pi^-\gamma N$
1280 ± 2		ABATZIS	94	OMEG	450 $pp \to pp2(\pi^+\pi^-)$
1282 ± 4		ARMSTRONG	93C	E760	$\overline{p}p \to \pi^0\eta\eta \to 6\gamma$
1270 ± 6 ±10		ARMSTRONG	92C	OMEG	300 $pp \to pp\pi^+\pi^-\gamma$
1281 ± 1		ARMSTRONG	89E	OMEG	300 $pp \to pp2(\pi^+\pi^-)$
1279 ± 6 ±10	16	BECKER	87	MRK3	$e^+e^- \to \phi K\overline{K}\pi$
1286 ± 9		GIDAL	87	MRK2	$e^+e^- \to e^+e^-\eta\pi^+\pi^-$
1287 ± 5	353	BITYUKOV	84B	SPEC	32 $\pi^- p \to K^+K^-\pi^0 n$
~ 1279		[6] TORNQVIST	82B	RVUE	
1275 ± 6	31	BROMBERG	80	SPEC	100 $\pi^- p \to K\overline{K}\pi X$
1288 ± 9	200	GURTU	79	HBC	4.2 $K^- p \to n\eta 2\pi$
~ 1275.0	46	[7] STANTON	79	CNTR	8.5 $\pi^- p \to n2\gamma 2\pi$
1271 ±10	34	CORDEN	78	OMEG	12–15 $\pi^- p \to K^+K^-\pi n$
1295 ±12	85	CORDEN	78	OMEG	12–15 $\pi^- p \to n5\pi$
1292 ±10	150	DEFOIX	72	HBC	0.7 $\overline{p}p \to 7\pi$

Meson Particle Listings

$f_1(1285)$

1280	± 3	500	[8] THUN	72	MMS	13.4 $\pi^- p$
1303	± 8		BARDADIN-...	71	HBC	8 $\pi^+ p \rightarrow p6\pi$
1283	± 6		BOESEBECK	71	HBC	16.0 $\pi p \rightarrow p5\pi$
1270	±10		CAMPBELL	69	DBC	2.7 $\pi^+ d$
1285	± 7		LORSTAD	69	HBC	0.7 $\overline{p}p$, 4,5-body
1290	± 7		D'ANDLAU	68	HBC	1.2 $\overline{p}p$, 5–6 body

[1] Using the $2\pi^+2\pi^-$ and $\pi^+\pi^-\eta$ modes of $f_1(1285)$ decay.
[2] The selected process is $J/\psi \rightarrow \omega a_0(980)\pi$.
[3] Supersedes ABATZIS 94, ARMSTRONG 89E.
[4] From partial wave analysis of $K^+\overline{K}{}^0\pi^-$ system.
[5] No systematic error given.
[6] From a unitarized quark-model calculation.
[7] From phase shift analysis of $\eta\pi^+\pi^-$ system.
[8] Seen in the missing mass spectrum.

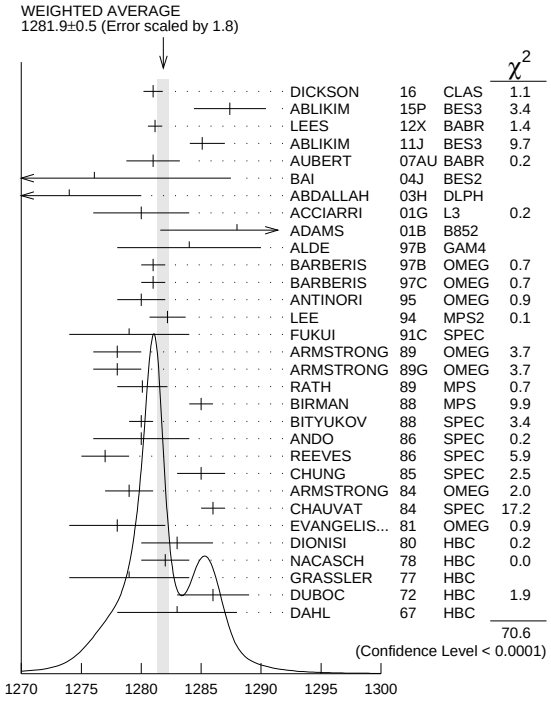

$f_1(1285)$ mass (MeV)

$f_1(1285)$ WIDTH

Only experiments giving width error less than 20 MeV are kept for averaging.

VALUE (MeV)	EVTS	DOCUMENT ID		TECN	COMMENT
22.7± 1.1 OUR AVERAGE		Error includes scale factor of 1.5. See the ideogram below.			
18.4± 1.4		DICKSON	16	CLAS	2.55 $\gamma p \rightarrow \eta\pi^+\pi^- p$
18.3± 6.3	87	ABLIKIM	15P	BES3	$J/\psi \rightarrow K^+K^-3\pi$
22.0± 3.1$^{+\ 2.0}_{-\ 1.5}$		[1] ABLIKIM	11J	BES3	$J/\psi \rightarrow \omega(\eta\pi^+\pi^-)$
35 ± 6 ± 4		AUBERT	07AU	BABR	10.6 $e^+e^- \rightarrow f_1(1285)\pi^+\pi^-\gamma$
40.0± 8.6± 9.3	203	BAI	04J	BES2	$J/\psi \rightarrow \gamma\gamma\pi^+\pi^-$
29 ±12	237	ABDALLAH	03H	DLPH	91.2 $e^+e^- \rightarrow K^0_S K^\pm\pi^\mp + X$
45 ± 9 ± 7	20k	ADAMS	01B	B852	18 GeV $\pi^- p \rightarrow K^+K^-\pi^0 n$
55 ±18	1400	ALDE	97B	GAM4	100 $\pi^- p \rightarrow \eta\pi^0\pi^0 n$
24 ± 3		BARBERIS	97B	OMEG	450 $pp \rightarrow pp2(\pi^+\pi^-)$
20 ± 2		BARBERIS	97C	OMEG	450 $pp \rightarrow pp K^0_S K^\pm\pi^\mp$
36 ± 5		[2] ANTINORI	95	OMEG	300,450 $pp \rightarrow pp2(\pi^+\pi^-)$
29.0± 4.1		LEE	94	MPS2	18 $\pi^- p \rightarrow K^+\overline{K}{}^0 2\pi^- p$
25 ± 4	140	ARMSTRONG	89	OMEG	300 $pp \rightarrow K\overline{K}\pi pp$
22 ± 2	4750	[3] BIRMAN	88	MPS	8 $\pi^- p \rightarrow K^+\overline{K}{}^0\pi^- n$
25 ± 4	504	BITYUKOV	88	SPEC	32.5 $\pi^- p \rightarrow K^+K^-\pi^0 n$
19 ± 5		ANDO	86	SPEC	8 $\pi^- p \rightarrow \eta\pi^+\pi^- n$
32 ± 8	420	REEVES	86	SPEC	6.6 $p\overline{p} \rightarrow KK\pi X$
22 ± 2		CHUNG	85	SPEC	8 $\pi^- p \rightarrow NK\overline{K}\pi$
32 ± 3	604	ARMSTRONG	84	OMEG	85 $\pi^+ p \rightarrow K\overline{K}\pi\pi p$, $pp \rightarrow K\overline{K}\pi pp$
24 ± 3		CHAUVAT	84	SPEC	ISR 31.5 pp
29 ±10	103	DIONISI	80	HBC	4 $\pi^- p \rightarrow K\overline{K}\pi n$
28.3± 6.7	320	NACASCH	78	HBC	0.7,0.76 $\overline{p}p \rightarrow K\overline{K}3\pi$

• • • We do not use the following data for averages, fits, limits, etc. • • •

32.4± 5.8	[4] AAIJ	14Y	LHCB	$\overline{B}{}^0_{(s)} \rightarrow J/\psi 2(\pi^+\pi^-)$
18.2± 1.2	[4] SOSA	99	SPEC	$pp \rightarrow p_{\rm slow}\ (K^0_S K^+\pi^-)\ p_{\rm fast}$
19.4± 1.5	[4] SOSA	99	SPEC	$pp \rightarrow p_{\rm slow}\ (K^0_S K^-\pi^+)\ p_{\rm fast}$
40 ± 5	ABATZIS	94	OMEG	450 $pp \rightarrow pp2(\pi^+\pi^-)$
31 ± 5	ARMSTRONG	89E	OMEG	300 $pp \rightarrow pp2(\pi^+\pi^-)$
41 ±12	ARMSTRONG	89G	OMEG	85 $\pi^+ p \rightarrow 4\pi\pi p$, $pp \rightarrow 4\pi pp$
17.9±10.9	60	RATH	89	MPS	21.4 $\pi^- p \rightarrow K^0_S K^0_S \pi^0 n$
14 $^{+20}_{-14}$ ±10	16	BECKER	87	MRK3	$e^+e^- \rightarrow \phi K\overline{K}\pi$
26 ±12		EVANGELIS...	81	OMEG	12 $\pi^- p \rightarrow \eta\pi^+\pi^-\pi^- p$
25 ±15	200	GURTU	79	HBC	4.2 $K^- p \rightarrow n\eta 2\pi$
~ 10		[5] STANTON	79	CNTR	8.5 $\pi^- p \rightarrow n2\gamma 2\pi$
24 ±18	210	GRASSLER	77	HBC	16 $\pi^\mp p$
28 ± 5	150	[6] DEFOIX	72	HBC	0.7 $\overline{p}p \rightarrow 7\pi$
46 ± 9	180	[6] DUBOC	72	HBC	1.2 $\overline{p}p \rightarrow 2K4\pi$
37 ± 5	500	[7] THUN	72	MMS	13.4 $\pi^- p$
10 ±10		BOESEBECK	71	HBC	16.0 $\pi p \rightarrow p5\pi$
30 ±15		CAMPBELL	69	DBC	2.7 $\pi^+ d$
60 ±15		[6] LORSTAD	69	HBC	0.7 $\overline{p}p$, 4,5-body
35 ±10		[6] DAHL	67	HBC	1.6–4.2 $\pi^- p$

[1] The selected process is $J/\psi \rightarrow \omega a_0(980)\pi$.
[2] Supersedes ABATZIS 94, ARMSTRONG 89E.
[3] From partial wave analysis of $K^+\overline{K}{}^0\pi^-$ system.
[4] No systematic error given.
[5] From phase shift analysis of $\eta\pi^+\pi^-$ system.
[6] Resolution is not unfolded.
[7] Seen in the missing mass spectrum.

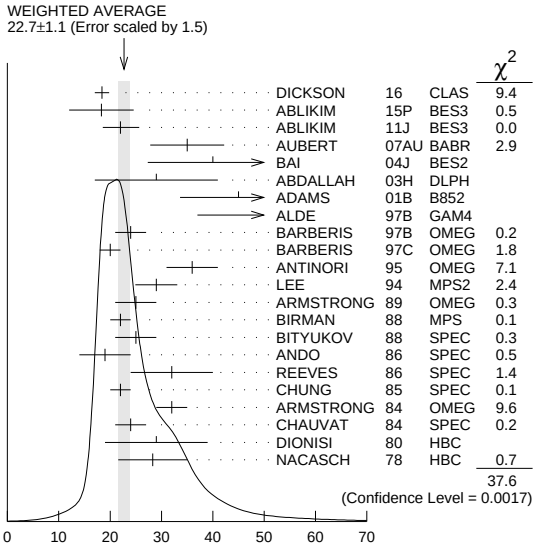

$f_1(1285)$ width (MeV)

$f_1(1285)$ DECAY MODES

	Mode	Fraction (Γ_i/Γ)	Scale factor/ Confidence level
Γ_1	4π	(33.5$^{+\ 2.0}_{-\ 1.8}$) %	S=1.3
Γ_2	$\pi^0\pi^0\pi^+\pi^-$	(22.3$^{+\ 1.3}_{-\ 1.2}$) %	S=1.3
Γ_3	$2\pi^+2\pi^-$	(11.2$^{+\ 0.7}_{-\ 0.6}$) %	S=1.3
Γ_4	$\rho^0\pi^+\pi^-$	(11.2$^{+\ 0.7}_{-\ 0.6}$) %	S=1.3
Γ_5	$\rho^0\rho^0$	seen	
Γ_6	$4\pi^0$	< 7 $\times 10^{-4}$	CL=90%
Γ_7	$\eta\pi^+\pi^-$	(35 ±15) %	
Γ_8	$\eta\pi\pi$	(52.0$^{+\ 1.8}_{-\ 2.1}$) %	S=1.2
Γ_9	$a_0(980)\pi$ [ignoring $a_0(980) \rightarrow K\overline{K}$]	(38 ± 4) %	
Γ_{10}	$\eta\pi\pi$ [excluding $a_0(980)\pi$]	(14 ± 4) %	
Γ_{11}	$K\overline{K}\pi$	(9.1± 0.4) %	S=1.1
Γ_{12}	$K\overline{K}^*(892)$	not seen	
Γ_{13}	$\pi^+\pi^-\pi^0$	(3.0± 0.9) $\times 10^{-3}$	
Γ_{14}	$\rho^\pm\pi^\mp$	< 3.1 $\times 10^{-3}$	CL=95%

Γ_{15}	$\gamma\rho^0$	(5.3± 1.2) %	S=2.9
Γ_{16}	$\phi\gamma$	(7.5± 2.7) $\times 10^{-4}$	
Γ_{17}	$\gamma\gamma^*$		
Γ_{18}	$\gamma\gamma$		

CONSTRAINED FIT INFORMATION

An overall fit to 7 branching ratios uses 19 measurements and one constraint to determine 5 parameters. The overall fit has a $\chi^2 =$ 33.5 for 15 degrees of freedom.

The following *off-diagonal* array elements are the correlation coefficients $\langle \delta x_i \delta x_j \rangle / (\delta x_i \cdot \delta x_j)$, in percent, from the fit to the branching fractions, $x_i \equiv \Gamma_i/\Gamma_{\rm total}$. The fit constrains the x_i whose labels appear in this array to sum to one.

x_9	−28			
x_{10}	−11	−88		
x_{11}	34	−11	−5	
x_{15}	−36	−7	−3	−34
	x_1	x_9	x_{10}	x_{11}

$f_1(1285)$ Γ(i)$\Gamma(\gamma\gamma)/\Gamma$(total)

$\Gamma(\eta\pi\pi) \times \Gamma(\gamma\gamma)/\Gamma_{\rm total}$ $\quad \Gamma_8\Gamma_{18}/\Gamma = (\Gamma_9+\Gamma_{10})\Gamma_{18}/\Gamma$

VALUE (keV)	CL%	DOCUMENT ID		TECN	COMMENT
<0.62	95	GIDAL	87	MRK2	$e^+e^- \to e^+e^-\eta\pi^+\pi^-$

$\Gamma(\eta\pi\pi) \times \Gamma(\gamma\gamma^*)/\Gamma_{\rm total}$ $\quad \Gamma_8\Gamma_{17}/\Gamma = (\Gamma_9+\Gamma_{10})\Gamma_{17}/\Gamma$

VALUE (keV)	EVTS	DOCUMENT ID		TECN	COMMENT
1.4 ±0.4 OUR AVERAGE		Error includes scale factor of 1.4.			
1.18±0.25±0.20	26	[1,2] AIHARA	88B	TPC	$e^+e^- \to e^+e^-\eta\pi^+\pi^-$
2.30±0.61±0.42		[1,3] GIDAL	87	MRK2	$e^+e^- \to e^+e^-\eta\pi^+\pi^-$
• • • We do not use the following data for averages, fits, limits, etc. • • •					
1.8 ±0.3 ±0.3	420	[4] ACHARD	02B	L3	183–209 $e^+e^- \to e^+e^-\eta\pi^+\pi^-$

[1] Assuming a ρ-pole form factor.
[2] Published value multiplied by $\eta\pi\pi$ branching ratio 0.49.
[3] Published value divided by 2 and multiplied by the $\eta\pi\pi$ branching ratio 0.49.
[4] Published value multiplied by the $\eta\pi\pi$ branching ratio 0.52.

$f_1(1285)$ BRANCHING RATIOS

$\Gamma(K\overline{K}\pi)/\Gamma(4\pi)$ $\quad \Gamma_{11}/\Gamma_1$

VALUE	DOCUMENT ID		TECN	COMMENT
0.272±0.016 OUR FIT	Error includes scale factor of 1.3.			
0.271±0.016 OUR AVERAGE	Error includes scale factor of 1.2.			
0.265±0.014	[1] BARBERIS	97C	OMEG	450 $pp \to pp K^0_S K^\pm\pi^\mp$
0.28 ±0.05	[2] ARMSTRONG	89E	OMEG	300 $pp \to pp f_1(1285)$
0.37 ±0.03 ±0.05	[3] ARMSTRONG	89G	OMEG	85 $\pi p \to 4\pi X$

[1] Using $2(\pi^+\pi^-)$ data from BARBERIS 97B.
[2] Assuming $\rho\pi\pi$ and $a_0(980)\pi$ intermediate states.
[3] 4π consistent with being entirely $\rho\pi\pi$.

$\Gamma(\pi^0\pi^0\pi^+\pi^-)/\Gamma_{\rm total}$ $\quad \Gamma_2/\Gamma = \frac{2}{3}\Gamma_1/\Gamma$

VALUE	DOCUMENT ID
$0.223^{+0.013}_{-0.012}$ **OUR FIT**	Error includes scale factor of 1.3.

$\Gamma(2\pi^+2\pi^-)/\Gamma_{\rm total}$ $\quad \Gamma_3/\Gamma = \frac{1}{3}\Gamma_1/\Gamma$

VALUE	DOCUMENT ID
$0.112^{+0.007}_{-0.006}$ **OUR FIT**	Error includes scale factor of 1.3.

$\Gamma(\rho^0\pi^+\pi^-)/\Gamma_{\rm total}$ $\quad \Gamma_4/\Gamma = \frac{1}{3}\Gamma_1/\Gamma$

VALUE	DOCUMENT ID
$0.112^{+0.007}_{-0.006}$ **OUR FIT**	Error includes scale factor of 1.3.

$\Gamma(\rho^0\pi^+\pi^-)/\Gamma(2\pi^+2\pi^-)$ $\quad \Gamma_4/\Gamma_3$

VALUE	DOCUMENT ID		TECN	COMMENT
• • • We do not use the following data for averages, fits, limits, etc. • • •				
1.0±0.4	GRASSLER	77	HBC	16 GeV $\pi^\pm p$

$\Gamma(\rho^0\rho^0)/\Gamma_{\rm total}$ $\quad \Gamma_5/\Gamma$

VALUE	DOCUMENT ID		COMMENT
seen	BARBERIS	00C	450 $pp \to p_f 4\pi p_s$

$\Gamma(4\pi^0)/\Gamma_{\rm total}$ $\quad \Gamma_6/\Gamma$

VALUE (units 10^{-4})	CL%	DOCUMENT ID		TECN	COMMENT
<7	90	ALDE	87	GAM4	100 $\pi^- p \to 4\pi^0 n$

$\Gamma(\pi^+\pi^-\pi^0)/\Gamma(\eta\pi^+\pi^-)$ $\quad \Gamma_{13}/\Gamma_7$

VALUE (%)	EVTS	DOCUMENT ID		TECN	COMMENT
0.86±0.16±0.20	2.3k	[1] DOROFEEV	11	VES	$\pi^- N \to \pi^- f_1(1285) N$

[1] Value obtained selecting the region corresponding to $f_0(980)$ in the $\pi^+\pi^-$ mass spectrum.

$\Gamma(\eta\pi\pi)/\Gamma_{\rm total}$ $\quad \Gamma_8/\Gamma = (\Gamma_9+\Gamma_{10})/\Gamma$

VALUE	DOCUMENT ID
$0.520^{+0.018}_{-0.021}$ **OUR FIT**	Error includes scale factor of 1.2.

$\Gamma(4\pi)/\Gamma(\eta\pi\pi)$ $\quad \Gamma_1/\Gamma_8 = \Gamma_1/(\Gamma_9+\Gamma_{10})$

VALUE	DOCUMENT ID		TECN	COMMENT
$0.64^{+0.06}_{-0.05}$ **OUR FIT**	Error includes scale factor of 1.2.			
0.41±0.14 OUR AVERAGE				
0.37±0.11±0.11	BOLTON	92	MRK3	$J/\psi \to \gamma f_1(1285)$
0.64±0.40	GURTU	79	HBC	4.2 $K^- p$
• • • We do not use the following data for averages, fits, limits, etc. • • •				
0.93±0.30	[1] GRASSLER	77	HBC	16 $\pi^\mp p$

[1] Assuming $\rho\pi\pi$ and $a_0(980)\pi$ intermediate states.

$\Gamma(2\pi^+2\pi^-)/\Gamma(\eta\pi\pi)$ $\quad \Gamma_3/\Gamma_8$

VALUE	DOCUMENT ID		TECN	COMMENT
0.28±0.02±0.02	[1] LEES	12X	BABR	$\tau^- \to \pi^- f_1(1285)\nu_\tau$

[1] Assuming B($f_1(1285) \to \pi\pi\eta$) = 3/2 B($f_1(1285) \to \pi^+\pi^-\eta$).

$\Gamma(a_0(980)\pi$ [ignoring $a_0(980) \to K\overline{K}$])$/\Gamma(\eta\pi\pi)$ $\quad \Gamma_9/\Gamma_8 = \Gamma_9/(\Gamma_9+\Gamma_{10})$

VALUE	CL%	DOCUMENT ID		TECN	COMMENT
0.72±0.08 OUR FIT					
0.72±0.07 OUR AVERAGE					
0.74±0.02±0.09		DICKSON	16	CLAS	$\gamma p \to f_1(1285) p$
0.72±0.15		GURTU	79	HBC	4.2 $K^- p$
$0.6\ ^{+0.3}_{-0.2}$		CORDEN	78	OMEG	12–15 $\pi^- p$
• • • We do not use the following data for averages, fits, limits, etc. • • •					
>0.69	95	ACHARD	02B	L3	183–209 $e^+e^- \to e^+e^-\eta\pi^+\pi^-$
0.28±0.07		ALDE	97B	GAM4	100 $\pi^- p \to \eta\pi^0\pi^0 n$
1.0 ±0.3		GRASSLER	77	HBC	16 $\pi^\mp p$

$\Gamma(K\overline{K}\pi)/\Gamma(\eta\pi\pi)$ $\quad \Gamma_{11}/\Gamma_8 = \Gamma_{11}/(\Gamma_9+\Gamma_{10})$

VALUE	DOCUMENT ID		TECN	COMMENT
0.176±0.012 OUR FIT	Error includes scale factor of 1.1.			
0.176±0.012 OUR AVERAGE				
0.216±0.010±0.031	DICKSON	16	CLAS	$\gamma p \to f_1(1285) p$
0.166±0.01 ±0.008	BARBERIS	98C	OMEG	450 $pp \to p_f f_1(1285) p_s$
0.42 ±0.15	GURTU	79	HBC	4.2 $K^- p$
0.5 ±0.2	[1] CORDEN	78	OMEG	12–15 $\pi^- p$
0.20 ±0.08	[2] DEFOIX	72	HBC	0.7 $\overline{p}p \to 7\pi$
0.16 ±0.08	CAMPBELL	69	DBC	2.7 $\pi^+ d$

[1] CORDEN 78 assumes low-mass $\eta\pi\pi$ region is dominantly 1^{++}. See BARBERIS 98C and MANAK 00A for discussion.
[2] $K\overline{K}$ system characterized by the $I = 1$ threshold enhancement. (See under $a_0(980)$).

$\Gamma(K\overline{K}^*(892))/\Gamma_{\rm total}$ $\quad \Gamma_{12}/\Gamma$

VALUE	DOCUMENT ID		TECN	COMMENT
not seen	NACASCH	78	HBC	0.7,0.76 $\overline{p}p \to K\overline{K}3\pi$
• • • We do not use the following data for averages, fits, limits, etc. • • •				
seen	[1] ACHARD	07	L3	183–209 $e^+e^- \to e^+e^- K^0_S K^\pm\pi^\mp$

[1] A clear signal of 19.8 ± 4.4 events observed at high Q^2.

$\Gamma(\pi^+\pi^-\pi^0)/\Gamma_{\rm total}$ $\quad \Gamma_{13}/\Gamma$

VALUE (%)	EVTS	DOCUMENT ID		TECN	COMMENT
0.30±0.055±0.074	2.3k	[1] DOROFEEV	11	VES	$\pi^- N \to \pi^- f_1(1285) N$

[1] Value obtained selecting the region corresponding to $f_0(980)$ in the $\pi^+\pi^-$ mass spectrum. The sytematic error includes the uncertainty on the partial width $f_1 \to \eta\pi\pi$ obtained from PDG 10 data.

$\Gamma(\rho^\pm\pi^\mp)/\Gamma_{\rm total}$ $\quad \Gamma_{14}/\Gamma$

VALUE (%)	CL%	DOCUMENT ID		TECN	COMMENT
<0.31	95	DOROFEEV	11	VES	$\pi^- N \to \pi^- f_1(1285) N$

$\Gamma(\gamma\rho^0)/\Gamma_{\rm total}$ $\quad \Gamma_{15}/\Gamma$

VALUE (units 10^{-2})	CL%	DOCUMENT ID		TECN	COMMENT
5.3±1.2 OUR FIT		Error includes scale factor of 2.9.			
2.8±0.7±0.6		AMELIN	95	VES	37 $\pi^- N \to \pi^-\pi^+\pi^-\gamma N$
• • • We do not use the following data for averages, fits, limits, etc. • • •					
<5	95	BITYUKOV	91B	SPEC	32 $\pi^- p \to \pi^+\pi^-\gamma n$

$\Gamma(\gamma\rho^0)/\Gamma(2\pi^+2\pi^-)$ $\quad \Gamma_{15}/\Gamma_3 = \Gamma_{15}/\frac{1}{3}\Gamma_1$

VALUE	DOCUMENT ID		TECN	COMMENT
0.48±0.13 OUR FIT	Error includes scale factor of 2.5.			
0.45±0.18	[1] COFFMAN	90	MRK3	$J/\psi \to \gamma\gamma\pi^+\pi^-$

[1] Using B($J/\psi \to \gamma f_1(1285) \to \gamma\gamma\rho^0$)=0.25 × 10^{-4} and B($J/\psi \to \gamma f_1(1285) \to \gamma 2\pi^+ 2\pi^-$)=0.55 × 10^{-4} given by MIR 88.

$\Gamma(\eta\pi\pi)/\Gamma(\gamma\rho^0)$ $\Gamma_8/\Gamma_{15} = (\Gamma_9+\Gamma_{10})/\Gamma_{15}$

VALUE	DOCUMENT ID		TECN	COMMENT
9.7±1.9 OUR FIT	Error includes scale factor of 2.4.			
8.5±2.0 OUR AVERAGE	Error includes scale factor of 2.2. See the ideogram below.			
21.3±4.4	DICKSON	16	CLAS	$\gamma p \to f_1(1285) p$
10.0±1.0±2.0	BARBERIS	98C	OMEG	450 $pp \to p_f f_1(1285) p_s$
7.5±1.0	[1] ARMSTRONG	92C	OMEG	300 $pp \to pp\pi^+\pi^-\gamma$, $pp\eta\pi^+\pi^-$

[1] Published value multiplied by 1.5.

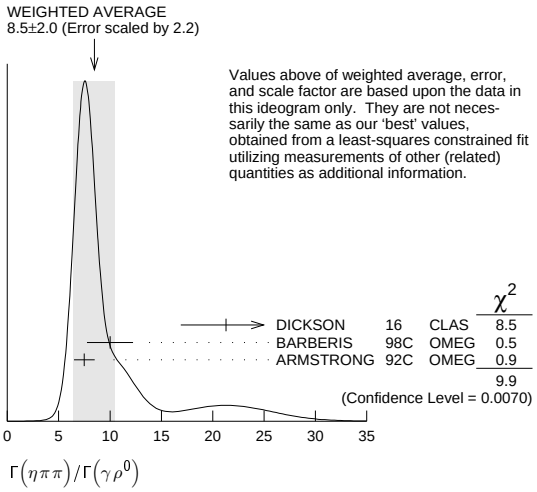

$\Gamma(\gamma\rho^0)/\Gamma(K\overline{K}\pi)$ Γ_{15}/Γ_{11}

VALUE	CL%	DOCUMENT ID		TECN	COMMENT
• • • We do not use the following data for averages, fits, limits, etc. • • •					
>0.035	90	[1] COFFMAN	90	MRK3	$J/\psi \to \gamma\gamma\pi^+\pi^-$

[1] Using B($J/\psi \to \gamma f_1(1285) \to \gamma\gamma\rho^0$)=0.25 × 10^{-4} and B($J/\psi \to \gamma f_1(1285) \to \gamma K\overline{K}\pi$)=< 0.72 × 10^{-3}.

$\Gamma(\phi\gamma)/\Gamma(K\overline{K}\pi)$ Γ_{16}/Γ_{11}

VALUE (units 10^{-2})	CL%	EVTS	DOCUMENT ID		TECN	COMMENT
0.82±0.21±0.20		19	BITYUKOV	88	SPEC	32.5 $\pi^- p \to K^+ K^- \pi^0 n$
• • • We do not use the following data for averages, fits, limits, etc. • • •						
<0.50	95		BARBERIS	98C	OMEG	450 $pp \to p_f f_1(1285) p_s$
<0.93	95		AMELIN	95	VES	37 $\pi^- N \to \pi^-\pi^+\pi^-\gamma N$

$f_1(1285)$ REFERENCES

DICKSON	16	PR C93 065202	R. Dickson *et al.*	(JLab CLAS Collab.)
ABLIKIM	15P	PR D92 012007	M. Ablikim *et al.*	(BES III Collab.)
AAIJ	14Y	PRL 112 091802	R. Aaij *et al.*	(LHCb Collab.)
LEES	12X	PR D86 092010	J.P. Lees *et al.*	(BABAR Collab.)
ABLIKIM	11J	PRL 107 182001	M. Ablikim *et al.*	(BES III Collab.)
DOROFEEV	11	EPJ A47 68	V. Dorofeev *et al.*	(SERP, MIPT)
PDG	10	JP G37 075021	K. Nakamura *et al.*	(PDG Collab.)
ACHARD	07	JHEP 0703 018	P. Achard *et al.*	(L3 Collab.)
AUBERT	07AU	PR D76 092005	B. Aubert *et al.*	(BABAR Collab.)
BAI	04J	PL B594 47	J.Z. Bai *et al.*	(BES Collab.)
ABDALLAH	03H	PL B569 129	J. Abdallah *et al.*	(DELPHI Collab.)
ACHARD	02B	PL B526 269	P. Achard *et al.*	(L3 Collab.)
ACCIARRI	01G	PL B501 1	M. Acciarri *et al.*	(L3 Collab.)
ADAMS	01B	PL B516 264	G.S. Adams *et al.*	(BNL E852 Collab.)
BARBERIS	00C	PL B471 440	D. Barberis *et al.*	(WA 102 Collab.)
MANAK	00A	PR D62 012003	J.J. Manak *et al.*	(BNL E852 Collab.)
SOSA	99	PRL 83 913	M. Sosa *et al.*	
BARBERIS	98C	PL B440 225	D. Barberis *et al.*	(WA 102 Collab.)
ALDE	97B	PAN 60 386	D. Alde *et al.*	(GAMS Collab.)
		Translated from YAF 60 458.		
BARBERIS	97B	PL B413 217	D. Barberis *et al.*	(WA 102 Collab.)
BARBERIS	97C	PL B413 225	D. Barberis *et al.*	(WA 102 Collab.)
AMELIN	95	ZPHY C66 71	D.V. Amelin *et al.*	(VES Collab.)
ANTINORI	95	PL B353 589	F. Antinori *et al.*	(ATHU, BARI, BIRM+)
ABATZIS	94	PL B324 509	S. Abatzis *et al.*	(ATHU, BARI, BIRM+)
LEE	94	PL B323 227	J.H. Lee *et al.*	(BNL, IND, KYUN, MASD+)
ARMSTRONG	93C	PL B307 394	T.A. Armstrong *et al.*	(FNAL, FERR, GENO+)
ARMSTRONG	92C	ZPHY C54 371	T.A. Armstrong *et al.*	(ATHU, BARI, BIRM+)
BOLTON	92	PL B278 495	T. Bolton *et al.*	(Mark III Collab.)
BITYUKOV	91B	SJNP 54 318	S.I. Bityukov *et al.*	(SERP)
		Translated from YAF 54 529.		
FUKUI	91C	PL B267 293	S. Fukui *et al.*	(SUGI, NAGO, KEK, KYOT+)
COFFMAN	90	PR D41 1410	D.M. Coffman *et al.*	(Mark III Collab.)
ARMSTRONG	89	PL B221 216	T.A. Armstrong *et al.*	(CERN, CDEF, BIRM+) JPC
ARMSTRONG	89E	PL B228 536	T.A. Armstrong, M. Benayoun	(ATHU, BARI, BIRM+)
ARMSTRONG	89G	ZPHY C43 55	T.A. Armstrong *et al.*	(CERN, BIRM, BARI+)
RATH	89	PR D40 693	M.G. Rath *et al.*	(NDAM, BRAN, BNL, CUNY+)
AIHARA	88B	PL B209 107	H. Aihara *et al.*	(TPC-2γ Collab.)
BIRMAN	88	PRL 61 1557	A. Birman *et al.*	(BNL, FSU, IND, MASD) JP
BITYUKOV	88	PL B203 327	S.I. Bityukov *et al.*	(SERP)
MIR	88	Photon-Photon 88, 126 Conference	R. Mir	(Mark III Collab.)
ALDE	87	PL B198 286	D.M. Alde *et al.*	(LANL, BRUX, SERP, LAPP)
BECKER	87	PRL 59 186	J.J. Becker *et al.*	(Mark III Collab.)
GIDAL	87	PRL 59 2012	G. Gidal *et al.*	(LBL, SLAC, HARV)
ANDO	86	PRL 57 1296	A. Ando *et al.*	(KEK, KYOT, NIRS, SAGA+) IJP
REEVES	86	PR D34 1960	D.F. Reeves *et al.*	(FLOR, BNL, IND+) JP
CHUNG	85	PRL 55 779	S.U. Chung *et al.*	(BNL, FLOR, IND+) JP
ARMSTRONG	84	PL 146B 273	T.A. Armstrong *et al.*	(ATHU, BARI, BIRM+) JP
BITYUKOV	84B	PL 144B 133	S.I. Bityukov *et al.*	(SERP)
CHAUVAT	84	PL 148B 382	P. Chauvat *et al.*	(CERN, CLER, UCLA+)
TORNQVIST	82B	NP B203 268	N.A. Tornqvist	(HELS)
EVANGELIS...	81	NP B178 197	C. Evangelista *et al.*	(BARI, BONN, CERN+)
BROMBERG	80	PR D22 1513	C.M. Bromberg *et al.*	(CIT, FNAL, ILLC+)
DIONISI	80	NP B169 1	C. Dionisi *et al.*	(CERN, MADR, CDEF+)
GURTU	79	NP B151 181	A. Gurtu *et al.*	(CERN, ZEEM, NIJM, OXF)
STANTON	79	PRL 42 346	N.R. Stanton *et al.*	(OSU, CARL, MCGI+) JP
CORDEN	78	NP B144 253	M.J. Corden *et al.*	(BIRM, RHEL, TELA+) JP
NACASCH	78	NP B135 203	R. Nacasch *et al.*	(PARIS, MADR, CERN)
GRASSLER	77	NP B121 189	H. Grassler *et al.*	(AACH3, BERL, BONN+)
DEFOIX	72	NP B44 125	C. Defoix *et al.*	(CDEF, CERN)
DUBOC	72	NP B46 429	J. Duboc *et al.*	(PARIS, LIVP)
THUN	72	PRL 28 1733	R. Thun *et al.*	(STON, NEAS)
BARDADIN-...	71	PR D4 2711	M. Bardadin-Otwinowska *et al.*	(WARS)
BOESEBECK	71	PL 34B 659	K. Boesebeck	(AACH, BERL, BONN, CERN, CRAC+)
CAMPBELL	69	PRL 22 1204	J.H. Campbell *et al.*	(PURD)
LORSTAD	69	NP B14 63	B. Lorstad *et al.*	(CDEF, CERN) JP
D'ANDLAU	68	NP B5 693	C. d'Andlau *et al.*	(CDEF, CERN, IRAD+) IJP
DAHL	67	PR 163 1377	O.I. Dahl *et al.*	(LRL) IJP

$\eta(1295)$ $I^G(J^{PC}) = 0^+(0^{-+})$

See also the mini-review under $\eta(1405)$

$\eta(1295)$ MASS

VALUE (MeV)	EVTS	DOCUMENT ID		TECN	COMMENT
1294±4 OUR AVERAGE	Error includes scale factor of 1.6. See the ideogram below.				
1302±9±8	20k	ADAMS	01B	B852	18 GeV $\pi^- p \to K^+ K^- \pi^0 n$
1282±5	9082	MANAK	00A	MPS	18 $\pi^- p \to \eta\pi^+\pi^- n$
1299±4	2100	ALDE	97B	GAM4	100 $\pi^- p \to \eta\pi^0\pi^0 n$
1295±4		FUKUI	91C	SPEC	8.95 $\pi^- p \to \eta\pi^+\pi^- n$
• • • We do not use the following data for averages, fits, limits, etc. • • •					
1264±8		[1] AUGUSTIN	90	DM2	$J/\psi \to \gamma\eta\pi^+\pi^-$
~ 1275		STANTON	79	CNTR	8.4 $\pi^- p \to n\eta 2\pi$

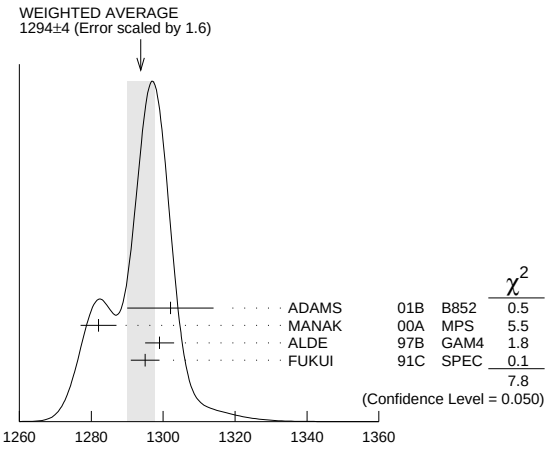

[1] PWA analysis of AUGUSTIN 92 assigns 0^{-+} quantum numbers to this state rather than 1^{++} as before.

$\eta(1295)$ WIDTH

VALUE (MeV)	EVTS	DOCUMENT ID		TECN	COMMENT
55± 5 OUR AVERAGE					
57±23±21	20k	ADAMS	01B	B852	18 GeV $\pi^- p \to K^+ K^- \pi^0 n$
66±13	9082	MANAK	00A	MPS	18 $\pi^- p \to \eta\pi^+\pi^- n$
53± 6		FUKUI	91C	SPEC	8.95 $\pi^- p \to \eta\pi^+\pi^- n$
• • • We do not use the following data for averages, fits, limits, etc. • • •					
<40	2100	ALDE	97B	GAM4	100 $\pi^- p \to \eta\pi^0\pi^0 n$
44±20		[2] AUGUSTIN	90	DM2	$J/\psi \to \gamma\eta\pi^+\pi^-$
~ 70		STANTON	79	CNTR	8.4 $\pi^- p \to n\eta 2\pi$

[2] PWA analysis of AUGUSTIN 92 assigns 0^{-+} quantum numbers to this state rather than 1^{++} as before.

$\eta(1295)$ DECAY MODES

	Mode	Fraction (Γ_i/Γ)
Γ_1	$\eta\pi^+\pi^-$	seen
Γ_2	$a_0(980)\pi$	seen
Γ_3	$\gamma\gamma$	
Γ_4	$\eta\pi^0\pi^0$	seen
Γ_5	$\eta(\pi\pi)_{S\text{-wave}}$	seen
Γ_6	$\sigma\eta$	
Γ_7	$K\overline{K}\pi$	

$\eta(1295)$ Γ(i)$\Gamma(\gamma\gamma)/\Gamma$(total)

$\Gamma(\eta\pi^+\pi^-) \times \Gamma(\gamma\gamma)/\Gamma_{\text{total}}$ $\Gamma_1\Gamma_3/\Gamma$

VALUE (keV)	CL%	DOCUMENT ID		TECN	COMMENT
<0.066	95	ACCIARRI	01G	L3	183–202 $e^+e^- \to e^+e^-\eta\pi^+\pi^-$
• • • We do not use the following data for averages, fits, limits, etc. • • •					
<0.6	90	AIHARA	88C	TPC	$e^+e^- \to e^+e^-\eta\pi^+\pi^-$
<0.3		ANTREASYAN	87	CBAL	$e^+e^- \to e^+e^-\eta\pi\pi$

$\Gamma(K\overline{K}\pi) \times \Gamma(\gamma\gamma)/\Gamma_{\text{total}}$ $\Gamma_7\Gamma_3/\Gamma$

VALUE (keV)	CL%	DOCUMENT ID		TECN	COMMENT
• • • We do not use the following data for averages, fits, limits, etc. • • •					
<0.014	90	[3,4] AHOHE	05	CLE2	10.6 $e^+e^- \to e^+e^- K^0_S K^\pm\pi^\mp$

[3] Using $\eta(1295)$ mass and width 1294 MeV and 55 MeV, respectively.
[4] Assuming three-body phase-space decay to $K^0_S K^\pm\pi^\mp$.

$\eta(1295)$ BRANCHING RATIOS

$\Gamma(a_0(980)\pi)/\Gamma_{\text{total}}$ Γ_2/Γ

VALUE	DOCUMENT ID		TECN	COMMENT
• • • We do not use the following data for averages, fits, limits, etc. • • •				
not seen	BERTIN	97	OBLX	0.0 $\overline{p}p \to K^\pm(K^0)\pi^\mp\pi^+\pi^-$
seen	BIRMAN	88	MPS	8 $\pi^-p \to K^+\overline{K}^0\pi^-n$
large	ANDO	86	SPEC	8 $\pi^-p \to \eta\pi^+\pi^-n$
large	STANTON	79	CNTR	8.4 $\pi^-p \to n\eta 2\pi$

$\Gamma(a_0(980)\pi)/\Gamma(\eta\pi^0\pi^0)$ Γ_2/Γ_4

VALUE	DOCUMENT ID		TECN	COMMENT
0.65±0.10	[5] ALDE	97B	GAM4	100 $\pi^-p \to \eta\pi^0\pi^0n$

[5] Assuming that $a_0(980)$ decays only to $\eta\pi$.

$\Gamma(\eta(\pi\pi)_{S\text{-wave}})/\Gamma(\eta\pi^0\pi^0)$ Γ_5/Γ_4

VALUE	DOCUMENT ID		TECN	COMMENT
0.35±0.10	ALDE	97B	GAM4	100 $\pi^-p \to \eta\pi^0\pi^0n$

$\Gamma(a_0(980)\pi)/\Gamma(\sigma\eta)$ Γ_2/Γ_6

VALUE	EVTS	DOCUMENT ID		TECN	COMMENT
0.48±0.22	9082	MANAK	00A	MPS	18 $\pi^-p \to \eta\pi^+\pi^-n$

$\eta(1295)$ REFERENCES

AHOHE	05	PR D71 072001	R. Ahohe *et al.*	(CLEO Collab.)
ACCIARRI	01G	PL B501 1	M. Acciarri *et al.*	(L3 Collab.)
ADAMS	01B	PL B516 264	G.S. Adams *et al.*	(BNL E852 Collab.)
MANAK	00A	PR D62 012003	J.J. Manak *et al.*	(BNL E852 Collab.)
ALDE	97B	PAN 60 386 Translated from YAF 60 458.	D. Alde *et al.*	(GAMS Collab.)
BERTIN	97	PL B400 226	A. Bertin *et al.*	(OBELIX Collab.)
AUGUSTIN	92	PR D46 1951	J.E. Augustin, G. Cosme	(DM2 Collab.)
FUKUI	91C	PL B267 293	S. Fukui *et al.*	(SUGI, NAGO, KEK, KYOT+)
AUGUSTIN	90	PR D42 10	J.E. Augustin *et al.*	(DM2 Collab.)
AIHARA	88C	PR D38 1	H. Aihara *et al.*	(TPC-2γ Collab.)
BIRMAN	88	PRL 61 1557	A. Birman *et al.*	(BNL, FSU, IND, MASD) JP
ANTREASYAN	87	PR D36 2633	D. Antreasyan *et al.*	(Crystal Ball Collab.)
ANDO	86	PRL 57 1296	A. Ando *et al.*	(KEK, KYOT, NIRS, SAGA+) IJP
STANTON	79	PRL 42 346	N.R. Stanton *et al.*	(OSU, CARL, MCGI+) JP

$\pi(1300)$

$I^G(J^{PC}) = 1^-(0^{-+})$

$\pi(1300)$ MASS

VALUE (MeV)	EVTS	DOCUMENT ID		TECN	COMMENT
1300±100 OUR ESTIMATE					
• • • We do not use the following data for averages, fits, limits, etc. • • •					
1128± 26±70		DARGENT	17	RVUE	$D^0 \to \pi^-\pi^+\pi^-\pi^+$
1345± 8±10	18k	[1] SCHEGELSKY	06	RVUE	$\gamma\gamma \to \pi^+\pi^-\pi^0$
1200± 40	90k	SALVINI	04	OBLX	$\overline{p}p \to 2\pi^+2\pi^-$
1343± 15±24		CHUNG	02	B852	18.3 $\pi^-p \to \pi^+\pi^-\pi^-p$
1375± 40		ABELE	01	CBAR	0.0 $\overline{p}d \to \pi^-4\pi^0p$
1275± 15		BERTIN	97D	OBLX	0.05 $\overline{p}p \to 2\pi^+2\pi^-$
~ 1114		ABELE	96	CBAR	0.0 $\overline{p}p \to 5\pi^0$
1190± 30		ZIELINSKI	84	SPEC	200 π^+ Z $\to$ Z3π
1240± 30		BELLINI	82	SPEC	40 π^-A $\to$ A3π
1273± 50		[2] AARON	81	RVUE	
1342± 20		BONESINI	81	OMEG	12 $\pi^-p \to p3\pi$
~ 1400		DAUM	81B	SPEC	63,94 π^-p

[1] From analysis of L3 data at 183–209 GeV.
[2] Uses multichannel Aitchison-Bowler model (BOWLER 75). Uses data from DAUM 80 and DANKOWYCH 81.

$\pi(1300)$ WIDTH

VALUE (MeV)	EVTS	DOCUMENT ID		TECN	COMMENT
200 to 600 OUR ESTIMATE					
• • • We do not use the following data for averages, fits, limits, etc. • • •					
314± 39±66		DARGENT	17	RVUE	$D^0 \to \pi^-\pi^+\pi^-\pi^+$
260± 20±30	18k	[3] SCHEGELSKY	06	RVUE	$\gamma\gamma \to \pi^+\pi^-\pi^0$
470±120	90k	SALVINI	04	OBLX	$\overline{p}p \to 2\pi^+2\pi^-$
449± 39±47		CHUNG	02	B852	18.3 $\pi^-p \to \pi^+\pi^-\pi^-p$
268± 50		ABELE	01	CBAR	0.0 $\overline{p}d \to \pi^-4\pi^0p$
218±100		BERTIN	97D	OBLX	0.05 $\overline{p}p \to 2\pi^+2\pi^-$
~ 340		ABELE	96	CBAR	0.0 $\overline{p}p \to 5\pi^0$
440± 80		ZIELINSKI	84	SPEC	200 π^+ Z $\to$ Z3π
360±120		BELLINI	82	SPEC	40 π^-A $\to$ A3π
580±100		[4] AARON	81	RVUE	
220± 70		BONESINI	81	OMEG	12 $\pi^-p \to p3\pi$
~ 600		DAUM	81B	SPEC	63,94 π^-p

[3] From analysis of L3 data at 183–209 GeV.
[4] Uses multichannel Aitchison-Bowler model (BOWLER 75). Uses data from DAUM 80 and DANKOWYCH 81.

$\pi(1300)$ DECAY MODES

	Mode	Fraction (Γ_i/Γ)
Γ_1	$\rho\pi$	seen
Γ_2	$\pi(\pi\pi)_{S\text{-wave}}$	seen
Γ_3	$\gamma\gamma$	

$\pi(1300)$ Γ(i)$\Gamma(\gamma\gamma)/\Gamma$(total)

$\Gamma(\rho\pi) \times \Gamma(\gamma\gamma)/\Gamma_{\text{total}}$ $\Gamma_1\Gamma_3/\Gamma$

VALUE (keV)	CL%	DOCUMENT ID		TECN	COMMENT
<0.085	90	ACCIARRI	97T	L3	$e^+e^- \to e^+e^-\pi^+\pi^-\pi^0$
• • • We do not use the following data for averages, fits, limits, etc. • • •					
<0.8	95	[5] SCHEGELSKY	06	RVUE	$\gamma\gamma \to \pi^+\pi^-\pi^0$
<0.54	90	ALBRECHT	97B	ARG	$e^+e^- \to e^+e^-\pi^+\pi^-\pi^0$

[5] From analysis of L3 data at 183–209 GeV.

$\pi(1300)$ BRANCHING RATIOS

$\Gamma(\pi(\pi\pi)_{S\text{-wave}})/\Gamma(\rho\pi)$ Γ_2/Γ_1

VALUE	CL%	EVTS	DOCUMENT ID		TECN	COMMENT
• • • We do not use the following data for averages, fits, limits, etc. • • •						
2.2 ±0.4		90k	SALVINI	04	OBLX	$\overline{p}p \to 2\pi^+2\pi^-$
seen			CHUNG	02	B852	18.3 $\pi^-p \to \pi^+2\pi^-p$
<0.15	90		ABELE	01	CBAR	0.0 $\overline{p}d \to \pi^-4\pi^0p$
2.12			[6] AARON	81	RVUE	

[6] Uses multichannel Aitchison-Bowler model (BOWLER 75). Uses data from DAUM 80 and DANKOWYCH 81.

$\pi(1300)$ REFERENCES

DARGENT	17	JHEP 1705 143	P. dArgent *et al.*	(HEID, BRIS)
SCHEGELSKY	06	EPJ A27 199	V.A. Schegelsky *et al.*	
SALVINI	04	EPJ C35 21	P. Salvini *et al.*	(OBELIX Collab.)
CHUNG	02	PR D65 072001	S.U. Chung *et al.*	(BNL E852 Collab.)
ABELE	01	EPJ C19 667	A. Abele *et al.*	(Crystal Barrel Collab.)
ACCIARRI	97T	PL B413 147	M. Acciarri *et al.*	(L3 Collab.)
ALBRECHT	97B	ZPHY C74 469	H. Albrecht *et al.*	(ARGUS Collab.)
BERTIN	97D	PL B414 220	A. Bertin *et al.*	(OBELIX Collab.)
ABELE	96	PL B380 453	A. Abele *et al.*	(Crystal Barrel Collab.)
ZIELINSKI	84	PR D30 1855	M. Zielinski *et al.*	(ROCH, MINN, FNAL)
BELLINI	82	PRL 48 1697	G. Bellini *et al.*	(MILA, BGNA, JINR)
AARON	81	PR D24 1207	R.A. Aaron, R.S. Longacre	(NEAS, BNL)
BONESINI	81	PL 103B 75	M. Bonesini *et al.*	(MILA, LIVP, DARE+)
DANKOWY...	81	PRL 46 580	J.A. Dankowych *et al.*	(TNTO, BNL, CARL+)
DAUM	81B	NP B182 269	C. Daum *et al.*	(AMST, CERN, CRAC, MPIM+)
DAUM	80	PL 89B 281	C. Daum *et al.*	(AMST, CERN, CRAC, MPIM+)
BOWLER	75	NP B97 227	M.G. Bowler *et al.*	(OXFTP, DARE)

Meson Particle Listings

$a_2(1320)$

$a_2(1320)$ $I^G(J^{PC}) = 1^-(2^{++})$

$a_2(1320)$ MASS

VALUE (MeV)	DOCUMENT ID

$1318.3^{+0.5}_{-0.6}$ OUR AVERAGE Includes data from the 4 datablocks that follow this one. Error includes scale factor of 1.2.

3π MODE

VALUE (MeV)	EVTS	DOCUMENT ID	TECN	CHG	COMMENT
The data in this block is included in the average printed for a previous datablock.					
$1319.0^{+1.0}_{-1.3}$ OUR AVERAGE Error includes scale factor of 1.4. See the ideogram below.					
1321 ± 1 $^{+0}_{-7}$	420k	ALEKSEEV 10	COMP		190 $\pi^- Pb \to \pi^-\pi^-\pi^+ Pb'$
1326 ± 2 ±2		CHUNG 02	B852		18.3 $\pi^- p \to \pi^+\pi^-\pi^- p$
1317 ± 3		BARBERIS 98B			450 $pp \to p_f \pi^+\pi^-\pi^0 p_s$
1323 ± 4 ±3		ACCIARRI 97T	L3		$e^+e^- \to e^+e^-\pi^+\pi^-\pi^0$
1320 ± 7		ALBRECHT 97B	ARG		$e^+e^- \to e^+e^-\pi^+\pi^-\pi^0$
1311.3± 1.6±3.0	72.4k	AMELIN 96	VES		36 $\pi^- p \to \pi^+\pi^-\pi^0 n$
1310 ± 5		ARMSTRONG 90	OMEG	0	300.0$pp \to pp\pi^+\pi^-\pi^0$
1323.8± 2.3	4022	AUGUSTIN 89	DM2	±	$J/\psi \to \rho^\pm a_2^\mp$
1320.6± 3.1	3562	AUGUSTIN 89	DM2	0	$J/\psi \to \rho^0 a_2^0$
1317 ± 2	25k	[1] DAUM 80C	SPEC	−	63,94 $\pi^- p \to 3\pi p$
1320 ±10	1097	[1] BALTAY 78B	HBC	+0	15 $\pi^+ p \to p4\pi$
1306 ± 8		FERRERSORIA 78	OMEG	−	9 $\pi^- p \to p3\pi$
1318 ± 7	1.6k	[1] EMMS 75	DBC	0	4 $\pi^+ n \to p(3\pi)^0$
1315 ± 5		[1] ANTIPOV 73C	CNTR	−	25,40 $\pi^- p \to p\eta\pi^-$
1306 ± 9	1580	CHALOUPKA 73	HBC	−	3.9 $\pi^- p$
• • • We do not use the following data for averages, fits, limits, etc. • • •					
1300 ± 2 ±4	18k	[2] SCHEGELSKY 06	RVUE	0	$\gamma\gamma \to \pi^+\pi^-\pi^0$
1305 ±14		CONDO 93	SHF		$\gamma p \to n\pi^+\pi^+\pi^-$
1310 ± 2		[1] EVANGELIS... 81	OMEG	−	12 $\pi^- p \to 3\pi p$
1343 ±11	490	BALTAY 78B	HBC	0	15 $\pi^+ p \to \Delta 3\pi$
1309 ± 5	5k	BINNIE 71	MMS	−	$\pi^- p$ near a_2 threshold
1299 ± 6	28k	BOWEN 71	MMS	−	5 $\pi^- p$
1300 ± 6	24k	BOWEN 71	MMS	+	5 $\pi^+ p$
1309 ± 4	17k	BOWEN 71	MMS	−	7 $\pi^- p$
1306 ± 4	941	ALSTON-... 70	HBC	+	7.0 $\pi^+ p \to 3\pi p$

[1] From a fit to $J^P = 2^+$ $\rho\pi$ partial wave.
[2] From analysis of L3 data at 183–209 GeV.

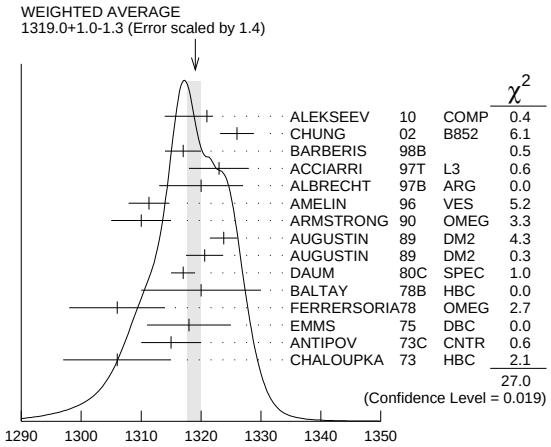

$a_2(1320)$ mass, 3π mode (MeV)

$K\overline{K}$ MODE

VALUE (MeV)	EVTS	DOCUMENT ID	TECN	CHG	COMMENT
The data in this block is included in the average printed for a previous datablock.					
1318.1± 0.7 OUR AVERAGE					
1319 ± 5	4700	[1,2] CLELAND 82B	SPEC	+	50 $\pi^+ p \to K^0_S K^+ p$
1324 ± 6	5200	[1,2] CLELAND 82B	SPEC	−	50 $\pi^- p \to K^0_S K^- p$
1320 ± 2	4000	CHABAUD 80	SPEC	−	17 π^-A $\to K^0_S K^-$A
1312 ± 4	11000	CHABAUD 78	SPEC	−	9.8 $\pi^- p \to K^- K^0_S p$
1316 ± 2	4730	CHABAUD 78	SPEC	−	18.8 $\pi^- p \to K^- K^0_S p$
1318 ± 1		[1,3] MARTIN 78D	SPEC	−	10 $\pi^- p \to K^0_S K^- p$
1320 ± 2	2724	MARGULIE 76	SPEC	−	23 $\pi^- p \to K^- K^0_S p$
1313 ± 4	730	FOLEY 72	CNTR	−	20.3 $\pi^- p \to K^- K^0_S p$
1319 ± 3	1500	[3] GRAYER 71	ASPK	−	17.2 $\pi^- p \to K^- K^0_S p$
• • • We do not use the following data for averages, fits, limits, etc. • • •					
1304 ±10	870	[4] SCHEGELSKY 06A	RVUE	0	$\gamma\gamma \to K^0_S K^0_S$
1330 ±11	1000	[1,2] CLELAND 82B	SPEC	+	30 $\pi^+ p \to K^0_S K^+ p$
1324 ± 5	350	HYAMS 78	ASPK	+	12.7 $\pi^+ p \to K^+ K^0_S p$

[1] From a fit to $J^P = 2^+$ partial wave.
[2] Number of events evaluated by us.
[3] Systematic error in mass scale subtracted.
[4] From analysis of L3 data at 91 and 183–209 GeV.

$\eta\pi$ MODE

VALUE (MeV)	EVTS	DOCUMENT ID	TECN	CHG	COMMENT
The data in this block is included in the average printed for a previous datablock.					
1317.7± 1.4 OUR AVERAGE					
1308 ± 9		BARBERIS 00H			450 $pp \to p_f \eta\pi^0 p_s$
1316 ± 9		BARBERIS 00H			450 $pp \to \Delta_f^{++}\eta\pi^- p_s$
1317 ± 1 ±2		THOMPSON 97	MPS		18 $\pi^- p \to \eta\pi^- p$
1315 ± 5 ±2		[1] AMSLER 94D	CBAR		0.0 $\overline{p}p \to \pi^0\pi^0\eta$
1325.1± 5.1		AOYAGI 93	BKEI		$\pi^- p \to \eta\pi^- p$
1317.7± 1.4±2.0		BELADIDZE 93	VES		37$\pi^- N \to \eta\pi^- N$
1323 ± 8	1000	[2] KEY 73	OSPK	−	6 $\pi^- p \to p\pi^-\eta$
• • • We do not use the following data for averages, fits, limits, etc. • • •					
1315 ±12		[3] ADOLPH 15	COMP		191 $\pi^- p \to \eta^{(\prime)}\pi^- p$
1309 ± 4		ANISOVICH 09	RVUE		$\overline{p}p$, πN
1324 ± 5		ARMSTRONG 93C	E760	0	$\overline{p}p \to \pi^0\eta\eta \to 6\gamma$
1336.2± 1.7	2561	DELFOSSE 81	SPEC	+	$\pi^\pm p \to p\pi^\pm\eta$
1330.7± 2.4	1653	DELFOSSE 81	SPEC	−	$\pi^\pm p \to p\pi^\pm\eta$
1324 ± 8	6200	[2,4] CONFORTO 73	OSPK	−	6 $\pi^- p \to p$MM$^-$

[1] The systematic error of 2 MeV corresponds to the spread of solutions.
[2] Error includes 5 MeV systematic mass-scale error.
[3] ADOLPH 15 value is derived from a Breit-Wigner fit with mass-dependent width taking the $\eta\pi$ and $\rho\pi$ channels into account.
[4] Missing mass with enriched MMS $= \eta\pi^-$, $\eta = 2\gamma$.

$\eta'\pi$ MODE

VALUE (MeV)	DOCUMENT ID	TECN	COMMENT
The data in this block is included in the average printed for a previous datablock.			
1322 ± 7 OUR AVERAGE			
1318 ± 8 $^{+3}_{-5}$	IVANOV 01	B852	18 $\pi^- p \to \eta'\pi^- p$
1327.0±10.7	BELADIDZE 93	VES	37$\pi^- N \to \eta'\pi^- N$

$a_2(1320)$ WIDTH

3π MODE

VALUE (MeV)	EVTS	DOCUMENT ID	TECN	CHG	COMMENT
$105.0^{+1.6}_{-1.9}$ OUR AVERAGE					
110 ± 2 $^{+2}_{-15}$	420k	ALEKSEEV 10	COMP		190 $\pi^- Pb \to \pi^-\pi^-\pi^+ Pb'$
108 ± 3 ±15		CHUNG 02	B852		18.3 $\pi^- p \to \pi^+\pi^-\pi^- p$
120 ±10		BARBERIS 98B			450 $pp \to p_f \pi^+\pi^-\pi^0 p_s$
105 ±10 ±11		ACCIARRI 97T	L3		$e^+e^- \to e^+e^-\pi^+\pi^-\pi^0$
120 ±10		ALBRECHT 97B	ARG		$e^+e^- \to e^+e^-\pi^+\pi^-\pi^0$
103.0± 6.0± 3.3	72.4k	AMELIN 96	VES		36 $\pi^- p \to \pi^+\pi^-\pi^0 n$
120 ±10		ARMSTRONG 90	OMEG	0	300.0$pp \to pp\pi^+\pi^-\pi^0$
107.0± 9.7	4022	AUGUSTIN 89	DM2	±	$J/\psi \to \rho^\pm a_2^\mp$
118.5±12.5	3562	AUGUSTIN 89	DM2	0	$J/\psi \to \rho^0 a_2^0$
97 ± 5		[1] EVANGELIS... 81	OMEG	−	12 $\pi^- p \to 3\pi p$
96 ± 9	25k	[1] DAUM 80C	SPEC	−	63,94 $\pi^- p \to 3\pi p$
110 ±15	1097	[1] BALTAY 78B	HBC	+0	15 $\pi^+ p \to p4\pi$
112 ±18	1.6k	[1] EMMS 75	DBC	0	4 $\pi^+ n \to p(3\pi)^0$
122 ±14	1.2k	[1,2] WAGNER 75	HBC	0	7 $\pi^+ p \to \Delta^{++}(3\pi)^0$
115 ±15		[1] ANTIPOV 73C	CNTR	−	25,40 $\pi^- p \to p\eta\pi^-$
99 ±15	1580	CHALOUPKA 73	HBC	−	3.9 $\pi^- p$
105 ± 5	28k	BOWEN 71	MMS	−	5 $\pi^- p$
99 ± 5	24k	BOWEN 71	MMS	+	5 $\pi^+ p$
103 ± 5	17k	BOWEN 71	MMS	−	7 $\pi^- p$
• • • We do not use the following data for averages, fits, limits, etc. • • •					
117 ± 6 ±20	18k	[3] SCHEGELSKY 06	RVUE	0	$\gamma\gamma \to \pi^+\pi^-\pi^0$

120	±40		CONDO	93	SHF		$\gamma p \to n\pi^+\pi^+\pi^-$	
115	±14	490	BALTAY	78B	HBC	0	15 $\pi^+ p \to \Delta 3\pi$	
72	±16	5k	BINNIE	71	MMS	−	$\pi^- p$ near a_2 threshold	
79	±12	941	ALSTON-...	70	HBC	+	7.0 $\pi^+ p \to 3\pi p$	

[1] From a fit to $J^P = 2^+$ $\rho\pi$ partial wave.
[2] Width errors enlarged by us to $4\Gamma/\sqrt{N}$; see the note with the $K^*(892)$ mass.
[3] From analysis of L3 data at 183–209 GeV.

$K\overline{K}$ AND $\eta\pi$ MODES

VALUE (MeV)	DOCUMENT ID
107 ±5 OUR ESTIMATE	
110.4±1.7 OUR AVERAGE	Includes data from the 2 datablocks that follow this one.

$K\overline{K}$ MODE

VALUE (MeV)	EVTS	DOCUMENT ID		TECN	CHG	COMMENT
The data in this block is included in the average printed for a previous datablock.						
109.8± 2.4 OUR AVERAGE						
112 ±20	4700	[1,2] CLELAND	82B	SPEC	+	50 $\pi^+ p \to K^0_S K^+ p$
120 ±25	5200	[1,2] CLELAND	82B	SPEC	−	50 $\pi^- p \to K^0_S K^- p$
106 ± 4	4000	CHABAUD	80	SPEC	−	17 π^- A $\to K^0_S K^-$ A
126 ±11	11000	CHABAUD	78	SPEC	−	9.8 $\pi^- p \to K^- K^0_S p$
101 ± 8	4730	CHABAUD	78	SPEC	−	18.8 $\pi^- p \to K^- K^0_S p$
113 ± 4		[1,3] MARTIN	78D	SPEC	−	10 $\pi^- p \to K^0_S K^- p$
105 ± 8	2724	[3] MARGULIE	76	SPEC	−	23 $\pi^- p \to K^- K^0_S p$
113 ±19	730	FOLEY	72	CNTR	−	20.3 $\pi^- p \to K^- K^0_S p$
123 ±13	1500	[3] GRAYER	71	ASPK	−	17.2 $\pi^- p \to K^- K^0_S p$
• • • We do not use the following data for averages, fits, limits, etc. • • •						
120 ±15	870	[4] SCHEGELSKY	06A	RVUE	0	$\gamma\gamma \to K^0_S K^0_S$
121 ±51	1000	[1,2] CLELAND	82B	SPEC	+	30 $\pi^+ p \to K^0_S K^+ p$
110 ±18	350	HYAMS	78	ASPK	+	12.7 $\pi^+ p \to K^+ K^0_S p$

[1] From a fit to $J^P = 2^+$ partial wave.
[2] Number of events evaluated by us.
[3] Width errors enlarged by us to $4\Gamma/\sqrt{N}$; see the note with the $K^*(892)$ mass.
[4] From analysis of L3 data at 91 and 183–209 GeV.

$\eta\pi$ MODE

VALUE (MeV)	EVTS	DOCUMENT ID		TECN	CHG	COMMENT
The data in this block is included in the average printed for a previous datablock.						
111.1± 2.4 OUR AVERAGE						
115 ±20		BARBERIS	00H			450 $pp \to p_f \eta\pi^0 p_s$
112 ±14		BARBERIS	00H			450 $pp \to \Delta^{++}_f \eta\pi^- p_s$
112 ± 3 ±2		[1] AMSLER	94D	CBAR		0.0 $\overline{p}p \to \pi^0\pi^0\eta$
103 ± 6 ±3		BELADIDZE	93	VES		37$\pi^- N \to \eta\pi^- N$
112.2± 5.7	2561	DELFOSSE	81	SPEC	+	$\pi^\pm p \to p\pi^\pm\eta$
116.6± 7.7	1653	DELFOSSE	81	SPEC	−	$\pi^\pm p \to p\pi^\pm\eta$
108 ± 9	1000	KEY	73	OSPK	−	6 $\pi^- p \to p\pi^-\eta$
• • • We do not use the following data for averages, fits, limits, etc. • • •						
119 ±14		[2] ADOLPH	15	COMP		191 $\pi^- p \to \eta^{(\prime)}\pi^- p$
110 ± 4		ANISOVICH	09	RVUE		$\overline{p}p$, πN
127 ± 2 ±2		[3] THOMPSON	97	MPS		18 $\pi^- p \to \eta\pi^- p$
118 ±10		ARMSTRONG	93C	E760	0	$\overline{p}p \to \pi^0\eta\eta \to 6\gamma$
104 ± 9	6200	[4] CONFORTO	73	OSPK	−	6 $\pi^- p \to p$MM$^-$

[1] The systematic error of 2 MeV corresponds to the spread of solutions.
[2] ADOLPH 15 value is derived from a Breit-Wigner fit with mass-dependent width taking the $\eta\pi$ and $\rho\pi$ channels into account.
[3] Resolution is not unfolded.
[4] Missing mass with enriched MMS = $\eta\pi^-$, $\eta = 2\gamma$.

$\eta'\pi$ MODE

VALUE (MeV)	DOCUMENT ID		TECN	COMMENT
119±25 OUR AVERAGE				
140±35±20	IVANOV	01	B852	18 $\pi^- p \to \eta'\pi^- p$
106±32	BELADIDZE	93	VES	37$\pi^- N \to \eta'\pi^- N$

$a_2(1320)$ DECAY MODES

	Mode	Fraction (Γ_i/Γ)	Scale factor/ Confidence level
Γ_1	3π	(70.1 ±2.7) %	S=1.2
Γ_2	$\rho(770)\pi$		
Γ_3	$f_2(1270)\pi$		
Γ_4	$\rho(1450)\pi$		
Γ_5	$\eta\pi$	(14.5 ±1.2) %	
Γ_6	$\omega\pi\pi$	(10.6 ±3.2) %	S=1.3
Γ_7	$K\overline{K}$	(4.9 ±0.8) %	
Γ_8	$\eta'(958)\pi$	(5.5 ±0.9) $\times 10^{-3}$	
Γ_9	$\pi^\pm\gamma$	(2.91±0.27) $\times 10^{-3}$	
Γ_{10}	$\gamma\gamma$	(9.4 ±0.7) $\times 10^{-6}$	
Γ_{11}	e^+e^-	< 5 $\times 10^{-9}$	CL=90%

CONSTRAINED FIT INFORMATION

An overall fit to 5 branching ratios uses 18 measurements and one constraint to determine 4 parameters. The overall fit has a χ^2 = 9.3 for 15 degrees of freedom.

The following *off-diagonal* array elements are the correlation coefficients $\langle \delta x_i \delta x_j \rangle / (\delta x_i \cdot \delta x_j)$, in percent, from the fit to the branching fractions, $x_i \equiv \Gamma_i/\Gamma_{\rm total}$. The fit constrains the x_i whose labels appear in this array to sum to one.

x_5	10		
x_6	−89	−46	
x_7	−1	−2	−24
	x_1	x_5	x_6

$a_2(1320)$ PARTIAL WIDTHS

$\Gamma(\eta\pi)$ Γ_5

VALUE (MeV)	EVTS	DOCUMENT ID		TECN	CHG	COMMENT
• • • We do not use the following data for averages, fits, limits, etc. • • •						
18.5±3.0	870	[1] SCHEGELSKY	06A	RVUE	0	$\gamma\gamma \to K^0_S K^0_S$

[1] From analysis of L3 data at 91 and 183–209 GeV, using $\Gamma(a_2(1320) \to \gamma\gamma) = 0.91$ keV and SU(3) relations.

$\Gamma(K\overline{K})$ Γ_7

VALUE (MeV)	EVTS	DOCUMENT ID		TECN	CHG	COMMENT
• • • We do not use the following data for averages, fits, limits, etc. • • •						
$7.0^{+2.0}_{-1.5}$	870	[1] SCHEGELSKY	06A	RVUE	0	$\gamma\gamma \to K^0_S K^0_S$

[1] From analysis of L3 data at 91 and 183–209 GeV, using $\Gamma(a_2(1320) \to \gamma\gamma) = 0.91$ keV and SU(3) relations.

$\Gamma(\pi^\pm\gamma)$ Γ_9

VALUE (keV)	EVTS	DOCUMENT ID		TECN	CHG	COMMENT
311± 25 OUR AVERAGE						
358± 6±42		[1] ADOLPH	14	COMP	−	190 π^-Pb $\to \pi^+\pi^-\pi^-$Pb$'$
284± 25±25	7.1k	MOLCHANOV	01	SELX		600 $\pi^- A \to \pi^+\pi^-\pi^- A$
295± 60		CIHANGIR	82	SPEC	+	200 π^+A
• • • We do not use the following data for averages, fits, limits, etc. • • •						
461±110		[2] MAY	77	SPEC	±	9.7 γA

[1] Primakoff reaction using $a_2(1320) \to 3\pi$ branching ratio of 70.1%.
[2] Assuming one-pion exchange.

$\Gamma(\gamma\gamma)$ Γ_{10}

VALUE (keV)	EVTS	DOCUMENT ID		TECN	CHG	COMMENT
1.00±0.06 OUR AVERAGE						
0.98±0.05±0.09		ACCIARRI	97T	L3		$e^+e^- \to e^+e^-\pi^+\pi^-\pi^0$
0.96±0.03±0.13		ALBRECHT	97B	ARG		$e^+e^- \to e^+e^-\pi^+\pi^-\pi^0$
1.26±0.26±0.18	36	BARU	90	MD1		$e^+e^- \to e^+e^-\pi^+\pi^-\pi^0$
1.00±0.07±0.15	415	BEHREND	90C	CELL	0	$e^+e^- \to e^+e^-\pi^+\pi^-\pi^0$
1.03±0.13±0.21		BUTLER	90	MRK2		$e^+e^- \to e^+e^-\pi^+\pi^-\pi^0$
1.01±0.14±0.22	85	OEST	90	JADE		$e^+e^- \to e^+e^-\pi^0\eta$
0.90±0.27±0.15	56	[1] ALTHOFF	86	TASS	0	$e^+e^- \to e^+e^-3\pi$
1.14±0.20±0.26		[2] ANTREASYAN	86	CBAL	0	$e^+e^- \to e^+e^-\pi^0\eta$
1.06±0.18±0.19		BERGER	84C	PLUT	0	$e^+e^- \to e^+e^-3\pi$
• • • We do not use the following data for averages, fits, limits, etc. • • •						
$0.81\pm0.19^{+0.42}_{-0.11}$	35	[1] BEHREND	82C	CELL	0	$e^+e^- \to e^+e^-3\pi$
0.77±0.18±0.27	22	[2] EDWARDS	82F	CBAL	0	$e^+e^- \to e^+e^-\pi^0\eta$

[1] From $\rho\pi$ decay mode.
[2] From $\eta\pi^0$ decay mode.

$\Gamma(e^+e^-)$ Γ_{11}

VALUE (eV)	CL%	DOCUMENT ID		TECN	COMMENT
< 0.56	90	ACHASOV	00K	SND	$e^+e^- \to \pi^0\pi^0$
• • • We do not use the following data for averages, fits, limits, etc. • • •					
<25	90	VOROBYEV	88	ND	$e^+e^- \to \pi^0\eta$

$a_2(1320)$ Γ(i)$\Gamma(\gamma\gamma)/\Gamma$(total)

$\Gamma(3\pi) \times \Gamma(\gamma\gamma)/\Gamma_{\rm total}$ $\Gamma_1\Gamma_{10}/\Gamma$

VALUE (keV)	EVTS	DOCUMENT ID		TECN	COMMENT
• • • We do not use the following data for averages, fits, limits, etc. • • •					
0.65±0.02±0.02	18k	[1] SCHEGELSKY	06	RVUE	$\gamma\gamma \to \pi^+\pi^-\pi^0$

[1] From analysis of L3 data at 183–209 GeV.

$\Gamma(\eta\pi) \times \Gamma(\gamma\gamma)/\Gamma_{total}$ $\Gamma_5\Gamma_{10}/\Gamma$

VALUE (keV)	DOCUMENT ID		TECN	COMMENT
• • • We do not use the following data for averages, fits, limits, etc. • • •				
$0.145^{+0.097}_{-0.034}$	[1] UEHARA	09A	BELL	$e^+e^- \to e^+e^-\eta\pi^0$

[1] From the D_2-wave. The fraction of the D_0-wave is $3.4^{+2.3}_{-1.1}$%.

$\Gamma(K\overline{K}) \times \Gamma(\gamma\gamma)/\Gamma_{total}$ $\Gamma_7\Gamma_{10}/\Gamma$

VALUE (keV)	DOCUMENT ID		TECN	COMMENT
0.126±0.007±0.028	[1] ALBRECHT	90G	ARG	$e^+e^- \to e^+e^-K^+K^-$
• • • We do not use the following data for averages, fits, limits, etc. • • •				
0.081±0.006±0.027	[2] ALBRECHT	90G	ARG	$e^+e^- \to e^+e^-K^+K^-$

[1] Using an incoherent background.
[2] Using a coherent background.

$a_2(1320)$ BRANCHING RATIOS

$[\Gamma(f_2(1270)\pi) + \Gamma(\rho(1450)\pi)]/\Gamma(\rho(770)\pi)$ $(\Gamma_3+\Gamma_4)/\Gamma_2$

VALUE	CL%	DOCUMENT ID		TECN	CHG	COMMENT
<0.12	90	ABRAMOVI...	70B	HBC	–	3.93 π^-p

$\Gamma(\eta\pi)/\Gamma(3\pi)$ Γ_5/Γ_1

VALUE	EVTS	DOCUMENT ID		TECN	CHG	COMMENT
0.207±0.018 OUR FIT						
0.213±0.020 OUR AVERAGE						
0.18 ±0.05		FORINO	76	HBC		11 π^-p
0.22 ±0.05	52	ANTIPOV	73	CNTR	–	40 π^-p
0.211±0.044	149	CHALOUPKA	73	HBC	–	3.9 π^-p
0.246±0.042	167	ALSTON-...	71	HBC	+	7.0 π^+p
0.25 ±0.09	15	BOECKMANN	70	HBC	+	5.0 π^+p
0.23 ±0.08	22	ASCOLI	68	HBC	–	5 π^-p
0.12 ±0.08		CHUNG	68	HBC	–	3.2 π^-p
0.22 ±0.09		CONTE	67	HBC	–	11.0 π^-p

$\Gamma(\omega\pi\pi)/\Gamma(3\pi)$ Γ_6/Γ_1

VALUE	EVTS	DOCUMENT ID		TECN	CHG	COMMENT
0.15±0.05 OUR FIT Error includes scale factor of 1.3.						
0.15±0.05 OUR AVERAGE Error includes scale factor of 1.3. See the ideogram below.						
0.28±0.09	60	DIAZ	74	DBC	0	6 π^+n
0.18±0.08		[1] KARSHON	74	HBC		Avg. of above two
0.10±0.05	279	[2] CHALOUPKA	73	HBC	–	3.9 π^-p
• • • We do not use the following data for averages, fits, limits, etc. • • •						
0.29±0.08	140	[1] KARSHON	74	HBC	0	4.9 π^+p
0.10±0.04	60	[1] KARSHON	74	HBC	+	4.9 π^+p
0.19±0.08		DEFOIX	73	HBC	0	0.7 $\overline{p}p$

[1] KARSHON 74 suggest an additional $I = 0$ state strongly coupled to $\omega\pi\pi$ which could explain discrepancies in branching ratios and masses. We use a central value and a systematic spread.
[2] Decays to $b_1(1040)\pi$, $b_1 \to \omega\pi$. Error increased to account for possible systematic errors of complicated analysis.

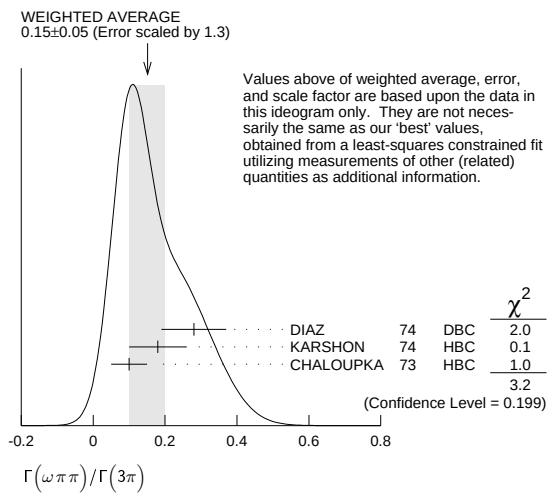

$\Gamma(K\overline{K})/\Gamma(3\pi)$ Γ_7/Γ_1

VALUE	EVTS	DOCUMENT ID		TECN	CHG	COMMENT
0.070±0.012 OUR FIT						
0.078±0.017		CHABAUD	78	RVUE		
• • • We do not use the following data for averages, fits, limits, etc. • • •						
0.011±0.003		[1] BERTIN	98B	OBLX		0.0 $\overline{p}p \to K^\pm K_S\pi^\mp$
0.056±0.014	50	[2] CHALOUPKA	73	HBC	–	3.9 π^-p
0.097±0.018	113	[2] ALSTON-...	71	HBC	+	7.0 π^+p
0.06 ±0.03		[2] ABRAMOVI...	70B	HBC	–	3.93 π^-p
0.054±0.022		[2] CHUNG	68	HBC	–	3.2 π^-p

[1] Using 4π data from BERTIN 97D.
[2] Included in CHABAUD 78 review.

$\Gamma(K\overline{K})/\Gamma(\eta\pi)$ Γ_7/Γ_5

VALUE	DOCUMENT ID		TECN	COMMENT
• • • We do not use the following data for averages, fits, limits, etc. • • •				
0.08±0.02	[1] BERTIN	98B	OBLX	0.0 $\overline{p}p \to K^\pm K_S\pi^\mp$

[1] Using $\eta\pi\pi$ data from AMSLER 94D.

$\Gamma(\eta\pi)/[\Gamma(3\pi) + \Gamma(\eta\pi) + \Gamma(K\overline{K})]$ $\Gamma_5/(\Gamma_1+\Gamma_5+\Gamma_7)$

VALUE	EVTS	DOCUMENT ID		TECN	CHG	COMMENT
0.162±0.012 OUR FIT						
0.140±0.028 OUR AVERAGE						
0.13 ±0.04		ESPIGAT	72	HBC	±	0.0 $\overline{p}p$
0.15 ±0.04	34	BARNHAM	71	HBC	+	3.7 π^+p

$\Gamma(K\overline{K})/[\Gamma(3\pi) + \Gamma(\eta\pi) + \Gamma(K\overline{K})]$ $\Gamma_7/(\Gamma_1+\Gamma_5+\Gamma_7)$

VALUE	EVTS	DOCUMENT ID		TECN	CHG	COMMENT
0.054±0.009 OUR FIT						
0.048±0.012 OUR AVERAGE						
0.05 ±0.02		TOET	73	HBC	+	5 π^+p
0.09 ±0.04		TOET	73	HBC	0	5 π^+p
0.03 ±0.02	8	[1] DAMERI	72	HBC	–	11 π^-p
0.06 ±0.03	17	BARNHAM	71	HBC	+	3.7 π^+p
• • • We do not use the following data for averages, fits, limits, etc. • • •						
0.020±0.004		[2] ESPIGAT	72	HBC	±	0.0 $\overline{p}p$

[1] Montanet agrees. Vlada.
[2] Not averaged because of discrepancy between masses from $K\overline{K}$ and $\rho\pi$ modes.

$\Gamma(\eta'(958)\pi)/\Gamma_{total}$ Γ_8/Γ

VALUE	CL%	DOCUMENT ID		TECN	CHG	COMMENT
• • • We do not use the following data for averages, fits, limits, etc. • • •						
<0.006	95	ALDE	92B	GAM2		38,100 $\pi^-p \to \eta'\pi^0 n$
<0.02	97	BARNHAM	71	HBC	+	3.7 π^+p
0.004±0.004		[1] BOESEBECK	68	HBC	+	8 π^+p

[1] No longer valid since $\Gamma(K\overline{K})/\Gamma(3\pi)$ value has changed (MORRISON 71).

$\Gamma(\eta'(958)\pi)/\Gamma(3\pi)$ Γ_8/Γ_1

VALUE	CL%	DOCUMENT ID		TECN	CHG	COMMENT
• • • We do not use the following data for averages, fits, limits, etc. • • •						
<0.011	90	EISENSTEIN	73	HBC	–	5 π^-p
<0.04		ALSTON-...	71	HBC	+	7.0 π^+p
$0.04^{+0.03}_{-0.04}$		BOECKMANN	70	HBC	0	5.0 π^+p

$\Gamma(\eta'(958)\pi)/\Gamma(\eta\pi)$ Γ_8/Γ_5

VALUE	DOCUMENT ID		TECN	COMMENT
0.038±0.005 OUR AVERAGE				
0.05 ±0.02	ADOLPH	15	COMP	191 $\pi^-p \to \eta^{(\prime)}\pi^-p$
0.032±0.009	ABELE	97C	CBAR	0.0 $\overline{p}p \to \pi^0\pi^0\eta'$
0.047±0.010±0.004	[1] BELADIDZE	93	VES	37$\pi^-N \to a_2^-N$
0.034±0.008±0.005	BELADIDZE	92	VES	36π^-C $\to a_2^-$C

[1] Using $B(\eta' \to \pi^+\pi^-\eta) = 0.441$, $B(\eta \to \gamma\gamma) = 0.389$ and $B(\eta \to \pi^+\pi^-\pi^0) = 0.236$.

$\Gamma(\pi^\pm\gamma)/\Gamma_{total}$ Γ_9/Γ

VALUE	DOCUMENT ID		TECN	COMMENT
• • • We do not use the following data for averages, fits, limits, etc. • • •				
$0.005^{+0.005}_{-0.003}$	[1] EISENBERG	72	HBC	4.3,5.25,7.5 γp

[1] Pion-exchange model used in this estimation.

$\Gamma(e^+e^-)/\Gamma_{total}$ Γ_{11}/Γ

VALUE (units 10^{-9})	CL%	DOCUMENT ID		TECN	COMMENT
• • • We do not use the following data for averages, fits, limits, etc. • • •					
<6	90	ACHASOV	00K	SND	$e^+e^- \to \pi^0\pi^0$

$a_2(1320)$ REFERENCES

ADOLPH	15	PL B740 303	M. Adolph *et al.*	(COMPASS Collab.)
ADOLPH	14	EPJ A50 79	C. Adolph *et al.*	(COMPASS Collab.)
ALEKSEEV	10	PRL 104 241803	M.G. Alekseev *et al.*	(COMPASS Collab.)
ANISOVICH	09	IJMP A24 2481	V.V. Anisovich, A.V. Sarantsev	
UEHARA	09A	PR D80 032001	S. Uehara *et al.*	(BELLE Collab.)
SCHEGELSKY	06	EPJ A27 199	V.A. Schegelsky *et al.*	
SCHEGELSKY	06A	EPJ A27 207	V.A. Schegelsky *et al.*	
CHUNG	02	PR D65 072001	S.U. Chung *et al.*	(BNL E852 Collab.)
IVANOV	01	PRL 86 3977	E.I. Ivanov *et al.*	(BNL E852 Collab.)
MOLCHANOV	01	PL B521 171	V.V. Molchanov *et al.*	(FNAL SELEX Collab.)
ACHASOV	00K	PL B492 8	M.N. Achasov *et al.*	(Novosibirsk SND Collab.)
BARBERIS	00H	PL B488 225	D. Barberis *et al.*	(WA 102 Collab.)
BARBERIS	98B	PL B422 399	D. Barberis *et al.*	(WA 102 Collab.)
BERTIN	98B	PL B434 180	A. Bertin *et al.*	(OBELIX Collab.)
ABELE	97C	PL B404 179	A. Abele *et al.*	(Crystal Barrel Collab.)

ACCIARRI	97T	PL B413 147	M. Acciarri *et al.*	(L3 Collab.)
ALBRECHT	97B	ZPHY C74 469	H. Albrecht *et al.*	(ARGUS Collab.)
THOMPSON	97	PRL 79 1630	D.R. Thompson *et al.*	(BNL E852 Collab.)
AMELIN	96	ZPHY C70 71	D.V. Amelin *et al.*	(SERP, TBIL)
AMSLER	94D	PL B333 277	C. Amsler *et al.*	(Crystal Barrel Collab.)
AOYAGI	93	PL B314 246	H. Aoyagi *et al.*	(BKEI Collab.)
ARMSTRONG	93C	PL B307 394	T.A. Armstrong *et al.*	(FNAL, FERR, GENO+)
BELADIDZE	93	PL B313 276	G.M. Beladidze *et al.*	(VES Collab.)
CONDO	93	PR D48 3045	G.T. Condo *et al.*	(SLAC Hybrid Collab.)
ALDE	92B	ZPHY C54 549	D.M. Alde *et al.*	(SERP, BELG, LANL, LAPP+)
BELADIDZE	92	ZPHY C54 235	G.M. Beladidze *et al.*	(VES Collab.)
ALBRECHT	90G	ZPHY C48 183	H. Albrecht *et al.*	(ARGUS Collab.)
ARMSTRONG	90	ZPHY C48 213	T.A. Armstrong, M. Benayoun, W. Beusch	(WA76 Coll.)
BARU	90	ZPHY C48 581	S.E. Baru *et al.*	(MD-1 Collab.)
BEHREND	90C	ZPHY C46 583	H.J. Behrend *et al.*	(CELLO Collab.)
BUTLER	90	PR D42 1368	F. Butler *et al.*	(Mark II Collab.)
OEST	90	ZPHY C47 343	T. Oest *et al.*	(JADE Collab.)
AUGUSTIN	89	NP B320 1	J.E. Augustin, G. Cosme	(DM2 Collab.)
VOROBYEV	88	SJNP 48 273	P.V. Vorobiev *et al.*	(NOVO)
		Translated from YAF 48 436.		
ALTHOFF	86	ZPHY C31 537	M. Althoff *et al.*	(TASSO Collab.)
ANTREASYAN	86	PR D33 1847	D. Antreasyan *et al.*	(Crystal Ball Collab.)
BERGER	84C	PL 149B 427	C. Berger *et al.*	(PLUTO Collab.)
BEHREND	82C	PL 114B 378	H.J. Behrend *et al.*	(CELLO Collab.)
Also		PL 125B 518 (erratum)	H.J. Behrend *et al.*	(CELLO Collab.)
CIHANGIR	82	PL 117B 123	S. Cihangir *et al.*	(FNAL, MINN, ROCH)
CLELAND	82B	NP B208 228	W.E. Cleland *et al.*	(DURH, GEVA, LAUS+)
EDWARDS	82F	PL 110B 82	C. Edwards *et al.*	(CIT, HARV, PRIN+)
DELFOSSE	81	NP B183 349	A. Delfosse *et al.*	(GEVA, LAUS)
EVANGELIS...	81	NP B178 197	C. Evangelista *et al.*	(BARI, BONN, CERN+)
CHABAUD	80	NP B175 189	V. Chabaud *et al.*	(CERN, MPIM, AMST)
DAUM	80C	PL 89B 276	C. Daum *et al.*	(AMST, CERN, CRAC, MPIM+) JP
BALTAY	78B	PR D17 62	C. Baltay *et al.*	(COLU, BING)
CHABAUD	78	NP B145 349	V. Chabaud *et al.*	(CERN, MPIM)
FERRERSORIA	78	PL 74B 287	A. Ferrer Soria *et al.*	(ORSAY, CERN, CDEF+)
HYAMS	78	NP B146 303	B.D. Hyams *et al.*	(CERN, MPIM, ATEN)
MARTIN	78D	PL 74B 417	A.D. Martin *et al.*	(DURH, GEVA) JP
MAY	77	PR D16 1983	E.N. May *et al.*	(ROCH, CORN)
FORINO	76	NC 35A 465	A. Forino *et al.*	(BGNA, FIRZ, GENO, MILA+)
MARGULIE	76	PR D14 667	M. Margulies *et al.*	(BNL, CUNY)
EMMS	75	PL 58B 117	M.J. Emms *et al.*	(BIRM, DURH, RHEL) JP
WAGNER	75	PL 58B 201	F. Wagner, M. Tabak, D.M. Chew	(LBL) JP
DIAZ	74	PRL 32 260	J. Diaz *et al.*	(CASE, CMU)
KARSHON	74	PRL 32 852	U. Karshon *et al.*	(REHO)
ANTIPOV	73	NP B63 175	Y.M. Antipov *et al.*	(CERN, SERP) JP
ANTIPOV	73C	NP B63 153	Y.M. Antipov *et al.*	(CERN, SERP) JP
CHALOUPKA	73	PL 44B 211	V. Chaloupka *et al.*	(CERN)
CONFORTO	73	PL 45B 154	G. Conforto *et al.*	(EFI, FNAL, TNTO+)
DEFOIX	73	PL 43B 141	C. Defoix *et al.*	(CDEF)
EISENSTEIN	73	PR D7 278	L. Eisenstein *et al.*	(ILL)
KEY	73	PRL 30 503	A.W. Key *et al.*	(TNTO, EFI, FNAL, WISC)
TOET	73	NP B63 248	D.Z. Toet *et al.*	(NIJM, BONN, DURH, TORI)
DAMERI	72	NC 9A 1	M. Dameri *et al.*	(GENO, MILA, SACL)
EISENBERG	72	PR D5 15	Y. Eisenberg *et al.*	(REHO, SLAC, TELA)
ESPIGAT	72	NP B36 93	P. Espigat *et al.*	(CERN, CDEF)
FOLEY	72	PR D6 747	K.J. Foley *et al.*	(BNL, CUNY)
ALSTON-...	71	PL 34B 156	M. Alston-Garnjost *et al.*	(LRL)
BARNHAM	71	PRL 26 1494	K.W.J. Barnham *et al.*	(LBL)
BINNIE	71	PL 36B 257	D.M. Binnie *et al.*	(LOIC, SHMP)
BOWEN	71	PRL 26 1663	D.R. Bowen *et al.*	(NEAS, STON)
GRAYER	71	PL 34B 333	G. Grayer *et al.*	(CERN, MPIM)
ABRAMOVI...	70B	NP B23 466	M. Abramovich *et al.*	(CERN) JP
ALSTON-...	70	PL 33B 607	M. Alston-Garnjost *et al.*	(LRL)
BOECKMANN	70	NP B16 221	K. Boeckmann *et al.*	(BONN, DURH, NIJM+)
ASCOLI	68	PRL 20 1321	G. Ascoli *et al.*	(ILL) JP
BOESEBECK	68	NP B4 501	K. Boesebeck *et al.*	(AACH, BERL, CERN)
CHUNG	68	PR 165 1491	S.U. Chung *et al.*	(LRL)
CONTE	67	NC 51A 175	F. Conte *et al.*	(GENO, HAMB, MILA, SACL)

$f_0(1370)$

$I^G(J^{PC}) = 0^+(0^{++})$

See also the mini-reviews on scalar mesons under $f_0(500)$ (see the index for the page number) and on non-$q\overline{q}$ candidates in PDG 06, Journal of Physics **G33** 1 (2006).

$f_0(1370)$ T-MATRIX POLE POSITION

Note that $\Gamma \approx 2\ \mathrm{Im}(\sqrt{s_{\mathrm{pole}}})$.

VALUE (MeV)	DOCUMENT ID		TECN	COMMENT
(1200–1500)−*i*(150–250) OUR ESTIMATE				
• • • We do not use the following data for averages, fits, limits, etc. • • •				
$(1290 \pm 50) - i(170^{+20}_{-40})$	[1] ANISOVICH	09	RVUE	0.0 $\overline{p}p$, πN
$(1373 \pm 15) - i(137 \pm 10)$	[2] BARGIOTTI	03	OBLX	$\overline{p}p$
$(1302 \pm 17) - i(166 \pm 18)$	[3] BARBERIS	00C		450 $pp \rightarrow p_f 4\pi p_s$
$(1312 \pm 25 \pm 10) - i(109 \pm 22 \pm 15)$	BARBERIS	99D	OMEG	450 $pp \rightarrow K^+K^-$, $\pi^+\pi^-$
$(1406 \pm 19) - i(80 \pm 6)$	[4] KAMINSKI	99	RVUE	$\pi\pi \rightarrow \pi\pi$, $K\overline{K}$, $\sigma\sigma$
$(1300 \pm 20) - i(120 \pm 20)$	ANISOVICH	98B	RVUE	Compilation
$(1290 \pm 15) - i(145 \pm 15)$	BARBERIS	97B	OMEG	450 $pp \rightarrow pp2(\pi^+\pi^-)$
$(1548 \pm 40) - i(560 \pm 40)$	BERTIN	97C	OBLX	0.0 $\overline{p}p \rightarrow \pi^+\pi^-\pi^0$
$(1380 \pm 40) - i(180 \pm 25)$	ABELE	96B	CBAR	0.0 $\overline{p}p \rightarrow \pi^0 K^0_L K^0_L$
$(1300 \pm 15) - i(115 \pm 8)$	BUGG	96	RVUE	
$(1330 \pm 50) - i(150 \pm 40)$	[5] AMSLER	95B	CBAR	$\overline{p}p \rightarrow 3\pi^0$
$(1360 \pm 35) - i(150–300)$	[5] AMSLER	95C	CBAR	$\overline{p}p \rightarrow \pi^0\eta\eta$
$(1390 \pm 30) - i(190 \pm 40)$	[6] AMSLER	95D	CBAR	$\overline{p}p \rightarrow 3\pi^0, \pi^0\eta\eta$, $\pi^0\pi^0\eta$
$1346 - i249$	[7,8] JANSSEN	95	RVUE	$\pi\pi \rightarrow \pi\pi$, $K\overline{K}$
$1214 - i168$	[8,9] TORNQVIST	95	RVUE	$\pi\pi \rightarrow \pi\pi$, $K\overline{K}$, $K\pi$, $\eta\pi$
$1364 - i139$	AMSLER	94D	CBAR	$\overline{p}p \rightarrow \pi^0\pi^0\eta$
$(1365^{+20}_{-55}) - i(134 \pm 35)$	ANISOVICH	94	CBAR	$\overline{p}p \rightarrow 3\pi^0, \pi^0\eta\eta$
$(1340 \pm 40) - i(127^{+30}_{-20})$	[10] BUGG	94	RVUE	$\overline{p}p \rightarrow 3\pi^0, \eta\eta\pi^0$, $\eta\pi^0\pi^0$
$(1430 \pm 5) - i(73 \pm 13)$	[11] KAMINSKI	94	RVUE	$\pi\pi \rightarrow \pi\pi$, $K\overline{K}$
$1420 - i220$	[12] AU	87	RVUE	$\pi\pi \rightarrow \pi\pi$, $K\overline{K}$

[1] Another pole is found at $(1510 \pm 130) - i\,(800^{+100}_{-150})$ MeV.
[2] Coupled channel analysis of $\pi^+\pi^-\pi^0$, $K^+K^-\pi^0$, and $K^\pm K^0_S\pi^\mp$.
[3] Average between $\pi^+\pi^-2\pi^0$ and $2(\pi^+\pi^-)$.
[4] T-matrix pole on sheet $---$.
[5] Supersedes ANISOVICH 94.
[6] Coupled-channel analysis of $\overline{p}p \rightarrow 3\pi^0$, $\pi^0\eta\eta$, and $\pi^0\pi^0\eta$ on sheet IV. Demonstrates explicitly that $f_0(500)$ and $f_0(1370)$ are two different poles.
[7] Analysis of data from FALVARD 88.
[8] The pole is on Sheet III. Demonstrates explicitly that $f_0(500)$ and $f_0(1370)$ are two different poles.
[9] Uses data from BEIER 72B, OCHS 73, HYAMS 73, GRAYER 74, ROSSELET 77, CASON 83, ASTON 88, and ARMSTRONG 91B. Coupled channel analysis with flavor symmetry and all light two-pseudoscalars systems.
[10] Reanalysis of ANISOVICH 94 data.
[11] T-matrix pole on sheet III.
[12] Analysis of data from OCHS 73,GRAYER 74, BECKER 79, and CASON 83.

$f_0(1370)$ BREIT-WIGNER MASS OR K-MATRIX POLE PARAMETER

VALUE (MeV)	DOCUMENT ID
1200 to 1500 OUR ESTIMATE	

$\pi\pi$ MODE

VALUE (MeV)	EVTS	DOCUMENT ID		TECN	COMMENT
• • • We do not use the following data for averages, fits, limits, etc. • • •					
1400 ± 40		[1] AUBERT	09L	BABR	$B^\pm \rightarrow \pi^\pm\pi^\pm\pi^\mp$
$1470^{+\ 6+\ 72}_{-\ 7-255}$		[2] UEHARA	08A	BELL	10.6 $e^+e^- \rightarrow e^+e^-\pi^0\pi^0$
1259 ± 55	2.6k	BONVICINI	07	CLEO	$D^+ \rightarrow \pi^-\pi^+\pi^+$
$1309 \pm 1 \pm 15$		[3] BUGG	07A	RVUE	0.0 $p\overline{p} \rightarrow 3\pi^0$
1449 ± 13	4.3k	[4] GARMASH	06	BELL	$B^+ \rightarrow K^+\pi^+\pi^-$
1350 ± 50		ABLIKIM	05	BES2	$J/\psi \rightarrow \phi\pi^+\pi^-$
$1265 \pm 30^{+\ 20}_{-\ 35}$		ABLIKIM	05Q	BES2	$\psi(2S) \rightarrow \gamma\pi^+\pi^-K^+K^-$
$1434 \pm 18 \pm 9$	848	AITALA	01A	E791	$D^+_s \rightarrow \pi^-\pi^+\pi^+$
1308 ± 10		BARBERIS	99B	OMEG	450 $pp \rightarrow p_s p_f \pi^+\pi^-$
1315 ± 50		BELLAZZINI	99	GAM4	450 $pp \rightarrow pp\pi^0\pi^0$
1315 ± 30		ALDE	98	GAM4	100 $\pi^-p \rightarrow \pi^0\pi^0 n$
1280 ± 55		BERTIN	98	OBLX	0.05–0.405 $\overline{n}p \rightarrow \pi^+\pi^+\pi^-$
1186		[5,6] TORNQVIST	95	RVUE	$\pi\pi \rightarrow \pi\pi$, $K\overline{K}$, $K\pi$, $\eta\pi$
1472 ± 12		ARMSTRONG	91	OMEG	300 $pp \rightarrow pp\pi\pi$, $ppK\overline{K}$
1275 ± 20		BREAKSTONE	90	SFM	62 $pp \rightarrow pp\pi^+\pi^-$
1420 ± 20		AKESSON	86	SPEC	63 $pp \rightarrow pp\pi^+\pi^-$
1256		FROGGATT	77	RVUE	$\pi^+\pi^-$ channel

[1] Breit-Wigner mass.
[2] Breit-Wigner mass. May also be the $f_0(1500)$.
[3] Reanalysis of ABELE 96C data.
[4] Also observed by GARMASH 07 in $B^0 \rightarrow K^0_S\pi^+\pi^-$ decays. Supersedes GARMASH 05.
[5] Uses data from BEIER 72B, OCHS 73, HYAMS 73, GRAYER 74, ROSSELET 77, CASON 83, ASTON 88, and ARMSTRONG 91B. Coupled channel analysis with flavor symmetry and all light two-pseudoscalars systems.
[6] Also observed by ASNER 00 in $\tau^- \rightarrow \pi^-\pi^0\pi^0\nu_\tau$ decays

$K\overline{K}$ MODE

VALUE (MeV)	EVTS	DOCUMENT ID		TECN	COMMENT
• • • We do not use the following data for averages, fits, limits, etc. • • •					
$1360 \pm 31 \pm 28$	430	[1,2] DOBBS	15		$J/\psi \rightarrow \gamma K^+K^-$
$1350 \pm 48 \pm 15$	168	[1,2] DOBBS	15		$\psi(2S) \rightarrow \gamma K^+K^-$
1440 ± 6		VLADIMIRSK...06		SPEC	40 $\pi^-p \rightarrow K^0_S K^0_S n$
1391 ± 10		TIKHOMIROV	03	SPEC	40.0 π^-C $\rightarrow K^0_S K^0_S K^0_L$ X
1440 ± 50		BOLONKIN	88	SPEC	40 $\pi^-p \rightarrow K^0_S K^0_S n$
1463 ± 9		ETKIN	82B	MPS	23 $\pi^-p \rightarrow n2K^0_S$
1425 ± 15		WICKLUND	80	SPEC	6 $\pi N \rightarrow K^+K^-N$
~ 1300		POLYCHRO...	79	STRC	7 $\pi^-p \rightarrow n2K^0_S$

[1] Using CLEO-c data but not authored by the CLEO Collaboration.
[2] From a fit to a Breit-Wigner line shape with fixed $\Gamma = 346$ MeV.

4π MODE $2(\pi\pi)_S$+$\rho\rho$

VALUE (MeV)	EVTS	DOCUMENT ID		TECN	COMMENT
• • • We do not use the following data for averages, fits, limits, etc. • • •					
1395 ± 40		ABELE	01	CBAR	0.0 $\overline{p}d \rightarrow \pi^-4\pi^0 p$
1374 ± 38		AMSLER	94	CBAR	0.0 $\overline{p}p \rightarrow \pi^+\pi^-3\pi^0$
1345 ± 12		ADAMO	93	OBLX	$\overline{n}p \rightarrow 3\pi^+2\pi^-$
1386 ± 30		GASPERO	93	DBC	0.0 $\overline{p}n \rightarrow 2\pi^+3\pi^-$
~ 1410	5751	[1] BETTINI	66	DBC	0.0 $\overline{p}n \rightarrow 2\pi^+3\pi^-$

[1] $\rho\rho$ dominant.

Meson Particle Listings

$f_0(1370)$

$\eta\eta$ MODE

VALUE (MeV)	DOCUMENT ID		TECN	COMMENT
• • • We do not use the following data for averages, fits, limits, etc. • • •				
$1262^{+51}_{-78}\pm\ 82\ {}^{-103}$	[1] UEHARA	10A	BELL	10.6 $e^+e^-\to e^+e^-\eta\eta$
1430	AMSLER	92	CBAR	0.0 $\overline{p}p\to\pi^0\eta\eta$
1220 ± 40	ALDE	86D	GAM4	100 $\pi^-p\to n2\eta$

[1] Breit-Wigner mass. May also be the $f_0(1500)$.

COUPLED CHANNEL MODE

VALUE (MeV)	DOCUMENT ID		TECN
• • • We do not use the following data for averages, fits, limits, etc. • • •			
1306 ± 20	[1] ANISOVICH	03	RVUE

[1] K-matrix pole from combined analysis of $\pi^-p\to\pi^0\pi^0n$, $\pi^-p\to K\overline{K}n$, $\pi^+\pi^-\to\pi^+\pi^-$, $\overline{p}p\to\pi^0\pi^0\pi^0$, $\pi^0\eta\eta$, $\pi^0\pi^0\eta$, $\pi^+\pi^-\pi^0$, $K^+K^-\pi^0$, $K^0_SK^0_S\pi^0$, $K^+K^0_S\pi^-$ at rest, $\overline{p}n\to\pi^-\pi^-\pi^+$, $K^0_SK^-\pi^0$, $K^0_SK^0_S\pi^-$ at rest.

$f_0(1370)$ BREIT-WIGNER WIDTH

VALUE (MeV)	DOCUMENT ID
200 to 500 OUR ESTIMATE	

$\pi\pi$ MODE

VALUE (MeV)	EVTS	DOCUMENT ID		TECN	COMMENT
• • • We do not use the following data for averages, fits, limits, etc. • • •					
$300\pm\ 80$		[1] AUBERT	09L	BABR	$B^\pm\to\pi^\pm\pi^\pm\pi^\mp$
$90^{+\ 2+\ 50}_{-\ 1-\ 22}$		[2] UEHARA	08A	BELL	10.6 $e^+e^-\to e^+e^-\pi^0\pi^0$
$298\pm\ 21$	2.6k	BONVICINI	07	CLEO	$D^+\to\pi^-\pi^+\pi^+$
$126\pm\ 25$	4286	[3] GARMASH	06	BELL	$B^+\to K^+\pi^+\pi^-$
$265\pm\ 40$		ABLIKIM	05	BES2	$J/\psi\to\phi\pi^+\pi^-$
$350\pm100^{+105}_{-\ 60}$		ABLIKIM	05Q	BES2	$\psi(2S)\to\gamma\pi^+\pi^-K^+K^-$
$173\pm\ 32\pm\ 6$	848	AITALA	01A	E791	$D^+_s\to\pi^-\pi^+\pi^+$
$222\pm\ 20$		BARBERIS	99B	OMEG	450 $pp\to p_sp_f\pi^+\pi^-$
$255\pm\ 60$		BELLAZZINI	99	GAM4	450 $pp\to pp\pi^0\pi^0$
$190\pm\ 50$		ALDE	98	GAM4	100 $\pi^-p\to\pi^0\pi^0n$
$323\pm\ 13$		BERTIN	98	OBLX	0.05–0.405 $\overline{n}p\to\pi^+\pi^+\pi^-$
350		[4,5] TORNQVIST	95	RVUE	$\pi\pi\to\pi\pi$, $K\overline{K}$, $K\pi$, $\eta\pi$
$195\pm\ 33$		ARMSTRONG	91	OMEG	300 $pp\to pp\pi\pi$, $pp K\overline{K}$
$285\pm\ 60$		BREAKSTONE	90	SFM	62 $pp\to pp\pi^+\pi^-$
$460\pm\ 50$		AKESSON	86	SPEC	63 $pp\to pp\pi^+\pi^-$
~ 400		[6] FROGGATT	77	RVUE	$\pi^+\pi^-$ channel

[1] The systematic errors are not reported.

[2] Breit-Wigner width. May also be the $f_0(1500)$.

[3] Also observed by GARMASH 07 in $B^0\to K^0_S\pi^+\pi^-$ decays. Supersedes GARMASH 05.

[4] Uses data from BEIER 72B, OCHS 73, HYAMS 73, GRAYER 74, ROSSELET 77, CASON 83, ASTON 88, and ARMSTRONG 91B. Coupled channel analysis with flavor symmetry and all light two-pseudoscalars systems.

[5] Also observed by ASNER 00 in $\tau^-\to\pi^-\pi^0\pi^0\nu_\tau$ decays

[6] Width defined as distance between 45 and 135° phase shift.

$K\overline{K}$ MODE

VALUE (MeV)	DOCUMENT ID		TECN	COMMENT
• • • We do not use the following data for averages, fits, limits, etc. • • •				
$121\pm\ 15$	VLADIMIRSK...06		SPEC	40 $\pi^-p\to K^0_SK^0_Sn$
$55\pm\ 26$	TIKHOMIROV	03	SPEC	40.0 π^-C $\to K^0_SK^0_SK^0_LX$
$250\pm\ 80$	BOLONKIN	88	SPEC	40 $\pi^-p\to K^0_SK^0_Sn$
$118^{+138}_{-\ 16}$	ETKIN	82B	MPS	23 $\pi^-p\to n2K^0_S$
$160\pm\ 30$	WICKLUND	80	SPEC	6 $\pi N\to K^+K^-N$
~ 150	POLYCHRO...	79	STRC	7 $\pi^-p\to n2K^0_S$

4π MODE $2(\pi\pi)_S+\rho\rho$

VALUE (MeV)	EVTS	DOCUMENT ID		TECN	COMMENT
• • • We do not use the following data for averages, fits, limits, etc. • • •					
275 ± 55		ABELE	01	CBAR	0.0 $\overline{p}d\to\pi^-4\pi^0p$
375 ± 61		AMSLER	94	CBAR	0.0 $\overline{p}p\to\pi^+\pi^-3\pi^0$
398 ± 26		ADAMO	93	OBLX	$\overline{n}p\to3\pi^+2\pi^-$
310 ± 50		GASPERO	93	DBC	0.0 $\overline{p}n\to2\pi^+3\pi^-$
$\sim\ 90$	5751	[1] BETTINI	66	DBC	0.0 $\overline{p}n\to2\pi^+3\pi^-$

[1] $\rho\rho$ dominant.

$\eta\eta$ MODE

VALUE (MeV)	DOCUMENT ID		TECN	COMMENT
• • • We do not use the following data for averages, fits, limits, etc. • • •				
$484^{+246+246}_{-170-263}$	[1] UEHARA	10A	BELL	10.6 $e^+e^-\to e^+e^-\eta\eta$
250	AMSLER	92	CBAR	0.0 $\overline{p}p\to\pi^0\eta\eta$
$320\pm\ 40$	ALDE	86D	GAM4	100 $\pi^-p\to n2\eta$

[1] Breit-Wigner width. May also be the $f_0(1500)$.

COUPLED CHANNEL MODE

VALUE (MeV)	DOCUMENT ID		TECN
• • • We do not use the following data for averages, fits, limits, etc. • • •			
147^{+30}_{-50}	[1] ANISOVICH	03	RVUE

[1] K-matrix pole from combined analysis of $\pi^-p\to\pi^0\pi^0n$, $\pi^-p\to K\overline{K}n$, $\pi^+\pi^-\to\pi^+\pi^-$, $\overline{p}p\to\pi^0\pi^0\pi^0$, $\pi^0\eta\eta$, $\pi^0\pi^0\eta$, $\pi^+\pi^-\pi^0$, $K^+K^-\pi^0$, $K^0_SK^0_S\pi^0$, $K^+K^0_S\pi^-$ at rest, $\overline{p}n\to\pi^-\pi^-\pi^+$, $K^0_SK^-\pi^0$, $K^0_SK^0_S\pi^-$ at rest.

$f_0(1370)$ DECAY MODES

	Mode	Fraction (Γ_i/Γ)
Γ_1	$\pi\pi$	seen
Γ_2	4π	seen
Γ_3	$4\pi^0$	seen
Γ_4	$2\pi^+2\pi^-$	seen
Γ_5	$\pi^+\pi^-2\pi^0$	seen
Γ_6	$\rho\rho$	dominant
Γ_7	$2(\pi\pi)_S$-wave	seen
Γ_8	$\pi(1300)\pi$	seen
Γ_9	$a_1(1260)\pi$	seen
Γ_{10}	$\eta\eta$	seen
Γ_{11}	$K\overline{K}$	seen
Γ_{12}	$K\overline{K}n\pi$	not seen
Γ_{13}	6π	not seen
Γ_{14}	$\omega\omega$	not seen
Γ_{15}	$\gamma\gamma$	seen
Γ_{16}	e^+e^-	not seen

$f_0(1370)$ PARTIAL WIDTHS

$\Gamma(\gamma\gamma)$ Γ_{15}

See $\gamma\gamma$ widths under $f_0(500)$ and MORGAN 90.

$\Gamma(e^+e^-)$ Γ_{16}

VALUE (eV)	CL%	DOCUMENT ID		TECN	COMMENT
<20	90	VOROBYEV	88	ND	$e^+e^-\to\pi^0\pi^0$

$f_0(1370)\ \Gamma(i)\Gamma(\gamma\gamma)/\Gamma(\text{total})$

$\Gamma(\eta\eta)\times\Gamma(\gamma\gamma)/\Gamma_{\text{total}}$ $\Gamma_{10}\Gamma_{15}/\Gamma$

VALUE (eV)	DOCUMENT ID		TECN	COMMENT
• • • We do not use the following data for averages, fits, limits, etc. • • •				
$121^{+133+169}_{-\ 53-106}$	[1] UEHARA	10A	BELL	10.6 $e^+e^-\to e^+e^-\eta\eta$

[1] Including interference with the $f'_2(1525)$ (parameters fixed to the values from the 2008 edition of this review, PDG 08) and $f_2(1270)$. May also be the $f_0(1500)$.

$f_0(1370)$ BRANCHING RATIOS

$\Gamma(\pi\pi)/\Gamma_{\text{total}}$ Γ_1/Γ

VALUE	CL%	DOCUMENT ID		TECN	COMMENT
• • • We do not use the following data for averages, fits, limits, etc. • • •					
<0.10	95	OCHS	13	RVUE	
0.26 ± 0.09		BUGG	96	RVUE	
<0.15		[1] AMSLER	94	CBAR	$\overline{p}p\to\pi^+\pi^-3\pi^0$
<0.06		GASPERO	93	DBC	0.0 $\overline{p}n\to$ hadrons

[1] Using AMSLER 95B ($3\pi^0$).

$\Gamma(4\pi)/\Gamma_{\text{total}}$ $\Gamma_2/\Gamma=(\Gamma_3+\Gamma_4+\Gamma_5)/\Gamma$

VALUE	DOCUMENT ID		TECN	COMMENT
• • • We do not use the following data for averages, fits, limits, etc. • • •				
>0.72	GASPERO	93	DBC	0.0 $\overline{p}n\to$ hadrons

$\Gamma(4\pi^0)/\Gamma(4\pi)$ Γ_3/Γ_2

VALUE	DOCUMENT ID		TECN	COMMENT
• • • We do not use the following data for averages, fits, limits, etc. • • •				
seen	ABELE	96	CBAR	0.0 $\overline{p}p\to5\pi^0$
0.068 ± 0.005	[1] GASPERO	93	DBC	0.0 $\overline{p}n\to$ hadrons

[1] Model-dependent evaluation.

$\Gamma(2\pi^+2\pi^-)/\Gamma(4\pi)$ $\Gamma_4/\Gamma_2=\Gamma_4/(\Gamma_3+\Gamma_4+\Gamma_5)$

VALUE	DOCUMENT ID		TECN	COMMENT
• • • We do not use the following data for averages, fits, limits, etc. • • •				
0.420 ± 0.014	[1] GASPERO	93	DBC	0.0 $\overline{p}n\to2\pi^+3\pi^-$

[1] Model-dependent evaluation.

$\Gamma(\pi^+\pi^-2\pi^0)/\Gamma(4\pi)$ $\Gamma_5/\Gamma_2=\Gamma_5/(\Gamma_3+\Gamma_4+\Gamma_5)$

VALUE	DOCUMENT ID		TECN	COMMENT
• • • We do not use the following data for averages, fits, limits, etc. • • •				
0.512±0.019	[1] GASPERO	93	DBC	0.0 $\overline{p}n \rightarrow$ hadrons

[1] Model-dependent evaluation.

$\Gamma(\rho\rho)/\Gamma(4\pi)$ Γ_6/Γ_2

VALUE	DOCUMENT ID		TECN	COMMENT
• • • We do not use the following data for averages, fits, limits, etc. • • •				
0.26±0.07	ABELE	01B	CBAR	0.0 $\overline{p}d \rightarrow 5\pi p$

$\Gamma(2(\pi\pi)_{S\text{-wave}})/\Gamma(\pi\pi)$ Γ_7/Γ_1

VALUE	DOCUMENT ID		TECN	COMMENT
• • • We do not use the following data for averages, fits, limits, etc. • • •				
5.6±2.6	[1] ABELE	01	CBAR	0.0 $\overline{p}d \rightarrow \pi^-4\pi^0 p$

[1] From the combined data of ABELE 96 and ABELE 96C.

$\Gamma(2(\pi\pi)_{S\text{-wave}})/\Gamma(4\pi)$ Γ_7/Γ_2

VALUE	DOCUMENT ID		TECN	COMMENT
• • • We do not use the following data for averages, fits, limits, etc. • • •				
0.51±0.09	ABELE	01B	CBAR	0.0 $\overline{p}d \rightarrow 5\pi p$

$\Gamma(\rho\rho)/\Gamma(2(\pi\pi)_{S\text{-wave}})$ Γ_6/Γ_7

VALUE	DOCUMENT ID		TECN	COMMENT
• • • We do not use the following data for averages, fits, limits, etc. • • •				
large	BARBERIS	00C		450 $pp \rightarrow p_f 4\pi p_s$
1.6 ±0.2	AMSLER	94	CBAR	$\overline{p}p \rightarrow \pi^+\pi^-3\pi^0$
∼ 0.65	GASPERO	93	DBC	0.0 $\overline{p}n \rightarrow$ hadrons

$\Gamma(\pi(1300)\pi)/\Gamma(4\pi)$ Γ_8/Γ_2

VALUE	DOCUMENT ID		TECN	COMMENT
• • • We do not use the following data for averages, fits, limits, etc. • • •				
0.17±0.06	ABELE	01B	CBAR	0.0 $\overline{p}d \rightarrow 5\pi p$

$\Gamma(a_1(1260)\pi)/\Gamma(4\pi)$ Γ_9/Γ_2

VALUE	DOCUMENT ID		TECN	COMMENT
• • • We do not use the following data for averages, fits, limits, etc. • • •				
0.06±0.02	ABELE	01B	CBAR	0.0 $\overline{p}d \rightarrow 5\pi p$

$\Gamma(\eta\eta)/\Gamma(4\pi)$ $\Gamma_{10}/\Gamma_2=\Gamma_{10}/(\Gamma_3+\Gamma_4+\Gamma_5)$

VALUE	DOCUMENT ID		TECN	COMMENT
• • • We do not use the following data for averages, fits, limits, etc. • • •				
$(28 \pm 11) \times 10^{-3}$	[1] ANISOVICH	02D	SPEC	Combined fit
$(4.7 \pm 2.0) \times 10^{-3}$	BARBERIS	00E		450 $pp \rightarrow p_f \eta\eta p_s$

[1] From a combined K-matrix analysis of Crystal Barrel (0. $p\overline{p} \rightarrow \pi^0\pi^0\pi^0$, $\pi^0\eta\eta$, $\pi^0\pi^0\eta$), GAMS ($\pi p \rightarrow \pi^0\pi^0 n$, $\eta\eta n$, $\eta\eta' n$), and BNL ($\pi p \rightarrow K\overline{K}n$) data.

$\Gamma(K\overline{K})/\Gamma_{\text{total}}$ Γ_{11}/Γ

VALUE	DOCUMENT ID		TECN	COMMENT
• • • We do not use the following data for averages, fits, limits, etc. • • •				
0.35±0.13	BUGG	96	RVUE	

$\Gamma(K\overline{K})/\Gamma(\pi\pi)$ Γ_{11}/Γ_1

VALUE	DOCUMENT ID		TECN	COMMENT
• • • We do not use the following data for averages, fits, limits, etc. • • •				
0.08±0.08	ABLIKIM	05	BES2	$J/\psi \rightarrow \phi\pi^+\pi^-$, ϕK^+K^-
0.91±0.20	[1] BARGIOTTI	03	OBLX	$\overline{p}p$
0.12±0.06	[2] ANISOVICH	02D	SPEC	Combined fit
0.46±0.15±0.11	BARBERIS	99D	OMEG	450 $pp \rightarrow K^+K^-, \pi^+\pi^-$

[1] Coupled channel analysis of $\pi^+\pi^-\pi^0$, $K^+K^-\pi^0$, and $K^\pm K^0_S\pi^\mp$.

[2] From a combined K-matrix analysis of Crystal Barrel (0. $p\overline{p} \rightarrow \pi^0\pi^0\pi^0$, $\pi^0\eta\eta$, $\pi^0\pi^0\eta$), GAMS ($\pi p \rightarrow \pi^0\pi^0 n$, $\eta\eta n$, $\eta\eta' n$), and BNL ($\pi p \rightarrow K\overline{K}n$) data.

$\Gamma(K\overline{K}n\pi)/\Gamma_{\text{total}}$ Γ_{12}/Γ

VALUE	DOCUMENT ID		TECN	COMMENT
• • • We do not use the following data for averages, fits, limits, etc. • • •				
<0.03	GASPERO	93	DBC	0.0 $\overline{p}n \rightarrow$ hadrons

$\Gamma(6\pi)/\Gamma_{\text{total}}$ Γ_{13}/Γ

VALUE	DOCUMENT ID		TECN	COMMENT
• • • We do not use the following data for averages, fits, limits, etc. • • •				
<0.22	GASPERO	93	DBC	0.0 $\overline{p}n \rightarrow$ hadrons

$\Gamma(\omega\omega)/\Gamma_{\text{total}}$ Γ_{14}/Γ

VALUE	DOCUMENT ID		TECN	COMMENT
• • • We do not use the following data for averages, fits, limits, etc. • • •				
<0.13	GASPERO	93	DBC	0.0 $\overline{p}n \rightarrow$ hadrons

$f_0(1370)$ REFERENCES

DOBBS	15	PR D91 052006	S. Dobbs *et al.* (NWES)
OCHS	13	JP G40 043001	W. Ochs
UEHARA	10A	PR D82 114031	S. Uehara *et al.* (BELLE Collab.)
ANISOVICH	09	IJMP A24 2481	V.V. Anisovich, A.V. Sarantsev
AUBERT	09L	PR D79 072006	B. Aubert *et al.* (BABAR Collab.)
PDG	08	PL B667 1	C. Amsler *et al.* (PDG Collab.)
UEHARA	08A	PR D78 052004	S. Uehara *et al.* (BELLE Collab.)
BONVICINI	07	PR D76 012001	G. Bonvicini *et al.* (CLEO Collab.)
BUGG	07A	JP G34 151	D.V. Bugg *et al.*
GARMASH	07	PR D75 012006	A. Garmash *et al.* (BELLE Collab.)
GARMASH	06	PRL 96 251803	A. Garmash *et al.* (BELLE Collab.)
PDG	06	JP G33 1	W.-M. Yao *et al.* (PDG Collab.)
VLADIMIRSK...	06	PAN 69 493	V.V. Vladimirsky *et al.* (ITEP, Moscow)
		Translated from YAF 69 515.	
ABLIKIM	05	PL B607 243	M. Ablikim *et al.* (BES Collab.)
ABLIKIM	05Q	PR D72 092002	M. Ablikim *et al.* (BES Collab.)
GARMASH	05	PR D71 092003	A. Garmash *et al.* (BELLE Collab.)
ANISOVICH	03	EPJ A16 229	V.V. Anisovich *et al.*
BARGIOTTI	03	EPJ C26 371	M. Bargiotti *et al.* (OBELIX Collab.)
TIKHOMIROV	03	PAN 66 828	G.D. Tikhomirov *et al.*
		Translated from YAF 66 860.	
ANISOVICH	02D	PAN 65 1545	V.V. Anisovich *et al.*
		Translated from YAF 65 1583.	
ABELE	01	EPJ C19 667	A. Abele *et al.* (Crystal Barrel Collab.)
ABELE	01B	EPJ C21 261	A. Abele *et al.* (Crystal Barrel Collab.)
AITALA	01A	PRL 86 765	E.M. Aitala *et al.* (FNAL E791 Collab.)
ASNER	00	PR D61 012002	D.M. Asner *et al.* (CLEO Collab.)
BARBERIS	00C	PL B471 440	D. Barberis *et al.* (WA 102 Collab.)
BARBERIS	00E	PL B479 59	D. Barberis *et al.* (WA 102 Collab.)
BARBERIS	99B	PL B453 316	D. Barberis *et al.* (Omega Expt.)
BARBERIS	99D	PL B462 462	D. Barberis *et al.* (Omega Expt.)
BELLAZZINI	99	PL B467 296	R. Bellazzini *et al.*
KAMINSKI	99	EPJ C9 141	R. Kaminski, L. Lesniak, B. Loiseau (CRAC, PARIN)
ALDE	98	EPJ A3 361	D. Alde *et al.* (GAM4 Collab.)
Also		PAN 62 405	D. Alde *et al.* (GAMS Collab.)
		Translated from YAF 62 446.	
ANISOVICH	98B	SPU 41 419	V.V. Anisovich *et al.*
		Translated from UFN 168 481.	
BERTIN	98	PR D57 55	A. Bertin *et al.* (OBELIX Collab.)
BARBERIS	97B	PL B413 217	D. Barberis *et al.* (WA 102 Collab.)
BERTIN	97C	PL B408 476	A. Bertin *et al.* (OBELIX Collab.)
ABELE	96	PL B380 453	A. Abele *et al.* (Crystal Barrel Collab.)
ABELE	96B	PL B385 425	A. Abele *et al.* (Crystal Barrel Collab.)
ABELE	96C	NP A609 562	A. Abele *et al.* (Crystal Barrel Collab.)
BUGG	96	NP B471 59	D.V. Bugg, A.V. Sarantsev, B.S. Zou (LOQM, PNPI)
AMSLER	95B	PL B342 433	C. Amsler *et al.* (Crystal Barrel Collab.)
AMSLER	95C	PL B353 571	C. Amsler *et al.* (Crystal Barrel Collab.)
AMSLER	95D	PL B355 425	C. Amsler *et al.* (Crystal Barrel Collab.)
JANSSEN	95	PR D52 2690	G. Janssen *et al.* (STON, ADLD, JULI)
TORNQVIST	95	ZPHY C68 647	N.A. Tornqvist (HELS)
AMSLER	94	PL B322 431	C. Amsler *et al.* (Crystal Barrel Collab.) JPC
AMSLER	94D	PL B333 277	C. Amsler *et al.* (Crystal Barrel Collab.)
ANISOVICH	94	PL B323 233	V.V. Anisovich *et al.* (Crystal Barrel Collab.) JPC
BUGG	94	PR D50 4412	D.V. Bugg *et al.* (LOQM)
KAMINSKI	94	PR D50 3145	R. Kaminski, L. Lesniak, J.P. Maillet (CRAC+)
ADAMO	93	NP A558 13C	A. Adamo *et al.* (OBELIX Collab.) JPC
GASPERO	93	NP A562 407	M. Gaspero (ROMA) JPC
AMSLER	92	PL B291 347	C. Amsler *et al.* (Crystal Barrel Collab.)
ARMSTRONG	91	ZPHY C51 351	T.A. Armstrong *et al.* (ATHU, BARI, BIRM+)
ARMSTRONG	91B	ZPHY C52 389	T.A. Armstrong *et al.* (ATHU, BARI, BIRM+)
BREAKSTONE	90	ZPHY C48 569	A.M. Breakstone *et al.* (ISU, BGNA, CERN+)
MORGAN	90	ZPHY C48 623	D. Morgan, M.R. Pennington (RAL, DURH)
ASTON	88	NP B296 493	D. Aston *et al.* (SLAC, NAGO, CINC, INUS)
BOLONKIN	88	NP B309 426	B.V. Bolonkin *et al.* (ITEP, SERP)
FALVARD	88	PR D38 2706	A. Falvard *et al.* (CLER, FRAS, LALO+)
VOROBYEV	88	SJNP 48 273	P.V. Vorobiev *et al.* (NOVO)
		Translated from YAF 48 436.	
AU	87	PR D35 1633	K.L. Au, D. Morgan, M.R. Pennington (DURH, RAL)
AKESSON	86	NP B264 154	T. Akesson *et al.* (Axial Field Spec. Collab.)
ALDE	86D	NP B269 485	D.M. Alde *et al.* (BELG, LAPP, SERP, CERN+)
CASON	83	PR D28 1586	N.M. Cason *et al.* (NDAM, ANL)
ETKIN	82B	PR D25 1786	A. Etkin *et al.* (BNL, CUNY, TUFTS, VAND)
WICKLUND	80	PRL 45 1469	A.B. Wicklund *et al.* (ANL)
BECKER	79	NP B151 46	H. Becker *et al.* (MPIM, CERN, ZEEM, CRAC)
POLYCHRO...	79	PR D19 1317	V.A. Polychronakos *et al.* (NDAM, ANL)
FROGGATT	77	NP B129 89	C.D. Froggatt, J.L. Petersen (GLAS, NORD)
ROSSELET	77	PR D15 574	L. Rosselet *et al.* (GEVA, SACL)
GRAYER	74	NP B75 189	G. Grayer *et al.* (CERN, MPIM)
HYAMS	73	NP B64 134	B.D. Hyams *et al.* (CERN, MPIM)
OCHS	73	Thesis	W. Ochs (MPIM, MUNI)
BEIER	72B	PRL 29 511	E.W. Beier *et al.* (PENN)
BETTINI	66	NC 42A 695	A. Bettini *et al.* (PADO, PISA)

$h_1(1380)$ $I^G(J^{PC}) = ?^-(1^{+-})$

OMITTED FROM SUMMARY TABLE

Seen in partial-wave analysis of the $K\overline{K}\pi$ system. Needs confirmation.

$h_1(1380)$ MASS

VALUE (MeV)	DOCUMENT ID		TECN	COMMENT
1407±12 OUR AVERAGE	Error includes scale factor of 1.5.			
1412± 4±8	ABLIKIM	15M	BES3	$\psi(2S) \rightarrow \gamma\chi_{c1,2} \rightarrow \gamma K^*\overline{K}$
1440±60	ABELE	97H	CBAR	$\overline{p}p \rightarrow K^0_L K^0_S \pi^0\pi^0$
1380±20	ASTON	88C	LASS	11 $K^-p \rightarrow K^0_S K^\pm\pi^\mp\Lambda$

$h_1(1380)$ WIDTH

VALUE (MeV)	DOCUMENT ID		TECN	COMMENT
89±23 OUR AVERAGE				
84±12±40	ABLIKIM	15M	BES3	$\psi(2S) \rightarrow \gamma\chi_{c1,2} \rightarrow \gamma K^*\overline{K}$
170±80	ABELE	97H	CBAR	$\overline{p}p \rightarrow K^0_L K^0_S \pi^0\pi^0$
80±30	ASTON	88C	LASS	11 $K^-p \rightarrow K^0_S K^\pm\pi^\mp\Lambda$

Meson Particle Listings

$h_1(1380)$, $\pi_1(1400)$, $\eta(1405)$

$h_1(1380)$ DECAY MODES

	Mode
Γ_1	$K\overline{K}^*(892)+$ c.c.

$h_1(1380)$ REFERENCES

ABLIKIM	15M	PR D91 112008	M. Ablikim *et al.*	(BES III Collab.)
ABELE	97H	PL B415 280	A. Abele *et al.*	(Crystal Barrel Collab.)
ASTON	88C	PL B201 573	D. Aston *et al.*	(SLAC, NAGO, CINC, INUS)

$\pi_1(1400)$

$I^G(J^{PC}) = 1^-(1^{-+})$

See also the mini-review under non-$q\overline{q}$ candidates in PDG 06, Journal of Physics **G33** 1 (2006).

$\pi_1(1400)$ MASS

VALUE (MeV)			EVTS	DOCUMENT ID		TECN	CHG	COMMENT
1354	**±25**	**OUR AVERAGE**		Error includes scale factor of 1.8. See the ideogram below.				
1257	±20	±25	23.5k	ADAMS	07B	B852		18 $\pi^- p \to \eta\pi^0 n$
1384	±20	±35	90k	SALVINI	04	OBLX		$\overline{p}p \to 2\pi^+ 2\pi^-$
1360	±25			ABELE	99	CBAR		0.0 $\overline{p}p \to \pi^0\pi^0\eta$
1400	±20	±20		ABELE	98B	CBAR		0.0 $\overline{p}n \to \pi^-\pi^0\eta$
1370	±16	$^{+50}_{-30}$		[1] THOMPSON	97	MPS		18 $\pi^- p \to \eta\pi^- p$
• • • We do not use the following data for averages, fits, limits, etc. • • •								
1323.1	± 4.6			[2] AOYAGI	93	BKEI		$\pi^- p \to \eta\pi^- p$
1406	±20			[3] ALDE	88B	GAM4	0	100 $\pi^- p \to \eta\pi^0 n$

[1] Natural parity exchange, questioned by DZIERBA 03.
[2] Unnatural parity exchange.
[3] Seen in the P_0-wave intensity of the $\eta\pi^0$ system, unnatural parity exchange.

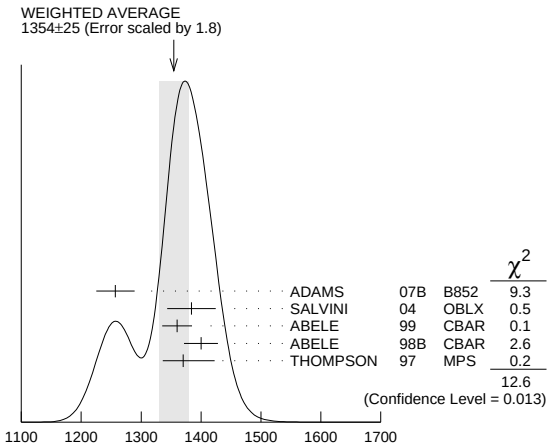

$\pi_1(1400)$ MASS (MeV)

$\pi_1(1400)$ WIDTH

VALUE (MeV)			EVTS	DOCUMENT ID		TECN	CHG	COMMENT
330	**±35**	**OUR AVERAGE**						
354	±64	± 58	23.5k	ADAMS	07B	B852		18 $\pi^- p \to \eta\pi^0 n$
378	±50	± 50	90k	SALVINI	04	OBLX		$\overline{p}p \to 2\pi^+ 2\pi^-$
220	±90			ABELE	99	CBAR		0.0 $\overline{p}p \to \pi^0\pi^0\eta$
310	±50	$^{+50}_{-30}$		ABELE	98B	CBAR		0.0 $\overline{p}n \to \pi^-\pi^0\eta$
385	±40	$^{+65}_{-105}$		[4] THOMPSON	97	MPS		18 $\pi^- p \to \eta\pi^- p$
• • • We do not use the following data for averages, fits, limits, etc. • • •								
143.2	±12.5			[5] AOYAGI	93	BKEI		$\pi^- p \to \eta\pi^- p$
180	±20			[6] ALDE	88B	GAM4	0	100 $\pi^- p \to \eta\pi^0 n$

[4] Resolution is not unfolded, natural parity exchange, questioned by DZIERBA 03.
[5] Unnatural parity exchange.
[6] Seen in the P_0-wave intensity of the $\eta\pi^0$ system, unnatural parity exchange.

$\pi_1(1400)$ DECAY MODES

	Mode	Fraction (Γ_i/Γ)
Γ_1	$\eta\pi^0$	seen
Γ_2	$\eta\pi^-$	seen
Γ_3	$\eta'\pi$	

$\pi_1(1400)$ BRANCHING RATIOS

$\Gamma(\eta\pi^0)/\Gamma_{\text{total}}$ Γ_1/Γ

VALUE	DOCUMENT ID		TECN	CHG	COMMENT
• • • We do not use the following data for averages, fits, limits, etc. • • •					
not seen	PROKOSHKIN	95B	GAM4		100 $\pi^- p \to \eta\pi^0 n$
not seen	[7] BUGG	94	RVUE		$\overline{p}p \to \eta 2\pi^0$
not seen	[8] APEL	81	NICE	0	40 $\pi^- p \to \eta\pi^0 n$

[7] Using Crystal Barrel data.
[8] A general fit allowing S, D, and P waves (including m=0) is not done because of limited statistics.

$\Gamma(\eta\pi^-)/\Gamma_{\text{total}}$ Γ_2/Γ

VALUE	DOCUMENT ID		TECN	COMMENT
• • • We do not use the following data for averages, fits, limits, etc. • • •				
possibly seen	BELADIDZE	93	VES	37 $\pi^- N \to \eta\pi^- N$

$\Gamma(\eta'\pi)/\Gamma(\eta\pi^0)$ Γ_3/Γ_1

VALUE	CL%	DOCUMENT ID		TECN	COMMENT
• • • We do not use the following data for averages, fits, limits, etc. • • •					
<0.80	95	BOUTEMEUR	90	GAM4	100 $\pi^- p \to 4\gamma n$

$\pi_1(1400)$ REFERENCES

ADAMS	07B	PL B657 27	G.S. Adams *et al.*	(BNL E852 Collab.)
PDG	06	JP G33 1	W.-M. Yao *et al.*	(PDG Collab.)
SALVINI	04	EPJ C35 21	P. Salvini *et al.*	(OBELIX Collab.)
DZIERBA	03	PR D67 094015	A.R. Dzierba *et al.*	
ABELE	99	PL B446 349	A. Abele *et al.*	(Crystal Barrel Collab.)
ABELE	98B	PL B423 175	A. Abele *et al.*	(Crystal Barrel Collab.)
THOMPSON	97	PRL 79 1630	D.R. Thompson *et al.*	(BNL E852 Collab.)
PROKOSHKIN	95B	PAN 58 606	Y.D. Prokoshkin, S.A. Sadovsky	(SERP)
		Translated from YAF 58 662.		
BUGG	94	PR D50 4412	D.V. Bugg *et al.*	(LOQM)
AOYAGI	93	PL B314 246	H. Aoyagi *et al.*	(BKEI Collab.)
BELADIDZE	93	PL B313 276	G.M. Beladidze *et al.*	(VES Collab.)
BOUTEMEUR	90	Hadron 89 Conf. p 119	M. Boutemeur, M. Poulet	(SERP, BELG, LANL+)
ALDE	88B	PL B205 397	D.M. Alde *et al.*	(SERP, BELG, LANL, LAPP) IGJPC
APEL	81	NP B193 269	W.D. Apel *et al.*	(SERP, CERN)

$\eta(1405)$

$I^G(J^{PC}) = 0^+(0^{-+})$

See also the $\eta(1475)$.

See the related review(s):
Pseudoscalar and Pseudovector Mesons in the 1400 MeV Region

$\eta(1405)$ MASS

VALUE (MeV)	DOCUMENT ID
1408.8±1.8 OUR AVERAGE	Includes data from the 2 datablocks that follow this one. Error includes scale factor of 2.1. See the ideogram below.

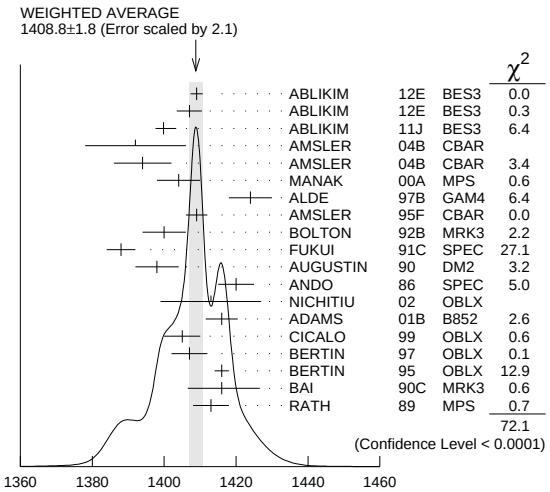

$\eta(1405)$ mass (MeV)

$\eta\pi\pi$ MODE

VALUE (MeV)	EVTS	DOCUMENT ID		TECN	COMMENT
The data in this block is included in the average printed for a previous datablock.					
1406.2± 2.3 OUR AVERAGE		Error includes scale factor of 2.2. See the ideogram below.			
1409.0± 1.7	743	ABLIKIM	12E	BES3	$J/\psi \to \gamma(\pi^+\pi^-\pi^0)$

1407.0± 3.5	198	ABLIKIM	12E	BES3	$J/\psi \to \gamma(\pi^0\pi^0\pi^0)$	
1399.8± $2.2^{+2.8}_{-0.1}$		[1] ABLIKIM	11J	BES3	$J/\psi \to \omega(\eta\pi^+\pi^-)$	
1392 ±14	900 ± 375	AMSLER	04B	CBAR	$0\,\overline{p}p \to \pi^+\pi^-\pi^+\pi^-\eta$	
1394 ± 8	6.6 ± 2.0k	AMSLER	04B	CBAR	$0\,\overline{p}p \to \pi^+\pi^-\pi^0\pi^0\eta$	
1404 ± 6	9082	MANAK	00A	MPS	$18\ \pi^-p \to \eta\pi^+\pi^-n$	
1424 ± 6	2200	ALDE	97B	GAM4	$100\ \pi^-p \to \eta\pi^0\pi^0n$	
1409 ± 3		AMSLER	95F	CBAR	$0\,\overline{p}p \to \pi^+\pi^-\pi^0\pi^0\eta$	
1400 ± 6		[2] BOLTON	92B	MRK3	$J/\psi \to \gamma\eta\pi^+\pi^-$	
1388 ± 4		FUKUI	91C	SPEC	$8.95\ \pi^-p \to \eta\pi^+\pi^-n$	
1398 ± 6	261	[3] AUGUSTIN	90	DM2	$J/\psi \to \gamma\eta\pi^+\pi^-$	
1420 ± 5		ANDO	86	SPEC	$8\ \pi^-p \to \eta\pi^+\pi^-n$	
• • • We do not use the following data for averages, fits, limits, etc. • • •						
1385 ± 7		BAI	99	BES	$J/\psi \to \gamma\eta\pi^+\pi^-$	

[1] The selected process is $J/\psi \to \omega a_0(980)\pi$.
[2] From fit to the $a_0(980)\pi\ 0^{-+}$ partial wave.
[3] Best fit with a single Breit Wigner.

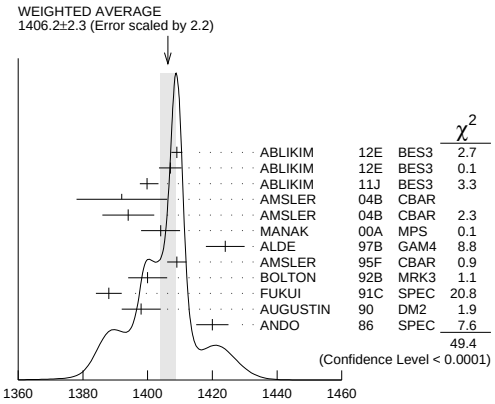

$\eta(1405)$ mass, $\eta\pi\pi$ mode (MeV)

$K\overline{K}\pi$ MODE ($a_0(980)\pi$ or direct $K\overline{K}\pi$)

VALUE (MeV)	EVTS	DOCUMENT ID	TECN	COMMENT
The data in this block is included in the average printed for a previous datablock.				

1413.9± 1.7 OUR AVERAGE Error includes scale factor of 1.1.

1413 ±14	3651	[1] NICHITIU	02	OBLX		
1416 ± 4 ±2	20k	ADAMS	01B	B852	18 GeV $\pi^-p \to K^+K^-\pi^0n$	
1405 ± 5		[2] CICALO	99	OBLX	$0\,\overline{p}p \to K^\pm K^0_S\pi^\mp\pi^+\pi^-$	
1407 ± 5		[2] BERTIN	97	OBLX	$0\,\overline{p}p \to K^\pm(K^0)\pi^\mp\pi^+\pi^-$	
1416 ± 2		[2] BERTIN	95	OBLX	$0\,\overline{p}p \to K\overline{K}\pi\pi\pi$	
1416 ± 8 $^{+7}_{-5}$	700	[3] BAI	90C	MRK3	$J/\psi \to \gamma K^0_S K^\pm\pi^\mp$	
1413 ± 5		[3] RATH	89	MPS	$21.4\ \pi^-p \to nK^0_S K^0_S\pi^0$	
• • • We do not use the following data for averages, fits, limits, etc. • • •						
1459 ± 5		[4] AUGUSTIN	92	DM2	$J/\psi \to \gamma K\overline{K}\pi$	

[1] Decaying dominantly directly to $K^+K^-\pi^0$.
[2] Decaying into $(K\overline{K})_S\pi$, $(K\pi)_S\overline{K}$, and $a_0(980)\pi$.
[3] From fit to the $a_0(980)\pi\ 0^{-+}$ partial wave. Cannot rule out a $a_0(980)\pi\ 1^{++}$ partial wave.
[4] Excluded from averaging because averaging would be meaningless.

$\pi\pi\gamma$ MODE

VALUE (MeV)	EVTS	DOCUMENT ID	TECN	COMMENT
1390±12	235 ± 91	AMSLER	04B CBAR	$0\,\overline{p}p \to \pi^+\pi^-\pi^+\pi^-\gamma$
• • • We do not use the following data for averages, fits, limits, etc. • • •				
1424±10±11	547	BAI	04J BES2	$J/\psi \to \gamma\gamma\pi^+\pi^-$
1401±18		[1,2] AUGUSTIN	90 DM2	$J/\psi \to \pi^+\pi^-\gamma\gamma$
1432± 8		[2] COFFMAN	90 MRK3	$J/\psi \to \pi^+\pi^-2\gamma$

[1] Best fit with a single Breit Wigner.
[2] This peak in the $\gamma\rho$ channel may not be related to the $\eta(1405)$.

4π MODE

VALUE (MeV)	EVTS	DOCUMENT ID	TECN	COMMENT
• • • We do not use the following data for averages, fits, limits, etc. • • •				
1420±20		BUGG	95 MRK3	$J/\psi \to \gamma\pi^+\pi^-\pi^+\pi^-$
1489±12	3270	[1] BISELLO	89B DM2	$J/\psi \to 4\pi\gamma$

[1] Estimated by us from various fits.

$K\overline{K}\pi$ MODE (unresolved)

VALUE (MeV)	EVTS	DOCUMENT ID	TECN	COMMENT
• • • We do not use the following data for averages, fits, limits, etc. • • •				
1452.7± 3.3	191	[1,2] ABLIKIM	13M BES3	$\psi(2S) \to \omega K K\pi$
1437.6± 3.2	249 ± 35	[1,2] ABLIKIM	08E BES2	$J/\psi \to \omega K^0_S K^+\pi^- +$ c.c.
1445.9± 5.7	62 ± 18	[1,2] ABLIKIM	08E BES2	$J/\psi \to \omega K^+K^-\pi^0$
1442 ±10	410	[1] BAI	98C BES	$J/\psi \to \gamma K^+K^-\pi^0$
1445 ± 8	693	[1] AUGUSTIN	90 DM2	$J/\psi \to \gamma K^0_S K^\pm\pi^\mp$
1433 ± 8	296	[1] AUGUSTIN	90 DM2	$J/\psi \to \gamma K^+K^-\pi^0$
1413 ± 8	500	[1] DUCH	89	ASTE	$\overline{p}p \to \pi^+\pi^-K^\pm\pi^\mp K^0$
1453 ± 7	170	[1] RATH	89	MPS	$21.4\ \pi^-p \to K^0_S K^0_S\pi^0n$
1419 ± 1	8800	[1] BIRMAN	88	MPS	$8\ \pi^-p \to K^+\overline{K}^0\pi^-n$
1424 ± 3	620	[1] REEVES	86	SPEC	$6.6\ p\overline{p} \to K\overline{K}\pi X$
1421 ± 2		[1] CHUNG	85	SPEC	$8\ \pi^-p \to K\overline{K}\pi n$
1440 $^{+20}_{-15}$	174	[1] EDWARDS	82E	CBAL	$J/\psi \to \gamma K^+K^-\pi^0$
1440 $^{+10}_{-15}$		[1] SCHARRE	80	MRK2	$J/\psi \to \gamma K^0_S K^\pm\pi^\mp$
1425 ± 7	800	[1,3] BAILLON	67	HBC	$0\,\overline{p}p \to K\overline{K}\pi\pi\pi$

[1] These experiments identify only one pseudoscalar in the 1400–1500 range. Data could also refer to $\eta(1475)$.
[2] Systematic uncertainty not evaluated.
[3] From best fit of 0^{-+} partial wave, 50% $K^*(892)K$, 50% $a_0(980)\pi$.

$\eta(1405)$ WIDTH

VALUE (MeV)	DOCUMENT ID
51.0±2.9 OUR AVERAGE Includes data from the 2 datablocks that follow this one. Error includes scale factor of 1.8. See the ideogram below.	

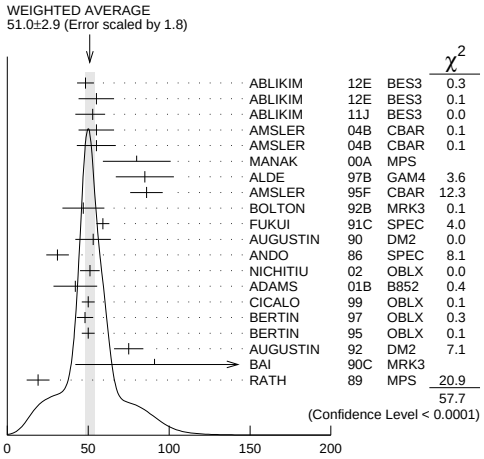

$\eta(1405)$ width (MeV)

$\eta\pi\pi$ MODE

VALUE (MeV)	EVTS	DOCUMENT ID	TECN	COMMENT
The data in this block is included in the average printed for a previous datablock.				

54 ± 4 OUR AVERAGE Error includes scale factor of 1.6. See the ideogram below.

48.3± 5.2	743	ABLIKIM	12E	BES3	$J/\psi \to \gamma(\pi^+\pi^-\pi^0)$	
55.0±11.0	198	ABLIKIM	12E	BES3	$J/\psi \to \gamma(\pi^0\pi^0\pi^0)$	
52.8± 7.6 $^{+0.1}_{-7.6}$		[1] ABLIKIM	11J	BES3	$J/\psi \to \omega(\eta\pi^+\pi^-)$	
55 ±11	900 ± 375	AMSLER	04B	CBAR	$0\,\overline{p}p \to \pi^+\pi^-\pi^+\pi^-\eta$	
55 ±12	6.6 ± 2.0k	AMSLER	04B	CBAR	$0\,\overline{p}p \to \pi^+\pi^-\pi^0\pi^0\gamma$	
80 ±21	9082	MANAK	00A	MPS	$18\ \pi^-p \to \eta\pi^+\pi^-n$	
85 ±18	2200	ALDE	97B	GAM4	$100\ \pi^-p \to \eta\pi^0\pi^0n$	
86 ±10		AMSLER	95F	CBAR	$0\,\overline{p}p \to \pi^+\pi^-\pi^0\pi^0\eta$	
47 ±13		[2] BOLTON	92B	MRK3	$J/\psi \to \gamma\eta\pi^+\pi^-$	
59 ± 4		FUKUI	91C	SPEC	$8.95\ \pi^-p \to \eta\pi^+\pi^-n$	
53 ±11		[3] AUGUSTIN	90	DM2	$J/\psi \to \gamma\eta\pi^+\pi^-$	
31 ± 7		ANDO	86	SPEC	$8\ \pi^-p \to \eta\pi^+\pi^-n$	

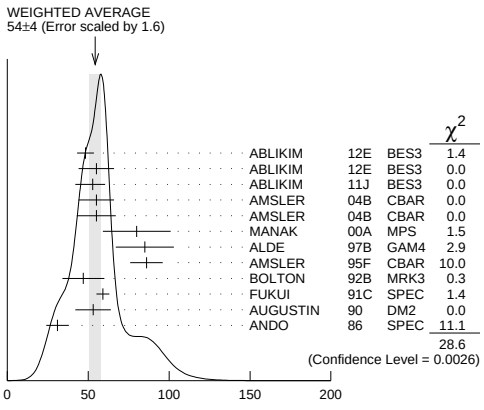

$\eta(1405)$ width $\eta\pi\pi$ mode (MeV)

Meson Particle Listings

$\eta(1405)$

[1] The selected process is $J/\psi \to \omega a_0(980)\pi$.
[2] From fit to the $a_0(980)\pi$ 0^{-+} partial wave.
[3] From $\eta\pi^+\pi^-$ mass distribution - mainly $a_0(980)\pi$ - no spin–parity determination available.

$K\overline{K}\pi$ MODE ($a_0(980)\pi$ or direct $K\overline{K}\pi$)

VALUE (MeV)	EVTS	DOCUMENT ID		TECN	COMMENT
The data in this block is included in the average printed for a previous datablock.					
48± 4 OUR AVERAGE	Error includes scale factor of 2.1. See the ideogram below.				
51± 6	3651	[1] NICHITIU	02	OBLX	
42±10± 9	20k	ADAMS	01B	B852	18 GeV $\pi^- p \to K^+K^-\pi^0 n$
50± 4		CICALO	99	OBLX	0 $\overline{p}p \to K^\pm K^0_S \pi^\mp \pi^+\pi^-$
48± 5		[2] BERTIN	97	OBLX	0.0 $\overline{p}p \to K^\pm(K^0)\pi^\mp\pi^+\pi^-$
50± 4		[2] BERTIN	95	OBLX	0 $\overline{p}p \to K\overline{K}\pi\pi\pi$
75± 9		AUGUSTIN	92	DM2	$J/\psi \to \gamma K\overline{K}\pi$
91^{+67+15}_{-31-38}		[3] BAI	90C	MRK3	$J/\psi \to \gamma K^0_S K^\pm\pi^\mp$
19± 7		[3] RATH	89	MPS	21.4 $\pi^- p \to n K^0_S K^0_S \pi^0$

[1] Decaying dominantly directly to $K^+K^-\pi^0$.
[2] Decaying into $(K\overline{K})_S\pi$, $(K\pi)_S\overline{K}$, and $a_0(980)\pi$.
[3] From fit to the $a_0(980)\pi$ 0^{-+} partial wave, but $a_0(980)\pi$ 1^{++} cannot be excluded.

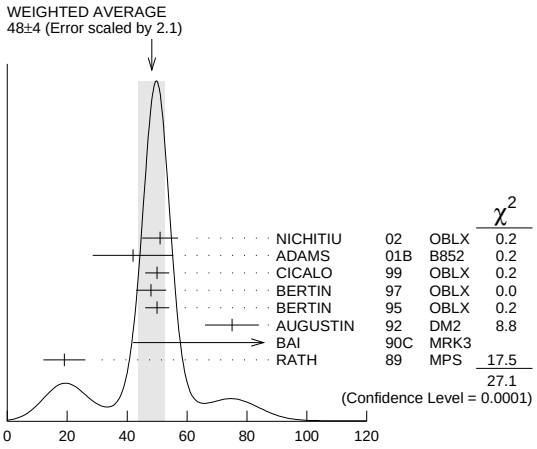

$\eta(1405)$ width $K\overline{K}\pi$ mode ($a_0(980)$ π dominant) (MeV)

$\pi\pi\gamma$ MODE

VALUE (MeV)	EVTS	DOCUMENT ID		TECN	COMMENT
64 ±18	235 ± 91	AMSLER	04B	CBAR	0 $\overline{p}p \to \pi^+\pi^-\pi^+\pi^-\gamma$
• • • We do not use the following data for averages, fits, limits, etc. • • •					
101.0± 8.8±8.8	547	BAI	04J	BES2	$J/\psi \to \gamma\gamma\pi^+\pi^-$
174 ±44		AUGUSTIN	90	DM2	$J/\psi \to \pi^+\pi^-\gamma\gamma$
90 ±26		[1] COFFMAN	90	MRK3	$J/\psi \to \pi^+\pi^-2\gamma$

[1] This peak in the $\gamma\rho$ channel may not be related to the $\eta(1405)$.

4π MODE

VALUE (MeV)	EVTS	DOCUMENT ID		TECN	COMMENT
• • • We do not use the following data for averages, fits, limits, etc. • • •					
160±30		BUGG	95	MRK3	$J/\psi \to \gamma\pi^+\pi^-\pi^+\pi^-$
144±13	3270	[1] BISELLO	89B	DM2	$J/\psi \to 4\pi\gamma$

[1] Estimated by us from various fits.

$K\overline{K}\pi$ MODE (unresolved)

VALUE (MeV)	EVTS	DOCUMENT ID		TECN	COMMENT
• • • We do not use the following data for averages, fits, limits, etc. • • •					
45.9± 8.2	191	[1,2] ABLIKIM	13M	BES3	$\psi(2S) \to \omega K K\pi$
48.9± 9.0	249 ± 35	[1,2] ABLIKIM	08E	BES2	$J/\psi \to \omega K^0_S K^+\pi^-$ + c.c.
34.2±18.5	62 ± 18	[1,2] ABLIKIM	08E	BES2	$J/\psi \to \omega K^+K^-\pi^0$
93 ±14	296	[1] AUGUSTIN	90	DM2	$J/\psi \to \gamma K^+K^-\pi^0$
105 ±10	693	[1] AUGUSTIN	90	DM2	$J/\psi \to \gamma K^0_S K^\pm\pi^\mp$
62 ±16	500	[1] DUCH	89	ASTE	$\overline{p}p \to K\overline{K}\pi\pi\pi$
100 ±11	170	[1] RATH	89	MPS	21.4 $\pi^- p \to K^0_S K^0_S \pi^0 n$
66 ± 2	8800	[1] BIRMAN	88	MPS	8 $\pi^- p \to K^+\overline{K}^0\pi^- n$
60 ±10	620	[1] REEVES	86	SPEC	6.6 $p\overline{p} \to K K\pi X$
60 ±10		[1] CHUNG	85	SPEC	8 $\pi^- p \to K\overline{K}\pi n$
$55\ ^{+20}_{-30}$	174	[1] EDWARDS	82E	CBAL	$J/\psi \to \gamma K^+K^-\pi^0$
$50\ ^{+30}_{-20}$		[1] SCHARRE	80	MRK2	$J/\psi \to \gamma K^0_S K^\pm\pi^\mp$
80 ±10	800	[1,3] BAILLON	67	HBC	0.0 $\overline{p}p \to K\overline{K}\pi\pi\pi$

[1] These experiments identify only one pseudoscalar in the 1400–1500 range. Data could also refer to $\eta(1475)$.
[2] Systematic uncertainty not evaluated.
[3] From best fit to 0^{-+} partial wave, 50% $K^*(892)K$, 50% $a_0(980)\pi$.

$\eta(1405)$ DECAY MODES

	Mode	Fraction (Γ_i/Γ)	Confidence level
Γ_1	$K\overline{K}\pi$	seen	
Γ_2	$\eta\pi\pi$	seen	
Γ_3	$a_0(980)\pi$	seen	
Γ_4	$\eta(\pi\pi)_S$-wave	seen	
Γ_5	$f_0(980)\pi^0 \to \pi^+\pi^-\pi^0$	not seen	
Γ_6	$f_0(980)\eta$	seen	
Γ_7	4π	seen	
Γ_8	$\rho\rho$	<58 %	99.85%
Γ_9	$\gamma\gamma$		
Γ_{10}	$\rho^0\gamma$	seen	
Γ_{11}	$\phi\gamma$		
Γ_{12}	$K^*(892)K$	seen	

$\eta(1405)$ Γ(i)$\Gamma(\gamma\gamma)/\Gamma$(total)

$\Gamma(K\overline{K}\pi) \times \Gamma(\gamma\gamma)/\Gamma_{total}$ $\Gamma_1\Gamma_9/\Gamma$

VALUE (keV)	CL%	DOCUMENT ID		TECN	COMMENT
• • • We do not use the following data for averages, fits, limits, etc. • • •					
<0.035	90	[1,2] AHOHE	05	CLE2	10.6 $e^+e^- \to e^+e^- K^0_S K^\pm\pi^\mp$

[1] Using $\eta(1405)$ mass and width 1410 MeV and 51 MeV, respectively.
[2] Assuming three-body phase-space decay to $K^0_S K^\pm\pi^\mp$.

$\Gamma(\eta\pi\pi) \times \Gamma(\gamma\gamma)/\Gamma_{total}$ $\Gamma_2\Gamma_9/\Gamma$

VALUE (keV)	CL%	DOCUMENT ID		TECN	COMMENT
<0.095	95	ACCIARRI	01G	L3	183–202 $e^+e^- \to e^+e^-\eta\pi^+\pi^-$

$\Gamma(\rho^0\gamma) \times \Gamma(\gamma\gamma)/\Gamma_{total}$ $\Gamma_{10}\Gamma_9/\Gamma$

VALUE (keV)	CL%	DOCUMENT ID		TECN	COMMENT
• • • We do not use the following data for averages, fits, limits, etc. • • •					
<1.5	95	ALTHOFF	84E	TASS	$e^+e^- \to e^+e^-\pi^+\pi^-\gamma$

$\eta(1405)$ BRANCHING RATIOS

$\Gamma(\eta\pi\pi)/\Gamma(K\overline{K}\pi)$ Γ_2/Γ_1

VALUE	CL%	DOCUMENT ID		TECN	COMMENT
• • • We do not use the following data for averages, fits, limits, etc. • • •					
1.09±0.48		[1] AMSLER	04B	CBAR	0 $\overline{p}p \to \pi^+\pi^-\pi^+\pi^-\eta$
<0.5	90	EDWARDS	83B	CBAL	$J/\psi \to \eta\pi\pi\gamma$
<1.1	90	SCHARRE	80	MRK2	$J/\psi \to \eta\pi\pi\gamma$
<1.5	95	FOSTER	68B	HBC	0.0 $\overline{p}p$

[1] Using the data of BAILLON 67 on $\overline{p}p \to K\overline{K}\pi$.

$\Gamma(\rho^0\gamma)/\Gamma(\eta\pi\pi)$ Γ_{10}/Γ_2

VALUE	DOCUMENT ID		TECN	COMMENT
0.111±0.064	AMSLER	04B	CBAR	0 $\overline{p}p$

$\Gamma(a_0(980)\pi)/\Gamma(K\overline{K}\pi)$ Γ_3/Γ_1

VALUE	EVTS	DOCUMENT ID		TECN	COMMENT
• • • We do not use the following data for averages, fits, limits, etc. • • •					
~ 0.15		[1] BERTIN	95	OBLX	0 $\overline{p}p \to K\overline{K}\pi\pi\pi$
~ 0.8	500	[1] DUCH	89	ASTE	$\overline{p}p \to \pi^+\pi^- K^\pm\pi^\mp K^0$
~ 0.75		[1] REEVES	86	SPEC	6.6 $p\overline{p} \to K K\pi X$

[1] Assuming that the $a_0(980)$ decays only into $K\overline{K}$.

$\Gamma(a_0(980)\pi)/\Gamma(\eta\pi\pi)$ Γ_3/Γ_2

VALUE	EVTS	DOCUMENT ID		TECN	COMMENT
• • • We do not use the following data for averages, fits, limits, etc. • • •					
0.29±0.10		ABELE	98E	CBAR	0 $p\overline{p} \to \eta\pi^0\pi^0\pi^0$
0.19±0.04	2200	[1] ALDE	97B	GAM4	100 $\pi^- p \to \eta\pi^0\pi^0 n$
0.56±0.04±0.03		[1] AMSLER	95F	CBAR	0 $\overline{p}p \to \pi^+\pi^-\pi^0\pi^0\eta$

[1] Assuming that the $a_0(980)$ decays only into $\eta\pi$.

$\Gamma(a_0(980)\pi)/\Gamma(\eta(\pi\pi)_{S\text{-wave}})$ Γ_3/Γ_4

VALUE	EVTS	DOCUMENT ID		TECN	COMMENT
• • • We do not use the following data for averages, fits, limits, etc. • • •					
0.91±0.12		ANISOVICH	01	SPEC	0.0 $\overline{p}p \to \eta\pi^+\pi^-\pi^+\pi^-$
0.15±0.04	9082	[1] MANAK	00A	MPS	18 $\pi^- p \to \eta\pi^+\pi^- n$
0.70±0.12±0.20		[2] BAI	99	BES	$J/\psi \to \gamma\eta\pi^+\pi^-$

[1] Statistical error only.
[2] Assuming that the $a_0(980)$ decays only into $\eta\pi$.

$\Gamma(\rho^0\gamma)/\Gamma(K\overline{K}\pi)$ Γ_{10}/Γ_1

VALUE	DOCUMENT ID		TECN	COMMENT
0.0152±0.0038	[1] COFFMAN	90	MRK3	$J/\psi \to \gamma\gamma\pi^+\pi^-$

[1] Using B($J/\psi \to \gamma\eta(1405) \to \gamma K\overline{K}\pi$)=4.2 × 10^{-3} and B($J/\psi \to \gamma\eta(1405) \to \gamma\gamma\rho^0$)=6.4 × 10^{-5} and assuming that the $\gamma\rho^0$ signal does not come from the $f_1(1420)$.

$\Gamma(\eta(\pi\pi)_{S\text{-wave}})/\Gamma(\eta\pi\pi)$ Γ_4/Γ_2

VALUE	EVTS	DOCUMENT ID	TECN	COMMENT
• • • We do not use the following data for averages, fits, limits, etc. • • •				
0.81±0.04	2200	ALDE 97B	GAM4	100 $\pi^- p \to \eta\pi^0\pi^0 n$

$\Gamma(f_0(980)\eta)/\Gamma(\eta\pi\pi)$ Γ_6/Γ_2

VALUE	DOCUMENT ID	TECN	COMMENT
• • • We do not use the following data for averages, fits, limits, etc. • • •			
0.32±0.07	[1] ANISOVICH 00	SPEC	0.9–1.2 $\overline{p}p \to \eta 3\pi^0$

[1] Using preliminary Crystal Barrel data.

$\Gamma(f_0(980)\pi^0 \to \pi^+\pi^-\pi^0)/\Gamma_{total}$ Γ_5/Γ

VALUE	DOCUMENT ID	TECN	COMMENT
not seen	[1] ABLIKIM 17AJ	BES3	$\psi(2S) \to \gamma\pi^+\pi^-\pi^0$

[1] ABLIKIM 17AJ reports B($\psi(2S) \to \gamma\eta(1405) \to \gamma f_0(980)\pi^0 \to \gamma\pi^+\pi^-\pi^0$) < 5.0 × 10^{-7}.

$\Gamma(\rho\rho)/\Gamma_{total}$ Γ_8/Γ

VALUE	CL%	DOCUMENT ID	TECN	COMMENT
<0.58	99.85	[1,2] AMSLER 04B	CBAR	0 $\overline{p}p$

[1] Assuming that the $\eta(1405)$ decays are saturated by the $\pi\pi\eta$, $K\overline{K}\pi$ and $\rho\rho$ modes.
[2] Using the data of BAILLON 67 on $\overline{p}p \to K\overline{K}\pi$.

$\Gamma(K^*(892)K)/\Gamma(a_0(980)\pi)$ Γ_{12}/Γ_3

VALUE	DOCUMENT ID	TECN	COMMENT
• • • We do not use the following data for averages, fits, limits, etc. • • •			
0.084±0.024	[1] ADAMS 01B	B852	18 GeV $\pi^- p \to K^+K^-\pi^0 n$

[1] Statistical error only.

$\Gamma(\phi\gamma)/\Gamma(\rho^0\gamma)$ Γ_{11}/Γ_{10}

VALUE	CL%	DOCUMENT ID	TECN	COMMENT
• • • We do not use the following data for averages, fits, limits, etc. • • •				
<0.77	95	[1] BAI 04J	BES2	$J/\psi \to \gamma\gamma K^+K^-$

[1] Calculated by us from B($J/\psi \to \eta(1405)\gamma \to \phi\gamma\gamma$) < 0.82 × 10^{-4} and B($J/\psi \to \eta(1405)\gamma \to \rho^0\gamma\gamma$) = (1.07 ± 0.17 ± 0.11) × 10^{-4}.

$\eta(1405)$ REFERENCES

ABLIKIM	17AJ	PR D96 112008	M. Ablikim *et al.*	(BES III Collab.)
ABLIKIM	13M	PR D87 092006	M. Ablikim *et al.*	(BES III Collab.)
ABLIKIM	12E	PRL 108 182001	M. Ablikim *et al.*	(BES III Collab.)
ABLIKIM	11J	PRL 107 182001	M. Ablikim *et al.*	(BES III Collab.)
ABLIKIM	08E	PR D77 032005	M. Ablikim *et al.*	(BES Collab.)
AHOHE	05	PR D71 072001	R. Ahohe *et al.*	(CLEO Collab.)
AMSLER	04B	EPJ C33 23	C. Amsler *et al.*	(Crystal Barrel Collab.)
BAI	04J	PL B594 47	J.Z. Bai *et al.*	(BES Collab.)
NICHITIU	02	PL B545 261	F. Nichitiu *et al.*	(OBELIX Collab.)
ACCIARRI	01G	PL B501 1	M. Acciarri *et al.*	(L3 Collab.)
ADAMS	01B	PL B516 264	G.S. Adams *et al.*	(BNL E852 Collab.)
ANISOVICH	01	NP A690 567	A.V. Anisovich *et al.*	
ANISOVICH	00	PL B472 168	A.V. Anisovich *et al.*	
MANAK	00A	PR D62 012003	J.J. Manak *et al.*	(BNL E852 Collab.)
BAI	99	PL B446 356	J.Z. Bai *et al.*	(BES Collab.)
CICALO	99	PL B462 453	C. Cicalo *et al.*	(OBELIX Collab.)
ABELE	98E	NP B514 45	A. Abele *et al.*	(Crystal Barrel Collab.)
BAI	98C	PL B440 217	J.Z. Bai *et al.*	(BES Collab.)
ALDE	97B	PAN 60 386	D. Alde *et al.*	(GAMS Collab.)
		Translated from YAF 60 458.		
BERTIN	97	PL B400 226	A. Bertin *et al.*	(OBELIX Collab.)
AMSLER	95F	PL B358 389	C. Amsler *et al.*	(Crystal Barrel Collab.)
BERTIN	95	PL B361 187	A. Bertin *et al.*	(OBELIX Collab.)
BUGG	95	PL B353 378	D.V. Bugg *et al.*	(LOQM, PNPI, WASH)
AUGUSTIN	92	PR D46 1951	J.E. Augustin, G. Cosme	(DM2 Collab.)
BOLTON	92B	PRL 69 1328	T. Bolton *et al.*	(Mark III Collab.)
FUKUI	91C	PL B267 293	S. Fukui *et al.*	(SUGI, NAGO, KEK, KYOT+)
AUGUSTIN	90	PR D42 10	J.E. Augustin *et al.*	(DM2 Collab.)
BAI	90C	PRL 65 2507	Z. Bai *et al.*	(Mark III Collab.)
COFFMAN	90	PR D41 1410	D.M. Coffman *et al.*	(Mark III Collab.)
BISELLO	89B	PR D39 701	G. Busetto *et al.*	(DM2 Collab.)
DUCH	89	ZPHY C45 223	K.D. Duch *et al.*	(ASTERIX Collab.) JP
RATH	89	PR D40 693	M.G. Rath *et al.*	(NDAM, BRAN, BNL, CUNY+)
BIRMAN	88	PRL 61 1557	A. Birman *et al.*	(BNL, FSU, IND, MASD) JP
ANDO	86	PRL 57 1296	A. Ando *et al.*	(KEK, KYOT, NIRS, SAGA+) IJP
REEVES	86	PR D34 1960	D.F. Reeves *et al.*	(FLOR, BNL, IND+) JP
CHUNG	85	PRL 55 779	S.U. Chung *et al.*	(BNL, FLOR, IND+) JP
ALTHOFF	84E	PL 147B 487	M. Althoff *et al.*	(TASSO Collab.)
EDWARDS	83B	PRL 51 859	C. Edwards *et al.*	(CIT, HARV, PRIN+)
EDWARDS	82E	PRL 49 259	C. Edwards *et al.*	(CIT, HARV, PRIN+)
Also		PRL 50 219	C. Edwards *et al.*	(CIT, HARV, PRIN+)
SCHARRE	80	PL 97B 329	D.L. Scharre *et al.*	(SLAC, LBL)
FOSTER	68B	NP B8 174	M. Foster *et al.*	(CERN, CDEF)
BAILLON	67	NC 50A 393	P.H. Baillon *et al.*	(CERN, CDEF, IRAD)

$a_1(1420)$

$I^G(J^{PC}) = 1^-(1^{++})$

OMITTED FROM SUMMARY TABLE

$a_1(1420)$ MASS

VALUE (MeV)	DOCUMENT ID	TECN	COMMENT
1414^{+15}_{-13}	[1] ADOLPH 15C	COMP	190 $\pi^- p \to \pi^-\pi^+\pi^- p$

[1] Using the isobar model and partial-wave analysis with 88 waves.

$a_1(1420)$ WIDTH

VALUE (MeV)	DOCUMENT ID	TECN	COMMENT
153^{+8}_{-23}	[1] ADOLPH 15C	COMP	190 $\pi^- p \to \pi^-\pi^+\pi^- p$

[1] Using the isobar model and partial-wave analysis with 88 waves.

$a_1(1420)$ DECAY MODES

	Mode	Fraction (Γ_i/Γ)
Γ_1	$f_0(980)\pi$	seen

$a_1(1420)$ BRANCHING RATIOS

$\Gamma(f_0(980)\pi)/\Gamma_{total}$ Γ_1/Γ

VALUE	DOCUMENT ID	TECN	COMMENT
seen	[1] ADOLPH 15C	COMP	190 $\pi^- p \to \pi^-\pi^+\pi^- p$

[1] Using the isobar model and partial-wave analysis with 88 waves.

$a_1(1420)$ REFERENCES

ADOLPH	15C	PRL 115 082001	C. Adolph *et al.*	(COMPASS Collab.)

$f_1(1420)$

$I^G(J^{PC}) = 0^+(1^{++})$

See the minireview under $\eta(1405)$.

$f_1(1420)$ MASS

VALUE (MeV)	EVTS	DOCUMENT ID	TECN	COMMENT
1426.4± 0.9 OUR AVERAGE		Error includes scale factor of 1.1.		
1434 ± 5 ± 5	133	[1] ACHARD 07	L3	183–209 $e^+e^- \to e^+e^- K^0_S K^\pm\pi^\mp$
1426 ± 6	711	ABDALLAH 03H	DLPH	91.2 $e^+e^- \to K^0_S K^\pm\pi^\mp + X$
1420 ±14	3651	NICHITIU 02	OBLX	
1428 ± 4 ± 2	20k	ADAMS 01B	B852	18 GeV $\pi^- p \to K^+K^-\pi^0 n$
1426 ± 1		BARBERIS 97C	OMEG	450 $pp \to pp K^0_S K^\pm\pi^\mp$
1425 ± 8		BERTIN 97	OBLX	0.0 $\overline{p}p \to K^\pm(K^0)\pi^\mp\pi^+\pi^-$
1435 ± 9		PROKOSHKIN 97B	GAM4	100 $\pi^- p \to \eta\pi^0\pi^0 n$
1430 ± 4		[2] ARMSTRONG 92E	OMEG	85,300 $\pi^+ p$, $pp \to \pi^+ p$, $pp(K\overline{K}\pi)$
1462 ±20		[3] AUGUSTIN 92	DM2	$J/\psi \to \gamma K\overline{K}\pi$
1443 $^{+7}_{-6}$ ± $^{3}_{2}$	1100	BAI 90C	MRK3	$J/\psi \to \gamma K^0_S K^\pm\pi^\mp$
1425 ±10	17	BEHREND 89	CELL	$\gamma\gamma \to K^0_S K^\pm\pi^\mp$
1442 ± 5 $^{+10}_{-17}$	111	BECKER 87	MRK3	e^+e^-, $\omega K\overline{K}\pi$
1423 ± 4		GIDAL 87B	MRK2	$e^+e^- \to e^+e^- K\overline{K}\pi$
1417 ±13	13	AIHARA 86C	TPC	$e^+e^- \to e^+e^- K\overline{K}\pi$
1422 ± 3		CHAUVAT 84	SPEC	ISR 31.5 pp
1440 ±10		[4] BROMBERG 80	SPEC	100 $\pi^- p \to K\overline{K}\pi$X
1426 ± 6	221	DIONISI 80	HBC	4 $\pi^- p \to K\overline{K}\pi n$
1420 ±20		DAHL 67	HBC	1.6–4.2 $\pi^- p$
• • • We do not use the following data for averages, fits, limits, etc. • • •				
1430.8± 0.9		[5] SOSA 99	SPEC	$pp \to p_{slow}(K^0_S K^+\pi^-)\, p_{fast}$
1433.4± 0.8		[5] SOSA 99	SPEC	$pp \to p_{slow}(K^0_S K^-\pi^+)\, p_{fast}$
1429 ± 3	389	ARMSTRONG 89	OMEG	300 $pp \to K\overline{K}pp$
1425 ± 2	1520	ARMSTRONG 84	OMEG	85 $\pi^+ p$, $pp \to (\pi^+, p)(K\overline{K}\pi)p$
~ 1420		BITYUKOV 84	SPEC	32 $K^- p \to K^+K^-\pi^0 Y$

[1] From a fit with a width fixed at 55 MeV.
[2] This result supersedes ARMSTRONG 84, ARMSTRONG 89.
[3] From fit to the $K^*(892)K$ 1^{++} partial wave.
[4] Mass error increased to account for $a_0(980)$ mass cut uncertainties.
[5] No systematic error given.

$f_1(1420)$ WIDTH

VALUE (MeV)	EVTS	DOCUMENT ID	TECN	COMMENT
54.9± 2.6 OUR AVERAGE				
51 ±14	711	ABDALLAH 03H	DLPH	91.2 $e^+e^- \to K^0_S K^\pm\pi^\mp + X$
61 ± 8	3651	NICHITIU 02	OBLX	

38	± 9	±6	20k	ADAMS	01B	B852	18 GeV $\pi^- p \to K^+ K^- \pi^0 n$
58	± 4			BARBERIS	97C	OMEG	450 $pp \to pp K^0_S K^\pm \pi^\mp$
45	±10			BERTIN	97	OBLX	0.0 $\overline{p}p \to K^\pm(K^0)\pi^\mp\pi^+\pi^-$
90	±25			PROKOSHKIN	97B	GAM4	100 $\pi^- p \to \eta\pi^0\pi^0 n$
58	±10		[6]	ARMSTRONG	92E	OMEG	85,300 $\pi^+ p$, $pp \to \pi^+ p$, $pp(K\overline{K}\pi)$
129	±41		[7]	AUGUSTIN	92	DM2	$J/\psi \to \gamma K\overline{K}\pi$
68	$^{+29}_{-18}$	$^{+8}_{-9}$	1100	BAI	90C	MRK3	$J/\psi \to \gamma K^0_S K^\pm\pi^\mp$
42	±22		17	BEHREND	89	CELL	$\gamma\gamma \to K^0_S K^\pm\pi^\mp$
40	$^{+17}_{-13}$	±5	111	BECKER	87	MRK3	$e^+e^- \to \omega K\overline{K}\pi$
35	$^{+47}_{-20}$		13	AIHARA	86C	TPC	$e^+e^- \to e^+e^- K\overline{K}\pi$
47	±10			CHAUVAT	84	SPEC	ISR 31.5 pp
62	±14			BROMBERG	80	SPEC	100 $\pi^- p \to K\overline{K}\pi X$
40	±15		221	DIONISI	80	HBC	4 $\pi^- p \to K\overline{K}\pi n$
60	±20			DAHL	67	HBC	1.6–4.2 $\pi^- p$
• • • We do not use the following data for averages, fits, limits, etc. • • •							
68.7	± 2.9			[8] SOSA	99	SPEC	$pp \to p_{\text{slow}}(K^0_S K^+\pi^-)\, p_{\text{fast}}$
58.8	± 3.3			[8] SOSA	99	SPEC	$pp \to p_{\text{slow}}(K^0_S K^-\pi^+)\, p_{\text{fast}}$
58	± 8		389	ARMSTRONG	89	OMEG	300 $pp \to K\overline{K}\pi pp$
62	± 5		1520	ARMSTRONG	84	OMEG	85 $\pi^+ p$, $pp \to (\pi^+, p)(K\overline{K}\pi)p$
~ 50				BITYUKOV	84	SPEC	32 $K^- p \to K^+ K^-\pi^0 Y$

[6] This result supersedes ARMSTRONG 84, ARMSTRONG 89.
[7] From fit to the $K^*(892)\,K$ 1^{++} partial wave.
[8] No systematic error given.

$f_1(1420)$ DECAY MODES

	Mode	Fraction (Γ_i/Γ)
Γ_1	$K\overline{K}\pi$	dominant
Γ_2	$K\overline{K}^*(892)+$ c.c.	dominant
Γ_3	$\eta\pi\pi$	possibly seen
Γ_4	$a_0(980)\pi$	
Γ_5	$\pi\pi\rho$	
Γ_6	4π	
Γ_7	$\rho^0\gamma$	
Γ_8	$\phi\gamma$	seen

$f_1(1420)$ $\Gamma(i)\Gamma(\gamma\gamma)/\Gamma(\text{total})$

$\Gamma(K\overline{K}\pi) \times \Gamma(\gamma\gamma^*)/\Gamma_{\text{total}}$

VALUE (keV)	CL%	EVTS		DOCUMENT ID		TECN	COMMENT
1.9±0.4 OUR AVERAGE							
3.2±0.6±0.7		133	[9,10]	ACHARD	07	L3	183–209 $e^+e^- \to e^+e^- K^0_S K^\pm\pi^\mp$
3.0±0.9±0.7			[11,12]	BEHREND	89	CELL	$e^+e^- \to e^+e^- K^0_S K\pi$
$2.3^{+1.0}_{-0.9}$±0.8				HILL	89	JADE	$e^+e^- \to e^+e^- K^\pm K^0_S\pi^\mp$
1.3±0.5±0.3				AIHARA	88B	TPC	$e^+e^- \to e^+e^- K^\pm K^0_S\pi^\mp$
1.6±0.7±0.3			[11,13]	GIDAL	87B	MRK2	$e^+e^- \to e^+e^- K\overline{K}\pi$
• • • We do not use the following data for averages, fits, limits, etc. • • •							
<8.0	95			JENNI	83	MRK2	$e^+e^- \to e^+e^- K\overline{K}\pi$

[9] From a fit with a width fixed at 55 MeV.
[10] The form factor parameter from the fit is 926 ± 78 MeV.
[11] Assume a ρ-pole form factor.
[12] A ϕ - pole form factor gives considerably smaller widths.
[13] Published value divided by 2.

$f_1(1420)$ BRANCHING RATIOS

$\Gamma(K\overline{K}^*(892)+\text{c.c.})/\Gamma(K\overline{K}\pi)$ Γ_2/Γ_1

VALUE	DOCUMENT ID		TECN	COMMENT
• • • We do not use the following data for averages, fits, limits, etc. • • •				
0.76±0.06	BROMBERG	80	SPEC	100 $\pi^- p \to K\overline{K}\pi X$
0.86±0.12	DIONISI	80	HBC	4 $\pi^- p \to K\overline{K}\pi n$

$\Gamma(\pi\pi\rho)/\Gamma(K\overline{K}\pi)$ Γ_5/Γ_1

VALUE	CL%	DOCUMENT ID		TECN	COMMENT
• • • We do not use the following data for averages, fits, limits, etc. • • •					
<0.3	95	CORDEN	78	OMEG	12–15 $\pi^- p$
<2.0		DAHL	67	HBC	1.6–4.2 $\pi^- p$

$\Gamma(\eta\pi\pi)/\Gamma(K\overline{K}\pi)$ Γ_3/Γ_1

VALUE	CL%	DOCUMENT ID		TECN	COMMENT
<0.1	95	ARMSTRONG	91B	OMEG	300 $pp \to pp\eta\pi^+\pi^-$
• • • We do not use the following data for averages, fits, limits, etc. • • •					
1.35±0.75		KOPKE	89	MRK3	$J/\psi \to \omega\eta\pi\pi(K\overline{K}\pi)$
<0.6	90	GIDAL	87	MRK2	$e^+e^- \to e^+e^-\eta\pi^+\pi^-$
<0.5	95	CORDEN	78	OMEG	12–15 $\pi^- p$
1.5 ±0.8		DEFOIX	72	HBC	0.7 $\overline{p}p$

$\Gamma(a_0(980)\pi)/\Gamma(\eta\pi\pi)$ Γ_4/Γ_3

VALUE	CL%	DOCUMENT ID		TECN	COMMENT
>0.1	90	PROKOSHKIN	97B	GAM4	100 $\pi^- p \to \eta\pi^0\pi^0 n$
• • • We do not use the following data for averages, fits, limits, etc. • • •					
not seen in either mode		ANDO	86	SPEC	8 $\pi^- p$
not seen in either mode		CORDEN	78	OMEG	12–15 $\pi^- p$
0.4±0.2		DEFOIX	72	HBC	0.7 $\overline{p}p \to 7\pi$

$\Gamma(4\pi)/\Gamma(K\overline{K}^*(892)+\text{c.c.})$ Γ_6/Γ_2

VALUE	CL%	DOCUMENT ID		TECN	COMMENT
• • • We do not use the following data for averages, fits, limits, etc. • • •					
<0.90	95	DIONISI	80	HBC	4 $\pi^- p$

$\Gamma(K\overline{K}\pi)/[\Gamma(K\overline{K}^*(892)+\text{c.c.})+\Gamma(a_0(980)\pi)]$ $\Gamma_1/(\Gamma_2+\Gamma_4)$

VALUE	DOCUMENT ID		TECN	COMMENT
• • • We do not use the following data for averages, fits, limits, etc. • • •				
0.65±0.27	[14] DIONISI	80	HBC	4 $\pi^- p$

[14] Calculated using $\Gamma(K\overline{K})/\Gamma(\eta\pi) = 0.24 \pm 0.07$ for $a_0(980)$ fractions.

$\Gamma(a_0(980)\pi)/\Gamma(K\overline{K}^*(892)+\text{c.c.})$ Γ_4/Γ_2

VALUE	CL%	DOCUMENT ID		TECN	COMMENT
0.04±0.01±0.01		BARBERIS	98C	OMEG	450 $pp \to p_f f_1(1420)\, p_s$
• • • We do not use the following data for averages, fits, limits, etc. • • •					
<0.04	68	ARMSTRONG	84	OMEG	85 $\pi^+ p$

$\Gamma(4\pi)/\Gamma(K\overline{K}\pi)$ Γ_6/Γ_1

VALUE	CL%	DOCUMENT ID		TECN	COMMENT
<0.62	95	ARMSTRONG	89G	OMEG	85 $\pi p \to 4\pi X$

$\Gamma(\rho^0\gamma)/\Gamma_{\text{total}}$ Γ_7/Γ

VALUE	CL%	DOCUMENT ID		TECN	COMMENT
<0.08	95	[15] ARMSTRONG	92C	SPEC	300 $pp \to pp\pi^+\pi^-\gamma$

[15] Using the data on the $\overline{K}K\pi$ mode from ARMSTRONG 89.

$\Gamma(\rho^0\gamma)/\Gamma(K\overline{K}\pi)$ Γ_7/Γ_1

VALUE	CL%	DOCUMENT ID		TECN	COMMENT
<0.02	95	BARBERIS	98C	OMEG	450 $pp \to p_f f_1(1420)\, p_s$

$\Gamma(\phi\gamma)/\Gamma(K\overline{K}\pi)$ Γ_8/Γ_1

VALUE	DOCUMENT ID		TECN	COMMENT
0.003±0.001±0.001	BARBERIS	98C	OMEG	450 $pp \to p_f f_1(1420)\, p_s$

$f_1(1420)$ REFERENCES

ACHARD	07	JHEP 0703 018	P. Achard *et al.*	(L3 Collab.)
ABDALLAH	03H	PL B569 129	J. Abdallah *et al.*	(DELPHI Collab.)
NICHITIU	02	PL B545 261	F. Nichitiu *et al.*	(OBELIX Collab.)
ADAMS	01B	PL B516 264	G.S. Adams *et al.*	(BNL E852 Collab.)
SOSA	99	PRL 83 913	M. Sosa *et al.*	
BARBERIS	98C	PL B440 225	D. Barberis *et al.*	(WA 102 Collab.)
BARBERIS	97C	PL B413 225	D. Barberis *et al.*	(WA 102 Collab.)
BERTIN	97	PL B400 226	A. Bertin *et al.*	(OBELIX Collab.)
PROKOSHKIN	97B	PD 42 298	Yu.D. Prokoshkin, S.A. Sadovsky	
		Translated from DANS 354 751.		
ARMSTRONG	92C	ZPHY C54 371	T.A. Armstrong *et al.*	(ATHU, BARI, BIRM+)
ARMSTRONG	92E	ZPHY C56 29	T.A. Armstrong *et al.*	(ATHU, BARI, BIRM+) JPC
AUGUSTIN	92	PR D46 1951	J.E. Augustin, G. Cosme	(DM2 Collab.)
ARMSTRONG	91B	ZPHY C52 389	T.A. Armstrong *et al.*	(ATHU, BARI, BIRM+)
BAI	90C	PRL 65 2507	Z. Bai *et al.*	(Mark III Collab.)
ARMSTRONG	89	PL B221 216	T.A. Armstrong *et al.*	(CERN, CDEF, BIRM+) JPC
ARMSTRONG	89G	ZPHY C43 55	T.A. Armstrong *et al.*	(CERN, BIRM, BARI+)
BEHREND	89	ZPHY C42 367	H.J. Behrend *et al.*	(CELLO Collab.)
HILL	89	ZPHY C42 355	P. Hill *et al.*	(JADE Collab.) JP
KOPKE	89	PRPL 174 67	L. Kopke *et al.*	(CERN)
AIHARA	88B	PL B209 107	H. Aihara *et al.*	(TPC-2γ Collab.)
BECKER	87	PRL 59 186	J.J. Becker *et al.*	(Mark III Collab.) JP
GIDAL	87	PRL 59 2012	G. Gidal *et al.*	(LBL, SLAC, HARV)
GIDAL	87B	PRL 59 2016	G. Gidal *et al.*	(LBL, SLAC, HARV)
AIHARA	86C	PRL 57 2500	H. Aihara *et al.*	(TPC-2γ Collab.) JP
ANDO	86	PRL 57 1296	A. Ando *et al.*	(KEK, KYOT, NIRS, SAGA+)
ARMSTRONG	84	PL 146B 273	T.A. Armstrong *et al.*	(ATHU, BARI, BIRM+) JP
BITYUKOV	84	SJNP 39 735	S. Bityukov *et al.*	(SERP)
		Translated from YAF 39 1165.		
CHAUVAT	84	PL 148B 382	P. Chauvat *et al.*	(CERN, CLER, UCLA+)
JENNI	83	PR D27 1031	P. Jenni *et al.*	(SLAC, LBL)
BROMBERG	80	PR D22 1513	C.M. Bromberg *et al.*	(CIT, FNAL, ILLC+)
DIONISI	80	NP B169 1	C. Dionisi *et al.*	(CERN, MADR, CDEF+) IJP
CORDEN	78	NP B144 253	M.J. Corden *et al.*	(BIRM, RHEL, TELA+)
DEFOIX	72	NP B44 125	C. Defoix *et al.*	(CDEF, CERN)
DAHL	67	PR 163 1377	O.I. Dahl *et al.*	(LRL) IJP
Also		PRL 14 1074	D.H. Miller *et al.*	(LRL, UCB)

$\omega(1420)$

$I^G(J^{PC}) = 0^-(1^{--})$

$\omega(1420)$ MASS

VALUE (MeV)	EVTS	DOCUMENT ID		TECN	COMMENT
(1400–1450) OUR ESTIMATE					
• • • We do not use the following data for averages, fits, limits, etc. • • •					
1418± 30± 10	824	[1] AKHMETSHIN	17A	CMD3	1.4–2.0 $e^+e^- \to \omega\eta$
1470± 50	13.1k	[2] AULCHENKO	15A	SND	1.05–1.80 $e^+e^- \to \pi^+\pi^-\pi^0$
1382± 23± 70		AUBERT	07AU	BABR	10.6 $e^+e^- \to \omega\pi^+\pi^-\gamma$
1350± 20± 20		AUBERT,B	04N	BABR	10.6 $e^+e^- \to \pi^+\pi^-\pi^0\gamma$
1400± 50±130	1.2M	[3] ACHASOV	03D	RVUE	0.44–2.00 $e^+e^- \to \pi^+\pi^-\pi^0$
1450± 10		[4] HENNER	02	RVUE	1.2–2.0 $e^+e^- \to \rho\pi, \omega\pi\pi$
1373± 70	177	[5] AKHMETSHIN	00D	CMD2	1.2–1.38 $e^+e^- \to \omega\pi^+\pi^-$
1370± 25	5095	ANISOVICH	00H	SPEC	0.0 $p\overline{p} \to \omega\pi^0\pi^0\pi^0$
1400^{+100}_{-200}		[6] ACHASOV	98H	RVUE	$e^+e^- \to \pi^+\pi^-\pi^0$
~ 1400		[7] ACHASOV	98H	RVUE	$e^+e^- \to \omega\pi^+\pi^-$
~ 1460		[8] ACHASOV	98H	RVUE	$e^+e^- \to K^+K^-$
1440± 70		[9] CLEGG	94	RVUE	
1419± 31	315	[10] ANTONELLI	92	DM2	1.34–2.4 $e^+e^- \to \rho\pi$

[1] From a fit of the interfering $\omega(1420)$ and $\omega(1650)$ with a relative phase of π and other parameters floating.
[2] From a fit with contributions from $\omega(782)$, $\phi(1020)$, $\omega(1420)$, and $\omega(1650)$.
[3] From the combined fit of ANTONELLI 92, ACHASOV 01E, ACHASOV 02E, and ACHASOV 03D data on the $\pi^+\pi^-\pi^0$ and ANTONELLI 92 on the $\omega\pi^+\pi^-$ final states. Supersedes ACHASOV 99E and ACHASOV 02E.
[4] Using results of CORDIER 81 and preliminary data of DOLINSKY 91 and ANTONELLI 92.
[5] Using the data of AKHMETSHIN 00D and ANTONELLI 92. The $\rho\pi$ dominance for the energy dependence of the $\omega(1420)$ and $\omega(1650)$ width assumed.
[6] Using data from BARKOV 87, DOLINSKY 91, and ANTONELLI 92.
[7] Using the data from ANTONELLI 92.
[8] Using the data from IVANOV 81 and BISELLO 88B.
[9] From a fit to two Breit-Wigner functions and using the data of DOLINSKY 91 and ANTONELLI 92.
[10] From a fit to two Breit-Wigner functions interfering between them and with the ω,ϕ tails with fixed $(+,-,+)$ phases.

$\omega(1420)$ WIDTH

VALUE (MeV)	EVTS	DOCUMENT ID		TECN	COMMENT
(180–250) OUR ESTIMATE					
• • • We do not use the following data for averages, fits, limits, etc. • • •					
104± 35± 10	824	[1] AKHMETSHIN	17A	CMD3	1.4–2.0 $e^+e^- \to \omega\eta$
880±170	13.1k	[2] AULCHENKO	15A	SND	1.05–1.80 $e^+e^- \to \pi^+\pi^-\pi^0$
130± 50±100		AUBERT	07AU	BABR	10.6 $e^+e^- \to \omega\pi^+\pi^-\gamma$
450± 70± 70		AUBERT,B	04N	BABR	10.6 $e^+e^- \to \pi^+\pi^-\pi^0\gamma$
870^{+500}_{-300}±450	1.2M	[3] ACHASOV	03D	RVUE	0.44–2.00 $e^+e^- \to \pi^+\pi^-\pi^0$
199± 15		[4] HENNER	02	RVUE	1.2–2.0 $e^+e^- \to \rho\pi, \omega\pi\pi$
188± 45	177	[5] AKHMETSHIN	00D	CMD2	1.2–1.38 $e^+e^- \to \omega\pi^+\pi^-$
360^{+100}_{-60}	5095	ANISOVICH	00H	SPEC	0.0 $p\overline{p} \to \omega\pi^0\pi^0\pi^0$
240± 70		[6] CLEGG	94	RVUE	
174± 59	315	[7] ANTONELLI	92	DM2	1.34–2.4 $e^+e^- \to \rho\pi$

[1] From a fit of the interfering $\omega(1420)$ and $\omega(1650)$ with a relative phase of π and other parameters floating.
[2] From a fit with contributions from $\omega(782)$, $\phi(1020)$, $\omega(1420)$, and $\omega(1650)$.
[3] From the combined fit of ANTONELLI 92, ACHASOV 01E, ACHASOV 02E, and ACHASOV 03D data on the $\pi^+\pi^-\pi^0$ and ANTONELLI 92 on the $\omega\pi^+\pi^-$ final states. Supersedes ACHASOV 99E and ACHASOV 02E.
[4] Using results of CORDIER 81 and preliminary data of DOLINSKY 91 and ANTONELLI 92.
[5] Using the data of AKHMETSHIN 00D and ANTONELLI 92. The $\rho\pi$ dominance for the energy dependence of the $\omega(1420)$ and $\omega(1650)$ width assumed.
[6] From a fit to two Breit-Wigner functions and using the data of DOLINSKY 91 and ANTONELLI 92.
[7] From a fit to two Breit-Wigner functions interfering between them and with the ω,ϕ tails with fixed $(+,-,+)$ phases.

$\omega(1420)$ DECAY MODES

	Mode	Fraction (Γ_i/Γ)
Γ_1	$\rho\pi$	dominant
Γ_2	$\omega\pi\pi$	seen
Γ_3	$\omega\eta$	
Γ_4	$b_1(1235)\pi$	seen
Γ_5	e^+e^-	seen
Γ_6	$\pi^0\gamma$	

$\omega(1420)$ $\Gamma(i)\Gamma(e^+e^-)/\Gamma^2$(total)

$\Gamma(\rho\pi)/\Gamma_{total} \times \Gamma(e^+e^-)/\Gamma_{total}$ $\quad \Gamma_1/\Gamma \times \Gamma_5/\Gamma$

VALUE (units 10^{-6})	EVTS	DOCUMENT ID		TECN	COMMENT
• • • We do not use the following data for averages, fits, limits, etc. • • •					
0.73 ±0.08	13.1k	[1] AULCHENKO	15A	SND	1.05–1.80 $e^+e^- \to \pi^+\pi^-\pi^0$
0.82 ±0.05 ±0.06		AUBERT,B	04N	BABR	10.6 $e^+e^- \to \pi^+\pi^-\pi^0\gamma$
0.65 ±0.13 ±0.21	1.2M	[2,3] ACHASOV	03D	RVUE	0.44–2.00 $e^+e^- \to \pi^+\pi^-\pi^0$
0.625±0.160		[4,5] CLEGG	94	RVUE	
0.466±0.178		[6,7] ANTONELLI	92	DM2	1.34–2.4 $e^+e^- \to \rho\pi$

[1] From a fit with contributions from $\omega(782)$, $\phi(1020)$, $\omega(1420)$, and $\omega(1650)$.
[2] Calculated by us from the cross section at the peak.
[3] From the combined fit of ANTONELLI 92, ACHASOV 01E, ACHASOV 02E, and ACHASOV 03D data on the $\pi^+\pi^-\pi^0$ and ANTONELLI 92 on the $\omega\pi^+\pi^-$ final states. Supersedes ACHASOV 99E and ACHASOV 02E.
[4] From a fit to two Breit-Wigner functions and using the data of DOLINSKY 91 and ANTONELLI 92.
[5] From the partial and leptonic width given by the authors.
[6] From a fit to two Breit-Wigner functions interfering between them and with the ω,ϕ tails with fixed $(+,-,+)$ phases.
[7] From the product of the leptonic width and partial branching ratio given by the authors.

$\Gamma(\omega\pi\pi)/\Gamma_{total} \times \Gamma(e^+e^-)/\Gamma_{total}$ $\quad \Gamma_2/\Gamma \times \Gamma_5/\Gamma$

VALUE (units 10^{-8})	DOCUMENT ID		TECN	COMMENT
• • • We do not use the following data for averages, fits, limits, etc. • • •				
19.7±5.7	AUBERT	07AU	BABR	10.6 $e^+e^- \to \omega\pi^+\pi^-\gamma$
1.9±1.9	[1] AKHMETSHIN	00D	CMD2	1.2–2.4 $e^+e^- \to \omega\pi^+\pi^-$

[1] Using the data of AKHMETSHIN 00D and ANTONELLI 92. The $\rho\pi$ dominance for the energy dependence of the $\omega(1420)$ and $\omega(1650)$ width assumed.

$\Gamma(\omega\eta)/\Gamma_{total} \times \Gamma(e^+e^-)/\Gamma_{total}$ $\quad \Gamma_3/\Gamma \times \Gamma_5/\Gamma$

VALUE (units 10^{-8})	EVTS	DOCUMENT ID		TECN	COMMENT
• • • We do not use the following data for averages, fits, limits, etc. • • •					
5.0±2.6±0.3	824	[1] AKHMETSHIN	17A	CMD3	1.4–2.0 $e^+e^- \to \omega\eta$
$1.6^{+0.9}_{-0.7}$	898	[2] ACHASOV	16B	SND	1.34–2.00 $e^+e^- \to \omega\eta$

[1] From a fit of the interfering $\omega(1420)$ and $\omega(1650)$ with a relative phase of π and other parameters floating. From an alternative fit $\Gamma(\omega(1420) \to \omega\eta)/\Gamma_{total} \times \Gamma(\omega(1420) \to e^+e^-) = 5.3 \pm 1.6$ eV.
[2] From a fit with contributions from $\omega(1420)$, $\omega(1650)$, and $\phi(1680)$. The mass and the width of $\omega(1420)$ are fixed to the 2014 edition (PDG 14) of this review.

$\Gamma(\pi^0\gamma)/\Gamma_{total} \times \Gamma(e^+e^-)/\Gamma_{total}$ $\quad \Gamma_6/\Gamma \times \Gamma_5/\Gamma$

VALUE (units 10^{-8})	DOCUMENT ID		TECN	COMMENT
• • • We do not use the following data for averages, fits, limits, etc. • • •				
$2.03^{+0.70}_{-0.75}$	[1] AKHMETSHIN	05	CMD2	0.60-1.38 $e^+e^- \to \pi^0\gamma$

[1] Using 1420 MeV and 220 MeV for the $\omega(1420)$ mass and width.

$\omega(1420)$ BRANCHING RATIOS

$\Gamma(\omega\pi\pi)/\Gamma_{total}$ $\quad \Gamma_2/\Gamma$

VALUE	DOCUMENT ID		TECN	COMMENT
• • • We do not use the following data for averages, fits, limits, etc. • • •				
0.301±0.029	[1] HENNER	02	RVUE	1.2–2.0 $e^+e^- \to \rho\pi, \omega\pi\pi$
possibly seen	AKHMETSHIN	00D	CMD2	$e^+e^- \to \omega\pi^+\pi^-$

$\Gamma(\omega\pi\pi)/\Gamma(b_1(1235)\pi)$ $\quad \Gamma_2/\Gamma_4$

VALUE	EVTS	DOCUMENT ID		TECN	COMMENT
• • • We do not use the following data for averages, fits, limits, etc. • • •					
0.60±0.16	5095	ANISOVICH	00H	SPEC	0.0 $p\overline{p} \to \omega\pi^0\pi^0\pi^0$

$\Gamma(\rho\pi)/\Gamma_{total}$ $\quad \Gamma_1/\Gamma$

VALUE	DOCUMENT ID		TECN	COMMENT
• • • We do not use the following data for averages, fits, limits, etc. • • •				
0.699±0.029	[1] HENNER	02	RVUE	1.2–2.0 $e^+e^- \to \rho\pi, \omega\pi\pi$

$\Gamma(e^+e^-)/\Gamma_{total}$ $\quad \Gamma_5/\Gamma$

VALUE (units 10^{-7})	EVTS	DOCUMENT ID		TECN	COMMENT
• • • We do not use the following data for averages, fits, limits, etc. • • •					
~ 6.6	1.2M	[2,3] ACHASOV	03D	RVUE	0.44–2.00 $e^+e^- \to \pi^+\pi^-\pi^0$
23 ±1		[1] HENNER	02	RVUE	1.2–2.0 $e^+e^- \to \rho\pi, \omega\pi\pi$

[1] Assuming that the $\omega(1420)$ decays into $\rho\pi$ and $\omega\pi\pi$ only.
[2] Calculated by us from the cross section at the peak.
[3] Assuming that the $\omega(1420)$ decays into $\rho\pi$ only.

$\omega(1420)$ REFERENCES

AKHMETSHIN 17A PL B773 150 R.R. Akhmetshin *et al.* (CMD-3 Collab.)
ACHASOV 16B PR D94 092002 M.N. Achasov *et al.* (SND Collab.)

AULCHENKO	15A	JETP 121 27 Translated from ZETF 148 34.	V.M. Aulchenko *et al.*	(SND Collab.)
PDG	14	CP C38 070001	K. Olive *et al.*	(PDG Collab.)
AUBERT	07AU	PR D76 092005	B. Aubert *et al.*	(BABAR Collab.)
AKHMETSHIN	05	PL B605 26	R.R. Akhmetshin *et al.*	(Novosibirsk CMD-2 Collab.)
AUBERT,B	04N	PR D70 072004	B. Aubert *et al.*	(BABAR Collab.)
ACHASOV	03D	PR D68 052006	M.N. Achasov *et al.*	(Novosibirsk SND Collab.)
ACHASOV	02E	PR D66 032001	M.N. Achasov *et al.*	(Novosibirsk SND Collab.)
HENNER	02	EPJ C26 3	V.K. Henner *et al.*	
ACHASOV	01E	PR D63 072002	M.N. Achasov *et al.*	(Novosibirsk SND Collab.)
AKHMETSHIN	00D	PL B489 125	R.R. Akhmetshin *et al.*	(Novosibirsk CMD-2 Collab.)
ANISOVICH	00H	PL B485 341	A.V. Anisovich *et al.*	
ACHASOV	99E	PL B462 365	M.N. Achasov *et al.*	(Novosibirsk SND Collab.)
ACHASOV	98H	PR D57 4334	N.N. Achasov, A.A. Kozhevnikov	
CLEGG	94	ZPHY C62 455	A.B. Clegg, A. Donnachie	(LANC, MCHS)
ANTONELLI	92	ZPHY C56 15	A. Antonelli *et al.*	(DM2 Collab.)
DOLINSKY	91	PRPL 202 99	S.I. Dolinsky *et al.*	(NOVO)
BISELLO	88B	ZPHY C39 13	D. Bisello *et al.*	(PADO, CLER, FRAS+)
BARKOV	87	JETPL 46 164 Translated from ZETFP 46 132.	L.M. Barkov *et al.*	(NOVO)
CORDIER	81	PL 106B 155	A. Cordier *et al.*	(ORSAY)
IVANOV	81	PL 107B 297	P.M. Ivanov *et al.*	(NOVO)

$f_2(1430)$

$I^G(J^{PC}) = 0^+(2^{++})$

OMITTED FROM SUMMARY TABLE

This entry lists nearby peaks observed in the D wave of the $K\overline{K}$ and $\pi^+\pi^-$ systems. Needs confirmation.

$f_2(1430)$ MASS

VALUE (MeV)	DOCUMENT ID		TECN	COMMENT
≈ 1430 OUR ESTIMATE				
• • • We do not use the following data for averages, fits, limits, etc. • • •				
1453± 4	[1] VLADIMIRSK...01		SPEC	40 $\pi^- p \to K^0_S K^0_S n$
1421± 5	AUGUSTIN	87	DM2	$J/\psi \to \gamma\pi^+\pi^-$
1480±50	AKESSON	86	SPEC	$pp \to pp\pi^+\pi^-$
1436^{+26}_{-16}	DAUM	84	CNTR	17–18 $\pi^- p \to K^+K^- n$
1412± 3	DAUM	84	CNTR	63 $\pi^- p \to K^0_S K^0_S n$, $K^+K^- n$
1439^{+5}_{-6}	[2] BEUSCH	67	OSPK	5,7,12 $\pi^- p \to K^0_S K^0_S n$

[1] $J^{PC} = 0^{++}$ or 2^{++}.
[2] Not seen by WETZEL 76.

$f_2(1430)$ WIDTH

VALUE (MeV)	DOCUMENT ID		TECN	COMMENT
• • • We do not use the following data for averages, fits, limits, etc. • • •				
13± 5	[3] VLADIMIRSK...01		SPEC	40 $\pi^- p \to K^0_S K^0_S n$
30± 9	AUGUSTIN	87	DM2	$J/\psi \to \gamma\pi^+\pi^-$
150±50	AKESSON	86	SPEC	$pp \to pp\pi^+\pi^-$
81^{+56}_{-29}	DAUM	84	CNTR	17–18 $\pi^- p \to K^+K^- n$
14± 6	DAUM	84	CNTR	63 $\pi^- p \to K^0_S K^0_S n$, $K^+K^- n$
43^{+17}_{-18}	[4] BEUSCH	67	OSPK	5,7,12 $\pi^- p \to K^0_S K^0_S n$

[3] $J^{PC} = 0^{++}$ or 2^{++}.
[4] Not seen by WETZEL 76.

$f_2(1430)$ DECAY MODES

	Mode
Γ_1	$K\overline{K}$
Γ_2	$\pi\pi$

$f_2(1430)$ REFERENCES

VLADIMIRSK...	01	PAN 64 1895 Translated from YAF 64 1979.	V.V. Vladimirsky *et al.*	
AUGUSTIN	87	ZPHY C36 369	J.E. Augustin *et al.*	(LALO, CLER, FRAS+)
AKESSON	86	NP B264 154	T. Akesson *et al.*	(Axial Field Spec. Collab.)
DAUM	84	ZPHY C23 339	C. Daum *et al.*	(AMST, CERN, CRAC, MPIM+) JP
WETZEL	76	NP B115 208	W. Wetzel *et al.*	(ETH, CERN, LOIC)
BEUSCH	67	PL 25B 357	W. Beusch *et al.*	(ETH, CERN)

$a_0(1450)$

$I^G(J^{PC}) = 1^-(0^{++})$

See minireview on scalar mesons under $f_0(500)$.

$a_0(1450)$ MASS

VALUE (MeV)	EVTS	DOCUMENT ID		TECN	COMMENT
1474 ±19 OUR AVERAGE					
1480 ±30		ABELE	98	CBAR	0.0 $\overline{p}p \to K^0_L K^\pm\pi^\mp$
1470 ±25		[1] AMSLER	95D	CBAR	0.0 $\overline{p}p \to \pi^0\pi^0\pi^0$, $\pi^0\eta\eta$, $\pi^0\pi^0\eta$
• • • We do not use the following data for averages, fits, limits, etc. • • •					
1458 ±14 ±15	190k	AAIJ	16N	LHCB	$D^0 \to K^0_S K^\pm\pi^\mp$
1515 ±30		[2] ANISOVICH	09	RVUE	0.0 $\overline{p}p$, πN
$1316.8^{+\ 0.7+24.7}_{-\ 1.0-\ 4.6}$		[3] UEHARA	09A	BELL	$\gamma\gamma \to \pi^0\eta$
1432 ±13 ±25		[4] BUGG	08A	RVUE	$\overline{p}p$
1477 ±10	80k	[5] UMAN	06	E835	5.2 $\overline{p}p \to \eta\eta\pi^0$
1441^{+40}_{-15}	35280	[2] BAKER	03	SPEC	$\overline{p}p \to \omega\pi^+\pi^-\pi^0$
1303 ±16		[6] BARGIOTTI	03	OBLX	$\overline{p}p$
1296 ±10		[7] AMSLER	02	CBAR	0.9 $\overline{p}p \to \pi^0\pi^0\eta$
1565 ±30		[7] ANISOVICH	98B	RVUE	Compilation
1290 ±10		[8] BERTIN	98B	OBLX	0.0 $\overline{p}p \to K^\pm K_S\pi^\mp$
1450 ±40		AMSLER	94D	CBAR	0.0 $\overline{p}p \to \pi^0\pi^0\eta$
1410 ±25		ETKIN	82C	MPS	23 $\pi^- p \to n2K^0_S$
~ 1300		MARTIN	78	SPEC	10 $K^\pm p \to K^0_S\pi p$
1255 ± 5		[9] CASON	76		

[1] Coupled-channel analysis of AMSLER 95B, AMSLER 95C, and AMSLER 94D.
[2] From the pole position.
[3] May be a different state.
[4] Using data from AMSLER 94D, ABELE 98, and BAKER 03. Supersedes BUGG 94.
[5] Statistical error only.
[6] Coupled channel analysis of $\pi^+\pi^-\pi^0$, $K^+K^-\pi^0$, and $K^\pm K^0_S\pi^\mp$.
[7] T-matrix pole.
[8] Not confirmed by BUGG 08A.
[9] Isospin 0 not excluded.

$a_0(1450)$ WIDTH

VALUE (MeV)	EVTS	DOCUMENT ID		TECN	COMMENT
265 ±13 OUR AVERAGE					
265 ±15		ABELE	98	CBAR	0.0 $\overline{p}p \to K^0_L K^\pm\pi^\mp$
265 ±30		[1] AMSLER	95D	CBAR	0.0 $\overline{p}p \to \pi^0\pi^0\pi^0$, $\pi^0\eta\eta$, $\pi^0\pi^0\eta$
• • • We do not use the following data for averages, fits, limits, etc. • • •					
282 ±12 ±13	190k	AAIJ	16N	LHCB	$D^0 \to K^0_S K^\pm\pi^\mp$
230 ±36		[2] ANISOVICH	09	RVUE	0.0 $\overline{p}p$, πN
$65.0^{+\ 2.1+99.1}_{-\ 5.4-32.6}$		[3] UEHARA	09A	BELL	$\gamma\gamma \to \pi^0\eta$
196 ±10 ±10		[4] BUGG	08A	RVUE	$\overline{p}p$
267 ±11	80k	[5] UMAN	06	E835	5.2 $\overline{p}p \to \eta\eta\pi^0$
110 ±14	35280	[2] BAKER	03	SPEC	$\overline{p}p \to \omega\pi^+\pi^-\pi^0$
92 ±16		[6] BARGIOTTI	03	OBLX	$\overline{p}p$
81 ±21		[7] AMSLER	02	CBAR	0.9 $\overline{p}p \to \pi^0\pi^0\eta$
292 ±40		[7] ANISOVICH	98B	RVUE	Compilation
80 ± 5		[8] BERTIN	98B	OBLX	0.0 $\overline{p}p \to K^\pm K_S\pi^\mp$
270 ±40		AMSLER	94D	CBAR	0.0 $\overline{p}p \to \pi^0\pi^0\eta$
230 ±30		ETKIN	82C	MPS	23 $\pi^- p \to n2K^0_S$
~ 250		MARTIN	78	SPEC	10 $K^\pm p \to K^0_S\pi p$
79 ±10		[9] CASON	76		

[1] Coupled-channel analysis of AMSLER 95B, AMSLER 95C, and AMSLER 94D.
[2] From the pole position.
[3] May be a different state.
[4] Using data from AMSLER 94D, ABELE 98, and BAKER 03. Supersedes BUGG 94.
[5] Statistical error only.
[6] Coupled channel analysis of $\pi^+\pi^-\pi^0$, $K^+K^-\pi^0$, and $K^\pm K^0_S\pi^\mp$.
[7] T-matrix pole.
[8] Not confirmed by BUGG 08A.
[9] Isospin 0 not excluded.

$a_0(1450)$ DECAY MODES

	Mode	Fraction (Γ_i/Γ)
Γ_1	$\pi\eta$	0.093±0.020
Γ_2	$\pi\eta'(958)$	0.033±0.017
Γ_3	$K\overline{K}$	0.082±0.028
Γ_4	$\omega\pi\pi$	**DEFINED AS 1**
Γ_5	$a_0(980)\pi\pi$	seen
Γ_6	$\gamma\gamma$	seen

$a_0(1450)$ Γ(i)Γ(γγ)/Γ(total)

$\Gamma(\pi\eta) \times \Gamma(\gamma\gamma)/\Gamma_{\text{total}}$ **$\Gamma_1\Gamma_6/\Gamma$**

VALUE (eV)	DOCUMENT ID		TECN	COMMENT
• • • We do not use the following data for averages, fits, limits, etc. • • •				
$432\pm6^{+1073}_{-\ 256}$	[1] UEHARA	09A	BELL	$\gamma\gamma \to \pi^0\eta$

[1] May be a different state.

$a_0(1450)$ BRANCHING RATIOS

$\Gamma(\pi\eta'(958))/\Gamma(\pi\eta)$ Γ_2/Γ_1

VALUE	DOCUMENT ID		TECN	COMMENT
0.35±0.16	[1] ABELE	98	CBAR	0.0 $\overline{p}p \to K_L^0 K^\pm \pi^\mp$
• • • We do not use the following data for averages, fits, limits, etc. • • •				
0.43±0.19	ABELE	97C	CBAR	0.0 $\overline{p}p \to \pi^0\pi^0\eta'$

[1] Using $\pi^0\eta$ from AMSLER 94D.

$\Gamma(K\overline{K})/\Gamma(\pi\eta)$ Γ_3/Γ_1

VALUE	DOCUMENT ID		TECN	COMMENT
0.88±0.23	[1] ABELE	98	CBAR	0.0 $\overline{p}p \to K_L^0 K^\pm \pi^\mp$

[1] Using $\pi^0\eta$ from AMSLER 94D.

$\Gamma(\omega\pi\pi)/\Gamma(\pi\eta)$ Γ_4/Γ_1

VALUE	EVTS	DOCUMENT ID		TECN	COMMENT
10.7±2.3	35280	[1] BAKER	03	SPEC	$\overline{p}p \to \omega\pi^+\pi^-\pi^0$

[1] Using results on $\overline{p}p \to a_0(1450)^0\pi^0$, $a_0(1450) \to \eta\pi^0$ from ABELE 96C and assuming the $\omega\rho$ mechanism for the $\omega\pi\pi$ state.

$\Gamma(a_0(980)\pi\pi)/\Gamma_{total}$ Γ_5/Γ

VALUE	DOCUMENT ID		TECN	COMMENT
seen	BUGG	08A	RVUE	$\overline{p}p$

$\Gamma(a_0(980)\pi\pi)/\Gamma(\pi\eta)$ Γ_5/Γ_1

VALUE	DOCUMENT ID		TECN	CHG	COMMENT
• • • We do not use the following data for averages, fits, limits, etc. • • •					
≤ 4.3	ANISOVICH	01	RVUE	0	$\overline{p}p \to \eta 2\pi^+ 2\pi^-$

$\Gamma(\gamma\gamma)/\Gamma_{total}$ Γ_6/Γ

VALUE	DOCUMENT ID		TECN	COMMENT
seen	[1] UEHARA	09A	BELL	$\gamma\gamma \to \pi^0\eta$

[1] May be a different state.

$a_0(1450)$ REFERENCES

AAIJ	16N	PR D93 052018	R. Aaij *et al.*	(LHCb Collab.)
ANISOVICH	09	IJMP A24 2481	V.V. Anisovich, A.V. Sarantsev	
UEHARA	09A	PR D80 032001	S. Uehara *et al.*	(BELLE Collab.)
BUGG	08A	PR D78 074023	D.V. Bugg	(LOQM)
UMAN	06	PR D73 052009	I. Uman *et al.*	(FNAL E835)
BAKER	03	PL B563 140	C.A. Baker *et al.*	
BARGIOTTI	03	EPJ C26 371	M. Bargiotti *et al.*	(OBELIX Collab.)
AMSLER	02	EPJ C23 29	C. Amsler *et al.*	
ANISOVICH	01	NP A690 567	A.V. Anisovich *et al.*	
ABELE	98	PR D57 3860	A. Abele *et al.*	(Crystal Barrel Collab.)
ANISOVICH	98B	SPU 41 419	V.V. Anisovich *et al.*	
		Translated from UFN 168 481.		
BERTIN	98B	PL B434 180	A. Bertin *et al.*	(OBELIX Collab.)
ABELE	97C	PL B404 179	A. Abele *et al.*	(Crystal Barrel Collab.)
ABELE	96C	NP A609 562	A. Abele *et al.*	(Crystal Barrel Collab.)
AMSLER	95B	PL B342 433	C. Amsler *et al.*	(Crystal Barrel Collab.)
AMSLER	95C	PL B353 571	C. Amsler *et al.*	(Crystal Barrel Collab.)
AMSLER	95D	PL B355 425	C. Amsler *et al.*	(Crystal Barrel Collab.)
AMSLER	94D	PL B333 277	C. Amsler *et al.*	(Crystal Barrel Collab.) IGJPC
BUGG	94	PR D50 4412	D.V. Bugg *et al.*	(LOQM)
ETKIN	82C	PR D25 2446	A. Etkin *et al.*	(BNL, CUNY, TUFTS, VAND)
MARTIN	78	NP B134 392	A.D. Martin *et al.*	(DURH, GEVA)
CASON	76	PRL 36 1485	N.M. Cason *et al.*	(NDAM, ANL)

$\rho(1450)$

$I^G(J^{PC}) = 1^+(1^{--})$

See our mini-review under the $\rho(1700)$.

$\rho(1450)$ MASS

VALUE (MeV)	DOCUMENT ID
1465±25 OUR ESTIMATE This is only an educated guess; the error given is larger than the error on the average of the published values.	

$\eta\rho^0$ MODE

VALUE (MeV)	EVTS	DOCUMENT ID		TECN	COMMENT
• • • We do not use the following data for averages, fits, limits, etc. • • •					
1500±10	7.4k	[1] ACHASOV	18	SND	1.22–2.00 $e^+e^- \to \eta\pi^+\pi^-$
1497±14		[2] AKHMETSHIN	01B	CMD2	$e^+e^- \to \eta\gamma$
1421±15		[3] AKHMETSHIN	00D	CMD2	$e^+e^- \to \eta\pi^+\pi^-$
1470±20		ANTONELLI	88	DM2	$e^+e^- \to \eta\pi^+\pi^-$
1446±10		FUKUI	88	SPEC	8.95 $\pi^-p \to \eta\pi^+\pi^-n$

[1] From the combined fit of AULCHENKO 15 and ACHASOV 18 in the model with the interfering $\rho(1450)$, $\rho(1700)$ and $\rho(2150)$ with the parameters of the $\rho(1450)$ and $\rho(1700)$ floating and the mass and width of the $\rho(2150)$ fixed at 2155 MeV and 320 MeV, respectively. The phases of the resonances are π, 0 and π, respectively.

[2] Using the data of AKHMETSHIN 01B on $e^+e^- \to \eta\gamma$, AKHMETSHIN 00D and ANTONELLI 88 on $e^+e^- \to \eta\pi^+\pi^-$.

[3] Using the data of ANTONELLI 88, DOLINSKY 91, and AKHMETSHIN 00D. The energy-independent width of the $\rho(1450)$ and $\rho(1700)$ mesons assumed.

$\omega\pi$ MODE

VALUE (MeV)	EVTS	DOCUMENT ID		TECN	COMMENT
• • • We do not use the following data for averages, fits, limits, etc. • • •					
1510± 7	10.2k	[1] ACHASOV	16D	SND	1.05–2.00 $e^+e^- \to \pi^0\pi^0\gamma$
$1544\pm22^{+11}_{-46}$	821	[2] MATVIENKO	15	BELL	$\overline{B}^0 \to D^{*+}\omega\pi^-$
1491±19	7815	[3] ACHASOV	13	SND	1.05–2.00 $e^+e^- \to \pi^0\pi^0\gamma$
1582±17±25	2382	[4] AKHMETSHIN	03B	CMD2	$e^+e \to \pi^0\pi^0\gamma$
$1349\pm25^{+10}_{-5}$	341	[5] ALEXANDER	01B	CLE2	$B \to D^{(*)}\omega\pi^-$
1523±10		[6] EDWARDS	00A	CLE2	$\tau^- \to \omega\pi^-\nu_\tau$
1463±25		[7] CLEGG	94	RVUE	
1250		[8] ASTON	80C	OMEG	20–70 $\gamma p \to \omega\pi^0 p$
1290±40		[8] BARBER	80C	SPEC	3–5 $\gamma p \to \omega\pi^0 p$

[1] From a phenomenological model based on vector meson dominance with interfering $\rho(770)$, $\rho(1450)$, and $\rho(1700)$. The $\rho(1700)$ mass and width are fixed at 1720 MeV and 250 MeV, respectively. Systematic uncertainties not estimated. Supersedes ACHASOV 13.

[2] Using Breit-Wigner parameterization of the $\rho(1450)$ and assuming equal probabilities of the $\rho(1450) \to \pi\pi$ and $\rho(1450) \to \omega\pi$ decays.

[3] From a phenomenological model based on vector meson dominance with the interfering $\rho(1450)$ and $\rho(1700)$ and their widths fixed at 400 and 250 MeV, respectively. Systematic uncertainty not estimated.

[4] Using the data of AKHMETSHIN 03B and BISELLO 91B assuming the $\omega\pi^0$ and $\pi^+\pi^-$ mass dependence of the total width. $\rho(1700)$ mass and width fixed at 1700 MeV and 240 MeV, respectively.

[5] Using Breit-Wigner parameterization of the $\rho(1450)$ and assuming the $\omega\pi^-$ mass dependence for the total width.

[6] Mass-independent width parameterization. $\rho(1700)$ mass and width fixed at 1700 MeV and 235 MeV respectively.

[7] Using data from BISELLO 91B, DOLINSKY 86 and ALBRECHT 87L.

[8] Not separated from $b_1(1235)$, not pure $J^P = 1^-$ effect.

4π MODE

VALUE (MeV)	DOCUMENT ID		TECN	COMMENT
• • • We do not use the following data for averages, fits, limits, etc. • • •				
1435±40	ABELE	01B	CBAR	0.0 $\overline{p}n \to 2\pi^-2\pi^0\pi^+$
1350±50	ACHASOV	97	RVUE	$e^+e^- \to 2(\pi^+\pi^-)$
1449± 4	[1] ARMSTRONG	89E	OMEG	300 $pp \to pp2(\pi^+\pi^-)$

[1] Not clear whether this observation has I=1 or 0.

$\pi\pi$ MODE

VALUE (MeV)			EVTS	DOCUMENT ID		TECN	COMMENT
• • • We do not use the following data for averages, fits, limits, etc. • • •							
1326.35± 3.46				[1] BARTOS	17	RVUE	$e^+e^- \to \pi^+\pi^-$
1342.31±46.62				[2] BARTOS	17A	RVUE	$e^+e^- \to \pi^+\pi^-$
1373.83±11.37				[3] BARTOS	17A	RVUE	$\tau^- \to \pi^-\pi^0\nu_\tau$
1429	±41		20K	[4] LEES	17C	BABR	$J/\psi \to \pi^+\pi^-\pi^0$
1350	±20	$+20$ -30	63.5k	[5] ABRAMOWICZ	12	ZEUS	$ep \to e\pi^+\pi^-p$
1493	±15			[6] LEES	12G	BABR	$e^+e^- \to \pi^+\pi^-\gamma$
1446	± 7	±28	5.4 M	[7,8] FUJIKAWA	08	BELL	$\tau^- \to \pi^-\pi^0\nu_\tau$
1328	±15			[9] SCHAEL	05C	ALEP	$\tau^- \to \pi^-\pi^0\nu_\tau$
1406	±15		87k	[7,10] ANDERSON	00A	CLE2	$\tau^- \to \pi^-\pi^0\nu_\tau$
~ 1368				[11] ABELE	99C	CBAR	0.0 $\overline{p}d \to \pi^+\pi^-\pi^-p$
1348	±33			BERTIN	98	OBLX	0.05–0.405 $\overline{p}p \to 2\pi^+\pi^-$
1411	±14			[12] ABELE	97	CBAR	$\overline{p}n \to \pi^-\pi^0\pi^0$
1370	$+90$ -70			ACHASOV	97	RVUE	$e^+e^- \to \pi^+\pi^-$
1359	±40			[10] BERTIN	97C	OBLX	0.0 $\overline{p}p \to \pi^+\pi^-\pi^0$
1282	±37			BERTIN	97D	OBLX	0.05 $\overline{p}p \to 2\pi^+2\pi^-$
1424	±25			BISELLO	89	DM2	$e^+e^- \to \pi^+\pi^-$
1265.5	±75.3			DUBNICKA	89	RVUE	$e^+e^- \to \pi^+\pi^-$
1292	±17			[13] KURDADZE	83	OLYA	0.64–1.4 $e^+e^- \to \pi^+\pi^-$

[1] Applies the Unitary & Analytic Model of the pion electromagnetic form factor of DUBNICKA 10 to analyze the data of LEES 12G and ABLIKIM 16C.

[2] Applies the Unitary & Analytic Model of the pion electromagnetic form factor of DUBNICKA 10 to analyze the data of ACHASOV 06, AKHMETSHIN 07, AUBERT 09AS, and AMBROSINO 11A.

[3] Applies the Unitary & Analytic Model of the pion electromagnetic form factor of DUBNICKA 10 to analyze the data of FUJIKAWA 08.

[4] From a Dalitz plot analysis in an isobar model with $\rho(1450)$ and $\rho(1700)$ masses and widths floating.

[5] Using the KUHN 90 parametrization of the pion form factor, neglecting $\rho-\omega$ interference.

[6] Using the GOUNARIS 68 parametrization of the pion form factor leaving the masses and widths of the $\rho(1450)$, $\rho(1700)$, and $\rho(2150)$ resonances as free parameters of the fit.

[7] From the GOUNARIS 68 parametrization of the pion form factor.

[8] $|F_\pi(0)|^2$ fixed to 1.

[9] From the combined fit of the τ^- data from ANDERSON 00A and SCHAEL 05C and e^+e^- data from the compilation of BARKOV 85, AKHMETSHIN 04, and ALOISIO 05. $\rho(1700)$ mass and width fixed at 1713 MeV and 235 MeV, respectively. Supersedes BARATE 97M.

[10] $\rho(1700)$ mass and width fixed at 1700 MeV and 235 MeV, respectively.

[11] $\rho(1700)$ mass and width fixed at 1780 MeV and 275 MeV respectively.

[12] T-matrix pole.

[13] Using for $\rho(1700)$ mass and width 1600 ± 20 and 300 ± 10 MeV respectively.

Meson Particle Listings

$\rho(1450)$

$K\overline{K}$ MODE

VALUE (MeV)	EVTS	DOCUMENT ID		TECN	CHG	COMMENT
• • • We do not use the following data for averages, fits, limits, etc. • • •						
1208 ±8 ±9	190k	[1] AAIJ	16N	LHCB		$D^0 \to K^0_S K^\pm \pi^\mp$
1422.8±6.5	27k	[2] ABELE	99D	CBAR	±	$0.0\ \overline{p}p \to K^+ K^- \pi^0$

[1] Using the GOUNARIS 68 parameterization with fixed width.
[2] K-matrix pole. Isospin not determined, could be $\omega(1420)$.

$K\overline{K}^*(892)$ + c.c. MODE

VALUE (MeV)	DOCUMENT ID	TECN	COMMENT
• • • We do not use the following data for averages, fits, limits, etc. • • •			
1505±19±7	AUBERT	08S	BABR $10.6\ e^+e^- \to K\overline{K}^*(892)\gamma$

$m_{\rho(1450)^0} - m_{\rho(1450)^\pm}$

VALUE (MeV)	DOCUMENT ID	TECN	COMMENT
• • • We do not use the following data for averages, fits, limits, etc. • • •			
−31.53±47.99	[1] BARTOS	17A	RVUE $e^+e^- \to \pi^+\pi^-$, $\tau^- \to \pi^-\pi^0\nu_\tau$

[1] Applies the Unitary & Analytic Model of the pion electromagnetic form factor of DUBNICKA 10 to analyze the data of ACHASOV 06, AKHMETSHIN 07, AUBERT 09AS, AMBROSINO 11A, and FUJIKAWA 08.

$\rho(1450)$ WIDTH

VALUE (MeV)	DOCUMENT ID
400±60 OUR ESTIMATE This is only an educated guess; the error given is larger than the error on the average of the published values.	

$\eta\rho^0$ MODE

VALUE (MeV)	EVTS	DOCUMENT ID		TECN	COMMENT
• • • We do not use the following data for averages, fits, limits, etc. • • •					
280±20	7.4k	[1] ACHASOV	18	SND	1.22–2.00 $e^+e^- \to \eta\pi^+\pi^-$
226±44		[2] AKHMETSHIN	01B	CMD2	$e^+e^- \to \eta\gamma$
211±31		[3] AKHMETSHIN	00D	CMD2	$e^+e^- \to \eta\pi^+\pi^-$
230±30		ANTONELLI	88	DM2	$e^+e^- \to \eta\pi^+\pi^-$
60±15		FUKUI	88	SPEC	$8.95\ \pi^- p \to \eta\pi^+\pi^- n$

[1] From the combined fit of AULCHENKO 15 and ACHASOV 18 in the model with the interfering $\rho(1450)$, $\rho(1700)$ and $\rho(2150)$ with the parameters of the $\rho(1450)$ and $\rho(1700)$ floating and the mass and width of the $\rho(2150)$ fixed at 2155 MeV and 320 MeV, respectively. The phases of the resonances are π, 0 and π, respectively.
[2] Using the data of AKHMETSHIN 01B on $e^+e^- \to \eta\gamma$, AKHMETSHIN 00D and ANTONELLI 88 on $e^+e^- \to \eta\pi^+\pi^-$.
[3] Using the data of ANTONELLI 88, DOLINSKY 91, and AKHMETSHIN 00D. The energy-independent width of the $\rho(1450)$ and $\rho(1700)$ mesons assumed.

$\omega\pi$ MODE

VALUE (MeV)	EVTS	DOCUMENT ID		TECN	COMMENT
• • • We do not use the following data for averages, fits, limits, etc. • • •					
440± 40	10.2k	[1] ACHASOV	16D	SND	1.05–2.00 $e^+e^- \to \pi^0\pi^0\gamma$
$303^{+\ 31+69}_{-\ 52-\ 7}$	821	[2] MATVIENKO	15	BELL	$\overline{B}^0 \to D^{*+}\omega\pi^-$
429± 42±10	2382	[3] AKHMETSHIN	03B	CMD2	$e^+e \to \pi^0\pi^0\gamma$
$547\pm\ 86^{+46}_{-45}$	341	[4] ALEXANDER	01B	CLE2	$B \to D^{(*)}\omega\pi^-$
400± 35		[5] EDWARDS	00A	CLE2	$\tau^- \to \omega\pi^-\nu_\tau$
311± 62		[6] CLEGG	94	RVUE	
300		[7] ASTON	80C	OMEG	20–70 $\gamma p \to \omega\pi^0 p$
320±100		[7] BARBER	80C	SPEC	3–5 $\gamma p \to \omega\pi^0 p$

[1] From a phenomenological model based on vector meson dominance with interfering $\rho(770)$, $\rho(1450)$, and $\rho(1700)$. The $\rho(1700)$ mass and width are fixed at 1720 MeV and 250 MeV, respectively. Systematic uncertainties not estimated. Supersedes ACHASOV 13.
[2] Using Breit-Wigner parameterization of the $\rho(1450)$ and assuming equal probabilities of the $\rho(1450) \to \pi\pi$ and $\rho(1450) \to \omega\pi$ decays.
[3] Using the data of AKHMETSHIN 03B and BISELLO 91B assuming the $\omega\pi^0$ and $\pi^+\pi^-$ mass dependence of the total width. $\rho(1700)$ mass and width fixed at 1700 MeV and 240 MeV, respectively.
[4] Using Breit-Wigner parameterization of the $\rho(1450)$ and assuming the $\omega\pi^-$ mass dependence for the total width.
[5] Mass-independent width parameterization. $\rho(1700)$ mass and width fixed at 1700 MeV and 235 MeV respectively.
[6] Using data from BISELLO 91B, DOLINSKY 86 and ALBRECHT 87L.
[7] Not separated from $b_1(1235)$, not pure $J^P = 1^-$ effect.

4π MODE

VALUE (MeV)	DOCUMENT ID	TECN	COMMENT
• • • We do not use the following data for averages, fits, limits, etc. • • •			
325±100	ABELE	01B	CBAR $0.0\ \overline{p}n \to 2\pi^-2\pi^0\pi^+$

$\pi\pi$ MODE

VALUE (MeV)	EVTS	DOCUMENT ID		TECN	COMMENT
• • • We do not use the following data for averages, fits, limits, etc. • • •					
324.13± 12.01		[1] BARTOS	17	RVUE	$e^+e^- \to \pi^+\pi^-$
492.17±138.38		[2] BARTOS	17A	RVUE	$e^+e^- \to \pi^+\pi^-$
340.87± 23.84		[3] BARTOS	17A	RVUE	$\tau^- \to \pi^-\pi^0\nu_\tau$
576 ± 29	20K	[4] LEES	17C	BABR	$J/\psi \to \pi^+\pi^-\pi^0$
460 ± 30 $^{+40}_{-45}$	63.5k	[5] ABRAMOWICZ	12	ZEUS	$ep \to e\pi^+\pi^- p$
427 ± 31		[6] LEES	12G	BABR	$e^+e^- \to \pi^+\pi^-\gamma$
434 ± 16 ±60	5.4M	[7,8] FUJIKAWA	08	BELL	$\tau^- \to \pi^-\pi^0\nu_\tau$
468 ± 41		[9] SCHAEL	05C	ALEP	$\tau^- \to \pi^-\pi^0\nu_\tau$
455 ± 41	87k	[7,10] ANDERSON	00A	CLE2	$\tau^- \to \pi^-\pi^0\nu_\tau$
∼ 374		[11] ABELE	99C	CBAR	$0.0\ \overline{p}d \to \pi^+\pi^-\pi^- p$
275 ± 10		BERTIN	98	OBLX	0.05–0.405 $\overline{n}p \to \pi^+\pi^+\pi^-$
343 ± 20		[12] ABELE	97	CBAR	$\overline{p}n \to \pi^-\pi^0\pi^0$
310 ± 40		[10] BERTIN	97C	OBLX	$0.0\ \overline{p}p \to \pi^+\pi^-\pi^0$
236 ± 36		BERTIN	97D	OBLX	$0.05\ \overline{p}p \to 2\pi^+2\pi^-$
269 ± 31		BISELLO	89	DM2	$e^+e^- \to \pi^+\pi^-$
391 ± 70		DUBNICKA	89	RVUE	$e^+e^- \to \pi^+\pi^-$
218 ± 46		[13] KURDADZE	83	OLYA	0.64–1.4 $e^+e^- \to \pi^+\pi^-$

[1] Applies the Unitary & Analytic Model of the pion electromagnetic form factor of DUBNICKA 10 to analyze the data of LEES 12G and ABLIKIM 16C.
[2] Applies the Unitary & Analytic Model of the pion electromagnetic form factor of DUBNICKA 10 to analyze the data of ACHASOV 06, AKHMETSHIN 07, AUBERT 09AS, and AMBROSINO 11A.
[3] Applies the Unitary & Analytic Model of the pion electromagnetic form factor of DUBNICKA 10 to analyze the data of FUJIKAWA 08.
[4] From a Dalitz plot analysis in an isobar model with $\rho(1450)$ and $\rho(1700)$ masses and widths floating.
[5] Using the KUHN 90 parametrization of the pion form factor, neglecting $\rho-\omega$ interference.
[6] Using the GOUNARIS 68 parametrization of the pion form factor leaving the masses and widths of the $\rho(1450)$, $\rho(1700)$, and $\rho(2150)$ resonances as free parameters of the fit.
[7] From the GOUNARIS 68 parametrization of the pion form factor.
[8] $|F_\pi(0)|^2$ fixed to 1.
[9] From the combined fit of the τ^- data from ANDERSON 00A and SCHAEL 05C and e^+e^- data from the compilation of BARKOV 85, AKHMETSHIN 04, and ALOISIO 05. $\rho(1700)$ mass and width fixed at 1713 MeV and 235 MeV, respectively. Supersedes BARATE 97M.
[10] $\rho(1700)$ mass and width fixed at 1700 MeV and 235 MeV, respectively.
[11] $\rho(1700)$ mass and width fixed at 1780 MeV and 275 MeV respectively.
[12] T-matrix pole.
[13] Using for $\rho(1700)$ mass and width 1600 ± 20 and 300 ± 10 MeV respectively.

$K\overline{K}$ MODE

VALUE (MeV)	EVTS	DOCUMENT ID		TECN	CHG	COMMENT
• • • We do not use the following data for averages, fits, limits, etc. • • •						
410 ±19 ±35	190k	[1] AAIJ	16N	LHCB		$D^0 \to K^0_S K^\pm \pi^\mp$
146.5±10.5	27k	[2] ABELE	99D	CBAR	±	$0.0\ \overline{p}p \to K^+ K^- \pi^0$

[1] Using the GOUNARIS 68 parameterization with fixed mass.
[2] K-matrix pole. Isospin not determined, could be $\omega(1420)$.

$K\overline{K}^*(892)$ + c.c. MODE

VALUE (MeV)	DOCUMENT ID	TECN	COMMENT
• • • We do not use the following data for averages, fits, limits, etc. • • •			
418±25±4	AUBERT	08S	BABR $10.6\ e^+e^- \to K\overline{K}^*(892)\gamma$

$\Gamma_{\rho(1450)^0} - \Gamma_{\rho(1450)^\pm}$

VALUE (MeV)	DOCUMENT ID	TECN	COMMENT
• • • We do not use the following data for averages, fits, limits, etc. • • •			
151.30±140.42	[1] BARTOS	17A	RVUE $e^+e^- \to \pi^+\pi^-$, $\tau^- \to \pi^-\pi^0\nu_\tau$

[1] Applies the Unitary & Analytic Model of the pion electromagnetic form factor of DUBNICKA 10 to analyze the data of ACHASOV 06, AKHMETSHIN 07, AUBERT 09AS, AMBROSINO 11A, and FUJIKAWA 08.

$\rho(1450)$ DECAY MODES

	Mode	Fraction (Γ_j/Γ)
Γ_1	$\pi\pi$	seen
Γ_2	$\pi^+\pi^-$	seen
Γ_3	4π	seen
Γ_4	$\omega\pi$	
Γ_5	$a_1(1260)\pi$	
Γ_6	$h_1(1170)\pi$	
Γ_7	$\pi(1300)\pi$	
Γ_8	$\rho\rho$	
Γ_9	$\rho(\pi\pi)_S$-wave	
Γ_{10}	e^+e^-	seen
Γ_{11}	$\eta\rho$	seen
Γ_{12}	$a_2(1320)\pi$	not seen
Γ_{13}	$K\overline{K}$	seen
Γ_{14}	K^+K^-	seen
Γ_{15}	$K\overline{K}^*(892)$ + c.c.	possibly seen
Γ_{16}	$\eta\gamma$	seen

Γ_{17}	$f_0(500)\gamma$	not seen
Γ_{18}	$f_0(980)\gamma$	not seen
Γ_{19}	$f_0(1370)\gamma$	not seen
Γ_{20}	$f_2(1270)\gamma$	not seen

$\rho(1450)$ Γ(i)$\Gamma(e^+e^-)/\Gamma$(total)

$\Gamma(\pi\pi) \times \Gamma(e^+e^-)/\Gamma_{total}$ $\Gamma_1\Gamma_{10}/\Gamma$

VALUE (keV)	DOCUMENT ID		TECN	COMMENT
• • • We do not use the following data for averages, fits, limits, etc. • • •				
0.12	[1] DIEKMAN	88	RVUE	$e^+e^- \to \pi^+\pi^-$
$0.027^{+0.015}_{-0.010}$	[2] KURDADZE	83	OLYA	0.64–1.4 $e^+e^- \to \pi^+\pi^-$

[1] Using total width = 235 MeV.
[2] Using for $\rho(1700)$ mass and width 1600 ± 20 and 300 ± 10 MeV respectively.

$\Gamma(\eta\rho) \times \Gamma(e^+e^-)/\Gamma_{total}$ $\Gamma_{11}\Gamma_{10}/\Gamma$

VALUE (eV)	DOCUMENT ID		TECN	COMMENT
• • • We do not use the following data for averages, fits, limits, etc. • • •				
74 ± 20	[1] AKHMETSHIN	00D	CMD2	$e^+e^- \to \eta\pi^+\pi^-$
91 ± 19	ANTONELLI	88	DM2	$e^+e^- \to \eta\pi^+\pi^-$

[1] Using the data of ANTONELLI 88, DOLINSKY 91, and AKHMETSHIN 00D. The energy-independent width of the $\rho(1450)$ and $\rho(1700)$ mesons assumed.

$\Gamma(\eta\gamma) \times \Gamma(e^+e^-)/\Gamma_{total}$ $\Gamma_{16}\Gamma_{10}/\Gamma$

VALUE (eV)	DOCUMENT ID		TECN	COMMENT
• • • We do not use the following data for averages, fits, limits, etc. • • •				
<16.4	[1] AKHMETSHIN	05	CMD2	0.60-1.38 $e^+e^- \to \eta\gamma$
2.2 ± 0.5 ± 0.3	[2] AKHMETSHIN	01B	CMD2	$e^+e^- \to \eta\gamma$

[1] From 2γ decay mode of η using 1465 MeV and 310 MeV for the $\rho(1450)$ mass and width. Recalculated by us.
[2] Using the data of AKHMETSHIN 01B on $e^+e^- \to \eta\gamma$, AKHMETSHIN 00D and ANTONELLI 88 on $e^+e^- \to \eta\pi^+\pi^-$. Recalculated by us using width of 226 MeV.

$\Gamma(K\overline{K}^*(892)+\text{c.c.}) \times \Gamma(e^+e^-)/\Gamma_{total}$ $\Gamma_{15}\Gamma_{10}/\Gamma$

VALUE (eV)	DOCUMENT ID		TECN	COMMENT
• • • We do not use the following data for averages, fits, limits, etc. • • •				
127 ± 15 ± 6	AUBERT	08S	BABR	10.6 $e^+e^- \to K\overline{K}^*(892)\gamma$

$\rho(1450)$ Γ(i)/Γ(total) × $\Gamma(e^+e^-)/\Gamma$(total)

$\Gamma(\omega\pi)/\Gamma_{total} \times \Gamma(e^+e^-)/\Gamma_{total}$ $\Gamma_4/\Gamma \times \Gamma_{10}/\Gamma$

VALUE (units 10^{-6})	EVTS	DOCUMENT ID		TECN	COMMENT
• • • We do not use the following data for averages, fits, limits, etc. • • •					
2.1 ± 0.4	10.2k	[1] ACHASOV	16D	SND	1.05–2.00 $e^+e^- \to \pi^0\pi^0\gamma$
5.3 ± 0.4	7815	[2] ACHASOV	13	SND	1.05–2.00 $e^+e^- \to \pi^0\pi^0\gamma$

[1] From a phenomenological model based on vector meson dominance with interfering $\rho(770)$, $\rho(1450)$, and $\rho(1700)$. The $\rho(1700)$ mass and width are fixed at 1720 MeV and 250 MeV, respectively. Systematic uncertainties not estimated. Supersedes ACHASOV 13.
[2] From a phenomenological model based on vector meson dominance with the interfering $\rho(1450)$ and $\rho(1700)$ and their widths fixed at 400 and 250 MeV, respectively. Systematic uncertainty not estimated.

$\Gamma(\eta\rho)/\Gamma_{total} \times \Gamma(e^+e^-)/\Gamma_{total}$ $\Gamma_{11}/\Gamma \times \Gamma_{10}/\Gamma$

VALUE (units 10^{-7})	EVTS	DOCUMENT ID		TECN	COMMENT
• • • We do not use the following data for averages, fits, limits, etc. • • •					
7.3 ± 0.3	7.4k	[1] ACHASOV	18	SND	1.22–2.00 $e^+e^- \to \eta\pi^+\pi^-$
$4.3^{+1.1}_{-0.9} \pm 0.2$	4.9k	[2] AULCHENKO	15	SND	1.22–2.00 $e^+e^- \to \eta\pi^+\pi^-$

[1] From the combined fit of AULCHENKO 15 and ACHASOV 18 in the model with the interfering $\rho(1450)$, $\rho(1700)$ and $\rho(2150)$ with the parameters of the $\rho(1450)$ and $\rho(1700)$ floating and the mass and width of the $\rho(2150)$ fixed at 2155 MeV and 320 MeV, respectively. The phases of the resonances are π, 0 and π, respectively.
[2] From a fit to the $e^+e^- \to \eta\pi^+\pi^-$ cross section with vector meson dominance model including $\rho(770)$, $\rho(1450)$, and $\rho(1700)$ decaying exclusively via $\eta\rho(770)$. Masses and widths of vector states are fixed to PDG 14. Coupling constants are assumed to be real.

$\Gamma(f_0(500)\gamma)/\Gamma_{total} \times \Gamma(e^+e^-)/\Gamma_{total}$ $\Gamma_{17}/\Gamma \times \Gamma_{10}/\Gamma$

VALUE (units 10^{-9})	CL%	DOCUMENT ID		TECN	COMMENT
<4.0	90	ACHASOV	11	SND	$e^+e^- \to \pi^0\pi^0\gamma$

$\Gamma(f_0(980)\gamma)/\Gamma_{total} \times \Gamma(e^+e^-)/\Gamma_{total}$ $\Gamma_{18}/\Gamma \times \Gamma_{10}/\Gamma$

VALUE (units 10^{-9})	CL%	DOCUMENT ID		TECN	COMMENT
<2.6	90	ACHASOV	11	SND	$e^+e^- \to \pi^0\pi^0\gamma$

$\Gamma(f_0(1370)\gamma)/\Gamma_{total} \times \Gamma(e^+e^-)/\Gamma_{total}$ $\Gamma_{19}/\Gamma \times \Gamma_{10}/\Gamma$

VALUE (units 10^{-9})	CL%	DOCUMENT ID		TECN	COMMENT
<3.5	90	ACHASOV	11	SND	$e^+e^- \to \pi^0\pi^0\gamma$

$\Gamma(f_2(1270)\gamma)/\Gamma_{total} \times \Gamma(e^+e^-)/\Gamma_{total}$ $\Gamma_{20}/\Gamma \times \Gamma_{10}/\Gamma$

VALUE (units 10^{-9})	CL%	DOCUMENT ID		TECN	COMMENT
<0.8	90	[1] ACHASOV	11	SND	$e^+e^- \to \pi^0\pi^0\gamma$

[1] Using Breit-Wigner parametrization of the $\rho(1450)$ with mass and width of 1465 MeV and 400 MeV, respectively.

$\rho(1450)$ BRANCHING RATIOS

$\Gamma(\pi\pi)/\Gamma(4\pi)$ Γ_1/Γ_3

VALUE	DOCUMENT ID		TECN	COMMENT
• • • We do not use the following data for averages, fits, limits, etc. • • •				
0.37 ± 0.10	[1,2] ABELE	01B	CBAR	0.0 $\overline{p}n \to 5\pi$

[1] $\omega\pi$ not included.
[2] Using ABELE 97.

$\Gamma(K^+K^-)/\Gamma(\pi^+\pi^-)$ Γ_{14}/Γ_2

VALUE (%)	EVTS	DOCUMENT ID		TECN	COMMENT
30.7 ± 8.4 ± 8.2	20K	[1] LEES	17C	BABR	$J/\psi \to h^+h^-\pi^0$

[1] From Dalitz plot analyses in isobar models.

$\Gamma(\omega\pi)/\Gamma_{total}$ Γ_4/Γ

VALUE	EVTS	DOCUMENT ID		TECN	COMMENT
• • • We do not use the following data for averages, fits, limits, etc. • • •					
seen	821	[1] MATVIENKO	15	BELL	$\overline{B}^0 \to D^{*+}\omega\pi^-$
seen	1.6k	ACHASOV	12	SND	$e^+e^- \to \pi^0\pi^0\gamma$
~ 0.21		CLEGG	94	RVUE	

[1] Using Breit-Wigner parameterization of the $\rho(1450)$ and assuming equal probabilities of the $\rho(1450) \to \pi\pi$ and $\rho(1450) \to \omega\pi$ decays.

$\Gamma(\pi\pi)/\Gamma(\omega\pi)$ Γ_1/Γ_4

VALUE	DOCUMENT ID		TECN
• • • We do not use the following data for averages, fits, limits, etc. • • •			
~ 0.32	CLEGG	94	RVUE

$\Gamma(\omega\pi)/\Gamma(4\pi)$ Γ_4/Γ_3

VALUE	DOCUMENT ID		TECN
• • • We do not use the following data for averages, fits, limits, etc. • • •			
<0.14	CLEGG	88	RVUE

$\Gamma(a_1(1260)\pi)/\Gamma(4\pi)$ Γ_5/Γ_3

VALUE	DOCUMENT ID		TECN	COMMENT
• • • We do not use the following data for averages, fits, limits, etc. • • •				
0.27 ± 0.08	[1] ABELE	01B	CBAR	0.0 $\overline{p}n \to 5\pi$

[1] $\omega\pi$ not included.

$\Gamma(h_1(1170)\pi)/\Gamma(4\pi)$ Γ_6/Γ_3

VALUE	DOCUMENT ID		TECN	COMMENT
• • • We do not use the following data for averages, fits, limits, etc. • • •				
0.08 ± 0.04	[1] ABELE	01B	CBAR	0.0 $\overline{p}n \to 5\pi$

[1] $\omega\pi$ not included.

$\Gamma(\pi(1300)\pi)/\Gamma(4\pi)$ Γ_7/Γ_3

VALUE	DOCUMENT ID		TECN	COMMENT
• • • We do not use the following data for averages, fits, limits, etc. • • •				
0.37 ± 0.13	[1] ABELE	01B	CBAR	0.0 $\overline{p}n \to 5\pi$

[1] $\omega\pi$ not included.

$\Gamma(\rho\rho)/\Gamma(4\pi)$ Γ_8/Γ_3

VALUE	DOCUMENT ID		TECN	COMMENT
• • • We do not use the following data for averages, fits, limits, etc. • • •				
0.11 ± 0.05	[1] ABELE	01B	CBAR	0.0 $\overline{p}n \to 5\pi$

[1] $\omega\pi$ not included.

$\Gamma(\rho(\pi\pi)_{S\text{-wave}})/\Gamma(4\pi)$ Γ_9/Γ_3

VALUE	DOCUMENT ID		TECN	COMMENT
• • • We do not use the following data for averages, fits, limits, etc. • • •				
0.17 ± 0.09	[1] ABELE	01B	CBAR	0.0 $\overline{p}n \to 5\pi$

[1] $\omega\pi$ not included.

$\Gamma(\eta\rho)/\Gamma_{total}$ Γ_{11}/Γ

VALUE	EVTS	DOCUMENT ID		TECN	COMMENT
seen	35	[1] ACHASOV	14	SND	1.15–2.00 $e^+e^- \to \eta\gamma$
• • • We do not use the following data for averages, fits, limits, etc. • • •					
<0.04		DONNACHIE	87B	RVUE	

[1] From a phenomenological model based on vector meson dominance with $\rho(1450)$ and $\phi(1680)$ masses and widths from the PDG 12.

Meson Particle Listings

$\rho(1450)$, $\eta(1475)$

$\Gamma(\eta\rho)/\Gamma(\omega\pi)$ Γ_{11}/Γ_4

VALUE	DOCUMENT ID		TECN	COMMENT
• • • We do not use the following data for averages, fits, limits, etc. • • •				
0.081 ± 0.020	[1,2] AULCHENKO	15	SND	1.22–2.00 $e^+e^- \to \eta\pi^+\pi^-$
~ 0.24	[3] DONNACHIE	91	RVUE	
>2	FUKUI	91	SPEC	8.95 $\pi^- p \to \omega\pi^0 n$

[1] From a fit to the $e^+e^- \to \eta\pi^+\pi^-$ cross section with vector meson dominance model including $\rho(770)$, $\rho(1450)$, and $\rho(1700)$ decaying exclusively via $\eta\rho(770)$. Masses and widths of vector states are fixed to PDG 14. Coupling constants are assumed to be real.
[2] Reports the inverse of the quoted value as 12.3 ± 3.1.
[3] Using data from BISELLO 91B, DOLINSKY 86 and ALBRECHT 87L.

$\Gamma(\pi\pi)/\Gamma(\eta\rho)$ Γ_1/Γ_{11}

VALUE	DOCUMENT ID		TECN	COMMENT
• • • We do not use the following data for averages, fits, limits, etc. • • •				
1.3 ± 0.4	[1] AULCHENKO	15	SND	1.22–2.00 $e^+e^- \to \eta\pi^+\pi^-$

[1] From a fit to the $e^+e^- \to \eta\pi^+\pi^-$ cross section with vector meson dominance model including $\rho(770)$, $\rho(1450)$, and $\rho(1700)$ decaying exclusively via $\eta\rho(770)$. Masses and widths of vector states are fixed to PDG 14. Coupling constants are assumed to be real.

$\Gamma(a_2(1320)\pi)/\Gamma_{\text{total}}$ Γ_{12}/Γ

VALUE	DOCUMENT ID		TECN	COMMENT
• • • We do not use the following data for averages, fits, limits, etc. • • •				
not seen	AMELIN	00	VES	37 $\pi^- p \to \eta\pi^+\pi^- n$

$\Gamma(K\overline{K})/\Gamma(\omega\pi)$ Γ_{13}/Γ_4

VALUE	DOCUMENT ID		TECN	
• • • We do not use the following data for averages, fits, limits, etc. • • •				
<0.08	[1] DONNACHIE	91	RVUE	

[1] Using data from BISELLO 91B, DOLINSKY 86 and ALBRECHT 87L.

$\Gamma(K\overline{K}^*(892)+\text{c.c.})/\Gamma_{\text{total}}$ Γ_{15}/Γ

VALUE	DOCUMENT ID		TECN	COMMENT
• • • We do not use the following data for averages, fits, limits, etc. • • •				
possibly seen	COAN	04	CLEO	$\tau^- \to K^-\pi^- K^+\nu_\tau$

$\Gamma(\eta\gamma)/\Gamma_{\text{total}}$ Γ_{16}/Γ

VALUE	EVTS	DOCUMENT ID		TECN	COMMENT
seen	35	[1] ACHASOV	14	SND	1.15–2.00 $e^+e^- \to \eta\gamma$

[1] From a phenomenological model based on vector meson dominance with $\rho(1450)$ and $\phi(1680)$ masses and widths from the PDG 12.

$\rho(1450)$ REFERENCES

ACHASOV	18	PR D97 012008	M.N. Achasov *et al.*	(SND Collab.)
BARTOS	17	PR D96 113004	E. Bartos *et al.*	
BARTOS	17A	IJMP A32 1750154	E. Bartos *et al.*	
LEES	17C	PR D95 072007	J.P. Lees *et al.*	(BABAR Collab)
AAIJ	16N	PR D93 052018	R. Aaij *et al.*	(LHCb Collab.)
ABLIKIM	16C	PL B753 629	M. Ablikim *et al.*	(BES III Collab.)
ACHASOV	16D	PR D94 112001	M.N. Achasov *et al.*	(SND Collab.)
AULCHENKO	15	PR D91 052013	V.M. Aulchenko *et al.*	(SND Collab.)
MATVIENKO	15	PR D92 012013	D. Matvienko *et al.*	(BELLE Collab.)
ACHASOV	14	PR D90 032002	M.N. Achasov *et al.*	(SND Collab.)
PDG	14	CP C38 070001	K. Olive *et al.*	(PDG Collab.)
ACHASOV	13	PR D88 054013	M.N. Achasov *et al.*	(SND Collab.)
ABRAMOWICZ	12	EPJ C72 1869	H. Abramowicz *et al.*	(ZEUS Collab.)
ACHASOV	12	JETPL 94 734	M.N. Achasov *et al.*	
		Translated from ZETFP 94 796.		
LEES	12G	PR D86 032013	J.P. Lees *et al.*	(BABAR Collab.)
PDG	12	PR D86 010001	J. Beringer *et al.*	(PDG Collab.)
ACHASOV	11	JETP 113 75	M.N. Achasov *et al.*	(SND Collab.)
		Translated from ZETF 140 87.		
AMBROSINO	11A	PL B700 102	F. Ambrosino *et al.*	(KLOE Collab.)
DUBNICKA	10	APS 60 1	S. Dubnicka, A.Z. Dubnickova	
AUBERT	09AS	PRL 103 231801	B. Aubert *et al.*	(BABAR Collab.)
AUBERT	08S	PR D77 092002	B. Aubert *et al.*	(BABAR Collab.)
FUJIKAWA	08	PR D78 072006	M. Fujikawa *et al.*	(BELLE Collab.)
AKHMETSHIN	07	PL B648 28	R.R. Akhmetshin *et al.*	(Novosibirsk CMD-2 Collab.)
ACHASOV	06	JETP 103 380	M.N. Achasov *et al.*	(Novosibirsk SND Collab.)
		Translated from ZETF 130 437.		
AKHMETSHIN	05	PL B605 26	R.R. Akhmetshin *et al.*	(Novosibirsk CMD-2 Collab.)
ALOISIO	05	PL B606 12	A. Aloisio *et al.*	(KLOE Collab.)
SCHAEL	05C	PRPL 421 191	S. Schael *et al.*	(ALEPH Collab.)
AKHMETSHIN	04	PL B578 285	R.R. Akhmetshin *et al.*	(Novosibirsk CMD-2 Collab.)
COAN	04	PRL 92 232001	T.E. Coan *et al.*	(CLEO Collab.)
AKHMETSHIN	03B	PL B562 173	R.R. Akhmetshin *et al.*	(Novosibirsk CMD-2 Collab.)
ABELE	01B	EPJ C21 261	A. Abele *et al.*	(Crystal Barrel Collab.)
AKHMETSHIN	01B	PL B509 217	R.R. Akhmetshin *et al.*	(Novosibirsk CMD-2 Collab.)
ALEXANDER	01B	PR D64 092001	J.P. Alexander *et al.*	(CLEO Collab.)
AKHMETSHIN	00D	PL B489 125	R.R. Akhmetshin *et al.*	(Novosibirsk CMD-2 Collab.)
AMELIN	00	NP A668 83	D. Amelin *et al.*	(VES Collab.)
ANDERSON	00A	PR D61 112002	S. Anderson *et al.*	(CLEO Collab.)
EDWARDS	00A	PR D61 072003	K.W. Edwards *et al.*	(CLEO Collab.)
ABELE	99C	PL B450 275	A. Abele *et al.*	(Crystal Barrel Collab.)
ABELE	99D	PL B468 178	A. Abele *et al.*	(Crystal Barrel Collab.)
BERTIN	98	PR D57 55	A. Bertin *et al.*	(OBELIX Collab.)
ABELE	97	PL B391 191	A. Abele *et al.*	(Crystal Barrel Collab.)
ACHASOV	97	PR D55 2663	N.N. Achasov *et al.*	(NOVM)
BARATE	97M	ZPHY C76 15	R. Barate *et al.*	(ALEPH Collab.)
BERTIN	97C	PL B408 476	A. Bertin *et al.*	(OBELIX Collab.)
BERTIN	97D	PL B414 220	A. Bertin *et al.*	(OBELIX Collab.)
CLEGG	94	ZPHY C62 455	A.B. Clegg, A. Donnachie	(LANC, MCHS)
BISELLO	91B	NPBPS B21 111	D. Bisello	(DM2 Collab.)
DOLINSKY	91	PRPL 202 99	S.I. Dolinsky *et al.*	(NOVO)
DONNACHIE	91	ZPHY C51 689	A. Donnachie, A.B. Clegg	(MCHS, LANC)
FUKUI	91	PL B257 241	S. Fukui *et al.*	(SUGI, NAGO, KEK, KYOT+)
KUHN	90	ZPHY C48 445	J.H. Kuhn *et al.*	(MPIM)
ARMSTRONG	89E	PL B228 536	T.A. Armstrong, M. Benayoun	(ATHU, BARI, BIRM+)
BISELLO	89	PL B220 321	D. Bisello *et al.*	(DM2 Collab.)
DUBNICKA	89	JP G15 1349	S. Dubnicka *et al.*	(JINR, SLOV)
ANTONELLI	88	PL B212 133	A. Antonelli *et al.*	(DM2 Collab.)
CLEGG	88	ZPHY C40 313	A.B. Clegg, A. Donnachie	(MCHS, LANC)
DIEKMAN	88	PRPL 159 99	B. Diekmann	(BONN)
FUKUI	88	PL B202 441	S. Fukui *et al.*	(SUGI, NAGO, KEK, KYOT+)
ALBRECHT	87L	PL B185 223	H. Albrecht *et al.*	(ARGUS Collab.)
DONNACHIE	87B	ZPHY C34 257	A. Donnachie, A.B. Clegg	(MCHS, LANC)
DOLINSKY	86	PL B174 453	S.I. Dolinsky *et al.*	(NOVO)
BARKOV	85	NP B256 365	L.M. Barkov *et al.*	(NOVO)
KURDADZE	83	JETPL 37 733	L.M. Kurdadze *et al.*	(NOVO)
		Translated from ZETFP 37 613.		
ASTON	80C	PL 92B 211	D. Aston	(BONN, CERN, EPOL, GLAS, LANC+)
BARBER	80C	ZPHY C4 169	D.P. Barber *et al.*	(DARE, LANC, SHEF)
GOUNARIS	68	PRL 21 244	G.J. Gounaris, J.J. Sakurai	

$\eta(1475)$ $I^G(J^{PC}) = 0^+(0^{-+})$

See also the $\eta(1405)$.

$\eta(1475)$ MASS

$K\overline{K}\pi$ MODE ($K^*(892)$ K dominant)

VALUE (MeV)	EVTS	DOCUMENT ID		TECN	COMMENT
1476± 4 OUR AVERAGE		Error includes scale factor of 1.3. See the ideogram below.			
$1469\pm14\pm13$	74	ACHARD	07	L3	183–209 $e^+e^- \to e^+e^- K^0_S K^\pm\pi^\mp$
1460 ± 19	3651	NICHITIU	02	OBLX	
$1485\pm 8\pm 5$	20k	ADAMS	01B	B852	18 GeV $\pi^- p \to K^+K^-\pi^0 n$
1500 ± 10		CICALO	99	OBLX	0 $\overline{p}p \to K^\pm K^0_S \pi^\mp\pi^+\pi^-$
1464 ± 10		BERTIN	97	OBLX	0 $\overline{p}p \to K^\pm(K^0)\pi^\mp\pi^+\pi^-$
1460 ± 10		BERTIN	95	OBLX	0 $\overline{p}p \to K\overline{K}\pi\pi\pi$
$1490^{+14+3}_{-\ 8-16}$	1100	BAI	90C	MRK3	$J/\psi \to \gamma K^0_S K^\pm\pi^\mp$
1475 ± 4		RATH	89	MPS	21.4 $\pi^- p \to n K^0_S K^0_S \pi^0$
• • • We do not use the following data for averages, fits, limits, etc. • • •					
$1565\pm\ 8^{+\ 0}_{-63}$		[1] ABLIKIM	15T	BES3	$J/\psi \to \gamma K^0_S K^0_S \eta$
1421 ± 14		AUGUSTIN	92	DM2	$J/\psi \to \gamma K\overline{K}\pi$

[1] Could also be the $\eta(1405)$.

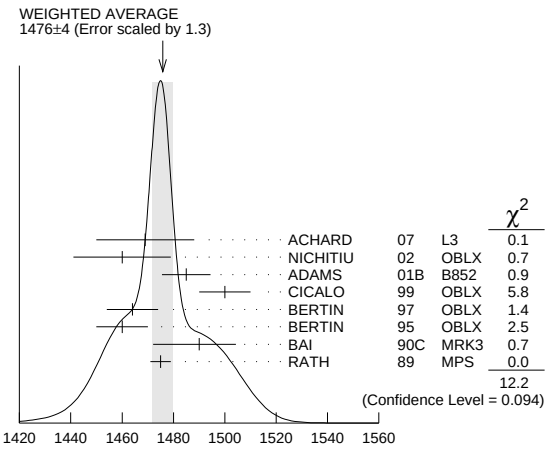

$\eta(1475)$ mass, $K\overline{K}\pi$ mode ($K^*(892)$ K dominant) (MeV)

$\eta(1475)$ WIDTH

$K\overline{K}\pi$ MODE ($K^*(892)$ K dominant)

VALUE (MeV)	EVTS	DOCUMENT ID		TECN	COMMENT
85± 9 OUR AVERAGE		Error includes scale factor of 1.5. See the ideogram below.			
$67\pm18\pm 7$	74	ACHARD	07	L3	183–209 $e^+e^- \to e^+e^- K^0_S K^\pm\pi^\mp$
120 ± 19	3651	NICHITIU	02	OBLX	
$98\pm18\pm 3$	20k	ADAMS	01B	B852	18 GeV $\pi^- p \to K^+K^-\pi^0 n$
100 ± 20		CICALO	99	OBLX	0 $\overline{p}p \to K^\pm K^0_S \pi^\mp\pi^+\pi^-$
105 ± 15		BERTIN	97	OBLX	0.0 $\overline{p}p \to K^\pm(K^0)\pi^\mp\pi^+\pi^-$
105 ± 15		BERTIN	95	OBLX	0 $\overline{p}p \to K\overline{K}\pi\pi\pi$
63 ± 18		AUGUSTIN	92	DM2	$J/\psi \to \gamma K\overline{K}\pi$
54^{+37+13}_{-21-24}		BAI	90C	MRK3	$J/\psi \to \gamma K^0_S K^\pm\pi^\mp$
51 ± 13		RATH	89	MPS	21.4 $\pi^- p \to n K^0_S K^0_S \pi^0$
• • • We do not use the following data for averages, fits, limits, etc. • • •					
54^{+14+21}_{-13-28}		[1] ABLIKIM	15T	BES3	$J/\psi \to \gamma K^0_S K^0_S \eta$

[1] Could also be the $\eta(1405)$.

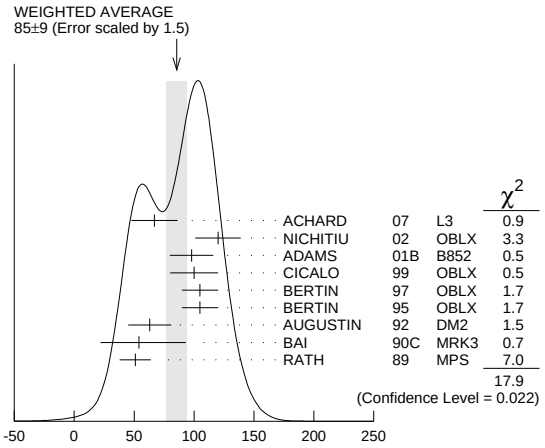

$\eta(1475)$ width $K\overline{K}\pi$ mode ($K^*(892)$ K dominant) (MeV)

$\eta(1475)$ DECAY MODES

	Mode	Fraction (Γ_i/Γ)
Γ_1	$K\overline{K}\pi$	dominant
Γ_2	$K\overline{K}^*(892)+$ c.c.	seen
Γ_3	$a_0(980)\pi$	seen
Γ_4	$\gamma\gamma$	seen
Γ_5	$K^0_S K^0_S \eta$	possibly seen

$\eta(1475)$ Γ(i)$\Gamma(\gamma\gamma)/\Gamma$(total)

$\Gamma(K\overline{K}\pi) \times \Gamma(\gamma\gamma)/\Gamma_{total}$ $\Gamma_1\Gamma_4/\Gamma$

VALUE (keV)	CL%	EVTS	DOCUMENT ID		TECN	COMMENT
0.23±0.05±0.05		74	[1] ACHARD	07	L3	183–209 $e^+e^- \to e^+e^- K^0_S K^\pm\pi^\mp$
• • • We do not use the following data for averages, fits, limits, etc. • • •						
< 0.089	90		[2,3] AHOHE	05	CLE2	10.6 $e^+e^- \to e^+e^- K^0_S K^\pm\pi^\mp$

[1] Supersedes ACCIARRI 01G. Compatible with K^*K decay. Using $B(K^0_S \to \pi^+\pi^-)=0.6895$.
[2] Using $\eta(1475)$ mass of 1481 MeV and width of 48 MeV. The upper limit increases to 0.140 keV if the world average value, 87 MeV, of the width is used.
[3] Assuming three-body phase-space decay to $K^0_S K^\pm\pi^\mp$.

$\eta(1475)$ BRANCHING RATIOS

$\Gamma(K\overline{K}^*(892)+$ c.c.$)/\Gamma(K\overline{K}\pi)$ Γ_2/Γ_1

VALUE	DOCUMENT ID		TECN	COMMENT
• • • We do not use the following data for averages, fits, limits, etc. • • •				
0.50±0.10	[1] BAILLON	67	HBC	0.0 $\overline{p}p \to K\overline{K}\pi\pi\pi$

[1] Data could also refer to $\eta(1405)$.

$\Gamma(K\overline{K}^*(892)+$ c.c.$)/[\Gamma(K\overline{K}^*(892)+$ c.c.$)+\Gamma(a_0(980)\pi)]$ $\Gamma_2/(\Gamma_2+\Gamma_3)$

VALUE	CL%	DOCUMENT ID	TECN	COMMENT
• • • We do not use the following data for averages, fits, limits, etc. • • •				
<0.25	90	EDWARDS	82E CBAL	$J/\psi \to K^+K^-\pi^0\gamma$

$\eta(1475)$ REFERENCES

ABLIKIM	15T	PRL 115 091803	M. Ablikim *et al.*	(BES III Collab.)
ACHARD	07	JHEP 0703 018	P. Achard *et al.*	(L3 Collab.)
AHOHE	05	PR D71 072001	R. Ahohe *et al.*	(CLEO Collab.)
NICHITIU	02	PL B545 261	F. Nichitiu *et al.*	(OBELIX Collab.)
ACCIARRI	01G	PL B501 1	M. Acciarri *et al.*	(L3 Collab.)
ADAMS	01B	PL B516 264	G.S. Adams *et al.*	(BNL E852 Collab.)
CICALO	99	PL B462 453	C. Cicalo *et al.*	(OBELIX Collab.)
BERTIN	97	PL B400 226	A. Bertin *et al.*	(OBELIX Collab.)
BERTIN	95	PL B361 187	A. Bertin *et al.*	(OBELIX Collab.)
AUGUSTIN	92	PR D46 1951	J.E. Augustin, G. Cosme	(DM2 Collab.)
BAI	90C	PRL 65 2507	Z. Bai *et al.*	(Mark III Collab.)
RATH	89	PR D40 693	M.G. Rath *et al.*	(NDAM, BRAN, BNL, CUNY+)
EDWARDS	82E	PRL 49 259	C. Edwards *et al.*	(CIT, HARV, PRIN+)
BAILLON	67	NC 50A 393	P.H. Baillon *et al.*	(CERN, CDEF, IRAD)

$f_0(1500)$ $I^G(J^{PC}) = 0^+(0^{++})$

See also the mini-reviews on scalar mesons under $f_0(500)$ (see the index for the page number) and on non-$q\overline{q}$ candidates in PDG 06, Journal of Physics **G33** 1 (2006).

$f_0(1500)$ MASS

VALUE (MeV)	EVTS	DOCUMENT ID		TECN	COMMENT
1504± 6 OUR AVERAGE		Error includes scale factor of 1.3. See the ideogram below.			
$1468^{+14}_{-15}\pm 23^{+}_{-}74$	5.5k	[1] ABLIKIM	13N	BES3	$e^+e^- \to J/\psi \to \gamma\eta\eta$
1466± 6± 20		ABLIKIM	06V	BES2	$e^+e^- \to J/\psi \to \gamma\pi^+\pi^-$
1515±12		[2] BARBERIS	00A		450 $pp \to p_f\eta\eta p_s$
1511± 9		[2,3] BARBERIS	00C		450 $pp \to p_f 4\pi p_s$
1510± 8		[2] BARBERIS	00E		450 $pp \to p_f\eta\eta p_s$
1522±25		BERTIN	98	OBLX	0.05–0.405 $\overline{n}p \to \pi^+\pi^+\pi^-$
1449±20		[2] BERTIN	97C	OBLX	0.0 $\overline{p}p \to \pi^+\pi^-\pi^0$
1515±20		ABELE	96B	CBAR	0.0 $\overline{p}p \to \pi^0 K^0_L K^0_L$
1500±15		[4] AMSLER	95B	CBAR	0.0 $\overline{p}p \to 3\pi^0$
1505±15		[5] AMSLER	95C	CBAR	0.0 $\overline{p}p \to \eta\eta\pi^0$
• • • We do not use the following data for averages, fits, limits, etc. • • •					
1447±16± 13	163	[6,7] DOBBS	15		$J/\psi \to \gamma\pi^+\pi^-$
1442± 9± 4	261	[6,7] DOBBS	15		$\psi(2S) \to \gamma\pi^+\pi^-$
1486±10		[2] ANISOVICH	09	RVUE	0.0 $\overline{p}p$, πN
1470±60	568	[8] KLEMPT	08	E791	$D^+_s \to \pi^-\pi^+\pi^+$
$1470^{+6}_{-7}{}^{+72}_{-255}$		[9] UEHARA	08A	BELL	10.6 $e^+e^- \to e^+e^-\pi^0\pi^0$
1495± 4		AMSLER	06	CBAR	0.9 $\overline{p}p \to K^+K^-\pi^0$
1539±20	9.9k	AUBERT	06O	BABR	$B^+ \to K^+K^+K^-$
1473± 5	80k	[10,11] UMAN	06	E835	5.2 $\overline{p}p \to \eta\eta\pi^0$
1478± 6		VLADIMIRSK...	06	SPEC	40 $\pi^-p \to K^0_S K^0_S n$
1493± 7		[10] BINON	05	GAMS	33 $\pi^-p \to \eta\eta n$
1524±14	1400	[12] GARMASH	05	BELL	$B^+ \to K^+K^+K^-$
1489^{+8}_{-4}		[13] ANISOVICH	03	RVUE	
1490±30		[10] ABELE	01	CBAR	0.0 $\overline{p}d \to \pi^-4\pi^0 p$
1497±10		[10] BARBERIS	99	OMEG	450 $pp \to p_s p_f K^+K^-$
1502±10		[10] BARBERIS	99B	OMEG	450 $pp \to p_s p_f \pi^+\pi^-$
1502±12± 10		[14] BARBERIS	99D	OMEG	450 $pp \to K^+K^-$, $\pi^+\pi^-$
1530±45		[10] BELLAZZINI	99	GAM4	450 $pp \to pp\pi^0\pi^0$
1505±18		[10] FRENCH	99		300 $pp \to p_f(K^+K^-)p_s$
1447±27		[15] KAMINSKI	99	RVUE	$\pi\pi \to \pi\pi$, $K\overline{K}$, $\sigma\sigma$
1580±80		[10] ALDE	98	GAM4	100 $\pi^-p \to \pi^0\pi^0 n$
1499± 8		[2] ANISOVICH	98B	RVUE	Compilation
~ 1520		REYES	98	SPEC	800 $pp \to p_s p_f K^0_S K^0_S$
1510±20		[2] BARBERIS	97B	OMEG	450 $pp \to pp2(\pi^+\pi^-)$
~ 1475		FRABETTI	97D	E687	$D^\pm_s \to \pi^\mp\pi^\pm\pi^\pm$
~ 1505		ABELE	96	CBAR	0.0 $\overline{p}p \to 5\pi^0$
1500± 8		[2] ABELE	96C	RVUE	Compilation
1460±20	120	[10] AMELIN	96B	VES	37 $\pi^-A \to \eta\eta\pi^-A$
1500± 8		BUGG	96	RVUE	
1500±10		[16] AMSLER	95D	CBAR	0.0 $\overline{p}p \to \pi^0\pi^0\pi^0$, $\pi^0\eta\eta$, $\pi^0\pi^0\eta$
1445± 5		[17] ANTINORI	95	OMEG	300,450 $pp \to pp2(\pi^+\pi^-)$
1497±30		[10] ANTINORI	95	OMEG	300,450 $pp \to pp\pi^+\pi^-$
~ 1505		BUGG	95	MRK3	$J/\psi \to \gamma\pi^+\pi^-\pi^+\pi^-$
1446± 5		[10] ABATZIS	94	OMEG	450 $pp \to pp2(\pi^+\pi^-)$
1545±25		[10] AMSLER	94E	CBAR	0.0 $\overline{p}p \to \pi^0\eta\eta'$
1520±25		[2,18] ANISOVICH	94	CBAR	0.0 $\overline{p}p \to 3\pi^0, \pi^0\eta\eta$
1505±20		[2,19] BUGG	94	RVUE	$\overline{p}p \to 3\pi^0, \eta\eta\pi^0, \eta\pi^0\pi^0$
1560±25		[10] AMSLER	92	CBAR	0.0 $\overline{p}p \to \pi^0\eta\eta$
1550±45± 30		[10] BELADIDZE	92C	VES	36 π^-Be $\to \pi^-\eta'\eta$Be
1449± 4		[10] ARMSTRONG	89E	OMEG	300 $pp \to pp2(\pi^+\pi^-)$
1610±20		[10] ALDE	88	GAM4	300 $\pi^-N \to \pi^-N2\eta$
~ 1525		ASTON	88D	LASS	11 $K^-p \to K^0_S K^0_S \Lambda$
1570±20	600	[10] ALDE	87	GAM4	100 $\pi^-p \to 4\pi^0 n$
1575±45		[20] ALDE	86D	GAM4	100 $\pi^-p \to 2\eta n$
1568±33		[10] BINON	84C	GAM2	38 $\pi^-p \to \eta\eta' n$
1592±25		[10] BINON	83	GAM2	38 $\pi^-p \to 2\eta n$
1525± 5		[10] GRAY	83	DBC	0.0 $\overline{p}N \to 3\pi$

[1] From partial wave analysis including all possible combinations of 0^{++}, 2^{++}, and 4^{++} resonances.
[2] T-matrix pole.
[3] Average between $\pi^+\pi^-2\pi^0$ and $2(\pi^+\pi^-)$.
[4] T-matrix pole, supersedes ANISOVICH 94.
[5] T-matrix pole, supersedes ANISOVICH 94 and AMSLER 92.
[6] Using CLEO-c data but not authored by the CLEO Collaboration.
[7] From a fit to a Breit-Wigner line shape with fixed $\Gamma = 109$ MeV.
[8] Reanalysis of AITALA 01A data. This state could also be $f_0(1370)$.
[9] Breit-Wigner mass. May also be the $f_0(1370)$.
[10] Breit-Wigner mass.
[11] Statistical error only.

Meson Particle Listings

$f_0(1500)$

[12] Breit-Wigner, solution 1, PWA ambiguous.
[13] K-matrix pole from combined analysis of $\pi^- p \to \pi^0\pi^0 n$, $\pi^- p \to K\overline{K}n$, $\pi^+\pi^- \to \pi^+\pi^-$, $\overline{p}p \to \pi^0\pi^0\pi^0$, $\pi^0\eta$, $\pi^0\pi^0\eta$, $\pi^+\pi^-\pi^0$, $K^+K^-\pi^0$, $K^0_S K^0_S \pi^0$, $K^+K^0_S\pi^-$ at rest, $\overline{p}n \to \pi^-\pi^-\pi^+$, $K^0_S K^-\pi^0$, $K^0_S K^0_S \pi^-$ at rest.
[14] Supersedes BARBERIS 99 and BARBERIS 99B.
[15] T-matrix pole on sheet $--+$.
[16] T-matrix pole. Coupled-channel analysis of AMSLER 95B, AMSLER 95C, and AMSLER 94D.
[17] Supersedes ABATZIS 94, ARMSTRONG 89E. Breit-Wigner mass.
[18] From a simultaneous analysis of the annihilations $\overline{p}p \to 3\pi^0, \pi^0\eta\eta$.
[19] Reanalysis of ANISOVICH 94 data.
[20] From central value and spread of two solutions. Breit-Wigner mass.

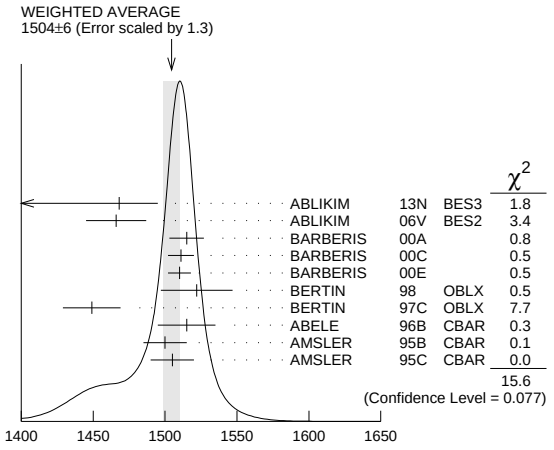

$f_0(1500)$ WIDTH

VALUE (MeV)	EVTS	DOCUMENT ID		TECN	COMMENT
109± 7 OUR AVERAGE					
$136^{+\ 41+\ 28}_{-\ 26-100}$	5.5k	[21] ABLIKIM	13N	BES3	$e^+e^- \to J/\psi \to \gamma\eta\eta$
$108^{+\ 14}_{-\ 11}\pm\ 25$		ABLIKIM	06V	BES2	$e^+e^- \to J/\psi \to \gamma\pi^+\pi^-$
110± 24		[22] BARBERIS	00A		450 $pp \to p_f\eta\eta p_s$
102± 18		[22,23] BARBERIS	00C		450 $pp \to p_f 4\pi p_s$
110± 16		[22] BARBERIS	00E		450 $pp \to p_f\eta\eta p_s$
108± 33		BERTIN	98	OBLX	0.05–0.405 $\overline{n}p \to \pi^+\pi^+\pi^-$
114± 30		[22] BERTIN	97C	OBLX	0.0 $\overline{p}p \to \pi^+\pi^-\pi^0$
105± 15		ABELE	96B	CBAR	0.0 $\overline{p}p \to \pi^0 K^0_L K^0_L$
120± 25		[24] AMSLER	95B	CBAR	0.0 $\overline{p}p \to 3\pi^0$
120± 30		[25] AMSLER	95C	CBAR	0.0 $\overline{p}p \to \eta\eta\pi^0$
• • • We do not use the following data for averages, fits, limits, etc. • • •					
114± 10		[22] ANISOVICH	09	RVUE	0.0 $\overline{p}p$, πN
$90^{+\ 2+\ 50}_{-\ 1-\ 22}$		[26] UEHARA	08A	BELL	10.6 $e^+e^- \to e^+e^-\pi^0\pi^0$
121± 8		AMSLER	06	CBAR	0.9 $\overline{p}p \to K^+K^-\pi^0$
257± 33	9.9k	AUBERT	06O	BABR	$B^+ \to K^+K^+K^-$
108± 9	80k	[27,28] UMAN	06	E835	5.2 $\overline{p}p \to \eta\eta\pi^0$
119± 10		VLADIMIRSK...	06	SPEC	40 $\pi^- p \to K^0_S K^0_S n$
90± 15		[27] BINON	05	GAMS	33 $\pi^- p \to \eta\eta n$
136± 23	1400	[29] GARMASH	05	BELL	$B^+ \to K^+K^+K^-$
102± 10		[30] ANISOVICH	03	RVUE	
140± 40		[27] ABELE	01	CBAR	0.0 $\overline{p}d \to \pi^- 4\pi^0 p$
104± 25		[27] BARBERIS	99	OMEG	450 $pp \to p_s p_f K^+K^-$
131± 15		[27] BARBERIS	99B	OMEG	450 $pp \to p_s p_f \pi^+\pi^-$
98± 18± 16		[31] BARBERIS	99D	OMEG	450 $pp \to K^+K^-, \pi^+\pi^-$
160± 50		[27] BELLAZZINI	99	GAM4	450 $pp \to pp\pi^0\pi^0$
100± 33		[27] FRENCH	99		300 $pp \to p_f(K^+K^-)p_s$
108± 46		[32] KAMINSKI	99	RVUE	$\pi\pi \to \pi\pi$, $K\overline{K}$, $\sigma\sigma$
280±100		[27] ALDE	98	GAM4	100 $\pi^- p \to \pi^0\pi^0 n$
130± 20		[22] ANISOVICH	98B	RVUE	Compilation
120± 35		[22] BARBERIS	97B	OMEG	450 $pp \to pp2(\pi^+\pi^-)$
~ 100		FRABETTI	97D	E687	$D^\pm_S \to \pi^\mp\pi^\pm\pi^\pm$
~ 169		ABELE	96	CBAR	0.0 $\overline{p}p \to 5\pi^0$
100± 30	120	[27] AMELIN	96B	VES	37 $\pi^- A \to \eta\eta\pi^- A$
132± 15		BUGG	96	RVUE	
154± 30		[33] AMSLER	95D	CBAR	0.0 $\overline{p}p \to \pi^0\pi^0\pi^0, \pi^0\eta\eta, \pi^0\pi^0\eta$
65± 10		[34] ANTINORI	95	OMEG	300,450 $pp \to pp2(\pi^+\pi^-)$
199± 30		[27] ANTINORI	95	OMEG	300,450 $pp \to pp\pi^+\pi^-$
56± 12		[27] ABATZIS	94	OMEG	450 $pp \to pp2(\pi^+\pi^-)$
100± 40		[27] AMSLER	94E	CBAR	0.0 $\overline{p}p \to \pi^0\eta\eta'$
$148^{+\ 20}_{-\ 25}$		[22,35] ANISOVICH	94	CBAR	0.0 $\overline{p}p \to 3\pi^0, \pi^0\eta\eta$
150± 20		[22,36] BUGG	94	RVUE	$\overline{p}p \to 3\pi^0, \eta\eta\pi^0, \eta\pi^0\pi^0$
245± 50		[27] AMSLER	92	CBAR	0.0 $\overline{p}p \to \pi^0\eta\eta$
153± 67± 50		[27] BELADIDZE	92C	VES	36 π^-Be $\to \pi^-\eta'\eta$Be
78± 18		[27] ARMSTRONG	89E	OMEG	300 $pp \to pp2(\pi^+\pi^-)$
170± 40		[27] ALDE	88	GAM4	300 $\pi^- N \to \pi^- N 2\eta$
150± 20	600	[27] ALDE	87	GAM4	100 $\pi^- p \to 4\pi^0 n$
265± 65		[37] ALDE	86D	GAM4	100 $\pi^- p \to 2\eta n$
260± 60		[27] BINON	84C	GAM2	38 $\pi^- p \to \eta\eta' n$
210± 40		[27] BINON	83	GAM2	38 $\pi^- p \to 2\eta n$
101± 13		[27] GRAY	83	DBC	0.0 $\overline{p}N \to 3\pi$

[21] From partial wave analysis including all possible combinations of 0^{++}, 2^{++}, and 4^{++} resonances.
[22] T-matrix pole.
[23] Average between $\pi^+\pi^- 2\pi^0$ and $2(\pi^+\pi^-)$.
[24] T-matrix pole, supersedes ANISOVICH 94.
[25] T-matrix pole, supersedes ANISOVICH 94 and AMSLER 92.
[26] Breit-Wigner width. May also be the $f_0(1370)$.
[27] Breit-Wigner width.
[28] Statistical error only.
[29] Breit-Wigner, solution 1, PWA ambiguous.
[30] K-matrix pole from combined analysis of $\pi^- p \to \pi^0\pi^0 n$, $\pi^- p \to K\overline{K}n$, $\pi^+\pi^- \to \pi^+\pi^-$, $\overline{p}p \to \pi^0\pi^0\pi^0$, $\pi^0\eta$, $\pi^0\pi^0\eta$, $\pi^+\pi^-\pi^0$, $K^+K^-\pi^0$, $K^0_S K^0_S\pi^0$, $K^+K^0_S\pi^-$ at rest, $\overline{p}n \to \pi^-\pi^-\pi^+$, $K^0_S K^-\pi^0$, $K^0_S K^0_S\pi^-$ at rest.
[31] Supersedes BARBERIS 99 and BARBERIS 99B.
[32] T-matrix pole on sheet $--+$.
[33] T-matrix pole. Coupled-channel analysis of AMSLER 95B, AMSLER 95C, and AMSLER 94D.
[34] Supersedes ABATZIS 94, ARMSTRONG 89E. Breit-Wigner mass.
[35] From a simultaneous analysis of the annihilations $\overline{p}p \to 3\pi^0, \pi^0\eta\eta$.
[36] Reanalysis of ANISOVICH 94 data.
[37] From central value and spread of two solutions. Breit-Wigner mass.

$f_0(1500)$ DECAY MODES

	Mode	Fraction (Γ_i/Γ)	Scale factor
Γ_1	$\pi\pi$	(34.9±2.3) %	1.2
Γ_2	$\pi^+\pi^-$	seen	
Γ_3	$2\pi^0$	seen	
Γ_4	4π	(49.5±3.3) %	1.2
Γ_5	$4\pi^0$	seen	
Γ_6	$2\pi^+2\pi^-$	seen	
Γ_7	$2(\pi\pi)$ s-wave	seen	
Γ_8	$\rho\rho$	seen	
Γ_9	$\pi(1300)\pi$	seen	
Γ_{10}	$a_1(1260)\pi$	seen	
Γ_{11}	$\eta\eta$	(5.1±0.9) %	1.4
Γ_{12}	$\eta\eta'(958)$	(1.9±0.8) %	1.7
Γ_{13}	$K\overline{K}$	(8.6±1.0) %	1.1
Γ_{14}	$\gamma\gamma$	not seen	

CONSTRAINED FIT INFORMATION

An overall fit to 6 branching ratios uses 10 measurements and one constraint to determine 5 parameters. The overall fit has a $\chi^2 = 11.4$ for 6 degrees of freedom.

The following *off-diagonal* array elements are the correlation coefficients $\langle \delta x_i \delta x_j \rangle / (\delta x_i \cdot \delta x_j)$, in percent, from the fit to the branching fractions, $x_i \equiv \Gamma_i/\Gamma_{\rm total}$. The fit constrains the x_i whose labels appear in this array to sum to one.

x_4	−83			
x_{11}	11	−52		
x_{12}	−5	−31	29	
x_{13}	39	−67	33	6
	x_1	x_4	x_{11}	x_{12}

$f_0(1500)$ Γ(i)$\Gamma(\gamma\gamma)/\Gamma$(total)

$\Gamma(\pi\pi) \times \Gamma(\gamma\gamma)/\Gamma_{\rm total}$ **$\Gamma_1\Gamma_{14}/\Gamma$**

VALUE (eV)	CL%	DOCUMENT ID		TECN	COMMENT
• • • We do not use the following data for averages, fits, limits, etc. • • •					
$33^{+12+1809}_{-\ 6-\ 21}$		[38] UEHARA	08A	BELL	10.6 $e^+e^- \to e^+e^-\pi^0\pi^0$
not seen		ACCIARRI	01H	L3	$\gamma\gamma \to K^0_S K^0_S$, $E^{ee}_{\rm cm}$= 91, 183–209 GeV
<460	95	BARATE	00E	ALEP	$\gamma\gamma \to \pi^+\pi^-$

[38] May also be the $f_0(1370)$. Multiplied by us by 3 to obtain the $\pi\pi$ value.

$f_0(1500)$ BRANCHING RATIOS

$\Gamma(\pi\pi)/\Gamma_{total}$ Γ_1/Γ

VALUE	DOCUMENT ID		TECN	
• • • We do not use the following data for averages, fits, limits, etc. • • •				
0.454±0.104	BUGG	96	RVUE	

$\Gamma(\pi^+\pi^-)/\Gamma_{total}$ Γ_2/Γ

VALUE	DOCUMENT ID		TECN	COMMENT
seen	BERTIN	98	OBLX	0.05–0.405 $\overline{n}p \rightarrow \pi^+\pi^+\pi^-$
• • • We do not use the following data for averages, fits, limits, etc. • • •				
possibly seen	FRABETTI	97D	E687	$D_s^\pm \rightarrow \pi^\mp\pi^\pm\pi^\pm$

$\Gamma(4\pi)/\Gamma(\pi\pi)$ Γ_4/Γ_1

VALUE	DOCUMENT ID		TECN	COMMENT
1.42±0.18 OUR FIT Error includes scale factor of 1.2.				
1.42±0.18 OUR AVERAGE Error includes scale factor of 1.2.				
1.37±0.16	BARBERIS	00D		450 $pp \rightarrow p_f 4\pi p_s$
2.1 ±0.6	[39] AMSLER	98	RVUE	
• • • We do not use the following data for averages, fits, limits, etc. • • •				
2.1 ±0.2	[40] ANISOVICH	02D	SPEC	Combined fit
3.4 ±0.8	[39] ABELE	96	CBAR	0.0 $\overline{p}p \rightarrow 5\pi^0$

$\Gamma(2(\pi\pi)_{S\text{-wave}})/\Gamma(\pi\pi)$ Γ_7/Γ_1

VALUE	DOCUMENT ID		TECN	COMMENT
• • • We do not use the following data for averages, fits, limits, etc. • • •				
0.42±0.26	[41] ABELE	01	CBAR	0.0 $\overline{p}d \rightarrow \pi^- 4\pi^0 p$

$\Gamma(2(\pi\pi)_{S\text{-wave}})/\Gamma(4\pi)$ Γ_7/Γ_4

VALUE	DOCUMENT ID		TECN	COMMENT
• • • We do not use the following data for averages, fits, limits, etc. • • •				
0.26±0.07	ABELE	01B	CBAR	0.0 $\overline{p}d \rightarrow 5\pi p$

$\Gamma(\rho\rho)/\Gamma(4\pi)$ Γ_8/Γ_4

VALUE	DOCUMENT ID		TECN	COMMENT
• • • We do not use the following data for averages, fits, limits, etc. • • •				
0.13±0.08	ABELE	01B	CBAR	0.0 $\overline{p}d \rightarrow 5\pi p$

$\Gamma(\rho\rho)/\Gamma(2(\pi\pi)_{S\text{-wave}})$ Γ_8/Γ_7

VALUE	DOCUMENT ID		COMMENT
• • • We do not use the following data for averages, fits, limits, etc. • • •			
3.3±0.5	BARBERIS	00C	450 $pp \rightarrow p_f \pi^+\pi^- 2\pi^0 p_s$
2.6±0.4	BARBERIS	00C	450 $pp \rightarrow p_f 2(\pi^+\pi^-) p_s$

$\Gamma(\pi(1300)\pi)/\Gamma(4\pi)$ Γ_9/Γ_4

VALUE	DOCUMENT ID		TECN	COMMENT
• • • We do not use the following data for averages, fits, limits, etc. • • •				
0.50±0.25	ABELE	01B	CBAR	0.0 $\overline{p}d \rightarrow 5\pi p$

$\Gamma(a_1(1260)\pi)/\Gamma(4\pi)$ Γ_{10}/Γ_4

VALUE	DOCUMENT ID		TECN	COMMENT
• • • We do not use the following data for averages, fits, limits, etc. • • •				
0.12±0.05	ABELE	01B	CBAR	0.0 $\overline{p}d \rightarrow 5\pi p$

$\Gamma(\eta\eta)/\Gamma_{total}$ Γ_{11}/Γ

VALUE	DOCUMENT ID		TECN	COMMENT
• • • We do not use the following data for averages, fits, limits, etc. • • •				
large	ALDE	88	GAM4	300 $\pi^- N \rightarrow \eta\eta\pi^- N$
large	BINON	83	GAM2	38 $\pi^- p \rightarrow 2\eta n$

$\Gamma(\eta\eta)/\Gamma(\pi\pi)$ Γ_{11}/Γ_1

VALUE	DOCUMENT ID		TECN	COMMENT
0.145±0.027 OUR FIT Error includes scale factor of 1.5.				
0.14 ±0.04 OUR AVERAGE Error includes scale factor of 1.7. See the ideogram below.				
0.080±0.033	AMSLER	02	CBAR	0.9 $\overline{p}p \rightarrow \pi^0\eta\eta, \pi^0\pi^0\pi^0$
0.18 ±0.03	BARBERIS	00E		450 $pp \rightarrow p_f \eta\eta p_s$
0.230±0.097	[42] AMSLER	95C	CBAR	0.0 $\overline{p}p \rightarrow \eta\eta\pi^0$
• • • We do not use the following data for averages, fits, limits, etc. • • •				
0.11 ±0.03	[40] ANISOVICH	02D	SPEC	Combined fit
0.078±0.013	[43] ABELE	96C	RVUE	Compilation
0.157±0.060	[44] AMSLER	95D	CBAR	0.0 $\overline{p}p \rightarrow \pi^0\pi^0\pi^0, \pi^0\eta\eta, \pi^0\pi^0\eta$

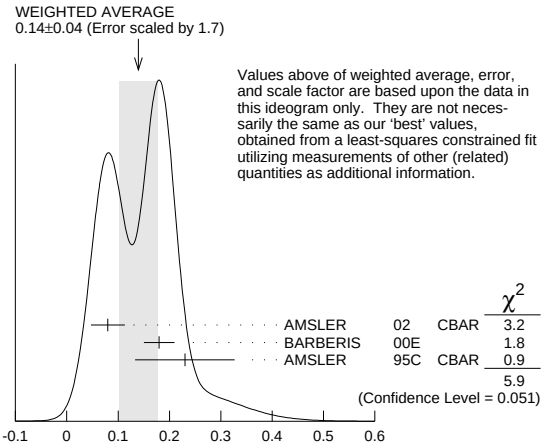

$\Gamma(\eta\eta)/\Gamma(\pi\pi)$ Γ_{11}/Γ_1

$\Gamma(4\pi^0)/\Gamma(\eta\eta)$ Γ_5/Γ_{11}

VALUE	DOCUMENT ID		TECN	COMMENT
• • • We do not use the following data for averages, fits, limits, etc. • • •				
0.8±0.3	ALDE	87	GAM4	100 $\pi^- p \rightarrow 4\pi^0 n$

$\Gamma(\eta\eta'(958))/\Gamma(\pi\pi)$ Γ_{12}/Γ_1

VALUE	DOCUMENT ID		TECN	COMMENT
0.055±0.024 OUR FIT Error includes scale factor of 1.8.				
0.095±0.026	BARBERIS	00A		450 $pp \rightarrow p_f \eta\eta p_s$
• • • We do not use the following data for averages, fits, limits, etc. • • •				
0.005±0.003	[40] ANISOVICH	02D	SPEC	Combined fit

$\Gamma(\eta\eta'(958))/\Gamma(\eta\eta)$ Γ_{12}/Γ_{11}

VALUE	DOCUMENT ID		TECN	COMMENT
0.38±0.16 OUR FIT Error includes scale factor of 1.9.				
0.29±0.10	[45] AMSLER	95C	CBAR	0.0 $\overline{p}p \rightarrow \eta\eta\pi^0$
• • • We do not use the following data for averages, fits, limits, etc. • • •				
0.05±0.03	[40] ANISOVICH	02D	SPEC	Combined fit
0.84±0.23	ABELE	96C	RVUE	Compilation
2.7 ±0.8	BINON	84C	GAM2	38 $\pi^- p \rightarrow \eta\eta' n$

$\Gamma(K\overline{K})/\Gamma_{total}$ Γ_{13}/Γ

VALUE	DOCUMENT ID		TECN
• • • We do not use the following data for averages, fits, limits, etc. • • •			
0.044±0.021	BUGG	96	RVUE

$\Gamma(K\overline{K})/\Gamma(\pi\pi)$ Γ_{13}/Γ_1

VALUE	DOCUMENT ID		TECN	COMMENT
0.246±0.026 OUR FIT				
0.241±0.028 OUR AVERAGE				
0.25 ±0.03	[46] BARGIOTTI	03	OBLX	$\overline{p}p$
0.19 ±0.07	[47] ABELE	98	CBAR	0.0 $\overline{p}p \rightarrow K_L^0 K^\pm \pi^\mp$
• • • We do not use the following data for averages, fits, limits, etc. • • •				
0.16 ±0.05	[40] ANISOVICH	02D	SPEC	Combined fit
0.33 ±0.03 ±0.07	BARBERIS	99D	OMEG	450 $pp \rightarrow K^+K^-, \pi^+\pi^-$
0.20 ±0.08	[48] ABELE	96B	CBAR	0.0 $\overline{p}p \rightarrow \pi^0 K_L^0 K_L^0$

$\Gamma(K\overline{K})/\Gamma(\eta\eta)$ Γ_{13}/Γ_{11}

VALUE	CL%	DOCUMENT ID		TECN	COMMENT
1.69±0.33 OUR FIT Error includes scale factor of 1.4.					
1.85±0.41		BARBERIS	00E		450 $pp \rightarrow p_f \eta\eta p_s$
• • • We do not use the following data for averages, fits, limits, etc. • • •					
1.5 ±0.6		[40] ANISOVICH	02D	SPEC	Combined fit
<0.4	90	[49] PROKOSHKIN	91	GAM4	300 $\pi^- p \rightarrow \pi^- p\eta\eta$
<0.6		[50] BINON	83	GAM2	38 $\pi^- p \rightarrow 2\eta n$

[39] Excluding $\rho\rho$ contribution to 4π.
[40] From a combined K-matrix analysis of Crystal Barrel (0. $p\overline{p} \rightarrow \pi^0\pi^0\pi^0$, $\pi^0\eta\eta$, $\pi^0\pi^0\eta$), GAMS ($\pi p \rightarrow \pi^0\pi^0 n$, $\eta\eta n$, $\eta\eta' n$), and BNL ($\pi p \rightarrow K\overline{K} n$) data.
[41] From the combined data of ABELE 96 and ABELE 96C.
[42] Using AMSLER 95B ($3\pi^0$).
[43] 2π width determined to be 60 ± 12 MeV.
[44] Coupled-channel analysis of AMSLER 95B, AMSLER 95C, and AMSLER 94D.
[45] Using AMSLER 94E ($\eta\eta'\pi^0$).
[46] Coupled channel analysis of $\pi^+\pi^-\pi^0$, $K^+K^-\pi^0$, and $K^\pm K_S^0 \pi^\mp$.
[47] Using $\pi^0\pi^0$ from AMSLER 95B.
[48] Using AMSLER 95B ($3\pi^0$), AMSLER 94C ($2\pi^0\eta$) and SU(3).
[49] Combining results of GAM4 with those of WA76 on $K\overline{K}$ central production.
[50] Using ETKIN 82B and COHEN 80.

Meson Particle Listings

$f_0(1500)$, $f_1(1510)$

$f_0(1500)$ REFERENCES

DOBBS	15	PR D91 052006	S. Dobbs *et al.*	(NWES)
ABLIKIM	13N	PR D87 092009	Ablikim M. *et al.*	(BES III Collab.)
ANISOVICH	09	IJMP A24 2481	V.V. Anisovich, A.V. Sarantsev	
KLEMPT	08	EPJ C55 39	E. Klempt, M. Matveev, A.V. Sarantsev	(BONN+)
UEHARA	08A	PR D78 052004	S. Uehara *et al.*	(BELLE Collab.)
ABLIKIM	06V	PL B642 441	M. Ablikim *et al.*	(BES Collab.)
AMSLER	06	PL B639 165	C. Amsler *et al.*	(CBAR Collab.)
AUBERT	06O	PR D74 032003	B. Aubert *et al.*	(BABAR Collab.)
PDG	06	JP G33 1	W.-M. Yao *et al.*	(PDG Collab.)
UMAN	06	PR D73 052009	I. Uman *et al.*	(FNAL E835)
VLADIMIRSK...	06	PAN 69 493	V.V. Vladimirsky *et al.*	(ITEP, Moscow)
		Translated from YAF 69 515.		
BINON	05	PAN 68 960	F. Binon *et al.*	
		Translated from YAF 68 998.		
GARMASH	05	PR D71 092003	A. Garmash *et al.*	(BELLE Collab.)
ANISOVICH	03	EPJ A16 229	V.V. Anisovich *et al.*	
BARGIOTTI	03	EPJ C26 371	M. Bargiotti *et al.*	(OBELIX Collab.)
AMSLER	02	EPJ C23 29	C. Amsler *et al.*	
ANISOVICH	02D	PAN 65 1545	V.V. Anisovich *et al.*	
		Translated from YAF 65 1583.		
ABELE	01	EPJ C19 667	A. Abele *et al.*	(Crystal Barrel Collab.)
ABELE	01B	EPJ C21 261	A. Abele *et al.*	(Crystal Barrel Collab.)
ACCIARRI	01H	PL B501 173	M. Acciarri *et al.*	(L3 Collab.)
AITALA	01A	PRL 86 765	E.M. Aitala *et al.*	(FNAL E791 Collab.)
BARATE	00E	PL B472 189	R. Barate *et al.*	(ALEPH Collab.)
BARBERIS	00A	PL B471 429	D. Barberis *et al.*	(WA 102 Collab.)
BARBERIS	00C	PL B471 440	D. Barberis *et al.*	(WA 102 Collab.)
BARBERIS	00D	PL B474 423	D. Barberis *et al.*	(WA 102 Collab.)
BARBERIS	00E	PL B479 59	D. Barberis *et al.*	(WA 102 Collab.)
BARBERIS	99	PL B453 305	D. Barberis *et al.*	(Omega Expt.)
BARBERIS	99B	PL B453 316	D. Barberis *et al.*	(Omega Expt.)
BARBERIS	99D	PL B462 462	D. Barberis *et al.*	(Omega Expt.)
BELLAZZINI	99	PL B467 296	R. Bellazzini *et al.*	
FRENCH	99	PL B460 213	B. French *et al.*	(WA76 Collab.)
KAMINSKI	99	EPJ C9 141	R. Kaminski, L. Lesniak, B. Loiseau	(CRAC, PARIN)
ABELE	98	PR D57 3860	A. Abele *et al.*	(Crystal Barrel Collab.)
ALDE	98	EPJ A3 361	D. Alde *et al.*	(GAM4 Collab.)
Also		PAN 62 405	D. Alde *et al.*	(GAMS Collab.)
		Translated from YAF 62 446.		
AMSLER	98	RMP 70 1293	C. Amsler	
ANISOVICH	98B	SPU 41 419	V.V. Anisovich *et al.*	
		Translated from UFN 168 481.		
BERTIN	98	PR D57 55	A. Bertin *et al.*	(OBELIX Collab.)
REYES	98	PRL 81 4079	M.A. Reyes *et al.*	
BARBERIS	97B	PL B413 217	D. Barberis *et al.*	(WA 102 Collab.)
BERTIN	97C	PL B408 476	A. Bertin *et al.*	(OBELIX Collab.)
FRABETTI	97D	PL B407 79	P.L. Frabetti *et al.*	(FNAL E687 Collab.)
ABELE	96	PL B380 453	A. Abele *et al.*	(Crystal Barrel Collab.)
ABELE	96B	PL B385 425	A. Abele *et al.*	(Crystal Barrel Collab.)
ABELE	96C	NP A609 562	A. Abele *et al.*	(Crystal Barrel Collab.)
AMELIN	96B	PAN 59 976	D.V. Amelin *et al.*	(SERP, TBIL)
		Translated from YAF 59 1021.		
BUGG	96	NP B471 59	D.V. Bugg, A.V. Sarantsev, B.S. Zou	(LOQM, PNPI)
AMSLER	95B	PL B342 433	C. Amsler *et al.*	(Crystal Barrel Collab.)
AMSLER	95C	PL B353 571	C. Amsler *et al.*	(Crystal Barrel Collab.)
AMSLER	95D	PL B355 425	C. Amsler *et al.*	(Crystal Barrel Collab.)
ANTINORI	95	PL B353 589	F. Antinori *et al.*	(ATHU, BARI, BIRM+)
BUGG	95	PL B353 378	D.V. Bugg *et al.*	(LOQM, PNPI, WASH)
ABATZIS	94	PL B324 509	S. Abatzis *et al.*	(ATHU, BARI, BIRM+)
AMSLER	94C	PL B327 425	C. Amsler *et al.*	(Crystal Barrel Collab.)
AMSLER	94D	PL B333 277	C. Amsler *et al.*	(Crystal Barrel Collab.)
AMSLER	94E	PL B340 259	C. Amsler *et al.*	(Crystal Barrel Collab.)
ANISOVICH	94	PL B323 233	V.V. Anisovich *et al.*	(Crystal Barrel Collab.)
BUGG	94	PR D50 4412	D.V. Bugg *et al.*	(LOQM)
AMSLER	92	PL B291 347	C. Amsler *et al.*	(Crystal Barrel Collab.)
BELADIDZE	92C	SJNP 55 1535	G.M. Beladidze, S.I. Bityukov, G.V. Borisov	(SERP+)
		Translated from YAF 55 2748.		
PROKOSHKIN	91	SPD 36 155	Y.D. Prokoshkin	(GAM2, GAM4 Collab.)
		Translated from DANS 316 900.		
ARMSTRONG	89E	PL B228 536	T.A. Armstrong, M. Benayoun	(ATHU, BARI, BIRM+)
ALDE	88	PL B201 160	D.M. Alde *et al.*	(SERP, BELG, LANL, LAPP+)
ASTON	88D	NP B301 525	D. Aston *et al.*	(SLAC, NAGO, CINC, INUS)
ALDE	87	PL B198 286	D.M. Alde *et al.*	(LANL, BRUX, SERP, LAPP)
ALDE	86D	NP B269 485	D.M. Alde *et al.*	(BELG, LAPP, SERP, CERN+)
BINON	84C	NC 80A 363	F.G. Binon *et al.*	(BELG, LAPP, SERP+)
BINON	83	NC 78A 313	F.G. Binon *et al.*	(BELG, LAPP, SERP+)
Also		SJNP 38 561	F.G. Binon *et al.*	(BELG, LAPP, SERP+)
		Translated from YAF 38 934.		
GRAY	83	PR D27 307	L. Gray *et al.*	(SYRA)
ETKIN	82B	PR D25 1786	A. Etkin *et al.*	(BNL, CUNY, TUFTS, VAND)
COHEN	80	PR D22 2595	D. Cohen *et al.*	(ANL)

$f_1(1510)$

$I^G(J^{PC}) = 0^+(1^{++})$

OMITTED FROM SUMMARY TABLE

See the minireview under $\eta(1405)$.

$f_1(1510)$ MASS

VALUE (MeV)	*EVTS*	*DOCUMENT ID*		*TECN*	*COMMENT*
1518± 5 OUR AVERAGE		Error includes scale factor of 1.7. See the ideogram below.			
1530±10		ASTON	88C	LASS	11 $K^- p \to K^0_S K^\pm \pi^\mp \Lambda$
1512± 4	600	[1] BIRMAN	88	MPS	8 $\pi^- p \to K^+ \overline{K}{}^0 \pi^- n$
1526± 6	271	GAVILLET	82	HBC	4.2 $K^- p \to \Lambda K K \pi$
• • • We do not use the following data for averages, fits, limits, etc. • • •					
~ 1525		[2] BAUER	93B		$\gamma\gamma^* \to \pi^+\pi^-\pi^0\pi^0$

[1] From partial wave analysis of $K^+ \overline{K}{}^0 \pi^-$ state.

[2] Not seen by AIHARA 88C in the $K^0_S K^\pm \pi^\mp$ final state.

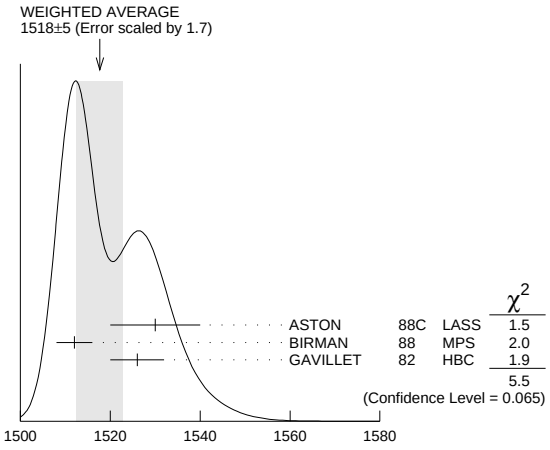

$f_1(1510)$ WIDTH

VALUE (MeV)	*EVTS*	*DOCUMENT ID*		*TECN*	*COMMENT*
73±25 OUR AVERAGE		Error includes scale factor of 2.5. See the ideogram below.			
100±40		ASTON	88C	LASS	11 $K^- p \to K^0_S K^\pm \pi^\mp \Lambda$
35±15	600	[3] BIRMAN	88	MPS	8 $\pi^- p \to K^+ \overline{K}{}^0 \pi^- n$
107±15	271	GAVILLET	82	HBC	4.2 $K^- p \to \Lambda K K \pi$

[3] From partial wave analysis of $K^+ \overline{K}{}^0 \pi^-$ state.

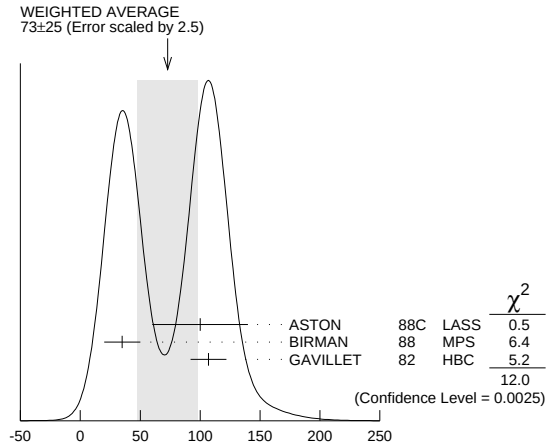

$f_1(1510)$ DECAY MODES

	Mode	Fraction (Γ_i/Γ)
Γ_1	$K\overline{K}^*(892)+$ c.c.	seen
Γ_2	$\pi^+\pi^-\eta'$	seen

$f_1(1510)$ BRANCHING RATIOS

$\Gamma(\pi^+\pi^-\eta')/\Gamma_{\text{total}}$ Γ_2/Γ

VALUE	*EVTS*	*DOCUMENT ID*		*TECN*	*COMMENT*
seen	230	ABLIKIM	11C	BES3	$J/\psi \to \gamma\pi^+\pi^-\eta'$

$f_1(1510)$ REFERENCES

ABLIKIM	11C	PRL 106 072002	M. Ablikim *et al.*	(BES III Collab.)
BAUER	93B	PR D48 3976	D.A. Bauer *et al.*	(SLAC)
AIHARA	88C	PR D38 1	H. Aihara *et al.*	(TPC-2γ Collab.)
ASTON	88C	PL B201 573	D. Aston *et al.*	(SLAC, NAGO, CINC, INUS) JP
BIRMAN	88	PRL 61 1557	A. Birman *et al.*	(BNL, FSU, IND, MASD) JP
GAVILLET	82	ZPHY C16 119	P. Gavillet *et al.*	(CERN, CDEF, PADO+)

$f_2'(1525)$

$I^G(J^{PC}) = 0^+(2^{++})$

$f_2'(1525)$ MASS

VALUE (MeV)	DOCUMENT ID
1525±5 OUR ESTIMATE	This is only an educated guess; the error given is larger than the error on the average of the published values.

PRODUCED BY PION BEAM

VALUE (MeV)	EVTS	DOCUMENT ID		TECN	COMMENT
• • • We do not use the following data for averages, fits, limits, etc. • • •					
1521±13		TIKHOMIROV	03	SPEC	40.0 π^- C → $K^0_S K^0_S K^0_L$ X
1547^{+10}_{-2}		[1] LONGACRE	86	MPS	22 $\pi^- p \to K^0_S K^0_S n$
1496^{+9}_{-8}		[2] CHABAUD	81	ASPK	6 $\pi^- p \to K^+ K^- n$
1497^{+8}_{-9}		CHABAUD	81	ASPK	18.4 $\pi^- p \to K^+ K^- n$
1492±29		GORLICH	80	ASPK	17 π^- p polarized → $K^+ K^- n$
1502±25		[3] CORDEN	79	OMEG	12–15 $\pi^- p \to \pi^+ \pi^- n$
1480	14	CRENNELL	66	HBC	6.0 $\pi^- p \to K^0_S K^0_S n$

PRODUCED BY $K^\pm$ BEAM

VALUE (MeV)	EVTS	DOCUMENT ID		TECN	COMMENT
1523.3± 1.1 OUR AVERAGE		Includes data from the datablock that follows this one.			
Error includes scale factor of 1.1.					
1526.8± 4.3		ASTON	88D	LASS	11 $K^- p \to K^0_S K^0_S \Lambda$
1504 ±12		BOLONKIN	86	SPEC	40 $K^- p \to K^0_S K^0_S Y$
1529 ± 3		ARMSTRONG	83B	OMEG	18.5 $K^- p \to K^- K^+ \Lambda$
1521 ± 6	650	AGUILAR-...	81B	HBC	4.2 $K^- p \to \Lambda K^+ K^-$
1521 ± 3	572	ALHARRAN	81	HBC	8.25 $K^- p \to \Lambda K \overline{K}$
1522 ± 6	123	BARREIRO	77	HBC	4.15 $K^- p \to \Lambda K^0_S K^0_S$
1528 ± 7	166	EVANGELIS...	77	OMEG	10 $K^- p \to K^+ K^- (\Lambda, \Sigma)$
1527 ± 3	120	BRANDENB...	76C	ASPK	13 $K^- p \to K^+ K^- (\Lambda, \Sigma)$
1519 ± 7	100	AGUILAR-...	72B	HBC	3.9,4.6 $K^- p \to K \overline{K} (\Lambda, \Sigma)$
• • • We do not use the following data for averages, fits, limits, etc. • • •					
1514 ± 8	61	BINON	07	GAMS	32.5 $K^- p \to \eta\eta(\Lambda/\Sigma^0)$
1513 ±10		[4] BARKOV	99	SPEC	40 $K^- p \to K^0_S K^0_S y$

PRODUCED IN e^+e^- ANNIHILATION AND PARTICLE DECAYS

VALUE (MeV)	EVTS	DOCUMENT ID		TECN	COMMENT
The data in this block is included in the average printed for a previous datablock.					
$1521.9^{+1.8}_{-1.5}$ OUR AVERAGE		Error includes scale factor of 1.1.			
$1522.2 \pm 2.8^{+5.3}_{-2.0}$		AAIJ	13AN	LHCB	$\overline{B}^0_s \to J/\psi K^+ K^-$
1513 ± 5 $^{+4}_{-10}$	5.5k	[5] ABLIKIM	13N	BES3	$e^+e^- \to J/\psi \to \gamma\eta\eta$
$1525.3^{+1.2}_{-1.4} \pm 3.7 \pm 2.1$		UEHARA	13	BELL	$\gamma\gamma \to K^0_S K^0_S$
1521 ± 5		ABLIKIM	05	BES2	$J/\psi \to \phi K^+ K^-$
1518 ± 1 ± 3		ABE	04	BELL	10.6 $e^+e^- \to e^+e^- K^+ K^-$
1519 ± 2 $^{+15}_{-5}$		BAI	03G	BES	$J/\psi \to \gamma K \overline{K}$
1523 ± 6	331	[6] ACCIARRI	01H	L3	91, 183–209 $e^+e^- \to e^+e^- K^0_S K^0_S$
1535 ± 5 ± 4		ABREU	96C	DLPH	$Z^0 \to K^+ K^-$ + X
1516 ± 5 $^{+9}_{-15}$		BAI	96C	BES	$J/\psi \to \gamma K^+ K^-$
1531.6±10.0		AUGUSTIN	88	DM2	$J/\psi \to \gamma K^+ K^-$
1515 ± 5		[7] FALVARD	88	DM2	$J/\psi \to \phi K^+ K^-$
1525 ±10 ±10		BALTRUSAIT...	87	MRK3	$J/\psi \to \gamma K^+ K^-$
• • • We do not use the following data for averages, fits, limits, etc. • • •					
1532 ± 3 ± 6	644	[8,9] DOBBS	15		$J/\psi \to \gamma K^+ K^-$
1557 ± 9 ± 3	113	[8,9] DOBBS	15		$\psi(2S) \to \gamma K^+ K^-$
1526 ± 7	29	[10] LEES	14H	BABR	$e^+e^- \to K^0_S K^0_S K^+ K^- \gamma$
1523 ± 5	870	[11] SCHEGELSKY	06A	RVUE	$\gamma\gamma \to K^0_S K^0_S$
1496 ± 2		[12] FALVARD	88	DM2	$J/\psi \to \phi K^+ K^-$

PRODUCED IN $\overline{p}p$ ANNIHILATION

VALUE (MeV)	DOCUMENT ID		TECN	COMMENT
• • • We do not use the following data for averages, fits, limits, etc. • • •				
1530±12	[13] ANISOVICH	09	RVUE	0.0 $\overline{p}p$, πN
1513± 4	AMSLER	06	CBAR	0.9 $\overline{p}p \to K^+ K^- \pi^0$
1508± 9	[14] AMSLER	02	CBAR	0.9 $\overline{p}p \to \pi^0\eta\eta$, $\pi^0\pi^0\pi^0$

CENTRAL PRODUCTION

VALUE (MeV)	DOCUMENT ID		TECN	COMMENT
1515±15	BARBERIS	99	OMEG	450 $pp \to p_s p_f K^+ K^-$

PRODUCED IN ep COLLISIONS

VALUE (MeV)	EVTS	DOCUMENT ID		TECN	COMMENT
$1512 \pm 3^{+1.4}_{-0.5}$		[15] CHEKANOV	08	ZEUS	$ep \to K^0_S K^0_S X$
• • • We do not use the following data for averages, fits, limits, etc. • • •					
1537^{+9}_{-8}	84	[16] CHEKANOV	04	ZEUS	$ep \to K^0_S K^0_S X$

[1] From a partial-wave analysis of data using a K-matrix formalism with 5 poles.
[2] CHABAUD 81 is a reanalysis of PAWLICKI 77 data.
[3] From an amplitude analysis where the $f_2'(1525)$ width and elasticity are in complete disagreement with the values obtained from $K\overline{K}$ channel, making the solution dubious.
[4] Systematic errors not estimated.
[5] From partial wave analysis including all possible combinations of 0^{++}, 2^{++}, and 4^{++} resonances.
[6] Supersedes ACCIARRI 95J.
[7] From an analysis ignoring interference with $f_0(1710)$.
[8] Using CLEO-c data but not authored by the CLEO Collaboration.
[9] From a fit to a Breit-Wigner line shape with fixed $\Gamma = 73$ MeV.
[10] From a fit to a Breit-Wigner line shape plus a second-order polynomial function. Systematic errors not evaluated.
[11] From analysis of L3 data at 91 and 183–209 GeV.
[12] From an analysis including interference with $f_0(1710)$.
[13] 4-poles, 5-channel K matrix fit.
[14] T-matrix pole.
[15] In the SU(3) based model with a specific interference pattern of the $f_2(1270)$, $a_2^0(1320)$, and $f_2'(1525)$ mesons incoherently added to the $f_0(1710)$ and non-resonant background.
[16] Systematic errors not estimated.

$f_2'(1525)$ WIDTH

VALUE (MeV)	DOCUMENT ID		COMMENT
73^{+6}_{-5} OUR FIT			
76±10	PDG	90	For fitting

PRODUCED BY PION BEAM

VALUE (MeV)	DOCUMENT ID		TECN	COMMENT
• • • We do not use the following data for averages, fits, limits, etc. • • •				
102±42	TIKHOMIROV	03	SPEC	40.0 π^- C → $K^0_S K^0_S K^0_L$ X
108^{+5}_{-2}	[17] LONGACRE	86	MPS	22 $\pi^- p \to K^0_S K^0_S n$
69^{+22}_{-16}	[18] CHABAUD	81	ASPK	6 $\pi^- p \to K^+ K^- n$
137^{+23}_{-21}	CHABAUD	81	ASPK	18.4 $\pi^- p \to K^+ K^- n$
150^{+83}_{-50}	GORLICH	80	ASPK	17 π^- p polarized → $K^+ K^- n$
165±42	[19] CORDEN	79	OMEG	12–15 $\pi^- p \to \pi^+ \pi^- n$
92^{+39}_{-22}	[20] POLYCHRO...	79	STRC	7 $\pi^- p \to n K^0_S K^0_S$

PRODUCED BY $K^\pm$ BEAM

VALUE (MeV)	EVTS	DOCUMENT ID		TECN	COMMENT
$81.4^{+2.2}_{-1.9}$ OUR AVERAGE		Includes data from the datablock that follows this one.			
90 ±12		ASTON	88D	LASS	11 $K^- p \to K^0_S K^0_S \Lambda$
73 ±18		BOLONKIN	86	SPEC	40 $K^- p \to K^0_S K^0_S Y$
83 ±15		ARMSTRONG	83B	OMEG	18.5 $K^- p \to K^- K^+ \Lambda$
85 ±16	650	AGUILAR-...	81B	HBC	4.2 $K^- p \to \Lambda K^+ K^-$
80 $^{+14}_{-11}$	572	ALHARRAN	81	HBC	8.25 $K^- p \to \Lambda K \overline{K}$
72 ±25	166	EVANGELIS...	77	OMEG	10 $K^- p \to K^+ K^- (\Lambda, \Sigma)$
69 ±22	100	AGUILAR-...	72B	HBC	3.9,4.6 $K^- p \to K \overline{K} (\Lambda, \Sigma)$
• • • We do not use the following data for averages, fits, limits, etc. • • •					
92 $^{+25}_{-16}$	61	BINON	07	GAMS	32.5 $K^- p \to \eta\eta(\Lambda/\Sigma^0)$
75 ±20		[21] BARKOV	99	SPEC	40 $K^- p \to K^0_S K^0_S y$
62 $^{+19}_{-14}$	123	BARREIRO	77	HBC	4.15 $K^- p \to \Lambda K^0_S K^0_S$
61 ± 8	120	BRANDENB...	76C	ASPK	13 $K^- p \to K^+ K^- (\Lambda, \Sigma)$

PRODUCED IN e^+e^- ANNIHILATION AND PARTICLE DECAYS

VALUE (MeV)	EVTS	DOCUMENT ID		TECN	COMMENT
The data in this block is included in the average printed for a previous datablock.					
$81.4^{+2.4}_{-2.0}$ OUR AVERAGE					
84 ± 6 $^{+10}_{-5}$		AAIJ	13AN	LHCB	$\overline{B}^0_s \to J/\psi K^+ K^-$
75 $^{+12}_{-10}$ $^{+16}_{-8}$	5.5k	[22] ABLIKIM	13N	BES3	$e^+e^- \to J/\psi \to \gamma\eta\eta$
$82.9^{+2.1}_{-2.2} \pm 3.3 \pm 2.0$		UEHARA	13	BELL	$\gamma\gamma \to K^0_S K^0_S$
77 ±15		ABLIKIM	05	BES2	$J/\psi \to \phi K^+ K^-$
82 ± 2 ± 3		ABE	04	BELL	10.6 $e^+e^- \to e^+e^- K^+ K^-$
75 ± 4 $^{+15}_{-5}$		BAI	03G	BES	$J/\psi \to \gamma K \overline{K}$
100 ±15	331	[23] ACCIARRI	01H	L3	91, 183–209 $e^+e^- \to e^+e^- K^0_S K^0_S$

Meson Particle Listings

$f_2'(1525)$

60	±20	±19	ABREU	96C	DLPH	$Z^0 \to K^+K^- + X$
60	±23	$^{+13}_{-20}$	BAI	96C	BES	$J/\psi \to \gamma K^+K^-$
103	±30		AUGUSTIN	88	DM2	$J/\psi \to \gamma K^+K^-$
62	±10		[24] FALVARD	88	DM2	$J/\psi \to \phi K^+K^-$
85	±35		BALTRUSAIT...87		MRK3	$J/\psi \to \gamma K^+K^-$

• • • We do not use the following data for averages, fits, limits, etc. • • •

37	±12	29	[25] LEES	14H	BABR	$e^+e^- \to K^0_S K^0_S K^+K^-\gamma$
104	±10	870	[26] SCHEGELSKY	06A	RVUE	$\gamma\gamma \to K^0_S K^0_S$
100	± 3		[27] FALVARD	88	DM2	$J/\psi \to \phi K^+K^-$

PRODUCED IN $\overline{p}p$ ANNIHILATION

VALUE (MeV)	DOCUMENT ID		TECN	COMMENT
79± 8	[28] AMSLER	02	CBAR	0.9 $\overline{p}p \to \pi^0\eta\eta, \pi^0\pi^0\pi^0$

• • • We do not use the following data for averages, fits, limits, etc. • • •

128±20	[29] ANISOVICH	09	RVUE	0.0 $\overline{p}p$, πN
76± 6	AMSLER	06	CBAR	0.9 $\overline{p}p \to K^+K^-\pi^0$

CENTRAL PRODUCTION

VALUE (MeV)	DOCUMENT ID		TECN	COMMENT
70±25	BARBERIS	99	OMEG	450 $pp \to p_s p_f K^+K^-$

PRODUCED IN ep COLLISIONS

VALUE (MeV)	EVTS	DOCUMENT ID		TECN	COMMENT
83± 9^{+5}_{-4}		[30] CHEKANOV	08	ZEUS	$ep \to K^0_S K^0_S X$

• • • We do not use the following data for averages, fits, limits, etc. • • •

50^{+34}_{-22}	84	[31] CHEKANOV	04	ZEUS	$ep \to K^0_S K^0_S X$

[17] From a partial-wave analysis of data using a K-matrix formalism with 5 poles.
[18] CHABAUD 81 is a reanalysis of PAWLICKI 77 data.
[19] From an amplitude analysis where the $f_2'(1525)$ width and elasticity are in complete disagreement with the values obtained from $K\overline{K}$ channel, making the solution dubious.
[20] From a fit to the D with $f_2(1270)$-$f_2'(1525)$ interference. Mass fixed at 1516 MeV.
[21] Systematic errors not estimated.
[22] From partial wave analysis including all possible combinations of 0^{++}, 2^{++}, and 4^{++} resonances.
[23] Supersedes ACCIARRI 95J.
[24] From an analysis ignoring interference with $f_0(1710)$.
[25] From a fit to a Breit-Wigner line shape plus a second-order polynomial function. Systematic errors not evaluated.
[26] From analysis of L3 data at 91 and 183–209 GeV.
[27] From an analysis including interference with $f_0(1710)$.
[28] T-matrix pole.
[29] 4-poles, 5-channel K matrix fit.
[30] In the SU(3) based model with a specific interference pattern of the $f_2(1270)$, $a_2^0(1320)$, and $f_2'(1525)$ mesons incoherently added to the $f_0(1710)$ and non-resonant background.
[31] Systematic errors not estimated.

$f_2'(1525)$ DECAY MODES

	Mode	Fraction (Γ_i/Γ)
Γ_1	$K\overline{K}$	(88.7 ±2.2) %
Γ_2	$\eta\eta$	(10.4 ±2.2) %
Γ_3	$\pi\pi$	(8.2 ±1.5) × 10^{-3}
Γ_4	$K\overline{K}^*(892)$ + c.c.	
Γ_5	$\pi K\overline{K}$	
Γ_6	$\pi\pi\eta$	
Γ_7	$\pi^+\pi^+\pi^-\pi^-$	
Γ_8	$\gamma\gamma$	(1.10±0.14) × 10^{-6}

CONSTRAINED FIT INFORMATION

An overall fit to the total width, 2 partial widths, a combination of partial widths obtained from integrated cross sections, and 3 branching ratios uses 17 measurements and one constraint to determine 5 parameters. The overall fit has a $\chi^2 = 14.3$ for 13 degrees of freedom.

The following *off-diagonal* array elements are the correlation coefficients $\langle \delta p_i \delta p_j \rangle / (\delta p_i \cdot \delta p_j)$, in percent, from the fit to parameters p_i, including the branching fractions, $x_i \equiv \Gamma_i/\Gamma_{total}$. The fit constrains the x_i whose labels appear in this array to sum to one.

x_2	−100			
x_3	−6	−1		
x_8	−6	6	1	
Γ	−23	23	−1	−56
	x_1	x_2	x_3	x_8

	Mode	Rate (MeV)
Γ_1	$K\overline{K}$	65 $^{+5}_{-4}$
Γ_2	$\eta\eta$	7.6 ±1.8
Γ_3	$\pi\pi$	0.60±0.12
Γ_8	$\gamma\gamma$	(8.1 ±0.9) × 10^{-5}

$f_2'(1525)$ PARTIAL WIDTHS

$\Gamma(K\overline{K})$ Γ_1

VALUE (MeV)	DOCUMENT ID		TECN	COMMENT
65 $^{+5}_{-4}$ OUR FIT				
63 $^{+6}_{-5}$	[32] LONGACRE	86	MPS	22 $\pi^-p \to K^0_S K^0_S n$

$\Gamma(\eta\eta)$ Γ_2

VALUE (MeV)	EVTS	DOCUMENT ID		TECN	COMMENT
7.6±1.8 OUR FIT					

• • • We do not use the following data for averages, fits, limits, etc. • • •

5.0±0.8	870	[33] SCHEGELSKY	06A	RVUE	$\gamma\gamma \to K^0_S K^0_S$
24 $^{+3}_{-1}$		[32] LONGACRE	86	MPS	22 $\pi^-p \to K^0_S K^0_S n$

$\Gamma(\pi\pi)$ Γ_3

VALUE (MeV)	EVTS	DOCUMENT ID		TECN	COMMENT
0.60±0.12 OUR FIT					
1.4 $^{+1.0}_{-0.5}$		[32] LONGACRE	86	MPS	22 $\pi^-p \to K^0_S K^0_S n$

• • • We do not use the following data for averages, fits, limits, etc. • • •

0.2 $^{+1.0}_{-0.2}$	870	[33] SCHEGELSKY	06A	RVUE	$\gamma\gamma \to K^0_S K^0_S$

$\Gamma(\gamma\gamma)$ Γ_8

VALUE (keV)	EVTS	DOCUMENT ID		TECN	COMMENT
0.081±0.009 OUR FIT					

• • • We do not use the following data for averages, fits, limits, etc. • • •

0.13 ±0.03	870	[33] SCHEGELSKY	06A	RVUE	$\gamma\gamma \to K^0_S K^0_S$

[32] From a partial-wave analysis of data using a K-matrix formalism with 5 poles.
[33] From analysis of L3 data at 91 and 183–209 GeV, using $\Gamma(f_2'(1525) \to K\overline{K}) = 68$ MeV and SU(3) relations.

$f_2'(1525)$ Γ(i)$\Gamma(\gamma\gamma)/\Gamma$(total)

$\Gamma(K\overline{K}) \times \Gamma(\gamma\gamma)/\Gamma_{total}$ $\Gamma_1\Gamma_8/\Gamma$

VALUE (keV)	EVTS	DOCUMENT ID		TECN	COMMENT
0.072 ±0.007 OUR FIT					
0.072 ±0.007 OUR AVERAGE					
0.048 $^{+0.067}_{-0.008}$ $^{+0.108}_{-0.012}$		UEHARA	13	BELL	$\gamma\gamma \to K^0_S K^0_S$
0.0564±0.0048±0.0116		ABE	04	BELL	10.6 $e^+e^- \to e^+e^- K^+K^-$
0.076 ±0.006 ±0.011	331	[34] ACCIARRI	01H	L3	$e^+e^- \to e^+e^- K^0_S K^0_S$
0.067 ±0.008 ±0.015		[35] ALBRECHT	90G	ARG	$e^+e^- \to e^+e^- K^+K^-$
0.11 $^{+0.03}_{-0.02}$ ±0.02		BEHREND	89C	CELL	$e^+e^- \to e^+e^- K^0_S K^0_S$
0.10 $^{+0.04}_{-0.03}$ $^{+0.03}_{-0.02}$		BERGER	88	PLUT	$e^+e^- \to e^+e^- K^0_S K^0_S$
0.12 ±0.07 ±0.04		[35] AIHARA	86B	TPC	$e^+e^- \to e^+e^- K^+K^-$
0.11 ±0.02 ±0.04		[35] ALTHOFF	83	TASS	$e^+e^- \to e^+e^- K\overline{K}$

• • • We do not use the following data for averages, fits, limits, etc. • • •

0.0314±0.0050±0.0077		[36] ALBRECHT	90G	ARG	$e^+e^- \to e^+e^- K^+K^-$

[34] Supersedes ACCIARRI 95J. From analysis of L3 data at 91 and 183–209 GeV,
[35] Using an incoherent background.
[36] Using a coherent background.

$f_2'(1525)$ BRANCHING RATIOS

$\Gamma(\eta\eta)/\Gamma_{total}$ Γ_2/Γ

VALUE	DOCUMENT ID		TECN	COMMENT

• • • We do not use the following data for averages, fits, limits, etc. • • •

seen	UEHARA	10A	BELL	10.6 $e^+e^- \to e^+e^-\eta\eta$	
0.10±0.03	[37] PROKOSHKIN	91	GAM4	300 $\pi^-p \to \pi^-p\eta\eta$	

[37] Combining results of GAM4 with those of WA76 on $K\overline{K}$ central production and results of CBAL, MRK3 and DM2 on $J/\psi \to \gamma\eta\eta$.

$\Gamma(\eta\eta)/\Gamma(K\overline{K})$ Γ_2/Γ_1

VALUE	CL%	EVTS	DOCUMENT ID		TECN	COMMENT
0.118±0.028 OUR FIT						
0.115±0.028 OUR AVERAGE						
0.119±0.015±0.036		61	[38] BINON	07	GAMS	32.5 $K^-p \to \eta\eta(\Lambda/\Sigma^0)$
0.11 ±0.04			[39] PROKOSHKIN	91	GAM4	300 $\pi^-p \to \pi^-p\eta\eta$

• • • We do not use the following data for averages, fits, limits, etc. • • •

< 0.14	90	BARBERIS	00E		450 $pp \to p_f\eta\eta p_s$
< 0.50		BARNES	67	HBC	4.6,5.0 K^-p

[38] Using the compilation of the cross sections for $f_2'(1525)$ production in K^-p collisions from ASTON 88D.

[39] Combining results of GAM4 with those of WA76 on $K\overline{K}$ central production and results of CBAL, MRK3 and DM2 on $J/\psi \to \gamma\eta\eta$.

$\Gamma(\pi\pi)/\Gamma_{total}$ Γ_3/Γ

VALUE	CL%	DOCUMENT ID		TECN	COMMENT
0.0082±0.0016 OUR FIT					
0.0075±0.0016 OUR AVERAGE					
0.007 ±0.002		COSTA	80	OMEG	10 $\pi^- p \to K^+ K^- n$
0.027 $^{+0.071}_{-0.013}$		[40] GORLICH	80	ASPK	17,18 $\pi^- p$
0.0075±0.0025		[40,41] MARTIN	79	RVUE	
• • • We do not use the following data for averages, fits, limits, etc. • • •					
<0.06	95	AGUILAR-...	81B	HBC	4.2 $K^- p \to \Lambda K^+ K^-$
0.19 ±0.03		CORDEN	79	OMEG	12–15 $\pi^- p \to \pi^+\pi^- n$
<0.045	95	BARREIRO	77	HBC	4.15 $K^- p \to \Lambda K^0_S K^0_S$
0.012 ±0.004		[40] PAWLICKI	77	SPEC	6 $\pi N \to K^+ K^- N$
<0.063	90	BRANDENB...	76C	ASPK	13 $K^- p \to K^+ K^- (\Lambda, \Sigma)$
<0.0086		[40] BEUSCH	75B	OSPK	8.9 $\pi^- p \to K^0 \overline{K}^0 n$

[40] Assuming that the $f_2'(1525)$ is produced by an one-pion exchange production mechanism.

[41] MARTIN 79 uses the PAWLICKI 77 data with different input value of the $f_2'(1525) \to K\overline{K}$ branching ratio.

$\Gamma(\pi\pi)/\Gamma(K\overline{K})$ Γ_3/Γ_1

VALUE	DOCUMENT ID		TECN	COMMENT
0.0092±0.0018 OUR FIT				
0.075 ±0.035	AUGUSTIN	87	DM2	$J/\psi \to \gamma\pi^+\pi^-$

$[\Gamma(K\overline{K}^*(892)+\text{c.c.}) + \Gamma(\pi K\overline{K})]/\Gamma(K\overline{K})$ $(\Gamma_4+\Gamma_5)/\Gamma_1$

VALUE	CL%	DOCUMENT ID		TECN	COMMENT
• • • We do not use the following data for averages, fits, limits, etc. • • •					
<0.35	95	AGUILAR-...	72B	HBC	3.9,4.6 $K^- p$
<0.4	67	AMMAR	67	HBC	

$\Gamma(\pi\pi\eta)/\Gamma(K\overline{K})$ Γ_6/Γ_1

VALUE	CL%	DOCUMENT ID		TECN	COMMENT
• • • We do not use the following data for averages, fits, limits, etc. • • •					
<0.41	95	AGUILAR-...	72B	HBC	3.9,4.6 $K^- p$
<0.3	67	AMMAR	67	HBC	

$\Gamma(\pi^+\pi^+\pi^-\pi^-)/\Gamma(K\overline{K})$ Γ_7/Γ_1

VALUE	CL%	DOCUMENT ID		TECN	COMMENT
• • • We do not use the following data for averages, fits, limits, etc. • • •					
<0.32	95	AGUILAR-...	72B	HBC	3.9,4.6 $K^- p$

$f_2'(1525)$ REFERENCES

DOBBS	15	PR D91 052006	S. Dobbs *et al.*	(NWES)
LEES	14H	PR D89 092002	J.P. Lees *et al.*	(BABAR Collab.)
AAIJ	13AN	PR D87 072004	R. Aaij *et al.*	(LHCb Collab.)
ABLIKIM	13N	PR D87 092009	Ablikim M. *et al.*	(BES III Collab.)
UEHARA	13	PTEP 2013 123C01	S. Uehara *et al.*	(BELLE Collab.)
UEHARA	10A	PR D82 114031	S. Uehara *et al.*	(BELLE Collab.)
ANISOVICH	09	IJMP A24 2481	V.V. Anisovich, A.V. Sarantsev	
CHEKANOV	08	PRL 101 112003	S. Chekanov *et al.*	(ZEUS Collab.)
BINON	07	PAN 70 1713	F. Binon *et al.*	(GAMS Collab.)
		Translated from YAF 70 1758.		
AMSLER	06	PL B639 165	C. Amsler *et al.*	(CBAR Collab.)
SCHEGELSKY	06A	EPJ A27 207	V.A. Schegelsky *et al.*	
ABLIKIM	05	PL B607 243	M. Ablikim *et al.*	(BES Collab.)
ABE	04	EPJ C32 323	K. Abe *et al.*	(BELLE Collab.)
CHEKANOV	04	PL B578 33	S. Chekanov *et al.*	(ZEUS Collab.)
BAI	03G	PR D68 052003	J.Z. Bai *et al.*	(BES Collab.)
TIKHOMIROV	03	PAN 66 828	G.D. Tikhomirov *et al.*	
		Translated from YAF 66 860.		
AMSLER	02	EPJ C23 29	C. Amsler *et al.*	
ACCIARRI	01H	PL B501 173	M. Acciarri *et al.*	(L3 Collab.)
BARBERIS	00E	PL B479 59	D. Barberis *et al.*	(WA 102 Collab.)
BARBERIS	99	PL B453 305	D. Barberis *et al.*	(Omega Expt.)
BARKOV	99	JETPL 70 248	B.P. Barkov *et al.*	
		Translated from ZETFP 70 242.		
ABREU	96C	PL B379 309	P. Abreu *et al.*	(DELPHI Collab.)
BAI	96C	PRL 77 3959	J.Z. Bai *et al.*	(BES Collab.)
ACCIARRI	95J	PL B363 118	M. Acciarri *et al.*	(L3 Collab.)
PROKOSHKIN	91	SPD 36 155	Y.D. Prokoshkin	(GAM2, GAM4 Collab.)
		Translated from DANS 316 900.		
ALBRECHT	90G	ZPHY C48 183	H. Albrecht *et al.*	(ARGUS Collab.)
PDG	90	PL B239 1	J.J. Hernandez *et al.*	(IFIC, BOST, CIT+)
BEHREND	89C	ZPHY C43 91	H.J. Behrend *et al.*	(CELLO Collab.)
ASTON	88D	NP B301 525	D. Aston *et al.*	(SLAC, NAGO, CINC, INUS)
AUGUSTIN	88	PRL 60 2238	J.E. Augustin *et al.*	(DM2 Collab.)
BERGER	88	ZPHY C37 329	C. Berger *et al.*	(PLUTO Collab.)
FALVARD	88	PR D38 2706	A. Falvard *et al.*	(CLER, FRAS, LALO+)
AUGUSTIN	87	ZPHY C36 369	J.E. Augustin *et al.*	(LALO, CLER, FRAS+)
BALTRUSAIT...	87	PR D35 2077	R.M. Baltrusaitis *et al.*	(Mark III Collab.)
AIHARA	86B	PRL 57 404	H. Aihara *et al.*	(TPC-2γ Collab.)
BOLONKIN	86	SJNP 43 776	B.V. Bolonkin *et al.*	(ITEP) JP
		Translated from YAF 43 1211.		
LONGACRE	86	PL B177 223	R.S. Longacre *et al.*	(BNL, BRAN, CUNY+)
ALTHOFF	83	PL 121B 216	M. Althoff *et al.*	(TASSO Collab.)
ARMSTRONG	83B	NP B224 193	T.A. Armstrong *et al.*	(BARI, BIRM, CERN+)
AGUILAR-...	81B	ZPHY C8 313	M. Aguilar-Benitez *et al.*	(CERN, CDEF+)
ALHARRAN	81	NP B191 26	S. Al-Harran *et al.*	(BIRM, CERN, GLAS+)
CHABAUD	81	APP B12 575	V. Chabaud *et al.*	(CERN, CRAC, MPIM)
COSTA	80	NP B175 402	G. Costa *et al.*	(BARI, BONN, CERN, GLAS+)
GORLICH	80	NP B174 16	L. Gorlich *et al.*	(CRAC, MPIM, CERN+)
CORDEN	79	NP B157 250	M.J. Corden *et al.*	(BIRM, RHEL, TELA+) JP
MARTIN	79	NP B158 520	A.D. Martin, E.N. Ozmutlu	(DURH)
POLYCHRO...	79	PR D19 1317	V.A. Polychronakos *et al.*	(NDAM, ANL)
BARREIRO	77	NP B121 237	F. Barreiro *et al.*	(CERN, AMST, NIJM+)
EVANGELIS...	77	NP B127 384	C. Evangelista *et al.*	(BARI, BONN, CERN+)
PAWLICKI	77	PR D15 3196	A.J. Pawlicki *et al.*	(ANL) IJP
BRANDENB...	76C	NP B104 413	G.W. Brandenburg *et al.*	(SLAC)
BEUSCH	75B	PL 60B 101	W. Beusch *et al.*	(CERN, ETH)
AGUILAR-...	72B	PR D6 29	M. Aguilar-Benitez *et al.*	(BNL)
AMMAR	67	PRL 19 1071	R. Ammar *et al.*	(NWES, ANL) JP
BARNES	67	PRL 19 964	V.E. Barnes *et al.*	(BNL, SYRA) IJPC
CRENNELL	66	PRL 16 1025	D.J. Crennell *et al.*	(BNL) I

$f_2(1565)$ $I^G(J^{PC}) = 0^+(2^{++})$

OMITTED FROM SUMMARY TABLE

Seen mostly in antinucleon-nucleon annihilation. Needs confirmation in other channels.

$f_2(1565)$ MASS

VALUE (MeV)	DOCUMENT ID		TECN	COMMENT
1562±13 OUR AVERAGE	Error includes scale factor of 2.1. See the ideogram below.			
1590±10	[1] AMELIN	06	VES	36 $\pi^- p \to \omega\omega n$
1552±13	[2] AMSLER	02	CBAR	0.9 $\overline{p}p \to \pi^0\eta\eta$, $\pi^0\pi^0\pi^0$
1550±10±20	AMELIN	00	VES	37 $\pi^- p \to \eta\pi^+\pi^- n$
1575±18	BERTIN	98	OBLX	0.05–0.405 $\overline{n}p \to \pi^+\pi^+\pi^-$
1507±15	[2] BERTIN	97C	OBLX	0.0 $\overline{p}p \to \pi^+\pi^-\pi^0$
1565±20	MAY	90	ASTE	0.0 $\overline{p}p \to \pi^+\pi^-\pi^0$
• • • We do not use the following data for averages, fits, limits, etc. • • •				
1560±15	[3] ANISOVICH	09	RVUE	0.0 $\overline{p}p$, πN
1598±11± 9	BAKER	99B	SPEC	0 $\overline{p}p \to \omega\omega\pi^0$
1534±20	[4] ABELE	96C	RVUE	Compilation
~ 1552	[5] AMSLER	95D	CBAR	0.0 $\overline{p}p \to \pi^0\pi^0\pi^0$, $\pi^0\eta\eta$, $\pi^0\pi^0\eta$
1598±72	BALOSHIN	95	SPEC	40 π^- C $\to K^0_S K^0_S$ X
1566 $^{+80}_{-50}$	[6] ANISOVICH	94	CBAR	0.0 $\overline{p}p \to 3\pi^0, \eta\eta\pi^0$
1502± 9	ADAMO	93	OBLX	$\overline{n}p \to \pi^+\pi^+\pi^-$
1488±10	[7] ARMSTRONG	93C	E760	$\overline{p}p \to \pi^0\eta\eta \to 6\gamma$
1508±10	[7] ARMSTRONG	93D	E760	$\overline{p}p \to 3\pi^0 \to 6\gamma$
1525±10	[7] ARMSTRONG	93D	E760	$\overline{p}p \to \eta\pi^0\pi^0 \to 6\gamma$
~ 1504	[8] WEIDENAUER	93	ASTE	0.0 $\overline{p}N \to 3\pi^-2\pi^+$
1540±15	[7] ADAMO	92	OBLX	$\overline{n}p \to \pi^+\pi^+\pi^-$
1515±10	[9] AKER	91	CBAR	0.0 $\overline{p}p \to 3\pi^0$
1477± 5	BRIDGES	86C	DBC	0.0 $\overline{p}N \to 3\pi^-2\pi^+$

[1] Supersedes the $\omega\omega$ state of BELADIDZE 92B earlier assigned to the $f_2(1640)$.

[2] T-matrix pole.

[3] On sheet II in a two-pole solution.

[4] T-matrix pole, large coupling to $\rho\rho$ and $\omega\omega$, could be $f_2(1640)$.

[5] Coupled-channel analysis of AMSLER 95B, AMSLER 95C, and AMSLER 94D.

[6] From a simultaneous analysis of the annihilations $\overline{p}p \to 3\pi^0, \pi^0\eta\eta$ including AKER 91 data.

[7] J^P not determined, could be partly $f_0(1500)$.

[8] J^P not determined.

[9] Superseded by AMSLER 95B.

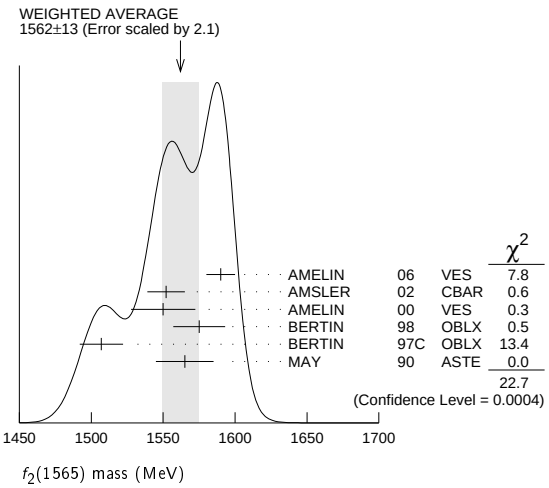

$f_2(1565)$ WIDTH

VALUE (MeV)	DOCUMENT ID		TECN	COMMENT
134± 8 OUR AVERAGE				
140± 11	[10] AMELIN	06	VES	36 $\pi^- p \to \omega\omega n$
113± 23	[11] AMSLER	02	CBAR	0.9 $\overline{p}p \to \pi^0\eta\eta$, $\pi^0\pi^0\pi^0$
130± 20±40	AMELIN	00	VES	37 $\pi^- p \to \eta\pi^+\pi^- n$
119± 24	BERTIN	98	OBLX	0.05–0.405 $\overline{n}p \to \pi^+\pi^+\pi^-$
130± 20	[11] BERTIN	97C	OBLX	0.0 $\overline{p}p \to \pi^+\pi^-\pi^0$
170± 40	MAY	90	ASTE	0.0 $\overline{p}p \to \pi^+\pi^-\pi^0$

Meson Particle Listings

$f_2(1565)$, $\rho(1570)$

• • • We do not use the following data for averages, fits, limits, etc. • • •

280± 40	[12] ANISOVICH	09	RVUE	0.0 $\overline{p}p$, πN	
180± 60	[13] ABELE	96C	RVUE	Compilation	
~ 142	[14] AMSLER	95D	CBAR	0.0 $\overline{p}p \to \pi^0\pi^0\pi^0$, $\pi^0\eta\eta$, $\pi^0\pi^0\eta$	
263±101	BALOSHIN	95	SPEC	40 π^- C $\to K^0_S K^0_S$ X	
$166^{+\ 80}_{-\ 20}$	[15] ANISOVICH	94	CBAR	0.0 $\overline{p}p \to 3\pi^0, \eta\eta\pi^0$	
130± 10	[16] ADAMO	93	OBLX	$\overline{n}p \to \pi^+\pi^+\pi^-$	
148± 27	[17] ARMSTRONG	93C	E760	$\overline{p}p \to \pi^0\eta\eta \to 6\gamma$	
103± 15	[17] ARMSTRONG	93D	E760	$\overline{p}p \to 3\pi^0 \to 6\gamma$	
111± 10	[17] ARMSTRONG	93D	E760	$\overline{p}p \to \eta\pi^0\pi^0 \to 6\gamma$	
~ 206	[18] WEIDENAUER	93	ASTE	0.0 $\overline{p}N \to 3\pi^-2\pi^+$	
132± 37	[17] ADAMO	92	OBLX	$\overline{n}p \to \pi^+\pi^+\pi^-$	
120± 10	[19] AKER	91	CBAR	0.0 $\overline{p}p \to 3\pi^0$	
116± 9	BRIDGES	86C	DBC	0.0 $\overline{p}N \to 3\pi^-2\pi^+$	

[10] Supersedes the $\omega\omega$ state of BELADIDZE 92B earlier assigned to the $f_2(1640)$.
[11] T-matrix pole.
[12] On sheet II in a two-pole solution.
[13] T-matrix pole, large coupling to $\rho\rho$ and $\omega\omega$, could be $f_2(1640)$.
[14] Coupled-channel analysis of AMSLER 95B, AMSLER 95C, and AMSLER 94D.
[15] From a simultaneous analysis of the annihilations $\overline{p}p \to 3\pi^0, \pi^0\eta\eta$ including AKER 91 data.
[16] Supersedes ADAMO 92.
[17] J^P not determined, could be partly $f_0(1500)$.
[18] J^P not determined.
[19] Superseded by AMSLER 95B.

$f_2(1565)$ DECAY MODES

	Mode	Fraction (Γ_i/Γ)
Γ_1	$\pi\pi$	seen
Γ_2	$\pi^+\pi^-$	seen
Γ_3	$\pi^0\pi^0$	seen
Γ_4	$\rho^0\rho^0$	seen
Γ_5	$2\pi^+2\pi^-$	seen
Γ_6	$\eta\eta$	seen
Γ_7	$a_2(1320)\pi$	
Γ_8	$\omega\omega$	seen
Γ_9	$K\overline{K}$	
Γ_{10}	$\gamma\gamma$	

$f_2(1565)$ PARTIAL WIDTHS

$\Gamma(\eta\eta)$ Γ_6

VALUE (MeV)	EVTS	DOCUMENT ID		TECN	COMMENT
• • • We do not use the following data for averages, fits, limits, etc. • • •					
1.2±0.3	870	[20] SCHEGELSKY	06A	RVUE	$\gamma\gamma \to K^0_S K^0_S$

$\Gamma(K\overline{K})$ Γ_9

VALUE (MeV)	EVTS	DOCUMENT ID		TECN	COMMENT
• • • We do not use the following data for averages, fits, limits, etc. • • •					
2.0±1.0	870	[20] SCHEGELSKY	06A	RVUE	$\gamma\gamma \to K^0_S K^0_S$

$\Gamma(\gamma\gamma)$ Γ_{10}

VALUE (keV)	EVTS	DOCUMENT ID		TECN	COMMENT
• • • We do not use the following data for averages, fits, limits, etc. • • •					
0.70±0.14	870	[20] SCHEGELSKY	06A	RVUE	$\gamma\gamma \to K^0_S K^0_S$

[20] From analysis of L3 data at 91 and 183–209 GeV, using $f_2(1565)$ mass of 1570 MeV, width of 160 MeV, $\Gamma(\pi\pi)$ = 25 MeV, and SU(3) relations.

$f_2(1565)$ BRANCHING RATIOS

$\Gamma(\pi\pi)/\Gamma_{total}$ Γ_1/Γ

VALUE	DOCUMENT ID		TECN	COMMENT
• • • We do not use the following data for averages, fits, limits, etc. • • •				
seen	BAKER	99B	SPEC	0 $\overline{p}p \to \omega\omega\pi^0$

$\Gamma(\pi^+\pi^-)/\Gamma_{total}$ Γ_2/Γ

VALUE	DOCUMENT ID		TECN	COMMENT
• • • We do not use the following data for averages, fits, limits, etc. • • •				
seen	BERTIN	98	OBLX	0.05–0.405 $\overline{n}p \to \pi^+\pi^+\pi^-$
not seen	[21] ANISOVICH	94B	RVUE	$\overline{p}p \to \pi^+\pi^-\pi^0$
seen	MAY	89	ASTE	$\overline{p}p \to \pi^+\pi^-\pi^0$

[21] ANISOVICH 94B is from a reanalysis of MAY 90.

$\Gamma(\pi^0\pi^0)/\Gamma_{total}$ Γ_3/Γ

VALUE	DOCUMENT ID		TECN	COMMENT
seen	AMSLER	95B	CBAR	0.0 $\overline{p}p \to 3\pi^0$

$\Gamma(\pi^+\pi^-)/\Gamma(\rho^0\rho^0)$ Γ_2/Γ_4

VALUE	DOCUMENT ID		TECN	COMMENT
• • • We do not use the following data for averages, fits, limits, etc. • • •				
0.042±0.013	BRIDGES	86B	DBC	$\overline{p}N \to 3\pi^-2\pi^+$

$\Gamma(\eta\eta)/\Gamma(\pi^0\pi^0)$ Γ_6/Γ_3

VALUE	DOCUMENT ID		TECN	COMMENT
• • • We do not use the following data for averages, fits, limits, etc. • • •				
0.024±0.005±0.012	[22] ARMSTRONG	93C	E760	$\overline{p}p \to \pi^0\eta\eta \to 6\gamma$

[22] J^P not determined, could be partly $f_0(1500)$.

$\Gamma(\omega\omega)/\Gamma_{total}$ Γ_8/Γ

VALUE	DOCUMENT ID		TECN	COMMENT
• • • We do not use the following data for averages, fits, limits, etc. • • •				
seen	BAKER	99B	SPEC	0 $\overline{p}p \to \omega\omega\pi^0$

$f_2(1565)$ REFERENCES

ANISOVICH	09	IJMP A24 2481	V.V. Anisovich, A.V. Sarantsev	
AMELIN	06	PAN 69 690 Translated from YAF 69 715.	D.V. Amelin *et al.*	(VES Collab.)
SCHEGELSKY	06A	EPJ A27 207	V.A. Schegelsky *et al.*	
AMSLER	02	EPJ C23 29	C. Amsler *et al.*	
AMELIN	00	NP A668 83	D. Amelin *et al.*	(VES Collab.)
BAKER	99B	PL B467 147	C.A. Baker *et al.*	
BERTIN	98	PR D57 55	A. Bertin *et al.*	(OBELIX Collab.)
BERTIN	97C	PL B408 476	A. Bertin *et al.*	(OBELIX Collab.)
ABELE	96C	NP A609 562	A. Abele *et al.*	(Crystal Barrel Collab.)
AMSLER	95B	PL B342 433	C. Amsler *et al.*	(Crystal Barrel Collab.)
AMSLER	95C	PL B353 571	C. Amsler *et al.*	(Crystal Barrel Collab.)
AMSLER	95D	PL B355 425	C. Amsler *et al.*	(Crystal Barrel Collab.)
BALOSHIN	95	PAN 58 46 Translated from YAF 58 50.	O.N. Baloshin *et al.*	(ITEP)
AMSLER	94D	PL B333 277	C. Amsler *et al.*	(Crystal Barrel Collab.)
ANISOVICH	94	PL B323 233	V.V. Anisovich *et al.*	(Crystal Barrel Collab.)
ANISOVICH	94B	PR D50 1972	V.V. Anisovich *et al.*	(LOQM)
ADAMO	93	NP A558 13C	A. Adamo *et al.*	(OBELIX Collab.)
ARMSTRONG	93C	PL B307 394	T.A. Armstrong *et al.*	(FNAL, FERR, GENO+)
ARMSTRONG	93D	PL B307 399	T.A. Armstrong *et al.*	(FNAL, FERR, GENO+)
WEIDENAUER	93	ZPHY C59 387	P. Weidenauer *et al.*	(ASTERIX Collab.)
ADAMO	92	PL B287 368	A. Adamo *et al.*	(OBELIX Collab.)
BELADIDZE	92B	ZPHY C54 367	G.M. Beladidze *et al.*	(VES Collab.)
AKER	91	PL B260 249	E. Aker *et al.*	(Crystal Barrel Collab.)
MAY	90	ZPHY C46 203	B. May *et al.*	(ASTERIX Collab.)
MAY	89	PL B225 450	B. May *et al.*	(ASTERIX Collab.) IJP
BRIDGES	86B	PRL 56 215	D.L. Bridges *et al.*	(SYRA, CASE)
BRIDGES	86C	PRL 57 1534	D.L. Bridges *et al.*	(SYRA)

$\rho(1570)$ $I^G(J^{PC}) = 1^+(1^{--})$

OMITTED FROM SUMMARY TABLE

May be an OZI-violating decay mode of $\rho(1700)$. See our mini-review under the $\rho(1700)$.

$\rho(1570)$ MASS

VALUE (MeV)	EVTS	DOCUMENT ID		TECN	COMMENT
1570±36±62	54	[1] AUBERT	08S	BABR	10.6 $e^+e^- \to \phi\pi^0\gamma$
• • • We do not use the following data for averages, fits, limits, etc. • • •					
1480±40		[2] BITYUKOV	87	SPEC	32.5 $\pi^-p \to \phi\pi^0 n$

[1] From the fit with two resonances.
[2] Systematic errors not estimated.

$\rho(1570)$ WIDTH

VALUE (MeV)	EVTS	DOCUMENT ID		TECN	COMMENT
144±75±43	54	[3] AUBERT	08S	BABR	10.6 $e^+e^- \to \phi\pi^0\gamma$
• • • We do not use the following data for averages, fits, limits, etc. • • •					
130±60		[4] BITYUKOV	87	SPEC	32.5 $\pi^-p \to \phi\pi^0 n$

[3] From the fit with two resonances.
[4] Systematic errors not estimated.

$\rho(1570)$ DECAY MODES

	Mode	Fraction (Γ_i/Γ)
Γ_1	e^+e^-	
Γ_2	$\phi\pi$	not seen
Γ_3	$\omega\pi$	

$\rho(1570)$ $\Gamma(i)\Gamma(e^+e^-)/\Gamma(total)$

$\Gamma(\phi\pi) \times \Gamma(e^+e^-)/\Gamma_{total}$ $\Gamma_2\Gamma_1/\Gamma$

VALUE (eV)	CL%	EVTS	DOCUMENT ID		TECN	COMMENT
3.5±0.9±0.3		54	[5] AUBERT	08S	BABR	10.6 $e^+e^- \to \phi\pi^0\gamma$
• • • We do not use the following data for averages, fits, limits, etc. • • •						
<70	90		[6] AULCHENKO	87B	ND	$e^+e^- \to K^0_S K^0_L \pi^0$

[5] From the fit with two resonances.

[6] Using mass and width of BITYUKOV 87.

$\rho(1570)$ BRANCHING RATIOS

$\Gamma(\phi\pi)/\Gamma_{total}$ — **Γ_2/Γ**

VALUE	DOCUMENT ID		TECN	COMMENT
not seen	ABELE	97H	CBAR	$\overline{p}p \rightarrow K^0_L K^0_S \pi^0 \pi^0$
• • • We do not use the following data for averages, fits, limits, etc. • • •				
<0.01	[7] DONNACHIE	91	RVUE	

[7] Using data from BISELLO 91B, DOLINSKY 86, and ALBRECHT 87L.

$\Gamma(\phi\pi)/\Gamma(\omega\pi)$ — **Γ_2/Γ_3**

VALUE	CL%	DOCUMENT ID		TECN	COMMENT
• • • We do not use the following data for averages, fits, limits, etc. • • •					
>0.5	95	BITYUKOV	87	SPEC	32.5 $\pi^- p \rightarrow \phi\pi^0 n$

$\rho(1570)$ REFERENCES

AUBERT	08S	PR D77 092002	B. Aubert *et al.*	(BABAR Collab.)
ABELE	97H	PL B415 280	A. Abele *et al.*	(Crystal Barrel Collab.)
BISELLO	91B	NPBPS B21 111	D. Bisello	(DM2 Collab.)
DONNACHIE	91	ZPHY C51 689	A. Donnachie, A.B. Clegg	(MCHS, LANC)
ALBRECHT	87L	PL B185 223	H. Albrecht *et al.*	(ARGUS Collab.)
AULCHENKO	87B	JETPL 45 145 Translated from ZETFP 45 118.	V.M. Aulchenko *et al.*	(NOVO)
BITYUKOV	87	PL B188 383	S.I. Bityukov *et al.*	(SERP)
DOLINSKY	86	PL B174 453	S.I. Dolinsky *et al.*	(NOVO)

$h_1(1595)$

$I^G(J^{PC}) = 0^-(1^{+-})$

OMITTED FROM SUMMARY TABLE

Seen in a partial-wave analysis of the $\omega\eta$ system produced in the reaction $\pi^- p \rightarrow \omega\eta n$ at 18 GeV/c.

$h_1(1595)$ MASS

VALUE (MeV)	DOCUMENT ID		TECN	COMMENT
$1594 \pm 15^{+10}_{-60}$	EUGENIO	01	SPEC	18 $\pi^- p \rightarrow \omega\eta n$

$h_1(1595)$ WIDTH

VALUE (MeV)	DOCUMENT ID		TECN	COMMENT
$384 \pm 60^{+70}_{-100}$	EUGENIO	01	SPEC	18 $\pi^- p \rightarrow \omega\eta n$

$h_1(1595)$ DECAY MODES

	Mode	Fraction (Γ_i/Γ)
Γ_1	$\omega\eta$	seen

$h_1(1595)$ REFERENCES

EUGENIO	01	PL B497 190	P. Eugenio *et al.*	

$\pi_1(1600)$

$I^G(J^{PC}) = 1^-(1^{-+})$

$\pi_1(1600)$ MASS

VALUE (MeV)	EVTS	DOCUMENT ID		TECN	COMMENT
1662^{+8}_{-9} OUR AVERAGE					
$1660 \pm 10^{+0}_{-64}$	420k	ALEKSEEV	10	COMP	190 $\pi^- Pb \rightarrow \pi^-\pi^-\pi^+ Pb'$
$1664 \pm 8 \pm 10$	145k	[1] LU	05	B852	18 $\pi^- p \rightarrow \omega\pi^-\pi^0 p$
$1709 \pm 24 \pm 41$	69k	[2] KUHN	04	B852	18 $\pi^- p \rightarrow \eta\pi^+\pi^-\pi^- p$
$1597 \pm 10^{+45}_{-10}$		[2] IVANOV	01	B852	18 $\pi^- p \rightarrow \eta'\pi^- p$
• • • We do not use the following data for averages, fits, limits, etc. • • •					
$1593 \pm 8^{+29}_{-47}$		[2,3] ADAMS	98B	B852	18.3 $\pi^- p \rightarrow \pi^+\pi^-\pi^- p$

[1] May be a different state: natural and unnatural parity exchanges.
[2] Natural parity exchange.
[3] Superseded by DZIERBA 06 excluding this state in a more refined PWA analysis, with 2.6 M events of $\pi^- p \rightarrow \pi^-\pi^-\pi^+ p$ and 3 M events of $\pi^- p \rightarrow \pi^-\pi^0\pi^0 p$ of E852 data.

$\pi_1(1600)$ WIDTH

VALUE (MeV)	EVTS	DOCUMENT ID		TECN	COMMENT
241 ± 40 OUR AVERAGE		Error includes scale factor of 1.4. See the ideogram below.			
$269 \pm 21^{+42}_{-64}$	420k	ALEKSEEV	10	COMP	190 $\pi^- Pb \rightarrow \pi^-\pi^-\pi^+ Pb'$
$185 \pm 25 \pm 28$	145k	[1] LU	05	B852	18 $\pi^- p \rightarrow \omega\pi^-\pi^0 p$
$403 \pm 80 \pm 115$	69k	[2] KUHN	04	B852	18 $\pi^- p \rightarrow \eta\pi^+\pi^-\pi^- p$
$340 \pm 40 \pm 50$		[2] IVANOV	01	B852	18 $\pi^- p \rightarrow \eta'\pi^- p$
• • • We do not use the following data for averages, fits, limits, etc. • • •					
$168 \pm 20^{+150}_{-12}$		[2,3] ADAMS	98B	B852	18.3 $\pi^- p \rightarrow \pi^+\pi^-\pi^- p$

[1] May be a different state: natural and unnatural parity exchanges.
[2] Natural parity exchange.
[3] Superseded by DZIERBA 06 excluding this state in a more refined PWA analysis, with 2.6 M events of $\pi^- p \rightarrow \pi^-\pi^-\pi^+ p$ and 3 M events of $\pi^- p \rightarrow \pi^-\pi^0\pi^0 p$ of E852 data.

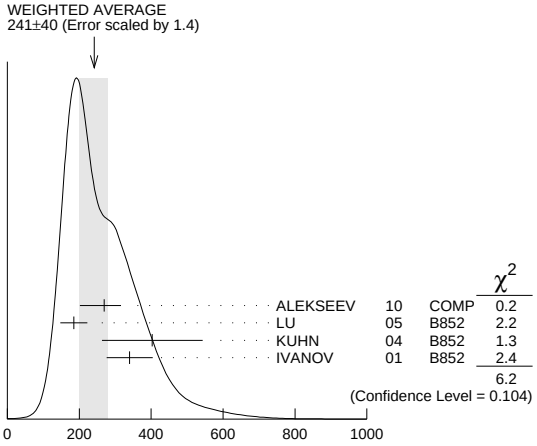

$\pi_1(1600)$ DECAY MODES

	Mode	Fraction (Γ_i/Γ)
Γ_1	$\pi\pi\pi$	seen
Γ_2	$\rho^0\pi^-$	seen
Γ_3	$f_2(1270)\pi^-$	not seen
Γ_4	$b_1(1235)\pi$	seen
Γ_5	$\eta'(958)\pi^-$	seen
Γ_6	$f_1(1285)\pi$	seen

$\pi_1(1600)$ BRANCHING RATIOS

$\Gamma(\rho^0\pi^-)/\Gamma_{total}$ — **Γ_2/Γ**

VALUE	DOCUMENT ID		TECN	COMMENT
seen	ALEKSEEV	10	COMP	190 $\pi^- Pb \rightarrow \pi^-\pi^-\pi^+ Pb'$
• • • We do not use the following data for averages, fits, limits, etc. • • •				
not seen	NOZAR	09	CLAS	$\gamma p \rightarrow 2\pi^+\pi^- n$
not seen	[1] DZIERBA	06	B852	18 $\pi^- p$

[1] From the PWA analysis of 2.6 M $\pi^- p \rightarrow \pi^-\pi^-\pi^+ p$ and 3 M events of $\pi^- p \rightarrow \pi^-\pi^0\pi^0 p$ of E852 data. Supersedes ADAMS 98B.

$\Gamma(f_2(1270)\pi^-)/\Gamma_{total}$ — **Γ_3/Γ**

VALUE	DOCUMENT ID		TECN	COMMENT
not seen	[1] DZIERBA	06	B852	18 $\pi^- p$

[1] From the PWA analysis of 2.6 M $\pi^- p \rightarrow \pi^-\pi^-\pi^+ p$ and 3 M events of $\pi^- p \rightarrow \pi^-\pi^0\pi^0 p$ of E852 data. Supersedes CHUNG 02.

$\Gamma(b_1(1235)\pi)/\Gamma_{total}$ — **Γ_4/Γ**

VALUE	EVTS	DOCUMENT ID		TECN	COMMENT
seen	35280	[1] BAKER	03	SPEC	$\overline{p}p \rightarrow \omega\pi^+\pi^-\pi^0$
• • • We do not use the following data for averages, fits, limits, etc. • • •					
seen	145k	LU	05	B852	18 $\pi^- p \rightarrow \omega\pi^-\pi^0 p$

[1] $B((b_1\pi)_{D-wave})/B((b_1\pi)_{S\text{-wave}}) = 0.3 \pm 0.1$.

$\Gamma(\eta'(958)\pi^-)/\Gamma_{total}$ — **Γ_5/Γ**

VALUE	DOCUMENT ID		TECN	COMMENT
seen	IVANOV	01	B852	18 $\pi^- p \rightarrow \eta'\pi^- p$

$\Gamma(f_1(1285)\pi)/\Gamma(\eta'(958)\pi^-)$ — **Γ_6/Γ_5**

VALUE	EVTS	DOCUMENT ID		TECN	COMMENT
3.80 ± 0.78	69k	[1] KUHN	04	B852	18 $\pi^- p \rightarrow \eta\pi^+\pi^-\pi^- p$

[1] Using $\eta'(958)\,\pi$ data from IVANOV 01.

$\pi_1(1600)$ REFERENCES

ALEKSEEV	10	PRL 104 241803	M.G. Alekseev *et al.*	(COMPASS Collab.)
NOZAR	09	PRL 102 102002	M. Nozar *et al.*	(JLab CLAS Collab.)

Meson Particle Listings

$\pi_1(1600)$, $a_1(1640)$, $f_2(1640)$

DZIERBA	06	PR D73 072001	A.R. Dzierba *et al.*	(BNL E852 Collab.)
LU	05	PRL 94 032002	M. Lu *et al.*	(BNL E852 Collab.)
KUHN	04	PL B595 109	J. Kuhn *et al.*	(BNL E852 Collab.)
BAKER	03	PL B563 140	C.A. Baker *et al.*	
CHUNG	02	PR D65 072001	S.U. Chung *et al.*	(BNL E852 Collab.)
IVANOV	01	PRL 86 3977	E.I. Ivanov *et al.*	(BNL E852 Collab.)
ADAMS	98B	PRL 81 5760	G.S. Adams *et al.*	(BNL E852 Collab.)

$a_1(1640)$

$I^G(J^{PC}) = 1^-(1^{++})$

OMITTED FROM SUMMARY TABLE

Seen in the amplitude analysis of the $3\pi^0$ system produced in $\overline{p}p \to 4\pi^0$. Possibly seen in the study of the hadronic structure in decay $\tau \to 3\pi\nu_\tau$ (ABREU 98G and ASNER 00). Needs confirmation.

$a_1(1640)$ MASS

VALUE (MeV)	EVTS	DOCUMENT ID		TECN	COMMENT
1654±19 OUR AVERAGE		Error includes scale factor of 1.3. See the ideogram below.			
1691±18±30		DARGENT	17	RVUE	$D^0 \to \pi^-\pi^+\pi^-\pi^+$
1630±20	35280	[1] BAKER	03	SPEC	$\overline{p}p \to \omega\pi^+\pi^-\pi^0$
1714± 9±36		CHUNG	02	B852	18.3 $\pi^-p \to \pi^+\pi^-\pi^-p$
1640±12±30		BAKER	99	SPEC	1.94 $\overline{p}p \to 4\pi^0$
• • • We do not use the following data for averages, fits, limits, etc. • • •					
1670±90		BELLINI	85	SPEC	40 $\pi^-A \to \pi^-\pi^+\pi^-A$

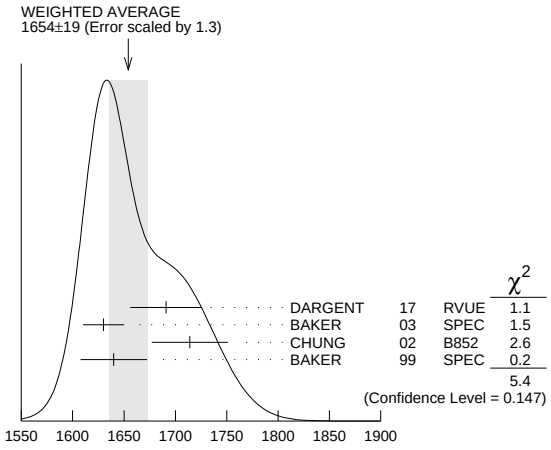

[1] Using the $a_1(1260)$ mass and width results of BOWLER 88.

$a_1(1640)$ WIDTH

VALUE (MeV)	EVTS	DOCUMENT ID		TECN	COMMENT
240± 27 OUR AVERAGE		Error includes scale factor of 1.2.			
171± 33±40		DARGENT	17	RVUE	$D^0 \to \pi^-\pi^+\pi^-\pi^+$
225± 30	35280	[2] BAKER	03	SPEC	$\overline{p}p \to \omega\pi^+\pi^-\pi^0$
308± 37±62		CHUNG	02	B852	18.3 $\pi^-p \to \pi^+\pi^-\pi^-p$
300± 22±40		BAKER	99	SPEC	1.94 $\overline{p}p \to 4\pi^0$
• • • We do not use the following data for averages, fits, limits, etc. • • •					
300±100		BELLINI	85	SPEC	40 $\pi^-A \to \pi^-\pi^+\pi^-A$

[2] Using the $a_1(1260)$ mass and width results of BOWLER 88.

$a_1(1640)$ DECAY MODES

	Mode	Fraction (Γ_i/Γ)
Γ_1	$\pi\pi\pi$	seen
Γ_2	$f_2(1270)\pi$	seen
Γ_3	$\sigma\pi$	seen
Γ_4	$\rho\pi$ $_{S-wave}$	seen
Γ_5	$\rho\pi$ $_{D-wave}$	seen
Γ_6	$\omega\pi\pi$	seen
Γ_7	$f_1(1285)\pi$	seen
Γ_8	$a_1(1260)\eta$	not seen

$a_1(1640)$ BRANCHING RATIOS

$\Gamma(f_2(1270)\pi)/\Gamma(\sigma\pi)$ Γ_2/Γ_3

VALUE	DOCUMENT ID		TECN	COMMENT
• • • We do not use the following data for averages, fits, limits, etc. • • •				
0.24±0.07	BAKER	99	SPEC	1.94 $\overline{p}p \to 4\pi^0$

$\Gamma(\rho\pi_{D-wave})/\Gamma_{total}$ Γ_5/Γ

VALUE	DOCUMENT ID		TECN	COMMENT
• • • We do not use the following data for averages, fits, limits, etc. • • •				
seen	CHUNG	02	B852	18.3 $\pi^-p \to \pi^+\pi^-\pi^-p$
seen	AMELIN	95B	VES	36 $\pi^-A \to \pi^+\pi^-\pi^-A$

$\Gamma(\omega\pi\pi)/\Gamma_{total}$ Γ_6/Γ

VALUE	EVTS	DOCUMENT ID		TECN	COMMENT
• • • We do not use the following data for averages, fits, limits, etc. • • •					
seen	35280	[3] BAKER	03	SPEC	$\overline{p}p \to \omega\pi^+\pi^-\pi^0$

$\Gamma(f_1(1285)\pi)/\Gamma_{total}$ Γ_7/Γ

VALUE	DOCUMENT ID		TECN	COMMENT
• • • We do not use the following data for averages, fits, limits, etc. • • •				
not seen	KUHN	04	B852	18 $\pi^-p \to \eta\pi^+\pi^-\pi^-p$
seen	LEE	94	MPS2	18 $\pi^-p \to K^+\overline{K}{}^0\pi^-\pi^-p$

$\Gamma(a_1(1260)\eta)/\Gamma_{total}$ Γ_8/Γ

VALUE	DOCUMENT ID	TECN	COMMENT
not seen	KUHN 04	B852	18 $\pi^-p \to \eta\pi^+\pi^-\pi^-p$

[3] Assuming the $\omega\rho$ mechanism for the $\omega\pi\pi$ state.

$a_1(1640)$ REFERENCES

DARGENT	17	JHEP 1705 143	P. dArgent *et al.*	(HEID, BRIS)
KUHN	04	PL B595 109	J. Kuhn *et al.*	(BNL E852 Collab.)
BAKER	03	PL B563 140	C.A. Baker *et al.*	
CHUNG	02	PR D65 072001	S.U. Chung *et al.*	(BNL E852 Collab.)
ASNER	00	PR D61 012002	D.M. Asner *et al.*	(CLEO Collab.)
BAKER	99	PL B449 114	C.A. Baker *et al.*	
ABREU	98G	PL B426 411	P. Abreu *et al.*	(DELPHI Collab.)
AMELIN	95B	PL B356 595	D.V. Amelin *et al.*	(SERP, TBIL)
LEE	94	PL B323 227	J.H. Lee *et al.*	(BNL, IND, KYUN, MASD+)
BOWLER	88	PL B209 99	M.G. Bowler	(OXF)
BELLINI	85	SJNP 41 781	D. Bellini *et al.*	
		Translated from YAF 41 1223.		

$f_2(1640)$

$I^G(J^{PC}) = 0^+(2^{++})$

OMITTED FROM SUMMARY TABLE

$f_2(1640)$ MASS

VALUE (MeV)	DOCUMENT ID		TECN	COMMENT
1639± 6 OUR AVERAGE	Error includes scale factor of 1.2.			
1620±16	BUGG	95	MRK3	$J/\psi \to \gamma\pi^+\pi^-\pi^+\pi^-$
1647± 7	ADAMO	92	OBLX	$\overline{n}p \to 3\pi^+2\pi^-$
1635± 7	ALDE	90	GAM2	38 $\pi^-p \to \omega\omega n$
• • • We do not use the following data for averages, fits, limits, etc. • • •				
1640± 5	AMSLER	06	CBAR	0.9 $\overline{p}p \to K^+K^-\pi^0$
1659± 6	VLADIMIRSK...06		SPEC	40 $\pi^-p \to K^0_S K^0_S n$
1643± 7	[1] ALDE	89B	GAM2	38 $\pi^-p \to \omega\omega n$

[1] Superseded by ALDE 90.

$f_2(1640)$ WIDTH

VALUE (MeV)	CL%	DOCUMENT ID		TECN	COMMENT
99^{+60}_{-40} OUR AVERAGE		Error includes scale factor of 2.9.			
140^{+60}_{-20}		BUGG	95	MRK3	$J/\psi \to \gamma\pi^+\pi^-\pi^+\pi^-$
58±20		ADAMO	92	OBLX	$\overline{n}p \to 3\pi^+2\pi^-$
• • • We do not use the following data for averages, fits, limits, etc. • • •					
44± 9		AMSLER	06	CBAR	0.9 $\overline{p}p \to K^+K^-\pi^0$
152±18		VLADIMIRSK...06		SPEC	40 $\pi^-p \to K^0_S K^0_S n$
< 70	90	ALDE	90	GAM2	38 $\pi^-p \to \omega\omega n$

$f_2(1640)$ DECAY MODES

	Mode	Fraction (Γ_i/Γ)
Γ_1	$\omega\omega$	seen
Γ_2	4π	seen
Γ_3	$K\overline{K}$	seen

$f_2(1640)$ BRANCHING RATIOS

$\Gamma(K\overline{K})/\Gamma_{total}$ Γ_3/Γ

VALUE	DOCUMENT ID		TECN	COMMENT
seen	AMSLER	06	CBAR	0.9 $\overline{p}p \to K^+K^-\pi^0$

$f_2(1640)$ REFERENCES

AMSLER	06	PL B639 165	C. Amsler *et al.*	(CBAR Collab.)
VLADIMIRSK...	06	PAN 69 493 Translated from YAF 69 515.	V.V. Vladimirsky *et al.*	(ITEP, Moscow)
BUGG	95	PL B353 378	D.V. Bugg *et al.*	(LOQM, PNPI, WASH) JP
ADAMO	92	PL B287 368	A. Adamo *et al.*	(OBELIX Collab.)
ALDE	90	PL B241 600	D.M. Alde *et al.*	(SERP, BELG, LANL, LAPP+)
ALDE	89B	PL B216 451	D.M. Alde *et al.*	(SERP, BELG, LANL, LAPP+) IGJPC

$\eta_2(1645)$

$I^G(J^{PC}) = 0^+(2^{-+})$

$\eta_2(1645)$ MASS

VALUE (MeV)	DOCUMENT ID		TECN	CHG	COMMENT
1617± 5 OUR AVERAGE					
1613± 8	BARBERIS	00B			450 $pp \to p_f \eta\pi^+\pi^- p_s$
1617± 8	BARBERIS	00C			450 $pp \to p_f 4\pi p_s$
1620±20	BARBERIS	97B	OMEG		450 $pp \to pp2(\pi^+\pi^-)$
1645±14±15	ADOMEIT	96	CBAR	0	1.94 $\overline{p}p \to \eta 3\pi^0$
• • • We do not use the following data for averages, fits, limits, etc. • • •					
1645± 6±20	ANISOVICH	00E	SPEC		0.9–1.94 $\overline{p}p \to \eta 3\pi^0$

$\eta_2(1645)$ WIDTH

VALUE (MeV)	DOCUMENT ID		TECN	CHG	COMMENT
181±11 OUR AVERAGE					
185±17	BARBERIS	00B			450 $pp \to p_f \eta\pi^+\pi^- p_s$
177±18	BARBERIS	00C			450 $pp \to p_f 4\pi p_s$
180±25	BARBERIS	97B	OMEG		450 $pp \to pp2(\pi^+\pi^-)$
180^{+40}_{-21}±25	ADOMEIT	96	CBAR	0	1.94 $\overline{p}p \to \eta 3\pi^0$
• • • We do not use the following data for averages, fits, limits, etc. • • •					
200±25	ANISOVICH	00E	SPEC		0.9–1.94 $\overline{p}p \to \eta 3\pi^0$

$\eta_2(1645)$ DECAY MODES

	Mode	Fraction (Γ_i/Γ)
Γ_1	$a_2(1320)\pi$	seen
Γ_2	$K\overline{K}\pi$	seen
Γ_3	$K^*\overline{K}$	seen
Γ_4	$\eta\pi^+\pi^-$	seen
Γ_5	$a_0(980)\pi$	seen
Γ_6	$f_2(1270)\eta$	not seen

$\eta_2(1645)$ BRANCHING RATIOS

$\Gamma(K\overline{K}\pi)/\Gamma(a_2(1320)\pi)$ Γ_2/Γ_1

VALUE	DOCUMENT ID		TECN	COMMENT
0.07±0.03	[1] BARBERIS	97C	OMEG	450 $pp \to pp K\overline{K}\pi$

[1] Using $2(\pi^+\pi^-)$ data from BARBERIS 97B.

$\Gamma(a_2(1320)\pi)/\Gamma(a_0(980)\pi)$ Γ_1/Γ_5

VALUE	DOCUMENT ID		TECN	COMMENT
13.1±2.3 OUR AVERAGE				
13.5±4.6	[2] ANISOVICH	11	SPEC	0.9–1.94 $p\overline{p}$
13.0±2.7	BARBERIS	00B		450 $pp \to p_f \eta\pi^+\pi^- p_s$

[2] Reanalysis of ADOMEIT 96 and ANISOVICH 00E.

$\Gamma(f_2(1270)\eta)/\Gamma_{total}$ Γ_6/Γ

VALUE	DOCUMENT ID		COMMENT
• • • We do not use the following data for averages, fits, limits, etc. • • •			
not seen	BARBERIS	00B	450 $pp \to p_f \eta\pi^+\pi^- p_s$

$\eta_2(1645)$ REFERENCES

ANISOVICH	11	EPJ C71 1511	A.V. Anisovich *et al.*	(LOQM, RAL, PNPI)
ANISOVICH	00E	PL B477 19	A.V. Anisovich *et al.*	
BARBERIS	00B	PL B471 435	D. Barberis *et al.*	(WA 102 Collab.)
BARBERIS	00C	PL B471 440	D. Barberis *et al.*	(WA 102 Collab.)
BARBERIS	97B	PL B413 217	D. Barberis *et al.*	(WA 102 Collab.)
BARBERIS	97C	PL B413 225	D. Barberis *et al.*	(WA 102 Collab.)
ADOMEIT	96	ZPHY C71 227	J. Adomeit *et al.*	(Crystal Barrel Collab.)

$\omega(1650)$

$I^G(J^{PC}) = 0^-(1^{--})$

$\omega(1650)$ MASS

VALUE (MeV)	EVTS	DOCUMENT ID		TECN	COMMENT
1670± 30 OUR ESTIMATE					
• • • We do not use the following data for averages, fits, limits, etc. • • •					
1671± 6±10	824	[1] AKHMETSHIN	17A	CMD3	1.4–2.0 $e^+e^- \to \omega\eta$
1660± 10	898	[2] ACHASOV	16B	SND	1.34–2.00 $e^+e^- \to \omega\eta$
1680± 10	13.1k	[3] AULCHENKO	15A	SND	1.05–1.80 $e^+e^- \to \pi^+\pi^-\pi^0$
1667± 13± 6		AUBERT	07AU	BABR	10.6 $e^+e^- \to \omega\pi^+\pi^-\gamma$
1645± 8	13	AUBERT	06D	BABR	10.6 $e^+e^- \to \omega\eta\gamma$
1660± 10± 2		AUBERT,B	04N	BABR	10.6 $e^+e^- \to \pi^+\pi^-\pi^0\gamma$
1770± 50±60	1.2M	[4] ACHASOV	03D	RVUE	0.44–2.00 $e^+e^- \to \pi^+\pi^-\pi^0$
1619± 5		[5] HENNER	02	RVUE	1.2–2.0 $e^+e^- \to \rho\pi$, $\omega\pi\pi$
1700± 20		EUGENIO	01	SPEC	18 $\pi^- p \to \omega\eta n$
1705± 26	612	[6] AKHMETSHIN	00D	CMD2	$e^+e^- \to \omega\pi^+\pi^-$
1820^{+190}_{-150}		[7] ACHASOV	98H	RVUE	$e^+e^- \to \pi^+\pi^-\pi^0$
$1840^{+100}_{-\ 70}$		[8] ACHASOV	98H	RVUE	$e^+e^- \to \omega\pi^+\pi^-$
1780^{+170}_{-300}		[9] ACHASOV	98H	RVUE	$e^+e^- \to K^+K^-$
~ 2100		[10] ACHASOV	98H	RVUE	$e^+e^- \to K^0_S K^\pm\pi^\mp$
1606± 9		[11] CLEGG	94	RVUE	
1662± 13	750	[12] ANTONELLI	92	DM2	1.34–2.4 $e^+e^- \to \rho\pi$, $\omega\pi\pi$
1670± 20		ATKINSON	83B	OMEG	20–70 $\gamma p \to 3\pi X$
1657± 13		CORDIER	81	DM1	$e^+e^- \to \omega 2\pi$
1679± 34	21	ESPOSITO	80	FRAM	$e^+e^- \to 3\pi$
1652± 17		COSME	79	OSPK	$e^+e^- \to 3\pi$

[1] From a fit of the interfering $\omega(1420)$ and $\omega(1650)$ with a relative phase of π and other parameters floating.
[2] From a fit with contributions from $\omega(1420)$, $\omega(1650)$, and $\phi(1680)$.
[3] From a fit with contributions from $\omega(782)$, $\phi(1020)$, $\omega(1420)$, and $\omega(1650)$.
[4] From the combined fit of ANTONELLI 92, ACHASOV 01E, ACHASOV 02E, and ACHASOV 03D data on the $\pi^+\pi^-\pi^0$ and ANTONELLI 92 on the $\omega\pi^+\pi^-$ final states. Supersedes ACHASOV 99E and ACHASOV 02E.
[5] Using results of CORDIER 81 and preliminary data of DOLINSKY 91 and ANTONELLI 92.
[6] Using the data of AKHMETSHIN 00D and ANTONELLI 92. The $\rho\pi$ dominance for the energy dependence of the $\omega(1420)$ and $\omega(1650)$ width assumed.
[7] Using data from BARKOV 87, DOLINSKY 91, and ANTONELLI 92.
[8] Using the data from ANTONELLI 92.
[9] Using the data from IVANOV 81 and BISELLO 88B.
[10] Using the data from BISELLO 91C.
[11] From a fit to two Breit-Wigner functions and using the data of DOLINSKY 91 and ANTONELLI 92.
[12] From the combined fit of the $\rho\pi$ and $\omega\pi\pi$ final states.

$\omega(1650)$ WIDTH

VALUE (MeV)	EVTS	DOCUMENT ID		TECN	COMMENT
315± 35 OUR ESTIMATE					
• • • We do not use the following data for averages, fits, limits, etc. • • •					
113± 9± 10	824	[1] AKHMETSHIN	17A	CMD3	1.4–2.0 $e^+e^- \to \omega\eta$
110± 20	898	[2] ACHASOV	16B	SND	1.34–2.00 $e^+e^- \to \omega\eta$
310± 30	13.1k	[3] AULCHENKO	15A	SND	1.05–1.80 $e^+e^- \to \pi^+\pi^-\pi^0$
222± 25± 20		AUBERT	07AU	BABR	10.6 $e^+e^- \to \omega\pi^+\pi^-\gamma$
114± 14	13	AUBERT	06D	BABR	10.6 $e^+e^- \to \omega\eta\gamma$
230± 30± 20		AUBERT,B	04N	BABR	10.6 $e^+e^- \to \pi^+\pi^-\pi^0\gamma$
490^{+200}_{-150}±130	1.2M	[4] ACHASOV	03D	RVUE	0.44–2.00 $e^+e^- \to \pi^+\pi^-\pi^0$
250± 14		[5] HENNER	02	RVUE	1.2–2.0 $e^+e^- \to \rho\pi, \omega\pi\pi$
250± 50		EUGENIO	01	SPEC	18 $\pi^- p \to \omega\eta n$
370± 25	612	[6] AKHMETSHIN	00D	CMD2	$e^+e^- \to \omega\pi^+\pi^-$
113± 20		[7] CLEGG	94	RVUE	
280± 24	750	[8] ANTONELLI	92	DM2	1.34–2.4 $e^+e^- \to \rho\pi, \omega\pi\pi$
160± 20		ATKINSON	83B	OMEG	20–70 $\gamma p \to 3\pi X$
136± 46		CORDIER	81	DM1	$e^+e^- \to \omega 2\pi$
99± 49	21	ESPOSITO	80	FRAM	$e^+e^- \to 3\pi$
42± 17		COSME	79	OSPK	$e^+e^- \to 3\pi$

[1] From a fit of the interfering $\omega(1420)$ and $\omega(1650)$ with a relative phase of π and other parameters floating.
[2] From a fit with contributions from $\omega(1420)$, $\omega(1650)$, and $\phi(1680)$.
[3] From a fit with contributions from $\omega(782)$, $\phi(1020)$, $\omega(1420)$, and $\omega(1650)$.
[4] From the combined fit of ANTONELLI 92, ACHASOV 01E, ACHASOV 02E, and ACHASOV 03D data on the $\pi^+\pi^-\pi^0$ and ANTONELLI 92 on the $\omega\pi^+\pi^-$ final states. Supersedes ACHASOV 99E and ACHASOV 02E.
[5] Using results of CORDIER 81 and preliminary data of DOLINSKY 91 and ANTONELLI 92.
[6] Using the data of AKHMETSHIN 00D and ANTONELLI 92. The $\rho\pi$ dominance for the energy dependence of the $\omega(1420)$ and $\omega(1650)$ width assumed.

[7] From a fit to two Breit-Wigner functions and using the data of DOLINSKY 91 and ANTONELLI 92.
[8] From the combined fit of the $\rho\pi$ and $\omega\pi\pi$ final states.

$\omega(1650)$ DECAY MODES

	Mode	Fraction (Γ_i/Γ)
Γ_1	$\rho\pi$	seen
Γ_2	$\omega\pi\pi$	seen
Γ_3	$\omega\eta$	seen
Γ_4	e^+e^-	seen

$\omega(1650)$ $\Gamma(i)\Gamma(e^+e^-)/\Gamma^2$(total)

$\Gamma(\rho\pi)/\Gamma_{total} \times \Gamma(e^+e^-)/\Gamma_{total}$ $\Gamma_1/\Gamma \times \Gamma_4/\Gamma$

VALUE (units 10^{-6})	EVTS	DOCUMENT ID		TECN	COMMENT
• • • We do not use the following data for averages, fits, limits, etc. • • •					
1.56 ±0.23	13.1k	[1] AULCHENKO	15A	SND	1.05–1.80 $e^+e^- \to \pi^+\pi^-\pi^0$
1.3 ±0.1 ±0.1		AUBERT,B	04N	BABR	10.6 $e^+e^- \to \pi^+\pi^-\pi^0\gamma$
1.2 $^{+0.4}_{-0.1}$ ±0.8	1.2M	[2,3] ACHASOV	03D	RVUE	0.44–2.00 $e^+e^- \to \pi^+\pi^-\pi^0$
0.921±0.230		[4,5] CLEGG	94	RVUE	
0.479±0.050	750	[6,7] ANTONELLI	92	DM2	1.34–2.4 $e^+e^- \to \rho\pi, \omega\pi\pi$

$\Gamma(\omega\pi\pi)/\Gamma_{total} \times \Gamma(e^+e^-)/\Gamma_{total}$ $\Gamma_2/\Gamma \times \Gamma_4/\Gamma$

VALUE (units 10^{-7})	EVTS	DOCUMENT ID		TECN	COMMENT
• • • We do not use the following data for averages, fits, limits, etc. • • •					
7.0 ±0.5		AUBERT	07AU	BABR	10.6 $e^+e^- \to \omega\pi^+\pi^-\gamma$
4.1 ±0.9 ±1.3	1.2M	[2,3] ACHASOV	03D	RVUE	0.44–2.00 $e^+e^- \to \pi^+\pi^-\pi^0$
5.40±0.95		[8] AKHMETSHIN	00D	CMD2	1.2–1.38 $e^+e^- \to \omega\pi^+\pi^-$
3.18±0.80		[4,5] CLEGG	94	RVUE	
6.07±0.61	750	[6,7] ANTONELLI	92	DM2	1.34–2.4 $e^+e^- \to \rho\pi, \omega\pi\pi$

$\Gamma(\omega\eta)/\Gamma_{total} \times \Gamma(e^+e^-)/\Gamma_{total}$ $\Gamma_3/\Gamma \times \Gamma_4/\Gamma$

VALUE (units 10^{-7})	CL%	EVTS	DOCUMENT ID		TECN	COMMENT
• • • We do not use the following data for averages, fits, limits, etc. • • •						
4.5±0.3±0.3		824	[9] AKHMETSHIN	17A	CMD3	1.4–2.0 $e^+e^- \to \omega\eta$
4.4±0.5		898	[10] ACHASOV	16B	SND	1.34–2.00 $e^+e^- \to \omega\eta$
5.7±0.6		13	AUBERT	06D	BABR	10.6 $e^+e^- \to \omega\eta\gamma$
<60	90		[11] AKHMETSHIN	03B	CMD2	$e^+e \to \eta\pi^0\gamma$

[1] From a fit with contributions from $\omega(782)$, $\phi(1020)$, $\omega(1420)$, and $\omega(1650)$.
[2] Calculated by us from the cross section at the peak.
[3] From the combined fit of ANTONELLI 92, ACHASOV 01E, ACHASOV 02E, and ACHASOV 03D data on the $\pi^+\pi^-\pi^0$ and ANTONELLI 92 on the $\omega\pi^+\pi^-$ final states. Supersedes ACHASOV 99E and ACHASOV 02E.
[4] From a fit to two Breit-Wigner functions and using the data of DOLINSKY 91 and ANTONELLI 92.
[5] From the partial and leptonic width given by the authors.
[6] From the combined fit of the $\rho\pi$ and $\omega\pi\pi$ final states.
[7] From the product of the leptonic width and partial branching ratio given by the authors.
[8] Using the data of AKHMETSHIN 00D and ANTONELLI 92. The $\rho\pi$ dominance for the energy dependence of the $\omega(1420)$ and $\omega(1650)$ width assumed.
[9] From a fit of the interfering $\omega(1420)$ and $\omega(1650)$ with a relative phase of π and other parameters floating. From an alternative fit $\Gamma(\omega(1650) \to \omega\eta)/\Gamma_{total} \times \Gamma(\omega(1650) \to e^+e^-) = 51 \pm 3$ eV.
[10] From a fit with contributions from $\omega(1420)$, $\omega(1650)$, and $\phi(1680)$.
[11] $\omega(1650)$ mass and width fixed at 1700 MeV and 250 MeV, respectively.

$\omega(1650)$ BRANCHING RATIOS

$\Gamma(\omega\pi\pi)/\Gamma_{total}$ Γ_2/Γ

VALUE	EVTS	DOCUMENT ID		TECN	COMMENT
• • • We do not use the following data for averages, fits, limits, etc. • • •					
~ 0.35	1.2M	[1] ACHASOV	03D	RVUE	0.44–2.00 $e^+e^- \to \pi^+\pi^-\pi^0$
0.620±0.014		[2] HENNER	02	RVUE	1.2–2.0 $e^+e^- \to \rho\pi, \omega\pi\pi$

$\Gamma(\rho\pi)/\Gamma_{total}$ Γ_1/Γ

VALUE	EVTS	DOCUMENT ID		TECN	COMMENT
• • • We do not use the following data for averages, fits, limits, etc. • • •					
~ 0.65	1.2M	[1] ACHASOV	03D	RVUE	0.44–2.00 $e^+e^- \to \pi^+\pi^-\pi^0$
0.380±0.014		[2] HENNER	02	RVUE	1.2–2.0 $e^+e^- \to \rho\pi, \omega\pi\pi$

$\Gamma(e^+e^-)/\Gamma_{total}$ Γ_4/Γ

VALUE (units 10^{-7})	EVTS	DOCUMENT ID		TECN	COMMENT
• • • We do not use the following data for averages, fits, limits, etc. • • •					
~ 18	1.2M	[2,3] ACHASOV	03D	RVUE	0.44–2.00 $e^+e^- \to \pi^+\pi^-\pi^0$
32±1		[2] HENNER	02	RVUE	1.2–2.0 $e^+e^- \to \rho\pi, \omega\pi\pi$

[1] From the combined fit of ANTONELLI 92, ACHASOV 01E, ACHASOV 02E, and ACHASOV 03D data on the $\pi^+\pi^-\pi^0$ and ANTONELLI 92 on the $\omega\pi^+\pi^-$ final states. Supersedes ACHASOV 99E and ACHASOV 02E.
[2] Assuming that the $\omega(1650)$ decays into $\rho\pi$ and $\omega\pi\pi$ only.
[3] Calculated by us from the cross section at the peak.

$\omega(1650)$ REFERENCES

AKHMETSHIN	17A	PL B773 150	R.R. Akhmetshin *et al.*	(CMD-3 Collab.)
ACHASOV	16B	PR D94 092002	M.N. Achasov *et al.*	(SND Collab.)
AULCHENKO	15A	JETP 121 27	V.M. Aulchenko *et al.*	(SND Collab.)
		Translated from ZETF 148 34.		
AUBERT	07AU	PR D76 092005	B. Aubert *et al.*	(BABAR Collab.)
AUBERT	06D	PR D73 052003	B. Aubert *et al.*	(BABAR Collab.)
AUBERT,B	04N	PR D70 072004	B. Aubert *et al.*	(BABAR Collab.)
ACHASOV	03D	PR D68 052006	M.N. Achasov *et al.*	(Novosibirsk SND Collab.)
AKHMETSHIN	03B	PL B562 173	R.R. Akhmetshin *et al.*	(Novosibirsk CMD-2 Collab.)
ACHASOV	02E	PR D66 032001	M.N. Achasov *et al.*	(Novosibirsk SND Collab.)
HENNER	02	EPJ C26 3	V.K. Henner *et al.*	
ACHASOV	01E	PR D63 072002	M.N. Achasov *et al.*	(Novosibirsk SND Collab.)
EUGENIO	01	PL B497 190	P. Eugenio *et al.*	
AKHMETSHIN	00D	PL B489 125	R.R. Akhmetshin *et al.*	(Novosibirsk CMD-2 Collab.)
ACHASOV	99E	PL B462 365	M.N. Achasov *et al.*	(Novosibirsk SND Collab.)
ACHASOV	98H	PR D57 4334	N.N. Achasov, A.A. Kozhevnikov	
CLEGG	94	ZPHY C62 455	A.B. Clegg, A. Donnachie	(LANC, MCHS)
ANTONELLI	92	ZPHY C56 15	A. Antonelli *et al.*	(DM2 Collab.)
BISELLO	91C	ZPHY C52 227	D. Bisello *et al.*	(DM2 Collab.)
DOLINSKY	91	PRPL 202 99	S.I. Dolinsky *et al.*	(NOVO)
BISELLO	88B	ZPHY C39 13	D. Bisello *et al.*	(PADO, CLER, FRAS+)
BARKOV	87	JETPL 46 164	L.M. Barkov *et al.*	(NOVO)
		Translated from ZETFP 46 132.		
ATKINSON	83B	PL 127B 132	M. Atkinson *et al.*	(BONN, CERN, GLAS+)
CORDIER	81	PL 106B 155	A. Cordier *et al.*	(ORSAY)
IVANOV	81	PL 107B 297	P.M. Ivanov *et al.*	(NOVO)
ESPOSITO	80	LNC 28 195	B. Esposito *et al.*	(FRAS, NAPL, PADO+)
COSME	79	NP B152 215	G. Cosme *et al.*	(IPN)

$\omega_3(1670)$

$I^G(J^{PC}) = 0^-(3^{--})$

$\omega_3(1670)$ MASS

VALUE (MeV)	EVTS	DOCUMENT ID		TECN	COMMENT
1667 ± 4 OUR AVERAGE					
1665.3± 5.2±4.5	23400	AMELIN	96	VES	36 $\pi^-p \to \pi^+\pi^-\pi^0 n$
1685 ±20	60	BAUBILLIER	79	HBC	8.2 K^-p backward
1673 ±12	430	[1,2] BALTAY	78E	HBC	15 $\pi^+p \to \Delta 3\pi$
1650 ±12		CORDEN	78B	OMEG	8–12 $\pi^-p \to N3\pi$
1669 ±11	600	[2] WAGNER	75	HBC	7 $\pi^+p \to \Delta^{++}3\pi$
1678 ±14	500	DIAZ	74	DBC	6 $\pi^+n \to p3\pi^0$
1660 ±13	200	DIAZ	74	DBC	6 $\pi^+n \to p\omega\pi^0\pi^0$
1679 ±17	200	MATTHEWS	71D	DBC	7.0 $\pi^+n \to p3\pi^0$
1670 ±20		KENYON	69	DBC	8 $\pi^+n \to p3\pi^0$
• • • We do not use the following data for averages, fits, limits, etc. • • •					
~ 1700	110	[1] CERRADA	77B	HBC	4.2 $K^-p \to \Lambda 3\pi$
1695 ±20		BARNES	69B	HBC	4.6 $K^-p \to \omega 2\pi X$
1636 ±20		ARMENISE	68B	DBC	5.1 $\pi^+n \to p3\pi^0$

[1] Phase rotation seen for $J^P = 3^-$ $\rho\pi$ wave.
[2] From a fit to $I(J^P) = 0(3^-)$ $\rho\pi$ partial wave.

$\omega_3(1670)$ WIDTH

VALUE (MeV)	EVTS	DOCUMENT ID		TECN	COMMENT
168±10 OUR AVERAGE					
149±19±7	23400	AMELIN	96	VES	36 $\pi^-p \to \pi^+\pi^-\pi^0 n$
160±80	60	[3] BAUBILLIER	79	HBC	8.2 K^-p backward
173±16	430	[4,5] BALTAY	78E	HBC	15 $\pi^+p \to \Delta 3\pi$
253±39		CORDEN	78B	OMEG	8–12 $\pi^-p \to N3\pi$
173±28	600	[3,5] WAGNER	75	HBC	7 $\pi^+p \to \Delta^{++}3\pi$
167±40	500	DIAZ	74	DBC	6 $\pi^+n \to p3\pi^0$
122±39	200	DIAZ	74	DBC	6 $\pi^+n \to p\omega\pi^0\pi^0$
155±40	200	[3] MATTHEWS	71D	DBC	7.0 $\pi^+n \to p3\pi^0$
• • • We do not use the following data for averages, fits, limits, etc. • • •					
90±20		BARNES	69B	HBC	4.6 $K^-p \to \omega 2\pi$
100±40		KENYON	69	DBC	8 $\pi^+n \to p3\pi^0$
112±60		ARMENISE	68B	DBC	5.1 $\pi^+n \to p3\pi^0$

[3] Width errors enlarged by us to $4\Gamma/\sqrt{N}$; see the note with the $K^*(892)$ mass.
[4] Phase rotation seen for $J^P = 3^-$ $\rho\pi$ wave.
[5] From a fit to $I(J^P) = 0(3^-)$ $\rho\pi$ partial wave.

$\omega_3(1670)$ DECAY MODES

	Mode	Fraction (Γ_i/Γ)
Γ_1	$\rho\pi$	seen
Γ_2	$\omega\pi\pi$	seen
Γ_3	$b_1(1235)\pi$	possibly seen

$\omega_3(1670)$ BRANCHING RATIOS

$\Gamma(\omega\pi\pi)/\Gamma(\rho\pi)$ Γ_2/Γ_1

VALUE	EVTS	DOCUMENT ID		TECN	COMMENT
• • • We do not use the following data for averages, fits, limits, etc. • • •					
0.71 ± 0.27	100	DIAZ	74	DBC	$6\ \pi^+ n \rightarrow\ p5\pi^0$

$\Gamma(b_1(1235)\pi)/\Gamma(\rho\pi)$ Γ_3/Γ_1

VALUE	DOCUMENT ID		TECN	COMMENT
possibly seen	DIAZ	74	DBC	$6\ \pi^+ n \rightarrow\ p5\pi^0$

$\Gamma(b_1(1235)\pi)/\Gamma(\omega\pi\pi)$ Γ_3/Γ_2

VALUE	CL%	DOCUMENT ID		TECN	COMMENT
• • • We do not use the following data for averages, fits, limits, etc. • • •					
>0.75	68	BAUBILLIER	79	HBC	$8.2\ K^- p$ backward

$\omega_3(1670)$ REFERENCES

AMELIN	96	ZPHY C70 71	D.V. Amelin *et al.*	(SERP, TBIL)
BAUBILLIER	79	PL 89B 131	M. Baubillier *et al.*	(BIRM, CERN, GLAS+)
BALTAY	78E	PRL 40 87	C. Baltay, C.V. Cautis, M. Kalelkar	(COLU) JP
CORDEN	78B	NP B138 235	M.J. Corden *et al.*	(BIRM, RHEL, TELA+)
CERRADA	77B	NP B126 241	M. Cerrada *et al.*	(AMST, CERN, NIJM+) JP
WAGNER	75	PL 58B 201	F. Wagner, M. Tabak, D.M. Chew	(LBL) JP
DIAZ	74	PRL 32 260	J. Diaz *et al.*	(CASE, CMU)
MATTHEWS	71D	PR D3 2561	J.A.J. Matthews *et al.*	(TNTO, WISC)
BARNES	69B	PRL 23 142	V.E. Barnes *et al.*	(BNL)
KENYON	69	PRL 23 146	I.R. Kenyon *et al.*	(BNL, UCND, ORNL)
ARMENISE	68B	PL 26B 336	N. Armenise *et al.*	(BARI, BGNA, FIRZ+)

$\pi_2(1670)$

$I^G(J^{PC}) = 1^-(2^{-+})$

$\pi_2(1670)$ MASS

VALUE (MeV)	EVTS	DOCUMENT ID		TECN	CHG	COMMENT
1672.2± 3.0 OUR AVERAGE		Error includes scale factor of 1.4. See the ideogram below.				
1658 ± 3 $^{+\ 24}_{-\ 8}$	420k	ALEKSEEV	10	COMP		$190\ \pi^- Pb \rightarrow \pi^-\pi^-\pi^+ Pb'$
1749 ±10 ±100	145k	LU	05	B852		$18\ \pi^- p \rightarrow \omega\pi^-\pi^0 p$
1676 ± 3 ± 8		[1] CHUNG	02	B852		$18.3\ \pi^- p \rightarrow \pi^+\pi^-\pi^- p$
1685 ±10 ± 30		[2] BARBERIS	01			$450\ pp \rightarrow p_f 3\pi^0 p_s$
1687 ± 9 ± 15		AMELIN	99	VES		$37\ \pi^- A \rightarrow \omega\pi^-\pi^0 A^*$
1669 ± 4		BARBERIS	98B			$450\ pp \rightarrow p_f \rho\pi p_s$
1670 ± 4		BARBERIS	98B			$450\ pp \rightarrow p_f f_2(1270)\pi p_s$
1730 ±20		[3] AMELIN	95B	VES		$36\ \pi^- A \rightarrow \pi^+\pi^-\pi^- A$
1690 ±14		[4] BERDNIKOV	94	VES		$37\ \pi^- A \rightarrow K^+K^-\pi^- A$
1710 ±20	700	ANTIPOV	87	SIGM	–	$50\ \pi^-$ Cu $\rightarrow \mu^+\mu^-\pi^-$ Cu
1676 ± 6		[4] EVANGELIS...	81	OMEG	–	$12\ \pi^- p \rightarrow 3\pi p$
1657 ±14		[4,5] DAUM	80D	SPEC	–	63–$94\ \pi p \rightarrow 3\pi$X
1662 ±10	2000	[4] BALTAY	77	HBC	+	$15\ \pi^+ p \rightarrow p3\pi$
• • • We do not use the following data for averages, fits, limits, etc. • • •						
1742 ±31 ± 49		ANTREASYAN	90	CBAL		$e^+e^- \rightarrow e^+e^-\pi^0\pi^0\pi^0$
1624 ±21		[1] BELLINI	85	SPEC		$40\ \pi^- A \rightarrow \pi^-\pi^+\pi^- A$
1622 ±35		[6] BELLINI	85	SPEC		$40\ \pi^- A \rightarrow \pi^-\pi^+\pi^- A$
1693 ±28		[7] BELLINI	85	SPEC		$40\ \pi^- A \rightarrow \pi^-\pi^+\pi^- A$
1710 ±20		[8] DAUM	81B	SPEC	–	$63{,}94\ \pi^- p$
1660 ±10		[4] ASCOLI	73	HBC	–	5–$25\ \pi^- p \rightarrow p\pi_2$

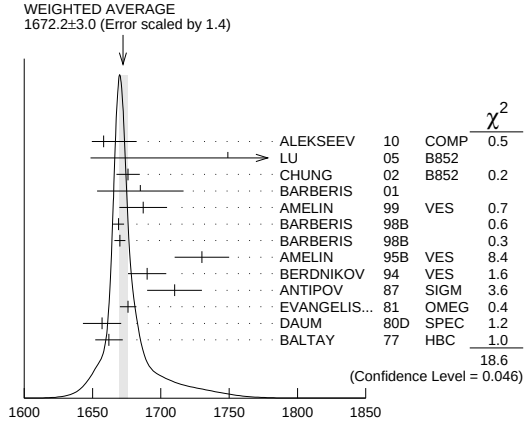

[1] From $f_2(1270)\pi$ decay.
[2] From a fit to the invariant mass distribution.
[3] From a fit to $J^{PC} = 2^{-+}$ $f_2(1270)\pi$, $f_0(1370)\pi$ waves.
[4] From a fit to $J^P = 2^-$ S-wave $f_2(1270)\pi$ partial wave.
[5] Clear phase rotation seen in 2^-S, 2^-P, 2^-D waves. We quote central value and spread of single-resonance fits to three channels.
[6] From $\rho\pi$ decay.
[7] From $\sigma\pi$ decay.
[8] From a two-resonance fit to four 2^-0^+ waves. This should not be averaged with all the single resonance fits.

$\pi_2(1670)$ WIDTH

VALUE (MeV)	EVTS	DOCUMENT ID		TECN	CHG	COMMENT
260± 9 OUR AVERAGE		Error includes scale factor of 1.2.				
271± $^{+\ 22}_{-\ 24}$	420k	ALEKSEEV	10	COMP		$190\ \pi^- Pb \rightarrow \pi^-\pi^-\pi^+ Pb'$
408± 60±250	145k	LU	05	B852		$18\ \pi^- p \rightarrow \omega\pi^-\pi^0 p$
254± 3± 31		[9] CHUNG	02	B852		$18.3\ \pi^- p \rightarrow \pi^+\pi^-\pi^- p$
265± 30± 40		[10] BARBERIS	01			$450\ pp \rightarrow p_f 3\pi^0 p_s$
168± 43± 53		AMELIN	99	VES		$37\ \pi^- A \rightarrow \omega\pi^-\pi^0 A^*$
268± 15		BARBERIS	98B			$450\ pp \rightarrow p_f \rho\pi p_s$
256± 15		BARBERIS	98B			$450\ pp \rightarrow p_f f_2(1270)\pi p_s$
310± 20		[11] AMELIN	95B	VES		$36\ \pi^- A \rightarrow \pi^+\pi^-\pi^- A$
190± 50		[12] BERDNIKOV	94	VES		$37\ \pi^- A \rightarrow K^+K^-\pi^- A$
170± 80	700	ANTIPOV	87	SIGM	–	$50\ \pi^-$ Cu $\rightarrow \mu^+\mu^-\pi^-$ Cu
260± 20		[12] EVANGELIS...	81	OMEG	–	$12\ \pi^- p \rightarrow 3\pi p$
219± 20		[12,13] DAUM	80D	SPEC	–	63–$94\ \pi p \rightarrow 3\pi$X
285± 60	2000	[12] BALTAY	77	HBC	+	$15\ \pi^+ p \rightarrow p3\pi$
• • • We do not use the following data for averages, fits, limits, etc. • • •						
236± 49± 36		ANTREASYAN	90	CBAL		$e^+e^- \rightarrow e^+e^-\pi^0\pi^0\pi^0$
304± 22		[9] BELLINI	85	SPEC		$40\ \pi^- A \rightarrow \pi^-\pi^+\pi^- A$
404±108		[14] BELLINI	85	SPEC		$40\ \pi^- A \rightarrow \pi^-\pi^+\pi^- A$
330± 90		[15] BELLINI	85	SPEC		$40\ \pi^- A \rightarrow \pi^-\pi^+\pi^- A$
312± 50		[16] DAUM	81B	SPEC	–	$63{,}94\ \pi^- p$
270± 60		[12] ASCOLI	73	HBC	–	5–$25\ \pi^- p \rightarrow p\pi_2$

[9] From $f_2(1270)\pi$ decay.
[10] From a fit to the invariant mass distribution.
[11] From a fit to $J^{PC} = 2^{-+}$ $f_2(1270)\pi$, $f_0(1370)\pi$ waves.
[12] From a fit to $J^P = 2^-$ $f_2(1270)\pi$ partial wave.
[13] Clear phase rotation seen in 2^-S, 2^-P, 2^-D waves. We quote central value and spread of single-resonance fits to three channels.
[14] From $\rho\pi$ decay.
[15] From $\sigma\pi$ decay.
[16] From a two-resonance fit to four 2^-0^+ waves. This should not be averaged with all the single resonance fits.

$\pi_2(1670)$ DECAY MODES

	Mode	Fraction (Γ_i/Γ)	Confidence level
Γ_1	3π	(95.8±1.4) %	
Γ_2	$\pi^+\pi^-\pi^0$		
Γ_3	$\pi^0\pi^0\pi^0$		
Γ_4	$f_2(1270)\pi$	(56.3±3.2) %	
Γ_5	$\rho\pi$	(31 ±4) %	
Γ_6	$\sigma\pi$	(10.9±3.4) %	
Γ_7	$\pi(\pi\pi)_S$-wave	(8.7±3.4) %	
Γ_8	$K\overline{K}^*(892)+$ c.c.	(4.2±1.4) %	
Γ_9	$\omega\rho$	(2.7±1.1) %	
Γ_{10}	$\pi^\pm\gamma$	(7.0±1.1) $\times 10^{-4}$	
Γ_{11}	$\gamma\gamma$	$<$ 2.8 $\times 10^{-7}$	90%
Γ_{12}	$\eta\pi$		
Γ_{13}	$\pi^\pm 2\pi^+ 2\pi^-$		
Γ_{14}	$\rho(1450)\pi$	$<$ 3.6 $\times 10^{-3}$	97.7%
Γ_{15}	$b_1(1235)\pi$	$<$ 1.9 $\times 10^{-3}$	97.7%
Γ_{16}	$\eta 3\pi$		
Γ_{17}	$f_1(1285)\pi$	possibly seen	
Γ_{18}	$a_2(1320)\pi$	not seen	

CONSTRAINED FIT INFORMATION

An overall fit to 4 branching ratios uses 6 measurements and one constraint to determine 4 parameters. The overall fit has a $\chi^2 =$ 1.9 for 3 degrees of freedom.

Meson Particle Listings

$\pi_2(1670)$

The following *off-diagonal* array elements are the correlation coefficients $\langle \delta x_i \delta x_j \rangle / (\delta x_i \cdot \delta x_j)$, in percent, from the fit to the branching fractions, $x_i \equiv \Gamma_i/\Gamma_{\text{total}}$. The fit constrains the x_i whose labels appear in this array to sum to one.

x_5	−53		
x_7	−29	−59	
x_8	−8	−21	−9
	x_4	x_5	x_7

$\pi_2(1670)$ PARTIAL WIDTHS

$\Gamma(\pi^\pm\gamma)$ Γ_{10}

VALUE (keV)	DOCUMENT ID		TECN	CHG	COMMENT
181±11±27	[17] ADOLPH	14	COMP	−	190 π^- Pb → $\pi^+\pi^-\pi^-$ Pb′

[17] Primakoff reaction. Assumes incoherent $f_2(1270)\pi$ contribution to 3π final state and uses B($\pi_2(1670)$ → $f_2\pi$) = 56%.

$\Gamma(\gamma\gamma)$ Γ_{11}

VALUE (keV)	CL%	DOCUMENT ID		TECN	CHG	COMMENT
<0.072	90	[18] ACCIARRI	97T	L3		e^+e^- → $e^+e^-\pi^+\pi^-\pi^0$
• • • We do not use the following data for averages, fits, limits, etc. • • •						
<0.19	90	[18] ALBRECHT	97B	ARG		e^+e^- → $e^+e^-\pi^+\pi^-\pi^0$
1.41 ±0.23±0.28		ANTREASYAN	90	CBAL	0	e^+e^- → $e^+e^-\pi^0\pi^0\pi^0$
0.8 ±0.3 ±0.12		[19] BEHREND	90C	CELL	0	e^+e^- → $e^+e^-\pi^+\pi^-\pi^0$
1.3 ±0.3 ±0.2		[20] BEHREND	90C	CELL	0	e^+e^- → $e^+e^-\pi^+\pi^-\pi^0$

[18] Decaying into $f_2(1270)\pi$ and $\rho\pi$.
[19] Constructive interference between $f_2(1270)\pi$,$\rho\pi$ and background.
[20] Incoherent Ansatz.

$\pi_2(1670)$ Γ(i)$\Gamma(\gamma\gamma)/\Gamma$(total)

$\Gamma(\pi^+\pi^-\pi^0) \times \Gamma(\gamma\gamma)/\Gamma_{\text{total}}$ $\Gamma_2\Gamma_{11}/\Gamma$

VALUE (keV)	CL%	DOCUMENT ID		TECN	COMMENT
<0.1	95	[21] SCHEGELSKY	06	RVUE	$\gamma\gamma$ → $\pi^+\pi^-\pi^0$

[21] From analysis of L3 data at 183–209 GeV.

$\pi_2(1670)$ BRANCHING RATIOS

$\Gamma(3\pi)/\Gamma_{\text{total}}$ $\Gamma_1/\Gamma = (\Gamma_4+\Gamma_5+\Gamma_7)/\Gamma$

VALUE	DOCUMENT ID
0.958±0.014 OUR FIT	

$\Gamma(\pi^0\pi^0\pi^0)/\Gamma(\pi^+\pi^-\pi^0)$ Γ_3/Γ_2

VALUE	DOCUMENT ID		COMMENT
0.29±0.03±0.05	[22] BARBERIS	01	450 pp → $p_f 3\pi^0 p_s$

$\Gamma(\rho\pi)/0.565\Gamma(f_2(1270)\pi)$ $\Gamma_5/0.565\Gamma_4$
(With $f_2(1270)$ → $\pi^+\pi^-$.)

VALUE	DOCUMENT ID		TECN	COMMENT
0.97±0.09 OUR AVERAGE	Error includes scale factor of 1.9.			
0.76±0.07±0.10	CHUNG	02	B852	18.3 π^-p → $\pi^+\pi^-\pi^-p$
1.01±0.05	BARBERIS	98B		450 pp → $p_f\pi^+\pi^-\pi^0 p_s$

$\Gamma(\sigma\pi)/\Gamma(f_2(1270)\pi)$ Γ_6/Γ_4

VALUE	DOCUMENT ID		TECN	COMMENT
0.19±0.06 OUR AVERAGE				
0.17±0.02±0.07	CHUNG	02	B852	18.3 π^-p → $\pi^+\pi^-\pi^-p$
0.24±0.10	[23,24] BAKER	99	SPEC	1.94 $\bar{p}p$ → $4\pi^0$

$\frac{1}{2}\Gamma(\rho\pi)/\Gamma(\pi^\pm\pi^+\pi^-)$ $\frac{1}{2}\Gamma_5/(0.565\Gamma_4+\frac{1}{2}\Gamma_5+0.624\Gamma_7)$

VALUE	DOCUMENT ID		TECN	CHG	COMMENT
0.29±0.04 OUR FIT					
0.29±0.05	[25] DAUM	81B	SPEC		63,94 π^-p
• • • We do not use the following data for averages, fits, limits, etc. • • •					
<0.3	BARTSCH	68	HBC	+	8 π^+p → $3\pi p$

$0.565\Gamma(f_2(1270)\pi)/\Gamma(\pi^\pm\pi^+\pi^-)$ $0.565\Gamma_4/(0.565\Gamma_4+\frac{1}{2}\Gamma_5+0.624\Gamma_7)$
(With $f_2(1270)$ → $\pi^+\pi^-$.)

VALUE	DOCUMENT ID		TECN	CHG	COMMENT
0.604±0.035 OUR FIT					
0.60 ±0.05 OUR AVERAGE	Error includes scale factor of 1.3.				
0.61 ±0.04	[25] DAUM	81B	SPEC		63,94 π^-p
0.76 $^{+0.24}_{-0.34}$	ARMENISE	69	DBC	+	5.1 π^+d → $d3\pi$
0.35 ±0.20	BALTAY	68	HBC	+	7–8.5 π^+p
• • • We do not use the following data for averages, fits, limits, etc. • • •					
0.59	BARTSCH	68	HBC	+	8 π^+p → $3\pi p$

$0.624\Gamma(\pi(\pi\pi)_{S\text{-wave}})/\Gamma(\pi^\pm\pi^+\pi^-)$ $0.624\Gamma_7/(0.565\Gamma_4+\frac{1}{2}\Gamma_5+0.624\Gamma_7)$
(With $(\pi\pi)_{S\text{-wave}}$ → $\pi^+\pi^-$.)

VALUE	DOCUMENT ID		TECN	COMMENT
0.10±0.04 OUR FIT				
0.10±0.05	[25] DAUM	81B	SPEC	63,94 π^-p

$\Gamma(K\overline{K}^*(892)+\text{c.c.})/\Gamma(f_2(1270)\pi)$ Γ_8/Γ_4

VALUE	DOCUMENT ID		TECN	CHG	COMMENT
0.075±0.025 OUR FIT					
0.075±0.025	[26] ARMSTRONG	82B	OMEG	−	16 π^-p → $K^+K^-\pi^-p$

$\Gamma(\omega\rho)/\Gamma_{\text{total}}$ Γ_9/Γ

VALUE	DOCUMENT ID		TECN	COMMENT
0.027±0.004±0.010	[27] AMELIN	99	VES	37 π^-A → $\omega\pi^-\pi^0 A^*$

$\Gamma(\eta\pi)/\Gamma(\pi^\pm\pi^+\pi^-)$ $\Gamma_{12}/(0.565\Gamma_4+\frac{1}{2}\Gamma_5+0.624\Gamma_7)$
(All η decays.)

VALUE	DOCUMENT ID		TECN	CHG	COMMENT
<0.09	BALTAY	68	HBC	+	7–8.5 π^+p
• • • We do not use the following data for averages, fits, limits, etc. • • •					
<0.10	CRENNELL	70	HBC	−	6 π^-p → $f_2\pi^-N$

$\Gamma(\pi^\pm 2\pi^+ 2\pi^-)/\Gamma(\pi^\pm\pi^+\pi^-)$ $\Gamma_{13}/(0.565\Gamma_4+\frac{1}{2}\Gamma_5+0.624\Gamma_7)$

VALUE	DOCUMENT ID		TECN	CHG	COMMENT
<0.10	CRENNELL	70	HBC	−	6 π^-p → $f_2\pi^-N$
<0.1	BALTAY	68	HBC	+	7,8.5 π^+p

$\Gamma(\rho(1450)\pi)/\Gamma_{\text{total}}$ Γ_{14}/Γ

VALUE	CL%	DOCUMENT ID		TECN	COMMENT
<0.0036	97.7	AMELIN	99	VES	37 π^-A → $\omega\pi^-\pi^0 A^*$

$\Gamma(b_1(1235)\pi)/\Gamma_{\text{total}}$ Γ_{15}/Γ

VALUE	CL%	DOCUMENT ID		TECN	COMMENT
<0.0019	97.7	AMELIN	99	VES	37 π^-A → $\omega\pi^-\pi^0 A^*$

$\Gamma(f_1(1285)\pi)/\Gamma_{\text{total}}$ Γ_{17}/Γ

VALUE	EVTS	DOCUMENT ID		TECN	COMMENT
possibly seen	69k	KUHN	04	B852	18 π^-p → $\eta\pi^+\pi^-\pi^-p$

$\Gamma(a_2(1320)\pi)/\Gamma_{\text{total}}$ Γ_{18}/Γ

VALUE	EVTS	DOCUMENT ID		TECN	COMMENT
not seen	69k	KUHN	04	B852	18 π^-p → $\eta\pi^+\pi^-\pi^-p$

***D*-wave/*S*-wave RATIO FOR $\pi_2(1670)$ → $f_2(1270)\pi$**

VALUE	DOCUMENT ID		TECN	COMMENT
−0.18±0.06	[23] BAKER	99	SPEC	1.94 $\bar{p}p$ → $4\pi^0$
• • • We do not use the following data for averages, fits, limits, etc. • • •				
0.22±0.10	[25] DAUM	81B	SPEC	63,94 π^-p

***F*-wave/*P*-wave RATIO FOR $\pi_2(1670)$ → $\rho\pi$**

VALUE	DOCUMENT ID		TECN	COMMENT
−0.72±0.07±0.14	CHUNG	02	B852	18.3 π^-p → $\pi^+\pi^-\pi^-p$

[22] Using BARBERIS 98B.
[23] Using preliminary CBAR data.
[24] With the $\sigma\pi$ in L=2 and the $f_2(1270)\pi$ in L=0.
[25] From a two-resonance fit to four 2^-0^+ waves.
[26] From a partial-wave analysis of $K^+K^-\pi^-$ system.
[27] Normalized to the B($\pi_2(1670)$ → $f_2\pi$).

$\pi_2(1670)$ REFERENCES

ADOLPH	14	EPJ A50 79	C. Adolph *et al.* (COMPASS Collab.)
ALEKSEEV	10	PRL 104 241803	M.G. Alekseev *et al.* (COMPASS Collab.)
SCHEGELSKY	06	EPJ A27 199	V.A. Schegelsky *et al.*
LU	05	PRL 94 032002	M. Lu *et al.* (BNL E852 Collab.)
KUHN	04	PL B595 109	J. Kuhn *et al.* (BNL E852 Collab.)
CHUNG	02	PR D65 072001	S.U. Chung *et al.* (BNL E852 Collab.)
BARBERIS	01	PL B507 14	D. Barberis *et al.*
AMELIN	99	PAN 62 445	D.V. Amelin *et al.* (VES Collab.)
		Translated from YAF 62 487.	
BAKER	99	PL B449 114	C.A. Baker *et al.*
BARBERIS	98B	PL B422 399	D. Barberis *et al.* (WA 102 Collab.)
ACCIARRI	97T	PL B413 147	M. Acciarri *et al.* (L3 Collab.)
ALBRECHT	97B	ZPHY C74 469	H. Albrecht *et al.* (ARGUS Collab.)
AMELIN	95B	PL B356 595	D.V. Amelin *et al.* (SERP, TBIL)
BERDNIKOV	94	PL B337 219	E.B. Berdnikov *et al.* (SERP, TBIL)
ANTREASYAN	90	ZPHY C48 561	D. Antreasyan *et al.* (Crystal Ball Collab.)
BEHREND	90C	ZPHY C46 583	H.J. Behrend *et al.* (CELLO Collab.)
ANTIPOV	87	EPL 4 403	Y.M. Antipov *et al.* (SERP, JINR, INRM+)
BELLINI	85	SJNP 41 781	D. Bellini *et al.*
		Translated from YAF 41 1223.	
ARMSTRONG	82B	NP B202 1	T.A. Armstrong, B. Baccari (AACH3, BARI, BONN+)
DAUM	81B	NP B182 269	C. Daum *et al.* (AMST, CERN, CRAC, MPIM+)
EVANGELIS...	81	NP B178 197	C. Evangelista *et al.* (BARI, BONN, CERN+)
Also		NP B186 594	C. Evangelista
DAUM	80D	PL 89B 285	C. Daum *et al.* (AMST, CERN, CRAC, MPIM+) JP
BALTAY	77	PRL 39 591	C. Baltay, C.V. Cautis, M. Kalelkar (COLU) JP
ASCOLI	73	PR D7 669	G. Ascoli (ILL, TNTO, GENO, HAMB, MILA+) JP

CRENNELL	70	PRL 24 781	D.J. Crennell *et al.*	(BNL)
ARMENISE	69	LNC 2 501	N. Armenise *et al.*	(BARI, BGNA, FIRZ)
BALTAY	68	PRL 20 887	C. Baltay *et al.*	(COLU, ROCH, RUTG, YALE)I
BARTSCH	68	NP B7 345	J. Bartsch *et al.*	(AACH, BERL, CERN)JP

$\phi(1680)$

$I^G(J^{PC}) = 0^-(1^{--})$

$\phi(1680)$ MASS

e^+e^- PRODUCTION

VALUE (MeV)	EVTS	DOCUMENT ID		TECN	COMMENT
1680±20 OUR ESTIMATE					
• • • We do not use the following data for averages, fits, limits, etc. • • •					
1674±12± 6	6.2k	[1] LEES	14H	BABR	$e^+e^- \to K^0_S K^0_L \gamma$
1733±10±10		[2] LEES	12F	BABR	10.6 $e^+e^- \to \phi\pi^+\pi^-\gamma$
1689± 7±10	4.8k	[3] SHEN	09	BELL	10.6 $e^+e^- \to K^+K^-\pi^+\pi^-\gamma$
1709±20±43		[4] AUBERT	08S	BABR	10.6 $e^+e^- \to$ hadrons
1623±20	948	[5] AKHMETSHIN	03	CMD2	1.05–1.38 $e^+e^- \to K^0_L K^0_S$
~ 1500		[6] ACHASOV	98H	RVUE	$e^+e^- \to \pi^+\pi^-\pi^0, \omega\pi^+\pi^-, K^+K^-$
~ 1900		[7] ACHASOV	98H	RVUE	$e^+e^- \to K^0_S K^\pm\pi^\mp$
1700±20		[8] CLEGG	94	RVUE	$e^+e^- \to K^+K^-, K^0_S K\pi$
1657±27	367	BISELLO	91C	DM2	$e^+e^- \to K^0_S K^\pm\pi^\mp$
1655±17		[9] BISELLO	88B	DM2	$e^+e^- \to K^+K^-$
1680±10		[10] BUON	82	DM1	$e^+e^- \to$ hadrons
1677±12		[11] MANE	82	DM1	$e^+e^- \to K^0_S K\pi$

[1] Using a vector meson dominance model with contribution from $\phi(1020)$, $\phi(1680)$, and higher mass excitations of $\rho(770)$ and $\omega(782)$.
[2] Using events with $\pi\pi$ invariant mass less than 0.85 GeV.
[3] From a fit with two incoherent Breit-Wigners.
[4] From the simultaneous fit to the $K\overline{K}^*(892)+$ c.c. and $\phi\eta$ data from AUBERT 08S using the results of AUBERT 07AK.
[5] From the combined fit of AKHMETSHIN 03 and MANE 81 also including ρ, ω, and ϕ. Neither isospin nor flavor structure known.
[6] Using data from IVANOV 81, BARKOV 87, BISELLO 88B, DOLINSKY 91, and ANTONELLI 92.
[7] Using the data from BISELLO 91C.
[8] Using BISELLO 88B and MANE 82 data.
[9] From global fit including ρ, ω, ϕ and $\rho(1700)$ assume mass 1570 MeV and width 510 MeV for ρ radial excitation.
[10] From global fit of ρ, ω, ϕ and their radial excitations to channels $\omega\pi^+\pi^-$, K^+K^-, $K^0_S K^0_L$, $K^0_S K^\pm\pi^\mp$. Assume mass 1570 MeV and width 510 MeV for ρ radial excitations, mass 1570 and width 500 MeV for ω radial excitation.
[11] Fit to one channel only, neglecting interference with ω, $\rho(1700)$.

PHOTOPRODUCTION

VALUE (MeV)	DOCUMENT ID		TECN	COMMENT
• • • We do not use the following data for averages, fits, limits, etc. • • •				
1753± 3	[12] LINK	02K	FOCS	20–160 $\gamma p \to K^+K^-p$
1726±22	[12] BUSENITZ	89	TPS	$\gamma p \to K^+K^-$X
1760±20	[12] ATKINSON	85C	OMEG	20–70 $\gamma p \to K\overline{K}$X
1690±10	[12] ASTON	81F	OMEG	25–70 $\gamma p \to K^+K^-$X

[12] We list here a state decaying into K^+K^- possibly different from $\phi(1680)$.

$p\overline{p}$ ANNIHILATION

VALUE (MeV)	DOCUMENT ID		TECN	COMMENT
• • • We do not use the following data for averages, fits, limits, etc. • • •				
1700±8	[13] AMSLER	06	CBAR	0.9 $\overline{p}p \to K^+K^-\pi^0$

[13] Could also be $\rho(1700)$.

$\phi(1680)$ WIDTH

e^+e^- PRODUCTION

VALUE (MeV)	EVTS	DOCUMENT ID		TECN	COMMENT
150±50 OUR ESTIMATE This is only an educated guess; the error given is larger than the error on the average of the published values.					
• • • We do not use the following data for averages, fits, limits, etc. • • •					
165±38± 70	6.2k	[14] LEES	14H	BABR	$e^+e^- \to K^0_S K^0_L \gamma$
300±15± 37		[15] LEES	12F	BABR	10.6 $e^+e^- \to \phi\pi^+\pi^-\gamma$
211±14± 19	4.8k	[16] SHEN	09	BELL	10.6 $e^+e^- \to K^+K^-\pi^+\pi^-\gamma$
322±77±160		[17] AUBERT	08S	BABR	10.6 $e^+e^- \to$ hadrons
139±60	948	[18] AKHMETSHIN	03	CMD2	1.05–1.38 $e^+e^- \to K^0_L K^0_S$
300±60		[19] CLEGG	94	RVUE	$e^+e^- \to K^+K^-, K^0_S K\pi$
146±55	367	BISELLO	91C	DM2	$e^+e^- \to K^0_S K^\pm\pi^\mp$
207±45		[20] BISELLO	88B	DM2	$e^+e^- \to K^+K^-$
185±22		[21] BUON	82	DM1	$e^+e^- \to$ hadrons
102±36		[22] MANE	82	DM1	$e^+e^- \to K^0_S K\pi$

[14] Using a vector meson dominance model with contribution from $\phi(1020)$, $\phi(1680)$, and higher mass excitations of $\rho(770)$ and $\omega(782)$.
[15] Using events with $\pi\pi$ invariant mass less than 0.85 GeV.
[16] From a fit with two incoherent Breit-Wigners.
[17] From the simultaneous fit to the $K\overline{K}^*(892)+$ c.c. and $\phi\eta$ data from AUBERT 08S using the results of AUBERT 07AK.
[18] From the combined fit of AKHMETSHIN 03 and MANE 81 also including ρ, ω, and ϕ. Neither isospin nor flavor structure known.
[19] Using BISELLO 88B and MANE 82 data.
[20] From global fit including ρ, ω, ϕ and $\rho(1700)$
[21] From global fit of ρ, ω, ϕ and their radial excitations to channels $\omega\pi^+\pi^-$, K^+K^-, $K^0_S K^0_L$, $K^0_S K^\pm\pi^\mp$. Assume mass 1570 MeV and width 510 MeV for ρ radial excitations, mass 1570 and width 500 MeV for ω radial excitation.
[22] Fit to one channel only, neglecting interference with ω, $\rho(1700)$.

PHOTOPRODUCTION

VALUE (MeV)	DOCUMENT ID		TECN	COMMENT
• • • We do not use the following data for averages, fits, limits, etc. • • •				
122±63	[23] LINK	02K	FOCS	20–160 $\gamma p \to K^+K^-p$
121±47	[23] BUSENITZ	89	TPS	$\gamma p \to K^+K^-$X
80±40	[23] ATKINSON	85C	OMEG	20–70 $\gamma p \to K\overline{K}$X
100±40	[23] ASTON	81F	OMEG	25–70 $\gamma p \to K^+K^-$X

[23] We list here a state decaying into K^+K^- possibly different from $\phi(1680)$.

$p\overline{p}$ ANNIHILATION

VALUE (MeV)	DOCUMENT ID		TECN	COMMENT
• • • We do not use the following data for averages, fits, limits, etc. • • •				
143±24	[24] AMSLER	06	CBAR	0.9 $\overline{p}p \to K^+K^-\pi^0$

[24] Could also be $\rho(1700)$.

$\phi(1680)$ DECAY MODES

	Mode	Fraction (Γ_i/Γ)
Γ_1	$K\overline{K}^*(892)+$ c.c.	dominant
Γ_2	$K^0_S K\pi$	seen
Γ_3	$K\overline{K}$	seen
Γ_4	$K^0_L K^0_S$	
Γ_5	e^+e^-	seen
Γ_6	$\omega\pi\pi$	not seen
Γ_7	$\phi\pi\pi$	
Γ_8	$K^+K^-\pi^+\pi^-$	seen
Γ_9	$\eta\phi$	seen
Γ_{10}	$\eta\gamma$	seen
Γ_{11}	$K^+K^-\pi^0$	

$\phi(1680)\ \Gamma(i)\Gamma(e^+e^-)/\Gamma(\text{total})$

This combination of a partial width with the partial width into e^+e^- and with the total width is obtained from the integrated cross section into channel (i) in e^+e^- annihilation. We list only data that have not been used to determine the partial width $\Gamma(i)$ or the branching ratio $\Gamma(i)/\text{total}$.

$\Gamma(K^0_L K^0_S) \times \Gamma(e^+e^-)/\Gamma_{\text{total}}$ $\quad \Gamma_4\Gamma_5/\Gamma$

VALUE (eV)	EVTS	DOCUMENT ID		TECN	COMMENT
• • • We do not use the following data for averages, fits, limits, etc. • • •					
14.3±2.4±6.2	6.2k	[25] LEES	14H	BABR	$e^+e^- \to K^0_S K^0_L \gamma$

[25] Using a vector meson dominance model with contribution from $\phi(1020)$, $\phi(1680)$, and higher mass excitations of $\rho(770)$ and $\omega(782)$.

$\Gamma(\phi\pi\pi) \times \Gamma(e^+e^-)/\Gamma_{\text{total}}$ $\quad \Gamma_7\Gamma_5/\Gamma$

VALUE (10^{-2} keV)	DOCUMENT ID		TECN	COMMENT
• • • We do not use the following data for averages, fits, limits, etc. • • •				
4.2±0.2±0.3	LEES	12F	BABR	10.6 $e^+e^- \to \phi\pi^+\pi^-\gamma$

$\phi(1680)\ \Gamma(i)\Gamma(e^+e^-)/\Gamma^2(\text{total})$

This combination of a branching ratio into channel (i) and branching ratio into e^+e^- is directly measured and obtained from the cross section at the peak. We list only data that have not been used to determine the branching ratio into (i) or e^+e^-.

$\Gamma(K^0_L K^0_S)/\Gamma_{\text{total}} \times \Gamma(e^+e^-)/\Gamma_{\text{total}}$ $\quad \Gamma_4/\Gamma \times \Gamma_5/\Gamma$

VALUE (units 10^{-6})	EVTS	DOCUMENT ID		TECN	COMMENT
• • • We do not use the following data for averages, fits, limits, etc. • • •					
0.131±0.059	948	[26] AKHMETSHIN	03	CMD2	1.05–1.38 $e^+e^- \to K^0_L K^0_S$

[26] From the combined fit of AKHMETSHIN 03 and MANE 81 also including ρ, ω, and ϕ. Neither isospin nor flavor structure known. Recalculated by us.

$\Gamma(K\overline{K}^*(892)+\text{c.c.})/\Gamma_{\text{total}} \times \Gamma(e^+e^-)/\Gamma_{\text{total}}$ $\quad \Gamma_1/\Gamma \times \Gamma_5/\Gamma$

VALUE (units 10^{-6})	EVTS	DOCUMENT ID		TECN	COMMENT
• • • We do not use the following data for averages, fits, limits, etc. • • •					
1.15±0.16±0.01		[27] AUBERT	08S	BABR	10.6 $e^+e^- \to K\overline{K}^*(892)\gamma +$ c.c.
3.29±1.57	367	[28] BISELLO	91C	DM2	1.35–2.40 $e^+e^- \to K^0_S K^\pm\pi^\mp$

[27] From the simultaneous fit to the $K\overline{K}^*(892)+$ c.c. and $\phi\eta$ data from AUBERT 08S using the results of AUBERT 07AK.
[28] Recalculated by us with the published value of $B(K\overline{K}^*(892)+$ c.c.$)\times\Gamma(e^+e^-)$.

$\Gamma(\phi\pi\pi)/\Gamma_{total}\times\Gamma(e^+e^-)/\Gamma_{total}$ $\Gamma_7/\Gamma\times\Gamma_5/\Gamma$

VALUE (units 10^{-7})	EVTS	DOCUMENT ID		TECN	COMMENT
• • • We do not use the following data for averages, fits, limits, etc. • • •					
$1.86\pm0.14\pm0.21$	4.8k	[29] SHEN	09	BELL	10.6 $e^+e^-\to K^+K^-\pi^+\pi^-\gamma$

[29] Multiplied by 3/2 to take into account the $\phi\pi^0\pi^0$ mode. Using $B(\phi\to K^+K^-)=(49.2\pm0.6)\%$.

$\Gamma(\eta\phi)/\Gamma_{total}\times\Gamma(e^+e^-)/\Gamma_{total}$ $\Gamma_9/\Gamma\times\Gamma_5/\Gamma$

VALUE (units 10^{-6})	DOCUMENT ID		TECN	COMMENT
• • • We do not use the following data for averages, fits, limits, etc. • • •				
$0.43\pm0.10\pm0.09$	[30] AUBERT	08S	BABR	10.6 $e^+e^-\to\phi\eta\gamma$

[30] From the simultaneous fit to the $K\overline{K}^*(892)+$ c.c. and $\phi\eta$ data from AUBERT 08S using the results of AUBERT 07AK.

$\phi(1680)$ BRANCHING RATIOS

$\Gamma(K\overline{K}^*(892)+\text{c.c.})/\Gamma(K^0_SK\pi)$ Γ_1/Γ_2

VALUE	DOCUMENT ID		TECN	COMMENT
dominant	MANE	82	DM1	$e^+e^-\to K^0_SK^\pm\pi^\mp$

$\Gamma(K\overline{K})/\Gamma(K\overline{K}^*(892)+\text{c.c.})$ Γ_3/Γ_1

VALUE	DOCUMENT ID		TECN	COMMENT
• • • We do not use the following data for averages, fits, limits, etc. • • •				
0.07 ± 0.01	BUON	82	DM1	e^+e^-

$\Gamma(\omega\pi\pi)/\Gamma(K\overline{K}^*(892)+\text{c.c.})$ Γ_6/Γ_1

VALUE	DOCUMENT ID		TECN	COMMENT
<0.10	BUON	82	DM1	e^+e^-

$\Gamma(\eta\phi)/\Gamma_{total}$ Γ_9/Γ

VALUE	EVTS	DOCUMENT ID		TECN	COMMENT
seen	35	[31] ACHASOV	14	SND	1.15–2.00 $e^+e^-\to\eta\gamma$

[31] From a phenomenological model based on vector meson dominance with $\rho(1450)$ and $\phi(1680)$ masses and widths from the PDG 12.

$\Gamma(\eta\phi)/\Gamma(K\overline{K}^*(892)+\text{c.c.})$ Γ_9/Γ_1

VALUE	DOCUMENT ID		TECN	COMMENT
• • • We do not use the following data for averages, fits, limits, etc. • • •				
≈ 0.37	[32] AUBERT	08S	BABR	10.6 $e^+e^-\to$ hadrons

[32] From the fit including data from AUBERT 07AK.

$\Gamma(\eta\gamma)/\Gamma_{total}$ Γ_{10}/Γ

VALUE	EVTS	DOCUMENT ID		TECN	COMMENT
seen	35	[33] ACHASOV	14	SND	1.15–2.00 $e^+e^-\to\eta\gamma$

[33] From a phenomenological model based on vector meson dominance with $\rho(1450)$ and $\phi(1680)$ masses and widths from the PDG 12.

$\phi(1680)$ REFERENCES

ACHASOV	14	PR D90 032002	M.N. Achasov *et al.*	(SND Collab.)
LEES	14H	PR D89 092002	J.P. Lees *et al.*	(BABAR Collab)
LEES	12F	PR D86 012008	J.P. Lees *et al.*	(BABAR Collab.)
PDG	12	PR D86 010001	J. Beringer *et al.*	(PDG Collab.)
SHEN	09	PR D80 031101	C.P. Shen *et al.*	(BELLE Collab.)
AUBERT	08S	PR D77 092002	B. Aubert *et al.*	(BABAR Collab.)
AUBERT	07AK	PR D76 012008	B. Aubert *et al.*	(BABAR Collab.)
AMSLER	06	PL B639 165	C. Amsler *et al.*	(CBAR Collab.)
AKHMETSHIN	03	PL B551 27	R.R. Akhmetshin *et al.*	(Novosibirsk CMD-2 Collab.)
Also		PAN 65 1222	E.V. Anashkin, V.M. Aulchenko, R.R. Akhmetshin	
		Translated from YAF 65 1255.		
LINK	02K	PL B545 50	J.M. Link *et al.*	(FNAL FOCUS Collab.)
ACHASOV	98H	PR D57 4334	N.N. Achasov, A.A. Kozhevnikov	
CLEGG	94	ZPHY C62 455	A.B. Clegg, A. Donnachie	(LANC, MCHS)
ANTONELLI	92	ZPHY C56 15	A. Antonelli *et al.*	(DM2 Collab.)
BISELLO	91C	ZPHY C52 227	D. Bisello *et al.*	(DM2 Collab.)
DOLINSKY	91	PRPL 202 99	S.I. Dolinsky *et al.*	(NOVO)
BUSENITZ	89	PR D40 1	J.K. Busenitz *et al.*	(ILL, FNAL)
BISELLO	88B	ZPHY C39 13	D. Bisello *et al.*	(PADO, CLER, FRAS+)
BARKOV	87	JETPL 46 164	L.M. Barkov *et al.*	(NOVO)
		Translated from ZETFP 46 132.		
ATKINSON	85C	ZPHY C27 233	M. Atkinson *et al.*	(BONN, CERN, GLAS+)
BUON	82	PL 118B 221	J. Buon *et al.*	(LALO, MONP)
MANE	82	PL 112B 178	F. Mane *et al.*	(LALO)
ASTON	81F	PL 104B 231	D. Aston	(BONN, CERN, EPOL, GLAS, LANC+)
IVANOV	81	PL 107B 297	P.M. Ivanov *et al.*	(NOVO)
MANE	81	PL 99B 261	F. Mane *et al.*	(ORSAY)

$\rho_3(1690)$

$I^G(J^{PC}) = 1^+(3^{--})$

$\rho_3(1690)$ MASS

VALUE (MeV)	DOCUMENT ID
1688.8±2.1 OUR AVERAGE	Includes data from the 5 datablocks that follow this one.

2π MODE

VALUE (MeV)	EVTS	DOCUMENT ID		TECN	CHG	COMMENT
The data in this block is included in the average printed for a previous datablock.						
1686± 4 OUR AVERAGE						
1677±14		EVANGELIS...	81	OMEG	−	12 $\pi^-p\to 2\pi p$
1679±11	476	BALTAY	78B	HBC	0	15 $\pi^+p\to\pi^+\pi^-n$
1678±12	175	[1] ANTIPOV	77	CIBS	0	25 $\pi^-p\to p3\pi$
1690± 7	600	[1] ENGLER	74	DBC	0	6 $\pi^+n\to\pi^+\pi^-p$
1693± 8		[2] GRAYER	74	ASPK	0	17 $\pi^-p\to\pi^+\pi^-n$
1678±12		MATTHEWS	71C	DBC	0	7 π^+N
• • • We do not use the following data for averages, fits, limits, etc. • • •						
1734±10		[3] CORDEN	79	OMEG		12–15 $\pi^-p\to n2\pi$
1692±12		[2,4] ESTABROOKS	75	RVUE		17 $\pi^-p\to\pi^+\pi^-n$
1737±23		ARMENISE	70	DBC	0	9 π^+N
1650±35	122	BARTSCH	70B	HBC	+	8 $\pi^+p\to N2\pi$
1687±21		STUNTEBECK	70	HDBC	0	8 π^-p, 5.4 π^+d
1683±13		ARMENISE	68	DBC	0	5.1 π^+d
1670±30		GOLDBERG	65	HBC	0	6 π^+d, 8 π^-p

[1] Mass errors enlarged by us to $\Gamma/\sqrt{N}$; see the note with the $K^*(892)$ mass.
[2] Uses same data as HYAMS 75.
[3] From a phase shift solution containing a $f_2'(1525)$ width two times larger than the $K\overline{K}$ result.
[4] From phase-shift analysis. Error takes account of spread of different phase-shift solutions.

$K\overline{K}$ AND $K\overline{K}\pi$ MODES

VALUE (MeV)	EVTS	DOCUMENT ID		TECN	CHG	COMMENT
The data in this block is included in the average printed for a previous datablock.						
1696± 4 OUR AVERAGE						
1699± 5		ALPER	80	CNTR	0	62 $\pi^-p\to K^+K^-n$
1698±12	6k	[5,6] MARTIN	78D	SPEC		10 $\pi p\to K^0_SK^-p$
1692± 6		BLUM	75	ASPK	0	18.4 $\pi^-p\to nK^+K^-$
1690±16		ADERHOLZ	69	HBC	+	8 $\pi^+p\to K\overline{K}\pi$
• • • We do not use the following data for averages, fits, limits, etc. • • •						
1694± 8		[7] COSTA	80	OMEG		10 $\pi^-p\to K^+K^-n$

[5] From a fit to $J^P=3^-$ partial wave.
[6] Systematic error on mass scale subtracted.
[7] They cannot distinguish between $\rho_3(1690)$ and $\omega_3(1670)$.

$(4\pi)^\pm$ MODE

VALUE (MeV)	EVTS	DOCUMENT ID		TECN	CHG	COMMENT
The data in this block is included in the average printed for a previous datablock.						
1686± 5 OUR AVERAGE Error includes scale factor of 1.1.						
1694± 6		[8] EVANGELIS...	81	OMEG	−	12 $\pi^-p\to p4\pi$
1665±15	177	BALTAY	78B	HBC	+	15 $\pi^+p\to p4\pi$
1670±10		THOMPSON	74	HBC	+	13 π^+p
1687±20		CASON	73	HBC	−	8,18.5 π^-p
1685±14		[9] CASON	73	HBC	−	8,18.5 π^-p
1680±40	144	BARTSCH	70B	HBC	+	8 $\pi^+p\to N4\pi$
1689±20	102	[9] BARTSCH	70B	HBC	+	8 $\pi^+p\to N2\rho$
1705±21		CASO	70	HBC	−	11.2 $\pi^-p\to n\rho2\pi$
• • • We do not use the following data for averages, fits, limits, etc. • • •						
1718±10		[10] EVANGELIS...	81	OMEG	−	12 $\pi^-p\to p4\pi$
1673± 9		[11] EVANGELIS...	81	OMEG	−	12 $\pi^-p\to p4\pi$
1733± 9	66	[9] KLIGER	74	HBC	−	4.5 $\pi^-p\to p4\pi$
1630±15		HOLMES	72	HBC	+	10–12 K^+p
1720±15		BALTAY	68	HBC	+	7, 8.5 π^+p

[8] From $\rho^-\rho^0$ mode, not independent of the other two EVANGELISTA 81 entries.
[9] From $\rho^\pm\rho^0$ mode.
[10] From $a_2(1320)^-\pi^0$ mode, not independent of the other two EVANGELISTA 81 entries.
[11] From $a_2(1320)^0\pi^-$ mode, not independent of the other two EVANGELISTA 81 entries.

$\omega\pi$ MODE

VALUE (MeV)	DOCUMENT ID		TECN	CHG	COMMENT
The data in this block is included in the average printed for a previous datablock.					
1681± 7 OUR AVERAGE					
1670±25	[12] ALDE	95	GAM2		38 $\pi^-p\to\omega\pi^0n$
1690±15	EVANGELIS...	81	OMEG	−	12 $\pi^-p\to\omega\pi p$
1666±14	GESSAROLI	77	HBC		11 $\pi^-p\to\omega\pi p$
1686± 9	THOMPSON	74	HBC	+	13 π^+p
• • • We do not use the following data for averages, fits, limits, etc. • • •					
1654±24	BARNHAM	70	HBC	+	10 $K^+p\to\omega\pi X$

[12] Supersedes ALDE 92C.

$\eta\pi^+\pi^-$ MODE

(For difficulties with MMS experiments, see the $a_2(1320)$ mini-review in the 1973 edition.)

VALUE (MeV)	DOCUMENT ID		TECN	CHG	COMMENT
The data in this block is included in the average printed for a previous datablock.					
1682±12 OUR AVERAGE					
1685±10±20	AMELIN	00	VES		37 $\pi^-p\to\eta\pi^+\pi^-n$
1680±15	FUKUI	88	SPEC	0	8.95 $\pi^-p\to\eta\pi^+\pi^-n$

• • • We do not use the following data for averages, fits, limits, etc. • • •

1700±47	[13] ANDERSON	69	MMS	–	16 $\pi^- p$ backward
1632±15	[13,14] FOCACCI	66	MMS	–	7–12 $\pi^- p \rightarrow p$MM
1700±15	[13,14] FOCACCI	66	MMS	–	7–12 $\pi^- p \rightarrow p$MM
1748±15	[13,14] FOCACCI	66	MMS	–	7–12 $\pi^- p \rightarrow p$MM

[13] Seen in 2.5–3 GeV/c $\overline{p}p$. $2\pi^+ 2\pi^-$, with 0, 1, 2 $\pi^+\pi^-$ pairs in ρ band not seen by OREN 74 (2.3 GeV/c $\overline{p}p$) with more statistics. (Jan. 1976)

[14] Not seen by BOWEN 72.

$\rho_3(1690)$ WIDTH

2π, $K\overline{K}$, AND $K\overline{K}\pi$ MODES

VALUE (MeV)	DOCUMENT ID
161±10 OUR AVERAGE	Includes data from the 5 datablocks that follow this one. Error includes scale factor of 1.5. See the ideogram below.

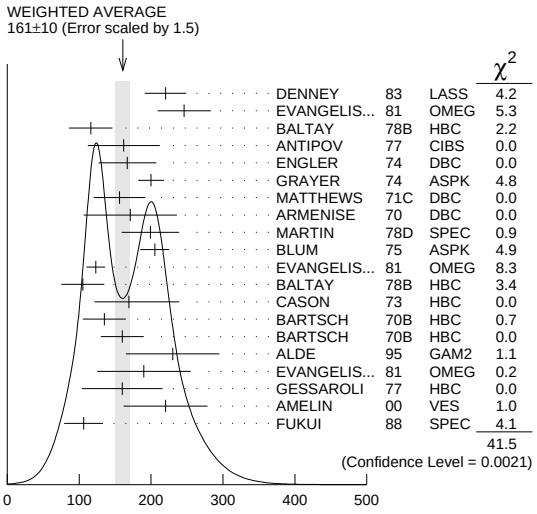

$\rho_3(1690)$ width, 2π, $K\overline{K}$, and $K\overline{K}\pi$ modes (MeV)

2π MODE

VALUE (MeV)	EVTS	DOCUMENT ID	TECN	CHG	COMMENT
The data in this block is included in the average printed for a previous datablock.					
186±14 OUR AVERAGE		Error includes scale factor of 1.3. See the ideogram below.			
220±29		DENNEY 83	LASS		10 $\pi^+ N$
246±37		EVANGELIS... 81	OMEG	–	12 $\pi^- p \rightarrow 2\pi p$
116±30	476	BALTAY 78B	HBC	0	15 $\pi^+ p \rightarrow \pi^+\pi^- n$
162±50	175	[15] ANTIPOV 77	CIBS	0	25 $\pi^- p \rightarrow p3\pi$
167±40	600	ENGLER 74	DBC	0	6 $\pi^+ n \rightarrow \pi^+\pi^- p$
200±18		[16] GRAYER 74	ASPK	0	17 $\pi^- p \rightarrow \pi^+\pi^- n$
156±36		MATTHEWS 71C	DBC	0	7 $\pi^+ N$
171±65		ARMENISE 70	DBC	0	9 $\pi^+ d$
• • • We do not use the following data for averages, fits, limits, etc. • • •					
322±35		[17] CORDEN 79	OMEG		12–15 $\pi^- p \rightarrow n2\pi$
240±30		[16,18] ESTABROOKS 75	RVUE		17 $\pi^- p \rightarrow \pi^+\pi^- n$
180±30	122	BARTSCH 70B	HBC	+	8 $\pi^+ p \rightarrow N2\pi$
267^{+72}_{-46}		STUNTEBECK 70	HDBC	0	8 $\pi^- p$, 5.4 $\pi^+ d$
188±49		ARMENISE 68	DBC	0	5.1 $\pi^+ d$
180±40		GOLDBERG 65	HBC	0	6 $\pi^+ d$, 8 $\pi^- p$

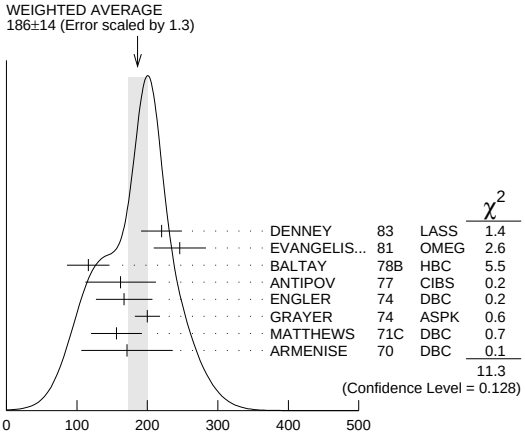

$\rho_3(1690)$ width, 2π mode (MeV)

[15] Width errors enlarged by us to $4\Gamma/\sqrt{N}$; see the note with the $K^*(892)$ mass.

[16] Uses same data as HYAMS 75 and BECKER 79.

[17] From a phase shift solution containing a $f_2'(1525)$ width two times larger than the $K\overline{K}$ result.

[18] From phase-shift analysis. Error takes account of spread of different phase-shift solutions.

$K\overline{K}$ AND $K\overline{K}\pi$ MODES

VALUE (MeV)	EVTS	DOCUMENT ID	TECN	CHG	COMMENT
The data in this block is included in the average printed for a previous datablock.					
204±18 OUR AVERAGE					
199±40	6000	[19] MARTIN 78D	SPEC		10 $\pi p \rightarrow K^0_S K^- p$
205±20		BLUM 75	ASPK	0	18.4 $\pi^- p \rightarrow nK^+ K^-$
• • • We do not use the following data for averages, fits, limits, etc. • • •					
219± 4		ALPER 80	CNTR	0	62 $\pi^- p \rightarrow K^+ K^- n$
186±11		[20] COSTA 80	OMEG		10 $\pi^- p \rightarrow K^+ K^- n$
112±60		ADERHOLZ 69	HBC	+	8 $\pi^+ p \rightarrow K\overline{K}\pi$

[19] From a fit to $J^P = 3^-$ partial wave.

[20] They cannot distinguish between $\rho_3(1690)$ and $\omega_3(1670)$.

$(4\pi)^\pm$ MODE

VALUE (MeV)	EVTS	DOCUMENT ID	TECN	CHG	COMMENT
The data in this block is included in the average printed for a previous datablock.					
129±10 OUR AVERAGE					
123±13		[21] EVANGELIS... 81	OMEG	–	12 $\pi^- p \rightarrow p4\pi$
105±30	177	BALTAY 78B	HBC	+	15 $\pi^+ p \rightarrow p4\pi$
169^{+70}_{-48}		CASON 73	HBC	–	8,18.5 $\pi^- p$
135±30	144	BARTSCH 70B	HBC	+	8 $\pi^+ p \rightarrow N4\pi$
160±30	102	BARTSCH 70B	HBC	+	8 $\pi^+ p \rightarrow N2\rho$
• • • We do not use the following data for averages, fits, limits, etc. • • •					
230±28		[22] EVANGELIS... 81	OMEG	–	12 $\pi^- p \rightarrow p4\pi$
184±33		[23] EVANGELIS... 81	OMEG	–	12 $\pi^- p \rightarrow p4\pi$
150	66	[24] KLIGER 74	HBC	–	4.5 $\pi^- p \rightarrow p4\pi$
106±25		THOMPSON 74	HBC	+	13 $\pi^+ p$
125^{+83}_{-35}		[24] CASON 73	HBC	–	8,18.5 $\pi^- p$
130±30		HOLMES 72	HBC	+	10–12 $K^+ p$
180±30	90	[24] BARTSCH 70B	HBC	+	8 $\pi^+ p \rightarrow Na_2\pi$
100±35		BALTAY 68	HBC	+	7, 8.5 $\pi^+ p$

[21] From $\rho^-\rho^0$ mode, not independent of the other two EVANGELISTA 81 entries.

[22] From $a_2(1320)^-\pi^0$ mode, not independent of the other two EVANGELISTA 81 entries.

[23] From $a_2(1320)^0\pi^-$ mode, not independent of the other two EVANGELISTA 81 entries.

[24] From $\rho^\pm\rho^0$ mode.

$\omega\pi$ MODE

VALUE (MeV)	DOCUMENT ID	TECN	CHG	COMMENT
The data in this block is included in the average printed for a previous datablock.				
190±40 OUR AVERAGE				
230±65	[25] ALDE 95	GAM2		38 $\pi^- p \rightarrow \omega\pi^0 n$
190±65	EVANGELIS... 81	OMEG	–	12 $\pi^- p \rightarrow \omega\pi p$
160±56	GESSAROLI 77	HBC		11 $\pi^- p \rightarrow \omega\pi p$
• • • We do not use the following data for averages, fits, limits, etc. • • •				
89±25	THOMPSON 74	HBC	+	13 $\pi^+ p$
130^{+73}_{-43}	BARNHAM 70	HBC	+	10 $K^+ p \rightarrow \omega\pi X$

[25] Supersedes ALDE 92C.

$\eta\pi^+\pi^-$ MODE

(For difficulties with MMS experiments, see the $a_2(1320)$ mini-review in the 1973 edition.)

VALUE (MeV)	DOCUMENT ID	TECN	CHG	COMMENT
The data in this block is included in the average printed for a previous datablock.				
126±40 OUR AVERAGE	Error includes scale factor of 1.8.			
220±30±50	AMELIN 00	VES		37 $\pi^- p \rightarrow \eta\pi^+\pi^- n$
106±27	FUKUI 88	SPEC	0	8.95 $\pi^- p \rightarrow \eta\pi^+\pi^- n$
• • • We do not use the following data for averages, fits, limits, etc. • • •				
195	[26] ANDERSON 69	MMS	–	16 $\pi^- p$ backward
< 21	[26,27] FOCACCI 66	MMS	–	7–12 $\pi^- p \rightarrow p$MM
< 30	[26,27] FOCACCI 66	MMS	–	7–12 $\pi^- p \rightarrow p$MM
< 38	[26,27] FOCACCI 66	MMS	–	7–12 $\pi^- p \rightarrow p$MM

[26] Seen in 2.5–3 GeV/c $\overline{p}p$. $2\pi^+ 2\pi^-$, with 0, 1, 2 $\pi^+\pi^-$ pairs in ρ^0 band not seen by OREN 74 (2.3 GeV/c $\overline{p}p$) with more statistics. (Jan. 1979)

[27] Not seen by BOWEN 72.

$\rho_3(1690)$ DECAY MODES

	Mode	Fraction (Γ_i/Γ)	Scale factor
Γ_1	4π	(71.1 ± 1.9) %	
Γ_2	$\pi^\pm\pi^+\pi^-\pi^0$	(67 ±22) %	
Γ_3	$\omega\pi$	(16 ± 6) %	
Γ_4	$\pi\pi$	(23.6 ± 1.3) %	

Meson Particle Listings

$\rho_3(1690)$

Γ_5	$K\overline{K}\pi$	(3.8 ± 1.2) %	
Γ_6	$K\overline{K}$	(1.58± 0.26) %	1.2
Γ_7	$\eta\pi^+\pi^-$	seen	
Γ_8	$\rho(770)\eta$	seen	
Γ_9	$\pi\pi\rho$ Excluding 2ρ and $a_2(1320)\pi$.	seen	
Γ_{10}	$a_2(1320)\pi$	seen	
Γ_{11}	$\rho\rho$	seen	
Γ_{12}	$\phi\pi$		
Γ_{13}	$\eta\pi$		
Γ_{14}	$\pi^\pm 2\pi^+ 2\pi^- \pi^0$		

CONSTRAINED FIT INFORMATION

An overall fit to 5 branching ratios uses 10 measurements and one constraint to determine 4 parameters. The overall fit has a $\chi^2 = 14.7$ for 7 degrees of freedom.

The following *off-diagonal* array elements are the correlation coefficients $\langle \delta x_i \delta x_j \rangle / (\delta x_i \cdot \delta x_j)$, in percent, from the fit to the branching fractions, $x_i \equiv \Gamma_i/\Gamma_{\rm total}$. The fit constrains the x_i whose labels appear in this array to sum to one.

x_4	−77		
x_5	−74	17	
x_6	−15	2	0
	x_1	x_4	x_5

$\rho_3(1690)$ BRANCHING RATIOS

$\Gamma(\pi\pi)/\Gamma_{\rm total$ — **Γ_4/Γ**

VALUE	DOCUMENT ID		TECN	CHG	COMMENT
0.236±0.013 OUR FIT					
0.243±0.013 OUR AVERAGE					
$0.259^{+0.018}_{-0.019}$	BECKER	79	ASPK	0	17 $\pi^- p$ polarized
0.23 ±0.02	CORDEN	79	OMEG		12–15 $\pi^- p \to n2\pi$
0.22 ±0.04	[28] MATTHEWS	71C	HDBC	0	7 $\pi^+ n \to \pi^- p$
• • • We do not use the following data for averages, fits, limits, etc. • • •					
0.245±0.006	[29] ESTABROOKS	75	RVUE		17 $\pi^- p \to \pi^+\pi^- n$

[28] One-pion-exchange model used in this estimation.
[29] From phase-shift analysis of HYAMS 75 data.

$\Gamma(\pi\pi)/\Gamma(\pi^\pm\pi^+\pi^-\pi^0)$ — **Γ_4/Γ_2**

VALUE	DOCUMENT ID		TECN	CHG	COMMENT
0.35±0.11	CASON	73	HBC	−	8,18.5 $\pi^- p$
• • • We do not use the following data for averages, fits, limits, etc. • • •					
<0.2	HOLMES	72	HBC	+	10–12 $K^+ p$
<0.12	BALLAM	71B	HBC	−	16 $\pi^- p$

$\Gamma(\pi\pi)/\Gamma(4\pi)$ — **Γ_4/Γ_1**

VALUE	DOCUMENT ID		TECN	CHG	COMMENT
0.332±0.026 OUR FIT Error includes scale factor of 1.1.					
0.30 ±0.10	BALTAY	78B	HBC	0	15 $\pi^+ p \to p4\pi$

$\Gamma(K\overline{K})/\Gamma(\pi\pi)$ — **Γ_6/Γ_4**

VALUE	DOCUMENT ID		TECN	CHG	COMMENT
0.067±0.011 OUR FIT Error includes scale factor of 1.2.					
$\mathbf{0.118^{+0.040}_{-0.032}}$ **OUR AVERAGE** Error includes scale factor of 1.7. See the ideogram below.					
$0.191^{+0.040}_{-0.037}$	GORLICH	80	ASPK	0	17,18 $\pi^- p$ polarized
0.08 ±0.03	BARTSCH	70B	HBC	+	8 $\pi^+ p$
$0.08^{+0.08}_{-0.03}$	CRENNELL	68B	HBC		6.0 $\pi^- p$

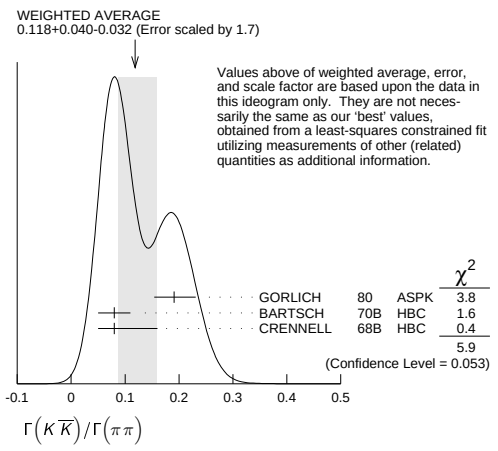

$\Gamma(K\overline{K}\pi)/\Gamma(\pi\pi)$ — **Γ_5/Γ_4**

VALUE	DOCUMENT ID		TECN	CHG	COMMENT
0.16±0.05 OUR FIT					
0.16±0.05	[30] BARTSCH	70B	HBC	+	8 $\pi^+ p$

[30] Increased by us to correspond to $B(\rho_3(1690) \to \pi\pi)$=0.24.

$[\Gamma(\pi\pi\rho) + \Gamma(a_2(1320)\pi) + \Gamma(\rho\rho)]/\Gamma(\pi^\pm\pi^+\pi^-\pi^0)$ — **$(\Gamma_9+\Gamma_{10}+\Gamma_{11})/\Gamma_2$**

VALUE	DOCUMENT ID		TECN	CHG	COMMENT
0.94±0.09 OUR AVERAGE					
0.96±0.21	BALTAY	78B	HBC	+	15 $\pi^+ p \to p4\pi$
0.88±0.15	BALLAM	71B	HBC	−	16 $\pi^- p$
1 ±0.15	BARTSCH	70B	HBC	+	8 $\pi^+ p$
consistent with 1	CASO	68	HBC	−	11 $\pi^- p$

$\Gamma(\rho\rho)/\Gamma(\pi^\pm\pi^+\pi^-\pi^0)$ — **Γ_{11}/Γ_2**

VALUE	EVTS	DOCUMENT ID		TECN	CHG	COMMENT
• • • We do not use the following data for averages, fits, limits, etc. • • •						
0.12±0.11		BALTAY	78B	HBC	+	15 $\pi^+ p \to p4\pi$
0.56	66	KLIGER	74	HBC	−	4.5 $\pi^- p \to p4\pi$
0.13±0.09		[31] THOMPSON	74	HBC	+	13 $\pi^+ p$
0.7 ±0.15		BARTSCH	70B	HBC	+	8 $\pi^+ p$

[31] $\rho\rho$ and $a_2(1320)\pi$ modes are indistinguishable.

$\Gamma(\rho\rho)/[\Gamma(\pi\pi\rho) + \Gamma(a_2(1320)\pi) + \Gamma(\rho\rho)]$ — **$\Gamma_{11}/(\Gamma_9+\Gamma_{10}+\Gamma_{11})$**

VALUE	DOCUMENT ID		TECN	CHG	COMMENT
• • • We do not use the following data for averages, fits, limits, etc. • • •					
0.48±0.16	CASO	68	HBC	−	11 $\pi^- p$

$\Gamma(a_2(1320)\pi)/\Gamma(\pi^\pm\pi^+\pi^-\pi^0)$ — **Γ_{10}/Γ_2**

VALUE	DOCUMENT ID		TECN	CHG	COMMENT
• • • We do not use the following data for averages, fits, limits, etc. • • •					
0.66±0.08	BALTAY	78B	HBC	+	15 $\pi^+ p \to p4\pi$
0.36±0.14	[32] THOMPSON	74	HBC	+	13 $\pi^+ p$
not seen	CASON	73	HBC	−	8,18.5 $\pi^- p$
0.6 ±0.15	BARTSCH	70B	HBC	+	8 $\pi^+ p$
0.6	BALTAY	68	HBC	+	7,8.5 $\pi^+ p$

[32] $\rho\rho$ and $a_2(1320)\pi$ modes are indistinguishable.

$\Gamma(\omega\pi)/\Gamma(\pi^\pm\pi^+\pi^-\pi^0)$ — **Γ_3/Γ_2**

VALUE	CL%	DOCUMENT ID		TECN	CHG	COMMENT
0.23±0.05 OUR AVERAGE Error includes scale factor of 1.2.						
0.33±0.07		THOMPSON	74	HBC	+	13 $\pi^+ p$
0.12±0.07		BALLAM	71B	HBC	−	16 $\pi^- p$
0.25±0.10		BALTAY	68	HBC	+	7,8.5 $\pi^+ p$
0.25±0.10		JOHNSTON	68	HBC	−	7.0 $\pi^- p$
• • • We do not use the following data for averages, fits, limits, etc. • • •						
<0.11	95	BALTAY	78B	HBC	+	15 $\pi^+ p \to p4\pi$
<0.09		KLIGER	74	HBC	−	4.5 $\pi^- p \to p4\pi$

$\Gamma(\phi\pi)/\Gamma(\pi^\pm\pi^+\pi^-\pi^0)$ — **Γ_{12}/Γ_2**

VALUE	DOCUMENT ID		TECN	CHG	COMMENT
• • • We do not use the following data for averages, fits, limits, etc. • • •					
<0.11	BALTAY	68	HBC	+	7,8.5 $\pi^+ p$

$\Gamma(\pi^\pm 2\pi^+ 2\pi^- \pi^0)/\Gamma(\pi^\pm\pi^+\pi^-\pi^0)$ — **Γ_{14}/Γ_2**

VALUE	DOCUMENT ID		TECN	CHG	COMMENT
• • • We do not use the following data for averages, fits, limits, etc. • • •					
<0.15	BALTAY	68	HBC	+	7,8.5 $\pi^+ p$

$\Gamma(\eta\pi)/\Gamma(\pi^\pm\pi^+\pi^-\pi^0)$ — **Γ_{13}/Γ_2**

VALUE	DOCUMENT ID		TECN	CHG	COMMENT
• • • We do not use the following data for averages, fits, limits, etc. • • •					
<0.02	THOMPSON	74	HBC	+	13 $\pi^+ p$

$\Gamma(K\overline{K})/\Gamma_{\rm total}$ — **Γ_6/Γ**

VALUE	DOCUMENT ID		TECN	CHG	COMMENT
0.0158±0.0026 OUR FIT Error includes scale factor of 1.2.					
0.0130±0.0024 OUR AVERAGE					
0.013 ±0.003	COSTA	80	OMEG	0	10 $\pi^- p \to K^+ K^- n$
0.013 ±0.004	[33] MARTIN	78B	SPEC	−	10 $\pi p \to K^0_S K^- p$

[33] From $(\Gamma_4\Gamma_6)^{1/2} = 0.056 \pm 0.034$ assuming $B(\rho_3(1690) \to \pi\pi) = 0.24$.

$\Gamma(\omega\pi)/[\Gamma(\omega\pi) + \Gamma(\rho\rho)]$ — **$\Gamma_3/(\Gamma_3+\Gamma_{11})$**

VALUE	DOCUMENT ID		TECN	CHG	COMMENT
• • • We do not use the following data for averages, fits, limits, etc. • • •					
0.22±0.08	CASON	73	HBC	−	8,18.5 $\pi^- p$

$\Gamma(\eta\pi^+\pi^-)/\Gamma_{\rm total}$ — **Γ_7/Γ**

VALUE	DOCUMENT ID		TECN	COMMENT
seen	FUKUI	88	SPEC	8.95 $\pi^- p \to \eta\pi^+\pi^- n$

$\Gamma(a_2(1320)\pi)/\Gamma(\rho(770)\eta)$ Γ_{10}/Γ_8

VALUE	DOCUMENT ID		TECN	COMMENT
5.5±2.0	AMELIN	00	VES	37 $\pi^- p \rightarrow \eta\pi^+\pi^- n$

$\rho_3(1690)$ REFERENCES

AMELIN	00	NP A668 83	D. Amelin *et al.*	(VES Collab.)
ALDE	95	ZPHY C66 379	D.M. Alde *et al.*	(GAMS Collab.) JP
ALDE	92C	ZPHY C54 553	D.M. Alde *et al.*	(BELG, SERP, KEK, LANL+)
FUKUI	88	PL B202 441	S. Fukui *et al.*	(SUGI, NAGO, KEK, KYOT+)
DENNEY	83	PR D28 2726	D.L. Denney *et al.*	(IOWA, MICH)
EVANGELIS...	81	NP B178 197	C. Evangelista *et al.*	(BARI, BONN, CERN+)
ALPER	80	PL 94B 422	B. Alper *et al.*	(AMST, CERN, CRAC, MPIM+)
COSTA	80	NP B175 402	G. Costa *et al.*	(BARI, BONN, CERN, GLAS+)
GORLICH	80	NP B174 16	L. Gorlich *et al.*	(CRAC, MPIM, CERN+)
BECKER	79	NP B151 46	H. Becker *et al.*	(MPIM, CERN, ZEEM, CRAC)
CORDEN	79	NP B157 250	M.J. Corden *et al.*	(BIRM, RHEL, TELA+) JP
BALTAY	78B	PR D17 62	C. Baltay *et al.*	(COLU, BING)
MARTIN	78B	NP B140 158	A.D. Martin *et al.*	(DURH, GEVA)
MARTIN	78D	PL 74B 417	A.D. Martin *et al.*	(DURH, GEVA)
ANTIPOV	77	NP B119 45	Y.M. Antipov *et al.*	(SERP, GEVA)
GESSAROLI	77	NP B126 382	R. Gessaroli *et al.*	(BGNA, FIRZ, GENO+)
BLUM	75	PL 57B 403	W. Blum *et al.*	(CERN, MPIM) JP
ESTABROOKS	75	NP B95 322	P.G. Estabrooks, A.D. Martin	(DURH)
HYAMS	75	NP B100 205	B.D. Hyams *et al.*	(CERN, MPIM)
ENGLER	74	PR D10 2070	A. Engler *et al.*	(CMU, CASE)
GRAYER	74	NP B75 189	G. Grayer *et al.*	(CERN, MPIM)
KLIGER	74	SJNP 19 428	G.K. Kliger *et al.*	(ITEP)
		Translated from YAF 19 839.		
OREN	74	NP B71 189	Y. Oren *et al.*	(ANL, OXF)
THOMPSON	74	NP B69 220	G. Thompson *et al.*	(PURD)
CASON	73	PR D7 1971	N.M. Cason *et al.*	(NDAM)
BOWEN	72	PRL 29 890	D.R. Bowen *et al.*	(NEAS, STON)
HOLMES	72	PR D6 3336	R. Holmes *et al.*	(ROCH)
BALLAM	71B	PR D3 2606	J. Ballam *et al.*	(SLAC)
MATTHEWS	71C	NP B33 1	J.A.J. Matthews *et al.*	(TNTO, WISC) JP
ARMENISE	70	LNC 4 199	N. Armenise *et al.*	(BARI, BGNA, FIRZ)
BARNHAM	70	PRL 24 1083	K.W.J. Barnham *et al.*	(BIRM)
BARTSCH	70B	NP B22 109	J. Bartsch *et al.*	(AACH, BERL, CERN)
CASO	70	LNC 3 707	C. Caso *et al.*	(GENO, HAMB, MILA, SACL)
STUNTEBECK	70	PL 32B 391	P.H. Stuntebeck *et al.*	(NDAM)
ADERHOLZ	69	NP B11 259	M. Aderholz *et al.*	(AACH3, BERL, CERN+)
ANDERSON	69	PRL 22 1390	E.W. Anderson *et al.*	(BNL, CMU)
ARMENISE	68	NC 54A 999	N. Armenise *et al.*	(BARI, BGNA, FIRZ+) I
BALTAY	68	PRL 20 887	C. Baltay *et al.*	(COLU, ROCH, RUTG, YALE) I
CASO	68	NC 54A 983	C. Caso *et al.*	(GENO, HAMB, MILA, SACL)
CRENNELL	68B	PL 28B 136	D.J. Crennell *et al.*	(BNL)
JOHNSTON	68	PRL 20 1414	T.F. Johnston *et al.*	(TNTO, WISC) IJP
FOCACCI	66	PRL 17 890	M.N. Focacci *et al.*	(CERN)
GOLDBERG	65	PL 17 354	M. Goldberg *et al.*	(CERN, EPOL, ORSAY+)

$\rho(1700)$

$I^G(J^{PC}) = 1^+(1^{--})$

See the related review(s):
$\rho(1450)$ and $\rho(1700)$

$\rho(1700)$ MASS

$\eta\rho^0$ AND $\pi^+\pi^-$ MODES

VALUE (MeV)	DOCUMENT ID
1720±20 OUR ESTIMATE	

$\eta\rho^0$ MODE

VALUE (MeV)	EVTS	DOCUMENT ID	TECN	COMMENT
The data in this block is included in the average printed for a previous datablock.				
• • • We do not use the following data for averages, fits, limits, etc. • • •				
1840±10	7.4k	[1] ACHASOV 18	SND	1.22–2.00 $e^+e^- \rightarrow \eta\pi^+\pi^-$
1740±20		ANTONELLI 88	DM2	$e^+e^- \rightarrow \eta\pi^+\pi^-$
1701±15		[2] FUKUI 88	SPEC	8.95 $\pi^- p \rightarrow \eta\pi^+\pi^- n$

[1] From the combined fit of AULCHENKO 15 and ACHASOV 18 in the model with the interfering $\rho(1450)$, $\rho(1700)$ and $\rho(2150)$ with the parameters of the $\rho(1450)$ and $\rho(1700)$ floating and the mass and width of the $\rho(2150)$ fixed at 2155 MeV and 320 MeV, respectively. The phases of the resonances are π, 0 and π, respectively.
[2] Assuming $\rho^+ f_0(1370)$ decay mode interferes with $a_1(1260)^+\pi$ background. From a two Breit-Wigner fit.

$\pi\pi$ MODE

VALUE (MeV)	EVTS	DOCUMENT ID	TECN	COMMENT
The data in this block is included in the average printed for a previous datablock.				
• • • We do not use the following data for averages, fits, limits, etc. • • •				
1770.54± 5.49		[1] BARTOS 17	RVUE	$e^+e^- \rightarrow \pi^+\pi^-$
1718.50±65.44		[2] BARTOS 17A	RVUE	$e^+e^- \rightarrow \pi^+\pi^-$
1766.80±52.36		[3] BARTOS 17A	RVUE	$\tau^- \rightarrow \pi^-\pi^0\nu_\tau$
1644 ±36	20K	[4] LEES 17C	BABR	$J/\psi \rightarrow \pi^+\pi^-\pi^0$
1780 ±20 $^{+15}_{-20}$	63.5k	[5] ABRAMOWICZ 12	ZEUS	$ep \rightarrow e\pi^+\pi^- p$
1861 ±17		[6] LEES 12G	BABR	$e^+e^- \rightarrow \pi^+\pi^-\gamma$
1728 ±17 ±89	5.4M	[7,8] FUJIKAWA 08	BELL	$\tau^- \rightarrow \pi^-\pi^0\nu_\tau$
1780 $^{+37}_{-29}$		[9] ABELE 97	CBAR	$\overline{p}n \rightarrow \pi^-\pi^0\pi^0$
1719 ±15		[9] BERTIN 97C	OBLX	0.0 $\overline{p}p \rightarrow \pi^+\pi^-\pi^0$
1730 ±30		CLEGG 94	RVUE	$e^+e^- \rightarrow \pi^+\pi^-$
1768 ±21		BISELLO 89	DM2	$e^+e^- \rightarrow \pi^+\pi^-$
1745.7 ±91.9		DUBNICKA 89	RVUE	$e^+e^- \rightarrow \pi^+\pi^-$
1546 ±26		GESHKEN... 89	RVUE	
1650		[10] ERKAL 85	RVUE	20–70 $\gamma p \rightarrow \gamma\pi$
1550 ±70		ABE 84B	HYBR	20 $\gamma p \rightarrow \pi^+\pi^- p$
1590 ±20		[11] ASTON 80	OMEG	20–70 $\gamma p \rightarrow p2\pi$
1600 ±10		[12] ATIYA 79B	SPEC	50 $\gamma C \rightarrow C2\pi$
1598 $^{+24}_{-22}$		BECKER 79	ASPK	17 $\pi^- p$ polarized
1659 ±25		[10] LANG 79	RVUE	
1575		[10] MARTIN 78C	RVUE	17 $\pi^- p \rightarrow \pi^+\pi^- n$
1610 ±30		[10] FROGGATT 77	RVUE	17 $\pi^- p \rightarrow \pi^+\pi^- n$
1590 ±20		[13] HYAMS 73	ASPK	17 $\pi^- p \rightarrow \pi^+\pi^- n$

[1] Applies the Unitary & Analytic Model of the pion electromagnetic form factor of DUBNICKA 10 to analyze the data of LEES 12G and ABLIKIM 16C.
[2] Applies the Unitary & Analytic Model of the pion electromagnetic form factor of DUBNICKA 10 to analyze the data of ACHASOV 06, AKHMETSHIN 07, AUBERT 09AS, and AMBROSINO 11A.
[3] Applies the Unitary & Analytic Model of the pion electromagnetic form factor of DUBNICKA 10 to analyze the data of FUJIKAWA 08.
[4] From a Dalitz plot analysis in an isobar model with $\rho(1450)$ and $\rho(1700)$ masses and widths floating.
[5] Using the KUHN 90 parametrization of the pion form factor, neglecting $\rho-\omega$ interference.
[6] Using the GOUNARIS 68 parametrization of the pion form factor leaving the masses and widths of the $\rho(1450)$, $\rho(1700)$, and $\rho(2150)$ resonances as free parameters of the fit.
[7] $|F_\pi(0)|^2$ fixed to 1.
[8] From the GOUNARIS 68 parametrization of the pion form factor.
[9] T-matrix pole.
[10] From phase shift analysis of HYAMS 73 data.
[11] Simple relativistic Breit-Wigner fit with constant width.
[12] An additional 40 MeV uncertainty in both the mass and width is present due to the choice of the background shape.
[13] Included in BECKER 79 analysis.

$\pi\omega$ MODE

VALUE (MeV)	EVTS	DOCUMENT ID		TECN	COMMENT
• • • We do not use the following data for averages, fits, limits, etc. • • •					
1708±41	7815	[1] ACHASOV	13	SND	1.05–2.00 $e^+e^- \rightarrow \pi^0\pi^0\gamma$
1550 to 1620		[2] ACHASOV	00I	SND	$e^+e^- \rightarrow \pi^0\pi^0\gamma$
1580 to 1710		[3] ACHASOV	00I	SND	$e^+e^- \rightarrow \pi^0\pi^0\gamma$
1710±90		ACHASOV	97	RVUE	$e^+e^- \rightarrow \omega\pi^0$

[1] From a phenomenological model based on vector meson dominance with the interfering $\rho(1450)$ and $\rho(1700)$ and their widths fixed at 400 and 250 MeV, respectively. Systematic uncertainty not estimated.
[2] Taking into account both $\rho(1450)$ and $\rho(1700)$ contributions. Using the data of ACHASOV 00I on $e^+e^- \rightarrow \omega\pi^0$ and of EDWARDS 00A on $\tau^- \rightarrow \omega\pi^-\nu_\tau$. $\rho(1450)$ mass and width fixed at 1400 MeV and 500 MeV respectively.
[3] Taking into account the $\rho(1700)$ contribution only. Using the data of ACHASOV 00I on $e^+e^- \rightarrow \omega\pi^0$ and of EDWARDS 00A on $\tau^- \rightarrow \omega\pi^-\nu_\tau$.

$K\overline{K}$ MODE

VALUE (MeV)	EVTS	DOCUMENT ID		TECN	CHG	COMMENT
1541 ±12 ±33	190k	[1] AAIJ	16N	LHCB		$D^0 \rightarrow K^0_S K^\pm\pi^\mp$
• • • We do not use the following data for averages, fits, limits, etc. • • •						
1740.8±22.2	27k	[2] ABELE	99D	CBAR	±	0.0 $\overline{p}p \rightarrow K^+K^-\pi^0$
1582 ±36	1600	CLELAND	82B	SPEC	±	50 $\pi p \rightarrow K^0_S K^\pm p$

[1] Using the GOUNARIS 68 parameterization with a fixed width. Value is average using different $K\pi$ S-wave parametrizations in fit.
[2] K-matrix pole. Isospin not determined, could be $\omega(1650)$ or $\phi(1680)$.

2 ($\pi^+\pi^-$) MODE

VALUE (MeV)	EVTS	DOCUMENT ID		TECN	COMMENT
• • • We do not use the following data for averages, fits, limits, etc. • • •					
1851 $^{+\ 27}_{-\ 24}$		ACHASOV 97		RVUE	$e^+e^- \rightarrow 2(\pi^+\pi^-)$
1570± 20		[1] CORDIER 82		DM1	$e^+e^- \rightarrow 2(\pi^+\pi^-)$
1520± 30		[2] ASTON 81E		OMEG	20–70 $\gamma p \rightarrow p4\pi$
1654± 25		[3] DIBIANCA 81		DBC	$\pi^+ d \rightarrow pp2(\pi^+\pi^-)$
1666± 39		[1] BACCI 80		FRAG	$e^+e^- \rightarrow 2(\pi^+\pi^-)$
1780	34	KILLIAN 80		SPEC	11 $e^- p \rightarrow 2(\pi^+\pi^-)$
1500		[4] ATIYA 79B		SPEC	50 $\gamma C \rightarrow C4\pi^\pm$
1570± 60	65	[5] ALEXANDER 75		HBC	7.5 $\gamma p \rightarrow p4\pi$
1550± 60		[2] CONVERSI 74		OSPK	$e^+e^- \rightarrow 2(\pi^+\pi^-)$
1550± 50	160	SCHACHT 74		STRC	5.5–9 $\gamma p \rightarrow p4\pi$
1450±100	340	SCHACHT 74		STRC	9–18 $\gamma p \rightarrow p4\pi$
1430± 50	400	BINGHAM 72B		HBC	9.3 $\gamma p \rightarrow p4\pi$

[1] Simple relativistic Breit-Wigner fit with model dependent width.
[2] Simple relativistic Breit-Wigner fit with constant width.
[3] One peak fit result.
[4] Parameters roughly estimated, not from a fit.
[5] Skew mass distribution compensated by Ross-Stodolsky factor.

$\pi^+\pi^-\pi^0\pi^0$ MODE

VALUE (MeV)	DOCUMENT ID	TECN	COMMENT
• • • We do not use the following data for averages, fits, limits, etc. • • •			
1660±30	ATKINSON 85B	OMEG	20–70 γp

Meson Particle Listings

$\rho(1700)$

$3(\pi^+\pi^-)$ AND $2(\pi^+\pi^-\pi^0)$ MODES

VALUE (MeV)	DOCUMENT ID		TECN	COMMENT
• • • We do not use the following data for averages, fits, limits, etc. • • •				
1730±34	[1] FRABETTI	04	E687	$\gamma p \to 3\pi^+ 3\pi^- p$
1783±15	CLEGG	90	RVUE	$e^+e^- \to 3(\pi^+\pi^-)2(\pi^+\pi^-\pi^0)$

[1] From a fit with two resonances with the JACOB 72 continuum.

$m_{\rho(1700)^0} - m_{\rho(1700)^\pm}$

VALUE (MeV)	DOCUMENT ID		TECN	COMMENT
• • • We do not use the following data for averages, fits, limits, etc. • • •				
−48.30±83.81	[1] BARTOS	17A	RVUE	$e^+e^- \to \pi^+\pi^-$, $\tau^- \to \pi^-\pi^0\nu_\tau$

[1] Applies the Unitary & Analytic Model of the pion electromagnetic form factor of DUBNICKA 10 to analyze the data of ACHASOV 06, AKHMETSHIN 07, AUBERT 09AS, AMBROSINO 11A, and FUJIKAWA 08.

$\rho(1700)$ WIDTH

$\eta\rho^0$ AND $\pi^+\pi^-$ MODES

VALUE (MeV)	DOCUMENT ID
250±100 OUR ESTIMATE	

$\eta\rho^0$ MODE

VALUE (MeV)	EVTS	DOCUMENT ID		TECN	COMMENT
The data in this block is included in the average printed for a previous datablock.					
• • • We do not use the following data for averages, fits, limits, etc. • • •					
132±40	7.4k	[1] ACHASOV	18	SND	1.22–2.00 $e^+e^- \to \eta\pi^+\pi^-$
150±30		ANTONELLI	88	DM2	$e^+e^- \to \eta\pi^+\pi^-$
282±44		[2] FUKUI	88	SPEC	8.95 $\pi^- p \to \eta\pi^+\pi^- n$

[1] From the combined fit of AULCHENKO 15 and ACHASOV 18 in the model with the interfering $\rho(1450)$, $\rho(1700)$ and $\rho(2150)$ with the parameters of the $\rho(1450)$ and $\rho(1700)$ floating and the mass and width of the $\rho(2150)$ fixed at 2155 MeV and 320 MeV, respectively. The phases of the resonances are π, 0 and π, respectively.

[2] Assuming $\rho^+ f_0(1370)$ decay mode interferes with $a_1(1260)^+\pi$ background. From a two Breit-Wigner fit.

$\pi\pi$ MODE

VALUE (MeV)	EVTS	DOCUMENT ID		TECN	COMMENT
The data in this block is included in the average printed for a previous datablock.					
• • • We do not use the following data for averages, fits, limits, etc. • • •					
268.98± 11.40		[1] BARTOS	17	RVUE	$e^+e^- \to \pi^+\pi^-$
489.58± 16.95		[2] BARTOS	17A	RVUE	$e^+e^- \to \pi^+\pi^-$
414.71±119.48		[3] BARTOS	17A	RVUE	$\tau^- \to \pi^-\pi^0\nu_\tau$
109 ± 19	20K	[4] LEES	17C	BABR	$J/\psi \to \pi^+\pi^-\pi^0$
310 $^{+25}_{-35}$	63.5k	[5] ABRAMOWICZ	12	ZEUS	$ep \to e\pi^+\pi^- p$
316 ± 26		[6] LEES	12G	BABR	$e^+e^- \to \pi^+\pi^-\gamma$
164 ± 21 $^{+89}_{-26}$	5.4M	[7,8] FUJIKAWA	08	BELL	$\tau^- \to \pi^-\pi^0\nu_\tau$
275 ± 45		[9] ABELE	97	CBAR	$\overline{p}n \to \pi^-\pi^0\pi^0$
310 ± 40		[9] BERTIN	97C	OBLX	0.0 $\overline{p}p \to \pi^+\pi^-\pi^0$
400 ±100		CLEGG	94	RVUE	$e^+e^- \to \pi^+\pi^-$
224 ± 22		BISELLO	89	DM2	$e^+e^- \to \pi^+\pi^-$
242.5 ±163.0		DUBNICKA	89	RVUE	$e^+e^- \to \pi^+\pi^-$
620 ± 60		GESHKEN...	89	RVUE	
<315		[10] ERKAL	85	RVUE	20–70 $\gamma p \to \gamma\pi$
280 $^{+30}_{-80}$		ABE	84B	HYBR	20 $\gamma p \to \pi^+\pi^- p$
230 ± 80		[11] ASTON	80	OMEG	20–70 $\gamma p \to p 2\pi$
283 ± 14		[12] ATIYA	79B	SPEC	50 γC → C2π
175 $^{+98}_{-53}$		BECKER	79	ASPK	17 $\pi^- p$ polarized
232 ± 34		[10] LANG	79	RVUE	
340		[10] MARTIN	78C	RVUE	17 $\pi^- p \to \pi^+\pi^- n$
300 ±100		[10] FROGGATT	77	RVUE	17 $\pi^- p \to \pi^+\pi^- n$
180 ± 50		[13] HYAMS	73	ASPK	17 $\pi^- p \to \pi^+\pi^- n$

[1] Applies the Unitary & Analytic Model of the pion electromagnetic form factor of DUBNICKA 10 to analyze the data of LEES 12G and ABLIKIM 16C.

[2] Applies the Unitary & Analytic Model of the pion electromagnetic form factor of DUBNICKA 10 to analyze the data of ACHASOV 06, AKHMETSHIN 07, AUBERT 09AS, and AMBROSINO 11A.

[3] Applies the Unitary & Analytic Model of the pion electromagnetic form factor of DUBNICKA 10 to analyze the data of FUJIKAWA 08.

[4] From a Dalitz plot analysis in an isobar model with $\rho(1450)$ and $\rho(1700)$ masses and widths floating.

[5] Using the KUHN 90 parametrization of the pion form factor, neglecting $\rho-\omega$ interference.

[6] Using the GOUNARIS 68 parametrization of the pion form factor leaving the masses and widths of the $\rho(1450)$, $\rho(1700)$, and $\rho(2150)$ resonances as free parameters of the fit.

[7] $|F_\pi(0)|^2$ fixed to 1.

[8] From the GOUNARIS 68 parametrization of the pion form factor.

[9] T-matrix pole.

[10] From phase shift analysis of HYAMS 73 data.

[11] Simple relativistic Breit-Wigner fit with constant width.

[12] An additional 40 MeV uncertainty in both the mass and width is present due to the choice of the background shape.

[13] Included in BECKER 79 analysis.

$K\overline{K}$ MODE

VALUE (MeV)	EVTS	DOCUMENT ID		TECN	CHG	COMMENT
• • • We do not use the following data for averages, fits, limits, etc. • • •						
187.2± 26.7	27k	[1] ABELE	99D	CBAR	±	0.0 $\overline{p}p \to K^+K^-\pi^0$
265 ±120	1600	CLELAND	82B	SPEC	±	50 $\pi p \to K^0_S K^\pm p$

[1] K-matrix pole. Isospin not determined, could be $\omega(1650)$ or $\phi(1680)$.

2 $(\pi^+\pi^-)$ MODE

VALUE (MeV)	EVTS	DOCUMENT ID		TECN	COMMENT
• • • We do not use the following data for averages, fits, limits, etc. • • •					
510± 40		[1] CORDIER	82	DM1	$e^+e^- \to 2(\pi^+\pi^-)$
400± 50		[2] ASTON	81E	OMEG	20–70 $\gamma p \to p4\pi$
400±146		[3] DIBIANCA	81	DBC	$\pi^+ d \to pp2(\pi^+\pi^-)$
700±160		[1] BACCI	80	FRAG	$e^+e^- \to 2(\pi^+\pi^-)$
100	34	KILLIAN	80	SPEC	11 $e^- p \to 2(\pi^+\pi^-)$
600		[4] ATIYA	79B	SPEC	50 γC → C4$\pi^\pm$
340±160	65	[5] ALEXANDER	75	HBC	7.5 $\gamma p \to p4\pi$
360±100		[2] CONVERSI	74	OSPK	$e^+e^- \to 2(\pi^+\pi^-)$
400±120	160	[6] SCHACHT	74	STRC	5.5–9 $\gamma p \to p4\pi$
850±200	340	[6] SCHACHT	74	STRC	9–18 $\gamma p \to p4\pi$
650±100	400	BINGHAM	72B	HBC	9.3 $\gamma p \to p4\pi$

[1] Simple relativistic Breit-Wigner fit with model-dependent width.

[2] Simple relativistic Breit-Wigner fit with constant width.

[3] One peak fit result.

[4] Parameters roughly estimated, not from a fit.

[5] Skew mass distribution compensated by Ross-Stodolsky factor.

[6] Width errors enlarged by us to $4\Gamma/\sqrt{N}$; see the note with the $K^*(892)$ mass.

$\pi^+\pi^-\pi^0\pi^0$ MODE

VALUE (MeV)	DOCUMENT ID		TECN	COMMENT
• • • We do not use the following data for averages, fits, limits, etc. • • •				
300±50	ATKINSON	85B	OMEG	20–70 γp

$\omega\pi^0$ MODE

VALUE (MeV)	DOCUMENT ID		TECN	COMMENT
• • • We do not use the following data for averages, fits, limits, etc. • • •				
350 to 580	[1] ACHASOV	00I	SND	$e^+e^- \to \pi^0\pi^0\gamma$
490 to 1040	[2] ACHASOV	00I	SND	$e^+e^- \to \pi^0\pi^0\gamma$

[1] Taking into account both $\rho(1450)$ and $\rho(1700)$ contributions. Using the data of ACHASOV 00I on $e^+e^- \to \omega\pi^0$ and of EDWARDS 00A on $\tau^- \to \omega\pi^-\nu_\tau$. $\rho(1450)$ mass and width fixed at 1400 MeV and 500 MeV respectively.

[2] Taking into account the $\rho(1700)$ contribution only. Using the data of ACHASOV 00I on $e^+e^- \to \omega\pi^0$ and of EDWARDS 00A on $\tau^- \to \omega\pi^-\nu_\tau$.

$3(\pi^+\pi^-)$ AND $2(\pi^+\pi^-\pi^0)$ MODES

VALUE (MeV)	DOCUMENT ID		TECN	COMMENT
• • • We do not use the following data for averages, fits, limits, etc. • • •				
315±100	[1] FRABETTI	04	E687	$\gamma p \to 3\pi^+ 3\pi^- p$
285± 20	CLEGG	90	RVUE	$e^+e^- \to 3(\pi^+\pi^-)2(\pi^+\pi^-\pi^0)$

[1] From a fit with two resonances with the JACOB 72 continuum.

$\Gamma_{\rho(1700)^0} - \Gamma_{\rho(1700)^\pm}$

VALUE (MeV)	DOCUMENT ID		TECN	COMMENT
• • • We do not use the following data for averages, fits, limits, etc. • • •				
74.87±120.67	[1] BARTOS	17A	RVUE	$e^+e^- \to \pi^+\pi^-, \tau^- \to \pi^-\pi^0\nu_\tau$

[1] Applies the Unitary & Analytic Model of the pion electromagnetic form factor of DUBNICKA 10 to analyze the data of ACHASOV 06, AKHMETSHIN 07, AUBERT 09AS, AMBROSINO 11A, and FUJIKAWA 08.

$\rho(1700)$ DECAY MODES

	Mode	Fraction (Γ_i/Γ)
Γ_1	4π	
Γ_2	$2(\pi^+\pi^-)$	large
Γ_3	$\rho\pi\pi$	dominant
Γ_4	$\rho^0\pi^+\pi^-$	large
Γ_5	$\rho^0\pi^0\pi^0$	
Γ_6	$\rho^\pm\pi^\mp\pi^0$	large
Γ_7	$a_1(1260)\pi$	seen
Γ_8	$h_1(1170)\pi$	seen
Γ_9	$\pi(1300)\pi$	seen
Γ_{10}	$\rho\rho$	seen
Γ_{11}	$\pi^+\pi^-$	seen
Γ_{12}	$\pi\pi$	seen
Γ_{13}	$K\overline{K}^*(892)+$ c.c.	seen
Γ_{14}	$\eta\rho$	seen

Γ_{15}	$a_2(1320)\pi$	not seen
Γ_{16}	$K\overline{K}$	seen
Γ_{17}	e^+e^-	seen
Γ_{18}	$\pi^0\omega$	seen

$\rho(1700)$ $\Gamma(i)\Gamma(e^+e^-)/\Gamma(\text{total})$

This combination of a partial width with the partial width into e^+e^- and with the total width is obtained from the cross-section into channel$_i$ in e^+e^- annihilation.

$\Gamma(2(\pi^+\pi^-)) \times \Gamma(e^+e^-)/\Gamma_{\text{total}}$ $\Gamma_2\Gamma_{17}/\Gamma$

VALUE (keV)	DOCUMENT ID		TECN	COMMENT
• • • We do not use the following data for averages, fits, limits, etc. • • •				
2.6 ±0.2	DELCOURT	81B	DM1	$e^+e^- \to 2(\pi^+\pi^-)$
2.83±0.42	BACCI	80	FRAG	$e^+e^- \to 2(\pi^+\pi^-)$

$\Gamma(\pi^+\pi^-) \times \Gamma(e^+e^-)/\Gamma_{\text{total}}$ $\Gamma_{11}\Gamma_{17}/\Gamma$

VALUE (keV)	DOCUMENT ID		TECN	COMMENT
• • • We do not use the following data for averages, fits, limits, etc. • • •				
0.13	[1] DIEKMAN	88	RVUE	$e^+e^- \to \pi^+\pi^-$
$0.029^{+0.016}_{-0.012}$	KURDADZE	83	OLYA	0.64–1.4 $e^+e^- \to \pi^+\pi^-$

[1] Using total width = 220 MeV.

$\Gamma(K\overline{K}^*(892)+\text{c.c.}) \times \Gamma(e^+e^-)/\Gamma_{\text{total}}$ $\Gamma_{13}\Gamma_{17}/\Gamma$

VALUE (keV)	DOCUMENT ID		TECN	COMMENT
• • • We do not use the following data for averages, fits, limits, etc. • • •				
0.305±0.071	[1] BIZOT	80	DM1	e^+e^-

[1] Model dependent.

$\Gamma(\eta\rho) \times \Gamma(e^+e^-)/\Gamma_{\text{total}}$ $\Gamma_{14}\Gamma_{17}/\Gamma$

VALUE (eV)	DOCUMENT ID		TECN	COMMENT
• • • We do not use the following data for averages, fits, limits, etc. • • •				
7±3	ANTONELLI	88	DM2	$e^+e^- \to \eta\pi^+\pi^-$

$\Gamma(K\overline{K}) \times \Gamma(e^+e^-)/\Gamma_{\text{total}}$ $\Gamma_{16}\Gamma_{17}/\Gamma$

VALUE (keV)	DOCUMENT ID		TECN	COMMENT
• • • We do not use the following data for averages, fits, limits, etc. • • •				
0.035±0.029	[1] BIZOT	80	DM1	e^+e^-

[1] Model dependent.

$\Gamma(\rho\pi\pi) \times \Gamma(e^+e^-)/\Gamma_{\text{total}}$ $\Gamma_3\Gamma_{17}/\Gamma$

VALUE (keV)	DOCUMENT ID		TECN	COMMENT
• • • We do not use the following data for averages, fits, limits, etc. • • •				
3.510±0.090	[1] BIZOT	80	DM1	e^+e^-

[1] Model dependent.

$\rho(1700)$ $\Gamma(i)/\Gamma(\text{total}) \times \Gamma(e^+e^-)/\Gamma(\text{total})$

$\Gamma(\pi^0\omega)/\Gamma_{\text{total}} \times \Gamma(e^+e^-)/\Gamma_{\text{total}}$ $\Gamma_{18}/\Gamma \times \Gamma_{17}/\Gamma$

VALUE (units 10^{-6})	EVTS	DOCUMENT ID		TECN	COMMENT
• • • We do not use the following data for averages, fits, limits, etc. • • •					
0.09±0.05	10.2k	[1] ACHASOV	16D	SND	1.05–2.00 $e^+e^- \to \pi^0\pi^0\gamma$
1.7 ±0.4	7815	[2] ACHASOV	13	SND	1.05–2.00 $e^+e^- \to \pi^0\pi^0\gamma$

[1] From a phenomenological model based on vector meson dominance with interfering $\rho(700)$, $\rho(1450)$, and $\rho(1700)$. The $\rho(1700)$ mass and width are fixed at 1720 MeV and 250 MeV, respectively. Systematic uncertainty not estimated. Supersedes ACHASOV 13.

[2] From a phenomenological model based on vector meson dominance with the interfering $\rho(1450)$ and $\rho(1700)$ and their widths fixed at 400 and 250 MeV, respectively. Systematic uncertainty not estimated.

$\Gamma(\eta\rho)/\Gamma_{\text{total}} \times \Gamma(e^+e^-)/\Gamma_{\text{total}}$ $\Gamma_{14}/\Gamma \times \Gamma_{17}/\Gamma$

VALUE (units 10^{-8})	EVTS	DOCUMENT ID		TECN	COMMENT
• • • We do not use the following data for averages, fits, limits, etc. • • •					
$8.3^{+3.8}_{-3.1}$	7.4k	[1] ACHASOV	18	SND	1.22–2.00 $e^+e^- \to \eta\pi^+\pi^-$

[1] From the combined fit of AULCHENKO 15 and ACHASOV 18 in the model with the interfering $\rho(1450)$, $\rho(1700)$ and $\rho(2150)$ with the parameters of the $\rho(1450)$ and $\rho(1700)$ floating and the mass and width of the $\rho(2150)$ fixed at 2155 MeV and 320 MeV, respectively. The phases of the resonances are π, 0 and π, respectively.

$\rho(1700)$ BRANCHING RATIOS

$\Gamma(\rho\pi\pi)/\Gamma(4\pi)$ Γ_3/Γ_1

VALUE	DOCUMENT ID		TECN	COMMENT
• • • We do not use the following data for averages, fits, limits, etc. • • •				
0.28±0.06	[1] ABELE	01B	CBAR	0.0 $\overline{p}n \to 5\pi$

[1] $\omega\pi$ not included.

$\Gamma(\rho^0\pi^+\pi^-)/\Gamma(2(\pi^+\pi^-))$ Γ_4/Γ_2

VALUE	EVTS	DOCUMENT ID		TECN	COMMENT
• • • We do not use the following data for averages, fits, limits, etc. • • •					
~ 1.0		DELCOURT	81B	DM1	$e^+e^- \to 2(\pi^+\pi^-)$
0.7 ±0.1	500	SCHACHT	74	STRC	5.5–18 $\gamma p \to p4\pi$
0.80		[1] BINGHAM	72B	HBC	9.3 $\gamma p \to p4\pi$

[1] The $\pi\pi$ system is in S-wave.

$\Gamma(\rho^0\pi^0\pi^0)/\Gamma(\rho^\pm\pi^\mp\pi^0)$ Γ_5/Γ_6

VALUE	DOCUMENT ID		TECN	CHG	COMMENT
• • • We do not use the following data for averages, fits, limits, etc. • • •					
<0.10	ATKINSON	85B	OMEG		20–70 γp
<0.15	ATKINSON	82	OMEG	0	20–70 $\gamma p \to p4\pi$

$\Gamma(a_1(1260)\pi)/\Gamma(4\pi)$ Γ_7/Γ_1

VALUE	DOCUMENT ID		TECN	COMMENT
• • • We do not use the following data for averages, fits, limits, etc. • • •				
0.16±0.05	[1] ABELE	01B	CBAR	0.0 $\overline{p}n \to 5\pi$

[1] $\omega\pi$ not included.

$\Gamma(h_1(1170)\pi)/\Gamma(4\pi)$ Γ_8/Γ_1

VALUE	DOCUMENT ID		TECN	COMMENT
• • • We do not use the following data for averages, fits, limits, etc. • • •				
0.17±0.06	[1] ABELE	01B	CBAR	0.0 $\overline{p}n \to 5\pi$

[1] $\omega\pi$ not included.

$\Gamma(\pi(1300)\pi)/\Gamma(4\pi)$ Γ_9/Γ_1

VALUE	DOCUMENT ID		TECN	COMMENT
• • • We do not use the following data for averages, fits, limits, etc. • • •				
0.30±0.10	[1] ABELE	01B	CBAR	0.0 $\overline{p}n \to 5\pi$

[1] $\omega\pi$ not included.

$\Gamma(\rho\rho)/\Gamma(4\pi)$ Γ_{10}/Γ_1

VALUE	DOCUMENT ID		TECN	COMMENT
• • • We do not use the following data for averages, fits, limits, etc. • • •				
0.09±0.03	[1] ABELE	01B	CBAR	0.0 $\overline{p}n \to 5\pi$

[1] $\omega\pi$ not included.

$\Gamma(\pi^+\pi^-)/\Gamma_{\text{total}}$ Γ_{11}/Γ

VALUE	DOCUMENT ID		TECN	COMMENT
• • • We do not use the following data for averages, fits, limits, etc. • • •				
$0.287^{+0.043}_{-0.042}$	BECKER	79	ASPK	17 π^-p polarized
0.15 to 0.30	[1] MARTIN	78C	RVUE	17 $\pi^-p \to \pi^+\pi^-n$
<0.20	[2] COSTA...	77B	RVUE	$e^+e^- \to 2\pi$, 4π
0.30 ±0.05	[1] FROGGATT	77	RVUE	17 $\pi^-p \to \pi^+\pi^-n$
<0.15	[3] EISENBERG	73	HBC	5 $\pi^+p \to \Delta^{++}2\pi$
0.25 ±0.05	[4] HYAMS	73	ASPK	17 $\pi^-p \to \pi^+\pi^-n$

[1] From phase shift analysis of HYAMS 73 data.
[2] Estimate using unitarity, time reversal invariance, Breit-Wigner.
[3] Estimated using one-pion-exchange model.
[4] Included in BECKER 79 analysis.

$\Gamma(\pi^+\pi^-)/\Gamma(2(\pi^+\pi^-))$ Γ_{11}/Γ_2

VALUE	DOCUMENT ID		TECN	COMMENT
• • • We do not use the following data for averages, fits, limits, etc. • • •				
0.13±0.05	ASTON	80	OMEG	20–70 $\gamma p \to p2\pi$
<0.14	[1] DAVIER	73	STRC	6–18 $\gamma p \to p4\pi$
<0.2	[2] BINGHAM	72B	HBC	9.3 $\gamma p \to p2\pi$

[1] Upper limit is estimate.
[2] 2σ upper limit.

$\Gamma(\pi\pi)/\Gamma(4\pi)$ Γ_{12}/Γ_1

VALUE	DOCUMENT ID		TECN	COMMENT
• • • We do not use the following data for averages, fits, limits, etc. • • •				
0.16±0.04	[1,2] ABELE	01B	CBAR	0.0 $\overline{p}n \to 5\pi$

[1] Using ABELE 97.
[2] $\omega\pi$ not included.

$\Gamma(K\overline{K}^*(892)+\text{c.c.})/\Gamma_{\text{total}}$ Γ_{13}/Γ

VALUE	DOCUMENT ID		TECN	COMMENT
• • • We do not use the following data for averages, fits, limits, etc. • • •				
possibly seen	COAN	04	CLEO	$\tau^- \to K^-\pi^-K^+\nu_\tau$

$\Gamma(K\overline{K}^*(892)+\text{c.c.})/\Gamma(2(\pi^+\pi^-))$ Γ_{13}/Γ_2

VALUE	DOCUMENT ID		TECN	COMMENT
• • • We do not use the following data for averages, fits, limits, etc. • • •				
0.15±0.03	[1] DELCOURT	81B	DM1	$e^+e^- \to \overline{K}K\pi$

[1] Assuming $\rho(1700)$ and ω radial excitations to be degenerate in mass.

Meson Particle Listings

$\rho(1700)$, $a_2(1700)$

$\Gamma(\eta\rho)/\Gamma_{\text{total}}$ Γ_{14}/Γ

VALUE	CL%	DOCUMENT ID		TECN	COMMENT
• • • We do not use the following data for averages, fits, limits, etc. • • •					
possibly seen		AKHMETSHIN	00D	CMD2	$e^+e^- \to \eta\pi^+\pi^-$
<0.04		DONNACHIE	87B	RVUE	
<0.02	58	ATKINSON	86B	OMEG	20–70 γp

$\Gamma(\eta\rho)/\Gamma(2(\pi^+\pi^-))$ Γ_{14}/Γ_2

VALUE	DOCUMENT ID		TECN	COMMENT
• • • We do not use the following data for averages, fits, limits, etc. • • •				
0.123 ± 0.027	DELCOURT	82	DM1	$e^+e^- \to \pi^+\pi^-$ MM
~ 0.1	ASTON	80	OMEG	20–70 γp

$\Gamma(\pi^+\pi^-\text{neutrals})/\Gamma(2(\pi^+\pi^-))$ $(\Gamma_5+\Gamma_6+0.714\Gamma_{14})/\Gamma_2$

VALUE	DOCUMENT ID		TECN	COMMENT
• • • We do not use the following data for averages, fits, limits, etc. • • •				
2.6 ± 0.4	[1] BALLAM	74	HBC	9.3 γp

[1] Upper limit. Background not subtracted.

$\Gamma(a_2(1320)\pi)/\Gamma_{\text{total}}$ Γ_{15}/Γ

VALUE	DOCUMENT ID		TECN	COMMENT
• • • We do not use the following data for averages, fits, limits, etc. • • •				
not seen	AMELIN	00	VES	37 $\pi^- p \to \eta\pi^+\pi^- n$

$\Gamma(K\overline{K})/\Gamma(2(\pi^+\pi^-))$ Γ_{16}/Γ_2

VALUE	CL%	DOCUMENT ID		TECN	CHG	COMMENT
• • • We do not use the following data for averages, fits, limits, etc. • • •						
0.015 ± 0.010		[1] DELCOURT	81B	DM1		$e^+e^- \to \overline{K}K$
<0.04	95	BINGHAM	72B	HBC	0	9.3 γp

[1] Assuming $\rho(1700)$ and ω radial excitations to be degenerate in mass.

$\Gamma(K\overline{K})/\Gamma(K\overline{K}^*(892)+\text{c.c.})$ Γ_{16}/Γ_{13}

VALUE	DOCUMENT ID		TECN	COMMENT
• • • We do not use the following data for averages, fits, limits, etc. • • •				
0.052 ± 0.026	BUON	82	DM1	$e^+e^- \to$ hadrons

$\Gamma(\pi^0\omega)/\Gamma_{\text{total}}$ Γ_{18}/Γ

VALUE	EVTS	DOCUMENT ID		TECN	COMMENT
• • • We do not use the following data for averages, fits, limits, etc. • • •					
not seen		MATVIENKO	15	BELL	$\overline{B}^0 \to D^{*+}\omega\pi^-$
seen	1.6k	ACHASOV	12	SND	$e^+e^- \to \pi^0\pi^0\gamma$
not seen	2382	AKHMETSHIN	03B	CMD2	$e^+e \to \pi^0\pi^0\gamma$
seen		ACHASOV	97	RVUE	$e^+e^- \to \omega\pi^0$

$\rho(1700)$ REFERENCES

ACHASOV	18	PR D97 012008	M.N. Achasov *et al.* (SND Collab.)
BARTOS	17	PR D96 113004	E. Bartos *et al.*
BARTOS	17A	IJMP A32 1750154	E. Bartos *et al.*
LEES	17C	PR D95 072007	J.P. Lees *et al.* (BABAR Collab)
AAIJ	16N	PR D93 052018	R. Aaij *et al.* (LHCb Collab.)
ABLIKIM	16C	PL B753 629	M. Ablikim *et al.* (BES III Collab.)
ACHASOV	16D	PR D94 112001	M.N. Achasov *et al.* (SND Collab.)
AULCHENKO	15	PR D91 052013	V.M. Aulchenko *et al.* (SND Collab.)
MATVIENKO	15	PR D92 012013	D. Matvienko *et al.* (BELLE Collab.)
ACHASOV	13	PR D88 054013	M.N. Achasov *et al.* (SND Collab.)
ABRAMOWICZ	12	EPJ C72 1869	H. Abramowicz *et al.* (ZEUS Collab.)
ACHASOV	12	JETPL 94 734	M.N. Achasov *et al.*
		Translated from ZETFP 94 796.	
LEES	12G	PR D86 032013	J.P. Lees *et al.* (BABAR Collab.)
AMBROSINO	11A	PL B700 102	F. Ambrosino *et al.* (KLOE Collab.)
DUBNICKA	10	APS 60 1	S. Dubnicka, A.Z. Dubnickova
AUBERT	09AS	PRL 103 231801	B. Aubert *et al.* (BABAR Collab.)
FUJIKAWA	08	PR D78 072006	M. Fujikawa *et al.* (BELLE Collab.)
AKHMETSHIN	07	PL B648 28	R.R. Akhmetshin *et al.* (Novosibirsk CMD-2 Collab.)
ACHASOV	06	JETP 103 380	M.N. Achasov *et al.* (Novosibirsk SND Collab.)
		Translated from ZETF 130 437.	
COAN	04	PRL 92 232001	T.E. Coan *et al.* (CLEO Collab.)
FRABETTI	04	PL B578 290	P.L. Frabetti *et al.* (FNAL E687 Collab.)
AKHMETSHIN	03B	PL B562 173	R.R. Akhmetshin *et al.* (Novosibirsk CMD-2 Collab.)
ABELE	01B	EPJ C21 261	A. Abele *et al.* (Crystal Barrel Collab.)
ACHASOV	00I	PL B486 29	M.N. Achasov *et al.* (Novosibirsk SND Collab.)
AKHMETSHIN	00D	PL B489 125	R.R. Akhmetshin *et al.* (Novosibirsk CMD-2 Collab.)
AMELIN	00	NP A668 83	D. Amelin *et al.* (VES Collab.)
EDWARDS	00A	PR D61 072003	K.W. Edwards *et al.* (CLEO Collab.)
ABELE	99D	PL B468 178	A. Abele *et al.* (Crystal Barrel Collab.)
ABELE	97	PL B391 191	A. Abele *et al.* (Crystal Barrel Collab.)
ACHASOV	97	PR D55 2663	N.N. Achasov *et al.* (NOVM)
BERTIN	97C	PL B408 476	A. Bertin *et al.* (OBELIX Collab.)
CLEGG	94	ZPHY C62 455	A.B. Clegg, A. Donnachie (LANC, MCHS)
CLEGG	90	ZPHY C45 677	A.B. Clegg, A. Donnachie (LANC, MCHS)
KUHN	90	ZPHY C48 445	J.H. Kuhn *et al.* (MPIM)
BISELLO	89	PL B220 321	D. Bisello *et al.* (DM2 Collab.)
DUBNICKA	89	JP G15 1349	S. Dubnicka *et al.* (JINR, SLOV)
GESHKEN...	89	ZPHY C45 351	B.V. Geshkenbein (ITEP)
ANTONELLI	88	PL B212 133	A. Antonelli *et al.* (DM2 Collab.)
DIEKMAN	88	PRPL 159 99	B. Diekmann (BONN)
FUKUI	88	PL B202 441	S. Fukui *et al.* (SUGI, NAGO, KEK, KYOT+)
DONNACHIE	87B	ZPHY C34 257	A. Donnachie, A.B. Clegg (MCHS, LANC)
ATKINSON	86B	ZPHY C30 531	M. Atkinson *et al.* (BONN, CERN, GLAS+)
ATKINSON	85B	ZPHY C26 499	M. Atkinson *et al.* (BONN, CERN, GLAS+)
ERKAL	85	ZPHY C29 485	C. Erkal, M.G. Olsson (WISC)
ABE	84B	PRL 53 751	K. Abe *et al.* (SLAC HFP Collab.)
KURDADZE	83	JETPL 37 733	L.M. Kurdadze *et al.* (NOVO)
		Translated from ZETFP 37 613.	
ATKINSON	82	PL 108B 55	M. Atkinson *et al.* (BONN, CERN, GLAS+)
BUON	82	PL 118B 221	J. Buon *et al.* (LALO, MONP)
CLELAND	82B	NP B208 228	W.E. Cleland *et al.* (DURH, GEVA, LAUS+)
CORDIER	82	PL 109B 129	A. Cordier *et al.* (LALO)
DELCOURT	82	PL 113B 93	B. Delcourt *et al.* (LALO)
ASTON	81E	NP B189 15	D. Aston (BONN, CERN, EPOL, GLAS, LANC+)
DELCOURT	81B	Bonn Conf. 205	B. Delcourt (ORSAY)
Also		PL 109B 129	A. Cordier *et al.* (LALO)
DIBIANCA	81	PR D23 595	F.A. di Bianca *et al.* (CASE, CMU)
ASTON	80	PL 92B 215	D. Aston (BONN, CERN, EPOL, GLAS, LANC+)
BACCI	80	PL 95B 139	C. Bacci *et al.* (ROMA, FRAS)
BIZOT	80	Madison Conf. 546	J.C. Bizot *et al.* (LALO, MONP)
KILLIAN	80	PR D21 3005	T.J. Killian *et al.* (CORN)
ATIYA	79B	PRL 43 1691	M.S. Atiya *et al.* (COLU, ILL, FNAL)
BECKER	79	NP B151 46	H. Becker *et al.* (MPIM, CERN, ZEEM, CRAC)
LANG	79	PR D19 956	C.B. Lang, A. Mas-Parareda (GRAZ)
MARTIN	78C	ANP 114 1	A.D. Martin, M.R. Pennington (CERN)
COSTA...	77B	PL 71B 345	B. Costa de Beauregard, B. Pire, T.N. Truong (EPOL)
FROGGATT	77	NP B129 89	C.D. Froggatt, J.L. Petersen (GLAS, NORD)
ALEXANDER	75	PL 57B 487	G. Alexander *et al.* (TELA)
BALLAM	74	NP B76 375	J. Ballam *et al.* (SLAC, LBL, MPIM)
CONVERSI	74	PL 52B 493	M. Conversi *et al.* (ROMA, FRAS)
SCHACHT	74	NP B81 205	P. Schacht *et al.* (MPIM)
DAVIER	73	NP B58 31	M. Davier *et al.* (SLAC)
EISENBERG	73	PL 43B 149	Y. Eisenberg *et al.* (REHO)
HYAMS	73	NP B64 134	B.D. Hyams *et al.* (CERN, MPIM)
BINGHAM	72B	PL 41B 635	H.H. Bingham *et al.* (LBL, UCB, SLAC) IGJP
JACOB	72	PR D5 1847	M. Jacob, R. Slansky
GOUNARIS	68	PRL 21 244	G.J. Gounaris, J.J. Sakurai

$a_2(1700)$

$I^G(J^{PC}) = 1^-(2^{++})$

OMITTED FROM SUMMARY TABLE

$a_2(1700)$ MASS

VALUE (MeV)	EVTS	DOCUMENT ID		TECN	CHG	COMMENT
1732± 9 OUR AVERAGE		Error includes scale factor of 1.2.				
$1726\pm12\pm25$		[1] ABLIKIM	17K	BES3		$\psi(2S) \to \gamma\eta\pi^+\pi^-$
$1737\pm 5\pm 7$		ABE	04	BELL		10.6 $e^+e^- \to e^+e^-K^+K^-$
1698 ± 44		[2] AMSLER	02	CBAR		0.9 $\overline{p}p \to \pi^0\eta\eta$
1660 ± 40		ABELE	99B	CBAR		1.94 $\overline{p}p \to \pi^0\eta\eta$
• • • We do not use the following data for averages, fits, limits, etc. • • •						
1675 ± 25		ANISOVICH	09	RVUE		0.0 $\overline{p}p$, πN
$1722\pm 9\pm15$	18k	[3] SCHEGELSKY	06	RVUE	0	$\gamma\gamma \to \pi^+\pi^-\pi^0$
1702 ± 7	80k	[4] UMAN	06	E835		5.2 $\overline{p}p \to \eta\eta\pi^0$
$1721\pm13\pm44$	145k	LU	05	B852		18 $\pi^-p \to \omega\pi^-\pi^0 p$
1767 ± 14	221	[5] ACCIARRI	01H	L3		$\gamma\gamma \to K^0_S K^0_S$, E^{ee}_{cm}= 91, 183–209 GeV
~ 1775		[6] GRYGOREV	99	SPEC		40 $\pi^-p \to K^0_S K^0_S n$
$1752\pm21\pm 4$		ACCIARRI	97T	L3		$\gamma\gamma \to \pi^+\pi^-\pi^0$

[1] From an amplitude analysis using an isobar model.
[2] T-matrix pole.
[3] From analysis of L3 data at 183–209 GeV.
[4] Statistical error only.
[5] Spin 2 dominant, isospin not determined, could also be I=1.
[6] Possibly two $J^P = 2^+$ resonances with isospins 0 and 1.

$a_2(1700)$ WIDTH

VALUE (MeV)	EVTS	DOCUMENT ID		TECN	CHG	COMMENT
193± 27 OUR AVERAGE		Error includes scale factor of 1.3. See the ideogram below.				
$190\pm 18\pm30$		[7] ABLIKIM	17K	BES3		$\psi(2S) \to \gamma\eta\pi^+\pi^-$
$151\pm 22\pm24$		ABE	04	BELL		10.6 $e^+e^- \to e^+e^-K^+K^-$
265 ± 55		[8] AMSLER	02	CBAR		0.9 $\overline{p}p \to \pi^0\eta\eta$
280 ± 70		ABELE	99B	CBAR		1.94 $\overline{p}p \to \pi^0\eta\eta$
• • • We do not use the following data for averages, fits, limits, etc. • • •						
$270^{+\ 50}_{-\ 20}$		ANISOVICH	09	RVUE		0.0 $\overline{p}p$, πN
$336\pm 20\pm20$	18k	[9] SCHEGELSKY	06	RVUE	0	$\gamma\gamma \to \pi^+\pi^-\pi^0$
417 ± 19	80k	[10] UMAN	06	E835		5.2 $\overline{p}p \to \eta\eta\pi^0$
$279\pm 49\pm66$	145k	LU	05	B852		18 $\pi^-p \to \omega\pi^-\pi^0 p$
187 ± 60	221	[11] ACCIARRI	01H	L3		$\gamma\gamma \to K^0_S K^0_S$, E^{ee}_{cm}= 91, 183–209 GeV
$150\pm110\pm34$		ACCIARRI	97T	L3		$\gamma\gamma \to \pi^+\pi^-\pi^0$

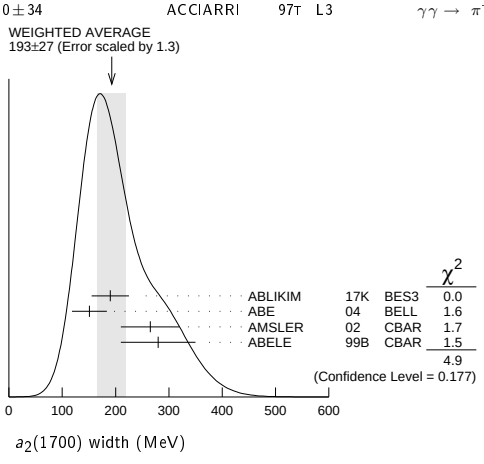

[7] From an amplitude analysis using an isobar model.
[8] T-matrix pole.
[9] From analysis of L3 data at 183–209 GeV.
[10] Statistical error only.
[11] Spin 2 dominant, isospin not determined, could also be I=1.

$a_2(1700)$ DECAY MODES

	Mode	Fraction (Γ_i/Γ)
Γ_1	$\eta\pi$	seen
Γ_2	$\gamma\gamma$	
Γ_3	$\rho\pi$	
Γ_4	$f_2(1270)\pi$	
Γ_5	$K\overline{K}$	seen
Γ_6	$\omega\pi^-\pi^0$	seen
Γ_7	$\omega\rho$	seen

$a_2(1700)$ PARTIAL WIDTHS

$\Gamma(\eta\pi)$ Γ_1

VALUE (MeV)	EVTS	DOCUMENT ID		TECN	COMMENT
• • • We do not use the following data for averages, fits, limits, etc. • • •					
9.5 ± 2.0	870	[12] SCHEGELSKY	06A	RVUE	$\gamma\gamma \to K^0_S K^0_S$

$\Gamma(\gamma\gamma)$ Γ_2

VALUE (keV)	EVTS	DOCUMENT ID		TECN	COMMENT
• • • We do not use the following data for averages, fits, limits, etc. • • •					
0.30 ± 0.05	870	[12] SCHEGELSKY	06A	RVUE	$\gamma\gamma \to K^0_S K^0_S$

$\Gamma(K\overline{K})$ Γ_5

VALUE (MeV)	EVTS	DOCUMENT ID		TECN	COMMENT
• • • We do not use the following data for averages, fits, limits, etc. • • •					
5.0 ± 3.0	870	[12] SCHEGELSKY	06A	RVUE	$\gamma\gamma \to K^0_S K^0_S$

[12] From analysis of L3 data at 91 and 183–209 GeV, using $a_2(1700)$ mass of 1730 MeV and width of 340 MeV, and SU(3) relations.

$a_2(1700)$ $\Gamma(i)\Gamma(\gamma\gamma)/\Gamma$(total)

$[\Gamma(\rho\pi) + \Gamma(f_2(1270)\pi)] \times \Gamma(\gamma\gamma)/\Gamma_{total}$ $(\Gamma_3+\Gamma_4)\Gamma_2/\Gamma$

VALUE (keV)	EVTS	DOCUMENT ID		TECN	COMMENT
0.29 ± 0.04 ± 0.02		ACCIARRI	97T	L3	$\gamma\gamma \to \pi^+\pi^-\pi^0$
• • • We do not use the following data for averages, fits, limits, etc. • • •					
$0.37^{+0.12}_{-0.08} \pm 0.10$	18k	[13] SCHEGELSKY	06	RVUE	$\gamma\gamma \to \pi^+\pi^-\pi^0$

$\Gamma(K\overline{K}) \times \Gamma(\gamma\gamma)/\Gamma_{total}$ $\Gamma_5\Gamma_2/\Gamma$

VALUE (eV)	DOCUMENT ID		TECN	COMMENT
• • • We do not use the following data for averages, fits, limits, etc. • • •				
20.6 ± 4.2 ± 4.6	[14] ABE	04	BELL	$10.6\ e^+e^- \to e^+e^- K^+K^-$
49 ± 11 ± 13	[15] ACCIARRI	01H	L3	$\gamma\gamma \to K^0_S K^0_S$, E^{ee}_{cm} = 91, 183–209 GeV

[13] From analysis of L3 data at 183–209 GeV.
[14] Assuming spin 2.
[15] Spin 2 dominant, isospin not determined, could also be I=1.

$a_2(1700)$ BRANCHING RATIOS

$\Gamma(\rho\pi)/\Gamma(f_2(1270)\pi)$ Γ_3/Γ_4

VALUE	EVTS	DOCUMENT ID		TECN	COMMENT
• • • We do not use the following data for averages, fits, limits, etc. • • •					
3.4 ± 0.4 ± 0.1	18k	[16] SCHEGELSKY	06	RVUE	$\gamma\gamma \to \pi^+\pi^-\pi^0$

[16] From analysis of L3 data at 183–209 GeV.

$a_2(1700)$ REFERENCES

ABLIKIM	17K	PR D95 032002	M. Ablikim *et al.*	(BES III Collab.)
ANISOVICH	09	IJMP A24 2481	V.V. Anisovich, A.V. Sarantsev	
SCHEGELSKY	06	EPJ A27 199	V.A. Schegelsky *et al.*	
SCHEGELSKY	06A	EPJ A27 207	V.A. Schegelsky *et al.*	
UMAN	06	PR D73 052009	I. Uman *et al.*	(FNAL E835)
LU	05	PRL 94 032002	M. Lu *et al.*	(BNL E852 Collab.)
ABE	04	EPJ C32 323	K. Abe *et al.*	(BELLE Collab.)
AMSLER	02	EPJ C23 29	C. Amsler *et al.*	
ACCIARRI	01H	PL B501 173	M. Acciarri *et al.*	(L3 Collab.)
ABELE	99B	EPJ C8 67	A. Abele *et al.*	(Crystal Barrel Collab.)
GRYGOREV	99	PAN 62 470	V.K. Grygorev *et al.*	
		Translated from YAF 62 513.		
ACCIARRI	97T	PL B413 147	M. Acciarri *et al.*	(L3 Collab.)

$f_0(1710)$ $I^G(J^{PC}) = 0^+(0^{++})$

See our mini-review in the 2004 edition of this *Review*, Physics Letters **B592** 1 (2004). See also the mini-review on scalar mesons under $f_0(500)$ (see the index for the page number).

$f_0(1710)$ MASS

VALUE (MeV)	EVTS	DOCUMENT ID		TECN	COMMENT
1723^{+6}_{-5} OUR AVERAGE		Error includes scale factor of 1.6. See the ideogram below.			
$1759 \pm 6\ ^{+14}_{-25}$	5.5k	[1] ABLIKIM	13N	BES3	$e^+e^- \to J/\psi \to \gamma\eta\eta$
$1750^{+6}_{-7}\ ^{+29}_{-18}$		UEHARA	13	BELL	$\gamma\gamma \to K^0_S K^0_S$
$1701 \pm 5\ ^{+9}_{-2}$	4k	[2] CHEKANOV	08	ZEUS	$ep \to K^0_S K^0_S X$
$1765^{+4}_{-3} \pm 13$		ABLIKIM	06V	BES2	$e^+e^- \to J/\psi \to \gamma\pi^+\pi^-$
$1760 \pm 15\ ^{+15}_{-10}$		[3] ABLIKIM	05Q	BES2	$\psi(2S) \to \gamma\pi^+\pi^- K^+K^-$
1738 ± 30		ABLIKIM	04E	BES2	$J/\psi \to \omega K^+K^-$
$1740 \pm 4\ ^{+10}_{-25}$		[4] BAI	03G	BES	$J/\psi \to \gamma K\overline{K}$
1740^{+30}_{-25}		[4] BAI	00A	BES	$J/\psi \to \gamma(\pi^+\pi^-\pi^+\pi^-)$
1698 ± 18		[5] BARBERIS	00E		$450\ pp \to p_f\eta\eta p_s$
1710 ± 12	±11	[6] BARBERIS	99D	OMEG	$450\ pp \to K^+K^-, \pi^+\pi^-$
1710 ± 25		[7] FRENCH	99		$300\ pp \to p_f(K^+K^-)p_s$
1707 ± 10		[8] AUGUSTIN	88	DM2	$J/\psi \to \gamma K^+K^-, K^0_S K^0_S$
1698 ± 15		[8] AUGUSTIN	87	DM2	$J/\psi \to \gamma\pi^+\pi^-$
1720 ± 10	±10	[9] BALTRUSAIT...	87	MRK3	$J/\psi \to \gamma K^+K^-$
1742 ± 15		[8] WILLIAMS	84	MPSF	$200\ \pi^- N \to 2K^0_S X$
1670 ± 50		BLOOM	83	CBAL	$J/\psi \to \gamma 2\eta$
• • • We do not use the following data for averages, fits, limits, etc. • • •					
1744 ± 7 ± 5	381	[10,11] DOBBS	15		$J/\psi \to \gamma\pi^+\pi^-$
1705 ± 11 ± 5	237	[10,11] DOBBS	15		$\psi(2S) \to \gamma\pi^+\pi^-$
1706 ± 4 ± 5	1.0k	[10,11] DOBBS	15		$J/\psi \to \gamma K^+K^-$
1690 ± 8 ± 3	349	[10,11] DOBBS	15		$\psi(2S) \to \gamma K^+K^-$
1750 ± 13		AMSLER	06	CBAR	$1.64\ \overline{p}p \to K^+K^-\pi^0$
1747 ± 5	80k	[12,13] UMAN	06	E835	$5.2\ \overline{p}p \to \eta\eta\pi^0$
1776 ± 15		VLADIMIRSK...	06	SPEC	$40\ \pi^- p \to K^0_S K^0_S n$
1790^{+40}_{-30}		[3] ABLIKIM	05	BES2	$J/\psi \to \phi\pi^+\pi^-$
1670 ± 20		[12] BINON	05	GAMS	$33\ \pi^- p \to \eta\eta n$
1726 ± 7	74	[13] CHEKANOV	04	ZEUS	$ep \to K^0_S K^0_S X$
1732 +15		[14] ANISOVICH	03	RVUE	
1682 ± 16		TIKHOMIROV	03	SPEC	$40.0\ \pi^- C \to K^0_S K^0_S K^0_L X$
1670 ± 26	3.6k	[4,15] NICHITIU	02	OBLX	
1770 ± 12		[16,17] ANISOVICH	99B	SPEC	$0.6\text{–}1.2\ p\overline{p} \to \eta\eta\pi^0$
1730 ± 15		[4] BARBERIS	99	OMEG	$450\ pp \to p_s p_f K^+K^-$
1750 ± 20		[4] BARBERIS	99B	OMEG	$450\ pp \to p_s p_f \pi^+\pi^-$
1750 ± 30		[18] ANISOVICH	98B	RVUE	Compilation
1720 ± 39		BAI	98H	BES	$J/\psi \to \gamma\pi^0\pi^0$
1775 ± 1.5	57	[19] BARKOV	98		$\pi^- p \to K^0_S K^0_S n$
1690 ± 11		[20] ABREU	96C	DLPH	$Z^0 \to K^+K^- + X$
$1696 \pm 5\ ^{+9}_{-34}$		[9] BAI	96C	BES	$J/\psi \to \gamma K^+K^-$
$1781 \pm 8\ ^{+10}_{-31}$		[4] BAI	96C	BES	$J/\psi \to \gamma K^+K^-$
1768 ± 14		BALOSHIN	95	SPEC	$40\ \pi^- C \to K^0_S K^0_S X$
1750 ± 15		[21] BUGG	95	MRK3	$J/\psi \to \gamma\pi^+\pi^-\pi^+\pi^-$
1620 ± 16		[9] BUGG	95	MRK3	$J/\psi \to \gamma\pi^+\pi^-\pi^+\pi^-$
1748 ± 10		[8] ARMSTRONG	93C	E760	$\overline{p}p \to \pi^0\eta\eta \to 6\gamma$
~ 1750		BREAKSTONE	93	SFM	$pp \to pp\pi^+\pi^-\pi^+\pi^-$
1744 ± 15		[22] ALDE	92D	GAM2	$38\ \pi^- p \to \eta\eta n$
1713 ± 10		[23] ARMSTRONG	89D	OMEG	$300\ pp \to pp K^+K^-$
1706 ± 10		[23] ARMSTRONG	89D	OMEG	$300\ pp \to pp K^0_S K^0_S$
1700 ± 15		[9] BOLONKIN	88	SPEC	$40\ \pi^- p \to K^0_S K^0_S n$
1720 ± 60		[4] BOLONKIN	88	SPEC	$40\ \pi^- p \to K^0_S K^0_S n$
1638 ± 10		[24] FALVARD	88	DM2	$J/\psi \to \phi K^+K^-, K^0_S K^0_S$
1690 ± 4		[25] FALVARD	88	DM2	$J/\psi \to \phi K^+K^-, K^0_S K^0_S$
1755 ± 8		[26] ALDE	86C	GAM2	$38\ \pi^- p \to n2\eta$
1730^{+2}_{-10}		[27] LONGACRE	86	RVUE	$22\ \pi^- p \to n2K^0_S$
1650 ± 50		BURKE	82	MRK2	$J/\psi \to \gamma 2\rho$
1640 ± 50		[28,29] EDWARDS	82D	CBAL	$J/\psi \to \gamma 2\eta$
1730 ± 10	±20	[30] ETKIN	82C	MPS	$23\ \pi^- p \to n2K^0_S$

[1] From partial wave analysis including all possible combinations of 0^{++}, 2^{++}, and 4^{++} resonances.
[2] In the SU(3) based model with a specific interference pattern of the $f_2(1270)$, $a_2^0(1320)$, and $f_2'(1525)$ mesons incoherently added to the $f_0(1710)$ and non-resonant background.
[3] This state may be different from $f_0(1710)$, see CLOSE 05.
[4] $J^P = 0^+$.
[5] T-matrix pole.

Meson Particle Listings

$f_0(1710)$

[6] Supersedes BARBERIS 99 and BARBERIS 99B.
[7] $J^P = 0^+$, supersedes by ARMSTRONG 89D.
[8] No J^{PC} determination.
[9] $J^P = 2^+$.
[10] Using CLEO-c data but not authored by the CLEO Collaboration.
[11] From a fit to a Breit-Wigner line shape with fixed $\Gamma = 135$ MeV.
[12] Breit-Wigner mass.
[13] Systematic errors not estimated.
[14] K-matrix pole, assuming $J^P = 0^+$, from combined analysis of $\pi^- p \to \pi^0\pi^0 n$, $\pi^- p \to K\overline{K} n$, $\pi^+\pi^- \to \pi^+\pi^-$, $\overline{p}p \to \pi^0\pi^0\pi^0$, $\pi^0\eta\eta$, $\pi^0\pi^0\eta$, $\pi^+\pi^-\pi^0$, $K^+K^-\pi^0$, $K^0_S K^0_S\pi^0$, $K^+K^0_S\pi^-$ at rest, $\overline{p}n \to \pi^-\pi^-\pi^+$, $K^0_S K^-\pi^0$, $K^0_S K^0_S\pi^-$ at rest.
[15] Decaying to $f_0(1370)\pi\pi$.
[16] $J^P = 0^+$.
[17] Not seen by AMSLER 02.
[18] T-matrix pole, assuming $J^P = 0^+$
[19] No J^{PC} determination.
[20] No J^{PC} determination, width not determined.
[21] From a fit to the 0^+ partial wave.
[22] ALDE 92D combines all the GAMS-2000 data.
[23] $J^P = 2^+$, superseded by FRENCH 99.
[24] From an analysis ignoring interference with $f_2'(1525)$.
[25] From an analysis including interference with $f_2'(1525)$.
[26] Superseded by ALDE 92D.
[27] Uses MRK3 data. From a partial-wave analysis of data using a K-matrix formalism with 5 poles, but assuming spin 2. Fit with constrained inelasticity.
[28] $J^P = 2^+$ preferred.
[29] From fit neglecting nearby $f_2'(1525)$. Replaced by BLOOM 83.
[30] Superseded by LONGACRE 86.

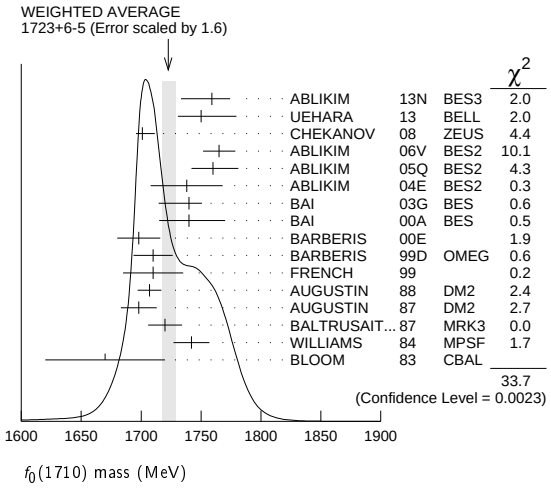

$f_0(1710)$ WIDTH

VALUE (MeV)			EVTS		DOCUMENT ID		TECN	COMMENT
139	**±**	**8**		**OUR AVERAGE**	Error includes scale factor of 1.1.			
172	± 10	$^{+32}_{-16}$	5.5k	[1] ABLIKIM	13N	BES3	$e^+e^- \to J/\psi \to \gamma\eta\eta$
139	$^{+11}_{-12}$	$^{+96}_{-50}$		UEHARA	13	BELL	$\gamma\gamma \to K^0_S K^0_S$
100	± 24	$^{+7}_{-22}$	4k	[2] CHEKANOV	08	ZEUS	$ep \to K^0_S K^0_S X$
145	± 8	±69		ABLIKIM	06V	BES2	$e^+e^- \to J/\psi \to \gamma\pi^+\pi^-$
125	± 25	$^{+10}_{-15}$		[3] ABLIKIM	05Q	BES2	$\psi(2S) \to \gamma\pi^+\pi^- K^+K^-$
125	± 20			ABLIKIM	04E	BES2	$J/\psi \to \omega K^+K^-$
166	$^{+5}_{-8}$	$^{+15}_{-10}$		[4] BAI	03G	BES	$J/\psi \to \gamma K\overline{K}$
120	$^{+50}_{-40}$			[4] BAI	00A	BES	$J/\psi \to \gamma(\pi^+\pi^-\pi^+\pi^-)$
120	± 26			[5] BARBERIS	00E		450 $pp \to p_f\eta\eta p_s$
126	± 16	±18		[6] BARBERIS	99D	OMEG	450 $pp \to K^+K^-, \pi^+\pi^-$
105	± 34			[7] FRENCH	99		300 $pp \to p_f(K^+K^-)p_s$
166.4	± 33.2			[8] AUGUSTIN	88	DM2	$J/\psi \to \gamma K^+K^-, K^0_S K^0_S$
136	± 28			[8] AUGUSTIN	87	DM2	$J/\psi \to \gamma\pi^+\pi^-$
130	± 20			[9] BALTRUSAIT...	87	MRK3	$J/\psi \to \gamma K^+K^-$
57	± 38			[10] WILLIAMS	84	MPSF	200 $\pi^- N \to 2K^0_S X$
160	± 80			BLOOM	83	CBAL	$J/\psi \to \gamma 2\eta$
• • • We do not use the following data for averages, fits, limits, etc. • • •								
148	$^{+40}_{-30}$			AMSLER	06	CBAR	1.64 $\overline{p}p \to K^+K^-\pi^0$
188	± 13		80k	[3,11] UMAN	06	E835	5.2 $\overline{p}p \to \eta\eta\pi^0$
250	± 30			VLADIMIRSK...	06	SPEC	40 $\pi^- p \to K^0_S K^0_S n$
270	$^{+60}_{-30}$			[12] ABLIKIM	05	BES2	$J/\psi \to \phi\pi^+\pi^-$
260	± 50			[3] BINON	05	GAMS	33 $\pi^- p \to \eta\eta n$
38	$^{+20}_{-14}$						
144	± 30						
320	$^{+50}_{-20}$						
102	± 26						
267	± 44		3651	[4,13] NICHITIU	02	OBLX	
220	± 40			[14,15] ANISOVICH	99B	SPEC	0.6–1.2 $p\overline{p} \to \eta\eta\pi^0$
100	± 25			[4] BARBERIS	99	OMEG	450 $pp \to p_s p_f K^+K^-$
160	± 30			[4] BARBERIS	99B	OMEG	450 $pp \to p_s p_f \pi^+\pi^-$
250	±140			[19] ANISOVICH	98B	RVUE	Compilation
30	± 7		57	[20] BARKOV	98		$\pi^- p \to K^0_S K^0_S n$
103	± 18	$^{+30}_{-11}$		[9] BAI	96C	BES	$J/\psi \to \gamma K^+K^-$
85	± 24	$^{+22}_{-19}$		[4] BAI	96C	BES	$J/\psi \to \gamma K^+K^-$
56	± 19			BALOSHIN	95	SPEC	40 π^- C $\to K^0_S K^0_S$ X
160	± 40			[21] BUGG	95	MRK3	$J/\psi \to \gamma\pi^+\pi^-\pi^+\pi^-$
160	$^{+60}_{-20}$			[9] BUGG	95	MRK3	$J/\psi \to \gamma\pi^+\pi^-\pi^+\pi^-$
264	± 25			[8] ARMSTRONG	93C	E760	$\overline{p}p \to \pi^0\eta\eta \to 6\gamma$
200	to 300			BREAKSTONE	93	SFM	$pp \to pp\pi^+\pi^-\pi^+\pi^-$
< 80	90% CL			[22] ALDE	92D	GAM2	38 $\pi^- p \to \eta\eta N^*$
181	± 30			[23] ARMSTRONG	89D	OMEG	300 $pp \to pp K^+K^-$
104	± 30			[23] ARMSTRONG	89D	OMEG	300 $pp \to pp K^0_S K^0_S$
30	± 20			[9] BOLONKIN	88	SPEC	40 $\pi^- p \to K^0_S K^0_S n$
350	±150			[4] BOLONKIN	88	SPEC	40 $\pi^- p \to K^0_S K^0_S n$
148	± 17			[24] FALVARD	88	DM2	$J/\psi \to \phi K^+K^-, K^0_S K^0_S$
184	± 6			[25] FALVARD	88	DM2	$J/\psi \to \phi K^+K^-, K^0_S K^0_S$
122	$^{+74}_{-15}$			[26] LONGACRE	86	RVUE	22 $\pi^- p \to n2K^0_S$
200	±100			BURKE	82	MRK2	$J/\psi \to \gamma 2\rho$
220	$^{+100}_{-70}$			[27,28] EDWARDS	82D	CBAL	$J/\psi \to \gamma 2\eta$
200	$^{+156}_{-9}$			[29] ETKIN	82B	MPS	23 $\pi^- p \to n2K^0_S$

[1] From partial wave analysis including all possible combinations of 0^{++}, 2^{++}, and 4^{++} resonances.
[2] In the SU(3) based model with a specific interference pattern of the $f_2(1270)$, $a_2^0(1320)$, and $f_2'(1525)$ mesons incoherently added to the $f_0(1710)$ and non-resonant background.
[3] Breit-Wigner width.
[4] $J^P = 0^+$.
[5] T-matrix pole.
[6] Supersedes BARBERIS 99 and BARBERIS 99B.
[7] $J^P = 0^+$, supersedes by ARMSTRONG 89D.
[8] No J^{PC} determination.
[9] $J^P = 2^+$.
[10] No J^{PC} determination.
[11] Systematic errors not estimated.
[12] This state may be different from $f_0(1710)$, see CLOSE 05.
[13] (Solution I)
[14] K-matrix pole, assuming $J^P = 0^+$, from combined analysis of $\pi^- p \to \pi^0\pi^0 n$, $\pi^- p \to K\overline{K} n$, $\pi^+\pi^- \to \pi^+\pi^-$, $\overline{p}p \to \pi^0\pi^0\pi^0$, $\pi^0\eta\eta$, $\pi^0\pi^0\eta$, $\pi^+\pi^-\pi^0$, $K^+K^-\pi^0$, $K^0_S K^0_S\pi^0$, $K^+K^0_S\pi^-$ at rest, $\overline{p}n \to \pi^-\pi^-\pi^+$, $K^0_S K^-\pi^0$, $K^0_S K^0_S\pi^-$ at rest.
[15] (Solution I)
[16] Decaying to $f_0(1370)\pi\pi$.
[17] $J^P = 0^+$.
[18] Not seen by AMSLER 02.
[19] T-matrix pole, assuming $J^P = 0^+$
[20] No J^{PC} determination.
[21] From a fit to the 0^+ partial wave.
[22] ALDE 92D combines all the GAMS-2000 data.
[23] $J^P = 2^+$, (0^+ excluded).
[24] From an analysis ignoring interference with $f_2'(1525)$.
[25] From an analysis including interference with $f_2'(1525)$.
[26] Uses MRK3 data. From a partial-wave analysis of data using a K-matrix formalism with 5 poles, but assuming spin 2. Fit with constrained inelasticity.
[27] $J^P = 2^+$ preferred.
[28] From fit neglecting nearby $f_2'(1525)$. Replaced by BLOOM 83.
[29] From an amplitude analysis of the $K^0_S K^0_S$ system, superseded by LONGACRE 86.

$f_0(1710)$ DECAY MODES

	Mode	Fraction (Γ_i/Γ)
Γ_1	$K\overline{K}$	seen
Γ_2	$\eta\eta$	seen
Γ_3	$\pi\pi$	seen
Γ_4	$\gamma\gamma$	
Γ_5	$\omega\omega$	seen

$f_0(1710)$ Γ(i)$\Gamma(\gamma\gamma)/\Gamma$(total)

$\Gamma(K\overline{K}) \times \Gamma(\gamma\gamma)/\Gamma_{\text{total}}$ $\qquad$ $\Gamma_1\Gamma_4/\Gamma$

VALUE (eV)	CL%	DOCUMENT ID		TECN	COMMENT
12^{+3+227}_{-2-8}		UEHARA	13	BELL	$\gamma\gamma \to K^0_S K^0_S$

• • • We do not use the following data for averages, fits, limits, etc. • • •

<480	95	ALBRECHT	90G	ARG	$\gamma\gamma \to K^+K^-$
<110	95	[1] BEHREND	89C	CELL	$\gamma\gamma \to K^0_S K^0_S$
<280	95	[1] ALTHOFF	85B	TASS	$\gamma\gamma \to K\overline{K}\pi$

[1] Assuming helicity 2.

$\Gamma(\pi\pi) \times \Gamma(\gamma\gamma)/\Gamma_{\text{total}}$ $\Gamma_3\Gamma_4/\Gamma$

VALUE (keV)	CL%	DOCUMENT ID		TECN	COMMENT
<0.82	95	[1] BARATE	00E	ALEP	$\gamma\gamma \to \pi^+\pi^-$

[1] Assuming spin 0.

$f_0(1710)$ BRANCHING RATIOS

$\Gamma(K\overline{K})/\Gamma_{\text{total}}$ Γ_1/Γ

VALUE	EVTS	DOCUMENT ID		TECN	COMMENT
• • • We do not use the following data for averages, fits, limits, etc. • • •					
seen	1004	[1] DOBBS	15		$J/\psi \to \gamma K^+K^-$
seen	349	[1] DOBBS	15		$\psi(2S) \to \gamma K^+K^-$
0.36 ± 0.12		ALBALADEJO	08	RVUE	
$0.38^{+0.09}_{-0.19}$		[2] LONGACRE	86	MPS	$22\ \pi^- p \to n 2K^0_S$

[1] Using CLEO-c data but not authored by the CLEO Collaboration.
[2] From a partial-wave analysis of data using a K-matrix formalism with 5 poles, but assuming spin 2. Fit with constrained inelasticity.

$\Gamma(\eta\eta)/\Gamma_{\text{total}}$ Γ_2/Γ

VALUE	DOCUMENT ID		TECN	COMMENT
• • • We do not use the following data for averages, fits, limits, etc. • • •				
0.22 ± 0.12	ALBALADEJO	08	RVUE	
$0.18^{+0.03}_{-0.13}$	[1] LONGACRE	86	RVUE	

[1] From a partial-wave analysis of data using a K-matrix formalism with 5 poles, but assuming spin 2. Fit with constrained inelasticity.

$\Gamma(\pi\pi)/\Gamma_{\text{total}}$ Γ_3/Γ

VALUE	EVTS	DOCUMENT ID		TECN	COMMENT
• • • We do not use the following data for averages, fits, limits, etc. • • •					
seen	381	[1] DOBBS	15		$J/\psi \to \gamma\pi^+\pi^-$
seen	237	[1] DOBBS	15		$\psi(2S) \to \gamma\pi^+\pi^-$
not seen		AMSLER	02	CBAR	$0.9\ \overline{p}p \to \pi^0\eta\eta,\ \pi^0\pi^0\pi^0$
$0.039^{+0.002}_{-0.024}$		[2] LONGACRE	86	RVUE	

[1] Using CLEO-c data but not authored by the CLEO Collaboration.
[2] From a partial-wave analysis of data using a K-matrix formalism with 5 poles, but assuming spin 2. Fit with constrained inelasticity.

$\Gamma(\pi\pi)/\Gamma(K\overline{K})$ Γ_3/Γ_1

VALUE	CL%	DOCUMENT ID		TECN	COMMENT
$\mathbf{0.41^{+0.11}_{-0.17}}$		ABLIKIM	06V	BES2	$e^+e^- \to J/\psi \to \gamma\pi^+\pi^-$
• • • We do not use the following data for averages, fits, limits, etc. • • •					
0.32 ± 0.14		ALBALADEJO	08	RVUE	
< 0.11	95	[1] ABLIKIM	04E	BES2	$J/\psi \to \omega K^+K^-$
$5.8\ ^{+9.1}_{-5.5}$		[2] ANISOVICH	02D	SPEC	Combined fit
$0.2\ \pm 0.024 \pm 0.036$		BARBERIS	99D	OMEG	$450\ pp \to K^+K^-, \pi^+\pi^-$
0.39 ± 0.14		ARMSTRONG	91	OMEG	$300\ pp \to pp\pi\pi,\ ppK\overline{K}$

[1] Using data from ABLIKIM 04A.
[2] From a combined K-matrix analysis of Crystal Barrel (0. $p\overline{p} \to \pi^0\pi^0\pi^0$, $\pi^0\eta\eta$, $\pi^0\pi^0\eta$), GAMS ($\pi p \to \pi^0\pi^0 n$, $\eta\eta n$, $\eta\eta' n$), and BNL ($\pi p \to K\overline{K}n$) data.

$\Gamma(\eta\eta)/\Gamma(K\overline{K})$ Γ_2/Γ_1

VALUE	CL%	DOCUMENT ID		TECN	COMMENT
0.48±0.15		BARBERIS	00E		$450\ pp \to p_f\eta\eta p_s$
• • • We do not use the following data for averages, fits, limits, etc. • • •					
$0.46^{+0.70}_{-0.38}$		[1] ANISOVICH	02D	SPEC	Combined fit
<0.02	90	[2] PROKOSHKIN	91	GA24	$300\ \pi^- p \to \pi^- p\eta\eta$

[1] From a combined K-matrix analysis of Crystal Barrel (0. $p\overline{p} \to \pi^0\pi^0\pi^0$, $\pi^0\eta\eta$, $\pi^0\pi^0\eta$), GAMS ($\pi p \to \pi^0\pi^0 n$, $\eta\eta n$, $\eta\eta' n$), and BNL ($\pi p \to K\overline{K}n$) data.
[2] Combining results of GAM4 with those of ARMSTRONG 89D.

$\Gamma(\omega\omega)/\Gamma_{\text{total}}$ Γ_5/Γ

VALUE	EVTS	DOCUMENT ID		TECN	COMMENT
seen	180	ABLIKIM	06H	BES	$J/\psi \to \gamma\omega\omega$

$f_0(1710)$ REFERENCES

DOBBS	15	PR D91 052006	S. Dobbs *et al.*	(NWES)
ABLIKIM	13N	PR D87 092009	Ablikim M. *et al.*	(BES III Collab.)
UEHARA	13	PTEP 2013 123C01	S. Uehara *et al.*	(BELLE Collab.)
ALBALADEJO	08	PRL 101 252002	M. Albaladejo, J.A. Oller	
CHEKANOV	08	PRL 101 112003	S. Chekanov *et al.*	(ZEUS Collab.)
ABLIKIM	06H	PR D73 112007	M. Ablikim *et al.*	(BES Collab.)
ABLIKIM	06V	PL B642 441	M. Ablikim *et al.*	(BES Collab.)
AMSLER	06	PL B639 165	C. Amsler *et al.*	(CBAR Collab.)
UMAN	06	PR D73 052009	I. Uman *et al.*	(FNAL E835)
VLADIMIRSK...	06	PAN 69 493 Translated from YAF 69 515.	V.V. Vladimirsky *et al.*	(ITEP, Moscow)
ABLIKIM	05	PL B607 243	M. Ablikim *et al.*	(BES Collab.)
ABLIKIM	05Q	PR D72 092002	M. Ablikim *et al.*	(BES Collab.)
BINON	05	PAN 68 960 Translated from YAF 68 998.	F. Binon *et al.*	
CLOSE	05	PR D71 094022	F.E. Close, Q. Zhao	
ABLIKIM	04A	PL B598 149	M. Ablikim *et al.*	(BES Collab.)
ABLIKIM	04E	PL B603 138	M. Ablikim *et al.*	(BES Collab.)
CHEKANOV	04	PL B578 33	S. Chekanov *et al.*	(ZEUS Collab.)
PDG	04	PL B592 1	S. Eidelman *et al.*	(PDG Collab.)
ANISOVICH	03	EPJ A16 229	V.V. Anisovich *et al.*	
BAI	03G	PR D68 052003	J.Z. Bai *et al.*	(BES Collab.)
TIKHOMIROV	03	PAN 66 828 Translated from YAF 66 860.	G.D. Tikhomirov *et al.*	
AMSLER	02	EPJ C23 29	C. Amsler *et al.*	
ANISOVICH	02D	PAN 65 1545 Translated from YAF 65 1583.	V.V. Anisovich *et al.*	
NICHITIU	02	PL B545 261	F. Nichitiu *et al.*	(OBELIX Collab.)
BAI	00A	PL B472 207	J.Z. Bai *et al.*	(BES Collab.)
BARATE	00E	PL B472 189	R. Barate *et al.*	(ALEPH Collab.)
BARBERIS	00E	PL B479 59	D. Barberis *et al.*	(WA 102 Collab.)
ANISOVICH	99B	PL B449 154	A.V. Anisovich *et al.*	
BARBERIS	99	PL B453 305	D. Barberis *et al.*	(Omega Expt.)
BARBERIS	99B	PL B453 316	D. Barberis *et al.*	(Omega Expt.)
BARBERIS	99D	PL B462 462	D. Barberis *et al.*	(Omega Expt.)
FRENCH	99	PL B460 213	B. French *et al.*	(WA76 Collab.)
ANISOVICH	98B	SPU 41 419 Translated from UFN 168 481.	V.V. Anisovich *et al.*	
BAI	98H	PRL 81 1179	J.Z. Bai *et al.*	(BES Collab.)
BARKOV	98	JETPL 68 764	B.P. Barkov *et al.*	
ABREU	96C	PL B379 309	P. Abreu *et al.*	(DELPHI Collab.)
BAI	96C	PRL 77 3959	J.Z. Bai *et al.*	(BES Collab.)
BALOSHIN	95	PAN 58 46 Translated from YAF 58 50.	O.N. Baloshin *et al.*	(ITEP)
BUGG	95	PL B353 378	D.V. Bugg *et al.*	(LOQM, PNPI, WASH)
ARMSTRONG	93C	PL B307 394	T.A. Armstrong *et al.*	(FNAL, FERR, GENO+)
BREAKSTONE	93	ZPHY C58 251	A.M. Breakstone *et al.*	(IOWA, CERN, DORT+)
ALDE	92D	PL B284 457	D.M. Alde *et al.*	(GAM2 Collab.)
Also		SJNP 54 451 Translated from YAF 54 745.	D.M. Alde *et al.*	(GAM2 Collab.)
ARMSTRONG	91	ZPHY C51 351	T.A. Armstrong *et al.*	(ATHU, BARI, BIRM+)
PROKOSHKIN	91	SPD 36 155 Translated from DANS 316 900.	Y.D. Prokoshkin	(GAM2, GAM4 Collab.)
ALBRECHT	90G	ZPHY C48 183	H. Albrecht *et al.*	(ARGUS Collab.)
ARMSTRONG	89D	PL B227 186	T.A. Armstrong, M. Benayoun	(ATHU, BARI, BIRM+)
BEHREND	89C	ZPHY C43 91	H.J. Behrend *et al.*	(CELLO Collab.)
AUGUSTIN	88	PRL 60 2238	J.E. Augustin *et al.*	(DM2 Collab.)
BOLONKIN	88	NP B309 426	B.V. Bolonkin *et al.*	(ITEP, SERP)
FALVARD	88	PR D38 2706	A. Falvard *et al.*	(CLER, FRAS, LALO+)
AUGUSTIN	87	ZPHY C36 369	J.E. Augustin *et al.*	(LALO, CLER, FRAS+)
BALTRUSAIT...	87	PR D35 2077	R.M. Baltrusaitis *et al.*	(Mark III Collab.)
ALDE	86C	PL B182 105	D.M. Alde *et al.*	(SERP, BELG, LANL, LAPP)
LONGACRE	86	PL B177 223	R.S. Longacre *et al.*	(BNL, BRAN, CUNY+)
ALTHOFF	85B	ZPHY C29 189	M. Althoff *et al.*	(TASSO Collab.)
WILLIAMS	84	PR D30 877	E.G.H. Williams *et al.*	(VAND, NDAM, TUFTS+)
BLOOM	83	ARNS 33 143	E.D. Bloom, C. Peck	(SLAC, CIT)
BURKE	82	PRL 49 632	D.L. Burke *et al.*	(LBL, SLAC)
EDWARDS	82D	PRL 48 458	C. Edwards *et al.*	(CIT, HARV, PRIN+)
ETKIN	82B	PR D25 1786	A. Etkin *et al.*	(BNL, CUNY, TUFTS, VAND)
ETKIN	82C	PR D25 2446	A. Etkin *et al.*	(BNL, CUNY, TUFTS, VAND)

$\eta(1760)$

$I^G(J^{PC}) = 0^+(0^{-+})$

OMITTED FROM SUMMARY TABLE

Seen by DM2 in the $\rho\rho$ system (BISELLO 89B). Structure in this region has been reported before in the same system (BALTRUSAITIS 86B) and in the $\omega\omega$ system (BALTRUSAITIS 85C, BISELLO 87).

$\eta(1760)$ MASS

VALUE (MeV)	EVTS	DOCUMENT ID		TECN	COMMENT
1751±15 OUR AVERAGE					
$1768^{+24}_{-25} \pm 10$	465	[1] ZHANG	12A	BELL	$e^+e^- \to e^+e^-\eta'\pi^+\pi^-$
$1744 \pm 10 \pm 15$	1045	[2] ABLIKIM	06H	BES	$J/\psi \to \gamma\omega\omega$
• • • We do not use the following data for averages, fits, limits, etc. • • •					
$1703^{+12}_{-11} \pm 2$		[3] ZHANG	12A	BELL	$e^+e^- \to e^+e^-\eta'\pi^+\pi^-$
1760 ± 11	320	[4] BISELLO	89B	DM2	$J/\psi \to 4\pi\gamma$

[1] From a single-resonance fit.
[2] From a partial wave analysis including $\eta(1760)$, $f_0(1710)$, $f_2(1640)$, and $f_2(1910)$.
[3] From a two-resonance fit.
[4] Estimated by us from various fits. Systematic uncertainties not estimated.

$\eta(1760)$ WIDTH

VALUE (MeV)	EVTS	DOCUMENT ID		TECN	COMMENT
240±30 OUR AVERAGE					
$224^{+62}_{-56} \pm 25$	465	[5] ZHANG	12A	BELL	$e^+e^- \to e^+e^-\eta'\pi^+\pi^-$
$244^{+24}_{-21} \pm 25$	1045	[6] ABLIKIM	06H	BES	$J/\psi \to \gamma\omega\omega$
• • • We do not use the following data for averages, fits, limits, etc. • • •					
$42^{+36}_{-22} \pm 15$		[7] ZHANG	12A	BELL	$e^+e^- \to e^+e^-\eta'\pi^+\pi^-$
60 ± 16	320	[8] BISELLO	89B	DM2	$J/\psi \to 4\pi\gamma$

[5] From a single-resonance fit.
[6] From a partial wave analysis including $\eta(1760)$, $f_0(1710)$, $f_2(1640)$, and $f_2(1910)$.
[7] From a two-resonance fit.

Meson Particle Listings

$\eta(1760)$, $\pi(1800)$

[8] Estimated by us from various fits. Systematic uncertainties not estimated.

$\eta(1760)$ DECAY MODES

	Mode	Fraction (Γ_i/Γ)
Γ_1	4π	
Γ_2	$2\pi^+2\pi^-$	seen
Γ_3	$\pi^+\pi^-2\pi^0$	seen
Γ_4	$\rho^0\rho^0$	seen
Γ_5	$\rho^+\rho^-$	seen
Γ_6	$2(\pi^+\pi^-\pi^0)$	
Γ_7	$\omega\omega$	seen
Γ_8	$\eta'\pi^+\pi^-$	seen
Γ_9	$\gamma\gamma$	seen

$\eta(1760)$ Γ(i)$\Gamma(\gamma\gamma)/\Gamma$(total)

$\Gamma(\eta'\pi^+\pi^-) \times \Gamma(\gamma\gamma)/\Gamma_{total}$ $\Gamma_8\Gamma_9/\Gamma$

VALUE (eV)	EVTS	DOCUMENT ID		TECN	COMMENT
$28.2^{+\ 7.9}_{-\ 7.5}\pm3.7$	465	[9] ZHANG	12A	BELL	$e^+e^- \to e^+e^-\eta'\pi^+\pi^-$

• • • We do not use the following data for averages, fits, limits, etc. • • •

$3.0^{+\ 2.0}_{-\ 1.2}\pm0.8$	52	[10] ZHANG	12A	BELL	$e^+e^- \to e^+e^-\eta'\pi^+\pi^-$
$18\ ^{+13}_{-10}\ \pm5$	315	[11] ZHANG	12A	BELL	$e^+e^- \to e^+e^-\eta'\pi^+\pi^-$

[9] From a single-resonance fit.
[10] From a two-resonance fit. For constructive interference with the $X(1835)$.
[11] From a two-resonance fit. For destructive interference with the $X(1835)$.

$\eta(1760)$ BRANCHING RATIOS

$\Gamma(2\pi^+2\pi^-)/\Gamma_{total}$ Γ_2/Γ

VALUE	DOCUMENT ID		TECN	COMMENT
seen	BISELLO	89B	DM2	$J/\psi \to \gamma 2\pi^+2\pi^-$

$\Gamma(\pi^+\pi^-2\pi^0)/\Gamma_{total}$ Γ_3/Γ

VALUE	DOCUMENT ID		TECN	COMMENT
seen	BISELLO	89B	DM2	$J/\psi \to \gamma\pi^+\pi^-2\pi^0$

$\Gamma(\rho^0\rho^0)/\Gamma_{total}$ Γ_4/Γ

VALUE	DOCUMENT ID		TECN	COMMENT
seen	BISELLO	89B	DM2	$J/\psi \to \gamma\rho^0\rho^0$
seen	BALTRUSAIT...86		MRK3	$J/\psi \to \gamma\rho^0\rho^0$

$\Gamma(\rho^+\rho^-)/\Gamma_{total}$ Γ_5/Γ

VALUE	DOCUMENT ID		TECN	COMMENT
seen	BISELLO	89B	DM2	$J/\psi \to \gamma\rho^+\rho^-$
seen	BALTRUSAIT...86		MRK3	$J/\psi \to \gamma\rho^+\rho^-$

$\Gamma(\omega\omega)/\Gamma_{total}$ Γ_7/Γ

VALUE	DOCUMENT ID		TECN	COMMENT
seen	BISELLO	87	DM2	$J/\psi \to \omega\omega$
seen	BALTRUSAIT...85C		MRK3	$J/\psi \to \gamma\omega\omega$

$\eta(1760)$ REFERENCES

ZHANG	12A	PR D86 052002	C.C. Zhang *et al.*	(BELLE Collab.)
ABLIKIM	06H	PR D73 112007	M. Ablikim *et al.*	(BES Collab.)
BISELLO	89B	PR D39 701	G. Busetto *et al.*	(DM2 Collab.)
BISELLO	87	PL B192 239	D. Bisello *et al.*	(PADO, CLER, FRAS+)
BALTRUSAIT...	86	PR D33 629	R.M. Baltrusaitis *et al.*	(Mark III Collab.)
BALTRUSAIT...	86B	PR D33 1222	R.M. Baltrusaitis *et al.*	(Mark III Collab.)
BALTRUSAIT...	85C	PRL 55 1723	R.M. Baltrusaitis *et al.*	(CIT, UCSC+)

$\pi(1800)$

$I^G(J^{PC}) = 1^-(0^{-+})$

See also minireview under non-$q\bar{q}$ candidates in PDG 06, Journal of Physics **G33** 1 (2006).

$\pi(1800)$ MASS

VALUE (MeV)	EVTS	DOCUMENT ID		TECN	CHG	COMMENT
1812±12 OUR AVERAGE		Error includes scale factor of 2.3. See the ideogram below.				
$1785\pm\ 9^{+12}_{-\ 6}$	420k	ALEKSEEV	10	COMP		190 $\pi^- Pb \to \pi^-\pi^-\pi^+ Pb'$
$1876\pm18\pm16$	4k	[1] EUGENIO	08	B852	–	18 $\pi^- p \to \eta\eta\pi^- p$
$1774\pm18\pm20$		[2] CHUNG	02	B852		18.3 $\pi^- p \to \pi^+\pi^-\pi^- p$
$1863\pm\ 9\pm10$		[3] CHUNG	02	B852		18.3 $\pi^- p \to \pi^+\pi^-\pi^- p$
$1840\pm10\pm10$	1200	AMELIN	96B	VES	–	37 $\pi^- A \to \eta\eta\pi^- A$
$1775\pm\ 7\pm10$		[4] AMELIN	95B	VES	–	36 $\pi^- A \to \pi^+\pi^-\pi^- A$
1790 ± 14		[5] BERDNIKOV	94	VES	–	37 $\pi^- A \to K^+K^-\pi^- A$
$1873\pm33\pm20$		BELADIDZE	92C	VES	–	36 π^- Be $\to \pi^-\eta'\eta$ Be
$1814\pm10\pm23$	426 ± 57	BITYUKOV	91	VES	–	36 π^- C $\to \pi^-\eta\eta$ C
1770 ± 30	1100	BELLINI	82	SPEC	–	40 π^- A $\to 3\pi$ A

• • • We do not use the following data for averages, fits, limits, etc. • • •

$1737\pm\ 5\pm15$		AMELIN	99	VES		37 $\pi^- A \to \omega\pi^-\pi^0 A^*$

[1] From a single-pole fit.
[2] In the $f_0(980)\pi$ wave.
[3] In the $f_0(500)\pi$ wave.
[4] From a fit to $J^{PC} = 0^{-+}$ $f_0(980)\pi$, $f_0(1370)\pi$ waves.
[5] From a fit to $J^{PC} = 0^{-+}$ $K_0^*(1430)K^-$ and $f_0(980)\pi^-$ waves.

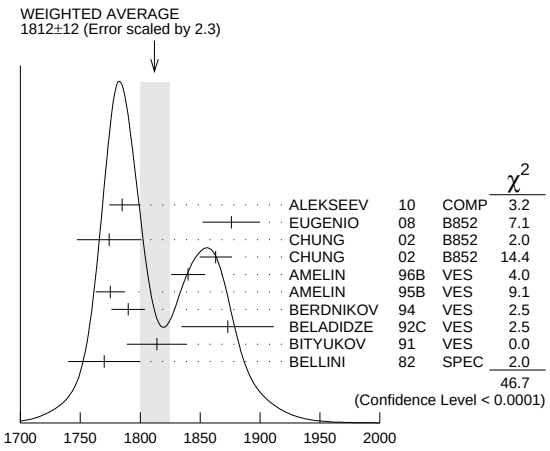

$\pi(1800)$ WIDTH

VALUE (MeV)	EVTS	DOCUMENT ID		TECN	CHG	COMMENT
208±12 OUR AVERAGE						
$208\pm22^{+21}_{-37}$	420k	ALEKSEEV	10	COMP		190 $\pi^- Pb \to \pi^-\pi^-\pi^+ Pb'$
$221\pm26\pm38$	4k	[6] EUGENIO	08	B852	–	18 $\pi^- p \to \eta\eta\pi^- p$
$223\pm48\pm50$		[7] CHUNG	02	B852		18.3 $\pi^- p \to \pi^+\pi^-\pi^- p$
$191\pm21\pm20$		[8] CHUNG	02	B852		18.3 $\pi^- p \to \pi^+\pi^-\pi^- p$
$210\pm30\pm30$	1200	AMELIN	96B	VES	–	37 $\pi^- A \to \eta\eta\pi^- A$
$190\pm15\pm15$		[9] AMELIN	95B	VES	–	36 $\pi^- A \to \pi^+\pi^-\pi^- A$
210 ± 70		[10] BERDNIKOV	94	VES	–	37 $\pi^- A \to K^+K^-\pi^- A$
$225\pm35\pm20$		BELADIDZE	92C	VES	–	36 π^- Be $\to \pi^-\eta'\eta$ Be
$205\pm18\pm32$	426 ± 57	BITYUKOV	91	VES	–	36 π^- C $\to \pi^-\eta\eta$ C
310 ± 50	1100	BELLINI	82	SPEC	–	40 π^- A $\to 3\pi$ A

• • • We do not use the following data for averages, fits, limits, etc. • • •

$259\pm19\pm\ 6$		AMELIN	99	VES		37 $\pi^- A \to \omega\pi^-\pi^0 A^*$

[6] From a single-pole fit.
[7] In the $f_0(980)\pi$ wave.
[8] In the $f_0(500)\pi$ wave.
[9] From a fit to $J^{PC} = 0^{-+}$ $f_0(980)\pi$, $f_0(1370)\pi$ waves.
[10] From a fit to $J^{PC} = 0^{-+}$ $K_0^*(1430)K^-$ and $f_0(980)\pi^-$ waves.

$\pi(1800)$ DECAY MODES

	Mode	Fraction (Γ_i/Γ)
Γ_1	$\pi^+\pi^-\pi^-$	seen
Γ_2	$f_0(500)\pi^-$	seen
Γ_3	$f_0(980)\pi^-$	seen
Γ_4	$f_0(1370)\pi^-$	seen
Γ_5	$f_0(1500)\pi^-$	not seen
Γ_6	$\rho\pi^-$	not seen
Γ_7	$\eta\eta\pi^-$	seen
Γ_8	$a_0(980)\eta$	seen
Γ_9	$a_2(1320)\eta$	not seen
Γ_{10}	$f_2(1270)\pi$	not seen
Γ_{11}	$f_0(1370)\pi^-$	not seen
Γ_{12}	$f_0(1500)\pi^-$	seen
Γ_{13}	$\eta\eta'(958)\pi^-$	seen
Γ_{14}	$K_0^*(1430)K^-$	seen
Γ_{15}	$K^*(892)K^-$	not seen

$\pi(1800)$ BRANCHING RATIOS

$\Gamma(f_0(980)\pi^-)/\Gamma(f_0(500)\pi^-)$ Γ_3/Γ_2

VALUE	DOCUMENT ID		TECN	COMMENT
0.44±0.08±0.38	[11] CHUNG	02	B852	18.3 $\pi^- p \to \pi^+\pi^-\pi^- p$

$\Gamma(f_0(980)\pi^-)/\Gamma(f_0(1370)\pi^-)$ Γ_3/Γ_4

VALUE	DOCUMENT ID		TECN	CHG	COMMENT
• • • We do not use the following data for averages, fits, limits, etc. • • •					
1.7±1.3	[12] AMELIN	95B	VES	–	36 $\pi^- A \to \pi^+\pi^-\pi^- A$

$\Gamma(f_0(1370)\pi^-)/\Gamma_{total}$ Γ_4/Γ

VALUE	DOCUMENT ID		TECN	CHG	COMMENT
seen	BELLINI	82	SPEC	–	40 π^-A → 3πA

$\Gamma(f_0(1500)\pi^-)/\Gamma_{total}$ Γ_5/Γ

VALUE	DOCUMENT ID		TECN	CHG	COMMENT
not seen	CHUNG	02	B852		18.3 $\pi^- p \to \pi^+\pi^-\pi^- p$

$\Gamma(\rho\pi^-)/\Gamma_{total}$ Γ_6/Γ

VALUE	DOCUMENT ID		TECN	CHG	COMMENT
not seen	BELLINI	82	SPEC	–	40 π^-A → 3πA

$\Gamma(\rho\pi^-)/\Gamma(f_0(980)\pi^-)$ Γ_6/Γ_3

VALUE	CL%	DOCUMENT ID		TECN	CHG	COMMENT
• • • We do not use the following data for averages, fits, limits, etc. • • •						
<0.25		CHUNG	02	B852		18.3 $\pi^- p \to \pi^+\pi^-\pi^- p$
<0.14	90	AMELIN	95B	VES	–	36 $\pi^- A \to \pi^+\pi^-\pi^- A$

$\Gamma(\eta\eta\pi^-)/\Gamma(\pi^+\pi^-\pi^-)$ Γ_7/Γ_1

VALUE	EVTS	DOCUMENT ID		TECN	CHG	COMMENT
• • • We do not use the following data for averages, fits, limits, etc. • • •						
0.5±0.1	1200	[12] AMELIN	96B	VES	–	37 $\pi^- A \to \eta\eta\pi^- A$

$\Gamma(a_2(1320)\eta)/\Gamma_{total}$ Γ_9/Γ

VALUE	DOCUMENT ID		TECN	COMMENT
not seen	EUGENIO	08	B852	18 $\pi^- p \to \eta\eta\pi^- p$

$\Gamma(f_2(1270)\pi)/\Gamma_{total}$ Γ_{10}/Γ

VALUE	DOCUMENT ID		TECN	COMMENT
not seen	EUGENIO	08	B852	18 $\pi^- p \to \eta\eta\pi^- p$

$\Gamma(f_0(1370)\pi^-)/\Gamma_{total}$ Γ_{11}/Γ

VALUE	DOCUMENT ID		TECN	COMMENT
not seen	EUGENIO	08	B852	18 $\pi^- p \to \eta\eta\pi^- p$

$\Gamma(f_0(1500)\pi^-)/\Gamma(a_0(980)\eta)$ Γ_{12}/Γ_8

VALUE	EVTS	DOCUMENT ID		TECN	CHG	COMMENT
• • • We do not use the following data for averages, fits, limits, etc. • • •						
0.48 ±0.17	4k	[12,13] EUGENIO	08	B852	–	18 $\pi^- p \to \eta\eta\pi^- p$
$0.030^{+0.014}_{-0.011}$		[12] ANISOVICH	01B	SPEC	0	0.6–1.94 $p\overline{p} \to \eta\eta\pi^0\pi^0$
0.08 ±0.03	1200	[12,14] AMELIN	96B	VES	–	37 $\pi^- A \to \eta\eta\pi^- A$

$\Gamma(\eta\eta'(958)\pi^-)/\Gamma(\eta\eta\pi^-)$ Γ_{13}/Γ_7

VALUE	EVTS	DOCUMENT ID		TECN	CHG	COMMENT
• • • We do not use the following data for averages, fits, limits, etc. • • •						
0.29±0.07		[12] BELADIDZE	92C	VES	–	36 π^-Be → $\pi^-\eta'\eta$Be
0.3 ±0.1	426 ± 57	[12] BITYUKOV	91	VES	–	36 π^-C → $\pi^-\eta\eta$C

$\Gamma(K_0^*(1430)K^-)/\Gamma_{total}$ Γ_{14}/Γ

VALUE	DOCUMENT ID		TECN	CHG	COMMENT
seen	BERDNIKOV	94	VES	–	37 $\pi^- A \to K^+K^-\pi^- A$

$\Gamma(K^*(892)K^-)/\Gamma_{total}$ Γ_{15}/Γ

VALUE	DOCUMENT ID		TECN	CHG	COMMENT
not seen	BERDNIKOV	94	VES	–	37 $\pi^- A \to K^+K^-\pi^- A$

[11] Assuming that $f_0(980)$ decays only to $\pi\pi$.
[12] Systematic errors not estimated.
[13] From a single-pole fit.
[14] Assuming that $f_0(1500)$ decays only to $\eta\eta$ and $a_0(980)$ decays only to $\eta\pi$.

$\pi(1800)$ REFERENCES

ALEKSEEV	10	PRL 104 241803	M.G. Alekseev *et al.*	(COMPASS Collab.)
EUGENIO	08	PL B660 466	P. Eugenio *et al.*	(BNL E852 Collab.)
PDG	06	JP G33 1	W.-M. Yao *et al.*	(PDG Collab.)
CHUNG	02	PR D65 072001	S.U. Chung *et al.*	(BNL E852 Collab.)
ANISOVICH	01B	PL B500 222	A.V. Anisovich *et al.*	
AMELIN	99	PAN 62 445 Translated from YAF 62 487.	D.V. Amelin *et al.*	(VES Collab.)
AMELIN	96B	PAN 59 976 Translated from YAF 59 1021.	D.V. Amelin *et al.*	(SERP, TBIL) IGJPC
AMELIN	95B	PL B356 595	D.V. Amelin *et al.*	(SERP, TBIL)
BERDNIKOV	94	PL B337 219	E.B. Berdnikov *et al.*	(SERP, TBIL)
BELADIDZE	92C	SJNP 55 1535 Translated from YAF 55 2748.	G.M. Beladidze, S.I. Bityukov, G.V. Borisov	(SERP+)
BITYUKOV	91	PL B268 137	S.I. Bityukov *et al.*	(SERP, TBIL)
BELLINI	82	PRL 48 1697	G. Bellini *et al.*	(MILA, BGNA, JINR)

$f_2(1810)$

$I^G(J^{PC}) = 0^+(2^{++})$

OMITTED FROM SUMMARY TABLE
Needs confirmation.

$f_2(1810)$ MASS

VALUE (MeV)	EVTS	DOCUMENT ID		TECN	COMMENT
1815±12 OUR AVERAGE		Error includes scale factor of 1.4. See the ideogram below.			
$1822^{+29}_{-24}{}^{+66}_{-57}$	5.5k	[1] ABLIKIM	13N	BES3	$e^+e^- \to J/\psi \to \gamma\eta\eta$
$1737\pm 9^{+198}_{-65}$		[2] UEHARA	10A	BELL	10.6 $e^+e^- \to e^+e^-\eta\eta$
1800±30	40	ALDE	88D	GAM4	300 $\pi^- p \to \pi^- p 4\pi^0$
1806±10	1600	ALDE	87	GAM4	100 $\pi^- p \to 4\pi^0 n$
1870±40		[3] ALDE	86D	GAM4	100 $\pi^- p \to \eta\eta n$
1857^{+35}_{-24}		[4] COSTA	80	OMEG	10 $\pi^- p \to K^+K^- n$
• • • We do not use the following data for averages, fits, limits, etc. • • •					
1858^{+18}_{-71}		[5] LONGACRE	86	RVUE	Compilation
1799±15		[6] CASON	82	STRC	8 $\pi^+ p \to \Delta^{++}\pi^0\pi^0$

[1] From partial wave analysis including all possible combinations of 0^{++}, 2^{++}, and 4^{++} resonances.
[2] Breit-Wigner mass.
[3] Seen in only one solution.
[4] Error increased by spread of two solutions. Included in LONGACRE 86 global analysis.
[5] From a partial-wave analysis of data using a K-matrix formalism with 5 poles. Includes compilation of several other experiments.
[6] From an amplitude analysis of the reaction $\pi^+\pi^- \to 2\pi^0$. The resonance in the $2\pi^0$ final state is not confirmed by PROKOSHKIN 97.

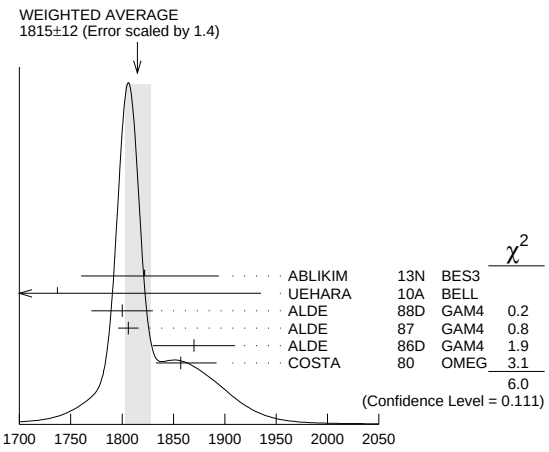

$f_2(1810)$ WIDTH

VALUE (MeV)	EVTS	DOCUMENT ID		TECN	COMMENT
197± 22 OUR AVERAGE		Error includes scale factor of 1.5. See the ideogram below.			
$229^{+52}_{-42}{}^{+88}_{-155}$	5.5k	[7] ABLIKIM	13N	BES3	$e^+e^- \to J/\psi \to \gamma\eta\eta$
$228^{+21}_{-20}{}^{+234}_{-153}$		[8] UEHARA	10A	BELL	10.6 $e^+e^- \to e^+e^-\eta\eta$
160± 30	40	ALDE	88D	GAM4	300 $\pi^- p \to \pi^- p 4\pi^0$
190± 20	1600	ALDE	87	GAM4	100 $\pi^- p \to 4\pi^0 n$
250± 30		[9] ALDE	86D	GAM4	100 $\pi^- p \to \eta\eta n$
185^{+102}_{-139}		[10] COSTA	80	OMEG	10 $\pi^- p \to K^+K^- n$
• • • We do not use the following data for averages, fits, limits, etc. • • •					
388^{+15}_{-21}		[11] LONGACRE	86	RVUE	Compilation
280^{+42}_{-35}		[12] CASON	82	STRC	8 $\pi^+ p \to \Delta^{++}\pi^0\pi^0$

[7] From partial wave analysis including all possible combinations of 0^{++}, 2^{++}, and 4^{++} resonances.
[8] Breit-Wigner width.
[9] Seen in only one solution.
[10] Error increased by spread of two solutions. Included in LONGACRE 86 global analysis.
[11] From a partial-wave analysis of data using a K-matrix formalism with 5 poles. Includes compilation of several other experiments.
[12] From an amplitude analysis of the reaction $\pi^+\pi^- \to 2\pi^0$. The resonance in the $2\pi^0$ final state is not confirmed by PROKOSHKIN 97.

Meson Particle Listings

$f_2(1810)$, $X(1835)$

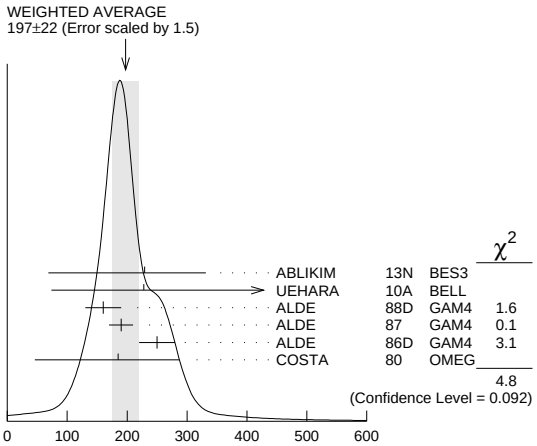

$f_2(1810)$ DECAY MODES

	Mode	Fraction (Γ_i/Γ)
Γ_1	$\pi\pi$	
Γ_2	$\eta\eta$	seen
Γ_3	$4\pi^0$	seen
Γ_4	K^+K^-	
Γ_5	$\gamma\gamma$	seen

$f_2(1810)$ $\Gamma(i)\Gamma(\gamma\gamma)/\Gamma(\text{total})$

$\Gamma(\eta\eta) \times \Gamma(\gamma\gamma)/\Gamma_{\text{total}}$ $\Gamma_2\Gamma_5/\Gamma$

VALUE (eV)	DOCUMENT ID		TECN	COMMENT
$5.2^{+0.9}_{-0.8}{}^{+37.3}_{-4.5}$	[13] UEHARA	10A	BELL	10.6 $e^+e^- \to e^+e^-\eta\eta$

[13] Including interference with the $f_2'(1525)$ (parameters fixed to the values from the 2008 edition of this review, PDG 08) and $f_2(1270)$. May also be the $f_0(1500)$.

$f_2(1810)$ BRANCHING RATIOS

$\Gamma(\pi\pi)/\Gamma_{\text{total}}$ Γ_1/Γ

VALUE	DOCUMENT ID		TECN	COMMENT
• • • We do not use the following data for averages, fits, limits, etc. • • •				
not seen	AMSLER	02	CBAR	0.9 $\bar{p}p \to \pi^0\eta\eta, \pi^0\pi^0\pi^0$
not seen	PROKOSHKIN	97	GAM2	38 $\pi^-p \to \pi^0\pi^0 n$
$0.21^{+0.02}_{-0.03}$	[14] LONGACRE	86	RVUE	Compilation
0.44 ± 0.03	[15] CASON	82	STRC	8 $\pi^+p \to \Delta^{++}\pi^0\pi^0$

[14] From a partial-wave analysis of data using a K-matrix formalism with 5 poles. Includes compilation of several other experiments.
[15] Included in LONGACRE 86 global analysis.

$\Gamma(\eta\eta)/\Gamma_{\text{total}}$ Γ_2/Γ

VALUE	DOCUMENT ID		TECN	COMMENT
seen	ABLIKIM	13N	BES3	PWA of $J/\psi \to \gamma\eta\eta$
• • • We do not use the following data for averages, fits, limits, etc. • • •				
$0.008^{+0.028}_{-0.003}$	[16] LONGACRE	86	RVUE	Compilation

[16] From a partial-wave analysis of data using a K-matrix formalism with 5 poles. Includes compilation of several other experiments.

$\Gamma(\pi\pi)/\Gamma(4\pi^0)$ Γ_1/Γ_3

VALUE	DOCUMENT ID		TECN	COMMENT
• • • We do not use the following data for averages, fits, limits, etc. • • •				
<0.75	ALDE	87	GAM4	100 $\pi^-p \to 4\pi^0 n$

$\Gamma(4\pi^0)/\Gamma(\eta\eta)$ Γ_3/Γ_2

VALUE	DOCUMENT ID		TECN	COMMENT
• • • We do not use the following data for averages, fits, limits, etc. • • •				
0.8 ± 0.3	ALDE	87	GAM4	100 $\pi^-p \to 4\pi^0 n$

$\Gamma(K^+K^-)/\Gamma_{\text{total}}$ Γ_4/Γ

VALUE	DOCUMENT ID		TECN	COMMENT
• • • We do not use the following data for averages, fits, limits, etc. • • •				
$0.003^{+0.019}_{-0.002}$	[17] LONGACRE	86	RVUE	Compilation
seen	COSTA	80	OMEG	10 $\pi^-p \to K^+K^-n$

[17] From a partial-wave analysis of data using a K-matrix formalism with 5 poles. Includes compilation of several other experiments.

$f_2(1810)$ REFERENCES

ABLIKIM	13N	PR D87 092009	Ablikim M. *et al.*	(BES III Collab.)
UEHARA	10A	PR D82 114031	S. Uehara *et al.*	(BELLE Collab.)
PDG	08	PL B667 1	C. Amsler *et al.*	(PDG Collab.)
AMSLER	02	EPJ C23 29	C. Amsler *et al.*	
PROKOSHKIN	97	PD 42 117	Y.D. Prokoshkin *et al.*	(SERP)
		Translated from DANS 353 323.		
ALDE	88D	SJNP 47 810	D.M. Alde *et al.*	(SERP, BELG, LANL, LAPP+)
		Translated from YAF 47 1273.		
ALDE	87	PL B198 286	D.M. Alde *et al.*	(LANL, BRUX, SERP, LAPP)
ALDE	86D	NP B269 485	D.M. Alde *et al.*	(BELG, LAPP, SERP, CERN+)
LONGACRE	86	PL B177 223	R.S. Longacre *et al.*	(BNL, BRAN, CUNY+)
CASON	82	PRL 48 1316	N.M. Cason *et al.*	(NDAM, ANL)
COSTA	80	NP B175 402	G. Costa *et al.*	(BARI, BONN, CERN, GLAS+)

$X(1835)$ $I^G(J^{PC}) = ?^?(0^{-+})$

OMITTED FROM SUMMARY TABLE

Could be a superposition of two states, one with small width appearing as threshold enhancement in $p\bar{p}$, the other one with a larger width, decaying into $\pi^+\pi^-\eta'$ and $K^0_S K^0_S \eta$. For the former ABLIKIM 12D determine $J^{PC} = 0^{-+}$.

$X(1835)$ MASS

VALUE (MeV)	EVTS	DOCUMENT ID		TECN	COMMENT
$1826.5^{+13.0}_{-3.4}$ OUR AVERAGE					
$1825.3\pm 2.4^{+17.3}_{-2.4}$		[1] ABLIKIM	16J	BES3	$J/\psi \to \gamma\pi^+\pi^-\eta'$
$1844 \pm 9 ^{+16}_{-25}$		ABLIKIM	15T	BES3	$J/\psi \to \gamma K^0_S K^0_S \eta$
• • • We do not use the following data for averages, fits, limits, etc. • • •					
$1909.5\pm15.9^{+9.4}_{-27.5}$		[2] ABLIKIM	16J	BES3	$J/\psi \to \gamma\pi^+\pi^-\eta'$
$1832 ^{+19}_{-5} \pm 26$		[3] ABLIKIM	12D	BES3	$J/\psi \to \gamma p\bar{p}$
$1836.5\pm 3.0^{+5.6}_{-2.1}$	4265	[4] ABLIKIM	11C	BES3	$J/\psi \to \gamma\pi^+\pi^-\eta'$
$1877.3\pm 6.3^{+3.4}_{-7.4}$		[5] ABLIKIM	11J	BES3	$J/\psi \to \omega(\eta\pi^+\pi^-)$
$1837 ^{+10}_{-12} ^{+9}_{-7}$	231	[6,7] ALEXANDER	10	CLEO	$J/\psi \to \gamma p\bar{p}$
$1833.7\pm 6.1\pm 2.7$	264	ABLIKIM	05R	BES2	$J/\psi \to \gamma\pi^+\pi^-\eta'$
1831 ± 7		[7,8] ABLIKIM	05R	BES2	$J/\psi \to \gamma p\bar{p}$
$1859 ^{+3}_{-10} ^{+5}_{-25}$		[7] BAI	03F	BES2	$J/\psi \to \gamma p\bar{p}$

[1] From a fit of the measured $\pi^+\pi^-\eta'$ lineshape that accounts for the abrupt distortion observed at the $p\bar{p}$ threshold through interference with a second previously unseen narrow resonance near 1870 MeV. The fit uses Breit-Wigner functions for the signal shapes and includes known backgrounds and contributors.
[2] Pole mass from a fit of the measured $\pi^+\pi^-\eta'$ lineshape to a Flatte formula that accounts for the abrupt distortion observed at the $p\bar{p}$ threshold; the fit also includes known backgrounds and contributors, as well as an *ad hoc* Breit-Wigner function ($M \approx$ 1919 MeV; $\Gamma \approx$ 51 MeV) that is required for a good fit.
[3] From the fit including final state interaction effects in isospin 0 S-wave according to SIBIRTSEV 05A. Supersedes ABLIKIM 10G.
[4] From a fit of the $\pi^+\pi^-\eta'$ mass distribution to a combination of $\gamma f_1(1510)$, $\gamma X(1835)$, and two unconfirmed states $\gamma X(2120)$, and $\gamma X(2370)$, for $M(p\bar{p}) < 2.8$ GeV, and accounting for backgrounds from non-η' events and $J/\psi \to \pi^0\pi^+\pi^-\eta'$.
[5] The selected process is $J/\psi \to \omega a_0(980)\pi$. This state may be due also to $\eta_2(1870)$ or to a combination of $X(1835)$ and $\eta_2(1870)$.
[6] From a fit of the $p\bar{p}$ mass distribution to a combination of $\gamma X(1835)$, γR with $M(R) = 2100$ MeV and $\Gamma(R) = 160$ MeV, and $\gamma p\bar{p}$ phase space, for $M(p\bar{p}) < 2.85$ GeV.
[7] Evidence for a threshold enhancement in the $p\bar{p}$ mass spectrum was also reported by ABE 02K, AUBERT,B 05L, and WANG 05A in $B^+ \to p\bar{p}K^+$, WANG 05A in $B^0 \to p\bar{p}K^0_S$, ABE 02W in $\overline{B}{}^0 \to p\bar{p}D^0$, DEL-AMO-SANCHEZ 12 in $B \to D(D^*)p\bar{p}(\pi)$, and WEI 08 in $B^+ \to p\bar{p}\pi^+$ decays. Not seen by ATHAR 06 in $\Upsilon(1S) \to p\bar{p}\gamma$.
[8] From the fit including final state interaction effects in isospin 0 S-wave according to SIBIRTSEV 05A. Systematic errors not estimated.

$X(1835)$ WIDTH

VALUE (MeV)	CL%	EVTS	DOCUMENT ID		TECN	COMMENT
$242 ^{+14}_{-15}$ OUR AVERAGE						
$245.2\pm13.1^{+4.6}_{-9.6}$			[1] ABLIKIM	16J	BES3	$J/\psi \to \gamma\pi^+\pi^-\eta'$
$192 ^{+20}_{-17} ^{+62}_{-43}$			ABLIKIM	15T	BES3	$J/\psi \to \gamma K^0_S K^0_S \eta$
• • • We do not use the following data for averages, fits, limits, etc. • • •						
$273.5\pm21.4^{+6.1}_{-64.0}$			[2] ABLIKIM	16J	BES3	$J/\psi \to \gamma\pi^+\pi^-\eta'$
< 76	90		[3] ABLIKIM	12D	BES3	$J/\psi \to \gamma p\bar{p}$
$190 \pm 9 ^{+38}_{-36}$		4265	[4] ABLIKIM	11C	BES3	$J/\psi \to \gamma\pi^+\pi^-\eta'$
$57 \pm 12 ^{+19}_{-4}$			[5] ABLIKIM	11J	BES3	$J/\psi \to \omega(\eta\pi^+\pi^-)$
$0 ^{+44}_{-0}$		231	[6,7] ALEXANDER	10	CLEO	$J/\psi \to \gamma p\bar{p}$
$67.7\pm20.3\pm 7.7$		264	ABLIKIM	05R	BES2	$J/\psi \to \gamma\pi^+\pi^-\eta'$

< 153	90	[7,8] ABLIKIM	05R	BES2	$J/\psi \to \gamma p\overline{p}$	
< 30		[7] BAI	03F	BES2	$J/\psi \to \gamma p\overline{p}$	

[1] From a fit of the measured $\pi^+\pi^-\eta'$ lineshape that accounts for the abrupt distortion observed at the $p\overline{p}$ threshold through interference with a second previously unseen narrow resonance near 1870 MeV. The fit uses Breit-Wigner functions for the signal shapes and includes known backgrounds and contributors.

[2] Pole width from a fit of the measured $\pi^+\pi^-\eta'$ lineshape to a Flatte formula that accounts for the abrupt distortion observed at the $p\overline{p}$ threshold; the fit also includes known backgrounds and contributors, as well as an *ad hoc* Breit-Wigner function ($M \approx$ 1919 MeV; $\Gamma \approx$ 51 MeV) that is required for a good fit.

[3] From the fit including final state interaction effects in isospin 0 S-wave according to SIBIRTSEV 05A. Supersedes ABLIKIM 10G.

[4] From a fit of the $\pi^+\pi^-\eta'$ mass distribution to a combination of $\gamma f_1(1510)$, $\gamma X(1835)$, and two unconfirmed states $\gamma X(2120)$, and $\gamma X(2370)$, for $M(p\overline{p}) < 2.8$ GeV, and accounting for backgrounds from non-η' events and $J/\psi \to \pi^0\pi^+\pi^-\eta'$.

[5] The selected process is $J/\psi \to \omega a_0(980)\pi$. This state may be due also to $\eta_2(1870)$ or to a combination of $X(1835)$ and $\eta_2(1870)$.

[6] From a fit of the $p\overline{p}$ mass distribution to a combination of $\gamma X(1835)$, γR with $M(R) = 2100$ MeV and $\Gamma(R) = 160$ MeV, and $\gamma p\overline{p}$ phase space, for $M(p\overline{p}) < 2.85$ GeV.

[7] Evidence for a threshold enhancement in the $p\overline{p}$ mass spectrum was also reported by ABE 02K, AUBERT,B 05L, and WANG 05A in $B^+ \to p\overline{p}K^+$, WANG 05A in $B^0 \to p\overline{p}K^0_S$, ABE 02W in $\overline{B}^0 \to p\overline{p}D^0$, DEL-AMO-SANCHEZ 12 in $B \to D(D^*)p\overline{p}(\pi)$, and WEI 08 in $B^+ \to p\overline{p}\pi^+$ decays. Not seen by ATHAR 06 in $\Upsilon(1S) \to p\overline{p}\gamma$.

[8] From the fit including final state interaction effects in isospin 0 S-wave according to SIBIRTSEV 05A. Systematic errors not estimated.

$X(1835)$ DECAY MODES

	Mode	Fraction (Γ_i/Γ)
Γ_1	$p\overline{p}$	seen
Γ_2	$\eta'\pi^+\pi^-$	seen
Γ_3	$\gamma\gamma$	
Γ_4	$K^0_S K^0_S \eta$	seen

$X(1835)$ $\Gamma(i)\Gamma(\gamma\gamma)/\Gamma(\text{total})$

$\Gamma(\eta'\pi^+\pi^-) \times \Gamma(\gamma\gamma)/\Gamma_{\text{total}}$ $\Gamma_2\Gamma_3/\Gamma$

VALUE (eV)	CL%	DOCUMENT ID		TECN	COMMENT
• • • We do not use the following data for averages, fits, limits, etc. • • •					
<35.6	90	[1] ZHANG	12A	BELL	$e^+e^- \to e^+e^-\eta'\pi^+\pi^-$
<83	90	[2] ZHANG	12A	BELL	$e^+e^- \to e^+e^-\eta'\pi^+\pi^-$

[1] From a two-resonance fit and constructive interference of the $\eta(1760)$ and $X(1835)$, a significance of 2.8 σ.

[2] From a two-resonance fit and destructive interference of the $\eta(1760)$ and $X(1835)$, a significance of 2.8 σ.

$X(1835)$ BRANCHING RATIOS

$\Gamma(p\overline{p})/\Gamma(\eta'\pi^+\pi^-)$ Γ_1/Γ_2

VALUE	DOCUMENT ID		TECN	COMMENT
• • • We do not use the following data for averages, fits, limits, etc. • • •				
0.333	ABLIKIM	05R	BES2	$J/\psi \to \gamma\pi^+\pi^-\eta'$

$\Gamma(\eta'\pi^+\pi^-)/\Gamma(K^0_S K^0_S \eta)$ Γ_2/Γ_4

VALUE	DOCUMENT ID		TECN	COMMENT
• • • We do not use the following data for averages, fits, limits, etc. • • •				
6.7 ± 1.8	[1] ABLIKIM	15T	BES3	$J/\psi \to \gamma K^0_S K^0_S \eta$

[1] Using resutls from ABLIKIM 05R.

$\Gamma(\eta'\pi^+\pi^-)/\Gamma_{\text{total}}$ Γ_2/Γ

VALUE	DOCUMENT ID		TECN	COMMENT
seen	[1] ABLIKIM	16J	BES3	$J/\psi \to \gamma\pi^+\pi^-\eta'$

[1] ABLIKIM 16J quotes B($J/\psi \to \gamma X(1835)$) $\times$ B($X(1835) \to \pi^+\pi^-\eta'$) = $(3.93 \pm 0.38^{+0.31}_{-0.84}) \times 10^{-4}$ from a fit of the measured $\pi^+\pi^-\eta'$ lineshape that accounts for the abrupt distortion observed at the $p\overline{p}$ threshold with a Flatte formula in addition to known backgrounds and contributors, as well as an *ad hoc* Breit-Wigner ($M \approx$ 1919 MeV; $\Gamma \approx$ 51 MeV) that is required for a good fit. Another explanation for the distortion provided by ABLIKIM 16J is that a second resonance near 1870 MeV interferes with the $X(1835)$; fits to this possibility yield product branching fraction values compatible with that shown within the respective systematic uncertainties.

$X(1835)$ REFERENCES

ABLIKIM	16J	PRL 117 042002	M. Ablikim *et al.*	(BES III Collab.)
ABLIKIM	15T	PRL 115 091803	M. Ablikim *et al.*	(BES III Collab.)
ABLIKIM	12D	PRL 108 112003	M. Ablikim *et al.*	(BES III Collab.) JPC
DEL-AMO-SA...	12	PR D85 092017	P. del Amo Sanchez *et al.*	(BABAR Collab.)
ZHANG	12A	PR D86 052002	C.C. Zhang *et al.*	(BELLE Collab.)
ABLIKIM	11C	PRL 106 072002	M. Ablikim *et al.*	(BES III Collab.)
ABLIKIM	11J	PRL 107 182001	M. Ablikim *et al.*	(BES III Collab.)
ABLIKIM	10G	CP C34 421	M. Ablikim *et al.*	(BES III Collab.)
ALEXANDER	10	PR D82 092002	J.P. Alexander *et al.*	(CLEO Collab.)
WEI	08	PL B659 80	J.-T. Wei *et al.*	(BELLE Collab.)
ATHAR	06	PR D73 032001	S.B. Athar *et al.*	(CLEO Collab.)
ABLIKIM	05R	PRL 95 262001	M. Ablikim *et al.*	(BES Collab.)
AUBERT,B	05L	PR D72 051101	B. Aubert *et al.*	(BABAR Collab.)
SIBIRTSEV	05A	PR D71 054010	A. Sibirtsev, J. Haidenbauer	
WANG	05A	PL B617 141	M.-Z. Wang *et al.*	(BELLE Collab.)
BAI	03F	PRL 91 022001	J.Z. Bai *et al.*	(BES II Collab.)
ABE	02K	PRL 88 181803	K. Abe *et al.*	(BELLE Collab.)
ABE	02W	PRL 89 151802	K. Abe *et al.*	(BELLE Collab.)

$X(1840)$

$I^G(J^{PC}) = ?^?(?^{??})$

OMITTED FROM SUMMARY TABLE

$X(1840)$ MASS

VALUE (MeV)	EVTS	DOCUMENT ID		TECN	COMMENT
$\mathbf{1842.2 \pm 4.2^{+7.1}_{-2.6}}$	0.6k	ABLIKIM	13U	BES3	$J/\psi \to \gamma 3(\pi^+\pi^-)$

$X(1840)$ WIDTH

VALUE (MeV)	EVTS	DOCUMENT ID		TECN	COMMENT
$\mathbf{83 \pm 14 \pm 11}$	0.6k	ABLIKIM	13U	BES3	$J/\psi \to \gamma 3(\pi^+\pi^-)$

$X(1840)$ DECAY MODES

	Mode	Fraction (Γ_i/Γ)
Γ_1	$3(\pi^+\pi^-)$	seen

$X(1840)$ BRANCHING RATIOS

$\Gamma(3(\pi^+\pi^-))/\Gamma_{\text{total}}$ Γ_1/Γ

VALUE	EVTS	DOCUMENT ID		TECN	COMMENT
seen	0.6k	ABLIKIM	13U	BES3	$J/\psi \to \gamma 3(\pi^+\pi^-)$

$X(1840)$ REFERENCES

ABLIKIM	13U	PR D88 091502	M. Ablikim *et al.*	(BES III Collab.)

$\phi_3(1850)$

$I^G(J^{PC}) = 0^-(3^{--})$

$\phi_3(1850)$ MASS

VALUE (MeV)	EVTS	DOCUMENT ID		TECN	COMMENT
1854 ± 7 OUR AVERAGE					
1855 ± 10		ASTON	88E	LASS	11 $K^-p \to K^-K^+\Lambda$, $K^0_S K^\pm\pi^\mp\Lambda$
1870^{+30}_{-20}	430	ARMSTRONG	82	OMEG	18.5 $K^-p \to K^-K^+\Lambda$
1850 ± 10	123	ALHARRAN	81B	HBC	8.25 $K^-p \to K\overline{K}\Lambda$

$\phi_3(1850)$ WIDTH

VALUE (MeV)	EVTS	DOCUMENT ID		TECN	COMMENT
$\mathbf{87^{+28}_{-23}}$ **OUR AVERAGE** Error includes scale factor of 1.2.					
64 ± 31		ASTON	88E	LASS	11 $K^-p \to K^-K^+\Lambda$, $K^0_S K^\pm\pi^\mp\Lambda$
160^{+90}_{-50}	430	ARMSTRONG	82	OMEG	18.5 $K^-p \to K^-K^+\Lambda$
80^{+40}_{-30}	123	ALHARRAN	81B	HBC	8.25 $K^-p \to K\overline{K}\Lambda$

$\phi_3(1850)$ DECAY MODES

	Mode	Fraction (Γ_i/Γ)
Γ_1	$K\overline{K}$	seen
Γ_2	$K\overline{K}^*(892) +$ c.c.	seen

$\phi_3(1850)$ BRANCHING RATIOS

$\Gamma(K\overline{K}^*(892) +$ c.c.$)/\Gamma(K\overline{K})$ Γ_2/Γ_1

VALUE	DOCUMENT ID		TECN	COMMENT
$\mathbf{0.55^{+0.85}_{-0.45}}$	ASTON	88E	LASS	11 $K^-p \to K^-K^+\Lambda$, $K^0_S K^\pm\pi^\mp\Lambda$
• • • We do not use the following data for averages, fits, limits, etc. • • •				
0.8 ± 0.4	ALHARRAN	81B	HBC	8.25 $K^-p \to K\overline{K}\pi\Lambda$

$\phi_3(1850)$ REFERENCES

ASTON	88E	PL B208 324	D. Aston *et al.*	(SLAC, NAGO, CINC, INUS) IGJPC
ARMSTRONG	82	PL 110B 77	T.A. Armstrong *et al.*	(BARI, BIRM, CERN+) JP
ALHARRAN	81B	PL 101B 357	S. Al-Harran *et al.*	(BIRM, CERN, GLAS+)

Meson Particle Listings

$\eta_2(1870)$, $\pi_2(1880)$, $\rho(1900)$

$\eta_2(1870)$

$I^G(J^{PC}) = 0^+(2^{-+})$

OMITTED FROM SUMMARY TABLE

Needs confirmation.

$\eta_2(1870)$ MASS

VALUE (MeV)	EVTS	DOCUMENT ID		TECN	COMMENT
1842± 8 OUR AVERAGE					
1835±12		BARBERIS	00B		450 $pp \to p_f \eta\pi^+\pi^- p_s$
1844±13		BARBERIS	00C		450 $pp \to p_f 4\pi p_s$
1840±25		BARBERIS	97B	OMEG	450 $pp \to pp2(\pi^+\pi^-)$
1875±20±35		ADOMEIT	96	CBAR	1.94 $\overline{p}p \to \eta 3\pi^0$
1881±32±40	26	KARCH	92	CBAL	$e^+e^- \to e^+e^-\eta\pi^0\pi^0$
• • • We do not use the following data for averages, fits, limits, etc. • • •					
1860± 5±15		ANISOVICH	00E	SPEC	0.9–1.94 $\overline{p}p \to \eta 3\pi^0$
1840±15		BAI	99	BES	$J/\psi \to \gamma\eta\pi^+\pi^-$

$\eta_2(1870)$ WIDTH

VALUE (MeV)	EVTS	DOCUMENT ID		TECN	COMMENT
225±14 OUR AVERAGE					
235±22		BARBERIS	00B		450 $pp \to p_f \eta\pi^+\pi^- p_s$
228±23		BARBERIS	00C		450 $pp \to p_f 4\pi p_s$
200±40		BARBERIS	97B	OMEG	450 $pp \to pp2(\pi^+\pi^-)$
200±25±45		ADOMEIT	96	CBAR	1.94 $\overline{p}p \to \eta 3\pi^0$
221±92±44	26	KARCH	92	CBAL	$e^+e^- \to e^+e^-\eta\pi^0\pi^0$
• • • We do not use the following data for averages, fits, limits, etc. • • •					
$250\pm25^{+50}_{-35}$		ANISOVICH	00E	SPEC	0.9–1.94 $\overline{p}p \to \eta 3\pi^0$
170±40		BAI	99	BES	$J/\psi \to \gamma\eta\pi^+\pi^-$

$\eta_2(1870)$ DECAY MODES

	Mode	Fraction (Γ_i/Γ)
Γ_1	$\eta\pi\pi$	
Γ_2	$a_2(1320)\pi$	
Γ_3	$f_2(1270)\eta$	
Γ_4	$a_0(980)\pi$	
Γ_5	$\gamma\gamma$	seen

$\eta_2(1870)$ BRANCHING RATIOS

$\Gamma(a_2(1320)\pi)/\Gamma(f_2(1270)\eta)$ Γ_2/Γ_3

VALUE	DOCUMENT ID		TECN	COMMENT
1.7 ±0.4 OUR AVERAGE				
1.60±0.40	[1] ANISOVICH	11	SPEC	0.9–1.94 $p\overline{p}$
20.4 ±6.6	BARBERIS	00B		450 $pp \to p_f \eta\pi^+\pi^- p_s$
4.1 ±2.3	ADOMEIT	96	CBAR	1.94 $\overline{p}p \to \eta 3\pi^0$

[1] Reanalysis of ADOMEIT 96 and ANISOVICH 00E.

$\Gamma(a_2(1320)\pi)/\Gamma(a_0(980)\pi)$ Γ_2/Γ_4

VALUE	DOCUMENT ID		COMMENT
32.6±12.6	BARBERIS	00B	450 $pp \to p_f \eta\pi^+\pi^- p_s$

$\Gamma(a_0(980)\pi)/\Gamma(f_2(1270)\eta)$ Γ_4/Γ_3

VALUE	DOCUMENT ID		TECN	COMMENT
0.48±0.45	[2] ANISOVICH	11	SPEC	0.9–1.94 $p\overline{p}$

[2] Reanalysis of ADOMEIT 96 and ANISOVICH 00E.

$\Gamma(\gamma\gamma)/\Gamma_{total}$ Γ_5/Γ

VALUE	DOCUMENT ID		TECN	COMMENT
seen	KARCH	92	CBAL	$e^+e^- \to e^+e^-\eta\pi^0\pi^0$

$\eta_2(1870)$ REFERENCES

ANISOVICH	11	EPJ C71 1511	A.V. Anisovich *et al.*	(LOQM, RAL, PNPI)
ANISOVICH	00E	PL B477 19	A.V. Anisovich *et al.*	
BARBERIS	00B	PL B471 435	D. Barberis *et al.*	(WA 102 Collab.)
BARBERIS	00C	PL B471 440	D. Barberis *et al.*	(WA 102 Collab.)
BAI	99	PL B446 356	J.Z. Bai *et al.*	(BES Collab.)
BARBERIS	97B	PL B413 217	D. Barberis *et al.*	(WA 102 Collab.)
ADOMEIT	96	ZPHY C71 227	J. Adomeit *et al.*	(Crystal Barrel Collab.)
KARCH	92	ZPHY C54 33	K. Karch *et al.*	(Crystal Ball Collab.)

$\pi_2(1880)$

$I^G(J^{PC}) = 1^-(2^{-+})$

$\pi(1880)$ MASS

VALUE (MeV)	EVTS	DOCUMENT ID		TECN	CHG	COMMENT
1895±16 OUR AVERAGE						
1929±24± 18	4k	EUGENIO	08	B852	–	18 $\pi^- p \to \eta\eta\pi^- p$
1876±11± 67	145k	LU	05	B852	–	18 $\pi^- p \to \omega\pi^-\pi^0 p$
2003±88±148	69k	KUHN	04	B852	–	18 $\pi^- p \to \eta\pi^+\pi^-\pi^- p$
1880±20		ANISOVICH	01B	SPEC	0	0.6–1.94 $\overline{p}p \to \eta\eta\pi^0\pi^0$

$\pi(1880)$ WIDTH

VALUE (MeV)	EVTS	DOCUMENT ID		TECN	CHG	COMMENT
235± 34 OUR AVERAGE						
323± 87± 43	4k	EUGENIO	08	B852	–	18 $\pi^- p \to \eta\eta\pi^- p$
146± 17± 62	145k	LU	05	B852	–	18 $\pi^- p \to \omega\pi^-\pi^0 p$
306±132±121	69k	KUHN	04	B852	–	18 $\pi^- p \to \eta\pi^+\pi^-\pi^- p$
255± 45		ANISOVICH	01B	SPEC	0	0.6–1.94 $\overline{p}p \to \eta\eta\pi^0\pi^0$

$\pi_2(1880)$ DECAY MODES

	Mode
Γ_1	$\eta\eta\pi^-$
Γ_2	$a_0(980)\eta$
Γ_3	$a_2(1320)\eta$
Γ_4	$f_0(1500)\pi$
Γ_5	$f_1(1285)\pi$
Γ_6	$\omega\pi^-\pi^0$

$\Gamma(a_2(1320)\eta)/\Gamma(f_1(1285)\pi)$ Γ_3/Γ_5

VALUE	EVTS	DOCUMENT ID		TECN	CHG	COMMENT
• • • We do not use the following data for averages, fits, limits, etc. • • •						
22.7±7.3	69k	KUHN	04	B852	–	18 $\pi^- p \to \eta\pi^+\pi^-\pi^- p$

$\Gamma(f_0(1500)\pi)/\Gamma(a_0(980)\eta)$ Γ_4/Γ_2

VALUE	DOCUMENT ID		TECN	CHG	COMMENT
• • • We do not use the following data for averages, fits, limits, etc. • • •					
$0.28^{+0.20}_{-0.15}$	[1] ANISOVICH	01B	SPEC	0	0.6–1.94 $\overline{p}p \to \eta\eta\pi^0\pi^0$

[1] Systematic errors not estimated.

$\pi_2(1880)$ REFERENCES

EUGENIO	08	PL B660 466	P. Eugenio *et al.*	(BNL E852 Collab.)
LU	05	PRL 94 032002	M. Lu *et al.*	(BNL E852 Collab.)
KUHN	04	PL B595 109	J. Kuhn *et al.*	(BNL E852 Collab.)
ANISOVICH	01B	PL B500 222	A.V. Anisovich *et al.*	

$\rho(1900)$

$I^G(J^{PC}) = 1^+(1^{--})$

OMITTED FROM SUMMARY TABLE

See our mini-review under the $\rho(1700)$.

$\rho(1900)$ MASS

VALUE (MeV)	EVTS	DOCUMENT ID		TECN	COMMENT
• • • We do not use the following data for averages, fits, limits, etc. • • •					
1909±17±25	54	[1] AUBERT	08S	BABR	10.6 $e^+e^- \to \phi\pi^0\gamma$
1880±30		AUBERT	06D	BABR	10.6 $e^+e^- \to 3\pi^+3\pi^-\gamma$
1860±20		AUBERT	06D	BABR	10.6 $e^+e^- \to 2(\pi^+\pi^-\pi^0)\gamma$
1910±10		[2,3] FRABETTI	04	E687	$\gamma p \to 3\pi^+3\pi^- p$
1870±10		ANTONELLI	96	SPEC	$e^+e^- \to$ hadrons

[1] From the fit with two resonances.
[2] From a fit with two resonances with the JACOB 72 continuum.
[3] Supersedes FRABETTI 01.

$\rho(1900)$ WIDTH

VALUE (MeV)	EVTS	DOCUMENT ID		TECN	COMMENT
• • • We do not use the following data for averages, fits, limits, etc. • • •					
48±17±2	54	[4] AUBERT	08S	BABR	10.6 $e^+e^- \to \phi\pi^0\gamma$
130±30		AUBERT	06D	BABR	10.6 $e^+e^- \to 3\pi^+3\pi^-\gamma$
160±20		AUBERT	06D	BABR	10.6 $e^+e^- \to 2(\pi^+\pi^-\pi^0)\gamma$
37±13		[5,6] FRABETTI	04	E687	$\gamma p \to 3\pi^+3\pi^- p$
10± 5		ANTONELLI	96	SPEC	$e^+e^- \to$ hadrons

[4] From the fit with two resonances.
[5] From a fit with two resonances with the JACOB 72 continuum.
[6] Supersedes FRABETTI 01.

$\rho(1900)$ $\Gamma(i)\Gamma(e^+e^-)/\Gamma^2(total)$

$\Gamma(\phi\pi)/\Gamma_{total} \times \Gamma(e^+e^-)/\Gamma_{total}$ $\Gamma_4/\Gamma \times \Gamma_6/\Gamma$

VALUE (units 10^{-8})	EVTS	DOCUMENT ID		TECN	COMMENT
• • • We do not use the following data for averages, fits, limits, etc. • • •					
4.2±1.2±0.8	54	[7] AUBERT	08S	BABR	10.6 $e^+e^- \to \phi\pi^0\gamma$

[7] From the fit with two resonances.

$\rho(1900)$ DECAY MODES

	Mode	Fraction (Γ_i/Γ)
Γ_1	6π	seen
Γ_2	$3\pi^+3\pi^-$	seen
Γ_3	$2\pi^+2\pi^-2\pi^0$	
Γ_4	$\phi\pi$	
Γ_5	hadrons	seen
Γ_6	e^+e^-	seen
Γ_7	$\overline{N}N$	not seen

$\rho(1900)$ BRANCHING RATIOS

$\Gamma(6\pi)/\Gamma_{total}$ — **Γ_1/Γ**

VALUE	EVTS	DOCUMENT ID		TECN	COMMENT
seen	8k	AKHMETSHIN	13	CMD3	$e^+e^- \to 3\pi^+3\pi^-$
not seen		AGNELLO	02	OBLX	$\overline{n}p \to 3\pi^+2\pi^-\pi^0$
seen		FRABETTI	01	E687	$\gamma p \to 3\pi^+3\pi^- p$
seen		ANTONELLI	96	SPEC	$e^+e^- \to$ hadrons

$\rho(1900)$ REFERENCES

AKHMETSHIN	13	PL B723 82	R.R. Akhmetshin *et al.*	(CMD-3 Collab.)
AUBERT	08S	PR D77 092002	B. Aubert *et al.*	(BABAR Collab.)
AUBERT	06D	PR D73 052003	B. Aubert *et al.*	(BABAR Collab.)
FRABETTI	04	PL B578 290	P.L. Frabetti *et al.*	(FNAL E687 Collab.)
AGNELLO	02	PL B527 39	M. Agnello *et al.*	(OBELIX Collab.)
FRABETTI	01	PL B514 240	P.L. Frabetti *et al.*	(FNAL E687 Collab.)
ANTONELLI	96	PL B365 427	A. Antonelli *et al.*	(FENICE Collab.)
JACOB	72	PR D5 1847	M. Jacob, R. Slansky	

$f_2(1910)$

$I^G(J^{PC}) = 0^+(2^{++})$

OMITTED FROM SUMMARY TABLE

We list here three different peaks with close masses and widths seen in the mass distributions of $\omega\omega$, $\eta\eta'$, and K^+K^- final states. ALDE 91B argues that they are of different nature.

$f_2(1910)$ MASS

$f_2(1910)$ $\omega\omega$ MODE

VALUE (MeV)		DOCUMENT ID		TECN	COMMENT
1903± 9 OUR AVERAGE	Error includes scale factor of 1.5. See the ideogram below.				
1890±10	[1]	AMELIN	06	VES	36 $\pi^- p \to \omega\omega n$
1934±20		ANISOVICH	00J	SPEC	
1897±11		BARBERIS	00F		450 $pp \to p_f\omega\omega p_s$
1924±14		ALDE	90	GAM2	38 $\pi^- p \to \omega\omega n$

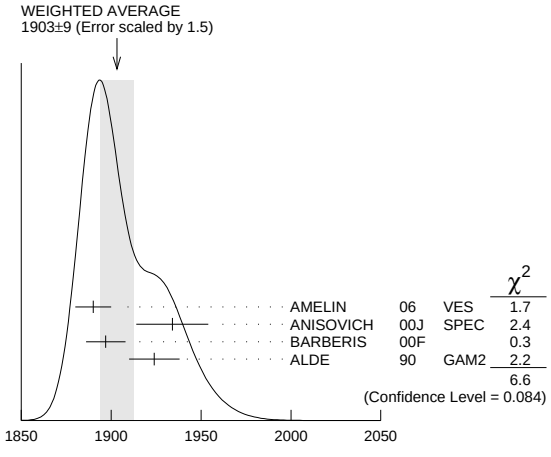

$f_2(1910)$ $\omega\omega$ MODE MASS (MeV)

[1] Supersedes BELADIDZE 92B.

$f_2(1910)$ $\eta\eta'$ MODE

VALUE (MeV)		DOCUMENT ID		TECN	COMMENT
1934±16	[2]	BARBERIS	00A		450 $pp \to p_f\eta\eta' p_s$
• • • We do not use the following data for averages, fits, limits, etc. • • •					
1911±10		ALDE	91B	GAM2	38 $\pi^- p \to \eta\eta' n$

[2] Also compatible with $J^{PC}=1^{-+}$.

$f_2(1910)$ K^+K^- MODE

VALUE (MeV)	DOCUMENT ID		TECN	COMMENT
• • • We do not use the following data for averages, fits, limits, etc. • • •				
1941±18	AMSLER	06	CBAR	1.64 $\overline{p}p \to K^+K^-\pi^0$

$f_2(1910)$ WIDTH

$f_2(1910)$ $\omega\omega$ MODE

VALUE (MeV)		DOCUMENT ID		TECN	COMMENT
196±31 OUR AVERAGE	Error includes scale factor of 2.3. See the ideogram below.				
165±19	[3]	AMELIN	06	VES	36 $\pi^- p \to \omega\omega n$
271±25		ANISOVICH	00J	SPEC	
202±32		BARBERIS	00F		450 $pp \to p_f\omega\omega p_s$
91±50		ALDE	90	GAM2	38 $\pi^- p \to \omega\omega n$

[3] Supersedes BELADIDZE 92B.

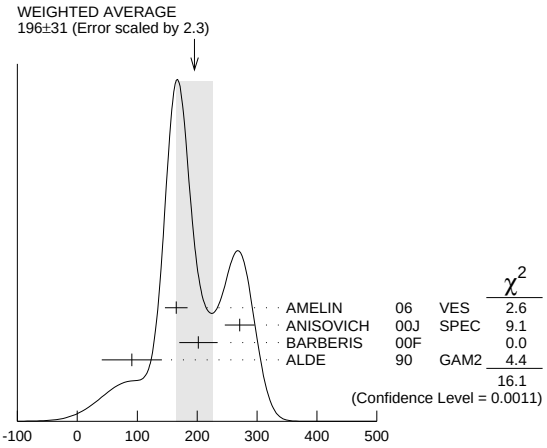

$f_2(1910)$ $\omega\omega$ MODE WIDTH(MeV)

$f_2(1910)$ $\eta\eta'$ MODE

VALUE (MeV)		DOCUMENT ID		TECN	COMMENT
141±41	[4]	BARBERIS	00A		450 $pp \to p_f\eta\eta' p_s$
• • • We do not use the following data for averages, fits, limits, etc. • • •					
90±35		ALDE	91B	GAM2	38 $\pi^- p \to \eta\eta' n$

[4] Also compatible with $J^{PC}=1^{-+}$.

$f_2(1910)$ K^+K^- MODE

VALUE (MeV)	DOCUMENT ID		TECN	COMMENT
• • • We do not use the following data for averages, fits, limits, etc. • • •				
120±40	AMSLER	06	CBAR	1.64 $\overline{p}p \to K^+K^-\pi^0$

$f_2(1910)$ DECAY MODES

	Mode	Fraction (Γ_i/Γ)
Γ_1	$\pi^0\pi^0$	
Γ_2	K^+K^-	seen
Γ_3	$K^0_S K^0_S$	
Γ_4	$\eta\eta$	seen
Γ_5	$\omega\omega$	seen
Γ_6	$\eta\eta'$	seen
Γ_7	$\eta'\eta'$	
Γ_8	$\rho\rho$	seen
Γ_9	$a_2(1320)\pi$	seen
Γ_{10}	$f_2(1270)\eta$	seen

$f_2(1910)$ BRANCHING RATIOS

$\Gamma(K^+K^-)/\Gamma_{total}$ — **Γ_2/Γ**

VALUE	DOCUMENT ID		TECN	COMMENT
seen	AMSLER	06	CBAR	1.64 $\overline{p}p \to K^+K^-\pi^0$

$\Gamma(\pi^0\pi^0)/\Gamma(\eta\eta')$ — **Γ_1/Γ_6**

VALUE	DOCUMENT ID		TECN	COMMENT
• • • We do not use the following data for averages, fits, limits, etc. • • •				
<0.1	ALDE	89	GAM2	38$\pi^- p \to \eta\eta' n$

Meson Particle Listings

$f_2(1910)$, $a_0(1950)$, $f_2(1950)$

$\Gamma(K^0_S K^0_S)/\Gamma(\eta\eta')$ Γ_3/Γ_6

VALUE	CL%	DOCUMENT ID		TECN	COMMENT
• • • We do not use the following data for averages, fits, limits, etc. • • •					
<0.066	90	BALOSHIN	86	SPEC	$40\pi p \to K^0_S K^0_S n$

$\Gamma(\eta\eta)/\Gamma(\eta\eta')$ Γ_4/Γ_6

VALUE	CL%	DOCUMENT ID		TECN	COMMENT
• • • We do not use the following data for averages, fits, limits, etc. • • •					
<0.05	90	ALDE	91B	GAM2	$38\ \pi^- p \to \eta\eta' n$

$\Gamma(\omega\omega)/\Gamma(\eta\eta')$ Γ_5/Γ_6

VALUE	DOCUMENT ID		TECN	COMMENT
• • • We do not use the following data for averages, fits, limits, etc. • • •				
2.6 ± 0.6	BARBERIS	00F		$450\ pp \to p_f \omega\omega p_s$

$\Gamma(\eta'\eta')/\Gamma_{\text{total}}$ Γ_7/Γ

VALUE	DOCUMENT ID		TECN	COMMENT
• • • We do not use the following data for averages, fits, limits, etc. • • •				
probably not seen	BARBERIS	00A		$450\ pp \to p_f \eta'\eta' p_s$
possibly seen	BELADIDZE	92D	VES	$37\ \pi^- p \to \eta'\eta' n$

$\Gamma(\rho\rho)/\Gamma(\omega\omega)$ Γ_8/Γ_5

VALUE	DOCUMENT ID		COMMENT
• • • We do not use the following data for averages, fits, limits, etc. • • •			
2.6 ± 0.4	BARBERIS	00F	$450\ pp \to p_f \omega\omega p_s$

$\Gamma(f_2(1270)\eta)/\Gamma(a_2(1320)\pi)$ Γ_{10}/Γ_9

VALUE	DOCUMENT ID		TECN	COMMENT
0.09±0.05	[5] ANISOVICH	11	SPEC	0.9–1.94 $p\overline{p}$

[5] Reanalysis of ADOMEIT 96 and ANISOVICH 00E.

$f_2(1910)$ REFERENCES

ANISOVICH	11	EPJ C71 1511	A.V. Anisovich *et al.*	(LOQM, RAL, PNPI)
AMELIN	06	PAN 69 690	D.V. Amelin *et al.*	(VES Collab.)
		Translated from YAF 69 715.		
AMSLER	06	PL B639 165	C. Amsler *et al.*	(CBAR Collab.)
ANISOVICH	00E	PL B477 19	A.V. Anisovich *et al.*	
ANISOVICH	00J	PL B491 47	A.V. Anisovich *et al.*	
BARBERIS	00A	PL B471 429	D. Barberis *et al.*	(WA 102 Collab.)
BARBERIS	00F	PL B484 198	D. Barberis *et al.*	(WA 102 Collab.)
ADOMEIT	96	ZPHY C71 227	J. Adomeit *et al.*	(Crystal Barrel Collab.)
BELADIDZE	92B	ZPHY C54 367	G.M. Beladidze *et al.*	(VES Collab.)
BELADIDZE	92D	ZPHY C57 13	G.M. Beladidze *et al.*	(VES Collab.)
ALDE	91B	SJNP 54 455	D.M. Alde *et al.*	(SERP, BELG, LANL, LAPP+)
		Translated from YAF 54 751.		
Also		PL B276 375	D.M. Alde *et al.*	(BELG, SERP, KEK, LANL+)
ALDE	90	PL B241 600	D.M. Alde *et al.*	(SERP, BELG, LANL, LAPP+)
ALDE	89	PL B216 447	D.M. Alde *et al.*	(SERP, BELG, LANL, LAPP)
Also		SJNP 48 1035	D.M. Alde *et al.*	(BELG, SERP, LANL, LAPP)
		Translated from YAF 48 1724.		
BALOSHIN	86	SJNP 43 959	O.N. Baloshin *et al.*	(ITEP)
		Translated from YAF 43 1487.		

$a_0(1950)$

$I^G(J^{PC}) = 1^-(0^{++})$

OMITTED FROM SUMMARY TABLE

Needs confirmation. Seen in $\gamma\gamma \to \eta_c(1S) \to K\overline{K}\pi$ by LEES 16A with significance 2.5 σ in $K^0_S K^\pm\pi^\mp$ and 4.2 σ in $K^+K^-\pi^0$. Spin-2 explanation ($a_2(1950)$) is not compatible with data.

$a_0(1950)$ MASS

VALUE (MeV)	EVTS	DOCUMENT ID		TECN	COMMENT
1931±14±22	12k	[1,2] LEES	16A	BABR	$\gamma\gamma \to \eta_c(1S) \to K\overline{K}\pi$
• • • We do not use the following data for averages, fits, limits, etc. • • •					
$1949\pm32\pm76$	8k	[1] LEES	16A	BABR	$\gamma\gamma \to \eta_c(1S) \to K^0_S K^\pm\pi^\mp$
$1927\pm15\pm23$	4k	[1] LEES	16A	BABR	$\gamma\gamma \to \eta_c(1S) \to K^+K^-\pi^0$

[1] From a model-independent partial wave analysis fit to a relativistic Breit-Wigner function with a floating width.
[2] WEighted average of the $K^0_S K^\pm$ and K^+K^- decay modes.

$a_0(1950)$ WIDTH

VALUE (MeV)	EVTS	DOCUMENT ID		TECN	COMMENT
271±22± 29	12k	[1,2] LEES	16A	BABR	$\gamma\gamma \to \eta_c(1S) \to K\overline{K}\pi$
• • • We do not use the following data for averages, fits, limits, etc. • • •					
$265\pm36\pm110$	8k	[1] LEES	16A	BABR	$\gamma\gamma \to \eta_c(1S) \to K^0_S K^\pm\pi^\mp$
$274\pm28\pm 30$	4k	[1] LEES	16A	BABR	$\gamma\gamma \to \eta_c(1S) \to K^+K^-\pi^0$

[1] From a model-independent partial wave analysis fit to a relativistic Breit-Wigner function with a floating mass.
[2] Weighted average of the $K^0_S K^\pm$ and K^+K^- decay modes.

$a_0(1950)$ DECAY MODES

	Mode	Fraction (Γ_i/Γ)
Γ_1	$K\overline{K}$	seen

$a_0(1950)$ BRANCHING RATIOS

$\Gamma(K\overline{K})/\Gamma_{\text{total}}$ Γ_1/Γ

VALUE	EVTS	DOCUMENT ID		TECN	COMMENT
seen	12k	[1] LEES	16A	BABR	$\gamma\gamma \to \eta_c(1S) \to K\overline{K}\pi$

[1] From a model-independent partial wave analysis.

$a_0(1950)$ REFERENCES

LEES	16A	PR D93 012005	J.P. Lees *et al.*	(BABAR Collab.)

$f_2(1950)$

$I^G(J^{PC}) = 0^+(2^{++})$

$f_2(1950)$ MASS

VALUE (MeV)	DOCUMENT ID		TECN	COMMENT
1944±12 OUR AVERAGE	Error includes scale factor of 1.5. See the ideogram below.			
1930 ± 25	[1] BINON	05	GAMS	$33\ \pi^- p \to \eta\eta n$
2010 ± 25	ANISOVICH	00J	SPEC	
1940 ± 50	BAI	00A	BES	$J/\psi \to \gamma(\pi^+\pi^-\pi^+\pi^-)$
1980 ± 22	[2] BARBERIS	00C		$450\ pp \to pp4\pi$
1940 ± 22	[3] BARBERIS	00C		$450\ pp \to pp2\pi2\pi^0$
1980 ± 50	ANISOVICH	99B	SPEC	1.35–1.94 $p\overline{p} \to \eta\eta\pi^0$
1960 ± 30	BARBERIS	97B	OMEG	$450\ pp \to pp2(\pi^+\pi^-)$
1918 ± 12	ANTINORI	95	OMEG	$300,450\ pp \to pp2(\pi^+\pi^-)$
• • • We do not use the following data for averages, fits, limits, etc. • • •				
2038^{+13+12}_{-11-73}	[4] UEHARA	09	BELL	$10.6\ e^+e^- \to e^+e^-\pi^0\pi^0$
$1980\pm\ 2\pm14$	ABE	04	BELL	$10.6\ e^+e^- \to e^+e^-K^+K^-$
1867 ± 46	[5] AMSLER	02	CBAR	$0.9\ \overline{p}p \to \pi^0\eta\eta,\ \pi^0\pi^0\pi^0$
~ 1990	[6] OAKDEN	94	RVUE	0.36–1.55 $\overline{p}p \to \pi\pi$
1950 ± 15	[7] ASTON	91	LASS	$11\ K^-p \to \Lambda K\overline{K}\pi\pi$

[1] First solution, PWA is ambiguous.
[2] Decaying into $\pi^+\pi^-2\pi^0$.
[3] Decaying into $2(\pi^+\pi^-)$.
[4] Taking into account $f_4(2050)$.
[5] T-matrix pole.
[6] From solution B of amplitude analysis of data on $\overline{p}p \to \pi\pi$. See however KLOET 96 who fit $\pi^+\pi^-$ only and find waves only up to $J = 3$ to be important but not significantly resonant.
[7] Cannot determine spin to be 2.

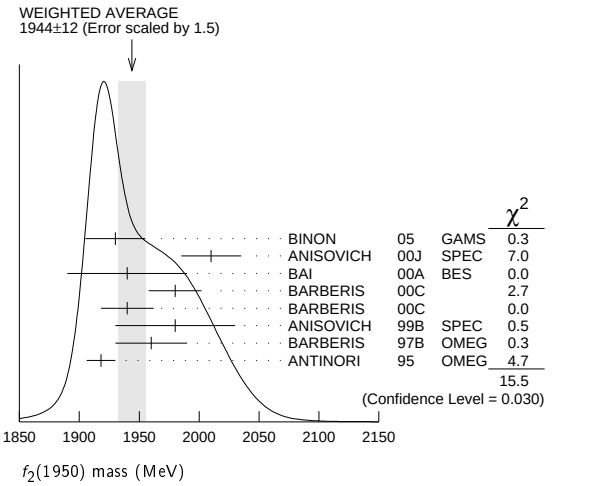

$f_2(1950)$ WIDTH

VALUE (MeV)	DOCUMENT ID		TECN	COMMENT
472± 18 OUR AVERAGE				
$450\pm\ 50$	[8] BINON	05	GAMS	$33\ \pi^- p \to \eta\eta n$
$495\pm\ 35$	ANISOVICH	00J	SPEC	
$380^{+120}_{-\ 90}$	BAI	00A	BES	$J/\psi \to \gamma(\pi^+\pi^-\pi^+\pi^-)$
$520\pm\ 50$	[9] BARBERIS	00C		$450\ pp \to pp4\pi$
$485\pm\ 55$	[10] BARBERIS	00C		$450\ pp \to pp4\pi$
500 ± 100	ANISOVICH	99B	SPEC	1.35–1.94 $p\overline{p} \to \eta\eta\pi^0$
$460\pm\ 40$	BARBERIS	97B	OMEG	$450\ pp \to pp2(\pi^+\pi^-)$
$390\pm\ 60$	ANTINORI	95	OMEG	$300,450\ pp \to pp2(\pi^+\pi^-)$

• • • We do not use the following data for averages, fits, limits, etc. • • •

$441^{+\ 27+\ 28}_{-\ 25-192}$	[11] UEHARA	09	BELL	10.6 $e^+e^- \to e^+e^-\pi^0\pi^0$	
$297 \pm 12 \pm 6$	ABE	04	BELL	10.6 $e^+e^- \to e^+e^-K^+K^-$	
385 ± 58	[12] AMSLER	02	CBAR	0.9 $\overline{p}p \to \pi^0\eta\eta$, $\pi^0\pi^0\pi^0$	
~ 100	[13] OAKDEN	94	RVUE	0.36–1.55 $\overline{p}p \to \pi\pi$	
250 ± 50	[14] ASTON	91	LASS	11 $K^-p \to \Lambda K\overline{K}\pi\pi$	

[8] First solution, PWA is ambiguous.
[9] Decaying into $\pi^+\pi^-2\pi^0$.
[10] Decaying into $2(\pi^+\pi^-)$.
[11] Taking into account $f_4(2050)$.
[12] T-matrix pole.
[13] From solution B of amplitude analysis of data on $\overline{p}p \to \pi\pi$. See however KLOET 96 who fit $\pi^+\pi^-$ only and find waves only up to $J = 3$ to be important but not significantly resonant.
[14] Cannot determine spin to be 2.

$f_2(1950)$ DECAY MODES

	Mode	Fraction (Γ_i/Γ)
Γ_1	$K^*(892)\overline{K}^*(892)$	seen
Γ_2	$\pi\pi$	
Γ_3	$\pi^+\pi^-$	seen
Γ_4	$\pi^0\pi^0$	seen
Γ_5	4π	seen
Γ_6	$\pi^+\pi^-\pi^+\pi^-$	
Γ_7	$a_2(1320)\pi$	
Γ_8	$f_2(1270)\pi\pi$	
Γ_9	$\eta\eta$	seen
Γ_{10}	$K\overline{K}$	seen
Γ_{11}	$\gamma\gamma$	seen
Γ_{12}	$p\overline{p}$	seen

$f_2(1950)$ Γ(i)$\Gamma(\gamma\gamma)/\Gamma$(total)

$\Gamma(K\overline{K}) \times \Gamma(\gamma\gamma)/\Gamma_{total}$ $\quad \Gamma_{10}\Gamma_{11}/\Gamma$

VALUE (eV)	DOCUMENT ID		TECN	COMMENT
• • • We do not use the following data for averages, fits, limits, etc. • • •				
$122 \pm 4 \pm 26$	[15] ABE	04	BELL	10.6 $e^+e^- \to e^+e^-K^+K^-$

[15] Assuming spin 2.

$\Gamma(\pi\pi) \times \Gamma(\gamma\gamma)/\Gamma_{total}$ $\quad \Gamma_2\Gamma_{11}/\Gamma$

VALUE	DOCUMENT ID		TECN	COMMENT
• • • We do not use the following data for averages, fits, limits, etc. • • •				
$162^{+\ 69+1137}_{-\ 42-\ 204}$	[16] UEHARA	09	BELL	10.6 $e^+e^- \to e^+e^-\pi^0\pi^0$

[16] Taking into account $f_4(2050)$.

$f_2(1950)$ BRANCHING RATIOS

$\Gamma(K^*(892)\overline{K}^*(892))/\Gamma_{total}$ $\quad \Gamma_1/\Gamma$

VALUE	DOCUMENT ID		TECN	CHG	COMMENT
seen	ASTON	91	LASS	0	11 $K^-p \to \Lambda K\overline{K}\pi\pi$

$\Gamma(a_2(1320)\pi)/\Gamma_{total}$ $\quad \Gamma_7/\Gamma$

VALUE	DOCUMENT ID		TECN	COMMENT
• • • We do not use the following data for averages, fits, limits, etc. • • •				
not seen	BARBERIS	00B		450 $pp \to p_f\eta\pi^+\pi^-p_s$
not seen	BARBERIS	00C		450 $pp \to p_f 4\pi p_s$
possibly seen	BARBERIS	97B	OMEG	450 $pp \to pp2(\pi^+\pi^-)$

$\Gamma(\eta\eta)/\Gamma(4\pi)$ $\quad \Gamma_9/\Gamma_5$

VALUE	CL%	DOCUMENT ID		COMMENT
• • • We do not use the following data for averages, fits, limits, etc. • • •				
$<5.0 \times 10^{-3}$	90	BARBERIS	00E	450 $pp \to p_f\eta\eta p_s$

$\Gamma(\eta\eta)/\Gamma(\pi^+\pi^-)$ $\quad \Gamma_9/\Gamma_3$

VALUE	DOCUMENT ID		TECN	COMMENT
0.14±0.05	AMSLER	02	CBAR	0.9 $\overline{p}p \to \pi^0\eta\eta$, $\pi^0\pi^0\pi^0$

$\Gamma(p\overline{p})/\Gamma_{total}$ $\quad \Gamma_{12}/\Gamma$

VALUE	EVTS	DOCUMENT ID		TECN	COMMENT
seen	111	ALEXANDER	10	CLEO	$\psi(2S) \to \gamma p\overline{p}$

$f_2(1950)$ REFERENCES

ALEXANDER	10	PR D82 092002	J.P. Alexander *et al.*	(CLEO Collab.)
UEHARA	09	PR D79 052009	S. Uehara *et al.*	(BELLE Collab.)
BINON	05	PAN 68 960 Translated from YAF 68 998.	F. Binon *et al.*	
ABE	04	EPJ C32 323	K. Abe *et al.*	(BELLE Collab.)
AMSLER	02	EPJ C23 29	C. Amsler *et al.*	
ANISOVICH	00J	PL B491 47	A.V. Anisovich *et al.*	
BAI	00A	PL B472 207	J.Z. Bai *et al.*	(BES Collab.)
BARBERIS	00B	PL B471 435	D. Barberis *et al.*	(WA 102 Collab.)
BARBERIS	00C	PL B471 440	D. Barberis *et al.*	(WA 102 Collab.)
BARBERIS	00E	PL B479 59	D. Barberis *et al.*	(WA 102 Collab.)
ANISOVICH	99B	PL B449 154	A.V. Anisovich *et al.*	
BARBERIS	97B	PL B413 217	D. Barberis *et al.*	(WA 102 Collab.)
KLOET	96	PR D53 6120	W.M. Kloet, F. Myhrer	(RUTG, NORD)
ANTINORI	95	PL B353 589	F. Antinori *et al.*	(ATHU, BARI, BIRM+) JP
OAKDEN	94	NP A574 731	M.N. Oakden, M.R. Pennington	(DURH)
ASTON	91	NPBPS B21 5	D. Aston *et al.*	(LASS Collab.)

$\rho_3(1990)$ $\quad I^G(J^{PC}) = 1^+(3^{--})$

OMITTED FROM SUMMARY TABLE

$\rho_3(1990)$ MASS

VALUE (MeV)	DOCUMENT ID		TECN	COMMENT
• • • We do not use the following data for averages, fits, limits, etc. • • •				
1982 ± 14	[1] ANISOVICH	02	SPEC	0.6–1.9 $p\overline{p} \to \omega\pi^0$, $\omega\eta\pi^0$, $\pi^+\pi^-$
~ 2007	HASAN	94	RVUE	$\overline{p}p \to \pi\pi$

[1] From the combined analysis of ANISOVICH 00J, ANISOVICH 01D, ANISOVICH 01E, and ANISOVICH 02.

$\rho_3(1990)$ WIDTH

VALUE (MeV)	DOCUMENT ID		TECN	COMMENT
• • • We do not use the following data for averages, fits, limits, etc. • • •				
188 ± 24	[2] ANISOVICH	02	SPEC	0.6–1.9 $p\overline{p} \to \omega\pi^0$, $\omega\eta\pi^0$, $\pi^+\pi^-$
~ 287	HASAN	94	RVUE	$\overline{p}p \to \pi\pi$

[2] From the combined analysis of ANISOVICH 00J, ANISOVICH 01D, ANISOVICH 01E, and ANISOVICH 02.

$\rho_3(1990)$ REFERENCES

ANISOVICH	02	PL B542 8	A.V. Anisovich *et al.*	
ANISOVICH	01D	PL B508 6	A.V. Anisovich *et al.*	
ANISOVICH	01E	PL B513 281	A.V. Anisovich *et al.*	
ANISOVICH	00J	PL B491 47	A.V. Anisovich *et al.*	
HASAN	94	PL B334 215	A. Hasan, D.V. Bugg	(LOQM)

$f_2(2010)$ $\quad I^G(J^{PC}) = 0^+(2^{++})$

$f_2(2010)$ MASS

VALUE (MeV)	DOCUMENT ID		TECN	COMMENT
$\mathbf{2011^{+\ 62}_{-\ 76}}$	[1] ETKIN	88	MPS	22 $\pi^-p \to \phi\phi n$
• • • We do not use the following data for averages, fits, limits, etc. • • •				
2005 ± 12	VLADIMIRSK...06		SPEC	40 $\pi^-p \to K^0_S K^0_S n$
1980 ± 20	[2] BOLONKIN	88	SPEC	40 $\pi^-p \to K^0_S K^0_S n$
$2050^{+\ 90}_{-\ 50}$	ETKIN	85	MPS	22 $\pi^-p \to 2\phi n$
$2120^{+\ 20}_{-120}$	LINDENBAUM	84	RVUE	
2160 ± 50	ETKIN	82	MPS	22 $\pi^-p \to 2\phi n$

[1] Includes data of ETKIN 85. The percentage of the resonance going into $\phi\phi$ 2^{++} S_2, D_2, and D_0 is 98^{+1}_{-3}, 0^{+1}_{-0}, and 2^{+2}_{-1}, respectively.
[2] Statistically very weak, only 1.4 s.d.

$f_2(2010)$ WIDTH

VALUE (MeV)	DOCUMENT ID		TECN	COMMENT
$\mathbf{202^{+\ 67}_{-\ 62}}$	[3] ETKIN	88	MPS	22 $\pi^-p \to \phi\phi n$
• • • We do not use the following data for averages, fits, limits, etc. • • •				
209 ± 32	VLADIMIRSK...06		SPEC	40 $\pi^-p \to K^0_S K^0_S n$
145 ± 50	[4] BOLONKIN	88	SPEC	40 $\pi^-p \to K^0_S K^0_S n$
$200^{+160}_{-\ 50}$	ETKIN	85	MPS	22 $\pi^-p \to 2\phi n$
$300^{+150}_{-\ 50}$	LINDENBAUM	84	RVUE	
310 ± 70	ETKIN	82	MPS	22 $\pi^-p \to 2\phi n$

[3] Includes data of ETKIN 85.
[4] Statistically very weak, only 1.4 s.d.

$f_2(2010)$ DECAY MODES

	Mode	Fraction (Γ_i/Γ)
Γ_1	$\phi\phi$	seen
Γ_2	$K\overline{K}$	seen

Meson Particle Listings

$f_2(2010)$, $f_0(2020)$, $a_4(2040)$

$f_2(2010)$ BRANCHING RATIOS

$\Gamma(K\overline{K})/\Gamma_{total}$ — **Γ_2/Γ**

VALUE	DOCUMENT ID	TECN	COMMENT
seen	VLADIMIRSK...06	SPEC	40 $\pi^- p \rightarrow K^0_S K^0_S n$

$f_2(2010)$ REFERENCES

VLADIMIRSK...	06	PAN 69 493	V.V. Vladimirsky *et al.*	(ITEP, Moscow)
		Translated from YAF 69 515.		
BOLONKIN	88	NP B309 426	B.V. Bolonkin *et al.*	(ITEP, SERP)
ETKIN	88	PL B201 568	A. Etkin *et al.*	(BNL, CUNY)
ETKIN	85	PL 165B 217	A. Etkin *et al.*	(BNL, CUNY)
LINDENBAUM	84	CNPP 13 285	S.J. Lindenbaum	(CUNY)
ETKIN	82	PRL 49 1620	A. Etkin *et al.*	(BNL, CUNY)
Also		Brighton Conf. 351	S.J. Lindenbaum	(BNL, CUNY)

$f_0(2020)$

$I^G(J^{PC}) = 0^+(0^{++})$

OMITTED FROM SUMMARY TABLE

Needs confirmation.

$f_0(2020)$ MASS

VALUE (MeV)	EVTS	DOCUMENT ID		TECN	COMMENT
1992±16		[1,2] BARBERIS	00C		450 $pp \rightarrow p_f 4\pi p_s$
• • • We do not use the following data for averages, fits, limits, etc. • • •					
2037± 8	80k	[3] UMAN	06	E835	5.2 $\overline{p}p \rightarrow \eta\eta\pi^0$
2040±38		ANISOVICH	00J	SPEC	
2010±60		ALDE	98	GAM4	100 $\pi^- p \rightarrow \pi^0\pi^0 n$
2020±35		BARBERIS	97B	OMEG	450 $pp \rightarrow pp2(\pi^+\pi^-)$

[1] Average between $\pi^+\pi^- 2\pi^0$ and $2(\pi^+\pi^-)$.
[2] T-matrix pole.
[3] Statistical error only.

$f_0(2020)$ WIDTH

VALUE (MeV)	EVTS	DOCUMENT ID		TECN	COMMENT
442± 60		[4,5] BARBERIS	00C		450 $pp \rightarrow p_f 4\pi p_s$
• • • We do not use the following data for averages, fits, limits, etc. • • •					
296± 17	80k	[6] UMAN	06	E835	5.2 $\overline{p}p \rightarrow \eta\eta\pi^0$
405± 40		ANISOVICH	00J	SPEC	
240±100		ALDE	98	GAM4	100 $\pi^- p \rightarrow \pi^0\pi^0 n$
410± 50		BARBERIS	97B	OMEG	450 $pp \rightarrow pp2(\pi^+\pi^-)$

[4] Average between $\pi^+\pi^- 2\pi^0$ and $2(\pi^+\pi^-)$.
[5] T-matrix pole.
[6] Statistical error only.

$f_0(2020)$ DECAY MODES

	Mode	Fraction (Γ_i/Γ)
Γ_1	$\rho\pi\pi$	seen
Γ_2	$\pi^0\pi^0$	seen
Γ_3	$\rho\rho$	seen
Γ_4	$\omega\omega$	seen
Γ_5	$\eta\eta$	seen

$f_0(2020)$ BRANCHING RATIOS

$\Gamma(\rho\rho)/\Gamma(\omega\omega)$ — **Γ_3/Γ_4**

VALUE	DOCUMENT ID		TECN	COMMENT
• • • We do not use the following data for averages, fits, limits, etc. • • •				
~ 3	BARBERIS	00F		450 $pp \rightarrow p_f \omega\omega p_s$

$\Gamma(\eta\eta)/\Gamma_{total}$ — **Γ_5/Γ**

VALUE	DOCUMENT ID		TECN	COMMENT
seen	UMAN	06	E835	5.2 $\overline{p}p \rightarrow \eta\eta\pi^0$

$f_0(2020)$ REFERENCES

UMAN	06	PR D73 052009	I. Uman *et al.*	(FNAL E835)
ANISOVICH	00J	PL B491 47	A.V. Anisovich *et al.*	
BARBERIS	00C	PL B471 440	D. Barberis *et al.*	(WA 102 Collab.)
BARBERIS	00F	PL B484 198	D. Barberis *et al.*	(WA 102 Collab.)
ALDE	98	EPJ A3 361	D. Alde *et al.*	(GAM4 Collab.)
Also		PAN 62 405	D. Alde *et al.*	(GAMS Collab.)
		Translated from YAF 62 446.		
BARBERIS	97B	PL B413 217	D. Barberis *et al.*	(WA 102 Collab.)

$a_4(2040)$

$I^G(J^{PC}) = 1^-(4^{++})$

$a_4(2040)$ MASS

VALUE (MeV)	EVTS	DOCUMENT ID		TECN	CHG	COMMENT
1995$^{+10}_{-8}$ OUR AVERAGE		Error includes scale factor of 1.1.				
1900$^{+80}_{-20}$		ADOLPH	15	COMP		191 $\pi^- p \rightarrow \eta^{(\prime)}\pi^- p$
1885±13$^{+50}_{-2}$	420k	ALEKSEEV	10	COMP		190 $\pi^- Pb \rightarrow \pi^-\pi^-\pi^+ Pb'$
1985±10±13	145k	LU	05	B852		18 $\pi^- p \rightarrow \omega\pi^-\pi^0 p$
1996±25±43		CHUNG	02	B852		18.3 $\pi^- p \rightarrow 3\pi p$
2005$^{+25}_{-45}$		[1] ANISOVICH	01F	SPEC		2.0 $\overline{p}p \rightarrow 3\pi^0, \pi^0\eta, \pi^0\eta'$
2000±40$^{+60}_{-20}$		IVANOV	01	B852		18 $\pi^- p \rightarrow \eta'\pi^- p$
1944± 8±50		[2] AMELIN	99	VES		37 $\pi^- A \rightarrow \omega\pi^-\pi^0 A^*$
2010±20		[3] DONSKOV	96	GAM2	0	38 $\pi^- p \rightarrow \eta\pi^0 n$
2040±30		[4] CLELAND	82B	SPEC	±	50 $\pi p \rightarrow K^0_S K^\pm p$
2030±50		[5] CORDEN	78C	OMEG	0	15 $\pi^- p \rightarrow 3\pi n$
• • • We do not use the following data for averages, fits, limits, etc. • • •						
2004± 6	80k	[6] UMAN	06	E835		5.2 $\overline{p}p \rightarrow \eta\eta\pi^0$
1903±10		[7] BALDI	78	SPEC	−	10 $\pi^- p \rightarrow p K^0_S K^-$

[1] From the combined analysis of ANISOVICH 99C, ANISOVICH 99E, and ANISOVICH 01F.
[2] May be a different state.
[3] From a simultaneous fit to the G_+ and G_0 wave intensities.
[4] From an amplitude analysis.
[5] $J^P = 4^+$ is favored, though $J^P = 2^+$ cannot be excluded.
[6] Statistical error only.
[7] From a fit to the Y^0_8 moment. Limited by phase space.

$a_4(2040)$ WIDTH

VALUE (MeV)	EVTS	DOCUMENT ID		TECN	CHG	COMMENT
257$^{+25}_{-23}$ OUR AVERAGE		Error includes scale factor of 1.3. See the ideogram below.				
300$^{+80}_{-100}$		ADOLPH	15	COMP		191 $\pi^- p \rightarrow \eta^{(\prime)}\pi^- p$
294± 25$^{+46}_{-19}$	420k	ALEKSEEV	10	COMP		190 $\pi^- Pb \rightarrow \pi^-\pi^-\pi^+ Pb'$
231± 30±46	145k	LU	05	B852		18 $\pi^- p \rightarrow \omega\pi^-\pi^0 p$
298± 81±85		CHUNG	02	B852		18.3 $\pi^- p \rightarrow 3\pi p$
180± 30		[1] ANISOVICH	01F	SPEC		2.0 $\overline{p}p \rightarrow 3\pi^0, \pi^0\eta, \pi^0\eta'$
350±100$^{+70}_{-50}$		IVANOV	01	B852		18 $\pi^- p \rightarrow \eta'\pi^- p$
324± 26±75		[2] AMELIN	99	VES		37 $\pi^- A \rightarrow \omega\pi^-\pi^0 A^*$
370± 80		[3] DONSKOV	96	GAM2	0	38 $\pi^- p \rightarrow \eta\pi^0 n$
380±150		[4] CLELAND	82B	SPEC	±	50 $\pi p \rightarrow K^0_S K^\pm p$
510±200		[5] CORDEN	78C	OMEG	0	15 $\pi^- p \rightarrow 3\pi n$
• • • We do not use the following data for averages, fits, limits, etc. • • •						
401± 16	80k	[6] UMAN	06	E835		5.2 $\overline{p}p \rightarrow \eta\eta\pi^0$
166± 43		[7] BALDI	78	SPEC	−	10 $\pi^- p \rightarrow p K^0_S K^-$

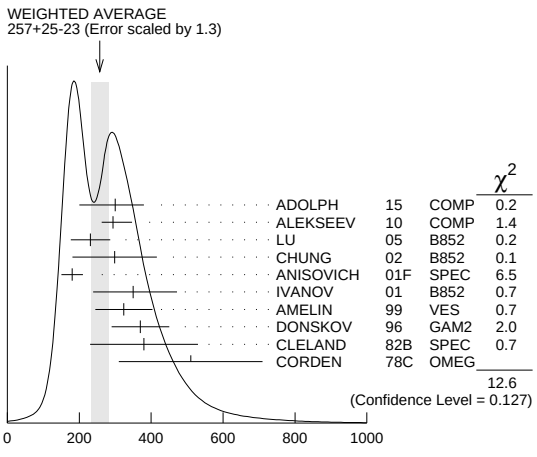

[1] From the combined analysis of ANISOVICH 99C, ANISOVICH 99E, and ANISOVICH 01F.
[2] May be a different state.
[3] From a simultaneous fit to the G_+ and G_0 wave intensities.
[4] From an amplitude analysis.

[5] $J^P = 4^+$ is favored, though $J^P = 2^+$ cannot be excluded.
[6] Statistical error only.
[7] From a fit to the Y_8^0 moment. Limited by phase space.

$a_4(2040)$ DECAY MODES

	Mode	Fraction (Γ_i/Γ)
Γ_1	$K\overline{K}$	seen
Γ_2	$\pi^+\pi^-\pi^0$	seen
Γ_3	$\rho\pi$	seen
Γ_4	$f_2(1270)\pi$	seen
Γ_5	$\omega\pi^-\pi^0$	seen
Γ_6	$\omega\rho$	seen
Γ_7	$\eta\pi$	seen
Γ_8	$\eta'(958)\pi$	seen

$a_4(2040)$ BRANCHING RATIOS

$\Gamma(K\overline{K})/\Gamma_{total}$ Γ_1/Γ

VALUE	DOCUMENT ID		TECN	CHG	COMMENT
seen	BALDI	78	SPEC	±	10 $\pi^- p \rightarrow K_S^0 K^- p$

$\Gamma(\pi^+\pi^-\pi^0)/\Gamma_{total}$ Γ_2/Γ

VALUE	DOCUMENT ID		TECN	CHG	COMMENT
seen	CORDEN	78C	OMEG	0	15 $\pi^- p \rightarrow 3\pi n$

$\Gamma(\rho\pi)/\Gamma(f_2(1270)\pi)$ Γ_3/Γ_4

VALUE	DOCUMENT ID		TECN	COMMENT
1.1±0.2±0.2	CHUNG	02	B852	18.3 $\pi^- p \rightarrow 3\pi p$

$\Gamma(\eta\pi)/\Gamma_{total}$ Γ_7/Γ

VALUE	DOCUMENT ID		TECN	CHG	COMMENT
seen	DONSKOV	96	GAM2	0	38 $\pi^- p \rightarrow \eta\pi^0 n$

$\Gamma(\eta'(958)\pi)/\Gamma(\eta\pi)$ Γ_8/Γ_7

VALUE	DOCUMENT ID		TECN	COMMENT
0.23±0.07	ADOLPH	15	COMP	191 $\pi^- p \rightarrow \eta^{(\prime)}\pi^- p$

$\Gamma(\omega\rho)/\Gamma_{total}$ Γ_6/Γ

VALUE	EVTS	DOCUMENT ID		TECN	COMMENT
seen	145k	LU	05	B852	18 $\pi^- p \rightarrow \omega\pi^-\pi^0 p$

$a_4(2040)$ REFERENCES

ADOLPH	15	PL B740 303	M. Adolph *et al.*	(COMPASS Collab.)
ALEKSEEV	10	PRL 104 241803	M.G. Alekseev *et al.*	(COMPASS Collab.)
UMAN	06	PR D73 052009	I. Uman *et al.*	(FNAL E835)
LU	05	PRL 94 032002	M. Lu *et al.*	(BNL E852 Collab.)
CHUNG	02	PR D65 072001	S.U. Chung *et al.*	(BNL E852 Collab.)
ANISOVICH	01F	PL B517 261	A.V. Anisovich *et al.*	
IVANOV	01	PRL 86 3977	E.I. Ivanov *et al.*	(BNL E852 Collab.)
AMELIN	99	PAN 62 445 Translated from YAF 62 487.	D.V. Amelin *et al.*	(VES Collab.)
ANISOVICH	99C	PL B452 173	A.V. Anisovich *et al.*	
ANISOVICH	99E	PL B452 187	A.V. Anisovich *et al.*	
DONSKOV	96	PAN 59 982 Translated from YAF 59 1027.	S.V. Donskov *et al.*	(GAMS Collab.) IGJPC
CLELAND	82B	NP B208 228	W.E. Cleland *et al.*	(DURH, GEVA, LAUS+)
BALDI	78	PL 74B 413	R. Baldi *et al.*	(GEVA) JP
CORDEN	78C	NP B136 77	M.J. Corden *et al.*	(BIRM, RHEL, TELA+) JP

$f_4(2050)$

$I^G(J^{PC}) = 0^+(4^{++})$

$f_4(2050)$ MASS

VALUE (MeV)	EVTS	DOCUMENT ID		TECN	COMMENT
2018±11 OUR AVERAGE		Error includes scale factor of 2.1. See the ideogram below.			
1960±15		AMELIN	06	VES	36 $\pi^- p \rightarrow \omega\omega n$
2005±10		[1] BINON	05	GAMS	33 $\pi^- p \rightarrow \eta\eta n$
1998±15		ALDE	98	GAM4	100 $\pi^- p \rightarrow \pi^0\pi^0 n$
2060±20		ALDE	90	GAM2	38 $\pi^- p \rightarrow \omega\omega n$
2038±30		AUGUSTIN	87	DM2	$J/\psi \rightarrow \gamma\pi^+\pi^-$
2086±15		BALTRUSAIT...	87	MRK3	$J/\psi \rightarrow \gamma\pi^+\pi^-$
2000±60		ALDE	86D	GAM4	100 $\pi^- p \rightarrow n2\eta$
2020±20	40k	[2] BINON	84B	GAM2	38 $\pi^- p \rightarrow n2\pi^0$
2015±28		[3] CASON	82	STRC	8 $\pi^+ p \rightarrow \Delta^{++}\pi^0\pi^0$
2031^{+25}_{-36}		ETKIN	82B	MPS	23 $\pi^- p \rightarrow n2K_S^0$
2020±30	700	APEL	75	NICE	40 $\pi^- p \rightarrow n2\pi^0$
2050±25		BLUM	75	ASPK	18.4 $\pi^- p \rightarrow nK^+K^-$
• • • We do not use the following data for averages, fits, limits, etc. • • •					
1966±25		[4] ANISOVICH	09	RVUE	0.0 $\overline{p}p$, πN
$1885^{+14+218}_{-13-25}$		[5] UEHARA	09	BELL	10.6 $e^+e^- \rightarrow e^+e^-\pi^0\pi^0$
2018± 6		ANISOVICH	00J	SPEC	2.0 $\overline{p}p \rightarrow \eta\pi^0\pi^0$, $\pi^0\pi^0$, $\eta\eta$, $\eta\eta'$, $\pi\pi$
~ 2000		[6] MARTIN	98	RVUE	$N\overline{N} \rightarrow \pi\pi$
~ 2010		[7] MARTIN	97	RVUE	$\overline{N}N \rightarrow \pi\pi$
~ 2040		[8] OAKDEN	94	RVUE	0.36–1.55 $\overline{p}p \rightarrow \pi\pi$
~ 1990		[9] OAKDEN	94	RVUE	0.36–1.55 $\overline{p}p \rightarrow \pi\pi$
1978± 5		[10] ALPER	80	CNTR	62 $\pi^- p \rightarrow K^+K^- n$
2040±10		[10] ROZANSKA	80	SPRK	18 $\pi^- p \rightarrow p\overline{p}n$
1935±13		[10] CORDEN	79	OMEG	12–15 $\pi^- p \rightarrow n2\pi$
1988± 7		EVANGELIS...	79B	OMEG	10 $\pi^- p \rightarrow K^+K^- n$
1922±14		[11] ANTIPOV	77	CIBS	25 $\pi^- p \rightarrow p3\pi$

[1] From the first PWA solution.
[2] From a partial-wave analysis of the data.
[3] From an amplitude analysis of the reaction $\pi^+\pi^- \rightarrow 2\pi^0$.
[4] K matrix pole.
[5] Taking into account the $f_2(1950)$. Helicity-2 production favored.
[6] Energy-dependent analysis.
[7] Single energy analysis.
[8] From solution A of amplitude analysis of data on $\overline{p}p \rightarrow \pi\pi$. See however KLOET 96 who fit $\pi^+\pi^-$ only and find waves only up to $J = 3$ to be important but not significantly resonant.
[9] From solution B of amplitude analysis of data on $\overline{p}p \rightarrow \pi\pi$. See however KLOET 96 who fit $\pi^+\pi^-$ only and find waves only up to $J = 3$ to be important but not significantly resonant.
[10] $I(J^P) = 0(4^+)$ from amplitude analysis assuming one-pion exchange.
[11] Width errors enlarged by us to $4\Gamma/\sqrt{N}$; see the note with the $K^*(892)$ mass.

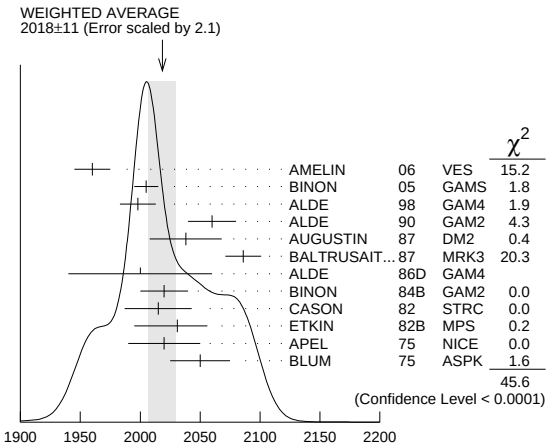

$f_4(2050)$ WIDTH

VALUE (MeV)	EVTS	DOCUMENT ID		TECN	COMMENT
237± 18 OUR AVERAGE		Error includes scale factor of 1.9. See the ideogram below.			
290± 20		AMELIN	06	VES	36 $\pi^- p \rightarrow \omega\omega n$
340± 80		[12] BINON	05	GAMS	33 $\pi^- p \rightarrow \eta\eta n$
395± 40		ALDE	98	GAM4	100 $\pi^- p \rightarrow \pi^0\pi^0 n$
170± 60		ALDE	90	GAM2	38 $\pi^- p \rightarrow \omega\omega n$
304± 60		AUGUSTIN	87	DM2	$J/\psi \rightarrow \gamma\pi^+\pi^-$
210± 63		BALTRUSAIT...	87	MRK3	$J/\psi \rightarrow \gamma\pi^+\pi^-$
400±100		ALDE	86D	GAM4	100 $\pi^- p \rightarrow n2\eta$
240± 40	40k	[13] BINON	84B	GAM2	38 $\pi^- p \rightarrow n2\pi^0$
190± 14		DENNEY	83	LASS	10 $\pi^+ n/\pi^+ p$
186^{+103}_{-58}		[14] CASON	82	STRC	8 $\pi^+ p \rightarrow \Delta^{++}\pi^0\pi^0$
305^{+36}_{-119}		ETKIN	82B	MPS	23 $\pi^- p \rightarrow n2K_S^0$
180± 60	700	APEL	75	NICE	40 $\pi^- p \rightarrow n2\pi^0$
225^{+120}_{-70}		BLUM	75	ASPK	18.4 $\pi^- p \rightarrow nK^+K^-$
• • • We do not use the following data for averages, fits, limits, etc. • • •					
260± 40		[15] ANISOVICH	09	RVUE	0.0 $\overline{p}p$, πN
453± 20^{+31}_{-129}		[16] UEHARA	09	BELL	10.6 $e^+e^- \rightarrow e^+e^-\pi^0\pi^0$
182± 7		ANISOVICH	00J	SPEC	2.0 $\overline{p}p \rightarrow \eta\pi^0\pi^0$, $\pi^0\pi^0$, $\eta\eta$, $\eta\eta'$, $\pi\pi$
~ 170		[17] MARTIN	98	RVUE	$N\overline{N} \rightarrow \pi\pi$
~ 200		[18] MARTIN	97	RVUE	$\overline{N}N \rightarrow \pi\pi$
~ 60		[19] OAKDEN	94	RVUE	0.36–1.55 $\overline{p}p \rightarrow \pi\pi$
~ 80		[20] OAKDEN	94	RVUE	0.36–1.55 $\overline{p}p \rightarrow \pi\pi$
243± 16		[21] ALPER	80	CNTR	62 $\pi^- p \rightarrow K^+K^- n$
140± 15		[21] ROZANSKA	80	SPRK	18 $\pi^- p \rightarrow p\overline{p}n$
263± 57		[21] CORDEN	79	OMEG	12–15 $\pi^- p \rightarrow n2\pi$
100± 28		EVANGELIS...	79B	OMEG	10 $\pi^- p \rightarrow K^+K^- n$
107± 56		[22] ANTIPOV	77	CIBS	25 $\pi^- p \rightarrow p3\pi$

[12] From the first PWA solution.

[13] From a partial-wave analysis of the data.
[14] From an amplitude analysis of the reaction $\pi^+\pi^- \to 2\pi^0$.
[15] K matrix pole.
[16] Taking into account the $f_2(1950)$. Helicity-2 production favored.
[17] Energy-dependent analysis.
[18] Single energy analysis.
[19] From solution A of amplitude analysis of data on $\bar{p}p \to \pi\pi$. See however KLOET 96 who fit $\pi^+\pi^-$ only and find waves only up to $J = 3$ to be important but not significantly resonant.
[20] From solution B of amplitude analysis of data on $\bar{p}p \to \pi\pi$. See however KLOET 96 who fit $\pi^+\pi^-$ only and find waves only up to $J = 3$ to be important but not significantly resonant.
[21] $I(J^P) = 0(4^+)$ from amplitude analysis assuming one-pion exchange.
[22] Width errors enlarged by us to $4\Gamma/\sqrt{N}$; see the note with the $K^*(892)$ mass.

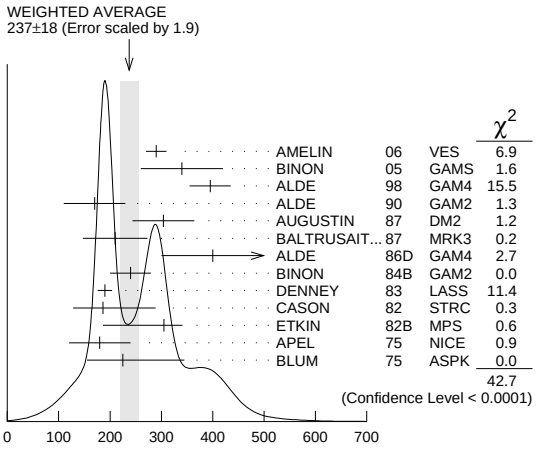

$f_4(2050)$ width (MeV)

$f_4(2050)$ DECAY MODES

	Mode	Fraction (Γ_i/Γ)
Γ_1	$\omega\omega$	seen
Γ_2	$\pi\pi$	(17.0 ± 1.5) %
Γ_3	$K\overline{K}$	$(\ 6.8^{+3.4}_{-1.8}) \times 10^{-3}$
Γ_4	$\eta\eta$	$(\ 2.1\pm0.8) \times 10^{-3}$
Γ_5	$4\pi^0$	$<\ 1.2$ %
Γ_6	$\gamma\gamma$	
Γ_7	$a_2(1320)\pi$	seen

$f_4(2050)$ $\Gamma(i)\Gamma(\gamma\gamma)/\Gamma(\text{total})$

$\Gamma(K\overline{K}) \times \Gamma(\gamma\gamma)/\Gamma_{\text{total}}$ $\quad \Gamma_3\Gamma_6/\Gamma$

VALUE (keV)	CL%	DOCUMENT ID		TECN	COMMENT
• • • We do not use the following data for averages, fits, limits, etc. • • •					
<0.29	95	ALTHOFF	85B	TASS	$\gamma\gamma \to K\overline{K}\pi$

$\Gamma(\pi\pi) \times \Gamma(\gamma\gamma)/\Gamma_{\text{total}}$ $\quad \Gamma_2\Gamma_6/\Gamma$

VALUE (eV)	CL%	EVTS	DOCUMENT ID		TECN	COMMENT
• • • We do not use the following data for averages, fits, limits, etc. • • •						
$23.1^{+3.6}_{-3.3}{}^{+70.5}_{-15.6}$			[23] UEHARA	09	BELL	$10.6\ e^+e^- \to e^+e^-\pi^0\pi^0$
<1100	95	13 ± 4	OEST	90	JADE	$e^+e^- \to e^+e^-\pi^0\pi^0$

[23] Taking into account the $f_2(1950)$. Helicity-2 production favored.

$f_4(2050)$ BRANCHING RATIOS

$\Gamma(\omega\omega)/\Gamma_{\text{total}}$ $\quad \Gamma_1/\Gamma$

VALUE	DOCUMENT ID		TECN	COMMENT
seen	AMELIN	06	VES	$36\ \pi^- p \to \omega\omega n$
• • • We do not use the following data for averages, fits, limits, etc. • • •				
not seen	BARBERIS	00F		$450\ pp \to p_f\omega\omega p_s$

$\Gamma(\omega\omega)/\Gamma(\pi\pi)$ $\quad \Gamma_1/\Gamma_2$

VALUE	DOCUMENT ID		TECN	COMMENT
1.5±0.3	ALDE	90	GAM2	$38\ \pi^- p \to \omega\omega n$

$\Gamma(\pi\pi)/\Gamma_{\text{total}}$ $\quad \Gamma_2/\Gamma$

VALUE	DOCUMENT ID		TECN	COMMENT
0.170±0.015 OUR AVERAGE				
0.18 ±0.03	[24] BINON	83C	GAM2	$38\ \pi^- p \to n4\gamma$
0.16 ±0.03	[24] CASON	82	STRC	$8\ \pi^+ p \to \Delta^{++}\pi^0\pi^0$
0.17 ±0.02	[24] CORDEN	79	OMEG	$12\text{–}15\ \pi^- p \to n2\pi$

[24] Assuming one pion exchange.

$\Gamma(K\overline{K})/\Gamma(\pi\pi)$ $\quad \Gamma_3/\Gamma_2$

VALUE	DOCUMENT ID		TECN	COMMENT
$0.04^{+0.02}_{-0.01}$	ETKIN	82B	MPS	$23\ \pi^- p \to n2K^0_S$

$\Gamma(\eta\eta)/\Gamma_{\text{total}}$ $\quad \Gamma_4/\Gamma$

VALUE (units 10^{-3})	DOCUMENT ID		TECN	COMMENT
2.1±0.8	ALDE	86D	GAM4	$100\ \pi^- p \to n4\gamma$

$\Gamma(4\pi^0)/\Gamma_{\text{total}}$ $\quad \Gamma_5/\Gamma$

VALUE	DOCUMENT ID		TECN	COMMENT
<0.012	ALDE	87	GAM4	$100\ \pi^- p \to 4\pi^0 n$

$\Gamma(a_2(1320)\pi)/\Gamma_{\text{total}}$ $\quad \Gamma_7/\Gamma$

VALUE	DOCUMENT ID		TECN	COMMENT
seen	AMELIN	00	VES	$37\ \pi^- p \to \eta\pi^+\pi^- n$

$f_4(2050)$ REFERENCES

ANISOVICH	09	IJMP A24 2481	V.V. Anisovich, A.V. Sarantsev	
UEHARA	09	PR D79 052009	S. Uehara *et al.*	(BELLE Collab.)
AMELIN	06	PAN 69 690	D.V. Amelin *et al.*	(VES Collab.)
		Translated from YAF 69 715.		
BINON	05	PAN 68 960	F. Binon *et al.*	
		Translated from YAF 68 998.		
AMELIN	00	NP A668 83	D. Amelin *et al.*	(VES Collab.)
ANISOVICH	00J	PL B491 47	A.V. Anisovich *et al.*	
BARBERIS	00F	PL B484 198	D. Barberis *et al.*	(WA 102 Collab.)
ALDE	98	EPJ A3 361	D. Alde *et al.*	(GAM4 Collab.)
Also		PAN 62 405	D. Alde *et al.*	(GAMS Collab.)
		Translated from YAF 62 446.		
MARTIN	98	PR C57 3492	B.R. Martin *et al.*	
MARTIN	97	PR C56 1114	B.R. Martin, G.C. Oades	(LOUC, AARH)
KLOET	96	PR D53 6120	W.M. Kloet, F. Myhrer	(RUTG, NORD)
OAKDEN	94	NP A574 731	M.N. Oakden, M.R. Pennington	(DURH)
ALDE	90	PL B241 600	D.M. Alde *et al.*	(SERP, BELG, LANL, LAPP+)
OEST	90	ZPHY C47 343	T. Oest *et al.*	(JADE Collab.)
ALDE	87	PL B198 286	D.M. Alde *et al.*	(LANL, BRUX, SERP, LAPP)
AUGUSTIN	87	ZPHY C36 369	J.E. Augustin *et al.*	(LALO, CLER, FRAS+)
BALTRUSAIT...	87	PR D35 2077	R.M. Baltrusaitis *et al.*	(Mark III Collab.)
ALDE	86D	NP B269 485	D.M. Alde *et al.*	(BELG, LAPP, SERP, CERN+)
ALTHOFF	85B	ZPHY C29 189	M. Althoff *et al.*	(TASSO Collab.)
BINON	84B	LNC 39 41	F.G. Binon *et al.*	(SERP, BELG, LAPP)
BINON	83C	SJNP 38 723	F.G. Binon *et al.*	(SERP, BRUX+)
		Translated from YAF 38 1199.		
DENNEY	83	PR D28 2726	D.L. Denney *et al.*	(IOWA, MICH)
CASON	82	PRL 48 1316	N.M. Cason *et al.*	(NDAM, ANL)
ETKIN	82B	PR D25 1786	A. Etkin *et al.*	(BNL, CUNY, TUFTS, VAND)
ALPER	80	PL 94B 422	B. Alper *et al.*	(AMST, CERN, CRAC, MPIM+)
ROZANSKA	80	NP B162 505	M. Rozanska *et al.*	(MPIM, CERN)
CORDEN	79	NP B157 250	M.J. Corden *et al.*	(BIRM, RHEL, TELA+) JP
EVANGELIS...	79B	NP B154 381	C. Evangelista *et al.*	(BARI, BONN, CERN+)
ANTIPOV	77	NP B119 45	Y.M. Antipov *et al.*	(SERP, GEVA)
APEL	75	PL 57B 398	W.D. Apel *et al.*	(KARLK, KARLE, PISA, SERP+) JP
BLUM	75	PL 57B 403	W. Blum *et al.*	(CERN, MPIM) JP

$\pi_2(2100)$ $\quad I^G(J^{PC}) = 1^-(2^{-+})$

OMITTED FROM SUMMARY TABLE
Needs confirmation.

$\pi_2(2100)$ MASS

VALUE (MeV)	DOCUMENT ID		TECN	COMMENT
2090± 29 OUR AVERAGE				
2090± 30	[1] AMELIN	95B	VES	$36\ \pi^- A \to \pi^+\pi^-\pi^- A$
2100±150	[2] DAUM	81B	CNTR	$63,94\ \pi^- p \to 3\pi X$

[1] From a fit to $J^{PC} = 2^{-+}$ $f_2(1270)\pi$, $(\pi\pi)_S\pi$ waves.
[2] From a two-resonance fit to four 2^-0^+ waves.

$\pi_2(2100)$ WIDTH

VALUE (MeV)	DOCUMENT ID		TECN	COMMENT
625± 50 OUR AVERAGE Error includes scale factor of 1.2.				
520±100	[3] AMELIN	95B	VES	$36\ \pi^- A \to \pi^+\pi^-\pi^- A$
651± 50	[4] DAUM	81B	CNTR	$63,94\ \pi^- p \to 3\pi X$

[3] From a fit to $J^{PC} = 2^{-+}$ $f_2(1270)\pi$, $(\pi\pi)_S\pi$ waves.
[4] From a two-resonance fit to four 2^-0^+ waves.

$\pi_2(2100)$ DECAY MODES

	Mode	Fraction (Γ_i/Γ)
Γ_1	3π	seen
Γ_2	$\rho\pi$	seen
Γ_3	$f_2(1270)\pi$	seen
Γ_4	$(\pi\pi)_S\pi$	seen

$\pi_2(2100)$ BRANCHING RATIOS

$\Gamma(\rho\pi)/\Gamma(3\pi)$ Γ_2/Γ_1

VALUE	DOCUMENT ID		TECN	COMMENT
0.19±0.05	[5] DAUM	81B	CNTR	63,94 $\pi^- p$

$\Gamma(f_2(1270)\pi)/\Gamma(3\pi)$ Γ_3/Γ_1

VALUE	DOCUMENT ID		TECN	COMMENT
0.36±0.09	[5] DAUM	81B	CNTR	63,94 $\pi^- p$

$\Gamma((\pi\pi)_S\pi)/\Gamma(3\pi)$ Γ_4/Γ_1

VALUE	DOCUMENT ID		TECN	COMMENT
0.45±0.07	[5] DAUM	81B	CNTR	63,94 $\pi^- p$

***D*-wave/*S*-wave RATIO FOR $\pi_2(2100) \to f_2(1270)\pi$**

VALUE	DOCUMENT ID		TECN	COMMENT
0.39±0.23	[5] DAUM	81B	CNTR	63,94 $\pi^- p$

[5] From a two-resonance fit to four 2^-0^+ waves.

$\pi_2(2100)$ REFERENCES

AMELIN	95B	PL B356 595	D.V. Amelin *et al.*	(SERP, TBIL)
DAUM	81B	NP B182 269	C. Daum *et al.*	(AMST, CERN, CRAC, MPIM+)

$f_0(2100)$

$I^G(J^{PC}) = 0^+(0^{++})$

OMITTED FROM SUMMARY TABLE

Needs confirmation.

$f_0(2100)$ MASS

VALUE (MeV)	EVTS	DOCUMENT ID		TECN	COMMENT
2101± 7 OUR AVERAGE					
$2081 \pm 13^{+24}_{-36}$	5.5k	[1] ABLIKIM	13N	BES3	$e^+e^- \to J/\psi \to \gamma\eta\eta$
2102±13		[2] ANISOVICH	00J	SPEC	2.0 $\overline{p}p \to \eta\pi^0\pi^0$, $\pi^0\pi^0$, $\eta\eta$, $\eta\eta'$, $\pi^+\pi^-$
2090±30		BAI	00A	BES	$J/\psi \to \gamma(\pi^+\pi^-\pi^+\pi^-)$
2105±10		ANISOVICH	99K	SPEC	0.6–1.94 $\overline{p}p \to \eta\eta$, $\eta\eta'$
• • • We do not use the following data for averages, fits, limits, etc. • • •					
2090±10± 6	529	[3,4] DOBBS	15		$J/\psi \to \gamma\pi^+\pi^-$
2099±17± 8	283	[3,4] DOBBS	15		$\psi(2S) \to \gamma\pi^+\pi^-$
2105± 8	80k	[5] UMAN	06	E835	5.2 $\overline{p}p \to \eta\eta\pi^0$
~ 2104		BUGG	95		$J/\psi \to \gamma\pi^+\pi^-\pi^+\pi^-$
~ 2122		HASAN	94	RVUE	$\overline{p}p \to \pi\pi$

[1] From partial wave analysis including all possible combinations of 0^{++}, 2^{++}, and 4^{++} resonances.
[2] Includes the data of ANISOVICH 00B indicating to exotic decay pattern.
[3] Using CLEO-c data but not authored by the CLEO Collaboration.
[4] From a fit to a Breit-Wigner line shape with fixed $\Gamma = 209$ MeV.
[5] Statistical error only.

$f_0(2100)$ WIDTH

VALUE (MeV)	EVTS	DOCUMENT ID		TECN	COMMENT
$\mathbf{224^{+\ 23}_{-\ 21}}$ **OUR AVERAGE**		Error includes scale factor of 1.3. See the ideogram below.			
$273^{+\ 27+70}_{-\ 24-23}$	5.5k	[6] ABLIKIM	13N	BES3	$e^+e^- \to J/\psi \to \gamma\eta\eta$
211± 29		[7] ANISOVICH	00J	SPEC	2.0 $\overline{p}p \to \eta\pi^0\pi^0$, $\pi^0\pi^0$, $\eta\eta$, $\eta\eta'$, $\pi^+\pi^-$
330±100		BAI	00A	BES	$J/\psi \to \gamma(\pi^+\pi^-\pi^+\pi^-)$
200± 25		ANISOVICH	99K	SPEC	0.6–1.94 $\overline{p}p \to \eta\eta$, $\eta\eta'$
• • • We do not use the following data for averages, fits, limits, etc. • • •					
236± 14	80k	[8] UMAN	06	E835	5.2 $\overline{p}p \to \eta\eta\pi^0$
~ 203		BUGG	95		$J/\psi \to \gamma\pi^+\pi^-\pi^+\pi^-$
~ 273		HASAN	94	RVUE	$\overline{p}p \to \pi\pi$

[6] From partial wave analysis including all possible combinations of 0^{++}, 2^{++}, and 4^{++} resonances.
[7] Includes the data of ANISOVICH 00B indicating to exotic decay pattern.
[8] Statistical error only.

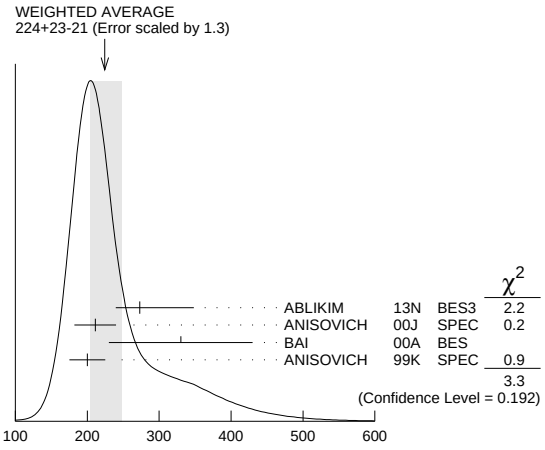

$f_0(2100)$ REFERENCES

DOBBS	15	PR D91 052006	S. Dobbs *et al.*	(NWES)
ABLIKIM	13N	PR D87 092009	Ablikim M. *et al.*	(BES III Collab.)
UMAN	06	PR D73 052009	I. Uman *et al.*	(FNAL E835)
ANISOVICH	00B	NP A662 319	A.V. Anisovich *et al.*	
ANISOVICH	00J	PL B491 47	A.V. Anisovich *et al.*	
BAI	00A	PL B472 207	J.Z. Bai *et al.*	(BES Collab.)
ANISOVICH	99K	PL B468 309	A.V. Anisovich *et al.*	
BUGG	95	PL B353 378	D.V. Bugg *et al.*	(LOQM, PNPI, WASH)
HASAN	94	PL B334 215	A. Hasan, D.V. Bugg	(LOQM)

$f_2(2150)$

$I^G(J^{PC}) = 0^+(2^{++})$

OMITTED FROM SUMMARY TABLE

This entry was previously called T_0.

$f_2(2150)$ MASS

$f_2(2150)$ MASS, COMBINED MODES (MeV)

VALUE (MeV)	EVTS	DOCUMENT ID		TECN	COMMENT
2157±12 OUR AVERAGE Includes data from the 2 datablocks that follow this one.					
• • • We do not use the following data for averages, fits, limits, etc. • • •					
2170± 6	80k	[1] UMAN	06	E835	5.2 $\overline{p}p \to \eta\eta\pi^0$

[1] Statistical error only.

$\eta\eta$ MODE

VALUE (MeV)	DOCUMENT ID		TECN	COMMENT
The data in this block is included in the average printed for a previous datablock.				
2157±12 OUR AVERAGE				
2151±16	BARBERIS	00E		450 $pp \to p_f\eta\eta p_s$
2175±20	PROKOSHKIN	95D	GAM4	300 $\pi^- N \to \pi^- N 2\eta$, 450 $pp \to pp2\eta$
2130±35	SINGOVSKI	94	GAM4	450 $pp \to pp2\eta$
• • • We do not use the following data for averages, fits, limits, etc. • • •				
2140±30	[2] ABELE	99B	CBAR	
2104±20	[3] ARMSTRONG	93C	E760	$\overline{p}p \to \pi^0\eta\eta \to 6\gamma$

[2] Spin not determined.
[3] No J^{PC} determination.

$\eta\pi\pi$ MODE

VALUE (MeV)	DOCUMENT ID		TECN	CHG	COMMENT
The data in this block is included in the average printed for a previous datablock.					
• • • We do not use the following data for averages, fits, limits, etc. • • •					
2135±20±45	[4] ADOMEIT	96	CBAR	0	1.94 $\overline{p}p \to \eta 3\pi^0$

[4] ANISOVICH 00E recommends to withdraw ADOMEIT 96 that assumed a single $J^P = 2^+$ resonance.

$\overline{p}p \to \pi\pi$

VALUE (MeV)	DOCUMENT ID		TECN	COMMENT
• • • We do not use the following data for averages, fits, limits, etc. • • •				
~ 2090	[5] OAKDEN	94	RVUE	0.36–1.55 $\overline{p}p \to \pi\pi$
~ 2120	[6] OAKDEN	94	RVUE	0.36–1.55 $\overline{p}p \to \pi\pi$
~ 2170	[7] MARTIN	80B	RVUE	
~ 2150	[7] MARTIN	80C	RVUE	
~ 2150	[8] DULUDE	78B	OSPK	1–2 $\overline{p}p \to \pi^0\pi^0$

[5] OAKDEN 94 makes an amplitude analysis of LEAR data on $\overline{p}p \to \pi\pi$ using a method based on Barrelet zeros. This is solution A. The amplitude analysis of HASAN 94 includes earlier data as well, and assume that the data can be parametrized in terms of towers of

Meson Particle Listings

$f_2(2150)$

nearly degenerate resonances on the leading Regge trajectory. See also KLOET 96 and MARTIN 97 who make related analyses.

[6] From solution B of amplitude analysis of data on $\overline{p}p \to \pi\pi$.

[7] $I(J^P) = 0(2^+)$ from simultaneous analysis of $p\overline{p} \to \pi^-\pi^+$ and $\pi^0\pi^0$.

[8] $I^G(J^P) = 0^+(2^+)$ from partial-wave amplitude analysis.

S-CHANNEL $\overline{p}p$, $\overline{N}N$ or $\overline{K}K$

VALUE (MeV)	DOCUMENT ID		TECN	CHG	COMMENT
• • • We do not use the following data for averages, fits, limits, etc. • • •					
$2139^{+\ 8}_{-\ 9}$	[9] EVANGELIS...	97	SPEC		0.6-2.4 $\overline{p}p \to K^0_S K^0_S$
~ 2190	[9] CUTTS	78B	CNTR		0.97–3 $\overline{p}p \to \overline{N}N$
2155 ± 15	[9,10] COUPLAND	77	CNTR	0	0.7–2.4 $\overline{p}p \to \overline{p}p$
2193 ± 2	[9,11] ALSPECTOR	73	CNTR		$\overline{p}p$ S channel

[9] Isospins 0 and 1 not separated.

[10] From a fit to the total elastic cross section.

[11] Referred to as T or T region by ALSPECTOR 73.

$K\overline{K}$ MODE

VALUE (MeV)	DOCUMENT ID		TECN	COMMENT
• • • We do not use the following data for averages, fits, limits, etc. • • •				
2200 ± 13	VLADIMIRSK...06		SPEC	40 $\pi^- p \to K^0_S K^0_S n$
2150 ± 20	ABLIKIM	04E	BES2	$J/\psi \to \omega K^+ K^-$
2130 ± 35	BARBERIS	99	OMEG	450 $pp \to p_s p_f K^+ K^-$

$f_2(2150)$ WIDTH

$f_2(2150)$ WIDTH, COMBINED MODES (MeV)

VALUE (MeV)	EVTS	DOCUMENT ID		TECN	COMMENT
152 ± 30 OUR AVERAGE Includes data from the 2 datablocks that follow this one. Error includes scale factor of 1.4. See the ideogram below.					
• • • We do not use the following data for averages, fits, limits, etc. • • •					
182 ± 11	80k	[12] UMAN	06	E835	5.2 $\overline{p}p \to \eta\eta\pi^0$

[12] Statistical error only.

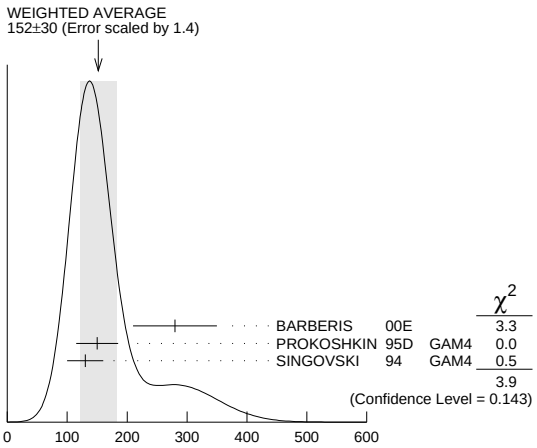

$f_2(2150)$ WIDTH, COMBINED MODES (MeV)

$\eta\eta$ MODE

VALUE (MeV)	DOCUMENT ID		TECN	COMMENT
The data in this block is included in the average printed for a previous datablock.				
152 ± 30 OUR AVERAGE Error includes scale factor of 1.4. See the ideogram below.				
280 ± 70	BARBERIS	00E		450 $pp \to p_f \eta\eta p_s$
150 ± 35	PROKOSHKIN	95D	GAM4	300 $\pi^- N \to \pi^- N 2\eta$, 450 $pp \to pp2\eta$
130 ± 30	SINGOVSKI	94	GAM4	450 $pp \to pp2\eta$
• • • We do not use the following data for averages, fits, limits, etc. • • •				
310 ± 50	[13] ABELE	99B	CBAR	
203 ± 10	[14] ARMSTRONG	93C	E760	$\overline{p}p \to \pi^0\eta\eta \to 6\gamma$

[13] Spin not determined.

[14] No J^{PC} determination.

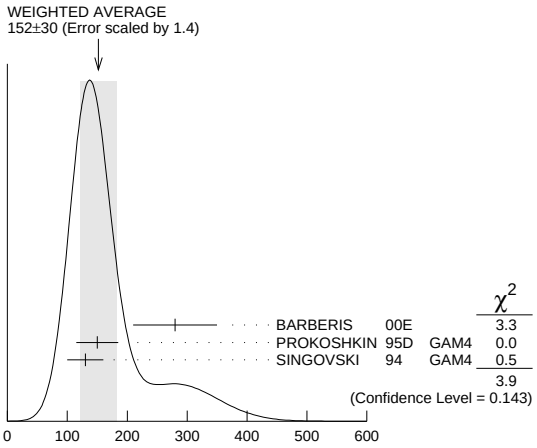

$f_2(2150)$ WIDTH, $\eta\eta$ MODE (MeV)

$\eta\pi\pi$ MODE

VALUE (MeV)	DOCUMENT ID		TECN	CHG	COMMENT
The data in this block is included in the average printed for a previous datablock.					
• • • We do not use the following data for averages, fits, limits, etc. • • •					
$250 \pm 25 \pm 45$	[15] ADOMEIT	96	CBAR	0	1.94 $\overline{p}p \to \eta 3\pi^0$

[15] ANISOVICH 00E recommends to withdraw ADOMEIT 96 that assumed a single $J^P = 2^+$ resonance.

$\overline{p}p \to \pi\pi$

VALUE (MeV)	DOCUMENT ID		TECN	COMMENT
250 OUR ESTIMATE				
• • • We do not use the following data for averages, fits, limits, etc. • • •				
~ 70	[16] OAKDEN	94	RVUE	0.36–1.55 $\overline{p}p \to \pi\pi$
~ 250	[17] MARTIN	80B	RVUE	
~ 250	[17] MARTIN	80C	RVUE	
~ 250	[18] DULUDE	78B	OSPK	1–2 $\overline{p}p \to \pi^0\pi^0$

[16] See however KLOET 96 who fit $\pi^+\pi^-$ only and find waves only up to $J = 3$ to be important but not significantly resonant.

[17] $I(J^P) = 0(2^+)$ from simultaneous analysis of $p\overline{p} \to \pi^-\pi^+$ and $\pi^0\pi^0$.

[18] $I^G(J^P) = 0^+(2^+)$ from partial-wave amplitude analysis.

S-CHANNEL $\overline{p}p$, $\overline{N}N$ or $\overline{K}K$

VALUE (MeV)	DOCUMENT ID		TECN	CHG	COMMENT
• • • We do not use the following data for averages, fits, limits, etc. • • •					
56^{+31}_{-16}	[19] EVANGELIS...	97	SPEC		0.6-2.4 $\overline{p}p \to K^0_S K^0_S$
135 ± 75	[20,21] COUPLAND	77	CNTR	0	0.7–2.4 $\overline{p}p \to \overline{p}p$
98 ± 8	[21] ALSPECTOR	73	CNTR		$\overline{p}p$ S channel

[19] Isospin 0 and 2 not separated.

[20] From a fit to the total elastic cross section.

[21] Isospins 0 and 1 not separated.

$K\overline{K}$ MODE

VALUE (MeV)	DOCUMENT ID		TECN	COMMENT
• • • We do not use the following data for averages, fits, limits, etc. • • •				
91 ± 62	VLADIMIRSK...06		SPEC	40 $\pi^- p \to K^0_S K^0_S n$
150 ± 30	ABLIKIM	04E	BES2	$J/\psi \to \omega K^+ K^-$
270 ± 50	BARBERIS	99	OMEG	450 $pp \to p_s p_f K^+ K^-$

$f_2(2150)$ DECAY MODES

	Mode	Fraction (Γ_i/Γ)
Γ_1	$\pi\pi$	
Γ_2	$\eta\eta$	seen
Γ_3	$K\overline{K}$	seen
Γ_4	$f_2(1270)\eta$	seen
Γ_5	$a_2(1320)\pi$	seen
Γ_6	$p\overline{p}$	seen

$f_2(2150)$ BRANCHING RATIOS

$\Gamma(K\overline{K})/\Gamma(\eta\eta)$ Γ_3/Γ_2

VALUE	CL%	DOCUMENT ID		TECN	COMMENT
1.28 ± 0.23		BARBERIS	00E		450 $pp \to p_f \eta\eta p_s$
• • • We do not use the following data for averages, fits, limits, etc. • • •					
<0.1	95	[22] PROKOSHKIN	95D	GAM4	300 $\pi^- N \to \pi^- N 2\eta$, 450 $pp \to pp2\eta$

[22] Using data from ARMSTRONG 89D.

$\Gamma(\pi\pi)/\Gamma(\eta\eta)$ Γ_1/Γ_2

VALUE	CL%	DOCUMENT ID	TECN	COMMENT
• • • We do not use the following data for averages, fits, limits, etc. • • •				
<0.33	95	[23] PROKOSHKIN 95D	GAM4	300 $\pi^- N \to \pi^- N 2\eta$, 450 $pp \to pp2\eta$

[23] Derived from a $\pi^0\pi^0/\eta\eta$ limit.

$\Gamma(f_2(1270)\eta)/\Gamma(a_2(1320)\pi)$ Γ_4/Γ_5

VALUE	DOCUMENT ID		TECN	COMMENT
0.79±0.11	[24] ADOMEIT	96	CBAR	1.94 $\overline{p}p \to \eta 3\pi^0$

[24] Using B($a_2(1320) \to \eta\pi$) = 0.145

$\Gamma(p\overline{p})/\Gamma_{total}$ Γ_6/Γ

VALUE	EVTS	DOCUMENT ID		TECN	COMMENT
seen	73	ALEXANDER	10	CLEO	$\psi(2S) \to \gamma p\overline{p}$

$f_2(2150)$ REFERENCES

ALEXANDER	10	PR D82 092002	J.P. Alexander *et al.* (CLEO Collab.)
UMAN	06	PR D73 052009	I. Uman *et al.* (FNAL E835)
VLADIMIRSK...	06	PAN 69 493	V.V. Vladimirsky *et al.* (ITEP, Moscow)
		Translated from YAF 69 515.	
ABLIKIM	04E	PL B603 138	M. Ablikim *et al.* (BES Collab.)
ANISOVICH	00E	PL B477 19	A.V. Anisovich *et al.*
BARBERIS	00E	PL B479 59	D. Barberis *et al.* (WA 102 Collab.)
ABELE	99B	EPJ C8 67	A. Abele *et al.* (Crystal Barrel Collab.)
BARBERIS	99	PL B453 305	D. Barberis *et al.* (Omega Expt.)
EVANGELIS...	97	PR D56 3803	C. Evangelista *et al.* (LEAR Collab.)
MARTIN	97	PR C56 1114	B.R. Martin, G.C. Oades (LOUC, AARH)
ADOMEIT	96	ZPHY C71 227	J. Adomeit *et al.* (Crystal Barrel Collab.)
KLOET	96	PR D53 6120	W.M. Kloet, F. Myhrer (RUTG, NORD)
PROKOSHKIN	95D	PD 40 495	Y.D. Prokoshkin (SERP) IGJPC
		Translated from DANS 344 469.	
HASAN	94	PL B334 215	A. Hasan, D.V. Bugg (LOQM)
OAKDEN	94	NP A574 731	M.N. Oakden, M.R. Pennington (DURH)
SINGOVSKI	94	NC A107 1911	A.V. Singovsky (SERP)
ARMSTRONG	93C	PL B307 394	T.A. Armstrong *et al.* (FNAL, FERR, GENO+)
ARMSTRONG	89D	PL B227 186	T.A. Armstrong, M. Benayoun (ATHU, BARI, BIRM+)
MARTIN	80B	NP B176 355	B.R. Martin, D. Morgan (LOUC, RHEL) JP
MARTIN	80C	NP B169 216	A.D. Martin, M.R. Pennington (DURH) JP
CUTTS	78B	PR D17 16	D. Cutts *et al.* (STON, WISC)
DULUDE	78B	PL 79B 335	R.S. Dulude *et al.* (BROW, MIT, BARI) JP
COUPLAND	77	PL 71B 460	M. Coupland *et al.* (LOQM, RHEL)
ALSPECTOR	73	PRL 30 511	J. Alspector *et al.* (RUTG, UPNJ)

$\rho(2150)$

$I^G(J^{PC}) = 1^+(1^{--})$

OMITTED FROM SUMMARY TABLE

This entry was previously called $T_1(2190)$. See our mini-review under the $\rho(1700)$.

$\rho(2150)$ MASS

e^+e^- PRODUCED

VALUE (MeV)	DOCUMENT ID		TECN	COMMENT
• • • We do not use the following data for averages, fits, limits, etc. • • •				
2254±22	[1] LEES	12G	BABR	$e^+e^- \to \pi^+\pi^-\gamma$
2150±40±50	AUBERT	07AU	BABR	10.6 $e^+e^- \to f_1(1285)\pi^+\pi^-\gamma$
1990±80	AUBERT	07AU	BABR	10.6 $e^+e^- \to \eta'\pi^+\pi^-\gamma$
2153±37	BIAGINI	91	RVUE	$e^+e^- \to \pi^+\pi^-$, K^+K^-
2110±50	[2] CLEGG	90	RVUE	$e^+e^- \to 3(\pi^+\pi^-)$, $2(\pi^+\pi^-\pi^0)$

$\overline{p}p \to \pi\pi$

VALUE (MeV)	DOCUMENT ID		TECN	COMMENT
• • • We do not use the following data for averages, fits, limits, etc. • • •				
~ 2191	HASAN	94	RVUE	$\overline{p}p \to \pi\pi$
~ 2070	[3] OAKDEN	94	RVUE	0.36–1.55 $\overline{p}p \to \pi\pi$
~ 2170	[4] MARTIN	80B	RVUE	
~ 2100	[4] MARTIN	80C	RVUE	

S-CHANNEL $\overline{N}N$

VALUE (MeV)	DOCUMENT ID		TECN	COMMENT
• • • We do not use the following data for averages, fits, limits, etc. • • •				
2110±35	[5] ANISOVICH	02	SPEC	0.6–1.9 $p\overline{p} \to \omega\pi^0$, $\omega\eta\pi^0$, $\pi^+\pi^-$
~ 2190	[6] CUTTS	78B	CNTR	0.97–3 $\overline{p}p \to \overline{N}N$
2155±15	[6,7] COUPLAND	77	CNTR	0.7–2.4 $\overline{p}p \to \overline{p}p$
2193± 2	[6,8] ALSPECTOR	73	CNTR	$\overline{p}p$ S channel
2190±10	[9] ABRAMS	70	CNTR	S channel $\overline{p}N$

$\pi^-p \to \omega\pi^0 n$

VALUE (MeV)	DOCUMENT ID		TECN	COMMENT
2155±21 OUR AVERAGE				
2140±30	ALDE	95	GAM2	38 $\pi^-p \to \omega\pi^0 n$
2170±30	ALDE	92C	GAM4	100 $\pi^-p \to \omega\pi^0 n$

[1] Using the GOUNARIS 68 parametrization of the pion form factor leaving the masses and widths of the $\rho(1450)$, $\rho(1700)$, and $\rho(2150)$ resonances as free parameters of the fit.
[2] Includes ATKINSON 85.
[3] See however KLOET 96 who fit $\pi^+\pi^-$ only and find waves only up to $J = 3$ to be important but not significantly resonant.
[4] $I(J^P) = 1(1^-)$ from simultaneous analysis of $p\overline{p} \to \pi^-\pi^+$ and $\pi^0\pi^0$.
[5] From the combined analysis of ANISOVICH 00J, ANISOVICH 01D, ANISOVICH 01E, and ANISOVICH 02.
[6] Isospins 0 and 1 not separated.
[7] From a fit to the total elastic cross section.
[8] Referred to as T or T region by ALSPECTOR 73.
[9] Seen as bump in $I = 1$ state. See also COOPER 68. PEASLEE 75 confirm $\overline{p}p$ results of ABRAMS 70, no narrow structure.

$\rho(2150)$ WIDTH

e^+e^- PRODUCED

VALUE (MeV)	DOCUMENT ID		TECN	COMMENT
• • • We do not use the following data for averages, fits, limits, etc. • • •				
109± 76	[10] LEES	12G	BABR	$e^+e^- \to \pi^+\pi^-\gamma$
350± 40±50	AUBERT	07AU	BABR	10.6 $e^+e^- \to f_1(1285)\pi^+\pi^-\gamma$
310±140	AUBERT	07AU	BABR	10.6 $e^+e^- \to \eta'\pi^+\pi^-\gamma$
389± 79	BIAGINI	91	RVUE	$e^+e^- \to \pi^+\pi^-$, K^+K^-
410±100	[11] CLEGG	90	RVUE	$e^+e^- \to 3(\pi^+\pi^-)$, $2(\pi^+\pi^-\pi^0)$

$\overline{p}p \to \pi\pi$

VALUE (MeV)	DOCUMENT ID		TECN	COMMENT
• • • We do not use the following data for averages, fits, limits, etc. • • •				
~ 296	HASAN	94	RVUE	$\overline{p}p \to \pi\pi$
~ 40	[12] OAKDEN	94	RVUE	0.36–1.55 $\overline{p}p \to \pi\pi$
~ 250	[13] MARTIN	80B	RVUE	
~ 200	[13] MARTIN	80C	RVUE	

S-CHANNEL $\overline{N}N$

VALUE (MeV)	DOCUMENT ID		TECN	COMMENT
• • • We do not use the following data for averages, fits, limits, etc. • • •				
230±50	[14] ANISOVICH	02	SPEC	0.6–1.9 $p\overline{p} \to \omega\pi^0$, $\omega\eta\pi^0$, $\pi^+\pi^-$
135±75	[15,16] COUPLAND	77	CNTR	0.7–2.4 $\overline{p}p \to \overline{p}p$
98± 8	[16] ALSPECTOR	73	CNTR	$\overline{p}p$ S channel
~ 85	[17] ABRAMS	70	CNTR	S channel $\overline{p}N$

$\pi^-p \to \omega\pi^0 n$

VALUE (MeV)	DOCUMENT ID		TECN	COMMENT
320±70	ALDE	95	GAM2	38 $\pi^-p \to \omega\pi^0 n$
• • • We do not use the following data for averages, fits, limits, etc. • • •				
~ 300	ALDE	92C	GAM4	100 $\pi^-p \to \omega\pi^0 n$

[10] Using the GOUNARIS 68 parametrization of the pion form factor leaving the masses and widths of the $\rho(1450)$, $\rho(1700)$, and $\rho(2150)$ resonances as free parameters of the fit.
[11] Includes ATKINSON 85.
[12] See however KLOET 96 who fit $\pi^+\pi^-$ only and find waves only up to $J = 3$ to be important but not significantly resonant.
[13] $I(J^P) = 1(1^-)$ from simultaneous analysis of $p\overline{p} \to \pi^-\pi^+$ and $\pi^0\pi^0$.
[14] From the combined analysis of ANISOVICH 00J, ANISOVICH 01D, ANISOVICH 01E, and ANISOVICH 02.
[15] From a fit to the total elastic cross section.
[16] Isospins 0 and 1 not separated.
[17] Seen as bump in $I = 1$ state. See also COOPER 68. PEASLEE 75 confirm $\overline{p}p$ results of ABRAMS 70, no narrow structure.

$\rho(2150)$ DECAY MODES

	Mode	Fraction (Γ_i/Γ)
Γ_1	e^+e^-	
Γ_2	$\pi^+\pi^-$	seen
Γ_3	K^+K^-	seen
Γ_4	$3(\pi^+\pi^-)$	seen
Γ_5	$2(\pi^+\pi^-\pi^0)$	seen
Γ_6	$\eta'\pi^+\pi^-$	seen
Γ_7	$f_1(1285)\pi^+\pi^-$	seen
Γ_8	$\omega\pi^0$	seen
Γ_9	$\omega\pi^0\eta$	seen
Γ_{10}	$p\overline{p}$	

$\rho(2150)$ $\Gamma(i)\Gamma(e^+e^-)/\Gamma^2(total)$

$\Gamma(f_1(1285)\pi^+\pi^-)/\Gamma_{total} \times \Gamma(e^+e^-)/\Gamma_{total}$ $\Gamma_7/\Gamma \times \Gamma_1/\Gamma$

VALUE (units 10^{-7})	DOCUMENT ID		TECN	COMMENT
3.1±0.6±0.5	[18] AUBERT	07AU	BABR	10.6 $e^+e^- \to f_1(1285)\pi^+\pi^-\gamma$

[18] Calculated by us from the reported value of cross section at the peak.

$\Gamma(\eta'\pi^+\pi^-)/\Gamma_{total} \times \Gamma(e^+e^-)/\Gamma_{total}$ $\Gamma_6/\Gamma \times \Gamma_1/\Gamma$

VALUE (units 10^{-8})	DOCUMENT ID		TECN	COMMENT
• • • We do not use the following data for averages, fits, limits, etc. • • •				
4.9±1.9	[19] AUBERT	07AU	BABR	10.6 $e^+e^- \to \eta'\pi^+\pi^-\gamma$

[19] Calculated by us from the reported value of cross section at the peak.

$\rho(2150)$ REFERENCES

LEES	12G	PR D86 032013	J.P. Lees *et al.*	(BABAR Collab.)
AUBERT	07AU	PR D76 092005	B. Aubert *et al.*	(BABAR Collab.)
ANISOVICH	02	PL B542 8	A.V. Anisovich *et al.*	
ANISOVICH	01D	PL B508 6	A.V. Anisovich *et al.*	
ANISOVICH	01E	PL B513 281	A.V. Anisovich *et al.*	
ANISOVICH	00J	PL B491 47	A.V. Anisovich *et al.*	
KLOET	96	PR D53 6120	W.M. Kloet, F. Myhrer	(RUTG, NORD)
ALDE	95	ZPHY C66 379	D.M. Alde *et al.*	(GAMS Collab.) JP
HASAN	94	PL B334 215	A. Hasan, D.V. Bugg	(LOQM)
OAKDEN	94	NP A574 731	M.N. Oakden, M.R. Pennington	(DURH)
ALDE	92C	ZPHY C54 553	D.M. Alde *et al.*	(BELG, SERP, KEK, LANL+)
BIAGINI	91	NC 104A 363	M.E. Biagini *et al.*	(FRAS, PRAG)
CLEGG	90	ZPHY C45 677	A.B. Clegg, A. Donnachie	(LANC, MCHS)
ATKINSON	85	ZPHY C29 333	M. Atkinson *et al.*	(BONN, CERN, GLAS+)
MARTIN	80B	NP B176 355	B.R. Martin, D. Morgan	(LOUC, RHEL) JP
MARTIN	80C	NP B169 216	A.D. Martin, M.R. Pennington	(DURH) JP
CUTTS	78B	PR D17 16	D. Cutts *et al.*	(STON, WISC)
COUPLAND	77	PL 71B 460	M. Coupland *et al.*	(LOQM, RHEL)
PEASLEE	75	PL 57B 189	D.C. Peaslee *et al.*	(CANB, BARI, BROW+)
ALSPECTOR	73	PRL 30 511	J. Alspector *et al.*	(RUTG, UPNJ)
ABRAMS	70	PR D1 1917	R.J. Abrams *et al.*	(BNL)
COOPER	68	PRL 20 1059	W.A. Cooper *et al.*	(ANL)
GOUNARIS	68	PRL 21 244	G.J. Gounaris, J.J. Sakurai	

$\phi(2170)$

$I^G(J^{PC}) = 0^-(1^{--})$

Observed by AUBERT,BE 06D in the initial-state radiation process $e^+e^- \to \phi f_0(980)\gamma$.

$\phi(2170)$ MASS

VALUE (MeV)	EVTS	DOCUMENT ID		TECN	COMMENT
2188±10 OUR AVERAGE		Error includes scale factor of 1.8. See the ideogram below.			
2200± 6± 5	471	ABLIKIM	15H	BES3	$J/\psi \to \eta\phi\pi^+\pi^-$
2180± 8± 8		[1,2] LEES	12F	BABR	10.6 $e^+e^- \to \phi\pi^+\pi^-\gamma$
2186±10± 6	52	ABLIKIM	08F	BES	$J/\psi \to \eta\phi f_0(980)$
2125±22±10	483	AUBERT	08S	BABR	10.6 $e^+e^- \to \phi\eta\gamma$
• • • We do not use the following data for averages, fits, limits, etc. • • •					
$2079\pm13^{+79}_{-28}$	4.8k	[3] SHEN	09	BELL	10.6 $e^+e^- \to K^+K^-\pi^+\pi^-\gamma$
2192±14	116	[4] AUBERT	07AK	BABR	10.6 $e^+e^- \to K^+K^-\pi^+\pi^-\gamma$
2169±20	149	[4] AUBERT	07AK	BABR	10.6 $e^+e^- \to K^+K^-\pi^0\pi^0\gamma$
2175±10±15	201	[2,5] AUBERT,BE	06D	BABR	10.6 $e^+e^- \to K^+K^-\pi\pi\gamma$

[1] Fit includes interference with the $\phi(1680)$.
[2] From the $\phi f_0(980)$ component.
[3] From a fit with two incoherent Breit-Wigners.
[4] From the $K^+K^- f_0(980)$ component.
[5] Superseded by LEES 12F.

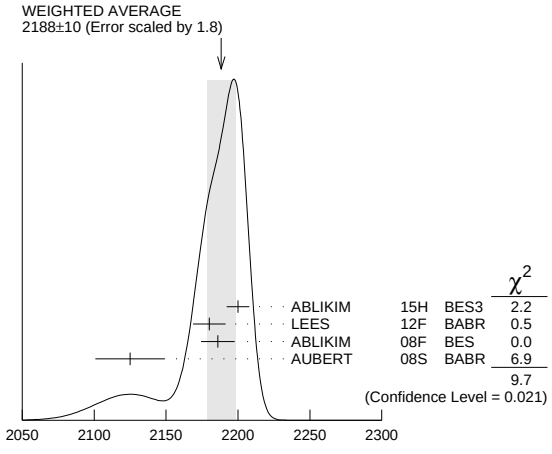

$\phi(2170)$ WIDTH

VALUE (MeV)	EVTS	DOCUMENT ID		TECN	COMMENT
83±12 OUR AVERAGE					
104±15±15	471	ABLIKIM	15H	BES3	$J/\psi \to \eta\phi\pi^+\pi^-$
77±15±10		[6,7] LEES	12F	BABR	10.6 $e^+e^- \to \phi\pi^+\pi^-\gamma$
65±23±17	52	ABLIKIM	08F	BES	$J/\psi \to \eta\phi f_0(980)$
61±50±13	483	AUBERT	08S	BABR	10.6 $e^+e^- \to \phi\eta\gamma$
• • • We do not use the following data for averages, fits, limits, etc. • • •					
$192\pm23^{+25}_{-61}$	4.8k	[8] SHEN	09	BELL	10.6 $e^+e^- \to K^+K^-\pi^+\pi^-\gamma$
71±21	116	[9] AUBERT	07AK	BABR	10.6 $e^+e^- \to K^+K^-\pi^+\pi^-\gamma$
102±27	149	[9] AUBERT	07AK	BABR	10.6 $e^+e^- \to K^+K^-\pi^0\pi^0\gamma$
58±16±20	201	[7,10] AUBERT,BE	06D	BABR	10.6 $e^+e^- \to K^+K^-\pi\pi\gamma$

[6] Fit includes interference with the $\phi(1680)$.
[7] From the $\phi f_0(980)$ component.
[8] From a fit with two incoherent Breit-Wigners.
[9] From the $K^+K^- f_0(980)$ component.
[10] Superseded by LEES 12F.

$\phi(2170)$ DECAY MODES

	Mode	Fraction (Γ_i/Γ)
Γ_1	e^+e^-	seen
Γ_2	$\phi\eta$	
Γ_3	$\phi\pi\pi$	
Γ_4	$\phi f_0(980)$	seen
Γ_5	$K^+K^-\pi^+\pi^-$	
Γ_6	$K^+K^- f_0(980) \to K^+K^-\pi^+\pi^-$	seen
Γ_7	$K^+K^-\pi^0\pi^0$	
Γ_8	$K^+K^- f_0(980) \to K^+K^-\pi^0\pi^0$	seen
Γ_9	$K^{*0}K^\pm\pi^\mp$	not seen
Γ_{10}	$K^*(892)^0\overline{K}^*(892)^0$	not seen

$\phi(2170)\ \Gamma(i)\Gamma(e^+e^-)/\Gamma(\text{total})$

$\Gamma(\phi\eta) \times \Gamma(e^+e^-)/\Gamma_{\text{total}}$ $\quad \Gamma_2\Gamma_1/\Gamma$

VALUE (eV)	EVTS	DOCUMENT ID		TECN	COMMENT
• • • We do not use the following data for averages, fits, limits, etc. • • •					
1.7±0.7±1.3	483	AUBERT	08S	BABR	10.6 $e^+e^- \to \phi\eta\gamma$

$\Gamma(\phi f_0(980)) \times \Gamma(e^+e^-)/\Gamma_{\text{total}}$ $\quad \Gamma_4\Gamma_1/\Gamma$

VALUE (eV)	EVTS	DOCUMENT ID		TECN	COMMENT
2.3±0.3±0.3		[11,12] LEES	12F	BABR	10.6 $e^+e^- \to \phi\pi^+\pi^-\gamma$
• • • We do not use the following data for averages, fits, limits, etc. • • •					
2.5±0.8±0.4	201	[12,13] AUBERT,BE	06D	BABR	10.6 $e^+e^- \to K^+K^-\pi\pi\gamma$

[11] From a fit with constructive interference with the $\phi(1680)$. In a fit with destructive interference, the value is larger by a factor of 12.
[12] From the $\phi f_0(980)$ component.
[13] Superseded by LEES 12F.

$\phi(2170)\ \Gamma(i)\Gamma(e^+e^-)/\Gamma^2(\text{total})$

$\Gamma(\phi\pi\pi)/\Gamma_{\text{total}} \times \Gamma(e^+e^-)/\Gamma_{\text{total}}$ $\quad \Gamma_3/\Gamma \times \Gamma_1/\Gamma$

VALUE (units 10^{-7})	EVTS	DOCUMENT ID		TECN	COMMENT
• • • We do not use the following data for averages, fits, limits, etc. • • •					
1.65±0.15±0.18	4.8k	[14] SHEN	09	BELL	10.6 $e^+e^- \to K^+K^-\pi^+\pi^-\gamma$

[14] Multiplied by 3/2 to take into account the $\phi\pi^0\pi^0$ mode. Using $B(\phi \to K^+K^-) = (49.2 \pm 0.6)\%$.

$\phi(2170)$ BRANCHING RATIOS

$\Gamma(K^+K^- f_0(980) \to K^+K^-\pi^+\pi^-)/\Gamma_{\text{total}}$ $\quad \Gamma_6/\Gamma$

VALUE	DOCUMENT ID		TECN	COMMENT
seen	AUBERT	07AK	BABR	10.6 $e^+e^- \to K^+K^-\pi^+\pi^-\gamma$

$\Gamma(K^+K^- f_0(980) \to K^+K^-\pi^0\pi^0)/\Gamma_{\text{total}}$ $\quad \Gamma_8/\Gamma$

VALUE	DOCUMENT ID		TECN	COMMENT
seen	AUBERT	07AK	BABR	10.6 $e^+e^- \to K^+K^-\pi^0\pi^0\gamma$

$\Gamma(K^{*0}K^\pm\pi^\mp)/\Gamma_{\text{total}}$ $\quad \Gamma_9/\Gamma$

VALUE	DOCUMENT ID		TECN	COMMENT
not seen	AUBERT	07AK	BABR	10.6 GeV e^+e^-

$\Gamma(K^*(892)^0\overline{K}^*(892)^0)/\Gamma_{\text{total}}$ $\quad \Gamma_{10}/\Gamma$

VALUE	DOCUMENT ID		TECN	COMMENT
not seen	ABLIKIM	10C	BES2	$J/\psi \to \eta K^+\pi^- K^-\pi^+$

$\phi(2170)$ REFERENCES

ABLIKIM	15H	PR D91 052017	M. Ablikim *et al.*	(BES III Collab.)
LEES	12F	PR D86 012008	J.P. Lees *et al.*	(BABAR Collab.)
ABLIKIM	10C	PL B685 27	M. Ablikim *et al.*	(BES II Collab.)
SHEN	09	PR D80 031101	C.P. Shen *et al.*	(BELLE Collab.)
ABLIKIM	08F	PRL 100 102003	M. Ablikim *et al.*	(BES Collab.)
AUBERT	08S	PR D77 092002	B. Aubert *et al.*	(BABAR Collab.)
AUBERT	07AK	PR D76 012008	B. Aubert *et al.*	(BABAR Collab.)
AUBERT,BE	06D	PR D74 091103	B. Aubert *et al.*	(BABAR Collab.)

$f_0(2200)$

$I^G(J^{PC}) = 0^+(0^{++})$

OMITTED FROM SUMMARY TABLE

Seen in $K^0_S K^0_S$ (AUGUSTIN 88), K^+K^- (ABLIKIM 05Q) and $\eta\eta$ (BINON 05) system. Not seen in $\Upsilon(1S)$ radiative decays (BARU 89).

$f_0(2200)$ MASS

VALUE (MeV)	EVTS	DOCUMENT ID		TECN	COMMENT
2189±13 OUR AVERAGE					
$2170\pm20^{+10}_{-15}$		ABLIKIM	05Q	BES2	$\psi(2S) \to \gamma\pi^+\pi^- K^+K^-$
2210±50		[1] BINON	05	GAMS	$33\ \pi^- p \to \eta\eta n$
2197±17		[2] AUGUSTIN	88	DM2	$J/\psi \to \gamma K^0_S K^0_S$
• • • We do not use the following data for averages, fits, limits, etc. • • •					
2206±12± 8	381	[3,4] DOBBS	15		$J/\psi \to \gamma K^+K^-$
2188±17±16	203	[3,4] DOBBS	15		$\psi(2S) \to \gamma K^+K^-$
~ 2122		HASAN	94	RVUE	$\overline{p}p \to \pi\pi$
~ 2321		HASAN	94	RVUE	$\overline{p}p \to \pi\pi$

[1] First solution, PWA is ambiguous.
[2] Cannot determine spin to be 0.
[3] Using CLEO-c data but not authored by the CLEO Collaboration.
[4] From a fit to a Breit-Wigner line shape with fixed Γ = 238 MeV.

$f_0(2200)$ WIDTH

VALUE (MeV)	DOCUMENT ID		TECN	COMMENT
238±50 OUR AVERAGE	Error includes scale factor of 1.2.			
$220\pm60^{+40}_{-45}$	ABLIKIM	05Q	BES2	$\psi(2S) \to \gamma\pi^+\pi^- K^+K^-$
380±90	[5] BINON	05	GAMS	$33\ \pi^- p \to \eta\eta n$
201±51	[6] AUGUSTIN	88	DM2	$J/\psi \to \gamma K^0_S K^0_S$
• • • We do not use the following data for averages, fits, limits, etc. • • •				
~ 273	HASAN	94	RVUE	$\overline{p}p \to \pi\pi$
~ 223	HASAN	94	RVUE	$\overline{p}p \to \pi\pi$

[5] First solution, PWA is ambiguous.
[6] Cannot determine spin to be 0.

$f_0(2200)$ REFERENCES

DOBBS	15	PR D91 052006	S. Dobbs *et al.*	(NWES)
ABLIKIM	05Q	PR D72 092002	M. Ablikim *et al.*	(BES Collab.)
BINON	05	PAN 68 960 Translated from YAF 68 998.	F. Binon *et al.*	
HASAN	94	PL B334 215	A. Hasan, D.V. Bugg	(LOQM)
BARU	89	ZPHY C42 505	S.E. Baru *et al.*	(NOVO)
AUGUSTIN	88	PRL 60 2238	J.E. Augustin *et al.*	(DM2 Collab.)

$f_J(2220)$

$I^G(J^{PC}) = 0^+(2^{++}$ or $4^{++})$

OMITTED FROM SUMMARY TABLE

Needs confirmation. See our mini-review in the 2004 edition of this *Review*, PDG 04.

$f_J(2220)$ MASS

VALUE (MeV)	EVTS	DOCUMENT ID		TECN	COMMENT
2231.1± 3.5 OUR AVERAGE					
2235 ± 4 ± 6	74	BAI	96B	BES	$e^+e^- \to J/\psi \to \gamma\pi^+\pi^-$
$2230\ ^{+\ 6}_{-\ 7}\ \pm16$	46	BAI	96B	BES	$e^+e^- \to J/\psi \to \gamma K^+K^-$
$2232\ ^{+\ 8}_{-\ 7}\ \pm15$	23	BAI	96B	BES	$e^+e^- \to J/\psi \to \gamma K^0_S K^0_S$
2235 ± 4 ± 5	32	BAI	96B	BES	$e^+e^- \to J/\psi \to \gamma p\overline{p}$
$2209\ ^{+17}_{-15}\ \pm10$		ASTON	88F	LASS	$11\ K^-p \to K^+K^-\Lambda$
2230 ±20		BOLONKIN	88	SPEC	$40\ \pi^- p \to K^0_S K^0_S n$
2220 ±10	41	[1] ALDE	86B	GA24	38–$100\ \pi p \to n\eta\eta'$
2230 ± 6 ±14	93	BALTRUSAIT...86D		MRK3	$e^+e^- \to \gamma K^+K^-$
2232 ± 7 ± 7	23	BALTRUSAIT...86D		MRK3	$e^+e^- \to \gamma K^0_S K^0_S$
• • • We do not use the following data for averages, fits, limits, etc. • • •					
2223.9± 2.5		[2] VLADIMIRSK...08		SPEC	$40\ \pi^- p \to K^0_S K^0_S n + m\pi^0$
2246 ±36		BAI	98H	BES	$J/\psi \to \gamma\pi^0\pi^0$

[1] ALDE 86B uses data from both the GAMS-2000 and GAMS-4000 detectors.
[2] $J^{PC} = 2^{++}$. Systematic uncertainties not evaluated

$f_J(2220)$ WIDTH

VALUE (MeV)	CL%	EVTS	DOCUMENT ID		TECN	COMMENT
$23^{+\ 8}_{-\ 7}$ OUR AVERAGE						
$19^{+\ 13}_{-\ 11}\pm12$		74	BAI	96B	BES	$e^+e^- \to J/\psi \to \gamma\pi^+\pi^-$
$20^{+\ 20}_{-\ 15}\pm17$		46	BAI	96B	BES	$e^+e^- \to J/\psi \to \gamma K^+K^-$
$20^{+\ 25}_{-\ 16}\pm14$		23	BAI	96B	BES	$e^+e^- \to J/\psi \to \gamma K^0_S K^0_S$
$15^{+\ 12}_{-\ 9}\pm\ 9$		32	BAI	96B	BES	$e^+e^- \to J/\psi \to \gamma p\overline{p}$
$60^{+107}_{-\ 57}$			ASTON	88F	LASS	$11\ K^-p \to K^+K^-\Lambda$
80± 30			BOLONKIN	88	SPEC	$40\ \pi^- p \to K^0_S K^0_S n$
$26^{+\ 20}_{-\ 16}\pm17$		93	BALTRUSAIT...86D		MRK3	$e^+e^- \to \gamma K^+K^-$
$18^{+\ 23}_{-\ 15}\pm10$		23	BALTRUSAIT...86D		MRK3	$e^+e^- \to \gamma K^0_S K^0_S$
• • • We do not use the following data for averages, fits, limits, etc. • • •						
8.6 ± 2.5			[1] VLADIMIRSK...08		SPEC	$40\ \pi^- p \to K^0_S K^0_S n + m\pi^0$
<80	90		ALDE	87C	GAM2	$38\ \pi^- p \to \eta'\eta n$

[1] $J^{PC} = 2^{++}$. Systematic uncertainties not evaluated

$f_J(2220)$ DECAY MODES

	Mode	Fraction (Γ_j/Γ)
Γ_1	$\pi\pi$	not seen
Γ_2	$\pi^+\pi^-$	not seen
Γ_3	$K\overline{K}$	not seen
Γ_4	$p\overline{p}$	not seen
Γ_5	$\gamma\gamma$	not seen
Γ_6	$\eta\eta'(958)$	seen
Γ_7	$\phi\phi$	not seen
Γ_8	$\eta\eta$	not seen

$f_J(2220)$ Γ(i)$\Gamma(\gamma\gamma)/\Gamma$(total)

$\Gamma(K\overline{K}) \times \Gamma(\gamma\gamma)/\Gamma_{\text{total}}$ $\quad \Gamma_3\Gamma_5/\Gamma$

VALUE (eV)	CL%	DOCUMENT ID		TECN	COMMENT
< 1.4	95	[1] ACCIARRI	01H	L3	$\gamma\gamma \to K^0_S K^0_S$, E^{ee}_{cm}= 91, 183–209 GeV
• • • We do not use the following data for averages, fits, limits, etc. • • •					
< 5.6	95	[1] GODANG	97	CLE2	$\gamma\gamma \to K^0_S K^0_S$
< 86	95	[1] ALBRECHT	90G	ARG	$\gamma\gamma \to K^+K^-$
<1000	95	[2] ALTHOFF	85B	TASS	$\gamma\gamma$, $K\overline{K}\pi$

$\Gamma(\pi\pi) \times \Gamma(\gamma\gamma)/\Gamma_{\text{total}}$ $\quad \Gamma_1\Gamma_5/\Gamma$

VALUE (eV)	CL%	DOCUMENT ID		TECN	COMMENT
<2.5	95	ALAM	98C	CLE2	$\gamma\gamma \to \pi^+\pi^-$

[1] Assuming $J^P = 2^+$.
[2] True for $J^P = 0^+$ and $J^P = 2^+$.

$f_J(2220)$ Γ(i)$\Gamma(p\overline{p})/\Gamma^2$(total)

$\Gamma(p\overline{p})/\Gamma_{\text{total}} \times \Gamma(\pi\pi)/\Gamma_{\text{total}}$ $\quad \Gamma_4/\Gamma \times \Gamma_1/\Gamma$

VALUE (units 10^{-5})	CL%	DOCUMENT ID		TECN	COMMENT
<18	95	[1] AMSLER	01	CBAR	1.4–1.5 $p\overline{p} \to \pi^0\pi^0$
• • • We do not use the following data for averages, fits, limits, etc. • • •					
<(11–42)	99	[2] HASAN	96	SPEC	1.35–1.55 $p\overline{p} \to \pi^+\pi^-$

$\Gamma(p\overline{p})/\Gamma_{\text{total}} \times \Gamma(\phi\phi)/\Gamma_{\text{total}}$ $\quad \Gamma_4/\Gamma \times \Gamma_7/\Gamma$

VALUE (units 10^{-5})	CL%	DOCUMENT ID		TECN	COMMENT
<6	95	[3] EVANGELIS...	98	SPEC	1.1–2.0 $p\overline{p} \to \phi\phi$

$\Gamma(p\overline{p})/\Gamma_{\text{total}} \times \Gamma(\eta\eta)/\Gamma_{\text{total}}$ $\quad \Gamma_4/\Gamma \times \Gamma_8/\Gamma$

VALUE (units 10^{-5})	CL%	DOCUMENT ID		TECN	COMMENT
<4	95	[1] AMSLER	01	CBAR	1.4–1.5 $p\overline{p} \to \eta\eta$

[1] For $J^P = 2^+$ in the mass range 2222–2240 MeV and the total width between 10 and 20 MeV.
[2] For $J^P = 2^+$ and $J^P = 4^+$ in the mass range 2220–2245 MeV and the total width of 15 MeV.
[3] For $J^P = 2^+$, the mass of 2235 MeV and the total width of 15 MeV.

Meson Particle Listings

$f_J(2220)$, $\eta(2225)$, $\rho_3(2250)$

$f_J(2220)$ BRANCHING RATIOS

$\Gamma(\pi\pi)/\Gamma_{total}$ — **Γ_1/Γ**

VALUE	DOCUMENT ID		COMMENT
not seen	[1] DOBBS	15	$J/\psi \to \gamma\pi\pi$
not seen	[1] DOBBS	15	$\psi(2S) \to \gamma\pi\pi$

[1] Using CLEO-c data but not authored by the CLEO Collaboration.

$\Gamma(K\overline{K})/\Gamma_{total}$ — **Γ_3/Γ**

VALUE	DOCUMENT ID		COMMENT
not seen	[1] DOBBS	15	$J/\psi \to \gamma K\overline{K}$
not seen	[1] DOBBS	15	$\psi(2S) \to \gamma K\overline{K}$

[1] Using CLEO-c data but not authored by the CLEO Collaboration.

$\Gamma(\pi\pi)/\Gamma(K\overline{K})$ — **Γ_1/Γ_3**

VALUE	DOCUMENT ID		TECN	COMMENT
1.0±0.5	BAI	96B	BES	$e^+e^- \to J/\psi \to \gamma 2\pi, K\overline{K}$

$\Gamma(p\overline{p})/\Gamma_{total}$ — **Γ_4/Γ**

VALUE (units 10^{-4})	CL%	DOCUMENT ID		TECN	COMMENT
• • • We do not use the following data for averages, fits, limits, etc. • • •					
not seen		[1] AUBERT	07AV	BABR	$B \to p\overline{p}K^{(*)}$
not seen		WANG	05A	BELL	$B^+ \to \overline{p}pK^+$
<3.0	95	[2] EVANGELIS...	97	SPEC	1.96–2.40 $\overline{p}p \to K^0_S K^0_S$
<1.1	99.7	[3] BARNES	93	SPEC	1.3–1.57 $\overline{p}p \to K^0_S K^0_S$
<2.6	99.7	[3] BARDIN	87	CNTR	1.3–1.5 $\overline{p}p \to K^+K^-$
<3.6	99.7	[3] SCULLI	87	CNTR	1.29–1.55 $\overline{p}p \to K^+K^-$

[1] Assuming $\Gamma < 30$ MeV.
[2] Assuming $\Gamma \sim 20$ MeV, $J^P = 2^+$ and B($f_J(2220) \to K\overline{K}$) = 100%.
[3] Assuming Γ = 30-35 MeV, $J^P = 2^+$ and B($f_J(2220) \to K\overline{K}$) = 100%.

$\Gamma(p\overline{p})/\Gamma(K\overline{K})$ — **Γ_4/Γ_3**

VALUE	DOCUMENT ID		TECN	COMMENT
0.17±0.09	BAI	96B	BES	$e^+e^- \to J/\psi \to \gamma p\overline{p}, K\overline{K}$

$f_J(2220)$ REFERENCES

DOBBS	15	PR D91 052006	S. Dobbs *et al.*	(NWES)
VLADIMIRSK...	08	PAN 71 2129	V.V. Vladimirsky *et al.*	(ITEP)
		Translated from YAF 71 2166.		
AUBERT	07AV	PR D76 092004	B. Aubert *et al.*	(BABAR Collab.)
WANG	05A	PL B617 141	M.-Z. Wang *et al.*	(BELLE Collab.)
PDG	04	PL B592 1	S. Eidelman *et al.*	(PDG Collab.)
ACCIARRI	01H	PL B501 173	M. Acciarri *et al.*	(L3 Collab.)
AMSLER	01	PL B520 175	C. Amsler *et al.*	(Crystal Barrel Collab.)
ALAM	98C	PRL 81 3328	M.S. Alam *et al.*	(CLEO Collab.)
BAI	98H	PRL 81 1179	J.Z. Bai *et al.*	(BES Collab.)
EVANGELIS...	98	PR D57 5370	C. Evangelista *et al.*	(JETSET Collab.)
EVANGELIS...	97	PR D56 3803	C. Evangelista *et al.*	(LEAR Collab.)
GODANG	97	PRL 79 3829	R. Godang *et al.*	(CLEO Collab.)
BAI	96B	PRL 76 3502	J.Z. Bai *et al.*	(BES Collab.)
HASAN	96	PL B388 376	A. Hasan, D.V. Bugg	(BRUN, LOQM)
BARNES	93	PL B309 469	P.D. Barnes *et al.*	(PS185 Collab.)
ALBRECHT	90G	ZPHY C48 183	H. Albrecht *et al.*	(ARGUS Collab.)
ASTON	88F	PL B215 199	D. Aston *et al.*	(SLAC, NAGO, CINC, INUS) JP
BOLONKIN	88	NP B309 426	B.V. Bolonkin *et al.*	(ITEP, SERP)
ALDE	87C	SJNP 45 255	D. Alde *et al.*	
		Translated from YAF 45 405.		
BARDIN	87	PL B195 292	G. Bardin *et al.*	(SACL, FERR, CERN, PADO+)
SCULLI	87	PRL 58 1715	J. Sculli *et al.*	(NYU, BNL)
ALDE	86B	PL B177 120	D.M. Alde *et al.*	(SERP, BELG, LANL, LAPP)
BALTRUSAIT...	86D	PRL 56 107	R.M. Baltrusaitis	(CIT, UCSC, ILL, SLAC+)
ALTHOFF	85B	ZPHY C29 189	M. Althoff *et al.*	(TASSO Collab.)

OTHER RELATED PAPERS

DEL-AMO-SA...	10O	PRL 105 172001	P. del Amo Sanchez *et al.*	(BABAR Collab.)

$\eta(2225)$

$I^G(J^{PC}) = 0^+(0^{-+})$

OMITTED FROM SUMMARY TABLE

Seen in $J/\psi \to \gamma\phi\phi$. Possibly seen in $B \to \phi\phi K$ by LEES 11A.

$\eta(2225)$ MASS

VALUE (MeV)	EVTS	DOCUMENT ID		TECN	COMMENT
2221^{+13}_{-10} OUR AVERAGE					
$2216^{+\ 4+21}_{-\ 5-11}$		[1] ABLIKIM	16N	BES3	$J/\psi \to \gamma K^+K^-K^+K^-$
2240^{+30+30}_{-20-20}	196 ± 19	ABLIKIM	08I	BES	$J/\psi \to \gamma K^+K^-K^0_S K^0_L$
2230±25±15		BAI	90B	MRK3	$J/\psi \to \gamma K^+K^-K^+K^-$
2214±20±13		BAI	90B	MRK3	$J/\psi \to \gamma K^+K^-K^0_S K^0_L$
• • • We do not use the following data for averages, fits, limits, etc. • • •					
~ 2220		BISELLO	86B	DM2	$J/\psi \to \gamma K^+K^-K^+K^-$

[1] From a partial wave analysis of $J/\psi \to \gamma\phi\phi$ that also finds significant signals for for $\eta(2100)$, 0^{-+} phase space, $f_0(2100)$, $f_2(2010)$, $f_2(2300)$, $f_2(2340)$, and a previously unseen 0^{-+} state $X(2500)$ (M = $2470^{+15}_{-19}{}^{+101}_{-\ 23}$ MeV, $\Gamma = 230^{+64}_{-35}{}^{+56}_{-33}$ MeV).

$\eta(2225)$ WIDTH

VALUE (MeV)	EVTS	DOCUMENT ID		TECN	COMMENT
$185^{+\ 40}_{-\ 20}$ OUR AVERAGE					
$185^{+\ 12+43}_{-\ 14-17}$		[1] ABLIKIM	16N	BES3	$J/\psi \to \gamma K^+K^-K^+K^-$
$190^{+\ 30+60}_{-\ 40}$	196 ± 19	ABLIKIM	08I	BES	$J/\psi \to \gamma K^+K^-K^0_S K^0_L$
$150^{+300}_{-\ 60}$±60		BAI	90B	MRK3	$J/\psi \to \gamma K^+K^-K^+K^-$
• • • We do not use the following data for averages, fits, limits, etc. • • •					
~ 80		BISELLO	86B	DM2	$J/\psi \to \gamma K^+K^-K^+K^-$

[1] From a partial wave analysis of $J/\psi \to \gamma\phi\phi$ that also finds significant signals for for $\eta(2100)$, 0^{-+} phase space, $f_0(2100)$, $f_2(2010)$, $f_2(2300)$, $f_2(2340)$, and a previously unseen 0^{-+} state $X(2500)$ (M = $2470^{+15}_{-19}{}^{+101}_{-\ 23}$ MeV, $\Gamma = 230^{+64}_{-35}{}^{+56}_{-33}$ MeV).

$\eta(2225)$ REFERENCES

ABLIKIM	16N	PR D93 112011	M. Ablikim	(BES III Collab.)
LEES	11A	PR D84 012001	J.P. Lees *et al.*	(BABAR Collab.)
ABLIKIM	08I	PL B662 330	M. Ablikim *et al.*	(BES Collab.)
BAI	90B	PRL 65 1309	Z. Bai *et al.*	(Mark III Collab.)
BISELLO	86B	PL B179 294	D. Bisello *et al.*	(DM2 Collab.)

$\rho_3(2250)$

$I^G(J^{PC}) = 1^+(3^{--})$

OMITTED FROM SUMMARY TABLE

Contains results mostly from formation experiments. For further production experiments see the Further States entry. See also $\rho(2150)$, $f_2(2150)$, $f_4(2300)$, $\rho_5(2350)$.

$\rho_3(2250)$ MASS

$\overline{p}p \to \pi\pi$ or $K\overline{K}$

VALUE (MeV)	DOCUMENT ID		TECN	CHG	COMMENT
• • • We do not use the following data for averages, fits, limits, etc. • • •					
~ 2232	HASAN	94	RVUE		$\overline{p}p \to \pi\pi$
~ 2090	[1] OAKDEN	94	RVUE		0.36–1.55 $\overline{p}p \to \pi\pi$
~ 2250	[2] MARTIN	80B	RVUE		
~ 2300	[2] MARTIN	80C	RVUE		
~ 2140	[3] CARTER	78B	CNTR	0	0.7–2.4 $\overline{p}p \to K^-K^+$
~ 2150	[4] CARTER	77	CNTR	0	0.7–2.4 $\overline{p}p \to \pi\pi$

[1] See however KLOET 96 who fit $\pi^+\pi^-$ only and find waves only up to $J = 3$ to be important but not significantly resonant.
[2] $I(J^P) = 1(3^-)$ from simultaneous analysis of $p\overline{p} \to \pi^-\pi^+$ and $\pi^0\pi^0$.
[3] $I = 0, 1$. $J^P = 3^-$ from Barrelet-zero analysis.
[4] $I(J^P) = 1(3^-)$ from amplitude analysis.

S-CHANNEL $\overline{N}N$

VALUE (MeV)	DOCUMENT ID		TECN	CHG	COMMENT
• • • We do not use the following data for averages, fits, limits, etc. • • •					
2260±20	[5] ANISOVICH	02	SPEC		0.6–1.9 $p\overline{p} \to \omega\pi^0$, $\omega\eta\pi^0$, $\pi^+\pi^-$
~ 2190	[6] CUTTS	78B	CNTR		0.97–3 $\overline{p}p \to \overline{N}N$
2155±15	[6,7] COUPLAND	77	CNTR	0	0.7–2.4 $\overline{p}p \to \overline{p}p$
2193± 2	[6,8] ALSPECTOR	73	CNTR		$\overline{p}p$ S channel
2190±10	[9] ABRAMS	70	CNTR		S channel $\overline{p}N$

[5] From the combined analysis of ANISOVICH 00J, ANISOVICH 01D, ANISOVICH 01E, and ANISOVICH 02.
[6] Isospins 0 and 1 not separated.
[7] From a fit to the total elastic cross section.
[8] Referred to as T or T' region by ALSPECTOR 73.
[9] Seen as bump in $I = 1$ state. See also COOPER 68. PEASLEE 75 confirm $\overline{p}p$ results of ABRAMS 70, no narrow structure.

$\pi^-p \to \eta\pi\pi$

VALUE (MeV)	DOCUMENT ID		TECN	COMMENT
• • • We do not use the following data for averages, fits, limits, etc. • • •				
2290±20±30	AMELIN	00	VES	37 $\pi^-p \to \eta\pi^+\pi^-n$

$\rho_3(2250)$ WIDTH

$\overline{p}p \to \pi\pi$ or $K\overline{K}$

VALUE (MeV)	DOCUMENT ID		TECN	CHG	COMMENT
• • • We do not use the following data for averages, fits, limits, etc. • • •					
~ 220	HASAN	94	RVUE		$\overline{p}p \to \pi\pi$
~ 60	[10] OAKDEN	94	RVUE		0.36–1.55 $\overline{p}p \to \pi\pi$
~ 250	[11] MARTIN	80B	RVUE		
~ 200	[11] MARTIN	80C	RVUE		
~ 150	[12] CARTER	78B	CNTR	0	0.7–2.4 $\overline{p}p \to K^-K^+$
~ 200	[13] CARTER	77	CNTR	0	0.7–2.4 $\overline{p}p \to \pi\pi$

[10] See however KLOET 96 who fit $\pi^+\pi^-$ only and find waves only up to $J = 3$ to be important but not significantly resonant.

[11] $I(J^P) = 1(3^-)$ from simultaneous analysis of $p\overline{p} \to \pi^-\pi^+$ and $\pi^0\pi^0$.
[12] $I = 0, 1$. $J^P = 3^-$ from Barrelet-zero analysis.
[13] $I(J^P) = 1(3^-)$ from amplitude analysis.

S-CHANNEL $\overline{N}N$

VALUE (MeV)	DOCUMENT ID		TECN	CHG	COMMENT
• • • We do not use the following data for averages, fits, limits, etc. • • •					
160±25	[14] ANISOVICH	02	SPEC		0.6–1.9 $p\overline{p} \to \omega\pi^0$, $\omega\eta\pi^0$, $\pi^+\pi^-$
135±75	[15,16] COUPLAND	77	CNTR	0	0.7–2.4 $\overline{p}p \to \overline{p}p$
98± 8	[16] ALSPECTOR	73	CNTR		$\overline{p}p$ S channel
~ 85	[17] ABRAMS	70	CNTR		S channel $\overline{p}N$

[14] From the combined analysis of ANISOVICH 00J, ANISOVICH 01D, ANISOVICH 01E, and ANISOVICH 02.
[15] From a fit to the total elastic cross section.
[16] Isospins 0 and 1 not separated.
[17] Seen as bump in $I = 1$ state. See also COOPER 68. PEASLEE 75 confirm $\overline{p}p$ results of ABRAMS 70, no narrow structure.

$\pi^- p \to \eta\pi\pi$

VALUE (MeV)	DOCUMENT ID		TECN	COMMENT
• • • We do not use the following data for averages, fits, limits, etc. • • •				
230±50±80	AMELIN	00	VES	37 $\pi^- p \to \eta\pi^+\pi^- n$

$\rho_3(2250)$ REFERENCES

ANISOVICH	02	PL B542 8	A.V. Anisovich et al.	
ANISOVICH	01D	PL B508 6	A.V. Anisovich et al.	
ANISOVICH	01E	PL B513 281	A.V. Anisovich et al.	
AMELIN	00	NP A668 83	D. Amelin et al.	(VES Collab.)
ANISOVICH	00J	PL B491 47	A.V. Anisovich et al.	
KLOET	96	PR D53 6120	W.M. Kloet, F. Myhrer	(RUTG, NORD)
HASAN	94	PL B334 215	A. Hasan, D.V. Bugg	(LOQM)
OAKDEN	94	NP A574 731	M.N. Oakden, M.R. Pennington	(DURH)
MARTIN	80B	NP B176 355	B.R. Martin, D. Morgan	(LOUC, RHEL) JP
MARTIN	80C	NP B169 216	A.D. Martin, M.R. Pennington	(DURH) JP
CARTER	78B	NP B141 467	A.A. Carter	(LOQM)
CUTTS	78B	PR D17 16	D. Cutts et al.	(STON, WISC)
CARTER	77	PL 67B 117	A.A. Carter et al.	(LOQM, RHEL) JP
COUPLAND	77	PL 71B 460	M. Coupland et al.	(LOQM, RHEL)
PEASLEE	75	PL 57B 189	D.C. Peaslee et al.	(CANB, BARI, BROW+)
ALSPECTOR	73	PRL 30 511	J. Alspector et al.	(RUTG, UPNJ)
ABRAMS	70	PR D1 1917	R.J. Abrams et al.	(BNL)
COOPER	68	PRL 20 1059	W.A. Cooper et al.	(ANL)

$f_2(2300)$

$I^G(J^{PC}) = 0^+(2^{++})$

$f_2(2300)$ MASS

VALUE (MeV)	DOCUMENT ID		TECN	COMMENT
2297±28	[1] ETKIN	88	MPS	22 $\pi^- p \to \phi\phi n$
• • • We do not use the following data for averages, fits, limits, etc. • • •				
$2243^{+\ 7}_{-\ 6}{}^{+\ 3}_{-29}$	UEHARA	13	BELL	$\gamma\gamma \to K^0_S K^0_S$
2270±12	VLADIMIRSK...06		SPEC	40 $\pi^- p \to K^0_S K^0_S n$
2327± 9± 6	ABE	04	BELL	10.6 $e^+e^- \to e^+e^- K^+K^-$
2231±10	BOOTH	86	OMEG	85 π^-Be $\to 2\phi$Be
$2220^{+\ 90}_{-\ 20}$	LINDENBAUM	84	RVUE	
2320±40	ETKIN	82	MPS	22 $\pi^- p \to 2\phi n$

[1] Includes data of ETKIN 85. The percentage of the resonance going into $\phi\phi$ 2^{++} S_2, D_2, and D_0 is $6^{+15}_{-\ 5}$, 25^{+18}_{-14}, and 69^{+16}_{-27}, respectively.

$f_2(2300)$ WIDTH

VALUE (MeV)	DOCUMENT ID		TECN	COMMENT
149±41	[2] ETKIN	88	MPS	22 $\pi^- p \to \phi\phi n$
• • • We do not use the following data for averages, fits, limits, etc. • • •				
$145 \pm 12^{+27}_{-34}$	UEHARA	13	BELL	$\gamma\gamma \to K^0_S K^0_S$
90±29	VLADIMIRSK...06		SPEC	40 $\pi^- p \to K^0_S K^0_S n$
275±36±20	ABE	04	BELL	10.6 $e^+e^- \to e^+e^- K^+K^-$
133±50	BOOTH	86	OMEG	85 π^-Be $\to 2\phi$Be
200±50	LINDENBAUM	84	RVUE	
220±70	ETKIN	82	MPS	22 $\pi^- p \to 2\phi n$

[2] Includes data of ETKIN 85.

$f_2(2300)$ DECAY MODES

	Mode	Fraction (Γ_i/Γ)
Γ_1	$\phi\phi$	seen
Γ_2	$K\overline{K}$	seen
Γ_3	$\gamma\gamma$	seen

$f_2(2300)$ Γ(i)$\Gamma(\gamma\gamma)/\Gamma$(total)

$\Gamma(K\overline{K}) \times \Gamma(\gamma\gamma)/\Gamma_{total}$				$\Gamma_2\Gamma_3/\Gamma$
VALUE (eV)	DOCUMENT ID		TECN	COMMENT
• • • We do not use the following data for averages, fits, limits, etc. • • •				
$3.2^{+0.5}_{-0.4} \pm 1.3$	UEHARA	13	BELL	$\gamma\gamma \to K^0_S K^0_S$
44 ±6 ±12	[3] ABE	04	BELL	10.6 $e^+e^- \to e^+e^- K^+K^-$

[3] Assuming spin 2.

$f_2(2300)$ REFERENCES

UEHARA	13	PTEP 2013 123C01	S. Uehara et al.	(BELLE Collab.)
VLADIMIRSK...	06	PAN 69 493 Translated from YAF 69 515.	V.V. Vladimirsky et al.	(ITEP, Moscow)
ABE	04	EPJ C32 323	K. Abe et al.	(BELLE Collab.)
ETKIN	88	PL B201 568	A. Etkin et al.	(BNL, CUNY)
BOOTH	86	NP B273 677	P.S.L. Booth et al.	(LIVP, GLAS, CERN)
ETKIN	85	PL 165B 217	A. Etkin et al.	(BNL, CUNY)
LINDENBAUM	84	CNPP 13 285	S.J. Lindenbaum	(CUNY)
ETKIN	82	PRL 49 1620	A. Etkin et al.	(BNL, CUNY)

$f_4(2300)$

$I^G(J^{PC}) = 0^+(4^{++})$

OMITTED FROM SUMMARY TABLE

This entry was previously called $U_0(2350)$. Contains results mostly from formation experiments. For further production experiments see the Further States entry. See also $\rho(2150)$, $f_2(2150)$, $\rho_3(2250)$, $\rho_5(2350)$.

$f_4(2300)$ MASS

$\overline{p}p \to \pi\pi$ or $\overline{K}K$

VALUE (MeV)	DOCUMENT ID		TECN	COMMENT
• • • We do not use the following data for averages, fits, limits, etc. • • •				
~ 2314	HASAN	94	RVUE	$\overline{p}p \to \pi\pi$
~ 2300	[1] MARTIN	80B	RVUE	
~ 2300	[1] MARTIN	80C	RVUE	
~ 2340	[2] CARTER	78B	CNTR	0.7–2.4 $\overline{p}p \to K^-K^+$
~ 2330	DULUDE	78B	OSPK	1–2 $\overline{p}p \to \pi^0\pi^0$
~ 2310	[3] CARTER	77	CNTR	0.7–2.4 $\overline{p}p \to \pi\pi$

[1] $I(J^P) = 0(4^+)$ from simultaneous analysis of $p\overline{p} \to \pi^-\pi^+$ and $\pi^0\pi^0$.
[2] $I(J^P) = 0(4^+)$ from Barrelet-zero analysis.
[3] $I(J^P) = 0(4^+)$ from amplitude analysis.

S-CHANNEL $\overline{p}p$ or $\overline{N}N$

VALUE (MeV)	DOCUMENT ID		TECN	COMMENT
• • • We do not use the following data for averages, fits, limits, etc. • • •				
2283±17	[4] ANISOVICH	00J	SPEC	
~ 2380	[5] CUTTS	78B	CNTR	0.97–3 $\overline{p}p \to \overline{N}N$
2345±15	[5,6] COUPLAND	77	CNTR	0.7–2.4 $\overline{p}p \to \overline{p}p$
2359± 2	[5,7] ALSPECTOR	73	CNTR	$\overline{p}p$ S channel
2375±10	ABRAMS	70	CNTR	S channel $\overline{N}N$

[4] From the combined analysis of ANISOVICH 99C and ANISOVICH 99F on $\overline{p}p \to \eta\pi^0\pi^0$, $\pi^0\pi^0$, $\eta\eta$, $\eta\eta'$, $\pi^+\pi^-$.
[5] Isospins 0 and 1 not separated.
[6] From a fit to the total elastic cross section.
[7] Referred to as U or U region by ALSPECTOR 73.

$\pi^- p \to \eta\pi\pi n$

VALUE (MeV)	DOCUMENT ID		TECN	COMMENT
• • • We do not use the following data for averages, fits, limits, etc. • • •				
2330±20±40	AMELIN	00	VES	37 $\pi^- p \to \eta\pi^+\pi^- n$

pp CENTRAL PRODUCTION

VALUE (MeV)	DOCUMENT ID		TECN	COMMENT
2320±60 OUR ESTIMATE				
• • • We do not use the following data for averages, fits, limits, etc. • • •				
2332±15	BARBERIS	00F		450 $pp \to p_f \omega\omega p_s$

$f_4(2300)$ WIDTH

$\overline{p}p \to \pi\pi$ or $\overline{K}K$

VALUE (MeV)	DOCUMENT ID		TECN	COMMENT
• • • We do not use the following data for averages, fits, limits, etc. • • •				
~ 278	HASAN	94	RVUE	$\overline{p}p \to \pi\pi$
~ 200	[8] MARTIN	80C	RVUE	
~ 150	[9] CARTER	78B	CNTR	0.7–2.4 $\overline{p}p \to K^-K^+$
~ 210	[10] CARTER	77	CNTR	0.7–2.4 $\overline{p}p \to \pi\pi$

[8] $I(J^P) = 0(4^+)$ from simultaneous analysis of $p\overline{p} \to \pi^-\pi^+$ and $\pi^0\pi^0$.
[9] $I(J^P) = 0(4^+)$ from Barrelet-zero analysis.
[10] $I(J^P) = 0(4^+)$ from amplitude analysis.

Meson Particle Listings

$f_4(2300)$, $f_0(2330)$, $f_2(2340)$, $\rho_5(2350)$

S-CHANNEL $\overline{p}p$ or $\overline{N}N$

VALUE (MeV)	DOCUMENT ID		TECN	COMMENT
• • • We do not use the following data for averages, fits, limits, etc. • • •				
310 ± 25	[11] ANISOVICH	00J	SPEC	
135^{+150}_{-65}	[12,13] COUPLAND	77	CNTR	0.7–2.4 $\overline{p}p \to \overline{p}p$
165^{+18}_{-8}	[13] ALSPECTOR	73	CNTR	$\overline{p}p$ S channel
~ 190	ABRAMS	70	CNTR	S channel $\overline{N}N$

[11] From the combined analysis of ANISOVICH 99C and ANISOVICH 99F on $\overline{p}p \to \eta\pi^0\pi^0$, $\pi^0\pi^0$, $\eta\eta$, $\eta\eta'$, $\pi^+\pi^-$.
[12] From a fit to the total elastic cross section.
[13] Isospins 0 and 1 not separated.

$\pi^- p \to \eta\pi\pi n$

VALUE (MeV)	DOCUMENT ID		TECN	COMMENT
• • • We do not use the following data for averages, fits, limits, etc. • • •				
$235 \pm 50 \pm 40$	AMELIN	00	VES	37 $\pi^- p \to \eta\pi^+\pi^- n$

pp CENTRAL PRODUCTION

VALUE (MeV)	DOCUMENT ID		COMMENT
250±80 OUR ESTIMATE			
• • • We do not use the following data for averages, fits, limits, etc. • • •			
260 ± 57	BARBERIS	00F	450 $pp \to p_f\omega\omega p_s$

$f_4(2300)$ DECAY MODES

	Mode	Fraction (Γ_i/Γ)
Γ_1	$\rho\rho$	seen
Γ_2	$\omega\omega$	seen
Γ_3	$\eta\pi\pi$	seen
Γ_4	$\pi\pi$	seen
Γ_5	$K\overline{K}$	seen
Γ_6	$N\overline{N}$	seen

$f_4(2300)$ BRANCHING RATIOS

$\Gamma(\rho\rho)/\Gamma(\omega\omega)$ **Γ_1/Γ_2**

VALUE	DOCUMENT ID		COMMENT
• • • We do not use the following data for averages, fits, limits, etc. • • •			
2.8 ± 0.5	BARBERIS	00F	450 $pp \to p_f\omega\omega p_s$

$f_4(2300)$ REFERENCES

AMELIN	00	NP A668 83	D. Amelin *et al.*	(VES Collab.)
ANISOVICH	00J	PL B491 47	A.V. Anisovich *et al.*	
BARBERIS	00F	PL B484 198	D. Barberis *et al.*	(WA 102 Collab.)
ANISOVICH	99C	PL B452 173	A.V. Anisovich *et al.*	
ANISOVICH	99F	NP A651 253	A.V. Anisovich *et al.*	
HASAN	94	PL B334 215	A. Hasan, D.V. Bugg	(LOQM)
MARTIN	80B	NP B176 355	B.R. Martin, D. Morgan	(LOUC, RHEL) JP
MARTIN	80C	NP B169 216	A.D. Martin, M.R. Pennington	(DURH) JP
CARTER	78B	NP B141 467	A.A. Carter	(LOQM)
CUTTS	78B	PR D17 16	D. Cutts *et al.*	(STON, WISC)
DULUDE	78B	PL 79B 335	R.S. Dulude *et al.*	(BROW, MIT, BARI) JP
CARTER	77	PL 67B 117	A.A. Carter *et al.*	(LOQM, RHEL) JP
COUPLAND	77	PL 71B 460	M. Coupland *et al.*	(LOQM, RHEL)
ALSPECTOR	73	PRL 30 511	J. Alspector *et al.*	(RUTG, UPNJ)
ABRAMS	70	PR D1 1917	R.J. Abrams *et al.*	(BNL)

$f_0(2330)$

$I^G(J^{PC}) = 0^+(0^{++})$

OMITTED FROM SUMMARY TABLE

$f_0(2330)$ MASS

VALUE (MeV)	DOCUMENT ID		TECN	COMMENT
• • • We do not use the following data for averages, fits, limits, etc. • • •				
2314 ± 25	[1] BUGG	04A	RVUE	
2337 ± 14	ANISOVICH	00J	SPEC	2.0 $\overline{p}p \to \pi\pi, \eta\eta$
~ 2321	HASAN	94	RVUE	$\overline{p}p \to \pi\pi$

[1] Partial wave analysis of the data on $p\overline{p} \to \overline{\Lambda}\Lambda$ from BARNES 00.

$f_0(2330)$ WIDTH

VALUE (MeV)	DOCUMENT ID		TECN	COMMENT
• • • We do not use the following data for averages, fits, limits, etc. • • •				
144 ± 20	[2] BUGG	04A	RVUE	
217 ± 33	ANISOVICH	00J	SPEC	2.0 $\overline{p}p \to \pi\pi, \eta\eta$
~ 223	HASAN	94	RVUE	$\overline{p}p \to \pi\pi$

[2] Partial wave analysis of the data on $p\overline{p} \to \overline{\Lambda}\Lambda$ from BARNES 00.

$f_0(2330)$ REFERENCES

BUGG	04A	EPJ C36 161	D.V. Bugg	
ANISOVICH	00J	PL B491 47	A.V. Anisovich *et al.*	
BARNES	00	PR C62 055203	P.D. Barnes *et al.*	
HASAN	94	PL B334 215	A. Hasan, D.V. Bugg	(LOQM)

$f_2(2340)$

$I^G(J^{PC}) = 0^+(2^{++})$

$f_2(2340)$ MASS

VALUE (MeV)	EVTS	DOCUMENT ID		TECN	COMMENT
2345^{+50}_{-40} OUR AVERAGE					
$2362^{+31+140}_{-30-63}$	5.5k	[1] ABLIKIM	13N	BES3	$e^+e^- \to J/\psi \to \gamma\eta\eta$
2339 ± 55		[2] ETKIN	88	MPS	22 $\pi^- p \to \phi\phi n$
• • • We do not use the following data for averages, fits, limits, etc. • • •					
2350 ± 7	80k	[3] UMAN	06	E835	5.2 $\overline{p}p \to \eta\eta\pi^0$
2392 ± 10		BOOTH	86	OMEG	85 π^-Be $\to 2\phi$Be
2360 ± 20		LINDENBAUM	84	RVUE	

[1] From partial wave analysis including all possible combinations of 0^{++}, 2^{++}, and 4^{++} resonances.
[2] Includes data of ETKIN 85. The percentage of the resonance going into $\phi\phi\, 2^{++}\, S_2$, D_2, and D_0 is 37 ± 19, 4^{+12}_{-4}, and 59^{+21}_{-19}, respectively.
[3] Statistical error only.

$f_2(2340)$ WIDTH

VALUE (MeV)	EVTS	DOCUMENT ID		TECN	COMMENT
322^{+70}_{-60} OUR AVERAGE					
$334^{+62+165}_{-54-100}$	5.5k	[4] ABLIKIM	13N	BES3	$e^+e^- \to J/\psi \to \gamma\eta\eta$
319^{+81}_{-69}		[5] ETKIN	88	MPS	22 $\pi^- p \to \phi\phi n$
• • • We do not use the following data for averages, fits, limits, etc. • • •					
218 ± 16	80k	[6] UMAN	06	E835	5.2 $\overline{p}p \to \eta\eta\pi^0$
198 ± 50		BOOTH	86	OMEG	85 π^-Be $\to 2\phi$Be
150^{+150}_{-50}		LINDENBAUM	84	RVUE	

[4] From partial wave analysis including all possible combinations of 0^{++}, 2^{++}, and 4^{++} resonances.
[5] Includes data of ETKIN 85.
[6] Statistical error only.

$f_2(2340)$ DECAY MODES

	Mode	Fraction (Γ_i/Γ)
Γ_1	$\phi\phi$	seen
Γ_2	$\eta\eta$	seen

$f_2(2340)$ BRANCHING RATIOS

$\Gamma(\eta\eta)/\Gamma_{\text{total}}$ **Γ_2/Γ**

VALUE	DOCUMENT ID		TECN	COMMENT
seen	UMAN	06	E835	5.2 $\overline{p}p \to \eta\eta\pi^0$

$f_2(2340)$ REFERENCES

ABLIKIM	13N	PR D87 092009	Ablikim M. *et al.*	(BES III Collab.)
UMAN	06	PR D73 052009	I. Uman *et al.*	(FNAL E835)
ETKIN	88	PL B201 568	A. Etkin *et al.*	(BNL, CUNY)
BOOTH	86	NP B273 677	P.S.L. Booth *et al.*	(LIVP, GLAS, CERN)
ETKIN	85	PL 165B 217	A. Etkin *et al.*	(BNL, CUNY)
LINDENBAUM	84	CNPP 13 285	S.J. Lindenbaum	(CUNY)

$\rho_5(2350)$

$I^G(J^{PC}) = 1^+(5^{--})$

OMITTED FROM SUMMARY TABLE

This entry was previously called $U_1(2400)$. See also $\rho(2150)$, $f_2(2150)$, $\rho_3(2250)$, $f_4(2300)$.

$\rho_5(2350)$ MASS

$\pi^- p \to \omega\pi^0 n$

VALUE (MeV)	DOCUMENT ID		TECN	COMMENT
2330 ± 35	ALDE	95	GAM2	38 $\pi^- p \to \omega\pi^0 n$

$\overline{p}p \to \pi\pi$ or $\overline{K}K$

VALUE (MeV)	DOCUMENT ID		TECN	CHG	COMMENT
• • • We do not use the following data for averages, fits, limits, etc. • • •					
~ 2303	HASAN	94	RVUE		$\overline{p}p \to \pi\pi$
~ 2300	[1] MARTIN	80B	RVUE		
~ 2250	[1] MARTIN	80C	RVUE		
~ 2500	[2] CARTER	78B	CNTR	0	0.7–2.4 $\overline{p}p \to K^-K^+$
~ 2480	[3] CARTER	77	CNTR	0	0.7–2.4 $\overline{p}p \to \pi\pi$

S-CHANNEL $\overline{N}N$

VALUE (MeV)	DOCUMENT ID		TECN	CHG	COMMENT
• • • We do not use the following data for averages, fits, limits, etc. • • •					
2300±45	[4] ANISOVICH	02	SPEC		0.6–1.9 $p\overline{p} \to \omega\pi^0$, $\omega\eta\pi^0$, $\pi^+\pi^-$
2295±30	ANISOVICH	00J	SPEC		
~ 2380	[5] CUTTS	78B	CNTR		0.97–3 $\overline{p}p \to \overline{N}N$
2345±15	[5,6] COUPLAND	77	CNTR	0	0.7–2.4 $\overline{p}p \to \overline{p}p$
2359± 2	[5,7] ALSPECTOR	73	CNTR		$\overline{p}p$ S channel
2350±10	[8] ABRAMS	70	CNTR		S channel $\overline{N}N$
2360±25	[9] OH	70B	HDBC	−0	$\overline{p}(pn)$, $K^*K2\pi$

$\pi^-p \to K^+K^-n$

VALUE (MeV)	DOCUMENT ID		TECN	CHG	COMMENT
• • • We do not use the following data for averages, fits, limits, etc. • • •					
2307±6	ALPER	80	CNTR	0	62 $\pi^-p \to K^+K^-n$

[1] $I(J^P) = 1(5^-)$ from simultaneous analysis of $p\overline{p} \to \pi^-\pi^+$ and $\pi^0\pi^0$.
[2] $I = 0(1)$; $J^P = 5^-$ from Barrelet-zero analysis.
[3] $I(J^P) = 1(5^-)$ from amplitude analysis.
[4] From the combined analysis of ANISOVICH 00J, ANISOVICH 01D, ANISOVICH 01E, and ANISOVICH 02.
[5] Isospins 0 and 1 not separated.
[6] From a fit to the total elastic cross section.
[7] Referred to as U or U region by ALSPECTOR 73.
[8] For $I = 1$ $\overline{N}N$.
[9] No evidence for this bump seen in the $\overline{p}p$ data of CHAPMAN 71B. Narrow state not confirmed by OH 73 with more data.

$\rho_5(2350)$ WIDTH

$\pi^-p \to \omega\pi^0 n$

VALUE (MeV)	DOCUMENT ID		TECN	COMMENT
400±100	ALDE	95	GAM2	38 $\pi^-p \to \omega\pi^0 n$

$\overline{p}p \to \pi\pi$ or $\overline{K}K$

VALUE (MeV)	DOCUMENT ID		TECN	CHG	COMMENT
• • • We do not use the following data for averages, fits, limits, etc. • • •					
~ 169	HASAN	94	RVUE		$\overline{p}p \to \pi\pi$
~ 250	[10] MARTIN	80B	RVUE		
~ 300	[10] MARTIN	80C	RVUE		
~ 150	[11] CARTER	78B	CNTR	0	0.7–2.4 $\overline{p}p \to K^-K^+$
~ 210	[12] CARTER	77	CNTR	0	0.7–2.4 $\overline{p}p \to \pi\pi$

S-CHANNEL $\overline{N}N$

VALUE (MeV)	DOCUMENT ID		TECN	CHG	COMMENT
• • • We do not use the following data for averages, fits, limits, etc. • • •					
260± 75	[13] ANISOVICH	02	SPEC		0.6–1.9 $p\overline{p} \to \omega\pi^0$, $\omega\eta\pi^0$, $\pi^+\pi^-$
235^{+65}_{-40}	ANISOVICH	00J	SPEC		
135^{+150}_{-65}	[14,15] COUPLAND	77	CNTR	0	0.7–2.4 $\overline{p}p \to \overline{p}p$
165^{+18}_{-8}	[15] ALSPECTOR	73	CNTR		$\overline{p}p$ S channel
< 60	[16] OH	70B	HDBC	−0	$\overline{p}(pn)$, $K^*K2\pi$
~ 140	ABRAMS	67C	CNTR		S channel $\overline{p}N$

$\pi^-p \to K^+K^-n$

VALUE (MeV)	DOCUMENT ID		TECN	CHG	COMMENT
• • • We do not use the following data for averages, fits, limits, etc. • • •					
245±20	ALPER	80	CNTR	0	62 $\pi^-p \to K^+K^-n$

[10] $I(J^P) = 1(5^-)$ from simultaneous analysis of $p\overline{p} \to \pi^-\pi^+$ and $\pi^0\pi^0$.
[11] $I = 0(1)$; $J^P = 5^-$ from Barrelet-zero analysis.
[12] $I(J^P) = 1(5^-)$ from amplitude analysis.
[13] From the combined analysis of ANISOVICH 00J, ANISOVICH 01D, ANISOVICH 01E, and ANISOVICH 02.
[14] From a fit to the total elastic cross section.
[15] Isospins 0 and 1 not separated.
[16] No evidence for this bump seen in the $\overline{p}p$ data of CHAPMAN 71B. Narrow state not confirmed by OH 73 with more data.

$\rho_5(2350)$ REFERENCES

ANISOVICH	02	PL B542 8	A.V. Anisovich *et al.*	
ANISOVICH	01D	PL B508 6	A.V. Anisovich *et al.*	
ANISOVICH	01E	PL B513 281	A.V. Anisovich *et al.*	
ANISOVICH	00J	PL B491 47	A.V. Anisovich *et al.*	
ALDE	95	ZPHY C66 379	D.M. Alde *et al.*	(GAMS Collab.) JP
HASAN	94	PL B334 215	A. Hasan, D.V. Bugg	(LOQM)
ALPER	80	PL 94B 422	B. Alper *et al.*	(AMST, CERN, CRAC, MPIM+)
MARTIN	80B	NP B176 355	B.R. Martin, D. Morgan	(LOUC, RHEL) JP
MARTIN	80C	NP B169 216	A.D. Martin, M.R. Pennington	(DURH) JP
CARTER	78B	NP B141 467	A.A. Carter	(LOQM)
CUTTS	78B	PR D17 16	D. Cutts *et al.*	(STON, WISC)
CARTER	77	PL 67B 117	A.A. Carter *et al.*	(LOQM, RHEL) JP
COUPLAND	77	PL 71B 460	M. Coupland *et al.*	(LOQM, RHEL)
ALSPECTOR	73	PRL 30 511	J. Alspector *et al.*	(RUTG, UPNJ)
OH	73	NP B51 57	B.Y. Oh *et al.*	(MSU)
CHAPMAN	71B	PR D4 1275	J.W. Chapman *et al.*	(MICH)
ABRAMS	70	PR D1 1917	R.J. Abrams *et al.*	(BNL)
OH	70B	PRL 24 1257	B.Y. Oh *et al.*	(MSU)
ABRAMS	67C	PRL 18 1209	R.J. Abrams *et al.*	(BNL)

$a_6(2450)$

$I^G(J^{PC}) = 1^-(6^{++})$

OMITTED FROM SUMMARY TABLE
Needs confirmation.

$a_6(2450)$ MASS

VALUE (MeV)	DOCUMENT ID		TECN	CHG	COMMENT
2450±130	[1] CLELAND	82B	SPEC	±	50 $\pi p \to K^0_S K^\pm p$

[1] From an amplitude analysis.

$a_6(2450)$ WIDTH

VALUE (MeV)	DOCUMENT ID		TECN	CHG	COMMENT
400±250	[2] CLELAND	82B	SPEC	±	50 $\pi p \to K^0_S K^\pm p$

[2] From an amplitude analysis.

$a_6(2450)$ DECAY MODES

	Mode
Γ_1	$K\overline{K}$

$a_6(2450)$ REFERENCES

CLELAND	82B	NP B208 228	W.E. Cleland *et al.*	(DURH, GEVA, LAUS+)

$f_6(2510)$

$I^G(J^{PC}) = 0^+(6^{++})$

OMITTED FROM SUMMARY TABLE
Needs confirmation.

$f_6(2510)$ MASS

VALUE (MeV)	DOCUMENT ID		TECN	COMMENT
2469±29 OUR AVERAGE	Error includes scale factor of 1.5. See the ideogram below.			
2485±40	[1] ANISOVICH	00J	SPEC	1.92–2.41 $p\overline{p}$
2420±30	ALDE	98	GAM4	100 $\pi^-p \to \pi^0\pi^0 n$
2510±30	BINON	84B	GAM2	38 $\pi^-p \to n2\pi^0$

[1] From the combined analysis of ANISOVICH 99C, ANISOVICH 99F, ANISOVICH 99J, ANISOVICH 99K, and ANISOVICH 00B.

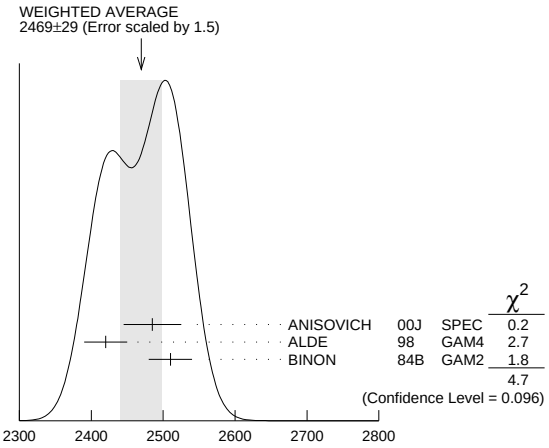

Meson Particle Listings

$f_6(2510)$

$f_6(2510)$ WIDTH

VALUE (MeV)	DOCUMENT ID		TECN	COMMENT
283±40 OUR AVERAGE	Error includes scale factor of 1.1.			
410±90	[2] ANISOVICH	00J	SPEC	1.92–2.41 $p\overline{p}$
270±60	ALDE	98	GAM4	100 $\pi^- p \rightarrow \pi^0\pi^0 n$
240±60	BINON	84B	GAM2	38 $\pi^- p \rightarrow n2\pi^0$

[2] From the combined analysis of ANISOVICH 99C, ANISOVICH 99F, ANISOVICH 99J, ANISOVICH 99K, and ANISOVICH 00B.

$f_6(2510)$ DECAY MODES

	Mode	Fraction (Γ_i/Γ)
Γ_1	$\pi\pi$	(6.0±1.0) %

$f_6(2510)$ BRANCHING RATIOS

$\Gamma(\pi\pi)/\Gamma_{total}$ **Γ_1/Γ**

VALUE	DOCUMENT ID		TECN	COMMENT
0.06±0.01	[3] BINON	83C	GAM2	38 $\pi^- p \rightarrow n4\gamma$

[3] Assuming one pion exchange and using data of BOLOTOV 74.

$f_6(2510)$ REFERENCES

ANISOVICH	00B	NP A662 319	A.V. Anisovich *et al.*	
ANISOVICH	00J	PL B491 47	A.V. Anisovich *et al.*	
ANISOVICH	99C	PL B452 173	A.V. Anisovich *et al.*	
ANISOVICH	99F	NP A651 253	A.V. Anisovich *et al.*	
ANISOVICH	99J	PL B471 271	A.V. Anisovich *et al.*	
ANISOVICH	99K	PL B468 309	A.V. Anisovich *et al.*	
ALDE	98	EPJ A3 361	D. Alde *et al.*	(GAM4 Collab.)
Also		PAN 62 405	D. Alde *et al.*	(GAMS Collab.)
		Translated from YAF 62 446.		
BINON	84B	LNC 39 41	F.G. Binon *et al.*	(SERP, BELG, LAPP) JP
BINON	83C	SJNP 38 723	F.G. Binon *et al.*	(SERP, BRUX+)
		Translated from YAF 38 1199.		
BOLOTOV	74	PL 52B 489	V.N. Bolotov *et al.*	(SERP)

OTHER LIGHT MESONS

Further States

OMITTED FROM SUMMARY TABLE

This section contains states observed by a single group or states poorly established that thus need confirmation.

QUANTUM NUMBERS, MASSES, WIDTHS, AND BRANCHING RATIOS

$X(360)$ $I^G(J^{PC}) = ?^?(?^{?+})$

MASS (MeV)	WIDTH (MeV)	EVTS	DOCUMENT ID		TECN	COMMENT
$360 \pm 7 \pm 9$	64 ± 18	2.3k	[1] ABRAAMYAN	09	CNTR	2.75 $dC \to \gamma\gamma X$

[1] Not seen in $pC \to \gamma\gamma X$ at 5.5 GeV/c.

$X(1070)$ $I^G(J^{PC}) = ?^?(0^{++})$

MASS (MeV)	WIDTH (MeV)	DOCUMENT ID		COMMENT
1072 ± 1	3.5 ± 0.5	[2] VLADIMIRSK...08		40 $\pi^- p \to K^0_S K^0_S n +$ mπ^0

[2] Supersedes GRIGOR'EV 05.

$X(1110)$ $I^G(J^{PC}) = 0^+(\text{even}^{++})$

MASS (MeV)	WIDTH (MeV)	DOCUMENT ID		TECN	COMMENT
1107 ± 4	$111 \pm 8 \pm 15$	DAFTARI	87	DBC	0. $\overline{p}n \to \rho^- \pi^+ \pi^-$

$f_0(1200\text{–}1600)$ $I^G(J^{PC}) = 0^+(0^{++})$

MASS (MeV)	WIDTH (MeV)	DOCUMENT ID		TECN	COMMENT
1323 ± 8	237 ± 20	VLADIMIRSK...06		SPEC	40 $\pi^- p \to K^0_S K^0_S n$
1480^{+100}_{-150}	1030^{+80}_{-170}	[3] ANISOVICH	03	SPEC	
1530^{+90}_{-250}	560 ± 40	[4] ANISOVICH	03	SPEC	

[3] K-matrix pole from combined analysis of $\pi^- p \to \pi^0\pi^0 n$, $\pi^- p \to K\overline{K} n$, $\pi^+\pi^- \to \pi^+\pi^-$, $\overline{p}p \to \pi^0\pi^0\pi^0$, $\pi^0\eta\eta$, $\pi^0\pi^0\eta$, $\pi^+\pi^-\pi^0$, $K^+K^-\pi^0$, $K^0_S K^0_S \pi^0$, $K^+K^0_S\pi^-$ at rest, $\overline{p}n \to \pi^-\pi^-\pi^+$, $K^0_S K^-\pi^0$, $K^0_S K^0_S \pi^-$ at rest.

[4] K-matrix pole from combined analysis of $\pi^- p \to \pi^0\pi^0 n$, $\pi^- p \to K\overline{K} n$, $\overline{p}p \to \pi^0\pi^0\pi^0$, $\pi^0\eta\eta$, $\pi^0\pi^0\eta$ at rest.

$X(1420)$ $I^G(J^{PC}) = 2^+(0^{++})$

MASS (MeV)	WIDTH (MeV)	DOCUMENT ID		TECN	COMMENT
1420 ± 20	160 ± 10	FILIPPI	00	OBLX	0 $\overline{n}p \to \pi^+\pi^+\pi^-$

$X(1545)$ $I^G(J^{PC}) = ?^?(?^{++})$

MASS (MeV)	WIDTH (MeV)	DOCUMENT ID		COMMENT
1545 ± 3	6.0 ± 2.5	[5] VLADIMIRSK...08		40 $\pi^- p \to K^0_S K^0_S n +$ mπ^0

[5] Supersedes VLADIMIRSKII 00.

$X(1575)$ $I^G(J^{PC}) = ?^?(1^{--})$

MASS (MeV)	WIDTH (MeV)	DOCUMENT ID		TECN	COMMENT
1576^{+49+98}_{-55-91}	$818^{+22+64}_{-23-133}$	[6] ABLIKIM	06S	BES	$J/\psi \to K^+K^-\pi^0$

[6] A broad peak observed at K^+K^- invariant mass. Mass and width above are its pole position. The observed branching ratio is $B(J/\psi \to X\pi^0)\, B(X \to K^+K^-) = (8.5 \pm 0.6^{+2.7}_{-3.6}) \times 10^{-4}$.

$X(1600)$ $I^G(J^{PC}) = 2^+(2^{++})$

MASS (MeV)	WIDTH (MeV)	DOCUMENT ID		TECN	COMMENT
1600 ± 100	400 ± 200	[7] ALBRECHT	91F	ARG	10.2 $e^+e^- \to e^+e^-2(\pi^+\pi^-)$

[7] Our estimate.

$X(1650)$ $I^G(J^{PC}) = 0^-(?^{?-})$

MASS (MeV)	WIDTH (MeV)	EVTS	DOCUMENT ID	TECN	COMMENT
1652 ± 7	<50	100	PROKOSHKIN 96	GAM2	32,38 $\pi p \to \omega\eta n$

$X(1730)$ $I^G(J^{PC}) = ?^?(?^{?+})$

MASS (MeV)	WIDTH (MeV)	EVTS	DOCUMENT ID	TECN	COMMENT
$1731.0 \pm 1.2 \pm 2.0$	$3.2 \pm 0.8 \pm 1.3$	58	VLADIMIRSK...07	SPEC	40 $\pi^- p \to K^0_S K^0_S X$

$X(1750)$ $I^G(J^{PC}) = ?^?(1^{--})$

MASS (MeV)	WIDTH (MeV)	DOCUMENT ID		TECN	COMMENT
$1753.5 \pm 1.5 \pm 2.3$	$122.2 \pm 6.2 \pm 8.0$	LINK	02K	FOCS	20–160 $\gamma p \to K^+K^- p$

$B(X(1750) \to \overline{K}^*(892)^0 K^0 \to K^\pm\pi^\mp K^0_S)/B(X(1750) \to K^+K^-)$

VALUE	CL%	DOCUMENT ID		TECN
<0.065	90	LINK	02K	FOCS

$B(X(1750) \to K^*(892)^\pm K^\mp \to K^0_S\pi^\pm K^\mp)/B(X(1750) \to K^+K^-)$

VALUE	CL%	DOCUMENT ID		TECN
<0.183	90	LINK	02K	FOCS

$f_2(1750)$ $I^G(J^{PC}) = 0^+(2^{++})$

MASS (MeV)	WIDTH (MeV)	EVTS	DOCUMENT ID		TECN	COMMENT
1755 ± 10	67 ± 12	870	[8] SCHEGELSKY	06A	RVUE	$\gamma\gamma \to K^0_S K^0_S$

$\Gamma(K\overline{K})$

VALUE (MeV)	EVTS	DOCUMENT ID		TECN	COMMENT
17 ± 5	870	[9] SCHEGELSKY	06A	RVUE	$\gamma\gamma \to K^0_S K^0_S$

$\Gamma(\gamma\gamma)$

VALUE (keV)	EVTS	DOCUMENT ID		TECN	COMMENT
0.13 ± 0.04	870	[9] SCHEGELSKY	06A	RVUE	$\gamma\gamma \to K^0_S K^0_S$

$\Gamma(\pi\pi)$

VALUE (MeV)	EVTS	DOCUMENT ID		TECN	COMMENT
1.3 ± 1.0	870	[9] SCHEGELSKY	06A	RVUE	$\gamma\gamma \to K^0_S K^0_S$

$\Gamma(\eta\eta)$

VALUE (MeV)	EVTS	DOCUMENT ID		TECN	COMMENT
2.0 ± 0.5	870	[9] SCHEGELSKY	06A	RVUE	$\gamma\gamma \to K^0_S K^0_S$

[8] From analysis of L3 data at 91 and 183–209 GeV.

[9] From analysis of L3 data at 91 and 183–209 GeV and using SU(3) relations.

$X(1775)$ $I^G(J^{PC}) = 1^-(?^{-+})$

MASS (MeV)	WIDTH (MeV)	DOCUMENT ID		TECN	COMMENT
1763 ± 20	192 ± 60	CONDO	91	SHF	$\gamma p \to (p\pi^+)(\pi^+\pi^-\pi^-)$
1787 ± 18	118 ± 60	CONDO	91	SHF	$\gamma p \to n\pi^+\pi^+\pi^-$

$f_0(1800)$ $I^G(J^{PC}) = 0^+(0^{++})$

MASS (MeV)	WIDTH (MeV)	DOCUMENT ID		TECN	COMMENT
$1795 \pm 7^{+23}_{-20}$	$95 \pm 10^{+78}_{-82}$	ABLIKIM	13J	BES3	$J/\psi \to \gamma\omega\phi$
$1812^{+19}_{-26} \pm 18$	$105 \pm 20 \pm 28$	[10] ABLIKIM	06J	BES2	$J/\psi \to \gamma\omega\phi$

[10] Not seen by LIU 09 in $B^\pm \to K^\pm\omega\phi$.

$X(1850 - 3100)$ $I^G(J^{PC}) = ?^?(1^{--})$

$\Gamma(e^+e^-)\cdot B(X \to \text{hadrons})$ (eV)	CL%	DOCUMENT ID		TECN	COMMENT
<120	90	[11] ANASHIN	11	KEDR	$e^+e^- \to$ hadrons

[11] This limit is center-of-mass energy dependent. We quote the most stringent one.

$X(1855)$ $I^G(J^{PC}) = ?^?(?^{??})$

MASS (MeV)	WIDTH (MeV)	DOCUMENT ID		TECN	COMMENT
1856.6 ± 5	20 ± 5	BRIDGES	86D	SPEC	0. $\overline{p}d \to \pi\pi N$

$X(1870)$ $I^G(J^{PC}) = ?^?(2^{??})$

MASS (MeV)	WIDTH (MeV)	DOCUMENT ID		TECN	COMMENT
1870 ± 40	250 ± 30	ALDE	86D	GAM4	100 $\pi^- p \to 2\eta$X

$a_3(1875)$ $I^G(J^{PC}) = 1^-(3^{++})$

MASS (MeV)	WIDTH (MeV)	DOCUMENT ID		TECN	COMMENT
$1874 \pm 43 \pm 96$	$385 \pm 121 \pm 114$	CHUNG	02	B852	18.3 $\pi^- p \to \pi^+\pi^-\pi^- p$

$B(a_3(1875) \to f_2(1270)\pi)/B(a_3(1875) \to \rho\pi)$

VALUE	DOCUMENT ID		TECN	COMMENT
0.8 ± 0.2	[12] CHUNG	02	B852	18.3 $\pi^- p \to \pi^+\pi^-\pi^- p$

[12] Using the observable fractions of 50.0% $\rho\pi$, 56.5% $f_2\pi$, and 11.8% $\rho_3\pi$.

$B(a_3(1875) \to \rho_3(1690)\pi)/B(a_3(1875) \to \rho\pi)$

VALUE	DOCUMENT ID		TECN	COMMENT
0.9 ± 0.3	[13] CHUNG	02	B852	18.3 $\pi^- p \to \pi^+\pi^-\pi^- p$

[13] Using the observable fractions of 50.0% $\rho\pi$, 56.5% $f_2\pi$, and 11.8% $\rho_3\pi$.

Meson Particle Listings

Further States

$a_1(1930)$ $I^G(J^{PC}) = 1^-(1^{++})$

MASS (MeV)	WIDTH (MeV)	DOCUMENT ID		TECN	COMMENT
1930^{+30}_{-70}	155 ± 45	ANISOVICH	01F	SPEC	2.0 $\overline{p}p \to 3\pi^0, \pi^0\eta, \pi^0\eta'$

$X(1935)$ $I^G(J^{PC}) = 1^+(1^{-?})$

MASS (MeV)	WIDTH (MeV)	DOCUMENT ID		TECN	COMMENT
1935 ± 20	215 ± 30	EVANGELIS...	79	OMEG	10,16 $\pi^- p \to \overline{p}pn$

$\rho_2(1940)$ $I^G(J^{PC}) = 1^+(2^{--})$

MASS (MeV)	WIDTH (MeV)	DOCUMENT ID		TECN	COMMENT
1940 ± 40	155 ± 40	[14] ANISOVICH	02	SPEC	0.6–1.9 $p\overline{p} \to \omega\pi^0$, $\omega\eta\pi^0$, $\pi^+\pi^-$

[14] From the combined analysis of ANISOVICH 00J, ANISOVICH 01D, ANISOVICH 01E, and ANISOVICH 02.

$\omega_3(1945)$ $I^G(J^{PC}) = 0^-(3^{--})$

MASS (MeV)	WIDTH (MeV)	DOCUMENT ID		TECN	COMMENT
1945 ± 20	115 ± 22	[15] ANISOVICH	02B	SPEC	0.6–1.9 $p\overline{p} \to \omega\eta, \omega\pi^0\pi^0$

[15] From the combined analysis of ANISOVICH 00D, ANISOVICH 01C, and ANISOVICH 02B.

$a_2(1950)$ $I^G(J^{PC}) = 1^-(2^{++})$

MASS (MeV)	WIDTH (MeV)	DOCUMENT ID		TECN	COMMENT
1950^{+30}_{-70}	180^{+30}_{-70}	[16] ANISOVICH	01F	SPEC	1.96–2.41 $\overline{p}p$

[16] From the combined analysis of ANISOVICH 99C, ANISOVICH 99E, and ANISOVICH 01F.

$\omega(1960)$ $I^G(J^{PC}) = 0^-(1^{--})$

MASS (MeV)	WIDTH (MeV)	DOCUMENT ID		TECN	COMMENT
1960 ± 25	195 ± 60	[17] ANISOVICH	02B	SPEC	0.6–1.9 $p\overline{p} \to \omega\eta, \omega\pi^0\pi^0$

[17] From the combined analysis of ANISOVICH 00D, ANISOVICH 01C, and ANISOVICH 02B.

$b_1(1960)$ $I^G(J^{PC}) = 1^+(1^{+-})$

MASS (MeV)	WIDTH (MeV)	DOCUMENT ID		TECN	COMMENT
1960 ± 35	230 ± 50	[18] ANISOVICH	02	SPEC	0.6–1.9 $p\overline{p} \to \omega\pi^0$, $\omega\eta\pi^0$, $\pi^+\pi^-$

[18] From the combined analysis of ANISOVICH 00J, ANISOVICH 01D, ANISOVICH 01E, and ANISOVICH 02.

$h_1(1965)$ $I^G(J^{PC}) = 0^-(1^{+-})$

MASS (MeV)	WIDTH (MeV)	DOCUMENT ID		TECN	COMMENT
1965 ± 45	345 ± 75	[19] ANISOVICH	02B	SPEC	0.6–1.9 $p\overline{p} \to \omega\eta, \omega\pi^0\pi^0$

[19] From the combined analysis of ANISOVICH 00D, ANISOVICH 01C, and ANISOVICH 02B.

$f_1(1970)$ $I^G(J^{PC}) = 0^+(1^{++})$

MASS (MeV)	WIDTH (MeV)	DOCUMENT ID		TECN
1971 ± 15	240 ± 45	ANISOVICH	00J	SPEC

$X(1970)$ $I^G(J^{PC}) = ?^?(?^{???})$

MASS (MeV)	WIDTH (MeV)	DOCUMENT ID		TECN	COMMENT
1970 ± 10	40 ± 20	CHLIAPNIK...	80	HBC	32 $K^+ p \to 2K^0_S 2\pi X$

$X(1975)$ $I^G(J^{PC}) = ?^?(?^{???})$

MASS (MeV)	WIDTH (MeV)	EVTS	DOCUMENT ID		TECN	COMMENT
1973 ± 15	80	30	CASO	70	HBC	11.2 $\pi^- p \to \rho 2\pi$

$\omega_2(1975)$ $I^G(J^{PC}) = 0^-(2^{--})$

MASS (MeV)	WIDTH (MeV)	DOCUMENT ID		TECN	COMMENT
1975 ± 20	175 ± 25	[20] ANISOVICH	02B	SPEC	0.6–1.9 $p\overline{p} \to \omega\eta, \omega\pi^0\pi^0$

[20] From the combined analysis of ANISOVICH 00D, ANISOVICH 01C, and ANISOVICH 02B.

$a_2(1990)$ $I^G(J^{PC}) = 1^-(2^{++})$

MASS (MeV)	WIDTH (MeV)	EVTS	DOCUMENT ID		TECN	COMMENT
$2050 \pm 10 \pm 40$	$190 \pm 22 \pm 100$	18k	[21] SCHEGELSKY	06	RVUE	$\gamma\gamma \to \pi^+\pi^-\pi^0$
$2003 \pm 10 \pm 19$	$249 \pm 23 \pm 32$		LU	05	B852	18 $\pi^- p \to \omega\pi^-\pi^0 p$

[21] From analysis of L3 data at 183–209 GeV.

$\Gamma(\gamma\gamma)\ \Gamma(\pi^+\pi^-\pi^0)$ / Γ(total)

VALUE (keV)	EVTS	DOCUMENT ID		TECN	COMMENT
$0.11 \pm 0.04 \pm 0.05$	18k	[22] SCHEGELSKY	06	RVUE	$\gamma\gamma \to \pi^+\pi^-\pi^0$

[22] From analysis of L3 data at 183–209 GeV.

$\rho(2000)$ $I^G(J^{PC}) = 1^+(1^{--})$

MASS (MeV)	WIDTH (MeV)	DOCUMENT ID		TECN	COMMENT
2000 ± 30	260 ± 45	[23] BUGG	04C	RVUE	Compilation
~ 1988	~ 244	HASAN	94	RVUE	$\overline{p}p \to \pi\pi$

[23] From the combined analysis of ANISOVICH 00J, ANISOVICH 01D, ANISOVICH 01E, and ANISOVICH 02.

$f_2(2000)$ $I^G(J^{PC}) = 0^+(2^{++})$

MASS (MeV)	WIDTH (MeV)	DOCUMENT ID		TECN	COMMENT
2001 ± 10	312 ± 32	ANISOVICH	00J	SPEC	
~ 1996	~ 134	HASAN	94	RVUE	$\overline{p}p \to \pi\pi$

$X(2000)$ $I^G(J^{PC}) = 1^-(?^?{}^+)$

MASS (MeV)	WIDTH (MeV)	DOCUMENT ID		TECN	CHG	COMMENT
1964 ± 35	225 ± 50	[24] ARMSTRONG	93D	E760		$\overline{p}p \to 3\pi^0 \to 6\gamma$
~ 2100	~ 500	[24] ANTIPOV	77	CIBS	$-$	25 $\pi^- p \to p\pi^-\rho_3$
2214 ± 15	355 ± 21	[25] BALTAY	77	HBC	0	15 $\pi^- p \to \Delta^{++}3\pi$
2080 ± 40	340 ± 80	KALELKAR	75	HBC	$+$	15 $\pi^+ p \to p\pi^+\rho_3$

[24] Cannot determine spin to be 3.
[25] BALTAY 77 favors $J^P = ,3^+$.

$X(2000)$ $I^G(J^{PC}) = ?^?(4^{++})$

MASS (MeV)	WIDTH (MeV)	DOCUMENT ID		TECN	COMMENT
$1998 \pm 3 \pm 5$	<15	VLADIMIRSK...03		SPEC	$\pi^- p \to K^0_S K^0_S MM$

$\pi_2(2005)$ $I^G(J^{PC}) = 1^-(2^{-+})$

MASS (MeV)	WIDTH (MeV)	EVTS	DOCUMENT ID		TECN	COMMENT
$1974 \pm 14 \pm 83$	$341 \pm 61 \pm 139$	145k	LU	05	B852	18 $\pi^- p \to \omega\pi^-\pi^0 p$
2005 ± 15	200 ± 40		ANISOVICH	01F	SPEC	2.0 $\overline{p}p \to 3\pi^0, \pi^0\eta, \pi^0\eta'$

$\eta(2010)$ $I^G(J^{PC}) = 0^+(0^{-+})$

MASS (MeV)	WIDTH (MeV)	DOCUMENT ID		TECN
2010^{+35}_{-60}	270 ± 60	ANISOVICH	00J	SPEC

$\pi_1(2015)$ $I^G(J^{PC}) = 1^-(1^{-+})$

MASS (MeV)	WIDTH (MeV)	EVTS	DOCUMENT ID		TECN	COMMENT
$2014 \pm 20 \pm 16$	$230 \pm 32 \pm 73$	145k	LU	05	B852	18 $\pi^- p \to \omega\pi^-\pi^0 p$
$2001 \pm 30 \pm 92$	$333 \pm 52 \pm 49$	69k	KUHN	04	B852	18 $\pi^- p \to \eta\pi^+\pi^-\pi^- p$

$a_0(2020)$ $I^G(J^{PC}) = 1^-(0^{++})$

MASS (MeV)	WIDTH (MeV)	DOCUMENT ID		TECN
2025 ± 30	330 ± 75	ANISOVICH	99C	SPEC

$X(2020)$ $I^G(J^{PC}) = ?^?(?^{??})$

MASS (MeV)	WIDTH (MeV)	DOCUMENT ID		TECN	COMMENT
2015 ± 3	10 ± 4	FERRER	99	RVUE	$\pi p \to pp\overline{p}\pi(\pi)$

$h_3(2025)$ $I^G(J^{PC}) = 0^-(3^{+-})$

MASS (MeV)	WIDTH (MeV)	DOCUMENT ID		TECN	COMMENT
2025 ± 20	145 ± 30	[26] ANISOVICH	02B	SPEC	0.6–1.9 $p\overline{p} \to \omega\eta, \omega\pi^0\pi^0$

[26] From the combined analysis of ANISOVICH 00D, ANISOVICH 01C, and ANISOVICH 02B.

$b_3(2030)$ $I^G(J^{PC}) = 1^+(3^{+-})$

MASS (MeV)	WIDTH (MeV)	DOCUMENT ID		TECN	COMMENT
2032 ± 12	117 ± 11	[27] ANISOVICH	02	SPEC	0.6–1.9 $p\overline{p} \to \omega\pi^0$, $\omega\eta\pi^0$, $\pi^+\pi^-$

[27] From the combined analysis of ANISOVICH 00J, ANISOVICH 01D, ANISOVICH 01E, and ANISOVICH 02.

$a_2(2030)$ $I^G(J^{PC}) = 1^-(2^{++})$

MASS (MeV)	WIDTH (MeV)	DOCUMENT ID		TECN	COMMENT
2030 ± 20	205 ± 30	[28] ANISOVICH	01F	SPEC	1.96–2.41 $\overline{p}p$

[28] From the combined analysis of ANISOVICH 99C, ANISOVICH 99E, and ANISOVICH 01F.

$a_3(2030)$ $I^G(J^{PC}) = 1^-(3^{++})$

MASS (MeV)	WIDTH (MeV)	DOCUMENT ID		TECN	COMMENT
2031 ± 12	150 ± 18	[29] ANISOVICH	01F	SPEC	1.96–2.41 $\overline{p}p$

[29] From the combined analysis of ANISOVICH 99C, ANISOVICH 99E, and ANISOVICH 01F.

$\eta_2(2030)$ $I^G(J^{PC}) = 0^+(2^{-+})$

MASS (MeV)	WIDTH (MeV)	DOCUMENT ID		TECN
$2030 \pm 5 \pm 15$	$205 \pm 10 \pm 15$	ANISOVICH	00E	SPEC

$B(a_2\pi)_{L=0}/B(a_2\pi)_{L=2}$

VALUE	DOCUMENT ID		TECN	COMMENT
0.05 ± 0.03	[30] ANISOVICH	11	SPEC	0.9–1.94 $p\overline{p}$

[30] Reanalysis of ADOMEIT 96 and ANISOVICH 00E.

$B(a_0\pi)/B(a_2\pi)_{L=2}$

VALUE	DOCUMENT ID		TECN	COMMENT
0.10 ± 0.08	[31] ANISOVICH	11	SPEC	0.9–1.94 $p\overline{p}$

[31] Reanalysis of ADOMEIT 96 and ANISOVICH 00E.

$B(f_2\eta)/B(a_2\pi)_{L=2}$

VALUE	DOCUMENT ID		TECN	COMMENT
0.13 ± 0.06	[32] ANISOVICH	11	SPEC	0.9–1.94 $p\overline{p}$

[32] Reanalysis of ADOMEIT 96 and ANISOVICH 00E.

$f_3(2050)$ $I^G(J^{PC}) = 0^+(3^{++})$

MASS (MeV)	WIDTH (MeV)	DOCUMENT ID		TECN	COMMENT
2048 ± 8	213 ± 34	ANISOVICH	00J	SPEC	2.0 $p\overline{p} \to \eta\pi^0\pi^0$

$f_0(2060)$ $I^G(J^{PC}) = 0^+(0^{++})$

MASS (MeV)	WIDTH (MeV)	DOCUMENT ID		TECN	COMMENT
~ 2050	~ 120	[33] OAKDEN	94	RVUE	0.36–1.55 $\overline{p}p \to \pi\pi$
~ 2060	~ 50	[33] OAKDEN	94	RVUE	0.36–1.55 $\overline{p}p \to \pi\pi$

[33] See SEMENOV 99 and KLOET 96.

$\pi(2070)$ $I^G(J^{PC}) = 1^-(0^{-+})$

MASS (MeV)	WIDTH (MeV)	DOCUMENT ID		TECN	COMMENT
2070 ± 35	310^{+100}_{-50}	ANISOVICH	01F	SPEC	2.0 $\overline{p}p \to 3\pi^0, \pi^0\eta, \pi^0\eta'$

$X(2075)$ $I^G(J^{PC}) = ?^?(?^{??})$

MASS (MeV)	WIDTH (MeV)	DOCUMENT ID		TECN	COMMENT
$2075 \pm 12 \pm 5$	$90 \pm 35 \pm 9$	[34] ABLIKIM	04J	BES2	$J/\psi \to K^- p\overline{\Lambda}$

[34] From a fit in the region $M_{p\overline{\Lambda}} - M_p - M_\Lambda < 150$ MeV. S-wave in the $p\overline{\Lambda}$ system preferred. A similar near-threshold enhancement in the $p\overline{\Lambda}$ system is observed in $B^+ \to p\overline{\Lambda D}^0$ by CHEN 11F.

$X(2080)$ $I^G(J^{PC}) = ?^?(?^{??})$

MASS (MeV)	WIDTH (MeV)	DOCUMENT ID		TECN	COMMENT
2080 ± 10	110 ± 20	KREYMER	80	STRC	13 $\pi^- d \to p\overline{p}n(n_s)$

$X(2080)$ $I^G(J^{PC}) = ?^?(3^{-?})$

MASS (MeV)	WIDTH (MeV)	DOCUMENT ID		TECN	COMMENT
2080 ± 10	190 ± 15	ROZANSKA	80	SPRK	18 $\pi^- p \to p\overline{p}n$

$a_1(2095)$ $I^G(J^{PC}) = 1^-(1^{++})$

MASS (MeV)	WIDTH (MeV)	EVTS	DOCUMENT ID		TECN	COMMENT
$2096 \pm 17 \pm 121$	$451 \pm 41 \pm 81$	69k	KUHN	04	B852	18 $\pi^- p \to \eta\pi^+\pi^-\pi^- p$

$B(a_1(2095) \to f_1(1285)\pi)$ / $B(a_1(2095) \to a_1(1260))$

VALUE	EVTS	DOCUMENT ID		TECN	COMMENT
3.18 ± 0.64	69k	KUHN	04	B852	18 $\pi^- p \to \eta\pi^+\pi^-\pi^- p$

$\eta(2100)$ $I^G(J^{PC}) = 0^+(0^{-+})$

MASS (MeV)	WIDTH (MeV)	EVTS	DOCUMENT ID		TECN	COMMENT
2050^{+30+75}_{-24-26}	$250^{+36+181}_{-30-164}$		[35] ABLIKIM	16N	BES3	$J/\psi \to \gamma K^+ K^- K^+ K^-$
2103 ± 50	187 ± 75	586	[36] BISELLO	89B	DM2	$J/\psi \to 4\pi\gamma$

[35] From a partial wave analysis of $J/\psi \to \gamma\phi\phi$, for which the primary signal is $\eta(2225) \to \phi\phi$, and that also finds significant signals for for 0^{-+} phase space, $f_0(2100)$, $f_2(2010)$, $f_2(2300)$, $f_2(2340)$, and a previously unseen 0^{-+} state $X(2500)$ ($M = 2470^{+15+101}_{-19-23}$ MeV, $\Gamma = 230^{+64+56}_{-35-33}$ MeV).

[36] ASTON 81B sees no peak, has 850 events in Ajinenko+Barth bins. ARESTOV 80 sees no peak.

$X(2100)$ $I^G(J^{PC}) = ?^?(0^{??})$

MASS (MeV)	WIDTH (MeV)	DOCUMENT ID		TECN	COMMENT
2100 ± 40	250 ± 40	ALDE	86D	GAM4	100 $\pi^- p \to 2\eta X$

$X(2110)$ $I^G(J^{PC}) = 1^+(3^{-?})$

MASS (MeV)	WIDTH (MeV)	DOCUMENT ID		TECN	COMMENT
2110 ± 10	330 ± 20	EVANGELIS...	79	OMEG	10,16 $\pi^- p \to \overline{p}pn$

$f_2(2140)$ $I^G(J^{PC}) = 0^+(2^{++})$

MASS (MeV)	WIDTH (MeV)	EVTS	DOCUMENT ID		TECN	COMMENT
2141 ± 12	49 ± 28	389	GREEN	86	MPSF	400 $pA \to 4KX$

$X(2150)$ $I^G(J^{PC}) = ?^?(2^{+?})$

MASS (MeV)	WIDTH (MeV)	DOCUMENT ID		TECN	COMMENT
2150 ± 10	260 ± 10	ROZANSKA	80	SPRK	18 $\pi^- p \to p\overline{p}n$

$a_2(2175)$ $I^G(J^{PC}) = 1^-(2^{++})$

MASS (MeV)	WIDTH (MeV)	DOCUMENT ID		TECN	COMMENT
2175 ± 40	310^{+90}_{-45}	ANISOVICH	01F	SPEC	2.0 $\overline{p}p \to 3\pi^0, \pi^0\eta, \pi^0\eta'$

$\eta(2190)$ $I^G(J^{PC}) = 0^+(0^{-+})$

MASS (MeV)	WIDTH (MeV)	DOCUMENT ID		TECN
2190 ± 50	850 ± 100	BUGG	99	BES

$\omega_2(2195)$ $I^G(J^{PC}) = 0^-(2^{--})$

MASS (MeV)	WIDTH (MeV)	DOCUMENT ID		TECN	COMMENT
2195 ± 30	225 ± 40	[37] ANISOVICH	02B	SPEC	0.6–1.9 $p\overline{p} \to \omega\eta, \omega\pi^0\pi^0$

[37] From the combined analysis of ANISOVICH 00D, ANISOVICH 01C, and ANISOVICH 02B.

$\omega(2205)$ $I^G(J^{PC}) = 0^-(1^{--})$

MASS (MeV)	WIDTH (MeV)	DOCUMENT ID		TECN	COMMENT
2205 ± 30	350 ± 90	[38] ANISOVICH	02B	SPEC	0.6–1.9 $p\overline{p} \to \omega\eta, \omega\pi^0\pi^0$

[38] From the combined analysis of ANISOVICH 00D, ANISOVICH 01C, and ANISOVICH 02B.

$X(2210)$ $I^G(J^{PC}) = ?^?(?^{??})$

MASS (MeV)	WIDTH (MeV)	DOCUMENT ID		TECN	COMMENT
2210^{+79}_{-21}	203^{+437}_{-87}	EVANGELIS...	79B	OMEG	10 $\pi^- p \to K^+ K^- n$

$X(2210)$ $I^G(J^{PC}) = ?^?(?^{??})$

MASS (MeV)	WIDTH (MeV)	DOCUMENT ID		TECN	COMMENT
2207 ± 22	130	CASO	70	HBC	11.2 $\pi^- p$

$h_1(2215)$ $I^G(J^{PC}) = 0^-(1^{+-})$

MASS (MeV)	WIDTH (MeV)	DOCUMENT ID		TECN	COMMENT
2215 ± 40	325 ± 55	[39] ANISOVICH	02B	SPEC	0.6–1.9 $p\overline{p} \to \omega\eta, \omega\pi^0\pi^0$

[39] From the combined analysis of ANISOVICH 00D, ANISOVICH 01C, and ANISOVICH 02B.

$\rho_2(2225)$ $I^G(J^{PC}) = 1^+(2^{--})$

MASS (MeV)	WIDTH (MeV)	DOCUMENT ID		TECN	COMMENT
2225 ± 35	335^{+100}_{-50}	[40] ANISOVICH	02	SPEC	0.6–1.9 $p\overline{p} \to \omega\pi^0, \omega\eta\pi^0, \pi^+\pi^-$

[40] From the combined analysis of ANISOVICH 00J, ANISOVICH 01D, ANISOVICH 01E, and ANISOVICH 02.

$\rho_4(2230)$ $I^G(J^{PC}) = 1^+(4^{--})$

MASS (MeV)	WIDTH (MeV)	DOCUMENT ID		TECN	COMMENT
2230 ± 25	210 ± 30	[41] ANISOVICH	02	SPEC	0.6–1.9 $p\overline{p} \to \omega\pi^0, \omega\eta\pi^0, \pi^+\pi^-$

[41] From the combined analysis of ANISOVICH 00J, ANISOVICH 01D, ANISOVICH 01E, and ANISOVICH 02.

$b_1(2240)$ $I^G(J^{PC}) = 1^+(1^{+-})$

MASS (MeV)	WIDTH (MeV)	DOCUMENT ID		TECN	COMMENT
2240 ± 35	320 ± 85	[42] ANISOVICH	02	SPEC	0.6–1.9 $p\overline{p} \to \omega\pi^0, \omega\eta\pi^0, \pi^+\pi^-$

[42] From the combined analysis of ANISOVICH 00J, ANISOVICH 01D, ANISOVICH 01E, and ANISOVICH 02.

$f_2(2240)$ $I^G(J^{PC}) = 0^+(2^{++})$

MASS (MeV)	WIDTH (MeV)	DOCUMENT ID		TECN	COMMENT
2240 ± 15	241 ± 30	[43] ANISOVICH	00J	SPEC	1.92–2.41 $p\overline{p}$
• • • We do not use the following data for averages, fits, limits, etc. • • •					
~ 2226	~ 226	HASAN	94	RVUE	$p\overline{p} \to \pi\pi$

[43] From the combined analysis of ANISOVICH 99C, ANISOVICH 99F, ANISOVICH 99J, ANISOVICH 99K, and ANISOVICH 00B. See also ANISOVICH 12.

$b_3(2245)$ $I^G(J^{PC}) = 1^+(3^{+-})$

MASS (MeV)	WIDTH (MeV)	DOCUMENT ID		TECN
2245 ± 50	320 ± 70	[44] BUGG	04C	RVUE

[44] From the combined analysis of ANISOVICH 00J, ANISOVICH 01D, ANISOVICH 01E, and ANISOVICH 02.

$\eta_2(2250)$ $I^G(J^{PC}) = 0^+(2^{-+})$

MASS (MeV)	WIDTH (MeV)	DOCUMENT ID		TECN
2248 ± 20	280 ± 20	ANISOVICH	00I	SPEC
2267 ± 14	290 ± 50	ANISOVICH	00J	SPEC

$\pi_4(2250)$ $I^G(J^{PC}) = 1^-(4^{-+})$

MASS (MeV)	WIDTH (MeV)	DOCUMENT ID		TECN	COMMENT
2250 ± 15	215 ± 25	ANISOVICH	01F	SPEC	2.0 $\overline{p}p \to 3\pi^0, \pi^0\eta, \pi^0\eta'$

$\omega_4(2250)$ $I^G(J^{PC}) = 0^-(4^{--})$

MASS (MeV)	WIDTH (MeV)	DOCUMENT ID		TECN	COMMENT
2250 ± 30	150 ± 50	[45] ANISOVICH	02B	SPEC	0.6–1.9 $p\overline{p} \to \omega\eta, \omega\pi^0\pi^0$

[45] From the combined analysis of ANISOVICH 00D, ANISOVICH 01C, and ANISOVICH 02B.

$\omega_5(2250)$ $I^G(J^{PC}) = 0^-(5^{--})$

MASS (MeV)	WIDTH (MeV)	DOCUMENT ID		TECN
2250 ± 70	320 ± 95	[46] BUGG	04	RVUE

[46] From the combined analysis of ANISOVICH 00D, ANISOVICH 01C, and ANISOVICH 02B.

$\omega_3(2255)$ $I^G(J^{PC}) = 0^-(3^{--})$

MASS (MeV)	WIDTH (MeV)	DOCUMENT ID		TECN	COMMENT
2255 ± 15	175 ± 30	[47] ANISOVICH	02B	SPEC	0.6–1.9 $p\overline{p} \to \omega\eta, \omega\pi^0\pi^0$

[47] From the combined analysis of ANISOVICH 00D, ANISOVICH 01C, and ANISOVICH 02B.

$a_4(2255)$ $I^G(J^{PC}) = 1^-(4^{++})$

MASS (MeV)	WIDTH (MeV)	DOCUMENT ID		TECN	COMMENT
2237 ± 5	291 ± 12	UMAN	06	E835	5.2 $\overline{p}p \to \eta\eta\pi^0$
2255 ± 40	330^{+110}_{-50}	[48] ANISOVICH	01F	SPEC	1.96–2.41 $\overline{p}p$

[48] From the combined analysis of ANISOVICH 99C, ANISOVICH 99E, and ANISOVICH 01F.

$a_2(2255)$ $I^G(J^{PC}) = 1^-(2^{++})$

MASS (MeV)	WIDTH (MeV)	DOCUMENT ID		TECN	COMMENT
2255 ± 20	230 ± 15	[49] ANISOVICH	01G	SPEC	1.96–2.41 $\overline{p}p$

[49] From the combined analysis of ANISOVICH 99C, ANISOVICH 99E, ANISOVICH 01F, and ANISOVICH 01G.

$X(2260)$ $I^G(J^{PC}) = 0^+(4^{+?})$

MASS (MeV)	WIDTH (MeV)	DOCUMENT ID		TECN	COMMENT
2260 ± 20	400 ± 100	EVANGELIS...	79	OMEG	10,16 $\pi^- p \to \overline{p}pn$

$\rho(2270)$ $I^G(J^{PC}) = 1^+(1^{--})$

MASS (MeV)	WIDTH (MeV)	DOCUMENT ID		TECN	COMMENT
2265 ± 40	325 ± 80	[50] ANISOVICH	02	SPEC	0.6–1.9 $p\overline{p} \to \omega\pi^0$, $\omega\eta\pi^0, \pi^+\pi^-$
2280 ± 50	440 ± 110	ATKINSON	85	OMEG	20–70 $\gamma p \to p\omega\pi^+\pi^-\pi^0$

[50] From the combined analysis of ANISOVICH 00J, ANISOVICH 01D, ANISOVICH 01E, and ANISOVICH 02.

$a_1(2270)$ $I^G(J^{PC}) = 1^-(1^{++})$

MASS (MeV)	WIDTH (MeV)	DOCUMENT ID		TECN	COMMENT
2270^{+55}_{-40}	305^{+70}_{-40}	ANISOVICH	01F	SPEC	2.0 $\overline{p}p \to 3\pi^0, \pi^0\eta, \pi^0\eta'$

$h_3(2275)$ $I^G(J^{PC}) = 0^-(3^{+-})$

MASS (MeV)	WIDTH (MeV)	DOCUMENT ID		TECN	COMMENT
2275 ± 25	190 ± 45	[51] ANISOVICH	02B	SPEC	0.6–1.9 $p\overline{p} \to \omega\eta, \omega\pi^0\pi^0$

[51] From the combined analysis of ANISOVICH 00D, ANISOVICH 01C, and ANISOVICH 02B.

$a_3(2275)$ $I^G(J^{PC}) = 1^-(3^{++})$

MASS (MeV)	WIDTH (MeV)	DOCUMENT ID		TECN	COMMENT
2275 ± 35	350^{+100}_{-50}	[52] ANISOVICH	01G	SPEC	1.96–2.41 $\overline{p}p$

[52] From the combined analysis of ANISOVICH 99C, ANISOVICH 99E, ANISOVICH 01F, and ANISOVICH 01G.

$\pi_2(2285)$ $I^G(J^{PC}) = 1^-(2^{-+})$

MASS (MeV)	WIDTH (MeV)	DOCUMENT ID		TECN	COMMENT
$2285 \pm 20 \pm 25$	$250 \pm 20 \pm 25$	[53] ANISOVICH	11	SPEC	0.9–1.94 $p\overline{p}$

[53] Reanalysis of ADOMEIT 96 and ANISOVICH 00E.

$\omega_3(2285)$ $I^G(J^{PC}) = 0^-(3^{--})$

MASS (MeV)	WIDTH (MeV)	DOCUMENT ID		TECN	COMMENT
2278 ± 28	224 ± 50	[54] BUGG	04A	RVUE	
2285 ± 60	230 ± 40	[55] ANISOVICH	02B	SPEC	0.6–1.9 $p\overline{p} \to \omega\eta, \omega\pi^0\pi^0$

[54] Partial wave analysis of the data on $p\overline{p} \to \overline{\Lambda}\Lambda$ from BARNES 00.
[55] From the combined analysis of ANISOVICH 00D, ANISOVICH 01C, and ANISOVICH 02B.

$\omega(2290)$ $I^G(J^{PC}) = 0^-(1^{--})$

MASS (MeV)	WIDTH (MeV)	DOCUMENT ID		TECN
2290 ± 20	275 ± 35	[56] BUGG	04A	RVUE

[56] Partial wave analysis of the data on $p\overline{p} \to \overline{\Lambda}\Lambda$ from BARNES 00.

$f_2(2295)$ $I^G(J^{PC}) = 0^+(2^{++})$

MASS (MeV)	WIDTH (MeV)	DOCUMENT ID		TECN	COMMENT
2293 ± 13	216 ± 37	[57] ANISOVICH	00J	SPEC	1.92–2.41 $p\overline{p}$

[57] From the combined analysis of ANISOVICH 99C, ANISOVICH 99F, ANISOVICH 99J, ANISOVICH 99K, and ANISOVICH 00B. See also ANISOVICH 12.

$f_3(2300)$ $I^G(J^{PC}) = 0^+(3^{++})$

MASS (MeV)	WIDTH (MeV)	DOCUMENT ID		TECN
2334 ± 25	200 ± 20	[58] BUGG	04A	RVUE

[58] Partial wave analysis of the data on $p\overline{p} \to \overline{\Lambda}\Lambda$ from BARNES 00.

$f_1(2310)$ $I^G(J^{PC}) = 0^+(1^{++})$

MASS (MeV)	WIDTH (MeV)	DOCUMENT ID		TECN
2310 ± 60	255 ± 70	ANISOVICH	00J	SPEC

$\eta(2320)$ $I^G(J^{PC}) = 0^+(0^{-+})$

MASS (MeV)	WIDTH (MeV)	DOCUMENT ID		TECN
2320 ± 15	230 ± 35	[59] ANISOVICH	00M	SPEC

[59] From the combined analysis of $\overline{p}p \to \eta\eta\eta$ from ANISOVICH 00M and $\overline{p}p \to \eta\pi^0\pi^0$ from ANISOVICH 00J.

$\eta_4(2330)$ $I^G(J^{PC}) = 0^+(4^{-+})$

MASS (MeV)	WIDTH (MeV)	DOCUMENT ID		TECN	COMMENT
2328 ± 38	240 ± 90	ANISOVICH	00J	SPEC	2.0 $p\overline{p} \to \eta\pi^0\pi^0$

$\omega(2330)$ $I^G(J^{PC}) = 0^-(1^{--})$

MASS (MeV)	WIDTH (MeV)	DOCUMENT ID		TECN	COMMENT
2330 ± 30	435 ± 75	ATKINSON	88	OMEG	25–50 $\gamma p \to \rho^\pm\rho^0\pi^\mp$

$X(2340)$ $I^G(J^{PC}) = ?^?(?^{??})$

MASS (MeV)	WIDTH (MeV)	EVTS	DOCUMENT ID		TECN	COMMENT
2340 ± 20	180 ± 60	126	[60] BALTAY	75	HBC	15 $\pi^+ p \to p5\pi$

[60] Dominant decay into $\rho^0\rho^0\pi^+$. BALTAY 78 finds confirmation in $2\pi^+\pi^-2\pi^0$ events which contain $\rho^+\rho^0\pi^0$ and $2\rho^+\pi^-$.

$\pi(2360)$ $I^G(J^{PC}) = 1^-(0^{-+})$

MASS (MeV)	WIDTH (MeV)	DOCUMENT ID		TECN	COMMENT
2360 ± 25	300^{+100}_{-50}	ANISOVICH	01F	SPEC	2.0 $\overline{p}p \to 3\pi^0, \pi^0\eta, \pi^0\eta'$

$X(2360)$ $I^G(J^{PC}) = ?^?(4^{+?})$

MASS (MeV)	WIDTH (MeV)	DOCUMENT ID		TECN	COMMENT
2360 ± 10	430 ± 30	ROZANSKA	80	SPRK	18 $\pi^- p \to p\overline{p}n$

$X(2440)$ $I^G(J^{PC}) = ?^?(5^{-?})$

MASS (MeV)	WIDTH (MeV)	DOCUMENT ID		TECN	COMMENT
2440 ± 10	310 ± 20	ROZANSKA	80	SPRK	18 $\pi^- p \to p\overline{p}n$

$X(2540)$ $I^G(J^{PC}) = 0^+(0^{++})$

MASS (MeV)	WIDTH (MeV)	DOCUMENT ID		TECN	COMMENT
$2539 \pm 14^{+38}_{-14}$	$274^{+77+126}_{-61-163}$	UEHARA	13	BELL	$\gamma\gamma \to K^0_S K^0_S$

$\Gamma(\gamma\gamma) \times B(K\overline{K})$

VALUE (eV)	DOCUMENT ID		TECN	COMMENT
40^{+9+17}_{-7-40}	UEHARA	13	BELL	$\gamma\gamma \to K^0_S K^0_S$

$X(2632)$ $I^G(J^{PC}) = ?^?(?^{??})$

MASS (MeV)	WIDTH (MeV)	DOCUMENT ID		TECN	COMMENT
2635.2 ± 3.3		[61] EVDOKIMOV	04	SELX	$X(2632) \to D^+_s \eta$
2631.6 ± 2.1	< 17	[62] EVDOKIMOV	04	SELX	$X(2632) \to D^0 K^+$

[61] From a mass difference to D^+_s of 666.9 ± 3.3 MeV.

[62] From a mass difference to D^0 of 767.0 ± 2.0 MeV.

$B(X(2632) \to D^0 K^+)/B(X(2632) \to D^+_s \eta)$

VALUE	DOCUMENT ID		TECN
0.14 ± 0.06	[63] EVDOKIMOV	04	SELX

[63] Possible interpretation of this decay pattern is discussed by YASUI 07.

$X(2680)$ $I^G(J^{PC}) = ?^?(?^{??})$

MASS (MeV)	WIDTH (MeV)	DOCUMENT ID		TECN	COMMENT
2676 ± 27	150	CASO	70	HBC	$11.2\ \pi^- p \to \rho^- \pi^+ \pi^- p$

$X(2710)$ $I^G(J^{PC}) = ?^?(6^{+?})$

MASS (MeV)	WIDTH (MeV)	DOCUMENT ID		TECN	COMMENT
2710 ± 20	170 ± 40	ROZANSKA	80	SPRK	$18\ \pi^- p \to p\overline{p} n$

$X(2750)$ $I^G(J^{PC}) = ?^?(7^{-?})$

MASS (MeV)	WIDTH (MeV)	DOCUMENT ID		TECN	COMMENT
2747 ± 32	195 ± 75	DENNEY	83	LASS	$10\ \pi^+ p \to K^+ K^- \pi^+ p$

$f_6(3100)$ $I^G(J^{PC}) = 0^+(6^{++})$

MASS (MeV)	WIDTH (MeV)	DOCUMENT ID		TECN	COMMENT
3100 ± 100	700 ± 130	BINON	05	GAMS	$33\ \pi^- p \to \eta\eta n$

$X(3250)$ $I^G(J^{PC}) = ?^?(?^{??})$ 3-Body Decays

MASS (MeV)	WIDTH (MeV)	DOCUMENT ID		TECN	COMMENT
3250 ± 8 ± 20	45 ± 18	ALEEV	93	BIS2	$X(3250) \to \Lambda\overline{p} K^+$
3265 ± 7 ± 20	40 ± 18	ALEEV	93	BIS2	$X(3250) \to \overline{\Lambda} p K^-$

$X(3250)$ $I^G(J^{PC}) = ?^?(?^{??})$ 4-Body Decays

MASS (MeV)	WIDTH (MeV)	DOCUMENT ID		TECN	COMMENT
3245 ± 8 ± 20	25 ± 11	ALEEV	93	BIS2	$X(3250) \to \Lambda\overline{p} K^+ \pi^\pm$
3250 ± 9 ± 20	50 ± 20	ALEEV	93	BIS2	$X(3250) \to \overline{\Lambda} p K^- \pi^\mp$
3270 ± 8 ± 20	25 ± 11	ALEEV	93	BIS2	$X(3250) \to K^0_S p\overline{p} K^\pm$

$X(3350)$ $I^G(J^{PC}) = ?^?(?^{??})$

MASS (MeV)	WIDTH (MeV)	EVTS	DOCUMENT ID		TECN	COMMENT
$3350^{+10}_{-20} \pm 20$	$70^{+40}_{-30} \pm 40$	50 ± 10	[64] GABYSHEV	06A	BELL	$B^- \to \Lambda^+_c \overline{p} \pi^-$

[64] A similar enhancement in the $\Lambda^+_c \overline{p}$ final state is also reported by BABAR collaboration in AUBERT 10H.

REFERENCES for Further States

ABLIKIM	16N	PR D93 112011	M. Ablikim	(BES III Collab.)
ABLIKIM	13J	PR D87 032008	M. Ablikim *et al.*	(BES III Collab.)
UEHARA	13	PTEP 2013 123C01	S. Uehara *et al.*	(BELLE Collab.)
ANISOVICH	12	PR D85 014001	A.V. Anisovich *et al.*	
ANASHIN	11	PL B703 543	V.V. Anashin *et al.*	(KEDR Collab.)
ANISOVICH	11	EPJ C71 1511	A.V. Anisovich *et al.*	(LOQM, RAL, PNPI)
CHEN	11F	PR D84 071501	P. Chen *et al.*	(BELLE Collab.)
AUBERT	10H	PR D82 031102	B. Aubert *et al.*	(BABAR Collab.)
ABRAAMYAN	09	PR C80 034001	Kh.U. Abraamyan *et al.*	
LIU	09	PR D79 071102	C. Liu *et al.*	(BELLE Collab.)
VLADIMIRSK...	08	PAN 71 2129	V.V. Vladimirsky *et al.*	(ITEP)
		Translated from YAF 71 2166.		
VLADIMIRSK...	07	PAN 70 1706	V. Vladimirsky *et al.*	
		Translated from YAF 70 1751.		
YASUI	07	PR D76 034009	S. Yasui, M. Oka	
ABLIKIM	06J	PRL 96 162002	M. Ablikim *et al.*	(BES Collab.)
ABLIKIM	06S	PRL 97 142002	M. Ablikim *et al.*	(BES Collab.)
GABYSHEV	06A	PRL 97 242001	N. Gabyshev *et al.*	(BELLE Collab.)
SCHEGELSKY	06	EPJ A27 199	V.A. Schegelsky *et al.*	
SCHEGELSKY	06A	EPJ A27 207	V.A. Schegelsky *et al.*	
UMAN	06	PR D73 052009	I. Uman *et al.*	(FNAL E835)
VLADIMIRSK...	06	PAN 69 493	V.V. Vladimirsky *et al.*	(ITEP, Moscow)
		Translated from YAF 69 515.		
BINON	05	PAN 68 960	F. Binon *et al.*	
		Translated from YAF 68 998.		
GRIGOR'EV	05	PAN 68 1271	V.K. Grigor'ev *et al.*	(ITEP)
		Translated from YAF 68 1324.		
LU	05	PRL 94 032002	M. Lu *et al.*	(BNL E852 Collab.)
ABLIKIM	04J	PRL 93 112002	M. Ablikim *et al.*	(BES Collab.)
BUGG	04	PL B595 556 (errat.)	D.V. Bugg	
BUGG	04A	EPJ C36 161	D.V. Bugg	
BUGG	04C	PRPL 397 257	D.V. Bugg	
EVDOKIMOV	04	PRL 93 242001	A.V. Evdokimov *et al.*	(SELEX Collab.)
KUHN	04	PL B595 109	J. Kuhn *et al.*	(BNL E852 Collab.)
ANISOVICH	03	EPJ A16 229	V.V. Anisovich *et al.*	
VLADIMIRSK...	03	PAN 66 700	V.V. Vladimirsky *et al.*	
		Translated from YAF 66 729.		
ANISOVICH	02	PL B542 8	A.V. Anisovich *et al.*	
ANISOVICH	02B	PL B542 19	A.V. Anisovich *et al.*	
CHUNG	02	PR D65 072001	S.U. Chung *et al.*	(BNL E852 Collab.)
LINK	02K	PL B545 50	J.M. Link *et al.*	(FNAL FOCUS Collab.)
ANISOVICH	01C	PL B507 23	A.V. Anisovich *et al.*	
ANISOVICH	01D	PL B508 6	A.V. Anisovich *et al.*	
ANISOVICH	01E	PL B513 281	A.V. Anisovich *et al.*	
ANISOVICH	01F	PL B517 261	A.V. Anisovich *et al.*	
ANISOVICH	01G	PL B517 273	A.V. Anisovich *et al.*	
ANISOVICH	00B	NP A662 319	A.V. Anisovich *et al.*	
ANISOVICH	00D	PL B476 15	A.V. Anisovich *et al.*	
ANISOVICH	00E	PL B477 19	A.V. Anisovich *et al.*	
ANISOVICH	00I	PL B491 40	A.V. Anisovich *et al.*	
ANISOVICH	00J	PL B491 47	A.V. Anisovich *et al.*	
ANISOVICH	00M	PL B496 145	A.V. Anisovich *et al.*	
BARNES	00	PR C62 055203	P.D. Barnes *et al.*	
FILIPPI	00	PL B495 284	A. Filippi *et al.*	(OBELIX Experiment)
VLADIMIRSKII	00	JETPL 72 486	V.V. Vladimirskii *et al.*	
		Translated from ZETFP 72 698.		
ANISOVICH	99C	PL B452 173	A.V. Anisovich *et al.*	
ANISOVICH	99E	PL B452 187	A.V. Anisovich *et al.*	
ANISOVICH	99F	NP A651 253	A.V. Anisovich *et al.*	
ANISOVICH	99J	PL B471 271	A.V. Anisovich *et al.*	
ANISOVICH	99K	PL B468 309	A.V. Anisovich *et al.*	
BUGG	99	PL B458 511	D.V. Bugg *et al.*	
FERRER	99	EPJ C10 249	A. Ferrer *et al.*	
SEMENOV	99	SPU 42 847	S.V. Semenov	
		Translated from UFN 42 937.		
ADOMEIT	96	ZPHY C71 227	J. Adomeit *et al.*	(Crystal Barrel Collab.)
KLOET	96	PR D53 6120	W.M. Kloet, F. Myhrer	(RUTG, NORD)
PROKOSHKIN	96	PD 41 247	Y.D. Prokoshkin, V.D. Samoilenko	(SERP)
		Translated from DANS 348 481.		
HASAN	94	PL B334 215	A. Hasan, D.V. Bugg	(LOQM)
OAKDEN	94	NP A574 731	M.N. Oakden, M.R. Pennington	(DURH)
ALEEV	93	PAN 56 1358	A.N. Aleev *et al.*	(BIS-2 Collab.)
		Translated from YAF 56 100.		
ARMSTRONG	93D	PL B307 399	T.A. Armstrong *et al.*	(FNAL, FERR, GENO+)
ALBRECHT	91F	ZPHY C50 1	H. Albrecht *et al.*	(ARGUS Collab.)
CONDO	91	PR D43 2787	G.T. Condo *et al.*	(SLAC Hybrid Collab.)
BISELLO	89B	PR D39 701	G. Busetto *et al.*	(DM2 Collab.)
ATKINSON	88	ZPHY C38 535	M. Atkinson *et al.*	(BONN, CERN, GLAS+)
DAFTARI	87	PRL 58 859	I.K. Daftari *et al.*	(SYRA)
ALDE	86D	NP B269 485	D.M. Alde *et al.*	(BELG, LAPP, SERP, CERN+)
BRIDGES	86D	PL B180 313	D.L. Bridges *et al.*	(SYRA, BNL, CASE+)
GREEN	86	PRL 56 1639	D.R. Green *et al.*	(FNAL, ARIZ, FSU+)
ATKINSON	85	ZPHY C29 333	M. Atkinson *et al.*	(BONN, CERN, GLAS+)
DENNEY	83	PR D28 2726	D.L. Denney *et al.*	(IOWA, MICH)
ASTON	81B	NP B189 205	D. Aston *et al.*	(BONN, CERN, EPOL, GLAS+)
ARESTOV	80	IHEP 80-165	Y.I. Arestov *et al.*	(SERP)
CHLIAPNIK...	80	ZPHY C3 285	P.V. Chliapnikov *et al.*	(SERP, BRUX, MONS)
KREYMER	80	PR D22 36	A.E. Kreymer *et al.*	(IND, PURD, SLAC+)
ROZANSKA	80	NP B162 505	M. Rozanska *et al.*	(MPIM, CERN)
EVANGELIS...	79	NP B153 253	C. Evangelista *et al.*	(BARI, BONN, CERN+)
EVANGELIS...	79B	NP B154 381	C. Evangelista *et al.*	(BARI, BONN, CERN+)
BALTAY	78	PR D17 52	C. Baltay *et al.*	(COLU, BING)
ANTIPOV	77	NP B119 45	Y.M. Antipov *et al.*	(SERP, GEVA)
BALTAY	77	PRL 39 591	C. Baltay, C.V. Cautis, M. Kalelkar	(COLU)
BALTAY	75	PRL 35 891	C. Baltay *et al.*	(COLU, BING)
KALELKAR	75	Thesis Nevis 207	M.S. Kalelkar	(COLU)
CASO	70	LNC 3 707	C. Caso *et al.*	(GENO, HAMB, MILA, SACL)

STRANGE MESONS
($S = \pm 1$, $C = B = 0$)

$K^+ = u\bar{s}$, $K^0 = d\bar{s}$, $\overline{K}^0 = \bar{d}s$, $K^- = \bar{u}s$, similarly for K^*'s

$K^{\pm}$ $I(J^P) = \frac{1}{2}(0^-)$

See the related review(s):
Charged Kaon Mass

$K^{\pm}$ MASS

VALUE (MeV)	DOCUMENT ID		TECN	CHG	COMMENT
493.677±0.016 OUR FIT	Error includes scale factor of 2.8.				
493.677±0.013 OUR AVERAGE	Error includes scale factor of 2.4. See the ideogram below.				
493.696±0.007	[1] DENISOV	91	CNTR	–	Kaonic atoms
493.636±0.011	[2] GALL	88	CNTR	–	Kaonic atoms
493.640±0.054	LUM	81	CNTR	–	Kaonic atoms
493.670±0.029	BARKOV	79	EMUL	±	$e^+e^- \to K^+K^-$
493.657±0.020	[2] CHENG	75	CNTR	–	Kaonic atoms
493.691±0.040	BACKENSTO...73		CNTR	–	Kaonic atoms
• • • We do not use the following data for averages, fits, limits, etc. • • •					
493.631±0.007	GALL	88	CNTR	–	K^- Pb (9→ 8)
493.675±0.026	GALL	88	CNTR	–	K^- Pb (11→ 10)
493.709±0.073	GALL	88	CNTR	–	K^- W (9→ 8)
493.806±0.095	GALL	88	CNTR	–	K^- W (11→ 10)
493.640±0.022±0.008	[3] CHENG	75	CNTR	–	K^- Pb (9→ 8)
493.658±0.019±0.012	[3] CHENG	75	CNTR	–	K^- Pb (10→ 9)
493.638±0.035±0.016	[3] CHENG	75	CNTR	–	K^- Pb (11→ 10)
493.753±0.042±0.021	[3] CHENG	75	CNTR	–	K^- Pb (12→ 11)
493.742±0.081±0.027	[3] CHENG	75	CNTR	–	K^- Pb (13→ 12)

[1] Error increased from 0.0059 based on the error analysis in IVANOV 92.
[2] This value is the authors' combination of all of the separate transitions listed for this paper.
[3] The CHENG 75 values for separate transitions were calculated from their Table 7 transition energies. The first error includes a 20% systematic error in the noncircular contaminant shift. The second error is due to a ±5 eV uncertainty in the theoretical transition energies.

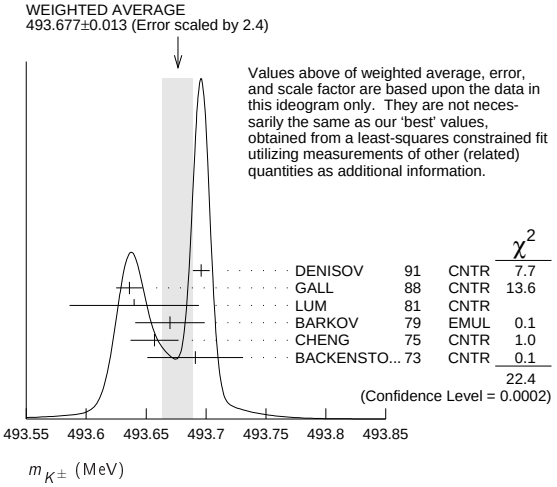

$m_{K^+} - m_{K^-}$

Test of CPT.

VALUE (MeV)	EVTS	DOCUMENT ID		TECN	CHG
−0.032±0.090	1.5M	[1] FORD	72	ASPK	±

[1] FORD 72 uses $m_{\pi^+} - m_{\pi^-} = +28 \pm 70$ keV.

$K^{\pm}$ MEAN LIFE

VALUE (10^{-8} s)	EVTS	DOCUMENT ID		TECN	CHG	COMMENT
1.2380±0.0020 OUR FIT	Error includes scale factor of 1.8.					
1.2379±0.0021 OUR AVERAGE	Error includes scale factor of 1.9. See the ideogram below.					
1.2347±0.0030	15M	[1] AMBROSINO	08	KLOE	±	$\phi \to K^+K^-$
1.2451±0.0030	250k	KOPTEV	95	CNTR		K at rest, U target
1.2368±0.0041	150k	KOPTEV	95	CNTR		K at rest, Cu target
1.2380±0.0016	3M	OTT	71	CNTR	+	K at rest
1.2272±0.0036		LOBKOWICZ	69	CNTR	+	K in flight
1.2443±0.0038		FITCH	65B	CNTR	+	K at rest
• • • We do not use the following data for averages, fits, limits, etc. • • •						
1.2415±0.0024	400k	[2] KOPTEV	95	CNTR		K at rest
1.221 ±0.011		FORD	67	CNTR	±	
1.231 ±0.011		BOYARSKI	62	CNTR	+	

[1] Result obtained by averaging the decay length and decay time analyses taking correlations into account.
[2] KOPTEV 95 report this weighted average of their U-target and Cu-target results, where they have weighted by $1/\sigma$ rather than $1/\sigma^2$.

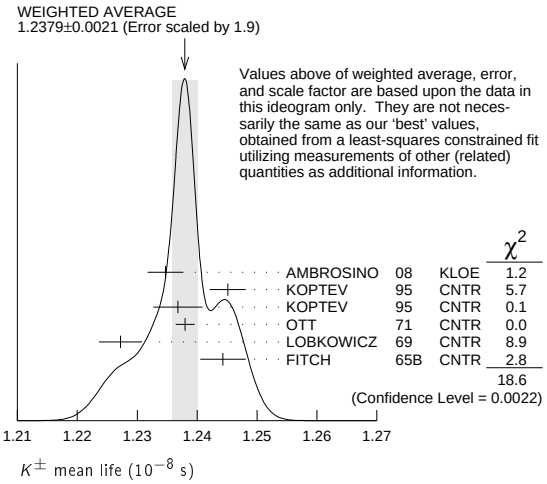

$(\tau_{K^+} - \tau_{K^-}) / \tau_{\text{average}}$

This quantity is a measure of CPT invariance in weak interactions.

VALUE (%)	DOCUMENT ID		TECN
0.10 ±0.09 OUR AVERAGE	Error includes scale factor of 1.2.		
−0.4 ±0.4	AMBROSINO	08	KLOE
0.090±0.078	LOBKOWICZ	69	CNTR
0.47 ±0.30	FORD	67	CNTR

See the related review(s):
Rare Kaon Decays

K^+ DECAY MODES

K^- modes are charge conjugates of the modes below.

	Mode	Fraction (Γ_i/Γ)	Scale factor/ Confidence level
	Leptonic and semileptonic modes		
Γ_1	$e^+\nu_e$	(1.582±0.007) × 10^{-5}	
Γ_2	$\mu^+\nu_\mu$	(63.56 ±0.11) %	S=1.2
Γ_3	$\pi^0 e^+ \nu_e$ Called K^+_{e3}.	(5.07 ±0.04) %	S=2.1
Γ_4	$\pi^0 \mu^+ \nu_\mu$ Called $K^+_{\mu 3}$.	(3.352±0.033) %	S=1.9
Γ_5	$\pi^0\pi^0 e^+\nu_e$	(2.55 ±0.04) × 10^{-5}	S=1.1
Γ_6	$\pi^+\pi^- e^+\nu_e$	(4.247±0.024) × 10^{-5}	
Γ_7	$\pi^+\pi^-\mu^+\nu_\mu$	(1.4 ±0.9) × 10^{-5}	
Γ_8	$\pi^0\pi^0\pi^0 e^+\nu_e$	< 3.5 × 10^{-6}	CL=90%
	Hadronic modes		
Γ_9	$\pi^+\pi^0$	(20.67 ±0.08) %	S=1.2
Γ_{10}	$\pi^+\pi^0\pi^0$	(1.760±0.023) %	S=1.1
Γ_{11}	$\pi^+\pi^+\pi^-$	(5.583±0.024) %	
	Leptonic and semileptonic modes with photons		
Γ_{12}	$\mu^+\nu_\mu\gamma$	[a,b] (6.2 ±0.8) × 10^{-3}	
Γ_{13}	$\mu^+\nu_\mu\gamma(\text{SD}^+)$	[c,d] (1.33 ±0.22) × 10^{-5}	
Γ_{14}	$\mu^+\nu_\mu\gamma(\text{SD}^+\text{INT})$	[c,d] < 2.7 × 10^{-5}	CL=90%
Γ_{15}	$\mu^+\nu_\mu\gamma(\text{SD}^- + \text{SD}^-\text{INT})$	[c,d] < 2.6 × 10^{-4}	CL=90%
Γ_{16}	$e^+\nu_e\gamma$	(9.4 ±0.4) × 10^{-6}	
Γ_{17}	$\pi^0 e^+\nu_e\gamma$	[a,b] (2.56 ±0.16) × 10^{-4}	
Γ_{18}	$\pi^0 e^+\nu_e\gamma(\text{SD})$	[c,d] < 5.3 × 10^{-5}	CL=90%
Γ_{19}	$\pi^0\mu^+\nu_\mu\gamma$	[a,b] (1.25 ±0.25) × 10^{-5}	
Γ_{20}	$\pi^0\pi^0 e^+\nu_e\gamma$	< 5 × 10^{-6}	CL=90%

Hadronic modes with photons or $\ell\overline{\ell}$ pairs

Γ_{21}	$\pi^+\pi^0\gamma$(INT)		$(-$ 4.2	$\pm$0.9	$)\times10^{-6}$	
Γ_{22}	$\pi^+\pi^0\gamma$(DE)	[a,e]	(6.0	$\pm$0.4	$)\times10^{-6}$	
Γ_{23}	$\pi^+\pi^0\pi^0\gamma$	[a,b]	(7.6	$^{+6.0}_{-3.0}$	$)\times10^{-6}$	
Γ_{24}	$\pi^+\pi^+\pi^-\gamma$	[a,b]	(1.04	$\pm$0.31	$)\times10^{-4}$	
Γ_{25}	$\pi^+\gamma\gamma$	[a]	(1.01	$\pm$0.06	$)\times10^{-6}$	
Γ_{26}	$\pi^+3\gamma$	[a]	< 1.0		$\times10^{-4}$	CL=90%
Γ_{27}	$\pi^+e^+e^-\gamma$		(1.19	$\pm$0.13	$)\times10^{-8}$	

Leptonic modes with $\ell\overline{\ell}$ pairs

Γ_{28}	$e^+\nu_e\nu\overline{\nu}$		< 6		$\times10^{-5}$	CL=90%
Γ_{29}	$\mu^+\nu_\mu\nu\overline{\nu}$		< 2.4		$\times10^{-6}$	CL=90%
Γ_{30}	$e^+\nu_e e^+e^-$		(2.48	$\pm$0.20	$)\times10^{-8}$	
Γ_{31}	$\mu^+\nu_\mu e^+e^-$		(7.06	$\pm$0.31	$)\times10^{-8}$	
Γ_{32}	$e^+\nu_e\mu^+\mu^-$		(1.7	$\pm$0.5	$)\times10^{-8}$	
Γ_{33}	$\mu^+\nu_\mu\mu^+\mu^-$		< 4.1		$\times10^{-7}$	CL=90%

Lepton family number (LF), Lepton number (L), $\Delta S=\Delta Q$ (SQ) violating modes, or $\Delta S=1$ weak neutral current ($S1$) modes

Γ_{34}	$\pi^+\pi^+e^-\overline{\nu}_e$	SQ	< 1.3		$\times10^{-8}$	CL=90%
Γ_{35}	$\pi^+\pi^+\mu^-\overline{\nu}_\mu$	SQ	< 3.0		$\times10^{-6}$	CL=95%
Γ_{36}	$\pi^+e^+e^-$	$S1$	(3.00	$\pm$0.09	$)\times10^{-7}$	
Γ_{37}	$\pi^+\mu^+\mu^-$	$S1$	(9.4	$\pm$0.6	$)\times10^{-8}$	S=2.6
Γ_{38}	$\pi^+\nu\overline{\nu}$	$S1$	(1.7	$\pm$1.1	$)\times10^{-10}$	
Γ_{39}	$\pi^+\pi^0\nu\overline{\nu}$	$S1$	< 4.3		$\times10^{-5}$	CL=90%
Γ_{40}	$\mu^-\nu e^+e^+$	LF	< 2.1		$\times10^{-8}$	CL=90%
Γ_{41}	$\mu^+\nu_e$	LF [f]	< 4		$\times10^{-3}$	CL=90%
Γ_{42}	$\pi^+\mu^+e^-$	LF	< 1.3		$\times10^{-11}$	CL=90%
Γ_{43}	$\pi^+\mu^-e^+$	LF	< 5.2		$\times10^{-10}$	CL=90%
Γ_{44}	$\pi^-\mu^+e^+$	L	< 5.0		$\times10^{-10}$	CL=90%
Γ_{45}	$\pi^-e^+e^+$	L	< 6.4		$\times10^{-10}$	CL=90%
Γ_{46}	$\pi^-\mu^+\mu^+$	L [f]	< 8.6		$\times10^{-11}$	CL=90%
Γ_{47}	$\mu^+\overline{\nu}_e$	L [f]	< 3.3		$\times10^{-3}$	CL=90%
Γ_{48}	$\pi^0e^+\overline{\nu}_e$	L	< 3		$\times10^{-3}$	CL=90%
Γ_{49}	$\pi^+\gamma$	[g]	< 2.3		$\times10^{-9}$	CL=90%

[a] See the Particle Listings below for the energy limits used in this measurement.

[b] Most of this radiative mode, the low-momentum γ part, is also included in the parent mode listed without γ's.

[c] Structure-dependent part.

[d] See the "Note on $\pi^\pm\to\ell^\pm\nu\gamma$ and $K^\pm\to\ell^\pm\nu\gamma$ Form Factors" in the $\pi^\pm$ Particle Listings for definitions and details.

[e] Direct-emission branching fraction.

[f] Derived from an analysis of neutrino-oscillation experiments.

[g] Violates angular-momentum conservation.

CONSTRAINED FIT INFORMATION

An overall fit to the mean life, a decay rate, and 15 branching ratios uses 35 measurements and one constraint to determine 8 parameters. The overall fit has a $\chi^2=53.4$ for 28 degrees of freedom.

The following *off-diagonal* array elements are the correlation coefficients $\langle\delta p_i\delta p_j\rangle/(\delta p_i\cdot\delta p_j)$, in percent, from the fit to parameters p_i, including the branching fractions, $x_i\equiv\Gamma_i/\Gamma_{\rm total}$. The fit constrains the x_i whose labels appear in this array to sum to one.

x_3	−66						
x_4	−64	90					
x_5	−12	−5	−5				
x_9	−67	0	−1	−6			
x_{10}	−13	−6	−5	91	−6		
x_{11}	−14	−6	−6	2	−7	2	
Γ	3	1	1	0	2	0	−24
	x_2	x_3	x_4	x_5	x_9	x_{10}	x_{11}

	Mode	Rate (10^8 s^{-1})	Scale factor
Γ_2	$\mu^+\nu_\mu$	0.5134 $\pm$0.0012	1.5
Γ_3	$\pi^0e^+\nu_e$ Called K^+_{e3}.	0.0410 $\pm$0.0004	2.1
Γ_4	$\pi^0\mu^+\nu_\mu$ Called $K^+_{\mu3}$.	0.02707 $\pm$0.00027	1.9
Γ_5	$\pi^0\pi^0e^+\nu_e$	$(2.059\ \pm0.029\ )\times10^{-5}$	1.1
Γ_9	$\pi^+\pi^0$	0.1670 $\pm$0.0007	1.3
Γ_{10}	$\pi^+\pi^0\pi^0$	0.01421 $\pm$0.00018	1.1
Γ_{11}	$\pi^+\pi^+\pi^-$	0.04510 $\pm$0.00019	

$K^\pm$ DECAY RATES

$\Gamma(\mu^+\nu_\mu)$ Γ_2

VALUE (10^6 s^{-1})	DOCUMENT ID		TECN	CHG
51.34 $\pm$0.12 OUR FIT Error includes scale factor of 1.5.				
• • • We do not use the following data for averages, fits, limits, etc. • • •				
51.2 $\pm$0.8	FORD	67	CNTR	$\pm$

$\Gamma(\pi^+\pi^+\pi^-)$ Γ_{11}

VALUE (10^6 s^{-1})	EVTS	DOCUMENT ID		TECN	CHG
4.510 $\pm$0.019 OUR FIT					
4.511 $\pm$0.024		[1] FORD	70	ASPK	
• • • We do not use the following data for averages, fits, limits, etc. • • •					
4.529 $\pm$0.032	3.2M	[1] FORD	70	ASPK	
4.496 $\pm$0.030		[1] FORD	67	CNTR	$\pm$

[1] First FORD 70 value is second FORD 70 combined with FORD 67.

K^+ BRANCHING RATIOS

Leptonic and semileptonic modes

$\Gamma(e^+\nu_e)/\Gamma(\mu^+\nu_\mu)$ Γ_1/Γ_2

See the note on "Decay Constants of Charged Pseudoscalar Mesons" in the D^+_s Listings.

VALUE (units 10^{-5})	EVTS	DOCUMENT ID		TECN	CHG
2.488 $\pm$0.009 OUR AVERAGE					
2.488 $\pm$0.007 $\pm$0.007	150k	[1] LAZZERONI	13	NA62	$\pm$
2.493 $\pm$0.025 $\pm$0.019	13.8K	[2] AMBROSINO	09E	KLOE	$\pm$
• • • We do not use the following data for averages, fits, limits, etc. • • •					
2.487 $\pm$0.011 $\pm$0.007	60k	[3] LAZZERONI	11	NA62	+
2.51 $\pm$0.15	404	HEINTZE	76	SPEC	+
2.37 $\pm$0.17	534	HEARD	75B	SPEC	+
2.42 $\pm$0.42	112	CLARK	72	OSPK	+

[1] LAZZERONI 13 uses full data sample collected from 2007 to 2008. This ratio is defined to be fully inclusive, including internal-bremsstrahlung.

[2] The ratio is defined to include internal-bremsstrahlung, ignoring direct-emission contributions. AMBROSINO 09E determined the ratio from the measurement of $\Gamma(K\to e\nu(\gamma)$, $E_\gamma<10$ MeV) / $\Gamma(K\to\mu\nu(\gamma))$. 89.8% of $K\to e\nu(\gamma)$ events had $E_\gamma<10$ MeV.

[3] This ratio is defined to be fully inclusive, including internal-bremsstrahlung.

$\Gamma(\mu^+\nu_\mu)/\Gamma_{\rm total}$ Γ_2/Γ

See the note on "Decay Constants of Charged Pseudoscalar Mesons" in the D^+_s Listings.

VALUE (units 10^{-2})	EVTS	DOCUMENT ID		TECN	CHG	COMMENT
63.56 $\pm$0.11 OUR FIT Error includes scale factor of 1.2.						
63.60 $\pm$0.16 OUR AVERAGE						
63.66 $\pm$0.09 $\pm$0.15	865k	[1] AMBROSINO	06A	KLOE	+	
63.24 $\pm$0.44	62k	CHIANG	72	OSPK	+	1.84 GeV/c K^+

[1] Fully inclusive. Used tagged kaons from ϕ decays.

$\Gamma(\pi^0e^+\nu_e)/\Gamma_{\rm total}$ Γ_3/Γ

VALUE (units 10^{-2})	EVTS	DOCUMENT ID		TECN	CHG	COMMENT
5.07 $\pm$0.04 OUR FIT Error includes scale factor of 2.1.						
4.94 $\pm$0.05 OUR AVERAGE						
4.965 $\pm$0.038 $\pm$0.037		[1] AMBROSINO	08A	KLOE	$\pm$	
4.86 $\pm$0.10	3516	CHIANG	72	OSPK	+	1.84 GeV/c K^+
• • • We do not use the following data for averages, fits, limits, etc. • • •						
4.7 $\pm$0.3	429	SHAKLEE	64	HLBC	+	
5.0 $\pm$0.5		ROE	61	HLBC	+	

[1] Depends on K^+ lifetime τ. AMBROSINO 08A uses PDG 06 value of $\tau=(1.2385\pm0.0024)\times10^{-8}$ sec. The correlation between K^+_{e3} and $K^+_{\mu3}$ branching fraction measurements is 62.7%.

$\Gamma(\pi^0e^+\nu_e)/\Gamma(\mu^+\nu_\mu)$ Γ_3/Γ_2

VALUE	EVTS	DOCUMENT ID		TECN	CHG
0.0798 $\pm$0.0008 OUR FIT Error includes scale factor of 1.9.					
• • • We do not use the following data for averages, fits, limits, etc. • • •					
0.069 $\pm$0.006	350	ZELLER	69	ASPK	+
0.0775 $\pm$0.0033	960	BOTTERILL	68C	ASPK	+
0.069 $\pm$0.006	561	GARLAND	68	OSPK	+
0.0791 $\pm$0.0054	295	[1] AUERBACH	67	OSPK	+

[1] AUERBACH 67 changed from 0.0797 $\pm$ 0.0054. See comment with ratio $\Gamma(\pi^0\mu^+\nu_\mu)/\Gamma(\mu^+\nu_\mu)$. The value 0.0785 $\pm$ 0.0025 given in AUERBACH 67 is an average of AUERBACH 67 $\Gamma(\pi^0e^+\nu_e)/\Gamma(\mu^+\nu_\mu)$ and CESTER 66 $\Gamma(\pi^0e^+\nu_e)/\left[\Gamma(\mu^+\nu_\mu)+\Gamma(\pi^+\pi^0)\right]$.

$\Gamma(\pi^0 e^+ \nu_e)/[\Gamma(\mu^+ \nu_\mu) + \Gamma(\pi^+ \pi^0)]$ $\Gamma_3/(\Gamma_2+\Gamma_9)$

VALUE (units 10^{-2})	EVTS	DOCUMENT ID		TECN	CHG
6.02±0.06 OUR FIT Error includes scale factor of 2.1.					
6.02±0.15 OUR AVERAGE					
6.16±0.22	5110	ESCHSTRUTH	68	OSPK	+
5.89±0.21	1679	CESTER	66	OSPK	+
• • • We do not use the following data for averages, fits, limits, etc. • • •					
5.92±0.65		[1] WEISSENBE...	76	SPEC	+

[1] Value calculated from WEISSENBERG 76 ($\pi^0 e\nu$), ($\mu\nu$), and ($\pi\pi^0$) values to eliminate dependence on our 1974 ($\pi 2\pi^0$) and ($\pi\pi^+\pi^-$) fractions.

$\Gamma(\pi^0 e^+ \nu_e)/[\Gamma(\pi^0 \mu^+ \nu_\mu) + \Gamma(\pi^+ \pi^0) + \Gamma(\pi^+ \pi^0 \pi^0)]$ $\Gamma_3/(\Gamma_4+\Gamma_9+\Gamma_{10})$

VALUE	EVTS	DOCUMENT ID		TECN	CHG
0.1967±0.0016 OUR FIT Error includes scale factor of 2.5.					
0.1962±0.0008±0.0035	71k	SHER	03	B865	+

$\Gamma(\pi^0 e^+ \nu_e)/\Gamma(\pi^+ \pi^0)$ Γ_3/Γ_9

VALUE	EVTS	DOCUMENT ID		TECN	CHG	COMMENT
0.2454±0.0023 OUR FIT Error includes scale factor of 2.6.						
0.2467±0.0011 OUR AVERAGE Error includes scale factor of 1.1.						
0.2423±0.0015±0.0037	31k	UVAROV	14	ISTR	−	ISTRA+
0.2470±0.0009±0.0004	87k	BATLEY	07A	NA48	±	
• • • We do not use the following data for averages, fits, limits, etc. • • •						
0.221 ±0.012	786	[1] LUCAS	73B	HBC	−	Dalitz pairs only

[1] LUCAS 73B gives N(K_{e3}) = 786 ± 3.1%, N(2π) = 3564 ± 3.1%. We use these values to obtain quoted result.

$\Gamma(\pi^0 e^+ \nu_e)/\Gamma(\pi^+ \pi^+ \pi^-)$ Γ_3/Γ_{11}

VALUE	EVTS	DOCUMENT ID		TECN	CHG
0.908±0.009 OUR FIT Error includes scale factor of 1.6.					
• • • We do not use the following data for averages, fits, limits, etc. • • •					
0.867±0.027	2768	BARMIN	87	XEBC	+
0.856±0.040	2827	BRAUN	75	HLBC	+
0.850±0.019	4385	[1] HAIDT	71	HLBC	+
0.846±0.021	4385	[1] EICHTEN	68	HLBC	+
0.94 ±0.09	854	BELLOTTI	67B	HLBC	
0.90 ±0.06	230	BORREANI	64	HBC	+

[1] HAIDT 71 is a reanalysis of EICHTEN 68. Not included in average because of large discrepancy in $\Gamma(\pi^0 \mu^+ \nu)/\Gamma(\pi^0 e^+ \nu)$ with more precise results.

$\Gamma(\pi^0 \mu^+ \nu_\mu)/\Gamma_{\text{total}}$ Γ_4/Γ

VALUE (units 10^{-2})	EVTS	DOCUMENT ID		TECN	CHG	COMMENT
3.352±0.033 OUR FIT Error includes scale factor of 1.9.						
3.24 ±0.04 OUR AVERAGE						
3.233±0.029±0.026		[1] AMBROSINO	08A	KLOE	±	
3.33 ±0.16	2345	CHIANG	72	OSPK	+	1.84 GeV/c K^+
• • • We do not use the following data for averages, fits, limits, etc. • • •						
2.8 ±0.4		[2] TAYLOR	59	EMUL	+	

[1] Depends on K^+ lifetime τ. AMBROSINO 08A uses PDG 06 value of $\tau = (1.2385 \pm 0.0024) \times 10^{-8}$ sec. The correlation between K^+_{e3} and $K^+_{\mu 3}$ branching fraction measurements is 62.7%.

[2] Earlier experiments not averaged.

$\Gamma(\pi^0 \mu^+ \nu_\mu)/\Gamma(\mu^+ \nu_\mu)$ Γ_4/Γ_2

VALUE	EVTS	DOCUMENT ID		TECN	CHG
0.0527±0.0006 OUR FIT Error includes scale factor of 1.8.					
• • • We do not use the following data for averages, fits, limits, etc. • • •					
0.054 ±0.009	240	ZELLER	69	ASPK	+
0.0480±0.0037	424	[1] GARLAND	68	OSPK	+
0.0486±0.0040	307	[2] AUERBACH	67	OSPK	+

[1] GARLAND 68 changed from 0.055 ± 0.004 in agreement with μ-spectrum calculation of GAILLARD 70 appendix B. L.G.Pondrom, (private communication 73).

[2] AUERBACH 67 changed from 0.0602 ± 0.0046 by erratum which brings the μ-spectrum calculation into agreement with GAILLARD 70 appendix B.

$\Gamma(\pi^0 \mu^+ \nu_\mu)/\Gamma(\pi^0 e^+ \nu_e)$ Γ_4/Γ_3

VALUE	EVTS	DOCUMENT ID		TECN	CHG	COMMENT
0.6608±0.0029 OUR FIT Error includes scale factor of 1.1.						
0.6618±0.0027 OUR AVERAGE						
0.663 ±0.003 ±0.001	77k	BATLEY	07A	NA48	±	
0.671 ±0.007 ±0.008	24k	HORIE	01	SPEC		
0.670 ±0.014		[1] HEINTZE	77	SPEC	+	
0.667 ±0.017	5601	BOTTERILL	68B	ASPK	+	
• • • We use the following data for averages but not for fits. • • •						
0.6511±0.0064		[2] AMBROSINO	08A	KLOE	±	
• • • We do not use the following data for averages, fits, limits, etc. • • •						
0.608 ±0.014	1585	[3] BRAUN	75	HLBC	+	
0.705 ±0.063	554	[4] LUCAS	73B	HBC	−	Dalitz pairs only
0.698 ±0.025	3480	[5] CHIANG	72	OSPK	+	1.84 GeV/c K^+
0.596 ±0.025		[6] HAIDT	71	HLBC	+	
0.604 ±0.022	1398	[6] EICHTEN	68	HLBC		
0.703 ±0.056	1509	CALLAHAN	66B	HLBC		

[1] HEINTZE 77 value from fit to λ_0. Assumes μ-e universality.

[2] Not used in the fit. This result enters the fit via correlation of K^+_{e3} and $K^+_{\mu 3}$ branching fraction measurements of AMBROSINO 08A.

[3] BRAUN 75 value is from form factor fit. Assumes μ-e universality.

[4] LUCAS 73B gives N($K_{\mu 3}$) = 554 ± 7.6%, N(K_{e3}) = 786 ± 3.1%. We divide.

[5] CHIANG 72 $\Gamma(\pi^0 \mu^+ \nu_\mu)/\Gamma(\pi^0 e^+ \nu_e)$ is statistically independent of CHIANG 72 $\Gamma(\pi^0 \mu^+ \nu_\mu)/\Gamma_{\text{total}}$ and $\Gamma(\pi^0 e^+ \nu_e)/\Gamma_{\text{total}}$.

[6] HAIDT 71 is a reanalysis of EICHTEN 68. Not included in average because of large discrepancy with more precise results.

$[\Gamma(\pi^0 \mu^+ \nu_\mu) + \Gamma(\pi^+ \pi^0)]/\Gamma_{\text{total}}$ $(\Gamma_4+\Gamma_9)/\Gamma$

We combine these two modes for experiments measuring them in xenon bubble chamber because of difficulties of separating them there.

VALUE (units 10^{-2})	EVTS	DOCUMENT ID		TECN	CHG
24.02±0.08 OUR FIT Error includes scale factor of 1.2.					
• • • We do not use the following data for averages, fits, limits, etc. • • •					
25.4 ±0.9	886	SHAKLEE	64	HLBC	+
23.4 ±1.1		ROE	61	HLBC	+

$\Gamma(\pi^0 \mu^+ \nu_\mu)/\Gamma(\pi^+ \pi^0)$ Γ_4/Γ_9

VALUE	EVTS	DOCUMENT ID		TECN	CHG
0.1637±0.0006±0.0003	77k	BATLEY	07A	NA48	±

$\Gamma(\pi^0 \mu^+ \nu_\mu)/\Gamma(\pi^+ \pi^+ \pi^-)$ Γ_4/Γ_{11}

VALUE	EVTS	DOCUMENT ID		TECN	CHG	COMMENT
0.600±0.007 OUR FIT Error includes scale factor of 1.6.						
• • • We do not use the following data for averages, fits, limits, etc. • • •						
0.503±0.019	1505	[1] HAIDT	71	HLBC	+	
0.510±0.017	1505	[1] EICHTEN	68	HLBC	+	
0.63 ±0.07	2845	[2] BISI	65B	BC	+	HBC+HLBC

[1] HAIDT 71 is a reanalysis of EICHTEN 68. Not included in average because of large discrepancy in $\Gamma(\pi^0 \mu^+ \nu)/\Gamma(\pi^0 e^+ \nu)$ with more precise results.

[2] Error enlarged for background problems. See GAILLARD 70.

$\Gamma(\pi^0 \pi^0 e^+ \nu_e)/\Gamma_{\text{total}}$ Γ_5/Γ

VALUE (units 10^{-5})	EVTS	DOCUMENT ID		TECN	CHG
2.55±0.04 OUR FIT Error includes scale factor of 1.1.					
2.54±0.89	10	BARMIN	88B	HLBC	+

$\Gamma(\pi^0 \pi^0 e^+ \nu_e)/\Gamma(\pi^+ \pi^0 \pi^0)$ Γ_5/Γ_{10}

VALUE (units 10^{-3})	EVTS	DOCUMENT ID		TECN	CHG
1.449±0.008 OUR FIT					
1.449±0.006±0.006	65.2k	[1] BATLEY	14A	NA48	±

[1] Data collected in 2003–2004. This leads to the scalar form factor $(1+\delta_{EM})\, f_s = 6.079 \pm 0.012 \pm 0.027 \pm 0.046$ where the last error is due to the normalizing decay mode uncertainty.

$\Gamma(\pi^0 \pi^0 e^+ \nu_e)/\Gamma(\pi^0 e^+ \nu_e)$ Γ_5/Γ_3

VALUE (units 10^{-4})	EVTS	DOCUMENT ID		TECN	CHG
5.03±0.09 OUR FIT Error includes scale factor of 1.2.					
4.1 $^{+1.0}_{-0.7}$ OUR AVERAGE					
4.2 $^{+1.0}_{-0.9}$	25	BOLOTOV	86B	CALO	−
3.8 $^{+5.0}_{-1.2}$	2	LJUNG	73	HLBC	+

$\Gamma(\pi^+ \pi^- e^+ \nu_e)/\Gamma(\pi^+ \pi^+ \pi^-)$ Γ_6/Γ_{11}

VALUE (units 10^{-4})	EVTS	DOCUMENT ID		TECN	CHG
7.606±0.029 OUR AVERAGE					
7.615±0.008±0.028	1.1M	[1] BATLEY	12	NA48	±
7.35 ±0.01 ±0.19	388k	[2] PISLAK	01	B865	
7.21 ±0.32	30k	ROSSELET	77	SPEC	+
• • • We do not use the following data for averages, fits, limits, etc. • • •					
7.36 ±0.68	500	BOURQUIN	71	ASPK	
7.0 ±0.9	106	SCHWEINB...	71	HLBC	+
5.83 ±0.63	269	ELY	69	HLBC	+

[1] BATLEY 12 uses data collected in 2003–2004. The result is inclusive of $K^\pm \to \pi^+\pi^- e^\pm \nu\gamma$ decays. Using PDG 12 value for $\Gamma(\pi^+\pi^-\pi^+)/\Gamma = (5.59 \pm 0.04) \times 10^{-2}$. BATLEY 12 obtains $B(\pi^+\pi^- e\nu) = (4.257 \pm 0.004 \pm 0.035) \times 10^{-5}$ where the syst. error is dominated by the error on the normalization mode.

[2] PISLAK 01 reports $\Gamma(\pi^+\pi^- e^+ \nu_e)/\Gamma_{\text{total}} = (4.109 \pm 0.008 \pm 0.110) \times 10^{-5}$ using the PDG 00 value $\Gamma(\pi^+\pi^+\pi^-)/\Gamma_{\text{total}} = (5.59 \pm 0.05) \times 10^{-2}$. We divide by the PDG value and unfold its error from the systematic error. PISLAK 03 and PISLAK 10A give additional details on the branching ratio measurement and give improved errors on the S-wave π-π scattering length: $a_0^0 = 0.235 \pm 0.013$ and $a_0^2 = -0.0410 \pm 0.0027$.

$\Gamma(\pi^+ \pi^- \mu^+ \nu_\mu)/\Gamma_{\text{total}}$ Γ_7/Γ

VALUE (units 10^{-5})	EVTS	DOCUMENT ID		TECN	CHG
• • • We do not use the following data for averages, fits, limits, etc. • • •					
0.77 $^{+0.54}_{-0.50}$	1	CLINE	65	FBC	+

$\Gamma(\pi^+\pi^-\mu^+\nu_\mu)/\Gamma(\pi^+\pi^+\pi^-)$ Γ_7/Γ_{11}

VALUE (units 10^{-4})	EVTS	DOCUMENT ID		TECN	CHG
2.57±1.55	7	BISI	67	DBC	+
• • • We do not use the following data for averages, fits, limits, etc. • • •					
~ 2.5	1	GREINER	64	EMUL	+

$\Gamma(\pi^0\pi^0\pi^0 e^+\nu_e)/\Gamma_{total}$ Γ_8/Γ

VALUE (units 10^{-6})	CL%	EVTS	DOCUMENT ID		TECN	CHG
<3.5	90	0	BOLOTOV	88	SPEC	−
• • • We do not use the following data for averages, fits, limits, etc. • • •						
<9	90	0	BARMIN	92	XEBC	+

Hadronic modes

$\Gamma(\pi^+\pi^0)/\Gamma_{total}$ Γ_9/Γ

VALUE (units 10^{-2})	EVTS	DOCUMENT ID		TECN	CHG	COMMENT
20.67±0.08 OUR FIT Error includes scale factor of 1.2.						
20.70±0.16 OUR AVERAGE Error includes scale factor of 1.8.						
20.65±0.05±0.08	1.4M	[1] AMBROSINO	08E	KLOE	+	$\phi \to K^+K^-$
21.18±0.28	16k	CHIANG	72	OSPK	+	1.84 GeV/c K^+
• • • We do not use the following data for averages, fits, limits, etc. • • •						
21.0 ±0.6		CALLAHAN	65	HLBC		See Γ_9/Γ_{11}

[1] Fully inclusive of final-state radiation. The branching ratio is evaluated using K^+ lifetime, τ= 12.385 ns.

$\Gamma(\pi^+\pi^0)/\Gamma(\pi^+\pi^+\pi^-)$ Γ_9/Γ_{11}

VALUE	EVTS	DOCUMENT ID		TECN	CHG
3.702±0.022 OUR FIT Error includes scale factor of 1.1.					
• • • We do not use the following data for averages, fits, limits, etc. • • •					
3.96 ±0.15	1045	CALLAHAN	66	FBC	+

$\Gamma(\pi^+\pi^0)/\Gamma(\mu^+\nu_\mu)$ Γ_9/Γ_2

VALUE	EVTS	DOCUMENT ID		TECN	CHG	COMMENT
0.3252±0.0016 OUR FIT Error includes scale factor of 1.2.						
0.3325±0.0032 OUR AVERAGE						
0.3329±0.0047±0.0010	45k	USHER	92	SPEC	+	$p\overline{p}$ at rest
0.3355±0.0057		[1] WEISSENBE...	76	SPEC	+	
0.3277±0.0065	4517	[2] AUERBACH	67	OSPK	+	
• • • We do not use the following data for averages, fits, limits, etc. • • •						
0.328 ±0.005	25k	[1] WEISSENBE...	74	STRC	+	
0.305 ±0.018	1600	ZELLER	69	ASPK	+	

[1] WEISSENBERG 76 revises WEISSENBERG 74.
[2] AUERBACH 67 changed from 0.3253 ± 0.0065. See comment with ratio $\Gamma(\pi^0\mu^+\nu_\mu)/\Gamma(\mu^+\nu_\mu)$.

$\Gamma(\pi^+\pi^0\pi^0)/\Gamma_{total}$ Γ_{10}/Γ

VALUE (units 10^{-2})	EVTS	DOCUMENT ID		TECN	CHG	COMMENT
1.760±0.023 OUR FIT Error includes scale factor of 1.1.						
1.775±0.028 OUR AVERAGE Error includes scale factor of 1.2.						
1.763±0.013±0.022		ALOISIO	04A	KLOE	±	
1.84 ±0.06	1307	CHIANG	72	OSPK	+	1.84 GeV/c K^+
• • • We do not use the following data for averages, fits, limits, etc. • • •						
1.53 ±0.11	198	[1] PANDOULAS	70	EMUL	+	
1.8 ±0.2	108	SHAKLEE	64	HLBC	+	
1.7 ±0.2		ROE	61	HLBC	+	
1.5 ±0.2		[2] TAYLOR	59	EMUL	+	

[1] Includes events of TAYLOR 59.
[2] Earlier experiments not averaged.

$\Gamma(\pi^+\pi^0\pi^0)/\Gamma(\pi^+\pi^0)$ Γ_{10}/Γ_9

VALUE	EVTS	DOCUMENT ID		TECN	CHG	COMMENT
0.0851±0.0012 OUR FIT Error includes scale factor of 1.1.						
• • • We do not use the following data for averages, fits, limits, etc. • • •						
0.081 ±0.005	574	[1] LUCAS	73B	HBC	−	Dalitz pairs only

[1] LUCAS 73B gives N($\pi 2\pi^0$) = 574 ± 5.9%, N(2π) = 3564 ± 3.1%. We quote 0.5N($\pi 2\pi^0$)/N(2π) where 0.5 is because only Dalitz pair π^0's were used.

$\Gamma(\pi^+\pi^0\pi^0)/\Gamma(\pi^+\pi^+\pi^-)$ Γ_{10}/Γ_{11}

VALUE	EVTS	DOCUMENT ID		TECN	CHG	COMMENT
0.315±0.004 OUR FIT Error includes scale factor of 1.1.						
0.303±0.009	2027	BISI	65	BC	+	HBC+HLBC
• • • We do not use the following data for averages, fits, limits, etc. • • •						
0.393±0.099	17	YOUNG	65	EMUL	+	

$\Gamma(\pi^+\pi^+\pi^-)/\Gamma_{total}$ Γ_{11}/Γ

VALUE (units 10^{-2})	EVTS	DOCUMENT ID		TECN	CHG	COMMENT
5.583±0.024 OUR FIT						
5.565±0.031±0.025	68K	[1] BABUSCI	14B	KLOE	+	
• • • We do not use the following data for averages, fits, limits, etc. • • •						
5.56 ±0.20	2330	[2] CHIANG	72	OSPK	+	1.84 GeV/c K^+
5.34 ±0.21	693	[3] PANDOULAS	70	EMUL	+	
5.71 ±0.15		DEMARCO	65	HBC		
6.0 ±0.4	44	YOUNG	65	EMUL	+	
5.54 ±0.12	2332	CALLAHAN	64	HLBC	+	
5.1 ±0.2	540	SHAKLEE	64	HLBC	+	
5.7 ±0.3		ROE	61	HLBC	+	

[1] Inclusive of final-state radiation. Result obtained from averaging two branching ratios: one from a sample with $K^- \to \mu\nu(\gamma)$ tagging and another with $K^- \to \pi^-\pi^0(\gamma)$ tagging.
[2] Value is not independent of CHIANG 72 $\Gamma(\mu^+\nu_\mu)/\Gamma_{total}$, $\Gamma(\pi^+\pi^0)/\Gamma_{total}$, $\Gamma(\pi^+\pi^0\pi^0)/\Gamma_{total}$, $\Gamma(\pi^0\mu^+\nu_\mu)/\Gamma_{total}$, and $\Gamma(\pi^0 e^+\nu_e)/\Gamma_{total}$.
[3] Includes events of TAYLOR 59.

Leptonic and semileptonic modes with photons

$\Gamma(\mu^+\nu_\mu\gamma)/\Gamma_{total}$ Γ_{12}/Γ

VALUE (units 10^{-3})	EVTS	DOCUMENT ID		TECN	CHG	COMMENT
6.2±0.8 OUR AVERAGE						
6.6±1.5		[1,2] DEMIDOV	90	XEBC		P(μ) <231.5 MeV/c
6.0±0.9		BARMIN	88	HLBC	+	P(μ) <231.5 MeV/c
• • • We do not use the following data for averages, fits, limits, etc. • • •						
3.5±0.8		[2,3] DEMIDOV	90	XEBC		E(γ) > 20 MeV
3.2±0.5	57	[4] BARMIN	88	HLBC	+	$E(\gamma)$ >20 MeV
5.4±0.3		[5] AKIBA	85	SPEC		P(μ) <231.5 MeV/c

[1] P(μ) cut given in DEMIDOV 90 paper, 235.1 MeV/c, is a misprint according to authors (private communication).
[2] DEMIDOV 90 quotes only inner bremsstrahlung (IB) part.
[3] Not independent of above DEMIDOV 90 value. Cuts differ.
[4] Not independent of above BARMIN 88 value. Cuts differ.
[5] Assumes μ-e universality and uses constraints from $K \to e\nu\gamma$.

$\Gamma(\mu^+\nu_\mu\gamma(\mathrm{SD}^+))/\Gamma_{total}$ Γ_{13}/Γ

Structure-dependent part with $+\gamma$ helicity (SD$^+$ term). See the "Note on $\pi^\pm \to \ell^\pm\nu\gamma$ and $K^\pm \to \ell^\pm\nu\gamma$ Form Factors" in the $\pi^\pm$ section of the Particle Data Listings above.

VALUE (units 10^{-5})	CL%	EVTS	DOCUMENT ID		TECN
1.33±0.12±0.18		2588	[1] ADLER	00B	B787
• • • We do not use the following data for averages, fits, limits, etc. • • •					
<3.0	90		AKIBA	85	SPEC

[1] ADLER 00B obtains the branching ratio by extrapolating the measurement in the kinematic region $E_\mu > 137$ MeV, $E_\gamma > 90$ MeV to the full SD$^+$ phase-space. Also reports $|F_V + F_A| = 0.165 \pm 0.007 \pm 0.011$ and $-0.04 < F_V - F_A < 0.24$ at 90% CL.

$\Gamma(\mu^+\nu_\mu\gamma(\mathrm{SD}^+\mathrm{INT}))/\Gamma_{total}$ Γ_{14}/Γ

Interference term between internal Bremsstrahlung and SD$^+$ term. See the "Note on $\pi^\pm \to \ell^\pm\nu\gamma$ and $K^\pm \to \ell^\pm\nu\gamma$ Form Factors" in the $\pi^\pm$ section of the Particle Data Listings above.

VALUE (units 10^{-5})	CL%	DOCUMENT ID		TECN
<2.7	90	AKIBA	85	SPEC

$\Gamma(\mu^+\nu_\mu\gamma(\mathrm{SD}^- + \mathrm{SD}^-\mathrm{INT}))/\Gamma_{total}$ Γ_{15}/Γ

Sum of structure-dependent part with $-\gamma$ helicity (SD$^-$ term) and interference term between internal Bremsstrahlung and SD$^-$ term. See the "Note on $\pi^\pm \to \ell^\pm\nu\gamma$ and $K^\pm \to \ell^\pm\nu\gamma$ Form Factors" in the $\pi^\pm$ section of the Particle Data Listings above.

VALUE (units 10^{-4})	CL%	DOCUMENT ID		TECN
<2.6	90	[1] AKIBA	85	SPEC

[1] Assumes μ-e universality and uses constraints from $K \to e\nu\gamma$.

$\Gamma(e^+\nu_e\gamma)/\Gamma(\mu^+\nu_\mu)$ Γ_{16}/Γ_2

VALUE (units 10^{-5})	EVTS	DOCUMENT ID		TECN	CHG	COMMENT
1.483±0.066±0.013	1.4K	[1] AMBROSINO	09E	KLOE	±	E_γ in 10–250 MeV, p_e > 200 MeV/c

[1] AMBROSINO 09E measured the differential width $dR_\gamma/dE_\gamma = (1/\Gamma(K \to \mu\nu))(d\Gamma(K \to e\nu\gamma)/dE_\gamma)$. Result obtained by integrating the differential width over E_γ from 10 to 250 MeV.

$\Gamma(\pi^0 e^+\nu_e\gamma)/\Gamma(\pi^0 e^+\nu_e)$ Γ_{17}/Γ_3

VALUE (units 10^{-2})	EVTS	DOCUMENT ID		TECN	CHG	COMMENT
0.505±0.032 OUR AVERAGE Error includes scale factor of 1.3. See the ideogram below.						
0.47 ±0.02 ±0.03	4476	[1] AKIMENKO	07	ISTR	−	$E_\gamma > 10$ MeV, 0.6 < cos($\theta_{e\gamma}$) < 0.9
0.46 ±0.08	82	[2] BARMIN	91	XEBC		$E_\gamma > 10$ MeV, 0.6 < cos($\theta_{e\gamma}$) < 0.9
0.56 ±0.04	192	[3] BOLOTOV	86B	CALO	−	$E_\gamma > 10$ MeV
• • • We do not use the following data for averages, fits, limits, etc. • • •						
1.81 ±0.03 ±0.07	4476	[1] AKIMENKO	07	ISTR	−	E_γ>10 MeV, $\theta_{e\gamma}$ >10°
0.63 ±0.02 ±0.03	4476	[1] AKIMENKO	07	ISTR	−	E_γ>30 MeV, $\theta_{e\gamma}$ >20°
1.51 ±0.25	82	[2] BARMIN	91	XEBC		$E_\gamma > 10$ MeV, cos($\theta_{e\gamma}$) < 0.98
0.48 ±0.20	16	[4] LJUNG	73	HLBC	+	$E_\gamma > 30$ MeV
0.22 $^{+0.15}_{-0.10}$		[4] LJUNG	73	HLBC	+	$E_\gamma > 30$ MeV
0.76 ±0.28	13	[5] ROMANO	71	HLBC		$E_\gamma > 10$ MeV
0.53 ±0.22		[5] ROMANO	71	HLBC	+	$E_\gamma > 30$ MeV
1.2 ±0.8		BELLOTTI	67	HLBC		$E_\gamma > 30$ MeV

[1] AKIMENKO 07 provides values for three kinematic regions. For averaging, we use value with $E_\gamma > 10$ MeV and $0.6 < \cos(\theta_{e\gamma}) < 0.9$.

[2] BARMIN 91 quotes branching ratio $\Gamma(K \to e\pi^0\nu\gamma)/\Gamma_{all}$. The measured normalization is $[\Gamma(K \to e\pi^0\nu) + \Gamma(K \to \pi^+\pi^+\pi^-)]$. For comparison with other experiments we used $\Gamma(K \to e\pi^0\nu)/\Gamma_{all} = 0.0482$ to calculate the values quoted here.

[3] $\cos(\theta_{e\gamma})$ between 0.6 and 0.9.

[4] First LJUNG 73 value is for $\cos(\theta_{e\gamma}) < 0.9$, second value is for $\cos(\theta_{e\gamma})$ between 0.6 and 0.9 for comparison with ROMANO 71.

[5] Both ROMANO 71 values are for $\cos(\theta_{e\gamma})$ between 0.6 and 0.9. Second value is for comparison with second LJUNG 73 value. We use lowest E_γ cut for Summary Table value. See ROMANO 71 for E_γ dependence.

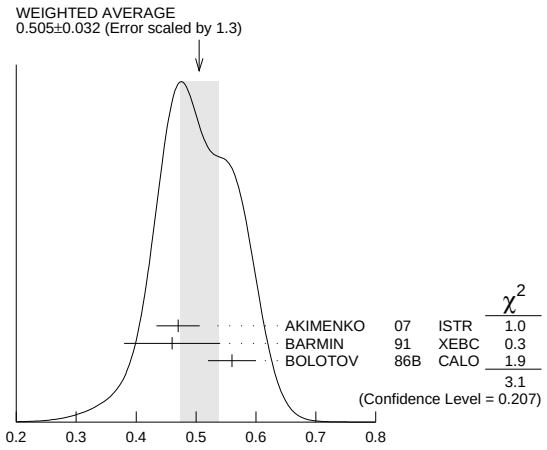

$\Gamma(\pi^0 e^+ \nu_e \gamma)/\Gamma(\pi^0 e^+ \nu_e)$ (units 10^{-2})

$\Gamma(\pi^0 e^+ \nu_e \gamma(\mathrm{SD}))/\Gamma_{total}$ Γ_{18}/Γ

Structure-dependent part.

VALUE (units 10^{-5})	CL%	DOCUMENT ID		TECN	CHG
<5.3	90	BOLOTOV	86B	CALO	−

$\Gamma(\pi^0 \mu^+ \nu_\mu \gamma)/\Gamma_{total}$ Γ_{19}/Γ

VALUE (units 10^{-5})	CL%	EVTS	DOCUMENT ID		TECN	CHG	COMMENT
1.25±0.25 OUR AVERAGE							
1.10±0.32±0.05		23	[1] ADLER	10	B787		$30 < E_\gamma < 60$ MeV
1.46±0.22±0.32		153	[2] TCHIKILEV	07	ISTR	−	$30 < E_\gamma < 60$ MeV
• • • We do not use the following data for averages, fits, limits, etc. • • •							
2.4 ±0.5 ±0.6		125	SHIMIZU	06	K470	+	$E_\gamma > 30$ MeV; $\Theta_{\mu\gamma} > 20°$
<6.1	90	0	LJUNG	73	HLBC	+	$E(\gamma) > 30$ MeV

[1] Value obtained from $B(K^+ \to \pi^0\mu^+\nu_\mu\gamma) = (2.51 \pm 0.74 \pm 0.12) \times 10^{-5}$ obtained in the kinematic region $E_\gamma > 20$ MeV, and then theoretical $K_{\mu 3\gamma}$ spectrum has been used. Also $B(K^+ \to \pi^0\mu^+\nu_\mu\gamma) = (1.58 \pm 0.46 \pm 0.08) \times 10^{-5}$, for $E_\gamma > 30$ MeV and $\theta_{\mu\gamma} > 20°$, was determined.

[2] Obtained from measuring $B(K_{\mu 3\gamma}) / B(K_{\mu 3})$ and using PDG 02 value $B(K_{\mu 3}) = 3.27\%$. $B(K_{\mu 3\gamma}) = (8.82 \pm 0.94 \pm 0.86) \times 10^{-5}$ is obtained for 5 MeV $< E_\gamma <$ 30 MeV.

$\Gamma(\pi^0\pi^0 e^+ \nu_e \gamma)/\Gamma_{total}$ Γ_{20}/Γ

VALUE (units 10^{-6})	CL%	EVTS	DOCUMENT ID	TECN	CHG	COMMENT
<5	90	0	BARMIN 92	XEBC	+	$E_\gamma > 10$ MeV

Hadronic modes with photons

$\Gamma(\pi^+\pi^0\gamma(\mathrm{INT}))/\Gamma_{total}$ Γ_{21}/Γ

The $K^+ \to \pi^+\pi^0\gamma$ differential decay rate can be described in terms of T_{π^+}, the charged pion kinetic energy, and $W^2 = (P_K \cdot P_\gamma)(P_{\pi^+} \cdot P_\gamma) / (m_K\, m_{\pi^+})^2$; then we can write $d^2\Gamma(K^+ \to \pi^+\pi^0\gamma) / (dT_{\pi^+}\, dW^2) = d^2\Gamma(K^+ \to \pi^+\pi^0\gamma)_{IB} / (dT_{\pi^+}\, dW^2)\, [1 + 2\cos(\pm\phi + \delta_1^1 - \delta_0^2)\, m_\pi^2\, m_K^2\, W^2\, X_E + m_\pi^4\, m_K^4\, (X_E^2 + X_M^2)\, W^4]$. The IB differential and total branching ratios are expressed in terms of the non-radiative experimental width $\Gamma(K^+ \to \pi^+\pi^0)$ by Low's theorem. Using PDG 10 $B(K^+ \to \pi^+\pi^0) = 0.2066 \pm 0.0008$, one obtains respectively $B(K^+ \to \pi^+\pi^0\gamma)_{IB}$ $(55 < T_{\pi^+} < 90$ MeV$) = 2.55 \times 10^{-4}$ and $B(K^+ \to \pi^+\pi^0\gamma)_{IB}$ $(0 < T_{\pi^+} < 80$ MeV$) = 1.80 \times 10^{-4}$. Fitting respectively the piece proportional to W^2 and the piece proportional to W^4, the interference contribution (INT), proportional to X_E, and the direct contribution (DE) proportional to $X_E^2 + X_M^2$ are extracted.

VALUE (units 10^{-6})	EVTS	DOCUMENT ID		TECN	CHG	COMMENT
−4.24±0.63±0.70	600k	[1] BATLEY	10A	NA48	±	T_{π^+} 0–80 MeV

[1] The cut on the photon energy implies $W^2 > 0.2$. BATLEY 10A obtains the INT and DE fractional branchings with respect to IB from a simultaneous kinematical fit of INT and DE and then we use the PDG 10 value for $B(K^+ \to \pi^+\pi^0) = 20.66 \pm 0.08$ to determine the IB. The INT and DE correlation coefficients −0.83. Assuming a constant electric amplitude, X_E, this INT value implies $X_E = -24 \pm 6$ GeV^{-4}.

$\Gamma(\pi^+\pi^0\gamma(\mathrm{DE}))/\Gamma_{total}$ Γ_{22}/Γ

Direct emission (DE) part of $\Gamma(\pi^+\pi^0\gamma)/\Gamma_{total}$, assuming that interference (INT) component is zero.

VALUE (units 10^{-6})	EVTS	DOCUMENT ID		TECN	CHG	COMMENT
5.99±0.27±0.25	600k	[1] BATLEY	10A	NA48	±	T_{π^+} 0–80 MeV
• • • We do not use the following data for averages, fits, limits, etc. • • •						
3.8 ±0.8 ±0.7	10k	ALIEV	06	K470	+	T_{π^+} 55–90 MeV
3.7 ±3.9 ±1.0	930	UVAROV	06	ISTR	−	T_{π^-} 55–90 MeV
3.2 ±1.3 ±1.0	4k	ALIEV	03	K470	+	T_{π^+} 55–90 MeV
6.1 ±2.5 ±1.9	4k	ALIEV	03	K470	+	T_{π^+} full range
4.7 ±0.8 ±0.3	20k	[2] ADLER	00C	B787	+	T_{π^+} 55–90 MeV
20.5 ±4.6 $^{+3.9}_{-2.3}$		BOLOTOV	87	WIRE	−	T_{π^-} 55–90 MeV
15.6 ±3.5 ±5.0		ABRAMS	72	ASPK	±	$T_{\pi^\pm}$ 55–90 MeV

[1] The cut on the photon energy implies $W^2 > 0.2$. BATLEY 10A obtains the INT and DE fractional branchings with respect to IB from a simultaneous kinematical fit of INT and DE and then we use the PDG 10 value for $B(K^+ \to \pi^+\pi^0) = 20.66 \pm 0.08$ to determine the IB. The INT and DE correlation coefficients −0.93. Assuming constant electric and magnetic amplitudes, X_E and X_M, these INTand DE values imply $X_E = -24 \pm 6$ GeV^{-4} and $X_M = -254 \pm 9$ GeV^{-4}.

[2] ADLER 00C measures the INT component to be $(-0.4 \pm 1.6)\%$ of the inner bremsstrahlung (IB) component.

$\Gamma(\pi^+\pi^0\pi^0\gamma)/\Gamma(\pi^+\pi^0\pi^0)$ Γ_{23}/Γ_{10}

VALUE (units 10^{-4})	DOCUMENT ID		TECN	CHG	COMMENT
4.3 $^{+3.2}_{-1.7}$	BOLOTOV	85	SPEC	−	$E(\gamma) > 10$ MeV

$\Gamma(\pi^+\pi^+\pi^-\gamma)/\Gamma_{total}$ Γ_{24}/Γ

VALUE (units 10^{-4})	EVTS	DOCUMENT ID		TECN	CHG	COMMENT
1.04±0.31 OUR AVERAGE						
1.10±0.48	7	BARMIN	89	XEBC		$E(\gamma) > 5$ MeV
1.0 ±0.4		STAMER	65	EMUL	+	$E(\gamma) > 11$ MeV

$\Gamma(\pi^+\gamma\gamma)/\Gamma_{total}$ Γ_{25}/Γ

VALUE (units 10^{-7})	CL%	EVTS	DOCUMENT ID		TECN	CHG	COMMENT
10.1 ±0.6 OUR AVERAGE							
10.03±0.51±0.24		215	[1] LAZZERONI	14	NA62	±	
11 ±3 ±1		31	[2] KITCHING	97	B787	+	
• • • We do not use the following data for averages, fits, limits, etc. • • •							
9.10±0.72±0.22		149	[3] BATLEY	14	NA48	±	
< 0.083	90		[4] ARTAMONOV	05	B949	+	$P_\pi > 213$ MeV/c
< 10	90	0	ATIYA	90B	B787	+	$T\pi$ 117–127 MeV
< 84	90	0	ASANO	82	CNTR	+	$T\pi$ 117–127 MeV
−420 ± 520		0	ABRAMS	77	SPEC	+	$T\pi < 92$ MeV
< 350	90	0	LJUNG	73	HLBC	+	6–102, 114–127 MeV
< 500	90	0	KLEMS	71	OSPK	+	$T\pi < 117$ MeV
−100 ± 600			CHEN	68	OSPK	+	$T\pi$ 60–90 MeV

[1] LAZZERONI 14 combines NA62 and NA48/2 results. The result for the full kinematic range is extrapolated from the model-independent branching fraction $(9.65 \pm 0.61 \pm 0.14) \times 10^{-7}$ for $(m_{\gamma\gamma}/m_K)^2 > 0.2$. The measured ChPT parameter $\hat{c} = 1.86 \pm 0.25$.

[2] KITCHING 97 is extrapolated from their model-independent branching fraction $(6.0 \pm 1.5 \pm 0.7) \times 10^{-7}$ for 100 MeV/c<P_{π^+} < 180 MeV/c using Chiral Perturbation Theory.

[3] BATLEY 14 uses data collected in 2003 and 2004. Branching ratio is obtained by determining the parameter $\hat{c} = 1.41 \pm 0.38 \pm 0.11$ and integrating the $\mathcal{O}(p^6)$ chiral spectrum. A model independent value for the branching ratio is also obtained $(8.77 \pm 0.87 \pm 0.17) \times 10^{-7}$ for kinematic range $(m_{\gamma\gamma}/m_K)^2 > 0.2$.

[4] ARTAMONOV 05 limit assumes ChPT with $\hat{c}$= 1.8 with unitarity corrections. With $\hat{c}$= 1.6 and no unitarity corrections they obtain < 2.3×10^{-8} at 90% CL. This partial branching ratio is predicted to be 6.10×10^{-9} and 0.49×10^{-9} for the cases with and without unitarity correction.

$\Gamma(\pi^+ 3\gamma)/\Gamma_{total}$ Γ_{26}/Γ

Values given here assume a phase space pion energy spectrum.

VALUE (units 10^{-4})	CL%	DOCUMENT ID		TECN	CHG	COMMENT
<1.0	90	ASANO	82	CNTR	+	$T(\pi)$ 117–127 MeV
• • • We do not use the following data for averages, fits, limits, etc. • • •						
<3.0	90	KLEMS	71	OSPK	+	$T(\pi) > 117$ MeV

$\Gamma(\pi^+ e^+ e^-\gamma)/\Gamma_{total}$ Γ_{27}/Γ

VALUE (units 10^{-8})	EVTS	DOCUMENT ID		TECN	COMMENT
1.19±0.12±0.04	113	[1] BATLEY	08	NA48	$m_{ee\gamma} > 260$ MeV

[1] BATLEY 08 also reports the Chiral Perturbation Theory parameter $\hat{c} = 0.9 \pm 0.45$ obtained using the shape of the $e^+e^-\gamma$ invariant mass spectrum. By extrapolating the theoretical amplitude to $m_{ee\gamma} < 260$ MeV, it obtains the inclusive $B(K^+ \to \pi^+e^+e^-\gamma) = (1.29 \pm 0.13 \pm 0.03) \times 10^{-8}$, where the first error is the combined statistical and systematic errors and the second error is from the uncertainty in $\hat{c}$.

Leptonic modes with $\ell\bar{\ell}$ pairs

$\Gamma(e^+\nu_e\nu\bar{\nu})/\Gamma(e^+\nu_e)$ Γ_{28}/Γ_1

VALUE	CL%	EVTS	DOCUMENT ID		TECN	CHG
<3.8	90	0	HEINTZE	79	SPEC	+

$\Gamma(\mu^+\nu_\mu\nu\bar{\nu})/\Gamma_{\text{total}}$ Γ_{29}/Γ

VALUE	CL%	DOCUMENT ID		TECN	CHG
$<2.4\times10^{-6}$	90	[1] ARTAMONOV	16	B949	+
• • • We do not use the following data for averages, fits, limits, etc. • • •					
$<6.0\times10^{-6}$	90	[2] PANG	73	CNTR	+

[1] ARTAMONOV 16 assumes Standard model μ spectrum. The search is performed in the muon momentum region between 130 and 175 MeV/c.
[2] PANG 73 assumes μ spectrum from ν-ν interaction of BARDIN 70.

$\Gamma(e^+\nu_e e^+ e^-)/\Gamma_{\text{total}}$ Γ_{30}/Γ

VALUE (units 10^{-8})	EVTS	DOCUMENT ID		TECN	CHG	COMMENT
2.48± 0.14±0.14	410	POBLAGUEV	02	B865	+	m_{ee} >150 MeV
• • • We do not use the following data for averages, fits, limits, etc. • • •						
20 ±20	4	DIAMANT-...	76	SPEC	+	$m_{e^+e^-}$ >140 MeV

$\Gamma(\mu^+\nu_\mu e^+ e^-)/\Gamma_{\text{total}}$ Γ_{31}/Γ

VALUE (units 10^{-8})	EVTS	DOCUMENT ID		TECN	CHG	COMMENT
7.06± 0.16±0.26	2.7k	POBLAGUEV	02	B865	+	m_{ee} >145 MeV
• • • We do not use the following data for averages, fits, limits, etc. • • •						
100 ±30	14	DIAMANT-...	76	SPEC	+	$m_{e^+e^-}$ >140 MeV

$\Gamma(e^+\nu_e\mu^+\mu^-)/\Gamma_{\text{total}}$ Γ_{32}/Γ

VALUE (units 10^{-8})	CL%	DOCUMENT ID		TECN
1.72±0.45		MA	06	B865
• • • We do not use the following data for averages, fits, limits, etc. • • •				
<50	90	ADLER	98	B787

$\Gamma(\mu^+\nu_\mu\mu^+\mu^-)/\Gamma_{\text{total}}$ Γ_{33}/Γ

VALUE (units 10^{-7})	CL%	DOCUMENT ID		TECN	CHG
<4.1	90	ATIYA	89	B787	+

Lepton Family number (LF), Lepton number (L), $\Delta S=\Delta Q$ (SQ) violating modes, or $\Delta S=1$ weak neutral current ($S1$) modes

$\Gamma(\pi^+\pi^+ e^-\bar{\nu}_e)/\Gamma_{\text{total}}$ Γ_{34}/Γ

Test of $\Delta S=\Delta Q$ rule.

VALUE (units 10^{-7})	CL%	EVTS	DOCUMENT ID		TECN	CHG
• • • We do not use the following data for averages, fits, limits, etc. • • •						
< 9.0	95	0	SCHWEINB...	71	HLBC	+
< 6.9	95	0	ELY	69	HLBC	+
<20.	95		BIRGE	65	FBC	+

$\Gamma(\pi^+\pi^+ e^-\bar{\nu}_e)/\Gamma(\pi^+\pi^- e^+\nu_e)$ Γ_{34}/Γ_6

Test of $\Delta S=\Delta Q$ rule.

VALUE (units 10^{-4})	CL%	EVTS	DOCUMENT ID		TECN
< 3	90	3	[1] BLOCH	76	SPEC
• • • We do not use the following data for averages, fits, limits, etc. • • •					
<130.	95	0	BOURQUIN	71	ASPK

[1] BLOCH 76 quotes 3.6×10^{-4} at CL = 95%, we convert.

$\Gamma(\pi^+\pi^+\mu^-\bar{\nu}_\mu)/\Gamma_{\text{total}}$ Γ_{35}/Γ

Test of $\Delta S=\Delta Q$ rule.

VALUE (units 10^{-6})	CL%	EVTS	DOCUMENT ID		TECN	CHG
<3.0	95	0	BIRGE	65	FBC	+

$\Gamma(\pi^+ e^+ e^-)/\Gamma_{\text{total}}$ Γ_{36}/Γ

Test for $\Delta S=1$ weak neutral current. Allowed by combined first-order weak and electromagnetic interactions.

VALUE (units 10^{-7})	EVTS	DOCUMENT ID		TECN	CHG
3.00±0.09 OUR AVERAGE					
3.11±0.04±0.12	7253	[1] BATLEY	09	NA48	±
2.94±0.05±0.14	10300	[2] APPEL	99	SPEC	+
2.75±0.23±0.13	500	[3] ALLIEGRO	92	SPEC	+
2.7 ±0.5	41	[4] BLOCH	75	SPEC	+

[1] Value extrapolated from a measurement in the region $z=(m_{ee}/m_K)^2$ >0.08. BATLEY 09 also evaluated the shape of the form factor using four different theoretical models.
[2] APPEL 99 establishes vector nature of this decay and determines form factor $f(Z)=f_0(1+\delta Z)$, $Z=M^2_{ee}/m^2_K$, δ=2.14 ± 0.13 ± 0.15.
[3] ALLIEGRO 92 assumes a vector interaction with a form factor given by $\lambda=0.105\pm0.035\pm0.015$ and a correlation coefficient of -0.82.
[4] BLOCH 75 assumes a vector interaction.

$\Gamma(\pi^+\mu^+\mu^-)/\Gamma_{\text{total}}$ Γ_{37}/Γ

Test for $\Delta S=1$ weak neutral current. Allowed by higher-order electroweak interactions.

VALUE (units 10^{-8})	CL%	EVTS	DOCUMENT ID		TECN	CHG	COMMENT
9.4 ±0.6 OUR AVERAGE Error includes scale factor of 2.6. See the ideogram below.							
9.62±0.21±0.13		3120	[1] BATLEY	11A	NA48	±	2003-04 data
9.8 ±1.0 ±0.5		110	[2] PARK	02	HYCP	±	
9.22±0.60±0.49		402	[3] MA	00	B865	+	
5.0 ±0.4 ±0.9		207	[4] ADLER	97C	B787	+	
• • • We do not use the following data for averages, fits, limits, etc. • • •							
9.7 ±1.2 ±0.4		65	PARK	02	HYCP	+	
10.0 ±1.9 ±0.7		35	PARK	02	HYCP	−	
<23	90		ATIYA	89	B787	+	

[1] BATLEY 11A also studies the form factor $f(z)$ dependence of the decay, described via single photon exchange: i) assuming a linear form factor, $f(z)=f_0(1+\delta z)$, $z=(M_{\mu\mu}/m_K)^2$, finding $f_0=0.470\pm0.040$ and $\delta=3.11\pm0.57$ and ii) assuming a linear form factor including π-π rescattering , $W_{\pi\pi}$, as in DAMBROSIO 98A, finding $f(z)=G_F\,m^2_K\,(a_+ + b_+ z)+W_{\pi\pi}(z)$, $a_+=-0.575\pm0.039$, $b_+=-0.813\pm0.145$.
[2] PARK 02 "±" result comes from combining $K^+\to\pi^+\mu^+\mu^-$ and $K^-\to\pi^-\mu^+\mu^-$, assuming CP is conserved.
[3] MA 00 establishes vector nature of this decay and determines form factor $f(z)=f_0(1+\delta z)$, $z=(M_{\mu\mu}/m_K)^2$, $\delta=2.45^{+1.30}_{-0.95}$.
[4] ADLER 97C gives systematic error 0.7×10^{-8} and theoretical uncertainty 0.6×10^{-8}, which we combine in quadrature to obtain our second error.

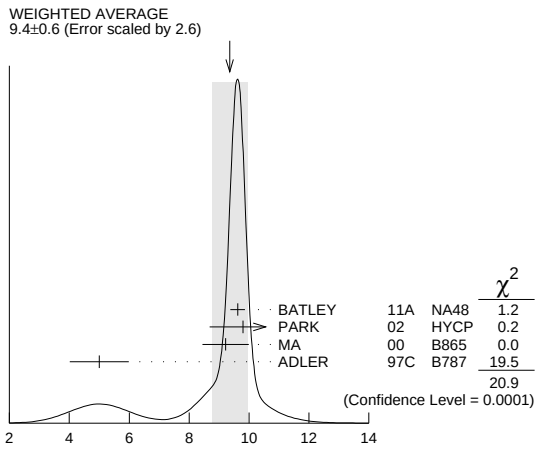

$\Gamma(\pi^+\mu^+\mu^-)/\Gamma_{\text{total}}$ Γ_{37}/Γ

$\Gamma(\pi^+\nu\bar{\nu})/\Gamma_{\text{total}}$ Γ_{38}/Γ

Test for $\Delta S=1$ weak neutral current. Allowed by higher-order electroweak interactions. Branching ratio values are extrapolated from the momentum or energy regions shown in the comments assuming Standard Model phase space except for those labeled "Scalar" or "Tensor" to indicate the assumed non-Standard-Model interaction.

VALUE (units 10^{-9})	CL%	EVTS	DOCUMENT ID		TECN	CHG	COMMENT
$0.173^{+0.115}_{-0.105}$		7	[1] ARTAMONOV	08	B949	+	$140<P_\pi<199$ MeV, $211<P_\pi<229$MeV
• • • We do not use the following data for averages, fits, limits, etc. • • •							
$0.789^{+0.926}_{-0.510}$		3	[2] ARTAMONOV	08	B949	+	$140<P_\pi<199$ MeV
< 2.2	90	1	[3] ADLER	04	B787	+	$211<P_\pi<229$ MeV
< 2.7	90		ADLER	04	B787	+	Scalar
< 1.8	90		ADLER	04	B787	+	Tensor
$0.147^{+0.130}_{-0.089}$		3	[4] ANISIMOVSK...	04	B949	+	$211<P_\pi<229$ MeV
$0.157^{+0.175}_{-0.082}$		2	ADLER	02	B787	+	$P_\pi>211$ MeV/c
< 4.2	90	1	ADLER	02C	B787	+	$140<P_\pi<195$ MeV
< 4.7	90		[5] ADLER	02C	B787	+	Scalar
< 2.5	90		[5] ADLER	02C	B787	+	Tensor
$0.15^{+0.34}_{-0.12}$		1	ADLER	00	B787		In ADLER 02
$0.42^{+0.97}_{-0.35}$		1	ADLER	97	B787		
< 2.4	90		ADLER	96	B787		
< 7.5	90		ATIYA	93	B787	+	$T(\pi)$ 115–127 MeV
< 5.2	90		[6] ATIYA	93	B787	+	
< 17	90	0	ATIYA	93B	B787	+	$T(\pi)$ 60–100 MeV
< 34	90		ATIYA	90	B787	+	
<140	90		ASANO	81B	CNTR	+	$T(\pi)$ 116–127 MeV

[1] Value obtained combining ANISIMOVSKY 04, ADLER 04, and the present ARTAMONOV 08 results.
[2] Observed 3 events with an estimated background of $0.93\pm0.17^{+0.32}_{-0.24}$. Signal-to-background ratio for each of these 3 events is 0.20, 0.42, and 0.47.
[3] Value obtained combining the previous result ADLER 02C with 1 event and the present result with 0 events to obtain an expected background 1.22 ± 0.24 events and 1 event observed.
[4] Value obtained combining the previous E787 result ADLER 02 with 2 events and the present E949 with 1 event. The additional event has a signal-to-background ratio 0.9. Superseded by ARTAMONOV 08.
[5] Superseded by ADLER 04.
[6] Combining ATIYA 93 and ATIYA 93B results. Superseded by ADLER 96.

Meson Particle Listings

$K^{\pm}$

$\Gamma(\pi^+\pi^0\nu\overline{\nu})/\Gamma_{\rm total}$ Γ_{39}/Γ

Test for $\Delta S = 1$ weak neutral current. Allowed by higher-order electroweak interactions.

VALUE (units 10^{-5})	CL%	DOCUMENT ID		TECN
<4.3	90	[1] ADLER	01	SPEC

[1] Search region defined by 90 MeV/c<P_{π^+} <188 MeV/c and 135 MeV<E_{π^0} <180 MeV.

$\Gamma(\mu^-\nu e^+ e^+)/\Gamma(\pi^+\pi^- e^+\nu_e)$ Γ_{40}/Γ_6

Test of lepton family number conservation.

VALUE (units 10^{-3})	CL%	EVTS	DOCUMENT ID		TECN	CHG
<0.5	90	0	[1] DIAMANT-...	76	SPEC	+

[1] DIAMANT-BERGER 76 quotes this result times our 1975 $\pi^+\pi^- e\nu$ BR ratio.

$\Gamma(\mu^+\nu_e)/\Gamma_{\rm total}$ Γ_{41}/Γ

Forbidden by lepton family number conservation.

VALUE	CL%	EVTS	DOCUMENT ID		TECN	COMMENT
<0.004	90	0	[1] LYONS	81	HLBC	200 GeV K^+ narrow band ν beam
• • • We do not use the following data for averages, fits, limits, etc. • • •						
<0.012	90		[1] COOPER	82	HLBC	Wideband ν beam

[1] COOPER 82 and LYONS 81 limits on ν_e observation are here interpreted as limits on lepton family number violation in the absence of mixing.

$\Gamma(\pi^+\mu^+ e^-)/\Gamma_{\rm total}$ Γ_{42}/Γ

Test of lepton family number conservation.

VALUE (units 10^{-10})	CL%	DOCUMENT ID		TECN	CHG
<0.13	90	[1] SHER	05	RVUE	+
• • • We do not use the following data for averages, fits, limits, etc. • • •					
<0.21	90	SHER	05	B865	+
<0.39	90	APPEL	00	B865	+
<2.1	90	LEE	90	SPEC	+

[1] This result combines SHER 05 1998 data, APPEL 00 1996 data, and data from BERGMAN 97 and PISLAK 97 theses, all from BNL-E865, with LEE 90 BNL-E777 data.

$\Gamma(\pi^+\mu^- e^+)/\Gamma_{\rm total}$ Γ_{43}/Γ

Test of lepton family number conservation.

VALUE (units 10^{-10})	CL%	EVTS	DOCUMENT ID		TECN	CHG
< 5.2	90	0	APPEL	00B	B865	+
• • • We do not use the following data for averages, fits, limits, etc. • • •						
<70	90	0	[1] DIAMANT-...	76	SPEC	+

[1] Measurement actually applies to the sum of the $\pi^+\mu^- e^+$ and $\pi^-\mu^+ e^+$ modes.

$\Gamma(\pi^-\mu^+ e^+)/\Gamma_{\rm total}$ Γ_{44}/Γ

Test of total lepton number conservation.

VALUE (units 10^{-10})	CL%	EVTS	DOCUMENT ID		TECN	CHG
< 5.0	90	0	APPEL	00B	B865	+
• • • We do not use the following data for averages, fits, limits, etc. • • •						
<70	90	0	[1] DIAMANT-...	76	SPEC	+

[1] Measurement actually applies to the sum of the $\pi^+\mu^- e^+$ and $\pi^-\mu^+ e^+$ modes.

$\Gamma(\pi^- e^+ e^+)/\Gamma_{\rm total}$ Γ_{45}/Γ

Test of total lepton number conservation.

VALUE	CL%	EVTS	DOCUMENT ID		TECN	CHG
<6.4 × 10^{-10}	90	0	APPEL	00B	B865	+
• • • We do not use the following data for averages, fits, limits, etc. • • •						
<9.2 × 10^{-9}	90	0	DIAMANT-...	76	SPEC	+
<1.5 × 10^{-5}			CHANG	68	HBC	−

$\Gamma(\pi^-\mu^+\mu^+)/\Gamma_{\rm total}$ Γ_{46}/Γ

Forbidden by total lepton number conservation.

VALUE	CL%	DOCUMENT ID		TECN	CHG
<8.6 × 10^{-11}	90	[1] BATLEY	17	NA48	±
• • • We do not use the following data for averages, fits, limits, etc. • • •					
<1.1 × 10^{-9}	90	BATLEY	11A	NA48	±
<3.0 × 10^{-9}	90	APPEL	00B	B865	+
<1.5 × 10^{-4}	90	[2] LITTENBERG	92	HBC	

[1] BATLEY 17 result is based on data taken in 2003 to 2004. Limits for two-body resonance X in $K^{\pm} \to \pi\mu\mu$ decays are also reported.
[2] LITTENBERG 92 is from retroactive data analysis of CHANG 68 bubble chamber data.

$\Gamma(\mu^+\overline{\nu}_e)/\Gamma_{\rm total}$ Γ_{47}/Γ

Forbidden by total lepton number conservation.

VALUE (units 10^{-3})	CL%	DOCUMENT ID		TECN	COMMENT
<3.3	90	[1] COOPER	82	HLBC	Wideband ν beam

[1] COOPER 82 limit on $\overline{\nu}_e$ observation is here interpreted as a limit on lepton number violation in the absence of mixing.

$\Gamma(\pi^0 e^+\overline{\nu}_e)/\Gamma_{\rm total}$ Γ_{48}/Γ

Forbidden by total lepton number conservation.

VALUE	CL%	DOCUMENT ID		TECN	COMMENT
<0.003	90	[1] COOPER	82	HLBC	Wideband ν beam

[1] COOPER 82 limit on $\overline{\nu}_e$ observation is here interpreted as a limit on lepton number violation in the absence of mixing.

$\Gamma(\pi^+\gamma)/\Gamma_{\rm total}$ Γ_{49}/Γ

Violates angular momentum conservation and gauge invariance. Current interest in this decay is as a search for non-commutative space-time effects as discussed in ARTAMONOV 05 and for exotic physics such as a vacuum expectation value of a new vector field, non-local Superstring effects, or departures from Lorentz invariance, as discussed in ADLER 02B.

VALUE (units 10^{-9})	CL%	DOCUMENT ID		TECN	CHG
< 2.3	90	ARTAMONOV	05	B949	+
• • • We do not use the following data for averages, fits, limits, etc. • • •					
< 360	90	ADLER	02B	B787	+
<1400	90	ASANO	82	CNTR	+
<4000	90	[1] KLEMS	71	OSPK	+

[1] Test of model of Selleri, Nuovo Cimento **60A** 291 (1969).

CPT VIOLATION TESTS IN $K^{\pm}$ DECAYS

$\Delta = (\Gamma(K^+) - \Gamma(K^-))\ /\ (\Gamma(K^+) + \Gamma(K^-))$

$\Delta(K^{\pm} \to \mu^{\pm}\nu_{\mu})$ RATE DIFFERENCE/SUM

VALUE (%)	DOCUMENT ID		TECN
−0.27±0.21	FORD	67	CNTR

$\Delta(K^{\pm} \to \pi^{\pm}\pi^0)$ RATE DIFFERENCE/SUM

VALUE (%)	DOCUMENT ID		TECN
0.4±0.6	HERZO	69	OSPK

CP VIOLATION TESTS IN $K^{\pm}$ DECAYS

$\Delta = (\Gamma(K^+) - \Gamma(K^-))\ /\ (\Gamma(K^+) + \Gamma(K^-))$

$\Delta(K^{\pm} \to \pi^{\pm} e^+ e^-)$ RATE DIFFERENCE/SUM

VALUE (units 10^{-2})	DOCUMENT ID		TECN
−2.2±1.5±0.6	[1] BATLEY	09	NA48

[1] This implies an upper limit of 2.1 × 10^{-2} at 90% CL.

$\Delta(K^{\pm} \to \pi^{\pm}\mu^+\mu^-)$ RATE DIFFERENCE/SUM

VALUE	DOCUMENT ID		TECN
0.010±0.023 OUR AVERAGE			
0.011±0.023	[1] BATLEY	11A	NA48
−0.02 ±0.11 ±0.04	PARK	02	HYCP

[1] This corresponds to the asymmetry upper limit of < 2.9 × 10^{-2} at 90% CL.

$\Delta(K^{\pm} \to \pi^{\pm}\pi^0\gamma)$ RATE DIFFERENCE/SUM

VALUE (units 10^{-3})	EVTS	DOCUMENT ID		TECN	CHG	COMMENT
0.0± 1.2 OUR AVERAGE						
0.0± 1.0±0.6	1M	[1] BATLEY	10A	NA48		
4 ±29	2461	SMITH	76	WIRE	±	E_{π} 55–90 MeV
5 ±20	4000	ABRAMS	73B	ASPK	±	E_{π} 51–100 MeV

[1] This value implies the upper bound for this asymmetry 1.5 × 10^{-3} at 90% CL.

$\Delta(K^{\pm} \to \pi^{\pm}\pi^+\pi^-)$ RATE DIFFERENCE/SUM

VALUE (%)	EVTS	DOCUMENT ID		TECN	CHG
0.04±0.06		[1] FORD	70	ASPK	
• • • We do not use the following data for averages, fits, limits, etc. • • •					
−0.01±0.08		[2] SMITH	73	ASPK	±
0.05±0.07	3.2M	[1] FORD	70	ASPK	
−0.25±0.45		FLETCHER	67	OSPK	
−0.02±0.11		[1] FORD	67	CNTR	

[1] First FORD 70 value is second FORD 70 combined with FORD 67.
[2] SMITH 73 value of $K^{\pm} \to \pi^{\pm}\pi^+\pi^-$ rate difference is derived from SMITH 73 value of $K^{\pm} \to \pi^{\pm}2\pi^0$ rate difference.

$\Delta(K^{\pm} \to \pi^{\pm}\pi^0\pi^0)$ RATE DIFFERENCE/SUM

VALUE (%)	EVTS	DOCUMENT ID		TECN	CHG
−0.02±0.28 OUR AVERAGE					
0.04±0.29		SMITH	73	ASPK	±
−0.6 ±0.9	1802	HERZO	69	OSPK	

T VIOLATION TESTS IN K^+ AND K^- DECAYS

P_T in $K^+ \to \pi^0\mu^+\nu_{\mu}$

T-violating muon polarization. Sensitive to new sources of *CP* violation beyond the Standard Model.

VALUE (units 10^{-3})	EVTS	DOCUMENT ID		TECN	CHG
−1.7±2.3±1.1		[1] ABE	04F	K246	+
• • • We do not use the following data for averages, fits, limits, etc. • • •					
−4.2±4.9±0.9	3.9M	ABE	99S	K246	+

[1] Includes three sets of data: 96-97 (ABE 99S), 98, and 99-00 totaling about three times the ABE 99S data sample. Corresponds to P_T < 5.0 × 10^{-3} at 90% CL.

P_T in $K^+ \to \mu^+\nu_{\mu}\gamma$

T-violating muon polarization. Sensitive to new sources of *CP* violation beyond the Standard Model.

VALUE (units 10^{-2})	EVTS	DOCUMENT ID		TECN	CHG
−0.64±1.85±0.10	114k	[1] ANISIMOVSK...03		K246	+

[1] Muons stopped and polarization measured from decay to positrons.

Im(ξ) in $K^+ \to \pi^0 \mu^+ \nu_\mu$ DECAY (from transverse μ pol.)

Test of T reversal invariance.

VALUE	EVTS	DOCUMENT ID		TECN	CHG	COMMENT
−0.006 ±0.008 OUR AVERAGE						
−0.0053±0.0071±0.0036		[1] ABE	04F	K246	+	
−0.016 ±0.025	20M	CAMPBELL	81	CNTR	+	Pol.
• • • We do not use the following data for averages, fits, limits, etc. • • •						
−0.013 ±0.016 ±0.003	3.9M	ABE	99S	CNTR	+	p_T K^+ at rest

[1] Includes three sets of data: 96-97 (ABE 99S), 98, and 99-00 totaling about three times the ABE 99S data sample. Corresponds to Im(ξ) < 0.016 at 90% CL.

See the related review(s):
Dalitz Plot Parameters for $K \to 3\pi$ Decays

ENERGY DEPENDENCE OF $K^{\pm}$ DALITZ PLOT

$|\text{matrix element}|^2 = 1 + gu + hu^2 + kv^2$
where $u = (s_3 - s_0) / m_\pi^2$ and $v = (s_2 - s_1) / m_\pi^2$

LINEAR COEFFICIENT g FOR $K^{\pm} \to \pi^{\pm}\pi^+\pi^-$

Some experiments use Dalitz variables x and y. In the comments we give a_y = coefficient of y term. See note above on "Dalitz Plot Parameters for $K \to 3\pi$ Decays." For discussion of the conversion of a_y to g, see the earlier version of the same note in the *Review* published in Physics Letters **111B** 70 (1982).

VALUE	EVTS	DOCUMENT ID		TECN	CHG	COMMENT
−0.21134±0.00017	471M	[1] BATLEY	07B	NA48	±	
• • • We do not use the following data for averages, fits, limits, etc. • • •						
−0.2221 ±0.0065	225k	DEVAUX	77	SPEC	+	a_y=.2814±.0082
−0.199 ±0.008	81k	[2] LUCAS	73	HBC	−	a_y=0.252±0.011
−0.2157 ±0.0028	750k	FORD	72	ASPK	+	a_y=.2734±.0035
−0.2186 ±0.0028	750k	FORD	72	ASPK	−	a_y=.2770±.0035
−0.200 ±0.009	39819	[3] HOFFMASTER	72	HLBC	+	
−0.196 ±0.012	17898	[4] GRAUMAN	70	HLBC	+	a_y=0.228±0.030
−0.193 ±0.010	50919	MAST	69	HBC	−	a_y=0.244±0.013
−0.218 ±0.016	9994	[5] BUTLER	68	HBC	+	a_y=0.277±0.020
−0.190 ±0.023	5778	[5,6] MOSCOSO	68	HBC	−	a_y=0.242±0.029
−0.22 ±0.024	5428	[5,6] ZINCHENKO	67	HBC	+	a_y=0.28 ± 0.03
−0.220 ±0.035	1347	[7] FERRO-LUZZI	61	HBC	−	a_y=0.28 ± 0.045

[1] Final state strong interaction and radiative corrections not included in the fit.
[2] Quadratic dependence is required by K_L^0 experiments.
[3] HOFFMASTER 72 includes GRAUMAN 70 data.
[4] Emulsion data added — all events included by HOFFMASTER 72.
[5] Experiments with large errors not included in average.
[6] Also includes DBC events.
[7] No radiative corrections included.

QUADRATIC COEFFICIENT h FOR $K^{\pm} \to \pi^{\pm}\pi^+\pi^-$

VALUE (units 10^{-2})	EVTS	DOCUMENT ID		TECN	CHG
1.848±0.040	471M	[1] BATLEY	07B	NA48	±
• • • We do not use the following data for averages, fits, limits, etc. • • •					
−0.06 ±1.43	225k	DEVAUX	77	SPEC	+
1.87 ±0.62	750k	FORD	72	ASPK	+
1.25 ±0.62	750k	FORD	72	ASPK	−
−0.9 ±1.4	39819	HOFFMASTER	72	HLBC	+
−0.1 ±1.2	50919	MAST	69	HBC	−

[1] Final state strong interaction and radiative corrections not included in the fit.

QUADRATIC COEFFICIENT k FOR $K^{\pm} \to \pi^{\pm}\pi^+\pi^-$

VALUE (units 10^{-3})	EVTS	DOCUMENT ID		TECN	CHG
− 4.63± 0.14	471M	[1] BATLEY	07B	NA48	±
• • • We do not use the following data for averages, fits, limits, etc. • • •					
−20.5 ± 3.9	225k	DEVAUX	77	SPEC	+
− 7.5 ± 1.9	750k	FORD	72	ASPK	+
− 8.3 ± 1.9	750k	FORD	72	ASPK	−
−10.5 ± 4.5	39819	HOFFMASTER	72	HLBC	+
−14 ±12	50919	MAST	69	HBC	−

[1] Final state strong interaction and radiative corrections not included in the fit.

$(g_+ - g_-) / (g_+ + g_-)$ FOR $K^{\pm} \to \pi^{\pm}\pi^+\pi^-$

This is a CP violating asymmetry between linear coefficients g_+ for $K^+ \to \pi^+\pi^+\pi^-$ decay and g_- for $K^- \to \pi^-\pi^+\pi^-$ decay.

VALUE (units 10^{-4})	EVTS	DOCUMENT ID		TECN
− 1.5± 1.5±1.6	3.1G	[1] BATLEY	07E	NA48
• • • We do not use the following data for averages, fits, limits, etc. • • •				
1.7± 2.1±2.0	1.7G	[2] BATLEY	06	NA48
−70.0±53	3.2M	FORD	70	ASPK

[1] BATLEY 07E includes data from BATLEY 06. Uses quadratic parametrization and value $g_+ + g_- = 2g$ from BATLEY 07B. This measurement neglects any possible charge asymmetries in higher order slope parameters h or k.
[2] This measurement neglects any possible charge asymmetries in higher order slope parameters h or k.

LINEAR COEFFICIENT g FOR $K^{\pm} \to \pi^{\pm}\pi^0\pi^0$

Unless otherwise stated, all experiments include terms quadratic in $(s_3 - s_0) / m^2_{\pi^+}$. See note above on "Dalitz Plot Parameters for $K \to 3\pi$ Decays."

See BATUSOV 98 for a discussion of the discrepancy between their result and others, especially BOLOTOV 86. At this time we have no way to resolve the discrepancy so we depend on the large scale factor as a warning.

VALUE	EVTS	DOCUMENT ID		TECN	CHG	COMMENT
0.626 ±0.007 OUR AVERAGE						
0.6259±0.0043±0.0093	493k	AKOPDZHAN..05B		TNF	±	
0.627 ±0.004 ±0.010	252k	[1,2] AJINENKO	03B	ISTR	−	
• • • We do not use the following data for averages, fits, limits, etc. • • •						
0.736 ±0.014 ±0.012	33k	BATUSOV	98	SPEC	+	
0.582 ±0.021	43k	BOLOTOV	86	CALO	−	
0.670 ±0.054	3263	BRAUN	76B	HLBC	+	
0.630 ±0.038	5635	SHEAFF	75	HLBC	+	
0.510 ±0.060	27k	SMITH	75	WIRE	+	
0.67 ±0.06	1365	AUBERT	72	HLBC	+	
0.544 ±0.048	4048	DAVISON	69	HLBC	+	Also emulsion

[1] Measured using in-flight decays of the 25 GeV negative secondary beam.
[2] They form new world averages $g_- = (0.617 \pm 0.018)$ and $g_+ = (0.684 \pm 0.033)$ which give $\Delta g_{\tau'} = 0.051 \pm 0.028$.

QUADRATIC COEFFICIENT h FOR $K^{\pm} \to \pi^{\pm}\pi^0\pi^0$

VALUE	EVTS	DOCUMENT ID		TECN	CHG	COMMENT
0.052 ±0.008 OUR AVERAGE						
0.0551±0.0044±0.0086	493k	AKOPDZHAN..05B		TNF	±	
0.046 ±0.004 ±0.012	252k	[1] AJINENKO	03B	ISTR	−	
• • • We do not use the following data for averages, fits, limits, etc. • • •						
0.128 ±0.015 ±0.024	33k	BATUSOV	98	SPEC	+	
0.037 ±0.024	43k	BOLOTOV	86	CALO	−	
0.152 ±0.082	3263	BRAUN	76B	HLBC	+	
0.041 ±0.030	5635	SHEAFF	75	HLBC	+	
0.009 ±0.040	27k	SMITH	75	WIRE	+	
−0.01 ±0.08	1365	AUBERT	72	HLBC	+	
0.026 ±0.050	4048	DAVISON	69	HLBC	+	Also emulsion

[1] Measured using in-flight decays of the 25 GeV negative secondary beam.

QUADRATIC COEFFICIENT k FOR $K^{\pm} \to \pi^{\pm}\pi^0\pi^0$

VALUE	EVTS	DOCUMENT ID		TECN	CHG
0.0054±0.0035 OUR AVERAGE Error includes scale factor of 2.5.					
0.0082±0.0011±0.0014	493k	AKOPDZHAN..05B		TNF	±
0.001 ±0.001 ±0.002	252k	[1] AJINENKO	03B	ISTR	−
• • • We do not use the following data for averages, fits, limits, etc. • • •					
0.0197±0.0045±0.0029	33k	BATUSOV	98	SPEC	+

[1] Measured using in-flight decays of the 25 GeV negative secondary beam.

$(g_+ - g_-) / (g_+ + g_-)$ FOR $K^{\pm} \to \pi^{\pm}\pi^0\pi^0$

A nonzero value for this quantity indicates CP violation.

VALUE (units 10^{-4})	EVTS	DOCUMENT ID		TECN
1.8± 1.8 OUR AVERAGE				
1.8± 1.7±0.6	91.3M	[1] BATLEY	07E	NA48
2 ±18 ±5	619k	[2] AKOPDZHAN..05		TNF
• • • We do not use the following data for averages, fits, limits, etc. • • •				
1.8± 2.2±1.3	47M	[3] BATLEY	06A	NA48

[1] BATLEY 07E includes data from BATLEY 06A. Uses quadratic parametrization and PDG 06 value $g = 0.626 \pm 0.007$ to obtain $g_+ - g_- = (2.2 \pm 2.1 \pm 0.7) \times 10^{-4}$. Neglects any possible charge asymmetries in higher order slope parameters h or k.
[2] Asymmetry obtained assuming that $g_+ + g_- = 2 \times 0.652$ (PDG 02) and that asymmetries in h and k are zero.
[3] Linear and quadratic slopes from PDG 04 are used. Any possible charge asymmetries in higher order slope parameters h or k are neglected.

ALTERNATIVE PARAMETRIZATIONS OF $K^{\pm} \to \pi^{\pm}\pi^0\pi^0$ DALITZ PLOT

The following functional form for the matrix element suggested by $\pi\pi$ rescattering in $K^+ \to \pi^+$"$\pi^+\pi^-$"$\to \pi^+\pi^0\pi^0$ is used for this fit (CABIBBO 04A, CABIBBO 05): Matrix element = $M_0 + M_1$ where $M_0 = 1 + (1/2)g_0\, u + (1/2)\, h'\, u^2 + (1/2)k_0\, v^2$ with $u = (s_3 - s_0)/(m_{\pi^+})^2$, $v = (s_2 - s_1)/(m_{\pi^+})^2$ and where M_1 takes into account the non-analytic piece due to pi pi rescattering amplitudes a_0 and a_2; The parameters g_0 and h' are related to the parameters g and h of the matrix element squared given in the previous section by the approximations $g_0 \sim g^{PDG}$ and $h' \sim h^{PDG} - (g/2)^2$ and $k_0 \sim k^{PDG}$.

In addition, we also consider the effective field theory framework of COLANGELO 06A and BISSEGGER 09 to extract g_{BB} and h'_{BB}.

LINEAR COEFFICIENT g_0 FOR $K^{\pm} \to \pi^{\pm}\pi^0\pi^0$

VALUE	EVTS	DOCUMENT ID		TECN	CHG
0.6525±0.0009±0.0033	60M	[1] BATLEY	09A	NA48	±
• • • We do not use the following data for averages, fits, limits, etc. • • •					
0.645 ±0.004 ±0.009	23M	[2] BATLEY	06B	NA48	±

[1] This fit is obtained with the CABIBBO 05 matrix element in the $2\pi^0$ invariant mass squared range $0.074094 < m^2_{2\pi^0} < 0.104244$ GeV^2. Electromagnetic corrections and CHPT constraints for $\pi\pi$ phase shifts (a_0 and a_2) have been used. Also measured $(a_0 - a_2)\, m_{\pi^+} = 0.2646 \pm 0.0021 \pm 0.0023$, where k_0 was kept fixed in the fit at -0.0099.

[2] Superseded by BATLEY 09A. This fit is obtained with the CABIBBO 05 matrix element in the $2\pi^0$ invariant mass squared range $0.074\ \text{GeV}^2 < m^2_{2\pi^0} < 0.097\ \text{GeV}^2$, assuming $k = 0$ (no term proportional to $(s_2 - s_1)^2$) and excluding the kinematic region around the cusp ($m^2_{2\pi^0} = (2m_{\pi^+})^2 \pm 0.000525$ GeV^2). Also π-π phase shifts a_0 and a_2 are measured: $(a_0 - a_2) m_{\pi^+} = 0.268 \pm 0.010 \pm 0.004 \pm 0.013$(external) and $a_2\, m_{\pi^+} = -0.041 \pm 0.022 \pm 0.014$.

QUADRATIC COEFFICIENT h' FOR $K^{\pm} \to \pi^{\pm}\pi^0\pi^0$

VALUE	EVTS	DOCUMENT ID		TECN	CHG
$-0.0433 \pm 0.0008 \pm 0.0026$	60M	[1] BATLEY	09A	NA48	$\pm$
• • • We do not use the following data for averages, fits, limits, etc. • • •					
$-0.047\ \pm 0.012\ \pm 0.011$	23M	[2] BATLEY	06B	NA48	$\pm$

[1] This fit is obtained with the CABIBBO 05 matrix element in the $2\pi^0$ invariant mass squared range $0.074094 < m^2_{2\pi^0} < 0.104244$ GeV^2. Electromagnetic corrections and CHPT constraints for $\pi\pi$ phase shifts (a_0 and a_2) have been used. Also measured $(a_0 - a_2)\, m_{\pi^+} = 0.2646 \pm 0.0021 \pm 0.0023$, where k_0 was kept fixed in the fit at -0.0099.

[2] Superseded by BATLEY 09A. This fit is obtained with the CABIBBO 05 matrix element in the $2\pi^0$ invariant mass squared range $0.074\ \text{GeV}^2 < m^2_{2\pi^0} < 0.097\ \text{GeV}^2$, assuming $k = 0$ (no term proportional to $(s_2 - s_1)^2$) and excluding the kinematic region around the cusp ($m^2_{2\pi^0} = (2m_{\pi^+})^2 \pm 0.000525$ GeV^2). Also π-π phase shifts a_0 and a_2 are measured: $(a_0 - a_2) m_{\pi^+} = 0.268 \pm 0.010 \pm 0.004 \pm 0.013$(external) and $a_2\, m_{\pi^+} = -0.041 \pm 0.022 \pm 0.014$.

QUADRATIC COEFFICIENT k_0 FOR $K^{\pm} \to \pi^{\pm}\pi^0\pi^0$

VALUE	EVTS	DOCUMENT ID		TECN	CHG
$0.0095 \pm 0.00017 \pm 0.00048$	60M	[1] BATLEY	09A	NA48	$\pm$

[1] Assumed $a_2\, m_{\pi^+} = -0.0044$ in the fit.

LINEAR COEFFICIENT g_{BB} FOR $K^{\pm} \to \pi^{\pm}\pi^0\pi^0$

VALUE	EVTS	DOCUMENT ID		TECN	CHG
$0.6219 \pm 0.0009 \pm 0.0033$	60M	[1] BATLEY	09A	NA48	$\pm$

[1] This fit is obtained using parametrizations of COLANGELO 06A and BISSEGGER 09 in the $2\pi^0$ invariant mass squared range $0.074094 < m^2_{2\pi^0} < 0.104244$ GeV^2. Electromagnetic corrections and CHPT constraints for $\pi\pi$ phase shifts (a_0 and a_2) have been used. Also measured $(a_0 - a_2)\, m_{\pi^+} = 0.2633 \pm 0.0024 \pm 0.0024$, where k_0 was kept fixed in the fit at 0.0085.

QUADRATIC COEFFICIENT h'_{BB} FOR $K^{\pm} \to \pi^{\pm}\pi^0\pi^0$

VALUE	EVTS	DOCUMENT ID		TECN	CHG
$-0.0520 \pm 0.0009 \pm 0.0026$	60M	[1] BATLEY	09A	NA48	$\pm$

[1] This fit is obtained using parametrizations of COLANGELO 06A and BISSEGGER 09 in the $2\pi^0$ invariant mass squared range $0.074094 < m^2_{2\pi^0} < 0.104244$ GeV^2. Electromagnetic corrections and CHPT constraints for $\pi\pi$ phase shifts (a_0 and a_2) have been used. Also measured $(a_0 - a_2)\, m_{\pi^+} = 0.2633 \pm 0.0024 \pm 0.0024$, where k_0 was kept fixed in the fit at 0.0085.

See the related review(s):

$K^{\pm}_{\ell 3}$ and $K^0_{\ell 3}$ Form Factors

$K^{\pm}_{\ell 3}$ FORM FACTORS

In the form factor comments, the following symbols are used.

f_+ and f_- are form factors for the vector matrix element.

f_S and f_T refer to the scalar and tensor term.

$f_0 = f_+ + f_-\, t/(m^2_{K^+} - m^2_{\pi^0})$.

t = momentum transfer to the π.

λ_+ and λ_0 are the linear expansion coefficients of f_+ and f_0:

$f_+(t) = f_+(0)\ (1 + \lambda_+\, t\, /m^2_{\pi^+})$

For quadratic expansion

$f_+(t) = f_+(0)\ (1 + \lambda'_+\, t\, /m^2_{\pi^+} + \frac{\lambda''_+}{2}\, t^2/m^4_{\pi^+})$

as used by KTeV. If there is a non-vanishing quadratic term, then λ_+ represents an average slope, which is then different from λ'_+.

NA48 and ISTRA quadratic expansion coefficients are converted with $\lambda'_+{}^{PDG} = \lambda_+{}^{NA48}$ and $\lambda''_+{}^{PDG} = 2\, \lambda'_+{}^{NA48}$

$\lambda'_+{}^{PDG} = (\frac{m_{\pi^+}}{m_{\pi^0}})^2\ \lambda_+{}^{ISTRA}$ and

$\lambda''_+{}^{PDG} = 2\,(\frac{m_{\pi^+}}{m_{\pi^0}})^4\ \lambda'_+{}^{ISTRA}$

ISTRA linear expansion coefficients are converted with $\lambda_+{}^{PDG} = (\frac{m_{\pi^+}}{m_{\pi^0}})^2\ \lambda_+{}^{ISTRA}$ and $\lambda_0{}^{PDG} = (\frac{m_{\pi^+}}{m_{\pi^0}})^2\ \lambda_0{}^{ISTRA}$

The pole parametrization is

$f_+(t) = f_+(0)\ (\frac{M_V^2}{M_V^2 - t}\ )$

$f_0(t) = f_0(0)\ (\frac{M_S^2}{M_S^2 - t}\ )$

where M_V and M_S are the vector and scalar pole masses.

The following abbreviations are used:

DP = Dalitz plot analysis.

PI = π spectrum analysis.

MU = μ spectrum analysis.

POL= μ polarization analysis.

BR = $K^{\pm}_{\mu 3}/K^{\pm}_{e3}$ branching ratio analysis.

E = positron or electron spectrum analysis.

RC = radiative corrections.

λ_+ (LINEAR ENERGY DEPENDENCE OF f_+ IN $K^{\pm}_{e3}$ DECAY)

These results are for a linear expansion only. See the next section for fits including a quadratic term. For radiative correction of the $K^{\pm}_{e3}$ Dalitz plot, see GINSBERG 67, BECHERRAWY 70, CIRIGLIANO 02, CIRIGLIANO 04, and ANDRE 07. Results labeled OUR FIT are discussed in the review "$K^{\pm}_{\ell 3}$ and $K^0_{\ell 3}$ Form Factors" above. For earlier, lower statistics results, see the 2004 edition of this review, Physics Letters **B592** 1 (2004).

VALUE (units 10^{-2})	EVTS	DOCUMENT ID		TECN	CHG	COMMENT
2.97 ±0.05 OUR FIT		Assuming μ-e universality				
2.98 ±0.05 OUR AVERAGE						
$3.044 \pm 0.083 \pm 0.074$	1.1M	AKOPDZANOV	09	TNF	$\pm$	
$2.966 \pm 0.050 \pm 0.034$	919k	[1] YUSHCHENKO	04B	ISTR	$-$	DP
2.78 ±0.26 ±0.30	41k	SHIMIZU	00	SPEC	+	DP
2.84 ±0.27 ±0.20	32k	[2] AKIMENKO	91	SPEC		PI, no RC
2.9 ±0.4	62k	[3] BOLOTOV	88	SPEC		PI, no RC
• • • We do not use the following data for averages, fits, limits, etc. • • •						
3.06 ±0.09 ±0.06	550k	[1,4] AJINENKO	03C	ISTR	$-$	DP
2.93 ±0.15 ±0.2	130k	[4] AJINENKO	02	SPEC		DP

[1] Rescaled to agree with our conventions as noted above.

[2] AKIMENKO 91 state that radiative corrections would raise λ_+ by 0.0013.

[3] BOLOTOV 88 state radiative corrections of GINSBERG 67 would raise λ_+ by 0.002.

[4] Superseded by YUSHCHENKO 04B.

λ_+ (LINEAR ENERGY DEPENDENCE OF f_+ IN $K^{\pm}_{\mu 3}$ DECAY)

Results labeled OUR FIT are discussed in the review "$K^{\pm}_{\ell 3}$ and $K^0_{\ell 3}$ Form Factors" above. For earlier, lower statistics results, see the 2004 edition of this review, Physics Letters **B592** 1 (2004).

VALUE (units 10^{-2})	EVTS	DOCUMENT ID		TECN	CHG	COMMENT
2.97±0.05 OUR FIT		Assuming μ-e universality				
2.96±0.17 OUR FIT		Not assuming μ-e universality				
2.96±0.14±0.10	540k	[1] YUSHCHENKO	04	ISTR	$-$	DP
• • • We do not use the following data for averages, fits, limits, etc. • • •						
3.21±0.45	112k	[2] AJINENKO	03	ISTR	$-$	DP

[1] Rescaled to agree with our conventions as noted above.

[2] Superseded by YUSHCHENKO 04.

λ_0 (LINEAR ENERGY DEPENDENCE OF f_0 IN $K^{\pm}_{\mu 3}$ DECAY)

Results labeled OUR FIT are discussed in the review "$K^{\pm}_{\ell 3}$ and $K^0_{\ell 3}$ Form Factors" above. For earlier, lower statistics results, see the 2004 edition of this review, Physics Letters **B592** 1 (2004).

VALUE (units 10^{-2})	$d\lambda_0/d\lambda_+$	EVTS	DOCUMENT ID		TECN	CHG	COMMENT
1.95±0.12 OUR FIT			Assuming μ-e universality				
1.96±0.13 OUR FIT			Not assuming μ-e universality				
+1.96±0.12±0.06	−0.348	540k	[1] YUSHCHENKO	04	ISTR	$-$	DP
• • • We do not use the following data for averages, fits, limits, etc. • • •							
+2.09±0.45	−0.46	112k	[2] AJINENKO	03	ISTR	$-$	DP
+1.9 ±0.64		24k	[3] HORIE	01	SPEC	+	BR
+1.9 ±1.0	+0.03	55k	[4] HEINTZE	77	SPEC	+	BR

[1] Rescaled to agree with our conventions as noted above.

[2] Superseded by YUSHCHENKO 04.

[3] HORIE 01 assumes μ-e universality in $K^{\pm}_{\ell 3}$ decay and uses SHIMIZU 00 value λ=0.0278± 0.0040 from $K^{\pm}_{e3}$ decay.

[4] HEINTZE 77 uses $\lambda_+ = 0.029 \pm 0.003$. $d\lambda_0/d\lambda_+$ estimated by us.

λ'_+ (LINEAR $K^{\pm}_{e3}$ FORM FACTOR FROM QUADRATIC FIT)

VALUE (units 10^{-2})	EVTS	DOCUMENT ID		TECN	CHG	COMMENT
2.485±0.163±0.034	919k	[1,2] YUSHCHENKO	04B	ISTR	$-$	DP
• • • We do not use the following data for averages, fits, limits, etc. • • •						
3.07 ±0.21	550k	[1,3] AJINENKO	03C	ISTR	$-$	DP

[1] Rescaled to agree with our conventions as noted above.

[2] YUSHCHENKO 04B λ'_+ and λ''_+ are strongly correlated with coefficient $\rho(\lambda'_+, \lambda''_+) = -0.95$.

[3] Superseded by YUSHCHENKO 04B.

λ''_+ (QUADRATIC $K^{\pm}_{e3}$ FORM FACTOR)

VALUE (units 10^{-2})	EVTS	DOCUMENT ID		TECN	CHG	COMMENT
0.192±0.062±0.071	919k	[1,2] YUSHCHENKO	04B	ISTR	$-$	DP

• • • We do not use the following data for averages, fits, limits, etc. • • •

−0.5	±0.7	±1.5	550k	[1,3]	AJINENKO	03C	ISTR	− DP

[1] Rescaled to agree with our conventions as noted above.
[2] YUSHCHENKO 04B λ'_+ and λ''_+ are strongly correlated with coefficient $\rho(\lambda'_+, \lambda''_+) = -0.95$.
[3] Superseded by YUSHCHENKO 04B.

$|f_S/f_+|$ FOR $K^{\pm}_{e3}$ DECAY

Ratio of scalar to f_+ couplings.

VALUE (units 10^{-2})	CL%	EVTS	DOCUMENT ID		TECN	CHG	COMMENT
−0.3 $^{+0.8}_{-0.7}$ OUR AVERAGE							
$-0.37^{+0.66}_{-0.56}\pm0.41$		919k	YUSHCHENKO	04B	ISTR	−	λ'_+, λ''_+, f_S fit
0.2 ±2.6 ±1.4		41k	SHIMIZU	00	SPEC	+	λ_+, f_S, f_T fit
• • • We do not use the following data for averages, fits, limits, etc. • • •							
$0.2\ ^{+2.0}_{-2.2}$ ±0.3		550k	[1] AJINENKO	03C	ISTR	−	λ_+, f_S, f_T fit
$-1.9\ ^{+2.5}_{-1.6}$		130k	[1] AJINENKO	02	SPEC		λ_+, f_S fit
7.0 ±1.6 ±1.6		32k	AKIMENKO	91	SPEC		λ_+, f_S, f_T, ϕ fit
0 ± 10		2827	[2] BRAUN	75	HLBC	+	
< 13	90	4017	CHIANG	72	OSPK	+	
14^{+3}_{-4}		2707	[2] STEINER	71	HLBC	+	λ_+, f_S, f_T, ϕ fit
< 23	90		BOTTERILL	68C	ASPK		
< 18	90		BELLOTTI	67B	HLBC		
< 30	95		KALMUS	67	HLBC	+	

[1] Superseded by YUSHCHENKO 04B.
[2] Statistical errors only.

$|f_T/f_+|$ FOR $K^{\pm}_{e3}$ DECAY

Ratio of tensor to f_+ couplings.

VALUE (units 10^{-2})	CL%	EVTS	DOCUMENT ID		TECN	CHG	COMMENT
− 1.2± 2.3 OUR AVERAGE							
− 1.2± 2.1± 1.1		919k	YUSHCHENKO	04B	ISTR	−	λ''_+,f_T fit
1 ±14 ± 9		41k	SHIMIZU	00	SPEC	+	λ_+, f_S, f_T fit
• • • We do not use the following data for averages, fits, limits, etc. • • •							
$2.1^{+6.4}_{-7.5}\pm$ 2.6		550k	[1] AJINENKO	03C	ISTR	−	λ_+, f_S, f_T fit
$-4.5^{+6.0}_{-5.7}$		130k	[1] AJINENKO	02	SPEC		λ_+, f_T fit
$53\ ^{+9}_{-10}$ ±10		32k	AKIMENKO	91	SPEC		λ_+, f_S, f_T, ϕ fit
7 ±37		2827	[2] BRAUN	75	HLBC	+	
< 75	90	4017	CHIANG	72	OSPK	+	
$24\ ^{+16}_{-14}$		2707	[2] STEINER	71	HLBC	+	λ_+, f_S, f_T, ϕ fit
< 58	90		BOTTERILL	68C	ASPK		
< 58	90		BELLOTTI	67B	HLBC		
< 110	95		KALMUS	67	HLBC	+	

[1] Superseded by YUSHCHENKO 04B.
[2] Statistical errors only.

f_S/f_+ FOR $K^{\pm}_{\mu3}$ DECAY

Ratio of scalar to f_+ couplings.

VALUE (units 10^{-2})	EVTS	DOCUMENT ID		TECN	CHG	COMMENT
0.17±0.14±0.54	540k	[1] YUSHCHENKO	04	ISTR	−	DP
• • • We do not use the following data for averages, fits, limits, etc. • • •						
0.4 ±0.5 ±0.5	112k	[2] AJINENKO	03	ISTR	−	DP

[1] The second error is the theoretical error from the uncertainty in the chiral perturbation theory prediction for λ_0, ±0.0053, combined in quadrature with the systematic error ±0.0009.
[2] The second error is the theoretical error from the uncertainty in the chiral perturbation theory prediction for λ_0. Superseded by YUSHCHENKO 04.

f_T/f_+ FOR $K^{\pm}_{\mu3}$ DECAY

Ratio of tensor to f_+ couplings.

VALUE (units 10^{-2})	EVTS	DOCUMENT ID		TECN	CHG	COMMENT
−0.07± 0.71±0.20	540k	YUSHCHENKO	04	ISTR	−	DP
• • • We do not use the following data for averages, fits, limits, etc. • • •						
−2.1 ± 2.8 ±1.4	112k	[1] AJINENKO	03	ISTR	−	DP
2 ±12	1585	BRAUN	75	HLBC		

[1] The second error is the theoretical error from the uncertainty in the chiral perturbation theory prediction for λ_0. Superseded by YUSHCHENKO 04.

$K^{\pm}_{\ell4}$ FORM FACTORS

Based on the parametrizations of AMOROS 99, the $K^{\pm}_{\ell4}$ form factors can be expressed as

$$F_s = f_s + f'_s\, q^2 + f''_s\, q^4 + f'_e\, S_e / 4m_\pi^2$$
$$F_p = f_p$$
$$G_p = g_p + g'_p\, q^2$$
$$H_p = h_p$$

where $q^2 = (S_\pi / 4m_\pi^2) - 1$, S_π is the invariant mass squared of the dipion, and S_e is the invariant mass squared of the dilepton.

f_s FOR $K^{\pm} \to \pi^+\pi^- e^{\pm}\nu$ DECAY

VALUE	EVTS	DOCUMENT ID			TECN	CHG
5.712±0.032 OUR AVERAGE						
5.705±0.003±0.035	1.1M	[1] BATLEY	12		NA48	±
5.75 ±0.02 ±0.08	400k	[2] PISLAK	03		B865	+

[1] BATLEY 12 uses data collected in 2003–2004. The result is obtained from a measurement of $\Gamma(\pi^+\pi^- e\nu)/\Gamma(\pi^+\pi^-\pi^+)$ and assumed PDG 12 value of $\Gamma(\pi^+\pi^-\pi^+)/\Gamma = (5.59 \pm 0.04) \times 10^{-2}$.
[2] Radiative corrections included. Using Roy equations and not including isospin breaking, PISLAK 03 obtains the following $\pi\pi$ scattering lengths $a_0^0 = 0.228 \pm 0.012 \pm 0.004\,^{+0.012}_{-0.016}$(theor.) and $a_0^2 = -0.0365 \pm 0.0023 \pm 0.0008\,^{+0.0031}_{-0.0026}$(theor.).

f'_s/f_s FOR $K^{\pm} \to \pi^+\pi^- e^{\pm}\nu$ DECAY

VALUE (units 10^{-2})	EVTS	DOCUMENT ID		TECN	CHG
15.2±0.7±0.5	1.13M	[1] BATLEY	10C	NA48	±
• • • We do not use the following data for averages, fits, limits, etc. • • •					
17.2±0.9±0.6	670k	[2] BATLEY	08A	NA48	±

[1] Radiative corrections included. Using Roy equations and including isospin breaking, BATLEY 10C obtains the following scattering lengths $a_0^0 = 0.2220 \pm 0.0128 \pm 0.0050 \pm 0.0037$ (theor.), $a_0^2 = -0.0432 \pm 0.0086 \pm 0.0034 \pm 0.0028$ (theor.). The correlation with $f''_s/f_s = -0.954$ and with $f'_e/f_s = 0.080$. Supersedes BATLEY 08A.
[2] Radiative corrections included. Using Roy equations and not including isospin breaking, BATLEY 08A obtains the following $\pi\pi$ scattering length $a_0^0 = 0.233 \pm 0.016 \pm 0.007$ $a_0^2 = -0.0471 \pm 0.011 \pm 0.004$.

f''_s/f_s FOR $K^{\pm} \to \pi^+\pi^- e^{\pm}\nu$ DECAY

VALUE (units 10^{-2})	EVTS	DOCUMENT ID		TECN	CHG
−7.3±0.7±0.6	1.13M	[1] BATLEY	10C	NA48	±
• • • We do not use the following data for averages, fits, limits, etc. • • •					
−9.0±0.9±0.7	670k	[2] BATLEY	08A	NA48	±

[1] Radiative corrections included. Using Roy equations and including isospin breaking, BATLEY 10C obtains the following scattering lengths $a_0^0 = 0.2220 \pm 0.0128 \pm 0.0050 \pm 0.0037$ (theor.), $a_0^2 = -0.0432 \pm 0.0086 \pm 0.0034 \pm 0.0028$ (theor.). The correlation with $f'_s/f_s = -0.954$ and with $f'_e/f_s = 0.019$. Supersedes BATLEY 08A.
[2] Radiative corrections included. Using Roy equations and not including isospin breaking, BATLEY 08A obtains the following $\pi\pi$ scattering length $a_0^0 = 0.233 \pm 0.016 \pm 0.007$ $a_0^2 = -0.0471 \pm 0.011 \pm 0.004$.

f'_e/f_s FOR $K^{\pm} \to \pi^+\pi^- e^{\pm}\nu$ DECAY

VALUE (units 10^{-2})	EVTS	DOCUMENT ID		TECN	CHG
6.8±0.6±0.7	1.13M	[1] BATLEY	10C	NA48	±
• • • We do not use the following data for averages, fits, limits, etc. • • •					
8.1±0.8±0.9	670k	[2] BATLEY	08A	NA48	±

[1] Radiative corrections included. Using Roy equations and including isospin breaking, BATLEY 10C obtains the following scattering lengths $a_0^0 = 0.2220 \pm 0.0128 \pm 0.0050 \pm 0.0037$ (theor.), $a_0^2 = -0.0432 \pm 0.0086 \pm 0.0034 \pm 0.0028$ (theor.). The correlation with $f'_s/f_s = 0.080$ and with $f''_s/f_s = 0.019$. Supersedes BATLEY 08A.
[2] Radiative corrections included. Using Roy equations and not including isospin breaking, BATLEY 08A obtains the following $\pi\pi$ scattering length $a_0^0 = 0.233 \pm 0.016 \pm 0.007$ $a_0^2 = -0.0471 \pm 0.011 \pm 0.004$.

f_p/f_s FOR $K^{\pm} \to \pi^+\pi^- e^{\pm}\nu$ DECAY

VALUE (units 10^{-2})	EVTS	DOCUMENT ID		TECN	CHG
−4.8±0.3±0.4	1.13M	[1] BATLEY	10C	NA48	±
• • • We do not use the following data for averages, fits, limits, etc. • • •					
−4.8±0.4±0.4	670k	[2] BATLEY	08A	NA48	±

[1] Radiative corrections included. Using Roy equations and including isospin breaking, BATLEY 10C obtains the following scattering lengths $a_0^0 = 0.2220 \pm 0.0128 \pm 0.0050 \pm 0.0037$ (theor.), $a_0^2 = -0.0432 \pm 0.0086 \pm 0.0034 \pm 0.0028$ (theor.). Supersedes BATLEY 08A.
[2] Radiative corrections included. Using Roy equations and not including isospin breaking, BATLEY 08A obtains the following $\pi\pi$ scattering length $a_0^0 = 0.233 \pm 0.016 \pm 0.007$ $a_0^2 = -0.0471 \pm 0.011 \pm 0.004$.

g_p/f_s FOR $K^{\pm} \to \pi^+\pi^- e^{\pm}\nu$ DECAY

VALUE (units 10^{-2})	EVTS	DOCUMENT ID		TECN	CHG
86.8±1.0±1.0	1.13M	[1] BATLEY	10C	NA48	±
• • • We do not use the following data for averages, fits, limits, etc. • • •					
87.3±1.3±1.2	670k	[2] BATLEY	08A	NA48	±
80.9±0.9±1.2	400k	[3] PISLAK	03	B865	±

[1] Radiative corrections included. Using Roy equations and including isospin breaking, BATLEY 10C obtains the following scattering lengths $a_0^0 = 0.2220 \pm 0.0128 \pm 0.0050 \pm 0.0037$ (theor.), $a_0^2 = -0.0432 \pm 0.0086 \pm 0.0034 \pm 0.0028$ (theor.). Supersedes BATLEY 08A. The correlation with $g'_p/f_s = -0.914$. Supersedes BATLEY 08A.

[2] Radiative corrections included. Using Roy equations and not including isospin breaking, BATLEY 08A obtains the following $\pi\pi$ scattering length $a_0^0 = 0.233 \pm 0.016 \pm 0.007$ $a_0^2 = -0.0471 \pm 0.011 \pm 0.004$.

[3] Radiative corrections included. Using Roy equations PISLAK 03 obtains the following scattering lengths $a_0^0 = 0.203 \pm 0.033 \pm 0.004$, $a_0^2 = -0.055 \pm 0.023 \pm 0.003$.

g'_p/f_s FOR $K^{\pm} \to \pi^+\pi^- e^{\pm}\nu$ DECAY

VALUE (units 10^{-2})	EVTS	DOCUMENT ID		TECN	CHG
8.9±1.7±1.3	1.13M	[1] BATLEY	10C	NA48	±
• • • We do not use the following data for averages, fits, limits, etc. • • •					
8.1±2.2±1.5	670k	[2] BATLEY	08A	NA48	±
12.0±1.9±0.7	400k	[3] PISLAK	03	B865	±

[1] Radiative corrections included. Using Roy equations and including isospin breaking, BATLEY 10C obtains the following scattering lengths $a_0^0 = 0.2220 \pm 0.0128 \pm 0.0050 \pm 0.0037$ (theor.), $a_0^2 = -0.0432 \pm 0.0086 \pm 0.0034 \pm 0.0028$ (theor.). The correlation with $g_p/f_s = -0.914$. Supersedes BATLEY 08A.

[2] Radiative corrections included. Using Roy equations and not including isospin breaking, BATLEY 08A obtains the following $\pi\pi$ scattering length $a_0^0 = 0.233 \pm 0.016 \pm 0.007$ $a_0^2 = -0.0471 \pm 0.011 \pm 0.004$.

[3] Radiative corrections included. Using Roy equations PISLAK 03 obtains the following scattering lengths $a_0^0 = 0.203 \pm 0.033 \pm 0.004$, $a_0^2 = -0.055 \pm 0.023 \pm 0.003$.

h_p/f_s FOR $K^{\pm} \to \pi^+\pi^- e^{\pm}\nu$ DECAY

VALUE (units 10^{-2})	EVTS	DOCUMENT ID		TECN	CHG
−39.8±1.5±0.8	1.13M	[1] BATLEY	10C	NA48	±
• • • We do not use the following data for averages, fits, limits, etc. • • •					
−41.1±1.9±0.8	670k	[2] BATLEY	08A	NA48	±
−51.3±3.3±3.5	400k	[3] PISLAK	03	B865	±

[1] Radiative corrections included. Using Roy equations and including isospin breaking, BATLEY 10C obtains the following scattering lengths $a_0^0 = 0.2220 \pm 0.0128 \pm 0.0050 \pm 0.0037$ (theor.), $a_0^2 = -0.0432 \pm 0.0086 \pm 0.0034 \pm 0.0028$ (theor.). Supersedes BATLEY 08A.

[2] Radiative corrections included. Using Roy equations and not including isospin breaking, BATLEY 08A obtains the following $\pi\pi$ scattering length $a_0^0 = 0.233 \pm 0.016 \pm 0.007$ $a_0^2 = -0.0471 \pm 0.011 \pm 0.004$.

[3] Radiative corrections included. Using Roy equations PISLAK 03 obtains the following scattering lengths $a_0^0 = 0.203 \pm 0.033 \pm 0.004$, $a_0^2 = -0.055 \pm 0.023 \pm 0.003$.

DECAY FORM FACTOR FOR $K^{\pm} \to \pi^0\pi^0 e^{\pm}\nu$

Given in BOLOTOV 86B, BARMIN 88B, and SHIMIZU 04.

$K^{\pm} \to \ell^{\pm}\nu\gamma$ FORM FACTORS

For definitions of the axial-vector F_A and vector F_V form factor, see the "Note on $\pi^{\pm} \to \ell^{\pm}\nu\gamma$ and $K^{\pm} \to \ell^{\pm}\nu\gamma$ Form Factors" in the $\pi^{\pm}$ section. In the kaon literature, often different definitions $a_K = F_A/m_K$ and $v_K = F_V/m_K$ are used.

$F_A + F_V$, SUM OF AXIAL-VECTOR AND VECTOR FORM FACTOR FOR $K \to e\nu_e\gamma$

VALUE	EVTS	DOCUMENT ID		TECN	COMMENT
0.133±0.008 OUR AVERAGE		Error includes scale factor of 1.3.			See the ideogram below.
0.125±0.007±0.001	1.4K	[1] AMBROSINO	09E	KLOE	E_γ in 10–250 MeV, $p_e > 200$ MeV/c
0.147±0.011	51	[2] HEINTZE	79	SPEC	
$0.150^{+0.018}_{-0.023}$	56	[3] HEARD	75	SPEC	

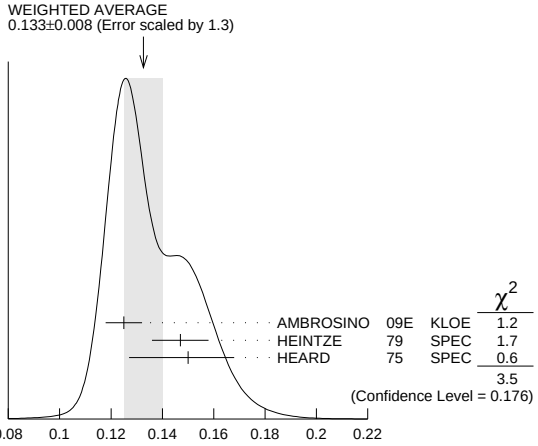

$F_A + F_V$, SUM OF AXIAL-VECTOR AND VECTOR FORM FACTOR FOR $K \to e\nu_e\gamma$

[1] AMBROSINO 09E measures the absolute value $|F_A + F_V|$ which is parametrized as $|F_A + F_V| = F_V\,(1 + \lambda(1-x)) + F_A$, $x = 2E_\gamma/m_K$. $(F_A + F_V)$ and λ are fit parameters. The fitted value of $\lambda = 0.38 \pm 0.20 \pm 0.02$ with a correlation of -0.93 between $(F_A + F_V)$ and λ.

[2] HEINTZE 79 quotes absolute value of $|F_A + F_V| \sin\theta_C$. We use $\sin\theta_C = V_{us} = 0.2205$.

[3] HEARD 75 quotes absolute value of $|F_A + F_V| \sin\theta_C$. We use $\sin\theta_C = V_{us} = 0.2205$.

$F_A + F_V$, SUM OF AXIAL-VECTOR AND VECTOR FORM FACTOR FOR $K \to \mu\nu_\mu\gamma$

VALUE	CL%	EVTS	DOCUMENT ID		TECN	CHG
0.165±0.007±0.011		2588	[1] ADLER	00B	B787	+
• • • We do not use the following data for averages, fits, limits, etc. • • •						
−1.2 to 1.1	90		DEMIDOV	90	XEBC	
< 0.23	90		[1] AKIBA	85	SPEC	

[1] Quotes absolute value. Sign not determined.

$F_A - F_V$, DIFFERENCE OF AXIAL-VECTOR AND VECTOR FORM FACTOR FOR $K \to e\nu_e\gamma$

VALUE	CL%	DOCUMENT ID		TECN
<0.49	90	[1] HEINTZE	79	SPEC

[1] HEINTZE 79 quotes $|F_A - F_V| < \sqrt{11}\,|F_A + F_V|$.

$F_A - F_V$, DIFFERENCE OF AXIAL-VECTOR AND VECTOR FORM FACTOR FOR $K \to \mu\nu_\mu\gamma$

VALUE	CL%	EVTS	DOCUMENT ID		TECN	CHG
−0.21±0.06		22K	DUK	11	ISTR	−
• • • We do not use the following data for averages, fits, limits, etc. • • •						
−0.24 to 0.04	90	2588	ADLER	00B	B787	+
−2.2 to 0.6	90		DEMIDOV	90	XEBC	
−2.5 to 0.3	90		AKIBA	85	SPEC	

$K^{\pm}$ CHARGE RADIUS

VALUE (fm)	DOCUMENT ID		COMMENT
0.560±0.031 OUR AVERAGE			
0.580±0.040	AMENDOLIA	86B	$Ke \to Ke$
0.530±0.050	DALLY	80	$Ke \to Ke$
• • • We do not use the following data for averages, fits, limits, etc. • • •			
0.620±0.037	BLATNIK	79	VMD + dispersion relations

K^+ LONGITUDINAL POLARIZATION OF EMITTED μ^+

VALUE	CL%	DOCUMENT ID		TECN	CHG	COMMENT
<−0.990	90	[1] AOKI	94	SPEC	+	
• • • We do not use the following data for averages, fits, limits, etc. • • •						
<−0.990	90	IMAZATO	92	SPEC	+	Repl. by AOKI 94
−0.970±0.047		[2] YAMANAKA	86	SPEC	+	
−1.0 ±0.1		[2] CUTTS	69	SPRK	+	
−0.96 ±0.12		[2] COOMBES	57	CNTR	+	

[1] AOKI 94 measures $\xi P_\mu = -0.9996 \pm 0.0030 \pm 0.0048$. The above limit is obtained by summing the statistical and systematic errors in quadrature, normalizing to the physically significant region ($|\xi P_\mu| < 1$) and assuming that ξ=1, its maximum value.

[2] Assumes ξ=1.

FORWARD-BACKWARD ASYMMETRY IN $K^{\pm}$ DECAYS

$$A_{FB}(K^{\pm}_{\pi\mu\mu}) = \frac{\Gamma(\cos(\theta_{K\mu})>0) - \Gamma(\cos(\theta_{K\mu})<0)}{\Gamma(\cos(\theta_{K\mu})>0) + \Gamma(\cos(\theta_{K\mu})<0)}$$

VALUE	CL%	DOCUMENT ID		TECN
$<2.3 \times 10^{-2}$	90	[1] BATLEY	11A	NA48

[1] BATLEY 11A gives a corresponding value of the asymmetry $A_{FB} = (-2.4 \pm 1.8) \times 10^{-2}$.

$K^{\pm}$ REFERENCES

BATLEY	17	PL B769 67	J.R. Batley *et al.*	(NA48/2 Collab.)
ARTAMONOV	16	PR D94 032012	A.V. Artamonov *et al.*	(BNL E949 Collab.)
BABUSCI	14B	PL B738 128	D. Babusci *et al.*	(KLOE, KLOE-2 Collab.)
BATLEY	14	PL B730 141	J.R. Batley *et al.*	(CERN NA48/2 Collab.)
BATLEY	14A	JHEP 1408 159	J.R. Batley *et al.*	(CERN NA48/2 Collab.)
LAZZERONI	14	PL B732 65	C. Lazzeroni *et al.*	(CERN NA62 Collab.)
UVAROV	14	PAN 77 725 Translated from YAF 77 765.	V.A. Uvarov *et al.*	(ISTRA+ Collab.)
LAZZERONI	13	PL B719 326	C. Lazzeroni *et al.*	(CERN NA62 Collab.)
BATLEY	12	PL B715 105	J.R. Batley *et al.*	(CERN NA48/2 Collab.)
PDG	12	PR D86 010001	J. Beringer *et al.*	(PDG Collab.)
BATLEY	11A	PL B697 107	J.R. Batley *et al.*	(CERN NA48/2 Collab.)
DUK	11	PL B695 59	V.A. Duk *et al.*	(ISTRA+ Collab.)
LAZZERONI	11	PL B698 105	C. Lazzeroni *et al.*	(CERN NA62 Collab.)
ADLER	10	PR D81 092001	S. Adler *et al.*	(BNL E787 Collab.)
BATLEY	10A	EPJ C68 75	J.R. Batley *et al.*	(CERN NA48/2 Collab.)
BATLEY	10C	EPJ C70 635	J.R. Batley *et al.*	(CERN NA48/2 Collab.)
PDG	10	JP G37 075021	K. Nakamura *et al.*	(PDG Collab.)
PISLAK	10A	PRL 105 019901E	S. Pislak *et al.*	(BNL E865 Collab.)
AKOPDZANOV	09	PAN 71 2074 Translated from YAF 71 2108.	G.A. Akopdzanov *et al.*	(IHEP)
AMBROSINO	09E	EPJ C64 627	F. Ambrosino *et al.*	(KLOE Collab.)
Also		EPJ C65 703 (errat.)	F. Ambrosino *et al.*	(KLOE Collab.)
BATLEY	09	PL B677 246	J.R. Batley *et al.*	(CERN NA48/2 Collab.)
BATLEY	09A	EPJ C64 589	J.R. Batley *et al.*	(CERN NA48/2 Collab.)
BISSEGGER	09	NP B806 178	M. Bissegger *et al.*	
AMBROSINO	08	JHEP 0801 073	F. Ambrosino *et al.*	(KLOE Collab.)
AMBROSINO	08A	JHEP 0802 098	F. Ambrosino *et al.*	(KLOE Collab.)
AMBROSINO	08E	PL B666 305	F. Ambrosino *et al.*	(KLOE Collab.)

See key on page 885

ARTAMONOV 08 PRL 101 191802 A.V. Artamonov *et al.* (BNL E949 Collab.)
Also PR D79 092004 A.V. Artamonov *et al.* (BNL E949 Collab.)
BATLEY 08 PL B659 493 J.R. Batley *et al.* (CERN NA48/2 Collab.)
BATLEY 08A EPJ C54 411 J.R. Batley *et al.* (CERN NA48/2 Collab.)
AKIMENKO 07 PAN 70 702 S.A. Akimenko *et al.* (ISTRA+ Collab.)
Translated from YAF 70 734.
ANDRE 07 ANP 322 2518 T. Andre (EFI)
BATLEY 07A EPJ C50 329 J.R. Batley *et al.* (CERN NA48/2 Collab.)
Also EPJ C52 1021 (errat.) J.R. Batley *et al.* (CERN NA48/2 Collab.)
BATLEY 07B PL B649 349 J.R. Batley *et al.* (CERN NA48/2 Collab.)
BATLEY 07E EPJ C52 875 J.R. Batley *et al.* (CERN NA48/2 Collab.)
TCHIKILEV 07 PAN 70 29 O.G. Tchikilev *et al.* (ISTRA+ Collab.)
ALIEV 06 EPJ C46 61 M.A. Aliev *et al.* (KEK E470 Collab.)
AMBROSINO 06A PL B632 76 F. Ambrosino *et al.* (KLOE Collab.)
BATLEY 06 PL B634 474 J.R. Batley *et al.* (CERN NA48/2 Collab.)
BATLEY 06A PL B638 22 J.R. Batley *et al.* (CERN NA48/2 Collab.)
Also PL B640 297 (errat.) J.R. Batley *et al.* (CERN NA48/2 Collab.)
BATLEY 06B PL B633 173 J.R. Batley *et al.* (CERN NA48/2 Collab.)
COLANGELO 06A PL B638 187 G. Colangelo *et al.*
MA 06 PR D73 037101 H. Ma *et al.* (BNL E865 Collab.)
PDG 06 JP G33 1 W.-M. Yao *et al.* (PDG Collab.)
SHIMIZU 06 PL B633 190 S. Shimizu *et al.* (KEK E470 Collab.)
UVAROV 06 PAN 69 26 V.A. Uvarov *et al.* (ISTRA+ Collab.)
AKOPDZHAN... 05 EPJ C40 343 G.A. Akopdzhanov *et al.* (IHEP)
Also PAN 68 948 G.A. Akopdzhanov *et al.* (IHEP)
Translated from YAF 68 986.
AKOPDZHAN... 05B JETPL 82 675 G.A. Akopdzhanov *et al.* (IHEP)
Translated from ZETFP 82 771.
ARTAMONOV 05 PL B623 192 A.V. Artamonov *et al.* (BNL E949 Collab.)
CABIBBO 05 JHEP 0503 021 N. Cabibbo, G. Isidori (CERN, ROMAI, FRAS)
SHER 05 PR D72 012005 A. Sher *et al.* (BNL E865 Collab.)
ABE 04F PRL 93 131601 M. Abe *et al.* (KEK E246 Collab.)
Also PR D73 072005 M. Abe *et al.* (KEK E246 Collab.)
ADLER 04 PR D70 037102 S. Adler *et al.* (BNL E787 Collab.)
ALOISIO 04A PL B597 139 A. Aloisio *et al.* (KLOE Collab.)
ANISIMOVSK... 04 PRL 93 031801 V.V. Anisimovsky *et al.* (BNL E949 Collab.)
Also PR D77 052003 S. Adler *et al.* (BNL E949 Collab.)
CABIBBO 04A PRL 93 121801 N. Cabibbo (CERN, ROMAI)
CIRIGLIANO 04 EPJ C35 53 V. Cirigliano, H. Neufeld, H. Pichl (CIT, VALE+)
PDG 04 PL B592 1 S. Eidelman *et al.* (PDG Collab.)
SHIMIZU 04 PR D70 037101 S. Shimizu *et al.* (KEK E470 Collab.)
YUSHCHENKO 04 PL B581 31 O.P. Yushchenko *et al.* (INRM, INRM)
YUSHCHENKO 04B PL B589 111 O.P. Yushchenko *et al.* (INRM)
AJINENKO 03 PAN 66 105 I.V. Ajinenko *et al.* (IHEP, INRM)
Translated from YAF 66 107.
AJINENKO 03B PL B567 159 I.V. Ajinenko *et al.* (IHEP, INRM)
AJINENKO 03C PL B574 14 I.V. Ajinenko *et al.* (IHEP, INRM)
ALIEV 03 PL B554 7 M.A. Aliev *et al.* (KEK E470 Collab.)
ANISIMOVSK... 03 PL B562 166 V.V. Anisimovsky *et al.*
PISLAK 03 PR D67 072004 S. Pislak *et al.* (BNL E865 Collab.)
Also PR D81 119903E S. Pislak *et al.* (BNL E865 Collab.)
SHER 03 PRL 91 261802 A. Sher *et al.* (BNL E865 Collab.)
ADLER 02 PRL 88 041803 S. Adler *et al.* (BNL E787 Collab.)
ADLER 02B PR D65 052009 S. Adler *et al.* (BNL E787 Collab.)
ADLER 02C PL B537 211 S. Adler *et al.* (BNL E787 Collab.)
AJINENKO 02 PAN 65 2064 I.V. Ajinenko *et al.* (IHEP, INRM)
Translated from YAF 65 2125.
CIRIGLIANO 02 EPJ C23 121 V. Cirigliano *et al.* (VIEN, VALE, MARS)
PARK 02 PRL 88 111801 H.K. Park *et al.* (FNAL HyperCP Collab.)
PDG 02 PR D66 010001 K. Hagiwara *et al.* (PDG Collab.)
POBLAGUEV 02 PRL 89 061803 A.A. Poblaguev *et al.* (BNL 865 Collab.)
ADLER 01 PR D63 032004 S. Adler *et al.* (BNL E787 Collab.)
HORIE 01 PL B513 311 K. Horie *et al.* (KEK E426 Collab.)
PISLAK 01 PRL 87 221801 S. Pislak *et al.* (BNL E865 Collab.)
Also PR D67 072004 S. Pislak *et al.* (BNL E865 Collab.)
Also PRL 105 019901E S. Pislak *et al.* (BNL E865 Collab.)
ADLER 00 PRL 84 3768 S. Adler *et al.* (BNL E787 Collab.)
ADLER 00B PR D61 052004 S. Adler *et al.* (BNL E787 Collab.)
ADLER 00C PRL 85 2256 S. Adler *et al.* (BNL E787 Collab.)
APPEL 00 PRL 85 4856 S. Adler *et al.* (BNL E787 Collab.)
Also PRL 85 2450 R. Appel *et al.* (BNL 865 Collab.)
Also Thesis, Yale Univ. D.R. Bergman
Also Thesis, Univ. Zurich S. Pislak
APPEL 00B PRL 85 2877 R. Appel *et al.* (BNL 865 Collab.)
MA 00 PRL 84 2580 H. Ma *et al.* (BNL 865 Collab.)
PDG 00 EPJ C15 1 D.E. Groom *et al.* (PDG Collab.)
SHIMIZU 00 PL B495 33 S. Shimizu *et al.* (KEK E246 Collab.)
ABE 99S PRL 83 4253 M. Abe *et al.* (KEK E246 Collab.)
AMOROS 99 JP G25 1607 G. Amoros, J. Bijnens (LUND, HELS)
APPEL 99 PRL 83 4482 R. Appel *et al.* (BNL 865 Collab.)
ADLER 98 PR D58 012003 S. Adler *et al.* (BNL E787 Collab.)
BATUSOV 98 NP B516 3 V.Y. Batusov *et al.*
DAMBROSIO 98A JHEP 9808 004 G. D'Ambrosio *et al.*
ADLER 97 PRL 79 2204 S. Adler *et al.* (BNL E787 Collab.)
ADLER 97C PRL 79 4756 S. Adler *et al.* (BNL E787 Collab.)
BERGMAN 97 Thesis, Yale Univ. D.R. Bergman
KITCHING 97 PRL 79 4079 P. Kitching *et al.* (BNL E787 Collab.)
PISLAK 97 Thesis, Univ. Zurich S. Pislak
ADLER 96 PRL 76 1421 S. Adler *et al.* (BNL E787 Collab.)
KOPTEV 95 JETPL 61 877 V.P. Koptev *et al.* (PNPI)
Translated from ZETFP 61 865.
AOKI 94 PR D50 69 M. Aoki *et al.* (INUS, KEK, TOKMS)
ATIYA 93 PRL 70 2521 M.S. Atiya *et al.* (BNL E787 Collab.)
Also PRL 71 305 (erratum) M.S. Atiya *et al.* (BNL E787 Collab.)
ATIYA 93B PR D48 1 M.S. Atiya *et al.* (BNL E787 Collab.)
ALLIEGRO 92 PRL 68 278 C. Alliegro *et al.* (BNL, FNAL, PSI+)
BARMIN 92 SJNP 55 547 V.V. Barmin *et al.* (ITEP)
Translated from YAF 55 976.
IMAZATO 92 PRL 69 877 J. Imazato *et al.* (KEK, INUS, TOKY+)
IVANOV 92 THESIS Yu.M. Ivanov (PNPI)
LITTENBERG 92 PRL 68 443 L.S. Littenberg, R.E. Shrock (BNL, STON)
USHER 92 PR D45 3961 T. Usher *et al.* (UCI)
AKIMENKO 91 PL B259 225 S.A. Akimenko *et al.* (SERP, JINR, TBIL+)
BARMIN 91 SJNP 53 606 V.V. Barmin *et al.* (ITEP)
Translated from YAF 53 981.
DENISOV 91 JETPL 54 558 A.S. Denisov *et al.* (PNPI)
Translated from ZETFP 54 557.
Also THESIS Yu.M. Ivanov (PNPI)
ATIYA 90 PRL 64 21 M.S. Atiya *et al.* (BNL E787 Collab.)
ATIYA 90B PRL 65 1188 M.S. Atiya *et al.* (BNL E787 Collab.)
DEMIDOV 90 SJNP 52 1006 V.S. Demidov *et al.* (ITEP)
Translated from YAF 52 1595.
LEE 90 PRL 64 165 A.M. Lee *et al.* (BNL, FNAL, VILL, WASH+)
ATIYA 89 PRL 63 2177 M.S. Atiya *et al.* (BNL E787 Collab.)
BARMIN 89 SJNP 50 421 V.V. Barmin *et al.* (ITEP)
Translated from YAF 50 679.
BARMIN 88 SJNP 47 643 V.V. Barmin *et al.* (ITEP)
Translated from YAF 47 1011.
BARMIN 88B SJNP 48 1032 V.V. Barmin *et al.* (ITEP)
Translated from YAF 48 1719.
BOLOTOV 88 JETPL 47 7 V.N. Bolotov *et al.* (ASCI)
Translated from ZETFP 47 8.
GALL 88 PRL 60 186 K.P. Gall *et al.* (BOST, MIT, WILL, CIT+)
BARMIN 87 SJNP 45 62 V.V. Barmin *et al.* (ITEP)
Translated from YAF 45 97.
BOLOTOV 87 SJNP 45 1023 V.N. Bolotov *et al.* (INRM)
Translated from YAF 45 1652.
AMENDOLIA 86B PL B178 435 S.R. Amendolia *et al.* (CERN NA7 Collab.)
BOLOTOV 86 SJNP 44 73 V.N. Bolotov *et al.* (INRM)
Translated from YAF 44 117.
BOLOTOV 86B SJNP 44 68 V.N. Bolotov *et al.* (INRM)
Translated from YAF 44 108.
YAMANAKA 86 PR D34 85 T. Yamanaka *et al.* (KEK, TOKY)
Also PRL 52 329 R.S. Hayano *et al.* (TOKY, KEK)
AKIBA 85 PR D32 2911 Y. Akiba *et al.* (TOKY, TINT, TSUK, KEK)
BOLOTOV 85 JETPL 42 481 V.N. Bolotov *et al.* (INRM)
Translated from ZETFP 42 390.
ASANO 82 PL 113B 195 Y. Asano *et al.* (KEK, TOKY, INUS, OSAK)
COOPER 82 PL 112B 97 A.M. Cooper *et al.* (RL)
PDG 82B PL 111B 70 M. Roos *et al.* (HELS, CIT, CERN)
ASANO 81B PL 107B 159 Y. Asano *et al.* (KEK, TOKY, INUS, OSAK)
CAMPBELL 81 PRL 47 1032 M.K. Campbell *et al.* (YALE, BNL)
Also PR D27 1056 S.R. Blatt *et al.* (YALE, BNL)
LUM 81 PR D23 2522 G.K. Lum *et al.* (LBL, NBS+)
LYONS 81 ZPHY C10 215 L. Lyons, C. Albajar, G. Myatt (OXF)
DALLY 80 PRL 45 232 E.B. Dally *et al.* (UCLA+)
BARKOV 79 NP B148 53 L.M. Barkov *et al.* (NOVO, KIAE)
BLATNIK 79 LNC 24 39 S. Blatnik, J. Stahov, C.B. Lang (TUZL, GRAZ)
HEINTZE 79 NP B149 365 J. Heintze *et al.* (HEIDP, CERN)
ABRAMS 77 PR D15 22 R.J. Abrams *et al.* (BNL)
DEVAUX 77 NP B126 11 B. Devaux *et al.* (SACL, GEVA)
HEINTZE 77 PL 70B 482 J. Heintze *et al.* (HEIDP, CERN)
ROSSELET 77 PR D15 574 L. Rosselet *et al.* (GEVA, SACL)
BLOCH 76 PL 60B 393 P. Bloch *et al.* (GEVA, SACL)
BRAUN 76B LNC 17 521 H.M. Braun *et al.* (AACH3, BARI, BELG+)
DIAMANT-... 76 PL 62B 485 A.M. Diamant-Berger *et al.* (SACL, GEVA)
HEINTZE 76 PL 60B 302 J. Heintze *et al.* (HEIDP)
SMITH 76 NP B109 173 K.M. Smith *et al.* (GLAS, LIVP, OXF+)
WEISSENBE... 76 NP B115 55 A.O. Weissenberg *et al.* (ITEP, LEBD)
BLOCH 75 PL 56B 201 P. Bloch *et al.* (SACL, GEVA)
BRAUN 75 NP B89 210 H.M. Braun *et al.* (AACH3, BARI, BRUX+)
CHENG 75 NP A254 381 S.C. Cheng *et al.* (COLU, YALE)
HEARD 75 PL 55B 324 K.S. Heard *et al.* (CERN, HEIDH)
HEARD 75B PL 55B 327 K.S. Heard *et al.* (CERN, HEIDH)
SHEAFF 75 PR D12 2570 M. Sheaff (WISC)
SMITH 75 NP B91 45 K.M. Smith *et al.* (GLAS, LIVP, OXF+)
WEISSENBE... 74 PL 48B 474 A.O. Weissenberg *et al.* (ITEP, LEBD)
ABRAMS 73B PRL 30 500 R.J. Abrams *et al.* (BNL)
BACKENSTO... 73 PL 43B 431 G. Backenstoss *et al.* (CERN, KARLK, KARLE+)
LJUNG 73 PR D8 1307 D. Ljung, D. Cline (WISC)
Also PRL 28 523 D. Ljung (WISC)
Also PRL 28 1287 D. Cline, D. Ljung (WISC)
Also PRL 23 326 U. Camerini *et al.* (WISC)
LUCAS 73 PR D8 719 P.W. Lucas, H.D. Taft, W.J. Willis (YALE)
LUCAS 73B PR D8 727 P.W. Lucas, H.D. Taft, W.J. Willis (YALE)
PANG 73 PR D8 1989 C.Y. Pang *et al.* (EFI, ARIZ, LBL)
Also PL 40B 699 G.D. Cable *et al.* (EFI, LBL)
SMITH 73 NP B60 411 K.M. Smith *et al.* (GLAS, LIVP, OXF+)
ABRAMS 72 PRL 29 1118 R.J. Abrams *et al.* (BNL)
AUBERT 72 NC 12A 509 B. Aubert *et al.* (ORSAY, BRUX, EPOL)
CHIANG 72 PR D6 1254 I.H. Chiang *et al.* (ROCH, WISC)
CLARK 72 PRL 29 1274 A.R. Clark *et al.* (LBL)
FORD 72 PL 38B 335 W.T. Ford *et al.* (PRIN)
HOFFMASTER 72 NP B36 1 S. Hoffmaster *et al.* (STEV, SETO, LEHI)
BOURQUIN 71 PL 36B 615 M.H. Bourquin *et al.* (GEVA, SACL)
HAIDT 71 PR D3 10 D. Haidt (AACH, BARI, CERN, EPOL, NIJM+)
Also PL 29B 691 D. Haidt *et al.* (AACH, BARI, CERN, EPOL+)
KLEMS 71 PR D4 66 J.H. Klems, R.H. Hildebrand, R. Stiening (CHIC+)
Also PRL 24 1086 J.H. Klems, R.H. Hildebrand, R. Stiening (LRL+)
Also PRL 25 473 J.H. Klems, R.H. Hildebrand, R. Stiening (LRL+)
OTT 71 PR D3 52 R.J. Ott, T.W. Pritchard (LOQM)
ROMANO 71 PL 36B 525 F. Romano *et al.* (BARI, CERN, ORSAY)
SCHWEINB... 71 PL 36B 246 W. Schweinberger (AACH, BELG, CERN, NIJM+)
STEINER 71 PL 36B 521 H.J. Steiner (AACH, BARI, CERN, EPOL, ORSAY+)
BARDIN 70 PL 32B 121 D.Y. Bardin, S.N. Bilenky, B.M. Pontecorvo (JINR)
BECHERRAWY 70 PR D1 1452 T. Becherrawy (ROCH)
FORD 70 PRL 25 1370 W.T. Ford *et al.* (PRIN)
GAILLARD 70 CERN 70-14 J.M. Gaillard, L.M. Chounet (CERN, ORSAY)
GRAUMAN 70 PR D1 1277 J. Grauman *et al.* (STEV, SETO, LEHI)
Also PRL 23 737 J.U. Grauman *et al.* (STEV, SETO, LEHI)
PANDOULAS 70 PR D2 1205 D. Pandoulas *et al.* (STEV, SETO)
CUTTS 69 PR 184 1380 D. Cutts *et al.* (LRL, MIT)
Also PRL 20 955 D. Cutts *et al.* (LRL, MIT)
DAVISON 69 PR 180 1333 D.C. Davison *et al.* (UCR)
ELY 69 PR 180 1319 R.P.J. Ely *et al.* (LOUC, WISC, LRL)
HERZO 69 PR 186 1403 D. Herzo *et al.* (ILL)
LOBKOWICZ 69 PR 185 1676 F. Lobkowicz *et al.* (ROCH, BNL)
Also PRL 17 548 F. Lobkowicz *et al.* (ROCH, BNL)
MAST 69 PR 183 1200 T.S. Mast *et al.* (LRL)
SELLERI 69 NC 60A 291 F. Selleri
ZELLER 69 PR 182 1420 M.E. Zeller *et al.* (UCLA, LRL)
BOTTERILL 68B PRL 21 766 D.R. Botterill *et al.* (OXF)
BOTTERILL 68C PR 174 1661 D.R. Botterill *et al.* (OXF)
BUTLER 68 UCRL 18420 W.D. Butler *et al.* (LRL)
CHANG 68 PRL 20 510 C.Y. Chang *et al.* (UMD, RUTG)
CHEN 68 PRL 20 73 M. Chen *et al.* (LRL, MIT)
EICHTEN 68 PL 27B 586 T. Eichten (AACH, BARI, CERN, EPOL, ORSAY+)
ESCHSTRUTH 68 PR 165 1487 P.T. Eschstruth *et al.* (PRIN, PENN)
GARLAND 68 PR 167 1225 R. Garland *et al.* (COLU, RUTG, WISC)
MOSCOSO 68 Thesis L. Moscoso (ORSAY)
AUERBACH 67 PR 155 1505 L.B. Auerbach *et al.* (PENN, PRIN)
Also PR D9 3216 L.B. Auerbach
Erratum.
BELLOTTI 67 Heidelberg Conf. E. Bellotti, A. Pullia (MILA)
BELLOTTI 67B NC 52A 1287 E. Bellotti, E. Fiorini, A. Pullia (MILA)
Also PL 20 690 E. Bellotti *et al.* (MILA)
BISI 67 PL 25B 572 V. Bisi *et al.* (TORI)
FLETCHER 67 PRL 19 98 C.R. Fletcher *et al.* (ILL)
FORD 67 PRL 18 1214 W.T. Ford *et al.* (PRIN)
GINSBERG 67 PR 162 1570 E.S. Ginsberg (MASB)
KALMUS 67 PR 159 1187 G.E. Kalmus, A. Kernan (LRL)
ZINCHENKO 67 Thesis Rutgers A.I. Zinchenko (RUTG)
CALLAHAN 66 NC 44A 90 A.C. Callahan (WISC)
CALLAHAN 66B PR 150 1153 A.C. Callahan *et al.* (WISC, LRL, UCR+)
CESTER 66 PL 21 343 R. Cester *et al.* (PPA)
See footnote 1 in AUERBACH 67.
Also PR 155 1505 L.B. Auerbach *et al.* (PENN, PRIN)
BIRGE 65 PR 139 B1600 R.W. Birge *et al.* (LRL, WISC)
BISI 65 NC 35 768 V. Bisi *et al.* (TORI)
BISI 65B PR 139 B1068 V. Bisi *et al.* (TORI)
CALLAHAN 65 PRL 15 129 A. Callahan, D. Cline (WISC)
CLINE 65 PL 15 293 D. Cline, W.F. Fry (WISC)
DEMARCO 65 PR 140 B1430 A. de Marco, C. Grosso, G. Rinaudo (TORI, CERN)
FITCH 65B PR 140 B1088 V.L. Fitch, C.A. Quarles, H.C. Wilkins (PRIN+)
STAMER 65 PR 138 B440 P. Stamer *et al.* (STEV)
YOUNG 65 Thesis UCRL 16362 P.S. Young (LRL)
Also PR 156 1464 P.S. Young, W.Z. Osborne, W.H. Barkas (LRL)
BORREANI 64 PL 12 123 G. Borreani, G. Rinaudo, A.E. Werbrouck (TORI)

CALLAHAN	64	PR 136 B1463	A. Callahan, R. March, R. Stark	(WISC)
GREINER	64	PRL 13 284	D.E. Greiner, W.Z. Osborne, W.H. Barkas	(LRL)
SHAKLEE	64	PR 136 B1423	F.S. Shaklee *et al.*	(MICH)
BOYARSKI	62	PR 128 2398	A.M. Boyarski *et al.*	(MIT)
FERRO-LUZZI	61	NC 22 1087	M. Ferro-Luzzi *et al.*	(LRL)
ROE	61	PRL 7 346	B.P. Roe *et al.*	(MICH, LRL)
TAYLOR	59	PR 114 359	S. Taylor *et al.*	(COLU)
COOMBES	57	PR 108 1348	C.A. Coombes *et al.*	(LBL)

OTHER RELATED PAPERS

LITTENBERG	93	ARNPS 43 729	L.S. Littenberg, G. Valencia	(BNL, FNAL)
	Rare and Radiative Kaon Decays			
RITCHIE	93	RMP 65 1149	J.L. Ritchie, S.G. Wojcicki	
	"Rare K Decays"			
BATTISTON	92	PRPL 214 293	R. Battiston *et al.*	(PGIA, CERN, TRSTT)
	Status and Perspectives of K Decay Physics			
BRYMAN	89	IJMP A4 79	D.A. Bryman	(TRIU)
	"Rare Kaon Decays"			
CHOUNET	72	PRPL 4C 199	L.M. Chounet, J.M. Gaillard, M.K. Gaillard	(ORSAY+)
FEARING	70	PR D2 542	H.W. Fearing, E. Fischbach, J. Smith	(STON, BOHR)
HAIDT	69B	PL 29B 696	D. Haidt *et al.*	(AACH, BARI, CERN, EPOL+)
CRONIN	68B	Vienna Conf. 241	J.W. Cronin	(PRIN)
	Rapporteur talk.			
WILLIS	67	Heidelberg Conf. 273	W.J. Willis	(YALE)
	Rapporteur talk.			
CABIBBO	66	Berkeley Conf. 33	N. Cabibbo	(CERN)
ADAIR	64	PL 12 67	R.K. Adair, L.B. Leipuner	(YALE, BNL)
CABIBBO	64	PL 9 352	N. Cabibbo, A. Maksymowicz	(CERN)
	Also	PL 11 360	N. Cabibbo, A. Maksymowicz	(CERN)
	Also	PL 14 72	N. Cabibbo, A. Maksymowicz	(CERN)
BIRGE	63	PRL 11 35	R.W. Birge *et al.*	(LRL, WISC, BARI)
BLOCK	62B	CERN Conf. 371	M.M. Block, L. Lendinara, L. Monari	(NWES, BGNA)
BRENE	61	NP 22 553	N. Brene, L. Egardt, B. Qvist	(NORD)

K^0

$I(J^P) = \frac{1}{2}(0^-)$

K^0 MASS

VALUE (MeV)	EVTS	DOCUMENT ID		TECN	COMMENT
497.611±0.013 OUR FIT Error includes scale factor of 1.2.					
497.611±0.013 OUR AVERAGE Error includes scale factor of 1.2.					
497.607±0.007±0.015	261k	[1] TOMARADZE	14		$\psi(2S) \to K^0_S X$
497.583±0.005±0.020	35k	AMBROSINO	07B	KLOE	$e^+e^- \to K^0_L K^0_S$
497.625±0.001±0.031	655k	LAI	02	NA48	K^0_L beam
497.661±0.033	3713	BARKOV	87B	CMD	$e^+e^- \to K^0_L K^0_S$
497.742±0.085	780	BARKOV	85B	CMD	$e^+e^- \to K^0_L K^0_S$
• • • We do not use the following data for averages, fits, limits, etc. • • •					
497.44 ±0.50		FITCH	67	OSPK	
498.9 ±0.5	4500	BALTAY	66	HBC	K^0 from $\overline{p}p$
497.44 ±0.33	2223	KIM	65B	HBC	K^0 from $\overline{p}p$
498.1 ±0.4		CHRISTENS...	64	OSPK	

[1] Obtained by analyzing CLEO-c data but not authored by the CLEO Collaboration.

$m_{K^0} - m_{K^\pm}$

VALUE (MeV)	EVTS	DOCUMENT ID		TECN	CHG	COMMENT
3.934±0.020 OUR FIT Error includes scale factor of 1.6.						
• • • We do not use the following data for averages, fits, limits, etc. • • •						
3.95 ±0.21	417	HILL	68B	DBC	+	$K^+ d \to K^0 pp$
3.90 ±0.25	9	BURNSTEIN	65	HBC	−	
3.71 ±0.35	7	KIM	65B	HBC	−	$K^- p \to n\overline{K}^0$
5.4 ±1.1		CRAWFORD	59	HBC	+	
3.9 ±0.6		ROSENFELD	59	HBC	−	

K^0 MEAN SQUARE CHARGE RADIUS

VALUE (fm^2)	EVTS	DOCUMENT ID		TECN	COMMENT
−0.077±0.010 OUR AVERAGE					
−0.077±0.007±0.011	5037	ABOUZAID	06	KTEV	$K^0_L \to \pi^+\pi^- e^+ e^-$
−0.090±0.021		LAI	03C	NA48	$K^0_L \to \pi^+\pi^- e^+ e^-$
−0.054±0.026		MOLZON	78		K_S regen. by electrons
• • • We do not use the following data for averages, fits, limits, etc. • • •					
−0.087±0.046		BLATNIK	79		VMD + dispersion relations
−0.050±0.130		FOETH	69B		K_S regen. by electrons

T-VIOLATION PARAMETER IN K^0-$\overline{K}^0$ MIXING

The asymmetry $A_T = \frac{\Gamma(\overline{K}^0 \to K^0) - \Gamma(K^0 \to \overline{K}^0)}{\Gamma(\overline{K}^0 \to K^0) + \Gamma(K^0 \to \overline{K}^0)}$ must vanish if T invariance holds.

ASYMMETRY A_T IN K^0-$\overline{K}^0$ MIXING

VALUE (units 10^{-3})	EVTS	DOCUMENT ID		TECN
6.6±1.3±1.0	640k	[1] ANGELOPO...	98E	CPLR

[1] ANGELOPOULOS 98E measures the asymmetry $A_T = [\Gamma(\overline{K}^0_{t=0} \to e^+\pi^-\nu_{t=\tau}) - \Gamma(K^0_{t=0} \to e^-\pi^+\overline{\nu}_{t=\tau})]/[\Gamma(\overline{K}^0_{t=0} \to e^+\pi^-\nu_{t=\tau}) + \Gamma(K^0_{t=0} \to e^-\pi^+\overline{\nu}_{t=\tau})]$ as a function of the neutral-kaon eigentime τ. The initial strangeness of the neutral kaon is tagged by the charge of the accompanying charged kaon in the reactions $p\overline{p} \to K^-\pi^+ K^0$ and $p\overline{p} \to K^+\pi^-\overline{K}^0$. The strangeness at the time of the decay is tagged by the lepton charge. The reported result is the average value of A_T over the interval $1\tau_S < \tau < 20\tau_S$. From this value of A_T ANGELOPOULOS 01B, assuming CPT invariance in the $e\pi\nu$ decay amplitude, determine the T-violating as $\Delta S = \Delta S$ conserving parameter (for its definition, see Review below) $4\mathrm{Re}(\epsilon) = (6.2 \pm 1.4 \pm 1.0) \times 10^{-3}$.

See the related review(s):
CPT Invariance Tests in Neutral Kaon Decay

CP-VIOLATION PARAMETERS

Re(ϵ)

VALUE (units 10^{-3})	DOCUMENT ID		TECN
1.596±0.013	[1] AMBROSINO	06H	KLOE
• • • We do not use the following data for averages, fits, limits, etc. • • •			
1.664±0.010	[2] LAI	05A	NA48

[1] AMBROSINO 06H uses Bell-Steinberger relations with the following measurements: B($K^0_L \to \pi^+\pi^-$) in AMBROSINO 06F, B($K^0_S \to \pi^0\pi^0\pi^0$) in AMBROSINO 05B, the K^0_S-semileptonic charge asymmetry in AMBROSINO 06E, and K^0-semileptonic results in ANGELOPOULOS 98F.
[2] LAI 05A values are obtained through unitarity (Bell-Steinberger relations), improving determination of η_{000} and combining other data from PDG 04 and APOSTOLAKIS 99B.

CPT-VIOLATION PARAMETERS

In K^0-$\overline{K}^0$ mixing, if CP-violating interactions include a T conserving part then

$$|K_S\rangle = [|K_1\rangle + (\epsilon+\delta)|K_2\rangle]/\sqrt{1+|\epsilon+\delta|^2}$$
$$|K_L\rangle = [|K_2\rangle + (\epsilon-\delta)|K_1\rangle]/\sqrt{1+|\epsilon-\delta|^2}$$

where

$$|K_1\rangle = [|K^0\rangle + |\overline{K}^0\rangle]/\sqrt{2}$$
$$|K_2\rangle = [|K^0\rangle - |\overline{K}^0\rangle]/\sqrt{2}$$

and

$$|\overline{K}^0\rangle = CP|K^0\rangle.$$

The parameter δ specifies the CPT-violating part.

Estimates of δ are given below assuming the validity of the $\Delta S = \Delta Q$ rule. See also THOMSON 95 for a test of CPT-symmetry conservation in K^0 decays using the Bell-Steinberger relation.

REAL PART OF δ

A nonzero value violates CPT invariance.

VALUE (units 10^{-4})	EVTS	DOCUMENT ID		TECN	COMMENT
2.51± 2.25		[1] ABOUZAID	11	KTEV	
• • • We do not use the following data for averages, fits, limits, etc. • • •					
2.3 ± 2.7		[2] AMBROSINO	06H	KLOE	
2.4 ± 2.8		[3] APOSTOLA...	99B	RVUE	
2.9 ± 2.6 ±0.6	1.3M	[4] ANGELOPO...	98F	CPLR	
180 ±200	6481	[5] DEMIDOV	95		$K_{\ell 3}$ reanalysis

[1] ABOUZAID 11 uses Bell-Steinberger relations.
[2] AMBROSINO 06H uses Bell-Steinberger relations with the following measurements: B($K^0_L \to \pi^+\pi^-$) in AMBROSINO 06F, B($K^0_S \to \pi^0\pi^0\pi^0$) in AMBROSINO 05B, the K^0_S-semileptonic charge asymmetry in AMBROSINO 06E, and K^0-semileptonic results in ANGELOPOULOS 98F.
[3] APOSTOLAKIS 99B assumes only unitarity and combines CPLEAR and other results.
[4] ANGELOPOULOS 98F use $\Delta S = \Delta Q$. If $\Delta S = \Delta Q$ is not assumed, they find $\mathrm{Re}\delta = (3.0 \pm 3.3 \pm 0.6) \times 10^{-4}$.
[5] DEMIDOV 95 reanalyzes data from HART 73 and NIEBERGALL 74.

IMAGINARY PART OF δ

A nonzero value violates CPT invariance.

VALUE (units 10^{-5})	EVTS	DOCUMENT ID		TECN	COMMENT
− 1.5± 1.6		[1] ABOUZAID	11	KTEV	
• • • We do not use the following data for averages, fits, limits, etc. • • •					
0.4± 2.1		[2] AMBROSINO	06H	KLOE	
− 0.2± 2.0		[3] LAI	05A	NA48	
2.4± 5.0		[4] APOSTOLA...	99B	RVUE	
− 90 ± 290 ±100	1.3M	[5] ANGELOPO...	98F	CPLR	
2100 ±3700	6481	[6] DEMIDOV	95		$K_{\ell 3}$ reanalysis

[1] ABOUZAID 11 uses Bell-Steinberger relations.
[2] AMBROSINO 06H uses Bell-Steinberger relations with the following measurements: B($K^0_L \to \pi^+\pi^-$) in AMBROSINO 06F, B($K^0_S \to \pi^0\pi^0\pi^0$) in AMBROSINO 05B, the K^0_S-semileptonic charge asymmetry in AMBROSINO 06E, and K^0-semileptonic results in ANGELOPOULOS 98F.
[3] LAI 05A values are obtained through unitarity (Bell-Steinberger relations), improving determination of η_{000} and combining other data from PDG 04 and APOSTOLAKIS 99B.
[4] APOSTOLAKIS 99B assumes only unitarity and combines CPLEAR and other results.
[5] If $\Delta S = \Delta Q$ is not assumed, ANGELOPOULOS 98F finds $\mathrm{Im}\delta = (-15 \pm 23 \pm 3) \times 10^{-3}$.
[6] DEMIDOV 95 reanalyzes data from HART 73 and NIEBERGALL 74.

Re(y)

A non-zero value would violate CPT invariance in $\Delta S = \Delta Q$ amplitude. Re(y) is the following combination of $K_{\ell 3}$ decay amplitudes:

$$\mathrm{Re(y)} = \mathrm{Re}\left(\frac{A(\overline{K}^0 \to e^-\pi^+\overline{\nu}_e)^* - A(K^0 \to e^+\pi^-\nu_e)}{A(\overline{K}^0 \to e^-\pi^+\overline{\nu}_e)^* + A(K^0 \to e^+\pi^-\nu_e)} \right)$$

VALUE (units 10^{-3})	EVTS	DOCUMENT ID		TECN
0.4±2.5	13k	[1] AMBROSINO	06E	KLOE
• • • We do not use the following data for averages, fits, limits, etc. • • •				
0.3±3.1		[2] APOSTOLA...	99B	CPLR

[1] They use the PDG 04 for the K^0_L semileptonic charge asymmetry and PDG 04 (*CP* review, *CPT* NOT ASSUMED) for Re(ϵ).

[2] Constrained by Bell-Steinberger (or unitarity) relation.

Re(x_-)

A non-zero value would violate *CPT* invariance in decay amplitudes with $\Delta S \neq \Delta Q$. x_-, used here to define Re(x_-), and x_+, used below in the $\Delta S = \Delta Q$ section are the following combinations of K_{e3} decay amplitudes:

$$x_\pm = \frac{1}{2}\left(\frac{A(\overline{K}^0 \to \pi^- e^+ \nu_e)}{A(K^0 \to \pi^- e^+ \nu_e)} \pm \frac{A(K^0 \to \pi^+ e^- \overline{\nu}_e)^*}{A(\overline{K}^0 \to \pi^+ e^- \overline{\nu}_e)^*} \right).$$

VALUE (units 10^{-3})	EVTS	DOCUMENT ID		TECN	COMMENT
−2.9± 2.0		[1] AMBROSINO	06H	KLOE	
• • • We do not use the following data for averages, fits, limits, etc. • • •					
−0.8± 2.5	13k	[2] AMBROSINO	06E	KLOE	
−0.5± 3.0		[3] APOSTOLA...	99B	CPLR	Strangeness tagged
2 ±13 ±3	650k	ANGELOPO...	98F	CPLR	Strangeness tagged

[1] AMBROSINO 06H uses Bell-Steinberger relations with the following measurements: $B(K^0_L \to \pi^+\pi^-)$ in AMBROSINO 06F, $B(K^0_S \to \pi^0\pi^0\pi^0)$ in AMBROSINO 05B, the K^0_S-semileptonic charge asymmetry in AMBROSINO 06E, and K^0-semileptonic results in ANGELOPOULOS 98F.

[2] Uses PDG 04 for the K^0_L semileptonic charge asymmetry and Re(δ) from CPLEAR, ANGELOPOULOS 98F.

[3] Constrained by Bell-Steinberger (or unitarity) relation.

$|m_{K^0} - m_{\overline{K}^0}| \,/\, m_{\text{average}}$

A test of *CPT* invariance. "Our Evaluation" is described in the "Tests of Conservation Laws" section. It assumes *CPT* invariance in the decay and neglects some contributions from decay channels other than $\pi\pi$.

VALUE	CL%	DOCUMENT ID		TECN
$< 6 \times 10^{-19}$	90	PDG	12	
• • • We do not use the following data for averages, fits, limits, etc. • • •				
$(-3 \pm 4) \times 10^{-18}$		[1] ANGELOPO...	99B	RVUE

[1] ANGELOPOULOS 99B assumes only unitarity and combines CPLEAR and other results.

$(\Gamma_{K^0} - \Gamma_{\overline{K}^0})/m_{\text{average}}$

A test of *CPT* invariance.

VALUE	DOCUMENT ID		TECN
$(7.8 \pm 8.4) \times 10^{-18}$	[1] ANGELOPO...	99B	RVUE

[1] ANGELOPOULOS 99B assumes only unitarity and combines CPLEAR with other results. Correlated with $(m_{K^0} - m_{\overline{K}^0}) \,/\, m_{\text{average}}$ with a correlation coefficient of −0.95.

TESTS OF $\Delta S = \Delta Q$ RULE

Re(x_+)

A non-zero value would violate the $\Delta S = \Delta Q$ rule in *CPT* conserving transitions. x_+ is defined above in the Re(x_-) section.

VALUE (units 10^{-3})	EVTS	DOCUMENT ID		TECN
−0.9± 3.0 OUR AVERAGE				
−2 ±10		[1] BATLEY	07D	NA48
−0.5± 3.6	13k	[2] AMBROSINO	06E	KLOE
−1.8± 6.1		[3] ANGELOPO...	98D	CPLR

[1] Result obtained from the measurement $\Gamma(K^0_S \to \pi e \nu) \,/\, \Gamma(K^0_L \to \pi e \nu) = 0.993 \pm 0.34$, neglecting possible *CPT* non-invariance and using PDG 06 values of $B(K^0_L \to \pi e \nu) = 0.4053 \pm 0.0015$, $\tau_L = (5.114 \pm 0.021) \times 10^{-8}$ s and $\tau_S = (0.8958 \pm 0.0005) \times 10^{-10}$ s.

[2] Re(x_+) can be shown to be equal to the following combination of rates:

$$\text{Re}(x_+) = \frac{1}{2} \frac{\Gamma(K^0_S \to \pi e \nu) - \Gamma(K^0_L \to \pi e \nu)}{\Gamma(K^0_S \to \pi e \nu) + \Gamma(K^0_L \to \pi e \nu)}$$

which is valid up to first order in terms violating *CPT* and/or the $\Delta S = \Delta Q$ rule.

[3] Obtained neglecting *CPT* violating amplitudes.

K^0 REFERENCES

TOMARADZE	14	PR D89 031501	A. Tomaradze *et al.*	(NWES, WAYN)
PDG	12	PR D86 010001	J. Beringer *et al.*	(PDG Collab.)
ABOUZAID	11	PR D83 092001	E. Abouzaid *et al.*	(FNAL KTeV Collab.)
AMBROSINO	07B	JHEP 0712 073	F. Ambrosino *et al.*	(KLOE Collab.)
BATLEY	07D	PL B653 145	J.R. Batley *et al.*	(CERN NA48 Collab.)
ABOUZAID	06	PRL 96 101801	E. Abouzaid *et al.*	(KTeV Collab.)
AMBROSINO	06E	PL B636 173	F. Ambrosino *et al.*	(KLOE Collab.)
AMBROSINO	06F	PL B638 140	F. Ambrosino *et al.*	(KLOE Collab.)
AMBROSINO	06H	JHEP 0612 011	F. Ambrosino *et al.*	(KLOE Collab.)
PDG	06	JP G33 1	W.-M. Yao *et al.*	(PDG Collab.)
AMBROSINO	05B	PL B619 61	F. Ambrosino *et al.*	(KLOE Collab.)
LAI	05A	PL B610 165	A. Lai *et al.*	(CERN NA48 Collab.)
PDG	04	PL B592 1	S. Eidelman *et al.*	(PDG Collab.)
LAI	03C	EPJ C30 33	A. Lai *et al.*	(CERN NA48 Collab.)
LAI	02	PL B533 196	A. Lai *et al.*	(CERN NA48 Collab.)
ANGELOPO...	01B	EPJ C22 55	A. Angelopoulos *et al.*	(CPLEAR Collab.)
ANGELOPO...	99B	PL B471 332	A. Angelopoulos *et al.*	(CPLEAR Collab.)
APOSTOLA...	99B	PL B456 297	A. Apostolakis *et al.*	(CPLEAR Collab.)
ANGELOPO...	98D	PL B444 38	A. Angelopoulos *et al.*	(CPLEAR Collab.)
Also		EPJ C22 55	A. Angelopoulos *et al.*	(CPLEAR Collab.)
ANGELOPO...	98E	PL B444 43	A. Angelopoulos *et al.*	(CPLEAR Collab.)
ANGELOPO...	98F	PL B444 52	A. Angelopoulos *et al.*	(CPLEAR Collab.)
Also		EPJ C22 55	A. Angelopoulos *et al.*	(CPLEAR Collab.)
DEMIDOV	95	PAN 58 968	V. Demidov, K. Gusev, E. Shabalin	(ITEP)
From YAF 58 1041.				
THOMSON	95	PR D51 1412	G.B. Thomson, Y. Zou	(RUTG)
BARKOV	87B	SJNP 46 630	L.M. Barkov *et al.*	(NOVO)
Translated from YAF 46 1088.				
BARKOV	85B	JETPL 42 138	L.M. Barkov *et al.*	(NOVO)
Translated from ZETFP 42 113.				
BLATNIK	79	LNC 24 39	S. Blatnik, J. Stahov, C.B. Lang	(TUZL, GRAZ)
MOLZON	78	PRL 41 1213	W.R. Molzon *et al.*	(EFI+)
NIEBERGALL	74	PL 49B 103	F. Niebergall *et al.*	(CERN, ORSAY, VIEN)
HART	73	NP B66 317	J.C. Hart *et al.*	(CAVE, RHEL)
FOETH	69B	PL 30B 276	H. Foeth *et al.*	(AACH, CERN, TORI)
HILL	68B	PR 168 1534	D.G. Hill *et al.*	(BNL, CMU)
FITCH	67	PR 164 1711	V.L. Fitch *et al.*	(PRIN)
BALTAY	66	PR 142 932	C. Baltay *et al.*	(YALE, BNL)
BURNSTEIN	65	PR 138 B895	R.A. Burnstein, H.A. Rubin	(UMD)
KIM	65B	PR 140 B1334	J.K. Kim, L. Kirsch, D. Miller	(COLU)
CHRISTENS...	64	PRL 13 138	J.H. Christenson *et al.*	(PRIN)
CRAWFORD	59	PRL 2 112	F.S. Crawford *et al.*	(LRL)
ROSENFELD	59	PRL 2 110	A.H. Rosenfeld, F.T. Solmitz, R.D. Tripp	(LRL)

K^0_S

$I(J^P) = \frac{1}{2}(0^-)$

K^0_S MEAN LIFE

For earlier measurements, beginning with BOLDT 58B, see our 1986 edition, Physics Letters **170B** 130 (1986).

OUR FIT is described in the note on "*CP* violation in K_L decays" in the K^0_L Particle Listings. The result labeled "OUR FIT Assuming *CPT*" ["OUR FIT Not assuming *CPT*"] includes all measurements except those with the comment "Not assuming *CPT*" ["Assuming *CPT*"]. Measurements with neither comment do not assume *CPT* and enter both fits.

VALUE (10^{-10} s)	EVTS	DOCUMENT ID		TECN	COMMENT
0.8954 ±0.0004 OUR FIT		Error includes scale factor of 1.1. Assuming *CPT*			
0.89564±0.00033 OUR FIT		Not assuming *CPT*			
0.89589±0.00070		[1,2] ABOUZAID	11	KTEV	Not assuming *CPT*
0.89623±0.00047		[1,3] ABOUZAID	11	KTEV	Assuming *CPT*
0.89562±0.00029±0.00043	20M	[4] AMBROSINO	11	KLOE	Not assuming *CPT*
0.89598±0.00048±0.00051	16M	LAI	02C	NA48	
0.8971 ±0.0021		BERTANZA	97	NA31	
0.8941 ±0.0014 ±0.0009		SCHWINGEN...	95	E773	Assuming *CPT*
0.8929 ±0.0016		GIBBONS	93	E731	Assuming *CPT*
• • • We do not use the following data for averages, fits, limits, etc. • • •					
0.8965 ±0.0007		[5] ALAVI-HARATI	03	KTEV	Assuming *CPT*
0.8958 ±0.0013		[6] ALAVI-HARATI	03	KTEV	Not assuming *CPT*
0.8920 ±0.0044	214k	GROSSMAN	87	SPEC	
0.905 ±0.007		[7] ARONSON	82B	SPEC	
0.881 ±0.009	26k	ARONSON	76	SPEC	
0.8926 ±0.0032 ±0.0002		[8] CARITHERS	75	SPEC	
0.8937 ±0.0048	6M	GEWENIGER	74B	ASPK	
0.8958 ±0.0045	50k	[9] SKJEGGEST...	72	HBC	
0.856 ±0.008	19994	[10] DONALD	68B	HBC	
0.872 ±0.009	20000	[9,10] HILL	68	DBC	

[1] The two ABOUZAID 11 values use the same full KTeV dataset from 1996, 1997, and 1999. The first enters the "assuming *CPT*" fit and the second enters the "not assuming *CPT*" fit.

[2] ABOUZAID 11 fit has Δm, τ_S, ϕ_ϵ, Re(ϵ'/ϵ), and Im(ϵ'/ϵ) as free parameters. See Im(ϵ'/ϵ) in the "K^0_L *CP* violation" section for correlation information.

[3] ABOUZAID 11 fit has Δm and τ_S free but constrains ϕ_ϵ to the Superweak value, i.e. assumes *CPT*. This τ_S value is correlated with their $\Delta m = m_{K^0_L} - m_{K^0_S}$ measurement in the K^0_L listings. The correlation coefficient $\rho(\tau_S, \Delta m) = -0.670$.

[4] Fit to the proper time distribution.

[5] This ALAVI-HARATI 03 fit has Δm and τ_S free but constrains ϕ_{+-} to the Superweak value, i.e. assumes *CPT*. This τ_S value is correlated with their $\Delta m = m_{K^0_L} - m_{K^0_S}$ measurement in the K^0_L listings. The correlation coefficient $\rho(\tau_S, \Delta m) = -0.396$. Superseded by ABOUZAID 11.

[6] This ALAVI-HARATI 03 fit has Δm, ϕ_{+-}, and τ_{K_S} free. See ϕ_{+-} in the "K_L *CP* violation" section for correlation information. Superseded by ABOUZAID 11.

[7] ARONSON 82 find that K^0_S mean life may depend on the kaon energy.

[8] CARITHERS 75 measures the Δm dependence of the total decay rate (inverse mean life) to be $\Gamma(K^0_S) = [(1.122 \pm 0.004) + 0.16(\Delta m - 0.5348)/\Delta m] 10^{10}$/s, or, in terms of mean life, CARITHERS 75 measures $\tau_S = (0.8913 \pm 0.0032) - 0.238\ [\Delta m - 0.5348]$ (10^{-10} s). We have adjusted the measurement to use our best values of ($\Delta m = 0.5293 \pm 0.0009$) ($10^{10}$ $\hbar$ s^{-1}). Our first error is their experiment's error and our second error is the systematic error from using our best values.

[9] HILL 68 has been changed by the authors from the published value (0.865 ± 0.009) because of a correction in the shift due to η_{+-}. SKJEGGESTAD 72 and HILL 68 give detailed discussions of systematics encountered in this type of experiment.

[10] Pre-1971 experiments are excluded from the average because of disagreement with later more precise experiments.

Meson Particle Listings

K^0_S

K^0_S DECAY MODES

	Mode		Fraction (Γ_i/Γ)	Scale factor/ Confidence level
	Hadronic modes			
Γ_1	$\pi^0\pi^0$		(30.69±0.05) %	
Γ_2	$\pi^+\pi^-$		(69.20±0.05) %	
Γ_3	$\pi^+\pi^-\pi^0$		$(3.5\ ^{+1.1}_{-0.9}) \times 10^{-7}$	
	Modes with photons or $\ell\bar{\ell}$ pairs			
Γ_4	$\pi^+\pi^-\gamma$	[a,b]	$(1.79\pm0.05) \times 10^{-3}$	
Γ_5	$\pi^+\pi^- e^+ e^-$		$(4.79\pm0.15) \times 10^{-5}$	
Γ_6	$\pi^0\gamma\gamma$	[a]	$(4.9\ \pm1.8\ ) \times 10^{-8}$	
Γ_7	$\gamma\gamma$		$(2.63\pm0.17) \times 10^{-6}$	S=3.0
	Semileptonic modes			
Γ_8	$\pi^\pm e^\mp \nu_e$	[c]	$(7.04\pm0.08) \times 10^{-4}$	
Γ_9	$\pi^\pm \mu^\mp \nu_\mu$	[c,d]	$(4.69\pm0.05) \times 10^{-4}$	
	***CP* violating (*CP*) and $\Delta S = 1$ weak neutral current (*S1*) modes**			
Γ_{10}	$3\pi^0$	*CP*	$< 2.6 \times 10^{-8}$	CL=90%
Γ_{11}	$\mu^+\mu^-$	*S1*	$< 8 \times 10^{-10}$	CL=90%
Γ_{12}	e^+e^-	*S1*	$< 9 \times 10^{-9}$	CL=90%
Γ_{13}	$\pi^0 e^+ e^-$	*S1*	[a] $(3.0\ ^{+1.5}_{-1.2}) \times 10^{-9}$	
Γ_{14}	$\pi^0\mu^+\mu^-$	*S1*	$(2.9\ ^{+1.5}_{-1.2}) \times 10^{-9}$	

[a] See the Particle Listings below for the energy limits used in this measurement.

[b] Most of this radiative mode, the low-momentum γ part, is also included in the parent mode listed without γ's.

[c] The value is for the sum of the charge states or particle/antiparticle states indicated.

[d] Not a measurement. Calculated as 0.666·B($\pi^\pm e^\mp \nu_e$).

CONSTRAINED FIT INFORMATION

An overall fit to 4 branching ratios uses 5 measurements and one constraint to determine 4 parameters. The overall fit has a χ^2 = 0.1 for 2 degrees of freedom.

The following *off-diagonal* array elements are the correlation coefficients $\langle \delta x_i \delta x_j \rangle / (\delta x_i \cdot \delta x_j)$, in percent, from the fit to the branching fractions, $x_i \equiv \Gamma_i/\Gamma_{\rm total}$. The fit constrains the x_i whose labels appear in this array to sum to one.

x_2	−100		
x_8	−6	3	
x_9	−6	3	100
	x_1	x_2	x_8

K^0_S DECAY RATES

$\Gamma(\pi^\pm e^\mp \nu_e)$ Γ_8

VALUE (10^6 s^{-1})	EVTS	DOCUMENT ID		TECN	COMMENT
• • • We do not use the following data for averages, fits, limits, etc. • • •					
8.1 ±1.6	75	[1] AKHMETSHIN	99	CMD2	Tagged K^0_S using $\phi \to K^0_L K^0_S$
7.50±0.08		[2] PDG	98		
seen		BURGUN	72	HBC	$K^+ p \to K^0 p \pi^+$
9.3 ±2.5		AUBERT	65	HLBC	ΔS=ΔQ, *CP* cons. not assumed

[1] AKHMETSHIN 99 is from a measured branching ratio B($K^0_S \to \pi e \nu_e$)= (7.2 ± 1.4) × 10^{-4} and $\tau_{K^0_S}$ = (0.8934 ± 0.0008) × 10^{-10} s. Not independent of measured branching ratio.

[2] PDG 98 from K^0_L measurements, assuming that $\Delta S = \Delta Q$ in K^0 decay so that $\Gamma(K^0_S \to \pi^\pm e^\mp \nu_e) = \Gamma(K^0_L \to \pi^\pm e^\mp \nu_e)$.

$\Gamma(\pi^\pm \mu^\mp \nu_\mu)$ Γ_9

VALUE (10^6 s^{-1})	DOCUMENT ID		
• • • We do not use the following data for averages, fits, limits, etc. • • •			
5.25±0.07	[1] PDG	98	

[1] PDG 98 from K^0_L measurements, assuming that $\Delta S = \Delta Q$ in K^0 decay so that $\Gamma(K^0_S \to \pi^\pm \mu^\mp \nu_\mu) = \Gamma(K^0_L \to \pi^\pm \mu^\mp \nu_\mu)$.

K^0_S BRANCHING RATIOS

Hadronic modes

$\Gamma(\pi^0\pi^0)/\Gamma_{\rm total}$ Γ_1/Γ

VALUE	EVTS	DOCUMENT ID		TECN
0.3069±0.0005 OUR FIT				
• • • We do not use the following data for averages, fits, limits, etc. • • •				
0.335 ±0.014	1066	BROWN	63	HLBC
0.288 ±0.021	198	CHRETIEN	63	HLBC
0.30 ±0.035		BROWN	61	HLBC

$\Gamma(\pi^+\pi^-)/\Gamma_{\rm total}$ Γ_2/Γ

VALUE	EVTS	DOCUMENT ID		TECN	COMMENT
0.6920±0.0005 OUR FIT					
• • • We do not use the following data for averages, fits, limits, etc. • • •					
0.670 ±0.010	3447	DOYLE	69	HBC	$\pi^- p \to \Lambda K^0$

$\Gamma(\pi^+\pi^-)/\Gamma(\pi^0\pi^0)$ Γ_2/Γ_1

VALUE	EVTS	DOCUMENT ID		TECN	COMMENT
2.255 ±0.005 OUR FIT					
2.2549±0.0054		[1] AMBROSINO	06C	KLOE	
• • • We do not use the following data for averages, fits, limits, etc. • • •					
2.2555±0.0012±0.0054		[2] AMBROSINO	06C	KLOE	
2.236 ±0.003 ±0.015	766k	[2] ALOISIO	02B	KLOE	
2.11 ±0.09	1315	EVERHART	76	WIRE	$\pi^- p \to \Lambda K^0$
2.169 ±0.094	16k	COWELL	74	OSPK	$\pi^- p \to \Lambda K^0$
2.16 ±0.08	4799	HILL	73	DBC	$K^+ d \to K^0 p p$
2.22 ±0.10	3068	[3] ALITTI	72	HBC	$K^+ p \to \pi^+ p K^0$
2.22 ±0.08	6380	MORSE	72B	DBC	$K^+ n \to K^0 p$
2.10 ±0.11	701	[4] NAGY	72	HLBC	$K^+ n \to K^0 p$
2.22 ±0.095	6150	[5] BALTAY	71	HBC	$K p \to K^0$ neutrals
2.282 ±0.043	7944	MOFFETT	70	OSPK	$K^+ n \to K^0 p$
2.12 ±0.17	267	[4] BOZOKI	69	HLBC	
2.285 ±0.055	3016	[6] GOBBI	69	OSPK	$K^+ n \to K^0 p$
2.10 ±0.06	3700	MORFIN	69	HLBC	$K^+ n \to K^0 p$

[1] This result combines AMBROSINO 06C KLOE 2001-02 data with ALOISIO 02B KLOE 2000 data. $K^0_S \to \pi^+\pi^-$ fully inclusive.

[2] Includes radiative decays $\pi^+\pi^-\gamma$.

[3] The directly measured quantity is $K^0_S \to \pi^+\pi^-$/all K^0 = 0.345 ± 0.005.

[4] NAGY 72 is a final result which includes BOZOKI 69.

[5] The directly measured quantity is $K^0_S \to \pi^+\pi^-$/all $\overline{K}^0$ = 0.345 ± 0.005.

[6] MOFFETT 70 is a final result which includes GOBBI 69.

$\Gamma(\pi^+\pi^-\pi^0)/\Gamma_{\rm total}$ Γ_3/Γ

VALUE (units 10^{-7})	EVTS	DOCUMENT ID		TECN	COMMENT
3.5 $^{+1.1}_{-0.9}$ OUR AVERAGE					
$4.7^{+2.2}_{-1.7}{}^{+1.7}_{-1.5}$		[1] BATLEY	05	NA48	
$2.5^{+1.3}_{-1.0}{}^{+0.5}_{-0.6}$	500k	[2] ADLER	97B	CPLR	
$4.8^{+2.2}_{-1.6}\pm1.1$		[3] ZOU	96	E621	
• • • We do not use the following data for averages, fits, limits, etc. • • •					
$4.1^{+2.5}_{-1.9}{}^{+0.5}_{-0.6}$		[4] ADLER	96E	CPLR	Sup. by ADLER 97B
$3.9^{+5.4}_{-1.8}{}^{+0.9}_{-0.7}$		[5] THOMSON	94	E621	Sup. by ZOU 96

[1] BATLEY 05 is obtained by measuring the interference parameters in K_S, $K_L \to \pi^+\pi^-\pi^0$: Re(λ) = 0.038 ± 0.008 ± 0.006 and Im(λ) = −0.013 ± 0.005 ± 0.004; the correlation coeff. between Re(λ) and Im(λ) is 0.66 (statistical only).

[2] ADLER 97B find the *CP*-conserving parameters Re(λ) = (28 ± 7 ± 3) × 10^{-3}, Im(λ) = (−10 ± 8 ± 2) × 10^{-3}. They estimate B($K^0_S \to \pi^+\pi^-\pi^0$) from Re($\lambda$) and the K^0_L decay parameters. See also ANGELOPOULOS 98C.

[3] ZOU 96 is from the the measured quantities $|\rho_{+-0}| = 0.039^{+0.009}_{-0.006} \pm 0.005$ and $\phi_\rho = (-9 \pm 18)^\circ$.

[4] ADLER 96E is from the measured quantities Re(λ) = 0.036 ± $0.010^{+0.002}_{-0.003}$ and Im(λ) consistent with zero. Note that the quantity λ is the same as ρ_{+-0} used in other footnotes.

[5] THOMSON 94 calculates this branching ratio from their measurements $|\rho_{+-0}| = 0.035^{+0.019}_{-0.011} \pm 0.004$ and $\phi_\rho = (-59 \pm 48)^\circ$ where $|\rho_{+-0}| e^{i\phi_\rho} = A(K^0_S \to \pi^+\pi^-\pi^0, I = 2)/A(K^0_L \to \pi^+\pi^-\pi^0)$.

Modes with photons or $\ell\bar{\ell}$ pairs

$\Gamma(\pi^+\pi^-\gamma)/\Gamma(\pi^+\pi^-)$ Γ_4/Γ_2

VALUE (units 10^{-3})	EVTS	DOCUMENT ID		TECN	COMMENT
2.59±0.08 OUR AVERAGE					
2.56±0.09	1286	RAMBERG	93	E731	p_γ >50 MeV/c
2.68±0.15		[1] TAUREG	76	SPEC	p_γ >50 MeV/c

• • • We do not use the following data for averages, fits, limits, etc. • • •

7.10±0.22	3723		RAMBERG	93	E731	p_γ >20 MeV/c
3.0 ±0.6	29	[2]	BOBISUT	74	HLBC	p_γ >40 MeV/c
2.8 ±0.6		[3]	BURGUN	73	HBC	p_γ >50 MeV/c

[1] TAUREG 76 find direct emission contribution <0.06, CL = 90%.
[2] BOBISUT 74 not included in average because p_γ cut differs. Estimates direct emission contribution to be 0.5 or less, CL = 95%.
[3] BURGUN 73 estimates that direct emission contribution is 0.3 ± 0.6.

$\Gamma(\pi^+\pi^-e^+e^-)/\Gamma_{total}$ Γ_5/Γ

VALUE (units 10^{-5})	EVTS	DOCUMENT ID		TECN	COMMENT
4.79±0.15 OUR AVERAGE					
4.83±0.11±0.14	23k	[1] BATLEY	11	NA48	2002 data
4.69±0.30	676	[2] LAI	03C	NA48	1998+1999 data
• • • We do not use the following data for averages, fits, limits, etc. • • •					
4.71±0.23±0.22	620	[2,3] LAI	03C	NA48	1999 data
4.5 ±0.7 ±0.4	56	LAI	00B	NA48	1998 data

[1] BATLEY 11 reports $[\Gamma(K^0_S \to \pi^+\pi^-e^+e^-)/\Gamma_{total}]$ / $[B(K^0_L \to \pi^+\pi^-\pi^0)]$ / $[B(\pi^0 \to e^+e^-\gamma)] = (3.28 \pm 0.06 \pm 0.04) \times 10^{-2}$ which we multiply by our best values $B(K^0_L \to \pi^+\pi^-\pi^0) = (12.54 \pm 0.05) \times 10^{-2}$, $B(\pi^0 \to e^+e^-\gamma) = (1.174 \pm 0.035) \times 10^{-2}$. Our first error is their experiment's error and our second error is the systematic error from using our best values. Also a limit on the absolute value of the interference between bremsstrahlung and E1 transition is given : $< 4 \times 10^{-7}$ at 90% C.L.
[2] Uses normalization BR($K_L \to \pi^+\pi^-\pi^0$)*BR($\pi^0 \to e^+e^-$) = $(1.505 \pm 0.047) \times 10^{-3}$ from our 2000 Edition.
[3] Second error is 0.16(syst) ± 0.15(norm) combined in quadrature.

$\Gamma(\pi^0\gamma\gamma)/\Gamma_{total}$ Γ_6/Γ

VALUE (units 10^{-8})	CL%	EVTS	DOCUMENT ID		TECN	COMMENT
4.9±1.6±0.9		17	[1] LAI	04	NA48	$m^2_{\gamma\gamma}/m^2_K > 0.2$
• • • We do not use the following data for averages, fits, limits, etc. • • •						
<33	90		LAI	03B	NA48	$m^2_{\gamma\gamma}/m^2_K > 0.2$

[1] Spectrum also measured and found consistent with the one generated by a constant matrix element.

$\Gamma(\gamma\gamma)/\Gamma_{total}$ Γ_7/Γ

VALUE (units 10^{-6})	CL%	EVTS	DOCUMENT ID		TECN	COMMENT
2.63 ±0.17 OUR AVERAGE			Error includes scale factor of 3.0.			
2.26 ±0.12 ±0.06		711	[1] AMBROSINO	08C	KLOE	$\phi \to K^0_S K^0_L$
2.713±0.063±0.005		7.5k	[2] LAI	03	NA48	
• • • We do not use the following data for averages, fits, limits, etc. • • •						
2.58 ±0.36 ±0.22		149	LAI	00	NA48	
2.2 ±1.1		16	[3] BARR	95B	NA31	
2.4 ±0.9		35	[4] BARR	95B	NA31	
< 13	90		BALATS	89	SPEC	
2.4 ±1.2		19	BURKHARDT	87	NA31	
<133	90		BARMIN	86B	XEBC	

[1] AMBROSINO 08C reports $(2.26 \pm 0.12 \pm 0.06) \times 10^{-6}$ from a measurement of $[\Gamma(K^0_S \to \gamma\gamma)/\Gamma_{total}] \times [B(K^0_S \to \pi^0\pi^0)]$ assuming $B(K^0_S \to \pi^0\pi^0) = (30.69 \pm 0.05) \times 10^{-2}$.
[2] LAI 03 reports $[\Gamma(K^0_S \to \gamma\gamma)/\Gamma_{total}] / [B(K^0_S \to \pi^0\pi^0)] = (8.84 \pm 0.18 \pm 0.10) \times 10^{-6}$ which we multiply by our best value $B(K^0_S \to \pi^0\pi^0) = (30.69 \pm 0.05) \times 10^{-2}$. Our first error is their experiment's error and our second error is the systematic error from using our best value.
[3] BARR 95B result is calculated using $B(K_L \to \gamma\gamma) = (5.86 \pm 0.17) \times 10^{-4}$.
[4] BARR 95B quotes this as the combined BARR 95B + BURKHARDT 87 result after rescaling BURKHARDT 87 to use same branching ratios and lifetimes as BARR 95B.

Semileptonic modes

$\Gamma(\pi^\pm e^\mp \nu_e)/\Gamma_{total}$ Γ_8/Γ

VALUE (units 10^{-4})	EVTS	DOCUMENT ID		TECN	COMMENT
7.04 ±0.08 OUR FIT					
7.04 ±0.08 OUR AVERAGE					
7.046±0.18±0.16		[1] BATLEY	07D	NA48	$K^0(\overline{K}^0)(t) \to \pi e\nu$
6.91 ±0.34±0.15	624	[2] ALOISIO	02	KLOE	Tagged K^0_S using $\phi \to K^0_L K^0_S$
• • • We use the following data for averages but not for fits. • • •					
7.05 ±0.09	13k	[3] AMBROSINO	06E	KLOE	Not fitted
• • • We do not use the following data for averages, fits, limits, etc. • • •					
7.2 ±1.4	75	AKHMETSHIN	99	CMD2	Tagged K^0_S using $\phi \to K^0_L K^0_S$

[1] Reconstructed from $K^0(\overline{K}^0)(t) \to \pi e\nu$ distributions using PDG values of $B(K^0_L \to \pi e\nu) = 0.4053 \pm 0.0015$, $\tau_L = (5.114 \pm 0.021) \times 10^{-8}$ s and $\tau_S = (0.8958 \pm 0.0005) \times 10^{-10}$ s.
[2] Uses the PDG 00 value for $B(K^0_S \to \pi^+\pi^-)$.
[3] Obtained by imposing $\Sigma_i B(K^0_S \to i) = 1$, where i runs over all the four branching ratios $\pi^+\pi^-$, $\pi^0\pi^0$, $\pi e\nu$, and $\pi\mu\nu$. Input value of $B(K^0_S \to \pi^+\pi^-)$ / $B(K^0_S \to \pi^0\pi^0)$ from AMBROSINO 06C is used. To derive $\Gamma(K^0_S \to \pi^+\mu\nu)$ / $\Gamma(K^0_S \to \pi^+e\nu)$, lepton universality is assumed, radiative corrections from ANDRE 07 are used, and phase space integrals are taken from KTeV, ALEXOPOULOS 04A. This branching fraction enters our fit via their $\Gamma(\pi^\pm e^\mp \nu_e)$ / $\Gamma(\pi^+\pi^-)$ branching ratio measurement.

$\Gamma(\pi^\pm \mu^\mp \nu_\mu)/\Gamma_{total}$ Γ_9/Γ

The PDG 06 value below has not been measured but is computed to be 0.666 times the $K_S \to \pi^\pm e^\mp \nu_e$ branching fraction. It is included in the fit that constrains the four branching ratios $\pi^+\pi^-$, $\pi^0\pi^0$, $\pi e\nu$, and $\pi\mu\nu$ to sum to 1. This treatment, used by AMBROSINO 06E, is preferable to our previous practice of constraining the $\pi^+\pi^-$ and $\pi^0\pi^0$ modes to sum to 1. The 0.666 factor is obtained from AMBROSINO 06E and assumes lepton universality, radiative corrections from ANDRE 07, and phase space integrals from KTeV, ALEXOPOULOS 04A.

VALUE (units 10^{-4})	DOCUMENT ID			COMMENT
4.69 ±0.06 OUR FIT				
4.691±0.001±0.056	[1] PDG	06		calculated from $\pi^\pm e^\mp \nu_e$

[1] The PDG 06 value is computed to be $B_{PDG06}(\pi\mu\nu) = 0.666\ B_{FIT}(\pi e\nu)$. The first error specifies the arbitrarily small error, 0.001×10^{-4}, on $B_{PDG06}(\pi\mu\nu)$ for fixed $B_{FIT}(\pi e\nu)$. The second error is that due to the uncertainty in $B_{FIT}(\pi e\nu)$.

$\Gamma(\pi^\pm e^\mp \nu_e)/\Gamma(\pi^+\pi^-)$ Γ_8/Γ_2

VALUE (units 10^{-4})	EVTS	DOCUMENT ID		TECN
10.18±0.12 OUR FIT				
10.19±0.11±0.07	13k	AMBROSINO	06E	KLOE

CP violating (*CP*) and $\Delta S = 1$ weak neutral current (*S1*) modes

$\Gamma(3\pi^0)/\Gamma_{total}$ Γ_{10}/Γ

Violates *CP* conservation.

VALUE (units 10^{-7})	CL%	EVTS	DOCUMENT ID		TECN	COMMENT
< 0.26	90	590M	[1] BABUSCI	13C	KLOE	$\phi \to K^0_L K^0_S$
• • • We do not use the following data for averages, fits, limits, etc. • • •						
< 1.2	90	37.8M	AMBROSINO	05B	KLOE	
< 7.4	90	4.9M	[2] LAI	05A	NA48	
<140	90	7M	ACHASOV	99D	SND	
<190	90	17300	[3] ANGELOPO...	98B	CPLR	
<370	90		BARMIN	83	HLBC	

[1] BABUSCI 13C uses 1.7 fb^{-1} of data of $\phi \to K^0_L K^0_S$ decays with K^0_L interaction in the calorimeter, collected from 2004 to 2005. No candidate events were found in the data with an expected background of $0.04^{+0.15}_{-0.03}$ events. Upper limit is obtained by normalizing to $K^0_S \to 2\pi^0$ decays.
[2] LAI 05A value is obtained from their bound on $|\eta_{000}|$ (not assuming *CPT*) and $B(K^0_L \to 3\pi^0) = 0.211 \pm 0.003$, and PDG 04 values for K^0_L and K^0_S lifetimes. If *CPT* is assumed then $B(K^0_S \to 3\pi^0)_{CPT} < 2.3 \times 10^{-7}$ at 90% CL
[3] ANGELOPOULOS 98B is from $Im(\eta_{000}) = -0.05 \pm 0.12 \pm 0.05$, assuming $Re(\eta_{000}) = Re(\epsilon) = 1.635 \times 10^{-3}$ and using the value $B(K^0_L \to \pi^0\pi^0\pi^0) = 0.2112 \pm 0.0027$.

$\Gamma(\mu^+\mu^-)/\Gamma_{total}$ Γ_{11}/Γ

Test for $\Delta S = 1$ weak neutral current. Allowed by first-order weak interaction combined with electromagnetic interaction.

VALUE	CL%	DOCUMENT ID		TECN
<8 × 10^{-10}	90	[1] AAIJ	17BQ	LHCB
• • • We do not use the following data for averages, fits, limits, etc. • • •				
<9 × 10^{-9}	90	[2] AAIJ	13G	LHCB
<3.2 × 10^{-7}	90	GJESDAL	73	ASPK
<7 × 10^{-6}	90	HYAMS	69B	OSPK

[1] AAIJ 17BQ uses 3.0 fb^{-1} of pp collisions at $\sqrt{s}$ = 7 and 8 TeV. The result utilizes the normalization mode branching fraction $B(K^0_S \to \pi^+\pi^-) = (69.20 \pm 0.05) \times 10^{-2}$ from PDG 16. Supersedes AAIJ 13G.
[2] AAIJ 13G uses 1.0 fb^{-1} of pp collisions at $\sqrt{s}$ = 7 TeV. They obtained $B(K^0_S \to \mu^+\mu^-) < 11 \times 10^{-9}$ at 95% C.L.

$\Gamma(e^+e^-)/\Gamma_{total}$ Γ_{12}/Γ

Test for $\Delta S = 1$ weak neutral current. Allowed by first-order weak interaction combined with electromagnetic interaction.

VALUE (units 10^{-7})	CL%	DOCUMENT ID		TECN	COMMENT
< 0.09	90	[1] AMBROSINO	09A	KLOE	$e^+e^- \to \phi \to K^0_S K^0_L$
• • • We do not use the following data for averages, fits, limits, etc. • • •					
< 1.4	90	ANGELOPO...	97	CPLR	
< 28	90	BLICK	94	CNTR	Hyperon facility
<100	90	BARMIN	86	XEBC	

[1] AMBROSINO 09A reports $< 0.09 \times 10^{-7}$ from a measurement of $[\Gamma(K^0_S \to e^+e^-)/\Gamma_{total}] / [B(K^0_S \to \pi^+\pi^-)]$ assuming $B(K^0_S \to \pi^+\pi^-) = (69.20 \pm 0.05) \times 10^{-2}$.

$\Gamma(\pi^0e^+e^-)/\Gamma_{total}$ Γ_{13}/Γ

Test for $\Delta S = 1$ weak neutral current. Allowed by first-order weak interaction combined with electromagnetic interaction.

VALUE (units 10^{-9})	CL%	EVTS	DOCUMENT ID		TECN	COMMENT
$3.0^{+1.5}_{-1.2}$±0.2		7	[1] BATLEY	03	NA48	m_{ee} >0.165 GeV
• • • We do not use the following data for averages, fits, limits, etc. • • •						
< 140	90		LAI	01	NA48	
< 1100	90	0	BARR	93B	NA31	
<45000	90		GIBBONS	88	E731	

[1] BATLEY 03 extrapolate also to the full kinematical region using a constant form factor and a vector matrix element. The resulting branching ratio is $(5.8^{+2.9}_{-2.4}) \times 10^{-9}$.

Meson Particle Listings

K^0_S

$\Gamma(\pi^0\mu^+\mu^-)/\Gamma_{total}$ Γ_{14}/Γ

Test for $\Delta S = 1$ weak neutral current. Allowed by first-order weak interaction combined with electromagnetic interaction.

VALUE (units 10^{-9})	EVTS	DOCUMENT ID		TECN	COMMENT
$2.9^{+1.5}_{-1.2}\pm0.2$	6	[1] BATLEY	04A	NA48	NA48/1 K^0_S beam

[1] Background estimate is $0.22^{+0.18}_{-0.11}$ events. Branching ratio assumes a vector matrix element and unit form factor.

K^0_S FORM FACTORS

For discussion, see note on $K_{\ell3}$ form factors in the $K^\pm$ section of the Particle Listings above. Because the semileptonic branching fraction is smaller in K^0_S than K^0_L by the ratio of the mean lives, the K^0_S semileptonic form factor has so far been measured only in the K_{e3} mode using the linear expansion $f_+(t) = f_+(0)\ (1 + \lambda_+ t\ /m^2_{\pi^+})$, which gives the vector form factor $f_+(t)$ relative to its value at $t = 0$.

λ_+ (LINEAR ENERGY DEPENDENCE OF f_+ IN K^0_{e3} DECAY)

VALUE (units 10^{-2})	EVTS	DOCUMENT ID		TECN
3.39 ± 0.41	15k	AMBROSINO	06E	KLOE

See the related review(s):

CP Violation in $K^0_S \to 3\pi$

CP-VIOLATION PARAMETERS IN K^0_S DECAY

$A_S = [\ \Gamma(K^0_S \to \pi^- e^+ \nu_e) - \Gamma(K^0_S \to \pi^+ e^- \bar{\nu}_e)\ ]\ /\ \text{SUM}$

Such asymmetry violates *CP*. If *CPT* is assumed then $A_S = 2\,\mathrm{Re}(\epsilon)$.

VALUE (units 10^{-3})	EVTS	DOCUMENT ID		TECN
$1.5\pm9.6\pm2.9$	13k	AMBROSINO	06E	KLOE

PARAMETERS FOR $K^0_S \to 3\pi$ DECAY

$\mathrm{Im}(\eta_{+-0})^2 = \Gamma(K^0_S \to \pi^+\pi^-\pi^0,\ CP\text{-violating})\ /\ \Gamma(K^0_L \to \pi^+\pi^-\pi^0)$

CPT assumed valid (i.e. $\mathrm{Re}(\eta_{+-0}) \simeq 0$).

VALUE	CL%	EVTS	DOCUMENT ID		TECN
• • • We do not use the following data for averages, fits, limits, etc. • • •					
<0.23	90	601	[1] BARMIN	85	HLBC
<0.12	90	384	METCALF	72	ASPK

[1] BARMIN 85 find $\mathrm{Re}(\eta_{+-0}) = (0.05 \pm 0.17)$ and $\mathrm{Im}(\eta_{+-0}) = (0.15 \pm 0.33)$. Includes events of BALDO-CEOLIN 75.

$\mathrm{Im}(\eta_{+-0}) = \mathrm{Im}(A(K^0_S \to \pi^+\pi^-\pi^0,\ CP\text{-violating})\ /\ A(K^0_L \to \pi^+\pi^-\pi^0))$

VALUE	EVTS	DOCUMENT ID		TECN	COMMENT
$-0.002\pm0.009^{+0.002}_{-0.001}$	500k	[1] ADLER	97B	CPLR	
• • • We do not use the following data for averages, fits, limits, etc. • • •					
$-0.002\pm0.018\pm0.003$	137k	[2] ADLER	96D	CPLR	Sup. by ADLER 97B
$-0.015\pm0.017\pm0.025$	272k	[3] ZOU	94	SPEC	

[1] ADLER 97B also find $\mathrm{Re}(\eta_{+-0}) = -0.002 \pm 0.007^{+0.004}_{-0.001}$. See also ANGELOPOULOS 98C.

[2] The ADLER 96D fit also yields $\mathrm{Re}(\eta_{+-0}) = 0.006 \pm 0.013 \pm 0.001$ with a correlation $+0.66$ between real and imaginary parts. Their results correspond to $|\eta_{+-0}| < 0.037$ with 90% CL.

[3] ZOU 94 use theoretical constraint $\mathrm{Re}(\eta_{+-0}) = \mathrm{Re}(\epsilon) = 0.0016$. Without this constraint they find $\mathrm{Im}(\eta_{+-0}) = 0.019 \pm 0.061$ and $\mathrm{Re}(\eta_{+-0}) = 0.019 \pm 0.027$.

$\mathrm{Im}(\eta_{000})^2 = \Gamma(K^0_S \to 3\pi^0)\ /\ \Gamma(K^0_L \to 3\pi^0)$

CPT assumed valid (i.e. $\mathrm{Re}(\eta_{000}) \simeq 0$). This limit determines branching ratio $\Gamma(3\pi^0)/\Gamma_{total}$ above.

VALUE	CL%	EVTS	DOCUMENT ID		TECN	COMMENT
• • • We do not use the following data for averages, fits, limits, etc. • • •						
<0.1	90	632	[1] BARMIN	83	HLBC	
<0.28	90		[2] GJESDAL	74B	SPEC	Indirect meas.

[1] BARMIN 83 find $\mathrm{Re}(\eta_{000}) = (-0.08 \pm 0.18)$ and $\mathrm{Im}(\eta_{000}) = (-0.05 \pm 0.27)$. Assuming *CPT* invariance they obtain the limit quoted above.

[2] GJESDAL 74B uses $K2\pi$, $K_{\mu3}$, and K_{e3} decay results, unitarity, and *CPT*. Calculates $|(\eta_{000})| = 0.26 \pm 0.20$. We convert to upper limit.

$\mathrm{Im}(\eta_{000}) = \mathrm{Im}(A(K^0_S \to \pi^0\pi^0\pi^0)/A(K^0_L \to \pi^0\pi^0\pi^0))$

$K^0_S \to \pi^0\pi^0\pi^0$ violates *CP* conservation, in contrast to $K^0_S \to \pi^+\pi^-\pi^0$ which has a *CP*-conserving part.

VALUE	EVTS	DOCUMENT ID		TECN	COMMENT
-0.001 ± 0.016 OUR AVERAGE					
$0.000\pm0.009\pm0.013$	4.9M	[1] LAI	05A	NA48	Assumes *CPT*
$-0.05\ \pm0.12\ \pm0.05$	17300	[2] ANGELOPO...	98B	CPLR	Assumes *CPT*

[1] LAI 05A assumes $\mathrm{Re}(\eta_{000})=\mathrm{Re}(\epsilon)=1.66 \times 10^{-3}$. The equivalent limit is $|\eta_{000}|_{CPT} < 0.025$ at 90% CL Without assuming *CPT* invariance, they obtain $\mathrm{Re}(\eta_{000})=-0.002 \pm 0.011 \pm 0.015$ and $\mathrm{Im}(\eta_{000})=-0.003 \pm 0.013 \pm 0.017$ with a statistical correlation coefficient of 0.77 and an overall correlation coefficient of 0.57 between imaginary and real part. The equivalent limit is $|\eta_{000}| < 0.045$ at 90% CL

[2] ANGELOPOULOS 98B assumes $\mathrm{Re}(\eta_{000}) = \mathrm{Re}(\epsilon) = 1.635 \times 10^{-3}$. Without assuming *CPT* invariance, they obtain $\mathrm{Re}(\eta_{000}) = 0.18 \pm 0.14 \pm 0.06$ and $\mathrm{Im}(\eta_{000}) = 0.15 \pm 0.20 \pm 0.03$.

$|\eta_{000}| = |A(K^0_S \to 3\pi^0)/A(K^0_L \to 3\pi^0)|$

A non-zero value violates CP invariance.

VALUE	CL%	EVTS	DOCUMENT ID		TECN
<0.0088	90	590M	BABUSCI	13C	KLOE
• • • We do not use the following data for averages, fits, limits, etc. • • •					
<0.018	90	37.8M	AMBROSINO	05B	KLOE
<0.045	90	4.9M	LAI	05A	NA48

DECAY-PLANE ASYMMETRY IN $\pi^+\pi^-e^+e^-$ DECAYS

This is the *CP*-violating asymmetry

$$A = \frac{N_{\sin\phi\cos\phi>0.0} - N_{\sin\phi\cos\phi<0.0}}{N_{\sin\phi\cos\phi>0.0} + N_{\sin\phi\cos\phi<0.0}}$$

where ϕ is the angle between the e^+e^- and $\pi^+\pi^-$ planes in the K^0_S rest frame.

CP asymmetry A in $K^0_S \to \pi^+\pi^-e^+e^-$

VALUE (%)	DOCUMENT ID		TECN	COMMENT
-0.4 ± 0.8 OUR AVERAGE				
-0.4 ± 0.8	[1] BATLEY	11	NA48	2002 data
-1.1 ± 4.1	LAI	03C	NA48	1998+1999 data
• • • We do not use the following data for averages, fits, limits, etc. • • •				
$0.5\pm4.0\pm1.6$	LAI	03C	NA48	1999 data

[1] The result is used to set the limit $A < 1.5\%$ at 90% C.L.

K^0_S REFERENCES

AAIJ	17BQ	EPJ C77 678	R. Aaij *et al.*	(LHCb Collab.)
PDG	16	CP C40 100001	C. Patrignani *et al.*	(PDG Collab.)
AAIJ	13G	JHEP 1301 090	R. Aaij *et al.*	(LHCb Collab.)
BABUSCI	13C	PL B723 54	D. Babusci *et al.*	(KLOE-2 Collab.)
ABOUZAID	11	PR D83 092001	E. Abouzaid *et al.*	(FNAL KTeV Collab.)
AMBROSINO	11	EPJ C71 1604	F. Ambrosino *et al.*	(KLOE Collab.)
BATLEY	11	PL B694 301	J.R. Batley *et al.*	(CERN NA48/1 Collab.)
AMBROSINO	09A	PL B672 203	F. Ambrosino *et al.*	(KLOE Collab.)
AMBROSINO	08C	JHEP 0805 051	F. Ambrosino *et al.*	(KLOE Collab.)
ANDRE	07	ANP 322 2518	T. Andre	(EFI)
BATLEY	07D	PL B653 145	J.R. Batley *et al.*	(CERN NA48 Collab.)
AMBROSINO	06C	EPJ C48 767	F. Ambrosino *et al.*	(KLOE Collab.)
AMBROSINO	06E	PL B636 173	F. Ambrosino *et al.*	(KLOE Collab.)
PDG	06	JP G33 1	W.-M. Yao *et al.*	(PDG Collab.)
AMBROSINO	05B	PL B619 61	F. Ambrosino *et al.*	(KLOE Collab.)
BATLEY	05	PL B630 31	J.R. Batley *et al.*	(NA48 Collab.)
LAI	05A	PL B610 165	A. Lai *et al.*	(CERN NA48 Collab.)
ALEXOPOU...	04A	PR D70 092007	T. Alexopoulos *et al.*	(FNAL KTeV Collab.)
BATLEY	04A	PL B599 197	J.R. Batley *et al.*	(NA48 Collab.)
LAI	04	PL B578 276	A. Lai *et al.*	(CERN NA48 Collab.)
PDG	04	PL B592 1	S. Eidelman *et al.*	(PDG Collab.)
ALAVI-HARATI	03	PR D67 012005	A. Alavi-Harati *et al.*	(FNAL KTeV Collab.)
Also		PR D70 079904 (errat.)	A. Alavi-Harati *et al.*	(FNAL KTeV Collab.)
BATLEY	03	PL B576 43	J.R. Batley *et al.*	(CERN NA48 Collab.)
LAI	03	PL B551 7	A. Lai *et al.*	(CERN NA48 Collab.)
LAI	03B	PL B556 105	A. Lai *et al.*	(CERN NA48 Collab.)
LAI	03C	EPJ C30 33	A. Lai *et al.*	(CERN NA48 Collab.)
ALOISIO	02	PL B535 37	A. Aloisio *et al.*	(KLOE Collab.)
ALOISIO	02B	PL B538 21	A. Aloisio *et al.*	(KLOE Collab.)
LAI	02C	PL B537 28	A. Lai *et al.*	(CERN NA48 Collab.)
LAI	01	PL B514 253	A. Lai *et al.*	(CERN NA48 Collab.)
LAI	00	PL B493 29	A. Lai *et al.*	(CERN NA48 Collab.)
LAI	00B	PL B496 137	A. Lai *et al.*	(CERN NA48 Collab.)
PDG	00	EPJ C15 1	D.E. Groom *et al.*	(PDG Collab.)
ACHASOV	99D	PL B459 674	M.N. Achasov *et al.*	
AKHMETSHIN	99	PL B456 90	R.R. Akhmetshin *et al.*	(Novosibirsk CMD-2 Collab.)
ANGELOPO...	98B	PL B425 391	A. Angelopoulos *et al.*	(CPLEAR Collab.)
ANGELOPO...	98C	EPJ C5 389	A. Angelopoulos *et al.*	(CPLEAR Collab.)
PDG	98	EPJ C3 1	C. Caso *et al.*	(PDG Collab.)
ADLER	97B	PL B407 193	R. Adler *et al.*	(CPLEAR Collab.)
ANGELOPO...	97	PL B413 232	A. Angelopoulos *et al.*	(CPLEAR Collab.)
BERTANZA	97	ZPHY C73 629	L. Bertanza (PISA, CERN, EDIN, MANZ, ORSAY+)	
ADLER	96D	PL B370 167	R. Adler *et al.*	(CPLEAR Collab.)
ADLER	96E	PL B374 313	R. Adler *et al.*	(CPLEAR Collab.)
ZOU	96	PL B369 362	Y. Zou *et al.*	(RUTG, MINN, MICH)
BARR	95B	PL B351 579	G.D. Barr *et al.*	(CERN, EDIN, MANZ, LALO+)
SCHWINGEN...	95	PRL 74 4376	B. Schwingenheuer *et al.*	(EFI, CHIC+)
BLICK	94	PL B334 234	A.M. Blick *et al.*	(SERP, JINR)
THOMSON	94	PL B337 411	G.B. Thomson *et al.*	(RUTG, MINN, MICH)
ZOU	94	PL B329 519	Y. Zou *et al.*	(RUTG, MINN, MICH)
BARR	93B	PL B304 381	G.D. Barr *et al.*	(CERN, EDIN, MANZ, LALO+)
GIBBONS	93	PRL 70 1199	L.K. Gibbons *et al.*	(FNAL E731 Collab.)
Also		PR D55 6625	L.K. Gibbons *et al.*	(FNAL E731 Collab.)
RAMBERG	93	PRL 70 2525	E. Ramberg *et al.*	(FNAL E731 Collab.)
BALATS	89	SJNP 49 828	M.Y. Balats *et al.*	(ITEP)
		Translated from YAF 49 1332.		
GIBBONS	88	PRL 61 2661	L.K. Gibbons *et al.*	(FNAL E731 Collab.)
BURKHARDT	87	PL B199 139	H. Burkhardt *et al.*	(CERN, EDIN, MANZ+)
GROSSMAN	87	PRL 59 18	N. Grossman *et al.*	(MINN, MICH, RUTG)
BARMIN	86	SJNP 44 622	V.V. Barmin *et al.*	(ITEP)
		Translated from YAF 44 965.		
BARMIN	86B	NC 96A 159	V.V. Barmin *et al.*	(ITEP, PADO)
PDG	86B	PL 170B 130	M. Aguilar-Benitez *et al.*	(CERN, CIT+)
BARMIN	85	NC 85A 67	V.V. Barmin *et al.*	(ITEP, PADO)
Also		SJNP 41 759	V.V. Barmin *et al.*	(ITEP)
		Translated from YAF 41 1187.		
BARMIN	83	PL 128B 129	V.V. Barmin *et al.*	(ITEP, PADO)
Also		SJNP 39 269	V.V. Barmin *et al.*	(ITEP, PADO)
		Translated from YAF 39 428.		
ARONSON	82	PRL 48 1078	S.H. Aronson *et al.*	(BNL, CHIC, STAN+)
ARONSON	82B	PRL 48 1306	S.H. Aronson *et al.*	(BNL, CHIC, PURD)
Also		PL 116B 73	E. Fischbach *et al.*	(PURD, BNL, CHIC)
Also		PR D28 476	S.H. Aronson *et al.*	(BNL, CHIC, PURD)
Also		PR D28 495	S.H. Aronson *et al.*	(BNL, CHIC, PURD)
ARONSON	76	NC 32A 236	S.H. Aronson *et al.*	(WISC, EFI, UCSD+)
EVERHART	76	PR D14 661	G.C. Everhart *et al.*	(PENN)

TAUREG	76	PL 65B 92	H. Taureg *et al.*	(HEIDH, CERN, DORT)
BALDO-...	75	NC 25A 688	M. Baldo-Ceolin *et al.*	(PADO, WISC)
CARITHERS	75	PRL 34 1244	W.C.J. Carithers *et al.*	(COLU, NYU)
BOBISUT	74	LNC 11 646	F. Bobisut *et al.*	(PADO)
COWELL	74	PR D10 2083	P.L. Cowell *et al.*	(STON, COLU)
GEWENIGER	74B	PL 48B 487	C. Geweniger *et al.*	(CERN, HEIDH)
GJESDAL	74B	PL 52B 119	S. Gjesdal *et al.*	(CERN, HEIDH)
BURGUN	73	PL 46B 481	G. Burgun *et al.*	(SACL, CERN)
GJESDAL	73	PL 44B 217	S. Gjesdal *et al.*	(CERN, HEIDH)
HILL	73	PR D8 1290	D.G. Hill *et al.*	(BNL, CMU)
ALITTI	72	PL 39B 568	J. Alitti, E. Lesquoy, A. Muller	(SACL)
BURGUN	72	NP B50 194	G. Burgun *et al.*	(SACL, CERN, OSLO)
METCALF	72	PL 40B 703	M. Metcalf *et al.*	(CERN, IPN, WIEN)
MORSE	72B	PRL 28 388	R. Morse *et al.*	(COLO, PRIN, UMD)
NAGY	72	NP B47 94	E. Nagy, F. Telbisz, G. Vesztergombi	(BUDA)
Also		NP B30 498	G. Bozoki *et al.*	(BUDA)
SKJEGGEST...	72	NP B48 343	O. Skjeggestad *et al.*	(OSLO, CERN, SACL)
BALTAY	71	PRL 27 1678	C. Baltay *et al.*	(COLU)
Also		Thesis Nevis 187	W.A. Cooper	(COLU)
MOFFETT	70	BAPS 15 512	R. Moffett *et al.*	(ROCH)
BOZOKI	69	PL 30B 498	G. Bozoki *et al.*	(BUDA)
DOYLE	69	Thesis UCRL 18139	J.C. Doyle	(LRL)
GOBBI	69	PRL 22 682	B. Gobbi *et al.*	(ROCH)
HYAMS	69B	PL 29B 521	B.D. Hyams *et al.*	(CERN, MPIM)
MORFIN	69	PRL 23 660	J.G. Morfin, D. Sinclair	(MICH)
DONALD	68B	PL 27B 58	R.A. Donald *et al.*	(LIVP, CERN, IPNP+)
HILL	68	PR 171 1418	D.G. Hill *et al.*	(BNL, CMU)
AUBERT	65	PL 17 59	B. Aubert *et al.*	(EPOL, ORSAY)
BROWN	63	PR 130 769	J.L. Brown *et al.*	(LRL, MICH)
CHRETIEN	63	PR 131 2208	M. Chretien *et al.*	(BRAN, BROW, HARV+)
BROWN	61	NC 19 1155	J.L. Brown *et al.*	(MICH)
BOLDT	58B	PRL 1 150	E. Boldt, D.O. Caldwell, Y. Pal	(MIT)

OTHER RELATED PAPERS

LITTENBERG	93	ARNPS 43 729	L.S. Littenberg, G. Valencia	(BNL, FNAL)
Rare and Radiative Kaon Decays				
BATTISTON	92	PRPL 214 293	R. Battiston *et al.*	(PGIA, CERN, TRSTT)
Status and Perspectives of K Decay Physics				
TRILLING	65B	UCRL 16473	G.N. Trilling	(LRL)
Updated from 1965 Argonne Conference, page 115.				
CRAWFORD	62	CERN Conf. 827	F.S. Crawford	(LRL)
FITCH	61	NC 22 1160	V.L. Fitch, P.A. Piroue, R.B. Perkins	(PRIN+)
GOOD	61	PR 124 1223	R.H. Good *et al.*	(LRL)
BIRGE	60	Rochester Conf. 601	R.W. Birge *et al.*	(LRL, WISC)
MULLER	60	PRL 4 418	F. Muller *et al.*	(LRL, BNL)

K^0_L

$I(J^P) = \frac{1}{2}(0^-)$

$m_{K^0_L} - m_{K^0_S}$

For earlier measurements, beginning with GOOD 61 and FITCH 61, see our 1986 edition, Physics Letters **170B** 132 (1986).

OUR FIT is described in the note on "CP violation in K_L decays" in the K^0_L Particle Listings. The result labeled "OUR FIT Assuming CPT" ["OUR FIT Not assuming CPT"] includes all measurements except those with the comment "Not assuming CPT" ["Assuming CPT"]. Measurements with neither comment do not assume CPT and enter both fits.

VALUE ($10^{10}\ \hbar\ s^{-1}$)		*DOCUMENT ID*		*TECN*	*COMMENT*
0.5293 ±0.0009 OUR FIT		Error includes scale factor of 1.3. Assuming CPT			
0.5289 ±0.0010 OUR FIT		Not assuming CPT			
0.52797±0.00195		[1,2] ABOUZAID	11	KTEV	Not assuming CPT
0.52699±0.00123		[1,3] ABOUZAID	11	KTEV	Assuming CPT
0.5240 ±0.0044	±0.0033	APOSTOLA...	99C	CPLR	K^0-$\overline{K}^0$ to $\pi^+\pi^-$
0.5297 ±0.0030	±0.0022	[4] SCHWINGEN...	95	E773	20–160 GeV K beams
0.5286 ±0.0028		[5] GIBBONS	93	E731	Assuming CPT
0.5257 ±0.0049	±0.0021	[4] GIBBONS	93C	E731	Not assuming CPT
0.5340 ±0.00255	±0.0015	[6] GEWENIGER	74C	SPEC	Gap method
0.5334 ±0.0040	±0.0015	[6,7] GJESDAL	74	SPEC	Assuming CPT
• • • We do not use the following data for averages, fits, limits, etc. • • •					
0.5261 ±0.0015		[8] ALAVI-HARATI	03	KTEV	Assuming CPT
0.5288 ±0.0043		[9] ALAVI-HARATI	03	KTEV	Not assuming CPT
0.5343 ±0.0063	±0.0025	[10] ANGELOPO...	01	CPLR	
0.5295 ±0.0020	±0.0003	[11] ANGELOPO...	98D	CPLR	Assuming CPT
0.5307 ±0.0013		[12] ADLER	96C	RVUE	
0.5274 ±0.0029	±0.0005	[11] ADLER	95	CPLR	Sup. by ANGELOPOULOS 98D
0.482 ±0.014		[13] ARONSON	82B	SPEC	E=30–110 GeV
0.534 ±0.007		[14] CARNEGIE	71	ASPK	Gap method
0.542 ±0.006		[14] ARONSON	70	ASPK	Gap method
0.542 ±0.006		CULLEN	70	CNTR	

[1] The two ABOUZAID 11 values use the same data. The first enters the "assuming CPT" fit and the second enters the "not assuming CPT" fit.

[2] ABOUZAID 11 fit has Δm, τ_S, ϕ_ϵ, Re(ϵ'/ϵ), and Im(ϵ'/ϵ) as free parameters. See Im(ϵ'/ϵ) in the "K^0_L CP violation" section for correlation information.

[3] ABOUZAID 11 fit has Δm and τ_S free but constrains ϕ_ϵ to the Superweak value, i.e. assumes CPT. See "K^0_S Mean Life" section for correlation information.

[4] Fits Δm and ϕ_{+-} simultaneously. GIBBONS 93C systematic error is from B. Winstein via private communication. 20–160 GeV K beams.

[5] GIBBONS 93 value assume $\phi_{+-} = \phi_{00} = \phi_{SW} = (43.7 \pm 0.2)°$, i.e. assumes CPT. 20–160 GeV K beams.

[6] These two experiments have a common systematic error due to the uncertainty in the momentum scale, as pointed out in WAHL 89.

[7] GJESDAL 74 uses charge asymmetry in $K^0_{\ell 3}$ decays.

[8] ALAVI-HARATI 03 fit Δm and $\tau_{K^0_S}$ simultaneously. ϕ_{+-} is constrained to the Superweak value, i.e. CPT is assumed. See "K^0_S Mean Life" section for correlation information. Superseded by ABOUZAID 11.

[9] ALAVI-HARATI 03 fit Δm, ϕ_{+-}, and τ_{K_S} simultaneously. See ϕ_{+-} in the "K_L CP violation" section for correlation information. Superseded by ABOUZAID 11.

[10] ANGELOPOULOS 01 uses strong interactions strangeness tagging at two different times.

[11] Uses $\overline{K}^0_{e3}$ and K^0_{e3} strangeness tagging at production and decay. Assumes CPT conservation on $\Delta S = -\Delta Q$ transitions.

[12] ADLER 96C is the result of a fit which includes nearly the same data as entered into the "OUR FIT" value above.

[13] ARONSON 82 find that Δm may depend on the kaon energy.

[14] ARONSON 70 and CARNEGIE 71 use K^0_S mean life = $(0.862 \pm 0.006) \times 10^{-10}$ s. We have not attempted to adjust these values for the subsequent change in the K^0_S mean life or in η_{+-}.

K^0_L MEAN LIFE

VALUE (10^{-8} s)	*EVTS*	*DOCUMENT ID*		*TECN*	*COMMENT*
5.116±0.021 OUR FIT	Error includes scale factor of 1.1.				
5.099±0.021 OUR AVERAGE					
5.072±0.011±0.035	13M	[1] AMBROSINO	06	KLOE	$\sum_i B_i = 1$
5.092±0.017±0.025	15M	AMBROSINO	05C	KLOE	
5.154±0.044	0.4M	VOSBURGH	72	CNTR	
• • • We do not use the following data for averages, fits, limits, etc. • • •					
5.15 ±0.14		DEVLIN	67	CNTR	

[1] AMBROSINO 06 uses $\phi \to K_L K_S$ with K_L tagged by $K_S \to \pi^+\pi^-$. The four major K_L BR's are measured, the small remainder ($\pi^+\pi^-$,$\pi^0\pi^0$,$\gamma\gamma$) is taken from PDG 04. This KLOE K_L lifetime is obtained by imposing $\sum_i B_i = 1$. The correlation matrix among the four measured K_L BR's and this K_L lifetime is

	K_{e3}	$K_{\mu 3}$	$3\pi^0$	$\pi^+\pi^-\pi^0$	τ_{K_L}
K_{e3}	1	−0.25	−0.56	−0.07	0.25
$K_{\mu 3}$		1	−0.43	−0.20	0.33
$3\pi^0$			1	−0.39	−0.21
$\pi^+\pi^-\pi^0$				1	−0.39
τ_{K_L}					1

These correlations are taken into account in our fit. The average of this KLOE mean life measurement and the independent KLOE measurement in AMBROSINO 05C is $(5.084 \pm 0.023) \times 10^{-8}$ s.

K^0_L DECAY MODES

Mode			Fraction (Γ_i/Γ)	Scale factor/ Confidence level
Semileptonic modes				
Γ_1	$\pi^\pm e^\mp \nu_e$ Called K^0_{e3}.	[a]	(40.55 ±0.11) %	S=1.7
Γ_2	$\pi^\pm \mu^\mp \nu_\mu$ Called $K^0_{\mu 3}$.	[a]	(27.04 ±0.07) %	S=1.1
Γ_3	$(\pi\mu\text{atom})\nu$		(1.05 ±0.11) × 10^{-7}	
Γ_4	$\pi^0\pi^\pm e^\mp \nu$	[a]	(5.20 ±0.11) × 10^{-5}	
Γ_5	$\pi^\pm e^\mp \nu e^+ e^-$	[a]	(1.26 ±0.04) × 10^{-5}	
Hadronic modes, including Charge conjugation×Parity Violating (CPV) modes				
Γ_6	$3\pi^0$		(19.52 ±0.12) %	S=1.6
Γ_7	$\pi^+\pi^-\pi^0$		(12.54 ±0.05) %	
Γ_8	$\pi^+\pi^-$	CPV [b]	(1.967±0.010) × 10^{-3}	S=1.5
Γ_9	$\pi^0\pi^0$	CPV	(8.64 ±0.06) × 10^{-4}	S=1.8
Semileptonic modes with photons				
Γ_{10}	$\pi^\pm e^\mp \nu_e \gamma$	[a,c,d]	(3.79 ±0.06) × 10^{-3}	
Γ_{11}	$\pi^\pm \mu^\mp \nu_\mu \gamma$		(5.65 ±0.23) × 10^{-4}	
Hadronic modes with photons or $\ell\overline{\ell}$ pairs				
Γ_{12}	$\pi^0\pi^0\gamma$		< 2.43 × 10^{-7}	CL=90%
Γ_{13}	$\pi^+\pi^-\gamma$	[c,d]	(4.15 ±0.15) × 10^{-5}	S=2.8
Γ_{14}	$\pi^+\pi^-\gamma$(DE)		(2.84 ±0.11) × 10^{-5}	S=2.0
Γ_{15}	$\pi^0 2\gamma$	[c]	(1.273±0.033) × 10^{-6}	
Γ_{16}	$\pi^0\gamma e^+ e^-$		(1.62 ±0.17) × 10^{-8}	
Other modes with photons or $\ell\overline{\ell}$ pairs				
Γ_{17}	2γ		(5.47 ±0.04) × 10^{-4}	S=1.1
Γ_{18}	3γ		< 7.4 × 10^{-8}	CL=90%
Γ_{19}	$e^+ e^-\gamma$		(9.4 ±0.4) × 10^{-6}	S=2.0
Γ_{20}	$\mu^+\mu^-\gamma$		(3.59 ±0.11) × 10^{-7}	S=1.3
Γ_{21}	$e^+ e^-\gamma\gamma$	[c]	(5.95 ±0.33) × 10^{-7}	
Γ_{22}	$\mu^+\mu^-\gamma\gamma$	[c]	(1.0 $^{+0.8}_{-0.6}$) × 10^{-8}	

Meson Particle Listings

K_L^0

Charge conjugation × Parity (*CP*) or Lepton Family number (*LF*) violating modes, or $\Delta S = 1$ weak neutral current (*S1*) modes

Γ_{23}	$\mu^+\mu^-$	*S1*		$(6.84 \pm 0.11) \times 10^{-9}$		
Γ_{24}	e^+e^-	*S1*		$(9 \,^{+6}_{-4}) \times 10^{-12}$		
Γ_{25}	$\pi^+\pi^- e^+e^-$	*S1*	[c]	$(3.11 \pm 0.19) \times 10^{-7}$		
Γ_{26}	$\pi^0\pi^0 e^+e^-$	*S1*		$< 6.6 \times 10^{-9}$		CL=90%
Γ_{27}	$\pi^0\pi^0\mu^+\mu^-$	*S1*		$< 9.2 \times 10^{-11}$		CL=90%
Γ_{28}	$\mu^+\mu^- e^+e^-$	*S1*		$(2.69 \pm 0.27) \times 10^{-9}$		
Γ_{29}	$e^+e^- e^+e^-$	*S1*		$(3.56 \pm 0.21) \times 10^{-8}$		
Γ_{30}	$\pi^0\mu^+\mu^-$	*CP,S1*	[e]	$< 3.8 \times 10^{-10}$		CL=90%
Γ_{31}	$\pi^0 e^+e^-$	*CP,S1*	[e]	$< 2.8 \times 10^{-10}$		CL=90%
Γ_{32}	$\pi^0\nu\overline{\nu}$	*CP,S1*	[f]	$< 2.6 \times 10^{-8}$		CL=90%
Γ_{33}	$\pi^0\pi^0\nu\overline{\nu}$	*S1*		$< 8.1 \times 10^{-7}$		CL=90%
Γ_{34}	$e^\pm\mu^\mp$	*LF*	[a]	$< 4.7 \times 10^{-12}$		CL=90%
Γ_{35}	$e^\pm e^\pm\mu^\mp\mu^\mp$	*LF*	[a]	$< 4.12 \times 10^{-11}$		CL=90%
Γ_{36}	$\pi^0\mu^\pm e^\mp$	*LF*	[a]	$< 7.6 \times 10^{-11}$		CL=90%
Γ_{37}	$\pi^0\pi^0\mu^\pm e^\mp$	*LF*		$< 1.7 \times 10^{-10}$		CL=90%

[a] The value is for the sum of the charge states or particle/antiparticle states indicated.

[b] This mode includes gammas from inner bremsstrahlung but not the direct emission mode $K_L^0 \to \pi^+\pi^-\gamma$(DE).

[c] See the Particle Listings below for the energy limits used in this measurement.

[d] Most of this radiative mode, the low-momentum γ part, is also included in the parent mode listed without γ's.

[e] Allowed by higher-order electroweak interactions.

[f] Violates *CP* in leading order. Test of direct *CP* violation since the indirect *CP*-violating and *CP*-conserving contributions are expected to be suppressed.

CONSTRAINED FIT INFORMATION

An overall fit to the mean life and 15 branching ratios uses 27 measurements and one constraint to determine 11 parameters. The overall fit has a $\chi^2 = 37.4$ for 17 degrees of freedom.

The following *off-diagonal* array elements are the correlation coefficients $\langle \delta p_i \delta p_j \rangle / (\delta p_i \cdot \delta p_j)$, in percent, from the fit to parameters p_i, including the branching fractions, $x_i \equiv \Gamma_i/\Gamma_{\text{total}}$. The fit constrains the x_i whose labels appear in this array to sum to one.

x_2	−21									
x_6	−77	−29								
x_7	−15	−20	−18							
x_8	53	−11	−47	4						
x_9	30	−23	−11	−12	64					
x_{13}	6	−1	−6	0	12	8				
x_{14}	6	−1	−6	0	11	7	93			
x_{17}	−46	−22	64	−14	−21	8	−3	−3		
x_{19}	−5	−2	7	−1	−3	−1	0	0	4	
Γ	−27	−9	24	15	−13	−6	−2	−2	15	2
	x_1	x_2	x_6	x_7	x_8	x_9	x_{13}	x_{14}	x_{17}	x_{19}

	Mode		Rate (10^8 s^{-1})	Scale factor
Γ_1	$\pi^\pm e^\mp\nu_e$ Called K_{e3}^0.	[a]	0.07927 ± 0.00034	1.1
Γ_2	$\pi^\pm\mu^\mp\nu_\mu$ Called $K_{\mu3}^0$.	[a]	0.05286 ± 0.00025	1.1
Γ_6	$3\pi^0$		0.03815 ± 0.00030	1.5
Γ_7	$\pi^+\pi^-\pi^0$		0.02451 ± 0.00015	
Γ_8	$\pi^+\pi^-$	[b]	$(3.844 \pm 0.023) \times 10^{-4}$	1.2
Γ_9	$\pi^0\pi^0$		$(1.690 \pm 0.013) \times 10^{-4}$	1.4
Γ_{13}	$\pi^+\pi^-\gamma$	[c,d]	$(8.11 \pm 0.29) \times 10^{-6}$	2.7
Γ_{14}	$\pi^+\pi^-\gamma$(DE)		$(5.55 \pm 0.21) \times 10^{-6}$	2.0
Γ_{17}	2γ		$(1.069 \pm 0.010) \times 10^{-4}$	1.2
Γ_{19}	$e^+e^-\gamma$		$(1.84 \pm 0.08) \times 10^{-6}$	1.9

K_L^0 DECAY RATES

$\Gamma(\pi^+\pi^-\pi^0)$ Γ_7

VALUE (10^6 s^{-1})	EVTS	DOCUMENT ID	TECN	COMMENT
2.451±0.015 OUR FIT				
• • • We do not use the following data for averages, fits, limits, etc. • • •				
2.32 $^{+0.13}_{-0.15}$	192	BALDO-...	75	HLBC Assumes *CP*
2.35 ±0.20	180	[1] JAMES	72	HBC Assumes *CP*
2.71 ±0.28	99	CHO	71	DBC Assumes *CP*
2.5 ±0.3	98	[1] JAMES	71	HBC Assumes *CP*
2.12 ±0.33	50	MEISNER	71	HBC Assumes *CP*
2.20 ±0.35	53	WEBBER	70	HBC Assumes *CP*
2.62 $^{+0.28}_{-0.27}$	136	BEHR	66	HLBC Assumes *CP*
3.26 ±0.77	18	ANDERSON	65	HBC
1.4 ±0.4	14	FRANZINI	65	HBC

[1] JAMES 72 is a final measurement and includes JAMES 71.

$\Gamma(\pi^\pm e^\mp\nu_e)$ Γ_1

VALUE (10^6 s^{-1})	EVTS	DOCUMENT ID	TECN	COMMENT
7.927±0.034 OUR FIT	Error includes scale factor of 1.1.			
• • • We do not use the following data for averages, fits, limits, etc. • • •				
7.81 ±0.56	620	CHAN	71	HBC
7.52 $^{+0.85}_{-0.72}$		AUBERT	65	HLBC $\Delta S = \Delta Q$, *CP* assumed

$\Gamma(\pi^\pm e^\mp\nu_e) + \Gamma(\pi^\pm\mu^\mp\nu_\mu)$ $(\Gamma_1+\Gamma_2)$

VALUE (10^6 s^{-1})	EVTS	DOCUMENT ID	TECN	COMMENT
13.21±0.05 OUR FIT				
• • • We do not use the following data for averages, fits, limits, etc. • • •				
12.4 ±0.7	410	[1] BURGUN	72	HBC $K^+p \to K^0p\pi^+$
8.47±1.69	126	[1] MANN	72	HBC $K^-p \to n\overline{K}^0$
13.1 ±1.3	252	[1] WEBBER	71	HBC $K^-p \to n\overline{K}^0$
11.6 ±0.9	393	[1,2] CHO	70	DBC $K^+n \to K^0p$
10.3 ±0.8	335	[2] HILL	67	DBC $K^+n \to K^0p$
9.85 $^{+1.15}_{-1.05}$	109	[1] FRANZINI	65	HBC

[1] Assumes $\Delta S = \Delta Q$ rule.
[2] CHO 70 includes events of HILL 67.

K_L^0 BRANCHING RATIOS

Semileptonic modes

$\Gamma(\pi^\pm e^\mp\nu_e)/\Gamma_{\text{total}}$ Γ_1/Γ

VALUE	EVTS	DOCUMENT ID	TECN
0.4055±0.0011 OUR FIT	Error includes scale factor of 1.7.		
0.4047±0.0028 OUR AVERAGE	Error includes scale factor of 3.1.		
0.4007±0.0005±0.0015	13M	[1] AMBROSINO 06	KLOE
0.4067±0.0011		[2] ALEXOPOU... 04	KTEV

[1] There are correlations between these five KLOE measurements: B($K_L \to \pi e\nu$), B($K_L \to \pi\mu\nu$), B($K_L \to 3\pi^0$), B($K_L \to \pi^+\pi^-\pi^0$), and τ_{K_L} measured in AMBROSINO 06. See the footnote for the τ_{K_L} measurement for the correlation matrix.

[2] ALEXOPOULOS 04 constrains $\sum_i B_i = 0.9993$ for the six major K_L branching fractions. The correlations among these branching fractions are taken into account in our fit. The correlation matrix is

	K_{e3}	$K_{\mu3}$	$3\pi^0$	$\pi^+\pi^-\pi^0$	$\pi^+\pi^-$	$\pi^0\pi^0$
K_{e3}	1					
$K_{\mu3}$	0.15	1				
$3\pi^0$	−0.77	−0.62	1			
$\pi^+\pi^-\pi^0$	0.18	0.08	−0.54	1		
$\pi^+\pi^-$	0.28	0.22	−0.48	0.49	1	
$\pi^0\pi^0$	−0.72	−0.54	0.89	−0.46	−0.39	1

$\Gamma(\pi^\pm\mu^\mp\nu_\mu)/\Gamma_{\text{total}}$ Γ_2/Γ

VALUE	EVTS	DOCUMENT ID	TECN
0.2704±0.0007 OUR FIT	Error includes scale factor of 1.1.		
0.2700±0.0008 OUR AVERAGE			
0.2698±0.0005±0.0015	13M	[1] AMBROSINO 06	KLOE
0.2701±0.0009		[2] ALEXOPOU... 04	KTEV

[1] There are correlations between these five KLOE measurements: B($K_L \to \pi e\nu$), B($K_L \to \pi\mu\nu$), B($K_L \to 3\pi^0$), B($K_L \to \pi^+\pi^-\pi^0$), and τ_{K_L} measured in AMBROSINO 06. See the footnote for the τ_{K_L} measurement for the correlation matrix.

[2] For correlations with other ALEXOPOULOS 04 measurements, see the footnote with their B($K_L \to \pi e\nu$) measurement.

$[\Gamma(\pi^\pm e^\mp\nu_e) + \Gamma(\pi^\pm\mu^\mp\nu_\mu)]/\Gamma_{\text{total}}$ $(\Gamma_1+\Gamma_2)/\Gamma$

VALUE	DOCUMENT ID
0.6760±0.0012 OUR FIT	Error includes scale factor of 1.6.

$\Gamma(\pi^\pm\mu^\mp\nu_\mu)/\Gamma(\pi^\pm e^\mp\nu_e)$ Γ_2/Γ_1

VALUE	EVTS	DOCUMENT ID	TECN	COMMENT
0.6669±0.0027 OUR FIT	Error includes scale factor of 1.2.			
0.666 ±0.004 OUR AVERAGE	Error includes scale factor of 1.6.			
• • • We use the following data for averages but not for fits. • • •				
0.6740±0.0059	13M	[1] AMBROSINO 06	KLOE	Not in fit
0.6640±0.0014±0.0022	394K	[2] ALEXOPOU... 04	KTEV	Not in fit

• • • We do not use the following data for averages, fits, limits, etc. • • •

0.702 ±0.011	33k	CHO	80	HBC
0.662 ±0.037	10k	WILLIAMS	74	ASPK
0.741 ±0.044	6700	BRANDENB...	73	HBC
0.662 ±0.030	1309	EVANS	73	HLBC
0.68 ±0.08	3548	BASILE	70	OSPK
0.71 ±0.05	770	BUDAGOV	68	HLBC

[1] AMBROSINO 06 enters the fit via their separate measurements of these two modes.
[2] ALEXOPOULOS 04 enters the fit via their separate measurements of these two modes.

$\Gamma((\pi\mu\text{atom})\nu)/\Gamma(\pi^\pm\mu^\mp\nu_\mu)$ Γ_3/Γ_2

VALUE (units 10^{-7})	EVTS	DOCUMENT ID		TECN
3.90±0.39	155	[1] ARONSON	86	SPEC
• • • We do not use the following data for averages, fits, limits, etc. • • •				
seen	18	COOMBES	76	WIRE

[1] ARONSON 86 quote theoretical value of $(4.31 \pm 0.08) \times 10^{-7}$.

$\Gamma(\pi^0\pi^\pm e^\mp\nu)/\Gamma_{\text{total}}$ Γ_4/Γ

VALUE (units 10^{-5})	CL%	EVTS	DOCUMENT ID		TECN
5.20±0.11 OUR AVERAGE					
5.21±0.07±0.09		5402	BATLEY	04	NA48
5.16±0.20±0.22		729	MAKOFF	93	E731
• • • We do not use the following data for averages, fits, limits, etc. • • •					
6.2 ±2.0		16	CARROLL	80C	SPEC
< 220	90		[1] DONALDSON	74	SPEC

[1] DONALDSON 74 uses $K_L^0 \to \pi^+\pi^-\pi^0/(\text{all } K_L^0)$ decays = 0.126.

$\Gamma(\pi^\pm e^\mp\nu e^+e^-)/\Gamma(\pi^+\pi^-\pi^0)$ Γ_5/Γ_7

VALUE (units 10^{-5})	EVTS	DOCUMENT ID		TECN	COMMENT
10.02±0.17±0.29	19k	[1] ABOUZAID	07C	KTEV	$M_{ee^*} > 5$ MeV, $E^*_{ee} > 30$ MeV

[1] E^*_{ee} is the energy of the e^+e^- pair in the kaon rest frame. ABOUZAID 07C reports $[\Gamma(K_L^0 \to \pi^\pm e^\mp\nu e^+e^-)/\Gamma(K_L^0 \to \pi^+\pi^-\pi^0)] / [B(\pi^0 \to e^+e^-\gamma)] = (8.54 \pm 0.07 \pm 0.13) \times 10^{-3}$ which we multiply by our best value $B(\pi^0 \to e^+e^-\gamma) = (1.174 \pm 0.035) \times 10^{-2}$. Our first error is their experiment's error and our second error is the systematic error from using our best value.

Hadronic modes, including Charge conjugation×Parity Violating (*CPV*) modes

$\Gamma(3\pi^0)/\Gamma_{\text{total}}$ Γ_6/Γ

VALUE	EVTS	DOCUMENT ID		TECN	COMMENT
0.1952±0.0012 OUR FIT	Error includes scale factor of 1.6.				
0.1969±0.0026 OUR AVERAGE	Error includes scale factor of 2.0.				
• • • We use the following data for averages but not for fits. • • •					
0.1997±0.0003±0.0019	13M	[1] AMBROSINO	06	KLOE	Not fitted
0.1945±0.0018		[1] ALEXOPOU...	04	KTEV	Not fitted

[1] We exclude these $B(K_L \to 3\pi^0)$ measurements from our fit because the authors have constrained K_L branching fractions to sum to one. It enters our fit via the other measurements from the experiment and their correlations, along with our constraint that the fitted branching fractions sum to one.

$\Gamma(3\pi^0)/\Gamma(\pi^\pm e^\mp\nu_e)$ Γ_6/Γ_1

VALUE	EVTS	DOCUMENT ID		TECN	COMMENT
0.481 ±0.004 OUR FIT	Error includes scale factor of 1.8.				
• • • We use the following data for averages but not for fits. • • •					
0.4782±0.0014±0.0053	209K	[1] ALEXOPOU...	04	KTEV	Not in fit
• • • We do not use the following data for averages, fits, limits, etc. • • •					
0.545 ±0.004 ±0.009	38k	KREUTZ	95	NA31	

[1] This measurement enters the fit via their separate measurements of these two modes.

$\Gamma(3\pi^0)/[\Gamma(\pi^\pm e^\mp\nu_e) + \Gamma(\pi^\pm\mu^\mp\nu_\mu) + \Gamma(\pi^+\pi^-\pi^0)]$ $\Gamma_6/(\Gamma_1+\Gamma_2+\Gamma_7)$

VALUE	EVTS	DOCUMENT ID		TECN	COMMENT
0.2436±0.0018 OUR FIT	Error includes scale factor of 1.6.				
• • • We do not use the following data for averages, fits, limits, etc. • • •					
0.251 ±0.014	549	BUDAGOV	68	HLBC	ORSAY measur.
0.277 ±0.021	444	BUDAGOV	68	HLBC	Ecole polytec.meas
$0.31\ ^{+0.07}_{-0.06}$	29	KULYUKINA	68	CC	
0.24 ±0.08	24	ANIKINA	64	CC	

$\Gamma(3\pi^0)/\Gamma(\pi^+\pi^-\pi^0)$ Γ_6/Γ_7

VALUE	EVTS	DOCUMENT ID		TECN	COMMENT
1.557±0.012 OUR FIT	Error includes scale factor of 1.3.				
• • • We use the following data for averages but not for fits. • • •					
1.582±0.027	13M	[1] AMBROSINO	06	KLOE	Not in fit
• • • We do not use the following data for averages, fits, limits, etc. • • •					
1.611±0.014±0.034	28k	KREUTZ	95	NA31	
1.65 ±0.07	883	BARMIN	72B	HLBC	Error statistical only
1.80 ±0.13	1010	BUDAGOV	68	HLBC	
2.0 ±0.6	188	ALEKSANYAN	64B	FBC	

[1] AMBROSINO 06 enters the fit via their separate measurements of these two modes.

$\Gamma(\pi^+\pi^-\pi^0)/\Gamma_{\text{total}}$ Γ_7/Γ

VALUE	EVTS	DOCUMENT ID		TECN
0.1254±0.0005 OUR FIT				
0.1255±0.0006 OUR AVERAGE				
0.1263±0.0004±0.0011	13M	[1] AMBROSINO	06	KLOE
0.1252±0.0007		[2] ALEXOPOU...	04	KTEV

[1] There are correlations between these five KLOE measurements: $B(K_L \to \pi e\nu)$, $B(K_L \to \pi\mu\nu)$, $B(K_L \to 3\pi^0)$, $B(K_L \to \pi^+\pi^-\pi^0)$, and τ_{K_L} measured in AMBROSINO 06. See the footnote for the τ_{K_L} measurement for the correlation matrix.
[2] For correlations with other ALEXOPOULOS 04 measurements, see the footnote with their $B(K_L \to \pi e\nu)$ measurement.

$\Gamma(\pi^+\pi^-\pi^0)/\Gamma(\pi^\pm e^\mp\nu_e)$ Γ_7/Γ_1

VALUE	EVTS	DOCUMENT ID		TECN	COMMENT
0.3092±0.0016 OUR FIT	Error includes scale factor of 1.1.				
• • • We use the following data for averages but not for fits. • • •					
0.3078±0.0005±0.0017	799K	[1] ALEXOPOU...	04	KTEV	Not in fit
• • • We do not use the following data for averages, fits, limits, etc. • • •					
0.336 ±0.003 ±0.007	28k	KREUTZ	95	NA31	

[1] This measurement enters the fit via their separate measurements for the two modes.

$\Gamma(\pi^+\pi^-\pi^0)/[\Gamma(\pi^\pm e^\mp\nu_e) + \Gamma(\pi^\pm\mu^\mp\nu_\mu) + \Gamma(\pi^+\pi^-\pi^0)]$ $\Gamma_7/(\Gamma_1+\Gamma_2+\Gamma_7)$

VALUE	EVTS	DOCUMENT ID		TECN	COMMENT
0.1565±0.0006 OUR FIT	Error includes scale factor of 1.1.				
• • • We do not use the following data for averages, fits, limits, etc. • • •					
0.163 ±0.003	6499	CHO	77	HBC	
0.1605±0.0038	1590	ALEXANDER	73B	HBC	
0.146 ±0.004	3200	BRANDENB...	73	HBC	
0.159 ±0.010	558	EVANS	73	HLBC	
0.167 ±0.016	1402	KULYUKINA	68	CC	
0.161 ±0.005		HOPKINS	67	HBC	
0.162 ±0.015	126	HAWKINS	66	HBC	
0.159 ±0.015	326	ASTBURY	65B	CC	
0.178 ±0.017	566	GUIDONI	65	HBC	
0.144 ±0.004	1729	HOPKINS	65	HBC	See HOPKINS 67

$\Gamma(\pi^+\pi^-)/\Gamma_{\text{total}}$ Γ_8/Γ

Violates *CP* conservation.

VALUE (units 10^{-3})	DOCUMENT ID		TECN
1.967±0.010 OUR FIT	Error includes scale factor of 1.5.		
1.975±0.012	[1] ALEXOPOU...	04	KTEV

[1] For correlations with other ALEXOPOULOS 04 measurements, see the footnote with their $B(K_L \to \pi e\nu)$ measurement.

$\Gamma(\pi^+\pi^-)/\Gamma(\pi^\pm e^\mp\nu_e)$ Γ_8/Γ_1

VALUE (units 10^{-3})	EVTS	DOCUMENT ID		TECN	COMMENT
4.849±0.020 OUR FIT	Error includes scale factor of 1.1.				
4.840±0.020 OUR AVERAGE					
4.826±0.022±0.016	47k	[1] LAI	07	NA48	
• • • We use the following data for averages but not for fits. • • •					
4.856±0.017±0.023	84k	[2] ALEXOPOU...	04	KTEV	Not in fit

[1] The LAI 07 central value of 4.835×10^{-3} has been reduced by 0.19% to 4.826×10^{-3} to subtract the contribution from the direct emission mode $K_L^0 \to \pi^+\pi^-\gamma(\text{DE})$.
[2] This measurement enters the fit via their separate measurements for the two modes.

$[\Gamma(\pi^+\pi^-) + \Gamma(\pi^+\pi^-\gamma(\text{DE}))]/\Gamma(\pi^\pm\mu^\mp\nu_\mu)$ $(\Gamma_8+\Gamma_{14})/\Gamma_2$

VALUE (units 10^{-3})	EVTS	DOCUMENT ID		TECN
7.38 ±0.04 OUR FIT	Error includes scale factor of 1.4.			
7.275±0.042±0.054	45k	[1] AMBROSINO	06F	KLOE

[1] Fully inclusive. Taking $B(K_L^0 \to \pi\mu\nu)$ from KLOE, AMBROSINO 06, $B(K_L^0 \to \pi^+\pi^- + \pi^+\pi^-\gamma(\text{DE})) = (1.963 \pm 0.012 \pm 0.017) \times 10^{-3}$ is obtained.

$\Gamma(\pi^+\pi^-)/[\Gamma(\pi^\pm e^\mp\nu_e) + \Gamma(\pi^\pm\mu^\mp\nu_\mu)]$ $\Gamma_8/(\Gamma_1+\Gamma_2)$

Violates *CP* conservation.

VALUE (units 10^{-3})	EVTS	DOCUMENT ID		TECN	COMMENT
2.909±0.013 OUR FIT	Error includes scale factor of 1.3.				
• • • We do not use the following data for averages, fits, limits, etc. • • •					
3.13 ±0.14	1687	COUPAL	85	SPEC	η_{+-}=2.28 ± 0.06
3.04 ±0.14	2703	DEVOE	77	SPEC	η_{+-}=2.25 ± 0.05
2.51 ±0.23	309	[1] DEBOUARD	67	OSPK	η_{+-}=2.00 ± 0.09
2.35 ±0.19	525	[1] FITCH	67	OSPK	η_{+-}=1.94 ± 0.08

[1] Old experiments excluded from fit. See subsection on η_{+-} in section on "PARAMETERS FOR $K_L^0 \to 2\pi$ DECAY" below for average η_{+-} of these experiments and for note on discrepancy.

$\Gamma(\pi^\pm e^\mp\nu_e)/\Gamma(2\text{ tracks})$ $\Gamma_1/(\Gamma_1+\Gamma_2+0.03508\Gamma_6+\Gamma_7+\Gamma_8)$

$\Gamma(2\text{ tracks}) = \Gamma(\pi^\pm e^\mp\nu_e) + \Gamma(\pi^\pm\mu^\mp\nu_\mu) + 0.03508\,\Gamma(3\pi^0) + \Gamma(\pi^+\pi^-\pi^0) + \Gamma(\pi^+\pi^-)$ where 0.03508 is the fraction of $3\pi^0$ events with one Dalitz decay ($\pi^0 \to \gamma e^+e^-$).

VALUE	EVTS	DOCUMENT ID		TECN
0.5006±0.0009 OUR FIT	Error includes scale factor of 1.3.			
0.4978±0.0035	6.8M	LAI	04B	NA48

$\Gamma(\pi^+\pi^-)/[\Gamma(\pi^\pm e^\mp\nu_e)+\Gamma(\pi^\pm\mu^\mp\nu_\mu)+\Gamma(\pi^+\pi^-\pi^0)]$ $\Gamma_8/(\Gamma_1+\Gamma_2+\Gamma_7)$

Violates CP conservation.

VALUE (units 10^{-3})	EVTS	DOCUMENT ID		TECN	COMMENT
2.454±0.011 OUR FIT		Error includes scale factor of 1.3.			
• • • We do not use the following data for averages, fits, limits, etc. • • •					
2.60 ±0.07	4200	[1] MESSNER	73	ASPK	$\eta_{+-} = 2.23 \pm 0.05$

[1] From same data as $\Gamma(\pi^+\pi^-)/\Gamma(\pi^+\pi^-\pi^0)$ MESSNER 73, but with different normalization.

$\Gamma(\pi^+\pi^-)/\Gamma(\pi^+\pi^-\pi^0)$ Γ_8/Γ_7

Violates CP conservation.

VALUE (units 10^{-2})	EVTS	DOCUMENT ID		TECN	COMMENT
1.568±0.010 OUR FIT		Error includes scale factor of 1.3.			
• • • We do not use the following data for averages, fits, limits, etc. • • •					
1.64 ±0.04	4200	MESSNER	73	ASPK	$\eta_{+-} = 2.23$

$\Gamma(\pi^0\pi^0)/\Gamma_{\text{total}}$ Γ_9/Γ

Violates CP conservation.

VALUE (units 10^{-3})	DOCUMENT ID		TECN
0.864±0.006 OUR FIT	Error includes scale factor of 1.8.		
0.865±0.012	[1] ALEXOPOU...	04	KTEV

[1] For correlations with other ALEXOPOULOS 04 measurements, see the footnote with their $B(K_L \to \pi e\nu)$ measurement.

$\Gamma(\pi^0\pi^0)/\Gamma(\pi^+\pi^-)$ Γ_9/Γ_8

Violates CP conservation.

VALUE	DOCUMENT ID	
0.4395±0.0023 OUR FIT	Error includes scale factor of 2.0.	
0.4390±0.0012	ETAFIT	16

$\Gamma(\pi^0\pi^0)/\Gamma(3\pi^0)$ Γ_9/Γ_6

Violates CP conservation.

VALUE (units 10^{-2})	EVTS	DOCUMENT ID		TECN	COMMENT
0.443 ±0.004 OUR FIT		Error includes scale factor of 2.1.			
• • • We use the following data for averages but not for fits. • • •					
0.4446±0.0016±0.0019	100K	[1] ALEXOPOU...	04	KTEV	Not in fit
• • • We do not use the following data for averages, fits, limits, etc. • • •					
0.37 ±0.08	29	BARMIN	70	HLBC	η_{00}=2.02 ± 0.23
0.32 ±0.15	30	BUDAGOV	70	HLBC	η_{00}=1.9 ± 0.5
0.46 ±0.11	57	BANNER	69	OSPK	η_{00}=2.2 ± 0.3

[1] This measurement enters the fit via their separate measurements for the two modes.

Semileptonic modes with photons

$\Gamma(\pi^\pm e^\mp\nu_e\gamma)/\Gamma(\pi^\pm e^\mp\nu_e)$ Γ_{10}/Γ_1

VALUE (units 10^{-2})	EVTS	DOCUMENT ID		TECN	COMMENT
0.935±0.015 OUR AVERAGE		Error includes scale factor of 1.9. See the ideogram below.			
0.924±0.023±0.016	9k	[1] AMBROSINO	08F	KLOE	E^*_γ >30 MeV, $\theta^*_{e\gamma}$ >20°
0.916±0.017	4309	[2] ALEXOPOU...	05	KTEV	E^*_γ >30 MeV, $\theta^*_{e\gamma}$ >20°
$0.964\pm0.008^{+0.011}_{-0.009}$	19K	LAI	05	NA48	E^*_γ >30 MeV, $\theta^*_{e\gamma}$ >20°
$0.908\pm0.008^{+0.013}_{-0.012}$	15k	ALAVI-HARATI	01J	KTEV	$E^*_\gamma \geq 30$ MeV, $\theta^*_{e\gamma} \geq 20°$
$0.934\pm0.036^{+0.055}_{-0.039}$	1384	LEBER	96	NA31	$E^*_\gamma \geq 30$ MeV, $\theta^*_{e\gamma} \geq 20°$

[1] Direct emission contribution measured $\langle X \rangle = -2.3 \pm 1.3 \pm 1.4$.

[2] Also measured cut E^*_γ >10 MeV, $\theta^*_{e\gamma}$ >0° 14221 evts: $\Gamma(\pi^\pm e^\mp\nu_e\gamma)$ / $\Gamma(\pi^\pm e^\mp\nu_e)$ = (4.942 ± 0.062)%.

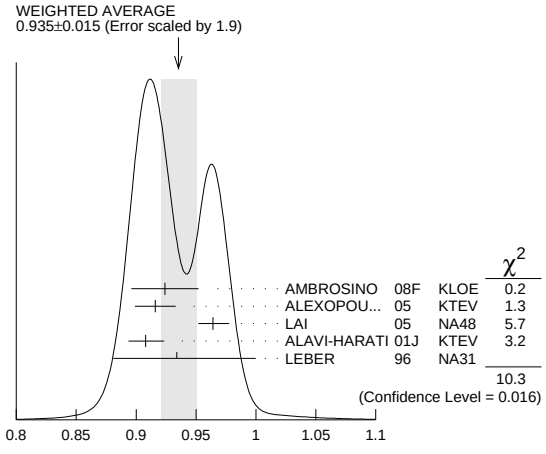

$\Gamma(\pi^\pm\mu^\mp\nu_\mu\gamma)/\Gamma(\pi^\pm\mu^\mp\nu_\mu)$ Γ_{11}/Γ_2

VALUE (units 10^{-3})	EVTS	DOCUMENT ID		TECN	COMMENT
2.09±0.08 OUR AVERAGE					
2.09±0.09		[1] ALEXOPOU...	05	KTEV	E^*_γ > 30 MeV
$2.08\pm0.17^{+0.16}_{-0.21}$	252	BENDER	98	NA48	$E^*_\gamma \geq 30$ MeV

[1] Also measured cut E^*_γ >10 MeV, 1385 evts: $\Gamma(\pi^\pm\mu^\mp\nu_\mu\gamma)$ / $\Gamma(\pi^\pm\mu^\mp\nu_\mu)$ = (0.530 ± 0.014 ± 0.012)%.

Hadronic modes with photons or $\ell\bar{\ell}$ pairs

$\Gamma(\pi^0\pi^0\gamma)/\Gamma_{\text{total}}$ Γ_{12}/Γ

VALUE (units 10^{-6})	CL%	DOCUMENT ID		TECN	COMMENT
< 0.243	90	ABOUZAID	08B	KTEV	$K^0_L \to \pi^0\pi^0_D\gamma, \pi^0_D \to ee\gamma$
• • • We do not use the following data for averages, fits, limits, etc. • • •					
< 5.6	90	BARR	94	NA31	
<230	90	ROBERTS	94	E799	

$\Gamma(\pi^+\pi^-\gamma)/\Gamma(\pi^+\pi^-\pi^0)$ Γ_{13}/Γ_7

For earlier limits see our 1992 edition Physical Review **D45** S1 (1992).

VALUE (units 10^{-4})	EVTS	DOCUMENT ID		TECN	COMMENT
• • • We do not use the following data for averages, fits, limits, etc. • • •					
1.23±0.13	516	[1,2] CARROLL	80B	SPEC	E^*_γ > 20 MeV
2.33±0.23	546	[1,3] CARROLL	80B	SPEC	
3.56±0.26	1062	[1,4] CARROLL	80B	SPEC	E^*_γ > 20 MeV

[1] CARROLL 80B quotes $B(\pi^+\pi^-\gamma)$ using normalization $B(\pi^+\pi^-\pi^0) = 0.1239$. We divide by this value to obtain their measured $\Gamma(\pi^+\pi^-\gamma)$ / $\Gamma(\pi^+\pi^-\pi^0)$.

[2] Internal Bremsstrahlung component only.

[3] Direct γ emission component only.

[4] Both IB and DE components.

$\Gamma(\pi^+\pi^-\gamma)/\Gamma(\pi^+\pi^-)$ Γ_{13}/Γ_8

VALUE (units 10^{-2})	EVTS	DOCUMENT ID		TECN	COMMENT
2.11±0.08 OUR FIT		Error includes scale factor of 2.9.			
2.11±0.08 OUR AVERAGE		Error includes scale factor of 2.9.			
2.08±0.02±0.02	8669	[1] ALAVI-HARATI	01B	KTEV	E^*_γ > 20 MeV
2.30±0.07	3136	RAMBERG	93	E731	E^*_γ > 20 MeV

[1] ALAVI-HARATI 01B includes both Direct Emission (DE) and Inner Bremsstrahlung (IB) processes.

$\Gamma(\pi^+\pi^-\gamma(\text{DE}))/\Gamma(\pi^+\pi^-\gamma)$ Γ_{14}/Γ_{13}

These values assume that $\Gamma(K^0_L \to \pi^+\pi^-\gamma) = \Gamma(K^0_L \to \pi^+\pi^-\gamma(\text{DE})) + \Gamma(K^0_L \to \pi^+\pi^-\gamma(\text{IB}))$, the sum of widths for the direct emission (DE) and inner bremsstrahlung (IE) processes, with no IB-DE interference. DE assumes a form factor as described in RAMBERG 93.

VALUE	EVTS	DOCUMENT ID		TECN	COMMENT
0.684±0.009 OUR FIT					
0.684±0.009 OUR AVERAGE					
0.689±0.021	111k	ABOUZAID	06A	KTEV	E^*_γ > 20 MeV
0.683±0.011	8669	ALAVI-HARATI	01B	KTEV	E^*_γ > 20 MeV
0.685±0.041	3136	RAMBERG	93	E731	E^*_γ > 20 MeV

$\Gamma(\pi^0 2\gamma)/\Gamma_{\text{total}}$ Γ_{15}/Γ

VALUE (units 10^{-6})	CL%	EVTS	DOCUMENT ID		TECN	COMMENT
1.273±0.033 OUR AVERAGE						
1.28 ±0.06 ±0.01		1.4k	[1] ABOUZAID	08	KTEV	
1.27 ±0.04 ±0.01		2.5k	[2] LAI	02B	NA48	
• • • We do not use the following data for averages, fits, limits, etc. • • •						
1.68 ±0.07 ±0.08		884	[3] ALAVI-HARATI	99B	KTEV	
1.7 ±0.2 ±0.2		63	[4] BARR	92	NA31	
1.86 ±0.60 ±0.60		60	PAPADIMITR...	91	E731	$m_{\gamma\gamma} > 280$ MeV
<5.1	90		PAPADIMITR...	91	E731	$m_{\gamma\gamma} < 264$ MeV
2.1 ±0.6		14	[5] BARR	90C	NA31	$m_{\gamma\gamma} > 280$ MeV

[1] ABOUZAID 08 reports $(1.29 \pm 0.03 \pm 0.05) \times 10^{-6}$ from a measurement of $[\Gamma(K^0_L \to \pi^0 2\gamma)/\Gamma_{\text{total}}] / [B(K^0_L \to \pi^0\pi^0)]$ assuming $B(K^0_L \to \pi^0\pi^0) = (8.69 \pm 0.04) \times 10^{-4}$, which we rescale to our best value $B(K^0_L \to \pi^0\pi^0) = (8.64 \pm 0.06) \times 10^{-4}$. Our first error is their experiment's error and our second error is the systematic error from using our best value.

[2] LAI 02B reports $[\Gamma(K^0_L \to \pi^0 2\gamma)/\Gamma_{\text{total}}] / [B(K^0_L \to \pi^0\pi^0)] = (1.467 \pm 0.032 \pm 0.032) \times 10^{-3}$ which we multiply by our best value $B(K^0_L \to \pi^0\pi^0) = (8.64 \pm 0.06) \times 10^{-4}$. Our first error is their experiment's error and our second error is the systematic error from using our best value. They also find that $B(\pi^0 2\gamma, m_{\gamma\gamma} < 110 \text{ MeV}) < 0.6 \times 10^{-8}$(90% CL).

[3] ALAVI-HARATI 99B finds that $\Gamma(\pi^0 2\gamma, m_{\gamma\gamma} < 240 \text{ MeV}))$ / $\Gamma(\pi^0 2\gamma) = (17.3 \pm 1.3 \pm 1.5)$%. Superseded by ABOUZAID 08.

[4] BARR 92 find that $\Gamma(\pi^0 2\gamma, m_{\gamma\gamma} < 240 \text{ MeV})/\Gamma(\pi^0 2\gamma) < 0.09$ (90% CL).

[5] BARR 90C superseded by BARR 92.

$\Gamma(\pi^0\gamma e^+ e^-)/\Gamma_{\text{total}}$ Γ_{16}/Γ

VALUE (units 10^{-8})	CL%	EVTS	DOCUMENT ID		TECN
1.62±0.14±0.09		125	[1] ABOUZAID	07D	KTEV
• • • We do not use the following data for averages, fits, limits, etc. • • •					
2.34±0.35±0.13		44	ALAVI-HARATI	01E	KTEV
<71	90	0	MURAKAMI	99	SPEC

[1] ABOUZAID 07D includes 1997 (ALAVI-HARATI 01E) and 1999 data. It measures the ratio of $B(K^0_L \to \pi^0\gamma e^+ e^-)$ / $B(K^0_L \to \pi^0\pi^0_D)$, where π^0_D is the Dalitz decaying π^0, and uses PDG 06 values $B(K^0_L \to \pi^0\pi^0) = (8.69 \pm 0.04) \times 10^{-4}$, and $B(\pi^0_D \to e^+ e^-\gamma) = (1.198 \pm 0.032) \times 10^{-2}$. Supersedes ALAVI-HARATI 01E result.

Other modes with photons or $\ell\bar{\ell}$ pairs

$\Gamma(2\gamma)/\Gamma_{\text{total}}$ Γ_{17}/Γ

VALUE (units 10^{-4})	EVTS	DOCUMENT ID		TECN	COMMENT
5.47±0.04 OUR FIT	Error includes scale factor of 1.1.				
• • • We do not use the following data for averages, fits, limits, etc. • • •					
4.54±0.84		[1] BANNER	72B	OSPK	
4.5 ±1.0	23	ENSTROM	71	OSPK	K_L^0 1.5–9 GeV/c
5.0 ±1.0		[2] REPELLIN	71	OSPK	
5.5 ±1.1	90	KUNZ	68	OSPK	Norm.to 3 π(C+N)

[1] This value uses $(\eta_{00}/\eta_{+-})^2 = 1.05 \pm 0.14$. In general, $\Gamma(2\gamma)/\Gamma_{\text{total}} = [(4.32 \pm 0.55) \times 10^{-4}][(\eta_{00}/\eta_{+-})^2]$.

[2] Assumes regeneration amplitude in copper at 2 GeV is 22 mb. To evaluate for a given regeneration amplitude and error, multiply by (regeneration amplitude/22mb)^2.

$\Gamma(2\gamma)/\Gamma(3\pi^0)$ Γ_{17}/Γ_6

VALUE (units 10^{-3})	EVTS	DOCUMENT ID		TECN	COMMENT
2.802±0.017 OUR FIT					
2.802±0.018 OUR AVERAGE					
2.79 ±0.02 ±0.02	27k	ADINOLFI	03	KLOE	
2.81 ±0.01 ±0.02		LAI	03	NA48	
• • • We do not use the following data for averages, fits, limits, etc. • • •					
2.13 ±0.43	28	BARMIN	71	HLBC	
2.24 ±0.28	115	BANNER	69	OSPK	
2.5 ±0.7	16	ARNOLD	68B	HLBC	Vacuum decay

$\Gamma(2\gamma)/\Gamma(\pi^0\pi^0)$ Γ_{17}/Γ_9

VALUE	EVTS	DOCUMENT ID		TECN
0.633±0.006 OUR FIT	Error includes scale factor of 1.4.			
0.632±0.004±0.008	110k	BURKHARDT	87	NA31

$\Gamma(3\gamma)/\Gamma_{\text{total}}$ Γ_{18}/Γ

VALUE	CL%	DOCUMENT ID		TECN
$<7.4 \times 10^{-8}$	90	[1] TUNG	11	K391
• • • We do not use the following data for averages, fits, limits, etc. • • •				
$<2.4 \times 10^{-7}$	90	[2] BARR	95C	NA31

[1] TUNG 11 reports the result assuming parity violating interaction and using 2005 data (Run-II and III). Assuming parity conserving or phase space interaction, the 90% upper limits obtained are 7.5×10^{-8} and 8.6×10^{-8}, respectively.

[2] Assumes a phase-space decay distribution.

$\Gamma(e^+e^-\gamma)/\Gamma_{\text{total}}$ Γ_{19}/Γ

VALUE (units 10^{-6})	EVTS	DOCUMENT ID		TECN
9.4±0.4 OUR FIT	Error includes scale factor of 2.0.			
10.0±0.5 OUR AVERAGE	Error includes scale factor of 1.5. See the ideogram below.			
10.6±0.2±0.4	6864	[1] FANTI	99B	NA48
9.2±0.5±0.5	1053	BARR	90B	NA31
$9.1 \pm 0.4^{+0.6}_{-0.5}$	919	OHL	90B	B845

[1] For FANTI 99B, the ±0.4 systematic error includes for uncertainties in the calculation, primarily uncertainties in the $\pi^0 \to e^+e^-\gamma$ and $K_L^0 \to \pi^0\pi^0$ branching ratios, evaluated using our 1999 Web edition values.

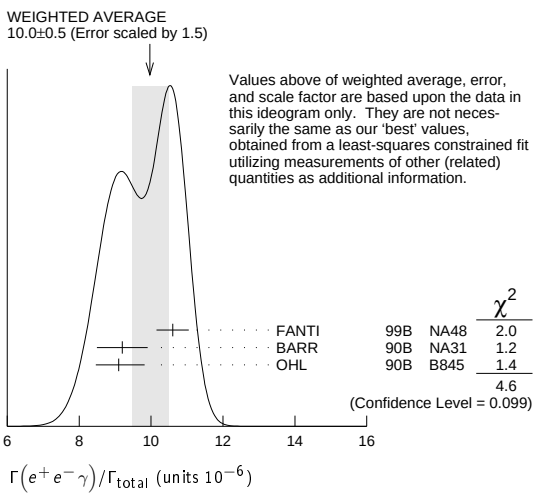

$\Gamma(e^+e^-\gamma)/\Gamma(3\pi^0)$ Γ_{19}/Γ_6

VALUE (units 10^{-5})	EVTS	DOCUMENT ID		TECN
4.82±0.21 OUR FIT	Error includes scale factor of 2.0.			
4.63±0.04±0.13	83k	[1] ABOUZAID	07B	KTEV

[1] ABOUZAID 07B reports $[\Gamma(K_L^0 \to e^+e^-\gamma)/\Gamma(K_L^0 \to 3\pi^0)] / [3\Gamma(\pi^0 \to 2\gamma)/\Gamma_{\text{total}} \times \Gamma(\pi^0 \to e^+e^-\gamma)/\Gamma_{\text{total}}] = (1.3302 \pm 0.0046 \pm 0.0103) \times 10^{-3}$ which we multiply by our best value $3\Gamma(\pi^0 \to 2\gamma)/\Gamma_{\text{total}} \times \Gamma(\pi^0 \to e^+e^-\gamma)/\Gamma_{\text{total}} = 0.0348 \pm 0.0010$. Our first error is their experiment's error and our second error is the systematic error from using our best value.

$\Gamma(\mu^+\mu^-\gamma)/\Gamma_{\text{total}}$ Γ_{20}/Γ

VALUE (units 10^{-7})	EVTS	DOCUMENT ID		TECN
3.59±0.11 OUR AVERAGE	Error includes scale factor of 1.3.			
3.62±0.04±0.08	9100	ALAVI-HARATI	01G	KTEV
3.4 ±0.6 ±0.4	45	FANTI	97	NA48
3.23±0.23±0.19	197	SPENCER	95	E799

$\Gamma(e^+e^-\gamma\gamma)/\Gamma_{\text{total}}$ Γ_{21}/Γ

VALUE (units 10^{-7})	EVTS	DOCUMENT ID		TECN	COMMENT
5.95±0.33 OUR AVERAGE					
5.84±0.15±0.32	1543	ALAVI-HARATI	01F	KTEV	$E^*_\gamma > 5$ MeV
$8.0 \pm 1.5 \ ^{+1.4}_{-1.2}$	40	SETZU	98	NA31	$E^*_\gamma > 5$ MeV
6.5 ±1.2 ±0.6	58	NAKAYA	94	E799	$E^*_\gamma > 5$ MeV
6.6 ±3.2		MORSE	92	B845	$E^*_\gamma > 5$ MeV

$\Gamma(\mu^+\mu^-\gamma\gamma)/\Gamma_{\text{total}}$ Γ_{22}/Γ

VALUE (units 10^{-9})	EVTS	DOCUMENT ID		TECN	COMMENT
$\mathbf{10.4^{+7.5}_{-5.9} \pm 0.7}$	4	ALAVI-HARATI	00E	KTEV	$m_{\gamma\gamma} \geq 1$ MeV/c^2

Charge conjugation × Parity (CP) or Lepton Family number (LF) violating modes, or $\Delta S = 1$ weak neutral current ($S1$) modes

$\Gamma(\mu^+\mu^-)/\Gamma(\pi^+\pi^-)$ Γ_{23}/Γ_8

Test for $\Delta S = 1$ weak neutral current. Allowed by higher-order electroweak interaction.

VALUE (units 10^{-6})	EVTS	DOCUMENT ID		TECN	COMMENT
3.48 ±0.05 OUR AVERAGE					
3.474±0.057	6210	AMBROSE	00	B871	
3.87 ±0.30	179	[1] AKAGI	95	SPEC	
3.38 ±0.17	707	HEINSON	95	B791	
• • • We do not use the following data for averages, fits, limits, etc. • • •					
3.9 ±0.3 ±0.1	178	[2] AKAGI	91B	SPEC	In AKAGI 95
3.45 ±0.18 ±0.13	368	[3] HEINSON	91	SPEC	In HEINSON 95
4.1 ±0.5	54	INAGAKI	89	SPEC	In AKAGI 91B
2.8 ±0.3 ±0.2	87	MATHIAZHA...	89B	SPEC	In HEINSON 91

[1] AKAGI 95 gives this number multiplied by the PDG 1992 average for $\Gamma(K_L^0 \to \pi^+\pi^-)/\Gamma(\text{total})$.

[2] AKAGI 91B give this number multiplied by the 1990 PDG average for $\Gamma(K_L^0 \to \pi^+\pi^-)/\Gamma(\text{total})$.

[3] HEINSON 91 give $\Gamma(K_L^0 \to \mu\mu)/\Gamma_{\text{total}}$. We divide out the $\Gamma(K_L^0 \to \pi^+\pi^-)/\Gamma_{\text{total}}$ PDG average which they used.

$\Gamma(e^+e^-)/\Gamma_{\text{total}}$ Γ_{24}/Γ

Test for $\Delta S = 1$ weak neutral current. Allowed by higher-order electroweak interaction.

VALUE (units 10^{-10})	CL%	EVTS	DOCUMENT ID		TECN
$\mathbf{0.087^{+0.057}_{-0.041}}$		4	AMBROSE	98	B871
• • • We do not use the following data for averages, fits, limits, etc. • • •					
<1.6	90	1	AKAGI	95	SPEC
<0.41	90	0	[1] ARISAKA	93B	B791

[1] ARISAKA 93B includes all events with <6 MeV radiated energy.

$\Gamma(\pi^+\pi^-e^+e^-)/\Gamma_{\text{total}}$ Γ_{25}/Γ

Test for $\Delta S = 1$ weak neutral current. Allowed by higher-order electroweak interaction.

VALUE (units 10^{-7})	CL%	EVTS	DOCUMENT ID		TECN	COMMENT
3.11±0.19 OUR AVERAGE						
3.08±0.09±0.18		1125	[1] LAI	03C	NA48	
3.2 ±0.6 ±0.4		37	ADAMS	98	KTEV	
4.4 ±1.3 ±0.5		13	TAKEUCHI	98	SPEC	
• • • We do not use the following data for averages, fits, limits, etc. • • •						
<4.6	90		NOMURA	97	SPEC	$m_{ee} > 4$ MeV

[1] LAI 03C second error is 0.15(syst)±0.10(norm) combined in quadrature. The normalization uses BR($K_L \to \pi^+\pi^-\pi^0$) * BR($\pi^0 \to e^+e^-$) = $(1.505 \pm 0.047) \times 10^{-3}$ from our 2000 Edition.

$\Gamma(\pi^0\pi^0e^+e^-)/\Gamma_{\text{total}}$ Γ_{26}/Γ

Test for $\Delta S = 1$ weak neutral current. Allowed by higher-order electroweak interaction.

VALUE (units 10^{-9})	CL%	EVTS	DOCUMENT ID		TECN
<6.6	90	1	ALAVI-HARATI	02C	E799

$\Gamma(\pi^0\pi^0\mu^+\mu^-)/\Gamma_{\text{total}}$ Γ_{27}/Γ

Test for $\Delta S = 1$ weak neutral current. Allowed by higher-order electroweak interaction.

VALUE	CL%	DOCUMENT ID		TECN
$<9.2 \times 10^{-11}$	90	[1] ABOUZAID	11A	E799

[1] ABOUZAID 11A also reports $B(K_L^0 \to \pi^0\pi^0X^0 \to \pi^0\pi^0\mu^+\mu^-) < 1.0 \times 10^{-10}$ at 90% C.L., where the X^0 is a possible new neutral boson that was reported by PARK 05 with a mass of 214.3 ± 0.5 MeV/c^2.

Meson Particle Listings

K_L^0

$\Gamma(\mu^+\mu^-e^+e^-)/\Gamma_{total}$ Γ_{28}/Γ

Test for $\Delta S = 1$ weak neutral current. Allowed by higher-order electroweak interaction.

VALUE (units 10^{-9})	CL%	EVTS	DOCUMENT ID		TECN	COMMENT
2.69±0.27 OUR AVERAGE						
2.69±0.24±0.12		131	[1] ALAVI-HARATI	03B	KTEV	
$2.9\ ^{+6.7}_{-2.4}$		1	GU	96	E799	
• • • We do not use the following data for averages, fits, limits, etc. • • •						
2.62±0.40±0.17		43	ALAVI-HARATI	01H	KTEV	Sup. by ALAVI-HARATI 03B
<4900	90		BALATS	83	SPEC	

[1] ALAVI-HARATI 03B also measures the linear slope $\alpha = -1.59 \pm 0.37$.

$\Gamma(e^+e^-e^+e^-)/\Gamma_{total}$ Γ_{29}/Γ

Test for $\Delta S = 1$ weak neutral current. Allowed by higher-order electroweak interaction.

VALUE (units 10^{-8})	EVTS	DOCUMENT ID		TECN	COMMENT
3.56±0.21 OUR AVERAGE					
3.30±0.24±0.25	200	[1] LAI	05B	NA48	
3.72±0.18±0.23	441	ALAVI-HARATI	01D	KTEV	
3.96±0.78±0.32	27	GU	94	E799	
3.07±1.25±0.26	6	VAGINS	93	B845	
• • • We do not use the following data for averages, fits, limits, etc. • • •					
6 ±2 ±1	18	[2] AKAGI	95	SPEC	m_{ee} >470 MeV
7 ±3 ±2	6	[2] AKAGI	95	SPEC	m_{ee} >470 MeV
10.4 ±3.7 ±1.1	8	[3] BARR	95	NA31	
6 ±2 ±1	18	AKAGI	93	CNTR	Sup. by AKAGI 95
4 ±3	2	BARR	91	NA31	Sup. by BARR 95

[1] LAI 05B uses 1998 and 1999 data. Data are normalized to the observed events of $K_L^0 \to \pi^+\pi^-\pi^0$ (π^0 into Dalitz pair) and PDG 04 values are used for $B(K_L^0 \to \pi^+\pi^-\pi^0)$ and $B(\pi^0 \to e^+e^-\gamma)$. The systematic error includes a normalization error of ±0.10.
[2] Values are for the total branching fraction, acceptance-corrected for the m_{ee} cuts shown.
[3] Distribution of angles between two e^+e^- pair planes favors CP=−1 for K_L^0.

$\Gamma(\pi^0\mu^+\mu^-)/\Gamma_{total}$ Γ_{30}/Γ

Violates CP in leading order. Test for $\Delta S = 1$ weak neutral current. Allowed by higher-order electroweak interaction.

VALUE (units 10^{-9})	CL%	EVTS	DOCUMENT ID		TECN
<0.38	90		ALAVI-HARATI	00D	KTEV
• • • We do not use the following data for averages, fits, limits, etc. • • •					
<5.1	90	0	HARRIS	93	E799

$\Gamma(\pi^0e^+e^-)/\Gamma_{total}$ Γ_{31}/Γ

Violates CP in leading order. Direct and indirect CP-violating contributions are expected to be comparable and to dominate the CP-conserving part. LAI 02B result suggests that CP-violation effects dominate. Test for $\Delta S = 1$ weak neutral current. Allowed by higher-order electroweak interaction.

VALUE (units 10^{-10})	CL%	EVTS	DOCUMENT ID		TECN	COMMENT
< 2.8	90		[1] ALAVI-HARATI	04A	KTEV	combined result
• • • We do not use the following data for averages, fits, limits, etc. • • •						
< 3.5	90		ALAVI-HARATI	04A	KTEV	
$0.0047\ ^{+0.0022}_{-0.0018}$			[2] LAI	02B	NA48	CP-conserving part
< 5.1	90	2	ALAVI-HARATI	01	KTEV	
0.01 to 0.02			ALAVI-HARATI	99B	KTEV	CP-conserving part
< 43	90	0	HARRIS	93B	E799	
< 75	90	0	BARKER	90	E731	
< 55	90	0	OHL	90	B845	
< 400	90		BARR	88	NA31	
<3200	90		JASTRZEM...	88	SPEC	

[1] Combined result of ALAVI-HARATI 04A 1999-2000 data set and ALAVI-HARATI 01 1997 data set.
[2] LAI 02B uses the absence of a signal in $K_L^0 \to \pi^0\gamma\gamma$ with $m(\gamma\gamma)<m(\pi^0)$ and their a_V value to predict this value.

$\Gamma(\pi^0\nu\overline{\nu})/\Gamma_{total}$ Γ_{32}/Γ

Violates CP in leading order. Test of direct CP violation since the indirect CP-violating and CP-conserving contributions are expected to be suppressed. Test of $\Delta S = 1$ weak neutral current.

VALUE (units 10^{-8})	CL%	EVTS	DOCUMENT ID		TECN
< 2.6	90		[1] AHN	10	K391
• • • We do not use the following data for averages, fits, limits, etc. • • •					
< 5.1	90	1	[2] AHN	17	KOTO
< 6.7	90		[3] AHN	08	K391
<21	90		[4] AHN	06	K391
<59	90		ALAVI-HARATI	00	KTEV
$< 1.6 \times 10^2$	90		ADAMS	99	KTEV
$< 5.8 \times 10^3$	90		WEAVER	94	E799
$< 2.2 \times 10^4$	90		GRAHAM	92	CNTR

[1] Obtained combining Run-2 (AHN 08) and Run-3 data.
[2] AHN 17 result is based on the first 100 hours of physics running in 2013. One candidate event was observed with an expected background of 0.34 ± 0.16 events. An upper limit of $< 3.7 \times 10^{-8}$ at the 90% C.L. for the $K_L \to \pi^0 X^0$ decay was also set, where X^0 is an invisible particle with a mass of 135 MeV/c^2.
[3] Value obtained using data from February to April 2005.
[4] Value obtained analyzing 10% of data of RUN 1 (performed in 2004).

$\Gamma(\pi^0\pi^0\nu\overline{\nu})/\Gamma_{total}$ Γ_{33}/Γ

VALUE	CL%	DOCUMENT ID		TECN
<8.1 × 10⁻⁷	90	[1] OGATA	11	K391
• • • We do not use the following data for averages, fits, limits, etc. • • •				
$<4.7 \times 10^{-5}$	90	[2] NIX	07	K391

[1] Using 2005 Run-I data. OGATA 11 also sets a limit on the $K_L^0 \to \pi^0\pi^0X \to$ invisible particles process: the limit on the branching fraction varied from 7.0×10^{-7} to 4.0×10^{-5} for the mass of X ranging from 50 to 200 MeV/c^2.
[2] Observed 1 event with expected background of 0.43 ± 0.35 events. NIX 07 also measured $B(K_L^0 \to \pi^0\pi^0P) < 1.2\times10^{-6}$ at 90% CL, where P is the pseudoscalar particle and $m_P < 100$ MeV.

$\Gamma(e^\pm\mu^\mp)/\Gamma_{total}$ Γ_{34}/Γ

Test of lepton family number conservation.

VALUE (units 10^{-11})	CL%	EVTS	DOCUMENT ID		TECN
<0.47	90		AMBROSE	98B	B871
• • • We do not use the following data for averages, fits, limits, etc. • • •					
<9.4	90	0	AKAGI	95	SPEC
<3.9	90	0	ARISAKA	93	B791
<3.3	90	0	[1] ARISAKA	93	B791

[1] This is the combined result of ARISAKA 93 and MATHIAZHAGAN 89.

$\Gamma(e^\pm e^\pm\mu^\mp\mu^\mp)/\Gamma_{total}$ Γ_{35}/Γ

Test of lepton family number conservation.

VALUE (units 10^{-11})	CL%	EVTS	DOCUMENT ID		TECN	COMMENT
< 4.12	90	0	ALAVI-HARATI	03B	KTEV	
• • • We do not use the following data for averages, fits, limits, etc. • • •						
< 12.3	90	0	[1] ALAVI-HARATI	01H	KTEV	Sup. by ALAVI-HARATI 03B
<610	90	0	[1] GU	96	E799	

[1] Assuming uniform phase space distribution.

$\Gamma(\pi^0\mu^\pm e^\mp)/\Gamma_{total}$ Γ_{36}/Γ

Test of lepton family number conservation.

VALUE (units 10^{-10})	CL%	DOCUMENT ID		TECN
< 0.76	90	ABOUZAID	08C	KTEV
• • • We do not use the following data for averages, fits, limits, etc. • • •				
<62	90	ARISAKA	98	E799

$\Gamma(\pi^0\pi^0\mu^\pm e^\mp)/\Gamma_{total}$ Γ_{37}/Γ

Test of lepton family number conservation.

VALUE (units 10^{-10})	CL%	DOCUMENT ID		TECN
<1.7	90	ABOUZAID	08C	KTEV

See the related review(s):
V_{ud}, V_{us} the Cabibbo Angle, and CKM Unitarity

ENERGY DEPENDENCE OF K_L^0 DALITZ PLOT

For discussion, see note on Dalitz plot parameters in the $K^\pm$ section of the Particle Listings above. For definitions of a_V, a_t, a_u, and a_y, see the earlier version of the same note in the 1982 edition of this *Review* published in Physics Letters **111B** 70 (1982).

$$|\text{matrix element}|^2 = 1 + gu + hu^2 + jv + kv^2 + fuv$$
where $u = (s_3 - s_0)\ /\ m_\pi^2$ and $v = (s_2 - s_1)\ /\ m_\pi^2$

LINEAR COEFFICIENT g FOR $K_L^0 \to \pi^+\pi^-\pi^0$

VALUE	EVTS	DOCUMENT ID		TECN	COMMENT
0.678 ±0.008 OUR AVERAGE Error includes scale factor of 1.5. See the ideogram below.					
0.6823±0.0044±0.0044	500k	ANGELOPO...	98C	CPLR	
0.681 ±0.024	6499	CHO	77	HBC	
0.620 ±0.023	4709	PEACH	77	HBC	
0.677 ±0.010	509k	MESSNER	74	ASPK	$a_y = -0.917 \pm 0.013$
• • • We do not use the following data for averages, fits, limits, etc. • • •					
0.69 ±0.07	192	[1] BALDO-...	75	HLBC	
0.590 ±0.022	56k	[1] BUCHANAN	75	SPEC	$a_u = -0.277 \pm 0.010$
0.619 ±0.027	20k	[1,2] BISI	74	ASPK	$a_t = -0.282 \pm 0.011$
0.612 ±0.032		[1] ALEXANDER	73B	HBC	
0.73 ±0.04	3200	[1] BRANDENB...	73	HBC	
0.608 ±0.043	1486	[1] KRENZ	72	HLBC	$a_t = -0.277 \pm 0.018$
0.650 ±0.012	29k	[1] ALBROW	70	ASPK	$a_y = -0.858 \pm 0.015$
0.593 ±0.022	36k	[1,3] BUCHANAN	70	SPEC	$a_u = -0.278 \pm 0.010$
0.664 ±0.056	4400	[1] SMITH	70	OSPK	$a_t = -0.306 \pm 0.024$
0.400 ±0.045	2446	[1] BASILE	68B	OSPK	$a_t = -0.188 \pm 0.020$
0.649 ±0.044	1350	[1] HOPKINS	67	HBC	$a_t = -0.294 \pm 0.018$
0.428 ±0.055	1198	[1] NEFKENS	67	OSPK	$a_u = -0.204 \pm 0.025$

[1] Quadratic dependence required by some experiments. (See sections on "QUADRATIC COEFFICIENT h" and "QUADRATIC COEFFICIENT k" below.) Correlations prevent us from averaging results of fits not including g, h, and k terms.
[2] BISI 74 value comes from quadratic fit with quad. term consistent with zero. g error is thus larger than if linear fit were used.

[3] BUCHANAN 70 result revised by BUCHANAN 75 to include radiative correlations and to use more reliable K^0_L momentum spectrum of second experiment (had same beam).

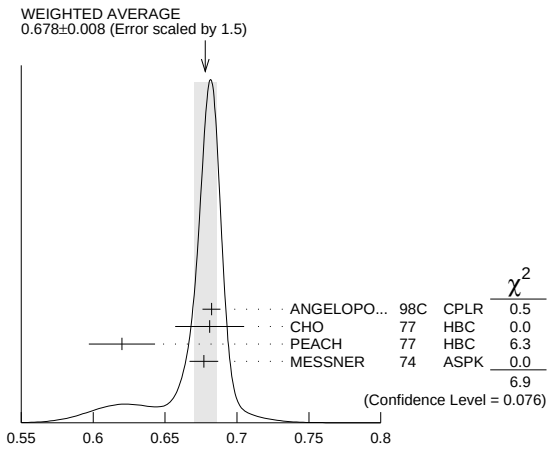

Linear coeff. g for $K^0_L \to \pi^+\pi^-\pi^0$ matrix element squared

QUADRATIC COEFFICIENT h FOR $K^0_L \to \pi^+\pi^-\pi^0$

VALUE	EVTS	DOCUMENT ID		TECN
0.076±0.006 OUR AVERAGE				
0.061±0.004±0.015	500k	ANGELOPO...	98C	CPLR
0.095±0.032	6499	CHO	77	HBC
0.048±0.036	4709	PEACH	77	HBC
0.079±0.007	509k	MESSNER	74	ASPK
• • • We do not use the following data for averages, fits, limits, etc. • • •				
−0.011±0.018	29k	[1] ALBROW	70	ASPK
0.043±0.052	4400	[1] SMITH	70	OSPK

See notes in section "LINEAR COEFFICIENT g FOR $K^0_L \to \pi^+\pi^-\pi^0$ |MATRIX ELEMENT|^2" above.

[1] Quadratic coefficients h and k required by some experiments. (See section on "QUADRATIC COEFFICIENT k" below.) Correlations prevent us from averaging results of fits not including g, h, and k terms.

QUADRATIC COEFFICIENT k FOR $K^0_L \to \pi^+\pi^-\pi^0$

VALUE	EVTS	DOCUMENT ID		TECN
0.0099±0.0015 OUR AVERAGE				
0.0104±0.0017±0.0024	500k	ANGELOPO...	98C	CPLR
0.024 ±0.010	6499	CHO	77	HBC
−0.008 ±0.012	4709	PEACH	77	HBC
0.0097±0.0018	509k	MESSNER	74	ASPK

LINEAR COEFFICIENT j FOR $K^0_L \to \pi^+\pi^-\pi^0$ (CP-VIOLATING TERM)

Listed in CP-violation section below.

QUADRATIC COEFFICIENT f FOR $K^0_L \to \pi^+\pi^-\pi^0$ (CP-VIOLATING TERM)

Listed in CP-violation section below.

QUADRATIC COEFFICIENT h FOR $K^0_L \to \pi^0\pi^0\pi^0$

We do not average measurements that do not account for the effect of final state rescattering.

VALUE (units 10^{-3})	EVTS	DOCUMENT ID		TECN
+0.59±0.20±1.16	68M	[1] ABOUZAID	08A	KTEV
• • • We do not use the following data for averages, fits, limits, etc. • • •				
−6.1 ±0.9 ±0.5	14.7M	[2] LAI	01B	NA48
−3.3 ±1.1 ±0.7	5M	[2,3] SOMALWAR	92	E731

[1] Result obtained using CI3pI model of CABIBBO 05 to include $\pi\pi$ rescattering effects. The systematic error includes an external error of 1.06×10^{-3} from the parametrization input of $(a_0 - a_2)\, m_{\pi^+} = 0.268 \pm 0.017$ from BATLEY 06B.

[2] LAI 01B and SOMALWAR 92 results do not include $\pi\pi$ final state rescattering effects.

[3] SOMALWAR 92 chose m_{π^+} as normalization to make it compatible with the Particle Data Group $K^0_L \to \pi^+\pi^-\pi^0$ definitions.

K^0_L FORM FACTORS

For discussion, see note on form factors in the $K^\pm$ section of the Particle Listings above.

In the form factor comments, the following symbols are used.

f_+ and f_- are form factors for the vector matrix element.

f_S and f_T refer to the scalar and tensor term.

$f_0(t) = f_+(t) + f_-(t)\ t/(m^2_{K^0} - m^2_{\pi^+})$.

t = momentum transfer to the π.

λ_+ and λ_0 are the linear expansion coefficients of f_+ and f_0:

$f_+(t) = f_+(0)\ (1 + \lambda_+\, t\, /m^2_{\pi^+})$

For quadratic expansion

$f_+(t) = f_+(0)\ (1 + \lambda'_+\, t\, /m^2_{\pi^+} + \frac{\lambda''_+}{2}\ t^2/m^4_{\pi^+})$

as used by KTeV. If there is a non-vanishing quadratic term, then λ_+ represents an average slope, which is then different from λ'_+.

NA48 (K_{e3}) and ISTRA quadratic expansion coefficients are converted with

$\lambda'_+{}^{PDG} = \lambda_+{}^{NA48}$ and $\lambda''_+{}^{PDG} = 2\,\lambda'_+{}^{NA48}$

$\lambda'_+{}^{PDG} = (\frac{m_{\pi^+}}{m_{\pi^0}})^2\ \lambda_+{}^{ISTRA}$ and

$\lambda''_+{}^{PDG} = 2\,(\frac{m_{\pi^+}}{m_{\pi^0}})^4\ \lambda'_+{}^{ISTRA}$

ISTRA linear expansion coefficients are converted with

$\lambda_+{}^{PDG} = (\frac{m_{\pi^+}}{m_{\pi^0}})^2\ \lambda_+{}^{ISTRA}$ and $\lambda_0{}^{PDG} = (\frac{m_{\pi^+}}{m_{\pi^0}})^2\ \lambda_0{}^{ISTRA}$

The pole parametrization is

$f_+(t) = f_+(0)\ (\frac{M_V^2}{M_V^2 - t}\ )$

$f_0(t) = f_0(0)\ (\frac{M_S^2}{M_S^2 - t}\ )$

where M_V and M_S are the vector and scalar pole masses.

The dispersive parametrization is

$f_+(t) = f_+(0)\ \exp[\ \frac{t}{m^2_\pi}\ (\Lambda_+ + H(t))\ ]$;

$f_0(t) = f_+(0)\ \exp[\ \frac{t}{m^2_K - m^2_\pi}\ (\ln[C] - G(t))\ ]$,

where Λ_+ is the slope parameter and $\ln[C] = \ln[\ f_0\ (m^2_K - m^2_\pi\ )\ ]$ is the logarithm of the scalar form factor at the Callan-Treiman point.

$H(t)$ and $G(t)$ are dispersive integrals.

The following abbreviations are used:

DP = Dalitz plot analysis.

PI = π spectrum analysis.

MU = μ spectrum analysis.

POL= μ polarization analysis.

BR = $K^0_{\mu 3}/K^0_{e3}$ branching ratio analysis.

E = positron or electron spectrum analysis.

RC = radiative corrections.

λ_+ (LINEAR ENERGY DEPENDENCE OF f_+ IN K^0_{e3} DECAY)

For radiative correction of K^0_{e3} DP, see GINSBERG 67, BECHERRAWY 70, CIRIGLIANO 02, CIRIGLIANO 04, and ANDRE 07. Results labeled OUR FIT are discussed in the review "$K^\pm_{\ell 3}$ and $K^0_{\ell 3}$ Form Factors" in the $K^\pm$ Listings. For earlier, lower statistics results, see the 2004 edition of this review, Physics Letters **B592** 1 (2004).

VALUE (units 10^{-2})	EVTS	DOCUMENT ID		TECN	COMMENT
2.82 ±0.04 OUR FIT	Error includes scale factor of 1.1. Assuming μ-e universality				
2.85 ±0.04 OUR AVERAGE					
2.86 ±0.05 ±0.04	2M	AMBROSINO	06D	KLOE	
2.832±0.037±0.043	1.9M	ALEXOPOU...	04A	KTEV	PI, no $\mu = e$
2.88 ±0.04 ±0.11	5.6M	[1] LAI	04C	NA48	DP
• • • We do not use the following data for averages, fits, limits, etc. • • •					
2.84 ±0.07 ±0.13	5.6M	[2] LAI	04C	NA48	DP
2.45 ±0.12 ±0.22	366k	APOSTOLA...	00	CPLR	DP
3.06 ±0.34	74k	BIRULEV	81	SPEC	DP
3.12 ±0.25	500k	GJESDAL	76	SPEC	DP
2.70 ±0.28	25k	BLUMENTHAL	75	SPEC	DP

[1] Results from linear fit and assuming only vector and axial couplings.

[2] Results from linear fit with $|f_S/f_+|$ and $|f_T/f_+|$ free.

λ_+ (LINEAR ENERGY DEPENDENCE OF f_+ IN $K^0_{\mu 3}$ DECAY)

Results labeled OUR FIT are discussed in the review "$K^\pm_{\ell 3}$ and $K^0_{\ell 3}$ Form Factors" in the $K^\pm$ Listings. For earlier, lower statistics results, see the 2004 edition of this review, Physics Letters **B592** 1 (2004).

VALUE (units 10^{-2})	EVTS	DOCUMENT ID		TECN	COMMENT
2.82 ±0.04 OUR FIT	Error includes scale factor of 1.1. Assuming μ-e universality				
2.71 ±0.10 OUR FIT	Error includes scale factor of 1.4. Not assuming μ-e universality				
2.67 ±0.06 ±0.08	2.3M	[1] LAI	07A	NA48	DP
2.745±0.088±0.063	1.5M	ALEXOPOU...	04A	KTEV	DP, no $\mu = e$
2.813±0.051	3.4M	ALEXOPOU...	04A	KTEV	PI, DP, $\mu = e$
3.0 ±0.3	1.6M	DONALDSON	74B	SPEC	DP
• • • We do not use the following data for averages, fits, limits, etc. • • •					
4.27 ±0.44	150k	BIRULEV	81	SPEC	DP

[1] LAI 07A gives a correlation −0.40 between their λ_0 and λ_+ measurements.

λ_0 (LINEAR ENERGY DEPENDENCE OF f_0 IN $K^0_{\mu 3}$ DECAY)

Wherever possible, we have converted the above values of $\xi(0)$ into values of λ_0 using the associated λ^μ_+ and $d\xi(0)/d\lambda_+$. Results labeled OUR FIT are discussed in the review "$K^\pm_{\ell 3}$ and $K^0_{\ell 3}$ Form Factors" in the $K^\pm$ Listings. For earlier, lower statistics results, see the 2004 edition of this review, Physics Letters **B592** 1 (2004).

VALUE (units 10^{-2})	$d\lambda_0/d\lambda_+$	EVTS	DOCUMENT ID		TECN	COMMENT
1.38 ±0.18 OUR FIT			Error includes scale factor of 2.2. Assuming μ-e universality			
1.42 ±0.23 OUR FIT			Error includes scale factor of 2.8. Not assuming μ-e universality			
1.17 ±0.07 ±0.10		2.3M	[1] LAI	07A	NA48	DP
1.657±0.125	−0.44	1.5M	[2] ALEXOPOU...	04A	KTEV	DP, no $\mu = e$
1.635±0.121	−0.85	3.4M	[3] ALEXOPOU...	04A	KTEV	PI, DP, $\mu = e$
+1.9 ±0.4	−0.47	1.6M	[4] DONALDSON	74B	SPEC	DP
• • • We do not use the following data for averages, fits, limits, etc. • • •						
3.41 ±0.67	unknown	150k	[5] BIRULEV	81	SPEC	DP

[1] LAI 07A gives a correlation −0.40 between their λ_0 and λ_+ measurements.
[2] ALEXOPOULOS 04A gives a correlation −0.38 between their λ_0 and λ_+ measurements.
[3] ALEXOPOULOS 04A gives a correlation −0.36 between their λ_0 and λ_+ measurements.
[4] DONALDSON 74B $d\lambda_0/d\lambda_+$ obtained from figure 18.
[5] BIRULEV 81 gives $d\lambda_0/d\lambda_+ = -1.5$, giving an unreasonably narrow error ellipse which dominates all other results. We use $d\lambda_0/d\lambda_+ = 0$.

λ'_+(LINEAR K^0_{e3} FORM FACTOR FROM QUADRATIC FIT)

VALUE (units 10^{-2})	EVTS	DOCUMENT ID		TECN	COMMENT
2.40 ±0.12 OUR FIT		Error includes scale factor of 1.2. Assuming μ-e universality			
2.49 ±0.13 OUR FIT		Error includes scale factor of 1.1. Not assuming μ-e universality			
2.48 ±0.17 OUR AVERAGE		Error includes scale factor of 1.5. See the ideogram below.			
2.55 ±0.15 ±0.10	2M	[1] AMBROSINO	06D	KLOE	
2.167±0.137±0.143	1.9M	[2] ALEXOPOU...	04A	KTEV	PI, no $\mu = e$
2.80 ±0.19 ±0.15	5.6M	[3] LAI	04C	NA48	DP

[1] We use AMBROSINO 06D result in the fit not assuming $\mu-e$ universality. This result enters the fit assuming $\mu-e$ universality via AMBROSINO 07C measurement of λ'_+ in $K_{\mu3}$ decays. AMBROSINO 06D gives a correlation −0.95 between their λ'_+ and λ''_+.
[2] ALEXOPOULOS 04A gives a correlation −0.97 between their λ'_+ and λ''_+.
[3] For LAI 04C we calculate a correlation −0.88 between their λ'_+ and λ''_+.

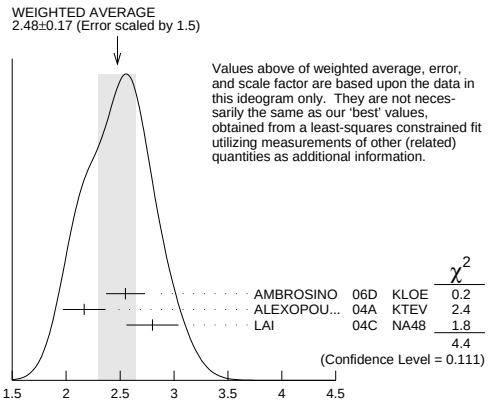

λ'_+(LINEAR K^0_{e3} FORM FACTOR FROM QUADRATIC FIT) (units 10^{-2})

λ''_+(QUADRATIC K^0_{e3} FORM FACTOR)

VALUE (units 10^{-2})	EVTS	DOCUMENT ID		TECN	COMMENT
0.20 ±0.05 OUR FIT		Error includes scale factor of 1.2. Assuming μ-e universality			
0.16 ±0.05 OUR FIT		Error includes scale factor of 1.1. Not assuming μ-e universality			
0.17 ±0.07 OUR AVERAGE		Error includes scale factor of 1.5. See the ideogram below.			
0.14 ±0.07 ±0.04	2M	[1] AMBROSINO	06D	KLOE	
0.287±0.057±0.053	1.9M	[2] ALEXOPOU...	04A	KTEV	PI, no $\mu = e$
0.04 ±0.08 ±0.04	5.6M	[3,4] LAI	04C	NA48	DP

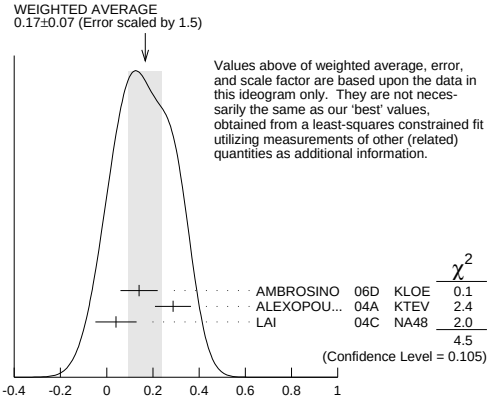

λ''_+(QUADRATIC K^0_{e3} FORM FACTOR) (units 10^{-2})

[1] We use AMBROSINO 06D result in the fit not assuming $\mu-e$ universality. This result enters the fit assuming $\mu-e$ universality via AMBROSINO 07C measurement of λ''_+ in $K_{\mu3}$ decays. AMBROSINO 06D gives a correlation −0.95 between their λ'_+ and λ''_+.
[2] ALEXOPOULOS 04A gives a correlation −0.97 between their λ'_+ and λ''_+.
[3] Values doubled to agree with PDG conventions described above.
[4] LAI 04C gives a correlation −0.88 between their λ'_+ and λ''_+.

λ'_+(LINEAR $K^0_{\mu3}$ FORM FACTOR FROM QUADRATIC FIT)

VALUE (units 10^{-2})	EVTS	DOCUMENT ID		TECN	COMMENT
2.40 ±0.12 OUR FIT		Error includes scale factor of 1.2. Assuming μ-e universality			
1.89 ±0.24 OUR FIT		Not assuming μ-e universality			
2.23 ±0.98 ±0.37	1.8M	[1] AMBROSINO	07C	KLOE	no $\mu = e$
2.56 ±0.15 ±0.09	3.8M	[1] AMBROSINO	07C	KLOE	$\mu = e$
2.05 ±0.22 ±0.24	2.3M	[1] LAI	07A	NA48	DP
1.703±0.319±0.177	1.5M	[1] ALEXOPOU...	04A	KTEV	DP, no $\mu = e$
2.064±0.175	3.4M	[1] ALEXOPOU...	04A	KTEV	PI, DP, $\mu = e$

[1] See section λ_0 below for correlations.

λ''_+(QUADRATIC $K^0_{\mu3}$ FORM FACTOR)

VALUE (units 10^{-2})	EVTS	DOCUMENT ID		TECN	COMMENT
0.20 ±0.05 OUR FIT		Error includes scale factor of 1.2. Assuming μ-e universality			
0.37 ±0.12 OUR FIT		Error includes scale factor of 1.3. Not assuming μ-e universality			
0.48 ±0.49 ±0.16	1.8M	[1] AMBROSINO	07C	KLOE	no $\mu = e$
0.15 ±0.07 ±0.04	3.8M	[1] AMBROSINO	07C	KLOE	$\mu = e$
0.26 ±0.09 ±0.10	2.3M	[1] LAI	07A	NA48	DP
0.443±0.131±0.072	1.5M	[1] ALEXOPOU...	04A	KTEV	DP, no $\mu = e$
0.320±0.069	3.4M	[1] ALEXOPOU...	04A	KTEV	PI, DP, $\mu = e$

[1] See section λ_0 below for correlations.

λ_0(LINEAR f_0 $K^0_{\mu3}$ FORM FACTOR FROM QUADRATIC FIT)

VALUE (units 10^{-2})	EVTS	DOCUMENT ID		TECN	COMMENT
1.16 ±0.09 OUR FIT		Error includes scale factor of 1.2. Assuming μ-e universality			
1.07 ±0.14 OUR FIT		Error includes scale factor of 1.3. Not assuming μ-e universality			
0.91 ±0.59 ±0.26	1.8M	[1] AMBROSINO	07C	KLOE	no $\mu = e$
1.54 ±0.18 ±0.13	3.8M	[2] AMBROSINO	07C	KLOE	$\mu = e$
0.95 ±0.11 ±0.08	2.3M	[3] LAI	07A	NA48	DP
1.281±0.136±0.122	1.5M	[4] ALEXOPOU...	04A	KTEV	DP, no $\mu = e$
1.372±0.131	3.4M	[5] ALEXOPOU...	04A	KTEV	PI, DP, $\mu = e$

[1] AMBROSINO 07C, not assuming μ-e universality, gives a correlation matrix

	λ'_+	λ''_+
λ''_+	−0.97	1
λ_0	0.81	−0.91

[2] AMBROSINO 07C, assuming μ-e universality, gives a correlation matrix

	λ'_+	λ''_+
λ''_+	−0.95	1
λ_0	0.29	−0.38

[3] LAI 07A gives a correlation matrix

	λ'_+	λ''_+
λ''_+	−0.96	1
λ_0	0.63	−0.73

[4] ALEXOPOULOS 04A, not assuming μ-e universality, gives a correlation matrix

	λ'_+	λ''_+	λ_0
λ'_+	1		
λ''_+	−0.96	1	
λ_0	0.65	−0.75	1

[5] ALEXOPOULOS 04A, assuming μ-e universality, gives a correlation matrix

	λ'_+	λ''_+	λ_0
λ'_+	1		
λ''_+	−0.97	1	
λ_0	0.34	−0.44	1

M^e_V (POLE MASS FOR K^0_{e3} DECAY)

VALUE (MeV)	EVTS	DOCUMENT ID		TECN	COMMENT
878 ± 6 OUR FIT		Error includes scale factor of 1.1. Assuming μ-e universality			
875 ± 5 OUR AVERAGE					
870 ± 6 ±7	2M	AMBROSINO	06D	KLOE	
881.03± 5.12±4.94	1.9M	ALEXOPOU...	04A	KTEV	PI, no $\mu = e$
859 ±18	5.6M	LAI	04C	NA48	

M^μ_V (POLE MASS FOR $K^0_{\mu3}$ DECAY)

VALUE (MeV)	EVTS	DOCUMENT ID		TECN	COMMENT
878 ± 6 OUR FIT		Error includes scale factor of 1.1. Assuming μ-e universality			
900 ±21 OUR FIT		Error includes scale factor of 1.7. Not assuming μ-e universality			
905 ± 9 ±17	2.3M	[1] LAI	07A	NA48	DP
889.19±12.81± 9.92	1.5M	[1] ALEXOPOU...	04A	KTEV	DP, no $\mu = e$
882.32± 6.54	3.4M	[1] ALEXOPOU...	04A	KTEV	PI, DP, $\mu = e$

[1] See section M^μ_S below for correlations.

M^{μ}_S (POLE MASS FOR $K^0_{\mu 3}$ DECAY)

VALUE (MeV)			EVTS	DOCUMENT ID		TECN	COMMENT
1252	**±90**	**OUR FIT**		Error includes scale factor of 2.6. Assuming μ-e universality			
1222	**±80**	**OUR FIT**		Error includes scale factor of 2.3. Not assuming μ-e universality			
1400	±46	±53	2.3M	[1] LAI	07A	NA48	DP
1167.14	±28.30	±31.04	1.5M	[2] ALEXOPOU...	04A	KTEV	PI, no $\mu = e$
1173.80	±39.47		3.4M	[3] ALEXOPOU...	04A	KTEV	PI, DP, $\mu = e$

[1] LAI 07A gives a correlation −0.47 between their M^{μ}_S and M^{μ}_V measurements, not assuming μ-e universality.
[2] ALEXOPOULOS 04A gives a correlation −0.46 between their M^{μ}_S and M^{μ}_V and measurements, not assuming μ-e universality.
[3] ALEXOPOULOS 04A gives a correlation −0.40 between their M^{μ}_S and M^{μ}_V and measurements, assuming μ-e universality.

Λ_+ (DISPERSIVE VECTOR FORM FACTOR FOR $K^0_{\mu 3}$ DECAY)

See the review on "$K^{\pm}_{\ell 3}$ and $K^0_{\ell 3}$ Form Factors" for details of the dispersive parametrization.

VALUE (units 10^{-1})			EVTS	DOCUMENT ID		TECN	COMMENT
0.251	**±0.006**	**OUR AVERAGE**		Error includes scale factor of 1.5. See the ideogram below.			
0.2509	±0.0035	±0.0043	3.4M	[1] ABOUZAID	10	KTEV	$\mu = e$
0.257	±0.004	±0.004	3.8M	[2] AMBROSINO	07C	KLOE	$\mu = e$
0.233	±0.005	±0.008	2.3M	[3] LAI	07A	NA48	DP

[1] Obtained from a sample of 1.9 M K_{e3} and 1.5 M $K_{\mu 3}$. The correlation between Λ_+ and ln(C) is −0.269.
[2] AMBROSINO 07C results include 2M K_{e3} events from AMBROSINO 06D. The correlation between Λ_+ and ln(C) is −0.26.
[3] LAI 07A gives a correlation −0.44 between their Λ_+ and ln(C) measurements.

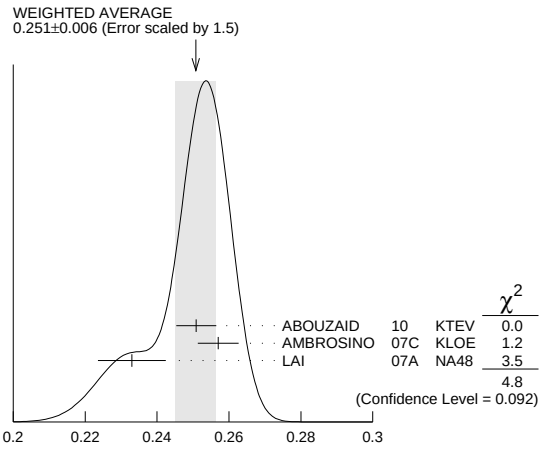

Λ_+ (DISPERSIVE VECTOR FORM FACTOR FOR $K^0_{\mu 3}$ DECAY) (units 10^{-1})

ln(C) (DISPERSIVE SCALAR FORM FACTOR FOR $K^0_{\mu 3}$ DECAY)

See the review on "$K^{\pm}_{\ell 3}$ and $K^0_{\ell 3}$ Form Factors" for details of the dispersive parametrization.

VALUE (units 10^{-1})			EVTS	DOCUMENT ID		TECN	COMMENT
1.75	**±0.18**	**OUR AVERAGE**		Error includes scale factor of 2.0. See the ideogram below.			
1.915	±0.078	±0.094	3.4M	[1] ABOUZAID	10	KTEV	$\mu = e$
2.04	±0.19	±0.15	3.8M	[2] AMBROSINO	07C	KLOE	$\mu = e$
1.438	±0.080	±0.112	2.3M	[3] LAI	07A	NA48	DP

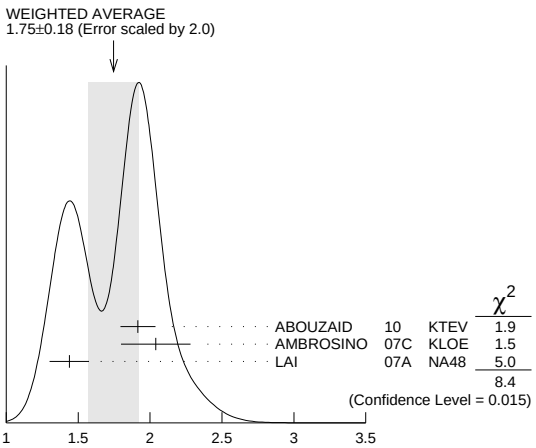

ln(C) (DISPERSIVE SCALAR FORM FACTOR FOR $K^0_{\mu 3}$ DECAY) (units 10^{-1})

[1] Obtained from a sample of 1.9 M K_{e3} and 1.5 M $K_{\mu 3}$. The correlation between Λ_+ and ln(C) is −0.269.
[2] AMBROSINO 07C results include 2M K_{e3} events from AMBROSINO 06D. We convert (Λ_+, Λ_0) to (Λ_+, ln(C)) parametrization using ln$(C) = (\Lambda_0 \cdot 11.713 + 0.0398) \pm 0.0041$, where the error is due to theory parametrization of the form factor. The correlation between Λ_+ and ln(C) is −0.26.
[3] LAI 07A gives a correlation −0.44 between their Λ_+ and ln(C) measurements.

$a_1(t_0, Q^2)$ FORM FACTOR PARAMETER

See HILL 06 for a definition of this parameter.

VALUE	EVTS	DOCUMENT ID		TECN
1.023±0.028±0.029	2M	[1] ABOUZAID	06C	KTEV

[1] Q^2= 2 GeV^2, $t_0 = 0.49\,(m_K - m_\pi)^2$. Correlation between a_1 and a_2: $\rho_{12} = -0.064$.

$a_2(t_0, Q^2)$ FORM FACTOR PARAMETER

See HILL 06 for a definition of this parameter.

VALUE	EVTS	DOCUMENT ID		TECN
0.75±1.58±1.47	2M	[1] ABOUZAID	06C	KTEV

[1] Q^2= 2 GeV^2, $t_0 = 0.49\,(m_K - m_\pi)^2$. Correlation between a_1 and a_2: $\rho_{12} = -0.064$.

$|f_S/f_+|$ FOR K^0_{e3} DECAY

Ratio of scalar to f_+ couplings.

VALUE (units 10^{-2})	CL%	EVTS	DOCUMENT ID		TECN	COMMENT
$\mathbf{1.5^{+0.7}_{-1.0}\pm1.2}$		5.6M	[1] LAI	04C	NA48	
• • • We do not use the following data for averages, fits, limits, etc. • • •						
<9.5	95	18k	HILL	78	STRC	
<7.	68	48k	BIRULEV	76	SPEC	See also BIRULEV 81
<4.	68	25k	BLUMENTHAL	75	SPEC	

[1] Results from linear fit with $|f_S/f_+|$ and $|f_T/f_+|$ free.

$|f_T/f_+|$ FOR K^0_{e3} DECAY

Ratio of tensor to f_+ couplings.

VALUE (units 10^{-2})	CL%	EVTS	DOCUMENT ID		TECN	COMMENT
$\mathbf{5^{+3}_{-4}\pm3}$		5.6M	[1] LAI	04C	NA48	
• • • We do not use the following data for averages, fits, limits, etc. • • •						
<40.	95	18k	HILL	78	STRC	
<34.	68	48k	BIRULEV	76	SPEC	See also BIRULEV 81
<23.	68	25k	BLUMENTHAL	75	SPEC	

[1] Results from linear fit with $|f_S/f_+|$ and $|f_T/f_+|$ free.

$|f_T/f_+|$ FOR $K^0_{\mu 3}$ DECAY

Ratio of tensor to f_+ couplings.

VALUE (units 10^{-2})	DOCUMENT ID		TECN
12.±12.	BIRULEV	81	SPEC

α_{K^*} DECAY FORM FACTOR FOR $K_L \to \ell^+\ell^-\gamma$, $K^0_L \to \ell^+\ell^-\ell'^+\ell'^-$

Average of all α_{K^*} measurements (from each of three datablocks following this one) assuming lepton universality.

VALUE	DOCUMENT ID
−0.205±0.022 OUR AVERAGE	Includes data from the 3 datablocks that follow this one. Error includes scale factor of 1.8. See the ideogram below.

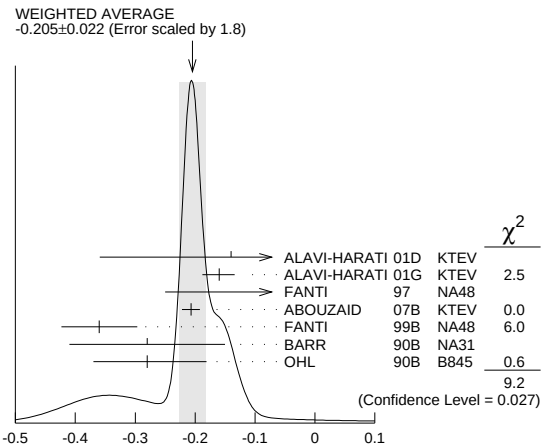

α_{K^*} DECAY FORM FACTOR FOR $K_L \to \ell^+\ell^-\gamma$, $K^0_L \to \ell^+\ell^-\ell'^+\ell'^-$

α_{K^*} DECAY FORM FACTOR FOR $K_L \to e^+e^-\gamma$

α_{K^*} is the constant in the model of BERGSTROM 83 which measures the relative strength of the vector-vector transition $K_L \to K^*\gamma$ with $K^* \to \rho, \omega, \phi \to \gamma^*$ and the pseudoscalar-pseudoscalar transition $K_L \to \pi, \eta, \eta' \to \gamma\gamma^*$.

Meson Particle Listings

K_L^0

VALUE	EVTS	DOCUMENT ID		TECN
The data in this block is included in the average printed for a previous datablock.				
−0.217±0.034 OUR AVERAGE	Error includes scale factor of 2.4.			
−0.207±0.012±0.009	83k	[1] ABOUZAID	07B	KTEV
−0.36 ±0.06 ±0.02	6864	FANTI	99B	NA48
−0.28 ±0.13		BARR	90B	NA31
$-0.280^{+0.099}_{-0.090}$		OHL	90B	B845

[1] ABOUZAID 07B measures $C\cdot\alpha_{K^*} = -0.517 \pm 0.030 \pm 0.022$. We assume $C = 2.5$, as in all other measurements.

α_{K^*} DECAY FORM FACTOR FOR $K_L \to \mu^+\mu^-\gamma$

α_{K^*} is the constant in the model of BERGSTROM 83 described in the previous section.

VALUE	EVTS	DOCUMENT ID		TECN
The data in this block is included in the average printed for a previous datablock.				
−0.158±0.027 OUR AVERAGE				
$-0.160^{+0.026}_{-0.028}$	9100	ALAVI-HARATI	01G	KTEV
$-0.04\ ^{+0.24}_{-0.21}$		FANTI	97	NA48

$\alpha_{K^*}^{\rm eff}$ DECAY FORM FACTOR FOR $K_L \to e^+e^-e^+e^-$

$\alpha_{K^*}^{\rm eff}$ is the parameter describing the relative strength of an intermediate pseudoscalar decay amplitude and a vector meson decay amplitude in the model of BERGSTROM 83. It takes into account both the radiative effects and the form factor. Since there are two e^+e^- pairs here compared with one in $e^+e^-\gamma$ decays, a factorized expression is used for the $e^+e^-e^+e^-$ decay form factor.

VALUE	EVTS	DOCUMENT ID		TECN
The data in this block is included in the average printed for a previous datablock.				
−0.14±0.16±0.15	441	ALAVI-HARATI	01D	KTEV

α_{DIP} DECAY FORM FACTOR FOR $K_L^0 \to \ell^+\ell^-\gamma$, $K_L^0 \to \ell^+\ell^-\ell'^+\ell'^-$

Average of all α_{DIP} measurements (from each of three datablocks following this one) assuming lepton universality.

VALUE	DOCUMENT ID
−1.69±0.08 OUR AVERAGE	Includes data from the 3 datablocks that follow this one. Error includes scale factor of 1.7.

α_{DIP} DECAY FORM FACTOR FOR $K_L^0 \to e^+e^-\gamma$

α_{DIP} parameter in $K_L^0 \to \gamma^*\gamma^*$ form factor by DAMBROSIO 98, motivated by vector meson dominance and a proper short distance behavior.

VALUE	EVTS	DOCUMENT ID		TECN
The data in this block is included in the average printed for a previous datablock.				
−1.729±0.043±0.028	83k	ABOUZAID	07B	KTEV

α_{DIP} DECAY FORM FACTOR FOR $K_L^0 \to \mu^+\mu^-\gamma$

α_{DIP} is a constant in the model of DAMBROSIO 98 described in the previous section.

VALUE	EVTS	DOCUMENT ID		TECN
The data in this block is included in the average printed for a previous datablock.				
−1.54±0.10	9100	ALAVI-HARATI	01G	KTEV

α_{DIP} DECAY FORM FACTOR FOR $K_L^0 \to e^+e^-\mu^+\mu^-$

α_{DIP} is a constant in the model of DAMBROSIO 98 described in the previous section.

VALUE	EVTS	DOCUMENT ID		TECN
The data in this block is included in the average printed for a previous datablock.				
−1.59±0.37	131	ALAVI-HARATI	03B	KTEV

a_1/a_2 FORM FACTOR FOR M1 DIRECT EMISSION AMPLITUDE

Form factor $= \tilde{g}_{M1}\left[1+\frac{a_1/a_2}{(M_\rho^2-M_K^2)+2M_K E_\gamma^*}\right]$ as described in ALAVI-HARATI 00B.

VALUE (GeV^2)	EVTS	DOCUMENT ID		TECN	COMMENT
−0.737±0.014 OUR AVERAGE					
−0.744±0.027±0.032	5241	[1] ABOUZAID	06	KTEV	$\pi^+\pi^-e^+e^-$
−0.738±0.007±0.018	111k	[2] ABOUZAID	06A	KTEV	$\pi^+\pi^+\gamma$
$-0.81\ ^{+0.07}_{-0.13}$ ±0.02		[3] LAI	03C	NA48	$\pi^+\pi^-e^+e^-$
−0.737±0.026±0.022		[4] ALAVI-HARATI	01B		$\pi^+\pi^-\gamma$
−0.720±0.028±0.009	1766	[5] ALAVI-HARATI	00B	KTEV	$\pi^+\pi^-e^+e^-$

[1] ABOUZAID 06 also measured $|\tilde{g}_{M1}| = 1.11 \pm 0.14$.
[2] ABOUZAID 06A also measured $|\tilde{g}_{M1}| = 1.198 \pm 0.035 \pm 0.086$.
[3] LAI 03C also measured $\tilde{g}_{M1} = 0.99^{+0.28}_{-0.27} \pm 0.07$.
[4] ALAVI-HARATI 01B fit gives χ^2/DOF = 38.8/27. Linear and quadratic fits give χ^2/DOF = 43.2/27 and 37.6/26 respectively.
[5] ALAVI-HARATI 00B also measured $|\tilde{g}_{M1}| = 1.35^{+0.20}_{-0.17} \pm 0.04$.

$\overline{f}_S$ DECAY FORM FACTOR FOR $K_L^0 \to \pi^\pm\pi^0 e^\mp\nu_e$

VALUE	DOCUMENT ID		TECN
0.049±0.011 OUR AVERAGE	Error includes scale factor of 1.7.		
0.052±0.006±0.002	BATLEY	04	NA48
0.010±0.016±0.017	MAKOFF	93	E731

$\overline{f}_P$ DECAY FORM FACTOR FOR $K_L^0 \to \pi^\pm\pi^0 e^\mp\nu_e$

VALUE	DOCUMENT ID		TECN
−0.052±0.012 OUR AVERAGE			
−0.051±0.011±0.005	BATLEY	04	NA48
−0.079±0.049±0.022	MAKOFF	93	E731

λ_g DECAY FORM FACTOR FOR $K_L^0 \to \pi^\pm\pi^0 e^\mp\nu_e$

VALUE	DOCUMENT ID		TECN
0.085±0.020 OUR AVERAGE			
0.087±0.019±0.006	BATLEY	04	NA48
0.014±0.087±0.070	MAKOFF	93	E731

$\overline{h}$ DECAY FORM FACTOR FOR $K_L^0 \to \pi^\pm\pi^0 e^\mp\nu_e$

VALUE	DOCUMENT ID		TECN
−0.30±0.13 OUR AVERAGE			
−0.32±0.12±0.07	BATLEY	04	NA48
−0.07±0.31±0.31	MAKOFF	93	E731

L_3 CHIRAL PERT. THEO. PARAM. FOR $K_L^0 \to \pi^\pm\pi^0 e^\mp\nu_e$

VALUE (units 10^{-3})	DOCUMENT ID		TECN
−3.96±0.28 OUR AVERAGE	Error includes scale factor of 1.6.		
−4.1 ±0.2	BATLEY	04	NA48
−3.4 ±0.4	[1] MAKOFF	93	E731

[1] MAKOFF 93 sign has been changed to negative to agree with the sign convention used in BATLEY 04.

a_V, VECTOR MESON EXCHANGE CONTRIBUTION

VALUE	EVTS	DOCUMENT ID		TECN	COMMENT
−0.43±0.06 OUR AVERAGE		Error includes scale factor of 1.5.			
−0.31±0.05±0.07	1.4k	[1] ABOUZAID	08	KTEV	
−0.46±0.03±0.04		LAI	02B	NA48	$K_L^0 \to \pi^0 2\gamma$
−0.67±0.21±0.12		ALAVI-HARATI	01E	KTEV	$K_L^0 \to \pi^0 e^+ e^-\gamma$
• • • We do not use the following data for averages, fits, limits, etc. • • •					
−0.72±0.05±0.06		[2] ALAVI-HARATI	99B	KTEV	$K_L^0 \to \pi^0 2\gamma$

[1] Using KTeV dataset collected in 1996, 1997, and 1999.
[2] Superseded by ABOUZAID 08.

See the related review(s):
CP Violation in K_L^0 Decays

CP-VIOLATION PARAMETERS IN K_L^0 DECAYS

CHARGE ASYMMETRY IN $K_{\ell 3}^0$ DECAYS

Such asymmetry violates *CP*. It is related to Re(ϵ).

A_L = weighted average of $A_L(\mu)$ and $A_L(e)$

In previous editions and in the literature the symbol used for this asymmetry was δ_L or δ. We use A_L for consistency with B^0 asymmetry notation and with recent K_S^0 notation.

VALUE (%)	EVTS	DOCUMENT ID		TECN	COMMENT
0.332±0.006 OUR AVERAGE		Includes data from the 2 datablocks that follow this one.			
0.333±0.050	33M	WILLIAMS	73	ASPK	$K_{\mu 3}+K_{e3}$

$A_L(\mu) = [\Gamma(\pi^-\mu^+\nu_\mu) - \Gamma(\pi^+\mu^-\overline{\nu}_\mu)]$/SUM

Only the combined value below is put into the Meson Summary Table.

VALUE (%)	EVTS	DOCUMENT ID		TECN
The data in this block is included in the average printed for a previous datablock.				
0.304±0.025 OUR AVERAGE				
0.313±0.029	15M	GEWENIGER	74	ASPK
0.278±0.051	7.7M	PICCIONI	72	ASPK
• • • We do not use the following data for averages, fits, limits, etc. • • •				
0.60 ±0.14	4.1M	MCCARTHY	73	CNTR
0.57 ±0.17	1M	[1] PACIOTTI	69	OSPK
0.403±0.134	1M	[1] DORFAN	67	OSPK

[1] PACIOTTI 69 is a reanalysis of DORFAN 67 and is corrected for $\mu^+\mu^-$ range difference in MCCARTHY 72.

$A_L(e) = [\Gamma(\pi^-e^+\nu_e) - \Gamma(\pi^+e^-\overline{\nu}_e)]$/SUM

Only the combined value below is put into the Meson Summary Table.

VALUE (%)	EVTS	DOCUMENT ID		TECN
The data in this block is included in the average printed for a previous datablock.				
0.334 ±0.007 OUR AVERAGE				
0.3322±0.0058±0.0047	298M	ALAVI-HARATI	02	
0.341 ±0.018	34M	GEWENIGER	74	ASPK
0.318 ±0.038	40M	FITCH	73	ASPK
0.346 ±0.033	10M	MARX	70	CNTR
• • • We do not use the following data for averages, fits, limits, etc. • • •				
0.36 ±0.18	600k	ASHFORD	72	ASPK
0.246 ±0.059	10M	[1] SAAL	69	CNTR
0.224 ±0.036	10M	[1] BENNETT	67	CNTR

[1] SAAL 69 is a reanalysis of BENNETT 67.

PARAMETERS FOR $K_L^0 \to 2\pi$ DECAY

$\eta_{+-} = A(K_L^0 \to \pi^+\pi^-) / A(K_S^0 \to \pi^+\pi^-)$
$\eta_{00} = A(K_L^0 \to \pi^0\pi^0) / A(K_S^0 \to \pi^0\pi^0)$

The fitted values of $|\eta_{+-}|$ and $|\eta_{00}|$ given below are the results of a fit to $|\eta_{+-}|$, $|\eta_{00}|$, $|\eta_{00}/\eta_{+-}|$, and Re(ϵ'/ϵ). Independent information on $|\eta_{+-}|$ and $|\eta_{00}|$ can be obtained from the fitted values of the $K^0_L \to \pi\pi$ and $K^0_S \to \pi\pi$ branching ratios and the K^0_L and K^0_S lifetimes. This information is included as data in the $|\eta_{+-}|$ and $|\eta_{00}|$ sections with a Document ID "BRFIT." See the note "*CP* violation in K_L decays" above for details.

$|\eta_{00}| = |A(K^0_L \to 2\pi^0) / A(K^0_S \to 2\pi^0)|$

VALUE (units 10^{-3})		DOCUMENT ID		TECN	COMMENT
2.220±0.011 OUR FIT	Error includes scale factor of 1.8.				
2.243±0.014		BRFIT	16		
• • • We do not use the following data for averages, fits, limits, etc. • • •					
2.47 ±0.31 ±0.24		ANGELOPO...	98	CPLR	
2.49 ±0.40		[1] ADLER	96B	CPLR	Sup. by ANGELOPOULOS 98
2.33 ±0.18		CHRISTENS...	79	ASPK	
2.71 ±0.37		[2] WOLFF	71	OSPK	Cu reg., 4γ's
2.95 ±0.63		[2] CHOLLET	70	OSPK	Cu reg., 4γ's

[1] Error is statistical only.

[2] CHOLLET 70 gives $|\eta_{00}| = (1.23 \pm 0.24)\times$(regeneration amplitude, 2 GeV/c Cu)/10000mb. WOLFF 71 gives $|\eta_{00}| = (1.13 \pm 0.12)\times$(regeneration amplitude, 2 GeV/c Cu)/10000mb. We compute both $|\eta_{00}|$ values for (regeneration amplitude, 2 GeV/c Cu) = 24 ± 2mb. This regeneration amplitude results from averaging over FAISSNER 69, extrapolated using optical-model calculations of Bohm et al., Physics Letters **27B** 594 (1968) and the data of BALATS 71. (From H. Faissner, private communication).

$|\eta_{+-}| = |A(K^0_L \to \pi^+\pi^-) / A(K^0_S \to \pi^+\pi^-)|$

VALUE (units 10^{-3})	EVTS	DOCUMENT ID		TECN	COMMENT
2.232±0.011 OUR FIT		Error includes scale factor of 1.8.			
2.226±0.007		BRFIT	16		
• • • We do not use the following data for averages, fits, limits, etc. • • •					
2.223±0.012		[1] LAI	07	NA48	
2.219±0.013		[2] AMBROSINO	06F	KLOE	
2.228±0.010		[3] ALEXOPOU...	04	KTEV	
2.286±0.023±0.026	70M	[4] APOSTOLA...	99C	CPLR	K^0-$\overline{K}^0$ asymmetry
2.310±0.043±0.031		[5] ADLER	95B	CPLR	K^0-$\overline{K}^0$ asymmetry
2.32 ±0.14 ±0.03	10^5	ADLER	92B	CPLR	K^0-$\overline{K}^0$ asymmetry
2.30 ±0.035		GEWENIGER	74B	ASPK	

[1] Value obtained from the NA48 measurements of $\Gamma(K^0_L \to \pi^+\pi^-)/\Gamma(K^0_L \to \pi e \nu_e)$ and $\tau_{K^0_S}$ and KLOE measurements of $B(K^0_S \to \pi^+\pi^-)$ and $\tau_{K^0_L}$. $\Gamma(K^0_L \to \pi^+\pi^-)$ is defined to include the inner bremsstrahlung component $\Gamma(K^0_L \to \pi^+\pi^-\gamma(IB))$ but exclude the direct emission component $B(K^0_S \to \pi^+\pi^-(DE))$. Their $|\eta_{+-}|$ value is not directly used in our fit, but enters the fit via their branching ratio and lifetime measurements.

[2] AMBROSINO 06F uses KLOE branching ratios and τ_L together with τ_S from PDG 04. Their $|\eta_{+-}|$ value is not directly used in our fit, but enters the fit via their branching ratio and lifetime measurements.

[3] ALEXOPOULOS 04 $|\eta_{+-}|$ uses their $K^0_L \to \pi\pi$ branching fractions, $\tau_S = (0.8963 \pm 0.0005)\times 10^{-10}$ s from the average of KTeV and NA48 τ_S measurements, and assumes that $\Gamma(K^0_S \to \pi\ell\nu_\ell) = \Gamma(K^0_L \to \pi\ell\nu_\ell)$ giving $B(K^0_S \to \pi\ell\nu_\ell) = 0.118\%$. Their η_{+-} is not directly used in our fit, but enters our fit via their branching ratio measurements.

[4] APOSTOLAKIS 99C report $(2.264 \pm 0.023 \pm 0.026 + 9.1[\tau_S - 0.8934]) \times 10^{-3}$. We evaluate for our 2006 best value $\tau_S = (0.8958 \pm 0.0005) \times 10^{-10}$ s.

[5] ADLER 95B report $(2.312 \pm 0.043 \pm 0.030 - 1[\Delta m - 0.5274] + 9.1[\tau_S - 0.8926]) \times 10^{-3}$. We evaluate for our 1996 best values $\Delta m = (0.5304 \pm 0.0014) \times 10^{-10}\ \hbar s^{-1}$ and $\tau_S = (0.8927 \pm 0.0009) \times 10^{-10}$ s. Superseded by APOSTOLAKIS 99C.

$|\epsilon| = (2|\eta_{+-}| + |\eta_{00}|)/3$

This expression is a very good approximation, good to about one part in 10^{-4} because of the small measured value of $\phi_{00} - \phi_{+-}$ and small theoretical ambiguities.

VALUE (units 10^{-3})	DOCUMENT ID	
2.228±0.011 OUR FIT	Error includes scale factor of 1.8.	

$|\eta_{00}/\eta_{+-}|$

VALUE	EVTS	DOCUMENT ID		TECN
0.9950±0.0007 OUR FIT		Error includes scale factor of 1.6.		
0.9930±0.0020 OUR AVERAGE				
0.9931±0.0020		[1,2] BARR	93D	NA31
0.9904±0.0084±0.0036		[3] WOODS	88	E731
• • • We do not use the following data for averages, fits, limits, etc. • • •				
0.9939±0.0013±0.0015	1M	[1] BARR	93D	NA31
0.9899±0.0020±0.0025		[1] BURKHARDT	88	NA31

[1] This is the square root of the ratio R given by BURKHARDT 88 and BARR 93D.

[2] This is the combined results from BARR 93D and BURKHARDT 88, taking into account a common systematic uncertainty of 0.0014.

[3] We calculate $|\eta_{00}/\eta_{+-}| = 1 - 3(\epsilon'/\epsilon)$ from WOODS 88 (ϵ'/ϵ) value.

$\mathrm{Re}(\epsilon'/\epsilon) = (1 - |\eta_{00}/\eta_{+-}|)/3$

We have neglected terms of order $\omega \cdot \mathrm{Re}(\epsilon'/\epsilon)$, where $\omega = \mathrm{Re}(A_2)/\mathrm{Re}(A_0) \simeq 1/22$. If included, this correction would lower Re(ϵ'/ϵ) by about 0.04×10^{-3}. See SOZZI 04.

VALUE (units 10^{-3})		DOCUMENT ID		TECN	COMMENT
1.66 ±0.23	**OUR FIT**	Error includes scale factor of 1.6.			
1.68 ±0.20	**OUR AVERAGE**	Error includes scale factor of 1.4. See the ideogram below.			
1.92 ±0.21		[1] ABOUZAID	11	KTEV	Assuming *CPT*
1.47 ±0.22		BATLEY	02	NA48	
0.74 ±0.52 ±0.29		GIBBONS	93B	E731	
• • • We use the following data for averages but not for fits. • • •					
2.3 ±0.65		[2,3] BARR	93D	NA31	
• • • We do not use the following data for averages, fits, limits, etc. • • •					
2.110±0.343		[1,4] ABOUZAID	11	KTEV	Not assuming *CPT*
2.07 ±0.28		ALAVI-HARATI	03	KTEV	In ABOUZAID 11
1.53 ±0.26		LAI	01C	NA48	Incl. in BATLEY 02
2.80 ±0.30 ±0.28		ALAVI-HARATI	99D	KTEV	In ALAVI-HARATI 03
1.85 ±0.45 ±0.58		FANTI	99C	NA48	In LAI 01C
2.0 ±0.7		[5] BARR	93D	NA31	
−0.4 ±1.4 ±0.6		PATTERSON	90	E731	in GIBBONS 93B
3.3 ±1.1		[5] BURKHARDT	88	NA31	
3.2 ±2.8 ±1.2		[2] WOODS	88	E731	

[1] The two ABOUZAID 11 values use the same data. The fits are performed with and without *CPT* invariance requirement.

[2] These values are derived from $|\eta_{00}/\eta_{+-}|$ measurements. They enter the average in this section but enter the fit via the $|\eta_{00}/\eta_{+-}|$ only.

[3] This is the combined results from BARR 93D and BURKHARDT 88, taking into account their common systematic uncertainty.

[4] We use ABOUZAID 11 Re(ϵ'/ϵ) value with *CPT* assumption in our fits for $|\eta_{+-}|$, $|\eta_{00}|$, and Re(ϵ'/ϵ).

[5] These values are derived from $|\eta_{00}/\eta_{+-}|$ measurements.

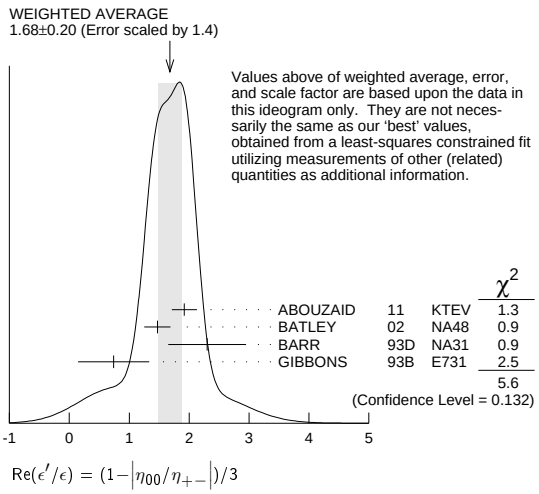

$\mathrm{Re}(\epsilon'/\epsilon) = (1 - |\eta_{00}/\eta_{+-}|)/3$

ϕ_{+-}, PHASE of η_{+-}

The dependence of the phase on Δm and τ_S is given for each experiment in the comments below, where Δm is the $K^0_L - K^0_S$ mass difference in units $10^{10}\ \hbar s^{-1}$ and τ_S is the K_S mean life in units 10^{-10} s. We also give the regeneration phase ϕ_f in the comments below.

OUR FIT is described in the note on "*CP* violation in K_L decays" in the K^0_L Particle Listings. Most experiments in this section are included in both the "Not Assuming *CPT*" and "Assuming *CPT*" fits. In the latter fit, they have little direct influence on ϕ_{+-} because their errors are large compared to that assuming *CPT*, but they influence Δm and τ_S through their dependencies on these parameters, which are given in the footnotes.

VALUE (°)	EVTS	DOCUMENT ID		TECN	COMMENT
43.51±0.05 OUR FIT		Error includes scale factor of 1.2. Assuming *CPT*			
43.4 ±0.5 OUR FIT		Error includes scale factor of 1.2. Not assuming *CPT*			
42.9 ±0.6 ±0.3	70M	[1] APOSTOLA...	99C	CPLR	K^0-$\overline{K}^0$ asymmetry
42.9 ±0.8 ±0.2		[2,3] SCHWINGEN...	95	E773	$CH_{1.1}$ regenerator
41.4 ±0.9 ±0.2		[3,4] GIBBONS	93	E731	B_4C regenerator
44.5 ±1.6 ±0.6		[5] CAROSI	90	NA31	Vacuum regen.
43.3 ±1.0 ±0.5		[6] GEWENIGER	74B	ASPK	Vacuum regen.
• • • We do not use the following data for averages, fits, limits, etc. • • •					
43.76±0.64		[7] ABOUZAID	11	KTEV	Not assuming *CPT*
44.12±0.72±1.20		[8] ALAVI-HARATI	03	KTEV	Not assuming *CPT*
42.5 ±0.4 ±0.3		[9,10] ADLER	96C	RVUE	
43.4 ±1.1 ±0.3		[11] ADLER	95B	CPLR	K^0-$\overline{K}^0$ asymmetry
42.3 ±4.4 ±1.4	100k	[12] ADLER	92B	CPLR	K^0-$\overline{K}^0$ asymmetry
47.7 ±2.0 ±0.9		[3,13] KARLSSON	90	E731	
44.3 ±2.8 ±0.2		[14] CARITHERS	75	SPEC	C regenerator

[1] APOSTOLAKIS 99C measures $\phi_{+-} = (43.19 \pm 0.53 \pm 0.28) + 300\ [\Delta m - 0.5301]$ (°). We have adjusted the measurement to use our best values of $(\Delta m = 0.5293 \pm 0.0009)$ $(10^{10}\ \hbar\ s^{-1})$. Our first error is their experiment's error and our second error is the systematic error from using our best values.

[2] SCHWINGENHEUER 95 measures $\phi_{+-} = (43.53 \pm 0.76) + 173\,[\Delta m - 0.5282] - 275\,[\tau_S - 0.8926]$ (°). We have adjusted the measurement to use our best values of ($\Delta m = 0.5293 \pm 0.0009$) ($10^{10}\ \hbar\ s^{-1}$), ($\tau_S = 0.8954 \pm 0.0004$) ($10^{-10}$ s). Our first error is their experiment's error and our second error is the systematic error from using our best values.

[3] These experiments measure ϕ_{+-}-ϕ_f and calculate the regeneration phase from the power law momentum dependence of the regeneration amplitude using analyticity and dispersion relations. SCHWINGENHEUER 95 [GIBBONS 93] includes a systematic error of 0.35° [0.5°] for uncertainties in their modeling of the regeneration amplitude.

[4] GIBBONS 93 measures $\phi_{+-} = (42.21 \pm 0.9) + 189\,[\Delta m - 0.5257] - 460\,[\tau_S - 0.8922]$ (°). We have adjusted the measurement to use our best values of ($\Delta m = 0.5293 \pm 0.0009$) ($10^{10}\ \hbar\ s^{-1}$), ($\tau_S = 0.8954 \pm 0.0004$) ($10^{-10}$ s). Our first error is their experiment's error and our second error is the systematic error from using our best values. This is actually reported in SCHWINGENHEUER 95, footnote 8. GIBBONS 93 reports ϕ_{+-} (42.2 ± 1.4)°. They measure ϕ_{+}-ϕ_f and calculate the regeneration phase ϕ_f from the power law momentum dependence of the regeneration amplitude using analyticity. An error of 0.6° is included for possible uncertainties in the regeneration phase.

[5] CAROSI 90 measures $\phi_{+-} = (46.9 \pm 1.4 \pm 0.7) + 579\,[\Delta m - 0.5351] + 303\,[\tau_S - 0.8922]$ (°). We have adjusted the measurement to use our best values of ($\Delta m = 0.5293 \pm 0.0009$) ($10^{10}\ \hbar\ s^{-1}$), ($\tau_S = 0.8954 \pm 0.0004$) ($10^{-10}$ s). Our first error is their experiment's error and our second error is the systematic error from using our best values.

[6] GEWENIGER 74B measures $\phi_{+-} = (49.4 \pm 1.0) + 565\,[\Delta m - 0.540]$ (°). We have adjusted the measurement to use our best values of ($\Delta m = 0.5293 \pm 0.0009$) ($10^{10}\ \hbar\ s^{-1}$). Our first error is their experiment's error and our second error is the systematic error from using our best values.

[7] Not independent of other phase parameters reported in ABOUZAID 11.

[8] ALAVI-HARATI 03 ϕ_{+-} is correlated with their $\Delta m = m_{K_L^0} - m_{K_S^0}$ and τ_{K_S} measurements in the K_L^0 and K_S^0 sections respectively. The correlation coefficients are $\rho(\phi_{+-},\Delta m) = +0.955$, $\rho(\phi_{+-},\tau_S) = -0.871$, and $\rho(\tau_S,\Delta m) = -0.840$. *CPT* is not assumed. Uses scintillator Pb regenerator. Superseded by ABOUZAID 11.

[9] ADLER 96C measures $\phi_{+-} = (43.82 \pm 0.41) + 339\,[\Delta m - 0.5307] - 252\,[\tau_S - 0.8922]$ (°). We have adjusted the measurement to use our best values of ($\Delta m = 0.5293 \pm 0.0009$) ($10^{10}\ \hbar\ s^{-1}$), ($\tau_S = 0.8954 \pm 0.0004$) ($10^{-10}$ s). Our first error is their experiment's error and our second error is the systematic error from using our best values.

[10] ADLER 96C is the result of a fit which includes nearly the same data as entered into the "OUR FIT" value in the 1996 edition of this Review (Physical Review **D54** 1 (1996)).

[11] ADLER 95B measures $\phi_{+-} = (42.7 \pm 0.9 \pm 0.6) + 316\,[\Delta m - 0.5274] + 30\,[\tau_S - 0.8926]$ (°). We have adjusted the measurement to use our best values of ($\Delta m = 0.5293 \pm 0.0009$) ($10^{10}\ \hbar\ s^{-1}$), ($\tau_S = 0.8954 \pm 0.0004$) ($10^{-10}$ s). Our first error is their experiment's error and our second error is the systematic error from using our best values.

[12] ADLER 92B quote separately two systematic errors: ±0.4 from their experiment and ±1.0 degrees due to the uncertainty in the value of Δm.

[13] KARLSSON 90 systematic error does not include regeneration phase uncertainty.

[14] CARITHERS 75 measures $\phi_{+-} = (45.5 \pm 2.8) + 224\,[\Delta m - 0.5348]$ (°). We have adjusted the measurement to use our best values of ($\Delta m = 0.5293 \pm 0.0009$) ($10^{10}\ \hbar\ s^{-1}$). Our first error is their experiment's error and our second error is the systematic error from using our best values. $\phi_f = -40.9 \pm 2.6$°.

ϕ_{00}, PHASE OF η_{00}

See comment in ϕ_{+-} header above for treatment of Δm and τ_S dependence, as well as for the inclusion of data in both the "Assuming *CPT*" and "Not Assuming *CPT*" fits.

OUR FIT is described in the note on "*CP* violation in K_L decays" in the K_L^0 Particle Listings.

VALUE (°)	DOCUMENT ID		TECN	COMMENT
43.52±0.05 OUR FIT	Error includes scale factor of 1.3. Assuming *CPT*			
43.7 ±0.6 OUR FIT	Error includes scale factor of 1.2. Not assuming *CPT*			
44.5 ±2.3 ±0.5	[1] CAROSI	90	NA31	
• • • We do not use the following data for averages, fits, limits, etc. • • •				
44.06±0.68	[2] ABOUZAID	11	KTEV	Not assuming *CPT*
41.7 ±5.9 ±0.2	[3] ANGELOPO...	98	CPLR	
50.8 ±7.1 ±1.7	[4] ADLER	96B	CPLR	Sup. by ANGELOPOULOS 98
47.4 ±1.4 ±0.9	[5] KARLSSON	90	E731	

[1] CAROSI 90 measures $\phi_{00} = (47.1 \pm 2.1 \pm 1.0) + 579\,[\Delta m - 0.5351] + 252\,[\tau_S - 0.8922]$ (°). We have adjusted the measurement to use our best values of ($\Delta m = 0.5293 \pm 0.0009$) ($10^{10}\ \hbar\ s^{-1}$), ($\tau_S = 0.8954 \pm 0.0004$) ($10^{-10}$ s). Our first error is their experiment's error and our second error is the systematic error from using our best values.

[2] Not independent of other phase parameters reported in ABOUZAID 11.

[3] ANGELOPOULOS 98 measures $\phi_{00} = (42.0 \pm 5.6 \pm 1.9) + 240\,[\Delta m - 0.5307]$ (°). We have adjusted the measurement to use our best values of ($\Delta m = 0.5293 \pm 0.0009$) ($10^{10}\ \hbar\ s^{-1}$). Our first error is their experiment's error and our second error is the systematic error from using our best values. The τ_S dependence is negligible.

[4] ADLER 96B identified initial neutral kaon individually as being a K^0 or a $\overline{K}^0$. The systematic uncertainty is ±1.5° combined in quadrature with ±0.8° due to Δm.

[5] KARLSSON 90 systematic error does not include regeneration phase uncertainty.

$\phi_\epsilon = (2\phi_{+-} + \phi_{00})/3$

This expression is a very good approximation, good to about 10^{-3} degrees because of the small measured values of $\phi_{00}-\phi_{+-}$ and Re ϵ'/ϵ, and small theoretical ambiguities.

VALUE (°)	DOCUMENT ID		TECN	COMMENT
43.52 ±0.05 OUR FIT	Error includes scale factor of 1.2. Assuming *CPT*			
43.5 ±0.5 OUR FIT	Error includes scale factor of 1.3. Not assuming *CPT*			
43.5164±0.0002±0.0518	[1] SUPERWEAK	16		Assuming *CPT*
43.86 ±0.63	[2] ABOUZAID	11	KTEV	Not assuming *CPT*

[1] SUPERWEAK 16 is a fake measurement used to impose the *CPT* or Superweak constraint $\phi_{+-} = \phi_{SW} = \tan^{-1}[2\,\frac{\Delta m}{\hbar}\,(\frac{\tau_S\tau_L}{\tau_L-\tau_S})]$. This "measurement" is linearized using values near the PDG 04 edition values of Δm, τ_S and τ_L, and then adjusted to our current values as described in the following "measurement". SUPERWEAK 16 measures $\phi_\epsilon = (43.50258 \pm 0.00021) + 54.1\,[\Delta m - 0.5289] + 32.0\,[\tau_S - 0.89564]$ (°). We have adjusted the measurement to use our best values of ($\Delta m = 0.5293 \pm 0.0009$) ($10^{10}\ \hbar\ s^{-1}$), ($\tau_S = 0.8954 \pm 0.0004$) ($10^{-10}$ s). Our first error is their experiment's error and our second error is the systematic error from using our best values.

[2] ABOUZAID 11 uses the full KTeV dataset collected in 1996, 1997, and 1999. See Im(ϵ'/ϵ) section for correlation information.

Im(ϵ'/ϵ) = $-(\phi_{00} - \phi_{+-})/3$

For small $|\epsilon'/\epsilon|$, Im(ϵ'/ϵ) is related to the phases of η_{00} and η_{+-} by the above expression.

VALUE (°)	DOCUMENT ID		TECN	COMMENT
−0.002 ±0.005 OUR FIT	Error includes scale factor of 1.7. Assuming *CPT*			
−0.11 ±0.11 OUR FIT	Not assuming *CPT*			
−0.0985±0.1157	[1] ABOUZAID	11	KTEV	Not assuming *CPT*

[1] ABOUZAID 11 uses the full KTeV dataset collected in 1996, 1997, and 1999. The fit has Δm, τ_S, ϕ_ϵ, Re(ϵ'/ϵ), and Im(ϵ'/ϵ) as free parameters. The reported value of Im(ϵ'/ϵ) = $(-17.20 \pm 20.20) \times 10^{-4}$ rad. The correlation coefficients are $\rho(\phi_\epsilon, \Delta m) = 0.828$, $\rho(\phi_\epsilon, \tau_S) = -0.765$, $\rho(\Delta m, \tau_S) = -0.858$, $\rho(\text{Im}(\epsilon'/\epsilon), \phi_\epsilon) = -0.041$, $\rho(\text{Im}(\epsilon'/\epsilon), \Delta m) = 0.026$, $\rho(\text{Im}(\epsilon'/\epsilon), \tau_S) = -0.010$.

DECAY-PLANE ASYMMETRY IN $\pi^+\pi^-e^+e^-$ DECAYS

This is the *CP*-violating asymmetry

$$A = \frac{N_{\sin\phi\cos\phi>0.0} - N_{\sin\phi\cos\phi<0.0}}{N_{\sin\phi\cos\phi>0.0} + N_{\sin\phi\cos\phi<0.0}}$$

where ϕ is the angle between the e^+e^- and $\pi^+\pi^-$ planes in the K_L^0 rest frame.

CP ASYMMETRY *A* in $K_L^0 \to \pi^+\pi^-e^+e^-$

VALUE (%)	DOCUMENT ID		TECN
13.7±1.5 OUR AVERAGE			
13.6±1.4±1.5	ABOUZAID	06	KTEV
14.2±3.0±1.9	LAI	03C	NA48
13.6±2.5±1.2	ALAVI-HARATI	00B	KTEV

PARAMETERS FOR $e^+e^-e^+e^-$ DECAYS

These are the *CP*-violating parameters in the ϕ distribution, where ϕ is the angle between the planes of the two e^+e^- pairs in the kaon rest frame:

$$d\Gamma/d\phi \propto 1 + \beta_{CP}\cos(2\phi) + \gamma_{CP}\sin(2\phi)$$

β_{CP} from $K_L^0 \to e^+e^-e^+e^-$

VALUE	EVTS	DOCUMENT ID		TECN	COMMENT
−0.19±0.07 OUR AVERAGE					
−0.13±0.10±0.03	200	[1] LAI	05B	NA48	
−0.23±0.09±0.02	441	ALAVI-HARATI	01D	KTEV	M_{ee} >8 MeV/c^2

[1] LAI 05B obtains $\beta_{CP} = -0.13 \pm 0.10$ (stat) if $\gamma_{CP} = 0$ is assumed.

γ_{CP} from $K_L^0 \to e^+e^-e^+e^-$

VALUE	EVTS	DOCUMENT ID		TECN	COMMENT
0.01±0.11 OUR AVERAGE	Error includes scale factor of 1.6.				
+0.13±0.10±0.03	200	LAI	05B	NA48	
−0.09±0.09±0.02	441	ALAVI-HARATI	01D	KTEV	M_{ee} >8 MeV/c^2

CHARGE ASYMMETRY IN $\pi^+\pi^-\pi^0$ DECAYS

These are *CP*-violating charge-asymmetry parameters, defined at beginning of section "LINEAR COEFFICIENT *g* FOR $K_L^0 \to \pi^+\pi^-\pi^0$ above.

See also note on Dalitz plot parameters in $K^\pm$ section and note on "*CP* violation in K_L decays" above.

LINEAR COEFFICIENT *j* FOR $K_L^0 \to \pi^+\pi^-\pi^0$

VALUE	EVTS	DOCUMENT ID		TECN	
0.0012±0.0008 OUR AVERAGE					
0.0010±0.0024±0.0030	500k	ANGELOPO...	98C	CPLR	
−0.001 ±0.011	6499	CHO	77		
0.001 ±0.003	4709	PEACH	77		
0.0013±0.0009	3M	SCRIBANO	70		
0.0 ±0.017	4400	SMITH	70	OSPK	
0.001 ±0.004	238k	BLANPIED	68		

QUADRATIC COEFFICIENT *f* FOR $K_L^0 \to \pi^+\pi^-\pi^0$

VALUE	EVTS	DOCUMENT ID		TECN
0.0045±0.0024±0.0059	500k	ANGELOPO...	98C	CPLR

PARAMETERS for $K^0_L \to \pi^+\pi^-\gamma$ DECAY

$|\eta_{+-\gamma}| = |A(K^0_L \to \pi^+\pi^-\gamma, CP \text{ violating})/A(K^0_S \to \pi^+\pi^-\gamma)|$

VALUE (units 10^{-3})	EVTS	DOCUMENT ID		TECN
2.35 ±0.07 OUR AVERAGE				
2.359±0.062±0.040	9045	MATTHEWS	95	E773
2.15 ±0.26 ±0.20	3671	RAMBERG	93B	E731

$\phi_{+-\gamma}$ = phase of $\eta_{+-\gamma}$

VALUE (°)	EVTS	DOCUMENT ID		TECN
44 ± 4 OUR AVERAGE				
43.8± 3.5± 1.9	9045	MATTHEWS	95	E773
72 ±23 ±17	3671	RAMBERG	93B	E731

$|\epsilon'_{+-\gamma}|/\epsilon$ for $K^0_L \to \pi^+\pi^-\gamma$

VALUE	CL%	EVTS	DOCUMENT ID		TECN
<0.3	90	3671	[1] RAMBERG	93B	E731

[1] RAMBERG 93B limit on $|\epsilon'_{+-\gamma}|/\epsilon$ assumes than any difference between η_{+-} and $\eta_{+-\gamma}$ is due to direct *CP* violation.

$|g_{E1}|$ for $K^0_L \to \pi^+\pi^-\gamma$

This parameter is the amplitude of the direct emission of a *CP* violating E1 electric dipole photon.

VALUE	CL%	EVTS	DOCUMENT ID		TECN	COMMENT
<0.21	90	111k	ABOUZAID	06A	KTEV	$E^*_\gamma > 20$ MeV

T VIOLATION TESTS IN K^0_L DECAYS

Im(ξ) in $K^0_{\mu 3}$ DECAY (from transverse μ pol.)

Test of *T* reversal invariance.

VALUE	EVTS	DOCUMENT ID		TECN	COMMENT
−0.007±0.026 OUR AVERAGE					
0.009±0.030	12M	MORSE	80	CNTR	Polarization
0.35 ±0.30	207k	[1] CLARK	77	SPEC	POL, t=0
−0.085±0.064	2.2M	[2] SANDWEISS	73	CNTR	POL, t=0
−0.02 ±0.08		LONGO	69	CNTR	POL, t=3.3
−0.2 ±0.6		ABRAMS	68B	OSPK	Polarization
• • • We do not use the following data for averages, fits, limits, etc. • • •					
0.012±0.026		SCHMIDT	79	CNTR	Repl. by MORSE 80

[1] CLARK 77 value has additional $\xi(0)$ dependence $+0.21\mathrm{Re}[\xi(0)]$.

[2] SANDWEISS 73 value corrected from value quoted in their paper due to new value of Re(ξ). See footnote 4 of SCHMIDT 79.

CPT-INVARIANCE TESTS IN K^0_L DECAYS

PHASE DIFFERENCE $\phi_{00} - \phi_{+-}$

Test of *CPT*.

OUR FIT is described in the note on "*CP* violation in K_L decays" in the K^0_L Particle Listings.

VALUE (°)	DOCUMENT ID		TECN	COMMENT
0.006±0.014 OUR FIT	Error includes scale factor of 1.7. Assuming *CPT*			
0.34 ±0.32 OUR FIT	Not assuming *CPT*			
0.006±0.008	[1] SUPERWEAK	16		Assuming *CPT*
−0.30 ±0.88	[2] SCHWINGEN...	95		Combined E731, E773
• • • We do not use the following data for averages, fits, limits, etc. • • •				
0.30 ±0.35	[3] ABOUZAID	11	KTEV	Not assuming *CPT*
0.39 ±0.22 ±0.45	[4] ALAVI-HARATI	03	KTEV	
0.62 ±0.71 ±0.75	SCHWINGEN...	95	E773	
−1.6 ±1.2	[5] GIBBONS	93	E731	
0.2 ±2.6 ±1.2	[6] CAROSI	90	NA31	
−0.3 ±2.4 ±1.2	KARLSSON	90	E731	

[1] SUPERWEAK 16 is a fake experiment to constrain $\phi_{00} - \phi_{+-}$ to a small value as described in the note "*CP* violation in K_L decays."

[2] This SCHWINGENHEUER 95 values is the combined result of SCHWINGENHEUER 95 and GIBBONS 93, accounting for correlated systematic errors.

[3] Not independent of other phase parameters reported in ABOUZAID 11.

[4] ALAVI-HARATI 03 fit Re(ϵ'/ϵ), Im(ϵ'/ϵ), Δm, τ_S, and ϕ_{+-} simultaneously, not assuming *CPT*. Phase difference is obtained from $\phi_{00} - \phi_{+-} \approx -3\mathrm{Im}(\epsilon'/\epsilon)$ for small $|\epsilon'/\epsilon|$. Superseded by ABOUZAID 11.

[5] GIBBONS 93 give detailed dependence of systematic error on lifetime (see the section on the K^0_S mean life) and mass difference (see the section on $m_{K^0_L} - m_{K^0_S}$).

[6] CAROSI 90 is excluded from the fit because it it is not independent of ϕ_{+-} and ϕ_{00} values.

PHASE DIFFERENCE $\phi_{+-} - \phi_{SW}$

Test of *CPT*. The Superweak phase $\phi_{SW} \equiv \tan^{-1}(2\Delta m/\Delta\Gamma)$ where $\Delta m = m_{K^0_L} - m_{K^0_S}$ and $\Delta\Gamma = \hbar(\tau_L - \tau_S)/(\tau_L\tau_S)$.

VALUE (°)	DOCUMENT ID		TECN
0.61±0.62±1.01	[1] ALAVI-HARATI	03	KTEV

[1] ALAVI-HARATI 03 fit is the same as their ϕ_{+-}, τ_{K_S}, Δm fit, except that the parameter $\phi_{+-} - \phi_{SW}$ is used in place of ϕ.

$\mathrm{Re}(\frac{2}{3}\eta_{+-} + \frac{1}{3}\eta_{00}) - \frac{A_L}{2}$

Test of *CPT*

VALUE (units 10^{-6})	DOCUMENT ID		TECN	COMMENT
−3±35	[1] ALAVI-HARATI	02	E799	Uses A_L from K_{e3} decays

[1] ALAVI-HARATI 02 uses PDG 00 values of η_{+-} and η_{00}.

$\Delta S = \Delta Q$ IN K^0 DECAYS

The relative amount of $\Delta S \neq \Delta Q$ component present is measured by the parameter x, defined as

$$x = A(\overline{K}^0 \to \pi^-\ell^+\nu)/A(K^0 \to \pi^-\ell^+\nu) \ .$$

We list Re{x} and Im{x} for K_{e3} and $K_{\mu 3}$ combined.

$x = A(\overline{K}^0 \to \pi^-\ell^+\nu)/A(K^0 \to \pi^-\ell^+\nu) = A(\Delta S{=}-\Delta Q)/A(\Delta S{=}\Delta Q)$

REAL PART OF x

VALUE	EVTS	DOCUMENT ID		TECN	COMMENT
−0.0018±0.0041±0.0045		ANGELOPO...	98D	CPLR	K_{e3} from K^0
• • • We do not use the following data for averages, fits, limits, etc. • • •					
$0.10\ ^{+0.18}_{-0.19}$	79	SMITH	75B	WIRE	$\pi^- p \to K^0\Lambda$
0.04 ±0.03	4724	NIEBERGALL	74	ASPK	$K^+p \to K^0p\pi^+$
−0.008 ±0.044	1757	FACKLER	73	OSPK	K_{e3} from K^0
−0.03 ±0.07	1367	HART	73	OSPK	K_{e3} from $K^0\Lambda$
−0.070 ±0.036	1079	MALLARY	73	OSPK	K_{e3} from $K^0\Lambda$X
0.03 ±0.06	410	[1] BURGUN	72	HBC	$K^+p \to K^0p\pi^+$
$0.04\ ^{+0.10}_{-0.13}$	100	[2] GRAHAM	72	OSPK	$K_{\mu 3}$ from $K^0\Lambda$
−0.05 ±0.09	442	[2] GRAHAM	72	OSPK	$\pi^- p \to K^0\Lambda$
$0.26\ ^{+0.10}_{-0.14}$	126	MANN	72	HBC	$K^-p \to n\overline{K}^0$
−0.13 ±0.11	342	[2] MANTSCH	72	OSPK	K_{e3} from $K^0\Lambda$
$0.04\ ^{+0.07}_{-0.08}$	222	[1] BURGUN	71	HBC	$K^+p \to K^0p\pi^+$
$0.25\ ^{+0.07}_{-0.09}$	252	WEBBER	71	HBC	$K^-p \to n\overline{K}^0$
0.12 ±0.09	215	[3] CHO	70	DBC	$K^+d \to K^0pp$
−0.020 ±0.025		[4] BENNETT	69	CNTR	Charge asym+ Cu regen.
$0.09\ ^{+0.14}_{-0.16}$	686	LITTENBERG	69	OSPK	$K^+n \to K^0p$
0.03 ±0.03		[4] BENNETT	68	CNTR	
$0.09\ ^{+0.07}_{-0.09}$	121	JAMES	68	HBC	$\overline{p}p$
$0.17\ ^{+0.16}_{-0.35}$	116	FELDMAN	67B	OSPK	$\pi^- p \to K^0\Lambda$
0.17 ±0.10	335	[3] HILL	67	DBC	$K^+d \to K^0pp$
$0.035\ ^{+0.11}_{-0.13}$	196	AUBERT	65	HLBC	K^+ charge exch.
$0.06\ ^{+0.18}_{-0.44}$	152	[5] BALDO-...	65	HLBC	K^+ charge exch.
−0.08 $^{+0.16}_{-0.28}$	109	[6] FRANZINI	65	HBC	$\overline{p}p$

[1] BURGUN 72 is a final result which includes BURGUN 71.

[2] First GRAHAM 72 value is second GRAHAM 72 value combined with MANTSCH 72.

[3] CHO 70 is analysis of unambiguous events in new data and HILL 67.

[4] BENNETT 69 is a reanalysis of BENNETT 68.

[5] BALDO-CEOLIN 65 gives x and θ converted by us to Re(x) and Im(x).

[6] FRANZINI 65 gives x and θ for Re(x) and Im(x). See SCHMIDT 67.

IMAGINARY PART OF x

Assumes $m_{K^0_L} - m_{K^0_S}$ positive. See Listings above.

VALUE	EVTS	DOCUMENT ID		TECN	COMMENT
0.0012±0.0019±0.0009	640k	ANGELOPO...	01B	CPLR	K_{e3} from K^0
• • • We do not use the following data for averages, fits, limits, etc. • • •					
0.0012±0.0019	640k	[1] ANGELOPO...	98E	CPLR	K_{e3} from K^0
$-0.10\ ^{+0.16}_{-0.19}$	79	SMITH	75B	WIRE	$\pi^- p \to K^0\Lambda$
−0.06 ±0.05	4724	NIEBERGALL	74	ASPK	$K^+p \to K^0p\pi^+$
−0.017 ±0.060	1757	FACKLER	73	OSPK	K_{e3} from K^0
0.09 ±0.07	1367	HART	73	OSPK	K_{e3} from $K^0\Lambda$
$0.107\ ^{+0.092}_{-0.074}$	1079	MALLARY	73	OSPK	K_{e3} from $K^0\Lambda$X
$0.07\ ^{+0.06}_{-0.07}$	410	[2] BURGUN	72	HBC	$K^+p \to K^0p\pi^+$
$0.12\ ^{+0.17}_{-0.16}$	100	[3] GRAHAM	72	OSPK	$K_{\mu 3}$ from $K^0\Lambda$
0.05 ±0.13	442	[3] GRAHAM	72	OSPK	$\pi^- p \to K^0\Lambda$
$0.21\ ^{+0.15}_{-0.12}$	126	MANN	72	HBC	$K^-p \to n\overline{K}^0$
−0.04 ±0.16	342	[3] MANTSCH	72	OSPK	K_{e3} from $K^0\Lambda$
$0.12\ ^{+0.08}_{-0.09}$	222	[2] BURGUN	71	HBC	$K^+p \to K^0p\pi^+$
0.0 ±0.08	252	WEBBER	71	HBC	$K^-p \to n\overline{K}^0$
−0.08 ±0.07	215	[4] CHO	70	DBC	$K^+d \to K^0pp$

Meson Particle Listings

K_L^0

-0.11	$^{+0.10}_{-0.11}$	686	LITTENBERG	69	OSPK	$K^+ n \to K^0 p$
$+0.22$	$^{+0.37}_{-0.29}$	121	JAMES	68	HBC	$\overline{p}p$
0.0	± 0.25	116	FELDMAN	67B	OSPK	$\pi^- p \to K^0 \Lambda$
-0.20	± 0.10	335	[4] HILL	67	DBC	$K^+ d \to K^0 pp$
-0.21	$^{+0.11}_{-0.15}$	196	AUBERT	65	HLBC	K^+ charge exch.
-0.44	$^{+0.32}_{-0.19}$	152	[5] BALDO-...	65	HLBC	K^+ charge exch.
$+0.24$	$^{+0.40}_{-0.30}$	109	[6] FRANZINI	65	HBC	$\overline{p}p$

[1] Superseded by ANGELOPOULOS 01B.
[2] BURGUN 72 is a final result which includes BURGUN 71.
[3] First GRAHAM 72 value is second GRAHAM 72 value combined with MANTSCH 72.
[4] Footnote 10 of HILL 67 should read $+0.58$, not -0.58 (private communication) CHO 70 is analysis of unambiguous events in new data and HILL 67.
[5] BALDO-CEOLIN 65 gives x and θ converted by us to Re(x) and Im(x).
[6] FRANZINI 65 gives x and θ for Re(x) and Im(x). See SCHMIDT 67.

K_L^0 REFERENCES

AHN 17 PTEP 2017 021C01 J.K. Ahn *et al.* (KOTO Collab.)
BRFIT 16 RPP 2016 edition C.-J. Lin (PDG Collab.)
ETAFIT 16 RPP 2016 edition C.-J. Lin (PDG Collab.)
SUPERWEAK 16 RPP 2016 edition C.-J. Lin (PDG Collab.)
ABOUZAID 11 PR D83 092001 E. Abouzaid *et al.* (FNAL KTeV Collab.)
ABOUZAID 11A PRL 107 201803 E. Abouzaid *et al.* (KTeV Collab.)
OGATA 11 PR D84 052009 R. Ogata *et al.* (KEK E391a Collab.)
TUNG 11 PR D83 031101 Y.C. Tung *et al.* (KEK E391a Collab.)
ABOUZAID 10 PR D81 052001 E. Abouzaid *et al.* (FNAL KTeV Collab.)
AHN 10 PR D81 072004 J.K. Ahn *et al.* (KEK E391a Collab.)
ABOUZAID 08 PR D77 112004 E. Abouzaid *et al.* (FNAL KTeV Collab.)
ABOUZAID 08A PR D78 032009 E. Abouzaid *et al.* (FNAL KTeV Collab.)
ABOUZAID 08B PR D78 032014 E. Abouzaid *et al.* (FNAL KTeV Collab.)
ABOUZAID 08C PRL 100 131803 E. Abouzaid *et al.* (FNAL KTeV Collab.)
AHN 08 PRL 100 201802 J.K. Ahn *et al.* (KEK E391a Collab.)
AMBROSINO 08F EPJ C55 539 F. Ambrosino *et al.* (KLOE Collab.)
ABOUZAID 07B PRL 99 051804 E. Abouzaid *et al.* (FNAL KTeV Collab.)
ABOUZAID 07C PRL 99 081803 E. Abouzaid *et al.* (FNAL KTeV Collab.)
ABOUZAID 07D PR D76 052001 E. Abouzaid *et al.* (FNAL KTeV Collab.)
AMBROSINO 07C JHEP 0712 105 F. Ambrosino *et al.* (KLOE Collab.)
ANDRE 07 ANP 322 2518 T. Andre (EFI)
LAI 07 PL B645 26 A. Lai *et al.* (CERN NA48 Collab.)
LAI 07A PL B647 341 A. Lai *et al.* (CERN NA48 Collab.)
NIX 07 PR D76 011101 J. Nix *et al.* (KEK E391a Collab.)
ABOUZAID 06 PRL 96 101801 E. Abouzaid *et al.* (KTeV Collab.)
ABOUZAID 06A PR D74 032004 E. Abouzaid *et al.* (KTeV Collab.)
Also PR D74 039905 (errat.) E. Abouzaid *et al.* (KTeV Collab.)
ABOUZAID 06C PR D74 097101 E. Abouzaid *et al.* (KTeV Collab.)
AHN 06 PR D74 051105 J.K. Ahn *et al.* (KEK E391a Collab.)
Also PR D74 079901 (errat.) J.K. Ahn *et al.* (KEK E391a Collab.)
AMBROSINO 06 PL B632 43 F. Ambrosino *et al.* (KLOE Collab.)
AMBROSINO 06D PL B636 166 F. Ambrosino *et al.* (KLOE Collab.)
AMBROSINO 06F PL B638 140 F. Ambrosino *et al.* (KLOE Collab.)
BATLEY 06B PL B633 173 J.R. Batley *et al.* (CERN NA48/2 Collab.)
HILL 06 PR D74 096006 R.J. Hill (FNAL)
PDG 06 JP G33 1 W.-M. Yao *et al.* (PDG Collab.)
ALEXOPOU... 05 PR D71 012001 T. Alexopoulos *et al.* (FNAL KTeV Collab.)
AMBROSINO 05C PL B626 15 F. Ambrosino *et al.* (KLOE Collab.)
CABIBBO 05 JHEP 0503 021 N. Cabibbo, G. Isidori (CERN, ROMAI, FRAS)
LAI 05 PL B605 247 A. Lai *et al.* (CERN NA48 Collab.)
LAI 05B PL B615 31 A. Lai *et al.* (CERN NA48 Collab.)
PARK 05 PRL 94 021801 H.K. Park *et al.* (FNAL HyperCP Collab.)
ALAVI-HARATI 04A PRL 93 021805 A. Alavi-Harati *et al.* (FNAL KTeV/E799 Collab.)
ALEXOPOU... 04 PR D70 092006 T. Alexopoulos *et al.* (FNAL KTeV Collab.)
ALEXOPOU... 04A PR D70 092007 T. Alexopoulos *et al.* (FNAL KTeV Collab.)
BATLEY 04 PL B595 75 J.R. Batley *et al.* (CERN NA48 Collab.)
CIRIGLIANO 04 EPJ C35 53 V. Cirigliano, H. Neufeld, H. Pichl (CIT, VALE+)
LAI 04B PL B602 41 A. Lai *et al.* (CERN NA48 Collab.)
LAI 04C PL B604 1 A. Lai *et al.* (CERN NA48 Collab.)
PDG 04 PL B592 1 S. Eidelman *et al.* (PDG Collab.)
SOZZI 04 EPJ C36 37 M. Sozzi (PISA)
ADINOLFI 03 PL B566 61 M. Adinolfi *et al.* (KLOE Collab.)
ALAVI-HARATI 03 PR D67 012005 A. Alavi-Harati *et al.* (FNAL KTeV Collab.)
Also PR D70 079904 (errat.) A. Alavi-Harati *et al.* (FNAL KTeV Collab.)
ALAVI-HARATI 03B PRL 90 141801 A. ALavi-Harati *et al.* (FNAL KTeV Collab.)
LAI 03 PL B551 7 A. Lai *et al.* (CERN NA48 Collab.)
LAI 03C EPJ C30 33 A. Lai *et al.* (CERN NA48 Collab.)
ALAVI-HARATI 02 PRL 88 181601 A. Alavi-Harati *et al.* (FNAL KTeV Collab.)
ALAVI-HARATI 02C PRL 89 211801 A. Alavi-Harati *et al.* (FNAL KTeV Collab.)
BATLEY 02 PL B544 97 J.R. Batley *et al.* (CERN NA48 Collab.)
CIRIGLIANO 02 EPJ C23 121 V. Cirigliano *et al.* (VIEN, VALE, MARS)
LAI 02B PL B536 229 A. Lai *et al.* (CERN NA48 Collab.)
ALAVI-HARATI 01 PRL 86 397 A. Alavi-Harati *et al.* (FNAL KTeV Collab.)
ALAVI-HARATI 01B PRL 86 761 A. Alavi-Harati *et al.* (FNAL KTeV Collab.)
ALAVI-HARATI 01D PRL 86 5425 A. Alavi-Harati *et al.* (FNAL KTeV Collab.)
ALAVI-HARATI 01E PRL 87 021801 A. Alavi-Harati *et al.* (FNAL KTeV Collab.)
ALAVI-HARATI 01F PR D64 012003 A. Alavi-Harati *et al.* (FNAL KTeV Collab.)
ALAVI-HARATI 01G PRL 87 071801 A. Alavi-Harati *et al.* (FNAL KTeV Collab.)
ALAVI-HARATI 01H PRL 87 111802 A. Alavi-Harati *et al.* (FNAL KTeV Collab.)
ALAVI-HARATI 01J PR D64 112004 A. Alavi-Harati *et al.* (FNAL KTeV Collab.)
ANGELOPO... 01 PL B503 49 A. Angelopoulos *et al.* (CPLEAR Collab.)
ANGELOPO... 01B EPJ C22 55 A. Angelopoulos *et al.* (CPLEAR Collab.)
LAI 01B PL B515 261 A. Lai *et al.* (CERN NA48 Collab.)
LAI 01C EPJ C22 231 A. Lai *et al.* (CERN NA48 Collab.)
ALAVI-HARATI 00 PR D61 072006 A. Alavi-Harati *et al.* (FNAL KTeV Collab.)
ALAVI-HARATI 00B PRL 84 408 A. Alavi-Harati *et al.* (FNAL KTeV Collab.)
ALAVI-HARATI 00D PRL 84 5279 A. Alavi-Harati *et al.* (FNAL KTeV Collab.)
ALAVI-HARATI 00E PR D62 112001 A. Alavi-Harati *et al.* (FNAL KTeV Collab.)
AMBROSE 00 PRL 84 1389 D. Ambrose *et al.* (BNL E871 Collab.)
APOSTOLA... 00 PL B473 186 A. Apostolakis *et al.* (CPLEAR Collab.)
PDG 00 EPJ C15 1 D.E. Groom *et al.* (PDG Collab.)
ADAMS 99 PL B447 240 J. Adams *et al.* (FNAL KTeV Collab.)
ALAVI-HARATI 99B PRL 83 917 A. Alavi-Harati *et al.* (FNAL KTeV Collab.)
ALAVI-HARATI 99D PRL 83 22 A. Alavi-Harati *et al.* (FNAL KTeV Collab.)
APOSTOLA... 99C PL B458 545 A. Apostolakis *et al.* (CPLEAR Collab.)
Also EPJ C18 41 A. Apostolakis *et al.* (CPLEAR Collab.)
FANTI 99B PL B458 553 V. Fanti *et al.* (CERN NA48 Collab.)
FANTI 99C PL B465 335 V. Fanti *et al.* (CERN NA48 Collab.)
MURAKAMI 99 PL B463 333 K. Murakami *et al.* (KEK E162 Collab.)
ADAMS 98 PRL 80 4123 J. Adams *et al.* (FNAL KTeV Collab.)
AMBROSE 98 PRL 81 4309 D. Ambrose *et al.* (BNL E871 Collab.)
AMBROSE 98B PRL 81 5734 D. Ambrose *et al.* (BNL E871 Collab.)
ANGELOPO... 98 PL B420 191 A. Angelopoulos *et al.* (CPLEAR Collab.)
ANGELOPO... 98C EPJ C5 389 A. Angelopoulos *et al.* (CPLEAR Collab.)
ANGELOPO... 98D PL B444 38 A. Angelopoulos *et al.* (CPLEAR Collab.)
Also EPJ C22 55 A. Angelopoulos *et al.* (CPLEAR Collab.)
ANGELOPO... 98E PL B444 43 A. Angelopoulos *et al.* (CPLEAR Collab.)
ARISAKA 98 PL B432 230 K. Arisaka *et al.* (FNAL E799 Collab.)
BENDER 98 PL B418 411 M. Bender *et al.* (CERN NA48 Collab.)
DAMBROSIO 98 PL B423 385 G. D'Ambrosio, G. Isidori, J. Portoles
SETZU 98 PL B420 205 M.G. Setzu *et al.*
TAKEUCHI 98 PL B443 409 Y. Takeuchi *et al.* (KYOT, KEK, HIRO)
FANTI 97 ZPHY C76 653 V. Fanti *et al.* (CERN NA48 Collab.)
NOMURA 97 PL B408 445 T. Nomura *et al.* (KYOT, KEK, HIRO)
ADLER 96B ZPHY C70 211 R. Adler *et al.* (CPLEAR Collab.)
ADLER 96C PL B369 367 R. Adler *et al.* (CPLEAR Collab.)
GU 96 PRL 76 4312 P. Gu *et al.* (RUTG, UCLA, EFI, COLO+)
LEBER 96 PL B369 69 F. Leber *et al.* (MANZ, CERN, EDIN, ORSAY+)
PDG 96 PR D54 1 R. M. Barnett *et al.* (PDG Collab.)
ADLER 95 PL B363 237 R. Adler *et al.* (CPLEAR Collab.)
ADLER 95B PL B363 243 R. Adler *et al.* (CPLEAR Collab.)
AKAGI 95 PR D51 2061 T. Akagi *et al.* (TOHOK, TOKY, KYOT, KEK)
BARR 95 ZPHY C65 361 G.D. Barr *et al.* (CERN, EDIN, MANZ, LALO+)
BARR 95C PL B358 399 G.D. Barr *et al.* (CERN, EDIN, MANZ, LALO+)
HEINSON 95 PR D51 985 A.P. Heinson *et al.* (BNL E791 Collab.)
KREUTZ 95 ZPHY C65 67 A. Kreutz *et al.* (SIEG, EDIN, MANZ, ORSAY+)
MATTHEWS 95 PRL 75 2803 J.N. Matthews *et al.* (RUTG, EFI, ELMT+)
SCHWINGEN... 95 PRL 74 4376 B. Schwingenheuer *et al.* (EFI, CHIC+)
SPENCER 95 PRL 74 3323 M.B. Spencer *et al.* (UCLA, EFI, COLO+)
BARR 94 PL B328 528 G.D. Barr *et al.* (CERN, EDIN, MANZ, LALO+)
GU 94 PRL 72 3000 P. Gu *et al.* (RUTG, UCLA, EFI, COLO+)
NAKAYA 94 PRL 73 2169 T. Nakaya *et al.* (OSAK, UCLA, EFI, COLU+)
ROBERTS 94 PR D50 1874 D. Roberts *et al.* (UCLA, EFI, COLU+)
WEAVER 94 PRL 72 3758 M. Weaver *et al.* (UCLA, EFI, COLU, ELMT+)
AKAGI 93 PR D47 2644 T. Akagi *et al.* (TOHOK, TOKY, KYOT, KEK)
ARISAKA 93 PRL 70 1049 K. Arisaka *et al.* (BNL E791 Collab.)
ARISAKA 93B PRL 71 3910 K. Arisaka *et al.* (BNL E791 Collab.)
BARR 93D PL B317 233 G.D. Barr *et al.* (CERN, EDIN, MANZ, LALO+)
GIBBONS 93 PRL 70 1199 L.K. Gibbons *et al.* (FNAL E731 Collab.)
Also PR D55 6625 L.K. Gibbons *et al.* (FNAL E731 Collab.)
GIBBONS 93B PRL 70 1203 L.K. Gibbons *et al.* (FNAL E731 Collab.)
GIBBONS 93C Thesis RX-1487 L.K. Gibbons (CHIC)
Also PR D55 6625 L.K. Gibbons *et al.* (FNAL E731 Collab.)
HARRIS 93 PRL 71 3914 D.A. Harris *et al.* (EFI, UCLA, COLO+)
HARRIS 93B PRL 71 3918 D.A. Harris *et al.* (EFI, UCLA, COLO+)
MAKOFF 93 PRL 70 1591 G. Makoff *et al.* (FNAL E731 Collab.)
Also PRL 75 2069 (erratum) G. Makoff *et al.*
RAMBERG 93 PRL 70 2525 E. Ramberg *et al.* (FNAL E731 Collab.)
RAMBERG 93B PRL 70 2529 E.J. Ramberg *et al.* (FNAL E731 Collab.)
VAGINS 93 PRL 71 35 M.R. Vagins *et al.* (BNL E845 Collab.)
ADLER 92B PL B286 180 R. Adler *et al.* (CPLEAR Collab.)
Also SJNP 55 840 R. Adler *et al.* (CPLEAR Collab.)
BARR 92 PL B284 440 G.D. Barr *et al.* (CERN, EDIN, MANZ, LALO+)
GRAHAM 92 PL B295 169 G.E. Graham *et al.* (FNAL E731 Collab.)
MORSE 92 PR D45 36 W.M. Morse *et al.* (BNL, YALE, VASS)
PDG 92 PR D45 S1 K. Hikasa *et al.* (KEK, LBL, BOST+)
SOMALWAR 92 PRL 68 2580 S.V. Somalwar *et al.* (FNAL E731 Collab.)
AKAGI 91B PRL 67 2618 T. Akagi *et al.* (TOHOK, TOKY, KYOT, KEK)
BARR 91 PL B259 389 G.D. Barr *et al.* (CERN, EDIN, MANZ, LALO+)
HEINSON 91 PR D44 1 A.P. Heinson *et al.* (UCI, UCLA, LANL+)
PAPADIMITR... 91 PR D44 573 V. Papadimitriou *et al.* (FNAL E731 Collab.)
BARKER 90 PR D41 3546 A.R. Barker *et al.* (FNAL E731 Collab.)
Also PRL 61 2661 L.K. Gibbons *et al.* (FNAL E731 Collab.)
BARR 90B PL B240 283 G.D. Barr *et al.* (CERN, EDIN, MANZ, LALO+)
BARR 90C PL B242 523 G.D. Barr *et al.* (CERN, EDIN, MANZ, LALO+)
CAROSI 90 PL B237 303 R. Carosi *et al.* (CERN, EDIN, MANZ, LALO+)
KARLSSON 90 PRL 64 2976 M. Karlsson *et al.* (FNAL E731 Collab.)
OHL 90 PRL 64 2755 K.E. Ohl *et al.* (BNL E845 Collab.)
OHL 90B PRL 65 1407 K.E. Ohl *et al.* (BNL E845 Collab.)
PATTERSON 90 PRL 64 1491 J.R. Patterson *et al.* (FNAL E731 Collab.)
INAGAKI 89 PR D40 1712 T. Inagaki *et al.* (KEK, TOKY, KYOT)
MATHIAZHA... 89 PRL 63 2181 C. Mathiazhagan *et al.* (UCI, UCLA, LANL+)
MATHIAZHA... 89B PRL 63 2185 C. Mathiazhagan *et al.* (UCI, UCLA, LANL+)
WAHL 89 CERN-EP/89-86 H. Wahl (CERN)
BARR 88 PL B214 303 G.D. Barr *et al.* (CERN, EDIN, MANZ, LALO+)
BURKHARDT 88 PL B206 169 H. Burkhardt *et al.* (CERN, EDIN, MANZ+)
JASTRZEM... 88 PRL 61 2300 E. Jastrzembski *et al.* (BNL, YALE)
WOODS 88 PRL 60 1695 M. Woods *et al.* (FNAL E731 Collab.)
BURKHARDT 87 PL B199 139 H. Burkhardt *et al.* (CERN, EDIN, MANZ+)
ARONSON 86 PR D33 3180 S.H. Aronson *et al.* (BNL, CHIC, STAN+)
Also PRL 48 1078 S.H. Aronson *et al.* (BNL, CHIC, STAN+)
PDG 86C PL 170B 132 M. Aguilar-Benitez *et al.* (CERN, CIT+)
COUPAL 85 PRL 55 566 D.P. Coupal *et al.* (CHIC, SACL)
BALATS 83 SJNP 38 556 M.Y. Balats *et al.* (ITEP)
Translated from YAF 38 927.
BERGSTROM 83 PL 131B 229 L. Bergstrom, E. Masso, P. Singer (CERN)
ARONSON 82 PRL 48 1078 S.H. Aronson *et al.* (BNL, CHIC, STAN+)
ARONSON 82B PRL 48 1306 S.H. Aronson *et al.* (BNL, CHIC, PURD)
Also PL 116B 73 E. Fischbach *et al.* (PURD, BNL, CHIC)
Also PR D28 476 S.H. Aronson *et al.* (BNL, CHIC, PURD)
Also PR D28 495 S.H. Aronson *et al.* (BNL, CHIC, PURD)
PDG 82B PL 111B 70 M. Roos *et al.* (HELS, CIT, CERN)
BIRULEV 81 NP B182 1 V.K. Birulev *et al.* (JINR)
Also SJNP 31 622 V.K. Birulev *et al.* (JINR)
Translated from YAF 31 1204.
CARROLL 80B PRL 44 529 A.S. Carroll *et al.* (BNL, ROCH)
CARROLL 80C PL 96B 407 A.S. Carroll *et al.* (BNL, ROCH)
CHO 80 PR D22 2688 Y. Cho *et al.* (ANL, CMU)
MORSE 80 PR D21 1750 W.M. Morse *et al.* (BNL, YALE)
CHRISTENS... 79 PRL 43 1209 J.H. Christenson *et al.* (NYU)
SCHMIDT 79 PRL 43 556 M.P. Schmidt *et al.* (YALE, BNL)
HILL 78 PL 73B 483 D.G. Hill *et al.* (BNL, SLAC, SBER)
CHO 77 PR D15 587 Y. Cho *et al.* (ANL, CMU)
CLARK 77 PR D15 553 A.R. Clark *et al.* (LBL)
Also Thesis LBL-4275 G. Shen (LBL)
DEVOE 77 PR D16 565 R. Devoe *et al.* (EFI, ANL)
PEACH 77 NP B127 399 K.J. Peach *et al.* (BGNA, EDIN, GLAS+)
BIRULEV 76 SJNP 24 178 V.K. Birulev *et al.* (JINR)
Translated from YAF 24 340.
COOMBES 76 PRL 37 249 R.W. Coombes *et al.* (STAN, NYU)
GJESDAL 76 NP B109 118 G. Gjesdal *et al.* (CERN, HEIDH)
BALDO-... 75 NC 25A 688 M. Baldo-Ceolin *et al.* (PADO, WISC)
BLUMENTHAL 75 PRL 34 164 R.B. Blumenthal *et al.* (PENN, CHIC, TEMP)
BUCHANAN 75 PR D11 457 C.D. Buchanan *et al.* (UCLA, SLAC, JHU)
CARITHERS 75 PRL 34 1244 W.C.J. Carithers *et al.* (COLU, NYU)
SMITH 75B Thesis UCSD unpub. J.G. Smith (UCSD)
BISI 74 PL 50B 504 V. Bisi, M.I. Ferrero (TORI)
DONALDSON 74 Thesis SLAC-0184 G. Donaldson (SLAC)
Also PR D14 2839 G. Donaldson *et al.* (SLAC)
DONALDSON 74B PR D9 2960 G. Donaldson *et al.* (SLAC, UCSC)
Also PRL 31 337 G. Donaldson *et al.* (SLAC, UCSC)
GEWENIGER 74 PL 48B 483 C. Geweniger *et al.* (CERN, HEIDH)
Also Thesis CERN Int. 74-4 V. Luth (CERN)
GEWENIGER 74B PL 48B 487 C. Geweniger *et al.* (CERN, HEIDH)
Also PL 52B 119 S. Gjesdal *et al.* (CERN, HEIDH)

GEWENIGER	74C	PL 52B 108	C. Geweniger *et al.*	(CERN, HEIDH)
GJESDAL	74	PL 52B 113	S. Gjesdal *et al.*	(CERN, HEIDH)
MESSNER	74	PRL 33 1458	R. Messner *et al.*	(COLO, SLAC, UCSC)
NIEBERGALL	74	PL 49B 103	F. Niebergall *et al.*	(CERN, ORSAY, VIEN)
WILLIAMS	74	PRL 33 240	H.H. Williams *et al.*	(BNL, YALE)
ALEXANDER	73B	NP B65 301	G. Alexander *et al.*	(TELA, HEID)
BRANDENB...	73	PR D8 1978	G.W. Brandenburg *et al.*	(SLAC)
EVANS	73	PR D7 36	G.R. Evans *et al.*	(EDIN, CERN)
Also		PRL 23 427	G.R. Evans *et al.*	(EDIN, CERN)
FACKLER	73	PRL 31 847	O. Fackler *et al.*	(MIT)
FITCH	73	PRL 31 1524	V.L. Fitch *et al.*	(PRIN)
Also		Thesis COO-3072-13	R.C. Webb	(PRIN)
HART	73	NP B66 317	J.C. Hart *et al.*	(CAVE, RHEL)
MALLARY	73	PR D7 1953	M.L. Mallary *et al.*	(CIT)
Also		PRL 25 1214	F.J. Sciulli *et al.*	(CIT)
MCCARTHY	73	PR D7 687	R.L. McCarthy *et al.*	(LBL)
Also		PL 42B 291	R.L. McCarthy *et al.*	(LBL)
Also		Thesis LBL-550	R.L. McCarthy	(LBL)
MESSNER	73	PRL 30 876	R. Messner *et al.*	(COLO, SLAC, UCSC)
SANDWEISS	73	PRL 30 1002	J. Sandweiss *et al.*	(YALE, ANL)
WILLIAMS	73	PRL 31 1521	H.H. Williams *et al.*	(BNL, YALE)
ASHFORD	72	PL 38B 47	V.A. Ashford *et al.*	(UCSD)
BANNER	72B	PRL 29 237	M. Banner *et al.*	(PRIN)
BARMIN	72B	SJNP 15 638 Translated from YAF 15 1152.	V.V. Barmin *et al.*	(ITEP)
BURGUN	72	NP B50 194	G. Burgun *et al.*	(SACL, CERN, OSLO)
GRAHAM	72	NC 9A 166	M.F. Graham *et al.*	(ILL, NEAS)
JAMES	72	NP B49 1	F. James *et al.*	(CERN, SACL, OSLO)
KRENZ	72	LNC 4 213	W. Krenz *et al.*	(AACH, CERN, EDIN)
MANN	72	PR D6 137	W.A. Mann *et al.*	(MASA, BNL, YALE)
MANTSCH	72	NC 9A 160	P.M. Mantsch *et al.*	(ILL, NEAS)
MCCARTHY	72	PL 42B 291	R.L. McCarthy *et al.*	(LBL)
PICCIONI	72	PRL 29 1412	R. Piccioni *et al.*	(SLAC)
Also		PR D9 2939	R. Piccioni *et al.*	(SLAC, UCSC, COLO)
VOSBURGH	72	PR D6 1834	K.G. Vosburgh *et al.*	(RUTG, MASA)
Also		PRL 26 866	K.G. Vosburgh *et al.*	(RUTG, MASA)
BALATS	71	SJNP 13 53 Translated from YAF 13 93.	M.Y. Balats *et al.*	(ITEP)
BARMIN	71	PL 35B 604	V.V. Barmin *et al.*	(ITEP)
BURGUN	71	LNC 2 1169	G. Burgun *et al.*	(SACL, CERN, OSLO)
CARNEGIE	71	PR D4 1	R.K. Carnegie *et al.*	(PRIN)
CHAN	71	Thesis LBL-350	J.H.S. Chan	(LBL)
CHO	71	PR D3 1557	Y. Cho *et al.*	(CMU, BNL, CASE)
ENSTROM	71	PR D4 2629	J. Enstrom *et al.*	(SLAC, STAN)
Also		Thesis SLAC-0125	J.E. Enstrom	(STAN)
JAMES	71	PL 35B 265	F. James *et al.*	(CERN, SACL, OSLO)
MEISNER	71	PR D3 59	G.W. Meisner *et al.*	(MASA, BNL, YALE)
REPELLIN	71	PL 36B 603	J.P. Repellin *et al.*	(ORSAY, CERN)
WEBBER	71	PR D3 64	B.R. Webber *et al.*	(LRL)
Also		PRL 21 498	B.R. Webber *et al.*	(LRL)
Also		Thesis UCRL 19226	B.R. Webber	(LRL)
WOLFF	71	PL 36B 517	B. Wolff *et al.*	(ORSAY, CERN)
ALBROW	70	PL 33B 516	M.G. Albrow *et al.*	(MCHS, DARE)
ARONSON	70	PRL 25 1057	S.H. Aronson *et al.*	(EFI, ILLC, SLAC)
BARMIN	70	PL 33B 377	V.V. Barmin *et al.*	(ITEP, JINR)
BASILE	70	PR D2 78	P. Basile *et al.*	(SACL)
BECHERRAWY	70	PR D1 1452	T. Becherrawy	(ROCH)
BUCHANAN	70	PL 33B 623	C.D. Buchanan *et al.*	(SLAC, JHU, UCLA)
Also		Private Comm.	A.J. Cox	
BUDAGOV	70	PR D2 815	I.A. Budagov *et al.*	(CERN, ORSAY, EPOL)
Also		PL 28B 215	I.A. Budagov *et al.*	(CERN, ORSAY, EPOL)
CHO	70	PR D1 3031	Y. Cho *et al.*	(CMU, BNL, CASE)
Also		PRL 19 668	D.G. Hill *et al.*	(BNL, CMU)
CHOLLET	70	PL 31B 658	J.C. Chollet *et al.*	(CERN)
CULLEN	70	PR 32B 523	M. Cullen *et al.*	(AACH, CERN, TORI)
MARX	70	PL 32B 219	J. Marx *et al.*	(COLU, HARV, CERN)
Also		Thesis Nevis 179	J. Marx	(COLU)
SCRIBANO	70	PL 32B 224	A. Scribano *et al.*	(PISA, COLU, HARV)
SMITH	70	PR 32B 133	R.C. Smith *et al.*	(UMD, BNL)
WEBBER	70	PR D1 1967	B.R. Webber *et al.*	(LRL)
Also		Thesis UCRL 19226	B.R. Webber	(LRL)
BANNER	69	PR 188 2033	M. Banner *et al.*	(PRIN)
Also		PRL 21 1103	M. Banner *et al.*	(PRIN)
Also		PRL 21 1107	J.W. Cronin, J.K. Liu, J.E. Pilcher	(PRIN)
BENNETT	69	PL 29B 317	S. Bennett *et al.*	(COLU, BNL)
FAISSNER	69	PL 30B 204	H. Faissner *et al.*	(AACH3, CERN, TORI)
LITTENBERG	69	PRL 22 654	L.S. Littenberg *et al.*	(UCSD)
LONGO	69	PR 181 1808	M.J. Longo, K.K. Young, J.A. Helland	(MICH, UCLA)
PACIOTTI	69	Thesis UCRL 19446	M.A. Paciotti	(LRL)
SAAL	69	Thesis	H.J. Saal	(COLU)
ABRAMS	68B	PR 176 1603	R.J. Abrams *et al.*	(ILL)
ARNOLD	68B	PL 28B 56	R.G. Arnold *et al.*	(CERN, ORSAY)
BASILE	68B	PL 28B 58	P. Basile *et al.*	(SACL)
BENNETT	68	PL 27B 244	S. Bennett *et al.*	(COLU, CERN)
BLANPIED	68	PRL 21 1650	W.A. Blanpied *et al.*	(CASE, HARV, MCGI)
BOHM	68B	PL 27B 594	A. Bohm *et al.*	
BUDAGOV	68	NC 57A 182	I.A. Budagov *et al.*	(CERN, ORSAY, IPNP)
Also		PL 28B 215	I.A. Budagov *et al.*	(CERN, ORSAY, EPOL)
JAMES	68	NP B8 365	F. James, H. Briand	(IPNP, CERN)
Also		PRL 21 257	J.A. Helland, M.J. Longo, K.K. Young	(UCLA, MICH)
KULYUKINA	68	JETP 26 20 Translated from ZETF 53 29.	L.A. Kulyukina *et al.*	(JINR)
KUNZ	68	Thesis PU-68-46	P.F. Kunz	(PRIN)
BENNETT	67	PRL 19 993	S. Bennett *et al.*	(COLU)
DEBOUARD	67	NC 52A 662	X. de Bouard *et al.*	(CERN)
Also		PL 15 58	X. de Bouard *et al.*	(CERN, ORSAY, MPIM)
DEVLIN	67	PRL 18 54	T.J. Devlin *et al.*	(PRIN, UMD)
Also		PR 169 1045	G.A. Sayer *et al.*	(UMD, PPA, PRIN)
DORFAN	67	PRL 19 987	D.E. Dorfan *et al.*	(SLAC, LRL)
FELDMAN	67B	PR 155 1611	L. Feldman *et al.*	(PENN)
FITCH	67	PR 164 1711	V.L. Fitch *et al.*	(PRIN)
GINSBERG	67	PR 162 1570	E.S. Ginsberg	(MASB)
HILL	67	PRL 19 668	D.G. Hill *et al.*	(BNL, CMU)
HOPKINS	67	PRL 19 185	H.W.K. Hopkins, T.C. Bacon, F.R. Eisler	(BNL)
NEFKENS	67	PR 157 1233	B.M.K. Nefkens *et al.*	(ILL)
SCHMIDT	67	Thesis Nevis 160	P. Schmidt	(COLU)
BEHR	66	PL 22 540	L. Behr *et al.*	(EPOL, MILA, PADO, ORSAY)
HAWKINS	66	PL 21 238	C.J.B. Hawkins	(YALE)
Also		PR 156 1444	C.J.B. Hawkins	(YALE)
ANDERSON	65	PRL 14 475	J.A. Anderson *et al.*	(LRL, WISC)
ASTBURY	65B	PL 18 175	P. Astbury *et al.*	(CERN, ZURI)
AUBERT	65	PL 17 59	B. Aubert *et al.*	(EPOL, ORSAY)
Also		PL 24B 75	J.P. Lowys *et al.*	(EPOL, ORSAY)
BALDO-...	65	NC 38 684	M. Baldo-Ceolin *et al.*	(PADO)
FRANZINI	65	PR 140 B127	P. Franzini *et al.*	(COLU, RUTG)
GUIDONI	65	Argonne Conf. 49	P. Guidoni *et al.*	(BNL, YALE)
HOPKINS	65	Argonne Conf. 67	H.W.K. Hopkins, T.C. Bacon, F. Eisler	(VAND+)
ALEKSANYAN	64B	Dubna Conf. 2 102	A.S. Aleksanyan *et al.*	(YERE)
Also		JETP 19 1019 Translated from ZETF 46 1504.	A.S. Aleksanyan *et al.*	(LEBD, MPEI, YERE)
ANIKINA	64	JETP 19 42 Translated from ZETF 46 59.	M.K. Anikina *et al.*	(GEOR, JINR)
FITCH	61	NC 22 1160	V.L. Fitch, P.A. Piroue, R.B. Perkins	(PRIN+)
GOOD	61	PR 124 1223	R.H. Good *et al.*	(LRL)

OTHER RELATED PAPERS

HAYAKAWA	93	PR D48 1150	M. Hayakawa, A.I. Sanda	(NAGO)
"Searching for *T*, *CP*, *CPT*, $\Delta S = \Delta Q$ Rule Violations in the Neutral *K* Meson System: A Guide"				
LITTENBERG	93	ARNPS 43 729	L.S. Littenberg, G. Valencia	(BNL, FNAL)
Rare and Radiative Kaon Decays				
RITCHIE	93	RMP 65 1149	J.L. Ritchie, S.G. Wojcicki	
"Rare *K* Decays"				
WINSTEIN	93	RMP 65 1113	B. Winstein, L. Wolfenstein	
"The Search for Direct *CP* Violation"				
BATTISTON	92	PRPL 214 293	R. Battiston *et al.*	(PGIA, CERN, TRSTT)
Status and Perspectives of *K* Decay Physics				
DIB	92	PR D46 2265	C.O. Dib, R.D. Peccei	(UCLA)
Tests of *CPT* conservation in the neutral kaon system.				
KLEINKNECHT	92	CNPP 20 281	K. Kleinknecht	(MANZ)
New Results on *CP* Violation in Decays of Neutral *K* Mesons.				
KLEINKNECHT	90	ZPHY C46 S57	K. Kleinknecht	(MANZ)
PEACH	90	JP G16 131	K.J. Peach	(EDIN)
BRYMAN	89	IJMP A4 79	D.A. Bryman	(TRIU)
"Rare Kaon Decays"				
KLEINKNECHT	76	ARNS 26 1	K. Kleinknecht	(DORT)
GINSBERG	73	PR D8 3887	E.S. Ginsberg, J. Smith	(MIT, STON)
GINSBERG	70	PR D1 229	E.S. Ginsberg	(HAIF)
HEUSSE	70	LNC 3 449	P. Heusse *et al.*	(ORSAY)
CRONIN	68C	Vienna Conf. 281	J.W. Cronin	(PRIN)
RUBBIA	67	PL 24B 531	C. Rubbia, J. Steinberger	(CERN, COLU)
Also		PL 23 167	C. Rubbia, J. Steinberger	(CERN, COLU)
Also		PL 20 207	C. Alff-Steinberger *et al.*	(CERN)
Also		PL 21 595	C. Alff-Steinberger *et al.*	(CERN)
AUERBACH	66	PR 149 1052	L.B. Auerbach *et al.*	(PENN)
Also		PRL 14 192	L.B. Auerbach *et al.*	(PENN)
FIRESTONE	66B	PRL 17 116	A. Firestone *et al.*	(YALE, BNL)
BEHR	65	Argonne Conf. 59	L. Behr *et al.*	(EPOL, MILA, PADO)
MESTVIRISH...	65	JINR P 2449	A.N. Mestvirishvili *et al.*	(JINR)
TRILLING	65B	UCRL 16473 Updated from 1965 Argonne Conference, page 115.	G.N. Trilling	(LRL)
JOVANOV...	63	BNL Conf. 42	J.V. Jovanovich *et al.*	(BNL, UMD)

$K^*_0(700)$

$I(J^P) = \frac{1}{2}(0^+)$

also known as κ; was $K^*_0(800)$

Needs confirmation. See the mini-review on scalar mesons under $f_0(500)$ (see the index for the page number).

$K^*_0(700)$ T-Matrix Pole $\sqrt{s}$

VALUE (MeV)	*DOCUMENT ID*		*TECN*	*COMMENT*
(630–730) − *i* (260–340) OUR EVALUATION				
• • • We do not use the following data for averages, fits, limits, etc. • • •				
$(670 \pm 18) - i\,(295 \pm 28)$	[1] PELAEZ	17	RVUE	
$(764 \pm 63^{+71}_{-54}) - i\,(306 \pm 149^{+143}_{-85})$	[2] ABLIKIM	11B	BES2	1.3k $J/\psi \to K^0_S K^0_S \pi^+\pi^-$
$(665 \pm 9) - i\,(268^{+21}_{-6})$	[3] GUO	11B	RVUE	
$(849 \pm 77^{+18}_{-14}) - i\,(256 \pm 40^{+46}_{-22})$	[2] ABLIKIM	10E	BES2	1.4k $J/\psi \to K^\pm K^0_S \pi^\mp \pi^0$
$(663 \pm 8 \pm 34) - i\,(329 \pm 5 \pm 22)$	[4] BUGG	10	RVUE	S-matrix pole
$(706.0 \pm 1.8 \pm 22.8) - i\,(319.4 \pm 2.2 \pm 20.2)$	[5] BONVICINI	08A	CLEO	141k $D^+ \to K^-\pi^+\pi^+$
$(841 \pm 30^{+81}_{-73}) - i\,(309 \pm 45^{+48}_{-72})$	[2] ABLIKIM	06C	BES2	25k $J/\psi \to \overline{K}^*(892)^0 K^+\pi^-$
$(750^{+30}_{-55}) - i\,(342 \pm 60)$	[6] BUGG	06	RVUE	
$(658 \pm 13) - i\,(279 \pm 12)$	[7] DESCOTES-G...	06	RVUE	$\pi K \to \pi K$
$(757 \pm 33) - i\,(279 \pm 41)$	[8] GUO	06	RVUE	
$(694 \pm 53) - i\,(303 \pm 30)$	[9] ZHOU	06	RVUE	$Kp \to K^-\pi^+ n$
$(754 \pm 22) - i\,(230 \pm 27)$	[10] PELAEZ	04A	RVUE	$K\pi \to K\pi$
$(594 \pm 79) - i\,(362 \pm 166)$	[9] ZHENG	04	RVUE	$K^- p \to K^-\pi^+ n$
$(722 \pm 60) - i\,(386 \pm 50)$	[9] BUGG	03	RVUE	11 $K^- p \to K^-\pi^+ n$
$(875 \pm 75) - i\,(335 \pm 110)$	[11] ISHIDA	97B	RVUE	11 $K^- p \to K^-\pi^+ n$
$727 - i\,263$	[12] VANBEVEREN	86	RVUE	

[1] Extracted from Forward Dispersion Relations using sequences of Pade approximants .
[2] Extracted from Breit-Wigner parameters.
[3] Fit to scattering phase shifts using UChPT amplitudes with explicit resonances.
[4] Supersedes BUGG 06. Combined analysis of ASTON 88, ABLIKIM 06C, AITALA 06, and LINK 09 using an s-dependent width with couplings to $K\pi$ and $K\eta'$, and the Adler zero near thresholds.
[5] From a complex pole included in the fit. Using parameters from the model that fits data best.
[6] Reanalysis of ASTON 88, AITALA 02, and ABLIKIM 06C using for the κ an s-dependent width with an Adler zero near threshold.
[7] Using Roy-Steiner equations (ROY 71) consistent with unitarity, analyticity and crossing symmetry constraints.
[8] From UChPT fitted to MERCER 71, BINGHAM 72 and ESTABROOKS 78. Amplitude shown to be consistent with data of ABLIKIM 06C.
[9] Reanalysis of ASTON 88 data.
[10] Reanalysis of data from LINGLIN 73, ESTABROOKS 78, and ASTON 88 using the Inverse Amplitude Method.
[11] Reanalysis of ASTON 88 using interfering Breit-Wigner amplitudes. Extracted from Breit-Wigner parameters.
[12] Unitarized Quark Model.

Meson Particle Listings

$K_0^*(700)$, $K^*(892)$

$K_0^*(700)$ Breit-Wigner Mass

VALUE (MeV)			EVTS	DOCUMENT ID		TECN	COMMENT
824	**±30**	**OUR AVERAGE**					
826	±49	$^{+49}_{-34}$	1.3k	[1] ABLIKIM	11B	BES2	$J/\psi \to K_S^0 K_S^0 \pi^+ \pi^-$
810	±68	$^{+15}_{-24}$	1.4k	[2] ABLIKIM	10E	BES2	$J/\psi \to K^\pm K_S^0 \pi^\mp \pi^0$
878	±23	$^{+64}_{-55}$	25k	[3] ABLIKIM	06C	BES2	$J/\psi \to \overline{K}^*(892)^0 K^+ \pi^-$
797	±19	±43	15k	[4,5] AITALA	02	E791	$D^+ \to K^- \pi^+ \pi^+$
• • • We do not use the following data for averages, fits, limits, etc. • • •							
888.0	± 1.9		141k	[6] BONVICINI	08A	CLEO	$D^+ \to K^- \pi^+ \pi^+$
856	±17	±13	54k	[7] LINK	07B	FOCS	$D^+ \to K^- \pi^+ \pi^+$
855	±15		0.6k	[8] CAWLFIELD	06A	CLEO	$D^0 \to K^+ K^- \pi^0$
905	$^{+65}_{-30}$			[9] ISHIDA	97B	RVUE	11 $K^- p \to K^- \pi^+ n$

[1] The Breit-Wigner parameters from a fit with seven intermediate resonances. The S-matrix pole position is $(764 \pm 63^{+71}_{-54}) - i\,(306 \pm 149^{+143}_{-85})$ MeV.
[2] From a fit including ten additional resonances and energy-independent Breit-Wigner width.
[3] A fit in the $K_0^*(700) + K^*(892) + K^*(1410)$ model with mass and width of the $K_0^*(700)$ from ABLIKIM 06C well describes the left slope of the $K_S^0\pi^-$ invariant mass spectrum in $\tau^- \to K_S^0 \pi^- \nu_\tau$ decay studied by EPIFANOV 07. Averaged value from different parameterizations.
[4] Not seen by KOPP 01 using 7070 events of $D^0 \to K^- \pi^+ \pi^0$. LINK 02E and LINK 05I show clear evidence for a constant non-resonant scalar amplitude rather than $K_0^*(700)$ in their high statistics analysis of $D^+ \to K^- \pi^+ \mu^+ \nu_\mu$.
[5] AUBERT 07T does not find evidence for the charged $K_0^*(700)$ using 11k events of $D^0 \to K^- K^+ \pi^0$.
[6] Using parameters from the model that fits data best.
[7] A Breit-Wigner mass and width.
[8] Breit-Wigner parameters. A significant S-wave can be also modeled as a non-resonant contribution.
[9] Reanalysis of ASTON 88 using interfering Breit-Wigner amplitudes.

$K_0^*(700)$ Breit-Wigner Width

VALUE (MeV)			EVTS	DOCUMENT ID		TECN	COMMENT
478	**± 50**	**OUR AVERAGE**					
449	±156	$^{+144}_{-81}$	1.3k	[1] ABLIKIM	11B	BES2	$J/\psi \to K_S^0 K_S^0 \pi^+ \pi^-$
536	± 87	$^{+106}_{-47}$	1.4k	[2] ABLIKIM	10E	BES2	$J/\psi \to K^\pm K_S^0 \pi^\mp \pi^0$
499	± 52	$^{+55}_{-87}$	25k	[3] ABLIKIM	06C	BES2	$J/\psi \to \overline{K}^*(892)^0 K^+ \pi^-$
410	± 43	± 87	15k	[4,5] AITALA	02	E791	$D^+ \to K^- \pi^+ \pi^+$
• • • We do not use the following data for averages, fits, limits, etc. • • •							
550.4	± 11.8		141k	[6] BONVICINI	08A	CLEO	$D^+ \to K^- \pi^+ \pi^+$
464	± 28	± 22	54k	[7] LINK	07B	FOCS	$D^+ \to K^- \pi^+ \pi^+$
251	± 48		0.6k	[8] CAWLFIELD	06A	CLEO	$D^0 \to K^+ K^- \pi^0$
545	$^{+235}_{-110}$			[9] ISHIDA	97B	RVUE	11 $K^- p \to K^- \pi^+ n$

[1] The Breit-Wigner parameters from a fit with seven intermediate resonances. The S-matrix pole position is $(764 \pm 63^{+71}_{-54}) - i\,(306 \pm 149^{+143}_{-85})$ MeV.
[2] From a fit including ten additional resonances and energy-independent Breit-Wigner width.
[3] A fit in the $K_0^*(700) + K^*(892) + K^*(1410)$ model with mass and width of the $K_0^*(700)$ from ABLIKIM 06C well describes the left slope of the $K_S^0\pi^-$ invariant mass spectrum in $\tau^- \to K_S^0 \pi^- \nu_\tau$ decay studied by EPIFANOV 07. Averaged value from different parameterizations.
[4] Not seen by KOPP 01 using 7070 events of $D^0 \to K^- \pi^+ \pi^0$. LINK 02E and LINK 05I show clear evidence for a constant non-resonant scalar amplitude rather than $K_0^*(700)$ in their high statistics analysis of $D^+ \to K^- \pi^+ \mu^+ \nu_\mu$.
[5] AUBERT 07T does not find evidence for the charged $K_0^*(700)$ using 11k events of $D^0 \to K^- K^+ \pi^0$.
[6] Using parameters from the model that fits data best.
[7] A Breit-Wigner mass and width.
[8] Statistical error only. A fit to the Dalitz plot including the $K_0^*(700)^\pm$, $K^*(892)^\pm$, and ϕ resonances modeled as Breit-Wigners. A significant S-wave can be also modeled as a non-resonant contribution.
[9] Reanalysis of ASTON 88 using interfering Breit-Wigner amplitudes.

$K_0^*(700)$ REFERENCES

PELAEZ	17	EPJ C77 91	J.R. Pelaez, A.Rodas, J.Ruiz de Elvira	
ABLIKIM	11B	PL B698 183	M. Ablikim *et al.*	(BES II Collab.)
GUO	11B	PR D84 034005	Z.-H. Guo, J.A. Oller	
ABLIKIM	10E	PL B693 88	M. Ablikim *et al.*	(BES II Collab.)
BUGG	10	PR D81 014002	D.V. Bugg	(LOQM)
LINK	09	PL B681 14	J.M. Link *et al.*	(FNAL FOCUS Collab.)
BONVICINI	08A	PR D78 052001	G. Bonvicini *et al.*	(CLEO Collab.)
AUBERT	07T	PR D76 011102	B. Aubert *et al.*	(BABAR Collab.)
EPIFANOV	07	PL B654 65	D. Epifanov *et al.*	(BELLE Collab.)
LINK	07B	PL B653 1	J.M. Link *et al.*	(FNAL FOCUS Collab.)
ABLIKIM	06C	PL B633 681	M. Ablikim *et al.*	(BES Collab.)
AITALA	06	PR D73 032004	E.M. Aitala *et al.*	(FNAL E791 Collab.)
Also		PR D74 059901 (errat.)	E.M. Aitala *et al.*	(FNAL E791 Collab.)
BUGG	06	PL B632 471	D.V. Bugg	(LOQM)
CAWLFIELD	06A	PR D74 031108	C. Cawlfield *et al.*	(CLEO Collab.)
DESCOTES-G...	06	EPJ C48 553	S. Descotes-Genon, B. Moussallam	
GUO	06	NP A773 78	F.K. Guo *et al.*	
ZHOU	06	NP A775 212	Z.Y. Zhou, H.Q. Zheng	
LINK	05I	PL B621 72	J.M. Link *et al.*	(FNAL FOCUS Collab.)
PELAEZ	04A	MPL A19 2879	J.R. Pelaez	
ZHENG	04	NP A733 235	H.Q. Zheng *et al.*	
BUGG	03	PL B572 1	D.V. Bugg	
AITALA	02	PRL 89 121801	E.M. Aitala *et al.*	(FNAL E791 Collab.)
LINK	02E	PL B535 43	J.M. Link *et al.*	(FNAL FOCUS Collab.)
KOPP	01	PR D63 092001	S. Kopp *et al.*	(CLEO Collab.)
ISHIDA	97B	PTP 98 621	S. Ishida *et al.*	
ASTON	88	NP B296 493	D. Aston *et al.*	(SLAC, NAGO, CINC, INUS)
VANBEVEREN	86	ZPHY C30 615	E. van Beveren *et al.*	(NIJM, BIEL)
ESTABROOKS	78	NP B133 490	P.G. Estabrooks *et al.*	(MCGI, CARL, DURH+)
LINGLIN	73	NP B55 408	D. Linglin	(CERN)
BINGHAM	72	NP B41 1	H.H. Bingham *et al.*	(International K^+ Collab.)
MERCER	71	NP B32 381	R. Mercer *et al.*	(JHU)
ROY	71	PL 36B 353	S.M. Roy	

$K^*(892)$

$I(J^P) = \frac{1}{2}(1^-)$

$K^*(892)$ MASS

CHARGED ONLY, HADROPRODUCED

VALUE (MeV)			EVTS	DOCUMENT ID		TECN	CHG	COMMENT
891.76±0.25 OUR AVERAGE								
893.2	±0.1	±1.0	190k	[1] AAIJ	16N	LHCB		$D^0 \to K_S^0 K^\pm \pi^\mp$
892.6	±0.5		5840	BAUBILLIER	84B	HBC	−	8.25 $K^- p \to \overline{K}^0 \pi^- p$
888	±3			NAPIER	84	SPEC	+	200 $\pi^- p \to 2K_S^0 X$
891	±1			NAPIER	84	SPEC	−	200 $\pi^- p \to 2K_S^0 X$
891.7	±2.1		3700	BARTH	83	HBC	+	70 $K^+ p \to K^0 \pi^+ X$
891	±1		4100	TOAFF	81	HBC	−	6.5 $K^- p \to \overline{K}^0 \pi^- p$
892.8	±1.6			AJINENKO	80	HBC	+	32 $K^+ p \to K^0 \pi^+ X$
890.7	±0.9		1800	AGUILAR-...	78B	HBC	±	0.76 $\overline{p}p \to K^\mp K_S^0 \pi^\pm$
886.6	±2.4		1225	BALAND	78	HBC	±	12 $\overline{p}p \to (K\pi)^\pm X$
891.7	±0.6		6706	COOPER	78	HBC	±	0.76 $\overline{p}p \to (K\pi)^\pm X$
891.9	±0.7		9000	[2] PALER	75	HBC	−	14.3 $K^- p \to (K\pi)^- X$
892.2	±1.5		4404	AGUILAR-...	71B	HBC	−	3.9,4.6 $K^- p \to (K\pi)^- p$
891	±2		1000	CRENNELL	69D	DBC	−	3.9 $K^- N \to K^0 \pi^- X$
890	±3.0		720	BARLOW	67	HBC	±	1.2 $\overline{p}p \to (K^0\pi)^\pm K^\mp$
889	±3.0		600	BARLOW	67	HBC	±	1.2 $\overline{p}p \to (K^0\pi)^\pm K\pi$
891	±2.3		620	[3] DEBAERE	67B	HBC	+	3.5 $K^+ p \to K^0 \pi^+ p$
891.0	±1.2		1700	[4] WOJCICKI	64	HBC	−	1.7 $K^- p \to \overline{K}^0 \pi^- p$
• • • We do not use the following data for averages, fits, limits, etc. • • •								
895.6	±0.8		4K	[5] LEES	17C	BABR		$J/\psi \to K_S^0 K^\pm \pi^\mp$
893.5	±1.1		27k	[6] ABELE	99D	CBAR	±	0.0 $\overline{p}p \to K^+ K^- \pi^0$
890.4	±0.2	±0.5	80k	[7] BIRD	89	LASS	−	11 $K^- p \to \overline{K}^0 \pi^- p$
890.0	±2.3		800	[3,4] CLELAND	82	SPEC	+	30 $K^+ p \to K_S^0 \pi^+ p$
896.0	±1.1		3200	[3,4] CLELAND	82	SPEC	+	50 $K^+ p \to K_S^0 \pi^+ p$
893	±1		3600	[3,4] CLELAND	82	SPEC	−	50 $K^+ p \to K_S^0 \pi^- p$
896.0	±1.9		380	DELFOSSE	81	SPEC	+	50 $K^\pm p \to K^\pm \pi^0 p$
886.0	±2.3		187	DELFOSSE	81	SPEC	−	50 $K^\pm p \to K^\pm \pi^0 p$
894.2	±2.0		765	[3] CLARK	73	HBC	−	3.13 $K^- p \to \overline{K}^0 \pi^- p$
894.3	±1.5		1150	[3,4] CLARK	73	HBC	−	3.3 $K^- p \to \overline{K}^0 \pi^- p$
892.0	±2.6		341	[3] SCHWEING...68		HBC	−	5.5 $K^- p \to \overline{K}^0 \pi^- p$

[1] Average of fit results with different parametrizations for the $K\pi$ S-wave.
[2] Inclusive reaction. Complicated background and phase-space effects.
[3] Mass errors enlarged by us to $\Gamma/\sqrt{N}$. See note.
[4] Number of events in peak reevaluated by us.
[5] From a Dalitz plot analysis in an isobar model with charged and neutral $K^*(892)$ masses and widths floating.
[6] K-matrix pole.
[7] From a partial wave amplitude analysis.

CHARGED ONLY, PRODUCED IN τ LEPTON DECAYS

VALUE (MeV)	EVTS	DOCUMENT ID		TECN	COMMENT
895.47±0.20±0.74	53k	[1] EPIFANOV	07	BELL	$\tau^- \to K_S^0 \pi^- \nu_\tau$
• • • We do not use the following data for averages, fits, limits, etc. • • •					
892.0 ±0.5		[2] BOITO	10	RVUE	$\tau^- \to K_S^0 \pi^- \nu_\tau$
892.0 ±0.9		[3,4] BOITO	09	RVUE	$\tau^- \to K_S^0 \pi^- \nu_\tau$
895.3 ±0.2		[4,5] JAMIN	08	RVUE	$\tau^- \to K_S^0 \pi^- \nu_\tau$
896.4 ±0.9	12k	[6] BONVICINI	02	CLEO	$\tau^- \to K^- \pi^0 \nu_\tau$
895 ±2		[7] BARATE	99R	ALEP	$\tau^- \to K^- \pi^0 \nu_\tau$

[1] From a fit in the $K_0^*(700) + K^*(892) + K^*(1410)$ model.
[2] From the pole position of the $K\pi$ vector form factor using EPIFANOV 07 and constraints from K_{l3} decays in ANTONELLI 10.
[3] From the pole position of the $K\pi$ vector form factor in the complex s-plane and using EPIFANOV 07 data.
[4] Systematic uncertainties not estimated.
[5] Reanalysis of EPIFANOV 07 using resonance chiral theory.
[6] Calculated by us from the shift by 4.7 ± 0.9 MeV (statistical uncertainty only) reported in BONVICINI 02 with respect to the world average value from PDG 00.
[7] With mass and width of the $K^*(1410)$ fixed at 1412 MeV and 227 MeV, respectively.

NEUTRAL ONLY

VALUE (MeV)	EVTS	DOCUMENT ID		TECN	COMMENT
895.55±0.20 OUR AVERAGE		Error includes scale factor of 1.7. See the ideogram below.			
894.68±0.25±0.05		[1] ABLIKIM	16F	BES3	$D^+ \to K^-\pi^+e^+\nu_e$
895.4 ±0.2 ±0.2	243k	[2] DEL-AMO-SA...	11I	BABR	$D^+ \to K^-\pi^+e^+\nu_e$
895.7 ±0.2 ±0.3	141k	[3] BONVICINI	08A	CLEO	$D^+ \to K^-\pi^+\pi^+$
$895.41\pm0.32^{+0.35}_{-0.43}$	18k	[4] LINK	05I	FOCS	$D^+ \to K^-\pi^+\mu^+\nu_\mu$
896 ±2		BARBERIS	98E	OMEG	450 $pp \to p_f p_s K^*\overline{K}^*$
895.9 ±0.5 ±0.2		ASTON	88	LASS	11 $K^-p \to K^-\pi^+n$
894.52±0.63	25k	[5] ATKINSON	86	OMEG	20–70 γp
894.63±0.76	20k	[5] ATKINSON	86	OMEG	20–70 γp
897 ±1	28k	EVANGELIS...	80	OMEG	10 $\pi^-p \to K^+\pi^-(\Lambda,\Sigma)$
898.4 ±1.4	1180	AGUILAR-...	78B	HBC	0.76 $\overline{p}p \to K^\mp K^0_S\pi^\pm$
894.9 ±1.6		WICKLUND	78	ASPK	3,4,6 $K^\pm N \to (K\pi)^0 N$
897.6 ±0.9		BOWLER	77	DBC	5.4 $K^+d \to K^+\pi^-pp$
895.5 ±1.0	3600	MCCUBBIN	75	HBC	3.6 $K^-p \to K^-\pi^+n$
897.1 ±0.7	22k	[5] PALER	75	HBC	14.3 $K^-p \to (K\pi)^0$ X
896.0 ±0.6	10k	FOX	74	RVUE	2 $K^-p \to K^-\pi^+n$
896.0 ±0.6		FOX	74	RVUE	2 $K^+n \to K^+\pi^-p$
896 ±2		[6] MATISON	74	HBC	12 $K^+p \to K^+\pi^-\Delta$
896 ±1	3186	LEWIS	73	HBC	2.1–2.7 $K^+p \to K\pi\pi p$
894.0 ±1.3		[6] LINGLIN	73	HBC	2–13 $K^+p \to K^+\pi^-\pi^+p$
898.4 ±1.3	1700	[7] BUCHNER	72	DBC	4.6 $K^+n \to K^+\pi^-p$
897.9 ±1.1	2934	[7] AGUILAR-...	71B	HBC	3.9,4.6 $K^-p \to K^-\pi^+n$
898.0 ±0.7	5362	[7] AGUILAR-...	71B	HBC	3.9,4.6 $K^-p \to K^-\pi^+\pi^-p$
895 ±1	4300	[8] HABER	70	DBC	3 $K^-N \to K^-\pi^+$ X
893.7 ±2.0	10k	DAVIS	69	HBC	12 $K^+p \to K^+\pi^-\pi^+p$
894.7 ±1.4	1040	[7] DAUBER	67B	HBC	2.0 $K^-p \to K^-\pi^+\pi^-p$
• • • We do not use the following data for averages, fits, limits, etc. • • •					
898.1 ±1.0	4K	[9] LEES	17C	BABR	$J/\psi \to K^0_S K^\pm\pi^\mp$
895.53±0.17		LEES	13F	BABR	$D^+ \to K^+K^-\pi^+$
894.9 ±0.5 ±0.7	14.4k	[10] MITCHELL	09A	CLEO	$D_s^+ \to K^+K^-\pi^+$
896.2 ±0.3	20k	[11] AUBERT	07AK	BABR	10.6 $e^+e^- \to K^{*0}K^\pm\pi^\mp\gamma$
900.7 ±1.1	5900	BARTH	83	HBC	70 $K^+p \to K^+\pi^-$X

[1] Taking also into account the $K_0^*(1430)^0$ and $K_2^*(1430)^0$.
[2] Taking into account the $K^*(892)^0$, S-wave and P-wave ($K^*(1410)^0$).
[3] From the isobar model with a complex pole for the κ.
[4] Fit to $K\pi$ mass spectrum includes a non-resonant scalar component.
[5] Inclusive reaction. Complicated background and phase-space effects.
[6] From pole extrapolation.
[7] Mass errors enlarged by us to $\Gamma/\sqrt{N}$. See note.
[8] Number of events in peak reevaluated by us.
[9] From a Dalitz plot analysis in an isobar model with charged and neutral $K^*(892)$ masses and widths floating.
[10] This value comes from a fit with χ^2 of 178/117.
[11] Systematic uncertainties not estimated.

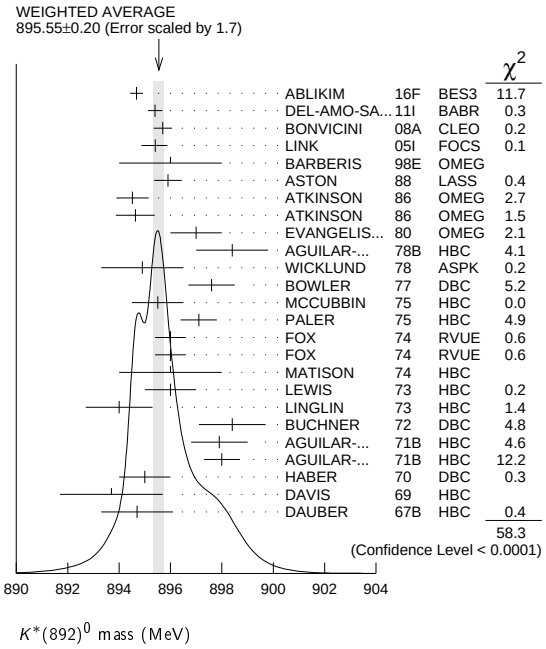

$K^*(892)$ MASSES AND MASS DIFFERENCES

Unrealistically small errors have been reported by some experiments. We use simple "realistic" tests for the minimum errors on the determination of a mass and width from a sample of N events:

$$\delta_{\min}(m) = \frac{\Gamma}{\sqrt{N}}, \quad \delta_{\min}(\Gamma) = 4\frac{\Gamma}{\sqrt{N}} \ . \tag{1}$$

We consistently increase unrealistic errors before averaging. For a detailed discussion, see the 1971 edition of this Note.

$m_{K^*(892)^0} - m_{K^*(892)^\pm}$

VALUE (MeV)	EVTS	DOCUMENT ID		TECN	CHG	COMMENT
6.7±1.2 OUR AVERAGE						
7.7±1.7	2980	AGUILAR-...	78B	HBC	±0	0.76 $\overline{p}p \to K^\mp K^0_S\pi^\pm$
5.7±1.7	7338	AGUILAR-...	71B	HBC	−0	3.9,4.6 K^-p
6.3±4.1	283	[1] BARASH	67B	HBC		0.0 $\overline{p}p$

[1] Number of events in peak reevaluated by us.

$K^*(892)$ RANGE PARAMETER

All from partial wave amplitude analyses.

VALUE (GeV^{-1})	EVTS	DOCUMENT ID		TECN	CHG	COMMENT
2.1 ±0.5 ±0.5	243k	[1] DEL-AMO-SA.	11I	BABR	0	$D^+ \to K^-\pi^+e^+\nu_e$
$3.96\pm0.54^{+1.31}_{-0.90}$	18k	[2] LINK	05I	FOCS	0	$D^+ \to K^-\pi^+\mu^+\nu_\mu$
3.4 ±0.7		ASTON	88	LASS	0	11 $K^-p \to K^-\pi^+n$
• • • We do not use the following data for averages, fits, limits, etc. • • •						
12.1 ±3.2 ±3.0		BIRD	89	LASS	−	11 $K^-p \to \overline{K}^0\pi^-p$

[1] Taking into account the $K^*(892)^0$, S-wave and P-wave ($K^*(1410)^0$).
[2] Fit to $K\pi$ mass spectrum includes a non-resonant scalar component.

$K^*(892)$ WIDTH

CHARGED ONLY, HADROPRODUCED

VALUE (MeV)	EVTS	DOCUMENT ID		TECN	CHG	COMMENT
50.3±0.8 OUR FIT						
50.3±0.8 OUR AVERAGE						
47.2±0.3±2.3	190k	[1] AAIJ	16N	LHCB		$D^0 \to K^0_S K^\pm\pi^\mp$
49 ±2	5840	BAUBILLIER	84B	HBC	−	8.25 $K^-p \to \overline{K}^0\pi^-p$
56 ±4		NAPIER	84	SPEC	−	200 $\pi^-p \to 2K^0_S$ X
51 ±2	4100	TOAFF	81	HBC	−	6.5 $K^-p \to \overline{K}^0\pi^-p$
50.5±5.6		AJINENKO	80	HBC	+	32 $K^+p \to K^0\pi^+$X
45.8±3.6	1800	AGUILAR-...	78B	HBC	±	0.76 $\overline{p}p \to K^\mp K^0_S\pi^\pm$
52.0±2.5	6706	[2] COOPER	78	HBC	±	0.76 $\overline{p}p \to (K\pi)^\pm$ X
52.1±2.2	9000	[3] PALER	75	HBC	−	14.3 $K^-p \to (K\pi)^-$ X
46.3±6.7	765	[2] CLARK	73	HBC	−	3.13 $K^-p \to \overline{K}^0\pi^-p$
48.2±5.7	1150	[2,4] CLARK	73	HBC	−	3.3 $K^-p \to \overline{K}^0\pi^-p$
54.3±3.3	4404	[2] AGUILAR-...	71B	HBC	−	3.9,4.6 $K^-p \to (K\pi)^-p$
46 ±5	1700	[2,4] WOJCICKI	64	HBC	−	1.7 $K^-p \to \overline{K}^0\pi^-p$
• • • We do not use the following data for averages, fits, limits, etc. • • •						
43.6±1.3	4K	[5] LEES	17C	BABR		$J/\psi \to K^0_S K^\pm\pi^\mp$
54.8±1.7	27k	[6] ABELE	99D	CBAR	±	0.0 $\overline{p}p \to K^+K^-\pi^0$
45.2±1 ±2	80k	[7] BIRD	89	LASS	−	11 $K^-p \to \overline{K}^0\pi^-p$
42.8±7.1	3700	BARTH	83	HBC	+	70 $K^+p \to K^0\pi^+$X
64.0±9.2	800	[2,4] CLELAND	82	SPEC	+	30 $K^+p \to K^0_S\pi^+p$
62.0±4.4	3200	[2,4] CLELAND	82	SPEC	+	50 $K^+p \to K^0_S\pi^+p$
55 ±4	3600	[2,4] CLELAND	82	SPEC	−	50 $K^+p \to K^0_S\pi^-p$
62.6±3.8	380	DELFOSSE	81	SPEC	+	50 $K^\pm p \to K^\pm\pi^0p$
50.5±3.9	187	DELFOSSE	81	SPEC	−	50 $K^\pm p \to K^\pm\pi^0p$

[1] Average of fit results with different parametrizations for the $K\pi$ S-wave.
[2] Width errors enlarged by us to $4\times\Gamma/\sqrt{N}$; see note.
[3] Inclusive reaction. Complicated background and phase-space effects.
[4] Number of events in peak reevaluated by us.
[5] From a Dalitz plot analysis in an isobar model with charged and neutral $K^*(892)$ masses and widths floating.
[6] K-matrix pole.
[7] From a partial wave amplitude analysis.

CHARGED ONLY, PRODUCED IN τ LEPTON DECAYS

VALUE (MeV)	EVTS	DOCUMENT ID		TECN	COMMENT
46.2±0.6±1.2	53k	[1] EPIFANOV	07	BELL	$\tau^- \to K^0_S\pi^-\nu_\tau$

Meson Particle Listings

$K^*(892)$

• • • We do not use the following data for averages, fits, limits, etc. • • •

46.5±1.1	[2] BOITO	10	RVUE	$\tau^- \to K^0_S \pi^- \nu_\tau$	
46.2±0.4	[3,4] BOITO	09	RVUE	$\tau^- \to K^0_S \pi^- \nu_\tau$	
47.5±0.4	[4,5] JAMIN	08	RVUE	$\tau^- \to K^0_S \pi^- \nu_\tau$	
55 ±8	[6] BARATE	99R	ALEP	$\tau^- \to K^- \pi^0 \nu_\tau$	

[1] From a fit in the $K^*_0(700) + K^*(892) + K^*(1410)$ model.
[2] From the pole position of the $K\pi$ vector form factor using EPIFANOV 07 and constraints from K_{l3} decays in ANTONELLI 10.
[3] From the pole position of the $K\pi$ vector form factor in the complex s-plane and using EPIFANOV 07 data.
[4] Systematic uncertainties not estimated.
[5] Reanalysis of EPIFANOV 07 using resonance chiral theory.
[6] With mass and width of the $K^*(1410)$ fixed at 1412 MeV and 227 MeV, respectively.

NEUTRAL ONLY

VALUE (MeV)	EVTS	DOCUMENT ID		TECN	COMMENT
47.3 ±0.5 OUR FIT	Error includes scale factor of 1.9.				
47.3 ±0.5 OUR AVERAGE	Error includes scale factor of 2.0. See the ideogram below.				
46.53±0.56±0.31		[1] ABLIKIM	16F	BES3	$D^+ \to K^- \pi^+ e^+ \nu_e$
46.5 ±0.3 ±0.2	243k	[2] DEL-AMO-SA...	11I	BABR	$D^+ \to K^- \pi^+ e^+ \nu_e$
45.3 ±0.5 ±0.6	141k	[3] BONVICINI	08A	CLEO	$D^+ \to K^- \pi^+ \pi^+$
$47.79 \pm 0.86 ^{+1.32}_{-1.06}$	18k	[4] LINK	05I	FOCS	$D^+ \to K^- \pi^+ \mu^+ \nu_\mu$
54 ±3		BARBERIS	98E	OMEG	450 $pp \to p_f p_s K^* \overline{K}^*$
50.8 ±0.8 ±0.9		ASTON	88	LASS	11 $K^- p \to K^- \pi^+ n$
46.5 ±4.3	5900	BARTH	83	HBC	70 $K^+ p \to K^+ \pi^- X$
54 ±2	28k	EVANGELIS...	80	OMEG	10 $\pi^- p \to K^+ \pi^- (\Lambda, \Sigma)$
45.9 ±4.8	1180	AGUILAR-...	78B	HBC	0.76 $\overline{p}p \to K^\mp K^0_S \pi^\pm$
51.2 ±1.7		WICKLUND	78	ASPK	3,4,6 $K^\pm N \to (K\pi)^0 N$
48.9 ±2.5		BOWLER	77	DBC	5.4 $K^+ d \to K^+ \pi^- pp$
48 $^{+3}_{-2}$	3600	MCCUBBIN	75	HBC	3.6 $K^- p \to K^- \pi^+ n$
50.6 ±2.5	22k	[5] PALER	75	HBC	14.3 $K^- p \to (K\pi)^0$ X
47 ±2	10k	FOX	74	RVUE	2 $K^- p \to K^- \pi^+ n$
51 ±2		FOX	74	RVUE	2 $K^+ n \to K^+ \pi^- p$
46.0 ±3.3	3186	[6] LEWIS	73	HBC	2.1–2.7 $K^+ p \to K \pi \pi p$
51.4 ±5.0	1700	[6] BUCHNER	72	DBC	4.6 $K^+ n \to K^+ \pi^- p$
55.8 $^{+4.2}_{-3.4}$	2934	[6] AGUILAR-...	71B	HBC	3.9,4.6 $K^- p \to K^- \pi^+ n$
48.5 ±2.7	5362	AGUILAR-...	71B	HBC	3.9,4.6 $K^- p \to K^- \pi^+ \pi^- p$
54.0 ±3.3	4300	[6,7] HABER	70	DBC	3 $K^- N \to K^- \pi^+ X$
53.2 ±2.1	10k	[6] DAVIS	69	HBC	12 $K^+ p \to K^+ \pi^- \pi^+ p$
44 ±5.5	1040	[6] DAUBER	67B	HBC	2.0 $K^- p \to K^- \pi^+ \pi^- p$

• • • We do not use the following data for averages, fits, limits, etc. • • •

52.6 ±1.7	4K	[8] LEES	17C	BABR	$J/\psi \to K^0_S K^\pm \pi^\mp$
44.90±0.30		LEES	13F	BABR	$D^+ \to K^+ K^- \pi^+$
45.7 ±1.1 ±0.5	14.4k	[9] MITCHELL	09A	CLEO	$D^+_s \to K^+ K^- \pi^+$
50.6 ±0.9	20k	[10] AUBERT	07AK	BABR	10.6 $e^+ e^- \to K^{*0} K^\pm \pi^\mp \gamma$

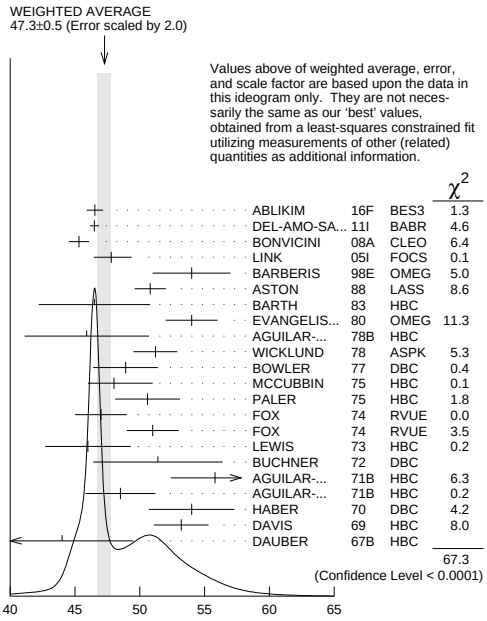

[1] Taking also into account the $K^*_0(1430)^0$ and $K^*_2(1430)^0$.
[2] Taking into account the $K^*(892)^0$, S-wave and P-wave ($K^*(1410)^0$).
[3] From the isobar model with a complex pole for the κ.
[4] Fit to $K\pi$ mass spectrum includes a non-resonant scalar component.
[5] Inclusive reaction. Complicated background and phase-space effects.
[6] Width errors enlarged by us to $4 \times \Gamma/\sqrt{N}$; see note.
[7] Number of events in peak reevaluated by us.
[8] From a Dalitz plot analysis in an isobar model with charged and neutral $K^*(892)$ masses and widths floating.
[9] This value comes from a fit with χ^2 of 178/117.
[10] Systematic uncertainties not estimated.

$K^*(892)$ DECAY MODES

	Mode	Fraction (Γ_i/Γ)	Confidence level
Γ_1	$K\pi$	~ 100 %	
Γ_2	$(K\pi)^\pm$	(99.900±0.009) %	
Γ_3	$(K\pi)^0$	(99.754±0.021) %	
Γ_4	$K^0\gamma$	(2.46 ±0.21) × 10^{-3}	
Γ_5	$K^\pm\gamma$	(1.00 ±0.09) × 10^{-3}	
Γ_6	$K\pi\pi$	< 7 × 10^{-4}	95%

CONSTRAINED FIT INFORMATION

An overall fit to the total width and a partial width uses 14 measurements and one constraint to determine 3 parameters. The overall fit has a $\chi^2 = 9.8$ for 12 degrees of freedom.

The following *off-diagonal* array elements are the correlation coefficients $\langle \delta p_i \delta p_j \rangle / (\delta p_i \cdot \delta p_j)$, in percent, from the fit to parameters p_i, including the branching fractions, $x_i \equiv \Gamma_i/\Gamma_{total}$. The fit constrains the x_i whose labels appear in this array to sum to one.

x_5	−100		
Γ	18	−18	
	x_2	x_5	

	Mode	Rate (MeV)
Γ_2	$(K\pi)^\pm$	50.2 ±0.8
Γ_5	$K^\pm\gamma$	0.050±0.005

CONSTRAINED FIT INFORMATION

An overall fit to the total width and a partial width uses 23 measurements and one constraint to determine 3 parameters. The overall fit has a $\chi^2 = 68.4$ for 21 degrees of freedom.

The following *off-diagonal* array elements are the correlation coefficients $\langle \delta p_i \delta p_j \rangle / (\delta p_i \cdot \delta p_j)$, in percent, from the fit to parameters p_i, including the branching fractions, $x_i \equiv \Gamma_i/\Gamma_{total}$. The fit constrains the x_i whose labels appear in this array to sum to one.

x_4	−100		
Γ	12	−12	
	x_3	x_4	

	Mode	Rate (MeV)	Scale factor
Γ_3	$(K\pi)^0$	47.2 ±0.5	1.9
Γ_4	$K^0\gamma$	0.117±0.010	

$K^*(892)$ PARTIAL WIDTHS

$\Gamma(K^0\gamma)$ **Γ_4**

VALUE (keV)	EVTS	DOCUMENT ID		TECN	CHG	COMMENT
116 ±10 OUR FIT						
116.5± 9.9	584	CARLSMITH	86	SPEC	0	$K^0_L A \to K^0_S \pi^0 A$

$\Gamma(K^\pm\gamma)$ **Γ_5**

VALUE (keV)	DOCUMENT ID		TECN	CHG	COMMENT
50± 5 OUR FIT					
50± 5 OUR AVERAGE					
48±11	BERG	83	SPEC	−	156 $K^- A \to \overline{K}\pi A$
51± 5	CHANDLEE	83	SPEC	+	200 $K^+ A \to K\pi A$

$K^*(892)$ BRANCHING RATIOS

$\Gamma(K^0\gamma)/\Gamma_{total}$ **Γ_4/Γ**

VALUE (units 10^{-3})	DOCUMENT ID		TECN	CHG	COMMENT
2.46±0.21 OUR FIT					
• • • We do not use the following data for averages, fits, limits, etc. • • •					
1.5 ±0.7	CARITHERS	75B	CNTR	0	8–16 $\overline{K}^0 A$

$\Gamma(K^\pm\gamma)/\Gamma_{total}$ Γ_5/Γ

VALUE (units 10^{-3})	CL%	DOCUMENT ID	TECN	CHG	COMMENT
1.00±0.09 OUR FIT					
• • • We do not use the following data for averages, fits, limits, etc. • • •					
<1.6	95	BEMPORAD 73	CNTR	+	10–16 K^+ A

$\Gamma(K\pi\pi)/\Gamma((K\pi)^\pm)$ Γ_6/Γ_2

VALUE	CL%	DOCUMENT ID	TECN	CHG	COMMENT
< 7 × 10^{-4}	95	JONGEJANS 78	HBC		4 $K^- p \to p\overline{K}^0 2\pi$
• • • We do not use the following data for averages, fits, limits, etc. • • •					
<20 × 10^{-4}		WOJCICKI 64	HBC	−	1.7 $K^- p \to \overline{K}^0 \pi^- p$

$K^*(892)$ REFERENCES

LEES	17C	PR D95 072007	J.P. Lees *et al.*	(BABAR Collab)
AAIJ	16N	PR D93 052018	R. Aaij *et al.*	(LHCb Collab.)
ABLIKIM	16F	PR D94 032001	M. Ablikim *et al.*	(BES III Collab.)
LEES	13F	PR D87 052010	J.P. Lees *et al.*	(BABAR Collab.)
DEL-AMO-SA...	11I	PR D83 072001	P. del Amo Sanchez *et al.*	(BABAR Collab.)
ANTONELLI	10	EPJ C69 399	M. Antonelli *et al.*	(FlaviaNet Working Group)
BOITO	10	JHEP 1009 031	D.R. Boito, R. Escribano, M. Jamin	(BARC)
BOITO	09	EPJ C59 821	D.R. Boito, R. Escribano, M. Jamin	
MITCHELL	09A	PR D79 072008	R.E. Mitchell *et al.*	(CLEO Collab.)
BONVICINI	08A	PR D78 052001	G. Bonvicini *et al.*	(CLEO Collab.)
JAMIN	08	PL B664 78	M. Jamin, A. Pich, J. Portoles	
AUBERT	07AK	PR D76 012008	B. Aubert *et al.*	(BABAR Collab.)
EPIFANOV	07	PL B654 65	D. Epifanov *et al.*	(BELLE Collab.)
LINK	05I	PL B621 72	J.M. Link *et al.*	(FNAL FOCUS Collab.)
BONVICINI	02	PRL 88 111803	G. Bonvicini *et al.*	(CLEO Collab.)
PDG	00	EPJ C15 1	D.E. Groom *et al.*	(PDG Collab.)
ABELE	99D	PL B468 178	A. Abele *et al.*	(Crystal Barrel Collab.)
BARATE	99R	EPJ C11 599	R. Barate *et al.*	(ALEPH Collab.)
BARBERIS	98E	PL B436 204	D. Barberis *et al.*	(Omega Expt.)
BIRD	89	SLAC-332	P.F. Bird	(SLAC)
ASTON	88	NP B296 493	D. Aston *et al.*	(SLAC, NAGO, CINC, INUS)
ATKINSON	86	ZPHY C30 521	M. Atkinson *et al.*	(BONN, CERN, GLAS+)
CARLSMITH	86	PRL 56 18	D. Carlsmith *et al.*	(EFI, SACL)
BAUBILLIER	84B	ZPHY C26 37	M. Baubillier *et al.*	(BIRM, CERN, GLAS+)
NAPIER	84	PL 149B 514	A. Napier *et al.*	(TUFTS, ARIZ, FNAL, FLOR+)
BARTH	83	NP B223 296	M. Barth *et al.*	(BRUX, CERN, GENO, MONS+)
BERG	83	Thesis UMI 83-21652	D.M. Berg	(ROCH)
CHANDLEE	83	PRL 51 168	C. Chandlee *et al.*	(ROCH, FNAL, MINN)
CLELAND	82	NP B208 189	W.E. Cleland *et al.*	(DURH, GEVA, LAUS+)
DELFOSSE	81	NP B183 349	A. Delfosse *et al.*	(GEVA, LAUS)
TOAFF	81	PR D23 1500	S. Toaff *et al.*	(ANL, KANS)
AJINENKO	80	ZPHY C5 177	I.V. Ajinenko *et al.*	(SERP, BRUX, MONS+)
EVANGELIS...	80	NP B165 383	C. Evangelista *et al.*	(BARI, BONN, CERN+)
AGUILAR-...	78B	NP B141 101	M. Aguilar-Benitez *et al.*	(MADR, TATA+)
BALAND	78	NP B140 220	J.F. Baland *et al.*	(MONS, BELG, CERN+)
COOPER	78	NP B136 365	A.M. Cooper *et al.*	(TATA, CERN, CDEF+)
JONGEJANS	78	NP B139 383	B. Jongejans *et al.*	(ZEEM, CERN, NIJM+)
WICKLUND	78	PR D17 1197	A.B. Wicklund *et al.*	(ANL)
BOWLER	77	NP B126 31	M.G. Bowler *et al.*	(OXF)
CARITHERS	75B	PRL 35 349	W.C.J. Carithers *et al.*	(ROCH, MCGI)
MCCUBBIN	75	NP B86 13	N.A. McCubbin, L. Lyons	(OXF)
PALER	75	NP B96 1	K. Paler *et al.*	(RHEL, SACL, EPOL)
FOX	74	NP B80 403	G.C. Fox, M.L. Griss	(CIT)
MATISON	74	PR D9 1872	M.J. Matison *et al.*	(LBL)
BEMPORAD	73	NP B51 1	C. Bemporad *et al.*	(CERN, ETH, LOIC)
CLARK	73	NP B54 432	A.G. Clark, L. Lyons, D. Radojicic	(OXF)
LEWIS	73	NP B60 283	P.H. Lewis *et al.*	(LOWC, LOIC, CDEF)
LINGLIN	73	NP B55 408	D. Linglin	(CERN)
BUCHNER	72	NP B45 333	K. Buchner *et al.*	(MPIM, CERN, BRUX)
AGUILAR-...	71B	PR D4 2583	M. Aguilar-Benitez, R.L. Eisner, J.B. Kinson	(BNL)
HABER	70	NP B17 289	B. Haber *et al.*	(REHO, SACL, BGNA, EPOL)
CRENNELL	69D	PRL 22 487	D.J. Crennell *et al.*	(BNL)
DAVIS	69	PRL 23 1071	P.J. Davis *et al.*	(LRL)
SCHWEING...	68	PR 166 1317	F. Schweingruber *et al.*	(ANL, NWES)
BARASH	67B	PR 156 1399	N. Barash *et al.*	(COLU)
BARLOW	67	NC 50A 701	J. Barlow *et al.*	(CERN, CDEF, IRAD, LIVP)
DAUBER	67B	PR 153 1403	P.M. Dauber *et al.*	(UCLA)
DEBAERE	67B	NC 51A 401	W. de Baere *et al.*	(BRUX, CERN)
WOJCICKI	64	PR 135 B484	S.G. Wojcicki	(LRL)

$K_1(1270)$ $I(J^P) = \frac{1}{2}(1^+)$

$K_1(1270)$ MASS

VALUE (MeV)	DOCUMENT ID
1272±7 OUR AVERAGE	Includes data from the 2 datablocks that follow this one.

PRODUCED BY K^-, BACKWARD SCATTERING, HYPERON EXCHANGE

VALUE (MeV)	EVTS	DOCUMENT ID	TECN	CHG	COMMENT
The data in this block is included in the average printed for a previous datablock.					
1275±10	700	GAVILLET 78	HBC	+	4.2 $K^- p \to \Xi^-(K\pi\pi)^+$

PRODUCED BY K BEAMS

VALUE (MeV)	DOCUMENT ID	TECN	CHG	COMMENT
The data in this block is included in the average printed for a previous datablock.				
1270±10	[1] DAUM 81C	CNTR	−	63 $K^- p \to K^- 2\pi p$
• • • We do not use the following data for averages, fits, limits, etc. • • •				
~ 1276	[2] TORNQVIST 82B	RVUE		
~ 1300	VERGEEST 79	HBC	−	4.2 $K^- p \to (\overline{K}\pi\pi)^- p$
1289±25	[3] CARNEGIE 77	ASPK	±	13 $K^\pm p \to (K\pi\pi)^\pm p$
~ 1300	BRANDENB... 76	ASPK	±	13 $K^\pm p \to (K\pi\pi)^\pm p$
~ 1270	OTTER 76	HBC	−	10,14,16 $K^- p \to (\overline{K}\pi\pi)^- p$
1260	DAVIS 72	HBC	+	12 $K^+ p$
1234±12	FIRESTONE 72B	DBC	+	12 $K^+ d$

[1] Well described in the chiral unitary approach of GENG 07 with two poles at 1195 and 1284 MeV and widths of 246 and 146 MeV, respectively.
[2] From a unitarized quark-model calculation.
[3] From a model-dependent fit with Gaussian background to BRANDENBURG 76 data.

PRODUCED BY BEAMS OTHER THAN K MESONS

VALUE (MeV)	EVTS	DOCUMENT ID	TECN	CHG	COMMENT
1248.1± 3.3±1.4		GULER 11	BELL		$B^+ \to J/\psi K^+\pi^+\pi^-$
• • • We do not use the following data for averages, fits, limits, etc. • • •					
1279 ±10	25k	[4] ABLIKIM 06C	BES2		$J/\psi \to \overline{K}^*(892)^0 K^+\pi^-$
1294 ±10	310	RODEBACK 81	HBC		4 $\pi^- p \to \Lambda K 2\pi$
1300	40	CRENNELL 72	HBC	0	4.5 $\pi^- p \to \Lambda K 2\pi$
1242 $^{+9}_{-10}$		[5] ASTIER 69	HBC	0	$\overline{p}p$
1300	45	CRENNELL 67	HBC	0	6 $\pi^- p \to \Lambda K 2\pi$

[4] Systematic errors not estimated.
[5] This was called the C meson.

PRODUCED IN τ LEPTON DECAYS

VALUE (MeV)	EVTS	DOCUMENT ID	TECN	CHG	COMMENT
1254±33±34	7k	ASNER 00B	CLEO	±	$\tau^- \to K^-\pi^+\pi^-\nu_\tau$

$K_1(1270)$ WIDTH

VALUE (MeV)	DOCUMENT ID
90±20 OUR ESTIMATE	This is only an educated guess; the error given is larger than the error on the average of the published values.
87± 7 OUR AVERAGE	Includes data from the 2 datablocks that follow this one.

PRODUCED BY K^-, BACKWARD SCATTERING, HYPERON EXCHANGE

VALUE (MeV)	EVTS	DOCUMENT ID	TECN	CHG	COMMENT
The data in this block is included in the average printed for a previous datablock.					
75±15	700	GAVILLET 78	HBC	+	4.2 $K^- p \to \Xi^- K\pi\pi$

PRODUCED BY K BEAMS

VALUE (MeV)	EVTS	DOCUMENT ID	TECN	CHG	COMMENT
The data in this block is included in the average printed for a previous datablock.					
90± 8		[6] DAUM 81C	CNTR	−	63 $K^- p \to K^- 2\pi p$
• • • We do not use the following data for averages, fits, limits, etc. • • •					
~ 150		VERGEEST 79	HBC	−	4.2 $K^- p \to (\overline{K}\pi\pi)^- p$
150±71		[7] CARNEGIE 77	ASPK	±	13 $K^\pm p \to (K\pi\pi)^\pm p$
~ 200		BRANDENB... 76	ASPK	±	13 $K^\pm p \to (K\pi\pi)^\pm p$
120		DAVIS 72	HBC	+	12 $K^+ p$
188±21		FIRESTONE 72B	DBC	+	12 $K^+ d$

[6] Well described in the chiral unitary approach of GENG 07 with two poles at 1195 and 1284 MeV and widths of 246 and 146 MeV, respectively.
[7] From a model-dependent fit with Gaussian background to BRANDENBURG 76 data.

PRODUCED BY BEAMS OTHER THAN K MESONS

VALUE (MeV)	EVTS	DOCUMENT ID	TECN	CHG	COMMENT
119.5± 5.2±6.7		GULER 11	BELL		$B^+ \to J/\psi K^+\pi^+\pi^-$
• • • We do not use the following data for averages, fits, limits, etc. • • •					
131 ±21	25k	[8] ABLIKIM 06C	BES2		$J/\psi \to \overline{K}^*(892)^0 K^+\pi^-$
66 ±15	310	RODEBACK 81	HBC		4 $\pi^- p \to \Lambda K 2\pi$
60	40	CRENNELL 72	HBC	0	4.5 $\pi^- p \to \Lambda K 2\pi$
127 $^{+7}_{-25}$		ASTIER 69	HBC	0	$\overline{p}p$
60	45	CRENNELL 67	HBC	0	6 $\pi^- p \to \Lambda K 2\pi$

[8] Systematic errors not estimated.

PRODUCED IN τ LEPTON DECAYS

VALUE (MeV)	EVTS	DOCUMENT ID	TECN	CHG	COMMENT
260 $^{+90}_{-70}$ ±80	7k	ASNER 00B	CLEO	±	$\tau^- \to K^-\pi^+\pi^-\nu_\tau$

$K_1(1270)$ DECAY MODES

	Mode	Fraction (Γ_i/Γ)
Γ_1	$K\rho$	(42 ±6) %
Γ_2	$K_0^*(1430)\pi$	(28 ±4) %
Γ_3	$K^*(892)\pi$	(16 ±5) %
Γ_4	$K\omega$	(11.0±2.0) %
Γ_5	$K f_0(1370)$	(3.0±2.0) %
Γ_6	γK^0	seen

$K_1(1270)$ PARTIAL WIDTHS

$\Gamma(K\rho)$ Γ_1

VALUE (MeV)	DOCUMENT ID	TECN	CHG	COMMENT
• • • We do not use the following data for averages, fits, limits, etc. • • •				
57±5	MAZZUCATO 79	HBC	+	4.2 $K^- p \to \Xi^-(K\pi\pi)^+$
75±6	CARNEGIE 77B	ASPK	±	13 $K^\pm p \to (K\pi\pi)^\pm p$

Meson Particle Listings

$K_1(1270)$, $K_1(1400)$

$\Gamma(K_0^*(1430)\pi)$ Γ_2

VALUE (MeV)	DOCUMENT ID	TECN	CHG	COMMENT
• • • We do not use the following data for averages, fits, limits, etc. • • •				
26±6	CARNEGIE 77B	ASPK	±	13 $K^\pm p \to (K\pi\pi)^\pm p$

$\Gamma(K^*(892)\pi)$ Γ_3

VALUE (MeV)	DOCUMENT ID	TECN	CHG	COMMENT
• • • We do not use the following data for averages, fits, limits, etc. • • •				
14±11	MAZZUCATO 79	HBC	+	4.2 $K^- p \to \Xi^-(K\pi\pi)^+$
2± 2	CARNEGIE 77B	ASPK	±	13 $K^\pm p \to (K\pi\pi)^\pm p$

$\Gamma(K\omega)$ Γ_4

VALUE (MeV)	DOCUMENT ID	TECN	CHG	COMMENT
• • • We do not use the following data for averages, fits, limits, etc. • • •				
4±4	MAZZUCATO 79	HBC	+	4.2 $K^- p \to \Xi^-(K\pi\pi)^+$
24±3	CARNEGIE 77B	ASPK	±	13 $K^\pm p \to (K\pi\pi)^\pm p$

$\Gamma(K f_0(1370))$ Γ_5

VALUE (MeV)	DOCUMENT ID	TECN	CHG	COMMENT
• • • We do not use the following data for averages, fits, limits, etc. • • •				
22±5	CARNEGIE 77B	ASPK	±	13 $K^\pm p \to (K\pi\pi)^\pm p$

$\Gamma(\gamma K^0)$ Γ_6

VALUE (keV)	DOCUMENT ID	TECN	COMMENT
73.2±6.1±28.3	ALAVI-HARATI 02B	KTEV	$K + A \to K^* + A$

$K_1(1270)$ BRANCHING RATIOS

$\Gamma(K\rho)/\Gamma_{total}$ Γ_1/Γ

VALUE	DOCUMENT ID	TECN	COMMENT
0.42 ±0.06	[9] DAUM 81C	CNTR	63 $K^- p \to K^- 2\pi p$
• • • We do not use the following data for averages, fits, limits, etc. • • •			
0.584±0.043	[10] GULER 11	BELL	$B^+ \to J/\psi K^+\pi^+\pi^-$
dominant	RODEBACK 81	HBC	4 $\pi^- p \to \Lambda K 2\pi$

$\Gamma(K_0^*(1430)\pi)/\Gamma_{total}$ Γ_2/Γ

VALUE	DOCUMENT ID	TECN	COMMENT
0.28 ±0.04	[9] DAUM 81C	CNTR	63 $K^- p \to K^- 2\pi p$
• • • We do not use the following data for averages, fits, limits, etc. • • •			
0.0201±0.0064	[10] GULER 11	BELL	$B^+ \to J/\psi K^+\pi^+\pi^-$

$\Gamma(K^*(892)\pi)/\Gamma_{total}$ Γ_3/Γ

VALUE	DOCUMENT ID	TECN	COMMENT
0.16 ±0.05	[9] DAUM 81C	CNTR	63 $K^- p \to K^- 2\pi p$
• • • We do not use the following data for averages, fits, limits, etc. • • •			
0.171±0.023	[10] GULER 11	BELL	$B^+ \to J/\psi K^+\pi^+\pi^-$

$\Gamma(K\omega)/\Gamma_{total}$ Γ_4/Γ

VALUE	DOCUMENT ID	TECN	COMMENT
0.11 ±0.02	[9] DAUM 81C	CNTR	63 $K^- p \to K^- 2\pi p$
• • • We do not use the following data for averages, fits, limits, etc. • • •			
0.225±0.052	[10] GULER 11	BELL	$B^+ \to J/\psi K^+\pi^+\pi^-$

$\Gamma(K\omega)/\Gamma(K\rho)$ Γ_4/Γ_1

VALUE	CL%	DOCUMENT ID	TECN	COMMENT
• • • We do not use the following data for averages, fits, limits, etc. • • •				
<0.30	95	RODEBACK 81	HBC	4 $\pi^- p \to \Lambda K 2\pi$

$\Gamma(K f_0(1370))/\Gamma_{total}$ Γ_5/Γ

VALUE	DOCUMENT ID	TECN	COMMENT
0.03±0.02	[9] DAUM 81C	CNTR	63 $K^- p \to K^- 2\pi p$

D-wave/S-wave RATIO FOR $K_1(1270) \to K^*(892)\pi$

VALUE	DOCUMENT ID	TECN	COMMENT
1.0±0.7	[9] DAUM 81C	CNTR	63 $K^- p \to K^- 2\pi p$

[9] Average from low and high t data.

[10] Assuming that decays are saturated by the $K\rho$, $K_0^*(1430)\pi$, $K^*(892)\pi$, $K\omega$ decay modes and neglecting interference between them. The values $B(\omega \to \pi^+\pi^-) = (1.53^{+0.11}_{-0.13})\%$ and $B(K_0^*(1430) \to K\pi) = (93 \pm 10)\%$ are used. Systematic uncertainties not estimated.

$K_1(1270)$ REFERENCES

GULER	11	PR D83 032005	H. Guler *et al.*	(BELLE Collab.)
GENG	07	PR D75 014017	L.S. Geng *et al.*	
ABLIKIM	06C	PL B633 681	M. Ablikim *et al.*	(BES Collab.)
ALAVI-HARATI	02B	PRL 89 072001	A. Alavi-Harati *et al.*	(FNAL KTeV Collab.)
ASNER	00B	PR D62 072006	D.M. Asner *et al.*	(CLEO Collab.)
TORNQVIST	82B	NP B203 268	N.A. Tornqvist	(HELS)
DAUM	81C	NP B187 1	C. Daum *et al.*	(AMST, CERN, CRAC, MPIM+)
RODEBACK	81	ZPHY C9 9	S. Rodeback *et al.*	(CERN, CDEF, MADR+)
MAZZUCATO	79	NP B156 532	M. Mazzucato *et al.*	(CERN, ZEEM, NIJM+)
VERGEEST	79	NP B158 265	J.S.M. Vergeest *et al.*	(NIJM, AMST, CERN+)
GAVILLET	78	PL 76B 517	P. Gavillet *et al.*	(AMST, CERN, NIJM+) JP
CARNEGIE	77	NP B127 509	R.K. Carnegie *et al.*	(SLAC)
CARNEGIE	77B	PL 68B 287	R.K. Carnegie *et al.*	(SLAC)
BRANDENB...	76	PRL 36 703	G.W. Brandenburg *et al.*	(SLAC) JP
OTTER	76	NP B106 77	G. Otter *et al.*	(AACH3, BERL, CERN, LOIC+) JP
CRENNELL	72	PR D6 1220	D.J. Crennell *et al.*	(BNL)
DAVIS	72	PR D5 2688	P.J. Davis *et al.*	(LBL)
FIRESTONE	72B	PR D5 505	A. Firestone *et al.*	(LBL)
ASTIER	69	NP B10 65	A. Astier *et al.*	(CDEF, CERN, IPNP, LIVP) IJP
CRENNELL	67	PRL 19 44	D.J. Crennell *et al.*	(BNL) I

$K_1(1400)$ $I(J^P) = \frac{1}{2}(1^+)$

$K_1(1400)$ MASS

VALUE (MeV)	EVTS	DOCUMENT ID	TECN	CHG	COMMENT
1403± 7 OUR AVERAGE					
1463±64±68	7k	ASNER 00B	CLEO	±	$\tau^- \to K^-\pi^+\pi^-\nu_\tau$
1373±14±18		[1] ASTON 87	LASS	0	11 $K^- p \to \overline{K}^0\pi^+\pi^- n$
1392±18		BAUBILLIER 82B	HBC	0	8.25 $K^- p \to K_S^0\pi^+\pi^- n$
1410±25		DAUM 81C	CNTR	−	63 $K^- p \to K^- 2\pi p$
1415±15		ETKIN 80	MPS	0	6 $K^- p \to \overline{K}^0\pi^+\pi^- n$
1404±10		[2] CARNEGIE 77	ASPK	±	13 $K^\pm p \to (K\pi\pi)^\pm p$
• • • We do not use the following data for averages, fits, limits, etc. • • •					
1418± 8	25k	[3] ABLIKIM 06C	BES2		$J/\psi \to \overline{K}^*(892)^0 K^+\pi^-$
~ 1350		[4] TORNQVIST 82B	RVUE		
~ 1400		VERGEEST 79	HBC	−	4.2 $K^- p \to (\overline{K}\pi\pi)^- p$
~ 1400		BRANDENB... 76	ASPK	±	13 $K^\pm p \to (K\pi\pi)^\pm p$
1420		DAVIS 72	HBC	+	12 $K^+ p$
1368±18		FIRESTONE 72B	DBC	+	12 $K^+ d$

[1] From partial-wave analysis of $K^0\pi^+\pi^-$ system.

[2] From a model-dependent fit with Gaussian background to BRANDENBURG 76 data.

[3] Systematic errors not estimated.

[4] From a unitarized quark-model calculation.

$K_1(1400)$ WIDTH

VALUE (MeV)	EVTS	DOCUMENT ID	TECN	CHG	COMMENT
174± 13 OUR AVERAGE Error includes scale factor of 1.6. See the ideogram below.					
300^{+370}_{-110}±140	7k	ASNER 00B	CLEO	±	$\tau^- \to K^-\pi^+\pi^-\nu_\tau$
188± 54± 60		[5] ASTON 87	LASS	0	11 $K^- p \to \overline{K}^0\pi^+\pi^- n$
276± 65		BAUBILLIER 82B	HBC	0	8.25 $K^- p \to K_S^0\pi^+\pi^- n$
195± 25		DAUM 81C	CNTR	−	63 $K^- p \to K^- 2\pi p$
180± 10		ETKIN 80	MPS	0	6 $K^- p \to \overline{K}^0\pi^+\pi^- n$
142± 16		[6] CARNEGIE 77	ASPK	±	13 $K^\pm p \to (K\pi\pi)^\pm p$
• • • We do not use the following data for averages, fits, limits, etc. • • •					
152± 16	25k	[7] ABLIKIM 06C	BES2		$J/\psi \to \overline{K}^*(892)^0 K^+\pi^-$
~ 200		VERGEEST 79	HBC	−	4.2 $K^- p \to (\overline{K}\pi\pi)^- p$
~ 160		BRANDENB... 76	ASPK	±	13 $K^\pm p \to (K\pi\pi)^\pm p$
80		DAVIS 72	HBC	+	12 $K^+ p$
241± 30		FIRESTONE 72B	DBC	+	12 $K^+ d$

[5] From partial-wave analysis of $K^0\pi^+\pi^-$ system.

[6] From a model-dependent fit with Gaussian background to BRANDENBURG 76 data.

[7] Systematic errors not estimated.

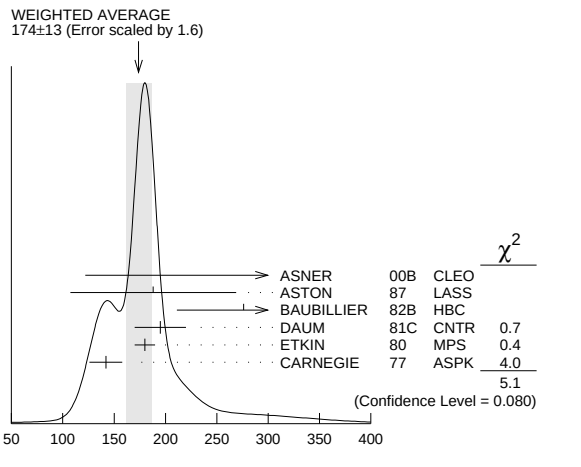

$K_1(1400)$ DECAY MODES

	Mode	Fraction (Γ_i/Γ)
Γ_1	$K^*(892)\pi$	(94 ±6) %
Γ_2	$K\rho$	(3.0±3.0) %
Γ_3	$Kf_0(1370)$	(2.0±2.0) %
Γ_4	$K\omega$	(1.0±1.0) %
Γ_5	$K_0^*(1430)\pi$	not seen
Γ_6	γK^0	seen

$K_1(1400)$ PARTIAL WIDTHS

$\Gamma(K^*(892)\pi)$ Γ_1

VALUE (MeV)	DOCUMENT ID		TECN	CHG	COMMENT
117±10	CARNEGIE	77	ASPK	±	13 $K^\pm p \to (K\pi\pi)^\pm p$

$\Gamma(K\rho)$ Γ_2

VALUE (MeV)	DOCUMENT ID		TECN	CHG	COMMENT
2±1	CARNEGIE	77	ASPK	±	13 $K^\pm p \to (K\pi\pi)^\pm p$

$\Gamma(K\omega)$ Γ_4

VALUE (MeV)	DOCUMENT ID		TECN	CHG	COMMENT
23±12	CARNEGIE	77	ASPK	±	13 $K^\pm p \to (K\pi\pi)^\pm p$

$\Gamma(\gamma K^0)$ Γ_6

VALUE (keV)	DOCUMENT ID		TECN	COMMENT
280.8±23.2±40.4	ALAVI-HARATI	02B	KTEV	$K + A \to K^* + A$

$K_1(1400)$ BRANCHING RATIOS

$\Gamma(K^*(892)\pi)/\Gamma_{total}$ Γ_1/Γ

VALUE	DOCUMENT ID		TECN	COMMENT
0.94±0.06	[8] DAUM	81C	CNTR	63 $K^- p \to K^- 2\pi p$

$\Gamma(K\rho)/\Gamma_{total}$ Γ_2/Γ

VALUE	DOCUMENT ID		TECN	COMMENT
0.03±0.03	[8] DAUM	81C	CNTR	63 $K^- p \to K^- 2\pi p$

$\Gamma(Kf_0(1370))/\Gamma_{total}$ Γ_3/Γ

VALUE	DOCUMENT ID		TECN	COMMENT
0.02±0.02	[8] DAUM	81C	CNTR	63 $K^- p \to K^- 2\pi p$

$\Gamma(K\omega)/\Gamma_{total}$ Γ_4/Γ

VALUE	DOCUMENT ID		TECN	COMMENT
0.01±0.01	[8] DAUM	81C	CNTR	63 $K^- p \to K^- 2\pi p$

$\Gamma(K_0^*(1430)\pi)/\Gamma_{total}$ Γ_5/Γ

VALUE	DOCUMENT ID		TECN	COMMENT
not seen	[8] DAUM	81C	CNTR	63 $K^- p \to K^- 2\pi p$

D-wave/S-wave RATIO FOR $K_1(1400) \to K^*(892)\pi$

VALUE	DOCUMENT ID		TECN	COMMENT
0.04±0.01	[8] DAUM	81C	CNTR	63 $K^- p \to K^- 2\pi p$

[8] Average from low and high t data.

$K_1(1400)$ REFERENCES

ABLIKIM	06C	PL B633 681	M. Ablikim *et al.*	(BES Collab.)
ALAVI-HARATI	02B	PRL 89 072001	A. Alavi-Harati *et al.*	(FNAL KTeV Collab.)
ASNER	00B	PR D62 072006	D.M. Asner *et al.*	(CLEO Collab.)
ASTON	87	NP B292 693	D. Aston *et al.*	(SLAC, NAGO, CINC, INUS)
BAUBILLIER	82B	NP B202 21	M. Baubillier *et al.*	(BIRM, CERN, GLAS+)
TORNQVIST	82B	NP B203 268	N.A. Tornqvist	(HELS)
DAUM	81C	NP B187 1	C. Daum *et al.*	(AMST, CERN, CRAC, MPIM+)
ETKIN	80	PR D22 42	A. Etkin *et al.*	(BNL, CUNY) JP
VERGEEST	79	NP B158 265	J.S.M. Vergeest *et al.*	(NIJM, AMST, CERN+)
CARNEGIE	77	NP B127 509	R.K. Carnegie *et al.*	(SLAC)
BRANDENB...	76	PRL 36 703	G.W. Brandenburg *et al.*	(SLAC) JP
DAVIS	72	PR D5 2688	P.J. Davis *et al.*	(LBL)
FIRESTONE	72B	PR D5 505	A. Firestone *et al.*	(LBL)

$K^*(1410)$

$I(J^P) = \frac{1}{2}(1^-)$

$K^*(1410)$ MASS

VALUE (MeV)	EVTS	DOCUMENT ID		TECN	CHG	COMMENT
1421± 9 OUR AVERAGE						
1437± 8±16	190k	[1] AAIJ	16N	LHCB		$D^0 \to (K_S^0\pi^\mp)K^\pm$
1426± 8±24	190k	[2] AAIJ	16N	LHCB		$D^0 \to K_S^0(K^\pm\pi^\mp)$
1380±21±19		ASTON	88	LASS	0	11 $K^- p \to K^-\pi^+ n$
1420± 7±10		ASTON	87	LASS	0	11 $K^- p \to \overline{K}^0\pi^+\pi^- n$
• • • We do not use the following data for averages, fits, limits, etc. • • •						
1276^{+72}_{-77}		[3,4] BOITO	09	RVUE		$\tau^- \to K_S^0\pi^-\nu_\tau$
1367±54		BIRD	89	LASS	–	11 $K^- p \to \overline{K}^0\pi^- p$
1474±25		BAUBILLIER	82B	HBC	0	8.25 $K^- p \to \overline{K}^0 2\pi n$
1500±30		ETKIN	80	MPS	0	6 $K^- p \to \overline{K}^0\pi^+\pi^- n$

[1] Using a parametrization for the $K\pi$ S-wave similar to ASTON 88 with fixed resonance width.
[2] Using a $K\pi$ S-wave parametrization with resonant and non-resonant contributions.
[3] From the pole position of the $K\pi$ vector form factor in the complex s-plane and using EPIFANOV 07 data.
[4] Systematic uncertainties not estimated.

$K^*(1410)$ WIDTH

VALUE (MeV)	EVTS	DOCUMENT ID		TECN	CHG	COMMENT
236± 18 OUR AVERAGE						
210± 20±60	190k	[1] AAIJ	16N	LHCB		$D^0 \to (K_S^0\pi^\mp)K^\pm$
270± 20±40	190k	[1] AAIJ	16N	LHCB		$D^0 \to K_S^0(K^\pm\pi^\mp)$
176± 52±22		ASTON	88	LASS	0	11 $K^- p \to K^-\pi^+ n$
240± 18±12		ASTON	87	LASS	0	11 $K^- p \to \overline{K}^0\pi^+\pi^- n$
• • • We do not use the following data for averages, fits, limits, etc. • • •						
198^{+61}_{-87}		[2,3] BOITO	09	RVUE		$\tau^- \to K_S^0\pi^-\nu_\tau$
114±101		BIRD	89	LASS	–	11 $K^- p \to \overline{K}^0\pi^- p$
275± 65		BAUBILLIER	82B	HBC	0	8.25 $K^- p \to \overline{K}^0 2\pi n$
500±100		ETKIN	80	MPS	0	6 $K^- p \to \overline{K}^0\pi^+\pi^- n$

[1] Using a $K\pi$ S-wave parametrization with resonant and non-resonant contributions.
[2] From the pole position of the $K\pi$ vector form factor in the complex s-plane and using EPIFANOV 07 data.
[3] Systematic uncertainties not estimated.

$K^*(1410)$ DECAY MODES

	Mode	Fraction (Γ_i/Γ)		Confidence level
Γ_1	$K^*(892)\pi$	> 40	%	95%
Γ_2	$K\pi$	(6.6±1.3)	%	
Γ_3	$K\rho$	< 7	%	95%
Γ_4	γK^0	< 2.2	$\times 10^{-4}$	90%

$K^*(1410)$ PARTIAL WIDTHS

$\Gamma(\gamma K^0)$ Γ_4

VALUE (keV)	CL%	DOCUMENT ID	TECN	COMMENT
<52.9	90	ALAVI-HARATI 02B	KTEV	$K + A \to K^* + A$

$K^*(1410)$ BRANCHING RATIOS

$\Gamma(K\rho)/\Gamma(K^*(892)\pi)$ Γ_3/Γ_1

VALUE	CL%	DOCUMENT ID		TECN	CHG	COMMENT
<0.17	95	ASTON	84	LASS	0	11 $K^- p \to \overline{K}^0 2\pi n$

$\Gamma(K\pi)/\Gamma(K^*(892)\pi)$ Γ_2/Γ_1

VALUE	CL%	DOCUMENT ID		TECN	CHG	COMMENT
<0.16	95	ASTON	84	LASS	0	11 $K^- p \to \overline{K}^0 2\pi n$

$\Gamma(K\pi)/\Gamma_{total}$ Γ_2/Γ

VALUE	DOCUMENT ID		TECN	CHG	COMMENT
0.066±0.010±0.008	ASTON	88	LASS	0	11 $K^- p \to K^-\pi^+ n$

$K^*(1410)$ REFERENCES

AAIJ	16N	PR D93 052018	R. Aaij *et al.*	(LHCb Collab.)
BOITO	09	EPJ C59 821	D.R. Boito, R. Escribano, M. Jamin	
EPIFANOV	07	PL B654 65	D. Epifanov *et al.*	(BELLE Collab.)
ALAVI-HARATI	02B	PRL 89 072001	A. Alavi-Harati *et al.*	(FNAL KTeV Collab.)
BIRD	89	SLAC-332	P.F. Bird	(SLAC)
ASTON	88	NP B296 493	D. Aston *et al.*	(SLAC, NAGO, CINC, INUS)
ASTON	87	NP B292 693	D. Aston *et al.*	(SLAC, NAGO, CINC, INUS)
ASTON	84	PL 149B 258	D. Aston *et al.*	(SLAC, CARL, OTTA) JP
BAUBILLIER	82B	NP B202 21	M. Baubillier *et al.*	(BIRM, CERN, GLAS+)
ETKIN	80	PR D22 42	A. Etkin *et al.*	(BNL, CUNY) JP

$K_0^*(1430)$

$I(J^P) = \frac{1}{2}(0^+)$

See our minireview in the 1994 edition and in this edition under the $f_0(500)$.

$K_0^*(1430)$ MASS

VALUE (MeV)	EVTS	DOCUMENT ID	TECN	COMMENT
1425 ±50 OUR ESTIMATE				

Meson Particle Listings

$K_0^*(1430)$, $K_2^*(1430)$

• • • We do not use the following data for averages, fits, limits, etc. • • •

1438	± 8	± 4	5.4k	[1] LEES	14E	BABR $\eta_c(1S) \to K^+K^-\eta/\pi^0$
1427	± 4	±13		[2] BUGG	10	RVUE S-matrix pole
1466.6	± 0.7	± 3.4	141k	[3] BONVICINI	08A	CLEO $D^+ \to K^-\pi^+\pi^+$
~ 1412				[4] LINK	07	FOCS $D^+ \to K^-K^+\pi^+$
1461.0	± 4.0	± 2.1	54k	[5] LINK	07B	FOCS $D^+ \to K^-\pi^+\pi^+$
1406	±29			[6] BUGG	06	RVUE
1435	± 6			[7] ZHOU	06	RVUE $Kp \to K^-\pi^+n$
1455	±20	±15		ABLIKIM	05Q	BES2 $\psi(2S) \to \gamma\pi^+\pi^-K^+K^-$
1456	± 8			[8] ZHENG	04	RVUE $K^-p \to K^-\pi^+n$
~ 1419				[9] BUGG	03	RVUE 11 $K^-p \to K^-\pi^+n$
~ 1440				[10] LI	03	RVUE 11 $K^-p \to K^-\pi^+n$
1459	± 9		15k	[11] AITALA	02	E791 $D^+ \to K^-\pi^+\pi^+$
~ 1440				[12] JAMIN	00	RVUE $Kp \to Kp$
1436	± 8			[13] BARBERIS	98E	OMEG 450 $pp \to p_f p_s K^+K^-\pi^+\pi^-$
1415	±25			[9] ANISOVICH	97C	RVUE 11 $K^-p \to K^-\pi^+n$
~ 1450				[14] TORNQVIST	96	RVUE $\pi\pi \to \pi\pi, K\overline{K}, K\pi$
1412	± 6			[15] ASTON	88	LASS 11 $K^-p \to K^-\pi^+n$
~ 1430				BAUBILLIER	84B	HBC 8.25 $K^-p \to \overline{K}^0\pi^-p$
~ 1425				[16] ESTABROOKS	78	ASPK 13 $K^\pm p \to K^\pm\pi^\pm(n,\Delta)$
~ 1450				MARTIN	78	SPEC 10 $K^\pm p \to K^0_S\pi p$

[1] Using both $\eta \to \gamma\gamma$ and $\eta \to \pi^+\pi^-\pi^0$. From a likelihood scan in the presence of several interfering scalar-meson resonances with fixed width $\Gamma(K_0^*(1430)) = 210$ MeV.
[2] S-Matrix pole. Supersedes BUGG 06. Combined analysis of ASTON 88, ABLIKIM 06C, AITALA 06, and LINK 09 using an s-dependent width with couplings to $K\pi$ and $K\eta'$, and the Adler zero near thresholds.
[3] From the isobar model with a complex pole for the κ.
[4] From a non-parametric analysis.
[5] A Breit-Wigner mass and width.
[6] S-matrix pole. Reanalysis of ASTON 88, AITALA 02, and ABLIKIM 06C including the κ with an s-dependent width and an Adler zero near threshold.
[7] S-matrix pole. Using ASTON 88 and assuming $K_0^*(700)$, $K_0^*(1950)$.
[8] Using ASTON 88 and assuming $K_0^*(700)$.
[9] T-matrix pole. Reanalysis of ASTON 88 data.
[10] Breit-Wigner fit. Using ASTON 88.
[11] Assuming a low-mass scalar $K\pi$ resonance, $\kappa(700)$.
[12] T-matrix pole. Using data from ESTABROOKS 78 and ASTON 88.
[13] J^P not determined, could be $K_2^*(1430)$.
[14] T-matrix pole.
[15] Uses a model for the background, without this background they get a mass 1340 MeV, where the phase shift passes 90°.
[16] Mass defined by pole position. From elastic $K\pi$ partial-wave analysis.

$K_0^*(1430)$ WIDTH

VALUE (MeV)	EVTS	DOCUMENT ID		TECN	COMMENT
270 ±80 OUR ESTIMATE					

• • • We do not use the following data for averages, fits, limits, etc. • • •

210	±20	±12	5.4k	[1] LEES	14E	BABR $\eta_c(1S) \to K^+K^-\eta/\pi^0$
270	±10	±40		[2] BUGG	10	RVUE S-matrix pole
174.2	± 1.9	± 3.2	141k	[3] BONVICINI	08A	CLEO $D^+ \to K^-\pi^+\pi^+$
~ 500				[4] LINK	07	FOCS $D^+ \to K^-K^+\pi^+$
177.0	± 8.0	± 3.4	54k	[5] LINK	07B	FOCS $D^+ \to K^-\pi^+\pi^+$
350	±40			[6] BUGG	06	RVUE
288	±22			[7] ZHOU	06	RVUE $Kp \to K^-\pi^+n$
270	±45	$^{+30}_{-35}$		ABLIKIM	05Q	BES2 $\psi(2S) \to \gamma\pi^+\pi^-K^+K^-$
217	±31			[8] ZHENG	04	RVUE $K^-p \to K^-\pi^+n$
~ 316				[9] BUGG	03	RVUE 11 $K^-p \to K^-\pi^+n$
~ 350				[10] LI	03	RVUE 11 $K^-p \to K^-\pi^+n$
175	±17		15k	[11] AITALA	02	E791 $D^+ \to K^-\pi^+\pi^+$
~ 300				[12] JAMIN	00	RVUE $Kp \to Kp$
196	±45			[13] BARBERIS	98E	OMEG 450 $pp \to p_f p_s K^+K^-\pi^+\pi^-$
330	±50			[9] ANISOVICH	97C	RVUE 11 $K^-p \to K^-\pi^+n$
~ 320				[14] TORNQVIST	96	RVUE $\pi\pi \to \pi\pi, K\overline{K}, K\pi$
294	±23			ASTON	88	LASS 11 $K^-p \to K^-\pi^+n$
~ 200				BAUBILLIER	84B	HBC 8.25 $K^-p \to \overline{K}^0\pi^-p$
200	to 300			[15] ESTABROOKS	78	ASPK 13 $K^\pm p \to K^\pm\pi^\pm(n,\Delta)$

[1] Using both $\eta \to \gamma\gamma$ and $\eta \to \pi^+\pi^-\pi^0$. From a likelihood scan in the presence of several interfering scalar-meson resonances with fixed mass $M(K_0^*(1430)) = 1435$ MeV.
[2] S-Matrix pole. Supersedes BUGG 06. Combined analysis of ASTON 88, ABLIKIM 06C, AITALA 06, and LINK 09 using an s-dependent width with couplings to $K\pi$ and $K\eta'$, and the Adler zero near thresholds.
[3] From the isobar model with a complex pole for the κ.
[4] From a non-parametric analysis.
[5] A Breit-Wigner mass and width.
[6] S-matrix pole. Reanalysis of ASTON 88, AITALA 02, and ABLIKIM 06C including the κ with an s-dependent width and an Adler zero near threshold.
[7] S-matrix pole. Using ASTON 88 and assuming $K_0^*(700)$, $K_0^*(1950)$.
[8] Using ASTON 88 and assuming $K_0^*(700)$.
[9] T-matrix pole. Reanalysis of ASTON 88 data.
[10] Breit-Wigner fit. Using ASTON 88.
[11] Assuming a low-mass scalar $K\pi$ resonance, $\kappa(700)$.
[12] T-matrix pole. Using data from ESTABROOKS 78 and ASTON 88.
[13] J^P not determined, could be $K_2^*(1430)$.
[14] T-matrix pole.
[15] From elastic $K\pi$ partial-wave analysis.

$K_0^*(1430)$ DECAY MODES

	Mode	Fraction (Γ_i/Γ)
Γ_1	$K\pi$	(93 ±10) %
Γ_2	$K\eta$	($8.6^{+\ 2.7}_{-\ 3.4}$) %
Γ_3	$K\eta'(958)$	seen

$K_0^*(1430)$ BRANCHING RATIOS

$\Gamma(K\pi)/\Gamma_{\text{total}}$ — **Γ_1/Γ**

VALUE	DOCUMENT ID		TECN	CHG	COMMENT
0.93±0.04±0.09	ASTON	88	LASS	0	11 $K^-p \to K^-\pi^+n$

$\Gamma(K\eta)/\Gamma(K\pi)$ — **Γ_2/Γ_1**

VALUE (%)	EVTS	DOCUMENT ID		TECN	COMMENT
9.2±2.5$^{+1.0}_{-2.5}$	5.4k	[1] LEES	14E	BABR	$\eta_c(1S) \to K^+K^-\eta/\pi^0$

[1] Using both $\eta \to \gamma\gamma$ and $\eta \to \pi^+\pi^-\pi^0$. From a Dalitz analysis in the presence of several interfering scalar-meson resonances.

$\Gamma(K\eta'(958))/\Gamma_{\text{total}}$ — **Γ_3/Γ**

VALUE	DOCUMENT ID		TECN	COMMENT
seen	ABLIKIM	14J	BES3	$\psi(2S) \to \gamma K^+K^-\eta'(958)$

$K_0^*(1430)$ REFERENCES

ABLIKIM	14J	PR D89 074030	M. Ablikim *et al.*	(BES III Collab.)
LEES	14E	PR D89 112004	J.P. Lees *et al.*	(BABAR Collab.)
BUGG	10	PR D81 014002	D.V. Bugg	(LOQM)
LINK	09	PL B681 14	J.M. Link *et al.*	(FNAL FOCUS Collab.)
BONVICINI	08A	PR D78 052001	G. Bonvicini *et al.*	(CLEO Collab.)
LINK	07	PL B648 156	J.M. Link *et al.*	(FNAL FOCUS Collab.)
LINK	07B	PL B653 1	J.M. Link *et al.*	(FNAL FOCUS Collab.)
ABLIKIM	06C	PL B633 681	M. Ablikim *et al.*	(BES Collab.)
AITALA	06	PR D73 032004	E.M. Aitala *et al.*	(FNAL E791 Collab.)
Also		PR D74 059901 (errat.)	E.M. Aitala *et al.*	(FNAL E791 Collab.)
BUGG	06	PL B632 471	D.V. Bugg	(LOQM)
ZHOU	06	NP A775 212	Z.Y. Zhou, H.Q. Zheng	
ABLIKIM	05Q	PR D72 092002	M. Ablikim *et al.*	(BES Collab.)
ZHENG	04	NP A733 235	H.Q. Zheng *et al.*	
BUGG	03	PL B572 1	D.V. Bugg	
LI	03	PR D67 034025	L. Li, B. Zou, G. Li	
AITALA	02	PRL 89 121801	E.M. Aitala *et al.*	(FNAL E791 Collab.)
JAMIN	00	NP B587 331	M. Jamin *et al.*	
BARBERIS	98E	PL B436 204	D. Barberis *et al.*	(Omega Expt.)
ANISOVICH	97C	PL B413 137	A.V. Anisovich, A.V. Sarantsev	
TORNQVIST	96	PRL 76 1575	N.A. Tornqvist, M. Roos	(HELS)
ASTON	88	NP B296 493	D. Aston *et al.*	(SLAC, NAGO, CINC, INUS)
BAUBILLIER	84B	ZPHY C26 37	M. Baubillier *et al.*	(BIRM, CERN, GLAS+)
ESTABROOKS	78	NP B133 490	P.G. Estabrooks *et al.*	(MCGI, CARL, DURH+)
MARTIN	78	NP B134 392	A.D. Martin *et al.*	(DURH, GEVA)

$K_2^*(1430)$

$I(J^P) = \frac{1}{2}(2^+)$

We consider that phase-shift analyses provide more reliable determinations of the mass and width.

$K_2^*(1430)$ MASS

CHARGED ONLY, WITH FINAL STATE $K\pi$

VALUE (MeV)	EVTS	DOCUMENT ID		TECN	CHG	COMMENT
1425.6± 1.5 OUR AVERAGE		Error includes scale factor of 1.1.				
1420 ± 4	1587	BAUBILLIER	84B	HBC	−	8.25 $K^-p \to \overline{K}^0\pi^-p$
1436 ± 5.5	400	[1,2] CLELAND	82	SPEC	+	30 $K^+p \to K^0_S\pi^+p$
1430 ± 3.2	1500	[1,2] CLELAND	82	SPEC	+	50 $K^+p \to K^0_S\pi^+p$
1430 ± 3.2	1200	[1,2] CLELAND	82	SPEC	−	50 $K^+p \to K^0_S\pi^-p$
1423 ± 5	935	TOAFF	81	HBC	−	6.5 $K^-p \to \overline{K}^0\pi^-p$
1428.0± 4.6		[3] MARTIN	78	SPEC	+	10 $K^\pm p \to K^0_S\pi p$
1423.8± 4.6		[3] MARTIN	78	SPEC	−	10 $K^\pm p \to K^0_S\pi p$
1420.0± 3.1	1400	AGUILAR-...	71B	HBC	−	3.9,4.6 K^-p
1425 ± 8.0	225	[1,2] BARNHAM	71C	HBC	+	$K^+p \to K^0\pi^+p$
1416 ±10	220	CRENNELL	69D	DBC	−	3.9 $K^-N \to \overline{K}^0\pi^-N$
1414 ±13.0	60	[1] LIND	69	HBC	+	9 $K^+p \to K^0\pi^+p$
1427 ±12	63	[1] SCHWEING...	68	HBC	−	5.5 $K^-p \to \overline{K}\pi N$
1423 ±11.0	39	[1] BASSANO	67	HBC	−	4.6–5.0 $K^-p \to \overline{K}^0\pi^-p$

• • • We do not use the following data for averages, fits, limits, etc. • • •

1423.4± 2 ±3	24809± 820	[4] BIRD	89	LASS	−	11 $K^-p \to \overline{K}^0\pi^-p$	

NEUTRAL ONLY

VALUE (MeV)	EVTS	DOCUMENT ID		TECN	COMMENT	
1432.4± 1.3 OUR AVERAGE						
1431.2± 1.8± 0.7		[5] ASTON	88	LASS	11 $K^-p \to K^-\pi^+n$	
1434 ± 4 ± 6		[5] ASTON	87	LASS	11 $K^-p \to \overline{K}^0\pi^+\pi^-n$	
1433 ± 6 ±10		[5] ASTON	84B	LASS	11 $K^-p \to \overline{K}^0 2\pi n$	
1471 ±12		[5] BAUBILLIER	82B	HBC	8.25 $K^-p \to nK^0_S\pi\pi$	
1428 ± 3		[5] ASTON	81C	LASS	11 $K^-p \to K^-\pi^+n$	
1434 ± 2		[5] ESTABROOKS	78	ASPK	13 $K^\pm p \to pK\pi$	
1440 ±10		[5] BOWLER	77	DBC	5.5 $K^+d \to K\pi pp$	
• • • We do not use the following data for averages, fits, limits, etc. • • •						
1428.5± 3.9	1786± 127	[6] AUBERT	07AK	BABR	10.6 $e^+e^- \to K^{*0}K^\pm\pi^\mp\gamma$	
1420 ± 7	300	HENDRICK	76	DBC	8.25 $K^+N \to K^+\pi N$	
1421.6± 4.2	800	MCCUBBIN	75	HBC	3.6 $K^-p \to K^-\pi^+n$	
1420.1± 4.3		[7] LINGLIN	73	HBC	2–13 $K^+p \to K^+\pi^-X$	
1419.1± 3.7	1800	AGUILAR-...	71B	HBC	3.9,4.6 K^-p	
1416 ± 6	600	CORDS	71	DBC	9 $K^+n \to K^+\pi^-p$	
1421.1± 2.6	2200	DAVIS	69	HBC	12 $K^+p \to K^+\pi^-X$	

[1] Errors enlarged by us to $\Gamma/\sqrt{N}$; see the note with the $K^*(892)$ mass.
[2] Number of events in peak re-evaluated by us.
[3] Systematic error added by us.
[4] From a partial wave amplitude analysis.
[5] From phase shift or partial-wave analysis.
[6] Systematic errors not estimated.
[7] From pole extrapolation, using world K^+p data summary tape.

$K_2^*(1430)$ WIDTH

CHARGED ONLY, WITH FINAL STATE $K\pi$

VALUE (MeV)	EVTS	DOCUMENT ID		TECN	CHG	COMMENT
98.5± 2.7 OUR FIT Error includes scale factor of 1.1.						
98.5± 2.9 OUR AVERAGE Error includes scale factor of 1.1.						
109 ±22	400	[8,9] CLELAND	82	SPEC	+	30 $K^+p \to K^0_S\pi^+p$
124 ±12.8	1500	[8,9] CLELAND	82	SPEC	+	50 $K^+p \to K^0_S\pi^+p$
113 ±12.8	1200	[8,9] CLELAND	82	SPEC	−	50 $K^+p \to K^0_S\pi^-p$
85 ±16	935	TOAFF	81	HBC	−	6.5 $K^-p \to \overline{K}^0\pi^-p$
96.5± 3.8		MARTIN	78	SPEC	+	10 $K^\pm p \to K^0_S\pi p$
97.7± 4.0		MARTIN	78	SPEC	−	10 $K^\pm p \to K^0_S\pi p$
$94.7^{+15.1}_{-12.5}$	1400	AGUILAR-...	71B	HBC	−	3.9,4.6 K^-p
• • • We do not use the following data for averages, fits, limits, etc. • • •						
98 ± 4 ±4	25k	[10] BIRD	89	LASS	−	11 $K^-p \to \overline{K}^0\pi^-p$

NEUTRAL ONLY

VALUE (MeV)	EVTS	DOCUMENT ID		TECN	COMMENT
109 ± 5 OUR AVERAGE Error includes scale factor of 1.9. See the ideogram below.					
116.5± 3.6± 1.7		[11] ASTON	88	LASS	11 $K^-p \to K^-\pi^+n$
129 ±15 ±15		[11] ASTON	87	LASS	11 $K^-p \to \overline{K}^0\pi^+\pi^-n$
131 ±24 ±20		[11] ASTON	84B	LASS	11 $K^-p \to \overline{K}^0 2\pi n$
143 ±34		[11] BAUBILLIER	82B	HBC	8.25 $K^-p \to nK^0_S\pi\pi$
98 ± 8		[11] ASTON	81C	LASS	11 $K^-p \to K^-\pi^+n$
140 ±30		[11] ETKIN	80	SPEC	6 $K^-p \to \overline{K}^0\pi^+\pi^-n$
98 ± 5		[11] ESTABROOKS	78	ASPK	13 $K^\pm p \to pK\pi$
• • • We do not use the following data for averages, fits, limits, etc. • • •					
113.7± 9.2	1786± 127	[12] AUBERT	07AK	BABR	10.6 $e^+e^- \to K^{*0}K^\pm\pi^\mp\gamma$
125 ±29	300	[8] HENDRICK	76	DBC	8.25 $K^+N \to K^+\pi N$
116 ±18	800	MCCUBBIN	75	HBC	3.6 $K^-p \to K^-\pi^+n$
61 ±14		[13] LINGLIN	73	HBC	2–13 $K^+p \to K^+\pi^-X$
$116.6^{+10.3}_{-15.5}$	1800	AGUILAR-...	71B	HBC	3.9,4.6 K^-p
144 ±24.0	600	[8] CORDS	71	DBC	9 $K^+n \to K^+\pi^-p$
101 ±10	2200	DAVIS	69	HBC	12 $K^+p \to K^+\pi^-\pi^+p$

[8] Errors enlarged by us to $4\Gamma/\sqrt{N}$; see the note with the $K^*(892)$ mass.
[9] Number of events in peak re-evaluated by us.
[10] From a partial wave amplitude analysis.
[11] From phase shift or partial-wave analysis.
[12] Systematic errors not estimated.
[13] From pole extrapolation, using world K^+p data summary tape.

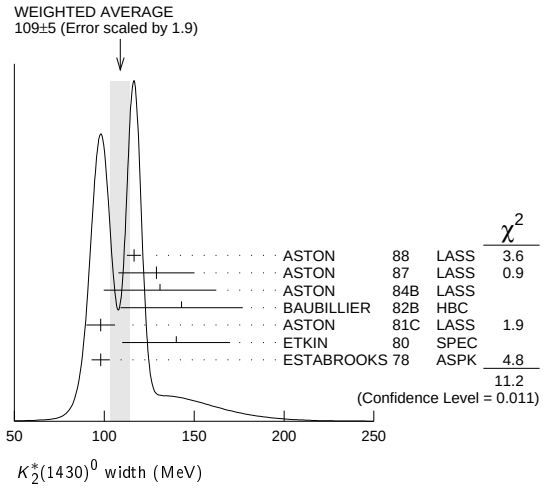

$K_2^*(1430)$ DECAY MODES

	Mode	Fraction (Γ_i/Γ)	Scale factor / Confidence level
Γ_1	$K\pi$	(49.9±1.2) %	
Γ_2	$K^*(892)\pi$	(24.7±1.5) %	
Γ_3	$K^*(892)\pi\pi$	(13.4±2.2) %	
Γ_4	$K\rho$	(8.7±0.8) %	S=1.2
Γ_5	$K\omega$	(2.9±0.8) %	
Γ_6	$K^+\gamma$	(2.4±0.5) $\times 10^{-3}$	S=1.1
Γ_7	$K\eta$	($1.5^{+3.4}_{-1.0}$) $\times 10^{-3}$	S=1.3
Γ_8	$K\omega\pi$	< 7.2 $\times 10^{-4}$	CL=95%
Γ_9	$K^0\gamma$	< 9 $\times 10^{-4}$	CL=90%

CONSTRAINED FIT INFORMATION

An overall fit to the total width, a partial width, and 10 branching ratios uses 31 measurements and one constraint to determine 8 parameters. The overall fit has a $\chi^2 = 20.2$ for 24 degrees of freedom.

The following *off-diagonal* array elements are the correlation coefficients $\langle \delta p_i \delta p_j \rangle / (\delta p_i \cdot \delta p_j)$, in percent, from the fit to parameters p_i, including the branching fractions, $x_i \equiv \Gamma_i/\Gamma_{\text{total}}$. The fit constrains the x_i whose labels appear in this array to sum to one.

	x_1	x_2	x_3	x_4	x_5	x_6	x_7
x_2	−9						
x_3	−40	−73					
x_4	−8	36	−52				
x_5	−11	−3	−26	−7			
x_6	−1	−1	−1	−1	0		
x_7	−4	−7	−5	−5	−2	0	
Γ	0	0	0	0	0	−13	0

	Mode	Rate (MeV)	Scale factor
Γ_1	$K\pi$	49.1 ±1.8	
Γ_2	$K^*(892)\pi$	24.3 ±1.6	
Γ_3	$K^*(892)\pi\pi$	13.2 ±2.2	
Γ_4	$K\rho$	8.5 ±0.8	1.2
Γ_5	$K\omega$	2.9 ±0.8	
Γ_6	$K^+\gamma$	0.24±0.05	1.1
Γ_7	$K\eta$	$0.15^{+0.33}_{-0.10}$	1.3

$K_2^*(1430)$ PARTIAL WIDTHS

$\Gamma(K^+\gamma)$ **Γ_6**

VALUE (keV)	DOCUMENT ID		TECN	CHG	COMMENT
241±50 OUR FIT Error includes scale factor of 1.1.					
240±45	CIHANGIR	82	SPEC	+	200 $K^+Z \to ZK^+\pi^0$, $ZK^0_S\pi^+$

$\Gamma(K^0\gamma)$ Γ_9

VALUE (keV)	CL%	DOCUMENT ID	TECN	CHG	COMMENT
< 5.4	90	ALAVI-HARATI 02B	KTEV		$K + A \to K^* + A$
• • • We do not use the following data for averages, fits, limits, etc. • • •					
<84	90	CARLSMITH 87	SPEC	0	60–200 $K_L^0 A \to K_S^0 \pi^0 A$

$K_2^*(1430)$ BRANCHING RATIOS

$\Gamma(K\pi)/\Gamma_{total}$ Γ_1/Γ

VALUE	DOCUMENT ID	TECN	CHG	COMMENT
0.499±0.012 OUR FIT				
0.488±0.014 OUR AVERAGE				
0.485±0.006±0.020	[14] ASTON 88	LASS	0	11 $K^- p \to K^- \pi^+ n$
0.49 ±0.02	[14] ESTABROOKS 78	ASPK	±	13 $K^\pm p \to p K \pi$

$\Gamma(K^*(892)\pi)/\Gamma(K\pi)$ Γ_2/Γ_1

VALUE	DOCUMENT ID	TECN	CHG	COMMENT
0.496±0.034 OUR FIT				
0.47 ±0.04 OUR AVERAGE				
0.44 ±0.09	ASTON 84B	LASS	0	11 $K^- p \to \overline{K}^0 2\pi n$
0.62 ±0.19	LAUSCHER 75	HBC	0	10,16 $K^- p \to K^- \pi^+ n$
0.54 ±0.16	DEHM 74	DBC	0	4.6 $K^+ N$
0.47 ±0.08	AGUILAR-... 71B	HBC		3.9,4.6 $K^- p$
0.47 ±0.10	BASSANO 67	HBC	−0	4.6,5.0 $K^- p$
0.45 ±0.13	BADIER 65C	HBC	−	3 $K^- p$

$\Gamma(K\omega)/\Gamma(K\pi)$ Γ_5/Γ_1

VALUE	DOCUMENT ID	TECN	CHG	COMMENT
0.059±0.017 OUR FIT				
0.070±0.035 OUR AVERAGE				
0.05 ±0.04	AGUILAR-... 71B	HBC		3.9,4.6 $K^- p$
0.13 ±0.07	BASSOMPIE... 69	HBC	0	5 $K^+ p$

$\Gamma(K\rho)/\Gamma(K\pi)$ Γ_4/Γ_1

VALUE	DOCUMENT ID	TECN	CHG	COMMENT
0.174±0.017 OUR FIT	Error includes scale factor of 1.2.			
$0.150^{+0.029}_{-0.017}$ OUR AVERAGE				
0.18 ±0.05	ASTON 84B	LASS	0	11 $K^- p \to \overline{K}^0 2\pi n$
0.02 $^{+0.10}_{-0.02}$	DEHM 74	DBC	0	4.6 $K^+ N$
0.16 ±0.05	AGUILAR-... 71B	HBC		3.9,4.6 $K^- p$
0.14 ±0.10	BASSANO 67	HBC	−0	4.6,5.0 $K^- p$
0.14 ±0.07	BADIER 65C	HBC	−	3 $K^- p$

$\Gamma(K\rho)/\Gamma(K^*(892)\pi)$ Γ_4/Γ_2

VALUE	DOCUMENT ID	TECN	CHG	COMMENT
0.350±0.031 OUR FIT	Error includes scale factor of 1.4.			
0.354±0.033 OUR AVERAGE	Error includes scale factor of 1.4. See the ideogram below.			
0.293±0.032±0.020	ASTON 87	LASS	0	11 $K^- p \to \overline{K}^0 \pi^+ \pi^- n$
0.38 ±0.09	BAUBILLIER 82B	HBC	0	8.25 $K^- p \to N K_S^0 \pi\pi$
0.39 ±0.03	DAUM 81C	CNTR		63 $K^- p \to K^- 2\pi p$

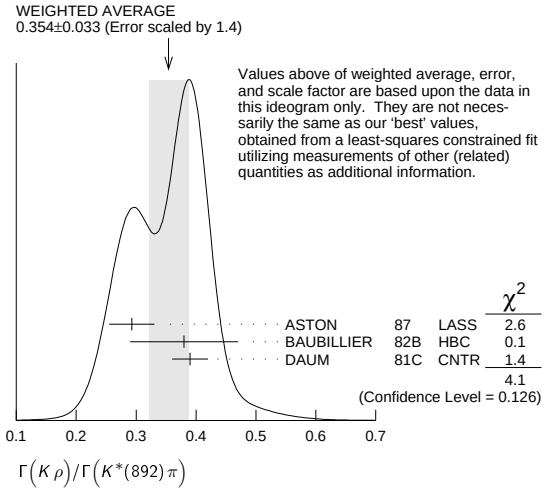

$\Gamma(K\omega)/\Gamma(K^*(892)\pi)$ Γ_5/Γ_2

VALUE	DOCUMENT ID	TECN	CHG	COMMENT
0.118±0.034 OUR FIT				
0.10 ±0.04	FIELD 67	HBC	−	3.8 $K^- p$

$\Gamma(K\eta)/\Gamma(K^*(892)\pi)$ Γ_7/Γ_2

VALUE	DOCUMENT ID	TECN	CHG	COMMENT
$0.006^{+0.014}_{-0.004}$ OUR FIT	Error includes scale factor of 1.2.			
0.07 ±0.04	FIELD 67	HBC	−	3.8 $K^- p$

$\Gamma(K\eta)/\Gamma(K\pi)$ Γ_7/Γ_1

VALUE	CL%	DOCUMENT ID	TECN	CHG	COMMENT
$0.0030^{+0.0070}_{-0.0020}$ OUR FIT		Error includes scale factor of 1.3.			
0 ±0.0056		[15] ASTON 88B	LASS	−	11 $K^- p \to K^- \eta p$
• • • We do not use the following data for averages, fits, limits, etc. • • •					
<0.04	95	AGUILAR-... 71B	HBC		3.9,4.6 $K^- p$
<0.065		[16] BASSOMPIE... 69	HBC		5.0 $K^+ p$
<0.02		BISHOP 69	HBC		3.5 $K^+ p$

$\Gamma(K^*(892)\pi\pi)/\Gamma_{total}$ Γ_3/Γ

VALUE	DOCUMENT ID	TECN	CHG	COMMENT
0.134±0.022 OUR FIT				
0.12 ±0.04	[17] GOLDBERG 76	HBC	−	3 $K^- p \to p \overline{K}^0 \pi\pi\pi$

$\Gamma(K^*(892)\pi\pi)/\Gamma(K\pi)$ Γ_3/Γ_1

VALUE	DOCUMENT ID	TECN	CHG	COMMENT
0.27±0.05 OUR FIT				
0.21±0.08	[16,17] JONGEJANS 78	HBC	−	4 $K^- p \to p \overline{K}^0 \pi\pi\pi$

$\Gamma(K\omega\pi)/\Gamma_{total}$ Γ_8/Γ

VALUE (units 10^{-3})	CL%	EVTS	DOCUMENT ID	TECN	COMMENT
<0.72	95	0	JONGEJANS 78	HBC	4 $K^- p \to p \overline{K}^0 4\pi$

[14] From phase shift analysis.
[15] ASTON 88B quote < 0.0092 at CL=95%. We convert this to a central value and 1 sigma error in order to be able to use it in our constrained fit.
[16] Restated by us.
[17] Assuming $\pi\pi$ system has isospin 1, which is supported by the data.

$K_2^*(1430)$ REFERENCES

AUBERT	07AK	PR D76 012008	B. Aubert *et al.* (BABAR Collab.)
ALAVI-HARATI	02B	PRL 89 072001	A. Alavi-Harati *et al.* (FNAL KTeV Collab.)
BIRD	89	SLAC-332	P.F. Bird (SLAC)
ASTON	88	NP B296 493	D. Aston *et al.* (SLAC, NAGO, CINC, INUS)
ASTON	88B	PL B201 169	D. Aston *et al.* (SLAC, NAGO, CINC, INUS)
ASTON	87	NP B292 693	D. Aston *et al.* (SLAC, NAGO, CINC, INUS)
CARLSMITH	87	PR D36 3502	D. Carlsmith *et al.* (EFI, SACL)
ASTON	84B	NP B247 261	D. Aston *et al.* (SLAC, CARL, OTTA)
BAUBILLIER	84B	ZPHY C26 37	M. Baubillier *et al.* (BIRM, CERN, GLAS+)
BAUBILLIER	82B	NP B202 21	M. Baubillier *et al.* (BIRM, CERN, GLAS+)
CIHANGIR	82	PL 117B 123	S. Cihangir *et al.* (FNAL, MINN, ROCH)
CLELAND	82	NP B208 189	W.E. Cleland *et al.* (DURH, GEVA, LAUS+)
ASTON	81C	PL 106B 235	D. Aston *et al.* (SLAC, CARL, OTTA) JP
DAUM	81C	NP B187 1	C. Daum *et al.* (AMST, CERN, CRAC, MPIM+)
TOAFF	81	PR D23 1500	S. Toaff *et al.* (ANL, KANS)
ETKIN	80	PR D22 42	A. Etkin *et al.* (BNL, CUNY) JP
ESTABROOKS	78	NP B133 490	P.G. Estabrooks *et al.* (MCGI, CARL, DURH+)
Also		PR D17 658	P.G. Estabrooks *et al.* (MCGI, CARL, DURH+)
JONGEJANS	78	NP B139 383	B. Jongejans *et al.* (ZEEM, CERN, NIJM+)
MARTIN	78	NP B134 392	A.D. Martin *et al.* (DURH, GEVA)
BOWLER	77	NP B126 31	M.G. Bowler *et al.* (OXF)
GOLDBERG	76	LNC 17 253	J. Goldberg (HAIF)
HENDRICK	76	NP B112 189	K. Hendrickx *et al.* (MONS, SACL, PARIS+)
LAUSCHER	75	NP B86 189	P. Lauscher *et al.* (ABCLV Collab.) JP
MCCUBBIN	75	NP B86 13	N.A. McCubbin, L. Lyons (OXF)
DEHM	74	NP B75 47	G. Dehm *et al.* (MPIM, BRUX, MONS, CERN)
LINGLIN	73	NP B55 408	D. Linglin (CERN)
AGUILAR-...	71B	PR D4 2583	M. Aguilar-Benitez, R.L. Eisner, J.B. Kinson (BNL)
BARNHAM	71C	NP B28 171	K.W.J. Barnham *et al.* (BIRM, GLAS)
CORDS	71	PR D4 1974	D. Cords *et al.* (PURD, UCD, IUPU)
BASSOMPIE...	69	NP B13 189	G. Bassompierre *et al.* (CERN, BRUX) JP
BISHOP	69	NP B9 403	J.M. Bishop *et al.* (WISC)
CRENNELL	69D	PRL 22 487	D.J. Crennell *et al.* (BNL)
DAVIS	69	PRL 23 1071	P.J. Davis *et al.* (LRL)
LIND	69	NP B14 1	V.G. Lind *et al.* (LRL) JP
SCHWEING...	68	PR 166 1317	F. Schweingruber *et al.* (ANL, NWES)
Also		Thesis	F.L. Schweingruber (NWES, NWES)
BASSANO	67	PRL 19 968	D. Bassano *et al.* (BNL, SYRA)
FIELD	67	PL 24B 638	J.H. Field *et al.* (UCSD)
BADIER	65C	PL 19 612	J. Badier *et al.* (EPOL, SACL, AMST)

$K(1460)$ $I(J^P) = \frac{1}{2}(0^-)$

OMITTED FROM SUMMARY TABLE
Observed in $K\pi\pi$ partial-wave analysis.

$K(1460)$ MASS

VALUE (MeV)	DOCUMENT ID	TECN	CHG	COMMENT
• • • We do not use the following data for averages, fits, limits, etc. • • •				
~ 1460	DAUM 81C	CNTR	−	63 $K^- p \to K^- 2\pi p$
~ 1400	[1] BRANDENB... 76B	ASPK	±	13 $K^\pm p \to K^+ 2\pi p$

[1] Coupled mainly to $K f_0(1370)$. Decay into $K^*(892)\pi$ seen.

$K(1460)$ WIDTH

VALUE (MeV)	DOCUMENT ID		TECN	CHG	COMMENT
• • • We do not use the following data for averages, fits, limits, etc. • • •					
~ 260	DAUM	81C	CNTR	–	63 $K^- p \to K^- 2\pi p$
~ 250	[2] BRANDENB...	76B	ASPK	±	13 $K^\pm p \to K^+ 2\pi p$

[2] Coupled mainly to $K f_0(1370)$. Decay into $K^*(892)\pi$ seen.

$K(1460)$ DECAY MODES

	Mode	Fraction (Γ_i/Γ)
Γ_1	$K^*(892)\pi$	seen
Γ_2	$K\rho$	seen
Γ_3	$K_0^*(1430)\pi$	seen

$K(1460)$ PARTIAL WIDTHS

$\Gamma(K^*(892)\pi)$ Γ_1

VALUE (MeV)	DOCUMENT ID	TECN	COMMENT
• • • We do not use the following data for averages, fits, limits, etc. • • •			
~ 109	DAUM	81C	CNTR 63 $K^- p \to K^- 2\pi p$

$\Gamma(K\rho)$ Γ_2

VALUE (MeV)	DOCUMENT ID	TECN	COMMENT
• • • We do not use the following data for averages, fits, limits, etc. • • •			
~ 34	DAUM	81C	CNTR 63 $K^- p \to K^- 2\pi p$

$\Gamma(K_0^*(1430)\pi)$ Γ_3

VALUE (MeV)	DOCUMENT ID	TECN	COMMENT
• • • We do not use the following data for averages, fits, limits, etc. • • •			
~ 117	DAUM	81C	CNTR 63 $K^- p \to K^- 2\pi p$

$K(1460)$ REFERENCES

DAUM	81C	NP B187 1	C. Daum *et al.*	(AMST, CERN, CRAC, MPIM+)
BRANDENB...	76B	PRL 36 1239	G.W. Brandenburg *et al.*	(SLAC) JP

$K_2(1580)$

$I(J^P) = \frac{1}{2}(2^-)$

OMITTED FROM SUMMARY TABLE

Seen in partial-wave analysis of the $K^-\pi^+\pi^-$ system. Needs confirmation.

$K_2(1580)$ MASS

VALUE (MeV)	DOCUMENT ID	CHG	COMMENT
• • • We do not use the following data for averages, fits, limits, etc. • • •			
~ 1580	OTTER	79 –	10,14,16 $K^- p$

$K_2(1580)$ WIDTH

VALUE (MeV)	DOCUMENT ID	CHG	COMMENT
• • • We do not use the following data for averages, fits, limits, etc. • • •			
~ 110	OTTER	79 –	10,14,16 $K^- p$

$K_2(1580)$ DECAY MODES

	Mode	Fraction (Γ_i/Γ)
Γ_1	$K^*(892)\pi$	seen
Γ_2	$K_2^*(1430)\pi$	possibly seen

$K_2(1580)$ BRANCHING RATIOS

$\Gamma(K^*(892)\pi)/\Gamma_{total}$ Γ_1/Γ

VALUE	DOCUMENT ID	TECN	CHG	COMMENT
seen	OTTER	79 HBC	–	10,14,16 $K^- p$
• • • We do not use the following data for averages, fits, limits, etc. • • •				
possibly seen	GULER	11 BELL		$B^+ \to J/\psi K^+\pi^+\pi^-$

$\Gamma(K_2^*(1430)\pi)/\Gamma_{total}$ Γ_2/Γ

VALUE	DOCUMENT ID	TECN	CHG	COMMENT
possibly seen	OTTER	79 HBC	–	10,14,16 $K^- p$

$K_2(1580)$ REFERENCES

GULER	11	PR D83 032005	H. Guler *et al.*	(BELLE Collab.)
OTTER	79	NP B147 1	G. Otter *et al.*	(AACH3, BERL, CERN, LOIC+) JP

$K(1630)$

$I(J^P) = \frac{1}{2}(?^?)$

OMITTED FROM SUMMARY TABLE

Seen as a narrow peak, compatible with the experimental resolution, in the invariant mass of the $K_S^0\pi^+\pi^-$ system produced in $\pi^- p$ interactions at high momentum transfers.

$K(1630)$ MASS

VALUE (MeV)	EVTS	DOCUMENT ID	TECN	COMMENT
1629±7	~ 75	KARNAUKHOV98	BC	16.0 $\pi^- p \to (K_S^0\pi^+\pi^-) X^+\pi^- X^0$

$K(1630)$ WIDTH

VALUE (MeV)	EVTS	DOCUMENT ID	TECN	COMMENT
16^{+19}_{-16}	~ 75	[1] KARNAUKHOV98	BC	16.0 $\pi^- p \to (K_S^0\pi^+\pi^-) X^+\pi^- X^0$

[1] Compatible with an experimental resolution of 14 ± 1 MeV.

$K(1630)$ DECAY MODES

	Mode
Γ_1	$K_S^0\pi^+\pi^-$

$K(1630)$ REFERENCES

KARNAUKHOV 98	PAN 61 203	V.M. Karnaukhov, C. Coca, V.I. Moroz	
	Translated from YAF 61 252.		

$K_1(1650)$

$I(J^P) = \frac{1}{2}(1^+)$

OMITTED FROM SUMMARY TABLE

This entry contains various peaks in strange meson systems ($K^+\phi$, $K\pi\pi$) reported in partial-wave analysis in the 1600–1900 mass region.

$K_1(1650)$ MASS

VALUE (MeV)	EVTS	DOCUMENT ID	TECN	CHG	COMMENT
1672±50 OUR AVERAGE		Error includes scale factor of 1.1.			
$1793\pm59^{+153}_{-101}$	4289	[1] AAIJ	17C LHCB		$B^+ \to J/\psi\phi K^+$
1650±50		FRAME	86 OMEG	+	13 $K^+ p \to \phi K^+ p$
• • • We do not use the following data for averages, fits, limits, etc. • • •					
~ 1840		ARMSTRONG	83 OMEG	–	18.5 $K^- p \to 3Kp$
~ 1800		DAUM	81C CNTR	–	63 $K^- p \to K^- 2\pi p$

[1] From an amplitude analysis of the decay $B^+ \to J/\psi\phi K^+$ with a significance of 7.6 σ.

$K_1(1650)$ WIDTH

VALUE (MeV)	EVTS	DOCUMENT ID	TECN	CHG	COMMENT
158± 50 OUR AVERAGE					
$365\pm157^{+138}_{-215}$	4289	[2] AAIJ	17C LHCB		$B^+ \to J/\psi\phi K^+$
150± 50		FRAME	86 OMEG	+	13 $K^+ p \to \phi K^+ p$
• • • We do not use the following data for averages, fits, limits, etc. • • •					
~ 250		DAUM	81C CNTR	–	63 $K^- p \to K^- 2\pi p$

[2] From an amplitude analysis of the decay $B^+ \to J/\psi\phi K^+$ with a significance of 7.6 σ.

$K_1(1650)$ DECAY MODES

	Mode
Γ_1	$K\pi\pi$
Γ_2	$K\phi$

$K_1(1650)$ REFERENCES

AAIJ	17C	PRL 118 022003	R. Aaij *et al.*	(LHCb Collab.)
Also		PR D95 012002	R. Aaij *et al.*	(LHCb Collab.)
FRAME	86	NP B276 667	D. Frame *et al.*	(GLAS)
ARMSTRONG	83	NP B221 1	T.A. Armstrong *et al.*	(BARI, BIRM, CERN+)
DAUM	81C	NP B187 1	C. Daum *et al.*	(AMST, CERN, CRAC, MPIM+)

Meson Particle Listings

$K^*(1680)$, $K_2(1770)$

$K^*(1680)$

$I(J^P) = \frac{1}{2}(1^-)$

$K^*(1680)$ MASS

VALUE (MeV)	EVTS	DOCUMENT ID		TECN	CHG	COMMENT
1718±18 OUR AVERAGE						
$1722\pm20^{+33}_{-109}$	4289	[1] AAIJ	17C	LHCB		$B^+ \to J/\psi\phi K^+$
1677±10± 32		ASTON	88	LASS	0	11 $K^-p \to K^-\pi^+n$
1735±10± 20		ASTON	87	LASS	0	11 $K^-p \to \overline{K}^0\pi^+\pi^-n$
• • • We do not use the following data for averages, fits, limits, etc. • • •						
1678±64		BIRD	89	LASS	–	11 $K^-p \to \overline{K}^0\pi^-p$
1800±70		ETKIN	80	MPS	0	6 $K^-p \to \overline{K}^0\pi^+\pi^-n$
~ 1650		ESTABROOKS	78	ASPK	0	13 $K^\pm p \to K^\pm\pi^\pm n$

[1] From an amplitude analysis of the decay $B^+ \to J/\psi\phi K^+$ with a significance of 8.5 σ.

$K^*(1680)$ WIDTH

VALUE (MeV)	EVTS	DOCUMENT ID		TECN	CHG	COMMENT
322±110 OUR AVERAGE		Error includes scale factor of 4.2.				
$354\pm 75^{+140}_{-181}$	4289	[2] AAIJ	17C	LHCB		$B^+ \to J/\psi\phi K^+$
205± 16± 34		ASTON	88	LASS	0	11 $K^-p \to K^-\pi^+n$
423± 18± 30		ASTON	87	LASS	0	11 $K^-p \to \overline{K}^0\pi^+\pi^-n$
• • • We do not use the following data for averages, fits, limits, etc. • • •						
454±270		BIRD	89	LASS	–	11 $K^-p \to \overline{K}^0\pi^-p$
170± 30		ETKIN	80	MPS	0	6 $K^-p \to \overline{K}^0\pi^+\pi^-n$
250 to 300		ESTABROOKS	78	ASPK	0	13 $K^\pm p \to K^\pm\pi^\pm n$

[2] From an amplitude analysis of the decay $B^+ \to J/\psi\phi K^+$ with a significance of 8.5 σ.

$K^*(1680)$ DECAY MODES

	Mode	Fraction (Γ_i/Γ)
Γ_1	$K\pi$	(38.7±2.5) %
Γ_2	$K\rho$	$(31.4^{+5.0}_{-2.1})$ %
Γ_3	$K^*(892)\pi$	$(29.9^{+2.2}_{-5.0})$ %
Γ_4	$K\phi$	seen

CONSTRAINED FIT INFORMATION

An overall fit to 4 branching ratios uses 4 measurements and one constraint to determine 3 parameters. The overall fit has a $\chi^2 = 2.9$ for 2 degrees of freedom.

The following *off-diagonal* array elements are the correlation coefficients $\langle \delta x_i \delta x_j \rangle / (\delta x_i \cdot \delta x_j)$, in percent, from the fit to the branching fractions, $x_i \equiv \Gamma_i/\Gamma_{\rm total}$. The fit constrains the x_i whose labels appear in this array to sum to one.

x_2	−36	
x_3	−39	−72
	x_1	x_2

$K^*(1680)$ BRANCHING RATIOS

$\Gamma(K\pi)/\Gamma_{\rm total}$ Γ_1/Γ

VALUE	DOCUMENT ID		TECN	CHG	COMMENT
0.387±0.026 OUR FIT					
0.388±0.014±0.022	ASTON	88	LASS	0	11 $K^-p \to K^-\pi^+n$

$\Gamma(K\pi)/\Gamma(K^*(892)\pi)$ Γ_1/Γ_3

VALUE	DOCUMENT ID		TECN	CHG	COMMENT
$\mathbf{1.30^{+0.23}_{-0.14}}$ **OUR FIT**					
2.8 ±1.1	ASTON	84	LASS	0	11 $K^-p \to \overline{K}^0 2\pi n$

$\Gamma(K\rho)/\Gamma(K\pi)$ Γ_2/Γ_1

VALUE	DOCUMENT ID		TECN	CHG	COMMENT
$\mathbf{0.81^{+0.14}_{-0.09}}$ **OUR FIT**					
1.2 ±0.4	ASTON	84	LASS	0	11 $K^-p \to \overline{K}^0 2\pi n$

$\Gamma(K\rho)/\Gamma(K^*(892)\pi)$ Γ_2/Γ_3

VALUE	DOCUMENT ID		TECN	CHG	COMMENT
$\mathbf{1.05^{+0.27}_{-0.11}}$ **OUR FIT**					
$\mathbf{0.97\pm0.09^{+0.30}_{-0.10}}$	ASTON	87	LASS	0	11 $K^-p \to \overline{K}^0\pi^+\pi^-n$

$\Gamma(K\phi)/\Gamma_{\rm total}$ Γ_4/Γ

VALUE	EVTS	DOCUMENT ID		TECN	COMMENT
seen	4289	[3] AAIJ	17C	LHCB	$B^+ \to J/\psi\phi K^+$

[3] From an amplitude analysis of the decay $B^+ \to J/\psi\phi K^+$ with a significance of 8.5 σ.

$K^*(1680)$ REFERENCES

AAIJ	17C	PRL 118 022003	R. Aaij *et al.*	(LHCb Collab.)
Also		PR D95 012002	R. Aaij *et al.*	(LHCb Collab.)
BIRD	89	SLAC-332	P.F. Bird	(SLAC)
ASTON	88	NP B296 493	D. Aston *et al.*	(SLAC, NAGO, CINC, INUS)
ASTON	87	NP B292 693	D. Aston *et al.*	(SLAC, NAGO, CINC, INUS)
ASTON	84	PL 149B 258	D. Aston *et al.*	(SLAC, CARL, OTTA) JP
ETKIN	80	PR D22 42	A. Etkin *et al.*	(BNL, CUNY) JP
ESTABROOKS	78	NP B133 490	P.G. Estabrooks *et al.*	(MCGI, CARL, DURH+) JP

$K_2(1770)$

$I(J^P) = \frac{1}{2}(2^-)$

See our mini-review in the 2004 edition of this *Review*, PDG 04.

$K_2(1770)$ MASS

VALUE (MeV)	EVTS	DOCUMENT ID		TECN	CHG	COMMENT
1773± 8 OUR AVERAGE						
$1777\pm35^{+122}_{-77}$	4289	[1] AAIJ	17C	LHCB		$B^+ \to J/\psi\phi K^+$
1773± 8		[2] ASTON	93	LASS		11 $K^-p \to K^-\omega p$
• • • We do not use the following data for averages, fits, limits, etc. • • •						
1743±15		TIKHOMIROV	03	SPEC		40.0 $\pi^-C \to K^0_S K^0_S K^0_L X$
1810±20		FRAME	86	OMEG	+	13 $K^+p \to \phi K^+p$
~ 1730		ARMSTRONG	83	OMEG	–	18.5 $K^-p \to 3Kp$
~ 1780		[3] DAUM	81C	CNTR	–	63 $K^-p \to K^-2\pi p$
1710±15	60	CHUNG	74	HBC	–	7.3 $K^-p \to K^-\omega p$
1767± 6		BLIEDEN	72	MMS	–	11–16 K^-p
1730±20	306	[4] FIRESTONE	72B	DBC	+	12 K^+d
1765±40		[5] COLLEY	71	HBC	+	10 $K^+p \to K2\pi N$
1740		DENEGRI	71	DBC	–	12.6 $K^-d \to \overline{K}2\pi d$
1745±20		AGUILAR-...	70C	HBC	–	4.6 K^-p
1780±15		BARTSCH	70C	HBC	–	10.1 K^-p
1760±15		LUDLAM	70	HBC	–	12.6 K^-p

[1] From an amplitude analysis of the decay $B^+ \to J/\psi\phi K^+$ with a significance of 5.0 σ.
[2] From a partial wave analysis of the $K^-\omega$ system.
[3] From a partial wave analysis of the $K^-2\pi$ system.
[4] Produced in conjunction with excited deuteron.
[5] Systematic errors added correspond to spread of different fits.

$K_2(1770)$ WIDTH

VALUE (MeV)	EVTS	DOCUMENT ID		TECN	CHG	COMMENT
186± 14 OUR AVERAGE						
$217\pm116^{+221}_{-154}$	4289	[6] AAIJ	17C	LHCB		$B^+ \to J/\psi\phi K^+$
186± 14		[7] ASTON	93	LASS		11 $K^-p \to K^-\omega p$
• • • We do not use the following data for averages, fits, limits, etc. • • •						
147± 70		TIKHOMIROV	03	SPEC		40.0 $\pi^-C \to K^0_S K^0_S K^0_L X$
140± 40		FRAME	86	OMEG	+	13 $K^+p \to \phi K^+p$
~ 220		ARMSTRONG	83	OMEG	–	18.5 $K^-p \to 3Kp$
~ 210		[8] DAUM	81C	CNTR	–	63 $K^-p \to K^-2\pi p$
110± 50	60	CHUNG	74	HBC	–	7.3 $K^-p \to K^-\omega p$
100± 26		BLIEDEN	72	MMS	–	11–16 K^-p
210± 30	306	[9] FIRESTONE	72B	DBC	+	12 K^+d
90± 70		[10] COLLEY	71	HBC	+	10 $K^+p \to K2\pi N$
130		DENEGRI	71	DBC	–	12.6 $K^-d \to \overline{K}2\pi d$
100± 50		AGUILAR-...	70C	HBC	–	4.6 K^-p
138± 40		BARTSCH	70C	HBC	–	10.1 K^-p
50^{+40}_{-20}		LUDLAM	70	HBC	–	12.6 K^-p

[6] From an amplitude analysis of the decay $B^+ \to J/\psi\phi K^+$ with a significance of 5.0 σ.
[7] From a partial wave analysis of the $K^-\omega$ system.
[8] From a partial wave analysis of the $K^-2\pi$ system.
[9] Produced in conjunction with excited deuteron.
[10] Systematic errors added correspond to spread of different fits.

$K_2(1770)$ DECAY MODES

	Mode	Fraction (Γ_i/Γ)
Γ_1	$K\pi\pi$	
Γ_2	$K_2^*(1430)\pi$	dominant
Γ_3	$K^*(892)\pi$	seen
Γ_4	$Kf_2(1270)$	seen
Γ_5	$Kf_0(980)$	
Γ_6	$K\phi$	seen
Γ_7	$K\omega$	seen

$K_2(1770)$ BRANCHING RATIOS

$\Gamma(K_2^*(1430)\pi)/\Gamma(K\pi\pi)$ Γ_2/Γ_1

($K_2^*(1430) \rightarrow K\pi$)

VALUE	DOCUMENT ID		TECN	CHG	COMMENT
• • • We do not use the following data for averages, fits, limits, etc. • • •					
~ 0.03	DAUM	81C	CNTR		63 $K^-p \rightarrow K^-2\pi p$
~ 1.0	[11] FIRESTONE	72B	DBC	+	12 K^+d
<1.0	COLLEY	71	HBC		10 K^+p
0.2 ±0.2	AGUILAR-...	70C	HBC	−	4.6 K^-p
<1.0	BARTSCH	70C	HBC	−	10.1 K^-p
1.0	BARBARO-...	69	HBC	+	12.0 K^+p

[11] Produced in conjunction with excited deuteron.

$\Gamma(K^*(892)\pi)/\Gamma(K\pi\pi)$ Γ_3/Γ_1

VALUE	DOCUMENT ID	TECN	COMMENT
• • • We do not use the following data for averages, fits, limits, etc. • • •			
~ 0.23	DAUM	81C	CNTR 63 $K^-p \rightarrow K^-2\pi p$

$\Gamma(Kf_2(1270))/\Gamma(K\pi\pi)$ Γ_4/Γ_1

($f_2(1270) \rightarrow \pi\pi$)

VALUE	DOCUMENT ID	TECN	COMMENT
• • • We do not use the following data for averages, fits, limits, etc. • • •			
~ 0.74	DAUM	81C	CNTR 63 $K^-p \rightarrow K^-2\pi p$

$\Gamma(Kf_0(980))/\Gamma_{total}$ Γ_5/Γ

VALUE	DOCUMENT ID	TECN	COMMENT
• • • We do not use the following data for averages, fits, limits, etc. • • •			
possibly seen	TIKHOMIROV 03	SPEC	40.0 $\pi^-C \rightarrow K_S^0K_S^0K_L^0X$

$\Gamma(K\phi)/\Gamma_{total}$ Γ_6/Γ

VALUE	EVTS	DOCUMENT ID		TECN	CHG	COMMENT
seen	4289	[12] AAIJ	17C	LHCB		$B^+ \rightarrow J/\psi\phi K^+$
seen		ARMSTRONG	83	OMEG	−	18.5 $K^-p \rightarrow K^-\phi N$

[12] From an amplitude analysis of the decay $B^+ \rightarrow J/\psi\phi K^+$ with a significance of 5.0 σ.

$\Gamma(K\omega)/\Gamma_{total}$ Γ_7/Γ

VALUE	DOCUMENT ID	TECN	CHG	COMMENT
seen	OTTER 81	HBC	±	8.25,10,16 $K^\pm p$
seen	CHUNG 74	HBC	−	7.3 $K^-p \rightarrow K^-\omega p$

$K_2(1770)$ REFERENCES

AAIJ	17C	PRL 118 022003	R. Aaij *et al.* (LHCb Collab.)
Also		PR D95 012002	R. Aaij *et al.* (LHCb Collab.)
PDG	04	PL B592 1	S. Eidelman *et al.* (PDG Collab.)
TIKHOMIROV	03	PAN 66 828	G.D. Tikhomirov *et al.*
		Translated from YAF 66 860.	
ASTON	93	PL B308 186	D. Aston *et al.* (SLAC, NAGO, CINC, INUS)
FRAME	86	NP B276 667	D. Frame *et al.* (GLAS)
ARMSTRONG	83	NP B221 1	T.A. Armstrong *et al.* (BARI, BIRM, CERN+)
DAUM	81C	NP B187 1	C. Daum *et al.* (AMST, CERN, CRAC, MPIM+)
OTTER	81	NP B181 1	G. Otter (AACH3, BERL, LOIC, VIEN, BIRM+)
CHUNG	74	PL 51B 413	S.U. Chung *et al.* (BNL)
BLIEDEN	72	PL 39B 668	H.R. Blieden *et al.* (STON, NEAS)
FIRESTONE	72B	PR D5 505	A. Firestone *et al.* (LBL)
COLLEY	71	NP B26 71	D.C. Colley *et al.* (BIRM, GLAS)
DENEGRI	71	NP B28 13	D. Denegri *et al.* (JHU) JP
AGUILAR-...	70C	PRL 25 54	M. Aguilar-Benitez *et al.* (BNL)
BARTSCH	70C	PL 33B 186	J. Bartsch *et al.* (AACH, BERL, CERN+)
LUDLAM	70	PR D2 1234	T. Ludlam, J. Sandweiss, A.J. Slaughter (YALE)
BARBARO-...	69	PRL 22 1207	A. Barbaro-Galtieri *et al.* (LRL)

$K_3^*(1780)$

$I(J^P) = \frac{1}{2}(3^-)$

$K_3^*(1780)$ MASS

VALUE (MeV)	EVTS	DOCUMENT ID		TECN	CHG	COMMENT
1776± 7 OUR AVERAGE	Error includes scale factor of 1.1.					
1781± 8± 4		[1] ASTON	88	LASS	0	11 $K^-p \rightarrow K^-\pi^+n$
1740±14±15		[1] ASTON	87	LASS	0	11 $K^-p \rightarrow \overline{K}^0\pi^+\pi^-n$
1779±11		[2] BALDI	76	SPEC	+	10 $K^+p \rightarrow K^0\pi^+p$
1776±26		[3] BRANDENB...	76D	ASPK	0	13 $K^\pm p \rightarrow K^\pm\pi^\mp N$
• • • We do not use the following data for averages, fits, limits, etc. • • •						
1720±10±15	6111	[4] BIRD	89	LASS	−	11 $K^-p \rightarrow \overline{K}^0\pi^-p$
1749±10		ASTON	88B	LASS	−	11 $K^-p \rightarrow K^-\eta p$
1780± 9	300	BAUBILLIER	84B	HBC	−	8.25 $K^-p \rightarrow \overline{K}^0\pi^-p$
1790±15		BAUBILLIER	82B	HBC	0	8.25 $K^-p \rightarrow K_S^0 2\pi N$
1784± 9	2060	CLELAND	82	SPEC	±	50 $K^+p \rightarrow K_S^0\pi^\pm p$
1786±15		[5] ASTON	81D	LASS	0	11 $K^-p \rightarrow K^-\pi^+n$
1762± 9	190	TOAFF	81	HBC	−	6.5 $K^-p \rightarrow \overline{K}^0\pi^-p$
1850±50		ETKIN	80	MPS	0	6 $K^-p \rightarrow \overline{K}^0\pi^+\pi^-$
1812±28		BEUSCH	78	OMEG		10 $K^-p \rightarrow \overline{K}^0\pi^+\pi^-n$
1786± 8		CHUNG	78	MPS	0	6 $K^-p \rightarrow K^-\pi^+n$

[1] From energy-independent partial-wave analysis.
[2] From a fit to Y_6^2 moment. $J^P = 3^-$ found.
[3] Confirmed by phase shift analysis of ESTABROOKS 78, yields $J^P = 3^-$.
[4] From a partial wave amplitude analysis.
[5] From a fit to the Y_6^0 moment.

$K_3^*(1780)$ WIDTH

VALUE (MeV)	EVTS	DOCUMENT ID		TECN	CHG	COMMENT
159±21 OUR AVERAGE	Error includes scale factor of 1.3. See the ideogram below.					
203±30± 8		[6] ASTON	88	LASS	0	11 $K^-p \rightarrow K^-\pi^+n$
171±42±20		[6] ASTON	87	LASS	0	11 $K^-p \rightarrow \overline{K}^0\pi^+\pi^-n$
135±22		[7] BALDI	76	SPEC	+	10 $K^+p \rightarrow K^0\pi^+p$
• • • We do not use the following data for averages, fits, limits, etc. • • •						
187±31±20	6111	[8] BIRD	89	LASS	−	11 $K^-p \rightarrow \overline{K}^0\pi^-p$
193^{+51}_{-37}		ASTON	88B	LASS	−	11 $K^-p \rightarrow K^-\eta p$
99±30	300	BAUBILLIER	84B	HBC	−	8.25 $K^-p \rightarrow \overline{K}^0\pi^-p$
~ 130		BAUBILLIER	82B	HBC	0	8.25 $K^-p \rightarrow K_S^0 2\pi N$
191±24	2060	CLELAND	82	SPEC	±	50 $K^+p \rightarrow K_S^0\pi^\pm p$
225±60		[9] ASTON	81D	LASS	0	11 $K^-p \rightarrow K^-\pi^+n$
~ 80	190	TOAFF	81	HBC	−	6.5 $K^-p \rightarrow \overline{K}^0\pi^-p$
240±50		ETKIN	80	MPS	0	6 $K^-p \rightarrow \overline{K}^0\pi^+\pi^-$
181±44		[10] BEUSCH	78	OMEG		10 $K^-p \rightarrow \overline{K}^0\pi^+\pi^-n$
96±31		CHUNG	78	MPS	0	6 $K^-p \rightarrow K^-\pi^+n$
270±70		[11] BRANDENB...	76D	ASPK	0	13 $K^\pm p \rightarrow K^\pm\pi^\mp N$

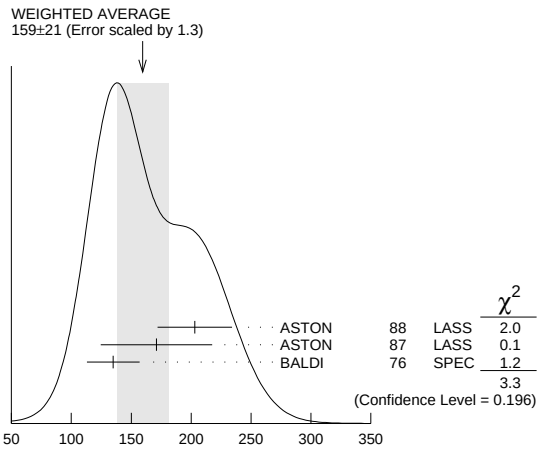

[6] From energy-independent partial-wave analysis.
[7] From a fit to Y_6^2 moment. $J^P = 3^-$ found.
[8] From a partial wave amplitude analysis.
[9] From a fit to Y_6^0 moment.
[10] Errors enlarged by us to $4\Gamma/\sqrt{N}$; see the note with the $K^*(892)$ mass.
[11] ESTABROOKS 78 find that BRANDENBURG 76D data are consistent with 175 MeV width. Not averaged.

Meson Particle Listings

$K_3^*(1780)$, $K_2(1820)$, $K(1830)$

$K_3^*(1780)$ DECAY MODES

	Mode	Fraction (Γ_i/Γ)	Confidence level
Γ_1	$K\rho$	(31 ± 9) %	
Γ_2	$K^*(892)\pi$	(20 ± 5) %	
Γ_3	$K\pi$	(18.8± 1.0) %	
Γ_4	$K\eta$	(30 ±13) %	
Γ_5	$K_2^*(1430)\pi$	< 16 %	95%

CONSTRAINED FIT INFORMATION

An overall fit to 3 branching ratios uses 4 measurements and one constraint to determine 4 parameters. The overall fit has a $\chi^2 = 0.0$ for 1 degrees of freedom.

The following *off-diagonal* array elements are the correlation coefficients $\langle \delta x_i \delta x_j \rangle / (\delta x_i \cdot \delta x_j)$, in percent, from the fit to the branching fractions, $x_i \equiv \Gamma_i/\Gamma_{\text{total}}$. The fit constrains the x_i whose labels appear in this array to sum to one.

x_2	85		
x_3	18	21	
x_4	−98	−94	−27
	x_1	x_2	x_3

$K_3^*(1780)$ BRANCHING RATIOS

$\Gamma(K\rho)/\Gamma(K^*(892)\pi)$ Γ_1/Γ_2

VALUE	DOCUMENT ID		TECN	CHG	COMMENT
1.52±0.23 OUR FIT					
1.52±0.21±0.10	ASTON	87	LASS	0	11 $K^-p \to \overline{K}^0\pi^+\pi^-n$

$\Gamma(K^*(892)\pi)/\Gamma(K\pi)$ Γ_2/Γ_3

VALUE	DOCUMENT ID		TECN	CHG	COMMENT
1.09±0.26 OUR FIT					
1.09±0.26	ASTON	84B	LASS	0	11 $K^-p \to \overline{K}^0 2\pi n$

$\Gamma(K\pi)/\Gamma_{\text{total}}$ Γ_3/Γ

VALUE	DOCUMENT ID		TECN	CHG	COMMENT
0.188±0.010 OUR FIT					
0.188±0.010 OUR AVERAGE					
0.187±0.008±0.008	ASTON	88	LASS	0	11 $K^-p \to K^-\pi^+n$
0.19 ±0.02	ESTABROOKS	78	ASPK	0	13 $K^\pm p \to K\pi N$

$\Gamma(K\eta)/\Gamma(K\pi)$ Γ_4/Γ_3

VALUE	DOCUMENT ID		TECN	CHG	COMMENT
1.6 ±0.7 OUR FIT					
• • • We do not use the following data for averages, fits, limits, etc. • • •					
0.41±0.050	[12] BIRD	89	LASS	–	11 $K^-p \to \overline{K}^0\pi^-p$
0.50±0.18	ASTON	88B	LASS	–	11 $K^-p \to K^-\eta p$

[12] This result supersedes ASTON 88B.

$\Gamma(K_2^*(1430)\pi)/\Gamma(K^*(892)\pi)$ Γ_5/Γ_2

VALUE	CL%	DOCUMENT ID		TECN	CHG	COMMENT
<0.78	95	ASTON	87	LASS	0	11 $K^-p \to \overline{K}^0\pi^+\pi^-n$

$K_3^*(1780)$ REFERENCES

BIRD	89	SLAC-332	P.F. Bird	(SLAC)
ASTON	88	NP B296 493	D. Aston *et al.*	(SLAC, NAGO, CINC, INUS)
ASTON	88B	PL B201 169	D. Aston *et al.*	(SLAC, NAGO, CINC, INUS) JP
ASTON	87	NP B292 693	D. Aston *et al.*	(SLAC, NAGO, CINC, INUS)
ASTON	84B	NP B247 261	D. Aston *et al.*	(SLAC, CARL, OTTA)
BAUBILLIER	84B	ZPHY C26 37	M. Baubillier *et al.*	(BIRM, CERN, GLAS+)
BAUBILLIER	82B	NP B202 21	M. Baubillier *et al.*	(BIRM, CERN, GLAS+)
CLELAND	82	NP B208 189	W.E. Cleland *et al.*	(DURH, GEVA, LAUS+)
ASTON	81D	PL 99B 502	D. Aston *et al.*	(SLAC, CARL, OTTA) JP
TOAFF	81	PR D23 1500	S. Toaff *et al.*	(ANL, KANS)
ETKIN	80	PR D22 42	A. Etkin *et al.*	(BNL, CUNY) JP
BEUSCH	78	PL 74B 282	W. Beusch *et al.*	(CERN, AACH3, ETH) JP
CHUNG	78	PRL 40 355	S.U. Chung *et al.*	(BNL, BRAN, CUNY+) JP
ESTABROOKS	78	NP B133 490	P.G. Estabrooks *et al.*	(MCGI, CARL, DURH+) JP
Also		PR D17 658	P.G. Estabrooks *et al.*	(MCGI, CARL, DURH+)
BALDI	76	PL 63B 344	R. Baldi *et al.*	(GEVA) JP
BRANDENB...	76D	PL 60B 478	G.W. Brandenburg *et al.*	(SLAC) JP

$K_2(1820)$ $I(J^P) = \frac{1}{2}(2^-)$

See our mini-review in the 2004 edition of this *Review* (PDG 04) under $K_2(1770)$.

$K_2(1820)$ MASS

VALUE (MeV)	EVTS	DOCUMENT ID		TECN	COMMENT
1819±12 OUR AVERAGE					
$1853 \pm 27^{+18}_{-35}$	4289	[1] AAIJ	17C	LHCB	$B^+ \to J/\psi\phi K^+$
1816±13		[2] ASTON	93	LASS	11 $K^-p \to K^-\omega p$
• • • We do not use the following data for averages, fits, limits, etc. • • •					
~ 1840		[3] DAUM	81C	CNTR	63 $K^-p \to K^-2\pi p$

[1] From an amplitude analysis of the decay $B^+ \to J/\psi\phi K^+$ with a significance of 3.0 σ.
[2] From a partial wave analysis of the $K^-\omega$ system.
[3] From a partial wave analysis of the $K^-2\pi$ system.

$K_2(1820)$ WIDTH

VALUE (MeV)	EVTS	DOCUMENT ID		TECN	COMMENT
264±34 OUR AVERAGE					
$167 \pm 58^{+82}_{-72}$	4289	[4] AAIJ	17C	LHCB	$B^+ \to J/\psi\phi K^+$
276±35		[5] ASTON	93	LASS	11 $K^-p \to K^-\omega p$
• • • We do not use the following data for averages, fits, limits, etc. • • •					
~ 230		[6] DAUM	81C	CNTR	63 $K^-p \to K^-2\pi p$

[4] From an amplitude analysis of the decay $B^+ \to J/\psi\phi K^+$ with a significance of 3.0 σ.
[5] From a partial wave analysis of the $K^-\omega$ system.
[6] From a partial wave analysis of the $K^-2\pi$ system.

$K_2(1820)$ DECAY MODES

	Mode	Fraction (Γ_i/Γ)
Γ_1	$K\pi\pi$	
Γ_2	$K_2^*(1430)\pi$	seen
Γ_3	$K^*(892)\pi$	seen
Γ_4	$Kf_2(1270)$	seen
Γ_5	$K\omega$	seen
Γ_6	$K\phi$	seen

$K_2(1820)$ BRANCHING RATIOS

$\Gamma(K_2^*(1430)\pi)/\Gamma(K\pi\pi)$ Γ_2/Γ_1

VALUE	DOCUMENT ID		TECN	COMMENT
• • • We do not use the following data for averages, fits, limits, etc. • • •				
~ 0.77	DAUM	81C	CNTR	63$K^-p \to \overline{K}2\pi p$

$\Gamma(K^*(892)\pi)/\Gamma(K\pi\pi)$ Γ_3/Γ_1

VALUE	DOCUMENT ID		TECN	COMMENT
• • • We do not use the following data for averages, fits, limits, etc. • • •				
~ 0.05	DAUM	81C	CNTR	63$K^-p \to \overline{K}2\pi p$

$\Gamma(Kf_2(1270))/\Gamma(K\pi\pi)$ Γ_4/Γ_1

VALUE	DOCUMENT ID		TECN	COMMENT
• • • We do not use the following data for averages, fits, limits, etc. • • •				
~ 0.18	DAUM	81C	CNTR	63$K^-p \to \overline{K}2\pi p$

$\Gamma(K\phi)/\Gamma_{\text{total}}$ Γ_6/Γ

VALUE	EVTS	DOCUMENT ID		TECN	COMMENT
seen	4289	[7] AAIJ	17C	LHCB	$B^+ \to J/\psi\phi K^+$

[7] From an amplitude analysis of the decay $B^+ \to J/\psi\phi K^+$ with a significance of 3.0 σ.

$K_2(1820)$ REFERENCES

AAIJ	17C	PRL 118 022003	R. Aaij *et al.*	(LHCb Collab.)
Also		PR D95 012002	R. Aaij *et al.*	(LHCb Collab.)
PDG	04	PL B592 1	S. Eidelman *et al.*	(PDG Collab.)
ASTON	93	PL B308 186	D. Aston *et al.*	(SLAC, NAGO, CINC, INUS)
DAUM	81C	NP B187 1	C. Daum *et al.*	(AMST, CERN, CRAC, MPIM+)

$K(1830)$ $I(J^P) = \frac{1}{2}(0^-)$

OMITTED FROM SUMMARY TABLE

Seen in partial-wave analysis of $K\phi$ system. Needs confirmation.

$K(1830)$ MASS

VALUE (MeV)	EVTS	DOCUMENT ID		TECN	CHG	COMMENT
$1874 \pm 43^{+59}_{-115}$	4289	[1] AAIJ	17C	LHCB		$B^+ \to J/\psi\phi K^+$
• • • We do not use the following data for averages, fits, limits, etc. • • •						
~ 1830		ARMSTRONG	83	OMEG	–	18.5 $K^-p \to 3Kp$

[1] From an amplitude analysis of the decay $B^+ \to J/\psi\phi K^+$ with a significance of 3.5 σ.

$K(1830)$ WIDTH

VALUE (MeV)	EVTS	DOCUMENT ID		TECN	CHG	COMMENT
$\mathbf{168 \pm 90^{+280}_{-104}}$	4289	[2] AAIJ	17C	LHCB		$B^+ \to J/\psi\phi K^+$
• • • We do not use the following data for averages, fits, limits, etc. • • •						
~ 250		ARMSTRONG	83	OMEG	–	18.5 $K^- p \to 3Kp$

[2] From an amplitude analysis of the decay $B^+ \to J/\psi\phi K^+$ with a significance of 3.5 σ.

$K(1830)$ DECAY MODES

	Mode
Γ_1	$K\phi$

$K(1830)$ REFERENCES

AAIJ	17C	PRL 118 022003	R. Aaij *et al.*	(LHCb Collab.)
Also		PR D95 012002	R. Aaij *et al.*	(LHCb Collab.)
ARMSTRONG	83	NP B221 1	T.A. Armstrong *et al.*	(BARI, BIRM, CERN+) JP

$K_0^*(1950)$

$I(J^P) = \frac{1}{2}(0^+)$

OMITTED FROM SUMMARY TABLE

Seen in partial-wave analysis of the $K^-\pi^+$ system. Needs confirmation.

$K_0^*(1950)$ MASS

VALUE (MeV)	DOCUMENT ID		TECN	CHG	COMMENT
1945 ± 10 ± 20	[1] ASTON	88	LASS	0	11 $K^- p \to K^-\pi^+ n$
• • • We do not use the following data for averages, fits, limits, etc. • • •					
1917 ± 12	[2] ZHOU	06	RVUE		$Kp \to K^-\pi^+ n$
1820 ± 40	[3] ANISOVICH	97C	RVUE		11 $K^- p \to K^-\pi^+ n$

[1] We take the central value of the two solutions and the larger error given.
[2] S-matrix pole. Using ASTON 88 and assuming $K_0^*(700)$, $K_0^*(1430)$.
[3] T-matrix pole. Reanalysis of ASTON 88 data.

$K_0^*(1950)$ WIDTH

VALUE (MeV)	DOCUMENT ID		TECN	CHG	COMMENT
201 ± 34 ± 79	[4] ASTON	88	LASS	0	11 $K^- p \to K^-\pi^+ n$
• • • We do not use the following data for averages, fits, limits, etc. • • •					
145 ± 38	[5] ZHOU	06	RVUE		$Kp \to K^-\pi^+ n$
250 ± 100	[6] ANISOVICH	97C	RVUE		11 $K^- p \to K^-\pi^+ n$

[4] We take the central value of the two solutions and the larger error given.
[5] S-matrix pole. Using ASTON 88 and assuming $K_0^*(700)$, $K_0^*(1430)$.
[6] T-matrix pole. Reanalysis of ASTON 88 data.

$K_0^*(1950)$ DECAY MODES

	Mode	Fraction (Γ_i/Γ)
Γ_1	$K\pi$	(52 ± 14) %

$K_0^*(1950)$ BRANCHING RATIOS

$\Gamma(K\pi)/\Gamma_{\text{total}}$ Γ_1/Γ

VALUE	DOCUMENT ID		TECN	CHG	COMMENT
0.52 ± 0.08 ± 0.12	[7] ASTON	88	LASS	0	11 $K^- p \to K^-\pi^+ n$
• • • We do not use the following data for averages, fits, limits, etc. • • •					
~ 0.60	[8] ZHOU	06	RVUE		$Kp \to K^-\pi^+ n$

[7] We take the central value of the two solutions and the larger error given.
[8] S-matrix pole. Using ASTON 88 and assuming $K_0^*(700)$, $K_0^*(1430)$.

$K_0^*(1950)$ REFERENCES

ZHOU	06	NP A775 212	Z.Y. Zhou, H.Q. Zheng
ANISOVICH	97C	PL B413 137	A.V. Anisovich, A.V. Sarantsev
ASTON	88	NP B296 493	D. Aston *et al.* (SLAC, NAGO, CINC, INUS)

$K_2^*(1980)$

$I(J^P) = \frac{1}{2}(2^+)$

OMITTED FROM SUMMARY TABLE

Needs confirmation.

$K_2^*(1980)$ MASS

VALUE (MeV)	EVTS	DOCUMENT ID		TECN	CHG	COMMENT
1974 ± 26 OUR AVERAGE						
$2073 \pm 94^{+245}_{-240}$	4289	[1] AAIJ	17C	LHCB		$B^+ \to J/\psi\phi K^+$
1973 ± 8 ± 25		ASTON	87	LASS	0	11 $K^- p \to \overline{K}^0\pi^+\pi^- n$
• • • We do not use the following data for averages, fits, limits, etc. • • •						
2020 ± 20		TIKHOMIROV	03	SPEC		40.0 π^- C $\to K_S^0 K_S^0 K_L^0$ X
1978 ± 40	241	BIRD	89	LASS	–	11 $K^- p \to \overline{K}^0\pi^- p$

[1] From an amplitude analysis of the decay $B^+ \to J/\psi\phi K^+$ with a significance of 5.4 σ.

$K_2^*(1980)$ WIDTH

VALUE (MeV)	EVTS	DOCUMENT ID		TECN	CHG	COMMENT
376 ± 70 OUR AVERAGE						
$678 \pm 311^{+1153}_{-559}$	4289	[2] AAIJ	17C	LHCB		$B^+ \to J/\psi\phi K^+$
373 ± 33 ± 60		ASTON	87	LASS	0	11 $K^- p \to \overline{K}^0\pi^+\pi^- n$
• • • We do not use the following data for averages, fits, limits, etc. • • •						
180 ± 70		TIKHOMIROV	03	SPEC		40.0 π^- C $\to K_S^0 K_S^0 K_L^0$ X
398 ± 47	241	BIRD	89	LASS	–	11 $K^- p \to \overline{K}^0\pi^- p$

[2] From an amplitude analysis of the decay $B^+ \to J/\psi\phi K^+$ with a significance of 5.4 σ.

$K_2^*(1980)$ DECAY MODES

	Mode	Fraction (Γ_i/Γ)
Γ_1	$K^*(892)\pi$	possibly seen
Γ_2	$K\rho$	possibly seen
Γ_3	$K f_2(1270)$	possibly seen
Γ_4	$K\phi$	seen

$K_2^*(1980)$ BRANCHING RATIOS

$\Gamma(K^*(892)\pi)/\Gamma_{\text{total}}$ Γ_1/Γ

VALUE	DOCUMENT ID		TECN	COMMENT
possibly seen	GULER	11	BELL	$B^+ \to J/\psi K^+\pi^+\pi^-$

$\Gamma(K\rho)/\Gamma_{\text{total}}$ Γ_2/Γ

VALUE	DOCUMENT ID		TECN	COMMENT
possibly seen	GULER	11	BELL	$B^+ \to J/\psi K^+\pi^+\pi^-$

$\Gamma(K\rho)/\Gamma(K^*(892)\pi)$ Γ_2/Γ_1

VALUE	DOCUMENT ID		TECN	CHG	COMMENT
1.49 ± 0.24 ± 0.09	ASTON	87	LASS	0	11 $K^- p \to \overline{K}^0\pi^+\pi^- n$

$\Gamma(K f_2(1270))/\Gamma_{\text{total}}$ Γ_3/Γ

VALUE	DOCUMENT ID		TECN	COMMENT
possibly seen	TIKHOMIROV	03	SPEC	40.0 π^- C $\to K_S^0 K_S^0 K_L^0$ X

$\Gamma(K\phi)/\Gamma_{\text{total}}$ Γ_4/Γ

VALUE	EVTS	DOCUMENT ID		TECN	COMMENT
seen	4289	[3] AAIJ	17C	LHCB	$B^+ \to J/\psi\phi K^+$

[3] From an amplitude analysis of the decay $B^+ \to J/\psi\phi K^+$ with a significance of 5.4 σ.

$K_2^*(1980)$ REFERENCES

AAIJ	17C	PRL 118 022003	R. Aaij *et al.*	(LHCb Collab.)
Also		PR D95 012002	R. Aaij *et al.*	(LHCb Collab.)
GULER	11	PR D83 032005	H. Guler *et al.*	(BELLE Collab.)
TIKHOMIROV	03	PAN 66 828 Translated from YAF 66 860.	G.D. Tikhomirov *et al.*	
BIRD	89	SLAC-332	P.F. Bird	(SLAC)
ASTON	87	NP B292 693	D. Aston *et al.*	(SLAC, NAGO, CINC, INUS)

$K_4^*(2045)$

$I(J^P) = \frac{1}{2}(4^+)$

$K_4^*(2045)$ MASS

VALUE (MeV)	EVTS	DOCUMENT ID		TECN	CHG	COMMENT
2045 ± 9 OUR AVERAGE	Error includes scale factor of 1.1.					
2062 ± 14 ± 13		[1] ASTON	86	LASS	0	11 $K^- p \to K^-\pi^+ n$
2039 ± 10	400	[2,3] CLELAND	82	SPEC	±	50 $K^+ p \to K_S^0\pi^\pm p$
2070^{+100}_{-40}		[4] ASTON	81C	LASS	0	11 $K^- p \to K^-\pi^+ n$
• • • We do not use the following data for averages, fits, limits, etc. • • •						
2079 ± 7	431	TORRES	86	MPSF		400 $pA \to 4KX$
2088 ± 20	650	BAUBILLIER	82	HBC	–	8.25 $K^- p \to K_S^0\pi^- p$
2115 ± 46	488	CARMONY	77	HBC	0	9 $K^+ d \to K^+\pi$'s X

Meson Particle Listings

$K_4^*(2045)$, $K_2(2250)$, $K_3(2320)$

[1] From a fit to all moments.
[2] From a fit to 8 moments.
[3] Number of events evaluated by us.
[4] From energy-independent partial-wave analysis.

$K_4^*(2045)$ WIDTH

VALUE (MeV)	EVTS	DOCUMENT ID		TECN	CHG	COMMENT
198± 30 OUR AVERAGE						
221± 48±27		[5] ASTON	86	LASS	0	11 $K^- p \to K^- \pi^+ n$
189± 35	400	[6,7] CLELAND	82	SPEC	±	50 $K^+ p \to K^0_S \pi^\pm p$
• • • We do not use the following data for averages, fits, limits, etc. • • •						
61± 58	431	TORRES	86	MPSF		400 $pA \to 4KX$
$170^{+100}_{-\ 50}$	650	BAUBILLIER	82	HBC	–	8.25 $K^- p \to K^0_S \pi^- p$
240^{+500}_{-100}		[8] ASTON	81C	LASS	0	11 $K^- p \to K^- \pi^+ n$
300±200		CARMONY	77	HBC	0	9 $K^+ d \to K^+ \pi$'s X

[5] From a fit to all moments.
[6] From a fit to 8 moments.
[7] Number of events evaluated by us.
[8] From energy-independent partial-wave analysis.

$K_4^*(2045)$ DECAY MODES

	Mode	Fraction (Γ_i/Γ)
Γ_1	$K\pi$	(9.9±1.2) %
Γ_2	$K^*(892)\pi\pi$	(9 ±5) %
Γ_3	$K^*(892)\pi\pi\pi$	(7 ±5) %
Γ_4	$\rho K\pi$	(5.7±3.2) %
Γ_5	$\omega K\pi$	(5.0±3.0) %
Γ_6	$\phi K\pi$	(2.8±1.4) %
Γ_7	$\phi K^*(892)$	(1.4±0.7) %

$K_4^*(2045)$ BRANCHING RATIOS

$\Gamma(K\pi)/\Gamma_{total}$ — **Γ_1/Γ**

VALUE	DOCUMENT ID		TECN	CHG	COMMENT
0.099±0.012	ASTON	88	LASS	0	11 $K^- p \to K^- \pi^+ n$

$\Gamma(K^*(892)\pi\pi)/\Gamma(K\pi)$ — **Γ_2/Γ_1**

VALUE	DOCUMENT ID		TECN	CHG	COMMENT
0.89±0.53	BAUBILLIER	82	HBC	–	8.25 $K^- p \to p K^0_S 3\pi$

$\Gamma(K^*(892)\pi\pi\pi)/\Gamma(K\pi)$ — **Γ_3/Γ_1**

VALUE	DOCUMENT ID		TECN	CHG	COMMENT
0.75±0.49	BAUBILLIER	82	HBC	–	8.25 $K^- p \to p K^0_S 3\pi$

$\Gamma(\rho K\pi)/\Gamma(K\pi)$ — **Γ_4/Γ_1**

VALUE	DOCUMENT ID		TECN	CHG	COMMENT
0.58±0.32	BAUBILLIER	82	HBC	–	8.25 $K^- p \to p K^0_S 3\pi$

$\Gamma(\omega K\pi)/\Gamma(K\pi)$ — **Γ_5/Γ_1**

VALUE	DOCUMENT ID		TECN	CHG	COMMENT
0.50±0.30	BAUBILLIER	82	HBC	–	8.25 $K^- p \to p K^0_S 3\pi$

$\Gamma(\phi K\pi)/\Gamma_{total}$ — **Γ_6/Γ**

VALUE	DOCUMENT ID		TECN	COMMENT
0.028±0.014	[9] TORRES	86	MPSF	400 $pA \to 4KX$

$\Gamma(\phi K^*(892))/\Gamma_{total}$ — **Γ_7/Γ**

VALUE	DOCUMENT ID		TECN	COMMENT
0.014±0.007	[9] TORRES	86	MPSF	400 $pA \to 4KX$

[9] Error determination is model dependent.

$K_4^*(2045)$ REFERENCES

ASTON	88	NP B296 493	D. Aston *et al.*	(SLAC, NAGO, CINC, INUS)
ASTON	86	PL B180 308	D. Aston *et al.*	(SLAC, NAGO, CINC, INUS)
TORRES	86	PR D34 707	S. Torres *et al.*	(VPI, ARIZ, FNAL, FSU+)
BAUBILLIER	82	PL 118B 447	M. Baubillier *et al.*	(BIRM, CERN, GLAS+)
CLELAND	82	NP B208 189	W.E. Cleland *et al.*	(DURH, GEVA, LAUS+)
ASTON	81C	PL 106B 235	D. Aston *et al.*	(SLAC, CARL, OTTA) JP
CARMONY	77	PR D16 1251	D.D. Carmony *et al.*	(PURD, UCD, IUPU)

$K_2(2250)$ $I(J^P) = \frac{1}{2}(2^-)$

OMITTED FROM SUMMARY TABLE

This entry contains various peaks in strange meson systems reported in the 2150–2260 MeV region, as well as enhancements seen in the antihyperon-nucleon system, either in the mass spectra or in the $J^P = 2^-$ wave.

$K_2(2250)$ MASS

VALUE (MeV)	EVTS	DOCUMENT ID		TECN	CHG	COMMENT
2247±17 OUR AVERAGE						
2200±40		[1] ARMSTRONG	83C	OMEG	–	18 $K^- p \to \Lambda\overline{p}X$
2235±50		[1] BAUBILLIER	81	HBC	–	8 $K^- p \to \Lambda\overline{p}X$
2260±20		[1] CLELAND	81	SPEC	±	50 $K^+ p \to \Lambda\overline{p}X$
• • • We do not use the following data for averages, fits, limits, etc. • • •						
2280±20		TIKHOMIROV	03	SPEC		40.0 $\overline{p}C \to K^0_S K^0_S K^0_L X$
2147± 4	37	CHLIAPNIK...	79	HBC	+	32 $K^+ p \to \overline{\Lambda} p X$
2240±20	20	LISSAUER	70	HBC		9 $K^+ p$

[1] $J^P = 2^-$ from moments analysis.

$K_2(2250)$ WIDTH

VALUE (MeV)	EVTS	DOCUMENT ID		TECN	CHG	COMMENT
180±30 OUR AVERAGE		Error includes scale factor of 1.4.				
150±30		[2] ARMSTRONG	83C	OMEG	–	18 $K^- p \to \Lambda\overline{p}X$
210±30		[2] CLELAND	81	SPEC	±	50 $K^+ p \to \Lambda\overline{p}X$
• • • We do not use the following data for averages, fits, limits, etc. • • •						
180±60		TIKHOMIROV	03	SPEC		40.0 $\overline{p}C \to K^0_S K^0_S K^0_L X$
~ 200		[2] BAUBILLIER	81	HBC	–	8 $K^- p \to \Lambda\overline{p}X$
~ 40	37	CHLIAPNIK...	79	HBC	+	32 $K^+ p \to \overline{\Lambda} p X$
80±20	20	LISSAUER	70	HBC		9 $K^+ p$

[2] $J^P = 2^-$ from moments analysis.

$K_2(2250)$ DECAY MODES

	Mode
Γ_1	$K\pi\pi$
Γ_2	$K f_2(1270)$
Γ_3	$K^*(892) f_0(980)$
Γ_4	$p\overline{\Lambda}$

$K_2(2250)$ REFERENCES

TIKHOMIROV	03	PAN 66 828 Translated from YAF 66 860.	G.D. Tikhomirov *et al.*	
ARMSTRONG	83C	NP B227 365	T.A. Armstrong *et al.*	(BARI, BIRM, CERN+)
BAUBILLIER	81	NP B183 1	M. Baubillier *et al.*	(BIRM, CERN, GLAS+) JP
CLELAND	81	NP B184 1	W.E. Cleland *et al.*	(PITT, GEVA, LAUS+) JP
CHLIAPNIK...	79	NP B158 253	P.V. Chliapnikov *et al.*	(CERN, BELG, MONS)
LISSAUER	70	NP B18 491	D. Lissauer *et al.*	(LBL)

$K_3(2320)$ $I(J^P) = \frac{1}{2}(3^+)$

OMITTED FROM SUMMARY TABLE

Seen in the $J^P = 3^+$ wave of the antihyperon-nucleon system. Needs confirmation.

$K_3(2320)$ MASS

VALUE (MeV)	DOCUMENT ID		TECN	CHG	COMMENT
2324±24 OUR AVERAGE					
2330±40	[1] ARMSTRONG	83C	OMEG	–	18 $K^- p \to \Lambda\overline{p}X$
2320±30	[1] CLELAND	81	SPEC	±	50 $K^+ p \to \Lambda\overline{p}X$

[1] $J^P = 3^+$ from moments analysis.

$K_3(2320)$ WIDTH

VALUE (MeV)	DOCUMENT ID		TECN	CHG	COMMENT
150±30	[2] ARMSTRONG	83C	OMEG	–	18 $K^- p \to \Lambda\overline{p}X$
• • • We do not use the following data for averages, fits, limits, etc. • • •					
~ 250	[2] CLELAND	81	SPEC	±	50 $K^+ p \to \Lambda\overline{p}X$

[2] $J^P = 3^+$ from moments analysis.

$K_3(2320)$ DECAY MODES

	Mode
Γ_1	$p\overline{\Lambda}$

$K_3(2320)$ REFERENCES

ARMSTRONG	83C	NP B227 365	T.A. Armstrong *et al.*	(BARI, BIRM, CERN+)
CLELAND	81	NP B184 1	W.E. Cleland *et al.*	(PITT, GEVA, LAUS+)

$K_5^*(2380)$

$I(J^P) = \frac{1}{2}(5^-)$

OMITTED FROM SUMMARY TABLE

Needs confirmation.

$K_5^*(2380)$ MASS

VALUE (MeV)	DOCUMENT ID		TECN	CHG	COMMENT
2382±14±19	[1] ASTON	86	LASS	0	11 $K^- p \rightarrow K^- \pi^+ n$

[1] From a fit to all the moments.

$K_5^*(2380)$ WIDTH

VALUE (MeV)	DOCUMENT ID		TECN	CHG	COMMENT
178±37±32	[2] ASTON	86	LASS	0	11 $K^- p \rightarrow K^- \pi^+ n$

[2] From a fit to all the moments.

$K_5^*(2380)$ DECAY MODES

	Mode	Fraction (Γ_i/Γ)
Γ_1	$K\pi$	(6.1±1.2) %

$K_5^*(2380)$ BRANCHING RATIOS

$\Gamma(K\pi)/\Gamma_{total}$ **Γ_1/Γ**

VALUE	DOCUMENT ID		TECN	CHG	COMMENT
0.061±0.012	ASTON	88	LASS	0	11 $K^- p \rightarrow K^- \pi^+ n$

$K_5^*(2380)$ REFERENCES

ASTON	88	NP B296 493	D. Aston *et al.*	(SLAC, NAGO, CINC, INUS)
ASTON	86	PL B180 308	D. Aston *et al.*	(SLAC, NAGO, CINC, INUS)

$K_4(2500)$

$I(J^P) = \frac{1}{2}(4^-)$

OMITTED FROM SUMMARY TABLE

Needs confirmation.

$K_4(2500)$ MASS

VALUE (MeV)	DOCUMENT ID		TECN	CHG	COMMENT
2490±20	[1] CLELAND	81	SPEC	±	50 $K^+ p \rightarrow \Lambda\overline{p}$

[1] $J^P = 4^-$ from moments analysis.

$K_4(2500)$ WIDTH

VALUE (MeV)	DOCUMENT ID		TECN	CHG	COMMENT
• • • We do not use the following data for averages, fits, limits, etc. • • •					
~ 250	[2] CLELAND	81	SPEC	±	50 $K^+ p \rightarrow \Lambda\overline{p}$

[2] $J^P = 4^-$ from moments analysis.

$K_4(2500)$ DECAY MODES

	Mode
Γ_1	$p\overline{\Lambda}$

$K_4(2500)$ REFERENCES

CLELAND	81	NP B184 1	W.E. Cleland *et al.*	(PITT, GEVA, LAUS+)

$K(3100)$

$I^G(J^{PC}) = ?^?(?^{??})$

OMITTED FROM SUMMARY TABLE

Narrow peak observed in several ($\Lambda\overline{p}$ + pions) and ($\overline{\Lambda}p$ + pions) states in Σ^- Be reactions by BOURQUIN 86 and in np and nA reactions by ALEEV 93. Not seen by BOEHNLEIN 91. If due to strong decays, this state has exotic quantum numbers (B=0,Q=+1,S=−1 for $\Lambda\overline{p}\pi^+\pi^+$ and $I \geq 3/2$ for $\Lambda\overline{p}\pi^-$). Needs confirmation.

$K(3100)$ MASS

VALUE (MeV)	DOCUMENT ID
≈ 3100 OUR ESTIMATE	

3-BODY DECAYS

VALUE (MeV)	DOCUMENT ID		TECN	COMMENT
3054±11 OUR AVERAGE				
3060± 7±20	[1] ALEEV	93	BIS2	$K(3100) \rightarrow \Lambda\overline{p}\pi^+$
3056± 7±20	[1] ALEEV	93	BIS2	$K(3100) \rightarrow \overline{\Lambda}p\pi^-$
3055± 8±20	[1] ALEEV	93	BIS2	$K(3100) \rightarrow \Lambda\overline{p}\pi^-$
3045± 8±20	[1] ALEEV	93	BIS2	$K(3100) \rightarrow \overline{\Lambda}p\pi^+$

4-BODY DECAYS

VALUE (MeV)	DOCUMENT ID		TECN	COMMENT
3059±11 OUR AVERAGE				
3067± 6±20	[1] ALEEV	93	BIS2	$K(3100) \rightarrow \Lambda\overline{p}\pi^+\pi^+$
3060± 8±20	[1] ALEEV	93	BIS2	$K(3100) \rightarrow \Lambda\overline{p}\pi^+\pi^-$
3055± 7±20	[1] ALEEV	93	BIS2	$K(3100) \rightarrow \overline{\Lambda}p\pi^-\pi^-$
3052± 8±20	[1] ALEEV	93	BIS2	$K(3100) \rightarrow \overline{\Lambda}p\pi^-\pi^+$
• • • We do not use the following data for averages, fits, limits, etc. • • •				
3105±30	BOURQUIN	86	SPEC	$K(3100) \rightarrow \Lambda\overline{p}\pi^+\pi^+$
3115±30	BOURQUIN	86	SPEC	$K(3100) \rightarrow \Lambda\overline{p}\pi^+\pi^-$

5-BODY DECAYS

VALUE (MeV)	DOCUMENT ID		TECN	COMMENT
• • • We do not use the following data for averages, fits, limits, etc. • • •				
3095±30	BOURQUIN	86	SPEC	$K(3100) \rightarrow \Lambda\overline{p}\pi^+\pi^+\pi^-$

[1] Supersedes ALEEV 90.

$K(3100)$ WIDTH

3-BODY DECAYS

VALUE (MeV)	DOCUMENT ID		TECN	COMMENT
• • • We do not use the following data for averages, fits, limits, etc. • • •				
42±16	[2] ALEEV	93	BIS2	$K(3100) \rightarrow \Lambda\overline{p}\pi^+$
36±15	[2] ALEEV	93	BIS2	$K(3100) \rightarrow \overline{\Lambda}p\pi^-$
50±18	[2] ALEEV	93	BIS2	$K(3100) \rightarrow \Lambda\overline{p}\pi^-$
30±15	[2] ALEEV	93	BIS2	$K(3100) \rightarrow \overline{\Lambda}p\pi^+$

4-BODY DECAYS

VALUE (MeV)	CL%	DOCUMENT ID		TECN	COMMENT
• • • We do not use the following data for averages, fits, limits, etc. • • •					
22± 8		[2] ALEEV	93	BIS2	$K(3100) \rightarrow \Lambda\overline{p}\pi^+\pi^+$
28±12		[2] ALEEV	93	BIS2	$K(3100) \rightarrow \Lambda\overline{p}\pi^+\pi^-$
32±15		[2] ALEEV	93	BIS2	$K(3100) \rightarrow \overline{\Lambda}p\pi^-\pi^-$
30±15		[2] ALEEV	93	BIS2	$K(3100) \rightarrow \overline{\Lambda}p\pi^-\pi^+$
<30	90	BOURQUIN	86	SPEC	$K(3100) \rightarrow \Lambda\overline{p}\pi^+\pi^+$
<80	90	BOURQUIN	86	SPEC	$K(3100) \rightarrow \Lambda\overline{p}\pi^+\pi^-$

5-BODY DECAYS

VALUE (MeV)	CL%	DOCUMENT ID		TECN	COMMENT
• • • We do not use the following data for averages, fits, limits, etc. • • •					
<30	90	BOURQUIN	86	SPEC	$K(3100) \rightarrow \Lambda\overline{p}\pi^+\pi^+\pi^-$

[2] Supersedes ALEEV 90.

$K(3100)$ DECAY MODES

	Mode
Γ_1	$K(3100)^0 \rightarrow \Lambda\overline{p}\pi^+$
Γ_2	$K(3100)^{--} \rightarrow \Lambda\overline{p}\pi^-$
Γ_3	$K(3100)^- \rightarrow \Lambda\overline{p}\pi^+\pi^-$
Γ_4	$K(3100)^+ \rightarrow \Lambda\overline{p}\pi^+\pi^+$
Γ_5	$K(3100)^0 \rightarrow \Lambda\overline{p}\pi^+\pi^+\pi^-$
Γ_6	$K(3100)^0 \rightarrow \Sigma(1385)^+\overline{p}$

$\Gamma(\Sigma(1385)^+\overline{p})/\Gamma(\Lambda\overline{p}\pi^+)$ **Γ_6/Γ_1**

VALUE	CL%	DOCUMENT ID		TECN	COMMENT
<0.04	90	ALEEV	93	BIS2	$K(3100)^0 \rightarrow \Sigma(1385)^+\overline{p}$

$K(3100)$ REFERENCES

ALEEV	93	PAN 56 1358 Translated from YAF 56 100.	A.N. Aleev *et al.*	(BIS-2 Collab.)
BOEHNLEIN	91	NPBPS B21 174	A. Boehnlein *et al.*	(FLOR, BNL, IND+)
ALEEV	90	ZPHY C47 533	A.N. Aleev *et al.*	(BIS-2 Collab.)
BOURQUIN	86	PL B172 113	M.H. Bourquin *et al.*	(GEVA, RAL, HEIDP+)

CHARMED MESONS ($C = \pm 1$)

$D^+ = c\overline{d}$, $D^0 = c\overline{u}$, $\overline{D}^0 = \overline{c}u$, $D^- = \overline{c}d$, similarly for D^*'s

$D^{\pm}$ $I(J^P) = \frac{1}{2}(0^-)$

$D^{\pm}$ MASS

The fit includes $D^{\pm}$, D^0, $D_s^{\pm}$, $D^{*\pm}$, D^{*0}, $D_s^{*\pm}$, $D_1(2420)^0$, $D_2^*(2460)^0$, and $D_{s1}(2536)^{\pm}$ mass and mass difference measurements.

VALUE (MeV)	EVTS	DOCUMENT ID		TECN	COMMENT
1869.65 ± 0.05 OUR FIT					
1869.5 ± 0.4 OUR AVERAGE					
1869.53 ± 0.49 ± 0.20	110 ± 15	ANASHIN	10A	KEDR	e^+e^- at $\psi(3770)$
1870.0 ± 0.5 ± 1.0	317	BARLAG	90C	ACCM	π^- Cu 230 GeV
1869.4 ± 0.6		[1] TRILLING	81	RVUE	e^+e^- 3.77 GeV
• • • We do not use the following data for averages, fits, limits, etc. • • •					
1875 ±10	9	ADAMOVICH	87	EMUL	Photoproduction
1860 ±16	6	ADAMOVICH	84	EMUL	Photoproduction
1863 ± 4		DERRICK	84	HRS	e^+e^- 29 GeV
1868.4 ± 0.5		[1] SCHINDLER	81	MRK2	e^+e^- 3.77 GeV
1874 ± 5		GOLDHABER	77	MRK1	D^0, D^+ recoil spectra
1868.3 ± 0.9		[1] PERUZZI	77	LGW	e^+e^- 3.77 GeV
1874 ±11		PICCOLO	77	MRK1	e^+e^- 4.03, 4.41 GeV
1876 ±15	50	PERUZZI	76	MRK1	$K^{\mp}\pi^{\pm}\pi^{\pm}$

[1] PERUZZI 77 and SCHINDLER 81 errors do not include the 0.13% uncertainty in the absolute SPEAR energy calibration. TRILLING 81 uses the high precision $J/\psi(1S)$ and $\psi(2S)$ measurements of ZHOLENTZ 80 to determine this uncertainty and combines the PERUZZI 77 and SCHINDLER 81 results to obtain the value quoted.

$D^{\pm}$ MEAN LIFE

Measurements with an error $> 100 \times 10^{-15}$ s have been omitted from the Listings.

VALUE (10^{-15} s)	EVTS	DOCUMENT ID		TECN	COMMENT
1040 ± 7 OUR AVERAGE					
1039.4 ± 4.3 ± 7.0	110k	LINK	02F	FOCS	γ nucleus, ≈ 180 GeV
$1033.6 \pm 22.1^{+9.9}_{-12.7}$	3.7k	BONVICINI	99	CLEO	$e^+e^- \approx \Upsilon(4S)$
1048 ±15 ±11	9k	FRABETTI	94D	E687	$D^+ \to K^-\pi^+\pi^+$
• • • We do not use the following data for averages, fits, limits, etc. • • •					
1075 ±40 ±18	2.4k	FRABETTI	91	E687	γ Be, $D^+ \to K^-\pi^+\pi^+$
1030 ±80 ±60	200	ALVAREZ	90	NA14	γ, $D^+ \to K^-\pi^+\pi^+$
$1050\ ^{+77}_{-72}$	317	[1] BARLAG	90C	ACCM	π^- Cu 230 GeV
1050 ±80 ±70	363	ALBRECHT	88I	ARG	e^+e^- 10 GeV
1090 ±30 ±25	2.9k	RAAB	88	E691	Photoproduction

[1] BARLAG 90C estimates the systematic error to be negligible.

D^+ DECAY MODES

Most decay modes (other than the semileptonic modes) that involve a neutral K meson are now given as K^0_S modes, not as $\overline{K}^0$ modes. Nearly always it is a K^0_S that is measured, and interference between Cabibbo-allowed and doubly Cabibbo-suppressed modes can invalidate the assumption that $2\Gamma(K^0_S) = \Gamma(\overline{K}^0)$.

	Mode	Fraction (Γ_i/Γ)		Scale factor / Confidence level
	Inclusive modes			
Γ_1	e^+ semileptonic	(16.07 ± 0.30)	%	
Γ_2	μ^+ anything	(17.6 ± 3.2)	%	
Γ_3	K^- anything	(25.7 ± 1.4)	%	
Γ_4	$\overline{K}^0$ anything + K^0 anything	(61 ± 5)	%	
Γ_5	K^+ anything	(5.9 ± 0.8)	%	
Γ_6	$\overline{K}^*(892)^-$ anything	(6 ± 5)	%	
Γ_7	$\overline{K}^*(892)^0$ anything	(23 ± 5)	%	
Γ_8	$K^*(892)^0$ anything	< 6.6	%	CL=90%
Γ_9	η anything	(6.3 ± 0.7)	%	
Γ_{10}	η' anything	(1.04 ± 0.18)	%	
Γ_{11}	ϕ anything	(1.03 ± 0.12)	%	
	Leptonic and semileptonic modes			
Γ_{12}	$e^+\nu_e$	< 8.8	$\times 10^{-6}$	CL=90%
Γ_{13}	$\gamma e^+\nu_e$	< 3.0	$\times 10^{-5}$	CL=90%
Γ_{14}	$\mu^+\nu_\mu$	(3.74 ± 0.17)	$\times 10^{-4}$	
Γ_{15}	$\tau^+\nu_\tau$	< 1.2	$\times 10^{-3}$	CL=90%
Γ_{16}	$\overline{K}^0 e^+\nu_e$	(8.73 ± 0.10)	%	
Γ_{17}	$\overline{K}^0\mu^+\nu_\mu$	(8.74 ± 0.19)	%	
Γ_{18}	$K^-\pi^+ e^+\nu_e$	(3.89 ± 0.13)	%	S=2.1
Γ_{19}	$\overline{K}^*(892)^0 e^+\nu_e$, $\overline{K}^*(892)^0 \to K^-\pi^+$	(3.66 ± 0.12)	%	
Γ_{20}	$(K^-\pi^+)$ [0.8–1.0]GeV $e^+\nu_e$	(3.39 ± 0.09)	%	
Γ_{21}	$(K^-\pi^+)_{S-wave}\, e^+\nu_e$	(2.28 ± 0.11)	$\times 10^{-3}$	
Γ_{22}	$\overline{K}^*(1410)^0 e^+\nu_e$, $\overline{K}^*(1410)^0 \to K^-\pi^+$	< 6	$\times 10^{-3}$	CL=90%
Γ_{23}	$\overline{K}^*_2(1430)^0 e^+\nu_e$, $\overline{K}^*_2(1430)^0 \to K^-\pi^+$	< 5	$\times 10^{-4}$	CL=90%
Γ_{24}	$K^-\pi^+ e^+\nu_e$ nonresonant	< 7	$\times 10^{-3}$	CL=90%
Γ_{25}	$K^-\pi^+\mu^+\nu_\mu$	(3.65 ± 0.34)	%	
Γ_{26}	$\overline{K}^*(892)^0\mu^+\nu_\mu$, $\overline{K}^*(892)^0 \to K^-\pi^+$	(3.52 ± 0.10)	%	
Γ_{27}	$K^-\pi^+\mu^+\nu_\mu$ nonresonant	(1.9 ± 0.5)	$\times 10^{-3}$	
Γ_{28}	$K^-\pi^+\pi^0\mu^+\nu_\mu$	< 1.5	$\times 10^{-3}$	CL=90%
Γ_{29}	$\pi^0 e^+\nu_e$	(3.72 ± 0.17)	$\times 10^{-3}$	S=2.0
Γ_{30}	$\eta e^+\nu_e$	(1.14 ± 0.10)	$\times 10^{-3}$	
Γ_{31}	$\rho^0 e^+\nu_e$	$(2.18^{+0.17}_{-0.25})$	$\times 10^{-3}$	
Γ_{32}	$\rho^0\mu^+\nu_\mu$	(2.4 ± 0.4)	$\times 10^{-3}$	
Γ_{33}	$\omega e^+\nu_e$	(1.69 ± 0.11)	$\times 10^{-3}$	
Γ_{34}	$\eta'(958)\, e^+\nu_e$	(2.2 ± 0.5)	$\times 10^{-4}$	
Γ_{35}	$\phi e^+\nu_e$	< 1.3	$\times 10^{-5}$	CL=90%
Γ_{36}	$D^0 e^+\nu_e$	< 1.0	$\times 10^{-4}$	CL=90%

Fractions of some of the following modes with resonances have already appeared above as submodes of particular charged-particle modes.

Γ_{37}	$\overline{K}^*(892)^0 e^+\nu_e$		(5.40 ± 0.10)	%	S=1.1
Γ_{38}	$\overline{K}^*(892)^0\mu^+\nu_\mu$		(5.25 ± 0.15)	%	
Γ_{39}	$\overline{K}^*_0(1430)^0\mu^+\nu_\mu$		< 2.3	$\times 10^{-4}$	CL=90%
Γ_{40}	$\overline{K}^*(1680)^0\mu^+\nu_\mu$		< 1.5	$\times 10^{-3}$	CL=90%
	Hadronic modes with a $\overline{K}$ or $\overline{K}K\overline{K}$				
Γ_{41}	$K^0_S\pi^+$		(1.47 ± 0.08)	%	S=3.0
Γ_{42}	$K^0_L\pi^+$		(1.46 ± 0.05)	%	
Γ_{43}	$K^-2\pi^+$	[a]	(8.98 ± 0.28)	%	S=2.2
Γ_{44}	$(K^-\pi^+)_{S-\text{wave}}\,\pi^+$		(7.20 ± 0.25)	%	
Γ_{45}	$\overline{K}^*_0(700)^0\pi^+$, $\overline{K}^*_0(700) \to K^-\pi^+$				
Γ_{46}	$\overline{K}^*_0(1430)^0\pi^+$, $\overline{K}^*_0(1430)^0 \to K^-\pi^+$	[b]	(1.19 ± 0.07)	%	
Γ_{47}	$\overline{K}^*(892)^0\pi^+$, $\overline{K}^*(892)^0 \to K^-\pi^+$		(10.0 ± 1.1)	$\times 10^{-3}$	
Γ_{48}	$\overline{K}^*(1410)^0\pi^+$, $\overline{K}^{*0} \to K^-\pi^+$		not seen		
Γ_{49}	$\overline{K}^*_2(1430)^0\pi^+$, $\overline{K}^*_2(1430)^0 \to K^-\pi^+$	[b]	(2.2 ± 0.7)	$\times 10^{-4}$	
Γ_{50}	$\overline{K}^*(1680)^0\pi^+$, $\overline{K}^*(1680)^0 \to K^-\pi^+$	[b]	(2.1 ± 1.0)	$\times 10^{-4}$	
Γ_{51}	$K^-(2\pi^+)_{I=2}$		(1.39 ± 0.26)	%	
Γ_{52}	$K^-2\pi^+$ nonresonant				
Γ_{53}	$K^0_S\pi^+\pi^0$	[a]	(7.05 ± 0.27)	%	
Γ_{54}	$K^0_S\rho^+$		$(5.9\ ^{+0.6}_{-0.4})$	%	
Γ_{55}	$K^0_S\rho(1450)^+$, $\rho^+ \to \pi^+\pi^0$		$(1.5\ ^{+1.1}_{-1.4})$	$\times 10^{-3}$	
Γ_{56}	$\overline{K}^*(892)^0\pi^+$, $\overline{K}^*(892)^0 \to K^0_S\pi^0$		(2.52 ± 0.31)	$\times 10^{-3}$	
Γ_{57}	$\overline{K}^*_0(1430)^0\pi^+$, $\overline{K}^*_0 \to K^0_S\pi^0$		(2.6 ± 0.9)	$\times 10^{-3}$	
Γ_{58}	$\overline{K}^*_0(1680)^0\pi^+$, $\overline{K}^{*0}_0 \to K^0_S\pi^0$		$(9\ ^{+7}_{-9})$	$\times 10^{-4}$	
Γ_{59}	$\overline{\kappa}^0\pi^+$, $\overline{\kappa}^0 \to K^0_S\pi^0$		$(5.4\ ^{+5.0}_{-3.5})$	$\times 10^{-3}$	
Γ_{60}	$K^0_S\pi^+\pi^0$ nonresonant		(3 ± 4)	$\times 10^{-3}$	
Γ_{61}	$K^0_S\pi^+\pi^0$ nonresonant and $\overline{\kappa}^0\pi^+$		$(1.31^{+0.21}_{-0.35})$	%	
Γ_{62}	$(K^0_S\pi^0)_{S-\text{wave}}\,\pi^+$		$(1.22^{+0.26}_{-0.32})$	%	
Γ_{63}	$K^-2\pi^+\pi^0$	[c]	(5.98 ± 0.23)	%	
Γ_{64}	$K^0_S 2\pi^+\pi^-$	[c]	(2.97 ± 0.11)	%	

Γ_{65}	$K^-3\pi^+\pi^-$	[a]	(5.5 ±0.5) × 10^{-3}	S=1.1
Γ_{66}	$\overline{K}^*(892)^0 2\pi^+\pi^-$, $\overline{K}^*(892)^0 \to K^-\pi^+$		(1.2 ±0.4) × 10^{-3}	
Γ_{67}	$\overline{K}^*(892)^0\rho^0\pi^+$, $\overline{K}^*(892)^0 \to K^-\pi^+$		(2.2 ±0.4) × 10^{-3}	
Γ_{68}	$\overline{K}^*(892)^0 a_1(1260)^+$	[d]	(8.9 ±1.8) × 10^{-3}	
Γ_{69}	$\overline{K}^*(892)^0 2\pi^+\pi^-$ no-ρ, $\overline{K}^*(892)^0 \to K^-\pi^+$			
Γ_{70}	$K^-\rho^0 2\pi^+$		(1.65±0.27) × 10^{-3}	
Γ_{71}	$K^-3\pi^+\pi^-$ nonresonant		(3.9 ±2.8) × 10^{-4}	
Γ_{72}	$K^+2K^0_S$		(2.54±0.13) × 10^{-3}	
Γ_{73}	$K^+K^-K^0_S\pi^+$		(2.3 ±0.5) × 10^{-4}	

Pionic modes

Γ_{74}	$\pi^+\pi^0$		(1.17±0.06) × 10^{-3}	
Γ_{75}	$2\pi^+\pi^-$		(3.13±0.19) × 10^{-3}	
Γ_{76}	$\rho^0\pi^+$		(8.0 ±1.4) × 10^{-4}	
Γ_{77}	$\pi^+(\pi^+\pi^-)_{S-\text{wave}}$		(1.75±0.16) × 10^{-3}	
Γ_{78}	$\sigma\pi^+$, $\sigma \to \pi^+\pi^-$		(1.32±0.12) × 10^{-3}	
Γ_{79}	$f_0(980)\pi^+$, $f_0(980) \to \pi^+\pi^-$		(1.50±0.32) × 10^{-4}	
Γ_{80}	$f_0(1370)\pi^+$, $f_0(1370) \to \pi^+\pi^-$		(8 ±4) × 10^{-5}	
Γ_{81}	$f_2(1270)\pi^+$, $f_2(1270) \to \pi^+\pi^-$		(4.8 ±0.8) × 10^{-4}	
Γ_{82}	$\rho(1450)^0\pi^+$, $\rho(1450)^0 \to \pi^+\pi^-$		< 8 × 10^{-5}	CL=95%
Γ_{83}	$f_0(1500)\pi^+$, $f_0(1500) \to \pi^+\pi^-$		(1.1 ±0.4) × 10^{-4}	
Γ_{84}	$f_0(1710)\pi^+$, $f_0(1710) \to \pi^+\pi^-$		< 5 × 10^{-5}	CL=95%
Γ_{85}	$f_0(1790)\pi^+$, $f_0(1790) \to \pi^+\pi^-$		< 6 × 10^{-5}	CL=95%
Γ_{86}	$(\pi^+\pi^+)_{S-\text{wave}}\pi^-$		< 1.2 × 10^{-4}	CL=95%
Γ_{87}	$2\pi^+\pi^-$ nonresonant		< 1.1 × 10^{-4}	CL=95%
Γ_{88}	$\pi^+2\pi^0$		(4.5 ±0.4) × 10^{-3}	
Γ_{89}	$2\pi^+\pi^-\pi^0$		(1.11±0.08) %	
Γ_{90}	$3\pi^+2\pi^-$		(1.59±0.16) × 10^{-3}	S=1.1
Γ_{91}	$\eta\pi^+$		(3.33±0.21) × 10^{-3}	S=1.4
Γ_{92}	$\eta\pi^+\pi^0$		(1.38±0.35) × 10^{-3}	
Γ_{93}	$\omega\pi^+$		(2.8 ±0.6) × 10^{-4}	
Γ_{94}	$\eta'(958)\pi^+$		(4.60±0.31) × 10^{-3}	
Γ_{95}	$\eta'(958)\pi^+\pi^0$		(1.6 ±0.5) × 10^{-3}	

Hadronic modes with a $K\overline{K}$ pair

Γ_{96}	$K^+K^0_S$		(2.83±0.16) × 10^{-3}	S=2.8
Γ_{97}	$K^+K^-\pi^+$	[a]	(9.51±0.34) × 10^{-3}	S=1.6
Γ_{98}	$\phi\pi^+$, $\phi \to K^+K^-$		(2.64±0.11) × 10^{-3}	
Γ_{99}	$K^+\overline{K}^*(892)^0$, $\overline{K}^*(892)^0 \to K^-\pi^+$		($2.44^{+0.11}_{-0.15}$) × 10^{-3}	
Γ_{100}	$K^+\overline{K}^*_0(1430)^0$, $\overline{K}^*_0(1430)^0 \to K^-\pi^+$		(1.79±0.34) × 10^{-3}	
Γ_{101}	$K^+\overline{K}^*_2(1430)^0$, $\overline{K}^*_2 \to K^-\pi^+$		($1.6^{+1.2}_{-0.8}$) × 10^{-4}	
Γ_{102}	$K^+\overline{K}^*_0(700)$, $\overline{K}^*_0 \to K^-\pi^+$		($6.7^{+3.4}_{-2.1}$) × 10^{-4}	
Γ_{103}	$a_0(1450)^0\pi^+$, $a^0_0 \to K^+K^-$		($4.4^{+7.0}_{-1.8}$) × 10^{-4}	
Γ_{104}	$\phi(1680)\pi^+$, $\phi \to K^+K^-$		($4.9^{+4.0}_{-1.9}$) × 10^{-5}	
Γ_{105}	$K^0_S K^0_S\pi^+$		(2.70±0.13) × 10^{-3}	
Γ_{106}	$K^+K^0_S\pi^+\pi^-$		(1.67±0.18) × 10^{-3}	
Γ_{107}	$K^0_S K^-2\pi^+$		(2.28±0.18) × 10^{-3}	
Γ_{108}	$K^+K^-2\pi^+\pi^-$		(2.2 ±1.2) × 10^{-4}	

A few poorly measured branching fractions:

Γ_{109}	$\phi\pi^+\pi^0$		(2.3 ±1.0) %	
Γ_{110}	$\phi\rho^+$		< 1.4 %	CL=90%
Γ_{111}	$K^+K^-\pi^+\pi^0$ non-ϕ		($1.5^{+0.7}_{-0.6}$) %	
Γ_{112}	$K^*(892)^+K^0_S$		(1.6 ±0.7) %	

Doubly Cabibbo-suppressed modes

Γ_{113}	$K^+\pi^0$		(1.81±0.27) × 10^{-4}	S=1.4
Γ_{114}	$K^+\eta$		(1.02±0.16) × 10^{-4}	
Γ_{115}	$K^+\eta'(958)$		(1.73±0.22) × 10^{-4}	
Γ_{116}	$K^+\pi^+\pi^-$		(5.19±0.26) × 10^{-4}	
Γ_{117}	$K^+\rho^0$		(2.0 ±0.5) × 10^{-4}	
Γ_{118}	$K^*(892)^0\pi^+$, $K^*(892)^0 \to K^+\pi^-$		(2.4 ±0.4) × 10^{-4}	
Γ_{119}	$K^+ f_0(980)$, $f_0(980) \to \pi^+\pi^-$		(4.6 ±2.8) × 10^{-5}	
Γ_{120}	$K^*_2(1430)^0\pi^+$, $K^*_2(1430)^0 \to K^+\pi^-$		(4.2 ±2.8) × 10^{-5}	
Γ_{121}	$K^+\pi^+\pi^-$ nonresonant		not seen	
Γ_{122}	$2K^+K^-$		(8.5 ±2.0) × 10^{-5}	

$\Delta C = 1$ weak neutral current ($C1$) modes, or Lepton Family number (LF) or Lepton number (L) violating modes

Γ_{123}	$\pi^+ e^+ e^-$	$C1$	< 1.1	× 10^{-6}	CL=90%
Γ_{124}	$\pi^+\phi$, $\phi \to e^+e^-$	[e]	($1.7^{+1.4}_{-0.9}$) × 10^{-6}		
Γ_{125}	$\pi^+\mu^+\mu^-$	$C1$	< 7.3	× 10^{-8}	CL=90%
Γ_{126}	$\pi^+\phi$, $\phi \to \mu^+\mu^-$	[e]	(1.8 ±0.8) × 10^{-6}		
Γ_{127}	$\rho^+\mu^+\mu^-$	$C1$	< 5.6	× 10^{-4}	CL=90%
Γ_{128}	$K^+e^+e^-$	[f]	< 1.0	× 10^{-6}	CL=90%
Γ_{129}	$K^+\mu^+\mu^-$	[f]	< 4.3	× 10^{-6}	CL=90%
Γ_{130}	$\pi^+e^+\mu^-$	LF	< 2.9	× 10^{-6}	CL=90%
Γ_{131}	$\pi^+e^-\mu^+$	LF	< 3.6	× 10^{-6}	CL=90%
Γ_{132}	$K^+e^+\mu^-$	LF	< 1.2	× 10^{-6}	CL=90%
Γ_{133}	$K^+e^-\mu^+$	LF	< 2.8	× 10^{-6}	CL=90%
Γ_{134}	π^-2e^+	L	< 1.1	× 10^{-6}	CL=90%
Γ_{135}	$\pi^-2\mu^+$	L	< 2.2	× 10^{-8}	CL=90%
Γ_{136}	$\pi^-e^+\mu^+$	L	< 2.0	× 10^{-6}	CL=90%
Γ_{137}	$\rho^-2\mu^+$	L	< 5.6	× 10^{-4}	CL=90%
Γ_{138}	K^-2e^+	L	< 9	× 10^{-7}	CL=90%
Γ_{139}	$K^-2\mu^+$	L	< 1.0	× 10^{-5}	CL=90%
Γ_{140}	$K^-e^+\mu^+$	L	< 1.9	× 10^{-6}	CL=90%
Γ_{141}	$K^*(892)^-2\mu^+$	L	< 8.5	× 10^{-4}	CL=90%

Γ_{142}	Unaccounted decay modes	(63.7 ±0.6) %	S=1.6

[a] The branching fraction for this mode may differ from the sum of the submodes that contribute to it, due to interference effects. See the relevant papers.

[b] These subfractions of the $K^-2\pi^+$ mode are uncertain: see the Particle Listings.

[c] Submodes of the $D^+ \to K^-2\pi^+\pi^0$ and $K^0_S 2\pi^+\pi^-$ modes were studied by ANJOS 92C and COFFMAN 92B, but with at most 142 events for the first mode and 229 for the second – not enough for precise results. With nothing new for 18 years, we refer to our 2008 edition, Physics Letters **B667** 1 (2008), for those results.

[d] The unseen decay modes of the resonances are included.

[e] This is *not* a test for the ΔC=1 weak neutral current, but leads to the $\pi^+\ell^+\ell^-$ final state.

[f] This mode is not a useful test for a ΔC=1 weak neutral current because both quarks must change flavor in this decay.

CONSTRAINED FIT INFORMATION

An overall fit to 22 branching ratios uses 33 measurements and one constraint to determine 14 parameters. The overall fit has a χ^2 = 45.6 for 20 degrees of freedom.

The following *off-diagonal* array elements are the correlation coefficients $\langle \delta x_i \delta x_j \rangle / (\delta x_i \cdot \delta x_j)$, in percent, from the fit to the branching fractions, $x_i \equiv \Gamma_i/\Gamma_{\text{total}}$. The fit constrains the x_i whose labels appear in this array to sum to one.

x_{18}	0									
x_{31}	0	0								
x_{37}	0	0	0							
x_{38}	8	0	0	0						
x_{41}	0	42	0	0	0					
x_{43}	0	72	0	0	0	59				
x_{65}	0	25	0	0	0	20	34			
x_{90}	0	23	0	0	0	19	32	77		
x_{91}	0	24	0	0	0	19	33	11	10	
x_{96}	0	40	0	0	0	85	56	19	18	18
x_{97}	0	63	0	0	0	52	88	30	28	29
x_{113}	0	13	0	0	0	11	19	6	6	6
x_{142}	−34	−72	−3	−18	−28	−61	−85	−39	−35	−31
	x_{17}	x_{18}	x_{31}	x_{37}	x_{38}	x_{41}	x_{43}	x_{65}	x_{90}	x_{91}

Meson Particle Listings

$D^{\pm}$

x_{97}	49		
x_{113}	10	16	
x_{142}	−57	−76	−16
	x_{96}	x_{97}	x_{113}

D^+ BRANCHING RATIOS

Some now-obsolete measurements have been omitted from these Listings.

c-quark decays

$\Gamma(c \to e^+ \text{anything})/\Gamma(c \to \text{anything})$

For the Summary Table, we only use the average of e^+ and μ^+ measurements from $Z^0 \to c\overline{c}$ decays; see the second data block below.

VALUE	EVTS	DOCUMENT ID		TECN	COMMENT
$0.103 \pm 0.009^{+0.009}_{-0.008}$	378	[1] ABBIENDI	99K	OPAL	$Z^0 \to c\overline{c}$

[1] ABBIENDI 99K uses the excess of right-sign over wrong-sign leptons opposite reconstructed $D^*(2010)^+ \to D^0\pi^+$ decays in $Z^0 \to c\overline{c}$.

$\Gamma(c \to \mu^+ \text{anything})/\Gamma(c \to \text{anything})$

For the Summary Table, we only use the average of e^+ and μ^+ measurements from $Z^0 \to c\overline{c}$ decays; see the next data block.

VALUE	EVTS	DOCUMENT ID		TECN	COMMENT
0.082 ± 0.005 OUR AVERAGE					
$0.073 \pm 0.008 \pm 0.002$	73	KAYIS-TOPAK.05		CHRS	ν_μ emulsion
$0.095 \pm 0.007^{+0.014}_{-0.013}$	2829	ASTIER	00D	NOMD	$\nu_\mu \text{Fe} \to \mu^-\mu^+\text{X}$
$0.090 \pm 0.007^{+0.007}_{-0.006}$	476	[1] ABBIENDI	99K	OPAL	$Z^0 \to c\overline{c}$
$0.086 \pm 0.017^{+0.008}_{-0.007}$	69	[2] ALBRECHT	92F	ARG	$e^+e^- \approx 10$ GeV
$0.078 \pm 0.009 \pm 0.012$		ONG	88	MRK2	e^+e^- 29 GeV
$0.078 \pm 0.015 \pm 0.02$		BARTEL	87	JADE	e^+e^- 34.6 GeV
$0.082 \pm 0.012^{+0.02}_{-0.01}$		ALTHOFF	84G	TASS	e^+e^- 34.5 GeV
• • • We do not use the following data for averages, fits, limits, etc. • • •					
$0.093 \pm 0.009 \pm 0.009$	88	KAYIS-TOPAK.02		CHRS	See KAYIS-TOPAKSU 05
$0.089 \pm 0.018 \pm 0.025$		BARTEL	85J	JADE	See BARTEL 87

[1] ABBIENDI 99K uses the excess of right-sign over wrong-sign leptons opposite reconstructed $D^*(2010)^+ \to D^0\pi^+$ decays in $Z^0 \to c\overline{c}$.
[2] ALBRECHT 92F uses the excess of right-sign over wrong-sign leptons in a sample of events tagged by fully reconstructed $D^*(2010)^+ \to D^0\pi^+$ decays.

$\Gamma(c \to \ell^+ \text{anything})/\Gamma(c \to \text{anything})$

This is an average (not a sum) of e^+ and μ^+ measurements.

VALUE	EVTS	DOCUMENT ID		TECN	COMMENT
0.096 ±0.004 OUR AVERAGE					
$0.0958 \pm 0.0042 \pm 0.0028$	1828	[1] ABREU	00O	DLPH	$Z^0 \to c\overline{c}$
$0.095 \pm 0.006^{+0.007}_{-0.006}$	854	[2] ABBIENDI	99K	OPAL	$Z^0 \to c\overline{c}$

[1] ABREU 00O uses leptons opposite fully reconstructed $D^*(2010)^+$, D^+, or D^0 mesons.
[2] ABBIENDI 99K uses the excess of right-sign over wrong-sign leptons opposite reconstructed $D^*(2010)^+ \to D^0\pi^+$ decays in $Z^0 \to c\overline{c}$.

$\Gamma(c \to D^*(2010)^+ \text{anything})/\Gamma(c \to \text{anything})$

VALUE	EVTS	DOCUMENT ID		TECN	COMMENT
$0.255 \pm 0.015 \pm 0.008$	2371	[1] ABREU	00O	DLPH	$Z^0 \to c\overline{c}$

[1] ABREU 00O uses slow pions opposite fully reconstructed $D^*(2010)^+$, D^+, or D^0 mesons as a signal of $D^*(2010)^-$ production.

Inclusive modes

$\Gamma(e^+ \text{semileptonic})/\Gamma_{\text{total}}$ Γ_1/Γ

The sum of our $\overline{K}^0 e^+\nu_e$, $\overline{K}^*(892)^0 e^+\nu_e$, $\pi^0 e^+\nu_e$, $\eta e^+\nu_e$, $\rho^0 e^+\nu_e$, and $\omega e^+\nu_e$ branching fractions is $15.3 \pm 0.4\%$.

VALUE (%)	EVTS	DOCUMENT ID		TECN	COMMENT
16.07±0.30 OUR AVERAGE					
$16.13 \pm 0.10 \pm 0.29$	26.2 ± 0.2k	[1] ASNER	10	CLEO	e^+e^- at 3774 MeV
$15.2 \pm 0.9 \pm 0.8$	521 ± 32	ABLIKIM	07G	BES2	$e^+e^- \approx \psi(3770)$
• • • We do not use the following data for averages, fits, limits, etc. • • •					
$16.13 \pm 0.20 \pm 0.33$	8798 ± 105	[2] ADAM	06A	CLEO	See ASNER 10
$17.0 \pm 1.9 \pm 0.7$	158	BALTRUSAIT...85B		MRK3	e^+e^- 3.77 GeV

[1] Using the D^+ and D^0 lifetimes, ASNER 10 finds that the ratio of the D^+ and D^0 semileptonic widths is $0.985 \pm 0.015 \pm 0.024$.
[2] Using the D^+ and D^0 lifetimes, ADAM 06A finds that the ratio of the D^+ and D^0 inclusive e^+ widths is $0.985 \pm 0.028 \pm 0.015$, consistent with the isospin-invariance prediction of 1.

$\Gamma(\mu^+ \text{anything})/\Gamma_{\text{total}}$ Γ_2/Γ

VALUE (%)	EVTS	DOCUMENT ID		TECN	COMMENT
$17.6 \pm 2.7 \pm 1.8$	100 ± 12	[1] ABLIKIM	08L	BES2	$e^+e^- \approx \psi(3772)$

[1] ABLIKIM 08L finds the ratio of $D^+ \to \mu^+X$ and $D^0 \to \mu^+X$ branching fractions to be $2.59 \pm 0.70 \pm 0.25$, in accord with the ratio of D^+ and D^0 lifetimes, 2.54 ± 0.02.

$\Gamma(K^- \text{anything})/\Gamma_{\text{total}}$ Γ_3/Γ

VALUE (%)	EVTS	DOCUMENT ID		TECN	COMMENT
25.7±1.4 OUR AVERAGE					
$24.7 \pm 1.3 \pm 1.2$	631 ± 33	ABLIKIM	07G	BES2	$e^+e^- \approx \psi(3770)$
$27.8^{+3.6}_{-3.1}$		BARLAG	92C	ACCM	π^- Cu 230 GeV
$27.1 \pm 2.3 \pm 2.4$		COFFMAN	91	MRK3	e^+e^- 3.77 GeV

$[\Gamma(\overline{K}^0 \text{anything}) + \Gamma(K^0 \text{anything})]/\Gamma_{\text{total}}$ Γ_4/Γ

VALUE (%)	EVTS	DOCUMENT ID		TECN	COMMENT
61 ±5 OUR AVERAGE					
$60.5 \pm 5.5 \pm 3.3$	244 ± 22	ABLIKIM	06U	BES2	e^+e^- at 3773 MeV
$61.2 \pm 6.5 \pm 4.3$		COFFMAN	91	MRK3	e^+e^- 3.77 GeV

$\Gamma(K^+ \text{anything})/\Gamma_{\text{total}}$ Γ_5/Γ

VALUE (%)	EVTS	DOCUMENT ID		TECN	COMMENT
5.9±0.8 OUR AVERAGE					
$6.1 \pm 0.9 \pm 0.4$	189 ± 27	ABLIKIM	07G	BES2	$e^+e^- \approx \psi(3770)$
$5.5 \pm 1.3 \pm 0.9$		COFFMAN	91	MRK3	e^+e^- 3.77 GeV

$\Gamma(K^*(892)^- \text{anything})/\Gamma_{\text{total}}$ Γ_6/Γ

VALUE (%)	EVTS	DOCUMENT ID		TECN	COMMENT
$5.7 \pm 5.2 \pm 0.7$	7.2 ± 6.5	ABLIKIM	06U	BES2	e^+e^- at 3773 MeV

$\Gamma(\overline{K}^*(892)^0 \text{anything})/\Gamma_{\text{total}}$ Γ_7/Γ

VALUE (%)	EVTS	DOCUMENT ID		TECN	COMMENT
$23.2 \pm 4.5 \pm 3.0$	189 ± 36	ABLIKIM	05P	BES	$e^+e^- \approx 3773$ MeV

$\Gamma(K^*(892)^0 \text{anything})/\Gamma_{\text{total}}$ Γ_8/Γ

VALUE (%)	CL%	DOCUMENT ID		TECN	COMMENT
<6.6	90	ABLIKIM	05P	BES	$e^+e^- \approx 3773$ MeV

$\Gamma(\eta \text{anything})/\Gamma_{\text{total}}$ Γ_9/Γ

This ratio includes η particles from η' decays.

VALUE (%)	EVTS	DOCUMENT ID		TECN	COMMENT
$6.3 \pm 0.5 \pm 0.5$	1972 ± 142	HUANG	06B	CLEO	e^+e^- at $\psi(3770)$

$\Gamma(\eta' \text{anything})/\Gamma_{\text{total}}$ Γ_{10}/Γ

VALUE (%)	EVTS	DOCUMENT ID		TECN	COMMENT
$1.04 \pm 0.16 \pm 0.09$	82 ± 13	HUANG	06B	CLEO	e^+e^- at $\psi(3770)$

$\Gamma(\phi \text{anything})/\Gamma_{\text{total}}$ Γ_{11}/Γ

VALUE (%)	EVTS	DOCUMENT ID		TECN	COMMENT
$1.03 \pm 0.10 \pm 0.07$	248 ± 21	HUANG	06B	CLEO	e^+e^- at $\psi(3770)$

Leptonic and semileptonic modes

$\Gamma(e^+\nu_e)/\Gamma_{\text{total}}$ Γ_{12}/Γ

VALUE	CL%	DOCUMENT ID		TECN	COMMENT
$<8.8 \times 10^{-6}$	90	EISENSTEIN	08	CLEO	e^+e^- at $\psi(3770)$
• • • We do not use the following data for averages, fits, limits, etc. • • •					
$<2.4 \times 10^{-5}$	90	ARTUSO	05A	CLEO	See EISENSTEIN 08

$\Gamma(\gamma e^+\nu_e)/\Gamma_{\text{total}}$ Γ_{13}/Γ

VALUE	CL%	DOCUMENT ID		TECN	COMMENT
$<3.0 \times 10^{-5}$	90	[1] ABLIKIM	17M	BES3	e^+e^- at 3.773 GeV

[1] This ABLIKIM 17M limit is for photons with energies greater than 10 MeV.

$\Gamma(\mu^+\nu_\mu)/\Gamma_{\text{total}}$ Γ_{14}/Γ

See the note on "Decay Constants of Charged Pseudoscalar Mesons" in the D_s^+ Listings.

VALUE (units 10^{-4})	EVTS	DOCUMENT ID		TECN	COMMENT
3.74± 0.17 OUR AVERAGE					
$3.71 \pm 0.19 \pm 0.06$	409 ± 21	[1] ABLIKIM	14F	BES3	e^+e^- at $\psi(3770)$
$3.82 \pm 0.32 \pm 0.09$	150 ± 12	[2] EISENSTEIN	08	CLEO	e^+e^- at $\psi(3770)$
• • • We do not use the following data for averages, fits, limits, etc. • • •					
$12.2^{+11.1}_{-5.3} \pm 1.0$	3	[3] ABLIKIM	05D	BES	$e^+e^- \approx 3.773$ GeV
$4.40 \pm 0.66^{+0.09}_{-0.12}$	47 ± 7	[4] ARTUSO	05A	CLEO	See EISENSTEIN 08
$3.5 \pm 1.4 \pm 0.6$	7	[5] BONVICINI	04A	CLEO	Incl. in ARTUSO 05A
$8^{+16}_{-5} \pm 5 \pm 2$	1	[6] BAI	98B	BES	$e^+e^- \to D^{*+}D^-$

[1] ABLIKIM 14F obtain $|V_{cd}| \cdot f_{D^+} = (45.75 \pm 1.20 \pm 0.39)$ MeV, and using $|V_{cd}| = 0.22520 \pm 0.00065$ gets $f_{D^+} = (203.2 \pm 5.3 \pm 1.8)$ MeV.
[2] EISENSTEIN 08, using the D^+ lifetime and assuming $|V_{cd}| = |V_{us}|$, gets $f_{D^+} = (205.8 \pm 8.5 \pm 2.5)$ MeV from this measurement.
[3] ABLIKIM 05D finds a background-subtracted 2.67 ± 1.74 $D^+ \to \mu^+\nu_\mu$ events, and from this obtains $f_{D^+} = 371^{+129}_{-119} \pm 25$ MeV.
[4] ARTUSO 05A obtains $f_{D^+} = 222.6 \pm 16.7^{+2.8}_{-3.4}$ MeV from this measurement.
[5] BONVICINI 04A finds eight events with an estimated background of one, and from the branching fraction obtains $f_{D^+} = 202 \pm 41 \pm 17$ MeV.
[6] BAI 98B obtains $f_{D^+} = (300^{+180}_{-150} \pm 80)$ MeV from this measurement.

$\Gamma(\tau^+\nu_\tau)/\Gamma_{total}$ Γ_{15}/Γ

VALUE	CL%	DOCUMENT ID		TECN	COMMENT
$<1.2\times10^{-3}$	90	EISENSTEIN	08	CLEO	e^+e^- at $\psi(3770)$
• • • We do not use the following data for averages, fits, limits, etc. • • •					
$<2.1\times10^{-3}$	90	RUBIN	06A	CLEO	See EISENSTEIN 08

$\Gamma(\overline{K}^0 e^+\nu_e)/\Gamma_{total}$ Γ_{16}/Γ

VALUE (%)	EVTS	DOCUMENT ID		TECN	COMMENT
8.73 ±0.10 OUR AVERAGE					
8.60 ±0.06 ±0.15	26k	ABLIKIM	17S	BES3	Using $\overline{K}^0\to\pi^+\pi^-$
8.59 ±0.14 ±0.21	5013	ABLIKIM	16V	BES3	Using $\overline{K}^0\to2\pi^0$
8.962±0.054±0.206	40k	[1] ABLIKIM	15AF	BES3	from $D^+\to K_L e^+\nu_e$
8.83 ±0.10 ±0.20	8.5k	[2] BESSON	09	CLEO	from $D^+\to K_S e^+\nu_e$
8.95 ±1.59 ±0.67	34	[3] ABLIKIM	05A	BES	from $D^+\to K_S e^+\nu_e$
• • • We do not use the following data for averages, fits, limits, etc. • • •					
8.53 ±0.13 ±0.23		[4] DOBBS	08	CLEO	See BESSON 09
8.71 ±0.38 ±0.37	545	HUANG	05B	CLEO	See DOBBS 08

[1] ABLIKIM 15AF report $\Gamma(D^+\to K_L e^+\nu_e)/\Gamma_{total}=(4.481\pm0.027\pm0.103)\%$. See also the form-factor parameters near the end of this D^+ Listing.

[2] See the form-factor parameters near the end of this D^+ Listing.

[3] The ABLIKIM 05A result together with the $D^0\to K^-e^+\nu_e$ branching fraction of ABLIKIM 04C and Particle Data Group lifetimes gives $\Gamma(D^0\to K^-e^+\nu_e)/\Gamma(D^+\to\overline{K}^0e^+\nu_e)=1.08\pm0.22\pm0.07$; isospin invariance predicts the ratio is 1.0.

[4] DOBBS 08 establishes $\left|\frac{V_{cd}}{V_{cs}}\cdot\frac{f_+^\pi(0)}{f_+^K(0)}\right|=0.188\pm0.008\pm0.002$ from the D^+ and D^0 decays to $\overline{K}e^+\nu_e$ and $\pi e^+\nu_e$. It also finds $\Gamma(D^0\to K^-e^+\nu_e)/\Gamma(D^+\to\overline{K}^0e^+\nu_e)=1.06\pm0.02\pm0.03$; isospin invariance predicts the ratio is 1.0.

$\Gamma(\overline{K}^0\mu^+\nu_\mu)/\Gamma_{total}$ Γ_{17}/Γ

VALUE (units 10^{-2})	EVTS	DOCUMENT ID		TECN	COMMENT
8.74±0.19 OUR FIT					
8.72±0.07±0.18	21k	ABLIKIM	16G	BES3	e^+e^- at 3773 MeV
• • • We do not use the following data for averages, fits, limits, etc. • • •					
10.3 ±2.3 ±0.8	29 ± 6	ABLIKIM	07	BES2	e^+e^- at 3773 MeV

$\Gamma(\overline{K}^0\mu^+\nu_\mu)/\Gamma(K^-2\pi^+)$ Γ_{17}/Γ_{43}

VALUE	EVTS	DOCUMENT ID	TECN	COMMENT
0.97 ±0.04 OUR FIT	Error includes scale factor of 1.5.			
1.019±0.076±0.065	555 ± 39	LINK	04E FOCS	γ nucleus, $\overline{E}_\gamma\approx180$ GeV

$\Gamma(K^-\pi^+e^+\nu_e)/\Gamma_{total}$ Γ_{18}/Γ

VALUE (units 10^{-2})	EVTS	DOCUMENT ID		TECN	COMMENT
3.89±0.13 OUR FIT	Error includes scale factor of 2.1.				
3.77±0.03±0.08	18.3k	ABLIKIM	16F	BES3	e^+e^- at $\psi(3770)$
• • • We do not use the following data for averages, fits, limits, etc. • • •					
3.50±0.75±0.27	29	ABLIKIM	06O	BES2	e^+e^- at 3773 MeV
$3.5\ ^{+1.2}_{-0.7}\ \pm0.4$	14	BAI	91	MRK3	$e^+e^-\approx$ 3.77 GeV

$\Gamma(K^-\pi^+e^+\nu_e)/\Gamma(K^-2\pi^+)$ Γ_{18}/Γ_{43}

VALUE	EVTS	DOCUMENT ID	TECN	COMMENT
0.433 ±0.011 OUR FIT	Error includes scale factor of 2.1.			
0.4380±0.0036±0.0042	70k±363	DEL-AMO-SA..11I	BABR	$e^+e^-\approx$ 10.6 GeV

$\Gamma(\overline{K}^*(892)^0e^+\nu_e)/\Gamma_{total}$ Γ_{37}/Γ

Unseen decay modes of $\overline{K}^*(892)^0$ are included. See the end of the D^+ Listings for measurements of $D^+\to\overline{K}^*(892)^0\ell^+\nu_\ell$ form-factor ratios.

VALUE (units 10^{-2})	EVTS	DOCUMENT ID		TECN	COMMENT
5.40±0.10 OUR FIT	Error includes scale factor of 1.1.				
5.40±0.10 OUR AVERAGE	Error includes scale factor of 1.1.				
5.31±0.05±0.12	16.2k	ABLIKIM	16F	BES3	e^+e^- at $\psi(3770)$
5.52±0.07±0.13	≈5k	BRIERE	10	CLEO	e^+e^- at $\psi(3770)$
• • • We do not use the following data for averages, fits, limits, etc. • • •					
5.06±1.21±0.40	28 ± 7	ABLIKIM	06O	BES2	e^+e^- at 3773 MeV
5.56±0.27±0.23	422 ± 21	[1] HUANG	05B	CLEO	e^+e^- at $\psi(3770)$

[1] HUANG 05B finds $\Gamma(D^0\to K^{*-}e^+\nu_e)/\Gamma(D^+\to\overline{K}^{*0}e^+\nu_e)=0.98\pm0.08\pm0.04$; isospin invariance predicts the ratio is 1.0.

$\Gamma((K^-\pi^+)_{[0.8\text{–}1.0]\text{GeV}}e^+\nu_e)/\Gamma_{total}$ Γ_{20}/Γ

VALUE (units 10^{-2})	EVTS	DOCUMENT ID	TECN	COMMENT
3.39±0.03±0.08	16.2k	ABLIKIM	16F BES3	e^+e^- at $\psi(3770)$

$\Gamma(\overline{K}^*(892)^0e^+\nu_e)/\Gamma(K^-2\pi^+)$ Γ_{37}/Γ_{43}

Unseen decay modes of the $\overline{K}^*(892)^0$ are included. See the end of the D^+ Listings for measurements of $D^+\to\overline{K}^*(892)^0\ell^+\nu_\ell$ form-factor ratios.

VALUE	EVTS	DOCUMENT ID	TECN	COMMENT
• • • We do not use the following data for averages, fits, limits, etc. • • •				
0.74±0.04±0.05		BRANDENB...	02 CLEO	$e^+e^-\approx\ \Upsilon(4S)$
0.62±0.15±0.09	35	ADAMOVICH	91 OMEG	π^- 340 GeV
0.55±0.08±0.10	880	ALBRECHT	91 ARG	$e^+e^-\approx$ 10.4 GeV
0.49±0.04±0.05		ANJOS	89B E691	Photoproduction

$\Gamma((K^-\pi^+)_{S\text{–}wave}e^+\nu_e)/\Gamma_{total}$ Γ_{21}/Γ

VALUE (units 10^{-3})	DOCUMENT ID		TECN	COMMENT
2.28±0.08±0.08	ABLIKIM	16F	BES3	e^+e^- at $\psi(3770)$

$\Gamma(\overline{K}^*(892)^0e^+\nu_e,\overline{K}^*(892)^0\to K^-\pi^+)/\Gamma(K^-\pi^+e^+\nu_e)$ Γ_{19}/Γ_{18}

VALUE (%)	DOCUMENT ID		TECN	COMMENT
93.94±0.27 OUR AVERAGE				
93.93±0.22±0.18	ABLIKIM	16F	BES3	e^+e^- at $\psi(3770)$
94.11±0.74±0.75	DEL-AMO-SA...11I		BABR	$e^+e^-\approx$ 10.6 GeV

$\Gamma((K^-\pi^+)_{S\text{–}wave}e^+\nu_e)/\Gamma(K^-\pi^+e^+\nu_e)$ Γ_{21}/Γ_{18}

VALUE (%)	DOCUMENT ID		TECN	COMMENT
5.89±0.17 OUR AVERAGE				
6.05±0.22±0.18	ABLIKIM	16F	BES3	e^+e^- at $\psi(3770)$
5.79±0.16±0.15	DEL-AMO-SA...11I		BABR	$e^+e^-\approx$ 10.6 GeV

$\Gamma(\overline{K}^*(1410)^0e^+\nu_e,\overline{K}^*(1410)^0\to K^-\pi^+)/\Gamma_{total}$ Γ_{22}/Γ

VALUE	CL%	DOCUMENT ID	TECN	COMMENT
$<6\times10^{-3}$	90	DEL-AMO-SA...11I	BABR	$e^+e^-\approx$ 10.6 GeV

$\Gamma(\overline{K}_2^*(1430)^0e^+\nu_e,\overline{K}_2^*(1430)^0\to K^-\pi^+)/\Gamma_{total}$ Γ_{23}/Γ

VALUE	CL%	DOCUMENT ID	TECN	COMMENT
$<5\times10^{-4}$	90	DEL-AMO-SA...11I	BABR	$e^+e^-\approx$ 10.6 GeV

$\Gamma(K^-\pi^+e^+\nu_e\text{ nonresonant})/\Gamma_{total}$ Γ_{24}/Γ

VALUE	CL%	DOCUMENT ID		TECN	COMMENT
<0.007	90	ANJOS	89B	E691	Photoproduction

$\Gamma(K^-\pi^+\mu^+\nu_\mu)/\Gamma(\overline{K}^0\mu^+\nu_\mu)$ Γ_{25}/Γ_{17}

VALUE	EVTS	DOCUMENT ID	TECN	COMMENT
0.417±0.030±0.023	555 ± 39	LINK	04E FOCS	γ nucleus, $\overline{E}_\gamma\approx180$ GeV

$\Gamma(\overline{K}^*(892)^0\mu^+\nu_\mu)/\Gamma_{total}$ Γ_{38}/Γ

VALUE (units 10^{-2})	EVTS	DOCUMENT ID	TECN	COMMENT
5.25±0.15 OUR FIT				
5.27±0.07±0.14	≈5k	BRIERE	10 CLEO	e^+e^- at $\psi(3770)$

$\Gamma(\overline{K}^*(892)^0\mu^+\nu_\mu)/\Gamma(\overline{K}^0\mu^+\nu_\mu)$ Γ_{38}/Γ_{17}

Unseen decay modes of the $\overline{K}^*(892)^0$ are included. See the end of the D^+ Listings for measurements of $D^+\to\overline{K}^*(892)^0\ell^+\nu_\ell$ form-factor ratios.

VALUE	EVTS	DOCUMENT ID	TECN	COMMENT
0.600±0.021 OUR FIT				
0.594±0.043±0.033	555 ± 39	LINK	04E FOCS	γ nucleus, $\overline{E}_\gamma\approx180$ GeV

$\Gamma(\overline{K}^*(892)^0\mu^+\nu_\mu)/\Gamma(K^-2\pi^+)$ Γ_{38}/Γ_{43}

Unseen decay modes of the $\overline{K}^*(892)^0$ are included. See the end of the D^+ Listings for measurements of $D^+\to\overline{K}^*(892)^0\ell^+\nu_\ell$ form-factor ratios.

VALUE	EVTS	DOCUMENT ID	TECN	COMMENT
0.584±0.025 OUR FIT	Error includes scale factor of 1.4.			
0.57 ±0.06 OUR AVERAGE	Error includes scale factor of 1.2.			
0.72 ±0.10 ±0.05		BRANDENB...	02 CLEO	$e^+e^-\approx\ \Upsilon(4S)$
0.56 ±0.04 ±0.06	875	FRABETTI	93E E687	γBe $\overline{E}_\gamma\approx$ 200 GeV
0.46 ±0.07 ±0.08	224	KODAMA	92C E653	π^- emulsion 600 GeV
• • • We do not use the following data for averages, fits, limits, etc. • • •				
0.602±0.010±0.021	12k	[1] LINK	02J FOCS	γ nucleus, ≈180 GeV

[1] This LINK 02J result includes the effects of an interference of a small S-wave $K^-\pi^+$ amplitude with the dominant $\overline{K}^{*0}$ amplitude. (The interference effect is reported in LINK 02E.) This result is redundant with results of LINK 04E elsewhere in these Listings.

$\Gamma(K^-\pi^+\mu^+\nu_\mu\text{ nonresonant})/\Gamma(K^-\pi^+\mu^+\nu_\mu)$ Γ_{27}/Γ_{25}

VALUE	EVTS	DOCUMENT ID	TECN	COMMENT
$0.0530\pm0.0074^{+0.0099}_{-0.0096}$	14k	LINK	05I FOCS	γ nucleus, $\overline{E}_\gamma\approx180$ GeV

$\Gamma(K^-\pi^+\pi^0\mu^+\nu_\mu)/\Gamma(K^-\pi^+\mu^+\nu_\mu)$ Γ_{28}/Γ_{25}

VALUE	CL%	DOCUMENT ID	TECN	COMMENT
<0.042	90	FRABETTI	93E E687	γBe $\overline{E}_\gamma\approx$ 200 GeV

$\Gamma(\overline{K}_0^*(1430)^0\mu^+\nu_\mu)/\Gamma(K^-\pi^+\mu^+\nu_\mu)$ Γ_{39}/Γ_{25}

Unseen decay modes of the $\overline{K}_0^*(1430)^0$ are included.

VALUE	CL%	DOCUMENT ID	TECN	COMMENT
<0.0064	90	LINK	05I FOCS	γ A, $\overline{E}_\gamma\approx180$ GeV

$\Gamma(\overline{K}^*(1680)^0\mu^+\nu_\mu)/\Gamma(K^-\pi^+\mu^+\nu_\mu)$ Γ_{40}/Γ_{25}

Unseen decay modes of the $\overline{K}^*(1680)^0$ are included.

VALUE	CL%	DOCUMENT ID	TECN	COMMENT
<0.04	90	LINK	05I FOCS	γ A, $\overline{E}_\gamma\approx180$ GeV

Meson Particle Listings

$D^{\pm}$

$\Gamma(\pi^0 e^+ \nu_e)/\Gamma_{total}$ Γ_{29}/Γ

VALUE (%)	EVTS	DOCUMENT ID		TECN	COMMENT
0.372±0.017 OUR AVERAGE		Error includes scale factor of 2.0.			
0.363±0.008±0.005	3.4k	ABLIKIM	17S	BES3	Using $\pi^0 \to 2\gamma$
0.405±0.016±0.009	838	[1] BESSON	09	CLEO	e^+e^- at $\psi(3770)$
• • • We do not use the following data for averages, fits, limits, etc. • • •					
0.373±0.022±0.013		[2] DOBBS	08	CLEO	See BESSON 09
0.44 ±0.06 ±0.03	63 ± 9	HUANG	05B	CLEO	See DOBBS 08

[1] See the form-factor parameters near the end of this D^+ Listing.

[2] DOBBS 08 establishes $|\frac{V_{cd}}{V_{cs}} \cdot \frac{f_+^{\pi}(0)}{f_+^{K}(0)}| = 0.188 \pm 0.008 \pm 0.002$ from the D^+ and D^0 decays to $\overline{K} e^+ \nu_e$ and $\pi e^+ \nu_e$. It finds $\Gamma(D^0 \to \pi^- e^+ \nu_e) / \Gamma(D^+ \to \pi^0 e^+ \nu_e) = 2.03 \pm 0.14 \pm 0.08$; isospin invariance predicts the ratio is 2.0.

$\Gamma(\eta e^+ \nu_e)/\Gamma_{total}$ Γ_{30}/Γ

VALUE (units 10^{-4})	EVTS	DOCUMENT ID		TECN	COMMENT
11.4±0.9±0.4		YELTON	11	CLEO	e^+e^- at $\psi(3770)$
• • • We do not use the following data for averages, fits, limits, etc. • • •					
13.3±2.0±0.6	46 ± 8	MITCHELL	09B	CLEO	See YELTON 11

$\Gamma(\rho^0 e^+ \nu_e)/\Gamma_{total}$ Γ_{31}/Γ

VALUE (units 10^{-3})	EVTS	DOCUMENT ID		TECN	COMMENT
$2.18^{+0.17}_{-0.25}$ OUR FIT					
$2.17\pm0.12^{+0.12}_{-0.22}$	447 ± 25	[1] DOBBS	13	CLEO	e^+e^- at $\psi(3770)$
• • • We do not use the following data for averages, fits, limits, etc. • • •					
2.1 ±0.4 ±0.1	27 ± 6	[2] HUANG	05B	CLEO	See DOBBS 13

[1] DOBBS 13 finds $\Gamma(D^0 \to \rho^- e^+ \nu_e) / 2\,\Gamma(D^+ \to \rho^0 e^+ \nu_e) = 1.03 \pm 0.09^{+0.08}_{-0.02}$; isospin invariance predicts the ratio is 1.0.

[2] HUANG 05B finds $\Gamma(D^0 \to \rho^- e^+ \nu_e) / 2\,\Gamma(D^+ \to \rho^0 e^+ \nu_e) = 1.2^{+0.4}_{-0.3} \pm 0.1$; isospin invariance predicts the ratio is 1.0.

$\Gamma(\rho^0 e^+ \nu_e)/\Gamma(\overline{K}^*(892)^0 e^+ \nu_e)$ Γ_{31}/Γ_{37}

VALUE	EVTS	DOCUMENT ID		TECN	COMMENT
$0.0404^{+0.0033}_{-0.0050}$ OUR FIT					
0.045 ±0.014 ±0.009	49	[1] AITALA	97	E791	π^- nucleus, 500 GeV

[1] AITALA 97 explicitly subtracts $D^+ \to \eta' e^+ \nu_e$ and other backgrounds to get this result.

$\Gamma(\rho^0 \mu^+ \nu_\mu)/\Gamma(\overline{K}^*(892)^0 \mu^+ \nu_\mu)$ Γ_{32}/Γ_{38}

VALUE	EVTS	DOCUMENT ID		TECN	COMMENT
0.045±0.007 OUR AVERAGE		Error includes scale factor of 1.1.			
0.041±0.006±0.004	320 ± 44	LINK	06B	FOCS	γ A, $\overline{E}_\gamma \approx$ 180 GeV
0.051±0.015±0.009	54	[1] AITALA	97	E791	π^- nucleus, 500 GeV
0.079±0.019±0.013	39	[2] FRABETTI	97	E687	γ Be, $\overline{E}_\gamma \approx$ 220 GeV

[1] AITALA 97 explicitly subtracts $D^+ \to \eta' \mu^+ \nu_\mu$ and other backgrounds to get this result.

[2] Because the reconstruction efficiency for photons is low, this FRABETTI 97 result also includes any $D^+ \to \eta' \mu^+ \nu_\mu \to \gamma \rho^0 \mu^+ \nu_\mu$ events in the numerator.

$\Gamma(\omega e^+ \nu_e)/\Gamma_{total}$ Γ_{33}/Γ

VALUE (units 10^{-3})	EVTS	DOCUMENT ID		TECN	COMMENT
1.69±0.11 OUR AVERAGE					
1.63±0.11±0.08	491 ± 32	ABLIKIM	15W	BES3	292 fb^{-1}, 3773 MeV
1.82±0.18±0.07	129 ± 13	DOBBS	13	CLEO	e^+e^- at $\psi(3770)$
• • • We do not use the following data for averages, fits, limits, etc. • • •					
1.6 $^{+0.7}_{-0.6}$ ±0.1	$7.6^{+3.3}_{-2.7}$	HUANG	05B	CLEO	See DOBBS 13

$\Gamma(\eta'(958) e^+ \nu_e)/\Gamma_{total}$ Γ_{34}/Γ

VALUE (units 10^{-4})	CL%	DOCUMENT ID		TECN	COMMENT
2.16±0.53±0.07		YELTON	11	CLEO	e^+e^- at $\psi(3770)$
• • • We do not use the following data for averages, fits, limits, etc. • • •					
<3.5	90	MITCHELL	09B	CLEO	See YELTON 11

$\Gamma(\phi e^+ \nu_e)/\Gamma_{total}$ Γ_{35}/Γ

Unseen decay modes of the ϕ are included.

VALUE	CL%	DOCUMENT ID		TECN	COMMENT
<1.3 $\times 10^{-5}$	90	ABLIKIM	15W	BES3	292 fb^{-1}, 3773 MeV
• • • We do not use the following data for averages, fits, limits, etc. • • •					
<0.9 $\times 10^{-4}$	90	YELTON	11	CLEO	e^+e^- at $\psi(3770)$
<1.6 $\times 10^{-4}$	90	MITCHELL	09B	CLEO	See YELTON 11
<0.0201	90	ABLIKIM	06P	BES2	e^+e^- at 3773 MeV
<0.0209	90	BAI	91	MRK3	e^+e^- at 3.77 GeV

$\Gamma(D^0 e^+ \nu_e)/\Gamma_{total}$ Γ_{36}/Γ

VALUE	CL%	DOCUMENT ID		TECN	COMMENT
<1.0 $\times 10^{-4}$	90	ABLIKIM	17AD	BES3	e^+e^- at 3.773 GeV

Hadronic modes with a $\overline{K}$ or $\overline{K}K\overline{K}$

$\Gamma(K^0_S \pi^+)/\Gamma_{total}$ Γ_{41}/Γ

VALUE (units 10^{-2})	EVTS	DOCUMENT ID		TECN	COMMENT
• • • We do not use the following data for averages, fits, limits, etc. • • •					
1.526±0.022±0.038		[1] DOBBS	07	CLEO	See MENDEZ 10
1.55 ±0.05 ±0.06	2.2k	[1] HE	05	CLEO	See DOBBS 07
1.6 ±0.3 ±0.1	161	ADLER	88C	MRK3	e^+e^- 3.77 GeV

[1] DOBBS 07 and HE 05 use single- and double-tagged events in an overall fit. DOBBS 07 supersedes HE 05.

$\Gamma(K^0_S \pi^+)/\Gamma(K^- 2\pi^+)$ Γ_{41}/Γ_{43}

VALUE	EVTS	DOCUMENT ID		TECN	COMMENT
0.164 ±0.007 OUR FIT		Error includes scale factor of 3.9.			
0.162 ±0.009 OUR AVERAGE		Error includes scale factor of 4.5.			
0.171 ±0.002 ±0.002		BONVICINI	14	CLEO	All CLEO-c runs
0.1530±0.0023±0.0016	10.6k	LINK	02B	FOCS	γ nucleus, $\overline{E}_\gamma \approx$ 180 GeV
• • • We do not use the following data for averages, fits, limits, etc. • • •					
0.1682±0.0012±0.0037	30k	MENDEZ	10	CLEO	See BONVICINI 14
0.174 ±0.012 ±0.011	473	[1] BISHAI	97	CLEO	$e^+e^- \approx \Upsilon(4S)$
0.137 ±0.015 ±0.016	264	ANJOS	90C	E691	Photoproduction

[1] See BISHAI 97 for an isospin analysis of $D^+ \to \overline{K}\pi$ amplitudes.

$\Gamma(K^0_L \pi^+)/\Gamma_{total}$ Γ_{42}/Γ

VALUE (units 10^{-2})	EVTS	DOCUMENT ID		TECN	COMMENT
1.460±0.040±0.035	2023 ± 54	[1] HE	08	CLEO	e^+e^- at $\psi(3770)$

[1] The difference of CLEO $D^+ \to K^0_S \pi^+$ and $K^0_L \pi^+$ branching fractions over the sum (DOBBS 07 and HE 08) is $+0.022 \pm 0.016 \pm 0.018$.

$\Gamma(K^- 2\pi^+)/\Gamma_{total}$ Γ_{43}/Γ

VALUE (units 10^{-2})	EVTS	DOCUMENT ID		TECN	COMMENT
8.98 ±0.28 OUR FIT		Error includes scale factor of 2.2.			
9.224±0.059±0.157		BONVICINI	14	CLEO	All CLEO-c runs
• • • We do not use the following data for averages, fits, limits, etc. • • •					
9.14 ±0.10 ±0.17		[1] DOBBS	07	CLEO	See BONVICINI 14
9.5 ±0.2 ±0.3	15.1k	[1] HE	05	CLEO	See DOBBS 07
9.3 ±0.6 ±0.8	1502	[2] BALEST	94	CLEO	$e^+e^- \approx \Upsilon(4S)$
6.4 $^{+1.5}_{-1.4}$		[3] BARLAG	92C	ACCM	π^- Cu 230 GeV
9.1 ±1.3 ±0.4	1164	ADLER	88C	MRK3	e^+e^- 3.77 GeV
9.1 ±1.9	239	[4] SCHINDLER	81	MRK2	e^+e^- 3.771 GeV

[1] DOBBS 07 and HE 05 use single- and double-tagged events in an overall fit. DOBBS 07 supersedes HE 05.

[2] BALEST 94 measures the ratio of $D^+ \to K^-\pi^+\pi^+$ and $D^0 \to K^-\pi^+$ branching fractions to be 2.35 ± 0.16 ± 0.16 and uses their absolute measurement of the $D^0 \to K^-\pi^+$ fraction (AKERIB 93).

[3] BARLAG 92C computes the branching fraction by topological normalization.

[4] SCHINDLER 81 (MARK-2) measures $\sigma(e^+e^- \to \psi(3770)) \times$ branching fraction to be 0.38 ± 0.05 nb. We use the MARK-3 (ADLER 88C) value of $\sigma = 4.2 \pm 0.6 \pm 0.3$ nb.

See the related review(s):
Review of Multibody Charm Analyses

$\Gamma((K^-\pi^+)_{S-wave}\pi^+)/\Gamma(K^- 2\pi^+)$ Γ_{44}/Γ_{43}

This is the "fit fraction" from the Dalitz-plot analysis. The $K^-\pi^+$ S-wave includes a broad scalar κ ($\overline{K}^*_0(700)$), the $\overline{K}^*_0(1430)^0$, and non-resonant background.

VALUE	DOCUMENT ID		TECN	COMMENT
0.801 ±0.012 OUR AVERAGE				
0.8024±0.0138±0.0043	[1] LINK	09	FOCS	MIPWA fit, 53k evts
0.838 ±0.038	[2] BONVICINI	08A	CLEO	QMIPWA fit, 141k evts
0.786 ±0.014 ±0.018	AITALA	06	E791	Dalitz fit, 15.1k events
• • • We do not use the following data for averages, fits, limits, etc. • • •				
0.8323±0.0150±0.0008	[3] LINK	07B	FOCS	See LINK 09

[1] This LINK 09 model-independent partial-wave analysis of the $K^-\pi^+$ S-wave slices the $K^-\pi^+$ mass range into 39 bins.

[2] The BONVICINI 08A QMIPWA (quasi-model-independent partial-wave analysis) of the $K^-\pi^+$ S-wave amplitude slices the $K^-\pi^+$ mass range into 26 bins but keeps the Breit-Wigner $\overline{K}^*_0(1430)^0$.

[3] This LINK 07B fit uses a K matrix. The $K^-\pi^+$ S-wave fit fraction given above breaks down into (207.3 ± 25.5 ± 12.4)% isospin-1/2 and (40.5 ± 9.6 ± 3.2)% isospin-3/2 — with large interference between the two. The isospin-1/2 component includes the κ (or $\overline{K}^*_0(700)^0$) and $\overline{K}^*_0(1430)^0$.

$\Gamma(\overline{K}^*_0(700)^0\pi^+, \overline{K}^*_0(700) \to K^-\pi^+)/\Gamma(K^- 2\pi^+)$ Γ_{45}/Γ_{43}

This is the "fit fraction" from the Dalitz-plot analysis.

VALUE	DOCUMENT ID		TECN	COMMENT
• • • We do not use the following data for averages, fits, limits, etc. • • •				
0.478±0.121±0.053	AITALA	02	E791	See AITALA 06

$\Gamma(\overline{K}^*(892)^0\pi^+, \overline{K}^*(892)^0 \to K^-\pi^+)/\Gamma(K^- 2\pi^+)$ Γ_{47}/Γ_{43}

This is the "fit fraction" from the Dalitz-plot analysis.

VALUE	DOCUMENT ID		TECN	COMMENT
0.111 ±0.012 OUR AVERAGE	Error includes scale factor of 3.7.			
0.1236±0.0034±0.0034	LINK	09	FOCS	MIPWA fit, 53k evts
0.0988±0.0046	BONVICINI	08A	CLEO	QMIPWA fit, 141k evts
0.119 ±0.002 ±0.020	AITALA	06	E791	Dalitz fit, 15.1k events

• • • We do not use the following data for averages, fits, limits, etc. • • •

$0.1361 \pm 0.0041 \pm 0.0030$	[1]	LINK	07B	FOCS	See LINK 09
$0.123 \pm 0.010 \pm 0.009$		AITALA	02	E791	See AITALA 06
$0.137 \pm 0.006 \pm 0.009$		FRABETTI	94G	E687	Dalitz fit, 8800 evts
$0.170 \pm 0.009 \pm 0.034$		ANJOS	93	E691	γBe 90–260 GeV
$0.14 \pm 0.04 \pm 0.04$		ALVAREZ	91B	NA14	Photoproduction
$0.13 \pm 0.01 \pm 0.07$		ADLER	87	MRK3	e^+e^- 3.77 GeV

[1] The statistical error on this LINK 07B value is corrected in LINK 09.

$\Gamma(\overline{K}^*(1410)^0\pi^+, \overline{K}^{*0} \to K^-\pi^+)/\Gamma(K^-2\pi^+)$ Γ_{48}/Γ_{43}

VALUE (units 10^{-3})	DOCUMENT ID		TECN	COMMENT
not seen	LINK	09	FOCS	MIPWA fit, 53k evts
not seen	BONVICINI	08A	CLEO	QMIPWA fit, 141k evts

• • • We do not use the following data for averages, fits, limits, etc. • • •

$4.8 \pm 2.1 \pm 1.7$	LINK	07B	FOCS	See LINK 09

$\Gamma(\overline{K}_0^*(1430)^0\pi^+, \overline{K}_0^*(1430)^0 \to K^-\pi^+)/\Gamma(K^-2\pi^+)$ Γ_{46}/Γ_{43}

This is the "fit fraction" from the Dalitz-plot analysis.

VALUE	DOCUMENT ID		TECN	COMMENT
0.1330 ± 0.0062	BONVICINI	08A	CLEO	QMIPWA fit, 141k evts

• • • We do not use the following data for averages, fits, limits, etc. • • •

$0.125 \pm 0.014 \pm 0.005$		AITALA	02	E791	See AITALA 06
$0.284 \pm 0.022 \pm 0.059$		FRABETTI	94G	E687	Dalitz fit, 8800 evts
$0.248 \pm 0.019 \pm 0.017$		ANJOS	93	E691	γBe 90–260 GeV

$\Gamma(\overline{K}_2^*(1430)^0\pi^+, \overline{K}_2^*(1430)^0 \to K^-\pi^+)/\Gamma(K^-2\pi^+)$ Γ_{49}/Γ_{43}

This is the "fit fraction" from the Dalitz-plot analysis.

VALUE (units 10^{-2})	DOCUMENT ID		TECN	COMMENT
0.24 ± 0.08 OUR AVERAGE	Error includes scale factor of 2.2. See the ideogram below.			
$0.58 \pm 0.10 \pm 0.06$	LINK	09	FOCS	MIPWA fit, 53k evts
0.204 ± 0.040	BONVICINI	08A	CLEO	QMIPWA fit, 141k evts
$0.2 \pm 0.1 \pm 0.1$	AITALA	06	E791	Dalitz fit, 15.1k events

• • • We do not use the following data for averages, fits, limits, etc. • • •

$0.39 \pm 0.09 \pm 0.05$	LINK	07B	FOCS	See LINK 09
$0.5 \pm 0.1 \pm 0.2$	AITALA	02	E791	See AITALA 06

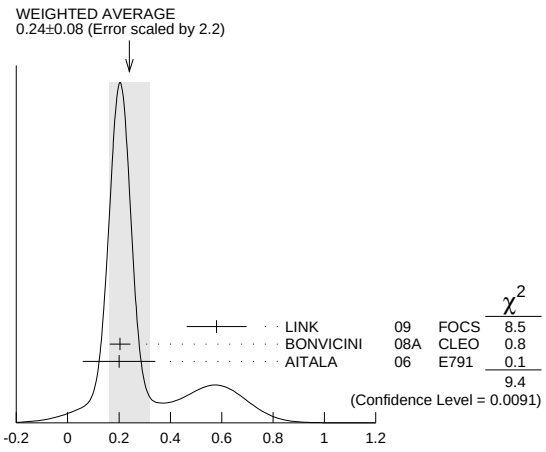

$\Gamma(\overline{K}_2^*(1430)^0\pi^+, \overline{K}_2^*(1430)^0 \to K^-\pi^+)/\Gamma(K^-2\pi^+)$ Γ_{49}/Γ_{43} (units 10^{-2})

$\Gamma(\overline{K}^*(1680)^0\pi^+, \overline{K}^*(1680)^0 \to K^-\pi^+)/\Gamma(K^-2\pi^+)$ Γ_{50}/Γ_{43}

This is the "fit fraction" from the Dalitz-plot analysis.

VALUE (units 10^{-2})	DOCUMENT ID		TECN	COMMENT
0.23 ± 0.12 OUR AVERAGE				
$1.75 \pm 0.62 \pm 0.54$	LINK	09	FOCS	MIPWA fit, 53k evts
0.196 ± 0.118	BONVICINI	08A	CLEO	QMIPWA fit, 141k evts
$1.2 \pm 0.6 \pm 1.2$	AITALA	06	E791	Dalitz fit, 15.1k events

• • • We do not use the following data for averages, fits, limits, etc. • • •

$1.90 \pm 0.63 \pm 0.43$		LINK	07B	FOCS	See LINK 09
$2.5 \pm 0.7 \pm 0.3$		AITALA	02	E791	See AITALA 06
$4.7 \pm 0.6 \pm 0.7$		FRABETTI	94G	E687	Dalitz fit, 8800 evts
$3.0 \pm 0.4 \pm 1.3$		ANJOS	93	E691	γBe 90–260 GeV

$\Gamma(K^-(2\pi^+)_{I=2})/\Gamma(K^-2\pi^+)$ Γ_{51}/Γ_{43}

VALUE	DOCUMENT ID		TECN	COMMENT
0.155 ± 0.028	BONVICINI	08A	CLEO	QMIPWA fit, 141k evts

$\Gamma(K^-2\pi^+ \text{ nonresonant})/\Gamma(K^-2\pi^+)$ Γ_{52}/Γ_{43}

This is the "fit fraction" from the Dalitz-plot analysis. Later analyses find little need for this decay mode.

VALUE	DOCUMENT ID		TECN	COMMENT

• • • We do not use the following data for averages, fits, limits, etc. • • •

$0.130 \pm 0.058 \pm 0.044$	AITALA	02	E791	See AITALA 06
$0.998 \pm 0.037 \pm 0.072$	FRABETTI	94G	E687	Dalitz fit, 8800 evts
$0.838 \pm 0.088 \pm 0.275$	ANJOS	93	E691	γBe 90–260 GeV
$0.79 \pm 0.07 \pm 0.15$	ADLER	87	MRK3	e^+e^- 3.77 GeV

$\Gamma(K_S^0\pi^+\pi^0)/\Gamma_{\text{total}}$ Γ_{53}/Γ

VALUE (units 10^{-2})	EVTS	DOCUMENT ID		TECN	COMMENT

• • • We do not use the following data for averages, fits, limits, etc. • • •

$6.99 \pm 0.09 \pm 0.25$		[1] DOBBS	07	CLEO	See BONVICINI 14
$7.2 \pm 0.2 \pm 0.4$	5.1k	[1] HE	05	CLEO	See DOBBS 07
$5.1 \pm 1.3 \pm 0.8$	159	ADLER	88C	MRK3	e^+e^- 3.77 GeV

[1] DOBBS 07 and HE 05 use single- and double-tagged events in an overall fit. DOBBS 07 supersedes HE 05.

$\Gamma(K_S^0\pi^+\pi^0)/\Gamma(K^-2\pi^+)$ Γ_{53}/Γ_{43}

VALUE	DOCUMENT ID		TECN	COMMENT
$0.785 \pm 0.007 \pm 0.016$	BONVICINI	14	CLEO	All CLEO-c runs

$\Gamma(K_S^0\rho^+)/\Gamma(K_S^0\pi^+\pi^0)$ Γ_{54}/Γ_{53}

This is the "fit fraction" from the Dalitz-plot analysis.

VALUE (units 10^{-2})	DOCUMENT ID		TECN	COMMENT
$83.4 \pm 2.2^{+\ 7.1}_{-\ 3.6}$	[1] ABLIKIM	14E	BES3	e^+e^- at $\psi(3770)$

• • • We do not use the following data for averages, fits, limits, etc. • • •

$68 \pm 8 \pm 12$	ADLER	87	MRK3	e^+e^- 3.77 GeV

[1] Fit fraction from Dalitz plot analysis of 142k $D^+ \to K_S^0\pi^+\pi^0$ events.

$\Gamma(K_S^0\rho(1450)^+, \rho^+ \to \pi^+\pi^0)/\Gamma(K_S^0\pi^+\pi^0)$ Γ_{55}/Γ_{53}

VALUE (%)	DOCUMENT ID		TECN	COMMENT
$2.1 \pm 0.3^{+1.6}_{-1.9}$	ABLIKIM	14E	BES3	e^+e^- at $\psi(3770)$

$\Gamma(\overline{K}^*(892)^0\pi^+, \overline{K}^*(892)^0 \to K_S^0\pi^0)/\Gamma(K_S^0\pi^+\pi^0)$ Γ_{56}/Γ_{53}

This is the "fit fraction" from the Dalitz-plot analysis.

VALUE (units 10^{-2})	DOCUMENT ID		TECN	COMMENT
$3.58 \pm 0.17^{+0.39}_{-0.38}$	[1] ABLIKIM	14E	BES3	e^+e^- at $\psi(3770)$

• • • We do not use the following data for averages, fits, limits, etc. • • •

$19 \pm 6 \pm 6$	ADLER	87	MRK3	e^+e^- 3.77 GeV

[1] Fit fraction from Dalitz plot analysis of 142k $D^+ \to K_S^0\pi^+\pi^0$ events.

$\Gamma(\overline{K}_0^*(1430)^0\pi^+, \overline{K}_0^{*0} \to K_S^0\pi^0)/\Gamma(K_S^0\pi^+\pi^0)$ Γ_{57}/Γ_{53}

VALUE (%)	DOCUMENT ID		TECN	COMMENT
$3.7 \pm 0.6 \pm 1.1$	ABLIKIM	14E	BES3	e^+e^- at $\psi(3770)$

$\Gamma(\overline{K}_0^*(1680)^0\pi^+, \overline{K}_0^{*0} \to K_S^0\pi^0)/\Gamma(K_S^0\pi^+\pi^0)$ Γ_{58}/Γ_{53}

VALUE (%)	DOCUMENT ID		TECN	COMMENT
$1.3 \pm 0.2^{+0.9}_{-1.3}$	ABLIKIM	14E	BES3	e^+e^- at $\psi(3770)$

$\Gamma(\overline{\kappa}^0\pi^+, \overline{\kappa}^0 \to K_S^0\pi^0)/\Gamma(K_S^0\pi^+\pi^0)$ Γ_{59}/Γ_{53}

VALUE (%)	DOCUMENT ID		TECN	COMMENT
$7.7 \pm 1.2^{+6.5}_{-4.8}$	ABLIKIM	14E	BES3	e^+e^- at $\psi(3770)$

$\Gamma(K_S^0\pi^+\pi^0 \text{ nonresonant})/\Gamma(K_S^0\pi^+\pi^0)$ Γ_{60}/Γ_{53}

This is the "fit fraction" from the Dalitz-plot analysis.

VALUE (units 10^{-2})	DOCUMENT ID		TECN	COMMENT
$4.6 \pm 0.7^{+5.4}_{-5.1}$	[1] ABLIKIM	14E	BES3	e^+e^- at $\psi(3770)$

• • • We do not use the following data for averages, fits, limits, etc. • • •

$13 \pm 7 \pm 8$	ADLER	87	MRK3	e^+e^- 3.77 GeV

[1] Fit fraction from Dalitz plot analysis of 142k $D^+ \to K_S^0\pi^+\pi^0$ events.

$\Gamma(K_S^0\pi^+\pi^0 \text{ nonresonant and } \overline{\kappa}^0\pi^+)/\Gamma(K_S^0\pi^+\pi^0)$ Γ_{61}/Γ_{53}

VALUE (%)	DOCUMENT ID		TECN	COMMENT
$18.6 \pm 1.7^{+2.3}_{-4.6}$	ABLIKIM	14E	BES3	e^+e^- at $\psi(3770)$

$\Gamma((K_S^0\pi^0)_{S\text{-wave}}\pi^+)/\Gamma(K_S^0\pi^+\pi^0)$ Γ_{62}/Γ_{53}

The numerator here is the coherent sum of the $\overline{K}_0^*(1430)^0\pi^+$, $\overline{\kappa}^0\pi^+$, and nonresonant contributions.

VALUE (%)	DOCUMENT ID		TECN	COMMENT
$17.3 \pm 1.4^{+3.4}_{-4.3}$	ABLIKIM	14E	BES3	e^+e^- at $\psi(3770)$

Meson Particle Listings

$D^{\pm}$

$\Gamma(K^-2\pi^+\pi^0)/\Gamma_{total}$ Γ_{63}/Γ

See our 2008 Review (Physics Letters **B667** 1 (2008)) for measurements of submodes of this mode. There is nothing new since 1992, and the two papers, ANJOS 92C, with 91 ± 12 events above background, and COFFMAN 92B, with 142 ± 20 such events, could not determine submode fractions with much accuracy.

VALUE (units 10^{-2})	EVTS	DOCUMENT ID		TECN	COMMENT
• • • We do not use the following data for averages, fits, limits, etc. • • •					
5.98±0.08±0.16		[1] DOBBS	07	CLEO	See BONVICINI 14
6.0 ±0.2 ±0.2	4.8k	[1] HE	05	CLEO	See DOBBS 07
5.8 ±1.2 ±1.2	142	COFFMAN	92B	MRK3	e^+e^- 3.77 GeV
$6.3\ ^{+1.4}_{-1.3}$ ±1.2	175	BALTRUSAIT...86E		MRK3	See COFFMAN 92B

[1] DOBBS 07 and HE 05 use single- and double-tagged events in an overall fit. DOBBS 07 supersedes HE 05.

$\Gamma(K^-2\pi^+\pi^0)/\Gamma(K^-2\pi^+)$ Γ_{63}/Γ_{43}

VALUE	DOCUMENT ID		TECN	COMMENT
0.666±0.006±0.014	BONVICINI	14	CLEO	All CLEO-c runs

$\Gamma(K^0_S2\pi^+\pi^-)/\Gamma_{total}$ Γ_{64}/Γ

See our 2008 Review (Physics Letters **B667** 1 (2008)) for measurements of submodes of this mode. There is nothing new since 1992, and the two papers, ANJOS 92C, with 229 ± 17 events above background, and COFFMAN 92B, with 209 ± 20 such events, could not determine submode fractions with much accuracy.

VALUE (units 10^{-2})	EVTS	DOCUMENT ID		TECN	COMMENT
• • • We do not use the following data for averages, fits, limits, etc. • • •					
3.122±0.046±0.096		[1] DOBBS	07	CLEO	See BONVICINI 14
3.2 ±0.1 ±0.2	3.2k	[1] HE	05	CLEO	See DOBBS 07
$2.1\ ^{+1.0}_{-0.9}$		[2] BARLAG	92C	ACCM	π^- Cu 230 GeV
3.3 ±0.8 ±0.2	168	ADLER	88C	MRK3	e^+e^- 3.77 GeV

[1] DOBBS 07 and HE 05 use single- and double-tagged events in an overall fit. DOBBS 07 supersedes HE 05.
[2] BARLAG 92C computes the branching fraction by topological normalization.

$\Gamma(K^0_S2\pi^+\pi^-)/\Gamma(K^-2\pi^+)$ Γ_{64}/Γ_{43}

VALUE	DOCUMENT ID		TECN	COMMENT
0.331±0.004±0.006	BONVICINI	14	CLEO	All CLEO-c runs

$\Gamma(K^-3\pi^+\pi^-)/\Gamma(K^-2\pi^+)$ Γ_{65}/Γ_{43}

VALUE	EVTS	DOCUMENT ID		TECN	COMMENT
0.061±0.005 OUR FIT Error includes scale factor of 1.1.					
0.062±0.008 OUR AVERAGE Error includes scale factor of 1.3.					
0.058±0.002±0.006	2923	LINK	03D	FOCS	γ A, $\overline{E}_\gamma \approx$ 180 GeV
0.077±0.008±0.010	239	FRABETTI	97C	E687	γBe, $\overline{E}_\gamma \approx$ 200 GeV
• • • We do not use the following data for averages, fits, limits, etc. • • •					
0.09 ±0.01 ±0.01	113	ANJOS	90D	E691	Photoproduction

$\Gamma(\overline{K}^*(892)^0\pi^+\pi^-, \overline{K}^*(892)^0 \to K^-\pi^+)/\Gamma(K^-3\pi^+\pi^-)$ Γ_{66}/Γ_{65}

VALUE	DOCUMENT ID		TECN	COMMENT
0.21±0.04±0.06	LINK	03D	FOCS	γ A, $\overline{E}_\gamma \approx$ 180 GeV

$\Gamma(\overline{K}^*(892)^0\rho^0\pi^+, \overline{K}^*(892)^0 \to K^-\pi^+)/\Gamma(K^-3\pi^+\pi^-)$ Γ_{67}/Γ_{65}

VALUE	DOCUMENT ID		TECN	COMMENT
0.40±0.03±0.06	LINK	03D	FOCS	γ A, $\overline{E}_\gamma \approx$ 180 GeV

$\Gamma(\overline{K}^*(892)^0\rho^0\pi^+, \overline{K}^*(892)^0 \to K^-\pi^+)/\Gamma(K^-2\pi^+)$ Γ_{67}/Γ_{43}

VALUE	DOCUMENT ID		TECN	COMMENT
• • • We do not use the following data for averages, fits, limits, etc. • • •				
0.016±0.007±0.004	FRABETTI	97C	E687	γBe, $\overline{E}_\gamma \approx$ 200 GeV

$\Gamma(\overline{K}^*(892)^0 2\pi^+\pi^-$ no-$\rho, \overline{K}^*(892)^0 \to K^-\pi^+)/\Gamma(K^-2\pi^+)$ Γ_{69}/Γ_{43}

VALUE	DOCUMENT ID		TECN	COMMENT
• • • We do not use the following data for averages, fits, limits, etc. • • •				
0.032±0.010±0.008	FRABETTI	97C	E687	γBe, $\overline{E}_\gamma \approx$ 200 GeV

$\Gamma(K^-\rho^0 2\pi^+)/\Gamma(K^-3\pi^+\pi^-)$ Γ_{70}/Γ_{65}

VALUE	DOCUMENT ID		TECN	COMMENT
0.30±0.04±0.01	LINK	03D	FOCS	γ A, $\overline{E}_\gamma \approx$ 180 GeV

$\Gamma(K^-\rho^0 2\pi^+)/\Gamma(K^-2\pi^+)$ Γ_{70}/Γ_{43}

VALUE	DOCUMENT ID		TECN	COMMENT
• • • We do not use the following data for averages, fits, limits, etc. • • •				
0.034±0.009±0.005	FRABETTI	97C	E687	γBe, $\overline{E}_\gamma \approx$ 200 GeV

$\Gamma(\overline{K}^*(892)^0 a_1(1260)^+)/\Gamma(K^-2\pi^+)$ Γ_{68}/Γ_{43}

Unseen decay modes of the $\overline{K}^*(892)^0$ and $a_1(1260)^+$ are included.

VALUE	DOCUMENT ID		TECN	COMMENT
0.099±0.008±0.018	LINK	03D	FOCS	γ A, $\overline{E}_\gamma \approx$ 180 GeV

$\Gamma(K^-3\pi^+\pi^-$ nonresonant$)/\Gamma(K^-3\pi^+\pi^-)$ Γ_{71}/Γ_{65}

VALUE	CL%	DOCUMENT ID		TECN	COMMENT
0.07 ±0.05±0.01		LINK	03D	FOCS	γ A, $\overline{E}_\gamma \approx$ 180 GeV
• • • We do not use the following data for averages, fits, limits, etc. • • •					
<0.026	90	FRABETTI	97C	E687	γBe, $\overline{E}_\gamma \approx$ 200 GeV

$\Gamma(K^+2K^0_S)/\Gamma_{total}$ Γ_{72}/Γ

VALUE (units 10^{-4})	EVTS	DOCUMENT ID		TECN	COMMENT
25.4±0.5±1.2	3551	ABLIKIM	17A	BES3	$e^+e^- \to \psi(3770)$

$\Gamma(K^+2K^0_S)/\Gamma(K^-2\pi^+)$ Γ_{72}/Γ_{43}

VALUE	EVTS	DOCUMENT ID		TECN	COMMENT
• • • We do not use the following data for averages, fits, limits, etc. • • •					
0.035±0.010±0.005	39 ± 9	ALBRECHT	94I	ARG	$e^+e^-\approx$ 10 GeV
0.085±0.018	70 ± 12	AMMAR	91	CLEO	$e^+e^- \approx$ 10.5 GeV

$\Gamma(K^+K^-K^0_S\pi^+)/\Gamma(K^0_S2\pi^+\pi^-)$ Γ_{73}/Γ_{64}

VALUE (units 10^{-3})	EVTS	DOCUMENT ID		TECN	COMMENT
7.7±1.5±0.9	35 ± 7	LINK	01C	FOCS	γ nucleus, $\overline{E}_\gamma \approx$ 180 GeV

Pionic modes

$\Gamma(\pi^+\pi^0)/\Gamma(K^-2\pi^+)$ Γ_{74}/Γ_{43}

VALUE (units 10^{-2})	EVTS	DOCUMENT ID		TECN	COMMENT
1.31±0.06 OUR AVERAGE					
1.29±0.04±0.05	2649 ± 76	MENDEZ	10	CLEO	e^+e^- at 3774 MeV
1.33±0.11±0.09	1229 ± 99	AUBERT,B	06F	BABR	$e^+e^- \approx \Upsilon(4S)$
1.44±0.19±0.10	171 ± 22	ARMS	04	CLEO	$e^+e^- \approx$ 10 GeV
• • • We do not use the following data for averages, fits, limits, etc. • • •					
1.33±0.07±0.06	914 ± 46	RUBIN	06	CLEO	See MENDEZ 10

$\Gamma(2\pi^+\pi^-)/\Gamma(K^-2\pi^+)$ Γ_{75}/Γ_{43}

VALUE (units 10^{-2})	EVTS	DOCUMENT ID		TECN	COMMENT
3.48±0.19 OUR AVERAGE Error includes scale factor of 1.4. See the ideogram below.					
3.52±0.11±0.12	3303 ± 95	RUBIN	06	CLEO	e^+e^- at $\psi(3770)$
4.1 ±1.1 ±0.3	85 ± 22	ABLIKIM	05F	BES	$e^+e^- \approx \psi(3770)$
$3.11\pm0.18\ ^{+0.16}_{-0.26}$	1172	AITALA	01B	E791	π^- nucleus, 500 GeV
4.3 ±0.3 ±0.3	236	FRABETTI	97D	E687	γ Be $\approx$ 200 GeV
3.5 ±0.7 ±0.3	83	ANJOS	89	E691	Photoproduction

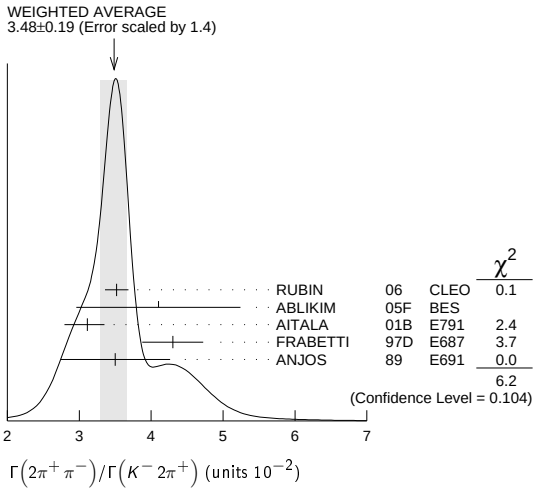

$\Gamma(\rho^0\pi^+)/\Gamma(2\pi^+\pi^-)$ Γ_{76}/Γ_{75}

This is the "fit fraction" from the Dalitz-plot analysis.

VALUE	DOCUMENT ID		TECN	COMMENT
0.25 ±0.04 OUR AVERAGE Error includes scale factor of 2.4. See the ideogram below.				
0.200 ±0.023 ±0.009	BONVICINI	07	CLEO	Dalitz fit, ≈ 2240 evts
0.3082±0.0314±0.0230	LINK	04	FOCS	Dalitz fit, 1527 ± 51 evts
0.336 ±0.032 ±0.022	AITALA	01B	E791	Dalitz fit, 1172 evts

See key on page 885

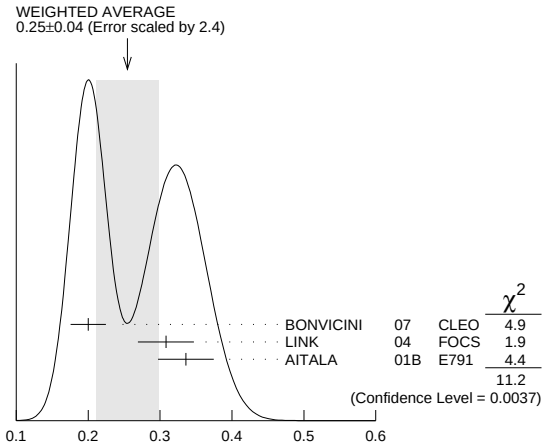

$\Gamma(\rho^0\pi^+)/\Gamma(2\pi^+\pi^-)$

$\Gamma(\pi^+(\pi^+\pi^-)_{S-\text{wave}})/\Gamma(2\pi^+\pi^-)$ Γ_{77}/Γ_{75}

This is the "fit fraction" from the Dalitz-plot analysis. See also the next three data blocks.

VALUE	DOCUMENT ID		TECN	COMMENT
0.5600±0.0324±0.0214	[1] LINK	04	FOCS	Dalitz fit, 1527 ± 51 evts

[1] LINK 04 borrows a K-matrix parametrization from ANISOVICH 03 of the full π-π S-wave isoscalar scattering amplitude to describe the $\pi^+\pi^-$ S-wave component of the $\pi^+\pi^+\pi^-$ state. The fit fraction given above is a sum over five f_0 mesons, the $f_0(980)$, $f_0(1300)$, $f_0(1200$–$1600)$, $f_0(1500)$, and $f_0(1750)$. See LINK 04 for details and discussion.

$\Gamma(\sigma\pi^+, \sigma\to\pi^+\pi^-)/\Gamma(2\pi^+\pi^-)$ Γ_{78}/Γ_{75}

This is the "fit fraction" from the Dalitz-plot analysis.

VALUE	DOCUMENT ID		TECN	COMMENT
0.422±0.027 OUR AVERAGE				
0.418±0.014±0.025	BONVICINI	07	CLEO	Dalitz fit, ≈ 2240 evts
0.463±0.090±0.021	AITALA	01B	E791	Dalitz fit, 1172 evts

$\Gamma(f_0(980)\pi^+, f_0(980)\to\pi^+\pi^-)/\Gamma(2\pi^+\pi^-)$ Γ_{79}/Γ_{75}

This is the "fit fraction" from the Dalitz-plot analysis.

VALUE	DOCUMENT ID		TECN	COMMENT
0.048±0.010 OUR AVERAGE	Error includes scale factor of 1.3.			
0.041±0.009±0.003	BONVICINI	07	CLEO	Dalitz fit, ≈ 2240 evts
0.062±0.013±0.004	AITALA	01B	E791	Dalitz fit, 1172 evts

$\Gamma(f_0(1370)\pi^+, f_0(1370)\to\pi^+\pi^-)/\Gamma(2\pi^+\pi^-)$ Γ_{80}/Γ_{75}

This is the "fit fraction" from the Dalitz-plot analysis.

VALUE	DOCUMENT ID		TECN	COMMENT
0.024±0.013 OUR AVERAGE				
0.026±0.018±0.006	BONVICINI	07	CLEO	Dalitz fit, ≈ 2240 evts
0.023±0.015±0.008	AITALA	01B	E791	Dalitz fit, 1172 evts

$\Gamma(f_2(1270)\pi^+, f_2(1270)\to\pi^+\pi^-)/\Gamma(2\pi^+\pi^-)$ Γ_{81}/Γ_{75}

This is the "fit fraction" from the Dalitz-plot analysis.

VALUE	DOCUMENT ID		TECN	COMMENT
0.154 ±0.025 OUR AVERAGE	Error includes scale factor of 1.9. See the ideogram below.			
0.182 ±0.026 ±0.007	BONVICINI	07	CLEO	Dalitz fit, ≈ 2240 evts
0.1174±0.0190±0.0029	LINK	04	FOCS	Dalitz fit, 1527 ± 51 evts
0.194 ±0.025 ±0.004	AITALA	01B	E791	Dalitz fit, 1172 evts

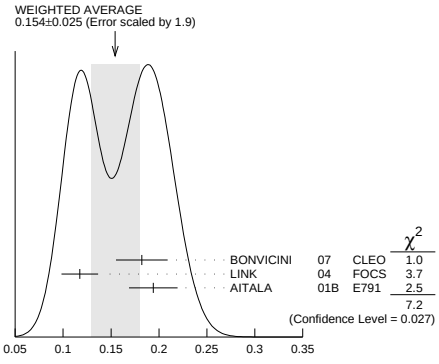

$\Gamma(f_2(1270)\pi^+, f_2(1270)\to\pi^+\pi^-)/\Gamma(2\pi^+\pi^-)$

$\Gamma(\rho(1450)^0\pi^+, \rho(1450)^0\to\pi^+\pi^-)/\Gamma(2\pi^+\pi^-)$ Γ_{82}/Γ_{75}

This is the "fit fraction" from the Dalitz-plot analysis.

VALUE	CL%	DOCUMENT ID		TECN	COMMENT
<0.024	95	BONVICINI	07	CLEO	Dalitz fit, ≈ 2240 evts
• • • We do not use the following data for averages, fits, limits, etc. • • •					
0.007±0.007±0.003		AITALA	01B	E791	Dalitz fit, 1172 evts

$\Gamma(f_0(1500)\pi^+, f_0(1500)\to\pi^+\pi^-)/\Gamma(2\pi^+\pi^-)$ Γ_{83}/Γ_{75}

This is the "fit fraction" from the Dalitz-plot analysis.

VALUE	DOCUMENT ID		TECN	COMMENT
0.034±0.010±0.008	BONVICINI	07	CLEO	Dalitz fit, ≈ 2240 evts

$\Gamma(f_0(1710)\pi^+, f_0(1710)\to\pi^+\pi^-)/\Gamma(2\pi^+\pi^-)$ Γ_{84}/Γ_{75}

This is the "fit fraction" from the Dalitz-plot analysis.

VALUE	CL%	DOCUMENT ID		TECN	COMMENT
<0.016	95	BONVICINI	07	CLEO	Dalitz fit, ≈ 2240 evts

$\Gamma(f_0(1790)\pi^+, f_0(1790)\to\pi^+\pi^-)/\Gamma(2\pi^+\pi^-)$ Γ_{85}/Γ_{75}

This is the "fit fraction" from the Dalitz-plot analysis.

VALUE	CL%	DOCUMENT ID		TECN	COMMENT
<0.02	95	BONVICINI	07	CLEO	Dalitz fit, ≈ 2240 evts

$\Gamma((\pi^+\pi^+)_{S-\text{wave}}\pi^-)/\Gamma(2\pi^+\pi^-)$ Γ_{86}/Γ_{75}

This is the "fit fraction" from the Dalitz-plot analysis.

VALUE	CL%	DOCUMENT ID		TECN	COMMENT
<0.037	95	BONVICINI	07	CLEO	Dalitz fit, ≈ 2240 evts

$\Gamma(2\pi^+\pi^-\text{ nonresonant})/\Gamma(2\pi^+\pi^-)$ Γ_{87}/Γ_{75}

This is the "fit fraction" from the Dalitz-plot analysis.

VALUE	CL%	DOCUMENT ID		TECN	COMMENT
<0.035	95	BONVICINI	07	CLEO	Dalitz fit, ≈ 2240 evts
• • • We do not use the following data for averages, fits, limits, etc. • • •					
0.078±0.060±0.027		AITALA	01B	E791	Dalitz fit, 1172 evts

$\Gamma(\pi^+2\pi^0)/\Gamma(K^-2\pi^+)$ Γ_{88}/Γ_{43}

VALUE (units 10^{-2})	EVTS	DOCUMENT ID		TECN	COMMENT
5.0±0.3±0.3	1535 ± 89	RUBIN	06	CLEO	e^+e^- at $\psi(3770)$

$\Gamma(2\pi^+\pi^-\pi^0)/\Gamma(K^-2\pi^+)$ Γ_{89}/Γ_{43}

VALUE (units 10^{-2})	EVTS	DOCUMENT ID		TECN	COMMENT
12.4±0.5±0.6	5701 ± 205	RUBIN	06	CLEO	e^+e^- at $\psi(3770)$

$\Gamma(\eta\pi^+)/\Gamma_{\text{total}}$ Γ_{91}/Γ

Unseen decay modes of the η are included.

VALUE (units 10^{-4})	EVTS	DOCUMENT ID		TECN	COMMENT
33.3±2.1 OUR FIT	Error includes scale factor of 1.4.				
30.7±2.2±1.3	258	ABLIKIM	16D	BES3	e^+e^- at 3773 MeV
• • • We do not use the following data for averages, fits, limits, etc. • • •					
34.3±1.4±1.7	1033±42	ARTUSO	08	CLEO	See MENDEZ 10

$\Gamma(\eta\pi^+)/\Gamma(K^-2\pi^+)$ Γ_{91}/Γ_{43}

Unseen decay modes of the η are included.

VALUE (units 10^{-2})	EVTS	DOCUMENT ID		TECN	COMMENT
3.71±0.23 OUR FIT	Error includes scale factor of 1.3.				
3.87±0.09±0.19	2940 ± 68	MENDEZ	10	CLEO	e^+e^- at 3774 MeV
• • • We do not use the following data for averages, fits, limits, etc. • • •					
3.81±0.26±0.21	377 ± 26	RUBIN	06	CLEO	See ARTUSO 08

$\Gamma(\omega\pi^+)/\Gamma_{\text{total}}$ Γ_{93}/Γ

Unseen decay modes of the ω are included.

VALUE (units 10^{-4})	CL%	EVTS	DOCUMENT ID		TECN	COMMENT
2.79±0.57±0.16		79	ABLIKIM	16D	BES3	e^+e^- at 3773 MeV
• • • We do not use the following data for averages, fits, limits, etc. • • •						
<3.4		90	RUBIN	06	CLEO	e^+e^- at $\psi(3770)$

$\Gamma(3\pi^+2\pi^-)/\Gamma(K^-2\pi^+)$ Γ_{90}/Γ_{43}

VALUE (units 10^{-2})	EVTS	DOCUMENT ID		TECN	COMMENT
1.77±0.17 OUR FIT					
1.73±0.20±0.17	732 ± 77	RUBIN	06	CLEO	e^+e^- at $\psi(3770)$
• • • We do not use the following data for averages, fits, limits, etc. • • •					
2.3 ±0.4 ±0.2	58	FRABETTI	97C	E687	γBe, $\overline{E}_\gamma \approx 200$ GeV

$\Gamma(3\pi^+2\pi^-)/\Gamma(K^-3\pi^+\pi^-)$ Γ_{90}/Γ_{65}

VALUE	EVTS	DOCUMENT ID		TECN	COMMENT
0.289±0.019 OUR FIT					
0.290±0.017±0.011	835	LINK	03D	FOCS	γ A, $\overline{E}_\gamma \approx 180$ GeV

$\Gamma(\eta\pi^+\pi^0)/\Gamma_{\text{total}}$ Γ_{92}/Γ

VALUE (units 10^{-4})	EVTS	DOCUMENT ID		TECN	COMMENT
13.8±3.1±1.6	149 ± 34	ARTUSO	08	CLEO	e^+e^- at $\psi(3770)$

$\Gamma(\eta'(958)\pi^+)/\Gamma_{\text{total}}$ Γ_{94}/Γ

Unseen decay modes of the $\eta'(958)$ are included.

VALUE (units 10^{-4})	EVTS	DOCUMENT ID		TECN	COMMENT
• • • We do not use the following data for averages, fits, limits, etc. • • •					
44.2±2.5±2.9	352 ± 20	ARTUSO	08	CLEO	See MENDEZ 10

Meson Particle Listings

$D^{\pm}$

$\Gamma(\eta'(958)\pi^+)/\Gamma(K^-2\pi^+)$ Γ_{94}/Γ_{43}

Unseen decay modes of the $\eta'(958)$ are included.

VALUE (units 10^{-2})	EVTS	DOCUMENT ID		TECN	COMMENT
5.12±0.17±0.25	1037 ± 35	MENDEZ	10	CLEO	e^+e^- at 3774 MeV

$\Gamma(\eta'(958)\pi^+\pi^0)/\Gamma_{total}$ Γ_{95}/Γ

Unseen decay modes of the $\eta'(958)$ are included.

VALUE (units 10^{-4})	EVTS	DOCUMENT ID		TECN	COMMENT
15.7±4.3±2.5	33 ± 9	ARTUSO	08	CLEO	e^+e^- at $\psi(3770)$

Hadronic modes with a $K\overline{K}$ pair

$\Gamma(K^+K^0_S)/\Gamma_{total}$ Γ_{96}/Γ

VALUE (units 10^{-3})	EVTS	DOCUMENT ID		TECN	COMMENT
• • • We do not use the following data for averages, fits, limits, etc. • • •					
3.14±0.09±0.08	1971±51	BONVICINI	08	CLEO	See MENDEZ 10

$\Gamma(K^+K^0_S)/\Gamma(K^0_S\pi^+)$ Γ_{96}/Γ_{41}

VALUE	EVTS	DOCUMENT ID		TECN	COMMENT
0.192 ±0.006 OUR FIT	Error includes scale factor of 2.6.				
0.1901±0.0024 OUR AVERAGE					
0.1899±0.0011±0.0022	101k±561	WON	09	BELL	e^+e^- at $\Upsilon(4S)$
0.1892±0.0155±0.0073	278 ± 21	ARMS	04	CLEO	$e^+e^-\approx$ 10 GeV
0.1996±0.0119±0.0096	949	LINK	02B	FOCS	γ A, $\overline{E}_\gamma\approx$180 GeV
• • • We do not use the following data for averages, fits, limits, etc. • • •					
0.222 ±0.037 ±0.013	63 ± 10	ABLIKIM	05F	BES	$e^+e^-\approx\psi(3770)$
0.222 ±0.041 ±0.019	70	BISHAI	97	CLEO	See ARMS 04
0.25 ±0.04 ±0.02	129	FRABETTI	95	E687	γBe $\overline{E}_\gamma\approx$200 GeV
0.271 ±0.065 ±0.039	69	ANJOS	90C	E691	γBe
0.317 ±0.086 ±0.048	31	BALTRUSAIT...85E		MRK3	e^+e^- 3.77 GeV
0.25 ±0.15	6	SCHINDLER	81	MRK2	e^+e^- 3.771 GeV

$\Gamma(K^+K^0_S)/\Gamma(K^-2\pi^+)$ Γ_{96}/Γ_{43}

VALUE (units 10^{-2})	EVTS	DOCUMENT ID		TECN	COMMENT
3.15±0.15 OUR FIT	Error includes scale factor of 3.2.				
3.35±0.06±0.07	5161±86	MENDEZ	10	CLEO	e^+e^- at 3774 MeV
• • • We do not use the following data for averages, fits, limits, etc. • • •					
3.02±0.18±0.15	949	[1] LINK	02B	FOCS	γ nucleus, $\overline{E}_\gamma\approx$ 180 GeV

[1] This LINK 02B result is redundant with a result in the previous datablock.

$\Gamma(K^+K^-\pi^+)/\Gamma_{total}$ Γ_{97}/Γ

VALUE (units 10^{-2})	EVTS	DOCUMENT ID		TECN	COMMENT
• • • We do not use the following data for averages, fits, limits, etc. • • •					
0.935±0.017±0.024		[1] DOBBS	07	CLEO	See BONVICINI 14
0.97 ±0.04 ±0.04	1250 ± 40	[1] HE	05	CLEO	See DOBBS 07

[1] DOBBS 07 and HE 05 use single- and double-tagged events in an overall fit. DOBBS 07 supersedes HE 05.

$\Gamma(K^+K^-\pi^+)/\Gamma(K^-2\pi^+)$ Γ_{97}/Γ_{43}

VALUE	EVTS	DOCUMENT ID		TECN	COMMENT
0.1059±0.0018 OUR FIT					
0.1059±0.0018 OUR AVERAGE					
0.106 ±0.002 ±0.003		BONVICINI	14	CLEO	All CLEO-c runs
0.117 ±0.013 ±0.007	181 ± 20	ABLIKIM	05F	BES	$e^+e^-\approx\psi(3770)$
0.107 ±0.001 ±0.002	43k	AUBERT	05S	BABR	$e^+e^-\approx\Upsilon(4S)$
0.093 ±0.010 $^{+0.008}_{-0.006}$		JUN	00	SELX	Σ^- nucleus, 600 GeV
0.0976±0.0042±0.0046		FRABETTI	95B	E687	γ Be, $\overline{E}_\gamma\approx$ 200 GeV

$\Gamma(\phi\pi^+, \phi\to K^+K^-)/\Gamma(K^+K^-\pi^+)$ Γ_{98}/Γ_{97}

This is the "fit fraction" from the Dalitz-plot analysis.

VALUE (%)	DOCUMENT ID		TECN	COMMENT
27.8±0.4 $^{+0.2}_{-0.5}$	RUBIN	08	CLEO	Dalitz fit, 19,458±163 evts
• • • We do not use the following data for averages, fits, limits, etc. • • •				
29.2±3.1±3.0	FRABETTI	95B	E687	Dalitz fit, 915 evts

$\Gamma(K^+\overline{K}^*(892)^0, \overline{K}^*(892)^0\to K^-\pi^+)/\Gamma(K^+K^-\pi^+)$ Γ_{99}/Γ_{97}

This is the "fit fraction" from the Dalitz-plot analysis.

VALUE (%)	DOCUMENT ID		TECN	COMMENT
25.7±0.5 $^{+0.4}_{-1.2}$	RUBIN	08	CLEO	Dalitz fit, 19,458±163 evts
• • • We do not use the following data for averages, fits, limits, etc. • • •				
30.1±2.0±2.5	FRABETTI	95B	E687	Dalitz fit, 915 evts

$\Gamma(K^+\overline{K}^*_0(1430)^0, \overline{K}^*_0(1430)^0\to K^-\pi^+)/\Gamma(K^+K^-\pi^+)$ Γ_{100}/Γ_{97}

This is the "fit fraction" from the Dalitz-plot analysis.

VALUE (%)	DOCUMENT ID		TECN	COMMENT
18.8±1.2 $^{+3.3}_{-3.4}$	RUBIN	08	CLEO	Dalitz fit, 19,458±163 evts
• • • We do not use the following data for averages, fits, limits, etc. • • •				
37.0±3.5±1.8	FRABETTI	95B	E687	Dalitz fit, 915 evts

$\Gamma(K^+\overline{K}^*_2(1430)^0, \overline{K}^*_2\to K^-\pi^+)/\Gamma(K^+K^-\pi^+)$ Γ_{101}/Γ_{97}

This is the "fit fraction" from the Dalitz-plot analysis.

VALUE (%)	DOCUMENT ID		TECN	COMMENT
1.7±0.4 $^{+1.2}_{-0.7}$	RUBIN	08	CLEO	Dalitz fit, 19,458±163 evts

$\Gamma(K^+\overline{K}^*_0(700), \overline{K}^*_0\to K^-\pi^+)/\Gamma(K^+K^-\pi^+)$ Γ_{102}/Γ_{97}

This is the "fit fraction" from the Dalitz-plot analysis.

VALUE (%)	DOCUMENT ID		TECN	COMMENT
7.0±0.8 $^{+3.5}_{-2.0}$	RUBIN	08	CLEO	Dalitz fit, 19,458±163 evts

$\Gamma(a_0(1450)^0\pi^+, a^0_0\to K^+K^-)/\Gamma(K^+K^-\pi^+)$ Γ_{103}/Γ_{97}

This is the "fit fraction" from the Dalitz-plot analysis.

VALUE (%)	DOCUMENT ID		TECN	COMMENT
4.6±0.6 $^{+7.2}_{-1.8}$	RUBIN	08	CLEO	Dalitz fit, 19,458±163 evts

$\Gamma(\phi(1680)\pi^+, \phi\to K^+K^-)/\Gamma(K^+K^-\pi^+)$ Γ_{104}/Γ_{97}

This is the "fit fraction" from the Dalitz-plot analysis.

VALUE (%)	DOCUMENT ID		TECN	COMMENT
0.51±0.11 $^{+0.37}_{-0.16}$	RUBIN	08	CLEO	Dalitz fit, 19,458±163 evts

$\Gamma(K^*(892)^+K^0_S)/\Gamma(K^0_S\pi^+)$ Γ_{112}/Γ_{41}

Unseen decay modes of the $K^*(892)^+$ are included.

VALUE	EVTS	DOCUMENT ID		TECN	COMMENT
1.1±0.3±0.4	67	FRABETTI	95	E687	γBe $\overline{E}_\gamma\approx$200 GeV

$\Gamma(K^0_SK^0_S\pi^+)/\Gamma_{total}$ Γ_{105}/Γ

VALUE (units 10^{-4})	EVTS	DOCUMENT ID		TECN	COMMENT
27.0±0.5±1.2	4897	ABLIKIM	17A	BES3	$e^+e^-\to\psi(3770)$

$\Gamma(\phi\pi^+\pi^0)/\Gamma_{total}$ Γ_{109}/Γ

Unseen decay modes of the ϕ are included.

VALUE	DOCUMENT ID		TECN	COMMENT
0.023±0.010	[1] BARLAG	92C	ACCM	π^- Cu 230 GeV

[1] BARLAG 92C computes the branching fraction using topological normalization.

$\Gamma(\phi\rho^+)/\Gamma(K^-2\pi^+)$ Γ_{110}/Γ_{43}

Unseen decay modes of the ϕ are included.

VALUE	CL%	DOCUMENT ID		TECN	COMMENT
<0.16	90	DAOUDI	92	CLEO	$e^+e^-\approx$ 10.5 GeV

$\Gamma(K^+K^-\pi^+\pi^0$ non-$\phi)/\Gamma_{total}$ Γ_{111}/Γ

VALUE	DOCUMENT ID		TECN	COMMENT
0.015 $^{+0.007}_{-0.006}$	[1] BARLAG	92C	ACCM	π^- Cu 230 GeV

[1] BARLAG 92C computes the branching fraction using topological normalization.

$\Gamma(K^+K^-\pi^+\pi^0$ non-$\phi)/\Gamma(K^-2\pi^+)$ Γ_{111}/Γ_{43}

VALUE	CL%	DOCUMENT ID		TECN	COMMENT
• • • We do not use the following data for averages, fits, limits, etc. • • •					
<0.25	90	ANJOS	89E	E691	Photoproduction

$\Gamma(K^+K^0_S\pi^+\pi^-)/\Gamma(K^0_S2\pi^+\pi^-)$ Γ_{106}/Γ_{64}

VALUE (units 10^{-2})	EVTS	DOCUMENT ID		TECN	COMMENT
5.62±0.39±0.40	469 ± 32	LINK	01C	FOCS	γ nucleus, $\overline{E}_\gamma\approx$ 180 GeV

$\Gamma(K^0_SK^-2\pi^+)/\Gamma(K^0_S2\pi^+\pi^-)$ Γ_{107}/Γ_{64}

VALUE (units 10^{-2})	EVTS	DOCUMENT ID		TECN	COMMENT
7.68±0.41±0.32	670 ± 35	LINK	01C	FOCS	γ nucleus, $\overline{E}_\gamma\approx$ 180 GeV

$\Gamma(K^+K^-2\pi^+\pi^-)/\Gamma(K^-3\pi^+\pi^-)$ Γ_{108}/Γ_{65}

VALUE	EVTS	DOCUMENT ID		TECN	COMMENT
0.040±0.009±0.019	38	LINK	03D	FOCS	γ A, $\overline{E}_\gamma\approx$ 180 GeV

Doubly Cabibbo-suppressed modes

$\Gamma(K^+\pi^0)/\Gamma_{total}$ Γ_{113}/Γ

VALUE (units 10^{-4})	EVTS	DOCUMENT ID		TECN	COMMENT
1.81±0.27 OUR FIT	Error includes scale factor of 1.4.				
2.52±0.47±0.26	189 ± 37	AUBERT,B	06F	BABR	$e^+e^-\approx\Upsilon(4S)$
• • • We do not use the following data for averages, fits, limits, etc. • • •					
2.28±0.36±0.17	148 ± 23	DYTMAN	06	CLEO	See MENDEZ 10

$\Gamma(K^+\pi^0)/\Gamma(K^-2\pi^+)$ Γ_{113}/Γ_{43}

VALUE (units 10^{-3})	EVTS	DOCUMENT ID		TECN	COMMENT
2.01±0.30 OUR FIT	Error includes scale factor of 1.4.				
1.9 ±0.2 ±0.1	343 ± 37	MENDEZ	10	CLEO	e^+e^- at 3774 MeV

$\Gamma(K^+\eta)/\Gamma(\eta\pi^+)$ Γ_{114}/Γ_{91}

VALUE (%)	EVTS	DOCUMENT ID		TECN	COMMENT
3.06±0.43±0.14	166 ± 23	WON	11	BELL	$e^+e^-\approx\Upsilon(4S)$

$\Gamma(K^+\eta)/\Gamma(K^-2\pi^+)$ Γ_{114}/Γ_{43}

Unseen decay modes of the η are included.

VALUE (units 10^{-2})	CL%	DOCUMENT ID		TECN	COMMENT
• • • We do not use the following data for averages, fits, limits, etc. • • •					
<0.15	90	MENDEZ	10	CLEO	e^+e^- at 3774 MeV

$\Gamma(K^+\eta'(958))/\Gamma(\eta'(958)\pi^+)$ Γ_{115}/Γ_{94}

VALUE (%)	EVTS	DOCUMENT ID		TECN	COMMENT
3.77±0.39±0.10	180 ± 19	WON	11	BELL	$e^+e^- \approx \Upsilon(4S)$

$\Gamma(K^+\eta'(958))/\Gamma(K^-2\pi^+)$ Γ_{115}/Γ_{43}

Unseen decay modes of the $\eta'(958)$ are included.

VALUE (units 10^{-2})	CL%	DOCUMENT ID		TECN	COMMENT
• • • We do not use the following data for averages, fits, limits, etc. • • •					
<0.20	90	MENDEZ	10	CLEO	e^+e^- at 3774 MeV

$\Gamma(K^+\pi^+\pi^-)/\Gamma(K^-2\pi^+)$ Γ_{116}/Γ_{43}

VALUE (units 10^{-3})	EVTS	DOCUMENT ID		TECN	COMMENT
5.77±0.22 OUR AVERAGE					
5.69±0.18±0.14	2638 ± 84	KO	09	BELL	e^+e^- at $\Upsilon(4S)$
6.5 ±0.8 ±0.4	189 ± 24	LINK	04F	FOCS	γ A, $\overline{E}_\gamma \approx 180$ GeV
7.7 ±1.7 ±0.8	59 ± 13	AITALA	97C	E791	π^- A, 500 GeV
7.2 ±2.3 ±1.7	21	FRABETTI	95E	E687	γBe, $\overline{E}_\gamma = 220$ GeV

$\Gamma(K^+\rho^0)/\Gamma(K^+\pi^+\pi^-)$ $\Gamma_{117}/\Gamma_{116}$

This is the "fit fraction" from the Dalitz-plot analysis.

VALUE	DOCUMENT ID		TECN	COMMENT
0.39 ±0.09 OUR AVERAGE				
0.3943±0.0787±0.0815	LINK	04F	FOCS	Dalitz fit, 189 evts
0.37 ±0.14 ±0.07	AITALA	97C	E791	Dalitz fit, 59 evts

$\Gamma(K^+ f_0(980), f_0(980) \to \pi^+\pi^-)/\Gamma(K^+\pi^+\pi^-)$ $\Gamma_{119}/\Gamma_{116}$

This is the "fit fraction" from the Dalitz-plot analysis.

VALUE	DOCUMENT ID		TECN	COMMENT
0.0892±0.0333±0.0412	LINK	04F	FOCS	Dalitz fit, 189 evts

$\Gamma(K^*(892)^0\pi^+, K^*(892)^0 \to K^+\pi^-)/\Gamma(K^+\pi^+\pi^-)$ $\Gamma_{118}/\Gamma_{116}$

This is the "fit fraction" from the Dalitz-plot analysis.

VALUE	DOCUMENT ID		TECN	COMMENT
0.47 ±0.08 OUR AVERAGE				
0.5220±0.0684±0.0638	LINK	04F	FOCS	Dalitz fit, 189 evts
0.35 ±0.14 ±0.01	AITALA	97C	E791	Dalitz fit, 59 evts

$\Gamma(K_2^*(1430)^0\pi^+, K_2^*(1430)^0 \to K^+\pi^-)/\Gamma(K^+\pi^+\pi^-)$ $\Gamma_{120}/\Gamma_{116}$

This is the "fit fraction" from the Dalitz-plot analysis.

VALUE	DOCUMENT ID		TECN	COMMENT
0.0803±0.0372±0.0391	LINK	04F	FOCS	Dalitz fit, 189 evts

$\Gamma(K^+\pi^+\pi^-\text{nonresonant})/\Gamma(K^+\pi^+\pi^-)$ $\Gamma_{121}/\Gamma_{116}$

This is the "fit fraction" from the Dalitz-plot analysis.

VALUE	DOCUMENT ID		TECN	COMMENT
• • • We do not use the following data for averages, fits, limits, etc. • • •				
0.36±0.14±0.07	[1] AITALA	97C	E791	Dalitz fit, 59 evts

[1] LINK 04F, with three times as many events, finds no need for a nonresonant amplitude.

$\Gamma(2K^+K^-)/\Gamma(K^-2\pi^+)$ Γ_{122}/Γ_{43}

VALUE (units 10^{-4})	EVTS	DOCUMENT ID		TECN	COMMENT
9.49±2.17±0.22	65	[1] LINK	02I	FOCS	γ nucleus, ≈ 180 GeV

[1] LINK 02I finds little evidence for ϕK^+ or $f_0(980)\,K^+$ submodes.

Rare or forbidden modes

$\Gamma(\pi^+e^+e^-)/\Gamma_{\text{total}}$ Γ_{123}/Γ

A test for the $\Delta C = 1$ weak neutral current. Allowed by higher-order electroweak interactions.

VALUE	CL%	DOCUMENT ID		TECN	COMMENT
$<1.1 \times 10^{-6}$	90	LEES	11G	BABR	$e^+e^- \approx \Upsilon(4S)$
• • • We do not use the following data for averages, fits, limits, etc. • • •					
$<5.9 \times 10^{-6}$	90	[1] RUBIN	10	CLEO	e^+e^- at $\psi(3770)$
$<7.4 \times 10^{-6}$	90	HE	05A	CLEO	See RUBIN 10
$<5.2 \times 10^{-5}$	90	AITALA	99G	E791	π^- N 500 GeV
$<1.1 \times 10^{-4}$	90	FRABETTI	97B	E687	γ Be, $\overline{E}_\gamma \approx 220$ GeV
$<6.6 \times 10^{-5}$	90	AITALA	96	E791	π^- N 500 GeV
$<2.5 \times 10^{-3}$	90	WEIR	90B	MRK2	e^+e^- 29 GeV
$<2.6 \times 10^{-3}$	90	HAAS	88	CLEO	e^+e^- 10 GeV

[1] This RUBIN 10 limit is for the e^+e^- mass in the continuum away from the $\phi(1020)$. See the next data block.

$\Gamma(\pi^+\phi, \phi \to e^+e^-)/\Gamma_{\text{total}}$ Γ_{124}/Γ

This is *not* a test for the $\Delta C = 1$ weak neutral current, but leads to the $\pi^+e^+e^-$ final state.

VALUE	EVTS	DOCUMENT ID		TECN	COMMENT
$(1.7^{+1.4}_{-0.9}\pm0.1) \times 10^{-6}$	4	[1] RUBIN	10	CLEO	e^+e^- at $\psi(3770)$
• • • We do not use the following data for averages, fits, limits, etc. • • •					
$(2.7^{+3.6}_{-1.8}\pm0.2) \times 10^{-6}$	2	HE	05A	CLEO	See RUBIN 10

[1] This RUBIN 10 result is consistent with the known $D^+ \to \phi\pi^+$ and $\phi \to e^+e^-$ fractions.

$\Gamma(\pi^+\mu^+\mu^-)/\Gamma_{\text{total}}$ Γ_{125}/Γ

A test for the $\Delta C = 1$ weak neutral current. Allowed by higher-order electroweak interactions.

VALUE	CL%	DOCUMENT ID		TECN	COMMENT
$<7.3 \times 10^{-8}$	90	AAIJ	13AF	LHCB	pp at 7 TeV
• • • We do not use the following data for averages, fits, limits, etc. • • •					
$<6.5 \times 10^{-6}$	90	LEES	11G	BABR	$e^+e^- \approx \Upsilon(4S)$
$<3.9 \times 10^{-6}$	90	[1] ABAZOV	08D	D0	$p\overline{p}$, $E_{\text{cm}} = 1.96$ TeV
$<8.8 \times 10^{-6}$	90	LINK	03F	FOCS	γ A, $\overline{E}_\gamma \approx 180$ GeV
$<1.5 \times 10^{-5}$	90	AITALA	99G	E791	π^- N 500 GeV
$<8.9 \times 10^{-5}$	90	FRABETTI	97B	E687	γ Be, $\overline{E}_\gamma \approx 220$ GeV
$<1.8 \times 10^{-5}$	90	AITALA	96	E791	π^- N 500 GeV
$<2.2 \times 10^{-4}$	90	KODAMA	95	E653	π^- emulsion 600 GeV
$<5.9 \times 10^{-3}$	90	WEIR	90B	MRK2	e^+e^- 29 GeV
$<2.9 \times 10^{-3}$	90	HAAS	88	CLEO	e^+e^- 10 GeV

[1] This ABAZOV 08D limit is for the $\mu^+\mu^-$ mass in the continuum away from the $\phi(1020)$. See the next data block.

$\Gamma(\pi^+\phi, \phi \to \mu^+\mu^-)/\Gamma_{\text{total}}$ Γ_{126}/Γ

This is *not* a test for the $\Delta C = 1$ weak neutral current, but leads to the $\pi^+\mu^+\mu^-$ final state.

VALUE	DOCUMENT ID		TECN	COMMENT
$(1.8\pm0.5\pm0.6) \times 10^{-6}$	[1] ABAZOV	08D	D0	$p\overline{p}$, $E_{\text{cm}} = 1.96$ TeV

[1] This ABAZOV 08D value is consistent with the known $D^+ \to \phi\pi^+$ and $\phi \to \mu^+\mu^-$ fractions.

$\Gamma(\rho^+\mu^+\mu^-)/\Gamma_{\text{total}}$ Γ_{127}/Γ

A test for the $\Delta C = 1$ weak neutral current. Allowed by higher-order electroweak interactions.

VALUE	CL%	DOCUMENT ID		TECN	COMMENT
$<5.6 \times 10^{-4}$	90	KODAMA	95	E653	π^- emulsion 600 GeV

$\Gamma(K^+e^+e^-)/\Gamma_{\text{total}}$ Γ_{128}/Γ

Both quarks would have to change flavor for this decay to occur.

VALUE	CL%	DOCUMENT ID		TECN	COMMENT
$<1.0 \times 10^{-6}$	90	LEES	11G	BABR	$e^+e^- \approx \Upsilon(4S)$
• • • We do not use the following data for averages, fits, limits, etc. • • •					
$<3.0 \times 10^{-6}$	90	RUBIN	10	CLEO	e^+e^- at $\psi(3770)$
$<6.2 \times 10^{-6}$	90	HE	05A	CLEO	See RUBIN 10
$<2.0 \times 10^{-4}$	90	AITALA	99G	E791	π^- N 500 GeV
$<2.0 \times 10^{-4}$	90	FRABETTI	97B	E687	γ Be, $\overline{E}_\gamma \approx 220$ GeV
$<4.8 \times 10^{-3}$	90	WEIR	90B	MRK2	e^+e^- 29 GeV

$\Gamma(K^+\mu^+\mu^-)/\Gamma_{\text{total}}$ Γ_{129}/Γ

Both quarks would have to change flavor for this decay to occur.

VALUE	CL%	DOCUMENT ID		TECN	COMMENT
$<4.3 \times 10^{-6}$	90	LEES	11G	BABR	$e^+e^- \approx \Upsilon(4S)$
• • • We do not use the following data for averages, fits, limits, etc. • • •					
$<9.2 \times 10^{-6}$	90	LINK	03F	FOCS	γ A, $\overline{E}_\gamma \approx 180$ GeV
$<4.4 \times 10^{-5}$	90	AITALA	99G	E791	π^- N 500 GeV
$<9.7 \times 10^{-5}$	90	FRABETTI	97B	E687	γ Be, $\overline{E}_\gamma \approx 220$ GeV
$<3.2 \times 10^{-4}$	90	KODAMA	95	E653	π^- emulsion 600 GeV
$<9.2 \times 10^{-3}$	90	WEIR	90B	MRK2	e^+e^- 29 GeV

$\Gamma(\pi^+e^+\mu^-)/\Gamma_{\text{total}}$ Γ_{130}/Γ

A test of lepton-family-number conservation.

VALUE	CL%	DOCUMENT ID		TECN	COMMENT
$<2.9 \times 10^{-6}$	90	LEES	11G	BABR	$e^+e^- \approx \Upsilon(4S)$
• • • We do not use the following data for averages, fits, limits, etc. • • •					
$<1.1 \times 10^{-4}$	90	FRABETTI	97B	E687	γ Be, $\overline{E}_\gamma \approx 220$ GeV
$<3.3 \times 10^{-3}$	90	WEIR	90B	MRK2	e^+e^- 29 GeV

$\Gamma(\pi^+e^-\mu^+)/\Gamma_{\text{total}}$ Γ_{131}/Γ

A test of lepton-family-number conservation.

VALUE	CL%	DOCUMENT ID		TECN	COMMENT
$<3.6 \times 10^{-6}$	90	LEES	11G	BABR	$e^+e^- \approx \Upsilon(4S)$
• • • We do not use the following data for averages, fits, limits, etc. • • •					
$<1.3 \times 10^{-4}$	90	FRABETTI	97B	E687	γ Be, $\overline{E}_\gamma \approx 220$ GeV
$<3.3 \times 10^{-3}$	90	WEIR	90B	MRK2	e^+e^- 29 GeV

$\Gamma(K^+e^+\mu^-)/\Gamma_{\text{total}}$ Γ_{132}/Γ

A test of lepton-family-number conservation.

VALUE	CL%	DOCUMENT ID		TECN	COMMENT
$<1.2 \times 10^{-6}$	90	LEES	11G	BABR	$e^+e^- \approx \Upsilon(4S)$
• • • We do not use the following data for averages, fits, limits, etc. • • •					
$<1.3 \times 10^{-4}$	90	FRABETTI	97B	E687	γ Be, $\overline{E}_\gamma \approx 220$ GeV
$<3.4 \times 10^{-3}$	90	WEIR	90B	MRK2	e^+e^- 29 GeV

Meson Particle Listings

$D^{\pm}$

$\Gamma(K^+ e^- \mu^+)/\Gamma_{total}$ Γ_{133}/Γ

A test of lepton-family-number conservation.

VALUE	CL%	DOCUMENT ID		TECN	COMMENT
$<2.8 \times 10^{-6}$	90	LEES	11G	BABR	$e^+e^- \approx \Upsilon(4S)$
• • • We do not use the following data for averages, fits, limits, etc. • • •					
$<1.2 \times 10^{-4}$	90	FRABETTI	97B	E687	γ Be, $\overline{E}_\gamma \approx$ 220 GeV
$<3.4 \times 10^{-3}$	90	WEIR	90B	MRK2	e^+e^- 29 GeV

$\Gamma(\pi^- 2e^+)/\Gamma_{total}$ Γ_{134}/Γ

A test of lepton-number conservation.

VALUE	CL%	DOCUMENT ID		TECN	COMMENT
$<1.1 \times 10^{-6}$	90	RUBIN	10	CLEO	e^+e^- at $\psi(3770)$
• • • We do not use the following data for averages, fits, limits, etc. • • •					
$<1.9 \times 10^{-6}$	90	LEES	11G	BABR	$e^+e^- \approx \Upsilon(4S)$
$<3.6 \times 10^{-6}$	90	HE	05A	CLEO	See RUBIN 10
$<9.6 \times 10^{-5}$	90	AITALA	99G	E791	π^- N 500 GeV
$<1.1 \times 10^{-4}$	90	FRABETTI	97B	E687	γ Be, $\overline{E}_\gamma \approx$ 220 GeV
$<4.8 \times 10^{-3}$	90	WEIR	90B	MRK2	e^+e^- 29 GeV

$\Gamma(\pi^- 2\mu^+)/\Gamma_{total}$ Γ_{135}/Γ

A test of lepton-number conservation.

VALUE	CL%	DOCUMENT ID		TECN	COMMENT
$<2.2 \times 10^{-8}$	90	AAIJ	13AF	LHCB	pp at 7 TeV
• • • We do not use the following data for averages, fits, limits, etc. • • •					
$<2.0 \times 10^{-6}$	90	LEES	11G	BABR	$e^+e^- \approx \Upsilon(4S)$
$<4.8 \times 10^{-6}$	90	LINK	03F	FOCS	γ A, $\overline{E}_\gamma \approx$ 180 GeV
$<1.7 \times 10^{-5}$	90	AITALA	99G	E791	π^- N 500 GeV
$<8.7 \times 10^{-5}$	90	FRABETTI	97B	E687	γ Be, $\overline{E}_\gamma \approx$ 220 GeV
$<2.2 \times 10^{-4}$	90	KODAMA	95	E653	π^- emulsion 600 GeV
$<6.8 \times 10^{-3}$	90	WEIR	90B	MRK2	e^+e^- 29 GeV

$\Gamma(\pi^- e^+ \mu^+)/\Gamma_{total}$ Γ_{136}/Γ

A test of lepton-number conservation.

VALUE	CL%	DOCUMENT ID		TECN	COMMENT
$<2.0 \times 10^{-6}$	90	LEES	11G	BABR	$e^+e^- \approx \Upsilon(4S)$
• • • We do not use the following data for averages, fits, limits, etc. • • •					
$<5.0 \times 10^{-5}$	90	AITALA	99G	E791	π^- N 500 GeV
$<1.1 \times 10^{-4}$	90	FRABETTI	97B	E687	γ Be, $\overline{E}_\gamma \approx$ 220 GeV
$<3.7 \times 10^{-3}$	90	WEIR	90B	MRK2	e^+e^- 29 GeV

$\Gamma(\rho^- 2\mu^+)/\Gamma_{total}$ Γ_{137}/Γ

A test of lepton-number conservation.

VALUE	CL%	DOCUMENT ID		TECN	COMMENT
$<5.6 \times 10^{-4}$	90	KODAMA	95	E653	π^- emulsion 600 GeV

$\Gamma(K^- 2e^+)/\Gamma_{total}$ Γ_{138}/Γ

A test of lepton-number conservation.

VALUE	CL%	DOCUMENT ID		TECN	COMMENT
$<0.9 \times 10^{-6}$	90	LEES	11G	BABR	$e^+e^- \approx \Upsilon(4S)$
• • • We do not use the following data for averages, fits, limits, etc. • • •					
$<3.5 \times 10^{-6}$	90	RUBIN	10	CLEO	e^+e^- at $\psi(3770)$
$<4.5 \times 10^{-6}$	90	HE	05A	CLEO	See RUBIN 10
$<1.2 \times 10^{-4}$	90	FRABETTI	97B	E687	γ Be, $\overline{E}_\gamma \approx$ 220 GeV
$<9.1 \times 10^{-3}$	90	WEIR	90B	MRK2	e^+e^- 29 GeV

$\Gamma(K^- 2\mu^+)/\Gamma_{total}$ Γ_{139}/Γ

A test of lepton-number conservation.

VALUE	CL%	DOCUMENT ID		TECN	COMMENT
$<10 \times 10^{-6}$	90	LEES	11G	BABR	$e^+e^- \approx \Upsilon(4S)$
• • • We do not use the following data for averages, fits, limits, etc. • • •					
$< 1.3 \times 10^{-5}$	90	LINK	03F	FOCS	γ A, $\overline{E}_\gamma \approx$ 180 GeV
$< 1.2 \times 10^{-4}$	90	FRABETTI	97B	E687	γ Be, $\overline{E}_\gamma \approx$ 220 GeV
$< 3.2 \times 10^{-4}$	90	KODAMA	95	E653	π^- emulsion 600 GeV
$< 4.3 \times 10^{-3}$	90	WEIR	90B	MRK2	e^+e^- 29 GeV

$\Gamma(K^- e^+ \mu^+)/\Gamma_{total}$ Γ_{140}/Γ

A test of lepton-number conservation.

VALUE	CL%	DOCUMENT ID		TECN	COMMENT
$<1.9 \times 10^{-6}$	90	LEES	11G	BABR	$e^+e^- \approx \Upsilon(4S)$
• • • We do not use the following data for averages, fits, limits, etc. • • •					
$<1.3 \times 10^{-4}$	90	FRABETTI	97B	E687	γ Be, $\overline{E}_\gamma \approx$ 220 GeV
$<4.0 \times 10^{-3}$	90	WEIR	90B	MRK2	e^+e^- 29 GeV

$\Gamma(K^*(892)^- 2\mu^+)/\Gamma_{total}$ Γ_{141}/Γ

A test of lepton-number conservation.

VALUE	CL%	DOCUMENT ID		TECN	COMMENT
$<8.5 \times 10^{-4}$	90	KODAMA	95	E653	π^- emulsion 600 GeV

$D^{\pm}$ CP-VIOLATING DECAY-RATE ASYMMETRIES

This is the difference between D^+ and D^- partial widths for the decay to state f, divided by the sum of the widths:
$A_{CP}(f) = [\Gamma(D^+ \to f) - \Gamma(D^- \to \overline{f})]/[\Gamma(D^+ \to f) + \Gamma(D^- \to \overline{f})]$.

$A_{CP}(\mu^{\pm}\nu)$ in $D^+ \to \mu^+\nu_\mu$, $D^- \to \mu^-\overline{\nu}_\mu$

VALUE (%)	DOCUMENT ID		TECN	COMMENT
$+8 \pm 8$	EISENSTEIN	08	CLEO	e^+e^- at $\psi(3770)$

$A_{CP}(K^0_L e^{\pm}\nu)$ in $D^+ \to K^0_L e^+\nu_e$, $D^- \to K^0_L e^-\overline{\nu}_e$

VALUE (%)	DOCUMENT ID		TECN	COMMENT
$-0.59 \pm 0.60 \pm 1.48$	ABLIKIM	15AF	BES3	e^+e^- 3773 MeV

$A_{CP}(K^0_S \pi^{\pm})$ in $D^{\pm} \to K^0_S \pi^{\pm}$

VALUE (%)	EVTS	DOCUMENT ID		TECN	COMMENT
-0.41 ± 0.09 OUR AVERAGE					
$-1.1 \pm 0.6 \pm 0.2$		BONVICINI	14	CLEO	All CLEO-c runs
$-0.363 \pm 0.094 \pm 0.067$	1738k	[1] KO	12A	BELL	$e^+e^- \approx \Upsilon$(nS)
$-0.44 \pm 0.13 \pm 0.10$	807k	DEL-AMO-SA..	11H	BABR	$e^+e^- \approx \Upsilon(4S)$
$-1.6 \pm 1.5 \pm 0.9$	10.6k	[2] LINK	02B	FOCS	γ nucleus, $\overline{E}_\gamma \approx$ 180 GeV
• • • We do not use the following data for averages, fits, limits, etc. • • •					
$-0.71 \pm 0.19 \pm 0.20$		KO	10	BELL	See KO 12A
$-1.3 \pm 0.7 \pm 0.3$	30k	MENDEZ	10	CLEO	See BONVICINI 14
$-0.6 \pm 1.0 \pm 0.3$		DOBBS	07	CLEO	See MENDEZ 10

[1] KO 12A finds that after subtracting the contribution due to $K^0 - \overline{K}^0$ mixing, the CP asymmetry due to the change of charm is $(-0.024 \pm 0.094 \pm 0.067)$%, consistent with zero.

[2] LINK 02B measures $N(D^+ \to K^0_S \pi^+)/N(D^+ \to K^-\pi^+\pi^+)$, the ratio of numbers of events observed, and similarly for the D^-.

$A_{CP}(K^{\mp}2\pi^{\pm})$ in $D^+ \to K^-2\pi^+$, $D^- \to K^+2\pi^-$

VALUE (%)	EVTS	DOCUMENT ID		TECN	COMMENT
-0.18 ± 0.16 OUR AVERAGE					
$-0.16 \pm 0.15 \pm 0.09$	2.3M	ABAZOV	14L	D0	$p\overline{p}$, $\sqrt{s} = 1.96$ TeV
$-0.3 \pm 0.2 \pm 0.4$		BONVICINI	14	CLEO	All CLEO-c runs
• • • We do not use the following data for averages, fits, limits, etc. • • •					
$-0.1 \pm 0.4 \pm 0.9$	231k	MENDEZ	10	CLEO	See BONVICINI 14
$-0.5 \pm 0.4 \pm 0.9$		DOBBS	07	CLEO	See MENDEZ 10

$A_{CP}(K^{\mp}\pi^{\pm}\pi^{\pm}\pi^0)$ in $D^+ \to K^-\pi^+\pi^+\pi^0$, $D^- \to K^+\pi^-\pi^-\pi^0$

VALUE (%)	DOCUMENT ID		TECN	COMMENT
$-0.3 \pm 0.6 \pm 0.4$	BONVICINI	14	CLEO	All CLEO-c runs
• • • We do not use the following data for averages, fits, limits, etc. • • •				
$1.0 \pm 0.9 \pm 0.9$	DOBBS	07	CLEO	See BONVICINI 14

$A_{CP}(K^0_S \pi^{\pm}\pi^0)$ in $D^+ \to K^0_S\pi^+\pi^0$, $D^- \to K^0_S\pi^-\pi^0$

VALUE (%)	DOCUMENT ID		TECN	COMMENT
$-0.1 \pm 0.7 \pm 0.2$	BONVICINI	14	CLEO	All CLEO-c runs
• • • We do not use the following data for averages, fits, limits, etc. • • •				
$0.3 \pm 0.9 \pm 0.3$	DOBBS	07	CLEO	See BONVICINI 14

$A_{CP}(K^0_S \pi^+\pi^+\pi^-)$ in $D^+ \to K^0_S\pi^+\pi^+\pi^-$, $D^- \to K^0_S\pi^-\pi^-\pi^+$

VALUE (%)	DOCUMENT ID		TECN	COMMENT
$0.0 \pm 1.2 \pm 0.3$	BONVICINI	14	CLEO	All CLEO-c runs
• • • We do not use the following data for averages, fits, limits, etc. • • •				
$0.1 \pm 1.1 \pm 0.6$	DOBBS	07	CLEO	See BONVICINI 14

$A_{CP}(\pi^{\pm}\pi^0)$ in $D^{\pm} \to \pi^{\pm}\pi^0$

VALUE (%)	EVTS	DOCUMENT ID		TECN	COMMENT
2.4 ± 1.2 OUR AVERAGE					
$2.31 \pm 1.24 \pm 0.23$	108k	BABU	18	BELL	At/near $\Upsilon(4S)$, $\Upsilon(5S)$
$2.9 \pm 2.9 \pm 0.3$	2.6k	MENDEZ	10	CLEO	e^+e^- at 3774 MeV

$A_{CP}(\pi^{\pm}\eta)$ in $D^{\pm} \to \pi^{\pm}\eta$

VALUE (%)	EVTS	DOCUMENT ID		TECN	COMMENT
1.0 ± 1.5 OUR AVERAGE Error includes scale factor of 1.4.					
$+1.74 \pm 1.13 \pm 0.19$		WON	11	BELL	$e^+e^- \approx \Upsilon(4S)$
$-2.0 \pm 2.3 \pm 0.3$	2.9k	MENDEZ	10	CLEO	e^+e^- at 3774 MeV

$A_{CP}(\pi^{\pm}\eta'(958))$ in $D^{\pm} \to \pi^{\pm}\eta'(958)$

VALUE (%)	EVTS	DOCUMENT ID		TECN	COMMENT
-0.6 ± 0.7 OUR AVERAGE					
$-0.61 \pm 0.72 \pm 0.54$	63k	AAIJ	17AF	LHCB	pp at 7, 8 TeV
$-0.12 \pm 1.12 \pm 0.17$		WON	11	BELL	$e^+e^- \approx \Upsilon(4S)$
$-4.0 \pm 3.4 \pm 0.3$	1.0k	MENDEZ	10	CLEO	e^+e^- at 3774 MeV

$A_{CP}(\overline{K}^0/K^0 K^{\pm})$ in $D^+ \to \overline{K}^0 K^+$, $D^- \to K^0 K^-$

VALUE (%)	EVTS	DOCUMENT ID		TECN	COMMENT
0.11 ± 0.17 OUR AVERAGE					
$0.03 \pm 0.17 \pm 0.14$	1.0M	[1] AAIJ	14BD	LHCB	pp at 7, 8 TeV
$0.08 \pm 0.28 \pm 0.14$	277k	KO	13	BELL	e^+e^- at $\Upsilon(4S)$
$0.46 \pm 0.36 \pm 0.25$	159k	LEES	13E	BABR	e^+e^- at $\Upsilon(4S)$

[1] AAIJ 14BD reports its result as $A_{CP}(D^{\pm} \to K^0_S \pi^{\pm})$ with *CP*-violation effects in the $K^0 - \overline{K}^0$ system subtracted. It also measures $A_{CP}(D^{\pm} \to \overline{K}^0/K^0 K^{\pm}) + A_{CP}(D^{\pm}_s \to \overline{K}^0/K^0 \pi^{\pm}) = (0.41 \pm 0.49 \pm 0.26)\%$.

$A_{CP}(K^0_S K^{\pm})$ in $D^{\pm} \to K^0_S K^{\pm}$

VALUE (%)	EVTS	DOCUMENT ID		TECN	COMMENT
−0.11±0.25 OUR AVERAGE					
−0.25±0.28±0.14	277k	KO	13	BELL	e^+e^- at Υ(nS)
0.13±0.36±0.25	159k	LEES	13E	BABR	e^+e^- at $\Upsilon(4S)$
−0.2 ±1.5 ±0.9	5.2k	MENDEZ	10	CLEO	e^+e^- at 3774 MeV
7.1 ±6.1 ±1.2	949	[1] LINK	02B	FOCS	γ nucleus, $\overline{E}_\gamma \approx 180$ GeV
• • • We do not use the following data for averages, fits, limits, etc. • • •					
−0.16±0.58±0.25		KO	10	BELL	$e^+e^- \approx \Upsilon(4S)$
6.9 ±6.0 ±1.5	949	[2] LINK	02B	FOCS	γ nucleus, $\overline{E}_\gamma \approx 180$ GeV

[1] LINK 02B measures $N(D^+ \to K^0_S K^+)/N(D^+ \to K^0_S \pi^+)$, the ratio of numbers of events observed, and similarly for the D^-.

[2] LINK 02B measures $N(D^+ \to K^0_S K^+)/N(D^+ \to K^-\pi^+\pi^+)$, the ratio of numbers of events observed, and similarly for the D^-.

$A_{CP}(K^+K^-\pi^{\pm})$ in $D^{\pm} \to K^+K^-\pi^{\pm}$

See also AAIJ 11G for a search for *CP* asymmetry in the $D^{\pm} \to K^+K^-\pi^{\pm}$ Dalitz plots using 370k decays and four different binning schemes. No evidence for *CP* asymmetry was found.

VALUE (%)	EVTS	DOCUMENT ID		TECN	COMMENT
0.37±0.29 OUR AVERAGE					
0.37±0.30±0.15	224k	[1] LEES	13F	BABR	e^+e^- at $\Upsilon(4S)$
−0.03±0.84±0.29		RUBIN	08	CLEO	e^+e^- at 3774 MeV
1.4 ±1.0 ±0.8	43k	[2] AUBERT	05S	BABR	e^+e^- at $\Upsilon(4S)$
0.6 ±1.1 ±0.5	14k	[3] LINK	00B	FOCS	
−1.4 ±2.9		[3] AITALA	97B	E791	$-0.062 < A_{CP} < +0.034$ (90% CL)
−3.1 ±6.8		[3] FRABETTI	94I	E687	$-0.14 < A_{CP} < +0.081$ (90% CL)
• • • We do not use the following data for averages, fits, limits, etc. • • •					
−0.1 ±0.9 ±0.4		[4] BONVICINI	14	CLEO	See RUBIN 08
−0.1 ±1.5 ±0.8		DOBBS	07	CLEO	See BONVICINI 14 and RUBIN 08

[1] This is the integrated *CP* asymmetry. LEES 13F also searches for *CP* asymmetries in four regions of the Dalitz plots (two of which are listed below); in comparisons of binned D^+ and D^- Dalitz plots; in parametrized fits to those plots, including 2-body submodes; and in comparisons of Legendre-polynomial distributions for the K^+K^- and $K^-\pi^+$ systems.

[2] AUBERT 05S measures $N(D^+ \to K^+K^-\pi^+)/N(D^+_s \to K^+K^-\pi^+)$, the ratio of the numbers of events observed, and similarly for the D^-.

[3] FRABETTI 94I, AITALA 98C, and LINK 00B measure $N(D^+ \to K^-K^+\pi^+)/N(D^+ \to K^-\pi^+\pi^+)$, the ratio of numbers of events observed, and similarly for the D^-.

[4] RUBIN 08 performs a dedicated analysis of this decay mode on the same dataset, with slightly better precision. We therefore take it that BONVICINI 14 does not supersede RUBIN 08's A_{CP} result.

$A_{CP}(K^{\pm}K^{*0})$ in $D^+ \to K^+\overline{K}^{*0}$, $D^- \to K^-K^{*0}$

VALUE (%)	EVTS	DOCUMENT ID		TECN	COMMENT
− 0.3± 0.4 OUR AVERAGE					
− 0.3± 0.4±0.2	73k	[1] LEES	13F	BABR	e^+e^- at $\Upsilon(4S)$
− 0.4± 2.0±0.6		RUBIN	08	CLEO	Fit-fraction asymmetry
+ 0.9± 1.7±0.7	11k	[2] AUBERT	05S	BABR	e^+e^- at $\Upsilon(4S)$
− 1.0± 5.0		[3] AITALA	97B	E791	$-0.092 < A_{CP} < +0.072$ (90% CL)
−12 ±13		[3] FRABETTI	94I	E687	$-0.33 < A_{CP} < +0.094$ (90% CL)

[1] This LEES 13F result is for the $K^{\mp}\pi^{\pm}$ mass-squared between 0.4 and 1.0 GeV^2, and does not actually separate out the K^*.

[2] AUBERT 05S measures $N(D^+ \to K^+\overline{K}^{*0})/N(D^+_s \to K^+K^-\pi^+)$, the ratio of the numbers of events observed, and similarly for the D^-.

[3] FRABETTI 94I and AITALA 97B measure $N(D^+ \to K^+\overline{K}^*(892)^0)/N(D^+ \to K^-\pi^+\pi^+)$, the ratio of numbers of events observed, and similarly for the D^-.

$A_{CP}(\phi\pi^{\pm})$ in $D^{\pm} \to \phi\pi^{\pm}$

VALUE (%)	EVTS	DOCUMENT ID		TECN	COMMENT
0.09±0.19 OUR AVERAGE Error includes scale factor of 1.2.					
−0.04±0.14±0.14	1.58M	AAIJ	13W	LHCB	pp at 7 TeV
−0.3 ±0.3 ±0.5	97k	[1] LEES	13F	BABR	e^+e^- at $\Upsilon(4S)$
+0.51±0.28±0.05	237k	STARIC	12	BELL	Mainly at $\Upsilon(4S)$
−1.8 ±1.6 $^{+0.2}_{-0.4}$		RUBIN	08	CLEO	Fit-fraction asymmetry
+0.2 ±1.5 ±0.6	10k	[2] AUBERT	05S	BABR	e^+e^- at $\Upsilon(4S)$
−2.8 ±3.6		[3] AITALA	97B	E791	$-0.087 < A_{CP} < +0.031$ (90% CL)
+6.6 ±8.6		[3] FRABETTI	94I	E687	$-0.075 < A_{CP} < +0.21$ (90% CL)

[1] This LEES 13F result is for the K^+K^- mass-squared less than 1.3 GeV^2 and the $K^{\mp}\pi^{\pm}$ mass-squared above 1.0 GeV^2, and does not actually separate out the ϕ.

[2] AUBERT 05S measures $N(D^+ \to \phi\pi^+)/N(D^+_s \to K^+K^-\pi^+)$, the ratio of the numbers of events observed, and similarly for the D^-.

[3] FRABETTI 94I and AITALA 97B measure $N(D^+ \to \phi\pi^+)/N(D^+ \to K^-\pi^+\pi^+)$, the ratio of numbers of events observed, and similarly for the D^-.

$A_{CP}(K^{\pm}K^*_0(1430)^0)$ in $D^+ \to K^+\overline{K}^*_0(1430)^0$, $D^- \to K^-K^*_0(1430)^0$

VALUE (%)	DOCUMENT ID		TECN	COMMENT
$+8 \pm 6^{+4}_{-2}$	RUBIN	08	CLEO	Fit-fraction asymmetry

$A_{CP}(K^{\pm}K^*_2(1430)^0)$ in $D^+ \to K^+\overline{K}^*_2(1430)^0$, $D^- \to K^-K^*_2(1430)^0$

VALUE (%)	DOCUMENT ID		TECN	COMMENT
$+43 \pm 19^{+5}_{-18}$	RUBIN	08	CLEO	Fit-fraction asymmetry

$A_{CP}(K^{\pm}K^*_0(700))$ in $D^+ \to K^+\overline{K}^*_0(700)$, $D^- \to K^-K^*_0(700)$

VALUE (%)	DOCUMENT ID		TECN	COMMENT
$-12 \pm 11^{+14}_{-6}$	RUBIN	08	CLEO	Fit-fraction asymmetry

$A_{CP}(a_0(1450)^0\pi^{\pm})$ in $D^{\pm} \to a_0(1450)^0\pi^{\pm}$

VALUE (%)	DOCUMENT ID		TECN	COMMENT
$-19 \pm 12^{+8}_{-11}$	RUBIN	08	CLEO	Fit-fraction asymmetry

$A_{CP}(\phi(1680)\pi^{\pm})$ in $D^{\pm} \to \phi(1680)\pi^{\pm}$

VALUE (%)	DOCUMENT ID		TECN	COMMENT
−9±22±14	RUBIN	08	CLEO	Fit-fraction asymmetry

$A_{CP}(\pi^+\pi^-\pi^{\pm})$ in $D^{\pm} \to \pi^+\pi^-\pi^{\pm}$

See also AAIJ 14C for a search for *CP* violation in $D^{\pm} \to \pi^+\pi^-\pi^{\pm}$ Dalitz plots using model-independent binned and unbinned methods. No evidence was found.

VALUE (%)	DOCUMENT ID		TECN	COMMENT
−1.7±4.2	[1] AITALA	97B	E791	$-0.086 < A_{CP} < +0.052$ (90% CL)

[1] AITALA 97B measure $N(D^+ \to \pi^+\pi^-\pi^+)/N(D^+ \to K^-\pi^+\pi^+)$, the ratio of numbers of events observed, and similarly for the D^-.

$A_{CP}(K^0_S K^{\pm}\pi^+\pi^-)$ in $D^{\pm} \to K^0_S K^{\pm}\pi^+\pi^-$

VALUE (%)	EVTS	DOCUMENT ID		TECN	COMMENT
−4.2±6.4±2.2	523 ± 32	LINK	05E	FOCS	γ A, $\overline{E}_\gamma \approx 180$ GeV

$A_{CP}(K^{\pm}\pi^0)$ in $D^{\pm} \to K^{\pm}\pi^0$

VALUE (%)	EVTS	DOCUMENT ID		TECN	COMMENT
−3.5±10.7±0.9	343 ± 37	MENDEZ	10	CLEO	e^+e^- at 3774 MeV

$D^{\pm}$ χ^2 TESTS OF *CP*-VIOLATION (*CPV*)

We list model-independent searches for local *CP* violation in phase-space distributions of multi-body decays.

Most of these searches divide phase space (Dalitz plot for 3-body decays, five-dimensional equivalent for 4-body decays) into bins, and perform a χ^2 test comparing normalised yields N_i, $\overline{N}_i$ in *CP*-conjugate bin pairs i: $\chi^2 = \Sigma_i (N_i - \alpha\,\overline{N}_i)/\sigma(N_i - \alpha\,\overline{N}_i)$. The factor $\alpha = (\Sigma_i N_i)/(\Sigma_i \overline{N}_i)$ removes the dependence on phase-space-integrated rate asymmetries. The result is used to obtain the probability (p-value) to obtain the measured χ^2 or larger under the assumption of CP conservation [AUBERT 08AO, BEDIAGA 09]. Alternative methods obtain p-values from other test variables based on unbinned analyses [WILLIAMS 11, AAIJ 14C]. Results can be combined using Fisher's method [MOSTELLER 48].

Local *CPV* in $D^{\pm} \to \pi^+\pi^-\pi^{\pm}$

p-value (%)	EVTS	DOCUMENT ID		TECN	COMMENT
78.1	3.1M	[1] AAIJ	14C	LHCB	χ^2

[1] AAIJ 14C uses binned and unbinned methods, and finds slightly better sensitivity with the former. We took the first value in the table of results for the binned method.

Local *CPV* in $D^{\pm} \to K^+K^-\pi^{\pm}$

p-value (%)	EVTS	DOCUMENT ID		TECN	COMMENT
31 OUR EVALUATION					
72	224k	LEES	13F	BABR	χ^2
12.7	370k	[1] AAIJ	11G	LHCB	χ^2

[1] AAIJ 11G publishes results for several binning schemes. We picked the first value in their table of results.

CP VIOLATING ASYMMETRIES OF *P*-ODD (*T*-ODD) MOMENTS

$A_{Tviol}(K^0_S K^{\pm}\pi^+\pi^-)$ in $D^{\pm} \to K^0_S K^{\pm}\pi^+\pi^-$

$C_T \equiv \vec{p}_{K^+} \cdot (\vec{p}_{\pi^+} \times \vec{p}_{\pi^-})$ is a parity-odd correlation of the K^+, π^+, and π^- momenta for the D^+. $\overline{C}_T \equiv \vec{p}_{K^-} \cdot (\vec{p}_{\pi^-} \times \vec{p}_{\pi^+})$ is the corresponding quantity for the D^-. Then

$A_T \equiv [\Gamma(C_T > 0) - \Gamma(C_T < 0)] \,/\, [\Gamma(C_T > 0) + \Gamma(C_T < 0)]$, and

$\overline{A}_T \equiv [\Gamma(-\overline{C}_T > 0) - \Gamma(-\overline{C}_T < 0)] \,/\, [\Gamma(-\overline{C}_T > 0) + \Gamma(-\overline{C}_T < 0)]$, and

$A_{Tviol} \equiv \frac{1}{2}(A_T - \overline{A}_T)$. C_T and $\overline{C}_T$ are commonly referred to as *T*-odd moments, because they are odd under *T* reversal. However, the *T*-conjugate process $K^0_S K^{\pm}\pi^+\pi^- \to D^{\pm}$ is not accessible, while the *P*-conjugate process is.

Meson Particle Listings

$D^{\pm}$

VALUE (units 10^{-3})	EVTS	DOCUMENT ID		TECN	COMMENT
−12.0±10.0± 4.6	21.2±0.4k	LEES	11E	BABR	$e^+e^- \approx \Upsilon(4S)$
• • • We do not use the following data for averages, fits, limits, etc. • • •					
23 ±62 ±22	523 ± 32	LINK	05E	FOCS	γ A, $\overline{E}_\gamma \approx 180$ GeV

$D^+ \to (\overline{K}^0/\pi^0/\eta/\omega/\rho^0/\overline{K}^{*0})\ell^+\nu_\ell$ FORM FACTORS

$f_+(0)|V_{cs}|$ in $D^+ \to \overline{K}^0\ell^+\nu_\ell$

VALUE	DOCUMENT ID		TECN	COMMENT
0.719 ±0.011 OUR AVERAGE	Error includes scale factor of 1.6. See the ideogram below.			
0.7053±0.0040±0.0112	ABLIKIM	17S	BES3	$K^0_S e^+\nu_e$ 2-parameter fit
0.737 ±0.006 ±0.009	[1] ABLIKIM	15AF	BES3	$K_L e^+\nu_e$ 3-parameter fit
0.707 ±0.010 ±0.009	[2] BESSON	09	CLEO	$K_S e^+\nu_e$ 3-parameter fit

[1] ABLIKIM 15AF finds 0.728 ± 0.006 ± 0.011 for a 2-parameter fit.
[2] BESSON 09 finds 0.716 ± 0.007 ± 0.009 for a 2-parameter fit.

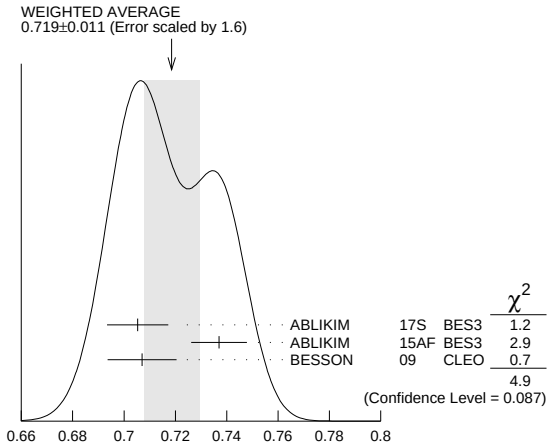

$f_+(0)|V_{cs}|$ in $D^+ \to \overline{K}^0\ell^+\nu_\ell$

$r_1 \equiv a_1/a_0$ in $D^+ \to \overline{K}^0\ell^+\nu_\ell$

VALUE	EVTS	DOCUMENT ID		TECN	COMMENT
−2.13±0.14 OUR AVERAGE					
−2.18±0.14±0.05		ABLIKIM	17S	BES3	$K^0_S e^+\nu_e$ 2-parameter fit
−2.23±0.42±0.53	40k	[1] ABLIKIM	15AF	BES3	$K_L e^+\nu_e$ 3-parameter fit
−1.66±0.44±0.10		[2] BESSON	09	CLEO	$K_S e^+\nu_e$ 3-parameter fit

[1] ABLIKIM 15AF finds $r_1 = -1.91 \pm 0.33 \pm 0.28$ for a 2-parameter fit.
[2] BESSON 09 finds $r_1 = -2.10 \pm 0.25 \pm 0.08$ for 2-parameter fit.

$r_2 \equiv a_2/a_0$ in $D^+ \to \overline{K}^0\ell^+\nu_\ell$

VALUE	EVTS	DOCUMENT ID		TECN	COMMENT
− 3±12 OUR AVERAGE	Error includes scale factor of 1.5.				
+11± 9±9	40k	ABLIKIM	15AF	BES3	$K_L e^+\nu_e$ 3-parameter fit
−14±11±1		BESSON	09	CLEO	$K_S e^+\nu_e$ 3-parameter fit

$f_+(0)|V_{cd}|$ in $D^+ \to \pi^0\ell^+\nu_\ell$

VALUE	DOCUMENT ID		TECN	COMMENT
0.1407±0.0025 OUR AVERAGE				
0.1400±0.0026±0.0007	ABLIKIM	17S	BES3	$\pi^0 e^+\nu_e$ 2-parameter fit
0.146 ±0.007 ±0.002	BESSON	09	CLEO	$\pi^0 e^+\nu_e$ 3-parameter fit

$r_1 \equiv a_1/a_0$ in $D^+ \to \pi^0\ell^+\nu_\ell$

VALUE	DOCUMENT ID		TECN	COMMENT
−2.00±0.13 OUR AVERAGE				
−2.01±0.13±0.02	ABLIKIM	17S	BES3	$\pi^0 e^+\nu_e$ 2-parameter fit
−1.37±0.88±0.24	BESSON	09	CLEO	$\pi^0 e^+\nu_e$ 3-parameter fit

$r_2 \equiv a_2/a_0$ in $D^+ \to \pi^0\ell^+\nu_\ell$

VALUE	DOCUMENT ID		TECN	COMMENT
−4±5±1	BESSON	09	CLEO	$\pi^0 e^+\nu_e$ 3-parameter fit

$f_+(0)|V_{cd}|$ in $D^+ \to \eta e^+\nu_e$

VALUE	DOCUMENT ID		TECN	COMMENT
0.086±0.006±0.001	YELTON	11	CLEO	z expansion

$r_1 \equiv a_1/a_0$ in $D^+ \to \eta e^+\nu_e$

VALUE	DOCUMENT ID		TECN	COMMENT
−1.83±2.23±0.28	YELTON	11	CLEO	z expansion

$r_v \equiv V(0)/A_1(0)$ in $D^+ \to \omega e^+\nu_e$

VALUE	DOCUMENT ID		TECN	COMMENT
1.24±0.09±0.06	ABLIKIM	15W	BES3	292 fb^{-1}, 3773 MeV

$r_2 \equiv A_2(0)/A_1(0)$ in $D^+ \to \omega e^+\nu_e$

VALUE	DOCUMENT ID		TECN	COMMENT
1.06±0.15±0.05	ABLIKIM	15W	BES3	292 fb^{-1}, 3773 MeV

$r_v \equiv V(0)/A_1(0)$ in $D^+, D^0 \to \rho e^+\nu_e$

VALUE	DOCUMENT ID		TECN	COMMENT
1.48±0.15±0.05	[1] DOBBS	13	CLEO	e^+e^- at $\psi(3770)$

[1] Uses both D^+ and D^0 events. Using PDG 10 values of V_{cd} and lifetimes, DOBBS 13 gets $A_1(0) = 0.56 \pm 0.01^{+0.02}_{-0.03}$, $A_2(0) = 0.47 \pm 0.06 \pm 0.04$, and $V(0) = 0.84 \pm 0.09^{+0.05}_{-0.06}$.

$r_2 \equiv A_2(0)/A_1(0)$ in $D^+, D^0 \to \rho e^+\nu_e$

VALUE	DOCUMENT ID		TECN	COMMENT
0.83±0.11±0.04	[1] DOBBS	13	CLEO	e^+e^- at $\psi(3770)$

[1] Uses both D^+ and D^0 events. Using PDG 10 values of V_{cd} and lifetimes, DOBBS 13 gets $A_1(0) = 0.56 \pm 0.01^{+0.02}_{-0.03}$, $A_2(0) = 0.47 \pm 0.06 \pm 0.04$, and $V(0) = 0.84 \pm 0.09^{+0.05}_{-0.06}$.

$r_v \equiv V(0)/A_1(0)$ in $D^+ \to \overline{K}^*(892)^0\ell^+\nu_\ell$

See also BRIERE 10 for $\overline{K}^*\ell^+\nu_\ell$ helicity-basis form-factor measurements.

VALUE	EVTS	DOCUMENT ID		TECN	COMMENT
1.49 ±0.05 OUR AVERAGE		Error includes scale factor of 2.1. See the ideogram below.			
1.411±0.058±0.007	16.2k	ABLIKIM	16F	BES3	$\overline{K}^*(892)^0 e^+\nu_e$
1.463±0.017±0.031		[1] DEL-AMO-SA...	11I	BABR	
1.504±0.057±0.039	15k	[2] LINK	02L	FOCS	$\overline{K}^*(892)^0\mu^+\nu_\mu$
1.45 ±0.23 ±0.07	763	ADAMOVICH	99	BEAT	$\overline{K}^*(892)^0\mu^+\nu_\mu$
1.90 ±0.11 ±0.09	3000	[3] AITALA	98B	E791	$\overline{K}^*(892)^0 e^+\nu_e$
1.84 ±0.11 ±0.09	3034	AITALA	98F	E791	$\overline{K}^*(892)^0\mu^+\nu_\mu$
1.74 ±0.27 ±0.28	874	FRABETTI	93E	E687	$\overline{K}^*(892)^0\mu^+\nu_\mu$
2.00 $^{+0.34}_{-0.32}$ ±0.16	305	KODAMA	92	E653	$\overline{K}^*(892)^0\mu^+\nu_\mu$
• • • We do not use the following data for averages, fits, limits, etc. • • •					
2.0 ±0.6 ±0.3	183	ANJOS	90E	E691	$\overline{K}^*(892)^0 e^+\nu_e$

[1] DEL-AMO-SANCHEZ 11I finds the pole mass $m_A = (2.63 \pm 0.10 \pm 0.13)$ GeV (m_V is fixed at 2 GeV).
[2] LINK 02L includes the effects of interference with an S-wave background. This much improves the goodness of fit, but does not much shift the values of the form factors.
[3] This is slightly different from the AITALA 98B value: see ref. [5] in AITALA 98F.

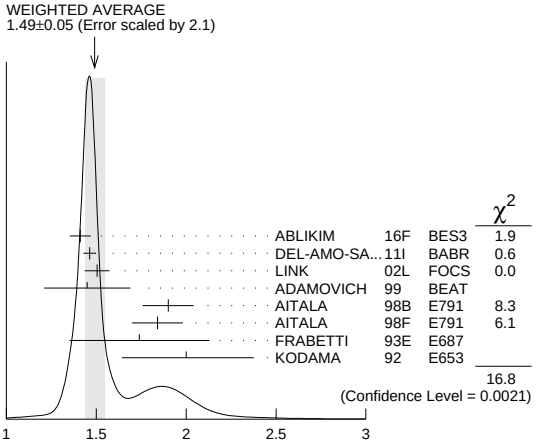

$r_v \equiv V(0)/A_1(0)$ in $D^+ \to \overline{K}^*(892)^0\ell^+\nu_\ell$

$r_2 \equiv A_2(0)/A_1(0)$ in $D^+ \to \overline{K}^*(892)^0\ell^+\nu_\ell$

See also BRIERE 10 for $\overline{K}^*\ell^+\nu_\ell$ helicity-basis form-factor measurements.

VALUE	EVTS	DOCUMENT ID		TECN	COMMENT
0.802±0.021 OUR AVERAGE					
0.788±0.042±0.008	16.2k	ABLIKIM	16F	BES3	$\overline{K}^*(892)^0 e^+\nu_e$
0.801±0.020±0.020		[1] DEL-AMO-SA...	11I	BABR	
0.875±0.049±0.064	15k	[2] LINK	02L	FOCS	$\overline{K}^*(892)^0\mu^+\nu_\mu$
1.00 ±0.15 ±0.03	763	ADAMOVICH	99	BEAT	$\overline{K}^*(892)^0\mu^+\nu_\mu$
0.71 ±0.08 ±0.09	3000	AITALA	98B	E791	$\overline{K}^*(892)^0 e^+\nu_e$
0.75 ±0.08 ±0.09	3034	AITALA	98F	E791	$\overline{K}^*(892)^0\mu^+\nu_\mu$
0.78 ±0.18 ±0.10	874	FRABETTI	93E	E687	$\overline{K}^*(892)^0\mu^+\nu_\mu$
0.82 $^{+0.22}_{-0.23}$ ±0.11	305	KODAMA	92	E653	$\overline{K}^*(892)^0\mu^+\nu_\mu$
• • • We do not use the following data for averages, fits, limits, etc. • • •					
0.0 ±0.5 ±0.2	183	ANJOS	90E	E691	$\overline{K}^*(892)^0 e^+\nu_e$

[1] DEL-AMO-SANCHEZ 11I finds the pole mass $m_A = (2.63 \pm 0.10 \pm 0.13)$ GeV (m_V is fixed at 2 GeV).
[2] LINK 02L includes the effects of interference with an S-wave background. This much improves the goodness of fit, but does not much shift the values of the form factors.

$r_3 \equiv A_3(0)/A_1(0)$ in $D^+ \to \overline{K}^*(892)^0 \ell^+ \nu_\ell$

See also BRIERE 10 for $\overline{K}^* \ell^+ \nu_\ell$ helicity-basis form-factor measurements.

VALUE	EVTS	DOCUMENT ID		TECN	COMMENT
0.04±0.33±0.29	3034	AITALA	98F	E791	$\overline{K}^*(892)^0 \mu^+ \nu_\mu$

Γ_L/Γ_T in $D^+ \to \overline{K}^*(892)^0 \ell^+ \nu_\ell$

See also BRIERE 10 for $\overline{K}^* \ell^+ \nu_\ell$ helicity-basis form-factor measurements.

VALUE	EVTS	DOCUMENT ID		TECN	COMMENT
1.13±0.08 OUR AVERAGE					
1.09±0.10±0.02	763	ADAMOVICH	99	BEAT	$\overline{K}^*(892)^0 \mu^+ \nu_\mu$
1.20±0.13±0.13	874	FRABETTI	93E	E687	$\overline{K}^*(892)^0 \mu^+ \nu_\mu$
1.18±0.18±0.08	305	KODAMA	92	E653	$\overline{K}^*(892)^0 \mu^+ \nu_\mu$
• • • We do not use the following data for averages, fits, limits, etc. • • •					
$1.8\ ^{+0.6}_{-0.4}\ \pm 0.3$	183	ANJOS	90E	E691	$\overline{K}^*(892)^0 e^+ \nu_e$

Γ_+/Γ_- in $D^+ \to \overline{K}^*(892)^0 \ell^+ \nu_\ell$

See also BRIERE 10 for $\overline{K}^* \ell^+ \nu_\ell$ helicity-basis form-factor measurements.

VALUE	EVTS	DOCUMENT ID		TECN	COMMENT
0.22±0.06 OUR AVERAGE Error includes scale factor of 1.6.					
0.28±0.05±0.02	763	ADAMOVICH	99	BEAT	$\overline{K}^*(892)^0 \mu^+ \nu_\mu$
0.16±0.05±0.02	305	KODAMA	92	E653	$\overline{K}^*(892)^0 \mu^+ \nu_\mu$
• • • We do not use the following data for averages, fits, limits, etc. • • •					
$0.15\ ^{+0.07}_{-0.05}\ \pm 0.03$	183	ANJOS	90E	E691	$\overline{K}^*(892)^0 e^+ \nu_e$

$D^{\pm}$ REFERENCES

BABU	18	PR D97 011101	V. Babu *et al.*	(BELLE Collab.)
AAIJ	17AF	PL B771 21	R. Aaij *et al.*	(LHCb Collab.)
ABLIKIM	17A	PL B765 231	M. Ablikim *et al.*	(BES III Collab.)
ABLIKIM	17AD	PR D96 092002	M. Ablikim *et al.*	(BES III Collab.)
ABLIKIM	17M	PR D95 071102	M. Ablikim *et al.*	(BES III Collab.)
ABLIKIM	17S	PR D96 012002	M. Ablikim *et al.*	(BES III Collab.)
ABLIKIM	16D	PRL 116 082001	M. Ablikim *et al.*	(BES III Collab.)
ABLIKIM	16F	PR D94 032001	M. Ablikim *et al.*	(BES III Collab.)
ABLIKIM	16G	EPJ C76 369	M. Ablikim *et al.*	(BES III Collab.)
ABLIKIM	16V	CP C40 113001	M. Ablikim *et al.*	(BES III Collab.)
ABLIKIM	15AF	PR D92 112008	M. Ablikim *et al.*	(BES III Collab.)
ABLIKIM	15W	PR D92 071101	M. Ablikiim *et al.*	(BES III Collab.)
AAIJ	14BD	JHEP 1410 025	R. Aaij *et al.*	(LHCb Collab.)
AAIJ	14C	PL B728 585	R. Aaij *et al.*	(LHCb Collab.)
ABAZOV	14L	PR D90 111102	V.M. Abazov *et al.*	(D0 Collab.)
ABLIKIM	14E	PR D89 052001	M. Ablikim *et al.*	(BES III Collab.)
ABLIKIM	14F	PR D89 051104	M. Ablikim *et al.*	(BES III Collab.)
BONVICINI	14	PR D89 072002	G. Bonvicini *et al.*	(CLEO Collab.)
AAIJ	13AF	PL B724 203	R. Aaij *et al.*	(LHCb Collab.)
AAIJ	13W	JHEP 1306 112	R. Aaij *et al.*	(LHCb Collab.)
DOBBS	13	PRL 110 131802	S. Dobbs *et al.*	(CLEO Collab.)
KO	13	JHEP 1302 098	B.R. Ko *et al.*	(BELLE Collab.)
LEES	13E	PR D87 052012	J.P. Lees *et al.*	(BABAR Collab.)
LEES	13F	PR D87 052010	J.P. Lees *et al.*	(BABAR Collab.)
KO	12A	PRL 109 119903 (errat.)	B.R. Ko *et al.*	(BELLE Collab.)
Also		PRL 109 021601	B.R. Ko *et al.*	(BELLE Collab.)
STARIC	12	PRL 108 071801	M. Staric *et al.*	(BELLE Collab.)
AAIJ	11G	PR D84 112008	R. Aaij *et al.*	(LHCb Collab.)
DEL-AMO-SA...	11H	PR D83 071103	P. del Amo Sanchez *et al.*	(BABAR Collab.)
DEL-AMO-SA...	11I	PR D83 072001	P. del Amo Sanchez *et al.*	(BABAR Collab.)
LEES	11E	PR D84 031103	J.P. Lees *et al.*	(BABAR Collab.)
LEES	11G	PR D84 072006	J.P. Lees *et al.*	(BABAR Collab.)
WILLIAMS	11	PR D84 054015	M. Williams	(LOIC)
WON	11	PRL 107 221801	E. Won *et al.*	(BELLE Collab.)
YELTON	11	PR D84 032001	J. Yelton *et al.*	(CLEO Collab.)
ANASHIN	10A	PL B686 84	V.V. Anashin *et al.*	(VEPP-4M KEDR Collab.)
ASNER	10	PR D81 052007	D.M. Asner *et al.*	(CLEO Collab.)
BRIERE	10	PR D81 112001	R.A. Briere *et al.*	(CLEO Collab.)
KO	10	PRL 104 181602	B.R. Ko *et al.*	(BELLE Collab.)
MENDEZ	10	PR D81 052013	H. Mendez *et al.*	(CLEO Collab.)
PDG	10	JP G37 075021	K. Nakamura *et al.*	(PDG Collab.)
RUBIN	10	PR D82 092007	P. Rubin *et al.*	(CLEO Collab.)
BEDIAGA	09	PR D80 096006	I. Bediaga *et al.*	(CBPF, NDAM)
BESSON	09	PR D80 032005	D. Besson *et al.*	(CLEO Collab.)
Also		PR D79 052010	J.Y. Ge *et al.*	(CLEO Collab.)
KO	09	PRL 102 221802	B.R. Ko *et al.*	(BELLE Collab.)
LINK	09	PL B681 14	J.M. Link *et al.*	(FNAL FOCUS Collab.)
MITCHELL	09B	PRL 102 081801	R.E. Mitchell *et al.*	(CLEO Collab.)
WON	09	PR D80 111101	E. Won *et al.*	(BELLE Collab.)
ABAZOV	08D	PRL 100 101801	V.M. Abazov *et al.*	(D0 Collab.)
ABLIKIM	08L	PL B665 16	M. Ablikim *et al.*	(BES Collab.)
ARTUSO	08	PR D77 092003	M. Artuso *et al.*	(CLEO Collab.)
AUBERT	08AO	PR D78 051102	B. Aubert *et al.*	(BABAR Collab.)
BONVICINI	08	PR D77 091106	G. Bonvicini *et al.*	(CLEO Collab.)
BONVICINI	08A	PR D78 052001	G. Bonvicini *et al.*	(CLEO Collab.)
DOBBS	08	PR D77 112005	S. Dobbs *et al.*	(CLEO Collab.)
Also		PRL 100 251802	D. Cronin-Hennessy *et al.*	(CLEO Collab.)
EISENSTEIN	08	PR D78 052003	B.I. Eisenstein *et al.*	(CLEO Collab.)
HE	08	PRL 100 091801	Q. He *et al.*	(CLEO Collab.)
PDG	08	PL B667 1	C. Amsler *et al.*	(PDG Collab.)
RUBIN	08	PR D78 072003	P. Rubin *et al.*	(CLEO Collab.)
ABLIKIM	07	PL B644 20	M. Ablikim *et al.*	(BES Collab.)
ABLIKIM	07G	PL B658 1	M. Ablikim *et al.*	(BES Collab.)
BONVICINI	07	PR D76 012001	G. Bonvicini *et al.*	(CLEO Collab.)
DOBBS	07	PR D76 112001	S. Dobbs *et al.*	(CLEO Collab.)
LINK	07B	PL B653 1	J.M. Link *et al.*	(FNAL FOCUS Collab.)
ABLIKIM	06O	EPJ C47 31	M. Ablikim *et al.*	(BES Collab.)
ABLIKIM	06P	EPJ C47 39	M. Ablikim *et al.*	(BES Collab.)
ABLIKIM	06U	PL B643 246	M. Ablikim *et al.*	(BES Collab.)
ADAM	06A	PRL 97 251801	N.E. Adam *et al.*	(CLEO Collab.)
AITALA	06	PR D73 032004	E.M. Aitala *et al.*	(FNAL E791 Collab.)
Also		PR D74 059901 (errat.)	E.M. Aitala *et al.*	(FNAL E791 Collab.)
AUBERT,B	06F	PR D74 011107	B. Aubert *et al.*	(BABAR Collab.)
DYTMAN	06	PR D74 071102	S.A. Dytman *et al.*	(CLEO Collab.)
HUANG	06B	PR D74 112005	G.S. Huang *et al.*	(CLEO Collab.)
LINK	06B	PL B637 32	J.M. Link *et al.*	(FNAL FOCUS Collab.)
RUBIN	06	PRL 96 081802	P. Rubin *et al.*	(CLEO Collab.)
RUBIN	06A	PR D73 112005	P. Rubin *et al.*	(CLEO Collab.)
ABLIKIM	05A	PL B608 24	M. Ablikim *et al.*	(BES Collab.)
ABLIKIM	05D	PL B610 183	M. Ablikim *et al.*	(BES Collab.)
ABLIKIM	05F	PL B622 6	M. Ablikim *et al.*	(BES Collab.)
ABLIKIM	05P	PL B625 196	M. Ablikim *et al.*	(BES Collab.)
ARTUSO	05A	PRL 95 251801	M. Artuso *et al.*	(CLEO Collab.)
AUBERT	05S	PR D71 091101	B. Aubert *et al.*	(BABAR Collab.)
HE	05	PRL 95 121801	Q. He *et al.*	(CLEO Collab.)
Also		PRL 96 199903 (errat.)	Q. He *et al.*	(CLEO Collab.)
HE	05A	PRL 95 221802	Q. He *et al.*	(CLEO Collab.)
HUANG	05B	PRL 95 181801	G.S. Huang *et al.*	(CLEO Collab.)
KAYIS-TOPAK...	05	PL B626 24	A. Kayis-Topaksu *et al.*	(CERN CHORUS Collab.)
LINK	05E	PL B622 239	J.M. Link *et al.*	(FNAL FOCUS Collab.)
LINK	05I	PL B621 72	J.M. Link *et al.*	(FNAL FOCUS Collab.)
ABLIKIM	04C	PL B597 39	M. Ablikim *et al.*	(BEPC BES Collab.)
ARMS	04	PR D69 071102	K. Arms *et al.*	(CLEO Collab.)
BONVICINI	04A	PR D70 112004	G. Bonvicini *et al.*	(CLEO Collab.)
LINK	04	PL B585 200	J.M. Link *et al.*	(FNAL FOCUS Collab.)
LINK	04E	PL B598 33	J.M. Link *et al.*	(FNAL FOCUS Collab.)
LINK	04F	PL B601 10	J.M. Link *et al.*	(FNAL FOCUS Collab.)
ANISOVICH	03	EPJ A16 229	V.V. Anisovich *et al.*	
LINK	03D	PL B561 225	J.M. Link *et al.*	(FNAL FOCUS Collab.)
LINK	03F	PL B572 21	J.M. Link *et al.*	(FNAL FOCUS Collab.)
AITALA	02	PRL 89 121801	E.M. Aitala *et al.*	(FNAL E791 Collab.)
BRANDENB...	02	PRL 89 222001	G. Brandenburg *et al.*	(CLEO Collab.)
KAYIS-TOPAK...	02	PL B549 48	A. Kayis-Topaksu *et al.*	(CERN CHORUS Collab.)
LINK	02B	PRL 88 041602	J.M. Link *et al.*	(FNAL FOCUS Collab.)
Also		PRL 88 159903 (errat.)	J.M. Link *et al.*	(FNAL FOCUS Collab.)
LINK	02E	PL B535 43	J.M. Link *et al.*	(FNAL FOCUS Collab.)
LINK	02F	PL B537 192	J.M. Link *et al.*	(FNAL FOCUS Collab.)
LINK	02I	PL B541 227	J.M. Link *et al.*	(FNAL FOCUS Collab.)
LINK	02J	PL B541 243	J.M. Link *et al.*	(FNAL FOCUS Collab.)
LINK	02L	PL B544 89	J.M. Link *et al.*	(FNAL FOCUS Collab.)
AITALA	01B	PRL 86 770	E.M. Aitala *et al.*	(FNAL E791 Collab.)
LINK	01C	PRL 87 162001	J.M. Link *et al.*	(FNAL FOCUS Collab.)
ABREU	00O	EPJ C12 209	P. Abreu *et al.*	(DELPHI Collab.)
ASTIER	00D	PL B486 35	P. Astier *et al.*	(CERN NOMAD Collab.)
JUN	00	PRL 84 1857	S.Y. Jun *et al.*	(FNAL SELEX Collab.)
LINK	00B	PL B491 232	J.M. Link *et al.*	(FNAL FOCUS Collab.)
Also		PL B495 443 (errat.)	J.M. Link *et al.*	(FNAL FOCUS Collab.)
ABBIENDI	99K	EPJ C8 573	G. Abbiendi *et al.*	(OPAL Collab.)
ADAMOVICH	99	EPJ C6 35	M. Adamovich *et al.*	(CERN BEATRICE Collab.)
AITALA	99G	PL B462 401	E.M. Aitala *et al.*	(FNAL E791 Collab.)
BONVICINI	99	PRL 82 4586	G. Bonvicini *et al.*	(CLEO Collab.)
AITALA	98B	PRL 80 1393	E.M. Aitala *et al.*	(FNAL E791 Collab.)
AITALA	98C	PL B421 405	E.M. Aitala *et al.*	(FNAL E791 Collab.)
AITALA	98F	PL B440 435	E.M. Aitala *et al.*	(FNAL E791 Collab.)
BAI	98B	PL B429 188	J.Z. Bai *et al.*	(BEPC BES Collab.)
AITALA	97	PL B397 325	E.M. Aitala *et al.*	(FNAL E791 Collab.)
AITALA	97B	PL B403 377	E.M. Aitala *et al.*	(FNAL E791 Collab.)
AITALA	97C	PL B404 187	E.M. Aitala *et al.*	(FNAL E791 Collab.)
BISHAI	97	PRL 78 3261	M. Bishai *et al.*	(CLEO Collab.)
FRABETTI	97	PL B391 235	P.L. Frabetti *et al.*	(FNAL E687 Collab.)
FRABETTI	97B	PL B398 239	P.L. Frabetti *et al.*	(FNAL E687 Collab.)
FRABETTI	97C	PL B401 131	P.L. Frabetti *et al.*	(FNAL E687 Collab.)
FRABETTI	97D	PL B407 79	P.L. Frabetti *et al.*	(FNAL E687 Collab.)
AITALA	96	PRL 76 364	E.M. Aitala *et al.*	(FNAL E791 Collab.)
FRABETTI	95	PL B346 199	P.L. Frabetti *et al.*	(FNAL E687 Collab.)
FRABETTI	95B	PL B351 591	P.L. Frabetti *et al.*	(FNAL E687 Collab.)
FRABETTI	95E	PL B359 403	P.L. Frabetti *et al.*	(FNAL E687 Collab.)
KODAMA	95	PL B345 85	K. Kodama *et al.*	(FNAL E653 Collab.)
ALBRECHT	94I	ZPHY C64 375	H. Albrecht *et al.*	(ARGUS Collab.)
BALEST	94	PRL 72 2328	R. Balest *et al.*	(CLEO Collab.)
FRABETTI	94D	PL B323 459	P.L. Frabetti *et al.*	(FNAL E687 Collab.)
FRABETTI	94G	PL B331 217	P.L. Frabetti *et al.*	(FNAL E687 Collab.)
FRABETTI	94I	PR D50 2953	P.L. Frabetti *et al.*	(FNAL E687 Collab.)
AKERIB	93	PRL 71 3070	D.S. Akerib *et al.*	(CLEO Collab.)
ANJOS	93	PR D48 56	J.C. Anjos *et al.*	(FNAL E691 Collab.)
FRABETTI	93E	PL B307 262	P.L. Frabetti *et al.*	(FNAL E687 Collab.)
ALBRECHT	92F	PL B278 202	H. Albrecht *et al.*	(ARGUS Collab.)
ANJOS	92C	PR D46 1941	J.C. Anjos *et al.*	(FNAL E691 Collab.)
BARLAG	92C	ZPHY C55 383	S. Barlag *et al.*	(ACCMOR Collab.)
Also		ZPHY C48 29	S. Barlag *et al.*	(ACCMOR Collab.)
COFFMAN	92B	PR D45 2196	D.M. Coffman *et al.*	(Mark III Collab.)
DAOUDI	92	PR D45 3965	M. Daoudi *et al.*	(CLEO Collab.)
KODAMA	92	PL B274 246	K. Kodama *et al.*	(FNAL E653 Collab.)
KODAMA	92C	PL B286 187	K. Kodama *et al.*	(FNAL E653 Collab.)
ADAMOVICH	91	PL B268 142	M.I. Adamovich *et al.*	(WA82 Collab.)
ALBRECHT	91	PL B255 634	H. Albrecht *et al.*	(ARGUS Collab.)
ALVAREZ	91B	ZPHY C50 11	M.P. Alvarez *et al.*	(CERN NA14/2 Collab.)
AMMAR	91	PR D44 3383	R. Ammar *et al.*	(CLEO Collab.)
BAI	91	PRL 66 1011	Z. Bai *et al.*	(Mark III Collab.)
COFFMAN	91	PL B263 135	D.M. Coffman *et al.*	(Mark III Collab.)
FRABETTI	91	PL B263 584	P.L. Frabetti *et al.*	(FNAL E687 Collab.)
ALVAREZ	90	ZPHY C47 539	M.P. Alvarez *et al.*	(CERN NA14/2 Collab.)
ANJOS	90C	PR D41 2705	J.C. Anjos *et al.*	(FNAL E691 Collab.)
ANJOS	90D	PR D42 2414	J.C. Anjos *et al.*	(FNAL E691 Collab.)
ANJOS	90E	PRL 65 2630	J.C. Anjos *et al.*	(FNAL E691 Collab.)
BARLAG	90C	ZPHY C46 563	S. Barlag *et al.*	(ACCMOR Collab.)
WEIR	90B	PR D41 1384	A.J. Weir *et al.*	(Mark II Collab.)
ANJOS	89	PRL 62 125	J.C. Anjos *et al.*	(FNAL E691 Collab.)
ANJOS	89B	PRL 62 722	J.C. Anjos *et al.*	(FNAL E691 Collab.)
ANJOS	89E	PL B223 267	J.C. Anjos *et al.*	(FNAL E691 Collab.)
ADLER	88C	PRL 60 89	J. Adler *et al.*	(Mark III Collab.)
ALBRECHT	88I	PL B210 267	H. Albrecht *et al.*	(ARGUS Collab.)
HAAS	88	PRL 60 1614	P. Haas *et al.*	(CLEO Collab.)
ONG	88	PRL 60 2587	R.A. Ong *et al.*	(Mark II Collab.)
RAAB	88	PR D37 2391	J.R. Raab *et al.*	(FNAL E691 Collab.)
ADAMOVICH	87	EPL 4 887	M.I. Adamovich *et al.*	(Photon Emulsion Collab.)
ADLER	87	PL B196 107	J. Adler *et al.*	(Mark III Collab.)
BARTEL	87	ZPHY C33 339	W. Bartel *et al.*	(JADE Collab.)
BALTRUSAIT...	86E	PRL 56 2140	R.M. Baltrusaitis *et al.*	(Mark III Collab.)
BALTRUSAIT...	85B	PRL 54 1976	R.M. Baltrusaitis *et al.*	(Mark III Collab.)
BALTRUSAIT...	85E	PRL 55 150	R.M. Baltrusaitis *et al.*	(Mark III Collab.)
BARTEL	85J	PL 163B 277	W. Bartel *et al.*	(JADE Collab.)
ADAMOVICH	84	PL 140B 119	M.I. Adamovich *et al.*	(CERN WA58 Collab.)
ALTHOFF	84G	ZPHY C22 219	M. Althoff *et al.*	(TASSO Collab.)
DERRICK	84	PRL 53 1971	M. Derrick *et al.*	(HRS Collab.)
SCHINDLER	81	PR D24 78	R.H. Schindler *et al.*	(Mark II Collab.)
TRILLING	81	PRPL 75 57	G.H. Trilling	(LBL, UCB) J
ZHOLENTZ	80	PL 96B 214	A.A. Zholents *et al.*	(NOVO)
Also		SJNP 34 814 Translated from YAF 34 1471.	A.A. Zholents *et al.*	(NOVO)
GOLDHABER	77	PL 69B 503	G. Goldhaber *et al.*	(Mark I Collab.)
PERUZZI	77	PRL 39 1301	I. Peruzzi *et al.*	(LGW Collab.)
PICCOLO	77	PL 70B 260	M. Piccolo *et al.*	(Mark I Collab.)
PERUZZI	76	PRL 37 569	I. Peruzzi *et al.*	(Mark I Collab.)
MOSTELLER	48	Am.Stat.3 No.5 30	R.A. Fisher, F. Mosteller	

OTHER RELATED PAPERS

RICHMAN	95	RMP 67 893	J.D. Richman, P.R. Burchat	(UCSB, STAN)
ROSNER	95	CNPP 21 369	J. Rosner	(CHIC)

Meson Particle Listings

D^0

D^0 $I(J^P) = \frac{1}{2}(0^-)$

D^0 MASS

The fit includes $D^\pm$, D^0, $D_s^\pm$, $D^{*\pm}$, D^{*0}, $D_s^{*\pm}$, $D_1(2420)^0$, $D_2^*(2460)^0$, and $D_{s1}(2536)^\pm$ mass and mass difference measurements.

Given the recent addition of much more precise measurements, we have omitted all those masses published up through 1990. See any Review before 2015 for those earlier results.

VALUE (MeV)	EVTS	DOCUMENT ID		TECN	COMMENT
1864.83 ±0.05 OUR FIT					
1864.84 ±0.05 OUR AVERAGE					
1864.845±0.025±0.057	63k	[1] TOMARADZE	14		$D^0 \to K^-2\pi^+\pi^-$
1864.75 ±0.15 ±0.11		AAIJ	13V	LHCB	$D^0 \to K^+2K^-\pi^+$
1864.841±0.048±0.063	4.3k	[2] LEES	13S	BABR	e^+e^- at $\Upsilon(4S)$
1865.30 ±0.33 ±0.23	0.1k	ANASHIN	10A	KEDR	e^+e^- at $\psi(3770)$
1864.847±0.150±0.095	0.3k	CAWLFIELD	07	CLEO	$D^0 \to K^0_S\phi$

[1] Obtained by analyzing CLEO-c data but not authored by the CLEO Collaboration. The largest source of error in the TOMARADZE 14 value is from the uncertainties in the K^- and K^0_S masses. The systematic error given above is the addition in quadrature of $\pm 0.022 \pm 0.053$ MeV, where the second error is from those mass uncertainties.

[2] The largest source of error in the LEES 13S value is from the uncertainty of the K^+ mass. The quoted systematic error is in fact $\pm 0.043 + 3\,(m_{K^+} - 493.677)$, in MeV.

$m_{D^\pm} - m_{D^0}$

The fit includes $D^\pm$, D^0, $D_s^\pm$, $D^{*\pm}$, D^{*0}, $D_s^{*\pm}$, $D_1(2420)^0$, $D_2^*(2460)^0$, and $D_{s1}(2536)^\pm$ mass and mass difference measurements.

VALUE (MeV)	DOCUMENT ID		TECN	COMMENT
4.822±0.015 OUR FIT				
4.76 ±0.12 ±0.07	AAIJ	13V	LHCB	$D^+ \to K^+K^-\pi^+$

D^0 MEAN LIFE

Measurements with an error $> 10 \times 10^{-15}$ s have been omitted from the average.

VALUE (10^{-15} s)	EVTS	DOCUMENT ID		TECN	COMMENT
410.1± 1.5 OUR AVERAGE					
409.6± 1.1± 1.5	210k	LINK	02F	FOCS	γ nucleus, ≈ 180 GeV
407.9± 6.0± 4.3	10k	KUSHNIR...	01	SELX	$K^-\pi^+$, $K^-\pi^+\pi^+\pi^-$
413 ± 3 ± 4	35k	AITALA	99E	E791	$K^-\pi^+$
408.5± 4.1$^{+3.5}_{-3.4}$	25k	BONVICINI	99	CLE2	$e^+e^- \approx \Upsilon(4S)$
413 ± 4 ± 3	16k	FRABETTI	94D	E687	$K^-\pi^+$, $K^-\pi^+\pi^+\pi^-$
• • • We do not use the following data for averages, fits, limits, etc. • • •					
424 ±11 ± 7	5118	FRABETTI	91	E687	$K^-\pi^+$, $K^-\pi^+\pi^+\pi^-$
417 ±18 ±15	890	ALVAREZ	90	NA14	$K^-\pi^+$, $K^-\pi^+\pi^+\pi^-$
388 $^{+23}_{-21}$	641	[1] BARLAG	90C	ACCM	π^- Cu 230 GeV
480 ±40 ±30	776	ALBRECHT	88I	ARG	e^+e^- 10 GeV
422 ± 8 ±10	4212	RAAB	88	E691	Photoproduction
420 ±50	90	BARLAG	87B	ACCM	K^- and π^- 200 GeV

[1] BARLAG 90C estimate systematic error to be negligible.

See the related review(s):
D^0 — $\overline{D}^0$ Mixing

$|m_{D_1^0} - m_{D_2^0}| = x\,\Gamma$

The D_1^0 and D_2^0 are the mass eigenstates of the D^0 meson, as described in the note on "D^0-$\overline{D}^0$ Mixing," above. The experiments usually present $x \equiv \Delta m/\Gamma$. Then $\Delta m = x\,\Gamma = x\,\hbar/\tau$.

"OUR EVALUATION" comes from CPV allowing averages provided by the Heavy Flavor Averaging Group, see the note on "D^0-$\overline{D}^0$ Mixing."

VALUE (10^{10} $\hbar$ s^{-1})	CL%	DOCUMENT ID		TECN	COMMENT
0.95$^{+0.41}_{-0.44}$ OUR EVALUATION					
0.8 ±0.7 OUR AVERAGE Error includes scale factor of 1.7. See the ideogram below.					
− 2.10±1.29±0.41		[1] AAIJ	17AO	LHCB	pp at 7, 8 TeV
3.7 ±2.9 ±1.5		[2] AAIJ	16V	LHCB	pp at 7 TeV
1.37±0.46$^{+0.18}_{-0.28}$		[3] LEES	16D	BABR	e^+e^-, 10.6 GeV
0.39±0.56±0.35		[4] KO	14	BELL	$e^+e^- \to \Upsilon(nS)$
		[5] PENG	14	BELL	$e^+e^- \to \Upsilon(nS)$
		[6] AALTONEN	13AE	CDF	$p\overline{p}$ at 1.96 TeV
		[7] DEL-AMO-SA...	10D	BABR	e^+e^-, 10.6 GeV
6.4 $^{+1.4}_{-1.7}$ ±1.0		[8] AAIJ	13CE	LHCB	Repl. by AAIJ 17AO
− 2 $^{+7}_{-6}$		[9] AAIJ	13N	LHCB	Repl. by AAIJ 13CE
1.98±0.73$^{+0.32}_{-0.41}$		[10] AUBERT	09AN	BABR	e^+e^- at 10.58 GeV
< 7	95	[11] LOWREY	09	CLEO	e^+e^- at $\psi(3770)$
−11 to +22		[12] ZHANG	07B	BELL	Repl. by PENG 14
< 11	90	[13] ZHANG	06	BELL	e^+e^-
< 30	90	[12] ASNER	05	CLEO	$e^+e^- \approx 10$ GeV
< 7	95	BITENC	05	BELL	
< 22	95	CAWLFIELD	05	CLEO	
< 23	95	[13] LI	05A	BELL	See ZHANG 06
< 11	95	[14] LINK	05H	FOCS	γ nucleus
< 7	95	AUBERT	04Q	BABR	
< 32	90	[13] AUBERT	03Z	BABR	e^+e^-, 10.6 GeV
< 24	90	[15] GODANG	00	CLE2	e^+e^-
< 21	90	[16,17] AITALA	98	E791	π^- nucleus, 500 GeV
		[18] AITALA	96C	E791	π^- nucleus, 500 GeV
		[17,19] ANJOS	88C	E691	Photoproduction

[1] The result was established with D^0 from prompt and secondary D^*. Based on 3 fb^{-1} of data collected at $\sqrt{s} = 7$, 8 TeV. Assumes no CP violation. Reported $x'^2 = (3.6 \pm 4.3) \times 10^{-5}$ and $y' = (5.23 \pm 0.84) \times 10^{-3}$, where $x' = x\cos(\delta) + y\sin(\delta)$, $y' = y\cos(\delta) - x\sin(\delta)$ and δ is the strong phase between the $D^0 \to K^+\pi^-$ and $\overline{D}^0 \to K^+\pi^-$.

[2] Model-independent measurement of the charm mixing parameters in the decay $D^0 \to K^0_S\pi^+\pi^-$ using 1.0 fb^{-1} of LHCb data at $\sqrt{s} = 7$ TeV.

[3] Time-dependent amplitude analysis of $D^0 \to \pi^+\pi^-\pi^0$.

[4] Based on 976 fb^{-1} of data collected at Υ(nS) resonances. Assumes no CP violation. Reported $x'^2 = (0.09 \pm 0.22) \times 10^{-3}$ and $y' = (4.6 \pm 3.4) \times 10^{-3}$, where $x' = x\cos(\delta) + y\sin(\delta)$, $y' = y\cos(\delta) - x\sin(\delta)$ and δ is the strong phase between $D^0 \to K^+\pi^-$ and $\overline{D}^0 \to K^+\pi^-$.

[5] The time-dependent Dalitz-plot analysis of $D^0 \to K^0_S\pi^+\pi^-$ is emplored. Decay-time information and interference on the Dalitz plot are used to distinguish doubly Cabibbo-suppressed decays from mixing and to measure the relative phase between $D^0 \to K^{*+}\pi^-$ and $\overline{D}^0 \to K^{*+}\pi^-$. This value allows CP violation and is sensitive to the sign of Δm.

[6] Based on 9.6 fb^{-1} of data collected at the Tevatron. Assumes no CP violation. Reported $x'^2 = (0.08 \pm 0.18) \times 10^{-3}$ and $y' = (4.3 \pm 4.3) \times 10^{-3}$, where $x' = x\cos(\delta) + y\sin(\delta)$, $y' = y\cos(\delta) - x\sin(\delta)$ and δ is the strong phase between the $D^0 \to K^+\pi^-$ and $\overline{D}^0 \to K^+\pi^-$.

[7] DEL-AMO-SANCHEZ 10D uses 540,800±800 $K^0_S\pi^+\pi^-$ and 79,900±300 $K^0_S K^+K^-$ events in a time-dependent amplitude analysis of the D^0 and $\overline{D}^0$ Dalitz plots. No evidence was found for CP violation, and the values here assume no such violation.

[8] Based on 3 fb^{-1} of data collected at $\sqrt{s} = 7$, 8 TeV. Assumes no CP violation. Reported $x'^2 = (5.5 \pm 4.9) \times 10^{-4}$ and $y' = (4.8 \pm 1.0) \times 10^{-3}$, where $x' = x\cos(\delta) + y\sin(\delta)$, $y' = y\cos(\delta) - x\sin(\delta)$ and δ is the strong phase between the $D^0 \to K^+\pi^-$ and $\overline{D}^0 \to K^+\pi^-$.

[9] Based on 1 fb^{-1} of data collected at $\sqrt{s} = 7$ TeV in 2011. Assumes no CP violation. Reported $x'^2 = (-0.9 \pm 1.3) \times 10^{-4}$ and $y' = (7.2 \pm 2.4) \times 10^{-3}$, where $x' = x\cos(\delta) + y\sin(\delta)$, $y' = y\cos(\delta) - x\sin(\delta)$ and δ is the strong phase between the $D^0 \to K^+\pi^-$ and $\overline{D}^0 \to K^+\pi^-$.

[10] The AUBERT 09AN values are inferred from the branching ratio $\Gamma(D^0 \to K^+\pi^-\pi^0$ via $\overline{D}^0)/\Gamma(D^0 \to K^-\pi^+\pi^0)$ given near the end of this Listings. Mixing is distinguished from DCS decays using decay-time information. Interference between mixing and DCS is allowed. The phase between $D^0 \to K^+\pi^-\pi^0$ and $\overline{D}^0 \to K^+\pi^-\pi^0$ is assumed to be small. The width difference here is y'', which is not the same as y_{CP} in the note on D^0-$\overline{D}^0$ mixing.

[11] LOWREY 09 uses quantum correlations in $e^+e^- \to D^0\overline{D}^0$ at the $\psi(3770)$. See below for coherence factors and average relative strong phases for both $D^0 \to K^-\pi^+\pi^0$ and $D^0 \to K^-\pi^-2\pi^+$. A fit that includes external measurements of charm mixing parameters gets $\Delta m = (2.34 \pm 0.61) \times 10^{10}$ $\hbar$ s^{-1}.

[12] The ASNER 05 and ZHANG 07B values are from the time-dependent Dalitz-plot analysis of $D^0 \to K^0_S\pi^+\pi^-$. Decay-time information and interference on the Dalitz plot are used to distinguish doubly Cabibbo-suppressed decays from mixing and to measure the relative phase between $D^0 \to K^{*+}\pi^-$ and $\overline{D}^0 \to K^{*+}\pi^-$. This value allows CP violation and is sensitive to the sign of Δm.

[13] The AUBERT 03Z, LI 05A, and ZHANG 06 limits are inferred from the D^0-$\overline{D}^0$ mixing ratio $\Gamma(K^+\pi^-$ (via $\overline{D}^0))/\Gamma(K^-\pi^+)$ given near the end of this D^0 Listings. Decay-time information is used to distinguish DCS decays from D^0-$\overline{D}^0$ mixing. The limit allows interference between the DCS and mixing ratios, and also allows CP violation. AUBERT 03Z assumes the strong phase between $D^0 \to K^+\pi^-$ and $\overline{D}^0 \to K^+\pi^-$ amplitudes is small; if an arbitrary phase is allowed, the limit degrades by 20%. The LI 05A and ZHANG 06 limits are valid for an arbitrary strong phase.

[14] This LINK 05H limit is inferred from the D^0-$\overline{D}^0$ mixing ratio $\Gamma(K^+\pi^-$ (via $\overline{D}^0))/\Gamma(K^-\pi^+)$ given near the end of this D^0 Listings. Decay-time information is used to distinguish DCS decays from D^0-$\overline{D}^0$ mixing. The limit allows interference between the DCS and mixing ratios, and also allows CP violation. The strong phase between $D^0 \to K^+\pi^-$ and $\overline{D}^0 \to K^+\pi^-$ is assumed to be small. If an arbitrary relative strong phase is allowed, the limit degrades by 25%.

[15] This GODANG 00 limit is inferred from the D^0-$\overline{D}^0$ mixing ratio $\Gamma(K^+\pi^-$ (via $\overline{D}^0))/\Gamma(K^-\pi^+)$ given near the end of this D^0 Listings. Decay-time information is used to distinguish DCS decays from D^0-$\overline{D}^0$ mixing. The limit allows interference between the DCS and mixing ratios, and also allows CP violation. The strong phase between $D^0 \to K^+\pi^-$ and $\overline{D}^0 \to K^+\pi^-$ is assumed to be small. If an arbitrary relative strong phase is allowed, the limit degrades by a factor of two.

[16] AITALA 98 allows interference between the doubly Cabibbo-suppressed and mixing amplitudes, and also allows *CP* violation in this term, but assumes that $A_D = A_R = 0$. See the note on "D^0-$\overline{D}^0$ Mixing," above.

[17] This limit is inferred from R_M for $f = K^+\pi^-$ and $f = K^+\pi^-\pi^+\pi^-$. See the note on "D^0-$\overline{D}^0$ Mixing," above. Decay-time information is used to distinguish doubly Cabibbo-suppressed decays from D^0-$\overline{D}^0$ mixing.

[18] This limit is inferred from R_M for $f = K^+\ell^-\overline{\nu}_\ell$. See the note on "$D^0$-$\overline{D}^0$ Mixing," above.

[19] ANJOS 88C assumes that $y = 0$. See the note on "D^0-$\overline{D}^0$ Mixing," above. Without this assumption, the limit degrades by about a factor of two.

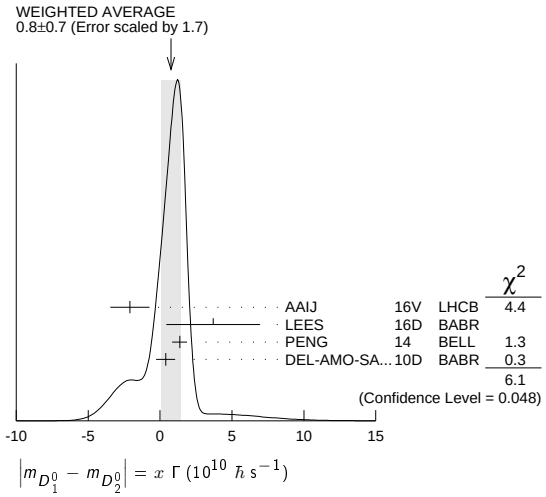

$(\Gamma_{D_1^0} - \Gamma_{D_2^0})/\Gamma = 2y$

The D_1^0 and D_2^0 are the mass eigenstates of the D^0 meson, as described in the note on "D^0-$\overline{D}^0$ Mixing," above.

Due to the strong phase difference between $D^0 \to K^+\pi^-$ and $\overline{D}^0 \to K^+\pi^-$, we exclude from the average those measurements of y' that are inferred from the D^0-$\overline{D}^0$ mixing ratio $\Gamma(K^+\pi^-$ via $\overline{D}^0)$ / $\Gamma(K^+\pi^-)$ given near the end of this D^0 Listings.

Some early results have been omitted. See our 2006 *Review* (Journal of Physics **G33** 1 (2006)).

"OUR EVALUATION" comes from CPV allowing averages provided by the Heavy Flavor Averaging Group, see the note on "D^0-$\overline{D}^0$ Mixing."

VALUE (units 10^{-2})	*EVTS*	*DOCUMENT ID*		*TECN*	*COMMENT*
$1.29^{+\ 0.14}_{-\ 0.18}$ OUR EVALUATION					
1.06 ± 0.26 OUR AVERAGE Error includes scale factor of 1.3. See the ideogram below.					
		[1] AAIJ	17AO	LHCB	pp at 7, 8 TeV
$0.06 \pm 0.92 \pm 0.26$		[2] AAIJ	16V	LHCB	pp at 7 TeV
$0.4 \pm 1.8 \pm 1.0$		[3] LEES	16D	BABR	e^+e^-, 10.6 GeV
$2.22 \pm 0.44 \pm 0.18$		[4] STARIC	16	BELL	$e^+e^- \to \Upsilon(nS)$
$-4.0 \pm 2.6 \pm 1.4$		[5] ABLIKIM	15D	BES3	e^+e^- at $\psi(3770)$
		[6] KO	14	BELL	$e^+e^- \to \Upsilon(nS)$
$0.60 \pm 0.30^{+0.10}_{-0.17}$		[7] PENG	14	BELL	$e^+e^- \to \Upsilon(nS)$
		[8] AALTONEN	13AE	CDF	$p\overline{p}$ at 1.96 TeV
$1.44 \pm 0.36 \pm 0.24$		[9] LEES	13	BABR	$e^+e^- \to \Upsilon(4S)$
$0.55 \pm 0.63 \pm 0.41$		[10] AAIJ	12K	LHCB	pp at 7 TeV
$1.14 \pm 0.40 \pm 0.30$		[11] DEL-AMO-SA...	10D	BABR	e^+e^-, 10.6 GeV
$0.22 \pm 1.22 \pm 1.04$		[12] ZUPANC	09	BELL	$e^+e^- \approx \Upsilon(4S)$
$-1.0 \pm 2.0\ ^{+1.4}_{-1.6}$	18k	[13] ABE	02I	BELL	$e^+e^- \approx \Upsilon(4S)$
$-2.4 \pm 5.0 \pm 2.8$	3393	[14] CSORNA	02	CLE2	$e^+e^- \approx \Upsilon(4S)$
$6.84 \pm 2.78 \pm 1.48$	10k	[13] LINK	00	FOCS	γ nucleus
$+1.6 \pm 5.8 \pm 2.1$		[13] AITALA	99E	E791	$K^-\pi^+$, K^+K^-
• • • We do not use the following data for averages, fits, limits, etc. • • •					
		[15] AAIJ	13CE	LHCB	Repl. by AAIJ 17AO
		[16] AAIJ	13N	LHCB	Repl. by AAIJ 13CE
$2.32 \pm 0.44 \pm 0.36$		[17] AUBERT	09AI	BABR	See LEES 13
$-0.12^{+\ 1.10}_{-\ 1.28} \pm 0.68$		[18] AUBERT	09AN	BABR	e^+e^- at 10.58 GeV
$1.4\ ^{+\ 4.8}_{-\ 5.4}$		[19] LOWREY	09	CLEO	e^+e^- at $\psi(3770)$
1.70 ± 1.52	12.7 ± 0.3k	[20] AALTONEN	08E	CDF	$p\overline{p}$, $\sqrt{s} = 1.96$ TeV
$2.06 \pm 0.66 \pm 0.38$		[21] AUBERT	08U	BABR	See AUBERT 09AI
$1.94 \pm 0.88 \pm 0.62$	4030 ± 90	[20] AUBERT	07W	BABR	$e^+e^- \approx 10.6$ GeV
$2.62 \pm 0.64 \pm 0.50$	160k	[22] STARIC	07	BELL	Repl. by STARIC 16
$0.74 \pm 0.50^{+0.20}_{-0.31}$	534k	[23] ZHANG	07B	BELL	Repl. by PENG 14
-0.7 ± 4.9	4k $\pm$ 88	[20,24] ZHANG	06	BELL	e^+e^-
$-3.0\ ^{+\ 5.0}_{-\ 4.8}\ ^{+1.6}_{-0.8}$		[23] ASNER	05	CLEO	$e^+e^- \approx 10$ GeV
-0.3 ± 5.7		[20,24] LI	05A	BELL	See ZHANG 06
$-5.2\ ^{+18.4}_{-16.8}$		[20,24] LINK	05H	FOCS	γ nucleus
$1.6 \pm 0.8\ ^{+1.0}_{-0.8}$	450k	[25] AUBERT	03P	BABR	See AUBERT 08U
$1.6\ ^{+\ 6.2}_{-12.8}$		[20,24] AUBERT	03Z	BABR	e^+e^-, 10.6 GeV
$-5.0\ ^{+\ 2.8}_{-\ 3.2} \pm 0.6$		[20] GODANG	00	CLE2	e^+e^-

[1] The result was established with D^0 from prompt and secondary D^*. Based on 3 fb^{-1} of data collected at $\sqrt{s} = 7$, 8 TeV. Assumes no *CP* violation. Reported $x'^2 = (3.6 \pm 4.3) \times 10^{-5}$ and $y' = (5.23 \pm 0.84) \times 10^{-3}$, where $x' = x\cos(\delta) + y\sin(\delta)$, $y' = y\cos(\delta) - x\sin(\delta)$ and δ is the strong phase between the $D^0 \to K^+\pi^-$ and $\overline{D}^0 \to K^+\pi^-$.

[2] Model-independent measurement of the charm mixing parameters in the decay $D^0 \to K^0_S\pi^+\pi^-$ using 1.0 fb^{-1} of LHCb data at $\sqrt{s} = 7$ TeV.

[3] Time-dependent amplitude analysis of $D^0 \to \pi^+\pi^-\pi^0$.

[4] An improved measurement of $\overline{D}^0 - D^0$ mixing and a search for *CP* violation in D^0 decays to *CP*-even final states K^+K^- and $\pi^+\pi^-$ using the final Belle data sample of 976 fb^{-1}.

[5] ABLIKIM 15D uses quantum correlations in $e^+e^- \to D^0\overline{D}^0$ at the $\psi(3770)$.

[6] Based on 976 fb^{-1} of data collected at $\Upsilon(nS)$ resonances. Assumes no *CP* violation. Reported $x'^2 = (0.09 \pm 0.22) \times 10^{-3}$ and $y' = (4.6 \pm 3.4) \times 10^{-3}$, where $x' = x\cos(\delta) + y\sin(\delta)$, $y' = y\cos(\delta) - x\sin(\delta)$ and δ is the strong phase between $D^0 \to K^+\pi^-$ and $\overline{D}^0 \to K^+\pi^-$.

[7] The time-dependent Dalitz-plot analysis of $D^0 \to K^0_S\pi^+\pi^-$ is emplored. Decay-time information and interference on the Dalitz plot are used to distinguish doubly Cabibbo-suppressed decays from mixing and to measure the relative phase between $D^0 \to K^{*+}\pi^-$ and $\overline{D}^0 \to K^{*+}\pi^-$. This value allows *CP* violation and is sensitive to the sign of Δm.

[8] Based on 9.6 fb^{-1} of data collected at the Tevatron. Assumes no *CP* violation. Reported $x'^2 = (0.08 \pm 0.18) \times 10^{-3}$ and $y' = (4.3 \pm 4.3) \times 10^{-3}$, where $x' = x\cos(\delta) + y\sin(\delta)$, $y' = y\cos(\delta) - x\sin(\delta)$ and δ is the strong phase between the $D^0 \to K^+\pi^-$ and $\overline{D}^0 \to K^+\pi^-$.

[9] Obtained $y_{CP} = (0.72 \pm 0.18 \pm 0.12)\%$ based on three effective D^0 lifetimes measured in $K^\mp\pi^\pm$, K^-K^+, and $\pi^-\pi^+$. We list $2y_{CP} = \Delta\Gamma/\Gamma$.

[10] Compared the lifetimes of D^0 decay to the *CP* eigenstate K^+K^- with D^0 decay to π^+K^-. The values here assume no *CP* violation.

[11] DEL-AMO-SANCHEZ 10D uses 540,800 $\pm$ 800 $K^0_S\pi^+\pi^-$ and 79,900 $\pm$ 300 $K^0_S K^+K^-$ events in a time-dependent amplitude analyses of the D^0 and $\overline{D}^0$ Dalitz plots. No evidence was found for *CP* violation, and the values here assume no such violation.

[12] ZUPANC 09 uses a method based on measuring the mean decay time of $D^0 \to K^0_S K^+K^-$ events for different K^+K^- mass intervals.

[13] LINK 00, AITALA 99E, and ABE 02I measure the lifetime difference between $D^0 \to K^-K^+$ (*CP* even) decays and $D^0 \to K^-\pi^+$ (*CP* mixed) decays, or $y_{CP} = [\Gamma(CP+) - \Gamma(CP-)]/[\Gamma(CP+) + \Gamma(CP-)]$. We list $2y_{CP} = \Delta\Gamma/\Gamma$.

[14] CSORNA 02 measures the lifetime difference between $D^0 \to K^-K^+$ and $\pi^-\pi^+$ (*CP* even) decays and $D^0 \to K^-\pi^+$ (*CP* mixed) decays, or $y_{CP} = [\Gamma(CP+) - \Gamma(CP-)]/[\Gamma(CP+) + \Gamma(CP-)]$. We list $2y_{CP} = \Delta\Gamma/\Gamma$.

[15] Based on 3 fb^{-1} of data collected at $\sqrt{s} = 7$, 8 TeV. Assumes no *CP* violation. Reported $x'^2 = (5.5 \pm 4.9) \times 10^{-4}$ and $y' = (4.8 \pm 1.0) \times 10^{-3}$, where $x' = x\cos(\delta) + y\sin(\delta)$, $y' = y\cos(\delta) - x\sin(\delta)$ and δ is the strong phase between the $D^0 \to K^+\pi^-$ and $\overline{D}^0 \to K^+\pi^-$.

[16] Based on 1 fb^{-1} of data collected at $\sqrt{s} = 7$ TeV in 2011. Assumes no *CP* violation. Reported $x'^2 = (-0.9 \pm 1.3) \times 10^{-4}$ and $y' = (7.2 \pm 2.4) \times 10^{-3}$, where $x' = x\cos(\delta) + y\sin(\delta)$, $y' = y\cos(\delta) - x\sin(\delta)$ and δ is the strong phase between the $D^0 \to K^+\pi^-$ and $\overline{D}^0 \to K^+\pi^-$.

[17] This combines the $y_{CP} = (\tau_{K\pi}/\tau_{KK}) - 1$ using untagged $K^-\pi^+$ and K^-K^+ events of AUBERT 09AI with the disjoint y_{CP} using tagged $K^-\pi^+$, K^-K^+, and $\pi^-\pi^+$ events of AUBERT 08U.

[18] The AUBERT 09AN values are inferred from the branching ratio $\Gamma(D^0 \to K^+\pi^-\pi^0$ via $\overline{D}^0)/\Gamma(D^0 \to K^-\pi^+\pi^0)$ given near the end of this Listings. Mixing is distinguished from DCS decays using decay-time information. Interference between mixing and DCS is allowed. The phase between $D^0 \to K^+\pi^-\pi^0$ and $\overline{D}^0 \to K^+\pi^-\pi^0$ is assumed to be small. The width difference here is y'', which is not the same as y_{CP} in the note on D^0-$\overline{D}^0$ mixing.

[19] LOWREY 09 uses quantum correlations in $e^+e^- \to D^0\overline{D}^0$ at the $\psi(3770)$. See below for coherence factors and average relative strong phases for both $D^0 \to K^-\pi^+\pi^0$ and $D^0 \to K^-\pi^-2\pi^+$. A fit that includes external measurements of charm mixing parameters gets $2y = (1.62 \pm 0.32) \times 10^{-2}$.

[20] The GODANG 00, AUBERT 03Z, LINK 05H, LI 05A, ZHANG 06, AUBERT 07W, and AALTONEN 08E limits are inferred from the D^0-$\overline{D}^0$ mixing ratio $\Gamma(K^+\pi^-$ (via $\overline{D}^0))/\Gamma(K^-\pi^+)$ given near the end of this D^0 Listings. Decay-time information is used to distinguish DCS decays from D^0-$\overline{D}^0$ mixing. The limits allow interference between the DCS and mixing ratios, and all except AUBERT 07W and AALTONEN 08E also allow *CP* violation. The phase between $D^0 \to K^+\pi^-$ and $\overline{D}^0 \to K^+\pi^-$ is assumed to be small. This is a measurement of y' and is not the same as the y_{CP} of our note above on "D^0-$\overline{D}^0$ Mixing."

[21] This value combines the results of AUBERT 08U and AUBERT 03P.

[22] STARIC 07 compares the lifetimes of D^0 decay to the *CP* eigenstates K^+K^- and $\pi^+\pi^-$ with D^0 decay to $K^-\pi^+$.

[23] The ASNER 05 and ZHANG 07B values are from the time-dependent Dalitz-plot analysis of $D^0 \to K^0_S\pi^+\pi^-$. Decay-time information and interference on the Dalitz plot are used to distinguish doubly Cabibbo-suppressed decays from mixing and to measure the

relative phase between $D^0 \to K^{*+}\pi^-$ and $\overline{D}^0 \to K^{*+}\pi^-$. This limit allows *CP* violation.

[24] The ranges of AUBERT 03Z, LINK 05H, LI 05A, and ZHANG 06 measurements are for 95% confidence level.

[25] AUBERT 03P measures $Y \equiv 2\tau^0/(\tau^+ + \tau^-) - 1$, where τ^0 is the $D^0 \to K^-\pi^+$ (and $\overline{D}^0 \to K^+\pi^-$) lifetime, and τ^+ and τ^- are the D^0 and $\overline{D}^0$ lifetimes to *CP*-even states (here K^-K^+ and $\pi^-\pi^+$). In the limit of *CP* conservation, $Y = y \equiv \Delta\Gamma/2\Gamma$ (we list $2y = \Delta\Gamma/\Gamma$). AUBERT 03P also uses $\tau^+ - \tau^-$ to get $\Delta Y = -0.008 \pm 0.006 \pm 0.002$.

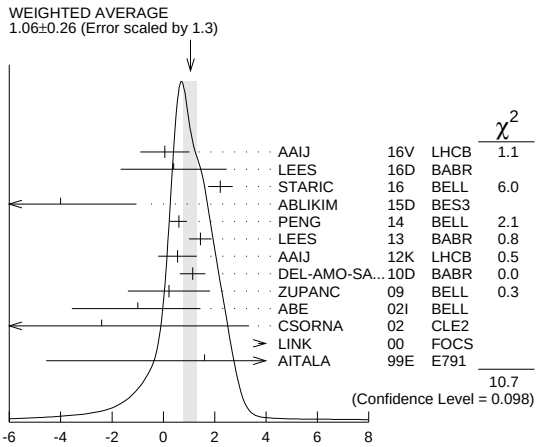

$(\Gamma_1 - \Gamma_2)/\Gamma = 2y$

|q/p|

The mass eigenstates D_1^0 and D_2^0 are related to the $C = \pm 1$ states by $|D_{1,2}> = p\,|D^0> + q\,|\overline{D}^0>$. See the note on "$D^0$–$\overline{D}^0$ Mixing" above.

"OUR EVALUATION" comes from CPV allowing averages provided by the Heavy Flavor Averaging Group. This would include as-yet-unpublished results, see the note on "D^0-$\overline{D}^0$ Mixing."

VALUE	DOCUMENT ID		TECN	COMMENT
$0.92^{+0.12}_{-0.09}$ OUR EVALUATION	HFAG fit; see the note on "D^0-$\overline{D}^0$ Mixing."			
$0.90^{+0.16+0.08}_{-0.15-0.06}$	[1] PENG	14	BELL	$e^+e^- \to \Upsilon(nS)$
	[2] AAIJ	13CE	LHCB	pp at 7, 8 TeV
• • • We do not use the following data for averages, fits, limits, etc. • • •				
$0.86^{+0.30+0.10}_{-0.29-0.08}$	[3] ZHANG	07B	BELL	Repl. by PENG 14

[1] The time-dependent Dalitz-plot analysis of $D^0 \to K^0_S\pi^+\pi^-$ is employed. Decay-time information and interference on the Dalitz plot are used to distinguish doubly Cabibbo-suppressed decays from mixing and to measure the relative phase between $D^0 \to K^{*+}\pi^-$ and $\overline{D}^0 \to K^{*+}\pi^-$. This value allows *CP* violation and is sensitive to the sign of Δm.

[2] Based on 3 fb^{-1} of data collected at $\sqrt{s} = 7$, 8 TeV. Allowing for *CP* violation, the direct *CP* violation in mixing is reported $0.75 < |q/p| < 1.24$ at the 68.3% CL for the $D^0 \to K^+\pi^-$ and $\overline{D}^0 \to K^+\pi^-$.

[3] The phase of p/q is $(-14^{+16}_{-18} \pm 5)^\circ$. The ZHANG 07B value is from the time-dependent Dalitz-plot analysis of $D^0 \to K^0_S\pi^+\pi^-$. Decay-time information and interference on the Dalitz plot are used to distinguish doubly Cabibbo-suppressed decays from mixing and to measure the relative phase between $D^0 \to K^{*+}\pi^-$ and $\overline{D}^0 \to K^{*+}\pi^-$. This value allows *CP* violation.

A_Γ

A_Γ is the decay-rate asymmetry for *CP*-even final states $A_\Gamma = (\overline{\tau}_+ - \tau_+)/(\overline{\tau}_+ + \tau_+)$. See the note on "$D^0$–$\overline{D}^0$ Mixing" above.

VALUE (units 10^{-3})	EVTS	DOCUMENT ID		TECN	COMMENT
-0.125 ± 0.526 OUR EVALUATION					
-0.32 ± 0.26 OUR AVERAGE					
$-0.30 \pm 0.32 \pm 0.10$	9.6M	[1] AAIJ	17AK	LHCB	pp at 7, 8 TeV
$0.46 \pm 0.58 \pm 0.12$	3.0M	[2] AAIJ	17AK	LHCB	pp at 7, 8 TeV
$-0.3 \pm 2.0 \pm 0.7$		[3] STARIC	16	BELL	$e^+e^- \to \Upsilon(nS)$
$-1.34 \pm 0.77\ ^{+0.26}_{-0.34}$	2.3M	[4] AAIJ	15AA	LHCB	pp at 7, 8 TeV
$-0.92 \pm 1.45\ ^{+0.25}_{-0.33}$	0.8M	[5] AAIJ	15AA	LHCB	pp at 7, 8 TeV
-1.2 ± 1.2	1.8M	[6] AALTONEN	14Q	CDF	$p\overline{p}$, $\sqrt{s} = 1.96$ TeV
$0.9 \pm 2.6 \pm 0.6$	0.7M	LEES	13	BABR	$e^+e^- \to \Upsilon(4S)$
$-5.9 \pm 5.9 \pm 2.1$		[1] AAIJ	12K	LHCB	pp at 7 TeV, 2010 data.
• • • We do not use the following data for averages, fits, limits, etc. • • •					
$-0.35 \pm 0.62 \pm 0.12$		[1] AAIJ	14AL	LHCB	Repl. by AAIJ 17AK
$0.33 \pm 1.06 \pm 0.14$		[2] AAIJ	14AL	LHCB	Repl. by AAIJ 17AK
$2.6 \pm 3.6 \pm 0.8$		AUBERT	08U	BABR	See LEES 13
$0.1 \pm 3.0 \pm 2.5$		STARIC	07	BELL	Repl. by STARIC 16
$8 \pm 6 \pm 2$		AUBERT	03P	BABR	$e^+e^- \approx \Upsilon(4S)$

[1] Measured using $D^{*+} \to D^0\pi^+$, $D^0 \to K^+K^-$ decays (and cc).

[2] Measured using $D^{*+} \to D^0\pi^+$, $D^0 \to \pi^+\pi^-$ decays (and cc).

[3] An improved measurement of $\overline{D}^0 - D^0$ mixing and a search for *CP* violation in D^0 decays to *CP*-even final states K^+K^- and $\pi^+\pi^-$ using the final Belle data sample of 976 fb^{-1}.

[4] Measured using $D^0 \to K^+K^-$ decays, with D^0 from partially reconstructed semileptonic B hadron decays.

[5] Measured using $D^0 \to \pi^+\pi^-$ decays, with D^0 from partially reconstructed semileptonic B hadron decays.

[6] Combined result from $D^0 \to K^+K^-$ and $D^0 \to \pi^+\pi^-$, with D^0 from $D^{*+} \to D^0\pi^+$ (and cc).

cos δ

δ is the $D^0 \to K^+\pi^-$ relative strong phase.

VALUE	DOCUMENT ID		TECN	COMMENT
0.97 ± 0.11 OUR AVERAGE				
$1.02 \pm 0.11 \pm 0.06$	[1] ABLIKIM	14C	BES3	$e^+e^- \to D^0\overline{D}^0$, 3.77 GeV
$0.81\ ^{+0.22+0.07}_{-0.18-0.05}$	[2] ASNER	12	CLEO	$e^+e^- \to D^0\overline{D}^0$, 3.77 GeV
• • • We do not use the following data for averages, fits, limits, etc. • • •				
$1.03^{+0.31}_{-0.17} \pm 0.06$	[3] ASNER	08	CLEO	Repl. by ASNER 12

[1] Uses quantum correlations in $e^+e^- \to D^0\overline{D}^0$ at the $\psi(3770)$ to measure the asymmetry of the branching fraction of $D^0 \to K^-\pi^+$ in *CP*-odd and *CP*-even eigenstates to be $(12.7 \pm 1.3 \pm 0.7)\%$. A fit that includes external measurements of charm mixing parameters finds the value quoted above.

[2] Uses quantum correlations in $e^+e^- \to D^0\overline{D}^0$ at the $\psi(3770)$, where decay rates of *CP*-tagged $K\pi$ final states depend on the strong phases between the decays of $D^0 \to K^+\pi^-$ and $\overline{D}^0 \to K^+\pi^-$. The measurements obtained $\sin(\delta) = -0.01 \pm 0.41 \pm 0.04$ and $|\delta| = (10^{+28+13}_{-53-00})^\circ$ as well. A fit that includes external measurements of charm mixing parameters finds $\cos(\delta) = 1.15^{+0.19+0.00}_{-0.17-0.08}$, $\sin(\delta) = 0.56^{+0.32+0.21}_{-0.31-0.20}$, and $|\delta| = (18^{+11}_{-17})^\circ$.

[3] ASNER 08 uses quantum correlations in $e^+e^- \to D^0\overline{D}^0$ at the $\psi(3770)$, where decay rates of *CP*-tagged $K\pi$ final states depend on $\cos\delta$ because of interfering amplitudes. The above measurement implies $|\delta| < 75^\circ$ with a confidence level of 95%. A fit that includes external measurements of charm mixing parameters finds $\cos\delta = 1.10 \pm 0.35 \pm 0.07$. See also the note on "$D^0$–$\overline{D}^0$ Mixing" p. 783 in our 2008 Review (PDG 08).

$D^0 \to K^-\pi^+\pi^0$ COHERENCE FACTOR $R_{K\pi\pi^0}$

See the note on 'D^0-$\overline{D}^0$ Mixing' for the definition. $R_{K\pi\pi^0}$ can have any value between 0 and 1. A value near 1 indicates the decay is dominated by a few intermediate states with limited interference.

VALUE	DOCUMENT ID		TECN	COMMENT
0.82 ± 0.06	[1,2] EVANS	16	CLEO	$e^+e^- \to D^0\overline{D}^0$ at $\psi(3770)$
• • • We do not use the following data for averages, fits, limits, etc. • • •				
0.82 ± 0.07	[1] LIBBY	14	CLEO	Repl. by EVANS 16
$0.78^{+0.11}_{-0.25}$	[3] LOWREY	09	CLEO	Repl. by LIBBY 14

[1] Uses quantum correlations in $e^+e^- \to D^0\overline{D}^0$ at the $\psi(3770)$, where the decay rates of *CP*-tagged $K^-\pi^+\pi^0$ final states depend on $R_{K\pi\pi^0}$ and $\delta^{K\pi\pi^0}$.

[2] A combined fit with a recent LHCb $D^0\overline{D}^0$ mixing results in AAIJ 16F is also reported to be 0.81 ± 0.06.

[3] LOWREY 09 uses quantum correlations in $e^+e^- \to D^0\overline{D}^0$ at the $\psi(3770)$, where the decay rates of *CP*-tagged $K^-\pi^+\pi^0$ final states depend on $R_{K\pi\pi^0}$ and $\delta^{K\pi\pi^0}$. A fit that includes external measurements of charm mixing parameters gets $R_{K\pi\pi^0} = 0.84 \pm 0.07$.

$D^0 \to K^-\pi^+\pi^0$ AVERAGE RELATIVE STRONG PHASE $\delta^{K\pi\pi^0}$

The quoted value of δ is based on the same sign *CP* phase of D^0 and $\overline{D}^0$ convention.

VALUE (°)	DOCUMENT ID		TECN	COMMENT
199^{+13}_{-14}	[1,2] EVANS	16	CLEO	$e^+e^- \to D^0\overline{D}^0$ at $\psi(3770)$
• • • We do not use the following data for averages, fits, limits, etc. • • •				
164^{+20}_{-14}	[1] LIBBY	14	CLEO	Repl. by EVANS 16
239^{+32}_{-28}	[3] LOWREY	09	CLEO	Repl. by LIBBY 14

[1] Uses quantum correlations in $e^+e^- \to D^0\overline{D}^0$ at the $\psi(3770)$, where the decay rates of *CP*-tagged $K^-\pi^+\pi^0$ final states depend on $R_{K\pi\pi^0}$ and $\delta^{K\pi\pi^0}$.

[2] A combined fit with a recent LHCB $D^0\overline{D}^0$ mixing results in AAIJ 16F is also reported to 198^{+14}_{-15} degree.

[3] LOWREY 09 uses quantum correlations in $e^+e^- \to D^0\overline{D}^0$ at the $\psi(3770)$, where the decay rates of *CP*-tagged $K^-\pi^+\pi^0$ final states depend on $R_{K\pi\pi^0}$ and $\delta^{K\pi\pi^0}$. A fit that includes external measurements of charm mixing parameters gets $\delta^{K\pi\pi^0} = (227^{+14}_{-17})^\circ$.

$D^0 \to K^-\pi^-2\pi^+$ COHERENCE FACTOR $R_{K3\pi}$

See the note on 'D^0-$\overline{D}^0$ Mixing' for the definition. $R_{K3\pi}$ can have any value between 0 and 1. A value near 1 indicates the decay is dominated by a few intermediate states with limited interference.

VALUE	DOCUMENT ID		TECN	COMMENT
$0.53^{+0.18}_{-0.21}$	[1,2] EVANS	16	CLEO	$e^+e^- \to D^0\overline{D}^0$ at $\psi(3770)$
• • • We do not use the following data for averages, fits, limits, etc. • • •				
$0.32^{+0.20}_{-0.28}$	[1] LIBBY	14	CLEO	Repl. by EVANS 16
$0.36^{+0.24}_{-0.30}$	[3] LOWREY	09	CLEO	Repl. by LIBBY 14

[1] Uses quantum correlations in $e^+e^- \to D^0\overline{D}^0$ at the $\psi(3770)$, where the decay rates of CP-tagged $K^-\pi^-2\pi^+$ final states depend on $R_{K3\pi}$ and $\delta^{K3\pi}$.

[2] A combined fit with a recent LHCb $D^0\overline{D}^0$ mixing results in AAIJ 16F is also reported to be $0.43^{+0.17}_{-0.13}$.

[3] LOWREY 09 uses quantum correlations in $e^+e^- \to D^0\overline{D}^0$ at the $\psi(3770)$, where the decay rates of CP-tagged $K^-\pi^-2\pi^+$ final states depend on $R_{K3\pi}$ and $\delta^{K3\pi}$. A fit that includes external measurements of charm mixing parameters gets $R_{K3\pi} = 0.33^{+0.26}_{-0.23}$.

$D^0 \to K^-\pi^-2\pi^+$ AVERAGE RELATIVE STRONG PHASE $\delta^{K3\pi}$

The quoted value of δ is based on the same sign CP phase of D^0 and $\overline{D}^0$ convention.

VALUE (°)		DOCUMENT ID		TECN	COMMENT
125^{+22}_{-14}	[1,2] EVANS	16	CLEO	$e^+e^- \to D^0\overline{D}^0$ at $\psi(3770)$	
• • • We do not use the following data for averages, fits, limits, etc. • • •					
255^{+21}_{-78}	[1] LIBBY	14	CLEO	Repl. by EVANS 16	
118^{+62}_{-53}	[3] LOWREY	09	CLEO	Repl. by LIBBY 14	

[1] Uses quantum correlations in $e^+e^- \to D^0\overline{D}^0$ at the $\psi(3770)$, where the decay rates of CP-tagged $K^-\pi^-2\pi^+$ final states depend on $R_{K3\pi}$ and $\delta^{K3\pi}$.

[2] A combined fit with a recent LHCb $D^0\overline{D}^0$ mixing results in AAIJ 16F is also reported to be $(128^{+28}_{-17})°$.

[3] LOWREY 09 uses quantum correlations in $e^+e^- \to D^0\overline{D}^0$ at the $\psi(3770)$, where the decay rates of CP-tagged $K^-\pi^-2\pi^+$ final states depend on $R_{K3\pi}$ and $\delta^{K3\pi}$. A fit that includes external measurements of charm mixing parameters gets $\delta^{K3\pi} = (114^{+26}_{-23})°$.

$D^0 \to K^-\pi^-2\pi^+$, $R_{K3\pi}$ ($y\cos\delta^{K3\pi} - x\sin\delta^{K3\pi}$)

VALUE (10^{-3} TeV^{-1})	EVTS	DOCUMENT ID		TECN	COMMENT
-3.0 ± 0.7	42.5k	[1] AAIJ	16F	LHCB	pp at 7, 8 TeV

[1] From a time-dependent analysis of D mixing in $D^0 \to K^+\pi^-\pi^+\pi^-$. This result uses external constraints on $R_M = 1/2\,(x^2 + y^2)$. Without such constraints, AAIJ 16F measure $(0.3 \pm 1.8) \times 10^{-3}$, with a large correlation coefficient to R_M.

$D^0 \to K^0_S K^+\pi^-$ COHERENCE FACTOR $R_{K^0_S K\pi}$

VALUE	DOCUMENT ID		TECN	COMMENT
0.70 ± 0.08	[1] INSLER	12	CLEO	$e^+e^- \to D^0\overline{D}^0$ at 3.77 GeV

[1] Uses quantum correlations in $e^+e^- \to D^0\overline{D}^0$ at the $\psi(3770)$, where the signal side D decays to $K^0_S K\pi$ and the tag-side D decays to $K\pi$, $K\pi\pi\pi$, $K\pi\pi^0$, and 10 additional CP-even, CP-odd, and mixed CP modes involving K^0_S or K^0_L.

$D^0 \to K^0_S K^+\pi^-$ AVERAGE RELATIVE STRONG PHASE $\delta^{K^0_S K\pi}$

The quoted value of δ is based on the same sign CP phase of D^0 and $\overline{D}^0$ convention.

VALUE (°)	DOCUMENT ID		TECN	COMMENT
0.1 ± 15.7	[1] INSLER	12	CLEO	$e^+e^- \to D^0\overline{D}^0$ at 3.77 GeV

[1] Uses quantum correlations in $e^+e^- \to D^0\overline{D}^0$ at the $\psi(3770)$, where the signal side D decays to $K^0_S K\pi$ and the tag-side D decays to $K\pi$, $K\pi\pi\pi$, $K\pi\pi^0$, and 10 additional CP-even, CP-odd, and mixed CP modes involving K^0_S or K^0_L.

$D^0 \to K^*K$ COHERENCE FACTOR R_{K^*K}

VALUE	DOCUMENT ID		TECN	COMMENT
0.94 ± 0.12	[1] INSLER	12	CLEO	$e^+e^- \to D^0\overline{D}^0$ at 3.77 GeV

[1] Uses quantum correlations in $e^+e^- \to D^0\overline{D}^0$ at the $\psi(3770)$, where the signal side D decays to $K^0_S K\pi$ and the tag-side D decays to $K\pi$, $K\pi\pi\pi$, $K\pi\pi^0$., and 10 additional CP-even, CP-odd, and mixed CP modes involving K^0_S or K^0_L.

$D^0 \to K^*K$ AVERAGE RELATIVE STRONG PHASE δ^{K^*K}

The quoted value of δ is based on the same sign CP phase of D^0 and $\overline{D}^0$ convention.

VALUE (°)	DOCUMENT ID		TECN	COMMENT
-16.6 ± 18.4	[1] INSLER	12	CLEO	$e^+e^- \to D^0\overline{D}^0$ at 3.77 GeV

[1] Uses quantum correlations in $e^+e^- \to D^0\overline{D}^0$ at the $\psi(3770)$, where the signal side D decays to $K^0_S K\pi$ and the tag-side D decays to $K\pi$, $K\pi\pi\pi$, $K\pi\pi^0$, and 10 additional CP-even, CP-odd, and mixed CP modes involving K^0_S or K^0_L.

D^0 DECAY MODES

Most decay modes (other than the semileptonic modes) that involve a neutral K meson are now given as K^0_S modes, not as $\overline{K}^0$ modes. Nearly always it is a K^0_S that is measured, and interference between Cabibbo-allowed and doubly Cabibbo-suppressed modes can invalidate the assumption that $2\Gamma(K^0_S) = \Gamma(\overline{K}^0)$.

	Mode		Fraction (Γ_i/Γ)	Scale factor/ Confidence level
	Topological modes			
Γ_1	0-prongs	[a]	(15 ± 6) %	
Γ_2	2-prongs		(70 ± 6) %	
Γ_3	4-prongs	[b]	(14.5 ± 0.5) %	
Γ_4	6-prongs	[c]	(6.4 ± 1.3) $\times 10^{-4}$	
	Inclusive modes			
Γ_5	e^+ anything	[d]	(6.49 ± 0.11) %	
Γ_6	μ^+ anything		(6.7 ± 0.6) %	
Γ_7	K^- anything		(54.7 ± 2.8) %	S=1.3
Γ_8	$\overline{K}^0$ anything + K^0 anything		(47 ± 4) %	
Γ_9	K^+ anything		(3.4 ± 0.4) %	
Γ_{10}	$K^*(892)^-$ anything		(15 ± 9) %	
Γ_{11}	$\overline{K}^*(892)^0$ anything		(9 ± 4) %	
Γ_{12}	$K^*(892)^+$ anything		< 3.6 %	CL=90%
Γ_{13}	$K^*(892)^0$ anything		(2.8 ± 1.3) %	
Γ_{14}	η anything		(9.5 ± 0.9) %	
Γ_{15}	η' anything		(2.48 ± 0.27) %	
Γ_{16}	ϕ anything		(1.05 ± 0.11) %	
Γ_{17}	invisibles		< 9.4 $\times 10^{-5}$	CL=90%
	Semileptonic modes			
Γ_{18}	$K^-\ell^+\nu_\ell$			
Γ_{19}	$K^-e^+\nu_e$		(3.530 ± 0.028) %	S=1.1
Γ_{20}	$K^-\mu^+\nu_\mu$		(3.31 ± 0.13) %	
Γ_{21}	$K^*(892)^-e^+\nu_e$		(2.15 ± 0.16) %	
Γ_{22}	$K^*(892)^-\mu^+\nu_\mu$		(1.86 ± 0.24) %	
Γ_{23}	$K^-\pi^0e^+\nu_e$		(1.6 $^{+\ 1.3}_{-\ 0.5}$) %	
Γ_{24}	$\overline{K}^0\pi^-e^+\nu_e$		(2.7 $^{+\ 0.9}_{-\ 0.7}$) %	
Γ_{25}	$K^-\pi^+\pi^-e^+\nu_e$		(2.8 $^{+\ 1.4}_{-\ 1.1}$) $\times 10^{-4}$	
Γ_{26}	$K_1(1270)^-e^+\nu_e$		(7.6 $^{+\ 4.0}_{-\ 3.1}$) $\times 10^{-4}$	
Γ_{27}	$K^-\pi^+\pi^-\mu^+\nu_\mu$		< 1.2 $\times 10^{-3}$	CL=90%
Γ_{28}	$(\overline{K}^*(892)\pi)^-\mu^+\nu_\mu$		< 1.4 $\times 10^{-3}$	CL=90%
Γ_{29}	$\pi^-e^+\nu_e$		(2.91 ± 0.04) $\times 10^{-3}$	S=1.1
Γ_{30}	$\pi^-\mu^+\nu_\mu$		(2.37 ± 0.24) $\times 10^{-3}$	
Γ_{31}	$\rho^-e^+\nu_e$		(1.77 ± 0.16) $\times 10^{-3}$	
	Hadronic modes with one $\overline{K}$			
Γ_{32}	$K^-\pi^+$		(3.89 ± 0.04) %	S=1.1
Γ_{33}	$K^0_S\pi^0$		(1.19 ± 0.04) %	
Γ_{34}	$K^0_L\pi^0$		(10.0 ± 0.7) $\times 10^{-3}$	
Γ_{35}	$K^0_S\pi^+\pi^-$	[e]	(2.75 ± 0.18) %	S=1.1
Γ_{36}	$K^0_S\rho^0$		(6.2 $^{+\ 0.6}_{-\ 0.8}$) $\times 10^{-3}$	
Γ_{37}	$K^0_S\omega$, $\omega \to \pi^+\pi^-$		(2.0 ± 0.6) $\times 10^{-4}$	
Γ_{38}	$K^0_S(\pi^+\pi^-)_{S-wave}$		(3.3 ± 0.7) $\times 10^{-3}$	
Γ_{39}	$K^0_S f_0(980)$, $f_0 \to \pi^+\pi^-$		(1.18 $^{+\ 0.40}_{-\ 0.23}$) $\times 10^{-3}$	
Γ_{40}	$K^0_S f_0(1370)$, $f_0 \to \pi^+\pi^-$		(2.7 $^{+\ 0.8}_{-\ 1.3}$) $\times 10^{-3}$	
Γ_{41}	$K^0_S f_2(1270)$, $f_2 \to \pi^+\pi^-$		(9 $^{+10}_{-\ 6}$) $\times 10^{-5}$	
Γ_{42}	$K^*(892)^-\pi^+$, $K^{*-} \to K^0_S\pi^-$		(1.62 $^{+\ 0.14}_{-\ 0.17}$) %	
Γ_{43}	$K^*_0(1430)^-\pi^+$, $K^{*-}_0 \to K^0_S\pi^-$		(2.63 $^{+\ 0.40}_{-\ 0.32}$) $\times 10^{-3}$	
Γ_{44}	$K^*_2(1430)^-\pi^+$, $K^{*-}_2 \to K^0_S\pi^-$		(3.3 $^{+\ 1.8}_{-\ 1.0}$) $\times 10^{-4}$	
Γ_{45}	$K^*(1680)^-\pi^+$, $K^{*-} \to K^0_S\pi^-$		(4.3 ± 3.5) $\times 10^{-4}$	
Γ_{46}	$K^*(892)^+\pi^-$, $K^{*+} \to K^0_S\pi^+$	[f]	(1.11 $^{+\ 0.60}_{-\ 0.33}$) $\times 10^{-4}$	
Γ_{47}	$K^*_0(1430)^+\pi^-$, $K^{*+}_0 \to K^0_S\pi^+$	[f]	< 1.4 $\times 10^{-5}$	CL=95%
Γ_{48}	$K^*_2(1430)^+\pi^-$, $K^{*+}_2 \to K^0_S\pi^+$	[f]	< 3.3 $\times 10^{-5}$	CL=95%
Γ_{49}	$K^0_S\pi^+\pi^-$ nonresonant		(2.5 $^{+\ 6.0}_{-\ 1.6}$) $\times 10^{-4}$	
Γ_{50}	$K^-\pi^+\pi^0$	[e]	(14.2 ± 0.5) %	S=1.9
Γ_{51}	$K^-\rho^+$		(11.1 ± 0.7) %	

Meson Particle Listings

D^0

Γ_{52}	$K^-\rho(1700)^+$, $\rho^+ \to \pi^+\pi^0$	(8.1 ± 1.7) $\times 10^{-3}$		
Γ_{53}	$K^*(892)^-\pi^+$, $K^*(892)^- \to K^-\pi^0$	(2.27 $^{+\ 0.40}_{-\ 0.20}$) %		
Γ_{54}	$\overline{K}^*(892)^0\pi^0$, $\overline{K}^*(892)^0 \to K^-\pi^+$	(1.93 ± 0.24) %		
Γ_{55}	$K_0^*(1430)^-\pi^+$, $K_0^{*-} \to K^-\pi^0$	(4.7 ± 2.2) $\times 10^{-3}$		
Γ_{56}	$\overline{K}_0^*(1430)^0\pi^0$, $\overline{K}_0^{*0} \to K^-\pi^+$	(5.8 $^{+\ 5.0}_{-\ 1.6}$) $\times 10^{-3}$		
Γ_{57}	$K^*(1680)^-\pi^+$, $K^{*-} \to K^-\pi^0$	(1.8 ± 0.7) $\times 10^{-3}$		
Γ_{58}	$K^-\pi^+\pi^0$ nonresonant	(1.14 $^{+\ 0.50}_{-\ 0.20}$) %		
Γ_{59}	$K_S^0 2\pi^0$	(9.1 ± 1.1) $\times 10^{-3}$		S=2.2
Γ_{60}	$K_S^0(2\pi^0)_{S-wave}$	(2.6 ± 0.7) $\times 10^{-3}$		
Γ_{61}	$\overline{K}^*(892)^0\pi^0$, $\overline{K}^{*0} \to K_S^0\pi^0$	(7.8 ± 0.7) $\times 10^{-3}$		
Γ_{62}	$\overline{K}^*(1430)^0\pi^0$, $\overline{K}^{*0} \to K_S^0\pi^0$	(4 ±23) $\times 10^{-5}$		
Γ_{63}	$\overline{K}^*(1680)^0\pi^0$, $\overline{K}^{*0} \to K_S^0\pi^0$	(1.0 ± 0.4) $\times 10^{-3}$		
Γ_{64}	$K_S^0 f_2(1270)$, $f_2 \to 2\pi^0$	(2.3 ± 1.1) $\times 10^{-4}$		
Γ_{65}	$2K_S^0$, one $K_S^0 \to 2\pi^0$	(3.2 ± 1.1) $\times 10^{-4}$		
Γ_{66}	$K_S^0 2\pi^0$ nonresonant			
Γ_{67}	$K^-2\pi^+\pi^-$	[e]	(8.11 ± 0.15) %	S=1.1
Γ_{68}	$K^-\pi^+\rho^0$ total		(6.77 ± 0.31) %	
Γ_{69}	$K^-\pi^+\rho^0$ 3-body		(6.0 ± 1.6) $\times 10^{-3}$	
Γ_{70}	$\overline{K}^*(892)^0\rho^0$, $\overline{K}^{*0} \to K^-\pi^+$		(10.0 ± 0.5) $\times 10^{-3}$	
Γ_{71}	$(\overline{K}^*(892)^0\rho^0)_{S-wave}$, $\overline{K}^*(892)^0 \to K^-\pi^+$		(5.8 ± 0.8) $\times 10^{-3}$	
Γ_{72}	$(\overline{K}^*(892)^0\rho^0)_{P-wave}$, $\overline{K}^*(892)^0 \to K^-\pi^+$		(1.86 ± 0.18) $\times 10^{-3}$	
Γ_{73}	$(\overline{K}^*(892)^0\rho^0)_{D-wave}$, $\overline{K}^*(892)^0 \to K^-\pi^+$		(6.6 ± 0.7) $\times 10^{-3}$	
Γ_{74}	$\overline{K}^*(892)^0\rho^0$ transverse, $\overline{K}^{*0} \to K^-\pi^+$		(1.2 ± 0.4) %	
Γ_{75}	$K^-a_1(1260)^+$, $a_1^+ \to \rho^0\pi^+$		(4.26 ± 0.32) %	
Γ_{76}	$K^-a_1(1260)^+$, $a_1(1260)^+ \to (\rho^0\pi^+)_{S-wave}$		(4.3 ± 0.4) %	
Γ_{77}	$K^-a_1(1260)^+$, $a_1(1260)^+ \to (\rho^0\pi^+)_{D-wave}$		(2.4 ± 1.1) $\times 10^{-4}$	
Γ_{78}	$K_1(1270)^-\pi^+$, $K_1^- \to K^-\pi^+\pi^-$ total		(5.4 ± 1.6) $\times 10^{-3}$	
Γ_{79}	$\overline{K}^*(892)^0\pi^+\pi^-$ total, $\overline{K}^*(892)^0 \to K^-\pi^+$			
Γ_{80}	$\overline{K}^*(892)^0\pi^+\pi^-$ 3-body, $\overline{K}^{*0} \to K^-\pi^+$		(5.9 ± 0.5) $\times 10^{-3}$	
Γ_{81}	$K_1(1270)^-\pi^+$, $K_1^- \to \overline{K}^*(892)^0\pi^-$, $\overline{K}^{*0} \to K^-\pi^+$		(6.5 ± 2.3) $\times 10^{-4}$	
Γ_{82}	$K_1(1270)^-\pi^+$, $K_1(1270)^- \to (\overline{K}^{*0}\pi^-)_{S-wave}$, $\overline{K}^*(892)^0 \to K^-\pi^+$		(8 ±11) $\times 10^{-5}$	
Γ_{83}	$K_1(1270)^-\pi^+$, $K_1(1270)^- \to (\overline{K}^{*0}\pi^-)_{D-wave}$, $\overline{K}^*(892)^0 \to K^-\pi^+$		(5.7 ± 2.3) $\times 10^{-4}$	
Γ_{84}	$K_1(1270)^-\pi^+$, $K_1(1270)^- \to (K^-\rho^0)_{S-wave}$		(2.8 ± 0.5) $\times 10^{-3}$	
Γ_{85}	$K^-2\pi^+\pi^-$ nonresonant		(1.78 ± 0.07) %	
Γ_{86}	$K_S^0\pi^+\pi^-\pi^0$	[g]	(5.1 ± 0.6) %	
Γ_{87}	$K_S^0\eta$, $\eta \to \pi^+\pi^-\pi^0$		(1.10 ± 0.07) $\times 10^{-3}$	
Γ_{88}	$K_S^0\omega$, $\omega \to \pi^+\pi^-\pi^0$		(9.9 ± 0.6) $\times 10^{-3}$	
Γ_{89}	$K^-\pi^+ 2\pi^0$			
Γ_{90}	$K^-2\pi^+\pi^-\pi^0$		(4.2 ± 0.4) %	
Γ_{91}	$\overline{K}^*(892)^0\pi^+\pi^-\pi^0$, $\overline{K}^{*0} \to K^-\pi^+$		(1.3 ± 0.6) %	
Γ_{92}	$K^-\pi^+\omega$, $\omega \to \pi^+\pi^-\pi^0$		(2.7 ± 0.5) %	
Γ_{93}	$\overline{K}^*(892)^0\omega$, $\overline{K}^{*0} \to K^-\pi^+$, $\omega \to \pi^+\pi^-\pi^0$		(6.5 ± 3.0) $\times 10^{-3}$	
Γ_{94}	$K_S^0\eta\pi^0$		(5.5 ± 1.1) $\times 10^{-3}$	
Γ_{95}	$K_S^0 a_0(980)$, $a_0 \to \eta\pi^0$		(6.5 ± 2.0) $\times 10^{-3}$	
Γ_{96}	$\overline{K}^*(892)^0\eta$, $\overline{K}^{*0} \to K_S^0\pi^0$		(1.6 ± 0.5) $\times 10^{-3}$	
Γ_{97}	$K_S^0 2\pi^+ 2\pi^-$		(2.61 ± 0.29) $\times 10^{-3}$	
Γ_{98}	$K_S^0\rho^0\pi^+\pi^-$, no $K^*(892)^-$		(1.0 ± 0.7) $\times 10^{-3}$	
Γ_{99}	$K^*(892)^-2\pi^+\pi^-$, $K^*(892)^- \to K_S^0\pi^-$, no ρ^0		(4 ± 7) $\times 10^{-4}$	
Γ_{100}	$K^*(892)^-\rho^0\pi^+$, $K^*(892)^- \to K_S^0\pi^-$		(1.6 ± 0.6) $\times 10^{-3}$	
Γ_{101}	$K_S^0 2\pi^+ 2\pi^-$ nonresonant		< 1.2 $\times 10^{-3}$	CL=90%
Γ_{102}	$\overline{K}^0\pi^+\pi^-2\pi^0$ (π^0)			
Γ_{103}	$K^-3\pi^+2\pi^-$		(2.2 ± 0.6) $\times 10^{-4}$	

Fractions of some of the following modes with resonances have already appeared above as submodes of particular charged-particle modes. These nine modes below are all corrected for unseen decays of the resonances.

Γ_{104}	$K_S^0\eta$		(4.80 ± 0.30) $\times 10^{-3}$	
Γ_{105}	$K_S^0\omega$		(1.11 ± 0.06) %	
Γ_{106}	$K_S^0\eta'(958)$		(9.4 ± 0.5) $\times 10^{-3}$	
Γ_{107}	$\overline{K}^*(892)^0\pi^+\pi^-\pi^0$		(1.9 ± 0.9) %	
Γ_{108}	$\overline{K}^*(892)^0\eta$			
Γ_{109}	$K^-\pi^+\omega$		(3.0 ± 0.6) %	
Γ_{110}	$\overline{K}^*(892)^0\omega$		(1.1 ± 0.5) %	
Γ_{111}	$K^-\pi^+\eta'(958)$		(7.5 ± 1.9) $\times 10^{-3}$	
Γ_{112}	$\overline{K}^*(892)^0\eta'(958)$		< 1.1 $\times 10^{-3}$	CL=90%

Hadronic modes with three K's

Γ_{113}	$K_S^0 K^+K^-$		(4.35 ± 0.32) $\times 10^{-3}$	
Γ_{114}	$K_S^0 a_0(980)^0$, $a_0^0 \to K^+K^-$		(2.9 ± 0.4) $\times 10^{-3}$	
Γ_{115}	$K^-a_0(980)^+$, $a_0^+ \to K^+K_S^0$		(5.8 ± 1.7) $\times 10^{-4}$	
Γ_{116}	$K^+a_0(980)^-$, $a_0^- \to K^-K_S^0$		< 1.1 $\times 10^{-4}$	CL=95%
Γ_{117}	$K_S^0 f_0(980)$, $f_0 \to K^+K^-$		< 9 $\times 10^{-5}$	CL=95%
Γ_{118}	$K_S^0\phi$, $\phi \to K^+K^-$		(2.00 ± 0.15) $\times 10^{-3}$	
Γ_{119}	$K_S^0 f_0(1370)$, $f_0 \to K^+K^-$		(1.7 ± 1.1) $\times 10^{-4}$	
Γ_{120}	$3K_S^0$		(7.5 ± 0.6) $\times 10^{-4}$	S=1.3
Γ_{121}	$K^+2K^-\pi^+$		(2.22 ± 0.31) $\times 10^{-4}$	
Γ_{122}	$K^+K^-\overline{K}^*(892)^0$, $\overline{K}^{*0} \to K^-\pi^+$		(4.4 ± 1.7) $\times 10^{-5}$	
Γ_{123}	$K^-\pi^+\phi$, $\phi \to K^+K^-$		(4.0 ± 1.7) $\times 10^{-5}$	
Γ_{124}	$\phi\overline{K}^*(892)^0$, $\phi \to K^+K^-$, $\overline{K}^{*0} \to K^-\pi^+$		(1.06 ± 0.20) $\times 10^{-4}$	
Γ_{125}	$K^+2K^-\pi^+$ nonresonant		(3.3 ± 1.5) $\times 10^{-5}$	
Γ_{126}	$2K_S^0 K^\pm\pi^\mp$		(5.8 ± 1.2) $\times 10^{-4}$	

Pionic modes

Γ_{127}	$\pi^+\pi^-$		(1.407± 0.025) $\times 10^{-3}$	S=1.1
Γ_{128}	$2\pi^0$		(8.22 ± 0.25) $\times 10^{-4}$	
Γ_{129}	$\pi^+\pi^-\pi^0$		(1.47 ± 0.06) %	S=2.1
Γ_{130}	$\rho^+\pi^-$		(10.0 ± 0.4) $\times 10^{-3}$	
Γ_{131}	$\rho^0\pi^0$		(3.81 ± 0.23) $\times 10^{-3}$	
Γ_{132}	$\rho^-\pi^+$		(5.08 ± 0.25) $\times 10^{-3}$	
Γ_{133}	$\rho(1450)^+\pi^-$, $\rho^+ \to \pi^+\pi^0$		(1.6 ± 2.0) $\times 10^{-5}$	
Γ_{134}	$\rho(1450)^0\pi^0$, $\rho^0 \to \pi^+\pi^-$		(4.4 ± 1.9) $\times 10^{-5}$	
Γ_{135}	$\rho(1450)^-\pi^+$, $\rho^- \to \pi^-\pi^0$		(2.6 ± 0.4) $\times 10^{-4}$	
Γ_{136}	$\rho(1700)^+\pi^-$, $\rho^+ \to \pi^+\pi^0$		(6.0 ± 1.5) $\times 10^{-4}$	
Γ_{137}	$\rho(1700)^0\pi^0$, $\rho^0 \to \pi^+\pi^-$		(7.3 ± 1.7) $\times 10^{-4}$	
Γ_{138}	$\rho(1700)^-\pi^+$, $\rho^- \to \pi^-\pi^0$		(4.7 ± 1.1) $\times 10^{-4}$	
Γ_{139}	$f_0(980)\pi^0$, $f_0 \to \pi^+\pi^-$		(3.7 ± 0.8) $\times 10^{-5}$	
Γ_{140}	$f_0(500)\pi^0$, $f_0 \to \pi^+\pi^-$		(1.20 ± 0.21) $\times 10^{-4}$	
Γ_{141}	$(\pi^+\pi^-)_{S-wave}\pi^0$			
Γ_{142}	$f_0(1370)\pi^0$, $f_0 \to \pi^+\pi^-$		(5.4 ± 2.1) $\times 10^{-5}$	
Γ_{143}	$f_0(1500)\pi^0$, $f_0 \to \pi^+\pi^-$		(5.7 ± 1.6) $\times 10^{-5}$	
Γ_{144}	$f_0(1710)\pi^0$, $f_0 \to \pi^+\pi^-$		(4.5 ± 1.6) $\times 10^{-5}$	
Γ_{145}	$f_2(1270)\pi^0$, $f_2 \to \pi^+\pi^-$		(1.94 ± 0.21) $\times 10^{-4}$	
Γ_{146}	$\pi^+\pi^-\pi^0$ nonresonant		(1.2 ± 0.4) $\times 10^{-4}$	
Γ_{147}	$3\pi^0$		< 3.5 $\times 10^{-4}$	CL=90%
Γ_{148}	$2\pi^+ 2\pi^-$		(7.45 ± 0.20) $\times 10^{-3}$	
Γ_{149}	$a_1(1260)^+\pi^-$, $a_1^+ \to 2\pi^+\pi^-$ total		(4.47 ± 0.31) $\times 10^{-3}$	
Γ_{150}	$a_1(1260)^+\pi^-$, $a_1^+ \to \rho^0\pi^+$ S-wave		(3.09 ± 0.21) $\times 10^{-3}$	
Γ_{151}	$a_1(1260)^+\pi^-$, $a_1^+ \to \rho^0\pi^+$ D-wave		(1.9 ± 0.5) $\times 10^{-4}$	
Γ_{152}	$a_1(1260)^+\pi^-$, $a_1^+ \to \sigma\pi^+$		(6.3 ± 0.7) $\times 10^{-4}$	
Γ_{153}	$a_1(1260)^-\pi^+$, $a_1^- \to \rho^0\pi^-$ S-wave		(2.3 ± 0.9) $\times 10^{-4}$	

Γ_{154}	$a_1(1260)^-\pi^+$, $a_1^- \to \sigma\pi^-$		(6.0 ± 3.3) $\times 10^{-5}$	
Γ_{155}	$\pi(1300)^+\pi^-$, $\pi(1300)^+ \to \sigma\pi^+$		(5.1 ± 2.6) $\times 10^{-4}$	
Γ_{156}	$\pi(1300)^-\pi^+$, $\pi(1300)^- \to \sigma\pi^-$		(2.2 ± 2.1) $\times 10^{-4}$	
Γ_{157}	$a_1(1640)^+\pi^-$, $a_1^+ \to \rho^0\pi^+$ D-wave		(3.1 ± 1.6) $\times 10^{-4}$	
Γ_{158}	$a_1(1640)^+\pi^-$, $a_1^+ \to \sigma\pi^+$		(1.8 ± 1.4) $\times 10^{-4}$	
Γ_{159}	$\pi_2(1670)^+\pi^-$, $\pi_2^+ \to f_2(1270)^0\pi^+$, $f_2^0 \to \pi^+\pi^-$		(2.0 ± 0.9) $\times 10^{-4}$	
Γ_{160}	$\pi_2(1670)^+\pi^-$, $\pi_2^+ \to \sigma\pi^+$		(2.6 ± 1.0) $\times 10^{-4}$	
Γ_{161}	$2\rho^0$ total		(1.83 ± 0.13) $\times 10^{-3}$	
Γ_{162}	$2\rho^0$, parallel helicities		(8.2 ± 3.2) $\times 10^{-5}$	
Γ_{163}	$2\rho^0$, perpendicular helicities		(4.8 ± 0.6) $\times 10^{-4}$	
Γ_{164}	$2\rho^0$, longitudinal helicities		(1.25 ± 0.10) $\times 10^{-3}$	
Γ_{165}	$2\rho(770)^0$, S-wave		(1.8 ± 1.2) $\times 10^{-4}$	
Γ_{166}	$2\rho(770)^0$, P-wave		(5.2 ± 1.3) $\times 10^{-4}$	
Γ_{167}	$2\rho(770)^0$, D-wave		(6.1 ± 3.0) $\times 10^{-4}$	
Γ_{168}	Resonant $(\pi^+\pi^-)\pi^+\pi^-$ 3-body total		(1.49 ± 0.12) $\times 10^{-3}$	
Γ_{169}	$\sigma\pi^+\pi^-$		(6.1 ± 0.9) $\times 10^{-4}$	
Γ_{170}	$\sigma\rho(770)^0$		(4.9 ± 2.5) $\times 10^{-4}$	
Γ_{171}	$f_0(980)\pi^+\pi^-$, $f_0 \to \pi^+\pi^-$		(1.8 ± 0.5) $\times 10^{-4}$	
Γ_{172}	$f_2(1270)\pi^+\pi^-$, $f_2 \to \pi^+\pi^-$		(3.7 ± 0.6) $\times 10^{-4}$	
Γ_{173}	$2f_2(1270)$, $f_2 \to \pi^+\pi^-$		(1.6 ± 1.8) $\times 10^{-4}$	
Γ_{174}	$f_0(1370)\sigma$, $f_0 \to \pi^+\pi^-$		(1.6 ± 0.5) $\times 10^{-3}$	
Γ_{175}	$\pi^+\pi^-2\pi^0$		(1.00 ± 0.09) %	
Γ_{176}	$\eta\pi^0$	[h]	(6.7 ± 0.6) $\times 10^{-4}$	
Γ_{177}	$\omega\pi^0$	[h]	(1.17 ± 0.35) $\times 10^{-4}$	
Γ_{178}	$2\pi^+2\pi^-\pi^0$		(4.2 ± 0.5) $\times 10^{-3}$	
Γ_{179}	$\eta\pi^+\pi^-$	[h]	(1.09 ± 0.16) $\times 10^{-3}$	
Γ_{180}	$\omega\pi^+\pi^-$	[h]	(1.6 ± 0.5) $\times 10^{-3}$	
Γ_{181}	$3\pi^+3\pi^-$		(4.2 ± 1.2) $\times 10^{-4}$	
Γ_{182}	$\eta'(958)\pi^0$		(9.0 ± 1.4) $\times 10^{-4}$	
Γ_{183}	$\eta'(958)\pi^+\pi^-$		(4.5 ± 1.7) $\times 10^{-4}$	
Γ_{184}	2η		(1.68 ± 0.20) $\times 10^{-3}$	
Γ_{185}	$\eta\eta'(958)$		(1.05 ± 0.26) $\times 10^{-3}$	

Hadronic modes with a $K\overline{K}$ pair

Γ_{186}	K^+K^-		(3.97 ± 0.07) $\times 10^{-3}$	S=1.4
Γ_{187}	$2K_S^0$		(1.70 ± 0.12) $\times 10^{-4}$	
Γ_{188}	$K_S^0K^-\pi^+$		(3.3 ± 0.5) $\times 10^{-3}$	S=1.1
Γ_{189}	$\overline{K}^*(892)^0K_S^0$, $\overline{K}^{*0} \to K^-\pi^+$		(8.1 ± 1.6) $\times 10^{-5}$	
Γ_{190}	$K^*(892)^+K^-$, $K^{*+} \to K_S^0\pi^+$		(1.86 ± 0.30) $\times 10^{-3}$	
Γ_{191}	$\overline{K}^*(1410)^0K_S^0$, $\overline{K}^{*0} \to K^-\pi^+$		(1.2 ± 1.8) $\times 10^{-4}$	
Γ_{192}	$K^*(1410)^+K^-$, $K^{*+} \to K_S^0\pi^+$		(3.1 ± 1.9) $\times 10^{-4}$	
Γ_{193}	$(K^-\pi^+)_{S-wave}K_S^0$		(5.9 ± 2.8) $\times 10^{-4}$	
Γ_{194}	$(K_S^0\pi^+)_{S-wave}K^-$		(3.8 ± 1.0) $\times 10^{-4}$	
Γ_{195}	$a_0(980)^-\pi^+$, $a_0^- \to K_S^0K^-$		(1.3 ± 1.4) $\times 10^{-4}$	
Γ_{196}	$a_0(1450)^-\pi^+$, $a_0^- \to K_S^0K^-$		(2.4 ± 2.0) $\times 10^{-5}$	
Γ_{197}	$a_2(1320)^-\pi^+$, $a_2^- \to K_S^0K^-$		(5 ± 5) $\times 10^{-6}$	
Γ_{198}	$\rho(1450)^-\pi^+$, $\rho^- \to K_S^0K^-$		(4.6 ± 2.5) $\times 10^{-5}$	
Γ_{199}	$K_S^0K^+\pi^-$		(2.13 ± 0.34) $\times 10^{-3}$	S=1.1
Γ_{200}	$K^*(892)^0K_S^0$, $K^{*0} \to K^+\pi^-$		(1.10 ± 0.21) $\times 10^{-4}$	
Γ_{201}	$K^*(892)^-K^+$, $K^{*-} \to K_S^0\pi^-$		(6.1 ± 1.0) $\times 10^{-4}$	
Γ_{202}	$K^*(1410)^0K_S^0$, $K^{*0} \to K^+\pi^+$		(5 ± 8) $\times 10^{-5}$	
Γ_{203}	$K^*(1410)^-K^+$, $K^{*-} \to K_S^0\pi^-$		(2.5 ± 2.0) $\times 10^{-4}$	
Γ_{204}	$(K^+\pi^-)_{S-wave}K_S^0$		(3.6 ± 1.9) $\times 10^{-4}$	
Γ_{205}	$(K_S^0\pi^-)_{S-wave}K^+$		(1.3 ± 0.6) $\times 10^{-4}$	
Γ_{206}	$a_0(980)^+\pi^-$, $a_0^+ \to K_S^0K^+$		(6 ± 4) $\times 10^{-4}$	
Γ_{207}	$a_0(1450)^+\pi^-$, $a_0^+ \to K_S^0K^+$		(3.2 ± 2.5) $\times 10^{-5}$	
Γ_{208}	$\rho(1700)^+\pi^-$, $\rho^+ \to K_S^0K^+$		(1.1 ± 0.6) $\times 10^{-5}$	
Γ_{209}	$K^+K^-\pi^0$		(3.37 ± 0.15) $\times 10^{-3}$	
Γ_{210}	$K^*(892)^+K^-$, $K^*(892)^+ \to K^+\pi^0$		(1.50 ± 0.07) $\times 10^{-3}$	
Γ_{211}	$K^*(892)^-K^+$, $K^*(892)^- \to K^-\pi^0$		(5.4 ± 0.4) $\times 10^{-4}$	
Γ_{212}	$(K^+\pi^0)_{S-wave}K^-$		(2.40 ± 0.17) $\times 10^{-3}$	
Γ_{213}	$(K^-\pi^0)_{S-wave}K^+$		(1.3 ± 0.5) $\times 10^{-4}$	
Γ_{214}	$f_0(980)\pi^0$, $f_0 \to K^+K^-$		(3.5 ± 0.6) $\times 10^{-4}$	
Γ_{215}	$\phi\pi^0$, $\phi \to K^+K^-$		(6.5 ± 0.4) $\times 10^{-4}$	
Γ_{216}	$K^+K^-\pi^0$ nonresonant			
Γ_{217}	$2K_S^0\pi^0$		< 5.9 $\times 10^{-4}$	
Γ_{218}	$K^+K^-\pi^+\pi^-$		(2.44 ± 0.11) $\times 10^{-3}$	
Γ_{219}	$\phi(\pi^+\pi^-)_{S-wave}$, $\phi \to K^+K^-$		(10 ± 5) $\times 10^{-5}$	
Γ_{220}	$(\phi\rho^0)_{S-wave}$, $\phi \to K^+K^-$		(6.8 ± 0.6) $\times 10^{-4}$	
Γ_{221}	$(\phi\rho^0)_{P-wave}$, $\phi \to K^+K^-$		(3.9 ± 1.9) $\times 10^{-5}$	
Γ_{222}	$(\phi\rho^0)_{D-wave}$, $\phi \to K^+K^-$		(4.1 ± 1.4) $\times 10^{-5}$	
Γ_{223}	$K^*(892)^0\overline{K}^*(892)^0$, $K^{*0} \to K^\pm\pi^\mp$			
Γ_{224}	$K^+K^-\rho^0$ 3-body			
Γ_{225}	$f_0(980)\pi^+\pi^-$, $f_0 \to K^+K^-$			
Γ_{226}	$(K^*(892)^0\overline{K}^*(892)^0)_{S-wave}$, $K^{*0} \to K^\pm\pi^\mp$		(1.1 ± 0.5) $\times 10^{-4}$	
Γ_{227}	$(K^*(892)^0\overline{K}^*(892)^0)_{P-wave}$, $K^* \to K^\pm\pi^\mp$		(9 ± 4) $\times 10^{-5}$	
Γ_{228}	$(K^*(892)^0\overline{K}^*(892)^0)_{D-wave}$, $K^* \to K^\pm\pi^\mp$		(9.7 ± 2.3) $\times 10^{-5}$	
Γ_{229}	$K^*(892)^0K^\mp\pi^\pm$ 3-body, $K^{*0} \to K^\pm\pi^\mp$			
Γ_{230}	$K^*(892)^0(K^-\pi^+)_{S-wave}$ 3-body, $K^{*0} \to K^+\pi^-$		(1.4 ± 0.6) $\times 10^{-4}$	
Γ_{231}	$(K^-\pi^+)_{P-wave}$, $(K^+\pi^-)_{S-wave}$			
Γ_{232}	$K_1(1270)^\pm K^\mp$, $K_1^\pm \to K^\pm\pi^+\pi^-$			
Γ_{233}	$K_1(1270)^+K^-$, $K_1^+ \to K^{*0}\pi^+$		(1.3 ± 0.9) $\times 10^{-4}$	
Γ_{234}	$K_1(1270)^+K^-$, $K_1^+ \to K^*(1430)^0\pi^+$, $K^{*0} \to K^+\pi^-$		(1.5 ± 0.5) $\times 10^{-4}$	
Γ_{235}	$K_1(1270)^+K^-$, $K_1^+ \to \rho^0K^+$		(2.2 ± 0.6) $\times 10^{-4}$	
Γ_{236}	$K_1(1270)^+K^-$, $K_1^+ \to \omega(782)K^+$, $\omega \to \pi^+\pi^-$		(1.5 ± 1.2) $\times 10^{-5}$	
Γ_{237}	$K_1(1270)^-K^+$, $K_1^- \to \overline{K}^{*0}\pi^-$			
Γ_{238}	$K_1(1270)^-K^+$, $K_1^- \to \rho^0K^-$		(1.3 ± 0.4) $\times 10^{-4}$	
Γ_{239}	$K_1(1400)^\pm K^\mp$, $K_1^\pm \to K^\pm\pi^+\pi^-$			
Γ_{240}	$K_1(1400)^+K^-$, $K_1^+ \to K^*(892)^0\pi^+$, $K^{*0} \to K^+\pi^-$		(3.0 ± 1.7) $\times 10^{-4}$	
Γ_{241}	$K^*(1410)^+K^-$, $K^{*+} \to K^{*0}\pi^+$			
Γ_{242}	$K^*(1410)^-K^+$, $K^{*-} \to \overline{K}^{*0}\pi^-$			
Γ_{243}	$K_1(1680)^+K^-$, $K_1^+ \to K^{*0}\pi^+$, $K^{*0} \to K^+\pi^-$		(8.8 ± 3.1) $\times 10^{-5}$	
Γ_{244}	$K^+K^-\pi^+\pi^-$ non-resonant		(2.7 ± 0.6) $\times 10^{-4}$	
Γ_{245}	$2K_S^0\pi^+\pi^-$		(1.20 ± 0.23) $\times 10^{-3}$	
Γ_{246}	$K_S^0K^-2\pi^+\pi^-$		< 1.4 $\times 10^{-4}$	CL=90%
Γ_{247}	$K^+K^-\pi^+\pi^-\pi^0$		(3.1 ± 2.0) $\times 10^{-3}$	

Other $K\overline{K}X$ modes. They include all decay modes of the ϕ, η, and ω.

Γ_{248}	$\phi\pi^0$			
Γ_{249}	$\phi\eta$		(1.4 ± 0.5) $\times 10^{-4}$	
Γ_{250}	$\phi\omega$		< 2.1 $\times 10^{-3}$	CL=90%

Radiative modes

Γ_{251}	$\rho^0\gamma$		(1.76 ± 0.31) $\times 10^{-5}$	
Γ_{252}	$\omega\gamma$		< 2.4 $\times 10^{-4}$	CL=90%
Γ_{253}	$\phi\gamma$		(2.74 ± 0.19) $\times 10^{-5}$	
Γ_{254}	$\overline{K}^*(892)^0\gamma$		(4.1 ± 0.7) $\times 10^{-4}$	

Meson Particle Listings

D^0

Doubly Cabibbo suppressed (DC) modes or $\Delta C = 2$ forbidden via mixing (C2M) modes

Γ_{255}	$K^+ \ell^- \overline{\nu}_\ell$ via $\overline{D}^0$		< 2.2	$\times 10^{-5}$	CL=90%
Γ_{256}	K^+ or $K^*(892)^+ e^- \overline{\nu}_e$ via $\overline{D}^0$		< 6	$\times 10^{-5}$	CL=90%
Γ_{257}	$K^+ \pi^-$	DC	(1.48 ± 0.07)	$\times 10^{-4}$	S=2.8
Γ_{258}	$K^+ \pi^-$ via DCS		(1.366 ± 0.028)	$\times 10^{-4}$	
Γ_{259}	$K^+ \pi^-$ via $\overline{D}^0$		< 1.6	$\times 10^{-5}$	CL=95%
Γ_{260}	$K^0_S \pi^+ \pi^-$ in $D^0 \to \overline{D}^0$		< 1.7	$\times 10^{-4}$	CL=95%
Γ_{261}	$K^*(892)^+ \pi^-$, $K^{*+} \to K^0_S \pi^+$	DC	$(1.11 \, {}^{+\ 0.60}_{-\ 0.33})$	$\times 10^{-4}$	
Γ_{262}	$K^*_0(1430)^+ \pi^-$, $K^{*+}_0 \to K^0_S \pi^+$	DC	< 1.4	$\times 10^{-5}$	
Γ_{263}	$K^*_2(1430)^+ \pi^-$, $K^{*+}_2 \to K^0_S \pi^+$	DC	< 3.3	$\times 10^{-5}$	
Γ_{264}	$K^+ \pi^- \pi^0$	DC	(3.01 ± 0.15)	$\times 10^{-4}$	
Γ_{265}	$K^+ \pi^- \pi^0$ via $\overline{D}^0$		(7.5 ± 0.5)	$\times 10^{-4}$	
Γ_{266}	$K^+ \pi^+ 2\pi^-$ via DCS		(2.45 ± 0.07)	$\times 10^{-4}$	
Γ_{267}	$K^+ \pi^+ 2\pi^-$	DC	(2.61 ± 0.06)	$\times 10^{-4}$	
Γ_{268}	$K^+ \pi^+ 2\pi^-$ via $\overline{D}^0$		(7.8 ± 2.9)	$\times 10^{-6}$	
Γ_{269}	$K^+ \pi^-$ or $K^+ \pi^+ 2\pi^-$ via $\overline{D}^0$				
Γ_{270}	μ^- anything via $\overline{D}^0$		< 4	$\times 10^{-4}$	CL=90%

$\Delta C = 1$ weak neutral current (C1) modes, Lepton Family number (LF) violating modes, Lepton (L) or Baryon (B) number violating modes

Γ_{271}	$\gamma\gamma$	C1	< 8.5	$\times 10^{-7}$	CL=90%
Γ_{272}	$e^+ e^-$	C1	< 7.9	$\times 10^{-8}$	CL=90%
Γ_{273}	$\mu^+ \mu^-$	C1	< 6.2	$\times 10^{-9}$	CL=90%
Γ_{274}	$\pi^0 e^+ e^-$	C1	< 4.5	$\times 10^{-5}$	CL=90%
Γ_{275}	$\pi^0 \mu^+ \mu^-$	C1	< 1.8	$\times 10^{-4}$	CL=90%
Γ_{276}	$\eta e^+ e^-$	C1	< 1.1	$\times 10^{-4}$	CL=90%
Γ_{277}	$\eta \mu^+ \mu^-$	C1	< 5.3	$\times 10^{-4}$	CL=90%
Γ_{278}	$\pi^+ \pi^- e^+ e^-$	C1	< 3.73	$\times 10^{-4}$	CL=90%
Γ_{279}	$\rho^0 e^+ e^-$	C1	< 1.0	$\times 10^{-4}$	CL=90%
Γ_{280}	$\pi^+ \pi^- \mu^+ \mu^-$	C1	(9.6 ± 1.2)	$\times 10^{-7}$	
Γ_{281}	$\pi^+ \pi^- \mu^+ \mu^-$ (non-res)		< 5.5	$\times 10^{-7}$	CL=90%
Γ_{282}	$\rho^0 \mu^+ \mu^-$	C1	< 2.2	$\times 10^{-5}$	CL=90%
Γ_{283}	$\omega e^+ e^-$	C1	< 1.8	$\times 10^{-4}$	CL=90%
Γ_{284}	$\omega \mu^+ \mu^-$	C1	< 8.3	$\times 10^{-4}$	CL=90%
Γ_{285}	$K^- K^+ e^+ e^-$	C1	< 3.15	$\times 10^{-4}$	CL=90%
Γ_{286}	$\phi e^+ e^-$	C1	< 5.2	$\times 10^{-5}$	CL=90%
Γ_{287}	$K^- K^+ \mu^+ \mu^-$	C1	(1.54 ± 0.32)	$\times 10^{-7}$	
Γ_{288}	$K^- K^+ \mu^+ \mu^-$ (non-res)		< 3.3	$\times 10^{-5}$	CL=90%
Γ_{289}	$\phi \mu^+ \mu^-$	C1	< 3.1	$\times 10^{-5}$	CL=90%
Γ_{290}	$\overline{K}^0 e^+ e^-$	[i]	< 1.1	$\times 10^{-4}$	CL=90%
Γ_{291}	$\overline{K}^0 \mu^+ \mu^-$	[i]	< 2.6	$\times 10^{-4}$	CL=90%
Γ_{292}	$K^- \pi^+ e^+ e^-$	C1	< 3.85	$\times 10^{-4}$	CL=90%
Γ_{293}	$\overline{K}^*(892)^0 e^+ e^-$	[i]	< 4.7	$\times 10^{-5}$	CL=90%
Γ_{294}	$K^- \pi^+ \mu^+ \mu^-$	C1	< 3.59	$\times 10^{-4}$	CL=90%
Γ_{295}	$K^- \pi^+ \mu^+ \mu^-$, $675 < m_{\mu\mu} < 875$ MeV		(4.2 ± 0.4)	$\times 10^{-6}$	
Γ_{296}	$\overline{K}^*(892)^0 \mu^+ \mu^-$	[i]	< 2.4	$\times 10^{-5}$	CL=90%
Γ_{297}	$\pi^+ \pi^- \pi^0 \mu^+ \mu^-$	C1	< 8.1	$\times 10^{-4}$	CL=90%
Γ_{298}	$\mu^\pm e^\mp$	LF	[j] < 1.3	$\times 10^{-8}$	CL=90%
Γ_{299}	$\pi^0 e^\pm \mu^\mp$	LF	[j] < 8.6	$\times 10^{-5}$	CL=90%
Γ_{300}	$\eta e^\pm \mu^\mp$	LF	[j] < 1.0	$\times 10^{-4}$	CL=90%
Γ_{301}	$\pi^+ \pi^- e^\pm \mu^\mp$	LF	[j] < 1.5	$\times 10^{-5}$	CL=90%
Γ_{302}	$\rho^0 e^\pm \mu^\mp$	LF	[j] < 4.9	$\times 10^{-5}$	CL=90%
Γ_{303}	$\omega e^\pm \mu^\mp$	LF	[j] < 1.2	$\times 10^{-4}$	CL=90%
Γ_{304}	$K^- K^+ e^\pm \mu^\mp$	LF	[j] < 1.8	$\times 10^{-4}$	CL=90%
Γ_{305}	$\phi e^\pm \mu^\mp$	LF	[j] < 3.4	$\times 10^{-5}$	CL=90%
Γ_{306}	$\overline{K}^0 e^\pm \mu^\mp$	LF	[j] < 1.0	$\times 10^{-4}$	CL=90%
Γ_{307}	$K^- \pi^+ e^\pm \mu^\mp$	LF	[j] < 5.53	$\times 10^{-4}$	CL=90%
Γ_{308}	$\overline{K}^*(892)^0 e^\pm \mu^\mp$	LF	[j] < 8.3	$\times 10^{-5}$	CL=90%
Γ_{309}	$2\pi^- 2e^+ +$ c.c.	L	< 1.12	$\times 10^{-4}$	CL=90%
Γ_{310}	$2\pi^- 2\mu^+ +$ c.c.	L	< 2.9	$\times 10^{-5}$	CL=90%
Γ_{311}	$K^- \pi^- 2e^+ +$ c.c.	L	< 2.06	$\times 10^{-4}$	CL=90%
Γ_{312}	$K^- \pi^- 2\mu^+ +$ c.c.	L	< 3.9	$\times 10^{-4}$	CL=90%
Γ_{313}	$2K^- 2e^+ +$ c.c.	L	< 1.52	$\times 10^{-4}$	CL=90%
Γ_{314}	$2K^- 2\mu^+ +$ c.c.	L	< 9.4	$\times 10^{-5}$	CL=90%
Γ_{315}	$\pi^- \pi^- e^+ \mu^+ +$ c.c.	L	< 7.9	$\times 10^{-5}$	CL=90%
Γ_{316}	$K^- \pi^- e^+ \mu^+ +$ c.c.	L	< 2.18	$\times 10^{-4}$	CL=90%
Γ_{317}	$2K^- e^+ \mu^+ +$ c.c.	L	< 5.7	$\times 10^{-5}$	CL=90%
Γ_{318}	$p e^-$	L,B	[k] < 1.0	$\times 10^{-5}$	CL=90%
Γ_{319}	$\overline{p} e^+$	L,B	[l] < 1.1	$\times 10^{-5}$	CL=90%
Γ_{320}	Unaccounted decay modes		(37.9 ± 1.3) %		S=1.1

[a] This value is obtained by subtracting the branching fractions for 2-, 4- and 6-prongs from unity.

[b] This is the sum of our $K^- 2\pi^+ \pi^-$, $K^- 2\pi^+ \pi^- \pi^0$, $\overline{K}^0 2\pi^+ 2\pi^-$, $K^+ 2K^- \pi^+$, $2\pi^+ 2\pi^-$, $2\pi^+ 2\pi^- \pi^0$, $K^+ K^- \pi^+ \pi^-$, and $K^+ K^- \pi^+ \pi^- \pi^0$, branching fractions.

[c] This is the sum of our $K^- 3\pi^+ 2\pi^-$ and $3\pi^+ 3\pi^-$ branching fractions.

[d] The branching fractions for the $K^- e^+ \nu_e$, $K^*(892)^- e^+ \nu_e$, $\pi^- e^+ \nu_e$, and $\rho^- e^+ \nu_e$ modes add up to 6.19 ± 0.17 %.

[e] The branching fraction for this mode may differ from the sum of the submodes that contribute to it, due to interference effects. See the relevant papers.

[f] This is a doubly Cabibbo-suppressed mode.

[g] Submodes of the $D^0 \to K^0_S \pi^+ \pi^- \pi^0$ mode with a K^* and/or ρ were studied by COFFMAN 92B, but with only 140 events. With nothing new for 18 years, we refer to our 2008 edition, Physics Letters **B667** 1 (2008), for those results.

[h] This branching fraction includes all the decay modes of the resonance in the final state.

[i] This mode is not a useful test for a ΔC=1 weak neutral current because both quarks must change flavor in this decay.

[j] The value is for the sum of the charge states or particle/antiparticle states indicated.

[k] This limit is for either D^0 or $\overline{D}^0$ to $p e^-$.

[l] This limit is for either D^0 or $\overline{D}^0$ to $\overline{p} e^+$.

CONSTRAINED FIT INFORMATION

An overall fit to 3 branching ratios uses 3 measurements and one constraint to determine 4 parameters. The overall fit has a $\chi^2 = 0.0$ for 0 degrees of freedom.

The following *off-diagonal* array elements are the correlation coefficients $\langle \delta x_i \delta x_j \rangle / (\delta x_i \cdot \delta x_j)$, in percent, from the fit to the branching fractions, $x_i \equiv \Gamma_i / \Gamma_{\rm total}$. The fit constrains the x_i whose labels appear in this array to sum to one.

x_2	−100		
x_3	−46	40	
x_4	0	0	0
	x_1	x_2	x_3

CONSTRAINED FIT INFORMATION

An overall fit to 55 branching ratios uses 114 measurements and one constraint to determine 32 parameters. The overall fit has a $\chi^2 = 108.1$ for 83 degrees of freedom.

The following *off-diagonal* array elements are the correlation coefficients $\langle \delta x_i \delta x_j \rangle / (\delta x_i \cdot \delta x_j)$, in percent, from the fit to the branching fractions, $x_i \equiv \Gamma_i / \Gamma_{total}$. The fit constrains the x_i whose labels appear in this array to sum to one.

	x_6	x_{19}	x_{20}	x_{21}	x_{29}	x_{30}	x_{32}	x_{33}	x_{35}	x_{50}
x_{19}	0									
x_{20}	20	3								
x_{21}	0	0	0							
x_{29}	0	1	1	0						
x_{30}	3	0	17	0	0					
x_{32}	3	16	16	2	4	3				
x_{33}	1	5	5	2	1	1	31			
x_{35}	0	2	2	15	0	0	11	14		
x_{50}	1	4	4	0	1	1	28	8	3	
x_{67}	2	9	9	1	2	2	55	17	6	15
x_{86}	0	1	1	6	0	0	4	5	38	1
x_{90}	0	2	2	0	0	0	10	3	1	3
x_{104}	1	3	3	0	1	0	16	5	2	4
x_{105}	0	0	0	1	0	0	0	1	5	0
x_{106}	1	3	3	3	1	0	18	7	19	5
x_{120}	0	0	0	3	0	0	2	3	20	1
x_{127}	2	9	9	1	2	2	57	17	6	16
x_{128}	0	1	1	0	0	0	9	3	1	2
x_{129}	1	4	4	0	1	1	24	7	3	82
x_{148}	1	6	6	1	1	1	37	11	4	10
x_{176}	0	1	1	0	0	0	7	2	1	2
x_{182}	0	1	1	0	0	0	6	2	1	2
x_{184}	0	1	1	0	0	0	9	3	1	2
x_{185}	0	1	1	0	0	0	4	1	0	1
x_{186}	2	9	9	1	2	2	55	17	6	15
x_{187}	0	1	1	0	0	0	6	2	1	2
x_{188}	0	1	1	5	0	0	5	5	34	1
x_{199}	0	1	1	5	0	0	5	5	34	1
x_{253}	0	2	2	0	1	0	15	4	2	4
x_{257}	1	3	3	0	1	1	21	7	2	6
x_{320}	−49	−8	−25	−18	−2	−6	−35	−18	−40	−51

	x_{67}	x_{86}	x_{90}	x_{104}	x_{105}	x_{106}	x_{120}	x_{127}	x_{128}	x_{129}
x_{86}	2									
x_{90}	13	0								
x_{104}	9	1	2							
x_{105}	0	12	0	0						
x_{106}	10	7	2	3	1					
x_{120}	1	8	0	0	1	4				
x_{127}	31	2	6	9	0	10	1			
x_{128}	5	0	1	1	0	2	0	5		
x_{129}	13	1	2	4	0	4	1	13	2	
x_{148}	50	2	7	6	0	7	1	21	3	9
x_{176}	4	0	1	1	0	1	0	4	1	2
x_{182}	4	0	1	1	0	1	0	4	1	2
x_{184}	5	0	1	1	0	2	0	5	1	2
x_{185}	2	0	0	1	0	1	0	2	0	1
x_{186}	30	2	6	9	0	10	1	31	5	13
x_{187}	3	0	1	1	0	1	0	3	1	1
x_{188}	3	13	1	1	2	7	7	3	0	1
x_{199}	3	13	1	1	2	7	7	3	0	1
x_{253}	8	1	2	2	0	3	0	8	1	3
x_{257}	12	1	2	4	0	4	0	12	2	5
x_{320}	−30	−55	−35	−8	−11	−16	−9	−20	−3	−43

	x_{148}	x_{176}	x_{182}	x_{184}	x_{185}	x_{186}	x_{187}	x_{188}	x_{199}	x_{253}
x_{176}	3									
x_{182}	2	0								
x_{184}	3	1	1							
x_{185}	1	0	0	0						
x_{186}	20	4	3	5	2					
x_{187}	2	0	0	1	0	3				
x_{188}	2	0	0	0	0	3	0			
x_{199}	2	0	0	0	0	3	0	100		
x_{253}	5	1	1	1	1	23	1	1	1	
x_{257}	8	2	1	2	1	12	1	1	1	3
x_{320}	−19	−3	−3	−5	−3	−20	−2	−20	−20	−5

	x_{257}
x_{320}	−7

D^0 BRANCHING RATIOS

Some older now obsolete results have been omitted from these Listings.

Topological modes

Γ(0-prongs)/Γ_{total} Γ_1/Γ

This value is obtained by subtracting the branching fractions for 2-, 4-, and 6-prongs from unity.

VALUE	DOCUMENT ID
0.15±0.06 OUR FIT	

Γ(4-prongs)/Γ(2-prongs) Γ_3/Γ_2

VALUE	EVTS	DOCUMENT ID		TECN	COMMENT
0.207±0.016 OUR FIT					
0.207±0.016±0.004	226	ONENGUT	05	CHRS	ν_μ emulsion, $\overline{E}_\nu \approx 27$ GeV

Γ(4-prongs)/Γ_{total} Γ_3/Γ

This is the sum of our $K^-2\pi^+\pi^-$, $K^-2\pi^+\pi^-\pi^0$, $\overline{K}^0 2\pi^+ 2\pi^-$, $K^+2K^-\pi^+$, $2\pi^+2\pi^-$, $2\pi^+2\pi^-\pi^0$, $K^+K^-\pi^+\pi^-$, and $K^+K^-\pi^+\pi^-\pi^0$ branching fractions.

VALUE	DOCUMENT ID	
0.145±0.005 OUR FIT		
0.145±0.005	PDG	12

Γ(6-prongs)/Γ_{total} Γ_4/Γ

This is the sum of our $K^-3\pi^+2\pi^-$ and $3\pi^+3\pi^-$ branching fractions.

VALUE (units 10^{-4})	EVTS	DOCUMENT ID		TECN	COMMENT
6.4± 1.3 OUR FIT					
6.4± 1.3		PDG	12		
• • • We do not use the following data for averages, fits, limits, etc. • • •					
$12\ ^{+13}_{-9}\ \pm 2$	3	ONENGUT	05	CHRS	ν_μ emulsion, $\overline{E}_\nu \approx 27$ GeV

Inclusive modes

$\Gamma(e^+ \text{anything})/\Gamma_{total}$ Γ_5/Γ

The branching fractions for the $K^- e^+ \nu_e$, $K^*(892)^- e^+ \nu_e$, $\pi^- e^+ \nu_e$, and $\rho^- e^+ \nu_e$ modes add up to 6.20 ± 0.17 %.

VALUE (%)	EVTS	DOCUMENT ID		TECN	COMMENT
6.49±0.11 OUR AVERAGE					
6.46±0.09±0.11	6584 ± 96	[1] ASNER	10	CLEO	e^+e^- at 3774 MeV
6.3 ±0.7 ±0.4	290 ± 32	ABLIKIM	07G	BES2	$e^+e^- \approx \psi(3770)$
6.46±0.17±0.13	2246 ± 57	ADAM	06A	CLEO	See ASNER 10
6.9 ±0.3 ±0.5	1670	ALBRECHT	96C	ARG	$e^+e^- \approx$ 10 GeV
6.64±0.18±0.29	4609	KUBOTA	96B	CLE2	$e^+e^- \approx \Upsilon(4S)$

[1] Using the D^+ and D^0 lifetimes, ASNER 10 finds that the ratio of the D^+ and D^0 semileptonic widths is 0.985 ± 0.015 ± 0.024.

$\Gamma(\mu^+ \text{anything})/\Gamma_{total}$ Γ_6/Γ

VALUE (%)	EVTS	DOCUMENT ID		TECN	COMMENT
6.7±0.6 OUR FIT					
6.4±0.8 OUR AVERAGE					
6.8±1.5±0.8	79 ± 10	[1] ABLIKIM	08L	BES2	$e^+e^- \approx \psi(3772)$
6.5±1.2±0.3	36	KAYIS-TOPAK...	05	CHRS	ν_μ emulsion
6.0±0.7±1.2	310	ALBRECHT	96C	ARG	$e^+e^- \approx$ 10 GeV

[1] ABLIKIM 08L finds the ratio of $D^+ \to \mu^+ X$ and $D^0 \to \mu^+ X$ branching fractions to be 2.59 ± 0.70 ± 0.25, in accord with the ratio of D^+ and D^0 lifetimes, 2.54 ± 0.02.

$\Gamma(K^- \text{anything})/\Gamma_{total}$ Γ_7/Γ

VALUE	EVTS	DOCUMENT ID		TECN	COMMENT
0.547±0.028 OUR AVERAGE Error includes scale factor of 1.3. See the ideogram below.					
0.578±0.016±0.032	2098 ± 59	ABLIKIM	07G	BES2	$e^+e^- \approx \psi(3770)$
$0.546\ ^{+0.039}_{-0.038}$		[1] BARLAG	92C	ACCM	π^- Cu 230 GeV
0.609±0.032±0.052		COFFMAN	91	MRK3	e^+e^- 3.77 GeV
0.42 ±0.08		AGUILAR-...	87E	HYBR	πp, pp 360, 400 GeV

0.55 ±0.11	121	SCHINDLER	81	MRK2	e^+e^- 3.771 GeV
0.35 ±0.10	19	VUILLEMIN	78	LGW	e^+e^- 3.772 GeV

[1] BARLAG 92C computes the branching fraction using topological normalization.

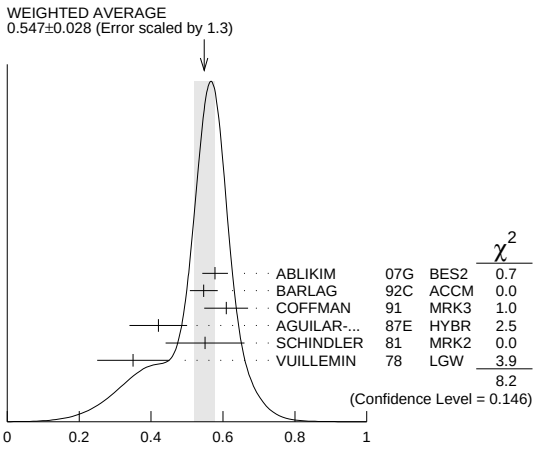

$[\Gamma(\overline{K}^0 \text{anything}) + \Gamma(K^0 \text{anything})]/\Gamma_{\text{total}}$ Γ_8/Γ

VALUE	EVTS	DOCUMENT ID	TECN	COMMENT
0.47 ±0.04 OUR AVERAGE				
0.476±0.048±0.030	250 ± 25	ABLIKIM	06U BES2	e^+e^- at 3773 MeV
0.455±0.050±0.032		COFFMAN	91 MRK3	e^+e^- 3.77 GeV

$\Gamma(K^+ \text{anything})/\Gamma_{\text{total}}$ Γ_9/Γ

VALUE	EVTS	DOCUMENT ID	TECN	COMMENT
0.034±0.004 OUR AVERAGE				
0.035±0.007±0.003	119 ± 23	ABLIKIM	07G BES2	$e^+e^- \approx \psi(3770)$
$0.034^{+0.007}_{-0.005}$		[1] BARLAG	92C ACCM	π^- Cu 230 GeV
0.028±0.009±0.004		COFFMAN	91 MRK3	e^+e^- 3.77 GeV
$0.03^{+0.05}_{-0.02}$		AGUILAR-...	87E HYBR	πp, pp 360, 400 GeV
0.08 ±0.03	25	SCHINDLER	81 MRK2	e^+e^- 3.771 GeV

[1] BARLAG 92C computes the branching fraction using topological normalization.

$\Gamma(K^*(892)^- \text{anything})/\Gamma_{\text{total}}$ Γ_{10}/Γ

VALUE	EVTS	DOCUMENT ID	TECN	COMMENT
0.153±0.083±0.019	28 ± 15	ABLIKIM	06U BES2	e^+e^- at 3773 MeV

$\Gamma(\overline{K}^*(892)^0 \text{anything})/\Gamma_{\text{total}}$ Γ_{11}/Γ

VALUE	EVTS	DOCUMENT ID	TECN	COMMENT
0.087±0.040±0.012	96 ± 44	ABLIKIM	05P BES	$e^+e^- \approx$ 3773 MeV

$\Gamma(K^*(892)^+ \text{anything})/\Gamma_{\text{total}}$ Γ_{12}/Γ

VALUE	CL%	DOCUMENT ID	TECN	COMMENT
<0.036	90	ABLIKIM	06U BES2	e^+e^- at 3773 MeV

$\Gamma(K^*(892)^0 \text{anything})/\Gamma_{\text{total}}$ Γ_{13}/Γ

VALUE	EVTS	DOCUMENT ID	TECN	COMMENT
0.028±0.012±0.004	31 ± 12	ABLIKIM	05P BES	$e^+e^- \approx$ 3773 MeV

$\Gamma(\eta \text{anything})/\Gamma_{\text{total}}$ Γ_{14}/Γ

This ratio includes η particles from η' decays.

VALUE (units 10^{-2})	EVTS	DOCUMENT ID	TECN	COMMENT
9.5±0.4±0.8	4463±197	HUANG	06B CLEO	e^+e^- at $\psi(3770)$

$\Gamma(\eta' \text{anything})/\Gamma_{\text{total}}$ Γ_{15}/Γ

VALUE (units 10^{-2})	EVTS	DOCUMENT ID	TECN	COMMENT
2.48±0.17±0.21	299 ± 21	HUANG	06B CLEO	e^+e^- at $\psi(3770)$

$\Gamma(\phi \text{anything})/\Gamma_{\text{total}}$ Γ_{16}/Γ

VALUE (units 10^{-2})	EVTS	DOCUMENT ID	TECN	COMMENT
1.05±0.08±0.07	368 ± 24	HUANG	06B CLEO	e^+e^- at $\psi(3770)$
• • • We do not use the following data for averages, fits, limits, etc. • • •				
$1.71^{+0.76}_{-0.71}\pm0.17$	9	BAI	00C BES	$e^+e^- \to D\overline{D}^*, D^*\overline{D}^*$

$\Gamma(\text{invisibles})/\Gamma_{\text{total}}$ Γ_{17}/Γ

VALUE	CL%	DOCUMENT ID	TECN	COMMENT
<9.4 × 10^{-5}	90	LAI	17 BELL	e^+e^- at Υ(nS), n=4,5

Semileptonic modes

$\Gamma(K^- e^+ \nu_e)/\Gamma_{\text{total}}$ Γ_{19}/Γ

VALUE (units 10^{-2})	EVTS	DOCUMENT ID	TECN	COMMENT
3.530±0.028 OUR FIT Error includes scale factor of 1.1.				
3.503±0.029 OUR AVERAGE				
3.505±0.014±0.033	71k	[1] ABLIKIM	15X BES3	2.92 fb^{-1}, 3.773 GeV
3.50 ±0.03 ±0.04	14.1k	[1] BESSON	09 CLEO	e^+e^- at $\psi(3770)$
3.45 ±0.10 ±0.19	1.3k	[2] WIDHALM	06 BELL	$e^+e^- \approx \Upsilon(4S)$
3.82 ±0.40 ±0.27	104	ABLIKIM	04C BES	e^+e^-, 3.773 GeV
3.4 ±0.5 ±0.4	55	ADLER	89 MRK3	e^+e^- 3.77 GeV
• • • We do not use the following data for averages, fits, limits, etc. • • •				
3.56 ±0.03 ±0.09		[3] DOBBS	08 CLEO	See BESSON 09
3.44 ±0.10 ±0.10	1.3k	COAN	05 CLEO	See DOBBS 08

[1] See the form-factor parameters near the end of this D^0 Listing.

[2] The $\pi^- e^+ \nu_e$ and $K^- e^+ \nu_e$ results of WIDHALM 06 give $|\frac{V_{cd}}{V_{cs}} \cdot \frac{f_+^\pi(0)}{f_+^K(0)}|^2 = 0.042 \pm 0.003 \pm 0.003$.

[3] DOBBS 08 establishes $|\frac{V_{cd}}{V_{cs}} \cdot \frac{f_+^\pi(0)}{f_+^K(0)}| = 0.188 \pm 0.008 \pm 0.002$ from the D^+ and D^0 decays to $\overline{K} e^+ \nu_e$ and $\pi e^+ \nu_e$.

$\Gamma(K^- e^+ \nu_e)/\Gamma(K^- \pi^+)$ Γ_{19}/Γ_{32}

VALUE	EVTS	DOCUMENT ID	TECN	COMMENT
0.907±0.011 OUR FIT Error includes scale factor of 1.2.				
0.930±0.013 OUR AVERAGE				
0.927±0.007±0.012	76k±323	[1] AUBERT	07BG BABR	$e^+e^- \approx \Upsilon(4S)$
0.978±0.027±0.044	2510	[2] BEAN	93C CLE2	$e^+e^- \approx \Upsilon(4S)$
0.90 ±0.06 ±0.06	584	[3] CRAWFORD	91B CLEO	$e^+e^- \approx$ 10.5 GeV
0.91 ±0.07 ±0.11	250	[4] ANJOS	89F E691	Photoproduction

[1] The event samples in this AUBERT 07BG result include radiative photons. The $D^0 \to K^- e^+ \nu_e$ form factor at $q^2 = 0$ is $f_+(0) = 0.727 \pm 0.007 \pm 0.005 \pm 0.007$.

[2] BEAN 93C uses $K^- \mu^+ \nu_\mu$ as well as $K^- e^+ \nu_e$ events and makes a small phase-space adjustment to the number of the μ^+ events to use them as e^+ events. A pole mass of $2.00 \pm 0.12 \pm 0.18$ GeV/c^2 is obtained from the q^2 dependence of the decay rate.

[3] CRAWFORD 91B uses $K^- e^+ \nu_e$ and $K^- \mu^+ \nu_\mu$ candidates to measure a pole mass of $2.1^{+0.4}_{-0.2}{}^{+0.3}_{-0.2}$ GeV/c^2 from the q^2 dependence of the decay rate.

[4] ANJOS 89F measures a pole mass of $2.1^{+0.4}_{-0.2} \pm 0.2$ GeV/c^2 from the q^2 dependence of the decay rate.

$\Gamma(K^- \mu^+ \nu_\mu)/\Gamma_{\text{total}}$ Γ_{20}/Γ

VALUE (units 10^{-2})	EVTS	DOCUMENT ID	TECN	COMMENT
3.31±0.13 OUR FIT				
3.45±0.10±0.21	1249 ± 43	WIDHALM	06 BELL	$e^+e^- \approx \Upsilon(4S)$

$\Gamma(K^- \mu^+ \nu_\mu)/\Gamma(\mu^+ \text{anything})$ Γ_{20}/Γ_6

VALUE	EVTS	DOCUMENT ID	TECN	COMMENT
0.50 ±0.05 OUR FIT				
0.472±0.051±0.040	232	KODAMA	94 E653	π^- emulsion 600 GeV
• • • We do not use the following data for averages, fits, limits, etc. • • •				
0.32 ±0.05 ±0.05	124	KODAMA	91 EMUL	pA 800 GeV

$\Gamma(K^- \mu^+ \nu_\mu)/\Gamma(K^- \pi^+)$ Γ_{20}/Γ_{32}

VALUE	EVTS	DOCUMENT ID	TECN	COMMENT
0.851±0.033 OUR FIT				
0.84 ±0.04 OUR AVERAGE				
0.852±0.034±0.028	1897	[1] FRABETTI	95G E687	γBe $\overline{E}_\gamma$= 220 GeV
0.82 ±0.13 ±0.13	338	[2] FRABETTI	93I E687	γBe $\overline{E}_\gamma$= 221 GeV
0.79 ±0.08 ±0.09	231	[3] CRAWFORD	91B CLEO	$e^+e^- \approx$ 10.5 GeV

[1] FRABETTI 95G extracts the ratio of form factors $f_-(0)/f_+(0) = -1.3^{+3.6}_{-3.4} \pm 0.6$, and measures a pole mass of $1.87^{+0.11}_{-0.08}{}^{+0.07}_{-0.06}$ GeV/c^2 from the q^2 dependence of the decay rate.

[2] FRABETTI 93I measures a pole mass of $2.1^{+0.7}_{-0.3}{}^{+0.7}_{-0.3}$ GeV/c^2 from the q^2 dependence of the decay rate.

[3] CRAWFORD 91B measures a pole mass of $2.00 \pm 0.12 \pm 0.18$ GeV/c^2 from the q^2 dependence of the decay rate.

$\Gamma(K^*(892)^- e^+ \nu_e)/\Gamma_{\text{total}}$ Γ_{21}/Γ

Both decay modes of the $K^*(892)^-$ are included.

VALUE (units 10^{-2})	EVTS	DOCUMENT ID	TECN	COMMENT
2.15±0.16 OUR FIT				
2.16±0.15±0.08	219 ± 16	[1] COAN	05 CLEO	e^+e^- at $\psi(3770)$

[1] COAN 05 uses both $K^-\pi^0$ and $K^0_S\pi^-$ events.

$\Gamma(K^*(892)^- e^+ \nu_e)/\Gamma(K^0_S \pi^+ \pi^-)$ Γ_{21}/Γ_{35}

Unseen decay modes of the $K^*(892)^-$ are included.

VALUE	EVTS	DOCUMENT ID	TECN	COMMENT
0.78±0.07 OUR FIT				
0.76±0.12±0.06	152	[1] BEAN	93C CLE2	$e^+e^- \approx \Upsilon(4S)$

[1] BEAN 93C uses $K^{*-} \mu^+ \nu_\mu$ as well as $K^{*-} e^+ \nu_e$ events and makes a small phase-space adjustment to the number of the μ^+ events to use them as e^+ events.

$\Gamma(K^*(892)^-\mu^+\nu_\mu)/\Gamma(K^0_S\pi^+\pi^-)$ Γ_{22}/Γ_{35}

Unseen decay modes of the $K^*(892)^-$ are included.

VALUE	EVTS	DOCUMENT ID		TECN	COMMENT
0.674±0.068±0.026	175 ± 17	[1] LINK	05B	FOCS	γ A, $\overline{E}_\gamma \approx$ 180 GeV

[1] LINK 05B finds that in $D^0 \to \overline{K}^0\pi^-\mu^+\nu_\mu$ the $\overline{K}^0\pi^-$ system is 6% in S-wave.

$\Gamma(K^-\pi^0 e^+\nu_e)/\Gamma_{\text{total}}$ Γ_{23}/Γ

VALUE	EVTS	DOCUMENT ID		TECN	COMMENT
$\mathbf{0.016^{+0.013}_{-0.005}\pm0.002}$	4	[1] BAI	91	MRK3	$e^+e^- \approx$ 3.77 GeV

[1] BAI 91 finds that a fraction $0.79^{+0.15}_{-0.17}{}^{+0.09}_{-0.03}$ of combined D^+ and D^0 decays to $\overline{K}\pi e^+\nu_e$ (24 events) are $\overline{K}^*(892)e^+\nu_e$. BAI 91 uses 56 $K^-e^+\nu_e$ events to measure a pole mass of $1.8 \pm 0.3 \pm 0.2$ GeV/c^2 from the q^2 dependence of the decay rate.

$\Gamma(\overline{K}^0\pi^-e^+\nu_e)/\Gamma_{\text{total}}$ Γ_{24}/Γ

VALUE (units 10^{-2})	EVTS	DOCUMENT ID		TECN	COMMENT
2.7 $^{+0.9}_{-0.7}$ OUR AVERAGE					
2.61±1.04±0.28	9 ± 3	ABLIKIM	06O	BES2	e^+e^- at 3773 MeV
2.8 $^{+1.7}_{-0.8}$ ±0.3	6	[1] BAI	91	MRK3	$e^+e^- \approx$ 3.77 GeV

[1] BAI 91 finds that a fraction $0.79^{+0.15}_{-0.17}{}^{+0.09}_{-0.03}$ of combined D^+ and D^0 decays to $\overline{K}\pi e^+\nu_e$ (24 events) are $\overline{K}^*(892)e^+\nu_e$.

$\Gamma(K^-\pi^+\pi^-e^+\nu_e)/\Gamma_{\text{total}}$ Γ_{25}/Γ

VALUE (units 10^{-4})	EVTS	DOCUMENT ID	TECN	COMMENT
$\mathbf{2.8^{+1.4}_{-1.1}\pm0.3}$	8	ARTUSO	07A	CLEO	e^+e^- at $\Upsilon(3770)$

$\Gamma(K_1(1270)^-e^+\nu_e)/\Gamma_{\text{total}}$ Γ_{26}/Γ

VALUE (units 10^{-4})	EVTS	DOCUMENT ID		TECN	COMMENT
$\mathbf{7.6^{+4.1}_{-3.0}\pm0.9}$	8	[1] ARTUSO	07A	CLEO	e^+e^- at $\Upsilon(3770)$

[1] This ARTUSO 07A result is corrected for all decay modes of the $K_1(1270)^-$.

$\Gamma(K^-\pi^+\pi^-\mu^+\nu_\mu)/\Gamma(K^-\mu^+\nu_\mu)$ Γ_{27}/Γ_{20}

VALUE	CL%	DOCUMENT ID	TECN	COMMENT
<0.037	90	KODAMA	93B	E653	π^- emulsion 600 GeV

$\Gamma((\overline{K}^*(892)\pi)^-\mu^+\nu_\mu)/\Gamma(K^-\mu^+\nu_\mu)$ Γ_{28}/Γ_{20}

VALUE	CL%	DOCUMENT ID		TECN	COMMENT
<0.043	90	[1] KODAMA	93B	E653	π^- emulsion 600 GeV

[1] KODAMA 93B searched in $K^-\pi^+\pi^-\mu^+\nu_\mu$, but the limit includes other $(\overline{K}^*(892)\pi)^-$ charge states.

$\Gamma(\pi^-e^+\nu_e)/\Gamma_{\text{total}}$ Γ_{29}/Γ

VALUE (units 10^{-2})	EVTS	DOCUMENT ID		TECN	COMMENT
0.291±0.004 OUR FIT	Error includes scale factor of 1.1.				
0.293±0.004 OUR AVERAGE					
0.295±0.004±0.003	6.3k	[1] ABLIKIM	15X	BES3	2.92 fb^{-1}, 3.773 GeV
0.288±0.008±0.003	1.3k	[1] BESSON	09	CLEO	e^+e^- at $\psi(3770)$
0.279±0.027±0.016	126	[2] WIDHALM	06	BELL	$e^+e^- \approx \Upsilon(4S)$
• • • We do not use the following data for averages, fits, limits, etc. • • •					
0.299±0.011±0.009		[3] DOBBS	08	CLEO	See BESSON 09
0.262±0.025±0.008	117	COAN	05	CLEO	See DOBBS 08

[1] See the form-factor parameters near the end of this D^0 Listing.

[2] The $\pi^-e^+\nu_e$ and $K^-e^+\nu_e$ results of WIDHALM 06 give $|\frac{V_{cd}}{V_{cs}}\cdot\frac{f_+^\pi(0)}{f_+^K(0)}|^2 = 0.042 \pm 0.003 \pm 0.003$.

[3] DOBBS 08 establishes $|\frac{V_{cd}}{V_{cs}}\cdot\frac{f_+^\pi(0)}{f_+^K(0)}| = 0.188 \pm 0.008 \pm 0.002$ from the D^+ and D^0 decays to $\overline{K}e^+\nu_e$ and $\pi e^+\nu_e$.

$\Gamma(\pi^-e^+\nu_e)/\Gamma(K^-e^+\nu_e)$ Γ_{29}/Γ_{19}

VALUE	EVTS	DOCUMENT ID		TECN	COMMENT
0.0823±0.0014 OUR FIT	Error includes scale factor of 1.1.				
0.085 ±0.007 OUR AVERAGE					
0.082 ±0.006 ±0.005		[1] HUANG	05	CLEO	$e^+e^- \approx \Upsilon(4S)$
0.101 ±0.020 ±0.003	91	[2] FRABETTI	96B	E687	γ Be, $\overline{E}_\gamma \approx$ 200 GeV
0.103 ±0.039 ±0.013	87	[3] BUTLER	95	CLE2	< 0.156 (90% CL)

[1] HUANG 05 uses both e and μ events, and makes a small correction to the μ events to make them effectively e events. This result gives $|\frac{V_{cd}}{V_{cs}}\cdot\frac{f_+^\pi(0)}{f_+^K(0)}|^2 = 0.038^{+0.006}_{-0.007}{}^{+0.005}_{-0.003}$.

[2] FRABETTI 96B uses both e and μ events, and makes a small correction to the μ events to make them effectively e events. This result gives $|\frac{V_{cd}}{V_{cs}}\cdot\frac{f_+^\pi(0)}{f_+^K(0)}|^2 = 0.050\pm0.011\pm0.002$.

[3] BUTLER 95 has 87 ± 33 $\pi^-e^+\nu_e$ events. The result gives $|\frac{V_{cd}}{V_{cs}}\cdot\frac{f_+^\pi(0)}{f_+^K(0)}|^2 = 0.052 \pm 0.020 \pm 0.007$.

$\Gamma(\pi^-e^+\nu_e)/\Gamma(K^-\pi^+)$ Γ_{29}/Γ_{32}

VALUE (units 10^{-2})	EVTS	DOCUMENT ID		TECN	COMMENT
7.47±0.13 OUR FIT	Error includes scale factor of 1.1.				
7.02±0.17±0.23	375k	[1] LEES	15F	BABR	347 fb^{-1}, 10.58 GeV

[1] See the form-factor parameters near the end of the D^0 Listing.

$\Gamma(\pi^-\mu^+\nu_\mu)/\Gamma_{\text{total}}$ Γ_{30}/Γ

VALUE (units 10^{-2})	EVTS	DOCUMENT ID		TECN	COMMENT
0.237±0.024 OUR FIT					
0.231±0.026±0.019	106 ± 13	WIDHALM	06	BELL	$e^+e^- \approx \Upsilon(4S)$

$\Gamma(\pi^-\mu^+\nu_\mu)/\Gamma(K^-\mu^+\nu_\mu)$ Γ_{30}/Γ_{20}

VALUE	EVTS	DOCUMENT ID		TECN	COMMENT
0.072±0.007 OUR FIT					
0.074±0.008±0.007	288 ± 29	[1] LINK	05	FOCS	γ A, $\overline{E}_\gamma \approx$ 180 GeV

[1] LINK 05 finds the form-factor ratio $|f_0^\pi(0)/f_0^K(0)|$ to be 0.85 ± 0.04 ± 0.04 ± 0.01.

$\Gamma(\rho^-e^+\nu_e)/\Gamma_{\text{total}}$ Γ_{31}/Γ

VALUE (units 10^{-3})	EVTS	DOCUMENT ID		TECN	COMMENT
1.77±0.12±0.10	305 ± 21	[1,2] DOBBS	13	CLEO	e^+e^- at $\psi(3770)$
• • • We do not use the following data for averages, fits, limits, etc. • • •					
1.94±0.39±0.13	31 ± 6	COAN	05	CLEO	See DOBBS 13

[1] DOBBS 13 finds $\Gamma(D^0 \to \rho^-e^+\nu_e)$ / 2 $\Gamma(D^+ \to \rho^0e^+\nu_e) = 1.03 \pm 0.09^{+0.08}_{-0.02}$; isospin invariance predicts the ratio is 1.0.

[2] See the D^+ Listings for $D \to \rho e^+\nu_e$ form factors.

Hadronic modes with a single $\overline{K}$

$\Gamma(K^-\pi^+)/\Gamma_{\text{total}}$ Γ_{32}/Γ

VALUE (units 10^{-2})	EVTS	DOCUMENT ID		TECN	COMMENT
3.89 ±0.04 OUR FIT	Error includes scale factor of 1.1.				
3.93 ±0.05 OUR AVERAGE	Error includes scale factor of 1.1.				
3.934±0.021±0.061		BONVICINI	14	CLEO	All CLEO-c runs
4.007±0.037±0.072	33.8k	AUBERT	08L	BABR	e^+e^- at $\Upsilon(4S)$
3.82 ±0.07 ±0.12		[1] ARTUSO	98	CLE2	CLEO average
3.90 ±0.09 ±0.12	5.4k	[2] BARATE	97C	ALEP	From Z decays
3.41 ±0.12 ±0.28	1.2k	[2] ALBRECHT	94F	ARG	$e^+e^- \approx \Upsilon(4S)$
3.62 ±0.34 ±0.44		[2] DECAMP	91J	ALEP	From Z decays
• • • We do not use the following data for averages, fits, limits, etc. • • •					
3.891±0.035±0.069		[3] DOBBS	07	CLEO	See BONVICINI 14
3.91 ±0.08 ±0.09	10.3k	[3] HE	05	CLEO	See DOBBS 07
3.81 ±0.15 ±0.16	1.2k	[4] ARTUSO	98	CLE2	e^+e^- at $\Upsilon(4S)$
3.69 ±0.11 ±0.16		[5] COAN	98	CLE2	See ARTUSO 98
4.5 ±0.6 ±0.4		[6] ALBRECHT	94	ARG	$e^+e^- \approx \Upsilon(4S)$
3.95 ±0.08 ±0.17	4.2k	[2,7] AKERIB	93	CLE2	See ARTUSO 98
4.5 ±0.8 ±0.5	56	[2] ABACHI	88	HRS	e^+e^- 29 GeV
4.2 ±0.4 ±0.4	0.9k	ADLER	88C	MRK3	e^+e^- 3.77 GeV
4.1 ±0.6	0.3k	[8] SCHINDLER	81	MRK2	e^+e^- 3.771 GeV
4.3 ±1.0	130	[9] PERUZZI	77	LGW	e^+e^- 3.77 GeV

[1] This combines the CLEO results of ARTUSO 98, COAN 98, and AKERIB 93.

[2] ABACHI 88, DECAMP 91J, AKERIB 93, ALBRECHT 94F, and BARATE 97C use $D^*(2010)^+ \to D^0\pi^+$ decays. The π^+ is both slow and of low p_T with respect to the event thrust axis or nearest jet ($\approx D^{*+}$ direction). The excess number of such π^+'s over background gives the number of $D^*(2010)^+ \to D^0\pi^+$ events, and the fraction with $D^0 \to K^-\pi^+$ gives the $D^0 \to K^-\pi^+$ branching fraction.

[3] DOBBS 07 and HE 05 use single- and double-tagged events in an overall fit. DOBBS 07 supersedes HE 05.

[4] ARTUSO 98, following ALBRECHT 94, uses D^0 mesons from $\overline{B}^0 \to D^*(2010)^+X\ell^-\overline{\nu}_\ell$ decays. Our average uses the CLEO average of this value with the values of COAN 98 and AKERIB 93.

[5] COAN 98 assumes that $\Gamma(B \to \overline{D}X\ell^+\nu)/\Gamma(B \to X\ell^+\nu) = 1.0 - 3|V_{ub}/V_{cb}|^2 - 0.010 \pm 0.005$, the last term accounting for $\overline{B} \to D_s^+KX\ell^-\overline{\nu}$. COAN 98 is included in the CLEO average in ARTUSO 98.

[6] ALBRECHT 94 uses D^0 mesons from $\overline{B}^0 \to D^{*+}\ell^-\overline{\nu}_\ell$ decays. This is a different set of events than used by ALBRECHT 94F.

[7] This AKERIB 93 value includes radiative corrections; without them, the value is 0.0391 ± 0.0008 ± 0.0017. AKERIB 93 is included in the CLEO average in ARTUSO 98.

[8] SCHINDLER 81 (MARK-2) measures $\sigma(e^+e^- \to \psi(3770)) \times$ branching fraction to be 0.24 ± 0.02 nb. We use the MARK-3 (ADLER 88C) value of $\sigma = 5.8 \pm 0.5 \pm 0.6$ nb.

[9] PERUZZI 77 (MARK-1) measures $\sigma(e^+e^- \to \psi(3770)) \times$ branching fraction to be 0.25 ± 0.05 nb. We use the MARK-3 (ADLER 88C) value of $\sigma = 5.8 \pm 0.5 \pm 0.6$ nb.

$\Gamma(K^0_S\pi^0)/\Gamma_{\text{total}}$ Γ_{33}/Γ

VALUE (units 10^{-2})	EVTS	DOCUMENT ID		TECN	COMMENT
• • • We do not use the following data for averages, fits, limits, etc. • • •					
1.240±0.017±0.056	614	HE	08	CLEO	See MENDEZ 10

$\Gamma(K^0_S\pi^0)/\Gamma(K^-\pi^+)$ Γ_{33}/Γ_{32}

VALUE	EVTS	DOCUMENT ID		TECN	COMMENT
• • • We do not use the following data for averages, fits, limits, etc. • • •					
0.68±0.12±0.11	119	ANJOS	92B	E691	γBe 80–240 GeV

$\Gamma(K^0_S\pi^0)/[\Gamma(K^-\pi^+)+\Gamma(K^+\pi^-)]$ $\Gamma_{33}/(\Gamma_{32}+\Gamma_{257})$

VALUE (units 10^{-2})	EVTS	DOCUMENT ID		TECN	COMMENT
30.4±0.9 OUR FIT					
30.4±0.3±0.9	20k	MENDEZ	10	CLEO	e^+e^- at 3774 MeV

$\Gamma(K^0_S\pi^0)/\Gamma(K^0_S\pi^+\pi^-)$ Γ_{33}/Γ_{35}

VALUE	EVTS	DOCUMENT ID		TECN	COMMENT
0.432±0.028 OUR FIT					
0.44 ±0.02 ±0.05	1942 ± 64	PROCARIO	93B	CLE2	e^+e^- 10.36–10.7 GeV
• • • We do not use the following data for averages, fits, limits, etc. • • •					
0.34 ±0.04 ±0.02	92	[1] ALBRECHT	92P	ARG	$e^+e^-\approx$ 10 GeV
0.36 ±0.04 ±0.08	104	KINOSHITA	91	CLEO	$e^+e^-\sim$ 10.7 GeV

[1] This value is calculated from numbers in Table 1 of ALBRECHT 92P.

$\Gamma(K^0_L\pi^0)/\Gamma_{\rm total}$ Γ_{34}/Γ

VALUE (units 10^{-2})	EVTS	DOCUMENT ID		TECN	COMMENT
0.998±0.049±0.048	1116	[1] HE	08	CLEO	e^+e^- at $\psi(3770)$

[1] The difference of HE 08 $D^0\to K^0_S\pi^0$ and $K^0_L\pi^0$ branching fractions over the sum is $0.108\pm0.025\pm0.024$. This is consistent with U-spin symmetry and the Cabibbo angle.

$\Gamma(K^0_S\pi^+\pi^-)/\Gamma_{\rm total}$ Γ_{35}/Γ

VALUE (units 10^{-2})	EVTS	DOCUMENT ID		TECN	COMMENT
• • • We do not use the following data for averages, fits, limits, etc. • • •					
2.52±0.20±0.25	284 ± 22	[1] ALBRECHT	94F	ARG	$e^+e^-\approx\Upsilon(4S)$
3.2 ±0.3 ±0.5		ADLER	87	MRK3	e^+e^- 3.77 GeV
2.6 ±0.8	32 ± 8	[2] SCHINDLER	81	MRK2	e^+e^- 3.771 GeV
4.0 ±1.2	28	[3] PERUZZI	77	LGW	e^+e^- 3.77 GeV

[1] See the footnote on the ALBRECHT 94F measurement of $\Gamma(K^-\pi^+)/\Gamma_{\rm total}$ for the method used.
[2] SCHINDLER 81 (MARK-2) measures $\sigma(e^+e^-\to\psi(3770))\times$ branching fraction to be 0.30 ± 0.08 nb. We use the MARK-3 (ADLER 88C) value of $\sigma=5.8\pm0.5\pm0.6$ nb.
[3] PERUZZI 77 (MARK-1) measures $\sigma(e^+e^-\to\psi(3770))\times$ branching fraction to be 0.46 ± 0.12 nb. We use the MARK-3 (ADLER 88C) value of $\sigma=5.8\pm0.5\pm0.6$ nb.

$\Gamma(K^0_S\pi^+\pi^-)/\Gamma(K^-\pi^+)$ Γ_{35}/Γ_{32}

VALUE	EVTS	DOCUMENT ID		TECN	COMMENT
0.71±0.05 OUR FIT Error includes scale factor of 1.1.					
0.81±0.05±0.08	856 ± 35	FRABETTI	94J	E687	γBe $\overline{E}_\gamma$=220 GeV
• • • We do not use the following data for averages, fits, limits, etc. • • •					
0.85±0.40	35	AVERY	80	SPEC	$\gamma N\to D^{*+}$
1.4 ±0.5	116	PICCOLO	77	MRK1	e^+e^- 4.03, 4.41 GeV

$\Gamma(K^0_S\rho^0)/\Gamma(K^0_S\pi^+\pi^-)$ Γ_{36}/Γ_{35}

This is the "fit fraction" from the Dalitz-plot analysis.

VALUE	DOCUMENT ID		TECN	COMMENT
$0.224^{+0.017}_{-0.023}$ OUR AVERAGE Error includes scale factor of 1.7.				
0.210±0.016	[1] AUBERT	08AL	BABR	Dalitz fit, ≈ 487 k evts
$0.264\pm0.009^{+0.010}_{-0.026}$	MURAMATSU	02	CLE2	Dalitz fit, 5299 evts
• • • We do not use the following data for averages, fits, limits, etc. • • •				
$0.267\pm0.011^{+0.009}_{-0.028}$	ASNER	04A	CLEO	See MURAMATSU 02
0.350±0.028±0.067	FRABETTI	94G	E687	Dalitz fit, 597 evts
0.227±0.032±0.009	ALBRECHT	93D	ARG	Dalitz fit, 440 evts
0.215±0.051±0.037	ANJOS	93	E691	γBe 90–260 GeV
0.20 ±0.06 ±0.03	FRABETTI	92B	E687	γ Be, $\overline{E}_\gamma$= 221 GeV
0.12 ±0.01 ±0.07	ADLER	87	MRK3	e^+e^- 3.77 GeV

[1] The error on this AUBERT 08AL value includes both statistical and systematic uncertainties; the latter dominates.

$\Gamma(K^0_S\omega,\ \omega\to\pi^+\pi^-)/\Gamma(K^0_S\pi^+\pi^-)$ Γ_{37}/Γ_{35}

This is the "fit fraction" from the Dalitz-plot analysis.

VALUE	DOCUMENT ID		TECN	COMMENT
0.0073±0.0020 OUR AVERAGE				
0.009 ±0.010	[1] AUBERT	08AL	BABR	Dalitz fit, ≈ 487 k evts
$0.0072\pm0.0018^{+0.0010}_{-0.0009}$	MURAMATSU	02	CLE2	Dalitz fit, 5299 evts
• • • We do not use the following data for averages, fits, limits, etc. • • •				
$0.0081\pm0.0019^{+0.0018}_{-0.0010}$	ASNER	04A	CLEO	See MURAMATSU 02

[1] The error on this AUBERT 08AL value includes both statistical and systematic uncertainties; the latter dominates.

$\Gamma(K^0_S(\pi^+\pi^-)_{S-wave})/\Gamma(K^0_S\pi^+\pi^-)$ Γ_{38}/Γ_{35}

This is the "fit fraction" from the Dalitz-plot analysis. The $(\pi^+\pi^-)_{S-wave}$ includes what in isobar models are the $f_0(980)$ and $f_0(1370)$; see the following two data blocks.

VALUE	DOCUMENT ID		TECN	COMMENT
0.119±0.026	[1] AUBERT	08AL	BABR	Dalitz fit, ≈ 487 k evts

[1] The error on this AUBERT 08AL value includes both statistical and systematic uncertainties; the latter dominates.

$\Gamma(K^0_S f_0(980),\ f_0\to\pi^+\pi^-)/\Gamma(K^0_S\pi^+\pi^-)$ Γ_{39}/Γ_{35}

Fit fraction from the Dalitz plot analyses.

VALUE	DOCUMENT ID		TECN	COMMENT
$0.043\pm0.005^{+0.012}_{-0.006}$	MURAMATSU	02	CLE2	Dalitz fit, 5299 evts
• • • We do not use the following data for averages, fits, limits, etc. • • •				
$0.042\pm0.005^{+0.011}_{-0.005}$	ASNER	04A	CLEO	See MURAMATSU 02
0.068±0.016±0.018	FRABETTI	94G	E687	Dalitz fit, 597 evts
0.046±0.018±0.006	ALBRECHT	93D	ARG	Dalitz fit, 440 evts

$\Gamma(K^0_S f_0(1370),\ f_0\to\pi^+\pi^-)/\Gamma(K^0_S\pi^+\pi^-)$ Γ_{40}/Γ_{35}

This is the "fit fraction" from the Dalitz-plot analysis.

VALUE	DOCUMENT ID		TECN	COMMENT
$0.099\pm0.011^{+0.028}_{-0.044}$	MURAMATSU	02	CLE2	Dalitz fit, 5299 evts
• • • We do not use the following data for averages, fits, limits, etc. • • •				
$0.098\pm0.014^{+0.026}_{-0.036}$	ASNER	04A	CLEO	See MURAMATSU 02
0.077±0.022±0.031	FRABETTI	94G	E687	Dalitz fit, 597 evts
0.082±0.028±0.013	ALBRECHT	93D	ARG	Dalitz fit, 440 evts

$\Gamma(K^0_S f_2(1270),\ f_2\to\pi^+\pi^-)/\Gamma(K^0_S\pi^+\pi^-)$ Γ_{41}/Γ_{35}

This is the "fit fraction" from the Dalitz-plot analysis.

VALUE	DOCUMENT ID		TECN	COMMENT
$0.0032^{+0.0035}_{-0.0022}$ OUR AVERAGE				
0.006 ±0.007	[1] AUBERT	08AL	BABR	Dalitz fit, ≈ 487 k evts
$0.0027\pm0.0015^{+0.0037}_{-0.0017}$	MURAMATSU	02	CLE2	Dalitz fit, 5299 evts
• • • We do not use the following data for averages, fits, limits, etc. • • •				
$0.0036\pm0.0022^{+0.0032}_{-0.0019}$	ASNER	04A	CLEO	See MURAMATSU 02
0.037 ±0.014 ±0.017	FRABETTI	94G	E687	Dalitz fit, 597 evts
0.050 ±0.021 ±0.008	ALBRECHT	93D	ARG	Dalitz fit, 440 evts

[1] The error on this AUBERT 08AL value includes both statistical and systematic uncertainties; the latter dominates.

$\Gamma(K^*(892)^-\pi^+,\ K^{*-}\to K^0_S\pi^-)/\Gamma(K^0_S\pi^+\pi^-)$ Γ_{42}/Γ_{35}

This is the "fit fraction" from the Dalitz-plot analysis.

VALUE	DOCUMENT ID		TECN	COMMENT
$0.588^{+0.034}_{-0.050}$ OUR AVERAGE Error includes scale factor of 2.0.				
0.557±0.028	[1] AUBERT	08AL	BABR	Dalitz fit, ≈ 487 k evts
$0.657\pm0.013^{+0.018}_{-0.040}$	MURAMATSU	02	CLE2	Dalitz fit, 5299 evts
• • • We do not use the following data for averages, fits, limits, etc. • • •				
$0.663\pm0.013^{+0.024}_{-0.043}$	ASNER	04A	CLEO	See MURAMATSU 02
0.625±0.036±0.026	FRABETTI	94G	E687	Dalitz fit, 597 evts
0.718±0.042±0.030	ALBRECHT	93D	ARG	Dalitz fit, 440 evts
0.480±0.097	ANJOS	93	E691	γBe 90–260 GeV
0.56 ±0.04 ±0.05	ADLER	87	MRK3	e^+e^- 3.77 GeV

[1] The error on this AUBERT 08AL value includes both statistical and systematic uncertainties; the latter dominates.

$\Gamma(K^*_0(1430)^-\pi^+,\ K^{*-}_0\to K^0_S\pi^-)/\Gamma(K^0_S\pi^+\pi^-)$ Γ_{43}/Γ_{35}

This is the "fit fraction" from the Dalitz-plot analysis.

VALUE	DOCUMENT ID		TECN	COMMENT
$0.095^{+0.014}_{-0.010}$ OUR AVERAGE				
0.102±0.015	[1] AUBERT	08AL	BABR	Dalitz fit, ≈ 487 k evts
$0.073\pm0.007^{+0.031}_{-0.011}$	MURAMATSU	02	CLE2	Dalitz fit, 5299 evts
• • • We do not use the following data for averages, fits, limits, etc. • • •				
$0.072\pm0.007^{+0.014}_{-0.013}$	ASNER	04A	CLEO	See MURAMATSU 02
0.109±0.027±0.029	FRABETTI	94G	E687	Dalitz fit, 597 evts
0.129±0.034±0.021	ALBRECHT	93D	ARG	Dalitz fit, 440 evts

[1] The error on this AUBERT 08AL value includes both statistical and systematic uncertainties; the latter dominates.

$\Gamma(K^*_2(1430)^-\pi^+,\ K^{*-}_2\to K^0_S\pi^-)/\Gamma(K^0_S\pi^+\pi^-)$ Γ_{44}/Γ_{35}

This is the "fit fraction" from the Dalitz-plot analysis.

VALUE	DOCUMENT ID		TECN	COMMENT
$0.0120^{+0.0070}_{-0.0035}$ OUR AVERAGE				
0.022 ±0.016	[1] AUBERT	08AL	BABR	Dalitz fit, ≈ 487 k evts
$0.011\pm0.002^{+0.007}_{-0.003}$	MURAMATSU	02	CLE2	Dalitz fit, 5299 evts
• • • We do not use the following data for averages, fits, limits, etc. • • •				
$0.011\pm0.002^{+0.005}_{-0.003}$	ASNER	04A	CLEO	See MURAMATSU 02

[1] The error on this AUBERT 08AL value includes both statistical and systematic uncertainties; the latter dominates.

$\Gamma(K^*(1680)^-\pi^+,\ K^{*-}\to K^0_S\pi^-)/\Gamma(K^0_S\pi^+\pi^-)$ Γ_{45}/Γ_{35}

This is the "fit fraction" from the Dalitz-plot analysis.

VALUE	DOCUMENT ID		TECN	COMMENT
0.016±0.013 OUR AVERAGE				
0.007±0.019	[1] AUBERT	08AL	BABR	Dalitz fit, ≈ 487 k evts
$0.022\pm0.004^{+0.018}_{-0.015}$	MURAMATSU	02	CLE2	Dalitz fit, 5299 evts

• • • We do not use the following data for averages, fits, limits, etc. • • •

$0.023 \pm 0.005 \pm 0.007$	ASNER	04A	CLEO	See MURAMATSU 02

[1] The error on this AUBERT 08AL value includes both statistical and systematic uncertainties; the latter dominates.

$\Gamma(K^*(892)^+\pi^-,\ K^{*+} \to K^0_S\pi^+)/\Gamma(K^0_S\pi^+\pi^-)$ Γ_{46}/Γ_{35}

This is the "fit fraction" from the Dalitz-plot analysis. This is a doubly Cabibbo-suppressed mode.

VALUE (units 10^{-3})	DOCUMENT ID		TECN	COMMENT
$4.0^{+2.0}_{-1.2}$ OUR AVERAGE				
4.6 ± 2.3	[1] AUBERT	08AL	BABR	Dalitz fit, $\approx$ 487 k evts
$3.4 \pm 1.3^{+4.1}_{-0.4}$	MURAMATSU	02	CLE2	Dalitz fit, 5299 evts
• • • We do not use the following data for averages, fits, limits, etc. • • •				
$3.4 \pm 1.3^{+3.6}_{-0.5}$	ASNER	04A	CLEO	See MURAMATSU 02

[1] The error on this AUBERT 08AL value includes both statistical and systematic uncertainties; the latter dominates.

$\Gamma(K^*_0(1430)^+\pi^-,\ K^{*+}_0 \to K^0_S\pi^+)/\Gamma(K^0_S\pi^+\pi^-)$ Γ_{47}/Γ_{35}

This is the "fit fraction" from the Dalitz-plot analysis. This is a doubly Cabibbo-suppressed mode.

VALUE	CL%	DOCUMENT ID		TECN	COMMENT
$< 5 \times 10^{-4}$	95	AUBERT	08AL	BABR	Dalitz fit, $\approx$ 487 k evts

$\Gamma(K^*_2(1430)^+\pi^-,\ K^{*+}_2 \to K^0_S\pi^+)/\Gamma(K^0_S\pi^+\pi^-)$ Γ_{48}/Γ_{35}

This is the "fit fraction" from the Dalitz-plot analysis. This is a doubly Cabibbo-suppressed mode.

VALUE	CL%	DOCUMENT ID		TECN	COMMENT
$< 1.2 \times 10^{-3}$	95	AUBERT	08AL	BABR	Dalitz fit, $\approx$ 487 k evts

$\Gamma(K^0_S\pi^+\pi^-$ nonresonant$)/\Gamma(K^0_S\pi^+\pi^-)$ Γ_{49}/Γ_{35}

This is the "fit fraction" from the Dalitz-plot analysis. Neither FRABETTI 94G nor ALBRECHT 93D (quoted in many of the earlier submodes of $K^0_S\pi^+\pi^-$) sees evidence for a nonresonant component.

VALUE	DOCUMENT ID		TECN	COMMENT
$0.009 \pm 0.004^{+0.020}_{-0.004}$	MURAMATSU	02	CLE2	Dalitz fit, 5299 evts
• • • We do not use the following data for averages, fits, limits, etc. • • •				
$0.007 \pm 0.007^{+0.021}_{-0.006}$	ASNER	04A	CLEO	See MURAMATSU 02
$0.263 \pm 0.024 \pm 0.041$	ANJOS	93	E691	γBe 90–260 GeV
$0.26 \pm 0.08 \pm 0.05$	FRABETTI	92B	E687	γ Be, $\overline{E}_\gamma = 221$ GeV
$0.33 \pm 0.05 \pm 0.10$	ADLER	87	MRK3	e^+e^- 3.77 GeV

$\Gamma(K^-\pi^+\pi^0)/\Gamma_{\text{total}}$ Γ_{50}/Γ

VALUE (units 10^{-2})	EVTS	DOCUMENT ID		TECN	COMMENT
• • • We do not use the following data for averages, fits, limits, etc. • • •					
$14.57 \pm 0.12 \pm 0.38$		[1] DOBBS	07	CLEO	See BONVICINI 14
$14.9 \pm 0.3 \pm 0.5$	19k	[1] HE	05	CLEO	See DOBBS 07
$13.3 \pm 1.2 \pm 1.3$	931	ADLER	88C	MRK3	e^+e^- 3.77 GeV
11.7 ± 4.3	37	[2] SCHINDLER	81	MRK2	e^+e^- 3.771 GeV

[1] DOBBS 07 and HE 05 use single- and double-tagged events in an overall fit. DOBBS 07 supersedes HE 05.

[2] SCHINDLER 81 (MARK-2) measures $\sigma(e^+e^- \to \psi(3770)) \times$ branching fraction to be 0.68 ± 0.23 nb. We use the MARK-3 (ADLER 88C) value of $\sigma = 5.8 \pm 0.5 \pm 0.6$ nb.

$\Gamma(K^-\pi^+\pi^0)/\Gamma(K^-\pi^+)$ Γ_{50}/Γ_{32}

VALUE	EVTS	DOCUMENT ID		TECN	COMMENT
3.65 ±0.13 OUR FIT Error includes scale factor of 2.1.					
3.76 ±0.10 OUR AVERAGE Error includes scale factor of 1.4. See the ideogram below.					
$3.802 \pm 0.022 \pm 0.073$		BONVICINI	14	CLEO	All CLEO-c runs
$3.81 \pm 0.07 \pm 0.26$	10k	BARISH	96	CLE2	$e^+e^- \approx \Upsilon(4S)$
$3.04 \pm 0.16 \pm 0.34$	931	[1] ALBRECHT	92P	ARG	$e^+e^- \approx 10$ GeV
$2.8 \pm 0.14 \pm 0.52$	1050	KINOSHITA	91	CLEO	$e^+e^- \sim 10.7$ GeV

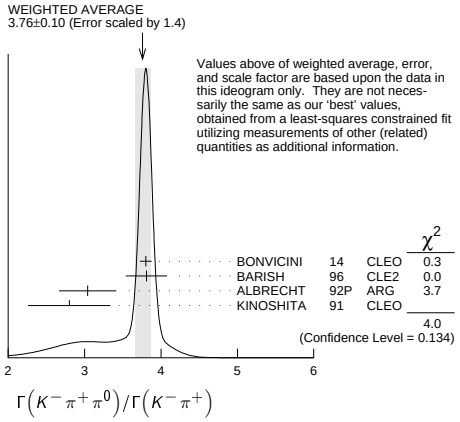

[1] This value is calculated from numbers in Table 1 of ALBRECHT 92P.

$\Gamma(K^-\rho^+)/\Gamma(K^-\pi^+\pi^0)$ Γ_{51}/Γ_{50}

This is the "fit fraction" from the Dalitz-plot analysis.

VALUE	DOCUMENT ID		TECN	COMMENT
0.78 ±0.04 OUR AVERAGE				
$0.788 \pm 0.019 \pm 0.048$	KOPP	01	CLE2	Dalitz fit, $\approx$ 7,000 evts
$0.765 \pm 0.041 \pm 0.054$	FRABETTI	94G	E687	Dalitz fit, 530 evts
• • • We do not use the following data for averages, fits, limits, etc. • • •				
$0.647 \pm 0.039 \pm 0.150$	ANJOS	93	E691	γBe 90–260 GeV
$0.81 \pm 0.03 \pm 0.06$	ADLER	87	MRK3	e^+e^- 3.77 GeV

$\Gamma(K^-\rho(1700)^+,\ \rho^+ \to \pi^+\pi^0)/\Gamma(K^-\pi^+\pi^0)$ Γ_{52}/Γ_{50}

This is the "fit fraction" from the Dalitz-plot analysis.

VALUE	DOCUMENT ID		TECN	COMMENT
$0.057 \pm 0.008 \pm 0.009$	KOPP	01	CLE2	Dalitz fit, $\approx$ 7,000 evts

$\Gamma(K^*(892)^-\pi^+,\ K^*(892)^- \to K^-\pi^0)/\Gamma(K^-\pi^+\pi^0)$ Γ_{53}/Γ_{50}

This is the "fit fraction" from the Dalitz-plot analysis.

VALUE	DOCUMENT ID		TECN	COMMENT
$0.160^{+0.025}_{-0.013}$ OUR AVERAGE				
$0.161 \pm 0.007^{+0.027}_{-0.011}$	KOPP	01	CLE2	Dalitz fit, $\approx$ 7,000 evts
$0.148 \pm 0.028 \pm 0.049$	FRABETTI	94G	E687	Dalitz fit, 530 evts
• • • We do not use the following data for averages, fits, limits, etc. • • •				
$0.084 \pm 0.011 \pm 0.012$	ANJOS	93	E691	γBe 90–260 GeV
$0.12 \pm 0.02 \pm 0.03$	ADLER	87	MRK3	e^+e^- 3.77 GeV

$\Gamma(\overline{K}^*(892)^0\pi^0,\ \overline{K}^*(892)^0 \to K^-\pi^+)/\Gamma(K^-\pi^+\pi^0)$ Γ_{54}/Γ_{50}

This is the "fit fraction" from the Dalitz-plot analysis.

VALUE	DOCUMENT ID		TECN	COMMENT
0.135 ±0.016 OUR AVERAGE				
$0.127 \pm 0.009 \pm 0.016$	KOPP	01	CLE2	Dalitz fit, $\approx$ 7,000 evts
$0.165 \pm 0.031 \pm 0.015$	FRABETTI	94G	E687	Dalitz fit, 530 evts
• • • We do not use the following data for averages, fits, limits, etc. • • •				
$0.142 \pm 0.018 \pm 0.024$	ANJOS	93	E691	γBe 90–260 GeV
$0.13 \pm 0.02 \pm 0.03$	ADLER	87	MRK3	e^+e^- 3.77 GeV

$\Gamma(K^*_0(1430)^-\pi^+,\ K^{*-}_0 \to K^-\pi^0)/\Gamma(K^-\pi^+\pi^0)$ Γ_{55}/Γ_{50}

This is the "fit fraction" from the Dalitz-plot analysis.

VALUE	DOCUMENT ID		TECN	COMMENT
0.033 ±0.006 ±0.014	KOPP	01	CLE2	Dalitz fit, $\approx$ 7,000 evts

$\Gamma(\overline{K}^*_0(1430)^0\pi^0,\ \overline{K}^{*0}_0 \to K^-\pi^+)/\Gamma(K^-\pi^+\pi^0)$ Γ_{56}/Γ_{50}

This is the "fit fraction" from the Dalitz-plot analysis.

VALUE	DOCUMENT ID		TECN	COMMENT
$0.041 \pm 0.006^{+0.032}_{-0.009}$	KOPP	01	CLE2	Dalitz fit, $\approx$ 7,000 evts

$\Gamma(K^*(1680)^-\pi^+,\ K^{*-} \to K^-\pi^0)/\Gamma(K^-\pi^+\pi^0)$ Γ_{57}/Γ_{50}

This is the "fit fraction" from the Dalitz-plot analysis.

VALUE	DOCUMENT ID		TECN	COMMENT
0.013 ±0.003 ±0.004	KOPP	01	CLE2	Dalitz fit, $\approx$ 7,000 evts

$\Gamma(K^-\pi^+\pi^0$ nonresonant$)/\Gamma(K^-\pi^+\pi^0)$ Γ_{58}/Γ_{50}

This is the "fit fraction" from the Dalitz-plot analysis.

VALUE	EVTS	DOCUMENT ID		TECN	COMMENT
$0.080^{+0.040}_{-0.014}$ OUR AVERAGE					
$0.075 \pm 0.009^{+0.056}_{-0.011}$		KOPP	01	CLE2	Dalitz fit, $\approx$ 7,000 evts
$0.101 \pm 0.033 \pm 0.040$		FRABETTI	94G	E687	Dalitz fit, 530 evts
• • • We do not use the following data for averages, fits, limits, etc. • • •					
$0.036 \pm 0.004 \pm 0.018$		ANJOS	93	E691	γBe 90–260 GeV
$0.09 \pm 0.02 \pm 0.04$		ADLER	87	MRK3	e^+e^- 3.77 GeV
0.51 ± 0.22	21	SUMMERS	84	E691	Photoproduction

$\Gamma(K^0_S 2\pi^0)/\Gamma_{\text{total}}$ Γ_{59}/Γ

VALUE (units 10^{-3})	EVTS	DOCUMENT ID		TECN	COMMENT
9.1 ±1.1 OUR AVERAGE Error includes scale factor of 2.2.					
$10.58 \pm 0.38 \pm 0.73$	1259	LOWREY	11	CLEO	$e^+e^- \approx 3.77$ GeV
$8.34 \pm 0.45 \pm 0.42$		ASNER	08	CLEO	$e^+e^- \to D^0\overline{D}^0$, 3.77 GeV

$\Gamma(K^0_S(2\pi^0)_{S-wave})/\Gamma(K^0_S 2\pi^0)$ Γ_{60}/Γ_{59}

VALUE (%)	DOCUMENT ID		TECN	COMMENT
28.9±6.3±3.1	LOWREY	11	CLEO	Dalitz analysis, 1259 evts

$\Gamma(\overline{K}^*(892)^0\pi^0,\ \overline{K}^{*0} \to K^0_S\pi^0)/\Gamma(K^0_S\pi^0)$ Γ_{61}/Γ_{33}

VALUE (%)	DOCUMENT ID		TECN	COMMENT
65.6± 5.3±2.5	LOWREY	11	CLEO	Dalitz analysis, 1259 evts
• • • We do not use the following data for averages, fits, limits, etc. • • •				
$55\ ^{+13}_{-10} \pm 7$	PROCARIO	93B	CLE2	Dalitz plot fit, 122 evts

$\Gamma(\overline{K}^*(1430)^0\pi^0,\ \overline{K}^{*0} \to K^0_S\pi^0)/\Gamma(K^0_S 2\pi^0)$ Γ_{62}/Γ_{59}

VALUE (%)	DOCUMENT ID		TECN	COMMENT
0.49±0.45±2.51	LOWREY	11	CLEO	Dalitz analysis, 1259 evts

$\Gamma(\overline{K}^*(1680)^0\pi^0,\ \overline{K}^{*0}\to K^0_S\pi^0)/\Gamma(K^0_S 2\pi^0)$ Γ_{63}/Γ_{59}

VALUE (%)	DOCUMENT ID		TECN	COMMENT
11.2±2.7±2.5	LOWREY	11	CLEO	Dalitz analysis, 1259 evts

$\Gamma(K^0_S f_2(1270),\ f_2\to 2\pi^0)/\Gamma(K^0_S 2\pi^0)$ Γ_{64}/Γ_{59}

VALUE (%)	DOCUMENT ID		TECN	COMMENT
2.48±0.91±0.78	LOWREY	11	CLEO	Dalitz analysis, 1259 evts

$\Gamma(2K^0_S,\text{one}\,K^0_S\to 2\pi^0)/\Gamma(K^0_S 2\pi^0)$ Γ_{65}/Γ_{59}

VALUE (%)	DOCUMENT ID		TECN	COMMENT
3.46±0.92±0.66	LOWREY	11	CLEO	Dalitz analysis, 1259 evts

$\Gamma(K^0_S 2\pi^0\,\text{nonresonant})/\Gamma(K^0_S\pi^0)$ Γ_{66}/Γ_{33}

VALUE	DOCUMENT ID		TECN	COMMENT
• • • We do not use the following data for averages, fits, limits, etc. • • •				
0.37±0.08±0.04	PROCARIO	93B	CLE2	Dalitz plot fit, 122 evts

$\Gamma(K^-2\pi^+\pi^-)/\Gamma_{\text{total}}$ Γ_{67}/Γ

VALUE (units 10^{-2})	EVTS	DOCUMENT ID		TECN	COMMENT
• • • We do not use the following data for averages, fits, limits, etc. • • •					
8.30±0.07±0.20		[1] DOBBS	07	CLEO	See BONVICINI 14
8.3 ±0.2 ±0.3	15k	[1] HE	05	CLEO	See DOBBS 07
7.9 ±1.5 ±0.9		[2] ALBRECHT	94	ARG	$e^+e^-\approx\Upsilon(4S)$
6.80±0.27±0.57	1.4k	[3] ALBRECHT	94F	ARG	$e^+e^-\approx\Upsilon(4S)$
9.1 ±0.8 ±0.8	992	ADLER	88C	MRK3	e^+e^- 3.77 GeV
11.7 ±2.5	185	[4] SCHINDLER	81	MRK2	e^+e^- 3.771 GeV
6.2 ±1.9	44	[5] PERUZZI	77	LGW	e^+e^- 3.77 GeV

[1] DOBBS 07 and HE 05 use single- and double-tagged events in an overall fit. DOBBS 07 supersedes HE 05.
[2] ALBRECHT 94 uses D^0 mesons from $\overline{B}^0\to D^{*+}\ell^-\overline{\nu}_\ell$ decays. This is a different set of events than used by ALBRECHT 94F.
[3] See the footnote on the ALBRECHT 94F measurement of $\Gamma(K^-\pi^+)/\Gamma_{\text{total}}$ for the method used.
[4] SCHINDLER 81 (MARK-2) measures $\sigma(e^+e^-\to\psi(3770))\times$ branching fraction to be 0.68 ± 0.11 nb. We use the MARK-3 (ADLER 88C) value of $\sigma = 5.8\pm0.5\pm0.6$ nb.
[5] PERUZZI 77 (MARK-1) measures $\sigma(e^+e^-\to\psi(3770))\times$ branching fraction to be 0.36 ± 0.10 nb. We use the MARK-3 (ADLER 88C) value of $\sigma = 5.8\pm0.5\pm0.6$ nb.

$\Gamma(K^-2\pi^+\pi^-)/\Gamma(K^-\pi^+)$ Γ_{67}/Γ_{32}

VALUE	EVTS	DOCUMENT ID		TECN	COMMENT
2.083±0.031 OUR FIT					
2.087±0.032 OUR AVERAGE					
2.106±0.013±0.032		BONVICINI	14	CLEO	All CLEO-c runs
1.94 ±0.07 $^{+0.09}_{-0.11}$		JUN	00	SELX	Σ^- nucleus, 600 GeV
1.7 ±0.2 ±0.2	1745	ANJOS	92C	E691	γBe 90–260 GeV
1.90 ±0.25 ±0.20	337	ALVAREZ	91B	NA14	Photoproduction
2.12 ±0.16 ±0.09		BORTOLETTO	88	CLEO	e^+e^- 10.55 GeV
2.17 ±0.28 ±0.23		ALBRECHT	85F	ARG	e^+e^- 10 GeV
• • • We do not use the following data for averages, fits, limits, etc. • • •					
2.0 ±0.9	48	BAILEY	86	ACCM	π^- Be fixed target
2.0 ±1.0	10	BAILEY	83B	SPEC	$\pi^-\text{Be}\to D^0$
2.2 ±0.8	214	PICCOLO	77	MRK1	e^+e^- 4.03, 4.41 GeV

$\Gamma(K^-\pi^+\rho^0\text{total})/\Gamma(K^-2\pi^+\pi^-)$ Γ_{68}/Γ_{67}

VALUE (units 10^{-2})	DOCUMENT ID		TECN	COMMENT
83.5±3.5 OUR AVERAGE				
80 ±3 ±5	ANJOS	92C	E691	1745 $K^-2\pi^+\pi^-$ evts
85.5±3.2±3.0	COFFMAN	92B	MRK3	1281 ± 45 $K^-2\pi^+\pi^-$ evts

$\Gamma(K^-\pi^+\rho^0\,3\text{-body})/\Gamma(K^-2\pi^+\pi^-)$ Γ_{69}/Γ_{67}

VALUE (units 10^{-2})	EVTS	DOCUMENT ID		TECN	COMMENT
7.4±2.0 OUR AVERAGE					
8.4±1.1±2.5	16k	ABLIKIM	17O	BES3	$D^0\to K^-2\pi^+\pi^-$
5 ±3 ±2		ANJOS	92C	E691	1745 $K^-2\pi^+\pi^-$ evts
8.4±2.2±4.0		COFFMAN	92B	MRK3	1281 ± 45 $K^-2\pi^+\pi^-$ evts

$\Gamma(\overline{K}^*(892)^0\rho^0,\ \overline{K}^{*0}\to K^-\pi^+)/\Gamma(K^-2\pi^+\pi^-)$ Γ_{70}/Γ_{67}

VALUE (units 10^{-2})	EVTS	DOCUMENT ID		TECN	COMMENT
12.3±0.6 OUR AVERAGE					
12.3±0.4±0.5	16k	ABLIKIM	17O	BES3	$D^0\to K^-2\pi^+\pi^-$
13 ±2 ±2		ANJOS	92C	E691	1745 $K^-2\pi^+\pi^-$ evts

$\Gamma(\overline{K}^*(892)^0\rho^0\,\text{transverse},\ \overline{K}^{*0}\to K^-\pi^+)/\Gamma(K^-2\pi^+\pi^-)$ Γ_{74}/Γ_{67}

VALUE	EVTS	DOCUMENT ID		TECN	COMMENT
0.142±0.016±0.05	1281	COFFMAN	92B	MRK3	$K^-2\pi^+\pi^-$ evts

$\Gamma((\overline{K}^*(892)^0\rho^0)_{S-wave},\ \overline{K}^*(892)^0\to K^-\pi^+)/\Gamma(K^-2\pi^+\pi^-)$ Γ_{71}/Γ_{67}

VALUE (units 10^{-2})	EVTS	DOCUMENT ID		TECN	COMMENT
7.1±0.9 OUR AVERAGE					
6.5±0.5±0.8	16k	ABLIKIM	17O	BES3	$D^0\to K^-2\pi^+\pi^-$
25 ±3 ±4	1.7k	ANJOS	92C	E691	$K^-2\pi^+\pi^-$

$\Gamma((\overline{K}^*(892)^0\rho^0)_{P-wave},\ \overline{K}^*(892)^0\to K^-\pi^+)/\Gamma(K^-2\pi^+\pi^-)$ Γ_{72}/Γ_{67}

VALUE (units 10^{-2})	EVTS	DOCUMENT ID		TECN	COMMENT
2.3±0.2±0.1	16k	ABLIKIM	17O	BES3	$D^0\to K^-2\pi^+\pi^-$

$\Gamma((\overline{K}^*(892)^0\rho^0)_{D-wave},\ \overline{K}^*(892)^0\to K^-\pi^+)/\Gamma(K^-2\pi^+\pi^-)$ Γ_{73}/Γ_{67}

VALUE (units 10^{-2})	EVTS	DOCUMENT ID		TECN	COMMENT
8.1±0.8 OUR AVERAGE					
7.9±0.4±0.7	16k	ABLIKIM	17O	BES3	$D^0\to K^-2\pi^+\pi^-$
17 ±3 ±4		ANJOS	92C	E691	1745 $K^-2\pi^+\pi^-$ evts

$\Gamma(K^-a_1(1260)^+,\ a_1^+\to\rho^0\pi^+)/\Gamma(K^-2\pi^+\pi^-)$ Γ_{75}/Γ_{67}

VALUE (%)	EVTS	DOCUMENT ID		TECN	COMMENT
53 ±4 OUR AVERAGE					
54.6±2.8± 3.7	16k	ABLIKIM	17O	BES3	$D^0\to K^-2\pi^+\pi^-$
47 ±5 ±10	1745	ANJOS	92C	E691	$K^-2\pi^+\pi^-$ evts
49.2±2.4± 8.0	1281	COFFMAN	92B	MRK3	$K^-2\pi^+\pi^-$ evts

$\Gamma(K^-a_1(1260)^+,\ a_1(1260)^+\to(\rho^0\pi^+)_{S-wave})/\Gamma(K^-2\pi^+\pi^-)$ Γ_{76}/Γ_{67}

VALUE (units 10^{-2})	EVTS	DOCUMENT ID		TECN	COMMENT
53.2±2.8±4.0	16k	ABLIKIM	17O	BES3	$D^0\to K^-2\pi^+\pi^-$

$\Gamma(K^-a_1(1260)^+,\ a_1(1260)^+\to(\rho^0\pi^+)_{D-wave})/\Gamma(K^-2\pi^+\pi^-)$ Γ_{77}/Γ_{67}

VALUE (units 10^{-2})	EVTS	DOCUMENT ID		TECN	COMMENT
0.3±0.1±0.1	16k	ABLIKIM	17O	BES3	$D^0\to K^-2\pi^+\pi^-$

$\Gamma(K_1(1270)^-\pi^+,\ K_1^-\to K^-\pi^+\pi^-\text{total})/\Gamma(K^-2\pi^+\pi^-)$ Γ_{78}/Γ_{67}

VALUE (%)	EVTS	DOCUMENT ID		TECN	COMMENT
6.6±1.9±0.3	1281	COFFMAN	92B	MRK3	$K^-2\pi^+\pi^-$ evts

$\Gamma(\overline{K}^*(892)^0\pi^+\pi^-\,3\text{-body},\ \overline{K}^{*0}\to K^-\pi^+)/\Gamma(K^-2\pi^+\pi^-)$ Γ_{80}/Γ_{67}

VALUE (units 10^{-2})	EVTS	DOCUMENT ID		TECN	COMMENT
7.3±0.6 OUR AVERAGE					
7.0±0.4±0.5	16k	ABLIKIM	17O	BES3	$D^0\to K^-2\pi^+\pi^-$
11 ±2 ±3	1745	ANJOS	92C	E691	$K^-2\pi^+\pi^-$ evts
14.0±1.8±4.0	1281	COFFMAN	92B	MRK3	$K^-2\pi^+\pi^-$ evts

$\Gamma(K_1(1270)^-\pi^+,\ K_1^-\to\overline{K}^*(892)^0\pi^-,\ \overline{K}^{*0}\to K^-\pi^+)/\Gamma(K^-2\pi^+\pi^-)$ Γ_{81}/Γ_{67}

VALUE (%)	EVTS	DOCUMENT ID		TECN	COMMENT
0.8±0.2±0.2	16k	ABLIKIM	17O	BES3	$D^0\to K^-2\pi^+\pi^-$

$\Gamma(K_1(1270)^-\pi^+,\ K_1(1270)^-\to(\overline{K}^{*0}\pi^-)_{S-wave},\ \overline{K}^*(892)^0\to K^-\pi^+)/\Gamma(K^-2\pi^+\pi^-)$ Γ_{82}/Γ_{67}

VALUE (units 10^{-2})	EVTS	DOCUMENT ID		TECN	COMMENT
0.1±0.1±0.1	16k	ABLIKIM	17O	BES3	$D^0\to K^-2\pi^+\pi^-$

$\Gamma(K_1(1270)^-\pi^+,\ K_1(1270)^-\to(\overline{K}^{*0}\pi^-)_{D-wave},\ \overline{K}^*(892)^0\to K^-\pi^+)/\Gamma(K^-2\pi^+\pi^-)$ Γ_{83}/Γ_{67}

VALUE (units 10^{-2})	EVTS	DOCUMENT ID		TECN	COMMENT
0.7±0.2±0.2	16k	ABLIKIM	17O	BES3	$D^0\to K^-2\pi^+\pi^-$

$\Gamma(K_1(1270)^-\pi^+,\ K_1(1270)^-\to(K^-\rho^0)_{S-wave})/\Gamma(K^-2\pi^+\pi^-)$ Γ_{84}/Γ_{67}

VALUE (units 10^{-2})	EVTS	DOCUMENT ID		TECN	COMMENT
3.4±0.3±0.5	16k	ABLIKIM	17O	BES3	$D^0\to K^-2\pi^+\pi^-$

$\Gamma(K^-2\pi^+\pi^-\,\text{nonresonant})/\Gamma(K^-2\pi^+\pi^-)$ Γ_{85}/Γ_{67}

VALUE (%)	EVTS	DOCUMENT ID		TECN	COMMENT
22.0±0.8 OUR AVERAGE					
21.9±0.6±0.6	16k	[1] ABLIKIM	17O	BES3	$D^0\to K^-2\pi^+\pi^-$
23 ±2 ±3	1.7k	ANJOS	92C	E691	$D^0\to K^-2\pi^+\pi^-$
24.2±2.5±6.0	1.2k	COFFMAN	92B	MRK3	$D^0\to K^-2\pi^+\pi^-$

[1] In addition to the 14 ABLIKIM 17O branching ratios we have listed, the paper gives 15 more ratios for mostly non-resonant modes. Four of the 15 have less than 2-standard-deviation significance. Here are some of the omitted modes, with S, P, V, A, and T for scalar, pseudo-scalar, vector, axial-vector, and tensor spin sub-structures: $\pi^+(K^-\rho^0)_P$, $\pi^+(K^-\rho^0)_V$, $\pi^+(\overline{K}^{*0}\pi^-)_P$, $\pi^+(\overline{K}^{*0}\pi^-)_V$, $\pi^+(\pi^-(K^-\pi^+)_{S-wave})_A$, $(K^-\pi^+)_V(\pi^+\pi^-)_S$, $(K^-\pi^+)_T(\pi^+\pi^-)_S\ldots$

$\Gamma(K^0_S\pi^+\pi^-\pi^0)/\Gamma_{\text{total}}$ Γ_{86}/Γ

VALUE (units 10^{-2})	EVTS	DOCUMENT ID		TECN	COMMENT
5.1±0.6 OUR FIT					
5.2±1.1±1.2	140	COFFMAN	92B	MRK3	e^+e^- 3.77 GeV
• • • We do not use the following data for averages, fits, limits, etc. • • •					
$6.7^{+1.6}_{-1.7}$		[1] BARLAG	92C	ACCM	π^- Cu 230 GeV

[1] BARLAG 92C computes the branching fraction using topological normalization.

$\Gamma(K^0_S\pi^+\pi^-\pi^0)/\Gamma(K^0_S\pi^+\pi^-)$ Γ_{86}/Γ_{35}

Branching fractions for submodes of this mode with narrow resonances (the η, ω, η') are fairly well determined (see below). COFFMAN 92B gives fractions of K^* and ρ submodes, but with only 140 ± 28 events above background could not determine them

with much accuracy. We omit those measurements here; they are in our 2008 Review (Physics Letters **B667** 1 (2008)).

VALUE	EVTS	DOCUMENT ID		TECN	COMMENT
1.85±0.20 OR FIT					
1.86±0.23 OR AVERAGE					
1.80±0.20±0.21	190	[1] ALBRECHT	92P	ARG	$e^+e^- \approx$ 10 GeV
2.8 ±0.8 ±0.8	46	ANJOS	92C	E691	γBe 90–260 GeV
1.85±0.26±0.30	158	KINOSHITA	91	CLEO	$e^+e^- \sim$ 10.7 GeV

[1] This value is calculated from numbers in Table 1 of ALBRECHT 92P.

$\Gamma(K^0_S\eta)/\Gamma_{total}$ — Γ_{104}/Γ

Unseen decay modes of the η are included.

VALUE (units 10^{-3})	DOCUMENT ID		TECN	COMMENT
• • • We do not use the following data for averages, fits, limits, etc. • • •				
4.42±0.15±0.28	ASNER	08	CLEO	See MENDEZ 10

$\Gamma(K^0_S\eta)/[\Gamma(K^-\pi^+)+\Gamma(K^+\pi^-)]$ — $\Gamma_{104}/(\Gamma_{32}+\Gamma_{257})$

Unseen decay modes of the η are included.

VALUE (units 10^{-2})	EVTS	DOCUMENT ID		TECN	COMMENT
12.3±0.8 OR FIT					
12.3±0.3±0.7	2864 ± 65	MENDEZ	10	CLEO	e^+e^- at 3774 MeV

$\Gamma(K^0_S\eta)/\Gamma(K^0_S\pi^0)$ — Γ_{104}/Γ_{33}

Unseen decay modes of the η are included.

VALUE	EVTS	DOCUMENT ID		TECN	COMMENT
• • • We do not use the following data for averages, fits, limits, etc. • • •					
0.32±0.04±0.03	225 ± 30	PROCARIO	93B	CLE2	$\eta \to \gamma\gamma$

$\Gamma(K^0_S\eta)/\Gamma(K^0_S\pi^+\pi^-)$ — Γ_{104}/Γ_{35}

Unseen decay modes of the η are included.

VALUE	EVTS	DOCUMENT ID		TECN	COMMENT
• • • We do not use the following data for averages, fits, limits, etc. • • •					
0.14±0.02±0.02	80 ± 12	PROCARIO	93B	CLE2	$\eta \to \pi^+\pi^-\pi^0$

$\Gamma(K^0_S\omega)/\Gamma_{total}$ — Γ_{105}/Γ

Unseen decay modes of the ω are included.

VALUE (%)	DOCUMENT ID		TECN	COMMENT
1.11±0.06 OR FIT				
1.12±0.04±0.05	ASNER	08	CLEO	$e^+e^- \to D^0\overline{D}^0$, 3.77 GeV

$\Gamma(K^0_S\omega)/\Gamma(K^-\pi^+)$ — Γ_{105}/Γ_{32}

Unseen decay modes of the ω are included.

VALUE	DOCUMENT ID		TECN	COMMENT
• • • We do not use the following data for averages, fits, limits, etc. • • •				
0.50±0.18±0.10	ALBRECHT	89D	ARG	e^+e^- 10 GeV

$\Gamma(K^0_S\omega)/\Gamma(K^0_S\pi^+\pi^-)$ — Γ_{105}/Γ_{35}

Unseen decay modes of the ω are included.

VALUE	EVTS	DOCUMENT ID		TECN	COMMENT
0.402±0.033 OR FIT Error includes scale factor of 1.1.					
0.33 ±0.09 OR AVERAGE Error includes scale factor of 1.1.					
0.29 ±0.08 ±0.05	16	[1] ALBRECHT	92P	ARG	$e^+e^- \approx$ 10 GeV
0.54 ±0.14 ±0.16	40	KINOSHITA	91	CLEO	$e^+e^- \sim$ 10.7 GeV

[1] This value is calculated from numbers in Table 1 of ALBRECHT 92P.

$\Gamma(K^0_S\omega)/\Gamma(K^0_S\pi^+\pi^-\pi^0)$ — Γ_{105}/Γ_{86}

Unseen decay modes of the ω are included.

VALUE	DOCUMENT ID		TECN	COMMENT
0.217±0.026 OR FIT				
0.220±0.048±0.0116	COFFMAN	92B	MRK3	1281 ± 45 $K^-2\pi^+\pi^-$ evts

$\Gamma(K^0_S\eta'(958))/[\Gamma(K^-\pi^+)+\Gamma(K^+\pi^-)]$ — $\Gamma_{106}/(\Gamma_{32}+\Gamma_{257})$

Unseen decay modes of the $\eta'(958)$ are included.

VALUE (units 10^{-2})	EVTS	DOCUMENT ID		TECN	COMMENT
23.9±1.3 OR FIT					
24.3±0.8±1.1	1321 ± 42	MENDEZ	10	CLEO	e^+e^- at 3774 MeV

$\Gamma(K^0_S\eta'(958))/\Gamma(K^0_S\pi^+\pi^-)$ — Γ_{106}/Γ_{35}

Unseen decay modes of the $\eta'(958)$ are included.

VALUE	EVTS	DOCUMENT ID		TECN	COMMENT
0.340±0.025 OR FIT					
0.32 ±0.04 OR AVERAGE					
0.31 ±0.02 ±0.04	594	PROCARIO	93B	CLE2	$\eta' \to \eta\pi^+\pi^-, \rho^0\gamma$
0.37 ±0.13 ±0.06	18	[1] ALBRECHT	92P	ARG	$e^+e^- \approx$ 10 GeV

[1] This value is calculated from numbers in Table 1 of ALBRECHT 92P.

$\Gamma(K^-\pi^+2\pi^0)/\Gamma_{total}$ — Γ_{89}/Γ

VALUE	EVTS	DOCUMENT ID		TECN	COMMENT
• • • We do not use the following data for averages, fits, limits, etc. • • •					
0.177±0.029		[1] BARLAG	92C	ACCM	π^- Cu 230 GeV
0.149±0.037±0.030	24	[2] ADLER	88C	MRK3	e^+e^- 3.77 GeV
$0.209^{+0.074}_{-0.043}$±0.012	9	[1] AGUILAR-...	87F	HYBR	πp, pp 360, 400 GeV

[1] AGUILAR-BENITEZ 87F and BARLAG 92C compute the branching fraction using topological normalization. They do not distinguish the presence of a third π^0, and thus are not included in the average.

[2] ADLER 88C uses an absolute normalization method finding this decay channel opposite a detected $\overline{D}^0 \to K^+\pi^-$ in pure $D\overline{D}$ events.

$\Gamma(K^-2\pi^+\pi^-\pi^0)/\Gamma(K^-\pi^+)$ — Γ_{90}/Γ_{32}

VALUE	EVTS	DOCUMENT ID		TECN	COMMENT
1.09±0.10 OR FIT					
0.98±0.11±0.11	225	[1] ALBRECHT	92P	ARG	$e^+e^- \approx$ 10 GeV

[1] This value is calculated from numbers in Table 1 of ALBRECHT 92P.

$\Gamma(K^-2\pi^+\pi^-\pi^0)/\Gamma(K^-2\pi^+\pi^-)$ — Γ_{90}/Γ_{67}

VALUE	EVTS	DOCUMENT ID		TECN	COMMENT
0.52±0.05 OR FIT					
0.56±0.07 OR AVERAGE					
$0.55\pm0.07^{+0.12}_{-0.09}$	167	KINOSHITA	91	CLEO	$e^+e^- \sim$ 10.7 GeV
0.57±0.06±0.05	180	ANJOS	90D	E691	Photoproduction

$\Gamma(\overline{K}^*(892)^0\pi^+\pi^-\pi^0)/\Gamma(K^-2\pi^+\pi^-\pi^0)$ — Γ_{107}/Γ_{90}

Unseen decay modes of the $\overline{K}^*(892)^0$ are included.

VALUE	DOCUMENT ID		TECN	COMMENT
0.45±0.15±0.15	ANJOS	90D	E691	Photoproduction

$\Gamma(\overline{K}^*(892)^0\eta)/\Gamma(K^-\pi^+)$ — Γ_{108}/Γ_{32}

Unseen decay modes of the $\overline{K}^*(892)^0$ and η are included.

VALUE	EVTS	DOCUMENT ID		TECN	COMMENT
• • • We do not use the following data for averages, fits, limits, etc. • • •					
$0.58\pm0.19^{+0.24}_{-0.28}$	46	KINOSHITA	91	CLEO	$e^+e^- \sim$ 10.7 GeV

$\Gamma(\overline{K}^*(892)^0\eta)/\Gamma(K^-\pi^+\pi^0)$ — Γ_{108}/Γ_{50}

Unseen decay modes of the $\overline{K}^*(892)^0$ and η are included.

VALUE	EVTS	DOCUMENT ID		TECN	COMMENT
• • • We do not use the following data for averages, fits, limits, etc. • • •					
0.13±0.02±0.03	214	PROCARIO	93B	CLE2	$\overline{K}^{*0}\eta \to K^-\pi^+/\gamma\gamma$

$\Gamma(K^0_S\eta\pi^0)/\Gamma(K^0_S\pi^0)$ — Γ_{94}/Γ_{33}

VALUE	EVTS	DOCUMENT ID		TECN	COMMENT
0.46±0.07±0.06	155 ± 22	[1] RUBIN	04	CLEO	$e^+e^- \approx$ 10 GeV

[1] The η here is detected in its $\gamma\gamma$ mode, but other η modes are included in the value given.

$\Gamma(K^0_S a_0(980), a_0 \to \eta\pi^0)/\Gamma(K^0_S\eta\pi^0)$ — Γ_{95}/Γ_{94}

This is the "fit fraction" from the Dalitz-plot analysis, with interference.

VALUE	DOCUMENT ID		TECN	COMMENT
1.19±0.09±0.26	[1] RUBIN	04	CLEO	Dalitz fit, 155 evts

[1] In addition to $K^0_S a_0(980)$ and $\overline{K}^*(892)^0\eta$ modes, RUBIN 04 finds a fit fraction of 0.246 ± 0.092 ± 0.091 for other, undetermined modes.

$\Gamma(\overline{K}^*(892)^0\eta, \overline{K}^{*0} \to K^0_S\pi^0)/\Gamma(K^0_S\eta\pi^0)$ — Γ_{96}/Γ_{94}

This is the "fit fraction" from the Dalitz-plot analysis, with interference.

VALUE	DOCUMENT ID		TECN	COMMENT
0.293±0.062±0.035	[1] RUBIN	04	CLEO	Dalitz fit, 155 evts

[1] See the note on RUBIN 04 in the preceding data block.

$\Gamma(K^-\pi^+\omega)/\Gamma(K^-\pi^+)$ — Γ_{109}/Γ_{32}

Unseen decay modes of the ω are included.

VALUE	EVTS	DOCUMENT ID		TECN	COMMENT
0.78±0.12±0.10	99	[1] ALBRECHT	92P	ARG	$e^+e^- \approx$ 10 GeV

[1] This value is calculated from numbers in Table 1 of ALBRECHT 92P.

$\Gamma(\overline{K}^*(892)^0\omega)/\Gamma(K^-\pi^+)$ — Γ_{110}/Γ_{32}

Unseen decay modes of the $\overline{K}^*(892)^0$ and ω are included.

VALUE	EVTS	DOCUMENT ID		TECN	COMMENT
0.28±0.11±0.04	17	[1] ALBRECHT	92P	ARG	$e^+e^- \approx$ 10 GeV

[1] This value is calculated from numbers in Table 1 of ALBRECHT 92P.

$\Gamma(K^-\pi^+\eta'(958))/\Gamma(K^-2\pi^+\pi^-)$ — Γ_{111}/Γ_{67}

Unseen decay modes of the $\eta'(958)$ are included.

VALUE	EVTS	DOCUMENT ID		TECN	COMMENT
0.093±0.014±0.019	286	PROCARIO	93B	CLE2	$\eta' \to \eta\pi^+\pi^-, \rho^0\gamma$

$\Gamma(\overline{K}^*(892)^0\eta'(958))/\Gamma(K^-\pi^+\eta'(958))$ — $\Gamma_{112}/\Gamma_{111}$

Unseen decay modes of the $\overline{K}^*(892)^0$ are included.

VALUE	CL%	DOCUMENT ID		TECN
<0.15	90	PROCARIO	93B	CLE2

$\Gamma(K^0_S2\pi^+2\pi^-)/\Gamma(K^0_S\pi^+\pi^-)$ — Γ_{97}/Γ_{35}

VALUE	EVTS	DOCUMENT ID		TECN	COMMENT
0.095±0.005±0.007	1283 ± 57	LINK	04D	FOCS	γ A, $\overline{E}_\gamma \approx$ 180 GeV
• • • We do not use the following data for averages, fits, limits, etc. • • •					
0.07 ±0.02 ±0.01	11	[1] ALBRECHT	92P	ARG	$e^+e^- \approx$ 10 GeV
0.149±0.026	56	AMMAR	91	CLEO	$e^+e^- \approx$ 10.5 GeV
0.18 ±0.07 ±0.04	6	ANJOS	90D	E691	Photoproduction

[1] This value is calculated from numbers in Table 1 of ALBRECHT 92P.

Meson Particle Listings

D^0

$\Gamma(K^0_S\rho^0\pi^+\pi^-, \text{no } K^*(892)^-)/\Gamma(K^0_S2\pi^+2\pi^-)$ Γ_{98}/Γ_{97}

VALUE	DOCUMENT ID		TECN	COMMENT
0.40±0.24±0.07	LINK	04D	FOCS	γ A, $\overline{E}_\gamma \approx 180$ GeV

$\Gamma(K^*(892)^-2\pi^+\pi^-,\ K^*(892)^- \to K^0_S\pi^-, \text{no } \rho^0)/\Gamma(K^0_S2\pi^+2\pi^-)$ Γ_{99}/Γ_{97}

VALUE	DOCUMENT ID		TECN	COMMENT
0.17±0.28±0.02	LINK	04D	FOCS	γ A, $\overline{E}_\gamma \approx 180$ GeV

$\Gamma(K^*(892)^-\rho^0\pi^+,\ K^*(892)^- \to K^0_S\pi^-)/\Gamma(K^0_S2\pi^+2\pi^-)$ Γ_{100}/Γ_{97}

VALUE	DOCUMENT ID		TECN	COMMENT
0.60±0.21±0.09	LINK	04D	FOCS	γ A, $\overline{E}_\gamma \approx 180$ GeV

$\Gamma(K^0_S2\pi^+2\pi^-\text{nonresonant})/\Gamma(K^0_S2\pi^+2\pi^-)$ Γ_{101}/Γ_{97}

VALUE	CL%	DOCUMENT ID		TECN	COMMENT
<0.46	90	LINK	04D	FOCS	γ A, $\overline{E}_\gamma \approx 180$ GeV

$\Gamma(K^-3\pi^+2\pi^-)/\Gamma(K^-2\pi^+\pi^-)$ Γ_{103}/Γ_{67}

VALUE (units 10^{-3})	EVTS	DOCUMENT ID		TECN	COMMENT
2.70±0.58±0.38	48 ± 10	LINK	04B	FOCS	γA, $\overline{E}_\gamma \approx 180$ GeV

Hadronic modes with three K's

$\Gamma(K^0_SK^+K^-)/\Gamma(K^0_S\pi^+\pi^-)$ Γ_{113}/Γ_{35}

VALUE	EVTS	DOCUMENT ID		TECN	COMMENT
0.158±0.001±0.005	14k±116	AUBERT,B	05J	BABR	$e^+e^- \approx \Upsilon(4S)$
• • • We do not use the following data for averages, fits, limits, etc. • • •					
0.20 ±0.05 ±0.04	47	FRABETTI	92B	E687	γ Be, $\overline{E}_\gamma$= 221 GeV
0.170±0.022	136	AMMAR	91	CLEO	$e^+e^- \approx$ 10.5 GeV
0.24 ±0.08		BEBEK	86	CLEO	e^+e^- near $\Upsilon(4S)$
0.185±0.055	52	ALBRECHT	85B	ARG	e^+e^- 10 GeV

$\Gamma(K^0_Sa_0(980)^0,\ a_0^0 \to K^+K^-)/\Gamma(K^0_SK^+K^-)$ $\Gamma_{114}/\Gamma_{113}$

This is the "fit fraction" from the Dalitz-plot analysis, with interference.

VALUE	DOCUMENT ID		TECN	COMMENT
0.664±0.016±0.070	AUBERT,B	05J	BABR	Dalitz fit, 12540 ± 112 evts

$\Gamma(K^-a_0(980)^+,\ a_0^+ \to K^+K^0_S)/\Gamma(K^0_SK^+K^-)$ $\Gamma_{115}/\Gamma_{113}$

This is the "fit fraction" from the Dalitz-plot analysis, with interference.

VALUE	DOCUMENT ID		TECN	COMMENT
0.134±0.011±0.037	AUBERT,B	05J	BABR	Dalitz fit, 12540 ± 112 evts

$\Gamma(K^+a_0(980)^-,\ a_0^- \to K^-K^0_S)/\Gamma(K^0_SK^+K^-)$ $\Gamma_{116}/\Gamma_{113}$

This is a doubly Cabibbo-suppressed mode.

VALUE	CL%	DOCUMENT ID		TECN	COMMENT
<0.025	95	AUBERT,B	05J	BABR	Dalitz fit, 12540 ± 112 evts

$\Gamma(K^0_Sf_0(980),\ f_0 \to K^+K^-)/\Gamma(K^0_SK^+K^-)$ $\Gamma_{117}/\Gamma_{113}$

VALUE	CL%	DOCUMENT ID		TECN	COMMENT
<0.021	95	AUBERT,B	05J	BABR	Dalitz fit, 12540 ± 112 evts

$\Gamma(K^0_S\phi,\ \phi \to K^+K^-)/\Gamma(K^0_SK^+K^-)$ $\Gamma_{118}/\Gamma_{113}$

This is the "fit fraction" from the Dalitz-plot analysis, with interference.

VALUE	DOCUMENT ID		TECN	COMMENT
0.459±0.007±0.007	AUBERT,B	05J	BABR	Dalitz fit, 12540 ± 112 evts

$\Gamma(K^0_Sf_0(1370),\ f_0 \to K^+K^-)/\Gamma(K^0_SK^+K^-)$ $\Gamma_{119}/\Gamma_{113}$

This is the "fit fraction" from the Dalitz-plot analysis, with interference.

VALUE	DOCUMENT ID		TECN	COMMENT
0.038±0.007±0.023	[1] AUBERT,B	05J	BABR	Dalitz fit, 12540 ± 112 evts

[1] AUBERT,B 05J calls the mode $K^0_Sf_0(1400)$, but insofar as it is seen here at all, it is certainly the same as $f_0(1370)$.

$\Gamma(3K^0_S)/\Gamma_{\text{total}}$ Γ_{120}/Γ

VALUE (units 10^{-4})	EVTS	DOCUMENT ID		TECN	COMMENT
7.5 ±0.6 OUR FIT	Error includes scale factor of 1.3.				
7.21±0.33±0.44	597	ABLIKIM	17A	BES3	$e^+e^- \to \psi(3770)$

$\Gamma(3K^0_S)/\Gamma(K^0_S\pi^+\pi^-)$ Γ_{120}/Γ_{35}

VALUE (units 10^{-2})	EVTS	DOCUMENT ID		TECN	COMMENT
2.74±0.25 OUR FIT	Error includes scale factor of 1.1.				
3.2 ±0.4 OUR AVERAGE					
3.58±0.54±0.52	170 ± 26	LINK	05A	FOCS	γBe, $\overline{E}_\gamma \approx 180$ GeV
2.78±0.38±0.48	61	ASNER	96B	CLE2	$e^+e^- \approx \Upsilon(4S)$
7.0 ±2.4 ±1.2	10 ± 3	FRABETTI	94J	E687	γBe, $\overline{E}_\gamma$=220 GeV
3.2 ±1.0	22	AMMAR	91	CLEO	$e^+e^- \approx$ 10.5 GeV
3.4 ±1.4 ±1.0	5	ALBRECHT	90C	ARG	$e^+e^- \approx$ 10 GeV

$\Gamma(K^+2K^-\pi^+)/\Gamma(K^-2\pi^+\pi^-)$ Γ_{121}/Γ_{67}

VALUE	EVTS	DOCUMENT ID		TECN	COMMENT
0.0027 ±0.0004 OUR AVERAGE	Error includes scale factor of 1.1.				
0.00257±0.00034±0.00024	143	LINK	03G	FOCS	γ A, $\overline{E}_\gamma \approx 180$ GeV
0.0054 ±0.0016 ±0.0008	18	AITALA	01D	E791	π^- A, 500 GeV
0.0028 ±0.0007 ±0.0001	20	FRABETTI	95C	E687	γ Be, $\overline{E}_\gamma \approx 200$ GeV

$\Gamma(\phi\overline{K}^*(892)^0,\ \phi \to K^+K^-,\ \overline{K}^{*0} \to K^-\pi^+)/\Gamma(K^+2K^-\pi^+)$ $\Gamma_{124}/\Gamma_{121}$

VALUE	DOCUMENT ID		TECN	COMMENT
0.48±0.06±0.01	LINK	03G	FOCS	γ A, $\overline{E}_\gamma \approx 180$ GeV

$\Gamma(K^-\pi^+\phi,\ \phi \to K^+K^-)/\Gamma(K^+2K^-\pi^+)$ $\Gamma_{123}/\Gamma_{121}$

VALUE	DOCUMENT ID		TECN	COMMENT
0.18±0.06±0.04	LINK	03G	FOCS	γ A, $\overline{E}_\gamma \approx 180$ GeV

$\Gamma(K^+K^-\overline{K}^*(892)^0,\ \overline{K}^{*0} \to K^-\pi^+)/\Gamma(K^+2K^-\pi^+)$ $\Gamma_{122}/\Gamma_{121}$

VALUE	DOCUMENT ID		TECN	COMMENT
0.20±0.07±0.02	LINK	03G	FOCS	γ A, $\overline{E}_\gamma \approx 180$ GeV

$\Gamma(K^+2K^-\pi^+\text{nonresonant})/\Gamma(K^+2K^-\pi^+)$ $\Gamma_{125}/\Gamma_{121}$

VALUE	DOCUMENT ID		TECN	COMMENT
0.15±0.06±0.02	LINK	03G	FOCS	γ A, $\overline{E}_\gamma \approx 180$ GeV

$\Gamma(2K^0_SK^\pm\pi^\mp)/\Gamma(K^0_S\pi^+\pi^-)$ Γ_{126}/Γ_{35}

VALUE (units 10^{-2})	EVTS	DOCUMENT ID		TECN	COMMENT
2.12±0.38±0.20	57 ± 10	LINK	05A	FOCS	γ Be, $\overline{E}_\gamma \approx 180$ GeV

Pionic modes

$\Gamma(\pi^+\pi^-)/\Gamma(K^-\pi^+)$ Γ_{127}/Γ_{32}

VALUE (units 10^{-2})	EVTS	DOCUMENT ID		TECN	COMMENT
3.62 ±0.05 OUR FIT					
3.59 ±0.06 OUR AVERAGE					
3.594±0.054±0.040	7334 ± 97	ACOSTA	05C	CDF	$p\overline{p}$, $\sqrt{s}$ = 1.96 TeV
3.53 ±0.12 ±0.06	3453	LINK	03	FOCS	γ A, $\overline{E}_\gamma \approx 180$ GeV
3.51 ±0.16 ±0.17	710	CSORNA	02	CLE2	$e^+e^- \approx \Upsilon(4S)$
4.0 ±0.2 ±0.3	2043	AITALA	98C	E791	π^- A, 500 GeV
• • • We do not use the following data for averages, fits, limits, etc. • • •					
3.62 ±0.10 ±0.08	2085 ± 54	RUBIN	06	CLEO	See MENDEZ 10
3.4 ±0.7 ±0.1	76 ± 15	ABLIKIM	05F	BES	$e^+e^- \approx \psi(3770)$
4.3 ±0.7 ±0.3	177	FRABETTI	94C	E687	γBe $\overline{E}_\gamma$= 220 GeV
3.48 ±0.30 ±0.23	227	SELEN	93	CLE2	$e^+e^- \approx \Upsilon(4S)$
5.5 ±0.8 ±0.5	120	ANJOS	91D	E691	Photoproduction
5.0 ±0.7 ±0.5	110	ALEXANDER	90	CLEO	e^+e^- 10.5–11 GeV

$\Gamma(\pi^+\pi^-)/[\Gamma(K^-\pi^+)+\Gamma(K^+\pi^-)]$ $\Gamma_{127}/(\Gamma_{32}+\Gamma_{257})$

VALUE (units 10^{-2})	EVTS	DOCUMENT ID		TECN	COMMENT
3.60±0.05 OUR FIT					
3.70±0.06±0.09	6210 ± 93	MENDEZ	10	CLEO	e^+e^- at 3774 MeV

$\Gamma(2\pi^0)/\Gamma_{\text{total}}$ Γ_{128}/Γ

VALUE (units 10^{-4})	EVTS	DOCUMENT ID		TECN	COMMENT
8.22±0.25 OUR FIT					
8.29±0.30 OUR AVERAGE					
8.24±0.21±0.30	6k	ABLIKIM	15F	BES3	e^+e^- at 3.773GeV
8.4 ±0.1 ±0.5	26k	LEES	12L	BABR	$e^+e^- \approx$ 10.58 GeV

$\Gamma(2\pi^0)/\Gamma(K^-\pi^+)$ Γ_{128}/Γ_{32}

VALUE (units 10^{-2})	EVTS	DOCUMENT ID		TECN	COMMENT
• • • We do not use the following data for averages, fits, limits, etc. • • •					
2.05±0.13±0.16	499 ± 32	RUBIN	06	CLEO	See MENDEZ 10
2.2 ±0.4 ±0.4	40	SELEN	93	CLE2	$e^+e^- \to \Upsilon(4S)$

$\Gamma(2\pi^0)/[\Gamma(K^-\pi^+)+\Gamma(K^+\pi^-)]$ $\Gamma_{128}/(\Gamma_{32}+\Gamma_{257})$

VALUE (units 10^{-2})	EVTS	DOCUMENT ID		TECN	COMMENT
2.11±0.07 OUR FIT					
2.06±0.07±0.10	1567 ± 54	MENDEZ	10	CLEO	e^+e^- at 3774 MeV

$\Gamma(\pi^+\pi^-\pi^0)/\Gamma(K^-\pi^+)$ Γ_{129}/Γ_{32}

VALUE (units 10^{-2})	EVTS	DOCUMENT ID		TECN	COMMENT
37.7±1.6 OUR FIT	Error includes scale factor of 2.2.				
34.4±0.5±1.2	11k±164	RUBIN	06	CLEO	e^+e^- at $\psi(3770)$

$\Gamma(\pi^+\pi^-\pi^0)/\Gamma(K^-\pi^+\pi^0)$ Γ_{129}/Γ_{50}

VALUE (units 10^{-2})	EVTS	DOCUMENT ID		TECN	COMMENT
10.32±0.25 OUR FIT	Error includes scale factor of 2.3.				
10.41±0.23 OUR AVERAGE	Error includes scale factor of 2.0.				
10.12±0.04±0.18	123k±490	ARINSTEIN	08	BELL	$e^+e^- \approx \Upsilon(4S)$
10.59±0.06±0.13	60k±343	AUBERT,B	06X	BABR	$e^+e^- \approx \Upsilon(4S)$

$\Gamma(\rho^+\pi^-)/\Gamma(\pi^+\pi^-\pi^0)$ $\Gamma_{130}/\Gamma_{129}$

This is the "fit fraction" from the Dalitz-plot analysis, with interference. See GASPERO 08 and BHATTACHARYA 10A for isospin decompositions of the $D^0 \to \pi^+\pi^0\pi^-$ Dalitz plot, both based on the amplitudes of AUBERT 07BJ. They quantify the conclusion that the final state is dominantly isospin 0.

VALUE (units 10^{-2})	DOCUMENT ID		TECN	COMMENT
68.1±0.6 OUR AVERAGE				
67.8±0.0±0.6	AUBERT	07BJ	BABR	Dalitz fit, 45k events
76.3±1.9±2.5	CRONIN-HEN...05		CLEO	$e^+e^- \approx$ 10 GeV

$\Gamma(\rho^0\pi^0)/\Gamma(\pi^+\pi^-\pi^0)$ $\Gamma_{131}/\Gamma_{129}$

This is the "fit fraction" from the Dalitz-plot analysis, with interference.

VALUE (units 10^{-2})	DOCUMENT ID		TECN	COMMENT
25.9±1.1 OUR AVERAGE				
26.2±0.5±1.1	AUBERT	07BJ	BABR	Dalitz fit, 45k events
24.4±2.0±2.1	CRONIN-HEN..05		CLEO	$e^+e^-\approx$ 10 GeV

$\Gamma(\rho^-\pi^+)/\Gamma(\pi^+\pi^-\pi^0)$ $\Gamma_{132}/\Gamma_{129}$

This is the "fit fraction" from the Dalitz-plot analysis, with interference.

VALUE (units 10^{-2})	DOCUMENT ID		TECN	COMMENT
34.6±0.8 OUR AVERAGE				
34.6±0.8±0.3	AUBERT	07BJ	BABR	Dalitz fit, 45k events
34.5±2.4±1.3	CRONIN-HEN..05		CLEO	$e^+e^-\approx$ 10 GeV

$\Gamma(\rho(1450)^+\pi^-,\ \rho^+\to\pi^+\pi^0)/\Gamma(\pi^+\pi^-\pi^0)$ $\Gamma_{133}/\Gamma_{129}$

VALUE (units 10^{-2})	DOCUMENT ID		TECN	COMMENT
0.11±0.07±0.12	AUBERT	07BJ	BABR	Dalitz fit, 45k events

$\Gamma(\rho(1450)^0\pi^0,\ \rho^0\to\pi^+\pi^-)/\Gamma(\pi^+\pi^-\pi^0)$ $\Gamma_{134}/\Gamma_{129}$

VALUE (units 10^{-2})	DOCUMENT ID		TECN	COMMENT
0.30±0.11±0.07	AUBERT	07BJ	BABR	Dalitz fit, 45k events

$\Gamma(\rho(1450)^-\pi^+,\ \rho^-\to\pi^-\pi^0)/\Gamma(\pi^+\pi^-\pi^0)$ $\Gamma_{135}/\Gamma_{129}$

VALUE (units 10^{-2})	DOCUMENT ID		TECN	COMMENT
1.79±0.22±0.12	AUBERT	07BJ	BABR	Dalitz fit, 45k events

$\Gamma(\rho(1700)^+\pi^-,\ \rho^+\to\pi^+\pi^0)/\Gamma(\pi^+\pi^-\pi^0)$ $\Gamma_{136}/\Gamma_{129}$

VALUE (units 10^{-2})	DOCUMENT ID		TECN	COMMENT
4.1±0.7±0.7	AUBERT	07BJ	BABR	Dalitz fit, 45k events

$\Gamma(\rho(1700)^0\pi^0,\ \rho^0\to\pi^+\pi^-)/\Gamma(\pi^+\pi^-\pi^0)$ $\Gamma_{137}/\Gamma_{129}$

VALUE (units 10^{-2})	DOCUMENT ID		TECN	COMMENT
5.0±0.6±1.0	AUBERT	07BJ	BABR	Dalitz fit, 45k events

$\Gamma(\rho(1700)^-\pi^+,\ \rho^-\to\pi^-\pi^0)/\Gamma(\pi^+\pi^-\pi^0)$ $\Gamma_{138}/\Gamma_{129}$

VALUE (units 10^{-2})	DOCUMENT ID		TECN	COMMENT
3.2±0.4±0.6	AUBERT	07BJ	BABR	Dalitz fit, 45k events

$\Gamma(f_0(980)\pi^0,\ f_0\to\pi^+\pi^-)/\Gamma(\pi^+\pi^-\pi^0)$ $\Gamma_{139}/\Gamma_{129}$

VALUE (units 10^{-2})	CL%	DOCUMENT ID		TECN	COMMENT
0.25 ±0.04±0.04		AUBERT	07BJ	BABR	Dalitz fit, 45k events
• • • We do not use the following data for averages, fits, limits, etc. • • •					
<0.026	95	[1] CRONIN-HEN..05		CLEO	$e^+e^-\approx$ 10 GeV

[1] The CRONIN-HENNESSY 05 fit here includes, in addition to the three $\rho\pi$ charged states, only the $f_0(980)\pi^0$ mode. See also the next entries for limits obtained in the same way for the $f_0(500)\pi^0$ mode and for an S-wave $\pi^+\pi^-$ parametrized using a K-matrix. Our $\rho\pi$ branching ratios, given above, use the fit with the K-matrix S wave.

$\Gamma(f_0(500)\pi^0,\ f_0\to\pi^+\pi^-)/\Gamma(\pi^+\pi^-\pi^0)$ $\Gamma_{140}/\Gamma_{129}$

The $f_0(500)$ is the σ.

VALUE (units 10^{-2})	CL%	DOCUMENT ID		TECN	COMMENT
0.82±0.10±0.10		AUBERT	07BJ	BABR	Dalitz fit, 45k events
• • • We do not use the following data for averages, fits, limits, etc. • • •					
<0.21	95	[1] CRONIN-HEN..05		CLEO	$e^+e^-\approx$ 10 GeV

[1] See the note on CRONIN-HENNESSY 05 in the proceeding data block.

$\Gamma((\pi^+\pi^-)_{S-wave}\pi^0)/\Gamma(\pi^+\pi^-\pi^0)$ $\Gamma_{141}/\Gamma_{129}$

VALUE	CL%	DOCUMENT ID		TECN	COMMENT
• • • We do not use the following data for averages, fits, limits, etc. • • •					
<0.019	95	[1] CRONIN-HEN..05		CLEO	$e^+e^-\approx$ 10 GeV

[1] See the note on CRONIN-HENNESSY 05 two data blocks up.

$\Gamma(f_0(1370)\pi^0,\ f_0\to\pi^+\pi^-)/\Gamma(\pi^+\pi^-\pi^0)$ $\Gamma_{142}/\Gamma_{129}$

VALUE (units 10^{-2})	DOCUMENT ID		TECN	COMMENT
0.37±0.11±0.09	AUBERT	07BJ	BABR	Dalitz fit, 45k events

$\Gamma(f_0(1500)\pi^0,\ f_0\to\pi^+\pi^-)/\Gamma(\pi^+\pi^-\pi^0)$ $\Gamma_{143}/\Gamma_{129}$

VALUE (units 10^{-2})	DOCUMENT ID		TECN	COMMENT
0.39±0.08±0.07	AUBERT	07BJ	BABR	Dalitz fit, 45k events

$\Gamma(f_0(1710)\pi^0,\ f_0\to\pi^+\pi^-)/\Gamma(\pi^+\pi^-\pi^0)$ $\Gamma_{144}/\Gamma_{129}$

VALUE (units 10^{-2})	DOCUMENT ID		TECN	COMMENT
0.31±0.07±0.08	AUBERT	07BJ	BABR	Dalitz fit, 45k events

$\Gamma(f_2(1270)\pi^0,\ f_2\to\pi^+\pi^-)/\Gamma(\pi^+\pi^-\pi^0)$ $\Gamma_{145}/\Gamma_{129}$

VALUE (units 10^{-2})	DOCUMENT ID		TECN	COMMENT
1.32±0.08±0.10	AUBERT	07BJ	BABR	Dalitz fit, 45k events

$\Gamma(\pi^+\pi^-\pi^0\text{nonresonant})/\Gamma(\pi^+\pi^-\pi^0)$ $\Gamma_{146}/\Gamma_{129}$

VALUE (units 10^{-2})	DOCUMENT ID		TECN	COMMENT
0.84±0.21±0.12	AUBERT	07BJ	BABR	Dalitz fit, 45k events

$\Gamma(3\pi^0)/\Gamma_{\text{total}}$ Γ_{147}/Γ

VALUE	CL%	DOCUMENT ID		TECN	COMMENT
<3.5 × 10^{-4}	90	RUBIN	06	CLEO	e^+e^- at $\psi(3770)$

$\Gamma(2\pi^+2\pi^-)/\Gamma(K^-\pi^+)$ Γ_{148}/Γ_{32}

VALUE (units 10^{-2})	EVTS	DOCUMENT ID		TECN	COMMENT
19.1±0.5 OUR FIT					
19.1±0.4±0.6	7331 ± 130	RUBIN	06	CLEO	e^+e^- at $\psi(3770)$

$\Gamma(2\pi^+2\pi^-)/\Gamma(K^-2\pi^+\pi^-)$ Γ_{148}/Γ_{67}

VALUE (units 10^{-2})	EVTS	DOCUMENT ID		TECN	COMMENT
9.19±0.22 OUR FIT					
9.20±0.26 OUR AVERAGE					
9.14±0.18±0.22	6360±115	LINK	07A	FOCS	γBe, $\overline{E}_\gamma\approx$ 180 GeV
7.9 ±1.8 ±0.5	162	ABLIKIM	05F	BES	$e^+e^-\approx\psi(3770)$
9.5 ±0.7 ±0.2	814	FRABETTI	95C	E687	γBe, $\overline{E}_\gamma\approx$ 200 GeV
10.2 ±1.3	345	AMMAR	91	CLEO	$e^+e^-\approx$ 10.5 GeV
• • • We do not use the following data for averages, fits, limits, etc. • • •					
11.5 ±2.3 ±1.6	64	ADAMOVICH	92	OMEG	π^- 340 GeV
10.8 ±2.4 ±0.8	79	FRABETTI	92	E687	γBe
9.6 ±1.8 ±0.7	66	ANJOS	91	E691	γBe 80–240 GeV

$\Gamma(a_1(1260)^+\pi^-,\ a_1^+\to 2\pi^+\pi^-\text{total})/\Gamma(2\pi^+2\pi^-)$ $\Gamma_{149}/\Gamma_{148}$

This is the fit fraction from the coherent amplitude analysis.

VALUE (units 10^{-2})	DOCUMENT ID		TECN	COMMENT
60.0±3.0±2.4	LINK	07A	FOCS	4-body fit, ≈ 5.7k evts

$\Gamma(a_1(1260)^+\pi^-,\ a_1^+\to\rho^0\pi^+ S\text{-wave})/\Gamma(2\pi^+2\pi^-)$ $\Gamma_{150}/\Gamma_{148}$

This is the fit fraction from the coherent amplitude analysis.

VALUE (units 10^{-2})	DOCUMENT ID		TECN	COMMENT
41.5±2.5 OUR AVERAGE				
38.1±2.3±3.6	[1] DARGENT	17		4-body fit, 7.3k 4π evts
43.3±2.5±1.9	LINK	07A	FOCS	4-body fit, ≈ 5.7k evts

[1] Obtained by analyzing CLEO-c data but not authored by the CLEO Collaboration.

$\Gamma(a_1(1260)^-\pi^+,\ a_1^-\to\rho^0\pi^- S\text{-wave})/\Gamma(2\pi^+2\pi^-)$ $\Gamma_{153}/\Gamma_{148}$

This is the fit fraction from a coherent amplitude analysis.

VALUE (units 10^{-2})	EVTS	DOCUMENT ID		COMMENT
3.1±0.6±1.0	7.3k	[1] DARGENT	17	4-body fit, 4π evts

[1] Obtained by analyzing CLEO-c data but not authored by the CLEO Collaboration.

$\Gamma(a_1(1260)^+\pi^-,\ a_1^+\to\rho^0\pi^+ D\text{-wave})/\Gamma(2\pi^+2\pi^-)$ $\Gamma_{151}/\Gamma_{148}$

This is the fit fraction from the coherent amplitude analysis.

VALUE (units 10^{-2})	DOCUMENT ID		TECN	COMMENT
2.5±0.5±0.4	[1] LINK	07A	FOCS	4-body fit, ≈ 5.7k evts

[1] DARGENT 17 using 7.3k events find this contribution negligible.

$\Gamma(a_1(1260)^+\pi^-,\ a_1^+\to\sigma\pi^+)/\Gamma(2\pi^+2\pi^-)$ $\Gamma_{152}/\Gamma_{148}$

This is the fit fraction from the coherent amplitude analysis.

VALUE (units 10^{-2})	DOCUMENT ID		TECN	COMMENT
8.4±0.9 OUR AVERAGE				
10.2±1.4±3.3	[1] DARGENT	17		7.3k 4-body fit, 4π evts
8.3±0.7±0.6	LINK	07A	FOCS	4-body fit, ≈ 5.7k evts

[1] Obtained by analyzing CLEO-c data but not authored by the CLEO Collaboration.

$\Gamma(a_1(1260)^-\pi^+,\ a_1^-\to\sigma\pi^-)/\Gamma(2\pi^+2\pi^-)$ $\Gamma_{154}/\Gamma_{148}$

This is the fit fraction from a coherent amplitude analysis.

VALUE (units 10^{-2})	EVTS	DOCUMENT ID		COMMENT
0.8±0.2±0.4	7.3k	[1] DARGENT	17	4-body fit, 4π evts

[1] Obtained by analyzing CLEO-c data but not authored by the CLEO Collaboration.

$\Gamma(\pi(1300)^+\pi^-,\ \pi(1300)^+\to\sigma\pi^+)/\Gamma(2\pi^+2\pi^-)$ $\Gamma_{155}/\Gamma_{148}$

This is the fit fraction from a coherent amplitude analysis.

VALUE (units 10^{-2})	EVTS	DOCUMENT ID		COMMENT
6.8±0.9±3.4	7.3k	[1] DARGENT	17	4-body fit, 4π evts

[1] Obtained by analyzing CLEO-c data but not authored by the CLEO Collaboration.

$\Gamma(\pi(1300)^-\pi^+,\ \pi(1300)^-\to\sigma\pi^-)/\Gamma(2\pi^+2\pi^-)$ $\Gamma_{156}/\Gamma_{148}$

This is the fit fraction from a coherent amplitude analysis.

VALUE (units 10^{-2})	EVTS	DOCUMENT ID		COMMENT
3.0±0.6±2.8	7.3k	[1] DARGENT	17	4-body fit, 4π evts

[1] Obtained by analyzing CLEO-c data but not authored by the CLEO Collaboration.

$\Gamma(a_1(1640)^+\pi^-,\ a_1^+\to\rho^0\pi^+ D\text{-wave})/\Gamma(2\pi^+2\pi^-)$ $\Gamma_{157}/\Gamma_{148}$

This is the fit fraction from a coherent amplitude analysis.

VALUE (units 10^{-2})	EVTS	DOCUMENT ID		COMMENT
4.2±0.6±2.0	7.3k	[1,2] DARGENT	17	4-body fit, 4π evts

[1] Obtained by analyzing CLEO-c data but not authored by the CLEO Collaboration.
[2] 4-body fit, 4π evts

Meson Particle Listings

D^0

$\Gamma(a_1(1640)^+\pi^-,\ a_1^+\to\sigma\pi^+)/\Gamma(2\pi^+2\pi^-)$ $\Gamma_{158}/\Gamma_{148}$

This is the fit fraction from a coherent amplitude analysis.

VALUE (units 10^{-2})	EVTS	DOCUMENT ID		COMMENT
2.4±0.7±1.7	7.3k	[1] DARGENT	17	4-body fit, 4π evts

[1] Obtained by analyzing CLEO-c data but not authored by the CLEO Collaboration.

$\Gamma(\pi_2(1670)^+\pi^-,\ \pi_2^+\to f_2(1270)^0\pi^+,\ f_2^0\to\pi^+\pi^-)/\Gamma(2\pi^+2\pi^-)$ $\Gamma_{159}/\Gamma_{148}$

This is the fit fraction from a coherent amplitude analysis.

VALUE (units 10^{-2})	EVTS	DOCUMENT ID		COMMENT
2.7±0.6±1.1	7.3k	[1] DARGENT	17	4-body fit, 4π evts

[1] Obtained by analyzing CLEO-c data but not authored by the CLEO Collaboration.

$\Gamma(\pi_2(1670)^+\pi^-,\ \pi_2^+\to\sigma\pi^+)/\Gamma(2\pi^+2\pi^-)$ $\Gamma_{160}/\Gamma_{148}$

This is the fit fraction from a coherent amplitude analysis.

VALUE (units 10^{-2})	EVTS	DOCUMENT ID		COMMENT
3.5±0.6±1.2	7.3k	[1] DARGENT	17	4-body fit, 4π evts

[1] Obtained by analyzing CLEO-c data but not authored by the CLEO Collaboration.

$\Gamma(2\rho^0\text{total})/\Gamma(2\pi^+2\pi^-)$ $\Gamma_{161}/\Gamma_{148}$

This is the fit fraction from the coherent amplitude analysis.

VALUE (units 10^{-2})	DOCUMENT ID		TECN	COMMENT
24.5±1.3±1.0	LINK	07A	FOCS	4-body fit, ≈ 5.7k evts

$\Gamma(2\rho^0,\text{parallel helicities})/\Gamma(2\pi^+2\pi^-)$ $\Gamma_{162}/\Gamma_{148}$

This is the fit fraction from the coherent amplitude analysis.

VALUE (units 10^{-2})	DOCUMENT ID		TECN	COMMENT
1.1±0.3±0.3	LINK	07A	FOCS	4-body fit, ≈ 5.7k evts

$\Gamma(2\rho^0,\text{perpendicular helicities})/\Gamma(2\pi^+2\pi^-)$ $\Gamma_{163}/\Gamma_{148}$

This is the fit fraction from the coherent amplitude analysis.

VALUE (units 10^{-2})	DOCUMENT ID		TECN	COMMENT
6.4±0.6±0.5	LINK	07A	FOCS	4-body fit, ≈ 5.7k evts

$\Gamma(2\rho^0,\text{longitudinal helicities})/\Gamma(2\pi^+2\pi^-)$ $\Gamma_{164}/\Gamma_{148}$

This is the fit fraction from the coherent amplitude analysis.

VALUE (units 10^{-2})	DOCUMENT ID		TECN	COMMENT
16.8±1.0±0.8	LINK	07A	FOCS	4-body fit, ≈ 5.7k evts

$\Gamma(2\rho(770)^0,\ S\text{-wave})/\Gamma(2\pi^+2\pi^-)$ $\Gamma_{165}/\Gamma_{148}$

This is the fit fraction from a coherent amplitude analysis.

VALUE (units 10^{-2})	EVTS	DOCUMENT ID		COMMENT
2.4±0.7±1.5	7.3k	[1] DARGENT	17	4-body fit, 4π evts

[1] Obtained by analyzing CLEO-c data but not authored by the CLEO Collaboration.

$\Gamma(2\rho(770)^0,\ P\text{-wave})/\Gamma(2\pi^+2\pi^-)$ $\Gamma_{166}/\Gamma_{148}$

This is the fit fraction from a coherent amplitude analysis.

VALUE (units 10^{-2})	EVTS	DOCUMENT ID		COMMENT
7.0±0.5±1.6	7.3k	[1] DARGENT	17	4-body fit, 4π evts

[1] Obtained by analyzing CLEO-c data but not authored by the CLEO Collaboration.

$\Gamma(2\rho(770)^0,\ D\text{-wave})/\Gamma(2\pi^+2\pi^-)$ $\Gamma_{167}/\Gamma_{148}$

This is the fit fraction from a coherent amplitude analysis.

VALUE (units 10^{-2})	EVTS	DOCUMENT ID		COMMENT
8.2±1.0±3.9	7.3k	[1] DARGENT	17	4-body fit, 4π evts

[1] Obtained by analyzing CLEO-c data but not authored by the CLEO Collaboration.

$\Gamma(\text{Resonant }(\pi^+\pi^-)\pi^+\pi^-\text{ 3-body total})/\Gamma(2\pi^+2\pi^-)$ $\Gamma_{168}/\Gamma_{148}$

This is the fit fraction from the coherent amplitude analysis.

VALUE (units 10^{-2})	DOCUMENT ID		TECN	COMMENT
20.0±1.2±1.0	LINK	07A	FOCS	4-body fit, ≈ 5.7k evts

$\Gamma(\sigma\pi^+\pi^-)/\Gamma(2\pi^+2\pi^-)$ $\Gamma_{169}/\Gamma_{148}$

This is the fit fraction from a coherent amplitude analysis.

VALUE (units 10^{-2})	DOCUMENT ID		TECN	COMMENT
8.2±0.9±0.7	LINK	07A	FOCS	4-body fit, ≈ 5.7k evts

$\Gamma(\sigma\rho(770)^0)/\Gamma(2\pi^+2\pi^-)$ $\Gamma_{170}/\Gamma_{148}$

This is the fit fraction from a coherent amplitude analysis.

VALUE (units 10^{-2})	EVTS	DOCUMENT ID		COMMENT
6.6±1.0±3.2	7.3k	[1] DARGENT	17	4-body fit, 4π evts

[1] Obtained by analyzing CLEO-c data but not authored by the CLEO Collaboration.

$\Gamma(f_0(1370)\sigma,\ f_0\to\pi^+\pi^-)/\Gamma(2\pi^+2\pi^-)$ $\Gamma_{174}/\Gamma_{148}$

This is the fit fraction from a coherent amplitude analysis.

VALUE (units 10^{-2})	EVTS	DOCUMENT ID		COMMENT
21.2±1.8±6.7	7.3k	[1] DARGENT	17	4-body fit, 4π evts

[1] Obtained by analyzing CLEO-c data but not authored by the CLEO Collaboration.

$\Gamma(f_0(980)\pi^+\pi^-,\ f_0\to\pi^+\pi^-)/\Gamma(2\pi^+2\pi^-)$ $\Gamma_{171}/\Gamma_{148}$

This is the fit fraction from a coherent amplitude analysis.

VALUE (units 10^{-2})	DOCUMENT ID		TECN	COMMENT
2.4±0.5±0.4	LINK	07A	FOCS	4-body fit, ≈ 5.7k evts

$\Gamma(f_2(1270)\pi^+\pi^-,\ f_2\to\pi^+\pi^-)/\Gamma(2\pi^+2\pi^-)$ $\Gamma_{172}/\Gamma_{148}$

This is the fit fraction from the coherent amplitude analysis.

VALUE (units 10^{-2})	DOCUMENT ID		TECN	COMMENT
4.9±0.6±0.5	LINK	07A	FOCS	4-body fit, ≈ 5.7k evts

$\Gamma(2f_2(1270),\ f_2\to\pi^+\pi^-)/\Gamma(2\pi^+2\pi^-)$ $\Gamma_{173}/\Gamma_{148}$

This is the fit fraction from a coherent amplitude analysis.

VALUE (units 10^{-2})	EVTS	DOCUMENT ID		COMMENT
2.1±0.5±2.3	7.3k	[1] DARGENT	17	4-body fit, 4π evts

[1] Obtained by analyzing CLEO-c data but not authored by the CLEO Collaboration.

$\Gamma(\pi^+\pi^-2\pi^0)/\Gamma(K^-\pi^+)$ Γ_{175}/Γ_{32}

VALUE (units 10^{-2})	EVTS	DOCUMENT ID		TECN	COMMENT
25.8±1.5±1.8	2724 ± 166	RUBIN	06	CLEO	e^+e^- at $\psi(3770)$

$\Gamma(\eta\pi^0)/\Gamma_{\text{total}}$ Γ_{176}/Γ

Unseen decay modes of the η are included.

VALUE (units 10^{-4})	EVTS	DOCUMENT ID		TECN	COMMENT
6.7±0.6 OUR FIT					
6.5±0.9±0.4	75	ABLIKIM	16D	BES3	e^+e^-, 3773 MeV
• • • We do not use the following data for averages, fits, limits, etc. • • •					
6.4±1.0±0.4	156 ± 24	ARTUSO	08	CLEO	See MENDEZ 10

$\Gamma(\eta\pi^0)/\Gamma(K^-\pi^+)$ Γ_{176}/Γ_{32}

Unseen decay modes of the η are included.

VALUE (units 10^{-2})	EVTS	DOCUMENT ID		TECN	COMMENT
• • • We do not use the following data for averages, fits, limits, etc. • • •					
1.47±0.34±0.11	62 ± 14	RUBIN	06	CLEO	See ARTUSO 08

$\Gamma(\eta\pi^0)/[\Gamma(K^-\pi^+)+\Gamma(K^+\pi^-)]$ $\Gamma_{176}/(\Gamma_{32}+\Gamma_{257})$

Unseen decay modes of the η are included.

VALUE (units 10^{-2})	EVTS	DOCUMENT ID		TECN	COMMENT
1.71±0.15 OUR FIT					
1.74±0.15±0.11	481 ± 40	MENDEZ	10	CLEO	e^+e^- at 3774 MeV

$\Gamma(\omega\pi^0)/\Gamma_{\text{total}}$ Γ_{177}/Γ

Unseen decay modes of the ω are included.

VALUE (units 10^{-4})	CL%	EVTS	DOCUMENT ID		TECN	COMMENT
1.17±0.34±0.07		45	ABLIKIM	16D	BES3	e^+e^-, 3773 MeV
• • • We do not use the following data for averages, fits, limits, etc. • • •						
<2.6	90		RUBIN	06	CLEO	e^+e^- at $\psi(3770)$

$\Gamma(2\pi^+2\pi^-\pi^0)/\Gamma(K^-\pi^+)$ Γ_{178}/Γ_{32}

VALUE (units 10^{-2})	EVTS	DOCUMENT ID		TECN	COMMENT
10.7±1.2±0.5	1614 ± 171	RUBIN	06	CLEO	e^+e^- at $\psi(3770)$

$\Gamma(\eta\pi^+\pi^-)/\Gamma_{\text{total}}$ Γ_{179}/Γ

Unseen decay modes of the η are included.

VALUE (units 10^{-4})	CL%	EVTS	DOCUMENT ID		TECN	COMMENT
10.9±1.3±0.9		257 ± 32	ARTUSO	08	CLEO	e^+e^- at $\psi(3770)$
• • • We do not use the following data for averages, fits, limits, etc. • • •						
<19	90		RUBIN	06	CLEO	e^+e^- at $\psi(3770)$

$\Gamma(\omega\pi^+\pi^-)/\Gamma(K^-\pi^+)$ Γ_{180}/Γ_{32}

Unseen decay modes of the ω are included.

VALUE (units 10^{-2})	EVTS	DOCUMENT ID		TECN	COMMENT
4.1±1.2±0.4	472 ± 132	RUBIN	06	CLEO	e^+e^- at $\psi(3770)$

$\Gamma(3\pi^+3\pi^-)/\Gamma(K^-2\pi^+\pi^-)$ Γ_{181}/Γ_{67}

VALUE (units 10^{-3})	EVTS	DOCUMENT ID		TECN	COMMENT
5.23±0.59±1.35	149 ± 17	LINK	04B	FOCS	γA, $\overline{E}_\gamma \approx 180$ GeV

$\Gamma(3\pi^+3\pi^-)/\Gamma(K^-3\pi^+2\pi^-)$ $\Gamma_{181}/\Gamma_{103}$

VALUE	DOCUMENT ID		TECN	COMMENT
• • • We do not use the following data for averages, fits, limits, etc. • • •				
1.93±047±0.48	[1] LINK	04B	FOCS	γA, $\overline{E}_\gamma \approx 180$ GeV

[1] This LINK 04B result is not independent of other results in these Listings.

$\Gamma(\eta'(958)\pi^0)/\Gamma_{\text{total}}$ Γ_{182}/Γ

Unseen decay modes of the $\eta'(958)$ are included.

VALUE (units 10^{-4})	EVTS	DOCUMENT ID		TECN	COMMENT
• • • We do not use the following data for averages, fits, limits, etc. • • •					
8.1±1.5±0.6	50 ± 9	ARTUSO	08	CLEO	See MENDEZ 10

$\Gamma(\eta'(958)\pi^0)/[\Gamma(K^-\pi^+)+\Gamma(K^+\pi^-)]$ $\Gamma_{182}/(\Gamma_{32}+\Gamma_{257})$

Unseen decay modes of the $\eta'(958)$ are included.

VALUE (units 10^{-2})	EVTS	DOCUMENT ID		TECN	COMMENT
2.3±0.4 OUR FIT					
2.3±0.3±0.2	159 ± 19	MENDEZ	10	CLEO	e^+e^- at 3774 MeV

$\Gamma(\eta'(958)\pi^+\pi^-)/\Gamma_{total}$ Γ_{183}/Γ

Unseen decay modes of the $\eta'(958)$ are included.

VALUE (units 10^{-4})	EVTS	DOCUMENT ID		TECN	COMMENT
4.5±1.6±0.5	21 ± 8	ARTUSO	08	CLEO	e^+e^- at $\psi(3770)$

$\Gamma(2\eta)/\Gamma_{total}$ Γ_{184}/Γ

Unseen decay modes of the η are included.

VALUE (units 10^{-4})	EVTS	DOCUMENT ID		TECN	COMMENT
• • • We do not use the following data for averages, fits, limits, etc. • • •					
16.7±1.4±1.3	255 ± 22	ARTUSO	08	CLEO	See MENDEZ 10

$\Gamma(2\eta)/[\Gamma(K^-\pi^+)+\Gamma(K^+\pi^-)]$ $\Gamma_{184}/(\Gamma_{32}+\Gamma_{257})$

Unseen decay modes of the η are included.

VALUE (units 10^{-2})	EVTS	DOCUMENT ID		TECN	COMMENT
4.3±0.5 OUR FIT					
4.3±0.3±0.4	430 ± 29	MENDEZ	10	CLEO	e^+e^- at 3774 MeV

$\Gamma(\eta\eta'(958))/\Gamma_{total}$ Γ_{185}/Γ

Unseen decay modes of the η and $\eta'(958)$ are included.

VALUE (units 10^{-4})	EVTS	DOCUMENT ID		TECN	COMMENT
• • • We do not use the following data for averages, fits, limits, etc. • • •					
12.6±2.5±1.1	46 ± 9	ARTUSO	08	CLEO	See MENDEZ 10

$\Gamma(\eta\eta'(958))/[\Gamma(K^-\pi^+)+\Gamma(K^+\pi^-)]$ $\Gamma_{185}/(\Gamma_{32}+\Gamma_{257})$

Unseen decay modes of the η and $\eta'(958)$ are included.

VALUE (units 10^{-2})	EVTS	DOCUMENT ID		TECN	COMMENT
2.7±0.7 OUR FIT					
2.7±0.6±0.3	66 ± 15	MENDEZ	10	CLEO	e^+e^- at 3774 MeV

Hadronic modes with a $K\overline{K}$ pair

$\Gamma(K^+K^-)/\Gamma_{total}$ Γ_{186}/Γ

VALUE (units 10^{-3})	EVTS	DOCUMENT ID		TECN	COMMENT
3.97±0.07 OUR FIT	Error includes scale factor of 1.4.				
• • • We do not use the following data for averages, fits, limits, etc. • • •					
4.08±0.08±0.09	4746 ± 74	BONVICINI	08	CLEO	See MENDEZ 10

$\Gamma(K^+K^-)/\Gamma(K^-\pi^+)$ Γ_{186}/Γ_{32}

VALUE	EVTS	DOCUMENT ID		TECN	COMMENT
0.1021±0.0015 OUR FIT	Error includes scale factor of 1.7.				
0.1010±0.0016 OUR AVERAGE	Error includes scale factor of 1.4. See the ideogram below.				
0.122 ±0.011 ±0.004	242 ± 20	ABLIKIM	05F	BES	$e^+e^- \approx \psi(3770)$
0.0992±0.0011±0.0012	16k±200	ACOSTA	05C	CDF	$p\overline{p}$, $\sqrt{s}$=1.96 TeV
0.0993±0.0014±0.0014	11k	LINK	03	FOCS	γ nucleus, $\overline{E}_\gamma \approx$ 180 GeV
0.1040±0.0033±0.0027	1900	CSORNA	02	CLE2	$e^+e^- \approx \Upsilon(4S)$
0.109 ±0.003 ±0.003	3317	AITALA	98C	E791	π^- nucleus, 500 GeV
0.116 ±0.007 ±0.007	1102	ASNER	96B	CLE2	$e^+e^- \approx \Upsilon(4S)$
0.109 ±0.007 ±0.009	581	FRABETTI	94C	E687	γBe $\overline{E}_\gamma$= 220 GeV
0.107 ±0.010 ±0.009	193	ANJOS	91D	E691	Photoproduction
0.117 ±0.010 ±0.007	249	ALEXANDER	90	CLEO	e^+e^- 10.5–11 GeV
• • • We do not use the following data for averages, fits, limits, etc. • • •					
0.107 ±0.029 ±0.015	103	ADAMOVICH	92	OMEG	π^- 340 GeV
0.138 ±0.027 ±0.010	155	FRABETTI	92	E687	γBe
0.16 ±0.05	34	ALVAREZ	91B	NA14	Photoproduction
0.10 ±0.02 ±0.01	131	ALBRECHT	90C	ARG	$e^+e^- \approx$ 10 GeV
0.122 ±0.018 ±0.012	118	BALTRUSAIT...85E		MRK3	e^+e^- 3.77 GeV
0.113 ±0.030		ABRAMS	79D	MRK2	e^+e^- 3.77 GeV

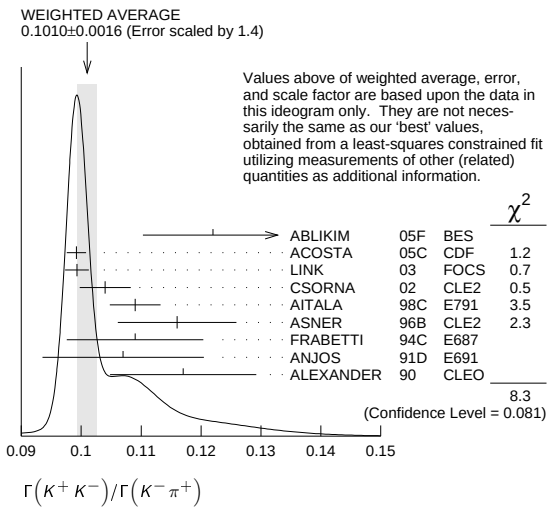

$\Gamma(K^+K^-)/[\Gamma(K^-\pi^+)+\Gamma(K^+\pi^-)]$ $\Gamma_{186}/(\Gamma_{32}+\Gamma_{257})$

VALUE (units 10^{-2})	EVTS	DOCUMENT ID		TECN	COMMENT
10.18±0.15 OUR FIT	Error includes scale factor of 1.7.				
10.41±0.11±0.12	13.8k	MENDEZ	10	CLEO	e^+e^- at 3774 MeV

$\Gamma(K^+K^-)/\Gamma(\pi^+\pi^-)$ $\Gamma_{186}/\Gamma_{127}$

The unused results here are redundant with $\Gamma(K^+K^-)/\Gamma(K^-\pi^+)$ and $\Gamma(\pi^+\pi^-)/\Gamma(K^-\pi^+)$ measurements by the same experiments.

VALUE	EVTS	DOCUMENT ID		TECN	COMMENT
• • • We do not use the following data for averages, fits, limits, etc. • • •					
2.760±0.040±0.034	7334	ACOSTA	05C	CDF	$p\overline{p}$, $\sqrt{s}$=1.96 TeV
2.81 ±0.10 ±0.06		LINK	03	FOCS	γ nucleus, $\overline{E}_\gamma \approx$ 180 GeV
2.96 ±0.16 ±0.15	710	CSORNA	02	CLE2	$e^+e^- \approx \Upsilon(4S)$
2.75 ±0.15 ±0.16		AITALA	98C	E791	π^- nucleus, 500 GeV
2.53 ±0.46 ±0.19		FRABETTI	94C	E687	γBe $\overline{E}_\gamma$= 220 GeV
2.23 ±0.81 ±0.46		ADAMOVICH	92	OMEG	π^- 340 GeV
1.95 ±0.34 ±0.22		ANJOS	91D	E691	Photoproduction
2.5 ±0.7		ALBRECHT	90C	ARG	$e^+e^- \approx$ 10 GeV
2.35 ±0.37 ±0.28		ALEXANDER	90	CLEO	e^+e^- 10.5–11 GeV

$\Gamma(2K_S^0)/\Gamma_{total}$ Γ_{187}/Γ

VALUE (units 10^{-4})	EVTS	DOCUMENT ID		TECN	COMMENT
1.70±0.12 OUR FIT					
1.67±0.11±0.11	576	ABLIKIM	17A	BES3	$e^+e^- \to \psi(3770)$
• • • We do not use the following data for averages, fits, limits, etc. • • •					
1.46±0.32±0.09	68 ± 15	BONVICINI	08	CLEO	See MENDEZ 10

$\Gamma(2K_S^0)/[\Gamma(K^-\pi^+)+\Gamma(K^+\pi^-)]$ $\Gamma_{187}/(\Gamma_{32}+\Gamma_{257})$

VALUE (units 10^{-2})	EVTS	DOCUMENT ID		TECN	COMMENT
0.436±0.030 OUR FIT					
0.41 ±0.04 ±0.02	215 ± 23	MENDEZ	10	CLEO	e^+e^- at 3774 MeV

$\Gamma(2K_S^0)/\Gamma(K_S^0\pi^+\pi^-)$ Γ_{187}/Γ_{35}

This is the same as $\Gamma(K^0\overline{K}^0)$ / $\Gamma(\overline{K}^0\pi^+\pi^-)$ because $D^0 \to K_S^0 K_L^0$ is forbidden by CP conservation.

VALUE	EVTS	DOCUMENT ID		TECN	COMMENT
0.0062±0.0006 OUR FIT					
0.0120±0.0022 OUR AVERAGE					
0.0144±0.0032±0.0016	79 ± 17	LINK	05A	FOCS	γ Be, $\overline{E}_\gamma \approx$ 180 GeV
0.0101±0.0022±0.0016	26	ASNER	96B	CLE2	$e^+e^- \approx \Upsilon(4S)$
0.039 ±0.013 ±0.013	20 ± 7	FRABETTI	94J	E687	γBe $\overline{E}_\gamma$=220 GeV
• • • We do not use the following data for averages, fits, limits, etc. • • •					
0.021 $^{+0.011}_{-0.008}$ ±0.002	5	ALEXANDER	90	CLEO	e^+e^- 10.5–11 GeV

$\Gamma(2K_S^0)/\Gamma(K_S^0\pi^0)$ Γ_{187}/Γ_{33}

VALUE (units 10^{-2})	EVTS	DOCUMENT ID		TECN	COMMENT
1.101±0.023±0.030	4.8k	DASH	17	BELL	At/near $\Upsilon(4S)$, $\Upsilon(5S)$

$\Gamma(K_S^0K^-\pi^+)/\Gamma(K^-\pi^+)$ Γ_{188}/Γ_{32}

VALUE	EVTS	DOCUMENT ID		TECN	COMMENT
0.084±0.013 OUR FIT	Error includes scale factor of 1.1.				
0.08 ±0.03		[1] ANJOS	91	E691	γBe 80–240 GeV

[1] The factor 100 at the top of column 2 of Table I of ANJOS 91 should be omitted.

$\Gamma(K_S^0K^-\pi^+)/\Gamma(K_S^0\pi^+\pi^-)$ Γ_{188}/Γ_{35}

VALUE	EVTS	DOCUMENT ID		TECN	COMMENT
0.118±0.017 OUR FIT	Error includes scale factor of 1.1.				
0.119±0.021 OUR AVERAGE	Error includes scale factor of 1.3.				
0.108±0.019	61	AMMAR	91	CLEO	$e^+e^- \approx$ 10.5 GeV
0.16 ±0.03 ±0.02	39	ALBRECHT	90C	ARG	$e^+e^- \approx$ 10 GeV

$\Gamma(\overline{K}^*(892)^0K_S^0, \overline{K}^{*0} \to K^-\pi^+)/\Gamma(K_S^0K^-\pi^+)$ $\Gamma_{189}/\Gamma_{188}$

Fit fraction from Dalitz plot analyses. The fraction for the $K_S^0\pi^+$ mass between 792 and 992 MeV is 0.370 ± 0.003 ± 0.012.

VALUE	EVTS	DOCUMENT ID		TECN	COMMENT
2.47±0.15±0.23	113k	[1] AAIJ	16N	LHCB	Dalitz plot fit

[1] AAIJ 16N gives results for two S-wave parameterisations. We take the values from the model with LASS parametrization, and the difference as a systematic uncertainty.

$\Gamma(K^*(892)^+K^-, K^{*+} \to K_S^0\pi^+)/\Gamma(K_S^0K^-\pi^+)$ $\Gamma_{190}/\Gamma_{188}$

Fit fraction from Dalitz plot analyses.

VALUE	EVTS	DOCUMENT ID		TECN	COMMENT
56.9±0.6±1.1	113k	[1] AAIJ	16N	LHCB	Dalitz plot fit

[1] AAIJ 16N gives results for two S-wave parameterisations. We take the values from the model with LASS parametrization, and the difference as a systematic uncertainty.

$\Gamma(\overline{K}^*(1410)^0K_S^0, \overline{K}^{*0} \to K^-\pi^+)/\Gamma(K_S^0K^-\pi^+)$ $\Gamma_{191}/\Gamma_{188}$

Fit fraction from Dalitz plot analyses.

VALUE (units 10^{-2})	EVTS	DOCUMENT ID		TECN	COMMENT
3.8±0.5±5.6	113k	[1] AAIJ	16N	LHCB	Dalitz plot fit

[1] AAIJ 16N gives results for two S-wave parameterisations. We take the values from the model with LASS parametrization, and the difference as a uncertainty (which in this case dominates)

$\Gamma(K^*(1410)^+ K^-,\ K^{*+} \to K^0_S\pi^+)/\Gamma(K^0_S K^-\pi^+)$ $\Gamma_{192}/\Gamma_{188}$

Fit fraction from Dalitz plot analyses.

VALUE (units 10^{-2})	EVTS	DOCUMENT ID		TECN	COMMENT
9.6±1.1±5.4	113k	[1] AAIJ	16N	LHCB	Dalitz plot fit

[1] AAIJ 16N gives results for two S-wave parameterisations. We take the values from the model with LASS parametrization, and the difference as a systematic uncertainty (which in this case dominates).

$\Gamma((K^-\pi^+)_{S-wave}\,K^0_S)/\Gamma(K^0_S K^-\pi^+)$ $\Gamma_{193}/\Gamma_{188}$

Fit fraction from Dalitz plot analyses.

VALUE (units 10^{-2})	EVTS	DOCUMENT ID		TECN	COMMENT
18±2±8	113k	[1] AAIJ	16N	LHCB	Dalitz plot fit

[1] AAIJ 16N gives results for two S-wave parameterisations. We take the values from the model with LASS parametrization, and the difference as a systematic uncertainty (which in this case dominates).

$\Gamma((K^0_S\pi^+)_{S-wave}\,K^-)/\Gamma(K^0_S K^-\pi^+)$ $\Gamma_{194}/\Gamma_{188}$

Fit fraction from Dalitz plot analyses.

VALUE (units 10^{-2})	EVTS	DOCUMENT ID		TECN	COMMENT
11.7±1.0±2.3	113k	[1] AAIJ	16N	LHCB	Dalitz plot fit

[1] AAIJ 16N gives results for two S-wave parameterisations. We take the values from the model with LASS parametrization, and the difference as a systematic uncertainty.

$\Gamma(a_0(980)^-\pi^+,\ a_0^- \to K^0_S K^-)/\Gamma(K^0_S K^-\pi^+)$ $\Gamma_{195}/\Gamma_{188}$

Fit fraction from Dalitz plot analyses.

VALUE (units 10^{-2})	EVTS	DOCUMENT ID		TECN	COMMENT
4.0±0.7±4.1	113k	[1] AAIJ	16N	LHCB	Dalitz plot fit

[1] AAIJ 16N gives results for two S-wave parameterisations. We take the values from the model with LASS parametrization, and the difference as a systematic uncertainty (which in this case dominates).

$\Gamma(a_0(1450)^-\pi^+,\ a_0^- \to K^0_S K^-)/\Gamma(K^0_S K^-\pi^+)$ $\Gamma_{196}/\Gamma_{188}$

Fit fraction from Dalitz plot analyses.

VALUE (units 10^{-2})	EVTS	DOCUMENT ID		TECN	COMMENT
0.74±0.15±0.57	113k	[1] AAIJ	16N	LHCB	Dalitz plot fit

[1] AAIJ 16N gives results for two S-wave parameterisations. We take the values from the model with LASS parametrization, and the difference as a systematic uncertainty (which in this case dominates).

$\Gamma(a_2(1320)^-\pi^+,\ a_2^- \to K^0_S K^-)/\Gamma(K^0_S K^-\pi^+)$ $\Gamma_{197}/\Gamma_{188}$

VALUE (units 10^{-2})	EVTS	DOCUMENT ID		TECN	COMMENT
0.15±0.06±0.14	113k	[1] AAIJ	16N	LHCB	Dalitz plot fit

[1] AAIJ 16N gives results for two S-wave parameterisations. We take the values from the model with LASS parametrization, and the difference as a systematic uncertainty.

$\Gamma(\rho(1450)^-\pi^+,\ \rho^- \to K^0_S K^-)/\Gamma(K^0_S K^-\pi^+)$ $\Gamma_{198}/\Gamma_{188}$

Fit fraction from Dalitz plot analyses.

VALUE (units 10^{-2})	EVTS	DOCUMENT ID		TECN	COMMENT
1.4±0.2±0.7	113k	[1] AAIJ	16N	LHCB	Dalitz plot fit

[1] AAIJ 16N gives results for two S-wave parameterisations. We take the values from the model with LASS parametrization, and the difference as a systematic uncertainty.

$\Gamma(K^0_S K^+\pi^-)/\Gamma(K^-\pi^+)$ Γ_{199}/Γ_{32}

VALUE	DOCUMENT ID		TECN	COMMENT
• • • We do not use the following data for averages, fits, limits, etc. • • •				
0.05±0.025	[1] ANJOS	91	E691	γBe 80–240 GeV

[1] The factor 100 at the top of column 2 of Table I of ANJOS 91 should be omitted.

$\Gamma(K^0_S K^+\pi^-)/\Gamma(K^0_S\pi^+\pi^-)$ Γ_{199}/Γ_{35}

VALUE	EVTS	DOCUMENT ID		TECN	COMMENT
• • • We do not use the following data for averages, fits, limits, etc. • • •					
0.098±0.020	55	AMMAR	91	CLEO	$e^+e^- \approx$ 10.5 GeV

$\Gamma(K^0_S K^+\pi^-)/\Gamma(K^0_S K^-\pi^+)$ $\Gamma_{199}/\Gamma_{188}$

VALUE	EVTS	DOCUMENT ID		TECN	COMMENT
0.654±0.007 OUR FIT					
0.654±0.007 OUR AVERAGE					
0.655±0.004±0.006	76k,113k	AAIJ	16N	LHCB	pp at 7, 8 TeV
0.592±0.044±0.018		INSLER	12	CLEO	$e^+e^- \to D^0\overline{D}^0$ at 3.77 GeV

$\Gamma(K^*(892)^0 K^0_S,\ K^{*0} \to K^+\pi^-)/\Gamma(K^0_S K^+\pi^-)$ $\Gamma_{200}/\Gamma_{199}$

Fit fraction from Dalitz plot analyses.

VALUE (units 10^{-2})	EVTS	DOCUMENT ID		TECN	COMMENT
5.17±0.21±0.47	76k	[1] AAIJ	16N	LHCB	Dalitz plot fit

[1] AAIJ 16N gives results for two S-wave parameterisations. We take the values from the model with LASS parametrization, and the difference as a systematic uncertainty.

$\Gamma(K^*(892)^- K^+,\ K^{*-} \to K^0_S\pi^-)/\Gamma(K^0_S K^+\pi^-)$ $\Gamma_{201}/\Gamma_{199}$

Fit fraction from Dalitz plot analyses.

VALUE (units 10^{-2})	EVTS	DOCUMENT ID		TECN	COMMENT
28.8±0.4±1.5	76k	[1] AAIJ	16N	LHCB	Dalitz plot fit

[1] AAIJ 16N gives results for two S-wave parameterisations. We take the values from the model with LASS parametrization, and the difference as a systematic uncertainty.

$\Gamma(K^*(1410)^0 K^0_S,\ K^{*0} \to K^+\pi^-)/\Gamma(K^0_S K^+\pi^-)$ $\Gamma_{202}/\Gamma_{199}$

Fit fraction from Dalitz plot analyses.

VALUE (units 10^{-2})	EVTS	DOCUMENT ID		TECN	COMMENT
2.2±0.6±3.7	76k	[1] AAIJ	16N	LHCB	Dalitz plot fit

[1] AAIJ 16N gives results for two S-wave parameterisations. We take the values from the model with LASS parametrization, and the difference as a systematic uncertainty (which in this case dominates).

$\Gamma(K^*(1410)^- K^+,\ K^{*-} \to K^0_S\pi^-)/\Gamma(K^0_S K^+\pi^-)$ $\Gamma_{203}/\Gamma_{199}$

Fit fraction from Dalitz plot analyses.

VALUE (units 10^{-2})	EVTS	DOCUMENT ID		TECN	COMMENT
11.9±1.5±9.1	76k	[1] AAIJ	16N	LHCB	Dalitz plot fit

[1] AAIJ 16N gives results for two S-wave parameterisations. We take the values from the model with LASS parametrization, and the difference as a systematic uncertainty (which in this case dominates).

$\Gamma((K^+\pi^-)_{S-wave}\,K^0_S)/\Gamma(K^0_S K^+\pi^-)$ $\Gamma_{204}/\Gamma_{199}$

Fit fraction from Dalitz plot analyses.

VALUE (units 10^{-2})	EVTS	DOCUMENT ID		TECN	COMMENT
17±2±8	76k	[1] AAIJ	16N	LHCB	Dalitz plot fit

[1] AAIJ 16N gives results for two S-wave parameterisations. We take the values from the model with LASS parametrization, and the difference as a systematic uncertainty.

$\Gamma((K^0_S\pi^-)_{S-wave}\,K^+)/\Gamma(K^0_S K^+\pi^-)$ $\Gamma_{205}/\Gamma_{199}$

Fit fraction from Dalitz plot analyses.

VALUE (units 10^{-2})	EVTS	DOCUMENT ID		TECN	COMMENT
6.3±0.9±2.3	76k	[1] AAIJ	16N	LHCB	Dalitz plot fit

[1] AAIJ 16N gives results for two S-wave parameterisations. We take the values from the model with LASS parametrization, and the difference as a systematic uncertainty.

$\Gamma(a_0(980)^+\pi^-,\ a_0^+ \to K^0_S K^+)/\Gamma(K^0_S K^+\pi^-)$ $\Gamma_{206}/\Gamma_{199}$

Fit fraction from Dalitz plot analyses.

VALUE (units 10^{-2})	EVTS	DOCUMENT ID		TECN	COMMENT
26±2±18	76k	[1] AAIJ	16N	LHCB	Dalitz plot fit

[1] AAIJ 16N gives results for two S-wave parameterisations. We take the values from the model with LASS parametrization, and the difference as a systematic uncertainty (which in this case dominates).

$\Gamma(a_0(1450)^+\pi^-,\ a_0^+ \to K^0_S K^+)/\Gamma(K^0_S K^+\pi^-)$ $\Gamma_{207}/\Gamma_{199}$

Fit fraction from Dalitz plot analyses.

VALUE (units 10^{-2})	EVTS	DOCUMENT ID		TECN	COMMENT
1.5±0.3±1.1	76k	[1] AAIJ	16N	LHCB	Dalitz plot fit

[1] AAIJ 16N gives results for two S-wave parameterisations. We take the values from the model with LASS parametrization, and the difference as a systematic uncertainty (which in this case dominates).

$\Gamma(\rho(1700)^+\pi^-,\ \rho^+ \to K^0_S K^+)/\Gamma(K^0_S K^+\pi^-)$ $\Gamma_{208}/\Gamma_{199}$

Fit fraction from Dalitz plot analyses.

VALUE (units 10^{-2})	EVTS	DOCUMENT ID		TECN	COMMENT
0.53±0.11±0.23	76k	[1] AAIJ	16N	LHCB	Dalitz plot fit

[1] AAIJ 16N gives results for two S-wave parameterisations. We take the values from the model with LASS parametrization, and the difference as a systematic uncertainty.

$\Gamma(K^*(892)^0 K^0_S,\ K^{*0} \to K^+\pi^-)/\Gamma(\overline{K}^*(892)^0 K^0_S,\ \overline{K}^{*0} \to K^-\pi^+)$ $\Gamma_{200}/\Gamma_{189}$

VALUE	CL%	DOCUMENT ID		TECN	COMMENT
0.356±0.034±0.007		[1] INSLER	12	CLEO	$e^+e^- \to D^0\overline{D}^0$, 3.77 GeV
• • • We do not use the following data for averages, fits, limits, etc. • • •					
<0.010	90	AMMAR	91	CLEO	$e^+e^- \approx$ 10.5 GeV

[1] Uses quantum correlations in $e^+e^- \to D^0\overline{D}^0$ at the $\psi(3770)$, where the signal side D decays to $K^0_S K\pi$ and the tag-side D decays to $K\pi$, $K\pi\pi\pi$, $K\pi\pi^0$, and 10 additional CP-even, CP-odd, and mixed CP modes involving K^0_S or K^0_L.

$\Gamma(K^+K^-\pi^0)/\Gamma(K^-\pi^+\pi^0)$ Γ_{209}/Γ_{50}

VALUE (units 10^{-2})	EVTS	DOCUMENT ID		TECN	COMMENT
2.37±0.03±0.04	11k±122	AUBERT,B	06X	BABR	$e^+e^- \approx \Upsilon(4S)$
• • • We do not use the following data for averages, fits, limits, etc. • • •					
0.95±0.26	151	ASNER	96B	CLE2	$e^+e^- \approx \Upsilon(4S)$

$\Gamma(K^*(892)^+ K^-,\ K^*(892)^+ \to K^+\pi^0)/\Gamma(K^+K^-\pi^0)$ $\Gamma_{210}/\Gamma_{209}$

This is the "fit fraction" from the Dalitz-plot analysis with interference.

VALUE (units 10^{-2})	DOCUMENT ID		TECN	COMMENT
44.4±0.8±0.6	AUBERT	07T	BABR	Dalitz fit II, 11k evts
• • • We do not use the following data for averages, fits, limits, etc. • • •				
46.1±3.1	[1] CAWLFIELD	06A	CLEO	Dalitz fit, 627 ± 30 evts

[1] The error on this CAWLFIELD 06A result is statistical only.

$\Gamma(K^*(892)^- K^+, K^*(892)^- \to K^-\pi^0)/\Gamma(K^+K^-\pi^0)$ $\Gamma_{211}/\Gamma_{209}$

This is the "fit fraction" from the Dalitz-plot analysis with interference.

VALUE (units 10^{-2})	DOCUMENT ID		TECN	COMMENT
15.9±0.7±0.6	AUBERT	07T	BABR	Dalitz fit II, 11k evts
• • • We do not use the following data for averages, fits, limits, etc. • • •				
12.3±2.2	[1] CAWLFIELD	06A	CLEO	Dalitz fit, 627 ± 30 evts

[1] The error on this CAWLFIELD 06A result is statistical only.

$\Gamma((K^+\pi^0)_{S-wave}K^-)/\Gamma(K^+K^-\pi^0)$ $\Gamma_{212}/\Gamma_{209}$

This is the "fit fraction" from the Dalitz-plot analysis with interference.

VALUE (units 10^{-2})	DOCUMENT ID		TECN	COMMENT
71.1±3.7±1.9	[1] AUBERT	07T	BABR	Dalitz fit II, 11k evts

[1] The only major difference between fits I and II in the AUBERT 07T analysis is in this mode, where the fit-I fraction is (16.3 ± 3.4 ± 2.1)%.

$\Gamma((K^-\pi^0)_{S-wave}K^+)/\Gamma(K^+K^-\pi^0)$ $\Gamma_{213}/\Gamma_{209}$

This is the "fit fraction" from the Dalitz-plot analysis with interference.

VALUE (units 10^{-2})	DOCUMENT ID		TECN	COMMENT
3.9±0.9±1.0	AUBERT	07T	BABR	Dalitz fit II, 11k evts

$\Gamma(f_0(980)\pi^0, f_0 \to K^+K^-)/\Gamma(K^+K^-\pi^0)$ $\Gamma_{214}/\Gamma_{209}$

This is the "fit fraction" from the Dalitz-plot analysis with interference.

VALUE (units 10^{-2})	DOCUMENT ID		TECN	COMMENT
10.5±1.1±1.2	[1] AUBERT	07T	BABR	Dalitz fit II, 11k evts

[1] When AUBERT 07T replace the $f_0(980)\pi^0$ mode with $a_0(980)\pi^0$, the fit fraction is a negligibly different (11.0 ± 1.5 ± 1.2)%.

$\Gamma(\phi\pi^0, \phi \to K^+K^-)/\Gamma(K^+K^-\pi^0)$ $\Gamma_{215}/\Gamma_{209}$

This is the "fit fraction" from the Dalitz-plot analysis with interference.

VALUE (units 10^{-2})	DOCUMENT ID		TECN	COMMENT
19.4±0.6±0.5	AUBERT	07T	BABR	Dalitz fit II, 11k evts
• • • We do not use the following data for averages, fits, limits, etc. • • •				
14.9±1.6	[1] CAWLFIELD	06A	CLEO	Dalitz fit, 627 ± 30 evts

[1] The error on this CAWLFIELD 06A result is statistical only.

$\Gamma(K^+K^-\pi^0\,\text{nonresonant})/\Gamma(K^+K^-\pi^0)$ $\Gamma_{216}/\Gamma_{209}$

This is the "fit fraction" from the Dalitz-plot analysis with interference.

VALUE	DOCUMENT ID		TECN	COMMENT
• • • We do not use the following data for averages, fits, limits, etc. • • •				
0.360±0.037	[1] CAWLFIELD	06A	CLEO	Dalitz fit, 627 ± 30 evts

[1] The error is statistical only. CAWLFIELD 06A also fits the Dalitz plot replacing this flat nonresonant background with broad S–wave $\kappa^\pm \to K^\pm\pi^0$ resonances. There is no significant improvement in the fit, and $K^{*\pm}K^\mp$ and $\phi\pi^0$ results are not much changed.

$\Gamma(2K_S^0\pi^0)/\Gamma_{\text{total}}$ Γ_{217}/Γ

VALUE	DOCUMENT ID		TECN	COMMENT
<0.00059	ASNER	96B	CLE2	$e^+e^- \approx \Upsilon(4S)$

$\Gamma(\phi\pi^0)/\Gamma(K^+K^-)$ $\Gamma_{248}/\Gamma_{186}$

VALUE	EVTS	DOCUMENT ID		TECN	COMMENT
• • • We do not use the following data for averages, fits, limits, etc. • • •					
0.194±0.006±0.009	1254	TAJIMA	04	BELL	e^+e^- at $\Upsilon(4S)$

$\Gamma(\phi\eta)/\Gamma(K^+K^-)$ $\Gamma_{249}/\Gamma_{186}$

VALUE (units 10^{-2})	EVTS	DOCUMENT ID		TECN	COMMENT
3.59±1.14±0.18	31	TAJIMA	04	BELL	e^+e^- at $\Upsilon(4S)$

$\Gamma(\phi\omega)/\Gamma_{\text{total}}$ Γ_{250}/Γ

VALUE	CL%	DOCUMENT ID		TECN	COMMENT
<0.0021	90	ALBRECHT	94I	ARG	$e^+e^-\approx$ 10 GeV

$\Gamma(K^+K^-\pi^+\pi^-)/\Gamma(K^-2\pi^+\pi^-)$ Γ_{218}/Γ_{67}

VALUE (units 10^{-2})	EVTS	DOCUMENT ID		TECN	COMMENT
3.00±0.13 OUR AVERAGE					
2.95±0.11±0.08	2669 ± 101	[1] LINK	05G	FOCS	γBe, $\overline{E}_\gamma \approx 180$ GeV
3.13±0.37±0.36	136 ± 15	AITALA	98D	E791	π^- nucleus, 500 GeV
3.5 ±0.4 ±0.2	244 ± 26	FRABETTI	95C	E687	γBe, $\overline{E}_\gamma \approx 200$ GeV
• • • We do not use the following data for averages, fits, limits, etc. • • •					
4.4 ±1.8 ±0.5	19 ± 8	ABLIKIM	05F	BES	$e^+e^- \approx \psi(3770)$
4.1 ±0.7 ±0.5	114 ± 20	ALBRECHT	94I	ARG	$e^+e^-\approx$ 10 GeV
3.14±1.0	89 ± 29	AMMAR	91	CLEO	$e^+e^- \approx$ 10.5 GeV
$2.8\ ^{+0.8}_{-0.7}$		ANJOS	91	E691	γBe 80–240 GeV

[1] LINK 05G uses a smaller, cleaner subset of 1279 ± 48 events for the amplitude analysis that gives the results in the next data blocks.

$\Gamma(\phi(\pi^+\pi^-)_{S-wave}, \phi \to K^+K^-)/\Gamma(K^+K^-\pi^+\pi^-)$ $\Gamma_{219}/\Gamma_{218}$

This is the fraction from a coherent amplitude analysis.

VALUE (%)	DOCUMENT ID		TECN	COMMENT
4.0±0.6±2.1	[1] DARGENT	17		4-body fit, 2.9k $KK\pi\pi$ evts
• • • We do not use the following data for averages, fits, limits, etc. • • •				
10.3±1.0±0.8	[2] ARTUSO	12	CLEO	Fitting 2959 evts.
1 ±1	LINK	05G	FOCS	Fits 1279 ± 48 evts.

[1] Obtained by analyzing CLEO data but not authored by the CLEO Collaboration.
[2] See DARGENT 17

$\Gamma((\phi\rho^0)_{S-wave}, \phi \to K^+K^-)/\Gamma(K^+K^-\pi^+\pi^-)$ $\Gamma_{220}/\Gamma_{218}$

This is the fraction from a coherent amplitude analysis.

VALUE (units 10^{-2})	EVTS	DOCUMENT ID		TECN	COMMENT
28.1±1.3±1.7	2.9k	[1,2] DARGENT	17		4-body fit, $KK\pi\pi$ evts
• • • We do not use the following data for averages, fits, limits, etc. • • •					
38.3±2.5±3.8		[1,3] ARTUSO	12	CLEO	Fitting 2959 evts.
29 ±2 ±1		LINK	05G	FOCS	Fits 1279 ± 48 evts.

[1] ARTUSO 12 and DARGENT 17 use the same dataset, but ARTUSO 12 uses a formulation for the D-wave component that is in fact a mix of S- and D-wave, while DARGENT 17 uses a pure D-wave. This explains the discrepancy in their $\rho\phi$ S- and D-wave components.
[2] Obtained by analyzing CLEO data but not authored by the CLEO Collaboration.
[3] See DARGENT 17

$\Gamma((\phi\rho^0)_{P-wave}, \phi \to K^+K^-)/\Gamma(K^+K^-\pi^+\pi^-)$ $\Gamma_{221}/\Gamma_{218}$

This is the fit fraction from a coherent amplitude analysis.

VALUE (units 10^{-2})	EVTS	DOCUMENT ID		COMMENT
1.6±0.3±0.7	2.9k	[1] DARGENT	17	4-body fit, $KK\pi\pi$ evts

[1] Obtained by analyzing CLEO data but not authored by the CLEO Collaboration.

$\Gamma((\phi\rho^0)_{D-wave}, \phi \to K^+K^-)/\Gamma(K^+K^-\pi^+\pi^-)$ $\Gamma_{222}/\Gamma_{218}$

VALUE (units 10^{-2})	EVTS	DOCUMENT ID		TECN	COMMENT
1.7±0.4±0.4	2.9k	[1,2] DARGENT	17		4-body fit, $KK\pi\pi$ evts
• • • We do not use the following data for averages, fits, limits, etc. • • •					
3.4±0.7±0.6		[1,3] ARTUSO	12	CLEO	Fitting 2959 evts.

[1] ARTUSO 12 use a formulation for the D-wave component that is in fact a mix of S- and D-wave, while DARGENT 17 uses a pure D-wave.
[2] Obtained by analyzing CLEO data but not authored by the CLEO Collaboration.
[3] See DARGENT 17

$\Gamma(K^+K^-\rho^0\,3\text{-body})/\Gamma(K^+K^-\pi^+\pi^-)$ $\Gamma_{224}/\Gamma_{218}$

This is the fraction from a coherent amplitude analysis.

VALUE (%)	DOCUMENT ID		TECN	COMMENT
• • • We do not use the following data for averages, fits, limits, etc. • • •				
2±2±2	LINK	05G	FOCS	Fits 1279 ± 48 evts.

$\Gamma(f_0(980)\pi^+\pi^-, f_0 \to K^+K^-)/\Gamma(K^+K^-\pi^+\pi^-)$ $\Gamma_{225}/\Gamma_{218}$

This is the fraction from a coherent amplitude analysis.

VALUE (%)	DOCUMENT ID		TECN	COMMENT
• • • We do not use the following data for averages, fits, limits, etc. • • •				
15±3±2	LINK	05G	FOCS	Fits 1279 ± 48 evts.

$\Gamma(K^*(892)^0\overline{K}^*(892)^0, K^{*0} \to K^\pm\pi^\mp)/\Gamma(K^+K^-\pi^+\pi^-)$ $\Gamma_{223}/\Gamma_{218}$

This is the fraction from a coherent amplitude analysis.

VALUE (%)	DOCUMENT ID		TECN	COMMENT
• • • We do not use the following data for averages, fits, limits, etc. • • •				
3±2±1	LINK	05G	FOCS	Fits 1279 ± 48 evts.

$\Gamma((K^*(892)^0\overline{K}^*(892)^0)_{S-wave}, K^{*0} \to K^\pm\pi^\mp)/\Gamma(K^+K^-\pi^+\pi^-)$ $\Gamma_{226}/\Gamma_{218}$

VALUE (units 10^{-2})	EVTS	DOCUMENT ID		TECN	COMMENT
4.5±0.8±2.0	2.9k	[1] DARGENT	17		4-body fit, $KK\pi\pi$ evts
• • • We do not use the following data for averages, fits, limits, etc. • • •					
6.1±0.8±0.9		[2] ARTUSO	12	CLEO	Fitting 2959 evts.

[1] Obtained by analyzing CLEO data but not authored by the CLEO Collaboration.
[2] See DARGENT 17

$\Gamma((K^*(892)^0\overline{K}^*(892)^0)_{P-wave}, K^* \to K^\pm\pi^\mp)/\Gamma(K^+K^-\pi^+\pi^-)$ $\Gamma_{227}/\Gamma_{218}$

This is the fit fraction from a coherent amplitude analysis.

VALUE (units 10^{-2})	EVTS	DOCUMENT ID		COMMENT
3.6±0.7±1.5	2.9k	[1] DARGENT	17	4-body fit, $KK\pi\pi$ evts

[1] Obtained by analyzing CLEO data but not authored by the CLEO Collaboration.

$\Gamma((K^*(892)^0\overline{K}^*(892)^0)_{D-wave}, K^* \to K^\pm\pi^\mp)/\Gamma(K^+K^-\pi^+\pi^-)$ $\Gamma_{228}/\Gamma_{218}$

This is the fit fraction from a coherent amplitude analysis.

VALUE (units 10^{-2})	EVTS	DOCUMENT ID		COMMENT
4.0±0.6±0.7	2.9k	[1] DARGENT	17	4-body fit, $KK\pi\pi$ evts

[1] Obtained by analyzing CLEO data but not authored by the CLEO Collaboration.

$\Gamma(K^*(892)^0 K^\mp\pi^\pm\,3\text{-body}, K^{*0} \to K^\pm\pi^\mp)/\Gamma(K^+K^-\pi^+\pi^-)$ $\Gamma_{229}/\Gamma_{218}$

This is the fraction from a coherent amplitude analysis.

VALUE (%)	DOCUMENT ID		TECN	COMMENT
• • • We do not use the following data for averages, fits, limits, etc. • • •				
11±2±1	LINK	05G	FOCS	Fits 1279 ± 48 evts.

Meson Particle Listings

D^0

$\Gamma(K^*(892)^0(K^-\pi^+)_{S-wave}$ 3-body, $K^{*0}\to K^+\pi^-)/\Gamma(K^+K^-\pi^+\pi^-)$ $\Gamma_{230}/\Gamma_{218}$

This is the fit fraction from a coherent amplitude analysis.

VALUE (units 10^{-2})	EVTS	DOCUMENT ID		COMMENT
5.8±1.2±2.1	2.9k	[1] DARGENT	17	4-body fit, $K K\pi\pi$ evts

[1] Obtained by analyzing CLEO data but not authored by the CLEO Collaboration.

$\Gamma((K^-\pi^+)_{P-wave}, (K^+\pi^-)_{S-wave})/\Gamma(K^+K^-\pi^+\pi^-)$ $\Gamma_{231}/\Gamma_{218}$

VALUE (%)	DOCUMENT ID		TECN	COMMENT
• • • We do not use the following data for averages, fits, limits, etc. • • •				
10.9±1.2±1.7	[1] ARTUSO	12	CLEO	Fitting 2959 evts.

[1] See DARGENT 17

$\Gamma(K_1(1270)^\pm K^\mp, K_1^\pm\to K^\pm\pi^+\pi^-)/\Gamma(K^+K^-\pi^+\pi^-)$ $\Gamma_{232}/\Gamma_{218}$

This is the fraction from a coherent amplitude analysis.

VALUE (%)	DOCUMENT ID		TECN	COMMENT
• • • We do not use the following data for averages, fits, limits, etc. • • •				
33±6±4	[1] LINK	05G	FOCS	Fits 1279 ± 48 evts.

[1] This LINK 05G value includes $K_1(1270)^\pm\to\rho^0K^\pm$, $\to K_0^*(1430)^0\pi^\pm$, and $K^*(892)^0\pi^\pm$.

$\Gamma(K_1(1270)^+K^-, K_1^+\to K^{*0}\pi^+)/\Gamma(K^+K^-\pi^+\pi^-)$ $\Gamma_{233}/\Gamma_{218}$

VALUE (%)	EVTS	DOCUMENT ID		TECN	COMMENT
5.5±1.4±3.4	2.9k	[1] DARGENT	17		4-body fit, $K K\pi\pi$ evts
• • • We do not use the following data for averages, fits, limits, etc. • • •					
7.3±0.8±1.9		[2] ARTUSO	12	CLEO	Fitting 2959 evts.

[1] Obtained by analyzing CLEO data but not authored by the CLEO Collaboration.
[2] See DARGENT 17

$\Gamma(K_1(1270)^+K^-, K_1^+\to K^*(1430)^0\pi^+, K^{*0}\to K^+\pi^-)/\Gamma(K^+K^-\pi^+\pi^-)$ $\Gamma_{234}/\Gamma_{218}$

This is the fit fraction from a coherent amplitude analysis.

VALUE (units 10^{-2})	EVTS	DOCUMENT ID		COMMENT
6.1±1.2±1.8	2.9k	[1] DARGENT	17	4-body fit, $K K\pi\pi$ evts

[1] Obtained by analyzing CLEO data but not authored by the CLEO Collaboration.

$\Gamma(K_1(1270)^+K^-, K_1^+\to\rho^0K^+)/\Gamma(K^+K^-\pi^+\pi^-)$ $\Gamma_{235}/\Gamma_{218}$

VALUE (units 10^{-2})	EVTS	DOCUMENT ID		TECN	COMMENT
9.1±1.5±1.9	2.9k	[1] DARGENT	17		4-body fit, $K K\pi\pi$ evts
• • • We do not use the following data for averages, fits, limits, etc. • • •					
4.7±0.7±0.8		[2] ARTUSO	12	CLEO	Fitting 2959 evts.

[1] Obtained by analyzing CLEO data but not authored by the CLEO Collaboration.
[2] see DARGENT 17

$\Gamma(K_1(1270)^+K^-, K_1^+\to\omega(782)K^+, \omega\to\pi^+\pi^-)/\Gamma(K^+K^-\pi^+\pi^-)$ $\Gamma_{236}/\Gamma_{218}$

This is the fit fraction from a coherent amplitude analysis.

VALUE (units 10^{-2})	EVTS	DOCUMENT ID		COMMENT
0.6±0.3±0.4	2.9k	[1] DARGENT	17	4-body fit, $K K\pi\pi$ evts

[1] Obtained by analyzing CLEO data but not authored by the CLEO Collaboration.

$\Gamma(K_1(1270)^-K^+, K_1^-\to\overline{K}^{*0}\pi^-)/\Gamma(K^+K^-\pi^+\pi^-)$ $\Gamma_{237}/\Gamma_{218}$

VALUE (%)	DOCUMENT ID		TECN	COMMENT
• • • We do not use the following data for averages, fits, limits, etc. • • •				
0.9±0.3±0.4	[1] ARTUSO	12	CLEO	Fitting 2959 evts.

[1] See DARGENT 17

$\Gamma(K_1(1270)^-K^+, K_1^-\to\rho^0K^-)/\Gamma(K^+K^-\pi^+\pi^-)$ $\Gamma_{238}/\Gamma_{218}$

VALUE (units 10^{-2})	EVTS	DOCUMENT ID		TECN	COMMENT
5.4±0.7±1.3	2.9k	[1] DARGENT	17		4-body fit, $K K\pi\pi$ evts
• • • We do not use the following data for averages, fits, limits, etc. • • •					
6.0±0.8±0.6		[2] ARTUSO	12	CLEO	Fitting 2959 evts.

[1] Obtained by analyzing CLEO data but not authored by the CLEO Collaboration.
[2] See DARGENT 17

$\Gamma(K_1(1400)^\pm K^\mp, K_1^\pm\to K^\pm\pi^+\pi^-)/\Gamma(K^+K^-\pi^+\pi^-)$ $\Gamma_{239}/\Gamma_{218}$

This is the fraction from a coherent amplitude analysis.

VALUE (%)	DOCUMENT ID		TECN	COMMENT
• • • We do not use the following data for averages, fits, limits, etc. • • •				
22±3±4	LINK	05G	FOCS	Fits 1279 ± 48 evts.

$\Gamma(K_1(1400)^+K^-, K_1^+\to K^*(892)^0\pi^+, K^{*0}\to K^+\pi^-)/\Gamma(K^+K^-\pi^+\pi^-)$ $\Gamma_{240}/\Gamma_{218}$

This is the fit fraction from a coherent amplitude analysis.

VALUE (units 10^{-2})	EVTS	DOCUMENT ID		COMMENT
12.4±2.6±6.3	2.9k	[1] DARGENT	17	4-body fit, $K K\pi\pi$ evts

[1] Obtained by analyzing CLEO data but not authored by the CLEO Collaboration.

$\Gamma(K^*(1410)^+K^-, K^{*+}\to K^{*0}\pi^+)/\Gamma(K^+K^-\pi^+\pi^-)$ $\Gamma_{241}/\Gamma_{218}$

VALUE (units 10^{-2})	DOCUMENT ID		TECN	COMMENT
• • • We do not use the following data for averages, fits, limits, etc. • • •				
4.2±0.7±0.8	[1,2] ARTUSO	12	CLEO	Fitting 2959 evts.

[1] DARGENT 17 find $K^*(1410)^+\pi^-$ and $K^*(1680)^+\pi^-$, which both peak outside the $D^0\to K K\pi\pi$ kinematic range, effectively indistinguishable; we list their result under $K^*(1680)^+\pi^-$.
[2] See DARGENT 17

$\Gamma(K^*(1410)^-K^+, K^{*-}\to\overline{K}^{*0}\pi^-)/\Gamma(K^+K^-\pi^+\pi^-)$ $\Gamma_{242}/\Gamma_{218}$

VALUE (units 10^{-2})	DOCUMENT ID		TECN	COMMENT
• • • We do not use the following data for averages, fits, limits, etc. • • •				
4.7±0.7±0.7	[1] ARTUSO	12	CLEO	Fitting 2959 evts.

[1] See DARGENT 17.

$\Gamma(K_1(1680)^+K^-, K_1^+\to K^{*0}\pi^+, K^{*0}\to K^+\pi^-)/\Gamma(K^+K^-\pi^+\pi^-)$ $\Gamma_{243}/\Gamma_{218}$

This is the fit fraction from a coherent amplitude analysis.

VALUE (units 10^{-2})	EVTS	DOCUMENT ID		COMMENT
3.6±0.8±1.0	2.9k	[1,2] DARGENT	17	4-body fit, $K K\pi\pi$ evts

[1] DARGENT 17 find $K^*(1410)^+\pi^-$ and $K^*(1680)^+\pi^-$, which both peak outside the $D^0\to K K\pi\pi$ kinematic range, effectively indistinguishable.
[2] Obtained by analyzing CLEO data but not authored by the CLEO Collaboration.

$\Gamma(K^+K^-\pi^+\pi^-$ non-resonant$)/\Gamma(K^+K^-\pi^+\pi^-)$ $\Gamma_{244}/\Gamma_{218}$

This is the fit fraction from a coherent amplitude analysis.

VALUE (units 10^{-2})	EVTS	DOCUMENT ID		COMMENT
11.1±1.2±2.2	2.9k	[1] DARGENT	17	4-body fit, $K K\pi\pi$ evts

[1] Obtained by analyzing CLEO data but not authored by the CLEO Collaboration.

$\Gamma(2K_S^0\pi^+\pi^-)/\Gamma(K_S^0\pi^+\pi^-)$ Γ_{245}/Γ_{35}

VALUE (units 10^{-2})	EVTS	DOCUMENT ID		TECN	COMMENT
4.3 ±0.8 OUR AVERAGE					
4.16±0.70±0.42	113 ± 21	LINK	05A	FOCS	γ Be, $\overline{E}_\gamma\approx$ 180 GeV
6.2 ±2.0 ±1.6	25	ALBRECHT	94I	ARG	$e^+e^-\approx$ 10 GeV

$\Gamma(K_S^0K^-2\pi^+\pi^-)/\Gamma(K_S^02\pi^+2\pi^-)$ Γ_{246}/Γ_{97}

VALUE	CL%	DOCUMENT ID		TECN	COMMENT
<0.054	90	LINK	04D	FOCS	γ A, $\overline{E}_\gamma\approx$ 180 GeV

$\Gamma(K^+K^-\pi^+\pi^-\pi^0)/\Gamma_{\text{total}}$ Γ_{247}/Γ

VALUE	DOCUMENT ID		TECN	COMMENT
0.0031±0.0020	[1] BARLAG	92C	ACCM	π^- Cu 230 GeV

[1] BARLAG 92C computes the branching fraction using topological normalization.

Radiative modes

$\Gamma(\rho^0\gamma)/\Gamma(\pi^+\pi^-)$ $\Gamma_{251}/\Gamma_{127}$

VALUE (units 10^{-2})	EVTS	DOCUMENT ID		TECN	COMMENT
1.25±0.21±0.05	500	NANUT	17	BELL	e^+e^- at Υ(nS), n=2,3,4,5

$\Gamma(\omega\gamma)/\Gamma_{\text{total}}$ Γ_{252}/Γ

VALUE	CL%	DOCUMENT ID		TECN
$<2.4\times10^{-4}$	90	ASNER	98	CLE2

$\Gamma(\phi\gamma)/\Gamma(K^+K^-)$ $\Gamma_{253}/\Gamma_{186}$

VALUE (units 10^{-3})	EVTS	DOCUMENT ID		TECN	COMMENT
6.9 ±0.5 OUR FIT					
6.88±0.47±0.21	524	NANUT	17	BELL	e^+e^- at Υ(nS), n=2,3,4,5
• • • We do not use the following data for averages, fits, limits, etc. • • •					
$6.31^{+1.70}_{-1.48}{}^{+0.30}_{-0.36}$	28	TAJIMA	04	BELL	See NANUT 17

$\Gamma(\phi\gamma)/\Gamma(K^-\pi^+)$ Γ_{253}/Γ_{32}

VALUE (units 10^{-4})	EVTS	DOCUMENT ID		TECN	COMMENT
7.1 ±0.5 OUR FIT					
7.15±0.78±0.69	243 ± 25	AUBERT	08AZ	BABR	$e^+e^-\approx$ 10.6 GeV

$\Gamma(\overline{K}^*(892)^0\gamma)/\Gamma(K^-\pi^+)$ Γ_{254}/Γ_{32}

VALUE (units 10^{-3})	EVTS	DOCUMENT ID		TECN	COMMENT
10.5 ±1.7 OUR AVERAGE	Error includes scale factor of 3.1.				
11.9 ±0.5 ±0.5	9.1k	NANUT	17	BELL	e^+e^- at Υ(nS), n=2,3,4,5
8.43±0.51±0.70	2.2k	AUBERT	08AZ	BABR	$e^+e^-\approx$ 10.6 GeV

Doubly Cabibbo-suppressed / Mixing modes

$\Gamma(K^+\ell^-\overline{\nu}_\ell$ via $\overline{D}^0)/\Gamma(K^-\ell^+\nu_\ell)$ Γ_{255}/Γ_{18}

This is a limit on R_M without the complications of possible doubly Cabibbo-suppressed decays that occur when using hadronic modes. For the limits on $|m_1 - m_2|$ and $(\Gamma_1 - \Gamma_2)/\Gamma$ that come from the best mixing limit, see near the beginning of these D^0 Listings.

VALUE	CL%	DOCUMENT ID		TECN	COMMENT
< 6.1 × 10⁻⁴	90	[1] BITENC	08	BELL	e^+e^-, 10.58 GeV
• • • We do not use the following data for averages, fits, limits, etc. • • •					
<50 × 10⁻⁴	90	[2] AITALA	96C	E791	π^- nucleus, 500 GeV

[1] The BITENC 08 right-sign sample includes about 15% of $D^0 \to K^-\pi^0\ell^+\nu_\ell$ and other decays.
[2] AITALA 96C uses $D^{*+} \to D^0\pi^+$ (and charge conjugate) decays to identify the charm at production and $D^0 \to K^-\ell^+\nu_\ell$ (and charge conjugate) decays to identify the charm at decay.

$\Gamma(K^+$ or $K^*(892)^+ e^-\overline{\nu}_e$ via $\overline{D}^0)/\left[\Gamma(K^-e^+\nu_e) + \Gamma(K^*(892)^-e^+\nu_e)\right]$ $\Gamma_{256}/(\Gamma_{19}+\Gamma_{21})$

This is a limit on R_M without the complications of possible doubly Cabibbo-suppressed decays that occur when using hadronic modes. The experiments use $D^{*+} \to D^0\pi^+$ (and charge conjugate) decays to identify the charm at production and the charge of the e to identify the charm at decay. These limits do not allow CP violation. For the limits on $|m_1 - m_2|$ and $(\Gamma_1 - \Gamma_2)/\Gamma$ that come from the best mixing limit, see near the beginning of these D^0 Listings.

VALUE	CL%	DOCUMENT ID		TECN	COMMENT
<0.001	90	BITENC	05	BELL	$e^+e^- \approx$ 10.6 GeV
• • • We do not use the following data for averages, fits, limits, etc. • • •					
−0.0013 <R< +0.0012	90	AUBERT	07AB	BABR	$e^+e^- \approx$ 10.58 GeV
<0.0078	90	CAWLFIELD	05	CLEO	$e^+e^- \approx$ 10.6 GeV
<0.0042	90	AUBERT,B	04Q	BABR	See AUBERT 07AB

$\Gamma(K^+\pi^-)/\Gamma(K^-\pi^+)$ Γ_{257}/Γ_{32}

This is R, the time-integrated wrong-sign rate compared to the right-sign rate. See the note on "D^0-$\overline{D}^0$ Mixing," near the start of the D^0 Listings.

The experiments here use the charge of the pion in $D^*(2010)^\pm \to (D^0$ or $\overline{D}^0)\,\pi^\pm$ decay to tell whether a D^0 or a $\overline{D}^0$ was born. The $D^0 \to K^+\pi^-$ decay can occur directly by doubly Cabibbo-suppressed (DCS) decay, or indirectly by $D^0 \to \overline{D}^0$ mixing followed by $\overline{D}^0 \to K^+\pi^-$ decay. Some of the experiments can use the decay-time information to disentangle the two mechanisms. Here, we list the experimental branching ratio, which if there is no mixing is the DCS ratio. See the next data block for values of the DCS ratio R_D, and the following data block for limits on the mixing ratio R_M. See the section on CP-violating asymmetries near the end of this D^0 Listing for values of A_D, and the note on "D^0-$\overline{D}^0$ Mixing" for limits on x' and y'.

Some early limits have been omitted from this Listing; see our 1998 edition (The European Physical Journal **C3** 1 (1998)) and our 2006 edition (Journal of Physics **G33** 1 (2006)).

VALUE (units 10^{-3})	EVTS	DOCUMENT ID		TECN	COMMENT
3.79±0.18 OUR FIT Error includes scale factor of 3.3.					
3.79±0.18 OUR AVERAGE Error includes scale factor of 3.3. See the ideogram below.					
4.15±0.10	12.7±0.3k	[1] AALTONEN	08E	CDF	$p\overline{p}$, $\sqrt{s}$ = 1.96 TeV
3.53±0.08±0.04	4030 ± 90	[2] AUBERT	07W	BABR	$e^+e^- \approx$ 10.6 GeV
3.77±0.08±0.05	4024 ± 88	[1] ZHANG	06	BELL	e^+e^-
• • • We do not use the following data for averages, fits, limits, etc. • • •					
4.05±0.21±0.11	2.0 ± 0.1k	[3] ABULENCIA	06X	CDF	See AALTONEN 08E
$3.81 \pm 0.17^{+0.08}_{-0.16}$	845 ± 40	[2] LI	05A	BELL	See ZHANG 06
$4.29^{+0.63}_{-0.61} \pm 0.27$	234	[4] LINK	05H	FOCS	γ nucleus
3.57±0.22±0.27		[5] AUBERT	03Z	BABR	See AUBERT 07W
4.04±0.85±0.25	149	[6] LINK	01	FOCS	γ nucleus
$3.32^{+0.63}_{-0.65} \pm 0.40$	45	[1] GODANG	00	CLE2	e^+e^-
$6.8\ ^{+3.4}_{-3.3}\ \pm 0.7$	34	[2] AITALA	98	E791	π^- nucl., 500 GeV

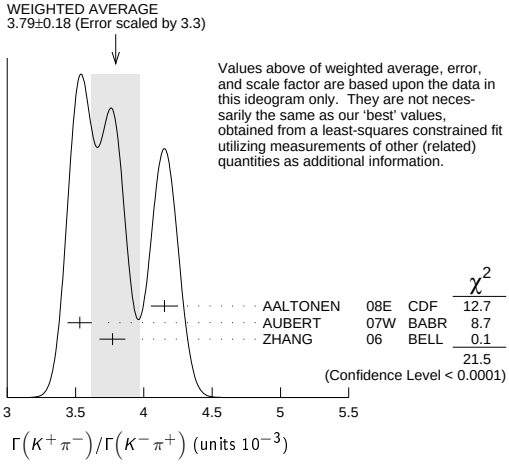

[1] GODANG 00, ZHANG 06, and AALTONEN 08E allow CP violation.
[2] AITALA 98, LI 05A, and AUBERT 07W assume no CP violation.
[3] This ABULENCIA 06X result assumes no mixing.
[4] This LINK 05H result assumes no mixing but allows CP violation. If neither mixing nor CP violation is allowed, $R = (4.29 \pm 0.63 \pm 0.28) \times 10^{-3}$.
[5] This AUBERT 03Z result allows CP violation. If CP violation is not allowed, $R = 0.00359 \pm 0.00020 \pm 0.00027$.
[6] This LINK 01 result assumes no mixing or CP violation.

$\Gamma(K^+\pi^-$ via DCS$)/\Gamma(K^-\pi^+)$ Γ_{258}/Γ_{32}

This is R_D, the doubly Cabibbo-suppressed ratio when mixing is allowed.

VALUE (units 10^{-3})	CL%	EVTS	DOCUMENT ID		TECN	COMMENT
3.51 ± 0.06 OUR AVERAGE Error includes scale factor of 1.3. See the ideogram below.						
3.533± 0.054		236k	[1] AAIJ	17AO	LHCB	pp at 7, 8 TeV
3.53 ± 0.13			[2] KO	14	BELL	$e^+e^- \to \Upsilon$(nS)
3.51 ± 0.35			[3] AALTONEN	13AE	CDF	$p\overline{p}$ at 1.96 TeV
3.04 ± 0.55		13k	AALTONEN	08E	CDF	$p\overline{p}$, $\sqrt{s}$ =1.96 TeV
3.03 ± 0.16 ±0.10		4.0k	[4] AUBERT	07W	BABR	$e^+e^- \approx$ 10.6 GeV
3.64 ± 0.17		4.0k	[5] ZHANG	06	BELL	e^+e^-
$5.17\ ^{+\ 1.47}_{-\ 1.58}$ ±0.76		234	[6] LINK	05H	FOCS	γ nucleus
4.8 ± 1.2 ±0.4		45	[7] GODANG	00	CLE2	e^+e^-
• • • We do not use the following data for averages, fits, limits, etc. • • •						
3.568± 0.066			[8] AAIJ	13CE	LHCB	pp at 7, 8 TeV
3.52 ± 0.15			[9] AAIJ	13N	LHCB	Repl. by AAIJ 13CE
2.87 ± 0.37		0.8k	LI	05A	BELL	See ZHANG 06
$2.3 < R_D < 5.2$	95		[10] AUBERT	03Z	BABR	See AUBERT 07W
$9.0\ ^{+12.0}_{-10.9}$ ±4.4		34	[11] AITALA	98	E791	π^- nucl., 500 GeV

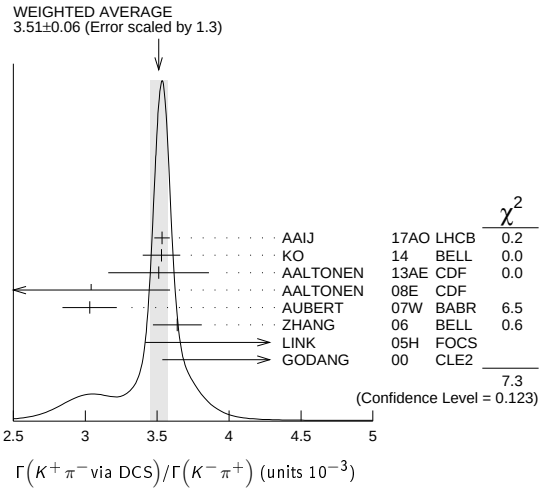

[1] The result was established with D^0 from prompt and secondary D^* assuming no CPV or no direct CPV.
[2] Based on 976 fb^{-1} of data collected at Y(nS) resonances. Assumes no CP violation.
[3] Based on 9.6 fb^{-1} of data collected at the Tevatron. Assumes no CP violation.
[4] Result is the same whether or not CP violation is allowed.
[5] This ZHANG 06 assumes no CP violation.
[6] This LINK 05H result allows CP violation. Allowing mixing but not CP violation, $R_D = (3.81\ ^{+1.67}_{-1.63} \pm 0.92) \times 10^{-3}$.
[7] This GODANG 00 result allows CP violation.
[8] Based on 3 fb^{-1} of data collected at $\sqrt{s}$ = 7, 8 TeV. Assumes no CP violation.
[9] Based on 1 fb^{-1} of data collected at $\sqrt{s}$ = 7 TeV in 2011. Assumes no CP violation.
[10] This AUBERT 03Z result allows CP violation. If only mixing is allowed, the 95% confidence level interval is $(2.4 < R_D < 4.9) \times 10^{-3}$.
[11] This AITALA 98 result assumes no CP violation.

$\Gamma(K^+\pi^-$ via $\overline{D}^0)/\Gamma(K^-\pi^+)$ Γ_{259}/Γ_{32}

This is R_M in the note on "D^0-$\overline{D}^0$ Mixing" near the start of the D^0 Listings. The experiments here (1) use the charge of the pion in $D^*(2010)^\pm \to (D^0$ or $\overline{D}^0)\,\pi^\pm$ decay to tell whether a D^0 or a $\overline{D}^0$ was born; and (2) use the decay-time distribution to disentangle doubly Cabibbo-suppressed decay and mixing. For the limits on $|m_1 - m_2|$ and $(\Gamma_1 - \Gamma_2)/\Gamma$ that come from the best mixing limit, see near the beginning of these D^0 Listings.

VALUE	CL%	DOCUMENT ID		TECN	COMMENT
<0.00040	95	[1] ZHANG	06	BELL	e^+e^-
• • • We do not use the following data for averages, fits, limits, etc. • • •					
<0.00046	95	[2] LI	05A	BELL	See ZHANG 06
<0.0063	95	[3] LINK	05H	FOCS	γ nucleus
<0.0013	95	[4] AUBERT	03Z	BABR	e^+e^-, 10.6 GeV
<0.00041	95	[5] GODANG	00	CLE2	e^+e^-
<0.0092	95	[6] BARATE	98W	ALEP	e^+e^- at Z^0
<0.005	90	[7] ANJOS	88C	E691	Photoproduction

[1] This ZHANG 06 result allows *CP* violation, but the result does not change if *CP* violation is not allowed.
[2] This LI 05A result allows *CP* violation. The limit becomes < 0.00042 (95% CL) if *CP* violation is not allowed.
[3] LINK 05H obtains the same result whether or not *CP* violation is allowed.
[4] This AUBERT 03Z result allows *CP* violation and assumes that the strong phase between $D^0 \to K^+\pi^-$ and $\overline{D}^0 \to K^+\pi^-$ is small, and limits only $D^0 \to \overline{D}^0$ transitions via off-shell intermediate states. The limit on transitions via on-shell intermediate states is 0.0016.
[5] This GODANG 00 result allows *CP* violation and assumes that the strong phase between $D^0 \to K^+\pi^-$ and $\overline{D}^0 \to K^+\pi^-$ is small, and limits only $D^0 \to \overline{D}^0$ transitions via off-shell intermediate states. The limit on transitions via on-shell intermediate states is 0.0017.
[6] This BARATE 98W result assumes no interference between the DCS and mixing amplitudes ($y' = 0$ in the note on "D^0-$\overline{D}^0$ Mixing" near the start of the D^0 Listings). When interference is allowed, the limit degrades to 0.036 (95%CL).
[7] This ANJOS 88C result assumes no interference between the DCS and mixing amplitudes ($y' = 0$ in the note on "D^0-$\overline{D}^0$ Mixing" near the start of the D^0 Listings). When interference is allowed, the limit degrades to 0.019.

$\Gamma(K^0_S\pi^+\pi^-$ in $D^0 \to \overline{D}^0)/\Gamma(K^0_S\pi^+\pi^-)$ Γ_{260}/Γ_{35}

This is R_M in the note on "D^0-$\overline{D}^0$ Mixing" near the start of the D^0 Listings. The experiments here (1) use the charge of the pion in $D^*(2010)^\pm \to (D^0$ or $\overline{D}^0)\,\pi^\pm$ decay to tell whether a D^0 or a $\overline{D}^0$ was born; and (2) use the decay-time distribution to disentangle doubly Cabibbo-suppressed decay and mixing. For the limits on $|m_1 - m_2|$ and $(\Gamma_1 - \Gamma_2)/\Gamma$ that come from the best mixing limit, see near the beginning of these D^0 Listings.

VALUE	CL%	DOCUMENT ID		TECN	COMMENT
<0.0063	95	[1] ASNER	05	CLEO	$e^+e^- \approx$ 10 GeV

[1] This ASNER 05 limit allows *CP* violation. If *CP* violation is not allowed, the limit is 0.0042 at 95% CL.

$\Gamma(K^+\pi^-\pi^0)/\Gamma(K^-\pi^+\pi^0)$ Γ_{264}/Γ_{50}

The experiments here use the charge of the pion in $D^*(2010)^\pm \to (D^0$ or $\overline{D}^0)\,\pi^\pm$ decay to tell whether a D^0 or a $\overline{D}^0$ was born. The $D^0 \to K^+\pi^-\pi^0$ decay can occur directly by doubly Cabibbo-suppressed (DCS) decay, or indirectly by $D^0 \to \overline{D}^0$ mixing followed by $\overline{D}^0 \to K^+\pi^-\pi^0$ decay.

VALUE (units 10^{-3})	EVTS	DOCUMENT ID		TECN	COMMENT
2.12±0.07 OUR AVERAGE					
2.01 ± 0.11		[1] EVANS	16	CLEO	$e^+e^- \to D^0\overline{D}^0$ at $\psi(3770)$
$2.14 \pm 0.08 \pm 0.08$	763	[2] AUBERT,B	06N	BABR	$e^+e^- \approx \Upsilon(4S)$
$2.29 \pm 0.15 \,^{+0.13}_{-0.09}$	1.9k	TIAN	05	BELL	$e^+e^- \approx \Upsilon(4S)$
$4.3 \,^{+1.1}_{-1.0} \pm 0.7$	38	BRANDENB...	01	CLE2	$e^+e^- \approx \Upsilon(4S)$

[1] A combined fit with a recent LHCb $D^0\overline{D}^0$ mixing results in AAIJ 16F is also reported to be $(2.00 \pm 0.11) \times 10^{-3}$.
[2] This AUBERT,B 06N result assumes no mixing.

$\Gamma(K^+\pi^-\pi^0$ via $\overline{D}^0)/\Gamma(K^-\pi^+\pi^0)$ Γ_{265}/Γ_{50}

This is R_M in the note on "D^0-$\overline{D}^0$ Mixing" near the start of the D^0 Listings. The experiments here (1) use the charge of the pion in $D^*(2010)^\pm \to (D^0$ or $\overline{D}^0)\,\pi^\pm$ decay to tell whether a D^0 or a $\overline{D}^0$ was born; and (2) use the decay-time distribution to disentangle doubly Cabibbo-suppressed decay and mixing. For the limits on $|m_1 - m_2|$ and $(\Gamma_1 - \Gamma_2)/\Gamma$ that come from the best mixing limit, see near the beginning of these D^0 Listings.

VALUE (units 10^{-3})	CL%	DOCUMENT ID	TECN	COMMENT
$5.25 \,^{+0.25}_{-0.31} \pm 0.12$		AUBERT	09AN BABR	e^+e^- at 10.58 GeV
• • • We do not use the following data for averages, fits, limits, etc. • • •				
<0.54	95	[1] AUBERT,B	06N BABR	$e^+e^- \approx \Upsilon(4S)$

[1] This AUBERT,B 06N limit assumes no *CP* violation. The measured value corresponding to the limit is $(2.3 \,^{+1.8}_{-1.4} \pm 0.4) \times 10^{-4}$. If *CP* violation is allowed, this becomes $(1.0 \,^{+2.2}_{-0.7} \pm 0.3) \times 10^{-4}$.

$\Gamma(K^+\pi^+2\pi^-$ via DCS$)/\Gamma(K^-2\pi^+\pi^-)$ Γ_{266}/Γ_{67}

VALUE (units 10^{-3})	EVTS	DOCUMENT ID		TECN	COMMENT
3.03 ±0.07 OUR AVERAGE					
3.025 ± 0.077	42k,11M	[1] AAIJ	16F	LHCB	pp at 7, 8 TeV
3.03 ± 0.13		[2] EVANS	16	CLEO	$e^+e^- \to D^0\overline{D}^0$ at $\psi(3770)$

[1] This result uses external input on the mixing parameters x, y. Without this input, the result is $(3.215 \pm 0.136) \times 10^{-3}$.
[2] A combined fit with a recent LHCb $D^0\overline{D}^0$ mixing results in AAIJ 16F is also reported to be $(3.01 \pm 0.07) \times 10^{-3}$.

$\Gamma(K^+\pi^+2\pi^-)/\Gamma(K^-2\pi^+\pi^-)$ Γ_{267}/Γ_{67}

The experiments here use the charge of the pion in $D^*(2010)^\pm \to (D^0$ or $\overline{D}^0)\,\pi^\pm$ decay to tell whether a D^0 or a $\overline{D}^0$ was born. The $D^0 \to K^+\pi^-\pi^+\pi^-$ decay can occur directly by doubly Cabibbo-suppressed (DCS) decay, or indirectly by $D^0 \to \overline{D}^0$ mixing followed by $\overline{D}^0 \to K^+\pi^-\pi^+\pi^-$ decay. Some of the experiments can use the decay-time information to disentangle the two mechanisms. Here, we list the experimental branching ratio, which if there is no mixing is the DCS ratio; in the next data block we give the limits on the mixing ratio.

Some early limits have been omitted from this Listing; see our 1998 edition (EPJ **C3** 1).

VALUE (units 10^{-3})	CL%	EVTS	DOCUMENT ID		TECN	COMMENT
3.22±0.05 OUR AVERAGE						
3.22 ± 0.05		42k,11M	[1] AAIJ	16F	LHCB	pp at 7, 8 TeV
$3.24 \pm 0.08 \pm 0.07$		3.3k	[2] WHITE	13	BELL	$e^+e^- \approx \Upsilon(4S)$
$4.4 \,^{+1.3}_{-1.2} \pm 0.4$		54	[2] DYTMAN	01	CLE2	$e^+e^- \approx \Upsilon(4S)$
$2.5 \,^{+3.6}_{-3.4} \pm 0.3$			[3] AITALA	98	E791	π^- nucl., 500 GeV
• • • We do not use the following data for averages, fits, limits, etc. • • •						
$3.20 \pm 0.18 \,^{+0.18}_{-0.13}$		1.7k	[2] TIAN	05	BELL	See WHITE 13
<18	90		[2] AMMAR	91	CLEO	$e^+e^- \approx$ 10.5 GeV
<18	90		[4] ANJOS	88C	E691	Photoproduction

[1] AAIJ 16F result comes from time-dependent analysis that uses external input on the mixing parameters x, y. Without this input, the result is $(3.29 \pm 0.08) \times 10^{-3}$.
[2] AMMAR 91 cannot and DYTMAN 01, TIAN 05 do not distinguish between doublyCabibbo-suppressed decay and D^0-$\overline{D}^0$ mixing.
[3] This AITALA 98result assumes no D^0-$\overline{D}^0$ mixing (R_M in the note on "D^0-$\overline{D}^0$ Mixing").It becomes $-0.0020 \,^{+0.0117}_{-0.0106} \pm 0.0035$ whenmixing is allowed and decay-time information is used todistinguish doubly Cabibbo-suppressed decays from mixing.
[4] ANJOS 88C uses decay-time information to distinguish doubly Cabibbo-suppressed (DCS) decays from D^0-$\overline{D}^0$ mixing. However, the result assumes no interference between the DCS and mixing amplitudes ($y' = 0$ in the note on "D^0-$\overline{D}^0$ Mixing" near the start of the D^0 Listings). When interference is allowed, the limit degrades to 0.033.

$\Gamma(K^+\pi^+2\pi^-$ via $\overline{D}^0)/\Gamma(K^-2\pi^+\pi^-)$ Γ_{268}/Γ_{67}

This is a D^0-$\overline{D}^0$ mixing limit. The experiments here (1) use the charge of the pion in $D^*(2010)^\pm \to (D^0$ or $\overline{D}^0)\,\pi^\pm$ decay to tell whether a D^0 or a $\overline{D}^0$ was born; and (2) use the decay-time distribution to disentangle doubly Cabibbo-suppressed decay and mixing. For the limits on $|m_{D^0_1} - m_{D^0_2}|$ and $(\Gamma_{D^0_1} - \Gamma_{D^0_2})/\Gamma_{D^0}$ that come from the best mixing limit, see near the beginning of these D^0 Listings.

VALUE (units 10^{-5})	CL%	DOCUMENT ID		TECN	COMMENT
9.6±3.6		[1] AAIJ	16F	LHCB	pp at 7, 8 TeV
• • • We do not use the following data for averages, fits, limits, etc. • • •					
<500	90	[2] ANJOS	88C	E691	Photoproduction

[1] AAIJ 16F result comes from an unconstrained decay-time dependent fit to the wrong-sign to right-sign decay rates ratio as $(x^2 + y^2)/2$.
[2] ANJOS 88C uses decay-time information to distinguish doubly Cabibbo-suppressed (DCS) decays from D^0-$\overline{D}^0$ mixing. However, the result assumes no interference between the DCS and mixing amplitudes ($y' = 0$ in the note on "D^0-$\overline{D}^0$ Mixing" near the start of the D^0 Listings). When interference is allowed, the limit degrades to 0.007.

$\Gamma(K^+\pi^-$ or $K^+\pi^+2\pi^-$ via $\overline{D}^0)/\Gamma(K^-\pi^+$ or $K^-2\pi^+\pi^-)$ Γ_{269}/Γ_0

This is a D^0-$\overline{D}^0$ mixing limit. For the limits on $|m_{D^0_1} - m_{D^0_2}|$ and $(\Gamma_{D^0_1} - \Gamma_{D^0_2})/\Gamma_{D^0}$ that come from the best mixing limit, see near the beginning of these D^0 Listings.

VALUE	CL%	DOCUMENT ID		TECN	COMMENT
• • • We do not use the following data for averages, fits, limits, etc. • • •					
<0.0085	90	[1] AITALA	98	E791	π^- nucleus, 500 GeV
<0.0037	90	[2] ANJOS	88C	E691	Photoproduction

[1] AITALA 98 uses decay-time information to distinguish doubly Cabibbo-suppressed decays from D^0-$\overline{D}^0$ mixing. The fit allows interference between the two amplitudes, and also allows *CP* violation in this term. The central value obtained is $0.0039 \,^{+0.0036}_{-0.0032} \pm 0.0016$. When interference is disallowed, the result becomes $0.0021 \pm 0.0009 \pm 0.0002$.
[2] This combines results of ANJOS 88C on $K^+\pi^-$ and $K^+\pi^-\pi^+\pi^-$ (via $\overline{D}^0$) reported in the data block above (see footnotes there). It assumes no interference.

$\Gamma(\mu^-$ anything via $\overline{D}^0)/\Gamma(\mu^+$ anything) Γ_{270}/Γ_6

This is a D^0-$\overline{D}^0$ mixing limit. See the somewhat better limits above.

VALUE	CL%	DOCUMENT ID	TECN	COMMENT
<0.0056	90	LOUIS	86 SPEC	π^- W 225 GeV
• • • We do not use the following data for averages, fits, limits, etc. • • •				
<0.012	90	BENVENUTI	85 CNTR	μC, 200 GeV
<0.044	90	BODEK	82 SPEC	π^-, pFe $\to D^0$

Rare or forbidden modes

$\Gamma(\gamma\gamma)/\Gamma_{\text{total}}$ Γ_{271}/Γ

$D^0 \to \gamma\gamma$ is a flavor-changing neutral-current decay, forbidden in the Standard Model at the tree level.

VALUE	CL%	DOCUMENT ID		TECN	COMMENT
$< 8.5 \times 10^{-7}$	90	NISAR	16	BELL	e^+e^- at $\Upsilon(4S)$, $\Upsilon(5S)$
• • • We do not use the following data for averages, fits, limits, etc. • • •					
$< 3.8 \times 10^{-6}$	90	ABLIKIM	15F	BES3	e^+e^- at 3.773 GeV
$< 2.2 \times 10^{-6}$	90	LEES	12L	BABR	$e^+e^- \approx$ 10.58 GeV
$<29 \times 10^{-6}$	90	COAN	03	CLE2	$e^+e^- \approx \Upsilon(4S)$

$\Gamma(e^+e^-)/\Gamma_{\text{total}}$ Γ_{272}/Γ

A test for the $\Delta C = 1$ weak neutral current. Allowed by first-order weak interaction combined with electromagnetic interaction.

VALUE	CL%	DOCUMENT ID		TECN	COMMENT
$<7.9 \times 10^{-8}$	90	PETRIC	10	BELL	$e^+e^- \approx \Upsilon(4S)$

• • • We do not use the following data for averages, fits, limits, etc. • • •

$<1.7 \times 10^{-7}$	90	LEES	12Q	BABR	$e^+e^- \approx$ 10.58 GeV
$<1.2 \times 10^{-6}$	90	AUBERT,B	04Y	BABR	$e^+e^- \approx \Upsilon(4S)$
$<8.19 \times 10^{-6}$	90	PRIPSTEIN	00	E789	p nucleus, 800 GeV
$<6.2 \times 10^{-6}$	90	AITALA	99G	E791	π^- N 500 GeV
$<1.3 \times 10^{-5}$	90	FREYBERGER	96	CLE2	$e^+e^- \approx \Upsilon(4S)$
$<1.3 \times 10^{-4}$	90	ADLER	88	MRK3	e^+e^- 3.77 GeV
$<1.7 \times 10^{-4}$	90	ALBRECHT	88G	ARG	e^+e^- 10 GeV
$<2.2 \times 10^{-4}$	90	HAAS	88	CLEO	e^+e^- 10 GeV

$\Gamma(\mu^+\mu^-)/\Gamma_{total}$ Γ_{273}/Γ

A test for the $\Delta C = 1$ weak neutral current. Allowed by first-order weak interaction combined with electromagnetic interaction.

VALUE	CL%	DOCUMENT ID		TECN	COMMENT
$<6.2 \times 10^{-9}$	90	AAIJ	13AI	LHCB	pp at 7 TeV

• • • We do not use the following data for averages, fits, limits, etc. • • •

0.6–8.1 $\times 10^{-7}$	90	[1]	LEES	12Q	BABR	$e^+e^- \approx$ 10.58 GeV
$<2.1 \times 10^{-7}$	90		AALTONEN	10X	CDF	$p\overline{p}$, $\sqrt{s} =$ 1.96 TeV
$<1.4 \times 10^{-7}$	90		PETRIC	10	BELL	$e^+e^- \approx \Upsilon(4S)$
$<2.0 \times 10^{-6}$	90		ABT	04	HERB	pA, 920 GeV
$<1.3 \times 10^{-6}$	90		AUBERT,B	04Y	BABR	$e^+e^- \approx \Upsilon(4S)$
$<2.5 \times 10^{-6}$	90		ACOSTA	03F	CDF	See AALTONEN 10X
$<1.56 \times 10^{-5}$	90		PRIPSTEIN	00	E789	p nucleus, 800 GeV
$<5.2 \times 10^{-6}$	90		AITALA	99G	E791	π^- N 500 GeV
$<4.1 \times 10^{-6}$	90		ADAMOVICH	97	BEAT	π^- Cu, W 350 GeV
$<4.2 \times 10^{-6}$	90		ALEXOPOU...	96	E771	p Si, 800 GeV
$<3.4 \times 10^{-5}$	90		FREYBERGER	96	CLE2	$e^+e^- \approx \Upsilon(4S)$
$<7.6 \times 10^{-6}$	90		ADAMOVICH	95	BEAT	See ADAMOVICH 97
$<4.4 \times 10^{-5}$	90		KODAMA	95	E653	π^- emulsion 600 GeV
$<3.1 \times 10^{-5}$	90	[2]	MISHRA	94	E789	-4.1 ± 4.8 events
$<7.0 \times 10^{-5}$	90		ALBRECHT	88G	ARG	e^+e^- 10 GeV
$<1.1 \times 10^{-5}$	90		LOUIS	86	SPEC	π^- W 225 GeV
$<3.4 \times 10^{-4}$	90		AUBERT	85	EMC	Deep inelast. $\mu^- N$

[1] LEES 12Q gives a 2-sided range.

[2] Here MISHRA 94 uses "the statistical approach advocated by the PDG." For an alternate approach, giving a limit of 9×10^{-6} at 90% confidence level, see the paper.

$\Gamma(\pi^0 e^+ e^-)/\Gamma_{total}$ Γ_{274}/Γ

A test for the $\Delta C = 1$ weak neutral current. Allowed by higher-order electroweak interactions.

VALUE	CL%	DOCUMENT ID	TECN	COMMENT
$<4.5 \times 10^{-5}$	90	FREYBERGER 96	CLE2	$e^+e^- \approx \Upsilon(4S)$

$\Gamma(\pi^0 \mu^+ \mu^-)/\Gamma_{total}$ Γ_{275}/Γ

A test for the ΔC=1 weak neutral current. Allowed by higher-order electroweak interactions.

VALUE	CL%	DOCUMENT ID		TECN	COMMENT
$<1.8 \times 10^{-4}$	90	KODAMA	95	E653	π^- emulsion 600 GeV

• • • We do not use the following data for averages, fits, limits, etc. • • •

$<5.4 \times 10^{-4}$	90	FREYBERGER	96	CLE2	$e^+e^- \approx \Upsilon(4S)$

$\Gamma(\eta e^+ e^-)/\Gamma_{total}$ Γ_{276}/Γ

A test for the $\Delta C = 1$ weak neutral current. Allowed by higher-order electroweak interactions.

VALUE	CL%	DOCUMENT ID	TECN	COMMENT
$<1.1 \times 10^{-4}$	90	FREYBERGER 96	CLE2	$e^+e^- \approx \Upsilon(4S)$

$\Gamma(\eta \mu^+ \mu^-)/\Gamma_{total}$ Γ_{277}/Γ

A test for the $\Delta C = 1$ weak neutral current. Allowed by higher-order electroweak interactions.

VALUE	CL%	DOCUMENT ID	TECN	COMMENT
$<5.3 \times 10^{-4}$	90	FREYBERGER 96	CLE2	$e^+e^- \approx \Upsilon(4S)$

$\Gamma(\pi^+\pi^- e^+ e^-)/\Gamma_{total}$ Γ_{278}/Γ

A test for the $\Delta C = 1$ weak neutral current. Allowed by higher-order electroweak interactions.

VALUE	CL%	DOCUMENT ID	TECN	COMMENT
$<3.73 \times 10^{-4}$	90	AITALA	01C	E791	π^- nucleus, 500 GeV

$\Gamma(\rho^0 e^+ e^-)/\Gamma_{total}$ Γ_{279}/Γ

A test for the $\Delta C = 1$ weak neutral current. Allowed by higher-order electroweak interactions.

VALUE	CL%	DOCUMENT ID		TECN	COMMENT
$<1.0 \times 10^{-4}$	90	[1]	FREYBERGER 96	CLE2	$e^+e^- \approx \Upsilon(4S)$

• • • We do not use the following data for averages, fits, limits, etc. • • •

$<1.24 \times 10^{-4}$	90	AITALA	01C	E791	π^- nucleus, 500 GeV
$<4.5 \times 10^{-4}$	90	HAAS	88	CLEO	e^+e^- 10 GeV

[1] This FREYBERGER 96 limit is obtained using a phase-space model. The limit changes to $< 1.8 \times 10^{-4}$ using a photon pole amplitude model.

$\Gamma(\pi^+\pi^-\mu^+\mu^-)/\Gamma_{total}$ Γ_{280}/Γ

A test for the $\Delta C = 1$ weak neutral current. Allowed by higher-order electroweak interactions.

VALUE (units 10^{-7})	EVTS	DOCUMENT ID		TECN	COMMENT
$9.64 \pm 0.48 \pm 1.10$	561	[1] AAIJ	17BG	LHCB	pp at 8 TeV

[1] The second AAIJ 17BG error is the systematic 0.51×10^{-7} and normalization 0.97×10^{-7} mode errors added in quadrature.

$\Gamma(\pi^+\pi^-\mu^+\mu^-\text{ (non-res)})/\Gamma_{total}$ Γ_{281}/Γ

VALUE	CL%	DOCUMENT ID		TECN	COMMENT
$<5.5 \times 10^{-7}$	90	[1] AAIJ	14B	LHCB	pp at 7 TeV

• • • We do not use the following data for averages, fits, limits, etc. • • •

$<3.0 \times 10^{-5}$	90		AITALA	01C	E791	π^- nucleus, 500 GeV

[1] AAIJ 14B measures this branching-fraction limit relative to the $\pi^+\pi^-\phi$, $\phi \to \mu^+\mu^-$ fraction. The above limit excludes the resonant ϕ, ω, and ρ regions, and then fills those gaps with a phase-space model.

$\Gamma(\rho^0\mu^+\mu^-)/\Gamma_{total}$ Γ_{282}/Γ

A test for the $\Delta C = 1$ weak neutral current. Allowed by higher-order electroweak interactions.

VALUE	CL%	DOCUMENT ID		TECN	COMMENT
$<2.2 \times 10^{-5}$	90	AITALA	01C	E791	π^- nucleus, 500 GeV

• • • We do not use the following data for averages, fits, limits, etc. • • •

$<4.9 \times 10^{-4}$	90	[1]	FREYBERGER	96	CLE2	$e^+e^- \approx \Upsilon(4S)$
$<2.3 \times 10^{-4}$	90		KODAMA	95	E653	π^- emulsion 600 GeV
$<8.1 \times 10^{-4}$	90		HAAS	88	CLEO	e^+e^- 10 GeV

[1] This FREYBERGER 96 limit is obtained using a phase-space model. The limit changes to $< 4.5 \times 10^{-4}$ using a photon pole amplitude model.

$\Gamma(\omega e^+ e^-)/\Gamma_{total}$ Γ_{283}/Γ

A test for the $\Delta C = 1$ weak neutral current. Allowed by higher-order electroweak interactions.

VALUE	CL%	DOCUMENT ID		TECN	COMMENT
$<1.8 \times 10^{-4}$	90	[1] FREYBERGER	96	CLE2	$e^+e^- \approx \Upsilon(4S)$

[1] This FREYBERGER 96 limit is obtained using a phase-space model. The limit changes to $< 2.7 \times 10^{-4}$ using a photon pole amplitude model.

$\Gamma(\omega\mu^+\mu^-)/\Gamma_{total}$ Γ_{284}/Γ

A test for the $\Delta C = 1$ weak neutral current. Allowed by higher-order electroweak interactions.

VALUE	CL%	DOCUMENT ID		TECN	COMMENT
$<8.3 \times 10^{-4}$	90	[1] FREYBERGER	96	CLE2	$e^+e^- \approx \Upsilon(4S)$

[1] This FREYBERGER 96 limit is obtained using a phase-space model. The limit changes to $< 6.5 \times 10^{-4}$ using a photon pole amplitude model.

$\Gamma(K^- K^+ e^+ e^-)/\Gamma_{total}$ Γ_{285}/Γ

A test for the $\Delta C = 1$ weak neutral current. Allowed by higher-order electroweak interactions.

VALUE	CL%	DOCUMENT ID		TECN	COMMENT
$<3.15 \times 10^{-4}$	90	AITALA	01C	E791	π^- nucleus, 500 GeV

$\Gamma(\phi e^+ e^-)/\Gamma_{total}$ Γ_{286}/Γ

A test for the $\Delta C = 1$ weak neutral current. Allowed by higher-order electroweak interactions.

VALUE	CL%	DOCUMENT ID		TECN	COMMENT
$<5.2 \times 10^{-5}$	90	[1] FREYBERGER	96	CLE2	$e^+e^- \approx \Upsilon(4S)$

• • • We do not use the following data for averages, fits, limits, etc. • • •

$<5.9 \times 10^{-5}$	90		AITALA	01C	E791	π^- nucleus, 500 GeV

[1] This FREYBERGER 96 limit is obtained using a phase-space model. The limit changes to $< 7.6 \times 10^{-5}$ using a photon pole amplitude model.

$\Gamma(K^- K^+ \mu^+ \mu^-)/\Gamma_{total}$ Γ_{287}/Γ

A test for the $\Delta C = 1$ weak neutral current. Allowed by higher-order electroweak interactions.

VALUE (units 10^{-7})	EVTS	DOCUMENT ID		TECN	COMMENT
$1.54 \pm 0.27 \pm 0.18$	34	[1] AAIJ	17BG	LHCB	pp at 8 TeV

[1] The second AAIJ 17BG error is the systematic 0.09×10^{-7} and normalization 0.16×10^{-7} mode errors added in quadrature.

$\Gamma(K^- K^+ \mu^+ \mu^-\text{ (non-res)})/\Gamma_{total}$ Γ_{288}/Γ

VALUE	CL%	DOCUMENT ID		TECN	COMMENT
$<3.3 \times 10^{-5}$	90	AITALA	01C	E791	π^- nucleus, 500 GeV

$\Gamma(\phi\mu^+\mu^-)/\Gamma_{total}$ Γ_{289}/Γ

A test for the $\Delta C = 1$ weak neutral current. Allowed by higher-order electroweak interactions.

VALUE	CL%	DOCUMENT ID		TECN	COMMENT
$<3.1 \times 10^{-5}$	90	AITALA	01C	E791	π^- nucleus, 500 GeV

• • • We do not use the following data for averages, fits, limits, etc. • • •

$<4.1 \times 10^{-4}$	90	[1]	FREYBERGER	96	CLE2	$e^+e^- \approx \Upsilon(4S)$

[1] This FREYBERGER 96 limit is obtained using a phase-space model. The limit changes to $< 2.4 \times 10^{-4}$ using a photon pole amplitude model.

$\Gamma(\overline{K}^0 e^+ e^-)/\Gamma_{total}$ Γ_{290}/Γ

Not a useful test for ΔC =1 weak neutral current because both quarks must change flavor.

VALUE	CL%	DOCUMENT ID		TECN	COMMENT
$<1.1 \times 10^{-4}$	90	FREYBERGER	96	CLE2	$e^+e^- \approx \Upsilon(4S)$

• • • We do not use the following data for averages, fits, limits, etc. • • •

$<1.7 \times 10^{-3}$	90		ADLER	89C	MRK3	e^+e^- 3.77 GeV

Meson Particle Listings

D^0

$\Gamma(\overline{K}^0\mu^+\mu^-)/\Gamma_{total}$ Γ_{291}/Γ

Not a useful test for $\Delta C=1$ weak neutral current because both quarks must change flavor.

VALUE	CL%	DOCUMENT ID		TECN	COMMENT
$<2.6\times10^{-4}$	90	KODAMA	95	E653	π^- emulsion 600 GeV
• • • We do not use the following data for averages, fits, limits, etc. • • •					
$<6.7\times10^{-4}$	90	FREYBERGER	96	CLE2	$e^+e^-\approx\ \Upsilon(4S)$

$\Gamma(K^-\pi^+e^+e^-)/\Gamma_{total}$ Γ_{292}/Γ

A test for the $\Delta C=1$ weak neutral current. Allowed by higher-order electroweak interactions.

VALUE	CL%	DOCUMENT ID		TECN	COMMENT
$<3.85\times10^{-4}$	90	AITALA	01C	E791	π^- nucleus, 500 GeV

$\Gamma(\overline{K}^*(892)^0e^+e^-)/\Gamma_{total}$ Γ_{293}/Γ

Not a useful test for $\Delta C=1$ weak neutral current because both quarks must change flavor.

VALUE	CL%	DOCUMENT ID		TECN	COMMENT
$<4.7\times10^{-5}$	90	AITALA	01C	E791	π^- nucleus, 500 GeV
• • • We do not use the following data for averages, fits, limits, etc. • • •					
$<1.4\times10^{-4}$	90	[1] FREYBERGER	96	CLE2	$e^+e^-\approx\ \Upsilon(4S)$

[1] This FREYBERGER 96 limit is obtained using a phase-space model. The limit changes to $<2.0\times10^{-4}$ using a photon pole amplitude model.

$\Gamma(K^-\pi^+\mu^+\mu^-, 675<m_{\mu\mu}<875\ \text{MeV})/\Gamma_{total}$ Γ_{295}/Γ

VALUE (units 10^{-6})	EVTS	DOCUMENT ID		TECN	COMMENT
$4.17\pm0.12\pm0.40$	2.4k	[1] AAIJ	16I	LHCB	pp at 8 TeV

[1] AAIJ 16I uses $B(D^0\to K^-\pi^+\pi^+\pi^-)=(8.287\pm0.043\pm0.200)\times10^{-2}$ value for the normalization mode.

$\Gamma(K^-\pi^+\mu^+\mu^-)/\Gamma_{total}$ Γ_{294}/Γ

A test for the $\Delta C=1$ weak neutral current. Allowed by higher-order electroweak interactions.

VALUE	CL%	DOCUMENT ID		TECN	COMMENT
$<3.59\times10^{-4}$	90	AITALA	01C	E791	π^- nucleus, 500 GeV

$\Gamma(\overline{K}^*(892)^0\mu^+\mu^-)/\Gamma_{total}$ Γ_{296}/Γ

Not a useful test for $\Delta C=1$ weak neutral current because both quarks must change flavor.

VALUE	CL%	DOCUMENT ID		TECN	COMMENT
$<2.4\ \times10^{-5}$	90	AITALA	01C	E791	π^- nucleus, 500 GeV
• • • We do not use the following data for averages, fits, limits, etc. • • •					
$<1.18\times10^{-3}$	90	[1] FREYBERGER	96	CLE2	$e^+e^-\approx\ \Upsilon(4S)$

[1] This FREYBERGER 96 limit is obtained using a phase-space model. The limit changes to $<1.0\times10^{-3}$ using a photon pole amplitude model.

$\Gamma(\pi^+\pi^-\pi^0\mu^+\mu^-)/\Gamma_{total}$ Γ_{297}/Γ

A test for the $\Delta C=1$ weak neutral current. Allowed by higher-order electroweak interactions.

VALUE	CL%	DOCUMENT ID		TECN	COMMENT
$<8.1\times10^{-4}$	90	KODAMA	95	E653	π^- emulsion 600 GeV

$\Gamma(\mu^\pm e^\mp)/\Gamma_{total}$ Γ_{298}/Γ

A test of lepton family number conservation.

VALUE	CL%	DOCUMENT ID		TECN	COMMENT
$<1.3\ \times10^{-8}$	90	AAIJ	16H	LHCB	pp at 7, 8 GeV
• • • We do not use the following data for averages, fits, limits, etc. • • •					
$<3.3\ \times10^{-7}$	90	LEES	12Q	BABR	$e^+e^-\approx$ 10.58 GeV
$<2.6\ \times10^{-7}$	90	PETRIC	10	BELL	$e^+e^-\approx\ \Upsilon(4S)$
$<8.1\ \times10^{-7}$	90	AUBERT,B	04Y	BABR	$e^+e^-\approx\ \Upsilon(4S)$
$<1.72\times10^{-5}$	90	PRIPSTEIN	00	E789	p nucleus, 800 GeV
$<8.1\ \times10^{-6}$	90	AITALA	99G	E791	π^-N 500 GeV
$<1.9\ \times10^{-5}$	90	[1] FREYBERGER	96	CLE2	$e^+e^-\approx\ \Upsilon(4S)$
$<1.0\ \times10^{-4}$	90	ALBRECHT	88G	ARG	e^+e^- 10 GeV
$<2.7\ \times10^{-4}$	90	HAAS	88	CLEO	e^+e^- 10 GeV
$<1.2\ \times10^{-4}$	90	BECKER	87C	MRK3	e^+e^- 3.77 GeV
$<9\ \times10^{-4}$	90	PALKA	87	SILI	200 GeV πp
$<21\ \times10^{-4}$	90	[2] RILES	87	MRK2	e^+e^- 29 GeV

[1] This is the corrected result given in the erratum to FREYBERGER 96.
[2] RILES 87 assumes $B(D\to K\pi)=3.0\%$ and has production model dependency.

$\Gamma(\pi^0e^\pm\mu^\mp)/\Gamma_{total}$ Γ_{299}/Γ

A test of lepton family number conservation. The value is for the sum of the two charge states.

VALUE	CL%	DOCUMENT ID		TECN	COMMENT
$<8.6\times10^{-5}$	90	FREYBERGER	96	CLE2	$e^+e^-\approx\ \Upsilon(4S)$

$\Gamma(\eta e^\pm\mu^\mp)/\Gamma_{total}$ Γ_{300}/Γ

A test of lepton family number conservation. The value is for the sum of the two charge states.

VALUE	CL%	DOCUMENT ID		TECN	COMMENT
$<1.0\times10^{-4}$	90	FREYBERGER	96	CLE2	$e^+e^-\approx\ \Upsilon(4S)$

$\Gamma(\pi^+\pi^-e^\pm\mu^\mp)/\Gamma_{total}$ Γ_{301}/Γ

A test of lepton family-number conservation. The value is for the sum of the two charge states.

VALUE	CL%	DOCUMENT ID		TECN	COMMENT
$<1.5\times10^{-5}$	90	AITALA	01C	E791	π^- nucleus, 500 GeV

$\Gamma(\rho^0e^\pm\mu^\mp)/\Gamma_{total}$ Γ_{302}/Γ

A test of lepton family number conservation. The value is for the sum of the two charge states.

VALUE	CL%	DOCUMENT ID		TECN	COMMENT
$<4.9\times10^{-5}$	90	[1] FREYBERGER	96	CLE2	$e^+e^-\approx\ \Upsilon(4S)$
• • • We do not use the following data for averages, fits, limits, etc. • • •					
$<6.6\times10^{-5}$	90	AITALA	01C	E791	π^- nucleus, 500 GeV

[1] This FREYBERGER 96 limit is obtained using a phase-space model. The limit changes to $<5.0\times10^{-5}$ using a photon pole amplitude model.

$\Gamma(\omega e^\pm\mu^\mp)/\Gamma_{total}$ Γ_{303}/Γ

A test of lepton family number conservation. The value is for the sum of the two charge states.

VALUE	CL%	DOCUMENT ID		TECN	COMMENT
$<1.2\times10^{-4}$	90	[1] FREYBERGER	96	CLE2	$e^+e^-\approx\ \Upsilon(4S)$

[1] This FREYBERGER 96 limit is obtained using a phase-space model. The same limit is obtained using a photon pole amplitude model.

$\Gamma(K^-K^+e^\pm\mu^\mp)/\Gamma_{total}$ Γ_{304}/Γ

A test of lepton family-number conservation. The value is for the sum of the two charge states.

VALUE	CL%	DOCUMENT ID		TECN	COMMENT
$<1.8\times10^{-4}$	90	AITALA	01C	E791	π^- nucleus, 500 GeV

$\Gamma(\phi e^\pm\mu^\mp)/\Gamma_{total}$ Γ_{305}/Γ

A test of lepton family number conservation. The value is for the sum of the two charge states.

VALUE	CL%	DOCUMENT ID		TECN	COMMENT
$<3.4\times10^{-5}$	90	[1] FREYBERGER	96	CLE2	$e^+e^-\approx\ \Upsilon(4S)$
• • • We do not use the following data for averages, fits, limits, etc. • • •					
$<4.7\times10^{-5}$	90	AITALA	01C	E791	π^- nucleus, 500 GeV

[1] This FREYBERGER 96 limit is obtained using a phase-space model. The limit changes to $<3.3\times10^{-5}$ using a photon pole amplitude model.

$\Gamma(\overline{K}^0e^\pm\mu^\mp)/\Gamma_{total}$ Γ_{306}/Γ

A test of lepton family number conservation. The value is for the sum of the two charge states.

VALUE	CL%	DOCUMENT ID		TECN	COMMENT
$<1.0\times10^{-4}$	90	FREYBERGER	96	CLE2	$e^+e^-\approx\ \Upsilon(4S)$

$\Gamma(K^-\pi^+e^\pm\mu^\mp)/\Gamma_{total}$ Γ_{307}/Γ

A test of lepton family-number conservation. The value is for the sum of the two charge states.

VALUE	CL%	DOCUMENT ID		TECN	COMMENT
$<5.53\times10^{-4}$	90	AITALA	01C	E791	π^- nucleus, 500 GeV

$\Gamma(\overline{K}^*(892)^0e^\pm\mu^\mp)/\Gamma_{total}$ Γ_{308}/Γ

A test of lepton family number conservation. The value is for the sum of the two charge states.

VALUE	CL%	DOCUMENT ID		TECN	COMMENT
$<8.3\times10^{-5}$	90	AITALA	01C	E791	π^- nucleus, 500 GeV
• • • We do not use the following data for averages, fits, limits, etc. • • •					
$<1.0\times10^{-4}$	90	[1] FREYBERGER	96	CLE2	$e^+e^-\approx\ \Upsilon(4S)$

[1] This FREYBERGER 96 limit is obtained using a phase-space model. The same limit is obtained using a photon pole amplitude model.

$\Gamma(2\pi^-2e^+ + \text{c.c.})/\Gamma_{total}$ Γ_{309}/Γ

A test of lepton-number conservation. The value is for the sum of the two charge states.

VALUE	CL%	DOCUMENT ID		TECN	COMMENT
$<1.12\times10^{-4}$	90	AITALA	01C	E791	π^- nucleus, 500 GeV

$\Gamma(2\pi^-2\mu^+ + \text{c.c.})/\Gamma_{total}$ Γ_{310}/Γ

A test of lepton-number conservation. The value is for the sum of the two charge states.

VALUE	CL%	DOCUMENT ID		TECN	COMMENT
$<2.9\times10^{-5}$	90	AITALA	01C	E791	π^- nucleus, 500 GeV

$\Gamma(K^-\pi^-2e^+ + \text{c.c.})/\Gamma_{total}$ Γ_{311}/Γ

A test of lepton-number conservation. The value is for the sum of the two charge states.

VALUE	CL%	DOCUMENT ID		TECN	COMMENT
$<2.06\times10^{-4}$	90	AITALA	01C	E791	π^- nucleus, 500 GeV

$\Gamma(K^-\pi^-2\mu^+ + \text{c.c.})/\Gamma_{total}$ Γ_{312}/Γ

A test of lepton-number conservation. The value is for the sum of the two charge states.

VALUE	CL%	DOCUMENT ID		TECN	COMMENT
$<3.9\times10^{-4}$	90	AITALA	01C	E791	π^- nucleus, 500 GeV

$\Gamma(2K^-2e^+ + \text{c.c.})/\Gamma_{\text{total}}$ Γ_{313}/Γ

A test of lepton-number conservation. The value is for the sum of the two charge states.

VALUE	CL%	DOCUMENT ID		TECN	COMMENT
$<1.52 \times 10^{-4}$	90	AITALA	01C	E791	π^- nucleus, 500 GeV

$\Gamma(2K^-2\mu^+ + \text{c.c.})/\Gamma_{\text{total}}$ Γ_{314}/Γ

A test of lepton-number conservation. The value is for the sum of the two charge states.

VALUE	CL%	DOCUMENT ID		TECN	COMMENT
$<9.4 \times 10^{-5}$	90	AITALA	01C	E791	π^- nucleus, 500 GeV

$\Gamma(\pi^-\pi^- e^+\mu^+ + \text{c.c.})/\Gamma_{\text{total}}$ Γ_{315}/Γ

A test of lepton-number conservation. The value is for the sum of the two charge states.

VALUE	CL%	DOCUMENT ID		TECN	COMMENT
$<7.9 \times 10^{-5}$	90	AITALA	01C	E791	π^- nucleus, 500 GeV

$\Gamma(K^-\pi^- e^+\mu^+ + \text{c.c.})/\Gamma_{\text{total}}$ Γ_{316}/Γ

A test of lepton-number conservation. The value is for the sum of the two charge states.

VALUE	CL%	DOCUMENT ID		TECN	COMMENT
$<2.18 \times 10^{-4}$	90	AITALA	01C	E791	π^- nucleus, 500 GeV

$\Gamma(2K^- e^+\mu^+ + \text{c.c.})/\Gamma_{\text{total}}$ Γ_{317}/Γ

A test of lepton-number conservation. The value is for the sum of the two charge states.

VALUE	CL%	DOCUMENT ID		TECN	COMMENT
$<5.7 \times 10^{-5}$	90	AITALA	01C	E791	π^- nucleus, 500 GeV

$\Gamma(pe^-)/\Gamma_{\text{total}}$ Γ_{318}/Γ

A test of baryon- and lepton-number conservation.

VALUE	CL%	DOCUMENT ID		TECN	COMMENT
$<1.0 \times 10^{-5}$	90	[1] RUBIN	09	CLEO	e^+e^- at $\psi(3770)$

[1] This RUBIN 09 limit is for either $D^0 \to pe^-$ or $\overline{D}^0 \to pe^-$ decay.

$\Gamma(\overline{p}e^+)/\Gamma_{\text{total}}$ Γ_{319}/Γ

A test of baryon- and lepton-number conservation.

VALUE	CL%	DOCUMENT ID		TECN	COMMENT
$<1.1 \times 10^{-5}$	90	[1] RUBIN	09	CLEO	e^+e^- at $\psi(3770)$

[1] This RUBIN 09 limit is for either $D^0 \to \overline{p}e^+$ or $\overline{D}^0 \to \overline{p}e^+$ decay.

D^0 CP-VIOLATING DECAY-RATE ASYMMETRIES

This is the difference between D^0 and $\overline{D}^0$ partial widths for the decay to state f, divided by the sum of the widths:
$A_{CP}(f) = [\Gamma(D^0 \to f) - \Gamma(\overline{D}^0 \to \overline{f})] / [\Gamma(D^0 \to f) + \Gamma(\overline{D}^0 \to \overline{f})]$.

$A_{CP}(K^+K^-)$ in $D^0, \overline{D}^0 \to K^+K^-$

VALUE (%)	EVTS	DOCUMENT ID		TECN	COMMENT
-0.07 ± 0.11 OUR AVERAGE					
$0.04 \pm 0.12 \pm 0.10$	4.56M	AAIJ	17M	LHCB	pp 7, 8 TeV
$-0.24 \pm 0.22 \pm 0.09$	476k	[1] AALTONEN	12B	CDF	$p\overline{p}$, $\sqrt{s}$=1.96 TeV
$0.00 \pm 0.34 \pm 0.13$	129k	[2] AUBERT	08M	BABR	$e^+e^- \approx$ 10.6 GeV
$-0.43 \pm 0.30 \pm 0.11$	120k	[3] STARIC	08	BELL	$e^+e^- \approx \Upsilon(4S)$
$+2.0 \pm 1.2 \pm 0.6$		[4] ACOSTA	05C	CDF	$p\overline{p}$, $\sqrt{s}$=1.96 TeV
$0.0 \pm 2.2 \pm 0.8$	3023	[4] CSORNA	02	CLE2	$e^+e^- \approx \Upsilon(4S)$
$-0.1 \pm 2.2 \pm 1.5$	3330	[4] LINK	00B	FOCS	
$-1.0 \pm 4.9 \pm 1.2$	609	[4] AITALA	98C	E791	$-0.093 < A_{CP} < +0.073$ (90% CL)

• • • We do not use the following data for averages, fits, limits, etc. • • •

$-0.06 \pm 0.15 \pm 0.10$	1.8M	[1] AAIJ	14AK	LHCB	See AAIJ 17M

[1] See also "D^0 CP-violating asymmetry differences" at the end of the CP-violating asymmetries.
[2] AUBERT 08M uses corrected numbers of events directly, not ratios with $K^\mp\pi^\pm$ events.
[3] STARIC 08 uses $D^0 \to K^-\pi^+$ and $\overline{D}^0 \to K^+\pi^-$ decays to correct for detector-induced asymmetries.
[4] AITALA 98C, LINK 00B, CSORNA 02, and ACOSTA 05C measure $N(D^0 \to K^+K^-)/N(D^0 \to K^-\pi^+)$, the ratio of numbers of events observed, and similarly for the $\overline{D}^0$.

$A_{CP}(K^0_S K^0_S)$ in $D^0, \overline{D}^0 \to K^0_S K^0_S$

VALUE (%)	EVTS	DOCUMENT ID		TECN	COMMENT
-0.4 ± 1.5 OUR AVERAGE					
$-0.02 \pm 1.53 \pm 0.17$	5.4k	[1] DASH	17	BELL	At/near $\Upsilon(4S)$, $\Upsilon(5S)$
$-2.9 \pm 5.2 \pm 2.2$	630	AAIJ	15AT	LHCB	pp at 7, 8 TeV
-23 ± 19	65	BONVICINI	01	CLE2	$e^+e^- \approx$ 10.6 GeV

[1] The systematic uncertainty is dominated by the uncertainty on A_{CP} in the control channel $D^0 \to K^0_S\pi^0$.

$A_{CP}(\pi^+\pi^-)$ in $D^0, \overline{D}^0 \to \pi^+\pi^-$

VALUE (%)	EVTS	DOCUMENT ID		TECN	COMMENT
0.13 ± 0.14 OUR AVERAGE					
$0.07 \pm 0.14 \pm 0.11$		[1] AAIJ	17M	LHCB	pp 7, 8 TeV
$0.22 \pm 0.24 \pm 0.11$	215k	[2] AALTONEN	12B	CDF	$p\overline{p}$, $\sqrt{s}$=1.96 TeV
$-0.24 \pm 0.52 \pm 0.22$	63.7k	[3] AUBERT	08M	BABR	$e^+e^- \approx$ 10.6 GeV
$0.43 \pm 0.52 \pm 0.12$	51k	[4] STARIC	08	BELL	$e^+e^- \approx \Upsilon(4S)$
$1.0 \pm 1.3 \pm 0.6$		[5] ACOSTA	05C	CDF	$p\overline{p}$, $\sqrt{s}$=1.96 TeV
$1.9 \pm 3.2 \pm 0.8$	1136	[5] CSORNA	02	CLE2	$e^+e^- \approx \Upsilon(4S)$
$4.8 \pm 3.9 \pm 2.5$	1177	[5] LINK	00B	FOCS	
$-4.9 \pm 7.8 \pm 3.0$	343	[5] AITALA	98C	E791	$-0.186 < A_{CP} < +0.088$ (90% CL)

• • • We do not use the following data for averages, fits, limits, etc. • • •

$-0.20 \pm 0.19 \pm 0.10$	774k	[2,6] AAIJ	14AK	LHCB	See AAIJ 17M

[1] AAIJ 17M value combines $\Delta A_{CP}(\pi\pi, KK)$ from AAIJ 16D, $A_{CP}(KK)$ from AAIJ 17M, and $A_{CP}(\pi\pi)$ from AAIJ 14AK.
[2] See also "D^0 CP-violating asymmetry differences" at the end of the CP-violating asymmetries.
[3] AUBERT 08M uses corrected numbers of events directly, not ratios with $K^\mp\pi^\pm$ events.
[4] STARIC 08 uses $D^0 \to K^-\pi^+$ and $\overline{D}^0 \to K^+\pi^-$ decays to correct for detector-induced asymmetries.
[5] AITALA 98C, LINK 00B, CSORNA 02, and ACOSTA 05C measure $N(D^0 \to \pi^+\pi^-)/N(D^0 \to K^-\pi^+)$, the ratio of numbers of events observed, and similarly for the $\overline{D}^0$.
[6] AAIJ 14AK uses $\Delta A_{CP}(\pi\pi, KK)$ and $A_{CP}(KK)$ reported in the same paper.

$A_{CP}(\pi^0\pi^0)$ in $D^0, \overline{D}^0 \to \pi^0\pi^0$

VALUE (%)	EVTS	DOCUMENT ID		TECN	COMMENT
0.0 ±0.6 OUR AVERAGE					
$-0.03 \pm 0.64 \pm 0.10$	34k	NISAR	14	BELL	e^+e^- at/near Υ's
0.1 ± 4.8	810	BONVICINI	01	CLE2	$e^+e^- \approx$ 10.6 GeV

$A_{CP}(\rho\gamma)$ in $D^0, \overline{D}^0 \to \rho\gamma$

VALUE (units 10^{-2})	DOCUMENT ID		TECN	COMMENT
$5.6 \pm 15.2 \pm 0.6$	NANUT	17	BELL	e^+e^- at Υ(nS), n=2,3,4,5

$A_{CP}(\phi\gamma)$ in $D^0, \overline{D}^0 \to \phi\gamma$

VALUE (units 10^{-2})	DOCUMENT ID		TECN	COMMENT
$-9.4 \pm 6.6 \pm 0.1$	NANUT	17	BELL	e^+e^- at Υ(nS), n=2,3,4,5

$A_{CP}(\overline{K}^*(892)^0\gamma)$ in $D^0, \overline{D}^0 \to \overline{K}^*(892)^0\gamma$

VALUE (units 10^{-2})	DOCUMENT ID		TECN	COMMENT
$-0.3 \pm 2.0 \pm 0.0$	NANUT	17	BELL	e^+e^- at Υ(nS), n=2,3,4,5

$A_{CP}(\pi^+\pi^-\pi^0)$ in $D^0, \overline{D}^0 \to \pi^+\pi^-\pi^0$

VALUE (%)	EVTS	DOCUMENT ID		TECN	COMMENT
0.3 ±0.4 OUR AVERAGE					
0.43 ± 1.30	123k±490	ARINSTEIN	08	BELL	$e^+e^- \approx \Upsilon(4S)$
$0.31 \pm 0.41 \pm 0.17$	80 ± .3k	[1] AUBERT	08AO	BABR	$e^+e^- \approx$ 10.6 GeV
$1 \; {}^{+9}_{-7} \pm 5$		CRONIN-HEN..05		CLEO	$e^+e^- \approx$ 10 GeV

[1] AUBERT 08AO report their result using a different sign convention.

$A_{CP}(\rho(770)^+\pi^- \to \pi^+\pi^-\pi^0)$ in $D^0 \to \rho^+\pi^-, \overline{D}^0 \to \rho^-\pi^+$

VALUE (%)	DOCUMENT ID		TECN	COMMENT
$+1.2 \pm 0.8 \pm 0.3$	AUBERT	08AO	BABR	Table 1, −Col.5/2×Col.2

$A_{CP}(\rho(770)^0\pi^0 \to \pi^+\pi^-\pi^0)$ in $D^0, \overline{D}^0 \to \rho^0\pi^0$

VALUE (%)	DOCUMENT ID		TECN	COMMENT
$-3.1 \pm 2.7 \pm 1.2$	AUBERT	08AO	BABR	Table 1, −Col.5/2×Col.2

$A_{CP}(\rho(770)^-\pi^+ \to \pi^+\pi^-\pi^0)$ in $D^0 \to \rho^-\pi^+, \overline{D}^0 \to \rho^+\pi^-$

VALUE (%)	DOCUMENT ID		TECN	COMMENT
$-1.0 \pm 1.6 \pm 0.7$	AUBERT	08AO	BABR	Table 1, −Col.5/2×Col.2

$A_{CP}(\rho(1450)^+\pi^- \to \pi^+\pi^-\pi^0)$ in $D^0 \to \rho(1450)^+\pi^-, \overline{D}^0 \to$ c.c.

VALUE (%)	DOCUMENT ID		TECN	COMMENT
$0 \pm 50 \pm 50$	AUBERT	08AO	BABR	Table 1, −Col.5/2×Col.2

$A_{CP}(\rho(1450)^0\pi^0 \to \pi^+\pi^-\pi^0)$ in $D^0, \overline{D}^0 \to \rho(1450)^0\pi^0$

VALUE (%)	DOCUMENT ID		TECN	COMMENT
$-17 \pm 33 \pm 17$	AUBERT	08AO	BABR	Table 1, −Col.5/2×Col.2

$A_{CP}(\rho(1450)^-\pi^+ \to \pi^+\pi^-\pi^0)$ in $D^0 \to \rho(1450)^-\pi^+, \overline{D}^0 \to$ c.c.

VALUE (%)	DOCUMENT ID		TECN	COMMENT
$+6 \pm 8 \pm 3$	AUBERT	08AO	BABR	Table 1, −Col.5/2×Col.2

$A_{CP}(\rho(1700)^+\pi^- \to \pi^+\pi^-\pi^0)$ in $D^0 \to \rho(1700)^+\pi^-, \overline{D}^0 \to$ c.c.

VALUE (%)	DOCUMENT ID		TECN	COMMENT
$-5 \pm 13 \pm 5$	AUBERT	08AO	BABR	Table 1, −Col.5/2×Col.2

$A_{CP}(\rho(1700)^0\pi^0 \to \pi^+\pi^-\pi^0)$ in $D^0, \overline{D}^0 \to \rho(1700)^0\pi^0$

VALUE (%)	DOCUMENT ID		TECN	COMMENT
$+13 \pm 8 \pm 3$	AUBERT	08AO	BABR	Table 1, −Col.5/2×Col.2

$A_{CP}(\rho(1700)^-\pi^+ \to \pi^+\pi^-\pi^0)$ in $D^0 \to \rho(1700)^-\pi^+, \overline{D}^0 \to$ c.c.

VALUE (%)	DOCUMENT ID		TECN	COMMENT
$+8 \pm 10 \pm 5$	AUBERT	08AO	BABR	Table 1, −Col.5/2×Col.2

$A_{CP}(f_0(980)\pi^0 \to \pi^+\pi^-\pi^0)$ in $D^0, \overline{D}^0 \to f_0(980)\pi^0$

VALUE (%)	DOCUMENT ID		TECN	COMMENT
$0 \pm 25 \pm 25$	AUBERT	08AO	BABR	Table 1, −Col.5/2×Col.2

$A_{CP}(f_0(1370)\pi^0 \to \pi^+\pi^-\pi^0)$ in $D^0, \overline{D}^0 \to f_0(1370)\pi^0$

VALUE (%)	DOCUMENT ID		TECN	COMMENT
+25±13±13	AUBERT	08AO	BABR	Table 1, −Col.5/2×Col.2

$A_{CP}(f_0(1500)\pi^0 \to \pi^+\pi^-\pi^0)$ in $D^0, \overline{D}^0 \to f_0(1500)\pi^0$

VALUE (%)	DOCUMENT ID		TECN	COMMENT
0±13±13	AUBERT	08AO	BABR	Table 1, −Col.5/2×Col.2

$A_{CP}(f_0(1710)\pi^0 \to \pi^+\pi^-\pi^0)$ in $D^0, \overline{D}^0 \to f_0(1710)\pi^0$

VALUE (%)	DOCUMENT ID		TECN	COMMENT
0±17±17	AUBERT	08AO	BABR	Table 1, −Col.5/2×Col.2

$A_{CP}(f_2(1270)\pi^0 \to \pi^+\pi^-\pi^0)$ in $D^0, \overline{D}^0 \to f_2(1270)\pi^0$

VALUE (%)	DOCUMENT ID		TECN	COMMENT
−4±4±4	AUBERT	08AO	BABR	Table 1, −Col.5/2×Col.2

$A_{CP}(\sigma(400)\pi^0 \to \pi^+\pi^-\pi^0)$ in $D^0, \overline{D}^0 \to \sigma(400)\pi^0$

VALUE (%)	DOCUMENT ID		TECN	COMMENT
+6±6±6	AUBERT	08AO	BABR	Table 1, −Col.5/2×Col.2

A_{CP}(nonresonant $\pi^+\pi^-\pi^0$) in $D^0, \overline{D}^0 \to$ nonresonant $\pi^+\pi^-\pi^0$

VALUE (%)	DOCUMENT ID		TECN	COMMENT
−13±19±13	AUBERT	08AO	BABR	Table 1, −Col.5/2×Col.2

$A_{CP}(2\pi^+2\pi^-)$ in $D^0, \overline{D}^0 \to 2\pi^+2\pi^-$

VALUE (%)	EVTS	DOCUMENT ID		COMMENT
0.54±1.04±0.51	7.3k	[1,2] DARGENT	17	e^+e^- at $\psi(3770)$

[1] Decay rate asymmetry integrated in decay time and across full 4π phase space.
[2] Obtained by analyzing CLEO-c data but not authored by the CLEO Collaboration.

$A_{CP}(a_1(1260)^+\pi^- \to 2\pi^+2\pi^-)$ in $D^0 \to a_1(1260)^+\pi^-, \overline{D}^0 \to$ c.c.

VALUE (%)	EVTS	DOCUMENT ID		COMMENT
4.7±2.6±4.9	7.3k	[1] DARGENT	17	4-body fit, 4π evts

[1] Obtained by analyzing CLEO-c data but not authored by the CLEO Collaboration.

$A_{CP}(a_1(1260)^-\pi^+ \to 2\pi^+2\pi^-)$ in $D^0 \to a_1(1260)^-\pi^+, \overline{D}^0 \to$ c.c.

VALUE (%)	EVTS	DOCUMENT ID		COMMENT
13.7±13.8±11.4	7.3k	[1] DARGENT	17	4-body fit, 4π evts

[1] Obtained by analyzing CLEO-c data but not authored by the CLEO Collaboration.

$A_{CP}(\pi(1300)^+\pi^- \to 2\pi^+2\pi^-)$ in $D^0 \to \pi(1300)^+\pi^-, \overline{D}^0 \to$ c.c.

VALUE (%)	EVTS	DOCUMENT ID		COMMENT
−1.6±12.9±6.7	7.3k	[1] DARGENT	17	4-body fit, 4π evts

[1] Obtained by analyzing CLEO-c data but not authored by the CLEO Collaboration.

$A_{CP}(\pi(1300)^-\pi^+ \to 2\pi^+2\pi^-)$ in $D^0 \to \pi(1300)^-\pi^+, \overline{D}^0 \to$ c.c.

VALUE (%)	EVTS	DOCUMENT ID		COMMENT
−5.6±11.9±27.7	7.3k	[1] DARGENT	17	4-body fit, 4π evts

[1] Obtained by analyzing CLEO-c data but not authored by the CLEO Collaboration.

$A_{CP}(a_1(1640)^+\pi^- \to 2\pi^+2\pi^-)$ in $D^0 \to a_1(1640)^+\pi^-, \overline{D}^0 \to$ c.c.

VALUE (%)	EVTS	DOCUMENT ID		COMMENT
8.6±17.8±19.3	7.3k	[1] DARGENT	17	4-body fit, 4π evts

[1] Obtained by analyzing CLEO-c data but not authored by the CLEO Collaboration.

$A_{CP}(\pi_2(1670)^+\pi^- \to 2\pi^+2\pi^-)$ in $D^0 \to \pi_2(1670)^+\pi^-, \overline{D}^0 \to$ c.c.

VALUE (%)	EVTS	DOCUMENT ID		COMMENT
7.3±15.1±10.4	7.3k	[1] DARGENT	17	4-body fit, 4π evts

[1] Obtained by analyzing CLEO-c data but not authored by the CLEO Collaboration.

$A_{CP}(\sigma f_0(1370) \to 2\pi^+2\pi^-)$ in $D^0, \overline{D}^0 \to \sigma f_0(1370)$

VALUE (%)	EVTS	DOCUMENT ID		COMMENT
−14.6±16.5±9.4	7.3k	[1] DARGENT	17	4-body fit, 4π evts

[1] Obtained by analyzing CLEO-c data but not authored by the CLEO Collaboration.

$A_{CP}(\sigma\rho(770)^0 \to 2\pi^+2\pi^-)$ in $D^0, \overline{D}^0 \to \sigma\rho(770)^0$

VALUE (%)	EVTS	DOCUMENT ID		COMMENT
2.5±16.8±20.8	7.3k	[1] DARGENT	17	4-body fit, 4π evts

[1] Obtained by analyzing CLEO-c data but not authored by the CLEO Collaboration.

$A_{CP}(2\rho(770)^0 \to 2\pi^+2\pi^-)$ in $D^0, \overline{D}^0 \to 2\rho(770)^0$

VALUE (%)	EVTS	DOCUMENT ID		COMMENT
−5.6±5.0±2.9	7.3k	[1] DARGENT	17	4-body fit, 4π evts

[1] Obtained by analyzing CLEO-c data but not authored by the CLEO Collaboration.

$A_{CP}(2f_2(1270) \to 2\pi^+2\pi^-)$ in $D^0, \overline{D}^0 \to 2f_2(1270)$

VALUE (%)	EVTS	DOCUMENT ID		COMMENT
−28.3±12.3±20.9	7.3k	[1] DARGENT	17	4-body fit, 4π evts

[1] Obtained by analyzing CLEO-c data but not authored by the CLEO Collaboration.

$A_{CP}(K^+K^-\pi^0)$ in $D^0, \overline{D}^0 \to K^+K^-\pi^0$

VALUE (%)	EVTS	DOCUMENT ID		TECN	COMMENT
−1.00±1.67±0.25	11 ± 0.11k	AUBERT	08AO	BABR	$e^+e^- \approx$ 10.6 GeV

$A_{CP}(K^*(892)^+K^- \to K^+K^-\pi^0)$ in $D^0 \to K^*(892)^+K^-, \overline{D}^0 \to$ c.c.

VALUE (%)	DOCUMENT ID		TECN	COMMENT
−0.9±1.2±0.4	[1] AUBERT	08AO	BABR	Table 1, −Col.5/2×Col.2

[1] AUBERT 08AO report their result using a different sign convention.

$A_{CP}(K^*(1410)^+K^- \to K^+K^-\pi^0)$ in $D^0 \to K^*(1410)^+K^-, \overline{D}^0 \to$ c.c.

VALUE (%)	DOCUMENT ID		TECN	COMMENT
−21±23±8	AUBERT	08AO	BABR	Table 1, −Col.5/2×Col.2

$A_{CP}((K^+\pi^0)_{S-wave}K^- \to K^+K^-\pi^0)$ in $D^0 \to (K^+\pi^0)_S K^-, \overline{D}^0 \to$ c.c.

VALUE (%)	DOCUMENT ID		TECN	COMMENT
+7±15±3	AUBERT	08AO	BABR	Table 1, −Col.5/2×Col.2

$A_{CP}(\phi(1020)\pi^0 \to K^+K^-\pi^0)$ in $D^0, \overline{D}^0 \to \phi(1020)\pi^0$

VALUE (%)	DOCUMENT ID		TECN	COMMENT
+1.1±2.1±0.5	AUBERT	08AO	BABR	Table 1, −Col.5/2×Col.2

$A_{CP}(f_0(980)\pi^0 \to K^+K^-\pi^0)$ in $D^0, \overline{D}^0 \to f_0(980)\pi^0$

VALUE (%)	DOCUMENT ID		TECN	COMMENT
−3±19±1	AUBERT	08AO	BABR	Table 1, −Col.5/2×Col.2

$A_{CP}(a_0(980)^0\pi^0 \to K^+K^-\pi^0)$ in $D^0, \overline{D}^0 \to a_0(980)^0\pi^0$

VALUE (%)	DOCUMENT ID		TECN	COMMENT
−5±16±2	[1] AUBERT	08AO	BABR	Table 1, −Col.5/2×Col.2

[1] This AUBERT 08AO value is obtained when the $a_0(980)^0$ replaces the $f_0(980)$ in the fit.

$A_{CP}(f_2'(1525)\pi^0 \to K^+K^-\pi^0)$ in $D^0, \overline{D}^0 \to f_2'(1525)\pi^0$

VALUE (%)	DOCUMENT ID		TECN	COMMENT
0±50±150	AUBERT	08AO	BABR	Table 1, −Col.5/2×Col.2

$A_{CP}(K^*(892)^-K^+ \to K^+K^-\pi^0)$ in $D^0 \to K^*(892)^-K^+, \overline{D}^0 \to$ c.c.

VALUE (%)	DOCUMENT ID		TECN	COMMENT
−5±4±1	AUBERT	08AO	BABR	Table 1, −Col.5/2×Col.2

$A_{CP}(K^*(1410)^-K^+ \to K^+K^-\pi^0)$ in $D^0 \to K^*(1410)^-K^+, \overline{D}^0 \to$ c.c.

VALUE (%)	DOCUMENT ID		TECN	COMMENT
−17±28±7	AUBERT	08AO	BABR	Table 1, −Col.5/2×Col.2

$A_{CP}((K^-\pi^0)_{S-wave}K^+ \to K^+K^-\pi^0)$ in $D^0 \to (K^-\pi^0)_S K^+, \overline{D}^0 \to$ c.c.

VALUE (%)	DOCUMENT ID		TECN	COMMENT
−7±40±8	AUBERT	08AO	BABR	Table 1, −Col.5/2×Col.2

$A_{CP}(K^0_S\pi^0)$ in $D^0, \overline{D}^0 \to K^0_S\pi^0$

VALUE (%)	EVTS	DOCUMENT ID		TECN	COMMENT
−0.20±0.17 OUR AVERAGE					
−0.21±0.16±0.07	467k	[1] NISAR	14	BELL	e^+e^- at/near Υ's
0.1 ±1.3	9099	BONVICINI	01	CLE2	$e^+e^- \approx$ 10.6 GeV
• • • We do not use the following data for averages, fits, limits, etc. • • •					
−0.28±0.19±0.10	326k	KO	11	BELL	See NISAR 14
−1.8 ±3.0		BARTELT	95	CLE2	See BONVICINI 01

[1] After subtracting CPV in $K^0 - \overline{K}^0$ mixing, NISAR 14 gets $A_{CP} = (+0.12 \pm 0.16 \pm 0.07)\%$.

$A_{CP}(K^0_S\eta)$ in $D^0, \overline{D}^0 \to K^0_S\eta$

VALUE (%)	EVTS	DOCUMENT ID		TECN	COMMENT
+0.54±0.51±0.16	46k	KO	11	BELL	$e^+e^- \approx \Upsilon(4S)$

$A_{CP}(K^0_S\eta')$ in $D^0, \overline{D}^0 \to K^0_S\eta'$

VALUE (%)	EVTS	DOCUMENT ID		TECN	COMMENT
+0.98±0.67±0.14	27k	KO	11	BELL	$e^+e^- \approx \Upsilon(4S)$

$A_{CP}(K^0_S\phi)$ in $D^0, \overline{D}^0 \to K^0_S\phi$

VALUE (%)	DOCUMENT ID		TECN	COMMENT
−2.8±9.4	BARTELT	95	CLE2	$-18.2 < A_{CP} < +12.6\%$ (90%CL)

$A_{CP}(K^\mp\pi^\pm)$ in $D^0 \to K^-\pi^+, \overline{D}^0 \to K^+\pi^-$

VALUE (%)	EVTS	DOCUMENT ID		TECN	COMMENT
0.3±0.3±0.6		BONVICINI	14	CLEO	All CLEO-c runs
• • • We do not use the following data for averages, fits, limits, etc. • • •					
+0.5±0.4±0.9	150k	MENDEZ	10	CLEO	See BONVICINI 14
−0.4±0.5±0.9		DOBBS	07	CLEO	See BONVICINI 14

$A_{CP}(K^\pm\pi^\mp)$ in $D^0 \to K^+\pi^-, \overline{D}^0 \to K^-\pi^+$

VALUE (%)	EVTS	DOCUMENT ID		TECN	COMMENT
− 0.9± 1.4 OUR AVERAGE					
− 1.7± 1.6		[1,2] AAIJ	17AO	LHCB	pp at 7,8 TeV
− 2.1± 5.2±1.5	4.0k	AUBERT	07W	BABR	$e^+e^- \approx$ 10.6 GeV
+ 2.3± 4.7	4.0k	[3] ZHANG	06	BELL	e^+e^-

$+18 \pm 14 \pm 4$		[4] LINK	05H	FOCS	γ nucleus
$+ 9.5 \pm 6.1 \pm 8.3$		[5] AUBERT	03Z	BABR	e^+e^-, 10.6 GeV
$+ 2 \ ^{+19}_{-20} \pm 1$	45	[6] GODANG	00	CLE2	e^+e^-
• • • We do not use the following data for averages, fits, limits, etc. • • •					
$- 0.7 \pm 1.9$		[1] AAIJ	13CE	LHCB	Repl. by AAIJ 17AO
$- 8.0 \pm 7.7$	0.8k	[7] LI	05A	BELL	See ZHANG 06

[1] Based on 3 fb^{-1} of data collected at $\sqrt{s}$ = 7, 8 TeV. Allowing for *CP* violation, the direct *CP*-violation in mixing is reported for the $D^0 \to K^+\pi^-$ and $\overline{D}{}^0 \to K^+\pi^-$.

[2] The *CPV* is derived from $A_{CP} = (R_D^+ - R_D^-)/(R_D^+ + R_D^-)$.

[3] This ZHANG 06 result allows mixing.

[4] This LINK 05H result assumes no mixing. If mixing is allowed, it becomes $0.13^{+0.33}_{-0.25} \pm 0.10$.

[5] This AUBERT 03Z limit assumes no mixing. If mixing is allowed, the 95% confidence-level interval is $(-2.8 < A_D < 4.9)\times10^{-3}$.

[6] This GODANG 00 result assumes no D^0-$\overline{D}{}^0$ mixing and becomes $-0.43 < A_{CP} < +0.34$ at 95% CL. If mixing is allowd $A_{CP} = -0.01^{+0.16}_{-0.17} \pm 0.01$.

[7] This LI 05A result allows mixing.

$A_{CP}(K^-\pi^+)$ in $D_{CP(\pm1)} \to K^\mp\pi^\pm$

$A_{CP}(K^-\pi^+) = [B(D_{CP(-)} \to K^-\pi^+ + \text{c.c.}) - B(D_{CP(+)} \to K^-\pi^+ + \text{c.c.})]$ / Sum

VALUE (%)	DOCUMENT ID		TECN	COMMENT
12.7±1.3±0.7	[1] ABLIKIM	14C	BES3	$e^+e^- \to D^0\overline{D}{}^0$, 3.77 GeV

[1] ABLIKIM 14C uses quantum correlations in $e^+e^- \to D^0\overline{D}{}^0$ at the $\psi(3770)$ to measure the asymmetry of the branching fraction of $D^0 \to K^-\pi^+$ in *CP*-odd and *CP*-even eigenstates. It then extracts the strong-phase difference $\delta_{K\pi}$.

$A_{CP}(K^\mp\pi^\pm\pi^0)$ in $D^0 \to K^-\pi^+\pi^0$, $\overline{D}{}^0 \to K^+\pi^-\pi^0$

VALUE (%)	DOCUMENT ID		TECN	COMMENT
0.1±0.5 OUR AVERAGE				
$0.1 \pm 0.3 \pm 0.4$	BONVICINI	14	CLEO	All CLEO-c runs
-3.1 ± 8.6	[1] KOPP	01	CLE2	$e^+e^- \approx$ 10.6 GeV
• • • We do not use the following data for averages, fits, limits, etc. • • •				
$0.2 \pm 0.4 \pm 0.8$	DOBBS	07	CLEO	See BONVICINI 14

[1] KOPP 01 fits separately the D^0 and $\overline{D}{}^0$ Dalitz plots and then calculates the integrated difference of normalized densities divided by the integrated sum.

$A_{CP}(K^\pm\pi^\mp\pi^0)$ in $D^0 \to K^+\pi^-\pi^0$, $\overline{D}{}^0 \to K^-\pi^+\pi^0$

VALUE (%)	EVTS	DOCUMENT ID		TECN	COMMENT
0 ± 5 OUR AVERAGE					
-0.6 ± 5.3	1978 ± 104	TIAN	05	BELL	$e^+e^- \approx \Upsilon(4S)$
$+9 \ ^{+25}_{-22}$	38	BRANDENB...	01	CLE2	$e^+e^- \approx \Upsilon(4S)$

$A_{CP}(K^0_S\pi^+\pi^-)$ in $D^0, \overline{D}{}^0 \to K^0_S\pi^+\pi^-$

VALUE (%)	EVTS	DOCUMENT ID		TECN	COMMENT
−0.1 ±0.8 OUR AVERAGE					
$-0.05 \pm 0.57 \pm 0.54$	350k	[1] AALTONEN	12AD	CDF	
$-0.9 \pm 2.1 \ ^{+1.6}_{-5.7}$	4854	[2] ASNER	04A	CLEO	$e^+e^- \approx$ 10 GeV

[1] This is the overall result of AALTONEN 12AD. Following are the 15 *CP* fit-fraction asymmetries from the amplitude analysis of the D^0 and $\overline{D}{}^0 \to K^0_S\pi^+\pi^-$ Dalitz plots.

[2] This is the overall result of ASNER 04A; *CP*-violating limits are also given below for each of the 10 resonant submodes found in an amplitude analysis of the D^0 and $\overline{D}{}^0 \to K^0_S\pi^+\pi^-$ Dalitz plots.

$A_{CP}(K^*(892)^\mp\pi^\pm \to K^0_S\pi^+\pi^-)$ in $D^0 \to K^{*-}\pi^+$, $\overline{D}{}^0 \to K^{*+}\pi^-$

VALUE (%)	DOCUMENT ID		TECN	COMMENT
+0.36±0.33±0.40	AALTONEN	12AD	CDF	Dalitz fit, ∼ 350k evts
• • • We do not use the following data for averages, fits, limits, etc. • • •				
$+2.5 \pm 1.9 \ ^{+3.3}_{-0.8}$	ASNER	04A	CLEO	Dalitz fit, 4854 evts

$A_{CP}(K^*(892)^\pm\pi^\mp \to K^0_S\pi^+\pi^-)$ in $D^0 \to K^{*+}\pi^-$, $\overline{D}{}^0 \to K^{*-}\pi^+$

This is a doubly Cabibbo-suppressed mode.

VALUE (%)	DOCUMENT ID		TECN	COMMENT
+ 1.0± 5.7± 2.1	AALTONEN	12AD	CDF	Dalitz fit, ∼ 350k evts
• • • We do not use the following data for averages, fits, limits, etc. • • •				
$-21 \pm 42 \pm 28$	ASNER	04A	CLEO	Dalitz fit, 4854 evts

$A_{CP}(K^0_S\rho^0 \to K^0_S\pi^+\pi^-)$ in $D^0 \to \overline{K}{}^0\rho^0$, $\overline{D}{}^0 \to K^0\rho^0$

VALUE (%)	DOCUMENT ID		TECN	COMMENT
−0.05±0.50±0.08	AALTONEN	12AD	CDF	Dalitz fit, ∼ 350k evts
• • • We do not use the following data for averages, fits, limits, etc. • • •				
$+3.1 \pm 3.8 \ ^{+2.7}_{-2.2}$	ASNER	04A	CLEO	Dalitz fit, 4854 evts

$A_{CP}(K^0_S\omega \to K^0_S\pi^+\pi^-)$ in $D^0 \to \overline{K}{}^0\omega$, $\overline{D}{}^0 \to K^0\omega$

VALUE (%)	DOCUMENT ID		TECN	COMMENT
−12.6± 6.0± 2.6	AALTONEN	12AD	CDF	Dalitz fit, ∼ 350k evts
• • • We do not use the following data for averages, fits, limits, etc. • • •				
$-26 \pm 24 \ ^{+22}_{-4}$	ASNER	04A	CLEO	Dalitz fit, 4854 evts

$A_{CP}(K^0_S f_0(980) \to K^0_S\pi^+\pi^-)$ in $D^0 \to \overline{K}{}^0 f_0(980)$, $\overline{D}{}^0 \to K^0 f_0(980)$

VALUE (%)	DOCUMENT ID		TECN	COMMENT
−0.4± 2.2± 1.6	AALTONEN	12AD	CDF	Dalitz fit, ∼ 350k evts
• • • We do not use the following data for averages, fits, limits, etc. • • •				
$-4.7 \pm 11.0 \ ^{+24.9}_{-8.8}$	ASNER	04A	CLEO	Dalitz fit, 4854 evts

$A_{CP}(K^0_S f_2(1270) \to K^0_S\pi^+\pi^-)$ in $D^0 \to \overline{K}{}^0 f_2(1270)$, $\overline{D}{}^0 \to K^0 f_2(1270)$

VALUE (%)	DOCUMENT ID		TECN	COMMENT
− 4.0± 3.4± 3.0	AALTONEN	12AD	CDF	Dalitz fit, ∼ 350k evts
• • • We do not use the following data for averages, fits, limits, etc. • • •				
$+34 \pm 51 \ ^{+33}_{-79}$	ASNER	04A	CLEO	Dalitz fit, 4854 evts

$A_{CP}(K^0_S f_0(1370) \to K^0_S\pi^+\pi^-)$ in $D^0 \to \overline{K}{}^0 f_0(1370)$, $\overline{D}{}^0 \to K^0 f_0(1370)$

VALUE (%)	DOCUMENT ID		TECN	COMMENT
− 0.5± 4.6± 7.7	AALTONEN	12AD	CDF	Dalitz fit, ∼ 350k evts
• • • We do not use the following data for averages, fits, limits, etc. • • •				
$+18 \pm 10 \ ^{+13}_{-22}$	ASNER	04A	CLEO	Dalitz fit, 4854 evts

$A_{CP}(K^0_S\rho^0(1450))$ in $D^0 \to \overline{K}{}^0\rho^0(1450)$, $\overline{D}{}^0 \to K^0\rho^0(1450)$

VALUE (%)	DOCUMENT ID		TECN	COMMENT
−4.1±5.2±8.1	AALTONEN	12AD	CDF	Dalitz fit, ∼ 350k evts

$A_{CP}(K^0_S f_0(600))$ in $D^0 \to \overline{K}{}^0 f_0(600)$, $\overline{D}{}^0 \to K^0 f_0(600)$

VALUE (%)	DOCUMENT ID		TECN	COMMENT
−2.7±2.7±3.6	AALTONEN	12AD	CDF	Dalitz fit, ∼ 350k evts

$A_{CP}(K^*(1410)^\mp\pi^\pm)$ in $D^0 \to K^*(1410)^-\pi^+$, $\overline{D}{}^0 \to K^*(1410)^+\pi^-$

VALUE (%)	DOCUMENT ID		TECN	COMMENT
−2.3±5.7±6.4	AALTONEN	12AD	CDF	Dalitz fit, ∼ 350k evts

$A_{CP}(K^*_0(1430)^\mp\pi^\pm \to K^0_S\pi^+\pi^-)$ in $D^0 \to K^*_0(1430)^-\pi^+$, $\overline{D}{}^0 \to$ c.c.

VALUE (%)	DOCUMENT ID		TECN	COMMENT
4.0± 2.4±3.8	AALTONEN	12AD	CDF	Dalitz fit, ∼ 350k evts
• • • We do not use the following data for averages, fits, limits, etc. • • •				
$-0.2 \pm 11.3 \ ^{+8.8}_{-5.0}$	ASNER	04A	CLEO	Dalitz fit, 4854 evts

$A_{CP}(K^*_0(1430)^\pm\pi^\mp)$ in $D^0 \to K^*_0(1430)^+\pi^-$, $\overline{D}{}^0 \to K^*_0(1430)^-\pi^+$

This is a doubly Cabibbo-suppressed mode.

VALUE (%)	DOCUMENT ID		TECN	COMMENT
+12±11±10	AALTONEN	12AD	CDF	Dalitz fit, ∼ 350k evts

$A_{CP}(K^*_2(1430)^\mp\pi^\pm \to K^0_S\pi^+\pi^-)$ in $D^0 \to K^*_2(1430)^-\pi^+$, $\overline{D}{}^0 \to$ c.c.

VALUE (%)	DOCUMENT ID		TECN	COMMENT
+2.9± 4.0± 4.1	AALTONEN	12AD	CDF	Dalitz fit, ∼ 350k evts
• • • We do not use the following data for averages, fits, limits, etc. • • •				
$-7 \pm 25 \ ^{+13}_{-26}$	ASNER	04A	CLEO	Dalitz fit, 4854 evts

$A_{CP}(K^*_2(1430)^\pm\pi^\mp)$ in $D^0 \to K^*_2(1430)^+\pi^-$, $\overline{D}{}^0 \to K^*_2(1430)^-\pi^+$

This is a doubly Cabibbo-suppressed mode.

VALUE (%)	DOCUMENT ID		TECN	COMMENT
−10±14±29	AALTONEN	12AD	CDF	Dalitz fit, ∼ 350k evts

$A_{CP}(K^*(1680)^\mp\pi^\pm \to K^0_S\pi^+\pi^-)$ in $D^0 \to K^*(1680)^-\pi^+$, $\overline{D}{}^0 \to$ c.c.

VALUE (%)	DOCUMENT ID		TECN	COMMENT
• • • We do not use the following data for averages, fits, limits, etc. • • •				
$-36 \pm 19 \ ^{+10}_{-35}$	ASNER	04A	CLEO	Dalitz fit, 4854 evts

$A_{CP}(K^-\pi^+\pi^+\pi^-)$ in $D^0 \to K^-\pi^+\pi^+\pi^-$, $\overline{D}{}^0 \to K^+\pi^-\pi^-\pi^+$

VALUE (%)	DOCUMENT ID		TECN	COMMENT
0.2±0.3±0.4	BONVICINI	14	CLEO	All CLEO-c runs
• • • We do not use the following data for averages, fits, limits, etc. • • •				
$+0.7 \pm 0.5 \pm 0.9$	DOBBS	07	CLEO	See BONVICINI 14

$A_{CP}(K^\pm\pi^\mp\pi^+\pi^-)$ in $D^0 \to K^+\pi^-\pi^+\pi^-$, $\overline{D}{}^0 \to K^-\pi^+\pi^+\pi^-$

VALUE (%)	EVTS	DOCUMENT ID		TECN	COMMENT
−1.8±4.4	1721 ± 75	TIAN	05	BELL	$e^+e^- \approx \Upsilon(4S)$

$A_{CP}(K^+K^-\pi^+\pi^-)$ in $D^0, \overline{D}{}^0 \to K^+K^-\pi^+\pi^-$

See also AAIJ 13BR for a search for *CP* violation in $D^0 \to K^+K^-\pi^+\pi^-$ in binned phase space. No evidence of *CP* violation was found.

VALUE (%)	EVTS	DOCUMENT ID		TECN	COMMENT
1.3 ±1.7 OUR AVERAGE					
$1.84 \pm 1.74 \pm 0.3$	2.9k	[1] DARGENT	17		e^+e^-
$-8.2 \pm 5.6 \pm 4.7$	828 ± 46	LINK	05E	FOCS	γ A, $\overline{E}_\gamma \approx$ 180 GeV

[1] Obtained by analyzing CLEO data but not authored by the CLEO Collaboration.

$A_{CP}(K_1^*(1270)^+ K^-) \to K^+K^-\pi^+\pi^-)$ in $D^0 \to K_1^*(1270)^+ K^-, \overline{D}^0 \to$ c.c.

Including the full $K_1^*(1270)^+$ phase space accessible in this decay chain, with its various resonance contributions.

VALUE (%)	EVTS	DOCUMENT ID		COMMENT
25.3±9.7±12.7	2.9k	[1] DARGENT	17	4-body fit, $KK\pi\pi$ evts

[1] Obtained by analyzing CLEO data but not authored by the CLEO Collaboration.

$A_{CP}(K_1^*(1270)^+ K^-) \to K^{*0}\pi^+ K^-)$ in $D^0 \to K_1^*(1270)^+ K^-, \overline{D}^0 \to$ c.c.

VALUE (%)	DOCUMENT ID		TECN	COMMENT
−0.7±10.4	ARTUSO	12	CLEO	Amplitude fit, 2959 evts.

$A_{CP}(K_1^*(1270)^- K^+ \to \overline{K}^{*0}\pi^- K^+)$ in $D^0 \to K_1^*(1270)^- K^+, \overline{D}^0 \to$ c.c.

VALUE (%)	DOCUMENT ID		TECN	COMMENT
−10.0±31.5	ARTUSO	12	CLEO	Amplitude fit, 2959 evts.

$A_{CP}(K_1^*(1270)^- K^+ \to K^+K^-\pi^+\pi^-)$ in $D^0 \to K_1^*(1270)^- K^+, \overline{D}^0 \to$ c.c.

Including the full $K_1^*(1270)^-$ phase space accessible in this decay chain, with its various resonance contributions.

VALUE (%)	EVTS	DOCUMENT ID		COMMENT
−50.4±12.0±16.1	2.9k	[1] DARGENT	17	4-body fit, $KK\pi\pi$ evts

[1] Obtained by analyzing CLEO data but not authored by the CLEO Collaboration.

$A_{CP}(K_1^*(1270)^+ K^-) \to \rho^0 K^+K^-)$ in $D^0 \to K_1^*(1270)^+ K^-, \overline{D}^0 \to$ c.c.

VALUE (%)	DOCUMENT ID		TECN	COMMENT
−6.5±16.9	ARTUSO	12	CLEO	Amplitude fit, 2959 evts.

$A_{CP}(K_1^*(1270)^- K^+ \to \rho^0 K^-K^+)$ in $D^0 \to K_1^*(1270)^- K^+, \overline{D}^0 \to$ c.c.

VALUE (%)	DOCUMENT ID		TECN	COMMENT
+9.6±12.9	ARTUSO	12	CLEO	Amplitude fit, 2959 evts.

$A_{CP}(K_1^*(1400)^+ K^-) \to K^+K^-\pi^+\pi^-)$ in $D^0 \to K_1^*(1400)^+ K^-, \overline{D}^0 \to$ c.c.

Including the full $K_1^*(1400)^+$ phase space accessible in this decay chain, with its various resonance contributions.

VALUE (%)	EVTS	DOCUMENT ID		COMMENT
9.2±15.2±20.3	2.9k	[1] DARGENT	17	4-body fit, $KK\pi\pi$ evts

[1] Obtained by analyzing CLEO data but not authored by the CLEO Collaboration.

$A_{CP}(K^*(1410)^+ K^-) \to K^{*0}\pi^+ K^-)$ in $D^0 \to K^*(1410)^+ K^-, \overline{D}^0 \to$ c.c.

VALUE (%)	DOCUMENT ID		TECN	COMMENT
−20.0±16.8	ARTUSO	12	CLEO	Amplitude fit, 2959 evts.

$A_{CP}(K^*(1410)^- K^+ \to \overline{K}^{*0}\pi^- K^+)$ in $D^0 \to K^*(1410)^- K^+, \overline{D}^0 \to$ c.c.

VALUE (%)	DOCUMENT ID		TECN	COMMENT
−1.1±13.7	ARTUSO	12	CLEO	Amplitude fit, 2959 evts.

$A_{CP}(K^*(1680)^+ K^- \to K^+K^-\pi^+\pi^-)$ in $D^0 \to K^*(1680)^+ K^-, \overline{D}^0 \to$ c.c.

Including the full $K^*(1680)^+$ phase space accessible in this decay chain, with its various resonance contributions.

VALUE (%)	EVTS	DOCUMENT ID		COMMENT
−17.1±21.8±18.5	2.9k	[1] DARGENT	17	4-body fit, $KK\pi\pi$ evts

[1] Obtained by analyzing CLEO data but not authored by the CLEO Collaboration.

$A_{CP}(K^{*0}\overline{K}^{*0})$ in $D^0, \overline{D}^0 \to K^{*0}\overline{K}^{*0}$

Including S, P, D wave

VALUE (%)	EVTS	DOCUMENT ID		COMMENT
−4.6±9.0±11.3	2.9k	[1] DARGENT	17	4-body fit, $KK\pi\pi$ evts

[1] Obtained by analyzing CLEO data but not authored by the CLEO Collaboration.

$A_{CP}(K^{*0}\overline{K}^{*0}$ S-wave) in $D^0, \overline{D}^0 \to K^{*0}\overline{K}^{*0}$ S-wave

VALUE (%)	DOCUMENT ID		TECN	COMMENT
+9.5±13.5	ARTUSO	12	CLEO	Amplitude fit, 2959 evts.

$A_{CP}(\phi\rho^0)$ in $D^0, \overline{D}^0 \to \phi\rho^0$

Including S, P, D wave

VALUE (%)	EVTS	DOCUMENT ID		COMMENT
1.5±4.6±8.0	2.9k	[1] DARGENT	17	4-body fit, $KK\pi\pi$ evts

[1] Obtained by analyzing CLEO data but not authored by the CLEO Collaboration.

$A_{CP}(\phi\rho^0$ S-wave) in $D^0, \overline{D}^0 \to \phi\rho^0$ S-wave

VALUE (%)	DOCUMENT ID		TECN	COMMENT
−2.7±5.3	ARTUSO	12	CLEO	Amplitude fit, 2959 evts.

$A_{CP}(\phi\rho^0$ D-wave) in $D^0, \overline{D}^0 \to \phi\rho^0$ D-wave

VALUE (%)	DOCUMENT ID		TECN	COMMENT
−37.1±19.0	ARTUSO	12	CLEO	Amplitude fit, 2959 evts.

$A_{CP}(\phi(\pi^+\pi^-)_{S-wave})$ in $D^0, \overline{D}^0 \to \phi(\pi^+\pi^-)_{S-wave}$

VALUE (%)	DOCUMENT ID		TECN	COMMENT
−4.0±18.0±44.6	[1] DARGENT	17		4-body fit, 2959 evts.

• • • We do not use the following data for averages, fits, limits, etc. • • •

−8.6±10.4	[2] ARTUSO	12	CLEO	Amplitude fit, 2959 evts.

[1] Obtained by analyzing CLEO data but not authored by the CLEO Collaboration.
[2] see DARGENT 17

$A_{CP}(K^*(892)^0(K^-\pi^+)_{S-wave})$ in $D^0, \overline{D}^0 \to K^*(892)^0(K^-\pi^+)_{S-wave}$

VALUE (%)	EVTS	DOCUMENT ID		COMMENT
−13.1±17.9±31.2	2.9k	[1] DARGENT	17	4-body fit, $KK\pi\pi$ evts

[1] Obtained by analyzing CLEO data but not authored by the CLEO Collaboration.

$A_{CP}(K^+K^-\pi^+\pi^-$ non-resonant) in $D^0, \overline{D}^0 \to K^+K^-\pi^+\pi^-$ non-resonant

VALUE (%)	DOCUMENT ID		COMMENT
+8.2±10.9±17.1	[1] DARGENT	17	4-body fit, 2.9k $KK\pi\pi$ evts

[1] Obtained by analyzing CLEO data but not authored by the CLEO Collaboration.

$A_{CP}((K^-\pi^+)_{P-wave}(K^+\pi^-)_{S-wave})$ in $D^0 \to (K^-\pi^+)_{P-wave}(K^+\pi^-)_{S-wave}, \overline{D}^0 \to$ c.c.

VALUE (%)	DOCUMENT ID		TECN	COMMENT
+2.7±10.6	ARTUSO	12	CLEO	Amplitude fit, 2959 evts.

D^0 CP-EVEN FRACTIONS

The CP-even fraction F_+, defined for self-conjugate final states, like the coherence factor is useful for measuring the unitary triangle angle γ in $B \to DK$ decays. A purely CP-even state has $F_+ = 1$, a CP-odd one has $F_+ = 0$. For details, see NAYAK 15.

CP-even fraction in $D^0 \to \pi^+\pi^-\pi^0$ decays

VALUE (%)	DOCUMENT ID		COMMENT
97.3±1.7	MALDE	15	Uses CLEO data
• • • We do not use the following data for averages, fits, limits, etc. • • •			
96.8±1.7±0.6	NAYAK	15	see MALDE 15

CP-even fraction in $D^0 \to K^+K^-\pi^0$ decays

VALUE (%)	DOCUMENT ID		COMMENT
73.2±5.5	MALDE	15	Uses CLEO data
• • • We do not use the following data for averages, fits, limits, etc. • • •			
73.1±5.8±2.1	NAYAK	15	see MALDE 15

CP-even fraction in $D^0 \to \pi^+\pi^-\pi^+\pi^-$ decays

VALUE (%)	DOCUMENT ID		TECN	COMMENT
73.7±2.8	MALDE	15	CLEO	amplitude model independent
• • • We do not use the following data for averages, fits, limits, etc. • • •				
72.9±0.9±1.8	[1,2] DARGENT	17		from amplitude model

[1] MALDE 15 and DARGENT 17 use different CLEO data sets, so in principle their results could be averaged. However, given the importance that model-independence has in the use of this value, we exclude the amplitude model-derived result from the average.
[2] Obtained by analyzing CLEO-c data but not authored by the CLEO Collaboration.

CP-even fraction in $D^0 \to K^+K^-\pi^+\pi^-$ decays

VALUE (%)	DOCUMENT ID		COMMENT
75.3±1.8±3.9	[1] DARGENT	17	from amplitude model

[1] Obtained by analyzing CLEO data but not authored by the CLEO Collaboration.

D^0 CP-VIOLATING ASYMMETRY DIFFERENCES

$\Delta A_{CP} = A_{CP}(K^+K^-) - A_{CP}(\pi^+\pi^-)$

CP violation in these modes can come from the decay amplitudes (direct) and/or from mixing or interference of mixing and decay (indirect). The difference ΔA_{CP} is primarily sensitive to the direct component, and only retains a second-order dependence on the indirect component for measurements where the mean decay time of the K^+K^- and $\pi^+\pi^-$ samples are not identical. The results below are averaged assuming the indirect component can be neglected.

VALUE (%)	EVTS	DOCUMENT ID		TECN	COMMENT
−0.12±0.13 OUR AVERAGE	Error includes scale factor of 1.8. See the ideogram below.				
−0.10±0.08±0.03	6.5M,2.2M	AAIJ	16D	LHCB	Time-integrated
0.14±0.16±0.08	2.2M,0.8M	AAIJ	14AK	LHCB	Time-integrated
−0.62±0.21±0.10		AALTONEN	12O	CDF	Time-integrated
0.24±0.62±0.26		[1] AUBERT	08M	BABR	Time-integrated
−0.86±0.60±0.07	120k	STARIC	08	BELL	Time-integrated
• • • We do not use the following data for averages, fits, limits, etc. • • •					
0.49±0.30±0.14	0.56M,0.22M	AAIJ	13AD	LHCB	See AAIJ 14AK
−0.82±0.21±0.11	1.4M,0.4M	AAIJ	12G	LHCB	See AAIJ 16D
−0.46±0.31±0.12		AALTONEN	12B	CDF	See AALTONEN 12O

[1] Calculated from the AUBERT 08M values of $A_{CP}(K^+K^-)$ and $A_{CP}(\pi^+\pi^-)$. The systematic error here combines the systematic errors in quadrature, and therefore somewhat over-estimates it.

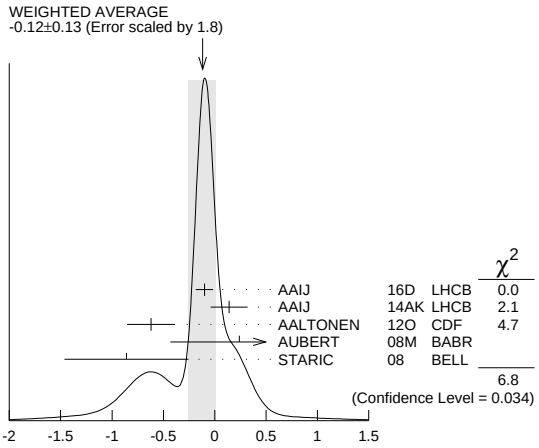

D^0 TESTS OF LOCAL *CP*-VIOLATION (*CPV*)

We list model-independent searches for local *CP* violation in phase-space distributions of multi-body decays.

Most of these searches divide phase space (Dalitz plot for 3-body decays, five-dimensional equivalent for 4-body decays) into bins, and perform a χ^2 test comparing normalised yields N_i, $\overline{N}_i$ in *CP*-conjugate bin pairs i: $\chi^2 = \Sigma_i (N_i - \alpha\,\overline{N}_i)/\sigma(N_i - \alpha\,\overline{N}_i)$. The factor $\alpha = (\Sigma_i N_i)/(\Sigma_i \overline{N}_i)$ removes the dependence on phase-space-integrated rate asymmetries. The result is used to obtain the probability (p-value) to obtain the measured χ^2 or larger under the assumption of CP conservation [AUBERT 08AO, BEDIAGA 09]. Alternative methods obtain p-values from other test variables based on unbinned analyses [WILLIAMS 11, AAIJ 14C]. Results can be combined using Fisher's method [MOSTELLER 48].

Local *CPV* in $D^0, \overline{D}^0 \to \pi^+\pi^-\pi^0$

p-value (%)	EVTS	DOCUMENT ID		TECN	COMMENT
4.9 OUR EVALUATION					
2.6	566k	[1] AAIJ	15A	LHCB	unbinned method
32.8	82k	AUBERT	08AO	BABR	χ^2

[1] Unusually, AAIJ 15A assigns an uncertainty on the p value of ±0.5%. This results from limited test statistics.

Local *CPV* in $D^0, \overline{D}^0 \to \pi^+\pi^-\pi^+\pi^-$

p-value (%)	EVTS	DOCUMENT ID		TECN	COMMENT
0.6±0.2	1.0M	[1] AAIJ	17AE	LHCB	unbinned, *P*-odd
• • • We do not use the following data for averages, fits, limits, etc. • • •					
4.6±0.5	1.0M	[2,3] AAIJ	17AE	LHCB	unbinned, *P*-even
41	330k	[2,4] AAIJ	13BR	LHCB	χ^2, *P*-even

[1] This AAIJ 17AE value tests *CP* Violation in *P*-odd variables.
[2] This value tests *CP* Violation in *P*-even variables.
[3] Not included in average as correlation to *P*-odd measurement using the same data is unclear.
[4] See AAIJ 17AE.

Local *CPV* in $D^0, \overline{D}^0 \to K^0_S\pi^+\pi^-$

p-value (%)	EVTS	DOCUMENT ID		TECN	COMMENT
96	350k	AALTONEN	12AD	CDF	χ^2

Local *CPV* in $D^0, \overline{D}^0 \to K^+K^-\pi^0$

p-value (%)	EVTS	DOCUMENT ID		TECN	COMMENT
16.6	11k	AUBERT	08AO	BABR	χ^2

Local *CPV* in $D^0, \overline{D}^0 \to K^+K^-\pi^+\pi^-$

p-value (%)	EVTS	DOCUMENT ID		TECN	COMMENT
9.1	57k	AAIJ	13BR	LHCB	χ^2

CP VIOLATING ASYMMETRIES OF *P*-ODD (*T*-ODD) MOMENTS

The *CP*-sensitive *P*-odd (*T*-odd) correlation in D^0, $\overline{D}^0$ decays. The D^0 and $\overline{D}^0$ are distinguished by the charge of the parent D^*: $D^{*+} \to D^0\pi^+$ and $D^{*-} \to \overline{D}^0\pi^-$.

$A_{Tviol}(K^+K^-\pi^+\pi^-)$ in $D^0, \overline{D}^0 \to K^+K^-\pi^+\pi^-$

$C_T \equiv \vec{p}_{K^+} \cdot (\vec{p}_{\pi^+} \times \vec{p}_{\pi^-})$ is a parity-odd correlation of the K^+, π^+, and π^- momenta (evaluated in the D^0 rest frame) for the D^0. $\overline{C}_T \equiv \vec{p}_{K^-} \cdot (\vec{p}_{\pi^-} \times \vec{p}_{\pi^+})$ is the corresponding quantity for the $\overline{D}^0$. Then
$A_T \equiv [\Gamma(C_T > 0) - \Gamma(C_T < 0)] \,/\, [\Gamma(C_T > 0) + \Gamma(C_T < 0)]$, and
$\overline{A}_T \equiv [\Gamma(-\overline{C}_T > 0) - \Gamma(-\overline{C}_T < 0)] \,/\, [\Gamma(-\overline{C}_T > 0) + \Gamma(-\overline{C}_T < 0)]$, and
$A_{Tviol} \equiv \frac{1}{2}(A_T - \overline{A}_T)$. C_T and $\overline{C}_T$ are commonly referred to as *T*-odd moments, because they are odd under *T* reversal. However, the *T*-conjugate process $K^+K^-\pi^+\pi^- \to D^0$ is not accessible, while the *P*-conjugate process is.

VALUE (units 10^{-3})	EVTS	DOCUMENT ID		TECN	COMMENT
1.7± 2.7 OUR AVERAGE					
1.8± 2.9± 0.4	171k	AAIJ	14BC	LHCB	$B \to D^0\mu^- X$
1.0± 5.1± 4.4	47k	DEL-AMO-SA...10		BABR	$e^+e^- \approx 10.6$ GeV
• • • We do not use the following data for averages, fits, limits, etc. • • •					
10 ±57 ±37	0.8k	LINK	05E	FOCS	γ A, $\overline{E}_\gamma \approx 180$ GeV

$A_{Tviol}(K_S\pi^+\pi^-\pi^0)$ in $D^0, \overline{D}^0 \to K_S\pi^+\pi^-\pi^0$

VALUE (units 10^{-3})	EVTS	DOCUMENT ID		TECN	COMMENT
$-0.28 \pm 1.38^{+0.23}_{-0.76}$	745k	[1] PRASANTH	17	BELL	e^+e^- at Υ(nS)'s

[1] PRASANTH 17 also measures A_{Tviol} in sub-regions of the $D^0 \to K_S\pi^+\pi^-\pi^0$ phase-space. No evidence of *T* violation is found.

D^0 *CPT*-VIOLATING DECAY-RATE ASYMMETRIES

$A_{CPT}(K^\mp\pi^\pm)$ in $D^0 \to K^-\pi^+$, $\overline{D}^0 \to K^+\pi^-$

$A_{CPT}(t)$ is defined in terms of the time-dependent decay probabilities $P(D^0 \to K^-\pi^+)$ and $\overline{P}(\overline{D}^0 \to K^+\pi^-)$ by $A_{CPT}(t) = (\overline{P} - P)/(\overline{P} + P)$. For small mixing parameters $x \equiv \Delta m/\Gamma$ and $y \equiv \Delta\Gamma/2\Gamma$ (as is the case), and times t, $A_{CPT}(t)$ reduces to $[\, y\, Re\,\xi - x\, Im\,\xi\,]\,\Gamma t$, where ξ is the *CPT*-violating parameter.

The following is actually $y\, Re\,\xi - x\, Im\,\xi$.

VALUE	DOCUMENT ID		TECN	COMMENT
0.0083±0.0065±0.0041	LINK	03B	FOCS	γ nucleus, $\overline{E}_\gamma \approx 180$ GeV

$D^0 \to K^*(892)^-\ell^+\nu_\ell$ FORM FACTORS

$r_V \equiv V(0)/A_1(0)$ in $D^0 \to K^*(892)^-\ell^+\nu_\ell$

VALUE	DOCUMENT ID		TECN	COMMENT
1.71±0.68±0.34	LINK	05B	FOCS	$K^*(892)^-\mu^+\nu_\mu$

$r_2 \equiv A_2(0)/A_1(0)$ in $D^0 \to K^*(892)^-\ell^+\nu_\ell$

VALUE	DOCUMENT ID		TECN	COMMENT
0.91±0.37±0.10	LINK	05B	FOCS	$K^*(892)^-\mu^+\nu_\mu$

$D^0 \to K^-/\pi^-\ell^+\nu_\ell$ FORM FACTORS

$f_+(0)$ in $D^0 \to K^-\ell^+\nu_\ell$

VALUE	EVTS	DOCUMENT ID		TECN	COMMENT
0.736 ±0.004 OUR AVERAGE					
0.7368±0.0026±0.0036	71k	ABLIKIM	15X	BES3	ℓ=e, 2-parameter fit
0.727 ±0.007 ±0.009		AUBERT	07BG	BABR	ℓ=e, 2-parameter fit

$f_+(0)|V_{cs}|$ in $D^0 \to K^-\ell^+\nu_\ell$

VALUE	EVTS	DOCUMENT ID		TECN	COMMENT
0.719 ±0.004 OUR AVERAGE					
0.7172±0.0025±0.0035	71k	[1] ABLIKIM	15X	BES3	ℓ=e, 2-parameter fit
0.726 ±0.008 ±0.004		BESSON	09	CLEO	ℓ=e, 3-parameter fit

[1] The 3-parameter fit yields 0.7195 ± 0.0035 ± 0.0041.

$r_1 \equiv a_1/a_0$ in $D^0 \to K^-\ell^+\nu_\ell$

VALUE	EVTS	DOCUMENT ID		TECN	COMMENT
−2.40±0.16 OUR AVERAGE					
−2.33±0.16±0.08	71k	[1] ABLIKIM	15X	BES3	ℓ=e, 3-parameter fit
−2.65±0.34±0.08		BESSON	09	CLEO	ℓ=e, 3-parameter fit

[1] The 2-parameter fit yields −2.23 ± 0.09 ± 0.06.

$r_2 \equiv a_2/a_0$ in $D^0 \to K^-\ell^+\nu_\ell$

VALUE	EVTS	DOCUMENT ID		TECN	COMMENT
5 ±4 OUR AVERAGE					
3.4±3.9±2.4	71k	ABLIKIM	15X	BES3	ℓ=e, 3-parameter fit
13 ±9 ±1		BESSON	09	CLEO	ℓ=e, 3-parameter fit

$f_+(0)$ in $D^0 \to \pi^-\ell^+\nu_\ell$

VALUE	EVTS	DOCUMENT ID		TECN	COMMENT
0.6372±0.0080±0.0044	6.3k	ABLIKIM	15X	BES3	ℓ=e, 2-parameter fit

$f_+(0)|V_{cd}|$ in $D^0 \to \pi^-\ell^+\nu_\ell$

VALUE	EVTS	DOCUMENT ID		TECN	COMMENT
0.1436±0.0026 OUR AVERAGE	Error includes scale factor of 1.5. See the ideogram below.				
0.1435±0.0018±0.0009	6.3k	[1] ABLIKIM	15X	BES3	ℓ=e, 2-parameter fit
0.1374±0.0038±0.0024	5.3k	[2] LEES	15F	BABR	ℓ=e, 3-parameter fit
0.152 ±0.005 ±0.001		BESSON	09	CLEO	ℓ=e, 3-parameter fit

[1] The 3-parameter fit yields 0.1420 ± 0.0024 ± 0.0010.
[2] LEES 15F reports a value 0.1374 ± 0.0038 ± 0.0022 ± 0.0009, where the last uncertainty is due to the uncertainties of the $D^0 \to K^-\pi^+$ branching fraction.

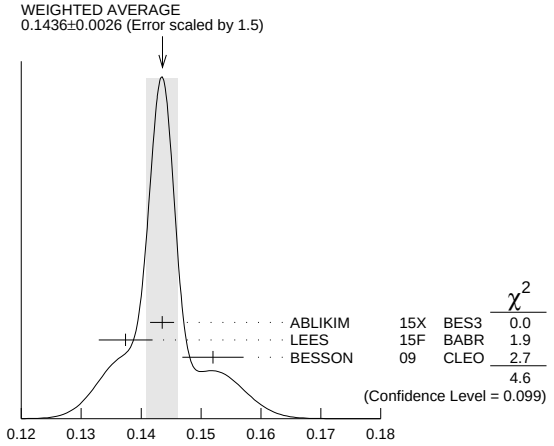

$f_+(0)\left|V_{cd}\right|$ in $D^0 \to \pi^- \ell^+ \nu_\ell$

$r_1 \equiv a_1/a_0$ in $D^0 \to \pi^- \ell^+ \nu_\ell$

VALUE	EVTS	DOCUMENT ID		TECN	COMMENT
−1.97±0.28 OUR AVERAGE		Error includes scale factor of 1.4. See the ideogram below.			
−1.84±0.22±0.07	6.3k	[1] ABLIKIM	15X	BES3	ℓ=e, 3-parameter fit
−1.31±0.70±0.43	5.3k	LEES	15F	BABR	ℓ=e, 3-parameter fit
−2.80±0.49±0.04		BESSON	09	CLEO	ℓ=e, 3-parameter fit

[1] The 2-parameter fit yields −2.04 ± 0.08 ± 0.03.

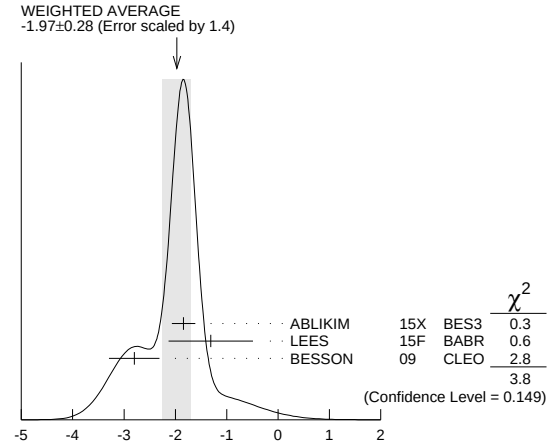

$r_1 \equiv a_1/a_0$ in $D^0 \to \pi^- \ell^+ \nu_\ell$

$r_2 \equiv a_1/a_0$ in $D^0 \to \pi^- \ell^+ \nu_\ell$

VALUE	EVTS	DOCUMENT ID		TECN	COMMENT
−0.2±2.2 OUR AVERAGE		Error includes scale factor of 1.7. See the ideogram below.			
−1.4±1.5±0.5	6.3k	ABLIKIM	15X	BES3	ℓ=e, 3-parameter fit
−4.2±4.0±1.9	5.3k	LEES	15F	BABR	ℓ=e, 3-parameter fit
6 ±3 ±0		BESSON	09	CLEO	ℓ=e, 3-parameter fit

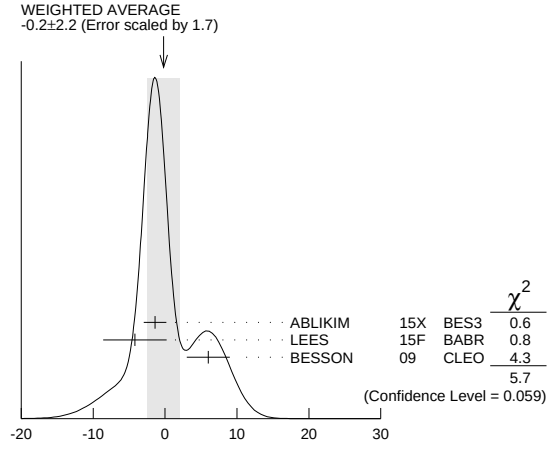

$r_2 \equiv a_1/a_0$ in $D^0 \to \pi^- \ell^+ \nu_\ell$

D^0 REFERENCES

AAIJ	17AE	PL B769 345	R. Aaij *et al.*	(LHCb Collab.)
AAIJ	17AK	PRL 118 261803	R. Aaij *et al.*	(LHCb Collab.)
AAIJ	17AO	PR D95 052004	R. Aaij *et al.*	(LHCb Collab.)
Also		PR D96 099907 (errat.)	R. Aaij *et al.*	(LHCb Collab.)
AAIJ	17BG	PRL 119 181805	R. Aaij *et al.*	(LHCb Collab.)
AAIJ	17M	PL B767 177	R. Aaij *et al.*	(LHCb Collab.)
ABLIKIM	17A	PL B765 231	M. Ablikim *et al.*	(BES III Collab.)
ABLIKIM	17O	PR D95 072010	M. Ablikim *et al.*	(BES III Collab.)
DARGENT	17	JHEP 1705 143	P. dArgent *et al.*	(HEID, BRIS)
DASH	17	PRL 119 171801	N. Dash *et al.*	(BELLE Collab.)
LAI	17	PR D95 011102	Y.-T. Lai *et al.*	(BELLE Collab.)
NANUT	17	PRL 118 051801	T. Nanut *et al.*	(BELLE Collab.)
PRASANTH	17	PR D95 091101	K. Prasanth *et al.*	(BELLE Collab.)
AAIJ	16D	PRL 116 191601	R. Aaij *et al.*	(LHCb Collab.)
AAIJ	16F	PRL 116 241801	R. Aaij *et al.*	(LHCb Collab.)
AAIJ	16H	PL B754 167	R. Aaij *et al.*	(LHCb Collab.)
AAIJ	16I	PL B757 558	R. Aaij *et al.*	(LHCb Collab.)
AAIJ	16N	PR D93 052018	R. Aaij *et al.*	(LHCb Collab.)
AAIJ	16V	JHEP 1604 033	R. Aaij *et al.*	(LHCb Collab.)
ABLIKIM	16D	PRL 116 082001	M. Ablikim *et al.*	(BES III Collab.)
EVANS	16	PL B757 520	T. Evans *et al.*	(OXF, BRIS, MADRA)
Also		PL B765 402 (errat.)	T. Evans *et al.*	(OXF, BRIS, MADRA)
LEES	16D	PR D93 112014	J.P. Lees *et al.*	(BABAR Collab.)
NISAR	16	PR D93 051102	N.K. Nisar *et al.*	(BELLE Collab.)
STARIC	16	PL B753 412	M. Staric *et al.*	(BELLE Collab.)
AAIJ	15A	PL B740 158	R. Aaij *et al.*	(LHCb Collab.)
AAIJ	15AA	JHEP 1504 043	R. Aaij *et al.*	(LHCb Collab.)
AAIJ	15AT	JHEP 1510 055	R. Aaij *et al.*	(LHCb Collab.)
ABLIKIM	15D	PL B744 339	M. Ablikim *et al.*	(BES III Collab.)
ABLIKIM	15F	PR D91 112015	M. Ablikim *et al.*	(BES III Collab.)
ABLIKIM	15X	PR D92 072012	M. Ablikiim *et al.*	(BES III Collab.)
LEES	15F	PR D91 052022	J.P. Lees *et al.*	(BABAR Collab.)
MALDE	15	PL B747 9	S. Malde *et al.*	(BRIS, CERN, MADRA, OXF+)
NAYAK	15	PL B740 1	M. Nayak *et al.*	(MADRA, OXF, CERN, CMU+)
AAIJ	14AK	JHEP 1407 041	R. Aaij *et al.*	(LHCb Collab.)
AAIJ	14AL	PRL 112 041801	R. Aaij *et al.*	(LHCb Collab.)
AAIJ	14B	PL B728 234	R. Aaij *et al.*	(LHCb Collab.)
AAIJ	14BC	JHEP 1410 005	R. Aaij *et al.*	(LHCb Collab.)
AAIJ	14C	PL B728 585	R. Aaij *et al.*	(LHCb Collab.)
AALTONEN	14Q	PR D90 111103	T. Aaltonen *et al.*	(CDF Collab.)
ABLIKIM	14C	PL B734 227	M. Ablikim *et al.*	(BES III Collab.)
BONVICINI	14	PR D89 072002	G. Bonvicini *et al.*	(CLEO Collab.)
KO	14	PRL 112 111801	B.R. Ko *et al.*	(BELLE Collab.)
LIBBY	14	PL B731 197	J. Libby *et al.*	(CLEO Collab.)
NISAR	14	PRL 112 211601	N.K. Nisar *et al.*	(BELLE Collab.)
PENG	14	PR D89 091103	T. Peng *et al.*	(BELLE Collab.)
TOMARADZE	14	PR D89 031501	A. Tomaradze *et al.*	(NWES, WAYN)
AAIJ	13AD	PL B723 33	R. Aaij *et al.*	(LHCb Collab.)
AAIJ	13AI	PL B725 15	R. Aaij *et al.*	(LHCb Collab.)
AAIJ	13BR	PL B726 623	R. Aaij *et al.*	(LHCb Collab.)
AAIJ	13CE	PRL 111 251801	R. Aaij *et al.*	(LHCb Collab.)
AAIJ	13N	PRL 110 101802	R. Aaij *et al.*	(LHCb Collab.)
AAIJ	13V	JHEP 1306 065	R. Aaij *et al.*	(LHCb Collab.)
AALTONEN	13AE	PRL 111 231802	T. Aaltonen *et al.*	(CDF Collab.)
DOBBS	13	PRL 110 131802	S. Dobbs *et al.*	(CLEO Collab.)
LEES	13	PR D87 012004	J.P. Lees *et al.*	(BABAR Collab.)
LEES	13S	PR D88 071104	J.P. Lees *et al.*	(BABAR Collab.)
WHITE	13	PR D88 051101	E. White *et al.*	(BELLE Collab.)
AAIJ	12G	PRL 108 111602	R. Aaij *et al.*	(LHCb Collab.)
AAIJ	12K	JHEP 1204 129	R. Aaij *et al.*	(LHCb Collab.)
AALTONEN	12AD	PR D86 032007	T. Aaltonen *et al.*	(CDF Collab.)
AALTONEN	12B	PR D85 012009	T. Aaltonen *et al.*	(CDF Collab.)
AALTONEN	12O	PRL 109 111801	T. Aaltonen *et al.*	(CDF Collab.)
ARTUSO	12	PR D85 122002	M. Artuso *et al.*	(CLEO Collab.)
ASNER	12	PR D86 112001	D.M. Asner	(CLEO Collab.)
INSLER	12	PR D85 092016	J. Insler *et al.*	(CLEO Collab.)
Also		PR D94 099905 (errat.)	J. Insler *et al.*	(CLEO Collab.)
LEES	12L	PR D85 091107	J.P. Lees *et al.*	(BABAR Collab.)
LEES	12Q	PR D86 032001	J.P. Lees *et al.*	(BABAR Collab.)
PDG	12	PR D86 010001	J. Beringer *et al.*	(PDG Collab.)
KO	11	PRL 106 211801	B.R. Ko *et al.*	(BELLE Collab.)
LOWREY	11	PR D84 092005	N. Lowrey *et al.*	(CLEO Collab.)
WILLIAMS	11	PR D84 054015	M. Williams	(LOIC)
AALTONEN	10X	PR D82 091105	T. Aaltonen *et al.*	(CDF Collab.)
ANASHIN	10A	PL B686 84	V.V. Anashin *et al.*	(VEPP-4M KEDR Collab.)
ASNER	10	PR D81 052007	D.M. Asner *et al.*	(CLEO Collab.)
BHATTACHAR..	10A	PR D81 096008	B. Bhattacharya, C.-W. Chiang, J.L. Rosner	(CHIC+)
DEL-AMO-SA...	10	PR D81 111103	P. del Amo Sanchez *et al.*	(BABAR Collab.)
DEL-AMO-SA...	10D	PRL 105 081803	P. del Amo Sanchez *et al.*	(BABAR Collab.)
MENDEZ	10	PR D81 052013	H. Mendez *et al.*	(CLEO Collab.)
PETRIC	10	PR D81 091102	M. Petric *et al.*	(BELLE Collab.)
AUBERT	09AI	PR D80 071103	B. Aubert *et al.*	(BABAR Collab.)
AUBERT	09AN	PRL 103 211801	B. Aubert *et al.*	(BABAR Collab.)
BEDIAGA	09	PR D80 096006	I. Bediaga *et al.*	(CBPF, NDAM)
BESSON	09	PR D80 032005	D. Besson *et al.*	(CLEO Collab.)
Also		PR D79 052010	J.Y. Ge *et al.*	(CLEO Collab.)
LOWREY	09	PR D80 031105	N. Lowrey *et al.*	(CLEO Collab.)
RUBIN	09	PR D79 097101	P. Rubin *et al.*	(CLEO Collab.)
ZUPANC	09	PR D80 052006	A. Zupanc *et al.*	(BELLE Collab.)
AALTONEN	08E	PRL 100 121802	T. Aaltonen *et al.*	(CDF Collab.)
ABLIKIM	08L	PL B665 16	M. Ablikim *et al.*	(BES Collab.)
ARINSTEIN	08	PL B662 102	K. Arinstein *et al.*	(BELLE Collab.)
ARTUSO	08	PR D77 092003	M. Artuso *et al.*	(CLEO Collab.)
ASNER	08	PR D78 012001	D.M. Asner *et al.*	(CLEO Collab.)
AUBERT	08AL	PR D78 034023	B. Aubert *et al.*	(BABAR Collab.)
AUBERT	08AO	PR D78 051102	B. Aubert *et al.*	(BABAR Collab.)
AUBERT	08AZ	PR D78 071101	B. Aubert *et al.*	(BABAR Collab.)
AUBERT	08L	PRL 100 051802	B. Aubert *et al.*	(BABAR Collab.)
AUBERT	08M	PRL 100 061803	B. Aubert *et al.*	(BABAR Collab.)
AUBERT	08U	PR D78 011105	B. Aubert *et al.*	(BABAR Collab.)
BITENC	08	PR D77 112003	U. Bitenc *et al.*	(BELLE Collab.)
BONVICINI	08	PR D77 091106	G. Bonvicini *et al.*	(CLEO Collab.)
DOBBS	08	PR D77 112005	S. Dobbs *et al.*	(CLEO Collab.)
Also		PRL 100 251802	D. Cronin-Hennessy *et al.*	(CLEO Collab.)
GASPERO	08	PR D78 014015	M. Gaspero *et al.*	(ROMA, CINN, TELA)
HE	08	PRL 100 091801	Q. He *et al.*	(CLEO Collab.)
PDG	08	PL B667 1	C. Amsler *et al.*	(PDG Collab.)
STARIC	08	PL B670 190	M. Staric *et al.*	(BELLE Collab.)
ABLIKIM	07G	PL B658 1	M. Ablikim *et al.*	(BES Collab.)
ARTUSO	07A	PRL 99 191801	M. Artuso *et al.*	(CLEO Collab.)
AUBERT	07AB	PR D76 014018	B. Aubert *et al.*	(BABAR Collab.)
AUBERT	07BG	PR D76 052005	B. Aubert *et al.*	(BABAR Collab.)
AUBERT	07BJ	PRL 99 251801	B. Aubert *et al.*	(BABAR Collab.)
AUBERT	07T	PR D76 011102	B. Aubert *et al.*	(BABAR Collab.)
AUBERT	07W	PRL 98 211802	B. Aubert *et al.*	(BABAR Collab.)
CAWLFIELD	07	PRL 98 092002	C. Cawlfield *et al.*	(CLEO Collab.)
DOBBS	07	PR D76 112001	S. Dobbs *et al.*	(CLEO Collab.)
LINK	07A	PR D75 052003	J.M. Link *et al.*	(FNAL FOCUS Collab.)
STARIC	07	PRL 98 211803	M. Staric *et al.*	(BELLE Collab.)
ZHANG	07B	PRL 99 131803	L.M. Zhang *et al.*	(BELLE Collab.)

ABLIKIM 06O EPJ C47 31 M. Ablikim *et al.* (BES Collab.)
ABLIKIM 06U PL B643 246 M. Ablikim *et al.* (BES Collab.)
ABULENCIA 06X PR D74 031109 A. Abulencia *et al.* (CDF Collab.)
ADAM 06A PRL 97 251801 N.E. Adam *et al.* (CLEO Collab.)
AUBERT,B 06N PRL 97 221803 B. Aubert *et al.* (BABAR Collab.)
AUBERT,B 06X PR D74 091102 B. Aubert *et al.* (BABAR Collab.)
CAWLFIELD 06A PR D74 031108 C. Cawlfield *et al.* (CLEO Collab.)
HUANG 06B PR D74 112005 G.S. Huang *et al.* (CLEO Collab.)
PDG 06 JP G33 1 W.-M. Yao *et al.* (PDG Collab.)
RUBIN 06 PRL 96 081802 P. Rubin *et al.* (CLEO Collab.)
WIDHALM 06 PRL 97 061804 L. Widhalm *et al.* (BELLE Collab.)
ZHANG 06 PRL 96 151801 L.M.. Zhang *et al.* (BELLE Collab.)
ABLIKIM 05F PL B622 6 M. Ablikim *et al.* (BES Collab.)
ABLIKIM 05P PL B625 196 M. Ablikim *et al.* (BES Collab.)
ACOSTA 05C PRL 94 122001 D. Acosta *et al.* (FNAL CDF Collab.)
ASNER 05 PR D72 012001 D.M. Asner *et al.* (CLEO Collab.)
AUBERT,B 05J PR D72 052008 B. Aubert *et al.* (BABAR Collab.)
BITENC 05 PR D72 071101 U. Bitenc *et al.* (BELLE Collab.)
CAWLFIELD 05 PR D71 077101 C. Cawlfield *et al.* (CLEO Collab.)
COAN 05 PRL 95 181802 T.E. Coan *et al.* (CLEO Collab.)
CRONIN-HEN... 05 PR D72 031102 D. Cronin-Hennessy *et al.* (CLEO Collab.)
HE 05 PRL 95 121801 Q. He *et al.* (CLEO Collab.)
Also PRL 96 199903 (errat.) Q. He *et al.* (CLEO Collab.)
HUANG 05 PRL 94 011802 G.S. Huang *et al.* (CLEO Collab.)
KAYIS-TOPAK... 05 PL B626 24 A. Kayis-Topaksu *et al.* (CERN CHORUS Collab.)
LI 05A PRL 94 071801 J. Li *et al.* (BELLE Collab.)
LINK 05 PL B607 51 J.M. Link *et al.* (FNAL FOCUS Collab.)
LINK 05A PL B607 59 J.M. Link *et al.* (FNAL FOCUS Collab.)
LINK 05B PL B607 67 J.M. Link *et al.* (FNAL FOCUS Collab.)
LINK 05E PL B622 239 J.M. Link *et al.* (FNAL FOCUS Collab.)
LINK 05G PL B610 225 J.M. Link *et al.* (FNAL FOCUS Collab.)
LINK 05H PL B618 23 J.M. Link *et al.* (FNAL FOCUS Collab.)
ONENGUT 05 PL B613 105 G. Onengut *et al.* (CERN CHORUS Collab.)
TIAN 05 PRL 95 231801 X.C. Tian *et al.* (BELLE Collab.)
ABLIKIM 04C PL B597 39 M. Ablikim *et al.* (BEPC BES Collab.)
ABT 04 PL B596 173 I. Abt *et al.* (HERA B Collab.)
ASNER 04A PR D70 091101 D.M. Asner *et al.* (CLEO Collab.)
AUBERT 04Q PR D69 051101 B. Aubert *et al.* (BABAR Collab.)
AUBERT,B 04Q PR D70 091102 B. Aubert *et al.* (BABAR Collab.)
AUBERT,B 04Y PRL 93 191801 B. Aubert *et al.* (BABAR Collab.)
LINK 04B PL B586 21 J.M. Link *et al.* (FNAL FOCUS Collab.)
LINK 04D PL B586 191 J.M. Link *et al.* (FNAL FOCUS Collab.)
RUBIN 04 PRL 93 111801 P. Rubin *et al.* (CLEO Collab.)
TAJIMA 04 PRL 92 101803 O. Tajima *et al.* (BELLE Collab.)
ACOSTA 03F PR D68 091101 D. Acosta *et al.* (CDF Collab.)
AUBERT 03P PRL 91 121801 B. Aubert *et al.* (BABAR Collab.)
AUBERT 03Z PRL 91 171801 B. Aubert *et al.* (BABAR Collab.)
COAN 03 PRL 90 101801 T.E. Coan *et al.* (CLEO Collab.)
LINK 03 PL B555 167 J.M. Link *et al.* (FNAL FOCUS Collab.)
LINK 03B PL B556 7 J.M. Link *et al.* (FNAL FOCUS Collab.)
LINK 03G PL B575 190 J.M. Link *et al.* (FNAL FOCUS Collab.)
ABE 02I PRL 88 162001 K. Abe *et al.* (KEK BELLE Collab.)
CSORNA 02 PR D65 092001 S.E. Csorna *et al.* (CLEO Collab.)
LINK 02F PL B537 192 J.M. Link *et al.* (FNAL FOCUS Collab.)
MURAMATSU 02 PRL 89 251802 H. Muramatsu *et al.* (CLEO Collab.)
Also PRL 90 059901 (errat.) H. Muramatsu *et al.* (CLEO Collab.)
AITALA 01C PR D64 112003 E.M. Aitala *et al.* (FNAL E791 Collab.)
AITALA 01D PR D64 112003 E.M. Aitala *et al.* (FNAL E791 Collab.)
BONVICINI 01 PR D63 071101 G. Bonvicini *et al.* (CLEO Collab.)
BRANDENB... 01 PRL 87 071802 G. Brandenburg *et al.* (CLEO Collab.)
DYTMAN 01 PR D64 111101 S.A. Dytman *et al.* (CLEO Collab.)
KOPP 01 PR D63 092001 S. Kopp *et al.* (CLEO Collab.)
KUSHNIR... 01 PRL 86 5243 A. Kushnirenko *et al.* (FNAL SELEX Collab.)
LINK 01 PRL 86 2955 J.M. Link *et al.* (FNAL FOCUS Collab.)
BAI 00C PR D62 052001 J.Z. Bai *et al.* (BEPC BES Collab.)
GODANG 00 PRL 84 5038 R. Godang *et al.* (CLEO Collab.)
JUN 00 PRL 84 1857 S.Y. Jun *et al.* (FNAL SELEX Collab.)
LINK 00 PL B485 62 J.M. Link *et al.* (FNAL FOCUS Collab.)
LINK 00B PL B491 232 J.M. Link *et al.* (FNAL FOCUS Collab.)
Also PL B495 443 (errat.) J.M. Link *et al.* (FNAL FOCUS Collab.)
PRIPSTEIN 00 PR D61 032005 D. Pripstein *et al.* (FNAL E789 Collab.)
AITALA 99E PRL 83 32 E.M. Aitala *et al.* (FNAL E791 Collab.)
AITALA 99G PL B462 401 E.M. Aitala *et al.* (FNAL E791 Collab.)
BONVICINI 99 PRL 82 4586 G. Bonvicini *et al.* (CLEO Collab.)
AITALA 98 PR D57 13 E.M. Aitala *et al.* (FNAL E791 Collab.)
AITALA 98C PL B421 405 E.M. Aitala *et al.* (FNAL E791 Collab.)
AITALA 98D PL B423 185 E.M. Aitala *et al.* (FNAL E791 Collab.)
ARTUSO 98 PRL 80 3193 M. Artuso *et al.* (CLEO Collab.)
ASNER 98 PR D58 092001 D.M. Asner *et al.* (CLEO Collab.)
BARATE 98W PL B436 211 R. Barate *et al.* (ALEPH Collab.)
COAN 98 PRL 80 1150 T.E. Coan *et al.* (CLEO Collab.)
PDG 98 EPJ C3 1 C. Caso *et al.* (PDG Collab.)
ADAMOVICH 97 PL B408 469 M.I. Adamovich *et al.* (CERN BEATRICE Collab.)
BARATE 97C PL B403 367 R. Barate *et al.* (ALEPH Collab.)
AITALA 96C PRL 77 2384 E.M. Aitala *et al.* (FNAL E791 Collab.)
ALBRECHT 96C PL B374 249 H. Albrecht *et al.* (ARGUS Collab.)
ALEXOPOU... 96 PRL 77 2380 T. Alexopoulos *et al.* (FNAL E771 Collab.)
ASNER 96B PR D54 4211 D.M. Asner *et al.* (CLEO Collab.)
BARISH 96 PL B373 334 B.C. Barish *et al.* (CLEO Collab.)
FRABETTI 96B PL B382 312 P.L. Frabetti *et al.* (FNAL E687 Collab.)
FREYBERGER 96 PRL 76 3065 A. Freyberger *et al.* (CLEO Collab.)
Also PRL 77 2147 (erratum) A. Freyberger *et al.* (CLEO Collab.)
KUBOTA 96B PR D54 2994 Y. Kubota *et al.* (CLEO Collab.)
ADAMOVICH 95 PL B353 563 M.I. Adamovich *et al.* (CERN BEATRICE Collab.)
BARTELT 95 PR D52 4860 J.E. Bartelt *et al.* (CLEO Collab.)
BUTLER 95 PR D52 2656 F. Butler *et al.* (CLEO Collab.)
FRABETTI 95C PL B354 486 P.L. Frabetti *et al.* (FNAL E687 Collab.)
FRABETTI 95G PL B364 127 P.L. Frabetti *et al.* (FNAL E687 Collab.)
KODAMA 95 PL B345 85 K. Kodama *et al.* (FNAL E653 Collab.)
ALBRECHT 94 PL B324 249 H. Albrecht *et al.* (ARGUS Collab.)
ALBRECHT 94F PL B340 125 H. Albrecht *et al.* (ARGUS Collab.)
ALBRECHT 94I ZPHY C64 375 H. Albrecht *et al.* (ARGUS Collab.)
FRABETTI 94C PL B321 295 P.L. Frabetti *et al.* (FNAL E687 Collab.)
FRABETTI 94D PL B323 459 P.L. Frabetti *et al.* (FNAL E687 Collab.)
FRABETTI 94G PL B331 217 P.L. Frabetti *et al.* (FNAL E687 Collab.)
FRABETTI 94J PL B340 254 P.L. Frabetti *et al.* (FNAL E687 Collab.)
KODAMA 94 PL B336 605 K. Kodama *et al.* (FNAL E653 Collab.)
MISHRA 94 PR D50 9 C.S. Mishra *et al.* (FNAL E789 Collab.)
AKERIB 93 PRL 71 3070 D.S. Akerib *et al.* (CLEO Collab.)
ALBRECHT 93D PL B308 435 H. Albrecht *et al.* (ARGUS Collab.)
ANJOS 93 PR D48 56 J.C. Anjos *et al.* (FNAL E691 Collab.)
BEAN 93C PL B317 647 A. Bean *et al.* (CLEO Collab.)
FRABETTI 93I PL B315 203 P.L. Frabetti *et al.* (FNAL E687 Collab.)
KODAMA 93B PL B313 260 K. Kodama *et al.* (FNAL E653 Collab.)
PROCARIO 93B PR D48 4007 M. Procario *et al.* (CLEO Collab.)
SELEN 93 PRL 71 1973 M.A. Selen *et al.* (CLEO Collab.)
ADAMOVICH 92 PL B280 163 M.I. Adamovich *et al.* (CERN WA82 Collab.)
ALBRECHT 92P ZPHY C56 7 H. Albrecht *et al.* (ARGUS Collab.)
ANJOS 92B PR D46 1 J.C. Anjos *et al.* (FNAL E691 Collab.)
ANJOS 92C PR D46 1941 J.C. Anjos *et al.* (FNAL E691 Collab.)
BARLAG 92C ZPHY C55 383 S. Barlag *et al.* (ACCMOR Collab.)
Also ZPHY C48 29 S. Barlag *et al.* (ACCMOR Collab.)
COFFMAN 92B PR D45 2196 D.M. Coffman *et al.* (Mark III Collab.)
Also PRL 64 2615 J. Adler *et al.* (Mark III Collab.)
FRABETTI 92 PL B281 167 P.L. Frabetti *et al.* (FNAL E687 Collab.)
FRABETTI 92B PL B286 195 P.L. Frabetti *et al.* (FNAL E687 Collab.)
ALVAREZ 91B ZPHY C50 11 M.P. Alvarez *et al.* (CERN NA14/2 Collab.)
AMMAR 91 PR D44 3383 R. Ammar *et al.* (CLEO Collab.)
ANJOS 91 PR D43 635 J.C. Anjos *et al.* (FNAL-TPS Collab.)
ANJOS 91D PR D44 3371 J.C. Anjos *et al.* (FNAL-TPS Collab.)
BAI 91 PRL 66 1011 Z. Bai *et al.* (Mark III Collab.)
COFFMAN 91 PL B263 135 D.M. Coffman *et al.* (Mark III Collab.)
CRAWFORD 91B PR D44 3394 G. Crawford *et al.* (CLEO Collab.)
DECAMP 91J PL B266 218 D. Decamp *et al.* (ALEPH Collab.)
FRABETTI 91 PL B263 584 P.L. Frabetti *et al.* (FNAL E687 Collab.)
KINOSHITA 91 PR D43 2836 K. Kinoshita *et al.* (CLEO Collab.)
KODAMA 91 PRL 66 1819 K. Kodama *et al.* (FNAL E653 Collab.)
ALBRECHT 90C ZPHY C46 9 H. Albrecht *et al.* (ARGUS Collab.)
ALEXANDER 90 PRL 65 1184 J. Alexander *et al.* (CLEO Collab.)
ALVAREZ 90 ZPHY C47 539 M.P. Alvarez *et al.* (CERN NA14/2 Collab.)
ANJOS 90D PR D42 2414 J.C. Anjos *et al.* (FNAL E691 Collab.)
BARLAG 90C ZPHY C46 563 S. Barlag *et al.* (ACCMOR Collab.)
ADLER 89 PRL 62 1821 J. Adler *et al.* (Mark III Collab.)
ADLER 89C PR D40 906 J. Adler *et al.* (Mark III Collab.)
ALBRECHT 89D ZPHY C43 181 H. Albrecht *et al.* (ARGUS Collab.)
ANJOS 89F PRL 62 1587 J.C. Anjos *et al.* (FNAL E691 Collab.)
ABACHI 88 PL B205 411 S. Abachi *et al.* (HRS Collab.)
ADLER 88 PR D37 2023 J. Adler *et al.* (Mark III Collab.)
ADLER 88C PRL 60 89 J. Adler *et al.* (Mark III Collab.)
ALBRECHT 88G PL B209 380 H. Albrecht *et al.* (ARGUS Collab.)
ALBRECHT 88I PL B210 267 H. Albrecht *et al.* (ARGUS Collab.)
ANJOS 88C PRL 60 1239 J.C. Anjos *et al.* (FNAL E691 Collab.)
BORTOLETTO 88 PR D37 1719 D. Bortoletto *et al.* (CLEO Collab.)
Also PR D39 1471 (erratum) D. Bortoletto *et al.* (CLEO Collab.)
HAAS 88 PRL 60 1614 P. Haas *et al.* (CLEO Collab.)
RAAB 88 PR D37 2391 J.R. Raab *et al.* (FNAL E691 Collab.)
ADLER 87 PL B196 107 J. Adler *et al.* (Mark III Collab.)
AGUILAR-... 87E ZPHY C36 551 M. Aguilar-Benitez *et al.* (LEBC-EHS Collab.)
Also ZPHY C40 321 M. Aguilar-Benitez *et al.* (LEBC-EHS Collab.)
AGUILAR-... 87F ZPHY C36 559 M. Aguilar-Benitez *et al.* (LEBC-EHS Collab.)
Also ZPHY C38 520 (erratum) M. Aguilar-Benitez *et al.* (LEBC-EHS Collab.)
BARLAG 87B ZPHY C37 17 S. Barlag *et al.* (ACCMOR Collab.)
BECKER 87C PL B193 147 J.J. Becker *et al.* (Mark III Collab.)
Also PL B198 590 (erratum) J.J. Becker *et al.* (Mark III Collab.)
PALKA 87 PL B189 238 H. Palka *et al.* (ACCMOR Collab.)
RILES 87 PR D35 2914 K. Riles *et al.* (Mark II Collab.)
BAILEY 86 ZPHY C30 51 R. Bailey *et al.* (ACCMOR Collab.)
BEBEK 86 PRL 56 1893 C. Bebek *et al.* (CLEO Collab.)
LOUIS 86 PRL 56 1027 W.C. Louis *et al.* (PRIN, CHIC, ISU)
ALBRECHT 85B PL 158B 525 H. Albrecht *et al.* (ARGUS Collab.)
ALBRECHT 85F PL 150B 235 H. Albrecht *et al.* (ARGUS Collab.)
AUBERT 85 PL 155B 461 J.J. Aubert *et al.* (EMC Collab.)
BALTRUSAIT... 85E PRL 55 150 R.M. Baltrusaitis *et al.* (Mark III Collab.)
BENVENUTI 85 PL 158B 531 A.C. Benvenuti *et al.* (BCDMS Collab.)
SUMMERS 84 PRL 52 410 D.J. Summers *et al.* (UCSB, CARL, COLO+)
BAILEY 83B PL 132B 237 R. Bailey *et al.* (ACCMOR Collab.)
BODEK 82 PL 113B 82 A. Bodek *et al.* (ROCH, CIT, CHIC, FNAL+)
SCHINDLER 81 PR D24 78 R.H. Schindler *et al.* (Mark II Collab.)
AVERY 80 PRL 44 1309 P. Avery *et al.* (ILL, FNAL, COLU)
ABRAMS 79D PRL 43 481 G.S. Abrams *et al.* (Mark II Collab.)
VUILLEMIN 78 PRL 41 1149 V. Vuillemin *et al.* (LGW Collab.)
PERUZZI 77 PRL 39 1301 I. Peruzzi *et al.* (LGW Collab.)
PICCOLO 77 PL 70B 260 M. Piccolo *et al.* (Mark I Collab.)
MOSTELLER 48 Am.Stat.3 No.5 30 R.A. Fisher, F. Mosteller

OTHER RELATED PAPERS

RICHMAN 95 RMP 67 893 J.D. Richman, P.R. Burchat (UCSB, STAN)
ROSNER 95 CNPP 21 369 J. Rosner (CHIC)

$D^*(2007)^0$

$I(J^P) = \frac{1}{2}(1^-)$
I, *J*, *P* need confirmation.

J consistent with 1, value 0 ruled out (NGUYEN 77).

$D^*(2007)^0$ MASS

The fit includes $D^\pm$, D^0, $D_s^\pm$, $D^{*\pm}$, D^{*0}, $D_s^{*\pm}$, $D_1(2420)^0$, $D_2^*(2460)^0$, and $D_{s1}(2536)^\pm$ mass and mass difference measurements.

VALUE (MeV)	*DOCUMENT ID*	*TECN*	*COMMENT*
2006.85 ± 0.05 OUR FIT Error includes scale factor of 1.1.			
• • • We do not use the following data for averages, fits, limits, etc. • • •			
2006 ±1.5	[1] GOLDHABER 77	MRK1	e^+e^-

[1] From simultaneous fit to $D^*(2010)^+$, $D^*(2007)^0$, D^+, and D^0.

$m_{D^*(2007)^0} - m_{D^0}$

The fit includes $D^\pm$, D^0, $D_s^\pm$, $D^{*\pm}$, D^{*0}, $D_s^{*\pm}$, $D_1(2420)^0$, $D_2^*(2460)^0$, and $D_{s1}(2536)^\pm$ mass and mass difference measurements.

VALUE (MeV)	*EVTS*	*DOCUMENT ID*	*TECN*	*COMMENT*
142.016 ± 0.030 OUR FIT Error includes scale factor of 1.5.				
142.016 ± 0.030 OUR AVERAGE Error includes scale factor of 1.5.				
142.007 ± 0.015 ± 0.014	10K	[2] TOMARADZE 15	CLEO	$e^+e^- \to$ hadrons
142.2 ±0.3 ±0.2	145	ALBRECHT 95F	ARG	$e^+e^- \to$ hadrons
142.12 ±0.05 ±0.05	1176	BORTOLETTO 92B	CLE2	$e^+e^- \to$ hadrons
• • • We do not use the following data for averages, fits, limits, etc. • • •				
142.2 ±2.0		SADROZINSKI 80	CBAL	$D^{*0} \to D^0\pi^0$
142.7 ±1.7		[3] GOLDHABER 77	MRK1	e^+e^-

[2] Obtained by analyzing CLEO-c data but not authored by the CLEO Collaboration . This value comes from the average of the results for two decay modes, $D^0 \to K^-\pi^+$ and $D^0 \to K^-\pi^+\pi^-\pi^+$.

[3] From simultaneous fit to $D^*(2010)^+$, $D^*(2007)^0$, D^+, and D^0.

$D^*(2007)^0$ WIDTH

VALUE (MeV)	CL%	DOCUMENT ID		TECN	COMMENT
<2.1	90	[4] ABACHI	88B	HRS	$D^{*0} \to D^+\pi^-$

[4] Assuming $m_{D^{*0}} = 2007.2 \pm 2.1$ MeV/c^2.

$D^*(2007)^0$ DECAY MODES

$\overline{D}{}^*(2007)^0$ modes are charge conjugates of modes below.

	Mode	Fraction (Γ_i/Γ)
Γ_1	$D^0\pi^0$	(64.7±0.9) %
Γ_2	$D^0\gamma$	(35.3±0.9) %

CONSTRAINED FIT INFORMATION

An overall fit to 2 branching ratios uses 5 measurements and one constraint to determine 2 parameters. The overall fit has a $\chi^2 = 2.5$ for 4 degrees of freedom.

The following *off-diagonal* array elements are the correlation coefficients $\langle \delta x_i \delta x_j \rangle / (\delta x_i \cdot \delta x_j)$, in percent, from the fit to the branching fractions, $x_i \equiv \Gamma_i/\Gamma_{\rm total}$. The fit constrains the x_i whose labels appear in this array to sum to one.

x_2	−100
	x_1

$D^*(2007)^0$ BRANCHING RATIOS

$\Gamma(D^0\pi^0)/\Gamma(D^0\gamma)$ Γ_1/Γ_2

VALUE	EVTS	DOCUMENT ID		TECN	COMMENT
1.83±0.07 OUR FIT	Error includes scale factor of 1.1.				
1.85±0.07 OUR AVERAGE					
1.90±0.07±0.05	4.9k	ABLIKIM	15B	BES3	10.6 $e^+e^- \to$ hadrons
1.74±0.02±0.13		AUBERT,BE	05G	BABR	10.6 $e^+e^- \to$ hadrons

$\Gamma(D^0\pi^0)/\Gamma_{\rm total}$ Γ_1/Γ

VALUE	EVTS	DOCUMENT ID		TECN	COMMENT
0.647±0.009 OUR FIT					
• • • We do not use the following data for averages, fits, limits, etc. • • •					
0.655±0.008±0.005	3.2k	[5] ABLIKIM	15B	BES3	$e^+e^- \to$ hadrons
0.635±0.003±0.017	69k	[5] AUBERT,BE	05G	BABR	10.6 $e^+e^- \to$ hadrons
0.596±0.035±0.028	858	[6] ALBRECHT	95F	ARG	$e^+e^- \to$ hadrons
0.636±0.023±0.033	1097	[6] BUTLER	92	CLE2	$e^+e^- \to$ hadrons

$\Gamma(D^0\gamma)/\Gamma_{\rm total}$ Γ_2/Γ

VALUE	EVTS	DOCUMENT ID		TECN	COMMENT
0.353±0.009 OUR FIT					
0.381±0.029 OUR AVERAGE					
0.404±0.035±0.028	456	[6] ALBRECHT	95F	ARG	$e^+e^- \to$ hadrons
0.364±0.023±0.033	621	[6] BUTLER	92	CLE2	$e^+e^- \to$ hadrons
0.37 ±0.08 ±0.08		ADLER	88D	MRK3	e^+e^-
• • • We do not use the following data for averages, fits, limits, etc. • • •					
0.345±0.008±0.005	1.8k	[5] ABLIKIM	15B	BES3	$e^+e^- \to$ hadrons
0.365±0.003±0.017	68k	[5] AUBERT,BE	05G	BABR	10.6 $e^+e^- \to$ hadrons
0.47 ±0.23		LOW	87	HRS	29 GeV e^+e^-
0.53 ±0.13		BARTEL	85G	JADE	e^+e^-, hadrons
0.47 ±0.12		COLES	82	MRK2	e^+e^-
0.45 ±0.15		GOLDHABER	77	MRK1	e^+e^-

[5] Derived from the ratio $\Gamma(D^0\pi^0)$ / $\Gamma(D^0\gamma)$ assuming that the branching fractions of $D^{*0} \to D^0\pi^0$ and $D^{*0} \to D^0\gamma$ decays sum to 100%

[6] The BUTLER 92 and ALBRECHT 95F branching ratios are not independent, they have been constrained by the authors to sum to 100%.

$D^*(2007)^0$ REFERENCES

ABLIKIM	15B	PR D91 031101	M. Ablikim *et al.*	(BES III Collab.)
TOMARADZE	15	PR D91 011102	A. Tomaradze *et al.*	(NWES)
AUBERT,BE	05G	PR D72 091101	B. Aubert *et al.*	(BABAR Collab.)
ALBRECHT	95F	ZPHY C66 63	H. Albrecht *et al.*	(ARGUS Collab.)
BORTOLETTO	92B	PRL 69 2046	D. Bortoletto *et al.*	(CLEO Collab.)
BUTLER	92	PRL 69 2041	F. Butler *et al.*	(CLEO Collab.)
ABACHI	88B	PL B212 533	S. Abachi *et al.*	(ANL, IND, MICH, PURD+)
ADLER	88D	PL B208 152	J. Adler *et al.*	(Mark III Collab.)
LOW	87	PL B183 232	E.H. Low *et al.*	(HRS Collab.)
BARTEL	85G	PL 161B 197	W. Bartel *et al.*	(JADE Collab.)
COLES	82	PR D26 2190	M.W. Coles *et al.*	(LBL, SLAC)
SADROZINSKI	80	Madison Conf. 681	H.F.W. Sadrozinski *et al.*	(PRIN, CIT+)
GOLDHABER	77	PL 69B 503	G. Goldhaber *et al.*	(Mark I Collab.)
NGUYEN	77	PRL 39 262	H.K. Nguyen *et al.*	(LBL, SLAC) J

$D^*(2010)^\pm$

$I(J^P) = \frac{1}{2}(1^-)$
I, J, P need confirmation.

$D^*(2010)^\pm$ MASS

The fit includes $D^\pm$, D^0, $D_s^\pm$, $D^{*\pm}$, D^{*0}, $D_s^{*\pm}$, $D_1(2420)^0$, $D_2^*(2460)^0$, and $D_{s1}(2536)^\pm$ mass and mass difference measurements.

VALUE (MeV)	DOCUMENT ID		TECN	CHG	COMMENT
2010.26±0.05 OUR FIT					
• • • We do not use the following data for averages, fits, limits, etc. • • •					
2008 ±3	[1] GOLDHABER	77	MRK1	±	e^+e^-
2008.6 ±1.0	[2] PERUZZI	77	LGW	±	e^+e^-

[1] From simultaneous fit to $D^*(2010)^+$, $D^*(2007)^0$, D^+, and D^0; not independent of FELDMAN 77B mass difference below.
[2] PERUZZI 77 mass not independent of FELDMAN 77B mass difference below and PERUZZI 77 D^0 mass value.

$m_{D^*(2010)^+} - m_{D^+}$

The fit includes $D^\pm$, D^0, $D_s^\pm$, $D^{*\pm}$, D^{*0}, $D_s^{*\pm}$, $D_1(2420)^0$, $D_2^*(2460)^0$, and $D_{s1}(2536)^\pm$ mass and mass difference measurements.

VALUE (MeV)	EVTS	DOCUMENT ID		TECN	COMMENT
140.603 ±0.015 OUR FIT					
140.602 ±0.014 OUR AVERAGE					
140.6010±0.0068±0.0129	151k	LEES	17F	BABR	$e^+e^- \to$ hadrons
140.64 ±0.08 ±0.06	620	BORTOLETTO	92B	CLE2	$e^+e^- \to$ hadrons

$m_{D^*(2010)^+} - m_{D^0}$

The fit includes $D^\pm$, D^0, $D_s^\pm$, $D^{*\pm}$, D^{*0}, $D_s^{*\pm}$, $D_1(2420)^0$, $D_2^*(2460)^0$, and $D_{s1}(2536)^\pm$ mass and mass difference measurements.

VALUE (MeV)	EVTS	DOCUMENT ID		TECN	COMMENT
145.4257±0.0017 OUR FIT					
145.4258±0.0020 OUR AVERAGE	Error includes scale factor of 1.2.				
145.4259±0.0004±0.0017	312.8k	LEES	13X	BABR	$D^{*\pm} \to D^0\pi^\pm \to (K\pi, K3\pi)\pi^\pm$
145.412 ±0.002 ±0.012		ANASTASSOV	02	CLE2	$D^{*\pm} \to D^0\pi^\pm \to (K\pi)\pi^\pm$
145.54 ±0.08	611	[3] ADINOLFI	99	BEAT	$D^{*\pm} \to D^0\pi^\pm$
145.45 ±0.02		[3] BREITWEG	99	ZEUS	$D^{*\pm} \to D^0\pi^\pm \to (K\pi)\pi^\pm$
145.42 ±0.05		[3] BREITWEG	99	ZEUS	$D^{*\pm} \to D^0\pi^\pm \to (K^-3\pi)\pi^\pm$
145.5 ±0.15	103	[4] ADLOFF	97B	H1	$D^{*\pm} \to D^0\pi^\pm$
145.44 ±0.08	152	[4] BREITWEG	97	ZEUS	$D^{*\pm} \to D^0\pi^\pm$, $D^0 \to K^-3\pi$
145.42 ±0.11	199	[4] BREITWEG	97	ZEUS	$D^{*\pm} \to D^0\pi^\pm$, $D^0 \to K^-\pi^+$
145.4 ±0.2	48	[4] DERRICK	95	ZEUS	$D^{*\pm} \to D^0\pi^\pm$
145.39 ±0.06 ±0.03		BARLAG	92B	ACCM	π^- 230 GeV
145.5 ±0.2	115	[4] ALEXANDER	91B	OPAL	$D^{*\pm} \to D^0\pi^\pm$
145.30 ±0.06		[4] DECAMP	91J	ALEP	$D^{*\pm} \to D^0\pi^\pm$
145.40 ±0.05 ±0.10		ABACHI	88B	HRS	$D^{*\pm} \to D^0\pi^\pm$
145.46 ±0.07 ±0.03		ALBRECHT	85F	ARG	$D^{*\pm} \to D^0\pi^+$
145.5 ±0.3	28	BAILEY	83	SPEC	$D^{*\pm} \to D^0\pi^\pm$
145.5 ±0.3	60	FITCH	81	SPEC	π^- A
145.3 ±0.5	30	FELDMAN	77B	MRK1	$D^{*+} \to D^0\pi^+$
• • • We do not use the following data for averages, fits, limits, etc. • • •					
145.4256±0.0006±0.0017	138.5k	LEES	13X	BABR	$D^{*\pm} \to D^0\pi^\pm \to (K^-\pi^+)\pi^\pm$
145.4266±0.0005±0.0019	174.3k	LEES	13X	BABR	$D^{*\pm} \to D^0\pi^\pm \to (K^-2\pi^+\pi^-)\pi^\pm$
145.44 ±0.09	122	[4] BREITWEG	97B	ZEUS	$D^{*\pm} \to D^0\pi^\pm$, $D^0 \to K^-\pi^+$
145.8 ±1.5	16	AHLEN	83	HRS	$D^{*+} \to D^0\pi^+$
145.1 ±1.8	12	BAILEY	83	SPEC	$D^{*\pm} \to D^0\pi^\pm$
145.1 ±0.5	14	BAILEY	83	SPEC	$D^{*\pm} \to D^0\pi^\pm$
145.5 ±0.5	14	YELTON	82	MRK2	29 $e^+e^- \to K^-\pi^+$
~ 145.5		AVERY	80	SPEC	γA
145.2 ±0.6	2	BLIETSCHAU	79	BEBC	νp

[3] Statistical errors only.
[4] Systematic error not evaluated.

$m_{D^*(2010)^+} - m_{D^*(2007)^0}$

VALUE (MeV)	DOCUMENT ID		TECN	COMMENT
• • • We do not use the following data for averages, fits, limits, etc. • • •				
2.6±1.8	[5] PERUZZI	77	LGW	e^+e^-

[5] Not independent of FELDMAN 77B mass difference above, PERUZZI 77 D^0 mass, and GOLDHABER 77 $D^*(2007)^0$ mass.

$D^*(2010)^\pm$ WIDTH

VALUE (keV)	CL%	EVTS	DOCUMENT ID		TECN	COMMENT
83.4±1.8 OUR AVERAGE						
83.3±1.2± 1.4		312.8k	[6] LEES	13X	BABR	$D^{*\pm} \to D^0\pi^\pm \to (K\pi, K3\pi)\pi^\pm$
96 ±4 ±22			[6] ANASTASSOV	02	CLE2	$D^{*\pm} \to D^0\pi^\pm \to (K\pi)\,\pi^\pm$
• • • We do not use the following data for averages, fits, limits, etc. • • •						
83.4±1.7± 1.5		138.5k	[6] LEES	13X	BABR	$D^{*\pm} \to D^0\pi^\pm \to (K^-\pi^+)\pi^\pm$
83.2±1.5± 2.6		174.3k	[6] LEES	13X	BABR	$D^{*\pm} \to D^0\pi^\pm \to (K^-2\pi^+\pi^-)\pi^\pm$
<131	90	110	BARLAG	92B	ACCM	π^- 230 GeV

[6] Ignoring the electromagnetic contribution from $D^{*\pm} \to D^\pm\gamma$.

$D^*(2010)^\pm$ DECAY MODES

$D^*(2010)^-$ modes are charge conjugates of the modes below.

	Mode	Fraction (Γ_i/Γ)
Γ_1	$D^0\pi^+$	(67.7±0.5) %
Γ_2	$D^+\pi^0$	(30.7±0.5) %
Γ_3	$D^+\gamma$	(1.6±0.4) %

CONSTRAINED FIT INFORMATION

An overall fit to 3 branching ratios uses 6 measurements and one constraint to determine 3 parameters. The overall fit has a $\chi^2 = 0.3$ for 4 degrees of freedom.

The following *off-diagonal* array elements are the correlation coefficients $\langle \delta x_i \delta x_j \rangle / (\delta x_i \cdot \delta x_j)$, in percent, from the fit to the branching fractions, $x_i \equiv \Gamma_i/\Gamma_{total}$. The fit constrains the x_i whose labels appear in this array to sum to one.

x_2	−62	
x_3	−43	−44
	x_1	x_2

$D^*(2010)^+$ BRANCHING RATIOS

$\Gamma(D^0\pi^+)/\Gamma_{total}$ Γ_1/Γ

VALUE	DOCUMENT ID		TECN	COMMENT
0.677 ±0.005 OUR FIT				
0.677 ±0.006 OUR AVERAGE				
0.6759±0.0029±0.0064	[7,8,9] BARTELT	98	CLE2	e^+e^-
0.688 ±0.024 ±0.013	ALBRECHT	95F	ARG	$e^+e^- \to$ hadrons
0.681 ±0.010 ±0.013	[7] BUTLER	92	CLE2	$e^+e^- \to$ hadrons
• • • We do not use the following data for averages, fits, limits, etc. • • •				
0.57 ±0.04 ±0.04	ADLER	88D	MRK3	e^+e^-
0.44 ±0.10	COLES	82	MRK2	e^+e^-
0.6 ±0.15	[9] GOLDHABER	77	MRK1	e^+e^-

$\Gamma(D^+\pi^0)/\Gamma_{total}$ Γ_2/Γ

VALUE	EVTS	DOCUMENT ID		TECN	COMMENT
0.307 ±0.005 OUR FIT					
0.3073±0.0013±0.0062		[7,8,9] BARTELT	98	CLE2	e^+e^-
• • • We do not use the following data for averages, fits, limits, etc. • • •					
0.312 ±0.011 ±0.008	1404	ALBRECHT	95F	ARG	$e^+e^- \to$ hadrons
0.308 ±0.004 ±0.008	410	[7] BUTLER	92	CLE2	$e^+e^- \to$ hadrons
0.26 ±0.02 ±0.02		ADLER	88D	MRK3	e^+e^-
0.34 ±0.07		COLES	82	MRK2	e^+e^-

$\Gamma(D^+\gamma)/\Gamma_{total}$ Γ_3/Γ

VALUE	CL%	EVTS	DOCUMENT ID		TECN	COMMENT
0.016 ±0.004 OUR FIT						
0.016 ±0.005 OUR AVERAGE						
0.0168±0.0042±0.0029			[7,8] BARTELT	98	CLE2	e^+e^-
0.011 ±0.014 ±0.016		12	[7] BUTLER	92	CLE2	$e^+e^- \to$ hadrons
• • • We do not use the following data for averages, fits, limits, etc. • • •						
<0.052	90		ALBRECHT	95F	ARG	$e^+e^- \to$ hadrons
0.17 ±0.05 ±0.05			ADLER	88D	MRK3	e^+e^-
0.22 ±0.12			[10] COLES	82	MRK2	e^+e^-

[7] The branching ratios are not independent, they have been constrained by the authors to sum to 100%.
[8] Systematic error includes theoretical error on the prediction of the ratio of hadronic modes.
[9] Assuming that isospin is conserved in the decay.
[10] Not independent of $\Gamma(D^0\pi^+)/\Gamma_{total}$ and $\Gamma(D^+\pi^0)/\Gamma_{total}$ measurement.

$D^*(2010)^\pm$ REFERENCES

LEES	17F	PRL 119 202003	J.P. Lees *et al.*	(BABAR Collab)
LEES	13X	PRL 111 111801	J.P. Lees *et al.*	(BABAR Collab.)
Also		PR D88 052003	J.P. Lees *et al.*	(BABAR Collab.)
Also		PR D88 079902 (errat.)	J.P. Lees *et al.*	(BABAR Collab.)
ANASTASSOV	02	PR D65 032003	A. Anastassov *et al.*	(CLEO Collab.)
ADINOLFI	99	NP B547 3	M. Adinolfi *et al.*	(Beatrice Collab.)
BREITWEG	99	EPJ C6 67	J. Breitweg *et al.*	(ZEUS Collab.)
BARTELT	98	PRL 80 3919	J. Bartelt *et al.*	(CLEO Collab.)
ADLOFF	97B	ZPHY C72 593	C. Adloff *et al.*	(H1 Collab.)
BREITWEG	97	PL B401 192	J. Breitweg *et al.*	(ZEUS Collab.)
BREITWEG	97B	PL B407 402	J. Breitweg *et al.*	(ZEUS Collab.)
ALBRECHT	95F	ZPHY C66 63	H. Albrecht *et al.*	(ARGUS Collab.)
DERRICK	95	PL B349 225	M. Derrick *et al.*	(ZEUS Collab.)
BARLAG	92B	PL B278 480	S. Barlag *et al.*	(ACCMOR Collab.)
BORTOLETTO	92B	PRL 69 2046	D. Bortoletto *et al.*	(CLEO Collab.)
BUTLER	92	PRL 69 2041	F. Butler *et al.*	(CLEO Collab.)
ALEXANDER	91B	PL B262 341	G. Alexander *et al.*	(OPAL Collab.)
DECAMP	91J	PL B266 218	D. Decamp *et al.*	(ALEPH Collab.)
ABACHI	88B	PL B212 533	S. Abachi *et al.*	(ANL, IND, MICH, PURD+)
ADLER	88D	PL B208 152	J. Adler *et al.*	(Mark III Collab.)
ALBRECHT	85F	PL 150B 235	H. Albrecht *et al.*	(ARGUS Collab.)
AHLEN	83	PRL 51 1147	S.P. Ahlen *et al.*	(ANL, IND, LBL+)
BAILEY	83	PL 132B 230	R. Bailey *et al.*	(AMST, BRIS, CERN, CRAC+)
COLES	82	PR D26 2190	M.W. Coles *et al.*	(LBL, SLAC)
YELTON	82	PRL 49 430	J.M. Yelton *et al.*	(SLAC, LBL, UCB+)
FITCH	81	PRL 46 761	V.L. Fitch *et al.*	(PRIN, SACL, TORI+)
AVERY	80	PRL 44 1309	P. Avery *et al.*	(ILL, FNAL, COLU)
BLIETSCHAU	79	PL 86B 108	J. Blietschau *et al.*	(AACH3, BONN, CERN+)
FELDMAN	77B	PRL 38 1313	G.J. Feldman *et al.*	(Mark I Collab.)
GOLDHABER	77	PL 69B 503	G. Goldhaber *et al.*	(Mark I Collab.)
PERUZZI	77	PRL 39 1301	I. Peruzzi *et al.*	(LGW Collab.)

$D_0^*(2400)^0$ $I(J^P) = \frac{1}{2}(0^+)$

$J^P = 0^+$ assignment favored (ABE 04D).

$D_0^*(2400)^0$ MASS

VALUE (MeV)	EVTS	DOCUMENT ID		TECN	COMMENT
2318±29 OUR AVERAGE Error includes scale factor of 1.7. See the ideogram below.					
2297± 8±20	3.4k	AUBERT	09AB	BABR	$B^- \to D^+\pi^-\pi^-$
2308±17±32		ABE	04D	BELL	$B^- \to D^+\pi^-\pi^-$
2407±21±35	9.8k	LINK	04A	FOCS	γ A

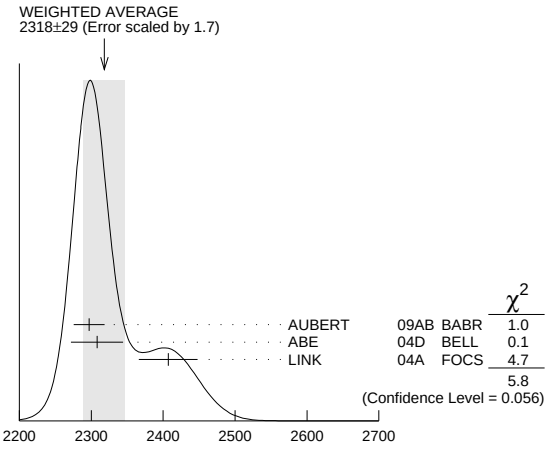

$D_0^*(2400)^0$ WIDTH

VALUE (MeV)	EVTS	DOCUMENT ID		TECN	COMMENT
267±40 OUR AVERAGE					
273±12±48	3.4k	AUBERT	09AB	BABR	$B^- \to D^+\pi^-\pi^-$
276±21±63		ABE	04D	BELL	$B^- \to D^+\pi^-\pi^-$
240±55±59	9.8k	LINK	04A	FOCS	γ A

$D_0^*(2400)^0$ DECAY MODES

	Mode	Fraction (Γ_i/Γ)
Γ_1	$D^+\pi^-$	seen

$D_0^*(2400)^0$ REFERENCES

AUBERT	09AB	PR D79 112004	B. Aubert *et al.*	(BABAR Collab.)
ABE	04D	PR D69 112002	K. Abe *et al.*	(BELLE Collab.)
LINK	04A	PL B586 11	J.M. Link *et al.*	(FOCUS Collab.)

Meson Particle Listings

$D_0^*(2400)^\pm$, $D_1(2420)^0$

$D_0^*(2400)^\pm$

$I(J^P) = \frac{1}{2}(0^+)$

OMITTED FROM SUMMARY TABLE

J, *P* need confirmation.

$D_0^*(2400)^\pm$ MASS

VALUE (MeV)	EVTS	DOCUMENT ID		TECN	COMMENT
2351± 7 OUR AVERAGE					
2360±15±30		[1] AAIJ	15X	LHCB	$B^0 \to \overline{D}^0 K^+\pi^-$
2349± 6± 4		[2] AAIJ	15Y	LHCB	$B^0 \to \overline{D}^0 \pi^+\pi^-$
2403±14±35	18.8k	LINK	04A	FOCS	γ A
• • • We do not use the following data for averages, fits, limits, etc. • • •					
2354± 7±11		[3] AAIJ	15Y	LHCB	$B^0 \to \overline{D}^0 \pi^+\pi^-$

[1] From the Dalitz plot analysis including various K^* and D^{**} mesons as well as broad structures in the $K\pi$ *S*-wave and the $D\pi$ *S*- and *P*-waves.
[2] Modeling the $\pi^+\pi^-$ *S*-wave with the Isobar formalism.
[3] Modeling the $\pi^+\pi^-$ *S*-wave with the K-matrix formalism.

$D_0^*(2400)^\pm$ WIDTH

VALUE (MeV)	EVTS	DOCUMENT ID		TECN	COMMENT
230±17 OUR AVERAGE Error includes scale factor of 1.1.					
255±26±51		[1] AAIJ	15X	LHCB	$B^0 \to \overline{D}^0 K^+\pi^-$
217±13±13		[2] AAIJ	15Y	LHCB	$B^0 \to \overline{D}^0 \pi^+\pi^-$
283±24±34	18.8k	LINK	04A	FOCS	γ A
• • • We do not use the following data for averages, fits, limits, etc. • • •					
230±15±21		[3] AAIJ	15Y	LHCB	$B^0 \to \overline{D}^0 \pi^+\pi^-$

[1] From the Dalitz plot analysis including various K^* and D^{**} mesons as well as broad structures in the $K\pi$ *S*-wave and the $D\pi$ *S*- and *P*-waves.
[2] Modeling the $\pi^+\pi^-$ *S*-wave with the Isobar formalism.
[3] Modeling the $\pi^+\pi^-$ *S*-wave with the K-matrix formalism.

$D_0^*(2400)^\pm$ DECAY MODES

	Mode	Fraction (Γ_i/Γ)
Γ_1	$D^0\pi^+$	seen

$D_0^*(2400)^\pm$ REFERENCES

AAIJ	15X	PR D92 012012	R. Aaij *et al.*	(LHCb Collab.)
AAIJ	15Y	PR D92 032002	R. Aaij *et al.*	(LHCb Collab.)
LINK	04A	PL B586 11	J.M. Link *et al.*	(FOCUS Collab.)

$D_1(2420)^0$

$I(J^P) = \frac{1}{2}(1^+)$

I needs confirmation.

$D_1(2420)^0$ MASS

The fit includes $D^\pm$, D^0, $D_s^\pm$, $D^{*\pm}$, D^{*0}, $D_s^{*\pm}$, $D_1(2420)^0$, $D_2^*(2460)^0$, and $D_{s1}(2536)^\pm$ mass and mass difference measurements.

VALUE (MeV)	EVTS	DOCUMENT ID		TECN	COMMENT
2420.8±0.5 OUR FIT Error includes scale factor of 1.3.					
2420.5±0.6 OUR AVERAGE Error includes scale factor of 1.3. See the ideogram below.					
2419.6±0.1±0.7	210k	AAIJ	13CC	LHCB	$pp \to D^{*+}\pi^- X$
$2423.1\pm1.5^{+0.4}_{-1.0}$	2.7k	[1] ABRAMOWICZ13		ZEUS	$e^\pm p \to D^{(*)+}\pi^- X$
2420.1±0.1±0.8	103k	DEL-AMO-SA...10P		BABR	$e^+e^- \to D^{*+}\pi^- X$
2426 ±3 ±1	151	ABE	05A	BELL	$B^- \to D^0\pi^+\pi^-\pi^-$
2421.4±1.5±0.9		[2] ABE	04D	BELL	$B^- \to D^{*+}\pi^-\pi^-$
$2421\ ^{+1}_{-2}$ ±2	286	AVERY	94C	CLE2	$e^+e^- \to D^{*+}\pi^- X$
2422 ±2 ±2	51	FRABETTI	94B	E687	γBe $\to D^{*+}\pi^- X$
2428 ±3 ±2	279	AVERY	90	CLEO	$e^+e^- \to D^{*+}\pi^- X$
2414 ±2 ±5	171	ALBRECHT	89H	ARG	$e^+e^- \to D^{*+}\pi^- X$
2428 ±8 ±5	171	ANJOS	89C	TPS	$\gamma N \to D^{*+}\pi^- X$
• • • We do not use the following data for averages, fits, limits, etc. • • •					
2420.5±2.1±0.9	3110±340	[3] CHEKANOV	09	ZEUS	$e^\pm p \to D^{*+}\pi^- X$
2421.7±0.7±0.6	7.5k	ABULENCIA	06A	CDF	1900 $p\overline{p} \to D^{*+}\pi^- X$
2425 ±3	235	[4] ABREU	98M	DLPH	e^+e^-

[1] From the combined fit of the $M(D^+\pi^-)$ and $M(D^{*+}\pi^-)$ distributions. and A_{D_2} fixed to the theoretical prediction of -1.
[2] Fit includes the contribution from $D_1^*(2430)^0$.
[3] Calculated using the mass difference $m(D_1^0) - m(D^{*+})_{PDG}$ reported below and $m(D^{*+})_{PDG} = 2010.27 \pm 0.17$ MeV. The 0.17 MeV uncertainty of the PDG mass value should be added to the experimental uncertainty of 0.9 MeV.
[4] No systematic error given.

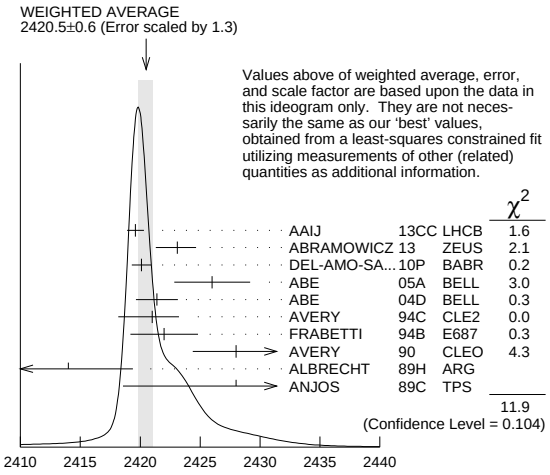

$D_1(2420)^0$ mass (MeV)

$m_{D_1^0} - m_{D^{*+}}$

The fit includes $D^\pm$, D^0, $D_s^\pm$, $D^{*\pm}$, D^{*0}, $D_s^{*\pm}$, $D_1(2420)^0$, $D_2^*(2460)^0$, and $D_{s1}(2536)^\pm$ mass and mass difference measurements.

VALUE	EVTS	DOCUMENT ID	TECN	COMMENT
410.6±0.5 OUR FIT Error includes scale factor of 1.3.				
411.5±0.8 OUR AVERAGE				
410.2±2.1±0.9	3110±340	CHEKANOV 09	ZEUS	$e^\pm p \to D^{*+}\pi^- X$
411.7±0.7±0.4	7.5k	ABULENCIA 06A	CDF	1900 $p\overline{p} \to D^{*+}\pi^- X$

$D_1(2420)^0$ WIDTH

VALUE (MeV)	EVTS	DOCUMENT ID		TECN	COMMENT
31.7± 2.5 OUR AVERAGE Error includes scale factor of 3.5. See the ideogram below.					
35.2± 0.4± 0.9	210k	AAIJ	13CC	LHCB	$pp \to D^{*+}\pi^- X$
$38.8\pm5.0^{+1.9}_{-5.4}$	2.7k	[1] ABRAMOWICZ13		ZEUS	$e^\pm p \to D^{(*)+}\pi^- X$
31.4± 0.5± 1.3	103k	DEL-AMO-SA...10P		BABR	$e^+e^- \to D^{*+}\pi^- X$
20.0± 1.7± 1.3	7.5k	ABULENCIA	06A	CDF	1900 $p\overline{p} \to D^{*+}\pi^- X$
24 ± 7 ± 8	151	ABE	05A	BELL	$B^- \to D^0\pi^+\pi^-\pi^-$
23.7± 2.7± 4.0		[2] ABE	04D	BELL	$B^- \to D^{*+}\pi^-\pi^-$
$20\ ^{+6}_{-5}$ ± 3	286	AVERY	94C	CLE2	$e^+e^- \to D^{*+}\pi^- X$
15 ± 8 ± 4	51	FRABETTI	94B	E687	γBe $\to D^{*+}\pi^- X$
$23\ ^{+8}_{-6}$ $^{+10}_{-3}$	279	AVERY	90	CLEO	$e^+e^- \to D^{*+}\pi^- X$
13 ± 6 $^{+10}_{-5}$	171	ALBRECHT	89H	ARG	$e^+e^- \to D^{*+}\pi^- X$
• • • We do not use the following data for averages, fits, limits, etc. • • •					
$53.2\pm7.2^{+3.3}_{-4.9}$	3110±340	CHEKANOV	09	ZEUS	$e^\pm p \to D^{*+}\pi^- X$
58 ±14 ±10	171	ANJOS	89C	TPS	$\gamma N \to D^{*+}\pi^- X$

[1] From the combined fit of the $M(D^+\pi^-)$ and $M(D^{*+}\pi^-)$ distributions. and A_{D_2} fixed to the theoretical prediction of -1.
[2] Fit includes the contribution from $D_1^*(2430)^0$.

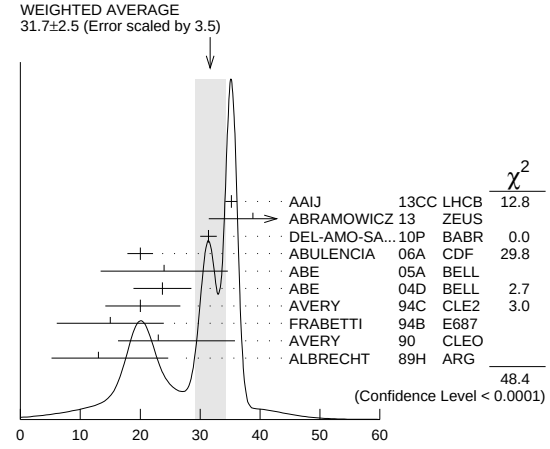

$D_1(2420)^0$ WIDTH (MeV)

$D_1(2420)^0$ DECAY MODES

$\overline{D}_1(2420)^0$ modes are charge conjugates of modes below.

	Mode	Fraction (Γ_i/Γ)
Γ_1	$D^*(2010)^+\pi^-$	seen
Γ_2	$D^0\pi^+\pi^-$	seen
Γ_3	$D^0\rho^0$	
Γ_4	$D^0 f_0(500)$	
Γ_5	$D_0^*(2400)^+\pi^-$	
Γ_6	$D^+\pi^-$	not seen
Γ_7	$D^{*0}\pi^+\pi^-$	not seen

$D_1(2420)^0$ BRANCHING RATIOS

$\Gamma(D^*(2010)^+\pi^-)/\Gamma_{total}$ Γ_1/Γ

VALUE	DOCUMENT ID		TECN	COMMENT
seen	ACKERSTAFF	97W	OPAL	$e^+e^- \to D^{*+}\pi^-X$
seen	AVERY	90	CLEO	$e^+e^- \to D^{*+}\pi^-X$
seen	ALBRECHT	89H	ARG	$e^+e^- \to D^{*+}\pi^-X$
seen	ANJOS	89C	TPS	$\gamma N \to D^{*+}\pi^-X$

$\Gamma(D^+\pi^-)/\Gamma(D^*(2010)^+\pi^-)$ Γ_6/Γ_1

VALUE	CL%	DOCUMENT ID		TECN	COMMENT
<0.24	90	AVERY	90	CLEO	$e^+e^- \to D^+\pi^-X$

$D_1(2420)^0$ POLARIZATION AMPLITUDE A_{D_1}

A polarization amplitude A_{D_1} is a parameter that depends on the initial polarization of the D_1 and is sensitive to a possible S-wave contribution to its decay. For D_1 decays the helicity angle, θ_h, distribution varies like $1 + A_{D_1}\cos^2\theta_h$, where θ_h is the angle in the D^* rest frame between the two pions emitted by the $D_1 \to D^*\pi$ and the $D^* \to D\pi$.

Unpolarized D_1 decaying purely via D-wave is predicted to give $A_{D_1} = 3$.

VALUE	EVTS	DOCUMENT ID		TECN	COMMENT
5.73±0.25 OUR AVERAGE					
$7.8\ ^{+6.7}_{-2.7}\ ^{+4.6}_{-1.8}$	2.7k	[1] ABRAMOWICZ13		ZEUS	$e^\pm p \to D^{(*)+}\pi^-X$
5.72±0.25	103k	DEL-AMO-SA...10P		BABR	$e^+e^- \to D^{*+}\pi^-X$
$5.9\ ^{+3.0}_{-1.7}\ ^{+2.4}_{-1.0}$		CHEKANOV	09	ZEUS	$e^\pm p \to D^{*+}\pi^-X$
• • • We do not use the following data for averages, fits, limits, etc. • • •					
3.30±0.48	210k	[2] AAIJ	13CC	LHCB	$pp \to D^{*+}\pi^-X$
3.8 ±0.6 ±0.8		[3] AUBERT	09Y	BABR	$B^+ \to D_1^0\ell^+\nu_\ell$
$2.74^{+1.40}_{-0.93}$		[4] AVERY	94C	CLE2	$e^+e^- \to D^{*+}\pi^-X$

[1] From the combined fit of the $M(D^+\pi^-)$ and $M(D^{*+}\pi^-)$ distributions. and A_{D_2} fixed to the theoretical prediction of -1. A pure D-wave not excluded although some S-wave mixing possible.
[2] Systematic uncertainty not estimated. Resonance parameters fixed.
[3] Assuming $\Gamma(\Upsilon(4S) \to B^+B^-)\ /\ \Gamma(\Upsilon(4S) \to B^0\overline{B}^0) = 1.065 \pm 0.026$ and equal partial widths and helicity angle distributions for charged and neutral D_1 mesons.
[4] Systematic uncertainties not estimated.

$D_1(2420)^0$ REFERENCES

AAIJ	13CC	JHEP 1309 145	R. Aaij *et al.*	(LHCb Collab.)
ABRAMOWICZ	13	NP B866 229	H. Abramowicz *et al.*	(ZEUS Collab.)
DEL-AMO-SA...	10P	PR D82 111101	P. del Amo Sanchez *et al.*	(BABAR Collab.)
AUBERT	09Y	PRL 103 051803	B. Aubert *et al.*	(BABAR Collab.)
CHEKANOV	09	EPJ C60 25	S. Chekanov *et al.*	(ZEUS Collab.)
ABULENCIA	06A	PR D73 051104	A. Abulencia *et al.*	(CDF Collab.)
ABE	05A	PRL 94 221805	K. Abe *et al.*	(BELLE Collab.)
ABE	04D	PR D69 112002	K. Abe *et al.*	(BELLE Collab.)
ABREU	98M	PL B426 231	P. Abreu *et al.*	(DELPHI Collab.)
ACKERSTAFF	97W	ZPHY C76 425	K. Ackerstaff *et al.*	(OPAL Collab.)
AVERY	94C	PL B331 236	P. Avery *et al.*	(CLEO Collab.)
FRABETTI	94B	PRL 72 324	P.L. Frabetti *et al.*	(FNAL E687 Collab.)
AVERY	90	PR D41 774	P. Avery, D. Besson	(CLEO Collab.)
ALBRECHT	89H	PL B232 398	H. Albrecht *et al.*	(ARGUS Collab.) JP
ANJOS	89C	PRL 62 1717	J.C. Anjos *et al.*	(FNAL E691 Collab.)

$D_1(2420)^\pm$

$I(J^P) = \frac{1}{2}(?^?)$
I needs confirmation.

OMITTED FROM SUMMARY TABLE
Seen in $D^*(2007)^0\pi^+$. $J^P = 0^+$ ruled out.

$D_1(2420)^\pm$ MASS

VALUE (MeV)	EVTS	DOCUMENT ID		TECN	COMMENT
2423.2±2.4 OUR AVERAGE Error includes scale factor of 1.5. See the ideogram below.					
$2421.9\pm4.7\ ^{+3.4}_{-1.2}$	759	[1] ABRAMOWICZ13		ZEUS	$e^\pm p \to D^{(*)0}\pi^+X$
2421 ±2 ±1	124	ABE	05A	BELL	$\overline{B}^0 \to D^+\pi^+\pi^-\pi^-$
2425 ±2 ±2	146	BERGFELD	94B	CLE2	$e^+e^- \to D^{*0}\pi^+X$
2443 ±7 ±5	190	ANJOS	89C	TPS	$\gamma N \to D^0\pi^+X^0$

[1] From the fit of the $M(D^0\pi^+)$ distribution. The widths of the D_1^+ and D_2^{*+} are fixed to 25 MeV and 37 MeV, and A_{D_1} and A_{D_2} are fixed to the theoretical predictions of 3 and -1, respectively.

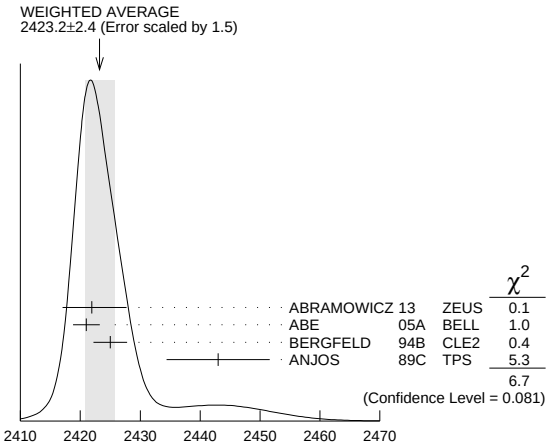

$m_{D_1^*(2420)^\pm} - m_{D_1^*(2420)^0}$

VALUE (MeV)	DOCUMENT ID		TECN	COMMENT
$\mathbf{4^{+2}_{-3}\pm3}$	BERGFELD	94B	CLE2	$e^+e^- \to$ hadrons

$D_1(2420)^\pm$ WIDTH

VALUE (MeV)	EVTS	DOCUMENT ID		TECN	COMMENT
25± 6 OUR AVERAGE					
21± 5±8	124	ABE	05A	BELL	$\overline{B}^0 \to D^+\pi^+\pi^-\pi^-$
$26^{+\ 8}_{-\ 7}\pm4$	146	BERGFELD	94B	CLE2	$e^+e^- \to D^{*0}\pi^+X$
41±19±8	190	ANJOS	89C	TPS	$\gamma N \to D^0\pi^+X^0$

$D_1(2420)^\pm$ DECAY MODES

$D_1^*(2420)^-$ modes are charge conjugates of modes below.

	Mode	Fraction (Γ_i/Γ)
Γ_1	$D^*(2007)^0\pi^+$	seen
Γ_2	$D^+\pi^+\pi^-$	seen
Γ_3	$D^+\rho^0$	
Γ_4	$D^+ f_0(500)$	
Γ_5	$D_0^*(2400)^0\pi^+$	
Γ_6	$D^0\pi^+$	not seen
Γ_7	$D^{*+}\pi^+\pi^-$	not seen

$D_1(2420)^\pm$ BRANCHING RATIOS

$\Gamma(D^*(2007)^0\pi^+)/\Gamma_{total}$ Γ_1/Γ

VALUE	DOCUMENT ID		TECN	COMMENT
seen	ANJOS	89C	TPS	$\gamma N \to D^0\pi^+X^0$

$\Gamma(D^0\pi^+)/\Gamma(D^*(2007)^0\pi^+)$ Γ_6/Γ_1

VALUE	CL%	DOCUMENT ID		TECN	COMMENT
• • • We do not use the following data for averages, fits, limits, etc. • • •					
<0.18	90	BERGFELD	94B	CLE2	$e^+e^- \to$ hadrons

$D_1(2420)^\pm$ POLARIZATION AMPLITUDE A_{D_1}

A polarization amplitude A_{D_1} is a parameter that depends on the initial polarization of the D_1 and is sensitive to a possible S-wave contribution to its decay. For D_1 decays the helicity angle, θ_h, distribution varies like $1 + A_{D_1}\cos^2\theta_h$, where θ_h is the angle in the D^* rest frame between the two pions emitted by the $D_1 \to D^*\pi$ and the $D^* \to D\pi$.

Unpolarized D_1 decaying purely via D-wave is predicted to give $A_{D_1} = 3$.

VALUE	DOCUMENT ID		TECN	COMMENT
• • • We do not use the following data for averages, fits, limits, etc. • • •				
3.8±0.6±0.8	[2] AUBERT	09Y	BABR	$B^0 \to D_1^-\ell^+\nu_\ell$

Meson Particle Listings

$D_1(2420)^{\pm}$, $D_1(2430)^0$, $D_2^*(2460)^0$

[2] Assuming $\Gamma(\Upsilon(4S) \to B^+B^-) / \Gamma(\Upsilon(4S) \to B^0\overline{B}^0) = 1.065 \pm 0.026$ and equal partial widths and helicity angle distributions for charged and neutral D_1 mesons.

$D_1(2420)^{\pm}$ REFERENCES

ABRAMOWICZ	13	NP B866 229	H. Abramowicz *et al.*	(ZEUS Collab.)
AUBERT	09Y	PRL 103 051803	B. Aubert *et al.*	(BABAR Collab.)
ABE	05A	PRL 94 221805	K. Abe *et al.*	(BELLE Collab.)
BERGFELD	94B	PL B340 194	T. Bergfeld *et al.*	(CLEO Collab.)
ANJOS	89C	PRL 62 1717	J.C. Anjos *et al.*	(FNAL E691 Collab.)

$D_1(2430)^0$

$I(J^P) = \frac{1}{2}(1^+)$

OMITTED FROM SUMMARY TABLE

$J = 1^+$ assignment favored (ABE 04D).

$D_1(2430)^0$ MASS

VALUE (MeV)	DOCUMENT ID		TECN	COMMENT
2427±26±25	ABE	04D	BELL	$B^- \to D^{*+}\pi^-\pi^-$
• • • We do not use the following data for averages, fits, limits, etc. • • •				
2477±28	[1] AUBERT	06L	BABR	$\overline{B}^0 \to D^{*+}\omega\pi^-$

[1] Systematic errors not estimated.

$D_1(2430)^0$ WIDTH

VALUE (MeV)	DOCUMENT ID		TECN	COMMENT
$384^{+107}_{-75}\pm74$	ABE	04D	BELL	$B^- \to D^{*+}\pi^-\pi^-$
• • • We do not use the following data for averages, fits, limits, etc. • • •				
266± 97	[2] AUBERT	06L	BABR	$\overline{B}^0 \to D^{*+}\omega\pi^-$

[2] Systematic errors not estimated.

$D_1(2430)^0$ DECAY MODES

	Mode	Fraction (Γ_i/Γ)
Γ_1	$D^*(2010)^+\pi^-$	seen

$D_1(2430)^0$ REFERENCES

AUBERT	06L	PR D74 012001	B. Aubert *et al.*	(BABAR Collab.)
ABE	04D	PR D69 112002	K. Abe *et al.*	(BELLE Collab.)

$D_2^*(2460)^0$

$I(J^P) = \frac{1}{2}(2^+)$

$J^P = 2^+$ assignment strongly favored (ALBRECHT 89B, ALBRECHT 89H), natural parity confirmed by the helicity analysis (DEL-AMO-SANCHEZ 10P). AAIJ 13CC confirms $J^P = 2^+$ and natural parity.

$D_2^*(2460)0$ MASS

The fit includes $D^{\pm}$, D^0, $D_s^{\pm}$, $D^{*\pm}$, D^{*0}, $D_s^{*\pm}$, $D_1(2420)^0$, $D_2^*(2460)^0$, and $D_{s1}(2536)^{\pm}$ mass and mass difference measurements.

VALUE (MeV)	EVTS		DOCUMENT ID		TECN	COMMENT
2460.7 ±0.4 OUR FIT Error includes scale factor of 3.1.						
2460.56±0.35 OUR AVERAGE Error includes scale factor of 2.6. See the ideogram below.						
2463.7 ±0.4 ±0.7	28k		[1] AAIJ	16AH	LHCB	$B^- \to D^+\pi^-\pi^-$
2460.4 ±0.4 ±1.2	82k		AAIJ	13CC	LHCB	$pp \to D^{*+}\pi^-X$
2460.4 ±0.1 ±0.1	675k		AAIJ	13CC	LHCB	$pp \to D^+\pi^-X$
2462.5 ±2.4 $^{+1.3}_{-1.1}$	2.3k		[2] ABRAMOWICZ	13	ZEUS	$e^{\pm}p \to D^{(*)+}\pi^-X$
2462.2 ±0.1 ±0.8	243k		DEL-AMO-SA...	10P	BABR	$e^+e^- \to D^+\pi^-X$
2460.4 ±1.2 ±2.2	3.4k		AUBERT	09AB	BABR	$B^- \to D^+\pi^-\pi^-$
2461.6 ±2.1 ±3.3			[3] ABE	04D	BELL	$B^- \to D^+\pi^-\pi^-$
2464.5 ±1.1 ±1.9	5.8k		[3] LINK	04A	FOCS	γ A
2465 ±3 ±3	486		AVERY	94C	CLE2	$e^+e^- \to D^+\pi^-$X
2453 ±3 ±2	128		FRABETTI	94B	E687	γBe $\to D^+\pi^-$X
2461 ±3 ±1	440		AVERY	90	CLEO	$e^+e^- \to D^{*+}\pi^-$X
2455 ±3 ±5	337		ALBRECHT	89B	ARG	$e^+e^- \to D^+\pi^-$X
2459 ±3 ±2	153		ANJOS	89C	TPS	$\gamma N \to D^+\pi^-$X
• • • We do not use the following data for averages, fits, limits, etc. • • •						
2469.1 ±3.7 $^{+1.2}_{-1.3}$	1.5k		[4] CHEKANOV	09	ZEUS	$e^{\pm}p \to D^{(*)+}\pi^-X$
2463.3 ±0.6 ±0.8	20k		ABULENCIA	06A	CDF	1900 $p\overline{p} \to D^+\pi^-X$
2461 ±6	126		[5] ABREU	98M	DLPH	e^+e^-
2466 ±7	1		ASRATYAN	95	BEBC	53,40 $\nu(\overline{\nu}) \to pX,dX$

[1] From the amplitude analysis in the model describing the $D^+\pi^-$ wave together with virtual contributions from the $D^*(2007)^0$ and B^{*0} states, and components corresponding to the $D_2^*(2460)^0$, $D_1^*(2680)^0$, $D_3^*(2760)^0$, and $D_2^*(3000)^0$ resonances.

[2] From the combined fit of the $M(D^+\pi^-)$ and $M(D^{*+}\pi^-)$ distributions. and A_{D_2} fixed to the theoretical prediction of -1.

[3] Fit includes the contribution from $D_0^*(2400)^0$.

[4] Calculated using the mass difference $m(D_2^{*0}) - m(D^{*+})_{PDG}$ reported below and $m(D^{*+})_{PDG} = 2010.27 \pm 0.17$ MeV. The 0.17 MeV uncertainty of the PDG mass value should be added to the experimental uncertainty of $^{+1.2}_{-1.3}$ MeV.

[5] No systematic error given.

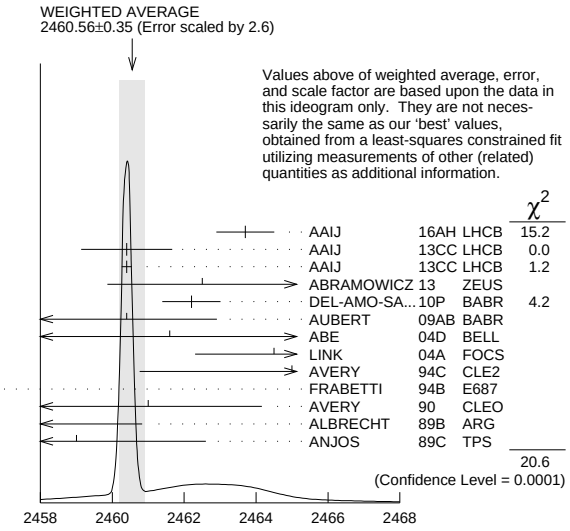

$m_{D_2^{*0}} - m_{D^+}$

The fit includes $D^{\pm}$, D^0, $D_s^{\pm}$, $D^{*\pm}$, D^{*0}, $D_s^{*\pm}$, $D_1(2420)^0$, $D_2^*(2460)^0$, and $D_{s1}(2536)^{\pm}$ mass and mass difference measurements.

VALUE (MeV)	EVTS	DOCUMENT ID		TECN	COMMENT
591.0±0.4 OUR FIT Error includes scale factor of 2.9.					
593.9±0.6±0.5	20k	ABULENCIA	06A	CDF	1900 $p\overline{p} \to D^+\pi^-X$

$m_{D_2^{*0}} - m_{D^{*+}}$

The fit includes $D^{\pm}$, D^0, $D_s^{\pm}$, $D^{*\pm}$, D^{*0}, $D_s^{*\pm}$, $D_1(2420)^0$, $D_2^*(2460)^0$, and $D_{s1}(2536)^{\pm}$ mass and mass difference measurements.

VALUE (MeV)	EVTS	DOCUMENT ID		TECN	COMMENT
450.4±0.4 OUR FIT Error includes scale factor of 2.9.					
$458.8\pm3.7^{+1.2}_{-1.3}$	1560±230	CHEKANOV	09	ZEUS	$e^{\pm}p \to D^{(*)+}\pi^-X$

$D_2^*(2460)^0$ WIDTH

VALUE (MeV)	EVTS		DOCUMENT ID		TECN	COMMENT
47.5± 1.1 OUR AVERAGE Error includes scale factor of 1.8. See the ideogram below.						
47.0± 0.8± 1.0	28k		[6] AAIJ	16AH	LHCB	$B^- \to D^+\pi^-\pi^-$
43.2± 1.2± 3.0	82k		AAIJ	13CC	LHCB	$pp \to D^{*+}\pi^-X$
45.6± 0.4± 1.1	675k		AAIJ	13CC	LHCB	$pp \to D^+\pi^-X$
46.6± 8.1± $^{5.9}_{3.8}$	2.3k		[7] ABRAMOWICZ	13	ZEUS	$e^{\pm}p \to D^{(*)+}\pi^-X$
50.5± 0.6± 0.7	243k		DEL-AMO-SA...	10P	BABR	$e^+e^- \to D^+\pi^-X$
41.8± 2.5± 2.9	3.4k		AUBERT	09AB	BABR	$B^- \to D^+\pi^-\pi^-$
49.2± 2.3± 1.3	20k		ABULENCIA	06A	CDF	1900 $p\overline{p} \to D^+\pi^-X$
45.6± 4.4± 6.7			[8] ABE	04D	BELL	$B^- \to D^+\pi^-\pi^-$
38.7± 5.3± 2.9	5.8k		[8] LINK	04A	FOCS	γ A
28 $^{+8}_{-7}$ ± 6	486		AVERY	94C	CLE2	$e^+e^- \to D^+\pi^-$X
25 ±10 ± 5	128		FRABETTI	94B	E687	γBe $\to D^+\pi^-$X
20 $^{+9}_{-12}$ $^{+9}_{-10}$	440		AVERY	90	CLEO	$e^+e^- \to D^{*+}\pi^-$X
15 $^{+13}_{-10}$ $^{+5}_{-10}$	337		ALBRECHT	89B	ARG	$e^+e^- \to D^+\pi^-$X
20 ±10 ± 5	153		ANJOS	89C	TPS	$\gamma N \to D^+\pi^-$X

[6] From the amplitude analysis in the model describing the $D^+\pi^-$ wave together with virtual contributions from the $D^*(2007)^0$ and B^{*0} states, and components corresponding to the $D_2^*(2460)^0$, $D_1^*(2680)^0$, $D_3^*(2760)^0$, and $D_2^*(3000)^0$ resonances.

[7] From the combined fit of the $M(D^+\pi^-)$ and $M(D^{*+}\pi^-)$ distributions. and A_{D_2} fixed to the theoretical prediction of -1.
[8] Fit includes the contribution from $D_0^*(2400)^0$.

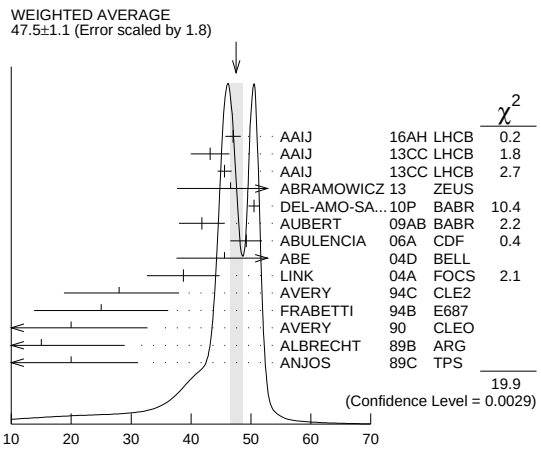

$D_2^*(2460)^0$ DECAY MODES

$\overline{D}_2^*(2460)^0$ modes are charge conjugates of modes below.

	Mode	Fraction (Γ_i/Γ)
Γ_1	$D^+\pi^-$	seen
Γ_2	$D^*(2010)^+\pi^-$	seen
Γ_3	$D^0\pi^+\pi^-$	not seen
Γ_4	$D^{*0}\pi^+\pi^-$	not seen

$D_2^*(2460)^0$ BRANCHING RATIOS

$\Gamma(D^+\pi^-)/\Gamma_{total}$ Γ_1/Γ

VALUE	EVTS	DOCUMENT ID		TECN	COMMENT
seen	3.4k	AUBERT	09AB	BABR	$B^- \to D^+\pi^-\pi^-$
seen	337	ALBRECHT	89B	ARG	$e^+e^- \to D^+\pi^-X$
seen		ANJOS	89C	TPS	$\gamma N \to D^+\pi^-X$

$\Gamma(D^*(2010)^+\pi^-)/\Gamma_{total}$ Γ_2/Γ

VALUE	DOCUMENT ID		TECN	COMMENT
seen	ACKERSTAFF	97W	OPAL	$e^+e^- \to D^{*+}\pi^-X$
seen	AVERY	90	CLEO	$e^+e^- \to D^{*+}\pi^-X$
seen	ALBRECHT	89H	ARG	$e^+e^- \to D^{*+}\pi^-X$

$\Gamma(D^+\pi^-)/\Gamma(D^*(2010)^+\pi^-)$ Γ_1/Γ_2

VALUE	EVTS	DOCUMENT ID		TECN	COMMENT
1.54±0.15 OUR AVERAGE					
1.4 ±0.3 ±0.3	2.3k	[9] ABRAMOWICZ13		ZEUS	$e^\pm p \to D^{(*)+}\pi^-X$
1.47±0.03±0.16	379k	DEL-AMO-SA...	10P	BABR	$e^+e^- \to D^{(*)+}\pi^-X$
2.8 ±0.8 $^{+0.5}_{-0.6}$	1560±230	CHEKANOV	09	ZEUS	$e^\pm p \to D^{(*)+}\pi^-X$
2.2 ±0.7 ±0.6		AVERY	94C	CLE2	$e^+e^- \to D^{*+}\pi^-X$
2.3 ±0.8		AVERY	90	CLEO	e^+e^-
3.0 ±1.1 ±1.5		ALBRECHT	89H	ARG	$e^+e^- \to D^{*+}\pi^-X$
• • • We do not use the following data for averages, fits, limits, etc. • • •					
1.9 ±0.5		ABE	04D	BELL	$B^- \to D^{(*)+}\pi^-\pi^-$

[9] From the combined fit of the $M(D^+\pi^-)$ and $M(D^{*+}\pi^-)$ distributions. and A_{D_2} fixed to the theoretical prediction of -1.

$\Gamma(D^+\pi^-)/[\Gamma(D^+\pi^-)+\Gamma(D^*(2010)^+\pi^-)]$ $\Gamma_1/(\Gamma_1+\Gamma_2)$

VALUE	EVTS	DOCUMENT ID		TECN	COMMENT
• • • We do not use the following data for averages, fits, limits, etc. • • •					
0.62±0.03±0.02	8414	[10] AUBERT	09Y	BABR	$B^+ \to D_2^{*0}\ell^+\nu_\ell$

[10] Assuming $\Gamma(\Upsilon(4S) \to B^+B^-) / \Gamma(\Upsilon(4S) \to B^0\overline{B}^0) = 1.065 \pm 0.026$ and equal partial widths for charged and neutral D_2^* mesons.

$D_2^*(2460)^0$ POLARIZATION AMPLITUDE A_{D_2}

A polarization amplitude A_{D_2} is a parameter that depends on the initial polarization of the D_2. For D_2 decays the helicity angle, θ_H, distribution varies like $1 + A_{D_2}\cos^2(\theta_H)$, where θ_H is the angle in the D^* rest frame between the two pions emitted by the $D_2 \to D^*\pi$ and $D^* \to D\pi$.

VALUE	EVTS	DOCUMENT ID		TECN	COMMENT
• • • We do not use the following data for averages, fits, limits, etc. • • •					
−1.16±0.35	2.3k	[11] ABRAMOWICZ13		ZEUS	$e^\pm p \to D^{(*)+}\pi^-X$
consistent with −1	243k	DEL-AMO-SA...	10P	BABR	$e^+e^- \to D^+\pi^-X$
$-0.74^{+0.49}_{-0.38}$		[12] AVERY	94C	CLE2	$e^+e^- \to D^{*+}\pi^-X$

[11] From the combined fit of the $M(D^+\pi^-)$ and $M(D^{*+}\pi^-)$ distributions.
[12] Systematic uncertainties not estimated.

$D_2^*(2460)^0$ REFERENCES

AAIJ	16AH	PR D94 072001	R. Aaij *et al.*	(LHCb Collab.)
AAIJ	13CC	JHEP 1309 145	R. Aaij *et al.*	(LHCb Collab.)
ABRAMOWICZ	13	NP B866 229	H. Abramowicz *et al.*	(ZEUS Collab.)
DEL-AMO-SA...	10P	PR D82 111101	P. del Amo Sanchez *et al.*	(BABAR Collab.)
AUBERT	09AB	PR D79 112004	B. Aubert *et al.*	(BABAR Collab.)
AUBERT	09Y	PRL 103 051803	B. Aubert *et al.*	(BABAR Collab.)
CHEKANOV	09	EPJ C60 25	S. Chekanov *et al.*	(ZEUS Collab.)
ABULENCIA	06A	PR D73 051104	A. Abulencia *et al.*	(CDF Collab.)
ABE	04D	PR D69 112002	K. Abe *et al.*	(BELLE Collab.)
LINK	04A	PL B586 11	J.M. Link *et al.*	(FOCUS Collab.)
ABREU	98M	PL B426 231	P. Abreu *et al.*	(DELPHI Collab.)
ACKERSTAFF	97W	ZPHY C76 425	K. Ackerstaff *et al.*	(OPAL Collab.)
ASRATYAN	95	ZPHY C68 43	A.E. Asratyan *et al.*	(BIRM, BELG, CERN+)
AVERY	94C	PL B331 236	P. Avery *et al.*	(CLEO Collab.)
FRABETTI	94B	PRL 72 324	P.L. Frabetti *et al.*	(FNAL E687 Collab.)
AVERY	90	PR D41 774	P. Avery, D. Besson	(CLEO Collab.)
ALBRECHT	89B	PL B221 422	H. Albrecht *et al.*	(ARGUS Collab.) JP
ALBRECHT	89H	PL B232 398	H. Albrecht *et al.*	(ARGUS Collab.) JP
ANJOS	89C	PRL 62 1717	J.C. Anjos *et al.*	(FNAL E691 Collab.)

$D_2^*(2460)^\pm$ $I(J^P) = \frac{1}{2}(2^+)$

$J^P = 2^+$ assignment strongly favored(ALBRECHT 89B).

$D_2^*(2460)^\pm$ MASS

VALUE (MeV)	EVTS	DOCUMENT ID		TECN	COMMENT
2465.4±1.3 OUR AVERAGE Error includes scale factor of 3.1. See the ideogram below.					
2465.6±1.8±1.3		[1] AAIJ	15X	LHCB	$B^0 \to \overline{D}^0K^+\pi^-$
2468.6±0.6±0.3		[2] AAIJ	15Y	LHCB	$B^0 \to \overline{D}^0\pi^+\pi^-$
2463.1±0.2±0.6	342k	AAIJ	13CC	LHCB	$pp \to D^0\pi^+X$
2460.6±4.4 $^{+3.6}_{-0.8}$	1371	[3] ABRAMOWICZ13		ZEUS	$e^\pm p \to D^{(*)0}\pi^+X$
2465.4±0.2±1.1	111k	[4] DEL-AMO-SA...	10P	BABR	$e^+e^- \to D^0\pi^+X$
2465.7±1.8 $^{+1.4}_{-4.8}$	2909	KUZMIN	07	BELL	e^+e^- → hadrons
2463 ±3 ±3	310	BERGFELD	94B	CLE2	$e^+e^- \to D^0\pi^+X$
2453 ±3 ±2	185	FRABETTI	94B	E687	γBe $\to D^0\pi^+X$
2469 ±4 ±6		ALBRECHT	89F	ARG	$e^+e^- \to D^0\pi^+X$
• • • We do not use the following data for averages, fits, limits, etc. • • •					
2468.1±0.6±0.5		[5] AAIJ	15Y	LHCB	$B^0 \to \overline{D}^0\pi^+\pi^-$
2467.6±1.5±0.8	3.5k	[6] LINK	04A	FOCS	γ A

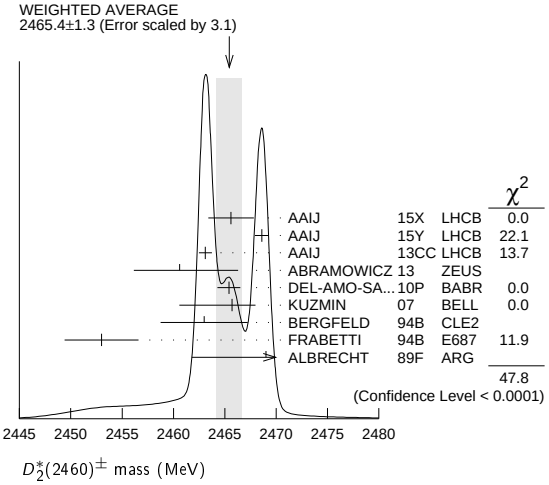

[1] From the Dalitz plot analysis including various K^* and D^{**} mesons as well as broad structures in the $K\pi$ S-wave and the $D\pi$ S- and P-waves.
[2] Modeling the $\pi^+\pi^-$ S-wave with the Isobar formalism.

Meson Particle Listings

$D_2^*(2460)^{\pm}$, $D(2550)^0$, $D_J^*(2600)$

[3] From the fit of the $M(D^0\pi^+)$ distribution. The widths of the D_1^+ and D_2^{*+} are fixed to 25 MeV and 37 MeV, and A_{D_1} and A_{D_2} are fixed to the theoretical predictions of 3 and -1, respectively.
[4] At a fixed width of 50.5 MeV.
[5] Modeling the $\pi^+\pi^-$ S-wave with the K-matrix formalism.
[6] Fit includes the contribution from $D_0^*(2400)^{\pm}$. Not independent of the corresponding mass difference measurement, $(m_{D_2^*(2460)^{\pm}}) - (m_{D_2^*(2460)^0})$.

$m_{D_2^*(2460)^{\pm}} - m_{D_2^*(2460)^0}$

VALUE (MeV)	DOCUMENT ID		TECN	COMMENT
2.4±1.7 OUR AVERAGE				
3.1±1.9±0.9	LINK	04A	FOCS	γ A
− 2 ±4 ±4	BERGFELD	94B	CLE2	$e^+e^- \to$ hadrons
0 ±4	FRABETTI	94B	E687	γBe $\to D\pi$X
14 ±5 ±8	ALBRECHT	89F	ARG	$e^+e^- \to D^0\pi^+$X

$D_2^*(2460)^{\pm}$ WIDTH

VALUE (MeV)	EVTS	DOCUMENT ID		TECN	COMMENT
46.7± 1.2 OUR AVERAGE					
46.0± 3.4±3.2		[1] AAIJ	15X	LHCB	$B^0 \to \overline{D}^0 K^+\pi^-$
47.3± 1.5±0.7		[2] AAIJ	15Y	LHCB	$B^0 \to \overline{D}^0\pi^+\pi^-$
48.6± 1.3±1.9	342k	AAIJ	13CC	LHCB	$pp \to D^0\pi^+X$
49.7± 3.8±6.4	2909	KUZMIN	07	BELL	$e^+e^- \to$ hadrons
34.1± 6.5±4.2	3.5k	[3] LINK	04A	FOCS	γ A
27 $^{+11}_{-8}$ ±5	310	BERGFELD	94B	CLE2	$e^+e^- \to D^0\pi^+$X
23 ± 9 ±5	185	FRABETTI	94B	E687	γBe $\to D^0\pi^+$X
• • • We do not use the following data for averages, fits, limits, etc. • • •					
46.0± 1.4±1.8		[4] AAIJ	15Y	LHCB	$B^0 \to \overline{D}^0\pi^+\pi^-$

[1] From the Dalitz plot analysis including various K^* and D^{**} mesons as well as broad structures in the $K\pi$ S-wave and the $D\pi$ S- and P-waves.
[2] Modeling the $\pi^+\pi^-$ S-wave with the Isobar formalism.
[3] Fit includes the contribution from $D_0^*(2400)^{\pm}$.
[4] Modeling the $\pi^+\pi^-$ S-wave with the K-matrix formalism.

$D_2^*(2460)^{\pm}$ DECAY MODES

$D_2^*(2460)^-$ modes are charge conjugates of modes below.

	Mode	Fraction (Γ_i/Γ)
Γ_1	$D^0\pi^+$	seen
Γ_2	$D^{*0}\pi^+$	seen
Γ_3	$D^+\pi^+\pi^-$	not seen
Γ_4	$D^{*+}\pi^+\pi^-$	not seen

$D_2^*(2460)^{\pm}$ BRANCHING RATIOS

$\Gamma(D^0\pi^+)/\Gamma_{\text{total}}$ Γ_1/Γ

VALUE	DOCUMENT ID		TECN	COMMENT
seen	ALBRECHT	89F	ARG	$e^+e^- \to D^0\pi^+$X

$\Gamma(D^0\pi^+)/\Gamma(D^{*0}\pi^+)$ Γ_1/Γ_2

VALUE	EVTS	DOCUMENT ID		TECN	COMMENT
1.2±0.4 OUR AVERAGE					
1.1±0.4 $^{+0.3}_{-0.2}$	1371	[1] ABRAMOWICZ13		ZEUS	$e^{\pm}p \to D^{(*)0}\pi^+X$
1.9±1.1±0.3		BERGFELD	94B	CLE2	$e^+e^- \to$ hadrons

[1] From the fit of the $M(D^0\pi^+)$ distribution. The widths of the D_1^+ and D_2^{*+} are fixed to 25 MeV and 37 MeV, and A_{D_1} and A_{D_2} are fixed to the theoretical predictions of 3 and -1, respectively.

$\Gamma(D^0\pi^+)/[\Gamma(D^0\pi^+)+\Gamma(D^{*0}\pi^+)]$ $\Gamma_1/(\Gamma_1+\Gamma_2)$

VALUE	EVTS	DOCUMENT ID		TECN	COMMENT
• • • We do not use the following data for averages, fits, limits, etc. • • •					
0.62±0.03±0.02	3361	[1] AUBERT	09Y	BABR	$\overline{B}^0 \to D_2^{*+}\ell^-\nu_\ell$

[1] Assuming $\Gamma(\Upsilon(4S) \to B^+B^-) / \Gamma(\Upsilon(4S) \to B^0\overline{B}^0) = 1.065 \pm 0.026$ and equal partial widths for charged and neutral D_2^* mesons.

$D_2^*(2460)^{\pm}$ REFERENCES

AAIJ	15X	PR D92 012012	R. Aaij *et al.*	(LHCb Collab.)
AAIJ	15Y	PR D92 032002	R. Aaij *et al.*	(LHCb Collab.)
AAIJ	13CC	JHEP 1309 145	R. Aaij *et al.*	(LHCb Collab.)
ABRAMOWICZ	13	NP B866 229	H. Abramowicz *et al.*	(ZEUS Collab.)
DEL-AMO-SA...	10P	PR D82 111101	P. del Amo Sanchez *et al.*	(BABAR Collab.)
AUBERT	09Y	PRL 103 051803	B. Aubert *et al.*	(BABAR Collab.)
KUZMIN	07	PR D76 012006	A. Kuzmin *et al.*	(BELLE Collab.)
LINK	04A	PL B586 11	J.M. Link *et al.*	(FOCUS Collab.)
BERGFELD	94B	PL B340 194	T. Bergfeld *et al.*	(CLEO Collab.)
FRABETTI	94B	PRL 72 324	P.L. Frabetti *et al.*	(FNAL E687 Collab.)
ALBRECHT	89B	PL B221 422	H. Albrecht *et al.*	(ARGUS Collab.)
ALBRECHT	89F	PL B231 208	H. Albrecht *et al.*	(ARGUS Collab.)

$D(2550)^0$ $I(J^P) = \frac{1}{2}(?^?)$

OMITTED FROM SUMMARY TABLE

Unnatural parity according to the helicity analysis of DEL-AMO-SANCHEZ 10P and AAIJ 13CC. DEL-AMO-SANCHEZ 10P suggests $J^P = 0^-$.

$D(2550)^0$ MASS

VALUE (MeV)	EVTS	DOCUMENT ID		TECN	COMMENT
2564 ±20 OUR AVERAGE		Error includes scale factor of 3.9.			
2579.5± 3.4±5.5	60k	AAIJ	13CC	LHCB	$pp \to D^{*+}\pi^-X$
2539.4± 4.5±6.8	34k	DEL-AMO-SA...10P		BABR	$e^+e^- \to D^{*+}\pi^-X$

$D(2550)^0$ WIDTH

VALUE (MeV)	EVTS	DOCUMENT ID		TECN	COMMENT
135 ±17 OUR AVERAGE					
177.5±17.8±46.0	60k	AAIJ	13CC	LHCB	$pp \to D^{*+}\pi^-X$
130 ±12 ±13	34k	DEL-AMO-SA...10P		BABR	$e^+e^- \to D^{*+}\pi^-X$

$D(2550)^0$ DECAY MODES

	Mode	Fraction (Γ_i/Γ)
Γ_1	$D^{*+}\pi^-$	seen

$D(2550)^0$ POLARIZATION AMPLITUDE A_{D_J}

A polarization amplitude A_{D_J} is a parameter that depends on the initial polarization of the D_J. For D_J decays the helicity angle, θ_H, distribution varies like $1 + A_{D_J}\cos^2(\theta_H)$, where θ_H is the angle in the D_J rest frame between the two pions emitted in the $D_J \to D^*\pi$ and $D^* \to D\pi$ decays.

VALUE	EVTS	DOCUMENT ID		TECN	COMMENT
• • • We do not use the following data for averages, fits, limits, etc. • • •					
4.2±1.3	60k	[1] AAIJ	13CC	LHCB	$pp \to D^{*+}\pi^-X$

[1] Systematic uncertainty not estimated.

$D(2550)^0$ REFERENCES

AAIJ	13CC	JHEP 1309 145	R. Aaij *et al.*	(LHCb Collab.)
DEL-AMO-SA...	10P	PR D82 111101	P. del Amo Sanchez *et al.*	(BABAR Collab.)

$D_J^*(2600)$ $I(J^P) = \frac{1}{2}(?^?)$

OMITTED FROM SUMMARY TABLE

was $D(2600)$

J^P consistent with natural parity (DEL-AMO-SANCHEZ 10P, AAIJ 13CC).

$D_J^*(2600)$ MASS

VALUE (MeV)	EVTS	DOCUMENT ID		TECN	CHG	COMMENT
2623 ±12 OUR AVERAGE		Error includes scale factor of 4.8. See the ideogram below.				
2681.1± 5.6±14.0	28k	[1] AAIJ	16AH	LHCB		$B^- \to D^+\pi^-\pi^-$
2649.2± 3.5± 3.5	51k	AAIJ	13CC	LHCB		$pp \to D^{*+}\pi^-X$
2608.7± 2.4± 2.5	26k	DEL-AMO-SA...10P		BABR	0	$e^+e^- \to D^+\pi^-X$
2621.3± 3.7± 4.2	13k	[2] DEL-AMO-SA...10P		BABR	+	$e^+e^- \to D^0\pi^+X$

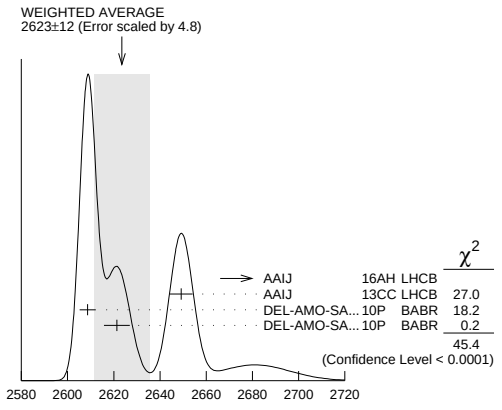

[1] From the amplitude analysis in the model describing the $D^+\pi^-$ wave together with virtual contributions from the $D^*(2007)^0$ and B^{*0} states, and components corresponding to the $D_2^*(2460)^0$, $D_1^*(2680)^0$, $D_3^*(2760)^0$, and $D_2^*(3000)^0$ resonances.

[2] At a fixed width of 93 MeV.

$D_J^*(2600)$ WIDTH

VALUE (MeV)	EVTS	DOCUMENT ID		TECN	COMMENT
139 ±31 OUR AVERAGE		Error includes scale factor of 3.2. See the ideogram below.			
186.7± 8.5±11.9	28k	[3] AAIJ	16AH	LHCB	$B^- \to D^+\pi^-\pi^-$
140.2±17.1±18.6	51k	AAIJ	13CC	LHCB	$pp \to D^{*+}\pi^- X$
93 ± 6 ±13	26k	DEL-AMO-SA...10P		BABR	$e^+e^- \to D^+\pi^- X$

[3] From the amplitude analysis in the model describing the $D^+\pi^-$ wave together with virtual contributions from the $D^*(2007)^0$ and B^{*0} states, and components corresponding to the $D_2^*(2460)^0$, $D_1^*(2680)^0$, $D_3^*(2760)^0$, and $D_2^*(3000)^0$ resonances.

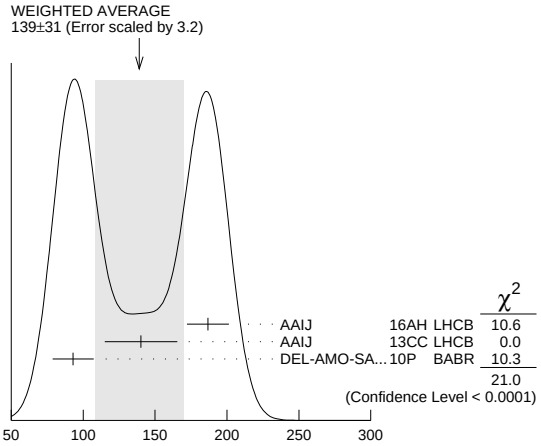

$D_J^*(2600)$ DECAY MODES

	Mode	Fraction (Γ_i/Γ)
Γ_1	$D\pi$	seen
Γ_2	$D^+\pi^-$	seen
Γ_3	$D^0\pi^\pm$	seen
Γ_4	$D^*\pi$	seen
Γ_5	$D^{*+}\pi^-$	seen

$D_J^*(2600)$ BRANCHING RATIOS

$\Gamma(D^+\pi^-)/\Gamma(D^{*+}\pi^-)$ Γ_2/Γ_5

VALUE	EVTS	DOCUMENT ID		TECN	COMMENT
0.32±0.02±0.09	76k	DEL-AMO-SA...10P		BABR	$e^+e^- \to D^{(*)+}\pi^- X$

$D_J^*(2600)$ REFERENCES

AAIJ	16AH	PR D94 072001	R. Aaij *et al.*	(LHCb Collab.)
AAIJ	13CC	JHEP 1309 145	R. Aaij *et al.*	(LHCb Collab.)
DEL-AMO-SA...	10P	PR D82 111101	P. del Amo Sanchez *et al.*	(BABAR Collab.)

$D^*(2640)^\pm$

$I(J^P) = \frac{1}{2}(?^?)$

OMITTED FROM SUMMARY TABLE

Seen in Z decays by ABREU 98M. Not seen by ABBIENDI 01N and CHEKANOV 09. Needs confirmation.

$D^*(2640)^\pm$ MASS

VALUE (MeV)	EVTS	DOCUMENT ID		TECN	COMMENT
2637±2±6	66 ± 14	ABREU	98M	DLPH	$e^+e^- \to D^{*+}\pi^+\pi^- X$

$D^*(2640)^\pm$ WIDTH

VALUE (MeV)	CL%	DOCUMENT ID		TECN	COMMENT
<15	95	ABREU	98M	DLPH	$e^+e^- \to D^{*+}\pi^+\pi^- X$

$D^*(2640)^+$ DECAY MODES

$D^*(2640)^-$ modes are charge conjugates of modes below.

	Mode	Fraction (Γ_i/Γ)
Γ_1	$D^*(2010)^+\pi^+\pi^-$	seen

$D^*(2640)^\pm$ REFERENCES

CHEKANOV	09	EPJ C60 25	S. Chekanov *et al.*	(ZEUS Collab.)
ABBIENDI	01N	EPJ C20 445	G. Abbiendi *et al.*	(OPAL Collab.)
ABREU	98M	PL B426 231	P. Abreu *et al.*	(DELPHI Collab.)

$D(2740)^0$

$I(J^P) = \frac{1}{2}(?^?)$

OMITTED FROM SUMMARY TABLE

J^P consistent with unnatural parity (AAIJ 13CC).

$D(2740)^0$ MASS

VALUE (MeV)	EVTS	DOCUMENT ID		TECN	COMMENT
2737.0±3.5±11.2	7.7k	AAIJ	13CC	LHCB	$pp \to D^{*+}\pi^- X$

$D(2740)^0$ WIDTH

VALUE (MeV)	EVTS	DOCUMENT ID		TECN	COMMENT
73.2±13.4±25.0	7.7k	AAIJ	13CC	LHCB	$pp \to D^{*+}\pi^- X$

$D(2740)^0$ DECAY MODES

	Mode	Fraction (Γ_i/Γ)
Γ_1	$D^{*+}\pi^-$	seen

$D(2740)^0$ POLARIZATION AMPLITUDE A_{D_J}

A polarization amplitude A_{D_J} is a parameter that depends on the initial polarization of the D_J. For D_J decays the helicity angle, θ_H, distribution varies like $1 + A_{D_J}\cos^2(\theta_H)$, where θ_H is the angle in the D_J rest frame between the two pions emitted in the $D_J \to D^*\pi$ and $D^* \to D\pi$ decays.

VALUE	EVTS	DOCUMENT ID		TECN	COMMENT
• • • We do not use the following data for averages, fits, limits, etc. • • •					
3.1±2.2	7.7k	[1] AAIJ	13CC	LHCB	$pp \to D^{*+}\pi^- X$

[1] Systematic uncertainty not estimated.

$D(2740)^0$ REFERENCES

AAIJ	13CC	JHEP 1309 145	R. Aaij *et al.*	(LHCb Collab.)

$D_3^*(2750)$

$I(J^P) = \frac{1}{2}(3^-)$

OMITTED FROM SUMMARY TABLE

J^P determined by AAIJ 15Y from the Dalitz plot analysis of $B^0 \to \overline{D}^0\pi^+\pi^-$ decays. J^P consistent with natural parity (AAIJ 13CC).

$D_3^*(2750)$ MASS

VALUE (MeV)	EVTS	DOCUMENT ID		TECN	CHG	COMMENT
2763.5± 3.4 OUR AVERAGE		Error includes scale factor of 2.2. See the ideogram below.				
2775.5± 4.5± 6.5	28k	[1] AAIJ	16AH	LHCB		$B^- \to D^+\pi^-\pi^-$
2798 ± 7 ± 7		[2] AAIJ	15Y	LHCB		$B^0 \to \overline{D}^0\pi^+\pi^-$
2761.1± 5.1± 6.5	14k	AAIJ	13CC	LHCB	0	$pp \to D^{*+}\pi^- X$
2760.1± 1.1± 3.7	56k	AAIJ	13CC	LHCB	0	$pp \to D^+\pi^- X$
2771.7± 1.7± 3.8	20k	AAIJ	13CC	LHCB	+	$pp \to D^0\pi^+ X$
2752.4± 1.7± 2.7	23.5k	[3] DEL-AMO-SA...	10P	BABR	0	$e^+e^- \to D^{*+}\pi^- X$
2763.3± 2.3± 2.3	11.3k	[3] DEL-AMO-SA...	10P	BABR	0	$e^+e^- \to D^+\pi^- X$
2769.7± 3.8± 1.5	5.7k	[3,4] DEL-AMO-SA...	10P	BABR	+	$e^+e^- \to D^0\pi^+ X$
• • • We do not use the following data for averages, fits, limits, etc. • • •						
2802 ±11 ±10		[5] AAIJ	15Y	LHCB		$B^0 \to \overline{D}^0\pi^+\pi^-$

[1] From the amplitude analysis in the model describing the $D^+\pi^-$ wave together with virtual contributions from the $D^*(2007)^0$ and B^{*0} states, and components corresponding to the $D_2^*(2460)^0$, $D_1^*(2680)^0$, $D_3^*(2760)^0$, and $D_2^*(3000)^0$ resonances.

[2] Modeling the $\pi^+\pi^-$ S-wave with the Isobar formalism.

[3] The states observed in the $D^*\pi$ and $D\pi$ final states are not necessarily the same.

[4] At a fixed width of 60.9 MeV.

[5] Modeling the $\pi^+\pi^-$ S-wave with the K-matrix formalism.

Meson Particle Listings

$D_3^*(2750)$, $D(3000)^0$

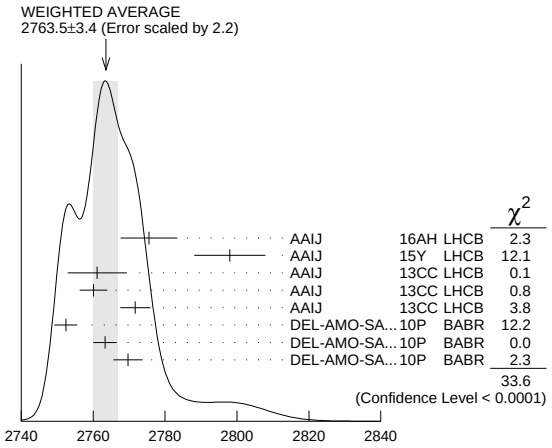

$D_3^*(2750)$ WIDTH

VALUE (MeV)	EVTS	DOCUMENT ID	TECN	CHG	COMMENT
66 ± 5 OUR AVERAGE					
95.3± 9.6±34.0	28k	[6] AAIJ	16AH LHCB		$B^- \to D^+\pi^-\pi^-$
105 ±18 ±24		[7] AAIJ	15Y LHCB		$B^0 \to \overline{D}^0\pi^+\pi^-$
74.4± 3.4±37.0	14k	AAIJ	13CC LHCB	0	$pp \to D^{*+}\pi^-X$
74.4± 3.4±19.1	56k	AAIJ	13CC LHCB	0	$pp \to D^+\pi^-X$
66.7± 6.6±10.5	20k	AAIJ	13CC LHCB	+	$pp \to D^0\pi^+X$
71 ± 6 ±11	23.5k	[8] DEL-AMO-SA..10P	BABR		$e^+e^- \to D^{*+}\pi^-X$
60.9± 5.1± 3.6	11.3k	[8] DEL-AMO-SA..10P	BABR		$e^+e^- \to D^+\pi^-X$
• • • We do not use the following data for averages, fits, limits, etc. • • •					
154 ±27 ±16		[9] AAIJ	15Y LHCB		$B^0 \to \overline{D}^0\pi^+\pi^-$

[6] From the amplitude analysis in the model describing the $D^+\pi^-$ wave together with virtual contributions from the $D^*(2007)^0$ and B^{*0} states, and components corresponding to the $D_2^*(2460)^0$, $D_1^*(2680)^0$, $D_3^*(2760)^0$, and $D_2^*(3000)^0$ resonances.
[7] Modeling the $\pi^+\pi^-$ S-wave with the Isobar formalism.
[8] The states observed in the $D^*\pi$ and $D\pi$ final states are not necessarily the same.
[9] Modeling the $\pi^+\pi^-$ S-wave with the K-matrix formalism.

$D_3^*(2750)$ DECAY MODES

	Mode	Fraction (Γ_i/Γ)
Γ_1	$D\pi$	seen
Γ_2	$D^+\pi^-$	seen
Γ_3	$D^0\pi^\pm$	seen
Γ_4	$D^*\pi$	seen
Γ_5	$D^{*+}\pi^-$	seen

$D_3^*(2750)$ BRANCHING RATIOS

$\Gamma(D^+\pi^-)/\Gamma(D^{*+}\pi^-)$ **Γ_2/Γ_5**

VALUE	EVTS	DOCUMENT ID	TECN	COMMENT
0.42±0.05±0.11	34.8k	[10] DEL-AMO-SA..10P	BABR	$e^+e^- \to D^{(*)+}\pi^-X$

[10] The states observed in the $D^*\pi$ and $D\pi$ final states are not necessarily the same.

$D_3^*(2750)$ POLARIZATION AMPLITUDE A_D

A polarization amplitude A_D is a parameter that depends on the initial polarization of the $D_3^*(2750)$. For $D_3^*(2750)$ decays the helicity angle, θ_H, distribution varies like $1 + A_D \cos(\theta_H)$, where θ_H is the angle in the D^* rest frame between the two pions emitted by the $D_3^*(2750) \to D^*\pi$ and $D^* \to D\pi$.

VALUE	EVTS	DOCUMENT ID	TECN	COMMENT
• • • We do not use the following data for averages, fits, limits, etc. • • •				
−0.33±0.28	23.5k	[11] DEL-AMO-SA..10P	BABR	$e^+e^- \to D^{*+}\pi^-X$

[11] Systematic uncertainties not estimated. The states observed in the $D^*\pi$ and $D\pi$ final states are not necessarily the same.

$D_3^*(2750)$ REFERENCES

AAIJ	16AH PR D94 072001	R. Aaij *et al.*		(LHCb Collab.)
AAIJ	15Y PR D92 032002	R. Aaij *et al.*		(LHCb Collab.) JP
AAIJ	13CC JHEP 1309 145	R. Aaij *et al.*		(LHCb Collab.)
DEL-AMO-SA...	10P PR D82 111101	P. del Amo Sanchez *et al.*		(BABAR Collab.)

$D(3000)^0$

$I(J^P) = \frac{1}{2}(?^?)$

OMITTED FROM SUMMARY TABLE

Both natural- and unnatural-parity components observed depending on the decay mode (AAIJ 13CC).

$D(3000)^0$ MASS

VALUE (MeV)	EVTS	DOCUMENT ID	TECN	COMMENT
3214 ±29 ±49	28k	[1] AAIJ	16AH LHCB	$B^- \to D^+\pi^-\pi^-$
• • • We do not use the following data for averages, fits, limits, etc. • • •				
2971.8± 8.7	9.5k	[2,3] AAIJ	13CC LHCB	$pp \to D^{*+}\pi^-X$
3008.1± 4.0	17.6k	[2,4] AAIJ	13CC LHCB	$pp \to D^+\pi^-X$

[1] From the amplitude analysis in the model describing the $D^+\pi^-$ wave together with virtual contributions from the $D^*(2007)^0$ and B^{*0} states, and components corresponding to the $D_2^*(2460)^0$, $D_1^*(2680)^0$, $D_3^*(2760)^0$, and $D_2^*(3000)^0$ resonances.
[2] Systematic uncertainty not estimated.
[3] Unnatural parity preferred.
[4] Natural parity state. A state $D(3000)^+$ is possibly seen in $D^0\pi^+$ final state.

$D(3000)^0$ WIDTH

VALUE (MeV)	EVTS	DOCUMENT ID	TECN	COMMENT
186 ±38 ±72	28k	[5] AAIJ	16AH LHCB	$B^- \to D^+\pi^-\pi^-$
• • • We do not use the following data for averages, fits, limits, etc. • • •				
188.1±44.8	9.5k	[6,7] AAIJ	13CC LHCB	$pp \to D^{*+}\pi^-X$
110.5±11.5	17.6k	[6,8] AAIJ	13CC LHCB	$pp \to D^+\pi^-X$

[5] From the amplitude analysis in the model describing the $D^+\pi^-$ wave together with virtual contributions from the $D^*(2007)^0$ and B^{*0} states, and components corresponding to the $D_2^*(2460)^0$, $D_1^*(2680)^0$, $D_3^*(2760)^0$, and $D_2^*(3000)^0$ resonances.
[6] Systematic uncertainty not estimated.
[7] Unnatural parity preferred.
[8] Natural parity state. A state $D(3000)^+$ is possibly seen in $D^0\pi^+$ final state.

$D(3000)^0$ DECAY MODES

	Mode	Fraction (Γ_i/Γ)
Γ_1	$D^{*+}\pi^-$	seen

$D(3000)^0$ POLARIZATION AMPLITUDE A_{D_J}

A polarization amplitude A_{D_J} is a parameter that depends on the initial polarization of the D_J. For D_J decays the helicity angle, θ_H, distribution varies like $1 + A_{D_J} \cos^2(\theta_H)$, where θ_H is the angle in the D_J rest frame between the two pions emitted in the $D_J \to D^*\pi$ and $D^* \to D\pi$ decays.

VALUE	EVTS	DOCUMENT ID	TECN	COMMENT
• • • We do not use the following data for averages, fits, limits, etc. • • •				
1.5±0.9	9.5k	[9] AAIJ	13CC LHCB	$pp \to D^{*+}\pi^-X$

[9] Systematic uncertainty not estimated.

$D(3000)^0$ REFERENCES

AAIJ	16AH PR D94 072001	R. Aaij *et al.*		(LHCb Collab.)
AAIJ	13CC JHEP 1309 145	R. Aaij *et al.*		(LHCb Collab.)

CHARMED, STRANGE MESONS ($C = S = \pm 1$)

$D_s^+ = c\bar{s}$, $D_s^- = \bar{c}s$, similarly for D_s^*'s

$D_s^\pm$

$I(J^P) = 0(0^-)$

The angular distributions of the decays of the ϕ and $\overline{K}^*(892)^0$ in the $\phi\pi^+$ and $K^+\overline{K}^*(892)^0$ modes strongly indicate that the spin is zero. The parity given is that expected of a $c\bar{s}$ ground state.

$D_s^\pm$ MASS

The fit includes $D^\pm$, D^0, $D_s^\pm$, $D^{*\pm}$, D^{*0}, $D_s^{*\pm}$, $D_1(2420)^0$, $D_2^*(2460)^0$, and $D_{s1}(2536)^\pm$ mass and mass difference measurements. Measurements of the $D_s^\pm$ mass with an error greater than 10 MeV are omitted from the fit and average. A number of early measurements have been omitted altogether.

VALUE (MeV)	EVTS	DOCUMENT ID		TECN	COMMENT
1968.34 ± 0.07 OUR FIT					
1969.0 ± 1.4 OUR AVERAGE		Error includes scale factor of 1.5. See the ideogram below.			
1967.0 ± 1.0 ± 1.0	54	BARLAG	90C	ACCM	π^- Cu 230 GeV
1969.3 ± 1.4 ± 1.4		ALBRECHT	88	ARG	e^+e^- 9.4–10.6 GeV
1972.7 ± 1.5 ± 1.0	21	BECKER	87B	SILI	200 GeV π, K, p
1972.4 ± 3.7 ± 3.7	27	BLAYLOCK	87	MRK3	e^+e^- 4.14 GeV
1963 ± 3 ± 3	30	DERRICK	85B	HRS	e^+e^- 29 GeV
1970 ± 5 ± 5	104	CHEN	83C	CLEO	e^+e^- 10.5 GeV
• • • We do not use the following data for averages, fits, limits, etc. • • •					
1968.3 ± 0.7 ± 0.7	290	[1] ANJOS	88	E691	Photoproduction
1980 ±15	6	USHIDA	86	EMUL	ν wideband
1973.6 ± 2.6 ± 3.0	163	ALBRECHT	85D	ARG	e^+e^- 10 GeV
1948 ±28 ±10	65	AIHARA	84D	TPC	e^+e^- 29 GeV
1975 ± 9 ±10	49	ALTHOFF	84	TASS	e^+e^- 14–25 GeV
1975 ± 4	3	BAILEY	84	ACCM	hadron$^+$ Be $\rightarrow \phi\pi^+ X$

[1] ANJOS 88 enters the fit via $m_{D_s^\pm} - m_{D^\pm}$ (see below).

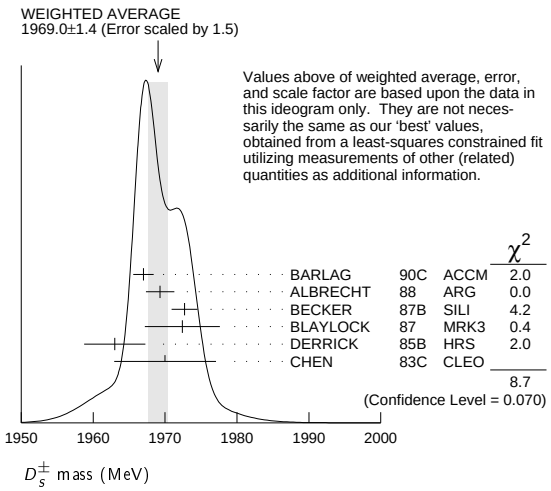

$m_{D_s^\pm} - m_{D^\pm}$

The fit includes $D^\pm$, D^0, $D_s^\pm$, $D^{*\pm}$, D^{*0}, $D_s^{*\pm}$, $D_1(2420)^0$, $D_2^*(2460)^0$, and $D_{s1}(2536)^\pm$ mass and mass difference measurements.

VALUE (MeV)	EVTS	DOCUMENT ID		TECN	COMMENT
98.69±0.05 OUR FIT					
98.69±0.05 OUR AVERAGE					
98.68±0.03±0.04		AAIJ	13V	LHCB	$D_s^+ \rightarrow K^+K^-\pi^+$
99.41±0.38±0.21		ACOSTA	03D	CDF2	$\overline{p}p$, $\sqrt{s}$= 1.96 TeV
98.4 ±0.1 ±0.3	48k	AUBERT	02G	BABR	$e^+e^- \approx \Upsilon(4S)$
99.5 ±0.6 ±0.3		BROWN	94	CLE2	$e^+e^- \approx \Upsilon(4S)$
98.5 ±1.5	555	CHEN	89	CLEO	e^+e^- 10.5 GeV
99.0 ±0.8	290	ANJOS	88	E691	Photoproduction

$D_s^\pm$ MEAN LIFE

Measurements with an error greater than 100×10^{-15} s or with fewer than 100 events have been omitted from the Listings.

VALUE (10^{-15} s)	EVTS	DOCUMENT ID		TECN	COMMENT
504 ± 4 OUR AVERAGE		Error includes scale factor of 1.2.			
506.4± 3.0± 1.7±1.7		[1] AAIJ	17AN	LHCB	pp at 7, 8 TeV
507.4± 5.5± 5.1	13.6k	LINK	05J	FOCS	$\Phi\pi^+$ and $\overline{K}^{*0}K^+$
472.5±17.2± 6.6	760	IORI	01	SELX	600 GeV Σ^-, π^-, p
518 ±14 ± 7	1662	AITALA	99	E791	π^- nucleus, 500 GeV
486.3±15.0$^{+\ 4.9}_{-\ 5.1}$	2167	[2] BONVICINI	99	CLE2	$e^+e^- \approx \Upsilon(4S)$
475 ±20 ± 7	900	FRABETTI	93F	E687	γBe, $\phi\pi^+$
500 ±60 ±30	104	FRABETTI	90	E687	γBe, $\phi\pi^+$
470 ±40 ±20	228	RAAB	88	E691	Photoproduction

[1] This AAIJ 17AN value is derived from the difference between the D_s^- and D^- widths. The 3rd uncertainty, $\pm 1.7 \times 10^{-15}$ s, arises from the uncertainty of the D^- width.
[2] BONVICINI 99 obtains 1.19 ± 0.04 for the ratio of D_s^+ to D^0 lifetimes.

D_s^+ DECAY MODES

Unless otherwise noted, the branching fractions for modes with a resonance in the final state include all the decay modes of the resonance. D_s^- modes are charge conjugates of the modes below.

	Mode		Fraction (Γ_i/Γ)		Scale factor / Confidence level
	Inclusive modes				
Γ_1	e^+ semileptonic	[a]	(6.5 ±0.4) %		
Γ_2	π^+ anything		(119.3 ±1.4) %		
Γ_3	π^- anything		(43.2 ±0.9) %		
Γ_4	π^0 anything		(123 ±7) %		
Γ_5	K^- anything		(18.7 ±0.5) %		
Γ_6	K^+ anything		(28.9 ±0.7) %		
Γ_7	K_S^0 anything		(19.0 ±1.1) %		
Γ_8	η anything	[b]	(29.9 ±2.8) %		
Γ_9	ω anything		(6.1 ±1.4) %		
Γ_{10}	η' anything	[c]	(10.3 ±1.4) %		S=1.1
Γ_{11}	$f_0(980)$ anything, $f_0 \rightarrow \pi^+\pi^-$		< 1.3	%	CL=90%
Γ_{12}	ϕ anything		(15.7 ±1.0) %		
Γ_{13}	K^+K^- anything		(15.8 ±0.7) %		
Γ_{14}	$K_S^0K^+$ anything		(5.8 ±0.5) %		
Γ_{15}	$K_S^0K^-$ anything		(1.9 ±0.4) %		
Γ_{16}	$2K_S^0$ anything		(1.70±0.32) %		
Γ_{17}	$2K^+$ anything		< 2.6	$\times 10^{-3}$	CL=90%
Γ_{18}	$2K^-$ anything		< 6	$\times 10^{-4}$	CL=90%
	Leptonic and semileptonic modes				
Γ_{19}	$e^+\nu_e$		< 8.3	$\times 10^{-5}$	CL=90%
Γ_{20}	$\mu^+\nu_\mu$		(5.50±0.23)	$\times 10^{-3}$	
Γ_{21}	$\tau^+\nu_\tau$		(5.48±0.23) %		
Γ_{22}	$K^+K^-e^+\nu_e$		—		
Γ_{23}	$\phi e^+\nu_e$	[d]	(2.39±0.16) %		S=1.3
Γ_{24}	$\phi\mu^+\nu_\mu$		(1.9 ±0.5) %		
Γ_{25}	$\eta e^+\nu_e + \eta'(958)e^+\nu_e$	[d]	(3.03±0.24) %		
Γ_{26}	$\eta e^+\nu_e$	[d]	(2.29±0.19) %		
Γ_{27}	$\eta'(958)e^+\nu_e$	[d]	(7.4 ±1.4)	$\times 10^{-3}$	
Γ_{28}	$\eta\mu^+\nu_\mu$		(2.4 ±0.5) %		
Γ_{29}	$\eta'(958)\mu^+\nu_\mu$		(1.1 ±0.5) %		
Γ_{30}	$\omega e^+\nu_e$	[e]	< 2.0	$\times 10^{-3}$	CL=90%
Γ_{31}	$K^0e^+\nu_e$		(3.9 ±0.9)	$\times 10^{-3}$	
Γ_{32}	$K^*(892)^0e^+\nu_e$	[d]	(1.8 ±0.4)	$\times 10^{-3}$	
Γ_{33}	$f_0(980)e^+\nu_e$, $f_0 \rightarrow \pi^+\pi^-$				
	Hadronic modes with a $K\overline{K}$ pair				
Γ_{34}	$K^+K_S^0$		(1.50±0.05) %		
Γ_{35}	$K^+\overline{K}^0$		(2.95±0.14) %		
Γ_{36}	$K^+K^-\pi^+$	[f]	(5.45±0.17) %		S=1.2
Γ_{37}	$\phi\pi^+$	[d,g]	(4.5 ±0.4) %		
Γ_{38}	$\phi\pi^+$, $\phi \rightarrow K^+K^-$	[g]	(2.27±0.08) %		
Γ_{39}	$K^+\overline{K}^*(892)^0$, $\overline{K}^{*0} \rightarrow K^-\pi^+$		(2.61±0.09) %		
Γ_{40}	$f_0(980)\pi^+$, $f_0 \rightarrow K^+K^-$		(1.15±0.32) %		
Γ_{41}	$f_0(1370)\pi^+$, $f_0 \rightarrow K^+K^-$		(7 ±5)	$\times 10^{-4}$	
Γ_{42}	$f_0(1710)\pi^+$, $f_0 \rightarrow K^+K^-$		(6.7 ±2.9)	$\times 10^{-4}$	
Γ_{43}	$K^+\overline{K}_0^*(1430)^0$, $\overline{K}_0^* \rightarrow K^-\pi^+$		(1.9 ±0.4)	$\times 10^{-3}$	
Γ_{44}	$K^+K_S^0\pi^0$		(1.52±0.22) %		

Γ_{45}	$2K_S^0\pi^+$		(7.7 $\pm$0.6) $\times 10^{-3}$			
Γ_{46}	$K^0\overline{K}^0\pi^+$		—			
Γ_{47}	$K^*(892)^+\overline{K}^0$	[d]	(5.4 $\pm$1.2) %			
Γ_{48}	$K^+K^-\pi^+\pi^0$		(6.3 $\pm$0.6) %			
Γ_{49}	$\phi\rho^+$	[d]	(8.4 $^{+1.9}_{-2.3}$) %			
Γ_{50}	$K_S^0K^-2\pi^+$		(1.68$\pm$0.10) %			
Γ_{51}	$K^*(892)^+\overline{K}^*(892)^0$	[d]	(7.2 $\pm$2.6) %			
Γ_{52}	$K^+K_S^0\pi^+\pi^-$		(1.00$\pm$0.08) %			
Γ_{53}	$K^+K^-2\pi^+\pi^-$		(8.7 $\pm$1.5) $\times 10^{-3}$			
Γ_{54}	$\phi2\pi^+\pi^-$	[d]	(1.21$\pm$0.16) %			
Γ_{55}	$K^+K^-\rho^0\pi^+$ non-ϕ		< 2.6	$\times 10^{-4}$		CL=90%
Γ_{56}	$\phi\rho^0\pi^+$, $\phi\to K^+K^-$		(6.5 $\pm$1.3) $\times 10^{-3}$			
Γ_{57}	$\phi a_1(1260)^+$, $\phi\to K^+K^-$, $a_1^+\to\rho^0\pi^+$		(7.5 $\pm$1.2) $\times 10^{-3}$			
Γ_{58}	$K^+K^-2\pi^+\pi^-$ nonresonant		(9 $\pm$7) $\times 10^{-4}$			
Γ_{59}	$2K_S^0\,2\pi^+\pi^-$		(9 $\pm$4) $\times 10^{-4}$			

Hadronic modes without K's

Γ_{60}	$\pi^+\pi^0$		< 3.5	$\times 10^{-4}$		CL=90%
Γ_{61}	$2\pi^+\pi^-$		(1.09$\pm$0.05) %			S=1.1
Γ_{62}	$\rho^0\pi^+$		(2.0 $\pm$1.2) $\times 10^{-4}$			
Γ_{63}	$\pi^+(\pi^+\pi^-)_{S-\text{wave}}$	[h]	(9.1 $\pm$0.4) $\times 10^{-3}$			
Γ_{64}	$f_0(980)\pi^+$, $f_0\to\pi^+\pi^-$					
Γ_{65}	$f_0(1370)\pi^+$, $f_0\to\pi^+\pi^-$					
Γ_{66}	$f_0(1500)\pi^+$, $f_0\to\pi^+\pi^-$					
Γ_{67}	$f_2(1270)\pi^+$, $f_2\to\pi^+\pi^-$		(1.10$\pm$0.20) $\times 10^{-3}$			
Γ_{68}	$\rho(1450)^0\pi^+$, $\rho^0\to\pi^+\pi^-$		(3.0 $\pm$2.0) $\times 10^{-4}$			
Γ_{69}	$\pi^+2\pi^0$		(6.5 $\pm$1.3) $\times 10^{-3}$			
Γ_{70}	$2\pi^+\pi^-\pi^0$		—			
Γ_{71}	$\eta\pi^+$	[d]	(1.70$\pm$0.09) %			S=1.1
Γ_{72}	$\omega\pi^+$	[d]	(2.4 $\pm$0.6) $\times 10^{-3}$			
Γ_{73}	$3\pi^+2\pi^-$		(8.0 $\pm$0.8) $\times 10^{-3}$			
Γ_{74}	$2\pi^+\pi^-2\pi^0$		—			
Γ_{75}	$\eta\rho^+$	[d]	(8.9 $\pm$0.8) %			
Γ_{76}	$\eta\pi^+\pi^0$		(9.2 $\pm$1.2) %			
Γ_{77}	$\omega\pi^+\pi^0$	[d]	(2.8 $\pm$0.7) %			
Γ_{78}	$3\pi^+2\pi^-\pi^0$		(4.9 $\pm$3.2) %			
Γ_{79}	$\omega2\pi^+\pi^-$	[d]	(1.6 $\pm$0.5) %			
Γ_{80}	$\eta'(958)\pi^+$	[c,d]	(3.94$\pm$0.25) %			
Γ_{81}	$3\pi^+2\pi^-2\pi^0$		—			
Γ_{82}	$\omega\eta\pi^+$	[d]	< 2.13	%		CL=90%
Γ_{83}	$\eta'(958)\rho^+$	[c,d]	(5.8 $\pm$1.5) %			
Γ_{84}	$\eta'(958)\pi^+\pi^0$		(5.6 $\pm$0.8) %			
Γ_{85}	$\eta'(958)\pi^+\pi^0$ nonresonant		< 5.1	%		CL=90%

Modes with one or three K's

Γ_{86}	$K^+\pi^0$		(6.3 $\pm$2.1) $\times 10^{-4}$			
Γ_{87}	$K_S^0\pi^+$		(1.22$\pm$0.06) $\times 10^{-3}$			
Γ_{88}	$K^+\eta$	[d]	(1.77$\pm$0.35) $\times 10^{-3}$			
Γ_{89}	$K^+\omega$	[d]	< 2.4	$\times 10^{-3}$		CL=90%
Γ_{90}	$K^+\eta'(958)$	[d]	(1.8 $\pm$0.6) $\times 10^{-3}$			
Γ_{91}	$K^+\pi^+\pi^-$		(6.6 $\pm$0.4) $\times 10^{-3}$			
Γ_{92}	$K^+\rho^0$		(2.5 $\pm$0.4) $\times 10^{-3}$			
Γ_{93}	$K^+\rho(1450)^0$, $\rho^0\to\pi^+\pi^-$		(7.0 $\pm$2.4) $\times 10^{-4}$			
Γ_{94}	$K^*(892)^0\pi^+$, $K^{*0}\to K^+\pi^-$		(1.42$\pm$0.24) $\times 10^{-3}$			
Γ_{95}	$K^*(1410)^0\pi^+$, $K^{*0}\to K^+\pi^-$		(1.24$\pm$0.29) $\times 10^{-3}$			
Γ_{96}	$K^*(1430)^0\pi^+$, $K^{*0}\to K^+\pi^-$		(5.0 $\pm$3.5) $\times 10^{-4}$			
Γ_{97}	$K^+\pi^+\pi^-$ nonresonant		(1.04$\pm$0.34) $\times 10^{-3}$			
Γ_{98}	$K^0\pi^+\pi^0$		(1.00$\pm$0.18) %			
Γ_{99}	$K_S^0\,2\pi^+\pi^-$		(3.0 $\pm$1.1) $\times 10^{-3}$			
Γ_{100}	$K^+\omega\pi^0$	[d]	< 8.2	$\times 10^{-3}$		CL=90%
Γ_{101}	$K^+\omega\pi^+\pi^-$	[d]	< 5.4	$\times 10^{-3}$		CL=90%
Γ_{102}	$K^+\omega\eta$	[d]	< 7.9	$\times 10^{-3}$		CL=90%
Γ_{103}	$2K^+K^-$		(2.18$\pm$0.21) $\times 10^{-4}$			
Γ_{104}	ϕK^+, $\phi\to K^+K^-$		(8.9 $\pm$2.0) $\times 10^{-5}$			

Doubly Cabibbo-suppressed modes

Γ_{105}	$2K^+\pi^-$		(1.27$\pm$0.13) $\times 10^{-4}$			
Γ_{106}	$K^+K^*(892)^0$, $K^{*0}\to K^+\pi^-$		(6.0 $\pm$3.4) $\times 10^{-5}$			

Baryon-antibaryon mode

Γ_{107}	$p\overline{n}$		(1.3 $\pm$0.4) $\times 10^{-3}$			

$\Delta C = 1$ weak neutral current ($C1$) modes, Lepton family number (LF), or Lepton number (L) violating modes

Γ_{108}	$\pi^+e^+e^-$		[i] < 1.3	$\times 10^{-5}$		CL=90%
Γ_{109}	$\pi^+\phi$, $\phi\to e^+e^-$		[j] (6 $^{+8}_{-4}$) $\times 10^{-6}$			
Γ_{110}	$\pi^+\mu^+\mu^-$		[i] < 4.1	$\times 10^{-7}$		CL=90%
Γ_{111}	$K^+e^+e^-$	$C1$	< 3.7	$\times 10^{-6}$		CL=90%
Γ_{112}	$K^+\mu^+\mu^-$	$C1$	< 2.1	$\times 10^{-5}$		CL=90%
Γ_{113}	$K^*(892)^+\mu^+\mu^-$	$C1$	< 1.4	$\times 10^{-3}$		CL=90%
Γ_{114}	$\pi^+e^+\mu^-$	LF	< 1.2	$\times 10^{-5}$		CL=90%
Γ_{115}	$\pi^+e^-\mu^+$	LF	< 2.0	$\times 10^{-5}$		CL=90%
Γ_{116}	$K^+e^+\mu^-$	LF	< 1.4	$\times 10^{-5}$		CL=90%
Γ_{117}	$K^+e^-\mu^+$	LF	< 9.7	$\times 10^{-6}$		CL=90%
Γ_{118}	π^-2e^+	L	< 4.1	$\times 10^{-6}$		CL=90%
Γ_{119}	$\pi^-2\mu^+$	L	< 1.2	$\times 10^{-7}$		CL=90%
Γ_{120}	$\pi^-e^+\mu^+$	L	< 8.4	$\times 10^{-6}$		CL=90%
Γ_{121}	K^-2e^+	L	< 5.2	$\times 10^{-6}$		CL=90%
Γ_{122}	$K^-2\mu^+$	L	< 1.3	$\times 10^{-5}$		CL=90%
Γ_{123}	$K^-e^+\mu^+$	L	< 6.1	$\times 10^{-6}$		CL=90%
Γ_{124}	$K^*(892)^-2\mu^+$	L	< 1.4	$\times 10^{-3}$		CL=90%

[a] This is the purely e^+ semileptonic branching fraction: the e^+ fraction from τ^+ decays has been subtracted off. The sum of our (non-τ) e^+ exclusive fractions — an $e^+\nu_e$ with an η, η', ϕ, K^0, or K^{*0} — is 5.99 $\pm$ 0.31 %.

[b] This fraction includes η from η' decays.

[c] The sum of our exclusive η' fractions — $\eta' e^+\nu_e$, $\eta'\mu^+\nu_\mu$, $\eta'\pi^+$, $\eta'\rho^+$, and $\eta' K^+$ — is 11.8 $\pm$ 1.6%.

[d] This branching fraction includes all the decay modes of the final-state resonance.

[e] A test for $u\overline{u}$ or $d\overline{d}$ content in the D_s^+. Neither Cabibbo-favored nor Cabibbo-suppressed decays can contribute, and ω–ϕ mixing is an unlikely explanation for any fraction above about 2×10^{-4}.

[f] The branching fraction for this mode may differ from the sum of the submodes that contribute to it, due to interference effects. See the relevant papers.

[g] We decouple the $D_s^+\to\phi\pi^+$ branching fraction obtained from mass projections (and used to get some of the other branching fractions) from the $D_s^+\to\phi\pi^+$, $\phi\to K^+K^-$ branching fraction obtained from the Dalitz-plot analysis of $D_s^+\to K^+K^-\pi^+$. That is, the ratio of these two branching fractions is not exactly the $\phi\to K^+K^-$ branching fraction 0.491.

[h] This is the average of a model-independent and a K-matrix parametrization of the $\pi^+\pi^-$ S-wave and is a sum over several f_0 mesons.

[i] This mode is not a useful test for a ΔC=1 weak neutral current because both quarks must change flavor in this decay.

[j] This is *not* a test for the ΔC=1 weak neutral current, but leads to the $\pi^+\ell^+\ell^-$ final state.

CONSTRAINED FIT INFORMATION

An overall fit to 13 branching ratios uses 16 measurements and one constraint to determine 10 parameters. The overall fit has a χ^2 = 4.8 for 7 degrees of freedom.

The following *off-diagonal* array elements are the correlation coefficients $\langle\delta x_i\delta x_j\rangle/(\delta x_i\cdot\delta x_j)$, in percent, from the fit to the branching fractions, $x_i \equiv \Gamma_i/\Gamma_{\text{total}}$. The fit constrains the x_i whose labels appear in this array to sum to one.

x_{36}	55							
x_{48}	15	27						
x_{50}	36	33	10					
x_{52}	24	26	9	38				
x_{61}	36	55	16	21	18			
x_{71}	16	0	−3	10	2	−1		
x_{72}	2	0	0	1	0	0	11	
x_{91}	21	19	3	13	7	10	12	1
	x_{34}	x_{36}	x_{48}	x_{50}	x_{52}	x_{61}	x_{71}	x_{72}

See the related review(s):

D_s^+ Branching Fractions

D_s^+ BRANCHING RATIOS

A number of older, now obsolete results have been omitted. They may be found in earlier editions.

Inclusive modes

$\Gamma(e^+ \text{semileptonic})/\Gamma_{total}$ Γ_1/Γ

This is the purely e^+ semileptonic branching fraction: the e^+ fraction from τ^+ decays has been subtracted off. The sum of our (non-τ) e^+ exclusive fractions — an $e^+\nu_e$ with an η, η', ϕ, K^0, or K^{*0} — is 5.99 ± 0.31 %.

VALUE (units 10^{-2})	EVTS	DOCUMENT ID		TECN	COMMENT
6.52±0.39±0.15	536 ± 29	[1] ASNER	10	CLEO	e^+e^- at 3774 MeV

[1] Using the D_s^+ and D^0 lifetimes, ASNER 10 finds that the ratio of the D_s^+ and D^0 semileptonic widths is 0.828 ± 0.051 ± 0.025.

$\Gamma(\pi^+ \text{anything})/\Gamma_{total}$ Γ_2/Γ

Events with two π^+'s count twice, etc. But π^+'s from $K_S^0 \to \pi^+\pi^-$ are not included.

VALUE (units 10^{-2})	DOCUMENT ID		TECN	COMMENT
119.3±1.2±0.7	DOBBS	09	CLEO	e^+e^- at 4170 MeV

$\Gamma(\pi^- \text{anything})/\Gamma_{total}$ Γ_3/Γ

Events with two π^-'s count twice, etc. But π^-'s from $K_S^0 \to \pi^+\pi^-$ are not included.

VALUE (units 10^{-2})	DOCUMENT ID		TECN	COMMENT
43.2±0.9±0.3	DOBBS	09	CLEO	e^+e^- at 4170 MeV

$\Gamma(\pi^0 \text{anything})/\Gamma_{total}$ Γ_4/Γ

Events with two π^0's count twice, etc. But π^0's from $K_S^0 \to 2\pi^0$ are not included.

VALUE (units 10^{-2})	DOCUMENT ID		TECN	COMMENT
123.4±3.8±5.3	DOBBS	09	CLEO	e^+e^- at 4170 MeV

$\Gamma(K^- \text{anything})/\Gamma_{total}$ Γ_5/Γ

VALUE (units 10^{-2})	DOCUMENT ID		TECN	COMMENT
18.7±0.5±0.2	DOBBS	09	CLEO	e^+e^- at 4170 MeV

$\Gamma(K^+ \text{anything})/\Gamma_{total}$ Γ_6/Γ

VALUE (units 10^{-2})	DOCUMENT ID		TECN	COMMENT
28.9±0.6±0.3	DOBBS	09	CLEO	e^+e^- at 4170 MeV

$\Gamma(K_S^0 \text{anything})/\Gamma_{total}$ Γ_7/Γ

VALUE (units 10^{-2})	DOCUMENT ID		TECN	COMMENT
19.0±1.0±0.4	DOBBS	09	CLEO	e^+e^- at 4170 MeV

$\Gamma(\eta \text{anything})/\Gamma_{total}$ Γ_8/Γ

This ratio includes η particles from η' decays.

VALUE (units 10^{-2})	EVTS	DOCUMENT ID		TECN	COMMENT
29.9±2.2±1.7		DOBBS	09	CLEO	e^+e^- at 4170 MeV
• • • We do not use the following data for averages, fits, limits, etc. • • •					
23.5±3.1±2.0	674 ± 91	HUANG	06B	CLEO	See DOBBS 09

$\Gamma(\omega \text{anything})/\Gamma_{total}$ Γ_9/Γ

VALUE (units 10^{-2})	DOCUMENT ID		TECN	COMMENT
6.1±1.4±0.3	DOBBS	09	CLEO	e^+e^- at 4170 MeV

$\Gamma(\eta' \text{anything})/\Gamma_{total}$ Γ_{10}/Γ

VALUE (units 10^{-2})	EVTS	DOCUMENT ID		TECN	COMMENT
10.3±1.4 OUR AVERAGE	Error includes scale factor of 1.1.				
8.8±1.8±0.5	68	ABLIKIM	15Z	BES3	482 pb^{-1}, 4009 MeV
11.7±1.7±0.7		DOBBS	09	CLEO	e^+e^- at 4170 MeV
• • • We do not use the following data for averages, fits, limits, etc. • • •					
8.7±1.9±0.8	68	HUANG	06B	CLEO	See DOBBS 09

$\Gamma(f_0(980) \text{anything}, f_0 \to \pi^+\pi^-)/\Gamma_{total}$ Γ_{11}/Γ

VALUE (units 10^{-2})	CL%	DOCUMENT ID		TECN	COMMENT
<1.3	90	DOBBS	09	CLEO	e^+e^- at 4170 MeV

$\Gamma(\phi \text{anything})/\Gamma_{total}$ Γ_{12}/Γ

VALUE (units 10^{-2})	EVTS	DOCUMENT ID		TECN	COMMENT
15.7±0.8±0.6		DOBBS	09	CLEO	e^+e^- at 4170 MeV
• • • We do not use the following data for averages, fits, limits, etc. • • •					
16.1±1.2±1.1	398 ± 27	HUANG	06B	CLEO	See DOBBS 09

$\Gamma(K^+K^- \text{anything})/\Gamma_{total}$ Γ_{13}/Γ

VALUE (units 10^{-2})	DOCUMENT ID		TECN	COMMENT
15.8±0.6±0.3	DOBBS	09	CLEO	e^+e^- at 4170 MeV

$\Gamma(K_S^0 K^+ \text{anything})/\Gamma_{total}$ Γ_{14}/Γ

VALUE (units 10^{-2})	DOCUMENT ID		TECN	COMMENT
5.8±0.5±0.1	DOBBS	09	CLEO	e^+e^- at 4170 MeV

$\Gamma(K_S^0 K^- \text{anything})/\Gamma_{total}$ Γ_{15}/Γ

VALUE (units 10^{-2})	DOCUMENT ID		TECN	COMMENT
1.9±0.4±0.1	DOBBS	09	CLEO	e^+e^- at 4170 MeV

$\Gamma(2K_S^0 \text{anything})/\Gamma_{total}$ Γ_{16}/Γ

VALUE (units 10^{-2})	DOCUMENT ID		TECN	COMMENT
1.7±0.3±0.1	DOBBS	09	CLEO	e^+e^- at 4170 MeV

$\Gamma(2K^+ \text{anything})/\Gamma_{total}$ Γ_{17}/Γ

VALUE (units 10^{-2})	CL%	DOCUMENT ID		TECN	COMMENT
<0.26	90	DOBBS	09	CLEO	e^+e^- at 4170 MeV

$\Gamma(2K^- \text{anything})/\Gamma_{total}$ Γ_{18}/Γ

VALUE (units 10^{-2})	CL%	DOCUMENT ID		TECN	COMMENT
<0.06	90	DOBBS	09	CLEO	e^+e^- at 4170 MeV

Leptonic and semileptonic modes

See the related review(s):

Leptonic Decays of Charged Pseudoscalar Mesons

$\Gamma(e^+\nu_e)/\Gamma_{total}$ Γ_{19}/Γ

VALUE	CL%	DOCUMENT ID		TECN	COMMENT
<0.83 × 10^{-4}	90	[1] ZUPANC	13	BELL	e^+e^- at $\Upsilon(4S), \Upsilon(5S)$
• • • We do not use the following data for averages, fits, limits, etc. • • •					
<2.3 × 10^{-4}	90	DEL-AMO-SA...10J		BABR	e^+e^-, 10.58 GeV
<1.2 × 10^{-4}	90	ALEXANDER	09	CLEO	e^+e^- at 4170 MeV
<1.3 × 10^{-4}	90	PEDLAR	07A	CLEO	See ALEXANDER 09

[1] ZUPANC 13 also gives the limit as < 1.0 × 10^{-4} at 95% CL.

$\Gamma(\mu^+\nu_\mu)/\Gamma_{total}$ Γ_{20}/Γ

See the note on "Decay Constants of Charged Pseudoscalar Mesons" above.

VALUE (units 10^{-3})	EVTS	DOCUMENT ID		TECN	COMMENT
5.50±0.23 OUR AVERAGE					
4.95±0.67±0.26	69	[1] ABLIKIM	16O	BES3	e^+e^- at 4.009 GeV
5.31±0.28±0.20	492 ± 26	[2] ZUPANC	13	BELL	e^+e^- at $\Upsilon(4S), \Upsilon(5S)$
6.02±0.38±0.34	275 ± 17	[3] DEL-AMO-SA...10J		BABR	e^+e^-, 10.58 GeV
5.65±0.45±0.17	235 ± 14	ALEXANDER	09	CLEO	e^+e^- at 4170 MeV
• • • We do not use the following data for averages, fits, limits, etc. • • •					
6.44±0.76±0.57	169 ± 18	[4] WIDHALM	08	BELL	See ZUPANC 13
5.94±0.66±0.31	88	[5] PEDLAR	07A	CLEO	See ALEXANDER 09
6.8 ±1.1 ±1.8	553	[6] HEISTER	02I	ALEP	Z decays

[1] ABLIKIM 16O value is constrained by the Standard Model ratio of $\Gamma(D_s^+ \to \tau^+\nu_\tau)/\Gamma(D_s^+ \to \mu^+\nu_\mu) = 9.76$; the unconstrained value is (0.517 ± 0.075 ± 0.021)%. The constrained value is used to obtain the decay constant, $f_{D_s^+}$ = (241.0 ± 16.3 ± 6.6) MeV.

[2] ZUPANC 13 uses both $\mu^+\nu$ and $\tau^+\nu$ events to get f_{D_s} = (255.5 ± 4.2 ± 5.1) MeV.

[3] DEL-AMO-SANCHEZ 10J uses $\mu^+\nu_\mu$ and $\tau^+\nu_\tau$ events together to get f_{D_s} = (258.6 ± 6.4 ± 7.5) MeV.

[4] WIDHALM 08 gets f_{D_s} = (275 ± 16 ± 12) MeV from the branching fraction.

[5] PEDLAR 07A also fits μ^+ and τ^+ events together and gets an effective $\mu^+\nu_\mu$ branching fraction of (6.38 ± 0.59 ± 0.33) × 10^{-3}

[6] This HEISTER 02I result is not actually an independent measurement of the absolute $\mu^+\nu_\mu$ branching fraction, but is in fact based on our $\phi\pi^+$ branching fraction of 3.6 ± 0.9%, so it cannot be included in our overall fit. HEISTER 02I combines its $D_s^+ \to \tau^+\nu_\tau$ and $\mu^+\nu_\mu$ branching fractions to get f_{D_s} = (285 ± 19 ± 40) MeV.

$\Gamma(\mu^+\nu_\mu)/\Gamma(\phi\pi^+)$ Γ_{20}/Γ_{37}

See the note on "Decay Constants of Charged Pseudoscalar Mesons" above.

VALUE	EVTS	DOCUMENT ID		TECN	COMMENT
• • • We do not use the following data for averages, fits, limits, etc. • • •					
0.143±0.018±0.006	489 ± 55	[1] AUBERT	07V	BABR	$e^+e^- \approx \Upsilon(4S)$
0.23 ±0.06 ±0.04	18	[2] ALEXANDROV	00	BEAT	π^- nucleus, 350 GeV
0.173±0.023±0.035	182	[3] CHADHA	98	CLE2	$e^+e^- \approx \Upsilon(4S)$
0.245±0.052±0.074	39	[4] ACOSTA	94	CLE2	See CHADHA 98

[1] AUBERT 07V gets $f_{D_s^+}$ = (283 ± 17 ± 16) MeV, using $\Gamma(D_s^+ \to \phi\pi^+)/\Gamma(\text{total})$ = (4.71 ± 0.46)%.

[2] ALEXANDROV 00 uses $f_D^2/f_{D_s}^2$ = 0.82 ± 0.09 from a lattice-gauge-theory calculation to get the relative numbers of $D^+ \to \mu^+\nu_\mu$ and $D_s^+ \to \mu^+\nu_\mu$ events. The present result leads to f_{D_s} = (323 ± 44 ± 36) MeV.

[3] CHADHA 98 obtains f_{D_s} = (280 ± 19 ± 28 ± 34) MeV from this measurement, using $\Gamma(D_s^+ \to \phi\pi^+)/\Gamma(\text{total})$ = 0.036 ± 0.009.

[4] ACOSTA 94 obtains f_{D_s} = (344 ± 37 ± 52 ± 42) MeV from this measurement, using $\Gamma(D_s^+ \to \phi\pi^+)/\Gamma(\text{total})$ = 0.037 ± 0.009.

$\Gamma(\tau^+\nu_\tau)/\Gamma_{\text{total}}$ Γ_{21}/Γ

See the note on "Decay Constants of Charged Pseudoscalar Mesons" above.

VALUE (units 10^{-2})	EVTS	DOCUMENT ID		TECN	COMMENT
5.48±0.23 OUR AVERAGE					
4.83±0.65±0.26	33	[1] ABLIKIM	16O	BES3	e^+e^- at 4.009 GeV
5.70±0.21 $^{+0.31}_{-0.30}$	2.2k	[2] ZUPANC	13	BELL	e^+e^- at $\Upsilon(4S)$, $\Upsilon(5S)$
4.96±0.37±0.57	748 ± 53	[3] DEL-AMO-SA...	10J	BABR	$e^-\overline{\nu}_e\nu_\tau$, $\mu^-\overline{\nu}_\mu\nu_\tau$
6.42±0.81±0.18	126 ± 16	[4] ALEXANDER	09	CLEO	$\tau^+ \to \pi^+\overline{\nu}_\tau$
5.52±0.57±0.21	155 ± 17	[4] NAIK	09A	CLEO	$\tau^+ \to \rho^+\overline{\nu}_\tau$
5.30±0.47±0.22	181 ± 16	[4] ONYISI	09	CLEO	$\tau^+ \to e^+\nu_e\overline{\nu}_\tau$
• • • We do not use the following data for averages, fits, limits, etc. • • •					
6.17±0.71±0.34	102	[5] ECKLUND	08	CLEO	See ONYISI 09
8.0 ±1.3 ±0.4	47	[5] PEDLAR	07A	CLEO	See ALEXANDER 09
5.79±0.77±1.84	881	[6] HEISTER	02I	ALEP	Z decays
7.0 ±2.1 ±2.0	22	[7] ABBIENDI	01L	OPAL	$D_s^{*+} \to \gamma D_s^+$ from Z's
7.4 ±2.8 ±2.4	16	[8] ACCIARRI	97F	L3	$D_s^{*+} \to \gamma D_s^+$ from Z's

[1] ABLIKIM 16O value is constrained by the Standard Model ratio of $\Gamma(D_s^+ \to \tau^+\nu_\tau)/\Gamma(D_s^+ \to \mu^+\nu_\mu)$ = 9.76; the unconstrained value is (3.28 ± 1.83 ± 0.37)%.

[2] ZUPANC 13 uses both $\mu^+\nu$ and $\tau^+\nu$ events to get f_{D_s} = (255.5 ± 4.2 ± 5.1) MeV.

[3] DEL-AMO-SANCHEZ 10J (with a small correction; see LEES 15D) uses $\mu^+\nu_\mu$ and $\tau^+\nu_\tau$ events together to get f_{D_s} = (259.9 ± 6.6 ± 7.6) MeV.

[4] ALEXANDER 09, NAIK 09A, and ONYISI 09 use different τ decay modes and are independent. The three papers combined give f_{D_s} = (259.7 ± 7.8 ± 3.4) MeV.

[5] ECKLUND 08 and PEDLAR 07A are independent: ECKLUND 08 uses $\tau^+ \to e^+\nu_e\overline{\nu}_\tau$ events, PEDLAR 07A uses $\tau^+ \to \pi^+\overline{\nu}_\tau$ events.

[6] HEISTER 02I combines its $D_s^+ \to \tau^+\nu_\tau$ and $\mu^+\nu_\mu$ branching fractions to get f_{D_s} = (285 ± 19 ± 40) MeV.

[7] This ABBIENDI 01L value gives a decay constant f_{D_s} of (286 ± 44 ± 41) MeV.

[8] The second ACCIARRI 97F error here combines in quadrature systematic (0.016) and normalization (0.018) errors. The branching fraction gives f_{D_s} = (309 ± 58 ± 33 ± 38) MeV.

$\Gamma(\tau^+\nu_\tau)/\Gamma(\mu^+\nu_\mu)$ Γ_{21}/Γ_{20}

VALUE	EVTS	DOCUMENT ID		TECN	COMMENT
• • • We do not use the following data for averages, fits, limits, etc. • • •					
10.73±0.69 $^{+0.56}_{-0.53}$	2.2k/492	[1] ZUPANC	13	BELL	e^+e^- at $\Upsilon(4S)$, $\Upsilon(5S)$
11.0 ±1.4 ±0.6	102	[2] ECKLUND	08	CLEO	See ONYISI 09

[1] This ZUPANC 13 ratio is not independent of the separate $\tau\nu$ and $\mu\nu$ fractions listed above.

[2] This ECKLUND 08 value also uses results from PEDLAR 07A, and it is not independent of other results in these Listings. Combined with earlier CLEO results, the decay constant f_{D_s} is 274 ± 10 ± 5 MeV.

$\Gamma(K^+K^-e^+\nu_e)/\Gamma(K^+K^-\pi^+)$ Γ_{22}/Γ_{36}

VALUE	DOCUMENT ID		TECN	COMMENT
• • • We do not use the following data for averages, fits, limits, etc. • • •				
0.558±0.007±0.016	[1] AUBERT	08AN	BABR	e^+e^- at $\Upsilon(4S)$

[1] This AUBERT 08AN ratio is only for the K^+K^- mass in the range 1.01–to–1.03 GeV in the numerator and 1.0095–to–1.0295 GeV in the denominator.

$\Gamma(\phi e^+\nu_e)/\Gamma_{\text{total}}$ Γ_{23}/Γ

See the end of the D_s^+ Listings for measurements of $D_s^+ \to \phi e^+\nu_e$ form factors. Unseen decay modes of the ϕ are included.

VALUE (units 10^{-2})	EVTS	DOCUMENT ID		TECN	COMMENT
2.39±0.16 OUR AVERAGE Error includes scale factor of 1.3. See the ideogram below.					
2.26±0.45±0.09	26	ABLIKIM	18A	BES3	e^+e^- at 4.009 GeV
2.14±0.17±0.08	207	HIETALA	15		Uses CLEO data
2.61±0.03±0.17	25k	AUBERT	08AN	BABR	e^+e^- at $\Upsilon(4S)$
• • • We do not use the following data for averages, fits, limits, etc. • • •					
2.36±0.23±0.13	106	ECKLUND	09	CLEO	See HIETALA 15
2.29±0.37±0.11	45	YELTON	09	CLEO	See ECKLUND 09

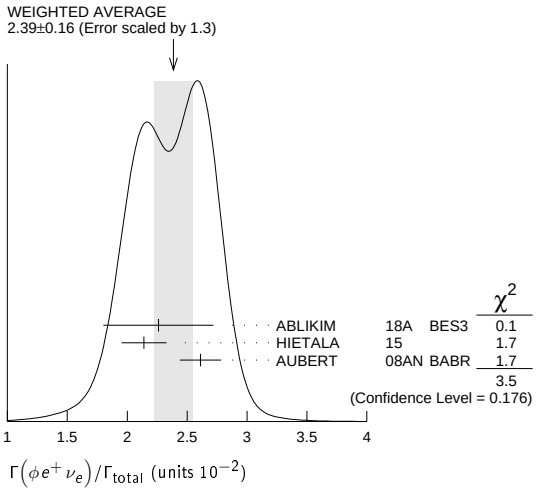

$\Gamma(\phi e^+\nu_e)/\Gamma(\phi\pi^+)$ Γ_{23}/Γ_{37}

As noted in the comment column, most of these measurements use $\phi\mu^+\nu_\mu$ events in addition to or instead of $\phi e^+\nu_e$ events.

VALUE	EVTS	DOCUMENT ID		TECN	COMMENT
• • • We do not use the following data for averages, fits, limits, etc. • • •					
0.540±0.033±0.048	793	LINK	02J	FOCS	Uses $\phi\mu^+\nu_\mu$
0.54 ±0.05 ±0.04	367	BUTLER	94	CLE2	Uses $\phi e^+\nu_e$ and $\phi\mu^+\nu_\mu$
0.58 ±0.17 ±0.07	97	FRABETTI	93G	E687	Uses $\phi\mu^+\nu_\mu$
0.57 ±0.15 ±0.15	104	ALBRECHT	91	ARG	Uses $\phi e^+\nu_e$
0.49 ±0.10 $^{+0.10}_{-0.14}$	54	ALEXANDER	90B	CLEO	Uses $\phi e^+\nu_e$ and $\phi\mu^+\nu_\mu$

$\Gamma(\phi\mu^+\nu_\mu)/\Gamma_{\text{total}}$ Γ_{24}/Γ

VALUE (%)	EVTS	DOCUMENT ID		TECN	COMMENT
1.94±0.53±0.09	22	ABLIKIM	18A	BES3	e^+e^- at 4.009 GeV

$\Gamma(\eta e^+\nu_e)/\Gamma_{\text{total}}$ Γ_{26}/Γ

Unseen decay modes of the η are included.

VALUE (units 10^{-2})	EVTS	DOCUMENT ID		TECN	COMMENT
2.29±0.19 OUR AVERAGE					
2.30±0.31±0.08	63	ABLIKIM	16T	BES3	e^+e^- at 4.009 GeV
2.28±0.14±0.19	358	HIETALA	15		Uses CLEO data
• • • We do not use the following data for averages, fits, limits, etc. • • •					
2.48±0.29±0.13	82	YELTON	09	CLEO	See HIETALA 15

$\Gamma(\eta e^+\nu_e)/\Gamma(\phi e^+\nu_e)$ Γ_{26}/Γ_{23}

Unseen decay modes of the η and the ϕ are included.

VALUE	EVTS	DOCUMENT ID		TECN	COMMENT
• • • We do not use the following data for averages, fits, limits, etc. • • •					
1.24±0.12±0.15	440	[1] BRANDENB...	95	CLE2	See HIETALA 15

[1] BRANDENBURG 95 uses both e^+ and μ^+ events and makes a phase-space adjustment to use the μ^+ events as e^+ events.

$\Gamma(\eta'(958)e^+\nu_e)/\Gamma_{\text{total}}$ Γ_{27}/Γ

Unseen decay modes of the $\eta'(958)$ are included.

VALUE (units 10^{-2})	EVTS	DOCUMENT ID		TECN	COMMENT
0.74±0.14 OUR AVERAGE					
0.93±0.30±0.05	14	ABLIKIM	16T	BES3	e^+e^- at 4170 MeV
0.68±0.15±0.06	20	HIETALA	15		Uses CLEO data
• • • We do not use the following data for averages, fits, limits, etc. • • •					
0.91±0.33±0.05	7.5	YELTON	09	CLEO	See HIETALA 15

$\Gamma(\eta'(958)e^+\nu_e)/\Gamma(\phi e^+\nu_e)$ Γ_{27}/Γ_{23}

Unseen decay modes of the resonances are included.

VALUE	EVTS	DOCUMENT ID		TECN	COMMENT
• • • We do not use the following data for averages, fits, limits, etc. • • •					
0.43±0.11±0.07	29	[1] BRANDENB...	95	CLE2	See HIETALA 15

[1] BRANDENBURG 95 uses both e^+ and μ^+ events and makes a phase-space adjustment to use the μ^+ events as e^+ events.

$[\Gamma(\eta e^+\nu_e) + \Gamma(\eta'(958)e^+\nu_e)]/\Gamma(\phi e^+\nu_e)$ $\Gamma_{25}/\Gamma_{23} = (\Gamma_{26}+\Gamma_{27})/\Gamma_{23}$

Unseen decay modes of the resonances are included.

VALUE	DOCUMENT ID		TECN	COMMENT
• • • We do not use the following data for averages, fits, limits, etc. • • •				
1.67±0.17±0.17	[1] BRANDENB...	95	CLE2	See HIETALA 15

[1] This BRANDENBURG 95 data is redundant with data in previous blocks.

$\Gamma(\eta\mu^+\nu_\mu)/\Gamma_{total}$ Γ_{28}/Γ

VALUE (%)	EVTS	DOCUMENT ID		TECN	COMMENT
2.42±0.46±0.11	44	ABLIKIM	18A	BES3	e^+e^- at 4.009 GeV

$\Gamma(\eta'(958)\mu^+\nu_\mu)/\Gamma_{total}$ Γ_{29}/Γ

VALUE (%)	EVTS	DOCUMENT ID		TECN	COMMENT
1.06±0.54±0.07	10	ABLIKIM	18A	BES3	e^+e^- at 4.009 GeV

$\Gamma(\omega e^+\nu_e)/\Gamma_{total}$ Γ_{30}/Γ

A test for $u\overline{u}$ or $d\overline{d}$ content in the D_s^+. Neither Cabibbo-favored nor Cabibbo-suppressed decays can contribute, and $\omega-\phi$ mixing is an unlikely explanation for any fraction above about 2×10^{-4}.

VALUE (%)	CL%	DOCUMENT ID		TECN	COMMENT
<0.20	90	MARTIN	11	CLEO	e^+e^- at 4170 MeV

$\Gamma(K^0e^+\nu_e)/\Gamma_{total}$ Γ_{31}/Γ

VALUE (units 10^{-2})	EVTS	DOCUMENT ID		TECN	COMMENT
0.39±0.08±0.03	42	HIETALA	15		Uses CLEO data
• • • We do not use the following data for averages, fits, limits, etc. • • •					
0.37±0.10±0.02	14	YELTON	09	CLEO	See HIETALA 15

$\Gamma(K^*(892)^0e^+\nu_e)/\Gamma_{total}$ Γ_{32}/Γ

Unseen decay modes of the $K^*(892)^0$ are included.

VALUE (units 10^{-2})	EVTS	DOCUMENT ID		TECN	COMMENT
0.18±0.04±0.01	32	HIETALA	15		Uses CLEO data
• • • We do not use the following data for averages, fits, limits, etc. • • •					
0.18±0.07±0.01	7.5	YELTON	09	CLEO	See HIETALA 15

$\Gamma(f_0(980)e^+\nu_e, f_0\to\pi^+\pi^-)/\Gamma_{total}$ Γ_{33}/Γ

VALUE (units 10^{-2})	EVTS	DOCUMENT ID		TECN	COMMENT
• • • We do not use the following data for averages, fits, limits, etc. • • •					
0.13±0.03±0.01	42	[1] HIETALA	15		Uses CLEO data
0.20±0.03±0.01	44	ECKLUND	09	CLEO	See HIETALA 15
0.13±0.04±0.01	13	YELTON	09	CLEO	See ECKLUND 09

[1] HIETALA 15 uses a tighter cut on the reconstructed $\pi^+\pi^-$ mass (±60 MeV around the f^0) than ECKLUND 09. It finds that applying the same tight cut to both analyses gives consistent results.

Hadronic modes with a $K\overline{K}$ pair

$\Gamma(K^+K_S^0)/\Gamma_{total}$ Γ_{34}/Γ

VALUE (units 10^{-2})	DOCUMENT ID		TECN	COMMENT
1.50±0.05 OUR FIT				
1.52±0.05±0.03	ONYISI	13	CLEO	e^+e^- at 4.17 GeV
• • • We do not use the following data for averages, fits, limits, etc. • • •				
1.49±0.07±0.05	[1] ALEXANDER	08	CLEO	See ONYISI 13

[1] ALEXANDER 08 uses single- and double-tagged events in an overall fit.

$\Gamma(K^+\overline{K}^0)/\Gamma_{total}$ Γ_{35}/Γ

VALUE (units 10^{-2})	EVTS	DOCUMENT ID		TECN	COMMENT
2.95±0.11±0.09	2.0k	[1] ZUPANC	13	BELL	e^+e^- at $\Upsilon(4S),\Upsilon(5S)$

[1] ZUPANC 13 finds the $\overline{K}^0$ from its missing-mass squared, not from $K_S^0\to\pi^+\pi^-$. The DCS ($D_s^+\to K^+K^0$) contribution to this fraction is estimated to be an order of magnitude below the statistical uncertainty.

$\Gamma(K^+K^-\pi^+)/\Gamma_{total}$ Γ_{36}/Γ

VALUE (units 10^{-2})	EVTS	DOCUMENT ID		TECN	COMMENT
5.45±0.17 OUR FIT Error includes scale factor of 1.2.					
5.44±0.18 OUR AVERAGE Error includes scale factor of 1.3. See the ideogram below.					
5.55±0.14±0.13		ONYISI	13	CLEO	e^+e^- at 4.17 GeV
5.06±0.15±0.21	4.1k	ZUPANC	13	BELL	e^+e^- at $\Upsilon(4S),\Upsilon(5S)$
5.78±0.20±0.30		DEL-AMO-SA...10J		BABR	e^+e^-, 10.58 GeV
• • • We do not use the following data for averages, fits, limits, etc. • • •					
5.50±0.23±0.16		[1] ALEXANDER	08	CLEO	See ONYISI 13

[1] ALEXANDER 08 uses single- and double-tagged events in an overall fit.

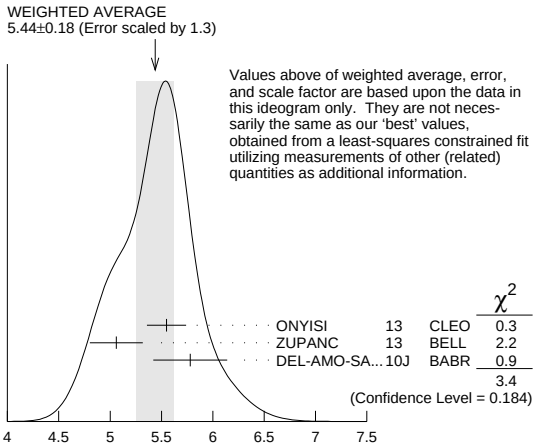

$\Gamma(\phi\pi^+)/\Gamma_{total}$ Γ_{37}/Γ

The results here are model-independent. For earlier, model-dependent results, see our PDG 06 edition. We decouple the $D_s^+\to\phi\pi^+$ branching fraction obtained from mass projections (and used to get some of the other branching fractions) from the $D_s^+\to\phi\pi^+$, $\phi\to K^+K^-$ branching fraction obtained from the Dalitz-plot analysis of $D_s^+\to K^+K^-\pi^+$. That is, the ratio of these two branching fractions is not exactly the $\phi\to K^+K^-$ branching fraction 0.491.

VALUE (units 10^{-2})	EVTS	DOCUMENT ID		TECN	COMMENT
4.5 ±0.4 OUR AVERAGE					
4.62±0.36±0.51		[1] AUBERT	06N	BABR	e^+e^- at $\Upsilon(4S)$
4.81±0.52±0.38	212±19	[2] AUBERT	05V	BABR	$e^+e^-\approx\Upsilon(4S)$
3.59±0.77±0.48		[3] ARTUSO	96	CLE2	e^+e^- at $\Upsilon(4S)$
• • • We do not use the following data for averages, fits, limits, etc. • • •					
3.9 $^{+5.1}_{-1.9}$ $^{+1.8}_{-1.1}$		[4] BAI	95C	BES	e^+e^- 4.03 GeV

[1] This AUBERT 06N measurement uses $\overline{B}^0\to D_s^{(*)-}D^{(*)+}$ and $B^-\to D_s^{(*)-}D^{(*)0}$ decays, including some from other papers. However, the result is independent of AUBERT 05V.

[2] AUBERT 05V uses the ratio of $B^0\to D^{*-}D_s^{*+}$ events seen in two different ways, in both of which the $D^{*-}\to\overline{D}^0\pi^-$ decay is fully reconstructed: (1) The $D_s^{*+}\to D_s^+\gamma$, $D_s^+\to\phi\pi^+$ decay is fully reconstructed. (2) The number of events in the D_s^+ peak in the missing mass spectrum against the $D^{*-}\gamma$ is measured.

[3] ARTUSO 96 uses partially reconstructed $\overline{B}^0\to D^{*+}D_s^{*-}$ decays to get a model-independent value for $\Gamma(D_s^-\to\phi\pi^-)/\Gamma(D^0\to K^-\pi^+)$ of $0.92\pm0.20\pm0.11$.

[4] BAI 95C uses $e^+e^-\to D_s^+D_s^-$ events in which one or both of the $D_s^\pm$ are observed to obtain the first model-independent measurement of the $D_s^+\to\phi\pi^+$ branching fraction, without assumptions about $\sigma(D_s^\pm)$. However, with only two "doubly-tagged" events, the statistical error is very large.

$\Gamma(\phi\pi^+,\phi\to K^+K^-)/\Gamma(K^+K^-\pi^+)$ Γ_{38}/Γ_{36}

This is the "fit fraction" from the Dalitz-plot analysis. We decouple the $D_s^+\to\phi\pi^+$ branching fraction obtained from mass projections (and used to get some of the other branching fractions) from the $D_s^+\to\phi\pi^+$, $\phi\to K^+K^-$ branching fraction obtained from the Dalitz-plot analysis of $D_s^+\to K^+K^-\pi^+$. That is, the ratio of these two branching fractions is not exactly the $\phi\to K^+K^-$ branching fraction 0.491.

VALUE (%)	DOCUMENT ID		TECN	COMMENT
41.6±0.8 OUR AVERAGE				
41.4±0.8±0.5	DEL-AMO-SA...11G		BABR	Dalitz fit, 96k±369 evts
42.2±1.6±0.3	MITCHELL	09A	CLEO	Dalitz fit, 12k evts
• • • We do not use the following data for averages, fits, limits, etc. • • •				
39.6±3.3±4.7	FRABETTI	95B	E687	Dalitz fit, 701 evts

$\Gamma(K^+\overline{K}^*(892)^0,\overline{K}^{*0}\to K^-\pi^+)/\Gamma(K^+K^-\pi^+)$ Γ_{39}/Γ_{36}

This is the "fit fraction" from the Dalitz-plot analysis.

VALUE (%)	DOCUMENT ID		TECN	COMMENT
47.8±0.6 OUR AVERAGE				
47.9±0.5±0.5	DEL-AMO-SA...11G		BABR	Dalitz fit, 96k±369 evts
47.4±1.5±0.4	MITCHELL	09A	CLEO	Dalitz fit, 12k evts
• • • We do not use the following data for averages, fits, limits, etc. • • •				
47.8±4.6±4.0	FRABETTI	95B	E687	Dalitz fit, 701 evts

$\Gamma(f_0(980)\pi^+,f_0\to K^+K^-)/\Gamma(K^+K^-\pi^+)$ Γ_{40}/Γ_{36}

This is the "fit fraction" from the Dalitz-plot analysis.

VALUE (%)	DOCUMENT ID		TECN	COMMENT
21 ±6 OUR AVERAGE Error includes scale factor of 3.5.				
16.4±0.7±2.0	DEL-AMO-SA...11G		BABR	Dalitz fit, 96k±369 evts
28.2±1.9±1.8	MITCHELL	09A	CLEO	Dalitz fit, 12k evts

• • • We do not use the following data for averages, fits, limits, etc. • • •

11.0±3.5±2.6	FRABETTI	95B	E687	Dalitz fit, 701 evts

$\Gamma(f_0(1370)\pi^+, f_0 \to K^+K^-)/\Gamma(K^+K^-\pi^+)$ Γ_{41}/Γ_{36}

This is the "fit fraction" from the Dalitz-plot analysis.

VALUE (%)	DOCUMENT ID		TECN	COMMENT
1.3±0.8 OUR AVERAGE	Error includes scale factor of 3.9.			
1.1±0.1±0.2	DEL-AMO-SA..11G		BABR	Dalitz fit, 96k±369 evts
4.3±0.6±0.5	MITCHELL	09A	CLEO	Dalitz fit, 12k evts

$\Gamma(f_0(1710)\pi^+, f_0 \to K^+K^-)/\Gamma(K^+K^-\pi^+)$ Γ_{42}/Γ_{36}

This is the "fit fraction" from the Dalitz-plot analysis.

VALUE (%)	DOCUMENT ID		TECN	COMMENT
1.2±0.5 OUR AVERAGE	Error includes scale factor of 3.8.			
1.1±0.1±0.1	DEL-AMO-SA..11G		BABR	Dalitz fit, 96k±369 evts
3.4±0.5±0.3	MITCHELL	09A	CLEO	Dalitz fit, 12k evts
• • • We do not use the following data for averages, fits, limits, etc. • • •				
3.4±2.3±3.5	FRABETTI	95B	E687	Dalitz fit, 701 evts

$\Gamma(K^+\overline{K}_0^*(1430)^0, \overline{K}_0^* \to K^-\pi^+)/\Gamma(K^+K^-\pi^+)$ Γ_{43}/Γ_{36}

This is the "fit fraction" from the Dalitz-plot analysis.

VALUE (%)	DOCUMENT ID		TECN	COMMENT
3.4±0.7 OUR AVERAGE	Error includes scale factor of 1.2.			
2.4±0.3±1.0	DEL-AMO-SA..11G		BABR	Dalitz fit, 96k±369 evts
3.9±0.5±0.5	MITCHELL	09A	CLEO	Dalitz fit, 12k evts
• • • We do not use the following data for averages, fits, limits, etc. • • •				
9.3±3.2±3.2	FRABETTI	95B	E687	Dalitz fit, 701 evts

$\Gamma(K^+K_S^0\pi^0)/\Gamma_{\text{total}}$ Γ_{44}/Γ

VALUE (units 10^{-2})	DOCUMENT ID		TECN	COMMENT
1.52±0.09±0.20	ONYISI	13	CLEO	e^+e^- at 4.17 GeV

$\Gamma(2K_S^0\pi^+)/\Gamma_{\text{total}}$ Γ_{45}/Γ

VALUE (units 10^{-2})	DOCUMENT ID		TECN	COMMENT
0.77±0.05±0.03	ONYISI	13	CLEO	e^+e^- at 4.17 GeV

$\Gamma(K^*(892)^+\overline{K}^0)/\Gamma(\phi\pi^+)$ Γ_{47}/Γ_{37}

Unseen decay modes of the resonances are included.

VALUE	DOCUMENT ID		TECN	COMMENT
1.20±0.21±0.13	CHEN	89	CLEO	e^+e^- 10 GeV

$\Gamma(K^+K^-\pi^+\pi^0)/\Gamma_{\text{total}}$ Γ_{48}/Γ

VALUE (units 10^{-2})	DOCUMENT ID		TECN	COMMENT
6.3 ±0.6 OUR FIT				
6.37±0.21±0.56	ONYISI	13	CLEO	e^+e^- at 4.17 GeV
• • • We do not use the following data for averages, fits, limits, etc. • • •				
5.65±0.29±0.40	[1] ALEXANDER	08	CLEO	See ONYISI 13

[1] ALEXANDER 08 uses single- and double-tagged events in an overall fit.

$\Gamma(\phi\rho^+)/\Gamma(\phi\pi^+)$ Γ_{49}/Γ_{37}

VALUE	EVTS	DOCUMENT ID		TECN	COMMENT
$\mathbf{1.86\pm0.26^{+0.29}_{-0.40}}$	253	AVERY	92	CLE2	$e^+e^- \simeq 10.5$ GeV

$\Gamma(K_S^0K^-2\pi^+)/\Gamma_{\text{total}}$ Γ_{50}/Γ

VALUE (units 10^{-2})	DOCUMENT ID		TECN	COMMENT
1.68±0.10 OUR FIT				
1.69±0.07±0.08	ONYISI	13	CLEO	e^+e^- at 4.17 GeV
• • • We do not use the following data for averages, fits, limits, etc. • • •				
1.64±0.10±0.07	[1] ALEXANDER	08	CLEO	See ONYISI 13

[1] ALEXANDER 08 uses single- and double-tagged events in an overall fit.

$\Gamma(K^*(892)^+\overline{K}^*(892)^0)/\Gamma(\phi\pi^+)$ Γ_{51}/Γ_{37}

Unseen decay modes of the resonances are included.

VALUE	DOCUMENT ID		TECN	COMMENT
1.6±0.4±0.4	ALBRECHT	92B	ARG	$e^+e^- \simeq 10.4$ GeV

$\Gamma(K^+K_S^0\pi^+\pi^-)/\Gamma_{\text{total}}$ Γ_{52}/Γ

VALUE (units 10^{-2})	DOCUMENT ID		TECN	COMMENT
1.00±0.08 OUR FIT				
1.03±0.06±0.08	ONYISI	13	CLEO	e^+e^- at 4.17 GeV

$\Gamma(K^+K_S^0\pi^+\pi^-)/\Gamma(K_S^0K^-2\pi^+)$ Γ_{52}/Γ_{50}

VALUE	EVTS	DOCUMENT ID		TECN	COMMENT
0.60 ±0.05 OUR FIT					
0.586±0.052±0.043	476	LINK	01C	FOCS	γ A, $\overline{E}_\gamma \approx 180$ GeV

$\Gamma(K^+K^-2\pi^+\pi^-)/\Gamma(K^+K^-\pi^+)$ Γ_{53}/Γ_{36}

VALUE	EVTS	DOCUMENT ID		TECN	COMMENT
0.160±0.027 OUR AVERAGE					
0.150±0.019±0.025	240	LINK	03D	FOCS	γ A, $\overline{E}_\gamma \approx 180$ GeV
0.188±0.036±0.040	75	FRABETTI	97C	E687	γBe, $\overline{E}_\gamma \approx 200$ GeV

$\Gamma(\phi2\pi^+\pi^-)/\Gamma(\phi\pi^+)$ Γ_{54}/Γ_{37}

VALUE	EVTS	DOCUMENT ID		TECN	COMMENT
0.269±0.027 OUR AVERAGE					
0.249±0.024±0.021	136	LINK	03D	FOCS	γ A, $\overline{E}_\gamma \approx 180$ GeV
0.28 ±0.06 ±0.01	40	FRABETTI	97C	E687	γBe, $\overline{E}_\gamma \approx 200$ GeV
0.58 ±0.21 ±0.10	21	FRABETTI	92	E687	γBe
0.42 ±0.13 ±0.07	19	ANJOS	88	E691	Photoproduction
1.11 ±0.37 ±0.28	62	ALBRECHT	85D	ARG	e^+e^- 10 GeV

$\Gamma(K^+K^-\rho^0\pi^+ \text{non-}\phi)/\Gamma(K^+K^-2\pi^+\pi^-)$ Γ_{55}/Γ_{53}

VALUE	CL%	DOCUMENT ID		TECN	COMMENT
<0.03	90	LINK	03D	FOCS	γ A, $\overline{E}_\gamma \approx 180$ GeV

$\Gamma(\phi\rho^0\pi^+, \phi \to K^+K^-)/\Gamma(K^+K^-2\pi^+\pi^-)$ Γ_{56}/Γ_{53}

VALUE	DOCUMENT ID		TECN	COMMENT
0.75±0.06±0.04	LINK	03D	FOCS	γ A, $\overline{E}_\gamma \approx 180$ GeV

$\Gamma(\phi a_1(1260)^+, \phi \to K^+K^-, a_1^+ \to \rho^0\pi^+)/\Gamma(K^+K^-\pi^+)$ Γ_{57}/Γ_{36}

VALUE	DOCUMENT ID		TECN	COMMENT
0.137±0.019±0.011	LINK	03D	FOCS	γ A, $\overline{E}_\gamma \approx 180$ GeV

$\Gamma(K^+K^-2\pi^+\pi^-\text{nonresonant})/\Gamma(K^+K^-2\pi^+\pi^-)$ Γ_{58}/Γ_{53}

VALUE	DOCUMENT ID		TECN	COMMENT
0.10±0.06±0.05	LINK	03D	FOCS	γ A, $\overline{E}_\gamma \approx 180$ GeV

$\Gamma(2K_S^0\pi^+\pi^-)/\Gamma(K_S^0K^-2\pi^+)$ Γ_{59}/Γ_{50}

VALUE	EVTS	DOCUMENT ID		TECN	COMMENT
0.051±0.015±0.015	37 ± 10	LINK	04D	FOCS	γ A, $\overline{E}_\gamma \approx 180$ GeV

Pionic modes

$\Gamma(\pi^+\pi^0)/\Gamma(K^+K_S^0)$ Γ_{60}/Γ_{34}

VALUE (units 10^{-2})	CL%	DOCUMENT ID		TECN	COMMENT
<2.3	90	MENDEZ	10	CLEO	e^+e^- at 4170 MeV
• • • We do not use the following data for averages, fits, limits, etc. • • •					
<4.1	90	ADAMS	07A	CLEO	See MENDEZ 10

$\Gamma(2\pi^+\pi^-)/\Gamma_{\text{total}}$ Γ_{61}/Γ

VALUE (units 10^{-2})	DOCUMENT ID		TECN	COMMENT
1.09±0.05 OUR FIT	Error includes scale factor of 1.1.			
1.11±0.04±0.04	ONYISI	13	CLEO	e^+e^- at 4.17 GeV
• • • We do not use the following data for averages, fits, limits, etc. • • •				
1.11±0.07±0.04	[1] ALEXANDER	08	CLEO	See ONYISI 13

[1] ALEXANDER 08 uses single- and double-tagged events in an overall fit.

$\Gamma(2\pi^+\pi^-)/\Gamma(K^+K^-\pi^+)$ Γ_{61}/Γ_{36}

VALUE	EVTS	DOCUMENT ID		TECN	COMMENT
0.201±0.007 OUR FIT					
0.199±0.004±0.009	≈ 10.5k	AUBERT	09O	BABR	$e^+e^- \approx 10.6$ GeV
• • • We do not use the following data for averages, fits, limits, etc. • • •					
0.265±0.041±0.031	98	FRABETTI	97D	E687	γ Be ≈ 200 GeV

$\Gamma(\rho^0\pi^+)/\Gamma(2\pi^+\pi^-)$ Γ_{62}/Γ_{61}

VALUE	CL%	DOCUMENT ID		TECN	COMMENT
0.018±0.005±0.010		AUBERT	09O	BABR	Dalitz fit, ≈ 10.5k evts
• • • We do not use the following data for averages, fits, limits, etc. • • •					
not seen		LINK	04	FOCS	Dalitz fit, 1475 ±50 evts
0.058±0.023±0.037		AITALA	01A	E791	Dalitz fit, 848 evts
<0.073	90	FRABETTI	97D	E687	γ Be ≈ 200 GeV

$\Gamma(\pi^+(\pi^+\pi^-)_{S\text{-wave}})/\Gamma(2\pi^+\pi^-)$ Γ_{63}/Γ_{61}

This is the "fit fraction" from the Dalitz-plot analysis. See also KLEMPT 08, which uses 568 $D_s^+ \to 3\pi$ decays (over 280 background events) from FNAL E791 to study various parametrizations of the decay amplitudes. The emphasis there is more on S-wave $\pi\pi$ decay products — 20 different solutions are given — than on D_s^+ fit fractions.

VALUE	DOCUMENT ID		TECN	COMMENT
0.833 ±0.020 OUR AVERAGE				
0.830 ±0.009 ±0.019	[1] AUBERT	09O	BABR	Dalitz fit, ≈ 10.5k evts
0.8704±0.0560±0.0438	[2] LINK	04	FOCS	Dalitz fit, 1475 ± 50 evts

[1] AUBERT 09O gives the amplitude and phase of the $\pi^+\pi^-$ S-wave in 29 $\pi^+\pi^-$ invariant-mass bins.

[2] LINK 04 borrows a K-matrix parametrization from ANISOVICH 03 of the full π-π S-wave isoscalar scattering amplitude to describe the $\pi^+\pi^-$ S-wave component of the $\pi^+\pi^+\pi^-$ state. The fit fraction given above is a sum over five f_0 mesons, the $f_0(980)$, $f_0(1300)$, $f_0(1200$–$1600)$, $f_0(1500)$, and $f_0(1750)$. See LINK 04 for details and discussion.

$\Gamma(f_0(980)\pi^+, f_0 \to \pi^+\pi^-)/\Gamma(2\pi^+\pi^-)$ Γ_{64}/Γ_{61}

This is the "fit fraction" from the Dalitz-plot analysis. See above for the full $\pi^+(\pi^+\pi^-)_{S-wave}$ fit fraction.

VALUE	DOCUMENT ID		TECN	COMMENT
• • • We do not use the following data for averages, fits, limits, etc. • • •				
0.565 ± 0.043 ± 0.047	AITALA	01A	E791	Dalitz fit, 848 evts
1.074 ± 0.140 ± 0.043	FRABETTI	97D	E687	γ Be ≈ 200 GeV

$\Gamma(f_0(1370)\pi^+, f_0 \to \pi^+\pi^-)/\Gamma(2\pi^+\pi^-)$ Γ_{65}/Γ_{61}

This is the "fit fraction" from the Dalitz-plot analysis. See above for the full $\pi^+(\pi^+\pi^-)_{S-wave}$ fit fraction.

VALUE	DOCUMENT ID		TECN	COMMENT
• • • We do not use the following data for averages, fits, limits, etc. • • •				
0.324 ± 0.077 ± 0.017	AITALA	01A	E791	Dalitz fit, 848 evts

$\Gamma(f_0(1500)\pi^+, f_0 \to \pi^+\pi^-)/\Gamma(2\pi^+\pi^-)$ Γ_{66}/Γ_{61}

This is the "fit fraction" from the Dalitz-plot analysis. See above for the full $\pi^+(\pi^+\pi^-)_{S-wave}$ fit fraction.

VALUE	DOCUMENT ID		TECN	COMMENT
• • • We do not use the following data for averages, fits, limits, etc. • • •				
0.274 ± 0.114 ± 0.019	[1] FRABETTI	97D	E687	γ Be ≈ 200 GeV

[1] FRABETTI 97D calls this mode $S(1475)\,\pi^+$, but finds the mass and width of this $S(1475)$ to be in excellent agreement with those of the $f_0(1500)$.

$\Gamma(f_2(1270)\pi^+, f_2 \to \pi^+\pi^-)/\Gamma(2\pi^+\pi^-)$ Γ_{67}/Γ_{61}

This is the "fit fraction" from the Dalitz-plot analysis.

VALUE	DOCUMENT ID		TECN	COMMENT
0.101 ±0.018 OUR AVERAGE				
0.101 ±0.015 ±0.011	AUBERT	09O	BABR	Dalitz fit, ≈ 10.5k evts
0.0974 ± 0.0449 ± 0.0294	LINK	04	FOCS	Dalitz fit, 1475 ± 50 evts
• • • We do not use the following data for averages, fits, limits, etc. • • •				
0.197 ±0.033 ±0.006	AITALA	01A	E791	Dalitz fit, 848 evts
0.123 ±0.056 ±0.018	FRABETTI	97D	E687	γ Be ≈ 200 GeV

$\Gamma(\rho(1450)^0\pi^+, \rho^0 \to \pi^+\pi^-)/\Gamma(2\pi^+\pi^-)$ Γ_{68}/Γ_{61}

This is the "fit fraction" from the Dalitz-plot analysis.

VALUE	DOCUMENT ID		TECN	COMMENT
0.027 ±0.018 OUR AVERAGE				
0.023 ±0.008 ±0.017	AUBERT	09O	BABR	Dalitz fit, ≈ 10.5k evts
0.0656 ± 0.0343 ± 0.0440	LINK	04	FOCS	Dalitz fit, 1475 ± 50 evts
• • • We do not use the following data for averages, fits, limits, etc. • • •				
0.044 ±0.021 ±0.002	AITALA	01A	E791	Dalitz fit, 848 evts

$\Gamma(\pi^+ 2\pi^0)/\Gamma_{total}$ Γ_{69}/Γ

VALUE (units 10^{-2})	EVTS	DOCUMENT ID		TECN	COMMENT
0.65 ± 0.13 ± 0.03	72 ± 16	NAIK	09A	CLEO	e^+e^- at 4170 MeV

$\Gamma(2\pi^+\pi^-\pi^0)/\Gamma(\phi\pi^+)$ Γ_{70}/Γ_{37}

VALUE	CL%	DOCUMENT ID		TECN	COMMENT
• • • We do not use the following data for averages, fits, limits, etc. • • •					
<3.3	90	ANJOS	89E	E691	Photoproduction

$\Gamma(\eta\pi^+)/\Gamma_{total}$ Γ_{71}/Γ

Unseen decay modes of the η are included.

VALUE (units 10^{-2})	EVTS	DOCUMENT ID		TECN	COMMENT
1.70 ± 0.09 OUR FIT Error includes scale factor of 1.1.					
1.71 ± 0.08 OUR AVERAGE					
1.67 ± 0.08 ± 0.06		ONYISI	13	CLEO	e^+e^- at 4.17 GeV
1.82 ± 0.14 ± 0.07	0.8k	ZUPANC	13	BELL	e^+e^- at $\Upsilon(4S), \Upsilon(5S)$
• • • We do not use the following data for averages, fits, limits, etc. • • •					
1.58 ± 0.11 ± 0.18		[1] ALEXANDER	08	CLEO	See ONYISI 13

[1] ALEXANDER 08 uses single- and double-tagged events in an overall fit.

$\Gamma(\eta\pi^+)/\Gamma(K^+K_S^0)$ Γ_{71}/Γ_{34}

Unseen decay modes of the η are included.

VALUE	EVTS	DOCUMENT ID	TECN	COMMENT
1.13 ±0.07 OUR FIT Error includes scale factor of 1.1.				
• • • We do not use the following data for averages, fits, limits, etc. • • •				
1.236 ± 0.043 ± 0.063	2587 ± 89	MENDEZ	10	CLEO	See ONYISI 13

$\Gamma(\eta\pi^+)/\Gamma(\phi\pi^+)$ Γ_{71}/Γ_{37}

Unseen decay modes of the resonances are included.

VALUE	EVTS	DOCUMENT ID		TECN	COMMENT
• • • We do not use the following data for averages, fits, limits, etc. • • •					
0.48 ± 0.03 ± 0.04	920	JESSOP	98	CLE2	$e^+e^- \approx \Upsilon(4S)$
0.54 ± 0.09 ± 0.06	165	ALEXANDER	92	CLE2	See JESSOP 98

$\Gamma(\omega\pi^+)/\Gamma_{total}$ Γ_{72}/Γ

Unseen decay modes of the ω are included.

VALUE (units 10^{-2})	EVTS	DOCUMENT ID		TECN	COMMENT
0.24 ± 0.06 OUR FIT					
0.21 ± 0.09 ± 0.01	6 ± 2.4	GE	09A	CLEO	e^+e^- at 4170 MeV

$\Gamma(\omega\pi^+)/\Gamma(\eta\pi^+)$ Γ_{72}/Γ_{71}

Unseen decay modes of the resonances are included.

VALUE	DOCUMENT ID		TECN	COMMENT
0.14 ± 0.04 OUR FIT				
0.16 ± 0.04 ± 0.03	BALEST	97	CLE2	$e^+e^- \approx \Upsilon(4S)$

$\Gamma(3\pi^+2\pi^-)/\Gamma(K^+K^-\pi^+)$ Γ_{73}/Γ_{36}

VALUE	EVTS	DOCUMENT ID		TECN	COMMENT
0.146 ± 0.014 OUR AVERAGE					
0.145 ± 0.011 ± 0.010	671	LINK	03D	FOCS	γ A, $\overline{E}_\gamma \approx$ 180 GeV
0.158 ± 0.042 ± 0.031	37	FRABETTI	97C	E687	γBe, $\overline{E}_\gamma \approx$ 200 GeV

$\Gamma(\eta\rho^+)/\Gamma_{total}$ Γ_{75}/Γ

Unseen decay modes of the η are included.

VALUE (units 10^{-2})	EVTS	DOCUMENT ID		TECN	COMMENT
8.9 ± 0.6 ± 0.5	328 ± 22	NAIK	09A	CLEO	$\eta \to 2\gamma$

$\Gamma(\eta\rho^+)/\Gamma(\phi\pi^+)$ Γ_{75}/Γ_{37}

Unseen decay modes of the resonances are included.

VALUE	EVTS	DOCUMENT ID		TECN	COMMENT
• • • We do not use the following data for averages, fits, limits, etc. • • •					
2.98 ± 0.20 ± 0.39	447	JESSOP	98	CLE2	$e^+e^- \approx \Upsilon(4S)$
$2.86 \pm 0.38^{+0.36}_{-0.38}$	217	AVERY	92	CLE2	See JESSOP 98

$\Gamma(\eta\pi^+\pi^0)/\Gamma_{total}$ Γ_{76}/Γ

VALUE (units 10^{-2})	DOCUMENT ID		TECN	COMMENT
9.2 ± 0.4 ± 1.1	ONYISI	13	CLEO	e^+e^- at 4.17 GeV

$\Gamma(\omega\pi^+\pi^0)/\Gamma_{total}$ Γ_{77}/Γ

Unseen decay modes of the ω are included.

VALUE (units 10^{-2})	EVTS	DOCUMENT ID		TECN	COMMENT
2.78 ± 0.65 ± 0.25	34 ± 7.9	GE	09A	CLEO	e^+e^- at 4170 MeV

$\Gamma(3\pi^+2\pi^-\pi^0)/\Gamma_{total}$ Γ_{78}/Γ

VALUE	DOCUMENT ID		TECN	COMMENT
$\mathbf{0.049^{+0.033}_{-0.030}}$	BARLAG	92C	ACCM	π^- 230 GeV

$\Gamma(\omega 2\pi^+\pi^-)/\Gamma_{total}$ Γ_{79}/Γ

Unseen decay modes of the ω are included.

VALUE (units 10^{-2})	EVTS	DOCUMENT ID		TECN	COMMENT
1.58 ± 0.45 ± 0.09	29 ± 8.2	GE	09A	CLEO	e^+e^- at 4170 MeV

$\Gamma(\eta'(958)\pi^+)/\Gamma_{total}$ Γ_{80}/Γ

Unseen decay modes of the $\eta'(958)$ are included.

VALUE (units 10^{-2})	DOCUMENT ID		TECN	COMMENT
3.94 ± 0.15 ± 0.20	ONYISI	13	CLEO	e^+e^- at 4.17 GeV
• • • We do not use the following data for averages, fits, limits, etc. • • •				
3.77 ± 0.25 ± 0.30	[1] ALEXANDER	08	CLEO	See ONYISI 13

[1] ALEXANDER 08 uses single- and double-tagged events in an overall fit.

$\Gamma(\eta'(958)\pi^+)/\Gamma(K^+K_S^0)$ Γ_{80}/Γ_{34}

Unseen decay modes of the $\eta'(958)$ are included.

VALUE	EVTS	DOCUMENT ID	TECN	COMMENT
• • • We do not use the following data for averages, fits, limits, etc. • • •				
2.654 ± 0.088 ± 0.139	1436 ± 47	MENDEZ	10	CLEO	See ONYISI 13

$\Gamma(\eta'(958)\pi^+)/\Gamma(\phi\pi^+)$ Γ_{80}/Γ_{37}

Unseen decay modes of the resonances are included.

VALUE	EVTS	DOCUMENT ID		TECN	COMMENT
• • • We do not use the following data for averages, fits, limits, etc. • • •					
1.03 ± 0.06 ± 0.07	537	JESSOP	98	CLE2	$e^+e^- \approx \Upsilon(4S)$
1.20 ± 0.15 ± 0.11	281	ALEXANDER	92	CLE2	See JESSOP 98
$2.5 \pm 1.0\ ^{+1.5}_{-0.4}$	22	ALVAREZ	91	NA14	Photoproduction
2.5 ±0.5 ±0.3	215	ALBRECHT	90D	ARG	$e^+e^- \approx 10.4$ GeV

$\Gamma(\omega\eta\pi^+)/\Gamma_{total}$ Γ_{82}/Γ

Unseen decay modes of the ω and η are included.

VALUE	CL%	DOCUMENT ID		TECN	COMMENT
$\mathbf{< 2.13 \times 10^{-2}}$	90	GE	09A	CLEO	e^+e^- at 4170 MeV

$\Gamma(\eta'(958)\rho^+)/\Gamma_{total}$ Γ_{83}/Γ

VALUE (units 10^{-2})	DOCUMENT ID		TECN	COMMENT
5.8 ± 1.4 ± 0.4	ABLIKIM	15Z	BES3	482 pb^{-1}, 4009 MeV

$\Gamma(\eta'(958)\rho^+)/\Gamma(\phi\pi^+)$ Γ_{83}/Γ_{37}

Unseen decay modes of the resonances are included.

VALUE	EVTS	DOCUMENT ID		TECN	COMMENT
• • • We do not use the following data for averages, fits, limits, etc. • • •					
2.78 ± 0.28 ± 0.30	137	[1] JESSOP	98	CLE2	$e^+e^- \approx \Upsilon(4S)$
$3.44 \pm 0.62^{+0.44}_{-0.46}$	68	AVERY	92	CLE2	See JESSOP 98

Meson Particle Listings

$D_s^{\pm}$

[1] This JESSOP 98 fraction, when combined with other η' fractions, greatly overshoots the inclusive η' fraction. See the measurement just above, which fits nicely.

$\Gamma(\eta'(958)\pi^+\pi^0)/\Gamma_{total}$ Γ_{84}/Γ

VALUE (units 10^{-2})	DOCUMENT ID		TECN	COMMENT
5.6±0.5±0.6	ONYISI	13	CLEO	e^+e^- at 4.17 GeV

$\Gamma(\eta'(958)\pi^+\pi^0$ nonresonant$)/\Gamma_{total}$ Γ_{85}/Γ

VALUE	CL%	DOCUMENT ID		TECN	COMMENT
<5.1 × 10^{-2}	90	ABLIKIM	15Z	BES3	482 pb^{-1}, 4009 MeV

Modes with one or three K's

$\Gamma(K^+\pi^0)/\Gamma(K^+K_S^0)$ Γ_{86}/Γ_{34}

VALUE (units 10^{-2})	EVTS	DOCUMENT ID		TECN	COMMENT
4.2±1.4±0.2	202 ± 70	MENDEZ	10	CLEO	e^+e^- at 4170 MeV
• • • We do not use the following data for averages, fits, limits, etc. • • •					
5.5±1.3±0.7	141 ± 34	ADAMS	07A	CLEO	See MENDEZ 10

$\Gamma(K_S^0\pi^+)/\Gamma(K^+K_S^0)$ Γ_{87}/Γ_{34}

VALUE (units 10^{-2})	EVTS	DOCUMENT ID		TECN	COMMENT
8.12±0.28 OUR AVERAGE					
8.5 ±0.7 ±0.2	393 ± 33	MENDEZ	10	CLEO	e^+e^- at 4170 MeV
8.03±0.24±0.19	17.6k±481	WON	09	BELL	e^+e^- at $\Upsilon(4S)$
10.4 ±2.4 ±1.4	113 ± 26	LINK	08	FOCS	γ A, $\overline{E}_\gamma \approx$ 180 GeV
• • • We do not use the following data for averages, fits, limits, etc. • • •					
8.2 ±0.9 ±0.2	206 ± 22	ADAMS	07A	CLEO	See MENDEZ 10

$\Gamma(K^+\eta)/\Gamma(K^+K_S^0)$ Γ_{88}/Γ_{34}

Unseen decay modes of the η are included.

VALUE (units 10^{-2})	EVTS	DOCUMENT ID		TECN	COMMENT
11.8±2.2±0.6	222 ± 41	MENDEZ	10	CLEO	e^+e^- at 4170 MeV

$\Gamma(K^+\eta)/\Gamma(\eta\pi^+)$ Γ_{88}/Γ_{71}

VALUE (units 10^{-2})	EVTS	DOCUMENT ID		TECN	COMMENT
• • • We do not use the following data for averages, fits, limits, etc. • • •					
8.9±1.5±0.4	113 ± 18	ADAMS	07A	CLEO	See MENDEZ 10

$\Gamma(K^+\omega)/\Gamma_{total}$ Γ_{89}/Γ

Unseen decay modes of the ω are included.

VALUE (units 10^{-2})	CL%	DOCUMENT ID		TECN	COMMENT
<0.24	90	GE	09A	CLEO	e^+e^- at 4170 MeV

$\Gamma(K^+\eta'(958))/\Gamma(K^+K_S^0)$ Γ_{90}/Γ_{34}

Unseen decay modes of the $\eta'(958)$ are included.

VALUE (units 10^{-2})	EVTS	DOCUMENT ID		TECN	COMMENT
11.8±3.6±0.7	56 ± 17	MENDEZ	10	CLEO	e^+e^- at 4170 MeV

$\Gamma(K^+\eta'(958))/\Gamma(\eta'(958)\pi^+)$ Γ_{90}/Γ_{80}

VALUE (units 10^{-2})	EVTS	DOCUMENT ID		TECN	COMMENT
• • • We do not use the following data for averages, fits, limits, etc. • • •					
4.2±1.3±0.3	28 ± 9	ADAMS	07A	CLEO	See MENDEZ 10

$\Gamma(K^+\pi^+\pi^-)/\Gamma_{total}$ Γ_{91}/Γ

VALUE (units 10^{-2})	DOCUMENT ID		TECN	COMMENT
0.66 ±0.04 OUR FIT				
0.654±0.033±0.025	ONYISI	13	CLEO	e^+e^- at 4.17 GeV
• • • We do not use the following data for averages, fits, limits, etc. • • •				
0.69 ±0.05 ±0.03	[1] ALEXANDER	08	CLEO	See ONYISI 13

[1] ALEXANDER 08 uses single- and double-tagged events in an overall fit.

$\Gamma(K^+\pi^+\pi^-)/\Gamma(K^+K^-\pi^+)$ Γ_{91}/Γ_{36}

VALUE	EVTS	DOCUMENT ID		TECN	COMMENT
0.120±0.007 OUR FIT Error includes scale factor of 1.1.					
0.127±0.007±0.014	567 ± 31	LINK	04F	FOCS	γ A, $\overline{E}_\gamma \approx$ 180 GeV

$\Gamma(K^+\rho^0)/\Gamma(K^+\pi^+\pi^-)$ Γ_{92}/Γ_{91}

This is the "fit fraction" from the Dalitz-plot analysis.

VALUE	DOCUMENT ID		TECN	COMMENT
0.3883±0.0531±0.0261	LINK	04F	FOCS	Dalitz fit, 567 evts

$\Gamma(K^+\rho(1450)^0, \rho^0 \to \pi^+\pi^-)/\Gamma(K^+\pi^+\pi^-)$ Γ_{93}/Γ_{91}

This is the "fit fraction" from the Dalitz-plot analysis.

VALUE	DOCUMENT ID		TECN	COMMENT
0.1062±0.0351±0.0104	LINK	04F	FOCS	Dalitz fit, 567 evts

$\Gamma(K^*(892)^0\pi^+, K^{*0} \to K^+\pi^-)/\Gamma(K^+\pi^+\pi^-)$ Γ_{94}/Γ_{91}

This is the "fit fraction" from the Dalitz-plot analysis.

VALUE	DOCUMENT ID		TECN	COMMENT
0.2164±0.0321±0.0114	LINK	04F	FOCS	Dalitz fit, 567 evts

$\Gamma(K^*(1410)^0\pi^+, K^{*0} \to K^+\pi^-)/\Gamma(K^+\pi^+\pi^-)$ Γ_{95}/Γ_{91}

This is the "fit fraction" from the Dalitz-plot analysis.

VALUE	DOCUMENT ID		TECN	COMMENT
0.1882±0.0403±0.0122	LINK	04F	FOCS	Dalitz fit, 567 evts

$\Gamma(K^*(1430)^0\pi^+, K^{*0} \to K^+\pi^-)/\Gamma(K^+\pi^+\pi^-)$ Γ_{96}/Γ_{91}

This is the "fit fraction" from the Dalitz-plot analysis.

VALUE	DOCUMENT ID		TECN	COMMENT
0.0765±0.0500±0.0170	LINK	04F	FOCS	Dalitz fit, 567 evts

$\Gamma(K^+\pi^+\pi^-$ nonresonant$)/\Gamma(K^+\pi^+\pi^-)$ Γ_{97}/Γ_{91}

This is the "fit fraction" from the Dalitz-plot analysis.

VALUE	DOCUMENT ID		TECN	COMMENT
0.1588±0.0492±0.0153	LINK	04F	FOCS	Dalitz fit, 567 evts

$\Gamma(K^0\pi^+\pi^0)/\Gamma_{total}$ Γ_{98}/Γ

VALUE (units 10^{-2})	EVTS	DOCUMENT ID		TECN	COMMENT
1.00±0.18±0.04	44 ± 8	NAIK	09A	CLEO	e^+e^- at 4170 MeV

$\Gamma(K_S^0 2\pi^+\pi^-)/\Gamma(K_S^0 K^- 2\pi^+)$ Γ_{99}/Γ_{50}

VALUE	EVTS	DOCUMENT ID		TECN	COMMENT
0.18±0.04±0.05	179 ± 36	LINK	08	FOCS	γ A, $\overline{E}_\gamma \approx$ 180 GeV

$\Gamma(K^+\omega\pi^0)/\Gamma_{total}$ Γ_{100}/Γ

Unseen decay modes of the ω are included.

VALUE (units 10^{-2})	CL%	DOCUMENT ID		TECN	COMMENT
<0.82	90	GE	09A	CLEO	e^+e^- at 4170 MeV

$\Gamma(K^+\omega\pi^+\pi^-)/\Gamma_{total}$ Γ_{101}/Γ

Unseen decay modes of the ω are included.

VALUE (units 10^{-2})	CL%	DOCUMENT ID		TECN	COMMENT
<0.54	90	GE	09A	CLEO	e^+e^- at 4170 MeV

$\Gamma(K^+\omega\eta)/\Gamma_{total}$ Γ_{102}/Γ

Unseen decay modes of the ω and η are included.

VALUE (units 10^{-2})	CL%	DOCUMENT ID		TECN	COMMENT
<0.79	90	GE	09A	CLEO	e^+e^- at 4170 MeV

$\Gamma(2K^+K^-)/\Gamma(K^+K^-\pi^+)$ Γ_{103}/Γ_{36}

VALUE (units 10^{-3})	EVTS	DOCUMENT ID		TECN	COMMENT
4.0 ±0.3 ±0.2	748 ± 60	DEL-AMO-SA...11G		BABR	$e^+e^- \approx \Upsilon(4S)$
• • • We do not use the following data for averages, fits, limits, etc. • • •					
$8.95 \pm 2.12^{+2.24}_{-2.31}$	31	LINK	02I	FOCS	γ A, ≈ 180 GeV

$\Gamma(\phi K^+, \phi \to K^+K^-)/\Gamma(2K^+K^-)$ $\Gamma_{104}/\Gamma_{103}$

VALUE	DOCUMENT ID		TECN	COMMENT
0.41±0.08±0.03	DEL-AMO-SA...11G		BABR	$e^+e^- \approx \Upsilon(4S)$

Doubly Cabibbo-suppressed modes

$\Gamma(2K^+\pi^-)/\Gamma(K^+K^-\pi^+)$ Γ_{105}/Γ_{36}

VALUE (units 10^{-3})	EVTS	DOCUMENT ID		TECN	COMMENT
2.33±0.23 OUR AVERAGE					
2.3 ±0.3 ±0.2	356 ± 52	DEL-AMO-SA...11G		BABR	$e^+e^- \approx \Upsilon(4S)$
2.29±0.28±0.12	281 ± 34	KO	09	BELL	e^+e^- at $\Upsilon(4S)$
5.2 ±1.7 ±1.1	27 ± 9	LINK	05K	FOCS	<0.78%, CL = 90%

$\Gamma(K^+K^*(892)^0, K^{*0} \to K^+\pi^-)/\Gamma(2K^+\pi^-)$ $\Gamma_{106}/\Gamma_{105}$

VALUE	DOCUMENT ID		TECN	COMMENT
0.47±0.22±0.15	DEL-AMO-SA...11G		BABR	$e^+e^- \approx \Upsilon(4S)$

Baryon-antibaryon mode

$\Gamma(p\overline{p})/\Gamma_{total}$ Γ_{107}/Γ

This is the only baryonic mode allowed kinematically.

VALUE (units 10^{-3})	EVTS	DOCUMENT ID		TECN	COMMENT
$1.30 \pm 0.36^{+0.12}_{-0.16}$	13.0 ± 3.6	ATHAR	08	CLEO	e^+e^-, $E_{cm} \approx$ 4170 MeV

Rare or forbidden modes

$\Gamma(\pi^+e^+e^-)/\Gamma_{total}$ Γ_{108}/Γ

This mode is not a useful test for a ΔC=1 weak neutral current because both quarks must change flavor in this decay.

VALUE	CL%	DOCUMENT ID		TECN	COMMENT
<13 × 10^{-6}	90	LEES	11G	BABR	$e^+e^- \approx \Upsilon(4S)$
• • • We do not use the following data for averages, fits, limits, etc. • • •					
< 2.2 × 10^{-5}	90	[1] RUBIN	10	CLEO	e^+e^- at 4170 MeV
<27 × 10^{-5}	90	AITALA	99G	E791	π^- N 500 GeV

[1] This RUBIN 10 limit is for the e^+e^- mass in the continuum away from the $\phi(1020)$. See the next data block.

$\Gamma(\pi^+\phi,\ \phi\to e^+e^-)/\Gamma_{total}$ Γ_{109}/Γ

This is *not* a test for the $\Delta C = 1$ weak neutral current, but leads to the $\pi^+e^+e^-$ final state.

VALUE	EVTS	DOCUMENT ID		TECN	COMMENT
$(6^{+8}_{-4}\pm1)\times10^{-6}$	3	RUBIN	10	CLEO	e^+e^- at 4170 MeV

$\Gamma(\pi^+\mu^+\mu^-)/\Gamma_{total}$ Γ_{110}/Γ

This mode is not a useful test for a ΔC=1 weak neutral current because both quarks must change flavor in this decay.

VALUE	CL%	DOCUMENT ID		TECN	COMMENT
$<4.1\times10^{-7}$	90	AAIJ	13AF	LHCB	pp at 7 TeV
• • • We do not use the following data for averages, fits, limits, etc. • • •					
$<4.3\times10^{-5}$	90	LEES	11G	BABR	$e^+e^-\approx\ \Upsilon(4S)$
$<2.6\times10^{-5}$	90	LINK	03F	FOCS	γ A, $\overline{E}_\gamma\approx$ 180 GeV
$<1.4\times10^{-4}$	90	AITALA	99G	E791	π^- N 500 GeV
$<4.3\times10^{-4}$	90	KODAMA	95	E653	π^- emulsion 600 GeV

$\Gamma(K^+e^+e^-)/\Gamma_{total}$ Γ_{111}/Γ

A test for the ΔC=1 weak neutral current. Allowed by higher-order electroweak interactions.

VALUE	CL%	DOCUMENT ID		TECN	COMMENT
$<3.7\times10^{-6}$	90	LEES	11G	BABR	$e^+e^-\approx\ \Upsilon(4S)$
• • • We do not use the following data for averages, fits, limits, etc. • • •					
$<5.2\times10^{-5}$	90	RUBIN	10	CLEO	e^+e^- at 4170 MeV
$<1.6\times10^{-3}$	90	AITALA	99G	E791	π^- N 500 GeV

$\Gamma(K^+\mu^+\mu^-)/\Gamma_{total}$ Γ_{112}/Γ

A test for the ΔC=1 weak neutral current. Allowed by higher-order electroweak interactions.

VALUE	CL%	DOCUMENT ID		TECN	COMMENT
$<21\ \times10^{-6}$	90	LEES	11G	BABR	$e^+e^-\approx\ \Upsilon(4S)$
• • • We do not use the following data for averages, fits, limits, etc. • • •					
$<3.6\times10^{-5}$	90	LINK	03F	FOCS	γ A, $\overline{E}_\gamma\approx$ 180 GeV
$<1.4\times10^{-4}$	90	AITALA	99G	E791	π^- N 500 GeV
$<5.9\times10^{-4}$	90	KODAMA	95	E653	π^- emulsion 600 GeV

$\Gamma(K^*(892)^+\mu^+\mu^-)/\Gamma_{total}$ Γ_{113}/Γ

A test for the ΔC=1 weak neutral current. Allowed by higher-order electroweak interactions.

VALUE	CL%	DOCUMENT ID		TECN	COMMENT
$<1.4\times10^{-3}$	90	KODAMA	95	E653	π^- emulsion 600 GeV

$\Gamma(\pi^+e^+\mu^-)/\Gamma_{total}$ Γ_{114}/Γ

A test of lepton-family-number conservation.

VALUE	CL%	DOCUMENT ID		TECN	COMMENT
$<12\times10^{-6}$	90	LEES	11G	BABR	$e^+e^-\approx\ \Upsilon(4S)$

$\Gamma(\pi^+e^-\mu^+)/\Gamma_{total}$ Γ_{115}/Γ

A test of lepton-family-number conservation.

VALUE	CL%	DOCUMENT ID		TECN	COMMENT
$<20\times10^{-6}$	90	LEES	11G	BABR	$e^+e^-\approx\ \Upsilon(4S)$

$\Gamma(K^+e^+\mu^-)/\Gamma_{total}$ Γ_{116}/Γ

A test of lepton-family-number conservation.

VALUE	CL%	DOCUMENT ID		TECN	COMMENT
$<14\times10^{-6}$	90	LEES	11G	BABR	$e^+e^-\approx\ \Upsilon(4S)$

$\Gamma(K^+e^-\mu^+)/\Gamma_{total}$ Γ_{117}/Γ

A test of lepton-family-number conservation.

VALUE	CL%	DOCUMENT ID		TECN	COMMENT
$<9.7\times10^{-6}$	90	LEES	11G	BABR	$e^+e^-\approx\ \Upsilon(4S)$

$\Gamma(\pi^-2e^+)/\Gamma_{total}$ Γ_{118}/Γ

A test of lepton-number conservation.

VALUE	CL%	DOCUMENT ID		TECN	COMMENT
$<4.1\times10^{-6}$	90	LEES	11G	BABR	$e^+e^-\approx\ \Upsilon(4S)$
• • • We do not use the following data for averages, fits, limits, etc. • • •					
$<1.8\times10^{-5}$	90	RUBIN	10	CLEO	e^+e^- at 4170 MeV
$<69\ \times10^{-5}$	90	AITALA	99G	E791	π^- N 500 GeV

$\Gamma(\pi^-2\mu^+)/\Gamma_{total}$ Γ_{119}/Γ

A test of lepton-number conservation.

VALUE	CL%	DOCUMENT ID		TECN	COMMENT
$<1.2\times10^{-7}$	90	AAIJ	13AF	LHCB	pp at 7 TeV
• • • We do not use the following data for averages, fits, limits, etc. • • •					
$<1.4\times10^{-5}$	90	LEES	11G	BABR	$e^+e^-\approx\ \Upsilon(4S)$
$<2.9\times10^{-5}$	90	LINK	03F	FOCS	γ A, $\overline{E}_\gamma\approx$ 180 GeV
$<8.2\times10^{-5}$	90	AITALA	99G	E791	π^- N 500 GeV
$<4.3\times10^{-4}$	90	KODAMA	95	E653	π^- emulsion 600 GeV

$\Gamma(\pi^-e^+\mu^+)/\Gamma_{total}$ Γ_{120}/Γ

A test of lepton-number conservation.

VALUE	CL%	DOCUMENT ID		TECN	COMMENT
$<8.4\times10^{-6}$	90	LEES	11G	BABR	$e^+e^-\approx\ \Upsilon(4S)$
• • • We do not use the following data for averages, fits, limits, etc. • • •					
$<7.3\times10^{-4}$	90	AITALA	99G	E791	π^- N 500 GeV

$\Gamma(K^-2e^+)/\Gamma_{total}$ Γ_{121}/Γ

A test of lepton-number conservation.

VALUE	CL%	DOCUMENT ID		TECN	COMMENT
$<5.2\times10^{-6}$	90	LEES	11G	BABR	$e^+e^-\approx\ \Upsilon(4S)$
• • • We do not use the following data for averages, fits, limits, etc. • • •					
$<1.7\times10^{-5}$	90	RUBIN	10	CLEO	e^+e^- at 4170 MeV
$<63\ \times10^{-5}$	90	AITALA	99G	E791	π^- N 500 GeV

$\Gamma(K^-2\mu^+)/\Gamma_{total}$ Γ_{122}/Γ

A test of lepton-number conservation.

VALUE	CL%	DOCUMENT ID		TECN	COMMENT
$<1.3\times10^{-5}$	90	LEES	11G	BABR	$e^+e^-\approx\ \Upsilon(4S)$
$<1.3\times10^{-5}$	90	LINK	03F	FOCS	γ A, $\overline{E}_\gamma\approx$ 180 GeV
• • • We do not use the following data for averages, fits, limits, etc. • • •					
$<1.8\times10^{-4}$	90	AITALA	99G	E791	π^- N 500 GeV
$<5.9\times10^{-4}$	90	KODAMA	95	E653	π^- emulsion 600 GeV

$\Gamma(K^-e^+\mu^+)/\Gamma_{total}$ Γ_{123}/Γ

A test of lepton-number conservation.

VALUE	CL%	DOCUMENT ID		TECN	COMMENT
$<6.1\times10^{-6}$	90	LEES	11G	BABR	$e^+e^-\approx\ \Upsilon(4S)$
• • • We do not use the following data for averages, fits, limits, etc. • • •					
$<6.8\times10^{-4}$	90	AITALA	99G	E791	π^- N 500 GeV

$\Gamma(K^*(892)^-2\mu^+)/\Gamma_{total}$ Γ_{124}/Γ

A test of lepton-number conservation.

VALUE	CL%	DOCUMENT ID		TECN	COMMENT
$<1.4\times10^{-3}$	90	KODAMA	95	E653	π^- emulsion 600 GeV

$D_s^+ - D_s^-$ *CP*-VIOLATING DECAY-RATE ASYMMETRIES

This is the difference between D_s^+ and D_s^- partial widths for the decay to state f, divided by the sum of the widths:
$A_{CP}(f) = [\Gamma(D_s^+\to f) - \Gamma(D_s^-\to \overline{f})] / [\Gamma(D_s^+\to f) + \Gamma(D_s^-\to \overline{f})]$.

$A_{CP}(\mu^\pm\nu)$ in $D_s^+\to\ \mu^+\nu$, $D_s^-\to\ \mu^-\overline{\nu}_\mu$

VALUE (%)	DOCUMENT ID		TECN	COMMENT
4.8±6.1	ALEXANDER	09	CLEO	e^+e^- at 4170 MeV

$A_{CP}(K^\pm K_S^0)$ in $D_s^\pm\to\ K^\pm K_S^0$

VALUE (%)	EVTS	DOCUMENT ID		TECN	COMMENT
0.08±0.26 OUR AVERAGE					
$-0.05\pm0.23\pm0.24$	288k	[1] LEES	13E	BABR	e^+e^- at $\Upsilon(4S)$
2.6 ±1.5 ±0.6		ONYISI	13	CLEO	e^+e^- at 4.17 GeV
$0.12\pm0.36\pm0.22$		KO	10	BELL	$e^+e^-\approx\ \Upsilon(4S)$
• • • We do not use the following data for averages, fits, limits, etc. • • •					
4.7 ±1.8 ±0.9	4.0k	MENDEZ	10	CLEO	See ONYISI 13
4.9 ±2.1 ±0.9		ALEXANDER	08	CLEO	See MENDEZ 10

[1] LEES 13E finds that after subtracting the contribution due to $K^0-\overline{K}^0$ mixing, the *CP* asymmetry is $(+0.28\pm0.23\pm0.24)$%.

$A_{CP}(K^+K^-\pi^\pm)$ in $D_s^\pm\to\ K^+K^-\pi^\pm$

VALUE (%)	DOCUMENT ID		TECN	COMMENT
−0.5±0.8±0.4	ONYISI	13	CLEO	e^+e^- at 4.17 GeV
• • • We do not use the following data for averages, fits, limits, etc. • • •				
$0.3\pm1.1\pm0.8$	ALEXANDER	08	CLEO	See ONYISI 13

$A_{CP}(\phi\pi^\pm)$ in $D_s^\pm\to\ \phi\pi^\pm$

VALUE (%)	DOCUMENT ID		TECN	COMMENT
−0.38±0.26±0.08	ABAZOV	14B	D0	$p\overline{p}$ at 1.96 TeV

$A_{CP}(K^\pm K_S^0\pi^0)$ in $D_s^\pm\to\ K^\pm K_S^0\pi^0$

VALUE (%)	DOCUMENT ID		TECN	COMMENT
−1.6±6.0±1.1	ONYISI	13	CLEO	e^+e^- at 4.17 GeV

$A_{CP}(2K_S^0\pi^\pm)$ in $D_s^\pm\to\ 2K_S^0\pi^\pm$

VALUE (%)	DOCUMENT ID		TECN	COMMENT
3.1±5.2±0.6	ONYISI	13	CLEO	e^+e^- at 4.17 GeV

$A_{CP}(K^+K^-\pi^\pm\pi^0)$ in $D_s^\pm\to\ K^+K^-\pi^\pm\pi^0$

VALUE (%)	DOCUMENT ID		TECN	COMMENT
0.0±2.7±1.2	ONYISI	13	CLEO	e^+e^- at 4.17 GeV
• • • We do not use the following data for averages, fits, limits, etc. • • •				
$-5.9\pm4.2\pm1.2$	ALEXANDER	08	CLEO	See ONYISI 13

$A_{CP}(K^\pm K_S^0\pi^+\pi^-)$ in $D_s^\pm\to\ K^\pm K_S^0\pi^+\pi^-$

VALUE (%)	DOCUMENT ID		TECN	COMMENT
−5.7±5.3±0.9	ONYISI	13	CLEO	e^+e^- at 4.17 GeV

Meson Particle Listings

$D_s^\pm$

$A_{CP}(K_S^0 K^\mp 2\pi^\pm)$ in $D_s^+ \to K_S^0 K^\mp 2\pi^\pm$

VALUE (%)	DOCUMENT ID		TECN	COMMENT
4.1±2.7±0.9	ONYISI	13	CLEO	e^+e^- at 4.17 GeV
• • • We do not use the following data for averages, fits, limits, etc. • • •				
−0.7±3.6±1.1	ALEXANDER	08	CLEO	See ONYISI 13

$A_{CP}(\pi^+\pi^-\pi^\pm)$ in $D_s^\pm \to \pi^+\pi^-\pi^\pm$

VALUE (%)	DOCUMENT ID		TECN	COMMENT
−0.7±3.0±0.6	ONYISI	13	CLEO	e^+e^- at 4.17 GeV
• • • We do not use the following data for averages, fits, limits, etc. • • •				
2.0±4.6±0.7	ALEXANDER	08	CLEO	See ONYISI 13

$A_{CP}(\pi^\pm\eta)$ in $D_s^\pm \to \pi^\pm\eta$

VALUE (%)	EVTS	DOCUMENT ID		TECN	COMMENT
1.1±3.0±0.8		ONYISI	13	CLEO	e^+e^- at 4.17 GeV
• • • We do not use the following data for averages, fits, limits, etc. • • •					
−4.6±2.9±0.3	2.5k	MENDEZ	10	CLEO	See ONYISI 13
−8.2±5.2±0.8		ALEXANDER	08	CLEO	See MENDEZ 10

$A_{CP}(\pi^\pm\eta')$ in $D_s^\pm \to \pi^\pm\eta'$

VALUE (%)	EVTS	DOCUMENT ID		TECN	COMMENT
−0.9 ±0.5 OUR AVERAGE					
−0.82±0.36±0.35	152k	AAIJ	17AF	LHCB	pp at 7, 8 TeV
−2.2 ±2.2 ±0.6		ONYISI	13	CLEO	e^+e^- at 4.17 GeV
• • • We do not use the following data for averages, fits, limits, etc. • • •					
−6.1 ±3.0 ±0.3	1.4k	MENDEZ	10	CLEO	See ONYISI 13
−5.5 ±3.7 ±1.2		ALEXANDER	08	CLEO	See MENDEZ 10

$A_{CP}(\eta\pi^\pm\pi^0)$ in $D_s^\pm \to \eta\pi^\pm\pi^0$

VALUE (%)	DOCUMENT ID		TECN	COMMENT
−0.5±3.9±2.0	ONYISI	13	CLEO	e^+e^- at 4.17 GeV

$A_{CP}(\eta'\pi^\pm\pi^0)$ in $D_s^\pm \to \eta'\pi^\pm\pi^0$

VALUE (%)	DOCUMENT ID		TECN	COMMENT
−0.4±7.4±1.9	ONYISI	13	CLEO	e^+e^- at 4.17 GeV

$A_{CP}(K^\pm\pi^0)$ in $D_s^\pm \to K^\pm\pi^0$

VALUE (%)	EVTS	DOCUMENT ID		TECN	COMMENT
−26.6±23.8±0.9	202 ± 70	MENDEZ	10	CLEO	e^+e^- at 4.170 MeV
• • • We do not use the following data for averages, fits, limits, etc. • • •					
2 ±29		ADAMS	07A	CLEO	See MENDEZ 10

$A_{CP}(\overline{K}^0/K^0\pi^\pm)$ in $D_s^+ \to \overline{K}^0\pi^+$, $D_s^- \to K^0\pi^-$

VALUE (%)	EVTS	DOCUMENT ID		TECN	COMMENT
0.4 ±0.5 OUR AVERAGE					
0.38±0.46±0.17	121k	[1] AAIJ	14BD	LHCB	pp at 7, 8 TeV
0.3 ±2.0 ±0.3	14k	LEES	13E	BABR	e^+e^- at $\Upsilon(4S)$
• • • We do not use the following data for averages, fits, limits, etc. • • •					
0.61±0.83±0.14	26k	AAIJ	13W	LHCB	See AAIJ 14BD

[1] AAIJ 14BD reports its result as $A_{CP}(D_s^\pm \to K_S^0 K^\pm)$ with CP-violation effects in the $K^0 - \overline{K}^0$ system subtracted. It also measures $A_{CP}(D^\pm \to \overline{K}^0/K^0K^\pm) + A_{CP}(D_s^\pm \to \overline{K}^0/K^0\pi^\pm) = (0.41 \pm 0.49 \pm 0.26)\%$.

$A_{CP}(K_S^0\pi^\pm)$ in $D_s^\pm \to K_S^0\pi^\pm$

VALUE (%)	EVTS	DOCUMENT ID		TECN	COMMENT
3.1 ± 2.6 OUR AVERAGE	Error includes scale factor of 1.7. See the ideogram below.				
0.6 ± 2.0 ±0.3	14k	LEES	13E	BABR	e^+e^- at $\Upsilon(4S)$
5.45± 2.50±0.33		KO	10	BELL	$e^+e^- \approx \Upsilon(4S)$
16.3 ± 7.3 ±0.3	0.4k	MENDEZ	10	CLEO	e^+e^- at 4170 MeV
• • • We do not use the following data for averages, fits, limits, etc. • • •					
27 ±11		ADAMS	07A	CLEO	See MENDEZ 10

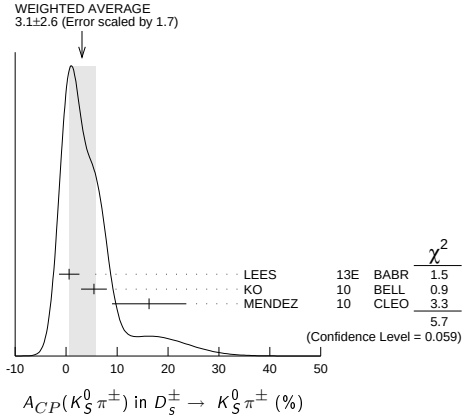

$A_{CP}(K^\pm\pi^+\pi^-)$ in $D_s^\pm \to K^\pm\pi^+\pi^-$

VALUE (%)	DOCUMENT ID		TECN	COMMENT
4.5±4.8±0.6	ONYISI	13	CLEO	e^+e^- at 4.17 GeV
• • • We do not use the following data for averages, fits, limits, etc. • • •				
11.2±7.0±0.9	ALEXANDER	08	CLEO	See ONYISI 13

$A_{CP}(K^\pm\eta)$ in $D_s^\pm \to K^\pm\eta$

VALUE (%)	EVTS	DOCUMENT ID		TECN	COMMENT
9.3±15.2±0.9	222 ± 41	MENDEZ	10	CLEO	e^+e^- at 4170 MeV
• • • We do not use the following data for averages, fits, limits, etc. • • •					
−20 ±18		ADAMS	07A	CLEO	See MENDEZ 10

$A_{CP}(K^\pm\eta'(958))$ in $D_s^\pm \to K^\pm\eta'(958)$

VALUE (%)	EVTS	DOCUMENT ID		TECN	COMMENT
6.0±18.9±0.9	56 ± 17	MENDEZ	10	CLEO	e^+e^- at 4170 MeV
• • • We do not use the following data for averages, fits, limits, etc. • • •					
−17 ±37		ADAMS	07A	CLEO	See MENDEZ 10

CP VIOLATING ASYMMETRIES OF P-ODD (T-ODD) MOMENTS

$A_{Tviol}(K_S^0 K^\pm\pi^+\pi^-)$ in $D_s^\pm \to K_S^0 K^\pm\pi^+\pi^-$

$C_T \equiv \vec{p}_{K^+} \cdot (\vec{p}_{\pi^+} \times \vec{p}_{\pi^-})$ is a parity-odd correlation of the K^+, π^+, and π^- momenta for the D_s^+. $\overline{C}_T \equiv \vec{p}_{K^-} \cdot (\vec{p}_{\pi^-} \times \vec{p}_{\pi^+})$ is the corresponding quantity for the D_s^-. Then

$A_T \equiv [\Gamma(C_T > 0) - \Gamma(C_T \leq 0)] \,/\, [\Gamma(C_T > 0) + \Gamma(C_T < 0)]$, and

$\overline{A}_T \equiv [\Gamma(-\overline{C}_T > 0) - \Gamma(-\overline{C}_T < 0)] \,/\, [\Gamma(-\overline{C}_T > 0) + \Gamma(-\overline{C}_T < 0)]$, and

$A_{Tviol} \equiv \frac{1}{2}(A_T - \overline{A}_T)$. C_T and $\overline{C}_T$ are commonly referred to as T-odd moments, because they are odd under T reversal. However, the T-conjugate process $K_S^0 K^\pm\pi^+\pi^- \to D_s^\pm$ is not accessible, while the P-conjugate process is.

VALUE (units 10^{-3})	EVTS	DOCUMENT ID		TECN	COMMENT
−13.6± 7.7± 3.4	29.8±0.3k	LEES	11E	BABR	$e^+e^- \approx \Upsilon(4S)$
• • • We do not use the following data for averages, fits, limits, etc. • • •					
−36 ±67 ±23	508 ± 34	LINK	05E	FOCS	γ A, $\overline{E}_\gamma \approx 180$ GeV

$D_s^+ \to \phi\ell^+\nu_\ell$ FORM FACTORS

$r_2 \equiv A_2(0)/A_1(0)$ in $D_s^+ \to \phi\ell^+\nu_\ell$

VALUE	EVTS	DOCUMENT ID		TECN	COMMENT
0.84 ±0.11 OUR AVERAGE	Error includes scale factor of 2.4.				
0.816±0.036±0.030	25±0.5k	[1] AUBERT	08AN	BABR	$\phi e^+\nu_e$
0.713±0.202±0.284	793	LINK	04C	FOCS	$\phi\mu^+\nu_\mu$
1.57 ±0.25 ±0.19	271	AITALA	99D	E791	$\phi e^+\nu_e$, $\phi\mu^+\nu_\mu$
1.4 ±0.5 ±0.3	308	AVERY	94B	CLE2	$\phi e^+\nu_e$
1.1 ±0.8 ±0.1	90	FRABETTI	94F	E687	$\phi\mu^+\nu_\mu$
2.1 $^{+0.6}_{-0.5}$ ±0.2	19	KODAMA	93	E653	$\phi\mu^+\nu_\mu$

[1] To compare with previous measurements, this AUBERT 08AN value is from a fit that fixes the pole masses at $m_A = 2.5$ GeV/c^2 and $m_V = 2.1$ GeV/c^2. A simultaneous fit to r_2, r_V, r_0 (a significant s-wave contribution) and m_A, gives $r_2 = 0.763 \pm 0.071 \pm 0.065$.

$r_V \equiv V(0)/A_1(0)$ in $D_s^+ \to \phi\ell^+\nu_\ell$

VALUE	EVTS	DOCUMENT ID		TECN	COMMENT
1.80 ±0.08 OUR AVERAGE					
1.807±0.046±0.065	25±0.5k	[1] AUBERT	08AN	BABR	$\phi e^+\nu_e$
1.549±0.250±0.148	793	LINK	04C	FOCS	$\phi\mu^+\nu_\mu$
2.27 ±0.35 ±0.22	271	AITALA	99D	E791	$\phi e^+\nu_e$, $\phi\mu^+\nu_\mu$
0.9 ±0.6 ±0.3	308	AVERY	94B	CLE2	$\phi e^+\nu_e$
1.8 ±0.9 ±0.2	90	FRABETTI	94F	E687	$\phi\mu^+\nu_\mu$
2.3 $^{+1.1}_{-0.9}$ ±0.4	19	KODAMA	93	E653	$\phi\mu^+\nu_\mu$

[1] To compare with previous measurements, this AUBERT 08AN value is from a fit that fixes the pole masses at $m_A = 2.5$ GeV/c^2 and $m_V = 2.1$ GeV/c^2. A simultaneous fit to r_2, r_V, r_0 (a significant s-wave contribution) and m_A, gives $r_V = 1.849 \pm 0.060 \pm 0.095$.

Γ_L/Γ_T in $D_s^+ \to \phi\ell^+\nu_\ell$

VALUE	EVTS	DOCUMENT ID		TECN	COMMENT
0.72±0.18 OUR AVERAGE					
1.0 ±0.3 ±0.2	308	AVERY	94B	CLE2	$\phi e^+\nu_e$
1.0 ±0.5 ±0.1	90	[1] FRABETTI	94F	E687	$\phi\mu^+\nu_\mu$
0.54±0.21±0.10	19	[1] KODAMA	93	E653	$\phi\mu^+\nu_\mu$

[1] FRABETTI 94F and KODAMA 93 evaluate Γ_L/Γ_T for a lepton mass of zero.

$D_s^\pm$ REFERENCES

ABLIKIM	18A	PR D97 012006	M. Ablikim *et al.*	(BES III Collab.)
AAIJ	17AF	PL B771 21	R. Aaij *et al.*	(LHCb Collab.)
AAIJ	17AN	PRL 119 101801	R. Aaij *et al.*	(LHCb Collab.)
ABLIKIM	16O	PR D94 072004	M. Ablikim *et al.*	(BES III Collab.)
ABLIKIM	16T	PR D94 112003	M. Ablikim *et al.*	(BES III Collab.)
ABLIKIM	15Z	PL B750 466	M. Ablikim *et al.*	(BES III Collab.)
HIETALA	15	PR D92 012009	J. Hietala *et al.*	(MINN, LUTH, OXF)
LEES	15D	PR D91 019901 (errat.)	J.P. Lees *et al.*	(BABAR Collab.)

AAIJ	14BD	JHEP 1410 025	R. Aaij *et al.*	(LHCb Collab.)
ABAZOV	14B	PRL 112 111804	V.M. Abazov *et al.*	(D0 Collab.)
AAIJ	13AF	PL B724 203	R. Aaij *et al.*	(LHCb Collab.)
AAIJ	13V	JHEP 1306 065	R. Aaij *et al.*	(LHCb Collab.)
AAIJ	13W	JHEP 1306 112	R. Aaij *et al.*	(LHCb Collab.)
LEES	13E	PR D87 052012	J.P. Lees *et al.*	(BABAR Collab.)
ONYISI	13	PR D88 032009	P.U.E. Onyisi *et al.*	(CLEO Collab.)
ZUPANC	13	JHEP 1309 139	A. Zupanc *et al.*	(BELLE Collab.)
DEL-AMO-SA...	11G	PR D83 052001	P. del Amo Sanchez *et al.*	(BABAR Collab.)
LEES	11E	PR D84 031103	J.P. Lees *et al.*	(BABAR Collab.)
LEES	11G	PR D84 072006	J.P. Lees *et al.*	(BABAR Collab.)
MARTIN	11	PR D84 012005	L. Martin *et al.*	(CLEO Collab.)
ASNER	10	PR D81 052007	D.M. Asner *et al.*	(CLEO Collab.)
DEL-AMO-SA...	10J	PR D82 091103	P. del Amo Sanchez *et al.*	(BABAR Collab.)
Also		PR D91 019901 (errat.)	J.P. Lees *et al.*	(BABAR Collab.)
KO	10	PRL 104 181602	B.R. Ko *et al.*	(BELLE Collab.)
MENDEZ	10	PR D81 052013	H. Mendez *et al.*	(CLEO Collab.)
RUBIN	10	PR D82 092007	P. Rubin *et al.*	(CLEO Collab.)
ALEXANDER	09	PR D79 052001	J.P. Alexander *et al.*	(CLEO Collab.)
AUBERT	09O	PR D79 032003	B. Aubert *et al.*	(BABAR Collab.)
DOBBS	09	PR D79 112008	S. Dobbs *et al.*	(CLEO Collab.)
ECKLUND	09	PR D80 052009	K.M. Ecklund *et al.*	(CLEO Collab.)
GE	09A	PR D80 051102	J.Y. Ge *et al.*	(CLEO Collab.)
KO	09	PRL 102 221802	B.R. Ko *et al.*	(BELLE Collab.)
MITCHELL	09A	PR D79 072008	R.E. Mitchell *et al.*	(CLEO Collab.)
NAIK	09A	PR D80 112004	P. Naik *et al.*	(CLEO Collab.)
ONYISI	09	PR D79 052002	P.U.E. Onyisi *et al.*	(CLEO Collab.)
WON	09	PR D80 111101	E. Won *et al.*	(BELLE Collab.)
YELTON	09	PR D80 052007	J. Yelton *et al.*	(CLEO Collab.)
ALEXANDER	08	PRL 100 161804	J.P. Alexander *et al.*	(CLEO Collab.)
ATHAR	08	PRL 100 181802	S.B. Athar *et al.*	(CLEO Collab.)
AUBERT	08AN	PR D78 051101	B. Aubert *et al.*	(BABAR Collab.)
ECKLUND	08	PRL 100 161801	K.M. Ecklund *et al.*	(CLEO Collab.)
KLEMPT	08	EPJ C55 39	E. Klempt, M. Matveev, A.V. Sarantsev	(BONN+)
LINK	08	PL B660 147	J.M. Link *et al.*	(FNAL FOCUS Collab.)
WIDHALM	08	PRL 100 241801	L. Widhalm *et al.*	(BELLE Collab.)
ADAMS	07A	PRL 99 191805	G.S. Adams *et al.*	(CLEO Collab.)
AUBERT	07V	PRL 98 141801	B. Aubert *et al.*	(BABAR Collab.)
PEDLAR	07A	PR D76 072002	T.K. Pedlar *et al.*	(CLEO Collab.)
Also		PRL 99 071802	M. Artuso *et al.*	(CLEO Collab.)
AUBERT	06N	PR D74 031103	B. Aubert *et al.*	(BABAR Collab.)
HUANG	06B	PR D74 112005	G.S. Huang *et al.*	(CLEO Collab.)
PDG	06	JP G33 1	W.-M. Yao *et al.*	(PDG Collab.)
AUBERT	05V	PR D71 091104	B. Aubert *et al.*	(BABAR Collab.)
LINK	05E	PL B622 239	J.M. Link *et al.*	(FNAL FOCUS Collab.)
LINK	05J	PRL 95 052003	J.M. Link *et al.*	(FNAL FOCUS Collab.)
LINK	05K	PL B624 166	J.M. Link *et al.*	(FNAL FOCUS Collab.)
LINK	04	PL B585 200	J.M. Link *et al.*	(FNAL FOCUS Collab.)
LINK	04C	PL B586 183	J.M. Link *et al.*	(FNAL FOCUS Collab.)
LINK	04D	PL B586 191	J.M. Link *et al.*	(FNAL FOCUS Collab.)
LINK	04F	PL B601 10	J.M. Link *et al.*	(FNAL FOCUS Collab.)
ACOSTA	03D	PR D68 072004	D. Acosta *et al.*	(FNAL CDF-II Collab.)
ANISOVICH	03	EPJ A16 229	V.V. Anisovich *et al.*	
LINK	03D	PL B561 225	J.M. Link *et al.*	(FNAL FOCUS Collab.)
LINK	03F	PL B572 21	J.M. Link *et al.*	(FNAL FOCUS Collab.)
AUBERT	02G	PR D65 091104	B. Aubert *et al.*	(BABAR Collab.)
HEISTER	02I	PL B528 1	A. Heister *et al.*	(ALEPH Collab.)
LINK	02I	PL B541 227	J.M. Link *et al.*	(FNAL FOCUS Collab.)
LINK	02J	PL B541 243	J.M. Link *et al.*	(FNAL FOCUS Collab.)
ABBIENDI	01L	PL B516 236	G. Abbiendi *et al.*	(OPAL Collab.)
AITALA	01A	PRL 86 765	E.M. Aitala *et al.*	(FNAL E791 Collab.)
IORI	01	PL B523 22	M. Iori *et al.*	(FNAL SELEX Collab.)
LINK	01C	PRL 87 162001	J.M. Link *et al.*	(FNAL FOCUS Collab.)
ALEXANDROV	00	PL B478 31	Y. Alexandrov *et al.*	(CERN BEATRICE Collab.)
AITALA	99	PL B445 449	E.M. Aitala *et al.*	(FNAL E791 Collab.)
AITALA	99D	PL B450 294	E.M. Aitala *et al.*	(FNAL E791 Collab.)
AITALA	99G	PL B462 401	E.M. Aitala *et al.*	(FNAL E791 Collab.)
BONVICINI	99	PRL 82 4586	G. Bonvicini *et al.*	(CLEO Collab.)
CHADHA	98	PR D58 032002	M. Chada *et al.*	(CLEO Collab.)
JESSOP	98	PR D58 052002	C.P. Jessop *et al.*	(CLEO Collab.)
ACCIARRI	97F	PL B396 327	M. Acciarri *et al.*	(L3 Collab.)
BALEST	97	PRL 79 1436	R. Balest *et al.*	(CLEO Collab.)
FRABETTI	97C	PL B401 131	P.L. Frabetti *et al.*	(FNAL E687 Collab.)
FRABETTI	97D	PL B407 79	P.L. Frabetti *et al.*	(FNAL E687 Collab.)
ARTUSO	96	PL B378 364	M. Artuso *et al.*	(CLEO Collab.)
BAI	95C	PR D52 3781	J.Z. Bai *et al.*	(BES Collab.)
BRANDENB...	95	PRL 75 3804	G.W. Brandenburg *et al.*	(CLEO Collab.)
FRABETTI	95B	PL B351 591	P.L. Frabetti *et al.*	(FNAL E687 Collab.)
KODAMA	95	PL B345 85	K. Kodama *et al.*	(FNAL E653 Collab.)
ACOSTA	94	PR D49 5690	D. Acosta *et al.*	(CLEO Collab.)
AVERY	94B	PL B337 405	P. Avery *et al.*	(CLEO Collab.)
BROWN	94	PR D50 1884	D. Brown *et al.*	(CLEO Collab.)
BUTLER	94	PL B324 255	F. Butler *et al.*	(CLEO Collab.)
FRABETTI	94F	PL B328 187	P.L. Frabetti *et al.*	(FNAL E687 Collab.)
FRABETTI	93F	PRL 71 827	P.L. Frabetti *et al.*	(FNAL E687 Collab.)
FRABETTI	93G	PL B313 253	P.L. Frabetti *et al.*	(FNAL E687 Collab.)
KODAMA	93	PL B309 483	K. Kodama *et al.*	(FNAL E653 Collab.)
ALBRECHT	92B	ZPHY C53 361	H. Albrecht *et al.*	(ARGUS Collab.)
ALEXANDER	92	PRL 68 1275	J. Alexander *et al.*	(CLEO Collab.)
AVERY	92	PRL 68 1279	P. Avery *et al.*	(CLEO Collab.)
BARLAG	92C	ZPHY C55 383	S. Barlag *et al.*	(ACCMOR Collab.)
Also		ZPHY C48 29	S. Barlag *et al.*	(ACCMOR Collab.)
FRABETTI	92	PL B281 167	P.L. Frabetti *et al.*	(FNAL E687 Collab.)
ALBRECHT	91	PL B255 634	H. Albrecht *et al.*	(ARGUS Collab.)
ALVAREZ	91	PL B255 639	M.P. Alvarez *et al.*	(CERN NA14/2 Collab.)
ALBRECHT	90D	PL B245 315	H. Albrecht *et al.*	(ARGUS Collab.)
ALEXANDER	90B	PRL 65 1531	J. Alexander *et al.*	(CLEO Collab.)
BARLAG	90C	ZPHY C46 563	S. Barlag *et al.*	(ACCMOR Collab.)
FRABETTI	90	PL B251 639	P.L. Frabetti *et al.*	(FNAL E687 Collab.)
ANJOS	89E	PL B223 267	J.C. Anjos *et al.*	(FNAL E691 Collab.)
CHEN	89	PL B226 192	W.Y. Chen *et al.*	(CLEO Collab.)
ALBRECHT	88	PL B207 349	H. Albrecht *et al.*	(ARGUS Collab.)
ANJOS	88	PRL 60 897	J.C. Anjos *et al.*	(FNAL E691 Collab.)
RAAB	88	PR D37 2391	J.R. Raab *et al.*	(FNAL E691 Collab.)
BECKER	87B	PL B184 277	H. Becker *et al.*	(NA11 and NA32 Collabs.)
BLAYLOCK	87	PRL 58 2171	G.T. Blaylock *et al.*	(Mark III Collab.)
USHIDA	86	PRL 56 1767	N. Ushida *et al.*	(FNAL E531 Collab.)
ALBRECHT	85D	PL 153B 343	H. Albrecht *et al.*	(ARGUS Collab.)
DERRICK	85B	PRL 54 2568	M. Derrick *et al.*	(HRS Collab.)
AIHARA	84D	PRL 53 2465	H. Aihara *et al.*	(TPC Collab.)
ALTHOFF	84	PL 136B 130	M. Althoff *et al.*	(TASSO Collab.)
BAILEY	84	PL 139B 320	R. Bailey *et al.*	(ACCMOR Collab.)
CHEN	83C	PRL 51 634	A. Chen *et al.*	(CLEO Collab.)

OTHER RELATED PAPERS

RICHMAN	95	RMP 67 893	J.D. Richman, P.R. Burchat	(UCSB, STAN)

$D_s^{*\pm}$

$I(J^P) = 0(?^?)$

J^P is natural, width and decay modes consistent with 1^-.

$D_s^{*\pm}$ MASS

The fit includes $D^{\pm}$, D^0, $D_s^{\pm}$, $D^{*\pm}$, D^{*0}, $D_s^{*\pm}$, $D_1(2420)^0$, $D_2^*(2460)^0$, and $D_{s1}(2536)^{\pm}$ mass and mass difference measurements.

VALUE (MeV)	DOCUMENT ID		TECN	COMMENT
2112.2±0.4 OUR FIT				
2106.6±2.1±2.7	[1] BLAYLOCK	87	MRK3	$e^+e^- \to D_s^{\pm}\gamma X$

[1] Assuming $D_s^{\pm}$ mass = 1968.7 ± 0.9 MeV.

$m_{D_s^{*\pm}} - m_{D_s^{\pm}}$

The fit includes $D^{\pm}$, D^0, $D_s^{\pm}$, $D^{*\pm}$, D^{*0}, $D_s^{*\pm}$, $D_1(2420)^0$, $D_2^*(2460)^0$, and $D_{s1}(2536)^{\pm}$ mass and mass difference measurements.

VALUE (MeV)	EVTS	DOCUMENT ID		TECN	COMMENT
143.8 ± 0.4 OUR FIT					
143.9 ± 0.4 OUR AVERAGE					
143.76± 0.39±0.40		GRONBERG	95	CLE2	e^+e^-
144.22± 0.47±0.37		BROWN	94	CLE2	e^+e^-
142.5 ± 0.8 ±1.5		[2] ALBRECHT	88	ARG	$e^+e^- \to D_s^{\pm}\gamma X$
139.5 ± 8.3 ±9.7	60	AIHARA	84D	TPC	$e^+e^- \to$ hadrons
• • • We do not use the following data for averages, fits, limits, etc. • • •					
143.0 ±18.0	8	ASRATYAN	85	HLBC	FNAL 15-ft, ν-^{2}H
110 ±46		BRANDELIK	79	DASP	$e^+e^- \to D_s^{\pm}\gamma X$

[2] Result includes data of ALBRECHT 84B.

$D_s^{*\pm}$ WIDTH

VALUE (MeV)	CL%	DOCUMENT ID		TECN	COMMENT
< 1.9	90	GRONBERG	95	CLE2	e^+e^-
< 4.5	90	ALBRECHT	88	ARG	$E_{\rm cm}^{ee}$ = 10.2 GeV
• • • We do not use the following data for averages, fits, limits, etc. • • •					
< 4.9	90	BROWN	94	CLE2	e^+e^-
<22	90	BLAYLOCK	87	MRK3	$e^+e^- \to D_s^{\pm}\gamma X$

D_s^{*+} DECAY MODES

D_s^{*-} modes are charge conjugates of the modes below.

	Mode	Fraction (Γ_i/Γ)
Γ_1	$D_s^+\gamma$	(93.5±0.7) %
Γ_2	$D_s^+\pi^0$	(5.8±0.7) %
Γ_3	$D_s^+e^+e^-$	(6.7±1.6) × 10^{-3}

CONSTRAINED FIT INFORMATION

An overall fit to 2 branching ratios uses 3 measurements and one constraint to determine 3 parameters. The overall fit has a χ^2 = 0.0 for 1 degrees of freedom.

The following *off-diagonal* array elements are the correlation coefficients $\langle \delta x_i \delta x_j \rangle / (\delta x_i \cdot \delta x_j)$, in percent, from the fit to the branching fractions, $x_i \equiv \Gamma_i/\Gamma_{\rm total}$. The fit constrains the x_i whose labels appear in this array to sum to one.

x_2	−97		
x_3	−19	−4	
	x_1	x_2	

D_s^{*+} BRANCHING RATIOS

$\Gamma(D_s^+\gamma)/\Gamma_{\rm total}$ Γ_1/Γ

VALUE	DOCUMENT ID		TECN	COMMENT
0.935±0.007 OUR FIT				
• • • We do not use the following data for averages, fits, limits, etc. • • •				
seen	ASRATYAN	91	HLBC	$\overline{\nu}_\mu$ Ne
seen	ALBRECHT	88	ARG	$e^+e^- \to D_s^{\pm}\gamma X$
seen	AIHARA	84D		
seen	ALBRECHT	84B		
seen	BRANDELIK	79		

$\Gamma(D_s^+\pi^0)/\Gamma(D_s^+\gamma)$ Γ_2/Γ_1

VALUE	DOCUMENT ID		TECN	COMMENT
0.062±0.008 OUR FIT				
0.062±0.008 OUR AVERAGE				
0.062±0.005±0.006	AUBERT,BE	05G	BABR	10.6 e^+e^- → hadrons
$0.062^{+0.020}_{-0.018}\pm0.022$	GRONBERG	95	CLE2	e^+e^-

$\Gamma(D_s^+e^+e^-)/\Gamma(D_s^+\gamma)$ Γ_3/Γ_1

VALUE (units 10^{-3})	EVTS	DOCUMENT ID	TECN	COMMENT
7.2±1.7 OUR FIT				
$\mathbf{7.2^{+1.5}_{-1.3}\pm1.0}$	38	CRONIN-HEN...12	CLEO	4.17 e^+e^- → hadrons

$D_s^{*\pm}$ REFERENCES

CRONIN-HEN...	12	PR D86 072005	D. Cronin-Hennessey *et al.*	(CLEO Collab.)
AUBERT,BE	05G	PR D72 091101	B. Aubert *et al.*	(BABAR Collab.)
GRONBERG	95	PRL 75 3232	J. Gronberg *et al.*	(CLEO Collab.)
BROWN	94	PR D50 1884	D. Brown *et al.*	(CLEO Collab.)
ASRATYAN	91	PL B257 525	A.E. Asratyan *et al.*	(ITEP, BELG, SACL+)
ALBRECHT	88	PL B207 349	H. Albrecht *et al.*	(ARGUS Collab.)
BLAYLOCK	87	PRL 58 2171	G.T. Blaylock *et al.*	(Mark III Collab.)
ASRATYAN	85	PL 156B 441	A.E. Asratyan *et al.*	(ITEP, SERP)
AIHARA	84D	PRL 53 2465	H. Aihara *et al.*	(TPC Collab.)
ALBRECHT	84B	PL 146B 111	H. Albrecht *et al.*	(ARGUS Collab.)
BRANDELIK	79	PL 80B 412	R. Brandelik *et al.*	(DASP Collab.)

$D_{s0}^*(2317)^\pm$

$I(J^P) = 0(0^+)$
J, P need confirmation.

AUBERT 06P and CHOI 15A do not observe neutral and doubly charged partners of the $D_{s0}^*(2317)^+$.

$D_{s0}^*(2317)^\pm$ MASS

The fit includes $D^\pm$, D^0, $D_s^\pm$, $D^{*\pm}$, D^{*0}, $D_s^{*\pm}$, $D_1(2420)^0$, $D_2^*(2460)^0$, and $D_{s1}(2536)^\pm$ mass and mass difference measurements.

VALUE (MeV)	EVTS	DOCUMENT ID		TECN	COMMENT
2317.7±0.6 OUR FIT Error includes scale factor of 1.1.					
2318.0±1.0 OUR AVERAGE Error includes scale factor of 1.4.					
2319.6±0.2±1.4	3180	AUBERT	06P	BABR	10.6 e^+e^- → $D_s^+\pi^0X$
2317.3±0.4±0.8	1022	[1] AUBERT	04E	BABR	10.6 e^+e^-
• • • We do not use the following data for averages, fits, limits, etc. • • •					
2317.2±1.3	88	[2] AUBERT,B	04S	BABR	$B \to D_{s0}^{(*)}(2317)^+\overline{D}^{(*)}$
2317.2±0.5±0.9	761	[3] MIKAMI	04	BELL	10.6 e^+e^-
2316.8±0.4±3.0	1267±53	[3,4] AUBERT	03G	BABR	10.6 e^+e^-
2317.6±1.3	273±33	[3,5] AUBERT	03G	BABR	10.6 e^+e^-
2319.8±2.1±2.0	24	[3] KROKOVNY	03B	BELL	10.6 e^+e^-

[1] Supersedes AUBERT 03G.
[2] Systematic errors not evaluated.
[3] Not independent of the corresponding $m_{D_{s0}^*(2317)} - m_{D_s}$.
[4] From $D_s^+ \to K^+K^-\pi^+$ decay.
[5] From $D_s^+ \to K^+K^-\pi^+\pi^0$ decay.

$m_{D_{s0}^*(2317)^\pm} - m_{D_s^\pm}$

The fit includes $D^\pm$, D^0, $D_s^\pm$, $D^{*\pm}$, D^{*0}, $D_s^{*\pm}$, $D_1(2420)^0$, $D_2^*(2460)^0$, and $D_{s1}(2536)^\pm$ mass and mass difference measurements.

VALUE (MeV)	EVTS	DOCUMENT ID		TECN	COMMENT
349.4±0.6 OUR FIT Error includes scale factor of 1.1.					
349.2±0.7 OUR AVERAGE					
348.7±0.5±0.7	761	MIKAMI	04	BELL	10.6 e^+e^-
350.0±1.2±1.0	135	BESSON	03	CLE2	10.6 e^+e^-
351.3±2.1±1.9	24	[6] KROKOVNY	03B	BELL	10.6 e^+e^-
• • • We do not use the following data for averages, fits, limits, etc. • • •					
349.6±0.4±3.0	1267	[7,8] AUBERT	03G	BABR	10.6 e^+e^-
350.2±1.3	273	[9,10] AUBERT	03G	BABR	10.6 e^+e^-

[6] Recalculated by us using $m_{D_s^+}$ = 1968.5 ± 0.6 MeV.
[7] From $D_s^+ \to K^+K^-\pi^+$ decay.
[8] Recalculated by us using $m_{D_s^+}$ = 1967.20 ± 0.03 MeV.
[9] From $D_s^+ \to K^+K^-\pi^+\pi^0$ decay.
[10] Recalculated by us using $m_{D_s^+}$ = 1967.4 ± 0.2 MeV. Systematic errors not estimated.

$D_{s0}^*(2317)^\pm$ WIDTH

VALUE (MeV)	CL%	EVTS	DOCUMENT ID		TECN	COMMENT
< 3.8	95	3180	AUBERT	06P	BABR	10.6 e^+e^- → $D_s^+\pi^0X$
• • • We do not use the following data for averages, fits, limits, etc. • • •						
< 4.6	90	761	MIKAMI	04	BELL	10.6 e^+e^-
<10			AUBERT	03G	BABR	10.6 e^+e^-
< 7	90	135	BESSON	03	CLE2	10.6 e^+e^-

$D_{s0}^*(2317)^\pm$ DECAY MODES

$D_{s0}^*(2317)^-$ modes are charge conjugates of modes below.

	Mode	Fraction (Γ_i/Γ)
Γ_1	$D_s^+\pi^0$	seen
Γ_2	$D_s^+\gamma$	
Γ_3	$D_s^*(2112)^+\gamma$	
Γ_4	$D_s^+\gamma\gamma$	
Γ_5	$D_s^*(2112)^+\pi^0$	
Γ_6	$D_s^+\pi^+\pi^-$	
Γ_7	$D_s^+\pi^0\pi^0$	not seen

$D_{s0}^*(2317)^\pm$ BRANCHING RATIOS

$\Gamma(D_s^+\pi^0)/\Gamma_{total}$ Γ_1/Γ

VALUE	EVTS	DOCUMENT ID		TECN	COMMENT
seen	1540±62	AUBERT	03G	BABR	10.6 e^+e^-

$\Gamma(D_s^+\gamma)/\Gamma(D_s^+\pi^0)$ Γ_2/Γ_1

VALUE	CL%	DOCUMENT ID		TECN	COMMENT
<0.05	90	MIKAMI	04	BELL	10.6 e^+e^-
• • • We do not use the following data for averages, fits, limits, etc. • • •					
<0.14	95	AUBERT	06P	BABR	10.6 e^+e^-
<0.052	90	BESSON	03	CLE2	10.6 e^+e^-

$\Gamma(D_s^*(2112)^+\gamma)/\Gamma(D_s^+\pi^0)$ Γ_3/Γ_1

VALUE	CL%	DOCUMENT ID		TECN	COMMENT
<0.059	90	BESSON	03	CLE2	10.6 e^+e^-
• • • We do not use the following data for averages, fits, limits, etc. • • •					
<0.16	95	AUBERT	06P	BABR	10.6 e^+e^-
<0.18	90	MIKAMI	04	BELL	10.6 e^+e^-

$\Gamma(D_s^+\gamma\gamma)/\Gamma(D_s^+\pi^0)$ Γ_4/Γ_1

VALUE	CL%	DOCUMENT ID		TECN	COMMENT
<0.18	95	AUBERT	06P	BABR	10.6 e^+e^-
• • • We do not use the following data for averages, fits, limits, etc. • • •					
not seen		AUBERT	03G	BABR	10.6 e^+e^-

$\Gamma(D_s^*(2112)^+\pi^0)/\Gamma(D_s^+\pi^0)$ Γ_5/Γ_1

VALUE	CL%	DOCUMENT ID		TECN	COMMENT
<0.11	90	BESSON	03	CLE2	10.6 e^+e^-

$\Gamma(D_s^+\pi^+\pi^-)/\Gamma(D_s^+\pi^0)$ Γ_6/Γ_1

VALUE	CL%	DOCUMENT ID		TECN	COMMENT
<0.004	90	MIKAMI	04	BELL	10.6 e^+e^-
• • • We do not use the following data for averages, fits, limits, etc. • • •					
<0.005	95	AUBERT	06P	BABR	10.6 e^+e^-
<0.019	90	BESSON	03	CLE2	10.6 e^+e^-

$\Gamma(D_s^+\pi^0\pi^0)/\Gamma(D_s^+\pi^0)$ Γ_7/Γ_1

VALUE	CL%	DOCUMENT ID		TECN	COMMENT
<0.25	95	AUBERT	06P	BABR	10.6 e^+e^-

$D_{s0}^*(2317)^\pm$ REFERENCES

CHOI	15A	PR D91 092011	S.-K. Choi *et al.*	(BELLE Collab.)
AUBERT	06P	PR D74 032007	B. Aubert *et al.*	(BABAR Collab.)
AUBERT	04E	PR D69 031101	B. Aubert *et al.*	(BABAR Collab.)
AUBERT,B	04S	PRL 93 181801	B. Aubert *et al.*	(BABAR Collab.)
MIKAMI	04	PRL 92 012002	Y. Mikami *et al.*	(BELLE Collab.)
AUBERT	03G	PRL 90 242001	B. Aubert *et al.*	(BABAR Collab.)
BESSON	03	PR D68 032002	D. Besson *et al.*	(CLEO Collab.)
KROKOVNY	03B	PRL 91 262002	P. Krokovny *et al.*	(BELLE Collab.)

$D_{s1}(2460)^{\pm}$

$I(J^P) = 0(1^+)$

$D_{s1}(2460)^{\pm}$ MASS

The fit includes $D^{\pm}$, D^0, $D_s^{\pm}$, $D^{*\pm}$, D^{*0}, $D_s^{*\pm}$, $D_1(2420)^0$, $D_2^*(2460)^0$, and $D_{s1}(2536)^{\pm}$ mass and mass difference measurements.

VALUE (MeV)	EVTS	DOCUMENT ID		TECN	COMMENT
2459.5±0.6 OUR FIT		Error includes scale factor of 1.1.			
2459.6±0.9 OUR AVERAGE		Error includes scale factor of 1.3.			
2460.1±0.2±0.8		[1] AUBERT	06P	BABR	10.6 e^+e^-
2458.0±1.0±1.0	195	AUBERT	04E	BABR	10.6 e^+e^-
• • • We do not use the following data for averages, fits, limits, etc. • • •					
2459.5±1.2±3.7	920	AUBERT	06P	BABR	10.6 $e^+e^- \to D_s^+\gamma X$
2458.6±1.0±2.5	560	AUBERT	06P	BABR	10.6 $e^+e^- \to D_s^+\pi^0\gamma X$
2460.2±0.2±0.8	123	AUBERT	06P	BABR	10.6 $e^+e^- \to D_s^+\pi^+\pi^- X$
2458.9±1.5	112	[2] AUBERT,B	04S	BABR	$B \to D_{s1}(2460)^+\overline{D}^{(*)}$
2461.1±1.6	139	[3] AUBERT,B	04S	BABR	$B \to D_{s1}(2460)^+\overline{D}^{(*)}$
2456.5±1.3±1.3	126	[4,5] MIKAMI	04	BELL	10.6 e^+e^-
2459.5±1.3±2.0	152	[6,7] MIKAMI	04	BELL	10.6 e^+e^-
2459.9±0.9±1.6	60	[6,7] MIKAMI	04	BELL	10.6 e^+e^-
2459.2±1.6±2.0	57	KROKOVNY	03B	BELL	10.6 e^+e^-

[1] The average of the values obtained from the $D_s^+\gamma$, $D_s^+\pi^0\gamma$, $D_s^+\pi^+\pi^-$ final state.

[2] Systematic errors not evaluated. From the decay to $D_s^{*+}\pi^0$.

[3] Systematic errors not evaluated. From the decay to $D_s^+\gamma$.

[4] Not independent of the corresponding $m_{D_{s1}(2460)^{\pm}} - m_{D_s^{*\pm}}$.

[5] Using $m_{D_s^{*+}} = 2112.4 \pm 0.7$ MeV.

[6] Not independent of the corresponding $m_{D_{s1}(2460)^{\pm}} - m_{D_s^{\pm}}$.

[7] Using $m_{D_s^+} = 1968.5 \pm 0.6$ MeV.

$m_{D_{s1}(2460)^{\pm}} - m_{D_s^{*\pm}}$

The fit includes $D^{\pm}$, D^0, $D_s^{\pm}$, $D^{*\pm}$, D^{*0}, $D_s^{*\pm}$, $D_1(2420)^0$, $D_2^*(2460)^0$, and $D_{s1}(2536)^{\pm}$ mass and mass difference measurements.

VALUE (MeV)	EVTS	DOCUMENT ID		TECN	COMMENT
347.3±0.7 OUR FIT		Error includes scale factor of 1.2.			
347.1±2.2 OUR AVERAGE		Error includes scale factor of 1.9. See the ideogram below.			
344.1±1.3±1.1	126	MIKAMI	04	BELL	10.6 e^+e^-
351.2±1.7±1.0	41	BESSON	03	CLE2	10.6 e^+e^-
346.8±1.6±1.9	57	[8] KROKOVNY	03B	BELL	10.6 e^+e^-

[8] Recalculated by us using $m_{D_s^{*+}} = 2112.4 \pm 0.7$ MeV.

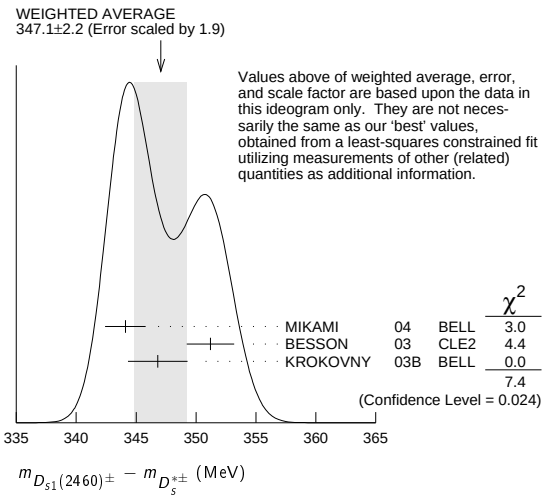

$m_{D_{s1}(2460)^{\pm}} - m_{D_s^{\pm}}$

The fit includes $D^{\pm}$, D^0, $D_s^{\pm}$, $D^{*\pm}$, D^{*0}, $D_s^{*\pm}$, $D_1(2420)^0$, $D_2^*(2460)^0$, and $D_{s1}(2536)^{\pm}$ mass and mass difference measurements.

VALUE (MeV)	EVTS	DOCUMENT ID		TECN	COMMENT
491.2±0.6 OUR FIT		Error includes scale factor of 1.1.			
491.3±1.4 OUR AVERAGE					
491.0±1.3±1.9	152	[9] MIKAMI	04	BELL	10.6 e^+e^-
491.4±0.9±1.5	60	[10] MIKAMI	04	BELL	10.6 e^+e^-

[9] From the decay to $D_s^{\pm}\gamma$.

[10] From the decay to $D_s^{\pm}\pi^+\pi^-$.

$D_{s1}(2460)^{\pm}$ WIDTH

VALUE (MeV)	CL%	EVTS	DOCUMENT ID		TECN	COMMENT
< 3.5	95	123	AUBERT	06P	BABR	10.6 $e^+e^- \to D_s^+\pi^+\pi^- X$
• • • We do not use the following data for averages, fits, limits, etc. • • •						
< 6.3	95	560	AUBERT	06P	BABR	10.6 $e^+e^- \to D_s^+\pi^0\gamma X$
<10		195	AUBERT	04E	BABR	10.6 e^+e^-
< 5.5	90	126	MIKAMI	04	BELL	10.6 e^+e^-
< 7	90	41	BESSON	03	CLE2	10.6 e^+e^-

$D_{s1}(2460)^+$ DECAY MODES

$D_{s1}(2460)^-$ modes are charge conjugates of the modes below.

	Mode	Fraction (Γ_i/Γ)	Scale factor/ Confidence level
Γ_1	$D_s^{*+}\pi^0$	(48 ±11) %	
Γ_2	$D_s^+\gamma$	(18 ± 4) %	
Γ_3	$D_s^+\pi^+\pi^-$	(4.3± 1.3) %	S=1.1
Γ_4	$D_s^{*+}\gamma$	< 8 %	CL=90%
Γ_5	$D_{s0}^*(2317)^+\gamma$	($3.7^{+5.0}_{-2.4}$) %	
Γ_6	$D_s^+\pi^0$		
Γ_7	$D_s^+\pi^0\pi^0$		
Γ_8	$D_s^+\gamma\gamma$		

CONSTRAINED FIT INFORMATION

An overall fit to 7 branching ratios uses 8 measurements and one constraint to determine 5 parameters. The overall fit has a $\chi^2 = 3.4$ for 4 degrees of freedom.

The following *off-diagonal* array elements are the correlation coefficients $\langle \delta x_i \delta x_j \rangle / (\delta x_i \cdot \delta x_j)$, in percent, from the fit to the branching fractions, $x_i \equiv \Gamma_i/\Gamma_{\text{total}}$. The fit constrains the x_i whose labels appear in this array to sum to one.

x_2	80		
x_3	68	62	
x_5	−3	25	26
	x_1	x_2	x_3

$D_{s1}(2460)^{\pm}$ BRANCHING RATIOS

$\Gamma(D_s^{*+}\pi^0)/\Gamma_{\text{total}}$ Γ_1/Γ

VALUE	EVTS	DOCUMENT ID		TECN	COMMENT
0.48±0.11 OUR FIT					
0.56±0.13±0.09		[11] AUBERT	06N	BABR	$B \to D_{s1}(2460)^-\overline{D}^{(*)}$
• • • We do not use the following data for averages, fits, limits, etc. • • •					
seen	41	BESSON	03	CLE2	10.6 e^+e^-

[11] Evaluated in AUBERT 06N including measurements from AUBERT,B 04S.

$\Gamma(D_s^+\gamma)/\Gamma_{\text{total}}$ Γ_2/Γ

VALUE	DOCUMENT ID		TECN	COMMENT
0.18±0.04 OUR FIT				
0.16±0.04±0.03	[12] AUBERT	06N	BABR	$B \to D_{s1}(2460)^-\overline{D}^{(*)}$

[12] Evaluated in AUBERT 06N including measurements from AUBERT,B 04S.

$\Gamma(D_s^+\gamma)/\Gamma(D_s^{*+}\pi^0)$ Γ_2/Γ_1

VALUE	CL%	EVTS	DOCUMENT ID		TECN	COMMENT
0.38 ±0.05 OUR FIT						
0.44 ±0.09 OUR AVERAGE						
0.55 ±0.13 ±0.08		152	MIKAMI	04	BELL	10.6 e^+e^-
0.38 ±0.11 ±0.04		38	KROKOVNY	03B	BELL	10.6 e^+e^-
• • • We do not use the following data for averages, fits, limits, etc. • • •						
0.274±0.045±0.020		251	[13] AUBERT,B	04S	BABR	$B \to D_{s1}(2460)^+\overline{D}^{(*)}$
< 0.49	90		BESSON	03	CLE2	10.6 e^+e^-

[13] Used by AUBERT 06N in their measurement of $B(D_s^{*-}\pi^0)$ and $B(D_s^-\gamma)$.

$\Gamma(D_s^+\pi^+\pi^-)/\Gamma(D_s^{*+}\pi^0)$ Γ_3/Γ_1

VALUE	CL%	EVTS	DOCUMENT ID		TECN	COMMENT
0.090±0.020 OUR FIT			Error includes scale factor of 1.2.			
0.14 ±0.04 ±0.02		60	MIKAMI	04	BELL	10.6 e^+e^-
• • • We do not use the following data for averages, fits, limits, etc. • • •						
<0.08	90		BESSON	03	CLE2	10.6 e^+e^-

Meson Particle Listings

$D_{s1}(2460)^{\pm}$, $D_{s1}(2536)^{\pm}$

$\Gamma(D_s^{*+}\gamma)/\Gamma(D_s^{*+}\pi^0)$ Γ_4/Γ_1

VALUE	CL%	DOCUMENT ID		TECN	COMMENT
<0.16	90	BESSON	03	CLE2	10.6 e^+e^-
• • • We do not use the following data for averages, fits, limits, etc. • • •					
<0.31	90	MIKAMI	04	BELL	10.6 e^+e^-

$\Gamma(D_{s0}^*(2317)^+\gamma)/\Gamma(D_s^{*+}\pi^0)$ Γ_5/Γ_1

VALUE	CL%	DOCUMENT ID		TECN	COMMENT
<0.22	95	AUBERT	04E	BABR	10.6 e^+e^-
• • • We do not use the following data for averages, fits, limits, etc. • • •					
<0.58	90	BESSON	03	CLE2	10.6 e^+e^-

$\Gamma(D_s^{*+}\pi^0)/[\Gamma(D_s^{*+}\pi^0)+\Gamma(D_{s0}^*(2317)^+\gamma)]$ $\Gamma_1/(\Gamma_1+\Gamma_5)$

VALUE	DOCUMENT ID		TECN	COMMENT
0.93±0.09 OUR FIT				
0.97±0.09±0.05	AUBERT	06P	BABR	10.6 e^+e^-

$\Gamma(D_s^+\gamma)/[\Gamma(D_s^{*+}\pi^0)+\Gamma(D_{s0}^*(2317)^+\gamma)]$ $\Gamma_2/(\Gamma_1+\Gamma_5)$

VALUE	DOCUMENT ID		TECN	COMMENT
0.35 ±0.04 OUR FIT				
0.337±0.036±0.038	AUBERT	06P	BABR	10.6 e^+e^-

$\Gamma(D_s^+\pi^+\pi^-)/[\Gamma(D_s^{*+}\pi^0)+\Gamma(D_{s0}^*(2317)^+\gamma)]$ $\Gamma_3/(\Gamma_1+\Gamma_5)$

VALUE	DOCUMENT ID		TECN	COMMENT
0.083±0.017 OUR FIT Error includes scale factor of 1.2.				
0.077±0.013±0.008	AUBERT	06P	BABR	10.6 e^+e^-

$\Gamma(D_s^{*+}\gamma)/[\Gamma(D_s^{*+}\pi^0)+\Gamma(D_{s0}^*(2317)^+\gamma)]$ $\Gamma_4/(\Gamma_1+\Gamma_5)$

VALUE	CL%	DOCUMENT ID		TECN	COMMENT
<0.24	95	AUBERT	06P	BABR	10.6 e^+e^-

$\Gamma(D_{s0}^*(2317)^+\gamma)/[\Gamma(D_s^{*+}\pi^0)+\Gamma(D_{s0}^*(2317)^+\gamma)]$ $\Gamma_5/(\Gamma_1+\Gamma_5)$

VALUE	CL%	DOCUMENT ID		TECN	COMMENT
<0.25	95	AUBERT	06P	BABR	10.6 e^+e^-

$\Gamma(D_s^+\pi^0)/[\Gamma(D_s^{*+}\pi^0)+\Gamma(D_{s0}^*(2317)^+\gamma)]$ $\Gamma_6/(\Gamma_1+\Gamma_5)$

VALUE	CL%	DOCUMENT ID		TECN	COMMENT
<0.042	95	AUBERT	06P	BABR	10.6 e^+e^-

$\Gamma(D_s^+\pi^0\pi^0)/[\Gamma(D_s^{*+}\pi^0)+\Gamma(D_{s0}^*(2317)^+\gamma)]$ $\Gamma_7/(\Gamma_1+\Gamma_5)$

VALUE	CL%	DOCUMENT ID		TECN	COMMENT
<0.68	95	AUBERT	06P	BABR	10.6 e^+e^-

$\Gamma(D_s^+\gamma\gamma)/[\Gamma(D_s^{*+}\pi^0)+\Gamma(D_{s0}^*(2317)^+\gamma)]$ $\Gamma_8/(\Gamma_1+\Gamma_5)$

VALUE	CL%	DOCUMENT ID		TECN	COMMENT
<0.33	95	AUBERT	06P	BABR	10.6 e^+e^-

$D_{s1}(2460)^{\pm}$ REFERENCES

AUBERT	06N	PR D74 031103	B. Aubert *et al.*	(BABAR Collab.)
AUBERT	06P	PR D74 032007	B. Aubert *et al.*	(BABAR Collab.)
AUBERT	04E	PR D69 031101	B. Aubert *et al.*	(BABAR Collab.)
AUBERT,B	04S	PRL 93 181801	B. Aubert *et al.*	(BABAR Collab.)
MIKAMI	04	PRL 92 012002	Y. Mikami *et al.*	(BELLE Collab.)
BESSON	03	PR D68 032002	D. Besson *et al.*	(CLEO Collab.)
KROKOVNY	03B	PRL 91 262002	P. Krokovny *et al.*	(BELLE Collab.)

$D_{s1}(2536)^{\pm}$

$I(J^P) = 0(1^+)$
J, P need confirmation.

Seen in $D^*(2010)^+K^0$, $D^*(2007)^0K^+$, and $D_s^+\pi^+\pi^-$. Not seen in D^+K^0 or D^0K^+. $J^P = 1^+$ assignment strongly favored.

$D_{s1}(2536)^{\pm}$ MASS

The fit includes $D^{\pm}$, D^0, $D_s^{\pm}$, $D^{*\pm}$, D^{*0}, $D_s^{*\pm}$, $D_1(2420)^0$, $D_2^*(2460)^0$, and $D_{s1}(2536)^{\pm}$ mass and mass difference measurements.

VALUE (MeV)	EVTS	DOCUMENT ID		TECN	COMMENT
2535.10±0.06 OUR FIT					
2535.18±0.24 OUR AVERAGE					
2535.7 ±0.6 ±0.5	46 ± 9	[1] ABAZOV	09G	D0	$B_s^0 \to D_{s1}^- \mu^+ \nu_\mu X$
2534.78±0.31±0.40	182	AUBERT	08B	BABR	$B \to \overline{D}^{(*)} D^* K$
2534.6 ±0.3 ±0.7	193	AUBERT	06P	BABR	10.6 $e^+e^- \to D_s^+\pi^+\pi^- X$
2535.3 ±0.7	92	[2] HEISTER	02B	ALEP	$e^+e^- \to D^{*+}K^0X$, $D^{*0}K^+X$
2534.2 ±1.2	9	ASRATYAN	94	BEBC	$\nu N \to D^*K^0X, D^{*0}K^{\pm}X$
2535 ±0.6 ±1	75	FRABETTI	94B	E687	γBe $\to D^{*+}K^0X$, $D^{*0}K^+X$
2535.3 ±0.2 ±0.5	134	ALEXANDER	93	CLE2	$e^+e^- \to D^{*0}K^+X$
2534.8 ±0.6 ±0.6	44	ALEXANDER	93	CLE2	$e^+e^- \to D^{*+}K^0X$
2535.2 ±0.5 ±1.5	28	ALBRECHT	92R	ARG	10.4 $e^+e^- \to D^{*0}K^+X$
2536.6 ±0.7 ±0.4		AVERY	90	CLEO	$e^+e^- \to D^{*+}K^0X$
2535.9 ±0.6 ±2.0		ALBRECHT	89E	ARG	$D_{s1}^* \to D^*(2010)K^0$
• • • We do not use the following data for averages, fits, limits, etc. • • •					
2534.1 ±0.6	116	[3] AUSHEV	11	BELL	$B \to D_{s1}(2536)^+ D^{(*)}$
2535.08±0.01±0.15	8038	[4] LEES	11B	BABR	10.6 $e^+e^- \to D^{*+}K_S^0X$
$2535.57^{+0.44}_{-0.41}\pm0.10$	236 ± 30	[5] CHEKANOV	09	ZEUS	$e^{\pm}p \to D^{*+}K_S^0X$, $D^{*0}K^+X$
2535 ± 28		[6] ASRATYAN	88	HLBC	$\nu N \to D_s\gamma\gamma X$

[1] Using the $D^*(2010)^{\pm}$ mass of 2010.0 ± 0.4 MeV from PDG 06.
[2] Calculated using $m(D^*(2010)^{\pm}) = 2010.0 \pm 0.5$ MeV, $m(D^*(2007)^0) = 2006.7 \pm 0.5$ MeV, and the mass difference below.
[3] Systematic uncertainties not evaluated.
[4] Calculated using the mass difference $m(D_{s1}^+) - m(D^{*+})_{PDG}$ below and $m(D^{*+})_{PDG}$ = 2010.25 ± 0.14 MeV. Assuming S-wave decay of the $D_{s1}(2536)$ to $D^{*+}K_S^0$, using a Breit-Wigner line shape corresponding to L=0.
[5] Calculated using the mass difference $m(D_{s1}^+) - m(D^{*+})_{PDG}$ reported below and $m(D^{*+})_{PDG}$ = 2010.27 ± 0.17 MeV.
[6] Not seen in D^*K.

$m_{D_{s1}(2536)^{\pm}} - m_{D_s^*(2111)}$

The fit includes $D^{\pm}$, D^0, $D_s^{\pm}$, $D^{*\pm}$, D^{*0}, $D_s^{*\pm}$, $D_1(2420)^0$, $D_2^*(2460)^0$, and $D_{s1}(2536)^{\pm}$ mass and mass difference measurements.

VALUE (MeV)	DOCUMENT ID		TECN	COMMENT
422.9± 0.4 OUR FIT				
424 ±28	ASRATYAN	88	HLBC	$D_s^{*\pm}\gamma$

$m_{D_{s1}(2536)^{\pm}} - m_{D^*(2010)^{\pm}}$

The fit includes $D^{\pm}$, D^0, $D_s^{\pm}$, $D^{*\pm}$, D^{*0}, $D_s^{*\pm}$, $D_1(2420)^0$, $D_2^*(2460)^0$, and $D_{s1}(2536)^{\pm}$ mass and mass difference measurements.

VALUE (MeV)	EVTS	DOCUMENT ID		TECN	COMMENT
524.84±0.04 OUR FIT					
524.84±0.04 OUR AVERAGE					
524.83±0.01±0.04	8038	[7] LEES	11B	BABR	10.6 $e^+e^- \to D^{*+}K_S^0X$
$525.30^{+0.44}_{-0.41}\pm0.10$	236 ± 30	CHEKANOV	09	ZEUS	$e^{\pm}p \to D^{*+}K_S^0X$, $D^{*0}K^+X$
525.3 ±0.6 ±0.1	41	HEISTER	02B	ALEP	$e^+e^- \to D^{*+}K^0X$

[7] Assuming S-wave decay of the $D_{s1}(2536)$ to $D^{*+}K_S^0$, using a Breit-Wigner line shape corresponding to L=0.

$m_{D_{s1}(2536)^{\pm}} - m_{D^*(2007)^0}$

The fit includes $D^{\pm}$, D^0, $D_s^{\pm}$, $D^{*\pm}$, D^{*0}, $D_s^{*\pm}$, $D_1(2420)^0$, $D_2^*(2460)^0$, and $D_{s1}(2536)^{\pm}$ mass and mass difference measurements.

VALUE (MeV)	EVTS	DOCUMENT ID		TECN	COMMENT
528.25±0.05 OUR FIT Error includes scale factor of 1.1.					
528.1 ±1.5 OUR AVERAGE					
528.7 ±1.9 ±0.5	51	HEISTER	02B	ALEP	$e^+e^- \to D^{*0}K^+X$
527.3 ±2.2	29	ACKERSTAFF	97W	OPAL	$e^+e^- \to D^{*0}K^+X$

$D_{s1}(2536)^{\pm}$ WIDTH

VALUE (MeV)	CL%	EVTS	DOCUMENT ID		TECN	COMMENT
0.92±0.03±0.04		8038	[8] LEES	11B	BABR	10.6 $e^+e^- \to D^{*+}K_S^0X$
• • • We do not use the following data for averages, fits, limits, etc. • • •						
0.75±0.23		116	[9] AUSHEV	11	BELL	$B \to D_{s1}(2536)^+ D^{(*)}$
< 2.5	95	193	AUBERT	06P	BABR	10.6 $e^+e^- \to D_s^+\pi^+\pi^-X$
< 3.2	90	75	FRABETTI	94B	E687	γBe $\to D^{*+}K^0X$, $D^{*0}K^+X$
< 2.3	90		ALEXANDER	93	CLEO	$e^+e^- \to D^{*0}K^+X$
< 3.9	90		ALBRECHT	92R	ARG	10.4 $e^+e^- \to D^{*0}K^+X$
< 5.44	90		AVERY	90	CLEO	$e^+e^- \to D^{*+}K^0X$
< 4.6	90		ALBRECHT	89E	ARG	$D_{s1}^* \to D^*(2010)K^0$

[8] Assuming S-wave decay of the $D_{s1}(2536)$ to $D^{*+}K_S^0$, using a Breit-Wigner line shape corresponding to L=0.
[9] Systematic uncertainties not evaluated.

$D_{s1}(2536)^+$ DECAY MODES

$D_{s1}(2536)^-$ modes are charge conjugates of the modes below.

	Mode	Fraction (Γ_i/Γ)	Confidence level
Γ_1	$D^*(2010)^+K^0$	0.85 ±0.12	
Γ_2	$(D^*(2010)^+K^0)_{S-wave}$	0.61 ±0.09	
Γ_3	$(D^*(2010)^+K^0)_{D-wave}$		
Γ_4	$D^+\pi^-K^+$	0.028±0.005	

Γ_5	$D^*(2007)^0 K^+$	**DEFINED AS 1**	
Γ_6	$D^+ K^0$	<0.34	90%
Γ_7	$D^0 K^+$	<0.12	90%
Γ_8	$D_s^{*+}\gamma$	possibly seen	
Γ_9	$D_s^+ \pi^+ \pi^-$	seen	

$D_{s1}(2536)^+$ BRANCHING RATIOS

$\Gamma(D^*(2007)^0 K^+)/\Gamma(D^*(2010)^+ K^0)$ Γ_5/Γ_1

VALUE	EVTS	DOCUMENT ID		TECN	COMMENT
1.18±0.16 OUR AVERAGE					
0.88±0.24±0.08	116	AUSHEV	11	BELL	$B \to D_{s1}(2536)^+ D^{(*)}$
2.3 ±0.6 ±0.3	236 ± 30	CHEKANOV	09	ZEUS	$e^{\pm} p \to D^{*+} K_S^0 X$, $D^{*0} K^+ X$
1.32±0.47±0.23	92	[10] HEISTER	02B	ALEP	$e^+ e^- \to D^{*+} K^0 X$, $D^{*0} K^+ X$
1.9 $^{+1.1}_{-0.9}$ ±0.4	35	[10] ACKERSTAFF	97W	OPAL	$e^+ e^- \to D^{*0} K^+ X$, $D^{*+} K^0 X$
1.1 ±0.3		ALEXANDER	93	CLEO	$e^+ e^- \to D^{*0} K^+ X, D^{*+} K^0 X$
1.4 ±0.3 ±0.2		[11] ALBRECHT	92R	ARG	10.4 $e^+ e^- \to D^{*0} K^+ X, D^{*+} K^0 X$

[10] Ratio of the production rates measured in Z^0 decays.
[11] Evaluated by us from published inclusive cross-sections.

$\Gamma((D^*(2010)^+ K^0)_{S-wave})/\Gamma(D^*(2010)^+ K^0)$ Γ_2/Γ_1

VALUE	EVTS	DOCUMENT ID		TECN	COMMENT
0.72±0.05±0.01	5485	BALAGURA	08	BELL	10.6 $e^+ e^- \to D^{*+} K^0 X$

$\Gamma(D^+ \pi^- K^+)/\Gamma(D^*(2010)^+ K^0)$ Γ_4/Γ_1

VALUE (units 10^{-2})	EVTS	DOCUMENT ID		TECN	COMMENT
3.27±0.18±0.37	1264	BALAGURA	08	BELL	10.6 $e^+ e^- \to D^+ \pi^- K^+ X$

$\Gamma(D^+ K^0)/\Gamma(D^*(2010)^+ K^0)$ Γ_6/Γ_1

VALUE	CL%	DOCUMENT ID		TECN	COMMENT
<0.40	90	ALEXANDER	93	CLEO	$e^+ e^- \to D^{*+} K^0 X$
<0.43	90	ALBRECHT	89E	ARG	$D_{s1}^* \to D^*(2010) K^0$

$\Gamma(D^0 K^+)/\Gamma(D^*(2007)^0 K^+)$ Γ_7/Γ_5

VALUE	CL%	DOCUMENT ID		TECN	COMMENT
<0.12	90	ALEXANDER	93	CLEO	$e^+ e^- \to D^{*0} K^+ X$

$\Gamma(D_s^{*+}\gamma)/\Gamma_{total}$ Γ_8/Γ

VALUE	DOCUMENT ID		TECN	COMMENT
possibly seen	ASRATYAN	88	HLBC	$\nu N \to D_s \gamma\gamma X$

$\Gamma(D_s^{*+}\gamma)/\Gamma(D^*(2007)^0 K^+)$ Γ_8/Γ_5

VALUE	CL%	DOCUMENT ID		TECN	COMMENT
<0.42	90	ALEXANDER	93	CLEO	$e^+ e^- \to D^{*0} K^+ X$

$\Gamma(D_s^+ \pi^+ \pi^-)/\Gamma_{total}$ Γ_9/Γ

VALUE	DOCUMENT ID		TECN	COMMENT
seen	AUBERT	06P	BABR	10.6 $e^+ e^- \to D_s^+ \pi^+ \pi^- X$

$D_{s1}(2536)^{\pm}$ REFERENCES

AUSHEV	11	PR D83 051102	T. Aushev *et al.*	(BELLE Collab.)
LEES	11B	PR D83 072003	J.P. Lees *et al.*	(BABAR Collab.)
ABAZOV	09G	PRL 102 051801	V.M. Abazov *et al.*	(D0 Collab.)
CHEKANOV	09	EPJ C60 25	S. Chekanov *et al.*	(ZEUS Collab.)
AUBERT	08B	PR D77 011102	B. Aubert *et al.*	(BABAR Collab.)
BALAGURA	08	PR D77 032001	V. Balagura *et al.*	(BELLE Collab.)
AUBERT	06P	PR D74 032007	B. Aubert *et al.*	(BABAR Collab.)
PDG	06	JP G33 1	W.-M. Yao *et al.*	(PDG Collab.)
HEISTER	02B	PL B526 34	A. Heister *et al.*	(ALEPH Collab.)
ACKERSTAFF	97W	ZPHY C76 425	K. Ackerstaff *et al.*	(OPAL Collab.)
ASRATYAN	94	ZPHY C61 563	A.E. Asratyan *et al.*	(BIRM, BELG, CERN+)
FRABETTI	94B	PRL 72 324	P.L. Frabetti *et al.*	(FNAL E687 Collab.)
ALEXANDER	93	PL B303 377	J. Alexander *et al.*	(CLEO Collab.)
ALBRECHT	92R	PL B297 425	H. Albrecht *et al.*	(ARGUS Collab.)
AVERY	90	PR D41 774	P. Avery, D. Besson	(CLEO Collab.)
ALBRECHT	89E	PL B230 162	H. Albrecht *et al.*	(ARGUS Collab.)
ASRATYAN	88	ZPHY C40 483	A.E. Asratyan *et al.*	(ITEP, SERP)

$D_{s2}^{*}(2573)$

$I(J^P) = 0(2^+)$

J^P is natural, width and decay modes consistent with 2^+.
AAIJ 14AW confirms $J^P = 2^+$.

$D_{s2}^{*}(2573)$ MASS

VALUE (MeV)	EVTS	DOCUMENT ID		TECN	COMMENT
2569.1 ±0.8 OUR AVERAGE		Error includes scale factor of 2.4. See the ideogram below.			
2568.39±0.29±0.26		AAIJ	14AW	LHCB	$B_s^0 \to \overline{D}^0 K^- \pi^+$
2569.4 ±1.6 ±0.5	82	AAIJ	11A	LHCB	$B_s \to D_{s2}^*(2573) \mu \overline{\nu} X$
2572.2 ±0.3 ±1.0		AUBERT,BE	06E	BABR	$e^+ e^- \to D K X$
2574.5 ±3.3 ±1.6		ALBRECHT	96	ARG	$e^+ e^- \to D^0 K^+ X$
2573.2 $^{+1.7}_{-1.6}$ ±0.9	217	KUBOTA	94	CLE2	$e^+ e^-$ ~ 10.5 GeV
• • • We do not use the following data for averages, fits, limits, etc. • • •					
2570.0 ±4.3	25	[1] EVDOKIMOV	04	SELX	600 $\Sigma^- A \to D^0 K^+ X$
2568.6 ±3.2	64	[2] HEISTER	02B	ALEP	$e^+ e^- \to D^0 K^+ X$

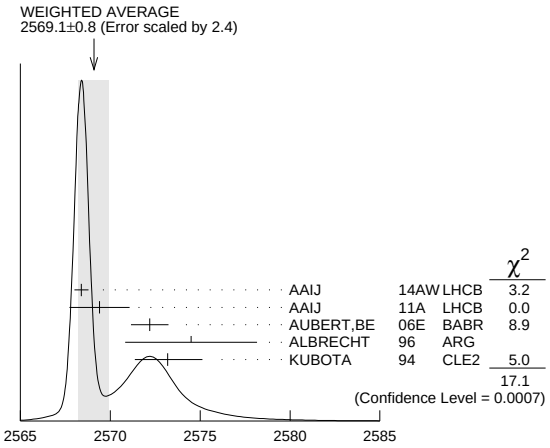

[1] Not independent of the mass difference below.
[2] Calculated using $m_{D^0} = 1864.5 \pm 0.5$ MeV and the mass difference below.

$m_{D_{s2}^*(2573)} - m_{D^0}$

VALUE (MeV)	EVTS	DOCUMENT ID		TECN	COMMENT
704 ±3 ±1	64	HEISTER	02B	ALEP	$e^+ e^- \to D^0 K^+ X$
• • • We do not use the following data for averages, fits, limits, etc. • • •					
705.4±4.3	25	[1] EVDOKIMOV	04	SELX	600 $\Sigma^- A \to D^0 K^+ X$

[1] Systematic errors not estimated.

$D_{s2}^{*}(2573)$ WIDTH

VALUE (MeV)	EVTS	DOCUMENT ID		TECN	COMMENT
16.9±0.8 OUR AVERAGE					
16.9±0.5±0.6		AAIJ	14AW	LHCB	$B_s^0 \to \overline{D}^0 K^- \pi^+$
12.1±4.5±1.6	82	AAIJ	11A	LHCB	$B_s \to D_{s2}^*(2573) \mu \overline{\nu} X$
27.1±0.6±5.6		AUBERT,BE	06E	BABR	$e^+ e^- \to D K X$
10.4±8.3±3.0		ALBRECHT	96	ARG	$e^+ e^- \to D^0 K^+ X$
16 $^{+5}_{-4}$ ±3	217	KUBOTA	94	CLE2	$e^+ e^-$ ~ 10.5 GeV
• • • We do not use the following data for averages, fits, limits, etc. • • •					
14 $^{+9}_{-6}$	25	[1] EVDOKIMOV	04	SELX	600 $\Sigma^- A \to D^0 K^+ X$

[1] Systematic errors not estimated.

$D_{s2}^{*}(2573)^+$ DECAY MODES

$D_{s2}^{*}(2573)^-$ modes are charge conjugates of the modes below.

	Mode	Fraction (Γ_i/Γ)
Γ_1	$D^0 K^+$	seen
Γ_2	$D^*(2007)^0 K^+$	not seen

$D_{s2}^{*}(2573)^+$ BRANCHING RATIOS

$\Gamma(D^0 K^+)/\Gamma_{total}$ Γ_1/Γ

VALUE	EVTS	DOCUMENT ID		TECN	CHG	COMMENT
seen	217	KUBOTA	94	CLE2	±	$e^+ e^-$ ~ 10.5 GeV

$\Gamma(D^*(2007)^0 K^+)/\Gamma(D^0 K^+)$ Γ_2/Γ_1

VALUE	CL%	DOCUMENT ID		TECN	CHG	COMMENT
<0.33	90	KUBOTA	94	CLE2	+	$e^+ e^-$ ~ 10.5 GeV

$D_{s2}^{*}(2573)$ REFERENCES

AAIJ	14AW	PRL 113 162001	R. Aaij *et al.*	(LHCb Collab.) JP
AAIJ	11A	PL B698 14	R. Aaij *et al.*	(LHCb Collab.)
AUBERT,BE	06E	PRL 97 222001	B. Aubert *et al.*	(BABAR Collab.)
EVDOKIMOV	04	PRL 93 242001	A.V. Evdokimov *et al.*	(SELEX Collab.)
HEISTER	02B	PL B526 34	A. Heister *et al.*	(ALEPH Collab.)

Meson Particle Listings

$D^*_{s2}(2573)$, $D^*_{s1}(2700)^\pm$, $D^*_{s1}(2860)^\pm$

ALBRECHT 96 ZPHY C69 405 H. Albrecht *et al.* (ARGUS Collab.)
KUBOTA 94 PRL 72 1972 Y. Kubota *et al.* (CLEO Collab.)

$D^*_{s1}(2700)^\pm$ $I(J^P) = 0(1^-)$

$D^*_{s1}(2700)^+$ MASS

VALUE (MeV)	EVTS	DOCUMENT ID		TECN	COMMENT
$2708.3^{+4.0}_{-3.4}$ OUR AVERAGE					
$2699\ ^{+14}_{-7}$		[1] LEES	15C	BABR	$B \to D D^0 K^+$
$2709.2 \pm 1.9 \pm 4.5$	52k	[2] AAIJ	12AU	LHCB	$pp \to (DK)^+ X$ at 7 TeV
$2710 \pm 2\ ^{+12}_{-7}$	10.4k	[3] AUBERT	09AR	BABR	$e^+e^- \to D^{(*)} KX$
$2708 \pm 9\ ^{+11}_{-10}$	182	BRODZICKA	08	BELL	$B^+ \to D^0 \overline{D}{}^0 K^+$
• • • We do not use the following data for averages, fits, limits, etc. • • •					
$2694 \pm 8\ ^{+13}_{-3}$		LEES	15C	BABR	$B^0 \to D^- D^0 K^+$
$2707 \pm 8 \pm 8$		LEES	15C	BABR	$B^+ \to \overline{D}{}^0 D^0 K^+$
$2688 \pm 4 \pm 3$		[4] AUBERT,BE	06E	BABR	$10.6\ e^+e^- \to DKX$

[1] From a combined analysis of $B^0 \to D^- D^0 K^+$ and $B^+ \to \overline{D}{}^0 D^0 K^+$.
[2] From the combined fit of the $D^+ K^0_S$ and $D^0 K^+$ modes in the model including the $D^*_{s2}(2573)^+$, $D^*_{s1}(2700)^+$ and spin-0 $D^*_{sJ}(2860)^+$.
[3] From simultaneous fits to the two DK mass spectra and to the total D^*K mass spectrum.
[4] Superseded by AUBERT 09AR.

$D^*_{s1}(2700)^+$ WIDTH

VALUE (MeV)	EVTS	DOCUMENT ID		TECN	COMMENT
120 ± 11 OUR AVERAGE					
$127\ ^{+24}_{-19}$		[5] LEES	15C	BABR	$B \to D D^0 K^+$
$115.8 \pm 7.3 \pm 12.1$	52k	[6] AAIJ	12AU	LHCB	$pp \to (DK)^+ X$ at 7 TeV
$149 \pm 7\ ^{+39}_{-52}$	10.4k	[7] AUBERT	09AR	BABR	$e^+e^- \to D^{(*)} KX$
$108 \pm 23\ ^{+36}_{-31}$	182	BRODZICKA	08	BELL	$B^+ \to D^0 \overline{D}{}^0 K^+$
• • • We do not use the following data for averages, fits, limits, etc. • • •					
$145 \pm 24\ ^{+22}_{-14}$		LEES	15C	BABR	$B^0 \to D^- D^0 K^+$
$113 \pm 21\ ^{+20}_{-16}$		LEES	15C	BABR	$B^+ \to \overline{D}{}^0 D^0 K^+$
$112 \pm 7 \pm 36$		[8] AUBERT,BE	06E	BABR	$10.6\ e^+e^- \to DKX$

[5] From a combined analysis of $B^0 \to D^- D^0 K^+$ and $B^+ \to \overline{D}{}^0 D^0 K^+$.
[6] From the combined fit of the $D^+ K^0_S$ and $D^0 K^+$ modes in the model including the $D^*_{s2}(2573)^+$, $D^*_{s1}(2700)^+$ and spin-0 $D^*_{sJ}(2860)^+$.
[7] From simultaneous fits to the two DK mass spectra and to the total D^*K mass spectrum.
[8] Superseded by AUBERT 09AR.

$D^*_{s1}(2700)^\pm$ DECAY MODES

	Mode
Γ_1	DK
Γ_2	$D^0 K^+$
Γ_3	$D^+ K^0_S$
Γ_4	D^*K
Γ_5	$D^{*0} K^+$
Γ_6	$D^{*+} K^0_S$

$D^*_{s1}(2700)^\pm$ BRANCHING RATIOS

$\Gamma(D^*K)/\Gamma(DK)$ Γ_4/Γ_1

VALUE	EVTS	DOCUMENT ID		TECN	COMMENT
$0.91 \pm 0.13 \pm 0.12$	10.4k	[9] AUBERT	09AR	BABR	$e^+e^- \to D^{(*)} KX$

[9] From the average of the corresponding ratios with $D^{(*)0} K^+$ and $D^{(*)+} K^0_S$.

$\Gamma(D^{*0}K^+)/\Gamma(D^0K^+)$ Γ_5/Γ_2

VALUE	EVTS	DOCUMENT ID		TECN	COMMENT
• • • We do not use the following data for averages, fits, limits, etc. • • •					
$0.88 \pm 0.14 \pm 0.14$	7716	[10] AUBERT	09AR	BABR	$e^+e^- \to D^{(*)} KX$

[10] From the $D^{*0} K^+$ and $D^0 K^+$, where $D^{*0} \to D^0 \pi^0$.

$\Gamma(D^{*+}K^0_S)/\Gamma(D^+K^0_S)$ Γ_6/Γ_3

VALUE	EVTS	DOCUMENT ID		TECN	COMMENT
• • • We do not use the following data for averages, fits, limits, etc. • • •					
$1.14 \pm 0.39 \pm 0.23$	2700	[11] AUBERT	09AR	BABR	$e^+e^- \to D^{(*)} KX$

[11] From the $D^{*+} K^0_S$ and $D^+ K^0_S$, where $D^{*+} \to D^+ \pi^0$.

$D^*_{s1}(2700)^\pm$ REFERENCES

LEES 15C PR D91 052002 J.P. Lees *et al.* (BABAR Collab.)
AAIJ 12AU JHEP 1210 151 R. Aaij *et al.* (LHCb Collab.)
AUBERT 09AR PR D80 092003 B. Aubert *et al.* (BABAR Collab.)
BRODZICKA 08 PRL 100 092001 J. Brodzicka *et al.* (BELLE Collab.)
AUBERT,BE 06E PRL 97 222001 B. Aubert *et al.* (BABAR Collab.)

$D^*_{s1}(2860)^\pm$ $I(J^P) = 0(1^-)$

OMITTED FROM SUMMARY TABLE

J^P consitent with 1^- from angular analysis of AAIJ 14AW. Observed by AUBERT,BE 06E and AUBERT 09AR in inclusive production of DK and D^*K in e^+e^- annihilation.

$D^*_{s1}(2860)^+$ MASS

VALUE (MeV)	EVTS	DOCUMENT ID		TECN	COMMENT
$2859 \pm 12 \pm 24$		[1] AAIJ	14AW	LHCB	$B^0_s \to \overline{D}{}^0 K^- \pi^+$
• • • We do not use the following data for averages, fits, limits, etc. • • •					
$2866.1 \pm 1.0 \pm 6.3$	36k	[2,3] AAIJ	12AU	LHCB	$pp \to (DK)^+ X$ at 7 TeV
$2862 \pm 2\ ^{+5}_{-2}$	3122	[3,4] AUBERT	09AR	BABR	$e^+e^- \to D^{(*)} KX$
$2856.6 \pm 1.5 \pm 5.0$		[5] AUBERT,BE	06E	BABR	$e^+e^- \to DKX$

[1] Separated from the spin-3 component $D^*_{s3}(2860)^-$ by a fit of the helicity angle of the $\overline{D}{}^0 K^-$ system, with a statistical significance of the spin-3 and spin-1 components in excess of 10 σ.
[2] From the combined fit of the $D^+ K^0_S$ and $D^0 K^+$ modes in the model including the $D^*_{s2}(2573)^+$, $D^*_{s1}(2700)^+$ and spin-0 $D^*_{sJ}(2860)^+$.
[3] Possible contribution from the $D^*_{s3}(2860)$ state.
[4] From simultaneous fits to the two DK mass spectra and to the total D^*K mass spectrum.
[5] Superseded by AUBERT 09AR.

$D^*_{s1}(2860)^+$ WIDTH

VALUE (MeV)	EVTS	DOCUMENT ID		TECN	COMMENT
$159 \pm 23 \pm 77$		[1] AAIJ	14AW	LHCB	$B^0_s \to \overline{D}{}^0 K^- \pi^+$
• • • We do not use the following data for averages, fits, limits, etc. • • •					
$69.9 \pm 3.2 \pm 6.6$	36k	[2,3] AAIJ	12AU	LHCB	$pp \to (DK)^+ X$ at 7 TeV
$48 \pm 3 \pm 6$	3122	[3,4] AUBERT	09AR	BABR	$e^+e^- \to D^{(*)} KX$
$47 \pm 7 \pm 10$		[5] AUBERT,BE	06E	BABR	$e^+e^- \to DKX$

[1] Separated from the spin-3 component $D^*_{s3}(2860)^-$ by a fit of the helicity angle of the $\overline{D}{}^0 K^-$ system, with a statistical significance of the spin-3 and spin-1 components in excess of 10 σ.
[2] From the combined fit of the $D^+ K^0_S$ and $D^0 K^+$ modes in the model including the $D^*_{s2}(2573)^+$, $D^*_{s1}(2700)^+$ and spin-0 $D^*_{sJ}(2860)^+$.
[3] Possible contribution from the $D^*_{s3}(2860)$ state.
[4] From simultaneous fits to the two DK mass spectra and to the total D^*K mass spectrum.
[5] Superseded by AUBERT 09AR.

$D^*_{s1}(2860)^\pm$ DECAY MODES

	Mode
Γ_1	DK
Γ_2	$D^0 K^+$
Γ_3	$D^+ K^0_S$
Γ_4	D^*K
Γ_5	$D^{*0} K^+$
Γ_6	$D^{*+} K^0_S$

$D^*_{s1}(2860)^\pm$ BRANCHING RATIOS

$\Gamma(D^*K)/\Gamma(DK)$ Γ_4/Γ_1

VALUE	EVTS	DOCUMENT ID		TECN	COMMENT
$1.10 \pm 0.15 \pm 0.19$	3122	[1] AUBERT	09AR	BABR	$e^+e^- \to D^{(*)} KX$

[1] From the average of the corresponding ratios with $D^{(*)0} K^+$ and $D^{(*)+} K^0_S$.

$\Gamma(D^{*0}K^+)/\Gamma(D^0K^+)$ Γ_5/Γ_2

VALUE	EVTS	DOCUMENT ID		TECN	COMMENT
• • • We do not use the following data for averages, fits, limits, etc. • • •					
$1.04 \pm 0.17 \pm 0.20$	2241	[1] AUBERT	09AR	BABR	$e^+e^- \to D^{(*)} KX$

[1] From the $D^{*0} K^+$ and $D^0 K^+$, where $D^{*0} \to D^0 \pi^0$.

$\Gamma(D^{*+}K_S^0)/\Gamma(D^+K_S^0)$ Γ_6/Γ_3

VALUE	EVTS	DOCUMENT ID		TECN	COMMENT
• • • We do not use the following data for averages, fits, limits, etc. • • •					
$1.38\pm0.35\pm0.49$	881	[1] AUBERT	09AR	BABR	$e^+e^- \to D^{(*)}KX$

[1] From the $D^{*+}K_S^0$ and $D^+K_S^0$, where $D^{*+} \to D^+\pi^0$.

$D_{s1}^*(2860)^\pm$ REFERENCES

AAIJ	14AW	PRL 113 162001	R. Aaij *et al.*	(LHCb Collab.) JP
AAIJ	12AU	JHEP 1210 151	R. Aaij *et al.*	(LHCb Collab.)
AUBERT	09AR	PR D80 092003	B. Aubert *et al.*	(BABAR Collab.)
AUBERT,BE	06E	PRL 97 222001	B. Aubert *et al.*	(BABAR Collab.)

$D_{s3}^*(2860)^\pm$ $I(J^P) = 0(3^-)$

OMITTED FROM SUMMARY TABLE

J^P consitent with 3^- from angular analysis of AAIJ 14AW.

$D_{s3}^*(2860)^+$ MASS

VALUE (MeV)	DOCUMENT ID		TECN	COMMENT
2860.5±2.6±6.5	[1] AAIJ	14AW	LHCB	$B_s^0 \to \overline{D}^0K^-\pi^+$

[1] Separated from the spin-1 component $D_{s1}^*(2860)^-$ by a fit of the helicity angle of the $\overline{D}^0K^-$ system, with a statistical significance of the spin-3 and spin-1 components in excess of 10 σ.

$D_{s3}^*(2860)^+$ WIDTH

VALUE (MeV)	DOCUMENT ID		TECN	COMMENT
53±7±7	[1] AAIJ	14AW	LHCB	$B_s^0 \to \overline{D}^0K^-\pi^+$

[1] Separated from the spin-1 component $D_{s1}^*(2860)^-$ by a fit of the helicity angle of the $\overline{D}^0K^-$ system, with a statistical significance of the spin-3 and spin-1 components in excess of 10 σ.

$D_{s3}^*(2860)^\pm$ REFERENCES

AAIJ	14AW	PRL 113 162001	R. Aaij *et al.*	(LHCb Collab.) JP

$D_{sJ}(3040)^\pm$ $I(J^P) = 0(?^?)$

OMITTED FROM SUMMARY TABLE

Observed by AUBERT 09AR in inclusive production of D^*K in e^+e^- annihilation.

$D_{sJ}(3040)^+$ MASS

VALUE (MeV)	DOCUMENT ID		TECN	COMMENT
$\mathbf{3044\pm8^{+30}_{-5}}$	AUBERT	09AR	BABR	$e^+e^- \to D^*KX$

$D_{sJ}(3040)^+$ WIDTH

VALUE (MeV)	DOCUMENT ID		TECN	COMMENT
$\mathbf{239\pm35^{+46}_{-42}}$	AUBERT	09AR	BABR	$e^+e^- \to D^*KX$

$D_{sJ}(3040)^\pm$ DECAY MODES

	Mode
Γ_1	D^*K
Γ_2	$D^{*0}K^+$
Γ_3	$D^{*+}K_S^0$

$D_{sJ}(3040)^\pm$ REFERENCES

AUBERT	09AR	PR D80 092003	B. Aubert *et al.*	(BABAR Collab.)

OTHER RELATED PAPERS

SUN	09	PR D80 074037	Z.-F. Sun, X. Liu	

BOTTOM MESONS ($B = \pm 1$)

$B^+ = u\overline{b}$, $B^0 = d\overline{b}$, $\overline{B}^0 = \overline{d}b$, $B^- = \overline{u}b$, similarly for B^*'s

B-particle organization

Many measurements of B decays involve admixtures of B hadrons. Previously we arbitrarily included such admixtures in the $B^{\pm}$ section, but because of their importance we have created two new sections: "$B^{\pm}/B^0$ Admixture" for $\Upsilon(4S)$ results and "$B^{\pm}/B^0/B_s^0/b$-baryon Admixture" for results at higher energies. Most inclusive decay branching fractions and χ_b at high energy are found in the Admixture sections. B^0-$\overline{B}^0$ mixing data are found in the B^0 section, while B_s^0-$\overline{B}_s^0$ mixing data and B-$\overline{B}$ mixing data for a B^0/B_s^0 admixture are found in the B_s^0 section. CP-violation data are found in the $B^{\pm}$, B^0, and $B^{\pm}$ B^0 Admixture sections. b-baryons are found near the end of the Baryon section. Recently, we also created a new section: "V_{cb} and V_{ub} CKM Matrix Elements."

The organization of the B sections is now as follows, where bullets indicate particle sections and brackets indicate reviews.

[Production and Decay of b-flavored Hadrons]
[A Short Note on HFLAV Activities]
- $B^{\pm}$
  - mass, mean life
  - branching fractions
  - polarization in $B^{\pm}$ decay
  - CP violation
- B^0
  - mass, mean life
  - branching fractions
  - [Polarization in B decay]
  - polarization in B^0 decay
  - [B-$\overline{B}$ Mixing]
  - B^0-$\overline{B}^0$ mixing
  - CP violation
- $B^{\pm}$ B^0 Admixture
  - branching fractions, CP violation
  - CP violation
- $B^{\pm}/B^0/B_s^0/b$-baryon Admixture
  - mean life
  - production fractions
  - branching fractions
  - χ_b at high energy
  - production fractions in hadronic Z decay
- V_{cb} and V_{ub} CKM Matrix Elements
  - [Determination of V_{cb} and V_{ub}]

- B^*
  - mass
- $B_1(5721)^0$
  - mass
- $B_J^*(5732)$
  - mass, width
- $B_2(5747)^0$
  - mass
- B_s^0
  - mass, mean life
  - branching fractions
  - polarization in B_s^0 decay
  - B_s^0-$\overline{B}_s^0$ mixing
- B_s^*
  - mass
- $B_{sJ}^*(5850)$
  - mass, width
- $B_c^{\pm}$
  - mass, mean life
  - branching fractions

At the end of Baryon Listings:
- Λ_b
  - mass, mean life
  - branching fractions
- Σ_b, Σ_b^*
  - mass
- Ξ_b^0, Ξ_b^-
  - mean life
- Ω_b^-
  - mass, mean life
  - branching fractions
- b-baryon Admixture
  - mean life
  - branching fractions

See the related review(s):
Production and Decay of b-flavored Hadrons
Heavy Flavor Averaging Group

$B^{\pm}$ $I(J^P) = \frac{1}{2}(0^-)$

Quantum numbers not measured. Values shown are quark-model predictions.

See also the $B^{\pm}/B^0$ ADMIXTURE and $B^{\pm}/B^0/B_s^0/b$-baryon ADMIXTURE sections.

$B^{\pm}$ MASS

The fit uses m_{B^+}, $(m_{B^0} - m_{B^+})$, and m_{B^0} to determine m_{B^+}, m_{B^0}, and the mass difference.

VALUE (MeV)	EVTS	DOCUMENT ID		TECN	COMMENT
5279.32±0.14 OUR FIT Error includes scale factor of 1.1.					
5279.25±0.26 OUR AVERAGE					
5279.38±0.11±0.33		[1] AAIJ	12E	LHCB	pp at 7 TeV
5279.10±0.41±0.36		[2] ACOSTA	06	CDF	$p\overline{p}$ at 1.96 TeV
5279.1 ±0.4 ±0.4	526	[3] CSORNA	00	CLE2	$e^+e^- \to \Upsilon(4S)$
5279.1 ±1.7 ±1.4	147	ABE	96B	CDF	$p\overline{p}$ at 1.8 TeV
• • • We do not use the following data for averages, fits, limits, etc. • • •					
5278.8 ±0.54±2.0	362	ALAM	94	CLE2	$e^+e^- \to \Upsilon(4S)$
5278.3 ±0.4 ±2.0		BORTOLETTO	92	CLEO	$e^+e^- \to \Upsilon(4S)$
5280.5 ±1.0 ±2.0		[4] ALBRECHT	90J	ARG	$e^+e^- \to \Upsilon(4S)$
5275.8 ±1.3 ±3.0	32	ALBRECHT	87C	ARG	$e^+e^- \to \Upsilon(4S)$
5278.2 ±1.8 ±3.0	12	[5] ALBRECHT	87D	ARG	$e^+e^- \to \Upsilon(4S)$
5278.6 ±0.8 ±2.0		BEBEK	87	CLEO	$e^+e^- \to \Upsilon(4S)$

[1] Uses $B^+ \to J/\psi K^+$ fully reconstructed decays.
[2] Uses exclusively reconstructed final states containing a $J/\psi \to \mu^+\mu^-$ decays.
[3] CSORNA 00 uses fully reconstructed 526 $B^+ \to J/\psi^{(\prime)} K^+$ events and invariant masses without beam constraint.
[4] ALBRECHT 90J assumes 10580 for $\Upsilon(4S)$ mass. Supersedes ALBRECHT 87C and ALBRECHT 87D.
[5] Found using fully reconstructed decays with $J/\psi(1S)$. ALBRECHT 87D assume $m_{\Upsilon(4S)}$ = 10577 MeV.

$B^{\pm}$ MEAN LIFE

See $B^{\pm}/B^0/B_s^0/b$-baryon ADMIXTURE section for data on B-hadron mean life averaged over species of bottom particles.

"OUR EVALUATION" is an average using rescaled values of the data listed below. The average and rescaling were performed by the Heavy Flavor Averaging Group (HFLAV) and are described at http://www.slac.stanford.edu/xorg/hflav/. The averaging/rescaling procedure takes into account correlations between the measurements and asymmetric lifetime errors.

VALUE (10^{-12} s)	EVTS	DOCUMENT ID		TECN	COMMENT
1.638±0.004 OUR EVALUATION					
1.637±0.004±0.003		AAIJ	14E	LHCB	pp at 7 TeV
1.639±0.009±0.009		[1] AALTONEN	11	CDF	$p\overline{p}$ at 1.96 TeV
1.663±0.023±0.015		[2] AALTONEN	11B	CDF	$p\overline{p}$ at 1.96 TeV
1.635±0.011±0.011		[3] ABE	05B	BELL	$e^+e^- \to \Upsilon(4S)$
1.624±0.014±0.018		[4] ABDALLAH	04E	DLPH	$e^+e^- \to Z$
1.636±0.058±0.025		[5] ACOSTA	02C	CDF	$p\overline{p}$ at 1.8 TeV
1.673±0.032±0.023		[6] AUBERT	01F	BABR	$e^+e^- \to \Upsilon(4S)$
1.648±0.049±0.035		[7] BARATE	00R	ALEP	$e^+e^- \to Z$
1.643±0.037±0.025		[8] ABBIENDI	99J	OPAL	$e^+e^- \to Z$
$1.637 \pm 0.058 ^{+0.045}_{-0.043}$		[7] ABE	98Q	CDF	$p\overline{p}$ at 1.8 TeV
1.66 ±0.06 ±0.03		[8] ACCIARRI	98S	L3	$e^+e^- \to Z$
1.66 ±0.06 ±0.05		[8] ABE	97J	SLD	$e^+e^- \to Z$
$1.58 ^{+0.21}_{-0.18} \pm 0.04 ^{+0.04}_{-0.03}$	94	[5] BUSKULIC	96J	ALEP	$e^+e^- \to Z$
1.61 ±0.16 ±0.12		[7,9] ABREU	95Q	DLPH	$e^+e^- \to Z$
1.72 ±0.08 ±0.06		[10] ADAM	95	DLPH	$e^+e^- \to Z$
1.52 ±0.14 ±0.09		[7] AKERS	95T	OPAL	$e^+e^- \to Z$

• • • We do not use the following data for averages, fits, limits, etc. • • •

$1.695 \pm 0.026 \pm 0.015$		[6] ABE	02H	BELL	Repl. by ABE 05B
$1.68 \pm 0.07 \pm 0.02$		[5] ABE	98B	CDF	Repl. by ACOSTA 02C
$1.56 \pm 0.13 \pm 0.06$		[7] ABE	96C	CDF	Repl. by ABE 98Q
$1.58 \pm 0.09 \pm 0.03$		[11] BUSKULIC	96J	ALEP	$e^+e^- \to Z$
$1.58 \pm 0.09 \pm 0.04$		[7] BUSKULIC	96J	ALEP	Repl. by BARATE 00R
1.70 ± 0.09		[12] ADAM	95	DLPH	$e^+e^- \to Z$
$1.61 \pm 0.16 \pm 0.05$	148	[5] ABE	94D	CDF	Repl. by ABE 98B
$1.30 \, {}^{+0.33}_{-0.29} \pm 0.16$	92	[7] ABREU	93D	DLPH	Sup. by ABREU 95Q
$1.56 \pm 0.19 \pm 0.13$	134	[10] ABREU	93G	DLPH	Sup. by ADAM 95
$1.51 \, {}^{+0.30}_{-0.28} \, {}^{+0.12}_{-0.14}$	59	[7] ACTON	93C	OPAL	Sup. by AKERS 95T
$1.47 \, {}^{+0.22}_{-0.19} \, {}^{+0.15}_{-0.14}$	77	[7] BUSKULIC	93D	ALEP	Sup. by BUSKULIC 96J

[1] Measured mean life using fully reconstructed decays ($J/\psi K^{(*)}$).
[2] Measured using $B^- \to D^0\pi^-$ with $D^0 \to K^-\pi^+$ events that were selected using a silicon vertex trigger.
[3] Measurement performed using a combined fit of *CP*-violation, mixing and lifetimes.
[4] Measurement performed using an inclusive reconstruction and B flavor identification technique.
[5] Measured mean life using fully reconstructed decays.
[6] Events are selected in which one B meson is fully reconstructed while the second B meson is reconstructed inclusively.
[7] Data analyzed using $D/D^*\ell$X event vertices.
[8] Data analyzed using charge of secondary vertex.
[9] ABREU 95Q assumes $B(B^0 \to D^{**-}\ell^+\nu_\ell) = 3.2 \pm 1.7\%$.
[10] Data analyzed using vertex-charge technique to tag B charge.
[11] Combined result of $D/D^*\ell$X analysis and fully reconstructed B analysis.
[12] Combined ABREU 95Q and ADAM 95 result.

τ_{B^+}/τ_{B^-}

VALUE	DOCUMENT ID		TECN	COMMENT
$1.002 \pm 0.004 \pm 0.002$	[1] AAIJ	14E	LHCB	pp at 7 TeV

[1] Measured using $B^{\pm} \to J/\psi K^{\pm}$ decays.

B^+ DECAY MODES

B^- modes are charge conjugates of the modes below. Modes which do not identify the charge state of the B are listed in the $B^{\pm}/B^0$ ADMIXTURE section.

The branching fractions listed below assume 50% $B^0\overline{B}{}^0$ and 50% B^+B^- production at the $\Upsilon(4S)$. We have attempted to bring older measurements up to date by rescaling their assumed $\Upsilon(4S)$ production ratio to 50:50 and their assumed D, D_s, D^*, and ψ branching ratios to current values whenever this would affect our averages and best limits significantly.

Indentation is used to indicate a subchannel of a previous reaction. All resonant subchannels have been corrected for resonance branching fractions to the final state so the sum of the subchannel branching fractions can exceed that of the final state.

For inclusive branching fractions, *e.g.*, $B \to D^{\pm}$anything, the values usually are multiplicities, not branching fractions. They can be greater than one.

	Mode		Fraction (Γ_i/Γ)	Scale factor/ Confidence level
	Semileptonic and leptonic modes			
Γ_1	$\ell^+\nu_\ell$ anything	[a]	(10.99 ± 0.28) %	
Γ_2	$e^+\nu_e X_c$		(10.8 ± 0.4) %	
Γ_3	$D\ell^+\nu_\ell$ anything		(8.4 ± 0.5) %	
Γ_4	$\overline{D}{}^0\ell^+\nu_\ell$	[a]	(2.20 ± 0.10) %	
Γ_5	$\overline{D}{}^0\tau^+\nu_\tau$		(7.7 ± 2.5) $\times 10^{-3}$	
Γ_6	$\overline{D}{}^*(2007)^0\ell^+\nu_\ell$	[a]	(4.88 ± 0.10) %	
Γ_7	$\overline{D}{}^*(2007)^0\tau^+\nu_\tau$		(1.88 ± 0.20) %	
Γ_8	$D^-\pi^+\ell^+\nu_\ell$		(4.1 ± 0.5) $\times 10^{-3}$	
Γ_9	$\overline{D}{}^*_0(2420)^0\ell^+\nu_\ell$, $\overline{D}{}^{*0}_0 \to D^-\pi^+$		(2.5 ± 0.5) $\times 10^{-3}$	
Γ_{10}	$\overline{D}{}^*_2(2460)^0\ell^+\nu_\ell$, $\overline{D}{}^{*0}_2 \to D^-\pi^+$		(1.53 ± 0.16) $\times 10^{-3}$	
Γ_{11}	$D^{(*)}\,n\pi\ell^+\nu_\ell (n \geq 1)$		(1.60 ± 0.22) %	
Γ_{12}	$D^{*-}\pi^+\ell^+\nu_\ell$		(6.1 ± 0.6) $\times 10^{-3}$	
Γ_{13}	$\overline{D}_1(2420)^0\ell^+\nu_\ell$, $\overline{D}{}^0_1 \to D^{*-}\pi^+$		(3.03 ± 0.20) $\times 10^{-3}$	
Γ_{14}	$\overline{D}{}'_1(2430)^0\ell^+\nu_\ell$, $\overline{D}{}'^0_1 \to D^{*-}\pi^+$		(2.7 ± 0.6) $\times 10^{-3}$	
Γ_{15}	$\overline{D}{}^*_2(2460)^0\ell^+\nu_\ell$, $\overline{D}{}^{*0}_2 \to D^{*-}\pi^+$		(1.01 ± 0.24) $\times 10^{-3}$	S=2.0
Γ_{16}	$\overline{D}{}^0\pi^+\pi^-\ell^+\nu_\ell$		(1.56 ± 0.34) $\times 10^{-3}$	
Γ_{17}	$\overline{D}{}^{*0}\pi^+\pi^-\ell^+\nu_\ell$		(7 ± 4) $\times 10^{-4}$	
Γ_{18}	$D_s^{(*)-}K^+\ell^+\nu_\ell$		(6.1 ± 1.0) $\times 10^{-4}$	
Γ_{19}	$D_s^-K^+\ell^+\nu_\ell$		($3.0 \, {}^{+1.4}_{-1.2}$) $\times 10^{-4}$	
Γ_{20}	$D_s^{*-}K^+\ell^+\nu_\ell$		(2.9 ± 1.9) $\times 10^{-4}$	
Γ_{21}	$\pi^0\ell^+\nu_\ell$		(7.80 ± 0.27) $\times 10^{-5}$	
Γ_{22}	$\pi^0 e^+\nu_e$			
Γ_{23}	$\eta\ell^+\nu_\ell$		(3.9 ± 0.5) $\times 10^{-5}$	
Γ_{24}	$\eta'\ell^+\nu_\ell$		(2.3 ± 0.8) $\times 10^{-5}$	
Γ_{25}	$\omega\ell^+\nu_\ell$	[a]	(1.19 ± 0.09) $\times 10^{-4}$	
Γ_{26}	$\omega\mu^+\nu_\mu$			
Γ_{27}	$\rho^0\ell^+\nu_\ell$	[a]	(1.58 ± 0.11) $\times 10^{-4}$	
Γ_{28}	$p\overline{p}\ell^+\nu_\ell$		($5.8 \, {}^{+2.6}_{-2.3}$) $\times 10^{-6}$	
Γ_{29}	$p\overline{p}\mu^+\nu_\mu$		< 8.5	$\times 10^{-6}$ CL=90%
Γ_{30}	$p\overline{p}e^+\nu_e$		($8.2 \, {}^{+4.0}_{-3.3}$) $\times 10^{-6}$	
Γ_{31}	$e^+\nu_e$		< 9.8	$\times 10^{-7}$ CL=90%
Γ_{32}	$\mu^+\nu_\mu$		< 1.0	$\times 10^{-6}$ CL=90%
Γ_{33}	$\tau^+\nu_\tau$		(1.09 ± 0.24) $\times 10^{-4}$	S=1.2
Γ_{34}	$\ell^+\nu_\ell\gamma$		< 3.5	$\times 10^{-6}$ CL=90%
Γ_{35}	$e^+\nu_e\gamma$		< 6.1	$\times 10^{-6}$ CL=90%
Γ_{36}	$\mu^+\nu_\mu\gamma$		< 3.4	$\times 10^{-6}$ CL=90%
	Inclusive modes			
Γ_{37}	D^0X		(8.6 ± 0.7) %	
Γ_{38}	$\overline{D}{}^0X$		(79 ± 4) %	
Γ_{39}	D^+X		(2.5 ± 0.5) %	
Γ_{40}	D^-X		(9.9 ± 1.2) %	
Γ_{41}	D_s^+X		($7.9 \, {}^{+1.4}_{-1.3}$) %	
Γ_{42}	D_s^-X		($1.10 \, {}^{+0.40}_{-0.32}$) %	
Γ_{43}	Λ_c^+X		($2.1 \, {}^{+0.9}_{-0.6}$) %	
Γ_{44}	$\overline{\Lambda}{}_c^-X$		($2.8 \, {}^{+1.1}_{-0.9}$) %	
Γ_{45}	$\overline{c}X$		(97 ± 4) %	
Γ_{46}	cX		($23.4 \, {}^{+2.2}_{-1.8}$) %	
Γ_{47}	$c/\overline{c}X$		(120 ± 6) %	
	D, D^*, or D_s modes			
Γ_{48}	$\overline{D}{}^0\pi^+$		(4.68 ± 0.13) $\times 10^{-3}$	
Γ_{49}	$D_{CP(+1)}\pi^+$	[b]	(2.05 ± 0.18) $\times 10^{-3}$	
Γ_{50}	$D_{CP(-1)}\pi^+$	[b]	(2.0 ± 0.4) $\times 10^{-3}$	
Γ_{51}	$\overline{D}{}^0\rho^+$		(1.34 ± 0.18) %	
Γ_{52}	$\overline{D}{}^0K^+$		(3.63 ± 0.12) $\times 10^{-4}$	
Γ_{53}	$D_{CP(+1)}K^+$	[b]	(1.80 ± 0.07) $\times 10^{-4}$	
Γ_{54}	$D_{CP(-1)}K^+$	[b]	(1.96 ± 0.18) $\times 10^{-4}$	
Γ_{55}	$[K^-\pi^+]_D K^+$	[c]	< 2.8	$\times 10^{-7}$ CL=90%
Γ_{56}	$[K^+\pi^-]_D K^+$	[c]	< 1.5	$\times 10^{-5}$ CL=90%
Γ_{57}	$[K^-\pi^+\pi^0]_D K^+$		seen	
Γ_{58}	$[K^+\pi^-\pi^0]_D K^+$		seen	
Γ_{59}	$[K^-\pi^+\pi^+\pi^-]_D K^+$		seen	
Γ_{60}	$[K^+\pi^-\pi^+\pi^-]_D K^+$		seen	
Γ_{61}	$[\pi^+\pi^+\pi^-\pi^-]K^+$			
Γ_{62}	$[\pi^+\pi^-\pi^+\pi^-]_D K^*(892)^+$			
Γ_{63}	$[K^-\pi^+]_D K^*(892)^+$	[c]		
Γ_{64}	$[K^+\pi^-]_D K^*(892)^+$	[c]		
Γ_{65}	$[K^-\pi^+\pi^-\pi^+]_D K^*(892)^+$			
Γ_{66}	$[K^+\pi^-\pi^+\pi^-]_D K^*(892)^+$			
Γ_{67}	$[K^-\pi^+]_D\pi^+$	[c]	(6.3 ± 1.1) $\times 10^{-7}$	
Γ_{68}	$[K^+\pi^-]_D\pi^+$		(1.78 ± 0.32) $\times 10^{-4}$	
Γ_{69}	$[K^-\pi^+\pi^0]_D\pi^+$		seen	
Γ_{70}	$[K^+\pi^-\pi^0]_D\pi^+$		seen	
Γ_{71}	$[K^-\pi^+\pi^+\pi^-]_D\pi^+$		seen	
Γ_{72}	$[K^+\pi^-\pi^+\pi^-]_D\pi^+$		seen	
Γ_{73}	$[K^-\pi^+]_{(D\,\pi)}\pi^+$			
Γ_{74}	$[K^+\pi^-]_{(D\,\pi)}\pi^+$			
Γ_{75}	$[K^-\pi^+]_{(D\,\gamma)}\pi^+$			
Γ_{76}	$[K^+\pi^-]_{(D\,\gamma)}\pi^+$			
Γ_{77}	$[K^-\pi^+]_{(D\,\pi)}K^+$			
Γ_{78}	$[K^+\pi^-]_{(D\,\pi)}K^+$			
Γ_{79}	$[K^-\pi^+]_{(D\,\gamma)}K^+$			
Γ_{80}	$[K^+\pi^-]_{(D\,\gamma)}K^+$			
Γ_{81}	$[\pi^+\pi^-\pi^0]_D K^-$		(4.6 ± 0.9) $\times 10^{-6}$	
Γ_{82}	$[K^0_S K^+\pi^-]_D K^+$		seen	
Γ_{83}	$[K^0_S K^-\pi^+]_D K^+$		seen	

Meson Particle Listings

$B^{\pm}$

Γ_{84}	$[K^*(892)^+ K^-]_D K^+$		seen					
Γ_{85}	$[K^0_S K^- \pi^+]_D \pi^+$		seen					
Γ_{86}	$[K^*(892)^+ K^-]_D \pi^+$		seen					
Γ_{87}	$[K^0_S K^+ \pi^-]_D \pi^+$		seen					
Γ_{88}	$[K^*(892)^- K^+]_D \pi^+$		seen					
Γ_{89}	$[K^+ K^- \pi^0]_D K^+$							
Γ_{90}	$[K^+ K^- \pi^0]_D \pi^+$							
Γ_{91}	$[\pi^+ \pi^- \pi^0]_D K^+$							
Γ_{92}	$[\pi^+ \pi^- \pi^0]_D \pi^+$							
Γ_{93}	$\overline{D}^0 K^*(892)^+$		(5.3	± 0.4	)	$\times 10^{-4}$		
Γ_{94}	$D_{CP(-1)} K^*(892)^+$	[b]	(2.7	± 0.8	)	$\times 10^{-4}$		
Γ_{95}	$D_{CP(+1)} K^*(892)^+$	[b]	(6.2	± 0.6	)	$\times 10^{-4}$		
Γ_{96}	$\overline{D}^0 K^+ \pi^+ \pi^-$		(5.2	± 2.1	)	$\times 10^{-4}$		
Γ_{97}	$[K^+ \pi^-]_D K^+ \pi^- \pi^+$							
Γ_{98}	$[K^- \pi^+]_D K^+ \pi^- \pi^+$							
Γ_{99}	$D_{CP(+1)} K^+ \pi^- \pi^+$							
Γ_{100}	$\overline{D}^0 K^+ \overline{K}^0$		(5.5	± 1.6	)	$\times 10^{-4}$		
Γ_{101}	$\overline{D}^0 K^+ \overline{K}^*(892)^0$		(7.5	± 1.7	)	$\times 10^{-4}$		
Γ_{102}	$\overline{D}^0 \pi^+ \pi^+ \pi^-$		(5.6	± 2.1	)	$\times 10^{-3}$		S=3.6
Γ_{103}	$[K^- \pi^+]_D \pi^+ \pi^- \pi^+$							
Γ_{104}	$\overline{D}^0 \pi^+ \pi^+ \pi^-$ nonresonant		(5	± 4	)	$\times 10^{-3}$		
Γ_{105}	$\overline{D}^0 \pi^+ \rho^0$		(4.2	± 3.0	)	$\times 10^{-3}$		
Γ_{106}	$\overline{D}^0 a_1(1260)^+$		(4	± 4	)	$\times 10^{-3}$		
Γ_{107}	$\overline{D}^0 \omega \pi^+$		(4.1	± 0.9	)	$\times 10^{-3}$		
Γ_{108}	$D^*(2010)^- \pi^+ \pi^+$		(1.35	± 0.22	)	$\times 10^{-3}$		
Γ_{109}	$D^*(2010)^- K^+ \pi^+$		(8.2	± 1.4	)	$\times 10^{-5}$		
Γ_{110}	$\overline{D}_1(2420)^0 \pi^+$, $\overline{D}_1^0 \to D^*(2010)^- \pi^+$		(5.2	± 2.2	)	$\times 10^{-4}$		
Γ_{111}	$D^- \pi^+ \pi^+$		(1.07	± 0.05	)	$\times 10^{-3}$		
Γ_{112}	$D^- K^+ \pi^+$		(7.7	± 0.5	)	$\times 10^{-5}$		
Γ_{113}	$D_0^*(2400)^0 K^+$, $D_0^{*0} \to D^- \pi^+$		(6.1	± 2.4	)	$\times 10^{-6}$		
Γ_{114}	$D_2^*(2460)^0 K^+$, $D_2^{*0} \to D^- \pi^+$		(2.32	± 0.23	)	$\times 10^{-5}$		
Γ_{115}	$D_1^*(2760)^0 K^+$, $D_1^{*0} \to D^- \pi^+$		(3.6	± 1.2	)	$\times 10^{-6}$		
Γ_{116}	$D^+ K^0$		< 2.9			$\times 10^{-6}$		CL=90%
Γ_{117}	$D^+ K^+ \pi^-$		(5.6	± 1.1	)	$\times 10^{-6}$		
Γ_{118}	$D_2^*(2460)^0 K^+$, $D_2^{*0} \to D^+ \pi^-$		< 6.3			$\times 10^{-7}$		CL=90%
Γ_{119}	$D^+ K^{*0}$		< 4.9			$\times 10^{-7}$		CL=90%
Γ_{120}	$D^+ \overline{K}^{*0}$		< 1.4			$\times 10^{-6}$		CL=90%
Γ_{121}	$\overline{D}^*(2007)^0 \pi^+$		(4.90	± 0.17	)	$\times 10^{-3}$		
Γ_{122}	$\overline{D}^{*0}_{CP(+1)} \pi^+$	[d]	(2.7	± 0.6	)	$\times 10^{-3}$		
Γ_{123}	$D^{*0}_{CP(-1)} \pi^+$	[d]	(2.4	± 0.9	)	$\times 10^{-3}$		
Γ_{124}	$\overline{D}^*(2007)^0 \omega \pi^+$		(4.5	± 1.2	)	$\times 10^{-3}$		
Γ_{125}	$\overline{D}^*(2007)^0 \rho^+$		(9.8	± 1.7	)	$\times 10^{-3}$		
Γ_{126}	$\overline{D}^*(2007)^0 K^+$		(3.97	$^{+0.31}_{-0.28}$	)	$\times 10^{-4}$		
Γ_{127}	$\overline{D}^{*0}_{CP(+1)} K^+$	[d]	(2.60	± 0.33	)	$\times 10^{-4}$		
Γ_{128}	$\overline{D}^{*0}_{CP(-1)} K^+$	[d]	(2.19	± 0.30	)	$\times 10^{-4}$		
Γ_{129}	$\overline{D}^*(2007)^0 K^*(892)^+$		(8.1	± 1.4	)	$\times 10^{-4}$		
Γ_{130}	$\overline{D}^*(2007)^0 K^+ \overline{K}^0$		< 1.06			$\times 10^{-3}$		CL=90%
Γ_{131}	$\overline{D}^*(2007)^0 K^+ \overline{K}^*(892)^0$		(1.5	± 0.4	)	$\times 10^{-3}$		
Γ_{132}	$\overline{D}^*(2007)^0 \pi^+ \pi^+ \pi^-$		(1.03	± 0.12	)	%		
Γ_{133}	$\overline{D}^*(2007)^0 a_1(1260)^+$		(1.9	± 0.5	)	%		
Γ_{134}	$\overline{D}^*(2007)^0 \pi^- \pi^+ \pi^+ \pi^0$		(1.8	± 0.4	)	%		
Γ_{135}	$\overline{D}^{*0} 3\pi^+ 2\pi^-$		(5.7	± 1.2	)	$\times 10^{-3}$		
Γ_{136}	$D^*(2010)^+ \pi^0$		< 3.6			$\times 10^{-6}$		
Γ_{137}	$D^*(2010)^+ K^0$		< 9.0			$\times 10^{-6}$		CL=90%
Γ_{138}	$D^*(2010)^- \pi^+ \pi^+ \pi^0$		(1.5	± 0.7	)	%		
Γ_{139}	$D^*(2010)^- \pi^+ \pi^+ \pi^+ \pi^-$		(2.6	± 0.4	)	$\times 10^{-3}$		
Γ_{140}	$\overline{D}^{**0} \pi^+$	[e]	(5.7	± 1.2	)	$\times 10^{-3}$		
Γ_{141}	$\overline{D}_1^*(2420)^0 \pi^+$		(1.5	± 0.6	)	$\times 10^{-3}$		S=1.3
Γ_{142}	$\overline{D}_1(2420)^0 \pi^+ \times$ B($\overline{D}_1^0 \to \overline{D}^0 \pi^+ \pi^-$)		(2.5	$^{+1.6}_{-1.4}$	)	$\times 10^{-4}$		S=3.9
Γ_{143}	$\overline{D}_1(2420)^0 \pi^+ \times$ B($\overline{D}_1^0 \to \overline{D}^0 \pi^+ \pi^-$ (nonresonant))		(2.2	± 1.0	)	$\times 10^{-4}$		
Γ_{144}	$\overline{D}_2^*(2462)^0 \pi^+ \times$ B($\overline{D}_2^*(2462)^0 \to D^- \pi^+$)		(3.56	± 0.24	)	$\times 10^{-4}$		
Γ_{145}	$\overline{D}_2^*(2462)^0 \pi^+ \times$B($\overline{D}_2^{*0} \to \overline{D}^0 \pi^- \pi^+$)		(2.2	± 1.0	)	$\times 10^{-4}$		
Γ_{146}	$\overline{D}_2^*(2462)^0 \pi^+ \times$B($\overline{D}_2^{*0} \to \overline{D}^0 \pi^- \pi^+$ (nonresonant))		< 1.7			$\times 10^{-4}$		CL=90%
Γ_{147}	$\overline{D}_2^*(2462)^0 \pi^+ \times$B($\overline{D}_2^{*0} \to D^*(2010)^- \pi^+$)		(2.2	± 1.1	)	$\times 10^{-4}$		
Γ_{148}	$\overline{D}_0^*(2400)^0 \pi^+ \times$ B($\overline{D}_0^*(2400)^0 \to D^- \pi^+$)		(6.4	± 1.4	)	$\times 10^{-4}$		
Γ_{149}	$\overline{D}_1(2421)^0 \pi^+ \times$ B($\overline{D}_1(2421)^0 \to D^{*-} \pi^+$)		(6.8	± 1.5	)	$\times 10^{-4}$		
Γ_{150}	$\overline{D}_2^*(2462)^0 \pi^+ \times$ B($\overline{D}_2^*(2462)^0 \to D^{*-} \pi^+$)		(1.8	± 0.5	)	$\times 10^{-4}$		
Γ_{151}	$\overline{D}_1'(2427)^0 \pi^+ \times$ B($\overline{D}_1'(2427)^0 \to D^{*-} \pi^+$)		(5.0	± 1.2	)	$\times 10^{-4}$		
Γ_{152}	$\overline{D}_1(2420)^0 \pi^+ \times$B($\overline{D}_1^0 \to \overline{D}^{*0} \pi^+ \pi^-$)		< 6			$\times 10^{-6}$		CL=90%
Γ_{153}	$\overline{D}_1^*(2420)^0 \rho^+$		< 1.4			$\times 10^{-3}$		CL=90%
Γ_{154}	$\overline{D}_2^*(2460)^0 \pi^+$		< 1.3			$\times 10^{-3}$		CL=90%
Γ_{155}	$\overline{D}_2^*(2460)^0 \pi^+ \times$B($\overline{D}_2^{*0} \to \overline{D}^{*0} \pi^+ \pi^-$)		< 2.2			$\times 10^{-5}$		CL=90%
Γ_{156}	$\overline{D}_1^*(2680)^0 \pi^+$, $\overline{D}_1^*(2680)^0 \to D^- \pi^+$		(8.4	± 2.1	)	$\times 10^{-5}$		
Γ_{157}	$\overline{D}_3^*(2760)^0 \pi^+$, $\overline{D}_3^*(2760)^0 \pi^+ \to D^- \pi^+$		(1.00	± 0.22	)	$\times 10^{-5}$		
Γ_{158}	$\overline{D}_2^*(3000)^0 \pi^+$, $\overline{D}_2^*(3000)^0 \pi^+ \to D^- \pi^+$		(2.0	± 1.4	)	$\times 10^{-6}$		
Γ_{159}	$\overline{D}_2^*(2460)^0 \rho^+$		< 4.7			$\times 10^{-3}$		CL=90%
Γ_{160}	$\overline{D}^0 D_s^+$		(9.0	± 0.9	)	$\times 10^{-3}$		
Γ_{161}	$D_{s0}^*(2317)^+ \overline{D}^0$, $D_{s0}^{*+} \to D_s^+ \pi^0$		(7.9	$^{+1.5}_{-1.3}$	)	$\times 10^{-4}$		
Γ_{162}	$D_{s0}(2317)^+ \overline{D}^0 \times$ B($D_{s0}(2317)^+ \to D_s^{*+} \gamma$)		< 7.6			$\times 10^{-4}$		CL=90%
Γ_{163}	$D_{s0}(2317)^+ \overline{D}^*(2007)^0 \times$ B($D_{s0}(2317)^+ \to D_s^+ \pi^0$)		(9	± 7	)	$\times 10^{-4}$		
Γ_{164}	$D_{sJ}(2457)^+ \overline{D}^0$		(3.1	$^{+1.0}_{-0.9}$	)	$\times 10^{-3}$		
Γ_{165}	$D_{sJ}(2457)^+ \overline{D}^0 \times$ B($D_{sJ}(2457)^+ \to D_s^+ \gamma$)		(4.6	$^{+1.3}_{-1.1}$	)	$\times 10^{-4}$		
Γ_{166}	$D_{sJ}(2457)^+ \overline{D}^0 \times$ B($D_{sJ}(2457)^+ \to D_s^+ \pi^+ \pi^-$)		< 2.2			$\times 10^{-4}$		CL=90%
Γ_{167}	$D_{sJ}(2457)^+ \overline{D}^0 \times$ B($D_{sJ}(2457)^+ \to D_s^+ \pi^0$)		< 2.7			$\times 10^{-4}$		CL=90%
Γ_{168}	$D_{sJ}(2457)^+ \overline{D}^0 \times$ B($D_{sJ}(2457)^+ \to D_s^{*+} \gamma$)		< 9.8			$\times 10^{-4}$		CL=90%
Γ_{169}	$D_{sJ}(2457)^+ \overline{D}^*(2007)^0$		(1.20	± 0.30	)	%		
Γ_{170}	$D_{sJ}(2457)^+ \overline{D}^*(2007)^0 \times$ B($D_{sJ}(2457)^+ \to D_s^+ \gamma$)		(1.4	$^{+0.7}_{-0.6}$	)	$\times 10^{-3}$		
Γ_{171}	$\overline{D}^0 D_{s1}(2536)^+ \times$ B($D_{s1}(2536)^+ \to D^*(2007)^0 K^+ + D^*(2010)^+ K^0$)		(4.0	± 1.0	)	$\times 10^{-4}$		
Γ_{172}	$\overline{D}^0 D_{s1}(2536)^+ \times$ B($D_{s1}(2536)^+ \to D^*(2007)^0 K^+$)		(2.2	± 0.7	)	$\times 10^{-4}$		
Γ_{173}	$\overline{D}^*(2007)^0 D_{s1}(2536)^+ \times$ B($D_{s1}(2536)^+ \to D^*(2007)^0 K^+$)		(5.5	± 1.6	)	$\times 10^{-4}$		
Γ_{174}	$\overline{D}^0 D_{s1}(2536)^+ \times$ B($D_{s1}(2536)^+ \to D^{*+} K^0$)		(2.3	± 1.1	)	$\times 10^{-4}$		
Γ_{175}	$\overline{D}^0 D_{sJ}(2700)^+ \times$ B($D_{sJ}(2700)^+ \to D^0 K^+$)		(5.6	± 1.8	)	$\times 10^{-4}$		S=1.7
Γ_{176}	$\overline{D}^{*0} D_{s1}(2536)^+$, $D_{s1}^+ \to D^{*+} K^0$		(3.9	± 2.6	)	$\times 10^{-4}$		
Γ_{177}	$\overline{D}^0 D_{sJ}(2573)^+$, $D_{sJ}^+ \to D^0 K^+$		(8	±15	)	$\times 10^{-6}$		
Γ_{178}	$\overline{D}^{*0} D_{sJ}(2573)$, $D_{sJ}^+ \to D^0 K^+$		< 2			$\times 10^{-4}$		CL=90%
Γ_{179}	$\overline{D}^*(2007)^0 D_{sJ}(2573)$, $D_{sJ}^+ \to D^0 K^+$		< 5			$\times 10^{-4}$		CL=90%
Γ_{180}	$\overline{D}^0 D_s^{*+}$		(7.6	± 1.6	)	$\times 10^{-3}$		
Γ_{181}	$\overline{D}^*(2007)^0 D_s^+$		(8.2	± 1.7	)	$\times 10^{-3}$		
Γ_{182}	$\overline{D}^*(2007)^0 D_s^{*+}$		(1.71	± 0.24	)	%		
Γ_{183}	$D_s^{(*)+} \overline{D}^{**0}$		(2.7	± 1.2	)	%		

See key on page 885

Γ_{184}	$\overline{D}^*(2007)^0 D^*(2010)^+$	(	8.1	± 1.7	) × 10^{-4}		
Γ_{185}	$\overline{D}^0 D^*(2010)^+ + \overline{D}^*(2007)^0 D^+$	<	1.30		%	CL=90%	
Γ_{186}	$\overline{D}^0 D^*(2010)^+$	(	3.9	± 0.5	) × 10^{-4}		
Γ_{187}	$\overline{D}^0 D^+$	(	3.8	± 0.4	) × 10^{-4}		
Γ_{188}	$\overline{D}^0 D^+ K^0$	(	1.55	± 0.21	) × 10^{-3}		
Γ_{189}	$D^+ \overline{D}^*(2007)^0$	(	6.3	± 1.7	) × 10^{-4}		
Γ_{190}	$\overline{D}^*(2007)^0 D^+ K^0$	(	2.1	± 0.5	) × 10^{-3}		
Γ_{191}	$\overline{D}^0 D^*(2010)^+ K^0$	(	3.8	± 0.4	) × 10^{-3}		
Γ_{192}	$\overline{D}^*(2007)^0 D^*(2010)^+ K^0$	(	9.2	± 1.2	) × 10^{-3}		
Γ_{193}	$\overline{D}^0 D^0 K^+$	(	1.45	± 0.33	) × 10^{-3}		S=2.6
Γ_{194}	$\overline{D}^*(2007)^0 D^0 K^+$	(	2.26	± 0.23	) × 10^{-3}		
Γ_{195}	$\overline{D}^0 D^*(2007)^0 K^+$	(	6.3	± 0.5	) × 10^{-3}		
Γ_{196}	$\overline{D}^*(2007)^0 D^*(2007)^0 K^+$	(	1.12	± 0.13	) %		
Γ_{197}	$D^- D^+ K^+$	(	2.2	± 0.7	) × 10^{-4}		
Γ_{198}	$D^- D^*(2010)^+ K^+$	(	6.3	± 1.1	) × 10^{-4}		
Γ_{199}	$D^*(2010)^- D^+ K^+$	(	6.0	± 1.3	) × 10^{-4}		
Γ_{200}	$D^*(2010)^- D^*(2010)^+ K^+$	(	1.32	± 0.18	) × 10^{-3}		
Γ_{201}	$(\overline{D}+\overline{D}^*)(D+D^*)K$	(	4.05	± 0.30	) %		
Γ_{202}	$D_s^+ \pi^0$	(	1.6	± 0.5	) × 10^{-5}		
Γ_{203}	$D_s^{*+} \pi^0$	<	2.6		× 10^{-4}	CL=90%	
Γ_{204}	$D_s^+ \eta$	<	4		× 10^{-4}	CL=90%	
Γ_{205}	$D_s^{*+} \eta$	<	6		× 10^{-4}	CL=90%	
Γ_{206}	$D_s^+ \rho^0$	<	3.0		× 10^{-4}	CL=90%	
Γ_{207}	$D_s^{*+} \rho^0$	<	4		× 10^{-4}	CL=90%	
Γ_{208}	$D_s^+ \omega$	<	4		× 10^{-4}	CL=90%	
Γ_{209}	$D_s^{*+} \omega$	<	6		× 10^{-4}	CL=90%	
Γ_{210}	$D_s^+ a_1(1260)^0$	<	1.8		× 10^{-3}	CL=90%	
Γ_{211}	$D_s^{*+} a_1(1260)^0$	<	1.3		× 10^{-3}	CL=90%	
Γ_{212}	$D_s^+ K^+ K^-$	(	7.1	± 1.1	) × 10^{-6}		
Γ_{213}	$D_s^+ \phi$	<	4.2		× 10^{-7}	CL=90%	
Γ_{214}	$D_s^{*+} \phi$	<	1.2		× 10^{-5}	CL=90%	
Γ_{215}	$D_s^+ \overline{K}^0$	<	8		× 10^{-4}	CL=90%	
Γ_{216}	$D_s^{*+} \overline{K}^0$	<	9		× 10^{-4}	CL=90%	
Γ_{217}	$D_s^+ \overline{K}^*(892)^0$	<	4.4		× 10^{-6}	CL=90%	
Γ_{218}	$D_s^+ K^{*0}$	<	3.5		× 10^{-6}	CL=90%	
Γ_{219}	$D_s^{*+} \overline{K}^*(892)^0$	<	3.5		× 10^{-4}	CL=90%	
Γ_{220}	$D_s^- \pi^+ K^+$	(	1.80	± 0.22	) × 10^{-4}		
Γ_{221}	$D_s^{*-} \pi^+ K^+$	(	1.45	± 0.24	) × 10^{-4}		
Γ_{222}	$D_s^- \pi^+ K^*(892)^+$	<	5		× 10^{-3}	CL=90%	
Γ_{223}	$D_s^{*-} \pi^+ K^*(892)^+$	<	7		× 10^{-3}	CL=90%	
Γ_{224}	$D_s^- K^+ K^+$	(	9.7	± 2.1	) × 10^{-6}		
Γ_{225}	$D_s^{*-} K^+ K^+$	<	1.5		× 10^{-5}	CL=90%	

Charmonium modes

Γ_{226}	$\eta_c K^+$	(	1.09	± 0.09	) × 10^{-3}		S=1.1
Γ_{227}	$\eta_c K^+,\ \eta_c \to K_S^0 K^{\mp}\pi^{\pm}$	(	2.7	± 0.6	) × 10^{-5}		
Γ_{228}	$\eta_c K^*(892)^+$	(	1.0	$^{+\ 0.5}_{-\ 0.4}$	) × 10^{-3}		
Γ_{229}	$\eta_c K^+ \pi^+ \pi^-$	<	3.9		× 10^{-4}	CL=90%	
Γ_{230}	$\eta_c K^+ \omega(782)$	<	5.3		× 10^{-4}	CL=90%	
Γ_{231}	$\eta_c K^+ \eta$	<	2.2		× 10^{-4}	CL=90%	
Γ_{232}	$\eta_c K^+ \pi^0$	<	6.2		× 10^{-5}	CL=90%	
Γ_{233}	$\eta_c(2S) K^+$	(	4.4	± 1.0	) × 10^{-4}		
Γ_{234}	$\eta_c(2S) K^+,\ \eta_c \to p\overline{p}$	(	3.5	± 0.8	) × 10^{-8}		
Γ_{235}	$\eta_c(2S) K^+,\ \eta_c \to K_S^0 K^{\mp}\pi^{\pm}$	(	3.4	$^{+\ 2.3}_{-\ 1.6}$	) × 10^{-6}		
Γ_{236}	$h_c(1P) K^+,\ h_c \to J/\psi\pi^+\pi^-$	<	3.4		× 10^{-6}	CL=90%	
Γ_{237}	$X(3730)^0 K^+,\ X^0 \to \eta_c \eta$	<	4.6		× 10^{-5}	CL=90%	
Γ_{238}	$X(3730)^0 K^+,\ X^0 \to \eta_c \pi^0$	<	5.7		× 10^{-6}	CL=90%	
Γ_{239}	$\chi_{c1}(3872) K^+$	<	2.6		× 10^{-4}	CL=90%	
Γ_{240}	$\chi_{c1}(3872) K^+,\ \chi_{c1} \to p\overline{p}$	<	5		× 10^{-9}	CL=95%	
Γ_{241}	$\chi_{c1}(3872) K^+,\ \chi_{c1} \to J/\psi\pi^+\pi^-$	(	8.6	± 0.8	) × 10^{-6}		
Γ_{242}	$\chi_{c1}(3872) K^+,\ \chi_{c1} \to J/\psi\gamma$	(	2.1	± 0.4	) × 10^{-6}		S=1.1
Γ_{243}	$\chi_{c1}(3872) K^+,\ \chi_{c1} \to \psi(2S)\gamma$	(	4	± 4	) × 10^{-6}		S=2.5
Γ_{244}	$\chi_{c1}(3872) K^+,\ \chi_{c1} \to J/\psi(1S)\eta$	<	7.7		× 10^{-6}	CL=90%	
Γ_{245}	$\chi_{c1}(3872) K^+,\ \chi_{c1} \to D^0\overline{D}^0$	<	6.0		× 10^{-5}	CL=90%	
Γ_{246}	$\chi_{c1}(3872) K^+,\ \chi_{c1} \to D^+ D^-$	<	4.0		× 10^{-5}	CL=90%	
Γ_{247}	$\chi_{c1}(3872) K^+,\ \chi_{c1} \to D^0\overline{D}^0\pi^0$	(	1.0	± 0.4	) × 10^{-4}		
Γ_{248}	$\chi_{c1}(3872) K^+,\ \chi_{c1} \to \overline{D}^{*0} D^0$	(	8.5	± 2.6	) × 10^{-5}		S=1.4
Γ_{249}	$\chi_{c1}(3872)^0 K^+,\ \chi_{c1}^0 \to \eta_c \pi^+\pi^-$	<	3.0		× 10^{-5}	CL=90%	
Γ_{250}	$\chi_{c1}(3872)^0 K^+,\ \chi_{c1}^0 \to \eta_c \omega(782)$	<	6.9		× 10^{-5}	CL=90%	
Γ_{251}	$\chi_{c1}(3872) K^+,\ \chi_{c1} \to \chi_{c1}(1P)\pi^+\pi^-$	<	1.5		× 10^{-6}	CL=90%	
Γ_{252}	$X(3915) K^+$	<	2.8		× 10^{-4}	CL=90%	
Γ_{253}	$X(3915)^0 K^+,\ X^0 \to \eta_c \eta$	<	4.7		× 10^{-5}	CL=90%	
Γ_{254}	$X(3915)^0 K^+,\ X^0 \to \eta_c \pi^0$	<	1.7		× 10^{-5}	CL=90%	
Γ_{255}	$X(4014)^0 K^+,\ X^0 \to \eta_c \eta$	<	3.9		× 10^{-5}	CL=90%	
Γ_{256}	$X(4014)^0 K^+,\ X^0 \to \eta_c \pi^0$	<	1.2		× 10^{-5}	CL=90%	
Γ_{257}	$Z_c(3900)^0 K^+,\ Z_c^0 \to \eta_c \pi^+\pi^-$	<	4.7		× 10^{-5}	CL=90%	
Γ_{258}	$X(4020)^0 K^+,\ X^0 \to \eta_c \pi^+\pi^-$	<	1.6		× 10^{-5}	CL=90%	
Γ_{259}	$\chi_{c1}(3872) K^*(892)^+,\ \chi_{c1} \to J/\psi\gamma$	<	4.8		× 10^{-6}	CL=90%	
Γ_{260}	$\chi_{c1}(3872) K^*(892)^+,\ \chi_{c1} \to \psi(2S)\gamma$	<	2.8		× 10^{-5}	CL=90%	
Γ_{261}	$\chi_{c1}(3872)^+ K^0,\ \chi_{c1}^+ \to J/\psi(1S)\pi^+\pi^0$	[f] <	6.1		× 10^{-6}	CL=90%	
Γ_{262}	$\chi_{c1}(3872) K^0\pi^+,\ \chi_{c1} \to J/\psi(1S)\pi^+\pi^-$	(	1.06	± 0.31	) × 10^{-5}		
Γ_{263}	$Z_c(4430)^+ K^0,\ Z_c^+ \to J/\psi\pi^+$	<	1.5		× 10^{-5}	CL=95%	
Γ_{264}	$Z_c(4430)^+ K^0,\ Z_c^+ \to \psi(2S)\pi^+$	<	4.7		× 10^{-5}	CL=95%	
Γ_{265}	$\psi(4260)^0 K^+,\ \psi^0 \to J/\psi\pi^+\pi^-$	<	2.9		× 10^{-5}	CL=95%	
Γ_{266}	$X(3915) K^+,\ X \to J/\psi\gamma$	<	1.4		× 10^{-5}	CL=90%	
Γ_{267}	$X(3930)^0 K^+,\ X^0 \to J/\psi\gamma$	<	2.5		× 10^{-6}	CL=90%	
Γ_{268}	$J/\psi(1S) K^+$	(	1.010	± 0.029	) × 10^{-3}		
Γ_{269}	$J/\psi(1S) K^0\pi^+$	(	1.14	± 0.11	) × 10^{-3}		
Γ_{270}	$J/\psi(1S) K^+\pi^+\pi^-$	(	8.1	± 1.3	) × 10^{-4}		S=2.5
Γ_{271}	$J/\psi(1S) K^+ K^- K^+$	(	3.37	± 0.29	) × 10^{-5}		
Γ_{272}	$X(3915) K^+,\ X \to p\overline{p}$	<	7.1		× 10^{-8}	CL=95%	
Γ_{273}	$J/\psi(1S) K^*(892)^+$	(	1.43	± 0.08	) × 10^{-3}		
Γ_{274}	$J/\psi(1S) K(1270)^+$	(	1.8	± 0.5	) × 10^{-3}		
Γ_{275}	$J/\psi(1S) K(1400)^+$	<	5		× 10^{-4}	CL=90%	
Γ_{276}	$J/\psi(1S)\eta K^+$	(	1.24	± 0.14	) × 10^{-4}		
Γ_{277}	$\chi_{c1-odd}(3872) K^+,\ \chi_{c1-odd} \to J/\psi\eta$	<	3.8		× 10^{-6}	CL=90%	
Γ_{278}	$\psi(4160) K^+,\ \psi \to J/\psi\eta$	<	7.4		× 10^{-6}	CL=90%	
Γ_{279}	$J/\psi(1S)\eta' K^+$	<	8.8		× 10^{-5}	CL=90%	
Γ_{280}	$J/\psi(1S)\phi K^+$	(	5.0	± 0.4	) × 10^{-5}		
Γ_{281}	$J/\psi(1S) K_1(1650),\ K_1 \to \phi K^+$	(	6	$^{+10}_{-\ 6}$	) × 10^{-6}		
Γ_{282}	$J/\psi(1S) K^*(1680)^+,\ K^* \to \phi K^+$	(	3.4	$^{+\ 1.9}_{-\ 2.2}$	) × 10^{-6}		
Γ_{283}	$J/\psi(1S) K_2^*(1980),\ K_2^* \to \phi K^+$	(	1.5	$^{+\ 0.9}_{-\ 0.5}$	) × 10^{-6}		
Γ_{284}	$J/\psi(1S) K(1830)^+,\ K(1830)^+ \to \phi K^+$	(	1.3	$^{+\ 1.3}_{-\ 1.1}$	) × 10^{-6}		
Γ_{285}	$\chi_{c1}(4140) K^+,\ \chi_{c1} \to J/\psi(1S)\phi$	(	10	± 4	) × 10^{-6}		
Γ_{286}	$\chi_{c1}(4274) K^+,\ \chi_{c1} \to J/\psi(1S)\phi$	(	3.6	$^{+\ 2.2}_{-\ 1.8}$	) × 10^{-6}		
Γ_{287}	$\chi_{c0}(4500) K^+,\ \chi_{c}^0 \to J/\psi(1S)\phi$	(	3.3	$^{+\ 2.1}_{-\ 1.7}$	) × 10^{-6}		
Γ_{288}	$\chi_{c0}(4700) K^+,\ \chi_{c0} \to J/\psi(1S)\phi$	(	6	$^{+\ 5}_{-\ 4}$	) × 10^{-6}		
Γ_{289}	$J/\psi(1S)\omega K^+$	(	3.20	$^{+\ 0.60}_{-\ 0.32}$	) × 10^{-4}		
Γ_{290}	$\chi_{c1}(3872) K^+,\ \chi_{c1} \to J/\psi\omega$	(	6.0	± 2.2	) × 10^{-6}		
Γ_{291}	$X(3915) K^+,\ X \to J/\psi\omega$	(	3.0	$^{+\ 0.9}_{-\ 0.7}$	) × 10^{-5}		
Γ_{292}	$J/\psi(1S)\pi^+$	(	3.88	± 0.12	) × 10^{-5}		
Γ_{293}	$J/\psi(1S)\pi^+\pi^+\pi^+\pi^-\pi^-$	(	1.17	± 0.13	) × 10^{-5}		
Γ_{294}	$\psi(2S)\pi^+\pi^+\pi^-$	(	1.9	± 0.4	) × 10^{-5}		
Γ_{295}	$J/\psi(1S)\rho^+$	(	5.0	± 0.8	) × 10^{-5}		
Γ_{296}	$J/\psi(1S)\pi^+\pi^0$ nonresonant	<	7.3		× 10^{-6}	CL=90%	
Γ_{297}	$J/\psi(1S) a_1(1260)^+$	<	1.2		× 10^{-3}	CL=90%	
Γ_{298}	$J/\psi(1S) p\overline{p}\pi^+$	<	5.0		× 10^{-7}	CL=90%	
Γ_{299}	$J/\psi(1S) p\overline{\Lambda}$	(	1.18	± 0.31	) × 10^{-5}		

Meson Particle Listings

$B^{\pm}$

Γ_{300}	$J/\psi(1S)\overline{\Sigma}^0 p$	$<$	1.1		$\times 10^{-5}$	CL=90%	
Γ_{301}	$J/\psi(1S)D^+$	$<$	1.2		$\times 10^{-4}$	CL=90%	
Γ_{302}	$J/\psi(1S)\overline{D}^0\pi^+$	$<$	2.5		$\times 10^{-5}$	CL=90%	
Γ_{303}	$\psi(2S)\pi^+$	(	2.44	$\pm$ 0.30	) $\times 10^{-5}$		
Γ_{304}	$\psi(2S)K^+$	(	6.21	$\pm$ 0.23	) $\times 10^{-4}$		
Γ_{305}	$\psi(2S)K^*(892)^+$	(	6.7	$\pm$ 1.4	) $\times 10^{-4}$		S=1.3
Γ_{306}	$\psi(2S)K^0\pi^+$						
Γ_{307}	$\psi(2S)K^+\pi^+\pi^-$	(	4.3	$\pm$ 0.5	) $\times 10^{-4}$		
Γ_{308}	$\psi(2S)\phi(1020)K^+$	(	4.0	$\pm$ 0.7	) $\times 10^{-6}$		
Γ_{309}	$\psi(3770)K^+$	(	4.9	$\pm$ 1.3	) $\times 10^{-4}$		
Γ_{310}	$\psi(3770)K+,\psi \to D^0\overline{D}^0$	(	1.5	$\pm$ 0.5	) $\times 10^{-4}$		S=1.4
Γ_{311}	$\psi(3770)K+,\psi \to D^+D^-$	(	9.4	$\pm$ 3.5	) $\times 10^{-5}$		
Γ_{312}	$\psi(3770)K^+,\ \psi \to p\overline{p}$	$<$	2		$\times 10^{-7}$	CL=95%	
Γ_{313}	$\psi(4040)K^+$	$<$	1.3		$\times 10^{-4}$	CL=90%	
Γ_{314}	$\psi(4160)K^+$	(	5.1	$\pm$ 2.7	) $\times 10^{-4}$		
Γ_{315}	$\psi(4160)K^+,\ \psi \to \overline{D}^0D^0$	(	8	$\pm$ 5	) $\times 10^{-5}$		
Γ_{316}	$\chi_{c0}\pi^+,\ \chi_{c0} \to \pi^+\pi^-$	$<$	1		$\times 10^{-7}$	CL=90%	
Γ_{317}	$\chi_{c0}K^+$	(	1.49	$^{+0.15}_{-0.14}$	) $\times 10^{-4}$		
Γ_{318}	$\chi_{c0}K^*(892)^+$	$<$	2.1		$\times 10^{-4}$	CL=90%	
Γ_{319}	$\chi_{c1}(1P)\pi^+$	(	2.2	$\pm$ 0.5	) $\times 10^{-5}$		
Γ_{320}	$\chi_{c1}(1P)K^+$	(	4.84	$\pm$ 0.23	) $\times 10^{-4}$		
Γ_{321}	$\chi_{c1}(1P)K^*(892)^+$	(	3.0	$\pm$ 0.6	) $\times 10^{-4}$		S=1.1
Γ_{322}	$\chi_{c1}(1P)K^0\pi^+$	(	5.8	$\pm$ 0.4	) $\times 10^{-4}$		
Γ_{323}	$\chi_{c1}(1P)K^+\pi^0$	(	3.29	$\pm$ 0.35	) $\times 10^{-4}$		
Γ_{324}	$\chi_{c1}(1P)K^+\pi^+\pi^-$	(	3.74	$\pm$ 0.30	) $\times 10^{-4}$		
Γ_{325}	$\chi_{c1}(2P)K^+,\ \chi_{c1}(2P) \to \pi^+\pi^-\chi_{c1}(1P)$	$<$	1.1		$\times 10^{-5}$	CL=90%	
Γ_{326}	$\chi_{c2}K^+$	(	1.1	$\pm$ 0.4	) $\times 10^{-5}$		
Γ_{327}	$\chi_{c2}K^*(892)^+$	$<$	1.2		$\times 10^{-4}$	CL=90%	
Γ_{328}	$\chi_{c2}K^0\pi^+$	(	1.16	$\pm$ 0.25	) $\times 10^{-4}$		
Γ_{329}	$\chi_{c2}K^+\pi^0$	$<$	6.2		$\times 10^{-5}$	CL=90%	
Γ_{330}	$\chi_{c2}K^+\pi^+\pi^-$	(	1.34	$\pm$ 0.19	) $\times 10^{-4}$		
Γ_{331}	$\chi_{c2}(3930)\pi^+,\ \chi_{c2} \to \pi^+\pi^-$	$<$	1		$\times 10^{-7}$	CL=90%	
Γ_{332}	$h_c(1P)K^+$	$<$	3.8		$\times 10^{-5}$	CL=90%	
Γ_{333}	$h_c(1P)K^+,\ h_c \to p\overline{p}$	$<$	6.4		$\times 10^{-8}$	CL=95%	

K or K^* modes

Γ_{334}	$K^0\pi^+$	(	2.37	$\pm$ 0.08	) $\times 10^{-5}$		
Γ_{335}	$K^+\pi^0$	(	1.29	$\pm$ 0.05	) $\times 10^{-5}$		
Γ_{336}	$\eta' K^+$	(	7.06	$\pm$ 0.25	) $\times 10^{-5}$		
Γ_{337}	$\eta' K^*(892)^+$	(	4.8	$^{+1.8}_{-1.6}$	) $\times 10^{-6}$		
Γ_{338}	$\eta' K_0^*(1430)^+$	(	5.2	$\pm$ 2.1	) $\times 10^{-6}$		
Γ_{339}	$\eta' K_2^*(1430)^+$	(	2.8	$\pm$ 0.5	) $\times 10^{-5}$		
Γ_{340}	ηK^+	(	2.4	$\pm$ 0.4	) $\times 10^{-6}$		S=1.7
Γ_{341}	$\eta K^*(892)^+$	(	1.93	$\pm$ 0.16	) $\times 10^{-5}$		
Γ_{342}	$\eta K_0^*(1430)^+$	(	1.8	$\pm$ 0.4	) $\times 10^{-5}$		
Γ_{343}	$\eta K_2^*(1430)^+$	(	9.1	$\pm$ 3.0	) $\times 10^{-6}$		
Γ_{344}	$\eta(1295)K^+ \times$ B($\eta(1295) \to \eta\pi\pi$)	(	2.9	$^{+0.8}_{-0.7}$	) $\times 10^{-6}$		
Γ_{345}	$\eta(1405)K^+ \times$ B($\eta(1405) \to \eta\pi\pi$)	$<$	1.3		$\times 10^{-6}$	CL=90%	
Γ_{346}	$\eta(1405)K^+ \times$ B($\eta(1405) \to K^*K$)	$<$	1.2		$\times 10^{-6}$	CL=90%	
Γ_{347}	$\eta(1475)K^+ \times$ B($\eta(1475) \to K^*K$)	(	1.38	$^{+0.21}_{-0.18}$	) $\times 10^{-5}$		
Γ_{348}	$f_1(1285)K^+$	$<$	2.0		$\times 10^{-6}$	CL=90%	
Γ_{349}	$f_1(1420)K^+ \times$ B($f_1(1420) \to \eta\pi\pi$)	$<$	2.9		$\times 10^{-6}$	CL=90%	
Γ_{350}	$f_1(1420)K^+ \times$ B($f_1(1420) \to K^*K$)	$<$	4.1		$\times 10^{-6}$	CL=90%	
Γ_{351}	$\phi(1680)K^+ \times$ B($\phi(1680) \to K^*K$)	$<$	3.4		$\times 10^{-6}$	CL=90%	
Γ_{352}	$f_0(1500)K^+$	(	3.7	$\pm$ 2.2	) $\times 10^{-6}$		
Γ_{353}	ωK^+	(	6.5	$\pm$ 0.4	) $\times 10^{-6}$		
Γ_{354}	$\omega K^*(892)^+$	$<$	7.4		$\times 10^{-6}$	CL=90%	
Γ_{355}	$\omega(K\pi)_0^{*+}$	(	2.8	$\pm$ 0.4	) $\times 10^{-5}$		
Γ_{356}	$\omega K_0^*(1430)^+$	(	2.4	$\pm$ 0.5	) $\times 10^{-5}$		
Γ_{357}	$\omega K_2^*(1430)^+$	(	2.1	$\pm$ 0.4	) $\times 10^{-5}$		
Γ_{358}	$a_0(980)^+K^0 \times$B($a_0(980)^+ \to \eta\pi^+$)	$<$	3.9		$\times 10^{-6}$	CL=90%	
Γ_{359}	$a_0(980)^0K^+ \times$B($a_0(980)^0 \to \eta\pi^0$)	$<$	2.5		$\times 10^{-6}$	CL=90%	
Γ_{360}	$K^*(892)^0\pi^+$	(	1.01	$\pm$ 0.08	) $\times 10^{-5}$		
Γ_{361}	$K^*(892)^+\pi^0$	(	6.8	$\pm$ 0.9	) $\times 10^{-6}$		
Γ_{362}	$K^+\pi^-\pi^+$	(	5.10	$\pm$ 0.29	) $\times 10^{-5}$		
Γ_{363}	$K^+\pi^-\pi^+$ nonresonant	(	1.63	$^{+0.21}_{-0.15}$	) $\times 10^{-5}$		
Γ_{364}	$\omega(782)K^+$	(	6	$\pm$ 9	) $\times 10^{-6}$		
Γ_{365}	$K^+f_0(980) \times$ B($f_0(980) \to \pi^+\pi^-$)	(	9.4	$^{+1.0}_{-1.2}$	) $\times 10^{-6}$		
Γ_{366}	$f_2(1270)^0K^+$	(	1.07	$\pm$ 0.27	) $\times 10^{-6}$		
Γ_{367}	$f_0(1370)^0K^+ \times$ B($f_0(1370)^0 \to \pi^+\pi^-$)	$<$	1.07		$\times 10^{-5}$	CL=90%	
Γ_{368}	$\rho^0(1450)K^+ \times$ B($\rho^0(1450) \to \pi^+\pi^-$)	$<$	1.17		$\times 10^{-5}$	CL=90%	
Γ_{369}	$f_2'(1525)K^+ \times$ B($f_2'(1525) \to \pi^+\pi^-$)	$<$	3.4		$\times 10^{-6}$	CL=90%	
Γ_{370}	$K^+\rho^0$	(	3.7	$\pm$ 0.5	) $\times 10^{-6}$		
Γ_{371}	$K_0^*(1430)^0\pi^+$	(	3.9	$^{+0.6}_{-0.5}$	) $\times 10^{-5}$		S=1.4
Γ_{372}	$K_0^*(1430)^+\pi^0$	(	1.19	$^{+0.20}_{-0.23}$	) $\times 10^{-5}$		
Γ_{373}	$K_2^*(1430)^0\pi^+$	(	5.6	$^{+2.2}_{-1.5}$	) $\times 10^{-6}$		
Γ_{374}	$K^*(1410)^0\pi^+$	$<$	4.5		$\times 10^{-5}$	CL=90%	
Γ_{375}	$K^*(1680)^0\pi^+$	$<$	1.2		$\times 10^{-5}$	CL=90%	
Γ_{376}	$K^+\pi^0\pi^0$	(	1.62	$\pm$ 0.19	) $\times 10^{-5}$		
Γ_{377}	$f_0(980)K^+ \times$ B($f_0 \to \pi^0\pi^0$)	(	2.8	$\pm$ 0.8	) $\times 10^{-6}$		
Γ_{378}	$K^-\pi^+\pi^+$	$<$	4.6		$\times 10^{-8}$	CL=90%	
Γ_{379}	$K^-\pi^+\pi^+$ nonresonant	$<$	5.6		$\times 10^{-5}$	CL=90%	
Γ_{380}	$K_1(1270)^0\pi^+$	$<$	4.0		$\times 10^{-5}$	CL=90%	
Γ_{381}	$K_1(1400)^0\pi^+$	$<$	3.9		$\times 10^{-5}$	CL=90%	
Γ_{382}	$K^0\pi^+\pi^0$	$<$	6.6		$\times 10^{-5}$	CL=90%	
Γ_{383}	$K^0\rho^+$	(	7.3	$^{+1.0}_{-1.2}$	) $\times 10^{-6}$		
Γ_{384}	$K^*(892)^+\pi^+\pi^-$	(	7.5	$\pm$ 1.0	) $\times 10^{-5}$		
Γ_{385}	$K^*(892)^+\rho^0$	(	4.6	$\pm$ 1.1	) $\times 10^{-6}$		
Γ_{386}	$K^*(892)^+f_0(980)$	(	4.2	$\pm$ 0.7	) $\times 10^{-6}$		
Γ_{387}	$a_1^+K^0$	(	3.5	$\pm$ 0.7	) $\times 10^{-5}$		
Γ_{388}	$b_1^+K^0 \times$ B($b_1^+ \to \omega\pi^+$)	(	9.6	$\pm$ 1.9	) $\times 10^{-6}$		
Γ_{389}	$K^*(892)^0\rho^+$	(	9.2	$\pm$ 1.5	) $\times 10^{-6}$		
Γ_{390}	$K_1(1400)^+\rho^0$	$<$	7.8		$\times 10^{-4}$	CL=90%	
Γ_{391}	$K_2^*(1430)^+\rho^0$	$<$	1.5		$\times 10^{-3}$	CL=90%	
Γ_{392}	$b_1^0K^+ \times$ B($b_1^0 \to \omega\pi^0$)	(	9.1	$\pm$ 2.0	) $\times 10^{-6}$		
Γ_{393}	$b_1^+K^{*0} \times$ B($b_1^+ \to \omega\pi^+$)	$<$	5.9		$\times 10^{-6}$	CL=90%	
Γ_{394}	$b_1^0K^{*+} \times$ B($b_1^0 \to \omega\pi^0$)	$<$	6.7		$\times 10^{-6}$	CL=90%	
Γ_{395}	$K^+\overline{K}^0$	(	1.31	$\pm$ 0.17	) $\times 10^{-6}$		S=1.2
Γ_{396}	$\overline{K}^0K^+\pi^0$	$<$	2.4		$\times 10^{-5}$	CL=90%	
Γ_{397}	$K^+K_S^0K_S^0$	(	1.08	$\pm$ 0.06	) $\times 10^{-5}$		
Γ_{398}	$f_0(980)K^+,\ f_0 \to K_S^0K_S^0$	(	1.47	$\pm$ 0.33	) $\times 10^{-5}$		
Γ_{399}	$f_0(1710)K^+,\ f_0 \to K_S^0K_S^0$	(	4.8	$^{+4.0}_{-2.6}$	) $\times 10^{-7}$		
Γ_{400}	$K^+K_S^0K_S^0$ nonresonant	(	2.0	$\pm$ 0.4	) $\times 10^{-5}$		
Γ_{401}	$K_S^0K_S^0\pi^+$	$<$	5.1		$\times 10^{-7}$	CL=90%	
Γ_{402}	$K^+K^-\pi^+$	(	5.2	$\pm$ 0.4	) $\times 10^{-6}$		
Γ_{403}	$K^+K^-\pi^+$ nonresonant	$<$	7.5		$\times 10^{-5}$	CL=90%	
Γ_{404}	$K^+\overline{K}^*(892)^0$	$<$	1.1		$\times 10^{-6}$	CL=90%	
Γ_{405}	$K^+\overline{K}_0^*(1430)^0$	$<$	2.2		$\times 10^{-6}$	CL=90%	
Γ_{406}	$K^+K^+\pi^-$	$<$	1.1		$\times 10^{-8}$	CL=90%	
Γ_{407}	$K^+K^+\pi^-$ nonresonant	$<$	8.79		$\times 10^{-5}$	CL=90%	
Γ_{408}	$f_2'(1525)K^+$	(	1.8	$\pm$ 0.5	) $\times 10^{-6}$		S=1.1
Γ_{409}	$K^+f_J(2220)$						
Γ_{410}	$K^{*+}\pi^+K^-$	$<$	1.18		$\times 10^{-5}$	CL=90%	
Γ_{411}	$K^*(892)^+K^*(892)^0$	(	9.1	$\pm$ 2.9	) $\times 10^{-7}$		
Γ_{412}	$K^{*+}K^+\pi^-$	$<$	6.1		$\times 10^{-6}$	CL=90%	
Γ_{413}	$K^+K^-K^+$	(	3.40	$\pm$ 0.14	) $\times 10^{-5}$		S=1.4
Γ_{414}	$K^+\phi$	(	8.8	$^{+0.7}_{-0.6}$	) $\times 10^{-6}$		S=1.1
Γ_{415}	$f_0(980)K^+ \times$ B($f_0(980) \to K^+K^-$)	(	9.4	$\pm$ 3.2	) $\times 10^{-6}$		
Γ_{416}	$a_2(1320)K^+ \times$ B($a_2(1320) \to K^+K^-$)	$<$	1.1		$\times 10^{-6}$	CL=90%	
Γ_{417}	$X_0(1550)K^+ \times$ B($X_0(1550) \to K^+K^-$)	(	4.3	$\pm$ 0.7	) $\times 10^{-6}$		
Γ_{418}	$\phi(1680)K^+ \times$ B($\phi(1680) \to K^+K^-$)	$<$	8		$\times 10^{-7}$	CL=90%	
Γ_{419}	$f_0(1710)K^+ \times$ B($f_0(1710) \to K^+K^-$)	(	1.1	$\pm$ 0.6	) $\times 10^{-6}$		
Γ_{420}	$K^+K^-K^+$ nonresonant	(	2.38	$^{+0.28}_{-0.50}$	) $\times 10^{-5}$		

See key on page 885

Γ_{421}	$K^*(892)^+ K^+ K^-$	(3.6	± 0.5	) $\times 10^{-5}$		
Γ_{422}	$K^*(892)^+ \phi$	(10.0	± 2.0	) $\times 10^{-6}$		S=1.7
Γ_{423}	$\phi (K\pi)_0^{*+}$	(8.3	± 1.6	) $\times 10^{-6}$		
Γ_{424}	$\phi K_1(1270)^+$	(6.1	± 1.9	) $\times 10^{-6}$		
Γ_{425}	$\phi K_1(1400)^+$	< 3.2		$\times 10^{-6}$		CL=90%
Γ_{426}	$\phi K^*(1410)^+$	< 4.3		$\times 10^{-6}$		CL=90%
Γ_{427}	$\phi K_0^*(1430)^+$	(7.0	± 1.6	) $\times 10^{-6}$		
Γ_{428}	$\phi K_2^*(1430)^+$	(8.4	± 2.1	) $\times 10^{-6}$		
Γ_{429}	$\phi K_2^*(1770)^+$	< 1.50		$\times 10^{-5}$		CL=90%
Γ_{430}	$\phi K_2^*(1820)^+$	< 1.63		$\times 10^{-5}$		CL=90%
Γ_{431}	$a_1^+ K^{*0}$	< 3.6		$\times 10^{-6}$		CL=90%
Γ_{432}	$K^+ \phi\phi$	(5.0	± 1.2	) $\times 10^{-6}$		S=2.3
Γ_{433}	$\eta'\eta' K^+$	< 2.5		$\times 10^{-5}$		CL=90%
Γ_{434}	$\omega\phi K^+$	< 1.9		$\times 10^{-6}$		CL=90%
Γ_{435}	$X(1812) K^+ \times B(X \to \omega\phi)$	< 3.2		$\times 10^{-7}$		CL=90%
Γ_{436}	$K^*(892)^+\gamma$	(3.92	± 0.22	) $\times 10^{-5}$		S=1.7
Γ_{437}	$K_1(1270)^+\gamma$	(4.4	$^{+0.7}_{-0.6}$	) $\times 10^{-5}$		
Γ_{438}	$\eta K^+\gamma$	(7.9	± 0.9	) $\times 10^{-6}$		
Γ_{439}	$\eta' K^+\gamma$	(2.9	$^{+1.0}_{-0.9}$	) $\times 10^{-6}$		
Γ_{440}	$\phi K^+\gamma$	(2.7	± 0.4	) $\times 10^{-6}$		S=1.2
Γ_{441}	$K^+\pi^-\pi^+\gamma$	(2.58	± 0.15	) $\times 10^{-5}$		S=1.3
Γ_{442}	$K^*(892)^0\pi^+\gamma$	(2.33	± 0.12	) $\times 10^{-5}$		
Γ_{443}	$K^+\rho^0\gamma$	(8.2	± 0.9	) $\times 10^{-6}$		
Γ_{444}	$(K^+\pi^-)_{NR}\pi^+\gamma$	(9.9	$^{+1.7}_{-2.0}$	) $\times 10^{-6}$		
Γ_{445}	$K^0\pi^+\pi^0\gamma$	(4.6	± 0.5	) $\times 10^{-5}$		
Γ_{446}	$K_1(1400)^+\gamma$	(10	$^{+5}_{-4}$	) $\times 10^{-6}$		
Γ_{447}	$K^*(1410)^+\gamma$	(2.7	$^{+0.8}_{-0.6}$	) $\times 10^{-5}$		
Γ_{448}	$K_0^*(1430)^0\pi^+\gamma$	(1.32	$^{+0.26}_{-0.32}$	) $\times 10^{-6}$		
Γ_{449}	$K_2^*(1430)^+\gamma$	(1.4	± 0.4	) $\times 10^{-5}$		
Γ_{450}	$K^*(1680)^+\gamma$	(6.7	$^{+1.7}_{-1.4}$	) $\times 10^{-5}$		
Γ_{451}	$K_3^*(1780)^+\gamma$	< 3.9		$\times 10^{-5}$		CL=90%
Γ_{452}	$K_4^*(2045)^+\gamma$	< 9.9		$\times 10^{-3}$		CL=90%

Light unflavored meson modes

Γ_{453}	$\rho^+\gamma$	(9.8	± 2.5	) $\times 10^{-7}$		
Γ_{454}	$\pi^+\pi^0$	(5.5	± 0.4	) $\times 10^{-6}$		S=1.2
Γ_{455}	$\pi^+\pi^+\pi^-$	(1.52	± 0.14	) $\times 10^{-5}$		
Γ_{456}	$\rho^0\pi^+$	(8.3	± 1.2	) $\times 10^{-6}$		
Γ_{457}	$\pi^+ f_0(980)$, $f_0 \to \pi^+\pi^-$	< 1.5		$\times 10^{-6}$		CL=90%
Γ_{458}	$\pi^+ f_2(1270)$	(1.6	$^{+0.7}_{-0.4}$	) $\times 10^{-6}$		
Γ_{459}	$\rho(1450)^0\pi^+$, $\rho^0 \to \pi^+\pi^-$	(1.4	$^{+0.6}_{-0.9}$	) $\times 10^{-6}$		
Γ_{460}	$f_0(1370)\pi^+$, $f_0 \to \pi^+\pi^-$	< 4.0		$\times 10^{-6}$		CL=90%
Γ_{461}	$f_0(500)\pi^+$, $f_0 \to \pi^+\pi^-$	< 4.1		$\times 10^{-6}$		CL=90%
Γ_{462}	$\pi^+\pi^-\pi^+$ nonresonant	(5.3	$^{+1.5}_{-1.1}$	) $\times 10^{-6}$		
Γ_{463}	$\pi^+\pi^0\pi^0$	< 8.9		$\times 10^{-4}$		CL=90%
Γ_{464}	$\rho^+\pi^0$	(1.09	± 0.14	) $\times 10^{-5}$		
Γ_{465}	$\pi^+\pi^-\pi^+\pi^0$	< 4.0		$\times 10^{-3}$		CL=90%
Γ_{466}	$\rho^+\rho^0$	(2.40	± 0.19	) $\times 10^{-5}$		
Γ_{467}	$\rho^+ f_0(980)$, $f_0 \to \pi^+\pi^-$	< 2.0		$\times 10^{-6}$		CL=90%
Γ_{468}	$a_1(1260)^+\pi^0$	(2.6	± 0.7	) $\times 10^{-5}$		
Γ_{469}	$a_1(1260)^0\pi^+$	(2.0	± 0.6	) $\times 10^{-5}$		
Γ_{470}	$\omega\pi^+$	(6.9	± 0.5	) $\times 10^{-6}$		
Γ_{471}	$\omega\rho^+$	(1.59	± 0.21	) $\times 10^{-5}$		
Γ_{472}	$\eta\pi^+$	(4.02	± 0.27	) $\times 10^{-6}$		
Γ_{473}	$\eta\rho^+$	(7.0	± 2.9	) $\times 10^{-6}$		S=2.8
Γ_{474}	$\eta'\pi^+$	(2.7	± 0.9	) $\times 10^{-6}$		S=1.9
Γ_{475}	$\eta'\rho^+$	(9.7	± 2.2	) $\times 10^{-6}$		
Γ_{476}	$\phi\pi^+$	< 1.5		$\times 10^{-7}$		CL=90%
Γ_{477}	$\phi\rho^+$	< 3.0		$\times 10^{-6}$		CL=90%
Γ_{478}	$a_0(980)^0\pi^+$, $a_0^0 \to \eta\pi^0$	< 5.8		$\times 10^{-6}$		CL=90%
Γ_{479}	$a_0(980)^+\pi^0$, $a_0^+ \to \eta\pi^+$	< 1.4		$\times 10^{-6}$		CL=90%
Γ_{480}	$\pi^+\pi^+\pi^+\pi^-\pi^-$	< 8.6		$\times 10^{-4}$		CL=90%
Γ_{481}	$\rho^0 a_1(1260)^+$	< 6.2		$\times 10^{-4}$		CL=90%
Γ_{482}	$\rho^0 a_2(1320)^+$	< 7.2		$\times 10^{-4}$		CL=90%
Γ_{483}	$b_1^0\pi^+$, $b_1^0 \to \omega\pi^0$	(6.7	± 2.0	) $\times 10^{-6}$		
Γ_{484}	$b_1^+\pi^0$, $b_1^+ \to \omega\pi^+$	< 3.3		$\times 10^{-6}$		CL=90%
Γ_{485}	$\pi^+\pi^+\pi^+\pi^-\pi^-\pi^0$	< 6.3		$\times 10^{-3}$		CL=90%
Γ_{486}	$b_1^+\rho^0$, $b_1^+ \to \omega\pi^+$	< 5.2		$\times 10^{-6}$		CL=90%
Γ_{487}	$a_1(1260)^+ a_1(1260)^0$	< 1.3		%		CL=90%
Γ_{488}	$b_1^0\rho^+$, $b_1^0 \to \omega\pi^0$	< 3.3		$\times 10^{-6}$		CL=90%

Charged particle ($h^{\pm}$) modes

$h^{\pm} = K^{\pm}$ or $\pi^{\pm}$

Γ_{489}	$h^+\pi^0$	(1.6	$^{+0.7}_{-0.6}$	) $\times 10^{-5}$		
Γ_{490}	ωh^+	(1.38	$^{+0.27}_{-0.24}$	) $\times 10^{-5}$		
Γ_{491}	$h^+ X^0$ (Familon)	< 4.9		$\times 10^{-5}$		CL=90%
Γ_{492}	$K^+ X^0$, $X^0 \to \mu^+\mu^-$	< 1		$\times 10^{-7}$		CL=95%

Baryon modes

Γ_{493}	$p\overline{p}\pi^+$	(1.62	± 0.20	) $\times 10^{-6}$		
Γ_{494}	$p\overline{p}\pi^+$ nonresonant	< 5.3		$\times 10^{-5}$		CL=90%
Γ_{495}	$p\overline{p}\pi^+\pi^+\pi^-$					
Γ_{496}	$p\overline{p}K^+$	(5.9	± 0.5	) $\times 10^{-6}$		S=1.5
Γ_{497}	$\Theta(1710)^{++}\overline{p}$, $\Theta^{++} \to pK^+$	[g] < 9.1		$\times 10^{-8}$		CL=90%
Γ_{498}	$f_J(2220) K^+$, $f_J \to p\overline{p}$	[g] < 4.1		$\times 10^{-7}$		CL=90%
Γ_{499}	$p\overline{\Lambda}(1520)$	(3.1	± 0.6	) $\times 10^{-7}$		
Γ_{500}	$p\overline{p}K^+$ nonresonant	< 8.9		$\times 10^{-5}$		CL=90%
Γ_{501}	$p\overline{p}K^*(892)^+$	(3.6	$^{+0.8}_{-0.7}$	) $\times 10^{-6}$		
Γ_{502}	$f_J(2220) K^{*+}$, $f_J \to p\overline{p}$	< 7.7		$\times 10^{-7}$		CL=90%
Γ_{503}	$p\overline{\Lambda}$	(2.4	$^{+1.0}_{-0.9}$	) $\times 10^{-7}$		
Γ_{504}	$p\overline{\Lambda}\gamma$	(2.4	$^{+0.5}_{-0.4}$	) $\times 10^{-6}$		
Γ_{505}	$p\overline{\Lambda}\pi^0$	(3.0	$^{+0.7}_{-0.6}$	) $\times 10^{-6}$		
Γ_{506}	$p\overline{\Sigma}(1385)^0$	< 4.7		$\times 10^{-7}$		CL=90%
Γ_{507}	$\Delta^+\overline{\Lambda}$	< 8.2		$\times 10^{-7}$		CL=90%
Γ_{508}	$p\overline{\Sigma}\gamma$	< 4.6		$\times 10^{-6}$		CL=90%
Γ_{509}	$p\overline{\Lambda}\pi^+\pi^-$	(5.9	± 1.1	) $\times 10^{-6}$		
Γ_{510}	$p\overline{\Lambda}\rho^0$	(4.8	± 0.9	) $\times 10^{-6}$		
Γ_{511}	$p\overline{\Lambda} f_2(1270)$	(2.0	± 0.8	) $\times 10^{-6}$		
Γ_{512}	$\Lambda\overline{\Lambda}\pi^+$	< 9.4		$\times 10^{-7}$		CL=90%
Γ_{513}	$\Lambda\overline{\Lambda}K^+$	(3.4	± 0.6	) $\times 10^{-6}$		
Γ_{514}	$\Lambda\overline{\Lambda}K^{*+}$	(2.2	$^{+1.2}_{-0.9}$	) $\times 10^{-6}$		
Γ_{515}	$\overline{\Delta}^0 p$	< 1.38		$\times 10^{-6}$		CL=90%
Γ_{516}	$\Delta^{++}\overline{p}$	< 1.4		$\times 10^{-7}$		CL=90%
Γ_{517}	$D^+ p\overline{p}$	< 1.5		$\times 10^{-5}$		CL=90%
Γ_{518}	$D^*(2010)^+ p\overline{p}$	< 1.5		$\times 10^{-5}$		CL=90%
Γ_{519}	$\overline{D}^0 p\overline{p}\pi^+$	(3.72	± 0.27	) $\times 10^{-4}$		
Γ_{520}	$\overline{D}^{*0} p\overline{p}\pi^+$	(3.73	± 0.32	) $\times 10^{-4}$		
Γ_{521}	$D^- p\overline{p}\pi^+\pi^-$	(1.66	± 0.30	) $\times 10^{-4}$		
Γ_{522}	$D^{*-} p\overline{p}\pi^+\pi^-$	(1.86	± 0.25	) $\times 10^{-4}$		
Γ_{523}	$p\overline{\Lambda}^0\overline{D}^0$	(1.43	± 0.32	) $\times 10^{-5}$		
Γ_{524}	$p\overline{\Lambda}^0\overline{D}^*(2007)^0$	< 5		$\times 10^{-5}$		CL=90%
Γ_{525}	$\overline{\Lambda}_c^- p\pi^+$	(2.3	± 0.4	) $\times 10^{-4}$		S=2.2
Γ_{526}	$\overline{\Lambda}_c^- \Delta(1232)^{++}$	< 1.9		$\times 10^{-5}$		CL=90%
Γ_{527}	$\overline{\Lambda}_c^- \Delta_X(1600)^{++}$	(4.7	± 1.0	) $\times 10^{-5}$		
Γ_{528}	$\overline{\Lambda}_c^- \Delta_X(2420)^{++}$	(3.8	± 0.9	) $\times 10^{-5}$		
Γ_{529}	$(\overline{\Lambda}_c^- p)_s \pi^+$	[h] (3.1	± 0.7	) $\times 10^{-5}$		
Γ_{530}	$\overline{\Sigma}_c(2520)^0 p$	< 3		$\times 10^{-6}$		CL=90%
Γ_{531}	$\overline{\Sigma}_c(2800)^0 p$	(2.7	± 0.9	) $\times 10^{-5}$		
Γ_{532}	$\overline{\Lambda}_c^- p\pi^+\pi^0$	(1.8	± 0.6	) $\times 10^{-3}$		
Γ_{533}	$\overline{\Lambda}_c^- p\pi^+\pi^+\pi^-$	(2.2	± 0.7	) $\times 10^{-3}$		
Γ_{534}	$\overline{\Lambda}_c^- p\pi^+\pi^+\pi^-\pi^0$	< 1.34		%		CL=90%
Γ_{535}	$\Lambda_c^+ \Lambda_c^- K^+$	(7.0	± 2.2	) $\times 10^{-4}$		
Γ_{536}	$\overline{\Sigma}_c(2455)^0 p$	(3.0	± 0.7	) $\times 10^{-5}$		
Γ_{537}	$\overline{\Sigma}_c(2455)^0 p\pi^0$	(3.5	± 1.1	) $\times 10^{-4}$		
Γ_{538}	$\overline{\Sigma}_c(2455)^0 p\pi^-\pi^+$	(3.5	± 1.1	) $\times 10^{-4}$		
Γ_{539}	$\overline{\Sigma}_c(2455)^{--} p\pi^+\pi^+$	(2.39	± 0.20	) $\times 10^{-4}$		
Γ_{540}	$\overline{\Lambda}_c(2593)^-/\overline{\Lambda}_c(2625)^- p\pi^+$	< 1.9		$\times 10^{-4}$		CL=90%
Γ_{541}	$\Xi_c^0\Lambda_c^+$, $\Xi_c^0 \to \Xi^+\pi^-$	(2.4	± 0.9	) $\times 10^{-5}$		S=1.4
Γ_{542}	$\Xi_c^0\Lambda_c^+$, $\Xi_c^0 \to \Lambda K^+\pi^-$	(2.1	± 0.9	) $\times 10^{-5}$		S=1.5

Lepton Family number (LF) or Lepton number (L) or Baryon number (B) violating modes, or/and $\Delta B = 1$ weak neutral current ($B1$) modes

Γ_{543}	$\pi^+\ell^+\ell^-$	$B1$	< 4.9		$\times 10^{-8}$		CL=90%
Γ_{544}	$\pi^+ e^+ e^-$	$B1$	< 8.0		$\times 10^{-8}$		CL=90%
Γ_{545}	$\pi^+\mu^+\mu^-$	$B1$	(1.76	± 0.23	) $\times 10^{-8}$		
Γ_{546}	$\pi^+\nu\overline{\nu}$	$B1$	< 1.4		$\times 10^{-5}$		CL=90%

Meson Particle Listings

$B^{\pm}$

Γ_{547}	$K^+\ell^+\ell^-$	*B1*	[a]	(4.51	± 0.23)	$\times 10^{-7}$		S=1.1
Γ_{548}	$K^+e^+e^-$	*B1*		(5.5	± 0.7)	$\times 10^{-7}$		
Γ_{549}	$K^+\mu^+\mu^-$	*B1*		(4.41	± 0.23)	$\times 10^{-7}$		S=1.2
Γ_{550}	$K^+\mu^+\mu^-$ nonresonant	*B1*		(4.37	± 0.27)	$\times 10^{-7}$		
Γ_{551}	$K^+\tau^+\tau^-$	*B1*		< 2.25		$\times 10^{-3}$	CL=90%	
Γ_{552}	$K^+\overline{\nu}\nu$	*B1*		< 1.6		$\times 10^{-5}$	CL=90%	
Γ_{553}	$\rho^+\nu\overline{\nu}$	*B1*		< 3.0		$\times 10^{-5}$	CL=90%	
Γ_{554}	$K^*(892)^+\ell^+\ell^-$	*B1*	[a]	(1.01	± 0.11)	$\times 10^{-6}$		S=1.1
Γ_{555}	$K^*(892)^+e^+e^-$	*B1*		(1.55	$^{+\ 0.40}_{-\ 0.31}$)	$\times 10^{-6}$		
Γ_{556}	$K^*(892)^+\mu^+\mu^-$	*B1*		(9.6	± 1.0)	$\times 10^{-7}$		
Γ_{557}	$K^*(892)^+\nu\overline{\nu}$	*B1*		< 4.0		$\times 10^{-5}$	CL=90%	
Γ_{558}	$K^+\pi^+\pi^-\mu^+\mu^-$	*B1*		(4.3	± 0.4)	$\times 10^{-7}$		
Γ_{559}	$\phi K^+\mu^+\mu^-$	*B1*		(7.9	$^{+\ 2.1}_{-\ 1.7}$)	$\times 10^{-8}$		
Γ_{560}	$\pi^+e^+\mu^-$	*LF*		< 6.4		$\times 10^{-3}$	CL=90%	
Γ_{561}	$\pi^+e^-\mu^+$	*LF*		< 6.4		$\times 10^{-3}$	CL=90%	
Γ_{562}	$\pi^+e^\pm\mu^\mp$	*LF*		< 1.7		$\times 10^{-7}$	CL=90%	
Γ_{563}	$\pi^+e^+\tau^-$	*LF*		< 7.4		$\times 10^{-5}$	CL=90%	
Γ_{564}	$\pi^+e^-\tau^+$	*LF*		< 2.0		$\times 10^{-5}$	CL=90%	
Γ_{565}	$\pi^+e^\pm\tau^\mp$	*LF*		< 7.5		$\times 10^{-5}$	CL=90%	
Γ_{566}	$\pi^+\mu^+\tau^-$	*LF*		< 6.2		$\times 10^{-5}$	CL=90%	
Γ_{567}	$\pi^+\mu^-\tau^+$	*LF*		< 4.5		$\times 10^{-5}$	CL=90%	
Γ_{568}	$\pi^+\mu^\pm\tau^\mp$	*LF*		< 7.2		$\times 10^{-5}$	CL=90%	
Γ_{569}	$K^+e^+\mu^-$	*LF*		< 9.1		$\times 10^{-8}$	CL=90%	
Γ_{570}	$K^+e^-\mu^+$	*LF*		< 1.3		$\times 10^{-7}$	CL=90%	
Γ_{571}	$K^+e^\pm\mu^\mp$	*LF*		< 9.1		$\times 10^{-8}$	CL=90%	
Γ_{572}	$K^+e^+\tau^-$	*LF*		< 4.3		$\times 10^{-5}$	CL=90%	
Γ_{573}	$K^+e^-\tau^+$	*LF*		< 1.5		$\times 10^{-5}$	CL=90%	
Γ_{574}	$K^+e^\pm\tau^\mp$	*LF*		< 3.0		$\times 10^{-5}$	CL=90%	
Γ_{575}	$K^+\mu^+\tau^-$	*LF*		< 4.5		$\times 10^{-5}$	CL=90%	
Γ_{576}	$K^+\mu^-\tau^+$	*LF*		< 2.8		$\times 10^{-5}$	CL=90%	
Γ_{577}	$K^+\mu^\pm\tau^\mp$	*LF*		< 4.8		$\times 10^{-5}$	CL=90%	
Γ_{578}	$K^*(892)^+e^+\mu^-$	*LF*		< 1.3		$\times 10^{-6}$	CL=90%	
Γ_{579}	$K^*(892)^+e^-\mu^+$	*LF*		< 9.9		$\times 10^{-7}$	CL=90%	
Γ_{580}	$K^*(892)^+e^\pm\mu^\mp$	*LF*		< 1.4		$\times 10^{-6}$	CL=90%	
Γ_{581}	$\pi^-e^+e^+$	*L*		< 2.3		$\times 10^{-8}$	CL=90%	
Γ_{582}	$\pi^-\mu^+\mu^+$	*L*		< 4.0		$\times 10^{-9}$	CL=95%	
Γ_{583}	$\pi^-e^+\mu^+$	*L*		< 1.5		$\times 10^{-7}$	CL=90%	
Γ_{584}	$\rho^-e^+e^+$	*L*		< 1.7		$\times 10^{-7}$	CL=90%	
Γ_{585}	$\rho^-\mu^+\mu^+$	*L*		< 4.2		$\times 10^{-7}$	CL=90%	
Γ_{586}	$\rho^-e^+\mu^+$	*L*		< 4.7		$\times 10^{-7}$	CL=90%	
Γ_{587}	$K^-e^+e^+$	*L*		< 3.0		$\times 10^{-8}$	CL=90%	
Γ_{588}	$K^-\mu^+\mu^+$	*L*		< 4.1		$\times 10^{-8}$	CL=90%	
Γ_{589}	$K^-e^+\mu^+$	*L*		< 1.6		$\times 10^{-7}$	CL=90%	
Γ_{590}	$K^*(892)^-e^+e^+$	*L*		< 4.0		$\times 10^{-7}$	CL=90%	
Γ_{591}	$K^*(892)^-\mu^+\mu^+$	*L*		< 5.9		$\times 10^{-7}$	CL=90%	
Γ_{592}	$K^*(892)^-e^+\mu^+$	*L*		< 3.0		$\times 10^{-7}$	CL=90%	
Γ_{593}	$D^-e^+e^+$	*L*		< 2.6		$\times 10^{-6}$	CL=90%	
Γ_{594}	$D^-e^+\mu^+$	*L*		< 1.8		$\times 10^{-6}$	CL=90%	
Γ_{595}	$D^-\mu^+\mu^+$	*L*		< 6.9		$\times 10^{-7}$	CL=95%	
Γ_{596}	$D^{*-}\mu^+\mu^+$	*L*		< 2.4		$\times 10^{-6}$	CL=95%	
Γ_{597}	$D_s^-\mu^+\mu^+$	*L*		< 5.8		$\times 10^{-7}$	CL=95%	
Γ_{598}	$\overline{D}^0\pi^-\mu^+\mu^+$	*L*		< 1.5		$\times 10^{-6}$	CL=95%	
Γ_{599}	$\Lambda^0\mu^+$	*L,B*		< 6		$\times 10^{-8}$	CL=90%	
Γ_{600}	Λ^0e^+	*L,B*		< 3.2		$\times 10^{-8}$	CL=90%	
Γ_{601}	$\overline{\Lambda}^0\mu^+$	*L,B*		< 6		$\times 10^{-8}$	CL=90%	
Γ_{602}	$\overline{\Lambda}^0e^+$	*L,B*		< 8		$\times 10^{-8}$	CL=90%	

[a] An ℓ indicates an e or a μ mode, not a sum over these modes.

[b] An $CP(\pm 1)$ indicates the $CP=+1$ and $CP=-1$ eigenstates of the D^0-$\overline{D}^0$ system.

[c] D denotes D^0 or $\overline{D}^0$.

[d] D^0_{CP+} decays into $D^0\pi^0$ with the D^0 reconstructed in CP-even eigenstates K^+K^- and $\pi^+\pi^-$.

[e] $\overline{D}^{**}$ represents an excited state with mass $2.2 < M < 2.8$ GeV/c^2.

[f] $\chi_{c1}(3872)^+$ is a hypothetical charged partner of the $\chi_{c1}(3872)$.

[g] $\Theta(1710)^{++}$ is a possible narrow pentaquark state and $G(2220)$ is a possible glueball resonance.

[h] $(\overline{\Lambda}_c^- p)_s$ denotes a low-mass enhancement near 3.35 GeV/c^2.

CONSTRAINED FIT INFORMATION

An overall fit to 3 branching ratios uses 6 measurements and one constraint to determine 3 parameters. The overall fit has a $\chi^2 = 3.7$ for 4 degrees of freedom.

The following *off-diagonal* array elements are the correlation coefficients $\langle \delta x_i \delta x_j \rangle / (\delta x_i \cdot \delta x_j)$, in percent, from the fit to the branching fractions, $x_i \equiv \Gamma_i/\Gamma_{\rm total}$. The fit constrains the x_i whose labels appear in this array to sum to one.

x_{395}	10	
	x_{334}	

CONSTRAINED FIT INFORMATION

An overall fit to 18 branching ratios uses 57 measurements and one constraint to determine 12 parameters. The overall fit has a $\chi^2 = 55.4$ for 46 degrees of freedom.

The following *off-diagonal* array elements are the correlation coefficients $\langle \delta x_i \delta x_j \rangle / (\delta x_i \cdot \delta x_j)$, in percent, from the fit to the branching fractions, $x_i \equiv \Gamma_i/\Gamma_{\rm total}$. The fit constrains the x_i whose labels appear in this array to sum to one.

x_7	33									
x_{48}	0	0								
x_{102}	0	0	7							
x_{142}	0	0	1	13						
x_{268}	0	0	0	0	0					
x_{273}	0	0	0	0	0	0				
x_{292}	0	0	0	0	0	93	0			
x_{304}	0	0	0	0	0	56	0	52		
x_{549}	0	0	0	0	0	13	0	13	8	
x_{556}	0	0	0	0	0	0	5	0	0	0
	x_6	x_7	x_{48}	x_{102}	x_{142}	x_{268}	x_{273}	x_{292}	x_{304}	x_{549}

B^+ BRANCHING RATIOS

$\Gamma(\ell^+\nu_\ell \text{anything})/\Gamma_{\rm total}$ Γ_1/Γ

"OUR EVALUATION" is an average using rescaled values of the data listed below. The average and rescaling were performed by the Heavy Flavor Averaging Group (HFLAV) and are described at http://www.slac.stanford.edu/xorg/hflav/. The averaging/rescaling procedure takes into account correlations between the measurements.

VALUE (units 10^{-2})	DOCUMENT ID		TECN	COMMENT
10.99±0.28 OUR EVALUATION				
10.76±0.32 OUR AVERAGE Error includes scale factor of 1.1.				
11.17±0.25±0.28	[1] URQUIJO	07	BELL	$e^+e^- \to \Upsilon(4S)$
10.28±0.26±0.39	[2] AUBERT,B	06Y	BABR	$e^+e^- \to \Upsilon(4S)$
10.25±0.57±0.65	[3] ARTUSO	97	CLE2	$e^+e^- \to \Upsilon(4S)$
• • • We do not use the following data for averages, fits, limits, etc. • • •				
11.15±0.26±0.41	[4] OKABE	05	BELL	Repl. by URQUIJO 07
10.1 ±1.8 ±1.5	ATHANAS	94	CLE2	Sup. by ARTUSO 97

[1] URQUIJO 07 report a measurement of (10.34 ± 023 ± 0.25)% for the partial branching fraction of $B^+ \to e^+\nu_e X_c$ decay with electron energy above 0.6 GeV. We converted the result to $B^+ \to e^+\nu_e X$ branching fraction.

[2] The measurements are obtained for charged and neutral B mesons partial rates of semileptonic decay to electrons with momentum above 0.6 GeV/c in the B rest frame. The best precision on the ratio is achieved for a momentum threshold of 1.0 GeV: $B(B^+ \to e^+\nu_e X) / B(B^0 \to e^+\nu_e X) = 1.074 \pm 0.041 \pm 0.026$.

[3] ARTUSO 97 uses partial reconstruction of $B \to D^*\ell\nu_\ell$ and inclusive semileptonic branching ratio from BARISH 96B (0.1049 ± 0.0017 ± 0.0043).

[4] The measurements are obtained for charged and neutral B mesons partial rates of semileptonic decay to electrons with momentum above 0.6 GeV/c in the B rest frame, and their ratio of $B(B^+ \to e^+\nu_e X)/B(B^0 \to e^+\nu_e X) = 1.08 \pm 0.05 \pm 0.02$.

$\Gamma(e^+\nu_e X_c)/\Gamma_{\rm total}$ Γ_2/Γ

VALUE (units 10^{-2})	DOCUMENT ID		TECN	COMMENT
10.79±0.25±0.27	[1] URQUIJO	07	BELL	$e^+e^- \to \Upsilon(4S)$

[1] Measure the independent B^+ and B^0 partial branching fractions with electron threshold energies of 0.4 GeV.

$\Gamma(\overline{D}^0\ell^+\nu_\ell)/\Gamma_{\rm total}$ Γ_4/Γ

"OUR EVALUATION" is an average using rescaled values of the data listed below. The average and rescaling were performed by the Heavy Flavor Averaging Group (HFLAV) and are described at http://www.slac.stanford.edu/xorg/hflav/. The averaging/rescaling procedure takes into account correlations between the measurements. $\ell = e$ or μ, not sum over e and μ modes.

VALUE (%)	DOCUMENT ID		TECN	COMMENT
2.20±0.10 OUR EVALUATION				
2.29±0.08 OUR AVERAGE				
2.29±0.08±0.09	[1] AUBERT	10	BABR	$e^+e^- \to \Upsilon(4S)$
2.34±0.03±0.13	AUBERT	09A	BABR	$e^+e^- \to \Upsilon(4S)$

2.21±0.13±0.19	[2] BARTELT	99	CLE2	$e^+e^- \to \Upsilon(4S)$	
1.6 ±0.6 ±0.3	[3] FULTON	91	CLEO	$e^+e^- \to \Upsilon(4S)$	
• • • We do not use the following data for averages, fits, limits, etc. • • •					
2.33±0.09±0.09	[1] AUBERT	08Q	BABR	Repl. by AUBERT 09A	
1.94±0.15±0.34	[4] ATHANAS	97	CLE2	Repl. by BARTELT 99	

[1] Uses a fully reconstructed B meson as a tag on the recoil side.
[2] Assumes equal production of B^+ and B^0 at the $\Upsilon(4S)$.
[3] FULTON 91 assumes equal production of $B^0\overline{B}^0$ and B^+B^- at the $\Upsilon(4S)$.
[4] ATHANAS 97 uses missing energy and missing momentum to reconstruct neutrino.

$\Gamma(\overline{D}^0\ell^+\nu_\ell)/\Gamma(\ell^+\nu_\ell\,\text{anything})$ Γ_4/Γ_1

VALUE	DOCUMENT ID		TECN	COMMENT
0.255±0.009±0.009	[1] AUBERT	10	BABR	$e^+e^- \to \Upsilon(4S)$

[1] Uses a fully reconstructed B meson on the recoil side.

$\Gamma(\overline{D}^0\ell^+\nu_\ell)/\Gamma(D\ell^+\nu_\ell\,\text{anything})$ Γ_4/Γ_3

VALUE	DOCUMENT ID		TECN	COMMENT
0.227±0.014±0.016	[1] AUBERT	07AN	BABR	$e^+e^- \to \Upsilon(4S)$

[1] Uses a fully reconstructed B meson on the recoil side.

$\Gamma(\overline{D}^0\tau^+\nu_\tau)/\Gamma_{\text{total}}$ Γ_5/Γ

VALUE (units 10^{-2})	DOCUMENT ID		TECN	COMMENT
0.77±0.22±0.12	[1] BOZEK	10	BELL	$e^+e^- \to \Upsilon(4S)$
• • • We do not use the following data for averages, fits, limits, etc. • • •				
0.67±0.37±0.13	[2] AUBERT	08N	BABR	Repl. by AUBERT 09S

[1] Assumes equal production of B^+ and B^0 at the $\Upsilon(4S)$.
[2] Uses a fully reconstructed B meson as a tag on the recoil side.

$\Gamma(\overline{D}^0\tau^+\nu_\tau)/\Gamma(\overline{D}^0\ell^+\nu_\ell)$ Γ_5/Γ_4

VALUE	DOCUMENT ID		TECN	COMMENT
0.429±0.082±0.052	[1,2] LEES	12D	BABR	$e^+e^- \to \Upsilon(4S)$
• • • We do not use the following data for averages, fits, limits, etc. • • •				
0.314±0.170±0.049	[1] AUBERT	09S	BABR	Repl. by LEES 12D

[1] Uses a fully reconstructed B meson as a tag on the recoil side.
[2] Uses $\tau^+ \to e^+\nu_e\overline{\nu}_\tau$ and $\tau^+ \to \mu^+\nu_\mu\overline{\nu}_\tau$ and e^+ or μ^+ as ℓ^+.

$\Gamma(\overline{D}^*(2007)^0\ell^+\nu_\ell)/\Gamma_{\text{total}}$ Γ_6/Γ

"OUR EVALUATION" is an average using rescaled values of the data listed below. The average and rescaling were performed by the Heavy Flavor Averaging Group (HFLAV) and are described at http://www.slac.stanford.edu/xorg/hflav/. The averaging/rescaling procedure takes into account correlations between the measurements. $\ell = e$ or μ, not sum over e and μ modes.

VALUE (%)	EVTS	DOCUMENT ID		TECN	COMMENT
4.88±0.10 OUR EVALUATION					
5.60±0.26 OUR FIT Error includes scale factor of 1.5.					
5.58±0.26 OUR AVERAGE Error includes scale factor of 1.5. See the ideogram below.					
5.40±0.02±0.21		AUBERT	09A	BABR	$e^+e^- \to \Upsilon(4S)$
5.56±0.08±0.41		[1] AUBERT	08AT	BABR	$e^+e^- \to \Upsilon(4S)$
6.50±0.20±0.43		[2] ADAM	03	CLE2	$e^+e^- \to \Upsilon(4S)$
6.6 ±1.6 ±1.5		[3] ALBRECHT	92C	ARG	$e^+e^- \to \Upsilon(4S)$
• • • We do not use the following data for averages, fits, limits, etc. • • •					
5.83±0.15±0.30		[4] AUBERT	08Q	BABR	Repl. by AUBERT 09A
6.50±0.20±0.43		[5] BRIERE	02	CLE2	$e^+e^- \to \Upsilon(4S)$
5.13±0.54±0.64	302	[6] BARISH	95	CLE2	Repl. by ADAM 03
seen	398	[7] SANGHERA	93	CLE2	$e^+e^- \to \Upsilon(4S)$
4.1 ±0.8 $^{+0.8}_{-0.9}$		[8] FULTON	91	CLEO	$e^+e^- \to \Upsilon(4S)$
7.0 ±1.8 ±1.4		[9] ANTREASYAN	90B	CBAL	$e^+e^- \to \Upsilon(4S)$

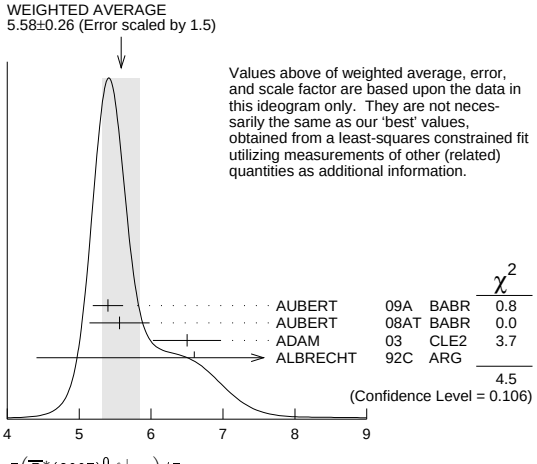

$\Gamma(\overline{D}^*(2007)^0\ell^+\nu_\ell)/\Gamma_{\text{total}}$ Γ_6/Γ

[1] Measured using the dependence of $B^- \to D^{*0}e^-\overline{\nu}_e$ decay differential rate and the form factor description by CAPRINI 98.
[2] Simultaneous measurements of both $B^0 \to D^*(2010)^-\ell\nu$ and $B^+ \to \overline{D}(2007)^0\ell\nu$.
[3] ALBRECHT 92C reports 0.058±0.014±0.013. We rescale using the method described in STONE 94 but with the updated PDG 94 $B(D^0 \to K^-\pi^+)$. Assumes equal production of $B^0\overline{B}^0$ and B^+B^- at the $\Upsilon(4S)$.
[4] Uses a fully reconstructed B meson as a tag on the recoil side.
[5] The results are based on the same analysis and data sample reported in ADAM 03.
[6] BARISH 95 use $B(D^0 \to K^-\pi^+) = (3.91 \pm 0.08 \pm 0.17)\%$ and $B(D^{*0} \to D^0\pi^0) = (63.6 \pm 2.3 \pm 3.3)\%$.
[7] Combining $\overline{D}^{*0}\ell^+\nu_\ell$ and $\overline{D}^{*-}\ell^+\nu_\ell$ SANGHERA 93 test $V-A$ structure and fit the decay angular distributions to obtain $A_{FB} = 3/4*(\Gamma^- - \Gamma^+)/\Gamma = 0.14 \pm 0.06 \pm 0.03$. Assuming a value of V_{cb}, they measure V, A_1, and A_2, the three form factors for the $D^*\ell\nu_\ell$ decay, where results are slightly dependent on model assumptions.
[8] Assumes equal production of $B^0\overline{B}^0$ and B^+B^- at the $\Upsilon(4S)$. Uncorrected for D and D^* branching ratio assumptions.
[9] ANTREASYAN 90B is average over B and $\overline{D}^*(2010)$ charge states.

$\Gamma(\overline{D}^*(2007)^0\ell^+\nu_\ell)/\Gamma(D\ell^+\nu_\ell\,\text{anything})$ Γ_6/Γ_3

VALUE	DOCUMENT ID		TECN	COMMENT
0.582±0.018±0.030	[1] AUBERT	07AN	BABR	$e^+e^- \to \Upsilon(4S)$

[1] Uses a fully reconstructed B meson on the recoil side.

$\Gamma(\overline{D}^*(2007)^0\tau^+\nu_\tau)/\Gamma_{\text{total}}$ Γ_7/Γ

VALUE (units 10^{-2})	DOCUMENT ID		TECN	COMMENT
1.88±0.20 OUR FIT				
$2.12^{+0.28}_{-0.27}$±0.29	[1] BOZEK	10	BELL	$e^+e^- \to \Upsilon(4S)$
• • • We do not use the following data for averages, fits, limits, etc. • • •				
2.25±0.48±0.28	[2] AUBERT	08N	BABR	Repl. by AUBERT 09S

[1] Assumes equal production of B^+ and B^0 at the $\Upsilon(4S)$.
[2] Uses a fully reconstructed B meson as a tag on the recoil side.

$\Gamma(\overline{D}^*(2007)^0\tau^+\nu_\tau)/\Gamma(\overline{D}^*(2007)^0\ell^+\nu_\ell)$ Γ_7/Γ_6

VALUE	DOCUMENT ID		TECN	COMMENT
0.335±0.034 OUR FIT				
0.322±0.032±0.022	[1,2] LEES	12D	BABR	$e^+e^- \to \Upsilon(4S)$
• • • We do not use the following data for averages, fits, limits, etc. • • •				
0.346±0.073±0.034	[1] AUBERT	09S	BABR	Repl. by LEES 12D

[1] Uses a fully reconstructed B meson as a tag on the recoil side.
[2] Uses $\tau^+ \to e^+\nu_e\overline{\nu}_\tau$ and $\tau^+ \to \mu^+\nu_\mu\overline{\nu}_\tau$ and e^+ or μ^+ as ℓ^+.

$\Gamma(D^-\pi^+\ell^+\nu_\ell)/\Gamma_{\text{total}}$ Γ_8/Γ

VALUE (units 10^{-3})	DOCUMENT ID		TECN	COMMENT
4.1±0.5 OUR AVERAGE				
4.2±0.6±0.3	[1] AUBERT	08Q	BABR	$e^+e^- \to \Upsilon(4S)$
4.1±0.6±0.2	[1,2] LIVENTSEV	08	BELL	$e^+e^- \to \Upsilon(4S)$
• • • We do not use the following data for averages, fits, limits, etc. • • •				
5.5±0.9±0.2	[3] LIVENTSEV	05	BELL	Repl. by LIVENTSEV 08

[1] Uses a fully reconstructed B meson as a tag on the recoil side.
[2] LIVENTSEV 08 reports $(4.0 \pm 0.4 \pm 0.6) \times 10^{-3}$ from a measurement of $[\Gamma(B^+ \to D^-\pi^+\ell^+\nu_\ell)/\Gamma_{\text{total}}] / [B(B^+ \to \overline{D}^0\ell^+\nu_\ell)]$ assuming $B(B^+ \to \overline{D}^0\ell^+\nu_\ell) = (2.15 \pm 0.22) \times 10^{-2}$, which we rescale to our best value $B(B^+ \to \overline{D}^0\ell^+\nu_\ell) = (2.20 \pm 0.10) \times 10^{-2}$. Our first error is their experiment's error and our second error is the systematic error from using our best value.
[3] LIVENTSEV 05 reports $[\Gamma(B^+ \to D^-\pi^+\ell^+\nu_\ell)/\Gamma_{\text{total}}] / [B(B^0 \to D^-\ell^+\nu_\ell)] = 0.25 \pm 0.03 \pm 0.03$ which we multiply by our best value $B(B^0 \to D^-\ell^+\nu_\ell) = (2.20 \pm 0.10) \times 10^{-2}$. Our first error is their experiment's error and our second error is the systematic error from using our best value.

$\Gamma(\overline{D}_0^*(2420)^0\ell^+\nu_\ell,\ \overline{D}_0^{*0} \to D^-\pi^+)/\Gamma_{\text{total}}$ Γ_9/Γ

VALUE (units 10^{-3})	DOCUMENT ID		TECN	COMMENT
2.5±0.5 OUR AVERAGE				
2.6±0.5±0.4	[1] AUBERT	08BL	BABR	$e^+e^- \to \Upsilon(4S)$
2.4±0.4±0.6	[1] LIVENTSEV	08	BELL	$e^+e^- \to \Upsilon(4S)$

[1] Uses a fully reconstructed B meson as a tag on the recoil side.

$\Gamma(\overline{D}_2^*(2460)^0\ell^+\nu_\ell,\ \overline{D}_2^{*0} \to D^-\pi^+)/\Gamma_{\text{total}}$ Γ_{10}/Γ

VALUE (units 10^{-3})	DOCUMENT ID		TECN	COMMENT
1.53±0.16 OUR AVERAGE				
1.42±0.15±0.15	[1] AUBERT	09Y	BABR	$e^+e^- \to \Upsilon(4S)$
1.5 ±0.2 ±0.2	[2] AUBERT	08BL	BABR	$e^+e^- \to \Upsilon(4S)$
2.2 ±0.3 ±0.4	[2] LIVENTSEV	08	BELL	$e^+e^- \to \Upsilon(4S)$

[1] Uses a simultaneous fit of all B semileptonic decays without full reconstruction of events. AUBERT 09Y reports $B(B^+ \to \overline{D}_2^*(2460)^0\ell^+\nu_\ell) \cdot B(\overline{D}_2^*(2460)^0 \to D^{(*)-}\pi^+) = (2.29 \pm 0.23 \pm 0.21) \times 10^{-3}$ and the authors have provided us the individual measurement.
[2] Uses a fully reconstructed B meson as a tag on the recoil side.

$\Gamma(D^{(*)}n\pi\ell^+\nu_\ell(n \geq 1))/\Gamma(D\ell^+\nu_\ell\,\text{anything})$ Γ_{11}/Γ_3

VALUE	DOCUMENT ID		TECN	COMMENT
0.191±0.013±0.019	[1] AUBERT	07AN	BABR	$e^+e^- \to \Upsilon(4S)$

[1] Uses a fully reconstructed B meson on the recoil side.

Meson Particle Listings

$B^{\pm}$

$\Gamma(D^{*-}\pi^+\ell^+\nu_\ell)/\Gamma_{\rm total}$ Γ_{12}/Γ

VALUE (units 10^{-3})	DOCUMENT ID		TECN	COMMENT
6.1±0.6 OUR AVERAGE				
5.9±0.5±0.4	[1] AUBERT	08Q	BABR	$e^+e^- \to \Upsilon(4S)$
6.5±1.0±0.3	[1,2] LIVENTSEV	08	BELL	$e^+e^- \to \Upsilon(4S)$
• • • We do not use the following data for averages, fits, limits, etc. • • •				
5.9±1.4±0.1	[3,4] LIVENTSEV	05	BELL	Repl. by LIVENTSEV 08

[1] Uses a fully reconstructed B meson as a tag on the recoil side.
[2] LIVENTSEV 08 reports $(6.4 \pm 0.8 \pm 0.9) \times 10^{-3}$ from a measurement of $[\Gamma(B^+ \to D^{*-}\pi^+\ell^+\nu_\ell)/\Gamma_{\rm total}]$ / $[{\rm B}(B^+ \to \overline{D}{}^0\ell^+\nu_\ell)]$ assuming ${\rm B}(B^+ \to \overline{D}{}^0\ell^+\nu_\ell) = (2.15 \pm 0.22) \times 10^{-2}$, which we rescale to our best value ${\rm B}(B^+ \to \overline{D}{}^0\ell^+\nu_\ell) = (2.20 \pm 0.10) \times 10^{-2}$. Our first error is their experiment's error and our second error is the systematic error from using our best value.
[3] Excludes D^{*+} contribution to $D\pi$ modes.
[4] LIVENTSEV 05 reports $[\Gamma(B^+ \to D^{*-}\pi^+\ell^+\nu_\ell)/\Gamma_{\rm total}]$ / $[{\rm B}(B^0 \to D^*(2010)^-\ell^+\nu_\ell)] = 0.12 \pm 0.02 \pm 0.02$ which we multiply by our best value ${\rm B}(B^0 \to D^*(2010)^-\ell^+\nu_\ell) = (4.88 \pm 0.10) \times 10^{-2}$. Our first error is their experiment's error and our second error is the systematic error from using our best value.

$\Gamma(\overline{D}_1(2420)^0\ell^+\nu_\ell, \overline{D}_1^0 \to D^{*-}\pi^+)/\Gamma_{\rm total}$ Γ_{13}/Γ

VALUE (units 10^{-3})	DOCUMENT ID		TECN	COMMENT
3.03±0.20 OUR AVERAGE				
2.97±0.17±0.17	[1] AUBERT	09Y	BABR	$e^+e^- \to \Upsilon(4S)$
2.9 ±0.3 ±0.3	[2] AUBERT	08BL	BABR	$e^+e^- \to \Upsilon(4S)$
4.2 ±0.7 ±0.7	[2] LIVENTSEV	08	BELL	$e^+e^- \to \Upsilon(4S)$
3.73±0.85±0.57	[3] ANASTASSOV	98	CLE2	$e^+e^- \to \Upsilon(4S)$

[1] Uses a simultaneous measurement of all B semileptonic decays without full reconstruction of events.
[2] Uses a fully reconstructed B meson as a tag on the recoil side.
[3] Assumes equal production of B^+ and B^0 at the $\Upsilon(4S)$.

$\Gamma(\overline{D}_1'(2430)^0\ell^+\nu_\ell, \overline{D}_1^{\prime 0} \to D^{*-}\pi^+)/\Gamma_{\rm total}$ Γ_{14}/Γ

VALUE (units 10^{-3})	CL%	DOCUMENT ID		TECN	COMMENT
2.7±0.4±0.5		[1] AUBERT	08BL	BABR	$e^+e^- \to \Upsilon(4S)$
• • • We do not use the following data for averages, fits, limits, etc. • • •					
<0.7	90	[1] LIVENTSEV	08	BELL	$e^+e^- \to \Upsilon(4S)$

[1] Uses a fully reconstructed B meson as a tag on the recoil side.

$\Gamma(\overline{D}_2^*(2460)^0\ell^+\nu_\ell, \overline{D}_2^{*0} \to D^{*-}\pi^+)/\Gamma_{\rm total}$ Γ_{15}/Γ

VALUE (units 10^{-3})	CL%	DOCUMENT ID		TECN	COMMENT
1.01±0.24 OUR AVERAGE		Error includes scale factor of 2.0.			
0.87±0.11±0.07		[1] AUBERT	09Y	BABR	$e^+e^- \to \Upsilon(4S)$
1.5 ±0.2 ±0.2		[2] AUBERT	08BL	BABR	$e^+e^- \to \Upsilon(4S)$
1.8 ±0.6 ±0.3		[2] LIVENTSEV	08	BELL	$e^+e^- \to \Upsilon(4S)$
• • • We do not use the following data for averages, fits, limits, etc. • • •					
<1.6	90	[3] ANASTASSOV	98	CLE2	$e^+e^- \to \Upsilon(4S)$

[1] Uses a simultaneous fit of all B semileptonic decays without full reconstruction of events. AUBERT 09Y reports ${\rm B}(B^+ \to \overline{D}_2^*(2460)^0\ell^+\nu_\ell) \cdot {\rm B}(\overline{D}_2^*(2460)^0 \to D^{(*)-}\pi^+) = (2.29 \pm 0.23 \pm 0.21) \times 10^{-3}$ and the authors have provided us the individual measurement.
[2] Uses a fully reconstructed B meson as a tag on the recoil side.
[3] Assumes equal production of B^+ and B^0 at the $\Upsilon(4S)$.

$\Gamma(\overline{D}^0\pi^+\pi^-\ell^+\nu_\ell)/\Gamma(\overline{D}^0\ell^+\nu_\ell)$ Γ_{16}/Γ_4

VALUE (units 10^{-2})	DOCUMENT ID		TECN	COMMENT
7.1±1.3±0.8	[1] LEES	16	BABR	$e^+e^- \to \Upsilon(4S)$

[1] Measurement used electrons and muons as leptons.

$\Gamma(\overline{D}^{*0}\pi^+\pi^-\ell^+\nu_\ell)/\Gamma(\overline{D}^*(2007)^0\ell^+\nu_\ell)$ Γ_{17}/Γ_6

VALUE (units 10^{-2})	DOCUMENT ID		TECN	COMMENT
1.4±0.7±0.4	[1] LEES	16	BABR	$e^+e^- \to \Upsilon(4S)$

[1] Measurement used electrons and muons as leptons.

$\Gamma(D_s^{(*)-}K^+\ell^+\nu_\ell)/\Gamma_{\rm total}$ Γ_{18}/Γ

VALUE (units 10^{-4})	DOCUMENT ID		TECN	COMMENT
6.1 ±1.0 OUR AVERAGE				
5.9 ±1.2 ±1.5	[1] STYPULA	12	BELL	$e^+e^- \to \Upsilon(4S)$
$6.13^{+1.04}_{-1.03}\pm0.67$	[1] DEL-AMO-SA...	11L	BABR	$e^+e^- \to \Upsilon(4S)$

[1] Assumes equal production of B^+ and B^0 at the $\Upsilon(4S)$.

$\Gamma(D_s^-K^+\ell^+\nu_\ell)/\Gamma_{\rm total}$ Γ_{19}/Γ

VALUE (units 10^{-4})	DOCUMENT ID		TECN	COMMENT
$\mathbf{3.0\pm0.9^{+1.1}_{-0.8}}$	[1] STYPULA	12	BELL	$e^+e^- \to \Upsilon(4S)$

[1] Assumes equal production of B^+ and B^0 at the $\Upsilon(4S)$.

$\Gamma(D_s^{*-}K^+\ell^+\nu_\ell)/\Gamma_{\rm total}$ Γ_{20}/Γ

VALUE (units 10^{-4})	DOCUMENT ID		TECN	COMMENT
$\mathbf{2.9\pm1.6^{+1.1}_{-1.0}}$	[1,2] STYPULA	12	BELL	$e^+e^- \to \Upsilon(4S)$

[1] Assumes equal production of B^+ and B^0 at the $\Upsilon(4S)$.
[2] STYPULA 12 provides also an upper limit of 0.56×10^{-3} at 90% CL for the same data. Also measures branching fraction of the combined modes of $D_s^-K^+\ell^+\nu_\ell$ and $D_s^{*-}K^+\ell^+\nu_\ell$ as ${\rm B}(B^+ \to D_s^{(*)-}K^+\ell^+\nu_\ell) = (5.9 \pm 1.2 \pm 1.5) \times 10^{-4}$.

$\Gamma(\pi^0\ell^+\nu_\ell)/\Gamma_{\rm total}$ Γ_{21}/Γ

"OUR EVALUATION" is an average using rescaled values of the data listed below. The average and rescaling were performed by the Heavy Flavor Averaging Group (HFLAV) and are described at http://www.slac.stanford.edu/xorg/hflav/. The averaging/rescaling procedure takes into account correlations between the measurements.

VALUE (units 10^{-4})	DOCUMENT ID		TECN	COMMENT
0.780±0.027 OUR EVALUATION				
0.748±0.029 OUR AVERAGE				
0.80 ±0.08 ±0.04	[1] SIBIDANOV	13	BELL	$e^+e^- \to \Upsilon(4S)$
0.77 ±0.04 ±0.03	[2] LEES	12AA	BABR	$e^+e^- \to \Upsilon(4S)$
0.705±0.025±0.035	[3] DEL-AMO-SA...	11C	BABR	$e^+e^- \to \Upsilon(4S)$
0.82 ±0.09 ±0.05	[3] AUBERT	08AV	BABR	$e^+e^- \to \Upsilon(4S)$
0.77 ±0.14 ±0.08	[4] HOKUUE	07	BELL	$e^+e^- \to \Upsilon(4S)$
• • • We do not use the following data for averages, fits, limits, etc. • • •				
0.74 ±0.05 ±0.10	[5] AUBERT,B	05O	BABR	Repl. by DEL-AMO-SANCHEZ 11C

[1] The signal events are tagged by a second B meson reconstructed in the fully hadronic decays.
[2] Uses loose neutrino reconstruction technique. Assumes ${\rm B}(\Upsilon(4S) \to B^+B^-) = (51.6 \pm 0.6)\%$ and ${\rm B}(\Upsilon(4S) \to B^0\overline{B}{}^0) = (48.4 \pm 0.6)\%$.
[3] Using the isospin symmetry relation, B^+ and B^0 branching fractions are combined.
[4] The signal events are tagged by a second B meson reconstructed in the semileptonic mode $B \to D^{(*)}\ell\nu_\ell$.
[5] B^+ and B^0 decays combined assuming isospin symmetry. Systematic errors include both experimental and form-factor uncertainties.

$\Gamma(\pi^0e^+\nu_e)/\Gamma_{\rm total}$ Γ_{22}/Γ

VALUE (units 10^{-4})	CL%	DOCUMENT ID		TECN	COMMENT
• • • We do not use the following data for averages, fits, limits, etc. • • •					
0.9±0.2±0.2		[1] ALEXANDER	96T	CLE2	$e^+e^- \to \Upsilon(4S)$
<22	90	ANTREASYAN	90B	CBAL	$e^+e^- \to \Upsilon(4S)$

[1] Derived based in the reported B^0 result by assuming isospin symmetry: $\Gamma(B^0 \to \pi^-\ell^+\nu) = 2\Gamma(B^+ \to \pi^0\ell^+\nu)$.

$\Gamma(\eta\ell^+\nu_\ell)/\Gamma_{\rm total}$ Γ_{23}/Γ

VALUE (units 10^{-4})	CL%	DOCUMENT ID		TECN	COMMENT
0.39±0.05 OUR AVERAGE					
0.42±0.11±0.03		[1] BELENO	17	BELL	$e^+e^- \to \Upsilon(4S)$
0.38±0.05±0.05		[2] LEES	12AA	BABR	$e^+e^- \to \Upsilon(4S)$
0.31±0.06±0.08		[2] AUBERT	09Q	BABR	$e^+e^- \to \Upsilon(4S)$
0.64±0.20±0.03		[3] AUBERT	08AV	BABR	$e^+e^- \to \Upsilon(4S)$
• • • We do not use the following data for averages, fits, limits, etc. • • •					
0.36±0.05±0.04		[2] DEL-AMO-SA...	11F	BABR	Repl. by LEES 12AA
<1.01	90	[4] ADAM	07	CLE2	$e^+e^- \to \Upsilon(4S)$
0.84±0.31±0.18		[5] ATHAR	03	CLE2	Repl. by ADAM 07

[1] Uses missing-mass technique by fully reconstructing the hadronic decay chain of the accompanying B.
[2] Uses loose neutrino reconstruction technique. Assumes ${\rm B}(\Upsilon(4S) \to B^+B^-) = (51.6 \pm 0.6)\%$ and ${\rm B}(\Upsilon(4S) \to B^0\overline{B}{}^0) = (48.4 \pm 0.6)\%$.
[3] Assumes equal production of B^+ and B^0 at the $\Upsilon(4S)$.
[4] The B^0 and B^+ results are combined assuming the isospin, B lifetimes, and relative charged/neutral B production at the $\Upsilon(4S)$.
[5] ATHAR 03 reports systematic errors 0.16 ± 0.09, which are experimental systematic and systematic due to model dependence. We combine these in quadrature.

$\Gamma(\eta'\ell^+\nu_\ell)/\Gamma_{\rm total}$ Γ_{24}/Γ

VALUE (units 10^{-4})	CL%	DOCUMENT ID		TECN	COMMENT
0.23±0.08 OUR AVERAGE					
0.24±0.08±0.03		[1] LEES	12AA	BABR	$e^+e^- \to \Upsilon(4S)$
$0.04\pm0.22^{+0.05}_{-0.02}$		[2] AUBERT	08AV	BABR	$e^+e^- \to \Upsilon(4S)$
2.66±0.80±0.56		[3] ADAM	07	CLE2	$e^+e^- \to \Upsilon(4S)$
• • • We do not use the following data for averages, fits, limits, etc. • • •					
<0.72	90	[4] BELENO	17	BELL	$e^+e^- \to \Upsilon(4S)$
0.24±0.08±0.03		[1] DEL-AMO-SA...	11F	BABR	Repl. by LEES 12AA

[1] Uses loose neutrino reconstruction technique. Assumes ${\rm B}(\Upsilon(4S) \to B^+B^-) = (51.6 \pm 0.6)\%$ and ${\rm B}(\Upsilon(4S) \to B^0\overline{B}{}^0) = (48.4 \pm 0.6)\%$.
[2] Assumes equal production of B^+ and B^0 at the $\Upsilon(4S)$.
[3] The B^0 and B^+ results are combined assuming the isospin, B lifetimes, and relative charged/neutral B production at the $\Upsilon(4S)$. Corresponds to 90% CL interval $(1.20\text{–}4.46) \times 10^{-4}$.
[4] Uses missing-mass technique by fully reconstructing the hadronic decay chain of the accompanying B.

$\Gamma(\omega\ell^+\nu_\ell)/\Gamma_{\rm total}$ Γ_{25}/Γ

$\ell = e$ or μ, not sum over e and μ modes.

VALUE (units 10^{-4})	CL%	DOCUMENT ID		TECN	COMMENT
1.19±0.09 OUR AVERAGE					
1.21±0.14±0.08		[1,2] LEES	13A	BABR	$e^+e^- \to \Upsilon(4S)$
1.35±0.21±0.11		[3] LEES	13T	BABR	$e^+e^- \to \Upsilon(4S)$

$1.07 \pm 0.16 \pm 0.07$		[4] SIBIDANOV	13	BELL	$e^+e^- \to \Upsilon(4S)$	
$1.19 \pm 0.16 \pm 0.09$		[2,5] LEES	12AA	BABR	$e^+e^- \to \Upsilon(4S)$	
$1.3 \pm 0.4 \pm 0.4$		[6] SCHWANDA	04	BELL	$e^+e^- \to \Upsilon(4S)$	
• • • We do not use the following data for averages, fits, limits, etc. • • •						
$1.14 \pm 0.16 \pm 0.08$		[2] AUBERT	09Q	BABR	Repl. by LEES 13A	
<2.1	90	[7] BEAN	93B	CLE2	$e^+e^- \to \Upsilon(4S)$	

[1] LEES 13A reports $(1.21 \pm 0.14 \pm 0.08) \times 10^{-4}$ from a measurement of $[\Gamma(B^+ \to \omega\ell^+\nu_\ell)/\Gamma_{\rm total}] \times [B(\omega(782) \to \pi^+\pi^-\pi^0)]$ assuming $B(\omega(782) \to \pi^+\pi^-\pi^0) = (89.2 \pm 0.7) \times 10^{-2}$.

[2] Uses $B(\Upsilon(4S) \to B^+B^-) = (51.6 \pm 0.6)\%$ and $B(\Upsilon(4S) \to B^0\overline{B}^0) = (48.4 \pm 0.6)\%$.

[3] Uses semileptonic tagging. Assumes $B(\omega \to \pi^+\pi^-\pi^0) = (89.2 \pm 0.7)\%$ and that the production ratio of B^+B^- to $B^0\overline{B}^0$ from $\Upsilon(4S)$ is 1.056 ± 0.028. The partial branching fractions in three bins of q^2 are also reported.

[4] The signal events are tagged by a second B meson reconstructed in the fully hadronic decays.

[5] Uses loose neutrino reconstruction technique.

[6] Assumes equal production of B^+ and B^0 at the $\Upsilon(4S)$.

[7] BEAN 93B limit set using ISGW Model. Using isospin and the quark model to combine $\Gamma(\rho^0\ell^+\nu_\ell)$ and $\Gamma(\rho^-\ell^+\nu_\ell)$ with this result, they obtain a limit $<(1.6\text{–}2.7) \times 10^{-4}$ at 90% CL for $B^+ \to \omega\ell^+\nu_\ell$. The range corresponds to the ISGW, WSB, and KS models. An upper limit on $|V_{ub}/V_{cb}| < 0.8\text{–}0.13$ at 90% CL is derived as well.

$\Gamma(\omega\mu^+\nu_\mu)/\Gamma_{\rm total}$ Γ_{26}/Γ

VALUE	DOCUMENT ID	TECN
• • • We do not use the following data for averages, fits, limits, etc. • • •		
seen	[1] ALBRECHT 91C	ARG

[1] In ALBRECHT 91C, one event is fully reconstructed providing evidence for the $b \to u$ transition.

$\Gamma(\rho^0\ell^+\nu_\ell)/\Gamma_{\rm total}$ Γ_{27}/Γ

$\ell = e$ or μ, not sum over e and μ modes.

"OUR EVALUATION" is an average using rescaled values of the data listed below. The average and rescaling were performed by the Heavy Flavor Averaging Group (HFLAV) and are described at http://www.slac.stanford.edu/xorg/hflav/. The averaging/rescaling procedure takes into account correlations between the measurements and asymmetric lifetime errors.

VALUE (units 10^{-4})	CL%	DOCUMENT ID		TECN	COMMENT
1.58 ± 0.11 OUR EVALUATION					
1.42 ± 0.23 OUR AVERAGE		Error includes scale factor of 2.4. See the ideogram below.			
$1.83 \pm 0.10 \pm 0.10$		[1] SIBIDANOV	13	BELL	$e^+e^- \to \Upsilon(4S)$
$0.94 \pm 0.08 \pm 0.14$		[2] DEL-AMO-SA...11C		BABR	$e^+e^- \to \Upsilon(4S)$
$1.33 \pm 0.23 \pm 0.18$		[3] HOKUUE	07	BELL	$e^+e^- \to \Upsilon(4S)$
$1.34 \pm 0.15 {}^{+0.28}_{-0.32}$		[4] BEHRENS	00	CLE2	$e^+e^- \to \Upsilon(4S)$
• • • We do not use the following data for averages, fits, limits, etc. • • •					
$1.16 \pm 0.11 \pm 0.30$		[2] AUBERT,B	05O	BABR	Repl. by DEL-AMO-SANCHEZ 11C
$1.40 \pm 0.21 {}^{+0.32}_{-0.33}$		[4] BEHRENS	00	CLE2	$e^+e^- \to \Upsilon(4S)$
$1.2 \pm 0.2 {}^{+0.3}_{-0.4}$		[4] ALEXANDER	96T	CLE2	$e^+e^- \to \Upsilon(4S)$
<2.1	90	[5] BEAN	93B	CLE2	$e^+e^- \to \Upsilon(4S)$

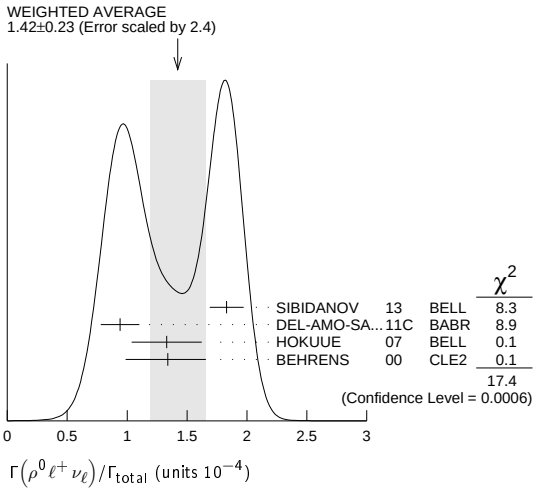

[1] The signal events are tagged by a second B meson reconstructed in the fully hadronic decays.

[2] B^+ and B^0 decays combined assuming isospin symmetry. Systematic errors include both experimental and form-factor uncertainties.

[3] The signal events are tagged by a second B meson reconstructed in the semileptonic mode $B \to D^{(*)}\ell\nu_\ell$.

[4] Derived based in the reported B^0 result by assuming isospin symmetry: $\Gamma(B^0 \to \rho^-\ell^+\nu) = 2\Gamma(B^+ \to \rho^0\ell^+\nu) \approx 2\Gamma(B^+ \to \omega\ell^+\nu)$.

[5] BEAN 93B limit set using ISGW Model. Using isospin and the quark model to combine $\Gamma(\omega^0\ell^+\nu_\ell)$ and $\Gamma(\rho^-\ell^+\nu_\ell)$ with this result, they obtain a limit $<(1.6\text{–}2.7) \times 10^{-4}$ at 90% CL for $B^+ \to \rho^0\ell^+\nu_\ell$. The range corresponds to the ISGW, WSB, and KS models. An upper limit on $|V_{ub}/V_{cb}| < 0.8\text{–}0.13$ at 90% CL is derived as well.

$\Gamma(p\overline{p}\ell^+\nu_\ell)/\Gamma_{\rm total}$ Γ_{28}/Γ

VALUE (units 10^{-6})	DOCUMENT ID		TECN	COMMENT
$5.8 {}^{+2.4}_{-2.1} \pm 0.9$	[1] TIEN	14	BELL	$e^+e^- \to \Upsilon(4S)$

[1] Assumes equal production of B^+ and B^0 at the $\Upsilon(4S)$.

$\Gamma(p\overline{p}\mu^+\nu_\mu)/\Gamma_{\rm total}$ Γ_{29}/Γ

VALUE	CL%	DOCUMENT ID		TECN	COMMENT
$<8.5 \times 10^{-6}$	90	[1] TIEN	14	BELL	$e^+e^- \to \Upsilon(4S)$

[1] Assumes equal production of B^+ and B^0 at the $\Upsilon(4S)$.

$\Gamma(p\overline{p}e^+\nu_e)/\Gamma_{\rm total}$ Γ_{30}/Γ

VALUE (units 10^{-6})	CL%	DOCUMENT ID		TECN	COMMENT
$8.2 {}^{+3.7}_{-3.2} \pm 0.6$		[1] TIEN	14	BELL	$e^+e^- \to \Upsilon(4S)$
• • • We do not use the following data for averages, fits, limits, etc. • • •					
<5200	90	[2] ADAM	03B	CLE2	$e^+e^- \to \Upsilon(4S)$

[1] Assumes equal production of B^+ and B^0 at the $\Upsilon(4S)$.

[2] Based on phase-space model; if $V\text{–}A$ model is used, the 90% CL upper limit becomes $< 1.2 \times 10^{-3}$.

$\Gamma(e^+\nu_e)/\Gamma_{\rm total}$ Γ_{31}/Γ

VALUE (units 10^{-6})	CL%	DOCUMENT ID		TECN	COMMENT
< 0.98	90	[1] SATOYAMA	07	BELL	$e^+e^- \to \Upsilon(4S)$
• • • We do not use the following data for averages, fits, limits, etc. • • •					
< 3.5	90	[2] YOOK	15	BELL	$e^+e^- \to \Upsilon(4S)$
< 8	90	[1] AUBERT	10E	BABR	$e^+e^- \to \Upsilon(4S)$
< 1.9	90	[1] AUBERT	09V	BABR	$e^+e^- \to \Upsilon(4S)$
< 5.2	90	[1] AUBERT	08AD	BABR	$e^+e^- \to \Upsilon(4S)$
<15	90	ARTUSO	95	CLE2	$e^+e^- \to \Upsilon(4S)$

[1] Assumes equal production of B^+ and B^0 at the $\Upsilon(4S)$.

[2] Assumes $B(\Upsilon(4S) \to B^+B^-) = 0.513 \pm 0.006$.

$\Gamma(\mu^+\nu_\mu)/\Gamma_{\rm total}$ Γ_{32}/Γ

VALUE (units 10^{-6})	CL%	DOCUMENT ID		TECN	COMMENT
< 1.0	90	[1] AUBERT	09V	BABR	$e^+e^- \to \Upsilon(4S)$
• • • We do not use the following data for averages, fits, limits, etc. • • •					
< 2.7	90	[2] YOOK	15	BELL	$e^+e^- \to \Upsilon(4S)$
<11	90	[1] AUBERT	10E	BABR	$e^+e^- \to \Upsilon(4S)$
< 5.6	90	[1] AUBERT	08AD	BABR	$e^+e^- \to \Upsilon(4S)$
< 1.7	90	[1] SATOYAMA	07	BELL	$e^+e^- \to \Upsilon(4S)$
< 6.6	90	AUBERT	04O	BABR	Repl. by AUBERT 09V
<21	90	ARTUSO	95	CLE2	$e^+e^- \to \Upsilon(4S)$

[1] Assumes equal production of B^+ and B^0 at the $\Upsilon(4S)$.

[2] Assumes $B(\Upsilon(4S) \to B^+B^-) = 0.513 \pm 0.006$.

$\Gamma(\tau^+\nu_\tau)/\Gamma_{\rm total}$ Γ_{33}/Γ

See the note on "Decay Constants of Charged Pseudoscalar Mesons" in the D_s^+ Listings.

VALUE (units 10^{-4})	CL%	DOCUMENT ID		TECN	COMMENT
1.09 ± 0.24 OUR AVERAGE		Error includes scale factor of 1.2.			
$1.25 \pm 0.28 \pm 0.27$		[1,2] KRONENBIT...	15	BELL	$e^+e^- \to \Upsilon(4S)$
$0.72 {}^{+0.27}_{-0.25} \pm 0.11$		[3] HARA	13	BELL	$e^+e^- \to \Upsilon(4S)$
$1.83 {}^{+0.53}_{-0.49} \pm 0.24$		[2,4] LEES	13K	BABR	$e^+e^- \to \Upsilon(4S)$
$1.7 \pm 0.8 \pm 0.2$		[2,5] AUBERT	10E	BABR	$e^+e^- \to \Upsilon(4S)$
• • • We do not use the following data for averages, fits, limits, etc. • • •					
$1.54 {}^{+0.38}_{-0.37} {}^{+0.29}_{-0.31}$		[2,6] HARA	10	BELL	Repl. by KRONENBIT-TER 15
$1.8 {}^{+0.9}_{-0.8} \pm 0.45$		[2,7] AUBERT	08D	BABR	Repl. by LEES 13K
$0.9 \pm 0.6 \pm 0.1$		[2,5] AUBERT	07AL	BABR	Repl. by AUBERT 10E
< 2.6	90	[2] AUBERT	06K	BABR	$e^+e^- \to \Upsilon(4S)$
$1.79 {}^{+0.56}_{-0.49} {}^{+0.46}_{-0.51}$		[2,7] IKADO	06	BELL	Repl. by HARA 13
< 4.2	90	[2] AUBERT,B	05B	BABR	Repl. by AUBERT 06K
< 8.3	90	[8] BARATE	01E	ALEP	$e^+e^- \to Z$
< 8.4	90	[2] BROWDER	01	CLE2	$e^+e^- \to \Upsilon(4S)$
< 5.7	90	[9] ACCIARRI	97F	L3	$e^+e^- \to Z$
<104	90	[10] ALBRECHT	95D	ARG	$e^+e^- \to \Upsilon(4S)$
< 22	90	ARTUSO	95	CLE2	$e^+e^- \to \Upsilon(4S)$
< 18	90	[11] BUSKULIC	95	ALEP	$e^+e^- \to Z$

[1] Requires one reconstructed semileptonic B decay $B^- \to D^{(*)0}\ell^-\overline{\nu}_\ell$ in the recoil.

[2] Assumes equal production of B^+ and B^0 at the $\Upsilon(4S)$.

[3] The authors combine their result with that from HARA 10 obtaining $B(B^- \to \tau^-\overline{\nu}_\tau) = (0.96 \pm 0.26) \times 10^{-4}$ and deriving $f_B\,|V_{ub}| = (7.4 \pm 0.8 \pm 0.5) \times 10^{-4}$ GeV.

[4] Requires a fully reconstructed hadronic B-decay in the recoil. Reports that this result combined with AUBERT 10E value gives $B(B^- \to \tau^- \overline{\nu}_\tau) = (1.79 \pm 0.48) \times 10^{-4}$.
[5] Requires one reconstructed semileptonic B decay $B^- \to D^0 \ell^- \overline{\nu}_\ell X$ in the recoil.
[6] Requires one reconstructed semileptonic B decay $B^- \to D^{(*)0} \ell^- \overline{\nu}_\ell X$ in the recoil.
[7] The analysis is based on a sample of events with one fully reconstructed tag B in a hadronic decay mode $B^- \to D^{(*)0} X^-$.
[8] The energy-flow and b-tagging algorithms were used.
[9] ACCIARRI 97F uses missing-energy technique and $f(b \to B^-) = (38.2 \pm 2.5)\%$.
[10] ALBRECHT 95D uses full reconstruction of one B decay as tag.
[11] BUSKULIC 95 uses same missing-energy technique as in $\overline{b} \to \tau^+ \nu_\tau X$, but analysis is restricted to endpoint region of missing-energy distribution.

$\Gamma(\ell^+ \nu_\ell \gamma)/\Gamma_{\text{total}}$ — Γ_{34}/Γ

VALUE	CL%	DOCUMENT ID		TECN	COMMENT
$< 3.5 \times 10^{-6}$	90	[1] HELLER	15	BELL	$e^+e^- \to \Upsilon(4S)$
• • • We do not use the following data for averages, fits, limits, etc. • • •					
$<15.6 \times 10^{-6}$	90	[1] AUBERT	09AT	BABR	$e^+e^- \to \Upsilon(4S)$

[1] Assumes equal production of B^+ and B^0 at the $\Upsilon(4S)$.

$\Gamma(e^+ \nu_e \gamma)/\Gamma_{\text{total}}$ — Γ_{35}/Γ

VALUE	CL%	DOCUMENT ID		TECN	COMMENT
$< 6.1 \times 10^{-6}$	90	[1] HELLER	15	BELL	$e^+e^- \to \Upsilon(4S)$
• • • We do not use the following data for averages, fits, limits, etc. • • •					
$< 17 \times 10^{-6}$	90	[1] AUBERT	09AT	BABR	$e^+e^- \to \Upsilon(4S)$
$<200 \times 10^{-6}$	90	[2] BROWDER	97	CLE2	$e^+e^- \to \Upsilon(4S)$

[1] Assumes equal production of B^+ and B^0 at the $\Upsilon(4S)$.
[2] BROWDER 97 uses the hermiticity of the CLEO II detector to reconstruct the neutrino energy and momentum.

$\Gamma(\mu^+ \nu_\mu \gamma)/\Gamma_{\text{total}}$ — Γ_{36}/Γ

VALUE	CL%	DOCUMENT ID		TECN	COMMENT
$< 3.4 \times 10^{-6}$	90	[1] HELLER	15	BELL	$e^+e^- \to \Upsilon(4S)$
• • • We do not use the following data for averages, fits, limits, etc. • • •					
$<24 \times 10^{-6}$	90	[1,2] AUBERT	09AT	BABR	$e^+e^- \to \Upsilon(4S)$
$<52 \times 10^{-6}$	90	[3] BROWDER	97	CLE2	$e^+e^- \to \Upsilon(4S)$

[1] Assumes equal production of B^+ and B^0 at the $\Upsilon(4S)$.
[2] Note that the value given by Aubert 2009 is 24 E-6 in the paper abstract, and 26 E-6 in the paper itself (Table I).
[3] BROWDER 97 uses the hermiticity of the CLEO II detector to reconstruct the neutrino energy and momentum.

$\Gamma(D^0 X)/\Gamma_{\text{total}}$ — Γ_{37}/Γ

VALUE	DOCUMENT ID		TECN	COMMENT
$0.086 \pm 0.006 \pm 0.004$	[1] AUBERT	07N	BABR	$e^+e^- \to \Upsilon(4S)$
• • • We do not use the following data for averages, fits, limits, etc. • • •				
$0.098 \pm 0.009 \pm 0.006$	[1] AUBERT,BE	04B	BABR	Repl. by AUBERT 07N

[1] Events are selected by completely reconstructing one B and searching for a reconstructed charmed particle in the rest of the event. The last error includes systematic and charm branching ratio uncertainties.

$\Gamma(\overline{D}^0 X)/\Gamma_{\text{total}}$ — Γ_{38}/Γ

VALUE	DOCUMENT ID		TECN	COMMENT
$0.786 \pm 0.016^{+0.034}_{-0.033}$	[1] AUBERT	07N	BABR	$e^+e^- \to \Upsilon(4S)$
• • • We do not use the following data for averages, fits, limits, etc. • • •				
$0.793 \pm 0.025^{+0.045}_{-0.044}$	[1] AUBERT,BE	04B	BABR	Repl. by AUBERT 07N

[1] Events are selected by completely reconstructing one B and searching for a reconstructed charmed particle in the rest of the event. The last error includes systematic and charm branching ratio uncertainties.

$\Gamma(D^0 X)/[\Gamma(D^0 X) + \Gamma(\overline{D}^0 X)]$ — $\Gamma_{37}/(\Gamma_{37}+\Gamma_{38})$

VALUE	DOCUMENT ID		TECN	COMMENT
$0.098 \pm 0.007 \pm 0.001$	AUBERT	07N	BABR	$e^+e^- \to \Upsilon(4S)$
• • • We do not use the following data for averages, fits, limits, etc. • • •				
$0.110 \pm 0.010 \pm 0.003$	AUBERT,BE	04B	BABR	Repl. by AUBERT 07N

$\Gamma(D^+ X)/\Gamma_{\text{total}}$ — Γ_{39}/Γ

VALUE	DOCUMENT ID		TECN	COMMENT
$0.025 \pm 0.005 \pm 0.002$	[1] AUBERT	07N	BABR	$e^+e^- \to \Upsilon(4S)$
• • • We do not use the following data for averages, fits, limits, etc. • • •				
$0.038 \pm 0.009 \pm 0.005$	[1] AUBERT,BE	04B	BABR	Repl. by AUBERT 07N

[1] Events are selected by completely reconstructing one B and searching for a reconstructed charmed particle in the rest of the event. The last error includes systematic and charm branching ratio uncertainties.

$\Gamma(D^- X)/\Gamma_{\text{total}}$ — Γ_{40}/Γ

VALUE	DOCUMENT ID		TECN	COMMENT
$0.099 \pm 0.008 \pm 0.009$	[1] AUBERT	07N	BABR	$e^+e^- \to \Upsilon(4S)$
• • • We do not use the following data for averages, fits, limits, etc. • • •				
$0.098 \pm 0.012 \pm 0.014$	[1] AUBERT,BE	04B	BABR	Repl. by AUBERT 07N

[1] Events are selected by completely reconstructing one B and searching for a reconstructed charmed particle in the rest of the event. The last error includes systematic and charm branching ratio uncertainties.

$\Gamma(D^+ X)/[\Gamma(D^+ X) + \Gamma(D^- X)]$ — $\Gamma_{39}/(\Gamma_{39}+\Gamma_{40})$

VALUE	DOCUMENT ID		TECN	COMMENT
$0.204 \pm 0.035 \pm 0.001$	AUBERT	07N	BABR	$e^+e^- \to \Upsilon(4S)$
• • • We do not use the following data for averages, fits, limits, etc. • • •				
$0.278 \pm 0.052 \pm 0.009$	AUBERT,BE	04B	BABR	Repl. by AUBERT 07N

$\Gamma(D_s^+ X)/\Gamma_{\text{total}}$ — Γ_{41}/Γ

VALUE	DOCUMENT ID		TECN	COMMENT
$0.079 \pm 0.006^{+0.013}_{-0.011}$	[1] AUBERT	07N	BABR	$e^+e^- \to \Upsilon(4S)$
• • • We do not use the following data for averages, fits, limits, etc. • • •				
$0.143 \pm 0.016^{+0.051}_{-0.034}$	[1] AUBERT,BE	04B	BABR	Repl. by AUBERT 07N

[1] Events are selected by completely reconstructing one B and searching for a reconstructed charmed particle in the rest of the event. The last error includes systematic and charm branching ratio uncertainties.

$\Gamma(D_s^- X)/\Gamma_{\text{total}}$ — Γ_{42}/Γ

VALUE	CL%	DOCUMENT ID		TECN	COMMENT
$0.011^{+0.004+0.002}_{-0.003-0.001}$		[1] AUBERT	07N	BABR	$e^+e^- \to \Upsilon(4S)$
• • • We do not use the following data for averages, fits, limits, etc. • • •					
<0.022	90	[1] AUBERT,BE	04B	BABR	Repl. by AUBERT 07N

[1] Events are selected by completely reconstructing one B and searching for a reconstructed charmed particle in the rest of the event. The last error includes systematic and charm branching ratio uncertainties.

$\Gamma(D_s^+ X)/[\Gamma(D_s^+ X) + \Gamma(D_s^- X)]$ — $\Gamma_{41}/(\Gamma_{41}+\Gamma_{42})$

VALUE	DOCUMENT ID		TECN	COMMENT
$0.884 \pm 0.038 \pm 0.002$	AUBERT	07N	BABR	$e^+e^- \to \Upsilon(4S)$
• • • We do not use the following data for averages, fits, limits, etc. • • •				
$0.966 \pm 0.039 \pm 0.012$	AUBERT,BE	04B	BABR	Repl. by AUBERT 07N

$\Gamma(D_s^- X)/[\Gamma(D_s^+ X) + \Gamma(D_s^- X)]$ — $\Gamma_{42}/(\Gamma_{41}+\Gamma_{42})$

VALUE	CL%	DOCUMENT ID		TECN	COMMENT
<0.126	90	AUBERT,BE	04B	BABR	$e^+e^- \to \Upsilon(4S)$

$\Gamma(\Lambda_c^+ X)/\Gamma_{\text{total}}$ — Γ_{43}/Γ

VALUE	DOCUMENT ID		TECN	COMMENT
$0.021 \pm 0.005^{+0.008}_{-0.004}$	[1] AUBERT	07N	BABR	$e^+e^- \to \Upsilon(4S)$
• • • We do not use the following data for averages, fits, limits, etc. • • •				
$0.029 \pm 0.008^{+0.011}_{-0.007}$	[1] AUBERT,BE	04B	BABR	Repl. by AUBERT 07N

[1] Events are selected by completely reconstructing one B and searching for a reconstructed charmed particle in the rest of the event. The last error includes systematic and charm branching ratio uncertainties.

$\Gamma(\overline{\Lambda}_c^- X)/\Gamma_{\text{total}}$ — Γ_{44}/Γ

VALUE	DOCUMENT ID		TECN	COMMENT
$0.028 \pm 0.005^{+0.010}_{-0.007}$	[1] AUBERT	07N	BABR	$e^+e^- \to \Upsilon(4S)$
• • • We do not use the following data for averages, fits, limits, etc. • • •				
$0.035 \pm 0.008^{+0.013}_{-0.009}$	[1] AUBERT,BE	04B	BABR	Repl. by AUBERT 07N

[1] Events are selected by completely reconstructing one B and searching for a reconstructed charmed particle in the rest of the event. The last error includes systematic and charm branching ratio uncertainties.

$\Gamma(\Lambda_c^+ X)/[\Gamma(\Lambda_c^+ X) + \Gamma(\overline{\Lambda}_c^- X)]$ — $\Gamma_{43}/(\Gamma_{43}+\Gamma_{44})$

VALUE	DOCUMENT ID		TECN	COMMENT
$0.427 \pm 0.071 \pm 0.001$	AUBERT	07N	BABR	$e^+e^- \to \Upsilon(4S)$
• • • We do not use the following data for averages, fits, limits, etc. • • •				
$0.452 \pm 0.090 \pm 0.003$	AUBERT,BE	04B	BABR	Repl. by AUBERT 07N

$\Gamma(\overline{c} X)/\Gamma_{\text{total}}$ — Γ_{45}/Γ

VALUE	DOCUMENT ID		TECN	COMMENT
$0.968 \pm 0.019^{+0.041}_{-0.039}$	[1] AUBERT	07N	BABR	$e^+e^- \to \Upsilon(4S)$
• • • We do not use the following data for averages, fits, limits, etc. • • •				
$0.983 \pm 0.030^{+0.054}_{-0.051}$	[1] AUBERT,BE	04B	BABR	Repl. by AUBERT 07N

[1] Events are selected by completely reconstructing one B and searching for a reconstructed charmed particle in the rest of the event. The last error includes systematic and charm branching ratio uncertainties.

$\Gamma(c X)/\Gamma_{\text{total}}$ — Γ_{46}/Γ

VALUE	DOCUMENT ID		TECN	COMMENT
$0.234 \pm 0.012^{+0.018}_{-0.014}$	[1] AUBERT	07N	BABR	$e^+e^- \to \Upsilon(4S)$
• • • We do not use the following data for averages, fits, limits, etc. • • •				
$0.330 \pm 0.022^{+0.055}_{-0.037}$	[1] AUBERT,BE	04B	BABR	Repl. by AUBERT 07N

[1] Events are selected by completely reconstructing one B and searching for a reconstructed charmed particle in the rest of the event. The last error includes systematic and charm branching ratio uncertainties.

$\Gamma(c/\bar{c}X)/\Gamma_{total}$ Γ_{47}/Γ

VALUE	DOCUMENT ID		TECN	COMMENT
$1.202\pm0.023^{+0.053}_{-0.049}$	[1] AUBERT	07N	BABR	$e^+e^- \to \Upsilon(4S)$
• • • We do not use the following data for averages, fits, limits, etc. • • •				
$1.313\pm0.037^{+0.088}_{-0.075}$	[1] AUBERT,BE	04B	BABR	Repl. by AUBERT 07N

[1] Events are selected by completely reconstructing one B and searching for a reconstructed charmed particle in the rest of the event. The last error includes systematic and charm branching ratio uncertainties.

$\Gamma(\overline{D}^0\pi^+)/\Gamma_{total}$ Γ_{48}/Γ

VALUE (units 10^{-3})	EVTS	DOCUMENT ID		TECN	COMMENT
4.68 ± 0.13 OUR FIT					
4.70 ± 0.13 OUR AVERAGE					
$4.34\pm0.10\pm0.23$		[1] KATO	18	BELL	$e^+e^- \to \Upsilon(4S)$
$4.90\pm0.07\pm0.22$		[2] AUBERT	07H	BABR	$e^+e^- \to \Upsilon(4S)$
$5.0\ \pm0.6\ \pm0.3$		[3] ABULENCIA	06J	CDF	$p\overline{p}$ at 1.96 TeV
$4.49\pm0.21\pm0.23$		[4] AUBERT,BE	06J	BABR	$e^+e^- \to \Upsilon(4S)$
$4.97\pm0.12\pm0.29$		[2,5] AHMED	02B	CLE2	$e^+e^- \to \Upsilon(4S)$
$5.0\ \pm0.7\ \pm0.6$	54	[6] BORTOLETTO	92	CLEO	$e^+e^- \to \Upsilon(4S)$
$5.4\ ^{+1.8}_{-1.5}\ ^{+1.2}_{-0.9}$	14	[7] BEBEK	87	CLEO	$e^+e^- \to \Upsilon(4S)$
• • • We do not use the following data for averages, fits, limits, etc. • • •					
$4.74\pm0.26\pm0.05$		[8] AUBERT,B	04P	BABR	Repl. by AUBERT 07H
$5.5\ \pm0.4\ \pm0.5$	304	[9] ALAM	94	CLE2	Repl. by AHMED 02B
$2.0\ \pm0.8\ \pm0.6$	12	[6] ALBRECHT	90J	ARG	$e^+e^- \to \Upsilon(4S)$
$1.9\ \pm1.0\ \pm0.6$	7	[10] ALBRECHT	88K	ARG	$e^+e^- \to \Upsilon(4S)$

[1] Measures absolute branching fractions using a missing-mass technique.
[2] Assumes equal production of B^+ and B^0 at the $\Upsilon(4S)$.
[3] ABULENCIA 06J reports $[\Gamma(B^+ \to \overline{D}^0\pi^+)/\Gamma_{total}] / [B(B^0 \to D^-\pi^+)] = 1.97 \pm 0.10 \pm 0.21$ which we multiply by our best value $B(B^0 \to D^-\pi^+) = (2.52 \pm 0.13) \times 10^{-3}$. Our first error is their experiment's error and our second error is the systematic error from using our best value.
[4] Uses a missing-mass method. Does not depend on D branching fractions or B^+/B^0 production rates.
[5] AHMED 02B reports an additional uncertainty on the branching ratios to account for 4.5% uncertainty on relative production of B^0 and B^+, which is not included here.
[6] Assumes equal production of B^+ and B^0 at the $\Upsilon(4S)$ and uses the MarkIII branching fractions for the D.
[7] BEBEK 87 value has been updated in BERKELMAN 91 to use same assumptions as noted for BORTOLETTO 92.
[8] AUBERT,B 04P reports $[\Gamma(B^+ \to \overline{D}^0\pi^+)/\Gamma_{total}] \times [B(D^0 \to K^-\pi^+)] = (1.846 \pm 0.032 \pm 0.097) \times 10^{-4}$ which we divide by our best value $B(D^0 \to K^-\pi^+) = (3.89 \pm 0.04) \times 10^{-2}$. Our first error is their experiment's error and our second error is the systematic error from using our best value.
[9] ALAM 94 assume equal production of B^+ and B^0 at the $\Upsilon(4S)$ and use the CLEOII absolute $B(D^0 \to K^-\pi^+)$ and the PDG 1992 $B(D^0 \to K^-\pi^+\pi^0)/B(D^0 \to K^-\pi^+)$ and $B(D^0 \to K^-2\pi^+\pi^-)/B(D^0 \to K^-\pi^+)$.
[10] ALBRECHT 88K assumes $B^0\overline{B}^0$:B^+B^- ratio is 45:55. Superseded by ALBRECHT 90J.

$\Gamma(\overline{D}^0\rho^+)/\Gamma_{total}$ Γ_{51}/Γ

VALUE	EVTS	DOCUMENT ID		TECN	COMMENT
0.0134 ± 0.0018 OUR AVERAGE					
$0.0135\pm0.0012\pm0.0015$	212	[1] ALAM	94	CLE2	$e^+e^- \to \Upsilon(4S)$
$0.013\ \pm0.004\ \pm0.004$	19	[2] ALBRECHT	90J	ARG	$e^+e^- \to \Upsilon(4S)$
• • • We do not use the following data for averages, fits, limits, etc. • • •					
$0.021\ \pm0.008\ \pm0.009$	10	[3] ALBRECHT	88K	ARG	$e^+e^- \to \Upsilon(4S)$

[1] ALAM 94 assume equal production of B^+ and B^0 at the $\Upsilon(4S)$ and use the CLEOII absolute $B(D^0 \to K^-\pi^+)$ and the PDG 1992 $B(D^0 \to K^-\pi^+\pi^0)/B(D^0 \to K^-\pi^+)$ and $B(D^0 \to K^-2\pi^+\pi^-)/B(D^0 \to K^-\pi^+)$.
[2] Assumes equal production of B^+ and B^0 at the $\Upsilon(4S)$ and uses the MarkIII branching fractions for the D.
[3] ALBRECHT 88K assumes $B^0\overline{B}^0$:B^+B^- ratio is 45:55.

$\Gamma(\overline{D}^0K^+)/\Gamma(\overline{D}^0\pi^+)$ Γ_{52}/Γ_{48}

VALUE (units 10^{-2})	DOCUMENT ID		TECN	COMMENT
$7.75\ \pm0.15$ OUR AVERAGE	Error includes scale factor of 2.1. See the ideogram below.			
$7.768\pm0.038\pm0.066$	[1] AAIJ	18A	LHCB	pp at 7, 8, 13 TeV
$6.77\ \pm0.23\ \pm0.30$	HORII	08	BELL	$e^+e^- \to \Upsilon(4S)$
$8.31\ \pm0.35\ \pm0.20$	AUBERT	04N	BABR	$e^+e^- \to \Upsilon(4S)$
$9.9\ ^{+1.4}_{-1.2}\ ^{+0.7}_{-0.6}$	BORNHEIM	03	CLE2	$e^+e^- \to \Upsilon(4S)$
• • • We do not use the following data for averages, fits, limits, etc. • • •				
$7.79\ \pm0.06\ \pm0.19$	AAIJ	16L	LHCB	pp at 7, 8 TeV
$7.93\ \pm0.10\ \pm0.18$	[2] AAIJ	16L	LHCB	pp at 7, 8 TeV
$7.71\ \pm0.17\ \pm0.26$	[2] AAIJ	13AE	LHCB	Repl. by AAIJ 16L
$7.74\ \pm0.12\ \pm0.19$	AAIJ	12M	LHCB	Repl. by AAIJ 16L
$9.4\ \pm0.9\ \pm0.7$	ABE	03D	BELL	Repl. by SWAIN 03
$7.7\ \pm0.5\ \pm0.6$	SWAIN	03	BELL	Repl. by HORII 08
$7.9\ \pm0.9\ \pm0.6$	ABE	01I	BELL	Repl. by ABE 03D
$5.5\ \pm1.4\ \pm0.5$	ATHANAS	98	CLE2	Repl. by BORNHEIM 03

[1] Supersedes AAIJ 16L.
[2] Uses $B^{\pm} \to [K^{\pm}\pi^{\mp}\pi^+\pi^-]_D h^{\pm}$ mode.

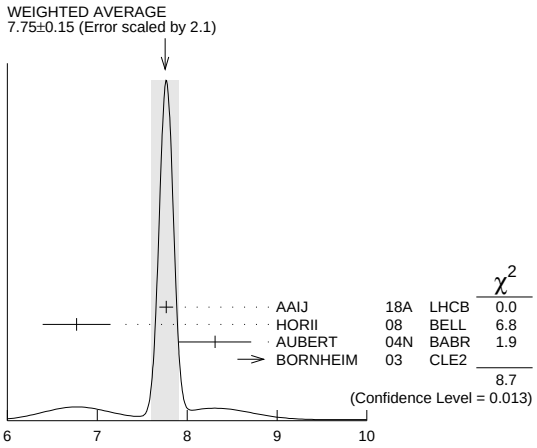

$\Gamma(D_{CP(+1)}K^+)/\Gamma(D_{CP(+1)}\pi^+)$ Γ_{53}/Γ_{49}

VALUE	DOCUMENT ID		TECN	COMMENT
0.088 ± 0.007 OUR AVERAGE				
$0.088\pm0.008\pm0.002$	[1,2] ABE	06	BELL	$e^+e^- \to \Upsilon(4S)$
$0.088\pm0.016\pm0.005$	[3] AUBERT	04N	BABR	$e^+e^- \to \Upsilon(4S)$
• • • We do not use the following data for averages, fits, limits, etc. • • •				
$0.125\pm0.036\pm0.010$	[3] ABE	03D	BELL	Repl. by SWAIN 03
$0.093\pm0.018\pm0.008$	[3] SWAIN	03	BELL	Repl. by ABE 06

[1] Reports a double ratio of $B(B^+ \to D_{CP(+1)}K^+)/B(B^+ \to D_{CP(+1)}\pi^+)$ and $B(B^+ \to \overline{D}^0K^+)/B(B^+ \to \overline{D}^0\pi^+)$, $1.13 \pm 0.16 \pm 0.08$. We multiply by our best value of $B(B^+ \to \overline{D}^0K^+)/B(B^+ \to \overline{D}^0\pi^+) = 0.083 \pm 0.006$. Our first error is their experiment's error and the second error is systematic error from using our best value.
[2] ABE 06 reports $[\Gamma(B^+ \to D_{CP(+1)}K^+)/\Gamma(B^+ \to D_{CP(+1)}\pi^+)] / [\Gamma(B^+ \to \overline{D}^0K^+)/\Gamma(B^+ \to \overline{D}^0\pi^+)] = 1.13 \pm 0.06 \pm 0.08$ which we multiply by our best value $\Gamma(B^+ \to \overline{D}^0K^+)/\Gamma(B^+ \to \overline{D}^0\pi^+) = 0.0775 \pm 0.0015$. Our first error is their experiment's error and our second error is the systematic error from using our best value.
[3] CP=+1 eigenstate of $D^0\overline{D}^0$ system is reconstructed via K^+K^- and $\pi^+\pi^-$.

$\Gamma(D_{CP(+1)}K^+)/\Gamma(\overline{D}^0K^+)$ Γ_{53}/Γ_{52}

VALUE	DOCUMENT ID		TECN	COMMENT
0.495 ± 0.007 OUR AVERAGE				
$0.494\pm0.008\pm0.006$	[1] AAIJ	18A	LHCB	pp at 7, 8, 13 TeV
$0.496\pm0.014\pm0.008$	[2] AAIJ	18A	LHCB	pp at 7, 8, 13 TeV
$0.489\pm0.010\pm0.009$	[3] AAIJ	16L	LHCB	pp at 7, 8 TeV
$0.65\ \pm0.12\ \pm0.06$	[4] AALTONEN	10A	CDF	$p\overline{p}$ at 1.96 TeV
$0.590\pm0.045\pm0.025$	[5] DEL-AMO-SA...10G		BABR	$e^+e^- \to \Upsilon(4S)$
• • • We do not use the following data for averages, fits, limits, etc. • • •				
$0.504\pm0.019\pm0.006$	[6] AAIJ	12M	LHCB	Repl. by AAIJ 16L
$0.53\ \pm0.05\ \pm0.025$	AUBERT	08AA	BABR	Repl. by DEL-AMO-SANCHEZ 10G
$0.45\ \pm0.06\ \pm0.02$	AUBERT	06J	BABR	Repl. by AUBERT 08AA

[1] Uses $D \to K^+K^-$ decay mode and reports $R_{CP+} = 0.988 \pm 0.015 \pm 0.011$ which we have divided by 2.
[2] Uses $D \to \pi^+\pi^-$ decay mode and reports $R_{CP+} = 0.992 \pm 0.027 \pm 0.015$ which we have divided by 2.
[3] AAIJ 16L reports $R_{CP+} = 0.978 \pm 0.019 \pm 0.018$ which we have divided by 2.
[4] Reports $R_{CP+} = 2\ (B(B^- \to D_{CP(+1)}K^-) + B(B^+ \to D_{CP(+1)}K^+)) / (B(B^- \to D^0K^-) + B(B^+ \to \overline{D}^0K^+)) = 1.30 \pm 0.24 \pm 0.12$ that we have divided by 2.
[5] Reports $R_{CP+} = 1.18 \pm 0.09 \pm 0.05$ that we have divided by 2.
[6] AAIJ 12M reports $R_{CP+} = 1.007 \pm 0.038 \pm 0.012$ which we have divided by 2.

$\Gamma(D_{CP(-1)}K^+)/\Gamma(D_{CP(-1)}\pi^+)$ Γ_{54}/Γ_{50}

VALUE	DOCUMENT ID		TECN	COMMENT
$0.097\pm0.016\pm0.007$	[1] ABE	06	BELL	$e^+e^- \to \Upsilon(4S)$
• • • We do not use the following data for averages, fits, limits, etc. • • •				
$0.119\pm0.028\pm0.006$	[2] ABE	03D	BELL	Repl. by SWAIN 03
$0.108\pm0.019\pm0.007$	[2] SWAIN	03	BELL	Repl. by ABE 06

[1] Reports a double ratio of $B(B^+ \to D_{CP(-1)}K^+)/B(B^+ \to D_{CP(-1)}\pi^+)$ and $B(B^+ \to \overline{D}^0K^+)/B(B^+ \to \overline{D}^0\pi^+)$, $1.17 \pm 0.14 \pm 0.14$. We multiply by our best value of $B(B^+ \to \overline{D}^0K^+)/B(B^+ \to \overline{D}^0\pi^+) = 0.083 \pm 0.006$. Our first error is their experiment's error and the second error is systematic error from using our best value.
[2] CP=−1 eigenstate of $D^0\overline{D}^0$ system is reconstructed via $K^0_S\pi^0$, $K^0_S\omega$, $K^0_S\phi$, $K^0_S\eta$, and $K^0_S\eta'$.

$\Gamma(D_{CP(-1)}K^+)/\Gamma(\overline{D}^0K^+)$ Γ_{54}/Γ_{52}

VALUE	DOCUMENT ID		TECN	COMMENT
$0.54\ \pm0.04\pm0.02$	[1] DEL-AMO-SA...10G		BABR	$e^+e^- \to \Upsilon(4S)$

• • • We do not use the following data for averages, fits, limits, etc. • • •

$0.515 \pm 0.05 \pm 0.025$		AUBERT	08AA	BABR	Repl. by DEL-AMO-SANCHEZ 10G
$0.43 \pm 0.05 \pm 0.02$		AUBERT	06J	BABR	Repl. by AUBERT 08AA

[1] Reports $R_{CP+} = 1.07 \pm 0.08 \pm 0.04$ that we have divided by 2.

$\Gamma([K^-\pi^+]_D K^+)/\Gamma_{\text{total}}$ Γ_{55}/Γ

VALUE	CL%	DOCUMENT ID		TECN	COMMENT
$< 2.8 \times 10^{-7}$	90	HORII	08	BELL	$e^+e^- \to \Upsilon(4S)$
• • • We do not use the following data for averages, fits, limits, etc. • • •					
$< 6.3 \times 10^{-7}$	90	SAIGO	05	BELL	$e^+e^- \to \Upsilon(4S)$

$\Gamma([K^-\pi^+]_D K^+)/\Gamma([K^+\pi^-]_D K^+)$ Γ_{55}/Γ_{56}

VALUE (units 10^{-3})	CL%	DOCUMENT ID		TECN	COMMENT
18.3 ± 1.4 OUR AVERAGE					
$18.8 \pm 1.1 \pm 1.0$		AAIJ	16L	LHCB	pp at 7, 8 TeV
$22.0 \pm 8.6 \pm 2.6$		[1] AALTONEN	11AJ	CDF	$p\overline{p}$ at 1.96 TeV
$16.3^{+4.4}_{-4.1} \pm 0.7 \pm 1.3$		HORII	11	BELL	$e^+e^- \to \Upsilon(4S)$
$11 \pm 6 \pm 2$		DEL-AMO-SA...10H		BABR	$e^+e^- \to \Upsilon(4S)$
• • • We do not use the following data for averages, fits, limits, etc. • • •					
$15.2 \pm 2.0 \pm 0.4$		AAIJ	12M	LHCB	Repl. by AAIJ 16L
$7.8^{+6.2}_{-5.7} \pm 2.0 \pm 2.8$		HORII	08	BELL	Repl. by HORII 11
< 29	90	[2] AUBERT	05G	BABR	Repl. by DEL-AMO-SANCHEZ 10H
< 44	90	[3] SAIGO	05	BELL	$e^+e^- \to \Upsilon(4S)$
< 26	90	[4] AUBERT,B	04L	BABR	Repl. by AUBERT 05G

[1] AALTONEN 11AJ also measures the ratio separately for B^+ ($R^+(K)$) and B^- ($R^-(K)$) and obtains: $R^+(K) = (42.6 \pm 13.7 \pm 2.8) \times 10^{-3}$, $R^-(K) = (3.8 \pm 10.3 \pm 2.7) \times 10^{-3}$.

[2] AUBERT 05G extract a constraint on the magnitude of the ratio of amplitudes $|A(B^+ \to D^0 K^+) / A(B^+ \to \overline{D}^0 K^+)| < 0.23$ at 90% CL (Bayesian). Similar measurements from $B^+ \to D^{*0} K^+$ are also reported.

[3] SAIGO 05 extract a constraint on the magnitude of the ratio of amplitudes $|A(B^+ \to D^0 K^+) / A(B^+ \to \overline{D}^0 K^+)| < 0.27$ at 90% CL.

[4] AUBERT,B 04L extract a constraint on the magnitude of the ratio of amplitudes $|A(B^+ \to D^0 K^+)/A(B^+ \to \overline{D}^0 K^+)| < 0.22$ at 90% CL.

$\Gamma([K^-\pi^+\pi^0]_D K^+)/\Gamma([K^+\pi^-\pi^0]_D K^+)$ Γ_{57}/Γ_{58}

VALUE (units 10^{-3})	CL%	DOCUMENT ID		TECN	COMMENT
16 ± 4 OUR AVERAGE					
$14.0 \pm 4.7 \pm 2.1$		[1] AAIJ	15W	LHCB	pp at 7, 8 TeV
$19.8 \pm 6.2 \pm 2.4$		NAYAK	13	BELL	$e^+e^- \to \Upsilon(4S)$
• • • We do not use the following data for averages, fits, limits, etc. • • •					
< 21	90	[2] LEES	11D	BABR	$e^+e^- \to \Upsilon(4S)$
< 39	95	[3] AUBERT	07BN	BABR	Repl. by LEES 11D

[1] Uses $D^0 \to K^-\pi^+\pi^0$ for the favored mode, and $D^0 \to K^+\pi^-\pi^0$ for the suppressed mode.

[2] Extracts a constraint on the magnitude of the ratio of amplitudes $|A(B^+ \to D^0 K^+)/A(B^+ \to \overline{D}^0 K^+)| < 0.13$ at 95% CL.

[3] Extracts a constraint on the magnitude of the ratio of amplitudes $|A(B^+ \to D^0 K^+)/A(B^+ \to \overline{D}^0 K^+)| < 0.19$ at 95% CL.

$\Gamma([K^-\pi^+\pi^+\pi^-]_D K^+)/\Gamma([K^+\pi^-\pi^+\pi^-]_D K^+)$ Γ_{59}/Γ_{60}

VALUE (units 10^{-2})	DOCUMENT ID		TECN	COMMENT
$1.40 \pm 0.15 \pm 0.06$	AAIJ	16L	LHCB	pp at 7, 8 TeV
• • • We do not use the following data for averages, fits, limits, etc. • • •				
1.24 ± 0.27	AAIJ	13AE	LHCB	Repl. by AAIJ 16L

$\Gamma([\pi^+\pi^+\pi^-\pi^-]K^+)/\Gamma([K^+\pi^-\pi^+\pi^-]_D K^+)$ Γ_{61}/Γ_{60}

VALUE	DOCUMENT ID		TECN	COMMENT
$0.975 \pm 0.037 \pm 0.019$	AAIJ	16L	LHCB	pp at 7, 8 TeV

$\Gamma([K^-\pi^+]_D K^*(892)^+)/\Gamma([K^+\pi^-]_D K^*(892)^+)$ Γ_{63}/Γ_{64}

VALUE	DOCUMENT ID		TECN	COMMENT
0.012 ± 0.004 OUR AVERAGE				
$0.011 \pm 0.004 \pm 0.001$	AAIJ	17BO	LHCB	pp at 7, 8, 13 TeV
$0.066 \pm 0.031 \pm 0.010$	AUBERT	09AJ	BABR	$e^+e^- \to \Upsilon(4S)$
• • • We do not use the following data for averages, fits, limits, etc. • • •				
$0.046 \pm 0.031 \pm 0.008$	AUBERT,B	05V	BABR	Repl. by AUBERT 09AJ

$\Gamma([K^-\pi^+\pi^-\pi^+]_D K^*(892)^+)/\Gamma([K^+\pi^-\pi^+\pi^-]_D K^*(892)^+)$ Γ_{65}/Γ_{66}

VALUE	DOCUMENT ID		TECN	COMMENT
$0.011 \pm 0.005 \pm 0.003$	AAIJ	17BO	LHCB	pp at 7, 8, 13 TeV

$\Gamma([\pi^+\pi^-\pi^+\pi^-]_D K^*(892)^+)/\Gamma([K^+\pi^-\pi^+\pi^-]_D K^*(892)^+)$ Γ_{62}/Γ_{66}

VALUE	DOCUMENT ID		TECN	COMMENT
$1.08 \pm 0.13 \pm 0.03$	AAIJ	17BO	LHCB	pp at 7, 8, 13 TeV

$\Gamma([K^-\pi^+]_D \pi^+)/\Gamma_{\text{total}}$ Γ_{67}/Γ

VALUE (units 10^{-7})	DOCUMENT ID		TECN	COMMENT
$6.29^{+1.02}_{-0.98} \pm 0.37 \pm 0.48$	HORII	08	BELL	$e^+e^- \to \Upsilon(4S)$
• • • We do not use the following data for averages, fits, limits, etc. • • •				
$6.6^{+1.9}_{-1.7} \pm 0.5$	SAIGO	05	BELL	Repl. by HORII 08

$\Gamma([K^-\pi^+]_D \pi^+)/\Gamma([K^+\pi^-]_D \pi^+)$ Γ_{67}/Γ_{68}

VALUE (units 10^{-3})	DOCUMENT ID		TECN	COMMENT
3.53 ± 0.14 OUR AVERAGE				
$3.60 \pm 0.12 \pm 0.09$	AAIJ	16L	LHCB	pp at 7, 8 TeV
$2.8 \pm 0.7 \pm 0.4$	[1] AALTONEN	11AJ	CDF	$p\overline{p}$ at 1.96 TeV
$3.28^{+0.38}_{-0.36} \pm 0.12 \pm 0.18$	HORII	11	BELL	$e^+e^- \to \Upsilon(4S)$
$3.3 \pm 0.6 \pm 0.4$	DEL-AMO-SA...10H		BABR	$e^+e^- \to \Upsilon(4S)$
• • • We do not use the following data for averages, fits, limits, etc. • • •				
$4.10 \pm 0.25 \pm 0.05$	AAIJ	12M	LHCB	Repl. by AAIJ 16L
$3.40^{+0.55}_{-0.53} \pm 0.15 \pm 0.22$	HORII	08	BELL	Repl. by HORII 11
$3.5^{+1.0}_{-0.9} \pm 0.2$	SAIGO	05	BELL	Repl. by HORII 08

[1] AALTONEN 11AJ also measures the ratio separately for B^+ ($R^+(\pi)$) and B^- ($R^-(\pi)$) and obtains: $R^+(\pi) = (2.4 \pm 1.0 \pm 0.4) \times 10^{-3}$, $R^-(K) = (3.1 \pm 1.1 \pm 0.4) \times 10^{-3}$.

$\Gamma([K^-\pi^+\pi^0]_D \pi^+)/\Gamma([K^+\pi^-\pi^0]_D \pi^+)$ Γ_{69}/Γ_{70}

VALUE (units 10^{-3})	DOCUMENT ID		TECN	COMMENT
2.2 ± 0.4 OUR AVERAGE				
$2.35 \pm 0.49 \pm 0.06$	[1] AAIJ	15W	LHCB	pp at 7, 8 TeV
$1.89 \pm 0.54^{+0.22}_{-0.25}$	NAYAK	13	BELL	$e^+e^- \to \Upsilon(4S)$

[1] Uses $D^0 \to K^-\pi^+\pi^0$ for the favored mode, and $D^0 \to K^+\pi^-\pi^0$ for the suppressed mode.

$\Gamma([K^-\pi^+\pi^+\pi^-]_D \pi^+)/\Gamma([K^+\pi^-\pi^+\pi^-]_D \pi^+)$ Γ_{71}/Γ_{72}

VALUE (units 10^{-3})	DOCUMENT ID		TECN	COMMENT
$3.77 \pm 0.18 \pm 0.06$	AAIJ	16L	LHCB	pp at 7, 8 TeV
• • • We do not use the following data for averages, fits, limits, etc. • • •				
3.7 ± 0.4	AAIJ	13AE	LHCB	Repl. by AAIJ 16L

$\Gamma([K^-\pi^+]_{(D\pi)}\pi^+)/\Gamma([K^+\pi^-]_{(D\pi)}\pi^+)$ Γ_{73}/Γ_{74}

VALUE (units 10^{-3})	DOCUMENT ID		TECN	COMMENT
$3.2 \pm 0.9 \pm 0.8$	DEL-AMO-SA...10H		BABR	$e^+e^- \to \Upsilon(4S)$

$\Gamma([K^-\pi^+]_{(D\gamma)}\pi^+)/\Gamma([K^+\pi^-]_{(D\gamma)}\pi^+)$ Γ_{75}/Γ_{76}

VALUE (units 10^{-3})	DOCUMENT ID		TECN	COMMENT
$2.7 \pm 1.4 \pm 2.2$	DEL-AMO-SA...10H		BABR	$e^+e^- \to \Upsilon(4S)$

$\Gamma([K^-\pi^+]_{(D\pi)}K^+)/\Gamma([K^+\pi^-]_{(D\pi)}K^+)$ Γ_{77}/Γ_{78}

VALUE (units 10^{-3})	DOCUMENT ID		TECN	COMMENT
$1.8 \pm 0.9 \pm 0.4$	DEL-AMO-SA...10H		BABR	$e^+e^- \to \Upsilon(4S)$

$\Gamma([K^-\pi^+]_{(D\gamma)}K^+)/\Gamma([K^+\pi^-]_{(D\gamma)}K^+)$ Γ_{79}/Γ_{80}

VALUE (units 10^{-3})	DOCUMENT ID		TECN	COMMENT
$1.3 \pm 1.4 \pm 0.8$	DEL-AMO-SA...10H		BABR	$e^+e^- \to \Upsilon(4S)$

$\Gamma([\pi^+\pi^-\pi^0]_D K^-)/\Gamma_{\text{total}}$ Γ_{81}/Γ

VALUE (units 10^{-6})	DOCUMENT ID		TECN	COMMENT
$4.6 \pm 0.8 \pm 0.4$	[1] AUBERT	07BJ	BABR	$e^+e^- \to \Upsilon(4S)$
• • • We do not use the following data for averages, fits, limits, etc. • • •				
$5.5 \pm 1.0 \pm 0.7$	[1] AUBERT,B	05T	BABR	Repl. by AUBERT 07BJ

[1] Assumes equal production of B^+ and B^0 at the $\Upsilon(4S)$.

$\Gamma([K^0_S K^+\pi^-]_D K^+)/\Gamma([K^0_S K^+\pi^-]_D \pi^+)$ Γ_{82}/Γ_{87}

VALUE	DOCUMENT ID		TECN	COMMENT
$0.092 \pm 0.009 \pm 0.004$	[1] AAIJ	14V	LHCB	pp at 7, 8 TeV

[1] The anaysis uses all of $D \to K^0_S K\pi$ Dalitz decays.

$\Gamma([K^0_S K^-\pi^+]_D K^+)/\Gamma([K^0_S K^-\pi^+]_D \pi^+)$ Γ_{83}/Γ_{85}

VALUE	DOCUMENT ID		TECN	COMMENT
$0.066 \pm 0.009 \pm 0.002$	[1] AAIJ	14V	LHCB	pp at 7, 8 TeV

[1] The anaysis uses all of $D \to K^0_S K\pi$ Dalitz decays.

$\Gamma([K^0_S K^-\pi^+]_D K^+)/\Gamma([K^0_S K^+\pi^-]_D \pi^+)$ Γ_{83}/Γ_{87}

VALUE	DOCUMENT ID		TECN	COMMENT
$0.084 \pm 0.011 \pm 0.003$	[1] AAIJ	14V	LHCB	pp at 7, 8 TeV

[1] The Analysis uses $D \to K^*(892)\,K \to K^0_S K\pi$ decays.

$\Gamma([K^*(892)^+K^-]_D K^+)/\Gamma([K^*(892)^-K^+]_D \pi^+)$ Γ_{84}/Γ_{88}

VALUE	DOCUMENT ID		TECN	COMMENT
$0.056 \pm 0.013 \pm 0.002$	[1] AAIJ	14V	LHCB	pp at 7, 8 TeV

[1] The Analysis uses $D \to K^*(892)\,K \to K^0_S K\pi$ decays.

$\Gamma([K^+K^-\pi^0]_D K^+)/\Gamma([K^+K^-\pi^0]_D \pi^+)$ Γ_{89}/Γ_{90}

VALUE	DOCUMENT ID		TECN	COMMENT
$0.95 \pm 0.22 \pm 0.05$	[1] AAIJ	15W	LHCB	pp at 7, 8 TeV

[1] Uses $D \to K^+K^-\pi^0$ mode.

$\Gamma([\pi^+\pi^-\pi^0]_D K^+)/\Gamma([\pi^+\pi^-\pi^0]_D\pi^+)$ Γ_{91}/Γ_{92}

VALUE	DOCUMENT ID		TECN	COMMENT
0.98±0.11±0.05	[1] AAIJ	15W	LHCB	pp at 7, 8 TeV

[1] Uses $D \to \pi^+\pi^-\pi^0$ mode.

$\Gamma([K^0_S K^+\pi^-]_D\pi^+)/\Gamma([K^0_S K^-\pi^+]_D\pi^+)$ Γ_{87}/Γ_{85}

VALUE	DOCUMENT ID		TECN	COMMENT
1.528±0.058±0.025	[1] AAIJ	14V	LHCB	pp at 7, 8 TeV

[1] The anaysis uses all of $D \to K^0_S K\pi$ Dalitz decays.

$\Gamma([K^*(892)^- K^+]_D\pi^+)/\Gamma([K^*(892)^+ K^-]_D\pi^+)$ Γ_{88}/Γ_{86}

VALUE	DOCUMENT ID		TECN	COMMENT
2.57±0.13±0.06	[1] AAIJ	14V	LHCB	pp at 7, 8 TeV

[1] The Analysis uses $D \to K^*(892)\,K \to K^0_S K\pi$ decays.

$\Gamma(\overline{D}^0 K^*(892)^+)/\Gamma_{\text{total}}$ Γ_{93}/Γ

VALUE (units 10^{-4})	DOCUMENT ID		TECN	COMMENT
5.3 ±0.4 OUR AVERAGE				
5.29±0.30±0.34	[1] AUBERT	06Z	BABR	$e^+e^- \to \Upsilon(4S)$
6.1 ±1.6 ±1.7	[1] MAHAPATRA	02	CLE2	$e^+e^- \to \Upsilon(4S)$
• • • We do not use the following data for averages, fits, limits, etc. • • •				
6.3 ±0.7 ±0.5	[1] AUBERT	04Q	BABR	Repl. by AUBERT 06Z

[1] Assumes equal production of B^+ and B^0 at the $\Upsilon(4S)$.

$\Gamma(D_{CP(-1)} K^*(892)^+)/\Gamma(\overline{D}^0 K^*(892)^+)$ Γ_{94}/Γ_{93}

VALUE	DOCUMENT ID		TECN	COMMENT
0.515±0.135±0.065	[1] AUBERT	09AJ	BABR	$e^+e^- \to \Upsilon(4S)$
• • • We do not use the following data for averages, fits, limits, etc. • • •				
0.325±0.13 ±0.04	[2] AUBERT,B	05U	BABR	Repl. by AUBERT 09AJ

[1] The authors report R_{CP-}= 1.03 ± 0.27 ± 0.13 which is, assuming CP conservation, twice the value of the quoted above branching ratio,

[2] The authors report R_{CP-}= 0.65 ± 0.26 ± 0.08 which is, assuming CP conservation, twice the value of the quoted above branching ratio.

$\Gamma(D_{CP(+1)} K^*(892)^+)/\Gamma(\overline{D}^0 K^*(892)^+)$ Γ_{95}/Γ_{93}

VALUE	DOCUMENT ID		TECN	COMMENT
1.16 ±0.07 OUR AVERAGE				
1.18 ±0.08 ±0.01	[1] AAIJ	17BO	LHCB	pp at 7, 8, 13 TeV
1.085±0.175±0.045	[2] AUBERT	09AJ	BABR	$e^+e^- \to \Upsilon(4S)$
• • • We do not use the following data for averages, fits, limits, etc. • • •				
0.98 ±0.20 ±0.055	[3] AUBERT,B	05U	BABR	Repl. by AUBERT 09AJ

[1] Measures the ratio separately for K^+K^- and $\pi^+\pi^-$ final states, $R_{KK} = 1.22\pm0.09\pm0.01$ and $R_{\pi\pi} = 1.08 \pm 0.14 \pm 0.03$, and combines the two results.

[2] The authors report R_{CP+}= 2.17 ± 0.35 ± 0.09 which is, assuming CP conservation, twice the value of the quoted above branching ratio,

[3] The authors report R_{CP+}= 1.96 ± 0.40 ± 0.11 which is, assuming CP conservation, twice the value of the quoted above branching ratio.

$\Gamma(\overline{D}^0 K^+\pi^+\pi^-)/\Gamma(\overline{D}^0\pi^+\pi^+\pi^-)$ Γ_{96}/Γ_{102}

VALUE (units 10^{-2})	DOCUMENT ID		TECN	COMMENT
9.4±1.3±0.9	AAIJ	12T	LHCB	pp at 7 TeV

$\Gamma(D_{CP(+1)} K^+\pi^-\pi^+)/\Gamma([K^+\pi^-]_D K^+\pi^-\pi^+)$ Γ_{99}/Γ_{97}

VALUE	DOCUMENT ID		TECN	COMMENT
1.040±0.064	AAIJ	15BC	LHCB	pp at 7, 8 TeV

$\Gamma([K^-\pi^+]_D K^+\pi^-\pi^+)/\Gamma([K^+\pi^-]_D K^+\pi^-\pi^+)$ Γ_{98}/Γ_{97}

VALUE (units 10^{-4})	DOCUMENT ID		TECN	COMMENT
85^{+36}_{-33}	AAIJ	15BC	LHCB	pp at 7, 8 TeV

$\Gamma(\overline{D}^0 K^+\overline{K}^0)/\Gamma_{\text{total}}$ Γ_{100}/Γ

VALUE (units 10^{-4})	DOCUMENT ID		TECN	COMMENT
5.5±1.4±0.8	[1] DRUTSKOY	02	BELL	$e^+e^- \to \Upsilon(4S)$

[1] Assumes equal production of B^+ and B^0 at the $\Upsilon(4S)$.

$\Gamma(\overline{D}^0 K^+\overline{K}^*(892)^0)/\Gamma_{\text{total}}$ Γ_{101}/Γ

VALUE (units 10^{-4})	DOCUMENT ID		TECN	COMMENT
7.5±1.3±1.1	[1] DRUTSKOY	02	BELL	$e^+e^- \to \Upsilon(4S)$

[1] Assumes equal production of B^+ and B^0 at the $\Upsilon(4S)$.

$\Gamma(\overline{D}^0\pi^+\pi^+\pi^-)/\Gamma_{\text{total}}$ Γ_{102}/Γ

VALUE	DOCUMENT ID		TECN	COMMENT
0.0056±0.0021 OUR FIT Error includes scale factor of 3.6.				
0.0115±0.0029±0.0021	[1] BORTOLETTO92		CLEO	$e^+e^- \to \Upsilon(4S)$

[1] BORTOLETTO 92 assumes equal production of B^+ and B^0 at the $\Upsilon(4S)$ and uses Mark III branching fractions for the D.

$\Gamma(\overline{D}^0\pi^+\pi^+\pi^-)/\Gamma(\overline{D}^0\pi^+)$ Γ_{102}/Γ_{48}

VALUE	DOCUMENT ID		TECN	COMMENT
1.2 ±0.4 OUR FIT Error includes scale factor of 3.7.				
1.27±0.06±0.11	AAIJ	11E	LHCB	pp at 7 TeV

$\Gamma([K^-\pi^+]_D\pi^+\pi^-\pi^+)/\Gamma([K^+\pi^-]_D K^+\pi^-\pi^+)$ Γ_{103}/Γ_{97}

VALUE (units 10^{-4})	DOCUMENT ID		TECN	COMMENT
42.7±5.6	AAIJ	15BC	LHCB	pp at 7, 8 TeV

$\Gamma(\overline{D}^0\pi^+\pi^+\pi^-$ nonresonant$)/\Gamma_{\text{total}}$ Γ_{104}/Γ

VALUE	DOCUMENT ID		TECN	COMMENT
0.0051±0.0034±0.0023	[1] BORTOLETTO92		CLEO	$e^+e^- \to \Upsilon(4S)$

[1] BORTOLETTO 92 assumes equal production of B^+ and B^0 at the $\Upsilon(4S)$ and uses Mark III branching fractions for the D.

$\Gamma(\overline{D}^0\pi^+\rho^0)/\Gamma_{\text{total}}$ Γ_{105}/Γ

VALUE	DOCUMENT ID		TECN	COMMENT
0.0042±0.0023±0.0020	[1] BORTOLETTO92		CLEO	$e^+e^- \to \Upsilon(4S)$

[1] BORTOLETTO 92 assumes equal production of B^+ and B^0 at the $\Upsilon(4S)$ and uses Mark III branching fractions for the D.

$\Gamma(\overline{D}^0 a_1(1260)^+)/\Gamma_{\text{total}}$ Γ_{106}/Γ

VALUE	DOCUMENT ID		TECN	COMMENT
0.0045±0.0019±0.0031	[1] BORTOLETTO92		CLEO	$e^+e^- \to \Upsilon(4S)$

[1] BORTOLETTO 92 assumes equal production of B^+ and B^0 at the $\Upsilon(4S)$ and uses Mark III branching fractions for the D.

$\Gamma(\overline{D}^0\omega\pi^+)/\Gamma_{\text{total}}$ Γ_{107}/Γ

VALUE	DOCUMENT ID		TECN	COMMENT
0.0041±0.0007±0.0006	[1] ALEXANDER	01B	CLE2	$e^+e^- \to \Upsilon(4S)$

[1] Assumes equal production of B^+ and B^0 at the $\Upsilon(4S)$. The signal is consistent with all observed $\omega\pi^+$ having proceeded through the ρ'^+ resonance at mass $1349 \pm 25^{+10}_{-5}$ MeV and width $547 \pm 86^{+46}_{-45}$ MeV.

$\Gamma(D^*(2010)^-\pi^+\pi^+)/\Gamma_{\text{total}}$ Γ_{108}/Γ

VALUE (units 10^{-3})	CL%	EVTS	DOCUMENT ID		TECN	COMMENT
1.35±0.22 OUR AVERAGE						
1.25±0.08±0.22			[1] ABE	04D	BELL	$e^+e^- \to \Upsilon(4S)$
1.9 ±0.7 ±0.3		14	[2] ALAM	94	CLE2	$e^+e^- \to \Upsilon(4S)$
2.6 ±1.4 ±0.7		11	[3] ALBRECHT	90J	ARG	$e^+e^- \to \Upsilon(4S)$
$2.4\ ^{+1.7}_{-1.6}\ ^{+1.0}_{-0.6}$		3	[4] BEBEK	87	CLEO	$e^+e^- \to \Upsilon(4S)$
• • • We do not use the following data for averages, fits, limits, etc. • • •						
<4.	90		[5] BORTOLETTO92		CLEO	$e^+e^- \to \Upsilon(4S)$
5. ±2. ±3.		7	[6] ALBRECHT	87C	ARG	$e^+e^- \to \Upsilon(4S)$

[1] Assumes equal production of B^+ and B^0 at the $\Upsilon(4S)$.

[2] ALAM 94 assume equal production of B^+ and B^0 at the $\Upsilon(4S)$ and use the CLEO II $B(D^*(2010)^+ \to D^0\pi^+)$ and absolute $B(D^0 \to K^-\pi^+)$ and the PDG 1992 $B(D^0 \to K^-\pi^+\pi^0)/B(D^0 \to K^-\pi^+)$ and $B(D^0 \to K^-2\pi^+\pi^-)/B(D^0 \to K^-\pi^+)$.

[3] Assumes equal production of B^+ and B^0 at the $\Upsilon(4S)$ and uses the Mark III branching fractions for the D.

[4] BEBEK 87 value has been updated in BERKELMAN 91 to use same assumptions as noted for BORTOLETTO 92.

[5] BORTOLETTO 92 assumes equal production of B^+ and B^0 at the $\Upsilon(4S)$ and uses Mark III branching fractions for the D and $D^*(2010)$. The authors also find the product branching fraction into $D^{**}\pi$ followed by $D^{**} \to D^*(2010)\pi$ to be $0.0014^{+0.0008}_{-0.0006} \pm 0.0003$ where D^{**} represents all orbitally excited D mesons.

[6] ALBRECHT 87C use PDG 86 branching ratios for D and $D^*(2010)$ and assume $B(\Upsilon(4S) \to B^+B^-) = 55\%$ and $B(\Upsilon(4S) \to B^0\overline{B}^0) = 45\%$. Superseded by ALBRECHT 90J.

$\Gamma(D^*(2010)^- K^+\pi^+)/\Gamma_{\text{total}}$ Γ_{109}/Γ

VALUE (units 10^{-5})	DOCUMENT ID		TECN	COMMENT
8.2±0.3±1.4	[1] AAIJ	17AR	LHCB	pp at 7 , 8 TeV

[1] The branching fraction of the normalization mode $B^+ \to D^{*-}\pi^+\pi^+$ is rescaled to the updated ratio of $\Upsilon(4S) \to B^+B^-$ to $\Upsilon(4S) \to B^0\overline{B}^0$ decay rates of 1.058 ± 0.024.

$\Gamma(D^*(2010)^- K^+\pi^+)/\Gamma(D^*(2010)^-\pi^+\pi^+)$ $\Gamma_{109}/\Gamma_{108}$

VALUE (units 10^{-2})	DOCUMENT ID		TECN	COMMENT
6.39±0.27±0.48	[1] AAIJ	17AR	LHCB	pp at 7, 8 TeV

[1] Uses $D^{*-} \to \overline{D}^0\pi^-$ and $\overline{D}^0 \to K^+\pi^-$ decays.

$\Gamma(\overline{D}_1(2420)^0\pi^+,\ \overline{D}^0_1 \to D^*(2010)^-\pi^+)/\Gamma(\overline{D}^0\pi^+\pi^+\pi^-)$ $\Gamma_{110}/\Gamma_{102}$

VALUE (units 10^{-2})	DOCUMENT ID		TECN	COMMENT
9.3±1.6±0.9	[1] AAIJ	11E	LHCB	pp at 7 TeV

[1] AAIJ 11E reports $(9.3 \pm 1.6 \pm 0.9) \times 10^{-2}$ from a measurement of $[\Gamma(B^+ \to \overline{D}_1(2420)^0\pi^+,\ \overline{D}^0_1 \to D^*(2010)^-\pi^+)/\Gamma(B^+ \to \overline{D}^0\pi^+\pi^+\pi^-)] \times [B(D^*(2010)^+ \to D^0\pi^+)]$ assuming $B(D^*(2010)^+ \to D^0\pi^+) = (67.7\pm0.5)\times10^{-2}$.

$\Gamma(D^-\pi^+\pi^+)/\Gamma_{\text{total}}$ Γ_{111}/Γ

VALUE (units 10^{-3})	CL%	EVTS	DOCUMENT ID		TECN	COMMENT
1.07±0.05 OUR AVERAGE						
1.08±0.03±0.05			[1] AUBERT	09AB	BABR	$e^+e^- \to \Upsilon(4S)$
1.02±0.04±0.15			[1] ABE	04D	BELL	$e^+e^- \to \Upsilon(4S)$

• • • We do not use the following data for averages, fits, limits, etc. • • •

<1.4	90	[2]	ALAM	94	CLE2	$e^+e^- \to \Upsilon(4S)$
<7	90	[3]	BORTOLETTO	92	CLEO	$e^+e^- \to \Upsilon(4S)$
$2.5\ ^{+4.1}_{-2.3}\ ^{+2.4}_{-0.8}$	1	[4]	BEBEK	87	CLEO	$e^+e^- \to \Upsilon(4S)$

[1] Assumes equal production of B^+ and B^0 at the $\Upsilon(4S)$.
[2] ALAM 94 assume equal production of B^+ and B^0 at the $\Upsilon(4S)$ and use the Mark III $B(D^+ \to K^-2\pi^+)$.
[3] BORTOLETTO 92 assumes equal production of B^+ and B^0 at the $\Upsilon(4S)$ and uses Mark III branching fractions for the D. The product branching fraction into $D_0^*(2340)\pi$ followed by $D_0^*(2340) \to D\pi$ is < 0.005 at 90%CL and into $D_2^*(2460)$ followed by $D_2^*(2460) \to D\pi$ is < 0.004 at 90%CL.
[4] BEBEK 87 assume the $\Upsilon(4S)$ decays 43% to $B^0\overline{B}^0$. $B(D^- \to K^+\pi^-\pi^-) = (9.1 \pm 1.3 \pm 0.4)\%$ is assumed.

$\Gamma(D^-K^+\pi^+)/\Gamma(D^-\pi^+\pi^+)$ $\Gamma_{112}/\Gamma_{111}$

VALUE (units 10^{-2})	DOCUMENT ID		TECN	COMMENT
7.20±0.19±0.21	AAIJ	15V	LHCB	pp at 7, 8 TeV

$\Gamma(D_0^*(2400)^0K^+,\ D_0^{*0} \to D^-\pi^+)/\Gamma_{\text{total}}$ Γ_{113}/Γ

VALUE (units 10^{-6})	DOCUMENT ID		TECN	COMMENT
6.1±1.9±1.5	[1] AAIJ	15V	LHCB	pp at 7, 8 TeV

[1] Performs the amplitude analysis by fitting the square-Dalitz-plot distribution.

$\Gamma(D_2^*(2460)^0K^+,\ D_2^{*0} \to D^-\pi^+)/\Gamma_{\text{total}}$ Γ_{114}/Γ

VALUE (units 10^{-6})	DOCUMENT ID		TECN	COMMENT
23.2±1.1±2.0	[1] AAIJ	15V	LHCB	pp at 7, 8 TeV

[1] Performs the amplitude analysis by fitting the square-Dalitz-plot distribution.

$\Gamma(D_1^*(2760)^0K^+,\ D_1^{*0} \to D^-\pi^+)/\Gamma_{\text{total}}$ Γ_{115}/Γ

VALUE (units 10^{-6})	DOCUMENT ID		TECN	COMMENT
3.6±0.9±0.8	[1] AAIJ	15V	LHCB	pp at 7, 8 TeV

[1] Performs the amplitude analysis by fitting the square-Dalitz-plot distribution.

$\Gamma(D^+K^0)/\Gamma_{\text{total}}$ Γ_{116}/Γ

VALUE (units 10^{-6})	CL%	DOCUMENT ID		TECN	COMMENT
<2.9	90	[1] DEL-AMO-SA...10K		BABR	$e^+e^- \to \Upsilon(4S)$
• • • We do not use the following data for averages, fits, limits, etc. • • •					
<5.0	90	[1] AUBERT,B	05E	BABR	Repl. by DEL-AMO-SANCHEZ 10K

[1] Assumes equal production of B^+ and B^0 at the $\Upsilon(4S)$.

$\Gamma(D^+K^+\pi^-)/\Gamma(D^-K^+\pi^+)$ $\Gamma_{117}/\Gamma_{112}$

VALUE (units 10^{-2})	DOCUMENT ID		TECN	COMMENT
7.3±1.2±0.7	AAIJ	16M	LHCB	pp at 7, 8 TeV

$\Gamma(D_2^*(2460)^0K^+,\ D_2^{*0} \to D^+\pi^-)/\Gamma_{\text{total}}$ Γ_{118}/Γ

VALUE	CL%	DOCUMENT ID		TECN	COMMENT
$<6.3 \times 10^{-7}$	90	AAIJ	16R	LHCB	pp at 7, 8 TeV

$\Gamma(D^+K^{*0})/\Gamma_{\text{total}}$ Γ_{119}/Γ

VALUE	CL%	DOCUMENT ID		TECN	COMMENT
$<4.9 \times 10^{-7}$	90	AAIJ	16M	LHCB	pp at 7, 8 TeV
• • • We do not use the following data for averages, fits, limits, etc. • • •					
$<1.8 \times 10^{-6}$	90	AAIJ	13R	LHCB	Repl. by AAIJ 16M
$<3.0 \times 10^{-6}$	90	[1] DEL-AMO-SA...10K		BABR	$e^+e^- \to \Upsilon(4S)$

[1] Assumes equal production of B^+ and B^0 at the $\Upsilon(4S)$.

$\Gamma(D^+\overline{K}^{*0})/\Gamma_{\text{total}}$ Γ_{120}/Γ

VALUE (units 10^{-6})	CL%	DOCUMENT ID		TECN	COMMENT
<1.4	90	AAIJ	13R	LHCB	pp at 7 TeV

$\Gamma(\overline{D}^*(2007)^0\pi^+)/\Gamma_{\text{total}}$ Γ_{121}/Γ

VALUE (units 10^{-3})	EVTS	DOCUMENT ID		TECN	COMMENT
4.90 ±0.17 OUR AVERAGE					
4.664±0.029±0.268		AAIJ	18A	LHCB	pp at 7, 8, 13 TeV
4.82 ±0.12 ±0.35		[1] KATO	18	BELL	$e^+e^- \to \Upsilon(4S)$
5.52 ±0.17 ±0.42		[2] AUBERT	07H	BABR	$e^+e^- \to \Upsilon(4S)$
5.3 ±0.4 ±0.1		[3,4] AUBERT,BE	06J	BABR	$e^+e^- \to \Upsilon(4S)$
4.34 ±0.47 ±0.18		[5] BRANDENB...	98	CLE2	$e^+e^- \to \Upsilon(4S)$
5.2 ±0.7 ±0.7	71	[6] ALAM	94	CLE2	$e^+e^- \to \Upsilon(4S)$
7.2 ±1.8 ±1.6		[7] BORTOLETTO	92	CLEO	$e^+e^- \to \Upsilon(4S)$
4.0 ±1.4 ±1.2	9	[7] ALBRECHT	90J	ARG	$e^+e^- \to \Upsilon(4S)$
• • • We do not use the following data for averages, fits, limits, etc. • • •					
2.7 ±4.4		[8] BEBEK	87	CLEO	$e^+e^- \to \Upsilon(4S)$

[1] Measures absolute branching fractions using a missing-mass technique.
[2] Assumes equal production of B^+ and B^0 at the $\Upsilon(4S)$.
[3] AUBERT,BE 06J reports $[\Gamma(B^+ \to \overline{D}^*(2007)^0\pi^+)/\Gamma_{\text{total}}] / [B(B^+ \to \overline{D}^0\pi^+)] = 1.14 \pm 0.07 \pm 0.04$ which we multiply by our best value $B(B^+ \to \overline{D}^0\pi^+) = (4.68 \pm 0.13) \times 10^{-3}$. Our first error is their experiment's error and our second error is the systematic error from using our best value.
[4] Uses a missing-mass method. Does not depend on D branching fractions or B^+/B^0 production rates.
[5] BRANDENBURG 98 assume equal production of B^+ and B^0 at $\Upsilon(4S)$ and use the D^* reconstruction technique. The first error is their experiment's error and the second error is the systematic error from the PDG 96 value of $B(D^* \to D\pi)$.
[6] ALAM 94 assume equal production of B^+ and B^0 at the $\Upsilon(4S)$ and use the CLEO II $B(D^*(2007)^0 \to D^0\pi^0)$ and absolute $B(D^0 \to K^-\pi^+)$ and the PDG 1992 $B(D^0 \to K^-\pi^+\pi^0)/B(D^0 \to K^-\pi^+)$ and $B(D^0 \to K^-2\pi^+\pi^-)/B(D^0 \to K^-\pi^+)$.
[7] Assumes equal production of B^+ and B^0 at the $\Upsilon(4S)$ and uses Mark III branching fractions for the D and $D^*(2010)$.
[8] This is a derived branching ratio, using the inclusive pion spectrum and other two-body B decays. BEBEK 87 assume the $\Upsilon(4S)$ decays 43% to $B^0\overline{B}^0$.

$\Gamma(\overline{D}^*(2007)^0\omega\pi^+)/\Gamma_{\text{total}}$ Γ_{124}/Γ

VALUE	DOCUMENT ID		TECN	COMMENT
0.0045±0.0010±0.0007	[1] ALEXANDER	01B	CLE2	$e^+e^- \to \Upsilon(4S)$

[1] Assumes equal production of B^+ and B^0 at the $\Upsilon(4S)$. The signal is consistent with all observed $\omega\pi^+$ having proceeded through the ρ'^+ resonance at mass $1349 \pm 25\ ^{+10}_{-\ 5}$ MeV and width $547 \pm 86^{+46}_{-45}$ MeV.

$\Gamma(\overline{D}^*(2007)^0\rho^+)/\Gamma_{\text{total}}$ Γ_{125}/Γ

VALUE	EVTS	DOCUMENT ID		TECN	COMMENT
0.0098±0.0017 OUR AVERAGE					
0.0098±0.0006±0.0017		[1] CSORNA	03	CLE2	$e^+e^- \to \Upsilon(4S)$
0.010 ±0.006 ±0.004	7	[2] ALBRECHT	90J	ARG	$e^+e^- \to \Upsilon(4S)$
• • • We do not use the following data for averages, fits, limits, etc. • • •					
0.0168±0.0021±0.0028	86	[3] ALAM	94	CLE2	$e^+e^- \to \Upsilon(4S)$

[1] Assumes equal production of B^0 and B^+ at the $\Upsilon(4S)$ resonance. The second error combines the systematic and theoretical uncertainties in quadrature. CSORNA 03 includes data used in ALAM 94. A full angular fit to three complex helicity amplitudes is performed.
[2] Assumes equal production of B^+ and B^0 at the $\Upsilon(4S)$ and uses Mark III branching fractions for the D and $D^*(2010)$.
[3] ALAM 94 assume equal production of B^+ and B^0 at the $\Upsilon(4S)$ and use the CLEO II $B(D^*(2007)^0 \to D^0\pi^0)$ and absolute $B(D^0 \to K^-\pi^+)$ and the PDG 1992 $B(D^0 \to K^-\pi^+\pi^0)/B(D^0 \to K^-\pi^+)$ and $B(D^0 \to K^-2\pi^+\pi^-)/B(D^0 \to K^-\pi^+)$. The nonresonant $\pi^+\pi^0$ contribution under the ρ^+ is negligible.

$\Gamma(\overline{D}^*(2007)^0K^+)/\Gamma_{\text{total}}$ Γ_{126}/Γ

VALUE (units 10^{-4})	DOCUMENT ID		TECN	COMMENT
$3.97^{+0.31}_{-0.28}$ OUR AVERAGE				
$3.98^{+0.28}_{-0.25}\pm0.13$	[1] AUBERT	05N	BABR	$e^+e^- \to \Upsilon(4S)$
3.8 ±1.0 ±0.1	[2] ABE	01I	BELL	$e^+e^- \to \Upsilon(4S)$

[1] AUBERT 05N reports $[\Gamma(B^+ \to \overline{D}^*(2007)^0K^+)/\Gamma_{\text{total}}] / [B(B^+ \to \overline{D}^*(2007)^0\pi^+)] = 0.0813 \pm 0.0040^{+0.0042}_{-0.0031}$ which we multiply by our best value $B(B^+ \to \overline{D}^*(2007)^0\pi^+) = (4.90 \pm 0.17) \times 10^{-3}$. Our first error is their experiment's error and our second error is the systematic error from using our best value.
[2] ABE 01I reports $[\Gamma(B^+ \to \overline{D}^*(2007)^0K^+)/\Gamma_{\text{total}}] / [B(B^+ \to \overline{D}^*(2007)^0\pi^+)] = 0.078 \pm 0.019 \pm 0.009$ which we multiply by our best value $B(B^+ \to \overline{D}^*(2007)^0\pi^+) = (4.90 \pm 0.17) \times 10^{-3}$. Our first error is their experiment's error and our second error is the systematic error from using our best value.

$\Gamma(\overline{D}^{*0}_{CP(+1)}K^+)/\Gamma_{\text{total}}$ Γ_{127}/Γ

VALUE (units 10^{-4})	DOCUMENT ID		TECN	COMMENT
$2.60\pm0.27^{+0.20}_{-0.18}$	[1] AUBERT	08BF	BABR	$e^+e^- \to \Upsilon(4S)$

[1] AUBERT 08BF reports $[\Gamma(B^+ \to \overline{D}^{*0}_{CP(+1)}K^+)/\Gamma_{\text{total}}] / [B(B^+ \to \overline{D}^*(2007)^0K^+)] = 0.655 \pm 0.065 \pm 0.020$ which we multiply by our best value $B(B^+ \to \overline{D}^*(2007)^0K^+) = (3.97^{+0.31}_{-0.28}) \times 10^{-4}$. Our first error is their experiment's error and our second error is the systematic error from using our best value.

$\Gamma(\overline{D}^*(2007)^0K^+)/\Gamma(\overline{D}^*(2007)^0\pi^+)$ $\Gamma_{126}/\Gamma_{121}$

VALUE (units 10^{-2})	DOCUMENT ID		TECN	COMMENT
7.930±0.110±0.560	AAIJ	18A	LHCB	pp at 7, 8, 13 TeV

$\Gamma(\overline{D}^{*0}_{CP(+1)}K^+)/\Gamma(\overline{D}^{*0}_{CP(+1)}\pi^+)$ $\Gamma_{127}/\Gamma_{122}$

VALUE	DOCUMENT ID		TECN	COMMENT
0.095±0.017 OUR AVERAGE				
0.11 ±0.02 ±0.02	[1] ABE	06	BELL	$e^+e^- \to \Upsilon(4S)$
0.086±0.021±0.007	[2] AUBERT	05N	BABR	$e^+e^- \to \Upsilon(4S)$

[1] Reports a double ratio of $B(B^+ \to D^{*0}_{CP(+1)}K^+)/B(B^+ \to D^{*0}_{CP(+1)}\pi^+)$ and $B(B^+ \to \overline{D}^{*0}K^+)/B(B^+ \to \overline{D}^{*0}\pi^+)$, $1.41 \pm 0.25 \pm 0.06$. We multiply by our best value of $B(B^+ \to \overline{D}^{*0}K^+)/B(B^+ \to \overline{D}^{*0}\pi^+) = 0.080 \pm 0.011$. Our first error is their experiment's error and the second error is systematic error from using our best value.
[2] Uses $D^{*0} \to D^0\pi^0$ with D^0 reconstructed in the CP-even eigenstates K^+K^- and $\pi^+\pi^-$.

$\Gamma(\overline{D}^{*0}_{CP(-1)}K^+)/\Gamma_{total}$ Γ_{128}/Γ

VALUE (units 10^{-4})	DOCUMENT ID		TECN	COMMENT
$2.19\pm0.25^{+0.17}_{-0.15}$	[1] AUBERT	08BF	BABR	$e^+e^-\to\Upsilon(4S)$

[1] AUBERT 08BF reports $[\Gamma(B^+\to\overline{D}^{*0}_{CP(-1)}K^+)/\Gamma_{total}]$ / $[B(B^+\to\overline{D}^*(2007)^0K^+)] = 0.55\pm0.06\pm0.02$ which we multiply by our best value $B(B^+\to\overline{D}^*(2007)^0K^+) = (3.97^{+0.31}_{-0.28})\times10^{-4}$. Our first error is their experiment's error and our second error is the systematic error from using our best value.

$\Gamma(\overline{D}^{*0}_{CP(-1)}K^+)/\Gamma(D^{*0}_{CP(-1)}\pi^+)$ $\Gamma_{128}/\Gamma_{123}$

VALUE	DOCUMENT ID		TECN	COMMENT
$0.09\pm0.03\pm0.01$	[1] ABE	06	BELL	$e^+e^-\to\Upsilon(4S)$

[1] Reports a double ratio of $B(B^+\to(D^*_{CP(-1)})^0K^+)/B(B^+\to(D^*_{CP(-1)})^0\pi^+)$ and $B(B^+\to\overline{D}^{*0}K^+)/B(B^+\to\overline{D}^{*0}\pi^+)$, $1.15\pm0.31\pm0.12$. We multiply by our best value of $B(B^+\to\overline{D}^{*0}K^+)/B(B^+\to\overline{D}^{*0}\pi^+) = 0.080\pm0.011$. Our first error is their experiment's error and the second error is systematic error from using our best value.

$\Gamma(\overline{D}^*(2007)^0K^*(892)^+)/\Gamma_{total}$ Γ_{129}/Γ

VALUE (units 10^{-4})	DOCUMENT ID		TECN	COMMENT
8.1 ± 1.4 OUR AVERAGE				
$8.3\pm1.1\pm1.0$	[1] AUBERT	04K	BABR	$e^+e^-\to\Upsilon(4S)$
$7.2\pm2.2\pm2.6$	[2] MAHAPATRA	02	CLE2	$e^+e^-\to\Upsilon(4S)$

[1] Assumes equal production of B^+ and B^0 at the $\Upsilon(4S)$.
[2] Assumes equal production of B^+ and B^0 at the $\Upsilon(4S)$ and an unpolarized final state.

$\Gamma(\overline{D}^*(2007)^0K^+\overline{K}^0)/\Gamma_{total}$ Γ_{130}/Γ

VALUE (units 10^{-4})	CL%	DOCUMENT ID		TECN	COMMENT
<10.6	90	[1] DRUTSKOY	02	BELL	$e^+e^-\to\Upsilon(4S)$

[1] Assumes equal production of B^+ and B^0 at the $\Upsilon(4S)$.

$\Gamma(\overline{D}^*(2007)^0K^+\overline{K}^*(892)^0)/\Gamma_{total}$ Γ_{131}/Γ

VALUE (units 10^{-4})	DOCUMENT ID		TECN	COMMENT
$15.3\pm3.1\pm2.9$	[1] DRUTSKOY	02	BELL	$e^+e^-\to\Upsilon(4S)$

[1] Assumes equal production of B^+ and B^0 at the $\Upsilon(4S)$.

$\Gamma(\overline{D}^*(2007)^0\pi^+\pi^+\pi^-)/\Gamma_{total}$ Γ_{132}/Γ

VALUE (units 10^{-2})	EVTS	DOCUMENT ID		TECN	COMMENT
1.03 ± 0.12 OUR AVERAGE					
$1.055\pm0.047\pm0.129$		[1] MAJUMDER	04	BELL	$e^+e^-\to\Upsilon(4S)$
$0.94\pm0.20\pm0.17$	48	[2,3] ALAM	94	CLE2	$e^+e^-\to\Upsilon(4S)$

[1] Assumes equal production of B^+ and B^0 at the $\Upsilon(4S)$.
[2] ALAM 94 assume equal production of B^+ and B^0 at the $\Upsilon(4S)$ and use the CLEO II $B(D^*(2007)^0\to D^0\pi^0)$ and absolute $B(D^0\to K^-\pi^+)$ and the PDG 1992 $B(D^0\to K^-\pi^+\pi^0)/B(D^0\to K^-\pi^+)$ and $B(D^0\to K^-2\pi^+\pi^-)/B(D^0\to K^-\pi^+)$.
[3] The three pion mass is required to be between 1.0 and 1.6 GeV consistent with an a_1 meson. (If this channel is dominated by a_1^+, the branching ratio for $\overline{D}^{*0}a_1^+$ is twice that for $\overline{D}^{*0}\pi^+\pi^+\pi^-$.)

$\Gamma(\overline{D}^*(2007)^0a_1(1260)^+)/\Gamma_{total}$ Γ_{133}/Γ

VALUE	DOCUMENT ID		TECN	COMMENT
$0.0188\pm0.0040\pm0.0034$	[1,2] ALAM	94	CLE2	$e^+e^-\to\Upsilon(4S)$

[1] ALAM 94 value is twice their $\Gamma(\overline{D}^*(2007)^0\pi^+\pi^+\pi^-)/\Gamma_{total}$ value based on their observation that the three pions are dominantly in the $a_1(1260)$ mass range 1.0 to 1.6 GeV.
[2] ALAM 94 assume equal production of B^+ and B^0 at the $\Upsilon(4S)$ and use the CLEO II $B(D^*(2007)^0\to D^0\pi^0)$ and absolute $B(D^0\to K^-\pi^+)$ and the PDG 1992 $B(D^0\to K^-\pi^+\pi^0)/B(D^0\to K^-\pi^+)$ and $B(D^0\to K^-2\pi^+\pi^-)/B(D^0\to K^-\pi^+)$.

$\Gamma(\overline{D}^*(2007)^0\pi^-\pi^+\pi^+\pi^0)/\Gamma_{total}$ Γ_{134}/Γ

VALUE	DOCUMENT ID		TECN	COMMENT
$0.0180\pm0.0024\pm0.0027$	[1] ALEXANDER	01B	CLE2	$e^+e^-\to\Upsilon(4S)$

[1] Assumes equal production of B^+ and B^0 at the $\Upsilon(4S)$. The signal is consistent with all observed $\omega\pi^+$ having proceeded through the ρ'^+ resonance at mass $1349\pm25^{+10}_{-5}$ MeV and width $547\pm86^{+46}_{-45}$ MeV.

$\Gamma(\overline{D}^{*0}3\pi^+2\pi^-)/\Gamma_{total}$ Γ_{135}/Γ

VALUE (units 10^{-3})	DOCUMENT ID		TECN	COMMENT
$5.67\pm0.91\pm0.85$	[1] MAJUMDER	04	BELL	$e^+e^-\to\Upsilon(4S)$

[1] Assumes equal production of B^+ and B^0 at the $\Upsilon(4S)$.

$\Gamma(D^*(2010)^+\pi^0)/\Gamma_{total}$ Γ_{136}/Γ

VALUE	CL%	DOCUMENT ID		TECN	COMMENT
$<3.6\times10^{-6}$		[1] IWABUCHI	08	BELL	$e^+e^-\to\Upsilon(4S)$
• • • We do not use the following data for averages, fits, limits, etc. • • •					
$<1.7\times10^{-4}$	90	[2] BRANDENB...	98	CLE2	$e^+e^-\to\Upsilon(4S)$

[1] Assumes equal production of B^+ and B^0 at the $\Upsilon(4S)$.
[2] BRANDENBURG 98 assume equal production of B^+ and B^0 at $\Upsilon(4S)$ and use the D^* partial reconstruction technique. The first error is their experiment's error and the second error is the systematic error from the PDG 96 value of $B(D^*\to D\pi)$.

$\Gamma(D^*(2010)^+K^0)/\Gamma_{total}$ Γ_{137}/Γ

VALUE	CL%	DOCUMENT ID		TECN	COMMENT
$<9.0\times10^{-6}$	90	[1] AUBERT,B	05E	BABR	$e^+e^-\to\Upsilon(4S)$
• • • We do not use the following data for averages, fits, limits, etc. • • •					
$<9.5\times10^{-5}$	90	[1] GRITSAN	01	CLE2	$e^+e^-\to\Upsilon(4S)$

[1] Assumes equal production of B^+ and B^0 at the $\Upsilon(4S)$.

$\Gamma(D^*(2010)^-\pi^+\pi^+\pi^0)/\Gamma_{total}$ Γ_{138}/Γ

VALUE	EVTS	DOCUMENT ID		TECN	COMMENT
$0.0152\pm0.0071\pm0.0001$	26	[1] ALBRECHT	90J	ARG	$e^+e^-\to\Upsilon(4S)$
• • • We do not use the following data for averages, fits, limits, etc. • • •					
$0.043\pm0.013\pm0.026$	24	[2] ALBRECHT	87C	ARG	$e^+e^-\to\Upsilon(4S)$

[1] ALBRECHT 90J reports $0.018\pm0.007\pm0.005$ from a measurement of $[\Gamma(B^+\to D^*(2010)^-\pi^+\pi^+\pi^0)/\Gamma_{total}]\times[B(D^*(2010)^+\to D^0\pi^+)]$ assuming $B(D^*(2010)^+\to D^0\pi^+) = 0.57\pm0.06$, which we rescale to our best value $B(D^*(2010)^+\to D^0\pi^+) = (67.7\pm0.5)\times10^{-2}$. Our first error is their experiment's error and our second error is the systematic error from using our best value. Assumes equal production of B^+ and B^0 at the $\Upsilon(4S)$ and uses Mark III branching fractions for the D.
[2] ALBRECHT 87C use PDG 86 branching ratios for D and $D^*(2010)$ and assume $B(\Upsilon(4S)\to B^+B^-) = 55\%$ and $B(\Upsilon(4S)\to B^0\overline{B}^0) = 45\%$. Superseded by ALBRECHT 90J.

$\Gamma(D^*(2010)^-\pi^+\pi^+\pi^+\pi^-)/\Gamma_{total}$ Γ_{139}/Γ

VALUE (units 10^{-3})	CL%	DOCUMENT ID		TECN	COMMENT
$2.56\pm0.26\pm0.33$		[1] MAJUMDER	04	BELL	$e^+e^-\to\Upsilon(4S)$
• • • We do not use the following data for averages, fits, limits, etc. • • •					
<10	90	[2] ALBRECHT	90J	ARG	$e^+e^-\to\Upsilon(4S)$

[1] Assumes equal production of B^+ and B^0 at the $\Upsilon(4S)$.
[2] Assumes equal production of B^+ and B^0 at the $\Upsilon(4S)$ and uses Mark III branching fractions for the D and $D^*(2010)$.

$\Gamma(\overline{D}^{**0}\pi^+)/\Gamma_{total}$ Γ_{140}/Γ

D^{**0} represents an excited state with mass $2.2 < M < 2.8$ GeV/c^2.

VALUE (units 10^{-3})	DOCUMENT ID		TECN	COMMENT
$5.7\pm1.2\pm0.2$	[1,2] AUBERT,BE	06J	BABR	$e^+e^-\to\Upsilon(4S)$

[1] AUBERT,BE 06J reports $[\Gamma(B^+\to\overline{D}^{**0}\pi^+)/\Gamma_{total}]$ / $[B(B^+\to\overline{D}^0\pi^+)] = 1.22\pm0.13\pm0.23$ which we multiply by our best value $B(B^+\to\overline{D}^0\pi^+) = (4.68\pm0.13)\times10^{-3}$. Our first error is their experiment's error and our second error is the systematic error from using our best value.
[2] Uses a missing-mass method. Does not depend on D branching fractions or B^+/B^0 production rates.

$\Gamma(\overline{D}_1^*(2420)^0\pi^+)/\Gamma_{total}$ Γ_{141}/Γ

VALUE	EVTS	DOCUMENT ID		TECN	COMMENT
0.0015 ± 0.0006 OUR AVERAGE		Error includes scale factor of 1.3.			
$0.0011\pm0.0005\pm0.0002$	8	[1] ALAM	94	CLE2	$e^+e^-\to\Upsilon(4S)$
$0.0025\pm0.0007\pm0.0006$		[2] ALBRECHT	94D	ARG	$e^+e^-\to\Upsilon(4S)$

[1] ALAM 94 assume equal production of B^+ and B^0 at the $\Upsilon(4S)$ and use the CLEO II $B(D^*(2010)^+\to D^0\pi^+)$ and absolute $B(D^0\to K^-\pi^+)$ and the PDG 1992 $B(D^0\to K^-\pi^+\pi^0)/B(D^0\to K^-\pi^+)$ and assuming $B(D_1(2420)^0\to D^*(2010)^+\pi^-) = 67\%$.
[2] ALBRECHT 94D assume equal production of B^+ and B^0 at the $\Upsilon(4S)$ and use the CLEO II $B(D^*(2010)^+\to D^0\pi^+)$ assuming $B(D_1(2420)^0\to D^*(2010)^+\pi^-) = 67\%$.

$\Gamma(\overline{D}_1(2420)^0\pi^+\times B(\overline{D}_1^0\to\overline{D}^0\pi^+\pi^-))/\Gamma_{total}$ Γ_{142}/Γ

VALUE (units 10^{-4})	DOCUMENT ID		TECN	COMMENT
$2.5^{+1.6}_{-1.4}$ OUR FIT	Error includes scale factor of 3.9.			
$1.85\pm0.29^{+0.35}_{-0.55}$	[1] ABE	05A	BELL	$e^+e^-\to\Upsilon(4S)$

[1] Assumes equal production of B^+ and B^0 at the $\Upsilon(4S)$.

$\Gamma(\overline{D}_1(2420)^0\pi^+\times B(\overline{D}_1^0\to\overline{D}^0\pi^+\pi^-))/\Gamma(\overline{D}^0\pi^+\pi^+\pi^-)$ $\Gamma_{142}/\Gamma_{102}$

VALUE (units 10^{-2})	DOCUMENT ID		TECN	COMMENT
$4.6^{+3.3}_{-2.7}$ OUR FIT	Error includes scale factor of 3.9.			
$10.3\pm1.5\pm0.9$	AAIJ	11E	LHCB	pp at 7 TeV

$\Gamma(\overline{D}_1(2420)^0\pi^+\times B(\overline{D}_1^0\to\overline{D}^0\pi^+\pi^-\text{ (nonresonant)}))/\Gamma(\overline{D}^0\pi^+\pi^+\pi^-)$ $\Gamma_{143}/\Gamma_{102}$

VALUE (units 10^{-2})	DOCUMENT ID		TECN	COMMENT
$4.0\pm0.7\pm0.5$	[1] AAIJ	11E	LHCB	pp at 7 TeV

[1] Excludes decays where $\overline{D}_1(2420)^0\to D*(2010)^-\pi^+$.

$\Gamma(\overline{D}_2^*(2462)^0\pi^+ \times B(\overline{D}_2^*(2462)^0 \to D^-\pi^+))/\Gamma_{total}$ Γ_{144}/Γ

VALUE (units 10^{-4})	DOCUMENT ID		TECN	COMMENT
3.56±0.24 OUR AVERAGE				
3.62±0.06±0.30	[1] AAIJ	16AH	LHCB	pp at 7, 8 TeV
3.5 ±0.2 ±0.4	[2] AUBERT	09AB	BABR	$e^+e^- \to \Upsilon(4S)$
3.4 ±0.3 ±0.72	[2] ABE	04D	BELL	$e^+e^- \to \Upsilon(4S)$

[1] Measured using a Dalitz plot analysis of $B^- \to D^+\pi^-\pi^-$ decays.
[2] Assumes equal production of B^+ and B^0 at the $\Upsilon(4S)$.

$\Gamma(\overline{D}_2^*(2462)^0\pi^+ \times B(\overline{D}_2^{*0} \to \overline{D}^0\pi^-\pi^+))/\Gamma(\overline{D}^0\pi^+\pi^+\pi^-)$ $\Gamma_{145}/\Gamma_{102}$

VALUE (units 10^{-2})	DOCUMENT ID		TECN	COMMENT
4.0±1.0±0.4	AAIJ	11E	LHCB	pp at 7 TeV

$\Gamma(\overline{D}_2^*(2462)^0\pi^+ \times B(\overline{D}_2^{*0} \to \overline{D}^0\pi^-\pi^+ \text{(nonresonant)}))/\Gamma(\overline{D}^0\pi^+\pi^+\pi^-)$ $\Gamma_{146}/\Gamma_{102}$

VALUE	CL%	DOCUMENT ID		TECN	COMMENT
<3.0 × 10^{-2}	90	[1] AAIJ	11E	LHCB	pp at 7 TeV

[1] Excludes decays where $\overline{D}_2^*(2462)^0 \to D^*(2010)^-\pi^+$.

$\Gamma(\overline{D}_2^*(2462)^0\pi^+ \times B(\overline{D}_2^{*0} \to D^*(2010)^-\pi^+))/\Gamma(\overline{D}^0\pi^+\pi^+\pi^-)$ $\Gamma_{147}/\Gamma_{102}$

VALUE (units 10^{-2})	DOCUMENT ID		TECN	COMMENT
3.9±1.2±0.4	[1] AAIJ	11E	LHCB	pp at 7 TeV

[1] Uses $B(D^*(2010)^+ \to D^0\pi^+) = (67.7 +- 0.5)\%$.

$\Gamma(\overline{D}_0^*(2400)^0\pi^+ \times B(\overline{D}_0^*(2400)^0 \to D^-\pi^+))/\Gamma_{total}$ Γ_{148}/Γ

VALUE (units 10^{-4})	DOCUMENT ID		TECN	COMMENT
6.4±1.4 OUR AVERAGE				
6.8±0.3±2.0	[1] AUBERT	09AB	BABR	$e^+e^- \to \Upsilon(4S)$
6.1±0.6±1.8	[1] ABE	04D	BELL	$e^+e^- \to \Upsilon(4S)$

[1] Assumes equal production of B^+ and B^0 at the $\Upsilon(4S)$.

$\Gamma(\overline{D}_1(2421)^0\pi^+ \times B(\overline{D}_1(2421)^0 \to D^{*-}\pi^+))/\Gamma_{total}$ Γ_{149}/Γ

VALUE (units 10^{-4})	DOCUMENT ID		TECN	COMMENT
6.8±0.7±1.3	[1] ABE	04D	BELL	$e^+e^- \to \Upsilon(4S)$

[1] Assumes equal production of B^+ and B^0 at the $\Upsilon(4S)$.

$\Gamma(\overline{D}_2^*(2462)^0\pi^+ \times B(\overline{D}_2^*(2462)^0 \to D^{*-}\pi^+))/\Gamma_{total}$ Γ_{150}/Γ

VALUE (units 10^{-4})	DOCUMENT ID		TECN	COMMENT
1.8±0.3±0.4	[1] ABE	04D	BELL	$e^+e^- \to \Upsilon(4S)$

[1] Assumes equal production of B^+ and B^0 at the $\Upsilon(4S)$.

$\Gamma(\overline{D}_1'(2427)^0\pi^+ \times B(\overline{D}_1'(2427)^0 \to D^{*-}\pi^+))/\Gamma_{total}$ Γ_{151}/Γ

VALUE (units 10^{-4})	DOCUMENT ID		TECN	COMMENT
5.0±0.4±1.1	[1] ABE	04D	BELL	$e^+e^- \to \Upsilon(4S)$

[1] Assumes equal production of B^+ and B^0 at the $\Upsilon(4S)$.

$\Gamma(\overline{D}_1(2420)^0\pi^+ \times B(\overline{D}_1^0 \to \overline{D}^{*0}\pi^+\pi^-))/\Gamma_{total}$ Γ_{152}/Γ

VALUE (units 10^{-4})	CL%	DOCUMENT ID		TECN	COMMENT
<0.06	90	[1] ABE	05A	BELL	$e^+e^- \to \Upsilon(4S)$

[1] Assumes equal production of B^+ and B^0 at the $\Upsilon(4S)$.

$\Gamma(\overline{D}_1^*(2420)^0\rho^+)/\Gamma_{total}$ Γ_{153}/Γ

VALUE	CL%	DOCUMENT ID		TECN	COMMENT
<0.0014	90	[1] ALAM	94	CLE2	$e^+e^- \to \Upsilon(4S)$

[1] ALAM 94 assume equal production of B^+ and B^0 at the $\Upsilon(4S)$ and use the CLEO II $B(D^*(2010)^+ \to D^0\pi^+)$ assuming $B(D_1(2420)^0 \to D^*(2010)^+\pi^-) = 67\%$.

$\Gamma(\overline{D}_2^*(2460)^0\pi^+)/\Gamma_{total}$ Γ_{154}/Γ

VALUE	CL%	DOCUMENT ID		TECN	COMMENT
<0.0013	90	[1] ALAM	94	CLE2	$e^+e^- \to \Upsilon(4S)$
• • • We do not use the following data for averages, fits, limits, etc. • • •					
<0.0028	90	[2] ALAM	94	CLE2	$e^+e^- \to \Upsilon(4S)$
<0.0023	90	[3] ALBRECHT	94D	ARG	$e^+e^- \to \Upsilon(4S)$

[1] ALAM 94 assume equal production of B^+ and B^0 at the $\Upsilon(4S)$ and use the Mark III $B(D^+ \to K^-2\pi^+)$ and $B(D_2^*(2460)^0 \to D^+\pi^-) = 30\%$.
[2] ALAM 94 assume equal production of B^+ and B^0 at the $\Upsilon(4S)$ and use the Mark III $B(D^+ \to K^-2\pi^+)$, the CLEO II $B(D^*(2010)^+ \to D^0\pi^+)$ and $B(D_2^*(2460)^0 \to D^*(2010)^+\pi^-) = 20\%$.
[3] ALBRECHT 94D assume equal production of B^+ and B^0 at the $\Upsilon(4S)$ and use the CLEO II $B(D^*(2010)^+ \to D^0\pi^+)$ and $B(D_2^*(2460)^0 \to D^*(2010)^+\pi^-) = 30\%$.

$\Gamma(\overline{D}_2^*(2460)^0\pi^+ \times B(\overline{D}_2^{*0} \to \overline{D}^{*0}\pi^+\pi^-))/\Gamma_{total}$ Γ_{155}/Γ

VALUE (units 10^{-4})	CL%	DOCUMENT ID		TECN	COMMENT
<0.22	90	[1] ABE	05A	BELL	$e^+e^- \to \Upsilon(4S)$

[1] Assumes equal production of B^+ and B^0 at the $\Upsilon(4S)$.

$\Gamma(\overline{D}_2^*(2460)^0\rho^+)/\Gamma_{total}$ Γ_{159}/Γ

VALUE	CL%	DOCUMENT ID		TECN	COMMENT
<0.0047	90	[1] ALAM	94	CLE2	$e^+e^- \to \Upsilon(4S)$
<0.005	90	[2] ALAM	94	CLE2	$e^+e^- \to \Upsilon(4S)$

[1] ALAM 94 assume equal production of B^+ and B^0 at the $\Upsilon(4S)$ and use the Mark III $B(D^+ \to K^-2\pi^+)$ and $B(D_2^*(2460)^0 \to D^+\pi^-) = 30\%$.
[2] ALAM 94 assume equal production of B^+ and B^0 at the $\Upsilon(4S)$ and use the Mark III $B(D^+ \to K^-2\pi^+)$, the CLEO II $B(D^*(2010)^+ \to D^0\pi^+)$ and $B(D_2^*(2460)^0 \to D^*(2010)^+\pi^-) = 20\%$.

$\Gamma(\overline{D}_1^*(2680)^0\pi^+, \overline{D}_1^*(2680)^0 \to D^-\pi^+)/\Gamma_{total}$ Γ_{156}/Γ

VALUE (units 10^{-4})	DOCUMENT ID		TECN	COMMENT
0.84±0.06±0.20	[1] AAIJ	16AH	LHCB	pp at 7, 8 TeV

[1] Measured using a Dalitz plot analysis of $B^+ \to D^-\pi^+\pi^+$ decays.

$\Gamma(\overline{D}_3^*(2760)^0\pi^+, \overline{D}_3^*(2760)^0\pi^+ \to D^-\pi^+)/\Gamma_{total}$ Γ_{157}/Γ

VALUE (units 10^{-5})	DOCUMENT ID		TECN	COMMENT
1.0±0.1±0.2	[1] AAIJ	16AH	LHCB	pp at 7, 8 TeV

[1] Measured using a Dalitz plot analysis of $B^+ \to D^-\pi^+\pi^+$ decays.

$\Gamma(\overline{D}_2^*(3000)^0\pi^+, \overline{D}_2^*(3000)^0\pi^+ \to D^-\pi^+)/\Gamma_{total}$ Γ_{158}/Γ

VALUE (units 10^{-6})	DOCUMENT ID		TECN	COMMENT
2±1±1	[1] AAIJ	16AH	LHCB	pp at 7, 8 TeV

[1] Measured using a Dalitz plot analysis of $B^+ \to D^-\pi^+\pi^+$ decays.

$\Gamma(\overline{D}^0 D_s^+)/\Gamma_{total}$ Γ_{160}/Γ

VALUE (units 10^{-3})	DOCUMENT ID		TECN	COMMENT
9.0±0.9 OUR AVERAGE				
8.6±0.2±1.1	[1] AAIJ	13AP	LHCB	pp at 7 TeV
9.5±2.0±0.8	[2] AUBERT	06N	BABR	$e^+e^- \to \Upsilon(4S)$
9.8±2.6±0.9	[3] GIBAUT	96	CLE2	$e^+e^- \to \Upsilon(4S)$
14 ±8 ±1	[4] ALBRECHT	92G	ARG	$e^+e^- \to \Upsilon(4S)$
13 ±6 ±1	[5] BORTOLETTO	90	CLEO	$e^+e^- \to \Upsilon(4S)$

[1] Uses $B(B^0 \to D^-D_s^+) = (7.2 \pm 0.8) \times 10^{-3}$.
[2] AUBERT 06N reports $(0.92 \pm 0.14 \pm 0.18) \times 10^{-2}$ from a measurement of $[\Gamma(B^+ \to \overline{D}^0 D_s^+)/\Gamma_{total}] \times [B(D_s^+ \to \phi\pi^+)]$ assuming $B(D_s^+ \to \phi\pi^+) = 0.0462 \pm 0.0062$, which we rescale to our best value $B(D_s^+ \to \phi\pi^+) = (4.5 \pm 0.4) \times 10^{-2}$. Our first error is their experiment's error and our second error is the systematic error from using our best value.
[3] GIBAUT 96 reports $0.0126 \pm 0.0022 \pm 0.0025$ from a measurement of $[\Gamma(B^+ \to \overline{D}^0 D_s^+)/\Gamma_{total}] \times [B(D_s^+ \to \phi\pi^+)]$ assuming $B(D_s^+ \to \phi\pi^+) = 0.035$, which we rescale to our best value $B(D_s^+ \to \phi\pi^+) = (4.5 \pm 0.4) \times 10^{-2}$. Our first error is their experiment's error and our second error is the systematic error from using our best value.
[4] ALBRECHT 92G reports $0.024 \pm 0.012 \pm 0.004$ from a measurement of $[\Gamma(B^+ \to \overline{D}^0 D_s^+)/\Gamma_{total}] \times [B(D_s^+ \to \phi\pi^+)]$ assuming $B(D_s^+ \to \phi\pi^+) = 0.027$, which we rescale to our best value $B(D_s^+ \to \phi\pi^+) = (4.5 \pm 0.4) \times 10^{-2}$. Our first error is their experiment's error and our second error is the systematic error from using our best value. Assumes PDG 1990 D^0 branching ratios, e.g., $B(D^0 \to K^-\pi^+) = 3.71 \pm 0.25\%$.
[5] BORTOLETTO 90 reports 0.029 ± 0.013 from a measurement of $[\Gamma(B^+ \to \overline{D}^0 D_s^+)/\Gamma_{total}] \times [B(D_s^+ \to \phi\pi^+)]$ assuming $B(D_s^+ \to \phi\pi^+) = 0.02$, which we rescale to our best value $B(D_s^+ \to \phi\pi^+) = (4.5 \pm 0.4) \times 10^{-2}$. Our first error is their experiment's error and our second error is the systematic error from using our best value.

$\Gamma(D_{s0}^*(2317)^+\overline{D}^0, D_{s0}^{*+} \to D_s^+\pi^0)/\Gamma_{total}$ Γ_{161}/Γ

VALUE (units 10^{-3})	DOCUMENT ID		TECN	COMMENT
$0.79^{+0.15}_{-0.13}$ OUR AVERAGE				
$0.79^{+0.17}_{-0.16}\pm0.02$	[1,2] CHOI	15A	BELL	$e^+e^- \to \Upsilon(4S)$
$0.80^{+0.35}_{-0.21}\pm0.07$	[2,3] AUBERT,B	04S	BABR	$e^+e^- \to \Upsilon(4S)$
• • • We do not use the following data for averages, fits, limits, etc. • • •				
$0.65^{+0.26}_{-0.24}\pm0.06$	[2,4] KROKOVNY	03B	BELL	Repl. by CHOI 15A

[1] CHOI 15A reports $(8.0^{+1.3}_{-1.2} \pm 1.1 \pm 0.4) \times 10^{-4}$ from a measurement of $[\Gamma(B^+ \to D_{s0}^*(2317)^+\overline{D}^0, D_{s0}^{*+} \to D_s^+\pi^0)/\Gamma_{total}] \times [B(D_s^+ \to K^+K^-\pi^+)]$ assuming $B(D_s^+ \to K^+K^-\pi^+) = (5.39 \pm 0.21) \times 10^{-2}$, which we rescale to our best value $B(D_s^+ \to K^+K^-\pi^+) = (5.45 \pm 0.17) \times 10^{-2}$. Our first error is their experiment's error and our second error is the systematic error from using our best value.
[2] Assumes equal production of B^+ and B^0 at the $\Upsilon(4S)$.
[3] AUBERT,B 04S reports $(1.0 \pm 0.3^{+0.4}_{-0.2}) \times 10^{-3}$ from a measurement of $[\Gamma(B^+ \to D_{s0}^*(2317)^+\overline{D}^0, D_{s0}^{*+} \to D_s^+\pi^0)/\Gamma_{total}] \times [B(D_s^+ \to \phi\pi^+)]$ assuming $B(D_s^+ \to \phi\pi^+) = 0.036 \pm 0.009$, which we rescale to our best value $B(D_s^+ \to \phi\pi^+) = (4.5 \pm 0.4) \times 10^{-2}$. Our first error is their experiment's error and our second error is the systematic error from using our best value.
[4] KROKOVNY 03B reports $(0.81^{+0.30}_{-0.27} \pm 0.24) \times 10^{-3}$ from a measurement of $[\Gamma(B^+ \to D_{s0}^*(2317)^+\overline{D}^0, D_{s0}^{*+} \to D_s^+\pi^0)/\Gamma_{total}] \times [B(D_s^+ \to \phi\pi^+)]$ assuming $B(D_s^+ \to$

$\phi\pi^+) = 0.036 \pm 0.009$, which we rescale to our best value $B(D_s^+ \to \phi\pi^+) = (4.5 \pm 0.4) \times 10^{-2}$. Our first error is their experiment's error and our second error is the systematic error from using our best value.

$\Gamma(D_{s0}(2317)^+ \overline{D}^0 \times B(D_{s0}(2317)^+ \to D_s^{*+}\gamma))/\Gamma_{total}$ Γ_{162}/Γ

VALUE (units 10^{-3})	CL%	DOCUMENT ID		TECN	COMMENT
<0.76	90	[1] KROKOVNY	03B	BELL	$e^+e^- \to \Upsilon(4S)$

[1] Assumes equal production of B^+ and B^0 at the $\Upsilon(4S)$.

$\Gamma(D_{s0}(2317)^+ \overline{D}^*(2007)^0 \times B(D_{s0}(2317)^+ \to D_s^+\pi^0))/\Gamma_{total}$ Γ_{163}/Γ

VALUE (units 10^{-3})	DOCUMENT ID		TECN	COMMENT
$0.9 \pm 0.6^{+0.4}_{-0.3}$	[1] AUBERT,B	04S	BABR	$e^+e^- \to \Upsilon(4S)$

[1] Assumes equal production of B^+ and B^0 at the $\Upsilon(4S)$.

$\Gamma(D_{sJ}(2457)^+ \overline{D}^0)/\Gamma_{total}$ Γ_{164}/Γ

VALUE (units 10^{-3})	DOCUMENT ID		TECN	COMMENT
$3.1^{+1.0}_{-0.9}$ OUR AVERAGE				
$4.3 \pm 1.6 \pm 1.3$	[1] AUBERT	06N	BABR	$e^+e^- \to \Upsilon(4S)$
$4.6^{+1.8}_{-1.6} \pm 1.0$	[2,3] AUBERT,B	04S	BABR	$e^+e^- \to \Upsilon(4S)$
$2.1^{+1.1}_{-0.9} \pm 0.5$	[2,4] KROKOVNY	03B	BELL	$e^+e^- \to \Upsilon(4S)$

[1] Uses a missing-mass method in the events that one of the B mesons is fully reconstructed.
[2] Assumes equal production of B^+ and B^0 at the $\Upsilon(4S)$.
[3] AUBERT,B 04S reports $[\Gamma(B^+ \to D_{sJ}(2457)^+\overline{D}^0)/\Gamma_{total}] \times [B(D_{s1}(2460)^+ \to D_s^{*+}\pi^0)] = (2.2^{+0.8}_{-0.7} \pm 0.3) \times 10^{-3}$ which we divide by our best value $B(D_{s1}(2460)^+ \to D_s^{*+}\pi^0) = (48 \pm 11) \times 10^{-2}$. Our first error is their experiment's error and our second error is the systematic error from using our best value.
[4] KROKOVNY 03B reports $[\Gamma(B^+ \to D_{sJ}(2457)^+\overline{D}^0)/\Gamma_{total}] \times [B(D_{s1}(2460)^+ \to D_s^{*+}\pi^0)] = (1.0^{+0.5}_{-0.4} \pm 0.1) \times 10^{-3}$ which we divide by our best value $B(D_{s1}(2460)^+ \to D_s^{*+}\pi^0) = (48 \pm 11) \times 10^{-2}$. Our first error is their experiment's error and our second error is the systematic error from using our best value.

$\Gamma(D_{sJ}(2457)^+ \overline{D}^0 \times B(D_{sJ}(2457)^+ \to D_s^+\gamma))/\Gamma_{total}$ Γ_{165}/Γ

VALUE (units 10^{-3})	DOCUMENT ID		TECN	COMMENT
$0.46^{+0.13}_{-0.11}$ OUR AVERAGE				
$0.48^{+0.19}_{-0.13} \pm 0.04$	[1,2] AUBERT,B	04S	BABR	$e^+e^- \to \Upsilon(4S)$
$0.45^{+0.15}_{-0.14} \pm 0.04$	[1,3] KROKOVNY	03B	BELL	$e^+e^- \to \Upsilon(4S)$

[1] Assumes equal production of B^+ and B^0 at the $\Upsilon(4S)$.
[2] AUBERT,B 04S reports $(0.6 \pm 0.2^{+0.2}_{-0.1}) \times 10^{-3}$ from a measurement of $[\Gamma(B^+ \to D_{sJ}(2457)^+\overline{D}^0 \times B(D_{sJ}(2457)^+ \to D_s^+\gamma))/\Gamma_{total}] \times [B(D_s^+ \to \phi\pi^+)]$ assuming $B(D_s^+ \to \phi\pi^+) = 0.036 \pm 0.009$, which we rescale to our best value $B(D_s^+ \to \phi\pi^+) = (4.5 \pm 0.4) \times 10^{-2}$. Our first error is their experiment's error and our second error is the systematic error from using our best value.
[3] KROKOVNY 03B reports $(0.56^{+0.16}_{-0.15} \pm 0.17) \times 10^{-3}$ from a measurement of $[\Gamma(B^+ \to D_{sJ}(2457)^+\overline{D}^0 \times B(D_{sJ}(2457)^+ \to D_s^+\gamma))/\Gamma_{total}] \times [B(D_s^+ \to \phi\pi^+)]$ assuming $B(D_s^+ \to \phi\pi^+) = 0.036 \pm 0.009$, which we rescale to our best value $B(D_s^+ \to \phi\pi^+) = (4.5 \pm 0.4) \times 10^{-2}$. Our first error is their experiment's error and our second error is the systematic error from using our best value.

$\Gamma(D_{sJ}(2457)^+ \overline{D}^0 \times B(D_{sJ}(2457)^+ \to D_s^+\pi^+\pi^-))/\Gamma_{total}$ Γ_{166}/Γ

VALUE (units 10^{-3})	CL%	DOCUMENT ID		TECN	COMMENT
<0.22	90	[1] KROKOVNY	03B	BELL	$e^+e^- \to \Upsilon(4S)$

[1] Assumes equal production of B^+ and B^0 at the $\Upsilon(4S)$.

$\Gamma(D_{sJ}(2457)^+ \overline{D}^0 \times B(D_{sJ}(2457)^+ \to D_s^+\pi^0))/\Gamma_{total}$ Γ_{167}/Γ

VALUE (units 10^{-3})	CL%	DOCUMENT ID		TECN	COMMENT
<0.27	90	[1] KROKOVNY	03B	BELL	$e^+e^- \to \Upsilon(4S)$

[1] Assumes equal production of B^+ and B^0 at the $\Upsilon(4S)$.

$\Gamma(D_{sJ}(2457)^+ \overline{D}^0 \times B(D_{sJ}(2457)^+ \to D_s^{*+}\gamma))/\Gamma_{total}$ Γ_{168}/Γ

VALUE (units 10^{-3})	CL%	DOCUMENT ID		TECN	COMMENT
<0.98	90	[1] KROKOVNY	03B	BELL	$e^+e^- \to \Upsilon(4S)$

[1] Assumes equal production of B^+ and B^0 at the $\Upsilon(4S)$.

$\Gamma(D_{sJ}(2457)^+ \overline{D}^*(2007)^0)/\Gamma_{total}$ Γ_{169}/Γ

VALUE (units 10^{-3})	DOCUMENT ID		TECN	COMMENT
12.0±3.0 OUR AVERAGE				
$11.2 \pm 2.6 \pm 2.0$	[1] AUBERT	06N	BABR	$e^+e^- \to \Upsilon(4S)$
$16\ ^{+8}_{-6}\ \pm 4$	[2,3] AUBERT,B	04S	BABR	$e^+e^- \to \Upsilon(4S)$

[1] Uses a missing-mass method in the events that one of the B mesons is fully reconstructed.
[2] AUBERT,B 04S reports $[\Gamma(B^+ \to D_{sJ}(2457)^+\overline{D}^*(2007)^0)/\Gamma_{total}] \times [B(D_{s1}(2460)^+ \to D_s^{*+}\pi^0)] = (7.6 \pm 1.7^{+3.2}_{-2.4}) \times 10^{-3}$ which we divide by our best value $B(D_{s1}(2460)^+ \to D_s^{*+}\pi^0) = (48 \pm 11) \times 10^{-2}$. Our first error is their experiment's error and our second error is the systematic error from using our best value.
[3] Assumes equal production of B^+ and B^0 at the $\Upsilon(4S)$.

$\Gamma(D_{sJ}(2457)^+ \overline{D}^*(2007)^0 \times B(D_{sJ}(2457)^+ \to D_s^+\gamma))/\Gamma_{total}$ Γ_{170}/Γ

VALUE (units 10^{-3})	DOCUMENT ID		TECN	COMMENT
$1.4 \pm 0.4^{+0.6}_{-0.4}$	[1] AUBERT,B	04S	BABR	$e^+e^- \to \Upsilon(4S)$

[1] Assumes equal production of B^+ and B^0 at the $\Upsilon(4S)$.

$\Gamma(\overline{D}^0 D_{s1}(2536)^+ \times B(D_{s1}(2536)^+ \to D^*(2007)^0 K^+))/\Gamma_{total}$ Γ_{172}/Γ

VALUE (units 10^{-4})	CL%	DOCUMENT ID		TECN	COMMENT
$2.16 \pm 0.52 \pm 0.45$		[1] AUBERT	08B	BABR	$e^+e^- \to \Upsilon(4S)$
• • • We do not use the following data for averages, fits, limits, etc. • • •					
<2	90	AUBERT	03X	BABR	Repl. by AUBERT 08B

[1] Assumes equal production of B^+ and B^0 at the $\Upsilon(4S)$.

$\Gamma(\overline{D}^0 D_{s1}(2536)^+ \times B(D_{s1}(2536)^+ \to D^*(2007)^0 K^+ + D^*(2010)^+ K^0))/\Gamma_{total}$ Γ_{171}/Γ

VALUE (units 10^{-4})	DOCUMENT ID		TECN	COMMENT
$3.97 \pm 0.85 \pm 0.56$	[1,2] AUSHEV	11	BELL	$e^+e^- \to \Upsilon(4S)$

[1] Uses $\Gamma(D^*(2007)^0 \to D^0\pi^0)\ /\ \Gamma(D^*(2007)^0 \to D^0\gamma) = 1.74 \pm 0.13$ and $\Gamma(D_{s1}(2536)^+ \to D^*(2007)^0 K^+)\ /\ \Gamma(D_{s1}(2536)^+ \to D^*(2010)^+ K^0) = 1.36 \pm 0.2$.
[2] Assumes equal production of B^+ and B^0 at the $\Upsilon(4S)$.

$\Gamma(\overline{D}^*(2007)^0 D_{s1}(2536)^+ \times B(D_{s1}(2536)^+ \to D^*(2007)^0 K^+))/\Gamma_{total}$ Γ_{173}/Γ

VALUE (units 10^{-4})	CL%	DOCUMENT ID		TECN	COMMENT
$5.46 \pm 1.17 \pm 1.04$		[1] AUBERT	08B	BABR	$e^+e^- \to \Upsilon(4S)$
• • • We do not use the following data for averages, fits, limits, etc. • • •					
<7	90	AUBERT	03X	BABR	Repl. by AUBERT 08B

[1] Assumes equal production of B^+ and B^0 at the $\Upsilon(4S)$.

$\Gamma(\overline{D}^0 D_{s1}(2536)^+ \times B(D_{s1}(2536)^+ \to D^{*+} K^0))/\Gamma_{total}$ Γ_{174}/Γ

VALUE (units 10^{-4})	DOCUMENT ID		TECN	COMMENT
$2.30 \pm 0.98 \pm 0.43$	[1] AUBERT	08B	BABR	$e^+e^- \to \Upsilon(4S)$

[1] Assumes equal production of B^+ and B^0 at the $\Upsilon(4S)$.

$\Gamma(\overline{D}^0 D_{sJ}(2700)^+ \times B(D_{sJ}(2700)^+ \to D^0 K^+))/\Gamma_{total}$ Γ_{175}/Γ

VALUE (units 10^{-4})	DOCUMENT ID		TECN	COMMENT
5.6 ±1.8 OUR AVERAGE Error includes scale factor of 1.7.				
$5.02 \pm 0.71 \pm 0.93$	[1] LEES	15C	BABR	$e^+e^- \to \Upsilon(4S)$
$11.3 \pm 2.2\ ^{+1.4}_{-2.8}$	[1] BRODZICKA	08	BELL	$e^+e^- \to \Upsilon(4S)$

[1] Assumes equal production of B^+ and B^0 at the $\Upsilon(4S)$.

$\Gamma(\overline{D}^{*0} D_{s1}(2536)^+,\ D_{s1}^+ \to D^{*+} K^0)/\Gamma_{total}$ Γ_{176}/Γ

VALUE (units 10^{-4})	DOCUMENT ID		TECN	COMMENT
$3.92 \pm 2.46 \pm 0.83$	[1] AUBERT	08B	BABR	$e^+e^- \to \Upsilon(4S)$

[1] Assumes equal production of B^+ and B^0 at the $\Upsilon(4S)$.

$\Gamma(\overline{D}^0 D_{sJ}(2573)^+,\ D_{sJ}^+ \to D^0 K^+)/\Gamma_{total}$ Γ_{177}/Γ

VALUE (units 10^{-4})	DOCUMENT ID		TECN	COMMENT
$0.08 \pm 0.14 \pm 0.05$	[1] LEES	15C	BABR	$e^+e^- \to \Upsilon(4S)$

[1] Assumes equal production of B^+ and B^0 at the $\Upsilon(4S)$.

$\Gamma(\overline{D}^{*0} D_{sJ}(2573),\ D_{sJ}^+ \to D^0 K^+)/\Gamma_{total}$ Γ_{178}/Γ

VALUE (units 10^{-4})	CL%	DOCUMENT ID		TECN	COMMENT
<2	90	AUBERT	03X	BABR	$e^+e^- \to \Upsilon(4S)$

$\Gamma(\overline{D}^*(2007)^0 D_{sJ}(2573),\ D_{sJ}^+ \to D^0 K^+)/\Gamma_{total}$ Γ_{179}/Γ

VALUE (units 10^{-4})	CL%	DOCUMENT ID		TECN	COMMENT
<5	90	AUBERT	03X	BABR	$e^+e^- \to \Upsilon(4S)$

$\Gamma(\overline{D}^0 D_s^{*+})/\Gamma_{total}$ Γ_{180}/Γ

VALUE	DOCUMENT ID		TECN	COMMENT
0.0076±0.0016 OUR AVERAGE				
$0.0079 \pm 0.0017 \pm 0.0007$	[1] AUBERT	06N	BABR	$e^+e^- \to \Upsilon(4S)$
$0.0068 \pm 0.0025 \pm 0.0006$	[2] GIBAUT	96	CLE2	$e^+e^- \to \Upsilon(4S)$
$0.010\ \pm 0.007\ \pm 0.001$	[3] ALBRECHT	92G	ARG	$e^+e^- \to \Upsilon(4S)$

[1] AUBERT 06N reports $(0.77 \pm 0.15 \pm 0.13) \times 10^{-2}$ from a measurement of $[\Gamma(B^+ \to \overline{D}^0 D_s^{*+})/\Gamma_{total}] \times [B(D_s^+ \to \phi\pi^+)]$ assuming $B(D_s^+ \to \phi\pi^+) = 0.0462 \pm 0.0062$, which we rescale to our best value $B(D_s^+ \to \phi\pi^+) = (4.5 \pm 0.4) \times 10^{-2}$. Our first error is their experiment's error and our second error is the systematic error from using our best value.
[2] GIBAUT 96 reports $0.0087 \pm 0.0027 \pm 0.0017$ from a measurement of $[\Gamma(B^+ \to \overline{D}^0 D_s^{*+})/\Gamma_{total}] \times [B(D_s^+ \to \phi\pi^+)]$ assuming $B(D_s^+ \to \phi\pi^+) = 0.035$, which we rescale to our best value $B(D_s^+ \to \phi\pi^+) = (4.5 \pm 0.4) \times 10^{-2}$. Our first error is

their experiment's error and our second error is the systematic error from using our best value.

[3] ALBRECHT 92G reports $0.016 \pm 0.012 \pm 0.003$ from a measurement of $[\Gamma(B^+ \to \overline{D}^0 D_s^{*+})/\Gamma_{\rm total}] \times [{\rm B}(D_s^+ \to \phi\pi^+)]$ assuming ${\rm B}(D_s^+ \to \phi\pi^+) = 0.027$, which we rescale to our best value ${\rm B}(D_s^+ \to \phi\pi^+) = (4.5 \pm 0.4) \times 10^{-2}$. Our first error is their experiment's error and our second error is the systematic error from using our best value. Assumes PDG 1990 D^0 branching ratios, e.g., ${\rm B}(D^0 \to K^-\pi^+) = 3.71 \pm 0.25\%$.

$\Gamma(\overline{D}^*(2007)^0 D_s^+)/\Gamma_{\rm total}$ Γ_{181}/Γ

VALUE	DOCUMENT ID		TECN	COMMENT
0.0082±0.0017 OUR AVERAGE				
$0.0078 \pm 0.0018 \pm 0.0007$	[1] AUBERT	06N	BABR	$e^+e^- \to \Upsilon(4S)$
$0.011 \pm 0.004 \pm 0.001$	[2] GIBAUT	96	CLE2	$e^+e^- \to \Upsilon(4S)$
$0.008 \pm 0.006 \pm 0.001$	[3] ALBRECHT	92G	ARG	$e^+e^- \to \Upsilon(4S)$

[1] AUBERT 06N reports $(0.76 \pm 0.15 \pm 0.13) \times 10^{-2}$ from a measurement of $[\Gamma(B^+ \to \overline{D}^*(2007)^0 D_s^+)/\Gamma_{\rm total}] \times [{\rm B}(D_s^+ \to \phi\pi^+)]$ assuming ${\rm B}(D_s^+ \to \phi\pi^+) = 0.0462 \pm 0.0062$, which we rescale to our best value ${\rm B}(D_s^+ \to \phi\pi^+) = (4.5 \pm 0.4) \times 10^{-2}$. Our first error is their experiment's error and our second error is the systematic error from using our best value.

[2] GIBAUT 96 reports $0.0140 \pm 0.0043 \pm 0.0035$ from a measurement of $[\Gamma(B^+ \to \overline{D}^*(2007)^0 D_s^+)/\Gamma_{\rm total}] \times [{\rm B}(D_s^+ \to \phi\pi^+)]$ assuming ${\rm B}(D_s^+ \to \phi\pi^+) = 0.035$, which we rescale to our best value ${\rm B}(D_s^+ \to \phi\pi^+) = (4.5 \pm 0.4) \times 10^{-2}$. Our first error is their experiment's error and our second error is the systematic error from using our best value.

[3] ALBRECHT 92G reports $0.013 \pm 0.009 \pm 0.002$ from a measurement of $[\Gamma(B^+ \to \overline{D}^*(2007)^0 D_s^+)/\Gamma_{\rm total}] \times [{\rm B}(D_s^+ \to \phi\pi^+)]$ assuming ${\rm B}(D_s^+ \to \phi\pi^+) = 0.027$, which we rescale to our best value ${\rm B}(D_s^+ \to \phi\pi^+) = (4.5 \pm 0.4) \times 10^{-2}$. Our first error is their experiment's error and our second error is the systematic error from using our best value. Assumes PDG 1990 D^0 and $D^*(2007)^0$ branching ratios, e.g., ${\rm B}(D^0 \to K^-\pi^+) = 3.71 \pm 0.25\%$ and ${\rm B}(D^*(2007)^0 \to D^0\pi^0) = 55 \pm 6\%$.

$\Gamma(\overline{D}^*(2007)^0 D_s^{*+})/\Gamma_{\rm total}$ Γ_{182}/Γ

VALUE	DOCUMENT ID		TECN	COMMENT
0.0171±0.0024 OUR AVERAGE				
$0.0167 \pm 0.0019 \pm 0.0015$	[1] AUBERT	06N	BABR	$e^+e^- \to \Upsilon(4S)$
$0.024 \pm 0.009 \pm 0.002$	[2] GIBAUT	96	CLE2	$e^+e^- \to \Upsilon(4S)$
$0.019 \pm 0.010 \pm 0.002$	[3] ALBRECHT	92G	ARG	$e^+e^- \to \Upsilon(4S)$

[1] AUBERT 06N reports $(1.62 \pm 0.22 \pm 0.18) \times 10^{-2}$ from a measurement of $[\Gamma(B^+ \to \overline{D}^*(2007)^0 D_s^{*+})/\Gamma_{\rm total}] \times [{\rm B}(D_s^+ \to \phi\pi^+)]$ assuming ${\rm B}(D_s^+ \to \phi\pi^+) = 0.0462 \pm 0.0062$, which we rescale to our best value ${\rm B}(D_s^+ \to \phi\pi^+) = (4.5 \pm 0.4) \times 10^{-2}$. Our first error is their experiment's error and our second error is the systematic error from using our best value.

[2] GIBAUT 96 reports $0.0310 \pm 0.0088 \pm 0.0065$ from a measurement of $[\Gamma(B^+ \to \overline{D}^*(2007)^0 D_s^{*+})/\Gamma_{\rm total}] \times [{\rm B}(D_s^+ \to \phi\pi^+)]$ assuming ${\rm B}(D_s^+ \to \phi\pi^+) = 0.035$, which we rescale to our best value ${\rm B}(D_s^+ \to \phi\pi^+) = (4.5 \pm 0.4) \times 10^{-2}$. Our first error is their experiment's error and our second error is the systematic error from using our best value.

[3] ALBRECHT 92G reports $0.031 \pm 0.016 \pm 0.005$ from a measurement of $[\Gamma(B^+ \to \overline{D}^*(2007)^0 D_s^{*+})/\Gamma_{\rm total}] \times [{\rm B}(D_s^+ \to \phi\pi^+)]$ assuming ${\rm B}(D_s^+ \to \phi\pi^+) = 0.027$, which we rescale to our best value ${\rm B}(D_s^+ \to \phi\pi^+) = (4.5 \pm 0.4) \times 10^{-2}$. Our first error is their experiment's error and our second error is the systematic error from using our best value. Assumes PDG 1990 D^0 and $D^*(2007)^0$ branching ratios, e.g., ${\rm B}(D^0 \to K^-\pi^+) = 3.71 \pm 0.25\%$ and ${\rm B}(D^*(2007)^0 \to D^0\pi^0) = 55 \pm 6\%$.

$\Gamma(D_s^{(*)+}\overline{D}^{**0})/\Gamma_{\rm total}$ Γ_{183}/Γ

VALUE	DOCUMENT ID		TECN	COMMENT
$(2.73 \pm 0.93 \pm 0.68) \times 10^{-2}$	[1] AHMED	00B	CLE2	$e^+e^- \to \Upsilon(4S)$

[1] AHMED 00B reports their experiment's uncertainties $(\pm 0.78 \pm 0.48 \pm 0.68)\%$, where the first error is statistical, the second is systematic, and the third is the uncertainty in the $D_S \to \phi\pi$ branching fraction. We combine the first two in quadrature.

$\Gamma(\overline{D}^*(2007)^0 D^*(2010)^+)/\Gamma_{\rm total}$ Γ_{184}/Γ

VALUE (units 10^{-4})	CL%	DOCUMENT ID		TECN	COMMENT
8.1±1.2±1.2		[1] AUBERT,B	06A	BABR	$e^+e^- \to \Upsilon(4S)$
• • • We do not use the following data for averages, fits, limits, etc. • • •					
<110	90	BARATE	98Q	ALEP	$e^+e^- \to Z$

[1] Assumes equal production of B^+ and B^0 at the $\Upsilon(4S)$.

$[\Gamma(\overline{D}^0 D^*(2010)^+) + \Gamma(\overline{D}^*(2007)^0 D^+)]/\Gamma_{\rm total}$ Γ_{185}/Γ

VALUE (units 10^{-4})	CL%	DOCUMENT ID	TECN	COMMENT
<130	90	BARATE	98Q ALEP	$e^+e^- \to Z$

$\Gamma(\overline{D}^0 D^*(2010)^+)/\Gamma_{\rm total}$ Γ_{186}/Γ

VALUE (units 10^{-4})	DOCUMENT ID		TECN	COMMENT
3.9 ±0.5 OUR AVERAGE				
$3.6 \pm 0.5 \pm 0.4$	[1] AUBERT,B	06A	BABR	$e^+e^- \to \Upsilon(4S)$
$4.57 \pm 0.71 \pm 0.56$	[1] MAJUMDER	05	BELL	$e^+e^- \to \Upsilon(4S)$

[1] Assumes equal production of B^+ and B^0 at the $\Upsilon(4S)$.

$\Gamma(\overline{D}^0 D^+)/\Gamma_{\rm total}$ Γ_{187}/Γ

VALUE (units 10^{-4})	CL%	DOCUMENT ID		TECN	COMMENT
3.8 ±0.4 OUR AVERAGE					
$3.85 \pm 0.31 \pm 0.38$		[1] ADACHI	08	BELL	$e^+e^- \to \Upsilon(4S)$
$3.8 \pm 0.6 \pm 0.5$		[1] AUBERT,B	06A	BABR	$e^+e^- \to \Upsilon(4S)$
• • • We do not use the following data for averages, fits, limits, etc. • • •					
$4.83 \pm 0.78 \pm 0.58$		[1] MAJUMDER	05	BELL	Repl. by ADACHI 08
<67	90	BARATE	98Q	ALEP	$e^+e^- \to Z$

[1] Assumes equal production of B^+ and B^0 at the $\Upsilon(4S)$.

$\Gamma(\overline{D}^0 D^+ K^0)/\Gamma_{\rm total}$ Γ_{188}/Γ

VALUE (units 10^{-3})	CL%	DOCUMENT ID		TECN	COMMENT
1.55±0.17±0.13		[1] DEL-AMO-SA...11B		BABR	$e^+e^- \to \Upsilon(4S)$
• • • We do not use the following data for averages, fits, limits, etc. • • •					
<2.8	90	[1] AUBERT	03X	BABR	Repl. by DEL-AMO-SANCHEZ 11B

[1] Assumes equal production of B^+ and B^0 at the $\Upsilon(4S)$.

$\Gamma(D^+\overline{D}^*(2007)^0)/\Gamma_{\rm total}$ Γ_{189}/Γ

VALUE (units 10^{-4})	DOCUMENT ID		TECN	COMMENT
6.3±1.4±1.0	[1] AUBERT,B	06A	BABR	$e^+e^- \to \Upsilon(4S)$

[1] Assumes equal production of B^+ and B^0 at the $\Upsilon(4S)$.

$\Gamma(\overline{D}^*(2007)^0 D^+ K^0)/\Gamma_{\rm total}$ Γ_{190}/Γ

VALUE (units 10^{-3})	CL%	DOCUMENT ID		TECN	COMMENT
2.06±0.38±0.30		[1] DEL-AMO-SA...11B		BABR	$e^+e^- \to \Upsilon(4S)$
• • • We do not use the following data for averages, fits, limits, etc. • • •					
<6.1	90	[1] AUBERT	03X	BABR	Repl. by DEL-AMO-SANCHEZ 11B

[1] Assumes equal production of B^+ and B^0 at the $\Upsilon(4S)$.

$\Gamma(\overline{D}^0 D^*(2010)^+ K^0)/\Gamma_{\rm total}$ Γ_{191}/Γ

VALUE (units 10^{-3})	DOCUMENT ID		TECN	COMMENT
3.81±0.31±0.23	[1] DEL-AMO-SA...11B		BABR	$e^+e^- \to \Upsilon(4S)$
• • • We do not use the following data for averages, fits, limits, etc. • • •				
$5.2\ ^{+1.0}_{-0.9} \pm 0.7$	[1] AUBERT	03X	BABR	Repl. by DEL-AMO-SANCHEZ 11B

[1] Assumes equal production of B^+ and B^0 at the $\Upsilon(4S)$.

$\Gamma(\overline{D}^*(2007)^0 D^*(2010)^+ K^0)/\Gamma_{\rm total}$ Γ_{192}/Γ

VALUE (units 10^{-3})	DOCUMENT ID		TECN	COMMENT
9.17±0.83±0.90	[1] DEL-AMO-SA...11B		BABR	$e^+e^- \to \Upsilon(4S)$
• • • We do not use the following data for averages, fits, limits, etc. • • •				
$7.8\ ^{+2.3}_{-2.1} \pm 1.4$	[1] AUBERT	03X	BABR	Repl. by DEL-AMO-SANCHEZ 11B

[1] Assumes equal production of B^+ and B^0 at the $\Upsilon(4S)$.

$\Gamma(\overline{D}^0 D^0 K^+)/\Gamma_{\rm total}$ Γ_{193}/Γ

VALUE (units 10^{-3})	DOCUMENT ID		TECN	COMMENT
1.45±0.33 OUR AVERAGE	Error includes scale factor of 2.6.			
$1.31 \pm 0.07 \pm 0.12$	[1] DEL-AMO-SA...11B		BABR	$e^+e^- \to \Upsilon(4S)$
$2.22 \pm 0.22\ ^{+0.26}_{-0.24}$	[1] BRODZICKA	08	BELL	$e^+e^- \to \Upsilon(4S)$
• • • We do not use the following data for averages, fits, limits, etc. • • •				
$1.17 \pm 0.21 \pm 0.15$	[1] CHISTOV	04	BELL	Repl. by BRODZICKA 08
$1.9 \pm 0.3 \pm 0.3$	[1] AUBERT	03X	BABR	Repl. by DEL-AMO-SANCHEZ 11B

[1] Assumes equal production of B^+ and B^0 at the $\Upsilon(4S)$.

$\Gamma(\overline{D}^*(2007)^0 D^0 K^+)/\Gamma_{\rm total}$ Γ_{194}/Γ

VALUE (units 10^{-3})	CL%	DOCUMENT ID		TECN	COMMENT
2.26±0.16±0.17		[1] DEL-AMO-SA...11B		BABR	$e^+e^- \to \Upsilon(4S)$
• • • We do not use the following data for averages, fits, limits, etc. • • •					
<3.8	90	[1] AUBERT	03X	BABR	Repl. by DEL-AMO-SANCHEZ 11B

[1] Assumes equal production of B^+ and B^0 at the $\Upsilon(4S)$.

$\Gamma(\overline{D}^0 D^*(2007)^0 K^+)/\Gamma_{\rm total}$ Γ_{195}/Γ

VALUE (units 10^{-3})	DOCUMENT ID		TECN	COMMENT
6.32±0.19±0.45	[1] DEL-AMO-SA...11B		BABR	$e^+e^- \to \Upsilon(4S)$
• • • We do not use the following data for averages, fits, limits, etc. • • •				
$4.7 \pm 0.7 \pm 0.7$	[1] AUBERT	03X	BABR	Repl. by DEL-AMO-SANCHEZ 11B

[1] Assumes equal production of B^+ and B^0 at the $\Upsilon(4S)$.

$\Gamma(\overline{D}^*(2007)^0 D^*(2007)^0 K^+)/\Gamma_{\rm total}$ Γ_{196}/Γ

VALUE (units 10^{-3})	DOCUMENT ID		TECN	COMMENT
11.23±0.36±1.26	[1] DEL-AMO-SA...11B		BABR	$e^+e^- \to \Upsilon(4S)$
• • • We do not use the following data for averages, fits, limits, etc. • • •				
$5.3\ ^{+1.1}_{-1.0} \pm 1.2$	[1] AUBERT	03X	BABR	Repl. by DEL-AMO-SANCHEZ 11B

[1] Assumes equal production of B^+ and B^0 at the $\Upsilon(4S)$.

$\Gamma(D^- D^+ K^+)/\Gamma_{total}$ Γ_{197}/Γ

VALUE (units 10^{-3})	CL%	DOCUMENT ID		TECN	COMMENT
0.22 ± 0.05 ± 0.05		[1] DEL-AMO-SA...11B	BABR		$e^+e^- \to \Upsilon(4S)$
• • • We do not use the following data for averages, fits, limits, etc. • • •					
<0.90	90	[1] CHISTOV	04	BELL	$e^+e^- \to \Upsilon(4S)$
<0.4	90	[1] AUBERT	03X	BABR	Repl. by DEL-AMO-SANCHEZ 11B

[1] Assumes equal production of B^+ and B^0 at the $\Upsilon(4S)$.

$\Gamma(D^- D^*(2010)^+ K^+)/\Gamma_{total}$ Γ_{198}/Γ

VALUE (units 10^{-3})	CL%	DOCUMENT ID		TECN	COMMENT
0.63 ± 0.09 ± 0.06		[1] DEL-AMO-SA...11B	BABR		$e^+e^- \to \Upsilon(4S)$
• • • We do not use the following data for averages, fits, limits, etc. • • •					
<0.7	90	[1] AUBERT	03X	BABR	Repl. by DEL-AMO-SANCHEZ 11B

[1] Assumes equal production of B^+ and B^0 at the $\Upsilon(4S)$.

$\Gamma(D^*(2010)^- D^+ K^+)/\Gamma_{total}$ Γ_{199}/Γ

VALUE (units 10^{-3})	DOCUMENT ID		TECN	COMMENT
0.60 ± 0.10 ± 0.08	[1] DEL-AMO-SA...11B	BABR		$e^+e^- \to \Upsilon(4S)$
• • • We do not use the following data for averages, fits, limits, etc. • • •				
1.5 ±0.3 ±0.2	[1] AUBERT	03X	BABR	Repl. by DEL-AMO-SANCHEZ 11B

[1] Assumes equal production of B^+ and B^0 at the $\Upsilon(4S)$.

$\Gamma(D^*(2010)^- D^*(2010)^+ K^+)/\Gamma_{total}$ Γ_{200}/Γ

VALUE (units 10^{-3})	CL%	DOCUMENT ID		TECN	COMMENT
1.32 ± 0.13 ± 0.12		[1] DEL-AMO-SA...11B	BABR		$e^+e^- \to \Upsilon(4S)$
• • • We do not use the following data for averages, fits, limits, etc. • • •					
<1.8	90	[1] AUBERT	03X	BABR	Repl. by DEL-AMO-SANCHEZ 11B

[1] Assumes equal production of B^+ and B^0 at the $\Upsilon(4S)$.

$\Gamma((\overline{D}+\overline{D}^*)(D+D^*)K)/\Gamma_{total}$ Γ_{201}/Γ

VALUE (units 10^{-2})	DOCUMENT ID		TECN	COMMENT
4.05 ± 0.11 ± 0.28	[1] DEL-AMO-SA...11B	BABR		$e^+e^- \to \Upsilon(4S)$
• • • We do not use the following data for averages, fits, limits, etc. • • •				
3.5 ±0.3 ±0.5	[1] AUBERT	03X	BABR	Repl. by DEL-AMO-SANCHEZ 11B

[1] Assumes equal production of B^+ and B^0 at the $\Upsilon(4S)$.

$\Gamma(D_s^+ \pi^0)/\Gamma_{total}$ Γ_{202}/Γ

VALUE (units 10^{-5})	CL%	DOCUMENT ID		TECN	COMMENT
$1.6^{+0.6}_{-0.5} \pm 0.1$		[1] AUBERT	07M	BABR	$e^+e^- \to \Upsilon(4S)$
• • • We do not use the following data for averages, fits, limits, etc. • • •					
<16	90	[2] ALEXANDER	93B	CLE2	$e^+e^- \to \Upsilon(4S)$

[1] AUBERT 07M reports $[\Gamma(B^+ \to D_s^+\pi^0)/\Gamma_{total}] \times [B(D_s^+ \to \phi\pi^+)] = (7.0^{+2.4}_{-2.1}{}^{+0.6}_{-0.8}) \times 10^{-7}$ which we divide by our best value $B(D_s^+ \to \phi\pi^+) = (4.5 \pm 0.4) \times 10^{-2}$. Our first error is their experiment's error and our second error is the systematic error from using our best value.

[2] ALEXANDER 93B reports $< 2.0 \times 10^{-4}$ from a measurement of $[\Gamma(B^+ \to D_s^+\pi^0)/\Gamma_{total}] \times [B(D_s^+ \to \phi\pi^+)]$ assuming $B(D_s^+ \to \phi\pi^+) = 0.037$, which we rescale to our best value $B(D_s^+ \to \phi\pi^+) = 4.5 \times 10^{-2}$.

$\left[\Gamma(D_s^+ \pi^0) + \Gamma(D_s^{*+} \pi^0)\right]/\Gamma_{total}$ $(\Gamma_{202}+\Gamma_{203})/\Gamma$

VALUE	CL%	DOCUMENT ID		TECN	COMMENT
$< 5 \times 10^{-4}$	90	[1] ALBRECHT	93E	ARG	$e^+e^- \to \Upsilon(4S)$

[1] ALBRECHT 93E reports $< 0.9 \times 10^{-3}$ from a measurement of $[\left[\Gamma(B^+ \to D_s^+\pi^0) + \Gamma(B^+ \to D_s^{*+}\pi^0)\right]/\Gamma_{total}] \times [B(D_s^+ \to \phi\pi^+)]$ assuming $B(D_s^+ \to \phi\pi^+) = 0.027$, which we rescale to our best value $B(D_s^+ \to \phi\pi^+) = 4.5 \times 10^{-2}$.

$\Gamma(D_s^{*+} \pi^0)/\Gamma_{total}$ Γ_{203}/Γ

VALUE	CL%	DOCUMENT ID		TECN	COMMENT
$< 2.6 \times 10^{-4}$	90	[1] ALEXANDER	93B	CLE2	$e^+e^- \to \Upsilon(4S)$

[1] ALEXANDER 93B reports $< 3.2 \times 10^{-4}$ from a measurement of $[\Gamma(B^+ \to D_s^{*+}\pi^0)/\Gamma_{total}] \times [B(D_s^+ \to \phi\pi^+)]$ assuming $B(D_s^+ \to \phi\pi^+) = 0.037$, which we rescale to our best value $B(D_s^+ \to \phi\pi^+) = 4.5 \times 10^{-2}$.

$\Gamma(D_s^+ \eta)/\Gamma_{total}$ Γ_{204}/Γ

VALUE	CL%	DOCUMENT ID		TECN	COMMENT
$< 4 \times 10^{-4}$	90	[1] ALEXANDER	93B	CLE2	$e^+e^- \to \Upsilon(4S)$

[1] ALEXANDER 93B reports $< 4.6 \times 10^{-4}$ from a measurement of $[\Gamma(B^+ \to D_s^+\eta)/\Gamma_{total}] \times [B(D_s^+ \to \phi\pi^+)]$ assuming $B(D_s^+ \to \phi\pi^+) = 0.037$, which we rescale to our best value $B(D_s^+ \to \phi\pi^+) = 4.5 \times 10^{-2}$.

$\Gamma(D_s^{*+} \eta)/\Gamma_{total}$ Γ_{205}/Γ

VALUE	CL%	DOCUMENT ID		TECN	COMMENT
$< 6 \times 10^{-4}$	90	[1] ALEXANDER	93B	CLE2	$e^+e^- \to \Upsilon(4S)$

[1] ALEXANDER 93B reports $< 7.5 \times 10^{-4}$ from a measurement of $[\Gamma(B^+ \to D_s^{*+}\eta)/\Gamma_{total}] \times [B(D_s^+ \to \phi\pi^+)]$ assuming $B(D_s^+ \to \phi\pi^+) = 0.037$, which we rescale to our best value $B(D_s^+ \to \phi\pi^+) = 4.5 \times 10^{-2}$.

$\Gamma(D_s^+ \rho^0)/\Gamma_{total}$ Γ_{206}/Γ

VALUE	CL%	DOCUMENT ID		TECN	COMMENT
$< 3.0 \times 10^{-4}$	90	[1] ALEXANDER	93B	CLE2	$e^+e^- \to \Upsilon(4S)$

[1] ALEXANDER 93B reports $< 3.7 \times 10^{-4}$ from a measurement of $[\Gamma(B^+ \to D_s^+\rho^0)/\Gamma_{total}] \times [B(D_s^+ \to \phi\pi^+)]$ assuming $B(D_s^+ \to \phi\pi^+) = 0.037$, which we rescale to our best value $B(D_s^+ \to \phi\pi^+) = 4.5 \times 10^{-2}$.

$\left[\Gamma(D_s^+ \rho^0) + \Gamma(D_s^+ \overline{K}^*(892)^0)\right]/\Gamma_{total}$ $(\Gamma_{206}+\Gamma_{217})/\Gamma$

VALUE	CL%	DOCUMENT ID		TECN	COMMENT
$< 2.0 \times 10^{-3}$	90	[1] ALBRECHT	93E	ARG	$e^+e^- \to \Upsilon(4S)$

[1] ALBRECHT 93E reports $< 3.4 \times 10^{-3}$ from a measurement of $[\left[\Gamma(B^+ \to D_s^+\rho^0) + \Gamma(B^+ \to D_s^+ \overline{K}^*(892)^0)\right]/\Gamma_{total}] \times [B(D_s^+ \to \phi\pi^+)]$ assuming $B(D_s^+ \to \phi\pi^+) = 0.027$, which we rescale to our best value $B(D_s^+ \to \phi\pi^+) = 4.5 \times 10^{-2}$.

$\Gamma(D_s^{*+} \rho^0)/\Gamma_{total}$ Γ_{207}/Γ

VALUE	CL%	DOCUMENT ID		TECN	COMMENT
$< 4 \times 10^{-4}$	90	[1] ALEXANDER	93B	CLE2	$e^+e^- \to \Upsilon(4S)$

[1] ALEXANDER 93B reports $< 4.8 \times 10^{-4}$ from a measurement of $[\Gamma(B^+ \to D_s^{*+}\rho^0)/\Gamma_{total}] \times [B(D_s^+ \to \phi\pi^+)]$ assuming $B(D_s^+ \to \phi\pi^+) = 0.037$, which we rescale to our best value $B(D_s^+ \to \phi\pi^+) = 4.5 \times 10^{-2}$.

$\left[\Gamma(D_s^{*+} \rho^0) + \Gamma(D_s^{*+} \overline{K}^*(892)^0)\right]/\Gamma_{total}$ $(\Gamma_{207}+\Gamma_{219})/\Gamma$

VALUE	CL%	DOCUMENT ID		TECN	COMMENT
$< 1.2 \times 10^{-3}$	90	[1] ALBRECHT	93E	ARG	$e^+e^- \to \Upsilon(4S)$

[1] ALBRECHT 93E reports $< 2.0 \times 10^{-3}$ from a measurement of $[\left[\Gamma(B^+ \to D_s^{*+}\rho^0) + \Gamma(B^+ \to D_s^{*+} \overline{K}^*(892)^0)\right]/\Gamma_{total}] \times [B(D_s^+ \to \phi\pi^+)]$ assuming $B(D_s^+ \to \phi\pi^+) = 0.027$, which we rescale to our best value $B(D_s^+ \to \phi\pi^+) = 4.5 \times 10^{-2}$.

$\Gamma(D_s^+ \omega)/\Gamma_{total}$ Γ_{208}/Γ

VALUE	CL%	DOCUMENT ID		TECN	COMMENT
$< 4 \times 10^{-4}$	90	[1] ALEXANDER	93B	CLE2	$e^+e^- \to \Upsilon(4S)$
• • • We do not use the following data for averages, fits, limits, etc. • • •					
$< 2.0 \times 10^{-3}$	90	[2] ALBRECHT	93E	ARG	$e^+e^- \to \Upsilon(4S)$

[1] ALEXANDER 93B reports $< 4.8 \times 10^{-4}$ from a measurement of $[\Gamma(B^+ \to D_s^+\omega)/\Gamma_{total}] \times [B(D_s^+ \to \phi\pi^+)]$ assuming $B(D_s^+ \to \phi\pi^+) = 0.037$, which we rescale to our best value $B(D_s^+ \to \phi\pi^+) = 4.5 \times 10^{-2}$.

[2] ALBRECHT 93E reports $< 3.4 \times 10^{-3}$ from a measurement of $[\Gamma(B^+ \to D_s^+\omega)/\Gamma_{total}] \times [B(D_s^+ \to \phi\pi^+)]$ assuming $B(D_s^+ \to \phi\pi^+) = 0.027$, which we rescale to our best value $B(D_s^+ \to \phi\pi^+) = 4.5 \times 10^{-2}$.

$\Gamma(D_s^{*+} \omega)/\Gamma_{total}$ Γ_{209}/Γ

VALUE	CL%	DOCUMENT ID		TECN	COMMENT
$< 6 \times 10^{-4}$	90	[1] ALEXANDER	93B	CLE2	$e^+e^- \to \Upsilon(4S)$
• • • We do not use the following data for averages, fits, limits, etc. • • •					
$< 1.1 \times 10^{-3}$	90	[2] ALBRECHT	93E	ARG	$e^+e^- \to \Upsilon(4S)$

[1] ALEXANDER 93B reports $< 6.8 \times 10^{-4}$ from a measurement of $[\Gamma(B^+ \to D_s^{*+}\omega)/\Gamma_{total}] \times [B(D_s^+ \to \phi\pi^+)]$ assuming $B(D_s^+ \to \phi\pi^+) = 0.037$, which we rescale to our best value $B(D_s^+ \to \phi\pi^+) = 4.5 \times 10^{-2}$.

[2] ALBRECHT 93E reports $< 1.9 \times 10^{-3}$ from a measurement of $[\Gamma(B^+ \to D_s^{*+}\omega)/\Gamma_{total}] \times [B(D_s^+ \to \phi\pi^+)]$ assuming $B(D_s^+ \to \phi\pi^+) = 0.027$, which we rescale to our best value $B(D_s^+ \to \phi\pi^+) = 4.5 \times 10^{-2}$.

$\Gamma(D_s^+ a_1(1260)^0)/\Gamma_{total}$ Γ_{210}/Γ

VALUE	CL%	DOCUMENT ID		TECN	COMMENT
$< 1.8 \times 10^{-3}$	90	[1] ALBRECHT	93E	ARG	$e^+e^- \to \Upsilon(4S)$

[1] ALBRECHT 93E reports $< 3.0 \times 10^{-3}$ from a measurement of $[\Gamma(B^+ \to D_s^+ a_1(1260)^0)/\Gamma_{total}] \times [B(D_s^+ \to \phi\pi^+)]$ assuming $B(D_s^+ \to \phi\pi^+) = 0.027$, which we rescale to our best value $B(D_s^+ \to \phi\pi^+) = 4.5 \times 10^{-2}$.

$\Gamma(D_s^{*+} a_1(1260)^0)/\Gamma_{total}$ Γ_{211}/Γ

VALUE	CL%	DOCUMENT ID		TECN	COMMENT
$< 1.3 \times 10^{-3}$	90	[1] ALBRECHT	93E	ARG	$e^+e^- \to \Upsilon(4S)$

[1] ALBRECHT 93E reports $< 2.2 \times 10^{-3}$ from a measurement of $[\Gamma(B^+ \to D_s^{*+} a_1(1260)^0)/\Gamma_{\text{total}}] \times [\text{B}(D_s^+ \to \phi\pi^+)]$ assuming $\text{B}(D_s^+ \to \phi\pi^+) = 0.027$, which we rescale to our best value $\text{B}(D_s^+ \to \phi\pi^+) = 4.5 \times 10^{-2}$.

$\Gamma(D_s^+ K^+ K^-)/\Gamma(\overline{D}^0 D_s^+)$ $\Gamma_{212}/\Gamma_{160}$

VALUE (units 10^{-4})		DOCUMENT ID		TECN	COMMENT
7.8±0.9±0.1	[1]	AAIJ	18B	LHCB	pp at 7, 8, 13 TeV

[1] AAIJ 18B reports $[\Gamma(B^+ \to D_s^+ K^+ K^-)/\Gamma(B^+ \to \overline{D}^0 D_s^+)] / [\text{B}(D^0 \to K^+ K^-)] = 0.197 \pm 0.015 \pm 0.017$ which we multiply by our best value $\text{B}(D^0 \to K^+ K^-) = (3.97 \pm 0.07) \times 10^{-3}$. Our first error is their experiment's error and our second error is the systematic error from using our best value.

$\Gamma(D_s^+ \phi)/\Gamma_{\text{total}}$ Γ_{213}/Γ

VALUE (units 10^{-6})	CL%		DOCUMENT ID		TECN	COMMENT
< 0.42	90	[1]	AAIJ	18B	LHCB	pp at 7, 8, 13 TeV
• • • We do not use the following data for averages, fits, limits, etc. • • •						
$1.7\ ^{+1.1}_{-0.7} \pm 0.2$		[2]	AAIJ	13R	LHCB	Repl. by AAIJ 18B
< 1.9	90	[3]	AUBERT	06F	BABR	$e^+e^- \to \Upsilon(4S)$
<1000	90	[4]	ALBRECHT	93E	ARG	$e^+e^- \to \Upsilon(4S)$
< 260	90	[5]	ALEXANDER	93B	CLE2	$e^+e^- \to \Upsilon(4S)$

[1] AAIJ 18B uses $B^+ \to D_s^+ \overline{D}^0$ decays for normalization.

[2] AAIJ 13R reports $(1.87\ ^{+1.25}_{-0.73} \pm 0.19 \pm 0.32) \times 10^{-6}$ from a measurement of $[\Gamma(B^+ \to D_s^+ \phi)/\Gamma_{\text{total}}] / [\text{B}(B^+ \to \overline{D}^0 D_s^+)]$ assuming $\text{B}(B^+ \to \overline{D}^0 D_s^+) = (10.0 \pm 1.7) \times 10^{-3}$, which we rescale to our best value $\text{B}(B^+ \to \overline{D}^0 D_s^+) = (9.0 \pm 0.9) \times 10^{-3}$. Our first error is their experiment's error and our second error is the systematic error from using our best value.

[3] Assumes equal production of B^+ and B^0 at the $\Upsilon(4S)$.

[4] ALBRECHT 93E reports $< 1.7 \times 10^{-3}$ from a measurement of $[\Gamma(B^+ \to D_s^+ \phi)/\Gamma_{\text{total}}] \times [\text{B}(D_s^+ \to \phi\pi^+)]$ assuming $\text{B}(D_s^+ \to \phi\pi^+) = 0.027$, which we rescale to our best value $\text{B}(D_s^+ \to \phi\pi^+) = 4.5 \times 10^{-2}$.

[5] ALEXANDER 93B reports $< 3.1 \times 10^{-4}$ from a measurement of $[\Gamma(B^+ \to D_s^+ \phi)/\Gamma_{\text{total}}] \times [\text{B}(D_s^+ \to \phi\pi^+)]$ assuming $\text{B}(D_s^+ \to \phi\pi^+) = 0.037$, which we rescale to our best value $\text{B}(D_s^+ \to \phi\pi^+) = 4.5 \times 10^{-2}$.

$\Gamma(D_s^{*+} \phi)/\Gamma_{\text{total}}$ Γ_{214}/Γ

VALUE	CL%		DOCUMENT ID		TECN	COMMENT
<1.2 × 10⁻⁵	90	[1]	AUBERT	06F	BABR	$e^+e^- \to \Upsilon(4S)$
• • • We do not use the following data for averages, fits, limits, etc. • • •						
$<1.3 \times 10^{-3}$	90	[2]	ALBRECHT	93E	ARG	$e^+e^- \to \Upsilon(4S)$
$<3.5 \times 10^{-4}$	90	[3]	ALEXANDER	93B	CLE2	$e^+e^- \to \Upsilon(4S)$

[1] Assumes equal production of B^+ and B^0 at the $\Upsilon(4S)$.

[2] ALBRECHT 93E reports $< 2.1 \times 10^{-3}$ from a measurement of $[\Gamma(B^+ \to D_s^{*+} \phi)/\Gamma_{\text{total}}] \times [\text{B}(D_s^+ \to \phi\pi^+)]$ assuming $\text{B}(D_s^+ \to \phi\pi^+) = 0.027$, which we rescale to our best value $\text{B}(D_s^+ \to \phi\pi^+) = 4.5 \times 10^{-2}$.

[3] ALEXANDER 93B reports $< 4.2 \times 10^{-4}$ from a measurement of $[\Gamma(B^+ \to D_s^{*+} \phi)/\Gamma_{\text{total}}] \times [\text{B}(D_s^+ \to \phi\pi^+)]$ assuming $\text{B}(D_s^+ \to \phi\pi^+) = 0.037$, which we rescale to our best value $\text{B}(D_s^+ \to \phi\pi^+) = 4.5 \times 10^{-2}$.

$\Gamma(D_s^+ \overline{K}^0)/\Gamma_{\text{total}}$ Γ_{215}/Γ

VALUE	CL%		DOCUMENT ID		TECN	COMMENT
<8 × 10⁻⁴	90	[1]	ALEXANDER	93B	CLE2	$e^+e^- \to \Upsilon(4S)$
• • • We do not use the following data for averages, fits, limits, etc. • • •						
$<1.5 \times 10^{-3}$	90	[2]	ALBRECHT	93E	ARG	$e^+e^- \to \Upsilon(4S)$

[1] ALEXANDER 93B reports $< 10.3 \times 10^{-4}$ from a measurement of $[\Gamma(B^+ \to D_s^+ \overline{K}^0)/\Gamma_{\text{total}}] \times [\text{B}(D_s^+ \to \phi\pi^+)]$ assuming $\text{B}(D_s^+ \to \phi\pi^+) = 0.037$, which we rescale to our best value $\text{B}(D_s^+ \to \phi\pi^+) = 4.5 \times 10^{-2}$.

[2] ALBRECHT 93E reports $< 2.5 \times 10^{-3}$ from a measurement of $[\Gamma(B^+ \to D_s^+ \overline{K}^0)/\Gamma_{\text{total}}] \times [\text{B}(D_s^+ \to \phi\pi^+)]$ assuming $\text{B}(D_s^+ \to \phi\pi^+) = 0.027$, which we rescale to our best value $\text{B}(D_s^+ \to \phi\pi^+) = 4.5 \times 10^{-2}$.

$\Gamma(D_s^{*+} \overline{K}^0)/\Gamma_{\text{total}}$ Γ_{216}/Γ

VALUE	CL%		DOCUMENT ID		TECN	COMMENT
<9 × 10⁻⁴	90	[1]	ALEXANDER	93B	CLE2	$e^+e^- \to \Upsilon(4S)$
• • • We do not use the following data for averages, fits, limits, etc. • • •						
$<1.9 \times 10^{-3}$	90	[2]	ALBRECHT	93E	ARG	$e^+e^- \to \Upsilon(4S)$

[1] ALEXANDER 93B reports $< 10.9 \times 10^{-4}$ from a measurement of $[\Gamma(B^+ \to D_s^{*+} \overline{K}^0)/\Gamma_{\text{total}}] \times [\text{B}(D_s^+ \to \phi\pi^+)]$ assuming $\text{B}(D_s^+ \to \phi\pi^+) = 0.037$, which we rescale to our best value $\text{B}(D_s^+ \to \phi\pi^+) = 4.5 \times 10^{-2}$.

[2] ALBRECHT 93E reports $< 3.1 \times 10^{-3}$ from a measurement of $[\Gamma(B^+ \to D_s^{*+} \overline{K}^0)/\Gamma_{\text{total}}] \times [\text{B}(D_s^+ \to \phi\pi^+)]$ assuming $\text{B}(D_s^+ \to \phi\pi^+) = 0.027$, which we rescale to our best value $\text{B}(D_s^+ \to \phi\pi^+) = 4.5 \times 10^{-2}$.

$\Gamma(D_s^+ \overline{K}^*(892)^0)/\Gamma_{\text{total}}$ Γ_{217}/Γ

VALUE	CL%		DOCUMENT ID		TECN	COMMENT
<4.4 × 10⁻⁶	90		AAIJ	13R	LHCB	pp at 7 TeV
• • • We do not use the following data for averages, fits, limits, etc. • • •						
$<4 \times 10^{-4}$	90	[1]	ALEXANDER	93B	CLE2	$e^+e^- \to \Upsilon(4S)$

[1] ALEXANDER 93B reports $< 4.4 \times 10^{-4}$ from a measurement of $[\Gamma(B^+ \to D_s^+ \overline{K}^*(892)^0)/\Gamma_{\text{total}}] \times [\text{B}(D_s^+ \to \phi\pi^+)]$ assuming $\text{B}(D_s^+ \to \phi\pi^+) = 0.037$, which we rescale to our best value $\text{B}(D_s^+ \to \phi\pi^+) = 4.5 \times 10^{-2}$.

$\Gamma(D_s^+ K^{*0})/\Gamma_{\text{total}}$ Γ_{218}/Γ

VALUE (units 10^{-6})	CL%	DOCUMENT ID		TECN	COMMENT
<3.5	90	AAIJ	13R	LHCB	pp at 7 TeV

$\Gamma(D_s^{*+} \overline{K}^*(892)^0)/\Gamma_{\text{total}}$ Γ_{219}/Γ

VALUE	CL%		DOCUMENT ID		TECN	COMMENT
<3.5 × 10⁻⁴	90	[1]	ALEXANDER	93B	CLE2	$e^+e^- \to \Upsilon(4S)$

[1] ALEXANDER 93B reports $< 4.3 \times 10^{-4}$ from a measurement of $[\Gamma(B^+ \to D_s^{*+} \overline{K}^*(892)^0)/\Gamma_{\text{total}}] \times [\text{B}(D_s^+ \to \phi\pi^+)]$ assuming $\text{B}(D_s^+ \to \phi\pi^+) = 0.037$, which we rescale to our best value $\text{B}(D_s^+ \to \phi\pi^+) = 4.5 \times 10^{-2}$.

$\Gamma(D_s^- \pi^+ K^+)/\Gamma_{\text{total}}$ Γ_{220}/Γ

VALUE (units 10^{-4})	CL%	DOCUMENT ID		TECN	COMMENT
1.80±0.22 OUR AVERAGE					
$1.71\ ^{+0.08}_{-0.07} \pm 0.25$		[1] WIECHCZYN...09		BELL	$e^+e^- \to \Upsilon(4S)$
$2.02 \pm 0.13 \pm 0.38$		[1] AUBERT	08G	BABR	$e^+e^- \to \Upsilon(4S)$
• • • We do not use the following data for averages, fits, limits, etc. • • •					
<7	90	[2] ALBRECHT	93E	ARG	$e^+e^- \to \Upsilon(4S)$

[1] Assumes equal production of B^+ and B^0 at the $\Upsilon(4S)$.

[2] ALBRECHT 93E reports $< 1.1 \times 10^{-3}$ from a measurement of $[\Gamma(B^+ \to D_s^- \pi^+ K^+)/\Gamma_{\text{total}}] \times [\text{B}(D_s^+ \to \phi\pi^+)]$ assuming $\text{B}(D_s^+ \to \phi\pi^+) = 0.027$, which we rescale to our best value $\text{B}(D_s^+ \to \phi\pi^+) = 4.5 \times 10^{-2}$.

$\Gamma(D_s^{*-} \pi^+ K^+)/\Gamma_{\text{total}}$ Γ_{221}/Γ

VALUE (units 10^{-4})	CL%	DOCUMENT ID		TECN	COMMENT
1.45±0.24 OUR AVERAGE					
$1.31\ ^{+0.13}_{-0.12} \pm 0.28$		[1] WIECHCZYN...09		BELL	$e^+e^- \to \Upsilon(4S)$
$1.67 \pm 0.16 \pm 0.35$		[1] AUBERT	08G	BABR	$e^+e^- \to \Upsilon(4S)$
• • • We do not use the following data for averages, fits, limits, etc. • • •					
<10	90	[2] ALBRECHT	93E	ARG	$e^+e^- \to \Upsilon(4S)$

[1] Assumes equal production of B^+ and B^0 at the $\Upsilon(4S)$.

[2] ALBRECHT 93E reports $< 1.6 \times 10^{-3}$ from a measurement of $[\Gamma(B^+ \to D_s^{*-} \pi^+ K^+)/\Gamma_{\text{total}}] \times [\text{B}(D_s^+ \to \phi\pi^+)]$ assuming $\text{B}(D_s^+ \to \phi\pi^+) = 0.027$, which we rescale to our best value $\text{B}(D_s^+ \to \phi\pi^+) = 4.5 \times 10^{-2}$.

$\Gamma(D_s^- \pi^+ K^*(892)^+)/\Gamma_{\text{total}}$ Γ_{222}/Γ

VALUE	CL%	DOCUMENT ID		TECN	COMMENT
<5 × 10⁻³	90	[1] ALBRECHT	93E	ARG	$e^+e^- \to \Upsilon(4S)$

[1] ALBRECHT 93E reports $< 8.6 \times 10^{-3}$ from a measurement of $[\Gamma(B^+ \to D_s^- \pi^+ K^*(892)^+)/\Gamma_{\text{total}}] \times [\text{B}(D_s^+ \to \phi\pi^+)]$ assuming $\text{B}(D_s^+ \to \phi\pi^+) = 0.027$, which we rescale to our best value $\text{B}(D_s^+ \to \phi\pi^+) = 4.5 \times 10^{-2}$.

$\Gamma(D_s^{*-} \pi^+ K^*(892)^+)/\Gamma_{\text{total}}$ Γ_{223}/Γ

VALUE	CL%	DOCUMENT ID		TECN	COMMENT
<7 × 10⁻³	90	[1] ALBRECHT	93E	ARG	$e^+e^- \to \Upsilon(4S)$

[1] ALBRECHT 93E reports $< 1.1 \times 10^{-2}$ from a measurement of $[\Gamma(B^+ \to D_s^{*-} \pi^+ K^*(892)^+)/\Gamma_{\text{total}}] \times [\text{B}(D_s^+ \to \phi\pi^+)]$ assuming $\text{B}(D_s^+ \to \phi\pi^+) = 0.027$, which we rescale to our best value $\text{B}(D_s^+ \to \phi\pi^+) = 4.5 \times 10^{-2}$.

$\Gamma(D_s^- K^+ K^+)/\Gamma_{\text{total}}$ Γ_{224}/Γ

VALUE (units 10^{-5})	DOCUMENT ID		TECN	COMMENT
0.97±0.21 OUR AVERAGE				
$0.93 \pm 0.22 \pm 0.10$	[1] WIECHCZYN...15		BELL	$e^+e^- \to \Upsilon(4S)$
$1.1\ \pm 0.4\ \pm 0.2$	[1] AUBERT	08G	BABR	$e^+e^- \to \Upsilon(4S)$

[1] Assumes equal production of B^+ and B^0 at the $\Upsilon(4S)$.

$\Gamma(D_s^- K^+ K^+)/\Gamma(D_s^- \pi^+ K^+)$ $\Gamma_{224}/\Gamma_{220}$

VALUE	DOCUMENT ID		TECN	COMMENT
0.054±0.013±0.006	WIECHCZYN...15		BELL	$e^+e^- \to \Upsilon(4S)$

$\Gamma(D_s^{*-} K^+ K^+)/\Gamma_{\text{total}}$ Γ_{225}/Γ

VALUE (units 10^{-4})	CL%	DOCUMENT ID		TECN	COMMENT
<0.15	90	[1] AUBERT	08G	BABR	$e^+e^- \to \Upsilon(4S)$

[1] Assumes equal production of B^+ and B^0 at the $\Upsilon(4S)$.

$\Gamma(\eta_c K^+)/\Gamma_{\text{total}}$ Γ_{226}/Γ

VALUE (units 10^{-3})	DOCUMENT ID		TECN	COMMENT
1.09±0.09 OUR AVERAGE	Error includes scale factor of 1.1.			
1.20±0.08±0.07	[1] KATO	18	BELL	$e^+e^- \to \Upsilon(4S)$
0.87±0.15	[1,2] AUBERT	06E	BABR	$e^+e^- \to \Upsilon(4S)$
$1.19^{+0.24}_{-0.19}{}^{+0.13}_{-0.12}$	[3] AUBERT,B	05L	BABR	$e^+e^- \to \Upsilon(4S)$
$1.25\pm0.14^{+0.39}_{-0.40}$	[4] FANG	03	BELL	$e^+e^- \to \Upsilon(4S)$
$0.69^{+0.26}_{-0.21}\pm0.22$	[5] EDWARDS	01	CLE2	$e^+e^- \to \Upsilon(4S)$
• • • We do not use the following data for averages, fits, limits, etc. • • •				
1.01±0.12±0.07	[2,6] AUBERT,B	04B	BABR	$e^+e^- \to \Upsilon(4S)$

[1] Measures absolute branching fractions using a missing-mass technique.
[2] The ratio of $B(B^{\pm} \to K^{\pm}\eta_c)\ B(\eta_c \to K\overline{K}\pi) = (7.4 \pm 0.5 \pm 0.7) \times 10^{-5}$ reported in AUBERT,B 04B and $B(B^{\pm} \to K^{\pm}\eta_c) = (8.7 \pm 1.5) \times 10^{-3}$ reported in AUBERT 06E contribute to the determination of $B(\eta_c \to K\overline{K}\pi)$, which is used by others for normalization.
[3] AUBERT,B 05L reports $[\Gamma(B^+ \to \eta_c K^+)/\Gamma_{\text{total}}] \times [B(\eta_c(1S) \to p\overline{p})] = (1.8^{+0.3}_{-0.2} \pm 0.2) \times 10^{-6}$ which we divide by our best value $B(\eta_c(1S) \to p\overline{p}) = (1.52 \pm 0.16) \times 10^{-3}$. Our first error is their experiment's error and our second error is the systematic error from using our best value.
[4] Assumes equal production of B^+ and B^0 at the $\Upsilon(4S)$.
[5] EDWARDS 01 assumes equal production of B^0 and B^+ at the $\Upsilon(4S)$. The correlated uncertainties (28.3)% from $B(J/\psi(1S) \to \gamma\eta_c)$ in those modes have been accounted for.
[6] AUBERT,B 04B reports $[\Gamma(B^+ \to \eta_c K^+)/\Gamma_{\text{total}}] \times [B(\eta_c(1S) \to K\overline{K}\pi)] = (0.074 \pm 0.005 \pm 0.007) \times 10^{-3}$ which we divide by our best value $B(\eta_c(1S) \to K\overline{K}\pi) = (7.3 \pm 0.5) \times 10^{-2}$. Our first error is their experiment's error and our second error is the systematic error from using our best value.

$\Gamma(B^+ \to \eta_c K^+)/\Gamma_{\text{total}} \times \Gamma(\eta_c(1S) \to \gamma\gamma)/\Gamma_{\text{total}}$ $\Gamma_{226}/\Gamma \times \Gamma^{\eta_c(1S)}_{48}/\Gamma^{\eta_c(1S)}$

VALUE (units 10^{-6})	DOCUMENT ID		TECN	COMMENT
$\mathbf{0.22^{+0.09}_{-0.07}{}^{+0.04}_{-0.02}}$	[1] WICHT	08	BELL	$e^+e^- \to \Upsilon(4S)$

[1] Assumes equal production of B^+ and B^0 at the $\Upsilon(4S)$.

$\Gamma(\eta_c K^+,\ \eta_c \to K^0_S K^{\mp}\pi^{\pm})/\Gamma_{\text{total}}$ Γ_{227}/Γ

VALUE (units 10^{-6})	DOCUMENT ID		TECN	COMMENT
$\mathbf{26.7\pm1.4^{+5.7}_{-5.5}}$	[1,2] VINOKUROVA 11		BELL	$e^+e^- \to \Upsilon(4S)$

[1] Assumes equal production of B^0 and B^+ from Upsilon(4S) decays.
[2] VINOKUROVA 11 reports $(26.7 \pm 1.4^{+2.9}_{-2.6} \pm 4.9) \times 10^{-6}$, where the first uncertainty is statistical, the second is due to systematics, and the third comes from interference of $\eta_c(1S) \to K^0_S K^{\pm}\pi^{\mp}$ with nonresonant $K^0_S K^{\pm}\pi^{\mp}$. We combined both systematic uncertainties to single values.

$\Gamma(\eta_c K^*(892)^+)/\Gamma_{\text{total}}$ Γ_{228}/Γ

VALUE (units 10^{-3})	DOCUMENT ID		TECN	COMMENT
$\mathbf{1.0^{+0.5}_{-0.4}\pm0.1}$	[1,2] AUBERT	07AV	BABR	$e^+e^- \to \Upsilon(4S)$

[1] AUBERT 07AV reports $[\Gamma(B^+ \to \eta_c K^*(892)^+)/\Gamma_{\text{total}}] \times [B(\eta_c(1S) \to p\overline{p})] = (1.57^{+0.56}_{-0.46}{}^{+0.45}_{-0.36}) \times 10^{-6}$ which we divide by our best value $B(\eta_c(1S) \to p\overline{p}) = (1.52 \pm 0.16) \times 10^{-3}$. Our first error is their experiment's error and our second error is the systematic error from using our best value.
[2] Assumes equal production of B^+ and B^0 at the $\Upsilon(4S)$.

$\Gamma(\eta_c K^+\pi^+\pi^-)/\Gamma_{\text{total}}$ Γ_{229}/Γ

VALUE	CL%	DOCUMENT ID	TECN	COMMENT
$\mathbf{<3.9\times10^{-4}}$	90	VINOKUROVA 15	BELL	$e^+e^- \to \Upsilon(4S)$

$\Gamma(\eta_c K^+\omega(782))/\Gamma_{\text{total}}$ Γ_{230}/Γ

VALUE	CL%	DOCUMENT ID	TECN	COMMENT
$\mathbf{<5.3\times10^{-4}}$	90	VINOKUROVA 15	BELL	$e^+e^- \to \Upsilon(4S)$

$\Gamma(\eta_c K^+\eta)/\Gamma_{\text{total}}$ Γ_{231}/Γ

VALUE	CL%	DOCUMENT ID	TECN	COMMENT
$\mathbf{<2.2\times10^{-4}}$	90	VINOKUROVA 15	BELL	$e^+e^- \to \Upsilon(4S)$

$\Gamma(\eta_c K^+\pi^0)/\Gamma_{\text{total}}$ Γ_{232}/Γ

VALUE	CL%	DOCUMENT ID	TECN	COMMENT
$\mathbf{<6.2\times10^{-5}}$	90	VINOKUROVA 15	BELL	$e^+e^- \to \Upsilon(4S)$

$\Gamma(\eta_c(2S) K^+)/\Gamma_{\text{total}}$ Γ_{233}/Γ

VALUE (units 10^{-4})	DOCUMENT ID		TECN	COMMENT
4.4±1.0 OUR AVERAGE				
4.8±1.1±0.3	[1] KATO	18	BELL	$e^+e^- \to \Upsilon(4S)$
3.4±1.8±0.3	[1] AUBERT	06E	BABR	$e^+e^- \to \Upsilon(4S)$

[1] Measures absolute branching fractions using a missing-mass technique.

$\Gamma(\eta_c(2S) K^+,\ \eta_c \to p\overline{p})/\Gamma_{\text{total}}$ Γ_{234}/Γ

VALUE (units 10^{-8})	CL%	DOCUMENT ID		TECN	COMMENT
$\mathbf{3.47\pm0.72\pm0.26}$		[1] AAIJ	17AD	LHCB	pp at 7 and 8 TeV
• • • We do not use the following data for averages, fits, limits, etc. • • •					
<10.6	95	[2] AAIJ	13S	LHCB	Repl. by AAIJ 17AD

[1] Measured relative to $B^+ \to J/\psi K^+$ decay with charmonia reconstructed in $p\overline{p}$ final state and using $B(B^+ \to J/\psi K^+) \times B(J/\psi \to p\overline{p}) = (2.17 \pm 0.08) \times 10^{-6}$. The last uncertainty includes the uncertainty of $B(B^+ \to J/\psi K^+) \times B(J/\psi \to p\overline{p})$.
[2] Measured relative to $B^+ \to J/\psi K^+$ decay with charmonia reconstructed in $p\overline{p}$ final state and using $B(B^+ \to J/\psi K^+) = (1.013 \pm 0.034) \times 10^{-3}$ and $B(J/\psi \to p\overline{p}) = (2.17 \pm 0.07) \times 10^{-3}$.

$\Gamma(B^+ \to h_c(1P) K^+)/\Gamma_{\text{total}} \times \Gamma(h_c(1P) \to \gamma\eta_c(1S))/\Gamma_{\text{total}}$ $\Gamma_{332}/\Gamma \times \Gamma^{h_c(1P)}_{9}/\Gamma^{h_c(1P)}$

VALUE (units 10^{-4})	CL%	DOCUMENT ID		TECN	COMMENT
<0.48	90	[1] AUBERT	08AB	BABR	$e^+e^- \to \Upsilon(4S)$

[1] Uses the production ratio of $(B^+B^-)/(B^0\overline{B}^0) = 1.026 \pm 0.032$ at $\Upsilon(4S)$.

$\Gamma(B^+ \to \eta_c(2S) K^+)/\Gamma_{\text{total}} \times \Gamma(\eta_c(2S) \to \gamma\gamma)/\Gamma_{\text{total}}$ $\Gamma_{233}/\Gamma \times \Gamma^{\eta_c(2S)}_{15}/\Gamma^{\eta_c(2S)}$

VALUE (units 10^{-6})	CL%	DOCUMENT ID		TECN	COMMENT
<0.18	90	[1] WICHT	08	BELL	$e^+e^- \to \Upsilon(4S)$

[1] Assumes equal production of B^+ and B^0 at the $\Upsilon(4S)$.

$\Gamma(\eta_c(2S) K^+,\ \eta_c \to K^0_S K^{\mp}\pi^{\pm})/\Gamma_{\text{total}}$ Γ_{235}/Γ

VALUE (units 10^{-6})	DOCUMENT ID		TECN	COMMENT
$\mathbf{3.4^{+2.2}_{-1.5}{}^{+0.5}_{-0.4}}$	[1,2] VINOKUROVA 11		BELL	$e^+e^- \to \Upsilon(4S)$

[1] Assumes equal production of B^0 and B^+ from Upsilon(4S) decays.
[2] The first uncertainty includes both statistical and interference effects while the second is due to systematics.

$\Gamma(J/\psi(1S) K^+)/\Gamma_{\text{total}}$ Γ_{268}/Γ

VALUE (units 10^{-4})	EVTS	DOCUMENT ID		TECN	COMMENT
10.10± 0.29 OUR FIT					
10.02± 0.33 OUR AVERAGE					
8.9 ± 0.6 ±0.5		[1] KATO	18	BELL	$e^+e^- \to \Upsilon(4S)$
8.1 ± 1.3 ±0.7		[1] AUBERT	06E	BABR	$e^+e^- \to \Upsilon(4S)$
10.61± 0.15±0.48		[2] AUBERT	05J	BABR	$e^+e^- \to \Upsilon(4S)$
10.4 ± 1.1 ±0.1		[3] AUBERT,B	05L	BABR	$e^+e^- \to \Upsilon(4S)$
10.1 ± 0.2 ±0.7		[2] ABE	03B	BELL	$e^+e^- \to \Upsilon(4S)$
10.2 ± 0.8 ±0.7		[2] JESSOP	97	CLE2	$e^+e^- \to \Upsilon(4S)$
9.24± 3.04±0.05		[4] BORTOLETTO	92	CLEO	$e^+e^- \to \Upsilon(4S)$
8.09± 3.50±0.04	6	[5] ALBRECHT	90J	ARG	$e^+e^- \to \Upsilon(4S)$
• • • We do not use the following data for averages, fits, limits, etc. • • •					
10.1 ± 0.3 ±0.5		[2] AUBERT	02	BABR	Repl. by AUBERT 05J
11.0 ± 1.5 ±0.9	59	[2] ALAM	94	CLE2	Repl. by JESSOP 97
22 ±10 ±2		BUSKULIC	92G	ALEP	$e^+e^- \to Z$
7 ± 4	3	[6] ALBRECHT	87D	ARG	$e^+e^- \to \Upsilon(4S)$
10 ± 7 ±2	3	[7] BEBEK	87	CLEO	$e^+e^- \to \Upsilon(4S)$
9 ± 5	3	[8] ALAM	86	CLEO	$e^+e^- \to \Upsilon(4S)$

[1] Measures absolute branching fractions using a missing-mass technique.
[2] Assumes equal production of B^+ and B^0 at the $\Upsilon(4S)$.
[3] AUBERT,B 05L reports $[\Gamma(B^+ \to J/\psi(1S) K^+)/\Gamma_{\text{total}}] \times [B(J/\psi(1S) \to p\overline{p})] = (2.2 \pm 0.2 \pm 0.1) \times 10^{-6}$ which we divide by our best value $B(J/\psi(1S) \to p\overline{p}) = (2.121 \pm 0.029) \times 10^{-3}$. Our first error is their experiment's error and our second error is the systematic error from using our best value.
[4] BORTOLETTO 92 reports $(8 \pm 2 \pm 2) \times 10^{-4}$ from a measurement of $[\Gamma(B^+ \to J/\psi(1S) K^+)/\Gamma_{\text{total}}] \times [B(J/\psi(1S) \to e^+e^-)]$ assuming $B(J/\psi(1S) \to e^+e^-) = 0.069 \pm 0.009$, which we rescale to our best value $B(J/\psi(1S) \to e^+e^-) = (5.971 \pm 0.032) \times 10^{-2}$. Our first error is their experiment's error and our second error is the systematic error from using our best value. Assumes equal production of B^+ and B^0 at the $\Upsilon(4S)$.
[5] ALBRECHT 90J reports $(7 \pm 3 \pm 1) \times 10^{-4}$ from a measurement of $[\Gamma(B^+ \to J/\psi(1S) K^+)/\Gamma_{\text{total}}] \times [B(J/\psi(1S) \to e^+e^-)]$ assuming $B(J/\psi(1S) \to e^+e^-) = 0.069 \pm 0.009$, which we rescale to our best value $B(J/\psi(1S) \to e^+e^-) = (5.971 \pm 0.032) \times 10^{-2}$. Our first error is their experiment's error and our second error is the systematic error from using our best value. Assumes equal production of B^+ and B^0 at the $\Upsilon(4S)$.
[6] ALBRECHT 87D assume $B^+B^-/B^0\overline{B}^0$ ratio is 55/45. Superseded by ALBRECHT 90J.
[7] BEBEK 87 value has been updated in BERKELMAN 91 to use same assumptions as noted for BORTOLETTO 92.
[8] ALAM 86 assumes $B^{\pm}/B^0$ ratio is 60/40.

$\Gamma(\eta_c K^+)/\Gamma(J/\psi(1S) K^+)$ $\Gamma_{226}/\Gamma_{268}$

VALUE	DOCUMENT ID		TECN	COMMENT
0.84±0.10 OUR AVERAGE				
$0.81\pm0.06^{+0.09}_{-0.08}$	[1] AAIJ	13S	LHCB	pp at 7 TeV
1.33±0.10±0.43	[2] AUBERT,B	04B	BABR	$e^+e^- \to \Upsilon(4S)$

[1] AAIJ 13S reports $[\Gamma(B^+ \to \eta_c K^+)/\Gamma(B^+ \to J/\psi(1S) K^+)] \times [B(\eta_c(1S) \to p\overline{p})] / [B(J/\psi(1S) \to p\overline{p})] = 0.578 \pm 0.035 \pm 0.026$ which we multiply or divide by our best values $B(\eta_c(1S) \to p\overline{p}) = (1.52 \pm 0.16) \times 10^{-3}$, $B(J/\psi(1S) \to p\overline{p}) = (2.121 \pm 0.029) \times 10^{-3}$. Our first error is their experiment's error and our second error is the systematic error from using our best values.

[2] Uses BABAR measurement of $B(B^+ \to J/\psi K^+) = (10.1 \pm 0.3 \pm 0.5) \times 10^{-4}$.

$\Gamma(B^+ \to J/\psi(1S) K^+)/\Gamma_{total} \times \Gamma(J/\psi(1S) \to \gamma\gamma)/\Gamma_{total}$ $\Gamma_{268}/\Gamma \times \Gamma_{269}^{J/\psi(1S)}/\Gamma^{J/\psi(1S)}$

VALUE (units 10^{-6})	CL%	DOCUMENT ID		TECN	COMMENT
<0.16	90	[1] WICHT	08	BELL	$e^+e^- \to \Upsilon(4S)$

[1] Assumes equal production of B^+ and B^0 at the $\Upsilon(4S)$.

$\Gamma(J/\psi(1S) K^+\pi^+\pi^-)/\Gamma_{total}$ Γ_{270}/Γ

VALUE (units 10^{-3})	CL%	EVTS	DOCUMENT ID		TECN	COMMENT
0.81 ±0.13 OUR AVERAGE Error includes scale factor of 2.5. See the ideogram below.						
0.716±0.010±0.060			[1] GULER	11	BELL	$e^+e^- \to \Upsilon(4S)$
1.16 ±0.07 ±0.09			[1] AUBERT	05R	BABR	$e^+e^- \to \Upsilon(4S)$
0.69 ±0.18 ±0.12			[2] ACOSTA	02F	CDF	$p\overline{p}$ 1.8 TeV
1.39 ±0.81 ±0.01			[3] BORTOLETTO	92	CLEO	$e^+e^- \to \Upsilon(4S)$
1.39 ±0.91 ±0.01		6	[4] ALBRECHT	87D	ARG	$e^+e^- \to \Upsilon(4S)$
• • • We do not use the following data for averages, fits, limits, etc. • • •						
<1.8	90		[5] ALBRECHT	90J	ARG	$e^+e^- \to \Upsilon(4S)$

[1] Assumes equal production of B^+ and B^0 at the $\Upsilon(4S)$.
[2] ACOSTA 02F uses as reference of $B(B \to J/\psi(1S) K^+) = (10.1 \pm 0.6) \times 10^{-4}$. The second error includes the systematic error and the uncertainties of the branching ratio.
[3] BORTOLETTO 92 reports $(1.2 \pm 0.6 \pm 0.4) \times 10^{-3}$ from a measurement of $[\Gamma(B^+ \to J/\psi(1S) K^+\pi^+\pi^-)/\Gamma_{total}] \times [B(J/\psi(1S) \to e^+e^-)]$ assuming $B(J/\psi(1S) \to e^+e^-) = 0.069 \pm 0.009$, which we rescale to our best value $B(J/\psi(1S) \to e^+e^-) = (5.971 \pm 0.032) \times 10^{-2}$. Our first error is their experiment's error and our second error is the systematic error from using our best value. Assumes equal production of B^+ and B^0 at the $\Upsilon(4S)$.
[4] ALBRECHT 87D reports $(1.2 \pm 0.8) \times 10^{-3}$ from a measurement of $[\Gamma(B^+ \to J/\psi(1S) K^+\pi^+\pi^-)/\Gamma_{total}] \times [B(J/\psi(1S) \to e^+e^-)]$ assuming $B(J/\psi(1S) \to e^+e^-) = 0.069 \pm 0.009$, which we rescale to our best value $B(J/\psi(1S) \to e^+e^-) = (5.971 \pm 0.032) \times 10^{-2}$. Our first error is their experiment's error and our second error is the systematic error from using our best value. They actually report 0.0011 ± 0.0007 assuming $B^+B^-/B^0\overline{B}^0$ ratio is 55/45. We rescale to 50/50. Analysis explicitly removes $B^+ \to \psi(2S) K^+$.
[5] ALBRECHT 90J reports $< 1.6 \times 10^{-3}$ from a measurement of $[\Gamma(B^+ \to J/\psi(1S) K^+\pi^+\pi^-)/\Gamma_{total}] \times [B(J/\psi(1S) \to e^+e^-)]$ assuming $B(J/\psi(1S) \to e^+e^-) = 0.069$, which we rescale to our best value $B(J/\psi(1S) \to e^+e^-) = 5.971 \times 10^{-2}$. Assumes equal production of B^+ and B^0 at the $\Upsilon(4S)$.

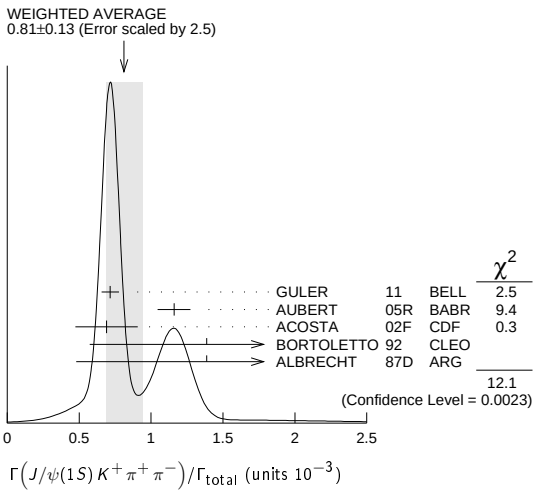

$\Gamma(J/\psi(1S) K^+K^-K^+)/\Gamma_{total}$ Γ_{271}/Γ

VALUE (units 10^{-6})	DOCUMENT ID		TECN	COMMENT
33.7±2.5±1.4	LEES	15	BABR	$e^+e^- \to \Upsilon(4S)$

$\Gamma(h_c(1P) K^+,\ h_c \to J/\psi\pi^+\pi^-)/\Gamma_{total}$ Γ_{236}/Γ

VALUE	CL%	DOCUMENT ID		TECN	COMMENT
<3.4 × 10⁻⁶	90	[1] AUBERT	05R	BABR	$e^+e^- \to \Upsilon(4S)$

[1] Assumes equal production of B^+ and B^0 at the $\Upsilon(4S)$.

$\Gamma(X(3730)^0 K^+,\ X^0 \to \eta_c\eta)/\Gamma_{total}$ Γ_{237}/Γ

VALUE	CL%	DOCUMENT ID		TECN	COMMENT
<4.6 × 10⁻⁵	90	VINOKUROVA	15	BELL	$e^+e^- \to \Upsilon(4S)$

$\Gamma(X(3730)^0 K^+,\ X^0 \to \eta_c\pi^0)/\Gamma_{total}$ Γ_{238}/Γ

VALUE	CL%	DOCUMENT ID		TECN	COMMENT
<5.7 × 10⁻⁶	90	VINOKUROVA	15	BELL	$e^+e^- \to \Upsilon(4S)$

$\Gamma(\chi_{c1}(3872) K^+)/\Gamma_{total}$ Γ_{239}/Γ

VALUE	CL%	DOCUMENT ID		TECN	COMMENT
<2.6 × 10⁻⁴	90	[1] KATO	18	BELL	$e^+e^- \to \Upsilon(4S)$
• • • We do not use the following data for averages, fits, limits, etc. • • •					
<3.2 × 10⁻⁴	90	[1] AUBERT	06E	BABR	$e^+e^- \to \Upsilon(4S)$

[1] Measures absolute branching fractions using a missing-mass technique.

$\Gamma(B^+ \to \chi_{c1}(3872) K^+)/\Gamma_{total} \times \Gamma(\chi_{c1}(3872) \to \gamma\gamma)/\Gamma_{total}$ $\Gamma_{239}/\Gamma \times \Gamma_7^{\chi_{c1}(3872)}/\Gamma^{\chi_{c1}(3872)}$

VALUE (units 10^{-6})	CL%	DOCUMENT ID		TECN	COMMENT
<0.24	90	[1] WICHT	08	BELL	$e^+e^- \to \Upsilon(4S)$

[1] Assumes equal production of B^+ and B^0 at the $\Upsilon(4S)$.

$\Gamma(\chi_{c1}(3872) K^+,\ \chi_{c1} \to J/\psi\pi^+\pi^-)/\Gamma_{total}$ Γ_{241}/Γ

VALUE (units 10^{-6})	DOCUMENT ID		TECN	COMMENT
8.6 ±0.8 OUR AVERAGE				
8.63±0.82±0.52	[1] CHOI	11	BELL	$e^+e^- \to \Upsilon(4S)$
8.4 ±1.5 ±0.7	[1] AUBERT	08Y	BABR	$e^+e^- \to \Upsilon(4S)$
• • • We do not use the following data for averages, fits, limits, etc. • • •				
10.1 ±2.5 ±1.0	[1] AUBERT	06	BABR	Repl. by AUBERT 08Y
12.8 ±4.1	[1] AUBERT	05R	BABR	Repl. by AUBERT 06
12.4 ±2.8 ±0.5	[2] CHOI	03	BELL	Repl. by CHOI 11

[1] Assumes equal production of B^+ and B^0 at the $\Upsilon(4S)$.
[2] CHOI 03 reports $[\Gamma(B^+ \to \chi_{c1}(3872) K^+,\ \chi_{c1} \to J/\psi\pi^+\pi^-)/\Gamma_{total}] / [B(B^+ \to \psi(2S) K^+)] = 0.0200 \pm 0.0038 \pm 0.0023$ which we multiply by our best value $B(B^+ \to \psi(2S) K^+) = (6.21 \pm 0.23) \times 10^{-4}$. Our first error is their experiment's error and our second error is the systematic error from using our best value.

$\Gamma(\chi_{c1}(3872) K^+,\ \chi_{c1} \to J/\psi\gamma)/\Gamma_{total}$ Γ_{242}/Γ

VALUE (units 10^{-6})	DOCUMENT ID		TECN	COMMENT
2.1 ±0.4 OUR AVERAGE Error includes scale factor of 1.1.				
$1.78^{+0.48}_{-0.44} \pm 0.12$	[1] BHARDWAJ	11	BELL	$e^+e^- \to \Upsilon(4S)$
2.8 ±0.8 ±0.1	[2] AUBERT	09B	BABR	$e^+e^- \to \Upsilon(4S)$
• • • We do not use the following data for averages, fits, limits, etc. • • •				
3.3 ±1.0 ±0.3	[1] AUBERT,BE	06M	BABR	Repl. by AUBERT 09B

[1] Assumes equal production of B^+ and B^0 at the $\Upsilon(4S)$.
[2] Uses $B(\Upsilon(4S) \to B^+B^-) = (51.6 \pm 0.6)\%$ and $B(\Upsilon(4S) \to B^0\overline{B}^0) = (48.4 \pm 0.6)\%$.

$\Gamma(\chi_{c1}(3872) K^*(892)^+,\ \chi_{c1} \to J/\psi\gamma)/\Gamma_{total}$ Γ_{259}/Γ

VALUE (units 10^{-6})	CL%	DOCUMENT ID		TECN	COMMENT
<4.8	90	[1] AUBERT	09B	BABR	$e^+e^- \to \Upsilon(4S)$

[1] Uses $B(\Upsilon(4S) \to B^+B^-) = (51.6 \pm 0.6)\%$ and $B(\Upsilon(4S) \to B^0\overline{B}^0) = (48.4 \pm 0.6)\%$.

$\Gamma(\chi_{c1}(3872) K^+,\ \chi_{c1} \to \psi(2S)\gamma)/\Gamma_{total}$ Γ_{243}/Γ

VALUE (units 10^{-6})	DOCUMENT ID		TECN	COMMENT
4 ±4 OUR AVERAGE Error includes scale factor of 2.5.				
$0.83^{+1.98}_{-1.83} \pm 0.44$	[1,2] BHARDWAJ	11	BELL	$e^+e^- \to \Upsilon(4S)$
9.5 ±2.7 ±0.6	[3] AUBERT	09B	BABR	$e^+e^- \to \Upsilon(4S)$

[1] BHARDWAJ 11 measurement is equivalent to a limit of $< 3.45 \times 10^{-6}$ at 90% CL.
[2] Assumes equal production of B^+ and B^0 at the $\Upsilon(4S)$.
[3] Uses $B(\Upsilon(4S) \to B^+B^-) = (51.6 \pm 0.6)\%$ and $B(\Upsilon(4S) \to B^0\overline{B}^0) = (48.4 \pm 0.6)\%$.

$\Gamma(\chi_{c1}(3872) K^*(892)^+,\ \chi_{c1} \to \psi(2S)\gamma)/\Gamma_{total}$ Γ_{260}/Γ

VALUE (units 10^{-6})	CL%	DOCUMENT ID		TECN	COMMENT
<28	90	[1] AUBERT	09B	BABR	$e^+e^- \to \Upsilon(4S)$

[1] Uses $B(\Upsilon(4S) \to B^+B^-) = (51.6 \pm 0.6)\%$ and $B(\Upsilon(4S) \to B^0\overline{B}^0) = (48.4 \pm 0.6)\%$.

$\Gamma(\chi_{c1}(3872) K^+,\ \chi_{c1} \to D^0\overline{D}^0)/\Gamma_{total}$ Γ_{245}/Γ

VALUE	CL%	DOCUMENT ID		TECN	COMMENT
<6.0 × 10⁻⁵	90	[1] CHISTOV	04	BELL	$e^+e^- \to \Upsilon(4S)$

[1] Assumes equal production of B^+ and B^0 at the $\Upsilon(4S)$.

$\Gamma(\chi_{c1}(3872) K^+,\ \chi_{c1} \to D^+D^-)/\Gamma_{total}$ Γ_{246}/Γ

VALUE	CL%	DOCUMENT ID		TECN	COMMENT
<4.0 × 10⁻⁵	90	[1] CHISTOV	04	BELL	$e^+e^- \to \Upsilon(4S)$

[1] Assumes equal production of B^+ and B^0 at the $\Upsilon(4S)$.

$\Gamma(\chi_{c1}(3872) K^+,\ \chi_{c1} \to D^0\overline{D}^0\pi^0)/\Gamma_{total}$ Γ_{247}/Γ

VALUE (units 10^{-4})	CL%	DOCUMENT ID		TECN	COMMENT
$1.02 \pm 0.31^{+0.21}_{-0.29}$		[1] GOKHROO	06	BELL	$e^+e^- \to \Upsilon(4S)$
• • • We do not use the following data for averages, fits, limits, etc. • • •					
<0.6	90	[2] CHISTOV	04	BELL	Repl. by GOKHROO 06

[1] Measure the near-threshold enhancements in the $(D^0\overline{D}^0\pi^0)$ system at a mass $3875.2 \pm 0.7^{+0.3}_{-1.6} \pm 0.8$ MeV/c^2.
[2] Assumes equal production of B^+ and B^0 at the $\Upsilon(4S)$.

$\Gamma(\chi_{c1}(3872)K^+,\ \chi_{c1}\to\overline{D}^{*0}D^0)/\Gamma_{\rm total}$ Γ_{248}/Γ

VALUE (units 10^{-4})		DOCUMENT ID		TECN	COMMENT
0.85±0.26 OUR AVERAGE	Error includes scale factor of 1.4.				
0.77±0.16±0.10		[1] AUSHEV	10	BELL	$e^+e^-\to\Upsilon(4S)$
1.67±0.36±0.47		[1] AUBERT	08B	BABR	$e^+e^-\to\Upsilon(4S)$

[1] Assumes equal production of B^+ and B^0 at the $\Upsilon(4S)$.

$\Gamma(\chi_{c1}(3872)^0K^+,\ \chi_{c1}^0\to\eta_c\pi^+\pi^-)/\Gamma_{\rm total}$ Γ_{249}/Γ

VALUE	CL%	DOCUMENT ID		TECN	COMMENT
<3.0 × 10⁻⁵	90	VINOKUROVA	15	BELL	$e^+e^-\to\Upsilon(4S)$

$\Gamma(\chi_{c1}(3872)^0K^+,\ \chi_{c1}^0\to\eta_c\omega(782))/\Gamma_{\rm total}$ Γ_{250}/Γ

VALUE	CL%	DOCUMENT ID		TECN	COMMENT
<6.9 × 10⁻⁵	90	VINOKUROVA	15	BELL	$e^+e^-\to\Upsilon(4S)$

$\Gamma(\chi_{c1}(3872)K^+,\ \chi_{c1}\to\chi_{c1}(1P)\pi^+\pi^-)/\Gamma_{\rm total}$ Γ_{251}/Γ

VALUE	CL%	DOCUMENT ID		TECN	COMMENT
<1.5 × 10⁻⁶	90	[1] BHARDWAJ	16	BELL	$e^+e^-\to\Upsilon(4S)$

[1] Assumes equal production of B^+ and B^0 at the $\Upsilon(4S)$.

$\Gamma(X(3915)K^+)/\Gamma_{\rm total}$ Γ_{252}/Γ

VALUE	CL%	DOCUMENT ID		TECN	COMMENT
<2.8 × 10⁻⁴	90	[1] KATO	18	BELL	$e^+e^-\to\Upsilon(4S)$

[1] Measures absolute branching fractions using a missing-mass technique.

$\Gamma(X(3915)^0K^+,\ X^0\to\eta_c\eta)/\Gamma_{\rm total}$ Γ_{253}/Γ

VALUE	CL%	DOCUMENT ID		TECN	COMMENT
<4.7 × 10⁻⁵	90	[1] VINOKUROVA	15	BELL	$e^+e^-\to\Upsilon(4S)$

[1] Upper limit is corrected in the Erratum.

$\Gamma(X(3915)^0K^+,\ X^0\to\eta_c\pi^0)/\Gamma_{\rm total}$ Γ_{254}/Γ

VALUE	CL%	DOCUMENT ID		TECN	COMMENT
<1.7 × 10⁻⁵	90	[1] VINOKUROVA	15	BELL	$e^+e^-\to\Upsilon(4S)$

[1] Upper limit is corrected in the Erratum.

$\Gamma(X(4014)^0K^+,\ X^0\to\eta_c\eta)/\Gamma_{\rm total}$ Γ_{255}/Γ

VALUE	CL%	DOCUMENT ID		TECN	COMMENT
<3.9 × 10⁻⁵	90	VINOKUROVA	15	BELL	$e^+e^-\to\Upsilon(4S)$

$\Gamma(X(4014)^0K^+,\ X^0\to\eta_c\pi^0)/\Gamma_{\rm total}$ Γ_{256}/Γ

VALUE	CL%	DOCUMENT ID		TECN	COMMENT
<1.2 × 10⁻⁵	90	VINOKUROVA	15	BELL	$e^+e^-\to\Upsilon(4S)$

$\Gamma(Z_c(3900)^0K^+,\ Z_c^0\to\eta_c\pi^+\pi^-)/\Gamma_{\rm total}$ Γ_{257}/Γ

VALUE	CL%	DOCUMENT ID		TECN	COMMENT
<4.7 × 10⁻⁵	90	VINOKUROVA	15	BELL	$e^+e^-\to\Upsilon(4S)$

$\Gamma(X(4020)^0K^+,\ X^0\to\eta_c\pi^+\pi^-)/\Gamma_{\rm total}$ Γ_{258}/Γ

VALUE	CL%	DOCUMENT ID		TECN	COMMENT
<1.6 × 10⁻⁵	90	VINOKUROVA	15	BELL	$e^+e^-\to\Upsilon(4S)$

$\Gamma(\chi_{c1}(3872)K^+,\ \chi_{c1}\to J/\psi(1S)\eta)/\Gamma_{\rm total}$ Γ_{244}/Γ

VALUE	CL%	DOCUMENT ID		TECN	COMMENT
<7.7 × 10⁻⁶	90	[1] AUBERT	04Y	BABR	$e^+e^-\to\Upsilon(4S)$

[1] Assumes equal production of B^+ and B^0 at the $\Upsilon(4S)$.

$\Gamma(\chi_{c1}(3872)^+K^0,\ \chi_{c1}^+\to J/\psi(1S)\pi^+\pi^0)/\Gamma_{\rm total}$ Γ_{261}/Γ

VALUE (units 10^{-6})	CL%	DOCUMENT ID		TECN	COMMENT
< 6.1	90	[1,2] CHOI	11	BELL	$e^+e^-\to\Upsilon(4S)$
• • • We do not use the following data for averages, fits, limits, etc. • • •					
<22	90	[3] AUBERT	05B	BABR	$e^+e^-\to\Upsilon(4S)$

[1] Assumes $\pi^+\pi^0$ originates from ρ^+.
[2] Assumes equal production of B^+ and B^0 at the $\Upsilon(4S)$.
[3] Assumes equal production of B^+ and B^0 at the $\Upsilon(4S)$. The isovector-X hypothesis is excluded with a likelihood test at 1×10^{-4} level.

$\Gamma(\chi_{c1}(3872)K^0\pi^+,\ \chi_{c1}\to J/\psi(1S)\pi^+\pi^-)/\Gamma_{\rm total}$ Γ_{262}/Γ

VALUE (units 10^{-6})	DOCUMENT ID		TECN	COMMENT
10.6±3.0±0.9	BALA	15	BELL	$e^+e^-\to\Upsilon(4S)$

$\Gamma(Z_c(4430)^+K^0,\ Z_c^+\to J/\psi\pi^+)/\Gamma_{\rm total}$ Γ_{263}/Γ

VALUE (units 10^{-5})	CL%	DOCUMENT ID		TECN	COMMENT
<1.5	95	[1] AUBERT	09AA	BABR	$e^+e^-\to\Upsilon(4S)$

[1] Assumes equal production of B^+ and B^0 at the $\Upsilon(4S)$.

$\Gamma(Z_c(4430)^+K^0,\ Z_c^+\to\psi(2S)\pi^+)/\Gamma_{\rm total}$ Γ_{264}/Γ

VALUE (units 10^{-5})	CL%	DOCUMENT ID		TECN	COMMENT
<4.7	95	[1] AUBERT	09AA	BABR	$e^+e^-\to\Upsilon(4S)$

[1] Assumes equal production of B^+ and B^0 at the $\Upsilon(4S)$.

$\Gamma(\psi(4260)^0K^+,\ \psi^0\to J/\psi\pi^+\pi^-)/\Gamma_{\rm total}$ Γ_{265}/Γ

VALUE (units 10^{-6})	CL%	DOCUMENT ID		TECN	COMMENT
<29	95	[1] AUBERT	06	BABR	$e^+e^-\to\Upsilon(4S)$

[1] Assumes equal production of B^+ and B^0 at the $\Upsilon(4S)$.

$\Gamma(X(3915)K^+,\ X\to J/\psi\gamma)/\Gamma_{\rm total}$ Γ_{266}/Γ

VALUE (units 10^{-6})	CL%	DOCUMENT ID		TECN	COMMENT
<14	90	[1] AUBERT,BE	06M	BABR	$e^+e^-\to\Upsilon(4S)$

[1] Assumes equal production of B^+ and B^0 at the $\Upsilon(4S)$.

$\Gamma(X(3930)^0K^+,\ X^0\to J/\psi\gamma)/\Gamma_{\rm total}$ Γ_{267}/Γ

VALUE (units 10^{-6})	CL%	DOCUMENT ID		TECN	COMMENT
<2.5	90	[1] AUBERT,BE	06M	BABR	$e^+e^-\to\Upsilon(4S)$

[1] Assumes equal production of B^+ and B^0 at the $\Upsilon(4S)$.

$\Gamma(J/\psi(1S)K^0\pi^+)/\Gamma_{\rm total}$ Γ_{269}/Γ

VALUE (units 10^{-3})	DOCUMENT ID		TECN	COMMENT
• • • We do not use the following data for averages, fits, limits, etc. • • •				
1.101±0.021	[1] AUBERT	09AA	BABR	$e^+e^-\to\Upsilon(4S)$

[1] Does not report systematic uncertainties.

$\Gamma(J/\psi(1S)K^*(892)^+)/\Gamma_{\rm total}$ Γ_{273}/Γ

For polarization information see the Listings at the end of the "B^0 Branching Ratios" section.

VALUE (units 10^{-3})	EVTS	DOCUMENT ID		TECN	COMMENT
1.43 ±0.08 OUR FIT					
1.43 ±0.08 OUR AVERAGE					
1.78 $^{+0.36}_{-0.32}$ ±0.02		[1,2] AUBERT	07AV	BABR	$e^+e^-\to\Upsilon(4S)$
1.454±0.047±0.097		[2] AUBERT	05J	BABR	$e^+e^-\to\Upsilon(4S)$
1.28 ±0.07 ±0.14		[2] ABE	02N	BELL	$e^+e^-\to\Upsilon(4S)$
1.41 ±0.23 ±0.24		[2] JESSOP	97	CLE2	$e^+e^-\to\Upsilon(4S)$
1.58 ±0.47 ±0.27		[3] ABE	96H	CDF	$p\overline{p}$ at 1.8 TeV
1.50 ±1.08 ±0.01		[4] BORTOLETTO	92	CLEO	$e^+e^-\to\Upsilon(4S)$
1.85 ±1.30 ±0.01	2	[5] ALBRECHT	90J	ARG	$e^+e^-\to\Upsilon(4S)$
• • • We do not use the following data for averages, fits, limits, etc. • • •					
1.37 ±0.09 ±0.11		[2] AUBERT	02	BABR	Repl. by AUBERT 05J
1.78 ±0.51 ±0.23	13	[2] ALAM	94	CLE2	Sup. by JESSOP 97

[1] AUBERT 07AV reports $[\Gamma(B^+\to J/\psi(1S)K^*(892)^+)/\Gamma_{\rm total}]\times[{\rm B}(J/\psi(1S)\to p\overline{p})] = (3.78^{+0.72}_{-0.64}{}^{+0.28}_{-0.23})\times10^{-6}$ which we divide by our best value ${\rm B}(J/\psi(1S)\to p\overline{p}) = (2.121\pm0.029)\times10^{-3}$. Our first error is their experiment's error and our second error is the systematic error from using our best value.
[2] Assumes equal production of B^+ and B^0 at the $\Upsilon(4S)$.
[3] ABE 96H assumes that ${\rm B}(B^+\to J/\psi K^+) = (1.02\pm0.14)\times10^{-3}$.
[4] BORTOLETTO 92 reports $(1.3\pm0.9\pm0.3)\times10^{-3}$ from a measurement of $[\Gamma(B^+\to J/\psi(1S)K^*(892)^+)/\Gamma_{\rm total}]\times[{\rm B}(J/\psi(1S)\to e^+e^-)]$ assuming ${\rm B}(J/\psi(1S)\to e^+e^-) = 0.069\pm0.009$, which we rescale to our best value ${\rm B}(J/\psi(1S)\to e^+e^-) = (5.971\pm0.032)\times10^{-2}$. Our first error is their experiment's error and our second error is the systematic error from using our best value. Assumes equal production of B^+ and B^0 at the $\Upsilon(4S)$.
[5] ALBRECHT 90J reports $(1.6\pm1.1\pm0.3)\times10^{-3}$ from a measurement of $[\Gamma(B^+\to J/\psi(1S)K^*(892)^+)/\Gamma_{\rm total}]\times[{\rm B}(J/\psi(1S)\to e^+e^-)]$ assuming ${\rm B}(J/\psi(1S)\to e^+e^-) = 0.069\pm0.009$, which we rescale to our best value ${\rm B}(J/\psi(1S)\to e^+e^-) = (5.971\pm0.032)\times10^{-2}$. Our first error is their experiment's error and our second error is the systematic error from using our best value. Assumes equal production of B^+ and B^0 at the $\Upsilon(4S)$.

$\Gamma(J/\psi(1S)K^*(892)^+)/\Gamma(J/\psi(1S)K^+)$ $\Gamma_{273}/\Gamma_{268}$

VALUE	DOCUMENT ID		TECN	COMMENT
1.39±0.09 OUR AVERAGE				
1.37±0.05±0.08	AUBERT	05J	BABR	$e^+e^-\to\Upsilon(4S)$
1.45±0.20±0.17	[1] JESSOP	97	CLE2	$e^+e^-\to\Upsilon(4S)$
1.92±0.60±0.17	ABE	96Q	CDF	$p\overline{p}$
• • • We do not use the following data for averages, fits, limits, etc. • • •				
1.37±0.10±0.08	[2] AUBERT	02	BABR	Repl. by AUBERT 05J

[1] JESSOP 97 assumes equal production of B^+ and B^0 at the $\Upsilon(4S)$. The measurement is actually measured as an average over kaon charged and neutral states.
[2] Assumes equal production of B^+ and B^0 at the $\Upsilon(4S)$.

$\Gamma(J/\psi(1S)K(1270)^+)/\Gamma_{\rm total}$ Γ_{274}/Γ

VALUE (units 10^{-3})	DOCUMENT ID		TECN	COMMENT
1.80±0.34±0.39	[1] ABE	01L	BELL	$e^+e^-\to\Upsilon(4S)$

[1] Uses the PDG value of ${\rm B}(B^+\to J/\psi(1S)K^+) = (1.00\pm0.10)\times10^{-3}$.

$\Gamma(J/\psi(1S)K(1400)^+)/\Gamma(J/\psi(1S)K(1270)^+)$ $\Gamma_{275}/\Gamma_{274}$

VALUE	CL%	DOCUMENT ID		TECN	COMMENT
<0.30	90	ABE	01L	BELL	$e^+e^-\to\Upsilon(4S)$

Meson Particle Listings

$B^{\pm}$

$\Gamma(J/\psi(1S)\eta K^+)/\Gamma_{\text{total}}$ Γ_{276}/Γ

VALUE (units 10^{-5})	DOCUMENT ID		TECN	COMMENT
12.4±1.4 OUR AVERAGE				
12.7±1.1±1.1	[1] IWASHITA	14	BELL	$e^+e^- \to \Upsilon(4S)$
10.8±2.3±2.4	[1] AUBERT	04Y	BABR	$e^+e^- \to \Upsilon(4S)$

[1] Assumes equal production of B^+ and B^0 at the $\Upsilon(4S)$.

$\Gamma(\chi_{c1-odd}(3872)K^+, \chi_{c1-odd} \to J/\psi\eta)/\Gamma_{\text{total}}$ Γ_{277}/Γ

VALUE	CL%	DOCUMENT ID		TECN	COMMENT
<3.8 × 10^{-6}	90	IWASHITA	14	BELL	$e^+e^- \to \Upsilon(4S)$

$\Gamma(\psi(4160)K^+, \psi \to J/\psi\eta)/\Gamma_{\text{total}}$ Γ_{278}/Γ

VALUE	CL%	DOCUMENT ID		TECN	COMMENT
<7.4 × 10^{-6}	90	IWASHITA	14	BELL	$e^+e^- \to \Upsilon(4S)$

$\Gamma(J/\psi(1S)\eta' K^+)/\Gamma_{\text{total}}$ Γ_{279}/Γ

VALUE (units 10^{-5})	CL%	DOCUMENT ID		TECN	COMMENT
<8.8	90	[1] XIE	07	BELL	$e^+e^- \to \Upsilon(4S)$

[1] Assumes equal production of B^+ and B^0 at the $\Upsilon(4S)$.

$\Gamma(J/\psi(1S)\phi K^+)/\Gamma_{\text{total}}$ Γ_{280}/Γ

VALUE (units 10^{-5})	DOCUMENT ID		TECN	COMMENT
5.0 ±0.4 OUR AVERAGE				
5.00±0.37±0.15	LEES	15	BABR	$e^+e^- \to \Upsilon(4S)$
4.4 ±1.4 ±0.5	[1] AUBERT	03O	BABR	$e^+e^- \to \Upsilon(4S)$
8.8 $^{+3.5}_{-3.0}$ ±1.3	[2] ANASTASSOV	00	CLE2	$e^+e^- \to \Upsilon(4S)$

[1] Assumes equal production of B^+ and B^0 at the $\Upsilon(4S)$.
[2] ANASTASSOV 00 finds 10 events on a background of 0.5 ± 0.2. Assumes equal production of B^0 and B^+ at the $\Upsilon(4S)$, a uniform Dalitz plot distribution, isotropic $J/\psi(1S)$ and ϕ decays, and $B(B^+ \to J/\psi(1S)\phi K^+) = B(B^0 \to J/\psi(1S)\phi K^0)$.

$\Gamma(J/\psi(1S)K_1(1650), K_1 \to \phi K^+)/\Gamma(J/\psi(1S)\phi K^+)$ $\Gamma_{281}/\Gamma_{280}$

VALUE	DOCUMENT ID		TECN	COMMENT
0.12±0.10 $^{+0.17}_{-0.06}$	[1] AAIJ	17	LHCB	pp at 7, 8 TeV

[1] Measured in amplitude analysis of $B^+ \to J/\psi(1S)\phi K^+$.

$\Gamma(J/\psi(1S)K^*(1680)^+, K^* \to \phi K^+)/\Gamma(J/\psi(1S)\phi K^+)$ $\Gamma_{282}/\Gamma_{280}$

VALUE (units 10^{-2})	DOCUMENT ID		TECN	COMMENT
6.7±1.9 $^{+3.2}_{-3.9}$	[1] AAIJ	17	LHCB	pp at 7, 8 TeV

[1] Measured in amplitude analysis of $B^+ \to J/\psi(1S)\phi K^+$.

$\Gamma(J/\psi(1S)K_2^*(1980), K_2^* \to \phi K^+)/\Gamma(J/\psi(1S)\phi K^+)$ $\Gamma_{283}/\Gamma_{280}$

VALUE (units 10^{-2})	DOCUMENT ID		TECN	COMMENT
2.9±0.8 $^{+1.7}_{-0.7}$	[1] AAIJ	17	LHCB	pp at 7, 8 TeV

[1] Measured in amplitude analysis of $B^+ \to J/\psi(1S)\phi K^+$.

$\Gamma(J/\psi(1S)K(1830)^+, K(1830)^+ \to \phi K^+)/\Gamma(J/\psi(1S)\phi K^+)$ $\Gamma_{284}/\Gamma_{280}$

VALUE (units 10^{-2})	DOCUMENT ID		TECN	COMMENT
2.6±1.1 $^{+2.3}_{-1.8}$	[1] AAIJ	17	LHCB	pp at 7, 8 TeV

[1] Measured in amplitude analysis of $B^+ \to J/\psi(1S)\phi K^+$.

$\Gamma(\chi_{c1}(4140)K^+, \chi_{c1} \to J/\psi(1S)\phi)/\Gamma(J/\psi(1S)\phi K^+)$ $\Gamma_{285}/\Gamma_{280}$

VALUE	CL%	DOCUMENT ID		TECN	COMMENT
0.19 ±0.08 OUR AVERAGE					
0.13 ±0.032 $^{+4.8}_{-2.0}$		[1] AAIJ	17	LHCB	pp at 7, 8 TeV
0.19 ±0.07 ±0.04		[2] ABAZOV	14A	D0	$p\overline{p}$ at 1.96 TeV
• • • We do not use the following data for averages, fits, limits, etc. • • •					
<0.133	90	LEES	15	BABR	$e^+e^- \to \Upsilon(4S)$
<0.07	90	[3] AAIJ	12AA	LHCB	pp at 7 TeV

[1] Measured in amplitude analysis of $B^+ \to J/\psi(1S)\phi K^+$.
[2] Reported a threshold enhancement in the $J/\psi\phi$ mass distribution consistent with the $\chi_{c1}(4140)$ state with a statistical significance of 3.1 standard deviations.
[3] Branching fractions are normalized to 382 ± 22 events of $B^+ \to J/\psi\phi K^+$.

$\Gamma(\chi_{c1}(4274)K^+, \chi_{c1} \to J/\psi(1S)\phi)/\Gamma(J/\psi(1S)\phi K^+)$ $\Gamma_{286}/\Gamma_{280}$

VALUE (units 10^{-2})	CL%	DOCUMENT ID		TECN	COMMENT
7.1±2.5 $^{+3.5}_{-2.4}$		[1] AAIJ	17	LHCB	pp at 7, 8 TeV
• • • We do not use the following data for averages, fits, limits, etc. • • •					
<18.1	90	LEES	15	BABR	$e^+e^- \to \Upsilon(4S)$
< 8	90	[2] AAIJ	12AA	LHCB	Repl. by AAIJ 17

[1] Measured in amplitude analysis of $B^+ \to J/\psi(1S)\phi K^+$.
[2] Branching fractions are normalized to 382 ± 22 events of $B^+ \to J/\psi\phi K^+$.

$\Gamma(\chi_{c0}(4500)K^+, \chi_c^0 \to J/\psi(1S)\phi)/\Gamma(J/\psi(1S)\phi K^+)$ $\Gamma_{287}/\Gamma_{280}$

VALUE (units 10^{-2})	DOCUMENT ID		TECN	COMMENT
6.6±2.4 $^{+3.5}_{-2.3}$	[1] AAIJ	17	LHCB	pp at 7, 8 TeV

[1] Measured in amplitude analysis of $B^+ \to J/\psi(1S)\phi K^+$.

$\Gamma(\chi_{c0}(4700)K^+, \chi_{c0} \to J/\psi(1S)\phi)/\Gamma(J/\psi(1S)\phi K^+)$ $\Gamma_{288}/\Gamma_{280}$

VALUE	DOCUMENT ID		TECN	COMMENT
0.12±0.05 $^{+0.09}_{-0.05}$	[1] AAIJ	17	LHCB	pp at 7, 8 TeV

[1] Measured in amplitude analysis of $B^+ \to J/\psi(1S)\phi K^+$.

$\Gamma(J/\psi(1S)\omega K^+)/\Gamma_{\text{total}}$ Γ_{289}/Γ

VALUE (units 10^{-4})	DOCUMENT ID		TECN	COMMENT
3.2±0.1 $^{+0.6}_{-0.3}$	[1] DEL-AMO-SA...10B		BABR	$e^+e^- \to \Upsilon(4S)$
• • • We do not use the following data for averages, fits, limits, etc. • • •				
3.5±0.2±0.4	[1] AUBERT	08W	BABR	Repl. by DEL-AMO-SANCHEZ 10B

[1] Assumes equal production of B^+ and B^0 at the $\Upsilon(4S)$.

$\Gamma(\chi_{c1}(3872)K^+, \chi_{c1} \to J/\psi\omega)/\Gamma_{\text{total}}$ Γ_{290}/Γ

VALUE (units 10^{-6})	DOCUMENT ID		TECN	COMMENT
6±2±1	[1] DEL-AMO-SA...10B		BABR	$e^+e^- \to \Upsilon(4S)$

[1] Assumes equal production of B^+ and B^0 at the $\Upsilon(4S)$.

$\Gamma(\chi_{c1}(3872)K^+, \chi_{c1} \to p\overline{p})/\Gamma_{\text{total}}$ Γ_{240}/Γ

VALUE	CL%	DOCUMENT ID		TECN	COMMENT
<0.5 × 10^{-8}	95	[1] AAIJ	17AD	LHCB	pp at 7 and 8 TeV
• • • We do not use the following data for averages, fits, limits, etc. • • •					
<1.7 × 10^{-8}	95	[2] AAIJ	13S	LHCB	Repl. by AAIJ 17AD

[1] Measured relative to $B^+ \to J/\psi K^+$ decay with charmonia reconstructed in $p\overline{p}$ final state and using $B(B^+ \to J/\psi K^+) \times B(J/\psi \to p\overline{p}) = (2.17 \pm 0.08) \times 10^{-6}$.
[2] Measured relative to $B^+ \to J/\psi K^+$ decay with charmonia reconstructed in $p\overline{p}$ final state and using $B(B^+ \to J/\psi K^+) = (1.013 \pm 0.034) \times 10^{-3}$ and $B(J/\psi \to p\overline{p}) = (2.17 \pm 0.07) \times 10^{-3}$.

$\Gamma(X(3915)K^+, X \to J/\psi\omega)/\Gamma_{\text{total}}$ Γ_{291}/Γ

VALUE (units 10^{-5})	DOCUMENT ID		TECN	COMMENT
3.0 $^{+0.7}_{-0.6}$ $^{+0.5}_{-0.3}$	[1] DEL-AMO-SA...10B		BABR	$e^+e^- \to \Upsilon(4S)$
• • • We do not use the following data for averages, fits, limits, etc. • • •				
4.9 $^{+1.0}_{-0.9}$ ±0.5	[1] AUBERT	08W	BABR	Repl. by DEL-AMO-SANCHEZ 10B

[1] Assumes equal production of B^+ and B^0 at the $\Upsilon(4S)$.

$\Gamma(X(3915)K^+, X \to p\overline{p})/\Gamma_{\text{total}}$ Γ_{272}/Γ

VALUE	CL%	DOCUMENT ID		TECN	COMMENT
<7.1 × 10^{-8}	95	[1] AAIJ	13S	LHCB	pp at 7 TeV

[1] Measured relative to $B^+ \to J/\psi K^+$ decay with charmonia reconstructed in $p\overline{p}$ final state and using $B(B^+ \to J/\psi K^+) = (1.013 \pm 0.034) \times 10^{-3}$ and $B(J/\psi \to p\overline{p}) = (2.17 \pm 0.07) \times 10^{-3}$.

$\Gamma(J/\psi(1S)\pi^+)/\Gamma_{\text{total}}$ Γ_{292}/Γ

VALUE	DOCUMENT ID		TECN	COMMENT
(3.88±0.12) × 10^{-5} OUR FIT				
(3.8 ±0.6 ±0.3) × 10^{-5}	[1] ABE	03B	BELL	$e^+e^- \to \Upsilon(4S)$

[1] Assumes equal production of B^+ and B^0 at the $\Upsilon(4S)$.

$\Gamma(J/\psi(1S)\pi^+)/\Gamma(J/\psi(1S)K^+)$ $\Gamma_{292}/\Gamma_{268}$

VALUE (units 10^{-2})	EVTS	DOCUMENT ID		TECN	COMMENT
3.85±0.04 OUR FIT					
3.85±0.04 OUR AVERAGE					
3.83±0.03±0.03		AAIJ	17O	LHCB	pp at 7, 8 TeV
3.5 ±0.3 ±1.2		AABOUD	16L	ATLS	pp at 7, 8 TeV
4.86±0.82±0.15		ABULENCIA	09	CDF	$p\overline{p}$ at 1.96 TeV
5.37±0.45±0.11		AUBERT	04P	BABR	$e^+e^- \to \Upsilon(4S)$
5.0 $^{+1.9}_{-1.7}$ ±0.1		ABE	96R	CDF	$p\overline{p}$ 1.8 TeV
5.2 ±2.4		BISHAI	96	CLE2	$e^+e^- \to \Upsilon(4S)$
• • • We do not use the following data for averages, fits, limits, etc. • • •					
3.83±0.11±0.07		AAIJ	12AC	LHCB	Repl. by AAIJ 17O
3.91±0.78±0.19		AUBERT	02F	BABR	Repl. by AUBERT 04P
4.3 ±2.3	5	[1] ALEXANDER	95	CLE2	Sup. by BISHAI 96

[1] Assumes equal production of B^+B^- and $B^0\overline{B}^0$ on $\Upsilon(4S)$.

$\Gamma(J/\psi(1S)\pi^+\pi^+\pi^+\pi^-\pi^-)/\Gamma(\psi(2S)K^+)$ $\Gamma_{293}/\Gamma_{304}$

VALUE (units 10^{-2})	DOCUMENT ID		TECN	COMMENT
1.88±0.17±0.09	[1] AAIJ	17K		pp at 7 and 8 TeV

[1] Contains also the contribution from $B^+ \to \psi(2S)[\to J/\psi\pi^+\pi^-]\pi^+\pi^+\pi^-$ decays.

$\Gamma(\psi(2S)\pi^+\pi^+\pi^-)/\Gamma(\psi(2S)K^+)$ $\Gamma_{294}/\Gamma_{304}$

VALUE (units 10^{-2})	DOCUMENT ID		TECN	COMMENT
3.04±0.50±0.26	AAIJ	17K	LHCB	pp at 7 and 8 TeV

$\Gamma(J/\psi(1S)\rho^+)/\Gamma_{total}$ Γ_{295}/Γ

VALUE (units 10^{-5})	CL%	DOCUMENT ID		TECN	COMMENT
5.0±0.7±0.3		[1] AUBERT	07AC	BABR	$e^+e^- \to \Upsilon(4S)$
• • • We do not use the following data for averages, fits, limits, etc. • • •					
<77	90	BISHAI	96	CLE2	$e^+e^- \to \Upsilon(4S)$

[1] Assumes equal production of B^+ and B^0 at the $\Upsilon(4S)$.

$\Gamma(J/\psi(1S)\pi^+\pi^0\,\text{nonresonant})/\Gamma_{total}$ Γ_{296}/Γ

VALUE (units 10^{-5})	CL%	DOCUMENT ID		TECN	COMMENT
<0.73	90	[1] AUBERT	07AC	BABR	$e^+e^- \to \Upsilon(4S)$

[1] Assumes equal production of B^+ and B^0 at the $\Upsilon(4S)$.

$\Gamma(J/\psi(1S)a_1(1260)^+)/\Gamma_{total}$ Γ_{297}/Γ

VALUE	CL%	DOCUMENT ID		TECN	COMMENT
<1.2 × 10^{-3}	90	BISHAI	96	CLE2	$e^+e^- \to \Upsilon(4S)$

$\Gamma(J/\psi(1S)p\overline{p}\pi^+)/\Gamma_{total}$ Γ_{298}/Γ

VALUE	CL%	DOCUMENT ID		TECN	COMMENT
<5.0 × 10^{-7}	90	[1] AAIJ	13Z	LHCB	pp at 7 TeV

[1] Uses $B(B_s^0 \to J/\psi(1S)\pi^+\pi^-) = (1.98 \pm 0.20) \times 10^{-4}$.

$\Gamma(J/\psi(1S)p\overline{\Lambda})/\Gamma_{total}$ Γ_{299}/Γ

VALUE (units 10^{-6})	CL%	DOCUMENT ID		TECN	COMMENT
11.8±3.1 OUR AVERAGE					
$11.7 \pm 2.8^{+1.8}_{-2.3}$		[1] XIE	05	BELL	$e^+e^- \to \Upsilon(4S)$
$12\ ^{+9}_{-6}$		[1] AUBERT	03K	BABR	$e^+e^- \to \Upsilon(4S)$
• • • We do not use the following data for averages, fits, limits, etc. • • •					
<41	90	ZANG	04	BELL	$e^+e^- \to \Upsilon(4S)$

[1] Assumes equal production of B^+ and B^0 at the $\Upsilon(4S)$.

$\Gamma(J/\psi(1S)\overline{\Sigma}^0 p)/\Gamma_{total}$ Γ_{300}/Γ

VALUE	CL%	DOCUMENT ID		TECN	COMMENT
<1.1 × 10^{-5}	90	[1] XIE	05	BELL	$e^+e^- \to \Upsilon(4S)$

[1] Assumes equal production of B^+ and B^0 at the $\Upsilon(4S)$.

$\Gamma(J/\psi(1S)D^+)/\Gamma_{total}$ Γ_{301}/Γ

VALUE (units 10^{-5})	CL%	DOCUMENT ID		TECN	COMMENT
<12	90	[1] AUBERT	05U	BABR	$e^+e^- \to \Upsilon(4S)$

[1] Assumes equal production of B^+ and B^0 at the $\Upsilon(4S)$.

$\Gamma(J/\psi(1S)\overline{D}^0\pi^+)/\Gamma_{total}$ Γ_{302}/Γ

VALUE (units 10^{-5})	CL%	DOCUMENT ID		TECN	COMMENT
<2.5	90	[1] ZHANG	05B	BELL	$e^+e^- \to \Upsilon(4S)$
• • • We do not use the following data for averages, fits, limits, etc. • • •					
<5.2	90	[1] AUBERT	05R	BABR	$e^+e^- \to \Upsilon(4S)$

[1] Assumes equal production of B^+ and B^0 at the $\Upsilon(4S)$.

$\Gamma(\psi(2S)\pi^+)/\Gamma_{total}$ Γ_{303}/Γ

VALUE (units 10^{-5})	DOCUMENT ID		TECN	COMMENT
2.44±0.22±0.20	[1] BHARDWAJ	08	BELL	$e^+e^- \to \Upsilon(4S)$

[1] Assumes equal production of B^+ and B^0 at the $\Upsilon(4S)$.

$\Gamma(\psi(2S)\pi^+)/\Gamma(\psi(2S)K^+)$ $\Gamma_{303}/\Gamma_{304}$

VALUE (units 10^{-2})	DOCUMENT ID		TECN	COMMENT
3.97±0.29 OUR AVERAGE				
3.95±0.40±0.12	AAIJ	12AC	LHCB	pp at 7 TeV
3.99±0.36±0.17	BHARDWAJ	08	BELL	$e^+e^- \to \Upsilon(4S)$

$\Gamma(\psi(2S)K^+)/\Gamma_{total}$ Γ_{304}/Γ

VALUE (units 10^{-4})	EVTS	DOCUMENT ID		TECN	COMMENT
6.21± 0.23 OUR FIT					
6.48± 0.34 OUR AVERAGE					
6.4 ± 1.0 ±0.4		[1] KATO	18	BELL	$e^+e^- \to \Upsilon(4S)$
6.65± 0.17±0.55		[2] GULER	11	BELL	$e^+e^- \to \Upsilon(4S)$
4.9 ± 1.6 ±0.4		[1] AUBERT	06E	BABR	$e^+e^- \to \Upsilon(4S)$
6.17± 0.32±0.44		[2] AUBERT	05J	BABR	$e^+e^- \to \Upsilon(4S)$
7.8 ± 0.7 ±0.9		[2] RICHICHI	01	CLE2	$e^+e^- \to \Upsilon(4S)$
18 ± 8 ±4	5	[2] ALBRECHT	90J	ARG	$e^+e^- \to \Upsilon(4S)$
• • • We do not use the following data for averages, fits, limits, etc. • • •					
6.9 ± 0.6		[2] ABE	03B	BELL	Repl. by GULER 11
6.4 ± 0.5 ±0.8		[2] AUBERT	02	BABR	Repl. by AUBERT 05J
6.1 ± 2.3 ±0.9	7	[2] ALAM	94	CLE2	Repl. by RICHICHI 01
<5 at 90% CL		[2] BORTOLETTO	92	CLEO	$e^+e^- \to \Upsilon(4S)$
22 ±17	3	[3] ALBRECHT	87D	ARG	$e^+e^- \to \Upsilon(4S)$

[1] Measures absolute branching fractions using a missing-mass technique.
[2] Assumes equal production of B^+ and B^0 at the $\Upsilon(4S)$.
[3] ALBRECHT 87D assume $B^+B^-/B^0\overline{B}^0$ ratio is 55/45. Superseded by ALBRECHT 90J.

$\Gamma(\psi(2S)K^+)/\Gamma(J/\psi(1S)K^+)$ $\Gamma_{304}/\Gamma_{268}$

VALUE	DOCUMENT ID		TECN	COMMENT
0.615±0.019 OUR FIT				
0.606±0.021 OUR AVERAGE				
0.59 ±0.11 ±0.02	[1] AAIJ	13S	LHCB	pp at 7 TeV
0.607±0.018±0.013	[2,3] AAIJ	12L	LHCB	pp at 7 TeV
0.63 ±0.05 ±0.08	ABAZOV	09Y	D0	$p\overline{p}$ at 1.96 TeV
0.558±0.082±0.056	ABE	98O	CDF	$p\overline{p}$ 1.8 TeV
• • • We do not use the following data for averages, fits, limits, etc. • • •				
0.64 ±0.06 ±0.07	[4] AUBERT	02	BABR	$e^+e^- \to \Upsilon(4S)$

[1] AAIJ 13S reports $[\Gamma(B^+ \to \psi(2S)K^+)/\Gamma(B^+ \to J/\psi(1S)K^+)] \times [B(\psi(2S) \to p\overline{p})] / [B(J/\psi(1S) \to p\overline{p})] = 0.080 \pm 0.012 \pm 0.009$ which we multiply or divide by our best values $B(\psi(2S) \to p\overline{p}) = (2.88 \pm 0.10) \times 10^{-4}$, $B(J/\psi(1S) \to p\overline{p}) = (2.121 \pm 0.029) \times 10^{-3}$. Our first error is their experiment's error and our second error is the systematic error from using our best values.
[2] AAIJ 12L reports $0.594 \pm 0.006 \pm 0.016 \pm 0.015$ from a measurement of $[\Gamma(B^+ \to \psi(2S)K^+)/\Gamma(B^+ \to J/\psi(1S)K^+)] \times [B(J/\psi(1S) \to e^+e^-)] / [B(\psi(2S) \to e^+e^-)]$ assuming $B(J/\psi(1S) \to e^+e^-) = (5.94 \pm 0.06) \times 10^{-2}$, $B(\psi(2S) \to e^+e^-) = (7.72 \pm 0.17) \times 10^{-3}$, which we rescale to our best values $B(J/\psi(1S) \to e^+e^-) = (5.971 \pm 0.032) \times 10^{-2}$, $B(\psi(2S) \to e^+e^-) = (7.93 \pm 0.17) \times 10^{-3}$. Our first error is their experiment's error and our second error is the systematic error from using our best values.
[3] Assumes $B(J/\psi \to \mu^+\mu^-) / B(\psi(2S) \to \mu^+\mu^-) = B(J/\psi \to e^+e^-) / B(\psi(2S) \to e^+e^-) = 7.69 \pm 0.19$.
[4] Assumes equal production of B^+ and B^0 at the $\Upsilon(4S)$.

$\Gamma(\psi(2S)K^*(892)^+)/\Gamma_{total}$ Γ_{305}/Γ

VALUE (units 10^{-4})	CL%	DOCUMENT ID		TECN	COMMENT
6.7 ±1.4 OUR AVERAGE		Error includes scale factor of 1.3.			
5.92±0.85±0.89		[1] AUBERT	05J	BABR	$e^+e^- \to \Upsilon(4S)$
9.2 ±1.9 ±1.2		[1] RICHICHI	01	CLE2	$e^+e^- \to \Upsilon(4S)$
• • • We do not use the following data for averages, fits, limits, etc. • • •					
<30	90	[1] ALAM	94	CLE2	Repl. by RICHICHI 01
<35	90	[1] BORTOLETTO	92	CLEO	$e^+e^- \to \Upsilon(4S)$
<49	90	[1] ALBRECHT	90J	ARG	$e^+e^- \to \Upsilon(4S)$

[1] Assumes equal production of B^+ and B^0 at the $\Upsilon(4S)$.

$\Gamma(\psi(2S)K^*(892)^+)/\Gamma(\psi(2S)K^+)$ $\Gamma_{305}/\Gamma_{304}$

VALUE	DOCUMENT ID		TECN	COMMENT
0.96±0.15±0.09	AUBERT	05J	BABR	$e^+e^- \to \Upsilon(4S)$

$\Gamma(\psi(2S)K^0\pi^+)/\Gamma_{total}$ Γ_{306}/Γ

VALUE (units 10^{-3})	DOCUMENT ID		TECN	COMMENT
• • • We do not use the following data for averages, fits, limits, etc. • • •				
0.588±0.034	[1] AUBERT	09AA	BABR	$e^+e^- \to \Upsilon(4S)$

[1] Does not report systematic uncertainties.

$\Gamma(\psi(2S)K^+\pi^+\pi^-)/\Gamma_{total}$ Γ_{307}/Γ

VALUE (units 10^{-4})	EVTS	DOCUMENT ID		TECN	COMMENT
4.3 ± 0.5 OUR AVERAGE					
4.31± 0.20±0.50		[1] GULER	11	BELL	$e^+e^- \to \Upsilon(4S)$
19 ±11 ±4	3	[1] ALBRECHT	90J	ARG	$e^+e^- \to \Upsilon(4S)$

[1] Assumes equal production of B^+ and B^0 at the $\Upsilon(4S)$.

$\Gamma(\psi(2S)\phi(1020)K^+)/\Gamma_{total}$ Γ_{308}/Γ

VALUE (units 10^{-6})	DOCUMENT ID		TECN	COMMENT
4.0±0.4±0.6	[1,2] KHACHATRY...17C		CMS	pp at 8 TeV

[1] Measured using $B^+ \to \psi(2S)K^+$ as a normalization channel. The second error represents total systematic uncertainties including those from branching fractions which were taken from PDG 16 as $B(\phi \to K^+K^-) = 0.489 \pm 0.005$ and $B(B^+ \to \psi(2S)K^+) = (6.26 \pm 0.24) \times 10^{-4}$.
[2] An upper limit on the fraction of the non-ϕ component in $B^+ \to \psi(2S)K^+K^-K^+$ decays is set as 0.26 at the 95% confidence level.

$\Gamma(\psi(3770)K^+)/\Gamma_{total}$ Γ_{309}/Γ

VALUE (units 10^{-3})	CL%	DOCUMENT ID		TECN	COMMENT
0.49±0.13 OUR AVERAGE					
3.5 ±2.5 ±0.3		[1] AUBERT	06E	BABR	$e^+e^- \to \Upsilon(4S)$
0.48±0.11±0.07		[2] CHISTOV	04	BELL	$e^+e^- \to \Upsilon(4S)$
• • • We do not use the following data for averages, fits, limits, etc. • • •					
<0.23	90	[1] KATO	18	BELL	$e^+e^- \to \Upsilon(4S)$

[1] Measures absolute branching fractions using a missing-mass technique.
[2] Assumes equal production of B^+ and B^0 at the $\Upsilon(4S)$.

$\Gamma(\psi(3770)K^+, \psi \to D^0\overline{D}^0)/\Gamma_{total}$ Γ_{310}/Γ

VALUE (units 10^{-4})	DOCUMENT ID		TECN	COMMENT
1.5 ±0.5 OUR AVERAGE	Error includes scale factor of 1.4.			
1.18±0.41±0.15	[1] LEES	15C	BABR	$e^+e^- \to \Upsilon(4S)$
2.2 ±0.5 ±0.3	[1] BRODZICKA	08	BELL	$e^+e^- \to \Upsilon(4S)$

Meson Particle Listings

$B^{\pm}$

• • • We do not use the following data for averages, fits, limits, etc. • • •

$1.41 \pm 0.30 \pm 0.22$	[1] AUBERT	08B	BABR	Repl. by LEES 15C	
$3.4 \pm 0.8 \pm 0.5$	[1] CHISTOV	04	BELL	Repl. by BRODZICKA 08	

[1] Assumes equal production of B^+ and B^0 at the $\Upsilon(4S)$.

$\Gamma(\psi(3770)K+, \psi \to D^+D^-)/\Gamma_{total}$ Γ_{311}/Γ

VALUE (units 10^{-4})	DOCUMENT ID		TECN	COMMENT
0.94 ± 0.35 OUR AVERAGE				
$0.84 \pm 0.32 \pm 0.21$	[1] AUBERT	08B	BABR	$e^+e^- \to \Upsilon(4S)$
$1.4 \pm 0.8 \pm 0.2$	[1] CHISTOV	04	BELL	$e^+e^- \to \Upsilon(4S)$

[1] Assumes equal production of B^+ and B^0 at the $\Upsilon(4S)$.

$\Gamma(\psi(3770)K^+, \psi \to p\overline{p})/\Gamma_{total}$ Γ_{312}/Γ

VALUE	CL%	DOCUMENT ID		TECN	COMMENT
$< 2 \times 10^{-7}$	95	[1] AAIJ	17AD	LHCB	pp at 7 and 8 TeV

[1] Measured relative to $B^+ \to J/\psi K^+$ decay with charmonia reconstructed in $p\overline{p}$ final state and using $B(B^+ \to J/\psi K^+) \times B(J/\psi \to p\overline{p}) = (2.17 \pm 0.08) \times 10^{-6}$.

$\Gamma(\psi(4040)K^+)/\Gamma_{total}$ Γ_{313}/Γ

VALUE	CL%	DOCUMENT ID		TECN	COMMENT
$< 1.3 \times 10^{-4}$	90	AAIJ	13BC	LHCB	pp at 7, 8 TeV
• • • We do not use the following data for averages, fits, limits, etc. • • •					
$< 3.0 \times 10^{-3}$	90	[1] IWASHITA	14	BELL	$e^+e^- \to \Upsilon(4S)$

[1] IWASHITA 14 reports $[\Gamma(B^+ \to \psi(4040)K^+)/\Gamma_{total}] \times [B(\psi(4040) \to J/\psi\eta)] < 15.5 \times 10^{-6}$ which we divide by our best value $B(\psi(4040) \to J/\psi\eta) = 5.2 \times 10^{-3}$.

$\Gamma(\psi(4160)K^+)/\Gamma_{total}$ Γ_{314}/Γ

VALUE (units 10^{-4})	DOCUMENT ID		TECN	COMMENT
$5.1^{+1.3+2.5}_{-1.2-2.4}$	[1] AAIJ	13BC	LHCB	pp at 7, 8 TeV

[1] AAIJ 13BC reports $[\Gamma(B^+ \to \psi(4160)K^+)/\Gamma_{total}] \times B(\psi(4160) \to \mu^+\mu^-) = (3.5^{+0.9}_{-0.8}) \times 10^{-9}$ which we devide by our best value $B(\psi(4160) \to e^+e^-) = (6.9 \pm 3.3) \times 10^{-6}$ assuming lepton universality. Our first error is their experiment's error and our second error is the systematic error from using our best value.

$\Gamma(\psi(4160)K^+, \psi \to \overline{D}^0D^0)/\Gamma_{total}$ Γ_{315}/Γ

VALUE (units 10^{-4})	DOCUMENT ID		TECN	COMMENT
$0.84 \pm 0.41 \pm 0.33$	[1] LEES	15C	BABR	$e^+e^- \to \Upsilon(4S)$

[1] Assumes equal production of B^+ and B^0 at the $\Upsilon(4S)$.

$\Gamma(\chi_{c0}\pi^+, \chi_{c0} \to \pi^+\pi^-)/\Gamma_{total}$ Γ_{316}/Γ

VALUE (units 10^{-5})	CL%	DOCUMENT ID		TECN	COMMENT
< 0.1	90	[1] AUBERT	09L	BABR	$e^+e^- \to \Upsilon(4S)$
• • • We do not use the following data for averages, fits, limits, etc. • • •					
< 0.3	90	[1] AUBERT,B	05G	BABR	Repl. by AUBERT 09L

[1] Assumes equal production of B^+ and B^0 at the $\Upsilon(4S)$.

$\Gamma(\chi_{c0}K^+)/\Gamma_{total}$ Γ_{317}/Γ

VALUE (units 10^{-4})	CL%	DOCUMENT ID		TECN	COMMENT
$1.49^{+0.15}_{-0.14}$ OUR AVERAGE					
$1.84 \pm 0.25 \pm 0.14$		[1,2] LEES	12O	BABR	$e^+e^- \to \Upsilon(4S)$
$1.68 \pm 0.32 \pm 0.16$		[1,3] LEES	12O	BABR	$e^+e^- \to \Upsilon(4S)$
$1.8 \pm 0.8 \pm 0.1$		[4] LEES	11I	BABR	$e^+e^- \to \Upsilon(4S)$
$1.23^{+0.28}_{-0.25} \pm 0.05$		[1,5] AUBERT	08AI	BABR	$e^+e^- \to \Upsilon(4S)$
$4.3 \pm 2.0 \pm 0.2$		[6] AUBERT,BE	06M	BABR	$e^+e^- \to \Upsilon(4S)$
$1.12 \pm 0.12^{+0.30}_{-0.20}$		[1] GARMASH	06	BELL	$e^+e^- \to \Upsilon(4S)$
• • • We do not use the following data for averages, fits, limits, etc. • • •					
< 3.3	90	[7] KATO	18	BELL	$e^+e^- \to \Upsilon(4S)$
< 2.7	95	[8] AAIJ	13S	LHCB	pp at 7 TeV
< 5	90	[1,9] WICHT	08	BELL	$e^+e^- \to \Upsilon(4S)$
< 1.8	90	[7] AUBERT	06E	BABR	$e^+e^- \to \Upsilon(4S)$
$1.84 \pm 0.32 \pm 0.31$		[1,10] AUBERT	06O	BABR	Repl. by LEES 12O
< 8.9	90	[1] AUBERT	05K	BABR	$e^+e^- \to \Upsilon(4S)$
$1.39 \pm 0.49 \pm 0.11$		[11] AUBERT,B	05N	BABR	Repl. by AUBERT 08AI
$1.96 \pm 0.35^{+2.00}_{-0.42}$		[1] GARMASH	05	BELL	Repl. by GARMASH 06
2.7 ± 0.7		[12] AUBERT	04T	BABR	Repl. by AUBERT,B 04P
$3.0 \pm 0.8 \pm 0.3$		[13] AUBERT,B	04P	BABR	Repl. by AUBERT,B 05N
$6.0^{+2.1}_{-1.8} \pm 1.1$		[14] ABE	02B	BELL	Repl. by GARMASH 05
< 4.8	90	[15] EDWARDS	01	CLE2	$e^+e^- \to \Upsilon(4S)$

[1] Assumes equal production of B^+ and B^0 at the $\Upsilon(4S)$.
[2] Measured in the $B^+ \to K^+K^-K^+$ decay.
[3] Measured in the $B^+ \to K^+K^0_SK^0_S$ decay.
[4] LEES 11I reports $[\Gamma(B^+ \to \chi_{c0}K^+)/\Gamma_{total}] \times [B(\chi_{c0}(1P) \to \pi\pi)] = (1.53 \pm 0.66 \pm 0.27) \times 10^{-6}$ which we divide by our best value $B(\chi_{c0}(1P) \to \pi\pi) = (8.51 \pm 0.33) \times 10^{-3}$. Our first error is their experiment's error and our second error is the systematic error from using our best value.
[5] AUBERT 08AI reports $(0.70 \pm 0.10^{+0.12}_{-0.10}) \times 10^{-6}$ for $B(B^+ \to \chi_{c0}K^+) \times B(\chi_{c0} \to \pi^+\pi^-)$. We compute $B(B^+ \to \chi_{c0}K^+)$ using the PDG value $B(\chi_{c0} \to \pi\pi)=(8.51 \pm 0.33) \times 10^{-3}$ and 2/3 for the $\pi^+\pi^-$ fraction. Our first error is their experiment's error and the second error is systematic error from using our best value.
[6] AUBERT,BE 06M reports $[\Gamma(B^+ \to \chi_{c0}K^+)/\Gamma_{total}] \times [B(\chi_{c0}(1P) \to \gamma J/\psi(1S))] = (6.1 \pm 2.6 \pm 1.1) \times 10^{-6}$ which we divide by our best value $B(\chi_{c0}(1P) \to \gamma J/\psi(1S)) = (1.40 \pm 0.05) \times 10^{-2}$. Our first error is their experiment's error and our second error is the systematic error from using our best value. The significance of the observed signal is 2.4 σ.
[7] Measures absolute branching fractions using a missing-mass technique.
[8] AAIJ 13S reports $[\Gamma(B^+ \to \chi_{c0}K^+)/\Gamma_{total}] \times [B(\chi_{c0}(1P) \to p\overline{p})] < 6 \times 10^{-8}$ which we divide by our best value $B(\chi_{c0}(1P) \to p\overline{p}) = 2.21 \times 10^{-4}$.
[9] WICHT 08 reports $[\Gamma(B^+ \to \chi_{c0}K^+)/\Gamma_{total}] \times [B(\chi_{c0}(1P) \to \gamma\gamma)] < 0.11 \times 10^{-6}$ which we divide by our best value $B(\chi_{c0}(1P) \to \gamma\gamma) = 2.04 \times 10^{-4}$.
[10] Measured in the $B^+ \to K^+K^-K^+$ decay.
[11] AUBERT,B 05N reports $(0.66 \pm 0.22 \pm 0.08) \times 10^{-6}$ for $B(B^+ \to \chi^0_cK^+) \times B(\chi^0_c \to \pi^+\pi^-)$. We compute $B(B^+ \to \chi^0_cK^+)$ using the PDG value $B(\chi^0_c \to \pi^+\pi^-) = (7.1 \pm 0.6) \times 10^{-3}$ and 2/3 for the $\pi^+\pi^-$ fraction.
[12] The measurement performed using decay channels $\chi_{c0} \to \pi^+\pi^-$ and $\chi_{c0} \to K^+K^-$. The ratio of the branching ratios for these channels is found to be consistent with world average.
[13] AUBERT 04P reports $B(B^+ \to \chi_{c0}K^+) \times B(\chi_{c0} \to \pi^+\pi^-) = (1.5 \pm 0.4 \pm 0.1) \times 10^{-6}$ and used PDG value of $B(\chi_{c0} \to \pi\pi) = (7.4 \pm 0.8) \times 10^{-3}$ and Clebsh-Gordan coefficient to compute $B(B^{\pm} -> \chi_{c0}K^+)$.
[14] ABE 02B measures the ratio of $B(B^+ \to \chi_{c0}K^+)/B(B^+ \to J/\psi(1S)K^+) = 0.60 + 0.21 - 0.18 \pm 0.05 \pm 0.08$, where the third error is due to the uncertainty in the $B(\chi_{c0} \to \pi^+\pi^-)$, and uses $B(B^+ \to J/\psi(1S)K^+) = (10.0 \pm 1.0) \times 10^{-4}$ to obtain the result.
[15] EDWARDS 01 assumes equal production of B^0 and B^+ at the $\Upsilon(4S)$. The correlated uncertainties (28.3)% from $B(J/\psi(1S) \to \gamma\eta_c)$ in those modes have been accounted for.

$\Gamma(\chi_{c0}K^*(892)^+)/\Gamma_{total}$ Γ_{318}/Γ

VALUE (units 10^{-4})	CL%	DOCUMENT ID		TECN	COMMENT
< 2.1	90	[1] AUBERT	08BD	BABR	$e^+e^- \to \Upsilon(4S)$
• • • We do not use the following data for averages, fits, limits, etc. • • •					
< 28.6	90	[1] AUBERT	05K	BABR	Repl. by AUBERT 08BD

[1] Assumes equal production of B^+ and B^0 at the $\Upsilon(4S)$.

$\Gamma(\chi_{c1}(1P)\pi^+)/\Gamma_{total}$ Γ_{319}/Γ

VALUE (units 10^{-5})	DOCUMENT ID		TECN	COMMENT
$2.2 \pm 0.4 \pm 0.3$	[1] KUMAR	06	BELL	$e^+e^- \to \Upsilon(4S)$

[1] Assumes equal production of B^+ and B^0 at the $\Upsilon(4S)$.

$\Gamma(\chi_{c1}(1P)K^+)/\Gamma_{total}$ Γ_{320}/Γ

VALUE (units 10^{-4})	EVTS	DOCUMENT ID		TECN	COMMENT
4.84 ± 0.23 OUR AVERAGE					
$5.8 \pm 0.9 \pm 0.5$		[1] KATO	18	BELL	$e^+e^- \to \Upsilon(4S)$
$4.94 \pm 0.11 \pm 0.33$		[2] BHARDWAJ	11	BELL	$e^+e^- \to \Upsilon(4S)$
$4.5 \pm 0.1 \pm 0.3$		[3] AUBERT	09B	BABR	$e^+e^- \to \Upsilon(4S)$
$8.1 \pm 1.4 \pm 0.7$		[1] AUBERT	06E	BABR	$e^+e^- \to \Upsilon(4S)$
$15.5 \pm 5.4 \pm 2.0$		[4] ACOSTA	02F	CDF	$p\overline{p}$ 1.8 TeV
• • • We do not use the following data for averages, fits, limits, etc. • • •					
$5.1 \pm 0.4 \pm 0.1$		[5] AUBERT,BE	06M	BABR	Repl. by AUBERT 09B
$4.49 \pm 0.19 \pm 0.53$		[2] SONI	06	BELL	Repl. by BHARDWAJ 11
$5.79 \pm 0.26 \pm 0.65$		[2] AUBERT	05J	BABR	Repl. by AUBERT,BE 06M
$6.0 \pm 0.9 \pm 0.2$		[6] AUBERT	02	BABR	Repl. by AUBERT 05J
$9.7 \pm 4.0 \pm 0.9$	6	[2] ALAM	94	CLE2	$e^+e^- \to \Upsilon(4S)$
$19 \pm 13 \pm 6$		[7] ALBRECHT	92E	ARG	$e^+e^- \to \Upsilon(4S)$

[1] Measures absolute branching fractions using a missing-mass technique.
[2] Assumes equal production of B^+ and B^0 at the $\Upsilon(4S)$.
[3] Uses $\chi_{c1,2} \to J/\psi\gamma$. Assumes $B(\Upsilon(4S) \to B^+B^-) = (51.6 \pm 0.6)\%$ and $B(\Upsilon(4S) \to B^0\overline{B}^0) = (48.4 \pm 0.6)\%$.
[4] ACOSTA 02F uses as reference of $B(B \to J/\psi(1S)K^+) = (10.1 \pm 0.6) \times 10^{-4}$. The second error includes the systematic error and the uncertainties of the branching ratio.
[5] AUBERT,BE 06M reports $[\Gamma(B^+ \to \chi_{c1}(1P)K^+)/\Gamma_{total}] \times [B(\chi_{c1}(1P) \to \gamma J/\psi(1S))] = (1.76 \pm 0.07 \pm 0.12) \times 10^{-4}$ which we divide by our best value $B(\chi_{c1}(1P) \to \gamma J/\psi(1S)) = (34.3 \pm 1.0) \times 10^{-2}$. Our first error is their experiment's error and our second error is the systematic error from using our best value.
[6] AUBERT 02 reports $(7.5 \pm 0.9 \pm 0.8) \times 10^{-4}$ from a measurement of $[\Gamma(B^+ \to \chi_{c1}(1P)K^+)/\Gamma_{total}] \times [B(\chi_{c1}(1P) \to \gamma J/\psi(1S))]$ assuming $B(\chi_{c1}(1P) \to \gamma J/\psi(1S)) = 0.273 \pm 0.016$, which we rescale to our best value $B(\chi_{c1}(1P) \to \gamma J/\psi(1S)) = (34.3 \pm 1.0) \times 10^{-2}$. Our first error is their experiment's error and our second error is the systematic error from using our best value. Assumes equal production of B^+ and B^0 at the $\Upsilon(4S)$.
[7] ALBRECHT 92E assumes no $\chi_{c2}(1P)$ production and $B(\Upsilon(4S) \to B^+B^-) = 50\%$.

$\Gamma(\chi_{c1}(1P)K^+)/\Gamma(J/\psi(1S)K^+)$ $\Gamma_{320}/\Gamma_{268}$

VALUE	DOCUMENT ID		TECN	COMMENT
$0.60 \pm 0.07 \pm 0.02$	[1] AUBERT	02	BABR	$e^+e^- \to \Upsilon(4S)$

[1] AUBERT 02 reports $0.75 \pm 0.08 \pm 0.05$ from a measurement of $[\Gamma(B^+ \to \chi_{c1}(1P)K^+)/\Gamma(B^+ \to J/\psi(1S)K^+)] \times [B(\chi_{c1}(1P) \to \gamma J/\psi(1S))]$ assuming $B(\chi_{c1}(1P) \to \gamma J/\psi(1S)) = 0.273 \pm 0.016$, which we rescale to our best value $B(\chi_{c1}(1P) \to \gamma J/\psi(1S)) = (34.3 \pm 1.0) \times 10^{-2}$. Our first error is their experiment's error and our

second error is the systematic error from using our best value. Assumes equal production of B^+ and B^0 at the $\Upsilon(4S)$.

$\Gamma(\chi_{c1}(1P)\pi^+)/\Gamma(\chi_{c1}(1P)K^+)$ $\Gamma_{319}/\Gamma_{320}$

VALUE	DOCUMENT ID		TECN	COMMENT
0.043±0.008±0.003	[1] KUMAR	06	BELL	$e^+e^- \to \Upsilon(4S)$

[1] Assumes equal production of B^+ and B^0 at the $\Upsilon(4S)$.

$\Gamma(\chi_{c1}(1P)K^*(892)^+)/\Gamma_{\text{total}}$ Γ_{321}/Γ

VALUE (units 10^{-4})	CL%	DOCUMENT ID		TECN	COMMENT
3.0 ±0.6 OUR AVERAGE		Error includes scale factor of 1.1.			
2.6 ±0.5 ±0.4		[1] AUBERT	09B	BABR	$e^+e^- \to \Upsilon(4S)$
4.05±0.59±0.95		[2] SONI	06	BELL	$e^+e^- \to \Upsilon(4S)$
• • • We do not use the following data for averages, fits, limits, etc. • • •					
2.94±0.95±0.98		[2] AUBERT	05J	BABR	Repl. by AUBERT 09B
<21	90	[2] ALAM	94	CLE2	$e^+e^- \to \Upsilon(4S)$

[1] Uses $\chi_{c1,2} \to J/\psi\gamma$. Assumes $B(\Upsilon(4S) \to B^+B^-) = (51.6\pm0.6)\%$ and $B(\Upsilon(4S) \to B^0\overline{B}^0) = (48.4 \pm 0.6)\%$.
[2] Assumes equal production of B^+ and B^0 at the $\Upsilon(4S)$.

$\Gamma(\chi_{c1}(1P)K^*(892)^+)/\Gamma(\chi_{c1}(1P)K^+)$ $\Gamma_{321}/\Gamma_{320}$

VALUE	DOCUMENT ID		TECN	COMMENT
0.51±0.17±0.16	AUBERT	05J	BABR	$e^+e^- \to \Upsilon(4S)$

$\Gamma(\chi_{c1}(1P)K^0\pi^+)/\Gamma_{\text{total}}$ Γ_{322}/Γ

VALUE (units 10^{-4})	DOCUMENT ID		TECN	COMMENT
5.75±0.26±0.32	[1] BHARDWAJ	16	BELL	$e^+e^- \to \Upsilon(4S)$

[1] Assumes equal production of B^+ and B^0 at the $\Upsilon(4S)$.

$\Gamma(\chi_{c1}(1P)K^0\pi^+)/\Gamma(J/\psi(1S)K^0\pi^+)$ $\Gamma_{322}/\Gamma_{269}$

VALUE	DOCUMENT ID		TECN	COMMENT
0.503±0.030±0.014	[1] LEES	12B	BABR	$e^+e^- \to \Upsilon(4S)$

[1] LEES 12B reports $0.501 \pm 0.024 \pm 0.028$ from a measurement of $[\Gamma(B^+ \to \chi_{c1}(1P)K^0\pi^+)/\Gamma(B^+ \to J/\psi(1S)K^0\pi^+)] \times [B(\chi_{c1}(1P) \to \gamma J/\psi(1S))]$ assuming $B(\chi_{c1}(1P) \to \gamma J/\psi(1S)) = (34.4 \pm 1.5) \times 10^{-2}$, which we rescale to our best value $B(\chi_{c1}(1P) \to \gamma J/\psi(1S)) = (34.3 \pm 1.0) \times 10^{-2}$. Our first error is their experiment's error and our second error is the systematic error from using our best value.

$\Gamma(\chi_{c1}(1P)K^+\pi^0)/\Gamma_{\text{total}}$ Γ_{323}/Γ

VALUE (units 10^{-4})	DOCUMENT ID		TECN	COMMENT
3.29±0.29±0.19	[1] BHARDWAJ	16	BELL	$e^+e^- \to \Upsilon(4S)$

[1] Assumes equal production of B^+ and B^0 at the $\Upsilon(4S)$.

$\Gamma(\chi_{c1}(1P)K^+\pi^+\pi^-)/\Gamma_{\text{total}}$ Γ_{324}/Γ

VALUE (units 10^{-4})	DOCUMENT ID		TECN	COMMENT
3.74±0.18±0.24	[1] BHARDWAJ	16	BELL	$e^+e^- \to \Upsilon(4S)$

[1] Assumes equal production of B^+ and B^0 at the $\Upsilon(4S)$.

$\Gamma(\chi_{c1}(2P)K^+, \chi_{c1}(2P) \to \pi^+\pi^-\chi_{c1}(1P))/\Gamma_{\text{total}}$ Γ_{325}/Γ

VALUE	CL%	DOCUMENT ID		TECN	COMMENT
<1.1 × 10⁻⁵	90	[1,2] BHARDWAJ	16	BELL	$e^+e^- \to \Upsilon(4S)$

[1] BHARDWAJ 16 analysis fixes mass and width of the $\chi_{c1}(2P)$ state to 3920 MeV and 20 MeV.
[2] Assumes equal production of B^+ and B^0 at the $\Upsilon(4S)$.

$\Gamma(\chi_{c2}K^+)/\Gamma_{\text{total}}$ Γ_{326}/Γ

VALUE (units 10^{-5})	CL%	DOCUMENT ID		TECN	COMMENT
$1.11^{+0.36}_{-0.34}\pm0.09$		[1] BHARDWAJ	11	BELL	$e^+e^- \to \Upsilon(4S)$
• • • We do not use the following data for averages, fits, limits, etc. • • •					
< 1.8	90	[2] AUBERT	09B	BABR	$e^+e^- \to \Upsilon(4S)$
<20	90	[3] AUBERT	06E	BABR	$e^+e^- \to \Upsilon(4S)$
< 2.9	90	[1] SONI	06	BELL	Repl. by BHARDWAJ 11
< 3.0	90	[1] AUBERT	05K	BABR	Repl. by AUBERT 06E

[1] Assumes equal production of B^+ and B^0 at the $\Upsilon(4S)$.
[2] Uses $\chi_{c1,2} \to J/\psi\gamma$. Assumes $B(\Upsilon(4S) \to B^+B^-) = (51.6\pm0.6)\%$ and $B(\Upsilon(4S) \to B^0\overline{B}^0) = (48.4 \pm 0.6)\%$.
[3] Perform measurements of absolute branching fractions using a missing mass technique.

$\Gamma(B^+ \to \chi_{c2}K^+)/\Gamma_{\text{total}} \times \Gamma(\chi_{c2}(1P) \to \gamma\gamma)/\Gamma_{\text{total}}$ $\Gamma_{326}/\Gamma \times \Gamma^{\chi_{c2}(1P)}_{89}/\Gamma_{\chi_{c2}(1P)}$

VALUE (units 10^{-6})	CL%	DOCUMENT ID		TECN	COMMENT
<0.09	90	[1] WICHT	08	BELL	$e^+e^- \to \Upsilon(4S)$

[1] Assumes equal production of B^+ and B^0 at the $\Upsilon(4S)$.

$\Gamma(\chi_{c2}K^*(892)^+)/\Gamma_{\text{total}}$ Γ_{327}/Γ

VALUE	CL%	DOCUMENT ID		TECN	COMMENT
<12 × 10⁻⁵	90	[1] AUBERT	09B	BABR	$e^+e^- \to \Upsilon(4S)$
• • • We do not use the following data for averages, fits, limits, etc. • • •					
<12.7 × 10⁻⁵	90	[2] SONI	06	BELL	$e^+e^- \to \Upsilon(4S)$
< 1.2 × 10⁻⁵	90	[2] AUBERT	05K	BABR	Repl. by AUBERT 09B

[1] Uses $\chi_{c1,2} \to J/\psi\gamma$. Assumes $B(\Upsilon(4S) \to B^+B^-) = (51.6\pm0.6)\%$ and $B(\Upsilon(4S) \to B^0\overline{B}^0) = (48.4 \pm 0.6)\%$.
[2] Assumes equal production of B^+ and B^0 at the $\Upsilon(4S)$.

$\Gamma(\chi_{c2}K^0\pi^+)/\Gamma_{\text{total}}$ Γ_{328}/Γ

VALUE (units 10^{-4})	DOCUMENT ID		TECN	COMMENT
1.16±0.22±0.12	[1] BHARDWAJ	16	BELL	$e^+e^- \to \Upsilon(4S)$

[1] Assumes equal production of B^+ and B^0 at the $\Upsilon(4S)$.

$\Gamma(\chi_{c2}K^+\pi^0)/\Gamma_{\text{total}}$ Γ_{329}/Γ

VALUE	CL%	DOCUMENT ID		TECN	COMMENT
<0.62 × 10⁻⁴	90	[1] BHARDWAJ	16	BELL	$e^+e^- \to \Upsilon(4S)$

[1] Assumes equal production of B^+ and B^0 at the $\Upsilon(4S)$.

$\Gamma(\chi_{c2}K^+\pi^+\pi^-)/\Gamma_{\text{total}}$ Γ_{330}/Γ

VALUE (units 10^{-4})	DOCUMENT ID		TECN	COMMENT
1.34±0.17±0.09	[1] BHARDWAJ	16	BELL	$e^+e^- \to \Upsilon(4S)$

[1] Assumes equal production of B^+ and B^0 at the $\Upsilon(4S)$.

$\Gamma(\chi_{c2}(3930)\pi^+, \chi_{c2} \to \pi^+\pi^-)/\Gamma_{\text{total}}$ Γ_{331}/Γ

VALUE (units 10^{-6})	CL%	DOCUMENT ID		TECN	COMMENT
<0.1	90	[1] AUBERT	09L	BABR	$e^+e^- \to \Upsilon(4S)$

[1] Assumes equal production of B^+ and B^0 at the $\Upsilon(4S)$.

$\Gamma(h_c(1P)K^+)/\Gamma_{\text{total}}$ Γ_{332}/Γ

VALUE (units 10^{-5})	CL%	DOCUMENT ID		TECN	COMMENT
<3.8	90	[1] FANG	06	BELL	$e^+e^- \to \Upsilon(4S)$

[1] Assumes equal production of B^+ and B^0 at the $\Upsilon(4S)$ and $B(h_c \to \eta_c\gamma) = 50\%$.

$\Gamma(h_c(1P)K^+, h_c \to p\overline{p})/\Gamma_{\text{total}}$ Γ_{333}/Γ

VALUE	CL%	DOCUMENT ID		TECN	COMMENT
<6.4 × 10⁻⁸	95	[1] AAIJ	13S	LHCB	pp at 7 TeV

[1] Measured relative to $B^+ \to J/\psi K^+$ decay with charmonia reconstructed in $p\overline{p}$ final state and using $B(B^+ \to J/\psi K^+) = (1.013 \pm 0.034) \times 10^{-3}$ and $B(J/\psi \to p\overline{p}) = (2.17 \pm 0.07) \times 10^{-3}$.

$\Gamma(K^0\pi^+)/\Gamma_{\text{total}}$ Γ_{334}/Γ

VALUE (units 10^{-6})	CL%	DOCUMENT ID		TECN	COMMENT
23.7 ± 0.8 OUR FIT					
23.8 ± 0.7 OUR AVERAGE					
23.97± 0.53±0.71		[1] DUH	13	BELL	$e^+e^- \to \Upsilon(4S)$
23.9 ± 1.1 ±1.0		[1] AUBERT,BE	06C	BABR	$e^+e^- \to \Upsilon(4S)$
$18.8\ ^{+\ 3.7}_{-\ 3.3}\ ^{+2.1}_{-1.8}$		[1] BORNHEIM	03	CLE2	$e^+e^- \to \Upsilon(4S)$
• • • We do not use the following data for averages, fits, limits, etc. • • •					
$22.8\ ^{+\ 0.8}_{-\ 0.7}$ ±1.3		[1] LIN	07	BELL	Repl. by DUH 13
26.0 ± 1.3 ±1.0		[1] AUBERT,BE	05E	BABR	Repl. by AUBERT,BE 06C
22.3 ± 1.7 ±1.1		[1] AUBERT	04M	BABR	Repl. by AUBERT,BE 05E
22.0 ± 1.9 ±1.1		[1] CHAO	04	BELL	Repl. by LIN 07
$19.4\ ^{+\ 3.1}_{-\ 3.0}$ ±1.6		[1] CASEY	02	BELL	Repl. by CHAO 04
$13.7\ ^{+\ 5.7}_{-\ 4.8}\ ^{+1.9}_{-1.8}$		[1] ABE	01H	BELL	Repl. by CASEY 02
$18.2\ ^{+\ 3.3}_{-\ 3.0}$ ±2.0		[1] AUBERT	01E	BABR	Repl. by AUBERT 04M
$18.2\ ^{+\ 4.6}_{-\ 4.0}$ ±1.6		[1] CRONIN-HEN..00		CLE2	Repl. by BORNHEIM 03
$23\ ^{+11}_{-10}$ ±3.6		GODANG	98	CLE2	Repl. by CRONIN-HENNESSY 00
< 48	90	ASNER	96	CLE2	Repl. by GODANG 98
<190	90	ALBRECHT	91B	ARG	$e^+e^- \to \Upsilon(4S)$
<100	90	[2] AVERY	89B	CLEO	$e^+e^- \to \Upsilon(4S)$
<680	90	AVERY	87	CLEO	$e^+e^- \to \Upsilon(4S)$

[1] Assumes equal production of B^+ and B^0 at the $\Upsilon(4S)$.
[2] AVERY 89B reports $< 9 \times 10^{-5}$ assuming the $\Upsilon(4S)$ decays 43% to $B^0\overline{B}^0$. We rescale to 50%.

$\Gamma(K^+\pi^0)/\Gamma_{\text{total}}$ Γ_{335}/Γ

VALUE (units 10^{-6})	CL%	DOCUMENT ID		TECN	COMMENT
12.9 ±0.5 OUR AVERAGE					
12.62±0.31±0.56		[1] DUH	13	BELL	$e^+e^- \to \Upsilon(4S)$
13.6 ±0.6 ±0.7		[1] AUBERT	07BC	BABR	$e^+e^- \to \Upsilon(4S)$
$12.9\ ^{+2.4}_{-2.2}\ ^{+1.2}_{-1.1}$		[1] BORNHEIM	03	CLE2	$e^+e^- \to \Upsilon(4S)$
• • • We do not use the following data for averages, fits, limits, etc. • • •					
12.4 ±0.5 ±0.6		[1] LIN	07A	BELL	Repl. by DUH 13
12.0 ±0.7 ±0.6		[1] AUBERT	05L	BABR	Repl. by AUBERT 07BC

Meson Particle Listings

$B^{\pm}$

$12.0 \pm 1.3 \, ^{+1.3}_{-0.9}$		[1] CHAO	04	BELL	Repl. by LIN 07A
$12.8 \, ^{+1.2}_{-1.1} \pm 1.0$		[1] AUBERT	03L	BABR	Repl. by AUBERT 05L
$13.0 \, ^{+2.5}_{-2.4} \pm 1.3$		[1] CASEY	02	BELL	Repl. by CHAO 04
$16.3 \, ^{+3.5}_{-3.3} \, ^{+1.6}_{-1.8}$		[1] ABE	01H	BELL	Repl. by CASEY 02
$10.8 \, ^{+2.1}_{-1.9} \pm 1.0$		[1] AUBERT	01E	BABR	Repl. by AUBERT 03L
$11.6 \, ^{+3.0}_{-2.7} \, ^{+1.4}_{-1.3}$		[1] CRONIN-HEN...00		CLE2	Repl. by BORNHEIM 03
<16	90	GODANG	98	CLE2	Repl. by CRONIN-HENNESSY 00
<14	90	ASNER	96	CLE2	Repl. by GODANG 98

[1] Assumes equal production of B^+ and B^0 at the $\Upsilon(4S)$.

$\Gamma(K^+\pi^0)/\Gamma(K^0\pi^+)$ $\Gamma_{335}/\Gamma_{334}$

VALUE	DOCUMENT ID		TECN	COMMENT
0.54±0.03±0.04	LIN	07A	BELL	$e^+e^- \to \Upsilon(4S)$
• • • We do not use the following data for averages, fits, limits, etc. • • •				
$2.38 \, ^{+0.98}_{-1.10} \, ^{+0.39}_{-0.26}$	ABE	01H	BELL	Repl. by LIN 07A

$\Gamma(\eta' K^+)/\Gamma_{\text{total}}$ Γ_{336}/Γ

VALUE (units 10^{-6})	DOCUMENT ID		TECN	COMMENT
70.6± 2.5 OUR AVERAGE				
$71.5 \pm 1.3 \pm 3.2$	[1] AUBERT	09AV	BABR	$e^+e^- \to \Upsilon(4S)$
$63 \, ^{+10}_{-9} \pm 2$	[1,2] WICHT	08	BELL	$e^+e^- \to \Upsilon(4S)$
$69.2 \pm 2.2 \pm 3.7$	[1] SCHUEMANN	06	BELL	$e^+e^- \to \Upsilon(4S)$
$80 \, ^{+10}_{-9} \pm 7$	[1] RICHICHI	00	CLE2	$e^+e^- \to \Upsilon(4S)$
• • • We do not use the following data for averages, fits, limits, etc. • • •				
$70.0 \pm 1.5 \pm 2.8$	[1] AUBERT	07AE	BABR	Repl. by AUBERT 09AV
$68.9 \pm 2.0 \pm 3.2$	[1] AUBERT	05M	BABR	Repl. by AUBERT 07AE
$76.9 \pm 3.5 \pm 4.4$	[1] AUBERT	03W	BABR	Repl. by AUBERT 05M
$79 \, ^{+12}_{-11} \pm 9$	[1] ABE	01M	BELL	Repl. by SCHUEMANN 06
$70 \pm 8 \pm 5$	[1] AUBERT	01G	BABR	Repl. by AUBERT 03W
$65 \, ^{+15}_{-14} \pm 9$	BEHRENS	98	CLE2	Repl. by RICHICHI 00

[1] Assumes equal production of B^+ and B^0 at the $\Upsilon(4S)$.

[2] WICHT 08 reports $[\Gamma(B^+ \to \eta' K^+)/\Gamma_{\text{total}}] \times [\text{B}(\eta'(958) \to \gamma\gamma)] = (1.40 \, ^{+0.16}_{-0.15} \, ^{+0.15}_{-0.12}) \times 10^{-6}$ which we divide by our best value $\text{B}(\eta'(958) \to \gamma\gamma) = (2.22 \pm 0.08) \times 10^{-2}$. Our first error is their experiment's error and our second error is the systematic error from using our best value.

$\Gamma(\eta' K^*(892)^+)/\Gamma_{\text{total}}$ Γ_{337}/Γ

VALUE (units 10^{-6})	CL%	DOCUMENT ID		TECN	COMMENT
$\mathbf{4.8 \, ^{+1.6}_{-1.4} \pm 0.8}$		[1] DEL-AMO-SA...10A		BABR	$e^+e^- \to \Upsilon(4S)$
• • • We do not use the following data for averages, fits, limits, etc. • • •					
$4.9 \, ^{+1.9}_{-1.7} \pm 0.8$		[1] AUBERT	07E	BABR	Repl. by DEL-AMO-SANCHEZ 10A
< 2.9	90	[1] SCHUEMANN	07	BELL	$e^+e^- \to \Upsilon(4S)$
<14	90	[1] AUBERT,B	04D	BABR	Repl. by AUBERT 07E
<35	90	[1] RICHICHI	00	CLE2	$e^+e^- \to \Upsilon(4S)$
<13	90	BEHRENS	98	CLE2	Repl. by RICHICHI 00

[1] Assumes equal production of B^+ and B^0 at the $\Upsilon(4S)$.

$\Gamma(\eta' K_0^*(1430)^+)/\Gamma_{\text{total}}$ Γ_{338}/Γ

VALUE (units 10^{-6})	DOCUMENT ID		TECN	COMMENT
5.2±1.9±1.0	[1] DEL-AMO-SA...10A		BABR	$e^+e^- \to \Upsilon(4S)$

[1] Assumes equal production of B^+ and B^0 at the $\Upsilon(4S)$.

$\Gamma(\eta' K_2^*(1430)^+)/\Gamma_{\text{total}}$ Γ_{339}/Γ

VALUE (units 10^{-6})	DOCUMENT ID		TECN	COMMENT
$\mathbf{28.0 \, ^{+4.6}_{-4.3} \pm 2.6}$	[1] DEL-AMO-SA...10A		BABR	$e^+e^- \to \Upsilon(4S)$

[1] Assumes equal production of B^+ and B^0 at the $\Upsilon(4S)$.

$\Gamma(\eta K^+)/\Gamma_{\text{total}}$ Γ_{340}/Γ

VALUE (units 10^{-6})	CL%	DOCUMENT ID		TECN	COMMENT
2.4 ±0.4 OUR AVERAGE		Error includes scale factor of 1.7.			
$2.12 \pm 0.23 \pm 0.11$		[1] HOI	12	BELL	$e^+e^- \to \Upsilon(4S)$
$2.94 \, ^{+0.39}_{-0.34} \pm 0.21$		[1] AUBERT	09AV	BABR	$e^+e^- \to \Upsilon(4S)$
$2.2 \, ^{+2.8}_{-2.2}$		[1] RICHICHI	00	CLE2	$e^+e^- \to \Upsilon(4S)$
• • • We do not use the following data for averages, fits, limits, etc. • • •					
$2.21 \, ^{+0.48}_{-0.42} \pm 0.01$		[1,2] WICHT	08	BELL	Repl. by HOI 12
$3.7 \pm 0.4 \pm 0.1$		[1] AUBERT	07AE	BABR	Repl. by AUBERT 09AV
$1.9 \pm 0.3 \, ^{+0.2}_{-0.1}$		[1] CHANG	07B	BELL	Repl. by HOI 12
$3.3 \pm 0.6 \pm 0.3$		[1] AUBERT,B	05K	BABR	Repl. by AUBERT 07AE
$2.1 \pm 0.6 \pm 0.2$		[1] CHANG	05A	BELL	Repl. by CHANG 07B
$3.4 \pm 0.8 \pm 0.2$		[1] AUBERT	04H	BABR	Repl. by AUBERT,B 05K
<14	90	BEHRENS	98	CLE2	Repl. by RICHICHI 00

[1] Assumes equal production of B^+ and B^0 at the $\Upsilon(4S)$.

[2] WICHT 08 reports $[\Gamma(B^+ \to \eta K^+)/\Gamma_{\text{total}}] \times [\text{B}(\eta \to 2\gamma)] = (0.87 \, ^{+0.16}_{-0.15} \, ^{+0.10}_{-0.07}) \times 10^{-6}$ which we divide by our best value $\text{B}(\eta \to 2\gamma) = (39.41 \pm 0.20) \times 10^{-2}$. Our first error is their experiment's error and our second error is the systematic error from using our best value.

$\Gamma(\eta K^*(892)^+)/\Gamma_{\text{total}}$ Γ_{341}/Γ

VALUE (units 10^{-6})	CL%	DOCUMENT ID		TECN	COMMENT
19.3±1.6 OUR AVERAGE					
$19.3 \, ^{+2.0}_{-1.9} \pm 1.5$		[1] WANG	07B	BELL	$e^+e^- \to \Upsilon(4S)$
$18.9 \pm 1.8 \pm 1.3$		[1] AUBERT,B	06H	BABR	$e^+e^- \to \Upsilon(4S)$
$26.4 \, ^{+9.6}_{-8.2} \pm 3.3$		[1] RICHICHI	00	CLE2	$e^+e^- \to \Upsilon(4S)$
• • • We do not use the following data for averages, fits, limits, etc. • • •					
$25.6 \pm 4.0 \pm 2.4$		[1] AUBERT,B	04D	BABR	Repl. by AUBERT,B 06H
<30	90	BEHRENS	98	CLE2	Repl. by RICHICHI 00

[1] Assumes equal production of B^+ and B^0 at the $\Upsilon(4S)$.

$\Gamma(\eta K_0^*(1430)^+)/\Gamma_{\text{total}}$ Γ_{342}/Γ

VALUE (units 10^{-6})	DOCUMENT ID		TECN	COMMENT
18.2±2.6±2.6	[1] AUBERT,B	06H	BABR	$e^+e^- \to \Upsilon(4S)$

[1] Assumes equal production of B^+ and B^0 at the $\Upsilon(4S)$.

$\Gamma(\eta K_2^*(1430)^+)/\Gamma_{\text{total}}$ Γ_{343}/Γ

VALUE (units 10^{-6})	DOCUMENT ID		TECN	COMMENT
9.1±2.7±1.4	[1] AUBERT,B	06H	BABR	$e^+e^- \to \Upsilon(4S)$

[1] Assumes equal production of B^+ and B^0 at the $\Upsilon(4S)$.

$\Gamma(\eta(1295)\, K^+ \times \text{B}(\eta(1295) \to \eta\pi\pi))/\Gamma_{\text{total}}$ Γ_{344}/Γ

VALUE (units 10^{-6})	DOCUMENT ID		TECN	COMMENT
$\mathbf{2.9 \, ^{+0.8}_{-0.7} \pm 0.2}$	[1] AUBERT	08X	BABR	$e^+e^- \to \Upsilon(4S)$

[1] Assumes equal production of B^+ and B^0 at the $\Upsilon(4S)$.

$\Gamma(\eta(1405)\, K^+ \times \text{B}(\eta(1405) \to \eta\pi\pi))/\Gamma_{\text{total}}$ Γ_{345}/Γ

VALUE (units 10^{-6})	CL%	DOCUMENT ID		TECN	COMMENT
<1.3	90	[1] AUBERT	08X	BABR	$e^+e^- \to \Upsilon(4S)$

[1] Assumes equal production of B^+ and B^0 at the $\Upsilon(4S)$.

$\Gamma(\eta(1405)\, K^+ \times \text{B}(\eta(1405) \to K^*K))/\Gamma_{\text{total}}$ Γ_{346}/Γ

VALUE (units 10^{-6})	CL%	DOCUMENT ID		TECN	COMMENT
<1.2	90	[1] AUBERT	08X	BABR	$e^+e^- \to \Upsilon(4S)$

[1] Assumes equal production of B^+ and B^0 at the $\Upsilon(4S)$.

$\Gamma(\eta(1475)\, K^+ \times \text{B}(\eta(1475) \to K^*K))/\Gamma_{\text{total}}$ Γ_{347}/Γ

VALUE (units 10^{-6})	DOCUMENT ID		TECN	COMMENT
$\mathbf{13.8 \, ^{+1.8}_{-1.7} \, ^{+1.0}_{-0.6}}$	[1] AUBERT	08X	BABR	$e^+e^- \to \Upsilon(4S)$

[1] Assumes equal production of B^+ and B^0 at the $\Upsilon(4S)$.

$\Gamma(f_1(1285)\, K^+)/\Gamma_{\text{total}}$ Γ_{348}/Γ

VALUE (units 10^{-6})	CL%	DOCUMENT ID		TECN	COMMENT
<2.0	90	[1] AUBERT	08X	BABR	$e^+e^- \to \Upsilon(4S)$

[1] Assumes equal production of B^+ and B^0 at the $\Upsilon(4S)$.

$\Gamma(f_1(1420)\, K^+ \times \text{B}(f_1(1420) \to \eta\pi\pi))/\Gamma_{\text{total}}$ Γ_{349}/Γ

VALUE (units 10^{-6})	CL%	DOCUMENT ID		TECN	COMMENT
<2.9	90	[1] AUBERT	08X	BABR	$e^+e^- \to \Upsilon(4S)$

[1] Assumes equal production of B^+ and B^0 at the $\Upsilon(4S)$.

$\Gamma(f_1(1420)\, K^+ \times \text{B}(f_1(1420) \to K^*K))/\Gamma_{\text{total}}$ Γ_{350}/Γ

VALUE (units 10^{-6})	CL%	DOCUMENT ID		TECN	COMMENT
<4.1	90	[1] AUBERT	08X	BABR	$e^+e^- \to \Upsilon(4S)$

[1] Assumes equal production of B^+ and B^0 at the $\Upsilon(4S)$.

$\Gamma(\phi(1680)\, K^+ \times \text{B}(\phi(1680) \to K^*K))/\Gamma_{\text{total}}$ Γ_{351}/Γ

VALUE (units 10^{-6})	CL%	DOCUMENT ID		TECN	COMMENT
<3.4	90	[1] AUBERT	08X	BABR	$e^+e^- \to \Upsilon(4S)$

[1] Assumes equal production of B^+ and B^0 at the $\Upsilon(4S)$.

$\Gamma(f_0(1500)\, K^+)/\Gamma_{\text{total}}$ Γ_{352}/Γ

VALUE (units 10^{-6})	CL%	DOCUMENT ID		TECN	COMMENT
3.7± 2.2 OUR AVERAGE					
$17 \pm 4 \pm 12$		[1] LEES	12O	BABR	$e^+e^- \to \Upsilon(4S)$
$20 \pm 10 \pm 27$		[2] LEES	12O	BABR	$e^+e^- \to \Upsilon(4S)$
$3.1 \, ^{+2.2}_{-2.3} \pm 0.2$		[3,4] AUBERT	08AI	BABR	$e^+e^- \to \Upsilon(4S)$

• • • We do not use the following data for averages, fits, limits, etc. • • •

<19	90	[4,5]	AUBERT,B	05N	BABR	Repl. by AUBERT 08AI

[1] Measured in the $B^+ \to K^+K^-K^+$ decay.
[2] Measured in the $B^+ \to K^+K^0_SK^0_S$ decay.
[3] AUBERT 08AI reports $B(B^+ \to f_0(1500)K^+) \cdot B(f_0(1500) \to \pi^+\pi^-) = (0.73 \pm 0.21^{+0.47}_{-0.48}) \times 10^{-6}$. We divide this result by our best value of $B(f_0(1500) \to \pi\pi) = (34.9 \pm 2.3) \times 10^{-2}$ multiplied by 2/3 to account for the $\pi^+\pi^-$ fraction. Our first quoted uncertainty is the combined experiment's uncertainty and our second is the systematic uncertainty from using out best value.
[4] Assumes equal production of B^+ and B^0 at the $\Upsilon(4S)$.
[5] AUBERT,B 05N reports $B(B^+ \to f_0(1500)K^+) \cdot B(f_0(1500) \to \pi^+\pi^-) < 4.4\times10^{-6}$. We divide this result by our best value of $B(f_0(1500) \to \pi\pi) = (34.9 \pm 2.3) \times 10^{-2}$ multiplied by 2/3 to account for the $\pi^+\pi^-$ fraction. Our first quoted uncertainty is the combined experiment's uncertainty and our second is the systematic uncertainty from using out best value.

$\Gamma(\omega K^+)/\Gamma_{total}$ Γ_{353}/Γ

VALUE (units 10^{-6})	CL%	DOCUMENT ID		TECN	COMMENT
6.5±0.4 OUR AVERAGE					
6.8±0.4±0.4		[1] CHOBANOVA	14	BELL	$e^+e^- \to \Upsilon(4S)$
6.3±0.5±0.3		[1] AUBERT	07AE	BABR	$e^+e^- \to \Upsilon(4S)$
$3.2^{+2.4}_{-1.9}\pm0.8$		[1] JESSOP	00	CLE2	$e^+e^- \to \Upsilon(4S)$

• • • We do not use the following data for averages, fits, limits, etc. • • •

6.1±0.6±0.4	[1] AUBERT,B	06E	BABR	AUBERT 07AE	
8.1±0.6±0.6	[1] JEN	06	BELL	Repl. by CHOBANOVA 14	
4.8±0.8±0.4	[1] AUBERT	04H	BABR	Repl. by AUBERT,B 06E	
$6.5^{+1.3}_{-1.2}\pm0.6$	[1] WANG	04A	BELL	Repl. by JEN 06	
$9.2^{+2.6}_{-2.3}\pm1.0$	[1] LU	02	BELL	Repl. by WANG 04A	
<4 90	[1] AUBERT	01G	BABR	$e^+e^- \to \Upsilon(4S)$	
$1.5^{+7}_{-6}\ \pm2$	[1] BERGFELD	98	CLE2	Repl. by JESSOP 00	

[1] Assumes equal production of B^+ and B^0 at the $\Upsilon(4S)$.

$\Gamma(\omega K^*(892)^+)/\Gamma_{total}$ Γ_{354}/Γ

VALUE (units 10^{-6})	CL%	DOCUMENT ID		TECN	COMMENT
< 7.4	90	[1] AUBERT	09H	BABR	$e^+e^- \to \Upsilon(4S)$

• • • We do not use the following data for averages, fits, limits, etc. • • •

< 3.4	90	[1] AUBERT,B	06T	BABR	Repl. by AUBERT 09H
< 7.4	90	[1] AUBERT	05O	BABR	Repl. by AUBERT,B 06T
<87	90	[1] BERGFELD	98	CLE2	

[1] Assumes equal production of B^+ and B^0 at the $\Upsilon(4S)$.

$\Gamma(\omega(K\pi)^{*+}_0)/\Gamma_{total}$ Γ_{355}/Γ

$(K\pi)^{*+}_0$ is the total S-wave composed of $K^*_0(1430)$ and nonresonant that are described using LASS shape.

VALUE (units 10^{-6})	DOCUMENT ID		TECN	COMMENT
27.5±3.0±2.6	[1] AUBERT	09H	BABR	$e^+e^- \to \Upsilon(4S)$

[1] Assumes equal production of B^+ and B^0 at the $\Upsilon(4S)$.

$\Gamma(\omega K^*_0(1430)^+)/\Gamma_{total}$ Γ_{356}/Γ

VALUE (units 10^{-6})	DOCUMENT ID		TECN	COMMENT
24.0±2.6±4.4	[1] AUBERT	09H	BABR	$e^+e^- \to \Upsilon(4S)$

[1] Assumes equal production of B^+ and B^0 at the $\Upsilon(4S)$.

$\Gamma(\omega K^*_2(1430)^+)/\Gamma_{total}$ Γ_{357}/Γ

VALUE (units 10^{-6})	DOCUMENT ID		TECN	COMMENT
21.5±3.6±2.4	[1] AUBERT	09H	BABR	$e^+e^- \to \Upsilon(4S)$

[1] Assumes equal production of B^+ and B^0 at the $\Upsilon(4S)$.

$\Gamma(a_0(980)^0K^+ \times B(a_0(980)^0 \to \eta\pi^0))/\Gamma_{total}$ Γ_{359}/Γ

VALUE (units 10^{-6})	CL%	DOCUMENT ID		TECN	COMMENT
<2.5	90	[1] AUBERT,BE	04	BABR	$e^+e^- \to \Upsilon(4S)$

[1] Assumes equal production of charged and neutral B mesons from $\Upsilon(4S)$ decays.

$\Gamma(a_0(980)^+K^0 \times B(a_0(980)^+ \to \eta\pi^+))/\Gamma_{total}$ Γ_{358}/Γ

VALUE (units 10^{-6})	CL%	DOCUMENT ID		TECN	COMMENT
<3.9	90	[1] AUBERT,BE	04	BABR	$e^+e^- \to \Upsilon(4S)$

[1] Assumes equal production of charged and neutral B mesons from $\Upsilon(4S)$ decays.

$\Gamma(K^*(892)^0\pi^+)/\Gamma_{total}$ Γ_{360}/Γ

VALUE (units 10^{-6})	CL%	DOCUMENT ID		TECN	COMMENT
10.1 ±0.8 OUR AVERAGE					
10.1 ±1.7 ±1.0		[1] LEES	17G	BABR	$e^+e^- \to \Upsilon(4S)$
$10.8\ \pm0.6\ ^{+1.2}_{-1.4}$		[2] AUBERT	08AI	BABR	$e^+e^- \to \Upsilon(4S)$
$9.67\pm0.64^{+0.81}_{-0.89}$		[2] GARMASH	06	BELL	$e^+e^- \to \Upsilon(4S)$

• • • We do not use the following data for averages, fits, limits, etc. • • •

$13.5\ \pm1.2\ ^{+0.8}_{-0.9}$	[2] AUBERT,B	05N	BABR	Repl. by AUBERT 08AI	
$9.8\ \pm0.9\ ^{+1.1}_{-1.2}$	[2] GARMASH	05	BELL	Repl. by GARMASH 06	
$15.5\ \pm1.8\ ^{+1.5}_{-4.0}$	[2,3] AUBERT,B	04P	BABR	Repl. by AUBERT,B 05N	
$19.4\ ^{+4.2}_{-3.9}\ ^{+4.1}_{-7.1}$	[4] GARMASH	02	BELL	Repl. by GARMASH 05	
<119	90 [5] ABE	00C	SLD	$e^+e^- \to Z$	
< 16	90 [2] JESSOP	00	CLE2	$e^+e^- \to \Upsilon(4S)$	
<390	90 [6] ADAM	96D	DLPH	$e^+e^- \to Z$	
< 41	90 ASNER	96	CLE2	Repl. by JESSOP 00	
<480	90 [6] ABREU	95N	DLPH	Sup. by ADAM 96D	
<170	90 ALBRECHT	91B	ARG	$e^+e^- \to \Upsilon(4S)$	
<150	90 [7] AVERY	89B	CLEO	$e^+e^- \to \Upsilon(4S)$	
<260	90 AVERY	87	CLEO	$e^+e^- \to \Upsilon(4S)$	

[1] Obtains the result from a Dalitz analysis of $B^+ \to K^0_S\pi^+\pi^0$ decays. The first error is statistical, the second combines all the systematic uncertainties reported in the paper, including signal modelling.
[2] Assumes equal production of B^+ and B^0 at the $\Upsilon(4S)$.
[3] AUBERT 04P also report a branching ratio for $B^+ \to$ "higher $K*$ resonances" π^+, $K* \to K^+\pi^-$, $(25.1 \pm 2.0^{+11.0}_{-5.7}) \times 10^{-6}$.
[4] Uses a reference decay mode $B^+ \to \overline{D}{}^0\pi^+$ and $\overline{D}{}^0 \to K^+\pi^-$ with $B(B^+ \to \overline{D}{}^0\pi^+) \cdot B(\overline{D}{}^0 \to K^+\pi^-) = (20.3 \pm 2.0) \times 10^{-5}$.
[5] ABE 00C assumes $B(Z \to b\overline{b})=(21.7 \pm 0.1)\%$ and the B fractions $f_{B^0}=f_{B^+}=(39.7^{+1.8}_{-2.2})\%$ and $f_{B_s}=(10.5^{+1.8}_{-2.2})\%$.
[6] Assumes a B^0, B^- production fraction of 0.39 and a B_s production fraction of 0.12.
[7] AVERY 89B reports $< 1.3 \times 10^{-4}$ assuming the $\Upsilon(4S)$ decays 43% to $B^0\overline{B}{}^0$. We rescale to 50%.

$\Gamma(K^*(892)^+\pi^0)/\Gamma_{total}$ Γ_{361}/Γ

VALUE (units 10^{-6})	CL%	DOCUMENT ID		TECN	COMMENT
6.8±0.9 OUR AVERAGE					
$6.4\pm0.9^{+0.4}_{-0.5}$		[1] LEES	17G	BABR	$e^+e^- \to \Upsilon(4S)$
8.2±1.5±1.1		[2] LEES	11I	BABR	$e^+e^- \to \Upsilon(4S)$

• • • We do not use the following data for averages, fits, limits, etc. • • •

6.9±2.0±1.3		[2] AUBERT	05X	BABR	Repl. by LEES 11I
<31	90	[2] JESSOP	00	CLE2	$e^+e^- \to \Upsilon(4S)$
<99	90	ASNER	96	CLE2	Repl. by JESSOP 00

[1] Obtains the result from a Dalitz analysis of $B^+ \to K^0_S\pi^+\pi^0$ decays. The first error is statistical, the second combines all the systematic uncertainties reported in the paper, including signal modelling.
[2] Assumes equal production of B^+ and B^0 at the $\Upsilon(4S)$.

$\Gamma(K^+\pi^-\pi^+)/\Gamma_{total}$ Γ_{362}/Γ

VALUE (units 10^{-6})	DOCUMENT ID		TECN	COMMENT
51.0±2.9 OUR AVERAGE				
54.4±1.1±4.6	[1] AUBERT	08AI	BABR	$e^+e^- \to \Upsilon(4S)$
48.8±1.1±3.6	[1] GARMASH	06	BELL	$e^+e^- \to \Upsilon(4S)$

• • • We do not use the following data for averages, fits, limits, etc. • • •

64.1±2.4±4.0	[1] AUBERT,B	05N	BABR	Repl. by AUBERT 08AI
46.6±2.1±4.3	[1] GARMASH	05	BELL	Repl. by GARMASH 06
53.6±3.1±5.1	[1] GARMASH	04	BELL	Repl. by GARMASH 05
59.1±3.8±3.2	[2] AUBERT	03M	BABR	Repl. by AUBERT,B 05N
55.6±5.8±7.7	[3] GARMASH	02	BELL	Repl. by GARMASH 04

[1] Assumes equal production of B^+ and B^0 at the $\Upsilon(4S)$.
[2] Assumes equal production of B^0 and B^+ at the $\Upsilon(4S)$; charm and charmonium contributions are subtracted, otherwise no assumptions about intermediate resonances.
[3] Uses a reference decay mode $B^+ \to \overline{D}{}^0\pi^+$ and $\overline{D}{}^0 \to K^+\pi^-$ with $B(B^+ \to \overline{D}{}^0\pi^+) \cdot B(\overline{D}{}^0 \to K^+\pi^-) = (20.3 \pm 2.0) \times 10^{-5}$.

$\Gamma(K^+\pi^-\pi^+ \text{nonresonant})/\Gamma_{total}$ Γ_{363}/Γ

VALUE (units 10^{-6})	CL%	DOCUMENT ID		TECN	COMMENT
$\mathbf{16.3^{+2.1}_{-1.5}}$ **OUR AVERAGE**					
$9.3\pm1.0^{+\ 6.9}_{-\ 1.7}$		[1,2] AUBERT	08AI	BABR	$e^+e^- \to \Upsilon(4S)$
$16.9\pm1.3^{+\ 1.7}_{-\ 1.6}$		[1] GARMASH	06	BELL	$e^+e^- \to \Upsilon(4S)$

• • • We do not use the following data for averages, fits, limits, etc. • • •

$2.9\pm0.6^{+\ 0.8}_{-\ 0.5}$	[1] AUBERT,B	05N	BABR	Repl. by AUBERT 08AI	
$17.3\pm1.7^{+17.2}_{-\ 8.0}$	[1] GARMASH	05	BELL	Repl. by GARMASH 06	
< 17	90 [1] AUBERT,B	04P	BABR	Repl. by AUBERT,B 05N	
<330	90 [3] ADAM	96D	DLPH	$e^+e^- \to Z$	
< 28	90 BERGFELD	96B	CLE2	$e^+e^- \to \Upsilon(4S)$	
<400	90 [3] ABREU	95N	DLPH	Sup. by ADAM 96D	
<330	90 ALBRECHT	91E	ARG	$e^+e^- \to \Upsilon(4S)$	
<190	90 [4] AVERY	89B	CLEO	$e^+e^- \to \Upsilon(4S)$	

[1] Assumes equal production of B^+ and B^0 at the $\Upsilon(4S)$.
[2] Calculate the total nonresonant contribution by combining the S-wave composed of $K^*_0(1430)$ and nonresonant that are described using LASS shape.

[3] Assumes a B^0, B^- production fraction of 0.39 and a B_s production fraction of 0.12.
[4] AVERY 89B reports $< 1.7 \times 10^{-4}$ assuming the $\Upsilon(4S)$ decays 43% to $B^0\overline{B}^0$. We rescale to 50%.

$\Gamma(\omega(782)K^+)/\Gamma_{total}$ Γ_{364}/Γ

VALUE (units 10^{-6})		DOCUMENT ID		TECN	COMMENT
$5.9^{+8.8}_{-9.0}{}^{+0.5}_{-0.4}$		[1,2] AUBERT	08AI	BABR	$e^+e^- \to \Upsilon(4S)$

[1] Assumes equal production of B^+ and B^0 at the $\Upsilon(4S)$.
[2] AUBERT 08AI reports $[\Gamma(B^+ \to \omega(782)K^+)/\Gamma_{total}] \times [B(\omega(782) \to \pi^+\pi^-)] = (0.09 \pm 0.13^{+0.036}_{-0.045}) \times 10^{-6}$ which we divide by our best value $B(\omega(782) \to \pi^+\pi^-) = (1.53^{+0.11}_{-0.13}) \times 10^{-2}$. Our first error is their experiment's error and our second error is the systematic error from using our best value.

$\Gamma(K^+ f_0(980) \times B(f_0(980) \to \pi^+\pi^-))/\Gamma_{total}$ Γ_{365}/Γ

VALUE (units 10^{-6})	CL%	DOCUMENT ID		TECN	COMMENT
$9.4\ ^{+1.0}_{-1.2}$ OUR AVERAGE					
$10.3 \pm 0.5\ ^{+2.0}_{-1.4}$		[1] AUBERT	08AI	BABR	$e^+e^- \to \Upsilon(4S)$
$8.78 \pm 0.82^{+0.85}_{-1.76}$		[1] GARMASH	06	BELL	$e^+e^- \to \Upsilon(4S)$
• • • We do not use the following data for averages, fits, limits, etc. • • •					
$9.47 \pm 0.97^{+0.62}_{-0.88}$		[1] AUBERT,B	05N	BABR	Repl. by AUBERT 08AI
$7.55 \pm 1.24^{+1.63}_{-1.18}$		[1] GARMASH	05	BELL	Repl. by GARMASH 06
$9.2 \pm 1.2\ ^{+2.1}_{-2.6}$		[2] AUBERT,B	04P	BABR	Repl. by AUBERT,B 05N
$9.6\ ^{+2.5}_{-2.3}\ ^{+3.7}_{-1.7}$		[3] GARMASH	02	BELL	Repl. by GARMASH 05
<80	90	[4] AVERY	89B	CLEO	$e^+e^- \to \Upsilon(4S)$

[1] Assumes equal production of B^+ and B^0 at the $\Upsilon(4S)$.
[2] AUBERT,B 04P also reports $B(B^+ \to$ "higher I^0 resonances" π^+, $f(980)^0 \to \pi^+\pi^-) = (3.2 \pm 1.2^{+6.0}_{-2.9}) \times 10^{-6}$.
[3] Uses a reference decay mode $B^+ \to \overline{D}{}^0\pi^+$ and $\overline{D}{}^0 \to K^+\pi^-$ with $B(B^+ \to \overline{D}{}^0\pi^+) \times B(\overline{D}{}^0 \to K^+\pi^-) = (20.3 \pm 2.0) \times 10^{-5}$. Only charged pions from the $f_0(980)$ are used.
[4] AVERY 89B reports $< 7 \times 10^{-5}$ assuming the $\Upsilon(4S)$ decays 43% to $B^0\overline{B}^0$. We rescale to 50%.

$\Gamma(f_2(1270)^0 K^+)/\Gamma_{total}$ Γ_{366}/Γ

VALUE (units 10^{-6})	CL%	DOCUMENT ID		TECN	COMMENT
1.07 ± 0.27 OUR AVERAGE					
$0.89^{+0.38}_{-0.33}{}^{+0.01}_{-0.03}$		[1,2] AUBERT	08AI	BABR	$e^+e^- \to \Upsilon(4S)$
$1.33 \pm 0.30^{+0.23}_{-0.34}$		[1] GARMASH	06	BELL	$e^+e^- \to \Upsilon(4S)$
• • • We do not use the following data for averages, fits, limits, etc. • • •					
<16	90	[3] AUBERT,B	05N	BABR	Repl. by AUBERT 08AI
< 2.3	90	[4] GARMASH	05	BELL	Repl. by GARMASH 06

[1] Assumes equal production of B^+ and B^0 at the $\Upsilon(4S)$.
[2] AUBERT 08AI reports $(0.50 \pm 0.15^{+0.15}_{-0.11}) \times 10^{-6}$ for $B(B^+ \to f_2(1270)K^+) \times B(f_2 \to \pi^+\pi^-)$. We compute $B(B^+ \to f_2(1270)K^+)$ using the PDG value $B(f_2(1270) \to \pi\pi) = (84.2^{+2.9}_{-0.9}) \times 10^{-2}$ and 2/3 for the $\pi^+\pi^-$ fraction. Our first error is their experiment's error and the second error is systematic error from using our best value.
[3] AUBERT,B 05N reports 8.9×10^{-6} at 90% CL for $B(B^+ \to f_2(1270)K^+) \times B(f_2(1270) \to \pi^+\pi^-)$. We rescaled it using the PDG value $B(f_2(1270) \to \pi\pi) = 84.7\%$ and 2/3 for the $\pi^+\pi^-$ fraction.
[4] GARMASH 05 reports 1.3×10^{-6} at 90% CL for $B(B^+ \to f_2(1270)K^+) \times B(f_2(1270) \to \pi^+\pi^-)$. We rescaled it using the PDG value $B(f_2(1270) \to \pi\pi) = 84.7\%$ and 2/3 for the $\pi^+\pi^-$ fraction.

$\Gamma(f_0(1370)^0 K^+ \times B(f_0(1370)^0 \to \pi^+\pi^-))/\Gamma_{total}$ Γ_{367}/Γ

VALUE	CL%	DOCUMENT ID		TECN	COMMENT
$<10.7 \times 10^{-6}$	90	[1] AUBERT,B	05N	BABR	$e^+e^- \to \Upsilon(4S)$

[1] Assumes equal production of B^+ and B^0 at the $\Upsilon(4S)$.

$\Gamma(\rho^0(1450)K^+ \times B(\rho^0(1450) \to \pi^+\pi^-))/\Gamma_{total}$ Γ_{368}/Γ

VALUE	CL%	DOCUMENT ID		TECN	COMMENT
$<11.7 \times 10^{-6}$	90	[1] AUBERT,B	05N	BABR	$e^+e^- \to \Upsilon(4S)$

[1] Assumes equal production of B^+ and B^0 at the $\Upsilon(4S)$.

$\Gamma(f_2'(1525)K^+ \times B(f_2'(1525) \to \pi^+\pi^-))/\Gamma_{total}$ Γ_{369}/Γ

VALUE	CL%	DOCUMENT ID		TECN	COMMENT
$<3.4 \times 10^{-6}$	90	[1] AUBERT,B	05N	BABR	$e^+e^- \to \Upsilon(4S)$

[1] Assumes equal production of B^+ and B^0 at the $\Upsilon(4S)$.

$\Gamma(K^+\rho^0)/\Gamma_{total}$ Γ_{370}/Γ

VALUE (units 10^{-6})	CL%	DOCUMENT ID		TECN	COMMENT
3.7 ± 0.5 OUR AVERAGE					
$3.56 \pm 0.45^{+0.57}_{-0.46}$		[1] AUBERT	08AI	BABR	$e^+e^- \to \Upsilon(4S)$
$3.89 \pm 0.47^{+0.43}_{-0.41}$		[1] GARMASH	06	BELL	$e^+e^- \to \Upsilon(4S)$
• • • We do not use the following data for averages, fits, limits, etc. • • •					
$5.07 \pm 0.75^{+0.55}_{-0.88}$		[1] AUBERT,B	05N	BABR	Repl. by AUBERT 08AI
$4.78 \pm 0.75^{+1.01}_{-0.97}$		[1] GARMASH	05	BELL	Repl. by GARMASH 06
< 6.2	90	[2] AUBERT,B	04P	BABR	Repl. by AUBERT,B 05N
< 12	90	[3] GARMASH	02	BELL	$e^+e^- \to \Upsilon(4S)$
< 86	90	[4] ABE	00C	SLD	$e^+e^- \to Z$
< 17	90	[1] JESSOP	00	CLE2	$e^+e^- \to \Upsilon(4S)$
<120	90	[5] ADAM	96D	DLPH	$e^+e^- \to Z$
< 19	90	ASNER	96	CLE2	Repl. by JESSOP 00
<190	90	[5] ABREU	95N	DLPH	Sup. by ADAM 96D
<180	90	ALBRECHT	91B	ARG	$e^+e^- \to \Upsilon(4S)$
< 80	90	[6] AVERY	89B	CLEO	$e^+e^- \to \Upsilon(4S)$
<260	90	AVERY	87	CLEO	$e^+e^- \to \Upsilon(4S)$

[1] Assumes equal production of B^+ and B^0 at the $\Upsilon(4S)$.
[2] AUBERT 04P reports a central value of $(3.9 \pm 1.2^{+1.3}_{-3.5}) \times 10^{-6}$ for this branching ratio.
[3] Uses a reference decay mode $B^+ \to \overline{D}{}^0\pi^+$ and $\overline{D}{}^0 \to K^+\pi^-$ with $B(B^+ \to \overline{D}{}^0\pi^+) \cdot B(\overline{D}{}^0 \to K^+\pi^-) = (20.3 \pm 2.0) \times 10^{-5}$.
[4] ABE 00C assumes $B(Z \to b\overline{b}) = (21.7 \pm 0.1)\%$ and the B fractions $f_{B^0} = f_{B^+} = (39.7^{+1.8}_{-2.2})\%$ and $f_{B_s} = (10.5^{+1.8}_{-2.2})\%$.
[5] Assumes production fractions $f_{B^0} = f_{B^-} = 0.39$ and $f_{B_s} = 0.12$.
[6] AVERY 89B reports $< 7 \times 10^{-5}$ assuming the $\Upsilon(4S)$ decays 43% to $B^0\overline{B}^0$. We rescale to 50%.

$\Gamma(K_0^*(1430)^0\pi^+)/\Gamma_{total}$ Γ_{371}/Γ

VALUE (units 10^{-6})	DOCUMENT ID		TECN	COMMENT
$39\ ^{+6}_{-5}$ OUR AVERAGE Error includes scale factor of 1.4. See the ideogram below.				
$34.6 \pm 3.3 \pm 4.6$	[1] LEES	17G	BABR	$e^+e^- \to \Upsilon(4S)$
$32.0 \pm 1.2^{+10.8}_{-6.0}$	[2] AUBERT	08AI	BABR	$e^+e^- \to \Upsilon(4S)$
$51.6 \pm 1.7^{+7.0}_{-7.5}$	[2] GARMASH	06	BELL	$e^+e^- \to \Upsilon(4S)$
• • • We do not use the following data for averages, fits, limits, etc. • • •				
$44.4 \pm 2.2 \pm 5.3$	[2,3] AUBERT,B	05N	BABR	Repl. by AUBERT 08AI
$45.0 \pm 2.9^{+15.0}_{-10.7}$	[2] GARMASH	05	BELL	Repl. by GARMASH 06

[1] Obtains the result from a Dalitz analysis of $B^+ \to K^0_S\pi^+\pi^0$ decays. The first error is statistical, the second combines all the systematic uncertainties reported in the paper, including signal modelling.
[2] Assumes equal production of B^+ and B^0 at the $\Upsilon(4S)$.
[3] See erratum: AUBERT,BE 06A.

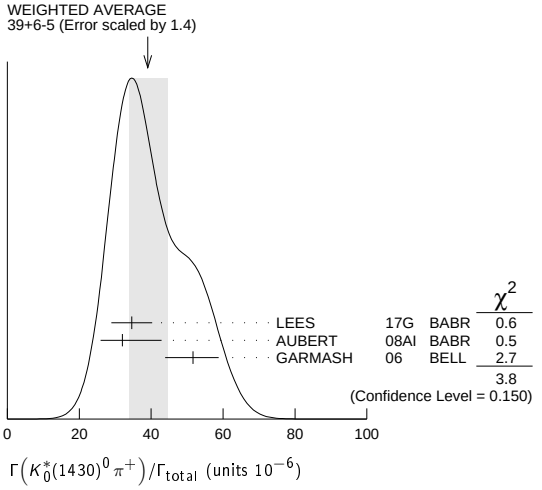

$\Gamma(K_2^*(1430)^0\pi^+)/\Gamma_{total}$ Γ_{373}/Γ

VALUE (units 10^{-6})	CL%	DOCUMENT ID		TECN	COMMENT
$5.6^{+2.2}_{-1.5} \pm 0.1$		[1,2] AUBERT	08AI	BABR	$e^+e^- \to \Upsilon(4S)$
• • • We do not use the following data for averages, fits, limits, etc. • • •					
< 23	90	[3] AUBERT,B	05N	BABR	Repl. by AUBERT 08AI
< 6.9	90	[4] GARMASH	05	BELL	$e^+e^- \to \Upsilon(4S)$
<680	90	ALBRECHT	91B	ARG	$e^+e^- \to \Upsilon(4S)$

[1] Assumes equal production of B^+ and B^0 at the $\Upsilon(4S)$.
[2] AUBERT 08AI reports $(1.85 \pm 0.41^{+0.61}_{-0.29}) \times 10^{-6}$ for $B(B^+ \to K_2^*(1430)^0\pi^+) \times B(K_2^*(1430)^0 \to K^+\pi^-)$. We compute $B(B^+ \to K_2^*(1430)^0\pi^+)$ using the PDG value $B(K_2^*(1430)^0 \to K\pi) = (49.9 \pm 1.2) \times 10^{-2}$ and 2/3 for the $K^+\pi^-$ fraction. Our first error is their experiment's error and the second error is systematic error from using our best value.

[3] AUBERT,B 05N reports 7.7×10^{-6} at 90% CL for $B(B^+ \to K_2^*(1430)^0\pi^+) \times B(K_2^*(1430)^0 \to K^+\pi^-)$. We rescaled it using the PDG value $B(K_2^*(1430)^0 \to K\pi) = 49.9\%$ and 2/3 for the $K^+\pi^-$ fraction.

[4] GARMASH 05 reports 2.3×10^{-6} at 90% CL for $B(B^+ \to K_2^*(1430)^0\pi^+) \times B(K_2^*(1430)^0 \to K^+\pi^-)$. We rescaled it using the PDG value $B(K_2^*(1430)^0 \to K\pi) = 49.9\%$ and 2/3 for the $K^+\pi^-$ mode.

$\Gamma(K_0^*(1430)^+\pi^0)/\Gamma_{total}$ Γ_{372}/Γ

VALUE (units 10^{-6})	DOCUMENT ID		TECN	COMMENT
$11.9 \pm 1.7^{+1.0}_{-1.6}$	[1] LEES	17G	BABR	$e^+e^- \to \Upsilon(4S)$

[1] Obtains the result from a Dalitz analysis of $B^+ \to K_S^0\pi^+\pi^0$ decays. The first error is statistical, the second combines all the systematic uncertainties reported in the paper, including signal modelling.

$\Gamma(K^*(1410)^0\pi^+)/\Gamma_{total}$ Γ_{374}/Γ

VALUE (units 10^{-6})	CL%	DOCUMENT ID		TECN	COMMENT
<45	90	[1] GARMASH	05	BELL	$e^+e^- \to \Upsilon(4S)$

[1] GARMASH 05 reports 2.0×10^{-6} at 90% CL for $B(B^+ \to K^*(1410)^0\pi^+) \times B(K^*(1410)^0 \to K^+\pi^-)$. We rescaled it using the PDG value $B(K^*(1410)^0 \to K\pi) = 6.6\%$ and 2/3 for the $K^+\pi^-$ mode.

$\Gamma(K^*(1680)^0\pi^+)/\Gamma_{total}$ Γ_{375}/Γ

VALUE (units 10^{-6})	CL%	DOCUMENT ID		TECN	COMMENT
<12	90	[1] GARMASH	05	BELL	$e^+e^- \to \Upsilon(4S)$
• • • We do not use the following data for averages, fits, limits, etc. • • •					
<15	90	[2] AUBERT,B	05N	BABR	$e^+e^- \to \Upsilon(4S)$

[1] GARMASH 05 reports 3.1×10^{-6} at 90% CL for $B(B^+ \to K^*(1680)^0\pi^+) \times B(K^*(1680)^0 \to K^+\pi^-)$. We rescaled it using the PDG value $B(K^*(1680)^0 \to K\pi) = 38.7\%$ and 2/3 for the $K^+\pi^-$ mode.

[2] AUBERT,B 05N reports 3.8×10^{-6} at 90% CL for $B(B^+ \to K^*(1680)^0\pi^+) \times B(K^*(1680)^0 \to K^+\pi^-)$. We rescaled it using the PDG value $B(K^*(1680)^0 \to K\pi) = 38.7\%$ and 2/3 for the $K^+\pi^-$ fraction.

$\Gamma(K^+\pi^0\pi^0)/\Gamma_{total}$ Γ_{376}/Γ

VALUE (units 10^{-6})	DOCUMENT ID		TECN	COMMENT
$16.2 \pm 1.2 \pm 1.5$	[1] LEES	11I	BABR	$e^+e^- \to \Upsilon(4S)$

[1] Assumes equal production of B^+ and B^0 at the $\Upsilon(4S)$.

$\Gamma(f_0(980)K^+ \times B(f_0 \to \pi^0\pi^0))/\Gamma_{total}$ Γ_{377}/Γ

VALUE (units 10^{-6})	DOCUMENT ID		TECN	COMMENT
$2.8 \pm 0.6 \pm 0.5$	[1] LEES	11I	BABR	$e^+e^- \to \Upsilon(4S)$

[1] Assumes equal production of B^+ and B^0 at the $\Upsilon(4S)$.

$\Gamma(K^-\pi^+\pi^+)/\Gamma_{total}$ Γ_{378}/Γ

VALUE	CL%	DOCUMENT ID		TECN	COMMENT
$<4.6 \times 10^{-8}$	90	AAIJ	17E	LHCB	pp at 7, 8 TeV
• • • We do not use the following data for averages, fits, limits, etc. • • •					
$<9.5 \times 10^{-7}$	90	[1] AUBERT	08BE	BABR	$e^+e^- \to \Upsilon(4S)$
$<4.5 \times 10^{-6}$	90	[1] GARMASH	04	BELL	$e^+e^- \to \Upsilon(4S)$
$<1.8 \times 10^{-6}$	90	[2] AUBERT	03M	BABR	Repl. by AUBERT 08BE
$<7.0 \times 10^{-6}$	90	[3] GARMASH	02	BELL	$e^+e^- \to \Upsilon(4S)$

[1] Assumes equal production of B^+ and B^0 at the $\Upsilon(4S)$.

[2] Assumes equal production of B^0 and B^+ at the $\Upsilon(4S)$; charm and charmonium contributions are subtracted, otherwise no assumptions about intermediate resonances.

[3] Uses a reference decay mode $B^+ \to \overline{D}^0\pi^+$ and $\overline{D}^0 \to K^+\pi^-$ with $B(B^+ \to \overline{D}^0\pi^+) \cdot B(\overline{D}^0 \to K^+\pi^-) = (20.3 \pm 2.0) \times 10^{-5}$.

$\Gamma(K^-\pi^+\pi^+ \text{nonresonant})/\Gamma_{total}$ Γ_{379}/Γ

VALUE (units 10^{-6})	CL%	DOCUMENT ID		TECN	COMMENT
<56	90	BERGFELD	96B	CLE2	$e^+e^- \to \Upsilon(4S)$

$\Gamma(K_1(1270)^0\pi^+)/\Gamma_{total}$ Γ_{380}/Γ

VALUE	CL%	DOCUMENT ID		TECN	COMMENT
$<4.0 \times 10^{-5}$	90	[1] AUBERT	10D	BABR	$e^+e^- \to \Upsilon(4S)$

[1] Assumes equal production of B^+ and B^0 at the $\Upsilon(4S)$.

$\Gamma(K_1(1400)^0\pi^+)/\Gamma_{total}$ Γ_{381}/Γ

VALUE	CL%	DOCUMENT ID		TECN	COMMENT
$<3.9 \times 10^{-5}$	90	[1] AUBERT	10D	BABR	$e^+e^- \to \Upsilon(4S)$
• • • We do not use the following data for averages, fits, limits, etc. • • •					
$<2.6 \times 10^{-3}$	90	ALBRECHT	91B	ARG	$e^+e^- \to \Upsilon(4S)$

[1] Assumes equal production of B^+ and B^0 at the $\Upsilon(4S)$.

$\Gamma(K^0\pi^+\pi^0)/\Gamma_{total}$ Γ_{382}/Γ

VALUE (units 10^{-6})	CL%	DOCUMENT ID		TECN	COMMENT
$31.8 \pm 1.8^{+6.3}_{-2.1}$		[1] LEES	17G	BABR	$e^+e^- \to \Upsilon(4S)$
<66	90	[2] ECKHART	02	CLE2	$e^+e^- \to \Upsilon(4S)$

[1] Obtains the result from a Dalitz analysis of $B^+ \to K_S^0\pi^+\pi^0$ decays. The first error is statistical, the second combines all the systematic uncertainties reported in the paper, including signal modelling.

[2] Assumes equal production of B^+ and B^0 at the $\Upsilon(4S)$.

$\Gamma(K^0\rho^+)/\Gamma_{total}$ Γ_{383}/Γ

VALUE (units 10^{-6})	CL%	DOCUMENT ID		TECN	COMMENT
$7.3^{+1.0}_{-1.2}$ OUR AVERAGE					
$6.5 \pm 1.1^{+0.8}_{-1.9}$		[1] LEES	17G	BABR	$e^+e^- \to \Upsilon(4S)$
$8.0^{+1.4}_{-1.3} \pm 0.6$		AUBERT	07Z	BABR	$e^+e^- \to \Upsilon(4S)$
• • • We do not use the following data for averages, fits, limits, etc. • • •					
<48	90	ASNER	96	CLE2	$e^+e^- \to \Upsilon(4S)$

[1] Obtains the result from a Dalitz analysis of $B^+ \to K_S^0\pi^+\pi^0$ decays. The first error is statistical, the second combines all the systematic uncertainties reported in the paper, including signal modelling.

$\Gamma(K^*(892)^+\pi^+\pi^-)/\Gamma_{total}$ Γ_{384}/Γ

VALUE (units 10^{-6})	CL%	DOCUMENT ID		TECN	COMMENT
$75.3 \pm 6.0 \pm 8.1$		[1] AUBERT,B	06U	BABR	$e^+e^- \to \Upsilon(4S)$
• • • We do not use the following data for averages, fits, limits, etc. • • •					
<1100	90	ALBRECHT	91E	ARG	$e^+e^- \to \Upsilon(4S)$

[1] Assumes equal production of B^+ and B^0 at the $\Upsilon(4S)$.

$\Gamma(K^*(892)^+\rho^0)/\Gamma_{total}$ Γ_{385}/Γ

VALUE (units 10^{-6})	CL%	DOCUMENT ID		TECN	COMMENT
$4.6 \pm 1.0 \pm 0.4$		[1] DEL-AMO-SA...11D		BABR	$e^+e^- \to \Upsilon(4S)$
• • • We do not use the following data for averages, fits, limits, etc. • • •					
< 6.1	90	[1] AUBERT,B	06G	BABR	Repl. by DEL-AMO-SANCHEZ 11D
$10.6^{+3.0}_{-2.6} \pm 2.4$		[1] AUBERT	03V	BABR	Repl. by AUBERT,B 06G
< 74	90	[2] GODANG	02	CLE2	$e^+e^- \to \Upsilon(4S)$
<900	90	ALBRECHT	91B	ARG	$e^+e^- \to \Upsilon(4S)$

[1] Assumes equal production of B^+ and B^0 at the $\Upsilon(4S)$.

[2] Assumes a helicity 00 configuration. For a helicity 11 configuration, the limit decreases to 4.9×10^{-5}.

$\Gamma(K^*(892)^+f_0(980))/\Gamma_{total}$ Γ_{386}/Γ

VALUE (units 10^{-6})	DOCUMENT ID		TECN	COMMENT
$4.2 \pm 0.6 \pm 0.3$	[1] DEL-AMO-SA...11D		BABR	$e^+e^- \to \Upsilon(4S)$
• • • We do not use the following data for averages, fits, limits, etc. • • •				
$5.2 \pm 1.2 \pm 0.5$	[1] AUBERT,B	06G	BABR	Repl. by DEL-AMO-SANCHEZ 11D

[1] Assumes equal production of B^+ and B^0 at the $\Upsilon(4S)$.

$\Gamma(a_1^+K^0)/\Gamma_{total}$ Γ_{387}/Γ

VALUE (units 10^{-6})	DOCUMENT ID		TECN	COMMENT
$34.9 \pm 5.0 \pm 4.4$	[1,2] AUBERT	08F	BABR	$e^+e^- \to \Upsilon(4S)$

[1] Assumes equal production of B^+ and B^0 at the $\Upsilon(4S)$.

[2] Assumes $a_1^{\pm}$ decays only to 3π and $B(a_1^{\pm} \to \pi^{\pm}\pi^{\mp}\pi^{\pm}) = 0.5$.

$\Gamma(b_1^+K^0 \times B(b_1^+ \to \omega\pi^+))/\Gamma_{total}$ Γ_{388}/Γ

VALUE (units 10^{-6})	DOCUMENT ID		TECN	COMMENT
$9.6 \pm 1.7 \pm 0.9$	[1] AUBERT	08AG	BABR	$e^+e^- \to \Upsilon(4S)$

[1] Assumes equal production of B^+ and B^0 at the $\Upsilon(4S)$.

$\Gamma(K^*(892)^0\rho^+)/\Gamma_{total}$ Γ_{389}/Γ

VALUE (units 10^{-6})	DOCUMENT ID		TECN	COMMENT
9.2 ± 1.5 OUR AVERAGE				
$9.6 \pm 1.7 \pm 1.5$	[1] AUBERT,B	06G	BABR	$e^+e^- \to \Upsilon(4S)$
$8.9 \pm 1.7 \pm 1.2$	[1] ZHANG	05D	BELL	$e^+e^- \to \Upsilon(4S)$

[1] Assumes equal production of B^+ and B^0 at the $\Upsilon(4S)$.

$\Gamma(K_1(1400)^+\rho^0)/\Gamma_{total}$ Γ_{390}/Γ

VALUE	CL%	DOCUMENT ID		TECN	COMMENT
$<7.8 \times 10^{-4}$	90	ALBRECHT	91B	ARG	$e^+e^- \to \Upsilon(4S)$

$\Gamma(K_2^*(1430)^+\rho^0)/\Gamma_{total}$ Γ_{391}/Γ

VALUE	CL%	DOCUMENT ID		TECN	COMMENT
$<1.5 \times 10^{-3}$	90	ALBRECHT	91B	ARG	$e^+e^- \to \Upsilon(4S)$

$\Gamma(b_1^0K^+ \times B(b_1^0 \to \omega\pi^0))/\Gamma_{total}$ Γ_{392}/Γ

VALUE (units 10^{-6})	DOCUMENT ID		TECN	COMMENT
$9.1 \pm 1.7 \pm 1.0$	[1] AUBERT	07BI	BABR	$e^+e^- \to \Upsilon(4S)$

[1] Assumes equal production of B^+ and B^0 at the $\Upsilon(4S)$.

$\Gamma(b_1^+K^{*0} \times B(b_1^+ \to \omega\pi^+))/\Gamma_{total}$ Γ_{393}/Γ

VALUE	CL%	DOCUMENT ID		TECN	COMMENT
$<5.9 \times 10^{-6}$	90	[1] AUBERT	09AF	BABR	$e^+e^- \to \Upsilon(4S)$

[1] Assumes equal production of B^+ and B^0 at the $\Upsilon(4S)$.

$\Gamma(b_1^0 K^{*+} \times B(b_1^0 \to \omega\pi^0))/\Gamma_{total}$ Γ_{394}/Γ

VALUE	CL%	DOCUMENT ID		TECN	COMMENT
$<6.7 \times 10^{-6}$	90	[1] AUBERT	09AF	BABR	$e^+e^- \to \Upsilon(4S)$

[1] Assumes equal production of B^+ and B^0 at the $\Upsilon(4S)$.

$\Gamma(K^+\overline{K}^0)/\Gamma_{total}$ Γ_{395}/Γ

VALUE (units 10^{-6})	CL%	DOCUMENT ID		TECN	COMMENT
1.31±0.17 OUR FIT Error includes scale factor of 1.2.					
1.19±0.18 OUR AVERAGE					
1.11±0.19±0.05		[1] DUH	13	BELL	$e^+e^- \to \Upsilon(4S)$
1.61±0.44±0.09		[1] AUBERT,BE	06C	BABR	$e^+e^- \to \Upsilon(4S)$
• • • We do not use the following data for averages, fits, limits, etc. • • •					
$1.22^{+0.32}_{-0.28}{}^{+0.13}_{-0.16}$		[1] LIN	07	BELL	Repl. by DUH 13
1.0 ±0.4 ±0.1		[1] ABE	05G	BELL	Repl. by LIN 07
1.5 ±0.5 ±0.1		[1] AUBERT,BE	05E	BABR	Repl. by AUBERT,BE 06C
< 2.5	90	[1] AUBERT	04M	BABR	Repl. by AUBERT,BE 05E
< 3.3	90	[1] CHAO	04	BELL	$e^+e^- \to \Upsilon(4S)$
< 3.3	90	[1] BORNHEIM	03	CLE2	$e^+e^- \to \Upsilon(4S)$
< 2.0	90	[1] CASEY	02	BELL	Repl. by CHAO 04
< 5.0	90	[1] ABE	01H	BELL	$e^+e^- \to \Upsilon(4S)$
< 2.4	90	[1] AUBERT	01E	BABR	$e^+e^- \to \Upsilon(4S)$
< 5.1	90	[1] CRONIN-HEN..00		CLE2	$e^+e^- \to \Upsilon(4S)$
<21	90	GODANG	98	CLE2	Repl. by CRONIN-HENNESSY 00

[1] Assumes equal production of B^+ and B^0 at the $\Upsilon(4S)$.

$\Gamma(K^+\overline{K}^0)/\Gamma(K^0\pi^+)$ $\Gamma_{395}/\Gamma_{334}$

VALUE	DOCUMENT ID		TECN	COMMENT
0.055±0.007 OUR FIT Error includes scale factor of 1.2.				
0.064±0.009±0.004	AAIJ	13BS	LHCB	pp at 7 TeV

$\Gamma(\overline{K}^0 K^+\pi^0)/\Gamma_{total}$ Γ_{396}/Γ

VALUE	CL%	DOCUMENT ID		TECN	COMMENT
$<24 \times 10^{-6}$	90	[1] ECKHART	02	CLE2	$e^+e^- \to \Upsilon(4S)$

[1] Assumes equal production of B^+ and B^0 at the $\Upsilon(4S)$.

$\Gamma(K^+ K_S^0 K_S^0)/\Gamma_{total}$ Γ_{397}/Γ

VALUE (units 10^{-6})	DOCUMENT ID		TECN	COMMENT
10.8±0.6 OUR AVERAGE				
10.6±0.5±0.3	[1,2] LEES	12O	BABR	$e^+e^- \to \Upsilon(4S)$
13.4±1.9±1.5	[1] GARMASH	04	BELL	$e^+e^- \to \Upsilon(4S)$
• • • We do not use the following data for averages, fits, limits, etc. • • •				
10.7±1.2±1.0	[1] AUBERT,B	04V	BABR	Repl. by LEES 12O

[1] Assumes equal production of B^+ and B^0 at the $\Upsilon(4S)$.
[2] All intermediate charmonium and charm resonances are removed, except of χ_{c0}.

$\Gamma(f_0(980) K^+,\ f_0 \to K_S^0 K_S^0)/\Gamma_{total}$ Γ_{398}/Γ

VALUE (units 10^{-6})	DOCUMENT ID		TECN	COMMENT
14.7±2.8±1.8	[1] LEES	12O	BABR	$e^+e^- \to \Upsilon(4S)$

[1] Assumes equal production of B^+ and B^0 at the $\Upsilon(4S)$.

$\Gamma(f_0(1710) K^+,\ f_0 \to K_S^0 K_S^0)/\Gamma_{total}$ Γ_{399}/Γ

VALUE (units 10^{-6})	DOCUMENT ID		TECN	COMMENT
$0.48^{+0.40}_{-0.24}$±0.11	[1] LEES	12O	BABR	$e^+e^- \to \Upsilon(4S)$

[1] Assumes equal production of B^+ and B^0 at the $\Upsilon(4S)$.

$\Gamma(K^+ K_S^0 K_S^0 \text{nonresonant})/\Gamma_{total}$ Γ_{400}/Γ

VALUE (units 10^{-6})	DOCUMENT ID		TECN	COMMENT
19.8±3.7±2.5	[1] LEES	12O	BABR	$e^+e^- \to \Upsilon(4S)$

[1] Assumes equal production of B^+ and B^0 at the $\Upsilon(4S)$.

$\Gamma(K_S^0 K_S^0 \pi^+)/\Gamma_{total}$ Γ_{401}/Γ

VALUE (units 10^{-6})	CL%	DOCUMENT ID		TECN	COMMENT
<0.51	90	[1] AUBERT	09J	BABR	$e^+e^- \to \Upsilon(4S)$
• • • We do not use the following data for averages, fits, limits, etc. • • •					
<3.2	90	[1] GARMASH	04	BELL	$e^+e^- \to \Upsilon(4S)$

[1] Assumes equal production of B^+ and B^0 at the $\Upsilon(4S)$.

$\Gamma(K^+ K^-\pi^+)/\Gamma_{total}$ Γ_{402}/Γ

VALUE (units 10^{-6})	CL%	DOCUMENT ID		TECN	COMMENT
5.2 ±0.4 OUR AVERAGE					
5.38±0.40±0.35		[1,2] HSU	17	BELL	$e^+e^- \to \Upsilon(4S)$
5.0 ±0.5 ±0.5		[2] AUBERT	07BB	BABR	$e^+e^- \to \Upsilon(4S)$
• • • We do not use the following data for averages, fits, limits, etc. • • •					
<13	90	[2] GARMASH	04	BELL	$e^+e^- \to \Upsilon(4S)$
< 6.3	90	[2,3] AUBERT	03M	BABR	Repl. by AUBERT 07BB
<12	90	[4] GARMASH	02	BELL	$e^+e^- \to \Upsilon(4S)$

[1] HSU 17 provides also measurement as a function of K^+K^- invariant mass.
[2] Assumes equal production of B^+ and B^0 at the $\Upsilon(4S)$.
[3] Charm and charmonium contributions are subtracted, otherwise no assumptions about intermediate resonances.
[4] Uses a reference decay mode $B^+ \to \overline{D}^0\pi^+$ and $\overline{D}^0 \to K^+\pi^-$ with $B(B^+ \to \overline{D}^0\pi^+)\cdot B(\overline{D}^0 \to K^+\pi^-) = (20.3 \pm 2.0) \times 10^{-5}$.

$\Gamma(K^+ K^-\pi^+ \text{nonresonant})/\Gamma_{total}$ Γ_{403}/Γ

VALUE (units 10^{-6})	CL%	DOCUMENT ID		TECN	COMMENT
<75	90	BERGFELD	96B	CLE2	$e^+e^- \to \Upsilon(4S)$

$\Gamma(K^+\overline{K}^*(892)^0)/\Gamma_{total}$ Γ_{404}/Γ

VALUE (units 10^{-6})	CL%	DOCUMENT ID		TECN	COMMENT
< 1.1	90	[1] AUBERT	07AR	BABR	$e^+e^- \to \Upsilon(4S)$
• • • We do not use the following data for averages, fits, limits, etc. • • •					
<129	90	ABBIENDI	00B	OPAL	$e^+e^- \to Z$
<138	90	[2] ABE	00C	SLD	$e^+e^- \to Z$
< 5.3	90	[1] JESSOP	00	CLE2	$e^+e^- \to \Upsilon(4S)$

[1] Assumes equal production of B^+ and B^0 at the $\Upsilon(4S)$.
[2] ABE 00C assumes $B(Z \to b\overline{b})$=(21.7 ± 0.1)% and the B fractions $f_{B^0}=f_{B^+}=(39.7^{+1.8}_{-2.2})$% and $f_{B_s}=(10.5^{+1.8}_{-2.2})$%.

$\Gamma(K^+\overline{K}_0^*(1430)^0)/\Gamma_{total}$ Γ_{405}/Γ

VALUE (units 10^{-6})	CL%	DOCUMENT ID		TECN	COMMENT
<2.2	90	[1] AUBERT	07AR	BABR	$e^+e^- \to \Upsilon(4S)$

[1] Assumes equal production of B^+ and B^0 at the $\Upsilon(4S)$.

$\Gamma(K^+ K^+\pi^-)/\Gamma_{total}$ Γ_{406}/Γ

VALUE	CL%	DOCUMENT ID		TECN	COMMENT
$<1.1 \times 10^{-8}$	90	AAIJ	17E	LHCB	pp at 7, 8 TeV
• • • We do not use the following data for averages, fits, limits, etc. • • •					
$<1.6 \times 10^{-7}$	90	[1] AUBERT	08BE	BABR	$e^+e^- \to \Upsilon(4S)$
$<2.4 \times 10^{-6}$	90	[1] GARMASH	04	BELL	$e^+e^- \to \Upsilon(4S)$
$<1.3 \times 10^{-6}$	90	[2] AUBERT	03M	BABR	Repl. by AUBERT 08BE
$<3.2 \times 10^{-6}$	90	[3] GARMASH	02	BELL	$e^+e^- \to \Upsilon(4S)$

[1] Assumes equal production of B^+ and B^0 at the $\Upsilon(4S)$.
[2] Assumes equal production of B^0 and B^+ at the $\Upsilon(4S)$; charm and charmonium contributions are subtracted, otherwise no assumptions about intermediate resonances.
[3] Uses a reference decay mode $B^+ \to \overline{D}^0\pi^+$ and $\overline{D}^0 \to K^+\pi^-$ with $B(B^+ \to \overline{D}^0\pi^+)\cdot B(\overline{D}^0 \to K^+\pi^-) = (20.3 \pm 2.0) \times 10^{-5}$.

$\Gamma(K^+ K^+\pi^- \text{nonresonant})/\Gamma_{total}$ Γ_{407}/Γ

VALUE (units 10^{-6})	CL%	DOCUMENT ID		TECN	COMMENT
<87.9	90	ABBIENDI	00B	OPAL	$e^+e^- \to Z$

$\Gamma(f_2'(1525) K^+)/\Gamma_{total}$ Γ_{408}/Γ

VALUE (units 10^{-6})	CL%	DOCUMENT ID		TECN	COMMENT
1.8 ±0.5 OUR AVERAGE Error includes scale factor of 1.1.					
1.56±0.36±0.30		[1,2] LEES	12O	BABR	$e^+e^- \to \Upsilon(4S)$
$2.8 \pm 0.9\ ^{+0.5}_{-0.4}$		[1,3] LEES	12O	BABR	$e^+e^- \to \Upsilon(4S)$
• • • We do not use the following data for averages, fits, limits, etc. • • •					
<8	90	[1,4] GARMASH	05	BELL	$e^+e^- \to \Upsilon(4S)$

[1] Assumes equal production of B^+ and B^0 at the $\Upsilon(4S)$.
[2] Measured in the $B^+ \to K^+K^-K^+$ decay.
[3] Measured in the $B^+ \to K^+K_S^0K_S^0$ decay.
[4] GARMASH 05 reports $B(B^+ \to f_2'(1525)\,K^+)\cdot B(f_2'(1525) \to K^+K^-) < 4.9\times10^{-6}$ at 90% CL. We divide this result by our best value of $B(f_2'(1525) \to K\overline{K}) = 88.7\times10^{-2}$ multiplied by 2/3 to account for the K^+K^- fraction.

$\Gamma(K^+ f_J(2220))/\Gamma_{total}$ Γ_{409}/Γ

VALUE (units 10^{-6})	DOCUMENT ID		TECN	COMMENT
not seen	[1] HUANG	03	BELL	$e^+e^- \to \Upsilon(4S)$

[1] No evidence is found for such decay and set a limit on $B(B^+ \to f_J(2220))\times B(f_J(2220) \to \phi\phi) < 1.2 \times 10^{-6}$ at 90%CL where the $f_J(2220)$ is a possible glueball state.

$\Gamma(K^{*+}\pi^+ K^-)/\Gamma_{total}$ Γ_{410}/Γ

VALUE (units 10^{-6})	CL%	DOCUMENT ID		TECN	COMMENT
<11.8	90	[1] AUBERT,B	06U	BABR	$e^+e^- \to \Upsilon(4S)$

[1] Assumes equal production of B^+ and B^0 at the $\Upsilon(4S)$.

$\Gamma(K^*(892)^+ K^*(892)^0)/\Gamma_{total}$ Γ_{411}/Γ

VALUE (units 10^{-6})	CL%	DOCUMENT ID		TECN	COMMENT
0.91 ± 0.29 OUR AVERAGE					
$0.77^{+0.35}_{-0.30} \pm 0.12$		[1] GOH	15	BELL	$e^+e^- \to \Upsilon(4S)$
$1.2 \pm 0.5 \pm 0.1$		[2] AUBERT	09F	BABR	$e^+e^- \to \Upsilon(4S)$
• • • We do not use the following data for averages, fits, limits, etc. • • •					
<71	90	[3] GODANG	02	CLE2	$e^+e^- \to \Upsilon(4S)$

[1] Signal significance is 2.7 standard deviations. This measurement corresponds to an upper limit of $< 1.31 \times 10^{-6}$ at 90% CL.
[2] Signal signicance is 3.7 standard deviations.
[3] Assumes a helicity 00 configuration. For a helicity 11 configuration, the limit decreases to 4.8×10^{-5}.

$\Gamma(K^{*+} K^+ \pi^-)/\Gamma_{total}$ Γ_{412}/Γ

VALUE (units 10^{-6})	CL%	DOCUMENT ID		TECN	COMMENT
<6.1	90	[1] AUBERT,B	06U	BABR	$e^+e^- \to \Upsilon(4S)$

[1] Assumes equal production of B^+ and B^0 at the $\Upsilon(4S)$.

$\Gamma(K^+ K^- K^+)/\Gamma_{total}$ Γ_{413}/Γ

VALUE (units 10^{-6})	CL%	DOCUMENT ID		TECN	COMMENT
34.0 ± 1.4 OUR AVERAGE		Error includes scale factor of 1.4.			
$34.6 \pm 0.6 \pm 0.9$		[1,2] LEES	12O	BABR	$e^+e^- \to \Upsilon(4S)$
$30.6 \pm 1.2 \pm 2.3$		[1] GARMASH	05	BELL	$e^+e^- \to \Upsilon(4S)$
• • • We do not use the following data for averages, fits, limits, etc. • • •					
$35.2 \pm 0.9 \pm 1.6$		[1] AUBERT	06O	BABR	Repl. by LEES 12O
$32.8 \pm 1.8 \pm 2.8$		[1] GARMASH	04	BELL	Repl. by GARMASH 05
$29.6 \pm 2.1 \pm 1.6$		[3] AUBERT	03M	BABR	Repl. by AUBERT 06O
$35.3 \pm 3.7 \pm 4.5$		[4] GARMASH	02	BELL	Repl. by GARMASH 04
<200	90	[5] ADAM	96D	DLPH	$e^+e^- \to Z$
<320	90	[5] ABREU	95N	DLPH	Sup. by ADAM 96D
<350	90	ALBRECHT	91E	ARG	$e^+e^- \to \Upsilon(4S)$

[1] Assumes equal production of B^+ and B^0 at the $\Upsilon(4S)$.
[2] All intermediate charmonium and charm resonances are removed, except of χ_{c0}.
[3] Assumes equal production of B^0 and B^+ at the $\Upsilon(4S)$; charm and charmonium contributions are subtracted, otherwise no assumptions about intermediate resonances.
[4] Uses a reference decay mode $B^+ \to \overline{D}^0 \pi^+$ and $\overline{D}^0 \to K^+\pi^-$ with $B(B^+ \to \overline{D}^0\pi^+) \cdot B(\overline{D}^0 \to K^+\pi^-) = (20.3 \pm 2.0) \times 10^{-5}$.
[5] Assumes B^0 and B^- production fractions of 0.39, and B_s production fraction of 0.12.

$\Gamma(K^+\phi)/\Gamma_{total}$ Γ_{414}/Γ

VALUE (units 10^{-6})	CL%	DOCUMENT ID		TECN	COMMENT
$8.8^{+0.7}_{-0.6}$ OUR AVERAGE		Error includes scale factor of 1.1.			
$9.2 \pm 0.4^{+0.7}_{-0.5}$		[1] LEES	12O	BABR	$e^+e^- \to \Upsilon(4S)$
$7.6 \pm 1.3 \pm 0.6$		[2] ACOSTA	05J	CDF	$p\overline{p}$ at 1.96 TeV
$9.60 \pm 0.92^{+1.05}_{-0.85}$		[1] GARMASH	05	BELL	$e^+e^- \to \Upsilon(4S)$
$5.5^{+2.1}_{-1.8} \pm 0.6$		[1] BRIERE	01	CLE2	$e^+e^- \to \Upsilon(4S)$
• • • We do not use the following data for averages, fits, limits, etc. • • •					
$8.4 \pm 0.7 \pm 0.7$		[1] AUBERT	06O	BABR	Repl. by LEES 12O
$10.0^{+0.9}_{-0.8} \pm 0.5$		[1] AUBERT	04A	BABR	Repl. by AUBERT 06O
$9.4 \pm 1.1 \pm 0.7$		[1] CHEN	03B	BELL	Repl. by GARMASH 05
$14.6^{+3.0}_{-2.8} \pm 2.0$		[3] GARMASH	02	BELL	Repl. by CHEN 03B
$7.7^{+1.6}_{-1.4} \pm 0.8$		[1] AUBERT	01D	BABR	$e^+e^- \to \Upsilon(4S)$
<144	90	[4] ABE	00C	SLD	$e^+e^- \to Z$
< 5	90	[1] BERGFELD	98	CLE2	
<280	90	[5] ADAM	96D	DLPH	$e^+e^- \to Z$
< 12	90	ASNER	96	CLE2	$e^+e^- \to \Upsilon(4S)$
<440	90	[6] ABREU	95N	DLPH	Sup. by ADAM 96D
<180	90	ALBRECHT	91B	ARG	$e^+e^- \to \Upsilon(4S)$
< 90	90	[7] AVERY	89B	CLEO	$e^+e^- \to \Upsilon(4S)$
<210	90	AVERY	87	CLEO	$e^+e^- \to \Upsilon(4S)$

[1] Assumes equal production of B^+ and B^0 at the $\Upsilon(4S)$.
[2] Uses $B(B^+ \to J/\psi K^+) = (1.00 \pm 0.04) \times 10^{-3}$ and $B(J/\psi \to \mu^+\mu^-) = 0.0588 \pm 0.0010$.
[3] Uses a reference decay mode $B^+ \to \overline{D}^0 \pi^+$ and $\overline{D}^0 \to K^+\pi^-$ with $B(B^+ \to \overline{D}^0\pi^+) \cdot B(\overline{D}^0 \to K^+\pi^-) = (20.3 \pm 2.0) \times 10^{-5}$.
[4] ABE 00C assumes $B(Z \to b\overline{b}) = (21.7 \pm 0.1)\%$ and the B fractions $f_{B^0} = f_{B^+} = (39.7^{+1.8}_{-2.2})\%$ and $f_{B_s} = (10.5^{+1.8}_{-2.2})\%$.
[5] ADAM 96D assumes $f_{B^0} = f_{B^-} = 0.39$ and $f_{B_s} = 0.12$.
[6] Assumes a B^0, B^- production fraction of 0.39 and a B_s production fraction of 0.12.
[7] AVERY 89B reports $< 8 \times 10^{-5}$ assuming the $\Upsilon(4S)$ decays 43% to $B^0\overline{B}^0$. We rescale to 50%.

$\Gamma(f_0(980) K^+ \times B(f_0(980) \to K^+K^-))/\Gamma_{total}$ Γ_{415}/Γ

VALUE (units 10^{-6})	CL%	DOCUMENT ID		TECN	COMMENT
$9.4 \pm 1.6 \pm 2.8$		[1] LEES	12O	BABR	$e^+e^- \to \Upsilon(4S)$
• • • We do not use the following data for averages, fits, limits, etc. • • •					
$6.5 \pm 2.5 \pm 1.6$		[1] AUBERT	06O	BABR	$e^+e^- \to \Upsilon(4S)$
<2.9	90	[1] GARMASH	05	BELL	$e^+e^- \to \Upsilon(4S)$

[1] Assumes equal production of B^+ and B^0 at the $\Upsilon(4S)$.

$\Gamma(a_2(1320) K^+ \times B(a_2(1320) \to K^+K^-))/\Gamma_{total}$ Γ_{416}/Γ

VALUE	CL%	DOCUMENT ID		TECN	COMMENT
$<1.1 \times 10^{-6}$	90	[1] GARMASH	05	BELL	$e^+e^- \to \Upsilon(4S)$

[1] Assumes equal production of B^+ and B^0 at the $\Upsilon(4S)$.

$\Gamma(X_0(1550) K^+ \times B(X_0(1550) \to K^+K^-))/\Gamma_{total}$ Γ_{417}/Γ

$X_0(1550)$ is a possible spin zero state near 1.55 GeV/c^2 invariant mass of K^+K^-.

VALUE (units 10^{-6})	DOCUMENT ID		TECN	COMMENT
$4.3 \pm 0.6 \pm 0.3$	[1] AUBERT	06O	BABR	$e^+e^- \to \Upsilon(4S)$

[1] Assumes equal production of B^+ and B^0 at the $\Upsilon(4S)$.

$\Gamma(\phi(1680) K^+ \times B(\phi(1680) \to K^+K^-))/\Gamma_{total}$ Γ_{418}/Γ

VALUE	CL%	DOCUMENT ID		TECN	COMMENT
$<0.8 \times 10^{-6}$	90	[1] GARMASH	05	BELL	$e^+e^- \to \Upsilon(4S)$

[1] Assumes equal production of B^+ and B^0 at the $\Upsilon(4S)$.

$\Gamma(f_0(1710) K^+ \times B(f_0(1710) \to K^+K^-))/\Gamma_{total}$ Γ_{419}/Γ

VALUE (units 10^{-6})	DOCUMENT ID		TECN	COMMENT
$1.12 \pm 0.25 \pm 0.50$	[1] LEES	12O	BABR	$e^+e^- \to \Upsilon(4S)$
• • • We do not use the following data for averages, fits, limits, etc. • • •				
$1.7 \pm 1.0 \pm 0.3$	[1] AUBERT	06O	BABR	Repl. by LEES 12O

[1] Assumes equal production of B^+ and B^0 at the $\Upsilon(4S)$.

$\Gamma(K^+K^-K^+ \text{nonresonant})/\Gamma_{total}$ Γ_{420}/Γ

VALUE (units 10^{-6})	CL%	DOCUMENT ID		TECN	COMMENT
$23.8^{+2.8}_{-5.0}$ OUR AVERAGE					
$22.8 \pm 2.7 \pm 7.6$		[1] LEES	12O	BABR	$e^+e^- \to \Upsilon(4S)$
$24.0 \pm 1.5^{+2.6}_{-6.0}$		[1] GARMASH	05	BELL	$e^+e^- \to \Upsilon(4S)$
• • • We do not use the following data for averages, fits, limits, etc. • • •					
$50.0 \pm 6.0 \pm 4.0$		[1] AUBERT	06O	BABR	Repl. by LEES 12O
<38	90	BERGFELD	96B	CLE2	$e^+e^- \to \Upsilon(4S)$

[1] Assumes equal production of B^+ and B^0 at the $\Upsilon(4S)$.

$\Gamma(K^*(892)^+ K^+ K^-)/\Gamma_{total}$ Γ_{421}/Γ

VALUE (units 10^{-6})	CL%	DOCUMENT ID		TECN	COMMENT
$36.2 \pm 3.3 \pm 3.6$		[1] AUBERT,B	06U	BABR	$e^+e^- \to \Upsilon(4S)$
• • • We do not use the following data for averages, fits, limits, etc. • • •					
<1600	90	ALBRECHT	91E	ARG	$e^+e^- \to \Upsilon(4S)$

[1] Assumes equal production of B^+ and B^0 at the $\Upsilon(4S)$.

$\Gamma(K^*(892)^+ \phi)/\Gamma_{total}$ Γ_{422}/Γ

VALUE (units 10^{-6})	CL%	DOCUMENT ID		TECN	COMMENT
10.0 ± 2.0 OUR AVERAGE		Error includes scale factor of 1.7.			
$11.2 \pm 1.0 \pm 0.9$		[1] AUBERT	07BA	BABR	$e^+e^- \to \Upsilon(4S)$
$6.7^{+2.1}_{-1.9} {}^{+0.7}_{-1.0}$		[1] CHEN	03B	BELL	$e^+e^- \to \Upsilon(4S)$
• • • We do not use the following data for averages, fits, limits, etc. • • •					
$12.7^{+2.2}_{-2.0} \pm 1.1$		[1] AUBERT	03V	BABR	Repl. by AUBERT 07BA
$9.7^{+4.2}_{-3.4} \pm 1.7$		[1] AUBERT	01D	BABR	Repl. by AUBERT 03V
< 22.5	90	[1] BRIERE	01	CLE2	$e^+e^- \to \Upsilon(4S)$
< 41	90	[1] BERGFELD	98	CLE2	
< 70	90	ASNER	96	CLE2	$e^+e^- \to \Upsilon(4S)$
<1300	90	ALBRECHT	91B	ARG	$e^+e^- \to \Upsilon(4S)$

[1] Assumes equal production of B^+ and B^0 at the $\Upsilon(4S)$.

$\Gamma(\phi(K\pi)_0^{*+})/\Gamma_{total}$ Γ_{423}/Γ

$(K\pi)_0^{*+}$ is the total S-wave composed of $K_0^*(1430)$ and nonresonant that are described using LASS shape.

VALUE (units 10^{-6})	DOCUMENT ID		TECN	COMMENT
$8.3 \pm 1.4 \pm 0.8$	[1] AUBERT	08BI	BABR	$e^+e^- \to \Upsilon(4S)$

[1] Assumes equal production of B^+ and B^0 at the $\Upsilon(4S)$.

$\Gamma(\phi K_1(1270)^+)/\Gamma_{total}$ Γ_{424}/Γ

VALUE (units 10^{-6})	DOCUMENT ID		TECN	COMMENT
$6.1 \pm 1.6 \pm 1.1$	[1] AUBERT	08BI	BABR	$e^+e^- \to \Upsilon(4S)$

[1] Assumes equal production of B^+ and B^0 at the $\Upsilon(4S)$.

$\Gamma(\phi K_1(1400)^+)/\Gamma_{total}$ Γ_{425}/Γ

VALUE (units 10^{-6})	CL%	DOCUMENT ID		TECN	COMMENT
< 3.2	90	[1] AUBERT	08BI	BABR	$e^+e^- \to \Upsilon(4S)$

• • • We do not use the following data for averages, fits, limits, etc. • • •

<1100	90	ALBRECHT	91B	ARG	$e^+e^- \to \Upsilon(4S)$

[1] Assumes equal production of B^+ and B^0 at the $\Upsilon(4S)$.

$\Gamma(\phi K^*(1410)^+)/\Gamma_{total}$ Γ_{426}/Γ

VALUE (units 10^{-6})	CL%	DOCUMENT ID		TECN	COMMENT
<4.3	90	[1] AUBERT	08BI	BABR	$e^+e^- \to \Upsilon(4S)$

[1] Assumes equal production of B^+ and B^0 at the $\Upsilon(4S)$.

$\Gamma(\phi K_0^*(1430)^+)/\Gamma_{total}$ Γ_{427}/Γ

VALUE (units 10^{-6})	DOCUMENT ID		TECN	COMMENT
7.0±1.3±0.9	[1] AUBERT	08BI	BABR	$e^+e^- \to \Upsilon(4S)$

[1] Assumes equal production of B^+ and B^0 at the $\Upsilon(4S)$.

$\Gamma(\phi K_2^*(1430)^+)/\Gamma_{total}$ Γ_{428}/Γ

VALUE (units 10^{-6})	CL%	DOCUMENT ID		TECN	COMMENT
8.4±1.8±1.0		[1] AUBERT	08BI	BABR	$e^+e^- \to \Upsilon(4S)$
• • • We do not use the following data for averages, fits, limits, etc. • • •					
<3400	90	ALBRECHT	91B	ARG	$e^+e^- \to \Upsilon(4S)$

[1] Assumes equal production of B^+ and B^0 at the $\Upsilon(4S)$.

$\Gamma(\phi K_2^*(1770)^+)/\Gamma_{total}$ Γ_{429}/Γ

VALUE (units 10^{-6})	CL%	DOCUMENT ID		TECN	COMMENT
<15.0	90	[1] AUBERT	08BI	BABR	$e^+e^- \to \Upsilon(4S)$

[1] Assumes equal production of B^+ and B^0 at the $\Upsilon(4S)$.

$\Gamma(\phi K_2^*(1820)^+)/\Gamma_{total}$ Γ_{430}/Γ

VALUE (units 10^{-6})	CL%	DOCUMENT ID		TECN	COMMENT
<16.3	90	[1] AUBERT	08BI	BABR	$e^+e^- \to \Upsilon(4S)$

[1] Assumes equal production of B^+ and B^0 at the $\Upsilon(4S)$.

$\Gamma(a_1^+ K^{*0})/\Gamma_{total}$ Γ_{431}/Γ

VALUE (units 10^{-6})	CL%	DOCUMENT ID		TECN	COMMENT
<3.6	90	[1,2] DEL-AMO-SA...10I		BABR	$e^+e^- \to \Upsilon(4S)$

[1] Assumes $B(a_1^{\pm} \to \pi^{\pm}\pi^{\mp}\pi^{\pm}) = 0.5$

[2] Assumes equal production of B^+ and B^0 at the $\Upsilon(4S)$.

$\Gamma(K^+\phi\phi)/\Gamma_{total}$ Γ_{432}/Γ

VALUE (units 10^{-6})	DOCUMENT ID		TECN	COMMENT
5.0±1.2 OUR AVERAGE Error includes scale factor of 2.3.				
$5.6 \pm 0.5 \pm 0.3$	[1] LEES	11A	BABR	$e^+e^- \to \Upsilon(4S)$
$2.6^{+1.1}_{-0.9} \pm 0.3$	[1] HUANG	03	BELL	$e^+e^- \to \Upsilon(4S)$
• • • We do not use the following data for averages, fits, limits, etc. • • •				
$7.5 \pm 1.0 \pm 0.7$	[1] AUBERT,BE	06H	BABR	Repl. by LEES 11A

[1] Assumes equal production of B^0 and B^+ at the $\Upsilon(4S)$ and for a $\phi\phi$ invariant mass below 2.85 GeV/c^2.

$\Gamma(\eta'\eta' K^+)/\Gamma_{total}$ Γ_{433}/Γ

VALUE (units 10^{-6})	CL%	DOCUMENT ID		TECN	COMMENT
<25	90	[1] AUBERT,B	06P	BABR	$e^+e^- \to \Upsilon(4S)$

[1] Assumes equal production of B^+ and B^0 at the $\Upsilon(4S)$.

$\Gamma(\omega\phi K^+)/\Gamma_{total}$ Γ_{434}/Γ

VALUE (units 10^{-6})	CL%	DOCUMENT ID		TECN	COMMENT
<1.9	90	[1] LIU	09	BELL	$e^+e^- \to \Upsilon(4S)$

[1] Assumes equal production of B^+ and B^0 at the $\Upsilon(4S)$.

$\Gamma(X(1812)\, K^+ \times B(X \to \omega\phi))/\Gamma_{total}$ Γ_{435}/Γ

VALUE (units 10^{-6})	CL%	DOCUMENT ID		TECN	COMMENT
<0.32	90	[1] LIU	09	BELL	$e^+e^- \to \Upsilon(4S)$

[1] Assumes equal production of B^+ and B^0 at the $\Upsilon(4S)$.

$\Gamma(K^*(892)^+\gamma)/\Gamma_{total}$ Γ_{436}/Γ

VALUE (units 10^{-5})	CL%	DOCUMENT ID		TECN	COMMENT
3.92±0.22 OUR AVERAGE Error includes scale factor of 1.7.					
$3.76 \pm 0.10 \pm 0.12$		[1] HORIGUCHI	17	BELL	$e^+e^- \to \Upsilon(4S)$
$4.22 \pm 0.14 \pm 0.16$		[2] AUBERT	09AO	BABR	$e^+e^- \to \Upsilon(4S)$
$3.76^{+0.89}_{-0.83} \pm 0.28$		[3] COAN	00	CLE2	$e^+e^- \to \Upsilon(4S)$
• • • We do not use the following data for averages, fits, limits, etc. • • •					
$3.87 \pm 0.28 \pm 0.26$		[4] AUBERT,BE	04A	BABR	Repl. by AUBERT 09AO
$4.25 \pm 0.31 \pm 0.24$		[3] NAKAO	04	BELL	Repl. by HORIGUCHI 17
$3.83 \pm 0.62 \pm 0.22$		[3] AUBERT	02C	BABR	Repl. by AUBERT,BE 04A
$5.7 \pm 3.1 \pm 1.1$		[5] AMMAR	93	CLE2	Repl. by COAN 00
< 55	90	[6] ALBRECHT	89G	ARG	$e^+e^- \to \Upsilon(4S)$
< 55	90	[6] AVERY	89B	CLEO	$e^+e^- \to \Upsilon(4S)$
<180	90	AVERY	87	CLEO	$e^+e^- \to \Upsilon(4S)$

[1] Uses $B(\Upsilon(4S) \to B^+B^-) = (51.4 \pm 0.6)\%$ and $B(\Upsilon(4S) \to B^0\overline{B}^0) = (48.6 \pm 0.6)\%$.

[2] Uses $B(\Upsilon(4S) \to B^+B^-) = (51.6 \pm 0.6)\%$ and $B(\Upsilon(4S) \to B^0\overline{B}^0) = (48.4 \pm 0.6)\%$.

[3] Assumes equal production of B^+ and B^0 at the $\Upsilon(4S)$.

[4] Uses the production ratio of charged and neutral B from $\Upsilon(4S)$ decays $R^{+/0} = 1.006 \pm 0.048$.

[5] AMMAR 93 observed 4.1 ± 2.3 events above background.

[6] Assumes the $\Upsilon(4S)$ decays 43% to $B^0\overline{B}^0$.

$\Gamma(K_1(1270)^+\gamma)/\Gamma_{total}$ Γ_{437}/Γ

VALUE (units 10^{-5})	CL%	DOCUMENT ID		TECN	COMMENT
4.4 $^{+0.7}_{-0.6}$ OUR AVERAGE					
$4.41^{+0.63}_{-0.44} \pm 0.58$		[1,2] DEL-AMO-SA...16		BABR	$e^+e^- \to \Upsilon(4S)$
$4.3 \pm 0.9 \pm 0.9$		[3] YANG	05	BELL	$e^+e^- \to \Upsilon(4S)$
• • • We do not use the following data for averages, fits, limits, etc. • • •					
< 9.9	90	[3] NISHIDA	02	BELL	Repl. by YANG 05
<730	90	[4] ALBRECHT	89G	ARG	$e^+e^- \to \Upsilon(4S)$

[1] Requires $M_{K\pi\pi} < 1.8$ GeV/c^2.

[2] Uses $B(\Upsilon(4S) \to B^+B^-) = 0.513 \pm 0.006$.

[3] Assumes equal production of B^+ and B^0 at the $\Upsilon(4S)$.

[4] ALBRECHT 89G reports < 0.0066 assuming the $\Upsilon(4S)$ decays 45% to $B^0\overline{B}^0$. We rescale to 50%.

$\Gamma(\eta K^+\gamma)/\Gamma_{total}$ Γ_{438}/Γ

VALUE (units 10^{-6})	DOCUMENT ID		TECN	COMMENT
7.9±0.9 OUR AVERAGE				
$7.7 \pm 1.0 \pm 0.4$	[1,2] AUBERT	09	BABR	$e^+e^- \to \Upsilon(4S)$
$8.4 \pm 1.5^{+1.2}_{-0.9}$	[2,3] NISHIDA	05	BELL	$e^+e^- \to \Upsilon(4S)$
• • • We do not use the following data for averages, fits, limits, etc. • • •				
$10.0 \pm 1.3 \pm 0.5$	[1,2] AUBERT,B	06M	BABR	Repl. by AUBERT 09

[1] $m_{\eta K} < 3.25$ GeV/c^2.

[2] Assumes equal production of B^+ and B^0 at the $\Upsilon(4S)$.

[3] $m_{\eta K} < 2.4$ GeV/c^2

$\Gamma(\eta' K^+\gamma)/\Gamma_{total}$ Γ_{439}/Γ

VALUE (units 10^{-6})	DOCUMENT ID		TECN	COMMENT
2.9 $^{+1.0}_{-0.9}$ OUR AVERAGE				
$3.6 \pm 1.2 \pm 0.4$	[1,2] WEDD	10	BELL	$e^+e^- \to \Upsilon(4S)$
$1.9^{+1.5}_{-1.2} \pm 0.1$	[1,3] AUBERT,B	06M	BABR	$e^+e^- \to \Upsilon(4S)$

[1] Assumes equal production of B^+ and B^0 at the $\Upsilon(4S)$.

[2] $m_{\eta' K} < 3.4$ GeV/c^2.

[3] Set the upper limit of 4.2×10^{-6} at 90% CL with $m_{\eta' K} < 3.25$ GeV/c^2.

$\Gamma(\phi K^+\gamma)/\Gamma_{total}$ Γ_{440}/Γ

VALUE (units 10^{-6})	DOCUMENT ID		TECN	COMMENT
2.7 ±0.4 OUR AVERAGE Error includes scale factor of 1.2.				
$2.48 \pm 0.30 \pm 0.24$	[1] SAHOO	11A	BELL	$e^+e^- \to \Upsilon(4S)$
$3.5 \pm 0.6 \pm 0.4$	[1] AUBERT	07Q	BABR	$e^+e^- \to \Upsilon(4S)$
• • • We do not use the following data for averages, fits, limits, etc. • • •				
$3.4 \pm 0.9 \pm 0.4$	[1] DRUTSKOY	04	BELL	Repl. by SAHOO 11A

[1] Assumes equal production of B^+ and B^0 at $\Upsilon(4S)$.

$\Gamma(K^+\pi^-\pi^+\gamma)/\Gamma_{total}$ Γ_{441}/Γ

VALUE (units 10^{-5})	DOCUMENT ID		TECN	COMMENT
2.58±0.15 OUR AVERAGE Error includes scale factor of 1.3. See the ideogram below.				
$2.45 \pm 0.09 \pm 0.12$	[1,2] DEL-AMO-SA...16		BABR	$e^+e^- \to \Upsilon(4S)$
$2.95 \pm 0.13 \pm 0.20$	[1,3] AUBERT	07R	BABR	$e^+e^- \to \Upsilon(4S)$
$2.50 \pm 0.18 \pm 0.22$	[3,4] YANG	05	BELL	$e^+e^- \to \Upsilon(4S)$
• • • We do not use the following data for averages, fits, limits, etc. • • •				
$2.4 \pm 0.5\ ^{+0.4}_{-0.2}$	[3,5] NISHIDA	02	BELL	Repl. by YANG 05

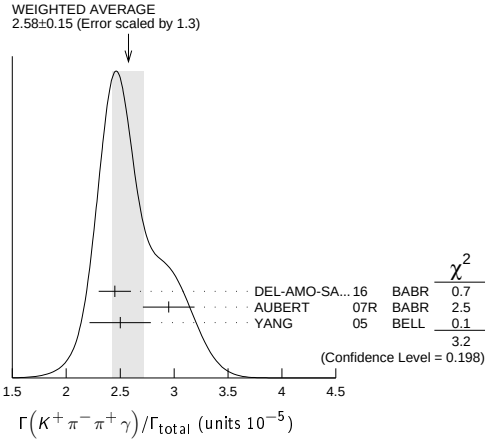

[1] $M_{K\pi\pi} < 1.8$ GeV/c^2.

[2] Uses B($\Upsilon(4S) \to B^+B^-$) = 0.513 ± 0.006.
[3] Assumes equal production of B^+ and B^0 at the $\Upsilon(4S)$.
[4] $M_{K\pi\pi} < 2.0$ GeV/c^2.
[5] $M_{K\pi\pi} < 2.4$ GeV/c^2.

$\Gamma(K^*(892)^0\pi^+\gamma)/\Gamma_{total}$ Γ_{442}/Γ

VALUE (units 10^{-5})	DOCUMENT ID		TECN	COMMENT
2.33±0.12 OUR AVERAGE				
$2.34 \pm 0.09^{+0.08}_{-0.07}$	[1,2] DEL-AMO-SA...16		BABR	$e^+e^- \to \Upsilon(4S)$
$2.0\ ^{+0.7}_{-0.6} \pm 0.2$	[3,4] NISHIDA	02	BELL	$e^+e^- \to \Upsilon(4S)$

[1] Requires $M_{K\pi\pi} < 1.8$ GeV/c^2.
[2] Uses B($\Upsilon(4S) \to B^+B^-$) = 0.513 ± 0.006.
[3] Assumes equal production of B^+ and B^0 at the $\Upsilon(4S)$.
[4] $M_{K\pi\pi} < 2.4$ GeV/c^2.

$\Gamma(K^+\rho^0\gamma)/\Gamma_{total}$ Γ_{443}/Γ

VALUE (units 10^{-6})	CL%	DOCUMENT ID		TECN	COMMENT
8.2±0.4±0.8		[1,2] DEL-AMO-SA...16		BABR	$e^+e^- \to \Upsilon(4S)$
• • • We do not use the following data for averages, fits, limits, etc. • • •					
<20	90	[3,4] NISHIDA	02	BELL	$e^+e^- \to \Upsilon(4S)$

[1] Requires $M_{K\pi\pi} < 1.8$ GeV/c^2.
[2] Uses B($\Upsilon(4S) \to B^+B^-$) = 0.513 ± 0.006.
[3] Assumes equal production of B^+ and B^0 at the $\Upsilon(4S)$.
[4] $M_{K\pi\pi} < 2.4$ GeV/c^2.

$\Gamma((K^+\pi^-)_{NR}\pi^+\gamma)/\Gamma_{total}$ Γ_{444}/Γ

VALUE (units 10^{-6})	CL%	DOCUMENT ID		TECN	COMMENT
$\mathbf{9.9 \pm 0.7^{+1.5}_{-1.9}}$		[1,2] DEL-AMO-SA...16		BABR	$e^+e^- \to \Upsilon(4S)$
• • • We do not use the following data for averages, fits, limits, etc. • • •					
<9.2	90	[3,4] NISHIDA	02	BELL	$e^+e^- \to \Upsilon(4S)$

[1] Requires $M_{K\pi\pi} < 1.8$ GeV/c^2.
[2] Uses B($\Upsilon(4S) \to B^+B^-$) = 0.513 ± 0.006.
[3] Assumes equal production of B^+ and B^0 at the $\Upsilon(4S)$.
[4] $M_{K\pi\pi} < 2.4$ GeV/c^2.

$\Gamma(K^0\pi^+\pi^0\gamma)/\Gamma_{total}$ Γ_{445}/Γ

VALUE (units 10^{-5})	DOCUMENT ID		TECN	COMMENT
4.56±0.42±0.31	[1,2] AUBERT	07R	BABR	$e^+e^- \to \Upsilon(4S)$

[1] $M_{K\pi\pi} < 1.8$ GeV/c^2.
[2] Assumes equal production of B^+ and B^0 at the $\Upsilon(4S)$.

$\Gamma(K_1(1400)^+\gamma)/\Gamma_{total}$ Γ_{446}/Γ

VALUE (units 10^{-6})	CL%	DOCUMENT ID		TECN	COMMENT
$\mathbf{9.7^{+4.6}_{-2.9} \pm 2.4}$		[1,2] DEL-AMO-SA...16		BABR	$e^+e^- \to \Upsilon(4S)$
• • • We do not use the following data for averages, fits, limits, etc. • • •					
< 15	90	[3] YANG	05	BELL	$e^+e^- \to \Upsilon(4S)$
< 50	90	[3] NISHIDA	02	BELL	Repl. by YANG 05
<2200	90	[4] ALBRECHT	89G	ARG	$e^+e^- \to \Upsilon(4S)$

[1] Requires $M_{K\pi\pi} < 1.8$ GeV/c^2.
[2] Uses B($\Upsilon(4S) \to B^+B^-$) = 0.513 ± 0.006.
[3] Assumes equal production of B^+ and B^0 at the $\Upsilon(4S)$.
[4] ALBRECHT 89G reports < 0.0020 assuming the $\Upsilon(4S)$ decays 45% to $B^0\overline{B}^0$. We rescale to 50%.

$\Gamma(K^*(1410)^+\gamma)/\Gamma_{total}$ Γ_{447}/Γ

VALUE (units 10^{-5})	DOCUMENT ID		TECN	COMMENT
$\mathbf{2.71^{+0.54}_{-0.48} \pm 0.59}$	[1,2] DEL-AMO-SA...16		BABR	$e^+e^- \to \Upsilon(4S)$

[1] Requires $M_{K\pi\pi} < 1.8$ GeV/c^2.
[2] Uses B($\Upsilon(4S) \to B^+B^-$) = 0.513 ± 0.006.

$\Gamma(K_0^*(1430)^0\pi^+\gamma)/\Gamma_{total}$ Γ_{448}/Γ

VALUE (units 10^{-5})	DOCUMENT ID		TECN	COMMENT
$\mathbf{1.32^{+0.09}_{-0.10} \pm 0.24 \pm 0.30}$	[1,2] DEL-AMO-SA...16		BABR	$e^+e^- \to \Upsilon(4S)$

[1] Requires $M_{K\pi\pi} < 1.8$ GeV/c^2.
[2] Uses B($\Upsilon(4S) \to B^+B^-$) = 0.513 ± 0.006.

$\Gamma(K_2^*(1430)^+\gamma)/\Gamma_{total}$ Γ_{449}/Γ

VALUE (units 10^{-5})	CL%	DOCUMENT ID		TECN	COMMENT
1.4 ±0.4 OUR AVERAGE					
$0.87^{+0.70}_{-0.53} \pm 0.87 \pm 1.04$		[1,2] DEL-AMO-SA...16		BABR	$e^+e^- \to \Upsilon(4S)$
$1.45 \pm 0.40 \pm 0.15$		[3] AUBERT,B	04U	BABR	$e^+e^- \to \Upsilon(4S)$
• • • We do not use the following data for averages, fits, limits, etc. • • •					
<140	90	[4] ALBRECHT	89G	ARG	$e^+e^- \to \Upsilon(4S)$

[1] Requires $M_{K\pi\pi} < 1.8$ GeV/c^2.
[2] Uses B($\Upsilon(4S) \to B^+B^-$) = 0.513 ± 0.006.
[3] Assumes equal production of B^+ and B^0 at the $\Upsilon(4S)$.
[4] ALBRECHT 89G reports < 0.0013 assuming the $\Upsilon(4S)$ decays 45% to $B^0\overline{B}^0$. We rescale to 50%.

$\Gamma(K^*(1680)^+\gamma)/\Gamma_{total}$ Γ_{450}/Γ

VALUE (units 10^{-5})	CL%	DOCUMENT ID		TECN	COMMENT
$\mathbf{6.67^{+0.93}_{-0.78} \pm 1.44 \pm 1.14}$		[1,2] DEL-AMO-SA...16		BABR	$e^+e^- \to \Upsilon(4S)$
• • • We do not use the following data for averages, fits, limits, etc. • • •					
<190	90	[3] ALBRECHT	89G	ARG	$e^+e^- \to \Upsilon(4S)$

[1] Requires $M_{K\pi\pi} < 1.8$ GeV/c^2.
[2] Uses B($\Upsilon(4S) \to B^+B^-$) = 0.513 ± 0.006.
[3] ALBRECHT 89G reports < 0.0017 assuming the $\Upsilon(4S)$ decays 45% to $B^0\overline{B}^0$. We rescale to 50%.

$\Gamma(K_3^*(1780)^+\gamma)/\Gamma_{total}$ Γ_{451}/Γ

VALUE (units 10^{-6})	CL%	DOCUMENT ID		TECN	COMMENT
< 39	90	[1,2] NISHIDA	05	BELL	$e^+e^- \to \Upsilon(4S)$
• • • We do not use the following data for averages, fits, limits, etc. • • •					
<5500	90	[3] ALBRECHT	89G	ARG	$e^+e^- \to \Upsilon(4S)$

[1] Assumes equal production of B^+ and B^0 at the $\Upsilon(4S)$.
[2] Uses B($K_3^*(1780) \to \eta K$) = $0.11^{+0.05}_{-0.04}$.
[3] ALBRECHT 89G reports < 0.005 assuming the $\Upsilon(4S)$ decays 45% to $B^0\overline{B}^0$. We rescale to 50%.

$\Gamma(K_4^*(2045)^+\gamma)/\Gamma_{total}$ Γ_{452}/Γ

VALUE	CL%	DOCUMENT ID		TECN	COMMENT
<0.0099	90	[1] ALBRECHT	89G	ARG	$e^+e^- \to \Upsilon(4S)$

[1] ALBRECHT 89G reports < 0.0090 assuming the $\Upsilon(4S)$ decays 45% to $B^0\overline{B}^0$. We rescale to 50%.

$\Gamma(\rho^+\gamma)/\Gamma_{total}$ Γ_{453}/Γ

VALUE (units 10^{-6})	CL%	DOCUMENT ID		TECN	COMMENT
0.98±0.25 OUR AVERAGE					
$1.20^{+0.42}_{-0.37} \pm 0.20$		[1] AUBERT	08BH	BABR	$e^+e^- \to \Upsilon(4S)$
$0.87^{+0.29}_{-0.27} {}^{+0.09}_{-0.11}$		[1] TANIGUCHI	08	BELL	$e^+e^- \to \Upsilon(4S)$
• • • We do not use the following data for averages, fits, limits, etc. • • •					
$1.10^{+0.37}_{-0.33} \pm 0.09$		[1] AUBERT	07L	BABR	Repl. by AUBERT 08BH
$0.55^{+0.42}_{-0.36} {}^{+0.09}_{-0.08}$		[1] MOHAPATRA	06	BELL	Repl. by TANIGUCHI 08
$0.9\ ^{+0.6}_{-0.5} \pm 0.1$	90	[1] AUBERT	05	BABR	Repl. by AUBERT 07L
< 2.2	90	[1] MOHAPATRA	05	BELL	$e^+e^- \to \Upsilon(4S)$
< 2.1	90	[1] AUBERT	04C	BABR	$e^+e^- \to \Upsilon(4S)$
<13	90	[1,2] COAN	00	CLE2	$e^+e^- \to \Upsilon(4S)$

[1] Assumes equal production of B^+ and B^0 at $\Upsilon(4S)$.
[2] No evidence for a nonresonant $K\pi\gamma$ contamination was seen; the central value assumes no contamination.

$\Gamma(\pi^+\pi^0)/\Gamma_{total}$ Γ_{454}/Γ

VALUE (units 10^{-6})	CL%	DOCUMENT ID		TECN	COMMENT
5.5 ±0.4 OUR AVERAGE		Error includes scale factor of 1.2.			
5.86±0.26±0.38		[1] DUH	13	BELL	$e^+e^- \to \Upsilon(4S)$
5.02±0.46±0.29		[1] AUBERT	07BC	BABR	$e^+e^- \to \Upsilon(4S)$
$4.6\ ^{+1.8}_{-1.6} \pm 0.6 \pm 0.7$		[1] BORNHEIM	03	CLE2	$e^+e^- \to \Upsilon(4S)$
• • • We do not use the following data for averages, fits, limits, etc. • • •					
6.5 ±0.4 ±0.4		[1] LIN	07A	BELL	Repl. by DUH 13
5.8 ±0.6 ±0.4		[1] AUBERT	05L	BABR	Repl. by AUBERT 07BC
5.0 ±1.2 ±0.5		[1] CHAO	04	BELL	Repl. by LIN 07A
$5.5\ ^{+1.0}_{-1.9} \pm 0.6$		[1] AUBERT	03L	BABR	Repl. by AUBERT 05L
$7.4\ ^{+2.3}_{-2.2} \pm 0.9$		[1] CASEY	02	BELL	Repl. by CHAO 04
< 13.4	90	[1] ABE	01H	BELL	$e^+e^- \to \Upsilon(4S)$
< 9.6	90	[1] AUBERT	01E	BABR	$e^+e^- \to \Upsilon(4S)$
< 12.7	90	[1] CRONIN-HEN...00		CLE2	$e^+e^- \to \Upsilon(4S)$
< 20	90	GODANG	98	CLE2	Repl. by CRONIN-HENNESSY 00
< 17	90	ASNER	96	CLE2	Repl. by GODANG 98
< 240	90	[1] ALBRECHT	90B	ARG	$e^+e^- \to \Upsilon(4S)$
<2300	90	[2] BEBEK	87	CLEO	$e^+e^- \to \Upsilon(4S)$

[1] Assumes equal production of B^+ and B^0 at the $\Upsilon(4S)$.
[2] BEBEK 87 assume the $\Upsilon(4S)$ decays 43% to $B^0\overline{B}^0$.

$\Gamma(\pi^+\pi^0)/\Gamma(K^0\pi^+)$ $\Gamma_{454}/\Gamma_{334}$

VALUE	DOCUMENT ID		TECN	COMMENT
0.285±0.02±0.02	LIN	07A	BELL	$e^+e^- \to \Upsilon(4S)$

$\Gamma(\pi^+\pi^+\pi^-)/\Gamma_{total}$ Γ_{455}/Γ

VALUE (units 10^{-6})	CL%	DOCUMENT ID		TECN	COMMENT
$\mathbf{15.2 \pm 0.6^{+1.3}_{-1.2}}$		[1] AUBERT	09L	BABR	$e^+e^- \to \Upsilon(4S)$

Meson Particle Listings

$B^{\pm}$

• • • We do not use the following data for averages, fits, limits, etc. • • •

16.2±1.2±0.9		[1] AUBERT,B	05G	BABR	Repl. by AUBERT 09L
10.9±3.3±1.6		[1] AUBERT	03M	BABR	Repl. by AUBERT 05G
<130	90	[2] ADAM	96D	DLPH	$e^+e^- \to Z$
<220	90	[3] ABREU	95N	DLPH	Sup. by ADAM 96D
<450	90	[4] ALBRECHT	90B	ARG	$e^+e^- \to \Upsilon(4S)$
<190	90	[5] BORTOLETTO	89	CLEO	$e^+e^- \to \Upsilon(4S)$

[1] Assumes equal production of B^0 and B^+ at the $\Upsilon(4S)$; charm and charmonium contributions are subtracted, otherwise no assumptions about intermediate resonances.
[2] ADAM 96D assumes $f_{B^0} = f_{B^-} = 0.39$ and $f_{B_s} = 0.12$.
[3] Assumes a B^0, B^- production fraction of 0.39 and a B_s production fraction of 0.12.
[4] ALBRECHT 90B limit assumes equal production of $B^0\overline{B}{}^0$ and B^+B^- at $\Upsilon(4S)$.
[5] BORTOLETTO 89 reports $< 1.7 \times 10^{-4}$ assuming the $\Upsilon(4S)$ decays 43% to $B^0\overline{B}{}^0$. We rescale to 50%.

$\Gamma(\rho^0\pi^+)/\Gamma_{total}$ Γ_{456}/Γ

VALUE (units 10^{-6})	CL%	DOCUMENT ID		TECN	COMMENT
8.3±1.2 OUR AVERAGE					
$8.1\pm0.7^{+1.3}_{-1.6}$		[1] AUBERT	09L	BABR	$e^+e^- \to \Upsilon(4S)$
$8.0^{+2.3}_{-2.0}\pm0.7$		[1] GORDON	02	BELL	$e^+e^- \to \Upsilon(4S)$
$10.4^{+3.3}_{-3.4}\pm2.1$		[1] JESSOP	00	CLE2	$e^+e^- \to \Upsilon(4S)$

• • • We do not use the following data for averages, fits, limits, etc. • • •

$8.8\pm1.0^{+0.6}_{-0.9}$		[1] AUBERT,B	05G	BABR	Repl. by AUBERT 09L
9.5±1.1±0.9		[1] AUBERT	04Z	BABR	Repl. by AUBERT 05G
< 83	90	[2] ABE	00C	SLD	$e^+e^- \to Z$
<160	90	[3] ADAM	96D	DLPH	$e^+e^- \to Z$
< 43	90	ASNER	96	CLE2	Repl. by JESSOP 00
<260	90	[4] ABREU	95N	DLPH	Sup. by ADAM 96D
<150	90	[1] ALBRECHT	90B	ARG	$e^+e^- \to \Upsilon(4S)$
<170	90	[5] BORTOLETTO	89	CLEO	$e^+e^- \to \Upsilon(4S)$
<230	90	[5] BEBEK	87	CLEO	$e^+e^- \to \Upsilon(4S)$
<600	90	GILES	84	CLEO	Repl. by BEBEK 87

[1] Assumes equal production of B^+ and B^0 at the $\Upsilon(4S)$.
[2] ABE 00C assumes $B(Z \to b\overline{b}) = (21.7 \pm 0.1)\%$ and the B fractions $f_{B^0} = f_{B^+} = (39.7^{+1.8}_{-2.2})\%$ and $f_{B_s} = (10.5^{+1.8}_{-2.2})\%$.
[3] ADAM 96D assumes $f_{B^0} = f_{B^-} = 0.39$ and $f_{B_s} = 0.12$.
[4] Assumes a B^0, B^- production fraction of 0.39 and a B_s production fraction of 0.12.
[5] Papers assume the $\Upsilon(4S)$ decays 43% to $B^0\overline{B}{}^0$. We rescale to 50%.

$[\Gamma(K^*(892)^0\pi^+) + \Gamma(\rho^0\pi^+)]/\Gamma_{total}$ $(\Gamma_{360}+\Gamma_{456})/\Gamma$

VALUE (units 10^{-6})	DOCUMENT ID		TECN	COMMENT
$\mathbf{170^{+120}_{-80}\pm20}$	[1] ADAM	96D	DLPH	$e^+e^- \to Z$

[1] ADAM 96D assumes $f_{B^0} = f_{B^-} = 0.39$ and $f_{B_s} = 0.12$.

$\Gamma(\pi^+ f_0(980),\ f_0 \to \pi^+\pi^-)/\Gamma_{total}$ Γ_{457}/Γ

VALUE (units 10^{-6})	CL%	DOCUMENT ID		TECN	COMMENT
< 1.5	90	[1] AUBERT	09L	BABR	$e^+e^- \to \Upsilon(4S)$

• • • We do not use the following data for averages, fits, limits, etc. • • •

< 3.0	90	[1] AUBERT,B	05G	BABR	Repl. by AUBERT 09L
<140	90	[2] BORTOLETTO	89	CLEO	$e^+e^- \to \Upsilon(4S)$

[1] Assumes equal production of B^+ and B^0 at the $\Upsilon(4S)$.
[2] BORTOLETTO 89 reports $< 1.2 \times 10^{-4}$ assuming the $\Upsilon(4S)$ decays 43% to $B^0\overline{B}{}^0$. We rescale to 50%.

$\Gamma(\pi^+ f_2(1270))/\Gamma_{total}$ Γ_{458}/Γ

VALUE (units 10^{-6})	CL%	DOCUMENT ID		TECN	COMMENT
$\mathbf{1.60^{+0.67}_{-0.44}{}^{+0.02}_{-0.06}}$		[1,2] AUBERT	09L	BABR	$e^+e^- \to \Upsilon(4S)$

• • • We do not use the following data for averages, fits, limits, etc. • • •

$4.10\pm1.28^{+0.04}_{-0.14}$		[2,3] AUBERT,B	05G	BABR	Repl. by AUBERT 09L
<240	90	[4] BORTOLETTO	89	CLEO	$e^+e^- \to \Upsilon(4S)$

[1] AUBERT 09L reports $[\Gamma(B^+ \to \pi^+ f_2(1270))/\Gamma_{total}] \times [B(f_2(1270) \to \pi^+\pi^-)] = (0.9 \pm 0.2 \pm 0.1^{+0.3}_{-0.1}) \times 10^{-6}$ which we divide by our best value $B(f_2(1270) \to \pi^+\pi^-) = (56.2^{+1.9}_{-0.6}) \times 10^{-2}$. Our first error is their experiment's error and our second error is the systematic error from using our best value.
[2] Assumes equal production of B^+ and B^0 at the $\Upsilon(4S)$.
[3] AUBERT,B 05G reports $[\Gamma(B^+ \to \pi^+ f_2(1270))/\Gamma_{total}] \times [B(f_2(1270) \to \pi^+\pi^-)] = (2.3 \pm 0.6 \pm 0.4) \times 10^{-6}$ which we divide by our best value $B(f_2(1270) \to \pi^+\pi^-) = (56.2^{+1.9}_{-0.6}) \times 10^{-2}$. Our first error is their experiment's error and our second error is the systematic error from using our best value.
[4] BORTOLETTO 89 reports $< 2.1 \times 10^{-4}$ assuming the $\Upsilon(4S)$ decays 43% to $B^0\overline{B}{}^0$. We rescale to 50%.

$\Gamma(\rho(1450)^0\pi^+,\ \rho^0 \to \pi^+\pi^-)/\Gamma_{total}$ Γ_{459}/Γ

VALUE (units 10^{-6})	CL%	DOCUMENT ID		TECN	COMMENT
$\mathbf{1.4\pm0.4^{+0.5}_{-0.8}}$		[1] AUBERT	09L	BABR	$e^+e^- \to \Upsilon(4S)$

• • • We do not use the following data for averages, fits, limits, etc. • • •

<2.3	90	[1] AUBERT,B	05G	BABR	Repl. by AUBERT 09L

[1] Assumes equal production of B^+ and B^0 at the $\Upsilon(4S)$.

$\Gamma(f_0(1370)\pi^+,\ f_0 \to \pi^+\pi^-)/\Gamma_{total}$ Γ_{460}/Γ

VALUE (units 10^{-6})	CL%	DOCUMENT ID		TECN	COMMENT
<4.0	90	[1] AUBERT	09L	BABR	$e^+e^- \to \Upsilon(4S)$

• • • We do not use the following data for averages, fits, limits, etc. • • •

<3.0	90	[1] AUBERT,B	05G	BABR	Repl. by AUBERT 09L

[1] Assumes equal production of B^+ and B^0 at the $\Upsilon(4S)$.

$\Gamma(f_0(500)\pi^+,\ f_0 \to \pi^+\pi^-)/\Gamma_{total}$ Γ_{461}/Γ

VALUE (units 10^{-6})	CL%	DOCUMENT ID		TECN	COMMENT
<4.1	90	[1] AUBERT,B	05G	BABR	$e^+e^- \to \Upsilon(4S)$

[1] Assumes equal production of B^+ and B^0 at the $\Upsilon(4S)$.

$\Gamma(\pi^+\pi^-\pi^+ \text{nonresonant})/\Gamma_{total}$ Γ_{462}/Γ

VALUE (units 10^{-6})	CL%	DOCUMENT ID		TECN	COMMENT
$\mathbf{5.3\pm0.7^{+1.3}_{-0.8}}$		[1] AUBERT	09L	BABR	$e^+e^- \to \Upsilon(4S)$

• • • We do not use the following data for averages, fits, limits, etc. • • •

< 4.6	90	[1] AUBERT,B	05G	BABR	Repl. by AUBERT 09L
<41	90	BERGFELD	96B	CLE2	$e^+e^- \to \Upsilon(4S)$

[1] Assumes equal production of B^+ and B^0 at the $\Upsilon(4S)$.

$\Gamma(\pi^+\pi^0\pi^0)/\Gamma_{total}$ Γ_{463}/Γ

VALUE	CL%	DOCUMENT ID		TECN	COMMENT
$\mathbf{<8.9 \times 10^{-4}}$	90	[1] ALBRECHT	90B	ARG	$e^+e^- \to \Upsilon(4S)$

[1] ALBRECHT 90B limit assumes equal production of $B^0\overline{B}{}^0$ and B^+B^- at $\Upsilon(4S)$.

$\Gamma(\rho^+\pi^0)/\Gamma_{total}$ Γ_{464}/Γ

VALUE (units 10^{-6})	CL%	DOCUMENT ID		TECN	COMMENT
10.9±1.4 OUR AVERAGE					
10.2±1.4±0.9		[1] AUBERT	07X	BABR	$e^+e^- \to \Upsilon(4S)$
$13.2\pm2.3^{+1.4}_{-1.9}$		[1] ZHANG	05A	BELL	$e^+e^- \to \Upsilon(4S)$

• • • We do not use the following data for averages, fits, limits, etc. • • •

10.9±1.9±1.9		[1] AUBERT	04Z	BABR	Repl. by AUBERT 07X
< 43	90	[1,2] JESSOP	00	CLE2	$e^+e^- \to \Upsilon(4S)$
< 77	90	ASNER	96	CLE2	Repl. by JESSOP 00
<550	90	[1] ALBRECHT	90B	ARG	$e^+e^- \to \Upsilon(4S)$

[1] Assumes equal production of B^+ and B^0 at the $\Upsilon(4S)$.
[2] Assumes no nonresonant contributions of $B^+ \to \pi^+\pi^0\pi^0$.

$\Gamma(\pi^+\pi^-\pi^+\pi^0)/\Gamma_{total}$ Γ_{465}/Γ

VALUE	CL%	DOCUMENT ID		TECN	COMMENT
$\mathbf{<4.0 \times 10^{-3}}$	90	[1] ALBRECHT	90B	ARG	$e^+e^- \to \Upsilon(4S)$

[1] ALBRECHT 90B limit assumes equal production of $B^0\overline{B}{}^0$ and B^+B^- at $\Upsilon(4S)$.

$\Gamma(\rho^+\rho^0)/\Gamma_{total}$ Γ_{466}/Γ

VALUE (units 10^{-6})	CL%	DOCUMENT ID		TECN	COMMENT
24.0±1.9 OUR AVERAGE					
23.7±1.4±1.4		[1] AUBERT	09G	BABR	$e^+e^- \to \Upsilon(4S)$
$31.7\pm7.1^{+3.8}_{-6.7}$		[1,2] ZHANG	03B	BELL	$e^+e^- \to \Upsilon(4S)$

• • • We do not use the following data for averages, fits, limits, etc. • • •

16.8±2.2±2.3		[1] AUBERT,BE	06G	BABR	Repl. by AUBERT 09G
$22.5^{+5.7}_{-5.4}\pm5.8$		[1] AUBERT	03V	BABR	Repl. by AUBERT,BE 06G
< 1000	90	[1] ALBRECHT	90B	ARG	$e^+e^- \to \Upsilon(4S)$

[1] Assumes equal production of B^+ and B^0 at the $\Upsilon(4S)$.
[2] The systematic error includes the error associated with the helicity-mix uncertainty.

$\Gamma(\rho^+ f_0(980),\ f_0 \to \pi^+\pi^-)/\Gamma_{total}$ Γ_{467}/Γ

VALUE (units 10^{-6})	CL%	DOCUMENT ID		TECN	COMMENT
<2.0	90	[1] AUBERT	09G	BABR	$e^+e^- \to \Upsilon(4S)$

• • • We do not use the following data for averages, fits, limits, etc. • • •

<1.9	90	[1] AUBERT,BE	06G	BABR	Repl. by AUBERT 09G

[1] Assumes equal production of B^+ and B^0 at the $\Upsilon(4S)$.

$\Gamma(a_1(1260)^+\pi^0)/\Gamma_{total}$ Γ_{468}/Γ

VALUE (units 10^{-6})	CL%	DOCUMENT ID		TECN	COMMENT
$\mathbf{26.4\pm5.4\pm4.1}$		[1,2] AUBERT	07BL	BABR	$e^+e^- \to \Upsilon(4S)$

• • • We do not use the following data for averages, fits, limits, etc. • • •

<1700	90	[1] ALBRECHT	90B	ARG	$e^+e^- \to \Upsilon(4S)$

[1] Assumes equal production of B^+ and B^0 at the $\Upsilon(4S)$.
[2] Assumes a_1^+ decays only to 3π and $B(a_1^+ \to \pi^\pm\pi^\mp\pi^+) = 0.5$.

$\Gamma(a_1(1260)^0\pi^+)/\Gamma_{total}$ Γ_{469}/Γ

VALUE (units 10^{-6})	CL%	DOCUMENT ID		TECN	COMMENT
20.4±4.7±3.4		[1,2] AUBERT	07BL	BABR	$e^+e^- \to \Upsilon(4S)$

• • • We do not use the following data for averages, fits, limits, etc. • • •

<900	90	[1] ALBRECHT	90B	ARG	$e^+e^- \to \Upsilon(4S)$	

[1] Assumes equal production of B^+ and B^0 at the $\Upsilon(4S)$.
[2] Assumes a_1^0 decays only to 3π and $B(a_1^+ \to \pi^\pm\pi^\mp\pi^0) = 1.0$.

$\Gamma(\omega\pi^+)/\Gamma_{total}$ Γ_{470}/Γ

VALUE (units 10^{-6})	CL%	DOCUMENT ID		TECN	COMMENT
6.9±0.5 OUR AVERAGE					
6.7±0.5±0.4		[1] AUBERT	07AE	BABR	$e^+e^- \to \Upsilon(4S)$
6.9±0.6±0.5		[1] JEN	06	BELL	$e^+e^- \to \Upsilon(4S)$
$11.3^{+3.3}_{-2.9}$±1.4		[1] JESSOP	00	CLE2	$e^+e^- \to \Upsilon(4S)$
• • • We do not use the following data for averages, fits, limits, etc. • • •					
6.1±0.7±0.4		[1] AUBERT,B	06E	BABR	Repl. by AUBERT 07AE
5.5±0.9±0.5		[1] AUBERT	04H	BABR	Repl. by AUBERT,B 06E
$5.7^{+1.4}_{-1.3}$±0.6		[1] WANG	04A	BELL	Repl. by JEN 06
$4.2^{+2.0}_{-1.8}$±0.5		[1] LU	02	BELL	Repl. by WANG 04A
$6.6^{+2.1}_{-1.8}$±0.7		[1] AUBERT	01G	BABR	Repl. by AUBERT 04H
< 23	90	[1] BERGFELD	98	CLE2	Repl. by JESSOP 00
<400	90	[1] ALBRECHT	90B	ARG	$e^+e^- \to \Upsilon(4S)$

[1] Assumes equal production of B^+ and B^0 at the $\Upsilon(4S)$.

$\Gamma(\omega\rho^+)/\Gamma_{total}$ Γ_{471}/Γ

VALUE (units 10^{-6})	CL%	DOCUMENT ID		TECN	COMMENT
15.9±1.6±1.4		[1] AUBERT	09H	BABR	$e^+e^- \to \Upsilon(4S)$
• • • We do not use the following data for averages, fits, limits, etc. • • •					
$10.6\pm2.1^{+1.6}_{-1.0}$		[1] AUBERT,B	06T	BABR	Repl. by AUBERT 09H
$12.6^{+3.7}_{-3.3}$±1.6		[1] AUBERT	05O	BABR	Repl. by AUBERT,B 06T
<61	90	[1] BERGFELD	98	CLE2	

[1] Assumes equal production of B^+ and B^0 at the $\Upsilon(4S)$.

$\Gamma(\eta\pi^+)/\Gamma_{total}$ Γ_{472}/Γ

VALUE (units 10^{-6})	CL%	DOCUMENT ID		TECN	COMMENT
4.02±0.27 OUR AVERAGE					
4.07±0.26±0.21		[1] HOI	12	BELL	$e^+e^- \to \Upsilon(4S)$
4.00±0.40±0.24		[1] AUBERT	09AV	BABR	$e^+e^- \to \Upsilon(4S)$
$1.2\ ^{+2.8}_{-1.2}$		[1] RICHICHI	00	CLE2	$e^+e^- \to \Upsilon(4S)$
• • • We do not use the following data for averages, fits, limits, etc. • • •					
5.0 ±0.5 ±0.3		[1] AUBERT	07AE	BABR	Repl. by AUBERT 09AV
4.2 ±0.4 ±0.2		[1] CHANG	07B	BELL	Repl. by HOI 12
5.1 ±0.6 ±0.3		[1] AUBERT,B	05K	BABR	Repl. by AUBERT 07AE
4.8 ±0.7 ±0.3		[1] CHANG	05A	BELL	Repl. by CHANG 07B
5.3 ±1.0 ±0.3		[1] AUBERT	04H	BABR	Repl. by AUBERT,B 05K
< 15	90	BEHRENS	98	CLE2	Repl. by RICHICHI 00
<700	90	[1] ALBRECHT	90B	ARG	$e^+e^- \to \Upsilon(4S)$

[1] Assumes equal production of B^+ and B^0 at the $\Upsilon(4S)$.

$\Gamma(\eta\rho^+)/\Gamma_{total}$ Γ_{473}/Γ

VALUE (units 10^{-6})	CL%	DOCUMENT ID		TECN	COMMENT
7.0±2.9 OUR AVERAGE Error includes scale factor of 2.8.					
9.9±1.2±0.8		[1] AUBERT	08AH	BABR	$e^+e^- \to \Upsilon(4S)$
$4.1^{+1.4}_{-1.3}$±0.4		[1] WANG	07B	BELL	$e^+e^- \to \Upsilon(4S)$
• • • We do not use the following data for averages, fits, limits, etc. • • •					
8.4±1.9±1.1		[1] AUBERT,B	05K	BABR	Repl. by AUBERT 08AH
<14	90	[1] AUBERT,B	04D	BABR	Repl. by AUBERT,B 05K
<15	90	[1] RICHICHI	00	CLE2	$e^+e^- \to \Upsilon(4S)$
<32	90	BEHRENS	98	CLE2	Repl. by RICHICHI 00

[1] Assumes equal production of B^+ and B^0 at the $\Upsilon(4S)$.

$\Gamma(\eta'\pi^+)/\Gamma_{total}$ Γ_{474}/Γ

VALUE (units 10^{-6})	CL%	DOCUMENT ID		TECN	COMMENT
2.7 ±0.9 OUR AVERAGE Error includes scale factor of 1.9.					
3.5 ±0.6 ±0.2		[1] AUBERT	09AV	BABR	$e^+e^- \to \Upsilon(4S)$
$1.76^{+0.67+0.15}_{-0.62-0.14}$		[1] SCHUEMANN	06	BELL	$e^+e^- \to \Upsilon(4S)$
• • • We do not use the following data for averages, fits, limits, etc. • • •					
3.9 ±0.7 ±0.3		[1] AUBERT	07AE	BABR	Repl. by AUBERT 09AV
4.0 ±0.8 ±0.4		[1] AUBERT,B	05K	BABR	Repl. by AUBERT 07AE
< 4.5	90	[1] AUBERT	04H	BABR	Repl. by AUBERT,B 05K
< 7.0	90	[1] ABE	01M	BELL	$e^+e^- \to \Upsilon(4S)$
<12	90	[1] AUBERT	01G	BABR	$e^+e^- \to \Upsilon(4S)$
<12	90	[1] RICHICHI	00	CLE2	$e^+e^- \to \Upsilon(4S)$
<31	90	BEHRENS	98	CLE2	Repl. by RICHICHI 00

[1] Assumes equal production of B^+ and B^0 at the $\Upsilon(4S)$.

$\Gamma(\eta'\rho^+)/\Gamma_{total}$ Γ_{475}/Γ

VALUE (units 10^{-6})	CL%	DOCUMENT ID		TECN	COMMENT
$\mathbf{9.7^{+1.9}_{-1.8}\pm1.1}$		[1] DEL-AMO-SA...10A		BABR	$e^+e^- \to \Upsilon(4S)$
• • • We do not use the following data for averages, fits, limits, etc. • • •					
$8.7^{+3.1+2.3}_{-2.8-1.3}$		[1] AUBERT	07E	BABR	Repl. by DEL-AMO-SANCHEZ 10A
< 5.8	90	[1] SCHUEMANN	07	BELL	$e^+e^- \to \Upsilon(4S)$
<22	90	[1] AUBERT,B	04D	BABR	Repl. by AUBERT 07E
<33	90	[1] RICHICHI	00	CLE2	$e^+e^- \to \Upsilon(4S)$
<47	90	BEHRENS	98	CLE2	Repl. by RICHICHI 00

[1] Assumes equal production of B^+ and B^0 at the $\Upsilon(4S)$.

$\Gamma(\phi\pi^+)/\Gamma_{total}$ Γ_{476}/Γ

VALUE (units 10^{-7})	CL%	DOCUMENT ID		TECN	COMMENT
< 1.5	90	[1] AAIJ	14A	LHCB	pp at 7 TeV
• • • We do not use the following data for averages, fits, limits, etc. • • •					
< 3.3	90	[2] KIM	12A	BELL	$e^+e^- \to \Upsilon(4S)$
< 2.4	90	[2] AUBERT,B	06C	BABR	$e^+e^- \to \Upsilon(4S)$
< 4.1	90	[2] AUBERT	04A	BABR	Repl. by AUBERT,B 06C
< 14	90	[2] AUBERT	01D	BABR	$e^+e^- \to \Upsilon(4S)$
<1530	90	[3] ABE	00C	SLD	$e^+e^- \to Z$
< 50	90	[2] BERGFELD	98	CLE2	

[1] Measures $B(B^+ \to \phi\pi^+)/B(B^+ \to \phi K^+) < 0.018$ at 90% C.L. and assumes $B(B^+ \to \phi K^+) = (8.8^{+0.7}_{-0.6}) \times 10^{-6}$.
[2] Assumes equal production of B^+ and B^0 at the $\Upsilon(4S)$.
[3] ABE 00C assumes $B(Z \to b\overline{b}) = (21.7 \pm 0.1)\%$ and the B fractions $f_{B^0} = f_{B^+} = (39.7^{+1.8}_{-2.2})\%$ and $f_{B_s} = (10.5^{+1.8}_{-2.2})\%$.

$\Gamma(\phi\rho^+)/\Gamma_{total}$ Γ_{477}/Γ

VALUE (units 10^{-6})	CL%	DOCUMENT ID		TECN	COMMENT
< 3.0	90	[1] AUBERT	08BK	BABR	$e^+e^- \to \Upsilon(4S)$
• • • We do not use the following data for averages, fits, limits, etc. • • •					
<16		[1] BERGFELD	98	CLE2	

[1] Assumes equal production of B^+ and B^0 at the $\Upsilon(4S)$.

$\Gamma(a_0(980)^0\pi^+,\ a_0^0 \to \eta\pi^0)/\Gamma_{total}$ Γ_{478}/Γ

VALUE (units 10^{-6})	CL%	DOCUMENT ID		TECN	COMMENT
<5.8	90	[1] AUBERT,BE	04	BABR	$e^+e^- \to \Upsilon(4S)$

[1] Assumes equal production of charged and neutral B mesons from $\Upsilon(4S)$ decays.

$\Gamma(a_0(980)^+\pi^0,\ a_0^+ \to \eta\pi^+)/\Gamma_{total}$ Γ_{479}/Γ

VALUE (units 10^{-6})	CL%	DOCUMENT ID		TECN	COMMENT
<1.4	90	[1] AUBERT	08A	BABR	$e^+e^- \to \Upsilon(4S)$

[1] Assumes equal production of B^+ and B^0 at the $\Upsilon(4S)$.

$\Gamma(\pi^+\pi^+\pi^+\pi^-\pi^-)/\Gamma_{total}$ Γ_{480}/Γ

VALUE	CL%	DOCUMENT ID		TECN	COMMENT
$<8.6 \times 10^{-4}$	90	[1] ALBRECHT	90B	ARG	$e^+e^- \to \Upsilon(4S)$

[1] ALBRECHT 90B limit assumes equal production of $B^0\overline{B}^0$ and B^+B^- at $\Upsilon(4S)$.

$\Gamma(\rho^0 a_1(1260)^+)/\Gamma_{total}$ Γ_{481}/Γ

VALUE	CL%	DOCUMENT ID		TECN	COMMENT
$<6.2 \times 10^{-4}$	90	[1] BORTOLETTO89		CLEO	$e^+e^- \to \Upsilon(4S)$
• • • We do not use the following data for averages, fits, limits, etc. • • •					
$<6.0 \times 10^{-4}$	90	[2] ALBRECHT	90B	ARG	$e^+e^- \to \Upsilon(4S)$
$<3.2 \times 10^{-3}$	90	[1] BEBEK	87	CLEO	$e^+e^- \to \Upsilon(4S)$

[1] BORTOLETTO 89 reports $< 5.4 \times 10^{-4}$ assuming the $\Upsilon(4S)$ decays 43% to $B^0\overline{B}^0$. We rescale to 50%.
[2] ALBRECHT 90B limit assumes equal production of $B^0\overline{B}^0$ and B^+B^- at $\Upsilon(4S)$.

$\Gamma(\rho^0 a_2(1320)^+)/\Gamma_{total}$ Γ_{482}/Γ

VALUE	CL%	DOCUMENT ID		TECN	COMMENT
$<7.2 \times 10^{-4}$	90	[1] BORTOLETTO89		CLEO	$e^+e^- \to \Upsilon(4S)$
• • • We do not use the following data for averages, fits, limits, etc. • • •					
$<2.6 \times 10^{-3}$	90	[2] BEBEK	87	CLEO	$e^+e^- \to \Upsilon(4S)$

[1] BORTOLETTO 89 reports $< 6.3 \times 10^{-4}$ assuming the $\Upsilon(4S)$ decays 43% to $B^0\overline{B}^0$. We rescale to 50%.
[2] BEBEK 87reports $< 2.3 \times 10^{-3}$ assuming the $\Upsilon(4S)$ decays 43% to $B^0\overline{B}^0$. We rescale to 50%.

$\Gamma(b_1^0\pi^+,\ b_1^0 \to \omega\pi^0)/\Gamma_{total}$ Γ_{483}/Γ

VALUE (units 10^{-6})	CL%	DOCUMENT ID		TECN	COMMENT
6.7±1.7±1.0		[1] AUBERT	07BI	BABR	$e^+e^- \to \Upsilon(4S)$

[1] Assumes equal production of B^+ and B^0 at the $\Upsilon(4S)$.

$\Gamma(b_1^+\pi^0,\ b_1^+ \to \omega\pi^+)/\Gamma_{total}$ Γ_{484}/Γ

VALUE (units 10^{-6})	CL%	DOCUMENT ID		TECN	COMMENT
<3.3	90	[1] AUBERT	08AG	BABR	$e^+e^- \to \Upsilon(4S)$

[1] Assumes equal production of B^+ and B^0 at the $\Upsilon(4S)$.

$\Gamma(\pi^+\pi^+\pi^+\pi^-\pi^-\pi^0)/\Gamma_{total}$ Γ_{485}/Γ

VALUE	CL%	DOCUMENT ID		TECN	COMMENT
$<6.3 \times 10^{-3}$	90	[1] ALBRECHT	90B	ARG	$e^+e^- \to \Upsilon(4S)$

[1] ALBRECHT 90B limit assumes equal production of $B^0\overline{B}^0$ and B^+B^- at $\Upsilon(4S)$.

$\Gamma(b_1^+\rho^0,\ b_1^+\to\omega\pi^+)/\Gamma_{\rm total}$ Γ_{486}/Γ

VALUE	CL%	DOCUMENT ID		TECN	COMMENT
$<5.2\times10^{-6}$	90	[1] AUBERT	09AF	BABR	$e^+e^-\to\Upsilon(4S)$

[1] Assumes equal production of B^+ and B^0 at the $\Upsilon(4S)$.

$\Gamma(b_1^0\rho^+,\ b_1^0\to\omega\pi^0)/\Gamma_{\rm total}$ Γ_{488}/Γ

VALUE	CL%	DOCUMENT ID		TECN	COMMENT
$<3.3\times10^{-6}$	90	[1] AUBERT	09AF	BABR	$e^+e^-\to\Upsilon(4S)$

[1] Assumes equal production of B^+ and B^0 at the $\Upsilon(4S)$.

$\Gamma(a_1(1260)^+a_1(1260)^0)/\Gamma_{\rm total}$ Γ_{487}/Γ

VALUE	CL%	DOCUMENT ID		TECN	COMMENT
$<1.3\times10^{-2}$	90	[1] ALBRECHT	90B	ARG	$e^+e^-\to\Upsilon(4S)$

[1] ALBRECHT 90B limit assumes equal production of $B^0\overline{B}^0$ and B^+B^- at $\Upsilon(4S)$.

$\Gamma(h^+\pi^0)/\Gamma_{\rm total}$ Γ_{489}/Γ

$h^+ = K^+$ or π^+

VALUE (units 10^{-6})	DOCUMENT ID		TECN	COMMENT
$16^{+6}_{-5}\pm3.6$	GODANG	98	CLE2	$e^+e^-\to\Upsilon(4S)$

$\Gamma(\omega h^+)/\Gamma_{\rm total}$ Γ_{490}/Γ

$h^+ = K^+$ or π^+

VALUE (units 10^{-6})	DOCUMENT ID		TECN	COMMENT
$13.8^{+2.7}_{-2.4}$ OUR AVERAGE				
$13.4^{+3.3}_{-2.9}\pm1.1$	[1] LU	02	BELL	$e^+e^-\to\Upsilon(4S)$
$14.3^{+3.6}_{-3.2}\pm2.0$	[1] JESSOP	00	CLE2	$e^+e^-\to\Upsilon(4S)$
• • • We do not use the following data for averages, fits, limits, etc. • • •				
$25\ ^{+8}_{-7}\ \pm3$	[1] BERGFELD	98	CLE2	Repl. by JESSOP 00

[1] Assumes equal production of B^+ and B^0 at the $\Upsilon(4S)$.

$\Gamma(h^+X^0(\text{Familon}))/\Gamma_{\rm total}$ Γ_{491}/Γ

VALUE (units 10^{-6})	CL%	DOCUMENT ID		TECN	COMMENT
<49	90	[1] AMMAR	01B	CLE2	$e^+e^-\to\Upsilon(4S)$

[1] AMMAR 01B searched for the two-body decay of the B meson to a massless neutral feebly-interacting particle X^0 such as the familon, the Nambu-Goldstone boson associated with a spontaneously broken global family symmetry.

$\Gamma(K^+X^0,\ X^0\to\mu^+\mu^-)/\Gamma_{\rm total}$ Γ_{492}/Γ

X^0 stands here for a long-lived scalar particle.

VALUE	CL%	DOCUMENT ID		TECN	COMMENT
$<1\times10^{-7}$	95	[1] AAIJ	17AQ	LHCB	pp at 7, 8 TeV

[1] AAIJ 17AQ searched for a long-lived scalar particle $X^0\to\mu^+\mu^-$ in the mass range 250–4700 MeV and lifetime range 0.1–1000 ps. The limit is between 10^{-7} and 2×10^{-10} in these ranges except in vetoed mass regions around K^0_S, J/ψ, $\psi(2S)$, and $\psi(3770)$.

$\Gamma(p\overline{p}\pi^+)/\Gamma_{\rm total}$ Γ_{493}/Γ

VALUE (units 10^{-6})	CL%	DOCUMENT ID		TECN	COMMENT
$1.62\pm\ 0.20$ OUR AVERAGE					
$1.60^{+\ 0.22}_{-\ 0.19}\pm\ 0.12$		[1,2,3] WEI	08	BELL	$e^+e^-\to\Upsilon(4S)$
$1.69\pm\ 0.29\pm\ 0.26$		[1] AUBERT	07AV	BABR	$e^+e^-\to\Upsilon(4S)$
• • • We do not use the following data for averages, fits, limits, etc. • • •					
$1.07\pm\ 0.11\pm\ 0.11$		[4] AAIJ	14AF	LHCB	pp at 7, 8 TeV
$3.06^{+\ 0.73}_{-\ 0.62}\pm\ 0.37$		[1,3] WANG	04	BELL	Repl. by WEI 08
$<\ 3.7$	90	[1,2] ABE	02K	BELL	Repl. by WANG 04
<500	90	[5] ABREU	95N	DLPH	Repl. by ADAM 96D
<160	90	[6] BEBEK	89	CLEO	$e^+e^-\to\Upsilon(4S)$
$570\ \ \pm150\ \ \pm210$		[7] ALBRECHT	88F	ARG	$e^+e^-\to\Upsilon(4S)$

[1] Assumes equal production of B^+ and B^0 at the $\Upsilon(4S)$.
[2] Explicitly vetoes resonant production of $p\overline{p}$ from Charmonium states.
[3] Also provides results with $m_{p\overline{p}}<2.85$ GeV/c^2 and angular asymmetry of $p\overline{p}$ system.
[4] Requires $m_{p\overline{p}}<2.85$ GeV/c^2.
[5] Assumes a B^0, B^- production fraction of 0.39 and a B_s production fraction of 0.12.
[6] BEBEK 89 reports $<1.4\times10^{-4}$ assuming the $\Upsilon(4S)$ decays 43% to $B^0\overline{B}^0$. We rescale to 50%.
[7] ALBRECHT 88F reports $(5.2\pm1.4\pm1.9)\times10^{-4}$ assuming the $\Upsilon(4S)$ decays 45% to $B^0\overline{B}^0$. We rescale to 50%.

$\Gamma(p\overline{p}\pi^+\text{nonresonant})/\Gamma_{\rm total}$ Γ_{494}/Γ

VALUE (units 10^{-6})	CL%	DOCUMENT ID		TECN	COMMENT
<53	90	BERGFELD	96B	CLE2	$e^+e^-\to\Upsilon(4S)$

$\Gamma(p\overline{p}\pi^+\pi^+\pi^-)/\Gamma_{\rm total}$ Γ_{495}/Γ

VALUE	CL%	DOCUMENT ID		TECN	COMMENT
• • • We do not use the following data for averages, fits, limits, etc. • • •					
$<5.2\times10^{-4}$	90	[1] ALBRECHT	88F	ARG	$e^+e^-\to\Upsilon(4S)$

[1] ALBRECHT 88F reports $<4.7\times10^{-4}$ assuming the $\Upsilon(4S)$ decays 45% to $B^0\overline{B}^0$. We rescale to 50%.

$\Gamma(p\overline{p}K^+)/\Gamma_{\rm total}$ Γ_{496}/Γ

VALUE (units 10^{-6})	DOCUMENT ID		TECN	COMMENT
$5.9\ \pm0.5$ OUR AVERAGE Error includes scale factor of 1.5.				
$5.54^{+0.27}_{-0.25}\pm0.36$	[1,2,3] WEI	08	BELL	$e^+e^-\to\Upsilon(4S)$
$6.7\ \pm0.5\ \pm0.4$	[1,3] AUBERT,B	05L	BABR	$e^+e^-\to\Upsilon(4S)$
• • • We do not use the following data for averages, fits, limits, etc. • • •				
$4.59^{+0.38}_{-0.34}\pm0.50$	[1,2,3] WANG	05A	BELL	Repl. by WEI 08
$5.66^{+0.67}_{-0.57}\pm0.62$	[1,2,3] WANG	04	BELL	Repl. by WANG 05A
$4.3\ ^{+1.1}_{-0.9}\ \pm0.5$	[1,2] ABE	02K	BELL	Repl. by WANG 04

[1] Assumes equal production of B^+ and B^0 at the $\Upsilon(4S)$.
[2] Explicitly vetoes resonant production of $p\overline{p}$ from Charmonium states.
[3] Provides also results with $m_{p\overline{p}}<2.85$ GeV/c^2 and angular asymmetry of $p\overline{p}$ system.

$\Gamma(p\overline{p}K^+)/\Gamma(J/\psi(1S)K^+)$ $\Gamma_{496}/\Gamma_{268}$

VALUE	DOCUMENT ID		TECN	COMMENT
$0.0104\pm0.0005\pm0.0001$	[1,2] AAIJ	13S	LHCB	pp at 7 TeV

[1] AAIJ 13S reports $[\Gamma(B^+\to p\overline{p}K^+)/\Gamma(B^+\to J/\psi(1S)K^+)]\ /\ [\mathrm{B}(J/\psi(1S)\to p\overline{p})] = 4.91\pm0.19\pm0.14$ which we multiply by our best value $\mathrm{B}(J/\psi(1S)\to p\overline{p}) = (2.121\pm0.029)\times10^{-3}$. Our first error is their experiment's error and our second error is the systematic error from using our best value.
[2] Measurement includes contribution where $p\overline{p}$ is produced in charmonia decays.

$\Gamma(\Theta(1710)^{++}\overline{p},\ \Theta^{++}\to pK^+)/\Gamma_{\rm total}$ Γ_{497}/Γ

VALUE (units 10^{-6})	CL%	DOCUMENT ID		TECN	COMMENT
<0.091	90	[1] WANG	05A	BELL	$e^+e^-\to\Upsilon(4S)$
• • • We do not use the following data for averages, fits, limits, etc. • • •					
<0.1	90	[1,2] AUBERT,B	05L	BABR	$e^+e^-\to\Upsilon(4S)$

[1] Assumes equal production of B^+ and B^0 at the $\Upsilon(4S)$.
[2] Provides upper limits depending on the pentaquark masses between 1.43 to 2.0 GeV/c^2.

$\Gamma(f_J(2220)K^+,\ f_J\to p\overline{p})/\Gamma_{\rm total}$ Γ_{498}/Γ

VALUE (units 10^{-6})	CL%	DOCUMENT ID		TECN	COMMENT
<0.41	90	[1] WANG	05A	BELL	$e^+e^-\to\Upsilon(4S)$

[1] Assumes equal production of B^+ and B^0 at the $\Upsilon(4S)$.

$\Gamma(p\overline{\Lambda}(1520))/\Gamma_{\rm total}$ Γ_{499}/Γ

VALUE (units 10^{-7})	CL%	DOCUMENT ID		TECN	COMMENT
$3.15\pm0.48\pm0.27$		[1] AAIJ	14AF	LHCB	pp at 7, 8 TeV
• • • We do not use the following data for averages, fits, limits, etc. • • •					
$3.9\ ^{+1.0}_{-0.9}\ \pm0.3$		[1] AAIJ	13AU	LHCB	Repl. by AAIJ 14AF
<15	90	[2] AUBERT,B	05L	BABR	$e^+e^-\to\Upsilon(4S)$

[1] Uses $\mathrm{B}(B^+\to J/\psi K^+) = (1.016\pm0.033)\times10^{-3}$, $\mathrm{B}(J/\psi\to p\overline{p}) = (2.17\pm0.07)\times10^{-3}$ and $\mathrm{B}(\Lambda(1520)\to K^-p) = 0.234\pm0.016$.
[2] Assumes equal production of B^+ and B^0 at the $\Upsilon(4S)$.

$\Gamma(p\overline{p}K^+\text{nonresonant})/\Gamma_{\rm total}$ Γ_{500}/Γ

VALUE (units 10^{-6})	CL%	DOCUMENT ID		TECN	COMMENT
<89	90	BERGFELD	96B	CLE2	$e^+e^-\to\Upsilon(4S)$

$\Gamma(p\overline{p}K^*(892)^+)/\Gamma_{\rm total}$ Γ_{501}/Γ

VALUE (units 10^{-6})	DOCUMENT ID		TECN	COMMENT
$3.6\ ^{+0.8}_{-0.7}$ OUR AVERAGE				
$3.38^{+0.73}_{-0.60}\pm0.39$	[1,2] CHEN	08C	BELL	$e^+e^-\to\Upsilon(4S)$
$5.3\ \pm1.5\ \pm1.3$	[2] AUBERT	07AV	BABR	$e^+e^-\to\Upsilon(4S)$
• • • We do not use the following data for averages, fits, limits, etc. • • •				
$10.3\ ^{+3.6}_{-2.8}\ ^{+1.3}_{-1.7}$	[2,3] WANG	04	BELL	Repl. by CHEN 08C

[1] Explicitly vetoes resonant production of $p\overline{p}$ from charmonium states.
[2] Assumes equal production of B^+ and B^0 at the $\Upsilon(4S)$.
[3] Explicitly vetoes resonant production of $p\overline{p}$ from charmonium states. The branching fraction for $M_{p\overline{p}}<2.85$ GeV/c^2 is also reported.

$\Gamma(f_J(2220)K^{*+},\ f_J\to p\overline{p})/\Gamma_{\rm total}$ Γ_{502}/Γ

VALUE (units 10^{-6})	CL%	DOCUMENT ID		TECN	COMMENT
<0.77	90	[1] AUBERT	07AV	BABR	$e^+e^-\to\Upsilon(4S)$

[1] Assumes equal production of B^+ and B^0 at the $\Upsilon(4S)$.

$\Gamma(p\overline{\Lambda})/\Gamma_{\rm total}$ Γ_{503}/Γ

VALUE (units 10^{-6})	CL%	DOCUMENT ID		TECN	COMMENT
$0.24^{+0.10}_{-0.08}\pm0.03$		[1] AAIJ	17R	LHCB	pp at 7, 8 TeV

• • • We do not use the following data for averages, fits, limits, etc. • • •

< 0.32	90	[2] TSAI	07	BELL	$e^+e^- \to \Upsilon(4S)$
< 0.49	90	[2] CHANG	05	BELL	Repl. by TSAI 07
< 1.5	90	[2] BORNHEIM	03	CLE2	$e^+e^- \to \Upsilon(4S)$
< 2.2	90	[2] ABE	02O	BELL	$e^+e^- \to \Upsilon(4S)$
< 2.6	90	[2] COAN	99	CLE2	$e^+e^- \to \Upsilon(4S)$
<60	90	[3] AVERY	89B	CLEO	$e^+e^- \to \Upsilon(4S)$
<93	90	[4] ALBRECHT	88F	ARG	$e^+e^- \to \Upsilon(4S)$

[1] Statistical significance of the signal is 4.1 standard deviations where the the normalisation is based on $B(B^+ \to K^0_S\pi^+) = (11.895 \pm 0.375) \times 10^{-06}$.

[2] Assumes equal production of B^+ and B^0 at the $\Upsilon(4S)$.

[3] AVERY 89B reports $< 5 \times 10^{-5}$ assuming the $\Upsilon(4S)$ decays 43% to $B^0\overline{B}^0$. We rescale to 50%.

[4] ALBRECHT 88F reports $< 8.5 \times 10^{-5}$ assuming the $\Upsilon(4S)$ decays 45% to $B^0\overline{B}^0$. We rescale to 50%.

$\Gamma(p\overline{\Lambda}\gamma)/\Gamma_{total}$ Γ_{504}/Γ

VALUE (units 10^{-6})	CL%	DOCUMENT ID		TECN	COMMENT
$\mathbf{2.45^{+0.44}_{-0.38} \pm 0.22}$		[1] WANG	07C	BELL	$e^+e^- \to \Upsilon(4S)$

• • • We do not use the following data for averages, fits, limits, etc. • • •

$2.16^{+0.58}_{-0.53} \pm 0.20$		[1] LEE	05	BELL	Repl. by WANG 07C
<3.9	90	[2] EDWARDS	03	CLE2	$e^+e^- \to \Upsilon(4S)$

[1] Assumes equal production of B^+ and B^0 at the $\Upsilon(4S)$.

[2] Corresponds to $E_\gamma > 1.5$ GeV. The limit changes to 3.3×10^{-6} for $E_\gamma > 2.0$ GeV.

$\Gamma(p\overline{\Lambda}\pi^0)/\Gamma_{total}$ Γ_{505}/Γ

VALUE (units 10^{-6})	DOCUMENT ID		TECN	COMMENT
$\mathbf{3.00^{+0.61}_{-0.53} \pm 0.33}$	[1] WANG	07C	BELL	$e^+e^- \to \Upsilon(4S)$

[1] Assumes equal production of B^+ and B^0 at the $\Upsilon(4S)$.

$\Gamma(p\overline{\Sigma}(1385)^0)/\Gamma_{total}$ Γ_{506}/Γ

VALUE (units 10^{-6})	CL%	DOCUMENT ID		TECN	COMMENT
<0.47	90	[1] WANG	07C	BELL	$e^+e^- \to \Upsilon(4S)$

[1] Assumes equal production of B^+ and B^0 at the $\Upsilon(4S)$.

$\Gamma(\Delta^+\overline{\Lambda})/\Gamma_{total}$ Γ_{507}/Γ

VALUE (units 10^{-6})	CL%	DOCUMENT ID		TECN	COMMENT
<0.82	90	[1] WANG	07C	BELL	$e^+e^- \to \Upsilon(4S)$

[1] Assumes equal production of B^+ and B^0 at the $\Upsilon(4S)$.

$\Gamma(p\overline{\Sigma}\gamma)/\Gamma_{total}$ Γ_{508}/Γ

VALUE (units 10^{-6})	CL%	DOCUMENT ID		TECN	COMMENT
<4.6	90	[1] LEE	05	BELL	$e^+e^- \to \Upsilon(4S)$

• • • We do not use the following data for averages, fits, limits, etc. • • •

<7.9	90	[2] EDWARDS	03	CLE2	$e^+e^- \to \Upsilon(4S)$

[1] Assumes equal production of B^+ and B^0 at the $\Upsilon(4S)$.

[2] Corresponds to $E_\gamma > 1.5$ GeV. The limit changes to 6.4×10^{-6} for $E_\gamma > 2.0$ GeV.

$\Gamma(p\overline{\Lambda}\pi^+\pi^-)/\Gamma_{total}$ Γ_{509}/Γ

VALUE (units 10^{-6})	CL%	DOCUMENT ID		TECN	COMMENT
$\mathbf{5.92^{+0.88}_{-0.84} \pm 0.69}$		[1] CHEN	09C	BELL	$e^+e^- \to \Upsilon(4S)$

• • • We do not use the following data for averages, fits, limits, etc. • • •

<200	90	[2] ALBRECHT	88F	ARG	$e^+e^- \to \Upsilon(4S)$

[1] Assumes equal production of B^+ and B^0 at the $\Upsilon(4S)$.

[2] ALBRECHT 88F reports $< 1.8 \times 10^{-4}$ assuming the $\Upsilon(4S)$ decays 45% to $B^0\overline{B}^0$. We rescale to 50%.

$\Gamma(p\overline{\Lambda}\rho^0)/\Gamma_{total}$ Γ_{510}/Γ

VALUE (units 10^{-6})	DOCUMENT ID		TECN	COMMENT
$\mathbf{4.78^{+0.67}_{-0.64} \pm 0.60}$	[1] CHEN	09C	BELL	$e^+e^- \to \Upsilon(4S)$

[1] Assumes equal production of B^+ and B^0 at the $\Upsilon(4S)$.

$\Gamma(p\overline{\Lambda}f_2(1270))/\Gamma_{total}$ Γ_{511}/Γ

VALUE (units 10^{-6})	DOCUMENT ID		TECN	COMMENT
$\mathbf{2.03^{+0.77}_{-0.72} \pm 0.27}$	[1] CHEN	09C	BELL	$e^+e^- \to \Upsilon(4S)$

[1] Assumes equal production of B^+ and B^0 at the $\Upsilon(4S)$.

$\Gamma(\Lambda\overline{\Lambda}\pi^+)/\Gamma_{total}$ Γ_{512}/Γ

VALUE (units 10^{-6})	CL%	DOCUMENT ID		TECN	COMMENT
<0.94	90	[1,2] CHANG	09	BELL	Repl. by CHANG 09

• • • We do not use the following data for averages, fits, limits, etc. • • •

<2.8	90	[2] LEE	04	BELL	$e^+e^- \to \Upsilon(4S)$

[1] For $m_{\Lambda\overline{\Lambda}} < 2.85$ GeV/c^2.

[2] Assumes equal production of B^+ and B^0 at the $\Upsilon(4S)$.

$\Gamma(\Lambda\overline{\Lambda}K^+)/\Gamma_{total}$ Γ_{513}/Γ

VALUE (units 10^{-6})	DOCUMENT ID		TECN	COMMENT
$\mathbf{3.38^{+0.41}_{-0.36} \pm 0.41}$	[1,2] CHANG	09	BELL	$e^+e^- \to \Upsilon(4S)$

• • • We do not use the following data for averages, fits, limits, etc. • • •

$2.91^{+0.9}_{-0.70} \pm 0.38$	[2] LEE	04	BELL	Repl. by CHANG 09

[1] Excluding charmonium events in $2.85 < m_{\Lambda\overline{\Lambda}} < 3.128$ GeV/c^2 and $3.315 < m_{\Lambda\overline{\Lambda}} < 3.735$ GeV/c^2. Measurements in various $m_{\Lambda\overline{\Lambda}}$ bins are also reported.

[2] Assumes equal production of B^+ and B^0 at the $\Upsilon(4S)$.

$\Gamma(\Lambda\overline{\Lambda}K^{*+})/\Gamma_{total}$ Γ_{514}/Γ

VALUE (units 10^{-6})	DOCUMENT ID		TECN	COMMENT
$\mathbf{2.19^{+1.13}_{-0.88} \pm 0.33}$	[1,2] CHANG	09	BELL	$e^+e^- \to \Upsilon(4S)$

[1] For $m_{\Lambda\overline{\Lambda}} < 2.85$ GeV/c^2.

[2] Assumes equal production of B^+ and B^0 at the $\Upsilon(4S)$.

$\Gamma(\overline{\Delta}^0 p)/\Gamma_{total}$ Γ_{515}/Γ

VALUE (units 10^{-6})	CL%	DOCUMENT ID		TECN	COMMENT
< 1.38	90	[1] WEI	08	BELL	$e^+e^- \to \Upsilon(4S)$

• • • We do not use the following data for averages, fits, limits, etc. • • •

<380	90	[2] BORTOLETTO	89	CLEO	$e^+e^- \to \Upsilon(4S)$

[1] Assumes equal production of B^+ and B^0 at the $\Upsilon(4S)$.

[2] BORTOLETTO 89 reports $< 3.3 \times 10^{-4}$ assuming the $\Upsilon(4S)$ decays 43% to $B^0\overline{B}^0$. We rescale to 50%.

$\Gamma(\Delta^{++}\overline{p})/\Gamma_{total}$ Γ_{516}/Γ

VALUE (units 10^{-6})	CL%	DOCUMENT ID		TECN	COMMENT
< 0.14	90	[1] WEI	08	BELL	$e^+e^- \to \Upsilon(4S)$

• • • We do not use the following data for averages, fits, limits, etc. • • •

<150	90	[2] BORTOLETTO	89	CLEO	$e^+e^- \to \Upsilon(4S)$

[1] Assumes equal production of B^+ and B^0 at the $\Upsilon(4S)$.

[2] BORTOLETTO 89 reports $< 1.3 \times 10^{-4}$ assuming the $\Upsilon(4S)$ decays 43% to $B^0\overline{B}^0$. We rescale to 50%.

$\Gamma(D^+p\overline{p})/\Gamma_{total}$ Γ_{517}/Γ

VALUE	CL%	DOCUMENT ID		TECN	COMMENT
$\mathbf{< 1.5 \times 10^{-5}}$	90	[1] ABE	02W	BELL	$e^+e^- \to \Upsilon(4S)$

[1] Assumes equal production of B^+ and B^0 at the $\Upsilon(4S)$.

$\Gamma(D^*(2010)^+p\overline{p})/\Gamma_{total}$ Γ_{518}/Γ

VALUE	CL%	DOCUMENT ID		TECN	COMMENT
$\mathbf{< 1.5 \times 10^{-5}}$	90	[1] ABE	02W	BELL	$e^+e^- \to \Upsilon(4S)$

[1] Assumes equal production of B^+ and B^0 at the $\Upsilon(4S)$.

$\Gamma(\overline{D}^0 p\overline{p}\pi^+)/\Gamma_{total}$ Γ_{519}/Γ

VALUE (units 10^{-4})	DOCUMENT ID		TECN	COMMENT
$\mathbf{3.72 \pm 0.11 \pm 0.25}$	[1,2] DEL-AMO-SA...12		BABR	$e^+e^- \to \Upsilon(4S)$

[1] Uses the values of D and D^* branching fractions from PDG 08.

[2] Assumes equal production of B^+ and B^0 at the $\Upsilon(4S)$.

$\Gamma(\overline{D}^{*0} p\overline{p}\pi^+)/\Gamma_{total}$ Γ_{520}/Γ

VALUE (units 10^{-4})	DOCUMENT ID		TECN	COMMENT
$\mathbf{3.73 \pm 0.17 \pm 0.27}$	[1,2] DEL-AMO-SA...12		BABR	$e^+e^- \to \Upsilon(4S)$

[1] Uses the values of D and D^* branching fractions from PDG 08.

[2] Assumes equal production of B^+ and B^0 at the $\Upsilon(4S)$.

$\Gamma(D^-p\overline{p}\pi^+\pi^-)/\Gamma_{total}$ Γ_{521}/Γ

VALUE (units 10^{-4})	DOCUMENT ID		TECN	COMMENT
$\mathbf{1.66 \pm 0.13 \pm 0.27}$	[1,2] DEL-AMO-SA...12		BABR	$e^+e^- \to \Upsilon(4S)$

[1] Uses the values of D and D^* branching fractions from PDG 08.

[2] Assumes equal production of B^+ and B^0 at the $\Upsilon(4S)$.

$\Gamma(D^{*-}p\overline{p}\pi^+\pi^-)/\Gamma_{total}$ Γ_{522}/Γ

VALUE (units 10^{-4})	DOCUMENT ID		TECN	COMMENT
$\mathbf{1.86 \pm 0.16 \pm 0.19}$	[1,2] DEL-AMO-SA...12		BABR	$e^+e^- \to \Upsilon(4S)$

[1] Uses the values of D and D^* branching fractions from PDG 08.

[2] Assumes equal production of B^+ and B^0 at the $\Upsilon(4S)$.

$\Gamma(p\overline{\Lambda}^0\overline{D}^0)/\Gamma_{total}$ Γ_{523}/Γ

VALUE (units 10^{-5})	DOCUMENT ID		TECN	COMMENT
$\mathbf{1.43^{+0.28}_{-0.25} \pm 0.18}$	[1,2] CHEN	11F	BELL	$e^+e^- \to \Upsilon(4S)$

[1] Uses $B(\Lambda \to p\pi^-) = 63.9 \pm 0.5\%$, $B(D^0 \to K^-\pi^+) = 3.89 \pm 0.05\%$, and $B(D^0 \to K^-\pi^+\pi^0) = 13.9 \pm 0.5\%$.

[2] Assumes equal production of B^0 and B^+ from Upsilon(4S) decays.

Meson Particle Listings

$B^{\pm}$

$\Gamma(p\overline{\Lambda}^0\overline{D}^*(2007)^0)/\Gamma_{\text{total}}$ Γ_{524}/Γ

VALUE (units 10^{-5})	CL%		DOCUMENT ID		TECN	COMMENT
<5	90	1,2,3	CHEN	11F	BELL	$e^+e^- \to \Upsilon(4S)$

[1] CHEN 11F reports $< 4.8 \times 10^{-5}$ from a measurement of $[\Gamma(B^+ \to p\overline{\Lambda}^0\overline{D}^*(2007)^0)/\Gamma_{\text{total}}] / [\text{B}(D^*(2007)^0 \to D^0\pi^0)]$ assuming $\text{B}(D^*(2007)^0 \to D^0\pi^0) = (61.9 \pm 2.9) \times 10^{-2}$, which we rescale to our best value $\text{B}(D^*(2007)^0 \to D^0\pi^0) = 64.7 \times 10^{-2}$.
[2] Uses $\text{B}(\Lambda \to p\pi^-) = 63.9 \pm 0.5\%$ and $\text{B}(D^0 \to K^-\pi^+) = 3.89 \pm 0.05\%$.
[3] Assumes equal production of B^0 and B^+ from Upsilon(4S) decays.

$\Gamma(\overline{\Lambda}_c^- p\pi^+)/\Gamma_{\text{total}}$ Γ_{525}/Γ

VALUE (units 10^{-4})		DOCUMENT ID		TECN	COMMENT
2.3 ±0.4 OUR AVERAGE		Error includes scale factor of 2.2.			See the ideogram below.
$2.73 \pm 0.16^{+0.15}_{-0.14}$	1,2	AUBERT	08BN	BABR	$e^+e^- \to \Upsilon(4S)$
$1.61 \pm 0.20^{+0.09}_{-0.08}$	1,3	GABYSHEV	06A	BELL	$e^+e^- \to \Upsilon(4S)$
1.9 ±0.5 ±0.1	1,4	DYTMAN	02	CLE2	$e^+e^- \to \Upsilon(4S)$
• • • We do not use the following data for averages, fits, limits, etc. • • •					
1.5 ±0.4 ±0.1	1,5	GABYSHEV	02	BELL	Repl. by GABYSHEV 06A
$6.2\ ^{+2.3}_{-2.0}$ ±1.6	1,6	FU	97	CLE2	Repl. by DYTMAN 02

[1] Assumes equal production of B^+ and B^0 at the $\Upsilon(4S)$.
[2] AUBERT 08BN reports $(3.4 \pm 0.1 \pm 0.9) \times 10^{-4}$ from a measurement of $[\Gamma(B^+ \to \overline{\Lambda}_c^- p\pi^+)/\Gamma_{\text{total}}] \times [\text{B}(\Lambda_c^+ \to pK^-\pi^+)]$ assuming $\text{B}(\Lambda_c^+ \to pK^-\pi^+) = (5.0 \pm 1.3) \times 10^{-2}$, which we rescale to our best value $\text{B}(\Lambda_c^+ \to pK^-\pi^+) = (6.23 \pm 0.33) \times 10^{-2}$. Our first error is their experiment's error and our second error is the systematic error from using our best value.
[3] GABYSHEV 06A reports $(2.01 \pm 0.15 \pm 0.20) \times 10^{-4}$ from a measurement of $[\Gamma(B^+ \to \overline{\Lambda}_c^- p\pi^+)/\Gamma_{\text{total}}] \times [\text{B}(\Lambda_c^+ \to pK^-\pi^+)]$ assuming $\text{B}(\Lambda_c^+ \to pK^-\pi^+) = 0.05$, which we rescale to our best value $\text{B}(\Lambda_c^+ \to pK^-\pi^+) = (6.23 \pm 0.33) \times 10^{-2}$. Our first error is their experiment's error and our second error is the systematic error from using our best value.
[4] DYTMAN 02 reports $(2.4\ ^{+0.63}_{-0.62}) \times 10^{-4}$ from a measurement of $[\Gamma(B^+ \to \overline{\Lambda}_c^- p\pi^+)/\Gamma_{\text{total}}] \times [\text{B}(\Lambda_c^+ \to pK^-\pi^+)]$ assuming $\text{B}(\Lambda_c^+ \to pK^-\pi^+) = 0.05$, which we rescale to our best value $\text{B}(\Lambda_c^+ \to pK^-\pi^+) = (6.23 \pm 0.33) \times 10^{-2}$. Our first error is their experiment's error and our second error is the systematic error from using our best value.
[5] GABYSHEV 02 reports $(1.87\ ^{+0.51}_{-0.49}) \times 10^{-4}$ from a measurement of $[\Gamma(B^+ \to \overline{\Lambda}_c^- p\pi^+)/\Gamma_{\text{total}}] \times [\text{B}(\Lambda_c^+ \to pK^-\pi^+)]$ assuming $\text{B}(\Lambda_c^+ \to pK^-\pi^+) = 0.05$, which we rescale to our best value $\text{B}(\Lambda_c^+ \to pK^-\pi^+) = (6.23 \pm 0.33) \times 10^{-2}$. Our first error is their experiment's error and our second error is the systematic error from using our best value.
[6] FU 97 uses PDG 96 values of Λ_c branching fraction.

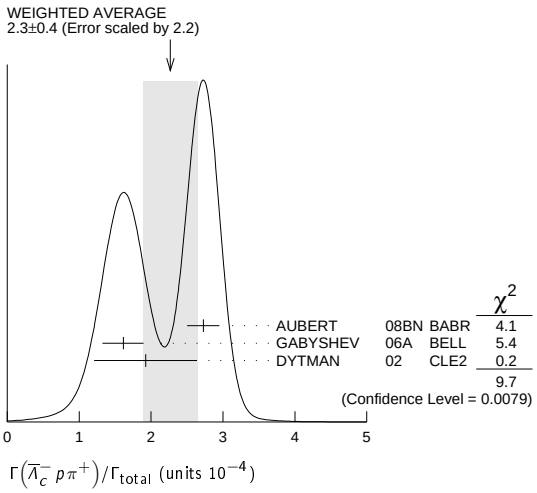

$\Gamma(\overline{\Lambda}_c^- \Delta(1232)^{++})/\Gamma_{\text{total}}$ Γ_{526}/Γ

VALUE (units 10^{-5})	CL%	DOCUMENT ID		TECN	COMMENT
<1.9	90	GABYSHEV	06A	BELL	$e^+e^- \to \Upsilon(4S)$

$\Gamma(\overline{\Lambda}_c^- \Delta_X(1600)^{++})/\Gamma_{\text{total}}$ Γ_{527}/Γ

VALUE (units 10^{-5})	DOCUMENT ID		TECN	COMMENT
$\mathbf{4.7 \pm 0.9\ ^{+0.3}_{-0.2}}$	[1] GABYSHEV	06A	BELL	$e^+e^- \to \Upsilon(4S)$

[1] GABYSHEV 06A reports $(5.9 \pm 1.0 \pm 0.6) \times 10^{-5}$ from a measurement of $[\Gamma(B^+ \to \overline{\Lambda}_c^- \Delta_X(1600)^{++})/\Gamma_{\text{total}}] \times [\text{B}(\Lambda_c^+ \to pK^-\pi^+)]$ assuming $\text{B}(\Lambda_c^+ \to pK^-\pi^+) = 0.05$, which we rescale to our best value $\text{B}(\Lambda_c^+ \to pK^-\pi^+) = (6.23 \pm 0.33) \times 10^{-2}$. Our first error is their experiment's error and our second error is the systematic error from using our best value.

$\Gamma(\overline{\Lambda}_c^- \Delta_X(2420)^{++})/\Gamma_{\text{total}}$ Γ_{528}/Γ

VALUE (units 10^{-5})	DOCUMENT ID		TECN	COMMENT
$\mathbf{3.8 \pm 0.9\ ^{+1.0}_{-0.8} \pm 0.2}$	[1] GABYSHEV	06A	BELL	$e^+e^- \to \Upsilon(4S)$

[1] GABYSHEV 06A reports $(4.7\ ^{+1.0}_{-0.9} \pm 0.4) \times 10^{-5}$ from a measurement of $[\Gamma(B^+ \to \overline{\Lambda}_c^- \Delta_X(2420)^{++})/\Gamma_{\text{total}}] \times [\text{B}(\Lambda_c^+ \to pK^-\pi^+)]$ assuming $\text{B}(\Lambda_c^+ \to pK^-\pi^+) = 0.05$, which we rescale to our best value $\text{B}(\Lambda_c^+ \to pK^-\pi^+) = (6.23 \pm 0.33) \times 10^{-2}$. Our first error is their experiment's error and our second error is the systematic error from using our best value.

$\Gamma((\overline{\Lambda}_c^- p)_s\pi^+)/\Gamma_{\text{total}}$ Γ_{529}/Γ

$(\overline{\Lambda}_c^- p)_s$ denotes a low-mass enhancement near 3.35 GeV/c^2.

VALUE (units 10^{-5})	DOCUMENT ID		TECN	COMMENT
$\mathbf{3.1\ ^{+0.7}_{-0.6} \pm 0.2}$	[1] GABYSHEV	06A	BELL	$e^+e^- \to \Upsilon(4S)$

[1] GABYSHEV 06A reports $(3.9\ ^{+0.8}_{-0.7} \pm 0.4) \times 10^{-5}$ from a measurement of $[\Gamma(B^+ \to (\overline{\Lambda}_c^- p)_s\pi^+)/\Gamma_{\text{total}}] \times [\text{B}(\Lambda_c^+ \to pK^-\pi^+)]$ assuming $\text{B}(\Lambda_c^+ \to pK^-\pi^+) = 0.05$, which we rescale to our best value $\text{B}(\Lambda_c^+ \to pK^-\pi^+) = (6.23 \pm 0.33) \times 10^{-2}$. Our first error is their experiment's error and our second error is the systematic error from using our best value.

$\Gamma(\Sigma_c(2520)^0 p)/\Gamma_{\text{total}}$ Γ_{530}/Γ

VALUE (units 10^{-5})	CL%		DOCUMENT ID		TECN	COMMENT
<0.3	90	1,2	AUBERT	08BN	BABR	$e^+e^- \to \Upsilon(4S)$
• • • We do not use the following data for averages, fits, limits, etc. • • •						
<2.7	90	1,2	GABYSHEV	06A	BELL	$e^+e^- \to \Upsilon(4S)$
<4.6	90	1,2	GABYSHEV	02	BELL	Repl. by GABYSHEV 06A

[1] Assumes equal production of B^+ and B^0 at the $\Upsilon(4S)$.
[2] Uses the value for $\Lambda_c \to pK^-\pi^+$ branching ratio (5.0 ± 1.3)%.

$\Gamma(\Sigma_c(2520)^0 p)/\Gamma(\overline{\Lambda}_c^- p\pi^+)$ $\Gamma_{530}/\Gamma_{525}$

VALUE (units 10^{-3})	CL%	DOCUMENT ID		TECN	COMMENT
<9	90	AUBERT	08BN	BABR	$e^+e^- \to \Upsilon(4S)$

$\Gamma(\Sigma_c(2800)^0 p)/\Gamma_{\text{total}}$ Γ_{531}/Γ

VALUE (units 10^{-5})	DOCUMENT ID		TECN	COMMENT
$\mathbf{2.7 \pm 0.8 \pm 0.4}$	[1] AUBERT	08BN	BABR	$e^+e^- \to \Upsilon(4S)$

[1] AUBERT 08BN reports $[\Gamma(B^+ \to \overline{\Sigma}_c(2800)^0 p)/\Gamma_{\text{total}}] / [\text{B}(B^+ \to \overline{\Lambda}_c^- p\pi^+)] = 0.117 \pm 0.023 \pm 0.024$ which we multiply by our best value $\text{B}(B^+ \to \overline{\Lambda}_c^- p\pi^+) = (2.3 \pm 0.4) \times 10^{-4}$. Our first error is their experiment's error and our second error is the systematic error from using our best value.

$\Gamma(\overline{\Lambda}_c^- p\pi^+\pi^0)/\Gamma_{\text{total}}$ Γ_{532}/Γ

VALUE (units 10^{-3})	CL%		DOCUMENT ID		TECN	COMMENT
$\mathbf{1.81 \pm 0.29 \pm 0.52}$		1,2	DYTMAN	02	CLE2	$e^+e^- \to \Upsilon(4S)$
• • • We do not use the following data for averages, fits, limits, etc. • • •						
<3.12	90	3	FU	97	CLE2	$e^+e^- \to \Upsilon(4S)$

[1] Assumes equal production of B^+ and B^0 at the $\Upsilon(4S)$.
[2] DYTMAN 02 measurement uses $\text{B}(\Lambda_c^- \to \overline{p}K^+\pi^-) = 5.0 \pm 1.3\%$. The second error includes the systematic and the uncertainty of the branching ratio.
[3] FU 97 uses PDG 96 values of Λ_c branching ratio.

$\Gamma(\overline{\Lambda}_c^- p\pi^+\pi^+\pi^-)/\Gamma_{\text{total}}$ Γ_{533}/Γ

VALUE (units 10^{-3})	CL%		DOCUMENT ID		TECN	COMMENT
$\mathbf{2.25 \pm 0.25\ ^{+0.63}_{-0.61}}$		1,2	DYTMAN	02	CLE2	$e^+e^- \to \Upsilon(4S)$
• • • We do not use the following data for averages, fits, limits, etc. • • •						
<1.46	90	3	FU	97	CLE2	$e^+e^- \to \Upsilon(4S)$

[1] Assumes equal production of B^+ and B^0 at the $\Upsilon(4S)$.
[2] DYTMAN 02 measurement uses $\text{B}(\Lambda_c^- \to \overline{p}K^+\pi^-) = 5.0 \pm 1.3\%$. The second error includes the systematic and the uncertainty of the branching ratio.
[3] FU 97 uses PDG 96 values of Λ_c branching ratio.

$\Gamma(\overline{\Lambda}_c^- p\pi^+\pi^+\pi^-\pi^0)/\Gamma_{\text{total}}$ Γ_{534}/Γ

VALUE	CL%		DOCUMENT ID		TECN	COMMENT
$\mathbf{< 1.34 \times 10^{-2}}$	90	1	FU	97	CLE2	$e^+e^- \to \Upsilon(4S)$

[1] FU 97 uses PDG 96 values of Λ_c branching ratio.

$\Gamma(\Lambda_c^+ \Lambda_c^- K^+)/\Gamma_{\text{total}}$ Γ_{535}/Γ

VALUE (units 10^{-4})		DOCUMENT ID		TECN	COMMENT
7.0 ±2.2 OUR AVERAGE					
9.2 ±4.5 ±0.5	1,2	AUBERT	08H	BABR	$e^+e^- \to \Upsilon(4S)$
6.3 ±2.5 ±0.3	2,3	GABYSHEV	06	BELL	$e^+e^- \to \Upsilon(4S)$

[1] AUBERT 08H reports $(1.14 \pm 0.15 \pm 0.62) \times 10^{-3}$ from a measurement of $[\Gamma(B^+ \to \Lambda_c^+ \Lambda_c^- K^+)/\Gamma_{\text{total}}] \times [\text{B}(\Lambda_c^+ \to pK^-\pi^+)]$ assuming $\text{B}(\Lambda_c^+ \to pK^-\pi^+) = (5.0 \pm 1.3) \times 10^{-2}$, which we rescale to our best value $\text{B}(\Lambda_c^+ \to pK^-\pi^+) = (6.23 \pm 0.33) \times$

10^{-2}. Our first error is their experiment's error and our second error is the systematic error from using our best value.

[2] Assumes equal production of B^+ and B^0 at the $\Upsilon(4S)$.

[3] GABYSHEV 06 reports $(7.9^{+1.0}_{-0.9} \pm 3.6) \times 10^{-4}$ from a measurement of $[\Gamma(B^+ \to \Lambda_c^+ \Lambda_c^- K^+)/\Gamma_{\rm total}] \times [B(\Lambda_c^+ \to p K^- \pi^+)]$ assuming $B(\Lambda_c^+ \to p K^- \pi^+) = (5.0 \pm 1.3) \times 10^{-2}$, which we rescale to our best value $B(\Lambda_c^+ \to p K^- \pi^+) = (6.23 \pm 0.33) \times 10^{-2}$. Our first error is their experiment's error and our second error is the systematic error from using our best value.

$\Gamma(\Sigma_c(2455)^0 p)/\Gamma_{\rm total}$ Γ_{536}/Γ

VALUE (units 10^{-5})	CL%	DOCUMENT ID		TECN	COMMENT
3.0±0.6±0.2		[1,2] GABYSHEV	06A	BELL	$e^+e^- \to \Upsilon(4S)$
• • • We do not use the following data for averages, fits, limits, etc. • • •					
<8	90	[1,3] DYTMAN	02	CLE2	$e^+e^- \to \Upsilon(4S)$
<9.3	90	[1,4] GABYSHEV	02	BELL	Repl. by GABYSHEV 06A

[1] Assumes equal production of B^+ and B^0 at the $\Upsilon(4S)$.

[2] GABYSHEV 06A reports $(3.7 \pm 0.7 \pm 0.4) \times 10^{-5}$ from a measurement of $[\Gamma(B^+ \to \overline{\Sigma}_c(2455)^0 p)/\Gamma_{\rm total}] \times [B(\Lambda_c^+ \to p K^- \pi^+)]$ assuming $B(\Lambda_c^+ \to p K^- \pi^+) = 0.05$, which we rescale to our best value $B(\Lambda_c^+ \to p K^- \pi^+) = (6.23 \pm 0.33) \times 10^{-2}$. Our first error is their experiment's error and our second error is the systematic error from using our best value.

[3] DYTMAN 02 measurement uses $B(\Lambda_c^- \to \overline{p} K^+ \pi^-) = 5.0 \pm 1.3\%$. The second error includes the systematic and the uncertainty of the branching ratio.

[4] Uses the value for $\Lambda_c \to p K^- \pi^+$ branching ratio $(5.0 \pm 1.3)\%$.

$\Gamma(\Sigma_c(2455)^0 p)/\Gamma(\Lambda_c^- p \pi^+)$ $\Gamma_{536}/\Gamma_{525}$

VALUE	DOCUMENT ID		TECN	COMMENT
0.123±0.012±0.008	[1] AUBERT	08BN	BABR	$e^+e^- \to \Upsilon(4S)$

[1] Assumes equal production of B^+ and B^0 at the $\Upsilon(4S)$.

$\Gamma(\Sigma_c(2455)^0 p\pi^0)/\Gamma_{\rm total}$ Γ_{537}/Γ

VALUE (units 10^{-4})	DOCUMENT ID		TECN	COMMENT
3.5±1.1±0.2	[1,2] DYTMAN	02	CLE2	$e^+e^- \to \Upsilon(4S)$

[1] DYTMAN 02 reports $(4.4 \pm 1.4) \times 10^{-4}$ from a measurement of $[\Gamma(B^+ \to \overline{\Sigma}_c(2455)^0 p\pi^0)/\Gamma_{\rm total}] \times [B(\Lambda_c^+ \to p K^- \pi^+)]$ assuming $B(\Lambda_c^+ \to p K^- \pi^+) = 0.05$, which we rescale to our best value $B(\Lambda_c^+ \to p K^- \pi^+) = (6.23 \pm 0.33) \times 10^{-2}$. Our first error is their experiment's error and our second error is the systematic error from using our best value.

[2] Assumes equal production of B^+ and B^0 at the $\Upsilon(4S)$.

$\Gamma(\Sigma_c(2455)^0 p\pi^-\pi^+)/\Gamma_{\rm total}$ Γ_{538}/Γ

VALUE (units 10^{-4})	DOCUMENT ID		TECN	COMMENT
3.5±1.0±0.2	[1,2] DYTMAN	02	CLE2	$e^+e^- \to \Upsilon(4S)$

[1] DYTMAN 02 reports $(4.4 \pm 1.3) \times 10^{-4}$ from a measurement of $[\Gamma(B^+ \to \overline{\Sigma}_c(2455)^0 p\pi^-\pi^+)/\Gamma_{\rm total}] \times [B(\Lambda_c^+ \to p K^- \pi^+)]$ assuming $B(\Lambda_c^+ \to p K^- \pi^+) = 0.05$, which we rescale to our best value $B(\Lambda_c^+ \to p K^- \pi^+) = (6.23 \pm 0.33) \times 10^{-2}$. Our first error is their experiment's error and our second error is the systematic error from using our best value.

[2] Assumes equal production of B^+ and B^0 at the $\Upsilon(4S)$.

$\Gamma(\Sigma_c(2455)^{--} p\pi^+\pi^+)/\Gamma_{\rm total}$ Γ_{539}/Γ

VALUE (units 10^{-4})	DOCUMENT ID		TECN	COMMENT
2.39±0.20 OUR AVERAGE				
2.39±0.16±0.13	[1,2] LEES	12Z	BABR	$e^+e^- \to \Upsilon(4S)$
2.2 ±0.8 ±0.1	[1,3] DYTMAN	02	CLE2	$e^+e^- \to \Upsilon(4S)$

[1] Assumes equal production of B^+ and B^0 at the $\Upsilon(4S)$.

[2] LEES 12Z reports $(2.98 \pm 0.16 \pm 0.15 \pm 0.77) \times 10^{-4}$ from a measurement of $[\Gamma(B^+ \to \overline{\Sigma}_c(2455)^{--} p\pi^+\pi^+)/\Gamma_{\rm total}] \times [B(\Lambda_c^+ \to p K^- \pi^+)]$ assuming $B(\Lambda_c^+ \to p K^- \pi^+) = (5.0 \pm 1.3) \times 10^{-2}$, which we rescale to our best value $B(\Lambda_c^+ \to p K^- \pi^+) = (6.23 \pm 0.33) \times 10^{-2}$. Our first error is their experiment's error and our second error is the systematic error from using our best value.

[3] DYTMAN 02 reports $(2.8 \pm 0.9 \pm 0.5 \pm 0.7) \times 10^{-4}$ from a measurement of $[\Gamma(B^+ \to \overline{\Sigma}_c(2455)^{--} p\pi^+\pi^+)/\Gamma_{\rm total}] \times [B(\Lambda_c^+ \to p K^- \pi^+)]$ assuming $B(\Lambda_c^+ \to p K^- \pi^+) = (5.0 \pm 1.3) \times 10^{-2}$, which we rescale to our best value $B(\Lambda_c^+ \to p K^- \pi^+) = (6.23 \pm 0.33) \times 10^{-2}$. Our first error is their experiment's error and our second error is the systematic error from using our best value.

$\Gamma(\overline{\Lambda}_c(2593)^-/\overline{\Lambda}_c(2625)^- p\pi^+)/\Gamma_{\rm total}$ Γ_{540}/Γ

VALUE	CL%	DOCUMENT ID		TECN	COMMENT
<1.9 × 10⁻⁴	90	[1,2] DYTMAN	02	CLE2	$e^+e^- \to \Upsilon(4S)$

[1] Assumes equal production of B^+ and B^0 at the $\Upsilon(4S)$.

[2] DYTMAN 02 measurement uses $B(\Lambda_c^- \to \overline{p} K^+ \pi^-) = 5.0 \pm 1.3\%$. The second error includes the systematic and the uncertainty of the branching ratio.

$\Gamma(\Xi_c^0 \Lambda_c^+, \Xi_c^0 \to \Xi^+\pi^-)/\Gamma_{\rm total}$ Γ_{541}/Γ

VALUE (units 10^{-5})	DOCUMENT ID		TECN	COMMENT
2.4±0.9 OUR AVERAGE Error includes scale factor of 1.4.				
2.0±0.7±0.1	[1,2] AUBERT	08H	BABR	$e^+e^- \to \Upsilon(4S)$
$4.5^{+1.8}_{-1.6}$±0.2	[2,3] CHISTOV	06A	BELL	$e^+e^- \to \Upsilon(4S)$

[1] AUBERT 08H reports $(2.51 \pm 0.89 \pm 0.61) \times 10^{-5}$ from a measurement of $[\Gamma(B^+ \to \Xi_c^0 \Lambda_c^+, \Xi_c^0 \to \Xi^+\pi^-)/\Gamma_{\rm total}] \times [B(\Lambda_c^+ \to p K^- \pi^+)]$ assuming $B(\Lambda_c^+ \to p K^- \pi^+) = (5.0 \pm 1.3) \times 10^{-2}$, which we rescale to our best value $B(\Lambda_c^+ \to p K^- \pi^+) = (6.23 \pm 0.33) \times 10^{-2}$. Our first error is their experiment's error and our second error is the systematic error from using our best value.

[2] Assumes equal production of B^+ and B^0 at the $\Upsilon(4S)$.

[3] CHISTOV 06A reports $(5.6^{+1.9}_{-1.5} \pm 1.9) \times 10^{-5}$ from a measurement of $[\Gamma(B^+ \to \Xi_c^0 \Lambda_c^+, \Xi_c^0 \to \Xi^+\pi^-)/\Gamma_{\rm total}] \times [B(\Lambda_c^+ \to p K^- \pi^+)]$ assuming $B(\Lambda_c^+ \to p K^- \pi^+) = (5.0 \pm 1.3) \times 10^{-2}$, which we rescale to our best value $B(\Lambda_c^+ \to p K^- \pi^+) = (6.23 \pm 0.33) \times 10^{-2}$. Our first error is their experiment's error and our second error is the systematic error from using our best value.

$\Gamma(\Xi_c^0 \Lambda_c^+, \Xi_c^0 \to \Lambda K^+\pi^-)/\Gamma_{\rm total}$ Γ_{542}/Γ

VALUE (units 10^{-5})	DOCUMENT ID		TECN	COMMENT
2.1±0.9 OUR AVERAGE Error includes scale factor of 1.5.				
1.4±0.8±0.1	[1,2] AUBERT	08H	BABR	$e^+e^- \to \Upsilon(4S)$
$3.2^{+1.1}_{-1.0}$±0.2	[2,3] CHISTOV	06A	BELL	$e^+e^- \to \Upsilon(4S)$

[1] AUBERT 08H reports $(1.70 \pm 0.93 \pm 0.53) \times 10^{-5}$ from a measurement of $[\Gamma(B^+ \to \Xi_c^0 \Lambda_c^+, \Xi_c^0 \to \Lambda K^+\pi^-)/\Gamma_{\rm total}] \times [B(\Lambda_c^+ \to p K^- \pi^+)]$ assuming $B(\Lambda_c^+ \to p K^- \pi^+) = (5.0 \pm 1.3) \times 10^{-2}$, which we rescale to our best value $B(\Lambda_c^+ \to p K^- \pi^+) = (6.23 \pm 0.33) \times 10^{-2}$. Our first error is their experiment's error and our second error is the systematic error from using our best value.

[2] Assumes equal production of B^+ and B^0 at the $\Upsilon(4S)$.

[3] CHISTOV 06A reports $(4.0^{+1.1}_{-0.9} \pm 1.3) \times 10^{-5}$ from a measurement of $[\Gamma(B^+ \to \Xi_c^0 \Lambda_c^+, \Xi_c^0 \to \Lambda K^+\pi^-)/\Gamma_{\rm total}] \times [B(\Lambda_c^+ \to p K^- \pi^+)]$ assuming $B(\Lambda_c^+ \to p K^- \pi^+) = (5.0 \pm 1.3) \times 10^{-2}$, which we rescale to our best value $B(\Lambda_c^+ \to p K^- \pi^+) = (6.23 \pm 0.33) \times 10^{-2}$. Our first error is their experiment's error and our second error is the systematic error from using our best value.

$\Gamma(\pi^+ \ell^+ \ell^-)/\Gamma_{\rm total}$ Γ_{543}/Γ

VALUE	CL%	DOCUMENT ID		TECN	COMMENT
<4.9 × 10⁻⁸	90	[1] WEI	08A	BELL	$e^+e^- \to \Upsilon(4S)$
• • • We do not use the following data for averages, fits, limits, etc. • • •					
<6.6 × 10⁻⁸	90	[1] LEES	13M	BABR	$e^+e^- \to \Upsilon(4S)$
<1.2 × 10⁻⁷	90	[1] AUBERT	07AG	BABR	$e^+e^- \to \Upsilon(4S)$

[1] Assumes equal production of B^+ and B^0 at the $\Upsilon(4S)$.

$\Gamma(\pi^+ e^+ e^-)/\Gamma_{\rm total}$ Γ_{544}/Γ

Test for ΔB=1 weak neutral current. Allowed by higher-order electroweak interactions.

VALUE	CL%	DOCUMENT ID		TECN	COMMENT
< 8.0 × 10⁻⁸	90	[1] WEI	08A	BELL	$e^+e^- \to \Upsilon(4S)$
• • • We do not use the following data for averages, fits, limits, etc. • • •					
<12.5 × 10⁻⁸	90	[1] LEES	13M	BABR	$e^+e^- \to \Upsilon(4S)$
<18 × 10⁻⁸	90	[1] AUBERT	07AG	BABR	$e^+e^- \to \Upsilon(4S)$
< 3.9 × 10⁻³	90	[2] WEIR	90B	MRK2	e^+e^- 29 GeV

[1] Assumes equal production of B^+ and B^0 at the $\Upsilon(4S)$.

[2] WEIR 90B assumes B^+ production cross section from LUND.

$\Gamma(\pi^+ \mu^+ \mu^-)/\Gamma_{\rm total}$ Γ_{545}/Γ

Test for ΔB=1 weak neutral current. Allowed by higher-order electroweak interactions.

VALUE (units 10^{-8})	CL%	DOCUMENT ID		TECN	COMMENT
1.76±0.22±0.05		[1] AAIJ	15AR	LHCB	pp at 7, 8 TeV
• • • We do not use the following data for averages, fits, limits, etc. • • •					
< 5.5	90	[2] LEES	13M	BABR	$e^+e^- \to \Upsilon(4S)$
2.3 ±0.6 ±0.1		AAIJ	12AY	LHCB	Repl. by AAIJ 15AR
< 6.9	90	[2] WEI	08A	BELL	$e^+e^- \to \Upsilon(4S)$
<28	90	[2] AUBERT	07AG	BABR	$e^+e^- \to \Upsilon(4S)$

[1] AAIJ 15AR reports $(1.83 \pm 0.24 \pm 0.05) \times 10^{-8}$ from a measurement of $[\Gamma(B^+ \to \pi^+\mu^+\mu^-)/\Gamma_{\rm total}] / [B(B^+ \to J/\psi(1S) K^+)] / [B(J/\psi(1S) \to \mu^+\mu^-)]$ assuming $B(B^+ \to J/\psi(1S) K^+) = (1.05 \pm 0.05) \times 10^{-3}$, $B(J/\psi(1S) \to \mu^+\mu^-) = (5.961 \pm 0.033) \times 10^{-2}$, which we rescale to our best values $B(B^+ \to J/\psi(1S) K^+) = (1.010 \pm 0.029) \times 10^{-3}$, $B(J/\psi(1S) \to \mu^+\mu^-) = (5.961 \pm 0.033) \times 10^{-2}$. Our first error is their experiment's error and our second error is the systematic error from using our best values.

[2] Assumes equal production of B^+ and B^0 at the $\Upsilon(4S)$.

$\Gamma(\pi^+ \mu^+ \mu^-)/\Gamma(K^+ \mu^+ \mu^-)$ $\Gamma_{545}/\Gamma_{549}$

VALUE	DOCUMENT ID		TECN	COMMENT
• • • We do not use the following data for averages, fits, limits, etc. • • •				
0.053±0.014±0.001	AAIJ	12AY	LHCB	Repl. by AAIJ 15AR

$\Gamma(\pi^+ \nu\overline{\nu})/\Gamma_{\rm total}$ Γ_{546}/Γ

Test for ΔB=1 weak neutral current. Allowed by higher-order electroweak interactions.

VALUE	CL%	DOCUMENT ID		TECN	COMMENT
<1.4 × 10⁻⁵	90	[1] GRYGIER	17	BELL	$e^+e^- \to \Upsilon(4S)$
• • • We do not use the following data for averages, fits, limits, etc. • • •					
<9.8 × 10⁻⁵	90	[1] LUTZ	13	BELL	$e^+e^- \to \Upsilon(4S)$
<1.7 × 10⁻⁴	90	[1] CHEN	07D	BELL	$e^+e^- \to \Upsilon(4S)$
<1.0 × 10⁻⁴	90	[1] AUBERT	05H	BABR	$e^+e^- \to \Upsilon(4S)$

[1] Assumes equal production of B^+ and B^0 at the $\Upsilon(4S)$.

Meson Particle Listings

$B^{\pm}$

$\Gamma(K^+\ell^+\ell^-)/\Gamma_{\text{total}}$ Γ_{547}/Γ

Test for ΔB=1 weak neutral current. Allowed by higher-order electroweak interactions.

VALUE (units 10^{-7})	DOCUMENT ID		TECN	COMMENT
4.51±0.23 OUR AVERAGE	Error includes scale factor of 1.1.			
4.36±0.15±0.18	[1] AAIJ	13H	LHCB	pp at 7 TeV
4.8 ±0.9 ±0.2	[2] AUBERT	09T	BABR	$e^+e^- \to \Upsilon(4S)$
5.3 $^{+0.6}_{-0.5}$ ±0.3	[2] WEI	09A	BELL	$e^+e^- \to \Upsilon(4S)$
• • • We do not use the following data for averages, fits, limits, etc. • • •				
3.8 $^{+0.9}_{-0.8}$ ±0.2	[2] AUBERT,B	06J	BABR	Repl. by AUBERT 09T
5.3 $^{+1.1}_{-1.0}$ ±0.3	[2] ISHIKAWA	03	BELL	Repl. by WEI 09A

[1] Uses B($B^+ \to J/\psi K^+ \to \mu^+\mu^- K^+$) = (6.01 ± 0.21) × 10^{-5}.
[2] Assumes equal production of B^+ and B^0 at the $\Upsilon(4S)$.

$\Gamma(K^+e^+e^-)/\Gamma_{\text{total}}$ Γ_{548}/Γ

Test for ΔB=1 weak neutral current. Allowed by higher-order electroweak interactions.

VALUE (units 10^{-7})	CL%	DOCUMENT ID		TECN	COMMENT
5.5±0.7 OUR AVERAGE					
5.1 $^{+1.2}_{-1.1}$ ±0.2		[1] AUBERT	09T	BABR	$e^+e^- \to \Upsilon(4S)$
5.7 $^{+0.9}_{-0.8}$ ±0.3		[1] WEI	09A	BELL	$e^+e^- \to \Upsilon(4S)$
• • • We do not use the following data for averages, fits, limits, etc. • • •					
4.2 $^{+1.2}_{-1.1}$ ±0.2		[1] AUBERT,B	06J	BABR	Repl. by AUBERT 09T
10.5 $^{+2.5}_{-2.2}$ ±0.7		[1] AUBERT	03U	BABR	Repl. by AUBERT,B 06J
6.3 $^{+1.9}_{-1.7}$ ±0.3		[2] ISHIKAWA	03	BELL	Repl. by WEI 09A
< 14	90	[1] ABE	02	BELL	$e^+e^- \to \Upsilon(4S)$
< 9	90	[1] AUBERT	02L	BABR	$e^+e^- \to \Upsilon(4S)$
< 24	90	[3] ANDERSON	01B	CLE2	$e^+e^- \to \Upsilon(4S)$
< 990	90	[4] ALBRECHT	91E	ARG	$e^+e^- \to \Upsilon(4S)$
<68000	90	[5] WEIR	90B	MRK2	e^+e^- 29 GeV
< 600	90	[6] AVERY	89B	CLEO	$e^+e^- \to \Upsilon(4S)$
< 2500	90	[7] AVERY	87	CLEO	$e^+e^- \to \Upsilon(4S)$

[1] Assumes equal production of B^+ and B^0 at the $\Upsilon(4S)$.
[2] Assumes equal production of B^0 and B^+ at $\Upsilon(4S)$. The second error is a total of systematic uncertainties including model dependence.
[3] The result is for di-lepton masses above 0.5 GeV.
[4] ALBRECHT 91E reports < 9.0 × 10^{-5} assuming the $\Upsilon(4S)$ decays 45% to $B^0\overline{B}^0$. We rescale to 50%.
[5] WEIR 90B assumes B^+ production cross section from LUND.
[6] AVERY 89B reports < 5 × 10^{-5} assuming the $\Upsilon(4S)$ decays 43% to $B^0\overline{B}^0$. We rescale to 50%.
[7] AVERY 87 reports < 2.1 × 10^{-4} assuming the $\Upsilon(4S)$ decays 40% to $B^0\overline{B}^0$. We rescale to 50%.

$\Gamma(K^+\mu^+\mu^-)/\Gamma_{\text{total}}$ Γ_{549}/Γ

Test for ΔB=1 weak neutral current. Allowed by higher-order electroweak interactions.

VALUE (units 10^{-7})	CL%	DOCUMENT ID		TECN	COMMENT
4.41±0.23 OUR FIT	Error includes scale factor of 1.2.				
4.36±0.27 OUR AVERAGE	Error includes scale factor of 1.3.				
4.29±0.07±0.21		[1] AAIJ	14M	LHCB	pp at 7, 8 TeV
4.1 $^{+1.6}_{-1.5}$ ±0.2		[2] AUBERT	09T	BABR	$e^+e^- \to \Upsilon(4S)$
5.3 $^{+0.8}_{-0.7}$ ±0.3		[2] WEI	09A	BELL	$e^+e^- \to \Upsilon(4S)$
• • • We do not use the following data for averages, fits, limits, etc. • • •					
4.36±0.15±0.18		[3] AAIJ	13H	LHCB	Repl. by AAIJ 14M
3.1 $^{+1.5}_{-1.2}$ ±0.3		[2] AUBERT,B	06J	BABR	Repl. by AUBERT 09T
0.7 $^{+1.9}_{-1.1}$ ±0.2		[2] AUBERT	03U	BABR	Repl. by AUBERT,B 06J
4.5 $^{+1.4}_{-1.2}$ ±0.3		[4] ISHIKAWA	03	BELL	Repl. by WEI 09A
9.8 $^{+4.6}_{-3.6}$ ±1.6		[2] ABE	02	BELL	Repl. by ISHIKAWA 03
< 12	90	[2] AUBERT	02L	BABR	$e^+e^- \to \Upsilon(4S)$
< 36.8	90	[5] ANDERSON	01B	CLE2	$e^+e^- \to \Upsilon(4S)$
< 52	90	[6] AFFOLDER	99B	CDF	$p\overline{p}$ at 1.8 TeV
< 100	90	[7] ABE	96L	CDF	Repl. by AFFOLDER 99B
< 2400	90	[8] ALBRECHT	91E	ARG	$e^+e^- \to \Upsilon(4S)$
<64000	90	[9] WEIR	90B	MRK2	e^+e^- 29 GeV
< 1700	90	[10] AVERY	89B	CLEO	$e^+e^- \to \Upsilon(4S)$
< 3800	90	[11] AVERY	87	CLEO	$e^+e^- \to \Upsilon(4S)$

[1] Uses B($B^+ \to J/\psi(1S) K^+$) = (0.998 ± 0.014 ± 0.040) × 10^{-3} for normalization.
[2] Assumes equal production of B^+ and B^0 at the $\Upsilon(4S)$.
[3] Uses B($B^+ \to J/\psi K^+ \to \mu^+\mu^- K^+$) = (6.01 ± 0.21) × 10^{-5}.
[4] Assumes equal production of B^0 and B^+ at $\Upsilon(4S)$. The second error is a total of systematic uncertainties including model dependence.
[5] The result is for di-lepton masses above 0.5 GeV.
[6] AFFOLDER 99B measured relative to $B^+ \to J/\psi(1S) K^+$.
[7] ABE 96L measured relative to $B^+ \to J/\psi(1S) K^+$ using PDG 94 branching ratios.
[8] ALBRECHT 91E reports < 2.2 × 10^{-4} assuming the $\Upsilon(4S)$ decays 45% to $B^0\overline{B}^0$. We rescale to 50%.
[9] WEIR 90B assumes B^+ production cross section from LUND.
[10] AVERY 89B reports < 1.5 × 10^{-4} assuming the $\Upsilon(4S)$ decays 43% to $B^0\overline{B}^0$. We rescale to 50%.
[11] AVERY 87 reports < 3.2 × 10^{-4} assuming the $\Upsilon(4S)$ decays 40% to $B^0\overline{B}^0$. We rescale to 50%.

$\Gamma(K^+\mu^+\mu^-\text{ nonresonant})/\Gamma_{\text{total}}$ Γ_{550}/Γ

VALUE (units 10^{-7})	DOCUMENT ID		TECN	COMMENT
4.37±0.15±0.23	[1] AAIJ	17Y	LHCB	pp at 7, 8 TeV

[1] Measured in amplitude analysis using model including short-distance $K^+\mu^+\mu^-$ and $\rho(770)$, $\omega(782)$, $\phi(1020)$, J/ψ, $\psi(2S)$, $\psi(3770)$, $\psi(4040)$, $\psi(4160)$, and $\psi(4415)$ contributions.

$\Gamma(K^+\tau^+\tau^-)/\Gamma_{\text{total}}$ Γ_{551}/Γ

VALUE	CL%	DOCUMENT ID		TECN	COMMENT
<2.25 × 10^{-3}	90	[1,2] LEES	17	BABR	$e^+e^- \to \Upsilon(4S)$

[1] Uses only leptonic decays of τ and the quoted limit combines the final states $K^+e^+e^-$, $K^+\mu^+\mu^-$, and $K^+e^\pm\mu^\mp$.
[2] If observed events are interpreted as a signal the branching fraction measurement becomes $(1.31^{+0.66+0.35}_{-0.61-0.25}) \times 10^{-3}$.

$\Gamma(K^+\mu^+\mu^-)/\Gamma(J/\psi(1S)K^+)$ $\Gamma_{549}/\Gamma_{268}$

VALUE (units 10^{-3})	DOCUMENT ID		TECN	COMMENT
0.437±0.024 OUR FIT	Error includes scale factor of 1.1.			
0.46 ±0.04 ±0.02	AALTONEN	11AI	CDF	$p\overline{p}$ at 1.96 TeV
• • • We do not use the following data for averages, fits, limits, etc. • • •				
0.38 ±0.05 ±0.02	AALTONEN	11L	CDF	Repl. by AALTONEN 11AI
0.59 ±0.15 ±0.03	AALTONEN	09B	CDF	Repl. by AALTONEN 11L

$\Gamma(K^+\overline{\nu}\nu)/\Gamma_{\text{total}}$ Γ_{552}/Γ

Test for ΔB=1 weak neutral current. Allowed by higher-order electroweak interactions.

VALUE	CL%	DOCUMENT ID		TECN	COMMENT
<1.6 × 10^{-5}	90	[1,2] LEES	13I	BABR	$e^+e^- \to \Upsilon(4S)$
• • • We do not use the following data for averages, fits, limits, etc. • • •					
<1.9 × 10^{-5}	90	[1,3] GRYGIER	17	BELL	$e^+e^- \to \Upsilon(4S)$
<5.5 × 10^{-5}	90	[1] LUTZ	13	BELL	$e^+e^- \to \Upsilon(4S)$
<1.3 × 10^{-5}	90	[1] DEL-AMO-SA10Q		BABR	Repl. by LEES 13I
<1.4 × 10^{-5}	90	[1] CHEN	07D	BELL	$e^+e^- \to \Upsilon(4S)$
<5.2 × 10^{-5}	90	[1] AUBERT	05H	BABR	$e^+e^- \to \Upsilon(4S)$
<2.4 × 10^{-4}	90	[1] BROWDER	01	CLE2	$e^+e^- \to \Upsilon(4S)$

[1] Assumes equal production of B^+ and B^0 at the $\Upsilon(4S)$.
[2] Also reported a limit < 3.7 × 10^{-5} at 90% CL obtained using a fully reconstructed hadronic B-tag evnets.
[3] The result was reported in arXiv:1702.03224, but missing from the publication by mistake.

$\Gamma(\rho^+\nu\overline{\nu})/\Gamma_{\text{total}}$ Γ_{553}/Γ

Test for $\Delta B = 1$ weak neutral current. Allowed by higher-order electroweak interaction.

VALUE	CL%	DOCUMENT ID		TECN	COMMENT
<3.0 × 10^{-5}	90	[1] GRYGIER	17	BELL	$e^+e^- \to \Upsilon(4S)$
• • • We do not use the following data for averages, fits, limits, etc. • • •					
<2.13 × 10^{-4}	90	[1] LUTZ	13	BELL	$e^+e^- \to \Upsilon(4S)$
<1.5 × 10^{-4}	90	[1] CHEN	07D	BELL	Repl. by LUTZ 13

[1] Assumes equal production of B^+ and B^0 at the $\Upsilon(4S)$.

$\Gamma(K^*(892)^+\ell^+\ell^-)/\Gamma_{\text{total}}$ Γ_{554}/Γ

Test for ΔB=1 weak neutral current. Allowed by higher-order electroweak interactions.

VALUE (units 10^{-7})	CL%	DOCUMENT ID		TECN	COMMENT
10.1 ±1.1 OUR AVERAGE	Error includes scale factor of 1.1.				
9.24±0.93±0.67		AAIJ	14M	LHCB	pp at 7, 8 TeV
14.0 $^{+4.0}_{-3.7}$ ±0.9		[1] AUBERT	09T	BABR	$e^+e^- \to \Upsilon(4S)$
12.4 $^{+2.3}_{-2.1}$ ±1.3		[1] WEI	09A	BELL	$e^+e^- \to \Upsilon(4S)$
• • • We do not use the following data for averages, fits, limits, etc. • • •					
11.6 ±1.9		[2] AAIJ	12AH	LHCB	Repl. by AAIJ 14M
7.3 $^{+5.0}_{-4.2}$ ±2.1		[1] AUBERT,B	06J	BABR	Repl. by AUBERT 09T
<22	90	[1] ISHIKAWA	03	BELL	$e^+e^- \to \Upsilon(4S)$

[1] Assumes equal production of B^+ and B^0 at the $\Upsilon(4S)$.
[2] Measured in $B^+ \to K^*(892)^+\mu^+\mu^-$ decays.

$\Gamma(K^*(892)^+e^+e^-)/\Gamma_{\text{total}}$ Γ_{555}/Γ

Test for ΔB=1 weak neutral current. Allowed by higher-order electroweak interactions.

VALUE (units 10^{-7})	CL%	DOCUMENT ID		TECN	COMMENT
15.5 $^{+4.0}_{-3.1}$ OUR AVERAGE					
13.8 $^{+4.7}_{-4.2}$ ±0.8		[1] AUBERT	09T	BABR	$e^+e^- \to \Upsilon(4S)$
17.3 $^{+5.0}_{-4.2}$ ±2.0		[1] WEI	09A	BELL	$e^+e^- \to \Upsilon(4S)$
• • • We do not use the following data for averages, fits, limits, etc. • • •					
7.5 $^{+7.6}_{-6.5}$ ±3.8		[1] AUBERT,B	06J	BABR	Repl. by AUBERT 09T
2.0 $^{+13.4}_{-8.7}$ ±2.8		[1] AUBERT	03U	BABR	$e^+e^- \to \Upsilon(4S)$
< 46	90	[2] ISHIKAWA	03	BELL	$e^+e^- \to \Upsilon(4S)$
< 89	90	[1] ABE	02	BELL	Repl. by ISHIKAWA 03

< 95	90	[1] AUBERT	02L	BABR	$e^+e^- \to \Upsilon(4S)$	
<6900	90	[3] ALBRECHT	91E	ARG	$e^+e^- \to \Upsilon(4S)$	

[1] Assumes equal production of B^+ and B^0 at the $\Upsilon(4S)$.
[2] Assumes equal production of B^0 and B^+ at $\Upsilon(4S)$. The second error is a total of systematic uncertainties including model dependence.
[3] ALBRECHT 91E reports $< 6.3 \times 10^{-4}$ assuming the $\Upsilon(4S)$ decays 45% to $B^0\overline{B}^0$. We rescale to 50%.

$\Gamma(K^*(892)^+\mu^+\mu^-)/\Gamma_{\text{total}}$ Γ_{556}/Γ

Test for ΔB=1 weak neutral current. Allowed by higher-order electroweak interactions.

VALUE (units 10^{-7})	CL%	DOCUMENT ID		TECN	COMMENT
9.6 ± 1.0 OUR FIT					
9.6 ± 1.1 OUR AVERAGE					
9.24± 0.93±0.67		[1] AAIJ	14M	LHCB	pp at 7, 8 TeV
$14.6\ ^{+\ 7.9}_{-\ 7.5} \pm 1.2$		[2] AUBERT	09T	BABR	$e^+e^- \to \Upsilon(4S)$
$11.1\ ^{+\ 3.2}_{-\ 2.7} \pm 1.0$		[2] WEI	09A	BELL	$e^+e^- \to \Upsilon(4S)$
• • • We do not use the following data for averages, fits, limits, etc. • • •					
11.6 ± 1.9		AAIJ	12AH	LHCB	Repl. by AAIJ 14M
$9.7\ ^{+\ 9.4}_{-\ 6.9} \pm 1.4$		[2] AUBERT,B	06J	BABR	Repl. by AUBERT 09T
$30.7\ ^{+25.8}_{-17.8} \pm 4.2$		[2] AUBERT	03U	BABR	$e^+e^- \to \Upsilon(4S)$
$6.5\ ^{+\ 6.9}_{-\ 5.3} \pm 1.5 \pm 1.6$		[3] ISHIKAWA	03	BELL	Repl. by WEI 09A
< 39	90	[2] ABE	02	BELL	Repl. by ISHIKAWA 03
<170	90	[2] AUBERT	02L	BABR	$e^+e^- \to \Upsilon(4S)$

[1] Uses $B(B^+ \to J/\psi(1S)K^*(892)^+) = (1.431 \pm 0.027 \pm 0.090) \times 10^{-3}$ for normalization.
[2] Assumes equal production of B^+ and B^0 at the $\Upsilon(4S)$.
[3] Assumes equal production of B^0 and B^+ at $\Upsilon(4S)$. The second error is a total of systematic uncertainties including model dependence. The 90% C.L. upper limit is 2.2×10^{-6}.

$\Gamma(K^*(892)^+\mu^+\mu^-)/\Gamma(J/\psi(1S)K^*(892)^+)$ $\Gamma_{556}/\Gamma_{273}$

VALUE (units 10^{-3})	DOCUMENT ID		TECN	COMMENT
0.67±0.08 OUR FIT				
0.67±0.22±0.04	AALTONEN	11AI	CDF	$p\overline{p}$ at 1.96 TeV

$\Gamma(K^*(892)^+\nu\overline{\nu})/\Gamma_{\text{total}}$ Γ_{557}/Γ

Test for $\Delta B = 1$ weak neutral current. Allowed by higher-order electroweak interaction.

VALUE	CL%	DOCUMENT ID		TECN	COMMENT
$< 4.0 \times 10^{-5}$	90	[1] LUTZ	13	BELL	$e^+e^- \to \Upsilon(4S)$
• • • We do not use the following data for averages, fits, limits, etc. • • •					
$< 6.1 \times 10^{-5}$	90	[1] GRYGIER	17	BELL	$e^+e^- \to \Upsilon(4S)$
$< 6.4 \times 10^{-5}$	90	[1,2] LEES	13I	BABR	$e^+e^- \to \Upsilon(4S)$
$< 8 \times 10^{-5}$	90	AUBERT	08BC	BABR	Repl. by LEES 13I
$< 1.4 \times 10^{-4}$	90	[1] CHEN	07D	BELL	$e^+e^- \to \Upsilon(4S)$

[1] Assumes equal production of B^+ and B^0 at the $\Upsilon(4S)$.
[2] Also reported a limit $< 11.6 \times 10^{-5}$ at 90% CL obtained using a fully reconstructed hadronic B-tag evnets.

$\Gamma(K^+\pi^+\pi^-\mu^+\mu^-)/\Gamma(\psi(2S)K^+)$ $\Gamma_{558}/\Gamma_{304}$

VALUE (units 10^{-4})	DOCUMENT ID		TECN	COMMENT
$6.95\ ^{+0.46}_{-0.43} \pm 0.34$	AAIJ	14AZ	LHCB	pp at 7, 8 TeV

$\Gamma(\phi K^+\mu^+\mu^-)/\Gamma(J/\psi(1S)\phi K^+)$ $\Gamma_{559}/\Gamma_{280}$

VALUE (units 10^{-3})	DOCUMENT ID		TECN	COMMENT
$1.58\ ^{+0.36}_{-0.32} \pm 0.19$	AAIJ	14AZ	LHCB	pp at 7, 8 TeV

$\Gamma(\pi^+e^+\mu^-)/\Gamma_{\text{total}}$ Γ_{560}/Γ

Test of lepton family number conservation.

VALUE	CL%	DOCUMENT ID		TECN	COMMENT
<0.0064	90	[1] WEIR	90B	MRK2	e^+e^- 29 GeV

[1] WEIR 90B assumes B^+ production cross section from LUND.

$\Gamma(\pi^+e^-\mu^+)/\Gamma_{\text{total}}$ Γ_{561}/Γ

Test of lepton family number conservation.

VALUE	CL%	DOCUMENT ID		TECN	COMMENT
<0.0064	90	[1] WEIR	90B	MRK2	e^+e^- 29 GeV

[1] WEIR 90B assumes B^+ production cross section from LUND.

$\Gamma(\pi^+e^\pm\mu^\mp)/\Gamma_{\text{total}}$ Γ_{562}/Γ

VALUE	CL%	DOCUMENT ID		TECN	COMMENT
$< 1.7 \times 10^{-7}$	90	[1] AUBERT	07AG	BABR	$e^+e^- \to \Upsilon(4S)$

[1] Assumes equal production of B^+ and B^0 at the $\Upsilon(4S)$.

$\Gamma(\pi^+e^+\tau^-)/\Gamma_{\text{total}}$ Γ_{563}/Γ

Test of lepton family number conservation.

VALUE (units 10^{-6})	CL%	DOCUMENT ID		TECN	COMMENT
<74	90	[1] LEES	12P	BABR	$e^+e^- \to \Upsilon(4S)$

[1] Uses a fully reconstructed hadronic B decay as a tag on the recoil side.

$\Gamma(\pi^+e^-\tau^+)/\Gamma_{\text{total}}$ Γ_{564}/Γ

Test of lepton family number conservation.

VALUE (units 10^{-6})	CL%	DOCUMENT ID		TECN	COMMENT
<20	90	[1] LEES	12P	BABR	$e^+e^- \to \Upsilon(4S)$

[1] Uses a fully reconstructed hadronic B decay as a tag on the recoil side.

$\Gamma(\pi^+e^\pm\tau^\mp)/\Gamma_{\text{total}}$ Γ_{565}/Γ

Test of lepton family number conservation.

VALUE (units 10^{-6})	CL%	DOCUMENT ID		TECN	COMMENT
<75	90	[1,2] LEES	12P	BABR	$e^+e^- \to \Upsilon(4S)$

[1] Assumes $B(B^+ \to h^+\ell^+\tau^-) = B(B^+ \to h^+\ell^-\tau^+)$.
[2] Uses a fully reconstructed hadronic B decay as a tag on the recoil side.

$\Gamma(\pi^+\mu^+\tau^-)/\Gamma_{\text{total}}$ Γ_{566}/Γ

Test of lepton family number conservation.

VALUE (units 10^{-6})	CL%	DOCUMENT ID		TECN	COMMENT
<62	90	[1] LEES	12P	BABR	$e^+e^- \to \Upsilon(4S)$

[1] Uses a fully reconstructed hadronic B decay as a tag on the recoil side.

$\Gamma(\pi^+\mu^-\tau^+)/\Gamma_{\text{total}}$ Γ_{567}/Γ

Test of lepton family number conservation.

VALUE (units 10^{-6})	CL%	DOCUMENT ID		TECN	COMMENT
<45	90	[1] LEES	12P	BABR	$e^+e^- \to \Upsilon(4S)$

[1] Uses a fully reconstructed hadronic B decay as a tag on the recoil side.

$\Gamma(\pi^+\mu^\pm\tau^\mp)/\Gamma_{\text{total}}$ Γ_{568}/Γ

Test of lepton family number conservation.

VALUE (units 10^{-6})	CL%	DOCUMENT ID		TECN	COMMENT
<72	90	[1,2] LEES	12P	BABR	$e^+e^- \to \Upsilon(4S)$

[1] Assumes $B(B^+ \to h^+\ell^+\tau^-) = B(B^+ \to h^+\ell^-\tau^+)$.
[2] Uses a fully reconstructed hadronic B decay as a tag on the recoil side.

$\Gamma(K^+e^+\mu^-)/\Gamma_{\text{total}}$ Γ_{569}/Γ

Test of lepton family number conservation.

VALUE (units 10^{-7})	CL%	DOCUMENT ID		TECN	COMMENT
<0.91	90	[1] AUBERT,B	06J	BABR	$e^+e^- \to \Upsilon(4S)$
• • • We do not use the following data for averages, fits, limits, etc. • • •					
<8	90	[1] AUBERT	02L	BABR	Repl. by AUBERT,B 06J
$< 6.4 \times 10^4$	90	[2] WEIR	90B	MRK2	e^+e^- 29 GeV

[1] Assumes equal production of B^+ and B^0 at the $\Upsilon(4S)$.
[2] WEIR 90B assumes B^+ production cross section from LUND.

$\Gamma(K^+e^-\mu^+)/\Gamma_{\text{total}}$ Γ_{570}/Γ

Test of lepton family number conservation.

VALUE (units 10^{-7})	CL%	DOCUMENT ID		TECN	COMMENT
<1.3	90	[1] AUBERT,B	06J	BABR	$e^+e^- \to \Upsilon(4S)$
• • • We do not use the following data for averages, fits, limits, etc. • • •					
$< 6.4 \times 10^4$	90	[2] WEIR	90B	MRK2	e^+e^- 29 GeV

[1] Assumes equal production of B^+ and B^0 at the $\Upsilon(4S)$.
[2] WEIR 90B assumes B^+ production cross section from LUND.

$\Gamma(K^+e^\pm\mu^\mp)/\Gamma_{\text{total}}$ Γ_{571}/Γ

VALUE (units 10^{-7})	CL%	DOCUMENT ID		TECN	COMMENT
<0.91	90	[1] AUBERT,B	06J	BABR	$e^+e^- \to \Upsilon(4S)$

[1] Assumes equal production of B^+ and B^0 at the $\Upsilon(4S)$.

$\Gamma(K^+e^+\tau^-)/\Gamma_{\text{total}}$ Γ_{572}/Γ

Test of lepton family number conservation.

VALUE (units 10^{-6})	CL%	DOCUMENT ID		TECN	COMMENT
<43	90	[1] LEES	12P	BABR	$e^+e^- \to \Upsilon(4S)$

[1] Uses a fully reconstructed hadronic B decay as a tag on the recoil side.

$\Gamma(K^+e^-\tau^+)/\Gamma_{\text{total}}$ Γ_{573}/Γ

Test of lepton family number conservation.

VALUE (units 10^{-6})	CL%	DOCUMENT ID		TECN	COMMENT
<15	90	[1] LEES	12P	BABR	$e^+e^- \to \Upsilon(4S)$

[1] Uses a fully reconstructed hadronic B decay as a tag on the recoil side.

$\Gamma(K^+e^\pm\tau^\mp)/\Gamma_{\text{total}}$ Γ_{574}/Γ

Test of lepton family number conservation.

VALUE (units 10^{-6})	CL%	DOCUMENT ID		TECN	COMMENT
<30	90	[1,2] LEES	12P	BABR	$e^+e^- \to \Upsilon(4S)$

[1] Assumes $B(B^+ \to h^+\ell^+\tau^-) = B(B^+ \to h^+\ell^-\tau^+)$.
[2] Uses a fully reconstructed hadronic B decay as a tag on the recoil side.

$\Gamma(K^+\mu^+\tau^-)/\Gamma_{\text{total}}$ Γ_{575}/Γ

Test of lepton family number conservation.

VALUE (units 10^{-6})	CL%	DOCUMENT ID		TECN	COMMENT
<45	90	[1] LEES	12P	BABR	$e^+e^- \to \Upsilon(4S)$

[1] Uses a fully reconstructed hadronic B decay as a tag on the recoil side.

Meson Particle Listings

$B^{\pm}$

$\Gamma(K^+\mu^-\tau^+)/\Gamma_{\text{total}}$ Γ_{576}/Γ

Test of lepton family number conservation.

VALUE (units 10^{-6})	CL%	DOCUMENT ID		TECN	COMMENT
<28	90	[1] LEES	12P	BABR	$e^+e^- \to \Upsilon(4S)$

[1] Uses a fully reconstructed hadronic B decay as a tag on the recoil side.

$\Gamma(K^+\mu^\pm\tau^\mp)/\Gamma_{\text{total}}$ Γ_{577}/Γ

Test of lepton family number conservation.

VALUE (units 10^{-6})	CL%	DOCUMENT ID		TECN	COMMENT
<48	90	[1,2] LEES	12P	BABR	$e^+e^- \to \Upsilon(4S)$
• • • We do not use the following data for averages, fits, limits, etc. • • •					
<77	90	[1] AUBERT	07AZ	BABR	Repl. by LEES 12P

[1] Uses a fully reconstructed hadronic B decay as a tag on the recoil side.
[2] Assumes $B(B^+ \to h^+\ell^+\tau^-) = B(B^+ \to h^+\ell^-\tau^+)$.

$\Gamma(K^*(892)^+e^+\mu^-)/\Gamma_{\text{total}}$ Γ_{578}/Γ

VALUE (units 10^{-7})	CL%	DOCUMENT ID		TECN	COMMENT
<13	90	[1] AUBERT,B	06J	BABR	$e^+e^- \to \Upsilon(4S)$

[1] Assumes equal production of B^+ and B^0 at the $\Upsilon(4S)$.

$\Gamma(K^*(892)^+e^-\mu^+)/\Gamma_{\text{total}}$ Γ_{579}/Γ

VALUE (units 10^{-7})	CL%	DOCUMENT ID		TECN	COMMENT
<9.9	90	[1] AUBERT,B	06J	BABR	$e^+e^- \to \Upsilon(4S)$

[1] Assumes equal production of B^+ and B^0 at the $\Upsilon(4S)$.

$\Gamma(K^*(892)^+e^\pm\mu^\mp)/\Gamma_{\text{total}}$ Γ_{580}/Γ

Test of lepton family number conservation.

VALUE	CL%	DOCUMENT ID		TECN	COMMENT
$<1.4\times10^{-6}$	90	[1] AUBERT,B	06J	BABR	$e^+e^- \to \Upsilon(4S)$
• • • We do not use the following data for averages, fits, limits, etc. • • •					
$<7.9\times10^{-6}$	90	[1] AUBERT	02L	BABR	Repl. by AUBERT,B 06J

[1] Assumes equal production of B^+ and B^0 at the $\Upsilon(4S)$.

$\Gamma(\pi^-e^+e^+)/\Gamma_{\text{total}}$ Γ_{581}/Γ

Test of total lepton number conservation.

VALUE	CL%	DOCUMENT ID		TECN	COMMENT
<2.3 $\times10^{-8}$	90	[1] LEES	12J	BABR	$e^+e^- \to \Upsilon(4S)$
• • • We do not use the following data for averages, fits, limits, etc. • • •					
$<1.6\times10^{-6}$	90	[1] EDWARDS	02B	CLE2	$e^+e^- \to \Upsilon(4S)$
<0.0039	90	[2] WEIR	90B	MRK2	e^+e^- 29 GeV

[1] Assumes equal production of B^+ and B^0 at the $\Upsilon(4S)$.
[2] WEIR 90B assumes B^+ production cross section from LUND.

$\Gamma(\pi^-\mu^+\mu^+)/\Gamma_{\text{total}}$ Γ_{582}/Γ

Test of total lepton number conservation.

VALUE	CL%	DOCUMENT ID		TECN	COMMENT
$< 4.0\times10^{-9}$	95	[1] AAIJ	14AC	LHCB	pp at 7, 8 TeV
• • • We do not use the following data for averages, fits, limits, etc. • • •					
$< 1.3\times10^{-8}$	95	[2] AAIJ	12AD	LHCB	Repl. by AAIJ 14AC
$< 4.4\times10^{-8}$	90	AAIJ	12C	LHCB	pp at 7 TeV
$<10.7\times10^{-8}$	90	[3] LEES	12J	BABR	$e^+e^- \to \Upsilon(4S)$
$< 1.4\times10^{-6}$	90	[3] EDWARDS	02B	CLE2	$e^+e^- \to \Upsilon(4S)$
$< 9.1\times10^{-3}$	90	[4] WEIR	90B	MRK2	e^+e^- 29 GeV

[1] Uses $B^+ \to J/\psi K^+$, $J/\psi \to \mu^+\mu^-$ mode for normalization. Obtains neutrino-mass-dependent upper limits in the range 0.4–4.0 $\times10^{-9}$. This limit is applicable for Majorana neutrino lifetime < 1 ps.
[2] Uses $B^+ \to J/\psi K^+$, $J/\psi \to \mu^+\mu^-$ mode for normalization. Obtains neutrino-mass-dependent upper limits in the range 0.4–1.0 $\times10^{-8}$.
[3] Assumes equal production of B^+ and B^0 at the $\Upsilon(4S)$.
[4] WEIR 90B assumes B^+ production cross section from LUND.

$\Gamma(\pi^-e^+\mu^+)/\Gamma_{\text{total}}$ Γ_{583}/Γ

Test of total lepton number conservation.

VALUE	CL%	DOCUMENT ID		TECN	COMMENT
<1.5 $\times10^{-7}$	90	[1] LEES	14A	BABR	$e^+e^- \to \Upsilon(4S)$
• • • We do not use the following data for averages, fits, limits, etc. • • •					
$<1.3\times10^{-6}$	90	[1] EDWARDS	02B	CLE2	$e^+e^- \to \Upsilon(4S)$
<0.0064	90	[2] WEIR	90B	MRK2	e^+e^- 29 GeV

[1] Assumes equal production of B^+ and B^0 at the $\Upsilon(4S)$.
[2] WEIR 90B assumes B^+ production cross section from LUND.

$\Gamma(\rho^-e^+e^+)/\Gamma_{\text{total}}$ Γ_{584}/Γ

Test of total lepton number conservation.

VALUE (units 10^{-6})	CL%	DOCUMENT ID		TECN	COMMENT
<0.17	90	[1] LEES	14A	BABR	$e^+e^- \to \Upsilon(4S)$
• • • We do not use the following data for averages, fits, limits, etc. • • •					
<2.6	90	[1] EDWARDS	02B	CLE2	$e^+e^- \to \Upsilon(4S)$

[1] Assumes equal production of B^+ and B^0 at the $\Upsilon(4S)$.

$\Gamma(\rho^-\mu^+\mu^+)/\Gamma_{\text{total}}$ Γ_{585}/Γ

Test of total lepton number conservation.

VALUE (units 10^{-6})	CL%	DOCUMENT ID		TECN	COMMENT
<0.42	90	LEES	14A	BABR	$e^+e^- \to \Upsilon(4S)$
• • • We do not use the following data for averages, fits, limits, etc. • • •					
<5.0	90	[1] EDWARDS	02B	CLE2	$e^+e^- \to \Upsilon(4S)$

[1] Assumes equal production of B^+ and B^0 at the $\Upsilon(4S)$.

$\Gamma(\rho^-e^+\mu^+)/\Gamma_{\text{total}}$ Γ_{586}/Γ

Test of total lepton number conservation.

VALUE (units 10^{-6})	CL%	DOCUMENT ID		TECN	COMMENT
<0.47	90	[1] LEES	14A	BABR	$e^+e^- \to \Upsilon(4S)$
• • • We do not use the following data for averages, fits, limits, etc. • • •					
<3.3	90	[1] EDWARDS	02B	CLE2	$e^+e^- \to \Upsilon(4S)$

[1] Assumes equal production of B^+ and B^0 at the $\Upsilon(4S)$.

$\Gamma(K^-e^+e^+)/\Gamma_{\text{total}}$ Γ_{587}/Γ

Test of total lepton number conservation.

VALUE	CL%	DOCUMENT ID		TECN	COMMENT
<3.0 $\times10^{-8}$	90	[1] LEES	12J	BABR	$e^+e^- \to \Upsilon(4S)$
• • • We do not use the following data for averages, fits, limits, etc. • • •					
$<1.0\times10^{-6}$	90	[1] EDWARDS	02B	CLE2	$e^+e^- \to \Upsilon(4S)$
<0.0039	90	[2] WEIR	90B	MRK2	e^+e^- 29 GeV

[1] Assumes equal production of B^+ and B^0 at the $\Upsilon(4S)$.
[2] WEIR 90B assumes B^+ production cross section from LUND.

$\Gamma(K^-\mu^+\mu^+)/\Gamma_{\text{total}}$ Γ_{588}/Γ

Test of total lepton number conservation.

VALUE	CL%	DOCUMENT ID		TECN	COMMENT
$<4.1\times10^{-8}$	90	AAIJ	12C	LHCB	pp at 7 TeV
• • • We do not use the following data for averages, fits, limits, etc. • • •					
$<6.7\times10^{-8}$	90	[1] LEES	12J	BABR	$e^+e^- \to \Upsilon(4S)$
$<1.8\times10^{-6}$	90	[1] EDWARDS	02B	CLE2	$e^+e^- \to \Upsilon(4S)$
$<9.1\times10^{-3}$	90	[2] WEIR	90B	MRK2	e^+e^- 29 GeV

[1] Assumes equal production of B^+ and B^0 at the $\Upsilon(4S)$.
[2] WEIR 90B assumes B^+ production cross section from LUND.

$\Gamma(K^-e^+\mu^+)/\Gamma_{\text{total}}$ Γ_{589}/Γ

Test of total lepton number conservation.

VALUE	CL%	DOCUMENT ID		TECN	COMMENT
<1.6 $\times10^{-7}$	90	[1] LEES	14A	BABR	$e^+e^- \to \Upsilon(4S)$
• • • We do not use the following data for averages, fits, limits, etc. • • •					
$<2.0\times10^{-6}$	90	[1] EDWARDS	02B	CLE2	$e^+e^- \to \Upsilon(4S)$
<0.0064	90	[2] WEIR	90B	MRK2	e^+e^- 29 GeV

[1] Assumes equal production of B^+ and B^0 at the $\Upsilon(4S)$.
[2] WEIR 90B assumes B^+ production cross section from LUND.

$\Gamma(K^*(892)^-e^+e^+)/\Gamma_{\text{total}}$ Γ_{590}/Γ

Test of total lepton number conservation.

VALUE (units 10^{-6})	CL%	DOCUMENT ID		TECN	COMMENT
<0.40	90	[1] LEES	14A	BABR	$e^+e^- \to \Upsilon(4S)$
• • • We do not use the following data for averages, fits, limits, etc. • • •					
<2.8	90	[1] EDWARDS	02B	CLE2	$e^+e^- \to \Upsilon(4S)$

[1] Assumes equal production of B^+ and B^0 at the $\Upsilon(4S)$.

$\Gamma(K^*(892)^-\mu^+\mu^+)/\Gamma_{\text{total}}$ Γ_{591}/Γ

Test of total lepton number conservation.

VALUE (units 10^{-6})	CL%	DOCUMENT ID		TECN	COMMENT
<0.59	90	[1] LEES	14A	BABR	$e^+e^- \to \Upsilon(4S)$
• • • We do not use the following data for averages, fits, limits, etc. • • •					
<8.3	90	[1] EDWARDS	02B	CLE2	$e^+e^- \to \Upsilon(4S)$

[1] Assumes equal production of B^+ and B^0 at the $\Upsilon(4S)$.

$\Gamma(K^*(892)^-e^+\mu^+)/\Gamma_{\text{total}}$ Γ_{592}/Γ

Test of total lepton number conservation.

VALUE (units 10^{-6})	CL%	DOCUMENT ID		TECN	COMMENT
<0.30	90	[1] LEES	14A	BABR	$e^+e^- \to \Upsilon(4S)$
• • • We do not use the following data for averages, fits, limits, etc. • • •					
<4.4	90	[1] EDWARDS	02B	CLE2	$e^+e^- \to \Upsilon(4S)$

[1] Assumes equal production of B^+ and B^0 at the $\Upsilon(4S)$.

$\Gamma(D^-e^+e^+)/\Gamma_{\text{total}}$ Γ_{593}/Γ

VALUE	CL%	DOCUMENT ID		TECN	COMMENT
$<2.6\times10^{-6}$	90	[1] LEES	14A	BABR	$e^+e^- \to \Upsilon(4S)$
$<2.6\times10^{-6}$	90	[1,2] SEON	11	BELL	$e^+e^- \to \Upsilon(4S)$

[1] Assumes equal production of B^0 and B^+ from Upsilon(4S) decays.
[2] Uses $D^- \to K^+\pi^-\pi^-$ mode and 3-body phase-space hypothesis for the signal decays.

$\Gamma(D^-e^+\mu^+)/\Gamma_{\text{total}}$ Γ_{594}/Γ

VALUE	CL%	DOCUMENT ID		TECN	COMMENT
$<1.8\times10^{-6}$	90	[1,2] SEON	11	BELL	$e^+e^- \to \Upsilon(4S)$

• • • We do not use the following data for averages, fits, limits, etc. • • •

$<2.1\times10^{-6}$	90	[1] LEES	14A	BABR	$e^+e^-\to\ \Upsilon(4S)$	

[1] Assumes equal production of B^0 and B^+ from Upsilon(4S) decays.
[2] Uses $D^-\to K^+\pi^-\pi^-$ mode and 3-body phase-space hypothesis for the signal decays.

$\Gamma(D^-\mu^+\mu^+)/\Gamma_{\rm total}$ Γ_{595}/Γ

VALUE	CL%	DOCUMENT ID		TECN	COMMENT
$<6.9\times10^{-7}$	95	[1] AAIJ	12AD	LHCB	pp at 7 TeV

• • • We do not use the following data for averages, fits, limits, etc. • • •

$<17\ \times10^{-7}$	90	[2] LEES	14A	BABR	$e^+e^-\to\ \Upsilon(4S)$	
$<1.1\times10^{-6}$	90	[2,3] SEON	11	BELL	$e^+e^-\to\ \Upsilon(4S)$	

[1] Uses $B^+\to\ \psi(2S)K^+$, $\psi(2S)\to\ J/\psi\pi^+\pi^-$ mode for normalization.
[2] Assumes equal production of B^0 and B^+ from Upsilon(4S) decays.
[3] Uses $D^-\to K^+\pi^-\pi^-$ mode and 3-body phase-space hypothesis for the signal decays.

$\Gamma(D^{*-}\mu^+\mu^+)/\Gamma_{\rm total}$ Γ_{596}/Γ

VALUE	CL%	DOCUMENT ID		TECN	COMMENT
$<2.4\times10^{-6}$	95	[1] AAIJ	12AD	LHCB	pp at 7 TeV

[1] Uses $B^+\to\ \psi(2S)K^+$, $\psi(2S)\to\ J/\psi\pi^+\pi^-$ mode for normalization.

$\Gamma(D_s^-\mu^+\mu^+)/\Gamma_{\rm total}$ Γ_{597}/Γ

VALUE	CL%	DOCUMENT ID		TECN	COMMENT
$<5.8\times10^{-7}$	95	[1] AAIJ	12AD	LHCB	pp at 7 TeV

[1] Uses $B^+\to\ \psi(2S)K^+$, $\psi(2S)\to\ J/\psi\pi^+\pi^-$ mode for normalization. Obtains neutrino-mass-dependent upper limits in the range 1.5–8.0 $\times10^{-7}$.

$\Gamma(\overline{D}{}^0\pi^-\mu^+\mu^+)/\Gamma_{\rm total}$ Γ_{598}/Γ

VALUE	CL%	DOCUMENT ID		TECN	COMMENT
$<1.5\times10^{-6}$	95	[1] AAIJ	12AD	LHCB	pp at 7 TeV

[1] Uses $B^+\to\ \psi(2S)K^+$, $\psi(2S)\to\ J/\psi\pi^+\pi^-$ mode for normalization. Obtains neutrino-mass-dependent upper limits in the range 0.3–1.5 $\times10^{-6}$.

$\Gamma(\Lambda^0\mu^+)/\Gamma_{\rm total}$ Γ_{599}/Γ

VALUE	CL%	DOCUMENT ID		TECN	COMMENT
$<6\times10^{-8}$	90	[1,2] DEL-AMO-SA...11K		BABR	$e^+e^-\to\ \Upsilon(4S)$

[1] DEL-AMO-SANCHEZ 11K reports $<6.1\times10^{-8}$ from a measurement of $[\Gamma(B^+\to\ \Lambda^0\mu^+)/\Gamma_{\rm total}]\times[{\rm B}(\Lambda\to\ p\pi^-)]$ assuming ${\rm B}(\Lambda\to\ p\pi^-)=(63.9\pm0.5)\times10^{-2}$.
[2] Uses ${\rm B}(\Upsilon(4S)\to\ B^0\overline{B}{}^0)=(51.6\pm0.6)\%$ and ${\rm B}(\Upsilon(4S)\to\ B^+B^-)=(48.4\pm0.6)\%$.

$\Gamma(\Lambda^0e^+)/\Gamma_{\rm total}$ Γ_{600}/Γ

VALUE	CL%	DOCUMENT ID		TECN	COMMENT
$<3.2\times10^{-8}$	90	[1,2] DEL-AMO-SA...11K		BABR	$e^+e^-\to\ \Upsilon(4S)$

[1] DEL-AMO-SANCHEZ 11K reports $<3.2\times10^{-8}$ from a measurement of $[\Gamma(B^+\to\ \Lambda^0e^+)/\Gamma_{\rm total}]\times[{\rm B}(\Lambda\to\ p\pi^-)]$ assuming ${\rm B}(\Lambda\to\ p\pi^-)=(63.9\pm0.5)\times10^{-2}$.
[2] Uses ${\rm B}(\Upsilon(4S)\to\ B^0\overline{B}{}^0)=(51.6\pm0.6)\%$ and ${\rm B}(\Upsilon(4S)\to\ B^+B^-)=(48.4\pm0.6)\%$.

$\Gamma(\overline{\Lambda}{}^0\mu^+)/\Gamma_{\rm total}$ Γ_{601}/Γ

VALUE	CL%	DOCUMENT ID		TECN	COMMENT
$<6\times10^{-8}$	90	[1,2] DEL-AMO-SA...11K		BABR	$e^+e^-\to\ \Upsilon(4S)$

[1] DEL-AMO-SANCHEZ 11K reports $<6.2\times10^{-8}$ from a measurement of $[\Gamma(B^+\to\ \overline{\Lambda}{}^0\mu^+)/\Gamma_{\rm total}]\times[{\rm B}(\Lambda\to\ p\pi^-)]$ assuming ${\rm B}(\Lambda\to\ p\pi^-)=(63.9\pm0.5)\times10^{-2}$.
[2] Uses ${\rm B}(\Upsilon(4S)\to\ B^0\overline{B}{}^0)=(51.6\pm0.6)\%$ and ${\rm B}(\Upsilon(4S)\to\ B^+B^-)=(48.4\pm0.6)\%$.

$\Gamma(\overline{\Lambda}{}^0e^+)/\Gamma_{\rm total}$ Γ_{602}/Γ

VALUE	CL%	DOCUMENT ID		TECN	COMMENT
$<8\times10^{-8}$	90	[1,2] DEL-AMO-SA...11K		BABR	$e^+e^-\to\ \Upsilon(4S)$

[1] DEL-AMO-SANCHEZ 11K reports $<8.1\times10^{-8}$ from a measurement of $[\Gamma(B^+\to\ \overline{\Lambda}{}^0e^+)/\Gamma_{\rm total}]\times[{\rm B}(\Lambda\to\ p\pi^-)]$ assuming ${\rm B}(\Lambda\to\ p\pi^-)=(63.9\pm0.5)\times10^{-2}$.
[2] Uses ${\rm B}(\Upsilon(4S)\to\ B^0\overline{B}{}^0)=(51.6\pm0.6)\%$ and ${\rm B}(\Upsilon(4S)\to\ B^+B^-)=(48.4\pm0.6)\%$.

POLARIZATION IN B^+ DECAY

In decays involving two vector mesons, one can distinguish among the states in which meson polarizations are both longitudinal (L) or both are transverse and parallel ($\|$) or perpendicular ($\perp$) to each other with the parameters Γ_L/Γ, $\Gamma_\perp/\Gamma$, and the relative phases $\phi_\|$ and $\phi_\perp$. See the definitions in the note on "Polarization in B Decays" review in the B^0 Particle Listings.

Γ_L/Γ in $B^+\to\ \overline{D}{}^{*0}\rho^+$

VALUE	DOCUMENT ID		TECN	COMMENT
$0.892\pm0.018\pm0.016$	CSORNA	03	CLE2	$e^+e^-\to\ \Upsilon(4S)$

Γ_L/Γ in $B^+\to\ \overline{D}{}^{*0}K^{*+}$

VALUE	DOCUMENT ID		TECN	COMMENT
$0.86\pm0.06\pm0.03$	AUBERT	04K	BABR	$e^+e^-\to\ \Upsilon(4S)$

Γ_L/Γ in $B^+\to\ J/\psi K^{*+}$

VALUE	DOCUMENT ID		TECN	COMMENT
$0.604\pm0.015\pm0.018$	ITOH	05	BELL	$e^+e^-\to\ \Upsilon(4S)$

$\Gamma_\perp/\Gamma$ in $B^+\to\ J/\psi K^{*+}$

VALUE	DOCUMENT ID		TECN	COMMENT
$0.180\pm0.014\pm0.010$	ITOH	05	BELL	$e^+e^-\to\ \Upsilon(4S)$

Γ_L/Γ in $B^+\to\ \omega K^{*+}$

VALUE	DOCUMENT ID		TECN	COMMENT
$0.41\pm0.18\pm0.05$	AUBERT	09H	BABR	$e^+e^-\to\ \Upsilon(4S)$

Γ_L/Γ in $B^+\to\ \omega K_2^*(1430)^+$

VALUE	DOCUMENT ID		TECN	COMMENT
$0.56\pm0.10\pm0.04$	AUBERT	09H	BABR	$e^+e^-\to\ \Upsilon(4S)$

Γ_L/Γ in $B^+\to\ K^{*+}\overline{K}{}^{*0}$

VALUE		DOCUMENT ID		TECN	COMMENT
$0.82^{+0.15}_{-0.21}$ OUR AVERAGE					
$1.06\pm0.30\pm0.14$	[1]	GOH	15	BELL	$e^+e^-\to\ \Upsilon(4S)$
$0.75^{+0.16}_{-0.26}\pm0.03$	[2,3]	AUBERT	09F	BABR	$e^+e^-\to\ \Upsilon(4S)$

[1] Signal significance 2.7 standard deviations.
[2] Signal significance 3.7 standard deviations.
[3] Assumes equal production of B^+ and B^0 at the $\Upsilon(4S)$.

Γ_L/Γ in $B^+\to\ \phi K^*(892)^+$

VALUE	DOCUMENT ID		TECN	COMMENT
0.50 ± 0.05 OUR AVERAGE				
$0.49\pm0.05\pm0.03$	AUBERT	07BA	BABR	$e^+e^-\to\ \Upsilon(4S)$
$0.52\pm0.08\pm0.03$	CHEN	05A	BELL	$e^+e^-\to\ \Upsilon(4S)$

• • • We do not use the following data for averages, fits, limits, etc. • • •

$0.46\pm0.12\pm0.03$	AUBERT	03V	BABR	Repl. by AUBERT 07BA	

$\Gamma_\perp/\Gamma$ in $B^+\to\ \phi K^{*+}$

VALUE	DOCUMENT ID		TECN	COMMENT
0.20 ± 0.05 OUR AVERAGE				
$0.21\pm0.05\pm0.02$	AUBERT	07BA	BABR	$e^+e^-\to\ \Upsilon(4S)$
$0.19\pm0.08\pm0.02$	CHEN	05A	BELL	$e^+e^-\to\ \Upsilon(4S)$

$\phi_\|$ in $B^+\to\ \phi K^{*+}$

VALUE (°)	DOCUMENT ID		TECN	COMMENT
2.34 ± 0.18 OUR AVERAGE				
$2.47\pm0.20\pm0.07$	AUBERT	07BA	BABR	$e^+e^-\to\ \Upsilon(4S)$
$2.10\pm0.28\pm0.04$	CHEN	05A	BELL	$e^+e^-\to\ \Upsilon(4S)$

$\phi_\perp$ in $B^+\to\ \phi K^{*+}$

VALUE (°)	DOCUMENT ID		TECN	COMMENT
2.58 ± 0.17 OUR AVERAGE				
$2.69\pm0.20\pm0.03$	AUBERT	07BA	BABR	$e^+e^-\to\ \Upsilon(4S)$
$2.31\pm0.30\pm0.07$	CHEN	05A	BELL	$e^+e^-\to\ \Upsilon(4S)$

$\delta_0(B^+\to\ \phi K^{*+})$

VALUE (rad)	DOCUMENT ID		TECN	COMMENT
$3.07\pm0.18\pm0.06$	AUBERT	07BA	BABR	$e^+e^-\to\ \Upsilon(4S)$

$A_{CP}^0(B^+\to\ \phi K^{*+})$

VALUE	DOCUMENT ID		TECN	COMMENT
$0.17\pm0.11\pm0.02$	AUBERT	07BA	BABR	$e^+e^-\to\ \Upsilon(4S)$

$A_{CP}^\perp(B^+\to\ \phi K^{*+})$

VALUE	DOCUMENT ID		TECN	COMMENT
$0.22\pm0.24\pm0.08$	AUBERT	07BA	BABR	$e^+e^-\to\ \Upsilon(4S)$

$\Delta\phi_\|(B^+\to\ \phi K^{*+})$

VALUE (rad)	DOCUMENT ID		TECN	COMMENT
$0.07\pm0.20\pm0.05$	AUBERT	07BA	BABR	$e^+e^-\to\ \Upsilon(4S)$

$\Delta\phi_\perp(B^+\to\ \phi K^{*+})$

VALUE (rad)	DOCUMENT ID		TECN	COMMENT
$0.19\pm0.20\pm0.07$	AUBERT	07BA	BABR	$e^+e^-\to\ \Upsilon(4S)$

$\Delta\delta_0(B^+\to\ \phi K^{*+})$

VALUE (rad)	DOCUMENT ID		TECN	COMMENT
$0.20\pm0.18\pm0.03$	AUBERT	07BA	BABR	$e^+e^-\to\ \Upsilon(4S)$

Γ_L/Γ in $B^+\to\ \phi K_1(1270)^+$

VALUE	DOCUMENT ID		TECN	COMMENT
$0.46^{+0.12}_{-0.13}\pm0.06$	AUBERT	08BI	BABR	$e^+e^-\to\ \Upsilon(4S)$

Γ_L/Γ in $B^+\to\ \phi K_2^*(1430)^+$

VALUE	DOCUMENT ID		TECN	COMMENT
$0.80^{+0.09}_{-0.10}\pm0.03$	AUBERT	08BI	BABR	$e^+e^-\to\ \Upsilon(4S)$

$\delta_0(B^+\to\ \phi K_2^*(1430)^+)$

VALUE (rad)	DOCUMENT ID		TECN	COMMENT
$3.59\pm0.19\pm0.12$	AUBERT	08BI	BABR	$e^+e^-\to\ \Upsilon(4S)$

Meson Particle Listings

$B^{\pm}$

$\Delta\delta_0(B^+ \to \phi K_2^*(1430)^+)$

VALUE (rad)	DOCUMENT ID		TECN	COMMENT
$-0.05 \pm 0.19 \pm 0.06$	AUBERT	08BI	BABR	$e^+e^- \to \Upsilon(4S)$

Γ_L/Γ in $B^+ \to \rho^0 K^*(892)^+$

VALUE	DOCUMENT ID		TECN	COMMENT
$0.78 \pm 0.12 \pm 0.03$	DEL-AMO-SA...11D		BABR	$e^+e^- \to \Upsilon(4S)$
• • • We do not use the following data for averages, fits, limits, etc. • • •				
$0.96^{+0.04}_{-0.15} \pm 0.04$	AUBERT	03V	BABR	Repl. by DEL-AMO-SANCHEZ 11D

$\Gamma_L/\Gamma(B^+ \to K^*(892)^0 \rho^+)$

VALUE	DOCUMENT ID		TECN	COMMENT
0.48±0.08 OUR AVERAGE				
$0.52 \pm 0.10 \pm 0.04$	AUBERT,B	06G	BABR	$e^+e^- \to \Upsilon(4S)$
$0.43 \pm 0.11^{+0.05}_{-0.02}$	ZHANG	05D	BELL	$e^+e^- \to \Upsilon(4S)$

Γ_L/Γ in $B^+ \to \rho^+\rho^0$

VALUE	DOCUMENT ID		TECN	COMMENT
0.950 ± 0.016 OUR AVERAGE				
$0.950 \pm 0.015 \pm 0.006$	AUBERT	09G	BABR	$e^+e^- \to \Upsilon(4S)$
$0.948 \pm 0.106 \pm 0.021$	ZHANG	03B	BELL	$e^+e^- \to \Upsilon(4S)$
• • • We do not use the following data for averages, fits, limits, etc. • • •				
$0.905 \pm 0.042^{+0.023}_{-0.027}$	AUBERT,BE	06G	BABR	Repl. by AUBERT 09G
$0.97\ ^{+0.03}_{-0.07} \pm 0.04$	AUBERT	03V	BABR	Repl. by AUBERT,BE 06G

Γ_L/Γ in $B^+ \to \omega\rho^+$

VALUE	DOCUMENT ID		TECN	COMMENT
$0.90 \pm 0.05 \pm 0.03$	AUBERT	09H	BABR	$e^+e^- \to \Upsilon(4S)$
• • • We do not use the following data for averages, fits, limits, etc. • • •				
$0.82 \pm 0.11 \pm 0.02$	AUBERT,B	06T	BABR	Repl. by AUBERT 09H
$0.88^{+0.12}_{-0.15} \pm 0.03$	AUBERT	05O	BABR	Repl. by AUBERT,B 06T

Γ_L/Γ in $B^+ \to p\overline{p}K^*(892)^+$

VALUE	DOCUMENT ID		TECN	COMMENT
$0.32 \pm 0.17 \pm 0.09$	CHEN	08C	BELL	$e^+e^- \to \Upsilon(4S)$

CP VIOLATION

A_{CP} is defined as

$$\frac{B(B^- \to \overline{f}) - B(B^+ \to f)}{B(B^- \to \overline{f}) + B(B^+ \to f)},$$

the *CP*-violation charge asymmetry of exclusive B^- and B^+ decay.

$A_{CP}(B^+ \to J/\psi(1S)K^+)$

VALUE (units 10^{-3})	DOCUMENT ID		TECN	COMMENT
1.8± 3.0 OUR AVERAGE	Error includes scale factor of 1.5. See the ideogram below.			
0.9± 2.7± 0.7	AAIJ	17AP	LHCB	pp at 7, 8 TeV
5.9± 3.6± 0.7	ABAZOV	13M	D0	$p\overline{p}$ at 1.96 TeV
− 7.6± 5.0± 2.2	SAKAI	10	BELL	$e^+e^- \to \Upsilon(4S)$
90 ±70 ±20	[1] WEI	08	BELL	$e^+e^- \to \Upsilon(4S)$
30 ±14 ±10	[2] AUBERT	05J	BABR	$e^+e^- \to \Upsilon(4S)$
18 ±43 ± 4	[3] BONVICINI	00	CLE2	$e^+e^- \to \Upsilon(4S)$
• • • We do not use the following data for averages, fits, limits, etc. • • •				
7.5± 6.1± 3.0	[4] ABAZOV	08O	D0	Repl. by ABAZOV 13M
30 ±15 ± 6	AUBERT	04P	BABR	Repl. by AUBERT 05J
− 26 ±22 ±17	ABE	03B	BELL	Repl. by SAKAI 10
3 ±30 ± 4	AUBERT	02F	BABR	Repl. by AUBERT 04P

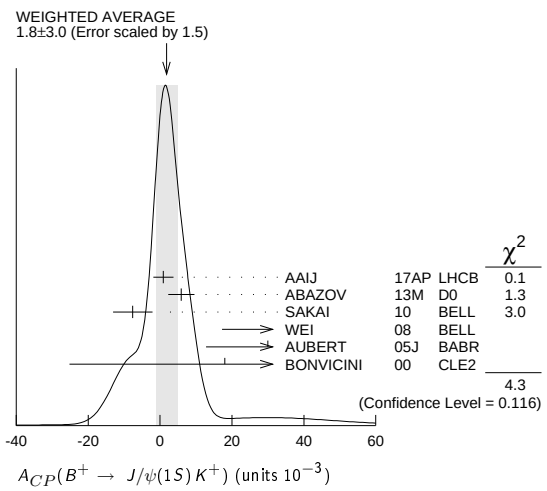

$A_{CP}(B^+ \to J/\psi(1S)K^+)$ (units 10^{-3})

[1] Uses $B^+ \to J/\psi K^+$, where $J/\psi \to p\overline{p}$.

[2] The result reported corresponds to $-A_{CP}$.

[3] A +0.3% correction is applied due to a slightly higher reconstruction efficiency for the positive kaons.

[4] Uses $J/\psi \to \mu^+\mu^-$ decay.

$A_{CP}(B^+ \to J/\psi(1S)\pi^+)$

VALUE (units 10^{-2})	DOCUMENT ID		TECN	COMMENT
1.8 ± 1.2 OUR AVERAGE	Error includes scale factor of 1.3.			
1.91± 0.89±0.16	[1] AAIJ	17O	LHCB	pp at 7, 8 TeV
− 4.2 ± 4.4 ±0.9	ABAZOV	13M	D0	$p\overline{p}$ at 1.96 TeV
12.3 ± 8.5 ±0.4	AUBERT	04P	BABR	$e^+e^- \to \Upsilon(4S)$
− 2.3 ±16.4 ±1.5	ABE	03B	BELL	$e^+e^- \to \Upsilon(4S)$
• • • We do not use the following data for averages, fits, limits, etc. • • •				
0.5 ± 2.7 ±1.1	[2] AAIJ	12AC	LHCB	Repl. by AAIJ 17O
− 9 ± 8 ±3	[3] ABAZOV	08O	D0	Repl. by ABAZOV 13M
1 ±22 ±1	AUBERT	02F	BABR	Repl. by AUBERT 04P

[1] Obtained by using LHCb measurement of $A_{CP}(B^+ \to J/\psi K^+) = (0.09 \pm 0.27 \pm 0.07) \times 10^{-2}$ of AAIJ 17AP.

[2] Uses $A_{CP}(B^+ \to J/\psi K^+) = 0.001 \pm 0.007$ to extract production asymmetry.

[3] Uses $J/\psi \to \mu^+\mu^-$ decay.

$A_{CP}(B^+ \to J/\psi\rho^+)$

VALUE	DOCUMENT ID		TECN	COMMENT
$-0.11 \pm 0.12 \pm 0.08$	AUBERT	07AC	BABR	$e^+e^- \to \Upsilon(4S)$

$A_{CP}(B^+ \to J/\psi K^*(892)^+)$

VALUE	DOCUMENT ID		TECN	COMMENT
$-0.048 \pm 0.029 \pm 0.016$	[1] AUBERT	05J	BABR	$e^+e^- \to \Upsilon(4S)$

[1] The result reported corresponds to $-A_{CP}$.

$A_{CP}(B^+ \to \eta_c K^+)$

VALUE	DOCUMENT ID		TECN	COMMENT
0.01 ±0.07 OUR AVERAGE	Error includes scale factor of 2.2.			
$0.040 \pm 0.034 \pm 0.004$	[1] AAIJ	14AF	LHCB	pp at 7, 8 TeV
$-0.16 \pm 0.08 \pm 0.02$	[1] WEI	08	BELL	$e^+e^- \to \Upsilon(4S)$
• • • We do not use the following data for averages, fits, limits, etc. • • •				
$0.046 \pm 0.057 \pm 0.007$	[1] AAIJ	13AU	LHCB	Repl. by AAIJ 14AF

[1] Uses $B^+ \to \eta_c K^+$, where $\eta_c \to p\overline{p}$.

$A_{CP}(B^+ \to \psi(2S)\pi^+)$

VALUE	DOCUMENT ID		TECN	COMMENT
0.03 ±0.06 OUR AVERAGE				
$0.048 \pm 0.090 \pm 0.011$	[1] AAIJ	12AC	LHCB	pp at 7 TeV
$0.022 \pm 0.085 \pm 0.016$	BHARDWAJ	08	BELL	$e^+e^- \to \Upsilon(4S)$

[1] Uses $A_{CP}(B^+ \to J/\psi K^+) = 0.001 \pm 0.007$ to extract production asymmetry.

$A_{CP}(B^+ \to \psi(2S)K^+)$

VALUE	DOCUMENT ID		TECN	COMMENT
0.012 ± 0.020 OUR AVERAGE	Error includes scale factor of 1.5. See the ideogram below.			
$0.092 \pm 0.058 \pm 0.004$	[1] AAIJ	14AF	LHCB	pp at 7, 8 TeV
$0.024 \pm 0.014 \pm 0.008$	[2] AAIJ	12AC	LHCB	pp at 7 TeV
$0.052 \pm 0.059 \pm 0.020$	AUBERT	05J	BABR	$e^+e^- \to \Upsilon(4S)$
$-0.042 \pm 0.020 \pm 0.017$	ABE	03B	BELL	$e^+e^- \to \Upsilon(4S)$
$0.02 \pm 0.091 \pm 0.01$	[3] BONVICINI	00	CLE2	$e^+e^- \to \Upsilon(4S)$
• • • We do not use the following data for averages, fits, limits, etc. • • •				
$-0.002 \pm 0.123 \pm 0.012$	[1,2] AAIJ	13AU	LHCB	Repl. by AAIJ 14AF

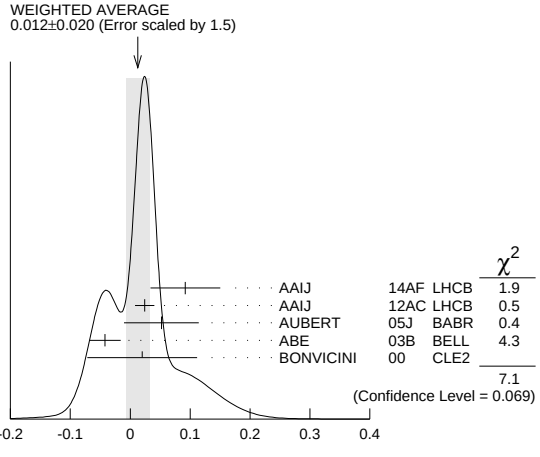

$A_{CP}(B^+ \to \psi(2S)K^+)$

[1] Uses $\psi(2S) \to p\overline{p}$ decays.

[2] Uses $A_{CP}(B^+ \to J/\psi K^+) = 0.001 \pm 0.007$ to extract production asymmetry.

[3] A +0.3% correction is applied due to a slightly higher reconstruction efficiency for the positive kaons.

$A_{CP}(B^+ \to \psi(2S)K^*(892)^+)$

VALUE	DOCUMENT ID		TECN	COMMENT
0.077±0.207±0.051	[1] AUBERT	05J	BABR	$e^+e^- \to \Upsilon(4S)$

[1] The result reported corresponds to $-A_{CP}$.

$A_{CP}(B^+ \to \chi_{c1}(1P)\pi^+)$

VALUE	DOCUMENT ID		TECN	COMMENT
0.07±0.18±0.02	KUMAR	06	BELL	$e^+e^- \to \Upsilon(4S)$

$A_{CP}(B^+ \to \chi_{c0}K^+)$

VALUE	DOCUMENT ID		TECN	COMMENT
−0.20 ±0.18 OUR AVERAGE	Error includes scale factor of 1.5. See the ideogram below.			
−0.96 ±0.37±0.04	LEES	11I	BABR	$e^+e^- \to \Upsilon(4S)$
−0.14 ±0.15 $^{+0.03}_{-0.06}$	AUBERT	08AI	BABR	$e^+e^- \to \Upsilon(4S)$
−0.065±0.20 $^{+0.035}_{-0.024}$	GARMASH	06	BELL	$e^+e^- \to \Upsilon(4S)$

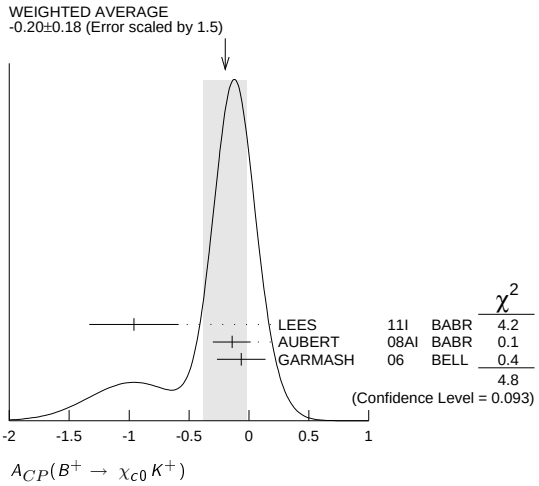

$A_{CP}(B^+ \to \chi_{c0}K^+)$

$A_{CP}(B^+ \to \chi_{c1}K^+)$

VALUE	DOCUMENT ID		TECN	COMMENT
−0.009±0.033 OUR AVERAGE				
−0.01 ±0.03 ±0.02	KUMAR	06	BELL	$e^+e^- \to \Upsilon(4S)$
−0.003±0.076±0.017	[1] AUBERT	05J	BABR	$e^+e^- \to \Upsilon(4S)$

[1] The result reported corresponds to $-A_{CP}$.

$A_{CP}(B^+ \to \chi_{c1}K^*(892)^+)$

VALUE	DOCUMENT ID		TECN	COMMENT
0.471±0.378±0.268	[1] AUBERT	05J	BABR	$e^+e^- \to \Upsilon(4S)$

[1] The result reported corresponds to $-A_{CP}$.

$A_{CP}(B^+ \to D^0\ell^+\nu_\ell)$

VALUE (units 10^{-2})	DOCUMENT ID		TECN	COMMENT
−0.14±0.14±0.14	[1] ABAZOV	17A	D0	$p\overline{p}$ at 1.96 TeV

[1] Uses $D^0 \to K^-\pi^+$ decays and f(B^+) = 0.56 ± 0.01 from 10.4 fb^{-1} of Run II data.

$A_{CP}(B^+ \to \overline{D}{}^0\pi^+)$

VALUE	DOCUMENT ID		TECN	COMMENT
−0.007±0.007 OUR AVERAGE				
−0.006±0.005±0.010	[1] AAIJ	13AE	LHCB	pp at 7 TeV
−0.008±0.008	ABE	06	BELL	$e^+e^- \to \Upsilon(4S)$

[1] Uses $B^\pm \to [K^\pm\pi^\mp\pi^+\pi^-]_D h^\pm$ mode.

$A_{CP}(B^+ \to D_{CP(+1)}\pi^+)$

VALUE	DOCUMENT ID		TECN	COMMENT
−0.0080±0.0026 OUR AVERAGE				
−0.008 ±0.003 ±0.002	[1] AAIJ	18A	LHCB	pp at 7, 8, 13 TeV
−0.008 ±0.006 ±0.002	[2] AAIJ	18A	LHCB	pp at 7, 8, 13 TeV
−0.0098±0.0043±0.0021	AAIJ	16L	LHCB	pp at 7, 8 TeV
0.035 ±0.024	ABE	06	BELL	$e^+e^- \to \Upsilon(4S)$

[1] Uses $D \to K^+K^-$ decay mode.
[2] Uses $D \to \pi^+\pi^-$ decay mode.

$A_{CP}(B^+ \to D_{CP(-1)}\pi^+)$

VALUE	DOCUMENT ID		TECN	COMMENT
0.017±0.026	ABE	06	BELL	$e^+e^- \to \Upsilon(4S)$

$A_{CP}([K^\mp\pi^\pm\pi^+\pi^-]_D\pi^+)$

VALUE	DOCUMENT ID		TECN	COMMENT
0.023±0.048±0.005	AAIJ	16L	LHCB	pp at 7, 8 TeV
• • • We do not use the following data for averages, fits, limits, etc. • • •				
0.13 ±0.10	AAIJ	13AE	LHCB	Repl. by AAIJ 16L

$A_{CP}(B^+ \to [\pi^+\pi^+\pi^-\pi^-]_D K^+)$

VALUE	DOCUMENT ID		TECN	COMMENT
0.100±0.034±0.018	AAIJ	16L	LHCB	pp at 7, 8 TeV

$A_{CP}(B^+ \to [\pi^+\pi^-\pi^+\pi^-]_D K^*(892)^+)$

VALUE	DOCUMENT ID		TECN	COMMENT
0.02±0.11±0.01	AAIJ	17BO	LHCB	pp at 7, 8, 13 TeV

$A_{CP}(B^+ \to \overline{D}{}^0K^+)$

VALUE	DOCUMENT ID		TECN	COMMENT
−0.017 ±0.005 OUR AVERAGE				
−0.019 ±0.005 ±0.002	[1] AAIJ	18A	LHCB	pp at 7, 8, 13 TeV
−0.0194±0.0072±0.0060	AAIJ	16L	LHCB	pp at 7, 8 TeV
0.010 ±0.026 ±0.005	[2] AAIJ	15W	LHCB	pp at 7, 8 TeV
0.066 ±0.036	ABE	06	BELL	$e^+e^- \to \Upsilon(4S)$
• • • We do not use the following data for averages, fits, limits, etc. • • •				
0.000 ±0.012 ±0.002	[3] AAIJ	16L	LHCB	pp at 7, 8 TeV
−0.029 ±0.020 ±0.018	[3] AAIJ	13AE	LHCB	Repl. by AAIJ 16L
0.003 ±0.080 ±0.037	[4] ABE	03D	BELL	Repl. by SWAIN 03
0.04 ±0.06 ±0.03	[5] SWAIN	03	BELL	Repl. by ABE 06

[1] Supersedes AAIJ 16L.
[2] Uses $D^0 \to K^-\pi^+\pi^0$ for the favored mode, and $D^0 \to K^+\pi^-\pi^0$ for the suppressed mode.
[3] Uses $B^\pm \to [K^\pm\pi^\mp\pi^+\pi^-]_D h^\pm$ mode.
[4] Corresponds to 90% confidence range $-0.15 < A_{CP} < 0.16$.
[5] Corresponds to 90% confidence range $-0.07 < A_{CP} < 0.15$.

$A_{CP}([K^\mp\pi^\pm\pi^+\pi^-]_D K^+)$

VALUE	DOCUMENT ID		TECN	COMMENT
−0.313±0.102±0.038	AAIJ	16L	LHCB	pp at 7, 8 TeV
• • • We do not use the following data for averages, fits, limits, etc. • • •				
−0.42 ±0.22	AAIJ	13AE	LHCB	Repl. by AAIJ 16L

$A_{CP}(B^+ \to [\pi^+\pi^+\pi^-\pi^-]_D\pi^+)$

VALUE (units 10^{-3})	DOCUMENT ID		TECN	COMMENT
−4.1±7.9±2.4	AAIJ	16L	LHCB	pp at 7, 8 TeV

$A_{CP}(B^+ \to [K^-\pi^+]_D K^+)$

VALUE	DOCUMENT ID		TECN	COMMENT
−0.58±0.21 OUR AVERAGE				
−0.82±0.44±0.09	AALTONEN	11AJ	CDF	$p\overline{p}$ at 1.96 TeV
−0.39 $^{+0.26}_{-0.28}$ ± 0.04 − 0.03	HORII	11	BELL	$e^+e^- \to \Upsilon(4S)$
−0.86±0.47 $^{+0.12}_{-0.16}$	DEL-AMO-SA...10H		BABR	$e^+e^- \to \Upsilon(4S)$
• • • We do not use the following data for averages, fits, limits, etc. • • •				
−0.1 $^{+0.8}_{-1.0}$ ±0.4	HORII	08	BELL	Repl. by HORII 11
+0.88 $^{+0.77}_{-0.62}$ ±0.06	SAIGO	05	BELL	Repl. by HORII 08

$A_{CP}(B^+ \to [K^-\pi^+\pi^0]_D K^+)$

VALUE	DOCUMENT ID		TECN	COMMENT
0.07±0.30 OUR AVERAGE	Error includes scale factor of 1.5.			
−0.20±0.27±0.04	[1] AAIJ	15W	LHCB	pp at 7, 8 TeV
0.41±0.30±0.05	NAYAK	13	BELL	$e^+e^- \to \Upsilon(4S)$

[1] Uses $D^0 \to K^-\pi^+\pi^0$ for the favored mode, and $D^0 \to K^+\pi^-\pi^0$ for the suppressed mode.

$A_{CP}(B^+ \to [K^+K^-\pi^0]_D K^+)$

VALUE	DOCUMENT ID		TECN	COMMENT
0.30±0.20±0.02	[1] AAIJ	15W	LHCB	pp at 7, 8 TeV

[1] Uses $D \to K^+K^-\pi^0$ mode.

$A_{CP}(B^+ \to [\pi^+\pi^-\pi^0]_D K^+)$

VALUE	DOCUMENT ID		TECN	COMMENT
0.054±0.091±0.011	[1] AAIJ	15W	LHCB	pp at 7, 8 TeV

[1] Uses $D \to \pi^+\pi^-\pi^0$ mode.

$A_{CP}(B^+ \to \overline{D}{}^0K^*(892)^+)$

VALUE	DOCUMENT ID		TECN	COMMENT
−0.007±0.019 OUR AVERAGE				
−0.004±0.023±0.008	[1] AAIJ	17BO	LHCB	pp at 7, 8, 13 TeV
−0.013±0.031±0.009	[2] AAIJ	17BO	LHCB	pp at 7, 8, 13 TeV

[1] Uses $B^\pm \to [K^\pm\pi^\mp]_D K^*(892)^\pm$ decay mode .
[2] Uses $B^\pm \to [K^\pm\pi^\mp\pi^+\pi^-]_D K^*(892)^\pm$ decay mode .

$A_{CP}(B^+ \to [K^-\pi^+]_{\overline{D}}K^*(892)^+)$

VALUE	DOCUMENT ID		TECN	COMMENT
−0.75±0.16 OUR AVERAGE				
−0.81±0.17±0.04	AAIJ	17BO	LHCB	pp at 7, 8, 13 TeV
−0.34±0.43±0.16	AUBERT	09AJ	BABR	$e^+e^- \to \Upsilon(4S)$

• • • We do not use the following data for averages, fits, limits, etc. • • •

$-0.22\pm0.61\pm0.17$	AUBERT,B	05V	BABR	Repl. by AUBERT 09AJ

$A_{CP}(B^+ \to [K^-\pi^+\pi^-\pi^+]_{\overline{D}} K^*(892)^+)$

VALUE	DOCUMENT ID		TECN	COMMENT
$-0.45\pm0.21\pm0.14$	AAIJ	17BO	LHCB	pp at 7, 8, 13 TeV

$A_{CP}(B^+ \to [K^-\pi^+]_D \pi^+)$

VALUE	DOCUMENT ID		TECN	COMMENT
0.00±0.09 OUR AVERAGE				
$0.13\pm0.25\pm0.02$	AALTONEN	11AJ	CDF	$p\overline{p}$ at 1.96 TeV
$-0.04\pm0.11^{+0.02}_{-0.01}$	HORII	11	BELL	$e^+e^- \to \Upsilon(4S)$
$0.03\pm0.17\pm0.04$	DEL-AMO-SA...	10H	BABR	$e^+e^- \to \Upsilon(4S)$

• • • We do not use the following data for averages, fits, limits, etc. • • •

$-0.02^{+0.15}_{-0.16}\pm0.04$	HORII	08	BELL	Repl. by HORII 11
$+0.30^{+0.29}_{-0.25}\pm0.06$	SAIGO	05	BELL	Repl. by HORII 08

$A_{CP}(B^+ \to [K^-\pi^+\pi^0]_D \pi^+)$

VALUE	DOCUMENT ID		TECN	COMMENT
0.35 ±0.16 OUR AVERAGE				
$0.438\pm0.190\pm0.011$	[1] AAIJ	15W	LHCB	pp at 7, 8 TeV
$0.16\ \pm0.27\ ^{+0.03}_{-0.04}$	NAYAK	13	BELL	$e^+e^- \to \Upsilon(4S)$

[1] Uses $D^0 \to K^-\pi^+\pi^0$ for the favored mode, and $D^0 \to K^+\pi^-\pi^0$ for the suppressed mode.

$A_{CP}(B^+ \to [K^+K^-\pi^0]_D \pi^+)$

VALUE	DOCUMENT ID		TECN	COMMENT
$-0.030\pm0.040\pm0.005$	[1] AAIJ	15W	LHCB	pp at 7, 8 TeV

[1] Uses $D \to K^+K^-$ mode.

$A_{CP}(B^+ \to [\pi^+\pi^-\pi^0]_D \pi^+)$

VALUE	DOCUMENT ID		TECN	COMMENT
$-0.016\pm0.020\pm0.004$	[1] AAIJ	15W	LHCB	pp at 7, 8 TeV

[1] Uses $D \to \pi^+\pi^-$ mode.

$A_{CP}(B^+ \to [K^-\pi^+]_{(D\pi)} \pi^+)$

VALUE	DOCUMENT ID		TECN	COMMENT
$-0.09\pm0.27\pm0.05$	DEL-AMO-SA...	10H	BABR	$e^+e^- \to \Upsilon(4S)$

$A_{CP}(B^+ \to [K^-\pi^+]_{(D\gamma)} \pi^+)$

VALUE	DOCUMENT ID		TECN	COMMENT
$-0.65\pm0.55\pm0.22$	DEL-AMO-SA...	10H	BABR	$e^+e^- \to \Upsilon(4S)$

$A_{CP}(B^+ \to [K^-\pi^+]_{(D\pi)} K^+)$

VALUE	DOCUMENT ID		TECN	COMMENT
$0.77\pm0.35\pm0.12$	DEL-AMO-SA...	10H	BABR	$e^+e^- \to \Upsilon(4S)$

$A_{CP}(B^+ \to [K^-\pi^+]_{(D\gamma)} K^+)$

VALUE	DOCUMENT ID		TECN	COMMENT
$0.36\pm0.94^{+0.25}_{-0.41}$	DEL-AMO-SA...	10H	BABR	$e^+e^- \to \Upsilon(4S)$

$A_{CP}(B^+ \to [\pi^+\pi^-\pi^0]_D K^+)$

VALUE	DOCUMENT ID		TECN	COMMENT
$-0.02\pm0.15\pm0.03$	[1] AUBERT	07BJ	BABR	$e^+e^- \to \Upsilon(4S)$

• • • We do not use the following data for averages, fits, limits, etc. • • •

$-0.02\pm0.16\pm0.03$	AUBERT,B	05T	BABR	Repl. by AUBERT 07BJ

[1] Uses a Dalitz plot analysis of $D^0 \to \pi^+\pi^-\pi^0$. Also reports the one-sigma regions: $0.06 < r_B < 0.78$, $-30^\circ < \gamma < 76^\circ$, and $-27^\circ < \delta < 78^\circ$.

$A_{CP}(B^+ \to [K^0_S K^+\pi^-]_D K^+)$

VALUE	DOCUMENT ID		TECN	COMMENT
$0.040\pm0.091\pm0.018$	[1] AAIJ	14V	LHCB	pp at 7, 8 TeV

[1] The anaysis uses all of $D \to K^0_S K\pi$ Dalitz decays.

$A_{CP}(B^+ \to [K^0_S K^-\pi^+]_D K^+)$

VALUE	DOCUMENT ID		TECN	COMMENT
$0.233\pm0.129\pm0.024$	[1] AAIJ	14V	LHCB	pp at 7, 8 TeV

[1] The anaysis uses all of $D \to K^0_S K\pi$ Dalitz decays.

$A_{CP}(B^+ \to [K^0_S K^-\pi^+]_D \pi^+)$

VALUE	DOCUMENT ID		TECN	COMMENT
$-0.052\pm0.029\pm0.017$	[1] AAIJ	14V	LHCB	pp at 7, 8 TeV

[1] The anaysis uses all of $D \to K^0_S K\pi$ Dalitz decays.

$A_{CP}(B^+ \to [K^0_S K^+\pi^-]_D \pi^+)$

VALUE	DOCUMENT ID		TECN	COMMENT
$-0.025\pm0.024\pm0.010$	[1] AAIJ	14V	LHCB	pp at 7, 8 TeV

[1] The anaysis uses all of $D \to K^0_S K\pi$ Dalitz decays.

$A_{CP}(B^+ \to [K^*(892)^- K^+]_D K^+)$

VALUE	DOCUMENT ID		TECN	COMMENT
$0.026\pm0.109\pm0.029$	[1] AAIJ	14V	LHCB	pp at 7, 8 TeV

[1] The Analysis uses $D \to K^*(892)\,K \to K^0_S K\pi$ decays.

$A_{CP}(B^+ \to [K^*(892)^+ K^-]_D K^+)$

VALUE	DOCUMENT ID		TECN	COMMENT
$0.336\pm0.208\pm0.026$	[1] AAIJ	14V	LHCB	pp at 7, 8 TeV

[1] The Analysis uses $D \to K^*(892)\,K \to K^0_S K\pi$ decays.

$A_{CP}(B^+ \to [K^*(892)^+ K^-]_D \pi^+)$

VALUE	DOCUMENT ID		TECN	COMMENT
$-0.054\pm0.043\pm0.017$	[1] AAIJ	14V	LHCB	pp at 7, 8 TeV

[1] The Analysis uses $D \to K^*(892)\,K \to K^0_S K\pi$ decays.

$A_{CP}(B^+ \to [K^*(892)^- K^+]_D \pi^+)$

VALUE	DOCUMENT ID		TECN	COMMENT
$-0.012\pm0.028\pm0.010$	[1] AAIJ	14V	LHCB	pp at 7, 8 TeV

[1] The Analysis uses $D \to K^*(892)\,K \to K^0_S K\pi$ decays.

$A_{CP}(B^+ \to D_{CP(+1)} K^+)$

VALUE	DOCUMENT ID		TECN	COMMENT
0.120±0.014 OUR AVERAGE	Error includes scale factor of 1.4. See the ideogram below.			
$0.126\pm0.014\pm0.002$	[1] AAIJ	18A	LHCB	pp at 7, 8, 13 TeV
$0.115\pm0.025\pm0.007$	[2] AAIJ	18A	LHCB	pp at 7, 8, 13 TeV
$0.097\pm0.018\pm0.009$	AAIJ	16L	LHCB	pp at 7, 8 TeV
$0.39\ \pm0.17\ \pm0.04$	AALTONEN	10A	CDF	$p\overline{p}$ at 1.96 TeV
$0.25\ \pm0.06\ \pm0.02$	[3] DEL-AMO-SA...	10G	BABR	$e^+e^- \to \Upsilon(4S)$
$0.06\ \pm0.14\ \pm0.05$	ABE	06	BELL	$e^+e^- \to \Upsilon(4S)$

• • • We do not use the following data for averages, fits, limits, etc. • • •

$0.145\pm0.032\pm0.010$	[4] AAIJ	12M	LHCB	Repl. by AAIJ 16L
$0.27\ \pm0.09\ \pm0.04$	AUBERT	08AA	BABR	Repl. by DEL-AMO-SANCHEZ 10G
$0.35\ \pm0.13\ \pm0.04$	AUBERT	06J	BABR	Repl. by AUBERT 08AA
$0.07\ \pm0.17\ \pm0.06$	AUBERT	04N	BABR	Repl. by AUBERT 06J
$0.29\ \pm0.26\ \pm0.05$	[5] ABE	03D	BELL	Repl. by SWAIN 03
$0.06\ \pm0.19\ \pm0.04$	[6] SWAIN	03	BELL	Repl. by ABE 06

[1] Uses $D \to K^+K^-$ decay mode.
[2] Uses $D \to \pi^+\pi^-$ decay mode.
[3] Reports the first evidence for direct CP violation in $B \to D\,K$ decays with 3.6 standard deviations.
[4] AAIJ 12M reports an evidence of direct CP violation in $B^\pm \to D\,K^\pm$ decays with a total significance of 5.8 σ.
[5] Corresponds to 90% confidence range $-0.14 < A_{CP} < 0.73$.
[6] Corresponds to 90% confidence range $-0.26 < A_{CP} < 0.38$.

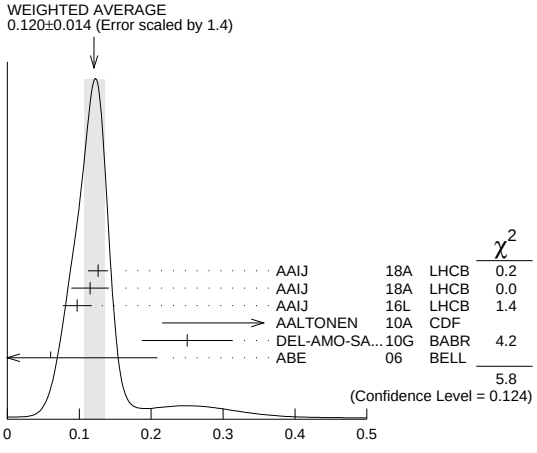

$A_{CP}(B^+ \to D_{CP(+1)} K^+)$

$A_{ADS}(B^+ \to D\,K^+)$

$A_{ADS}(B^+ \to D\,K^+) = \dfrac{(R_K^- - R_K^+)}{(R_K^- + R_K^+)}$ where

$R_K^- = \Gamma(B^- \to [K^+\pi^-]_D K^-) / \Gamma(B^- \to [K^-\pi^+]_D K^-)$ and

$R_K^+ = \Gamma(B^+ \to [K^-\pi^+]_D K^+) / \Gamma(B^+ \to [K^+\pi^-]_D K^+)$

VALUE	DOCUMENT ID		TECN	COMMENT
$-0.403\pm0.056\pm0.011$	AAIJ	16L	LHCB	pp at 7, 8 TeV

• • • We do not use the following data for averages, fits, limits, etc. • • •

$-0.52\ \pm0.15\ \pm0.02$	AAIJ	12M	LHCB	Repl. by AAIJ 16L

$A_{ADS}(B^+ \to D\pi^+)$

$A_{ADS}(B^+ \to D\pi^+) = \frac{(R_\pi^- - R_\pi^+)}{(R_\pi^- + R_\pi^+)}$ where

$R_\pi^- = \Gamma(B^- \to [K^+\pi^-]_D\pi^-) / \Gamma(B^- \to [K^-\pi^+]_D\pi^-)$ and

$R_\pi^+ = \Gamma(B^+ \to [K^-\pi^+]_D\pi^+) / \Gamma(B^+ \to [K^+\pi^-]_D\pi^+)$

VALUE	DOCUMENT ID		TECN	COMMENT
0.100±0.031±0.009	AAIJ	16L	LHCB	pp at 7, 8 TeV
• • • We do not use the following data for averages, fits, limits, etc. • • •				
0.143±0.062±0.011	AAIJ	12M	LHCB	Repl. by AAIJ 16L

$A_{ADS}(B^+ \to [K^-\pi^+]_D K^+\pi^-\pi^+)$

VALUE	DOCUMENT ID		TECN	COMMENT
$-0.33^{+0.36}_{-0.34}$	AAIJ	15BC	LHCB	pp at 7, 8 TeV

$A_{ADS}(B^+ \to [K^-\pi^+]_D\pi^+\pi^-\pi^+)$

VALUE	DOCUMENT ID		TECN	COMMENT
−0.013±0.087	AAIJ	15BC	LHCB	pp at 7, 8 TeV

$A_{CP}(B^+ \to D_{CP(-1)}K^+)$

VALUE	DOCUMENT ID		TECN	COMMENT
−0.10±0.07 OUR AVERAGE				
−0.09±0.07±0.02	DEL-AMO-SA...10G		BABR	$e^+e^- \to \Upsilon(4S)$
−0.12±0.14±0.05	ABE	06	BELL	$e^+e^- \to \Upsilon(4S)$
• • • We do not use the following data for averages, fits, limits, etc. • • •				
−0.09±0.09±0.02	AUBERT	08AA	BABR	Repl. by DEL-AMO-SANCHEZ 10G
−0.06±0.13±0.04	AUBERT	06J	BABR	Repl. by AUBERT 08AA
−0.22±0.24±0.04	[1] ABE	03D	BELL	Repl. by SWAIN 03
−0.19±0.17±0.05	[2] SWAIN	03	BELL	Repl. by ABE 06

[1] Corresponds to 90% confidence range $-0.62 < A_{CP} < 0.18$.
[2] Corresponds to 90% confidence range $-0.47 < A_{CP} < 0.11$.

$A_{CP}(B^+ \to [K^+K^-]_D K^+\pi^-\pi^+)$

VALUE	DOCUMENT ID		TECN	COMMENT
−0.045±0.064±0.011	AAIJ	15BC	LHCB	pp at 7, 8 TeV

$A_{CP}(B^+ \to [\pi^+\pi^-]_D K^+\pi^-\pi^+)$

VALUE	DOCUMENT ID		TECN	COMMENT
−0.054±0.101±0.011	AAIJ	15BC	LHCB	pp at 7, 8 TeV

$A_{CP}(B^+ \to [K^-\pi^+]_D K^+\pi^-\pi^+)$

VALUE	DOCUMENT ID		TECN	COMMENT
0.013±0.019±0.013	AAIJ	15BC	LHCB	pp at 7, 8 TeV

$A_{CP}(B^+ \to [K^+K^-]_D\pi^+\pi^-\pi^+)$

VALUE	DOCUMENT ID		TECN	COMMENT
−0.019±0.011±0.010	AAIJ	15BC	LHCB	pp at 7, 8 TeV

$A_{CP}(B^+ \to [\pi^+\pi^-]_D\pi^+\pi^-\pi^+)$

VALUE	DOCUMENT ID		TECN	COMMENT
−0.013±0.016±0.010	AAIJ	15BC	LHCB	pp at 7, 8 TeV

$A_{CP}(B^+ \to [K^-\pi^+]_D\pi^+\pi^-\pi^+)$

VALUE	DOCUMENT ID		TECN	COMMENT
−0.002±0.003±0.011	AAIJ	15BC	LHCB	pp at 7, 8 TeV

$A_{CP}(B^+ \to \overline{D}^{*0}\pi^+)$

VALUE	DOCUMENT ID		TECN	COMMENT
0.0010±0.0028 OUR AVERAGE				
0.000 ±0.006 ±0.001	[1] AAIJ	18A	LHCB	pp at 7, 8, 13 TeV
0.002 ±0.003 ±0.001	[2] AAIJ	18A	LHCB	pp at 7, 8, 13 TeV
−0.014 ±0.015	ABE	06	BELL	$e^+e^- \to \Upsilon(4S)$

[1] Uses $D^{*0} \to D^0\gamma$ decay mode.
[2] Uses $D^{*0} \to D^0\pi^0$ decay mode.

$A_{CP}(B^+ \to (D^*_{CP(+1)})^0\pi^+)$

VALUE	DOCUMENT ID		TECN	COMMENT
0.016±0.010 OUR AVERAGE Error includes scale factor of 1.2.				
−0.003±0.017±0.002	[1] AAIJ	18A	LHCB	pp at 7, 8, 13 TeV
0.025±0.010±0.003	[2] AAIJ	18A	LHCB	pp at 7, 8, 13 TeV
−0.021±0.045	ABE	06	BELL	$e^+e^- \to \Upsilon(4S)$

[1] Uses $D^{*0} \to D^0\gamma$ decay mode.
[2] Uses $D^{*0} \to D^0\pi^0$ decay mode.

$A_{CP}(B^+ \to (D^*_{CP(-1)})^0\pi^+)$

VALUE	DOCUMENT ID		TECN	COMMENT
−0.090±0.051	ABE	06	BELL	$e^+e^- \to \Upsilon(4S)$

$A_{CP}(B^+ \to D^{*0}K^+)$

VALUE	DOCUMENT ID		TECN	COMMENT
−0.001±0.011 OUR AVERAGE Error includes scale factor of 1.1.				
0.001±0.021±0.007	[1] AAIJ	18A	LHCB	pp at 7, 8, 13 TeV
0.006±0.012±0.004	[2] AAIJ	18A	LHCB	pp at 7, 8, 13 TeV
−0.06 ±0.04 ±0.01	AUBERT	08BF	BABR	$e^+e^- \to \Upsilon(4S)$
−0.089±0.086	ABE	06	BELL	$e^+e^- \to \Upsilon(4S)$

[1] Uses $D^{*0} \to D^0\gamma$ decay mode.
[2] Uses $D^{*0} \to D^0\pi^0$ decay mode.

$A_{CP}(B^+ \to D^{*0}_{CP(+1)}K^+)$

VALUE	DOCUMENT ID		TECN	COMMENT
−0.11 ±0.08 OUR AVERAGE Error includes scale factor of 2.7. See the ideogram below.				
0.276±0.094±0.047	[1] AAIJ	18A	LHCB	pp at 7, 8, 13 TeV
−0.151±0.033±0.011	[2] AAIJ	18A	LHCB	pp at 7, 8, 13 TeV
−0.11 ±0.09 ±0.01	AUBERT	08BF	BABR	$e^+e^- \to \Upsilon(4S)$
−0.20 ±0.22 ±0.04	ABE	06	BELL	$e^+e^- \to \Upsilon(4S)$
• • • We do not use the following data for averages, fits, limits, etc. • • •				
−0.10 ±0.23 $^{+0.03}_{-0.04}$	AUBERT	05N	BABR	Repl. by AUBERT 08BF

[1] Uses $D^{*0} \to D^0\gamma$ decay mode.
[2] Uses $D^{*0} \to D^0\pi^0$ decay mode.

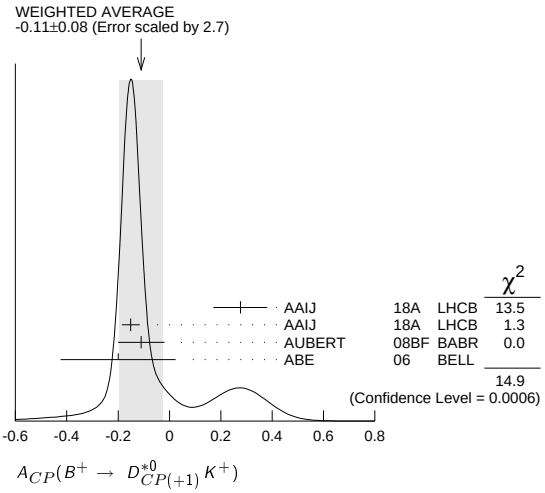

$A_{CP}(B^+ \to D^{*0}_{CP(+1)}K^+)$

$A_{CP}(B^+ \to D^*_{CP(-1)}K^+)$

VALUE	DOCUMENT ID		TECN	COMMENT
0.07±0.10 OUR AVERAGE				
+0.06±0.10±0.02	AUBERT	08BF	BABR	$e^+e^- \to \Upsilon(4S)$
+0.13±0.30±0.08	ABE	06	BELL	$e^+e^- \to \Upsilon(4S)$

$A_{CP}(B^+ \to D_{CP(+1)}K^*(892)^+)$

VALUE	DOCUMENT ID		TECN	COMMENT
0.08±0.06 OUR AVERAGE				
0.08±0.06±0.01	[1] AAIJ	17BO	LHCB	pp at 7, 8, 13 TeV
0.09±0.13±0.06	AUBERT	09AJ	BABR	$e^+e^- \to \Upsilon(4S)$
• • • We do not use the following data for averages, fits, limits, etc. • • •				
−0.08±0.19±0.08	AUBERT,B	05U	BABR	Repl. by AUBERT 09AJ

[1] Measures the asymmetry separately for K^+K^- and $\pi^+\pi^-$ final states, $A(KK) = 0.06 \pm 0.07 \pm 0.01$and $A(\pi\pi) = 0.15 \pm 0.13 \pm 0.02$, and combines the two results.

$A_{CP}(B^+ \to D_{CP(-1)}K^*(892)^+)$

VALUE	DOCUMENT ID		TECN	COMMENT
−0.23±0.21±0.07	AUBERT	09AJ	BABR	$e^+e^- \to \Upsilon(4S)$
• • • We do not use the following data for averages, fits, limits, etc. • • •				
−0.26±0.40±0.12	AUBERT,B	05U	BABR	Repl. by AUBERT 09AJ

$A_{CP}(B^+ \to D_s^+\phi)$

VALUE	DOCUMENT ID		TECN	COMMENT
−0.01±0.41±0.03	AAIJ	13R	LHCB	pp at 7 TeV

$A_{CP}(B^+ \to D^{*+}\overline{D}^{*0})$

VALUE	DOCUMENT ID		TECN	COMMENT
−0.15±0.11±0.02	AUBERT,B	06A	BABR	$e^+e^- \to \Upsilon(4S)$

$A_{CP}(B^+ \to D^{*+}\overline{D}^0)$

VALUE	DOCUMENT ID		TECN	COMMENT
−0.06±0.13±0.02	AUBERT,B	06A	BABR	$e^+e^- \to \Upsilon(4S)$

$A_{CP}(B^+ \to D^+\overline{D}^{*0})$

VALUE	DOCUMENT ID		TECN	COMMENT
0.13±0.18±0.04	AUBERT,B	06A	BABR	$e^+e^- \to \Upsilon(4S)$

Meson Particle Listings

$B^{\pm}$

$A_{CP}(B^+ \to D^+\overline{D}^0)$

VALUE	DOCUMENT ID		TECN	COMMENT
-0.03 ± 0.07 OUR AVERAGE				
$0.00\pm0.08\pm0.02$	ADACHI	08	BELL	$e^+e^- \to \Upsilon(4S)$
$-0.13\pm0.14\pm0.02$	AUBERT,B	06A	BABR	$e^+e^- \to \Upsilon(4S)$

$A_{CP}(B^+ \to K^0_S\pi^+)$

VALUE	DOCUMENT ID		TECN	COMMENT
-0.017 ± 0.016 OUR AVERAGE				
$-0.022\pm0.025\pm0.010$	AAIJ	13BS	LHCB	pp at 7 TeV
$-0.011\pm0.021\pm0.006$	DUH	13	BELL	$e^+e^- \to \Upsilon(4S)$
$-0.029\pm0.039\pm0.010$	[1] AUBERT,BE	06C	BABR	$e^+e^- \to \Upsilon(4S)$
$0.18\ \pm0.24$	[2] CHEN	00	CLE2	$e^+e^- \to \Upsilon(4S)$
• • • We do not use the following data for averages, fits, limits, etc. • • •				
$0.03\ \pm0.03\ \pm0.01$	LIN	07	BELL	Repl. by DUH 13
$-0.09\ \pm0.05\ \pm0.01$	[3] AUBERT,BE	05E	BABR	Repl. by AUBERT,BE 06C
$0.05\ \pm0.05\ \pm0.01$	[4] CHAO	05A	BELL	Repl. by LIN 07
$-0.05\ \pm0.08\ \pm0.01$	[5] AUBERT	04M	BABR	Repl. by AUBERT,BE 05E
$0.07\ ^{+0.09}_{-0.08}\ ^{+0.01}_{-0.03}$	[6] UNNO	03	BELL	Repl. by CHAO 05A
$0.46\ \pm0.15\ \pm0.02$	[7] CASEY	02	BELL	Repl. by UNNO 03
$0.098^{+0.430}_{-0.343}{}^{+0.020}_{-0.063}$	[8] ABE	01K	BELL	Repl. by CASEY 02
$-0.21\ \pm0.18\ \pm0.03$	[9] AUBERT	01E	BABR	Repl. by AUBERT 04M

[1] Corresponds to 90% confidence range $-0.092 < A_{CP} < 0.036$.
[2] Corresponds to 90% confidence range $-0.22 < A_{CP} < 0.56$.
[3] Corresponds to 90% confidence range $-0.16 < A_{CP} < -0.02$.
[4] Corresponds to 90% confidence range $-0.04 < A_{CP} < 0.13$.
[5] Corresponds to 90% confidence range $-0.18 < A_{CP} < 0.08$.
[6] Corresponds to 90% confidence range $-0.10 < A_{CP} < +0.22$.
[7] Corresponds to 90% confidence range $+0.19 < A_{CP} < +0.72$.
[8] Corresponds to 90% confidence range $-0.53 < A_{CP} < 0.82$.
[9] Corresponds to 90% confidence range $-0.51 < A_{CP} < 0.09$.

$A_{CP}(B^+ \to K^+\pi^0)$

VALUE	DOCUMENT ID		TECN	COMMENT
0.037 ± 0.021 OUR AVERAGE				
$0.043\pm0.024\pm0.002$	DUH	13	BELL	$e^+e^- \to \Upsilon(4S)$
$0.030\pm0.039\pm0.010$	AUBERT	07BC	BABR	$e^+e^- \to \Upsilon(4S)$
$-0.29\ \pm0.23$	[1] CHEN	00	CLE2	$e^+e^- \to \Upsilon(4S)$
• • • We do not use the following data for averages, fits, limits, etc. • • •				
$0.07\ \pm0.03\ \pm0.01$	LIN	08	BELL	Repl. by DUH 13
$0.06\ \pm0.06\ \pm0.01$	[2] AUBERT	05L	BABR	Repl. by AUBERT 07BC
$0.06\ \pm0.06\ \pm0.02$	[2] CHAO	05A	BELL	Repl. by CHAO 04B
$0.04\ \pm0.05\ \pm0.02$	[3] CHAO	04B	BELL	Repl. by LIN 08
$-0.09\ \pm0.09\ \pm0.01$	[4] AUBERT	03L	BABR	Repl. by AUBERT 05L
$-0.02\ \pm0.19\ \pm0.02$	[5] CASEY	02	BELL	Repl. by CHAO 04B
$-0.059^{+0.222}_{-0.196}{}^{+0.055}_{-0.017}$	[6] ABE	01K	BELL	Repl. by CASEY 02
$0.00\ \pm0.18\ \pm0.04$	[7] AUBERT	01E	BABR	Repl. by AUBERT 03L

[1] Corresponds to 90% confidence range $-0.67 < A_{CP} < 0.09$.
[2] Corresponds to a 90% CL interval of $-0.06 < A_{CP} < 0.18$.
[3] Corresponds to 90% CL interval of $-0.05 < A_{CP} < 0.13$.
[4] Corresponds to 90% confidence range $-0.24 < A_{CP} < 0.06$.
[5] Corresponds to 90% confidence range $-0.35 < A_{CP} < +0.30$.
[6] Corresponds to 90% confidence range $-0.40 < A_{CP} < 0.36$.
[7] Corresponds to 90% confidence range $-0.30 < A_{CP} < +0.30$.

$A_{CP}(B^+ \to \eta' K^+)$

VALUE	DOCUMENT ID		TECN	COMMENT
0.004 ± 0.011 OUR AVERAGE				
$-0.002\pm0.012\pm0.006$	[1] AAIJ	15O	LHCB	pp at 7, 8 TeV
$0.008^{+0.017}_{-0.018}\pm0.009$	AUBERT	09AV	BABR	$e^+e^- \to \Upsilon(4S)$
$0.028\pm0.028\pm0.021$	SCHUEMANN	06	BELL	$e^+e^- \to \Upsilon(4S)$
$0.03\ \pm0.12$	[2] CHEN	00	CLE2	$e^+e^- \to \Upsilon(4S)$
• • • We do not use the following data for averages, fits, limits, etc. • • •				
$0.010\pm0.022\pm0.006$	AUBERT	07AE	BABR	Repl. by AUBERT 09AV
$0.033\pm0.028\pm0.005$	[3] AUBERT	05M	BABR	Repl. by AUBERT 07AE
$0.037\pm0.045\pm0.011$	[4] AUBERT	03W	BABR	Repl. by AUBERT 05M
$-0.11\ \pm0.11\ \pm0.02$	[5] AUBERT	02E	BABR	Repl. by AUBERT 05M
$-0.015\pm0.070\pm0.009$	[6] CHEN	02B	BELL	Repl. by SCHUEMANN 06
$0.06\ \pm0.15\ \pm0.01$	[7] ABE	01M	BELL	Repl. by CHEN 02B

[1] Obtained using $A_{CP}(B^{\pm} \to J/\psi K^{\pm}) = (0.3 \pm 0.6) \times 10^{-2}$.
[2] Corresponds to 90% confidence range $-0.17 < A_{CP} < 0.23$.
[3] Corresponds to 90% confidence range $-0.012 < A_{CP} < 0.078$.
[4] Corresponds to 90% confidence range $-0.04 < A_{CP} < 0.11$.
[5] Corresponds to 90% confidence range $-0.28 < A_{CP} < 0.07$.
[6] Corresponds to 90% confidence range $-0.13 < A_{CP} < 0.10$.
[7] Corresponds to 90% confidence range $-0.20 < A_{CP} < 0.32$.

$A_{CP}(B^+ \to \eta' K^*(892)^+)$

VALUE	DOCUMENT ID		TECN	COMMENT
$-0.26\pm0.27\pm0.02$	DEL-AMO-SA...10A		BABR	$e^+e^- \to \Upsilon(4S)$
• • • We do not use the following data for averages, fits, limits, etc. • • •				
$-0.30^{+0.33}_{-0.37}\pm0.02$	[1] AUBERT	07E	BABR	Repl. by DEL-AMO-SANCHEZ 10A

[1] Reports A_{CP} with the opposite sign convention.

$A_{CP}(B^+ \to \eta' K_0^*(1430)^+)$

VALUE	DOCUMENT ID		TECN	COMMENT
$0.06\pm0.20\pm0.02$	DEL-AMO-SA...10A		BABR	$e^+e^- \to \Upsilon(4S)$

$A_{CP}(B^+ \to \eta' K_2^*(1430)^+)$

VALUE	DOCUMENT ID		TECN	COMMENT
$0.15\pm0.13\pm0.02$	DEL-AMO-SA...10A		BABR	$e^+e^- \to \Upsilon(4S)$

$A_{CP}(B^+ \to \eta K^+)$

VALUE	DOCUMENT ID		TECN	COMMENT
-0.37 ± 0.08 OUR AVERAGE				
$-0.38\pm0.11\pm0.01$	HOI	12	BELL	$e^+e^- \to \Upsilon(4S)$
$-0.36\pm0.11\pm0.03$	AUBERT	09AV	BABR	$e^+e^- \to \Upsilon(4S)$
• • • We do not use the following data for averages, fits, limits, etc. • • •				
$-0.22\pm0.11\pm0.01$	AUBERT	07AE	BABR	Repl. by AUBERT 09AV
$-0.39\pm0.16\pm0.03$	CHANG	07B	BELL	Repl. by HOI 12
$-0.20\pm0.15\pm0.01$	AUBERT,B	05K	BABR	Repl. by AUBERT 07AE
$-0.49\pm0.31\pm0.07$	CHANG	05A	BELL	Repl. by CHANG 07B
$-0.52\pm0.24\pm0.01$	AUBERT	04H	BABR	Repl. by AUBERT,B 05K

$A_{CP}(B^+ \to \eta K^*(892)^+)$

VALUE	DOCUMENT ID		TECN	COMMENT
0.02 ± 0.06 OUR AVERAGE				
$0.03\pm0.10\pm0.01$	WANG	07B	BELL	$e^+e^- \to \Upsilon(4S)$
$0.01\pm0.08\pm0.02$	AUBERT,B	06H	BABR	$e^+e^- \to \Upsilon(4S)$
• • • We do not use the following data for averages, fits, limits, etc. • • •				
$0.13\pm0.14\pm0.02$	AUBERT,B	04D	BABR	Repl. by AUBERT,B 06H

$A_{CP}(B^+ \to \eta K_0^*(1430)^+)$

VALUE	DOCUMENT ID		TECN	COMMENT
$0.05\pm0.13\pm0.02$	AUBERT,B	06H	BABR	$e^+e^- \to \Upsilon(4S)$

$A_{CP}(B^+ \to \eta K_2^*(1430)^+)$

VALUE	DOCUMENT ID		TECN	COMMENT
$-0.45\pm0.30\pm0.02$	AUBERT,B	06H	BABR	$e^+e^- \to \Upsilon(4S)$

$A_{CP}(B^+ \to \omega K^+)$

VALUE	DOCUMENT ID		TECN	COMMENT
-0.02 ± 0.04 OUR AVERAGE				
$-0.03\pm0.04\pm0.01$	CHOBANOVA	14	BELL	$e^+e^- \to \Upsilon(4S)$
$-0.01\pm0.07\pm0.01$	AUBERT	07AE	BABR	$e^+e^- \to \Upsilon(4S)$
• • • We do not use the following data for averages, fits, limits, etc. • • •				
$0.05\pm0.09\pm0.01$	AUBERT,B	06E	BABR	Repl. by AUBERT 07AE
$0.05^{+0.08}_{-0.07}\pm0.01$	JEN	06	BELL	Repl. by CHOBANOVA 14
$-0.09\pm0.17\pm0.01$	AUBERT	04H	BABR	Repl. by AUBERT,B 06E
$0.06^{+0.21}_{-0.18}\pm0.01$	[1] WANG	04A	BELL	Repl. by JEN 06
$-0.21\pm0.28\pm0.03$	[2] LU	02	BELL	Repl. by WANG 04A

[1] Corresponds to 90% CL interval $0.15 < A_{CP} < 0.90$
[2] Corresponds to 90% confidence range $-0.70 < A_{CP} < +0.38$.

$A_{CP}(B^+ \to \omega K^{*+})$

VALUE	DOCUMENT ID		TECN	COMMENT
$+0.29\pm0.35\pm0.02$	AUBERT	09H	BABR	$e^+e^- \to \Upsilon(4S)$

$A_{CP}(B^+ \to \omega (K\pi)_0^{*+})$

VALUE	DOCUMENT ID		TECN	COMMENT
$-0.10\pm0.09\pm0.02$	AUBERT	09H	BABR	$e^+e^- \to \Upsilon(4S)$

$A_{CP}(B^+ \to \omega K_2^*(1430)^+)$

VALUE	DOCUMENT ID		TECN	COMMENT
$+0.14\pm0.15\pm0.02$	AUBERT	09H	BABR	$e^+e^- \to \Upsilon(4S)$

$A_{CP}(B^+ \to K^{*0}\pi^+)$

VALUE	DOCUMENT ID		TECN	COMMENT
$-0.04\ \pm0.09$ OUR AVERAGE	Error includes scale factor of 2.1.			
$-0.12\ \pm0.21\ ^{+0.08}_{-0.14}$	[1] LEES	17G	BABR	$e^+e^- \to \Upsilon(4S)$
$0.032\pm0.052^{+0.016}_{-0.013}$	AUBERT	08AI	BABR	$e^+e^- \to \Upsilon(4S)$
$-0.149\pm0.064\pm0.022$	GARMASH	06	BELL	$e^+e^- \to \Upsilon(4S)$
• • • We do not use the following data for averages, fits, limits, etc. • • •				
$0.068\pm0.078^{+0.070}_{-0.067}$	AUBERT,B	05N	BABR	Repl. by AUBERT 08AI

[1] Obtains the result from a Dalitz analysis of $B^+ \to K^0_S\pi^+\pi^0$ decays. The first error is statistical, the second combines all the systematic uncertainties reported in the paper, including signal modelling.

$A_{CP}(B^+ \to K^*(892)^+\pi^0)$

VALUE	DOCUMENT ID		TECN	COMMENT
-0.39 ± 0.21 OUR AVERAGE	Error includes scale factor of 1.6.			
$-0.52\pm0.14^{+0.06}_{-0.05}$	[1] LEES	17G	BABR	$e^+e^- \to \Upsilon(4S)$
$-0.06\pm0.24\pm0.04$	LEES	11I	BABR	$e^+e^- \to \Upsilon(4S)$
• • • We do not use the following data for averages, fits, limits, etc. • • •				
$0.04\pm0.29\pm0.05$	AUBERT	05X	BABR	Repl. by LEES 11I

[1] Obtains the result from a Dalitz analysis of $B^+ \to K^0_S\pi^+\pi^0$ decays. The first error is statistical, the second combines all the systematic uncertainties reported in the paper, including signal modelling.

$A_{CP}(B^+ \to K^+\pi^-\pi^+)$

VALUE	DOCUMENT ID		TECN	COMMENT
0.027 ± 0.008 OUR AVERAGE				
$0.025\pm0.004\pm0.008$	[1] AAIJ	14BO	LHCB	pp at 7, 8 TeV
$0.028\pm0.020\pm0.023$	AUBERT	08AI	BABR	$e^+e^- \to \Upsilon(4S)$
$0.049\pm0.026\pm0.020$	GARMASH	06	BELL	$e^+e^- \to \Upsilon(4S)$
• • • We do not use the following data for averages, fits, limits, etc. • • •				
$0.032\pm0.008\pm0.008$	AAIJ	13AZ	LHCB	Repl. by AAIJ 14BO
$-0.013\pm0.037\pm0.011$	AUBERT,B	05N	BABR	Repl. by AUBERT 08AI
$0.01\ \pm0.07\ \pm0.03$	AUBERT	03M	BABR	Repl. by AUBERT,B 05N

[1] AAIJ 14BO reports also CP asymmetries in restricted regions of phase space.

$A_{CP}(B^+ \to K^+K^-K^+ \text{nonresonant})$

VALUE	DOCUMENT ID		TECN	COMMENT
$0.060\pm0.044\pm0.019$	LEES	12O	BABR	$e^+e^- \to \Upsilon(4S)$

$A_{CP}(B^+ \to f(980)^0K^+)$

VALUE	DOCUMENT ID		TECN	COMMENT
$-0.08\pm0.08\pm0.04$	[1] LEES	12O	BABR	$e^+e^- \to \Upsilon(4S)$

[1] Measured in the $B^+ \to K^+K^-K^+$ decay.

$A_{CP}(B^+ \to f_2(1270)K^+)$

VALUE	DOCUMENT ID		TECN	COMMENT
$-0.68^{+0.19}_{-0.17}$ OUR AVERAGE				
$-0.85\pm0.22^{+0.26}_{-0.13}$	AUBERT	08AI	BABR	$e^+e^- \to \Upsilon(4S)$
$-0.59\pm0.22\pm0.036$	GARMASH	06	BELL	$e^+e^- \to \Upsilon(4S)$

$A_{CP}(B^+ \to f_0(1500)K^+)$

VALUE	DOCUMENT ID		TECN	COMMENT
$0.28\pm0.26^{+0.15}_{-0.14}$	AUBERT	08AI	BABR	$e^+e^- \to \Upsilon(4S)$

$A_{CP}(B^+ \to f_2'(1525)^0K^+)$

VALUE	DOCUMENT ID		TECN	COMMENT
$-0.08\ ^{+0.05}_{-0.04}$ OUR AVERAGE				
$0.18\ \pm0.18\ \pm0.04$	[1] LEES	11I	BABR	$e^+e^- \to \Upsilon(4S)$
$-0.106\pm0.050^{+0.036}_{-0.015}$	AUBERT	08AI	BABR	$e^+e^- \to \Upsilon(4S)$
$-0.077\pm0.065^{+0.046}_{-0.026}$	GARMASH	06	BELL	$e^+e^- \to \Upsilon(4S)$
• • • We do not use the following data for averages, fits, limits, etc. • • •				
$0.14\ \pm0.10\ \pm0.04$	[2] LEES	12O	BABR	$e^+e^- \to \Upsilon(4S)$
$-0.31\ \pm0.25\ \pm0.08$	[3] AUBERT	06O	BABR	Repl. by LEES 12O
$0.088\pm0.095^{+0.097}_{-0.056}$	AUBERT,B	05N	BABR	Repl. by AUBERT 08AI

[1] Measured in $B^+ \to f_0K^+$ with $f_0 \to \pi^0\pi^0$ decay.

[2] Measured in the $B^+ \to K^+K^-K^+$ decay assuming $A_{CP}(B^+ \to f_2'(1525)^0K^+) = A_{CP}(B^+ \to f_0(1500)^0K^+) = A_{CP}(B^+ \to f_0(1710)^0K^+)$

[3] Measured in the $B^+ \to K^+K^-K^+$ decay.

$A_{CP}(B^+ \to \rho^0K^+)$

VALUE	DOCUMENT ID		TECN	COMMENT
0.37 ± 0.10 OUR AVERAGE				
$0.44\pm0.10^{+0.06}_{-0.14}$	AUBERT	08AI	BABR	$e^+e^- \to \Upsilon(4S)$
$0.30\pm0.11^{+0.11}_{-0.04}$	GARMASH	06	BELL	$e^+e^- \to \Upsilon(4S)$
• • • We do not use the following data for averages, fits, limits, etc. • • •				
$0.32\pm0.13^{+0.10}_{-0.08}$	AUBERT,B	05N	BABR	Repl. by AUBERT 08AI

$A_{CP}(B^+ \to K^0\pi^+\pi^0)$

VALUE	DOCUMENT ID		TECN	COMMENT
$0.07\pm0.05\pm0.04$	[1] LEES	17G	BABR	$e^+e^- \to \Upsilon(4S)$

[1] Obtains the result from a Dalitz analysis of $B^+ \to K^0_S\pi^+\pi^0$ decays. The first error is statistical, the second combines all the systematic uncertainties reported in the paper, including signal modelling.

$A_{CP}(B^+ \to K_0^*(1430)^0\pi^+)$

VALUE	DOCUMENT ID		TECN	COMMENT
0.061 ± 0.032 OUR AVERAGE				
$0.14\ \pm0.10\ ^{+0.14}_{-0.06}$	[1] LEES	17G	BABR	$e^+e^- \to \Upsilon(4S)$
$0.032\pm0.035^{+0.034}_{-0.028}$	AUBERT	08AI	BABR	$e^+e^- \to \Upsilon(4S)$
$0.076\pm0.038^{+0.028}_{-0.022}$	GARMASH	06	BELL	$e^+e^- \to \Upsilon(4S)$
• • • We do not use the following data for averages, fits, limits, etc. • • •				
$-0.064\pm0.032^{+0.023}_{-0.026}$	AUBERT,B	05N	BABR	Repl. by AUBERT 08AI

[1] Obtains the result from a Dalitz analysis of $B^+ \to K^0_S\pi^+\pi^0$ decays. The first error is statistical, the second combines all the systematic uncertainties reported in the paper, including signal modelling.

$A_{CP}(B^+ \to K_0^*(1430)^+\pi^0)$

VALUE	DOCUMENT ID		TECN	COMMENT
$0.26\pm0.12^{+0.14}_{-0.08}$	[1] LEES	17G	BABR	$e^+e^- \to \Upsilon(4S)$

[1] Obtains the result from a Dalitz analysis of $B^+ \to K^0_S\pi^+\pi^0$ decays. The first error is statistical, the second combines all the systematic uncertainties reported in the paper, including signal modelling.

$A_{CP}(B^+ \to K_2^*(1430)^0\pi^+)$

VALUE	DOCUMENT ID		TECN	COMMENT
$0.05\pm0.23^{+0.18}_{-0.08}$	AUBERT	08AI	BABR	$e^+e^- \to \Upsilon(4S)$

$A_{CP}(B^+ \to K^+\pi^0\pi^0)$

VALUE	DOCUMENT ID		TECN	COMMENT
$-0.06\pm0.06\pm0.04$	LEES	11I	BABR	$e^+e^- \to \Upsilon(4S)$

$A_{CP}(B^+ \to K^0\rho^+)$

VALUE	DOCUMENT ID		TECN	COMMENT
-0.03 ± 0.15 OUR AVERAGE				
$0.21\pm0.19^{+0.24}_{-0.20}$	[1] LEES	17G	BABR	$e^+e^- \to \Upsilon(4S)$
$-0.12\pm0.17\pm0.02$	AUBERT	07Z	BABR	$e^+e^- \to \Upsilon(4S)$

[1] Obtains the result from a Dalitz analysis of$B^+ \to K^0_S\pi^+\pi^0$ decays. The first error is statistical, the second combines all the systematic uncertainties reported in the paper, including signal modelling.

$A_{CP}(B^+ \to K^{*+}\pi^+\pi^-)$

VALUE	DOCUMENT ID		TECN	COMMENT
$0.07\pm0.07\pm0.04$	AUBERT,B	06U	BABR	$e^+e^- \to \Upsilon(4S)$

$A_{CP}(B^+ \to \rho^0K^*(892)^+)$

VALUE	DOCUMENT ID		TECN	COMMENT
$0.31\pm0.13\pm0.03$	DEL-AMO-SA...11D		BABR	$e^+e^- \to \Upsilon(4S)$
• • • We do not use the following data for averages, fits, limits, etc. • • •				
$0.20^{+0.32}_{-0.29}\pm0.04$	AUBERT	03V	BABR	Repl. by DEL-AMO-SANCHEZ 11D

$A_{CP}(B^+ \to K^*(892)^+f_0(980))$

VALUE	DOCUMENT ID		TECN	COMMENT
$-0.15\pm0.12\pm0.03$	DEL-AMO-SA...11D		BABR	$e^+e^- \to \Upsilon(4S)$
• • • We do not use the following data for averages, fits, limits, etc. • • •				
$-0.34\pm0.21\pm0.03$	AUBERT,B	06G	BABR	Repl. by DEL-AMO-SANCHEZ 11D

$A_{CP}(B^+ \to a_1^+K^0)$

VALUE	DOCUMENT ID		TECN	COMMENT
$+0.12\pm0.11\pm0.02$	AUBERT	08F	BABR	$e^+e^- \to \Upsilon(4S)$

$A_{CP}(B^+ \to b_1^+K^0)$

VALUE	DOCUMENT ID		TECN	COMMENT
$-0.03\pm0.15\pm0.02$	AUBERT	08AG	BABR	$e^+e^- \to \Upsilon(4S)$

$A_{CP}(B^+ \to K^*(892)^0\rho^+)$

VALUE	DOCUMENT ID		TECN	COMMENT
$-0.01\pm0.16\pm0.02$	AUBERT,B	06G	BABR	$e^+e^- \to \Upsilon(4S)$

$A_{CP}(B^+ \to b_1^0K^+)$

VALUE	DOCUMENT ID		TECN	COMMENT
$-0.46\pm0.20\pm0.02$	AUBERT	07BI	BABR	$e^+e^- \to \Upsilon(4S)$

$A_{CP}(B^+ \to K^0K^+)$

VALUE	DOCUMENT ID		TECN	COMMENT
$0.04\ \pm0.14$ OUR AVERAGE				
$0.014\pm0.168\pm0.002$	DUH	13	BELL	$e^+e^- \to \Upsilon(4S)$
$0.10\ \pm0.26\ \pm0.03$	[1] AUBERT,BE	06C	BABR	$e^+e^- \to \Upsilon(4S)$
• • • We do not use the following data for averages, fits, limits, etc. • • •				
$0.13\ ^{+0.23}_{-0.24}\ \pm0.02$	LIN	07	BELL	Repl. by DUH 13
$0.15\ \pm0.33\ \pm0.03$	[2] AUBERT,BE	05E	BABR	Repl. by AUBERT,BE 06C

[1] Corresponds to 90% confidence range $-0.31 < A_{CP} < 0.54$.

[2] Corresponds to 90% confidence range $-0.43 < A_{CP} < 0.68$.

Meson Particle Listings

$B^{\pm}$

$A_{CP}(B^+ \to K^0_S K^+)$

VALUE	DOCUMENT ID		TECN	COMMENT
$-0.21 \pm 0.14 \pm 0.01$	AAIJ	13BS	LHCB	pp at 7 TeV

$A_{CP}(B^+ \to K^+ K^0_S K^0_S)$

VALUE	DOCUMENT ID		TECN	COMMENT
$0.04^{+0.04}_{-0.05} \pm 0.02$	LEES	12O	BABR	$e^+e^- \to \Upsilon(4S)$
• • • We do not use the following data for averages, fits, limits, etc. • • •				
$-0.04 \pm 0.11 \pm 0.02$	[1] AUBERT,B	04V	BABR	Repl. by LEES 12O

[1] Corresponds to 90% confidence range $-0.23 < A_{CP} < 0.15$.

$A_{CP}(B^+ \to K^+ K^- \pi^+)$

VALUE	DOCUMENT ID		TECN	COMMENT
-0.122 ± 0.021 OUR AVERAGE				
$-0.170 \pm 0.073 \pm 0.017$	[1] HSU	17	BELL	$e^+e^- \to \Upsilon(4S)$
$-0.123 \pm 0.017 \pm 0.014$	[2] AAIJ	14BO	LHCB	pp at 7, 8 TeV
$0.00 \pm 0.10 \pm 0.03$	AUBERT	07BB	BABR	$e^+e^- \to \Upsilon(4S)$
• • • We do not use the following data for averages, fits, limits, etc. • • •				
$-0.141 \pm 0.040 \pm 0.019$	[3] AAIJ	14	LHCB	Repl. by AAIJ 14BO

[1] HSU 17 provides also measurement as a function of K^+K^- invariant mass.
[2] AAIJ 14BO reports also *CP* asymmetries in restricted regions of phase space.
[3] AAIJ 14 reports $A_{CP}(B^+ \to K^+ K^- \pi^+) = -0.648 \pm 0.070 \pm 0.013 \pm 0.007$ in the Dalitz plot region of $m^2_{K^+K^-} < 1.5$ GeV^2/c^4. The third uncertainty is due to the *CP* asymmetry of the $B^{\pm} \to J/\psi K^{\pm}$ reference mode uncertainty.

$A_{CP}(B^+ \to K^+ K^- K^+)$

VALUE	DOCUMENT ID		TECN	COMMENT
-0.033 ± 0.008 OUR AVERAGE				
$-0.036 \pm 0.004 \pm 0.007$	[1] AAIJ	14BO	LHCB	pp at 7, 8 TeV
$-0.017^{+0.019}_{-0.014} \pm 0.014$	[2] LEES	12O	BABR	$e^+e^- \to \Upsilon(4S)$
• • • We do not use the following data for averages, fits, limits, etc. • • •				
$-0.043 \pm 0.009 \pm 0.008$	AAIJ	13AZ	LHCB	Repl. by AAIJ 14BO
$-0.017 \pm 0.026 \pm 0.015$	AUBERT	06O	BABR	Repl. by LEES 12O
$0.02 \pm 0.07 \pm 0.03$	AUBERT	03M	BABR	Repl. by AUBERT 06O

[1] AAIJ 14BO reports also *CP* asymmetries in restricted regions of phase space.
[2] All intermediate charmonium and charm resonances are removed, except of χ_{c0}.

$A_{CP}(B^+ \to \phi K^+)$

VALUE	DOCUMENT ID		TECN	COMMENT
0.024 ± 0.028 OUR AVERAGE	Error includes scale factor of 2.3.			
$0.017 \pm 0.011 \pm 0.006$	[1] AAIJ	15O	LHCB	pp at 7, 8 TeV
$0.128 \pm 0.044 \pm 0.013$	LEES	12O	BABR	$e^+e^- \to \Upsilon(4S)$
$-0.07 \pm 0.17\ ^{+0.03}_{-0.02}$	ACOSTA	05J	CDF	$p\overline{p}$ at 1.96 TeV
$0.01 \pm 0.12 \pm 0.05$	[2] CHEN	03B	BELL	$e^+e^- \to \Upsilon(4S)$
• • • We do not use the following data for averages, fits, limits, etc. • • •				
$0.022 \pm 0.021 \pm 0.009$	AAIJ	14A	LHCB	Repl. by AAIJ 15O
$0.00 \pm 0.08 \pm 0.02$	AUBERT	06O	BABR	Repl. by LEES 12O
$0.04 \pm 0.09 \pm 0.01$	[3] AUBERT	04A	BABR	Repl. by AUBERT 06O
$-0.05 \pm 0.20 \pm 0.03$	[4] AUBERT	02E	BABR	$e^+e^- \to \Upsilon(4S)$

[1] Obtained using $A_{CP}(B^{\pm} \to J/\psi K^{\pm}) = (0.3 \pm 0.6) \times 10^{-2}$.
[2] Corresponds to 90% confidence range $-0.20 < A_{CP} < 0.22$.
[3] Corresponds to 90% confidence range $-0.10 < A_{CP} < 0.18$.
[4] Corresponds to 90% confidence range $-0.37 < A_{CP} < 0.28$.

$A_{CP}(B^+ \to X_0(1550) K^+)$

VALUE	DOCUMENT ID		TECN	COMMENT
$-0.04 \pm 0.07 \pm 0.02$	[1] AUBERT	06O	BABR	$e^+e^- \to \Upsilon(4S)$

[1] Measured in the $B^+ \to K^+K^-K^+$ decay.

$A_{CP}(B^+ \to K^{*+} K^+ K^-)$

VALUE	DOCUMENT ID		TECN	COMMENT
$0.11 \pm 0.08 \pm 0.03$	AUBERT,B	06U	BABR	$e^+e^- \to \Upsilon(4S)$

$A_{CP}(B^+ \to \phi K^*(892)^+)$

VALUE	DOCUMENT ID		TECN	COMMENT
-0.01 ± 0.08 OUR AVERAGE				
$0.00 \pm 0.09 \pm 0.04$	AUBERT	07BA	BABR	$e^+e^- \to \Upsilon(4S)$
$-0.02 \pm 0.14 \pm 0.03$	[1] CHEN	05A	BELL	$e^+e^- \to \Upsilon(4S)$
• • • We do not use the following data for averages, fits, limits, etc. • • •				
$0.16 \pm 0.17 \pm 0.03$	AUBERT	03V	BABR	Repl. by AUBERT 07BA
$-0.13 \pm 0.29^{+0.08}_{-0.11}$	[2] CHEN	03B	BELL	Repl. by CHEN 05A
$-0.43^{+0.36}_{-0.30} \pm 0.06$	[3] AUBERT	02E	BABR	Repl. by AUBERT 03V

[1] Corresponds to 90% confidence range $-0.25 < A_{CP} < 0.22$.
[2] Corresponds to 90% confidence range $-0.64 < A_{CP} < 0.36$.
[3] Corresponds to 90% confidence range $-0.88 < A_{CP} < 0.18$.

$A_{CP}(B^+ \to \phi(K\pi)^{*+}_0)$

VALUE	DOCUMENT ID		TECN	COMMENT
$0.04 \pm 0.15 \pm 0.04$	AUBERT	08BI	BABR	$e^+e^- \to \Upsilon(4S)$

$A_{CP}(B^+ \to \phi K_1(1270)^+)$

VALUE	DOCUMENT ID		TECN	COMMENT
$0.15 \pm 0.19 \pm 0.05$	AUBERT	08BI	BABR	$e^+e^- \to \Upsilon(4S)$

$A_{CP}(B^+ \to \phi K^*_2(1430)^+)$

VALUE	DOCUMENT ID		TECN	COMMENT
$-0.23 \pm 0.19 \pm 0.06$	AUBERT	08BI	BABR	$e^+e^- \to \Upsilon(4S)$

$A_{CP}(B^+ \to K^+ \phi\phi)$

VALUE	DOCUMENT ID		TECN	COMMENT
$-0.10 \pm 0.08 \pm 0.02$	[1] LEES	11A	BABR	$e^+e^- \to \Upsilon(4S)$

[1] $m_{\phi\phi} < 2.85$ GeV/c^2.

$A_{CP}(B^+ \to K^+[\phi\phi]_{\eta_c})$

VALUE	DOCUMENT ID		TECN	COMMENT
$0.09 \pm 0.10 \pm 0.02$	[1] LEES	11A	BABR	$e^+e^- \to \Upsilon(4S)$

[1] $m_{\phi\phi}$ is consistent with η_c mass [2.94, 3.02] GeV/c^2.

$A_{CP}(B^+ \to K^*(892)^+\gamma)$

VALUE	DOCUMENT ID		TECN	COMMENT
0.014 ± 0.018 OUR AVERAGE				
$0.011 \pm 0.023 \pm 0.003$	[1] HORIGUCHI	17	BELL	$e^+e^- \to \Upsilon(4S)$
$0.018 \pm 0.028 \pm 0.007$	AUBERT	09AO	BABR	$e^+e^- \to \Upsilon(4S)$

[1] Uses B($\Upsilon(4S) \to B^+B^-$) = (51.4 ± 0.6)% and B($\Upsilon(4S) \to B^0\overline{B}^0$) = (48.6 ± 0.6)%.

$A_{CP}(B^+ \to \eta K^+\gamma)$

VALUE	DOCUMENT ID		TECN	COMMENT
-0.12 ± 0.07 OUR AVERAGE				
$-0.09 \pm 0.10 \pm 0.01$	[1] AUBERT	09	BABR	$e^+e^- \to \Upsilon(4S)$
$-0.16 \pm 0.09 \pm 0.06$	[2] NISHIDA	05	BELL	$e^+e^- \to \Upsilon(4S)$
• • • We do not use the following data for averages, fits, limits, etc. • • •				
$-0.09 \pm 0.12 \pm 0.01$	[1] AUBERT,B	06M	BABR	Repl. by AUBERT 09

[1] $m_{\eta K} < 3.25$ GeV/c^2.
[2] $m_{\eta K} < 2.4$ GeV/c^2

$A_{CP}(B^+ \to \phi K^+\gamma)$

VALUE	DOCUMENT ID		TECN	COMMENT
-0.13 ± 0.11 OUR AVERAGE	Error includes scale factor of 1.1.			
$-0.03 \pm 0.11 \pm 0.08$	SAHOO	11A	BELL	$e^+e^- \to \Upsilon(4S)$
$-0.26 \pm 0.14 \pm 0.05$	AUBERT	07Q	BABR	$e^+e^- \to \Upsilon(4S)$

$A_{CP}(B^+ \to \rho^+\gamma)$

VALUE	DOCUMENT ID		TECN	COMMENT
$-0.11 \pm 0.32 \pm 0.09$	TANIGUCHI	08	BELL	$e^+e^- \to \Upsilon(4S)$

$A_{CP}(B^+ \to \pi^+\pi^0)$

VALUE	DOCUMENT ID		TECN	COMMENT
0.03 ± 0.04 OUR AVERAGE				
$0.025 \pm 0.043 \pm 0.007$	DUH	13	BELL	$e^+e^- \to \Upsilon(4S)$
$0.03 \pm 0.08 \pm 0.01$	AUBERT	07BC	BABR	$e^+e^- \to \Upsilon(4S)$
• • • We do not use the following data for averages, fits, limits, etc. • • •				
$0.07 \pm 0.06 \pm 0.01$	LIN	08	BELL	Repl. by DUH 13
$-0.01 \pm 0.10 \pm 0.02$	[1] AUBERT	05L	BABR	Repl. by AUBERT 07BC
$0.00 \pm 0.10 \pm 0.02$	[2] CHAO	05A	BELL	Repl. by CHAO 04B
$-0.02 \pm 0.10 \pm 0.01$	[3] CHAO	04B	BELL	Repl. by LIN 08
$-0.03\ ^{+0.18}_{-0.17} \pm 0.02$	[4] AUBERT	03L	BABR	Repl. by AUBERT 05L
$0.30 \pm 0.30\ ^{+0.06}_{-0.04}$	[5] CASEY	02	BELL	Repl. by CHAO 04B

[1] Corresponds to a 90% CL interval of $-0.19 < A_{CP} < 0.21$.
[2] Corresponds to a 90% CL interval of $-0.17 < A_{CP} < 0.16$.
[3] This corresponds to 90% CL interval of $-0.18 < A_{CP} < 0.14$.
[4] Corresponds to 90% confidence range $-0.32 < A_{CP} < 0.27$.
[5] Corresponds to 90% confidence range $-0.23 < A_{CP} < +0.86$.

$A_{CP}(B^+ \to \pi^+\pi^-\pi^+)$

VALUE	DOCUMENT ID		TECN	COMMENT
0.057 ± 0.013 OUR AVERAGE				
$0.058 \pm 0.008 \pm 0.011$	[1] AAIJ	14BO	LHCB	pp at 7, 8 TeV
$0.032 \pm 0.044^{+0.040}_{-0.037}$	AUBERT	09L	BABR	$e^+e^- \to \Upsilon(4S)$
• • • We do not use the following data for averages, fits, limits, etc. • • •				
$0.117 \pm 0.021 \pm 0.011$	[2] AAIJ	14	LHCB	Repl. by AAIJ 14BO
$-0.007 \pm 0.077 \pm 0.025$	AUBERT,B	05G	BABR	Repl. by AUBERT 09L
$-0.39 \pm 0.33 \pm 0.12$	AUBERT	03M	BABR	Repl. by AUBERT 05G

[1] AAIJ 14BO reports also *CP* asymmetries in restricted regions of phase space.
[2] AAIJ 14 reports $A_{CP}(B^+ \to \pi^+\pi^-\pi^+) = 0.584 \pm 0.082 \pm 0.027 \pm 0.007$ in the Dalitz plot region of $m^2_{\pi^+\pi^-} > 15$ GeV^2/c^4 or $m^2_{\pi^+\pi^-} < 0.4$ GeV^2/c^4. The third uncertainty is due to the *CP* asymmetry of the $B^{\pm} \to J/\psi K^{\pm}$ reference mode uncertainty.

$A_{CP}(B^+ \to \rho^0\pi^+)$

VALUE	DOCUMENT ID		TECN	COMMENT
$0.18 \pm 0.07\ ^{+0.05}_{-0.15}$	AUBERT	09L	BABR	$e^+e^- \to \Upsilon(4S)$

• • • We do not use the following data for averages, fits, limits, etc. • • •

$-0.074 \pm 0.120^{+0.035}_{-0.055}$	AUBERT,B	05G	BABR	Repl. by AUBERT 09L
$-0.19 \pm 0.11 \pm 0.02$	AUBERT	04Z	BABR	Repl. by AUBERT,B 05G

$A_{CP}(B^+ \to f_2(1270)\pi^+)$

VALUE	DOCUMENT ID	TECN	COMMENT
$0.41 \pm 0.25\ ^{+0.18}_{-0.15}$	AUBERT	09L	BABR $e^+e^- \to \Upsilon(4S)$

• • • We do not use the following data for averages, fits, limits, etc. • • •

$-0.004 \pm 0.247^{+0.028}_{-0.032}$	AUBERT,B	05G	BABR	Repl. by AUBERT 09L

$A_{CP}(B^+ \to \rho^0(1450)\pi^+)$

VALUE	DOCUMENT ID	TECN	COMMENT
$-0.06 \pm 0.28^{+0.23}_{-0.40}$	AUBERT	09L	BABR $e^+e^- \to \Upsilon(4S)$

$A_{CP}(B^+ \to f_0(1370)\pi^+)$

VALUE	DOCUMENT ID	TECN	COMMENT
$0.72 \pm 0.15 \pm 0.16$	AUBERT	09L	BABR $e^+e^- \to \Upsilon(4S)$

$A_{CP}(B^+ \to \pi^+\pi^-\pi^+$ nonresonant)

VALUE	DOCUMENT ID	TECN	COMMENT
$-0.14 \pm 0.14^{+0.18}_{-0.08}$	AUBERT	09L	BABR $e^+e^- \to \Upsilon(4S)$

$A_{CP}(B^+ \to \rho^+\pi^0)$

VALUE	DOCUMENT ID	TECN	COMMENT
0.02 ± 0.11 OUR AVERAGE			
$-0.01 \pm 0.13 \pm 0.02$	AUBERT	07X	BABR $e^+e^- \to \Upsilon(4S)$
$0.06 \pm 0.17^{+0.04}_{-0.05}$	ZHANG	05A	BELL $e^+e^- \to \Upsilon(4S)$

• • • We do not use the following data for averages, fits, limits, etc. • • •

$0.24 \pm 0.16 \pm 0.06$	AUBERT	04Z	BABR	Repl. by AUBERT 07X

$A_{CP}(B^+ \to \rho^+\rho^0)$

VALUE	DOCUMENT ID	TECN	COMMENT
-0.05 ± 0.05 OUR AVERAGE			
$-0.054 \pm 0.055 \pm 0.010$	AUBERT	09G	BABR $e^+e^- \to \Upsilon(4S)$
$0.00 \pm 0.22 \pm 0.03$	ZHANG	03B	BELL $e^+e^- \to \Upsilon(4S)$

• • • We do not use the following data for averages, fits, limits, etc. • • •

$-0.12 \pm 0.13 \pm 0.10$	AUBERT,BE	06G	BABR	Repl. by AUBERT 09G
$-0.19 \pm 0.23 \pm 0.03$	AUBERT	03V	BABR	Repl. by AUBERT,BE 06G

$A_{CP}(B^+ \to \omega\pi^+)$

VALUE	DOCUMENT ID	TECN	COMMENT
-0.04 ± 0.06 OUR AVERAGE			
$-0.02 \pm 0.08 \pm 0.01$	AUBERT	07AE	BABR $e^+e^- \to \Upsilon(4S)$
$-0.02 \pm 0.09 \pm 0.01$	JEN	06	BELL $e^+e^- \to \Upsilon(4S)$
-0.34 ± 0.25	[1] CHEN	00	CLE2 $e^+e^- \to \Upsilon(4S)$

• • • We do not use the following data for averages, fits, limits, etc. • • •

$-0.01 \pm 0.10 \pm 0.01$	AUBERT,B	06E	BABR	Repl. by AUBERT 07AE
$0.03 \pm 0.16 \pm 0.01$	AUBERT	04H	BABR	Repl. by AUBERT,B 06E
$0.50^{+0.23}_{-0.20} \pm 0.02$	[2] WANG	04A	BELL	Repl. by JEN 06
$-0.01^{+0.29}_{-0.31} \pm 0.03$	[3] AUBERT	02E	BABR	Repl. by AUBERT 04H

[1] Corresponds to 90% confidence range $-0.75 < A_{CP} < 0.07$.

[2] Corresponds to 90% CL interval -0.25< A_{CP} <0.41

[3] Corresponds to 90% confidence range $-0.50 < A_{CP} < 0.46$.

$A_{CP}(B^+ \to \omega\rho^+)$

VALUE	DOCUMENT ID	TECN	COMMENT
$-0.20 \pm 0.09 \pm 0.02$	AUBERT	09H	BABR $e^+e^- \to \Upsilon(4S)$

• • • We do not use the following data for averages, fits, limits, etc. • • •

$0.04 \pm 0.18 \pm 0.02$	AUBERT,B	06T	BABR	Repl. by AUBERT 09H
$0.05 \pm 0.26 \pm 0.02$	AUBERT	05O	BABR	Repl. by AUBERT,B 06T

$A_{CP}(B^+ \to \eta\pi^+)$

VALUE	DOCUMENT ID	TECN	COMMENT
-0.14 ± 0.07 OUR AVERAGE	Error includes scale factor of 1.4.		
$-0.19 \pm 0.06 \pm 0.01$	HOI	12	BELL $e^+e^- \to \Upsilon(4S)$
$-0.03 \pm 0.09 \pm 0.03$	AUBERT	09AV	BABR $e^+e^- \to \Upsilon(4S)$

• • • We do not use the following data for averages, fits, limits, etc. • • •

$-0.08 \pm 0.10 \pm 0.01$	AUBERT	07AE	BABR	Repl. by AUBERT 09AV
$-0.23 \pm 0.09 \pm 0.02$	CHANG	07B	BELL	Repl. by HOI 12
$-0.13 \pm 0.12 \pm 0.01$	AUBERT,B	05K	BABR	Repl. by AUBERT 07AE
$0.07 \pm 0.15 \pm 0.03$	CHANG	05A	BELL	Repl. by CHANG 07B
$-0.44 \pm 0.18 \pm 0.01$	AUBERT	04H	BABR	Repl. by AUBERT,B 05K

$A_{CP}(B^+ \to \eta\rho^+)$

VALUE	DOCUMENT ID	TECN	COMMENT
0.11 ± 0.11 OUR AVERAGE			
$0.13 \pm 0.11 \pm 0.02$	AUBERT	08AH	BABR $e^+e^- \to \Upsilon(4S)$
$-0.04^{+0.34}_{-0.32} \pm 0.01$	WANG	07B	BELL $e^+e^- \to \Upsilon(4S)$

• • • We do not use the following data for averages, fits, limits, etc. • • •

$0.02 \pm 0.18 \pm 0.02$	AUBERT,B	05K	BABR	Repl. by AUBERT 08AH

$A_{CP}(B^+ \to \eta'\pi^+)$

VALUE	DOCUMENT ID	TECN	COMMENT
0.06 ± 0.16 OUR AVERAGE			
$0.03 \pm 0.17 \pm 0.02$	AUBERT	09AV	BABR $e^+e^- \to \Upsilon(4S)$
$0.20^{+0.37}_{-0.36} \pm 0.04$	SCHUEMANN	06	BELL $e^+e^- \to \Upsilon(4S)$

• • • We do not use the following data for averages, fits, limits, etc. • • •

$0.21 \pm 0.17 \pm 0.01$	AUBERT	07AE	BABR	Repl. by AUBERT 09AV
$0.14 \pm 0.16 \pm 0.01$	AUBERT,B	05K	BABR	Repl. by AUBERT 07AE

$A_{CP}(B^+ \to \eta'\rho^+)$

VALUE	DOCUMENT ID	TECN	COMMENT
$0.26 \pm 0.17 \pm 0.02$	DEL-AMO-SA...10A	BABR	$e^+e^- \to \Upsilon(4S)$

• • • We do not use the following data for averages, fits, limits, etc. • • •

$0.04 \pm 0.28 \pm 0.02$	[1] AUBERT	07E	BABR	Repl. by DEL-AMO-SANCHEZ 10A

[1] Reports A_{CP} with the opposite sign convention.

$A_{CP}(B^+ \to b_1^0\pi^+)$

VALUE	DOCUMENT ID	TECN	COMMENT
$+0.05 \pm 0.16 \pm 0.02$	AUBERT	07BI	BABR $e^+e^- \to \Upsilon(4S)$

$A_{CP}(B^+ \to p\bar{p}\pi^+)$

VALUE	DOCUMENT ID	TECN	COMMENT
0.00 ± 0.04 OUR AVERAGE			
$-0.02 \pm 0.05 \pm 0.02$	[1] WEI	08	BELL $e^+e^- \to \Upsilon(4S)$
$+0.04 \pm 0.07 \pm 0.04$	AUBERT	07AV	BABR $e^+e^- \to \Upsilon(4S)$

• • • We do not use the following data for averages, fits, limits, etc. • • •

$-0.16 \pm 0.22 \pm 0.01$	WANG	04	BELL	Repl. by WEI 08

[1] Requires $m_{p\bar{p}} < 2.85$ GeV/c^2.

$A_{CP}(B^+ \to p\bar{p}K^+)$

VALUE	DOCUMENT ID	TECN	COMMENT
0.00 ± 0.04 OUR AVERAGE	Error includes scale factor of 2.2.		
$0.021 \pm 0.020 \pm 0.004$	[1] AAIJ	14AF	LHCB pp at 7, 8 TeV
$-0.17 \pm 0.10 \pm 0.02$	[1] WEI	08	BELL $e^+e^- \to \Upsilon(4S)$
$-0.16\ ^{+0.07}_{-0.08} \pm 0.04$	[1] AUBERT,B	05L	BABR $e^+e^- \to \Upsilon(4S)$

• • • We do not use the following data for averages, fits, limits, etc. • • •

$-0.047 \pm 0.036 \pm 0.007$	[1] AAIJ	13AU	LHCB	Repl. by AAIJ 14AF
$-0.05 \pm 0.11 \pm 0.01$	WANG	04	BELL	Repl. by WEI 08

[1] Requires $m_{p\bar{p}} < 2.85$ GeV/c^2.

$A_{CP}(B^+ \to p\bar{p}K^*(892)^+)$

VALUE	DOCUMENT ID	TECN	COMMENT
0.21 ± 0.16 OUR AVERAGE	Error includes scale factor of 1.4.		
$-0.01 \pm 0.19 \pm 0.02$	CHEN	08C	BELL $e^+e^- \to \Upsilon(4S)$
$+0.32 \pm 0.13 \pm 0.05$	AUBERT	07AV	BABR $e^+e^- \to \Upsilon(4S)$

$A_{CP}(B^+ \to p\bar{\Lambda}\gamma)$

VALUE	DOCUMENT ID	TECN	COMMENT
$+0.17 \pm 0.16 \pm 0.05$	WANG	07C	BELL $e^+e^- \to \Upsilon(4S)$

$A_{CP}(B^+ \to p\bar{\Lambda}\pi^0)$

VALUE	DOCUMENT ID	TECN	COMMENT
$+0.01 \pm 0.17 \pm 0.04$	WANG	07C	BELL $e^+e^- \to \Upsilon(4S)$

$A_{CP}(B^+ \to K^+\ell^+\ell^-)$

VALUE	DOCUMENT ID	TECN	COMMENT
-0.02 ± 0.08 OUR AVERAGE			
$-0.03 \pm 0.14 \pm 0.01$	[1] LEES	12S	BABR $e^+e^- \to \Upsilon(4S)$
$-0.18 \pm 0.18 \pm 0.01$	AUBERT	09T	BABR $e^+e^- \to \Upsilon(4S)$
$+0.04 \pm 0.10 \pm 0.02$	WEI	09A	BELL $e^+e^- \to \Upsilon(4S)$

• • • We do not use the following data for averages, fits, limits, etc. • • •

$-0.07 \pm 0.22 \pm 0.02$	AUBERT,B	06J	BABR	Repl. by AUBERT 09T

[1] Measured in the union of $0.10 < q^2 < 8.12$ GeV$^2/c^4$ and $q^2 > 10.11$ GeV$^2/c^4$. LEES 12S reports also individual measurements $A_{CP}(B^+ \to K^+\ell^+\ell^-) = 0.02 \pm 0.18 \pm 0.01$ for $0.10 < q^2 < 8.12$ GeV$^2/c^4$ and $A_{CP}(B^+ \to K^+\ell^+\ell^-) = -0.06^{+0.22}_{-0.21} \pm 0.01$ for $q^2 > 10.11$ GeV$^2/c^4$.

$A_{CP}(B^+ \to K^+e^+e^-)$

VALUE	DOCUMENT ID	TECN	COMMENT
$+0.14 \pm 0.14 \pm 0.03$	WEI	09A	BELL $e^+e^- \to \Upsilon(4S)$

$A_{CP}(B^+ \to K^+\mu^+\mu^-)$

VALUE	DOCUMENT ID	TECN	COMMENT
0.011 ± 0.017 OUR AVERAGE			
$0.012 \pm 0.017 \pm 0.001$	AAIJ	14AN	LHCB pp at 7, 8 TeV
$-0.05 \pm 0.13 \pm 0.03$	WEI	09A	BELL $e^+e^- \to \Upsilon(4S)$

• • • We do not use the following data for averages, fits, limits, etc. • • •

$0.000 \pm 0.033 \pm 0.009$	AAIJ	13BN	LHCB	Repl. by AAIJ 14AN

Meson Particle Listings

$B^{\pm}$

$A_{CP}(B^+ \to \pi^+\mu^+\mu^-)$

VALUE	DOCUMENT ID		TECN	COMMENT
$-0.11 \pm 0.12 \pm 0.01$	AAIJ	15AR	LHCB	pp at 7, 8 TeV

$A_{CP}(B^+ \to K^{*+}\ell^+\ell^-)$

VALUE	DOCUMENT ID		TECN	COMMENT
-0.09 ± 0.14 OUR AVERAGE				
$0.01^{+0.26}_{-0.24} \pm 0.02$	AUBERT	09T	BABR	$e^+e^- \to \Upsilon(4S)$
$-0.13^{+0.17}_{-0.16} \pm 0.01$	WEI	09A	BELL	$e^+e^- \to \Upsilon(4S)$
• • • We do not use the following data for averages, fits, limits, etc. • • •				
$0.03 \pm 0.23 \pm 0.03$	AUBERT,B	06J	BABR	Repl. by AUBERT 09T

$A_{CP}(B^+ \to K^*e^+e^-)$

VALUE	DOCUMENT ID		TECN	COMMENT
$-0.14^{+0.23}_{-0.22} \pm 0.02$	WEI	09A	BELL	$e^+e^- \to \Upsilon(4S)$

$A_{CP}(B^+ \to K^*\mu^+\mu^-)$

VALUE	DOCUMENT ID		TECN	COMMENT
$-0.12 \pm 0.24 \pm 0.02$	WEI	09A	BELL	$e^+e^- \to \Upsilon(4S)$

CP VIOLATION PARAMETERS IN $B^+ \to DK^+$ AND SIMILAR DECAYS

The parameters r_{B^+} and δ_{B^+} are the magnitude ratio and strong phase difference between the amplitudes of $A(B^+ \to \overline{D}^{(*)0} K^{(*)+})$ and $A(B^- \to D^{(*)0} K^{(*)-})$. The measured observables are defined as $x_\pm = r_{B^+} \cos(\delta_{B^+} \pm \gamma)$ and $y_\pm = r_{B^+} \sin(\delta_{B^+} \pm \gamma)$, and can be used to measure the CKM angle γ.

"OUR EVALUATION" is provided by the Heavy Flavor Averaging Group (HFLAV). It is derived from combinations of their results on $B^+ \to DK^+$ and related processes.

γ

For angle $\gamma(\phi_3)$ of the CKM unitarity triangle, see the review on "*CP* Violation" in the Reviews section.

VALUE (°)	CL%	DOCUMENT ID		TECN	COMMENT
$73.5^{+\ 4.3}_{-\ 5.0}$ OUR EVALUATION					
• • • We do not use the following data for averages, fits, limits, etc. • • •					
$80\ ^{+21}_{-22}$		[1] AAIJ	16AA	LHCB	Repl. by AAIJ 16Z
$72.2^{+\ 6.8}_{-\ 7.3}$		[2] AAIJ	16AQ	LHCB	pp at 7, 8 TeV
71 ± 20		[3,4] AAIJ	16Z	LHCB	pp at 7, 8 TeV
$74\ ^{+20}_{-19}$		AAIJ	15BC	LHCB	pp at 7, 8 TeV
$63.5^{+\ 7.2}_{-\ 6.7}$		[5,6] AAIJ	15K	LHCB	pp at 7, 8 TeV
$62\ ^{+15}_{-14}$		[7] AAIJ	14BA	LHCB	pp at 7, 8 TeV
$84\ ^{+49}_{-42}$		[8] AAIJ	14BE	LHCB	Repl. by AAIJ 14BA
$115\ ^{+28}_{-43}$		[9] AAIJ	14BF	LHCB	pp at 7 TeV
$72.6^{+\ 9.7}_{-17.2}$		[10] AAIJ	13AK	LHCB	pp at 7 TeV
$69\ ^{+17}_{-16}$		[11] LEES	13B	BABR	$e^+e^- \to \Upsilon(4S)$
$44\ ^{+43}_{-38}$		[12,13] AAIJ	12AQ	LHCB	Repl. by AAIJ 13AK
$77.3^{+15.1}_{-14.9} \pm 5.9$		[13,14] AIHARA	12	BELL	$e^+e^- \to \Upsilon(4S)$
$68 \pm 14 \pm 5$		[15] DEL-AMO-SA...	10F	BABR	Repl. by LEES 13B
7 to 173	95	[16] DEL-AMO-SA...	10G	BABR	$e^+e^- \to \Upsilon(4S)$
$78.4^{+10.8}_{-11.6} \pm 9.6$		[17] POLUEKTOV	10	BELL	$e^+e^- \to \Upsilon(4S)$
162 ± 56		[18] AUBERT	09R	BABR	$e^+e^- \to \Upsilon(4S)$
$76\ ^{+22}_{-23} \pm 7.1$		[19] AUBERT	08AL	BABR	Repl. by DEL-AMO-SANCHEZ 10F
$53\ ^{+15}_{-18} \pm 10$		[20] POLUEKTOV	06	BELL	Repl. by POLUEKTOV 10
$70 \pm 31\ ^{+18}_{-15}$		[21] AUBERT,B	05Y	BABR	Repl. by AUBERT 08AL
$77\ ^{+17}_{-19} \pm 17$		[22] POLUEKTOV	04	BELL	Repl. by POLUEKTOV 06

[1] Uses Dalitz plot analysis of $D \to K^0_S\pi^+\pi^-$ decays coming from $B^0 \to DK^*(892)^0$ modes. Measures $r_{B^0} = 0.39 \pm 0.13$, and $\delta_{B^0} = 197^{+24}_{-20}$ degrees.

[2] A combination of measurements from analyses of time-integrated $B^+ \to DK^+$, $B^0 \to DK^{(*)0}$, $B^0 \to DK^+\pi^-$, and $B^+ \to DK^+\pi^+\pi^-$ tree-level decays. In addition, results from a time-dependent analysis of $B^0_s \to D_sK$ decays are included.

[3] A model-independent binned Dalitz plot analysis of the decays $B^0 \to DK^{*0}$, with $D \to K^0_S\pi^+\pi^-$ and $D \to K^0_SK^+K^-$. The results cannot be combined with the model-dependent analysis of the same dataset reported in AAIJ 16AA.

[4] Angle γ required to satisfy $0 < \gamma < 180$ degrees.

[5] Obtained by measuring time-dependent *CP* asymmetry in $B^0_s \to K^+K^-$ and using a U-spin relation between $B^0_s \to K^+K^-$ and $B^0 \to \pi^+\pi^-$.

[6] Results are also presented using additional inputs on $B^0 \to \pi^0\pi^0$ and $B^+ \to \pi^+\pi^0$ decays from other experiments and isospin symmetry assumptions. The dependence of the results on the maximum allowed amount of U-spin breaking up to 50% is also included.

[7] Uses binned Dalitz plot analysis of $B^+ \to DK^+$ decays, with $D \to K^0_S\pi^+\pi^-$ and $D \to K^0_SK^+K^-$. Strong phase measurements from CLEO-c (LIBBY 10) of the D decay over the Dalitz plot are used as input. Solution that satisfies $0 < \gamma < 180$ is chosen.

[8] AAIJ 14BE uses model-dependent analysis of $D \to K^0_S\pi^+\pi^-$ amplitudes. The model is the same as in DEL-AMO-SANCHEZ 10F.

[9] Measured in $B^0_s \to D^\mp_s K^\pm$ decays, constraining $-2\beta_s$ by the measurement of $\phi_s = 0.01 \pm 0.07 \pm 0.0$ from AAIJ 13AR. The value is modulo 180° at 68% CL.

[10] Presents a confidence region $55.4° < \gamma < 82.3°$ at 68% CL with best fit value 72.6° and includes both statistical and systematic uncertainties. The corresponding 95% CL is $40.2\ ° < \gamma < 92.7°$. The value is determined from combination of measuremets using D meson decaying to K^+K^-, $\pi^+\pi^-$, $K^\pm\pi^\mp$, $K^0_S\pi^+\pi^-$, $K^0_SK^+K^-$, and $K^\pm\pi^\mp\pi^\pm\pi^\mp$. Combines $B^\pm \to DK^\pm$ and $B^\pm \to D\pi^\pm$.

[11] Reports combination of published measurements using GGSZ, GLW, and ADS methods. Reports also 2σ range of 41–102° and a 5.9σ significance for $\gamma(B^+ \to D^{(*)0}K^{(*)+}) \neq 0$ hypothesis.

[12] Reports combined statistical and systematic uncertainties.

[13] Uses binned Dalitz plot of $\overline{D}^0 \to K^0_S\pi^+\pi^-$ decays from $B^+ \to \overline{D}^0K^+$. Measurement of strong phases in $\overline{D}^0 \to K^0_S\pi^+\pi^-$ Dalitz plot from LIBBY 10 is used as input.

[14] We combined the systematics in quadrature. The authors report separately the contribution to the systematic uncertainty due to the uncertainty on the bin-averaged strong phase difference between D^0 and $\overline{D}^0$ amplitudes.

[15] Uses Dalitz plot analysis of $\overline{D}^0 \to K^0_S\pi^+\pi^-$, $K^0_SK^+K^-$ decays from $B^+ \to D^{(*)}K^+$, DK^{*+} modes. The corresponding two standard deviation interval for γ is $39° < \gamma < 98°$. CP conservation in the combined result is ruled out with a significance of 3.5 standard deviations.

[16] Reports confidence intervals for the CKM angle γ from the measured values of the GLW parameters using $B^\pm \to DK^\pm$ decays with D mesons decaying to non-*CP*($K\pi$), *CP*-even (K^+K^-, $\pi^+\pi^-$), and *CP*-odd ($K^0_S\pi^0$, $K^0_S\omega$) states.

[17] Uses Dalitz plot analysis of $\overline{D}^0 \to K^0_S\pi^+\pi^-$ decays from $B^+ \to D^{(*)}K^+$ modes. The corresponding two standard deviation interval for γ is $54.2° < \gamma < 100.5°$. CP conservation in the combined result is ruled out with a significance of 3.5 standard deviations.

[18] Uses Dalitz plot analysis of $D^0 \to K^0_S\pi^+\pi^-$ decays coming from $B^0 \to D^0K^{*0}$ modes. The corresponding 95% CL interval is $77° < \gamma < 247°$. A 180 degree ambiguity is implied.

[19] Uses Dalitz plot analysis of $\overline{D}^0 \to K^0_S\pi^+\pi^-$ and $\overline{D}^0 \to K^0_SK^+K^-$ decays coming from $B^\pm \to D^{(*)}K^{(*)\pm}$ modes. The corresponding two standard deviation interval is $29° < \gamma < 122°$.

[20] Uses a Dalitz plot analysis of the $\overline{D}^0 \to K^0_S\pi^+\pi^-$ decays; Combines the DK^+, D^*K^+ and DK^{*+} modes. The corresponding two standard deviations interval for gamma is $8° < \gamma < 111°$.

[21] Uses a Dalitz plot analysis of neutral $D \to K^0_S\pi^+\pi^-$ decays coming from $B^\pm \to DK^\pm$ and $B^\pm \to D^{*0}K^\pm$ followed by $D^{*0} \to D\pi^0$, $D\gamma$. The corresponding two standard deviations interval for gamma is $12° < \gamma < 137°$. AUBERT,B 05Y also reports the amplitude ratios and the strong phases.

[22] Uses a Dalitz plot analysis of the 3-body $D \to K^0_S\pi^+\pi^-$ decays coming from $B^\pm \to DK^\pm$ and $B^\pm \to D^*K^\pm$ followed by $D^* \to D\pi^0$; here we use D to denote that the neutral D meson produced in the decay is an admixture of D^0 and $\overline{D}^0$. The corresponding two standard deviations interval for γ is $26^\circ < \gamma < 126^\circ$. POLUEKTOV 04 also reports the amplitude ratios and the strong phases.

$r_B(B^+ \to D^0K^+)$

r_B and δ_B are the amplitude ratio and relative strong phase between the amplitudes of $A(B^+ \to D^0K^+)$ and $A(B^+ \to \overline{D}^0K^+)$,

VALUE	CL%	DOCUMENT ID		TECN	COMMENT
0.103 ± 0.005 OUR EVALUATION					
0.095 ± 0.008 OUR AVERAGE					
$0.080^{+0.019}_{-0.021}$		[1] AAIJ	14BA	LHCB	pp at 7, 8 TeV
0.097 ± 0.011		[2] AAIJ	13AE	LHCB	pp at 7 TeV
$0.092^{+0.013}_{-0.012}$		[3] LEES	13B	BABR	$e^+e^- \to \Upsilon(4S)$
$0.160^{+0.040+0.051}_{-0.038-0.015}$		[4] POLUEKTOV	10	BELL	$e^+e^- \to \Upsilon(4S)$
• • • We do not use the following data for averages, fits, limits, etc. • • •					
0.06 ± 0.04		[5] AAIJ	14BE	LHCB	Repl. by AAIJ 14BA
0.07 ± 0.04		[6,7] AAIJ	12AQ	LHCB	pp at 7 TeV
$0.145 \pm 0.030 \pm 0.015$		[7,8] AIHARA	12	BELL	$e^+e^- \to \Upsilon(4S)$
< 0.13	90	[9] LEES	11D	BABR	$e^+e^- \to \Upsilon(4S)$
$0.096 \pm 0.029 \pm 0.006$		[10] DEL-AMO-SA...	10F	BABR	Repl. by LEES 13B
$0.095^{+0.051}_{-0.041}$		[11] DEL-AMO-SA...	10H	BABR	Repl. by LEES 13B
$0.086 \pm 0.032 \pm 0.015$		[12] AUBERT	08AL	BABR	Repl. by DEL-AMO-SANCHEZ 10F
< 0.19	90	HORII	08	BELL	$e^+e^- \to \Upsilon(4S)$
$0.159^{+0.054}_{-0.050} \pm 0.050$		[13] POLUEKTOV	06	BELL	Repl. by POLUEKTOV 10
$0.12 \pm 0.08 \pm 0.05$		[14] AUBERT,B	05Y	BABR	Repl. by AUBERT 08AL

[1] Uses binned Dalitz plot analysis of $B^+ \to DK^+$ decays, with $D \to K^0_S\pi^+\pi^-$ and $D \to K^0_SK^+K^-$. Strong phase measurements from CLEO-c (LIBBY 10) of the D decay over the Dalitz plot are used as input.

[2] Uses $B^\pm \to [K^\pm\pi^\mp\pi^+\pi^-]_Dh^\pm$ mode.

[3] Reports combination of published measurements using GGSZ, GLW, and ADS methods.

[4] Uses Dalitz plot analysis of $\overline{D}^0 \to K^0_S\pi^+\pi^-$ decays from $B^+ \to D^0K^+$ modes. The corresponding two standard deviation interval is $0.084 < r_B < 0.239$.
[5] AAIJ 14BE uses model-dependent analysis of $D \to K^0_S\pi^+\pi^-$ amplitudes. The model is the same as in DEL-AMO-SANCHEZ 10F.
[6] Reports combined statistical and systematic uncertainties.
[7] Uses binned Dalitz plot of $\overline{D}^0 \to K^0_S\pi^+\pi^-$ decays from $B^+ \to \overline{D}^0K^+$. Measurement of strong phases in $\overline{D}^0 \to K^0_S\pi^+\pi^-$ Dalitz plot from LIBBY 10 is used as input.
[8] We combined the systematics in quadrature. The authors report separately the contribution to the systematic uncertainty due to the uncertainty on the bin-averaged strong phase difference between D^0 and $\overline{D}^0$ amplitudes.
[9] Uses decays of neutral D to $K^-\pi^+\pi^0$.
[10] Uses Dalitz plot analysis of $\overline{D}^0 \to K^0_S\pi^+\pi^-$, $K^0_SK^+K^-$ decays from $B^+ \to D^{(*)}K^{(*)+}$ modes. The corresponding two standard deviation interval is $0.037 < r_B < 0.155$.
[11] Uses the Cabibbo suppressed decay of $B^+ \to \overline{D}K^+$ followed by $\overline{D} \to K^-\pi^+$.
[12] Uses Dalitz plot analysis of $\overline{D}^0 \to K^0_S\pi^+\pi^-$ and $\overline{D}^0 \to K^0_SK^+K^-$ decays coming from $B^\pm \to D^{(*)}K^{(*)\pm}$ modes.
[13] Uses a Dalitz plot analysis of the $\overline{D}^0 \to K^0_S\pi^+\pi^-$ decays; Combines the DK^+, D^*K^+ and DK^{*+} modes.
[14] Uses a Dalitz analysis of neutral D decays to $K^0_S\pi^+\pi^-$ in the processes $B^\pm \to D^{(*)}K^\pm$, $D^* \to D\pi^0$, $D\gamma$.

$\delta_B(B^+ \to D^0K^+)$

VALUE (°)	DOCUMENT ID		TECN	COMMENT
$136.9^{+\ 4.6}_{-\ 5.2}$ OUR EVALUATION				
123 ±10 OUR AVERAGE				
$134\ ^{+14}_{-15}$	[1] AAIJ	14BA	LHCB	pp at 7, 8 TeV
$105\ ^{+16}_{-17}$	[2] LEES	13B	BABR	$e^+e^- \to \Upsilon(4S)$
$136.7^{+13.0}_{-15.8}\pm23.2$	[3] POLUEKTOV	10	BELL	$e^+e^- \to \Upsilon(4S)$
• • • We do not use the following data for averages, fits, limits, etc. • • •				
$115\ ^{+41}_{-51}$	[4] AAIJ	14BE	LHCB	Repl. by AAIJ 14BA
$137\ ^{+35}_{-46}$	[5,6] AAIJ	12AQ	LHCB	pp at 7 TeV
$129.9\pm15.0\pm\ 6.0$	[6,7] AIHARA	12	BELL	$e^+e^- \to \Upsilon(4S)$
$119\ ^{+19}_{-20}\ \pm\ 4$	[8] DEL-AMO-SA...10F		BABR	Repl. by LEES 13B
$109\ ^{+27}_{-30}\ \pm\ 8$	[9] AUBERT	08AL	BABR	Repl. by DEL-AMO-SANCHEZ 10F
$145.7^{+19.0}_{-19.7}\pm23.1$	[10] POLUEKTOV	06	BELL	Repl. by POLUEKTOV 10
$104\ \pm45\ ^{+23}_{-32}$	[11] AUBERT,B	05Y	BABR	Repl. by AUBERT 08AL

[1] Uses binned Dalitz plot analysis of $B^+ \to DK^+$ decays, with $D \to K^0_S\pi^+\pi^-$ and $D \to K^0_SK^+K^-$. Strong phase measurements from CLEO-c (LIBBY 10) of the D decay over the Dalitz plot are used as input.
[2] Reports combination of published measurements using GGSZ, GLW, and ADS methods.
[3] Uses Dalitz plot analysis of $\overline{D}^0 \to K^0_S\pi^+\pi^-$ decays from $B^+ \to \overline{D}^0K^+$ modes. The corresponding two standard deviation interval is $102.2° < \delta_B < 162.3°$.
[4] AAIJ 14BE uses model-dependent analysis of $D \to K^0_S\pi^+\pi^-$ amplitudes. The model is the same as in DEL-AMO-SANCHEZ 10F.
[5] Reports combined statistical and systematic uncertainties.
[6] Uses binned Dalitz plot of $\overline{D}^0 \to K^0_S\pi^+\pi^-$ decays from $B^+ \to \overline{D}^0K^+$. Measurement of strong phases in $\overline{D}^0 \to K^0_S\pi^+\pi^-$ Dalitz plot from LIBBY 10 is used as input.
[7] We combined the systematics in quadrature. The authors report separately the contribution to the systematic uncertainty due to the uncertainty on the bin-averaged strong phase difference between D^0 and $\overline{D}^0$ amplitudes.
[8] Uses Dalitz plot analysis of $\overline{D}^0 \to K^0_S\pi^+\pi^-$, $K^0_SK^+K^-$ decays from $B^+ \to D^{(*)}K^{(*)+}$ modes. The corresponding two standard deviation interval is $75° < \delta_B < 157°$.
[9] Uses Dalitz plot analysis of $\overline{D}^0 \to K^0_S\pi^+\pi^-$ and $\overline{D}^0 \to K^0_SK^+K^-$ decays coming from $B^\pm \to D^{(*)}K^{(*)\pm}$ modes.
[10] Uses a Dalitz plot analysis of the $\overline{D}^0 \to K^0_S\pi^+\pi^-$ decays; Combines the DK^+, D^*K^+ and DK^{*+} modes.
[11] Uses a Dalitz analysis of neutral D decays to $K^0_S\pi^+\pi^-$ in the processes $B^\pm \to D^{(*)}K^\pm$, $D^* \to D\pi^0$, $D\gamma$.

$r_B(B^+ \to \overline{D}^0K^{*+})$

r_B and δ_B are the amplitude ratio and relative strong phase between the amplitudes of $A_{CP}(B^+ \to D^0K^{*+})$ and $A_{CP}(B^+ \to \overline{D}^0K^{*+})$,

VALUE	DOCUMENT ID		TECN	COMMENT
$0.075^{+0.017}_{-0.018}$ OUR EVALUATION				
0.17 ±0.11 OUR AVERAGE Error includes scale factor of 2.3.				
$0.143^{+0.048}_{-0.049}$	[1] LEES	13B	BABR	$e^+e^- \to \Upsilon(4S)$
$0.564^{+0.216}_{-0.155}\pm0.093$	[2] POLUEKTOV	06	BELL	$e^+e^- \to \Upsilon(4S)$
• • • We do not use the following data for averages, fits, limits, etc. • • •				
$0.166^{+0.073}_{-0.069}$	[3] DEL-AMO-SA...10F		BABR	Repl. by LEES 13B
0.31 ±0.07	[4] AUBERT	09AJ	BABR	Repl. by LEES 13B
$0.181^{+0.088}_{-0.108}\pm0.042$	[5] AUBERT	08AL	BABR	Repl. by AUBERT 09AJ

[1] Reports combination of published measurements using GGSZ, GLW, and ADS methods.
[2] Uses a Dalitz plot analysis of the $\overline{D}^0 \to K^0_S\pi^+\pi^-$ decays; Combines the DK^+, D^*K^+ and DK^{*+} modes.
[3] DEL-AMO-SANCHEZ 10F reports $r_B \cdot k = 0.149^{+0.066}_{-0.062}$ for k = 0.9.
[4] Obtained by combining the GLW and ADS methods. The 2-sigma range corresponds to [0.17, 0.43].
[5] Uses Dalitz plot analysis of $\overline{D}^0 \to K^0_S\pi^+\pi^-$ and $\overline{D}^0 \to K^0_SK^+K^-$ decays coming from $B^\pm \to D^{(*)}K^{(*)\pm}$ modes.

$\delta_B(B^+ \to D^0K^{*+})$

VALUE (°)	DOCUMENT ID		TECN	COMMENT
$106\ ^{+18}_{-26}$ OUR EVALUATION				
155 ±70 OUR AVERAGE Error includes scale factor of 2.0.				
101 ±43	[1] LEES	13B	BABR	$e^+e^- \to \Upsilon(4S)$
$242.6^{+20.2}_{-23.2}\pm49.4$	[2] POLUEKTOV	06	BELL	$e^+e^- \to \Upsilon(4S)$
• • • We do not use the following data for averages, fits, limits, etc. • • •				
111 ±32	DEL-AMO-SA...10F		BABR	Repl. by LEES 13B
$104\ ^{+39}_{-37}\ \pm18$	[3] AUBERT	08AL	BABR	Repl. by LEES 13B

[1] Reports combination of published measurements using GGSZ, GLW, and ADS methods.
[2] Uses a Dalitz plot analysis of the $\overline{D}^0 \to K^0_S\pi^+\pi^-$ decays; Combines the DK^+, D^*K^+ and DK^{*+} modes.
[3] Uses Dalitz plot analysis of $\overline{D}^0 \to K^0_S\pi^+\pi^-$ and $\overline{D}^0 \to K^0_SK^+K^-$ decays coming from $B^\pm \to D^{(*)}K^{(*)\pm}$ modes.

$r^*_B(B^+ \to D^{*0}K^+)$

r^*_B and δ^*_B are the amplitude ratio and relative strong phase between the amplitudes of $A(B^+ \to D^{*0}K^+)$ and $A(B^+ \to \overline{D}^{*0}K^+)$,

VALUE	DOCUMENT ID		TECN	COMMENT
$0.142^{+0.019}_{-0.020}$ OUR EVALUATION				
$0.114^{+0.023}_{-0.040}$ OUR AVERAGE Error includes scale factor of 1.2.				
$0.106^{+0.019}_{-0.036}$	[1] LEES	13B	BABR	$e^+e^- \to \Upsilon(4S)$
$0.196^{+0.072}_{-0.069}{}^{+0.064}_{-0.017}$	[2] POLUEKTOV	10	BELL	$e^+e^- \to \Upsilon(4S)$
• • • We do not use the following data for averages, fits, limits, etc. • • •				
$0.133^{+0.042}_{-0.039}\pm0.013$	[3] DEL-AMO-SA...10F		BABR	Repl. by LEES 13B
$0.096^{+0.035}_{-0.051}$	[4] DEL-AMO-SA...10H		BABR	Repl. by LEES 13B
$0.135\pm0.050\pm0.012$	[5] AUBERT	08AL	BABR	Repl. by DEL-AMO-SANCHEZ 10F
$0.175^{+0.108}_{-0.099}\pm0.050$	[6] POLUEKTOV	06	BELL	Repl. by POLUEKTOV 10
0.17 ±0.10 ±0.04	[7] AUBERT,B	05Y	BABR	Repl. by AUBERT 08AL

[1] Reports combination of published measurements using GGSZ, GLW, and ADS methods.
[2] Uses Dalitz plot analysis of $\overline{D}^0 \to K^0_S\pi^+\pi^-$ decays from $B^+ \to D^{*0}K^+$ modes. The corresponding two standard deviation interval is $0.061 < r^*_B < 0.271$.
[3] Uses Dalitz plot analysis of $\overline{D}^0 \to K^0_S\pi^+\pi^-$, $K^0_SK^+K^-$ decays from $B^+ \to D^{(*)}K^{(*)+}$ modes. The corresponding two standard deviation interval is $0.049 < r^*_B < 0.215$.
[4] Uses the Cabibbo suppressed decay of $B^+ \to \overline{D}^*K^+$ followed by $\overline{D}^* \to \overline{D}\pi^0$ or $\overline{D}\gamma$, and $\overline{D} \to K^-\pi^+$.
[5] Uses Dalitz plot analysis of $\overline{D}^0 \to K^0_S\pi^+\pi^-$ and $\overline{D}^0 \to K^0_SK^+K^-$ decays coming from $B^\pm \to D^{(*)}K^{(*)\pm}$ modes.
[6] Uses a Dalitz plot analysis of the $\overline{D}^0 \to K^0_S\pi^+\pi^-$ decays; Combines the DK^+, D^*K^+ and DK^{*+} modes.
[7] Uses a Dalitz analysis of neutral D decays to $K^0_S\pi^+\pi^-$ in the processes $B^\pm \to D^{(*)}K^\pm$, $D^* \to D\pi^0$, $D\gamma$.

$\delta^*_B(B^+ \to D^{*0}K^+)$

VALUE (°)	DOCUMENT ID		TECN	COMMENT
$321\ ^{+\ 8}_{-\ 9}$ OUR EVALUATION				
$310\ ^{+22}_{-28}$ OUR AVERAGE Error includes scale factor of 1.3.				
$294\ ^{+21}_{-31}$	[1] LEES	13B	BABR	$e^+e^- \to \Upsilon(4S)$
$341.9^{+18.0}_{-19.6}\pm23.1$	[2] POLUEKTOV	10	BELL	$e^+e^- \to \Upsilon(4S)$
• • • We do not use the following data for averages, fits, limits, etc. • • •				
278 ±21 ± 6	[3] DEL-AMO-SA...10F		BABR	Repl. by LEES 13B
$297\ ^{+27}_{-29}\ \pm\ 6.4$	[4] AUBERT	08AL	BABR	Repl. by DEL-AMO-SANCHEZ 10F
$302.0^{+33.8}_{-35.1}\pm23.7$	[5] POLUEKTOV	06	BELL	Repl. by POLUEKTOV 10
$296\ \pm41\ ^{+20}_{-19}$	[6] AUBERT,B	05Y	BABR	Repl. by AUBERT 08AL

[1] Reports combination of published measurements using GGSZ, GLW, and ADS methods. We added 360° to the value of $(-66^{+21}_{-31})°$ quoted by LEES 13B.
[2] Uses Dalitz plot analysis of $\overline{D}^0 \to K^0_S\pi^+\pi^-$ decays from $B^+ \to D^*K^+$ modes. The corresponding two standard deviation interval is $296.5° < \delta^*_B < 382.7°$.

[3] Uses Dalitz plot analysis of $\overline{D}^0 \to K^0_S\pi^+\pi^-$, $K^0_S K^+K^-$ decays from $B^+ \to D^{(*)}K^{(*)+}$ modes. The corresponding two standard deviation interval is $236^\circ < \delta^*_B < 322^\circ$.
[4] Uses Dalitz plot analysis of $\overline{D}^0 \to K^0_S\pi^+\pi^-$ and $\overline{D}^0 \to K^0_S K^+K^-$ decays coming from $B^\pm \to D^{(*)}K^{(*)\pm}$ modes.
[5] Uses a Dalitz plot analysis of the $\overline{D}^0 \to K^0_S\pi^+\pi^-$ decays; Combines the DK^+, D^*K^+ and DK^{*+} modes.
[6] Uses a Dalitz analysis of neutral D decays to $K^0_S\pi^+\pi^-$ in the processes $B^\pm \to D^{(*)}K^\pm$, $D^* \to D\pi^0$, $D\gamma$.

PARTIAL BRANCHING FRACTIONS

B($B^+ \to K^{*+}\ell^+\ell^-$) ($q^2 < 2.0$ GeV$^2/c^4$)

VALUE (units 10^{-7})	DOCUMENT ID		TECN	COMMENT
1.4 ±0.5 OUR AVERAGE				
$1.37^{+0.60}_{-0.58}$	AAIJ	12AH	LHCB	pp at 7 TeV
1.30±0.98±0.14	AALTONEN	11AI	CDF	$p\overline{p}$ at 1.96 TeV

B($B^+ \to K^{*+}\ell^+\ell^-$) ($2.0 < q^2 < 4.3$ GeV$^2/c^4$)

VALUE (units 10^{-7})	DOCUMENT ID		TECN	COMMENT
1.1 ±0.5 OUR AVERAGE				
$1.24^{+0.60}_{-0.55}$	AAIJ	12AH	LHCB	pp at 7 TeV
0.71±1.00±0.15	AALTONEN	11AI	CDF	$p\overline{p}$ at 1.96 TeV

B($B^+ \to K^{*+}\ell^+\ell^-$) ($4.3 < q^2 < 8.68$ GeV$^2/c^4$)

VALUE (units 10^{-7})	DOCUMENT ID		TECN	COMMENT
$2.4\ ^{+0.8}_{-0.7}$ OUR AVERAGE				
$2.50^{+0.88}_{-0.74}$	AAIJ	12AH	LHCB	pp at 7 TeV
1.71±1.58±0.49	AALTONEN	11AI	CDF	$p\overline{p}$ at 1.96 TeV

B($B^+ \to K^{*+}\ell^+\ell^-$) ($10.09 < q^2 < 12.86$ GeV$^2/c^4$)

VALUE (units 10^{-7})	DOCUMENT ID		TECN	COMMENT
2.1 ±0.6 OUR AVERAGE				
$2.13^{+0.72}_{-0.66}$	AAIJ	12AH	LHCB	pp at 7 TeV
1.97±0.99±0.22	AALTONEN	11AI	CDF	$p\overline{p}$ at 1.96 TeV

B($B^+ \to K^{*+}\ell^+\ell^-$) ($14.18 < q^2 < 16.0$ GeV$^2/c^4$)

VALUE (units 10^{-7})	DOCUMENT ID		TECN	COMMENT
$0.86^{+0.40}_{-0.32}$ OUR AVERAGE				
$1.00^{+0.47}_{-0.38}$	AAIJ	12AH	LHCB	pp at 7 TeV
0.52±0.61±0.09	AALTONEN	11AI	CDF	$p\overline{p}$ at 1.96 TeV

B($B^+ \to K^{*+}\ell^+\ell^-$) ($15.0 < q^2 < 19.0$ GeV$^2/c^4$)

VALUE (units 10^{-7})	DOCUMENT ID		TECN	COMMENT
$1.58^{+0.32}_{-0.29}$±0.11	[1] AAIJ	14M	LHCB	pp at 7, 8 TeV

[1] Uses B($B^+ \to J/\psi(1S)K^*(892)^+$) = (1.431 ± 0.027 ± 0.090) × 10^{-3} for normalization and $\mu^+\mu^-$ as a lepton pair.

B($B^+ \to K^{*+}\ell^+\ell^-$) ($q^2 > 16.0$ GeV$^2/c^4$)

VALUE (units 10^{-7})	DOCUMENT ID		TECN	COMMENT
1.3 ±0.4 OUR AVERAGE				
1.25±0.46	AAIJ	12AH	LHCB	pp at 7 TeV
1.57±0.96±0.17	AALTONEN	11AI	CDF	$p\overline{p}$ at 1.96 TeV

B($B^+ \to K^{*+}\ell^+\ell^-$) ($1.0 < q^2 < 6.0$ GeV$^2/c^4$)

VALUE (units 10^{-7})	DOCUMENT ID		TECN	COMMENT
1.8 ±0.4 OUR AVERAGE				
$1.79^{+0.41}_{-0.37}$±0.13	[1] AAIJ	14M	LHCB	pp at 7, 8 TeV
2.57±1.61±0.40	AALTONEN	11AI	CDF	$p\overline{p}$ at 1.96 TeV
• • • We do not use the following data for averages, fits, limits, etc. • • •				
$2.90^{+0.90}_{-0.85}$	AAIJ	12AH	LHCB	Repl. by AAIJ 14M

[1] Uses B($B^+ \to J/\psi(1S)K^*(892)^+$) = (1.431 ± 0.027 ± 0.090) × 10^{-3} for normalization and $\mu^+\mu^-$ as a lepton pair. Measured in $1.1 < q^2 < 6.0$ GeV$^2/c^4$.

B($B^+ \to K^{*+}\ell^+\ell^-$) ($0.0 < q^2 < 4.3$ GeV$^2/c^4$)

VALUE (units 10^{-7})	DOCUMENT ID		TECN	COMMENT
2.01±1.39±0.27	AALTONEN	11AI	CDF	$p\overline{p}$ at 1.96 TeV

B($B^+ \to K^+\ell^+\ell^-$) ($q^2 < 2.0$ GeV$^2/c^4$)

VALUE (units 10^{-7})	DOCUMENT ID		TECN	COMMENT
0.51 ±0.08 OUR AVERAGE	Error includes scale factor of 1.5.			
0.556±0.053±0.027	[1] AAIJ	13H	LHCB	pp at 7 TeV
0.36 ±0.11 ±0.03	AALTONEN	11AI	CDF	$p\overline{p}$ at 1.96 TeV

[1] Measured in $0.05 < q^2 < 2.0$ GeV$^2/c^4$ range.

B($B^+ \to K^+\ell^+\ell^-$) ($2.0 < q^2 < 4.3$ GeV$^2/c^4$)

VALUE (units 10^{-7})	DOCUMENT ID		TECN	COMMENT
0.60 ±0.07 OUR AVERAGE	Error includes scale factor of 1.3.			
0.573±0.053±0.023	AAIJ	13H	LHCB	pp at 7 TeV
0.80 ±0.15 ±0.05	AALTONEN	11AI	CDF	$p\overline{p}$ at 1.96 TeV

B($B^+ \to K^+\ell^+\ell^-$) ($4.3 < q^2 < 8.68$ GeV$^2/c^4$)

VALUE (units 10^{-7})	DOCUMENT ID		TECN	COMMENT
1.03 ±0.07 OUR AVERAGE				
1.003±0.070±0.039	AAIJ	13H	LHCB	pp at 7 TeV
1.18 ±0.19 ±0.09	AALTONEN	11AI	CDF	$p\overline{p}$ at 1.96 TeV

B($B^+ \to K^+\ell^+\ell^-$) ($10.09 < q^2 < 12.86$ GeV$^2/c^4$)

VALUE (units 10^{-7})	DOCUMENT ID		TECN	COMMENT
0.58 ±0.05 OUR AVERAGE				
0.565±0.050±0.022	AAIJ	13H	LHCB	pp at 7 TeV
0.68 ±0.12 ±0.05	AALTONEN	11AI	CDF	$p\overline{p}$ at 1.96 TeV

B($B^+ \to K^+\ell^+\ell^-$) ($14.18 < q^2 < 16.0$ GeV$^2/c^4$)

VALUE (units 10^{-7})	DOCUMENT ID		TECN	COMMENT
0.40 ±0.05 OUR AVERAGE	Error includes scale factor of 1.4.			
0.377±0.036±0.015	AAIJ	13H	LHCB	pp at 7 TeV
0.53 ±0.10 ±0.03	AALTONEN	11AI	CDF	$p\overline{p}$ at 1.96 TeV

B($B^+ \to K^+\ell^+\ell^-$) ($16.0 < q^2 < 18.0$ GeV$^2/c^4$)

VALUE (units 10^{-7})	DOCUMENT ID		TECN	COMMENT
0.354±0.036±0.018	AAIJ	13H	LHCB	pp at 7 TeV

B($B^+ \to K^+\ell^+\ell^-$) ($18.0 < q^2 < 22.0$ GeV$^2/c^4$)

F_H is a fractional contribution of (pseudo) scalar and tensor amplitudes to the decay width in the massless muon approximation.

VALUE (units 10^{-7})	DOCUMENT ID		TECN	COMMENT
0.312±0.040±0.016	AAIJ	13H	LHCB	pp at 7 TeV

B($B^+ \to K^+\ell^+\ell^-$) ($15.0 < q^2 < 22.0$ GeV$^2/c^4$)

VALUE (units 10^{-7})	DOCUMENT ID		TECN	COMMENT
0.85±0.03±0.04	[1] AAIJ	14M	LHCB	pp at 7, 8 TeV

[1] Uses B($B^+ \to J/\psi(1S)K^+$) = (0.998 ± 0.014 ± 0.040) × 10^{-3} for normalization and $\mu^+\mu^-$ as a lepton pair.

B($B^+ \to K^+\ell^+\ell^-$) ($16.0 < q^2$ GeV$^2/c^4$)

VALUE (units 10^{-7})	DOCUMENT ID		TECN	COMMENT
0.48±0.11±0.03	AALTONEN	11AI	CDF	$p\overline{p}$ at 1.96 TeV

B($B^+ \to K^+\ell^+\ell^-$) ($1.0 < q^2 < 6.0$ GeV$^2/c^4$)

VALUE (units 10^{-7})	DOCUMENT ID		TECN	COMMENT
1.26 ±0.10 OUR AVERAGE	Error includes scale factor of 1.6. See the ideogram below.			
$1.56\ ^{+0.19}_{-0.15}\ ^{+0.06}_{-0.04}$	[1] AAIJ	14AR	LHCB	pp at 7, 8 TeV
1.19 ±0.034±0.059	[2] AAIJ	14M	LHCB	pp at 7, 8 TeV
1.41 ±0.20 ±0.10	AALTONEN	11AI	CDF	$p\overline{p}$ at 1.96 TeV
• • • We do not use the following data for averages, fits, limits, etc. • • •				
1.205±0.085±0.070	AAIJ	13H	LHCB	Repl. by AAIJ 14M

[1] Measured by taking the ratio of the branching fraction from $B^+ \to K^+e^+e^-$ and $B^+ \to J/\psi(e^+e^-)K^+$ decays and multiplying it by the measured value of $B^+ \to J/\psi K^+$ and $J/\psi \to e^+e^-$ as in PDG 12 update. The branching fraction of $B^+ \to K^+e^+e^-$ is determined in the region $1 < q^2 < 6$ GeV$^2/c^4$.
[2] Uses B($B^+ \to J/\psi(1S)K^+$) = (0.998 ± 0.014 ± 0.040) × 10^{-3} for normalization and $\mu^+\mu^-$ for leptons. Measured for $1.1 < q^2 < 6.0$ GeV$^2/c^4$.

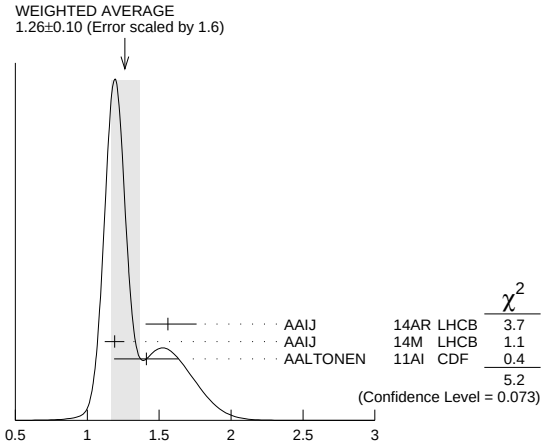

B($B^+ \to K^+\ell^+\ell^-$) ($1.0 < q^2 < 6.0$ GeV$^2/c^4$) (units 10^{-7})

B($B^+ \to K^+\mu^+\mu^-$) / B($B^+ \to K^+e^+e^-$) ($1.0 < q^2 < 6.0$ GeV$^2/c^4$)

VALUE	DOCUMENT ID		TECN	COMMENT
$0.745^{+0.090}_{-0.074}$±0.036	[1] AAIJ	14AR	LHCB	pp at 7, 8 TeV

[1] The ratio is determined using the ratio of the relative branching fractions of the decays $B^+ \to K^+\ell^+\ell^-$ and $B^+ \to J/\psi(\to \ell^+\ell^-)K^+$, with $\ell = e, \mu$.

B($B^+ \to K^+\ell^+\ell^-$) ($0.0 < q^2 < 4.3$ GeV$^2/c^4$)

VALUE (units 10^{-7})	DOCUMENT ID		TECN	COMMENT
1.13±0.19±0.08	AALTONEN	11AI	CDF	$p\overline{p}$ at 1.96 TeV

B($B^+ \to K^+\pi^+\pi^-\mu^+\mu^-$) ($1.00 < q^2 < 6.00$ GeV$^2/c^4$)

VALUE (units 10^{-7})	DOCUMENT ID		TECN	COMMENT
$1.38^{+0.15}_{-0.14}\pm0.08$	AAIJ	14AZ	LHCB	pp at 7, 8 TeV

B($B^+ \to K^+\pi^+\pi^-\mu^+\mu^-$) ($0.10 < q^2 < 2.00$ GeV$^2/c^4$)

VALUE (units 10^{-7})	DOCUMENT ID		TECN	COMMENT
$1.33^{+0.13}_{-0.12}\pm0.09$	AAIJ	14AZ	LHCB	pp at 7, 8 TeV

B($B^+ \to K^+\pi^+\pi^-\mu^+\mu^-$) ($2.00 < q^2 < 4.30$ GeV$^2/c^4$)

VALUE (units 10^{-8})	DOCUMENT ID		TECN	COMMENT
$5.38^{+0.94}_{-0.87}\pm0.35$	AAIJ	14AZ	LHCB	pp at 7, 8 TeV

B($B^+ \to K^+\pi^+\pi^-\mu^+\mu^-$) ($4.30 < q^2 < 8.68$ GeV$^2/c^4$)

VALUE (units 10^{-7})	DOCUMENT ID		TECN	COMMENT
$1.01^{+0.12}_{-0.13}\pm0.09$	AAIJ	14AZ	LHCB	pp at 7, 8 TeV

B($B^+ \to K^+\pi^+\pi^-\mu^+\mu^-$) ($10.09 < q^2 < 12.86$ GeV$^2/c^4$)

VALUE (units 10^{-8})	DOCUMENT ID		TECN	COMMENT
$5.07^{+0.94}_{-0.89}\pm0.47$	AAIJ	14AZ	LHCB	pp at 7, 8 TeV

B($B^+ \to K^+\pi^+\pi^-\mu^+\mu^-$) ($14.18 < q^2 < 19.00$ GeV$^2/c^4$)

VALUE (units 10^{-8})	DOCUMENT ID		TECN	COMMENT
$0.48^{+0.39}_{-0.29}\pm0.05$	AAIJ	14AZ	LHCB	pp at 7, 8 TeV

B($B^+ \to \pi^+\mu^+\mu^-$)/B($B^+ \to K^+\mu^+\mu^-$) ($1.00 < q^2 < 6.00$ GeV$^2/c^4$)

VALUE (units 10^{-2})	DOCUMENT ID		TECN	COMMENT
3.8±0.9±0.1	AAIJ	15AR	LHCB	pp at 7, 8 TeV

B($B^+ \to \pi^+\mu^+\mu^-$) ($1.00 < q^2 < 6.00$ GeV$^2/c^4$)

VALUE (units 10^{-9})	DOCUMENT ID		TECN	COMMENT
$4.55^{+1.05}_{-1.00}\pm0.15$	AAIJ	15AR	LHCB	pp at 7, 8 TeV

B($B^+ \to \pi^+\mu^+\mu^-$) ($15.00 < q^2 < 22.00$ GeV$^2/c^4$)

VALUE (units 10^{-9})	DOCUMENT ID		TECN	COMMENT
$3.29^{+0.84}_{-0.70}\pm0.07$	AAIJ	15AR	LHCB	pp at 7, 8 TeV

B($B^+ \to \pi^+\mu^+\mu^-$)/B($B^+ \to K^+\mu^+\mu^-$) ($15.0 < q^2 < 22.0$ GeV$^2/c^4$)

VALUE (units 10^{-2})	DOCUMENT ID		TECN	COMMENT
3.7±0.8±0.1	AAIJ	15AR	LHCB	pp at 7, 8 TeV

$A_{FB}(B^+ \to K^+\mu^+\mu^-)$ ($1.1 < q^2 < 6.0$ GeV$^2/c^4$)

A_{FB} is the forward-backward angular asymmetry of the lepton pair in $B \to K^{(*)}\ell^+\ell^-$ decay as defined in B^+, B^0 admixture particle listings.

VALUE	DOCUMENT ID		TECN	COMMENT
0.005±0.015±0.010	[1] AAIJ	14O	LHCB	pp at 7,8 TeV
• • • We do not use the following data for averages, fits, limits, etc. • • •				
$0.02\ ^{+0.05}_{-0.03}\ ^{+0.02}_{-0.01}$	AAIJ	13H	LHCB	Repl. by AAIJ 14O

[1] AAIJ 14O reports 68% C.L. interval, which we encode as midpoint with uncertainty as half of the width of interval.

$A_{FB}(B^+ \to K^+\mu^+\mu^-)$ ($15.0 < q^2 < 22.0$ GeV$^2/c^4$)

VALUE	DOCUMENT ID		TECN	COMMENT
−0.015±0.015±0.01	[1] AAIJ	14O	LHCB	pp at 7, 8 TeV

[1] AAIJ 14O reports 68% C.L. interval, which we encode as midpoint with uncertainty as half of the width of interval.

$F_H(B^+ \to K^+\mu^+\mu^-)$ ($1.1 < q^2 < 6.0$ GeV$^2/c^4$)

F_H is a fractional contribution of (pseudo) scalar and tensor amplitudes to the decay width in the massless muon approximation.

VALUE	DOCUMENT ID		TECN	COMMENT
0.03±0.03±0.02	[1] AAIJ	14O	LHCB	pp at 7, 8 TeV
• • • We do not use the following data for averages, fits, limits, etc. • • •				
$0.05\ ^{+0.08}_{-0.05}\ ^{+0.04}_{-0.02}$	AAIJ	13H	LHCB	Repl. by AAIJ 14O

[1] AAIJ 14O reports 68% C.L. interval, which we encode as midpoint with uncertainty as half of the width of interval.

$F_H(B^+ \to K^+\mu^+\mu^-)$ ($15.0 < q^2 < 22.0$ GeV$^2/c^4$)

F_H is a fractional contribution of (pseudo) scalar and tensor amplitudes to the decay width in the massless muon approximation.

VALUE	DOCUMENT ID		TECN	COMMENT
0.035±0.035±0.02	[1] AAIJ	14O	LHCB	pp at 7, 8 TeV

[1] AAIJ 14O reports 68% C.L. interval, which we encode as midpoint with uncertainty as half of the width of interval.

FORWARD-BACKWARD ASYMMETRIES

The forward-backward assymmetry is defined as A_{FB} = [N($q_{FB} > 0$) − N($q_{FB} < 0$)] / [N($q_{FB} > 0$) + N($q_{FB} < 0$)], where $q_{FB} = -q_B \cdot \mathrm{sgn}(\eta_B)$ with q_B as the B hadron electric charge, η_B as its pseudorapidity, and sgn(η_B) as a sign function of η_B.

$A_{FB}(B^{\pm} \to J/\psi K^{\pm})$

VALUE (units 10^{-2})	DOCUMENT ID		TECN	COMMENT
−0.24±0.41±0.19	ABAZOV	15	D0	$p\overline{p}$ at 1.96 TeV

$A_P(B^+) = [\sigma(B^-) - \sigma(B^+)] / [\sigma(B^-) + \sigma(B^+)]$

Production asymmetries

VALUE (units 10^{-3})	DOCUMENT ID		TECN	COMMENT
−5.2±1.9 OUR AVERAGE				
−4.1±4.9±1.0	[1] AAIJ	17AP	LHCB	pp at 7 TeV
−5.3±3.1±1.0	[1] AAIJ	17AP	LHCB	pp at 8 TeV
−2.3±2.4±3.7	[2] AAIJ	17BF	LHCB	pp at 7 TeV
−7.4±1.5±3.2	[2] AAIJ	17BF	LHCB	pp at 8 TeV

[1] AAIJ 17AP uses $B^+ \to \overline{D}^0\pi^+$ decays with B^+ transverse momenta p_T and rapidities y in the region of $2 < p_T < 30$ GeV/c and $2.1 < y < 4.5$.

[2] AAIJ 17BF uses $B^+ \to J/\psi K^+$ decays with B^+ transverse momenta p_T and rapidities y in the region of $0 < p_T < 30$ GeV/c and $2.1 < y < 4.5$.

$B^{\pm}$ REFERENCES

AAIJ	18A	PL B777 16	R. Aaij *et al.*	(LHCb Collab.)
AAIJ	18B	JHEP 1801 131	R. Aaij *et al.*	(LHCb Collab.)
KATO	18	PR D97 012005	Y. Kato *et al.*	(BELLE Collab.)
AAIJ	17	PR D95 012002	R. Aaij *et al.*	(LHCb Collab.)
AAIJ	17AD	PL B769 305	R. Aaij *et al.*	(LHCb Collab.)
AAIJ	17AP	PR D95 052005	R. Aaij *et al.*	(LHCb Collab.)
AAIJ	17AQ	PR D95 071101	R. Aaij *et al.*	(LHCb Collab.)
AAIJ	17AR	PR D96 011101	R. Aaij *et al.*	(LHCb Collab.)
AAIJ	17BF	PL B774 139	R. Aaij *et al.*	(LHCb Collab.)
AAIJ	17BO	JHEP 1711 156	R. Aaij *et al.*	(LHCb Collab.)
AAIJ	17E	PL B765 307	R. Aaij *et al.*	(LHCb Collab.)
AAIJ	17K	EPJ C77 72	R. Aaij *et al.*	(LHCb Collab.)
AAIJ	17O	JHEP 1703 036	R. Aaij *et al.*	(LHCb Collab.)
AAIJ	17R	JHEP 1704 162	R. Aaij *et al.*	(LHCb Collab.)
AAIJ	17Y	EPJ C77 161	R. Aaij *et al.*	(LHCb Collab.)
ABAZOV	17A	PR D95 031101	V.M. Abazov *et al.*	(D0 Collab.)
BELENO	17	PR D96 091102	C. Beleno *et al.*	(BELLE Collab.)
GRYGIER	17	PR D96 091101	J. Grygier *et al.*	(BELLE Collab.)
HORIGUCHI	17	PRL 119 191802	T. Horiguchi *et al.*	(BELLE Collab.)
HSU	17	PR D96 031101	C.-L. Hsu *et al.*	(BELLE Collab.)
KHACHATRY...	17C	PL B764 66	V. Khachatryan *et al.*	(CMS Collab.)
LEES	17	PRL 118 031802	J.P. Lees *et al.*	(BABAR Collab)
LEES	17G	PR D96 072001	J.P. Lees *et al.*	(BABAR Collab)
AABOUD	16L	EPJ C76 513	M. Aaboud *et al.*	(ATLAS Collab.)
AAIJ	16AA	JHEP 1608 137	R. Aaij *et al.*	(LHCb Collab.)
AAIJ	16AH	PR D94 072001	R. Aaij *et al.*	(LHCb Collab.)
AAIJ	16AQ	JHEP 1612 087	R. Aaij *et al.*	(LHCb Collab.)
AAIJ	16L	PL B760 117	R. Aaij *et al.*	(LHCb Collab.)
AAIJ	16M	PR D93 051101	R. Aaij *et al.*	(LHCb Collab.)
AAIJ	16R	PR D93 119902	R. Aaij *et al.*	(LHCb Collab.)
AAIJ	16Z	JHEP 1606 131	R. Aaij *et al.*	(LHCb Collab.)
BHARDWAJ	16	PR D93 052016	V. Bhardwaj *et al.*	(BELLE Collab.)
DEL-AMO-SA...	16	PR D93 052013	P. del Amo Sanchez *et al.*	(BABAR Collab.)
LEES	16	PRL 116 041801	J.P. Lees *et al.*	(BABAR Collab.)
PDG	16	CP C40 100001	C. Patrignani *et al.*	(PDG Collab.)
AAIJ	15AR	JHEP 1510 034	R. Aaij *et al.*	(LHCb Collab.)
AAIJ	15BC	PR D92 112005	R. Aaij *et al.*	(LHCb Collab.)
AAIJ	15K	PL B741 1	R. Aaij *et al.*	(LHCb Collab.)
AAIJ	15O	PRL 115 051801	R. Aaij *et al.*	(LHCb Collab.)
AAIJ	15V	PR D91 092002	R. Aaij *et al.*	(LHCb Collab.)
Also		PR D93 119901 (errat.)	R. Aaij *et al.*	(LHCb Collab.)
AAIJ	15W	PR D91 112014	R. Aaij *et al.*	(LHCb Collab.)
ABAZOV	15	PRL 114 051803	V.M. Abazov *et al.*	(D0 Collab.)
BALA	15	PR D91 051101	A. Bala *et al.*	(BELLE Collab.)
CHOI	15A	PR D91 092011	S.-K. Choi *et al.*	(BELLE Collab.)
GOH	15	PR D91 071101	Y.M. Goh *et al.*	(BELLE Collab.)
HELLER	15	PR D91 112009	A. Heller *et al.*	(BELLE Collab.)
KRONENBIT...	15	PR D92 051102	B. Kronenbitter *et al.*	(BELLE Collab.)
LEES	15	PR D91 012003	J.P. Lees *et al.*	(BABAR Collab.)
LEES	15C	PR D91 052002	J.P. Lees *et al.*	(BABAR Collab.)
VINOKUROVA	15	JHEP 1506 132	A. Vinokurova *et al.*	(BELLE Collab.)
Also		JHEP 1702 088 (errat.)	A. Vinokurova *et al.*	(BELLE Collab.)
WIECHCZYN...	15	PR D91 032008	J. Wiechczynski *et al.*	(BELLE Collab.)
YOOK	15	PR D91 052016	Y. Yook *et al.*	(BELLE Collab.)
AAIJ	14	PRL 112 011801	R. Aaij *et al.*	(LHCb Collab.)
AAIJ	14A	PL B728 85	R. Aaij *et al.*	(LHCb Collab.)
AAIJ	14AC	PRL 112 131802	R. Aaij *et al.*	(LHCb Collab.)
AAIJ	14AF	PRL 113 141801	R. Aaij *et al.*	(LHCb Collab.)
AAIJ	14AN	JHEP 1409 177	R. Aaij *et al.*	(LHCb Collab.)
AAIJ	14AR	PRL 113 151601	R. Aaij *et al.*	(LHCb Collab.)
AAIJ	14AZ	JHEP 1410 064	R. Aaij *et al.*	(LHCb Collab.)
AAIJ	14BA	JHEP 1410 097	R. Aaij *et al.*	(LHCb Collab.)
AAIJ	14BE	NP B888 169	R. Aaij *et al.*	(LHCb Collab.)
AAIJ	14BF	JHEP 1411 060	R. Aaij *et al.*	(LHCb Collab.)
AAIJ	14BO	PR D90 112004	R. Aaij *et al.*	(LHCb Collab.)
AAIJ	14E	JHEP 1404 114	R. Aaij *et al.*	(LHCb Collab.)
AAIJ	14M	JHEP 1406 133	R. Aaij *et al.*	(LHCb Collab.)
AAIJ	14O	JHEP 1405 082	R. Aaij *et al.*	(LHCb Collab.)
AAIJ	14V	PL B733 36	R. Aaij *et al.*	(LHCb Collab.)
ABAZOV	14A	PR D89 012004	V.M. Abazov *et al.*	(D0 Collab.)
CHOBANOVA	14	PR D90 012002	V. Chobanova *et al.*	(BELLE Collab.)
IWASHITA	14	PTEP 2014 043C01	T. Iwashita *et al.*	(BELLE Collab.)
LEES	14A	PR D89 011102	J.P. Lees *et al.*	(BABAR Collab.)
TIEN	14	PR D89 011101	K.-J. Tien *et al.*	(BELLE Collab.)

Meson Particle Listings

$B^{\pm}$

AAIJ 13AE PL B723 44 R. Aaij *et al.* (LHCb Collab.)
AAIJ 13AK PL B726 151 R. Aaij *et al.* (LHCb Collab.)
AAIJ 13AP PR D87 092007 R. Aaij *et al.* (LHCb Collab.)
AAIJ 13AR PR D87 112010 R. Aaij *et al.* (LHCb Collab.)
AAIJ 13AU PR D88 052015 R. Aaij *et al.* (LHCb Collab.)
AAIJ 13AZ PRL 111 101801 R. Aaij *et al.* (LHCb Collab.)
AAIJ 13BC PRL 111 112003 R. Aaij *et al.* (LHCb Collab.)
AAIJ 13BN PRL 111 151801 R. Aaij *et al.* (LHCb Collab.)
AAIJ 13BS PL B726 646 R. Aaij *et al.* (LHCb Collab.)
AAIJ 13H JHEP 1302 105 R. Aaij *et al.* (LHCb Collab.)
AAIJ 13R JHEP 1302 043 R. Aaij *et al.* (LHCb Collab.)
AAIJ 13S EPJ C73 2462 R. Aaij *et al.* (LHCb Collab.)
AAIJ 13Z JHEP 1309 006 R. Aaij *et al.* (LHCb Collab.)
ABAZOV 13M PRL 110 241801 V.M. Abazov *et al.* (D0 Collab.)
DUH 13 PR D87 031103 Y. T. Duh *et al.* (BELLE Collab.)
HARA 13 PRL 110 131801 K. Hara *et al.* (BELLE Collab.)
LEES 13A PR D87 032004 J.P. Lees *et al.* (BABAR Collab.)
LEES 13B PR D87 052015 J.P. Lees *et al.* (BABAR Collab.)
LEES 13I PR D87 112005 J.P. Lees *et al.* (BABAR Collab.)
LEES 13K PR D88 031102 J.P. Lees *et al.* (BABAR Collab.)
LEES 13M PR D88 032012 J.P. Lees *et al.* (BABAR Collab.)
LEES 13T PR D88 072006 J.P. Lees *et al.* (BABAR Collab.)
LUTZ 13 PR D87 111103 O. Lutz *et al.* (BELLE Collab.)
NAYAK 13 PR D88 091104 M. Nayak *et al.* (BELLE Collab.)
SIBIDANOV 13 PR D88 032005 A. Sibidanov *et al.* (BELLE Collab.)
AAIJ 12AA PR D85 091103 R. Aaij *et al.* (LHCb Collab.)
AAIJ 12AC PR D85 091105 R. Aaij *et al.* (LHCb Collab.)
AAIJ 12AD PR D85 112004 R. Aaij *et al.* (LHCb Collab.)
AAIJ 12AH JHEP 1207 133 R. Aaij *et al.* (LHCb Collab.)
AAIJ 12AQ PL B718 43 R. Aaij *et al.* (LHCb Collab.)
AAIJ 12AY JHEP 1212 125 R. Aaij *et al.* (LHCb Collab.)
AAIJ 12C PRL 108 101601 R. Aaij *et al.* (LHCb Collab.)
AAIJ 12E PL B708 241 R. Aaij *et al.* (LHCb Collab.)
AAIJ 12L EPJ C72 2118 R. Aaij *et al.* (LHCb Collab.)
AAIJ 12M PL B712 203 R. Aaij *et al.* (LHCb Collab.)
Also PL B713 351 (errat.) R. Aaij *et al.* (LHCb Collab.)
AAIJ 12T PRL 108 161801 R. Aaij *et al.* (LHCb Collab.)
AIHARA 12 PR D85 112014 H. Aihara *et al.* (BELLE Collab.)
DEL-AMO-SA... 12 PR D85 092017 P. del Amo Sanchez *et al.* (BABAR Collab.)
HOI 12 PRL 108 031801 C.-T. Hoi *et al.* (BELLE Collab.)
KIM 12A PR D86 031101 J.H. Kim *et al.* (BELLE Collab.)
LEES 12AA PR D86 092004 J.P. Lees *et al.* (BABAR Collab.)
LEES 12B PR D85 052003 J.P. Lees *et al.* (BABAR Collab.)
LEES 12D PRL 109 101802 J.P. Lees *et al.* (BABAR Collab.)
Also PR D88 072012 J.P. Lees *et al.* (BABAR Collab.)
LEES 12J PR D85 071103 J.P. Lees *et al.* (BABAR Collab.)
LEES 12O PR D85 112010 J.P. Lees *et al.* (BABAR Collab.)
LEES 12P PR D86 012004 J.P. Lees *et al.* (BABAR Collab.)
LEES 12S PR D86 032012 J.P. Lees *et al.* (BABAR Collab.)
LEES 12Z PR D86 091102 J.P. Lees *et al.* (BABAR Collab.)
PDG 12 PR D86 010001 J. Beringer *et al.* (PDG Collab.)
STYPULA 12 PR D86 072007 J. Stypula *et al.* (BELLE Collab.)
AAIJ 11E PR D84 092001 R. Aaij *et al.* (LHCb Collab.)
Also PR D85 039904 (errat.) R. Aaij *et al.* (LHCb Collab.)
AALTONEN 11 PRL 106 121804 T. Aaltonen *et al.* (CDF Collab.)
AALTONEN 11AI PRL 107 201802 T. Aaltonen *et al.* (CDF Collab.)
AALTONEN 11AJ PR D84 091504 T. Aaltonen *et al.* (CDF Collab.)
AALTONEN 11B PR D83 032008 T. Aaltonen *et al.* (CDF Collab.)
AALTONEN 11L PRL 106 161801 T. Aaltonen *et al.* (CDF Collab.)
AUSHEV 11 PR D83 051102 T. Aushev *et al.* (BELLE Collab.)
BHARDWAJ 11 PRL 107 091803 V. Bhardwaj *et al.* (BELLE Collab.)
CHEN 11F PR D84 071501 P. Chen *et al.* (BELLE Collab.)
CHOI 11 PR D84 052004 S.-K. Choi *et al.* (BELLE Collab.)
DEL-AMO-SA... 11B PR D83 032004 P. del Amo Sanchez *et al.* (BABAR Collab.)
DEL-AMO-SA... 11C PR D83 032007 P. del Amo Sanchez *et al.* (BABAR Collab.)
DEL-AMO-SA... 11D PR D83 051101 P. del Amo Sanchez *et al.* (BABAR Collab.)
DEL-AMO-SA... 11F PR D83 052011 P. del Amo Sanchez *et al.* (BABAR Collab.)
DEL-AMO-SA... 11K PR D83 091101 P. del Amo Sanchez *et al.* (BABAR Collab.)
DEL-AMO-SA... 11L PRL 107 041804 P. del Amo Sanchez *et al.* (BABAR Collab.)
GULER 11 PR D83 032005 H. Guler *et al.* (BELLE Collab.)
HORII 11 PRL 106 231803 Y. Horii *et al.* (BELLE Collab.)
LEES 11A PR D84 012001 J.P. Lees *et al.* (BABAR Collab.)
LEES 11D PR D84 012002 J.P. Lees *et al.* (BABAR Collab.)
LEES 11I PR D84 092007 J.P. Lees *et al.* (BABAR Collab.)
SAHOO 11A PR D84 071101 H. Sahoo *et al.* (BELLE Collab.)
SEON 11 PR D84 071106 O. Seon *et al.* (BELLE Collab.)
VINOKUROVA 11 PL B706 139 A. Vinokurova *et al.* (BELLE Collab.)
AALTONEN 10A PR D81 031105 T. Aaltonen *et al.* (CDF Collab.)
AUBERT 10 PRL 104 011802 B. Aubert *et al.* (BABAR Collab.)
AUBERT 10D PR D81 052009 B. Aubert *et al.* (BABAR Collab.)
AUBERT 10E PR D81 051101 B. Aubert *et al.* (BABAR Collab.)
AUSHEV 10 PR D81 031103 T. Aushev *et al.* (BELLE Collab.)
BOZEK 10 PR D82 072005 A. BOZEK *et al.* (BELLE Collab.)
DEL-AMO-SA... 10A PR D82 011502 P. del Amo Sanchez *et al.* (BABAR Collab.)
DEL-AMO-SA... 10B PR D82 011101 P. del Amo Sanchez *et al.* (BABAR Collab.)
DEL-AMO-SA... 10F PRL 105 121801 P. del Amo Sanchez *et al.* (BABAR Collab.)
DEL-AMO-SA... 10G PR D82 072004 P. del Amo Sanchez *et al.* (BABAR Collab.)
DEL-AMO-SA... 10H PR D82 072006 P. del Amo Sanchez *et al.* (BABAR Collab.)
DEL-AMO-SA... 10I PR D82 091101 P. del Amo Sanchez *et al.* (BABAR Collab.)
DEL-AMO-SA... 10K PR D82 092006 P. del Amo Sanchez *et al.* (BABAR Collab.)
DEL-AMO-SA... 10Q PR D82 112002 P. del Amo Sanchez *et al.* (BABAR Collab.)
HARA 10 PR D82 071101 K. Hara *et al.* (BELLE Collab.)
LIBBY 10 PR D82 112006 J. Libby *et al.* (CLEO Collab.)
POLUEKTOV 10 PR D81 112002 A. Poluektov *et al.* (BELLE Collab.)
SAKAI 10 PR D82 091104 K. Sakai *et al.* (BELLE Collab.)
WEDD 10 PR D81 111104 R. Wedd *et al.* (BELLE Collab.)
AALTONEN 09B PR D79 011104 T. Aaltonen *et al.* (CDF Collab.)
ABAZOV 09Y PR D79 111102 V.M. Abazov *et al.* (D0 Collab.)
ABULENCIA 09 PR D79 112003 A. Abulencia *et al.* (CDF Collab.)
AUBERT 09 PR D79 011102 B. Aubert *et al.* (BABAR Collab.)
AUBERT 09A PR D79 012002 B. Aubert *et al.* (BABAR Collab.)
AUBERT 09AA PR D79 112001 B. Aubert *et al.* (BABAR Collab.)
AUBERT 09AB PR D79 112004 B. Aubert *et al.* (BABAR Collab.)
AUBERT 09AF PR D80 051101 B. Aubert *et al.* (BABAR Collab.)
AUBERT 09AJ PR D80 092001 B. Aubert *et al.* (BABAR Collab.)
AUBERT 09AO PRL 103 211802 B. Aubert *et al.* (BABAR Collab.)
AUBERT 09AT PR D80 111105 B. Aubert *et al.* (BABAR Collab.)
AUBERT 09AV PR D80 112002 B. Aubert *et al.* (BABAR Collab.)
AUBERT 09B PRL 102 132001 B. Aubert *et al.* (BABAR Collab.)
AUBERT 09F PR D79 051102 B. Aubert *et al.* (BABAR Collab.)
AUBERT 09G PRL 102 141802 B. Aubert *et al.* (BABAR Collab.)
AUBERT 09H PR D79 052005 B. Aubert *et al.* (BABAR Collab.)
AUBERT 09J PR D79 051101 B. Aubert *et al.* (BABAR Collab.)
AUBERT 09L PR D79 072006 B. Aubert *et al.* (BABAR Collab.)
AUBERT 09Q PR D79 052011 B. Aubert *et al.* (BABAR Collab.)
AUBERT 09R PR D79 072003 B. Aubert *et al.* (BABAR Collab.)
AUBERT 09S PR D79 092002 B. Aubert *et al.* (BABAR Collab.)
AUBERT 09T PRL 102 091803 B. Aubert *et al.* (BABAR Collab.)
Also EPAPS Document No. E-PRLTAO-102-060910 (BABAR Collab.)
AUBERT 09V PR D79 091101 B. Aubert *et al.* (BABAR Collab.)
AUBERT 09Y PRL 103 051803 B. Aubert *et al.* (BABAR Collab.)
CHANG 09 PR D79 052006 Y.-W. Chang *et al.* (BELLE Collab.)
CHEN 09C PR D80 111103 P. Chen *et al.* (BELLE Collab.)
LIU 09 PR D79 071102 C. Liu *et al.* (BELLE Collab.)
WEI 09A PRL 103 171801 J.-T. Wei *et al.* (BELLE Collab.)
Also EPAPS Supplement EPAPS_appendix.pdf (BELLE Collab.)
WIECHCZYN... 09 PR D80 052005 J. Wiechczynski *et al.* (BELLE Collab.)
ABAZOV 08O PRL 100 211802 V.M. Abazov *et al.* (D0 Collab.)
ADACHI 08 PR D77 091101 I. Adachi *et al.* (BELLE Collab.)
AUBERT 08A PR D77 011101 B. Aubert *et al.* (BABAR Collab.)
AUBERT 08AA PR D77 111102 B. Aubert *et al.* (BABAR Collab.)
AUBERT 08AB PR D78 012006 B. Aubert *et al.* (BABAR Collab.)
AUBERT 08AD PR D77 091104 B. Aubert *et al.* (BABAR Collab.)
AUBERT 08AG PR D78 011104 B. Aubert *et al.* (BABAR Collab.)
AUBERT 08AH PR D78 011107 B. Aubert *et al.* (BABAR Collab.)
AUBERT 08AI PR D78 012004 B. Aubert *et al.* (BABAR Collab.)
AUBERT 08AL PR D78 034023 B. Aubert *et al.* (BABAR Collab.)
AUBERT 08AT PRL 100 231803 B. Aubert *et al.* (BABAR Collab.)
AUBERT 08AV PRL 101 081801 B. Aubert *et al.* (BABAR Collab.)
AUBERT 08B PR D77 011102 B. Aubert *et al.* (BABAR Collab.)
AUBERT 08BC PR D78 072007 B. Aubert *et al.* (BABAR Collab.)
AUBERT 08BD PR D78 091101 B. Aubert *et al.* (BABAR Collab.)
AUBERT 08BE PR D78 091102 B. Aubert *et al.* (BABAR Collab.)
AUBERT 08BF PR D78 092002 B. Aubert *et al.* (BABAR Collab.)
AUBERT 08BH PR D78 112001 B. Aubert *et al.* (BABAR Collab.)
AUBERT 08BI PRL 101 161801 B. Aubert *et al.* (BABAR Collab.)
AUBERT 08BK PRL 101 201801 B. Aubert *et al.* (BABAR Collab.)
AUBERT 08BL PRL 101 261802 B. Aubert *et al.* (BABAR Collab.)
AUBERT 08BN PR D78 112003 B. Aubert *et al.* (BABAR Collab.)
AUBERT 08D PR D77 011107 B. Aubert *et al.* (BABAR Collab.)
AUBERT 08F PRL 100 051803 B. Aubert *et al.* (BABAR Collab.)
AUBERT 08G PRL 100 171803 B. Aubert *et al.* (BABAR Collab.)
AUBERT 08H PR D77 031101 B. Aubert *et al.* (BABAR Collab.)
AUBERT 08N PRL 100 021801 B. Aubert *et al.* (BABAR Collab.)
Also PR D79 092002 B. Aubert *et al.* (BABAR Collab.)
AUBERT 08Q PRL 100 151802 B. Aubert *et al.* (BABAR Collab.)
AUBERT 08W PRL 101 082001 B. Aubert *et al.* (BABAR Collab.)
AUBERT 08X PRL 101 091801 B. Aubert *et al.* (BABAR Collab.)
AUBERT 08Y PR D77 111101 B. Aubert *et al.* (BABAR Collab.)
BHARDWAJ 08 PR D78 051104 V. Bhardwaj *et al.* (BELLE Collab.)
BRODZICKA 08 PRL 100 092001 J. Brodzicka *et al.* (BELLE Collab.)
CHEN 08C PRL 100 251801 J.-H. Chen *et al.* (BELLE Collab.)
HORII 08 PR D78 071901 Y. Horii *et al.* (BELLE Collab.)
IWABUCHI 08 PRL 101 041601 M. Iwabuchi *et al.* (BELLE Collab.)
LIN 08 NAT 452 332 S.-W. Lin *et al.* (BELLE Collab.)
LIVENTSEV 08 PR D77 091503 D. Liventsev *et al.* (BELLE Collab.)
PDG 08 PL B667 1 C. Amsler *et al.* (PDG Collab.)
TANIGUCHI 08 PRL 101 111801 N. Taniguchi *et al.* (BELLE Collab.)
WEI 08 PL B659 80 J.-T. Wei *et al.* (BELLE Collab.)
WEI 08A PR D78 011101 J.-T. Wei *et al.* (BELLE Collab.)
WICHT 08 PL B662 323 J. Wicht *et al.* (BELLE Collab.)
ADAM 07 PRL 99 041802 N.E. Adam *et al.* (CLEO Collab.)
Also PR D76 012007 D.M. Asner *et al.* (CLEO Collab.)
AUBERT 07AC PR D76 031101 B. Aubert *et al.* (BABAR Collab.)
AUBERT 07AE PR D76 031103 B. Aubert *et al.* (BABAR Collab.)
AUBERT 07AG PRL 99 051801 B. Aubert *et al.* (BABAR Collab.)
AUBERT 07AL PR D76 052002 B. Aubert *et al.* (BABAR Collab.)
AUBERT 07AN PR D76 051101 B. Aubert *et al.* (BABAR Collab.)
AUBERT 07AR PR D76 071103 B. Aubert *et al.* (BABAR Collab.)
AUBERT 07AV PR D76 092004 B. Aubert *et al.* (BABAR Collab.)
AUBERT 07AZ PRL 99 201801 B. Aubert *et al.* (BABAR Collab.)
AUBERT 07BA PRL 99 201802 B. Aubert *et al.* (BABAR Collab.)
AUBERT 07BB PRL 99 221801 B. Aubert *et al.* (BABAR Collab.)
AUBERT 07BC PR D76 091102 B. Aubert *et al.* (BABAR Collab.)
AUBERT 07BI PRL 99 241803 B. Aubert *et al.* (BABAR Collab.)
AUBERT 07BJ PRL 99 251801 B. Aubert *et al.* (BABAR Collab.)
AUBERT 07BL PRL 99 261801 B. Aubert *et al.* (BABAR Collab.)
AUBERT 07BN PR D76 111101 B. Aubert *et al.* (BABAR Collab.)
AUBERT 07E PRL 98 051802 B. Aubert *et al.* (BABAR Collab.)
AUBERT 07H PR D75 031101 B. Aubert *et al.* (BABAR Collab.)
AUBERT 07L PRL 98 151802 B. Aubert *et al.* (BABAR Collab.)
AUBERT 07M PRL 98 171801 B. Aubert *et al.* (BABAR Collab.)
AUBERT 07N PR D75 072002 B. Aubert *et al.* (BABAR Collab.)
AUBERT 07Q PR D75 051102 B. Aubert *et al.* (BABAR Collab.)
AUBERT 07R PRL 98 211804 B. Aubert *et al.* (BABAR Collab.)
Also PRL 100 189903E B. Aubert *et al.* (BABAR Collab.)
Also PRL 100 199905E B. Aubert *et al.* (BABAR Collab.)
AUBERT 07X PR D75 091103 B. Aubert *et al.* (BABAR Collab.)
AUBERT 07Z PR D76 011103 B. Aubert *et al.* (BABAR Collab.)
CHANG 07B PR D75 071104 P. Chang *et al.* (BELLE Collab.)
CHEN 07D PRL 99 221802 K.-F. Chen *et al.* (BELLE Collab.)
HOKUUE 07 PL B648 139 T. Hokuue *et al.* (BELLE Collab.)
LIN 07 PRL 98 181804 S.-W. Lin *et al.* (BELLE Collab.)
LIN 07A PRL 99 121601 S.-W. Lin *et al.* (BELLE Collab.)
SATOYAMA 07 PL B647 67 N. Satoyama *et al.* (BELLE Collab.)
SCHUEMANN 07 PR D75 092002 J. Schuemann *et al.* (BELLE Collab.)
TSAI 07 PR D75 111101 Y.-T. Tsai *et al.* (BELLE Collab.)
URQUIJO 07 PR D75 032001 P. Urquijo *et al.* (BELLE Collab.)
WANG 07B PR D75 092005 C.H. Wang *et al.* (BELLE Collab.)
WANG 07C PR D76 052004 M.-Z. Wang *et al.* (BELLE Collab.)
XIE 07 PR D75 017101 Q.L. Xie *et al.* (BELLE Collab.)
ABE 06 PR D73 051106 K. Abe *et al.* (BELLE Collab.)
ABULENCIA 06J PRL 96 191801 A. Abulencia *et al.* (CDF Collab.)
ACOSTA 06 PRL 96 202001 D. Acosta *et al.* (CDF Collab.)
AUBERT 06 PR D73 011101 B. Aubert *et al.* (BABAR Collab.)
AUBERT 06E PRL 96 052002 B. Aubert *et al.* (BABAR Collab.)
AUBERT 06F PR D73 011103 B. Aubert *et al.* (BABAR Collab.)
AUBERT 06J PR D73 051105 B. Aubert *et al.* (BABAR Collab.)
AUBERT 06K PR D73 057101 B. Aubert *et al.* (BABAR Collab.)
AUBERT 06N PR D74 031103 B. Aubert *et al.* (BABAR Collab.)
AUBERT 06O PR D74 032003 B. Aubert *et al.* (BABAR Collab.)
AUBERT 06Z PR D73 111104 B. Aubert *et al.* (BABAR Collab.)
AUBERT,B 06A PR D73 112004 B. Aubert *et al.* (BABAR Collab.)
AUBERT,B 06C PR D74 011102 B. Aubert *et al.* (BABAR Collab.)
AUBERT,B 06E PR D74 011106 B. Aubert *et al.* (BABAR Collab.)
AUBERT,B 06G PRL 97 201801 B. Aubert *et al.* (BABAR Collab.)
AUBERT,B 06H PRL 97 201802 B. Aubert *et al.* (BABAR Collab.)
AUBERT,B 06J PR D73 092001 B. Aubert *et al.* (BABAR Collab.)
AUBERT,B 06M PR D74 031102 B. Aubert *et al.* (BABAR Collab.)
AUBERT,B 06P PR D74 031105 B. Aubert *et al.* (BABAR Collab.)
AUBERT,B 06T PR D74 051102 B. Aubert *et al.* (BABAR Collab.)
AUBERT,B 06U PR D74 051104 B. Aubert *et al.* (BABAR Collab.)
AUBERT,B 06Y PR D74 091105 B. Aubert *et al.* (BABAR Collab.)
AUBERT,BE 06A PR D74 099903 (errat.) B. Aubert *et al.* (BABAR Collab.)
AUBERT,BE 06C PRL 97 171805 B. Aubert *et al.* (BABAR Collab.)
AUBERT,BE 06G PRL 97 261801 B. Aubert *et al.* (BABAR Collab.)
AUBERT,BE 06H PRL 97 261803 B. Aubert *et al.* (BABAR Collab.)
AUBERT,BE 06J PR D74 111102 B. Aubert *et al.* (BABAR Collab.)
AUBERT,BE 06M PR D74 071101 B. Aubert *et al.* (BABAR Collab.)
CHISTOV 06A PR D74 111105 R. Chistov *et al.* (BELLE Collab.)
FANG 06 PR D74 012007 F. Fang *et al.* (BELLE Collab.)
GABYSHEV 06 PRL 97 202003 N. Gabyshev *et al.* (BELLE Collab.)
GABYSHEV 06A PRL 97 242001 N. Gabyshev *et al.* (BELLE Collab.)
GARMASH 06 PRL 96 251803 A. Garmash *et al.* (BELLE Collab.)

See key on page 885

GOKHROO 06 PRL 97 162002 G. Gokhroo *et al.* (BELLE Collab.)
IKADO 06 PRL 97 251802 K. Ikado *et al.* (BELLE Collab.)
JEN 06 PR D74 111101 C.-M. Jen *et al.* (BELLE Collab.)
KUMAR 06 PR D74 051103 R. Kumar *et al.* (BELLE Collab.)
MOHAPATRA 06 PRL 96 221601 D. Mohapatra *et al.* (BELLE Collab.)
POLUEKTOV 06 PR D73 112009 A. Poluektov *et al.* (BELLE Collab.)
SCHUEMANN 06 PRL 97 061802 J. Schuemann *et al.* (BELLE Collab.)
SONI 06 PL B634 155 N. Soni *et al.* (BELLE Collab.)
ABE 05A PRL 94 221805 K. Abe *et al.* (BELLE Collab.)
ABE 05B PR D71 072003 K. Abe *et al.* (BELLE Collab.)
Also PR D71 079903 (errat.) K. Abe *et al.* (BELLE Collab.)
ABE 05G PRL 95 231802 K. Abe *et al.* (BELLE Collab.)
ACOSTA 05J PRL 95 031801 D. Acosta *et al.* (CDF Collab.)
AUBERT 05 PRL 94 011801 B. Aubert *et al.* (BABAR Collab.)
AUBERT 05B PR D71 031501 B. Aubert *et al.* (BABAR Collab.)
AUBERT 05G PR D72 032004 B. Aubert *et al.* (BABAR Collab.)
AUBERT 05H PRL 94 101801 B. Aubert *et al.* (BABAR Collab.)
AUBERT 05J PRL 94 141801 B. Aubert *et al.* (BABAR Collab.)
AUBERT 05K PRL 94 171801 B. Aubert *et al.* (BABAR Collab.)
AUBERT 05L PRL 94 181802 B. Aubert *et al.* (BABAR Collab.)
AUBERT 05M PRL 94 191802 B. Aubert *et al.* (BABAR Collab.)
AUBERT 05N PR D71 031102 B. Aubert *et al.* (BABAR Collab.)
AUBERT 05O PR D71 031103 B. Aubert *et al.* (BABAR Collab.)
AUBERT 05R PR D71 071103 B. Aubert *et al.* (BABAR Collab.)
AUBERT 05U PR D71 091103 B. Aubert *et al.* (BABAR Collab.)
AUBERT 05X PR D71 111101 B. Aubert *et al.* (BABAR Collab.)
AUBERT,B 05B PRL 95 041804 B. Aubert *et al.* (BABAR Collab.)
AUBERT,B 05E PR D72 011102 B. Aubert *et al.* (BABAR Collab.)
AUBERT,B 05G PR D72 052002 B. Aubert *et al.* (BABAR Collab.)
AUBERT,B 05K PRL 95 131803 B. Aubert *et al.* (BABAR Collab.)
AUBERT,B 05L PR D72 051101 B. Aubert *et al.* (BABAR Collab.)
AUBERT,B 05N PR D72 072003 B. Aubert *et al.* (BABAR Collab.)
Also PR D74 099903 (errat.) B. Aubert *et al.* (BABAR Collab.)
AUBERT,B 05O PR D72 051102 B. Aubert *et al.* (BABAR Collab.)
AUBERT,B 05T PR D72 071102 B. Aubert *et al.* (BABAR Collab.)
AUBERT,B 05U PR D72 071103 B. Aubert *et al.* (BABAR Collab.)
AUBERT,B 05V PR D72 071104 B. Aubert *et al.* (BABAR Collab.)
AUBERT,B 05Y PRL 95 121802 B. Aubert *et al.* (BABAR Collab.)
AUBERT,BE 05E PRL 95 221801 B. Aubert *et al.* (BABAR Collab.)
CHANG 05 PR D71 072007 M.-C. Chang *et al.* (BELLE Collab.)
CHANG 05A PR D71 091106 P. Chang *et al.* (BELLE Collab.)
CHAO 05A PR D71 031502 Y. Chao *et al.* (BELLE Collab.)
CHEN 05A PRL 94 221804 K.-F. Chen *et al.* (BELLE Collab.)
GARMASH 05 PR D71 092003 A. Garmash *et al.* (BELLE Collab.)
ITOH 05 PRL 95 091601 R. Itoh *et al.* (BELLE Collab.)
LEE 05 PRL 95 061802 Y.-J. Lee *et al.* (BELLE Collab.)
LIVENTSEV 05 PR D72 051109 D. Liventsev *et al.* (BELLE Collab.)
MAJUMDER 05 PRL 95 041803 G. Majumder *et al.* (BELLE Collab.)
MOHAPATRA 05 PR D72 011101 D. Mohapatra *et al.* (BELLE Collab.)
NISHIDA 05 PL B610 23 S. Nishida *et al.* (BELLE Collab.)
OKABE 05 PL B614 27 T. Okabe *et al.* (BELLE Collab.)
SAIGO 05 PRL 94 091601 M. Saigo *et al.* (BELLE Collab.)
WANG 05A PL B617 141 M.-Z. Wang *et al.* (BELLE Collab.)
XIE 05 PR D72 051105 Q.L. Xie *et al.* (BELLE Collab.)
YANG 05 PRL 94 111802 H. Yang *et al.* (BELLE Collab.)
ZHANG 05A PRL 94 031801 J. Zhang *et al.* (BELLE Collab.)
ZHANG 05B PR D71 091107 L.M. Zhang *et al.* (BELLE Collab.)
ZHANG 05D PRL 95 141801 J. Zhang *et al.* (BELLE Collab.)
ABDALLAH 04E EPJ C33 307 J. Abdallah *et al.* (DELPHI Collab.)
ABE 04D PR D69 112002 K. Abe *et al.* (BELLE Collab.)
AUBERT 04A PR D69 011102 B. Aubert *et al.* (BABAR Collab.)
AUBERT 04C PRL 92 111801 B. Aubert *et al.* (BABAR Collab.)
AUBERT 04H PRL 92 061801 B. Aubert *et al.* (BABAR Collab.)
AUBERT 04K PRL 92 141801 B. Aubert *et al.* (BABAR Collab.)
AUBERT 04M PRL 92 201802 B. Aubert *et al.* (BABAR Collab.)
AUBERT 04N PRL 92 202002 B. Aubert *et al.* (BABAR Collab.)
AUBERT 04O PRL 92 221803 B. Aubert *et al.* (BABAR Collab.)
AUBERT 04P PRL 92 241802 B. Aubert *et al.* (BABAR Collab.)
AUBERT 04Q PR D69 051101 B. Aubert *et al.* (BABAR Collab.)
AUBERT 04T PR D69 071103 B. Aubert *et al.* (BABAR Collab.)
AUBERT 04Y PRL 93 041801 B. Aubert *et al.* (BABAR Collab.)
AUBERT 04Z PRL 93 051802 B. Aubert *et al.* (BABAR Collab.)
AUBERT,B 04B PR D70 011101 B. Aubert *et al.* (BABAR Collab.)
AUBERT,B 04D PR D70 032006 B. Aubert *et al.* (BABAR Collab.)
AUBERT,B 04L PRL 93 131804 B. Aubert *et al.* (BABAR Collab.)
AUBERT,B 04P PR D70 092001 B. Aubert *et al.* (BABAR Collab.)
AUBERT,B 04S PRL 93 181801 B. Aubert *et al.* (BABAR Collab.)
AUBERT,B 04U PR D70 091105 B. Aubert *et al.* (BABAR Collab.)
AUBERT,B 04V PRL 93 181805 B. Aubert *et al.* (BABAR Collab.)
AUBERT,BE 04 PR D70 111102 B. Aubert *et al.* (BABAR Collab.)
AUBERT,BE 04A PR D70 112006 B. Aubert *et al.* (BABAR Collab.)
AUBERT,BE 04B PR D70 091106 B. Aubert *et al.* (BABAR Collab.)
CHAO 04 PR D69 111102 Y. Chao *et al.* (BELLE Collab.)
CHAO 04B PRL 93 191802 Y. Chao *et al.* (BELLE Collab.)
CHISTOV 04 PRL 93 051803 R. Chistov *et al.* (BELLE Collab.)
DRUTSKOY 04 PRL 92 051801 A. Drutskoy *et al.* (BELLE Collab.)
GARMASH 04 PR D69 012001 A. Garmash *et al.* (BELLE Collab.)
LEE 04 PRL 93 211801 Y.-J. Lee *et al.* (BELLE Collab.)
MAJUMDER 04 PR D70 111103 G. Majumder *et al.* (BELLE Collab.)
NAKAO 04 PR D69 112001 M. Nakao *et al.* (BELLE Collab.)
POLUEKTOV 04 PR D70 072003 A. Poluektov *et al.* (BELLE Collab.)
SCHWANDA 04 PRL 93 131803 C. Schwanda *et al.* (BELLE Collab.)
WANG 04 PRL 92 131801 M.Z. Wang *et al.* (BELLE Collab.)
WANG 04A PR D70 012001 C.H. Wang *et al.* (BELLE Collab.)
ZANG 04 PR D69 017101 S.L. Zang *et al.* (BELLE Collab.)
ABE 03B PR D67 032003 K. Abe *et al.* (BELLE Collab.)
ABE 03D PRL 90 131803 K. Abe *et al.* (BELLE Collab.)
ADAM 03 PR D67 032001 N.E. Adam *et al.* (CLEO Collab.)
ADAM 03B PR D68 012004 N.E. Adam *et al.* (CLEO Collab.)
ATHAR 03 PR D68 072003 S.B. Athar *et al.* (CLEO Collab.)
AUBERT 03K PRL 90 231801 B. Aubert *et al.* (BABAR Collab.)
AUBERT 03L PRL 91 021801 B. Aubert *et al.* (BABAR Collab.)
AUBERT 03M PRL 91 051801 B. Aubert *et al.* (BABAR Collab.)
AUBERT 03O PRL 91 071801 B. Aubert *et al.* (BABAR Collab.)
AUBERT 03U PRL 91 221802 B. Aubert *et al.* (BABAR Collab.)
AUBERT 03V PRL 91 171802 B. Aubert *et al.* (BABAR Collab.)
AUBERT 03W PRL 91 161801 B. Aubert *et al.* (BABAR Collab.)
AUBERT 03X PR D68 092001 B. Aubert *et al.* (BABAR Collab.)
BORNHEIM 03 PR D68 052002 A. Bornheim *et al.* (CLEO Collab.)
CHEN 03B PRL 91 201801 K.-F. Chen *et al.* (BELLE Collab.)
CHOI 03 PRL 91 262001 S.-K. Choi *et al.* (BELLE Collab.)
CSORNA 03 PR D67 112002 S.E. Csorna *et al.* (CLEO Collab.)
EDWARDS 03 PR D68 011102 K.W. Edwards *et al.* (CLEO Collab.)
FANG 03 PRL 90 071801 F. Fang *et al.* (BELLE Collab.)
HUANG 03 PRL 91 241802 H.-C. Huang *et al.* (BELLE Collab.)
ISHIKAWA 03 PRL 91 261601 A. Ishikawa *et al.* (BELLE Collab.)
KROKOVNY 03B PRL 91 262002 P. Krokovny *et al.* (BELLE Collab.)
SWAIN 03 PR D68 051101 S.K. Swain *et al.* (BELLE Collab.)
UNNO 03 PR D68 011103 Y. Unno *et al.* (BELLE Collab.)
ZHANG 03B PRL 91 221801 J. Zhang *et al.* (BELLE Collab.)
ABE 02 PRL 88 021801 K. Abe *et al.* (BELLE Collab.)
ABE 02B PRL 88 031802 K. Abe *et al.* (BELLE Collab.)
ABE 02H PRL 88 171801 K. Abe *et al.* (BELLE Collab.)
ABE 02K PRL 88 181803 K. Abe *et al.* (BELLE Collab.)
ABE 02N PL B538 11 K. Abe *et al.* (BELLE Collab.)
ABE 02O PR D65 091103 K. Abe *et al.* (BELLE Collab.)
ABE 02W PRL 89 151802 K. Abe *et al.* (BELLE Collab.)
ACOSTA 02C PR D65 092009 D. Acosta *et al.* (CDF Collab.)
ACOSTA 02F PR D66 052005 D. Acosta *et al.* (CDF Collab.)
AHMED 02B PR D66 031101 S. Ahmed *et al.* (CLEO Collab.)
AUBERT 02 PR D65 032001 B. Aubert *et al.* (BABAR Collab.)
AUBERT 02C PRL 88 101805 B. Aubert *et al.* (BABAR Collab.)
AUBERT 02E PR D65 051101 B. Aubert *et al.* (BABAR Collab.)
AUBERT 02F PR D65 091101 B. Aubert *et al.* (BABAR Collab.)
AUBERT 02L PRL 88 241801 B. Aubert *et al.* (BABAR Collab.)
BRIERE 02 PRL 89 081803 R. Briere *et al.* (CLEO Collab.)
CASEY 02 PR D66 092002 B.C.K. Casey *et al.* (BELLE Collab.)
CHEN 02B PL B546 196 K.-F. Chen *et al.* (BELLE Collab.)
DRUTSKOY 02 PL B542 171 A. Drutskoy *et al.* (BELLE Collab.)
DYTMAN 02 PR D66 091101 S.A. Dytman *et al.* (CLEO Collab.)
ECKHART 02 PRL 89 251801 E. Eckhart *et al.* (CLEO Collab.)
EDWARDS 02B PR D65 111102 K.W. Edwards *et al.* (CLEO Collab.)
GABYSHEV 02 PR D66 091102 N. Gabyshev *et al.* (BELLE Collab.)
GARMASH 02 PR D65 092005 A. Garmash *et al.* (BELLE Collab.)
GODANG 02 PRL 88 021802 R. Godang *et al.* (CLEO Collab.)
GORDON 02 PL B542 183 A. Gordon *et al.* (BELLE Collab.)
LU 02 PRL 89 191801 R.-S. Lu *et al.* (BELLE Collab.)
MAHAPATRA 02 PRL 88 101803 R. Mahapatra *et al.* (CLEO Collab.)
NISHIDA 02 PRL 89 231801 S. Nishida *et al.* (BELLE Collab.)
ABE 01H PRL 87 101801 K. Abe *et al.* (BELLE Collab.)
ABE 01I PRL 87 111801 K. Abe *et al.* (BELLE Collab.)
ABE 01K PR D64 071101 K. Abe *et al.* (BELLE Collab.)
ABE 01L PRL 87 161601 K. Abe *et al.* (BELLE Collab.)
ABE 01M PL B517 309 K. Abe *et al.* (BELLE Collab.)
ALEXANDER 01B PR D64 092001 J.P. Alexander *et al.* (CLEO Collab.)
AMMAR 01B PRL 87 271801 R. Ammar *et al.* (CLEO Collab.)
ANDERSON 01B PRL 87 181803 S. Anderson *et al.* (CLEO Collab.)
AUBERT 01D PRL 87 151801 B. Aubert *et al.* (BABAR Collab.)
AUBERT 01E PRL 87 151802 B. Aubert *et al.* (BABAR Collab.)
AUBERT 01F PRL 87 201803 B. Aubert *et al.* (BABAR Collab.)
AUBERT 01G PRL 87 221802 B. Aubert *et al.* (BABAR Collab.)
BARATE 01E EPJ C19 213 R. Barate *et al.* (ALEPH Collab.)
BRIERE 01 PRL 86 3718 R.A. Briere *et al.* (CLEO Collab.)
BROWDER 01 PRL 86 2950 T.E. Browder *et al.* (CLEO Collab.)
EDWARDS 01 PRL 86 30 K.W. Edwards *et al.* (CLEO Collab.)
GRITSAN 01 PR D64 077501 A. Gritsan *et al.* (CLEO Collab.)
RICHICHI 01 PR D63 031103 S.J. Richichi *et al.* (CLEO Collab.)
ABBIENDI 00B PL B476 233 G. Abbiendi *et al.* (OPAL Collab.)
ABE 00C PR D62 071101 K. Abe *et al.* (SLD Collab.)
AHMED 00B PR D62 112003 S. Ahmed *et al.* (CLEO Collab.)
ANASTASSOV 00 PRL 84 1393 A. Anastassov *et al.* (CLEO Collab.)
BARATE 00R PL B492 275 R. Barate *et al.* (ALEPH Collab.)
BEHRENS 00 PR D61 052001 B.H. Behrens *et al.* (CLEO Collab.)
BONVICINI 00 PRL 84 5940 G. Bonvicini *et al.* (CLEO Collab.)
CHEN 00 PRL 85 525 S. Chen *et al.* (CLEO Collab.)
COAN 00 PRL 84 5283 T.E. Coan *et al.* (CLEO Collab.)
CRONIN-HEN... 00 PRL 85 515 D. Cronin-Hennessy *et al.* (CLEO Collab.)
CSORNA 00 PR D61 111101 S.E. Csorna *et al.* (CLEO Collab.)
JESSOP 00 PRL 85 2881 C.P. Jessop *et al.* (CLEO Collab.)
RICHICHI 00 PRL 85 520 S.J. Richichi *et al.* (CLEO Collab.)
ABBIENDI 99J EPJ C12 609 G. Abbiendi *et al.* (OPAL Collab.)
AFFOLDER 99B PRL 83 3378 T. Affolder *et al.* (CDF Collab.)
BARTELT 99 PRL 82 3746 J. Bartelt *et al.* (CLEO Collab.)
COAN 99 PR D59 111101 T.E. Coan *et al.* (CLEO Collab.)
ABE 98B PR D57 5382 F. Abe *et al.* (CDF Collab.)
ABE 98O PR D58 072001 F. Abe *et al.* (CDF Collab.)
ABE 98Q PR D58 092002 F. Abe *et al.* (CDF Collab.)
ACCIARRI 98S PL B438 417 M. Acciarri *et al.* (L3 Collab.)
ANASTASSOV 98 PRL 80 4127 A. Anastassov *et al.* (CLEO Collab.)
ATHANAS 98 PRL 80 5493 M. Athanas *et al.* (CLEO Collab.)
BARATE 98Q EPJ C4 387 R. Barate *et al.* (ALEPH Collab.)
BEHRENS 98 PRL 80 3710 B.H. Behrens *et al.* (CLEO Collab.)
BERGFELD 98 PRL 81 272 T. Bergfeld *et al.* (CLEO Collab.)
BRANDENB... 98 PRL 80 2762 G. Brandenbrug *et al.* (CLEO Collab.)
CAPRINI 98 NP B530 153 I. Caprini, L. Lellouch, M. Neubert (BCIP, CERN)
GODANG 98 PRL 80 3456 R. Godang *et al.* (CLEO Collab.)
ABE 97J PRL 79 590 K. Abe *et al.* (SLD Collab.)
ACCIARRI 97F PL B396 327 M. Acciarri *et al.* (L3 Collab.)
ARTUSO 97 PL B399 321 M. Artuso *et al.* (CLEO Collab.)
ATHANAS 97 PRL 79 2208 M. Athanas *et al.* (CLEO Collab.)
BROWDER 97 PR D56 11 T. Browder *et al.* (CLEO Collab.)
FU 97 PRL 79 3125 X. Fu *et al.* (CLEO Collab.)
JESSOP 97 PRL 79 4533 C.P. Jessop *et al.* (CLEO Collab.)
ABE 96B PR D53 3496 F. Abe *et al.* (CDF Collab.)
ABE 96C PRL 76 4462 F. Abe *et al.* (CDF Collab.)
ABE 96H PRL 76 2015 F. Abe *et al.* (CDF Collab.)
ABE 96L PRL 76 4675 F. Abe *et al.* (CDF Collab.)
ABE 96Q PR D54 6596 F. Abe *et al.* (CDF Collab.)
ABE 96R PRL 77 5176 F. Abe *et al.* (CDF Collab.)
ADAM 96D ZPHY C72 207 W. Adam *et al.* (DELPHI Collab.)
ALEXANDER 96T PRL 77 5000 J.P. Alexander *et al.* (CLEO Collab.)
ASNER 96 PR D53 1039 D.M. Asner *et al.* (CLEO Collab.)
BARISH 96B PRL 76 1570 B.C. Barish *et al.* (CLEO Collab.)
BERGFELD 96B PRL 77 4503 T. Bergfeld *et al.* (CLEO Collab.)
BISHAI 96 PL B369 186 M. Bishai *et al.* (CLEO Collab.)
BUSKULIC 96J ZPHY C71 31 D. Buskulic *et al.* (ALEPH Collab.)
GIBAUT 96 PR D53 4734 D. Gibaut *et al.* (CLEO Collab.)
PDG 96 PR D54 1 R. M. Barnett *et al.* (PDG Collab.)
ABREU 95N PL B357 255 P. Abreu *et al.* (DELPHI Collab.)
ABREU 95Q ZPHY C68 13 P. Abreu *et al.* (DELPHI Collab.)
ADAM 95 ZPHY C68 363 W. Adam *et al.* (DELPHI Collab.)
AKERS 95T ZPHY C67 379 R. Akers *et al.* (OPAL Collab.)
ALBRECHT 95D PL B353 554 H. Albrecht *et al.* (ARGUS Collab.)
ALEXANDER 95 PL B341 435 J. Alexander *et al.* (CLEO Collab.)
Also PL B347 469 (erratum) J. Alexander *et al.* (CLEO Collab.)
ARTUSO 95 PRL 75 785 M. Artuso *et al.* (CLEO Collab.)
BARISH 95 PR D51 1014 B.C. Barish *et al.* (CLEO Collab.)
BUSKULIC 95 PL B343 444 D. Buskulic *et al.* (ALEPH Collab.)
ABE 94D PRL 72 3456 F. Abe *et al.* (CDF Collab.)
ALAM 94 PR D50 43 M.S. Alam *et al.* (CLEO Collab.)
ALBRECHT 94D PL B335 526 H. Albrecht *et al.* (ARGUS Collab.)
ATHANAS 94 PRL 73 3503 M. Athanas *et al.* (CLEO Collab.)
Also PRL 74 3090 (erratum) M. Athanas *et al.* (CLEO Collab.)
PDG 94 PR D50 1173 L. Montanet *et al.* (CERN, LBL, BOST+)
STONE 94 HEPSY 93-11 S. Stone
Published in B Decays, 2nd Edition, World Scientific, Singapore
ABREU 93D ZPHY C57 181 P. Abreu *et al.* (DELPHI Collab.)
ABREU 93G PL B312 253 P. Abreu *et al.* (DELPHI Collab.)
ACTON 93C PL B307 247 P.D. Acton *et al.* (OPAL Collab.)
ALBRECHT 93E ZPHY C60 11 H. Albrecht *et al.* (ARGUS Collab.)
ALEXANDER 93B PL B319 365 J. Alexander *et al.* (CLEO Collab.)
AMMAR 93 PRL 71 674 R. Ammar *et al.* (CLEO Collab.)
BEAN 93B PRL 70 2681 A. Bean *et al.* (CLEO Collab.)

Meson Particle Listings

$B^{\pm}$, B^0

BUSKULIC	93D	PL B307 194	D. Buskulic *et al.*	(ALEPH Collab.)
Also		PL B325 537 (erratum)	D. Buskulic *et al.*	(ALEPH Collab.)
SANGHERA	93	PR D47 791	S. Sanghera *et al.*	(CLEO Collab.)
ALBRECHT	92C	PL B275 195	H. Albrecht *et al.*	(ARGUS Collab.)
ALBRECHT	92E	PL B277 209	H. Albrecht *et al.*	(ARGUS Collab.)
ALBRECHT	92G	ZPHY C54 1	H. Albrecht *et al.*	(ARGUS Collab.)
BORTOLETTO	92	PR D45 21	D. Bortoletto *et al.*	(CLEO Collab.)
BUSKULIC	92G	PL B295 396	D. Buskulic *et al.*	(ALEPH Collab.)
ALBRECHT	91B	PL B254 288	H. Albrecht *et al.*	(ARGUS Collab.)
ALBRECHT	91C	PL B255 297	H. Albrecht *et al.*	(ARGUS Collab.)
ALBRECHT	91E	PL B262 148	H. Albrecht *et al.*	(ARGUS Collab.)
BERKELMAN	91	ARNPS 41 1	K. Berkelman, S. Stone	(CORN, SYRA)
"Decays of B Mesons"				
FULTON	91	PR D43 651	R. Fulton *et al.*	(CLEO Collab.)
ALBRECHT	90B	PL B241 278	H. Albrecht *et al.*	(ARGUS Collab.)
ALBRECHT	90J	ZPHY C48 543	H. Albrecht *et al.*	(ARGUS Collab.)
ANTREASYAN	90B	ZPHY C48 553	D. Antreasyan *et al.*	(Crystal Ball Collab.)
BORTOLETTO	90	PRL 64 2117	D. Bortoletto *et al.*	(CLEO Collab.)
Also		PR D45 21	D. Bortoletto *et al.*	(CLEO Collab.)
WEIR	90B	PR D41 1384	A.J. Weir *et al.*	(Mark II Collab.)
ALBRECHT	89G	PL B229 304	H. Albrecht *et al.*	(ARGUS Collab.)
AVERY	89B	PL B223 470	P. Avery *et al.*	(CLEO Collab.)
BEBEK	89	PRL 62 8	C. Bebek *et al.*	(CLEO Collab.)
BORTOLETTO	89	PRL 62 2436	D. Bortoletto *et al.*	(CLEO Collab.)
ALBRECHT	88F	PL B209 119	H. Albrecht *et al.*	(ARGUS Collab.)
ALBRECHT	88K	PL B215 424	H. Albrecht *et al.*	(ARGUS Collab.)
ALBRECHT	87C	PL B185 218	H. Albrecht *et al.*	(ARGUS Collab.)
ALBRECHT	87D	PL B199 451	H. Albrecht *et al.*	(ARGUS Collab.)
AVERY	87	PL B183 429	P. Avery *et al.*	(CLEO Collab.)
BEBEK	87	PR D36 1289	C. Bebek *et al.*	(CLEO Collab.)
ALAM	86	PR D34 3279	M.S. Alam *et al.*	(CLEO Collab.)
PDG	86	PL 170B 1	M. Aguilar-Benitez *et al.*	(CERN, CIT+)
GILES	84	PR D30 2279	R. Giles *et al.*	(CLEO Collab.)

B^0

$I(J^P) = \frac{1}{2}(0^-)$

Quantum numbers not measured. Values shown are quark-model predictions.

See also the $B^{\pm}/B^0$ ADMIXTURE and $B^{\pm}/B^0/B_s^0$/b-baryon ADMIXTURE sections.

See the Note "Production and Decay of b-flavored Hadrons" at the beginning of the $B^{\pm}$ Particle Listings and the Note on "B^0-$\overline{B}^0$ Mixing" near the end of the B^0 Particle Listings.

B^0 MASS

The fit uses m_{B^+}, $(m_{B^0} - m_{B^+})$, and m_{B^0} to determine m_{B^+}, m_{B^0}, and the mass difference.

VALUE (MeV)	EVTS	DOCUMENT ID		TECN	COMMENT
5279.63±0.15 OUR FIT Error includes scale factor of 1.1.					
5279.55±0.26 OUR AVERAGE					
5279.6 ±0.2 ±1.0		[1] AAD	13U	ATLS	pp at 7 TeV
5279.58±0.15±0.28		[2] AAIJ	12E	LHCB	pp at 7 TeV
5279.63±0.53±0.33		[3] ACOSTA	06	CDF	$p\overline{p}$ at 1.96 TeV
5279.1 ±0.7 ±0.3	135	[4] CSORNA	00	CLE2	$e^+e^- \to \Upsilon(4S)$
5281.3 ±2.2 ±1.4	51	ABE	96B	CDF	$p\overline{p}$ at 1.8 TeV
• • • We do not use the following data for averages, fits, limits, etc. • • •					
5279.2 ±0.54±2.0	340	ALAM	94	CLE2	$e^+e^- \to \Upsilon(4S)$
5278.0 ±0.4 ±2.0		BORTOLETTO	92	CLEO	$e^+e^- \to \Upsilon(4S)$
5279.6 ±0.7 ±2.0	40	[5] ALBRECHT	90J	ARG	$e^+e^- \to \Upsilon(4S)$
5278.2 ±1.0 ±3.0	40	ALBRECHT	87C	ARG	$e^+e^- \to \Upsilon(4S)$
5279.5 ±1.6 ±3.0	7	[6] ALBRECHT	87D	ARG	$e^+e^- \to \Upsilon(4S)$
5280.6 ±0.8 ±2.0		BEBEK	87	CLEO	$e^+e^- \to \Upsilon(4S)$

[1] Measured with $B_d^0 \to J/\psi(\mu^+\mu^-)\, K_S^0(\pi^+\pi^-)$ decays.
[2] Uses $B^0 \to J/\psi K^0$ fully reconstructed decays.
[3] Uses exclusively reconstructed final states containing a $J/\psi \to \mu^+\mu^-$ decays.
[4] CSORNA 00 uses fully reconstructed 135 $B^0 \to J/\psi^{(\prime)} K_S^0$ events and invariant masses without beam constraint.
[5] ALBRECHT 90J assumes 10580 for $\Upsilon(4S)$ mass. Supersedes ALBRECHT 87C and ALBRECHT 87D.
[6] Found using fully reconstructed decays with J/ψ. ALBRECHT 87D assume $m_{\Upsilon(4S)} =$ 10577 MeV.

$m_{B^0} - m_{B^+}$

VALUE (MeV)	DOCUMENT ID		TECN	COMMENT
0.31±0.06 OUR FIT				
0.32±0.05 OUR AVERAGE				
0.20±0.17±0.11	[1] AAIJ	12E	LHCB	pp at 7 TeV
0.33±0.05±0.03	[2] AUBERT	08AF	BABR	$e^+e^- \to \Upsilon(4S)$
0.53±0.67±0.14	[3] ACOSTA	06	CDF	$p\overline{p}$ at 1.96 TeV
0.41±0.25±0.19	ALAM	94	CLE2	$e^+e^- \to \Upsilon(4S)$
−0.4 ±0.6 ±0.5	BORTOLETTO	92	CLEO	$e^+e^- \to \Upsilon(4S)$
−0.9 ±1.2 ±0.5	ALBRECHT	90J	ARG	$e^+e^- \to \Upsilon(4S)$
2.0 ±1.1 ±0.3	[4] BEBEK	87	CLEO	$e^+e^- \to \Upsilon(4S)$

[1] Uses exclusively reconstructed final states containing a $J/\psi \to \mu^+\mu^-$ decay.
[2] Uses the B-momentum distributions in the e^+e^- rest frame.
[3] Uses exclusively reconstructed final states containing a $J/\psi \to \mu^+\mu^-$ decays.
[4] BEBEK 87 actually measure the difference between half of $E_{\rm cm}$ and the $B^{\pm}$ or B^0 mass, so the $m_{B^0} - m_{B^{\pm}}$ is more accurate. Assume $m_{\Upsilon(4S)} =$ 10580 MeV.

$m_{B_H^0} - m_{B_L^0}$

See the B^0-$\overline{B}^0$ MIXING PARAMETERS section near the end of these B^0 Listings.

B^0 MEAN LIFE

See $B^{\pm}/B^0/B_s^0$/b-baryon ADMIXTURE section for data on B-hadron mean life averaged over species of bottom particles.

"OUR EVALUATION" is an average using rescaled values of the data listed below. The average and rescaling were performed by the Heavy Flavor Averaging Group (HFLAV) and are described at http://www.slac.stanford.edu/xorg/hflav/. The averaging/rescaling procedure takes into account correlations between the measurements and asymmetric lifetime errors.

VALUE (10^{-12} s)	EVTS	DOCUMENT ID		TECN	COMMENT
1.520±0.004 OUR EVALUATION					
1.534±0.019±0.021		[1] ABAZOV	15A	D0	$p\overline{p}$ at 1.96 TeV
1.499±0.013±0.005		[2] AAIJ	14E	LHCB	pp at 7 TeV
1.524±0.006±0.004		[3] AAIJ	14E	LHCB	pp at 7 TeV
1.524±0.011±0.004		[4] AAIJ	14R	LHCB	pp at 7 TeV
1.509±0.012±0.018		[5] AAD	13U	ATLS	pp at 7 TeV
1.508±0.025±0.043		[2] ABAZOV	12U	D0	$p\overline{p}$ at 1.96 TeV
1.507±0.010±0.008		[6] AALTONEN	11	CDF	$p\overline{p}$ at 1.96 TeV
1.414±0.018±0.034		[7] ABAZOV	09E	D0	$p\overline{p}$ at 1.96 TeV
$1.504 \pm 0.013 ^{+0.018}_{-0.013}$		[8] AUBERT	06G	BABR	$e^+e^- \to \Upsilon(4S)$
1.534±0.008±0.010		[9] ABE	05B	BELL	$e^+e^- \to \Upsilon(4S)$
1.531±0.021±0.031		[10] ABDALLAH	04E	DLPH	$e^+e^- \to Z$
$1.523 ^{+0.024}_{-0.023} \pm 0.022$		[11] AUBERT	03C	BABR	$e^+e^- \to \Upsilon(4S)$
1.533±0.034±0.038		[12] AUBERT	03H	BABR	$e^+e^- \to \Upsilon(4S)$
1.497±0.073±0.032		[13] ACOSTA	02C	CDF	$p\overline{p}$ at 1.8 TeV
1.529±0.012±0.029		[14] AUBERT	02H	BABR	$e^+e^- \to \Upsilon(4S)$
1.546±0.032±0.022		[15] AUBERT	01F	BABR	$e^+e^- \to \Upsilon(4S)$
1.541±0.028±0.023		[14] ABBIENDI,G	00B	OPAL	$e^+e^- \to Z$
1.518±0.053±0.034		[16] BARATE	00R	ALEP	$e^+e^- \to Z$
1.523±0.057±0.053		[17] ABBIENDI	99J	OPAL	$e^+e^- \to Z$
$1.474 \pm 0.039 ^{+0.052}_{-0.051}$		[16] ABE	98Q	CDF	$p\overline{p}$ at 1.8 TeV
1.52 ±0.06 ±0.04		[17] ACCIARRI	98S	L3	$e^+e^- \to Z$
1.64 ±0.08 ±0.08		[17] ABE	97J	SLD	$e^+e^- \to Z$
1.532±0.041±0.040		[18] ABREU	97F	DLPH	$e^+e^- \to Z$
$1.25 ^{+0.15}_{-0.13} \pm 0.05$	121	[13] BUSKULIC	96J	ALEP	$e^+e^- \to Z$
$1.49 ^{+0.17}_{-0.15} ^{+0.08}_{-0.06}$		[19] BUSKULIC	96J	ALEP	$e^+e^- \to Z$
$1.61 ^{+0.14}_{-0.13} \pm 0.08$		[16,20] ABREU	95Q	DLPH	$e^+e^- \to Z$
1.63 ±0.14 ±0.13		[21] ADAM	95	DLPH	$e^+e^- \to Z$
1.53 ±0.12 ±0.08		[16,22] AKERS	95T	OPAL	$e^+e^- \to Z$
• • • We do not use the following data for averages, fits, limits, etc. • • •					
$1.501 ^{+0.078}_{-0.074} \pm 0.050$		[2] ABAZOV	07S	D0	Repl. by ABAZOV 12U
1.524±0.030±0.016		[2] ABULENCIA	07A	CDF	Repl. by AALTONEN 11
$1.473 ^{+0.052}_{-0.050} \pm 0.023$		[7] ABAZOV	05B	D0	Repl. by ABAZOV 05W
$1.40 ^{+0.11}_{-0.10} \pm 0.03$		[2] ABAZOV	05C	D0	Repl. by ABAZOV 07S
1.530±0.043±0.023		[7] ABAZOV	05W	D0	Repl. by ABAZOV 09E
1.54 ±0.05 ±0.02		[23] ACOSTA	05	CDF	Repl. by AALTONEN 11
1.554±0.030±0.019		[15] ABE	02H	BELL	Repl. by ABE 05B
1.58 ±0.09 ±0.02		[13] ABE	98B	CDF	Repl. by ACOSTA 02C
1.54 ±0.08 ±0.06		[16] ABE	96C	CDF	Repl. by ABE 98Q
1.55 ±0.06 ±0.03		[24] BUSKULIC	96J	ALEP	$e^+e^- \to Z$
1.61 ±0.07 ±0.04		[16] BUSKULIC	96J	ALEP	Repl. by BARATE 00R
1.62 ±0.12		[25] ADAM	95	DLPH	$e^+e^- \to Z$
1.57 ±0.18 ±0.08	121	[13] ABE	94D	CDF	Repl. by ABE 98B
$1.17 ^{+0.29}_{-0.23} \pm 0.16$	96	[16] ABREU	93D	DLPH	Sup. by ABREU 95Q
1.55 ±0.25 ±0.18	76	[21] ABREU	93G	DLPH	Sup. by ADAM 95
$1.51 ^{+0.24}_{-0.23} ^{+0.12}_{-0.14}$	78	[16] ACTON	93C	OPAL	Sup. by AKERS 95T
$1.52 ^{+0.20}_{-0.18} ^{+0.07}_{-0.13}$	77	[16] BUSKULIC	93D	ALEP	Sup. by BUSKULIC 96J
$1.20 ^{+0.52}_{-0.36} ^{+0.16}_{-0.14}$	15	[26] WAGNER	90	MRK2	$E_{\rm cm}^{ee} = 29$ GeV
$0.82 ^{+0.57}_{-0.37} \pm 0.27$		[27] AVERILL	89	HRS	$E_{\rm cm}^{ee} = 29$ GeV

[1] Measured using $B^0 \to D^-\mu^+\nu X$ decays.
[2] Measured mean life using $B^0 \to J/\psi K_S^0$ decays.
[3] Measured using $B^0 \to J/\psi K^{*0}$ decays.
[4] Measured using $B^0 \to K^+\pi^-$ decays.
[5] Measured with $B_d^0 \to J/\psi(\mu^+\mu^-)\, K_S^0(\pi^+\pi^-)$ decays.
[6] Measured mean life using fully reconstructed decays ($J/\psi K^{(*)}$).
[7] Measured mean life using $B^0 \to J/\psi K^{*0}$ decays.
[8] Measured using a simultaneous fit of the B^0 lifetime and $\overline{B}^0 B^0$ oscillation frequency Δm_d in the partially reconstructed $B^0 \to D^{*-}\ell\nu$ decays.

[9] Measurement performed using a combined fit of *CP*-violation, mixing and lifetimes.
[10] Measurement performed using an inclusive reconstruction and B flavor identification technique.
[11] AUBERT 03C uses a sample of approximately 14,000 exclusively reconstructed $B^0 \to D^*(2010)^- \ell\nu$ and simultaneously measures the lifetime and oscillation frequency.
[12] Measurement performed with decays $B^0 \to D^{*-}\pi^+$ and $B^0 \to D^{*-}\rho^+$ using a partial reconstruction technique.
[13] Measured mean life using fully reconstructed decays.
[14] Data analyzed using partially reconstructed $\overline{B}^0 \to D^{*+}\ell^-\overline{\nu}$ decays.
[15] Events are selected in which one B meson is fully reconstructed while the second B meson is reconstructed inclusively.
[16] Data analyzed using $D/D^*\ell$X event vertices.
[17] Data analyzed using charge of secondary vertex.
[18] Data analyzed using inclusive $D/D^*\ell X$.
[19] Measured mean life using partially reconstructed $D^{*-}\pi^+$X vertices.
[20] ABREU 95Q assumes B($B^0 \to D^{**-}\ell^+\nu_\ell$) = 3.2 ± 1.7%.
[21] Data analyzed using vertex-charge technique to tag B charge.
[22] AKERS 95T assumes B($B^0 \to D_s^{(*)}D^{0(*)}$) = 5.0 ± 0.9% to find B^+/B^0 yield.
[23] Measured using the time-dependent angular analysis of $B^0_d \to J/\psi K^{*0}$ decays.
[24] Combined result of $D/D^*\ell$x analysis, fully reconstructed B analysis, and partially reconstructed $D^{*-}\pi^+$X analysis.
[25] Combined ABREU 95Q and ADAM 95 result.
[26] WAGNER 90 tagged B^0 mesons by their decays into $D^{*-}e^+\nu$ and $D^{*-}\mu^+\nu$ where the D^{*-} is tagged by its decay into $\pi^-\overline{D}^0$.
[27] AVERILL 89 is an estimate of the B^0 mean lifetime assuming that $B^0 \to D^{*+}$+ X always.

$\tau_{B^0}/\tau_{\overline{B}^0}$

VALUE	DOCUMENT ID		TECN	COMMENT
1.000±0.008±0.009	[1] AAIJ	14E	LHCB	pp at 7 TeV

[1] Measured using $B^0 \to J/\psi K^{*0}$ decays.

MEAN LIFE RATIO τ_{B^+}/τ_{B^0}

τ_{B^+}/τ_{B^0} (direct measurements)

"OUR EVALUATION" is an average using rescaled values of the data listed below. The average and rescaling were performed by the Heavy Flavor Averaging Group (HFLAV) and are described at http://www.slac.stanford.edu/xorg/hflav/. The averaging/rescaling procedure takes into account correlations between the measurements and asymmetric lifetime errors.

VALUE	EVTS	DOCUMENT ID		TECN	COMMENT
1.076±0.004 OUR EVALUATION					
1.074±0.005±0.003		[1] AAIJ	14E	LHCB	pp at 7 TeV
1.088±0.009±0.004		[2] AALTONEN	11	CDF	$p\overline{p}$ at 1.96 TeV
1.080±0.016±0.014		[3] ABAZOV	05D	D0	$p\overline{p}$ at 1.96 TeV
1.066±0.008±0.008		[4] ABE	05B	BELL	$e^+e^- \to \Upsilon(4S)$
1.060±0.021±0.024		[5] ABDALLAH	04E	DLPH	$e^+e^- \to Z$
1.093±0.066±0.028		[6] ACOSTA	02C	CDF	$p\overline{p}$ at 1.8 TeV
1.082±0.026±0.012		[7] AUBERT	01F	BABR	$e^+e^- \to \Upsilon(4S)$
1.085±0.059±0.018		[3] BARATE	00R	ALEP	$e^+e^- \to Z$
1.079±0.064±0.041		[8] ABBIENDI	99J	OPAL	$e^+e^- \to Z$
1.110±0.056 $^{+0.033}_{-0.030}$		[3] ABE	98Q	CDF	$p\overline{p}$ at 1.8 TeV
1.09 ±0.07 ±0.03		[8] ACCIARRI	98S	L3	$e^+e^- \to Z$
1.01 ±0.07 ±0.06		[8] ABE	97J	SLD	$e^+e^- \to Z$
1.27 $^{+0.23}_{-0.19}$ $^{+0.03}_{-0.02}$		[6] BUSKULIC	96J	ALEP	$e^+e^- \to Z$
1.00 $^{+0.17}_{-0.15}$ ±0.10		[3,9] ABREU	95Q	DLPH	$e^+e^- \to Z$
1.06 $^{+0.13}_{-0.11}$ ±0.10		[10] ADAM	95	DLPH	$e^+e^- \to Z$
0.99 ±0.14 $^{+0.05}_{-0.04}$		[3,11] AKERS	95T	OPAL	$e^+e^- \to Z$
• • • We do not use the following data for averages, fits, limits, etc. • • •					
1.091±0.023±0.014		[7] ABE	02H	BELL	Repl. by ABE 05B
1.06 ±0.07 ±0.02		[6] ABE	98B	CDF	Repl. by ACOSTA 02C
1.01 ±0.11 ±0.02		[3] ABE	96C	CDF	Repl. by ABE 98Q
1.03 ±0.08 ±0.02		[12] BUSKULIC	96J	ALEP	$e^+e^- \to Z$
0.98 ±0.08 ±0.03		[3] BUSKULIC	96J	ALEP	Repl. by BARATE 00R
1.02 ±0.16 ±0.05	269	[6] ABE	94D	CDF	Repl. by ABE 98B
1.11 $^{+0.51}_{-0.39}$ ±0.11	188	[3] ABREU	93D	DLPH	Sup. by ABREU 95Q
1.01 $^{+0.29}_{-0.22}$ ±0.12	253	[10] ABREU	93G	DLPH	Sup. by ADAM 95
1.0 $^{+0.33}_{-0.25}$ ±0.08	130	ACTON	93C	OPAL	Sup. by AKERS 95T
0.96 $^{+0.19}_{-0.15}$ $^{+0.18}_{-0.12}$	154	[3] BUSKULIC	93D	ALEP	Sup. by BUSKULIC 96J

[1] Measured using $B \to J/\psi K^{(*)}$ decays.
[2] Measured mean life using fully reconstructed decays ($J/\psi K^{(*)}$).
[3] Data analyzed using $D/D^*\mu$X vertices.
[4] Measurement performed using a combined fit of *CP*-violation, mixing and lifetimes.
[5] Measurement performed using an inclusive reconstruction and B flavor identification technique.
[6] Measured using fully reconstructed decays.
[7] Events are selected in which one B meson is fully reconstructed while the second B meson is reconstructed inclusively.
[8] Data analyzed using charge of secondary vertex.
[9] ABREU 95Q assumes B($B^0 \to D^{**-}\ell^+\nu_\ell$) = 3.2 ± 1.7%.
[10] Data analyzed using vertex-charge technique to tag B charge.
[11] AKERS 95T assumes B($B^0 \to D_s^{(*)}D^{0(*)}$) = 5.0 ± 0.9% to find B^+/B^0 yield.
[12] Combined result of $D/D^*\ell$X analysis and fully reconstructed B analysis.

τ_{B^+}/τ_{B^0} (inferred from branching fractions)

These measurements are inferred from the branching fractions for semileptonic decay or other spectator-dominated decays by assuming that the rates for such decays are equal for B^0 and B^+. We do not use measurements which assume equal production of B^0 and B^+ because of the large uncertainty in the production ratio.

"OUR EVALUATION" has been obtained by the Heavy Flavor Averaging Group (HFLAV) by taking into account correlations between measurements.

VALUE	CL%	EVTS	DOCUMENT ID		TECN	COMMENT
1.076±0.034 OUR EVALUATION						
1.07 ±0.04 OUR AVERAGE						
1.07 ±0.04 ±0.03			URQUIJO	07	BELL	$e^+e^- \to \Upsilon(4S)$
1.067±0.041±0.033			AUBERT,B	06Y	BABR	$e^+e^- \to \Upsilon(4S)$
• • • We do not use the following data for averages, fits, limits, etc. • • •						
0.95 $^{+0.117}_{-0.080}$±0.091			[1] ARTUSO	97	CLE2	$e^+e^- \to \Upsilon(4S)$
1.15 ±0.17 ±0.06			[2] JESSOP	97	CLE2	$e^+e^- \to \Upsilon(4S)$
0.93 ±0.18 ±0.12			[3] ATHANAS	94	CLE2	Sup. by ARTUSO 97
0.91 ±0.27 ±0.21			[4] ALBRECHT	92C	ARG	$e^+e^- \to \Upsilon(4S)$
1.0 ±0.4		29	[4,5] ALBRECHT	92G	ARG	$e^+e^- \to \Upsilon(4S)$
0.89 ±0.19 ±0.13			[4] FULTON	91	CLEO	$e^+e^- \to \Upsilon(4S)$
1.00 ±0.23 ±0.14			[4] ALBRECHT	89L	ARG	$e^+e^- \to \Upsilon(4S)$
0.49 to 2.3	90		[6] BEAN	87B	CLEO	$e^+e^- \to \Upsilon(4S)$

[1] ARTUSO 97 uses partial reconstruction of $B \to D^*\ell\nu_\ell$ and independent of B^0 and B^+ production fraction.
[2] Assumes equal production of B^+ and B^0 at the $\Upsilon(4S)$.
[3] ATHANAS 94 uses events tagged by fully reconstructed B^- decays and partially or fully reconstructed B^0 decays.
[4] Assumes equal production of B^0 and B^+.
[5] ALBRECHT 92G data analyzed using $B \to D_s\overline{D}$, $D_s\overline{D}^*$, $D_s^*\overline{D}$, $D_s^*\overline{D}^*$ events.
[6] BEAN 87B assume the fraction of $B^0\overline{B}^0$ events at the $\Upsilon(4S)$ is 0.41.

$\Delta\Gamma_{B^0_d}$ / $\Gamma_{B^0_d}$

$\Gamma_{B^0_d}$ and $\Delta\Gamma_{B^0_d}$ are the decay rate average and difference between two B^0_d *CP* eigenstates (light − heavy). The λ_{CP} characterizes B^0 and $\overline{B}^0$ decays to states of charmonium plus K^0_L, see the review on "*CP* Violation" in the reviews section.

"OUR EVALUATION" has been obtained by the Heavy Flavor Averaging Group (HFLAV) by taking into account correlations between measurements.

VALUE (units 10^{-2})	CL%	DOCUMENT ID		TECN	COMMENT
− 0.2 ±1.0 OUR EVALUATION					
− 0.2 ±1.1 OUR AVERAGE					
− 0.1 ±1.1 ±0.9		[1] AABOUD	16G	ATLS	pp at 7, 8 TeV
− 4.4 ±2.5 ±1.1		[2] AAIJ	14E	LHCB	pp at 7 TeV
1.7 ±1.8 ±1.1		[3] HIGUCHI	12	BELL	$e^+e^- \to \Upsilon(4S)$
0.8 ±3.7 ±1.8		[4] AUBERT,B	04C	BABR	$e^+e^- \to \Upsilon(4S)$
0 ±9		[5] ABDALLAH	03B	DLPH	$e^+e^- \to Z$
• • • We do not use the following data for averages, fits, limits, etc. • • •					
0.50±1.38		ABAZOV	14	D0	$p\overline{p}$ at 1.96 TeV
< 80	95	[6] BEHRENS	00B	CLE2	$e^+e^- \to \Upsilon(4S)$

[1] Measured from the ratio of decay time distributions of $B^0 \to J/\psi K^0_S$ and $B^0 \to J/\psi K^{*0}$ decays.
[2] Measured using the effective lifetimes of $B^0 \to J/\psi K^0_S$ and $B^0 \to J/\psi K^{*0}$ decays.
[3] Reports $-\Delta\Gamma_d/\Gamma_d$ using $B^0 \to J/\psi K^0_S$, $J/\psi K^0_L$, $D^-\pi^+$, $D^{*-}\pi^+$, $D^{*-}\rho^+$, and $D^{*-}\ell^+\nu$ decays.
[4] Corresponds to 90% confidence range [−0.084, 0.068].
[5] Used the measured τ_{B^0} = 1.55 ± 0.03 ps. Corresponds to an upper limit of < 0.18 at 95% C.L.
[6] BEHRENS 00B uses high-momentum lepton tags and partially reconstructed $\overline{B}^0 \to D^{*+}\pi^-$, ρ^- decays to determine the flavor of the B meson. Assumes Δ_{md}=0.478 ± 0.018 ps^{-1} and τ_{B^0}=1.548 ± 0.032 ps.

B^0 DECAY MODES

$\overline{B}^0$ modes are charge conjugates of the modes below. Reactions indicate the weak decay vertex and do not include mixing. Modes which do not identify the charge state of the B are listed in the $B^\pm/B^0$ ADMIXTURE section.

The branching fractions listed below assume 50% $B^0\overline{B}^0$ and 50% B^+B^- production at the $\Upsilon(4S)$. We have attempted to bring older measurements up to date by rescaling their assumed $\Upsilon(4S)$ production ratio to 50:50 and their assumed D, D_S, D^*, and ψ branching ratios to current values whenever this would affect our averages and best limits significantly.

Meson Particle Listings

B^0

Indentation is used to indicate a subchannel of a previous reaction. All resonant subchannels have been corrected for resonance branching fractions to the final state so the sum of the subchannel branching fractions can exceed that of the final state.

For inclusive branching fractions, *e.g.*, $B \to D^{\pm}$ anything, the values usually are multiplicities, not branching fractions. They can be greater than one.

	Mode		Fraction (Γ_i/Γ)	Scale factor / Confidence level
Γ_1	$\ell^+ \nu_\ell$ anything	[a]	(10.33 ± 0.28) %	
Γ_2	$e^+ \nu_e X_c$		(10.1 ± 0.4) %	
Γ_3	$D \ell^+ \nu_\ell$ anything		(9.1 ± 0.8) %	
Γ_4	$D^- \ell^+ \nu_\ell$	[a]	(2.20 ± 0.10) %	
Γ_5	$D^- \tau^+ \nu_\tau$		(1.03 ± 0.22) %	
Γ_6	$D^*(2010)^- \ell^+ \nu_\ell$	[a]	(4.88 ± 0.10) %	
Γ_7	$D^*(2010)^- \tau^+ \nu_\tau$		(1.67 ± 0.13) %	S=1.1
Γ_8	$\overline{D}^0 \pi^- \ell^+ \nu_\ell$		(4.3 ± 0.6) $\times 10^{-3}$	
Γ_9	$D_0^*(2400)^- \ell^+ \nu_\ell$, $D_0^{*-} \to \overline{D}^0 \pi^-$		(3.0 ± 1.2) $\times 10^{-3}$	S=1.8
Γ_{10}	$D_2^*(2460)^- \ell^+ \nu_\ell$, $D_2^{*-} \to \overline{D}^0 \pi^-$		(1.21 ± 0.33) $\times 10^{-3}$	S=1.8
Γ_{11}	$\overline{D}^{(*)}$ n$\pi \ell^+ \nu_\ell$ (n $\geq$ 1)		(2.3 ± 0.4) %	
Γ_{12}	$\overline{D}^{*0} \pi^- \ell^+ \nu_\ell$		(4.9 ± 0.8) $\times 10^{-3}$	
Γ_{13}	$D_1(2420)^- \ell^+ \nu_\ell$, $D_1^- \to \overline{D}^{*0} \pi^-$		(2.80 ± 0.28) $\times 10^{-3}$	
Γ_{14}	$D_1'(2430)^- \ell^+ \nu_\ell$, $D_1'^- \to \overline{D}^{*0} \pi^-$		(3.1 ± 0.9) $\times 10^{-3}$	
Γ_{15}	$D_2^*(2460)^- \ell^+ \nu_\ell$, $D_2^{*-} \to \overline{D}^{*0} \pi^-$		(6.8 ± 1.2) $\times 10^{-4}$	
Γ_{16}	$D^- \pi^+ \pi^- \ell^+ \nu_\ell$		(1.3 ± 0.5) $\times 10^{-3}$	
Γ_{17}	$D^{*-} \pi^+ \pi^- \ell^+ \nu_\ell$		(1.4 ± 0.5) $\times 10^{-3}$	
Γ_{18}	$\rho^- \ell^+ \nu_\ell$	[a]	(2.94 ± 0.21) $\times 10^{-4}$	
Γ_{19}	$\pi^- \ell^+ \nu_\ell$	[a]	(1.50 ± 0.06) $\times 10^{-4}$	
Γ_{20}	$\pi^- \mu^+ \nu_\mu$			
Γ_{21}	$\pi^- \tau^+ \nu_\tau$		< 2.5 $\times 10^{-4}$	CL=90%
	Inclusive modes			
Γ_{22}	$K^{\pm}$ anything		(78 ± 8) %	
Γ_{23}	$D^0 X$		(8.1 ± 1.5) %	
Γ_{24}	$\overline{D}^0 X$		(47.4 ± 2.8) %	
Γ_{25}	$D^+ X$		< 3.9 %	CL=90%
Γ_{26}	$D^- X$		(36.9 ± 3.3) %	
Γ_{27}	$D_s^+ X$		(10.3 $^{+2.1}_{-1.8}$) %	
Γ_{28}	$D_s^- X$		< 2.6 %	CL=90%
Γ_{29}	$\Lambda_c^+ X$		< 3.1 %	CL=90%
Γ_{30}	$\overline{\Lambda}_c^- X$		(5.0 $^{+2.1}_{-1.5}$) %	
Γ_{31}	$\overline{c} X$		(95 ± 5) %	
Γ_{32}	$c X$		(24.6 ± 3.1) %	
Γ_{33}	$\overline{c}/c X$		(119 ± 6) %	
	D, D^*, or D_s modes			
Γ_{34}	$D^- \pi^+$		(2.52 ± 0.13) $\times 10^{-3}$	S=1.1
Γ_{35}	$D^- \rho^+$		(7.9 ± 1.3) $\times 10^{-3}$	
Γ_{36}	$D^- K^0 \pi^+$		(4.9 ± 0.9) $\times 10^{-4}$	
Γ_{37}	$D^- K^*(892)^+$		(4.5 ± 0.7) $\times 10^{-4}$	
Γ_{38}	$D^- \omega \pi^+$		(2.8 ± 0.6) $\times 10^{-3}$	
Γ_{39}	$D^- K^+$		(1.86 ± 0.20) $\times 10^{-4}$	
Γ_{40}	$D^- K^+ \pi^+ \pi^-$		(3.5 ± 0.8) $\times 10^{-4}$	
Γ_{41}	$D^- K^+ \overline{K}^0$		< 3.1 $\times 10^{-4}$	CL=90%
Γ_{42}	$D^- K^+ \overline{K}^*(892)^0$		(8.8 ± 1.9) $\times 10^{-4}$	
Γ_{43}	$\overline{D}^0 \pi^+ \pi^-$		(8.8 ± 0.5) $\times 10^{-4}$	
Γ_{44}	$D^*(2010)^- \pi^+$		(2.74 ± 0.13) $\times 10^{-3}$	
Γ_{45}	$\overline{D}^0 K^+ K^-$		(4.9 ± 1.2) $\times 10^{-5}$	
Γ_{46}	$D^- \pi^+ \pi^+ \pi^-$		(6.0 ± 0.7) $\times 10^{-3}$	S=1.1
Γ_{47}	($D^- \pi^+ \pi^+ \pi^-$) nonresonant		(3.9 ± 1.9) $\times 10^{-3}$	
Γ_{48}	$D^- \pi^+ \rho^0$		(1.1 ± 1.0) $\times 10^{-3}$	
Γ_{49}	$D^- a_1(1260)^+$		(6.0 ± 3.3) $\times 10^{-3}$	
Γ_{50}	$D^*(2010)^- \pi^+ \pi^0$		(1.5 ± 0.5) %	
Γ_{51}	$D^*(2010)^- \rho^+$		(2.2 $^{+1.8}_{-2.7}$) $\times 10^{-3}$	S=5.2
Γ_{52}	$D^*(2010)^- K^+$		(2.12 ± 0.15) $\times 10^{-4}$	
Γ_{53}	$D^*(2010)^- K^0 \pi^+$		(3.0 ± 0.8) $\times 10^{-4}$	
Γ_{54}	$D^*(2010)^- K^*(892)^+$		(3.3 ± 0.6) $\times 10^{-4}$	
Γ_{55}	$D^*(2010)^- K^+ \overline{K}^0$		< 4.7 $\times 10^{-4}$	CL=90%
Γ_{56}	$D^*(2010)^- K^+ \overline{K}^*(892)^0$		(1.29 ± 0.33) $\times 10^{-3}$	
Γ_{57}	$D^*(2010)^- \pi^+ \pi^+ \pi^-$		(7.21 ± 0.29) $\times 10^{-3}$	
Γ_{58}	($D^*(2010)^- \pi^+ \pi^+ \pi^-$) nonresonant		(0.0 ± 2.5) $\times 10^{-3}$	
Γ_{59}	$D^*(2010)^- \pi^+ \rho^0$		(5.7 ± 3.2) $\times 10^{-3}$	
Γ_{60}	$D^*(2010)^- a_1(1260)^+$		(1.30 ± 0.27) %	
Γ_{61}	$\overline{D}_1(2420)^0 \pi^- \pi^+$, $\overline{D}_1^0 \to D^{*-} \pi^+$		(1.47 ± 0.35) $\times 10^{-4}$	
Γ_{62}	$D^*(2010)^- K^+ \pi^- \pi^+$		(4.7 ± 0.4) $\times 10^{-4}$	
Γ_{63}	$D^*(2010)^- \pi^+ \pi^+ \pi^- \pi^0$		(1.76 ± 0.27) %	
Γ_{64}	$D^{*-} 3\pi^+ 2\pi^-$		(4.7 ± 0.9) $\times 10^{-3}$	
Γ_{65}	$\overline{D}^*(2010)^- \omega \pi^+$		(2.46 ± 0.18) $\times 10^{-3}$	S=1.2
Γ_{66}	$D_1(2430)^0 \omega$, $D_1^0 \to D^{*-} \pi^+$		(2.7 $^{+0.8}_{-0.4}$) $\times 10^{-4}$	
Γ_{67}	$\overline{D}^{*-} \rho(1450)^+$		(1.07 $^{+0.40}_{-0.34}$) $\times 10^{-3}$	
Γ_{68}	$\overline{D}_1(2420)^0 \omega$		(7.0 ± 2.2) $\times 10^{-5}$	
Γ_{69}	$\overline{D}_2^*(2460)^0 \omega$		(4.0 ± 1.4) $\times 10^{-5}$	
Γ_{70}	$\overline{D}^{*-} b_1(1235)^-$, $b_1^- \to \omega \pi^-$		< 7 $\times 10^{-5}$	CL=90%
Γ_{71}	$\overline{D}^{**-} \pi^+$	[b]	(1.9 ± 0.9) $\times 10^{-3}$	
Γ_{72}	$D_1(2420)^- \pi^+$, $D_1^- \to D^- \pi^+ \pi^-$		(9.9 $^{+2.0}_{-2.5}$) $\times 10^{-5}$	
Γ_{73}	$D_1(2420)^- \pi^+$, $D_1^- \to D^{*-} \pi^+ \pi^-$		< 3.3 $\times 10^{-5}$	CL=90%
Γ_{74}	$\overline{D}_2^*(2460)^- \pi^+$, $(D_2^*)^- \to D^0 \pi^-$		(2.38 ± 0.16) $\times 10^{-4}$	
Γ_{75}	$\overline{D}_0^*(2400)^- \pi^+$, $(D_0^*)^- \to D^0 \pi^-$		(7.6 ± 0.8) $\times 10^{-5}$	
Γ_{76}	$D_2^*(2460)^- \pi^+$, $(D_2^*)^- \to D^{*-} \pi^+ \pi^-$		< 2.4 $\times 10^{-5}$	CL=90%
Γ_{77}	$\overline{D}_2^*(2460)^- \rho^+$		< 4.9 $\times 10^{-3}$	CL=90%
Γ_{78}	$D^0 \overline{D}^0$		(1.4 ± 0.7) $\times 10^{-5}$	
Γ_{79}	$D^{*0} \overline{D}^0$		< 2.9 $\times 10^{-4}$	CL=90%
Γ_{80}	$D^- D^+$		(2.11 ± 0.18) $\times 10^{-4}$	
Γ_{81}	$D^{\pm} D^{*\mp}$ (CP-averaged)		(6.1 ± 0.6) $\times 10^{-4}$	
Γ_{82}	$D^- D_s^+$		(7.2 ± 0.8) $\times 10^{-3}$	
Γ_{83}	$D^*(2010)^- D_s^+$		(8.0 ± 1.1) $\times 10^{-3}$	
Γ_{84}	$D^- D_s^{*+}$		(7.4 ± 1.6) $\times 10^{-3}$	
Γ_{85}	$D^*(2010)^- D_s^{*+}$		(1.77 ± 0.14) %	
Γ_{86}	$D_{s0}(2317)^- K^+$, $D_{s0}^- \to D_s^- \pi^0$		(4.2 ± 1.4) $\times 10^{-5}$	
Γ_{87}	$D_{s0}(2317)^- \pi^+$, $D_{s0}^- \to D_s^- \pi^0$		< 2.5 $\times 10^{-5}$	CL=90%
Γ_{88}	$D_{sJ}(2457)^- K^+$, $D_{sJ}^- \to D_s^- \pi^0$		< 9.4 $\times 10^{-6}$	CL=90%
Γ_{89}	$D_{sJ}(2457)^- \pi^+$, $D_{sJ}^- \to D_s^- \pi^0$		< 4.0 $\times 10^{-6}$	CL=90%
Γ_{90}	$D_s^- D_s^+$		< 3.6 $\times 10^{-5}$	CL=90%
Γ_{91}	$D_s^{*-} D_s^+$		< 1.3 $\times 10^{-4}$	CL=90%
Γ_{92}	$D_s^{*-} D_s^{*+}$		< 2.4 $\times 10^{-4}$	CL=90%
Γ_{93}	$D_{s0}^*(2317)^+ D^-$, $D_{s0}^{*+} \to D_s^+ \pi^0$		(1.09 ± 0.16) $\times 10^{-3}$	
Γ_{94}	$D_{s0}(2317)^+ D^-$, $D_{s0}^+ \to D_s^{*+} \gamma$		< 9.5 $\times 10^{-4}$	CL=90%
Γ_{95}	$D_{s0}(2317)^+ D^*(2010)^-$, $D_{s0}^+ \to D_s^+ \pi^0$		(1.5 ± 0.6) $\times 10^{-3}$	
Γ_{96}	$D_{sJ}(2457)^+ D^-$		(3.5 ± 1.1) $\times 10^{-3}$	
Γ_{97}	$D_{sJ}(2457)^+ D^-$, $D_{sJ}^+ \to D_s^+ \gamma$		(6.5 $^{+1.7}_{-1.4}$) $\times 10^{-4}$	
Γ_{98}	$D_{sJ}(2457)^+ D^-$, $D_{sJ}^+ \to D_s^{*+} \gamma$		< 6.0 $\times 10^{-4}$	CL=90%
Γ_{99}	$D_{sJ}(2457)^+ D^-$, $D_{sJ}^+ \to D_s^+ \pi^+ \pi^-$		< 2.0 $\times 10^{-4}$	CL=90%
Γ_{100}	$D_{sJ}(2457)^+ D^-$, $D_{sJ}^+ \to D_s^+ \pi^0$		< 3.6 $\times 10^{-4}$	CL=90%
Γ_{101}	$D^*(2010)^- D_{sJ}(2457)^+$		(9.3 ± 2.2) $\times 10^{-3}$	
Γ_{102}	$D_{sJ}(2457)^+ D^*(2010)$, $D_{sJ}^+ \to D_s^+ \gamma$		(2.3 $^{+0.9}_{-0.7}$) $\times 10^{-3}$	
Γ_{103}	$D^- D_{s1}(2536)^+$, $D_{s1}^+ \to D^{*0} K^+ + D^{*+} K^0$		(2.8 ± 0.7) $\times 10^{-4}$	
Γ_{104}	$D^- D_{s1}(2536)^+$, $D_{s1}^+ \to D^{*0} K^+$		(1.7 ± 0.6) $\times 10^{-4}$	
Γ_{105}	$D^- D_{s1}(2536)^+$, $D_{s1}^+ \to D^{*+} K^0$		(2.6 ± 1.1) $\times 10^{-4}$	

See key on page 885

Γ_{106}	$D^*(2010)^- D_{s1}(2536)^+$, $D_{s1}^+ \to D^{*0} K^+ + D^{*+} K^0$	(5.0 ± 1.4)	$\times 10^{-4}$		
Γ_{107}	$D^*(2010)^- D_{s1}(2536)^+$, $D_{s1}^+ \to D^{*0} K^+$	(3.3 ± 1.1)	$\times 10^{-4}$		
Γ_{108}	$D^{*-} D_{s1}(2536)^+$, $D_{s1}^+ \to D^{*+} K^0$	(5.0 ± 1.7)	$\times 10^{-4}$		
Γ_{109}	$D^- D_{sJ}(2573)^+$, $D_{sJ}^+ \to D^0 K^+$	(3.4 ± 1.8)	$\times 10^{-5}$		
Γ_{110}	$D^*(2010)^- D_{sJ}(2573)^+$, $D_{sJ}^+ \to D^0 K^+$	< 2	$\times 10^{-4}$	CL=90%	
Γ_{111}	$D^- D_{sJ}(2700)^+$, $D_{sJ}^+ \to D^0 K^+$	(7.1 ± 1.2)	$\times 10^{-4}$		
Γ_{112}	$D^+ \pi^-$	(7.4 ± 1.3)	$\times 10^{-7}$		
Γ_{113}	$D_s^+ \pi^-$	(2.16 ± 0.26)	$\times 10^{-5}$		
Γ_{114}	$D_s^{*+} \pi^-$	(2.1 ± 0.4)	$\times 10^{-5}$		S=1.4
Γ_{115}	$D_s^+ \rho^-$	< 2.4	$\times 10^{-5}$	CL=90%	
Γ_{116}	$D_s^{*+} \rho^-$	(4.1 ± 1.3)	$\times 10^{-5}$		
Γ_{117}	$D_s^+ a_0^-$	< 1.9	$\times 10^{-5}$	CL=90%	
Γ_{118}	$D_s^{*+} a_0^-$	< 3.6	$\times 10^{-5}$	CL=90%	
Γ_{119}	$D_s^+ a_1(1260)^-$	< 2.1	$\times 10^{-3}$	CL=90%	
Γ_{120}	$D_s^{*+} a_1(1260)^-$	< 1.7	$\times 10^{-3}$	CL=90%	
Γ_{121}	$D_s^+ a_2^-$	< 1.9	$\times 10^{-4}$	CL=90%	
Γ_{122}	$D_s^{*+} a_2^-$	< 2.0	$\times 10^{-4}$	CL=90%	
Γ_{123}	$D_s^- K^+$	(2.7 ± 0.5)	$\times 10^{-5}$		S=2.7
Γ_{124}	$D_s^{*-} K^+$	(2.19 ± 0.30)	$\times 10^{-5}$		
Γ_{125}	$D_s^- K^*(892)^+$	(3.5 ± 1.0)	$\times 10^{-5}$		
Γ_{126}	$D_s^{*-} K^*(892)^+$	($3.2 \pm^{1.5}_{1.3}$)	$\times 10^{-5}$		
Γ_{127}	$D_s^- \pi^+ K^0$	(9.7 ± 1.4)	$\times 10^{-5}$		
Γ_{128}	$D_s^{*-} \pi^+ K^0$	< 1.10	$\times 10^{-4}$	CL=90%	
Γ_{129}	$D_s^- K^+ \pi^+ \pi^-$	(1.7 ± 0.5)	$\times 10^{-4}$		
Γ_{130}	$D_s^- \pi^+ K^*(892)^0$	< 3.0	$\times 10^{-3}$	CL=90%	
Γ_{131}	$D_s^{*-} \pi^+ K^*(892)^0$	< 1.6	$\times 10^{-3}$	CL=90%	
Γ_{132}	$\overline{D}{}^0 K^0$	(5.2 ± 0.7)	$\times 10^{-5}$		
Γ_{133}	$\overline{D}{}^0 K^+ \pi^-$	(8.8 ± 1.7)	$\times 10^{-5}$		
Γ_{134}	$\overline{D}{}^0 K^*(892)^0$	(4.5 ± 0.6)	$\times 10^{-5}$		
Γ_{135}	$\overline{D}{}^0 K^*(1410)^0$	< 6.7	$\times 10^{-5}$	CL=90%	
Γ_{136}	$\overline{D}{}^0 K_0^*(1430)^0$	(7 ± 7)	$\times 10^{-6}$		
Γ_{137}	$\overline{D}{}^0 K_2^*(1430)^0$	(2.1 ± 0.9)	$\times 10^{-5}$		
Γ_{138}	$D_0^*(2400)^-$, $D_0^{*-} \to \overline{D}{}^0 \pi^-$	(1.9 ± 0.9)	$\times 10^{-5}$		
Γ_{139}	$D_2^*(2460)^- K^+$, $D_2^{*-} \to \overline{D}{}^0 \pi^-$	(2.03 ± 0.35)	$\times 10^{-5}$		
Γ_{140}	$D_3^*(2760)^- K^+$, $D_3^{*-} \to \overline{D}{}^0 \pi^-$	< 1.0	$\times 10^{-6}$	CL=90%	
Γ_{141}	$\overline{D}{}^0 K^+ \pi^-$ non-resonant	< 3.7	$\times 10^{-5}$	CL=90%	
Γ_{142}	$[K^+ K^-]_D K^*(892)^0$				
Γ_{143}	$[\pi^+ \pi^-]_D K^*(892)^0$				
Γ_{144}	$\overline{D}{}^0 \pi^0$	(2.63 ± 0.14)	$\times 10^{-4}$		
Γ_{145}	$\overline{D}{}^0 \rho^0$	(3.21 ± 0.21)	$\times 10^{-4}$		
Γ_{146}	$\overline{D}{}^0 f_2$	(1.56 ± 0.21)	$\times 10^{-4}$		
Γ_{147}	$\overline{D}{}^0 \eta$	(2.36 ± 0.32)	$\times 10^{-4}$		S=2.5
Γ_{148}	$\overline{D}{}^0 \eta'$	(1.38 ± 0.16)	$\times 10^{-4}$		S=1.3
Γ_{149}	$\overline{D}{}^0 \omega$	(2.54 ± 0.16)	$\times 10^{-4}$		
Γ_{150}	$D^0 \phi$	< 1.16	$\times 10^{-5}$	CL=90%	
Γ_{151}	$D^0 K^+ \pi^-$	(5.3 ± 3.2)	$\times 10^{-6}$		
Γ_{152}	$D^0 K^*(892)^0$	< 1.1	$\times 10^{-5}$	CL=90%	
Γ_{153}	$\overline{D}{}^{*0} \gamma$	< 2.5	$\times 10^{-5}$	CL=90%	
Γ_{154}	$\overline{D}{}^*(2007)^0 \pi^0$	(2.2 ± 0.6)	$\times 10^{-4}$		S=2.6
Γ_{155}	$\overline{D}{}^*(2007)^0 \rho^0$	< 5.1	$\times 10^{-4}$	CL=90%	
Γ_{156}	$\overline{D}{}^*(2007)^0 \eta$	(2.3 ± 0.6)	$\times 10^{-4}$		S=2.8
Γ_{157}	$\overline{D}{}^*(2007)^0 \eta'$	(1.40 ± 0.22)	$\times 10^{-4}$		
Γ_{158}	$\overline{D}{}^*(2007)^0 \pi^+ \pi^-$	(6.2 ± 2.2)	$\times 10^{-4}$		
Γ_{159}	$\overline{D}{}^*(2007)^0 K^0$	(3.6 ± 1.2)	$\times 10^{-5}$		
Γ_{160}	$\overline{D}{}^*(2007)^0 K^*(892)^0$	< 6.9	$\times 10^{-5}$	CL=90%	
Γ_{161}	$D^*(2007)^0 K^*(892)^0$	< 4.0	$\times 10^{-5}$	CL=90%	
Γ_{162}	$D^*(2007)^0 \pi^+ \pi^+ \pi^- \pi^-$	(2.7 ± 0.5)	$\times 10^{-3}$		
Γ_{163}	$D^*(2010)^+ D^*(2010)^-$	(8.0 ± 0.6)	$\times 10^{-4}$		
Γ_{164}	$\overline{D}{}^*(2007)^0 \omega$	(3.6 ± 1.1)	$\times 10^{-4}$		S=3.1
Γ_{165}	$D^*(2010)^+ D^-$	(6.1 ± 1.5)	$\times 10^{-4}$		S=1.6
Γ_{166}	$D^*(2007)^0 \overline{D}{}^*(2007)^0$	< 9	$\times 10^{-5}$	CL=90%	
Γ_{167}	$D^- D^0 K^+$	(1.07 ± 0.11)	$\times 10^{-3}$		
Γ_{168}	$D^- D^*(2007)^0 K^+$	(3.5 ± 0.4)	$\times 10^{-3}$		
Γ_{169}	$D^*(2010)^- D^0 K^+$	(2.47 ± 0.21)	$\times 10^{-3}$		
Γ_{170}	$D^*(2010)^- D^*(2007)^0 K^+$	(1.06 ± 0.09) %			
Γ_{171}	$D^- D^+ K^0$	(7.5 ± 1.7)	$\times 10^{-4}$		
Γ_{172}	$D^*(2010)^- D^+ K^0 + D^- D^*(2010)^+ K^0$	(6.4 ± 0.5)	$\times 10^{-3}$		
Γ_{173}	$D^*(2010)^- D^*(2010)^+ K^0$	(8.1 ± 0.7)	$\times 10^{-3}$		
Γ_{174}	$D^{*-} D_{s1}(2536)^+$, $D_{s1}^+ \to D^{*+} K^0$	(8.0 ± 2.4)	$\times 10^{-4}$		
Γ_{175}	$\overline{D}{}^0 D^0 K^0$	(2.7 ± 1.1)	$\times 10^{-4}$		
Γ_{176}	$\overline{D}{}^0 D^*(2007)^0 K^0 + \overline{D}{}^*(2007)^0 D^0 K^0$	(1.1 ± 0.5)	$\times 10^{-3}$		
Γ_{177}	$\overline{D}{}^*(2007)^0 D^*(2007)^0 K^0$	(2.4 ± 0.9)	$\times 10^{-3}$		
Γ_{178}	$(\overline{D} + \overline{D}{}^*)(D + D^*) K$	(3.68 ± 0.26) %			

Charmonium modes

Γ_{179}	$\eta_c K^0$	(7.9 ± 1.2)	$\times 10^{-4}$		
Γ_{180}	$\eta_c K^*(892)^0$	(6.9 ± 0.9)	$\times 10^{-4}$		
Γ_{181}	$\eta_c(2S) K^{*0}$	< 3.9	$\times 10^{-4}$	CL=90%	
Γ_{182}	$h_c(1P) K^{*0}$	< 4	$\times 10^{-4}$	CL=90%	
Γ_{183}	$J/\psi(1S) K^0$	(8.73 ± 0.32)	$\times 10^{-4}$		
Γ_{184}	$J/\psi(1S) K^+ \pi^-$	(1.15 ± 0.05)	$\times 10^{-3}$		
Γ_{185}	$J/\psi(1S) K^*(892)^0$	(1.27 ± 0.05)	$\times 10^{-3}$		
Γ_{186}	$J/\psi(1S) \eta K_S^0$	(5.4 ± 0.9)	$\times 10^{-5}$		
Γ_{187}	$J/\psi(1S) \eta' K_S^0$	< 2.5	$\times 10^{-5}$	CL=90%	
Γ_{188}	$J/\psi(1S) \phi K^0$	(4.9 ± 1.0)	$\times 10^{-5}$		S=1.3
Γ_{189}	$J/\psi(1S) \omega K^0$	(2.3 ± 0.4)	$\times 10^{-4}$		
Γ_{190}	$\chi_{c1}(3872) K^0$, $\chi_{c1} \to J/\psi\omega$	(6.0 ± 3.2)	$\times 10^{-6}$		
Γ_{191}	$X(3915)$, $X \to J/\psi\omega$	(2.1 ± 0.9)	$\times 10^{-5}$		
Γ_{192}	$J/\psi(1S) K(1270)^0$	(1.3 ± 0.5)	$\times 10^{-3}$		
Γ_{193}	$J/\psi(1S) \pi^0$	(1.76 ± 0.16)	$\times 10^{-5}$		S=1.1
Γ_{194}	$J/\psi(1S) \eta$	(1.08 ± 0.23)	$\times 10^{-5}$		S=1.5
Γ_{195}	$J/\psi(1S) \pi^+ \pi^-$	(3.96 ± 0.17)	$\times 10^{-5}$		
Γ_{196}	$J/\psi(1S) \pi^+ \pi^-$ nonresonant	< 1.2	$\times 10^{-5}$	CL=90%	
Γ_{197}	$J/\psi(1S) f_0(500)$, $f_0 \to \pi\pi$	($8.0 \pm^{1.1}_{0.9}$)	$\times 10^{-6}$		
Γ_{198}	$J/\psi(1S) f_2$	(3.3 ± 0.5)	$\times 10^{-6}$		S=1.5
Γ_{199}	$J/\psi(1S) \rho^0$	($2.55 \pm^{0.18}_{0.16}$)	$\times 10^{-5}$		
Γ_{200}	$J/\psi(1S) f_0(980)$, $f_0 \to \pi^+ \pi^-$	< 1.1	$\times 10^{-6}$	CL=90%	
Γ_{201}	$J/\psi(1S) \rho(1450)^0$, $\rho^0 \to \pi\pi$	($2.9 \pm^{1.6}_{0.7}$)	$\times 10^{-6}$		
Γ_{202}	$J/\psi\rho(1700)^0$, $\rho^0 \to \pi^+ \pi^-$	(2.0 ± 1.3)	$\times 10^{-6}$		
Γ_{203}	$J/\psi(1S) \omega$	($1.8 \pm^{0.7}_{0.5}$)	$\times 10^{-5}$		
Γ_{204}	$J/\psi(1S) K^+ K^-$	(2.51 ± 0.35)	$\times 10^{-6}$		
Γ_{205}	$J/\psi(1S) a_0(980)$, $a_0 \to K^+ K^-$	(4.7 ± 3.4)	$\times 10^{-7}$		
Γ_{206}	$J/\psi(1S) \phi$	< 1.9	$\times 10^{-7}$	CL=90%	
Γ_{207}	$J/\psi(1S) \eta'(958)$	(7.6 ± 2.4)	$\times 10^{-6}$		
Γ_{208}	$J/\psi(1S) K^0 \pi^+ \pi^-$	(4.4 ± 0.4)	$\times 10^{-4}$		
Γ_{209}	$J/\psi(1S) K^0 K^- \pi^+ +$ c.c.	< 2.1	$\times 10^{-5}$	CL=90%	
Γ_{210}	$J/\psi(1S) K^0 K^+ K^-$	(2.5 ± 0.7)	$\times 10^{-5}$		S=1.8
Γ_{211}	$J/\psi(1S) K^0 K^\pm \pi^\mp$				
Γ_{212}	$J/\psi(1S) K^0 \rho^0$	(5.4 ± 3.0)	$\times 10^{-4}$		
Γ_{213}	$J/\psi(1S) K^*(892)^+ \pi^-$	(8 ± 4)	$\times 10^{-4}$		
Γ_{214}	$J/\psi(1S) \pi^+ \pi^- \pi^+ \pi^-$	(1.43 ± 0.12)	$\times 10^{-5}$		
Γ_{215}	$J/\psi(1S) f_1(1285)$	(8.2 ± 2.1)	$\times 10^{-6}$		
Γ_{216}	$J/\psi(1S) K^*(892)^0 \pi^+ \pi^-$	(6.6 ± 2.2)	$\times 10^{-4}$		
Γ_{217}	$\chi_{c1}(3872)^- K^+$	< 5	$\times 10^{-4}$	CL=90%	
Γ_{218}	$\chi_{c1}(3872)^- K^+$, $\chi_{c1}(3872)^- \to J/\psi(1S) \pi^- \pi^0$	[c] < 4.2	$\times 10^{-6}$	CL=90%	
Γ_{219}	$\chi_{c1}(3872) K^0$, $\chi_{c1} \to J/\psi \pi^+ \pi^-$	(4.3 ± 1.3)	$\times 10^{-6}$		
Γ_{220}	$\chi_{c1}(3872) K^0$, $\chi_{c1} \to J/\psi\gamma$	< 2.4	$\times 10^{-6}$	CL=90%	
Γ_{221}	$\chi_{c1}(3872) K^*(892)^0$, $\chi_{c1} \to J/\psi\gamma$	< 2.8	$\times 10^{-6}$	CL=90%	
Γ_{222}	$\chi_{c1}(3872) K^0$, $\chi_{c1} \to \psi(2S)\gamma$	< 6.62	$\times 10^{-6}$	CL=90%	
Γ_{223}	$\chi_{c1}(3872) K^*(892)^0$, $\chi_{c1} \to \psi(2S)\gamma$	< 4.4	$\times 10^{-6}$	CL=90%	
Γ_{224}	$\chi_{c1}(3872) K^0$, $\chi_{c1} \to D^0 \overline{D}{}^0 \pi^0$	(1.7 ± 0.8)	$\times 10^{-4}$		
Γ_{225}	$\chi_{c1}(3872) K^0$, $\chi_{c1} \to \overline{D}{}^{*0} D^0$	(1.2 ± 0.4)	$\times 10^{-4}$		
Γ_{226}	$\chi_{c1}(3872) K^+ \pi^-$, $\chi_{c1} \to J/\psi \pi^+ \pi^-$	(7.9 ± 1.4)	$\times 10^{-6}$		
Γ_{227}	$\chi_{c1}(3872) K^*(892)^0$, $\chi_{c1} \to J/\psi \pi^+ \pi^-$	(4.0 ± 1.5)	$\times 10^{-6}$		

Γ_{228}	$Z_c(4430)^\pm K^\mp,\ Z_c^\pm \to \psi(2S)\pi^\pm$	(	$6.0\ ^{+\ 3.0}_{-\ 2.4}$)	$\times 10^{-5}$	
Γ_{229}	$Z_c(4430)^\pm K^\mp,\ Z_c^\pm \to J/\psi\pi^\pm$	(	$5.4\ ^{+\ 4.0}_{-\ 1.2}$)	$\times 10^{-6}$	
Γ_{230}	$Z_c(3900)^\pm K^\mp,\ Z_c^\pm \to J/\psi\pi^\pm$	<	9	$\times 10^{-7}$	
Γ_{231}	$Z_c(4200)^\pm K^\mp,\ X^\pm \to J/\psi\pi^\pm$	(	$2.2\ ^{+\ 1.3}_{-\ 0.8}$)	$\times 10^{-5}$	
Γ_{232}	$J/\psi(1S)\,p\overline{p}$	<	5.2	$\times 10^{-7}$	CL=90%
Γ_{233}	$J/\psi(1S)\gamma$	<	1.5	$\times 10^{-6}$	CL=90%
Γ_{234}	$J/\psi(1S)\overline{D}^0$	<	1.3	$\times 10^{-5}$	CL=90%
Γ_{235}	$\psi(2S)\pi^0$	(	$1.17\pm\ 0.19$)	$\times 10^{-5}$	
Γ_{236}	$\psi(2S)K^0$	(	$5.8\ \pm\ 0.5$)	$\times 10^{-4}$	
Γ_{237}	$\psi(3770)K^0,\ \psi \to \overline{D}^0 D^0$	<	1.23	$\times 10^{-4}$	CL=90%
Γ_{238}	$\psi(3770)K^0,\ \psi \to D^- D^+$	<	1.88	$\times 10^{-4}$	CL=90%
Γ_{239}	$\psi(2S)\pi^+\pi^-$	(	$2.22\pm\ 0.35$)	$\times 10^{-5}$	
Γ_{240}	$\psi(2S)K^+\pi^-$	(	$5.8\ \pm\ 0.4$)	$\times 10^{-4}$	
Γ_{241}	$\psi(2S)K^*(892)^0$	(	$5.9\ \pm\ 0.4$)	$\times 10^{-4}$	
Γ_{242}	$\chi_{c0}K^0$	(	$1.46\pm\ 0.27$)	$\times 10^{-4}$	
Γ_{243}	$\chi_{c0}K^*(892)^0$	(	$1.7\ \pm\ 0.4$)	$\times 10^{-4}$	
Γ_{244}	$\chi_{c1}\pi^0$	(	$1.12\pm\ 0.28$)	$\times 10^{-5}$	
Γ_{245}	$\chi_{c1}K^0$	(	$3.93\pm\ 0.27$)	$\times 10^{-4}$	
Γ_{246}	$\chi_{c1}\pi^-K^+$	(	$4.97\pm\ 0.30$)	$\times 10^{-4}$	
Γ_{247}	$\chi_{c1}K^*(892)^0$	(	$2.38\pm\ 0.19$)	$\times 10^{-4}$	S=1.2
Γ_{248}	$X(4051)^-K^+,\ X^- \to \chi_{c1}\pi^-$	(	$3.0\ ^{+\ 4.0}_{-\ 1.8}$)	$\times 10^{-5}$	
Γ_{249}	$X(4248)^-K^+,\ X^- \to \chi_{c1}\pi^-$	(	$4.0\ ^{+20.0}_{-\ 1.0}$)	$\times 10^{-5}$	
Γ_{250}	$\chi_{c1}\pi^+\pi^-K^0$	(	$3.2\ \pm\ 0.5$)	$\times 10^{-4}$	
Γ_{251}	$\chi_{c1}\pi^-\pi^0K^+$	(	$3.5\ \pm\ 0.6$)	$\times 10^{-4}$	
Γ_{252}	$\chi_{c2}K^0$	<	1.5	$\times 10^{-5}$	CL=90%
Γ_{253}	$\chi_{c2}K^*(892)^0$	(	$4.9\ \pm\ 1.2$)	$\times 10^{-5}$	S=1.1
Γ_{254}	$\chi_{c2}\pi^-K^+$	(	$7.2\ \pm\ 1.0$)	$\times 10^{-5}$	
Γ_{255}	$\chi_{c2}\pi^+\pi^-K^0$	<	1.70	$\times 10^{-4}$	CL=90%
Γ_{256}	$\chi_{c2}\pi^-\pi^0K^+$	<	7.4	$\times 10^{-5}$	CL=90%

K or K^* modes

Γ_{257}	$K^+\pi^-$	(	$1.96\pm\ 0.05$)	$\times 10^{-5}$	
Γ_{258}	$K^0\pi^0$	(	$9.9\ \pm\ 0.5$)	$\times 10^{-6}$	
Γ_{259}	$\eta' K^0$	(	$6.6\ \pm\ 0.4$)	$\times 10^{-5}$	S=1.4
Γ_{260}	$\eta' K^*(892)^0$	(	$2.8\ \pm\ 0.6$)	$\times 10^{-6}$	
Γ_{261}	$\eta' K_0^*(1430)^0$	(	$6.3\ \pm\ 1.6$)	$\times 10^{-6}$	
Γ_{262}	$\eta' K_2^*(1430)^0$	(	$1.37\pm\ 0.32$)	$\times 10^{-5}$	
Γ_{263}	ηK^0	(	$1.23^{+\ 0.27}_{-\ 0.24}$)	$\times 10^{-6}$	
Γ_{264}	$\eta K^*(892)^0$	(	$1.59\pm\ 0.10$)	$\times 10^{-5}$	
Γ_{265}	$\eta K_0^*(1430)^0$	(	$1.10\pm\ 0.22$)	$\times 10^{-5}$	
Γ_{266}	$\eta K_2^*(1430)^0$	(	$9.6\ \pm\ 2.1$)	$\times 10^{-6}$	
Γ_{267}	ωK^0	(	$4.8\ \pm\ 0.4$)	$\times 10^{-6}$	
Γ_{268}	$a_0(980)^0 K^0,\ a_0^0 \to \eta\pi^0$	<	7.8	$\times 10^{-6}$	CL=90%
Γ_{269}	$b_1^0 K^0,\ b_1^0 \to \omega\pi^0$	<	7.8	$\times 10^{-6}$	CL=90%
Γ_{270}	$a_0(980)^\pm K^\mp,\ a_0^\pm \to \eta\pi^\pm$	<	1.9	$\times 10^{-6}$	CL=90%
Γ_{271}	$b_1^- K^+,\ b_1^- \to \omega\pi^-$	(	$7.4\ \pm\ 1.4$)	$\times 10^{-6}$	
Γ_{272}	$b_1^0 K^{*0},\ b_1^0 \to \omega\pi^0$	<	8.0	$\times 10^{-6}$	CL=90%
Γ_{273}	$b_1^- K^{*+},\ b_1^- \to \omega\pi^-$	<	5.0	$\times 10^{-6}$	CL=90%
Γ_{274}	$a_0(1450)^\pm K^\mp,\ a_0^\pm \to \eta\pi^\pm$	<	3.1	$\times 10^{-6}$	CL=90%
Γ_{275}	$K_S^0 X^0$(Familon)	<	5.3	$\times 10^{-5}$	CL=90%
Γ_{276}	$\omega K^*(892)^0$	(	$2.0\ \pm\ 0.5$)	$\times 10^{-6}$	
Γ_{277}	$\omega(K\pi)_0^{*0}$	(	$1.84\pm\ 0.25$)	$\times 10^{-5}$	
Γ_{278}	$\omega K_0^*(1430)^0$	(	$1.60\pm\ 0.34$)	$\times 10^{-5}$	
Γ_{279}	$\omega K_2^*(1430)^0$	(	$1.01\pm\ 0.23$)	$\times 10^{-5}$	
Γ_{280}	$\omega K^+\pi^-$ nonresonant	(	$5.1\ \pm\ 1.0$)	$\times 10^{-6}$	
Γ_{281}	$K^+\pi^-\pi^0$	(	$3.78\pm\ 0.32$)	$\times 10^{-5}$	
Γ_{282}	$K^+\rho^-$	(	$7.0\ \pm\ 0.9$)	$\times 10^{-6}$	
Γ_{283}	$K^+\rho(1450)^-$	(	$2.4\ \pm\ 1.2$)	$\times 10^{-6}$	
Γ_{284}	$K^+\rho(1700)^-$	(	$6\ \pm\ 7$)	$\times 10^{-7}$	
Γ_{285}	$(K^+\pi^-\pi^0)$ non-resonant	(	$2.8\ \pm\ 0.6$)	$\times 10^{-6}$	
Γ_{286}	$(K\pi)_0^{*+}\pi^-,\ (K\pi)_0^{*+} \to K^+\pi^0$	(	$3.4\ \pm\ 0.5$)	$\times 10^{-5}$	
Γ_{287}	$(K\pi)_0^{*0}\pi^0,\ (K\pi)_0^{*0} \to K^+\pi^-$	(	$8.6\ \pm\ 1.7$)	$\times 10^{-6}$	
Γ_{288}	$K_2^*(1430)^0\pi^0$	<	4.0	$\times 10^{-6}$	CL=90%
Γ_{289}	$K^*(1680)^0\pi^0$	<	7.5	$\times 10^{-6}$	CL=90%
Γ_{290}	$K_x^{*0}\pi^0$	[d] (	$6.1\ \pm\ 1.6$)	$\times 10^{-6}$	
Γ_{291}	$K^0\pi^+\pi^-$	(	$4.94\pm\ 0.18$)	$\times 10^{-5}$	
Γ_{292}	$K^0\pi^+\pi^-$ non-resonant	(	$1.47^{+\ 0.40}_{-\ 0.26}$)	$\times 10^{-5}$	S=2.1
Γ_{293}	$K^0\rho^0$	(	$4.7\ \pm\ 0.6$)	$\times 10^{-6}$	
Γ_{294}	$K^*(892)^+\pi^-$	(	$8.4\ \pm\ 0.8$)	$\times 10^{-6}$	
Γ_{295}	$K_0^*(1430)^+\pi^-$	(	$3.3\ \pm\ 0.7$)	$\times 10^{-5}$	S=2.0
Γ_{296}	$K_x^{*+}\pi^-$	[d] (	$5.1\ \pm\ 1.6$)	$\times 10^{-6}$	
Γ_{297}	$K^*(1410)^+\pi^-,\ K^{*+} \to K^0\pi^+$	<	3.8	$\times 10^{-6}$	CL=90%
Γ_{298}	$f_0(980)K^0,\ f_0 \to \pi^+\pi^-$	(	$7.0\ \pm\ 0.9$)	$\times 10^{-6}$	
Γ_{299}	$f_2(1270)K^0$	(	$2.7\ ^{+\ 1.3}_{-\ 1.2}$)	$\times 10^{-6}$	
Γ_{300}	$f_x(1300)K0, f_x \to \pi^+\pi^-$	(	$1.8\ \pm\ 0.7$)	$\times 10^{-6}$	
Γ_{301}	$K^*(892)^0\pi^0$	(	$3.3\ \pm\ 0.6$)	$\times 10^{-6}$	
Γ_{302}	$K_2^*(1430)^+\pi^-$	<	6	$\times 10^{-6}$	CL=90%
Γ_{303}	$K^*(1680)^+\pi^-$	<	1.0	$\times 10^{-5}$	CL=90%
Γ_{304}	$K^+\pi^-\pi^+\pi^-$	[e] <	2.3	$\times 10^{-4}$	CL=90%
Γ_{305}	$\rho^0 K^+\pi^-$	(	$2.8\ \pm\ 0.7$)	$\times 10^{-6}$	
Γ_{306}	$f_0(980)K^+\pi^-,\ f_0 \to \pi\pi$	(	$1.4\ ^{+\ 0.5}_{-\ 0.6}$)	$\times 10^{-6}$	
Γ_{307}	$K^+\pi^-\pi^+\pi^-$ nonresonant	<	2.1	$\times 10^{-6}$	CL=90%
Γ_{308}	$K^*(892)^0\pi^+\pi^-$	(	$5.5\ \pm\ 0.5$)	$\times 10^{-5}$	
Γ_{309}	$K^*(892)^0\rho^0$	(	$3.9\ \pm\ 1.3$)	$\times 10^{-6}$	S=1.9
Γ_{310}	$K^*(892)^0 f_0(980),\ f_0 \to \pi\pi$	(	$3.9\ ^{+\ 2.1}_{-\ 1.8}$)	$\times 10^{-6}$	S=3.9
Γ_{311}	$K_1(1270)^+\pi^-$	<	3.0	$\times 10^{-5}$	CL=90%
Γ_{312}	$K_1(1400)^+\pi^-$	<	2.7	$\times 10^{-5}$	CL=90%
Γ_{313}	$a_1(1260)^- K^+$	[e] (	$1.6\ \pm\ 0.4$)	$\times 10^{-5}$	
Γ_{314}	$K^*(892)^+\rho^-$	(	$1.03\pm\ 0.26$)	$\times 10^{-5}$	
Γ_{315}	$K_0^*(1430)^+\rho^-$	(	$2.8\ \pm\ 1.2$)	$\times 10^{-5}$	
Γ_{316}	$K_1(1400)^0\rho^0$	<	3.0	$\times 10^{-3}$	CL=90%
Γ_{317}	$K_0^*(1430)^0\rho^0$	(	$2.7\ \pm\ 0.6$)	$\times 10^{-5}$	
Γ_{318}	$K_0^*(1430)^0 f_0(980),\ f_0 \to \pi\pi$	(	$2.7\ \pm\ 0.9$)	$\times 10^{-6}$	
Γ_{319}	$K_2^*(1430)^0 f_0(980),\ f_0 \to \pi\pi$	(	$8.6\ \pm\ 2.0$)	$\times 10^{-6}$	
Γ_{320}	K^+K^-	(	$7.8\ \pm\ 1.5$)	$\times 10^{-8}$	
Γ_{321}	$K^0\overline{K}^0$	(	$1.21\pm\ 0.16$)	$\times 10^{-6}$	
Γ_{322}	$K^0K^-\pi^+$	(	$6.2\ \pm\ 0.7$)	$\times 10^{-6}$	
Γ_{323}	$K^*(892)^\pm K^\mp$	<	4	$\times 10^{-7}$	CL=90%
Γ_{324}	$\overline{K}^{*0}K^0 + K^{*0}\overline{K}^0$	<	9.6	$\times 10^{-7}$	CL=90%
Γ_{325}	$K^+K^-\pi^0$	(	$2.2\ \pm\ 0.6$)	$\times 10^{-6}$	
Γ_{326}	$K_S^0 K_S^0\pi^0$	<	9	$\times 10^{-7}$	CL=90%
Γ_{327}	$K_S^0 K_S^0\eta$	<	1.0	$\times 10^{-6}$	CL=90%
Γ_{328}	$K_S^0 K_S^0\eta'$	<	2.0	$\times 10^{-6}$	CL=90%
Γ_{329}	$K^0K^+K^-$	(	$2.67\pm\ 0.11$)	$\times 10^{-5}$	
Γ_{330}	$K^0\phi$	(	$7.3\ \pm\ 0.7$)	$\times 10^{-6}$	
Γ_{331}	$f_0(980)K^0,\ f_0 \to K^+K^-$	(	$7.0\ ^{+\ 3.5}_{-\ 3.0}$)	$\times 10^{-6}$	
Γ_{332}	$f_0(1500)K^0$	(	$1.3\ ^{+\ 0.7}_{-\ 0.5}$)	$\times 10^{-5}$	
Γ_{333}	$f_2'(1525)^0 K^0$	(	$3\ ^{+\ 5}_{-\ 4}$)	$\times 10^{-7}$	
Γ_{334}	$f_0(1710)K^0,\ f_0 \to K^+K^-$	(	$4.4\ \pm\ 0.9$)	$\times 10^{-6}$	
Γ_{335}	$K^0K^+K^-$ nonresonant	(	$3.3\ \pm\ 1.0$)	$\times 10^{-5}$	
Γ_{336}	$K_S^0 K_S^0 K_S^0$	(	$6.0\ \pm\ 0.5$)	$\times 10^{-6}$	S=1.1
Γ_{337}	$f_0(980)K^0,\ f_0 \to K_S^0 K_S^0$	(	$2.7\ \pm\ 1.8$)	$\times 10^{-6}$	
Γ_{338}	$f_0(1710)K^0,\ f_0 \to K_S^0 K_S^0$	(	$5.0\ ^{+\ 5.0}_{-\ 2.6}$)	$\times 10^{-7}$	
Γ_{339}	$f_2(2010)K^0,\ f_2 \to K_S^0 K_S^0$	(	$5\ \pm\ 6$)	$\times 10^{-7}$	
Γ_{340}	$K_S^0 K_S^0 K_S^0$ nonresonant	(	$1.33\pm\ 0.31$)	$\times 10^{-5}$	
Γ_{341}	$K_S^0 K_S^0 K_L^0$	<	1.6	$\times 10^{-5}$	CL=90%
Γ_{342}	$K^*(892)^0K^+K^-$	(	$2.75\pm\ 0.26$)	$\times 10^{-5}$	
Γ_{343}	$K^*(892)^0\phi$	(	$1.00\pm\ 0.05$)	$\times 10^{-5}$	
Γ_{344}	$K^+K^-\pi^+\pi^-$ nonresonant	<	7.17	$\times 10^{-5}$	CL=90%
Γ_{345}	$K^*(892)^0K^-\pi^+$	(	$4.5\ \pm\ 1.3$)	$\times 10^{-6}$	
Γ_{346}	$K^*(892)^0\overline{K}^*(892)^0$	(	$8\ \pm\ 5$)	$\times 10^{-7}$	S=2.2
Γ_{347}	$K^+K^+\pi^-\pi^-$ nonresonant	<	6.0	$\times 10^{-6}$	CL=90%
Γ_{348}	$K^*(892)^0K^+\pi^-$	<	2.2	$\times 10^{-6}$	CL=90%
Γ_{349}	$K^*(892)^0K^*(892)^0$	<	2	$\times 10^{-7}$	CL=90%
Γ_{350}	$K^*(892)^+K^*(892)^-$	<	2.0	$\times 10^{-6}$	CL=90%
Γ_{351}	$K_1(1400)^0\phi$	<	5.0	$\times 10^{-3}$	CL=90%
Γ_{352}	$\phi(K\pi)_0^{*0}$	(	$4.3\ \pm\ 0.4$)	$\times 10^{-6}$	
Γ_{353}	$\phi(K\pi)_0^{*0}$ $(1.60<m_{K\pi}<2.15)$	[f] <	1.7	$\times 10^{-6}$	CL=90%
Γ_{354}	$K_0^*(1430)^0K^-\pi^+$	<	3.18	$\times 10^{-5}$	CL=90%
Γ_{355}	$K_0^*(1430)^0\overline{K}^*(892)^0$	<	3.3	$\times 10^{-6}$	CL=90%
Γ_{356}	$K_0^*(1430)^0\overline{K}_0^*(1430)^0$	<	8.4	$\times 10^{-6}$	CL=90%
Γ_{357}	$K_0^*(1430)^0\phi$	(	$3.9\ \pm\ 0.8$)	$\times 10^{-6}$	
Γ_{358}	$K_0^*(1430)^0K^*(892)^0$	<	1.7	$\times 10^{-6}$	CL=90%
Γ_{359}	$K_0^*(1430)^0K_0^*(1430)^0$	<	4.7	$\times 10^{-6}$	CL=90%

See key on page 885

Γ_{360}	$K^*(1680)^0\phi$	<	3.5	$\times 10^{-6}$	CL=90%	
Γ_{361}	$K^*(1780)^0\phi$	<	2.7	$\times 10^{-6}$	CL=90%	
Γ_{362}	$K^*(2045)^0\phi$	<	1.53	$\times 10^{-5}$	CL=90%	
Γ_{363}	$K_2^*(1430)^0\rho^0$	<	1.1	$\times 10^{-3}$	CL=90%	
Γ_{364}	$K_2^*(1430)^0\phi$	(	6.8 ± 0.9)	$\times 10^{-6}$	S=1.2	
Γ_{365}	$K^0\phi\phi$	(	4.5 ± 0.9)	$\times 10^{-6}$		
Γ_{366}	$\eta'\eta'K^0$	<	3.1	$\times 10^{-5}$	CL=90%	
Γ_{367}	$\eta K^0\gamma$	(	7.6 ± 1.8)	$\times 10^{-6}$		
Γ_{368}	$\eta' K^0\gamma$	<	6.4	$\times 10^{-6}$	CL=90%	
Γ_{369}	$K^0\phi\gamma$	(	2.7 ± 0.7)	$\times 10^{-6}$		
Γ_{370}	$K^+\pi^-\gamma$	(	4.6 ± 1.4)	$\times 10^{-6}$		
Γ_{371}	$K^*(892)^0\gamma$	(	4.18 ± 0.25)	$\times 10^{-5}$	S=2.1	
Γ_{372}	$K^*(1410)\gamma$	<	1.3	$\times 10^{-4}$	CL=90%	
Γ_{373}	$K^+\pi^-\gamma$ nonresonant	<	2.6	$\times 10^{-6}$	CL=90%	
Γ_{374}	$K^*(892)^0X(214)$, $X \to \mu^+\mu^-$	[g] <	2.26	$\times 10^{-8}$	CL=90%	
Γ_{375}	$K^0\pi^+\pi^-\gamma$	(	1.99 ± 0.18)	$\times 10^{-5}$		
Γ_{376}	$K^+\pi^-\pi^0\gamma$	(	4.1 ± 0.4)	$\times 10^{-5}$		
Γ_{377}	$K_1(1270)^0\gamma$	<	5.8	$\times 10^{-5}$	CL=90%	
Γ_{378}	$K_1(1400)^0\gamma$	<	1.2	$\times 10^{-5}$	CL=90%	
Γ_{379}	$K_2^*(1430)^0\gamma$	(	1.24 ± 0.24)	$\times 10^{-5}$		
Γ_{380}	$K^*(1680)^0\gamma$	<	2.0	$\times 10^{-3}$	CL=90%	
Γ_{381}	$K_3^*(1780)^0\gamma$	<	8.3	$\times 10^{-5}$	CL=90%	
Γ_{382}	$K_4^*(2045)^0\gamma$	<	4.3	$\times 10^{-3}$	CL=90%	

Light unflavored meson modes

Γ_{383}	$\rho^0\gamma$	(	8.6 ± 1.5)	$\times 10^{-7}$		
Γ_{384}	$\rho^0X(214)$, $X \to \mu^+\mu^-$	[g] <	1.73	$\times 10^{-8}$	CL=90%	
Γ_{385}	$\omega\gamma$	(	$4.4\ ^{+\ 1.8}_{-\ 1.6}$)	$\times 10^{-7}$		
Γ_{386}	$\phi\gamma$	<	1.0	$\times 10^{-7}$	CL=90%	
Γ_{387}	$\pi^+\pi^-$	(	5.12 ± 0.19)	$\times 10^{-6}$		
Γ_{388}	$\pi^0\pi^0$	(	1.59 ± 0.26)	$\times 10^{-6}$	S=1.4	
Γ_{389}	$\eta\pi^0$	(	4.1 ± 1.7)	$\times 10^{-7}$		
Γ_{390}	$\eta\eta$	<	1.0	$\times 10^{-6}$	CL=90%	
Γ_{391}	$\eta'\pi^0$	(	1.2 ± 0.6)	$\times 10^{-6}$	S=1.7	
Γ_{392}	$\eta'\eta'$	<	1.7	$\times 10^{-6}$	CL=90%	
Γ_{393}	$\eta'\eta$	<	1.2	$\times 10^{-6}$	CL=90%	
Γ_{394}	$\eta'\rho^0$	<	1.3	$\times 10^{-6}$	CL=90%	
Γ_{395}	$\eta' f_0(980)$, $f_0 \to \pi^+\pi^-$	<	9	$\times 10^{-7}$	CL=90%	
Γ_{396}	$\eta\rho^0$	<	1.5	$\times 10^{-6}$	CL=90%	
Γ_{397}	$\eta f_0(980)$, $f_0 \to \pi^+\pi^-$	<	4	$\times 10^{-7}$	CL=90%	
Γ_{398}	$\omega\eta$	(	$9.4\ ^{+\ 4.0}_{-\ 3.1}$)	$\times 10^{-7}$		
Γ_{399}	$\omega\eta'$	(	$1.0\ ^{+\ 0.5}_{-\ 0.4}$)	$\times 10^{-6}$		
Γ_{400}	$\omega\rho^0$	<	1.6	$\times 10^{-6}$	CL=90%	
Γ_{401}	$\omega f_0(980)$, $f_0 \to \pi^+\pi^-$	<	1.5	$\times 10^{-6}$	CL=90%	
Γ_{402}	$\omega\omega$	(	1.2 ± 0.4)	$\times 10^{-6}$		
Γ_{403}	$\phi\pi^0$	<	1.5	$\times 10^{-7}$	CL=90%	
Γ_{404}	$\phi\eta$	<	5	$\times 10^{-7}$	CL=90%	
Γ_{405}	$\phi\eta'$	<	5	$\times 10^{-7}$	CL=90%	
Γ_{406}	$\phi\pi^+\pi^-$	(	1.8 ± 0.5)	$\times 10^{-7}$		
Γ_{407}	$\phi\rho^0$	<	3.3	$\times 10^{-7}$	CL=90%	
Γ_{408}	$\phi f_0(980)$, $f_0 \to \pi^+\pi^-$	<	3.8	$\times 10^{-7}$	CL=90%	
Γ_{409}	$\phi\omega$	<	7	$\times 10^{-7}$	CL=90%	
Γ_{410}	$\phi\phi$	<	2.8	$\times 10^{-8}$	CL=90%	
Γ_{411}	$a_0(980)^\pm\pi^\mp$, $a_0^\pm \to \eta\pi^\pm$	<	3.1	$\times 10^{-6}$	CL=90%	
Γ_{412}	$a_0(1450)^\pm\pi^\mp$, $a_0^\pm \to \eta\pi^\pm$	<	2.3	$\times 10^{-6}$	CL=90%	
Γ_{413}	$\pi^+\pi^-\pi^0$	<	7.2	$\times 10^{-4}$	CL=90%	
Γ_{414}	$\rho^0\pi^0$	(	2.0 ± 0.5)	$\times 10^{-6}$		
Γ_{415}	$\rho^\mp\pi^\pm$	[h] (	2.30 ± 0.23)	$\times 10^{-5}$		
Γ_{416}	$\pi^+\pi^-\pi^+\pi^-$	<	1.12	$\times 10^{-5}$	CL=90%	
Γ_{417}	$\rho^0\pi^+\pi^-$	<	8.8	$\times 10^{-6}$	CL=90%	
Γ_{418}	$\rho^0\rho^0$	(	9.6 ± 1.5)	$\times 10^{-7}$		
Γ_{419}	$f_0(980)\pi^+\pi^-$, $f_0 \to \pi^+\pi^-$	<	3.0	$\times 10^{-6}$	CL=90%	
Γ_{420}	$\rho^0 f_0(980)$, $f_0 \to \pi^+\pi^-$	(	7.8 ± 2.5)	$\times 10^{-7}$		
Γ_{421}	$f_0(980) f_0(980)$, $f_0 \to \pi^+\pi^-$, $f_0 \to \pi^+\pi^-$	<	1.9	$\times 10^{-7}$	CL=90%	
Γ_{422}	$f_0(980) f_0(980)$, $f_0 \to \pi^+\pi^-$, $f_0 \to K^+K^-$	<	2.3	$\times 10^{-7}$	CL=90%	
Γ_{423}	$a_1(1260)^\mp\pi^\pm$	[h] (	2.6 ± 0.5)	$\times 10^{-5}$	S=1.9	
Γ_{424}	$a_2(1320)^\mp\pi^\pm$	[h] <	6.3	$\times 10^{-6}$	CL=90%	
Γ_{425}	$\pi^+\pi^-\pi^0\pi^0$	<	3.1	$\times 10^{-3}$	CL=90%	
Γ_{426}	$\rho^+\rho^-$	(	2.77 ± 0.19)	$\times 10^{-5}$		
Γ_{427}	$a_1(1260)^0\pi^0$	<	1.1	$\times 10^{-3}$	CL=90%	
Γ_{428}	$\omega\pi^0$	<	5	$\times 10^{-7}$	CL=90%	
Γ_{429}	$\pi^+\pi^+\pi^-\pi^-\pi^0$	<	9.0	$\times 10^{-3}$	CL=90%	
Γ_{430}	$a_1(1260)^+\rho^-$	<	6.1	$\times 10^{-5}$	CL=90%	
Γ_{431}	$a_1(1260)^0\rho^0$	<	2.4	$\times 10^{-3}$	CL=90%	
Γ_{432}	$b_1^\mp\pi^\pm$, $b_1^\mp \to \omega\pi^\mp$	(	1.09 ± 0.15)	$\times 10^{-5}$		
Γ_{433}	$b_1^0\pi^0$, $b_1^0 \to \omega\pi^0$	<	1.9	$\times 10^{-6}$	CL=90%	
Γ_{434}	$b_1^-\rho^+$, $b_1^- \to \omega\pi^-$	<	1.4	$\times 10^{-6}$	CL=90%	
Γ_{435}	$b_1^0\rho^0$, $b_1^0 \to \omega\pi^0$	<	3.4	$\times 10^{-6}$	CL=90%	
Γ_{436}	$\pi^+\pi^+\pi^+\pi^-\pi^-\pi^-$	<	3.0	$\times 10^{-3}$	CL=90%	
Γ_{437}	$a_1(1260)^+a_1(1260)^-$, $a_1^+ \to 2\pi^+\pi^-$, $a_1^- \to 2\pi^-\pi^+$	(	1.18 ± 0.31)	$\times 10^{-5}$		
Γ_{438}	$\pi^+\pi^+\pi^+\pi^-\pi^-\pi^-\pi^0$	<	1.1	%	CL=90%	

Baryon modes

Γ_{439}	$p\overline{p}$	(	1.25 ± 0.32)	$\times 10^{-8}$		
Γ_{440}	$p\overline{p}\pi^+\pi^-$	(	2.87 ± 0.19)	$\times 10^{-6}$		
Γ_{441}	$p\overline{p}K^+\pi^-$	(	6.3 ± 0.5)	$\times 10^{-6}$		
Γ_{442}	$p\overline{p}K^0$	(	2.66 ± 0.32)	$\times 10^{-6}$		
Γ_{443}	$\Theta(1540)^+\overline{p}$, $\Theta^+ \to pK_S^0$	[i] <	5	$\times 10^{-8}$	CL=90%	
Γ_{444}	$f_J(2220)K^0$, $f_J \to p\overline{p}$	<	4.5	$\times 10^{-7}$	CL=90%	
Γ_{445}	$p\overline{p}K^*(892)^0$	(	$1.24^{+\ 0.28}_{-\ 0.25}$)	$\times 10^{-6}$		
Γ_{446}	$f_J(2220)K_0^*$, $f_J \to p\overline{p}$	<	1.5	$\times 10^{-7}$	CL=90%	
Γ_{447}	$p\overline{p}K^+K^-$	(	1.21 ± 0.32)	$\times 10^{-7}$		
Γ_{448}	$p\overline{\Lambda}\pi^-$	(	3.14 ± 0.29)	$\times 10^{-6}$		
Γ_{449}	$p\overline{\Lambda}\pi^-\gamma$	<	6.5	$\times 10^{-7}$	CL=90%	
Γ_{450}	$p\overline{\Sigma}(1385)^-$	<	2.6	$\times 10^{-7}$	CL=90%	
Γ_{451}	$\Delta^0\overline{\Lambda}$	<	9.3	$\times 10^{-7}$	CL=90%	
Γ_{452}	$p\overline{\Lambda}K^-$	<	8.2	$\times 10^{-7}$	CL=90%	
Γ_{453}	$p\overline{\Lambda}D^-$	(	2.5 ± 0.4)	$\times 10^{-5}$		
Γ_{454}	$p\overline{\Lambda}D^{*-}$	(	3.4 ± 0.8)	$\times 10^{-5}$		
Γ_{455}	$p\overline{\Sigma}^0\pi^-$	<	3.8	$\times 10^{-6}$	CL=90%	
Γ_{456}	$\overline{\Lambda}\Lambda$	<	3.2	$\times 10^{-7}$	CL=90%	
Γ_{457}	$\overline{\Lambda}\Lambda K^0$	(	$4.8\ ^{+\ 1.0}_{-\ 0.9}$)	$\times 10^{-6}$		
Γ_{458}	$\overline{\Lambda}\Lambda K^{*0}$	(	$2.5\ ^{+\ 0.9}_{-\ 0.8}$)	$\times 10^{-6}$		
Γ_{459}	$\overline{\Lambda}\Lambda D^0$	(	$1.00^{+\ 0.30}_{-\ 0.26}$)	$\times 10^{-5}$		
Γ_{460}	$D^0\Sigma^0\overline{\Lambda}$ + c.c.	<	3.1	$\times 10^{-5}$	CL=90%	
Γ_{461}	$\Delta^0\overline{\Delta}^0$	<	1.5	$\times 10^{-3}$	CL=90%	
Γ_{462}	$\Delta^{++}\overline{\Delta}^{--}$	<	1.1	$\times 10^{-4}$	CL=90%	
Γ_{463}	$\overline{D}^0 p\overline{p}$	(	1.04 ± 0.07)	$\times 10^{-4}$		
Γ_{464}	$D_s^-\overline{\Lambda}p$	(	2.8 ± 0.9)	$\times 10^{-5}$		
Γ_{465}	$\overline{D}^*(2007)^0 p\overline{p}$	(	9.9 ± 1.1)	$\times 10^{-5}$		
Γ_{466}	$D^*(2010)^- p\overline{n}$	(	1.4 ± 0.4)	$\times 10^{-3}$		
Γ_{467}	$D^- p\overline{p}\pi^+$	(	3.32 ± 0.31)	$\times 10^{-4}$		
Γ_{468}	$D^*(2010)^- p\overline{p}\pi^+$	(	4.7 ± 0.5)	$\times 10^{-4}$	S=1.2	
Γ_{469}	$\overline{D}^0 p\overline{p}\pi^+\pi^-$	(	3.0 ± 0.5)	$\times 10^{-4}$		
Γ_{470}	$\overline{D}^{*0} p\overline{p}\pi^+\pi^-$	(	1.9 ± 0.5)	$\times 10^{-4}$		
Γ_{471}	$\Theta_c\overline{p}\pi^+$, $\Theta_c \to D^- p$	<	9	$\times 10^{-6}$	CL=90%	
Γ_{472}	$\Theta_c\overline{p}\pi^+$, $\Theta_c \to D^{*-} p$	<	1.4	$\times 10^{-5}$	CL=90%	
Γ_{473}	$\overline{\Sigma}_c^{--}\Delta^{++}$	<	8	$\times 10^{-4}$	CL=90%	
Γ_{474}	$\overline{\Lambda}_c^- p\pi^+\pi^-$	(	1.03 ± 0.14)	$\times 10^{-3}$	S=1.3	
Γ_{475}	$\overline{\Lambda}_c^- p$	(	1.55 ± 0.18)	$\times 10^{-5}$		
Γ_{476}	$\overline{\Lambda}_c^- p\pi^0$	(	1.56 ± 0.19)	$\times 10^{-4}$		
Γ_{477}	$\overline{\Sigma}_c(2455)^- p$	<	2.4	$\times 10^{-5}$		
Γ_{478}	$\overline{\Lambda}_c^- p\pi^+\pi^-\pi^0$	<	5.07	$\times 10^{-3}$	CL=90%	
Γ_{479}	$\overline{\Lambda}_c^- p\pi^+\pi^-\pi^+\pi^-$	<	2.74	$\times 10^{-3}$	CL=90%	
Γ_{480}	$\overline{\Lambda}_c^- p\pi^+\pi^-$ (nonresonant)	(	5.5 ± 1.0)	$\times 10^{-4}$	S=1.3	
Γ_{481}	$\overline{\Sigma}_c(2520)^{--} p\pi^+$	(	1.03 ± 0.18)	$\times 10^{-4}$		
Γ_{482}	$\overline{\Sigma}_c(2520)^0 p\pi^-$	<	3.1	$\times 10^{-5}$	CL=90%	
Γ_{483}	$\overline{\Sigma}_c(2455)^0 p\pi^-$	(	1.08 ± 0.16)	$\times 10^{-4}$		
Γ_{484}	$\overline{\Sigma}_c(2455)^0 N^0$, $N^0 \to p\pi^-$	(	6.4 ± 1.7)	$\times 10^{-5}$		
Γ_{485}	$\overline{\Sigma}_c(2455)^{--} p\pi^+$	(	1.85 ± 0.24)	$\times 10^{-4}$		
Γ_{486}	$\Lambda_c^- pK^+\pi^-$	(	3.5 ± 0.7)	$\times 10^{-5}$		
Γ_{487}	$\overline{\Sigma}_c(2455)^{--} pK^+$, $\overline{\Sigma}_c^{--} \to \overline{\Lambda}_c^-\pi^-$	(	8.9 ± 2.6)	$\times 10^{-6}$		
Γ_{488}	$\Lambda_c^- pK^*(892)^0$	<	2.42	$\times 10^{-5}$	CL=90%	
Γ_{489}	$\Lambda_c^- pK^+K^-$	(	2.0 ± 0.4)	$\times 10^{-5}$		
Γ_{490}	$\Lambda_c^- p\phi$	<	1.0	$\times 10^{-5}$	CL=90%	
Γ_{491}	$\Lambda_c^- p\overline{p}p$	<	2.8	$\times 10^{-6}$		
Γ_{492}	$\overline{\Lambda}_c^- \Lambda K^+$	(	4.7 ± 1.1)	$\times 10^{-5}$		
Γ_{493}	$\overline{\Lambda}_c^- \Lambda_c^+$	<	1.6	$\times 10^{-5}$	CL=95%	

Meson Particle Listings

B^0

Γ_{494}	$\overline{\Lambda}_c(2593)^- / \overline{\Lambda}_c(2625)^- p$		<	1.1	$\times 10^{-4}$	CL=90%
Γ_{495}	$\overline{\Xi}_c^- \Lambda_c^+$, $\overline{\Xi}_c^- \to \overline{\Xi}^+ \pi^- \pi^-$		(	1.8 ± 1.8)	$\times 10^{-5}$	S=2.2
Γ_{496}	$\Lambda_c^+ \Lambda_c^- K^0$		(	4.3 ± 2.3)	$\times 10^{-4}$	

Lepton Family number (LF) or Lepton number (L) or Baryon number (B) violating modes, or/and $\Delta B = 1$ weak neutral current ($B1$) modes

Γ_{497}	$\gamma\gamma$	$B1$	<	3.2	$\times 10^{-7}$	CL=90%
Γ_{498}	$e^+ e^-$	$B1$	<	8.3	$\times 10^{-8}$	CL=90%
Γ_{499}	$e^+ e^- \gamma$	$B1$	<	1.2	$\times 10^{-7}$	CL=90%
Γ_{500}	$\mu^+ \mu^-$	$B1$	(	$1.6 \pm {}^{1.6}_{1.4}$)	$\times 10^{-10}$	S=1.9
Γ_{501}	$\mu^+ \mu^- \gamma$	$B1$	<	1.6	$\times 10^{-7}$	CL=90%
Γ_{502}	$\mu^+ \mu^- \mu^+ \mu^-$	$B1$	<	6.9	$\times 10^{-10}$	CL=95%
Γ_{503}	SP, $S \to \mu^+ \mu^-$, $P \to \mu^+ \mu^-$	$B1$	[j] <	6.0	$\times 10^{-10}$	CL=95%
Γ_{504}	$\tau^+ \tau^-$	$B1$	<	2.1	$\times 10^{-3}$	CL=95%
Γ_{505}	$\pi^0 \ell^+ \ell^-$	$B1$	<	5.3	$\times 10^{-8}$	CL=90%
Γ_{506}	$\pi^0 e^+ e^-$	$B1$	<	8.4	$\times 10^{-8}$	CL=90%
Γ_{507}	$\pi^0 \mu^+ \mu^-$	$B1$	<	6.9	$\times 10^{-8}$	CL=90%
Γ_{508}	$\eta \ell^+ \ell^-$	$B1$	<	6.4	$\times 10^{-8}$	CL=90%
Γ_{509}	$\eta e^+ e^-$	$B1$	<	1.08	$\times 10^{-7}$	CL=90%
Γ_{510}	$\eta \mu^+ \mu^-$	$B1$	<	1.12	$\times 10^{-7}$	CL=90%
Γ_{511}	$\pi^0 \nu \overline{\nu}$	$B1$	<	9	$\times 10^{-6}$	CL=90%
Γ_{512}	$K^0 \ell^+ \ell^-$	$B1$	[a]	$3.1 \pm {}^{0.8}_{0.7}$	$\times 10^{-7}$	
Γ_{513}	$K^0 e^+ e^-$	$B1$		$1.6 \pm {}^{1.0}_{0.8}$	$\times 10^{-7}$	
Γ_{514}	$K^0 \mu^+ \mu^-$	$B1$		3.39 ± 0.34	$\times 10^{-7}$	
Γ_{515}	$K^0 \nu \overline{\nu}$	$B1$	<	2.6	$\times 10^{-5}$	CL=90%
Γ_{516}	$\rho^0 \nu \overline{\nu}$	$B1$	<	4.0	$\times 10^{-5}$	CL=90%
Γ_{517}	$K^*(892)^0 \ell^+ \ell^-$	$B1$	[a]	$9.9 \pm {}^{1.2}_{1.1}$	$\times 10^{-7}$	
Γ_{518}	$K^*(892)^0 e^+ e^-$	$B1$		$1.03 \pm {}^{0.19}_{0.17}$	$\times 10^{-6}$	
Γ_{519}	$K^*(892)^0 \mu^+ \mu^-$	$B1$		9.4 ± 0.5	$\times 10^{-7}$	
Γ_{520}	$K^*(892)^0 \chi$, $\chi \to \mu^+ \mu^-$	$B1$				
Γ_{521}	$\pi^+ \pi^- \mu^+ \mu^-$	$B1$		2.1 ± 0.5	$\times 10^{-8}$	
Γ_{522}	$K^*(892)^0 \nu \overline{\nu}$	$B1$	<	1.8	$\times 10^{-5}$	CL=90%
Γ_{523}	invisible	$B1$	<	2.4	$\times 10^{-5}$	CL=90%
Γ_{524}	$\nu \overline{\nu} \gamma$	$B1$	<	1.7	$\times 10^{-5}$	CL=90%
Γ_{525}	$\phi \nu \overline{\nu}$	$B1$	<	1.27	$\times 10^{-4}$	CL=90%
Γ_{526}	$e^\pm \mu^\mp$	LF	[h] <	2.8	$\times 10^{-9}$	CL=90%
Γ_{527}	$\pi^0 e^\pm \mu^\mp$	LF	<	1.4	$\times 10^{-7}$	CL=90%
Γ_{528}	$K^0 e^\pm \mu^\mp$	LF	<	2.7	$\times 10^{-7}$	CL=90%
Γ_{529}	$K^*(892)^0 e^+ \mu^-$	LF	<	5.3	$\times 10^{-7}$	CL=90%
Γ_{530}	$K^*(892)^0 e^- \mu^+$	LF	<	3.4	$\times 10^{-7}$	CL=90%
Γ_{531}	$K^*(892)^0 e^\pm \mu^\mp$	LF	<	5.8	$\times 10^{-7}$	CL=90%
Γ_{532}	$e^\pm \tau^\mp$	LF	[h] <	2.8	$\times 10^{-5}$	CL=90%
Γ_{533}	$\mu^\pm \tau^\mp$	LF	[h] <	2.2	$\times 10^{-5}$	CL=90%
Γ_{534}	$\Lambda_c^+ \mu^-$	L,B	<	1.4	$\times 10^{-6}$	CL=90%
Γ_{535}	$\Lambda_c^+ e^-$	L,B	<	4	$\times 10^{-6}$	CL=90%

[a] An ℓ indicates an e or a μ mode, not a sum over these modes.

[b] $\overline{D}^{**}$ represents an excited state with mass $2.2 < M < 2.8$ GeV/c^2.

[c] $\chi_{c1}(3872)^+$ is a hypothetical charged partner of the $\chi_{c1}(3872)$.

[d] Stands for the possible candidates of $K^*(1410)$, $K_0^*(1430)$ and $K_2^*(1430)$.

[e] B^0 and B_s^0 contributions not separated. Limit is on weighted average of the two decay rates.

[f] This decay refers to the coherent sum of resonant and nonresonant $J^P = 0^+$ $K\pi$ components with $1.60 < m_{K\pi} < 2.15$ GeV/c^2.

[g] $X(214)$ is a hypothetical particle of mass 214 MeV/c^2 reported by the HyperCP experiment, Physical Review Letters **94** 021801 (2005)

[h] The value is for the sum of the charge states or particle/antiparticle states indicated.

[i] $\Theta(1540)^+$ denotes a possible narrow pentaquark state.

[j] Here S and P are the hypothetical scalar and pseudoscalar particles with masses of 2.5 GeV/c^2 and 214.3 MeV/c^2, respectively.

CONSTRAINED FIT INFORMATION

An overall fit to 34 branching ratios uses 85 measurements and one constraint to determine 22 parameters. The overall fit has a $\chi^2 = 63.6$ for 64 degrees of freedom.

The following *off-diagonal* array elements are the correlation coefficients $\langle \delta x_i \delta x_j \rangle / (\delta x_i \cdot \delta x_j)$, in percent, from the fit to the branching fractions, $x_i \equiv \Gamma_i / \Gamma_{\rm total}$. The fit constrains the x_i whose labels appear in this array to sum to one.

	x_6	x_7	x_{34}	x_{46}	x_{72}	x_{123}	x_{183}	x_{185}	x_{236}	x_{241}
x_7	56									
x_{34}	0	0								
x_{46}	0	0	43							
x_{72}	0	0	6	13						
x_{123}	0	0	10	4	1					
x_{183}	0	0	0	0	0	0				
x_{185}	0	0	0	0	0	0	0			
x_{236}	0	0	0	0	0	0	0	0		
x_{241}	0	0	0	0	0	0	0	0	19	
x_{247}	0	0	0	0	0	0	0	29	0	0
x_{253}	0	0	0	0	0	0	0	6	0	0
x_{257}	0	0	0	0	0	0	0	0	0	0
x_{291}	0	0	0	0	0	0	0	0	0	0
x_{322}	0	0	0	0	0	0	0	0	0	0
x_{329}	0	0	0	0	0	0	0	0	0	0
x_{343}	0	0	0	0	0	0	0	0	0	0
x_{387}	0	0	0	0	0	0	0	0	0	0
x_{418}	0	0	0	0	0	0	0	0	0	0
x_{514}	0	0	0	0	0	0	4	0	0	0
x_{519}	0	0	0	0	0	0	0	15	0	0

	x_{247}	x_{253}	x_{257}	x_{291}	x_{322}	x_{329}	x_{343}	x_{387}	x_{418}	x_{514}
x_{253}	22									
x_{257}	0	0								
x_{291}	0	0	0							
x_{322}	0	0	0	21						
x_{329}	0	0	0	28	6					
x_{343}	0	0	0	0	0	0				
x_{387}	0	0	27	0	0	0	0			
x_{418}	0	0	0	0	0	0	20	0		
x_{514}	0	0	0	0	0	0	0	0	0	
x_{519}	4	1	0	0	0	0	0	0	0	0

B^0 BRANCHING RATIOS

For branching ratios in which the charge of the decaying B is not determined, see the $B^\pm$ section.

$\Gamma(\ell^+ \nu_\ell \text{anything})/\Gamma_{\rm total}$ Γ_1/Γ

"OUR EVALUATION" is an average using rescaled values of the data listed below. The average and rescaling were performed by the Heavy Flavor Averaging Group (HFLAV) and are described at http://www.slac.stanford.edu/xorg/hflav/. The averaging/rescaling procedure takes into account correlations between the measurements.

VALUE (units 10^{-2})	DOCUMENT ID		TECN	COMMENT
10.33±0.28 OUR EVALUATION				
10.14±0.30 OUR AVERAGE	Error includes scale factor of 1.1.			
10.46±0.30±0.23	[1] URQUIJO	07	BELL	$e^+e^- \to \Upsilon(4S)$
9.64±0.27±0.33	[2] AUBERT,B	06Y	BABR	$e^+e^- \to \Upsilon(4S)$
10.78±0.60±0.69	[3] ARTUSO	97	CLE2	$e^+e^- \to \Upsilon(4S)$
9.3 ±1.1 ±1.5	ALBRECHT	94	ARG	$e^+e^- \to \Upsilon(4S)$
9.9 ±3.0 ±0.9	HENDERSON	92	CLEO	$e^+e^- \to \Upsilon(4S)$
• • • We do not use the following data for averages, fits, limits, etc. • • •				
10.32±0.36±0.35	[4] OKABE	05	BELL	Repl. by URQUIJO 07
10.9 ±0.7 ±1.1	ATHANAS	94	CLE2	Sup. by ARTUSO 97

[1] URQUIJO 07 report a measurement of (9.80 ± 0.29 ± 0.21)% for the partial branching fraction of $B \to e\nu_e X_c$ decay with electron energy above 0.6 GeV. We converted the result to $B \to e\nu_e X$ branching fraction.

[2] The measurements are obtained for charged and neutral B mesons partial rates of semileptonic decay to electrons with momentum above 0.6 GeV/c in the B rest frame. The best precision on the ratio is achieved for a momentum threshold of 1.0 GeV: $B(B^+ \to e^+\nu_e X) / B(B^0 \to e^+\nu_e X) = 1.074 \pm 0.041 \pm 0.026$.

[3] ARTUSO 97 uses partial reconstruction of $B \to D^* \ell \nu_\ell$ and inclusive semileptonic branching ratio from BARISH 96B (0.1049 ± 0.0017 ± 0.0043).

[4] The measurements are obtained for charged and neutral B mesons partial rates of semileptonic decay to electrons with momentum above 0.6 GeV/c in the B rest frame, and their ratio of $B(B^+ \to e^+\nu_e X)/B(B^0 \to e^+\nu_e X) = 1.08 \pm 0.05 \pm 0.02$.

$\Gamma(e^+ \nu_e X_c)/\Gamma_{\rm total}$ Γ_2/Γ

VALUE (units 10^{-2})	DOCUMENT ID		TECN	COMMENT
10.08±0.30±0.22	[1] URQUIJO	07	BELL	$e^+e^- \to \Upsilon(4S)$

[1] Measure the independent B^+ and B^0 partial branching fractions with electron threshold energies of 0.4 GeV.

$\Gamma(D^-\ell^+\nu_\ell)/\Gamma_{\rm total}$ Γ_4/Γ

ℓ denotes e or μ, not the sum.

"OUR EVALUATION" is an average using rescaled values of the data listed below. The average and rescaling were performed by the Heavy Flavor Averaging Group (HFLAV) and are described at http://www.slac.stanford.edu/xorg/hflav/. The averaging/rescaling procedure takes into account correlations between the measurements.

VALUE (%)	DOCUMENT ID		TECN	COMMENT
2.20±0.10 OUR EVALUATION				
2.25±0.08 OUR AVERAGE				
2.31±0.03±0.11	[1] GLATTAUER	16	BELL	$e^+e^-\to\Upsilon(4S)$
2.21±0.11±0.11	[2] AUBERT	10	BABR	$e^+e^-\to\Upsilon(4S)$
2.09±0.13±0.18	[3] BARTELT	99	CLE2	$e^+e^-\to\Upsilon(4S)$
2.35±0.20±0.44	[4] BUSKULIC	97	ALEP	$e^+e^-\to Z$
• • • We do not use the following data for averages, fits, limits, etc. • • •				
2.21±0.11±0.12	[2] AUBERT	08Q	BABR	Repl. by AUBERT 10
2.13±0.12±0.39	ABE	02E	BELL	Repl. by GLATTAUER 16
1.87±0.15±0.32	[5] ATHANAS	97	CLE2	Repl. by BARTELT 99
1.8 ±0.6 ±0.3	[6] FULTON	91	CLEO	$e^+e^-\to\Upsilon(4S)$
2.0 ±0.7 ±0.6	[7] ALBRECHT	89J	ARG	$e^+e^-\to\Upsilon(4S)$

[1] Uses a fully reconstructed B meson as a tag on the recoil side while the other, on the signal side, is partially reconstructed from $B\to D\ell\nu$.
[2] Uses a fully reconstructed B meson as a tag on the recoil side.
[3] Assumes equal production of B^+ and B^0 at the $\Upsilon(4S)$.
[4] BUSKULIC 97 assumes fraction (B^+) = fraction (B^0) = (37.8 ± 2.2)% and PDG 96 values for B lifetime and branching ratio of D^* and D decays.
[5] ATHANAS 97 uses missing energy and missing momentum to reconstruct neutrino.
[6] FULTON 91 assumes assuming equal production of B^0 and B^+ at the $\Upsilon(4S)$ and uses Mark III D and D^* branching ratios.
[7] ALBRECHT 89J reports 0.018 ± 0.006 ± 0.005. We rescale using the method described in STONE 94 but with the updated PDG 94 B($D^0\to K^-\pi^+$).

$\Gamma(D^-\ell^+\nu_\ell)/\Gamma(\ell^+\nu_\ell\,\text{anything})$ Γ_4/Γ_1

VALUE	DOCUMENT ID		TECN	COMMENT
0.230±0.011±0.011	[1] AUBERT	10	BABR	$e^+e^-\to\Upsilon(4S)$

[1] Uses a fully reconstructed B meson on the recoil side.

$\Gamma(D^-\ell^+\nu_\ell)/\Gamma(D\ell^+\nu_\ell\,\text{anything})$ Γ_4/Γ_3

VALUE	DOCUMENT ID		TECN	COMMENT
0.215±0.016±0.013	[1] AUBERT	07AN	BABR	$e^+e^-\to\Upsilon(4S)$

[1] Uses a fully reconstructed B meson on the recoil side.

$\Gamma(D^-\tau^+\nu_\tau)/\Gamma_{\rm total}$ Γ_5/Γ

VALUE (units 10^{-2})	DOCUMENT ID		TECN	COMMENT
• • • We do not use the following data for averages, fits, limits, etc. • • •				
1.04±0.35±0.18	[1] AUBERT	08N	BABR	Repl. by AUBERT 09S

[1] Uses a fully reconstructed B meson as a tag on the recoil side.

$\Gamma(D^-\tau^+\nu_\tau)/\Gamma(D^-\ell^+\nu_\ell)$ Γ_5/Γ_4

VALUE	DOCUMENT ID		TECN	COMMENT
0.469±0.084±0.053	[1,2] LEES	12D	BABR	$e^+e^-\to\Upsilon(4S)$
• • • We do not use the following data for averages, fits, limits, etc. • • •				
0.489±0.165±0.069	[1] AUBERT	09S	BABR	Repl. by LEES 12D

[1] Uses a fully reconstructed B meson as a tag on the recoil side.
[2] Uses $\tau^+\to e^+\nu_e\overline{\nu}_\tau$ and $\tau^+\to\mu^+\nu_\mu\overline{\nu}_\tau$ and e^+ or μ^+ as ℓ^+.

$\Gamma(D^*(2010)^-\ell^+\nu_\ell)/\Gamma_{\rm total}$ Γ_6/Γ

"OUR EVALUATION" is an average using rescaled values of the data listed below. The average and rescaling were performed by the Heavy Flavor Averaging Group (HFLAV) and are described at http://www.slac.stanford.edu/xorg/hflav/. The averaging/rescaling procedure takes into account correlations between the measurements.

VALUE (%)	EVTS	DOCUMENT ID		TECN	COMMENT
4.88±0.10 OUR EVALUATION		This value assumes isospin symmetry.			
5.10±0.23 OUR FIT		Error includes scale factor of 1.6.			
5.09±0.22 OUR AVERAGE		Error includes scale factor of 1.6. See the ideogram below.			
4.58±0.03±0.26		[1] DUNGEL	10	BELL	$e^+e^-\to\Upsilon(4S)$
5.49±0.16±0.25		[2] AUBERT	08Q	BABR	$e^+e^-\to\Upsilon(4S)$
4.69±0.04±0.34		[3] AUBERT	08R	BABR	$e^+e^-\to\Upsilon(4S)$
5.90±0.22±0.50		[4] ABDALLAH	04D	DLPH	$e^+e^-\to Z^0$
6.09±0.19±0.40		[5] ADAM	03	CLE2	$e^+e^-\to\Upsilon(4S)$
$4.70\pm0.13^{+0.36}_{-0.31}$		[6] ABREU	01H	DLPH	$e^+e^-\to Z$
5.26±0.20±0.46		[7] ABBIENDI	00Q	OPAL	$e^+e^-\to Z$
5.53±0.26±0.52		[8] BUSKULIC	97	ALEP	$e^+e^-\to Z$
• • • We do not use the following data for averages, fits, limits, etc. • • •					
$4.90\pm0.07^{+0.36}_{-0.35}$		[4] AUBERT	05E	BABR	Repl. by AUBERT 08R
5.39±0.11±0.34		[9] ABDALLAH	04D	DLPH	$e^+e^-\to Z^0$
4.59±0.23±0.40		[10] ABE	02F	BELL	Repl. by DUNGEL 10
6.09±0.19±0.40		[11] BRIERE	02	CLE2	$e^+e^-\to\Upsilon(4S)$
5.08±0.21±0.66		[12] ACKERSTAFF	97G	OPAL	Repl. by ABBIENDI 00Q
5.52±0.17±0.68		[13] ABREU	96P	DLPH	Repl. by ABREU 01H
4.49±0.32±0.39	376	[14] BARISH	95	CLE2	Repl. by ADAM 03
5.18±0.30±0.62	410	[15] BUSKULIC	95N	ALEP	Sup. by BUSKULIC 97
4.5 ±0.3 ±0.4		[16] ALBRECHT	94	ARG	$e^+e^-\to\Upsilon(4S)$
4.7 ±0.5 ±0.5	235	[17] ALBRECHT	93	ARG	$e^+e^-\to\Upsilon(4S)$
seen	398	[18] SANGHERA	93	CLE2	$e^+e^-\to\Upsilon(4S)$
7.0 ±1.8 ±1.4		[19] ANTREASYAN	90B	CBAL	$e^+e^-\to\Upsilon(4S)$
		[20] ALBRECHT	89C	ARG	$e^+e^-\to\Upsilon(4S)$
6.0 ±1.0 ±1.4		[21] ALBRECHT	89J	ARG	$e^+e^-\to\Upsilon(4S)$
4.0 ±0.4 ±0.6		[22] BORTOLETTO	89B	CLEO	$e^+e^-\to\Upsilon(4S)$
7.0 ±1.2 ±1.9	47	[23] ALBRECHT	87J	ARG	$e^+e^-\to\Upsilon(4S)$

[1] Uses fully reconstructed $D^{*-}\ell^+\nu$ events (ℓ = e or μ).
[2] Uses a fully reconstructed B meson as a tag on the recoil side.
[3] Measured using fully reconstructed D^* sample and a simultaneous fit to the Caprini-Lellouch-Neubert form factor parameters: $\rho^2 = 1.191\pm0.048\pm0.028$, $R_1(1) = 1.429\pm0.061\pm0.044$, and $R_2(1) = 0.827\pm0.038\pm0.022$.
[4] Measured using fully reconstructed D^* sample.
[5] Uses the combined fit of both $B^0\to D^*(2010)^-\ell\nu$ and $B^+\to\overline{D}(2007)^0\ell\nu$ samples.
[6] ABREU 01H measured using about 5000 partial reconstructed D^* sample.
[7] ABBIENDI 00Q assumes the fraction B($b\to B^0$)= $(39.7^{+1.8}_{-2.2})$%. This result is an average of two methods using exclusive and partial D^* reconstruction.
[8] BUSKULIC 97 assumes fraction (B^+) = fraction (B^0) = (37.8 ± 2.2)% and PDG 96 values for B lifetime and D^* and D branching fractions.
[9] Combines with previous partial reconstructed D^* measurement.
[10] Assumes equal production of B^+ and B^0 at the $\Upsilon(4S)$.
[11] The results are based on the same analysis and data sample reported in ADAM 03.
[12] ACKERSTAFF 97G assumes fraction (B^+) = fraction (B^0) = (37.8±2.2)% and PDG 96 values for B lifetime and branching ratio of D^* and D decays.
[13] ABREU 96P result is the average of two methods using exclusive and partial D^* reconstruction.
[14] BARISH 95 use B($D^0\to K^-\pi^+$) = (3.91 ± 0.08 ± 0.17)% and B($D^{*+}\to D^0\pi^+$) = (68.1 ± 1.0 ± 1.3)%.
[15] BUSKULIC 95N assumes fraction (B^+) = fraction (B^0) = 38.2 ± 1.3 ± 2.2% and τ_{B^0} = 1.58 ± 0.06 ps. $\Gamma(D^{*-}\ell^+\nu_\ell)$/total = [5.18 − 0.13(fraction(B^0)−38.2)−1.5(τ_{B^0} − 1.58)]%.
[16] ALBRECHT 94 assumes B($D^{*+}\to D^0\pi^+$) = 68.1 ± 1.0 ± 1.3%. Uses partial reconstruction of D^{*+} and is independent of D^0 branching ratios.
[17] ALBRECHT 93 reports 0.052 ± 0.005 ± 0.006. We rescale using the method described in STONE 94 but with the updated PDG 94 B($D^0\to K^-\pi^+$). We have taken their average e and μ value. They also obtain $\alpha = 2*\Gamma^0/(\Gamma^- + \Gamma^+) - 1 = 1.1\pm0.4\pm0.2$, $A_{AF} = 3/4*(\Gamma^- - \Gamma^+)/\Gamma = 0.2\pm0.08\pm0.06$ and a value of $|V_{cb}|$ = 0.036–0.045 depending on model assumptions.
[18] Combining $\overline{D}^{*0}\ell^+\nu_\ell$ and $\overline{D}^{*-}\ell^+\nu_\ell$ SANGHERA 93 test $V-A$ structure and fit the decay angular distributions to obtain $A_{FB} = 3/4*(\Gamma^- - \Gamma^+)/\Gamma = 0.14\pm0.06\pm0.03$. Assuming a value of V_{cb}, they measure V, A_1, and A_2, the three form factors for the $D^*\ell\nu_\ell$ decay, where results are slightly dependent on model assumptions.
[19] ANTREASYAN 90B is average over B and $\overline{D}^*(2010)$ charge states.
[20] The measurement of ALBRECHT 89C suggests a D^* polarization γ_L/γ_T of 0.85 ± 0.45. or $\alpha = 0.7\pm0.9$.
[21] ALBRECHT 89J is ALBRECHT 87J value rescaled using B($D^*(2010)^-\to D^0\pi^-$) = 0.57 ± 0.04 ± 0.04. Superseded by ALBRECHT 93.
[22] We have taken average of the the BORTOLETTO 89B values for electrons and muons, 0.046 ± 0.005 ± 0.007. We rescale using the method described in STONE 94 but with the updated PDG 94 B($D^0\to K^-\pi^+$). The measurement suggests a D^* polarization parameter value $\alpha = 0.65\pm0.66\pm0.25$.
[23] ALBRECHT 87J assume μ-e universality, the B($\Upsilon(4S)\to B^0\overline{B}^0$) = 0.45, the B($D^0\to K^-\pi^+$) = (0.042 ± 0.004 ± 0.004), and the B($D^*(2010)^-\to D^0\pi^-$) = 0.49 ± 0.08. Superseded by ALBRECHT 89J.

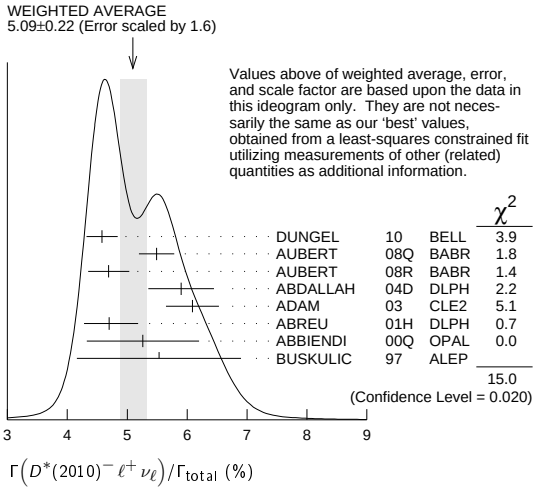

$\Gamma(D^*(2010)^-\ell^+\nu_\ell)/\Gamma(D\ell^+\nu_\ell\,\text{anything})$ Γ_6/Γ_3

VALUE	DOCUMENT ID		TECN	COMMENT
0.537±0.031±0.036	[1] AUBERT	07AN	BABR	$e^+e^-\to\Upsilon(4S)$

[1] Uses a fully reconstructed B meson on the recoil side.

Meson Particle Listings

B^0

$\Gamma(D^*(2010)^-\tau^+\nu_\tau)/\Gamma_{\text{total}}$ Γ_7/Γ

VALUE (units 10^{-2})	DOCUMENT ID		TECN	COMMENT
1.67±0.13 OUR FIT Error includes scale factor of 1.1.				
$2.02^{+0.40}_{-0.37}\pm0.37$	[1] MATYJA	07	BELL	$e^+e^-\to\Upsilon(4S)$
• • • We do not use the following data for averages, fits, limits, etc. • • •				
$1.11\pm0.51\pm0.06$	[2] AUBERT	08N	BABR	Repl. by AUBERT 09S

[1] Observed in the recoil of the accompanying B meson.
[2] Uses a fully reconstructed B meson as a tag on the recoil side.

$\Gamma(D^*(2010)^-\tau^+\nu_\tau)/\Gamma(D^*(2010)^-\ell^+\nu_\ell)$ Γ_7/Γ_6

VALUE	DOCUMENT ID		TECN	COMMENT
0.328±0.022 OUR FIT				
0.325±0.022 OUR AVERAGE				
$0.302\pm0.030\pm0.011$	[1] SATO	16B	BELL	$e^+e^-\to\Upsilon(4S)$
$0.336\pm0.027\pm0.030$	[2] AAIJ	15Q	LHCB	pp at 7, 8 TeV
$0.355\pm0.039\pm0.021$	[3,4] LEES	12D	BABR	$e^+e^-\to\Upsilon(4S)$
• • • We do not use the following data for averages, fits, limits, etc. • • •				
$0.207\pm0.095\pm0.008$	[3] AUBERT	09S	BABR	Repl. by LEES 12D

[1] Uses semileptonic B decay events for tagging and $\tau^+\to\ell^+\nu_\ell\overline{\nu}_\tau$ mode.
[2] Uses $\tau^+\to\mu^+\nu_\mu\overline{\nu}_\tau$ and μ^+ as ℓ^+.
[3] Uses a fully reconstructed B meson as a tag on the recoil side.
[4] Uses $\tau^+\to e^+\nu_e\overline{\nu}_\tau$ and $\tau^+\to\mu^+\nu_\mu\overline{\nu}_\tau$ and e^+ or μ^+ as ℓ^+.

$\Gamma(\overline{D}^0\pi^-\ell^+\nu_\ell)/\Gamma_{\text{total}}$ Γ_8/Γ

VALUE (units 10^{-3})	DOCUMENT ID		TECN	COMMENT
4.3±0.6 OUR AVERAGE				
$4.3\pm0.8\pm0.3$	[1] AUBERT	08Q	BABR	$e^+e^-\to\Upsilon(4S)$
$4.4\pm0.9\pm0.2$	[1,2] LIVENTSEV	08	BELL	$e^+e^-\to\Upsilon(4S)$
• • • We do not use the following data for averages, fits, limits, etc. • • •				
$3.3\pm0.9\pm0.1$	[3] LIVENTSEV	05	BELL	Repl. by LIVENTSEV 08

[1] Uses a fully reconstructed B meson as a tag on the recoil side.
[2] LIVENTSEV 08 reports $(4.2\pm0.7\pm0.6)\times10^{-3}$ from a measurement of $[\Gamma(B^0\to\overline{D}^0\pi^-\ell^+\nu_\ell)/\Gamma_{\text{total}}]$ / $[\mathrm{B}(B^0\to D^-\ell^+\nu_\ell)]$ assuming $\mathrm{B}(B^0\to D^-\ell^+\nu_\ell)=(2.12\pm0.20)\times10^{-2}$, which we rescale to our best value $\mathrm{B}(B^0\to D^-\ell^+\nu_\ell)=(2.20\pm0.10)\times10^{-2}$. Our first error is their experiment's error and our second error is the systematic error from using our best value.
[3] LIVENTSEV 05 reports $[\Gamma(B^0\to\overline{D}^0\pi^-\ell^+\nu_\ell)/\Gamma_{\text{total}}]$ / $[\mathrm{B}(B^+\to\overline{D}^0\ell^+\nu_\ell)]=0.15\pm0.03\pm0.03$ which we multiply by our best value $\mathrm{B}(B^+\to\overline{D}^0\ell^+\nu_\ell)=(2.20\pm0.10)\times10^{-2}$. Our first error is their experiment's error and our second error is the systematic error from using our best value.

$\Gamma(D_0^*(2400)^-\ell^+\nu_\ell,\ D_0^{*-}\to\overline{D}^0\pi^-)/\Gamma_{\text{total}}$ Γ_9/Γ

VALUE (units 10^{-3})	DOCUMENT ID		TECN	COMMENT
3.0±1.2 OUR AVERAGE Error includes scale factor of 1.8.				
$4.4\pm0.8\pm0.6$	[1] AUBERT	08BL	BABR	$e^+e^-\to\Upsilon(4S)$
$2.0\pm0.7\pm0.5$	[1] LIVENTSEV	08	BELL	$e^+e^-\to\Upsilon(4S)$

[1] Uses a fully reconstructed B meson as a tag on the recoil side.

$\Gamma(D_2^*(2460)^-\ell^+\nu_\ell,\ D_2^{*-}\to\overline{D}^0\pi^-)/\Gamma_{\text{total}}$ Γ_{10}/Γ

VALUE (units 10^{-3})	DOCUMENT ID		TECN	COMMENT
1.21±0.33 OUR AVERAGE Error includes scale factor of 1.8.				
$1.10\pm0.17\pm0.08$	[1] AUBERT	09Y	BABR	$e^+e^-\to\Upsilon(4S)$
$2.2\ \pm0.4\ \pm0.4$	[2] LIVENTSEV	08	BELL	$e^+e^-\to\Upsilon(4S)$

[1] Uses a simultaneous fit of all B semileptonic decays without full reconstruction of events. AUBERT 09Y reports $\mathrm{B}(B^0\to\overline{D}_2^*(2460)^-\ell^+\nu_\ell)\cdot\mathrm{B}(\overline{D}_2^*(2460)^-\to\overline{D}^{(*)0}\pi^-)=(1.77\pm0.26\pm0.11)\times10^{-3}$ and the authors have provided us the individual measurement.
[2] Uses a fully reconstructed B meson as a tag on the recoil side.

$\Gamma(\overline{D}^{(*)}n\pi\ell^+\nu_\ell(n\geq1))/\Gamma(D\ell^+\nu_\ell\,\text{anything})$ Γ_{11}/Γ_3

VALUE	DOCUMENT ID		TECN	COMMENT
0.248±0.032±0.030	[1] AUBERT	07AN	BABR	$e^+e^-\to\Upsilon(4S)$

[1] Uses a fully reconstructed B meson on the recoil side.

$\Gamma(\overline{D}^{*0}\pi^-\ell^+\nu_\ell)/\Gamma_{\text{total}}$ Γ_{12}/Γ

VALUE (units 10^{-3})	DOCUMENT ID		TECN	COMMENT
4.9±0.8 OUR AVERAGE				
$4.8\pm0.8\pm0.4$	[1] AUBERT	08Q	BABR	$e^+e^-\to\Upsilon(4S)$
$5.8\pm2.3\pm0.3$	[1,2] LIVENTSEV	08	BELL	$e^+e^-\to\Upsilon(4S)$
• • • We do not use the following data for averages, fits, limits, etc. • • •				
$4.9\pm1.1\pm0.1$	[3,4] LIVENTSEV	05	BELL	Repl. by LIVENTSEV 08

[1] Uses a fully reconstructed B meson as a tag on the recoil side.
[2] LIVENTSEV 08 reports $(5.6\pm2.1\pm0.8)\times10^{-3}$ from a measurement of $[\Gamma(B^0\to\overline{D}^{*0}\pi^-\ell^+\nu_\ell)/\Gamma_{\text{total}}]$ / $[\mathrm{B}(B^0\to D^-\ell^+\nu_\ell)]$ assuming $\mathrm{B}(B^0\to D^-\ell^+\nu_\ell)=(2.12\pm0.20)\times10^{-2}$, which we rescale to our best value $\mathrm{B}(B^0\to D^-\ell^+\nu_\ell)=(2.20\pm0.10)\times10^{-2}$. Our first error is their experiment's error and our second error is the systematic error from using our best value.
[3] Excludes D^{*+} contribution to $D\pi$ modes.
[4] LIVENTSEV 05 reports $[\Gamma(B^0\to\overline{D}^{*0}\pi^-\ell^+\nu_\ell)/\Gamma_{\text{total}}]$ / $[\mathrm{B}(B^+\to\overline{D}^*(2007)^0\ell^+\nu_\ell)]=0.10\pm0.02\pm0.01$ which we multiply by our best value $\mathrm{B}(B^+\to\overline{D}^*(2007)^0\ell^+\nu_\ell)=(4.88\pm0.10)\times10^{-2}$. Our first error is their experiment's error and our second error is the systematic error from using our best value.

$\Gamma(D_1(2420)^-\ell^+\nu_\ell,\ D_1^-\to\overline{D}^{*0}\pi^-)/\Gamma_{\text{total}}$ Γ_{13}/Γ

VALUE (units 10^{-3})	DOCUMENT ID		TECN	COMMENT
2.80±0.28 OUR AVERAGE				
$2.78\pm0.24\pm0.25$	[1] AUBERT	09Y	BABR	$e^+e^-\to\Upsilon(4S)$
$2.7\ \pm0.4\ \pm0.3$	[2] AUBERT	08BL	BABR	$e^+e^-\to\Upsilon(4S)$
$5.4\ \pm1.9\ \pm0.9$	[2] LIVENTSEV	08	BELL	$e^+e^-\to\Upsilon(4S)$

[1] Uses a simultaneous measurement of all B semileptonic decays without full reconstruction of events.
[2] Uses a fully reconstructed B meson as a tag on the recoil side.

$\Gamma(D_1'(2430)^-\ell^+\nu_\ell,\ D_1'^-\to\overline{D}^{*0}\pi^-)/\Gamma_{\text{total}}$ Γ_{14}/Γ

VALUE (units 10^{-3})	CL%	DOCUMENT ID		TECN	COMMENT
3.1±0.7±0.5		[1] AUBERT	08BL	BABR	$e^+e^-\to\Upsilon(4S)$
• • • We do not use the following data for averages, fits, limits, etc. • • •					
<5.0	90	[1] LIVENTSEV	08	BELL	$e^+e^-\to\Upsilon(4S)$

[1] Uses a fully reconstructed B meson as a tag on the recoil side.

$\Gamma(D_2^*(2460)^-\ell^+\nu_\ell,\ D_2^{*-}\to\overline{D}^{*0}\pi^-)/\Gamma_{\text{total}}$ Γ_{15}/Γ

VALUE (units 10^{-3})	CL%	DOCUMENT ID		TECN	COMMENT
0.68±0.12 OUR AVERAGE					
$0.67\pm0.12\pm0.05$		[1] AUBERT	09Y	BABR	$e^+e^-\to\Upsilon(4S)$
$0.7\ \pm0.2\ \pm0.2$		[2] AUBERT	08BL	BABR	$e^+e^-\to\Upsilon(4S)$
• • • We do not use the following data for averages, fits, limits, etc. • • •					
<3.0	90	[2] LIVENTSEV	08	BELL	$e^+e^-\to\Upsilon(4S)$

[1] Uses a simultaneous fit of all B semileptonic decays without full reconstruction of events. AUBERT 09Y reports $\mathrm{B}(B^0\to\overline{D}_2^*(2460)^-\ell^+\nu_\ell)\cdot\mathrm{B}(\overline{D}_2^*(2460)^-\to\overline{D}^{(*)0}\pi^-)=(1.77\pm0.26\pm0.11)\times10^{-3}$ and the authors have provided us the individual measurement.
[2] Uses a fully reconstructed B meson as a tag on the recoil side.

$\Gamma(D^-\pi^+\pi^-\ell^+\nu_\ell)/\Gamma(D^-\ell^+\nu_\ell)$ Γ_{16}/Γ_4

VALUE (units 10^{-2})	DOCUMENT ID		TECN	COMMENT
5.8±1.8±1.2	[1] LEES	16	BABR	$e^+e^-\to\Upsilon(4S)$

[1] Measurement used electrons and muons as leptons.

$\Gamma(D^{*-}\pi^+\pi^-\ell^+\nu_\ell)/\Gamma(D^*(2010)^-\ell^+\nu_\ell)$ Γ_{17}/Γ_6

VALUE (units 10^{-2})	DOCUMENT ID		TECN	COMMENT
2.8±0.8±0.6	[1] LEES	16	BABR	$e^+e^-\to\Upsilon(4S)$

[1] Measurement used electrons and muons as leptons.

$\Gamma(\rho^-\ell^+\nu_\ell)/\Gamma_{\text{total}}$ Γ_{18}/Γ

$\ell=e$ or μ, not sum over e and μ modes.

"OUR EVALUATION" has been obtained by the Heavy Flavor Averaging Group (HFLAV) by including both B^0 and B^+ decays. The average assumes equality of the semileptonic decay width for these isospin conjugate states.

VALUE (units 10^{-4})	CL%	DOCUMENT ID		TECN	COMMENT
2.94±0.11±0.18 OUR EVALUATION					
2.45±0.32 OUR AVERAGE Error includes scale factor of 1.6. See the ideogram below.					
$3.22\pm0.27\pm0.24$		[1] SIBIDANOV	13	BELL	$e^+e^-\to\Upsilon(4S)$
$1.75\pm0.15\pm0.27$		[2] DEL-AMO-SA..11C		BABR	$e^+e^-\to\Upsilon(4S)$
$2.93\pm0.37\pm0.37$		[3] ADAM	07	CLE2	$e^+e^-\to\Upsilon(4S)$
$2.17\pm0.54\pm0.32$		[4] HOKUUE	07	BELL	$e^+e^-\to\Upsilon(4S)$
$2.57\pm0.29^{+0.53}_{-0.62}$		[5] BEHRENS	00	CLE2	$e^+e^-\to\Upsilon(4S)$
• • • We do not use the following data for averages, fits, limits, etc. • • •					
$2.14\pm0.21\pm0.56$		[2] AUBERT,B	05O	BABR	Repl. by DEL-AMO-SANCHEZ 11C
$2.17\pm0.34^{+0.62}_{-0.68}$		[6] ATHAR	03	CLE2	Repl. by ADAM 07
$3.29\pm0.42\pm0.72$		[7] AUBERT	03E	BABR	Repl. by AUBERT,B 05O
$2.69\pm0.41^{+0.61}_{-0.64}$		[8] BEHRENS	00	CLE2	$e^+e^-\to\Upsilon(4S)$
$2.5\ \pm0.4\ ^{+0.7}_{-0.9}$		[9] ALEXANDER	96T	CLE2	Repl. by BEHRENS 00
<4.1	90	[10] BEAN	93B	CLE2	$e^+e^-\to\Upsilon(4S)$

[1] The signal events are tagged by a second B meson reconstructed in the fully hadronic decays.
[2] B^+ and B^0 decays combined assuming isospin symmetry. Systematic errors include both experimental and form-factor uncertainties.
[3] The B^0 and B^+ results are combined assuming the isospin, B lifetimes, and relative charged/neutral B production at the $\Upsilon(4S)$.
[4] The signal events are tagged by a second B meson reconstructed in the semileptonic mode $B\to D^{(*)}\ell\nu_\ell$.
[5] Averaging with ALEXANDER 96T results including experimental and theoretical correlations considered, BEHRENS 00 reports systematic errors $^{+0.33}_{-0.46}\pm0.41$, where the second error is theoretical model dependence. We combine these in quadrature.
[6] ATHAR 03 reports systematic errors $^{+0.47}_{-0.50}\pm0.41\pm0.01$, which are experimental systematic, systematic due to residual form-factor uncertainties in the signal, and systematic due to residual form-factor uncertainties in the cross-feed modes, respectively. We combine these in quadrature.
[7] Uses isospin constraints and extrapolation to all electron energies according to five different form-factor calculations. The second error combines the systematic and theoretical uncertainties in quadrature.

[8] BEHRENS 00 reports $^{+0.35}_{-0.40} \pm 0.50$, where the second error is the theoretical model dependence. We combine these in quadrature. B^+ and B^0 decays combined using isospin symmetry: $\Gamma(B^0 \to \rho^- \ell^+ \nu) = 2\Gamma(B^+ \to \rho^0 \ell^+ \nu) \approx 2\Gamma(B^+ \to \omega \ell^+ \nu)$. No evidence for $\omega \ell \nu$ is reported.

[9] ALEXANDER 96T reports $^{+0.5}_{-0.7} \pm 0.5$ where the second error is the theoretical model dependence. We combine these in quadrature. B^+ and B^0 decays combined using isospin symmetry: $\Gamma(B^0 \to \rho^- \ell^+ \nu) = 2\Gamma(B^+ \to \rho^0 \ell^+ \nu) \approx 2\Gamma(B^+ \to \omega \ell^+ \nu)$. No evidence for $\omega \ell \nu$ is reported.

[10] BEAN 93B limit set using ISGW Model. Using isospin and the quark model to combine $\Gamma(\rho^0 \ell^+ \nu_\ell)$ and $\Gamma(\omega \ell^+ \nu_\ell)$ with this result, they obtain a limit $< (1.6\text{–}2.7) \times 10^{-4}$ at 90% CL for $B^+ \to (\omega \text{or } \rho^0) \ell^+ \nu_\ell$. The range corresponds to the ISGW, WSB, and KS models. An upper limit on $|V_{ub}/V_{cb}| < 0.08\text{–}0.13$ at 90% CL is derived as well.

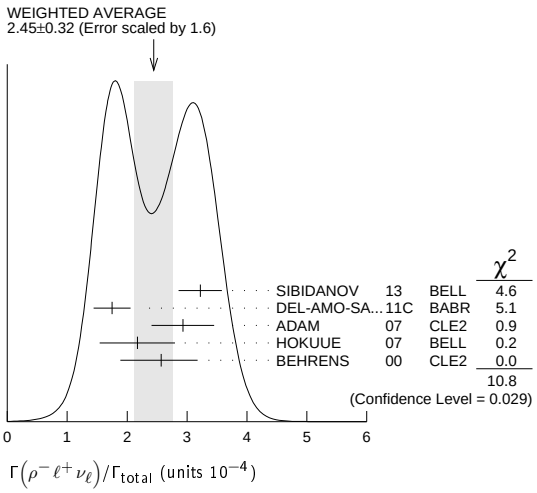

$\Gamma(\pi^- \ell^+ \nu_\ell)/\Gamma_{total}$ Γ_{19}/Γ

"OUR EVALUATION" is provided by the Heavy Flavor Averaging Group (HFLAV) and the procedure is described at http://www.slac.stanford.edu/xorg/hflav/.

VALUE (units 10^{-4})	DOCUMENT ID		TECN	COMMENT
1.50±0.06 OUR EVALUATION				
1.46±0.04 OUR AVERAGE				
1.49±0.09±0.07	[1] SIBIDANOV	13	BELL	$e^+e^- \to \Upsilon(4S)$
1.47±0.05±0.06	[2,3] LEES	12AA	BABR	$e^+e^- \to \Upsilon(4S)$
1.41±0.05±0.07	[4] DEL-AMO-SA...	11C	BABR	$e^+e^- \to \Upsilon(4S)$
1.49±0.04±0.07	[2] HA	11	BELL	$e^+e^- \to \Upsilon(4S)$
1.54±0.17±0.09	[4] AUBERT	08AV	BABR	$e^+e^- \to \Upsilon(4S)$
1.37±0.15±0.11	[5,6] ADAM	07	CLE2	$e^+e^- \to \Upsilon(4S)$
1.38±0.19±0.14	[7] HOKUUE	07	BELL	$e^+e^- \to \Upsilon(4S)$
• • • We do not use the following data for averages, fits, limits, etc. • • •				
1.42±0.05±0.08	[2] DEL-AMO-SA...	11F	BABR	Repl. by LEES 12AA
1.46±0.07±0.08	[8] AUBERT	07J	BABR	Repl. by DEL-AMO-SANCHEZ 11F
1.33±0.17±0.11	[9] AUBERT,B	06K	BABR	Repl. by AUBERT 08AV
1.38±0.10±0.18	[10] AUBERT,B	05O	BABR	Repl. by DEL-AMO-SANCHEZ 11C
1.33±0.18±0.13	[11] ATHAR	03	CLE2	Repl. by ADAM 07
1.8 ±0.4 ±0.4	[12] ALEXANDER	96T	CLE2	Repl. by ATHAR 03

[1] The signal events are tagged by a second B meson reconstructed in the fully hadronic decays.

[2] Uses loose neutrino reconstruction technique. Assumes $B(\Upsilon(4S) \to B^+B^-) = (51.6 \pm 0.6)\%$ and $B(\Upsilon(4S) \to B^0\overline{B}^0) = (48.4 \pm 0.6)\%$.

[3] Reports also a branching fraction value $B(B^0 \to \pi^- \ell^+ \nu) = (1.45 \pm 0.04 \pm 0.06) \times 10^{-4}$ from the decays of B^+ and B^0 that are combined using the isospin symmetry relation.

[4] Using the isospin symmetry relation, B^+ and B^0 branching fractions are combined.

[5] The B^0 and B^+ results are combined assuming the isospin, B lifetimes, and relative charged/neutral B production at the $\Upsilon(4S)$.

[6] Also report the rate for $q^2 > 16$ GeV^2 of $(0.41 \pm 0.08 \pm 0.04) \times 10^{-4}$ from which they obtain $|V_{ub}| = 3.6 \pm 0.4 \pm 0.2^{+0.6}_{-0.4}$ (last error is from theory).

[7] The signal events are tagged by a second B meson reconstructed in the semileptonic mode $B \to D^{(*)} \ell \nu_\ell$.

[8] The analysis uses events in which the signal B decays are reconstructed with an innovative loose neutrino reconstruction technique.

[9] The signals are tagged by a second B meson reconstructed in a semileptonic or hadronic decay. The B^0 and B^+ results are combined assuming the isospin symmetry.

[10] B^+ and B^0 decays combined assuming isospin symmetry. Systematic errors include both experimental and form-factor uncertainties.

[11] ATHAR 03 reports systematic errors $0.11 \pm 0.01 \pm 0.07$, which are experimental systematic, systematic due to residual form-factor uncertainties in the signal, and systematic due to residual form-factor uncertainties in the cross-feed modes, respectively. We combine these in quadrature.

[12] ALEXANDER 96T gives systematic errors $\pm 0.3 \pm 0.2$ where the second error reflects the estimated model dependence. We combine these in quadrature. Assumes isospin symmetry: $\Gamma(B^0 \to \pi^- \ell^+ \nu) = 2 \times \Gamma(B^+ \to \pi^0 \ell^+ \nu)$.

$\Gamma(\pi^- \mu^+ \nu_\mu)/\Gamma_{total}$ Γ_{20}/Γ

VALUE	DOCUMENT ID		TECN	
• • • We do not use the following data for averages, fits, limits, etc. • • •				
seen	[1] ALBRECHT	91C	ARG	

[1] In ALBRECHT 91C, one event is fully reconstructed providing evidence for the $b \to u$ transition.

$\Gamma(\pi^- \tau^+ \nu_\tau)/\Gamma_{total}$ Γ_{21}/Γ

VALUE	CL%	DOCUMENT ID		TECN	COMMENT
<2.5 × 10⁻⁴	90	[1] HAMER	16	BELL	$e^+e^- \to \Upsilon(4S)$

[1] Assumes equal production of B^+ and B^0 at the $\Upsilon(4S)$.

$\Gamma(K^\pm \text{anything})/\Gamma_{total}$ Γ_{22}/Γ

VALUE	DOCUMENT ID		TECN	COMMENT
0.78±0.08	[1] ALBRECHT	96D	ARG	$e^+e^- \to \Upsilon(4S)$

[1] Average multiplicity.

$\Gamma(D^0 X)/\Gamma_{total}$ Γ_{23}/Γ

VALUE	DOCUMENT ID		TECN	COMMENT
0.081±0.014±0.005	[1] AUBERT	07N	BABR	$e^+e^- \to \Upsilon(4S)$
• • • We do not use the following data for averages, fits, limits, etc. • • •				
0.063±0.019±0.005	[1] AUBERT,BE	04B	BABR	Repl. by AUBERT 07N

[1] Events are selected by completely reconstructing one B and searching for a reconstructed charmed particle in the rest of the event. The last error includes systematic and charm branching ratio uncertainties.

$\Gamma(\overline{D}^0 X)/\Gamma_{total}$ Γ_{24}/Γ

VALUE	DOCUMENT ID		TECN	COMMENT
0.474±0.020$^{+0.020}_{-0.019}$	[1] AUBERT	07N	BABR	$e^+e^- \to \Upsilon(4S)$
• • • We do not use the following data for averages, fits, limits, etc. • • •				
0.511±0.031±0.028	[1] AUBERT,BE	04B	BABR	Repl. by AUBERT 07N

[1] Events are selected by completely reconstructing one B and searching for a reconstructed charmed particle in the rest of the event. The last error includes systematic and charm branching ratio uncertainties.

$\Gamma(D^0 X)/[\Gamma(D^0 X) + \Gamma(\overline{D}^0 X)]$ $\Gamma_{23}/(\Gamma_{23}+\Gamma_{24})$

VALUE	DOCUMENT ID		TECN	COMMENT
0.146±0.022±0.006	AUBERT	07N	BABR	$e^+e^- \to \Upsilon(4S)$
• • • We do not use the following data for averages, fits, limits, etc. • • •				
0.110±0.031±0.008	AUBERT,BE	04B	BABR	Repl. by AUBERT 07N

$\Gamma(D^+ X)/\Gamma_{total}$ Γ_{25}/Γ

VALUE	CL%	DOCUMENT ID		TECN	COMMENT
<0.039	90	[1] AUBERT	07N	BABR	$e^+e^- \to \Upsilon(4S)$
• • • We do not use the following data for averages, fits, limits, etc. • • •					
<0.051	90	[1] AUBERT,BE	04B	BABR	Repl. by AUBERT 07N

[1] Events are selected by completely reconstructing one B and searching for a reconstructed charmed particle in the rest of the event. The last error includes systematic and charm branching ratio uncertainties.

$\Gamma(D^- X)/\Gamma_{total}$ Γ_{26}/Γ

VALUE	DOCUMENT ID		TECN	COMMENT
0.369±0.016$^{+0.030}_{-0.027}$	[1] AUBERT	07N	BABR	$e^+e^- \to \Upsilon(4S)$
• • • We do not use the following data for averages, fits, limits, etc. • • •				
0.397±0.030$^{+0.040}_{-0.038}$	[1] AUBERT,BE	04B	BABR	Repl. by AUBERT 07N

[1] Events are selected by completely reconstructing one B and searching for a reconstructed charmed particle in the rest of the event. The last error includes systematic and charm branching ratio uncertainties.

$\Gamma(D^+ X)/[\Gamma(D^+ X) + \Gamma(D^- X)]$ $\Gamma_{25}/(\Gamma_{25}+\Gamma_{26})$

VALUE	DOCUMENT ID		TECN	COMMENT
0.058±0.028±0.006	AUBERT	07N	BABR	$e^+e^- \to \Upsilon(4S)$
• • • We do not use the following data for averages, fits, limits, etc. • • •				
0.055±0.040±0.006	AUBERT,BE	04B	BABR	Repl. by AUBERT 07N

$\Gamma(D_s^+ X)/\Gamma_{total}$ Γ_{27}/Γ

VALUE	DOCUMENT ID		TECN	COMMENT
0.103±0.012$^{+0.017}_{-0.014}$	[1] AUBERT	07N	BABR	$e^+e^- \to \Upsilon(4S)$
• • • We do not use the following data for averages, fits, limits, etc. • • •				
0.109±0.021$^{+0.039}_{-0.024}$	[1] AUBERT,BE	04B	BABR	Repl. by AUBERT 07N

[1] Events are selected by completely reconstructing one B and searching for a reconstructed charmed particle in the rest of the event. The last error includes systematic and charm branching ratio uncertainties.

$\Gamma(D_s^- X)/\Gamma_{total}$ Γ_{28}/Γ

VALUE	CL%	DOCUMENT ID		TECN	COMMENT
<0.026	90	[1] AUBERT	07N	BABR	$e^+e^- \to \Upsilon(4S)$
• • • We do not use the following data for averages, fits, limits, etc. • • •					
<0.087	90	[1] AUBERT,BE	04B	BABR	Repl. by AUBERT 07N

[1] Events are selected by completely reconstructing one B and searching for a reconstructed charmed particle in the rest of the event. The last error includes systematic and charm branching ratio uncertainties.

$\Gamma(D_s^+X)/[\Gamma(D_s^+X)+\Gamma(D_s^-X)]$ $\Gamma_{27}/(\Gamma_{27}+\Gamma_{28})$

VALUE	DOCUMENT ID		TECN	COMMENT
0.879±0.066±0.005	AUBERT	07N	BABR	$e^+e^- \to \Upsilon(4S)$
• • • We do not use the following data for averages, fits, limits, etc. • • •				
0.733±0.092±0.010	AUBERT,BE	04B	BABR	Repl. by AUBERT 07N

$\Gamma(\Lambda_c^+X)/\Gamma_{\text{total}}$ Γ_{29}/Γ

VALUE	CL%	DOCUMENT ID		TECN	COMMENT
<0.031	90	[1] AUBERT	07N	BABR	$e^+e^- \to \Upsilon(4S)$
• • • We do not use the following data for averages, fits, limits, etc. • • •					
<0.038	90	[1] AUBERT,BE	04B	BABR	Repl. by AUBERT 07N

[1] Events are selected by completely reconstructing one B and searching for a reconstructed charmed particle in the rest of the event. The last error includes systematic and charm branching ratio uncertainties.

$\Gamma(\overline{\Lambda}_c^-X)/\Gamma_{\text{total}}$ Γ_{30}/Γ

VALUE	DOCUMENT ID		TECN	COMMENT
0.05 ±0.010$^{+0.019}_{-0.011}$	[1] AUBERT	07N	BABR	$e^+e^- \to \Upsilon(4S)$
• • • We do not use the following data for averages, fits, limits, etc. • • •				
0.049±0.017$^{+0.018}_{-0.011}$	[1] AUBERT,BE	04B	BABR	Repl. by AUBERT 07N

[1] Events are selected by completely reconstructing one B and searching for a reconstructed charmed particle in the rest of the event. The last error includes systematic and charm branching ratio uncertainties.

$\Gamma(\Lambda_c^+X)/[\Gamma(\Lambda_c^+X)+\Gamma(\overline{\Lambda}_c^-X)]$ $\Gamma_{29}/(\Gamma_{29}+\Gamma_{30})$

VALUE	DOCUMENT ID		TECN	COMMENT
0.243$^{+0.119}_{-0.121}$±0.003	AUBERT	07N	BABR	$e^+e^- \to \Upsilon(4S)$
• • • We do not use the following data for averages, fits, limits, etc. • • •				
0.286±0.142±0.007	AUBERT,BE	04B	BABR	Repl. by AUBERT 07N

$\Gamma(\overline{c}X)/\Gamma_{\text{total}}$ Γ_{31}/Γ

VALUE	DOCUMENT ID		TECN	COMMENT
0.947±0.030$^{+0.045}_{-0.040}$	[1] AUBERT	07N	BABR	$e^+e^- \to \Upsilon(4S)$
• • • We do not use the following data for averages, fits, limits, etc. • • •				
1.039±0.051$^{+0.063}_{-0.058}$	[1] AUBERT,BE	04B	BABR	Repl. by AUBERT 07N

[1] Events are selected by completely reconstructing one B and searching for a reconstructed charmed particle in the rest of the event. The last error includes systematic and charm branching ratio uncertainties.

$\Gamma(cX)/\Gamma_{\text{total}}$ Γ_{32}/Γ

VALUE	DOCUMENT ID		TECN	COMMENT
0.246±0.024$^{+0.021}_{-0.017}$	[1] AUBERT	07N	BABR	$e^+e^- \to \Upsilon(4S)$
• • • We do not use the following data for averages, fits, limits, etc. • • •				
0.237±0.036$^{+0.041}_{-0.027}$	[1] AUBERT,BE	04B	BABR	Repl. by AUBERT 07N

[1] Events are selected by completely reconstructing one B and searching for a reconstructed charmed particle in the rest of the event. The last error includes systematic and charm branching ratio uncertainties.

$\Gamma(\overline{c}/cX)/\Gamma_{\text{total}}$ Γ_{33}/Γ

VALUE	DOCUMENT ID		TECN	COMMENT
1.193±0.030$^{+0.053}_{-0.049}$	[1] AUBERT	07N	BABR	$e^+e^- \to \Upsilon(4S)$
• • • We do not use the following data for averages, fits, limits, etc. • • •				
1.276±0.062$^{+0.088}_{-0.074}$	[1] AUBERT,BE	04B	BABR	Repl. by AUBERT 07N

[1] Events are selected by completely reconstructing one B and searching for a reconstructed charmed particle in the rest of the event. The last error includes systematic and charm branching ratio uncertainties.

$\Gamma(D^-\pi^+)/\Gamma_{\text{total}}$ Γ_{34}/Γ

VALUE (units 10^{-3})	EVTS	DOCUMENT ID		TECN	COMMENT
2.52±0.13 OUR FIT Error includes scale factor of 1.1.					
2.68±0.13 OUR AVERAGE					
2.55±0.05±0.16		[1] AUBERT	07H	BABR	$e^+e^- \to \Upsilon(4S)$
3.03±0.23±0.23		[2] AUBERT,BE	06J	BABR	$e^+e^- \to \Upsilon(4S)$
2.68±0.12±0.24		[1,3] AHMED	02B	CLE2	$e^+e^- \to \Upsilon(4S)$
2.7 ±0.6 ±0.5		[4] BORTOLETTO	92	CLEO	$e^+e^- \to \Upsilon(4S)$
4.8 ±1.1 ±1.1	22	[5] ALBRECHT	90J	ARG	$e^+e^- \to \Upsilon(4S)$
5.1 $^{+2.8}_{-2.5}$ $^{+1.3}_{-1.2}$	4	[6] BEBEK	87	CLEO	$e^+e^- \to \Upsilon(4S)$
• • • We do not use the following data for averages, fits, limits, etc. • • •					
2.90±0.21±0.16		[1,7] AUBERT,B	04O	BABR	Repl. by AUBERT 07H
2.9 ±0.4 ±0.1	81	[8] ALAM	94	CLE2	Repl. by AHMED 02B
3.1 ±1.3 ±1.0	7	[5] ALBRECHT	88K	ARG	$e^+e^- \to \Upsilon(4S)$

[1] Assumes equal production of B^+ and B^0 at the $\Upsilon(4S)$.
[2] Uses a missing-mass method. Does not depend on D branching fractions or B^+/B^0 production rates.
[3] AHMED 02B reports an additional uncertainty on the branching ratios to account for 4.5% uncertainty on relative production of B^0 and B^+, which is not included here.
[4] BORTOLETTO 92 assumes equal production of B^+ and B^0 at the $\Upsilon(4S)$ and uses MarkIII branching fractions for the D.
[5] ALBRECHT 88K assumes $B^0\overline{B}^0$:B^+B^- production ratio is 45:55. Superseded by ALBRECHT 90J which assumes 50:50.
[6] BEBEK 87 value has been updated in BERKELMAN 91 to use same assumptions as noted for BORTOLETTO 92.
[7] AUBERT,B 04O reports $[\Gamma(B^0 \to D^-\pi^+)/\Gamma_{\text{total}}] \times [B(D^+ \to K^0_S\pi^+)] = (42.7 \pm 2.1 \pm 2.2) \times 10^{-6}$ which we divide by our best value $B(D^+ \to K^0_S\pi^+) = (1.47 \pm 0.08) \times 10^{-2}$. Our first error is their experiment's error and our second error is the systematic error from using our best value.
[8] ALAM 94 reports $[\Gamma(B^0 \to D^-\pi^+)/\Gamma_{\text{total}}] \times [B(D^+ \to K^-2\pi^+)] = (0.265 \pm 0.032 \pm 0.023) \times 10^{-3}$ which we divide by our best value $B(D^+ \to K^-2\pi^+) = (8.98 \pm 0.28) \times 10^{-2}$. Our first error is their experiment's error and our second error is the systematic error from using our best value. Assumes equal production of B^+ and B^0 at the $\Upsilon(4S)$.

$\Gamma(D^-\ell^+\nu_\ell)/\Gamma(D^-\pi^+)$ Γ_4/Γ_{34}

VALUE	DOCUMENT ID		TECN	COMMENT
9.9±1.0±0.9	AALTONEN	09E	CDF	$p\overline{p}$ at 1.96 TeV

$\Gamma(D^-\rho^+)/\Gamma_{\text{total}}$ Γ_{35}/Γ

VALUE	EVTS	DOCUMENT ID		TECN	COMMENT
0.0079±0.0013 OUR AVERAGE					
0.0078±0.0013±0.0002	79	[1] ALAM	94	CLE2	$e^+e^- \to \Upsilon(4S)$
0.009 ±0.005 ±0.003	9	[2] ALBRECHT	90J	ARG	$e^+e^- \to \Upsilon(4S)$
• • • We do not use the following data for averages, fits, limits, etc. • • •					
0.022 ±0.012 ±0.009	6	[2] ALBRECHT	88K	ARG	$e^+e^- \to \Upsilon(4S)$

[1] ALAM 94 reports $[\Gamma(B^0 \to D^-\rho^+)/\Gamma_{\text{total}}] \times [B(D^+ \to K^-2\pi^+)] = 0.000704 \pm 0.000096 \pm 0.000070$ which we divide by our best value $B(D^+ \to K^-2\pi^+) = (8.98 \pm 0.28) \times 10^{-2}$. Our first error is their experiment's error and our second error is the systematic error from using our best value. Assumes equal production of B^+ and B^0 at the $\Upsilon(4S)$.
[2] ALBRECHT 88K assumes $B^0\overline{B}^0$:B^+B^- production ratio is 45:55. Superseded by ALBRECHT 90J which assumes 50:50.

$\Gamma(D^-K^0\pi^+)/\Gamma_{\text{total}}$ Γ_{36}/Γ

VALUE (units 10^{-4})	DOCUMENT ID		TECN	COMMENT
4.9±0.7±0.5	[1] AUBERT,BE	05B	BABR	$e^+e^- \to \Upsilon(4S)$

[1] Assumes equal production of B^+ and B^0 at the $\Upsilon(4S)$.

$\Gamma(D^-K^*(892)^+)/\Gamma_{\text{total}}$ Γ_{37}/Γ

VALUE (units 10^{-4})	DOCUMENT ID		TECN	COMMENT
4.5±0.7 OUR AVERAGE				
4.6±0.6±0.5	[1] AUBERT,BE	05B	BABR	$e^+e^- \to \Upsilon(4S)$
3.7±1.5±1.0	[1] MAHAPATRA	02	CLE2	$e^+e^- \to \Upsilon(4S)$

[1] Assumes equal production of B^+ and B^0 at the $\Upsilon(4S)$.

$\Gamma(D^-\omega\pi^+)/\Gamma_{\text{total}}$ Γ_{38}/Γ

VALUE	DOCUMENT ID		TECN	COMMENT
0.0028±0.0005±0.0004	[1] ALEXANDER	01B	CLE2	$e^+e^- \to \Upsilon(4S)$

[1] Assumes equal production of B^+ and B^0 at the $\Upsilon(4S)$. The signal is consistent with all observed $\omega\pi^+$ having proceeded through the ρ'^+ resonance at mass 1349 ± 25$^{+10}_{-5}$ MeV and width 547 ± 86$^{+46}_{-45}$ MeV.

$\Gamma(D^-K^+)/\Gamma_{\text{total}}$ Γ_{39}/Γ

VALUE (units 10^{-4})	DOCUMENT ID		TECN	COMMENT
1.86±0.20 OUR AVERAGE				
1.89±0.19±0.10	[1] AAIJ	11F	LHCB	pp at 7 TeV
1.7 ±0.4 ±0.1	[2] ABE	01I	BELL	$e^+e^- \to \Upsilon(4S)$

[1] AAIJ 11F reports $(2.01 \pm 0.18 \pm 0.14) \times 10^{-4}$ from a measurement of $[\Gamma(B^0 \to D^-K^+)/\Gamma_{\text{total}}] / [B(B^0 \to D^-\pi^+)]$ assuming $B(B^0 \to D^-\pi^+) = (2.68 \pm 0.13) \times 10^{-3}$, which we rescale to our best value $B(B^0 \to D^-\pi^+) = (2.52 \pm 0.13) \times 10^{-3}$. Our first error is their experiment's error and our second error is the systematic error from using our best value.
[2] ABE 01I reports $[\Gamma(B^0 \to D^-K^+)/\Gamma_{\text{total}}] / [B(B^0 \to D^-\pi^+)] = (6.8 \pm 1.5 \pm 0.7) \times 10^{-2}$ which we multiply by our best value $B(B^0 \to D^-\pi^+) = (2.52 \pm 0.13) \times 10^{-3}$. Our first error is their experiment's error and our second error is the systematic error from using our best value.

$\Gamma(D^-K^+)/\Gamma(D^-\pi^+)$ Γ_{39}/Γ_{34}

VALUE (units 10^{-2})	DOCUMENT ID		TECN	COMMENT
8.22±0.11±0.25	AAIJ	13P	LHCB	pp at 7 TeV

$\Gamma(D^-K^+\pi^+\pi^-)/\Gamma(D^-\pi^+\pi^+\pi^-)$ Γ_{40}/Γ_{46}

VALUE (units 10^{-2})	DOCUMENT ID		TECN	COMMENT
5.9±1.1±0.5	AAIJ	12T	LHCB	pp at 7 TeV

$\Gamma(D^- K^+ \overline{K}^0)/\Gamma_{total}$ Γ_{41}/Γ

VALUE (units 10^{-4})	CL%	DOCUMENT ID		TECN	COMMENT
<3.1	90	[1] DRUTSKOY	02	BELL	$e^+e^- \to \Upsilon(4S)$

[1] Assumes equal production of B^+ and B^0 at the $\Upsilon(4S)$.

$\Gamma(D^- K^+ \overline{K}^*(892)^0)/\Gamma_{total}$ Γ_{42}/Γ

VALUE (units 10^{-4})	DOCUMENT ID		TECN	COMMENT
8.8±1.1±1.5	[1] DRUTSKOY	02	BELL	$e^+e^- \to \Upsilon(4S)$

[1] Assumes equal production of B^+ and B^0 at the $\Upsilon(4S)$.

$\Gamma(\overline{D}^0 \pi^+ \pi^-)/\Gamma_{total}$ Γ_{43}/Γ

VALUE (units 10^{-4})	CL%	EVTS	DOCUMENT ID		TECN	COMMENT
8.8 ±0.5 OUR AVERAGE						
8.95±0.15±0.52			[1] AAIJ	15Y	LHCB	pp at 7, 8 TeV
8.4 ±0.4 ±0.8			[2] KUZMIN	07	BELL	$e^+e^- \to \Upsilon(4S)$
• • • We do not use the following data for averages, fits, limits, etc. • • •						
8.0 ±0.6 ±1.5			[2,3] SATPATHY	03	BELL	Repl. by KUZMIN 07
< 16	90		[2] ALAM	94	CLE2	$e^+e^- \to \Upsilon(4S)$
< 70	90		[4] BORTOLETTO	92	CLEO	$e^+e^- \to \Upsilon(4S)$
<340	90		[5] BEBEK	87	CLEO	$e^+e^- \to \Upsilon(4S)$
700 ± 500		5	[6] BEHRENDS	83	CLEO	$e^+e^- \to \Upsilon(4S)$

[1] The second uncertainty combines in quadrature all systematic uncertainties quoted in the paper. AAIJ 15Y reports $B(B^0 \to \overline{D}^0\pi^+\pi^-) = (8.46 \pm 0.14 \pm 0.49) \times 10^{-4}$ in the kinematic region $m(\overline{D}^0\pi^\pm) > 2.1$ GeV which we corrected to the full phase-space dividing by 0.945 from Belle.

[2] Assumes equal production of B^+ and B^0 at the $\Upsilon(4S)$.

[3] No assumption about the intermediate mechanism is made in the analysis.

[4] BORTOLETTO 92 assumes equal production of B^+ and B^0 at the $\Upsilon(4S)$ and uses Mark III branching fractions for the D. The product branching fraction into $D_0^*(2340)\pi$ followed by $D_0^*(2340) \to D^0\pi$ is < 0.0001 at 90% CL and into $D_2^*(2460)$ followed by $D_2^*(2460) \to D^0\pi$ is < 0.0004 at 90% CL.

[5] BEBEK 87 assume the $\Upsilon(4S)$ decays 43% to $B^0\overline{B}^0$. We rescale to 50%. $B(D^0 \to K^-\pi^+) = (4.2 \pm 0.4 \pm 0.4)\%$ and $B(D^0 \to K^-\pi^+\pi^+\pi^-) = (9.1 \pm 0.8 \pm 0.8)\%$ were used.

[6] Corrected by us using assumptions: $B(D^0 \to K^-\pi^+) = (0.042 \pm 0.006)$ and $B(\Upsilon(4S) \to B^0\overline{B}^0) = 50\%$. The product branching ratio is $B(B^0 \to \overline{D}^0\pi^+\pi^-)B(\overline{D}^0 \to K^+\pi^-) = (0.39 \pm 0.26) \times 10^{-2}$.

$\Gamma(D^*(2010)^-\pi^+)/\Gamma_{total}$ Γ_{44}/Γ

VALUE (units 10^{-3})	EVTS	DOCUMENT ID		TECN	COMMENT
2.74±0.13 OUR AVERAGE					
2.79±0.08±0.17		[1] AUBERT	07H	BABR	$e^+e^- \to \Upsilon(4S)$
2.50±0.34±0.13		[2,3] AUBERT,BE	06J	BABR	$e^+e^- \to \Upsilon(4S)$
2.81±0.24±0.05		[4] BRANDENB...	98	CLE2	$e^+e^- \to \Upsilon(4S)$
2.6 ±0.3 ±0.4	82	[5] ALAM	94	CLE2	$e^+e^- \to \Upsilon(4S)$
3.37±0.96±0.02		[6] BORTOLETTO	92	CLEO	$e^+e^- \to \Upsilon(4S)$
2.36±0.88±0.02	12	[7] ALBRECHT	90J	ARG	$e^+e^- \to \Upsilon(4S)$
$2.36^{+1.50}_{-1.10}\pm0.02$	5	[8] BEBEK	87	CLEO	$e^+e^- \to \Upsilon(4S)$
• • • We do not use the following data for averages, fits, limits, etc. • • •					
10 ±4 ±1	8	[9] AKERS	94J	OPAL	$e^+e^- \to Z$
2.7 ±1.4 ±1.0	5	[10] ALBRECHT	87C	ARG	$e^+e^- \to \Upsilon(4S)$
3.5 ±2 ±2		[11] ALBRECHT	86F	ARG	$e^+e^- \to \Upsilon(4S)$
17 ±5 ±5	41	[12] GILES	84	CLEO	$e^+e^- \to \Upsilon(4S)$

[1] Assumes equal production of B^+ and B^0 at the $\Upsilon(4S)$.

[2] AUBERT,BE 06J reports $[\Gamma(B^0 \to D^*(2010)^-\pi^+)/\Gamma_{total}] / [B(B^0 \to D^-\pi^+)] = 0.99 \pm 0.11 \pm 0.08$ which we multiply by our best value $B(B^0 \to D^-\pi^+) = (2.52 \pm 0.13) \times 10^{-3}$. Our first error is their experiment's error and our second error is the systematic error from using our best value.

[3] Uses a missing-mass method. Does not depend on D branching fractions or B^+/B^0 production rates.

[4] BRANDENBURG 98 assume equal production of B^+ and B^0 at $\Upsilon(4S)$ and use the D^* reconstruction technique. The first error is their experiment's error and the second error is the systematic error from the PDG 96 value of $B(D^* \to D\pi)$.

[5] ALAM 94 assume equal production of B^+ and B^0 at the $\Upsilon(4S)$ and use the CLEO II $B(D^*(2010)^+ \to D^0\pi^+)$ and absolute $B(D^0 \to K^-\pi^+)$ and the PDG 1992 $B(D^0 \to K^-\pi^+\pi^0)/B(D^0 \to K^-\pi^+)$ and $B(D^0 \to K^-2\pi^+\pi^-)/B(D^0 \to K^-\pi^+)$.

[6] BORTOLETTO 92 reports $(4.0 \pm 1.0 \pm 0.7) \times 10^{-3}$ from a measurement of $[\Gamma(B^0 \to D^*(2010)^-\pi^+)/\Gamma_{total}] \times [B(D^*(2010)^+ \to D^0\pi^+)]$ assuming $B(D^*(2010)^+ \to D^0\pi^+) = 0.57 \pm 0.06$, which we rescale to our best value $B(D^*(2010)^+ \to D^0\pi^+) = (67.7 \pm 0.5) \times 10^{-2}$. Our first error is their experiment's error and our second error is the systematic error from using our best value. Assumes equal production of B^+ and B^0 at the $\Upsilon(4S)$ and uses Mark III branching fractions for the D.

[7] ALBRECHT 90J reports $(2.8 \pm 0.9 \pm 0.6) \times 10^{-3}$ from a measurement of $[\Gamma(B^0 \to D^*(2010)^-\pi^+)/\Gamma_{total}] \times [B(D^*(2010)^+ \to D^0\pi^+)]$ assuming $B(D^*(2010)^+ \to D^0\pi^+) = 0.57 \pm 0.06$, which we rescale to our best value $B(D^*(2010)^+ \to D^0\pi^+) = (67.7 \pm 0.5) \times 10^{-2}$. Our first error is their experiment's error and our second error is the systematic error from using our best value. Assumes equal production of B^+ and B^0 at the $\Upsilon(4S)$ and uses Mark III branching fractions for the D.

[8] BEBEK 87 reports $(2.8^{+1.5}_{-1.2}{}^{+1.0}_{-0.6}) \times 10^{-3}$ from a measurement of $[\Gamma(B^0 \to D^*(2010)^-\pi^+)/\Gamma_{total}] \times [B(D^*(2010)^+ \to D^0\pi^+)]$ assuming $B(D^*(2010)^+ \to D^0\pi^+) = 0.57 \pm 0.06$, which we rescale to our best value $B(D^*(2010)^+ \to D^0\pi^+) = (67.7 \pm 0.5) \times 10^{-2}$. Our first error is their experiment's error and our second error is the systematic error from using our best value. Updated in BERKELMAN 91 to use same assumptions as noted for BORTOLETTO 92 and ALBRECHT 90J.

[9] Assumes $B(Z \to b\overline{b}) = 0.217$ and 38% B_d production fraction.

[10] ALBRECHT 87C use PDG 86 branching ratios for D and $D^*(2010)$ and assume $B(\Upsilon(4S) \to B^+B^-) = 55\%$ and $B(\Upsilon(4S) \to B^0\overline{B}^0) = 45\%$. Superseded by ALBRECHT 90J.

[11] ALBRECHT 86F uses pseudomass that is independent of D^0 and D^+ branching ratios.

[12] Assumes $B(D^*(2010)^+ \to D^0\pi^+) = 0.60^{+0.08}_{-0.15}$. Assumes $B(\Upsilon(4S) \to B^0\overline{B}^0) = 0.40 \pm 0.02$ Does not depend on D branching ratios.

$\Gamma(D^*(2010)^-\ell^+\nu_\ell)/\Gamma(D^*(2010)^-\pi^+)$ Γ_6/Γ_{44}

VALUE	DOCUMENT ID		TECN	COMMENT
16.5±2.3±1.1	AALTONEN	09E	CDF	$p\overline{p}$ at 1.96 TeV

$\Gamma(\overline{D}^0 K^+ K^-)/\Gamma(\overline{D}^0\pi^+\pi^-)$ Γ_{45}/Γ_{43}

VALUE	DOCUMENT ID		TECN	COMMENT
0.056±0.011±0.007	AAIJ	12AM	LHCB	pp at 7 TeV

$\Gamma(D^-\pi^+\pi^+\pi^-)/\Gamma_{total}$ Γ_{46}/Γ

VALUE	DOCUMENT ID		TECN	COMMENT
0.0060±0.0007 OUR FIT Error includes scale factor of 1.1.				
0.0080±0.0021±0.0014	[1] BORTOLETTO	92	CLEO	$e^+e^- \to \Upsilon(4S)$

[1] BORTOLETTO 92 assumes equal production of B^+ and B^0 at the $\Upsilon(4S)$ and uses Mark III branching fractions for the D.

$\Gamma(D^-\pi^+\pi^+\pi^-)/\Gamma(D^-\pi^+)$ Γ_{46}/Γ_{34}

VALUE	DOCUMENT ID		TECN	COMMENT
2.39±0.23 OUR FIT				
2.38±0.11±0.21	AAIJ	11E	LHCB	pp at 7 TeV

$\Gamma((D^-\pi^+\pi^+\pi^-)\text{ nonresonant})/\Gamma_{total}$ Γ_{47}/Γ

VALUE	DOCUMENT ID		TECN	COMMENT
0.0039±0.0014±0.0013	[1] BORTOLETTO	92	CLEO	$e^+e^- \to \Upsilon(4S)$

[1] BORTOLETTO 92 assumes equal production of B^+ and B^0 at the $\Upsilon(4S)$ and uses Mark III branching fractions for the D.

$\Gamma(D^-\pi^+\rho^0)/\Gamma_{total}$ Γ_{48}/Γ

VALUE	DOCUMENT ID		TECN	COMMENT
0.0011±0.0009±0.0004	[1] BORTOLETTO	92	CLEO	$e^+e^- \to \Upsilon(4S)$

[1] BORTOLETTO 92 assumes equal production of B^+ and B^0 at the $\Upsilon(4S)$ and uses Mark III branching fractions for the D.

$\Gamma(D^- a_1(1260)^+)/\Gamma_{total}$ Γ_{49}/Γ

VALUE	DOCUMENT ID		TECN	COMMENT
0.0060±0.0022±0.0024	[1] BORTOLETTO	92	CLEO	$e^+e^- \to \Upsilon(4S)$

[1] BORTOLETTO 92 assumes equal production of B^+ and B^0 at the $\Upsilon(4S)$ and uses Mark III branching fractions for the D.

$\Gamma(D^*(2010)^-\pi^+\pi^0)/\Gamma_{total}$ Γ_{50}/Γ

VALUE	EVTS	DOCUMENT ID		TECN	COMMENT
0.0152±0.0052±0.0001	51	[1] ALBRECHT	90J	ARG	$e^+e^- \to \Upsilon(4S)$
• • • We do not use the following data for averages, fits, limits, etc. • • •					
0.015 ±0.008 ±0.008	8	[2] ALBRECHT	87C	ARG	$e^+e^- \to \Upsilon(4S)$

[1] ALBRECHT 90J reports $0.018 \pm 0.004 \pm 0.005$ from a measurement of $[\Gamma(B^0 \to D^*(2010)^-\pi^+\pi^0)/\Gamma_{total}] \times [B(D^*(2010)^+ \to D^0\pi^+)]$ assuming $B(D^*(2010)^+ \to D^0\pi^+) = 0.57 \pm 0.06$, which we rescale to our best value $B(D^*(2010)^+ \to D^0\pi^+) = (67.7 \pm 0.5) \times 10^{-2}$. Our first error is their experiment's error and our second error is the systematic error from using our best value. Assumes equal production of B^+ and B^0 at the $\Upsilon(4S)$ and uses Mark III branching fractions for the D.

[2] ALBRECHT 87C use PDG 86 branching ratios for D and $D^*(2010)$ and assume $B(\Upsilon(4S) \to B^+B^-) = 55\%$ and $B(\Upsilon(4S) \to B^0\overline{B}^0) = 45\%$. Superseded by ALBRECHT 90J.

$\Gamma(D^*(2010)^-\rho^+)/\Gamma_{total}$ Γ_{51}/Γ

VALUE (units 10^{-3})	EVTS	DOCUMENT ID		TECN	COMMENT
2.2 $\pm^{1.8}_{2.7}$ OUR AVERAGE Error includes scale factor of 5.2.					
$1.48\pm\ 0.27^{+\ 0.26}_{-\ 0.57}$		[1,2] MATVIENKO	15	BELL	$e^+e^- \to \Upsilon(4S)$
6.8 ± 0.3 ± 0.9		[1,3] CSORNA	03	CLE2	$e^+e^- \to \Upsilon(4S)$
16.0 ±11.3 ± 0.1		[4] BORTOLETTO	92	CLEO	$e^+e^- \to \Upsilon(4S)$
5.89± 3.52± 0.04	19	[5] ALBRECHT	90J	ARG	$e^+e^- \to \Upsilon(4S)$
• • • We do not use the following data for averages, fits, limits, etc. • • •					
7.4 ± 1.0 ± 1.4	76	[6,7] ALAM	94	CLE2	$e^+e^- \to \Upsilon(4S)$
81 ±29 $^{+59}_{-24}$	19	[8] CHEN	85	CLEO	$e^+e^- \to \Upsilon(4S)$

[1] Assumes equal production of B^0 and B^+ at the $\Upsilon(4S)$ resonance.

[2] The second uncertainty combines in quadrature the systematic and model uncertainties.

[3] The second error combines the systematic and theoretical uncertainties in quadrature. CSORNA 03 includes data used in ALAM 94. A full angular fit to three complex helicity amplitudes is performed.

[4] BORTOLETTO 92 reports $0.019 \pm 0.008 \pm 0.011$ from a measurement of $[\Gamma(B^0 \to D^*(2010)^-\rho^+)/\Gamma_{total}] \times [B(D^*(2010)^+ \to D^0\pi^+)]$ assuming $B(D^*(2010)^+ \to D^0\pi^+) = 0.57 \pm 0.06$, which we rescale to our best value $B(D^*(2010)^+ \to D^0\pi^+)$

$= (67.7 \pm 0.5) \times 10^{-2}$. Our first error is their experiment's error and our second error is the systematic error from using our best value. Assumes equal production of B^+ and B^0 at the $\Upsilon(4S)$ and uses MarkIII branching fractions for the D.

[5] ALBRECHT 90J reports $0.007 \pm 0.003 \pm 0.003$ from a measurement of $[\Gamma(B^0 \to D^*(2010)^- \rho^+)/\Gamma_{total}] \times [B(D^*(2010)^+ \to D^0\pi^+)]$ assuming $B(D^*(2010)^+ \to D^0\pi^+) = 0.57 \pm 0.06$, which we rescale to our best value $B(D^*(2010)^+ \to D^0\pi^+) = (67.7 \pm 0.5) \times 10^{-2}$. Our first error is their experiment's error and our second error is the systematic error from using our best value. Assumes equal production of B^+ and B^0 at the $\Upsilon(4S)$ and uses MarkIII branching fractions for the D.

[6] ALAM 94 assume equal production of B^+ and B^0 at the $\Upsilon(4S)$ and use the CLEOII $B(D^*(2010)^+ \to D^0\pi^+)$ and absolute $B(D^0 \to K^-\pi^+)$ and the PDG 1992 $B(D^0 \to K^-\pi^+\pi^0)/B(D^0 \to K^-\pi^+)$ and $B(D^0 \to K^-2\pi^+\pi^-)/B(D^0 \to K^-\pi^+)$.

[7] This decay is nearly completely longitudinally polarized, $\Gamma_L/\Gamma = (93 \pm 5 \pm 5)\%$, as expected from the factorization hypothesis (ROSNER 90). The nonresonant $\pi^+\pi^0$ contribution under the ρ^+ is less than 9% at 90% CL.

[8] Uses $B(D^* \to D^0\pi^+) = 0.6 \pm 0.15$ and $B(\Upsilon(4S) \to B^0\overline{B}^0) = 0.4$. Does not depend on D branching ratios.

$\Gamma(D^*(2010)^- K^+)/\Gamma_{total}$ Γ_{52}/Γ

VALUE (units 10^{-4})	DOCUMENT ID		TECN	COMMENT
2.12±0.15 OUR AVERAGE				
2.13±0.12±0.10	[1] AUBERT	06A	BABR	$e^+e^- \to \Upsilon(4S)$
2.0 ±0.4 ±0.1	[2] ABE	01I	BELL	$e^+e^- \to \Upsilon(4S)$

[1] AUBERT 06A reports $[\Gamma(B^0 \to D^*(2010)^- K^+)/\Gamma_{total}] / [B(B^0 \to D^*(2010)^-\pi^+)] = 0.0776 \pm 0.0034 \pm 0.0029$ which we multiply by our best value $B(B^0 \to D^*(2010)^-\pi^+) = (2.74 \pm 0.13) \times 10^{-3}$. Our first error is their experiment's error and our second error is the systematic error from using our best value.

[2] ABE 01I reports $[\Gamma(B^0 \to D^*(2010)^- K^+)/\Gamma_{total}] / [B(B^0 \to D^*(2010)^-\pi^+)] = 0.074 \pm 0.015 \pm 0.006$ which we multiply by our best value $B(B^0 \to D^*(2010)^-\pi^+) = (2.74 \pm 0.13) \times 10^{-3}$. Our first error is their experiment's error and our second error is the systematic error from using our best value.

$\Gamma(D^*(2010)^- K^+)/\Gamma(D^*(2010)^-\pi^+)$ Γ_{52}/Γ_{44}

VALUE	DOCUMENT ID		TECN	COMMENT
(7.76±0.34±0.26) × 10^{-2}	AAIJ	13AO	LHCB	pp at 7 TeV

$\Gamma(D^*(2010)^- K^0\pi^+)/\Gamma_{total}$ Γ_{53}/Γ

VALUE (units 10^{-4})	DOCUMENT ID		TECN	COMMENT
3.0±0.7±0.3	[1] AUBERT,BE	05B	BABR	$e^+e^- \to \Upsilon(4S)$

[1] Assumes equal production of B^+ and B^0 at the $\Upsilon(4S)$.

$\Gamma(D^*(2010)^- K^*(892)^+)/\Gamma_{total}$ Γ_{54}/Γ

VALUE (units 10^{-4})	DOCUMENT ID		TECN	COMMENT
3.3±0.6 OUR AVERAGE				
3.2±0.6±0.3	[1] AUBERT,BE	05B	BABR	$e^+e^- \to \Upsilon(4S)$
3.8±1.3±0.8	[2] MAHAPATRA	02	CLE2	$e^+e^- \to \Upsilon(4S)$

[1] Assumes equal production of B^+ and B^0 at the $\Upsilon(4S)$.

[2] Assumes equal production of B^+ and B^0 at the $\Upsilon(4S)$ and an unpolarized final state.

$\Gamma(D^*(2010)^- K^+\overline{K}^0)/\Gamma_{total}$ Γ_{55}/Γ

VALUE (units 10^{-4})	CL%	DOCUMENT ID		TECN	COMMENT
<4.7	90	[1] DRUTSKOY	02	BELL	$e^+e^- \to \Upsilon(4S)$

[1] Assumes equal production of B^+ and B^0 at the $\Upsilon(4S)$.

$\Gamma(D^*(2010)^- K^+\overline{K}^*(892)^0)/\Gamma_{total}$ Γ_{56}/Γ

VALUE (units 10^{-4})	DOCUMENT ID		TECN	COMMENT
12.9±2.2±2.5	[1] DRUTSKOY	02	BELL	$e^+e^- \to \Upsilon(4S)$

[1] Assumes equal production of B^+ and B^0 at the $\Upsilon(4S)$.

$\Gamma(D^*(2010)^-\pi^+\pi^+\pi^-)/\Gamma_{total}$ Γ_{57}/Γ

VALUE (units 10^{-3})	CL%	DOCUMENT ID		TECN	COMMENT
7.21±0.29 OUR AVERAGE					
7.26±0.11± 0.31		[1] LEES	16H	BABR	$e^+e^- \to \Upsilon(4S)$
6.81±0.23± 0.72		[2] MAJUMDER	04	BELL	$e^+e^- \to \Upsilon(4S)$
6.3 ±1.0 ± 1.1		[3,4] ALAM	94	CLE2	$e^+e^- \to \Upsilon(4S)$
13.4 ±3.6 ± 0.1		[5] BORTOLETTO	92	CLEO	$e^+e^- \to \Upsilon(4S)$
10.1 ±4.1 ± 0.1		[6] ALBRECHT	90J	ARG	$e^+e^- \to \Upsilon(4S)$
• • • We do not use the following data for averages, fits, limits, etc. • • •					
33 ±9 ±16		[7] ALBRECHT	87C	ARG	$e^+e^- \to \Upsilon(4S)$
<42	90	[8] BEBEK	87	CLEO	$e^+e^- \to \Upsilon(4S)$

[1] Assumes $B(\Upsilon(4S) \to B^0\overline{B}^0) = 0.486 \pm 0.006$.

[2] Assumes equal production of B^+ and B^0 at the $\Upsilon(4S)$.

[3] ALAM 94 assume equal production of B^+ and B^0 at the $\Upsilon(4S)$ and use the CLEOII $B(D^*(2010)^+ \to D^0\pi^+)$ and absolute $B(D^0 \to K^-\pi^+)$ and the PDG 1992 $B(D^0 \to K^-\pi^+\pi^0)/B(D^0 \to K^-\pi^+)$ and $B(D^0 \to K^-2\pi^+\pi^-)/B(D^0 \to K^-\pi^+)$.

[4] The three pion mass is required to be between 1.0 and 1.6 GeV consistent with an a_1 meson. (If this channel is dominated by a_1^+, the branching ratio for $\overline{D}^{*-}a_1^+$ is twice that for $\overline{D}^{*-}\pi^+\pi^+\pi^-$.)

[5] BORTOLETTO 92 reports $0.0159 \pm 0.0028 \pm 0.0037$ from a measurement of $[\Gamma(B^0 \to D^*(2010)^-\pi^+\pi^+\pi^-)/\Gamma_{total}] \times [B(D^*(2010)^+ \to D^0\pi^+)]$ assuming $B(D^*(2010)^+ \to D^0\pi^+) = 0.57 \pm 0.06$, which we rescale to our best value $B(D^*(2010)^+ \to D^0\pi^+) = (67.7 \pm 0.5) \times 10^{-2}$. Our first error is their experiment's error and our second error is the systematic error from using our best value. Assumes equal production of B^+ and B^0 at the $\Upsilon(4S)$ and uses MarkIII branching fractions for the D.

[6] ALBRECHT 90J reports $0.012 \pm 0.003 \pm 0.004$ from a measurement of $[\Gamma(B^0 \to D^*(2010)^-\pi^+\pi^+\pi^-)/\Gamma_{total}] \times [B(D^*(2010)^+ \to D^0\pi^+)]$ assuming $B(D^*(2010)^+ \to D^0\pi^+) = 0.57 \pm 0.06$, which we rescale to our best value $B(D^*(2010)^+ \to D^0\pi^+) = (67.7 \pm 0.5) \times 10^{-2}$. Our first error is their experiment's error and our second error is the systematic error from using our best value. Assumes equal production of B^+ and B^0 at the $\Upsilon(4S)$ and uses MarkIII branching fractions for the D.

[7] ALBRECHT 87C use PDG 86 branching ratios for D and $D^*(2010)$ and assume $B(\Upsilon(4S) \to B^+B^-) = 55\%$ and $B(\Upsilon(4S) \to B^0\overline{B}^0) = 45\%$. Superseded by ALBRECHT 90J.

[8] BEBEK 87 value has been updated in BERKELMAN 91 to use same assumptions as noted for BORTOLETTO 92.

$\Gamma((D^*(2010)^-\pi^+\pi^+\pi^-)$ nonresonant$)/\Gamma_{total}$ Γ_{58}/Γ

VALUE	DOCUMENT ID		TECN	COMMENT
0.0000±0.0019±0.0016	[1] BORTOLETTO 92		CLEO	$e^+e^- \to \Upsilon(4S)$

[1] BORTOLETTO 92 assumes equal production of B^+ and B^0 at the $\Upsilon(4S)$ and uses MarkIII branching fractions for the D and $D^*(2010)$.

$\Gamma(D^*(2010)^-\pi^+\rho^0)/\Gamma_{total}$ Γ_{59}/Γ

VALUE	DOCUMENT ID		TECN	COMMENT
0.00573±0.00317±0.00004	[1] BORTOLETTO 92		CLEO	$e^+e^- \to \Upsilon(4S)$

[1] BORTOLETTO 92 reports $0.0068 \pm 0.0032 \pm 0.0021$ from a measurement of $[\Gamma(B^0 \to D^*(2010)^-\pi^+\rho^0)/\Gamma_{total}] \times [B(D^*(2010)^+ \to D^0\pi^+)]$ assuming $B(D^*(2010)^+ \to D^0\pi^+) = 0.57 \pm 0.06$, which we rescale to our best value $B(D^*(2010)^+ \to D^0\pi^+) = (67.7 \pm 0.5) \times 10^{-2}$. Our first error is their experiment's error and our second error is the systematic error from using our best value. Assumes equal production of B^+ and B^0 at the $\Upsilon(4S)$ and uses MarkIII branching fractions for the D.

$\Gamma(D^*(2010)^- a_1(1260)^+)/\Gamma_{total}$ Γ_{60}/Γ

VALUE	DOCUMENT ID		TECN	COMMENT
0.0130±0.0027 OUR AVERAGE				
0.0126±0.0020±0.0022	[1,2] ALAM	94	CLE2	$e^+e^- \to \Upsilon(4S)$
0.0152±0.0070±0.0001	[3] BORTOLETTO	92	CLEO	$e^+e^- \to \Upsilon(4S)$

[1] ALAM 94 value is twice their $\Gamma(D^*(2010)^-\pi^+\pi^+\pi^-)/\Gamma_{total}$ value based on their observation that the three pions are dominantly in the $a_1(1260)$ mass range 1.0 to 1.6 GeV.

[2] ALAM 94 assume equal production of B^+ and B^0 at the $\Upsilon(4S)$ and use the CLEOII $B(D^*(2010)^+ \to D^0\pi^+)$ and absolute $B(D^0 \to K^-\pi^+)$ and the PDG 1992 $B(D^0 \to K^-\pi^+\pi^0)/B(D^0 \to K^-\pi^+)$ and $B(D^0 \to K^-2\pi^+\pi^-)/B(D^0 \to K^-\pi^+)$.

[3] BORTOLETTO 92 reports $0.018 \pm 0.006 \pm 0.006$ from a measurement of $[\Gamma(B^0 \to D^*(2010)^- a_1(1260)^+)/\Gamma_{total}] \times [B(D^*(2010)^+ \to D^0\pi^+)]$ assuming $B(D^*(2010)^+ \to D^0\pi^+) = 0.57 \pm 0.06$, which we rescale to our best value $B(D^*(2010)^+ \to D^0\pi^+) = (67.7 \pm 0.5) \times 10^{-2}$. Our first error is their experiment's error and our second error is the systematic error from using our best value. Assumes equal production of B^+ and B^0 at the $\Upsilon(4S)$ and uses MarkIII branching fractions for the D.

$\Gamma(\overline{D}_1(2420)^0\pi^-\pi^+, \overline{D}_1^0 \to D^{*-}\pi^+)/\Gamma(D^*(2010)^-\pi^+\pi^+\pi^-)$ Γ_{61}/Γ_{57}

VALUE	DOCUMENT ID		TECN	COMMENT
(2.04±0.42±0.22) × 10^{-2}	AAIJ	13AO	LHCB	pp at 7 TeV

$\Gamma(D^*(2010)^- K^+\pi^-\pi^+)/\Gamma(D^*(2010)^-\pi^+\pi^+\pi^-)$ Γ_{62}/Γ_{57}

VALUE	DOCUMENT ID		TECN	COMMENT
(6.47±0.37±0.35) × 10^{-2}	AAIJ	13AO	LHCB	pp at 7 TeV

$\Gamma(D^*(2010)^-\pi^+\pi^+\pi^-\pi^0)/\Gamma_{total}$ Γ_{63}/Γ

VALUE	EVTS	DOCUMENT ID		TECN	COMMENT
0.0176±0.0027 OUR AVERAGE					
0.0172±0.0014±0.0024		[1] ALEXANDER	01B	CLE2	$e^+e^- \to \Upsilon(4S)$
0.0345±0.0181±0.0003	28	[2] ALBRECHT	90J	ARG	$e^+e^- \to \Upsilon(4S)$

[1] Assumes equal production of B^+ and B^0 at the $\Upsilon(4S)$. The signal is consistent with all observed $\omega\pi^+$ having proceeded through the ρ'^+ resonance at mass $1349 \pm 25^{+10}_{-5}$ MeV and width $547 \pm 86^{+46}_{-45}$ MeV.

[2] ALBRECHT 90J reports $0.041 \pm 0.015 \pm 0.016$ from a measurement of $[\Gamma(B^0 \to D^*(2010)^-\pi^+\pi^+\pi^-\pi^0)/\Gamma_{total}] \times [B(D^*(2010)^+ \to D^0\pi^+)]$ assuming $B(D^*(2010)^+ \to D^0\pi^+) = 0.57 \pm 0.06$, which we rescale to our best value $B(D^*(2010)^+ \to D^0\pi^+) = (67.7 \pm 0.5) \times 10^{-2}$. Our first error is their experiment's error and our second error is the systematic error from using our best value. Assumes equal production of B^+ and B^0 at the $\Upsilon(4S)$ and uses MarkIII branching fractions for the D.

$\Gamma(D^{*-}3\pi^+2\pi^-)/\Gamma_{total}$ Γ_{64}/Γ

VALUE (units 10^{-3})	DOCUMENT ID		TECN	COMMENT
4.72±0.59±0.71	[1] MAJUMDER	04	BELL	$e^+e^- \to \Upsilon(4S)$

[1] Assumes equal production of B^+ and B^0 at the $\Upsilon(4S)$.

$\Gamma(\overline{D}^*(2010)^-\omega\pi^+)/\Gamma_{total}$ Γ_{65}/Γ

VALUE (units 10^{-3})	DOCUMENT ID		TECN	COMMENT
2.46±0.18 OUR AVERAGE	Error includes scale factor of 1.2.			
2.31±0.11±0.14	[1] MATVIENKO	15	BELL	$e^+e^- \to \Upsilon(4S)$
2.88±0.21±0.31	[1] AUBERT	06L	BABR	$e^+e^- \to \Upsilon(4S)$
2.9 ±0.3 ±0.4	[1,2] ALEXANDER	01B	CLE2	$e^+e^- \to \Upsilon(4S)$

[1] Assumes equal production of B^+ and B^0 at the $\Upsilon(4S)$.
[2] The signal is consistent with all observed $\omega\pi^+$ having proceeded through the ρ'^+ resonance at mass $1349 \pm 25^{+10}_{-5}$ MeV and width $547 \pm 86^{+46}_{-45}$ MeV.

$\Gamma(D_1(2430)^0\omega,\ D_1^0 \to D^{*-}\pi^+)/\Gamma_{total}$ Γ_{66}/Γ

VALUE (units 10^{-4})	DOCUMENT ID		TECN	COMMENT
$2.7^{+0.8}_{-0.4}$ OUR AVERAGE				
$2.5 \pm 0.4^{+0.8}_{-0.2}$	[1,2] MATVIENKO	15	BELL	$e^+e^- \to \Upsilon(4S)$
4.1±1.2±1.1	[3] AUBERT	06L	BABR	$e^+e^- \to \Upsilon(4S)$

[1] Assumes equal production of B^+ and B^0.
[2] The measurement is obtained by amplitude analysis of $B^0 \to D^{*-}\omega\pi^+$. The second uncertainty combines in quadrature experimental systematic and model uncertainties.
[3] Obtained by fitting the events with $\cos\theta_{D^*} < 0.5$ and scaling up the result by a factor of 4/3. No interference effects between $B^0 \to D_1'\omega$ and $D^*\omega\pi$ are assumed.

$\Gamma(\overline{D}^{*-}\rho(1450)^+)/\Gamma_{total}$ Γ_{67}/Γ

VALUE (units 10^{-3})	DOCUMENT ID		TECN	COMMENT
$1.07^{+0.15+0.40}_{-0.31-0.13}$	[1,2] MATVIENKO	15	BELL	$e^+e^- \to \Upsilon(4S)$

[1] Obtained by amplitude analysis of $\overline{B}^0 \to D^{*-}\omega\pi^+$. The second uncertainty combines in qudrature experimental systematic and model uncertainties.
[2] Assumes equal production of B^0 and B^+ at $\Upsilon(4S)$.

$\Gamma(\overline{D}_1(2420)^0\omega)/\Gamma_{total}$ Γ_{68}/Γ

VALUE (units 10^{-4})	DOCUMENT ID		TECN	COMMENT
0.7±0.2±0.1	[1,2] MATVIENKO	15	BELL	$e^+e^- \to \Upsilon(4S)$

[1] Obtained by amplitude analysis of $\overline{B}^0 \to D^{*-}\omega\pi^+$. The second uncertainty combines in qudrature experimental systematic and model uncertainties.
[2] Assumes equal production of B^0 and B^+ at $\Upsilon(4S)$.

$\Gamma(\overline{D}_2^*(2460)^0\omega)/\Gamma_{total}$ Γ_{69}/Γ

VALUE (units 10^{-4})	DOCUMENT ID		TECN	COMMENT
0.4±0.1±0.1	[1,2] MATVIENKO	15	BELL	$e^+e^- \to \Upsilon(4S)$

[1] Obtained by amplitude analysis of $\overline{B}^0 \to D^{*-}\omega\pi^+$. The second uncertainty combines in qudrature experimental systematic and model uncertainties.
[2] Assumes equal production of B^0 and B^+ at $\Upsilon(4S)$.

$\Gamma(\overline{D}^{*-}b_1(1235)^-,\ b_1^- \to \omega\pi^-)/\Gamma_{total}$ Γ_{70}/Γ

VALUE	CL%	DOCUMENT ID		TECN	COMMENT
$<0.7 \times 10^{-4}$	90	[1] MATVIENKO	15	BELL	$e^+e^- \to \Upsilon(4S)$

[1] Assumes equal production of B^0 and B^+ at $\Upsilon(4S)$.

$\Gamma(\overline{D}^{**-}\pi^+)/\Gamma_{total}$ Γ_{71}/Γ

D^{**-} represents an excited state with mass $2.2 < M < 2.8$ GeV/c^2.

VALUE (units 10^{-3})	DOCUMENT ID		TECN	COMMENT
1.9±0.9±0.1	[1,2] AUBERT,BE	06J	BABR	$e^+e^- \to \Upsilon(4S)$

[1] AUBERT,BE 06J reports $[\Gamma(B^0 \to \overline{D}^{**-}\pi^+)/\Gamma_{total}] / [B(B^0 \to D^-\pi^+)] = 0.77 \pm 0.22 \pm 0.29$ which we multiply by our best value $B(B^0 \to D^-\pi^+) = (2.52 \pm 0.13) \times 10^{-3}$. Our first error is their experiment's error and our second error is the systematic error from using our best value.
[2] Uses a missing-mass method. Does not depend on D branching fractions or B^+/B^0 production rates.

$\Gamma(D_1(2420)^-\pi^+,\ D_1^- \to D^-\pi^+\pi^-)/\Gamma_{total}$ Γ_{72}/Γ

VALUE (units 10^{-4})	DOCUMENT ID		TECN	COMMENT
$0.99^{+0.20}_{-0.25}$ OUR FIT				
$0.89 \pm 0.15^{+0.17}_{-0.32}$	[1] ABE	05A	BELL	$e^+e^- \to \Upsilon(4S)$

[1] Assumes equal production of B^+ and B^0 at the $\Upsilon(4S)$.

$\Gamma(D_1(2420)^-\pi^+,\ D_1^- \to D^-\pi^+\pi^-)/\Gamma(D^-\pi^+\pi^+\pi^-)$ Γ_{72}/Γ_{46}

VALUE (units 10^{-2})	DOCUMENT ID		TECN	COMMENT
$1.65^{+0.35}_{-0.40}$ OUR FIT				
2.1 ±0.5 $^{+0.3}_{-0.5}$	AAIJ	11E	LHCB	pp at 7 TeV

$\Gamma(D_1(2420)^-\pi^+,\ D_1^- \to D^{*-}\pi^+\pi^-)/\Gamma_{total}$ Γ_{73}/Γ

VALUE (units 10^{-4})	CL%	DOCUMENT ID		TECN	COMMENT
<0.33	90	[1] ABE	05A	BELL	$e^+e^- \to \Upsilon(4S)$

[1] Assumes equal production of B^+ and B^0 at the $\Upsilon(4S)$.

$\Gamma(D^*(2010)^-\pi^+\pi^+\pi^-)/\Gamma(D^*(2010)^-\pi^+)$ Γ_{57}/Γ_{44}

VALUE	DOCUMENT ID		TECN	COMMENT
2.64±0.04±0.13	AAIJ	13AO	LHCB	pp at 7 TeV

$\Gamma(\overline{D}_2^*(2460)^-\pi^+,\ (D_2^*)^- \to D^0\pi^-)/\Gamma_{total}$ Γ_{74}/Γ

VALUE (units 10^{-4})	CL%	DOCUMENT ID		TECN	COMMENT
2.38±0.16 OUR AVERAGE					
2.44±0.07±0.16		[1] AAIJ	15Y	LHCB	pp at 7, 8 TeV
2.15±0.17±0.31		[2,3] KUZMIN	07	BELL	$e^+e^- \to \Upsilon(4S)$
• • • We do not use the following data for averages, fits, limits, etc. • • •					
<14.7	90	[2] ALAM	94	CLE2	$e^+e^- \to \Upsilon(4S)$

[1] Result obtained using the isobar formalism. The second uncertainty combines in quadrature all systematic uncertainties quoted in the paper.
[2] Assumes equal production of B^+ and B^0 at the $\Upsilon(4S)$.
[3] Our second uncertainty combines systematics and model errors quoted in the paper.

$\Gamma(\overline{D}_0^*(2400)^-\pi^+,\ (D_0^*)^- \to D^0\pi^-)/\Gamma_{total}$ Γ_{75}/Γ

VALUE (units 10^{-4})	DOCUMENT ID		TECN	COMMENT
0.76±0.08 OUR AVERAGE				
0.77±0.05±0.06	[1] AAIJ	15Y	LHCB	pp at 7, 8 TeV
0.60±0.13±0.27	[2,3] KUZMIN	07	BELL	$e^+e^- \to \Upsilon(4S)$

[1] Result obtained using the isobar formalism. The second uncertainty combines in quadrature all systematic uncertainties quoted in the paper.
[2] Assumes equal production of B^+ and B^0 at the $\Upsilon(4S)$.
[3] Our second uncertainty combines systematics and model errors quoted in the paper.

$\Gamma(D_2^*(2460)^-\pi^+,\ (D_2^*)^- \to D^{*-}\pi^+\pi^-)/\Gamma_{total}$ Γ_{76}/Γ

VALUE (units 10^{-4})	CL%	DOCUMENT ID		TECN	COMMENT
<0.24	90	[1] ABE	05A	BELL	$e^+e^- \to \Upsilon(4S)$

[1] Assumes equal production of B^+ and B^0 at the $\Upsilon(4S)$.

$\Gamma(\overline{D}_2^*(2460)^-\rho^+)/\Gamma_{total}$ Γ_{77}/Γ

VALUE	CL%	DOCUMENT ID		TECN	COMMENT
<0.0049	90	[1] ALAM	94	CLE2	$e^+e^- \to \Upsilon(4S)$

[1] ALAM 94 assumes equal production of B^+ and B^0 at the $\Upsilon(4S)$ and use the CLEO II absolute $B(D^0 \to K^-\pi^+)$ and $B(D_2^*(2460)^+ \to D^0\pi^+) = 30\%$.

$\Gamma(D^0\overline{D}^0)/\Gamma_{total}$ Γ_{78}/Γ

VALUE (units 10^{-4})	CL%	DOCUMENT ID		TECN	COMMENT
0.14±0.06±0.03		[1] AAIJ	13AP	LHCB	pp at 7 TeV
• • • We do not use the following data for averages, fits, limits, etc. • • •					
<0.43	90	[2] ADACHI	08	BELL	$e^+e^- \to \Upsilon(4S)$
<0.6	90	[2] AUBERT,B	06A	BABR	$e^+e^- \to \Upsilon(4S)$

[1] Uses $B(B^0 \to D^-D^+) = (2.11 \pm 0.31) \times 10^{-4}$ and $B(B^+ \to \overline{D}^0 D_s^+) = (10.1 \pm 1.7) \times 10^{-3}$.
[2] Assumes equal production of B^+ and B^0 at the $\Upsilon(4S)$.

$\Gamma(D^{*0}\overline{D}^0)/\Gamma_{total}$ Γ_{79}/Γ

VALUE (units 10^{-4})	CL%	DOCUMENT ID		TECN	COMMENT
<2.9	90	[1] AUBERT,B	06A	BABR	$e^+e^- \to \Upsilon(4S)$

[1] Assumes equal production of B^+ and B^0 at the $\Upsilon(4S)$.

$\Gamma(D^-D^+)/\Gamma_{total}$ Γ_{80}/Γ

VALUE (units 10^{-4})	CL%	DOCUMENT ID		TECN	COMMENT
2.11±0.18 OUR AVERAGE					
2.12±0.16±0.18		[1] ROHRKEN	12	BELL	$e^+e^- \to \Upsilon(4S)$
1.97±0.20±0.20		[1] FRATINA	07	BELL	$e^+e^- \to \Upsilon(4S)$
2.8 ±0.4 ±0.5		[1] AUBERT,B	06A	BABR	$e^+e^- \to \Upsilon(4S)$
• • • We do not use the following data for averages, fits, limits, etc. • • •					
1.91±0.51±0.30		[1] MAJUMDER	05	BELL	Repl. by FRATINA 07
< 9.4	90	[1] LIPELES	00	CLE2	$e^+e^- \to \Upsilon(4S)$
<59	90	BARATE	98Q	ALEP	$e^+e^- \to Z$
<12	90	ASNER	97	CLE2	$e^+e^- \to \Upsilon(4S)$

[1] Assumes equal production of B^+ and B^0 at the $\Upsilon(4S)$.

$\Gamma(D^\pm D^{*\mp}(CP\text{-averaged}))/\Gamma_{total}$ Γ_{81}/Γ

VALUE (units 10^{-4})	DOCUMENT ID		TECN	COMMENT
6.14±0.29±0.50	[1] ROHRKEN	12	BELL	$e^+e^- \to \Upsilon(4S)$

[1] Assumes equal production of B^+ and B^0 at the $\Upsilon(4S)$.

$\Gamma(D^-D_s^+)/\Gamma_{total}$ Γ_{82}/Γ

VALUE	EVTS	DOCUMENT ID		TECN	COMMENT
0.0072±0.0008 OUR AVERAGE					
0.0073±0.0004±0.0007		[1] ZUPANC	07	BELL	$e^+e^- \to \Upsilon(4S)$
0.0066±0.0014±0.0006		[2] AUBERT	06N	BABR	$e^+e^- \to \Upsilon(4S)$
0.0068±0.0024±0.0006		[3] GIBAUT	96	CLE2	$e^+e^- \to \Upsilon(4S)$
0.010 ±0.009 ±0.001		[4] ALBRECHT	92G	ARG	$e^+e^- \to \Upsilon(4S)$
0.0053±0.0030±0.0005		[5] BORTOLETTO	92	CLEO	$e^+e^- \to \Upsilon(4S)$
• • • We do not use the following data for averages, fits, limits, etc. • • •					
0.012 ±0.007	3	[6] BORTOLETTO	90	CLEO	$e^+e^- \to \Upsilon(4S)$

[1] ZUPANC 07 reports $(7.5 \pm 0.2 \pm 1.1) \times 10^{-3}$ from a measurement of $[\Gamma(B^0 \to D^- D_s^+)/\Gamma_{\text{total}}] \times [B(D_s^+ \to \phi\pi^+)]$ assuming $B(D_s^+ \to \phi\pi^+) = (4.4 \pm 0.6) \times 10^{-2}$, which we rescale to our best value $B(D_s^+ \to \phi\pi^+) = (4.5 \pm 0.4) \times 10^{-2}$. Our first error is their experiment's error and our second error is the systematic error from using our best value.

[2] AUBERT 06N reports $(0.64 \pm 0.13 \pm 0.10) \times 10^{-2}$ from a measurement of $[\Gamma(B^0 \to D^- D_s^+)/\Gamma_{\text{total}}] \times [B(D_s^+ \to \phi\pi^+)]$ assuming $B(D_s^+ \to \phi\pi^+) = 0.0462 \pm 0.0062$, which we rescale to our best value $B(D_s^+ \to \phi\pi^+) = (4.5 \pm 0.4) \times 10^{-2}$. Our first error is their experiment's error and our second error is the systematic error from using our best value.

[3] GIBAUT 96 reports $0.0087 \pm 0.0024 \pm 0.0020$ from a measurement of $[\Gamma(B^0 \to D^- D_s^+)/\Gamma_{\text{total}}] \times [B(D_s^+ \to \phi\pi^+)]$ assuming $B(D_s^+ \to \phi\pi^+) = 0.035$, which we rescale to our best value $B(D_s^+ \to \phi\pi^+) = (4.5 \pm 0.4) \times 10^{-2}$. Our first error is their experiment's error and our second error is the systematic error from using our best value.

[4] ALBRECHT 92G reports $0.017 \pm 0.013 \pm 0.006$ from a measurement of $[\Gamma(B^0 \to D^- D_s^+)/\Gamma_{\text{total}}] \times [B(D_s^+ \to \phi\pi^+)]$ assuming $B(D_s^+ \to \phi\pi^+) = 0.027$, which we rescale to our best value $B(D_s^+ \to \phi\pi^+) = (4.5 \pm 0.4) \times 10^{-2}$. Our first error is their experiment's error and our second error is the systematic error from using our best value. Assumes PDG 1990 D^+ branching ratios, e.g., $B(D^+ \to K^- 2\pi^+) = 7.7 \pm 1.0\%$.

[5] BORTOLETTO 92 reports $0.0080 \pm 0.0045 \pm 0.0030$ from a measurement of $[\Gamma(B^0 \to D^- D_s^+)/\Gamma_{\text{total}}] \times [B(D_s^+ \to \phi\pi^+)]$ assuming $B(D_s^+ \to \phi\pi^+) = 0.030 \pm 0.011$, which we rescale to our best value $B(D_s^+ \to \phi\pi^+) = (4.5 \pm 0.4) \times 10^{-2}$. Our first error is their experiment's error and our second error is the systematic error from using our best value. Assumes equal production of B^+ and B^0 at the $\Upsilon(4S)$ and uses Mark III branching fractions for the D.

[6] BORTOLETTO 90 assume $B(D_s \to \phi\pi^+) = 2\%$. Superseded by BORTOLETTO 92.

$\Gamma(D^*(2010)^- D_s^+)/\Gamma_{\text{total}}$ Γ_{83}/Γ

VALUE	EVTS	DOCUMENT ID		TECN	COMMENT
0.0080±0.0011 OUR AVERAGE					
0.0073±0.0013±0.0007		[1] AUBERT	06N	BABR	$e^+e^- \to \Upsilon(4S)$
0.0083±0.0015±0.0007		[2] AUBERT	03I	BABR	$e^+e^- \to \Upsilon(4S)$
0.0088±0.0017±0.0008		[3] AHMED	00B	CLE2	$e^+e^- \to \Upsilon(4S)$
0.008 ±0.006 ±0.001		[4] ALBRECHT	92G	ARG	$e^+e^- \to \Upsilon(4S)$
0.011 ±0.006 ±0.001		[5] BORTOLETTO	92	CLEO	$e^+e^- \to \Upsilon(4S)$
• • • We do not use the following data for averages, fits, limits, etc. • • •					
0.0072±0.0022±0.0006		[6] GIBAUT	96	CLE2	Repl. by AHMED 00B
0.024 ±0.014	3	[7] BORTOLETTO	90	CLEO	$e^+e^- \to \Upsilon(4S)$

[1] AUBERT 06N reports $(0.71 \pm 0.13 \pm 0.09) \times 10^{-2}$ from a measurement of $[\Gamma(B^0 \to D^*(2010)^- D_s^+)/\Gamma_{\text{total}}] \times [B(D_s^+ \to \phi\pi^+)]$ assuming $B(D_s^+ \to \phi\pi^+) = 0.0462 \pm 0.0062$, which we rescale to our best value $B(D_s^+ \to \phi\pi^+) = (4.5 \pm 0.4) \times 10^{-2}$. Our first error is their experiment's error and our second error is the systematic error from using our best value.

[2] AUBERT 03I reports $0.0103 \pm 0.0014 \pm 0.0013$ from a measurement of $[\Gamma(B^0 \to D^*(2010)^- D_s^+)/\Gamma_{\text{total}}] \times [B(D_s^+ \to \phi\pi^+)]$ assuming $B(D_s^+ \to \phi\pi^+) = 0.036$, which we rescale to our best value $B(D_s^+ \to \phi\pi^+) = (4.5 \pm 0.4) \times 10^{-2}$. Our first error is their experiment's error and our second error is the systematic error from using our best value.

[3] AHMED 00B reports $0.0110 \pm 0.0018 \pm 0.0011$ from a measurement of $[\Gamma(B^0 \to D^*(2010)^- D_s^+)/\Gamma_{\text{total}}] \times [B(D_s^+ \to \phi\pi^+)]$ assuming $B(D_s^+ \to \phi\pi^+) = 0.036$, which we rescale to our best value $B(D_s^+ \to \phi\pi^+) = (4.5 \pm 0.4) \times 10^{-2}$. Our first error is their experiment's error and our second error is the systematic error from using our best value.

[4] ALBRECHT 92G reports $0.014 \pm 0.010 \pm 0.003$ from a measurement of $[\Gamma(B^0 \to D^*(2010)^- D_s^+)/\Gamma_{\text{total}}] \times [B(D_s^+ \to \phi\pi^+)]$ assuming $B(D_s^+ \to \phi\pi^+) = 0.027$, which we rescale to our best value $B(D_s^+ \to \phi\pi^+) = (4.5 \pm 0.4) \times 10^{-2}$. Our first error is their experiment's error and our second error is the systematic error from using our best value. Assumes PDG 1990 D^+ and $D^*(2010)^+$ branching ratios, e.g., $B(D^0 \to K^-\pi^+) = 3.71 \pm 0.25\%$, $B(D^+ \to K^- 2\pi^+) = 7.1 \pm 1.0\%$, and $B(D^*(2010)^+ \to D^0\pi^+) = 55 \pm 4\%$.

[5] BORTOLETTO 92 reports $0.016 \pm 0.009 \pm 0.006$ from a measurement of $[\Gamma(B^0 \to D^*(2010)^- D_s^+)/\Gamma_{\text{total}}] \times [B(D_s^+ \to \phi\pi^+)]$ assuming $B(D_s^+ \to \phi\pi^+) = 0.030 \pm 0.011$, which we rescale to our best value $B(D_s^+ \to \phi\pi^+) = (4.5 \pm 0.4) \times 10^{-2}$. Our first error is their experiment's error and our second error is the systematic error from using our best value. Assumes equal production of B^+ and B^0 at the $\Upsilon(4S)$ and uses Mark III branching fractions for the D and $D^*(2010)$.

[6] GIBAUT 96 reports $0.0093 \pm 0.0023 \pm 0.0016$ from a measurement of $[\Gamma(B^0 \to D^*(2010)^- D_s^+)/\Gamma_{\text{total}}] \times [B(D_s^+ \to \phi\pi^+)]$ assuming $B(D_s^+ \to \phi\pi^+) = 0.035$, which we rescale to our best value $B(D_s^+ \to \phi\pi^+) = (4.5 \pm 0.4) \times 10^{-2}$. Our first error is their experiment's error and our second error is the systematic error from using our best value.

[7] BORTOLETTO 90 assume $B(D_s \to \phi\pi^+) = 2\%$. Superseded by BORTOLETTO 92.

$\Gamma(D^- D_s^{*+})/\Gamma_{\text{total}}$ Γ_{84}/Γ

VALUE	DOCUMENT ID		TECN	COMMENT
0.0074±0.0016 OUR AVERAGE				
0.0071±0.0016±0.0006	[1] AUBERT	06N	BABR	$e^+e^- \to \Upsilon(4S)$
0.0078±0.0032±0.0007	[2] GIBAUT	96	CLE2	$e^+e^- \to \Upsilon(4S)$
0.016 ±0.012 ±0.001	[3] ALBRECHT	92G	ARG	$e^+e^- \to \Upsilon(4S)$

[1] AUBERT 06N reports $(0.69 \pm 0.16 \pm 0.09) \times 10^{-2}$ from a measurement of $[\Gamma(B^0 \to D^- D_s^{*+})/\Gamma_{\text{total}}] \times [B(D_s^+ \to \phi\pi^+)]$ assuming $B(D_s^+ \to \phi\pi^+) = 0.0462 \pm 0.0062$, which we rescale to our best value $B(D_s^+ \to \phi\pi^+) = (4.5 \pm 0.4) \times 10^{-2}$. Our first error is their experiment's error and our second error is the systematic error from using our best value.

[2] GIBAUT 96 reports $0.0100 \pm 0.0035 \pm 0.0022$ from a measurement of $[\Gamma(B^0 \to D^- D_s^{*+})/\Gamma_{\text{total}}] \times [B(D_s^+ \to \phi\pi^+)]$ assuming $B(D_s^+ \to \phi\pi^+) = 0.035$, which we rescale to our best value $B(D_s^+ \to \phi\pi^+) = (4.5 \pm 0.4) \times 10^{-2}$. Our first error is their experiment's error and our second error is the systematic error from using our best value.

[3] ALBRECHT 92G reports $0.027 \pm 0.017 \pm 0.009$ from a measurement of $[\Gamma(B^0 \to D^- D_s^{*+})/\Gamma_{\text{total}}] \times [B(D_s^+ \to \phi\pi^+)]$ assuming $B(D_s^+ \to \phi\pi^+) = 0.027$, which we rescale to our best value $B(D_s^+ \to \phi\pi^+) = (4.5 \pm 0.4) \times 10^{-2}$. Our first error is their experiment's error and our second error is the systematic error from using our best value. Assumes PDG 1990 D^+ branching ratios, e.g., $B(D^+ \to K^- 2\pi^+) = 7.7 \pm 1.0\%$.

$\Gamma(D^*(2010)^- D_s^{*+})/\Gamma_{\text{total}}$ Γ_{85}/Γ

VALUE	DOCUMENT ID		TECN	COMMENT
0.0177±0.0014 OUR AVERAGE				
0.0173±0.0018±0.0015	[1] AUBERT	06N	BABR	$e^+e^- \to \Upsilon(4S)$
0.0188±0.0009±0.0017	[2] AUBERT	05V	BABR	$e^+e^- \to \Upsilon(4S)$
0.0158±0.0027±0.0014	[3] AUBERT	03I	BABR	$e^+e^- \to \Upsilon(4S)$
0.015 ±0.004 ±0.001	[4] AHMED	00B	CLE2	$e^+e^- \to \Upsilon(4S)$
0.016 ±0.009 ±0.001	[5] ALBRECHT	92G	ARG	$e^+e^- \to \Upsilon(4S)$
• • • We do not use the following data for averages, fits, limits, etc. • • •				
0.016 ±0.005 ±0.001	[6] GIBAUT	96	CLE2	Repl. by AHMED 00B

[1] AUBERT 06N reports $(1.68 \pm 0.21 \pm 0.19) \times 10^{-2}$ from a measurement of $[\Gamma(B^0 \to D^*(2010)^- D_s^{*+})/\Gamma_{\text{total}}] \times [B(D_s^+ \to \phi\pi^+)]$ assuming $B(D_s^+ \to \phi\pi^+) = 0.0462 \pm 0.0062$, which we rescale to our best value $B(D_s^+ \to \phi\pi^+) = (4.5 \pm 0.4) \times 10^{-2}$. Our first error is their experiment's error and our second error is the systematic error from using our best value.

[2] A partial reconstruction technique is used and the result is independent of the particle decay rate of D_S^+ meson. It also provides a model-independent determination of $B(D_S^+ \to \phi\pi^+) = (4.81 \pm 0.52 \pm 0.38)\%$.

[3] AUBERT 03I reports $0.0197 \pm 0.0015 \pm 0.0030$ from a measurement of $[\Gamma(B^0 \to D^*(2010)^- D_s^{*+})/\Gamma_{\text{total}}] \times [B(D_s^+ \to \phi\pi^+)]$ assuming $B(D_s^+ \to \phi\pi^+) = 0.036$, which we rescale to our best value $B(D_s^+ \to \phi\pi^+) = (4.5 \pm 0.4) \times 10^{-2}$. Our first error is their experiment's error and our second error is the systematic error from using our best value.

[4] AHMED 00B reports $0.0182 \pm 0.0037 \pm 0.0025$ from a measurement of $[\Gamma(B^0 \to D^*(2010)^- D_s^{*+})/\Gamma_{\text{total}}] \times [B(D_s^+ \to \phi\pi^+)]$ assuming $B(D_s^+ \to \phi\pi^+) = 0.036$, which we rescale to our best value $B(D_s^+ \to \phi\pi^+) = (4.5 \pm 0.4) \times 10^{-2}$. Our first error is their experiment's error and our second error is the systematic error from using our best value.

[5] ALBRECHT 92G reports $0.026 \pm 0.014 \pm 0.006$ from a measurement of $[\Gamma(B^0 \to D^*(2010)^- D_s^{*+})/\Gamma_{\text{total}}] \times [B(D_s^+ \to \phi\pi^+)]$ assuming $B(D_s^+ \to \phi\pi^+) = 0.027$, which we rescale to our best value $B(D_s^+ \to \phi\pi^+) = (4.5 \pm 0.4) \times 10^{-2}$. Our first error is their experiment's error and our second error is the systematic error from using our best value. Assumes PDG 1990 D^+ and $D^*(2010)^+$ branching ratios, e.g., $B(D^0 \to K^-\pi^+) = 3.71 \pm 0.25\%$, $B(D^+ \to K^- 2\pi^+) = 7.1 \pm 1.0\%$, and $B(D^*(2010)^+ \to D^0\pi^+) = 55 \pm 4\%$.

[6] GIBAUT 96 reports $0.0203 \pm 0.0050 \pm 0.0036$ from a measurement of $[\Gamma(B^0 \to D^*(2010)^- D_s^{*+})/\Gamma_{\text{total}}] \times [B(D_s^+ \to \phi\pi^+)]$ assuming $B(D_s^+ \to \phi\pi^+) = 0.035$, which we rescale to our best value $B(D_s^+ \to \phi\pi^+) = (4.5 \pm 0.4) \times 10^{-2}$. Our first error is their experiment's error and our second error is the systematic error from using our best value.

$\left[\Gamma(D^*(2010)^- D_s^+) + \Gamma(D^*(2010)^- D_s^{*+})\right]/\Gamma_{\text{total}}$ $(\Gamma_{83}+\Gamma_{85})/\Gamma$

VALUE (units 10^{-2})	EVTS	DOCUMENT ID		TECN	COMMENT
2.5 ±0.4 OUR AVERAGE					
2.40±0.35±0.22		[1] AUBERT	03I	BABR	$e^+e^- \to \Upsilon(4S)$
3.3 ±0.9 ±0.3	22	[2] BORTOLETTO	90	CLEO	$e^+e^- \to \Upsilon(4S)$

[1] AUBERT 03I reports $(3.00 \pm 0.19 \pm 0.39) \times 10^{-2}$ from a measurement of $\left[\left[\Gamma(B^0 \to D^*(2010)^- D_s^+) + \Gamma(B^0 \to D^*(2010)^- D_s^{*+})\right]/\Gamma_{\text{total}}\right] \times [B(D_s^+ \to \phi\pi^+)]$ assuming $B(D_s^+ \to \phi\pi^+) = 0.036$, which we rescale to our best value $B(D_s^+ \to \phi\pi^+) = (4.5 \pm 0.4) \times 10^{-2}$. Our first error is their experiment's error and our second error is the systematic error from using our best value.

[2] BORTOLETTO 90 reports $(7.5 \pm 2.0) \times 10^{-2}$ from a measurement of $\left[\left[\Gamma(B^0 \to D^*(2010)^- D_s^+) + \Gamma(B^0 \to D^*(2010)^- D_s^{*+})\right]/\Gamma_{\text{total}}\right] \times [B(D_s^+ \to \phi\pi^+)]$ assuming $B(D_s^+ \to \phi\pi^+) = 0.02$, which we rescale to our best value $B(D_s^+ \to \phi\pi^+) = (4.5 \pm 0.4) \times 10^{-2}$. Our first error is their experiment's error and our second error is the systematic error from using our best value.

$\Gamma(D_{s0}(2317)^- K^+,\ D_{s0}^- \to D_s^- \pi^0)/\Gamma_{\text{total}}$ Γ_{86}/Γ

VALUE (units 10^{-5})	DOCUMENT ID		TECN	COMMENT
$4.2^{+1.4}_{-1.3}\pm0.4$	[1] DRUTSKOY	05	BELL	$e^+e^- \to \Upsilon(4S)$

[1] DRUTSKOY 05 reports $(5.3^{+1.5}_{-1.3} \pm 1.6) \times 10^{-5}$ from a measurement of $[\Gamma(B^0 \to D_{s0}(2317)^- K^+,\ D_{s0}^- \to D_s^- \pi^0)/\Gamma_{\text{total}}] \times [B(D_s^+ \to \phi\pi^+)]$ assuming $B(D_s^+ \to$

$\phi\pi^+) = 0.036 \pm 0.009$, which we rescale to our best value $B(D_s^+ \to \phi\pi^+) = (4.5 \pm 0.4) \times 10^{-2}$. Our first error is their experiment's error and our second error is the systematic error from using our best value.

$\Gamma(D_{s0}(2317)^- \pi^+,\ D_{s0}^- \to D_s^- \pi^0)/\Gamma_{total}$ Γ_{87}/Γ

VALUE (units 10^{-5})	CL%	DOCUMENT ID		TECN	COMMENT
<2.5	90	[1] DRUTSKOY	05	BELL	$e^+e^- \to \Upsilon(4S)$

[1] Assumes equal production of B^+ and B^0 at the $\Upsilon(4S)$.

$\Gamma(D_{sJ}(2457)^- K^+,\ D_{sJ}^- \to D_s^- \pi^0)/\Gamma_{total}$ Γ_{88}/Γ

VALUE (units 10^{-5})	CL%	DOCUMENT ID		TECN	COMMENT
<0.94	90	[1] DRUTSKOY	05	BELL	$e^+e^- \to \Upsilon(4S)$

[1] Assumes equal production of B^+ and B^0 at the $\Upsilon(4S)$.

$\Gamma(D_{sJ}(2457)^- \pi^+,\ D_{sJ}^- \to D_s^- \pi^0)/\Gamma_{total}$ Γ_{89}/Γ

VALUE (units 10^{-5})	CL%	DOCUMENT ID		TECN	COMMENT
<0.40	90	[1] DRUTSKOY	05	BELL	$e^+e^- \to \Upsilon(4S)$

[1] Assumes equal production of B^+ and B^0 at the $\Upsilon(4S)$.

$\Gamma(D_s^- D_s^+)/\Gamma_{total}$ Γ_{90}/Γ

VALUE	CL%	DOCUMENT ID		TECN	COMMENT
$< 3.6 \times 10^{-5}$	90	[1] ZUPANC	07	BELL	$e^+e^- \to \Upsilon(4S)$
• • • We do not use the following data for averages, fits, limits, etc. • • •					
$<10 \quad \times 10^{-5}$	90	[1] AUBERT,BE	05F	BABR	$e^+e^- \to \Upsilon(4S)$

[1] Assumes equal production of B^+ and B^0 at the $\Upsilon(4S)$.

$\Gamma(D_s^{*-} D_s^+)/\Gamma_{total}$ Γ_{91}/Γ

VALUE	CL%	DOCUMENT ID		TECN	COMMENT
$<1.3 \times 10^{-4}$	90	[1] AUBERT,BE	05F	BABR	$e^+e^- \to \Upsilon(4S)$

[1] Assumes equal production of B^+ and B^0 at the $\Upsilon(4S)$.

$\Gamma(D_s^{*-} D_s^{*+})/\Gamma_{total}$ Γ_{92}/Γ

VALUE	CL%	DOCUMENT ID		TECN	COMMENT
$<2.4 \times 10^{-4}$	90	[1] AUBERT,BE	05F	BABR	$e^+e^- \to \Upsilon(4S)$

[1] Assumes equal production of B^+ and B^0 at the $\Upsilon(4S)$.

$\Gamma(D_{s0}^*(2317)^+ D^-,\ D_{s0}^{*+} \to D_s^+ \pi^0)/\Gamma_{total}$ Γ_{93}/Γ

VALUE (units 10^{-3})	DOCUMENT ID		TECN	COMMENT
1.09±0.16 OUR AVERAGE				
$1.02 \pm 0.16 \pm 0.05$	[1,2] CHOI	15A	BELL	$e^+e^- \to \Upsilon(4S)$
$1.4\ ^{+0.5}_{-0.4} \pm 0.1$	[2,3] AUBERT,B	04S	BABR	$e^+e^- \to \Upsilon(4S)$
• • • We do not use the following data for averages, fits, limits, etc. • • •				
$0.69^{+0.29}_{-0.24} \pm 0.06$	[2,4] KROKOVNY	03B	BELL	Repl. by CHOI 15A

[1] CHOI 15A reports $(10.2^{+1.3}_{-1.2} \pm 1.0 \pm 0.4) \times 10^{-4}$ from a measurement of $[\Gamma(B^0 \to D_{s0}^*(2317)^+ D^-,\ D_{s0}^{*+} \to D_s^+ \pi^0)/\Gamma_{total}] \times [B(D_s^+ \to K^+K^-\pi^+)]$ × $[B(D^+ \to K^-2\pi^+)]$ assuming $B(D_s^+ \to K^+K^-\pi^+) = (5.39 \pm 0.21) \times 10^{-2}$,$B(D^+ \to K^-2\pi^+) = (9.13 \pm 0.19) \times 10^{-2}$, which we rescale to our best values $B(D_s^+ \to K^+K^-\pi^+) = (5.45 \pm 0.17) \times 10^{-2}$, $B(D^+ \to K^-2\pi^+) = (8.98 \pm 0.28) \times 10^{-2}$. Our first error is their experiment's error and our second error is the systematic error from using our best values.

[2] Assumes equal production of B^+ and B^0 at the $\Upsilon(4S)$.

[3] AUBERT,B 04S reports $(1.8 \pm 0.4^{+0.7}_{-0.5}) \times 10^{-3}$ from a measurement of $[\Gamma(B^0 \to D_{s0}^*(2317)^+ D^-,\ D_{s0}^{*+} \to D_s^+ \pi^0)/\Gamma_{total}] \times [B(D_s^+ \to \phi\pi^+)]$ assuming $B(D_s^+ \to \phi\pi^+) = 0.036 \pm 0.009$, which we rescale to our best value $B(D_s^+ \to \phi\pi^+) = (4.5 \pm 0.4) \times 10^{-2}$. Our first error is their experiment's error and our second error is the systematic error from using our best value.

[4] KROKOVNY 03B reports $(0.86^{+0.33}_{-0.26} \pm 0.26) \times 10^{-3}$ from a measurement of $[\Gamma(B^0 \to D_{s0}^*(2317)^+ D^-,\ D_{s0}^{*+} \to D_s^+ \pi^0)/\Gamma_{total}] \times [B(D_s^+ \to \phi\pi^+)]$ assuming $B(D_s^+ \to \phi\pi^+) = 0.036 \pm 0.009$, which we rescale to our best value $B(D_s^+ \to \phi\pi^+) = (4.5 \pm 0.4) \times 10^{-2}$. Our first error is their experiment's error and our second error is the systematic error from using our best value.

$\Gamma(D_{s0}(2317)^+ D^-,\ D_{s0}^{*+} \to D_s^{*+}\gamma)/\Gamma_{total}$ Γ_{94}/Γ

VALUE (units 10^{-3})	CL%	DOCUMENT ID		TECN	COMMENT
<0.95	90	[1] KROKOVNY	03B	BELL	$e^+e^- \to \Upsilon(4S)$

[1] Assumes equal production of B^+ and B^0 at the $\Upsilon(4S)$.

$\Gamma(D_{s0}(2317)^+ D^*(2010)^-,\ D_{s0}^{+} \to D_s^+ \pi^0)/\Gamma_{total}$ Γ_{95}/Γ

VALUE (units 10^{-3})	DOCUMENT ID		TECN	COMMENT
$1.5 \pm 0.4^{+0.5}_{-0.4}$	[1] AUBERT,B	04S	BABR	$e^+e^- \to \Upsilon(4S)$

[1] Assumes equal production of B^+ and B^0 at the $\Upsilon(4S)$.

$\Gamma(D_{sJ}(2457)^+ D^-)/\Gamma_{total}$ Γ_{96}/Γ

VALUE (units 10^{-3})	DOCUMENT ID		TECN	COMMENT
3.5±1.1 OUR AVERAGE				
$2.6 \pm 1.5 \pm 0.7$	[1] AUBERT	06N	BABR	$e^+e^- \to \Upsilon(4S)$
$4.8^{+2.2}_{-1.6} \pm 1.1$	[2,3] AUBERT,B	04S	BABR	$e^+e^- \to \Upsilon(4S)$
$3.9^{+1.5}_{-1.3} \pm 0.9$	[2,4] KROKOVNY	03B	BELL	$e^+e^- \to \Upsilon(4S)$

[1] Uses a missing-mass method in the events that one of the B mesons is fully reconstructed.

[2] Assumes equal production of B^+ and B^0 at the $\Upsilon(4S)$.

[3] AUBERT,B 04S reports $[\Gamma(B^0 \to D_{sJ}(2457)^+ D^-)/\Gamma_{total}] \times [B(D_{s1}(2460)^+ \to D_s^{*+}\pi^0)] = (2.3^{+1.0}_{-0.7} \pm 0.3) \times 10^{-3}$ which we divide by our best value $B(D_{s1}(2460)^+ \to D_s^{*+}\pi^0) = (48 \pm 11) \times 10^{-2}$. Our first error is their experiment's error and our second error is the systematic error from using our best value.

[4] KROKOVNY 03B reports $[\Gamma(B^0 \to D_{sJ}(2457)^+ D^-)/\Gamma_{total}] \times [B(D_{s1}(2460)^+ \to D_s^{*+}\pi^0)] = (1.9^{+0.7}_{-0.6} \pm 0.2) \times 10^{-3}$ which we divide by our best value $B(D_{s1}(2460)^+ \to D_s^{*+}\pi^0) = (48 \pm 11) \times 10^{-2}$. Our first error is their experiment's error and our second error is the systematic error from using our best value.

$\Gamma(D_{sJ}(2457)^+ D^-,\ D_{sJ}^+ \to D_s^+\gamma)/\Gamma_{total}$ Γ_{97}/Γ

VALUE (units 10^{-3})	DOCUMENT ID		TECN	COMMENT
$0.65^{+0.17}_{-0.14}$ OUR AVERAGE				
$0.64^{+0.24}_{-0.16} \pm 0.06$	[1,2] AUBERT,B	04S	BABR	$e^+e^- \to \Upsilon(4S)$
$0.66^{+0.21}_{-0.19} \pm 0.06$	[1,3] KROKOVNY	03B	BELL	$e^+e^- \to \Upsilon(4S)$

[1] Assumes equal production of B^+ and B^0 at the $\Upsilon(4S)$.

[2] AUBERT,B 04S reports $(0.8 \pm 0.2^{+0.3}_{-0.2}) \times 10^{-3}$ from a measurement of $[\Gamma(B^0 \to D_{sJ}(2457)^+ D^-,\ D_{sJ}^+ \to D_s^+\gamma)/\Gamma_{total}] \times [B(D_s^+ \to \phi\pi^+)]$ assuming $B(D_s^+ \to \phi\pi^+) = 0.036 \pm 0.009$, which we rescale to our best value $B(D_s^+ \to \phi\pi^+) = (4.5 \pm 0.4) \times 10^{-2}$. Our first error is their experiment's error and our second error is the systematic error from using our best value.

[3] KROKOVNY 03B reports $(0.82^{+0.22}_{-0.19} \pm 0.25) \times 10^{-3}$ from a measurement of $[\Gamma(B^0 \to D_{sJ}(2457)^+ D^-,\ D_{sJ}^+ \to D_s^+\gamma)/\Gamma_{total}] \times [B(D_s^+ \to \phi\pi^+)]$ assuming $B(D_s^+ \to \phi\pi^+) = 0.036 \pm 0.009$, which we rescale to our best value $B(D_s^+ \to \phi\pi^+) = (4.5 \pm 0.4) \times 10^{-2}$. Our first error is their experiment's error and our second error is the systematic error from using our best value.

$\Gamma(D_{sJ}(2457)^+ D^-,\ D_{sJ}^+ \to D_s^{*+}\gamma)/\Gamma_{total}$ Γ_{98}/Γ

VALUE (units 10^{-3})	CL%	DOCUMENT ID		TECN	COMMENT
<0.60	90	[1] KROKOVNY	03B	BELL	$e^+e^- \to \Upsilon(4S)$

[1] Assumes equal production of B^+ and B^0 at the $\Upsilon(4S)$.

$\Gamma(D_{sJ}(2457)^+ D^-,\ D_{sJ}^+ \to D_s^+\pi^+\pi^-)/\Gamma_{total}$ Γ_{99}/Γ

VALUE (units 10^{-3})	CL%	DOCUMENT ID		TECN	COMMENT
<0.20	90	[1] KROKOVNY	03B	BELL	$e^+e^- \to \Upsilon(4S)$

[1] Assumes equal production of B^+ and B^0 at the $\Upsilon(4S)$.

$\Gamma(D_{sJ}(2457)^+ D^-,\ D_{sJ}^+ \to D_s^+\pi^0)/\Gamma_{total}$ Γ_{100}/Γ

VALUE (units 10^{-3})	CL%	DOCUMENT ID		TECN	COMMENT
<0.36	90	[1] KROKOVNY	03B	BELL	$e^+e^- \to \Upsilon(4S)$

[1] Assumes equal production of B^+ and B^0 at the $\Upsilon(4S)$.

$\Gamma(D^*(2010)^- D_{sJ}(2457)^+)/\Gamma_{total}$ Γ_{101}/Γ

VALUE (units 10^{-3})	DOCUMENT ID		TECN	COMMENT
9.3±2.2 OUR AVERAGE				
$8.8 \pm 2.0 \pm 1.4$	[1] AUBERT	06N	BABR	$e^+e^- \to \Upsilon(4S)$
$11\ ^{+5}_{-4} \pm 3$	[2,3] AUBERT,B	04S	BABR	$e^+e^- \to \Upsilon(4S)$

[1] Uses a missing-mass method in the events that one of the B mesons is fully reconstructed.

[2] AUBERT,B 04S reports $[\Gamma(B^0 \to D^*(2010)^- D_{sJ}(2457)^+)/\Gamma_{total}] \times [B(D_{s1}(2460)^+ \to D_s^{*+}\pi^0)] = (5.5 \pm 1.2^{+2.2}_{-1.6}) \times 10^{-3}$ which we divide by our best value $B(D_{s1}(2460)^+ \to D_s^{*+}\pi^0) = (48 \pm 11) \times 10^{-2}$. Our first error is their experiment's error and our second error is the systematic error from using our best value.

[3] Assumes equal production of B^+ and B^0 at the $\Upsilon(4S)$.

$\Gamma(D_{sJ}(2457)^+ D^*(2010),\ D_{sJ}^+ \to D_s^+\gamma)/\Gamma_{total}$ Γ_{102}/Γ

VALUE (units 10^{-3})	DOCUMENT ID		TECN	COMMENT
$2.3 \pm 0.3^{+0.9}_{-0.6}$	[1] AUBERT,B	04S	BABR	$e^+e^- \to \Upsilon(4S)$

[1] Assumes equal production of B^+ and B^0 at the $\Upsilon(4S)$.

$\left[\Gamma(D^- D_{s1}(2536)^+,\ D_{s1}^+ \to D^{*0} K^+) + \Gamma(D^{*+} K^0)\right]/\Gamma_{total}$ $\Gamma_{103}/\Gamma = (\Gamma_{104}+\Gamma_{105})/\Gamma$

VALUE (units 10^{-4})	DOCUMENT ID		TECN	COMMENT
$2.75 \pm 0.62 \pm 0.36$	[1,2] AUSHEV	11	BELL	$e^+e^- \to \Upsilon(4S)$

[1] Uses $\Gamma(D^*(2007)^0 \to D^0\pi^0)\ /\ \Gamma(D^*(2007)^0 \to D^0\gamma) = 1.74 \pm 0.13$ and $\Gamma(D_{s1}(2536)^+ \to D^*(2007)^0 K^+)\ /\ \Gamma(D_{s1}(2536)^+ \to D^*(2010)^+ K^0) = 1.36 \pm 0.2$.

[2] Assumes equal production of B^+ and B^0 at the $\Upsilon(4S)$.

Meson Particle Listings

B^0

$\Gamma(D^- D_{s1}(2536)^+,\ D_{s1}^+ \to D^{*0} K^+)/\Gamma_{\text{total}}$ Γ_{104}/Γ

VALUE (units 10^{-4})	CL%	DOCUMENT ID		TECN	COMMENT
1.71±0.48±0.32		[1] AUBERT	08B	BABR	$e^+e^- \to \Upsilon(4S)$
• • • We do not use the following data for averages, fits, limits, etc. • • •					
<5	90	AUBERT	03X	BABR	Repl. by AUBERT 08B

[1] Assumes equal production of B^+ and B^0 at the $\Upsilon(4S)$.

$\Gamma(D^- D_{s1}(2536)^+,\ D_{s1}^+ \to D^{*+} K^0)/\Gamma_{\text{total}}$ Γ_{105}/Γ

VALUE (units 10^{-4})	DOCUMENT ID		TECN	COMMENT
2.61±1.03±0.31	[1] AUBERT	08B	BABR	$e^+e^- \to \Upsilon(4S)$

[1] Assumes equal production of B^+ and B^0 at the $\Upsilon(4S)$.

$\left[\Gamma(D^*(2010)^- D_{s1}(2536)^+,\ D_{s1}^+ \to D^{*0} K^+) + \Gamma(D^{*+} K^0)\right]/\Gamma_{\text{total}}$ $\Gamma_{106}/\Gamma = (\Gamma_{107}+\Gamma_{108})/\Gamma$

VALUE (units 10^{-4})	DOCUMENT ID		TECN	COMMENT
5.01±1.21±0.70	[1,2] AUSHEV	11	BELL	$e^+e^- \to \Upsilon(4S)$

[1] Uses $\Gamma(D^*(2007)^0 \to D^0\pi^0)$ / $\Gamma(D^*(2007)^0 \to D^0\gamma) = 1.74 \pm 0.13$ and $\Gamma(D_{s1}(2536)^+ \to D^*(2007)^0 K^+)$ / $\Gamma(D_{s1}(2536)^+ \to D^*(2010)^+ K^0) = 1.36 \pm 0.2$.

[2] Assumes equal production of B^+ and B^0 at the $\Upsilon(4S)$.

$\Gamma(D^*(2010)^- D_{s1}(2536)^+,\ D_{s1}^+ \to D^{*0} K^+)/\Gamma_{\text{total}}$ Γ_{107}/Γ

VALUE (units 10^{-4})	CL%	DOCUMENT ID		TECN	COMMENT
3.32±0.88±0.66		[1] AUBERT	08B	BABR	$e^+e^- \to \Upsilon(4S)$
• • • We do not use the following data for averages, fits, limits, etc. • • •					
<7	90	AUBERT	03X	BABR	Repl. by AUBERT 08B

[1] Assumes equal production of B^+ and B^0 at the $\Upsilon(4S)$.

$\Gamma(D^{*-} D_{s1}(2536)^+,\ D_{s1}^+ \to D^{*+} K^0)/\Gamma_{\text{total}}$ Γ_{108}/Γ

VALUE (units 10^{-4})	DOCUMENT ID		TECN	COMMENT
5.00±1.51±0.67	[1] AUBERT	08B	BABR	$e^+e^- \to \Upsilon(4S)$

[1] Assumes equal production of B^+ and B^0 at the $\Upsilon(4S)$.

$\Gamma(D^- D_{sJ}(2573)^+,\ D_{sJ}^+ \to D^0 K^+)/\Gamma_{\text{total}}$ Γ_{109}/Γ

VALUE (units 10^{-5})	CL%	DOCUMENT ID		TECN	COMMENT
3.4±1.7±0.5		[1] LEES	15C	BABR	$e^+e^- \to \Upsilon(4S)$
• • • We do not use the following data for averages, fits, limits, etc. • • •					
<10	90	AUBERT	03X	BABR	$e^+e^- \to \Upsilon(4S)$

[1] Assumes equal production of B^+ and B^0 at the $\Upsilon(4S)$.

$\Gamma(D^*(2010)^- D_{sJ}(2573)^+,\ D_{sJ}^+ \to D^0 K^+)/\Gamma_{\text{total}}$ Γ_{110}/Γ

VALUE (units 10^{-4})	CL%	DOCUMENT ID		TECN	COMMENT
<2	90	AUBERT	03X	BABR	$e^+e^- \to \Upsilon(4S)$

$\Gamma(D^- D_{sJ}(2700)^+,\ D_{sJ}^+ \to D^0 K^+)/\Gamma_{\text{total}}$ Γ_{111}/Γ

VALUE (units 10^{-4})	DOCUMENT ID		TECN	COMMENT
7.14±0.96±0.69	[1] LEES	15C	BABR	$e^+e^- \to \Upsilon(4S)$

[1] Assumes equal production of B^+ and B^0 at the $\Upsilon(4S)$.

$\Gamma(D^+\pi^-)/\Gamma_{\text{total}}$ Γ_{112}/Γ

VALUE (units 10^{-7})	DOCUMENT ID		TECN	COMMENT
7.4±1.2±0.4	[1,2] DAS	10	BELL	$e^+e^- \to \Upsilon(4S)$

[1] DAS 10 reports $[\Gamma(B^0 \to D^+\pi^-)/\Gamma_{\text{total}}]$ / $[\mathrm{B}(B^0 \to D^-\pi^+)] = (2.92 \pm 0.38 \pm 0.31) \times 10^{-4}$ which we multiply by our best value $\mathrm{B}(B^0 \to D^-\pi^+) = (2.52 \pm 0.13) \times 10^{-3}$. Our first error is their experiment's error and our second error is the systematic error from using our best value.

[2] Derived using $\tan(\theta_C)\ f_D/f_{D_s} \sqrt{B(B^0 \to D_s^+\pi^-)/B(B^0 \to D^-\pi^+)}$ by assuming the flavor SU(3) symmetry, where θ_C is the Cabibbo angle, f_D (f_{D_s}) is the D (D_s) meson decay constant.

$\Gamma(D_s^+\pi^-)/\Gamma_{\text{total}}$ Γ_{113}/Γ

VALUE (units 10^{-6})	CL%	DOCUMENT ID		TECN	COMMENT
21.6±2.6 OUR AVERAGE					
19.9±2.6±1.8		[1] DAS	10	BELL	$e^+e^- \to \Upsilon(4S)$
25 ±4 ±2		[1] AUBERT	08AJ	BABR	$e^+e^- \to \Upsilon(4S)$
• • • We do not use the following data for averages, fits, limits, etc. • • •					
14.0±3.5±1.3		[2] AUBERT	07K	BABR	Repl. by AUBERT 08AJ
25 $^{+9}_{-7}$ ±2		[3] AUBERT	03D	BABR	Repl. by AUBERT 07K
19 $^{+9}_{-7}$ ±2		[4] KROKOVNY	02	BELL	Repl. by DAS 10
< 220	90	[5] ALEXANDER	93B	CLE2	$e^+e^- \to \Upsilon(4S)$
<1300	90	[6] BORTOLETTO	90	CLEO	$e^+e^- \to \Upsilon(4S)$

[1] Assumes equal production of B^+ and B^0 at the $\Upsilon(4S)$.

[2] AUBERT 07K reports $[\Gamma(B^0 \to D_s^+\pi^-)/\Gamma_{\text{total}}] \times [\mathrm{B}(D_s^+ \to \phi\pi^+)] = (0.63 \pm 0.15 \pm 0.05) \times 10^{-6}$ which we divide by our best value $\mathrm{B}(D_s^+ \to \phi\pi^+) = (4.5 \pm 0.4) \times 10^{-2}$. Our first error is their experiment's error and our second error is the systematic error from using our best value.

[3] AUBERT 03D reports $[\Gamma(B^0 \to D_s^+\pi^-)/\Gamma_{\text{total}}] \times [\mathrm{B}(D_s^+ \to \phi\pi^+)] = (1.13 \pm 0.33 \pm 0.21) \times 10^{-6}$ which we divide by our best value $\mathrm{B}(D_s^+ \to \phi\pi^+) = (4.5 \pm 0.4) \times 10^{-2}$. Our first error is their experiment's error and our second error is the systematic error from using our best value.

[4] KROKOVNY 02 reports $[\Gamma(B^0 \to D_s^+\pi^-)/\Gamma_{\text{total}}] \times [\mathrm{B}(D_s^+ \to \phi\pi^+)] = (0.86 \,^{+0.37}_{-0.30} \pm 0.11) \times 10^{-6}$ which we divide by our best value $\mathrm{B}(D_s^+ \to \phi\pi^+) = (4.5 \pm 0.4) \times 10^{-2}$. Our first error is their experiment's error and our second error is the systematic error from using our best value.

[5] ALEXANDER 93B reports $< 270 \times 10^{-6}$ from a measurement of $[\Gamma(B^0 \to D_s^+\pi^-)/\Gamma_{\text{total}}] \times [\mathrm{B}(D_s^+ \to \phi\pi^+)]$ assuming $\mathrm{B}(D_s^+ \to \phi\pi^+) = 0.037$, which we rescale to our best value $\mathrm{B}(D_s^+ \to \phi\pi^+) = 4.5 \times 10^{-2}$.

[6] BORTOLETTO 90 assume $\mathrm{B}(D_s \to \phi\pi^+) = 2\%$.

$\left[\Gamma(D_s^+\pi^-) + \Gamma(D_s^- K^+)\right]/\Gamma_{\text{total}}$ $(\Gamma_{113}+\Gamma_{123})/\Gamma$

VALUE	CL%	DOCUMENT ID		TECN	COMMENT
<1.0 × 10⁻³	90	[1] ALBRECHT	93E	ARG	$e^+e^- \to \Upsilon(4S)$

[1] ALBRECHT 93E reports $< 1.7 \times 10^{-3}$ from a measurement of $\left[\left[\Gamma(B^0 \to D_s^+\pi^-) + \Gamma(B^0 \to D_s^- K^+)\right]/\Gamma_{\text{total}}\right] \times [\mathrm{B}(D_s^+ \to \phi\pi^+)]$ assuming $\mathrm{B}(D_s^+ \to \phi\pi^+) = 0.027$, which we rescale to our best value $\mathrm{B}(D_s^+ \to \phi\pi^+) = 4.5 \times 10^{-2}$.

$\Gamma(D_s^{*+}\pi^-)/\Gamma_{\text{total}}$ Γ_{114}/Γ

VALUE (units 10^{-5})	CL%	DOCUMENT ID		TECN	COMMENT
2.1 ±0.4 OUR AVERAGE		Error includes scale factor of 1.4.			
1.75±0.34±0.20		[1] JOSHI	10	BELL	$e^+e^- \to \Upsilon(4S)$
2.6 $^{+0.5}_{-0.4}$ ±0.2		[1] AUBERT	08AJ	BABR	$e^+e^- \to \Upsilon(4S)$
• • • We do not use the following data for averages, fits, limits, etc. • • •					
2.9 ±0.7 ±0.3		[2] AUBERT	07K	BABR	Repl. by AUBERT 08AJ
< 4.1	90	AUBERT	03D	BABR	Repl. by AUBERT 07K
<40	90	[3] ALEXANDER	93B	CLE2	$e^+e^- \to \Upsilon(4S)$

[1] Assumes equal production of B^+ and B^0 at the $\Upsilon(4S)$.

[2] AUBERT 07K reports $[\Gamma(B^0 \to D_s^{*+}\pi^-)/\Gamma_{\text{total}}] \times [\mathrm{B}(D_s^+ \to \phi\pi^+)] = (1.32 \pm 0.27 \pm 0.15) \times 10^{-6}$ which we divide by our best value $\mathrm{B}(D_s^+ \to \phi\pi^+) = (4.5 \pm 0.4) \times 10^{-2}$. Our first error is their experiment's error and our second error is the systematic error from using our best value.

[3] ALEXANDER 93B reports $< 44 \times 10^{-5}$ from a measurement of $[\Gamma(B^0 \to D_s^{*+}\pi^-)/\Gamma_{\text{total}}] \times [\mathrm{B}(D_s^+ \to \phi\pi^+)]$ assuming $\mathrm{B}(D_s^+ \to \phi\pi^+) = 0.037$, which we rescale to our best value $\mathrm{B}(D_s^+ \to \phi\pi^+) = 4.5 \times 10^{-2}$.

$\left[\Gamma(D_s^{*+}\pi^-) + \Gamma(D_s^{*-} K^+)\right]/\Gamma_{\text{total}}$ $(\Gamma_{114}+\Gamma_{124})/\Gamma$

VALUE	CL%	DOCUMENT ID		TECN	COMMENT
<7 × 10⁻⁴	90	[1] ALBRECHT	93E	ARG	$e^+e^- \to \Upsilon(4S)$

[1] ALBRECHT 93E reports $< 1.2 \times 10^{-3}$ from a measurement of $\left[\left[\Gamma(B^0 \to D_s^{*+}\pi^-) + \Gamma(B^0 \to D_s^{*-} K^+)\right]/\Gamma_{\text{total}}\right] \times [\mathrm{B}(D_s^+ \to \phi\pi^+)]$ assuming $\mathrm{B}(D_s^+ \to \phi\pi^+) = 0.027$, which we rescale to our best value $\mathrm{B}(D_s^+ \to \phi\pi^+) = 4.5 \times 10^{-2}$.

$\Gamma(D_s^+\rho^-)/\Gamma_{\text{total}}$ Γ_{115}/Γ

VALUE (units 10^{-5})	CL%	DOCUMENT ID		TECN	COMMENT
< 2.4	90	[1] AUBERT	08AJ	BABR	$e^+e^- \to \Upsilon(4S)$
• • • We do not use the following data for averages, fits, limits, etc. • • •					
<130	90	[2] ALBRECHT	93E	ARG	$e^+e^- \to \Upsilon(4S)$
< 50	90	[3] ALEXANDER	93B	CLE2	$e^+e^- \to \Upsilon(4S)$

[1] Assumes equal production of B^+ and B^0 at the $\Upsilon(4S)$.

[2] ALBRECHT 93E reports $< 2.2 \times 10^{-3}$ from a measurement of $[\Gamma(B^0 \to D_s^+\rho^-)/\Gamma_{\text{total}}] \times [\mathrm{B}(D_s^+ \to \phi\pi^+)]$ assuming $\mathrm{B}(D_s^+ \to \phi\pi^+) = 0.027$, which we rescale to our best value $\mathrm{B}(D_s^+ \to \phi\pi^+) = 4.5 \times 10^{-2}$.

[3] ALEXANDER 93B reports $< 6.6 \times 10^{-4}$ from a measurement of $[\Gamma(B^0 \to D_s^+\rho^-)/\Gamma_{\text{total}}] \times [\mathrm{B}(D_s^+ \to \phi\pi^+)]$ assuming $\mathrm{B}(D_s^+ \to \phi\pi^+) = 0.037$, which we rescale to our best value $\mathrm{B}(D_s^+ \to \phi\pi^+) = 4.5 \times 10^{-2}$.

$\Gamma(D_s^{*+}\rho^-)/\Gamma_{\text{total}}$ Γ_{116}/Γ

VALUE (units 10^{-5})	CL%	DOCUMENT ID		TECN	COMMENT
4.1 $^{+1.3}_{-1.2}$ ±0.4		[1] AUBERT	08AJ	BABR	$e^+e^- \to \Upsilon(4S)$
• • • We do not use the following data for averages, fits, limits, etc. • • •					
<150	90	[2] ALBRECHT	93E	ARG	$e^+e^- \to \Upsilon(4S)$
< 60	90	[3] ALEXANDER	93B	CLE2	$e^+e^- \to \Upsilon(4S)$

[1] Assumes equal production of B^+ and B^0 at the $\Upsilon(4S)$.

[2] ALBRECHT 93E reports $< 2.5 \times 10^{-3}$ from a measurement of $[\Gamma(B^0 \to D_s^{*+}\rho^-)/\Gamma_{\text{total}}] \times [\mathrm{B}(D_s^+ \to \phi\pi^+)]$ assuming $\mathrm{B}(D_s^+ \to \phi\pi^+) = 0.027$, which we rescale to our best value $\mathrm{B}(D_s^+ \to \phi\pi^+) = 4.5 \times 10^{-2}$.

[3] ALEXANDER 93B reports $< 7.4 \times 10^{-4}$ from a measurement of $[\Gamma(B^0 \to D_s^{*+}\rho^-)/\Gamma_{\text{total}}] \times [\mathrm{B}(D_s^+ \to \phi\pi^+)]$ assuming $\mathrm{B}(D_s^+ \to \phi\pi^+) = 0.037$, which we rescale to our best value $\mathrm{B}(D_s^+ \to \phi\pi^+) = 4.5 \times 10^{-2}$.

$\Gamma(D_s^+ a_0^-)/\Gamma_{total}$ Γ_{117}/Γ

VALUE (units 10^{-5})	CL%	DOCUMENT ID		TECN	COMMENT
<1.9	90	[1] AUBERT	06X	BABR	$e^+e^- \to \Upsilon(4S)$

[1] Assumes equal production of B^+ and B^0 at the $\Upsilon(4S)$.

$\Gamma(D_s^{*+} a_0^-)/\Gamma_{total}$ Γ_{118}/Γ

VALUE (units 10^{-5})	CL%	DOCUMENT ID		TECN	COMMENT
<3.6	90	[1] AUBERT	06X	BABR	$e^+e^- \to \Upsilon(4S)$

[1] Assumes equal production of B^+ and B^0 at the $\Upsilon(4S)$.

$\Gamma(D_s^+ a_1(1260)^-)/\Gamma_{total}$ Γ_{119}/Γ

VALUE	CL%	DOCUMENT ID		TECN	COMMENT
$<2.1 \times 10^{-3}$	90	[1] ALBRECHT	93E	ARG	$e^+e^- \to \Upsilon(4S)$

[1] ALBRECHT 93E reports $< 3.5 \times 10^{-3}$ from a measurement of $[\Gamma(B^0 \to D_s^+ a_1(1260)^-)/\Gamma_{total}] \times [B(D_s^+ \to \phi\pi^+)]$ assuming $B(D_s^+ \to \phi\pi^+) = 0.027$, which we rescale to our best value $B(D_s^+ \to \phi\pi^+) = 4.5 \times 10^{-2}$.

$\Gamma(D_s^{*+} a_1(1260)^-)/\Gamma_{total}$ Γ_{120}/Γ

VALUE	CL%	DOCUMENT ID		TECN	COMMENT
$<1.7 \times 10^{-3}$	90	[1] ALBRECHT	93E	ARG	$e^+e^- \to \Upsilon(4S)$

[1] ALBRECHT 93E reports $< 2.9 \times 10^{-3}$ from a measurement of $[\Gamma(B^0 \to D_s^{*+} a_1(1260)^-)/\Gamma_{total}] \times [B(D_s^+ \to \phi\pi^+)]$ assuming $B(D_s^+ \to \phi\pi^+) = 0.027$, which we rescale to our best value $B(D_s^+ \to \phi\pi^+) = 4.5 \times 10^{-2}$.

$\Gamma(D_s^+ a_2^-)/\Gamma_{total}$ Γ_{121}/Γ

VALUE (units 10^{-5})	CL%	DOCUMENT ID		TECN	COMMENT
<19	90	[1] AUBERT	06X	BABR	$e^+e^- \to \Upsilon(4S)$

[1] Assumes equal production of B^+ and B^0 at the $\Upsilon(4S)$.

$\Gamma(D_s^{*+} a_2^-)/\Gamma_{total}$ Γ_{122}/Γ

VALUE (units 10^{-5})	CL%	DOCUMENT ID		TECN	COMMENT
<20	90	[1] AUBERT	06X	BABR	$e^+e^- \to \Upsilon(4S)$

[1] Assumes equal production of B^+ and B^0 at the $\Upsilon(4S)$.

$\Gamma(D_s^- K^+)/\Gamma_{total}$ Γ_{123}/Γ

VALUE (units 10^{-6})	CL%	DOCUMENT ID		TECN	COMMENT
27 ± 5 OUR FIT Error includes scale factor of 2.7.					
22 ± 5 OUR AVERAGE Error includes scale factor of 1.8.					
19.1± 2.4±1.7		[1] DAS	10	BELL	$e^+e^- \to \Upsilon(4S)$
29 ± 4 ±2		[1] AUBERT	08AJ	BABR	$e^+e^- \to \Upsilon(4S)$
• • • We do not use the following data for averages, fits, limits, etc. • • •					
27 ± 5 ±2		[2] AUBERT	07K	BABR	Repl. by AUBERT 08AJ
26 ±10 ±2		[3] AUBERT	03D	BABR	Repl. by AUBERT 07K
36 $^{+11}_{-10}$ ±3		[4] KROKOVNY	02	BELL	Repl. by DAS 10
< 190	90	[5] ALEXANDER	93B	CLE2	$e^+e^- \to \Upsilon(4S)$
<1300	90	[6] BORTOLETTO	90	CLEO	$e^+e^- \to \Upsilon(4S)$

[1] Assumes equal production of B^+ and B^0 at the $\Upsilon(4S)$.

[2] AUBERT 07K reports $[\Gamma(B^0 \to D_s^- K^+)/\Gamma_{total}] \times [B(D_s^+ \to \phi\pi^+)] = (1.21 \pm 0.17 \pm 0.11) \times 10^{-6}$ which we divide by our best value $B(D_s^+ \to \phi\pi^+) = (4.5 \pm 0.4) \times 10^{-2}$. Our first error is their experiment's error and our second error is the systematic error from using our best value.

[3] AUBERT 03D reports $[\Gamma(B^0 \to D_s^- K^+)/\Gamma_{total}] \times [B(D_s^+ \to \phi\pi^+)] = (1.16 \pm 0.36 \pm 0.24) \times 10^{-6}$ which we divide by our best value $B(D_s^+ \to \phi\pi^+) = (4.5 \pm 0.4) \times 10^{-2}$. Our first error is their experiment's error and our second error is the systematic error from using our best value.

[4] KROKOVNY 02 reports $[\Gamma(B^0 \to D_s^- K^+)/\Gamma_{total}] \times [B(D_s^+ \to \phi\pi^+)] = (1.61^{+0.45}_{-0.38} \pm 0.21) \times 10^{-6}$ which we divide by our best value $B(D_s^+ \to \phi\pi^+) = (4.5 \pm 0.4) \times 10^{-2}$. Our first error is their experiment's error and our second error is the systematic error from using our best value.

[5] ALEXANDER 93B reports $< 230 \times 10^{-6}$ from a measurement of $[\Gamma(B^0 \to D_s^- K^+)/\Gamma_{total}] \times [B(D_s^+ \to \phi\pi^+)]$ assuming $B(D_s^+ \to \phi\pi^+) = 0.037$, which we rescale to our best value $B(D_s^+ \to \phi\pi^+) = 4.5 \times 10^{-2}$.

[6] BORTOLETTO 90 assume $B(D_s \to \phi\pi^+) = 2\%$.

$\Gamma(D_s^{*-} K^+)/\Gamma_{total}$ Γ_{124}/Γ

VALUE (units 10^{-5})	CL%	DOCUMENT ID		TECN	COMMENT
2.19±0.30 OUR AVERAGE					
2.02±0.33±0.22		[1] JOSHI	10	BELL	$e^+e^- \to \Upsilon(4S)$
2.4 ±0.4 ±0.2		[1] AUBERT	08AJ	BABR	$e^+e^- \to \Upsilon(4S)$
• • • We do not use the following data for averages, fits, limits, etc. • • •					
2.2 ±0.6 ±0.2		[2] AUBERT	07K	BABR	Repl. by AUBERT 08AJ
< 2.5	90	AUBERT	03D	BABR	Repl. by AUBERT 07K
<14	90	[3] ALEXANDER	93B	CLE2	$e^+e^- \to \Upsilon(4S)$

[1] Assumes equal production of B^+ and B^0 at the $\Upsilon(4S)$.

[2] AUBERT 07K reports $[\Gamma(B^0 \to D_s^{*-} K^+)/\Gamma_{total}] \times [B(D_s^+ \to \phi\pi^+)] = (0.97 \pm 0.24 \pm 0.12) \times 10^{-6}$ which we divide by our best value $B(D_s^+ \to \phi\pi^+) = (4.5 \pm 0.4) \times 10^{-2}$. Our first error is their experiment's error and our second error is the systematic error from using our best value.

[3] ALEXANDER 93B reports $< 17 \times 10^{-5}$ from a measurement of $[\Gamma(B^0 \to D_s^{*-} K^+)/\Gamma_{total}] \times [B(D_s^+ \to \phi\pi^+)]$ assuming $B(D_s^+ \to \phi\pi^+) = 0.037$, which we rescale to our best value $B(D_s^+ \to \phi\pi^+) = 4.5 \times 10^{-2}$.

$\Gamma(D_s^- K^+)/\Gamma(D^-\pi^+)$ Γ_{123}/Γ_{34}

VALUE (units 10^{-2})	DOCUMENT ID		TECN	COMMENT
1.09±0.19 OUR FIT Error includes scale factor of 2.6.				
1.29±0.05±0.08	AAIJ	15AC	LHCB	pp at 7, 8 TeV

$\Gamma(D_s^- K^*(892)^+)/\Gamma_{total}$ Γ_{125}/Γ

VALUE (units 10^{-5})	CL%	DOCUMENT ID		TECN	COMMENT
$3.5^{+1.0}_{-0.9} \pm 0.4$		[1] AUBERT	08AJ	BABR	$e^+e^- \to \Upsilon(4S)$
• • • We do not use the following data for averages, fits, limits, etc. • • •					
<280	90	[2] ALBRECHT	93E	ARG	$e^+e^- \to \Upsilon(4S)$
< 80	90	[3] ALEXANDER	93B	CLE2	$e^+e^- \to \Upsilon(4S)$

[1] Assumes equal production of B^+ and B^0 at the $\Upsilon(4S)$.

[2] ALBRECHT 93E reports $< 4.6 \times 10^{-3}$ from a measurement of $[\Gamma(B^0 \to D_s^- K^*(892)^+)/\Gamma_{total}] \times [B(D_s^+ \to \phi\pi^+)]$ assuming $B(D_s^+ \to \phi\pi^+) = 0.027$, which we rescale to our best value $B(D_s^+ \to \phi\pi^+) = 4.5 \times 10^{-2}$.

[3] ALEXANDER 93B reports $< 9.7 \times 10^{-4}$ from a measurement of $[\Gamma(B^0 \to D_s^- K^*(892)^+)/\Gamma_{total}] \times [B(D_s^+ \to \phi\pi^+)]$ assuming $B(D_s^+ \to \phi\pi^+) = 0.037$, which we rescale to our best value $B(D_s^+ \to \phi\pi^+) = 4.5 \times 10^{-2}$.

$\Gamma(D_s^{*-} K^*(892)^+)/\Gamma_{total}$ Γ_{126}/Γ

VALUE (units 10^{-5})	CL%	DOCUMENT ID		TECN	COMMENT
$3.2^{+1.4}_{-1.2} \pm 0.4$		[1] AUBERT	08AJ	BABR	$e^+e^- \to \Upsilon(4S)$
• • • We do not use the following data for averages, fits, limits, etc. • • •					
<350	90	[2] ALBRECHT	93E	ARG	$e^+e^- \to \Upsilon(4S)$
< 90	90	[3] ALEXANDER	93B	CLE2	$e^+e^- \to \Upsilon(4S)$

[1] Assumes equal production of B^+ and B^0 at the $\Upsilon(4S)$.

[2] ALBRECHT 93E reports $< 5.8 \times 10^{-3}$ from a measurement of $[\Gamma(B^0 \to D_s^{*-} K^*(892)^+)/\Gamma_{total}] \times [B(D_s^+ \to \phi\pi^+)]$ assuming $B(D_s^+ \to \phi\pi^+) = 0.027$, which we rescale to our best value $B(D_s^+ \to \phi\pi^+) = 4.5 \times 10^{-2}$.

[3] ALEXANDER 93B reports $< 11.0 \times 10^{-4}$ from a measurement of $[\Gamma(B^0 \to D_s^{*-} K^*(892)^+)/\Gamma_{total}] \times [B(D_s^+ \to \phi\pi^+)]$ assuming $B(D_s^+ \to \phi\pi^+) = 0.037$, which we rescale to our best value $B(D_s^+ \to \phi\pi^+) = 4.5 \times 10^{-2}$.

$\Gamma(D_s^- \pi^+ K^0)/\Gamma_{total}$ Γ_{127}/Γ

VALUE (units 10^{-4})	CL%	DOCUMENT ID		TECN	COMMENT
0.97±0.14 OUR AVERAGE					
0.94±0.12±0.10		[1] WIECHCZYN...15		BELL	$e^+e^- \to \Upsilon(4S)$
1.10±0.26±0.20		[1] AUBERT	08G	BABR	$e^+e^- \to \Upsilon(4S)$
• • • We do not use the following data for averages, fits, limits, etc. • • •					
<40	90	[2] ALBRECHT	93E	ARG	$e^+e^- \to \Upsilon(4S)$

[1] Assumes equal production of B^+ and B^0 at the $\Upsilon(4S)$.

[2] ALBRECHT 93E reports $< 7.3 \times 10^{-3}$ from a measurement of $[\Gamma(B^0 \to D_s^- \pi^+ K^0)/\Gamma_{total}] \times [B(D_s^+ \to \phi\pi^+)]$ assuming $B(D_s^+ \to \phi\pi^+) = 0.027$, which we rescale to our best value $B(D_s^+ \to \phi\pi^+) = 4.5 \times 10^{-2}$.

$\Gamma(D_s^{*-} \pi^+ K^0)/\Gamma_{total}$ Γ_{128}/Γ

VALUE (units 10^{-4})	CL%	DOCUMENT ID		TECN	COMMENT
< 1.10	90	[1] AUBERT	08G	BABR	$e^+e^- \to \Upsilon(4S)$
• • • We do not use the following data for averages, fits, limits, etc. • • •					
<25	90	[2] ALBRECHT	93E	ARG	$e^+e^- \to \Upsilon(4S)$

[1] Assumes equal production of B^+ and B^0 at the $\Upsilon(4S)$.

[2] ALBRECHT 93E reports $< 4.2 \times 10^{-3}$ from a measurement of $[\Gamma(B^0 \to D_s^{*-} \pi^+ K^0)/\Gamma_{total}] \times [B(D_s^+ \to \phi\pi^+)]$ assuming $B(D_s^+ \to \phi\pi^+) = 0.027$, which we rescale to our best value $B(D_s^+ \to \phi\pi^+) = 4.5 \times 10^{-2}$.

$\Gamma(D_s^- K^+ \pi^+ \pi^-)/\Gamma_{total}$ Γ_{129}/Γ

VALUE (units 10^{-4})	DOCUMENT ID		TECN	COMMENT
1.73±0.32±0.35	[1] AAIJ	12AX	LHCB	pp at 7 TeV

[1] AAIJ 12AX reports $[\Gamma(B^0 \to D_s^- K^+ \pi^+ \pi^-)/\Gamma_{total}] / [B(B_s^0 \to D_s^- K^+ \pi^+ \pi^-)] = 0.54 \pm 0.07 \pm 0.07$ which we multiply by our best value $B(B_s^0 \to D_s^- K^+ \pi^+ \pi^-) = (3.2 \pm 0.6) \times 10^{-4}$. Our first error is their experiment's error and our second error is the systematic error from using our best value.

$\Gamma(D_s^- \pi^+ K^*(892)^0)/\Gamma_{total}$ Γ_{130}/Γ

VALUE	CL%	DOCUMENT ID		TECN	COMMENT
$<3.0 \times 10^{-3}$	90	[1] ALBRECHT	93E	ARG	$e^+e^- \to \Upsilon(4S)$

[1] ALBRECHT 93E reports $< 5.0 \times 10^{-3}$ from a measurement of $[\Gamma(B^0 \to D_s^- \pi^+ K^*(892)^0)/\Gamma_{total}] \times [B(D_s^+ \to \phi\pi^+)]$ assuming $B(D_s^+ \to \phi\pi^+) = 0.027$, which we rescale to our best value $B(D_s^+ \to \phi\pi^+) = 4.5 \times 10^{-2}$.

$\Gamma(D_s^{*-}\pi^+ K^*(892)^0)/\Gamma_{total}$ Γ_{131}/Γ

VALUE	CL%	DOCUMENT ID		TECN	COMMENT
$<1.6 \times 10^{-3}$	90	[1] ALBRECHT	93E	ARG	$e^+e^- \to \Upsilon(4S)$

[1] ALBRECHT 93E reports $< 2.7 \times 10^{-3}$ from a measurement of $[\Gamma(B^0 \to D_s^{*-} \pi^+ K^*(892)^0)/\Gamma_{total}] \times [B(D_s^+ \to \phi\pi^+)]$ assuming $B(D_s^+ \to \phi\pi^+) = 0.027$, which we rescale to our best value $B(D_s^+ \to \phi\pi^+) = 4.5 \times 10^{-2}$.

$\Gamma(\overline{D}^0 K^0)/\Gamma_{total}$ Γ_{132}/Γ

VALUE (units 10^{-5})	DOCUMENT ID		TECN	COMMENT
5.2±0.7 OUR AVERAGE				
$5.3 \pm 0.7 \pm 0.3$	[1] AUBERT,B	06L	BABR	$e^+e^- \to \Upsilon(4S)$
$5.0^{+1.3}_{-1.2} \pm 0.6$	[1] KROKOVNY	03	BELL	$e^+e^- \to \Upsilon(4S)$

[1] Assumes equal production of B^+ and B^0 at the $\Upsilon(4S)$.

$\Gamma(\overline{D}^0 K^+\pi^-)/\Gamma_{total}$ Γ_{133}/Γ

VALUE (units 10^{-6})	DOCUMENT ID		TECN	COMMENT
88±15±9	[1] AUBERT	06A	BABR	$e^+e^- \to \Upsilon(4S)$

[1] Assumes equal production of B^+ and B^0 at the $\Upsilon(4S)$.

$\Gamma(\overline{D}^0 K^+\pi^-)/\Gamma(\overline{D}^0\pi^+\pi^-)$ Γ_{133}/Γ_{43}

VALUE	DOCUMENT ID		TECN	COMMENT
0.106±0.007±0.008	AAIJ	13AQ	LHCB	pp at 7 TeV

$\Gamma(\overline{D}^0 K^*(892)^0)/\Gamma_{total}$ Γ_{134}/Γ

VALUE (units 10^{-5})	DOCUMENT ID		TECN	COMMENT
4.5±0.6 OUR AVERAGE				
$5.4 \pm 0.3 \pm 1.1$	[1,2] AAIJ	15X	LHCB	pp at 7, 8 TeV
$4.0 \pm 0.7 \pm 0.3$	[3] AUBERT,B	06L	BABR	$e^+e^- \to \Upsilon(4S)$
$4.8^{+1.1}_{-1.0} \pm 0.5$	[3] KROKOVNY	03	BELL	$e^+e^- \to \Upsilon(4S)$
• • • We do not use the following data for averages, fits, limits, etc. • • •				
$5.7 \pm 0.9 \pm 0.6$	[3] AUBERT	06A	BABR	Repl. by AUBERT,B 06L

[1] AAIJ 15X reports $(5.13 \pm 0.20 \pm 0.15 \pm 0.24 \pm 0.60) \times 10^{-5}$ from a measurement of $[\Gamma(B^0 \to \overline{D}^0 K^*(892)^0)/\Gamma_{total}] \times [B(B^0 \to \overline{D}^0 K^+\pi^-)]$ assuming $B(B^0 \to \overline{D}^0 K^+\pi^-) = (9.2 \pm 0.6 \pm 0.7 \pm 0.6) \times 10^{-5}$, which we rescale to our best value $B(B^0 \to \overline{D}^0 K^+\pi^-) = (8.8 \pm 1.7) \times 10^{-5}$. Our first error is their experiment's error and our second error is the systematic error from using our best value.

[2] Measured via amplitude analysis of $B^0 \to \overline{D}^0 K^+\pi^-$, which excludes contribution from decay via $D^*(2010)^-$ resonance.

[3] Assumes equal production of B^+ and B^0 at the $\Upsilon(4S)$.

$\Gamma(\overline{D}^0 K^*(1410)^0)/\Gamma_{total}$ Γ_{135}/Γ

VALUE	CL%	DOCUMENT ID		TECN	COMMENT
$<6.7 \times 10^{-5}$	90	[1] AAIJ	15X	LHCB	pp at 7, 8 TeV

[1] Measured via amplitude analysis of $B^0 \to \overline{D}^0 K^+\pi^-$, which excludes contribution from decay via $D^*(2010)^-$ resonance.

$\Gamma(\overline{D}^0 K_0^*(1430)^0)/\Gamma_{total}$ Γ_{136}/Γ

VALUE (units 10^{-5})	DOCUMENT ID		TECN	COMMENT
0.7±0.7±0.1	[1,2] AAIJ	15X	LHCB	pp at 7, 8 TeV

[1] AAIJ 15X reports $(0.71 \pm 0.27 \pm 0.33 \pm 0.47 \pm 0.08) \times 10^{-5}$ from a measurement of $[\Gamma(B^0 \to \overline{D}^0 K_0^*(1430)^0)/\Gamma_{total}] \times [B(B^0 \to \overline{D}^0 K^+\pi^-)]$ assuming $B(B^0 \to \overline{D}^0 K^+\pi^-) = (9.2 \pm 0.6 \pm 0.7 \pm 0.6) \times 10^{-5}$, which we rescale to our best value $B(B^0 \to \overline{D}^0 K^+\pi^-) = (8.8 \pm 1.7) \times 10^{-5}$. Our first error is their experiment's error and our second error is the systematic error from using our best value.

[2] Measured via amplitude analysis of $B^0 \to \overline{D}^0 K^+\pi^-$, which excludes contribution from decay via $D^*(2010)^-$ resonance.

$\Gamma(\overline{D}^0 K_2^*(1430)^0)/\Gamma_{total}$ Γ_{137}/Γ

VALUE (units 10^{-5})	DOCUMENT ID		TECN	COMMENT
2.1±0.8±0.4	[1,2] AAIJ	15X	LHCB	pp at 7, 8 TeV

[1] AAIJ 15X reports $(2.04 \pm 0.45 \pm 0.30 \pm 0.54 \pm 0.25) \times 10^{-5}$ from a measurement of $[\Gamma(B^0 \to \overline{D}^0 K_2^*(1430)^0)/\Gamma_{total}] \times [B(B^0 \to \overline{D}^0 K^+\pi^-)]$ assuming $B(B^0 \to \overline{D}^0 K^+\pi^-) = (9.2 \pm 0.6 \pm 0.7 \pm 0.6) \times 10^{-5}$, which we rescale to our best value $B(B^0 \to \overline{D}^0 K^+\pi^-) = (8.8 \pm 1.7) \times 10^{-5}$. Our first error is their experiment's error and our second error is the systematic error from using our best value.

[2] Measured via amplitude analysis of $B^0 \to \overline{D}^0 K^+\pi^-$, which excludes contribution from decay via $D^*(2010)^-$ resonance.

$\Gamma(D_0^*(2400)^-,\ D_0^{*-} \to \overline{D}^0\pi^-)/\Gamma_{total}$ Γ_{138}/Γ

VALUE (units 10^{-5})	DOCUMENT ID		TECN	COMMENT
1.9±0.8±0.4	[1,2] AAIJ	15X	LHCB	pp at 7, 8 TeV

[1] AAIJ 15X reports $(1.77 \pm 0.26 \pm 0.19 \pm 0.67 \pm 0.20) \times 10^{-5}$ from a measurement of $[\Gamma(B^0 \to D_0^*(2400)^-,\ D_0^{*-} \to \overline{D}^0\pi^-)/\Gamma_{total}] \times [B(B^0 \to \overline{D}^0 K^+\pi^-)]$ assuming $B(B^0 \to \overline{D}^0 K^+\pi^-) = (9.2 \pm 0.6 \pm 0.7 \pm 0.6) \times 10^{-5}$, which we rescale to our best value $B(B^0 \to \overline{D}^0 K^+\pi^-) = (8.8 \pm 1.7) \times 10^{-5}$. Our first error is their experiment's error and our second error is the systematic error from using our best value.

[2] Measured via amplitude analysis of $B^0 \to \overline{D}^0 K^+\pi^-$, which excludes contribution from decay via $D^*(2010)^-$ resonance.

$\Gamma(D_2^*(2460)^- K^+,\ D_2^{*-} \to \overline{D}^0\pi^-)/\Gamma_{total}$ Γ_{139}/Γ

VALUE (units 10^{-6})	DOCUMENT ID		TECN	COMMENT
20.3±3.5 OUR AVERAGE				
$22 \pm 2 \pm 4$	[1,2] AAIJ	15X	LHCB	pp at 7, 8 TeV
$18.3 \pm 4.0 \pm 3.1$	[3] AUBERT	06A	BABR	$e^+e^- \to \Upsilon(4S)$

[1] AAIJ 15X reports $(2.12 \pm 0.10 \pm 0.11 \pm 0.11 \pm 0.25) \times 10^{-5}$ from a measurement of $[\Gamma(B^0 \to D_2^*(2460)^- K^+,\ D_2^{*-} \to \overline{D}^0\pi^-)/\Gamma_{total}] \times [B(B^0 \to \overline{D}^0 K^+\pi^-)]$ assuming $B(B^0 \to \overline{D}^0 K^+\pi^-) = (9.2 \pm 0.6 \pm 0.7 \pm 0.6) \times 10^{-5}$, which we rescale to our best value $B(B^0 \to \overline{D}^0 K^+\pi^-) = (8.8 \pm 1.7) \times 10^{-5}$. Our first error is their experiment's error and our second error is the systematic error from using our best value.

[2] Measured via amplitude analysis of $B^0 \to \overline{D}^0 K^+\pi^-$, which excludes contribution from decay via $D^*(2010)^-$ resonance.

[3] Assumes equal production of B^+ and B^0 at the $\Upsilon(4S)$.

$\Gamma(D_3^*(2760)^- K^+,\ D_3^{*-} \to \overline{D}^0\pi^-)/\Gamma_{total}$ Γ_{140}/Γ

VALUE	CL%	DOCUMENT ID		TECN	COMMENT
$<0.10 \times 10^{-5}$	90	[1] AAIJ	15X	LHCB	pp at 7, 8 TeV

[1] Measured via amplitude analysis of $B^0 \to \overline{D}^0 K^+\pi^-$, which excludes contribution from decay via $D^*(2010)^-$ resonance.

$\Gamma(\overline{D}^0 K^+\pi^-$ non-resonant$)/\Gamma_{total}$ Γ_{141}/Γ

VALUE (units 10^{-6})	CL%	DOCUMENT ID		TECN	COMMENT
<37	90	[1] AUBERT	06A	BABR	$e^+e^- \to \Upsilon(4S)$

[1] Assumes equal production of B^+ and B^0 at the $\Upsilon(4S)$.

$\Gamma([K^+K^-]_D K^*(892)^0)/\Gamma(\overline{D}^0 K^*(892)^0)$ $\Gamma_{142}/\Gamma_{134}$

VALUE	DOCUMENT ID		TECN	COMMENT
• • • We do not use the following data for averages, fits, limits, etc. • • •				
$1.05^{+0.17}_{-0.15} \pm 0.04$	AAIJ	14BN	LHCB	Repl. by AAIJ 16S
$1.36^{+0.37}_{-0.32} \pm 0.07$	AAIJ	13L	LHCB	Repl. by AAIJ 14BN

$\Gamma([\pi^+\pi^-]_D K^*(892)^0)/\Gamma(\overline{D}^0 K^*(892)^0)$ $\Gamma_{143}/\Gamma_{134}$

VALUE	DOCUMENT ID		TECN	COMMENT
• • • We do not use the following data for averages, fits, limits, etc. • • •				
$1.21^{+0.28}_{-0.25} \pm 0.05$	AAIJ	14BN	LHCB	Repl. by AAIJ 16S

$\Gamma(\overline{D}^0\pi^0)/\Gamma_{total}$ Γ_{144}/Γ

VALUE (units 10^{-4})	CL%	DOCUMENT ID		TECN	COMMENT
2.63±0.14 OUR AVERAGE					
$2.69 \pm 0.09 \pm 0.13$		[1] LEES	11M	BABR	$e^+e^- \to \Upsilon(4S)$
$2.25 \pm 0.14 \pm 0.35$		[1] BLYTH	06	BELL	$e^+e^- \to \Upsilon(4S)$
$2.74^{+0.36}_{-0.32} \pm 0.55$		[1] COAN	02	CLE2	$e^+e^- \to \Upsilon(4S)$
• • • We do not use the following data for averages, fits, limits, etc. • • •					
$2.9 \pm 0.2 \pm 0.3$		[1] AUBERT	04B	BABR	Repl. by LEES 11M
$3.1 \pm 0.4 \pm 0.5$		[1] ABE	02J	BELL	Repl. by BLYTH 06
<1.2	90	[2] NEMATI	98	CLE2	Repl. by COAN 02
<4.8	90	[3] ALAM	94	CLE2	Repl. by NEMATI 98

[1] Assumes equal production of B^+ and B^0 at the $\Upsilon(4S)$.

[2] NEMATI 98 assumes equal production of B^+ and B^0 at the $\Upsilon(4S)$ and use the PDG 96 values for D^0, D^{*0}, η, η', and ω branching fractions.

[3] ALAM 94 assume equal production of B^+ and B^0 at the $\Upsilon(4S)$ and use the CLEO II absolute $B(D^0 \to K^-\pi^+)$ and the PDG 1992 $B(D^0 \to K^-\pi^+\pi^0)/B(D^0 \to K^-\pi^+)$ and $B(D^0 \to K^-2\pi^+\pi^-)/B(D^0 \to K^-\pi^+)$.

$\Gamma(\overline{D}^0\rho^0)/\Gamma_{total}$ Γ_{145}/Γ

VALUE (units 10^{-4})	CL%	DOCUMENT ID		TECN	COMMENT
3.21±0.21 OUR AVERAGE					
$3.21 \pm 0.10 \pm 0.21$		[1] AAIJ	15Y	LHCB	pp at 7, 8 TeV
$3.19 \pm 0.20 \pm 0.45$		[2,3] KUZMIN	07	BELL	$e^+e^- \to \Upsilon(4S)$
• • • We do not use the following data for averages, fits, limits, etc. • • •					
$2.9 \pm 1.0 \pm 0.4$		[2] SATPATHY	03	BELL	Repl. by KUZMIN 07
< 3.9	90	[4] NEMATI	98	CLE2	$e^+e^- \to \Upsilon(4S)$
< 5.5	90	[5] ALAM	94	CLE2	Repl. by NEMATI 98
< 6.0	90	[6] BORTOLETTO	92	CLEO	$e^+e^- \to \Upsilon(4S)$
<27.0	90	[7] ALBRECHT	88K	ARG	$e^+e^- \to \Upsilon(4S)$

[1] Measured using isobar formalism in the decay chain $B^0 \to \overline{D}^0\rho(770)$, $\rho \to \pi^+\pi^-$ assuming $B(\rho(770) \to \pi^+\pi^-) = 1$. The second uncertainty combines in quadrature all systematic uncertainties quoted in the paper.

[2] Assumes equal production of B^+ and B^0 at the $\Upsilon(4S)$.

[3] Our second uncertainty combines systematics and model errors quoted in the paper.

[4] NEMATI 98 assumes equal production of B^+ and B^0 at the $\Upsilon(4S)$ and use the PDG 96 values for D^0, D^{*0}, η, η', and ω branching fractions.

[5] ALAM 94 assume equal production of B^+ and B^0 at the $\Upsilon(4S)$ and use the CLEO II absolute $B(D^0 \to K^-\pi^+)$ and the PDG 1992 $B(D^0 \to K^-\pi^+\pi^0)/B(D^0 \to K^-\pi^+)$ and $B(D^0 \to K^-2\pi^+\pi^-)/B(D^0 \to K^-\pi^+)$.

See key on page 885

[6] BORTOLETTO 92 assumes equal production of B^+ and B^0 at the $\Upsilon(4S)$ and uses Mark III branching fractions for the D.
[7] ALBRECHT 88K reports < 0.003 assuming $B^0\overline{B}^0$:B^+B^- production ratio is 45:55. We rescale to 50%.

$\Gamma(\overline{D}^0 f_2)/\Gamma_{total}$ Γ_{146}/Γ

VALUE (units 10^{-4})		DOCUMENT ID		TECN	COMMENT
1.56±0.21 OUR AVERAGE					
1.68±0.11±0.21		[1] AAIJ	15Y	LHCB	pp at 7, 8 TeV
1.20±0.18±0.38		[2,3] KUZMIN	07	BELL	$e^+e^- \to \Upsilon(4S)$

[1] Result obtained using the isobar formalism. The second uncertainty combines in quadrature all systematic uncertainties quoted in the paper. Measured in the decay chain $B^0 \to \overline{D}^0 f_2(1270)$, $f_2 \to \pi^+\pi^-$.
[2] Assumes equal production of B^+ and B^0 at the $\Upsilon(4S)$.
[3] Our second uncertainty combines systematics and model errors quoted in the paper.

$\Gamma(\overline{D}^0\eta)/\Gamma_{total}$ Γ_{147}/Γ

VALUE (units 10^{-4})	CL%	DOCUMENT ID		TECN	COMMENT
2.36±0.32 OUR AVERAGE		Error includes scale factor of 2.5.			
2.53±0.09±0.11		[1] LEES	11M	BABR	$e^+e^- \to \Upsilon(4S)$
1.77±0.16±0.21		[1] BLYTH	06	BELL	$e^+e^- \to \Upsilon(4S)$
• • • We do not use the following data for averages, fits, limits, etc. • • •					
2.5 ±0.2 ±0.3		[1] AUBERT	04B	BABR	Repl. by LEES 11M
1.4 $^{+0.5}_{-0.4}$ ±0.3		[1] ABE	02J	BELL	Repl. by BLYTH 06
<1.3	90	[2] NEMATI	98	CLE2	$e^+e^- \to \Upsilon(4S)$
<6.8	90	[3] ALAM	94	CLE2	Repl. by NEMATI 98

[1] Assumes equal production of B^+ and B^0 at the $\Upsilon(4S)$.
[2] NEMATI 98 assumes equal production of B^+ and B^0 at the $\Upsilon(4S)$ and use the PDG 96 values for D^0, D^{*0}, η, η', and ω branching fractions.
[3] ALAM 94 assume equal production of B^+ and B^0 at the $\Upsilon(4S)$ and use the CLEO II absolute B($D^0 \to K^-\pi^+$) and the PDG 1992 B($D^0 \to K^-\pi^+\pi^0$)/B($D^0 \to K^-\pi^+$) and B($D^0 \to K^-2\pi^+\pi^-$)/B($D^0 \to K^-\pi^+$).

$\Gamma(\overline{D}^0\eta')/\Gamma_{total}$ Γ_{148}/Γ

VALUE (units 10^{-4})	CL%	DOCUMENT ID		TECN	COMMENT
1.38±0.16 OUR AVERAGE		Error includes scale factor of 1.3.			
1.48±0.13±0.07		[1] LEES	11M	BABR	$e^+e^- \to \Upsilon(4S)$
1.14±0.20 $^{+0.10}_{-0.13}$		[1] SCHUMANN	05	BELL	$e^+e^- \to \Upsilon(4S)$
• • • We do not use the following data for averages, fits, limits, etc. • • •					
1.7 ±0.4 ±0.2		[1] AUBERT	04B	BABR	Repl. by LEES 11M
<9.4	90	[2] NEMATI	98	CLE2	$e^+e^- \to \Upsilon(4S)$
<8.6	90	[3] ALAM	94	CLE2	Repl. by NEMATI 98

[1] Assumes equal production of B^+ and B^0 at the $\Upsilon(4S)$.
[2] NEMATI 98 assumes equal production of B^+ and B^0 at the $\Upsilon(4S)$ and use the PDG 96 values for D^0, D^{*0}, η, η', and ω branching fractions.
[3] ALAM 94 assume equal production of B^+ and B^0 at the $\Upsilon(4S)$ and use the CLEO II absolute B($D^0 \to K^-\pi^+$) and the PDG 1992 B($D^0 \to K^-\pi^+\pi^0$)/B($D^0 \to K^-\pi^+$) and B($D^0 \to K^-2\pi^+\pi^-$)/B($D^0 \to K^-\pi^+$).

$\Gamma(\overline{D}^0\eta')/\Gamma(\overline{D}^0\eta)$ $\Gamma_{148}/\Gamma_{147}$

VALUE	DOCUMENT ID		TECN	COMMENT
0.54±0.07±0.01	LEES	11M	BABR	$e^+e^- \to \Upsilon(4S)$
• • • We do not use the following data for averages, fits, limits, etc. • • •				
0.7 ±0.2 ±0.1	AUBERT	04B	BABR	Repl. by LEES 11M

$\Gamma(\overline{D}^0\omega)/\Gamma_{total}$ Γ_{149}/Γ

VALUE (units 10^{-4})	CL%	DOCUMENT ID		TECN	COMMENT
2.54±0.16 OUR AVERAGE					
2.75±0.72±0.35		[1] AAIJ	15Y	LHCB	pp at 7, 8 TeV
2.57±0.11±0.14		[2] LEES	11M	BABR	$e^+e^- \to \Upsilon(4S)$
2.37±0.23±0.28		[2] BLYTH	06	BELL	$e^+e^- \to \Upsilon(4S)$
• • • We do not use the following data for averages, fits, limits, etc. • • •					
3.0 ±0.3 ±0.4		[2] AUBERT	04B	BABR	Repl. by LEES 11M
1.8 ±0.5 $^{+0.4}_{-0.3}$		[2] ABE	02J	BELL	Repl. by BLYTH 06
<5.1	90	[3] NEMATI	98	CLE2	$e^+e^- \to \Upsilon(4S)$
<6.3	90	[4] ALAM	94	CLE2	Repl. by NEMATI 98

[1] Result obtained using the isobar model. The second uncertainty combines in quadrature all systematic uncertainties quoted in the paper.
[2] Assumes equal production of B^+ and B^0 at the $\Upsilon(4S)$.
[3] NEMATI 98 assumes equal production of B^+ and B^0 at the $\Upsilon(4S)$ and use the PDG 96 values for D^0, D^{*0}, η, η', and ω branching fractions.
[4] ALAM 94 assume equal production of B^+ and B^0 at the $\Upsilon(4S)$ and use the CLEO II absolute B($D^0 \to K^-\pi^+$) and the PDG 1992 B($D^0 \to K^-\pi^+\pi^0$)/B($D^0 \to K^-\pi^+$) and B($D^0 \to K^-2\pi^+\pi^-$)/B($D^0 \to K^-\pi^+$).

$\Gamma(D^0\phi)/\Gamma_{total}$ Γ_{150}/Γ

VALUE (units 10^{-6})	CL%	DOCUMENT ID		TECN	COMMENT
<11.6	90	[1] AUBERT	07AO	BABR	$e^+e^- \to \Upsilon(4S)$

[1] Assumes equal production of B^+ and B^0 at the $\Upsilon(4S)$.

$\Gamma(D^0K^+\pi^-)/\Gamma_{total}$ Γ_{151}/Γ

VALUE (units 10^{-6})	CL%	DOCUMENT ID		TECN	COMMENT
• • • We do not use the following data for averages, fits, limits, etc. • • •					
<19	90	[1] AUBERT	06A	BABR	Repl. by AUBERT 09AE

[1] Assumes equal production of B^+ and B^0 at the $\Upsilon(4S)$.

$\Gamma(D^0K^+\pi^-)/\Gamma(\overline{D}^0K^+\pi^-)$ $\Gamma_{151}/\Gamma_{133}$

VALUE	DOCUMENT ID		TECN	COMMENT
0.060±0.034 OUR AVERAGE				
0.045 $^{+0.056}_{-0.050}$ $^{+0.028}_{-0.018}$	[1,2] NEGISHI	12	BELL	$e^+e^- \to \Upsilon(4S)$
0.068±0.042	[3] AUBERT	09AE	BABR	$e^+e^- \to \Upsilon(4S)$

[1] Assumes equal production of B^0 and B^+ at $\Upsilon(4S)$.
[2] Uses $D^0 \to K^-\pi^+$ mode. Restricts $K^+\pi^-$ mass within ±50 MeV of the nominal K^{*0} mass. Corresponds to the upper limit, < 0.16 at 95% CL.
[3] Reports a signal at the level of 2.5 standard deviations after combining results from $D^0 \to K^+\pi^-$, $K^+\pi^-\pi^0$, and $K^+\pi^-\pi^+\pi^-$.

$\Gamma(D^0K^*(892)^0)/\Gamma_{total}$ Γ_{152}/Γ

VALUE (units 10^{-5})	CL%	DOCUMENT ID		TECN	COMMENT
<1.1	90	[1] AUBERT,B	06L	BABR	$e^+e^- \to \Upsilon(4S)$
• • • We do not use the following data for averages, fits, limits, etc. • • •					
<1.8	90	[1] KROKOVNY	03	BELL	$e^+e^- \to \Upsilon(4S)$

[1] Assumes equal production of B^+ and B^0 at the $\Upsilon(4S)$.

$\Gamma(\overline{D}^{*0}\gamma)/\Gamma_{total}$ Γ_{153}/Γ

VALUE	CL%	DOCUMENT ID		TECN	COMMENT
<2.5 × 10^{-5}	90	[1] AUBERT,B	05Q	BABR	$e^+e^- \to \Upsilon(4S)$
• • • We do not use the following data for averages, fits, limits, etc. • • •					
<5.0 × 10^{-5}	90	[1] ARTUSO	00	CLE2	$e^+e^- \to \Upsilon(4S)$

[1] Assumes equal production of B^+ and B^0 at the $\Upsilon(4S)$.

$\Gamma(\overline{D}^*(2007)^0\pi^0)/\Gamma_{total}$ Γ_{154}/Γ

VALUE (units 10^{-4})	CL%	DOCUMENT ID		TECN	COMMENT
2.2 ±0.6 OUR AVERAGE		Error includes scale factor of 2.6. See the ideogram below.			
3.05±0.14±0.28		[1] LEES	11M	BABR	$e^+e^- \to \Upsilon(4S)$
1.39±0.18±0.26		[1] BLYTH	06	BELL	$e^+e^- \to \Upsilon(4S)$
2.20 $^{+0.59}_{-0.52}$ ±0.79		[1] COAN	02	CLE2	$e^+e^- \to \Upsilon(4S)$
• • • We do not use the following data for averages, fits, limits, etc. • • •					
2.9 ±0.4 ±0.5		[1] AUBERT	04B	BABR	Repl. by LEES 11M
2.7 $^{+0.8}_{-0.7}$ $^{+0.5}_{-0.6}$		[1] ABE	02J	BELL	Repl. by BLYTH 06
<4.4	90	[2] NEMATI	98	CLE2	Repl. by COAN 02
<9.7	90	[3] ALAM	94	CLE2	Repl. by NEMATI 98

[1] Assumes equal production of B^+ and B^0 at the $\Upsilon(4S)$.
[2] NEMATI 98 assumes equal production of B^+ and B^0 at the $\Upsilon(4S)$ and use the PDG 96 values for D^0, D^{*0}, η, η', and ω branching fractions.
[3] ALAM 94 assume equal production of B^+ and B^0 at the $\Upsilon(4S)$ and use the CLEO II B($D^*(2007)^0 \to D^0\pi^0$) and absolute B($D^0 \to K^-\pi^+$) and the PDG 1992 B($D^0 \to K^-\pi^+\pi^0$)/B($D^0 \to K^-\pi^+$) and B($D^0 \to K^-2\pi^+\pi^-$)/B($D^0 \to K^-\pi^+$).

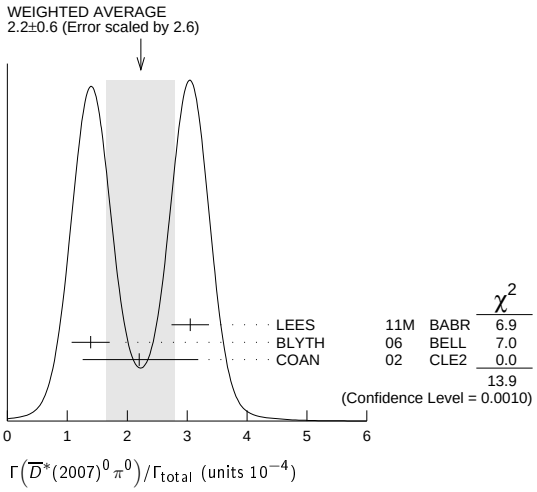

$\Gamma(\overline{D}^0\pi^0)/\Gamma(\overline{D}^*(2007)^0\pi^0)$ $\Gamma_{144}/\Gamma_{154}$

VALUE	DOCUMENT ID		TECN	COMMENT
0.90±0.08 OUR AVERAGE				
0.88±0.05±0.06	LEES	11M	BABR	$e^+e^- \to \Upsilon(4S)$
1.62±0.23±0.35	BLYTH	06	BELL	$e^+e^- \to \Upsilon(4S)$
• • • We do not use the following data for averages, fits, limits, etc. • • •				
1.0 ±0.1 ±0.2	AUBERT	04B	BABR	Repl. by LEES 11M

Meson Particle Listings

B^0

$\Gamma(\overline{D}^*(2007)^0\rho^0)/\Gamma_{total}$ Γ_{155}/Γ

VALUE	CL%	DOCUMENT ID		TECN	COMMENT
<5.1 $\times 10^{-4}$	90	[1] SATPATHY	03	BELL	$e^+e^- \to \Upsilon(4S)$
• • • We do not use the following data for averages, fits, limits, etc. • • •					
<0.00056	90	[2] NEMATI	98	CLE2	$e^+e^- \to \Upsilon(4S)$
<0.00117	90	[3] ALAM	94	CLE2	Repl. by NEMATI 98

[1] Assumes equal production of B^+ and B^0 at the $\Upsilon(4S)$.
[2] NEMATI 98 assumes equal production of B^+ and B^0 at the $\Upsilon(4S)$ and use the PDG 96 values for D^0, D^{*0}, η, η', and ω branching fractions.
[3] ALAM 94 assume equal production of B^+ and B^0 at the $\Upsilon(4S)$ and use the CLEO II $B(D^*(2007)^0 \to D^0\pi^0)$ and absolute $B(D^0 \to K^-\pi^+)$ and the PDG 1992 $B(D^0 \to K^-\pi^+\pi^0)/B(D^0 \to K^-\pi^+)$ and $B(D^0 \to K^-2\pi^+\pi^-)/B(D^0 \to K^-\pi^+)$.

$\Gamma(\overline{D}^*(2007)^0\eta)/\Gamma_{total}$ Γ_{156}/Γ

VALUE (units 10^{-4})	CL%	DOCUMENT ID		TECN	COMMENT
2.3 ±0.6 OUR AVERAGE		Error includes scale factor of 2.8.			
2.69±0.14±0.23		[1] LEES	11M	BABR	$e^+e^- \to \Upsilon(4S)$
1.40±0.28±0.26		[1] BLYTH	06	BELL	$e^+e^- \to \Upsilon(4S)$
• • • We do not use the following data for averages, fits, limits, etc. • • •					
2.6 ±0.4 ±0.4		[1] AUBERT	04B	BABR	Repl. by LEES 11M
<4.6	90	[1] ABE	02J	BELL	$e^+e^- \to \Upsilon(4S)$
<2.6	90	[2] NEMATI	98	CLE2	$e^+e^- \to \Upsilon(4S)$
<6.9	90	[3] ALAM	94	CLE2	Repl. by NEMATI 98

[1] Assumes equal production of B^+ and B^0 at the $\Upsilon(4S)$.
[2] NEMATI 98 assumes equal production of B^+ and B^0 at the $\Upsilon(4S)$ and use the PDG 96 values for D^0, D^{*0}, η, η', and ω branching fractions.
[3] ALAM 94 assume equal production of B^+ and B^0 at the $\Upsilon(4S)$ and use the CLEO II $B(D^*(2007)^0 \to D^0\pi^0)$ and absolute $B(D^0 \to K^-\pi^+)$ and the PDG 1992 $B(D^0 \to K^-\pi^+\pi^0)/B(D^0 \to K^-\pi^+)$ and $B(D^0 \to K^-2\pi^+\pi^-)/B(D^0 \to K^-\pi^+)$.

$\Gamma(\overline{D}^0\eta)/\Gamma(\overline{D}^*(2007)^0\eta)$ $\Gamma_{147}/\Gamma_{156}$

VALUE	DOCUMENT ID		TECN	COMMENT
0.99±0.10 OUR AVERAGE				
0.97±0.07±0.07	LEES	11M	BABR	$e^+e^- \to \Upsilon(4S)$
1.27±0.29±0.25	BLYTH	06	BELL	$e^+e^- \to \Upsilon(4S)$
• • • We do not use the following data for averages, fits, limits, etc. • • •				
0.9 ±0.2 ±0.1	AUBERT	04B	BABR	Repl. by LEES 11M

$\Gamma(\overline{D}^*(2007)^0\eta')/\Gamma(\overline{D}^*(2007)^0\eta)$ $\Gamma_{157}/\Gamma_{156}$

VALUE	DOCUMENT ID		TECN	COMMENT
0.61±0.14±0.02	LEES	11M	BABR	$e^+e^- \to \Upsilon(4S)$
• • • We do not use the following data for averages, fits, limits, etc. • • •				
0.5 ±0.3 ±0.1	AUBERT	04B	BABR	Repl. by LEES 11M

$\Gamma(\overline{D}^*(2007)^0\eta')/\Gamma_{total}$ Γ_{157}/Γ

VALUE (units 10^{-4})	CL%	DOCUMENT ID		TECN	COMMENT
1.40±0.22 OUR AVERAGE					
1.48±0.22±0.13		[1] LEES	11M	BABR	$e^+e^- \to \Upsilon(4S)$
1.21±0.34±0.22		[1] SCHUMANN	05	BELL	$e^+e^- \to \Upsilon(4S)$
• • • We do not use the following data for averages, fits, limits, etc. • • •					
1.3 ±0.7 ±0.2		[1,2] AUBERT	04B	BABR	Repl. by LEES 11M
<14	90	BRANDENB...	98	CLE2	$e^+e^- \to \Upsilon(4S)$
<19	90	[3] NEMATI	98	CLE2	$e^+e^- \to \Upsilon(4S)$
<27	90	[4] ALAM	94	CLE2	Repl. by NEMATI 98

[1] Assumes equal production of B^+ and B^0 at the $\Upsilon(4S)$.
[2] Reports an upper limit $< 2.6 \times 10^{-4}$ at 90% CL.
[3] NEMATI 98 assumes equal production of B^+ and B^0 at the $\Upsilon(4S)$ and use the PDG 96 values for D^0, D^{*0}, η, η', and ω branching fractions.
[4] ALAM 94 assume equal production of B^+ and B^0 at the $\Upsilon(4S)$ and use the CLEO II $B(D^*(2007)^0 \to D^0\pi^0)$ and absolute $B(D^0 \to K^-\pi^+)$ and the PDG 1992 $B(D^0 \to K^-\pi^+\pi^0)/B(D^0 \to K^-\pi^+)$ and $B(D^0 \to K^-2\pi^+\pi^-)/B(D^0 \to K^-\pi^+)$.

$\Gamma(\overline{D}^0\eta')/\Gamma(\overline{D}^*(2007)^0\eta')$ $\Gamma_{148}/\Gamma_{157}$

VALUE	DOCUMENT ID		TECN	COMMENT
0.96±0.18±0.06	LEES	11M	BABR	$e^+e^- \to \Upsilon(4S)$
• • • We do not use the following data for averages, fits, limits, etc. • • •				
1.3 ±0.8 ±0.2	AUBERT	04B	BABR	Repl. by LEES 11M

$\Gamma(\overline{D}^*(2007)^0\pi^+\pi^-)/\Gamma_{total}$ Γ_{158}/Γ

VALUE	DOCUMENT ID		TECN	COMMENT
(6.2±1.2±1.8) $\times 10^{-4}$	[1,2] SATPATHY	03	BELL	$e^+e^- \to \Upsilon(4S)$

[1] Assumes equal production of B^+ and B^0 at the $\Upsilon(4S)$.
[2] No assumption about the intermediate mechanism is made in the analysis.

$\Gamma(\overline{D}^*(2007)^0K^0)/\Gamma_{total}$ Γ_{159}/Γ

VALUE (units 10^{-5})	CL%	DOCUMENT ID		TECN	COMMENT
3.6±1.2±0.3		[1] AUBERT,B	06L	BABR	$e^+e^- \to \Upsilon(4S)$
• • • We do not use the following data for averages, fits, limits, etc. • • •					
<6.6	90	[1] KROKOVNY	03	BELL	$e^+e^- \to \Upsilon(4S)$

[1] Assumes equal production of B^+ and B^0 at the $\Upsilon(4S)$.

$\Gamma(\overline{D}^*(2007)^0K^*(892)^0)/\Gamma_{total}$ Γ_{160}/Γ

VALUE	CL%	DOCUMENT ID		TECN	COMMENT
<6.9 $\times 10^{-5}$	90	[1] KROKOVNY	03	BELL	$e^+e^- \to \Upsilon(4S)$

[1] Assumes equal production of B^+ and B^0 at the $\Upsilon(4S)$.

$\Gamma(D^*(2007)^0K^*(892)^0)/\Gamma_{total}$ Γ_{161}/Γ

VALUE	CL%	DOCUMENT ID		TECN	COMMENT
<4.0 $\times 10^{-5}$	90	[1] KROKOVNY	03	BELL	$e^+e^- \to \Upsilon(4S)$

[1] Assumes equal production of B^+ and B^0 at the $\Upsilon(4S)$.

$\Gamma(D^*(2007)^0\pi^+\pi^+\pi^-\pi^-)/\Gamma_{total}$ Γ_{162}/Γ

VALUE (units 10^{-3})	DOCUMENT ID		TECN	COMMENT
2.7 ±0.5 OUR AVERAGE				
2.60±0.47±0.37	[1] MAJUMDER	04	BELL	$e^+e^- \to \Upsilon(4S)$
3.0 ±0.7 ±0.6	[1] EDWARDS	02	CLE2	$e^+e^- \to \Upsilon(4S)$

[1] Assumes equal production of B^+ and B^0 at the $\Upsilon(4S)$.

$\Gamma(D^*(2007)^0\pi^+\pi^+\pi^-\pi^-)/\Gamma(D^*(2010)^-\pi^+\pi^+\pi^-\pi^0)$ Γ_{162}/Γ_{63}

VALUE	DOCUMENT ID		TECN	COMMENT
0.17±0.04±0.02	[1] EDWARDS	02	CLE2	$e^+e^- \to \Upsilon(4S)$

[1] Assumes equal production of B^+ and B^0 at the $\Upsilon(4S)$.

$\Gamma(D^*(2010)^+D^*(2010)^-)/\Gamma_{total}$ Γ_{163}/Γ

VALUE (units 10^{-4})	CL%	DOCUMENT ID		TECN	COMMENT
8.0 ±0.6 OUR AVERAGE					
7.82±0.38±0.63		[1] KRONENBIT...	12	BELL	$e^+e^- \to \Upsilon(4S)$
8.1 ±0.6 ±1.0		[1] AUBERT,B	06A	BABR	$e^+e^- \to \Upsilon(4S)$
9.9 $^{+4.2}_{-3.3}$ ±1.2		[1] LIPELES	00	CLE2	$e^+e^- \to \Upsilon(4S)$
• • • We do not use the following data for averages, fits, limits, etc. • • •					
8.1 ±0.8 ±1.1		[1] MIYAKE	05	BELL	Repl. by KRONENBIT-TER 12
8.3 ±1.6 ±1.2		[1,2] AUBERT	02M	BABR	Repl. by AUBERT,B 06B
6.2 $^{+4.0}_{-2.9}$ ±1.0		[3] ARTUSO	99	CLE2	Repl. by LIPELES 00
<61	90	[4] BARATE	98Q	ALEP	$e^+e^- \to Z$
<22	90	[5] ASNER	97	CLE2	Repl. by ARTUSO 99

[1] Assumes equal production of B^+ and B^0 at the $\Upsilon(4S)$.
[2] AUBERT 02M also assumes the measured CP-odd fraction of the final states is 0.22 ± 0.18 ± 0.03.
[3] ARTUSO 99 uses $B(\Upsilon(4S) \to B^0\overline{B}^0)$=(48 ± 4)%.
[4] BARATE 98Q (ALEPH) observes 2 events with an expected background of 0.10 ± 0.03 which corresponds to a branching ratio of $(2.3^{+1.9}_{-1.2} \pm 0.4) \times 10^{-3}$.
[5] ASNER 97 at CLEO observes 1 event with an expected background of 0.022 ± 0.011. This corresponds to a branching ratio of $(5.3^{+7.1}_{-3.7} \pm 1.0) \times 10^{-4}$.

$\Gamma(\overline{D}^*(2007)^0\omega)/\Gamma_{total}$ Γ_{164}/Γ

VALUE (units 10^{-4})	CL%	DOCUMENT ID		TECN	COMMENT
3.6 ±1.1 OUR AVERAGE		Error includes scale factor of 3.1.			
4.55±0.24±0.39		[1] LEES	11M	BABR	$e^+e^- \to \Upsilon(4S)$
2.29±0.39±0.40		[1] BLYTH	06	BELL	$e^+e^- \to \Upsilon(4S)$
• • • We do not use the following data for averages, fits, limits, etc. • • •					
4.2 ±0.7 ±0.9	90	[1] AUBERT	04B	BABR	Repl. by LEES 11M
< 7.9	90	[1] ABE	02J	BELL	$e^+e^- \to \Upsilon(4S)$
< 7.4	90	[2] NEMATI	98	CLE2	$e^+e^- \to \Upsilon(4S)$
<21	90	[3] ALAM	94	CLE2	Repl. by NEMATI 98

[1] Assumes equal production of B^+ and B^0 at the $\Upsilon(4S)$.
[2] NEMATI 98 assumes equal production of B^+ and B^0 at the $\Upsilon(4S)$ and use the PDG 96 values for D^0, D^{*0}, η, η', and ω branching fractions.
[3] ALAM 94 assume equal production of B^+ and B^0 at the $\Upsilon(4S)$ and use the CLEO II $B(D^*(2007)^0 \to D^0\pi^0)$ and absolute $B(D^0 \to K^-\pi^+)$ and the PDG 1992 $B(D^0 \to K^-\pi^+\pi^0)/B(D^0 \to K^-\pi^+)$ and $B(D^0 \to K^-2\pi^+\pi^-)/B(D^0 \to K^-\pi^+)$.

$\Gamma(\overline{D}^0\omega)/\Gamma(\overline{D}^*(2007)^0\omega)$ $\Gamma_{149}/\Gamma_{164}$

VALUE	DOCUMENT ID		TECN	COMMENT
0.58±0.06 OUR AVERAGE				
0.56±0.04±0.04	LEES	11M	BABR	$e^+e^- \to \Upsilon(4S)$
1.04±0.20±0.17	BLYTH	06	BELL	$e^+e^- \to \Upsilon(4S)$
• • • We do not use the following data for averages, fits, limits, etc. • • •				
0.7 ±0.1 ±0.1	AUBERT	04B	BABR	Repl. by LEES 11M

$\Gamma(D^*(2010)^+D^-)/\Gamma_{total}$ Γ_{165}/Γ

VALUE (units 10^{-4})	CL%	DOCUMENT ID		TECN	COMMENT
6.1±1.5 OUR AVERAGE		Error includes scale factor of 1.6.			
5.7±0.7±0.7		[1] AUBERT,B	06A	BABR	$e^+e^- \to \Upsilon(4S)$
11.7±2.6 $^{+2.2}_{-2.5}$		[1,2] ABE	02Q	BELL	$e^+e^- \to \Upsilon(4S)$
• • • We do not use the following data for averages, fits, limits, etc. • • •					
8.8±1.0±1.3		[1] AUBERT	03J	BABR	Repl. by AUBERT,B 06B
14.8±3.8 $^{+2.8}_{-3.1}$		[1,3] ABE	02Q	BELL	$e^+e^- \to \Upsilon(4S)$
< 6.3	90	[1] LIPELES	00	CLE2	$e^+e^- \to \Upsilon(4S)$

<56	90	BARATE	98Q ALEP	$e^+e^- \to Z$	
<18	90	ASNER	97 CLE2	$e^+e^- \to \Upsilon(4S)$	

[1] Assumes equal production of B^+ and B^0 at the $\Upsilon(4S)$.
[2] The measurement is performed using fully reconstructed D^* and D^+ decays.
[3] The measurement is performed using a partial reconstruction technique for the D^* and fully reconstructed D^+ decays as a cross check.

$\Gamma(D^*(2007)^0\overline{D}{}^*(2007)^0)/\Gamma_{total}$ Γ_{166}/Γ

VALUE (units 10^{-4})	CL%	DOCUMENT ID		TECN	COMMENT
< 0.9	90	[1] AUBERT,B	06A	BABR	$e^+e^- \to \Upsilon(4S)$
• • • We do not use the following data for averages, fits, limits, etc. • • •					
<270	90	BARATE	98Q	ALEP	$e^+e^- \to Z$

[1] Assumes equal production of B^+ and B^0 at the $\Upsilon(4S)$.

$\Gamma(D^-D^0K^+)/\Gamma_{total}$ Γ_{167}/Γ

VALUE (units 10^{-3})	DOCUMENT ID		TECN	COMMENT
1.07±0.07±0.09	[1] DEL-AMO-SA...11B		BABR	$e^+e^- \to \Upsilon(4S)$
• • • We do not use the following data for averages, fits, limits, etc. • • •				
1.7 ±0.3 ±0.3	[1] AUBERT	03X	BABR	Repl. by DEL-AMO-SANCHEZ 11B

[1] Assumes equal production of B^+ and B^0 at the $\Upsilon(4S)$.

$\Gamma(D^-D^*(2007)^0K^+)/\Gamma_{total}$ Γ_{168}/Γ

VALUE (units 10^{-3})	DOCUMENT ID		TECN	COMMENT
3.46±0.18±0.37	[1] DEL-AMO-SA...11B		BABR	$e^+e^- \to \Upsilon(4S)$
• • • We do not use the following data for averages, fits, limits, etc. • • •				
4.6 ±0.7 ±0.7	[1] AUBERT	03X	BABR	Repl. by DEL-AMO-SANCHEZ 11B

[1] Assumes equal production of B^+ and B^0 at the $\Upsilon(4S)$.

$\Gamma(D^*(2010)^-D^0K^+)/\Gamma_{total}$ Γ_{169}/Γ

VALUE (units 10^{-3})	DOCUMENT ID		TECN	COMMENT
2.47±0.10±0.18	[1] DEL-AMO-SA...11B		BABR	$e^+e^- \to \Upsilon(4S)$
• • • We do not use the following data for averages, fits, limits, etc. • • •				
$3.1\ ^{+0.4}_{-0.3}\ \pm0.4$	[1] AUBERT	03X	BABR	Repl. by DEL-AMO-SANCHEZ 11B

[1] Assumes equal production of B^+ and B^0 at the $\Upsilon(4S)$.

$\Gamma(D^*(2010)^-D^*(2007)^0K^+)/\Gamma_{total}$ Γ_{170}/Γ

VALUE (units 10^{-3})	DOCUMENT ID		TECN	COMMENT
10.6±0.33±0.86	[1] DEL-AMO-SA...11B		BABR	$e^+e^- \to \Upsilon(4S)$
• • • We do not use the following data for averages, fits, limits, etc. • • •				
11.8±1.0 ±1.7	[1] AUBERT	03X	BABR	Repl. by DEL-AMO-SANCHEZ 11B

[1] Assumes equal production of B^+ and B^0 at the $\Upsilon(4S)$.

$\Gamma(D^-D^+K^0)/\Gamma_{total}$ Γ_{171}/Γ

VALUE (units 10^{-3})	CL%	DOCUMENT ID		TECN	COMMENT
0.75±0.12±0.12		[1] DEL-AMO-SA...11B		BABR	$e^+e^- \to \Upsilon(4S)$
• • • We do not use the following data for averages, fits, limits, etc. • • •					
<1.7	90	[1] AUBERT	03X	BABR	Repl. by DEL-AMO-SANCHEZ 11B

[1] Assumes equal production of B^+ and B^0 at the $\Upsilon(4S)$.

$[\Gamma(D^*(2010)^-D^+K^0)+\Gamma(D^-D^*(2010)^+K^0)]/\Gamma_{total}$ Γ_{172}/Γ

VALUE (units 10^{-3})	DOCUMENT ID		TECN	COMMENT
6.41±0.36±0.39	[1] DEL-AMO-SA...11B		BABR	$e^+e^- \to \Upsilon(4S)$
• • • We do not use the following data for averages, fits, limits, etc. • • •				
6.5 ±1.2 ±1.0	[1] AUBERT	03X	BABR	Repl. by DEL-AMO-SANCHEZ 11B

[1] Assumes equal production of B^+ and B^0 at the $\Upsilon(4S)$.

$\Gamma(D^*(2010)^-D^*(2010)^+K^0)/\Gamma_{total}$ Γ_{173}/Γ

VALUE (units 10^{-3})	DOCUMENT ID		TECN	COMMENT
8.1 ±0.7 OUR AVERAGE				
8.26±0.43±0.67	[1] DEL-AMO-SA...11B		BABR	$e^+e^- \to \Upsilon(4S)$
6.8 ±0.8 ±1.4	[1,2] DALSENO	07	BELL	$e^+e^- \to \Upsilon(4S)$
8.8 ±0.8 ±1.4	[1,2] AUBERT,B	06Q	BABR	$e^+e^- \to \Upsilon(4S)$
• • • We do not use the following data for averages, fits, limits, etc. • • •				
$8.8\ ^{+1.5}_{-1.4}\ \pm1.3$	[1] AUBERT	03X	BABR	Repl. by AUBERT,B 06Q

[1] Assumes equal production of B^+ and B^0 at the $\Upsilon(4S)$.
[2] The result is rescaled by a factor of 2 to convert from K^0_S to K^0.

$\Gamma(D^{*-}D_{s1}(2536)^+,\ D^+_{s1}\to D^{*+}K^0)/\Gamma_{total}$ Γ_{174}/Γ

VALUE (units 10^{-4})	DOCUMENT ID		TECN	COMMENT
8.0±2.4 OUR AVERAGE				
$7.6\ ^{+4.8}_{-4.2}\ ^{+1.6}_{-1.4}$	[1,2] DALSENO	07	BELL	$e^+e^- \to \Upsilon(4S)$
8.2±2.6±1.2	[1,2] AUBERT,B	06Q	BABR	$e^+e^- \to \Upsilon(4S)$

[1] Assumes equal production of B^+ and B^0 at the $\Upsilon(4S)$.
[2] The result is rescaled by a factor of 2 to convert from K^0_S to K^0.

$\Gamma(\overline{D}{}^0D^0K^0)/\Gamma_{total}$ Γ_{175}/Γ

VALUE (units 10^{-3})	CL%	DOCUMENT ID		TECN	COMMENT
0.27±0.10±0.05		[1] DEL-AMO-SA...11B		BABR	$e^+e^- \to \Upsilon(4S)$
• • • We do not use the following data for averages, fits, limits, etc. • • •					
<1.4	90	[1] AUBERT	03X	BABR	Repl. by DEL-AMO-SANCHEZ 11B

[1] Assumes equal production of B^+ and B^0 at the $\Upsilon(4S)$.

$[\Gamma(\overline{D}{}^0D^*(2007)^0K^0)+\Gamma(\overline{D}{}^*(2007)^0D^0K^0)]/\Gamma_{total}$ Γ_{176}/Γ

VALUE (units 10^{-3})	CL%	DOCUMENT ID		TECN	COMMENT
1.08±0.32±0.36		[1] DEL-AMO-SA...11B		BABR	$e^+e^- \to \Upsilon(4S)$
• • • We do not use the following data for averages, fits, limits, etc. • • •					
<3.7	90	[1] AUBERT	03X	BABR	Repl. by DEL-AMO-SANCHEZ 11B

[1] Assumes equal production of B^+ and B^0 at the $\Upsilon(4S)$.

$\Gamma(\overline{D}{}^*(2007)^0D^*(2007)^0K^0)/\Gamma_{total}$ Γ_{177}/Γ

VALUE (units 10^{-3})	CL%	DOCUMENT ID		TECN	COMMENT
2.40±0.55±0.67		[1] DEL-AMO-SA...11B		BABR	$e^+e^- \to \Upsilon(4S)$
• • • We do not use the following data for averages, fits, limits, etc. • • •					
<6.6	90	[1] AUBERT	03X	BABR	Repl. by DEL-AMO-SANCHEZ 11B

[1] Assumes equal production of B^+ and B^0 at the $\Upsilon(4S)$.

$\Gamma((\overline{D}+\overline{D}{}^*)(D+D^*)K)/\Gamma_{total}$ Γ_{178}/Γ

VALUE (units 10^{-2})	DOCUMENT ID		TECN	COMMENT
3.68±0.10±0.24	[1] DEL-AMO-SA...11B		BABR	$e^+e^- \to \Upsilon(4S)$
• • • We do not use the following data for averages, fits, limits, etc. • • •				
4.3 ±0.3 ±0.6	[1] AUBERT	03X	BABR	Repl. by DEL-AMO-SANCHEZ 11B

[1] Assumes equal production of B^+ and B^0 at the $\Upsilon(4S)$.

$\Gamma(\eta_cK^0)/\Gamma_{total}$ Γ_{179}/Γ

VALUE (units 10^{-3})	DOCUMENT ID		TECN	COMMENT
0.79±0.12 OUR AVERAGE				
$0.55\ ^{+0.19}_{-0.17}\ \pm0.06$	[1,2] AUBERT	07AV	BABR	$e^+e^- \to \Upsilon(4S)$
0.89±0.15±0.06	[1,3] AUBERT,B	04B	BABR	$e^+e^- \to \Upsilon(4S)$
$1.23\pm0.23\ ^{+0.40}_{-0.41}$	[1] FANG	03	BELL	$e^+e^- \to \Upsilon(4S)$
$1.09\ ^{+0.55}_{-0.42}\pm0.33$	[4] EDWARDS	01	CLE2	$e^+e^- \to \Upsilon(4S)$

[1] Assumes equal production of B^+ and B^0 at the $\Upsilon(4S)$.
[2] AUBERT 07AV reports $[\Gamma(B^0\to\eta_cK^0)/\Gamma_{total}]\times[B(\eta_c(1S)\to p\overline{p})] = (0.83\ ^{+0.28}_{-0.26}\pm 0.05)\times10^{-6}$ which we divide by our best value $B(\eta_c(1S)\to p\overline{p}) = (1.52\pm0.16)\times10^{-3}$. Our first error is their experiment's error and our second error is the systematic error from using our best value.
[3] AUBERT,B 04B reports $[\Gamma(B^0\to\eta_cK^0)/\Gamma_{total}]\times[B(\eta_c(1S)\to K\overline{K}\pi)] = (0.0648\pm 0.0085\pm0.0071)\times10^{-3}$ which we divide by our best value $B(\eta_c(1S)\to K\overline{K}\pi) = (7.3\pm0.5)\times10^{-2}$. Our first error is their experiment's error and our second error is the systematic error from using our best value.
[4] EDWARDS 01 assumes equal production of B^0 and B^+ at the $\Upsilon(4S)$. The correlated uncertainties (28.3)% from $B(J/\psi(1S)\to\gamma\eta_c)$ in those modes have been accounted for.

$\Gamma(\eta_cK^0)/\Gamma(J/\psi(1S)K^0)$ $\Gamma_{179}/\Gamma_{183}$

VALUE	DOCUMENT ID		TECN	COMMENT
1.39±0.20±0.45	[1] AUBERT,B	04B	BABR	$e^+e^- \to \Upsilon(4S)$

[1] Uses BABAR measurement of $B(B^0\to J/\psi K^0) = (8.5\pm0.5\pm0.6)\times10^{-4}$.

$\Gamma(\eta_cK^*(892)^0)/\Gamma_{total}$ Γ_{180}/Γ

VALUE (units 10^{-3})	DOCUMENT ID		TECN	COMMENT
0.69±0.09 OUR AVERAGE				
0.67±0.08±0.05	[1,2] AUBERT	08AB	BABR	$e^+e^- \to \Upsilon(4S)$
$0.68\ ^{+0.21}_{-0.19}\pm0.07$	[3,4] AUBERT	07AV	BABR	$e^+e^- \to \Upsilon(4S)$
$1.62\pm0.32\ ^{+0.55}_{-0.60}$	[4] FANG	03	BELL	$e^+e^- \to \Upsilon(4S)$

[1] AUBERT 08AB reports $[\Gamma(B^0\to\eta_cK^*(892)^0)/\Gamma_{total}]\ /\ [B(B^+\to\eta_cK^+)] = 0.62\pm 0.06\pm0.05$ which we multiply by our best value $B(B^+\to\eta_cK^+) = (1.09\pm0.09)\times10^{-3}$. Our first error is their experiment's error and our second error is the systematic error from using our best value.
[2] Uses the production ratio of $(B^+B^-)/(B^0\overline{B}{}^0) = 1.026\pm0.032$ at $\Upsilon(4S)$.
[3] AUBERT 07AV reports $[\Gamma(B^0\to\eta_cK^*(892)^0)/\Gamma_{total}]\times[B(\eta_c(1S)\to p\overline{p})] = (1.03\ ^{+0.27}_{-0.24}\pm0.17)\times10^{-6}$ which we divide by our best value $B(\eta_c(1S)\to p\overline{p}) = (1.52\pm0.16)\times10^{-3}$. Our first error is their experiment's error and our second error is the systematic error from using our best value.
[4] Assumes equal production of B^+ and B^0 at the $\Upsilon(4S)$.

$\Gamma(\eta_c(2S)K^{*0})/\Gamma_{total}$ Γ_{181}/Γ

VALUE (units 10^{-4})	CL%	DOCUMENT ID		TECN	COMMENT
<3.9	90	[1] AUBERT	08AB	BABR	$e^+e^- \to \Upsilon(4S)$

[1] Uses the production ratio of $(B^+B^-)/(B^0\overline{B}^0) = 1.026 \pm 0.032$ at $\Upsilon(4S)$.

$\Gamma(B^0 \to h_c(1P)K^{*0})/\Gamma_{\rm total} \times \Gamma(h_c(1P) \to \gamma\eta_c(1S))/\Gamma_{\rm total}$ $\Gamma_{182}/\Gamma \times \Gamma_9^{h_c(1P)}/\Gamma^{h_c(1P)}$

VALUE (units 10^{-4})	CL%	DOCUMENT ID		TECN	COMMENT
<2.2	90	[1] AUBERT	08AB	BABR	$e^+e^- \to \Upsilon(4S)$

[1] Uses the production ratio of $(B^+B^-)/(B^0\overline{B}^0) = 1.026 \pm 0.032$ at $\Upsilon(4S)$.

$\Gamma(\eta_c K^*(892)^0)/\Gamma(\eta_c K^0)$ $\Gamma_{180}/\Gamma_{179}$

VALUE	DOCUMENT ID		TECN	COMMENT
$\mathbf{1.33 \pm 0.36^{+0.24}_{-0.33}}$	FANG	03	BELL	$e^+e^- \to \Upsilon(4S)$

$\Gamma(J/\psi(1S)K^0)/\Gamma_{\rm total}$ Γ_{183}/Γ

VALUE (units 10^{-4})	CL%	EVTS	DOCUMENT ID		TECN	COMMENT
8.73±0.32 OUR FIT						
8.72±0.32 OUR AVERAGE						
$8.8\ ^{+1.4}_{-1.3} \pm 0.1$			[1,2] AUBERT	07AV	BABR	$e^+e^- \to \Upsilon(4S)$
$8.69 \pm 0.22 \pm 0.30$			[2] AUBERT	05J	BABR	$e^+e^- \to \Upsilon(4S)$
$7.9 \pm 0.4 \pm 0.9$			[2] ABE	03B	BELL	$e^+e^- \to \Upsilon(4S)$
$9.5 \pm 0.8 \pm 0.6$			[2] AVERY	00	CLE2	$e^+e^- \to \Upsilon(4S)$
$11.5 \pm 2.3 \pm 1.7$			[3] ABE	96H	CDF	$p\overline{p}$ at 1.8 TeV
$6.93 \pm 4.07 \pm 0.04$			[4] BORTOLETTO	92	CLEO	$e^+e^- \to \Upsilon(4S)$
$9.24 \pm 7.21 \pm 0.05$		2	[5] ALBRECHT	90J	ARG	$e^+e^- \to \Upsilon(4S)$
• • • We do not use the following data for averages, fits, limits, etc. • • •						
$8.3 \pm 0.4 \pm 0.5$			[2] AUBERT	02	BABR	Repl. by AUBERT 05J
$8.5\ ^{+1.4}_{-1.2} \pm 0.6$			[2] JESSOP	97	CLE2	Repl. by AVERY 00
$7.5 \pm 2.4 \pm 0.8$		10	[4] ALAM	94	CLE2	Sup. by JESSOP 97
<50	90		ALAM	86	CLEO	$e^+e^- \to \Upsilon(4S)$

[1] AUBERT 07AV reports $[\Gamma(B^0 \to J/\psi(1S)K^0)/\Gamma_{\rm total}] \times [B(J/\psi(1S) \to p\overline{p})] = (1.87^{+0.28}_{-0.26} \pm 0.07) \times 10^{-6}$ which we divide by our best value $B(J/\psi(1S) \to p\overline{p}) = (2.121 \pm 0.029) \times 10^{-3}$. Our first error is their experiment's error and our second error is the systematic error from using our best value.

[2] Assumes equal production of B^+ and B^0 at the $\Upsilon(4S)$.

[3] ABE 96H assumes that $B(B^+ \to J/\psi K^+) = (1.02 \pm 0.14) \times 10^{-3}$.

[4] BORTOLETTO 92 reports $(6 \pm 3 \pm 2) \times 10^{-4}$ from a measurement of $[\Gamma(B^0 \to J/\psi(1S)K^0)/\Gamma_{\rm total}] \times [B(J/\psi(1S) \to e^+e^-)]$ assuming $B(J/\psi(1S) \to e^+e^-) = 0.069 \pm 0.009$, which we rescale to our best value $B(J/\psi(1S) \to e^+e^-) = (5.971 \pm 0.032) \times 10^{-2}$. Our first error is their experiment's error and our second error is the systematic error from using our best value. Assumes equal production of B^+ and B^0 at the $\Upsilon(4S)$.

[5] ALBRECHT 90J reports $(8 \pm 6 \pm 2) \times 10^{-4}$ from a measurement of $[\Gamma(B^0 \to J/\psi(1S)K^0)/\Gamma_{\rm total}] \times [B(J/\psi(1S) \to e^+e^-)]$ assuming $B(J/\psi(1S) \to e^+e^-) = 0.069 \pm 0.009$, which we rescale to our best value $B(J/\psi(1S) \to e^+e^-) = (5.971 \pm 0.032) \times 10^{-2}$. Our first error is their experiment's error and our second error is the systematic error from using our best value. Assumes equal production of B^+ and B^0 at the $\Upsilon(4S)$.

$\Gamma(J/\psi(1S)K^+\pi^-)/\Gamma_{\rm total}$ Γ_{184}/Γ

VALUE (units 10^{-3})	CL%	DOCUMENT ID		TECN	COMMENT
1.15 ±0.05 OUR AVERAGE					
$1.15 \pm 0.01 \pm 0.05$		CHILIKIN	14	BELL	$\overline{B}^0 \to J/\psi K^-\pi^+$
$1.16 \pm 0.56 \pm 0.01$		[1] BORTOLETTO	92	CLEO	$e^+e^- \to \Upsilon(4S)$
• • • We do not use the following data for averages, fits, limits, etc. • • •					
1.079 ± 0.011		[2] AUBERT	09AA	BABR	$e^+e^- \to \Upsilon(4S)$
<1.3	90	[3] ALBRECHT	87D	ARG	$e^+e^- \to \Upsilon(4S)$
<6.3	90	GILES	84	CLEO	$e^+e^- \to \Upsilon(4S)$

[1] BORTOLETTO 92 reports $(1.0 \pm 0.4 \pm 0.3) \times 10^{-3}$ from a measurement of $[\Gamma(B^0 \to J/\psi(1S)K^+\pi^-)/\Gamma_{\rm total}] \times [B(J/\psi(1S) \to e^+e^-)]$ assuming $B(J/\psi(1S) \to e^+e^-) = 0.069 \pm 0.009$, which we rescale to our best value $B(J/\psi(1S) \to e^+e^-) = (5.971 \pm 0.032) \times 10^{-2}$. Our first error is their experiment's error and our second error is the systematic error from using our best value. Assumes equal production of B^+ and B^0 at the $\Upsilon(4S)$.

[2] Does not report systematic uncertainties.

[3] ALBRECHT 87D assume $B^+B^-/B^0\overline{B}^0$ ratio is 55/45. $K\pi$ system is specifically selected as nonresonant.

$\Gamma(J/\psi(1S)K^*(892)^0)/\Gamma_{\rm total}$ Γ_{185}/Γ

VALUE (units 10^{-3})	EVTS	DOCUMENT ID		TECN	COMMENT
1.27 ±0.05 OUR FIT					
1.28 ±0.05 OUR AVERAGE					
$1.19 \pm 0.01 \pm 0.08$		CHILIKIN	14	BELL	$\overline{B}^0 \to J/\psi K^-\pi^+$
$1.33\ ^{+0.22}_{-0.21} \pm 0.02$		[1,2] AUBERT	07AV	BABR	$e^+e^- \to \Upsilon(4S)$
$1.309 \pm 0.026 \pm 0.077$		[2] AUBERT	05J	BABR	$e^+e^- \to \Upsilon(4S)$
$1.29 \pm 0.05 \pm 0.13$		[2] ABE	02N	BELL	$e^+e^- \to \Upsilon(4S)$
$1.74 \pm 0.20 \pm 0.18$		[3] ABE	98O	CDF	$p\overline{p}$ 1.8 TeV
$1.32 \pm 0.17 \pm 0.17$		[4] JESSOP	97	CLE2	$e^+e^- \to \Upsilon(4S)$
$1.27 \pm 0.65 \pm 0.01$		[5] BORTOLETTO	92	CLEO	$e^+e^- \to \Upsilon(4S)$
$1.27 \pm 0.60 \pm 0.01$	6	[6] ALBRECHT	90J	ARG	$e^+e^- \to \Upsilon(4S)$
$4.04 \pm 1.81 \pm 0.02$	5	[7] BEBEK	87	CLEO	$e^+e^- \to \Upsilon(4S)$
• • • We do not use the following data for averages, fits, limits, etc. • • •					
$1.24 \pm 0.05 \pm 0.09$		[2] AUBERT	02	BABR	Repl. by AUBERT 05J
$1.36 \pm 0.27 \pm 0.22$		[8] ABE	96H	CDF	Sup. by ABE 98O
$1.69 \pm 0.31 \pm 0.18$	29	[9] ALAM	94	CLE2	Sup. by JESSOP 97
		[10] ALBRECHT	94G	ARG	$e^+e^- \to \Upsilon(4S)$
4.0 ± 0.30		[11] ALBAJAR	91E	UA1	$E_{\rm cm}^{p\overline{p}} = 630$ GeV
3.3 ± 0.18	5	[12] ALBRECHT	87D	ARG	$e^+e^- \to \Upsilon(4S)$
4.1 ± 0.18	5	[13] ALAM	86	CLEO	Repl. by BEBEK 87

[1] AUBERT 07AV reports $[\Gamma(B^0 \to J/\psi(1S)K^*(892)^0)/\Gamma_{\rm total}] \times [B(J/\psi(1S) \to p\overline{p})] = (2.82^{+0.30+0.36}_{-0.28-0.35}) \times 10^{-6}$ which we divide by our best value $B(J/\psi(1S) \to p\overline{p}) = (2.121 \pm 0.029) \times 10^{-3}$. Our first error is their experiment's error and our second error is the systematic error from using our best value.

[2] Assumes equal production of B^+ and B^0 at the $\Upsilon(4S)$.

[3] ABE 98O reports $[B(B^0 \to J/\psi(1S)K^*(892)^0)]/[B(B^+ \to J/\psi(1S)K^+)] = 1.76 \pm 0.14 \pm 0.15$. We multiply by our best value $B(B^+ \to J/\psi(1S)K^+) = (9.9 \pm 1.0) \times 10^{-4}$. Our first error is their experiment's error and our second error is the systematic error from using our best value.

[4] Assumes equal production of B^+ and B^0 at the $\Upsilon(4S)$.

[5] BORTOLETTO 92 reports $(1.1 \pm 0.5 \pm 0.3) \times 10^{-3}$ from a measurement of $[\Gamma(B^0 \to J/\psi(1S)K^*(892)^0)/\Gamma_{\rm total}] \times [B(J/\psi(1S) \to e^+e^-)]$ assuming $B(J/\psi(1S) \to e^+e^-) = 0.069 \pm 0.009$, which we rescale to our best value $B(J/\psi(1S) \to e^+e^-) = (5.971 \pm 0.032) \times 10^{-2}$. Our first error is their experiment's error and our second error is the systematic error from using our best value. Assumes equal production of B^+ and B^0 at the $\Upsilon(4S)$.

[6] ALBRECHT 90J reports $(1.1 \pm 0.5 \pm 0.2) \times 10^{-3}$ from a measurement of $[\Gamma(B^0 \to J/\psi(1S)K^*(892)^0)/\Gamma_{\rm total}] \times [B(J/\psi(1S) \to e^+e^-)]$ assuming $B(J/\psi(1S) \to e^+e^-) = 0.069 \pm 0.009$, which we rescale to our best value $B(J/\psi(1S) \to e^+e^-) = (5.971 \pm 0.032) \times 10^{-2}$. Our first error is their experiment's error and our second error is the systematic error from using our best value. Assumes equal production of B^+ and B^0 at the $\Upsilon(4S)$.

[7] BEBEK 87 reports $(3.5 \pm 1.6 \pm 0.3) \times 10^{-3}$ from a measurement of $[\Gamma(B^0 \to J/\psi(1S)K^*(892)^0)/\Gamma_{\rm total}] \times [B(J/\psi(1S) \to e^+e^-)]$ assuming $B(J/\psi(1S) \to e^+e^-) = 0.069 \pm 0.009$, which we rescale to our best value $B(J/\psi(1S) \to e^+e^-) = (5.971 \pm 0.032) \times 10^{-2}$. Our first error is their experiment's error and our second error is the systematic error from using our best value. Updated in BORTOLETTO 92 to use the same assumptions.

[8] ABE 96H assumes that $B(B^+ \to J/\psi K^+) = (1.02 \pm 0.14) \times 10^{-3}$.

[9] The neutral and charged B events together are predominantly longitudinally polarized, $\Gamma_L/\Gamma = 0.080 \pm 0.08 \pm 0.05$. This can be compared with a prediction using HQET, 0.73 (KRAMER 92). This polarization indicates that the $B \to \psi K^*$ decay is dominated by the $CP = -1$ CP eigenstate. Assumes equal production of B^+ and B^0 at the $\Upsilon(4S)$.

[10] ALBRECHT 94G measures the polarization in the vector-vector decay to be predominantly longitudinal, $\Gamma_T/\Gamma = 0.03 \pm 0.16 \pm 0.15$ making the neutral decay a CP eigenstate when the K^{*0} decays through $K_S^0\pi^0$.

[11] ALBAJAR 91E assumes B_d^0 production fraction of 36%.

[12] ALBRECHT 87D assume $B^+B^-/B^0\overline{B}^0$ ratio is 55/45. Superseded by ALBRECHT 90J.

[13] ALAM 86 assumes $B^\pm/B^0$ ratio is 60/40. The observation of the decay $B^+ \to J/\psi K^*(892)^+$ (HAAS 85) has been retracted in this paper.

$\Gamma(J/\psi(1S)K^*(892)^0)/\Gamma(J/\psi(1S)K^0)$ $\Gamma_{185}/\Gamma_{183}$

VALUE	DOCUMENT ID		TECN	COMMENT
1.50±0.09 OUR AVERAGE				
$1.51 \pm 0.05 \pm 0.08$	AUBERT	05J	BABR	$e^+e^- \to \Upsilon(4S)$
$1.39 \pm 0.36 \pm 0.10$	ABE	96Q	CDF	$p\overline{p}$
• • • We do not use the following data for averages, fits, limits, etc. • • •				
$1.49 \pm 0.10 \pm 0.08$	[1] AUBERT	02	BABR	Repl. by AUBERT 05J

[1] Assumes equal production of B^+ and B^0 at the $\Upsilon(4S)$.

$\Gamma(J/\psi(1S)\eta K_S^0)/\Gamma_{\rm total}$ Γ_{186}/Γ

VALUE (units 10^{-5})	DOCUMENT ID		TECN	COMMENT
5.4 ±0.9 OUR AVERAGE				
$5.22 \pm 0.78 \pm 0.49$	[1] IWASHITA	14	BELL	$e^+e^- \to \Upsilon(4S)$
$8.4 \pm 2.6 \pm 2.7$	[1] AUBERT	04Y	BABR	$e^+e^- \to \Upsilon(4S)$

[1] Assumes equal production of B^+ and B^0 at the $\Upsilon(4S)$.

$\Gamma(J/\psi(1S)\eta' K_S^0)/\Gamma_{\rm total}$ Γ_{187}/Γ

VALUE (units 10^{-5})	CL%	DOCUMENT ID		TECN	COMMENT
<2.5	90	[1] XIE	07	BELL	$e^+e^- \to \Upsilon(4S)$

[1] Assumes equal production of B^+ and B^0 at the $\Upsilon(4S)$.

$\Gamma(J/\psi(1S)\omega K^0)/\Gamma_{\rm total}$ Γ_{189}/Γ

VALUE (units 10^{-4})	DOCUMENT ID		TECN	COMMENT
2.3±0.3±0.3	[1] DEL-AMO-SA...10B		BABR	$e^+e^- \to \Upsilon(4S)$
• • • We do not use the following data for averages, fits, limits, etc. • • •				
$3.1 \pm 0.6 \pm 0.3$	[1] AUBERT	08W	BABR	Repl. by DEL-AMO-SANCHEZ 10B

[1] Assumes equal production of B^+ and B^0 at the $\Upsilon(4S)$.

$\Gamma(\chi_{c1}(3872)K^0, \chi_{c1} \to J/\psi\omega)/\Gamma_{\rm total}$ Γ_{190}/Γ

VALUE (units 10^{-6})	DOCUMENT ID		TECN	COMMENT
6±3±1	[1] DEL-AMO-SA...10B		BABR	$e^+e^- \to \Upsilon(4S)$

[1] Assumes equal production of B^+ and B^0 at the $\Upsilon(4S)$.

$\Gamma(X(3915),\ X \to J/\psi\omega)/\Gamma_{total}$ Γ_{191}/Γ

VALUE (units 10^{-5})	DOCUMENT ID	TECN	COMMENT
2.1±0.9±0.3	[1] DEL-AMO-SA...10B	BABR	$e^+e^- \to \Upsilon(4S)$
• • • We do not use the following data for averages, fits, limits, etc. • • •			
$1.3^{+1.3}_{-1.1}\pm0.2$	[1,2] AUBERT	08W BABR	Repl. by DEL-AMO-SANCHEZ 10B

[1] Assumes equal production of B^+ and B^0 at the $\Upsilon(4S)$.
[2] Corresponds to upper limit of 3.9×10^{-5} at 90% CL.

$\Gamma(J/\psi(1S)\phi K^0)/\Gamma_{total}$ Γ_{188}/Γ

VALUE (units 10^{-5})	DOCUMENT ID	TECN	COMMENT
4.9 ±1.0 OUR AVERAGE	Error includes scale factor of 1.3.		
4.43±0.76±0.19	LEES	15 BABR	$e^+e^- \to \Upsilon(4S)$
10.2 ±3.8 ±1.0	[1] AUBERT	03O BABR	$e^+e^- \to \Upsilon(4S)$
$8.8\ ^{+3.5}_{-3.0}\ \pm1.3$	[2] ANASTASSOV 00	CLE2	$e^+e^- \to \Upsilon(4S)$

[1] Assumes equal production of B^+ and B^0 at the $\Upsilon(4S)$.
[2] ANASTASSOV 00 finds 10 events on a background of 0.5 ± 0.2. Assumes equal production of B^0 and B^+ at the $\Upsilon(4S)$, a uniform Dalitz plot distribution, isotropic $J/\psi(1S)$ and ϕ decays, and $B(B^+ \to J/\psi(1S)\phi K^+) = B(B^0 \to J/\psi(1S)\phi K^0)$.

$\Gamma(J/\psi(1S)K(1270)^0)/\Gamma_{total}$ Γ_{192}/Γ

VALUE (units 10^{-3})	DOCUMENT ID	TECN	COMMENT
1.30±0.34±0.32	[1] ABE	01L BELL	$e^+e^- \to \Upsilon(4S)$

[1] Assumes equal production of B^+ and B^0 at the $\Upsilon(4S)$ and uses the PDG value of $B(B^+ \to J/\psi(1S)K^+) = (1.00\pm0.10)\times10^{-3}$.

$\Gamma(J/\psi(1S)\pi^0)/\Gamma_{total}$ Γ_{193}/Γ

VALUE (units 10^{-5})	CL%	DOCUMENT ID	TECN	COMMENT
1.76±0.16 OUR AVERAGE		Error includes scale factor of 1.1.		
1.69±0.14±0.07		[1] AUBERT	08AU BABR	$e^+e^- \to \Upsilon(4S)$
2.3 ±0.5 ±0.2		[1] ABE	03B BELL	$e^+e^- \to \Upsilon(4S)$
$2.5\ ^{+1.1}_{-0.9}\ \pm0.2$		[1] AVERY	00 CLE2	$e^+e^- \to \Upsilon(4S)$
• • • We do not use the following data for averages, fits, limits, etc. • • •				
1.94±0.22±0.17		[1] AUBERT,B	06B BABR	Repl. by AUBERT 08AU
2.0 ±0.6 ±0.2		[1] AUBERT	02 BABR	Repl. by AUBERT,B 06B
< 32	90	[2] ACCIARRI	97C L3	
< 5.8	90	BISHAI	96 CLE2	Sup. by AVERY 00
<690	90	[1] ALEXANDER	95 CLE2	Sup. by BISHAI 96

[1] Assumes equal production of B^+ and B^0 at the $\Upsilon(4S)$.
[2] ACCIARRI 97C assumes B^0 production fraction (39.5 ± 4.0%) and B_s (12.0 ± 3.0%).

$\Gamma(J/\psi(1S)\eta)/\Gamma_{total}$ Γ_{194}/Γ

VALUE (units 10^{-6})	CL%	DOCUMENT ID	TECN	COMMENT
10.8±2.3 OUR AVERAGE		Error includes scale factor of 1.5.		
7.3±2.5±1.3		[1] AAIJ	15D LHCB	pp at 7, 8 TeV
$12.3^{+1.8}_{-1.7}\pm0.7$		[2,3] CHANG	12 BELL	$e^+e^- \to \Upsilon(4S)$
• • • We do not use the following data for averages, fits, limits, etc. • • •				
9.5±1.7±0.8		[3] CHANG	07A BELL	Repl. by CHANG 12
< 27	90	[3] AUBERT	03O BABR	$e^+e^- \to \Upsilon(4S)$
<1200	90	[4] ACCIARRI	97C L3	

[1] AAIJ 15D reports $[\Gamma(B^0 \to J/\psi(1S)\eta)/\Gamma_{total}] / [B(B_s^0 \to J/\psi(1S)\eta)] = (1.85 \pm 0.61 \pm 0.14)\times10^{-2}$ which we multiply by our best value $B(B_s^0 \to J/\psi(1S)\eta) = (4.0 \pm 0.7)\times10^{-4}$. Our first error is their experiment's error and our second error is the systematic error from using our best value.
[2] Reconstructs η in $\gamma\gamma$ and $\pi^+\pi^-\pi^0$ decays.
[3] Assumes equal production of B^+ and B^0 at the $\Upsilon(4S)$.
[4] ACCIARRI 97C assumes B^0 production fraction (39.5 ± 4.0%) and B_S (12.0 ± 3.0%).

$\Gamma(J/\psi(1S)\pi^+\pi^-)/\Gamma_{total}$ Γ_{195}/Γ

VALUE (units 10^{-5})	DOCUMENT ID	TECN	COMMENT
3.96±0.17 OUR AVERAGE			
3.94±0.14±0.11	[1,2] AAIJ	13M LHCB	pp at 7 TeV
4.6 ±0.7 ±0.6	[3] AUBERT	03B BABR	$e^+e^- \to \Upsilon(4S)$

[1] AAIJ 13M reports $(3.97\pm0.09\pm0.11\pm0.16)\times10^{-5}$ from a measurement of $[\Gamma(B^0 \to J/\psi(1S)\pi^+\pi^-)/\Gamma_{total}] / [B(B^+ \to J/\psi(1S)K^+)] = (1.018\pm0.042)\times10^{-3}$, which we rescale to our best value $B(B^+ \to J/\psi(1S)K^+) = (1.010\pm0.029)\times10^{-3}$. Our first error is their experiment's error and our second error is the systematic error from using our best value.
[2] AAIJ 13M does not report correlations between various measurements of the $J/\psi\pi\pi$ final state.
[3] Assumes equal production of B^+ and B^0 at the $\Upsilon(4S)$.

$\Gamma(J/\psi(1S)\pi^+\pi^-\ \text{nonresonant})/\Gamma_{total}$ Γ_{196}/Γ

VALUE (units 10^{-5})	CL%	DOCUMENT ID	TECN	COMMENT
<1.2	90	[1] AUBERT	07AC BABR	$e^+e^- \to \Upsilon(4S)$

[1] Assumes equal production of B^+ and B^0 at the $\Upsilon(4S)$.

$\Gamma(J/\psi(1S)f_0(500),\ f_0 \to \pi\pi)/\Gamma_{total}$ Γ_{197}/Γ

VALUE (units 10^{-6})	DOCUMENT ID	TECN	COMMENT
$8.0^{+1.1}_{-0.9}$ OUR AVERAGE			
$8.8\pm0.5^{+1.1}_{-1.5}$	[1] AAIJ	14X LHCB	pp at 7, 8 TeV
$6.4^{+2.5}_{-1.1}\pm0.3$	[2,3] AAIJ	13M LHCB	pp at 7 TeV

[1] AAIJ 14X uses Dalitz plot analysis of $B^0 \to J/\psi\pi^+\pi^-$.
[2] AAIJ 13M reports $(6.4 \pm 0.8^{+2.4}_{-0.8})\times10^{-6}$ from a measurement of $[\Gamma(B^0 \to J/\psi(1S)f_0(500),\ f_0 \to \pi\pi)/\Gamma_{total}] / [B(B^0 \to J/\psi(1S)\pi^+\pi^-)]$ assuming $B(B^0 \to J/\psi(1S)\pi^+\pi^-) = (3.97\pm0.09\pm0.11\pm0.16)\times10^{-5}$, which we rescale to our best value $B(B^0 \to J/\psi(1S)\pi^+\pi^-) = (3.96\pm0.17)\times10^{-5}$. Our first error is their experiment's error and our second error is the systematic error from using our best value.
[3] AAIJ 13M does not report correlations between various measurements of the $J/\psi\pi\pi$ final state. Measured in Dalitz plot like analysis of $B^0 \to J/\psi\pi^+\pi^-$.

$\Gamma(J/\psi(1S)f_2)/\Gamma_{total}$ Γ_{198}/Γ

VALUE (units 10^{-5})	CL%	DOCUMENT ID	TECN	COMMENT
0.33±0.05 OUR AVERAGE		Error includes scale factor of 1.5.		
$0.30\pm0.03^{+0.02}_{-0.03}$		[1] AAIJ	14X LHCB	pp at 7, 8 TeV
0.41±0.06±0.02		[2,3] AAIJ	13M LHCB	pp at 7 TeV
• • • We do not use the following data for averages, fits, limits, etc. • • •				
<0.5	90	[4,5] AUBERT	07AC BABR	$e^+e^- \to \Upsilon(4S)$

[1] AAIJ 14X uses Dalitz plot analysis of $B^0 \to J/\psi\pi^+\pi^-$.
[2] AAIJ 13M reports $[\Gamma(B^0 \to J/\psi(1S)f_2)/\Gamma_{total}] \times [B(f_2(1270) \to \pi\pi)] = (3.5\pm0.4\pm0.4)\times10^{-6}$ from a measurement of $[\Gamma(B^0 \to J/\psi(1S)f_2)/\Gamma_{total}] \times [B(f_2(1270) \to \pi\pi)] / [B(B^0 \to J/\psi(1S)\pi^+\pi^-)]$ assuming $B(B^0 \to J/\psi(1S)\pi^+\pi^-) = (3.97\pm0.09\pm0.11\pm0.16)\times10^{-5}$, which we rescale to our best values $B(f_2(1270) \to \pi\pi) = (84.2^{+2.9}_{-0.9})\times10^{-2}$, $B(B^0 \to J/\psi(1S)\pi^+\pi^-) = (3.96\pm0.17)\times10^{-5}$. Our first error is their experiment's error and our second error is the systematic error from using our best values.
[3] AAIJ 13M does not report correlations between various measurements of the $J/\psi\pi\pi$ final state. Measured in Dalitz plot like analysis of $B^0 \to J/\psi\pi^+\pi^-$.
[4] AUBERT 07AC reports $[\Gamma(B^0 \to J/\psi(1S)f_2)/\Gamma_{total}] \times [B(f_2(1270) \to \pi\pi)] < 0.46\times10^{-5}$ which we divide by our best value $B(f_2(1270) \to \pi\pi) = 84.2\times10^{-2}$.
[5] Assumes equal production of B^+ and B^0 at the $\Upsilon(4S)$.

$\Gamma(J/\psi(1S)\rho^0)/\Gamma_{total}$ Γ_{199}/Γ

VALUE (units 10^{-5})	CL%	DOCUMENT ID	TECN	COMMENT
$2.55^{+0.18}_{-0.16}$ OUR AVERAGE				
$2.50\pm0.10^{+0.18}_{-0.15}$		[1] AAIJ	14X LHCB	pp at 7, 8 TeV
2.7 ±0.3 ±0.2		[2] AUBERT	07AC BABR	$e^+e^- \to \Upsilon(4S)$
• • • We do not use the following data for averages, fits, limits, etc. • • •				
$2.48^{+0.22}_{-0.23}\pm0.11$		[3,4] AAIJ	13M LHCB	Repl. by AAIJ 14X
1.6 ±0.6 ±0.4		[2] AUBERT	03B BABR	Repl. by AUBERT 07AC
<25	90	BISHAI	96 CLE2	$e^+e^- \to \Upsilon(4S)$

[1] AAIJ 14X uses Dalitz plot analysis of $B^0 \to J/\psi\pi^+\pi^-$. We assume $B(\rho(770)^0 \to \pi^+\pi^-) = 100\%$.
[2] Assumes equal production of B^+ and B^0 at the $\Upsilon(4S)$.
[3] AAIJ 13M reports $(2.49^{+0.20+0.16}_{-0.13-0.23})\times10^{-5}$ from a measurement of $[\Gamma(B^0 \to J/\psi(1S)\rho^0)/\Gamma_{total}] / [B(B^0 \to J/\psi(1S)\pi^+\pi^-)]$ assuming $B(B^0 \to J/\psi(1S)\pi^+\pi^-) = (3.97\pm0.09\pm0.11\pm0.16)\times10^{-5}$, which we rescale to our best value $B(B^0 \to J/\psi(1S)\pi^+\pi^-) = (3.96\pm0.17)\times10^{-5}$. Our first error is their experiment's error and our second error is the systematic error from using our best value.
[4] AAIJ 13M does not report correlations between various measurements of the $J/\psi\pi\pi$ final state. Measured in Dalitz plot like analysis of $B^0 \to J/\psi\pi^+\pi^-$. Assumes $B(\rho(770)^0 \to \pi\pi) = 100\%$.

$\Gamma(J/\psi(1S)f_0(980),\ f_0 \to \pi^+\pi^-)/\Gamma_{total}$ Γ_{200}/Γ

VALUE	CL%	DOCUMENT ID	TECN	COMMENT
$<1.1\times10^{-6}$	90	[1] AAIJ	13M LHCB	pp at 7 TeV

[1] AAIJ 13M does not provide correlations between various measurements of the $J/\psi\pi^+\pi^-$ final state. The measurements were obtained from a Dalitz plot like analysis of $B^0 \to J/\psi\pi^+\pi^-$. Also reports $\Gamma(J/\psi(1S)f_0(980),\ f_0 \to \pi^+\pi^-)/\Gamma_{total} = (6.1^{+3.1+1.7}_{-2.0-1.4})\times10^{-6}$.

$\Gamma(J/\psi(1S)\rho(1450)^0,\ \rho^0 \to \pi\pi)/\Gamma_{total}$ Γ_{201}/Γ

VALUE (units 10^{-6})	DOCUMENT ID	TECN	COMMENT
$2.9^{+1.6}_{-0.7}$ OUR AVERAGE			
4.6±1.1±1.9	[1] AAIJ	14X LHCB	pp at 7, 8 TeV
$2.1^{+2.4}_{-0.7}\pm0.1$	[2,3] AAIJ	13M LHCB	pp at 7 TeV

[1] AAIJ 14X uses Dalitz plot analysis of $B^0 \to J/\psi\pi^+\pi^-$.
[2] AAIJ 13M reports $(2.1^{+1.0+2.2}_{-0.6-0.4})\times10^{-6}$ from a measurement of $[\Gamma(B^0 \to J/\psi(1S)\rho(1450)^0,\ \rho^0 \to \pi\pi)/\Gamma_{total}] / [B(B^0 \to J/\psi(1S)\pi^+\pi^-)]$ assuming $B(B^0 \to J/\psi(1S)\pi^+\pi^-) = (3.97\pm0.09\pm0.11\pm0.16)\times10^{-5}$, which we rescale

to our best value $B(B^0 \to J/\psi(1S)\pi^+\pi^-) = (3.96 \pm 0.17) \times 10^{-5}$. Our first error is their experiment's error and our second error is the systematic error from using our best value.

[3] AAIJ 13M does not report correlations between various measurements of the $J/\psi\pi\pi$ final state. Measured in Dalitz plot like analysis of $B^0 \to J/\psi\pi^+\pi^-$.

$\Gamma(J/\psi\rho(1700)^0,\ \rho^0 \to \pi^+\pi^-)/\Gamma_{total}$ Γ_{202}/Γ

VALUE (units 10^{-6})	DOCUMENT ID		TECN	COMMENT
2.0±0.5±1.2	[1] AAIJ	14X	LHCB	pp at 7, 8 TeV

[1] AAIJ 14X uses Dalitz plot analysis of $B^0 \to J/\psi\pi^+\pi^-$.

$\Gamma(J/\psi(1S)\omega)/\Gamma_{total}$ Γ_{203}/Γ

VALUE (units 10^{-5})	CL%	DOCUMENT ID		TECN	COMMENT
$\mathbf{1.8^{+0.7}_{-0.5}\pm0.1}$		[1] AAIJ	14X	LHCB	pp at 7, 8 TeV
• • • We do not use the following data for averages, fits, limits, etc. • • •					
<27	90	BISHAI	96	CLE2	$e^+e^- \to \Upsilon(4S)$

[1] AAIJ 14X reports $[\Gamma(B^0 \to J/\psi(1S)\omega)/\Gamma_{total}] \times [B(\omega(782) \to \pi^+\pi^-)] = (2.7^{+0.8+0.7}_{-0.6-0.5}) \times 10^{-7}$ which we divide by our best value $B(\omega(782) \to \pi^+\pi^-) = (1.53^{+0.11}_{-0.13}) \times 10^{-2}$. Our first error is their experiment's error and our second error is the systematic error from using our best value.

$\Gamma(J/\psi(1S)\omega)/\Gamma(J/\psi(1S)\rho^0)$ $\Gamma_{203}/\Gamma_{199}$

VALUE	DOCUMENT ID		TECN	COMMENT
$\mathbf{0.61^{+0.24+0.31}_{-0.14-0.16}}$	[1,2] AAIJ	13M	LHCB	pp at 7 TeV

[1] AAIJ 13M reports $0.61^{+0.24+0.31}_{-0.14-0.16}$ from a measurement of $[\Gamma(B^0 \to J/\psi(1S)\omega)/\Gamma(B^0 \to J/\psi(1S)\rho^0)] \times [B(\omega(782) \to \pi^+\pi^-)]$ assuming $B(\omega(782) \to \pi^+\pi^-) = (1.53^{+0.11}_{-0.13}) \times 10^{-2}$.

[2] AAIJ 13M does not report correlations between various measurements of the $J/\psi\pi\pi$ final state. Measured in Dalitz plot like analysis of $B^0 \to J/\psi\pi^+\pi^-$. Assumes $B(\rho(770)^0 \to \pi\pi) = 100\%$.

$\Gamma(J/\psi(1S)\omega)/\Gamma(J/\psi(1S)\rho^0)$ $\Gamma_{203}/\Gamma_{199}$

VALUE	DOCUMENT ID		TECN	COMMENT
$\mathbf{0.89\pm0.19^{+0.07}_{-0.13}}$	AAIJ	13A	LHCB	pp at 7 TeV

$\Gamma(J/\psi(1S)K^+K^-)/\Gamma_{total}$ Γ_{204}/Γ

VALUE (units 10^{-6})	DOCUMENT ID		TECN	COMMENT
2.51±0.35±0.07	[1] AAIJ	13BT	LHCB	pp at 7 TeV

[1] AAIJ 13BT reports $(2.53 \pm 0.31 \pm 0.19) \times 10^{-6}$ from a measurement of $[\Gamma(B^0 \to J/\psi(1S)K^+K^-)/\Gamma_{total}] / [B(B^+ \to J/\psi(1S)K^+)]$ assuming $B(B^+ \to J/\psi(1S)K^+) = (1.018 \pm 0.042) \times 10^{-3}$, which we rescale to our best value $B(B^+ \to J/\psi(1S)K^+) = (1.010 \pm 0.029) \times 10^{-3}$. Our first error is their experiment's error and our second error is the systematic error from using our best value.

$\Gamma(J/\psi(1S)a_0(980),\ a_0 \to K^+K^-)/\Gamma_{total}$ Γ_{205}/Γ

VALUE (units 10^{-6})	DOCUMENT ID		TECN	COMMENT
0.470±0.331±0.072	[1] AAIJ	13BT	LHCB	pp at 7 TeV

[1] AAIJ 13BT uses $B(\overline{B}^0 \to J/\psi K^+K^-) = (2.53 \pm 0.31 \pm 0.19) \times 10^{-6}$ to derive this result. It also reports the equivalent upper limit of $< 9.0 \times 10^{-7}$ at 90% CL.

$\Gamma(J/\psi(1S)\phi)/\Gamma_{total}$ Γ_{206}/Γ

VALUE (units 10^{-6})	CL%	DOCUMENT ID		TECN	COMMENT
<0.19	90	[1] AAIJ	13BT	LHCB	pp at 7 TeV
• • • We do not use the following data for averages, fits, limits, etc. • • •					
<1.01	90	LEES	15	BABR	$e^+e^- \to \Upsilon(4S)$
<0.94	90	[2] LIU	08I	BELL	$e^+e^- \to \Upsilon(4S)$
<9.2	90	[2] AUBERT	03O	BABR	$e^+e^- \to \Upsilon(4S)$

[1] AAIJ 13BT uses $B(B^0 \to J/\psi(1S)K^+K^-) = (2.53 \pm 0.31 \pm 0.19) \times 10^{-6}$ and $B(\phi \to K^+K^-) = (48.9 \pm 0.5)\%$ to obtain this result.

[2] Assumes equal production of B^+ and B^0 at the $\Upsilon(4S)$.

$\Gamma(J/\psi(1S)\eta'(958))/\Gamma_{total}$ Γ_{207}/Γ

VALUE (units 10^{-6})	CL%	DOCUMENT ID		TECN	COMMENT
7.6±2.2±1.0		[1] AAIJ	15D	LHCB	pp at 7, 8 TeV
• • • We do not use the following data for averages, fits, limits, etc. • • •					
< 7.4	90	[2,3] CHANG	12	BELL	$e^+e^- \to \Upsilon(4S)$
<63	90	[3] AUBERT	03O	BABR	$e^+e^- \to \Upsilon(4S)$

[1] AAIJ 15D reports $[\Gamma(B^0 \to J/\psi(1S)\eta'(958))/\Gamma_{total}] / [B(B^0_s \to J/\psi(1S)\eta')] = (2.28 \pm 0.65 \pm 0.16) \times 10^{-2}$ which we multiply by our best value $B(B^0_s \to J/\psi(1S)\eta') = (3.3 \pm 0.4) \times 10^{-4}$. Our first error is their experiment's error and our second error is the systematic error from using our best value.

[2] Reconstructs $\eta'(985)$ in $(etapi + pi)^-$ and $\rho(770)$ decays.

[3] Assumes equal production of B^+ and B^0 at the $\Upsilon(4S)$.

$\Gamma(J/\psi(1S)\eta)/\Gamma(J/\psi(1S)\eta'(958))$ $\Gamma_{194}/\Gamma_{207}$

VALUE	DOCUMENT ID		TECN	COMMENT
1.111±0.475±0.062	[1] AAIJ	15D	LHCB	pp at 7, 8 TeV

[1] Uses $J/\psi \to \mu^+\mu^-$, $\eta' \to \rho^0\gamma$, and $\eta' \to \eta\pi^+\pi^-$ decays.

$\Gamma(J/\psi(1S)K^0\pi^+\pi^-)/\Gamma(J/\psi(1S)K^0)$ $\Gamma_{208}/\Gamma_{183}$

VALUE	DOCUMENT ID		TECN	COMMENT
0.50 ±0.04 OUR AVERAGE				
0.493±0.034±0.027	AAIJ	14L	LHCB	pp at 7 TeV
1.24 ±0.40 ±0.15	AFFOLDER	02B	CDF	$p\overline{p}$ 1.8 TeV

$\Gamma(J/\psi(1S)K^0K^+K^-)/\Gamma_{total}$ Γ_{210}/Γ

VALUE (units 10^{-6})	DOCUMENT ID		TECN	COMMENT
25 ±7 OUR AVERAGE Error includes scale factor of 1.8.				
34.9±6.7±1.5	LEES	15	BABR	$e^+e^- \to \Upsilon(4S)$
20.2±4.3±1.9	[1] AAIJ	14L	LHCB	pp at 7 TeV

[1] Measured with $B(B^0 \to J/\psi K^0_S K^+K^-)$ / $B(B^0 \to J/\psi K^0_S)$ using PDG 12 for the involved branching fractions.

$\Gamma(J/\psi(1S)K^0K^-\pi^+ + \text{c.c.})/\Gamma_{total}$ Γ_{209}/Γ

VALUE	CL%	DOCUMENT ID		TECN	COMMENT
<21 × 10⁻⁶	90	[1] AAIJ	14L	LHCB	pp at 7 TeV

[1] Measured with $B(B^0 \to J/\psi K^0_S K^\pm\pi^\mp)$ / $B(B^0 \to J/\psi K^0_S\pi^+\pi^-)$ using PDG 12 values for the involved branching fractions.

$\Gamma(J/\psi(1S)K^0\rho^0)/\Gamma_{total}$ Γ_{212}/Γ

VALUE (units 10^{-4})	DOCUMENT ID		TECN	COMMENT
5.4±2.9±0.9	[1] AFFOLDER	02B	CDF	$p\overline{p}$ 1.8 TeV

[1] Uses $B^0 \to J/\psi(1S)K^0_S$ decay as a reference and $B(B^0 \to J/\psi(1S)K^0) = 8.3 \times 10^{-4}$.

$\Gamma(J/\psi(1S)K^*(892)^+\pi^-)/\Gamma_{total}$ Γ_{213}/Γ

VALUE (units 10^{-4})	DOCUMENT ID		TECN	COMMENT
7.7±4.1±1.3	[1] AFFOLDER	02B	CDF	$p\overline{p}$ 1.8 TeV

[1] Uses $B^0 \to J/\psi(1S)K^0_S$ decay as a reference and $B(B^0 \to J/\psi(1S)K^0) = 8.3 \times 10^{-4}$.

$\Gamma(J/\psi(1S)\pi^+\pi^-\pi^+\pi^-)/\Gamma(J/\psi(1S)\pi^+\pi^-)$ $\Gamma_{214}/\Gamma_{195}$

VALUE	DOCUMENT ID		TECN	COMMENT
0.361±0.017±0.021	[1] AAIJ	14Y	LHCB	pp at 7, 8 TeV

[1] Excludes contributions from $\psi(2S)$ and $\chi_{c1}(3872)$ decaying to $J/\psi(1S)\pi^+\pi^-$.

$\Gamma(J/\psi(1S)f_1(1285))/\Gamma_{total}$ Γ_{215}/Γ

VALUE (units 10^{-6})	DOCUMENT ID		TECN	COMMENT
$\mathbf{8.2\pm2.0^{+0.4}_{-0.5}}$	[1] AAIJ	14Y	LHCB	pp at 7, 8 TeV

[1] AAIJ 14Y reports $(8.37 \pm 1.95^{+0.71}_{-0.66} \pm 0.35) \times 10^{-6}$ from a measurement of $[\Gamma(B^0 \to J/\psi(1S)f_1(1285))/\Gamma_{total}] \times [B(f_1(1285) \to 2\pi^+2\pi^-)]$ assuming $B(f_1(1285) \to 2\pi^+2\pi^-) = 0.11^{+0.007}_{-0.006}$, which we rescale to our best value $B(f_1(1285) \to 2\pi^+2\pi^-) = (11.2^{+0.7}_{-0.6}) \times 10^{-2}$. Our first error is their experiment's error and our second error is the systematic error from using our best value.

$\Gamma(J/\psi(1S)K^*(892)^0\pi^+\pi^-)/\Gamma_{total}$ Γ_{216}/Γ

VALUE (units 10^{-4})	DOCUMENT ID		TECN	COMMENT
6.6±1.9±1.1	[1] AFFOLDER	02B	CDF	$p\overline{p}$ 1.8 TeV

[1] Uses $B^0 \to J/\psi(1S)K^*(892)^0$ decay as a reference and $B(B^0 \to J/\psi(1S)K^0) = 12.4 \times 10^{-4}$.

$\Gamma(\chi_{c1}(3872)^-K^+)/\Gamma_{total}$ Γ_{217}/Γ

VALUE	CL%	DOCUMENT ID		TECN	COMMENT
<5 × 10⁻⁴	90	[1] AUBERT	06E	BABR	$e^+e^- \to \Upsilon(4S)$

[1] Perform measurements of absolute branching fractions using a missing mass technique.

$\Gamma(\chi_{c1}(3872)^-K^+,\ \chi_{c1}(3872)^- \to J/\psi(1S)\pi^-\pi^0)/\Gamma_{total}$ Γ_{218}/Γ

VALUE (units 10^{-6})	CL%	DOCUMENT ID		TECN	COMMENT
<4.2	90	[1,2] CHOI	11	BELL	$e^+e^- \to \Upsilon(4S)$
• • • We do not use the following data for averages, fits, limits, etc. • • •					
<5.4	90	[2,3] AUBERT	05B	BABR	$e^+e^- \to \Upsilon(4S)$

[1] Assumes $\pi^+\pi^0$ originates from ρ^+.

[2] Assumes equal production of B^+ and B^0 at the $\Upsilon(4S)$.

[3] The isovector-X hypothesis is excluded with a likelihood test at 1×10^{-4} level.

$\Gamma(\chi_{c1}(3872)K^0,\ \chi_{c1} \to J/\psi\pi^+\pi^-)/\Gamma_{total}$ Γ_{219}/Γ

VALUE (units 10^{-6})	CL%	DOCUMENT ID		TECN	COMMENT
4.3±1.2±0.4		[1,2] CHOI	11	BELL	$e^+e^- \to \Upsilon(4S)$
• • • We do not use the following data for averages, fits, limits, etc. • • •					
< 6.0	90	[2] AUBERT	08Y	BABR	$e^+e^- \to \Upsilon(4S)$
<10.3	90	[2,3] AUBERT	06	BABR	Repl. by AUBERT 08Y

[1] CHOI 11 reports $[\Gamma(B^0 \to \chi_{c1}(3872)K^0,\ \chi_{c1} \to J/\psi\pi^+\pi^-)/\Gamma_{total}] / [B(B^+ \to \chi_{c1}(3872)K^+,\ \chi_{c1} \to J/\psi\pi^+\pi^-)] = 0.50 \pm 0.14 \pm 0.04$ which we multiply by our best value $B(B^+ \to \chi_{c1}(3872)K^+,\ \chi_{c1} \to J/\psi\pi^+\pi^-) = (8.6 \pm 0.8) \times 10^{-6}$. Our first error is their experiment's error and our second error is the systematic error from using our best value.

[2] Assumes equal production of B^+ and B^0 at the $\Upsilon(4S)$.

[3] The lower limit is also given to be 1.34×10^{-6} at 90% CL.

$\Gamma(\chi_{c1}(3872)K^0,\ \chi_{c1}\to J/\psi\gamma)/\Gamma_{\rm total}$ Γ_{220}/Γ

VALUE (units 10^{-6})	CL%	DOCUMENT ID		TECN	COMMENT
<2.4	90	[1] BHARDWAJ	11	BELL	$e^+e^-\to\ \Upsilon(4S)$
• • • We do not use the following data for averages, fits, limits, etc. • • •					
<4.9	90	[2] AUBERT	09B	BABR	$e^+e^-\to\ \Upsilon(4S)$

[1] Assumes equal production of B^+ and B^0 at the $\Upsilon(4S)$.
[2] Uses B($\Upsilon(4S)\to B^+B^-$) = (51.6 ± 0.6)% and B($\Upsilon(4S)\to B^0\overline{B}^0$) = (48.4 ± 0.6)%.

$\Gamma(\chi_{c1}(3872)K^*(892)^0,\ \chi_{c1}\to J/\psi\gamma)/\Gamma_{\rm total}$ Γ_{221}/Γ

VALUE (units 10^{-6})	CL%	DOCUMENT ID		TECN	COMMENT
<2.8	90	[1] AUBERT	09B	BABR	$e^+e^-\to\ \Upsilon(4S)$

[1] Uses B($\Upsilon(4S)\to B^+B^-$) = (51.6 ± 0.6)% and B($\Upsilon(4S)\to B^0\overline{B}^0$) = (48.4 ± 0.6)%.

$\Gamma(\chi_{c1}(3872)K^0,\ \chi_{c1}\to\psi(2S)\gamma)/\Gamma_{\rm total}$ Γ_{222}/Γ

VALUE (units 10^{-6})	CL%	DOCUMENT ID		TECN	COMMENT
< 6.62	90	[1] BHARDWAJ	11	BELL	$e^+e^-\to\ \Upsilon(4S)$
• • • We do not use the following data for averages, fits, limits, etc. • • •					
<19	90	[2] AUBERT	09B	BABR	$e^+e^-\to\ \Upsilon(4S)$

[1] Assumes equal production of B^+ and B^0 at the $\Upsilon(4S)$.
[2] Uses B($\Upsilon(4S)\to B^+B^-$) = (51.6 ± 0.6)% and B($\Upsilon(4S)\to B^0\overline{B}^0$) = (48.4 ± 0.6)%.

$\Gamma(\chi_{c1}(3872)K^*(892)^0,\ \chi_{c1}\to\psi(2S)\gamma)/\Gamma_{\rm total}$ Γ_{223}/Γ

VALUE (units 10^{-6})	CL%	DOCUMENT ID		TECN	COMMENT
<4.4	90	[1] AUBERT	09B	BABR	$e^+e^-\to\ \Upsilon(4S)$

[1] Uses B($\Upsilon(4S)\to B^+B^-$) = (51.6 ± 0.6)% and B($\Upsilon(4S)\to B^0\overline{B}^0$) = (48.4 ± 0.6)%.

$\Gamma(\chi_{c1}(3872)K^0,\ \chi_{c1}\to D^0\overline{D}^0\pi^0)/\Gamma_{\rm total}$ Γ_{224}/Γ

VALUE (units 10^{-4})	DOCUMENT ID		TECN	COMMENT
$1.66\pm0.70^{+0.32}_{-0.37}$	[1] GOKHROO	06	BELL	$e^+e^-\to\ \Upsilon(4S)$

[1] Measure the near-threshold enhancements in the $(D^0\overline{D}^0\pi^0)$ system at a mass $3875.2\pm0.7^{+0.3}_{-1.6}\pm0.8$ MeV/c^2.

$\Gamma(\chi_{c1}(3872)K^0,\ \chi_{c1}\to\overline{D}^{*0}D^0)/\Gamma_{\rm total}$ Γ_{225}/Γ

VALUE (units 10^{-4})		DOCUMENT ID		TECN	COMMENT
1.2 ±0.4 OUR AVERAGE					
0.97±0.46±0.13	[1]	AUSHEV	10	BELL	$e^+e^-\to\ \Upsilon(4S)$
2.22±1.05±0.42	[1,2]	AUBERT	08B	BABR	$e^+e^-\to\ \Upsilon(4S)$

[1] Assumes equal production of B^+ and B^0 at the $\Upsilon(4S)$.
[2] This result is equivalent to the the 90% CL upper limit of 4.37×10^{-4}

$\Gamma(\chi_{c1}(3872)K^+\pi^-,\ \chi_{c1}\to J/\psi\pi^+\pi^-)/\Gamma_{\rm total}$ Γ_{226}/Γ

VALUE (units 10^{-6})	DOCUMENT ID		TECN	COMMENT
7.9±1.3±0.4	[1] BALA	15	BELL	$e^+e^-\to\ \Upsilon(4S)$

[1] Assumes equal production of B^+ and B^0 at the $\Upsilon(4S)$.

$\Gamma(\chi_{c1}(3872)K^*(892)^0,\ \chi_{c1}\to J/\psi\pi^+\pi^-)/\Gamma_{\rm total}$ Γ_{227}/Γ

VALUE (units 10^{-6})	DOCUMENT ID		TECN	COMMENT
4.0±1.5±0.3	BALA	15	BELL	$e^+e^-\to\ \Upsilon(4S)$

$\Gamma(Z_c(4430)^\pm K^\mp,\ Z_c^\pm\to\psi(2S)\pi^\pm)/\Gamma_{\rm total}$ Γ_{228}/Γ

VALUE (units 10^{-5})	CL%	DOCUMENT ID		TECN	COMMENT
$6.0^{+1.7+2.5}_{-2.0-1.4}$		CHILIKIN	13	BELL	$e^+e^-\to\ \Upsilon(4S)$
• • • We do not use the following data for averages, fits, limits, etc. • • •					
<3.1	95	[1] AUBERT	09AA	BABR	$e^+e^-\to\ \Upsilon(4S)$
$3.2^{+1.8+5.3}_{-0.9-1.6}$		[1] MIZUK	09	BELL	$e^+e^-\to\ \Upsilon(4S)$
4.1±1.0±1.4	[1,2]	CHOI	08	BELL	Repl. by MIZUK 09

[1] Assumes equal production of B^+ and B^0 at the $\Upsilon(4S)$.
[2] Establishes the $(Z_C4430)^+$ with a significance of 6.5 sigma. Needs confirmation.

$\Gamma(Z_c(4430)^\pm K^\mp,\ Z_c^\pm\to J/\psi\pi^\pm)/\Gamma_{\rm total}$ Γ_{229}/Γ

VALUE (units 10^{-6})	CL%	DOCUMENT ID		TECN	COMMENT
$5.4^{+4.0+1.1}_{-1.0-0.6}$		CHILIKIN	14	BELL	$\overline{B}^0\to\ J/\psi K^-\pi^+$
• • • We do not use the following data for averages, fits, limits, etc. • • •					
<4	95	[1] AUBERT	09AA	BABR	$e^+e^-\to\ \Upsilon(4S)$

[1] Assumes equal production of B^+ and B^0 at the $\Upsilon(4S)$.

$\Gamma(Z_c(3900)^\pm K^\mp,\ Z_c^\pm\to J/\psi\pi^\pm)/\Gamma_{\rm total}$ Γ_{230}/Γ

VALUE	DOCUMENT ID		TECN	COMMENT
$<9\times10^{-7}$	CHILIKIN	14	BELL	$\overline{B}^0\to\ J/\psi K^-\pi^+$

$\Gamma(Z_c(4200)^\pm K^\mp,\ X^\pm\to J/\psi\pi^\pm)/\Gamma_{\rm total}$ Γ_{231}/Γ

VALUE (units 10^{-5})	DOCUMENT ID		TECN	COMMENT
$2.2^{+0.7+1.1}_{-0.5-0.6}$	CHILIKIN	14	BELL	$\overline{B}^0\to\ J/\psi K^-\pi^+$

$\Gamma(J/\psi(1S)p\overline{p})/\Gamma_{\rm total}$ Γ_{232}/Γ

VALUE	CL%	DOCUMENT ID		TECN	COMMENT
$<5.2\times10^{-7}$	90	[1] AAIJ	13Z	LHCB	pp at 7 TeV
• • • We do not use the following data for averages, fits, limits, etc. • • •					
$<8.3\times10^{-7}$	90	[2] XIE	05	BELL	$e^+e^-\to\ \Upsilon(4S)$
$<1.9\times10^{-6}$	90	[2] AUBERT	03K	BABR	$e^+e^-\to\ \Upsilon(4S)$

[1] Uses B($B_s^0\to\ J/\psi(1S)\pi^+\pi^-$) = (1.98 ± 0.20) × 10^{-4}.
[2] Assumes equal production of B^+ and B^0 at the $\Upsilon(4S)$.

$\Gamma(J/\psi(1S)\gamma)/\Gamma_{\rm total}$ Γ_{233}/Γ

VALUE (units 10^{-6})	CL%	DOCUMENT ID		TECN	COMMENT
<1.5	90	[1] AAIJ	15BB	LHCB	pp at 7, 8 TeV
• • • We do not use the following data for averages, fits, limits, etc. • • •					
<1.6	90	[2] AUBERT,B	04T	BABR	$e^+e^-\to\ \Upsilon(4S)$

[1] Branching fractions of normalization modes $B^0\to\ J/\psi\gamma X$ taken from PDG 14. Uses $f_s/f_d = 0.259\pm0.015$.
[2] Assumes equal production of B^+ and B^0 at the $\Upsilon(4S)$.

$\Gamma(J/\psi(1S)\overline{D}^0)/\Gamma_{\rm total}$ Γ_{234}/Γ

VALUE (units 10^{-5})	CL%	DOCUMENT ID		TECN	COMMENT
<1.3	90	[1] AUBERT	05U	BABR	$e^+e^-\to\ \Upsilon(4S)$
• • • We do not use the following data for averages, fits, limits, etc. • • •					
<2.0	90	[1] ZHANG	05B	BELL	$e^+e^-\to\ \Upsilon(4S)$

[1] Assumes equal production of B^+ and B^0 at the $\Upsilon(4S)$.

$\Gamma(\psi(2S)\pi^0)/\Gamma_{\rm total}$ Γ_{235}/Γ

VALUE (units 10^{-5})	DOCUMENT ID		TECN	COMMENT
1.17±0.17±0.08	[1] CHOBANOVA	16	BELL	$e^+e^-\to\ \Upsilon(4S)$

[1] Assumes equal production of B^+ and B^0 at the $\Upsilon(4S)$.

$\Gamma(\psi(2S)K^0)/\Gamma_{\rm total}$ Γ_{236}/Γ

VALUE (units 10^{-4})	CL%	DOCUMENT ID		TECN	COMMENT
5.8 ±0.5 OUR FIT					
5.8 ±0.5 OUR AVERAGE					
4.7 ±0.7 ±0.7		[1] AAIJ	14L	LHCB	pp at 7 TeV
6.46±0.65±0.51		[2] AUBERT	05J	BABR	$e^+e^-\to\ \Upsilon(4S)$
6.7 ±1.1		[2] ABE	03B	BELL	$e^+e^-\to\ \Upsilon(4S)$
5.0 ±1.1 ±0.6		[2] RICHICHI	01	CLE2	$e^+e^-\to\ \Upsilon(4S)$
• • • We do not use the following data for averages, fits, limits, etc. • • •					
6.9 ±1.1 ±1.1		[2] AUBERT	02	BABR	Repl. by AUBERT 05J
< 8	90	[2] ALAM	94	CLE2	$e^+e^-\to\ \Upsilon(4S)$
<15	90	[2] BORTOLETTO	92	CLEO	$e^+e^-\to\ \Upsilon(4S)$
<28	90	[2] ALBRECHT	90J	ARG	$e^+e^-\to\ \Upsilon(4S)$

[1] Measured with B($B^0\to\ \psi(2S)K_S^0$) × B($\psi(2S)\to\ J/\psi\pi^+\pi^-$) / B($B^0\to\ J/\psi K_S^0$) using PDG 12 values for the involved branching fractions.
[2] Assumes equal production of B^+ and B^0 at the $\Upsilon(4S)$.

$\Gamma(\psi(2S)K^0)/\Gamma(J/\psi(1S)K^0)$ $\Gamma_{236}/\Gamma_{183}$

VALUE	DOCUMENT ID		TECN	COMMENT
0.82±0.13±0.12	[1] AUBERT	02	BABR	$e^+e^-\to\ \Upsilon(4S)$

[1] Assumes equal production of B^+ and B^0 at the $\Upsilon(4S)$.

$\Gamma(\psi(3770)K^0,\ \psi\to\overline{D}^0D^0)/\Gamma_{\rm total}$ Γ_{237}/Γ

VALUE (units 10^{-4})	CL%	DOCUMENT ID		TECN	COMMENT
<1.23	90	[1] AUBERT	08B	BABR	$e^+e^-\to\ \Upsilon(4S)$

[1] Assumes equal production of B^+ and B^0 at the $\Upsilon(4S)$.

$\Gamma(\psi(3770)K^0,\ \psi\to D^-D^+)/\Gamma_{\rm total}$ Γ_{238}/Γ

VALUE (units 10^{-4})	CL%	DOCUMENT ID		TECN	COMMENT
<1.88	90	[1] AUBERT	08B	BABR	$e^+e^-\to\ \Upsilon(4S)$

[1] Assumes equal production of B^+ and B^0 at the $\Upsilon(4S)$.

$\Gamma(\psi(2S)\pi^+\pi^-)/\Gamma(J/\psi(1S)\pi^+\pi^-)$ $\Gamma_{239}/\Gamma_{195}$

VALUE	DOCUMENT ID		TECN	COMMENT
0.56±0.07±0.05	[1] AAIJ	13AA	LHCB	pp at 7 TeV

[1] Assuming lepton universality for dimuon decay modes of J/ψ and $\psi(2S)$ mesons, the ratio B($J/\psi\to\ \mu^+\mu^-$)/B($\psi(2S)\to\ \mu^+\mu^-$) = B($J/\psi\to\ e^+e^-$)/B($\psi(2S)\to\ e^+e^-$) = 7.69 ± 0.19 was used.

$\Gamma(\psi(2S)K^+\pi^-)/\Gamma_{\rm total}$ Γ_{240}/Γ

VALUE (units 10^{-4})	CL%	DOCUMENT ID		TECN	COMMENT
5.80±0.39		[1,2] CHILIKIN	13	BELL	$e^+e^-\to\ \Upsilon(4S)$
• • • We do not use the following data for averages, fits, limits, etc. • • •					
5.57±0.16		[3] AUBERT	09AA	BABR	$e^+e^-\to\ \Upsilon(4S)$
5.68±0.13±0.42		[2] MIZUK	09	BELL	$e^+e^-\to\ \Upsilon(4S)$
<10	90	[2] ALBRECHT	90J	ARG	$e^+e^-\to\ \Upsilon(4S)$

[1] Combines measurements with $\psi(2S)\to\ \ell^+\ell^-$ with measurement from MIZUK 09 which uses $\psi(2S)\to\ J/\psi\pi^+\pi^-$.
[2] Assumes equal production of B^+ and B^0 at the $\Upsilon(4S)$.

[3] Does not report systematic uncertainties.

$\Gamma(\psi(2S)K^*(892)^0)/\Gamma_{total}$ Γ_{241}/Γ

VALUE (units 10^{-4})	CL%	DOCUMENT ID		TECN	COMMENT
5.9 ±0.4 OUR FIT					
6.0 $^{+0.5}_{-0.7}$ OUR AVERAGE		Error includes scale factor of 1.1.			
$5.55^{+0.22+0.41}_{-0.23-0.84}$		[1] CHILIKIN	13	BELL	$e^+e^- \to \Upsilon(4S)$
6.49±0.59±0.97		[1] AUBERT	05J	BABR	$e^+e^- \to \Upsilon(4S)$
7.6 ±1.1 ±1.0		[1] RICHICHI	01	CLE2	$e^+e^- \to \Upsilon(4S)$
9.0 ±2.2 ±0.9		[2] ABE	98O	CDF	$p\overline{p}$ 1.8 TeV
• • • We do not use the following data for averages, fits, limits, etc. • • •					
$5.52^{+0.35+0.53}_{-0.32-0.58}$		[1] MIZUK	09	BELL	$e^+e^- \to \Upsilon(4S)$
<19	90	[1] ALAM	94	CLE2	Repl. by RICHICHI 01
14 ±8 ±4		[1] BORTOLETTO	92	CLEO	$e^+e^- \to \Upsilon(4S)$
<23	90	[1] ALBRECHT	90J	ARG	$e^+e^- \to \Upsilon(4S)$

[1] Assumes equal production of B^+ and B^0 at the $\Upsilon(4S)$.
[2] ABE 98O reports $[B(B^0 \to \psi(2S)K^*(892)^0)]/[B(B^+ \to J/\psi(1S)K^+)] = 0.908 \pm 0.194 \pm 0.10$. We multiply by our best value $B(B^+ \to J/\psi(1S)K^+) = (9.9 \pm 1.0) \times 10^{-4}$. Our first error is their experiment's error and our second error is the systematic error from using our best value.

$\Gamma(\psi(2S)K^*(892)^0)/\Gamma(J/\psi(1S)K^*(892)^0)$ $\Gamma_{241}/\Gamma_{185}$

VALUE		DOCUMENT ID		TECN	COMMENT
0.487±0.018±0.011	[1,2]	AAIJ	12L	LHCB	pp at 7 TeV

[1] AAIJ 12L reports $0.476 \pm 0.014 \pm 0.010 \pm 0.012$ from a measurement of $[\Gamma(B^0 \to \psi(2S)K^*(892)^0)/\Gamma(B^0 \to J/\psi(1S)K^*(892)^0)] \times [B(J/\psi(1S) \to e^+e^-)] / [B(\psi(2S) \to e^+e^-)]$ assuming $B(J/\psi(1S) \to e^+e^-) = (5.94 \pm 0.06) \times 10^{-2}$, $B(\psi(2S) \to e^+e^-) = (7.72 \pm 0.17) \times 10^{-3}$, which we rescale to our best values $B(J/\psi(1S) \to e^+e^-) = (5.971 \pm 0.032) \times 10^{-2}$, $B(\psi(2S) \to e^+e^-) = (7.93 \pm 0.17) \times 10^{-3}$. Our first error is their experiment's error and our second error is the systematic error from using our best values.
[2] Assumes $B(J/\psi \to \mu^+\mu^-) / B(\psi(2S) \to \mu^+\mu^-) = B(J/\psi \to e^+e^-) / B(\psi(2S) \to e^+e^-) = 7.69 \pm 0.19$.

$\Gamma(\psi(2S)K^*(892)^0)/\Gamma(\psi(2S)K^0)$ $\Gamma_{241}/\Gamma_{236}$

VALUE	DOCUMENT ID		TECN	COMMENT
1.02±0.10 OUR FIT				
1.00±0.14±0.09	AUBERT	05J	BABR	$e^+e^- \to \Upsilon(4S)$

$\Gamma(\chi_{c0}K^0)/\Gamma_{total}$ Γ_{242}/Γ

VALUE (units 10^{-6})	CL%	DOCUMENT ID		TECN	COMMENT
146± 27 OUR AVERAGE					
$145^{+103}_{-85} \pm 8$		[1,2] LEES	12I	BABR	$e^+e^- \to \Upsilon(4S)$
148± 30±13		[1,3] LEES	12O	BABR	$e^+e^- \to \Upsilon(4S)$
$142^{+55}_{-44} \pm 22$		[1,4] AUBERT	09AU	BABR	$e^+e^- \to \Upsilon(4S)$
• • • We do not use the following data for averages, fits, limits, etc. • • •					
< 113	90	[4] GARMASH	07	BELL	$e^+e^- \to \Upsilon(4S)$
<1240	90	[1] AUBERT	05K	BABR	$e^+e^- \to \Upsilon(4S)$
< 500	90	[5] EDWARDS	01	CLE2	$e^+e^- \to \Upsilon(4S)$

[1] Assumes equal production of B^+ and B^0 at the $\Upsilon(4S)$.
[2] LEES 12I reports $[\Gamma(B^0 \to \chi_{c0}K^0)/\Gamma_{total}] \times [B(\chi_{c0}(1P) \to K^0_S K^0_S)] = (0.46^{+0.25}_{-0.17} \pm 0.21) \times 10^{-6}$ which we divide by our best value $B(\chi_{c0}(1P) \to K^0_S K^0_S) = (3.16 \pm 0.17) \times 10^{-3}$. Our first error is their experiment's error and our second error is the systematic error from using our best value.
[3] Measured in the $B^0 \to K^0_S K^+ K^-$ decay.
[4] Uses Dalitz plot analysis of the $B^0 \to K^0\pi^+\pi^-$ final state decays.
[5] EDWARDS 01 assumes equal production of B^0 and B^+ at the $\Upsilon(4S)$. The correlated uncertainties (28.3)% from $B(J/\psi(1S) \to \gamma\eta_c)$ in those modes have been accounted for.

$\Gamma(\chi_{c0}K^*(892)^0)/\Gamma_{total}$ Γ_{243}/Γ

VALUE (units 10^{-4})	CL%	DOCUMENT ID		TECN	COMMENT
1.7±0.3±0.2		[1] AUBERT	08BD	BABR	$e^+e^- \to \Upsilon(4S)$
• • • We do not use the following data for averages, fits, limits, etc. • • •					
<7.7	90	[1] AUBERT	05K	BABR	Repl. by AUBERT 08BD

[1] Assumes equal production of B^+ and B^0 at the $\Upsilon(4S)$.

$\Gamma(\chi_{c1}\pi^0)/\Gamma_{total}$ Γ_{244}/Γ

VALUE (units 10^{-5})	DOCUMENT ID		TECN	COMMENT
1.12±0.25±0.12	[1] KUMAR	08	BELL	$e^+e^- \to \Upsilon(4S)$

[1] Assumes equal production of B^+ and B^0 at the $\Upsilon(4S)$.

$\Gamma(\chi_{c1}K^0)/\Gamma_{total}$ Γ_{245}/Γ

VALUE (units 10^{-4})	CL%	DOCUMENT ID		TECN	COMMENT
3.93±0.27 OUR AVERAGE					
$3.78^{+0.17}_{-0.16} \pm 0.33$		[1] BHARDWAJ	11	BELL	$e^+e^- \to \Upsilon(4S)$
4.2 ±0.3 ±0.3		[2] AUBERT	09B	BABR	$e^+e^- \to \Upsilon(4S)$
3.1 $^{+1.5}_{-1.1}$ ±0.1		[3] AVERY	00	CLE2	$e^+e^- \to \Upsilon(4S)$
• • • We do not use the following data for averages, fits, limits, etc. • • •					
3.51±0.33±0.45		[1] SONI	06	BELL	Repl. by BHARDWAJ 11
4.53±0.41±0.51		[1] AUBERT	05J	BABR	Repl. by AUBERT 09B
4.3 ±1.4 ±0.1		[4] AUBERT	02	BABR	Repl. by AUBERT 05J
<27	90	[1] ALAM	94	CLE2	$e^+e^- \to \Upsilon(4S)$

[1] Assumes equal production of B^+ and B^0 at the $\Upsilon(4S)$.
[2] Uses $\chi_{c1,2} \to J/\psi\gamma$. Assumes $B(\Upsilon(4S) \to B^+B^-) = (51.6 \pm 0.6)\%$ and $B(\Upsilon(4S) \to B^0\overline{B}^0) = (48.4 \pm 0.6)\%$.
[3] AVERY 00 reports $(3.9^{+1.9}_{-1.3} \pm 0.4) \times 10^{-4}$ from a measurement of $[\Gamma(B^0 \to \chi_{c1}K^0)/\Gamma_{total}] \times [B(\chi_{c1}(1P) \to \gamma J/\psi(1S))]$ assuming $B(\chi_{c1}(1P) \to \gamma J/\psi(1S)) = 0.273 \pm 0.016$, which we rescale to our best value $B(\chi_{c1}(1P) \to \gamma J/\psi(1S)) = (34.3 \pm 1.0) \times 10^{-2}$. Our first error is their experiment's error and our second error is the systematic error from using our best value. Assumes equal production of B^+ and B^0 at the $\Upsilon(4S)$.
[4] AUBERT 02 reports $(5.4 \pm 1.4 \pm 1.1) \times 10^{-4}$ from a measurement of $[\Gamma(B^0 \to \chi_{c1}K^0)/\Gamma_{total}] \times [B(\chi_{c1}(1P) \to \gamma J/\psi(1S))]$ assuming $B(\chi_{c1}(1P) \to \gamma J/\psi(1S)) = 0.273 \pm 0.016$, which we rescale to our best value $B(\chi_{c1}(1P) \to \gamma J/\psi(1S)) = (34.3 \pm 1.0) \times 10^{-2}$. Our first error is their experiment's error and our second error is the systematic error from using our best value. Assumes equal production of B^+ and B^0 at the $\Upsilon(4S)$.

$\Gamma(\chi_{c1}K^0)/\Gamma(J/\psi(1S)K^0)$ $\Gamma_{245}/\Gamma_{183}$

VALUE	DOCUMENT ID		TECN	COMMENT
0.53±0.16±0.01	[1] AUBERT	02	BABR	$e^+e^- \to \Upsilon(4S)$

[1] AUBERT 02 reports $0.66 \pm 0.11 \pm 0.17$ from a measurement of $[\Gamma(B^0 \to \chi_{c1}K^0)/\Gamma(B^0 \to J/\psi(1S)K^0)] \times [B(\chi_{c1}(1P) \to \gamma J/\psi(1S))]$ assuming $B(\chi_{c1}(1P) \to \gamma J/\psi(1S)) = 0.273 \pm 0.016$, which we rescale to our best value $B(\chi_{c1}(1P) \to \gamma J/\psi(1S)) = (34.3 \pm 1.0) \times 10^{-2}$. Our first error is their experiment's error and our second error is the systematic error from using our best value. Assumes equal production of B^+ and B^0 at the $\Upsilon(4S)$.

$\Gamma(\chi_{c1}\pi^-K^+)/\Gamma_{total}$ Γ_{246}/Γ

VALUE (units 10^{-4})	DOCUMENT ID		TECN	COMMENT
4.97±0.12±0.28	[1] BHARDWAJ	16	BELL	$e^+e^- \to \Upsilon(4S)$
• • • We do not use the following data for averages, fits, limits, etc. • • •				
3.83±0.10±0.39	[1] MIZUK	08	BELL	Repl. by BHARDWAJ 16

[1] Assumes equal production of B^+ and B^0 at the $\Upsilon(4S)$.

$\Gamma(\chi_{c1}\pi^-K^+)/\Gamma(J/\psi(1S)K^+\pi^-)$ $\Gamma_{246}/\Gamma_{184}$

VALUE	DOCUMENT ID		TECN
0.476±0.021±0.013	[1] LEES	12B	BABR

[1] LEES 12B reports $0.474 \pm 0.013 \pm 0.026$ from a measurement of $[\Gamma(B^0 \to \chi_{c1}\pi^-K^+)/\Gamma(B^0 \to J/\psi(1S)K^+\pi^-)] \times [B(\chi_{c1}(1P) \to \gamma J/\psi(1S))]$ assuming $B(\chi_{c1}(1P) \to \gamma J/\psi(1S)) = (34.4 \pm 1.5) \times 10^{-2}$, which we rescale to our best value $B(\chi_{c1}(1P) \to \gamma J/\psi(1S)) = (34.3 \pm 1.0) \times 10^{-2}$. Our first error is their experiment's error and our second error is the systematic error from using our best value.

$\Gamma(\chi_{c1}K^*(892)^0)/\Gamma_{total}$ Γ_{247}/Γ

VALUE (units 10^{-4})	CL%	DOCUMENT ID		TECN	COMMENT
2.38±0.19 OUR FIT		Error includes scale factor of 1.2.			
$2.22^{+0.40}_{-0.31}$ OUR AVERAGE		Error includes scale factor of 1.6.			
2.5 ±0.2 ±0.2		[1] AUBERT	09B	BABR	$e^+e^- \to \Upsilon(4S)$
$1.73^{+0.15+0.34}_{-0.12-0.22}$		[2] MIZUK	08	BELL	$e^+e^- \to \Upsilon(4S)$
• • • We do not use the following data for averages, fits, limits, etc. • • •					
3.14±0.34±0.72		[2] SONI	06	BELL	Repl. by MIZUK 08
3.27±0.42±0.64		[2] AUBERT	05J	BABR	Repl. by AUBERT 09B
3.8 ±1.3 ±0.1		[3] AUBERT	02	BABR	Repl. by AUBERT 05J
<21	90	[4] ALAM	94	CLE2	$e^+e^- \to \Upsilon(4S)$

[1] Uses $\chi_{c1,2} \to J/\psi\gamma$. Assumes $B(\Upsilon(4S) \to B^+B^-) = (51.6 \pm 0.6)\%$ and $B(\Upsilon(4S) \to B^0\overline{B}^0) = (48.4 \pm 0.6)\%$.
[2] Assumes equal production of B^+ and B^0 at the $\Upsilon(4S)$.
[3] AUBERT 02 reports $(4.8 \pm 1.4 \pm 0.9) \times 10^{-4}$ from a measurement of $[\Gamma(B^0 \to \chi_{c1}K^*(892)^0)/\Gamma_{total}] \times [B(\chi_{c1}(1P) \to \gamma J/\psi(1S))]$ assuming $B(\chi_{c1}(1P) \to \gamma J/\psi(1S)) = 0.273 \pm 0.016$, which we rescale to our best value $B(\chi_{c1}(1P) \to \gamma J/\psi(1S)) = (34.3 \pm 1.0) \times 10^{-2}$. Our first error is their experiment's error and our second error is the systematic error from using our best value. Assumes equal production of B^+ and B^0 at the $\Upsilon(4S)$.
[4] BORTOLETTO 92 assumes equal production of B^+ and B^0 at the $\Upsilon(4S)$.

$\Gamma(\chi_{c1}K^*(892)^0)/\Gamma(J/\psi(1S)K^*(892)^0)$ $\Gamma_{247}/\Gamma_{185}$

VALUE (units 10^{-2})	DOCUMENT ID		TECN	COMMENT
18.8±1.5 OUR FIT	Error includes scale factor of 1.1.			
19.8±1.1±1.5	[1] AAIJ	13AC	LHCB	pp at 7 TeV

[1] Uses $B(\chi_{c1} \to J/\psi\gamma) = (34.4 \pm 1.5)\%$.

$\Gamma(\chi_{c1}K^*(892)^0)/\Gamma(\chi_{c1}K^0)$ $\Gamma_{247}/\Gamma_{245}$

VALUE	DOCUMENT ID		TECN	COMMENT
0.72±0.11±0.12	AUBERT	05J	BABR	$e^+e^- \to \Upsilon(4S)$
• • • We do not use the following data for averages, fits, limits, etc. • • •				
0.89±0.34±0.17	[1] AUBERT	02	BABR	Repl. by AUBERT 05J

[1] Assumes equal production of B^+ and B^0 at the $\Upsilon(4S)$.

$\Gamma(X(4051)^- K^+, X^- \to \chi_{c1}\pi^-)/\Gamma_{\rm total}$ Γ_{248}/Γ

VALUE (units 10^{-5})	CL%	DOCUMENT ID		TECN	COMMENT
$3.0^{+1.5}_{-0.8}{}^{+3.7}_{-1.6}$		[1] MIZUK	08	BELL	$e^+e^- \to \Upsilon(4S)$
• • • We do not use the following data for averages, fits, limits, etc. • • •					
<1.8	90	[1,2] LEES	12B	BABR	

[1] Assumes equal production of B^+ and B^0 at the $\Upsilon(4S)$.
[2] Uses $\chi_{c1} \to J/\psi\gamma$ mode. Uses $\chi_{c1} \to J/\psi\gamma$ mode. Finds a good description of the data without this $B^0 \to X(4051)^+ K^-$ decay mode in a fit.

$\Gamma(X(4248)^- K^+, X^- \to \chi_{c1}\pi^-)/\Gamma_{\rm total}$ Γ_{249}/Γ

VALUE (units 10^{-5})	CL%	DOCUMENT ID		TECN	COMMENT
$4.0^{+2.3}_{-0.9}{}^{+19.7}_{-0.5}$		[1] MIZUK	08	BELL	$e^+e^- \to \Upsilon(4S)$
• • • We do not use the following data for averages, fits, limits, etc. • • •					
<4.0	90	[1,2] LEES	12B	BABR	

[1] Assumes equal production of B^+ and B^0 at the $\Upsilon(4S)$.
[2] Uses $\chi_{c1} \to J/\psi\gamma$ mode. Finds a good description of the data without this $B^0 \to X(4248)^+ K^-$ decay mode in a fit.

$\Gamma(\chi_{c1}\pi^+\pi^- K^0)/\Gamma_{\rm total}$ Γ_{250}/Γ

VALUE (units 10^{-4})	DOCUMENT ID		TECN	COMMENT
$3.16 \pm 0.35 \pm 0.32$	[1] BHARDWAJ	16	BELL	$e^+e^- \to \Upsilon(4S)$

[1] Assumes equal production of B^+ and B^0 at the $\Upsilon(4S)$.

$\Gamma(\chi_{c1}\pi^-\pi^0 K^+)/\Gamma_{\rm total}$ Γ_{251}/Γ

VALUE (units 10^{-4})	DOCUMENT ID		TECN	COMMENT
$3.52 \pm 0.52 \pm 0.24$	[1] BHARDWAJ	16	BELL	$e^+e^- \to \Upsilon(4S)$

[1] Assumes equal production of B^+ and B^0 at the $\Upsilon(4S)$.

$\Gamma(\chi_{c2} K^0)/\Gamma_{\rm total}$ Γ_{252}/Γ

VALUE	CL%	DOCUMENT ID		TECN	COMMENT
$<1.5 \times 10^{-5}$	90	[1] BHARDWAJ	11	BELL	$e^+e^- \to \Upsilon(4S)$
• • • We do not use the following data for averages, fits, limits, etc. • • •					
$<2.8 \times 10^{-5}$	90	[2] AUBERT	09B	BABR	$e^+e^- \to \Upsilon(4S)$
$<2.6 \times 10^{-5}$	90	[1] SONI	06	BELL	Repl. by BHARDWAJ 11
$<4.1 \times 10^{-5}$	90	[1] AUBERT	05K	BABR	$e^+e^- \to \Upsilon(4S)$

[1] Assumes equal production of B^+ and B^0 at the $\Upsilon(4S)$.
[2] Uses $\chi_{c1,2} \to J/\psi\gamma$. Assumes $B(\Upsilon(4S) \to B^+B^-) = (51.6 \pm 0.6)\%$ and $B(\Upsilon(4S) \to B^0\overline{B}{}^0) = (48.4 \pm 0.6)\%$.

$\Gamma(\chi_{c2} K^*(892)^0)/\Gamma_{\rm total}$ Γ_{253}/Γ

VALUE (units 10^{-5})	CL%	DOCUMENT ID		TECN	COMMENT
4.9 ± 1.2 OUR FIT Error includes scale factor of 1.1.					
$6.6 \pm 1.8 \pm 0.5$		[1] AUBERT	09B	BABR	$e^+e^- \to \Upsilon(4S)$
• • • We do not use the following data for averages, fits, limits, etc. • • •					
<7.1	90	[2] SONI	06	BELL	$e^+e^- \to \Upsilon(4S)$
<3.6	90	[2] AUBERT	05K	BABR	Repl. by AUBERT 09B

[1] Uses $\chi_{c1,2} \to J/\psi\gamma$. Assumes $B(\Upsilon(4S) \to B^+B^-) = (51.6 \pm 0.6)\%$ and $B(\Upsilon(4S) \to B^0\overline{B}{}^0) = (48.4 \pm 0.6)\%$.
[2] Assumes equal production of B^+ and B^0 at the $\Upsilon(4S)$.

$\Gamma(\chi_{c2} K^*(892)^0)/\Gamma(\chi_{c1} K^*(892)^0)$ $\Gamma_{253}/\Gamma_{247}$

VALUE (units 10^{-2})	DOCUMENT ID		TECN	COMMENT
20 ± 5 OUR FIT Error includes scale factor of 1.1.				
$17.1 \pm 5.0 \pm 2.0$	[1] AAIJ	13AC	LHCB	pp at 7 TeV

[1] Uses $B(\chi_{c1} \to J/\psi\gamma)/B(\chi_{c2} \to J/\psi\gamma) = 1.76 \pm 0.11$.

$\Gamma(\chi_{c2}\pi^- K^+)/\Gamma_{\rm total}$ Γ_{254}/Γ

VALUE (units 10^{-4})	DOCUMENT ID		TECN	COMMENT
$0.72 \pm 0.09 \pm 0.05$	[1] BHARDWAJ	16	BELL	$e^+e^- \to \Upsilon(4S)$

[1] Assumes equal production of B^+ and B^0 at the $\Upsilon(4S)$.

$\Gamma(\chi_{c2}\pi^+\pi^- K^0)/\Gamma_{\rm total}$ Γ_{255}/Γ

VALUE	CL%	DOCUMENT ID		TECN	COMMENT
$<1.70 \times 10^{-4}$	90	[1] BHARDWAJ	16	BELL	$e^+e^- \to \Upsilon(4S)$

[1] Assumes equal production of B^+ and B^0 at the $\Upsilon(4S)$.

$\Gamma(\chi_{c2}\pi^-\pi^0 K^+)/\Gamma_{\rm total}$ Γ_{256}/Γ

VALUE	CL%	DOCUMENT ID		TECN	COMMENT
$<0.74 \times 10^{-4}$	90	[1] BHARDWAJ	16	BELL	$e^+e^- \to \Upsilon(4S)$

[1] Assumes equal production of B^+ and B^0 at the $\Upsilon(4S)$.

$\Gamma(K^+\pi^-)/\Gamma_{\rm total}$ Γ_{257}/Γ

VALUE (units 10^{-6})	CL%	DOCUMENT ID		TECN	COMMENT
19.6 ± 0.5 OUR FIT					
19.6 ± 0.5 OUR AVERAGE					
$20.00 \pm 0.34 \pm 0.60$		[1] DUH	13	BELL	$e^+e^- \to \Upsilon(4S)$
$19.1 \pm 0.6 \pm 0.6$		[1] AUBERT	07B	BABR	$e^+e^- \to \Upsilon(4S)$
$18.0\ ^{+\ 2.3}_{-\ 2.1}\ ^{+1.2}_{-0.9}$		[1] BORNHEIM	03	CLE2	$e^+e^- \to \Upsilon(4S)$
• • • We do not use the following data for averages, fits, limits, etc. • • •					
$19.9 \pm 0.4 \pm 0.8$		[1] LIN	07A	BELL	Repl. by DUH 13
$18.5 \pm 1.0 \pm 0.7$		[1] CHAO	04	BELL	Repl. by LIN 07A
$17.9 \pm 0.9 \pm 0.7$		[1] AUBERT	02Q	BABR	Repl. by AUBERT 07B
$22.5 \pm 1.9 \pm 1.8$		[1] CASEY	02	BELL	Repl. by CHAO 04
$19.3\ ^{+\ 3.4}_{-\ 3.2}\ ^{+1.5}_{-0.6}$		[1] ABE	01H	BELL	Repl. by CASEY 02
$16.7 \pm 1.6 \pm 1.3$		[1] AUBERT	01E	BABR	Repl. by AUBERT 02Q
< 66	90	[2] ABE	00C	SLD	$e^+e^- \to Z$
$17.2\ ^{+\ 2.5}_{-\ 2.4} \pm 1.2$		[1] CRONIN-HEN...	00	CLE2	Repl. by BORNHEIM 03
$15\ ^{+\ 5.}_{-\ 4} \pm 1.4$		GODANG	98	CLE2	Repl. by CRONIN-HENNESSY 00
$24\ ^{+17}_{-11} \pm 2$		[3] ADAM	96D	DLPH	$e^+e^- \to Z$
< 17	90	ASNER	96	CLE2	Sup. by ADAM 96D
< 30	90	[4] BUSKULIC	96V	ALEP	$e^+e^- \to Z$
< 90	90	[5] ABREU	95N	DLPH	Sup. by ADAM 96D
< 81	90	[6] AKERS	94L	OPAL	$e^+e^- \to Z$
< 26	90	[7] BATTLE	93	CLE2	$e^+e^- \to \Upsilon(4S)$
<180	90	ALBRECHT	91B	ARG	$e^+e^- \to \Upsilon(4S)$
< 90	90	[8] AVERY	89B	CLEO	$e^+e^- \to \Upsilon(4S)$
<320	90	AVERY	87	CLEO	$e^+e^- \to \Upsilon(4S)$

[1] Assumes equal production of B^+ and B^0 at the $\Upsilon(4S)$.
[2] ABE 00C assumes $B(Z \to b\overline{b}) = (21.7 \pm 0.1)\%$ and the B fractions $f_{B^0} = f_{B^+} = (39.7^{+1.8}_{-2.2})\%$ and $f_{B_s} = (10.5^{+1.8}_{-2.2})\%$.
[3] ADAM 96D assumes $f_{B^0} = f_{B^-} = 0.39$ and $f_{B_s} = 0.12$. Contributions from B^0 and B_s decays cannot be separated. Limits are given for the weighted average of the decay rates for the two neutral B mesons.
[4] BUSKULIC 96V assumes PDG 96 production fractions for B^0, B^+, B_s, b baryons.
[5] Assumes a B^0, B^- production fraction of 0.39 and a B_s production fraction of 0.12. Contributions from B^0 and B_s^0 decays cannot be separated. Limits are given for the weighted average of the decay rates for the two neutral B mesons.
[6] Assumes $B(Z \to b\overline{b}) = 0.217$ and B_d^0 (B_s^0) fraction 39.5% (12%).
[7] BATTLE 93 assumes equal production of $B^0\overline{B}{}^0$ and B^+B^- at $\Upsilon(4S)$.
[8] Assumes the $\Upsilon(4S)$ decays 43% to $B^0\overline{B}{}^0$.

$\Gamma(K^+\pi^-)/\Gamma(K^0\pi^0)$ $\Gamma_{257}/\Gamma_{258}$

VALUE	DOCUMENT ID		TECN	COMMENT
$2.16 \pm 0.16 \pm 0.16$	LIN	07A	BELL	$e^+e^- \to \Upsilon(4S)$
• • • We do not use the following data for averages, fits, limits, etc. • • •				
$1.20^{+0.50}_{-0.58}{}^{+0.22}_{-0.32}$	[1] ABE	01H	BELL	Repl. by LIN 07A

[1] Assumes equal production of B^+ and B^0 at the $\Upsilon(4S)$.

$[\Gamma(K^+\pi^-) + \Gamma(\pi^+\pi^-)]/\Gamma_{\rm total}$ $(\Gamma_{257}+\Gamma_{387})/\Gamma$

VALUE (units 10^{-6})	EVTS	DOCUMENT ID		TECN	COMMENT
19 ± 6 OUR AVERAGE					
$28^{+15}_{-10} \pm 20$		[1] ADAM	96D	DLPH	$e^+e^- \to Z$
$18^{+\ 6+\ 3}_{-\ 5-\ 4}$	17.2	ASNER	96	CLE2	$e^+e^- \to \Upsilon(4S)$
• • • We do not use the following data for averages, fits, limits, etc. • • •					
$24^{+\ 8}_{-\ 7} \pm 2$		[2] BATTLE	93	CLE2	$e^+e^- \to \Upsilon(4S)$

[1] ADAM 96D assumes $f_{B^0} = f_{B^-} = 0.39$ and $f_{B_s} = 0.12$. Contributions from B^0 and B_s decays cannot be separated. Limits are given for the weighted average of the decay rates for the two neutral B mesons.
[2] BATTLE 93 assumes equal production of $B^0\overline{B}{}^0$ and B^+B^- at $\Upsilon(4S)$.

$\Gamma(K^0\pi^0)/\Gamma_{\rm total}$ Γ_{258}/Γ

VALUE (units 10^{-6})	CL%	DOCUMENT ID		TECN	COMMENT
9.9 ± 0.5 OUR AVERAGE					
$9.68 \pm 0.46 \pm 0.50$		[1] DUH	13	BELL	$e^+e^- \to \Upsilon(4S)$
$10.1 \pm 0.6 \pm 0.4$		[1] LEES	13D	BABR	$e^+e^- \to \Upsilon(4S)$
$12.8\ ^{+4.0}_{-3.3}\ ^{+1.7}_{-1.4}$		[1] BORNHEIM	03	CLE2	$e^+e^- \to \Upsilon(4S)$
• • • We do not use the following data for averages, fits, limits, etc. • • •					
$8.7 \pm 0.5 \pm 0.6$		[1] FUJIKAWA	10A	BELL	Repl. by DUH 13
$10.3 \pm 0.7 \pm 0.6$		[1] AUBERT	08E	BABR	Repl. by LEES 13D
$9.2 \pm 0.7 \pm 0.6$		[1] LIN	07A	BELL	Repl. by FUJIKAWA 10A
$11.4 \pm 0.9 \pm 0.6$		[1] AUBERT	05Y	BABR	Repl. by AUBERT 08E
$11.4 \pm 1.7 \pm 0.8$		[1] AUBERT	04M	BABR	Repl. by AUBERT 05Y
$11.7 \pm 2.3\ ^{+1.2}_{-1.3}$		[1] CHAO	04	BELL	Repl. by LIN 07A
$8.0\ ^{+3.3}_{-3.1} \pm 1.6$		[1] CASEY	02	BELL	Repl. by CHAO 04
$16.0\ ^{+7.2}_{-5.9}\ ^{+2.5}_{-2.7}$		[1] ABE	01H	BELL	Repl. by CASEY 02
$8.2\ ^{+3.1}_{-2.7} \pm 1.2$		[1] AUBERT	01E	BABR	Repl. by AUBERT 04M
$14.6\ ^{+5.9}_{-5.1}\ ^{+2.4}_{-3.3}$		[1] CRONIN-HEN...	00	CLE2	Repl. by BORNHEIM 03
<41	90	GODANG	98	CLE2	Repl. by CRONIN-HENNESSY 00
<40	90	ASNER	96	CLE2	Rep. by GODANG 98

[1] Assumes equal production of B^+ and B^0 at the $\Upsilon(4S)$.

$\Gamma(\eta' K^0)/\Gamma_{total}$ Γ_{259}/Γ

VALUE (units 10^{-6})	DOCUMENT ID		TECN	COMMENT
66 ± 4 OUR AVERAGE	Error includes scale factor of 1.4.			
$68.5 \pm 2.2 \pm 3.1$	[1] AUBERT	09AV	BABR	$e^+e^- \to \Upsilon(4S)$
$58.9^{+3.6}_{-3.5} \pm 4.3$	[1] SCHUEMANN	06	BELL	$e^+e^- \to \Upsilon(4S)$
$89^{+18}_{-16} \pm 9$	[1] RICHICHI	00	CLE2	$e^+e^- \to \Upsilon(4S)$
• • • We do not use the following data for averages, fits, limits, etc. • • •				
$66.6 \pm 2.6 \pm 2.8$	[1] AUBERT	07AE	BABR	Repl. by AUBERT 09AV
$67.4 \pm 3.3 \pm 3.2$	[1] AUBERT	05M	BABR	AUBERT 07AE
$60.6 \pm 5.6 \pm 4.6$	[1] AUBERT	03W	BABR	Repl. by AUBERT 05M
$55^{+19}_{-16} \pm 8$	[1] ABE	01M	BELL	Repl. by SCHUEMANN 06
$42^{+13}_{-11} \pm 4$	[1] AUBERT	01G	BABR	Repl. by AUBERT 03W
$47^{+27}_{-20} \pm 9$	BEHRENS	98	CLE2	Repl. by RICHICHI 00

[1] Assumes equal production of B^+ and B^0 at the $\Upsilon(4S)$.

$\Gamma(\eta' K^*(892)^0)/\Gamma_{total}$ Γ_{260}/Γ

VALUE (units 10^{-6})	CL%	DOCUMENT ID		TECN	COMMENT
2.8 ± 0.6 OUR AVERAGE					
$2.6 \pm 0.7 \pm 0.2$		[1] SATO	14	BELL	$e^+e^- \to \Upsilon(4S)$
$3.1^{+0.9}_{-0.8} \pm 0.3$		[1] DEL-AMO-SA...10A		BABR	$e^+e^- \to \Upsilon(4S)$
• • • We do not use the following data for averages, fits, limits, etc. • • •					
$3.8 \pm 1.1 \pm 0.5$		[1] AUBERT	07E	BABR	Repl. by DEL-AMO-SANCHEZ 10A
< 2.6	90	[1] SCHUEMANN	07	BELL	$e^+e^- \to \Upsilon(4S)$
< 7.6	90	[1] AUBERT,B	04D	BABR	Repl. by AUBERT 07E
<24	90	[1] RICHICHI	00	CLE2	$e^+e^- \to \Upsilon(4S)$
<39	90	BEHRENS	98	CLE2	Repl. by RICHICHI 00

[1] Assumes equal production of B^+ and B^0 at the $\Upsilon(4S)$.

$\Gamma(\eta' K_0^*(1430)^0)/\Gamma_{total}$ Γ_{261}/Γ

VALUE (units 10^{-6})	DOCUMENT ID		TECN	COMMENT
$6.3 \pm 1.3 \pm 0.9$	[1] DEL-AMO-SA...10A		BABR	$e^+e^- \to \Upsilon(4S)$

[1] Assumes equal production of B^+ and B^0 at the $\Upsilon(4S)$.

$\Gamma(\eta' K_2^*(1430)^0)/\Gamma_{total}$ Γ_{262}/Γ

VALUE (units 10^{-6})	DOCUMENT ID		TECN	COMMENT
$13.7^{+3.0}_{-2.9} \pm 1.2$	[1] DEL-AMO-SA...10A		BABR	$e^+e^- \to \Upsilon(4S)$

[1] Assumes equal production of B^+ and B^0 at the $\Upsilon(4S)$.

$\Gamma(\eta K^0)/\Gamma_{total}$ Γ_{263}/Γ

VALUE (units 10^{-6})	CL%	DOCUMENT ID		TECN	COMMENT
$1.23^{+0.27}_{-0.24}$ OUR AVERAGE					
$1.27^{+0.33}_{-0.29} \pm 0.08$		[1] HOI	12	BELL	$e^+e^- \to \Upsilon(4S)$
$1.15^{+0.43}_{-0.38} \pm 0.09$		[1] AUBERT	09AV	BABR	$e^+e^- \to \Upsilon(4S)$
• • • We do not use the following data for averages, fits, limits, etc. • • •					
< 1.9	90	[1] CHANG	07B	BELL	Repl. by HOI 12
< 2.9	90	[1] AUBERT,B	06V	BABR	$e^+e^- \to \Upsilon(4S)$
< 2.5	90	[1] AUBERT,B	05K	BABR	$e^+e^- \to \Upsilon(4S)$
< 2.0	90	[1] CHANG	05A	BELL	Repl. by CHANG 07B
< 5.2	90	[1] AUBERT	04H	BABR	Repl. by AUBERT,B 05K
< 9.3	90	[1] RICHICHI	00	CLE2	$e^+e^- \to \Upsilon(4S)$
<33	90	BEHRENS	98	CLE2	Repl. by RICHICHI 00

[1] Assumes equal production of B^+ and B^0 at the $\Upsilon(4S)$.

$\Gamma(\eta K^*(892)^0)/\Gamma_{total}$ Γ_{264}/Γ

VALUE (units 10^{-6})	CL%	DOCUMENT ID		TECN	COMMENT
15.9 ± 1.0 OUR AVERAGE					
$15.2 \pm 1.2 \pm 1.0$		[1] WANG	07B	BELL	$e^+e^- \to \Upsilon(4S)$
$16.5 \pm 1.1 \pm 0.8$		[1] AUBERT,B	06H	BABR	$e^+e^- \to \Upsilon(4S)$
$13.8^{+5.5}_{-4.6} \pm 1.6$		[1] RICHICHI	00	CLE2	$e^+e^- \to \Upsilon(4S)$
• • • We do not use the following data for averages, fits, limits, etc. • • •					
$18.6 \pm 2.3 \pm 1.2$		[1] AUBERT,B	04D	BABR	Repl. by AUBERT,B 06H
<30	90	BEHRENS	98	CLE2	Repl. by RICHICHI 00

[1] Assumes equal production of B^+ and B^0 at the $\Upsilon(4S)$.

$\Gamma(\eta K_0^*(1430)^0)/\Gamma_{total}$ Γ_{265}/Γ

VALUE (units 10^{-6})	DOCUMENT ID		TECN	COMMENT
$11.0 \pm 1.6 \pm 1.5$	[1] AUBERT,B	06H	BABR	$e^+e^- \to \Upsilon(4S)$

[1] Assumes equal production of B^+ and B^0 at the $\Upsilon(4S)$.

$\Gamma(\eta K_2^*(1430)^0)/\Gamma_{total}$ Γ_{266}/Γ

VALUE (units 10^{-6})	DOCUMENT ID		TECN	COMMENT
$9.6 \pm 1.8 \pm 1.1$	[1] AUBERT,B	06H	BABR	$e^+e^- \to \Upsilon(4S)$

[1] Assumes equal production of B^+ and B^0 at the $\Upsilon(4S)$.

$\Gamma(\omega K^0)/\Gamma_{total}$ Γ_{267}/Γ

VALUE (units 10^{-6})	CL%	DOCUMENT ID		TECN	COMMENT
4.8 ± 0.4 OUR AVERAGE					
$4.5 \pm 0.4 \pm 0.3$		[1] CHOBANOVA	14	BELL	$e^+e^- \to \Upsilon(4S)$
$5.4 \pm 0.8 \pm 0.3$		[1] AUBERT	07AE	BABR	$e^+e^- \to \Upsilon(4S)$
$10.0^{+5.4}_{-4.2} \pm 1.4$		[1] JESSOP	00	CLE2	$e^+e^- \to \Upsilon(4S)$
• • • We do not use the following data for averages, fits, limits, etc. • • •					
$6.2 \pm 1.0 \pm 0.4$		[1] AUBERT,B	06E	BABR	Repl. by AUBERT 07AE
$4.4^{+0.8}_{-0.7} \pm 0.4$		[1] JEN	06	BELL	Repl. by CHOBANOVA 14
$5.9^{+1.6}_{-1.3} \pm 0.5$		[1] AUBERT	04H	BABR	Repl. by AUBERT,B 06E
$4.0^{+1.9}_{-1.6} \pm 0.5$		[1] WANG	04A	BELL	Repl. by JEN 06
<13	90	[1] AUBERT	01G	BABR	Repl. by AUBERT 04H
<57	90	[1] BERGFELD	98	CLE2	Repl. by JESSOP 00

[1] Assumes equal production of B^+ and B^0 at the $\Upsilon(4S)$.

$\Gamma(a_0(980)^0 K^0,\ a_0^0 \to \eta\pi^0)/\Gamma_{total}$ Γ_{268}/Γ

VALUE (units 10^{-6})	CL%	DOCUMENT ID		TECN	COMMENT
<7.8	90	[1] AUBERT,BE	04	BABR	$e^+e^- \to \Upsilon(4S)$

[1] Assumes equal production of charged and neutral B mesons at $\Upsilon(4S)$.

$\Gamma(b_1^0 K^0,\ b_1^0 \to \omega\pi^0)/\Gamma_{total}$ Γ_{269}/Γ

VALUE (units 10^{-6})	CL%	DOCUMENT ID		TECN	COMMENT
<7.8	90	[1] AUBERT	08AG	BABR	$e^+e^- \to \Upsilon(4S)$

[1] Assumes equal production of B^+ and B^0 at the $\Upsilon(4S)$.

$\Gamma(a_0(980)^\pm K^\mp,\ a_0^\pm \to \eta\pi^\pm)/\Gamma_{total}$ Γ_{270}/Γ

VALUE (units 10^{-6})	CL%	DOCUMENT ID		TECN	COMMENT
<1.9	90	[1] AUBERT	07Y	BABR	$e^+e^- \to \Upsilon(4S)$
• • • We do not use the following data for averages, fits, limits, etc. • • •					
<2.1	90	[1] AUBERT,BE	04	BABR	Repl. by AUBERT 07Y

[1] Assumes equal production of B^+ and B^0 at the $\Upsilon(4S)$.

$\Gamma(b_1^- K^+,\ b_1^- \to \omega\pi^-)/\Gamma_{total}$ Γ_{271}/Γ

VALUE (units 10^{-6})	DOCUMENT ID		TECN	COMMENT
$7.4 \pm 1.0 \pm 1.0$	[1] AUBERT	07BI	BABR	$e^+e^- \to \Upsilon(4S)$

[1] Assumes equal production of B^+ and B^0 at the $\Upsilon(4S)$.

$\Gamma(b_1^0 K^{*0},\ b_1^0 \to \omega\pi^0)/\Gamma_{total}$ Γ_{272}/Γ

VALUE	CL%	DOCUMENT ID		TECN	COMMENT
$<8.0 \times 10^{-6}$	90	[1] AUBERT	09AF	BABR	$e^+e^- \to \Upsilon(4S)$

[1] Assumes equal production of B^+ and B^0 at the $\Upsilon(4S)$.

$\Gamma(b_1^- K^{*+},\ b_1^- \to \omega\pi^-)/\Gamma_{total}$ Γ_{273}/Γ

VALUE	CL%	DOCUMENT ID		TECN	COMMENT
$<5.0 \times 10^{-6}$	90	[1] AUBERT	09AF	BABR	$e^+e^- \to \Upsilon(4S)$

[1] Assumes equal production of B^+ and B^0 at the $\Upsilon(4S)$.

$\Gamma(a_0(1450)^\pm K^\mp,\ a_0^\pm \to \eta\pi^\pm)/\Gamma_{total}$ Γ_{274}/Γ

VALUE (units 10^{-6})	CL%	DOCUMENT ID		TECN	COMMENT
<3.1	90	[1] AUBERT	07Y	BABR	$e^+e^- \to \Upsilon(4S)$

[1] Assumes equal production of B^+ and B^0 at the $\Upsilon(4S)$.

$\Gamma(K_S^0 X^0(\text{Familon}))/\Gamma_{total}$ Γ_{275}/Γ

VALUE (units 10^{-6})	CL%	DOCUMENT ID		TECN	COMMENT
<53	90	[1] AMMAR	01B	CLE2	$e^+e^- \to \Upsilon(4S)$

[1] AMMAR 01B searched for the two-body decay of the B meson to a massless neutral feebly-interacting particle X^0 such as the familon, the Nambu-Goldstone boson associated with a spontaneously broken global family symmetry.

$\Gamma(\omega K^*(892)^0)/\Gamma_{total}$ Γ_{276}/Γ

VALUE (units 10^{-6})	CL%	DOCUMENT ID		TECN	COMMENT
2.0 ± 0.5 OUR AVERAGE					
$2.2 \pm 0.6 \pm 0.2$		[1] AUBERT	09H	BABR	$e^+e^- \to \Upsilon(4S)$
$1.8 \pm 0.7 \pm 0.3$		[1] GOLDENZWE...08		BELL	$e^+e^- \to \Upsilon(4S)$
• • • We do not use the following data for averages, fits, limits, etc. • • •					
< 4.2	90	[1] AUBERT,B	06T	BABR	Repl. by AUBERT 09H
< 6.0	90	[1] AUBERT	05O	BABR	Repl. by AUBERT,B 06T
<23	90	[1] BERGFELD	98	CLE2	

[1] Assumes equal production of B^+ and B^0 at the $\Upsilon(4S)$.

$\Gamma(\omega(K\pi)_0^{*0})/\Gamma_{total}$ Γ_{277}/Γ

$(K\pi)_0^{*0}$ is the total S-wave composed of $K_0^*(1430)$ and nonresonant that are described using LASS shape.

VALUE (units 10^{-6})	DOCUMENT ID		TECN	COMMENT
$18.4 \pm 1.8 \pm 1.7$	[1] AUBERT	09H	BABR	$e^+e^- \to \Upsilon(4S)$

[1] Assumes equal production of B^+ and B^0 at the $\Upsilon(4S)$.

See key on page 885

$\Gamma(\omega K_0^*(1430)^0)/\Gamma_{total}$ Γ_{278}/Γ

VALUE (units 10^{-6})	DOCUMENT ID		TECN	COMMENT
16.0±1.6±3.0	[1] AUBERT	09H	BABR	$e^+e^- \to \Upsilon(4S)$

[1] Assumes equal production of B^+ and B^0 at the $\Upsilon(4S)$.

$\Gamma(\omega K_2^*(1430)^0)/\Gamma_{total}$ Γ_{279}/Γ

VALUE (units 10^{-6})	DOCUMENT ID		TECN	COMMENT
10.1±2.0±1.1	[1] AUBERT	09H	BABR	$e^+e^- \to \Upsilon(4S)$

[1] Assumes equal production of B^+ and B^0 at the $\Upsilon(4S)$.

$\Gamma(\omega K^+\pi^-$ nonresonant$)/\Gamma_{total}$ Γ_{280}/Γ

VALUE (units 10^{-6})	DOCUMENT ID		TECN	COMMENT
5.1±0.7±0.7	[1,2] GOLDENZWE..08		BELL	$e^+e^- \to \Upsilon(4S)$

[1] Assumes equal production of B^+ and B^0 at the $\Upsilon(4S)$.
[2] For the $K\pi$ mass range 0.755–1.250 GeV/c^2, excluding $K^*(892)$.

$\Gamma(K^+\pi^-\pi^0)/\Gamma_{total}$ Γ_{281}/Γ

VALUE (units 10^{-6})	CL%	DOCUMENT ID		TECN	COMMENT
37.8±3.2 OUR AVERAGE					
$38.5 \pm 1.0 \pm 3.9$		[1,2] LEES	11	BABR	$e^+e^- \to \Upsilon(4S)$
$36.6^{+4.2}_{-4.3} \pm 3.0$		[1] CHANG	04	BELL	$e^+e^- \to \Upsilon(4S)$
• • • We do not use the following data for averages, fits, limits, etc. • • •					
$35.7^{+2.6}_{-1.5} \pm 2.2$		[1] AUBERT	08AQ	BABR	Repl. by LEES 11
<40	90	[1] ECKHART	02	CLE2	$e^+e^- \to \Upsilon(4S)$

[1] Assumes equal production of B^+ and B^0 at the $\Upsilon(4S)$.
[2] Uses Dalitz plot analysis of $B^0 \to K^+\pi^-\pi^0$ decays.

$\Gamma(K^+\rho^-)/\Gamma_{total}$ Γ_{282}/Γ

VALUE (units 10^{-6})	CL%	DOCUMENT ID		TECN	COMMENT
7.0±0.9 OUR AVERAGE					
$6.6 \pm 0.5 \pm 0.8$		[1,2] LEES	11	BABR	$e^+e^- \to \Upsilon(4S)$
$15.1^{+3.4}_{-3.3} {}^{+2.4}_{-2.6}$		[1] CHANG	04	BELL	$e^+e^- \to \Upsilon(4S)$
• • • We do not use the following data for averages, fits, limits, etc. • • •					
$8.0^{+0.8}_{-1.3} \pm 0.6$		[1] AUBERT	08AQ	BABR	Repl. by LEES 11
$7.3^{+1.3}_{-1.2} \pm 1.3$		[1] AUBERT	03T	BABR	Repl. by AUBERT 08AQ
<32	90	[1] JESSOP	00	CLE2	$e^+e^- \to \Upsilon(4S)$
<35	90	ASNER	96	CLE2	Repl. by JESSOP 00

[1] Assumes equal production of B^+ and B^0 at the $\Upsilon(4S)$.
[2] Uses Dalitz plot analysis of $B^0 \to K^+\pi^-\pi^0$ decays.

$\Gamma(K^+\rho(1450)^-)/\Gamma_{total}$ Γ_{283}/Γ

VALUE (units 10^{-6})	CL%	DOCUMENT ID		TECN	COMMENT
2.4±1.0±0.6		[1,2] LEES	11	BABR	$e^+e^- \to \Upsilon(4S)$
• • • We do not use the following data for averages, fits, limits, etc. • • •					
<2.1	90	[1] AUBERT	08AQ	BABR	Repl. by LEES 11

[1] Assumes equal production of B^+ and B^0 at the $\Upsilon(4S)$.
[2] Uses Dalitz plot analysis of $B^0 \to K^+\pi^-\pi^0$ decays.

$\Gamma(K^+\rho(1700)^-)/\Gamma_{total}$ Γ_{284}/Γ

VALUE (units 10^{-6})	CL%	DOCUMENT ID		TECN	COMMENT
0.6±0.6±0.4		[1,2] LEES	11	BABR	$e^+e^- \to \Upsilon(4S)$
• • • We do not use the following data for averages, fits, limits, etc. • • •					
<1.1	90	[1] AUBERT	08AQ	BABR	Repl. by LEES 11

[1] Assumes equal production of B^+ and B^0 at the $\Upsilon(4S)$.
[2] Uses Dalitz plot analysis of $B^0 \to K^+\pi^-\pi^0$ decays.

$\Gamma((K^+\pi^-\pi^0)$ non-resonant$)/\Gamma_{total}$ Γ_{285}/Γ

VALUE (units 10^{-6})	CL%	DOCUMENT ID		TECN	COMMENT
2.8±0.5±0.4		[1,2] LEES	11	BABR	$e^+e^- \to \Upsilon(4S)$
• • • We do not use the following data for averages, fits, limits, etc. • • •					
$4.4 \pm 0.9 \pm 0.5$		[1] AUBERT	08AQ	BABR	Repl. by LEES 11
<9.4	90	[1] CHANG	04	BELL	$e^+e^- \to \Upsilon(4S)$

[1] Assumes equal production of B^+ and B^0 at the $\Upsilon(4S)$.
[2] Uses Dalitz plot analysis of $B^0 \to K^+\pi^-\pi^0$ decays. The quoted value is only for the flat part of the non-resonant component.

$\Gamma((K\pi)_0^{*+}\pi^-,\ (K\pi)_0^{*+} \to K^+\pi^0)/\Gamma_{total}$ Γ_{286}/Γ

$(K\pi)_0^{*+}$ is the total S-wave composed of $K_0^*(1430)$ and nonresonant that are described using LASS shape.

VALUE (units 10^{-6})	DOCUMENT ID		TECN	COMMENT
34.2±2.4±4.1	[1,2] LEES	11	BABR	$e^+e^- \to \Upsilon(4S)$
• • • We do not use the following data for averages, fits, limits, etc. • • •				
$9.4^{+1.1}_{-1.3} {}^{+2.3}_{-2.1}$	[1] AUBERT	08AQ	BABR	Repl. by LEES 11

[1] Assumes equal production of B^+ and B^0 at the $\Upsilon(4S)$.
[2] Uses Dalitz plot analysis of $B^0 \to K^+\pi^-\pi^0$ decays.

$\Gamma((K\pi)_0^{*0}\pi^0,\ (K\pi)_0^{*0} \to K^+\pi^-)/\Gamma_{total}$ Γ_{287}/Γ

$(K\pi)_0^{*0}$ is the total S-wave composed of $K_0^*(1430)$ and nonresonant that are described using LASS shape.

VALUE (units 10^{-6})	DOCUMENT ID		TECN	COMMENT
8.6±1.1±1.3	[1,2] LEES	11	BABR	$e^+e^- \to \Upsilon(4S)$
• • • We do not use the following data for averages, fits, limits, etc. • • •				
$8.7^{+1.1}_{-0.9} {}^{+2.8}_{-2.6}$	[1] AUBERT	08AQ	BABR	Repl. by LEES 11

[1] Assumes equal production of B^+ and B^0 at the $\Upsilon(4S)$.
[2] Uses Dalitz plot analysis of $B^0 \to K^+\pi^-\pi^0$ decays.

$\Gamma(K_2^*(1430)^0\pi^0)/\Gamma_{total}$ Γ_{288}/Γ

VALUE (units 10^{-6})	CL%	DOCUMENT ID		TECN	COMMENT
<4.0	90	[1] AUBERT	08AQ	BABR	$e^+e^- \to \Upsilon(4S)$

[1] Assumes equal production of B^+ and B^0 at the $\Upsilon(4S)$.

$\Gamma(K^*(1680)^0\pi^0)/\Gamma_{total}$ Γ_{289}/Γ

VALUE (units 10^{-6})	CL%	DOCUMENT ID		TECN	COMMENT
<7.5	90	[1] AUBERT	08AQ	BABR	$e^+e^- \to \Upsilon(4S)$

[1] Assumes equal production of B^+ and B^0 at the $\Upsilon(4S)$.

$\Gamma(K_X^{*0}\pi^0)/\Gamma_{total}$ Γ_{290}/Γ

K_X^{*0} stands for the possible candidates of $K^*(1410)$, $K_0^*(1430)$ and $K_2^*(1430)$.

VALUE (units 10^{-6})	DOCUMENT ID		TECN	COMMENT
6.1$^{+1.6}_{-1.5}$ $^{+0.5}_{-0.6}$	[1] CHANG	04	BELL	$e^+e^- \to \Upsilon(4S)$

[1] Assumes equal production of B^+ and B^0 at the $\Upsilon(4S)$.

$\Gamma(K^0\pi^+\pi^-)/\Gamma_{total}$ Γ_{291}/Γ

VALUE (units 10^{-6})	CL%	DOCUMENT ID		TECN	COMMENT
49.4± 1.8 OUR FIT					
49.6± 2.0 OUR AVERAGE					
$50.2 \pm 1.5 \pm 1.8$		[1] AUBERT	09AU	BABR	$e^+e^- \to \Upsilon(4S)$
$47.5 \pm 2.4 \pm 3.7$		[2] GARMASH	07	BELL	$e^+e^- \to \Upsilon(4S)$
$50\ ^{+10}_{-9}\ \pm 7$		[1] ECKHART	02	CLE2	$e^+e^- \to \Upsilon(4S)$
• • • We do not use the following data for averages, fits, limits, etc. • • •					
$43.0 \pm 2.3 \pm 2.3$		[1] AUBERT	06I	BABR	Repl. by AUBERT 09AU
$43.7 \pm 3.8 \pm 3.4$		[1] AUBERT,B	04O	BABR	Repl. by AUBERT 06I
$45.4 \pm 5.2 \pm 5.9$		[1] GARMASH	04	BELL	Repl. by GARMASH 07
<440	90	ALBRECHT	91E	ARG	$e^+e^- \to \Upsilon(4S)$

[1] Assumes equal production of B^+ and B^0 at the $\Upsilon(4S)$.
[2] Uses Dalitz plot analysis of the $B^0 \to K^0\pi^+\pi^-$ final state decays.

$\Gamma(K^0\pi^+\pi^-$ non-resonant$)/\Gamma_{total}$ Γ_{292}/Γ

VALUE (units 10^{-6})	DOCUMENT ID		TECN	COMMENT
14.7$^{+4.0}_{-2.6}$ OUR AVERAGE Error includes scale factor of 2.1.				
$11.1^{+2.5}_{-1.0} \pm 0.9$	[1] AUBERT	09AU	BABR	$e^+e^- \to \Upsilon(4S)$
$19.9 \pm 2.5^{+1.7}_{-2.0}$	[2] GARMASH	07	BELL	$e^+e^- \to \Upsilon(4S)$

[1] Assumes equal production of B^+ and B^0 at the $\Upsilon(4S)$.
[2] Uses Dalitz plot analysis of the $B^0 \to K^0\pi^+\pi^-$ final state decays.

$\Gamma(K^0\rho^0)/\Gamma_{total}$ Γ_{293}/Γ

VALUE (units 10^{-6})	CL%	DOCUMENT ID		TECN	COMMENT
4.7±0.6 OUR AVERAGE					
$4.4^{+0.7}_{-0.6} \pm 0.3$		[1] AUBERT	09AU	BABR	$e^+e^- \to \Upsilon(4S)$
$6.1 \pm 1.0^{+1.1}_{-1.2}$		[2] GARMASH	07	BELL	$e^+e^- \to \Upsilon(4S)$
• • • We do not use the following data for averages, fits, limits, etc. • • •					
$4.9 \pm 0.8 \pm 0.9$		[1] AUBERT	07F	BABR	Repl. by AUBERT 09AU
<39	90	ASNER	96	CLEO	$e^+e^- \to \Upsilon(4S)$
<320	90	ALBRECHT	91B	ARG	$e^+e^- \to \Upsilon(4S)$
<500	90	[3] AVERY	89B	CLEO	$e^+e^- \to \Upsilon(4S)$
<64000	90	[4] AVERY	87	CLEO	$e^+e^- \to \Upsilon(4S)$

[1] Assumes equal production of B^+ and B^0 at the $\Upsilon(4S)$.
[2] Uses Dalitz plot analysis of the $B^0 \to K^0\pi^+\pi^-$ final state decays.
[3] AVERY 89B reports $< 5.8 \times 10^{-4}$ assuming the $\Upsilon(4S)$ decays 43% to $B^0\overline{B}{}^0$. We rescale to 50%.
[4] AVERY 87 reports < 0.08 assuming the $\Upsilon(4S)$ decays 40% to $B^0\overline{B}{}^0$. We rescale to 50%.

$\Gamma(K^*(892)^+\pi^-)/\Gamma_{total}$ Γ_{294}/Γ

VALUE (units 10^{-6})	CL%	DOCUMENT ID		TECN	COMMENT
8.4±0.8 OUR AVERAGE					
$8.0 \pm 1.1 \pm 0.8$		[1,2] LEES	11	BABR	$e^+e^- \to \Upsilon(4S)$
$8.3^{+0.9}_{-0.8} \pm 0.8$		[2,3] AUBERT	09AU	BABR	$e^+e^- \to \Upsilon(4S)$
$8.4 \pm 1.1^{+1.0}_{-0.9}$		[3] GARMASH	07	BELL	$e^+e^- \to \Upsilon(4S)$
$16\ ^{+6}_{-5}\ \pm 2$		[2] ECKHART	02	CLE2	$e^+e^- \to \Upsilon(4S)$

• • • We do not use the following data for averages, fits, limits, etc. • • •

$12.6^{+2.7}_{-1.6}\pm0.9$		[1,2] AUBERT	08AQ	BABR	Repl. by LEES 11	
$11.0\pm1.5\pm0.71$		[2] AUBERT	06I	BABR	Repl. by AUBERT 09AU	
$12.9\pm2.4\pm1.4$		[2] AUBERT,B	04O	BABR	Repl. by AUBERT 06I	
$14.8^{+4.6+2.8}_{-4.4-1.3}$		[2] CHANG	04	BELL	Repl. by GARMASH 07	
<72	90	ASNER	96	CLE2	$e^+e^-\to\Upsilon(4S)$	
<620	90	ALBRECHT	91B	ARG	$e^+e^-\to\Upsilon(4S)$	
<380	90	[4] AVERY	89B	CLEO	$e^+e^-\to\Upsilon(4S)$	
<560	90	[5] AVERY	87	CLEO	$e^+e^-\to\Upsilon(4S)$	

[1] Uses Dalitz plot analysis of $B^0\to K^+\pi^-\pi^0$ decays.
[2] Assumes equal production of B^+ and B^0 at the $\Upsilon(4S)$.
[3] Uses Dalitz plot analysis of the $B^0\to K^0\pi^+\pi^-$ final state decays.
[4] AVERY 89B reports $<4.4\times10^{-4}$ assuming the $\Upsilon(4S)$ decays 43% to $B^0\overline{B}^0$. We rescale to 50%.
[5] AVERY 87 reports $<7\times10^{-4}$ assuming the $\Upsilon(4S)$ decays 40% to $B^0\overline{B}^0$. We rescale to 50%.

$\Gamma(K_0^*(1430)^+\pi^-)/\Gamma_{\text{total}}$ Γ_{295}/Γ

VALUE (units 10^{-6})		DOCUMENT ID		TECN	COMMENT
33 ±7 OUR AVERAGE	Error includes scale factor of 2.0.				
$29.9^{+2.3}_{-1.7}\pm3.6$		[1,2] AUBERT	09AU	BABR	$e^+e^-\to\Upsilon(4S)$
$49.7\pm3.8^{+6.8}_{-8.2}$		[2] GARMASH	07	BELL	$e^+e^-\to\Upsilon(4S)$

[1] Assumes equal production of B^+ and B^0 at the $\Upsilon(4S)$.
[2] Uses Dalitz plot analysis of the $B^0\to K^0\pi^+\pi^-$ final state decays.

$\Gamma(K_x^{*+}\pi^-)/\Gamma_{\text{total}}$ Γ_{296}/Γ

K_x^{*+} stands for the possible candidates of $K^*(1410)$, $K_0^*(1430)$ and $K_2^*(1430)$.

VALUE (units 10^{-6})	DOCUMENT ID		TECN	COMMENT
$\mathbf{5.1\pm1.5^{+0.6}_{-0.7}}$	[1] CHANG	04	BELL	$e^+e^-\to\Upsilon(4S)$

[1] Assumes equal production of B^+ and B^0 at the $\Upsilon(4S)$.

$\Gamma(K^*(1410)^+\pi^-,\ K^{*+}\to K^0\pi^+)/\Gamma_{\text{total}}$ Γ_{297}/Γ

VALUE (units 10^{-6})	CL%	DOCUMENT ID		TECN	COMMENT
<3.8	90	[1] GARMASH	07	BELL	$e^+e^-\to\Upsilon(4S)$

[1] Uses Dalitz plot analysis of the $B^0\to K^0\pi^+\pi^-$ final state decays.

$\Gamma(f_0(980)K^0,\ f_0\to\pi^+\pi^-)/\Gamma_{\text{total}}$ Γ_{298}/Γ

VALUE (units 10^{-6})	CL%	DOCUMENT ID		TECN	COMMENT
7.0±0.9 OUR AVERAGE					
$6.9\pm0.8\pm0.6$		[1] AUBERT	09AU	BABR	$e^+e^-\to\Upsilon(4S)$
$7.6\pm1.7^{+0.9}_{-1.3}$		[2] GARMASH	07	BELL	$e^+e^-\to\Upsilon(4S)$

• • • We do not use the following data for averages, fits, limits, etc. • • •

$5.5\pm0.7\pm0.6$		[1] AUBERT	06I	BABR	Repl. by AUBERT 09AU	
<360	90	[3] AVERY	89B	CLEO	$e^+e^-\to\Upsilon(4S)$	

[1] Assumes equal production of B^+ and B^0 at the $\Upsilon(4S)$.
[2] Uses Dalitz plot analysis of the $B^0\to K^0\pi^+\pi^-$ final state decays.
[3] AVERY 89B reports $<4.2\times10^{-4}$ assuming the $\Upsilon(4S)$ decays 43% to $B^0\overline{B}^0$. We rescale to 50%.

$\Gamma(f_2(1270)K^0)/\Gamma_{\text{total}}$ Γ_{299}/Γ

VALUE (units 10^{-6})	CL%	DOCUMENT ID		TECN	COMMENT
$\mathbf{2.7^{+1.0}_{-0.8}\pm0.9}$		[1] AUBERT	09AU	BABR	$e^+e^-\to\Upsilon(4S)$

• • • We do not use the following data for averages, fits, limits, etc. • • •

<2.5	90	[2] GARMASH	07	BELL	$e^+e^-\to\Upsilon(4S)$

[1] Assumes equal production of B^+ and B^0 at the $\Upsilon(4S)$.
[2] GARMASH 07 reports $B(B^0\to f_2(1270)K^0)\times B(f_2(1270)\to\pi^+\pi^-)<1.4\times10^{-6}$ using Dalitz plot analysis. We compute $B(B^0\to f_2(1270)K^0)$ using the PDG value $B(f_2(1270)\to\pi\pi)=84.2\times10^{-2}$ and 2/3 for the $\pi^+\pi^-$ fraction.

$\Gamma(f_x(1300)K0,f_x\to\pi^+\pi^-)/\Gamma_{\text{total}}$ Γ_{300}/Γ

VALUE (units 10^{-6})	DOCUMENT ID		TECN	COMMENT
$\mathbf{1.81^{+0.55}_{-0.45}\pm0.48}$	[1] AUBERT	09AU	BABR	$e^+e^-\to\Upsilon(4S)$

[1] Assumes equal production of B^+ and B^0 at the $\Upsilon(4S)$.

$\Gamma(K^*(892)^0\pi^0)/\Gamma_{\text{total}}$ Γ_{301}/Γ

VALUE (units 10^{-6})	CL%	DOCUMENT ID		TECN	COMMENT
3.3±0.5±0.4		[1,2] LEES	11	BABR	$e^+e^-\to\Upsilon(4S)$

• • • We do not use the following data for averages, fits, limits, etc. • • •

$3.6\pm0.7\pm0.4$		[1,2] AUBERT	08AQ	BABR	Repl. by LEES 11	
<3.5	90	[2] CHANG	04	BELL	$e^+e^-\to\Upsilon(4S)$	
<3.6	90	JESSOP	00	CLE2	$e^+e^-\to\Upsilon(4S)$	
<28	90	ASNER	96	CLE2	Repl. by JESSOP 00	

[1] Uses Dalitz plot analysis of $B^0\to K^+\pi^-\pi^0$ decays.
[2] Assumes equal production of B^+ and B^0 at the $\Upsilon(4S)$.

$\Gamma(K_2^*(1430)^+\pi^-)/\Gamma_{\text{total}}$ Γ_{302}/Γ

VALUE (units 10^{-6})	CL%	DOCUMENT ID		TECN	COMMENT
< 6	90	[1] GARMASH	07	BELL	$e^+e^-\to\Upsilon(4S)$

• • • We do not use the following data for averages, fits, limits, etc. • • •

<16.2	90	[2,3] AUBERT	08AQ	BABR	$e^+e^-\to\Upsilon(4S)$	
<18	90	[3] GARMASH	04	BELL	Repl. by GARMASH 07	
<2600	90	ALBRECHT	91B	ARG	$e^+e^-\to\Upsilon(4S)$	

[1] GARMASH 07 reports $B(B^0\to K_2^*(1430)^+\pi^-)\times B(K_2^{*+}\to K^0\pi^+)<2.1\times10^{-6}$ using Dalitz plot analysis. We compute $B(B^0\to K_2^*(1430)^+\pi^-)$ using the PDG value $B(K_2^*(1430)\to K\pi)=49.9\times10^{-2}$ and 2/3 for the $K^0\pi^+$ fraction.
[2] Uses Dalitz plot analysis of $B^0\to K^+\pi^-\pi^0$ decays.
[3] Assumes equal production of B^+ and B^0 at the $\Upsilon(4S)$.

$\Gamma(K^*(1680)^+\pi^-)/\Gamma_{\text{total}}$ Γ_{303}/Γ

VALUE (units 10^{-6})	CL%	DOCUMENT ID		TECN	COMMENT
<10	90	[1] GARMASH	07	BELL	$e^+e^-\to\Upsilon(4S)$

• • • We do not use the following data for averages, fits, limits, etc. • • •

<25	90	[2,3] AUBERT	08AQ	BABR	$e^+e^-\to\Upsilon(4S)$	

[1] GARMASH 07 reports $B(B^0\to K^*(1680)^+\pi^-)\times B(K^{*+}\to K^0\pi^+)<2.6\times10^{-6}$ using Dalitz plot analysis. We compute $B(B^0\to K^*(1680)^+\pi^-)$ using the PDG value $B(K^*(1680)\to K\pi)=38.7\times10^{-2}$ and 2/3 for the $K^0\pi^+$ fraction.
[2] Uses Dalitz plot analysis of $B^0\to K^+\pi^-\pi^0$ decays.
[3] Assumes equal production of B^+ and B^0 at the $\Upsilon(4S)$.

$\Gamma(K^+\pi^-\pi^+\pi^-)/\Gamma_{\text{total}}$ Γ_{304}/Γ

VALUE	CL%	DOCUMENT ID		TECN	COMMENT
$\mathbf{<2.3\times10^{-4}}$	90	[1] ADAM	96D	DLPH	$e^+e^-\to Z$

• • • We do not use the following data for averages, fits, limits, etc. • • •

$<2.1\times10^{-4}$	90	[2] ABREU	95N	DLPH	Sup. by ADAM 96D	

[1] ADAM 96D assumes $f_{B^0}=f_{B^-}=0.39$ and $f_{B_s}=0.12$. Contributions from B^0 and B_s decays cannot be separated. Limits are given for the weighted average of the decay rates for the two neutral B mesons.
[2] Assumes a B^0, B^- production fraction of 0.39 and a B_s production fraction of 0.12. Contributions from B^0 and B_s^0 decays cannot be separated. Limits are given for the weighted average of the decay rates for the two neutral B mesons.

$\Gamma(\rho^0K^+\pi^-)/\Gamma_{\text{total}}$ Γ_{305}/Γ

VALUE (units 10^{-6})	DOCUMENT ID		TECN	COMMENT
2.8±0.5±0.5	[1,2] KYEONG	09	BELL	$e^+e^-\to\Upsilon(4S)$

[1] Assumes equal production of B^+ and B^0 at the $\Upsilon(4S)$.
[2] Required $0.75<m_{K^+\pi^-}<1.20$ GeV/c^2.

$\Gamma(f_0(980)K^+\pi^-,\ f_0\to\pi\pi)/\Gamma_{\text{total}}$ Γ_{306}/Γ

VALUE (units 10^{-6})	DOCUMENT ID		TECN	COMMENT
$\mathbf{1.4\pm0.4^{+0.3}_{-0.4}}$	[1,2] KYEONG	09	BELL	$e^+e^-\to\Upsilon(4S)$

[1] Assumes equal production of B^+ and B^0 at the $\Upsilon(4S)$.
[2] Required $0.75<m_{K^+K^-}<1.2$ GeV/c^2.

$\Gamma(K^+\pi^-\pi^+\pi^-\text{ nonresonant})/\Gamma_{\text{total}}$ Γ_{307}/Γ

VALUE	CL%	DOCUMENT ID		TECN	COMMENT
$\mathbf{<2.1\times10^{-6}}$	90	[1,2] KYEONG	09	BELL	$e^+e^-\to\Upsilon(4S)$

[1] Assumes equal production of B^+ and B^0 at the $\Upsilon(4S)$.
[2] Required $0.55<m_{\pi^+\pi^-}<1.42$ and $0.75<m_{K^+\pi^-}<1.20$ GeV/c^2.

$\Gamma(K^*(892)^0\pi^+\pi^-)/\Gamma_{\text{total}}$ Γ_{308}/Γ

VALUE (units 10^{-6})	CL%	DOCUMENT ID		TECN	COMMENT
54.5±2.9±4.3		[1] AUBERT	07AS	BABR	$e^+e^-\to\Upsilon(4S)$

• • • We do not use the following data for averages, fits, limits, etc. • • •

$4.5^{+1.1+0.9}_{-1.0-1.6}$		[1,2] KYEONG	09	BELL	$e^+e^-\to\Upsilon(4S)$
<1400	90	ALBRECHT	91E	ARG	$e^+e^-\to\Upsilon(4S)$

[1] Assumes equal production of B^+ and B^0 at the $\Upsilon(4S)$.
[2] Required $0.55<m_{\pi^+\pi^-}<1.42$ GeV/c^2.

$\Gamma(K^*(892)^0\rho^0)/\Gamma_{\text{total}}$ Γ_{309}/Γ

VALUE (units 10^{-6})	CL%	DOCUMENT ID		TECN	COMMENT
3.9±1.3 OUR AVERAGE	Error includes scale factor of 1.9.				
$5.1\pm0.6^{+0.6}_{-0.8}$		[1] LEES	12K	BABR	$e^+e^-\to\Upsilon(4S)$
$2.1^{+0.8+0.9}_{-0.7-0.5}$		[1] KYEONG	09	BELL	$e^+e^-\to\Upsilon(4S)$

• • • We do not use the following data for averages, fits, limits, etc. • • •

$5.6\pm0.9\pm1.3$		[1] AUBERT,B	06G	BABR	Repl. by LEES 12K	
<34	90	[2] GODANG	02	CLE2	$e^+e^-\to\Upsilon(4S)$	
<286	90	[3] ABE	00C	SLD	$e^+e^-\to Z$	
<460	90	ALBRECHT	91B	ARG	$e^+e^-\to\Upsilon(4S)$	
<580	90	[4] AVERY	89B	CLEO	$e^+e^-\to\Upsilon(4S)$	
<960	90	[5] AVERY	87	CLEO	$e^+e^-\to\Upsilon(4S)$	

[1] Assumes equal production of B^+ and B^0 at the $\Upsilon(4S)$.
[2] Assumes a helicity 00 configuration. For a helicity 11 configuration, the limit decreases to 2.4×10^{-5}.

[3] ABE 00C assumes B($Z \to b\overline{b}$)=(21.7 ± 0.1)% and the B fractions $f_{B^0}=f_{B^+}=(39.7^{+1.8}_{-2.2})$% and $f_{B_s}=(10.5^{+1.8}_{-2.2})$%.

[4] AVERY 89B reports $< 6.7\times10^{-4}$ assuming the $\Upsilon(4S)$ decays 43% to $B^0\overline{B}^0$. We rescale to 50%.

[5] AVERY 87 reports $< 1.2\times10^{-3}$ assuming the $\Upsilon(4S)$ decays 40% to $B^0\overline{B}^0$. We rescale to 50%.

$\Gamma(K^*(892)^0 f_0(980),\ f_0\to\pi\pi)/\Gamma_{total}$ Γ_{310}/Γ

VALUE (units 10^{-6})	CL%	DOCUMENT ID		TECN	COMMENT
$3.9^{+2.1}_{-1.8}$ OUR AVERAGE		Error includes scale factor of 3.9.			
$5.7\pm0.6\pm0.4$		[1] LEES	12K	BABR	$e^+e^-\to\Upsilon(4S)$
$1.4^{+0.6}_{-0.5}{}^{+0.6}_{-0.4}$		[1,2] KYEONG	09	BELL	$e^+e^-\to\Upsilon(4S)$
• • • We do not use the following data for averages, fits, limits, etc. • • •					
< 4.3	90	[1] AUBERT,B	06G	BABR	$e^+e^-\to\Upsilon(4S)$
<170	90	[3] AVERY	89B	CLEO	$e^+e^-\to\Upsilon(4S)$

[1] Assumes equal production of B^+ and B^0 at the $\Upsilon(4S)$.

[2] The upper limit is 2.2×10^{-6} at 90% CL.

[3] AVERY 89B reports $< 2.0\times10^{-4}$ assuming the $\Upsilon(4S)$ decays 43% to $B^0\overline{B}^0$. We rescale to 50%.

$\Gamma(K_1(1270)^+\pi^-)/\Gamma_{total}$ Γ_{311}/Γ

VALUE	CL%	DOCUMENT ID		TECN	COMMENT
$<3.0\times10^{-5}$	90	[1] AUBERT	10D	BABR	$e^+e^-\to\Upsilon(4S)$

[1] Assumes equal production of B^+ and B^0 at the $\Upsilon(4S)$.

$\Gamma(K_1(1400)^+\pi^-)/\Gamma_{total}$ Γ_{312}/Γ

VALUE	CL%	DOCUMENT ID		TECN	COMMENT
$<2.7\times10^{-5}$	90	[1] AUBERT	10D	BABR	$e^+e^-\to\Upsilon(4S)$
• • • We do not use the following data for averages, fits, limits, etc. • • •					
$<1.1\times10^{-3}$	90	ALBRECHT	91B	ARG	$e^+e^-\to\Upsilon(4S)$

[1] Assumes equal production of B^+ and B^0 at the $\Upsilon(4S)$.

$\Gamma(a_1(1260)^- K^+)/\Gamma_{total}$ Γ_{313}/Γ

VALUE (units 10^{-6})	CL%	DOCUMENT ID		TECN	COMMENT
$16.3\pm2.9\pm2.3$		[1,2] AUBERT	08F	BABR	$e^+e^-\to\Upsilon(4S)$
• • • We do not use the following data for averages, fits, limits, etc. • • •					
<230	90	[3] ADAM	96D	DLPH	$e^+e^-\to Z$
<390	90	[4] ABREU	95N	DLPH	Sup. by ADAM 96D

[1] Assumes equal production of B^+ and B^0 at the $\Upsilon(4S)$.

[2] Assumes $a_1^\pm$ decays only to 3π and B($a_1^\pm\to\pi^\pm\pi^\mp\pi^\pm$) = 0.5.

[3] ADAM 96D assumes $f_{B^0}=f_{B^-}=0.39$ and $f_{B_s}=0.12$. Contributions from B^0 and B_s decays cannot be separated. Limits are given for the weighted average of the decay rates for the two neutral B mesons.

[4] Assumes a B^0, B^- production fraction of 0.39 and a B_s production fraction of 0.12. Contributions from B^0 and B_s^0 decays cannot be separated. Limits are given for the weighted average of the decay rates for the two neutral B mesons.

$\Gamma(K^*(892)^+\rho^-)/\Gamma_{total}$ Γ_{314}/Γ

VALUE (units 10^{-6})	CL%	DOCUMENT ID		TECN	COMMENT
$10.3\pm2.3\pm1.3$		[1] LEES	12K	BABR	$e^+e^-\to\Upsilon(4S)$
• • • We do not use the following data for averages, fits, limits, etc. • • •					
<12.0	90	[1] AUBERT,B	06G	BABR	Repl. by LEES 12K

[1] Assumes equal production of B^+ and B^0 at the $\Upsilon(4S)$.

$\Gamma(K_0^*(1430)^+\rho^-)/\Gamma_{total}$ Γ_{315}/Γ

VALUE (units 10^{-6})	DOCUMENT ID		TECN	COMMENT
$28\pm10\pm6$	[1] LEES	12K	BABR	$e^+e^-\to\Upsilon(4S)$

[1] Assumes equal production of B^+ and B^0 at the $\Upsilon(4S)$.

$\Gamma(K_1(1400)^0\rho^0)/\Gamma_{total}$ Γ_{316}/Γ

VALUE	CL%	DOCUMENT ID		TECN	COMMENT
$<3.0\times10^{-3}$	90	ALBRECHT	91B	ARG	$e^+e^-\to\Upsilon(4S)$

$\Gamma(K_0^*(1430)^0\rho^0)/\Gamma_{total}$ Γ_{317}/Γ

VALUE (units 10^{-6})	DOCUMENT ID		TECN	COMMENT
$27\pm4\pm4$	[1] LEES	12K	BABR	$e^+e^-\to\Upsilon(4S)$

[1] Assumes equal production of B^+ and B^0 at the $\Upsilon(4S)$.

$\Gamma(K_0^*(1430)^0 f_0(980),\ f_0\to\pi\pi)/\Gamma_{total}$ Γ_{318}/Γ

VALUE (units 10^{-6})	DOCUMENT ID		TECN	COMMENT
$2.7\pm0.7\pm0.6$	[1] LEES	12K	BABR	$e^+e^-\to\Upsilon(4S)$

[1] Assumes equal production of B^+ and B^0 at the $\Upsilon(4S)$.

$\Gamma(K_2^*(1430)^0 f_0(980),\ f_0\to\pi\pi)/\Gamma_{total}$ Γ_{319}/Γ

VALUE (units 10^{-6})	DOCUMENT ID		TECN	COMMENT
$8.6\pm1.7\pm1.0$	[1] LEES	12K	BABR	$e^+e^-\to\Upsilon(4S)$

[1] Assumes equal production of B^+ and B^0 at the $\Upsilon(4S)$.

$\Gamma(K^+K^-)/\Gamma_{total}$ Γ_{320}/Γ

VALUE (units 10^{-8})	CL%	DOCUMENT ID		TECN	COMMENT
$7.80\pm1.27\pm0.84$		[1] AAIJ	17G	LHCB	pp at 7 and 8 TeV
• • • We do not use the following data for averages, fits, limits, etc. • • •					
$10\pm8\pm4$		[2,3] DUH	13	BELL	$e^+e^-\to\Upsilon(4S)$
$12^{+8}_{-7}\pm1$		[4] AAIJ	12AR	LHCB	Repl. by AAIJ 17G
$23\pm10\pm10$		[5] AALTONEN	12L	CDF	$p\overline{p}$ at 1.96 TeV
< 70	90	[6] AALTONEN	09C	CDF	Repl. by AALTONEN 12L
< 50	90	[3] AUBERT	07B	BABR	$e^+e^-\to\Upsilon(4S)$
< 41	90	[3] LIN	07	BELL	Repl. by DUH 13
< 180	90	[7] ABULENCIA,A	06D	CDF	Repl. by AALTONEN 09C
< 37	90	ABE	05G	BELL	Repl. by LIN 07
< 70	90	CHAO	04	BELL	$e^+e^-\to\Upsilon(4S)$
< 80	90	[3] BORNHEIM	03	CLE2	$e^+e^-\to\Upsilon(4S)$
< 60	90	[3] AUBERT	02Q	BABR	$e^+e^-\to\Upsilon(4S)$
< 90	90	[3] CASEY	02	BELL	$e^+e^-\to\Upsilon(4S)$
< 270	90	[3] ABE	01H	BELL	$e^+e^-\to\Upsilon(4S)$
< 250	90	[3] AUBERT	01E	BABR	$e^+e^-\to\Upsilon(4S)$
< 6600	90	[8] ABE	00C	SLD	$e^+e^-\to Z$
< 190	90	[3] CRONIN-HEN..	00	CLE2	$e^+e^-\to\Upsilon(4S)$
< 430	90	GODANG	98	CLE2	Repl. by CRONIN-HENNESSY 00
< 4600		[9] ADAM	96D	DLPH	$e^+e^-\to Z$
< 400	90	ASNER	96	CLE2	Repl. by GODANG 98
< 1800	90	[10] BUSKULIC	96V	ALEP	$e^+e^-\to Z$
<12000	90	[11] ABREU	95N	DLPH	Sup. by ADAM 96D
< 700	90	[3] BATTLE	93	CLE2	$e^+e^-\to\Upsilon(4S)$

[1] Supercedes results of AAIJ 12AR.

[2] DUH 13 reports also for the same data B($B^0\to K^+K^-$) $< 0.20\times10^{-6}$ at 90% CL.

[3] Assumes equal production of B^+ and B^0 at the $\Upsilon(4S)$.

[4] AAIJ 12AR reports $[\Gamma(B^0\to K^+K^-)/\Gamma_{total}]$ / $[\mathrm{B}(B_s^0\to K^+K^-)]$ / $[\Gamma(\overline{b}\to B_s^0)/\Gamma(\overline{b}\to B^0)] = 0.018^{+0.008}_{-0.007}\pm0.009$ which we multiply by our best values B($B_s^0\to K^+K^-$) = $(2.59\pm0.17)\times10^{-5}$, $\Gamma(\overline{b}\to B_s^0)/\Gamma(\overline{b}\to B^0) = 0.250\pm0.012$. Our first error is their experiment's error and our second error is the systematic error from using our best values.

[5] Reported a central value of $(0.23\pm0.10\pm0.10)\times10^{-6}$ using B($B^0\to K^+\pi^-$) = $(19.4\pm0.6)\times10^{-6}$.

[6] Obtains this result from B(K^+K^-)/B($K^+\pi^-$) = 0.020 ± 0.008 ± 0.006, assuming B($B^0\to K^+\pi^-$) = $(19.4\pm0.6)\times10^{-6}$.

[7] ABULENCIA,A 06D obtains this from $\Gamma(K^+K^-)/\Gamma(K^+\pi^-) < 0.10$ at 90% CL, assuming B($B^0\to K^+\pi^-$) = $(18.9\pm0.7)\times10^{-6}$.

[8] ABE 00C assumes B($Z\to b\overline{b}$)=(21.7 ± 0.1)% and the B fractions $f_{B^0}=f_{B^+}=(39.7^{+1.8}_{-2.2})$% and $f_{B_s}=(10.5^{+1.8}_{-2.2})$%.

[9] ADAM 96D assumes $f_{B^0}=f_{B^-}=0.39$ and $f_{B_s}=0.12$. Contributions from B^0 and B_s decays cannot be separated. Limits are given for the weighted average of the decay rates for the two neutral B mesons.

[10] BUSKULIC 96V assumes PDG 96 production fractions for B^0, B^+, B_s, b baryons.

[11] Assumes a B^0, B^- production fraction of 0.39 and a B_s production fraction of 0.12. Contributions from B^0 and B_s^0 decays cannot be separated. Limits are given for the weighted average of the decay rates for the two neutral B mesons.

$\Gamma(K^0\overline{K}^0)/\Gamma_{total}$ Γ_{321}/Γ

VALUE (units 10^{-6})	CL%	DOCUMENT ID		TECN	COMMENT
1.21 ± 0.16 OUR AVERAGE					
$1.26\pm0.19\pm0.05$		[1] DUH	13	BELL	$e^+e^-\to\Upsilon(4S)$
$1.08\pm0.28\pm0.11$		[1] AUBERT,BE	06C	BABR	$e^+e^-\to\Upsilon(4S)$
• • • We do not use the following data for averages, fits, limits, etc. • • •					
$0.87^{+0.25}_{-0.20}\pm0.09$		[1] LIN	07	BELL	Repl. by DUH 13
$0.8\ \pm0.3\ \pm0.9$		[1] ABE	05G	BELL	Repl. by LIN 07
$1.19^{+0.40}_{-0.35}\pm0.13$		[1] AUBERT,BE	05E	BABR	Repl. by AUBERT,BE 06C
< 1.8	90	[1] AUBERT	04M	BABR	$e^+e^-\to\Upsilon(4S)$
< 1.5	90	[1] CHAO	04	BELL	Repl. by ABE 05G
< 3.3	90	[1] BORNHEIM	03	CLE2	$e^+e^-\to\Upsilon(4S)$
< 4.1	90	[1] CASEY	02	BELL	$e^+e^-\to\Upsilon(4S)$
<17	90	GODANG	98	CLE2	$e^+e^-\to\Upsilon(4S)$

[1] Assumes equal production of B^+ and B^0 at the $\Upsilon(4S)$.

$\Gamma(K^0K^-\pi^+)/\Gamma_{total}$ Γ_{322}/Γ

VALUE (units 10^{-6})	CL%	DOCUMENT ID		TECN	COMMENT
6.2 ± 0.7 OUR FIT					
$6.4\pm1.0\pm0.6$		[1] DEL-AMO-SA...10E		BABR	$e^+e^-\to\Upsilon(4S)$
• • • We do not use the following data for averages, fits, limits, etc. • • •					
<18	90	[1] GARMASH	04	BELL	$e^+e^-\to\Upsilon(4S)$
<21	90	[1] ECKHART	02	CLE2	$e^+e^-\to\Upsilon(4S)$

[1] Assumes equal production of B^+ and B^0 at the $\Upsilon(4S)$.

$\Gamma(K^*(892)^\pm K^\mp)/\Gamma_{total}$ Γ_{323}/Γ

VALUE	CL%	DOCUMENT ID		TECN	COMMENT
$<0.4\times10^{-6}$	90	AAIJ	14BM	LHCB	pp at 7 TeV

$\Gamma(K^0 K^- \pi^+)/\Gamma(K^0 \pi^+ \pi^-)$ $\Gamma_{322}/\Gamma_{291}$

VALUE	DOCUMENT ID		TECN	COMMENT
0.125±0.014 OUR FIT				
0.123±0.009±0.015	AAIJ	17BP	LHCB	pp at 7, 8 TeV
• • • We do not use the following data for averages, fits, limits, etc. • • •				
0.128±0.017±0.009	AAIJ	13BP	LHCB	Repl. by AAIJ 17BP

$[\Gamma(\overline{K}^{*0} K^0) + \Gamma(K^{*0} \overline{K}^0)]/\Gamma_{\text{total}}$ Γ_{324}/Γ

VALUE (units 10^{-6})	CL%	DOCUMENT ID		TECN	COMMENT
<0.96	90	[1] AAIJ	16	LHCB	pp at 7 TeV
• • • We do not use the following data for averages, fits, limits, etc. • • •					
<1.9	90	[2] AUBERT,BE	06N	BABR	$e^+e^- \to \Upsilon(4S)$

[1] Assumes $B(B^0 \to K^0\pi^+\pi^-) = (4.96 \pm 0.20) \times 10^{-5}$.
[2] Assumes equal production of B^+ and B^0 at the $\Upsilon(4S)$.

$\Gamma(K^+ K^- \pi^0)/\Gamma_{\text{total}}$ Γ_{325}/Γ

VALUE (units 10^{-6})	CL%	DOCUMENT ID		TECN	COMMENT
2.17±0.60±0.24		[1] GAUR	13	BELL	$e^+e^- \to \Upsilon(4S)$
• • • We do not use the following data for averages, fits, limits, etc. • • •					
<19	90	[1] ECKHART	02	CLE2	$e^+e^- \to \Upsilon(4S)$

[1] Assumes equal production of B^+ and B^0 at the $\Upsilon(4S)$.

$\Gamma(K^0_S K^0_S \pi^0)/\Gamma_{\text{total}}$ Γ_{326}/Γ

VALUE	CL%	DOCUMENT ID		TECN	COMMENT
<0.9 × 10⁻⁶	90	[1] AUBERT	09AD	BABR	$e^+e^- \to \Upsilon(4S)$

[1] Assumes equal production of B^+ and B^0 at the $\Upsilon(4S)$.

$\Gamma(K^0_S K^0_S \eta)/\Gamma_{\text{total}}$ Γ_{327}/Γ

VALUE	CL%	DOCUMENT ID		TECN	COMMENT
<1.0 × 10⁻⁶	90	[1] AUBERT	09AD	BABR	$e^+e^- \to \Upsilon(4S)$

[1] Assumes equal production of B^+ and B^0 at the $\Upsilon(4S)$.

$\Gamma(K^0_S K^0_S \eta')/\Gamma_{\text{total}}$ Γ_{328}/Γ

VALUE	CL%	DOCUMENT ID		TECN	COMMENT
<2.0 × 10⁻⁶	90	[1] AUBERT	09AD	BABR	$e^+e^- \to \Upsilon(4S)$

[1] Assumes equal production of B^+ and B^0 at the $\Upsilon(4S)$.

$\Gamma(K^0 K^+ K^-)/\Gamma_{\text{total}}$ Γ_{329}/Γ

VALUE (units 10^{-6})	CL%	DOCUMENT ID		TECN	COMMENT
26.7±1.1 OUR FIT					
26.6±1.2 OUR AVERAGE					
26.5±0.9±0.8		[1,2] LEES	12O	BABR	$e^+e^- \to \Upsilon(4S)$
28.3±3.3±4.0		[1] GARMASH	04	BELL	$e^+e^- \to \Upsilon(4S)$
• • • We do not use the following data for averages, fits, limits, etc. • • •					
23.8±2.0±1.6		[1] AUBERT,B	04V	BABR	Repl. by LEES 12O
<1300	90	ALBRECHT	91E	ARG	$e^+e^- \to \Upsilon(4S)$

[1] Assumes equal production of B^+ and B^0 at the $\Upsilon(4S)$.
[2] All intermediate charmonium and charm resonances are removed, except of χ_{c0}.

$\Gamma(K^0 K^+ K^-)/\Gamma(K^0 \pi^+ \pi^-)$ $\Gamma_{329}/\Gamma_{291}$

VALUE	DOCUMENT ID		TECN	COMMENT
0.541±0.025 OUR FIT				
0.549±0.018±0.033	AAIJ	17BP	LHCB	pp at 7, 8 TeV
• • • We do not use the following data for averages, fits, limits, etc. • • •				
0.385±0.031±0.023	AAIJ	13BP	LHCB	Repl. by AAIJ 17BP

$\Gamma(K^0\phi)/\Gamma_{\text{total}}$ Γ_{330}/Γ

VALUE (units 10^{-6})	CL%	DOCUMENT ID		TECN	COMMENT
7.3±0.7 OUR AVERAGE					
$7.1 \pm 0.6 \,^{+0.4}_{-0.3}$		[1] LEES	12O	BABR	$e^+e^- \to \Upsilon(4S)$
$9.0 \,^{+2.2}_{-1.8} \pm 0.7$		[1] CHEN	03B	BELL	$e^+e^- \to \Upsilon(4S)$
• • • We do not use the following data for averages, fits, limits, etc. • • •					
$8.4 \,^{+1.5}_{-1.3} \pm 0.5$		[1] AUBERT	04A	BABR	Repl. by LEES 12O
$8.1 \,^{+3.1}_{-2.5} \pm 0.8$		[1] AUBERT	01D	BABR	$e^+e^- \to \Upsilon(4S)$
< 12.3	90	[1] BRIERE	01	CLE2	$e^+e^- \to \Upsilon(4S)$
< 31	90	[1] BERGFELD	98	CLE2	
< 88	90	ASNER	96	CLE2	$e^+e^- \to \Upsilon(4S)$
< 720	90	ALBRECHT	91B	ARG	$e^+e^- \to \Upsilon(4S)$
< 420	90	[2] AVERY	89B	CLEO	$e^+e^- \to \Upsilon(4S)$
<1000	90	[3] AVERY	87	CLEO	$e^+e^- \to \Upsilon(4S)$

[1] Assumes equal production of B^+ and B^0 at the $\Upsilon(4S)$.
[2] AVERY 89B reports $< 4.9 \times 10^{-4}$ assuming the $\Upsilon(4S)$ decays 43% to $B^0\overline{B}^0$. We rescale to 50%.
[3] AVERY 87 reports $< 1.3 \times 10^{-3}$ assuming the $\Upsilon(4S)$ decays 40% to $B^0\overline{B}^0$. We rescale to 50%.

$\Gamma(f_0(980) K^0,\ f_0 \to K^+ K^-)/\Gamma_{\text{total}}$ Γ_{331}/Γ

VALUE (units 10^{-6})	DOCUMENT ID		TECN	COMMENT
$\mathbf{7.0 \,^{+2.6}_{-1.8} \pm 2.4}$	[1] LEES	12O	BABR	$e^+e^- \to \Upsilon(4S)$

[1] Assumes equal production of B^+ and B^0 at the $\Upsilon(4S)$.

$\Gamma(f_0(1500) K^0)/\Gamma_{\text{total}}$ Γ_{332}/Γ

VALUE (units 10^{-6})	DOCUMENT ID		TECN	COMMENT
$\mathbf{13.3 \,^{+5.8}_{-4.4} \pm 3.2}$	[1] LEES	12O	BABR	$e^+e^- \to \Upsilon(4S)$

[1] Assumes equal production of B^+ and B^0 at the $\Upsilon(4S)$.

$\Gamma(f_2'(1525)^0 K^0)/\Gamma_{\text{total}}$ Γ_{333}/Γ

VALUE (units 10^{-6})	DOCUMENT ID		TECN	COMMENT
$\mathbf{0.29 \,^{+0.27}_{-0.18} \pm 0.36}$	[1] LEES	12O	BABR	$e^+e^- \to \Upsilon(4S)$

[1] Assumes equal production of B^+ and B^0 at the $\Upsilon(4S)$.

$\Gamma(f_0(1710) K^0,\ f_0 \to K^+ K^-)/\Gamma_{\text{total}}$ Γ_{334}/Γ

VALUE (units 10^{-6})	DOCUMENT ID		TECN	COMMENT
4.4±0.7±0.5	[1] LEES	12O	BABR	$e^+e^- \to \Upsilon(4S)$

[1] Assumes equal production of B^+ and B^0 at the $\Upsilon(4S)$.

$\Gamma(K^0 K^+ K^-$ nonresonant$)/\Gamma_{\text{total}}$ Γ_{335}/Γ

VALUE (units 10^{-6})	DOCUMENT ID		TECN	COMMENT
33±5±9	[1] LEES	12O	BABR	$e^+e^- \to \Upsilon(4S)$

[1] Assumes equal production of B^+ and B^0 at the $\Upsilon(4S)$.

$\Gamma(K^0_S K^0_S K^0_S)/\Gamma_{\text{total}}$ Γ_{336}/Γ

VALUE (units 10^{-6})	DOCUMENT ID		TECN	COMMENT
6.0 ±0.5 OUR AVERAGE Error includes scale factor of 1.1.				
6.19±0.48±0.19	[1] LEES	12I	BABR	$e^+e^- \to \Upsilon(4S)$
$4.2 \,^{+1.6}_{-1.3} \pm 0.8$	[1] GARMASH	04	BELL	$e^+e^- \to \Upsilon(4S)$
• • • We do not use the following data for averages, fits, limits, etc. • • •				
$6.9 \,^{+0.9}_{-0.8} \pm 0.6$	[1] AUBERT,B	05	BABR	Repl. by LEES 12I

[1] Assumes equal production of B^+ and B^0 at the $\Upsilon(4S)$.

$\Gamma(f_0(980) K^0,\ f_0 \to K^0_S K^0_S)/\Gamma_{\text{total}}$ Γ_{337}/Γ

VALUE (units 10^{-6})	DOCUMENT ID		TECN	COMMENT
$\mathbf{2.7 \,^{+1.3}_{-1.2} \pm 1.3}$	[1,2] LEES	12I	BABR	$e^+e^- \to \Upsilon(4S)$

[1] Assumes equal production of B^+ and B^0 at the $\Upsilon(4S)$.
[2] Uses Dalitz plot analysis of the $B^0 \to K^0_S K^0_S K^0_S$ decay.

$\Gamma(f_0(1710) K^0,\ f_0 \to K^0_S K^0_S)/\Gamma_{\text{total}}$ Γ_{338}/Γ

VALUE (units 10^{-6})	DOCUMENT ID		TECN	COMMENT
$\mathbf{0.50 \,^{+0.46}_{-0.24} \pm 0.11}$	[1,2] LEES	12I	BABR	$e^+e^- \to \Upsilon(4S)$

[1] Assumes equal production of B^+ and B^0 at the $\Upsilon(4S)$.
[2] Uses Dalitz plot analysis of the $B^0 \to K^0_S K^0_S K^0_S$ decay.

$\Gamma(f_2(2010) K^0,\ f_2 \to K^0_S K^0_S)/\Gamma_{\text{total}}$ Γ_{339}/Γ

VALUE (units 10^{-6})	DOCUMENT ID		TECN	COMMENT
$\mathbf{0.54 \,^{+0.21}_{-0.20} \pm 0.52}$	[1,2] LEES	12I	BABR	$e^+e^- \to \Upsilon(4S)$

[1] Assumes equal production of B^+ and B^0 at the $\Upsilon(4S)$.
[2] Uses Dalitz plot analysis of the $B^0 \to K^0_S K^0_S K^0_S$ decay.

$\Gamma(K^0_S K^0_S K^0_S$ nonresonant$)/\Gamma_{\text{total}}$ Γ_{340}/Γ

VALUE (units 10^{-6})	DOCUMENT ID		TECN	COMMENT
$\mathbf{13.3 \,^{+2.2}_{-2.3} \pm 2.2}$	[1,2] LEES	12I	BABR	$e^+e^- \to \Upsilon(4S)$

[1] Assumes equal production of B^+ and B^0 at the $\Upsilon(4S)$.
[2] Uses Dalitz plot analysis of the $B^0 \to K^0_S K^0_S K^0_S$ decay.

$\Gamma(K^0_S K^0_S K^0_L)/\Gamma_{\text{total}}$ Γ_{341}/Γ

VALUE (units 10^{-6})	CL%	DOCUMENT ID		TECN	COMMENT
<16	90	[1] AUBERT,B	06R	BABR	$e^+e^- \to \Upsilon(4S)$

[1] Assumes equal production of B^+ and B^0 at the $\Upsilon(4S)$.

$\Gamma(K^*(892)^0 K^+ K^-)/\Gamma_{\text{total}}$ Γ_{342}/Γ

VALUE (units 10^{-6})	CL%	DOCUMENT ID		TECN	COMMENT
27.5±1.3±2.2		[1] AUBERT	07AS	BABR	$e^+e^- \to \Upsilon(4S)$
• • • We do not use the following data for averages, fits, limits, etc. • • •					
<610	90	ALBRECHT	91E	ARG	$e^+e^- \to \Upsilon(4S)$

[1] Assumes equal production of B^+ and B^0 at the $\Upsilon(4S)$.

$\Gamma(K^*(892)^0\phi)/\Gamma_{\text{total}}$ Γ_{343}/Γ

VALUE (units 10^{-6})	CL%	DOCUMENT ID		TECN	COMMENT
10.0±0.5 OUR FIT					
10.0±0.5 OUR AVERAGE					
10.4±0.5±0.6		[1] PRIM	13	BELL	$e^+e^- \to \Upsilon(4S)$
9.7±0.5±0.5		[1] AUBERT	08BG	BABR	$e^+e^- \to \Upsilon(4S)$
$11.5 \,^{+4.5}_{-3.7} \,^{+1.8}_{-1.7}$		[1] BRIERE	01	CLE2	$e^+e^- \to \Upsilon(4S)$

• • • We do not use the following data for averages, fits, limits, etc. • • •

$9.2\pm0.7\pm0.6$		[1] AUBERT	07D	BABR	Repl. by AUBERT 08BG	
$9.2\pm0.9\pm0.5$		[1] AUBERT,B	04W	BABR	Repl. by AUBERT 07D	
$11.2\pm1.3\pm0.8$		[1] AUBERT	03V	BABR	Repl. by AUBERT,B 04W	
$10.0^{+1.6}_{-1.5}{}^{+0.7}_{-0.8}$		[1] CHEN	03B	BELL	Repl. by PRIM 13	
$8.7^{+2.5}_{-2.1}\pm1.1$		[1] AUBERT	01D	BABR	Repl. by AUBERT 03V	
<384	90	[2] ABE	00C	SLD	$e^+e^-\to Z$	
< 21	90	[1] BERGFELD	98	CLE2		
< 43	90	ASNER	96	CLE2	$e^+e^-\to\Upsilon(4S)$	
<320	90	ALBRECHT	91B	ARG	$e^+e^-\to\Upsilon(4S)$	
<380	90	[3] AVERY	89B	CLEO	$e^+e^-\to\Upsilon(4S)$	
<380	90	[4] AVERY	87	CLEO	$e^+e^-\to\Upsilon(4S)$	

[1] Assumes equal production of B^+ and B^0 at the $\Upsilon(4S)$.
[2] ABE 00C assumes $B(Z\to b\overline{b})=(21.7\pm0.1)\%$ and the B fractions $f_{B^0}=f_{B^+}=(39.7^{+1.8}_{-2.2})\%$ and $f_{B_s}=(10.5^{+1.8}_{-2.2})\%$.
[3] AVERY 89B reports $<4.4\times10^{-4}$ assuming the $\Upsilon(4S)$ decays 43% to $B^0\overline{B}{}^0$. We rescale to 50%.
[4] AVERY 87 reports $<4.7\times10^{-4}$ assuming the $\Upsilon(4S)$ decays 40% to $B^0\overline{B}{}^0$. We rescale to 50%.

$\Gamma(K^+K^-\pi^+\pi^-\text{ nonresonant})/\Gamma_{\text{total}}$ Γ_{344}/Γ

VALUE (units 10^{-6})	CL%	DOCUMENT ID		TECN	COMMENT
<71.7	90	[1,2] CHIANG	10	BELL	$e^+e^-\to\Upsilon(4S)$

[1] Measured in the range $0.7<m_{K\pi}<1.7$ and corrected using PS assumption for the full $K\pi$ mass range.
[2] Assumes equal production of B^+ and B^0 at the $\Upsilon(4S)$.

$\Gamma(K^*(892)^0K^-\pi^+)/\Gamma_{\text{total}}$ Γ_{345}/Γ

VALUE (units 10^{-6})		DOCUMENT ID		TECN	COMMENT
4.5 ±1.3 OUR AVERAGE					
$2.11^{+5.63}_{-5.26}{}^{+4.85}_{-4.75}$		[1,2] CHIANG	10	BELL	$e^+e^-\to\Upsilon(4S)$
4.6 ±1.1 ±0.8		[2] AUBERT	07AS	BABR	$e^+e^-\to\Upsilon(4S)$

[1] Measured in the range $0.7<m_{K\pi}<1.7$ and corrected using PS assumption for the full $K\pi$ mass range. The quoted result is equivalent to the upper limit of $<13.9\times10^{-6}$ at 90% CL.
[2] Assumes equal production of B^+ and B^0 at the $\Upsilon(4S)$.

$\Gamma(K^*(892)^0\overline{K}{}^*(892)^0)/\Gamma_{\text{total}}$ Γ_{346}/Γ

VALUE (units 10^{-6})	CL%	DOCUMENT ID		TECN	COMMENT
0.8 ±0.5 OUR AVERAGE		Error includes scale factor of 2.2.			
$0.26^{+0.33}_{-0.29}{}^{+0.10}_{-0.08}$		[1,2] CHIANG	10	BELL	$e^+e^-\to\Upsilon(4S)$
$1.28^{+0.35}_{-0.30}\pm0.11$		[2] AUBERT	08I	BABR	$e^+e^-\to\Upsilon(4S)$

• • • We do not use the following data for averages, fits, limits, etc. • • •

< 22	90	[3] GODANG	02	CLE2	$e^+e^-\to\Upsilon(4S)$	
<469	90	[4] ABE	00C	SLD	$e^+e^-\to Z$	

[1] Measured in the range $0.7<m_{K\pi}<1.7$ and corrected using PS assumption for the full $K\pi$ mass range. The quoted result is equivalent to the upper limit of $<0.8\times10^{-6}$ at 90% CL.
[2] Assumes equal production of B^+ and B^0 at the $\Upsilon(4S)$.
[3] Assumes a helicity 00 configuration. For a helicity 11 configuration, the limit decreases to 1.9×10^{-5}.
[4] ABE 00C assumes $B(Z\to b\overline{b})=(21.7\pm0.1)\%$ and the B fractions $f_{B^0}=f_{B^+}=(39.7^{+1.8}_{-2.2})\%$ and $f_{B_s}=(10.5^{+1.8}_{-2.2})\%$.

$\Gamma(K^+K^+\pi^-\pi^-\text{ nonresonant})/\Gamma_{\text{total}}$ Γ_{347}/Γ

VALUE (units 10^{-6})	CL%	DOCUMENT ID		TECN	COMMENT
<6.0	90	[1] CHIANG	10	BELL	$e^+e^-\to\Upsilon(4S)$

[1] Assumes equal production of B^+ and B^0 at the $\Upsilon(4S)$.

$\Gamma(K^*(892)^0K^+\pi^-)/\Gamma_{\text{total}}$ Γ_{348}/Γ

VALUE (units 10^{-6})	CL%	DOCUMENT ID		TECN	COMMENT
<2.2	90	[1] AUBERT	07AS	BABR	$e^+e^-\to\Upsilon(4S)$

• • • We do not use the following data for averages, fits, limits, etc. • • •

<7.6	90	[1] CHIANG	10	BELL	$e^+e^-\to\Upsilon(4S)$	

[1] Assumes equal production of B^+ and B^0 at the $\Upsilon(4S)$.

$\Gamma(K^*(892)^0K^*(892)^0)/\Gamma_{\text{total}}$ Γ_{349}/Γ

VALUE (units 10^{-6})	CL%	DOCUMENT ID		TECN	COMMENT
< 0.2	90	[1] CHIANG	10	BELL	$e^+e^-\to\Upsilon(4S)$

• • • We do not use the following data for averages, fits, limits, etc. • • •

< 0.41	90	[1] AUBERT	08I	BABR	$e^+e^-\to\Upsilon(4S)$	
<37	90	[2] GODANG	02	CLE2	$e^+e^-\to\Upsilon(4S)$	

[1] Assumes equal production of B^+ and B^0 at the $\Upsilon(4S)$.
[2] Assumes a helicity 00 configuration. For a helicity 11 configuration, the limit decreases to 2.9×10^{-5}.

$\Gamma(K^*(892)^+K^*(892)^-)/\Gamma_{\text{total}}$ Γ_{350}/Γ

VALUE (units 10^{-6})	CL%	DOCUMENT ID		TECN	COMMENT
< 2.0	90	[1] AUBERT	08AP	BABR	$e^+e^-\to\Upsilon(4S)$

• • • We do not use the following data for averages, fits, limits, etc. • • •

<141	90	[2] GODANG	02	CLE2	$e^+e^-\to\Upsilon(4S)$	

[1] Assumes equal production of B^+ and B^0 at the $\Upsilon(4S)$.
[2] Assumes a helicity 00 configuration. For a helicity 11 configuration, the limit decreases to 8.9×10^{-5}.

$\Gamma(K_1(1400)^0\phi)/\Gamma_{\text{total}}$ Γ_{351}/Γ

VALUE	CL%	DOCUMENT ID		TECN	COMMENT
<5.0 × 10⁻³	90	ALBRECHT	91B	ARG	$e^+e^-\to\Upsilon(4S)$

$\Gamma(\phi(K\pi)_0^{*0})/\Gamma_{\text{total}}$ Γ_{352}/Γ

This decay refers to the coherent sum of resonant and nonresonant $J^P=0^+$ $K\pi$ components with $1.13<m_{K\pi}<1.53$ GeV/c^2.

VALUE (units 10^{-6})		DOCUMENT ID		TECN	COMMENT
4.3±0.4 OUR AVERAGE					
$4.3\pm0.4\pm0.4$		[1] PRIM	13	BELL	$e^+e^-\to\Upsilon(4S)$
$4.3\pm0.6\pm0.4$		[1] AUBERT	08BG	BABR	$e^+e^-\to\Upsilon(4S)$

• • • We do not use the following data for averages, fits, limits, etc. • • •

$5.0\pm0.8\pm0.3$		[1] AUBERT	07D	BABR	Repl. by AUBERT 08BG	

[1] Assumes equal production of B^+ and B^0 at the $\Upsilon(4S)$.

$\Gamma(\phi(K\pi)_0^{*0}(1.60<m_{K\pi}<2.15))/\Gamma_{\text{total}}$ Γ_{353}/Γ

This decay refers to the coherent sum of resonant and nonresonant $J^P=0^+$ $K\pi$ components with $1.60<m_{K\pi}<2.15$ GeV/c^2.

VALUE (units 10^{-6})	CL%	DOCUMENT ID		TECN	COMMENT
<1.7	90	[1] AUBERT	07AO	BABR	$e^+e^-\to\Upsilon(4S)$

[1] Assumes equal production of B^+ and B^0 at the $\Upsilon(4S)$.

$\Gamma(K_0^*(1430)^0K^-\pi^+)/\Gamma_{\text{total}}$ Γ_{354}/Γ

VALUE (units 10^{-6})	CL%	DOCUMENT ID		TECN	COMMENT
<31.8	90	[1,2] CHIANG	10	BELL	$e^+e^-\to\Upsilon(4S)$

[1] Measured in the range $0.7<m_{K\pi}<1.7$ and corrected using PS assumption for the full $K\pi$ mass range.
[2] Assumes equal production of B^+ and B^0 at the $\Upsilon(4S)$.

$\Gamma(K_0^*(1430)^0\overline{K}{}^*(892)^0)/\Gamma_{\text{total}}$ Γ_{355}/Γ

VALUE (units 10^{-6})	CL%	DOCUMENT ID		TECN	COMMENT
<3.3	90	[1,2] CHIANG	10	BELL	$e^+e^-\to\Upsilon(4S)$

[1] Measured in the range $0.7<m_{K\pi}<1.7$ and corrected using PS assumption for the full $K\pi$ mass range.
[2] Assumes equal production of B^+ and B^0 at the $\Upsilon(4S)$.

$\Gamma(K_0^*(1430)^0\overline{K}{}_0^*(1430)^0)/\Gamma_{\text{total}}$ Γ_{356}/Γ

VALUE (units 10^{-6})	CL%	DOCUMENT ID		TECN	COMMENT
<8.4	90	[1,2] CHIANG	10	BELL	$e^+e^-\to\Upsilon(4S)$

[1] Measured in the range $0.7<m_{K\pi}<1.7$ and corrected using PS assumption for the full $K\pi$ mass range.
[2] Assumes equal production of B^+ and B^0 at the $\Upsilon(4S)$.

$\Gamma(K_0^*(1430)^0\phi)/\Gamma_{\text{total}}$ Γ_{357}/Γ

VALUE (units 10^{-6})		DOCUMENT ID		TECN	COMMENT
3.9±0.5±0.6		[1] AUBERT	08BG	BABR	$e^+e^-\to\Upsilon(4S)$

• • • We do not use the following data for averages, fits, limits, etc. • • •

$4.6\pm0.7\pm0.6$		[1] AUBERT	07D	BABR	Repl. by AUBERT 08BG	
seen		[2] AUBERT,B	04W	BABR	Repl. by AUBERT 07D	

[1] Assumes equal production of B^+ and B^0 at the $\Upsilon(4S)$.
[2] Observed 181 ± 17 events with statistical significance greater than 10 σ.

$\Gamma(K_0^*(1430)^0K^*(892)^0)/\Gamma_{\text{total}}$ Γ_{358}/Γ

VALUE (units 10^{-6})	CL%	DOCUMENT ID		TECN	COMMENT
<1.7	90	[1] CHIANG	10	BELL	$e^+e^-\to\Upsilon(4S)$

[1] Assumes equal production of B^+ and B^0 at the $\Upsilon(4S)$.

$\Gamma(K_0^*(1430)^0K_0^*(1430)^0)/\Gamma_{\text{total}}$ Γ_{359}/Γ

VALUE (units 10^{-6})	CL%	DOCUMENT ID		TECN	COMMENT
<4.7	90	[1] CHIANG	10	BELL	$e^+e^-\to\Upsilon(4S)$

[1] Assumes equal production of B^+ and B^0 at the $\Upsilon(4S)$.

$\Gamma(K^*(1680)^0\phi)/\Gamma_{\text{total}}$ Γ_{360}/Γ

VALUE (units 10^{-6})	CL%	DOCUMENT ID		TECN	COMMENT
<3.5	90	[1] AUBERT	07AO	BABR	$e^+e^-\to\Upsilon(4S)$

[1] Assumes equal production of B^+ and B^0 at the $\Upsilon(4S)$.

$\Gamma(K^*(1780)^0\phi)/\Gamma_{\text{total}}$ Γ_{361}/Γ

VALUE (units 10^{-6})	CL%	DOCUMENT ID		TECN	COMMENT
<2.7	90	[1] AUBERT	07AO	BABR	$e^+e^-\to\Upsilon(4S)$

[1] Assumes equal production of B^+ and B^0 at the $\Upsilon(4S)$.

$\Gamma(K^*(2045)^0\phi)/\Gamma_{total}$ Γ_{362}/Γ

VALUE (units 10^{-6})	CL%	DOCUMENT ID		TECN	COMMENT
<15.3	90	[1] AUBERT	07AO	BABR	$e^+e^- \to \Upsilon(4S)$

[1] Assumes equal production of B^+ and B^0 at the $\Upsilon(4S)$.

$\Gamma(K_2^*(1430)^0\rho^0)/\Gamma_{total}$ Γ_{363}/Γ

VALUE (units 10^{-6})	CL%	DOCUMENT ID		TECN	COMMENT
<1.1 × 10³	90	ALBRECHT	91B	ARG	$e^+e^- \to \Upsilon(4S)$

$\Gamma(K_2^*(1430)^0\phi)/\Gamma_{total}$ Γ_{364}/Γ

VALUE (units 10^{-6})	CL%	DOCUMENT ID		TECN	COMMENT
6.8±0.9 OUR AVERAGE		Error includes scale factor of 1.2.			
$5.5^{+0.9}_{-0.7}\pm1.0$		[1] PRIM	13	BELL	$e^+e^- \to \Upsilon(4S)$
7.5±0.9±0.5		[1] AUBERT	08BG	BABR	$e^+e^- \to \Upsilon(4S)$
• • • We do not use the following data for averages, fits, limits, etc. • • •					
7.8±1.1±0.6		[1] AUBERT	07D	BABR	Repl. by AUBERT 08BG
seen		[2] AUBERT,B	04W	BABR	Repl. by AUBERT 07D
<1400	90	ALBRECHT	91B	ARG	$e^+e^- \to \Upsilon(4S)$

[1] Assumes equal production of B^+ and B^0 at the $\Upsilon(4S)$.
[2] The angular distribution of $B \to \phi K^*(1430)$ provides evidence with statistical significance of 3.2 σ.

$\Gamma(K^0\phi\phi)/\Gamma_{total}$ Γ_{365}/Γ

VALUE (units 10^{-6})	DOCUMENT ID		TECN	COMMENT
4.5±0.8±0.3	[1] LEES	11A	BABR	$e^+e^- \to \Upsilon(4S)$
• • • We do not use the following data for averages, fits, limits, etc. • • •				
$4.1^{+1.7}_{-1.4}\pm0.4$	[1] AUBERT,BE	06H	BABR	Repl. by LEES 11A

[1] Assumes equal production of B^0 and B^+ at the $\Upsilon(4S)$ and for a $\phi\phi$ invariant mass below 2.85 GeV/c^2.

$\Gamma(\eta'\eta' K^0)/\Gamma_{total}$ Γ_{366}/Γ

VALUE (units 10^{-6})	CL%	DOCUMENT ID		TECN	COMMENT
<31	90	[1] AUBERT,B	06P	BABR	$e^+e^- \to \Upsilon(4S)$

[1] Assumes equal production of B^+ and B^0 at the $\Upsilon(4S)$.

$\Gamma(\eta K^0\gamma)/\Gamma_{total}$ Γ_{367}/Γ

VALUE (units 10^{-6})	DOCUMENT ID		TECN	COMMENT
7.6±1.8 OUR AVERAGE				
$7.1^{+2.1}_{-2.0}\pm0.4$	[1,2] AUBERT	09	BABR	$e^+e^- \to \Upsilon(4S)$
$8.7^{+3.1}_{-2.7}{}^{+1.9}_{-1.6}$	[2,3] NISHIDA	05	BELL	$e^+e^- \to \Upsilon(4S)$
• • • We do not use the following data for averages, fits, limits, etc. • • •				
$11.3^{+2.8}_{-1.6}\pm0.6$	[1,2] AUBERT,B	06M	BABR	Repl. by AUBERT 09

[1] $m_{\eta K} < 3.25$ GeV/c^2.
[2] Assumes equal production of B^+ and B^0 at the $\Upsilon(4S)$.
[3] $m_{\eta K} < 2.4$ GeV/c^2

$\Gamma(\eta' K^0\gamma)/\Gamma_{total}$ Γ_{368}/Γ

VALUE (units 10^{-6})	CL%	DOCUMENT ID		TECN	COMMENT
<6.4	90	[1,2] WEDD	10	BELL	$e^+e^- \to \Upsilon(4S)$
• • • We do not use the following data for averages, fits, limits, etc. • • •					
<6.6	90	[1,3] AUBERT,B	06M	BABR	$e^+e^- \to \Upsilon(4S)$

[1] Assumes equal production of B^+ and B^0 at the $\Upsilon(4S)$.
[2] $m_{\eta' K} < 3.4$ GeV/c^2.
[3] $m_{\eta' K} < 3.25$ GeV/c^2.

$\Gamma(K^0\phi\gamma)/\Gamma_{total}$ Γ_{369}/Γ

VALUE (units 10^{-6})	CL%	DOCUMENT ID		TECN	COMMENT
2.74±0.60±0.32		[1] SAHOO	11A	BELL	$e^+e^- \to \Upsilon(4S)$
• • • We do not use the following data for averages, fits, limits, etc. • • •					
<2.7	90	[1] AUBERT	07Q	BABR	$e^+e^- \to \Upsilon(4S)$
<8.3	90	[1] DRUTSKOY	04	BELL	$e^+e^- \to \Upsilon(4S)$

[1] Assumes equal production of B^+ and B^0 at $\Upsilon(4S)$.

$\Gamma(K^+\pi^-\gamma)/\Gamma_{total}$ Γ_{370}/Γ

VALUE	DOCUMENT ID		TECN	COMMENT
$(4.6^{+1.3}_{-1.2}{}^{+0.5}_{-0.7})\times10^{-6}$	[1,2] NISHIDA	02	BELL	$e^+e^- \to \Upsilon(4S)$

[1] Assumes equal production of B^+ and B^0 at the $\Upsilon(4S)$.
[2] 1.25 GeV/c^2 $< M_{K\pi} <$ 1.6 GeV/c^2

$\Gamma(K^*(892)^0\gamma)/\Gamma_{total}$ Γ_{371}/Γ

VALUE (units 10^{-6})	CL%	DOCUMENT ID		TECN	COMMENT
41.8± 2.5 OUR AVERAGE		Error includes scale factor of 2.1.			
39.6± 0.7±1.4		[1] HORIGUCHI	17	BELL	$e^+e^- \to \Upsilon(4S)$
44.7± 1.0±1.6		[2] AUBERT	09AO	BABR	$e^+e^- \to \Upsilon(4S)$
$45.5^{+7.2}_{-6.8}\pm3.4$		[3] COAN	00	CLE2	$e^+e^- \to \Upsilon(4S)$
• • • We do not use the following data for averages, fits, limits, etc. • • •					
39.2± 2.0±2.4		[4] AUBERT,BE	04A	BABR	Repl. by AUBERT 09AO
40.1± 2.1±1.7		[5] NAKAO	04	BELL	Repl. by HORIGUCHI 17
< 110	90	ACOSTA	02G	CDF	$p\overline{p}$ at 1.8 TeV
42.3± 4.0±2.2		[5] AUBERT	02C	BABR	Repl. by AUBERT,BE 04A
< 210	90	[6] ADAM	96D	DLPH	$e^+e^- \to Z$
40 ±17 ±8		[7] AMMAR	93	CLE2	Repl. by COAN 00
< 420	90	ALBRECHT	89G	ARG	$e^+e^- \to \Upsilon(4S)$
< 240	90	[8] AVERY	89B	CLEO	$e^+e^- \to \Upsilon(4S)$
<2100	90	AVERY	87	CLEO	$e^+e^- \to \Upsilon(4S)$

[1] Uses B($\Upsilon(4S) \to B^+B^-$) = (51.4±0.6)% and B($\Upsilon(4S) \to B^0\overline{B}^0$) = (48.6±0.6)%.
[2] Uses B($\Upsilon(4S) \to B^+B^-$) = (51.6±0.6)% and B($\Upsilon(4S) \to B^0\overline{B}^0$) = (48.4±0.6)%.
[3] Assumes equal production of B^+ and B^0 at the $\Upsilon(4S)$. No evidence for a nonresonant $K\pi\gamma$ contamination was seen; the central value assumes no contamination.
[4] Uses the production ratio of charged and neutral B from $\Upsilon(4S)$ decays $R^{+/0} = 1.006 \pm 0.048$.
[5] Assumes equal production of B^+ and B^0 at the $\Upsilon(4S)$.
[6] ADAM 96D assumes $f_{B^0} = f_{B^-} = 0.39$ and $f_{B_s} = 0.12$.
[7] AMMAR 93 observed 6.6 ± 2.8 events above background.
[8] AVERY 89B reports $< 2.8 \times 10^{-4}$ assuming the $\Upsilon(4S)$ decays 43% to $B^0\overline{B}^0$. We rescale to 50%.

$\Gamma(K^*(1410)\gamma)/\Gamma_{total}$ Γ_{372}/Γ

VALUE	CL%	DOCUMENT ID		TECN	COMMENT
<1.3 × 10⁻⁴	90	[1] NISHIDA	02	BELL	$e^+e^- \to \Upsilon(4S)$

[1] Assumes equal production of B^+ and B^0 at the $\Upsilon(4S)$.

$\Gamma(K^+\pi^-\gamma$ nonresonant$)/\Gamma_{total}$ Γ_{373}/Γ

VALUE	CL%	DOCUMENT ID		TECN	COMMENT
<2.6 × 10⁻⁶	90	[1,2] NISHIDA	02	BELL	$e^+e^- \to \Upsilon(4S)$

[1] Assumes equal production of B^+ and B^0 at the $\Upsilon(4S)$.
[2] 1.25 GeV/c^2 $< M_{K\pi} <$ 1.6 GeV/c^2

$\Gamma(K^*(892)^0X(214), X \to \mu^+\mu^-)/\Gamma_{total}$ Γ_{374}/Γ

$X(214)$ is a hypothetical particle of mass 214 MeV/c^2 reported by the HyperCP experiment (PARK 05)

VALUE (units 10^{-8})	CL%	DOCUMENT ID		TECN	COMMENT
<2.26	90	[1,2] HYUN	10	BELL	$e^+e^- \to \Upsilon(4S)$

[1] Assumes equal production of B^+ and B^0 at the $\Upsilon(4S)$.
[2] Based on scalar nature of X particle. With a vector X assumption, the upper limit is 2.27×10^{-8}.

$\Gamma(K^0\pi^+\pi^-\gamma)/\Gamma_{total}$ Γ_{375}/Γ

VALUE (units 10^{-5})	DOCUMENT ID		TECN	COMMENT
1.99±0.18 OUR AVERAGE				
$2.05\pm0.20^{+0.26}_{-0.22}$	[1,2] DEL-AMO-SA...16		BABR	$e^+e^- \to \Upsilon(4S)$
1.85±0.21±0.12	[1,3] AUBERT	07R	BABR	$e^+e^- \to \Upsilon(4S)$
2.40±0.4 ±0.3	[3,4] YANG	05	BELL	$e^+e^- \to \Upsilon(4S)$

[1] $M_{K\pi\pi} < 1.8$ GeV/c^2.
[2] Uses B($\Upsilon(4S) \to B^+B^-$) = 0.513 ± 0.006.
[3] Assumes equal production of B^+ and B^0 at the $\Upsilon(4S)$.
[4] $M_{K\pi\pi} < 2.0$ GeV/c^2.

$\Gamma(K^+\pi^-\pi^0\gamma)/\Gamma_{total}$ Γ_{376}/Γ

VALUE (units 10^{-5})	DOCUMENT ID		TECN	COMMENT
4.07±0.22±0.31	[1,2] AUBERT	07R	BABR	$e^+e^- \to \Upsilon(4S)$

[1] $M_{K\pi\pi} < 1.8$ GeV/c^2.
[2] Assumes equal production of B^+ and B^0 at the $\Upsilon(4S)$.

$\Gamma(K_1(1270)^0\gamma)/\Gamma_{total}$ Γ_{377}/Γ

VALUE (units 10^{-5})	CL%	DOCUMENT ID		TECN	COMMENT
< 5.8	90	[1] YANG	05	BELL	$e^+e^- \to \Upsilon(4S)$
• • • We do not use the following data for averages, fits, limits, etc. • • •					
<700	90	[2] ALBRECHT	89G	ARG	$e^+e^- \to \Upsilon(4S)$

[1] Assumes equal production of B^+ and B^0 at the $\Upsilon(4S)$.
[2] ALBRECHT 89G reports < 0.0078 assuming the $\Upsilon(4S)$ decays 45% to $B^0\overline{B}^0$. We rescale to 50%.

$\Gamma(K_1(1400)^0\gamma)/\Gamma_{total}$ Γ_{378}/Γ

VALUE (units 10^{-5})	CL%	DOCUMENT ID		TECN	COMMENT
< 1.2	90	[1] YANG	05	BELL	$e^+e^- \to \Upsilon(4S)$
• • • We do not use the following data for averages, fits, limits, etc. • • •					
<430	90	[2] ALBRECHT	89G	ARG	$e^+e^- \to \Upsilon(4S)$

[1] Assumes equal production of B^+ and B^0 at the $\Upsilon(4S)$.
[2] ALBRECHT 89G reports < 0.0048 assuming the $\Upsilon(4S)$ decays 45% to $B^0\overline{B}^0$. We rescale to 50%.

$\Gamma(K_2^*(1430)^0\gamma)/\Gamma_{total}$ Γ_{379}/Γ

VALUE (units 10^{-5})	CL%	DOCUMENT ID		TECN	COMMENT
1.24±0.24 OUR AVERAGE					
1.22±0.25±0.10		[1] AUBERT,B	04U	BABR	$e^+e^- \to \Upsilon(4S)$
1.3 ±0.5 ±0.1		[1] NISHIDA	02	BELL	$e^+e^- \to \Upsilon(4S)$
• • • We do not use the following data for averages, fits, limits, etc. • • •					
<40	90	[2] ALBRECHT	89G	ARG	$e^+e^- \to \Upsilon(4S)$

[1] Assumes equal production of B^+ and B^0 at the $\Upsilon(4S)$.
[2] ALBRECHT 89G reports $< 4.4 \times 10^{-4}$ assuming the $\Upsilon(4S)$ decays 45% to $B^0\overline{B}^0$. We rescale to 50%.

$\Gamma(K^*(1680)^0\gamma)/\Gamma_{total}$ Γ_{380}/Γ

VALUE	CL%	DOCUMENT ID		TECN	COMMENT
<0.0020	90	[1] ALBRECHT	89G	ARG	$e^+e^- \to \Upsilon(4S)$

[1] ALBRECHT 89G reports < 0.0022 assuming the $\Upsilon(4S)$ decays 45% to $B^0\overline{B}^0$. We rescale to 50%.

$\Gamma(K_3^*(1780)^0\gamma)/\Gamma_{total}$ Γ_{381}/Γ

VALUE (units 10^{-5})	CL%	DOCUMENT ID		TECN	COMMENT
< 83	90	[1,2] NISHIDA	05	BELL	$e^+e^- \to \Upsilon(4S)$
• • • We do not use the following data for averages, fits, limits, etc. • • •					
<10000	90	[3] ALBRECHT	89G	ARG	$e^+e^- \to \Upsilon(4S)$

[1] Assumes equal production of B^+ and B^0 at the $\Upsilon(4S)$.
[2] Uses $B(K_3^*(1780) \to \eta K) = 0.11^{+0.05}_{-0.04}$.
[3] ALBRECHT 89G reports < 0.011 assuming the $\Upsilon(4S)$ decays 45% to $B^0\overline{B}^0$. We rescale to 50%.

$\Gamma(K_4^*(2045)^0\gamma)/\Gamma_{total}$ Γ_{382}/Γ

VALUE	CL%	DOCUMENT ID		TECN	COMMENT
<0.0043	90	[1] ALBRECHT	89G	ARG	$e^+e^- \to \Upsilon(4S)$

[1] ALBRECHT 89G reports < 0.0048 assuming the $\Upsilon(4S)$ decays 45% to $B^0\overline{B}^0$. We rescale to 50%.

$\Gamma(\rho^0\gamma)/\Gamma_{total}$ Γ_{383}/Γ

VALUE (units 10^{-6})	CL%	DOCUMENT ID		TECN	COMMENT
0.86±0.15 OUR AVERAGE					
$0.97^{+0.24}_{-0.22}\pm0.06$		[1] AUBERT	08BH	BABR	$e^+e^- \to \Upsilon(4S)$
$0.78^{+0.17+0.09}_{-0.16-0.10}$		[1] TANIGUCHI	08	BELL	$e^+e^- \to \Upsilon(4S)$
• • • We do not use the following data for averages, fits, limits, etc. • • •					
$0.79^{+0.22}_{-0.20}\pm0.06$		[1] AUBERT	07L	BABR	Repl. by AUBERT 08BH
$1.25^{+0.37+0.07}_{-0.33-0.06}$		[1] MOHAPATRA	06	BELL	Repl. by TANIGUCHI 08
0.0 ±0.2 ±0.1	90	[1] AUBERT	05	BABR	Repl. by AUBERT 07L
< 0.8	90	[1] MOHAPATRA	05	BELL	$e^+e^- \to \Upsilon(4S)$
< 1.2	90	[1] AUBERT	04C	BABR	$e^+e^- \to \Upsilon(4S)$
<17	90	[1] COAN	00	CLE2	$e^+e^- \to \Upsilon(4S)$

[1] Assumes equal production of B^+ and B^0 at the $\Upsilon(4S)$.

$\Gamma(\rho^0 X(214),\ X \to \mu^+\mu^-)/\Gamma_{total}$ Γ_{384}/Γ

$X(214)$ is a hypothetical particle of mass 214 MeV/c^2 reported by the HyperCP experiment (PARK 05)

VALUE (units 10^{-8})	CL%	DOCUMENT ID		TECN	COMMENT
<1.73	90	[1,2] HYUN	10	BELL	$e^+e^- \to \Upsilon(4S)$

[1] Assumes equal production of B^+ and B^0 at the $\Upsilon(4S)$.
[2] The result is the same for a scalar or vector X particle.

$\Gamma(\rho^0\gamma)/\Gamma(K^*(892)^0\gamma)$ $\Gamma_{383}/\Gamma_{371}$

VALUE (units 10^{-2})	DOCUMENT ID	TECN	COMMENT
$\mathbf{2.06^{+0.45+0.14}_{-0.43-0.16}}$	TANIGUCHI 08	BELL	$e^+e^- \to \Upsilon(4S)$

$\Gamma(\omega\gamma)/\Gamma_{total}$ Γ_{385}/Γ

VALUE (units 10^{-6})	CL%	DOCUMENT ID		TECN	COMMENT
$\mathbf{0.44^{+0.18}_{-0.16}}$ **OUR AVERAGE**					
$0.50^{+0.27}_{-0.23}\pm0.09$		[1] AUBERT	08BH	BABR	$e^+e^- \to \Upsilon(4S)$
$0.40^{+0.19}_{-0.17}\pm0.13$		[1] TANIGUCHI	08	BELL	$e^+e^- \to \Upsilon(4S)$
• • • We do not use the following data for averages, fits, limits, etc. • • •					
$0.40^{+0.24}_{-0.20}\pm0.05$		[1] AUBERT	07L	BABR	Repl. by AUBERT 08BH
$0.56^{+0.34+0.05}_{-0.27-0.10}$		[1] MOHAPATRA	06	BELL	Repl. by TANIGUCHI 08
<1.0	90	[1] AUBERT	05	BABR	Repl. by AUBERT 07L
<0.8	90	[1] MOHAPATRA	05	BELL	Repl. by MOHAPATRA 06
<1.0	90	[1] AUBERT	04C	BABR	$e^+e^- \to \Upsilon(4S)$
<9.2	90	[1] COAN	00	CLE2	$e^+e^- \to \Upsilon(4S)$

[1] Assumes equal production of B^+ and B^0 at the $\Upsilon(4S)$.

$\Gamma(\phi\gamma)/\Gamma_{total}$ Γ_{386}/Γ

VALUE	CL%	DOCUMENT ID		TECN	COMMENT
$\mathbf{<1.0\times10^{-7}}$	90	[1] KING	16	BELL	$e^+e^- \to \Upsilon(4S)$
• • • We do not use the following data for averages, fits, limits, etc. • • •					
$<8.5\times10^{-7}$	90	[1] AUBERT,BE	05C	BABR	$e^+e^- \to \Upsilon(4S)$
$<3.3\times10^{-6}$	90	[1] COAN	00	CLE2	$e^+e^- \to \Upsilon(4S)$

[1] Assumes equal production of B^+ and B^0 at the $\Upsilon(4S)$.

$\Gamma(\pi^+\pi^-)/\Gamma_{total}$ Γ_{387}/Γ

VALUE (units 10^{-6})	CL%	DOCUMENT ID		TECN	COMMENT
5.12±0.19 OUR FIT					
5.13±0.24 OUR AVERAGE					
5.04±0.21±0.18		[1] DUH	13	BELL	$e^+e^- \to \Upsilon(4S)$
5.5 ±0.4 ±0.3		[1] AUBERT	07B	BABR	$e^+e^- \to \Upsilon(4S)$
$4.5\ ^{+1.4}_{-1.2}\ ^{+0.5}_{-0.4}$		[1] BORNHEIM	03	CLE2	$e^+e^- \to \Upsilon(4S)$
• • • We do not use the following data for averages, fits, limits, etc. • • •					
5.1 ±0.2 ±0.2		[1] LIN	07A	BELL	Repl. by DUH 13
4.4 ±0.6 ±0.3		[1] CHAO	04	BELL	Repl. by LIN 07A
4.7 ±0.6 ±0.2		[1] AUBERT	02Q	BABR	Repl. by AUBERT 07B
5.4 ±1.2 ±0.5		[1] CASEY	02	BELL	Repl. by CHAO 04
$5.6\ ^{+2.3}_{-2.0}\ ^{+0.4}_{-0.5}$		[1] ABE	01H	BELL	Repl. by CASEY 02
4.1 ±1.0 ±0.7		[1] AUBERT	01E	BABR	Repl. by AUBERT 02Q
< 67	90	[2] ABE	00C	SLD	$e^+e^- \to Z$
$4.3\ ^{+1.6}_{-1.4}$ ±0.5		[1] CRONIN-HEN..	00	CLE2	Repl. by BORNHEIM 03
< 15	90	GODANG	98	CLE2	Repl. by CRONIN-HENNESSY 00
< 45	90	[3] ADAM	96D	DLPH	$e^+e^- \to Z$
< 20	90	ASNER	96	CLE2	Repl. by GODANG 98
< 41	90	[4] BUSKULIC	96V	ALEP	$e^+e^- \to Z$
< 55	90	[5] ABREU	95N	DLPH	Sup. by ADAM 96D
< 47	90	[6] AKERS	94L	OPAL	$e^+e^- \to Z$
< 29	90	[1] BATTLE	93	CLE2	$e^+e^- \to \Upsilon(4S)$
<130	90	[1] ALBRECHT	90B	ARG	$e^+e^- \to \Upsilon(4S)$
< 77	90	[7] BORTOLETTO	89	CLEO	$e^+e^- \to \Upsilon(4S)$
<260	90	[7] BEBEK	87	CLEO	$e^+e^- \to \Upsilon(4S)$
<500	90	GILES	84	CLEO	$e^+e^- \to \Upsilon(4S)$

[1] Assumes equal production of B^+ and B^0 at the $\Upsilon(4S)$.
[2] ABE 00C assumes $B(Z \to b\overline{b})$=(21.7 ± 0.1)% and the B fractions $f_{B^0}=f_{B^+}=(39.7^{+1.8}_{-2.2})$% and $f_{B_s}=(10.5^{+1.8}_{-2.2})$%.
[3] ADAM 96D assumes $f_{B^0} = f_{B^-} = 0.39$ and $f_{B_s} = 0.12$.
[4] BUSKULIC 96V assumes PDG 96 production fractions for B^0, B^+, B_s, b baryons.
[5] Assumes a B^0, B^- production fraction of 0.39 and a B_s production fraction of 0.12.
[6] Assumes $B(Z \to b\overline{b}) = 0.217$ and B_d^0 (B_s^0) fraction 39.5% (12%).
[7] Paper assumes the $\Upsilon(4S)$ decays 43% to $B^0\overline{B}^0$. We rescale to 50%.

$\Gamma(\pi^+\pi^-)/\Gamma(K^+\pi^-)$ $\Gamma_{387}/\Gamma_{257}$

VALUE	DOCUMENT ID		TECN	COMMENT
0.261±0.010 OUR FIT				
0.261±0.015 OUR AVERAGE				
0.262±0.009±0.017	AAIJ	12AR	LHCB	pp at 7 TeV
0.259±0.017±0.016	AALTONEN	11N	CDF	$p\overline{p}$ at 1.96 TeV
• • • We do not use the following data for averages, fits, limits, etc. • • •				
0.21 ±0.05 ±0.03	ABULENCIA,A	06D	CDF	Repl. by AALTONEN 11N

$\Gamma(\pi^0\pi^0)/\Gamma_{total}$ Γ_{388}/Γ

VALUE (units 10^{-6})	CL%	DOCUMENT ID		TECN	COMMENT
1.59±0.26 OUR AVERAGE		Error includes scale factor of 1.4.			
1.31±0.19±0.19		[1] JULIUS	17	BELL	$e^+e^- \to \Upsilon(4S)$
1.83±0.21±0.13		[1] LEES	13D	BABR	$e^+e^- \to \Upsilon(4S)$
• • • We do not use the following data for averages, fits, limits, etc. • • •					
1.47±0.25±0.12		[1] AUBERT	07BC	BABR	Repl. by LEES 13D
1.17±0.32±0.10		[1] AUBERT	05L	BABR	Repl. by AUBERT 07BC
$2.3\ ^{+0.4}_{-0.5}\ ^{+0.2}_{-0.3}$		[1] CHAO	05	BELL	Repl. by JULIUS 17
< 3.6	90	[1] AUBERT	03L	BABR	$e^+e^- \to \Upsilon(4S)$
2.1 ±0.6 ±0.3		[1] AUBERT	03S	BABR	Repl. by AUBERT 05L
< 4.4	90	[1] BORNHEIM	03	CLE2	$e^+e^- \to \Upsilon(4S)$
1.7 ±0.6 ±0.2		[1] LEE	03	BELL	Repl. by CHAO 05
< 5.7	90	[1] ASNER	02	CLE2	$e^+e^- \to \Upsilon(4S)$
< 6.4	90	[1] CASEY	02	BELL	$e^+e^- \to \Upsilon(4S)$
< 9.3	90	GODANG	98	CLE2	Repl. by ASNER 02
< 9.1	90	ASNER	96	CLE2	Repl. by GODANG 98
<60	90	[2] ACCIARRI	95H	L3	$e^+e^- \to Z$

[1] Assumes equal production of B^+ and B^0 at the $\Upsilon(4S)$.
[2] ACCIARRI 95H assumes $f_{B^0} = 39.5 \pm 4.0$ and $f_{B_s} = 12.0 \pm 3.0$%.

$\Gamma(\eta\pi^0)/\Gamma_{total}$ Γ_{389}/Γ

VALUE (units 10^{-6})	CL%	DOCUMENT ID		TECN	COMMENT
$\mathbf{0.41^{+0.17+0.05}_{-0.15-0.07}}$		[1,2] PAL	15	BELL	$e^+e^- \to \Upsilon(4S)$

• • • We do not use the following data for averages, fits, limits, etc. • • •

< 1.5	90	[2] AUBERT	08AH	BABR	$e^+e^- \to \Upsilon(4S)$	
< 1.3	90	[2] AUBERT	06W	BABR	Repl. by AUBERT 08AH	
< 2.5	90	[2] CHANG	05A	BELL	Repl. by PAL 15	
< 2.5	90	[2] AUBERT,B	04D	BABR	Repl. by AUBERT 06W	
< 2.9	90	[2] RICHICHI	00	CLE2	$e^+e^- \to \Upsilon(4S)$	
< 8	90	BEHRENS	98	CLE2	Repl. by RICHICHI 00	
< 250	90	[3] ACCIARRI	95H	L3	$e^+e^- \to Z$	
<1800	90	[2] ALBRECHT	90B	ARG	$e^+e^- \to \Upsilon(4S)$	

[1] PAL 15 signal significance is 3.0 standard deviations. The measurement corresponds to 90% CL upper limit of $< 6.5 \times 10^{-7}$.
[2] Assumes equal production of B^+ and B^0 at the $\Upsilon(4S)$.
[3] ACCIARRI 95H assumes $f_{B^0} = 39.5 \pm 4.0$ and $f_{B_s} = 12.0 \pm 3.0\%$.

$\Gamma(\eta\eta)/\Gamma_{total}$ Γ_{390}/Γ

VALUE (units 10^{-6})	CL%	DOCUMENT ID		TECN	COMMENT
< 1.0	90	[1] AUBERT	09AV	BABR	$e^+e^- \to \Upsilon(4S)$

• • • We do not use the following data for averages, fits, limits, etc. • • •

< 1.8	90	[1] AUBERT,B	06V	BABR	Repl. by AUBERT 09AV	
< 2.0	90	[1] CHANG	05A	BELL	$e^+e^- \to \Upsilon(4S)$	
< 2.8	90	[1] AUBERT,B	04X	BABR	$e^+e^- \to \Upsilon(4S)$	
< 18	90	BEHRENS	98	CLE2	$e^+e^- \to \Upsilon(4S)$	
<410	90	[2] ACCIARRI	95H	L3	$e^+e^- \to Z$	

[1] Assumes equal production of B^+ and B^0 at the $\Upsilon(4S)$.
[2] ACCIARRI 95H assumes $f_{B^0} = 39.5 \pm 4.0$ and $f_{B_s} = 12.0 \pm 3.0\%$.

$\Gamma(\eta'\pi^0)/\Gamma_{total}$ Γ_{391}/Γ

VALUE (units 10^{-6})	CL%	DOCUMENT ID		TECN	COMMENT
1.2±0.6 OUR AVERAGE		Error includes scale factor of 1.7.			
0.9±0.4±0.1		[1] AUBERT	08AH	BABR	$e^+e^- \to \Upsilon(4S)$
2.8±1.0±0.3		[1] SCHUEMANN	06	BELL	$e^+e^- \to \Upsilon(4S)$

• • • We do not use the following data for averages, fits, limits, etc. • • •

$0.8^{+0.8}_{-0.6}\pm0.1$		[1] AUBERT	06W	BABR	Repl. by AUBERT 08AH	
$1.0^{+1.4}_{-1.0}\pm0.8$	90	[1] AUBERT,B	04D	BABR	Repl. by AUBERT 06W	
< 5.7	90	[1] RICHICHI	00	CLE2	$e^+e^- \to \Upsilon(4S)$	
<11	90	BEHRENS	98	CLE2	Repl. by RICHICHI 00	

[1] Assumes equal production of B^+ and B^0 at the $\Upsilon(4S)$.

$\Gamma(\eta'\eta')/\Gamma_{total}$ Γ_{392}/Γ

VALUE (units 10^{-6})	CL%	DOCUMENT ID		TECN	COMMENT
< 1.7	90	[1] AUBERT	09AV	BABR	$e^+e^- \to \Upsilon(4S)$

• • • We do not use the following data for averages, fits, limits, etc. • • •

< 6.5	90	[1] SCHUEMANN	07	BELL	$e^+e^- \to \Upsilon(4S)$	
< 2.4	90	[1] AUBERT,B	06V	BABR	Repl. by AUBERT 09AV	
<10	90	[1] AUBERT,B	04X	BABR	Repl. by AUBERT,B 06V	
<47	90	BEHRENS	98	CLE2	$e^+e^- \to \Upsilon(4S)$	

[1] Assumes equal production of B^+ and B^0 at the $\Upsilon(4S)$.

$\Gamma(\eta'\eta)/\Gamma_{total}$ Γ_{393}/Γ

VALUE (units 10^{-6})	CL%	DOCUMENT ID		TECN	COMMENT
< 1.2	90	[1] AUBERT	08AH	BABR	$e^+e^- \to \Upsilon(4S)$

• • • We do not use the following data for averages, fits, limits, etc. • • •

< 4.5	90	[1] SCHUEMANN	07	BELL	$e^+e^- \to \Upsilon(4S)$	
< 1.7	90	[1] AUBERT	06W	BABR	Repl. by AUBERT 08AH	
< 4.6	90	[1] AUBERT,B	04X	BABR	$e^+e^- \to \Upsilon(4S)$	
<27	90	BEHRENS	98	CLE2	$e^+e^- \to \Upsilon(4S)$	

[1] Assumes equal production of B^+ and B^0 at the $\Upsilon(4S)$.

$\Gamma(\eta'\rho^0)/\Gamma_{total}$ Γ_{394}/Γ

VALUE (units 10^{-6})	CL%	DOCUMENT ID		TECN	COMMENT
< 1.3	90	[1] SCHUEMANN	07	BELL	$e^+e^- \to \Upsilon(4S)$

• • • We do not use the following data for averages, fits, limits, etc. • • •

< 2.8	90	[1] DEL-AMO-SA...10A		BABR	$e^+e^- \to \Upsilon(4S)$	
< 3.7	90	AUBERT	07E	BABR	Repl. by DEL-AMO-SANCHEZ 10A	
< 4.3	90	[1] AUBERT,B	04D	BABR	Repl. by AUBERT 07E	
<12	90	[1] RICHICHI	00	CLE2	$e^+e^- \to \Upsilon(4S)$	
<23	90	BEHRENS	98	CLE2	Repl. by RICHICHI 00	

[1] Assumes equal production of B^+ and B^0 at the $\Upsilon(4S)$.

$\Gamma(\eta' f_0(980),\ f_0 \to \pi^+\pi^-)/\Gamma_{total}$ Γ_{395}/Γ

VALUE (units 10^{-6})	CL%	DOCUMENT ID		TECN	COMMENT
<0.9	90	[1] DEL-AMO-SA...10A		BABR	$e^+e^- \to \Upsilon(4S)$

• • • We do not use the following data for averages, fits, limits, etc. • • •

<1.5	90	AUBERT	07E	BABR	Repl. by DEL-AMO-SANCHEZ 10A

[1] Assumes equal production of B^+ and B^0 at the $\Upsilon(4S)$.

$\Gamma(\eta\rho^0)/\Gamma_{total}$ Γ_{396}/Γ

VALUE (units 10^{-6})	CL%	DOCUMENT ID		TECN	COMMENT
< 1.5	90	[1] AUBERT	07Y	BABR	$e^+e^- \to \Upsilon(4S)$

• • • We do not use the following data for averages, fits, limits, etc. • • •

< 1.9	90	[1] WANG	07B	BELL	$e^+e^- \to \Upsilon(4S)$	
< 1.5	90	[1] AUBERT,B	04D	BABR	Repl. by AUBERT 07Y	
<10	90	[1] RICHICHI	00	CLE2	$e^+e^- \to \Upsilon(4S)$	
<13	90	BEHRENS	98	CLE2	Repl. by RICHICHI 00	

[1] Assumes equal production of B^+ and B^0 at the $\Upsilon(4S)$.

$\Gamma(\eta f_0(980),\ f_0 \to \pi^+\pi^-)/\Gamma_{total}$ Γ_{397}/Γ

VALUE (units 10^{-6})	CL%	DOCUMENT ID		TECN	COMMENT
<0.4	90	[1] AUBERT	07Y	BABR	$e^+e^- \to \Upsilon(4S)$

[1] Assumes equal production of B^+ and B^0 at the $\Upsilon(4S)$.

$\Gamma(\omega\eta)/\Gamma_{total}$ Γ_{398}/Γ

VALUE (units 10^{-6})	CL%	DOCUMENT ID		TECN	COMMENT
$\mathbf{0.94^{+0.35}_{-0.30}\pm0.09}$		[1] AUBERT	09AV	BABR	$e^+e^- \to \Upsilon(4S)$

• • • We do not use the following data for averages, fits, limits, etc. • • •

< 1.9	90	[1] AUBERT,B	05K	BABR	Repl. by AUBERT 09AV	
$4.0\ ^{+1.3}_{-1.2}\ \pm0.4$		[1] AUBERT,B	04X	BABR	Repl. by AUBERT,B 05K	
<12	90	[1] BERGFELD	98	CLE2		

[1] Assumes equal production of B^+ and B^0 at the $\Upsilon(4S)$.

$\Gamma(\omega\eta')/\Gamma_{total}$ Γ_{399}/Γ

VALUE (units 10^{-6})	CL%	DOCUMENT ID		TECN	COMMENT
$\mathbf{1.01^{+0.46}_{-0.38}\pm0.09}$		[1] AUBERT	09AV	BABR	$e^+e^- \to \Upsilon(4S)$

• • • We do not use the following data for averages, fits, limits, etc. • • •

< 2.2	90	[1] SCHUEMANN	07	BELL	$e^+e^- \to \Upsilon(4S)$	
< 2.8	90	[1] AUBERT,B	04X	BABR	$e^+e^- \to \Upsilon(4S)$	
<60	90	[1] BERGFELD	98	CLE2		

[1] Assumes equal production of B^+ and B^0 at the $\Upsilon(4S)$.

$\Gamma(\omega\rho^0)/\Gamma_{total}$ Γ_{400}/Γ

VALUE (units 10^{-6})	CL%	DOCUMENT ID		TECN	COMMENT
< 1.6	90	[1] AUBERT	09H	BABR	$e^+e^- \to \Upsilon(4S)$

• • • We do not use the following data for averages, fits, limits, etc. • • •

< 1.5	90	[1] AUBERT,B	06T	BABR	Repl. by AUBERT 09H	
< 3.3	90	[1] AUBERT	05O	BABR	Repl. by AUBERT,B 06T	
<11	90	[1] BERGFELD	98	CLE2		

[1] Assumes equal production of B^+ and B^0 at the $\Upsilon(4S)$.

$\Gamma(\omega f_0(980),\ f_0 \to \pi^+\pi^-)/\Gamma_{total}$ Γ_{401}/Γ

VALUE (units 10^{-6})	CL%	DOCUMENT ID		TECN	COMMENT
<1.5	90	[1] AUBERT	09H	BABR	$e^+e^- \to \Upsilon(4S)$

• • • We do not use the following data for averages, fits, limits, etc. • • •

<1.5	90	[1] AUBERT,B	06T	BABR	Repl. by AUBERT 09H	

[1] Assumes equal production of B^+ and B^0 at the $\Upsilon(4S)$.

$\Gamma(\omega\omega)/\Gamma_{total}$ Γ_{402}/Γ

VALUE (units 10^{-6})	CL%	DOCUMENT ID		TECN	COMMENT
$\mathbf{1.2\pm0.3^{+0.3}_{-0.2}}$		[1] LEES	14	BABR	$e^+e^- \to \Upsilon(4S)$

• • • We do not use the following data for averages, fits, limits, etc. • • •

< 4.0	90	[1] AUBERT,B	06T	BABR	Repl. by LEES 14	
<19	90	[1] BERGFELD	98	CLE2		

[1] Assumes equal production of B^+ and B^0 at the $\Upsilon(4S)$.

$\Gamma(\phi\pi^0)/\Gamma_{total}$ Γ_{403}/Γ

VALUE (units 10^{-6})	CL%	DOCUMENT ID		TECN	COMMENT
<0.15	90	[1] KIM	12A	BELL	$e^+e^- \to \Upsilon(4S)$

• • • We do not use the following data for averages, fits, limits, etc. • • •

<0.28	90	[1] AUBERT,B	06C	BABR	$e^+e^- \to \Upsilon(4S)$	
<1.0	90	[1] AUBERT,B	04D	BABR	Repl. by AUBERT,B 06C	
<5	90	[1] BERGFELD	98	CLE2		

[1] Assumes equal production of B^+ and B^0 at the $\Upsilon(4S)$.

$\Gamma(\phi\eta)/\Gamma_{total}$ Γ_{404}/Γ

VALUE (units 10^{-6})	CL%	DOCUMENT ID		TECN	COMMENT
<0.5	90	[1] AUBERT	09AV	BABR	$e^+e^- \to \Upsilon(4S)$

• • • We do not use the following data for averages, fits, limits, etc. • • •

<0.6	90	[1] AUBERT,B	06V	BABR	Repl. by AUBERT 09AV	
<1.0	90	[1] AUBERT,B	04X	BABR	Repl. by AUBERT,B 06V	
<9	90	[1] BERGFELD	98	CLE2		

[1] Assumes equal production of B^+ and B^0 at the $\Upsilon(4S)$.

$\Gamma(\phi\eta')/\Gamma_{total}$ Γ_{405}/Γ

VALUE (units 10^{-6})	CL%	DOCUMENT ID		TECN	COMMENT
< 0.5	90	[1] SCHUEMANN	07	BELL	$e^+e^- \to \Upsilon(4S)$

• • • We do not use the following data for averages, fits, limits, etc. • • •

< 1.1	90	[1] AUBERT	09AV	BABR	$e^+e^- \to \Upsilon(4S)$	
< 1.0	90	[1] AUBERT,B	06V	BABR	Repl. by AUBERT 09AV	
< 4.5	90	[1] AUBERT,B	04X	BABR	Repl. by AUBERT,B 06V	
<31	90	[1] BERGFELD	98	CLE2		

[1] Assumes equal production of B^+ and B^0 at the $\Upsilon(4S)$.

$\Gamma(\phi\pi^+\pi^-)/\Gamma_{total}$ Γ_{406}/Γ

VALUE (units 10^{-7})	DOCUMENT ID		TECN	COMMENT
1.82±0.25±0.43	[1] AAIJ	17A	LHCB	pp at 7, 8 TeV

[1] Signal evidence is 4.5 standard deviations.

$\Gamma(\phi\rho^0)/\Gamma_{total}$ Γ_{407}/Γ

VALUE (units 10^{-6})	CL%	DOCUMENT ID		TECN	COMMENT
< 0.33	90	[1] AUBERT	08BK	BABR	$e^+e^- \to \Upsilon(4S)$
• • • We do not use the following data for averages, fits, limits, etc. • • •					
<156	90	[2] ABE	00C	SLD	$e^+e^- \to Z$
< 13	90	[1] BERGFELD	98	CLE2	

[1] Assumes equal production of B^+ and B^0 at the $\Upsilon(4S)$.
[2] ABE 00C assumes $B(Z \to b\overline{b})=(21.7 \pm 0.1)\%$ and the B fractions $f_{B^0}=f_{B^+}=(39.7^{+1.8}_{-2.2})\%$ and $f_{B_s}=(10.5^{+1.8}_{-2.2})\%$.

$\Gamma(\phi f_0(980),\ f_0 \to \pi^+\pi^-)/\Gamma_{total}$ Γ_{408}/Γ

VALUE (units 10^{-6})	CL%	DOCUMENT ID		TECN	COMMENT
<0.38	90	[1] AUBERT	08BK	BABR	$e^+e^- \to \Upsilon(4S)$

[1] Assumes equal production of B^+ and B^0 at the $\Upsilon(4S)$.

$\Gamma(\phi\omega)/\Gamma_{total}$ Γ_{409}/Γ

VALUE (units 10^{-6})	CL%	DOCUMENT ID		TECN	COMMENT
< 0.7	90	[1] LEES	14	BABR	$e^+e^- \to \Upsilon(4S)$
• • • We do not use the following data for averages, fits, limits, etc. • • •					
< 1.2	90	[1] AUBERT,B	06T	BABR	Repl. by LEES 14
<21	90	[1] BERGFELD	98	CLE2	

[1] Assumes equal production of B^+ and B^0 at the $\Upsilon(4S)$.

$\Gamma(\phi\phi)/\Gamma_{total}$ Γ_{410}/Γ

VALUE	CL%	DOCUMENT ID		TECN	COMMENT
<2.8 $\times 10^{-8}$	90	AAIJ	15AS	LHCB	pp at 7, 8 TeV
• • • We do not use the following data for averages, fits, limits, etc. • • •					
<2 $\times 10^{-7}$	90	[1] AUBERT	08BK	BABR	$e^+e^- \to \Upsilon(4S)$
<1.5 $\times 10^{-6}$	90	[1] AUBERT,B	04X	BABR	Repl. by AUBERT 08BK
<3.21 $\times 10^{-4}$	90	[2] ABE	00C	SLD	$e^+e^- \to Z$
<1.2 $\times 10^{-5}$	90	[1] BERGFELD	98	CLE2	
<3.9 $\times 10^{-5}$	90	ASNER	96	CLE2	$e^+e^- \to \Upsilon(4S)$

[1] Assumes equal production of B^+ and B^0 at the $\Upsilon(4S)$.
[2] ABE 00C assumes $B(Z \to b\overline{b})=(21.7 \pm 0.1)\%$ and the B fractions $f_{B^0}=f_{B^+}=(39.7^{+1.8}_{-2.2})\%$ and $f_{B_s}=(10.5^{+1.8}_{-2.2})\%$.

$\Gamma(a_0(980)^\pm\pi^\mp,\ a_0^\pm \to \eta\pi^\pm)/\Gamma_{total}$ Γ_{411}/Γ

VALUE (units 10^{-6})	CL%	DOCUMENT ID		TECN	COMMENT
<3.1	90	[1] AUBERT	07Y	BABR	$e^+e^- \to \Upsilon(4S)$
• • • We do not use the following data for averages, fits, limits, etc. • • •					
<5.1	90	[1] AUBERT,BE	04	BABR	Repl. by AUBERT 07Y

[1] Assumes equal production of B^+ and B^0 at the $\Upsilon(4S)$.

$\Gamma(a_0(1450)^\pm\pi^\mp,\ a_0^\pm \to \eta\pi^\pm)/\Gamma_{total}$ Γ_{412}/Γ

VALUE (units 10^{-6})	CL%	DOCUMENT ID		TECN	COMMENT
<2.3	90	[1] AUBERT	07Y	BABR	$e^+e^- \to \Upsilon(4S)$

[1] Assumes equal production of B^+ and B^0 at the $\Upsilon(4S)$.

$\Gamma(\pi^+\pi^-\pi^0)/\Gamma_{total}$ Γ_{413}/Γ

VALUE	CL%	DOCUMENT ID		TECN	COMMENT
<7.2 $\times 10^{-4}$	90	[1] ALBRECHT	90B	ARG	$e^+e^- \to \Upsilon(4S)$

[1] ALBRECHT 90B limit assumes equal production of $B^0\overline{B}^0$ and B^+B^- at $\Upsilon(4S)$.

$\Gamma(\rho^0\pi^0)/\Gamma_{total}$ Γ_{414}/Γ

VALUE (units 10^{-6})	CL%	DOCUMENT ID		TECN	COMMENT
2.0 ±0.5 OUR AVERAGE					
3.0 ±0.5 ±0.7		[1,2] KUSAKA	08	BELL	$e^+e^- \to \Upsilon(4S)$
1.4 ±0.6 ±0.3		[1] AUBERT	04Z	BABR	$e^+e^- \to \Upsilon(4S)$
$1.6\ ^{+2.0}_{-1.4}$ ±0.8		[1] JESSOP	00	CLEO	$e^+e^- \to \Upsilon(4S)$
• • • We do not use the following data for averages, fits, limits, etc. • • •					
$3.12^{+0.88}_{-0.82}{}^{+0.60}_{-0.76}$		[1] DRAGIC	06	BELL	Repl. by KUSAKA 08
5.1 ±1.6 ±0.9		DRAGIC	04	BELL	Repl. by DRAGIC 06
< 5.3	90	[1] GORDON	02	BELL	Repl. by DRAGIC 04
< 24	90	ASNER	96	CLEO	Repl. by JESSOP 00
<400	90	[1] ALBRECHT	90B	ARG	$e^+e^- \to \Upsilon(4S)$

[1] Assumes equal production of B^+ and B^0 at the $\Upsilon(4S)$.
[2] This is the first measurement that excludes contributions from $\rho(1450)$ and $\rho(1570)$ resonances.

$\Gamma(\rho^\mp\pi^\pm)/\Gamma_{total}$ Γ_{415}/Γ

VALUE (units 10^{-6})	CL%	DOCUMENT ID		TECN	COMMENT
23.0±2.3 OUR AVERAGE					
22.6±1.1±4.4		[1,2] KUSAKA	08	BELL	$e^+e^- \to \Upsilon(4S)$
22.6±1.8±2.2		[1] AUBERT	03T	BABR	$e^+e^- \to \Upsilon(4S)$
$27.6^{+8.4}_{-7.4}$ ±4.2		[1] JESSOP	00	CLE2	$e^+e^- \to \Upsilon(4S)$
• • • We do not use the following data for averages, fits, limits, etc. • • •					
$20.8^{+6.0}_{-6.3}{}^{+2.8}_{-3.1}$		[1] GORDON	02	BELL	Repl. by KUSAKA 08
< 88	90	ASNER	96	CLE2	Repl. by JESSOP 00
< 520	90	[1] ALBRECHT	90B	ARG	$e^+e^- \to \Upsilon(4S)$
<5200	90	[3] BEBEK	87	CLEO	$e^+e^- \to \Upsilon(4S)$

[1] Assumes equal production of B^+ and B^0 at the $\Upsilon(4S)$.
[2] This is the first measurement that excludes contributions from $\rho(1450)$ and $\rho(1570)$ resonances.
[3] BEBEK 87 reports $< 6.1\times10^{-3}$ assuming the $\Upsilon(4S)$ decays 43% to $B^0\overline{B}^0$. We rescale to 50%.

$\Gamma(\pi^+\pi^-\pi^+\pi^-)/\Gamma_{total}$ Γ_{416}/Γ

VALUE	CL%	DOCUMENT ID		TECN	COMMENT
<11.2 $\times 10^{-6}$	90	[1] VANHOEFER	14	BELL	$e^+e^- \to \Upsilon(4S)$
• • • We do not use the following data for averages, fits, limits, etc. • • •					
<23.1 $\times 10^{-6}$	90	[1] AUBERT	08BB	BABR	$e^+e^- \to \Upsilon(4S)$
<19.3 $\times 10^{-6}$	90	[1] CHIANG	08	BELL	Repl. by VANHOEFER 14
< 2.3 $\times 10^{-4}$	90	[2] ADAM	96D	DLPH	$e^+e^- \to Z$
< 2.8 $\times 10^{-4}$	90	[3] ABREU	95N	DLPH	Sup. by ADAM 96D
< 6.7 $\times 10^{-4}$	90	[1] ALBRECHT	90B	ARG	$e^+e^- \to \Upsilon(4S)$

[1] Assumes equal production of B^+ and B^0 at the $\Upsilon(4S)$.
[2] ADAM 96D assumes $f_{B^0} = f_{B^-} = 0.39$ and $f_{B_s} = 0.12$.
[3] Assumes a B^0, B^- production fraction of 0.39 and a B_s production fraction of 0.12.

$\Gamma(\rho^0\pi^+\pi^-)/\Gamma_{total}$ Γ_{417}/Γ

VALUE (units 10^{-6})	CL%	DOCUMENT ID		TECN	COMMENT
< 8.8	90	[1] AUBERT	08BB	BABR	$e^+e^- \to \Upsilon(4S)$
• • • We do not use the following data for averages, fits, limits, etc. • • •					
<12.0	90	[1] VANHOEFER	14	BELL	$e^+e^- \to \Upsilon(4S)$
<12.0	90	[1] CHIANG	08	BELL	Repl. by VANHOEFER 14

[1] Assumes equal production of B^+ and B^0 at the $\Upsilon(4S)$.

$\Gamma(\rho^0\rho^0)/\Gamma_{total}$ Γ_{418}/Γ

VALUE (units 10^{-6})	CL%	DOCUMENT ID		TECN	COMMENT
0.96±0.15 OUR FIT					
0.97±0.24 OUR AVERAGE					
1.02±0.30±0.15		[1,2] VANHOEFER	14	BELL	$e^+e^- \to \Upsilon(4S)$
0.92±0.32±0.14		[2] AUBERT	08BB	BABR	$e^+e^- \to \Upsilon(4S)$
• • • We do not use the following data for averages, fits, limits, etc. • • •					
$0.4\ \pm0.4\ ^{+0.2}_{-0.3}$		[2] CHIANG	08	BELL	Repl. by VANHOEFER 14
1.07±0.33±0.19		[2] AUBERT	07G	BABR	Repl. by AUBERT 08BB
< 1.1	90	[2] AUBERT	05I	BABR	Repl. by AUBERT 07G
< 2.1	90	[2] AUBERT	03V	BABR	Repl. by AUBERT 05I
< 18	90	[3] GODANG	02	CLE2	$e^+e^- \to \Upsilon(4S)$
<136	90	[4] ABE	00C	SLD	$e^+e^- \to Z$
<280	90	[2] ALBRECHT	90B	ARG	$e^+e^- \to \Upsilon(4S)$
<290	90	[5] BORTOLETTO	89	CLEO	$e^+e^- \to \Upsilon(4S)$
<430	90	[5] BEBEK	87	CLEO	$e^+e^- \to \Upsilon(4S)$

[1] Signal significance 3.4 standard deviations.
[2] Assumes equal production of B^+ and B^0 at the $\Upsilon(4S)$.
[3] Assumes a helicity 00 configuration. For a helicity 11 configuration, the limit decreases to 1.4×10^{-5}.
[4] ABE 00C assumes $B(Z \to b\overline{b})=(21.7 \pm 0.1)\%$ and the B fractions $f_{B^0}=f_{B^+}=(39.7^{+1.8}_{-2.2})\%$ and $f_{B_s}=(10.5^{+1.8}_{-2.2})\%$.
[5] Paper assumes the $\Upsilon(4S)$ decays 43% to $B^0\overline{B}^0$. We rescale to 50%.

$\Gamma(\rho^0\rho^0)/\Gamma(K^*(892)^0\phi)$ $\Gamma_{418}/\Gamma_{343}$

VALUE (units 10^{-2})	DOCUMENT ID		TECN	COMMENT
9.5±1.5 OUR FIT				
9.4±1.7±0.9	AAIJ	15T	LHCB	pp at 7, 8 TeV

$\Gamma(f_0(980)\pi^+\pi^-,\ f_0 \to \pi^+\pi^-)/\Gamma_{total}$ Γ_{419}/Γ

VALUE	CL%	DOCUMENT ID		TECN	COMMENT
<3.0 $\times 10^{-6}$	90	[1] VANHOEFER	14	BELL	$e^+e^- \to \Upsilon(4S)$
• • • We do not use the following data for averages, fits, limits, etc. • • •					
<3.8 $\times 10^{-6}$	90	[1] CHIANG	08	BELL	$e^+e^- \to \Upsilon(4S)$

[1] Assumes equal production of B^+ and B^0 at the $\Upsilon(4S)$.

$\Gamma(\rho^0 f_0(980),\ f_0 \to \pi^+\pi^-)/\Gamma_{total}$ Γ_{420}/Γ

VALUE (units 10^{-7})	CL%	DOCUMENT ID		TECN	COMMENT
7.8±2.2±1.1		[1,2] VANHOEFER	14	BELL	$e^+e^- \to \Upsilon(4S)$

• • • We do not use the following data for averages, fits, limits, etc. • • •

<8.1	90	AAIJ	15T	LHCB	pp at 7, 8 TeV
<4.0	90	[2] AUBERT	08BB	BABR	$e^+e^- \to \Upsilon(4S)$
<3	90	[2] CHIANG	08	BELL	Repl. by VANHOEFER 14
<5.3	90	[2] AUBERT	07G	BABR	Repl. by AUBERT 08BB

[1] Signal significance of 3.1 standard deviations.
[2] Assumes equal production of B^+ and B^0 at the $\Upsilon(4S)$.

$\Gamma(f_0(980)\,f_0(980),\ f_0 \to \pi^+\pi^-,\ f_0 \to \pi^+\pi^-)/\Gamma_{total}$ Γ_{421}/Γ

VALUE (units 10^{-6})	CL%	DOCUMENT ID		TECN	COMMENT
<0.19	90	[1] AUBERT	08BB	BABR	$e^+e^- \to \Upsilon(4S)$

• • • We do not use the following data for averages, fits, limits, etc. • • •

<0.2	90	[1] VANHOEFER	14	BELL	$e^+e^- \to \Upsilon(4S)$
<0.1	90	[1] CHIANG	08	BELL	Repl. by VANHOEFER 14
<0.16	90	[1] AUBERT	07G	BABR	Repl. by AUBERT 08BB

[1] Assumes equal production of B^+ and B^0 at the $\Upsilon(4S)$.

$\Gamma(f_0(980)\,f_0(980),\ f_0 \to \pi^+\pi^-,\ f_0 \to K^+K^-)/\Gamma_{total}$ Γ_{422}/Γ

VALUE (units 10^{-6})	CL%	DOCUMENT ID		TECN	COMMENT
<0.23	90	[1] AUBERT	08BK	BABR	$e^+e^- \to \Upsilon(4S)$

[1] Assumes equal production of B^+ and B^0 at the $\Upsilon(4S)$.

$\Gamma(a_1(1260)^{\mp}\pi^{\pm})/\Gamma_{total}$ Γ_{423}/Γ

VALUE (units 10^{-6})	CL%	DOCUMENT ID		TECN	COMMENT
26 ±5 OUR AVERAGE		Error includes scale factor of 1.9.			
22.2±2.0±2.8		[1,2] DALSENO	12	BELL	$e^+e^- \to \Upsilon(4S)$
33.2±3.8±3.0		[2,3] AUBERT	06V	BABR	$e^+e^- \to \Upsilon(4S)$

• • • We do not use the following data for averages, fits, limits, etc. • • •

< 630	90	[2] ALBRECHT	90B	ARG	$e^+e^- \to \Upsilon(4S)$
< 490	90	[4] BORTOLETTO	89	CLEO	$e^+e^- \to \Upsilon(4S)$
<1000	90	[4] BEBEK	87	CLEO	$e^+e^- \to \Upsilon(4S)$

[1] DALSENO 12 reports $B(B^0 \to a_1^{\pm}\pi^{\mp})\ B(a_1^{\pm} \to \pi^{\pm}\pi^+\pi^-) = (11.1 \pm 1.0 \pm 1.4) \times 10^{-6}$ which we rescaled assuming $a_1(1260)$ decays only to 3π and $B(a_1^{\pm} \to \pi^{\pm}\pi^+\pi^-) = 0.5$.
[2] Assumes equal production of B^+ and B^0 at the $\Upsilon(4S)$.
[3] Assumes $a_1(1260)$ decays only to 3π and $B(a_1^{\pm} \to \pi^{\pm}\pi^{\mp}\pi^{\pm}) = 0.5$.
[4] Paper assumes the $\Upsilon(4S)$ decays 43% to $B^0\overline{B}^0$. We rescale to 50%.

$\Gamma(a_2(1320)^{\mp}\pi^{\pm})/\Gamma_{total}$ Γ_{424}/Γ

VALUE	CL%	DOCUMENT ID		TECN	COMMENT
$<6.3 \times 10^{-6}$	90	[1] DALSENO	12	BELL	$e^+e^- \to \Upsilon(4S)$

• • • We do not use the following data for averages, fits, limits, etc. • • •

$<3.0 \times 10^{-4}$	90	[2] BORTOLETTO	89	CLEO	$e^+e^- \to \Upsilon(4S)$
$<1.4 \times 10^{-3}$	90	[2] BEBEK	87	CLEO	$e^+e^- \to \Upsilon(4S)$

[1] DALSENO 12 reports $B(B^0 \to a_2^{\pm}\pi^{\mp})\ B(a_2^{\pm} \to \pi^{\pm}\pi^+\pi^-) < 2.2 \times 10^{-6}$ which we rescaled using $B(a_2^{\pm} \to \pi^{\pm}\pi^+\pi^-) = 1/2\ B(a_2^{\pm} \to 3\pi) = 0.35 \pm 0.013$.
[2] Paper assumes the $\Upsilon(4S)$ decays 43% to $B^0\overline{B}^0$. We rescale to 50%.

$\Gamma(\pi^+\pi^-\pi^0\pi^0)/\Gamma_{total}$ Γ_{425}/Γ

VALUE	CL%	DOCUMENT ID		TECN	COMMENT
$<3.1 \times 10^{-3}$	90	[1] ALBRECHT	90B	ARG	$e^+e^- \to \Upsilon(4S)$

[1] ALBRECHT 90B limit assumes equal production of $B^0\overline{B}^0$ and B^+B^- at $\Upsilon(4S)$.

$\Gamma(\rho^+\rho^-)/\Gamma_{total}$ Γ_{426}/Γ

VALUE (units 10^{-6})	CL%	DOCUMENT ID		TECN	COMMENT
27.7±1.9 OUR AVERAGE					
28.3±1.5±1.5		[1] VANHOEFER	16	BELL	$e^+e^- \to \Upsilon(4S)$
$25.5 \pm 2.1 {}^{+3.6}_{-3.9}$		[1] AUBERT	07BF	BABR	$e^+e^- \to \Upsilon(4S)$

• • • We do not use the following data for averages, fits, limits, etc. • • •

$22.8 \pm 3.8 {}^{+2.3}_{-2.6}$	[1] SOMOV	06	BELL	Repl. by VANHOEFER 16
$25 \ {}^{+7}_{-6} \ {}^{+5}_{-6}$	[1] AUBERT	04G	BABR	Repl. by AUBERT,B 04R
30 ±4 ±5	[1,2] AUBERT,B	04R	BABR	Repl. by AUBERT 07BF
<2200 90	[1] ALBRECHT	90B	ARG	$e^+e^- \to \Upsilon(4S)$

[1] Assumes equal production of B^+ and B^0 at the $\Upsilon(4S)$.
[2] The quoted result is obtained after combining with AUBERT 04G result by AUBERT 04R alone gives $(33 \pm 4 \pm 5) \times 10^{-6}$.

$\Gamma(a_1(1260)^0\pi^0)/\Gamma_{total}$ Γ_{427}/Γ

VALUE	CL%	DOCUMENT ID		TECN	COMMENT
$<1.1 \times 10^{-3}$	90	[1] ALBRECHT	90B	ARG	$e^+e^- \to \Upsilon(4S)$

[1] ALBRECHT 90B limit assumes equal production of $B^0\overline{B}^0$ and B^+B^- at $\Upsilon(4S)$.

$\Gamma(\omega\pi^0)/\Gamma_{total}$ Γ_{428}/Γ

VALUE (units 10^{-6})	CL%	DOCUMENT ID		TECN	COMMENT
< 0.5	90	[1] AUBERT	08AH	BABR	$e^+e^- \to \Upsilon(4S)$

• • • We do not use the following data for averages, fits, limits, etc. • • •

< 2.0	90	[1] JEN	06	BELL	$e^+e^- \to \Upsilon(4S)$
< 1.2	90	[1] AUBERT,B	04D	BABR	Repl. by AUBERT 08AH
< 1.9	90	[1] WANG	04A	BELL	$e^+e^- \to \Upsilon(4S)$
< 3	90	[1] AUBERT	01G	BABR	$e^+e^- \to \Upsilon(4S)$
< 5.5	90	[1] JESSOP	00	CLE2	$e^+e^- \to \Upsilon(4S)$
< 14	90	[1] BERGFELD	98	CLE2	Repl. by JESSOP 00
<460	90	[2] ALBRECHT	90B	ARG	$e^+e^- \to \Upsilon(4S)$

[1] Assumes equal production of B^+ and B^0 at the $\Upsilon(4S)$.
[2] ALBRECHT 90B limit assumes equal production of $B^0\overline{B}^0$ and B^+B^- at $\Upsilon(4S)$.

$\Gamma(\pi^+\pi^+\pi^-\pi^-\pi^0)/\Gamma_{total}$ Γ_{429}/Γ

VALUE	CL%	DOCUMENT ID		TECN	COMMENT
$<9.0 \times 10^{-3}$	90	[1] ALBRECHT	90B	ARG	$e^+e^- \to \Upsilon(4S)$

[1] ALBRECHT 90B limit assumes equal production of $B^0\overline{B}^0$ and B^+B^- at $\Upsilon(4S)$.

$\Gamma(a_1(1260)^+\rho^-)/\Gamma_{total}$ Γ_{430}/Γ

VALUE (units 10^{-6})	CL%	DOCUMENT ID		TECN	COMMENT
< 61	90	[1,2] AUBERT,B	06O	BABR	$e^+e^- \to \Upsilon(4S)$

• • • We do not use the following data for averages, fits, limits, etc. • • •

<3400	90	[1] ALBRECHT	90B	ARG	$e^+e^- \to \Upsilon(4S)$

[1] Assumes equal production of B^+ and B^0 at the $\Upsilon(4S)$.
[2] Assumes $a_1(1260)$ decays only to 3π and $B(a_1^{\pm} \to \pi^{\pm}\pi^{\mp}\pi^{\pm}) = 0.5$.

$\Gamma(a_1(1260)^0\rho^0)/\Gamma_{total}$ Γ_{431}/Γ

VALUE	CL%	DOCUMENT ID		TECN	COMMENT
$<2.4 \times 10^{-3}$	90	[1] ALBRECHT	90B	ARG	$e^+e^- \to \Upsilon(4S)$

[1] ALBRECHT 90B limit assumes equal production of $B^0\overline{B}^0$ and B^+B^- at $\Upsilon(4S)$.

$\Gamma(b_1^{\mp}\pi^{\pm},\ b_1^{\mp} \to \omega\pi^{\mp})/\Gamma_{total}$ Γ_{432}/Γ

VALUE (units 10^{-6})	DOCUMENT ID		TECN	COMMENT
10.9±1.2±0.9	[1] AUBERT	07BI	BABR	$e^+e^- \to \Upsilon(4S)$

[1] Assumes equal production of B^+ and B^0 at the $\Upsilon(4S)$.

$\Gamma(b_1^0\pi^0,\ b_1^0 \to \omega\pi^0)/\Gamma_{total}$ Γ_{433}/Γ

VALUE (units 10^{-6})	CL%	DOCUMENT ID		TECN	COMMENT
<1.9	90	[1] AUBERT	08AG	BABR	$e^+e^- \to \Upsilon(4S)$

[1] Assumes equal production of B^+ and B^0 at the $\Upsilon(4S)$.

$\Gamma(b_1^-\rho^+,\ b_1^- \to \omega\pi^-)/\Gamma_{total}$ Γ_{434}/Γ

VALUE	CL%	DOCUMENT ID		TECN	COMMENT
$<1.4 \times 10^{-6}$	90	[1] AUBERT	09AF	BABR	$e^+e^- \to \Upsilon(4S)$

[1] Assumes equal production of B^+ and B^0 at the $\Upsilon(4S)$.

$\Gamma(b_1^0\rho^0,\ b_1^0 \to \omega\pi^0)/\Gamma_{total}$ Γ_{435}/Γ

VALUE	CL%	DOCUMENT ID		TECN	COMMENT
$<3.4 \times 10^{-6}$	90	[1] AUBERT	09AF	BABR	$e^+e^- \to \Upsilon(4S)$

[1] Assumes equal production of B^+ and B^0 at the $\Upsilon(4S)$.

$\Gamma(\pi^+\pi^+\pi^+\pi^-\pi^-\pi^-)/\Gamma_{total}$ Γ_{436}/Γ

VALUE	CL%	DOCUMENT ID		TECN	COMMENT
$<3.0 \times 10^{-3}$	90	[1] ALBRECHT	90B	ARG	$e^+e^- \to \Upsilon(4S)$

[1] ALBRECHT 90B limit assumes equal production of $B^0\overline{B}^0$ and B^+B^- at $\Upsilon(4S)$.

$\Gamma(a_1(1260)^+a_1(1260)^-,\ a_1^+ \to 2\pi^+\pi^-,\ a_1^- \to 2\pi^-\pi^+)/\Gamma_{total}$ Γ_{437}/Γ

VALUE (units 10^{-6})	CL%	DOCUMENT ID		TECN	COMMENT
11.8±2.6±1.6		[1] AUBERT	09AL	BABR	$e^+e^- \to \Upsilon(4S)$

• • • We do not use the following data for averages, fits, limits, etc. • • •

<6000	90	[1] ALBRECHT	90B	ARG	$e^+e^- \to \Upsilon(4S)$
<2800	90	[2] BORTOLETTO	89	CLEO	$e^+e^- \to \Upsilon(4S)$

[1] Assumes equal production of $B^0\overline{B}^0$ and B^+B^- at $\Upsilon(4S)$.
[2] BORTOLETTO 89 reports $< 3.2 \times 10^{-3}$ assuming the $\Upsilon(4S)$ decays 43% to $B^0\overline{B}^0$. We rescale to 50%.

$\Gamma(\pi^+\pi^+\pi^+\pi^-\pi^-\pi^-\pi^0)/\Gamma_{total}$ Γ_{438}/Γ

VALUE	CL%	DOCUMENT ID		TECN	COMMENT
$<1.1 \times 10^{-2}$	90	[1] ALBRECHT	90B	ARG	$e^+e^- \to \Upsilon(4S)$

[1] ALBRECHT 90B limit assumes equal production of $B^0\overline{B}^0$ and B^+B^- at $\Upsilon(4S)$.

$\Gamma(p\overline{p})/\Gamma_{total}$ Γ_{439}/Γ

VALUE (units 10^{-8})	CL%	DOCUMENT ID		TECN	COMMENT
$1.25 \pm 0.27 \pm 0.18$		[1] AAIJ	17BJ	LHCB	pp at 7 and 8 TeV

• • • We do not use the following data for averages, fits, limits, etc. • • •

$1.47 {}^{+0.62}_{-0.51} {}^{+0.35}_{-0.14}$	[2] AAIJ	13BQ	LHCB	Repl. by AAIJ 17BJ
< 11	90	[3] TSAI	07	BELL	$e^+e^- \to \Upsilon(4S)$
< 41	90	[3] CHANG	05	BELL	$e^+e^- \to \Upsilon(4S)$
< 27	90	[3] AUBERT	04U	BABR	$e^+e^- \to \Upsilon(4S)$
< 140	90	[3] BORNHEIM	03	CLE2	$e^+e^- \to \Upsilon(4S)$
< 120	90	[3] ABE	02O	BELL	$e^+e^- \to \Upsilon(4S)$
< 700	90	[3] COAN	99	CLE2	$e^+e^- \to \Upsilon(4S)$
< 1800	90	[4] BUSKULIC	96V	ALEP	$e^+e^- \to Z$
<35000	90	[5] ABREU	95N	DLPH	Sup. by ADAM 96D

< 3400	90	[6] BORTOLETTO	89	CLEO	$e^+e^- \to \Upsilon(4S)$	
<12000	90	[7] ALBRECHT	88F	ARG	$e^+e^- \to \Upsilon(4S)$	
<17000	90	[6] BEBEK	87	CLEO	$e^+e^- \to \Upsilon(4S)$	

[1] Uses normalization mode $B(B^0 \to K^+\pi^-) = (19.6 \pm 0.5) \times 10^{-6}$.
[2] Uses normalization mode $B(B^0 \to K^+\pi^-) = (19.55 \pm 0.54) \times 10^{-6}$.
[3] Assumes equal production of B^+ and B^0 at the $\Upsilon(4S)$.
[4] BUSKULIC 96V assumes PDG 96 production fractions for B^0, B^+, B_s, b baryons.
[5] Assumes a B^0, B^- production fraction of 0.39 and a B_s production fraction of 0.12.
[6] Paper assumes the $\Upsilon(4S)$ decays 43% to $B^0\overline{B}^0$. We rescale to 50%.
[7] ALBRECHT 88F reports $< 1.3 \times 10^{-4}$ assuming the $\Upsilon(4S)$ decays 45% to $B^0\overline{B}^0$. We rescale to 50%.

$\Gamma(p\overline{p}\pi^+\pi^-)/\Gamma_{\text{total}}$ Γ_{440}/Γ

VALUE (units 10^{-6})	CL%	DOCUMENT ID		TECN	COMMENT
2.87± 0.15± 0.11		[1,2] AAIJ	17BD	LHCB	pp at 7, 8 TeV
• • • We do not use the following data for averages, fits, limits, etc. • • •					
<950	90	[3] ABREU	95N	DLPH	Sup. by ADAM 96D
<250	90	[4] BEBEK	89	CLEO	$e^+e^- \to \Upsilon(4S)$
540 ±180 ±200		[5] ALBRECHT	88F	ARG	$e^+e^- \to \Upsilon(4S)$

[1] AAIJ 17BD reports $[\Gamma(B^0 \to p\overline{p}\pi^+\pi^-)/\Gamma_{\text{total}}] / [B(B^0 \to J/\psi(1S)K^*(892)^0)] / [B(J/\psi(1S) \to p\overline{p})] / [B(K^*(892) \to (K\pi)^\pm)] = 1.07 \pm 0.04 \pm 0.04$ which we multiply by our best values $B(B^0 \to J/\psi(1S)K^*(892)^0) = (1.27 \pm 0.05) \times 10^{-3}$, $B(J/\psi(1S) \to p\overline{p}) = (2.121 \pm 0.029) \times 10^{-3}$, $B(K^*(892) \to (K\pi)^\pm) = (99.900 \pm 0.009) \times 10^{-2}$. Our first error is their experiment's error and our second error is the systematic error from using our best values.
[2] The branching ratio is given for $m_{p\overline{p}} < 2.85$ GeV.
[3] Assumes a B^0, B^- production fraction of 0.39 and a B_s production fraction of 0.12.
[4] BEBEK 89 reports $< 2.9 \times 10^{-4}$ assuming the $\Upsilon(4S)$ decays 43% to $B^0\overline{B}^0$. We rescale to 50%.
[5] ALBRECHT 88F reports $6.0 \pm 2.0 \pm 2.2$ assuming the $\Upsilon(4S)$ decays 45% to $B^0\overline{B}^0$. We rescale to 50%.

$\Gamma(p\overline{p}\pi^+\pi^-)/\Gamma(p\overline{p}K^+\pi^-)$ $\Gamma_{440}/\Gamma_{441}$

VALUE	DOCUMENT ID		TECN	COMMENT
• • • We do not use the following data for averages, fits, limits, etc. • • •				
$0.46 \pm 0.02 \pm 0.02$	[1] AAIJ	17BD	LHCB	pp at 7, 8 TeV

[1] The ratio is given for $m_{p\overline{p}} < 2.85$ GeV.

$\Gamma(p\overline{p}K^0)/\Gamma_{\text{total}}$ Γ_{442}/Γ

VALUE (units 10^{-6})	CL%	DOCUMENT ID		TECN	COMMENT
2.66±0.32 OUR AVERAGE					
$2.51^{+0.35}_{-0.29} \pm 0.21$		[1,2] CHEN	08C	BELL	$e^+e^- \to \Upsilon(4S)$
3.0 ±0.5 ±0.3		[2] AUBERT	07AV	BABR	$e^+e^- \to \Upsilon(4S)$
• • • We do not use the following data for averages, fits, limits, etc. • • •					
$2.40^{+0.64}_{-0.44} \pm 0.28$		[2,3,4] WANG	05A	BELL	Repl. by CHEN 08C
$1.88^{+0.77}_{-0.60} \pm 0.23$		[2,3,5] WANG	04	BELL	Repl. by WANG 05A
<7.2	90	[2,3] ABE	02K	BELL	Repl. by WANG 04

[1] Explicitly vetoes resonant production of $p\overline{p}$ from charmonium states.
[2] Assumes equal production of B^+ and B^0 at the $\Upsilon(4S)$.
[3] Explicitly vetoes resonant production of $p\overline{p}$ from charmonium states and pK^0 production from Λ_c.
[4] Provides also results with $M_{p\overline{p}} < 2.85$ GeV/c^2 and angular asymmetry of $p\overline{p}$ system.
[5] The branching fraction for $M_{p\overline{p}} < 2.85$ is also reported.

$\Gamma(\Theta(1540)^+\overline{p},\ \Theta^+ \to pK^0_S)/\Gamma_{\text{total}}$ Γ_{443}/Γ

VALUE (units 10^{-6})	CL%	DOCUMENT ID		TECN	COMMENT
<0.05	90	[1] AUBERT	07AV	BABR	$e^+e^- \to \Upsilon(4S)$
• • • We do not use the following data for averages, fits, limits, etc. • • •					
<0.23	90	[1] WANG	05A	BELL	$e^+e^- \to \Upsilon(4S)$

[1] Assumes equal production of B^+ and B^0 at the $\Upsilon(4S)$.

$\Gamma(f_J(2220)K^0,\ f_J \to p\overline{p})/\Gamma_{\text{total}}$ Γ_{444}/Γ

VALUE (units 10^{-6})	CL%	DOCUMENT ID		TECN	COMMENT
<0.45	90	[1] AUBERT	07AV	BABR	$e^+e^- \to \Upsilon(4S)$

[1] Assumes equal production of B^+ and B^0 at the $\Upsilon(4S)$.

$\Gamma(p\overline{p}K^+\pi^-)/\Gamma_{\text{total}}$ Γ_{441}/Γ

VALUE (units 10^{-6})	DOCUMENT ID		TECN	COMMENT
6.3±0.5±0.2	[1,2] AAIJ	17BD	LHCB	pp at 7, 8 TeV

[1] AAIJ 17BD reports $[\Gamma(B^0 \to p\overline{p}K^+\pi^-)/\Gamma_{\text{total}}] / [B(B^0 \to J/\psi(1S)K^*(892)^0)] / [B(J/\psi(1S) \to p\overline{p})] / [B(K^*(892) \to (K\pi)^\pm)] = 2.34 \pm 0.12 \pm 0.12$ which we multiply by our best values $B(B^0 \to J/\psi(1S)K^*(892)^0) = (1.27 \pm 0.05) \times 10^{-3}$, $B(J/\psi(1S) \to p\overline{p}) = (2.121 \pm 0.029) \times 10^{-3}$, $B(K^*(892) \to (K\pi)^\pm) = (99.900 \pm 0.009) \times 10^{-2}$. Our first error is their experiment's error and our second error is the systematic error from using our best values.
[2] The branching ratio is given for $m_{p\overline{p}} < 2.85$ GeV.

$\Gamma(p\overline{p}K^*(892)^0)/\Gamma_{\text{total}}$ Γ_{445}/Γ

VALUE (units 10^{-6})	CL%	DOCUMENT ID		TECN	COMMENT
$1.24^{+0.28}_{-0.25}$ OUR AVERAGE					
$1.18^{+0.29}_{-0.25} \pm 0.11$		[1,2] CHEN	08C	BELL	$e^+e^- \to \Upsilon(4S)$
$1.47 \pm 0.45 \pm 0.40$		[2] AUBERT	07AV	BABR	$e^+e^- \to \Upsilon(4S)$
• • • We do not use the following data for averages, fits, limits, etc. • • •					
<7.6	90	[2] WANG	04	BELL	$e^+e^- \to \Upsilon(4S)$

[1] Explicitly vetoes resonant production of $p\overline{p}$ from charmonium states.
[2] Assumes equal production of B^+ and B^0 at the $\Upsilon(4S)$.

$\Gamma(f_J(2220)K^*_0,\ f_J \to p\overline{p})/\Gamma_{\text{total}}$ Γ_{446}/Γ

VALUE (units 10^{-6})	CL%	DOCUMENT ID		TECN	COMMENT
<0.15	90	[1] AUBERT	07AV	BABR	$e^+e^- \to \Upsilon(4S)$

[1] Assumes equal production of B^+ and B^0 at the $\Upsilon(4S)$.

$\Gamma(p\overline{p}K^+K^-)/\Gamma_{\text{total}}$ Γ_{447}/Γ

VALUE (units 10^{-8})	DOCUMENT ID		TECN	COMMENT
12.1±3.1±0.5	[1,2] AAIJ	17BD	LHCB	pp at 7, 8 TeV

[1] AAIJ 17BD reports $[\Gamma(B^0 \to p\overline{p}K^+K^-)/\Gamma_{\text{total}}] / [B(B^0 \to J/\psi(1S)K^*(892)^0)] / [B(J/\psi(1S) \to p\overline{p})] / [B(K^*(892) \to (K\pi)^\pm)] = 0.045 \pm 0.011 \pm 0.004$ which we multiply by our best values $B(B^0 \to J/\psi(1S)K^*(892)^0) = (1.27 \pm 0.05) \times 10^{-3}$, $B(J/\psi(1S) \to p\overline{p}) = (2.121 \pm 0.029) \times 10^{-3}$, $B(K^*(892) \to (K\pi)^\pm) = (99.900 \pm 0.009) \times 10^{-2}$. Our first error is their experiment's error and our second error is the systematic error from using our best values.
[2] The branching ratio is given for $m_{p\overline{p}} < 2.85$ GeV.

$\Gamma(p\overline{p}K^+K^-)/\Gamma(p\overline{p}K^+\pi^-)$ $\Gamma_{447}/\Gamma_{441}$

VALUE (%)	DOCUMENT ID		TECN	COMMENT
• • • We do not use the following data for averages, fits, limits, etc. • • •				
$1.9 \pm 0.5 \pm 0.2$	[1] AAIJ	17BD	LHCB	pp at 7, 8 TeV

[1] The ratio is given for $m_{p\overline{p}} < 2.85$ GeV.

$\Gamma(p\overline{\Lambda}\pi^-)/\Gamma_{\text{total}}$ Γ_{448}/Γ

VALUE (units 10^{-6})	CL%	DOCUMENT ID		TECN	COMMENT
3.14±0.29 OUR AVERAGE					
$3.07 \pm 0.31 \pm 0.23$		[1] AUBERT	09AC	BABR	$e^+e^- \to \Upsilon(4S)$
$3.23^{+0.33}_{-0.29} \pm 0.29$		[1] WANG	07C	BELL	$e^+e^- \to \Upsilon(4S)$
• • • We do not use the following data for averages, fits, limits, etc. • • •					
$2.62^{+0.44}_{-0.40} \pm 0.31$		[1,2] WANG	05A	BELL	Repl. by WANG 07C
$3.97^{+1.00}_{-0.80} \pm 0.56$		[1] WANG	03	BELL	Repl. by WANG 05A
< 13	90	[1] COAN	99	CLE2	$e^+e^- \to \Upsilon(4S)$
<180	90	[3] ALBRECHT	88F	ARG	$e^+e^- \to \Upsilon(4S)$

[1] Assumes equal production of B^+ and B^0 at the $\Upsilon(4S)$.
[2] Provides also results with $M_{p\overline{p}} < 2.85$ GeV/c^2 and angular asymmetry of $p\overline{\Lambda}$ system.
[3] ALBRECHT 88F reports $< 2.0 \times 10^{-4}$ assuming the $\Upsilon(4S)$ decays 45% to $B^0\overline{B}^0$. We rescale to 50%.

$\Gamma(p\overline{\Lambda}\pi^-\gamma)/\Gamma_{\text{total}}$ Γ_{449}/Γ

VALUE	CL%	DOCUMENT ID		TECN	COMMENT
<6.5 × 10⁻⁷	90	[1] LAI	14	BELL	$e^+e^- \to \Upsilon(4S)$

[1] Assumes equal production of B^+ and B^0 at the $\Upsilon(4S)$.

$\Gamma(p\overline{\Sigma}(1385)^-)/\Gamma_{\text{total}}$ Γ_{450}/Γ

VALUE (units 10^{-6})	CL%	DOCUMENT ID		TECN	COMMENT
<0.26	90	[1] WANG	07C	BELL	$e^+e^- \to \Upsilon(4S)$

[1] Assumes equal production of B^+ and B^0 at the $\Upsilon(4S)$.

$\Gamma(\Delta^0\overline{\Lambda})/\Gamma_{\text{total}}$ Γ_{451}/Γ

VALUE (units 10^{-6})	CL%	DOCUMENT ID		TECN	COMMENT
<0.93	90	[1] WANG	07C	BELL	$e^+e^- \to \Upsilon(4S)$

[1] Assumes equal production of B^+ and B^0 at the $\Upsilon(4S)$.

$\Gamma(p\overline{\Lambda}K^-)/\Gamma_{\text{total}}$ Γ_{452}/Γ

VALUE (units 10^{-6})	CL%	DOCUMENT ID		TECN	COMMENT
<0.82	90	[1] WANG	03	BELL	$e^+e^- \to \Upsilon(4S)$

[1] Assumes equal production of B^+ and B^0 at the $\Upsilon(4S)$.

$\Gamma(p\overline{\Lambda}D^-)/\Gamma_{\text{total}}$ Γ_{453}/Γ

VALUE (units 10^{-6})	DOCUMENT ID		TECN	COMMENT
25.1±2.6±3.5	[1] CHANG	15	BELL	$e^+e^- \to \Upsilon(4S)$

[1] Assumes equal production of B^+ and B^0 at the $\Upsilon(4S)$.

$\Gamma(p\overline{\Lambda}D^{*-})/\Gamma_{\text{total}}$ Γ_{454}/Γ

VALUE (units 10^{-6})	DOCUMENT ID		TECN	COMMENT
33.6±6.3±4.4	[1] CHANG	15	BELL	$e^+e^- \to \Upsilon(4S)$

[1] Assumes equal production of B^+ and B^0 at the $\Upsilon(4S)$.

$\Gamma(p\overline{\Sigma}^0\pi^-)/\Gamma_{total}$ Γ_{455}/Γ

VALUE	CL%	DOCUMENT ID		TECN	COMMENT
$<3.8\times10^{-6}$	90	[1] WANG	03	BELL	$e^+e^-\to\Upsilon(4S)$

[1] Assumes equal production of B^+ and B^0 at the $\Upsilon(4S)$.

$\Gamma(\overline{\Lambda}\Lambda)/\Gamma_{total}$ Γ_{456}/Γ

VALUE (units 10^{-6})	CL%	DOCUMENT ID		TECN	COMMENT
<0.32	90	[1] TSAI	07	BELL	$e^+e^-\to\Upsilon(4S)$
• • • We do not use the following data for averages, fits, limits, etc. • • •					
<0.69	90	[1] CHANG	05	BELL	Repl. by TSAI 07
<1.2	90	[1] BORNHEIM	03	CLE2	$e^+e^-\to\Upsilon(4S)$
<1.0	90	[1] ABE	02O	BELL	Repl. by CHANG 05
<3.9	90	[1] COAN	99	CLE2	$e^+e^-\to\Upsilon(4S)$

[1] Assumes equal production of B^+ and B^0 at the $\Upsilon(4S)$.

$\Gamma(\overline{\Lambda}\Lambda K^0)/\Gamma_{total}$ Γ_{457}/Γ

VALUE (units 10^{-6})	DOCUMENT ID		TECN	COMMENT
$4.76^{+0.84}_{-0.68}\pm0.61$	[1,2] CHANG	09	BELL	$e^+e^-\to\Upsilon(4S)$

[1] Excluding charmonium events in $2.85 < m_{\Lambda\overline{\Lambda}} < 3.128$ GeV/c^2 and $3.315 < m_{\Lambda\overline{\Lambda}} < 3.735$ GeV/c^2. Measurements in various $m_{\Lambda\overline{\Lambda}}$ bins are also reported.
[2] Assumes equal production of B^+ and B^0 at the $\Upsilon(4S)$.

$\Gamma(\overline{\Lambda}\Lambda K^{*0})/\Gamma_{total}$ Γ_{458}/Γ

VALUE (units 10^{-6})	DOCUMENT ID		TECN	COMMENT
$2.46^{+0.87}_{-0.72}\pm0.34$	[1,2] CHANG	09	BELL	$e^+e^-\to\Upsilon(4S)$

[1] Excluding charmonium events in $2.85 < m_{\Lambda\overline{\Lambda}} < 3.128$ GeV/c^2 and $3.315 < m_{\Lambda\overline{\Lambda}} < 3.735$ GeV/c^2. Measurements in various $m_{\Lambda\overline{\Lambda}}$ bins are also reported.
[2] Assumes equal production of B^+ and B^0 at the $\Upsilon(4S)$.

$\Gamma(\overline{\Lambda}\Lambda D^0)/\Gamma_{total}$ Γ_{459}/Γ

VALUE (units 10^{-5})	DOCUMENT ID		TECN	COMMENT
$1.00^{+0.30}_{-0.26}$ OUR AVERAGE				
$0.98^{+0.29}_{-0.26}\pm0.19$	[1,2] LEES	14B	BABR	$e^+e^-\to\Upsilon(4S)$
$1.05^{+0.57}_{-0.44}\pm0.14$	[2] CHANG	09	BELL	$e^+e^-\to\Upsilon(4S)$

[1] Evidence for 3.4 st. dev. signal significance.
[2] Assumes equal production of B^+ and B^0 at the $\Upsilon(4S)$.

$\Gamma(D^0\Sigma^0\overline{\Lambda}+\text{c.c.})/\Gamma_{total}$ Γ_{460}/Γ

VALUE	CL%	DOCUMENT ID		TECN	COMMENT
$<3.1\times10^{-5}$	90	[1,2] LEES	14B	BABR	$e^+e^-\to\Upsilon(4S)$

[1] Here $\Sigma^0\to\Lambda\gamma$.
[2] Assumes equal production of B^+ and B^0 at the $\Upsilon(4S)$.

$\Gamma(\Delta^0\overline{\Delta}^0)/\Gamma_{total}$ Γ_{461}/Γ

VALUE	CL%	DOCUMENT ID		TECN	COMMENT
<0.0015	90	[1] BORTOLETTO89		CLEO	$e^+e^-\to\Upsilon(4S)$

[1] BORTOLETTO 89 reports < 0.0018 assuming $\Upsilon(4S)$ decays 43% to $B^0\overline{B}^0$. We rescale to 50%.

$\Gamma(\Delta^{++}\overline{\Delta}^{--})/\Gamma_{total}$ Γ_{462}/Γ

VALUE	CL%	DOCUMENT ID		TECN	COMMENT
$<1.1\times10^{-4}$	90	[1] BORTOLETTO89		CLEO	$e^+e^-\to\Upsilon(4S)$

[1] BORTOLETTO 89 reports $< 1.3\times10^{-4}$ assuming $\Upsilon(4S)$ decays 43% to $B^0\overline{B}^0$. We rescale to 50%.

$\Gamma(\overline{D}^0p\overline{p})/\Gamma_{total}$ Γ_{463}/Γ

VALUE (units 10^{-4})	DOCUMENT ID		TECN	COMMENT
1.04 ± 0.07 OUR AVERAGE				
$1.02\pm0.04\pm0.06$	[1,2] DEL-AMO-SA...12		BABR	$e^+e^-\to\Upsilon(4S)$
$1.18\pm0.15\pm0.16$	[2] ABE	02W	BELL	$e^+e^-\to\Upsilon(4S)$
• • • We do not use the following data for averages, fits, limits, etc. • • •				
$1.13\pm0.06\pm0.08$	[2] AUBERT,B	06S	BABR	Repl. by DEL-AMO-SANCHEZ 12

[1] Uses the values of D and D^* branching fractions from PDG 08.
[2] Assumes equal production of B^+ and B^0 at the $\Upsilon(4S)$.

$\Gamma(D_s^-\overline{\Lambda}p)/\Gamma_{total}$ Γ_{464}/Γ

VALUE (units 10^{-5})	DOCUMENT ID		TECN	COMMENT
$2.8\pm0.8\pm0.3$	[1,2] MEDVEDEVA	07	BELL	$e^+e^-\to\Upsilon(4S)$

[1] Assumes equal production of B^+ and B^0 at the $\Upsilon(4S)$.
[2] MEDVEDEVA 07 reports $(2.9\pm0.7\pm0.5\pm0.4)\times10^{-5}$ from a measurement of $[\Gamma(B^0\to D_s^-\overline{\Lambda}p)/\Gamma_{total}]\times[B(D_s^+\to\phi\pi^+)]$ assuming $B(D_s^+\to\phi\pi^+)=(4.4\pm0.6)\times10^{-2}$, which we rescale to our best value $B(D_s^+\to\phi\pi^+)=(4.5\pm0.4)\times10^{-2}$. Our first error is their experiment's error and our second error is the systematic error from using our best value.

$\Gamma(\overline{D}^*(2007)^0p\overline{p})/\Gamma_{total}$ Γ_{465}/Γ

VALUE (units 10^{-4})	DOCUMENT ID		TECN	COMMENT
0.99 ± 0.11 OUR AVERAGE				
$0.97\pm0.07\pm0.09$	[1,2] DEL-AMO-SA...12		BABR	$e^+e^-\to\Upsilon(4S)$
$1.20^{+0.33}_{-0.29}\pm0.21$	[2] ABE	02W	BELL	$e^+e^-\to\Upsilon(4S)$
• • • We do not use the following data for averages, fits, limits, etc. • • •				
$1.01\pm0.10\pm0.09$	[2] AUBERT,B	06S	BABR	Repl. by DEL-AMO-SANCHEZ 12

[1] Uses the values of D and D^* branching fractions from PDG 08.
[2] Assumes equal production of B^+ and B^0 at the $\Upsilon(4S)$.

$\Gamma(D^*(2010)^-p\overline{n})/\Gamma_{total}$ Γ_{466}/Γ

VALUE (units 10^{-4})	DOCUMENT ID		TECN	COMMENT
$14.5^{+3.4}_{-3.0}\pm2.7$	[1] ANDERSON	01	CLE2	$e^+e^-\to\Upsilon(4S)$

[1] Assumes equal production of B^+ and B^0 at the $\Upsilon(4S)$.

$\Gamma(D^-p\overline{p}\pi^+)/\Gamma_{total}$ Γ_{467}/Γ

VALUE (units 10^{-4})	DOCUMENT ID		TECN	COMMENT
$3.32\pm0.10\pm0.29$	[1,2] DEL-AMO-SA...12		BABR	$e^+e^-\to\Upsilon(4S)$
• • • We do not use the following data for averages, fits, limits, etc. • • •				
$3.38\pm0.14\pm0.29$	[2] AUBERT,B	06S	BABR	Repl. by DEL-AMO-SANCHEZ 12

[1] Uses the values of D and D^* branching fractions from PDG 08.
[2] Assumes equal production of B^+ and B^0 at the $\Upsilon(4S)$.

$\Gamma(D^*(2010)^-p\overline{p}\pi^+)/\Gamma_{total}$ Γ_{468}/Γ

VALUE (units 10^{-4})	DOCUMENT ID		TECN	COMMENT
4.7 ± 0.5 OUR AVERAGE Error includes scale factor of 1.2.				
$4.55\pm0.16\pm0.39$	[1,2] DEL-AMO-SA...12		BABR	$e^+e^-\to\Upsilon(4S)$
$6.5^{+1.3}_{-1.2}\pm1.0$	[2] ANDERSON	01	CLE2	$e^+e^-\to\Upsilon(4S)$
• • • We do not use the following data for averages, fits, limits, etc. • • •				
$4.81\pm0.22\pm0.44$	[2] AUBERT,B	06S	BABR	Repl. by DEL-AMO-SANCHEZ 12

[1] Uses the values of D and D^* branching fractions from PDG 08.
[2] Assumes equal production of B^+ and B^0 at the $\Upsilon(4S)$.

$\Gamma(\overline{D}^0p\overline{p}\pi^+\pi^-)/\Gamma_{total}$ Γ_{469}/Γ

VALUE (units 10^{-4})	DOCUMENT ID		TECN	COMMENT
$2.99\pm0.21\pm0.45$	[1,2] DEL-AMO-SA...12		BABR	$e^+e^-\to\Upsilon(4S)$

[1] Uses the values of D and D^* branching fractions from PDG 08.
[2] Assumes equal production of B^+ and B^0 at the $\Upsilon(4S)$.

$\Gamma(\overline{D}^{*0}p\overline{p}\pi^+\pi^-)/\Gamma_{total}$ Γ_{470}/Γ

VALUE (units 10^{-4})	DOCUMENT ID		TECN	COMMENT
$1.91\pm0.36\pm0.29$	[1,2] DEL-AMO-SA...12		BABR	$e^+e^-\to\Upsilon(4S)$

[1] Uses the values of D and D^* branching fractions from PDG 08.
[2] Assumes equal production of B^+ and B^0 at the $\Upsilon(4S)$.

$\Gamma(\Theta_c\overline{p}\pi^+,\ \Theta_c\to D^-p)/\Gamma_{total}$ Γ_{471}/Γ

VALUE (units 10^{-6})	CL%	DOCUMENT ID		TECN	COMMENT
<9	90	[1] AUBERT,B	06S	BABR	$e^+e^-\to\Upsilon(4S)$

[1] Assumes equal production of B^+ and B^0 at the $\Upsilon(4S)$.

$\Gamma(\Theta_c\overline{p}\pi^+,\ \Theta_c\to D^{*-}p)/\Gamma_{total}$ Γ_{472}/Γ

VALUE (units 10^{-6})	CL%	DOCUMENT ID		TECN	COMMENT
<14	90	[1] AUBERT,B	06S	BABR	$e^+e^-\to\Upsilon(4S)$

[1] Assumes equal production of B^+ and B^0 at the $\Upsilon(4S)$.

$\Gamma(\overline{\Sigma}_c^{--}\Delta^{++})/\Gamma_{total}$ Γ_{473}/Γ

VALUE	CL%	DOCUMENT ID		TECN	COMMENT
$<8\times10^{-4}$	90	[1] PROCARIO	94	CLE2	$e^+e^-\to\Upsilon(4S)$

[1] PROCARIO 94 reports < 0.0012 from a measurement of $[\Gamma(B^0\to\overline{\Sigma}_c^{--}\Delta^{++})/\Gamma_{total}]\times[B(\Lambda_c^+\to pK^-\pi^+)]$ assuming $B(\Lambda_c^+\to pK^-\pi^+)=0.043$, which we rescale to our best value $B(\Lambda_c^+\to pK^-\pi^+)=6.23\times10^{-2}$.

$\Gamma(\overline{\Lambda}_c^-p\pi^+\pi^-)/\Gamma_{total}$ Γ_{474}/Γ

VALUE (units 10^{-3})	DOCUMENT ID		TECN	COMMENT
1.03 ± 0.14 OUR AVERAGE Error includes scale factor of 1.3. See the ideogram below.				
$1.23\pm0.05\pm0.33$	[1,2] LEES	13H	BABR	$e^+e^-\to\Upsilon(4S)$
$0.90\pm0.11\pm0.05$	[1,3] PARK	07	BELL	$e^+e^-\to\Upsilon(4S)$
$1.34^{+0.22}_{-0.20}\pm0.07$	[4] DYTMAN	02	CLE2	$e^+e^-\to\Upsilon(4S)$
• • • We do not use the following data for averages, fits, limits, etc. • • •				
$0.88\pm0.16\pm0.05$	[5] GABYSHEV	02	BELL	Repl. by PARK 07
$1.33^{+0.46}_{-0.42}\pm0.37$	[6] FU	97	CLE2	Repl. by DYTMAN 02

[1] Assumes equal production of B^+ and B^0 at the $\Upsilon(4S)$.
[2] Uses $\Lambda_c^+\to pK^-\pi^+$ mode. The second error includes the uncertainty of the branching fraction of the Λ_c decay, $B(\Lambda_c^+\to pK^-\pi^+)=(5.0\pm1.3)\%$.

[3] PARK 07 reports $(11.2 \pm 0.5 \pm 3.2) \times 10^{-4}$ from a measurement of $[\Gamma(B^0 \to \overline{\Lambda}_c^- p\pi^+\pi^-)/\Gamma_{\rm total}] \times [B(\Lambda_c^+ \to pK^-\pi^+)]$ assuming $B(\Lambda_c^+ \to pK^-\pi^+) = (5.0 \pm 1.3) \times 10^{-2}$, which we rescale to our best value $B(\Lambda_c^+ \to pK^-\pi^+) = (6.23 \pm 0.33) \times 10^{-2}$. Our first error is their experiment's error and our second error is the systematic error from using our best value.

[4] DYTMAN 02 reports $(1.67^{+0.27}_{-0.25}) \times 10^{-3}$ from a measurement of $[\Gamma(B^0 \to \overline{\Lambda}_c^- p\pi^+\pi^-)/\Gamma_{\rm total}] \times [B(\Lambda_c^+ \to pK^-\pi^+)]$ assuming $B(\Lambda_c^+ \to pK^-\pi^+) = 0.05$, which we rescale to our best value $B(\Lambda_c^+ \to pK^-\pi^+) = (6.23 \pm 0.33) \times 10^{-2}$. Our first error is their experiment's error and our second error is the systematic error from using our best value.

[5] GABYSHEV 02 reports $(1.1 \pm 0.2) \times 10^{-3}$ from a measurement of $[\Gamma(B^0 \to \overline{\Lambda}_c^- p\pi^+\pi^-)/\Gamma_{\rm total}] \times [B(\Lambda_c^+ \to pK^-\pi^+)]$ assuming $B(\Lambda_c^+ \to pK^-\pi^+) = 0.05$, which we rescale to our best value $B(\Lambda_c^+ \to pK^-\pi^+) = (6.23 \pm 0.33) \times 10^{-2}$. Our first error is their experiment's error and our second error is the systematic error from using our best value.

[6] FU 97 uses PDG 96 values of Λ_c branching fraction.

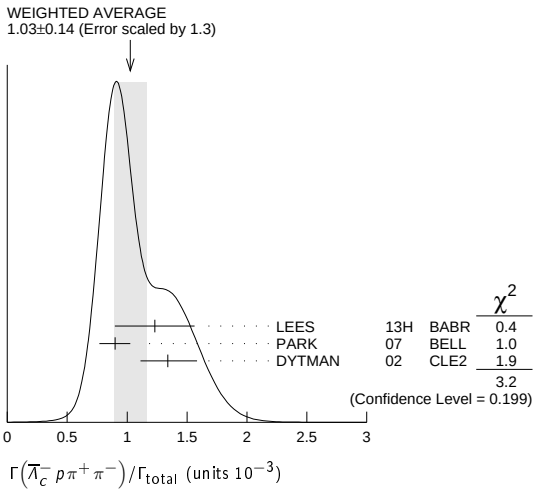

$\Gamma(\overline{\Lambda}_c^- p)/\Gamma_{\rm total}$ Γ_{475}/Γ

VALUE (units 10^{-5})	CL%	DOCUMENT ID		TECN	COMMENT
1.55±0.18 OUR AVERAGE					
1.52±0.17±0.08		[1,2] AUBERT	08BN	BABR	$e^+e^- \to \Upsilon(4S)$
$2.19^{+0.56}_{-0.49}\pm0.65$		[1,3] GABYSHEV	03	BELL	$e^+e^- \to \Upsilon(4S)$
• • • We do not use the following data for averages, fits, limits, etc. • • •					
$2.10^{+0.67+0.77}_{-0.55-0.46}$		[1,4] AUBERT	07AV	BABR	Repl. by AUBERT 08BN
< 9	90	[1,5] DYTMAN	02	CLE2	$e^+e^- \to \Upsilon(4S)$
< 3.1	90	[1,4] GABYSHEV	02	BELL	$e^+e^- \to \Upsilon(4S)$
<21	90	[6] FU	97	CLE2	$e^+e^- \to \Upsilon(4S)$

[1] Assumes equal production of B^+ and B^0 at the $\Upsilon(4S)$.

[2] AUBERT 08BN reports $(1.89 \pm 0.21 \pm 0.49) \times 10^{-5}$ from a measurement of $[\Gamma(B^0 \to \overline{\Lambda}_c^- p)/\Gamma_{\rm total}] \times [B(\Lambda_c^+ \to pK^-\pi^+)]$ assuming $B(\Lambda_c^+ \to pK^-\pi^+) = (5.0 \pm 1.3) \times 10^{-2}$, which we rescale to our best value $B(\Lambda_c^+ \to pK^-\pi^+) = (6.23 \pm 0.33) \times 10^{-2}$. Our first error is their experiment's error and our second error is the systematic error from using our best value.

[3] The second error for GABYSHEV 03 includes the systematic and the error of $\Lambda_c \to \overline{p}K^+\pi^-$ decay branching fraction.

[4] Uses the value for $\Lambda_c \to pK^-\pi^+$ branching ratio $(5.0 \pm 1.3)\%$.

[5] DYTMAN 02 measurement uses $B(\Lambda_c^- \to \overline{p}K^+\pi^-) = 5.0 \pm 1.3\%$. The second error includes the systematic and the uncertainty of the branching ratio.

[6] FU 97 uses PDG 96 values of Λ_c branching ratio.

$\Gamma(\overline{\Lambda}_c^- p\pi^0)/\Gamma_{\rm total}$ Γ_{476}/Γ

VALUE (units 10^{-4})	CL%	DOCUMENT ID		TECN	COMMENT
$\mathbf{1.56\pm0.17^{+0.09}_{-0.08}}$		[1,2] AUBERT	10H	BABR	$e^+e^- \to \Upsilon(4S)$
• • • We do not use the following data for averages, fits, limits, etc. • • •					
<5.9	90	[3] FU	97	CLE2	$e^+e^- \to \Upsilon(4S)$

[1] AUBERT 10H reports $(1.94 \pm 0.17 \pm 0.52) \times 10^{-4}$ from a measurement of $[\Gamma(B^0 \to \overline{\Lambda}_c^- p\pi^0)/\Gamma_{\rm total}] \times [B(\Lambda_c^+ \to pK^-\pi^+)]$ assuming $B(\Lambda_c^+ \to pK^-\pi^+) = (5.0 \pm 1.3) \times 10^{-2}$, which we rescale to our best value $B(\Lambda_c^+ \to pK^-\pi^+) = (6.23 \pm 0.33) \times 10^{-2}$. Our first error is their experiment's error and our second error is the systematic error from using our best value.

[2] Assumes equal production of B^+ and B^0 at the $\Upsilon(4S)$.

[3] FU 97 uses PDG 96 values of Λ_c branching ratio.

$\Gamma(\Lambda_c^- pK^+K^-)/\Gamma_{\rm total}$ Γ_{489}/Γ

VALUE (units 10^{-5})	DOCUMENT ID		TECN	COMMENT
2.0±0.4±0.1	[1,2] LEES	15B	BABR	$e^+e^- \to \Upsilon(4S)$

[1] LEES 15B reports $[\Gamma(B^0 \to \Lambda_c^- pK^+K^-)/\Gamma_{\rm total}] \times [B(\Lambda_c^+ \to pK^-\pi^+)] = (12.5 \pm 2.0 \pm 1.0) \times 10^{-7}$ which we divide by our best value $B(\Lambda_c^+ \to pK^-\pi^+) = (6.23 \pm 0.33) \times 10^{-2}$. Our first error is their experiment's error and our second error is the systematic error from using our best value.

[2] Assumes equal production of B^+ and B^0 at the $\Upsilon(4S)$.

$\Gamma(\Lambda_c^- p\phi)/\Gamma_{\rm total}$ Γ_{490}/Γ

VALUE	CL%	DOCUMENT ID		TECN	COMMENT
$\mathbf{<1.0\times10^{-5}}$	90	[1,2] LEES	15B	BABR	$e^+e^- \to \Upsilon(4S)$

[1] LEES 15B reports $< 1.2 \times 10^{-5}$ from a measurement of $[\Gamma(B^0 \to \Lambda_c^- p\phi)/\Gamma_{\rm total}] \times [B(\Lambda_c^+ \to pK^-\pi^+)]$ assuming $B(\Lambda_c^+ \to pK^-\pi^+) = (5.0 \pm 1.3) \times 10^{-2}$, which we rescale to our best value $B(\Lambda_c^+ \to pK^-\pi^+) = 6.23 \times 10^{-2}$.

[2] Assumes equal production of B^+ and B^0 at the $\Upsilon(4S)$.

$\Gamma(\Sigma_c(2455)^- p)/\Gamma_{\rm total}$ Γ_{477}/Γ

VALUE (units 10^{-6})	DOCUMENT ID		TECN	COMMENT
<24	[1,2] AUBERT	10H	BABR	$e^+e^- \to \Upsilon(4S)$

[1] AUBERT 10H reports $[\Gamma(B^0 \to \Sigma_c(2455)^- p)/\Gamma_{\rm total}] \times [B(\Lambda_c^+ \to pK^-\pi^+)] < 1.5 \times 10^{-6}$ which we divide by our best value $B(\Lambda_c^+ \to pK^-\pi^+) = 6.23 \times 10^{-2}$.

[2] Assumes equal production of B^+ and B^0 at the $\Upsilon(4S)$.

$\Gamma(\overline{\Lambda}_c^- p\pi^+\pi^-\pi^0)/\Gamma_{\rm total}$ Γ_{478}/Γ

VALUE	CL%	DOCUMENT ID		TECN	COMMENT
$\mathbf{<5.07\times10^{-3}}$	90	[1] FU	97	CLE2	$e^+e^- \to \Upsilon(4S)$

[1] FU 97 uses PDG 96 values of Λ_c branching ratio.

$\Gamma(\overline{\Lambda}_c^- p\pi^+\pi^-\pi^+\pi^-)/\Gamma_{\rm total}$ Γ_{479}/Γ

VALUE	CL%	DOCUMENT ID		TECN	COMMENT
$\mathbf{<2.74\times10^{-3}}$	90	[1] FU	97	CLE2	$e^+e^- \to \Upsilon(4S)$

[1] FU 97 uses PDG 96 values of Λ_c branching ratio.

$\Gamma(\overline{\Lambda}_c^- p\pi^+\pi^-(\text{nonresonant}))/\Gamma_{\rm total}$ Γ_{480}/Γ

VALUE (units 10^{-4})	DOCUMENT ID		TECN	COMMENT
5.5±1.0 OUR AVERAGE Error includes scale factor of 1.3.				
7.9±0.4±2.0	[1,2] LEES	13H	BABR	$e^+e^- \to \Upsilon(4S)$
5.1±0.8±0.3	[1,3] PARK	07	BELL	$e^+e^- \to \Upsilon(4S)$

[1] Assumes equal production of B^+ and B^0 at the $\Upsilon(4S)$.

[2] Uses $\Lambda_c^+ \to pK^-\pi^+$ mode. The second error includes the uncertainty of the branching fraction of the Λ_c decay, $B(\Lambda_c^+ \to pK^-\pi^+) = (5.0 \pm 1.3)\%$.

[3] PARK 07 reports $(6.4 \pm 0.4 \pm 1.9) \times 10^{-4}$ from a measurement of $[\Gamma(B^0 \to \overline{\Lambda}_c^- p\pi^+\pi^-(\text{nonresonant}))/\Gamma_{\rm total}] \times [B(\Lambda_c^+ \to pK^-\pi^+)]$ assuming $B(\Lambda_c^+ \to pK^-\pi^+) = (5.0 \pm 1.3) \times 10^{-2}$, which we rescale to our best value $B(\Lambda_c^+ \to pK^-\pi^+) = (6.23 \pm 0.33) \times 10^{-2}$. Our first error is their experiment's error and our second error is the systematic error from using our best value.

$\Gamma(\overline{\Sigma}_c(2520)^{--} p\pi^+)/\Gamma_{\rm total}$ Γ_{481}/Γ

VALUE (units 10^{-4})	DOCUMENT ID		TECN	COMMENT
1.03±0.18 OUR AVERAGE				
1.15±0.10±0.30	[1,2] LEES	13H	BABR	$e^+e^- \to \Upsilon(4S)$
0.96±0.22±0.05	[1,3] PARK	07	BELL	$e^+e^- \to \Upsilon(4S)$
• • • We do not use the following data for averages, fits, limits, etc. • • •				
1.3 ±0.5 ±0.1	[4] GABYSHEV	02	BELL	Repl. by PARK 07

[1] Assumes equal production of B^+ and B^0 at the $\Upsilon(4S)$.

[2] Uses $\Lambda_c^+ \to pK^-\pi^+$ mode. The second error includes the uncertainty of the branching fraction of the Λ_c decay, $B(\Lambda_c^+ \to pK^-\pi^+) = (5.0 \pm 1.3)\%$.

[3] PARK 07 reports $(1.2 \pm 0.1 \pm 0.4) \times 10^{-4}$ from a measurement of $[\Gamma(B^0 \to \overline{\Sigma}_c(2520)^{--} p\pi^+)/\Gamma_{\rm total}] \times [B(\Lambda_c^+ \to pK^-\pi^+)]$ assuming $B(\Lambda_c^+ \to pK^-\pi^+) = (5.0 \pm 1.3) \times 10^{-2}$, which we rescale to our best value $B(\Lambda_c^+ \to pK^-\pi^+) = (6.23 \pm 0.33) \times 10^{-2}$. Our first error is their experiment's error and our second error is the systematic error from using our best value.

[4] GABYSHEV 02 reports $(1.63^{+0.64}_{-0.58}) \times 10^{-4}$ from a measurement of $[\Gamma(B^0 \to \overline{\Sigma}_c(2520)^{--} p\pi^+)/\Gamma_{\rm total}] \times [B(\Lambda_c^+ \to pK^-\pi^+)]$ assuming $B(\Lambda_c^+ \to pK^-\pi^+) = 0.05$, which we rescale to our best value $B(\Lambda_c^+ \to pK^-\pi^+) = (6.23 \pm 0.33) \times 10^{-2}$. Our first error is their experiment's error and our second error is the systematic error from using our best value.

$\Gamma(\overline{\Sigma}_c(2520)^0 p\pi^-)/\Gamma_{\rm total}$ Γ_{482}/Γ

VALUE	CL%	DOCUMENT ID		TECN	COMMENT
$\mathbf{<0.31\times10^{-4}}$	90	[1,2] LEES	13H	BABR	$e^+e^- \to \Upsilon(4S)$
• • • We do not use the following data for averages, fits, limits, etc. • • •					
$<0.38\times10^{-4}$	90	[1] PARK	07	BELL	$e^+e^- \to \Upsilon(4S)$
$<1.21\times10^{-4}$	90	[1,2] GABYSHEV	02	BELL	Repl. by PARK 07

[1] Assumes equal production of B^+ and B^0 at the $\Upsilon(4S)$.

[2] Uses the value for $\Lambda_c \to pK^-\pi^+$ branching ratio (5.0 ± 1.3)%.

$\Gamma(\Sigma_c(2455)^0 N^0,\ N^0 \to p\pi^-)/\Gamma_{total}$ Γ_{484}/Γ

N^0 is the $N(1440)$ P_{11} or $N(1535)$ S_{11} or an admixture of the two baryonic states.

VALUE (units 10^{-4})		DOCUMENT ID		TECN	COMMENT
$\mathbf{0.64 \pm 0.16^{+0.04}_{-0.03}}$	[1,2]	KIM	08	BELL	$e^+e^- \to \Upsilon(4S)$

[1] Assumes equal production of B^+ and B^0 at the $\Upsilon(4S)$.
[2] KIM 08 reports $(0.80 \pm 0.15 \pm 0.25) \times 10^{-4}$ from a measurement of $[\Gamma(B^0 \to \overline{\Sigma}_c(2455)^0 N^0,\ N^0 \to p\pi^-)/\Gamma_{total}] \times [B(\Lambda_c^+ \to pK^-\pi^+)]$ assuming $B(\Lambda_c^+ \to pK^-\pi^+) = (5.0 \pm 1.3) \times 10^{-2}$, which we rescale to our best value $B(\Lambda_c^+ \to pK^-\pi^+) = (6.23 \pm 0.33) \times 10^{-2}$. Our first error is their experiment's error and our second error is the systematic error from using our best value.

$\Gamma(\overline{\Sigma}_c(2455)^0 p\pi^-)/\Gamma_{total}$ Γ_{483}/Γ

VALUE (units 10^{-4})	CL%	DOCUMENT ID		TECN	COMMENT
1.08 ± 0.16 OUR AVERAGE					
0.91 ± 0.07 ± 0.24		[1,2] LEES	13H	BABR	$e^+e^- \to \Upsilon(4S)$
1.12 ± 0.21 ± 0.06		[1,3] PARK	07	BELL	$e^+e^- \to \Upsilon(4S)$
1.8 ± 0.6 ± 0.1		[4] DYTMAN	02	CLE2	$e^+e^- \to \Upsilon(4S)$
• • • We do not use the following data for averages, fits, limits, etc. • • •					
$0.39^{+0.37}_{-0.33} \pm 0.02$	90	[5] GABYSHEV	02	BELL	Repl. by PARK 07

[1] Assumes equal production of B^+ and B^0 at the $\Upsilon(4S)$.
[2] Uses $\Lambda_c^+ \to pK^-\pi^+$ mode. The second error includes the uncertainty of the branching fraction of the Λ_c decay, $B(\Lambda_c^+ \to pK^-\pi^+) = (5.0 \pm 1.3)\%$.
[3] PARK 07 reports $(1.4 \pm 0.2 \pm 0.4) \times 10^{-4}$ from a measurement of $[\Gamma(B^0 \to \overline{\Sigma}_c(2455)^0 p\pi^-)/\Gamma_{total}] \times [B(\Lambda_c^+ \to pK^-\pi^+)]$ assuming $B(\Lambda_c^+ \to pK^-\pi^+) = (5.0 \pm 1.3) \times 10^{-2}$, which we rescale to our best value $B(\Lambda_c^+ \to pK^-\pi^+) = (6.23 \pm 0.33) \times 10^{-2}$. Our first error is their experiment's error and our second error is the systematic error from using our best value.
[4] DYTMAN 02 reports $(2.2 \pm 0.7) \times 10^{-4}$ from a measurement of $[\Gamma(B^0 \to \overline{\Sigma}_c(2455)^0 p\pi^-)/\Gamma_{total}] \times [B(\Lambda_c^+ \to pK^-\pi^+)]$ assuming $B(\Lambda_c^+ \to pK^-\pi^+) = 0.05$, which we rescale to our best value $B(\Lambda_c^+ \to pK^-\pi^+) = (6.23 \pm 0.33) \times 10^{-2}$. Our first error is their experiment's error and our second error is the systematic error from using our best value.
[5] GABYSHEV 02 reports $(0.48^{+0.46}_{-0.41}) \times 10^{-4}$ from a measurement of $[\Gamma(B^0 \to \overline{\Sigma}_c(2455)^0 p\pi^-)/\Gamma_{total}] \times [B(\Lambda_c^+ \to pK^-\pi^+)]$ assuming $B(\Lambda_c^+ \to pK^-\pi^+) = 0.05$, which we rescale to our best value $B(\Lambda_c^+ \to pK^-\pi^+) = (6.23 \pm 0.33) \times 10^{-2}$. Our first error is their experiment's error and our second error is the systematic error from using our best value.

$\Gamma(\Sigma_c(2455)^{--} p\pi^+)/\Gamma_{total}$ Γ_{485}/Γ

VALUE (units 10^{-4})		DOCUMENT ID		TECN	COMMENT
1.85 ± 0.24 OUR AVERAGE					
2.13 ± 0.10 ± 0.56	[1,2]	LEES	13H	BABR	$e^+e^- \to \Upsilon(4S)$
1.69 ± 0.26 ± 0.09	[1,3]	PARK	07	BELL	$e^+e^- \to \Upsilon(4S)$
3.0 ± 0.9 ± 0.2	[4]	DYTMAN	02	CLE2	$e^+e^- \to \Upsilon(4S)$
• • • We do not use the following data for averages, fits, limits, etc. • • •					
1.9 ± 0.6 ± 0.1	[5]	GABYSHEV	02	BELL	Repl. by PARK 07

[1] Assumes equal production of B^+ and B^0 at the $\Upsilon(4S)$.
[2] Uses $\Lambda_c^+ \to pK^-\pi^+$ mode. The second error includes the uncertainty of the branching fraction of the Λ_c decay, $B(\Lambda_c^+ \to pK^-\pi^+) = (5.0 \pm 1.3)\%$.
[3] PARK 07 reports $(2.1 \pm 0.2 \pm 0.6) \times 10^{-4}$ from a measurement of $[\Gamma(B^0 \to \overline{\Sigma}_c(2455)^{--} p\pi^+)/\Gamma_{total}] \times [B(\Lambda_c^+ \to pK^-\pi^+)]$ assuming $B(\Lambda_c^+ \to pK^-\pi^+) = (5.0 \pm 1.3) \times 10^{-2}$, which we rescale to our best value $B(\Lambda_c^+ \to pK^-\pi^+) = (6.23 \pm 0.33) \times 10^{-2}$. Our first error is their experiment's error and our second error is the systematic error from using our best value.
[4] DYTMAN 02 reports $(3.7 \pm 1.1) \times 10^{-4}$ from a measurement of $[\Gamma(B^0 \to \overline{\Sigma}_c(2455)^{--} p\pi^+)/\Gamma_{total}] \times [B(\Lambda_c^+ \to pK^-\pi^+)]$ assuming $B(\Lambda_c^+ \to pK^-\pi^+) = 0.05$, which we rescale to our best value $B(\Lambda_c^+ \to pK^-\pi^+) = (6.23 \pm 0.33) \times 10^{-2}$. Our first error is their experiment's error and our second error is the systematic error from using our best value.
[5] GABYSHEV 02 reports $(2.38^{+0.75}_{-0.69}) \times 10^{-4}$ from a measurement of $[\Gamma(B^0 \to \overline{\Sigma}_c(2455)^{--} p\pi^+)/\Gamma_{total}] \times [B(\Lambda_c^+ \to pK^-\pi^+)]$ assuming $B(\Lambda_c^+ \to pK^-\pi^+) = 0.05$, which we rescale to our best value $B(\Lambda_c^+ \to pK^-\pi^+) = (6.23 \pm 0.33) \times 10^{-2}$. Our first error is their experiment's error and our second error is the systematic error from using our best value.

$\Gamma(\Lambda_c^- pK^+\pi^-)/\Gamma_{total}$ Γ_{486}/Γ

VALUE (units 10^{-5})		DOCUMENT ID		TECN	COMMENT
3.5 ± 0.7 ± 0.2	[1,2]	AUBERT	09AG	BABR	$e^+e^- \to \Upsilon(4S)$

[1] AUBERT 09AG reports $(4.33 \pm 0.82 \pm 0.33 \pm 1.13) \times 10^{-5}$ from a measurement of $[\Gamma(B^0 \to \Lambda_c^- pK^+\pi^-)/\Gamma_{total}] \times [B(\Lambda_c^+ \to pK^-\pi^+)]$ assuming $B(\Lambda_c^+ \to pK^-\pi^+) = (5.0 \pm 1.3) \times 10^{-2}$, which we rescale to our best value $B(\Lambda_c^+ \to pK^-\pi^+) = (6.23 \pm 0.33) \times 10^{-2}$. Our first error is their experiment's error and our second error is the systematic error from using our best value.
[2] Assumes equal production of B^+ and B^0 at the $\Upsilon(4S)$.

$\Gamma(\overline{\Sigma}_c(2455)^{--} pK^+,\ \overline{\Sigma}_c^{--} \to \overline{\Lambda}_c^- \pi^-)/\Gamma_{total}$ Γ_{487}/Γ

VALUE (units 10^{-5})		DOCUMENT ID		TECN	COMMENT
0.89 ± 0.25 ± 0.05	[1,2]	AUBERT	09AG	BABR	$e^+e^- \to \Upsilon(4S)$

[1] AUBERT 09AG reports $(1.11 \pm 0.30 \pm 0.09 \pm 0.29) \times 10^{-5}$ from a measurement of $[\Gamma(B^0 \to \overline{\Sigma}_c(2455)^{--} pK^+,\ \overline{\Sigma}_c^{--} \to \overline{\Lambda}_c^- \pi^-)/\Gamma_{total}] \times [B(\Lambda_c^+ \to pK^-\pi^+)]$ assuming $B(\Lambda_c^+ \to pK^-\pi^+) = (5.0 \pm 1.3) \times 10^{-2}$, which we rescale to our best value $B(\Lambda_c^+ \to pK^-\pi^+) = (6.23 \pm 0.33) \times 10^{-2}$. Our first error is their experiment's error and our second error is the systematic error from using our best value.
[2] Assumes equal production of B^+ and B^0 at the $\Upsilon(4S)$.

$\Gamma(\Lambda_c^- pK^*(892)^0)/\Gamma_{total}$ Γ_{488}/Γ

VALUE (units 10^{-5})	CL%	DOCUMENT ID		TECN	COMMENT
< 2.42	90	[1] AUBERT	09AG	BABR	$e^+e^- \to \Upsilon(4S)$

[1] Assumes equal production of B^+ and B^0 at the $\Upsilon(4S)$.

$\Gamma(\Lambda_c^- p\overline{p}p)/\Gamma_{total}$ Γ_{491}/Γ

VALUE (units 10^{-6})		DOCUMENT ID		TECN	COMMENT
< 2.8	[1]	LEES	14C	BABR	$e^+e^- \to \Upsilon(4S)$

[1] Assumes equal production of B^+ and B^0 at the $\Upsilon(4S)$ and $B(\Lambda_c^+ \to pK^-\pi^+) = 0.050 \pm 0.013$.

$\Gamma(\overline{\Lambda}_c^- \Lambda K^+)/\Gamma_{total}$ Γ_{492}/Γ

VALUE (units 10^{-5})		DOCUMENT ID		TECN	COMMENT
4.7 ± 1.0 ± 0.3	[1,2]	LEES	11F	BABR	$e^+e^- \to \Upsilon(4S)$

[1] Assumes equal production of B^0 and B^+ from Upsilon(4S) decays.
[2] LEES 11F reports $(3.8 \pm 0.8 \pm 0.2 \pm 1.0) \times 10^{-5}$ from a measurement of $[\Gamma(B^0 \to \overline{\Lambda}_c^- \Lambda K^+)/\Gamma_{total}] / [B(\Lambda_c^+ \to pK^-\pi^+)] / [B(\Lambda \to p\pi^-)]$ assuming $B(\Lambda_c^+ \to pK^-\pi^+) = (5.0 \pm 1.3) \times 10^{-2}$, $B(\Lambda \to p\pi^-) = (63.9 \pm 0.5) \times 10^{-2}$, which we rescale to our best values $B(\Lambda_c^+ \to pK^-\pi^+) = (6.23 \pm 0.33) \times 10^{-2}$, $B(\Lambda \to p\pi^-) = (63.9 \pm 0.5) \times 10^{-2}$. Our first error is their experiment's error and our second error is the systematic error from using our best values. The reported uncertainties are statistical, systematic, and $\overline{\Lambda}_c^-$ branching fraction uncertainty.

$\Gamma(\overline{\Lambda}_c^- \Lambda_c^+)/\Gamma_{total}$ Γ_{493}/Γ

VALUE (units 10^{-5})	CL%	DOCUMENT ID		TECN	COMMENT
< 1.6	95	[1] AAIJ	14AA	LHCB	pp at 7 TeV
• • • We do not use the following data for averages, fits, limits, etc. • • •					
< 6.2	90	[2] UCHIDA	08	BELL	$e^+e^- \to \Upsilon(4S)$

[1] Uses $B(\overline{B}^0 \to D^+ D_s^-) = (7.2 \pm 0.8) \times 10^{-3}$.
[2] Assumes equal production of B^+ and B^0 at the $\Upsilon(4S)$.

$\Gamma(\overline{\Lambda}_c(2593)^- / \overline{\Lambda}_c(2625)^- p)/\Gamma_{total}$ Γ_{494}/Γ

VALUE	CL%	DOCUMENT ID		TECN	COMMENT
< 1.1 × 10^-4	90	[1,2] DYTMAN	02	CLE2	$e^+e^- \to \Upsilon(4S)$

[1] Assumes equal production of B^+ and B^0 at the $\Upsilon(4S)$.
[2] DYTMAN 02 measurement uses $B(\Lambda_c^- \to \overline{p}K^+\pi^-) = 5.0 \pm 1.3\%$. The second error includes the systematic and the uncertainty of the branching ratio.

$\Gamma(\Xi_c^- \Lambda_c^+,\ \Xi_c^- \to \Xi^+\pi^-\pi^-)/\Gamma_{total}$ Γ_{495}/Γ

VALUE (units 10^{-5})		DOCUMENT ID		TECN	COMMENT
1.8 ± 1.8 OUR AVERAGE Error includes scale factor of 2.2.					
1.2 ± 0.9 ± 0.1	[1,2]	AUBERT	08H	BABR	$e^+e^- \to \Upsilon(4S)$
$7.5^{+3.4}_{-2.7} \pm 0.4$	[2,3]	CHISTOV	06A	BELL	$e^+e^- \to \Upsilon(4S)$

[1] AUBERT 08H reports $(1.5 \pm 1.07 \pm 0.44) \times 10^{-5}$ from a measurement of $[\Gamma(B^0 \to \Xi_c^- \Lambda_c^+,\ \Xi_c^- \to \Xi^+\pi^-\pi^-)/\Gamma_{total}] \times [B(\Lambda_c^+ \to pK^-\pi^+)]$ assuming $B(\Lambda_c^+ \to pK^-\pi^+) = (5.0 \pm 1.3) \times 10^{-2}$, which we rescale to our best value $B(\Lambda_c^+ \to pK^-\pi^+) = (6.23 \pm 0.33) \times 10^{-2}$. Our first error is their experiment's error and our second error is the systematic error from using our best value.
[2] Assumes equal production of B^+ and B^0 at the $\Upsilon(4S)$.
[3] CHISTOV 06A reports $(9.3^{+3.7}_{-2.8} \pm 3.1) \times 10^{-5}$ from a measurement of $[\Gamma(B^0 \to \Xi_c^- \Lambda_c^+,\ \Xi_c^- \to \Xi^+\pi^-\pi^-)/\Gamma_{total}] \times [B(\Lambda_c^+ \to pK^-\pi^+)]$ assuming $B(\Lambda_c^+ \to pK^-\pi^+) = (5.0 \pm 1.3) \times 10^{-2}$, which we rescale to our best value $B(\Lambda_c^+ \to pK^-\pi^+) = (6.23 \pm 0.33) \times 10^{-2}$. Our first error is their experiment's error and our second error is the systematic error from using our best value.

$\Gamma(\Lambda_c^+ \Lambda_c^- K^0)/\Gamma_{total}$ Γ_{496}/Γ

VALUE (units 10^{-4})		DOCUMENT ID		TECN	COMMENT
4.3 ± 2.3 OUR AVERAGE					
3.1 ± 2.9 ± 0.2	[1,2]	AUBERT	08H	BABR	$e^+e^- \to \Upsilon(4S)$
$6.3^{+3.8}_{-3.6} \pm 0.3$	[2,3]	GABYSHEV	06	BELL	$e^+e^- \to \Upsilon(4S)$

[1] AUBERT 08H reports $(0.38 \pm 0.31 \pm 0.21) \times 10^{-3}$ from a measurement of $[\Gamma(B^0 \to \Lambda_c^+ \Lambda_c^- K^0)/\Gamma_{total}] \times [B(\Lambda_c^+ \to pK^-\pi^+)]$ assuming $B(\Lambda_c^+ \to pK^-\pi^+) = (5.0 \pm 1.3) \times 10^{-2}$, which we rescale to our best value $B(\Lambda_c^+ \to pK^-\pi^+) = (6.23 \pm 0.33) \times 10^{-2}$. Our first error is their experiment's error and our second error is the systematic error from using our best value.
[2] Assumes equal production of B^+ and B^0 at the $\Upsilon(4S)$.

[3] GABYSHEV 06 reports $(7.9^{+2.9}_{-2.3} \pm 4.3) \times 10^{-4}$ from a measurement of $[\Gamma(B^0 \to \Lambda_c^+ \Lambda_c^- K^0)/\Gamma_{\rm total}] \times [{\rm B}(\Lambda_c^+ \to p K^- \pi^+)]$ assuming ${\rm B}(\Lambda_c^+ \to p K^- \pi^+) = (5.0 \pm 1.3) \times 10^{-2}$, which we rescale to our best value ${\rm B}(\Lambda_c^+ \to p K^- \pi^+) = (6.23 \pm 0.33) \times 10^{-2}$. Our first error is their experiment's error and our second error is the systematic error from using our best value.

$\Gamma(\gamma\gamma)/\Gamma_{\rm total}$ Γ_{497}/Γ

Test for ΔB=1 weak neutral current. Allowed by higher-order electroweak interactions.

VALUE	CL%	DOCUMENT ID		TECN	COMMENT
$<3.2 \times 10^{-7}$	90	[1] DEL-AMO-SA...11A		BABR	$e^+e^- \to \Upsilon(4S)$
• • • We do not use the following data for averages, fits, limits, etc. • • •					
$<6.2 \times 10^{-7}$	90	[1] VILLA	06	BELL	$e^+e^- \to \Upsilon(4S)$
$<1.7 \times 10^{-6}$	90	[1] AUBERT	01I	BABR	$e^+e^- \to \Upsilon(4S)$
$<3.9 \times 10^{-5}$	90	[2] ACCIARRI	95I	L3	$e^+e^- \to Z$

[1] Assumes equal production of B^+ and B^0 at the $\Upsilon(4S)$.
[2] ACCIARRI 95I assumes $f_{B^0} = 39.5 \pm 4.0$ and $f_{B_s} = 12.0 \pm 3.0\%$.

$\Gamma(e^+e^-)/\Gamma_{\rm total}$ Γ_{498}/Γ

Test for ΔB=1 weak neutral current. Allowed by higher-order electroweak interactions.

VALUE	CL%	DOCUMENT ID		TECN	COMMENT
$< 8.3 \times 10^{-8}$	90	AALTONEN	09P	CDF	$p\overline{p}$ at 1.96 TeV
• • • We do not use the following data for averages, fits, limits, etc. • • •					
$<11.3 \times 10^{-8}$	90	[1] AUBERT	08P	BABR	$e^+e^- \to \Upsilon(4S)$
$< 6.1 \times 10^{-8}$	90	[1] AUBERT	05W	BABR	Repl. by AUBERT 08P
$< 1.9 \times 10^{-7}$	90	[1] CHANG	03	BELL	$e^+e^- \to \Upsilon(4S)$
$< 8.3 \times 10^{-7}$	90	[1] BERGFELD	00B	CLE2	$e^+e^- \to \Upsilon(4S)$
$< 1.4 \times 10^{-5}$	90	[2] ACCIARRI	97B	L3	$e^+e^- \to Z$
$< 5.9 \times 10^{-6}$	90	AMMAR	94	CLE2	Repl. by BERGFELD 00B
$< 2.6 \times 10^{-5}$	90	[3] AVERY	89B	CLEO	$e^+e^- \to \Upsilon(4S)$
$< 7.6 \times 10^{-5}$	90	[4] ALBRECHT	87D	ARG	$e^+e^- \to \Upsilon(4S)$
$< 6.4 \times 10^{-5}$	90	[5] AVERY	87	CLEO	$e^+e^- \to \Upsilon(4S)$
$< 3 \times 10^{-4}$	90	GILES	84	CLEO	Repl. by AVERY 87

[1] Assumes equal production of B^+ and B^0 at the $\Upsilon(4S)$.
[2] ACCIARRI 97B assume PDG 96 production fractions for B^+, B^0, B_s, and Λ_b.
[3] AVERY 89B reports $< 3 \times 10^{-5}$ assuming the $\Upsilon(4S)$ decays 43% to $B^0\overline{B}^0$. We rescale to 50%.
[4] ALBRECHT 87D reports $< 8.5 \times 10^{-5}$ assuming the $\Upsilon(4S)$ decays 45% to $B^0\overline{B}^0$. We rescale to 50%.
[5] AVERY 87 reports $< 8 \times 10^{-5}$ assuming the $\Upsilon(4S)$ decays 40% to $B^0\overline{B}^0$. We rescale to 50%.

$\Gamma(e^+e^-\gamma)/\Gamma_{\rm total}$ Γ_{499}/Γ

Test for ΔB=1 weak neutral current. Allowed by higher-order electroweak interactions.

VALUE	CL%	DOCUMENT ID	TECN	COMMENT
$<1.2 \times 10^{-7}$	90	AUBERT 08C	BABR	$e^+e^- \to \Upsilon(4S)$

$\Gamma(\mu^+\mu^-)/\Gamma_{\rm total}$ Γ_{500}/Γ

Test for ΔB=1 weak neutral current. Allowed by higher-order electroweak interactions.

VALUE (units 10^{-9})	CL%	DOCUMENT ID		TECN	COMMENT
$0.16^{+0.16}_{-0.14}$ OUR AVERAGE Error includes scale factor of 1.9. See the ideogram below.					
$0.15^{+0.12+0.02}_{-0.10-0.01}$		[1] AAIJ	17AI	LHCB	pp at 7, 8, 13 TeV
-0.25 ± 0.20		[2] AABOUD	16L	ATLS	pp at 7, 8 TeV
$0.39^{+0.16}_{-0.14}$		[3] KHACHATRY...15BE		LHC	pp at 7, 8 TeV
• • • We do not use the following data for averages, fits, limits, etc. • • •					
< 0.80	90	[4] AAIJ	13B	LHCB	Repl. by AAIJ 13BA
< 0.63	90	[5] AAIJ	13BA	LHCB	Repl. by KHACHATRYAN 15BE
< 3.8	90	[6] AALTONEN	13F	CDF	$p\overline{p}$ at 1.96 TeV
< 0.92	90	[7] CHATRCHYAN	13AW	CMS	pp at 7, 8 TeV
< 2.6	90	[4] AAIJ	12A	LHCB	Repl. by AAIJ 12W
< 0.81	90	[8] AAIJ	12W	LHCB	Repl. by AAIJ 13B
< 1.4	90	[8] CHATRCHYAN	12A	CMS	pp at 7 TeV
< 12	90	[9] AAIJ	11B	LHCB	Repl. by AAIJ 12A
< 5.0	90	[8] AALTONEN	11AG	CDF	$p\overline{p}$ at 1.96 TeV
< 3.7	90	[8] CHATRCHYAN	11T	CMS	Repl. by CHATRCHYAN 12A

[1] Corresponds to a 95% CL upper limit of $< 0.34 \times 10^{-9}$.
[2] This value is obtained from a profile-likelihood fit, see Fig. 9. It corresponds to an uppper limit of $< 0.42 \times 10^{-9}$ at 95% C.L.
[3] Derived from the combined fit to CMS and LHCb data. Uncertainty includes both statistical and systematic component. Also reports ${\rm B}(B^0 \to \mu^+\mu^-)/{\rm B}(B_s \to \mu^+\mu^-) = 0.14^{+0.08}_{-0.06}$.
[4] Uses ${\rm B}(B^+ \to J/\psi K^+ \to \mu^+\mu^- K^+) = (6.01 \pm 0.21) \times 10^{-5}$ and ${\rm B}(B^0 \to K^+\pi^-) = (1.94 \pm 0.06) \times 10^{-5}$ for normalization.
[5] Reports also a limit of $< 7.4 \times 10^{-10}$ at 95% CL. Uses normalization modes $B^+ \to J/\psi K^+ \to \mu^+\mu^- K^+$ and $B^0 \to K^+\pi^-$.
[6] Uses normalization mode ${\rm B}(B^+ \to J/\psi K^+) = (10.22 \pm 0.35) \times 10^{-4}$.
[7] Uses ${\rm B}(B^+ \to J/\psi K^+ \to \mu^+\mu^- K^+) = (6.0 \pm 0.2) \times 10^{-5}$ for normalization.
[8] Uses ${\rm B}(B^+ \to J/\psi K^+ \to \mu^+\mu^- K^+) = (6.01 \pm 0.21) \times 10^{-5}$.
[9] Uses B production ratio $f(\overline{b} \to B^+)/f(\overline{b} \to B_s^0) = 3.71 \pm 0.47$ and three normalization modes.

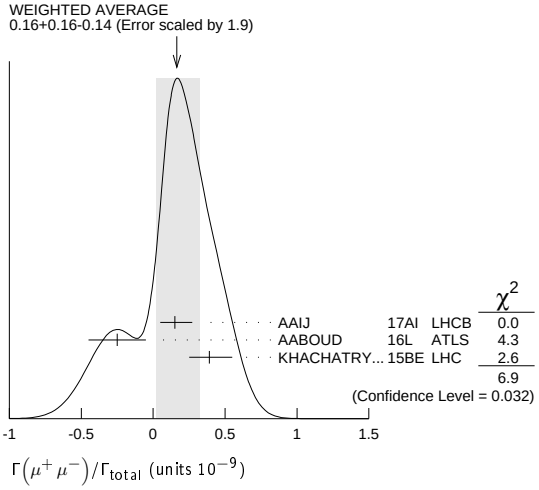

$\Gamma(\mu^+\mu^-\gamma)/\Gamma_{\rm total}$ Γ_{501}/Γ

Test for ΔB=1 weak neutral current. Allowed by higher-order electroweak interactions.

VALUE	CL%	DOCUMENT ID	TECN	COMMENT
$<1.6 \times 10^{-7}$	90	AUBERT 08C	BABR	$e^+e^- \to \Upsilon(4S)$

$\Gamma(\tau^+\tau^-)/\Gamma_{\rm total}$ Γ_{504}/Γ

Test for ΔB=1 weak neutral current. Allowed by higher-order electroweak interactions.

VALUE	CL%	DOCUMENT ID		TECN	COMMENT
$<2.1 \times 10^{-3}$	95	[1] AAIJ	17AJ	LHCB	pp at 7, 8 TeV
• • • We do not use the following data for averages, fits, limits, etc. • • •					
$<4.1 \times 10^{-3}$	90	[2] AUBERT	06S	BABR	$e^+e^- \to \Upsilon(4S)$

[1] Assuming no contribution from $B_s^0 \to \tau^+\tau^-$.
[2] Assumes equal production of B^+ and B^0 at the $\Upsilon(4S)$.

$\Gamma(\mu^+\mu^-\mu^+\mu^-)/\Gamma_{\rm total}$ Γ_{502}/Γ

VALUE	CL%	DOCUMENT ID	TECN	COMMENT
$<6.9 \times 10^{-10}$	95	AAIJ 17N	LHCB	pp at 7, 8 TeV
• • • We do not use the following data for averages, fits, limits, etc. • • •				
$<5.3 \times 10^{-9}$	90	[1] AAIJ 13AW	LHCB	Repl. by AAIJ 17N

[1] Also reports a limit of $< 6.6 \times 10^{-9}$ at 95% CL.

$\Gamma(SP, S \to \mu^+\mu^-, P \to \mu^+\mu^-)/\Gamma_{\rm total}$ Γ_{503}/Γ

Here S and P are the hypothetical scalar and pseudoscalar particles with masses of 2.5 GeV/c^2 and 214.3 MeV/c^2, respectively.

VALUE	CL%	DOCUMENT ID	TECN	COMMENT
$<6.0 \times 10^{-10}$	95	AAIJ 17N	LHCB	pp at 7, 8 TeV
• • • We do not use the following data for averages, fits, limits, etc. • • •				
$<5.1 \times 10^{-9}$	90	[1] AAIJ 13AW	LHCB	Repl. by AAIJ 17N

[1] Also reports a limit of $< 6.3 \times 10^{-9}$ at 95% CL.

$\Gamma(\pi^0\ell^+\ell^-)/\Gamma_{\rm total}$ Γ_{505}/Γ

VALUE	CL%	DOCUMENT ID		TECN	COMMENT
$<5.3 \times 10^{-8}$	90	[1] LEES	13M	BABR	$e^+e^- \to \Upsilon(4S)$
• • • We do not use the following data for averages, fits, limits, etc. • • •					
$<1.5 \times 10^{-7}$	90	[1] WEI	08A	BELL	$e^+e^- \to \Upsilon(4S)$
$<1.2 \times 10^{-7}$	90	[1] AUBERT	07AG	BABR	Repl. by LEES 13M

[1] Assumes equal production of B^+ and B^0 at the $\Upsilon(4S)$.

$\Gamma(\pi^0\nu\overline{\nu})/\Gamma_{\rm total}$ Γ_{511}/Γ

Test for $\Delta B = 1$ weak neutral current. Allowed by higher-order electroweak interaction.

VALUE	CL%	DOCUMENT ID		TECN	COMMENT
$<0.9 \times 10^{-5}$	90	[1] GRYGIER	17	BELL	$e^+e^- \to \Upsilon(4S)$
• • • We do not use the following data for averages, fits, limits, etc. • • •					
$<6.9 \times 10^{-5}$	90	[1] LUTZ	13	BELL	$e^+e^- \to \Upsilon(4S)$
$<2.2 \times 10^{-4}$	90	[1] CHEN	07D	BELL	Repl. by LUTZ 13

[1] Assumes equal production of B^+ and B^0 at the $\Upsilon(4S)$.

$\Gamma(\pi^0 e^+ e^-)/\Gamma_{\rm total}$ Γ_{506}/Γ

VALUE	CL%	DOCUMENT ID		TECN	COMMENT
$<8.4 \times 10^{-8}$	90	[1] LEES	13M	BABR	$e^+e^- \to \Upsilon(4S)$
• • • We do not use the following data for averages, fits, limits, etc. • • •					
$<2.3 \times 10^{-7}$	90	[1] WEI	08A	BELL	$e^+e^- \to \Upsilon(4S)$
$<1.4 \times 10^{-7}$	90	[1] AUBERT	07AG	BABR	Repl. by LEES 13M

[1] Assumes equal production of B^+ and B^0 at the $\Upsilon(4S)$.

$\Gamma(\pi^0\mu^+\mu^-)/\Gamma_{\rm total}$ Γ_{507}/Γ

VALUE	CL%	DOCUMENT ID		TECN	COMMENT
$<6.9 \times 10^{-8}$	90	[1] LEES	13M	BABR	$e^+e^- \to \Upsilon(4S)$

• • • We do not use the following data for averages, fits, limits, etc. • • •

$<1.8\times10^{-7}$	90	[1] WEI	08A	BELL	$e^+e^-\to\ \Upsilon(4S)$	
$<5.1\times10^{-7}$	90	[1] AUBERT	07AG	BABR	$e^+e^-\to\ \Upsilon(4S)$	

[1] Assumes equal production of B^+ and B^0 at the $\Upsilon(4S)$.

$\Gamma(\eta\ell^+\ell^-)/\Gamma_{total}$ Γ_{508}/Γ

VALUE	CL%	DOCUMENT ID		TECN	COMMENT
$<6.4\times10^{-8}$	90	[1] LEES	13M	BABR	$e^+e^-\to\ \Upsilon(4S)$

[1] Assumes equal production of B^+ and B^0 at the $\Upsilon(4S)$.

$\Gamma(\eta e^+e^-)/\Gamma_{total}$ Γ_{509}/Γ

VALUE	CL%	DOCUMENT ID		TECN	COMMENT
$<10.8\times10^{-8}$	90	[1] LEES	13M	BABR	$e^+e^-\to\ \Upsilon(4S)$

[1] Assumes equal production of B^+ and B^0 at the $\Upsilon(4S)$.

$\Gamma(\eta\mu^+\mu^-)/\Gamma_{total}$ Γ_{510}/Γ

VALUE	CL%	DOCUMENT ID		TECN	COMMENT
$<11.2\times10^{-8}$	90	[1] LEES	13M	BABR	$e^+e^-\to\ \Upsilon(4S)$

[1] Assumes equal production of B^+ and B^0 at the $\Upsilon(4S)$.

$\Gamma(K^0\ell^+\ell^-)/\Gamma_{total}$ Γ_{512}/Γ

VALUE (units 10^{-7})	CL%	DOCUMENT ID		TECN	COMMENT
$3.1^{+0.8}_{-0.7}$ OUR AVERAGE					
$2.1^{+1.5}_{-1.3}\pm0.2$		[1] AUBERT	09T	BABR	$e^+e^-\to\ \Upsilon(4S)$
$3.4^{+0.9}_{-0.8}\pm0.2$		[1] WEI	09A	BELL	$e^+e^-\to\ \Upsilon(4S)$
• • • We do not use the following data for averages, fits, limits, etc. • • •					
$2.9^{+1.6}_{-1.3}\pm0.3$		[1] AUBERT,B	06J	BABR	Repl. by AUBERT 09T
<6.8	90	[1] ISHIKAWA	03	BELL	$e^+e^-\to\ \Upsilon(4S)$

[1] Assumes equal production of B^0 and B^+ at $\Upsilon(4S)$.

$\Gamma(K^0e^+e^-)/\Gamma_{total}$ Γ_{513}/Γ

Test for ΔB=1 weak neutral current. Allowed by higher-order electroweak interactions.

VALUE (units 10^{-7})	CL%	DOCUMENT ID		TECN	COMMENT
$1.6^{+1.0}_{-0.8}$ OUR AVERAGE					
$0.8^{+1.5}_{-1.2}\pm0.1$		[1] AUBERT	09T	BABR	$e^+e^-\to\ \Upsilon(4S)$
$2.0^{+1.4}_{-1.0}\pm0.1$		[1] WEI	09A	BELL	$e^+e^-\to\ \Upsilon(4S)$
• • • We do not use the following data for averages, fits, limits, etc. • • •					
$1.3^{+1.6}_{-1.1}\pm0.2$		[1] AUBERT,B	06J	BABR	Repl. by AUBERT 09T
$-\ 2.1^{+2.3}_{-1.6}\pm0.8$		[1] AUBERT	03U	BABR	$e^+e^-\to\ \Upsilon(4S)$
$<\ 5.4$	90	[2] ISHIKAWA	03	BELL	$e^+e^-\to\ \Upsilon(4S)$
$<\ 27$	90	[1] ABE	02	BELL	Repl. by ISHIKAWA 03
$<\ 38$	90	[1] AUBERT	02L	BABR	$e^+e^-\to\ \Upsilon(4S)$
$<\ 84.5$	90	[3] ANDERSON	01B	CLE2	$e^+e^-\to\ \Upsilon(4S)$
$<\ 3000$	90	ALBRECHT	91E	ARG	$e^+e^-\to\ \Upsilon(4S)$
$<\ 5200$	90	[4] AVERY	87	CLEO	$e^+e^-\to\ \Upsilon(4S)$

[1] Assumes equal production of B^+ and B^0 at the $\Upsilon(4S)$.
[2] Assumes equal production of B^0 and B^+ at $\Upsilon(4S)$.
[3] The result is for di-lepton masses above 0.5 GeV.
[4] AVERY 87 reports $<6.5\times10^{-4}$ assuming the $\Upsilon(4S)$ decays 40% to $B^0\overline{B}^0$. We rescale to 50%.

$\Gamma(K^0\nu\overline{\nu})/\Gamma_{total}$ Γ_{515}/Γ

Test for $\Delta B=1$ weak neutral current. Allowed by higher-order electroweak interaction.

VALUE	CL%	DOCUMENT ID		TECN	COMMENT
$<2.6\times10^{-5}$	90	[1] GRYGIER	17	BELL	$e^+e^-\to\ \Upsilon(4S)$
• • • We do not use the following data for averages, fits, limits, etc. • • •					
$<4.9\times10^{-5}$	90	[1,2] LEES	13I	BABR	$e^+e^-\to\ \Upsilon(4S)$
$<19.4\times10^{-5}$	90	[1] LUTZ	13	BELL	$e^+e^-\to\ \Upsilon(4S)$
$<5.6\times10^{-5}$	90	[1] DEL-AMO-SA...10Q		BABR	Repl. by LEES 13I
$<1.6\times10^{-4}$	90	[1] CHEN	07D	BELL	$e^+e^-\to\ \Upsilon(4S)$

[1] Assumes equal production of B^+ and B^0 at the $\Upsilon(4S)$.
[2] Also reported a limit $<8.1\times10^{-5}$ at 90% CL obtained using a fully reconstructed hadronic B-tag evnets.

$\Gamma(\rho^0\nu\overline{\nu})/\Gamma_{total}$ Γ_{516}/Γ

Test for $\Delta B=1$ weak neutral current. Allowed by higher-order electroweak interaction.

VALUE	CL%	DOCUMENT ID		TECN	COMMENT
$<4.0\ \times10^{-5}$	90	[1] GRYGIER	17	BELL	$e^+e^-\to\ \Upsilon(4S)$
• • • We do not use the following data for averages, fits, limits, etc. • • •					
$<2.08\times10^{-4}$	90	[1] LUTZ	13	BELL	$e^+e^-\to\ \Upsilon(4S)$
$<4.4\ \times10^{-4}$	90	[1] CHEN	07D	BELL	Repl. by LUTZ 13

[1] Assumes equal production of B^+ and B^0 at the $\Upsilon(4S)$.

$\Gamma(K^0\mu^+\mu^-)/\Gamma_{total}$ Γ_{514}/Γ

Test for $\Delta B=1$ weak neutral current. Allowed by higher-order electroweak interactions.

VALUE (units 10^{-7})	CL%	DOCUMENT ID		TECN	COMMENT
3.39 ± 0.34 OUR FIT					
$3.4\ \pm0.4$ OUR AVERAGE					
$3.27\pm0.34\pm0.17$		[1] AAIJ	14M	LHCB	pp at 7, 8 TeV
$4.9\ ^{+2.9}_{-2.5}\ \pm0.3$		[2] AUBERT	09T	BABR	$e^+e^-\to\ \Upsilon(4S)$
$4.4\ ^{+1.3}_{-1.1}\ \pm0.3$		[2] WEI	09A	BELL	$e^+e^-\to\ \Upsilon(4S)$
• • • We do not use the following data for averages, fits, limits, etc. • • •					
$3.1\ ^{+0.7}_{-0.6}$		AAIJ	12AH	LHCB	Repl. by AAIJ 14M
$5.9\ ^{+3.3}_{-2.6}\ \pm0.7$		[2] AUBERT,B	06J	BABR	Repl. by AUBERT 09T
$1.63^{+0.82}_{-0.63}\pm0.14$		[2] AUBERT	03U	BABR	Repl. by AUBERT,B 06J
$5.6\ ^{+2.9}_{-2.3}\ \pm0.5$		[3] ISHIKAWA	03	BELL	Repl. by WEI 09A
<33	90	[2] ABE	02	BELL	Repl. by ISHIKAWA 03
<36	90	AUBERT	02L	BABR	$e^+e^-\to\ \Upsilon(4S)$
<66.4	90	[4] ANDERSON	01B	CLE2	$e^+e^-\to\ \Upsilon(4S)$
<5200	90	ALBRECHT	91E	ARG	$e^+e^-\to\ \Upsilon(4S)$
<3600	90	[5] AVERY	87	CLEO	$e^+e^-\to\ \Upsilon(4S)$

[1] Uses $B(B^0\to\ J/\psi(1S)K^0)=(0.928\pm0.013\pm0.037)\times10^{-3}$ for normalization.
[2] Assumes equal production of B^+ and B^0 at the $\Upsilon(4S)$.
[3] Assumes equal production of B^0 and B^+ at $\Upsilon(4S)$. The second error is a total of systematic uncertainties including model dependence.
[4] The result is for di-lepton masses above 0.5 GeV.
[5] AVERY 87 reports $<4.5\times10^{-4}$ assuming the $\Upsilon(4S)$ decays 40% to $B^0\overline{B}^0$. We rescale to 50%.

$\Gamma(K^0\mu^+\mu^-)/\Gamma(J/\psi(1S)K^0)$ $\Gamma_{514}/\Gamma_{183}$

VALUE (units 10^{-3})	DOCUMENT ID		TECN	COMMENT
0.39 ± 0.04 OUR FIT				
$0.37\pm0.12\pm0.02$	AALTONEN	11AI	CDF	$p\overline{p}$ at 1.96 TeV

$\Gamma(K^*(892)^0\ell^+\ell^-)/\Gamma_{total}$ Γ_{517}/Γ

Test for $\Delta B=1$ weak neutral current. Allowed by higher-order electroweak interactions.

VALUE (units 10^{-7})	DOCUMENT ID		TECN	COMMENT
$9.9^{+1.2}_{-1.1}$ OUR AVERAGE				
$10.3^{+2.2}_{-2.1}\pm0.7$	[1] AUBERT	09T	BABR	$e^+e^-\to\ \Upsilon(4S)$
$9.7^{+1.3}_{-1.1}\pm0.7$	[1] WEI	09A	BELL	$e^+e^-\to\ \Upsilon(4S)$
• • • We do not use the following data for averages, fits, limits, etc. • • •				
$8.1^{+2.1}_{-1.9}\pm0.9$	[1] AUBERT,B	06J	BABR	Repl. by AUBERT 09T
$11.7^{+3.0}_{-2.7}\pm0.9$	[1] ISHIKAWA	03	BELL	Repl. by WEI 09A

[1] Assumes equal production of B^0 and B^+ at $\Upsilon(4S)$.

$\Gamma(K^*(892)^0e^+e^-)/\Gamma_{total}$ Γ_{518}/Γ

Test for $\Delta B=1$ weak neutral current. Allowed by higher-order electroweak interactions.

VALUE (units 10^{-7})	CL%	DOCUMENT ID		TECN	COMMENT
$10.3^{+1.9}_{-1.7}$ OUR AVERAGE					
$8.6^{+2.6}_{-2.4}\pm0.5$		[1] AUBERT	09T	BABR	$e^+e^-\to\ \Upsilon(4S)$
$11.8^{+2.7}_{-2.2}\pm0.9$		[1] WEI	09A	BELL	$e^+e^-\to\ \Upsilon(4S)$
• • • We do not use the following data for averages, fits, limits, etc. • • •					
$10.4^{+3.3}_{-2.9}\pm1.1$		[1] AUBERT,B	06J	BABR	Repl. by AUBERT 09T
$11.1^{+5.6}_{-4.7}\pm1.1$		[1] AUBERT	03U	BABR	$e^+e^-\to\ \Upsilon(4S)$
$<\ 24$	90	[2] ISHIKAWA	03	BELL	$e^+e^-\to\ \Upsilon(4S)$
$<\ 64$	90	[1] ABE	02	BELL	Repl. by ISHIKAWA 03
$<\ 67$	90	[1] AUBERT	02L	BABR	$e^+e^-\to\ \Upsilon(4S)$
<2900	90	ALBRECHT	91E	ARG	$e^+e^-\to\ \Upsilon(4S)$

[1] Assumes equal production of B^+ and B^0 at the $\Upsilon(4S)$.
[2] Assumes equal production of B^0 and B^+ at $\Upsilon(4S)$.

$\Gamma(K^*(892)^0\mu^+\mu^-)/\Gamma_{total}$ Γ_{519}/Γ

Test for $\Delta B=1$ weak neutral current. Allowed by higher-order electroweak interactions.

VALUE (units 10^{-7})	CL%	DOCUMENT ID		TECN	COMMENT
$9.4\ \pm0.5$ OUR FIT					
$9.4\ \pm0.6$ OUR AVERAGE					
$9.04^{+0.16}_{-0.15}\pm0.62$		[1] AAIJ	17Q	LHCB	pp at 7, 8 TeV
$13.5\ ^{+4.0}_{-3.7}\ \pm1.0$		[2] AUBERT	09T	BABR	$e^+e^-\to\ \Upsilon(4S)$
$10.6\ ^{+1.9}_{-1.4}\ \pm0.7$		[2] WEI	09A	BELL	$e^+e^-\to\ \Upsilon(4S)$
• • • We do not use the following data for averages, fits, limits, etc. • • •					
$10.36^{+0.18}_{-0.17}\pm0.71$		[1] AAIJ	16AO	LHCB	Repl. by AAIJ 17Q
$8.7\ ^{+3.8}_{-3.3}\ \pm1.2$		[2] AUBERT,B	06J	BABR	Repl. by AUBERT 09T

$8.6\ ^{+7.9}_{-5.8}\ \pm1.1$		[2] AUBERT	03U	BABR	Repl. by AUBERT,B 06J
$13.3\ ^{+4.2}_{-3.7}\ \pm1.1$		[3] ISHIKAWA	03	BELL	Repl. by WEI 09A
<42	90	[2] ABE	02	BELL	$e^+e^- \to \Upsilon(4S)$
<33	90	AUBERT	02L	BABR	$e^+e^- \to \Upsilon(4S)$
<40	90	[4] AFFOLDER	99B	CDF	$p\overline{p}$ at 1.8 TeV

[1] Uses $B(B^0 \to J/\psi K^*(892)^0) = (1.19 \pm 0.01 \pm 0.08) \times 10^{-3}$. The second error is the total systematic uncertainty.
[2] Assumes equal production of B^+ and B^0 at the $\Upsilon(4S)$.
[3] Assumes equal production of B^0 and B^+ at $\Upsilon(4S)$. The second error is a total of systematic uncertainties including model dependence.
[4] AFFOLDER 99B measured relative to $B^0 \to J/\psi(1S) K^*(892)^0$.

$\Gamma(K^*(892)^0\mu^+\mu^-)/\Gamma(J/\psi(1S)K^*(892)^0)$ $\Gamma_{519}/\Gamma_{185}$

VALUE (units 10^{-3})	DOCUMENT ID		TECN	COMMENT
0.75±0.05 OUR FIT				
0.77±0.08±0.03	AALTONEN	11AI	CDF	$p\overline{p}$ at 1.96 TeV
• • • We do not use the following data for averages, fits, limits, etc. • • •				
0.80±0.10±0.06	AALTONEN	11L	CDF	Repl. by AALTONEN 11AI
0.61±0.23±0.07	AALTONEN	09B	CDF	Repl. by AALTONEN 11L

$\Gamma(K^*(892)^0\chi,\ \chi \to \mu^+\mu^-)/\Gamma_{\text{total}}$ Γ_{520}/Γ

VALUE	CL%	DOCUMENT ID		TECN	COMMENT
< ~ 10^{-9}	95	[1] AAIJ	15AZ	LHCB	pp at 7, 8 TeV

[1] The limt is obtained as a function of di-muon mass. A normalizing mode branching fraction value of $B(B^0 \to K^{*0}\mu^+\mu^-) = (1.6 \pm 0.3) \times 10^{-7}$ is used.

$\Gamma(\pi^+\pi^-\mu^+\mu^-)/\Gamma_{\text{total}}$ Γ_{521}/Γ

VALUE (units 10^{-8})	DOCUMENT ID		TECN	COMMENT
2.1±0.5±0.1	[1] AAIJ	15S	LHCB	pp at 7, 8 TeV

[1] AAIJ 15S reports $(2.11 \pm 0.51 \pm 0.15 \pm 0.16) \times 10^{-8}$ from a measurement of $[\Gamma(B^0 \to \pi^+\pi^-\mu^+\mu^-)/\Gamma_{\text{total}}] / [B(B^0 \to J/\psi(1S)K^*(892)^0)]$ assuming $B(B^0 \to J/\psi(1S)K^*(892)^0) = (1.3 \pm 0.1) \times 10^{-3}$, which we rescale to our best value $B(B^0 \to J/\psi(1S)K^*(892)^0) = (1.27 \pm 0.05) \times 10^{-3}$. Our first error is their experiment's error and our second error is the systematic error from using our best value.

$\Gamma(K^*(892)^0\nu\overline{\nu})/\Gamma_{\text{total}}$ Γ_{522}/Γ

Test for ΔB=1 weak neutral current. Allowed by higher-order electroweak interactions.

VALUE	CL%	DOCUMENT ID		TECN	COMMENT
<1.8 × 10^{-5}	90	[1] GRYGIER	17	BELL	$e^+e^- \to \Upsilon(4S)$
• • • We do not use the following data for averages, fits, limits, etc. • • •					
<1.2 × 10^{-4}	90	[1,2] LEES	13I	BABR	$e^+e^- \to \Upsilon(4S)$
<5.5 × 10^{-5}	90	[1] LUTZ	13	BELL	$e^+e^- \to \Upsilon(4S)$
<1.2 × 10^{-4}	90	AUBERT	08BC	BABR	Repl. by LEES 13I
<3.4 × 10^{-4}	90	[1] CHEN	07D	BELL	$e^+e^- \to \Upsilon(4S)$
<1.0 × 10^{-3}	90	[3] ADAM	96D	DLPH	$e^+e^- \to Z$

[1] Assumes equal production of B^+ and B^0 at the $\Upsilon(4S)$.
[2] Also reported a limit < 9.3 × 10^{-5} at 90% CL obtained using a fully reconstructed hadronic B-tag evnets.
[3] ADAM 96D assumes $f_{B^0} = f_{B^-} = 0.39$ and $f_{B_s} = 0.12$.

$\Gamma(\text{invisible})/\Gamma_{\text{total}}$ Γ_{523}/Γ

VALUE (units 10^{-5})	CL%	DOCUMENT ID		TECN	COMMENT
< 2.4	90	[1] LEES	12T	BABR	$e^+e^- \to \Upsilon(4S)$
• • • We do not use the following data for averages, fits, limits, etc. • • •					
<13	90	[2] HSU	12	BELL	$e^+e^- \to \Upsilon(4S)$
<22	90	[1] AUBERT,B	04J	BABR	$e^+e^- \to \Upsilon(4S)$

[1] Uses the fully reconstructed $B^0 \to D^{(*)-}\ell^+\nu_\ell$ events as a tag.
[2] Identified by fully reconstructing a hadronic decay of the accompanying B meson and requiring no other particles in the event.

$\Gamma(\nu\overline{\nu}\gamma)/\Gamma_{\text{total}}$ Γ_{524}/Γ

VALUE (units 10^{-5})	CL%	DOCUMENT ID		TECN	COMMENT
<1.7	90	[1] LEES	12T	BABR	$e^+e^- \to \Upsilon(4S)$
• • • We do not use the following data for averages, fits, limits, etc. • • •					
<4.7	90	[1] AUBERT,B	04J	BABR	Repl. by LEES 12T

[1] Uses the fully reconstructed $B^0 \to D^{(*)-}\ell^+\nu_\ell$ events as a tag.

$\Gamma(\phi\nu\overline{\nu})/\Gamma_{\text{total}}$ Γ_{525}/Γ

Test for $\Delta B = 1$ weak neutral current. Allowed by higher-order electroweak interaction.

VALUE	CL%	DOCUMENT ID		TECN	COMMENT
<1.27 × 10^{-4}	90	[1] LUTZ	13	BELL	$e^+e^- \to \Upsilon(4S)$
• • • We do not use the following data for averages, fits, limits, etc. • • •					
<5.8 × 10^{-5}	90	[1] CHEN	07D	BELL	Repl. by LUTZ 13

[1] Assumes equal production of B^+ and B^0 at the $\Upsilon(4S)$.

$\Gamma(e^\pm\mu^\mp)/\Gamma_{\text{total}}$ Γ_{526}/Γ

Test of lepton family number conservation. Allowed by higher-order electroweak interactions.

VALUE	CL%	DOCUMENT ID		TECN	COMMENT
< 2.8 × 10^{-9}	90	[1] AAIJ	13BM	LHCB	pp at 7 TeV
• • • We do not use the following data for averages, fits, limits, etc. • • •					
< 6.4 × 10^{-8}	90	AALTONEN	09P	CDF	$p\overline{p}$ at 1.96 TeV
< 9.2 × 10^{-8}	90	[2] AUBERT	08P	BABR	$e^+e^- \to \Upsilon(4S)$
< 1.8 × 10^{-7}	90	[2] AUBERT	05W	BABR	$e^+e^- \to \Upsilon(4S)$
< 1.7 × 10^{-7}	90	[2] CHANG	03	BELL	$e^+e^- \to \Upsilon(4S)$
<15 × 10^{-7}	90	[2] BERGFELD	00B	CLE2	$e^+e^- \to \Upsilon(4S)$
< 3.5 × 10^{-6}	90	ABE	98V	CDF	$p\overline{p}$ at 1.8 TeV
< 1.6 × 10^{-5}	90	[3] ACCIARRI	97B	L3	$e^+e^- \to Z$
< 5.9 × 10^{-6}	90	AMMAR	94	CLE2	$e^+e^- \to \Upsilon(4S)$
< 3.4 × 10^{-5}	90	[4] AVERY	89B	CLEO	$e^+e^- \to \Upsilon(4S)$
< 4.5 × 10^{-5}	90	[5] ALBRECHT	87D	ARG	$e^+e^- \to \Upsilon(4S)$
< 7.7 × 10^{-5}	90	[6] AVERY	87	CLEO	$e^+e^- \to \Upsilon(4S)$
< 3 × 10^{-4}	90	GILES	84	CLEO	Repl. by AVERY 87

[1] Uses normalization mode $B(B^0 \to K^+\pi^-) = (19.4 \pm 0.6) \times 10^{-6}$.
[2] Assumes equal production of B^+ and B^0 at the $\Upsilon(4S)$.
[3] ACCIARRI 97B assume PDG 96 production fractions for B^+, B^0, B_s, and Λ_b.
[4] Paper assumes the $\Upsilon(4S)$ decays 43% to $B^0\overline{B}^0$. We rescale to 50%.
[5] ALBRECHT 87D reports < 5 × 10^{-5} assuming the $\Upsilon(4S)$ decays 45% to $B^0\overline{B}^0$. We rescale to 50%.
[6] AVERY 87 reports < 9 × 10^{-5} assuming the $\Upsilon(4S)$ decays 40% to $B^0\overline{B}^0$. We rescale to 50%.

$\Gamma(\pi^0 e^\pm\mu^\mp)/\Gamma_{\text{total}}$ Γ_{527}/Γ

VALUE	CL%	DOCUMENT ID		TECN	COMMENT
<1.4 × 10^{-7}	90	[1] AUBERT	07AG	BABR	$e^+e^- \to \Upsilon(4S)$

[1] Assumes equal production of B^+ and B^0 at the $\Upsilon(4S)$.

$\Gamma(K^0 e^\pm\mu^\mp)/\Gamma_{\text{total}}$ Γ_{528}/Γ

Test of lepton family number conservation.

VALUE (units 10^{-7})	CL%	DOCUMENT ID		TECN	COMMENT
< 2.7	90	[1] AUBERT,B	06J	BABR	$e^+e^- \to \Upsilon(4S)$
• • • We do not use the following data for averages, fits, limits, etc. • • •					
<40	90	[1] AUBERT	02L	BABR	Repl. by AUBERT,B 06J

[1] Assumes equal production of B^+ and B^0 at the $\Upsilon(4S)$.

$\Gamma(K^*(892)^0 e^+\mu^-)/\Gamma_{\text{total}}$ Γ_{529}/Γ

VALUE (units 10^{-7})	CL%	DOCUMENT ID		TECN	COMMENT
<5.3	90	[1] AUBERT,B	06J	BABR	$e^+e^- \to \Upsilon(4S)$

[1] Assumes equal production of B^0 and B^+ at $\Upsilon(4S)$.

$\Gamma(K^*(892)^0 e^-\mu^+)/\Gamma_{\text{total}}$ Γ_{530}/Γ

VALUE (units 10^{-7})	CL%	DOCUMENT ID		TECN	COMMENT
<3.4	90	[1] AUBERT,B	06J	BABR	$e^+e^- \to \Upsilon(4S)$

[1] Assumes equal production of B^0 and B^+ at $\Upsilon(4S)$.

$\Gamma(K^*(892)^0 e^\pm\mu^\mp)/\Gamma_{\text{total}}$ Γ_{531}/Γ

Test of lepton family number conservation.

VALUE (units 10^{-7})	CL%	DOCUMENT ID		TECN	COMMENT
< 5.8	90	[1] AUBERT,B	06J	BABR	$e^+e^- \to \Upsilon(4S)$
• • • We do not use the following data for averages, fits, limits, etc. • • •					
<34	90	[1] AUBERT	02L	BABR	Repl. by AUBERT,B 06J

[1] Assumes equal production of B^+ and B^0 at the $\Upsilon(4S)$.

$\Gamma(e^\pm\tau^\mp)/\Gamma_{\text{total}}$ Γ_{532}/Γ

Test of lepton family number conservation. Allowed by higher-order electroweak interactions.

VALUE	CL%	DOCUMENT ID		TECN	COMMENT
<2.8 × 10^{-5}	90	[1] AUBERT	08AD	BABR	$e^+e^- \to \Upsilon(4S)$
• • • We do not use the following data for averages, fits, limits, etc. • • •					
<1.1 × 10^{-4}	90	BORNHEIM	04	CLE2	$e^+e^- \to \Upsilon(4S)$
<5.3 × 10^{-4}	90	AMMAR	94	CLE2	Repl. by BORNHEIM 04

[1] Assumes equal production of B^+ and B^0 at the $\Upsilon(4S)$.

$\Gamma(\mu^\pm\tau^\mp)/\Gamma_{\text{total}}$ Γ_{533}/Γ

Test of lepton family number conservation. Allowed by higher-order electroweak interactions.

VALUE	CL%	DOCUMENT ID		TECN	COMMENT
<2.2 × 10^{-5}	90	[1] AUBERT	08AD	BABR	$e^+e^- \to \Upsilon(4S)$
• • • We do not use the following data for averages, fits, limits, etc. • • •					
<3.8 × 10^{-5}	90	BORNHEIM	04	CLE2	$e^+e^- \to \Upsilon(4S)$
<8.3 × 10^{-4}	90	AMMAR	94	CLE2	Repl. by BORNHEIM 04

[1] Assumes equal production of B^+ and B^0 at the $\Upsilon(4S)$.

$\Gamma(\Lambda_c^+\mu^-)/\Gamma_{\text{total}}$ Γ_{534}/Γ

VALUE	CL%	DOCUMENT ID		TECN	COMMENT
<1.4 × 10^{-6}	90	[1,2] DEL-AMO-SA...11K		BABR	$e^+e^- \to \Upsilon(4S)$

[1] DEL-AMO-SANCHEZ 11K reports < 180 × 10^{-8} from a measurement of $[\Gamma(B^0 \to \Lambda_c^+\mu^-)/\Gamma_{\text{total}}] \times [B(\Lambda_c^+ \to pK^-\pi^+)]$ assuming $B(\Lambda_c^+ \to pK^-\pi^+) = (5.0 \pm 1.3) \times 10^{-2}$, which we rescale to our best value $B(\Lambda_c^+ \to pK^-\pi^+) = 6.23 \times 10^{-2}$.
[2] Uses $B(\Upsilon(4S) \to B^0\overline{B}^0) = (51.6 \pm 0.6)\%$ and $B(\Upsilon(4S) \to B^+B^-) = (48.4 \pm 0.6)\%$.

Meson Particle Listings

B^0

$\Gamma(\Lambda_c^+ e^-)/\Gamma_{total}$ Γ_{535}/Γ

VALUE	CL%	DOCUMENT ID		TECN	COMMENT
$<4 \times 10^{-6}$	90	1,2 DEL-AMO-SA...11K		BABR	$e^+e^- \to \Upsilon(4S)$

[1] DEL-AMO-SANCHEZ 11K reports $< 520 \times 10^{-8}$ from a measurement of $[\Gamma(B^0 \to \Lambda_c^+ e^-)/\Gamma_{total}] \times [B(\Lambda_c^+ \to p K^- \pi^+)]$ assuming $B(\Lambda_c^+ \to p K^- \pi^+) = (5.0 \pm 1.3) \times 10^{-2}$, which we rescale to our best value $B(\Lambda_c^+ \to p K^- \pi^+) = 6.23 \times 10^{-2}$.

[2] Uses $B(\Upsilon(4S) \to B^0 \overline{B}^0) = (51.6 \pm 0.6)\%$ and $B(\Upsilon(4S) \to B^+ B^-) = (48.4 \pm 0.6)\%$.

B_s^0 CROSS-PARTICLE BRANCHING RATIOS

$\Gamma([K^+K^-]_D K^*(892)^0)/\Gamma_{total} \times B(B_s^0 \to [K^+K^-]_D K^*(892)^0)$ $\Gamma_{142}/\Gamma \times B$

VALUE	DOCUMENT ID		TECN	COMMENT
$0.10 \pm 0.02 \pm 0.01$	AAIJ	14BN	LHCB	pp at 7, 8 TeV

$\Gamma([\pi^+\pi^-]_D K^*(892)^0)/\Gamma_{total} \times B(B_s^0 \to [\pi^+\pi^-]_D K^*(892)^0)$ $\Gamma_{143}/\Gamma \times B$

VALUE	DOCUMENT ID		TECN	COMMENT
$0.15 \pm 0.04 \pm 0.01$	AAIJ	14BN	LHCB	pp at 7, 8 TeV

See the related review(s):
Polarization in B Decays

POLARIZATION IN B^0 DECAY

In decays involving two vector mesons, one can distinguish among the states in which meson polarizations are both longitudinal (L) or both are transverse and parallel ($\|$) or perpendicular ($\perp$) to each other with the parameters Γ_L/Γ, $\Gamma_\perp/\Gamma$, and the relative phases $\phi_\|$ and $\phi_\perp$. See the definitions in the note on "Polarization in B Decays" review in the B^0 Particle Listings.

Γ_L/Γ in $B^0 \to J/\psi(1S) K^*(892)^0$

VALUE	EVTS	DOCUMENT ID		TECN	COMMENT
0.571 ± 0.007 OUR AVERAGE					
$0.572 \pm 0.006 \pm 0.014$		[1] AAIJ	13AT	LHCB	pp at 7 TeV
$0.587 \pm 0.011 \pm 0.013$		[2] ABAZOV	09E	D0	$p\overline{p}$ at 1.96 TeV
$0.556 \pm 0.009 \pm 0.010$		[3] AUBERT	07AD	BABR	$e^+e^- \to \Upsilon(4S)$
$0.562 \pm 0.026 \pm 0.018$		ACOSTA	05	CDF	$p\overline{p}$ at 1.96 TeV
$0.574 \pm 0.012 \pm 0.009$		ITOH	05	BELL	$e^+e^- \to \Upsilon(4S)$
$0.59 \pm 0.06 \pm 0.01$		[4] AFFOLDER	00N	CDF	$p\overline{p}$ at 1.8 TeV
$0.52 \pm 0.07 \pm 0.04$		[5] JESSOP	97	CLE2	$e^+e^- \to \Upsilon(4S)$
$0.65 \pm 0.10 \pm 0.04$	65	ABE	95Z	CDF	$p\overline{p}$ at 1.8 TeV
$0.97 \pm 0.16 \pm 0.15$	13	[6] ALBRECHT	94G	ARG	$e^+e^- \to \Upsilon(4S)$
• • • We do not use the following data for averages, fits, limits, etc. • • •					
$0.566 \pm 0.012 \pm 0.005$		[3] AUBERT	05P	BABR	Repl. by AUBERT 07AD
$0.62 \pm 0.02 \pm 0.03$		[7] ABE	02N	BELL	Repl. by ITOH 05
$0.597 \pm 0.028 \pm 0.024$		[8] AUBERT	01H	BABR	Repl. by AUBERT 07AD
$0.80 \pm 0.08 \pm 0.05$	42	[6] ALAM	94	CLE2	Sup. by JESSOP 97

[1] AAIJ 13AT obtains $\Gamma_\|/\Gamma = 0.227 \pm 0.004 \pm 0.011$. The relation $1 = (\Gamma_L + \Gamma_\perp + \Gamma_\|)/\Gamma$ is used to obtain Γ_L/Γ.

[2] Measured the angular and lifetime parameters for the time-dependent angular untagged decays $B_d^0 \to J/\psi K^{*0}$ and $B_s^0 \to J/\psi\phi$.

[3] Obtained by combining the B^0 and B^+ modes.

[4] AFFOLDER 00N measurements are based on 190 B^0 candidates obtained from a data sample of 89 pb^{-1}. The P-wave fraction is found to be $0.13^{+0.12}_{-0.09} \pm 0.06$.

[5] JESSOP 97 is the average over a mixture of B^0 and B^+ decays. The P-wave fraction is found to be $0.16 \pm 0.08 \pm 0.04$.

[6] Averaged over an admixture of B^0 and B^+ decays.

[7] Averaged over an admixture of B^0 and B^+ decays and the P wave fraction is $(19 \pm 2 \pm 3)\%$.

[8] Averaged over an admixture of B^0 and B^- decays and the P wave fraction is $(16.0 \pm 3.2 \pm 1.4) \times 10^{-2}$.

$\Gamma_\perp/\Gamma$ in $B^0 \to J/\psi K^{*0}$

VALUE	DOCUMENT ID		TECN	COMMENT
0.211 ± 0.008 OUR AVERAGE	Error includes scale factor of 1.3.			See the ideogram below.
$0.201 \pm 0.004 \pm 0.008$	AAIJ	13AT	LHCB	pp at 7 TeV
$0.230 \pm 0.013 \pm 0.025$	[1] ABAZOV	09E	D0	$p\overline{p}$ at 1.96 TeV
$0.233 \pm 0.010 \pm 0.005$	[2] AUBERT	07AD	BABR	$e^+e^- \to \Upsilon(4S)$
$0.215 \pm 0.032 \pm 0.006$	ACOSTA	05	CDF	$p\overline{p}$ at 1.96 TeV
$0.195 \pm 0.012 \pm 0.008$	ITOH	05	BELL	$e^+e^- \to \Upsilon(4S)$

[1] Measured the angular and lifetime parameters for the time-dependent angular untagged decays $B_d^0 \to J/\psi K^{*0}$ and $B_s^0 \to J/\psi\phi$.

[2] Obtained by combining the B^0 and B^+ modes.

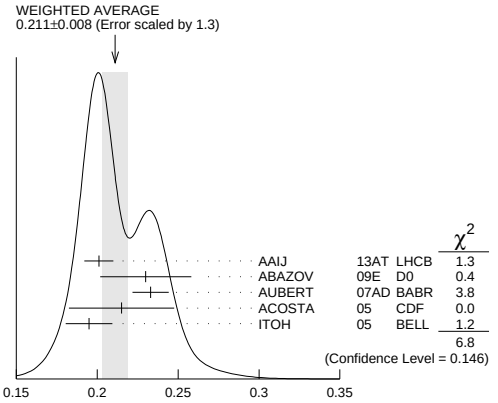

$\Gamma_\perp/\Gamma$ in $B^0 \to J/\psi K^{*0}$

$\phi_\|$ in $B^0 \to J/\psi K^{*0}$

VALUE (rad)	DOCUMENT ID		TECN	COMMENT
-2.92 ± 0.04 OUR AVERAGE	Error includes scale factor of 1.3.			See the ideogram below.
$-2.94 \pm 0.02 \pm 0.03$	AAIJ	13AT	LHCB	pp at 7 TeV
$-2.69 \pm 0.08 \pm 0.11$	[1] ABAZOV	09E	D0	$p\overline{p}$ at 1.96 TeV
$-2.93 \pm 0.08 \pm 0.04$	[2] AUBERT	07AD	BABR	$e^+e^- \to \Upsilon(4S)$

[1] Obtained $\phi_\|$ as $\delta_2 - \delta_1$, assuming they are uncorrelated.

[2] Obtained by combining the B^0 and B^+ modes.

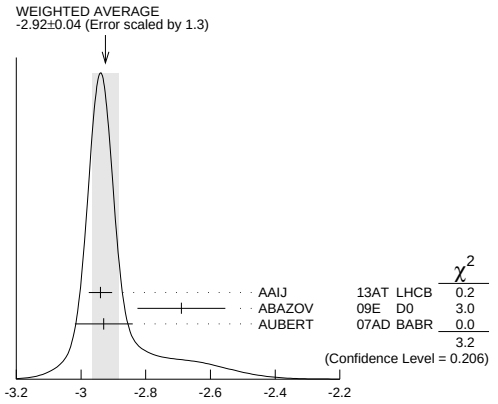

$\phi_\|$ in $B^0 \to J/\psi K^{*0}$ (rad)

$\phi_\perp$ in $B^0 \to J/\psi K^{*0}$

VALUE (rad)	DOCUMENT ID		TECN	COMMENT
2.96 ± 0.05 OUR AVERAGE	Error includes scale factor of 2.2.			See the ideogram below.
$2.94 \pm 0.02 \pm 0.02$	AAIJ	13AT	LHCB	pp at 7 TeV
$3.21 \pm 0.06 \pm 0.06$	ABAZOV	09E	D0	$p\overline{p}$ at 1.96 TeV
$2.91 \pm 0.05 \pm 0.03$	[1] AUBERT	07AD	BABR	$e^+e^- \to \Upsilon(4S)$

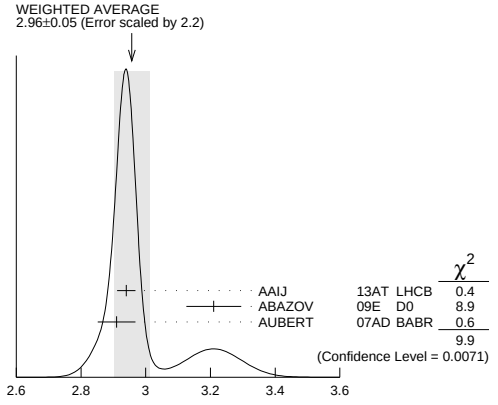

$\phi_\perp$ in $B^0 \to J/\psi K^{*0}$ (rad)

[1] Obtained by combining the B^0 and B^+ modes.

Γ_L/Γ in $B^0 \to \psi(2S) K^*(892)^0$

VALUE	DOCUMENT ID		TECN	COMMENT
$0.463^{+0.028}_{-0.040}$ OUR AVERAGE				
$0.455^{+0.031}_{-0.029}{}^{+0.014}_{-0.049}$	CHILIKIN	13	BELL	$e^+e^- \to \Upsilon(4S)$
$0.48 \pm 0.05 \pm 0.02$	[1] AUBERT	07AD	BABR	$e^+e^- \to \Upsilon(4S)$
$0.45 \pm 0.11 \pm 0.04$	[2] RICHICHI	01	CLE2	$e^+e^- \to \Upsilon(4S)$
• • • We do not use the following data for averages, fits, limits, etc. • • •				
$0.448^{+0.040}_{-0.027}{}^{+0.040}_{-0.053}$	MIZUK	09	BELL	$e^+e^- \to \Upsilon(4S)$

[1] Obtained by combining the B^0 and B^+ modes.
[2] Averages between charged and neutral B mesons.

$\Gamma_\perp/\Gamma$ in $B^0 \to \psi(2S) K^{*0}$

VALUE	DOCUMENT ID		TECN	COMMENT
$0.30 \pm 0.06 \pm 0.02$	[1] AUBERT	07AD	BABR	$e^+e^- \to \Upsilon(4S)$

[1] Obtained by combining the B^0 and B^+ modes.

$\phi_\parallel$ in $B^0 \to \psi(2S) K^{*0}$

VALUE (rad)	DOCUMENT ID		TECN	COMMENT
$-2.8 \pm 0.4 \pm 0.1$	[1] AUBERT	07AD	BABR	$e^+e^- \to \Upsilon(4S)$

[1] Obtained by combining the B^0 and B^+ modes.

$\phi_\perp$ in $B^0 \to \psi(2S) K^{*0}$

VALUE (rad)	DOCUMENT ID		TECN	COMMENT
$2.8 \pm 0.3 \pm 0.1$	[1] AUBERT	07AD	BABR	$e^+e^- \to \Upsilon(4S)$

[1] Obtained by combining the B^0 and B^+ modes.

Γ_L/Γ in $B^0 \to \chi_{c1} K^*(892)^0$

VALUE	DOCUMENT ID		TECN	COMMENT
$0.83\ ^{+0.06}_{-0.08}$ OUR AVERAGE Error includes scale factor of 1.3.				
$0.947^{+0.038}_{-0.048}{}^{+0.046}_{-0.099}$	MIZUK	08	BELL	$e^+e^- \to \Upsilon(4S)$
$0.77 \pm 0.07 \pm 0.04$	[1] AUBERT	07AD	BABR	$e^+e^- \to \Upsilon(4S)$

[1] Obtained by combining the B^0 and B^+ modes.

$\Gamma_\perp/\Gamma$ in $B^0 \to \chi_{c1} K^*(892)^0$

VALUE	DOCUMENT ID		TECN	COMMENT
$0.03 \pm 0.04 \pm 0.02$	[1] AUBERT	07AD	BABR	$e^+e^- \to \Upsilon(4S)$

[1] Obtained by combining the B^0 and B^+ modes.

$\phi_\parallel$ in $B^0 \to \chi_{c1} K^*(892)^0$

VALUE (rad)	DOCUMENT ID		TECN	COMMENT
$0.0 \pm 0.3 \pm 0.1$	[1] AUBERT	07AD	BABR	$e^+e^- \to \Upsilon(4S)$

[1] Obtained by combining the B^0 and B^+ modes.

Γ_L/Γ in $B^0 \to D_s^{*+} D^{*-}$

VALUE	DOCUMENT ID		TECN	COMMENT
0.52 ± 0.05 OUR AVERAGE				
$0.519 \pm 0.050 \pm 0.028$	[1] AUBERT	03I	BABR	$e^+e^- \to \Upsilon(4S)$
$0.506 \pm 0.139 \pm 0.036$	AHMED	00B	CLE2	$e^+e^- \to \Upsilon(4S)$

[1] Measurement performed using partial reconstruction of D^{*-} decay.

Γ_L/Γ in $B^0 \to D^{*-} \rho^+$

VALUE	EVTS	DOCUMENT ID		TECN	COMMENT
$0.885 \pm 0.016 \pm 0.012$		CSORNA	03	CLE2	$e^+e^- \to \Upsilon(4S)$
• • • We do not use the following data for averages, fits, limits, etc. • • •					
$0.93 \pm 0.05 \pm 0.05$	76	ALAM	94	CLE2	$e^+e^- \to \Upsilon(4S)$

Γ_L/Γ in $B^0 \to D_s^{*+} \rho^-$

VALUE	DOCUMENT ID		TECN	COMMENT
$0.84^{+0.26}_{-0.28} \pm 0.13$	[1] AUBERT	08AJ	BABR	$e^+e^- \to \Upsilon(4S)$

[1] Assumes equal production of B^+ and B^0 at the $\Upsilon(4S)$.

Γ_L/Γ in $B^0 \to D_s^{*+} K^{*-}$

VALUE	DOCUMENT ID		TECN	COMMENT
$0.92^{+0.37}_{-0.31} \pm 0.07$	[1] AUBERT	08AJ	BABR	$e^+e^- \to \Upsilon(4S)$

[1] Assumes equal production of B^+ and B^0 at the $\Upsilon(4S)$.

Γ_L/Γ in $B^0 \to D^{*+} D^{*-}$

VALUE	DOCUMENT ID		TECN	COMMENT
$0.624 \pm 0.029 \pm 0.011$	KRONENBIT...12		BELL	$e^+e^- \to \Upsilon(4S)$
• • • We do not use the following data for averages, fits, limits, etc. • • •				
$0.57 \pm 0.08 \pm 0.02$	MIYAKE	05	BELL	Repl. by KRONENBITTER 12

$\Gamma_\perp/\Gamma$ in $B^0 \to D^{*+} D^{*-}$

VALUE	DOCUMENT ID		TECN	COMMENT
0.147 ± 0.019 OUR AVERAGE				
$0.138 \pm 0.024 \pm 0.006$	KRONENBIT...12		BELL	$e^+e^- \to \Upsilon(4S)$
$0.158 \pm 0.028 \pm 0.006$	AUBERT	09C	BABR	$e^+e^- \to \Upsilon(4S)$
• • • We do not use the following data for averages, fits, limits, etc. • • •				
$0.125 \pm 0.043 \pm 0.023$	VERVINK	09	BELL	Repl. by KRONENBITTER 12
$0.143 \pm 0.034 \pm 0.008$	AUBERT	07BO	BABR	Repl. by AUBERT 09C
$0.125 \pm 0.044 \pm 0.007$	AUBERT,BE	05A	BABR	Repl. by AUBERT 07BO
$0.19 \pm 0.08 \pm 0.01$	MIYAKE	05	BELL	Repl. by VERVINK 09
$0.063 \pm 0.055 \pm 0.009$	AUBERT	03Q	BABR	Repl. by AUBERT,BE 05A

Γ_L/Γ in $B^0 \to \overline{D}^{*0} \omega$

VALUE	DOCUMENT ID		TECN	COMMENT
$0.665 \pm 0.047 \pm 0.015$	LEES	11M	BABR	$e^+e^- \to \Upsilon(4S)$

Γ_L/Γ in $B^0 \to \overline{D}_1(2430)^0 \omega$

VALUE (%)	DOCUMENT ID		TECN	COMMENT
$63.0 \pm 9.1^{+6.5}_{-6.0}$	[1,2] MATVIENKO	15	BELL	$e^+e^- \to \Upsilon(4S)$

[1] Obtained by amplitude analysis of $\overline{B}^0 \to D^{*-}\omega\pi^+$. The second uncertainty combines in qudrature experimental systematic and model uncertainties.
[2] Assumes equal production of B^0 and B^+ at $\Upsilon(4S)$.

Γ_L/Γ in $B^0 \to \overline{D}_1(2420)^0 \omega$

VALUE (%)	DOCUMENT ID		TECN	COMMENT
$67.1 \pm 11.7^{+2.3}_{-5.0}$	[1,2] MATVIENKO	15	BELL	$e^+e^- \to \Upsilon(4S)$

[1] Obtained by amplitude analysis of $\overline{B}^0 \to D^{*-}\omega\pi^+$. The second uncertainty combines in qudrature experimental systematic and model uncertainties.
[2] Assumes equal production of B^0 and B^+ at $\Upsilon(4S)$.

Γ_L/Γ in $B^0 \to \overline{D}_2^*(2460)^0 \omega$

VALUE (%)	DOCUMENT ID		TECN	COMMENT
$76.0^{+18.3}_{-\ 8.5}{}^{+3.5}_{-2.8}$	[1,2] MATVIENKO	15	BELL	$e^+e^- \to \Upsilon(4S)$

[1] Obtained by amplitude analysis of $\overline{B}^0 \to D^{*-}\omega\pi^+$. The second uncertainty combines in qudrature experimental systematic and model uncertainties.
[2] Assumes equal production of B^0 and B^+ at $\Upsilon(4S)$.

Γ_L/Γ in $B^0 \to D^{*-}\omega\pi^+$

VALUE	DOCUMENT ID		TECN	COMMENT
$0.654 \pm 0.042 \pm 0.016$	[1] AUBERT	06L	BABR	$e^+e^- \to \Upsilon(4S)$

[1] Invariant mass of the $[\omega\pi]$ system is restricted in the region 1.1 and 1.9 GeV.

Γ_L/Γ in $B^0 \to \omega K^{*0}$

VALUE	DOCUMENT ID		TECN	COMMENT
0.69 ± 0.13 OUR AVERAGE				
$0.72 \pm 0.14 \pm 0.02$	AUBERT	09H	BABR	$e^+e^- \to \Upsilon(4S)$
$0.56 \pm 0.29^{+0.18}_{-0.08}$	GOLDENZWE...08		BELL	$e^+e^- \to \Upsilon(4S)$

Γ_L/Γ in $B^0 \to \omega K_2^*(1430)^0$

VALUE	DOCUMENT ID		TECN	COMMENT
$0.45 \pm 0.12 \pm 0.02$	AUBERT	09H	BABR	$e^+e^- \to \Upsilon(4S)$

Γ_L/Γ in $B^0 \to K^{*0}\overline{K}^{*0}$

VALUE	DOCUMENT ID		TECN	COMMENT
$0.80^{+0.10}_{-0.12} \pm 0.06$	AUBERT	08I	BABR	$e^+e^- \to \Upsilon(4S)$

Γ_L/Γ in $B^0 \to \phi K^*(892)^0$

VALUE	DOCUMENT ID		TECN	COMMENT
0.497 ± 0.017 OUR AVERAGE				
$0.497 \pm 0.019 \pm 0.015$	AAIJ	14AM	LHCB	pp at 7 TeV
$0.499 \pm 0.030 \pm 0.018$	PRIM	13	BELL	$e^+e^- \to \Upsilon(4S)$
$0.494 \pm 0.034 \pm 0.013$	AUBERT	08BG	BABR	$e^+e^- \to \Upsilon(4S)$
• • • We do not use the following data for averages, fits, limits, etc. • • •				
$0.506 \pm 0.040 \pm 0.015$	AUBERT	07D	BABR	Repl. by AUBERT 08BG
$0.45 \pm 0.05 \pm 0.02$	CHEN	05A	BELL	Repl. by PRIM 13
$0.52 \pm 0.05 \pm 0.02$	[1] AUBERT,B	04W	BABR	Repl. by AUBERT 07D
$0.65 \pm 0.07 \pm 0.02$	AUBERT	03V	BABR	Repl. by AUBERT,B 04W
$0.41 \pm 0.10 \pm 0.04$	CHEN	03B	BELL	Repl. by CHEN 05A

[1] AUBERT,B 04W also measures the fraction of parity-odd transverse contribution $f_\perp = 0.22 \pm 0.05 \pm 0.02$ and the phases of the parity-even and parity-odd transverse amplitudes relative to the longitudinal amplitude.

$\Gamma_\perp/\Gamma$ in $B^0 \to \phi K^*(892)^0$

VALUE	DOCUMENT ID		TECN	COMMENT
0.224 ± 0.015 OUR AVERAGE				
$0.221 \pm 0.016 \pm 0.013$	AAIJ	14AM	LHCB	pp at 7 TeV
$0.238 \pm 0.026 \pm 0.008$	PRIM	13	BELL	$e^+e^- \to \Upsilon(4S)$
$0.212 \pm 0.032 \pm 0.013$	AUBERT	08BG	BABR	$e^+e^- \to \Upsilon(4S)$
• • • We do not use the following data for averages, fits, limits, etc. • • •				
$0.227 \pm 0.038 \pm 0.013$	AUBERT	07D	BABR	Repl. by AUBERT 08BG
$0.31\ ^{+0.06}_{-0.05} \pm 0.02$	[1] CHEN	05A	BELL	Repl. by PRIM 13
$0.22 \pm 0.05 \pm 0.02$	AUBERT,B	04W	BABR	Repl. by AUBERT 07D

[1] This quantity was recalculated by the BELLE authors from numbers in the original paper.

$\phi_\parallel$ in $B^0 \to \phi K^*(892)^0$

VALUE (rad)	DOCUMENT ID	TECN	COMMENT
2.43 ±0.11 OUR AVERAGE	Error includes scale factor of 1.8. See the ideogram below.		
2.562±0.069±0.040	AAIJ	14AM LHCB	pp at 7 TeV
2.23 ±0.10 ±0.02	PRIM	13 BELL	$e^+e^- \to \Upsilon(4S)$
2.40 ±0.13 ±0.08	AUBERT	08BG BABR	$e^+e^- \to \Upsilon(4S)$
• • • We do not use the following data for averages, fits, limits, etc. • • •			
2.31 ±0.14 ±0.08	AUBERT	07D BABR	Repl. by AUBERT 08BG
$2.40\ ^{+0.28}_{-0.24}$ ±0.07	[1] CHEN	05A BELL	Repl. by PRIM 13
$2.34\ ^{+0.23}_{-0.20}$ ±0.05	AUBERT,B	04W BABR	Repl. by AUBERT 07D

[1] This quantity was recalculated by the BELLE authors from numbers in the original paper.

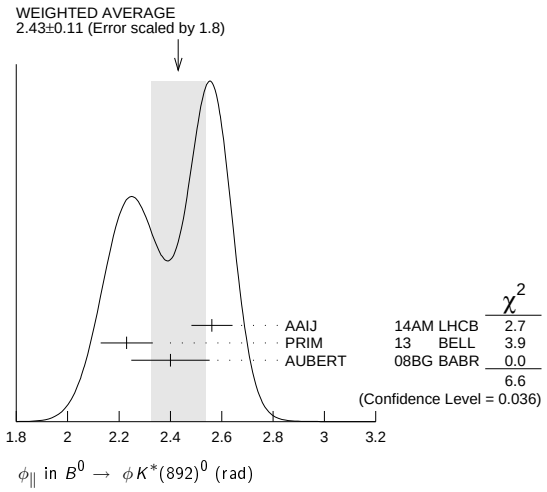

$\phi_\perp$ in $B^0 \to \phi K^*(892)^0$

VALUE (rad)	DOCUMENT ID	TECN	COMMENT
2.53 ±0.09 OUR AVERAGE	Error includes scale factor of 1.7. See the ideogram below.		
2.633±0.062±0.037	AAIJ	14AM LHCB	pp at 7 TeV
2.37 ±0.10 ±0.04	PRIM	13 BELL	$e^+e^- \to \Upsilon(4S)$
2.35 ±0.13 ±0.09	AUBERT	08BG BABR	$e^+e^- \to \Upsilon(4S)$
• • • We do not use the following data for averages, fits, limits, etc. • • •			
2.24 ±0.15 ±0.09	AUBERT	07D BABR	Repl. by AUBERT 08BG
2.51 ±0.25 ±0.06	[1] CHEN	05A BELL	Repl. by PRIM 13
2.47 ±0.25 ±0.05	AUBERT,B	04W BABR	Repl. by AUBERT 07D

[1] This quantity was recalculated by the BELLE authors from numbers in the original paper.

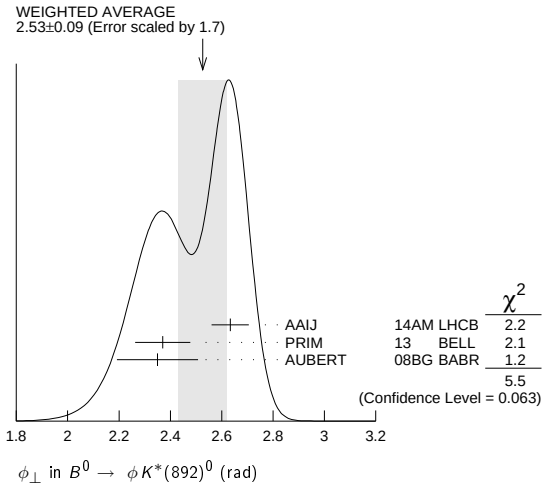

$\delta_0(B^0 \to \phi K^*(892)^0)$

VALUE (rad)	DOCUMENT ID	TECN	COMMENT
2.88±0.10 OUR AVERAGE			
2.91±0.10±0.08	PRIM	13 BELL	$e^+e^- \to \Upsilon(4S)$
2.82±0.15±0.09	AUBERT	08BG BABR	$e^+e^- \to \Upsilon(4S)$
• • • We do not use the following data for averages, fits, limits, etc. • • •			
2.78±0.17±0.09	AUBERT	07D BABR	Repl. by AUBERT 08BG

A^0_{CP} in $B^0 \to \phi K^*(892)^0$

VALUE	DOCUMENT ID	TECN	COMMENT
−0.007±0.030 OUR AVERAGE			
−0.003±0.038±0.005	AAIJ	14AM LHCB	pp at 7 TeV
−0.030±0.061±0.007	PRIM	13 BELL	$e^+e^- \to \Upsilon(4S)$
0.01 ±0.07 ±0.02	AUBERT	08BG BABR	$e^+e^- \to \Upsilon(4S)$
• • • We do not use the following data for averages, fits, limits, etc. • • •			
−0.03 ±0.08 ±0.02	AUBERT	07D BABR	Repl. by AUBERT 08BG
0.13 ±0.12 ±0.04	[1] CHEN	05A BELL	Repl. by PRIM 13
−0.06 ±0.10 ±0.01	AUBERT,B	04W BABR	Repl. by AUBERT 07D

[1] This quantity was recalculated by the BELLE authors from numbers in the original paper.

$A^\perp_{CP}$ in $B^0 \to \phi K^*(892)^0$

VALUE	DOCUMENT ID	TECN	COMMENT
−0.02 ±0.06 OUR AVERAGE			
0.047±0.074±0.009	AAIJ	14AM LHCB	pp at 7 TeV
−0.14 ±0.11 ±0.01	PRIM	13 BELL	$e^+e^- \to \Upsilon(4S)$
−0.04 ±0.15 ±0.06	AUBERT	08BG BABR	$e^+e^- \to \Upsilon(4S)$
• • • We do not use the following data for averages, fits, limits, etc. • • •			
−0.03 ±0.16 ±0.05	AUBERT	07D BABR	Repl. by AUBERT 08BG
−0.20 ±0.18 ±0.04	[1] CHEN	05A BELL	Repl. by PRIM 13
−0.10 ±0.24 ±0.05	AUBERT,B	04W BABR	Repl. by AUBERT 07D

[1] This quantity was recalculated by the BELLE authors from numbers in the original paper.

$\Delta\phi_\parallel$ in $B^0 \to \phi K^*(892)^0$

VALUE (rad)	DOCUMENT ID	TECN	COMMENT
0.05 ±0.05 OUR AVERAGE			
0.045±0.069±0.015	AAIJ	14AM LHCB	pp at 7 TeV
−0.02 ±0.10 ±0.01	PRIM	13 BELL	$e^+e^- \to \Upsilon(4S)$
0.22 ±0.12 ±0.08	AUBERT	08BG BABR	$e^+e^- \to \Upsilon(4S)$
• • • We do not use the following data for averages, fits, limits, etc. • • •			
0.24 ±0.14 ±0.08	AUBERT	07D BABR	Repl. by AUBERT 08BG
−0.32 ±0.27 ±0.07	[1] CHEN	05A BELL	Repl. by PRIM 13
$0.27\ ^{+0.20}_{-0.23}$ ±0.05	AUBERT,B	04W BABR	Repl. by AUBERT 07D

[1] This quantity was recalculated by the BELLE authors from numbers in the original paper.

$\Delta\phi_\perp$ in $B^0 \to \phi K^*(892)^0$

VALUE (rad)	DOCUMENT ID	TECN	COMMENT
0.08 ±0.05 OUR AVERAGE			
0.062±0.062±0.005	AAIJ	14AM LHCB	pp at 7 TeV
0.05 ±0.10 ±0.02	PRIM	13 BELL	$e^+e^- \to \Upsilon(4S)$
0.21 ±0.13 ±0.08	AUBERT	08BG BABR	$e^+e^- \to \Upsilon(4S)$
• • • We do not use the following data for averages, fits, limits, etc. • • •			
0.19 ±0.15 ±0.08	AUBERT	07D BABR	Repl. by AUBERT 08BG
−0.30 ±0.25 ±0.06	[1] CHEN	05A BELL	Repl. by PRIM 13
0.36 ±0.25 ±0.05	AUBERT,B	04W BABR	Repl. by AUBERT 07D

[1] This quantity was recalculated by the BELLE authors from numbers in the original paper.

$\Delta\delta_0(B^0 \to \phi K^*(892)^0)$

VALUE (rad)	DOCUMENT ID	TECN	COMMENT
0.13±0.09 OUR AVERAGE			
0.08±0.10±0.01	PRIM	13 BELL	$e^+e^- \to \Upsilon(4S)$
0.27±0.14±0.08	AUBERT	08BG BABR	$e^+e^- \to \Upsilon(4S)$
• • • We do not use the following data for averages, fits, limits, etc. • • •			
0.21±0.17±0.08	AUBERT	07D BABR	Repl. by AUBERT 08BG

$\Delta\phi_{00}(B^0 \to \phi K_0^*(1430)^0)$

VALUE (rad)	DOCUMENT ID	TECN	COMMENT
0.28±0.42±0.04	AUBERT	08BG BABR	$e^+e^- \to \Upsilon(4S)$

Γ_L/Γ in $B^0 \to \phi K_2^*(1430)^0$

VALUE	DOCUMENT ID	TECN	COMMENT
$\mathbf{0.913\ ^{+0.028}_{-0.050}}$ **OUR AVERAGE**			
$0.918\ ^{+0.029}_{-0.060}$ ±0.012	PRIM	13 BELL	$e^+e^- \to \Upsilon(4S)$
$0.901\ ^{+0.046}_{-0.058}$ ±0.037	AUBERT	08BG BABR	$e^+e^- \to \Upsilon(4S)$
• • • We do not use the following data for averages, fits, limits, etc. • • •			
$0.853\ ^{+0.061}_{-0.069}$ ±0.036	AUBERT	07D BABR	Repl. by AUBERT 08BG

$\Gamma_\perp/\Gamma$ in $B^0 \to \phi K_2^*(1430)^0$

VALUE	DOCUMENT ID	TECN	COMMENT
$\mathbf{0.027\ ^{+0.031}_{-0.025}}$ **OUR AVERAGE**	Error includes scale factor of 1.1.		
$0.056\ ^{+0.050}_{-0.035}$ ±0.009	PRIM	13 BELL	$e^+e^- \to \Upsilon(4S)$
$0.002\ ^{+0.018}_{-0.002}$ ±0.031	AUBERT	08BG BABR	$e^+e^- \to \Upsilon(4S)$
• • • We do not use the following data for averages, fits, limits, etc. • • •			
$0.045\ ^{+0.049}_{-0.040}$ ±0.013	AUBERT	07D BABR	Repl. by AUBERT 08BG

$\phi_\parallel$ in $B^0 \to \phi K_2^*(1430)^0$

VALUE (rad)	DOCUMENT ID		TECN	COMMENT
4.0 ±0.4 OUR AVERAGE				
3.76±2.88±1.32	PRIM	13	BELL	$e^+e^- \to \Upsilon(4S)$
3.96±0.38±0.06	AUBERT	08BG	BABR	$e^+e^- \to \Upsilon(4S)$
• • • We do not use the following data for averages, fits, limits, etc. • • •				
2.90±0.39±0.06	AUBERT	07D	BABR	Repl. by AUBERT 08BG

$\phi_\perp$ in $B^0 \to \phi K_2^*(1430)^0$

VALUE (rad)	DOCUMENT ID		TECN	COMMENT
$4.45^{+0.43}_{-0.38}\pm0.13$	PRIM	13	BELL	$e^+e^- \to \Upsilon(4S)$
• • • We do not use the following data for averages, fits, limits, etc. • • •				
$5.72^{+0.55}_{-0.87}\pm0.11$	AUBERT	07D	BABR	Repl. by AUBERT 08BG

$\delta_0(B^0 \to \phi K_2^*(1430)^0)$

VALUE (rad)	DOCUMENT ID		TECN	COMMENT
3.46±0.14 OUR AVERAGE				
3.53±0.11±0.19	PRIM	13	BELL	$e^+e^- \to \Upsilon(4S)$
3.41±0.13±0.13	AUBERT	08BG	BABR	$e^+e^- \to \Upsilon(4S)$
• • • We do not use the following data for averages, fits, limits, etc. • • •				
$3.54^{+0.12}_{-0.14}\pm0.06$	AUBERT	07D	BABR	Repl. by AUBERT 08BG

A_{CP}^0 in $B^0 \to \phi K_2^*(1430)^0$

VALUE	DOCUMENT ID		TECN	COMMENT
−0.03 ±0.04 OUR AVERAGE				
$-0.016^{+0.066}_{-0.051}\pm0.008$	PRIM	13	BELL	$e^+e^- \to \Upsilon(4S)$
−0.05 ±0.06 ±0.01	AUBERT	08BG	BABR	$e^+e^- \to \Upsilon(4S)$

$A_{CP}^\perp$ in $B^0 \to \phi K_2^*(1430)^0$

VALUE	DOCUMENT ID		TECN	COMMENT
$\mathbf{-0.01^{+0.85}_{-0.67}\pm0.09}$	PRIM	13	BELL	$e^+e^- \to \Upsilon(4S)$

$\Delta\phi_\parallel(B^0 \to \phi K_2^*(1430)^0)$

VALUE (rad)	DOCUMENT ID		TECN	COMMENT
−0.9 ±0.4 OUR AVERAGE				
−0.02±1.08±1.01	PRIM	13	BELL	$e^+e^- \to \Upsilon(4S)$
−1.00±0.38±0.09	AUBERT	08BG	BABR	$e^+e^- \to \Upsilon(4S)$

$\Delta\phi_\perp(B^0 \to \phi K_2^*(1430)^0)$

VALUE	DOCUMENT ID		TECN	COMMENT
−0.19±0.42±0.11	PRIM	13	BELL	$e^+e^- \to \Upsilon(4S)$

$\Delta\delta_0$ in $B^0 \to \phi K_2^*(1430)^0$

VALUE (rad)	DOCUMENT ID		TECN	COMMENT
0.08±0.09 OUR AVERAGE				
0.06±0.11±0.02	PRIM	13	BELL	$e^+e^- \to \Upsilon(4S)$
0.11±0.13±0.06	AUBERT	08BG	BABR	$e^+e^- \to \Upsilon(4S)$

Γ_L/Γ in $B^0 \to K^*(892)^0\rho^0$

VALUE	DOCUMENT ID		TECN	COMMENT
0.40±0.08±0.11	LEES	12K	BABR	$e^+e^- \to \Upsilon(4S)$
• • • We do not use the following data for averages, fits, limits, etc. • • •				
0.57±0.09±0.08	AUBERT,B	06G	BABR	Repl. by LEES 12K

Γ_L/Γ in $B^0 \to K^{*+}\rho^-$

VALUE	DOCUMENT ID		TECN	COMMENT
0.38±0.13±0.03	LEES	12K	BABR	$e^+e^- \to \Upsilon(4S)$

Γ_L/Γ in $B^0 \to \rho^+\rho^-$

VALUE	DOCUMENT ID		TECN	COMMENT
$\mathbf{0.990^{+0.021}_{-0.019}}$ **OUR AVERAGE**				
0.988±0.012±0.023	VANHOEFER	16	BELL	$e^+e^- \to \Upsilon(4S)$
$0.992\pm0.024^{+0.026}_{-0.013}$	AUBERT	07BF	BABR	$e^+e^- \to \Upsilon(4S)$
• • • We do not use the following data for averages, fits, limits, etc. • • •				
$0.941^{+0.034}_{-0.040}\pm0.030$	SOMOV	06	BELL	Repl. by VANHOEFER 16
$0.978\pm0.014^{+0.021}_{-0.029}$	AUBERT,B	05C	BABR	Repl. by AUBERT 07BF
$0.98\ ^{+0.02}_{-0.08}\ \pm0.03$	AUBERT	04G	BABR	Repl. by AUBERT,B 04R
$0.99\ \pm0.03\ ^{+0.04}_{-0.03}$	AUBERT,B	04R	BABR	Repl. by AUBERT,B 05C

Γ_L/Γ in $B^0 \to \rho^0\rho^0$

VALUE	DOCUMENT ID		TECN	COMMENT
$\mathbf{0.71\ ^{+0.08}_{-0.09}}$ **OUR AVERAGE** Error includes scale factor of 1.6. See the ideogram below.				
$0.745\ ^{+0.048}_{-0.058}\pm0.034$	AAIJ	15T	LHCB	pp at 7, 8 TeV
$0.21\ ^{+0.18}_{-0.22}\ \pm0.15$	VANHOEFER	14	BELL	$e^+e^- \to \Upsilon(4S)$
$0.75\ ^{+0.11}_{-0.14}\ \pm0.05$	AUBERT	08BB	BABR	$e^+e^- \to \Upsilon(4S)$
• • • We do not use the following data for averages, fits, limits, etc. • • •				
0.87 ±0.13 ±0.04	AUBERT	07G	BABR	Repl. by AUBERT 08BB

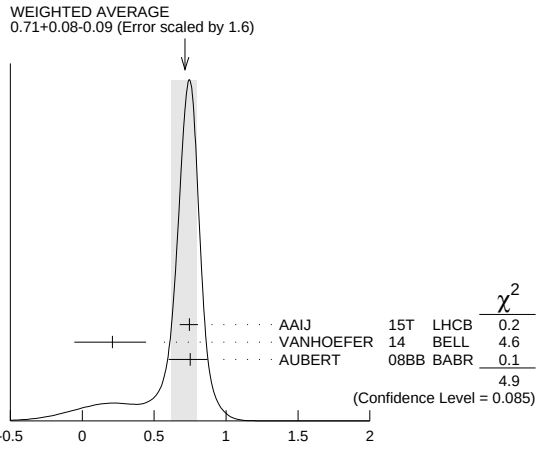

Γ_L/Γ in $B^0 \to \rho^0\rho^0$

Γ_L/Γ in $B^0 \to a_1(1260)^+ a_1(1260)^-$

VALUE	DOCUMENT ID		TECN	COMMENT
0.31±0.22±0.10	AUBERT	09AL	BABR	$e^+e^- \to \Upsilon(4S)$

Γ_L/Γ in $B^0 \to p\bar{p}K^*(892)^0$

VALUE	DOCUMENT ID		TECN	COMMENT
1.01±0.13±0.03	CHEN	08C	BELL	$e^+e^- \to \Upsilon(4S)$

Γ_L/Γ in $B^0 \to \Lambda\bar{\Lambda}K^*(892)^0$

VALUE	DOCUMENT ID		TECN	COMMENT
0.60±0.22±0.08	CHANG	09	BELL	$e^+e^- \to \Upsilon(4S)$

Γ_L/Γ in $B^0 \to K^*(892)^0 e^+e^-$ ($0.002 < q^2 < 1.120$ GeV$^2/c^4$)

VALUE	DOCUMENT ID		TECN	COMMENT
0.16±0.06±0.03	AAIJ	15Z	LHCB	pp at 7, 8 TeV

$A_T^{(2)}$ in $B^0 \to K^*(892)^0 e^+e^-$ ($0.002 < q^2 < 1.120$ GeV$^2/c^4$)

VALUE	DOCUMENT ID		TECN	COMMENT
−0.23±0.23±0.05	AAIJ	15Z	LHCB	pp at 7, 8 TeV

A_T^{Im} in $B^0 \to K^*(892)^0 e^+e^-$ ($0.002 < q^2 < 1.120$ GeV$^2/c^4$)

VALUE	DOCUMENT ID		TECN	COMMENT
0.14±0.22±0.05	AAIJ	15Z	LHCB	pp at 7, 8 TeV

A_T^{Re} in $B^0 \to K^*(892)^0 e^+e^-$ ($0.002 < q^2 < 1.120$ GeV$^2/c^4$)

Related to A_{FB}, F_L by $A_T^{Re} = (4/3)\, A_{FB} / (1 - F_L)$.

VALUE	DOCUMENT ID		TECN	COMMENT
0.10±0.18±0.05	AAIJ	15Z	LHCB	pp at 7, 8 TeV

See the related review(s):

B^0 — $\overline{B}^0$ Mixing

B^0-$\overline{B}^0$ MIXING PARAMETERS

For a discussion of B^0-$\overline{B}^0$ mixing see the note on "B^0-$\overline{B}^0$ Mixing" in the B^0 Particle Listings above.

χ_d is a measure of the time-integrated B^0-$\overline{B}^0$ mixing probability that a produced $B^0(\overline{B}^0)$ decays as a $\overline{B}^0(B^0)$. Mixing violates $\Delta B \neq 2$ rule.

$$\chi_d = \frac{x_d^2}{2(1+x_d^2)}$$

$$x_d = \frac{\Delta m_{B^0}}{\Gamma_{B^0}} = (m_{B_H^0} - m_{B_L^0})\,\tau_{B^0}\ ,$$

where H, L stand for heavy and light states of two B^0 CP eigenstates and $\tau_{B^0} = \frac{1}{0.5(\Gamma_{B_H^0}+\Gamma_{B_L^0})}$.

χ_d

This B^0-$\overline{B}^0$ mixing parameter is the probability (integrated over time) that a produced B^0 (or $\overline{B}^0$) decays as a $\overline{B}^0$ (or B^0), e.g. for inclusive lepton decays

Meson Particle Listings

B^0

χ_d = $\Gamma(B^0 \to \ell^- X$ (via $\overline{B}^0$))/$\Gamma(B^0 \to \ell^\pm X)$
= $\Gamma(\overline{B}^0 \to \ell^+ X$ (via B^0))/$\Gamma(\overline{B}^0 \to \ell^\pm X)$
Where experiments have measured the parameter $r = \chi/(1-\chi)$, we have converted to χ. Mixing violates the $\Delta B \neq 2$ rule.

Note that the measurement of χ at energies higher than the $\Upsilon(4S)$ have not separated χ_d from χ_S where the subscripts indicate $B^0(\overline{b}d)$ or $B_s^0(\overline{b}s)$. They are listed in the $B^\pm/B^0/B_s^0$/b-baryon ADMIXTURE section.

The experiments at $\Upsilon(4S)$ make an assumption about the $B^0\overline{B}^0$ fraction and about the ratio of the $B^\pm$ and B^0 semileptonic branching ratios (usually that it equals one).

"OUR EVALUATION" is an average using rescaled values of the data listed below. The average and rescaling were performed by the Heavy Flavor Averaging Group (HFLAV) and are described at http://www.slac.stanford.edu/xorg/hflav/. The averaging/rescaling procedure takes into account correlations between the measurements, includes χ_d calculated from Δm_{B^0} and τ_{B^0}.

VALUE	CL%	DOCUMENT ID		TECN	COMMENT
0.1860±0.0011 OUR EVALUATION					
0.182 ±0.015 OUR AVERAGE					
0.198 ±0.013 ±0.014		[1] BEHRENS	00B	CLE2	$e^+e^- \to \Upsilon(4S)$
0.16 ±0.04 ±0.04		[2] ALBRECHT	94	ARG	$e^+e^- \to \Upsilon(4S)$
0.149 ±0.023 ±0.022		[3] BARTELT	93	CLE2	$e^+e^- \to \Upsilon(4S)$
0.171 ±0.048		[4] ALBRECHT	92L	ARG	$e^+e^- \to \Upsilon(4S)$
• • • We do not use the following data for averages, fits, limits, etc. • • •					
0.20 ±0.13 ±0.12		[5] ALBRECHT	96D	ARG	$e^+e^- \to \Upsilon(4S)$
0.19 ±0.07 ±0.09		[6] ALBRECHT	96D	ARG	$e^+e^- \to \Upsilon(4S)$
0.24 ±0.12		[7] ELSEN	90	JADE	e^+e^- 35–44 GeV
0.158 $^{+0.052}_{-0.059}$		ARTUSO	89	CLEO	$e^+e^- \to \Upsilon(4S)$
0.17 ±0.05		[8] ALBRECHT	87I	ARG	$e^+e^- \to \Upsilon(4S)$
<0.19	90	[9] BEAN	87B	CLEO	$e^+e^- \to \Upsilon(4S)$
<0.27	90	[10] AVERY	84	CLEO	$e^+e^- \to \Upsilon(4S)$

[1] BEHRENS 00B uses high-momentum lepton tags and partially reconstructed $\overline{B}^0 \to D^{*+}\pi^-, \rho^-$ decays to determine the flavor of the B meson.
[2] ALBRECHT 94 reports r=0.194 ± 0.062 ± 0.054. We convert to χ for comparison. Uses tagged events (lepton + pion from D^*).
[3] BARTELT 93 analysis performed using tagged events (lepton+pion from D^*). Using dilepton events they obtain $0.157 \pm 0.016^{+0.033}_{-0.028}$.
[4] ALBRECHT 92L is a combined measurement employing several lepton-based techniques. It uses all previous ARGUS data in addition to new data and therefore supersedes ALBRECHT 87I. A value of $r = 20.6 \pm 7.0\%$ is directly measured. The value can be used to measure $x = \Delta M/\Gamma = 0.72 \pm 0.15$ for the B_d meson. Assumes $f_{+-}/f_0 = 1.0 \pm 0.05$ and uses $\tau_{B^\pm}/\tau_{B^0} = (0.95 \pm 0.14)$ (f_{+-}/f_0).
[5] Uses $D^{*+}K^\pm$ correlations.
[6] Uses $(D^{*+}\ell^-)$ $K^\pm$ correlations.
[7] These experiments see a combination of B_s and B_d mesons.
[8] ALBRECHT 87I is inclusive measurement with like-sign dileptons, with tagged B decays plus leptons, and one fully reconstructed event. Measures r=0.21 ± 0.08. We convert to χ for comparison. Superseded by ALBRECHT 92L.
[9] BEAN 87B measured $r <$ 0.24; we converted to χ.
[10] Same-sign dilepton events. Limit assumes semileptonic BR for B^+ and B^0 equal. If $B^0/B^\pm$ ratio <0.58, no limit exists. The limit was corrected in BEAN 87B from $r <$ 0.30 to $r <$ 0.37. We converted this limit to χ.

$\Delta m_{B^0} = m_{B^0_H} - m_{B^0_L}$

Δm_{B^0} is a measure of 2π times the B^0-$\overline{B}^0$ oscillation frequency in time-dependent mixing experiments.

The second "OUR EVALUATION" is an average using rescaled values of the data listed below. The average and rescaling were performed by the Heavy Flavor Averaging Group (HFLAV) and are described at http://www.slac.stanford.edu/xorg/hflav/. The averaging/rescaling procedure takes into account correlations between the measurements.

The first "OUR EVALUATION", also provided by the HFLAV, includes Δm_d calculated from χ_d measured at $\Upsilon(4S)$.

VALUE (10^{12} $\hbar$ s^{-1})	DOCUMENT ID		TECN	COMMENT
0.5064±0.0019 OUR EVALUATION First				
0.5065±0.0019 OUR EVALUATION Second				
0.5050 ± 0.0021 ± 0.0010	[1] AAIJ	16AV	LHCB	pp at 7, 8 TeV
0.503 ± 0.011 ± 0.013	[2] AAIJ	13CF	LHCB	pp at 7 TeV
0.5156 ± 0.0051 ± 0.0033	[3] AAIJ	13F	LHCB	pp at 7 TeV
0.499 ± 0.032 ± 0.003	[4] AAIJ	12I	LHCB	pp at 7 TeV
0.506 ± 0.020 ± 0.016	[5] ABAZOV	06W	D0	$p\overline{p}$ at 1.96 TeV
0.511 ± 0.007 $^{+0.007}_{-0.006}$	[6] AUBERT	06G	BABR	$e^+e^- \to \Upsilon(4S)$
0.511 ± 0.005 ± 0.006	[7] ABE	05B	BELL	$e^+e^- \to \Upsilon(4S)$
0.531 ± 0.025 ± 0.007	[8] ABDALLAH	03B	DLPH	$e^+e^- \to Z$
0.492 ± 0.018 ± 0.013	[9] AUBERT	03C	BABR	$e^+e^- \to \Upsilon(4S)$
0.503 ± 0.008 ± 0.010	[10] HASTINGS	03	BELL	$e^+e^- \to \Upsilon(4S)$
0.509 ± 0.017 ± 0.020	[11] ZHENG	03	BELL	$e^+e^- \to \Upsilon(4S)$
0.516 ± 0.016 ± 0.010	[12] AUBERT	02I	BABR	$e^+e^- \to \Upsilon(4S)$
0.493 ± 0.012 ± 0.009	[13] AUBERT	02J	BABR	$e^+e^- \to \Upsilon(4S)$
0.497 ± 0.024 ± 0.025	[14] ABBIENDI,G	00B	OPAL	$e^+e^- \to Z$
0.503 ± 0.064 ± 0.071	[15] ABE	99K	CDF	$p\overline{p}$ at 1.8 TeV
0.500 ± 0.052 ± 0.043	[16] ABE	99Q	CDF	$p\overline{p}$ at 1.8 TeV
0.516 ± 0.099 $^{+0.029}_{-0.035}$	[17] AFFOLDER	99C	CDF	$p\overline{p}$ at 1.8 TeV
0.471 $^{+0.078}_{-0.068}$ $^{+0.033}_{-0.034}$	[18] ABE	98C	CDF	$p\overline{p}$ at 1.8 TeV
0.458 ± 0.046 ± 0.032	[19] ACCIARRI	98D	L3	$e^+e^- \to Z$
0.437 ± 0.043 ± 0.044	[20] ACCIARRI	98D	L3	$e^+e^- \to Z$
0.472 ± 0.049 ± 0.053	[21] ACCIARRI	98D	L3	$e^+e^- \to Z$
0.523 ± 0.072 ± 0.043	[22] ABREU	97N	DLPH	$e^+e^- \to Z$
0.493 ± 0.042 ± 0.027	[20] ABREU	97N	DLPH	$e^+e^- \to Z$
0.499 ± 0.053 ± 0.015	[23] ABREU	97N	DLPH	$e^+e^- \to Z$
0.480 ± 0.040 ± 0.051	[19] ABREU	97N	DLPH	$e^+e^- \to Z$
0.444 ± 0.029 $^{+0.020}_{-0.017}$	[20] ACKERSTAFF	97U	OPAL	$e^+e^- \to Z$
0.430 ± 0.043 $^{+0.028}_{-0.030}$	[19] ACKERSTAFF	97V	OPAL	$e^+e^- \to Z$
0.482 ± 0.044 ± 0.024	[24] BUSKULIC	97D	ALEP	$e^+e^- \to Z$
0.404 ± 0.045 ± 0.027	[20] BUSKULIC	97D	ALEP	$e^+e^- \to Z$
0.452 ± 0.039 ± 0.044	[19] BUSKULIC	97D	ALEP	$e^+e^- \to Z$
0.539 ± 0.060 ± 0.024	[25] ALEXANDER	96V	OPAL	$e^+e^- \to Z$
0.567 ± 0.089 $^{+0.029}_{-0.023}$	[26] ALEXANDER	96V	OPAL	$e^+e^- \to Z$
• • • We do not use the following data for averages, fits, limits, etc. • • •				
0.516 ± 0.016 ± 0.010	[27] AUBERT	02N	BABR	$e^+e^- \to \Upsilon(4S)$
0.494 ± 0.012 ± 0.015	[28] HARA	02	BELL	Repl. by ABE 05B
0.528 ± 0.017 ± 0.011	[29] TOMURA	02	BELL	Repl. by ABE 05B
0.463 ± 0.008 ± 0.016	[13] ABE	01D	BELL	Repl. by HASTINGS 03
0.444 ± 0.028 ± 0.028	[30] ACCIARRI	98D	L3	$e^+e^- \to Z$
0.497 ± 0.035	[31] ABREU	97N	DLPH	$e^+e^- \to Z$
0.467 ± 0.022 $^{+0.017}_{-0.015}$	[32] ACKERSTAFF	97V	OPAL	$e^+e^- \to Z$
0.446 ± 0.032	[33] BUSKULIC	97D	ALEP	$e^+e^- \to Z$
0.531 $^{+0.050}_{-0.046}$ ± 0.078	[34] ABREU	96Q	DLPH	Sup. by ABREU 97N
0.496 $^{+0.055}_{-0.051}$ ± 0.043	[19] ACCIARRI	96E	L3	Repl. by ACCIARRI 98D
0.548 ± 0.050 $^{+0.023}_{-0.019}$	[35] ALEXANDER	96V	OPAL	$e^+e^- \to Z$
0.496 ± 0.046	[36] AKERS	95J	OPAL	Repl. by ACKERSTAFF 97V
0.462 $^{+0.040}_{-0.053}$ $^{+0.052}_{-0.035}$	[19] AKERS	95J	OPAL	Repl. by ACKERSTAFF 97V
0.50 ± 0.12 ± 0.06	[22] ABREU	94M	DLPH	Sup. by ABREU 97N
0.508 ± 0.075 ± 0.025	[25] AKERS	94C	OPAL	Repl. by ALEXANDER 96V
0.57 ± 0.11 ± 0.02	[26] AKERS	94H	OPAL	Repl. by ALEXANDER 96V
0.50 $^{+0.07}_{-0.06}$ $^{+0.11}_{-0.10}$	[19] BUSKULIC	94B	ALEP	Sup. by BUSKULIC 97D
0.52 $^{+0.10}_{-0.11}$ $^{+0.04}_{-0.03}$	[26] BUSKULIC	93K	ALEP	Sup. by BUSKULIC 97D

[1] Uses semileptonic decays of $B^0 \to D^-\mu^+\nu_\mu X$ and $B^0 \to D^{(*)-}\mu^+\nu_\mu X$, where the D mesons are reconstructed in $D^- \to K^+\pi^-\pi^-$ and $D^{(*)-} \to \overline{D}^0\pi^-$ with $\overline{D}^0 \to K^+\pi^-$.
[2] Uses semileptonic decays of $B^0 \to D^-\mu^+\nu_\mu X$ where the D^- mesons are reconstructed in $D^- \to K^+K^-\pi^-$.
[3] Measured using $B^0 \to D^-\pi^+$ and $B^0 \to J/\psi K^*(892)^0$ decays.
[4] Measured using $B^0 \to D^-\pi^+$.
[5] Uses opposite-side flavor-tagging with $B \to D^{(*)}\mu\nu_\mu X$ events.
[6] Measured using a simultaneous fit of the B^0 lifetime and $\overline{B}^0B^0$ oscillation frequency Δm_d in the partially reconstructed $B^0 \to D^{*-}\ell\nu$ decays.
[7] Measurement performed using a combined fit of CP-violation, mixing and lifetimes.
[8] Events with a high transverse momentum lepton were removed and an inclusively reconstructed vertex was required.
[9] AUBERT 03C uses a sample of approximately 14,000 exclusively reconstructed $B^0 \to D^*(2010)^-\ell\nu$ and simultaneously measures the lifetime and oscillation frequency.
[10] HASTINGS 03 measurement based on the time evolution of dilepton events. It also reports $f_+/f_0 = 1.01 \pm 0.03 \pm 0.09$ and CPT violation parameters in B^0-$\overline{B}^0$ mixing.
[11] ZHENG 03 data analyzed using partially reconstructed $\overline{B}^0 \to D^{*-}\pi^+$ decay and a flavor tag based on the charge of the lepton from the accompanying B decay.
[12] Uses a tagged sample of fully-reconstructed neutral B decays at $\Upsilon(4S)$.
[13] Measured based on the time evolution of dilepton events in $\Upsilon(4S)$ decays.
[14] Data analyzed using partially reconstructed $\overline{B}^0 \to D^{*+}\ell^-\overline{\nu}$ decay and a combination of flavor tags from the rest of the event.
[15] Uses di-muon events.
[16] Uses jet-charge and lepton-flavor tagging.
[17] Uses $\ell^- D^{*+} -\ell$ events.
[18] Uses π-B in the same side.
[19] Uses ℓ-ℓ.
[20] Uses ℓ-$Q_{\rm hem}$.
[21] Uses ℓ-ℓ with impact parameters.
[22] Uses $D^{*\pm}$-$Q_{\rm hem}$.
[23] Uses $\pi_s^\pm\ell$-$Q_{\rm hem}$.
[24] Uses $D^{*\pm}$-ℓ/$Q_{\rm hem}$.
[25] Uses $D^{*\pm}\ell$-$Q_{\rm hem}$.
[26] Uses $D^{*\pm}$-ℓ.
[27] AUBERT 02N result based on the same analysis and data sample reported in AUBERT 02I.
[28] Uses a tagged sample of B^0 decays reconstructed in the mode $B^0 \to D^*\ell\nu$.
[29] Uses a tagged sample of fully-reconstructed hadronic B^0 decays at $\Upsilon(4S)$.
[30] ACCIARRI 98D combines results from ℓ-ℓ, ℓ-$Q_{\rm hem}$, and ℓ-ℓ with impact parameters.
[31] ABREU 97N combines results from $D^{*\pm}$-$Q_{\rm hem}$, ℓ-$Q_{\rm hem}$, $\pi_s^\pm\ell$-$Q_{\rm hem}$, and ℓ-ℓ.
[32] ACKERSTAFF 97V combines results from ℓ-ℓ, ℓ-$Q_{\rm hem}$, D^*-ℓ, and $D^{*\pm}$-$Q_{\rm hem}$.

[33] BUSKULIC 97D combines results from $D^{*\pm}$-ℓ/$Q_{\rm hem}$, ℓ-$Q_{\rm hem}$, and ℓ-ℓ.
[34] ABREU 96Q analysis performed using lepton, kaon, and jet-charge tags.
[35] ALEXANDER 96V combines results from $D^{*\pm}$-ℓ and $D^{*\pm}$ ℓ-$Q_{\rm hem}$.
[36] AKERS 95J combines results from charge measurement, $D^{*\pm}$ ℓ-$Q_{\rm hem}$ and ℓ-ℓ.

$x_d = \Delta m_{B^0}/\Gamma_{B^0}$

The second "OUR EVALUATION" is an average using rescaled values of the data listed below. The average and rescaling were performed by the Heavy Flavor Averaging Group (HFLAV) and are described at http://www.slac.stanford.edu/xorg/hflav/. The averaging/rescaling procedure takes into account correlations between the measurements.

The first "OUR EVALUATION", also provided by the HFLAV, includes χ_d measured at $\Upsilon(4S)$.

VALUE	DOCUMENT ID
0.770±0.004 OUR EVALUATION	First
0.770±0.004 OUR EVALUATION	Second

Re(λ_{CP} / $|\lambda_{CP}|$) Re(z)

The λ_{CP} characterizes B^0 and $\overline{B}^0$ decays to states of charmonium plus K^0_L. Parameter z is used to describe CPT violation in mixing, see the review on "CP Violation" in the reviews section.

VALUE	DOCUMENT ID		TECN	COMMENT
0.047±0.022±0.003	[1] LEES	16E	BABR	$e^+e^- \to \Upsilon(4S)$
• • • We do not use the following data for averages, fits, limits, etc. • • •				
0.014±0.035±0.034	[2] AUBERT,B	04C	BABR	Repl. by LEES 16E

[1] The first uncertainty is the uncertainty from Re(z) and the second uncertainty is from Re($\lambda/|\lambda|$).
[2] Corresponds to 90% confidence range [−0.072, 0.101].

$\Delta\Gamma$ Re(z)

VALUE	DOCUMENT ID		TECN	COMMENT
−0.0071±0.0039±0.0020	AUBERT	06T	BABR	$e^+e^- \to \Upsilon(4S)$

Re(z)

VALUE (units 10^{-2})	DOCUMENT ID		TECN	COMMENT
−4 ± 4 OUR AVERAGE Error includes scale factor of 1.4.				
−6.5 ± 2.8±1.4	[1] LEES	16E	BABR	$e^+e^- \to \Upsilon(4S)$
1.9 ± 3.7±3.3	[2] HIGUCHI	12	BELL	$e^+e^- \to \Upsilon(4S)$
• • • We do not use the following data for averages, fits, limits, etc. • • •				
0 ±12 ±1	[3] HASTINGS	03	BELL	Repl. by HIGUCHI 12

[1] Measurement uses decays $B^0/\overline{B}^0 \to c\overline{c}K^0_S/K^0_L$.
[2] Measured using $B^0 \to J/\psi K^0_S$, $J/\psi K^0_L$, $D^-\pi^+$, $D^{*-}\pi^+$, $D^{*-}\rho^+$, and $D^{*-}\ell^+\nu$ decays.
[3] Measured using inclusive dilepton events from B^0 decay.

Im(z)

VALUE (units 10^{-2})	DOCUMENT ID		TECN	COMMENT
−0.8 ±0.4 OUR AVERAGE				
1.0 ±3.0 ±1.3	[1] LEES	16E	BABR	$e^+e^- \to \Upsilon(4S)$
−0.57±0.33±0.33	[2] HIGUCHI	12	BELL	$e^+e^- \to \Upsilon(4S)$
−1.39±0.73±0.32	[3] AUBERT	06T	BABR	$e^+e^- \to \Upsilon(4S)$
• • • We do not use the following data for averages, fits, limits, etc. • • •				
3.8 ±2.9 ±2.5	[4] AUBERT,B	04C	BABR	Repl. by AUBERT 06T
−3 ±1 ±3	[5] HASTINGS	03	BELL	Repl. by HIGUCHI 12

[1] Measurement uses decays $B^0/\overline{B}^0 \to c\overline{c}K^0_S/K^0_L$.
[2] Measured using $B^0 \to J/\psi K^0_S$, $J/\psi K^0_L$, $D^-\pi^+$, $D^{*-}\pi^+$, $D^{*-}\rho^+$, and $D^{*-}\ell^+\nu$ decays.
[3] Measurement uses $B^0/\overline{B}^0 \to \ell^+X/\ell^-X$ decays. Assuming $\Delta\Gamma = 0$, the result becomes Im(z) = $(-0.37 \pm 0.54) \times 10^{-2}$.
[4] Corresponds to 90% confidence range [−0.028, 0.104].
[5] Measured using inclusive dilepton events from B^0 decay.

CP VIOLATION PARAMETERS

Re(ϵ_{B^0})/(1+$|\epsilon_{B^0}|^2$)

CP impurity in B^0_d system. It is obtained from either $a_{\ell\ell}$, the charge asymmetry in like-sign dilepton events or a_{cp}, the time-dependent asymmetry of inclusive B^0 and $\overline{B}^0$ decays.

"OUR EVALUATION" is an average obtained by the Heavy Flavor Averaging Group (HFLAV) and described at http://www.slac.stanford.edu/xorg/hflav/. It is the result of a fit to B_d and B_s CP asymmetries, which includes the B_d measurements listed below and the B_s measurements listed in the B_s section, taking into account correlations between those measurements.

VALUE (units 10^{-3})	DOCUMENT ID		TECN	COMMENT
− 0.5 ± 0.4 OUR EVALUATION				
− 0.1 ± 0.4 OUR AVERAGE				
− 0.05 ± 0.48 ±0.75	[1] AAIJ	15F	LHCB	pp at 7, 8 TeV
− 0.975 ± 0.875 ±0.475	[2] LEES	15A	BABR	$e^+e^- \to \Upsilon(4S)$
1.55 ± 1.05	[3] ABAZOV	14	D0	$p\overline{p}$ at 1.96 TeV
0.15 ± 0.42 $^{+0.94}_{-0.81}$	[4] LEES	13N	BABR	$e^+e^- \to \Upsilon(4S)$
− 1.7 ± 1.1 ±0.4	[5] ABAZOV	12AC	D0	$p\overline{p}$ at 1.96 TeV
0.4 ± 1.3 ±0.9	[6] AUBERT	06T	BABR	$e^+e^- \to \Upsilon(4S)$
− 0.3 ± 2.0 ±2.1	[7] NAKANO	06	BELL	$e^+e^- \to \Upsilon(4S)$
3.5 ±10.3 ±1.5	[8] JAFFE	01	CLE2	$e^+e^- \to \Upsilon(4S)$
• • • We do not use the following data for averages, fits, limits, etc. • • •				
− 0.3 ± 1.3	[9] ABAZOV	11U	D0	Repl. by ABAZOV 14
− 2.3 ± 1.1 ±0.8	[10] ABAZOV	06S	D0	Repl. by ABAZOV 11U
−14.7 ± 6.7 ±5.7	[11] AUBERT,B	04C	BABR	Repl. by AUBERT 06T
1.2 ± 2.9 ±3.6	[2] AUBERT	02K	BABR	Repl. by LEES 15A
− 3.2 ± 6.5	[12] BARATE	01D	ALEP	$e^+e^- \to Z$
4 ±18 ±3	[13] BEHRENS	00B	CLE2	Repl. by JAFFE 01
1.2 ±13.8 ±3.2	[14] ABBIENDI	99J	OPAL	$e^+e^- \to Z$
2 ± 7 ±3	[15] ACKERSTAFF	97U	OPAL	$e^+e^- \to Z$
< 45	[16] BARTELT	93	CLE2	$e^+e^- \to \Upsilon(4S)$

[1] AAIJ 15F uses semileptonic B^0 decays in the inclusive final states $D^-\mu^+$ and $D^{*-}\mu^+$, where the D^- meson decays into the $K^+\pi^-\pi^-$ final state, and the D^{*-} meson into the $\overline{D}^0(\to K^+\pi^-)\pi^-$ final state. Reports $A^d_{SL} = (-0.02 \pm 0.19 \pm 0.30)\%$, which equals to 4Re($\epsilon_{B^0}$)/(1+$|\epsilon_{B^0}|^2$).
[2] Uses the charge asymmetry in like-sign dilepton events. LEES 15A reports $A^d_{SL} = (-3.9 \pm 3.5 \pm 1.9) \times 10^{-3}$.
[3] ABAZOV 14 uses the dimuon charge asymmetry with different impact parameters from which it reports $A^d_{SL} = (-0.62 \pm 0.42) \times 10^{-2}$.
[4] Uses $B^0 \to D^{*-}X\ell^+\nu_\ell$ and a kaon-tagged sample which yields measurement of $A^d_{SL} = (0.06 \pm 0.17^{+0.38}_{-0.32})\%$, corresponding to $\Delta_{CP} = 1-|q/p| = (0.29 \pm 0.84^{+1.88}_{-1.61}) \times 10^{-3}$.
[5] ABAZOV 12AC uses $B^0 \to D^-\mu^+X$ and $B^0 \to D^*(2010)^-\mu^+X$ decays without initial state flavor tagging which yields measurement of $A^d_{SL} = (6.8 \pm 4.5 \pm 1.4) \times 10^{-3}$.
[6] AUBERT 06T reports $|q/p|-1 = (-0.8 \pm 2.7 \pm 1.9) \times 10^{-3}$. We convert to $(1-|q/p|^2)/4$.
[7] Uses the charge asymmetry in like-sign dilepton events and reports $|q/p| = 1.0005 \pm 0.0040 \pm 0.0043$.
[8] JAFFE 01 finds $a_{\ell\ell} = 0.013 \pm 0.050 \pm 0.005$ and combines with the previous BEHRENS 00B independent measurement.
[9] ABAZOV 11U uses the dimuon charge asymmetry with different impact parameters from which it reports $A^d_{SL} = (-1.2 \pm 5.2) \times 10^{-3}$.
[10] Uses the dimuon charge asymmetry.
[11] AUBERT 04C reports $|q/p| = 1.029 \pm 0.013 \pm 0.011$ and we converted it to (1- $|q/p|^2$)/4.
[12] BARATE 01D measured by investigating time-dependent asymmetries in semileptonic and fully inclusive B^0_d decays.
[13] BEHRENS 00B uses high-momentum lepton tags and partially reconstructed $\overline{B}^0 \to D^{*+}\pi^-$, ρ^- decays to determine the flavor of the B meson.
[14] Data analyzed using the time-dependent asymmetry of inclusive B^0 decay. The production flavor of B^0 mesons is determined using both the jet charge and the charge of secondary vertex in the opposite hemisphere.
[15] ACKERSTAFF 97U assumes CPT and is based on measuring the charge asymmetry in a sample of B^0 decays defined by lepton and $Q_{\rm hem}$ tags. If CPT is not invoked, Re(ϵ_B) = $-0.006 \pm 0.010 \pm 0.006$ is found. The indirect CPT violation parameter is determined to Im(δB) = $-0.020 \pm 0.016 \pm 0.006$.
[16] BARTELT 93 finds $a_{\ell\ell} = 0.031 \pm 0.096 \pm 0.032$ which corresponds to $|a_{\ell\ell}| < 0.18$, which yields the above |Re(ϵ_{B^0})/(1+$|\epsilon_{B^0}|^2$)|.

$A_{T/CP}$

$A_{T/CP}$ is defined as

$$\frac{P(\overline{B}^0 \to B^0) - P(B^0 \to \overline{B}^0)}{P(\overline{B}^0 \to B^0) + P(B^0 \to \overline{B}^0)},$$

the CPT invariant asymmetry between the oscillation probabilities P($\overline{B}^0 \to B^0$) and P($B^0 \to \overline{B}^0$).

VALUE	DOCUMENT ID		TECN	COMMENT
0.005±0.012±0.014	[1] AUBERT	02K	BABR	$e^+e^- \to \Upsilon(4S)$

[1] AUBERT 02K uses the charge asymmetry in like-sign dilepton events.

$A_{CP}(B^0 \to D^*(2010)^+D^-)$

A_{CP} is defined as

$$\frac{B(\overline{B}^0 \to \overline{f}) - B(B^0 \to f)}{B(\overline{B}^0 \to \overline{f}) + B(B^0 \to f)},$$

the CP-violation charge asymmetry of exclusive B^0 and $\overline{B}^0$ decay.

VALUE	DOCUMENT ID		TECN	COMMENT
0.037±0.034 OUR AVERAGE				
0.06 ±0.05 ±0.02	ROHRKEN	12	BELL	$e^+e^- \to \Upsilon(4S)$
0.008±0.048±0.013	AUBERT	09C	BABR	$e^+e^- \to \Upsilon(4S)$
0.07 ±0.08 ±0.04	[1] AUSHEV	04	BELL	$e^+e^- \to \Upsilon(4S)$
• • • We do not use the following data for averages, fits, limits, etc. • • •				
−0.12 ±0.06 ±0.02	AUBERT	07AI	BABR	Repl. by AUBERT 09C
−0.03 ±0.10 ±0.02	AUBERT,B	06A	BABR	Repl. by AUBERT 07AI
−0.03 ±0.11 ±0.05	AUBERT	03J	BABR	Repl. by AUBERT,B 06B

[1] Combines results from fully and partially reconstructed $B^0 \to D^{*\pm}D^{\mp}$ decays.

$A_{CP}(B^0 \to [K^+K^-]_D K^*(892)^0)$

VALUE	DOCUMENT ID		TECN	COMMENT
• • • We do not use the following data for averages, fits, limits, etc. • • •				
−0.20±0.15±0.02	AAIJ	14BN	LHCB	Repl. by AAIJ 16S
−0.45±0.23±0.02	AAIJ	13L	LHCB	Repl. by AAIJ 14BN

$A_{CP}(B^0 \to [K^+\pi^-]_D K^*(892)^0)$

VALUE	DOCUMENT ID		TECN	COMMENT
−0.03±0.04±0.02	AAIJ	14BN	LHCB	pp at 7, 8 TeV

• • • We do not use the following data for averages, fits, limits, etc. • • •

$-0.08 \pm 0.08 \pm 0.01$	AAIJ	13L	LHCB	Repl. by AAIJ 14BN

$R_d^+ = \Gamma(B^0 \to [\pi^+ K^-]_D K^{*0}) / \Gamma(B^0 \to [\pi^- K^+]_D K^{*0})$

VALUE	DOCUMENT ID		TECN	COMMENT
0.06±0.03±0.01	AAIJ	14BN	LHCB	pp at 7, 8 TeV

$R_d^- = \Gamma(\overline{B}^0 \to [\pi^- K^+]_D K^{*0}) / \Gamma(\overline{B}^0 \to [\pi^+ K^-]_D K^{*0})$

VALUE	DOCUMENT ID		TECN	COMMENT
0.06±0.03±0.01	AAIJ	14BN	LHCB	pp at 7, 8 TeV

$A_{CP}(B^0 \to [\pi^+\pi^-]_D K^*(892)^0)$

VALUE	DOCUMENT ID		TECN	COMMENT
• • • We do not use the following data for averages, fits, limits, etc. • • •				
$-0.09 \pm 0.22 \pm 0.02$	AAIJ	14BN	LHCB	Repl. by AAIJ 16S

A_{CP} $(B^0 \to K^+\pi^-)$

VALUE	DOCUMENT ID		TECN	COMMENT
−0.082±0.006 OUR AVERAGE				
$-0.083 \pm 0.013 \pm 0.004$	AALTONEN	14P	CDF	$p\overline{p}$ at 1.96 TeV
$-0.080 \pm 0.007 \pm 0.003$	AAIJ	13AX	LHCB	pp at 7 TeV
$-0.069 \pm 0.014 \pm 0.007$	DUH	13	BELL	$e^+e^- \to \Upsilon(4S)$
$-0.107 \pm 0.016 \,^{+\,0.006}_{-\,0.004}$	LEES	13D	BABR	$e^+e^- \to \Upsilon(4S)$
-0.04 ± 0.16	[1] CHEN	00	CLE2	$e^+e^- \to \Upsilon(4S)$
• • • We do not use the following data for averages, fits, limits, etc. • • •				
$-0.088 \pm 0.011 \pm 0.008$	AAIJ	12V	LHCB	Repl. by AAIJ 13AX
$-0.086 \pm 0.023 \pm 0.009$	AALTONEN	11N	CDF	Repl. by AALTONEN 14P
$-0.094 \pm 0.018 \pm 0.008$	LIN	08	BELL	Repl. by DUH 13
$-0.107 \pm 0.018 \,^{+\,0.007}_{-\,0.004}$	AUBERT	07AF	BABR	Repl. by LEES 13D
$-0.013 \pm 0.078 \pm 0.012$	ABULENCIA,A	06D	CDF	Repl. by AALTONEN 11N
$-0.088 \pm 0.035 \pm 0.013$	[2] CHAO	05A	BELL	Repl. by CHAO 04B
$-0.133 \pm 0.030 \pm 0.009$	[3] AUBERT,B	04K	BABR	Repl. by AUBERT 07AF
$-0.101 \pm 0.025 \pm 0.005$	[4] CHAO	04B	BELL	Repl. by LIN 08
$-0.07 \pm 0.08 \pm 0.02$	[5] AUBERT	02D	BABR	Repl. by AUBERT 02Q
$-0.102 \pm 0.050 \pm 0.016$	[6] AUBERT	02Q	BABR	Repl. by AUBERT,B 04K
$-0.06 \pm 0.09 \,^{+\,0.01}_{-\,0.02}$	[7] CASEY	02	BELL	Repl. by CHAO 04B
$0.044 \,^{+\,0.186}_{-\,0.167} \,^{+\,0.018}_{-\,0.021}$	[8] ABE	01K	BELL	Repl. by CASEY 02
$-0.19 \pm 0.10 \pm 0.03$	[9] AUBERT	01E	BABR	Repl. by AUBERT 02Q

[1] Corresponds to 90% confidence range $-0.30 < A_{CP} < 0.22$.
[2] Corresponds to a 90% CL interval of $-0.15 < A_{CP} < -0.03$.
[3] Based on a total signal yield of $N(K^-\pi^+) + N(K^+\pi^-) = 1606 \pm 51$ events.
[4] CHAO 04B reports significance of 3.9 standard deviation for deviation of A_{CP} from zero.
[5] Corresponds to 90% confidence range $-0.21 < A_{CP} < 0.07$.
[6] Corresponds to 90% confidence range $-0.188 < A_{CP} < -0.016$.
[7] Corresponds to 90% confidence range $-0.21 < A_{CP} < +0.09$.
[8] Corresponds to 90% confidence range $-0.25 < A_{CP} < 0.37$.
[9] Corresponds to 90% confidence range $-0.35 < A_{CP} < -0.03$.

$A_{CP}(B^0 \to \eta' K^*(892)^0)$

VALUE	DOCUMENT ID		TECN	COMMENT
−0.07±0.18 OUR AVERAGE				
$-0.22 \pm 0.29 \pm 0.07$	SATO	14	BELL	$e^+e^- \to \Upsilon(4S)$
$0.02 \pm 0.23 \pm 0.02$	DEL-AMO-SA...10A		BABR	$e^+e^- \to \Upsilon(4S)$
• • • We do not use the following data for averages, fits, limits, etc. • • •				
$0.08 \pm 0.25 \pm 0.02$	[1] AUBERT	07E	BABR	Repl. by DEL-AMO-SANCHEZ 10A

[1] Reports A_{CP} with the opposite sign convention.

$A_{CP}(B^0 \to \eta' K_0^*(1430)^0)$

VALUE	DOCUMENT ID	TECN	COMMENT
−0.19±0.17±0.02	DEL-AMO-SA...10A	BABR	$e^+e^- \to \Upsilon(4S)$

$A_{CP}(B^0 \to \eta' K_2^*(1430)^0)$

VALUE	DOCUMENT ID	TECN	COMMENT
0.14±0.18±0.02	DEL-AMO-SA...10A	BABR	$e^+e^- \to \Upsilon(4S)$

$A_{CP}(B^0 \to \eta K^*(892)^0)$

VALUE	DOCUMENT ID		TECN	COMMENT
0.19±0.05 OUR AVERAGE				
$0.17 \pm 0.08 \pm 0.01$	WANG	07B	BELL	$e^+e^- \to \Upsilon(4S)$
$0.21 \pm 0.06 \pm 0.02$	AUBERT,B	06H	BABR	$e^+e^- \to \Upsilon(4S)$
• • • We do not use the following data for averages, fits, limits, etc. • • •				
$0.02 \pm 0.11 \pm 0.02$	AUBERT,B	04D	BABR	Repl. by AUBERT,B 06H

$A_{CP}(B^0 \to \eta K_0^*(1430)^0)$

VALUE	DOCUMENT ID	TECN	COMMENT
0.06±0.13±0.02	AUBERT,B 06H	BABR	$e^+e^- \to \Upsilon(4S)$

$A_{CP}(B^0 \to \eta K_2^*(1430)^0)$

VALUE	DOCUMENT ID	TECN	COMMENT
−0.07±0.19±0.02	AUBERT,B 06H	BABR	$e^+e^- \to \Upsilon(4S)$

$A_{CP}(B^0 \to b_1 K^+)$

VALUE	DOCUMENT ID		TECN	COMMENT
−0.07±0.12±0.02	AUBERT	07BI	BABR	$e^+e^- \to \Upsilon(4S)$

$A_{CP}(B^0 \to \omega K^{*0})$

VALUE	DOCUMENT ID		TECN	COMMENT
0.45±0.25±0.02	AUBERT	09H	BABR	$e^+e^- \to \Upsilon(4S)$

$A_{CP}(B^0 \to \omega (K\pi)_0^{*0})$

VALUE	DOCUMENT ID		TECN	COMMENT
−0.07±0.09±0.02	AUBERT	09H	BABR	$e^+e^- \to \Upsilon(4S)$

$A_{CP}(B^0 \to \omega K_2^*(1430)^0)$

VALUE	DOCUMENT ID		TECN	COMMENT
−0.37±0.17±0.02	AUBERT	09H	BABR	$e^+e^- \to \Upsilon(4S)$

$A_{CP}(B^0 \to K^+\pi^-\pi^0)$

VALUE (units 10^{-2})	DOCUMENT ID		TECN	COMMENT
0 ± 6 OUR AVERAGE				
$-3.0 \,^{+\,4.5}_{-\,5.1} \pm 5.5$	[1] AUBERT	08AQ	BABR	$e^+e^- \to \Upsilon(4S)$
$7 \pm 11 \pm 1$	[2] CHANG	04	BELL	$e^+e^- \to \Upsilon(4S)$

[1] Uses Dalitz plot analysis of $B^0 \to K^+\pi^-\pi^0$ decays.
[2] Corresponds to 90% confidence range $-0.12 < A^{CP} < 0.26$.

$A_{CP}(B^0 \to \rho^- K^+)$

VALUE	DOCUMENT ID		TECN	COMMENT
0.20±0.11 OUR AVERAGE				
$0.20 \pm 0.09 \pm 0.08$	[1] LEES	11	BABR	$e^+e^- \to \Upsilon(4S)$
$0.22 \,^{+\,0.22}_{-\,0.23} \,^{+\,0.06}_{-\,0.02}$	[2] CHANG	04	BELL	$e^+e^- \to \Upsilon(4S)$
• • • We do not use the following data for averages, fits, limits, etc. • • •				
$0.11 \,^{+\,0.14}_{-\,0.15} \pm 0.07$	[1] AUBERT	08AQ	BABR	Repl. by LEES 11
$-0.28 \pm 0.17 \pm 0.08$	[3] AUBERT	03T	BABR	Repl. by AUBERT 08AQ

[1] Uses Dalitz plot analysis of $B^0 \to K^+\pi^-\pi^0$ decays.
[2] Corresponds to 90% confidence range $-0.18 < A_{CP} < 0.64$.
[3] The result reported corresponds to $-A_{CP}$.

$A_{CP}(B^0 \to \rho(1450)^- K^+)$

VALUE	DOCUMENT ID		TECN	COMMENT
−0.10±0.32±0.09	[1] LEES	11	BABR	$e^+e^- \to \Upsilon(4S)$

[1] Uses Dalitz plot analysis of $B^0 \to K^+\pi^-\pi^0$ decays.

$A_{CP}(B^0 \to \rho(1700)^- K^+)$

VALUE	DOCUMENT ID		TECN	COMMENT
−0.36±0.57±0.23	[1] LEES	11	BABR	$e^+e^- \to \Upsilon(4S)$

[1] Uses Dalitz plot analysis of $B^0 \to K^+\pi^-\pi^0$ decays.

$A_{CP}(B^0 \to K^+\pi^-\pi^0$ nonresonant)

VALUE	DOCUMENT ID		TECN	COMMENT
0.10±0.16±0.08	[1] LEES	11	BABR	$e^+e^- \to \Upsilon(4S)$
• • • We do not use the following data for averages, fits, limits, etc. • • •				
$0.23 \,^{+\,0.19}_{-\,0.27} \,^{+\,0.11}_{-\,0.10}$	[1] AUBERT	08AQ	BABR	Repl. by LEES 11

[1] Uses Dalitz plot analysis of $B^0 \to K^+\pi^-\pi^0$ decays. The quoted value is only for the flat part of the non-resonant component.

$A_{CP}(B^0 \to K^0\pi^+\pi^-)$

VALUE	DOCUMENT ID		TECN	COMMENT
−0.01±0.05±0.01	[1] AUBERT	09AU	BABR	$e^+e^- \to \Upsilon(4S)$

[1] Uses Dalitz plot analysis of $B^0 \to K^0\pi^+\pi^-$ decays and the first of two equivalent solutions is used.

$A_{CP}(B^0 \to K^*(892)^+\pi^-)$

VALUE	DOCUMENT ID		TECN	COMMENT
−0.22±0.06 OUR AVERAGE				
$-0.29 \pm 0.11 \pm 0.02$	[1] LEES	11	BABR	$e^+e^- \to \Upsilon(4S)$
$-0.21 \pm 0.10 \pm 0.02$	[2,3] AUBERT	09AU	BABR	$e^+e^- \to \Upsilon(4S)$
$-0.21 \pm 0.11 \pm 0.07$	[4] DALSENO	09	BELL	$e^+e^- \to \Upsilon(4S)$
$0.26 \,^{+\,0.33}_{-\,0.34} \,^{+\,0.10}_{-\,0.08}$	[5] EISENSTEIN	03	CLE2	$e^+e^- \to \Upsilon(4S)$
• • • We do not use the following data for averages, fits, limits, etc. • • •				
$-0.19 \,^{+\,0.20}_{-\,0.15} \pm 0.04$	[1] AUBERT	08AQ	BABR	Repl. by LEES 11
$-0.11 \pm 0.14 \pm 0.05$	[2] AUBERT	06I	BABR	Repl. by AUBERT 09AU
$0.23 \pm 0.18 \,^{+\,0.09}_{-\,0.06}$	AUBERT,B	04O	BABR	Repl. by AUBERT 06I

[1] Uses Dalitz plot analysis of $B^0 \to K^+\pi^-\pi^0$ decays.
[2] Uses Dalitz plot analysis of $B^0 \to K^0\pi^+\pi^-$ decays.
[3] The first of two equivalent solutions is used.
[4] Uses Dalitz plot analysis of $B^0 \to K^0\pi^+\pi^-$ decays and the first of two consistent solutions that may be preferred.
[5] Corresponds to 90% confidence range $-0.31 < A_{CP} < 0.78$.

See key on page 885

$A_{CP}(B^0 \to (K\pi)_0^{*+}\pi^-)$

VALUE	DOCUMENT ID		TECN	COMMENT
0.09±0.07 OUR AVERAGE				
0.07±0.14±0.01	[1] LEES	11	BABR	$e^+e^- \to \Upsilon(4S)$
0.09±0.07±0.03	[2] AUBERT	09AU	BABR	$e^+e^- \to \Upsilon(4S)$
• • • We do not use the following data for averages, fits, limits, etc. • • •				
$0.17^{+0.11}_{-0.16}\pm0.22$	[1] AUBERT	08AQ	BABR	Repl. by LEES 11

[1] Uses Dalitz plot analysis of $B^0 \to K^+\pi^-\pi^0$ decays.
[2] Uses Dalitz plot analysis of $B^0 \to K^0\pi^+\pi^-$ decays and the first of two equivalent solutions is used.

$A_{CP}(B^0 \to (K\pi)_0^{*0}\pi^0)$

VALUE	DOCUMENT ID		TECN	COMMENT
−0.15±0.10±0.04	[1] LEES	11	BABR	$e^+e^- \to \Upsilon(4S)$
• • • We do not use the following data for averages, fits, limits, etc. • • •				
$-0.22\pm0.12^{+0.30}_{-0.29}$	[1] AUBERT	08AQ	BABR	Repl. by LEES 11

[1] Uses Dalitz plot analysis of $B^0 \to K^+\pi^-\pi^0$ decays.

$A_{CP}(B^0 \to K^{*0}\pi^0)$

VALUE	DOCUMENT ID		TECN	COMMENT
−0.15±0.12±0.04	[1] LEES	11	BABR	$e^+e^- \to \Upsilon(4S)$
• • • We do not use the following data for averages, fits, limits, etc. • • •				
$-0.09^{+0.21}_{-0.24}\pm0.09$	[1] AUBERT	08AQ	BABR	Repl. by LEES 11

[1] Uses Dalitz plot analysis of $B^0 \to K^+\pi^-\pi^0$ decays.

$A_{CP}(B^0 \to K^*(892)^0\pi^+\pi^-)$

VALUE	DOCUMENT ID		TECN	COMMENT
0.07±0.04±0.03	AUBERT	07AS	BABR	$e^+e^- \to \Upsilon(4S)$

$A_{CP}(B^0 \to K^*(892)^0\rho^0)$

VALUE	DOCUMENT ID		TECN	COMMENT
−0.06±0.09±0.02	LEES	12K	BABR	$e^+e^- \to \Upsilon(4S)$
• • • We do not use the following data for averages, fits, limits, etc. • • •				
0.09±0.19±0.02	AUBERT,B	06G	BABR	Repl. by LEES 12K

$A_{CP}(B^0 \to K^{*0}f_0(980))$

VALUE	DOCUMENT ID		TECN	COMMENT
0.07±0.10±0.02	LEES	12K	BABR	$e^+e^- \to \Upsilon(4S)$
• • • We do not use the following data for averages, fits, limits, etc. • • •				
−0.17±0.28±0.02	AUBERT,B	06G	BABR	Repl. by LEES 12K

$A_{CP}(B^0 \to K^{*+}\rho^-)$

VALUE	DOCUMENT ID		TECN	COMMENT
0.21±0.15±0.02	LEES	12K	BABR	$e^+e^- \to \Upsilon(4S)$

$A_{CP}(B^0 \to K^*(892)^0K^+K^-)$

VALUE	DOCUMENT ID		TECN	COMMENT
0.01±0.05±0.02	AUBERT	07AS	BABR	$e^+e^- \to \Upsilon(4S)$

$A_{CP}(B^0 \to a_1^-K^+)$

VALUE	DOCUMENT ID		TECN	COMMENT
−0.16±0.12±0.01	AUBERT	08F	BABR	$e^+e^- \to \Upsilon(4S)$

$A_{CP}(B^0 \to K^0K^0)$

VALUE	DOCUMENT ID		TECN	COMMENT
$-0.58^{+0.73}_{-0.66}\pm0.04$	LIN	07	BELL	$e^+e^- \to \Upsilon(4S)$

$A_{CP}(B^0 \to K^*(892)^0\phi)$

VALUE	DOCUMENT ID		TECN	COMMENT
0.00 ±0.04 OUR AVERAGE				
−0.007±0.048±0.021	PRIM	13	BELL	$e^+e^- \to \Upsilon(4S)$
0.01 ±0.06 ±0.03	AUBERT	08BG	BABR	$e^+e^- \to \Upsilon(4S)$
• • • We do not use the following data for averages, fits, limits, etc. • • •				
−0.03 ±0.07 ±0.03	AUBERT	07D	BABR	Repl. by AUBERT 08BG
0.02 ±0.09 ±0.02	[1] CHEN	05A	BELL	Repl. by PRIM 13
−0.01 ±0.09 ±0.02	AUBERT,B	04W	BABR	Repl. by AUBERT 07D
0.04 ±0.12 ±0.02	AUBERT	03V	BABR	Repl. by AUBERT 04W
0.07 ±0.15 $^{+0.05}_{-0.03}$	[2] CHEN	03B	BELL	Repl. by CHEN 05A
0.00 ±0.27 ±0.03	[3] AUBERT	02E	BABR	Repl. by AUBERT 03V

[1] Corresponds to 90% confidence range $-0.14 < A_{CP} < 0.17$.
[2] Corresponds to 90% confidence range $-0.18 < A_{CP} < 0.33$.
[3] Corresponds to 90% confidence range $-0.44 < A_{CP} < 0.44$.

$A_{CP}(B^0 \to K^*(892)^0K^-\pi^+)$

VALUE	DOCUMENT ID		TECN	COMMENT
0.22±0.33±0.20	AUBERT	07AS	BABR	$e^+e^- \to \Upsilon(4S)$

$A_{CP}(B^0 \to \phi(K\pi)_0^{*0})$

VALUE	DOCUMENT ID		TECN	COMMENT
0.12 ±0.08 OUR AVERAGE				
0.093±0.094±0.017	PRIM	13	BELL	$e^+e^- \to \Upsilon(4S)$
0.20 ±0.14 ±0.06	AUBERT	08BG	BABR	$e^+e^- \to \Upsilon(4S)$
• • • We do not use the following data for averages, fits, limits, etc. • • •				
0.17 ±0.15 ±0.03	AUBERT	07D	BABR	Repl. by AUBERT 08BG

$A_{CP}(B^0 \to \phi K_2^*(1430)^0)$

VALUE	DOCUMENT ID		TECN	COMMENT
−0.11 ±0.10 OUR AVERAGE				
$-0.155^{+0.152}_{-0.133}\pm0.033$	PRIM	13	BELL	$e^+e^- \to \Upsilon(4S)$
−0.08 ±0.12 ±0.05	AUBERT	08BG	BABR	$e^+e^- \to \Upsilon(4S)$
• • • We do not use the following data for averages, fits, limits, etc. • • •				
−0.12 ±0.14 ±0.04	AUBERT	07D	BABR	Repl. by AUBERT 08BG

$A_{CP}(B^0 \to K^*(892)^0\gamma)$

VALUE	DOCUMENT ID		TECN	COMMENT
−0.006±0.011 OUR AVERAGE				
−0.013±0.017±0.004	[1] HORIGUCHI	17	BELL	$e^+e^- \to \Upsilon(4S)$
0.008±0.017±0.009	AAIJ	13	LHCB	pp at 7 TeV
−0.016±0.022±0.007	AUBERT	09AO	BABR	$e^+e^- \to \Upsilon(4S)$

[1] Uses $B(\Upsilon(4S) \to B^+B^-) = (51.4 \pm 0.6)\%$ and $B(\Upsilon(4S) \to B^0\overline{B}^0) = (48.6 \pm 0.6)\%$.

$A_{CP}(B^0 \to K_2^*(1430)^0\gamma)$

VALUE	DOCUMENT ID		TECN	COMMENT
−0.08±0.15±0.01	AUBERT,B	04U	BABR	$e^+e^- \to \Upsilon(4S)$

$A_{CP}(B^0 \to \rho^+\pi^-)$

VALUE	DOCUMENT ID		TECN	COMMENT
0.13±0.06 OUR AVERAGE Error includes scale factor of 1.1.				
$0.09^{+0.05}_{-0.06}\pm0.04$	[1] LEES	13J	BABR	$e^+e^- \to \Upsilon(4S)$
0.21±0.08±0.04	[1] KUSAKA	07	BELL	$e^+e^- \to \Upsilon(4S)$
• • • We do not use the following data for averages, fits, limits, etc. • • •				
0.03±0.07±0.04	AUBERT	07AA	BABR	Repl. by LEES 13J
$-0.02\pm0.16^{+0.05}_{-0.02}$	WANG	05	BELL	Repl. by KUSAKA 07
−0.18±0.08±0.03	AUBERT	03T	BABR	Repl. by AUBERT 07AA

[1] Uses time-dependent Dalitz plot analysis of $B^0 \to \pi^+\pi^-\pi^0$ decays.

$A_{CP}(B^0 \to \rho^-\pi^+)$

VALUE	DOCUMENT ID		TECN	COMMENT
−0.08±0.08 OUR AVERAGE				
$-0.12\pm0.08^{+0.04}_{-0.05}$	[1] LEES	13J	BABR	$e^+e^- \to \Upsilon(4S)$
0.08±0.16±0.11	[1] KUSAKA	07	BELL	$e^+e^- \to \Upsilon(4S)$
• • • We do not use the following data for averages, fits, limits, etc. • • •				
$-0.37\pm0.16^{+0.09}_{-0.10}$	AUBERT	07AA	BABR	Repl. by LEES 13J
$-0.53\pm0.29^{+0.09}_{-0.04}$	WANG	05	BELL	Repl. by KUSAKA 07

[1] Uses time-dependent Dalitz plot analysis of $B^0 \to \pi^+\pi^-\pi^0$ decays.

$A_{CP}(B^0 \to a_1(1260)^\pm\pi^\mp)$

VALUE	DOCUMENT ID		TECN	COMMENT
−0.07±0.06 OUR AVERAGE				
−0.06±0.05±0.07	DALSENO	12	BELL	$e^+e^- \to \Upsilon(4S)$
−0.07±0.07±0.02	AUBERT	07O	BABR	$e^+e^- \to \Upsilon(4S)$

$A_{CP}(B^0 \to b_1^-\pi^+)$

VALUE	DOCUMENT ID		TECN	COMMENT
−0.05±0.10±0.02	AUBERT	07BI	BABR	$e^+e^- \to \Upsilon(4S)$

$A_{CP}(B^0 \to p\overline{p}K^*(892)^0)$

VALUE	DOCUMENT ID		TECN	COMMENT
0.05±0.12 OUR AVERAGE				
−0.08±0.20±0.02	CHEN	08C	BELL	$e^+e^- \to \Upsilon(4S)$
0.11±0.13±0.06	AUBERT	07AV	BABR	$e^+e^- \to \Upsilon(4S)$

$A_{CP}(B^0 \to p\overline{\Lambda}\pi^-)$

VALUE	DOCUMENT ID		TECN	COMMENT
0.04±0.07 OUR AVERAGE				
0.10±0.10±0.02	AUBERT	09AC	BABR	$e^+e^- \to \Upsilon(4S)$
−0.02±0.10±0.03	WANG	07C	BELL	$e^+e^- \to \Upsilon(4S)$

$A_{CP}(B^0 \to K^{*0}\ell^+\ell^-)$

VALUE	DOCUMENT ID		TECN	COMMENT
−0.05±0.10 OUR AVERAGE				
0.02±0.20±0.02	AUBERT	09T	BABR	$e^+e^- \to \Upsilon(4S)$
−0.08±0.12±0.02	WEI	09A	BELL	$e^+e^- \to \Upsilon(4S)$

$A_{CP}(B^0 \to K^{*0}e^+e^-)$

VALUE	DOCUMENT ID		TECN	COMMENT
−0.21±0.19±0.02	WEI	09A	BELL	$e^+e^- \to \Upsilon(4S)$

$A_{CP}(B^0 \to K^{*0}\mu^+\mu^-)$

VALUE	DOCUMENT ID		TECN	COMMENT
−0.034±0.024 OUR AVERAGE				
−0.035±0.024±0.003	AAIJ	14AN	LHCB	pp at 7, 8 TeV
0.00 ±0.15 ±0.03	WEI	09A	BELL	$e^+e^- \to \Upsilon(4S)$
• • • We do not use the following data for averages, fits, limits, etc. • • •				
−0.072±0.040±0.005	AAIJ	13E	LHCB	Repl. by AAIJ 14AN

$C_{D^*(2010)^-D^+}$ $(B^0 \to D^*(2010)^- D^+)$

VALUE	DOCUMENT ID		TECN	COMMENT
−0.01±0.11 OUR AVERAGE				
−0.13±0.16±0.05	[1] ROHRKEN	12	BELL	$e^+e^- \to \Upsilon(4S)$
0.00±0.17±0.03	AUBERT	09C	BABR	$e^+e^- \to \Upsilon(4S)$
0.23±0.25±0.06	[2] AUSHEV	04	BELL	$e^+e^- \to \Upsilon(4S)$
• • • We do not use the following data for averages, fits, limits, etc. • • •				
0.23±0.15±0.04	AUBERT	07AI	BABR	Repl. by AUBERT 09C
0.17±0.24±0.04	AUBERT,B	05Z	BABR	Repl. by AUBERT 07AI
−0.22±0.37±0.10	AUBERT	03J	BABR	Repl. by AUBERT,B 05Z

[1] ROHRKEN 12 reports the measurements of C = −0.01 ± 0.11 ± 0.04 and ΔC = 0.12 ± 0.11 ± 0.03 such that $C_{D^*(2010)^-D^+}$ = C − ΔC .

[2] Combines results from fully and partially reconstructed $B^0 \to D^{*\pm}D^{\mp}$ decays.

$S_{D^*(2010)^-D^+}$ $(B^0 \to D^*(2010)^- D^+)$

VALUE	DOCUMENT ID		TECN	COMMENT
−0.72±0.15 OUR AVERAGE				
−0.65±0.22±0.07	[1] ROHRKEN	12	BELL	$e^+e^- \to \Upsilon(4S)$
−0.73±0.23±0.050	AUBERT	09C	BABR	$e^+e^- \to \Upsilon(4S)$
−0.96±0.43±0.12	[2] AUSHEV	04	BELL	$e^+e^- \to \Upsilon(4S)$
• • • We do not use the following data for averages, fits, limits, etc. • • •				
−0.44±0.22±0.06	AUBERT	07AI	BABR	Repl. by AUBERT 09C
−0.29±0.33±0.07	AUBERT,B	05Z	BABR	Repl. by AUBERT 07AI
−0.24±0.69±0.12	AUBERT	03J	BABR	Repl. by AUBERT,B 05Z

[1] ROHRKEN 12 reports the measurements of S = −0.78 ± 0.15 ± 0.05 and ΔS = −0.13 ± 0.15 ± 0.04 such that $S_{D^*(2010)^+D^-}$ = S − ΔS.

[2] Combines results from fully and partially reconstructed $B^0 \to D^{*\pm}D^{\mp}$ decays.

$C_{D^*(2010)^+D^-}$ $(B^0 \to D^*(2010)^+ D^-)$

VALUE	DOCUMENT ID		TECN	COMMENT
0.00±0.13 OUR AVERAGE	Error includes scale factor of 1.3. See the ideogram below.			
0.11±0.14±0.06	[1] ROHRKEN	12	BELL	$e^+e^- \to \Upsilon(4S)$
0.08±0.17±0.04	AUBERT	09C	BABR	$e^+e^- \to \Upsilon(4S)$
−0.37±0.22±0.06	[2] AUSHEV	04	BELL	$e^+e^- \to \Upsilon(4S)$
• • • We do not use the following data for averages, fits, limits, etc. • • •				
0.18±0.15±0.04	AUBERT	07AI	BABR	Repl. by AUBERT 09C
0.09±0.25±0.06	AUBERT,B	05Z	BABR	Repl. by AUBERT 07AI
−0.47±0.40±0.12	AUBERT	03J	BABR	Repl. by AUBERT,B 05Z

[1] ROHRKEN 12 reports the measurements of C = −0.01 ± 0.11 ± 0.04 and ΔC = 0.12 ± 0.11 ± 0.03 such that $C_{D^*(2010)^+D^-}$ = C + ΔC .

[2] Combines results from fully and partially reconstructed $B^0 \to D^{*\pm}D^{\mp}$ decays.

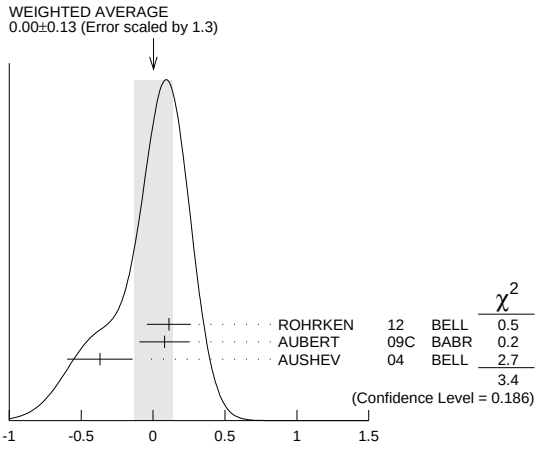

$C_{D^*(2010)^+D^-}$ $(B^0 \to D^*(2010)^+ D^-)$

$S_{D^*(2010)^+D^-}$ $(B^0 \to D^*(2010)^+ D^-)$

VALUE	DOCUMENT ID		TECN	COMMENT
−0.73±0.14 OUR AVERAGE				
−0.90±0.21±0.07	[1] ROHRKEN	12	BELL	$e^+e^- \to \Upsilon(4S)$
−0.62±0.21±0.03	AUBERT	09C	BABR	$e^+e^- \to \Upsilon(4S)$
−0.55±0.39±0.12	[2] AUSHEV	04	BELL	$e^+e^- \to \Upsilon(4S)$
• • • We do not use the following data for averages, fits, limits, etc. • • •				
−0.79±0.21±0.06	AUBERT	07AI	BABR	Repl. by AUBERT 09C
−0.54±0.35±0.07	AUBERT,B	05Z	BABR	Repl. by AUBERT 07AI
−0.82±0.75±0.14	AUBERT	03J	BABR	Repl. by AUBERT,B 05Z

[1] ROHRKEN 12 reports the measurements of S = −0.78 ± 0.15 ± 0.05 and ΔS = −0.13 ± 0.15 ± 0.04 such that $S_{D^*(2010)^+D^-}$ = S + ΔS.

[2] Combines results from fully and partially reconstructed $B^0 \to D^{*\pm}D^{\mp}$ decays.

$C_{D^{*+}D^{*-}}$ $(B^0 \to D^{*+} D^{*-})$

VALUE	DOCUMENT ID		TECN	COMMENT
0.01±0.09 OUR AVERAGE	Error includes scale factor of 1.6. See the ideogram below.			
−0.15±0.08±0.04	[1,2] KRONENBIT...	12	BELL	$e^+e^- \to \Upsilon(4S)$
+0.15±0.09±0.04	[3] LEES	12AF	BABR	$e^+e^- \to \Upsilon(4S)$
0.05±0.09±0.02	AUBERT	09C	BABR	$e^+e^- \to \Upsilon(4S)$
• • • We do not use the following data for averages, fits, limits, etc. • • •				
−0.15±0.13±0.04	[2] VERVINK	09	BELL	Repl. by KRONENBITTER 12
−0.02±0.11±0.02	[1] AUBERT	07BO	BABR	Repl. by AUBERT 09C
0.26±0.26±0.06	[2] MIYAKE	05	BELL	Repl. by VERVINK 09
0.28±0.23±0.02	[4] AUBERT	03Q	BABR	Repl. by AUBERT 07BO

[1] Assumes both CP-even and CP-odd states having the CP asymmetry.

[2] Belle Collab. quotes $A_{D^{*+}D^{*-}}$ which is equal to $-C_{D^{*+}D^{*-}}$.

[3] Measured partially reconstructed candidates when one D^0 meson is not excplicitely reconstructed. Analysis does not separate CP-even and CP-odd component.

[4] AUBERT 03Q reports $|\lambda|$=0.75 ± 0.19 ± 0.02 and Im(λ)=0.05 ± 0.29 ± 0.10. We convert them to S and C parameters taking into account correlations.

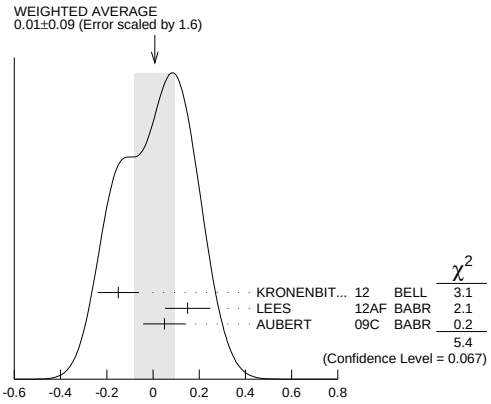

$C_{D^{*+}D^{*-}}$ $(B^0 \to D^{*+} D^{*-})$

$S_{D^{*+}D^{*-}}$ $(B^0 \to D^{*+} D^{*-})$

VALUE	DOCUMENT ID		TECN	COMMENT
−0.59±0.14 OUR AVERAGE	Error includes scale factor of 1.8. See the ideogram below.			
−0.79±0.13±0.03	[1] KRONENBIT...	12	BELL	$e^+e^- \to \Upsilon(4S)$
−0.34±0.12±0.05	[2] LEES	12AF	BABR	$e^+e^- \to \Upsilon(4S)$
−0.70±0.16±0.03	[1] AUBERT	09C	BABR	$e^+e^- \to \Upsilon(4S)$
• • • We do not use the following data for averages, fits, limits, etc. • • •				
$-0.96\pm0.25^{+0.13}_{-0.16}$	VERVINK	09	BELL	Repl. by KRONENBITTER 12
−0.66±0.19±0.04	[1] AUBERT	07BO	BABR	Repl. by AUBERT 09C
−0.75±0.56±0.12	MIYAKE	05	BELL	Repl. by VERVINK 09
0.06±0.37±0.13	[3] AUBERT	03Q	BABR	Repl. by AUBERT 07BO

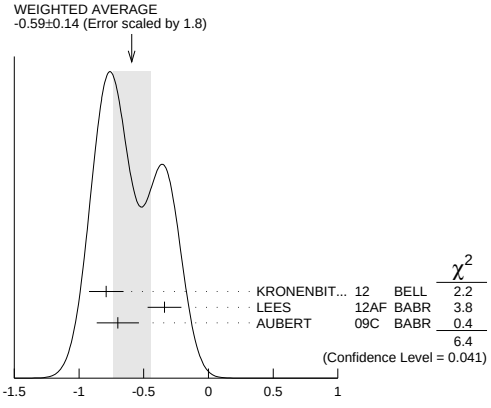

$S_{D^{*+}D^{*-}}$ $(B^0 \to D^{*+} D^{*-})$

[1] Assumes both CP-even and CP-odd states having the CP asymmetry.

[2] Measured partially reconstructed candidates when one D^0 meson is not excplicitely reconstructed. Analysis does not separate CP-even and CP-odd component.
[3] AUBERT 03Q reports $|\lambda|=0.75 \pm 0.19 \pm 0.02$ and $\mathrm{Im}(\lambda)=0.05 \pm 0.29 \pm 0.10$. We convert them to S and C parameters taking into account correlations.

C_+ ($B^0 \to D^{*+} D^{*-}$)

See the note in the $C_{\pi\pi}$ datablock, but for CP even final state.

VALUE	DOCUMENT ID		TECN	COMMENT
0.00±0.10 OUR AVERAGE	Error includes scale factor of 1.6. See the ideogram below.			
−0.18±0.10±0.05	[1] KRONENBIT...	12	BELL	$e^+e^- \to \Upsilon(4S)$
+0.15±0.09±0.04	[2] LEES	12AF	BABR	$e^+e^- \to \Upsilon(4S)$
0.00±0.12±0.02	AUBERT	09C	BABR	$e^+e^- \to \Upsilon(4S)$
• • • We do not use the following data for averages, fits, limits, etc. • • •				
−0.05±0.14±0.02	AUBERT	07BO	BABR	Repl. by AUBERT 09C
0.06±0.17±0.03	[3] AUBERT,BE	05A	BABR	Repl. by AUBERT 07BO

[1] Belle Collab. quotes $A_{D^{*+}D^{*-}}$ which is equal to $-C_{D^{*+}D^{*-}}$.
[2] Measured partially reconstructed candidates when one D^0 meson is not excplicitely reconstructed. Extracted under assumption of equal C_+ and C_-.
[3] AUBERT,BE 05A reports a CP-odd fraction $R_\perp = 0.125 \pm 0.044 \pm 0.007$.

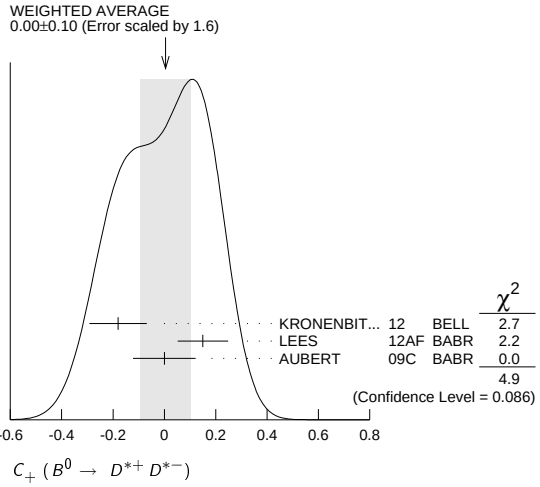

C_+ ($B^0 \to D^{*+} D^{*-}$)

S_+ ($B^0 \to D^{*+} D^{*-}$)

See the note in the $S_{\pi\pi}$ datablock, but for CP even final state.

VALUE	DOCUMENT ID		TECN	COMMENT
−0.73±0.09 OUR AVERAGE				
−0.81±0.13±0.03	KRONENBIT...	12	BELL	$e^+e^- \to \Upsilon(4S)$
−0.49±0.18±0.08	[1] LEES	12AF	BABR	$e^+e^- \to \Upsilon(4S)$
−0.76±0.16±0.04	AUBERT	09C	BABR	$e^+e^- \to \Upsilon(4S)$
• • • We do not use the following data for averages, fits, limits, etc. • • •				
−0.72±0.19±0.05	AUBERT	07BO	BABR	Repl. by AUBERT 09C
−0.75±0.25±0.03	[2] AUBERT,BE	05A	BABR	Repl. by AUBERT 07BO

[1] Measured partially reconstructed candidates when one D^0 meson is not excplicitely reconstructed. Analysis does not separate CP-even and CP-odd component. Value is obtained from $S = -0.34 \pm 0.12 \pm 0.05$ using $S = S_+ (1 - 2R_\perp)$ with $R_\perp = 0.158 \pm 0.029$.
[2] AUBERT,BE 05A reports a CP-odd fraction $R_\perp = 0.125 \pm 0.044 \pm 0.007$.

C_- ($B^0 \to D^{*+} D^{*-}$)

See the note in the $C_{\pi\pi}$ datablock, but for CP odd final state.

VALUE	DOCUMENT ID		TECN	COMMENT
0.19±0.31 OUR AVERAGE				
0.05±0.39±0.08	[1] KRONENBIT...	12	BELL	$e^+e^- \to \Upsilon(4S)$
0.41±0.49±0.08	AUBERT	09C	BABR	$e^+e^- \to \Upsilon(4S)$
• • • We do not use the following data for averages, fits, limits, etc. • • •				
0.23±0.67±0.10	AUBERT	07BO	BABR	Repl. by AUBERT 09C
−0.20±0.96±0.11	[2] AUBERT,BE	05A	BABR	Repl. by AUBERT 07BO

[1] Belle Collab. quotes $A_{D^{*+}D^{*-}}$ which is equal to $-C_{D^{*+}D^{*-}}$.
[2] AUBERT,BE 05A reports a CP-odd fraction $R_\perp = 0.125 \pm 0.044 \pm 0.007$.

S_- ($B^0 \to D^{*+} D^{*-}$)

See the note in the $S_{\pi\pi}$ datablock, but for CP odd final state.

VALUE	DOCUMENT ID		TECN	COMMENT
0.1 ±1.6 OUR AVERAGE	Error includes scale factor of 3.5.			
1.52±0.62±0.12	KRONENBIT...	12	BELL	$e^+e^- \to \Upsilon(4S)$
−1.80±0.70±0.16	AUBERT	09C	BABR	$e^+e^- \to \Upsilon(4S)$
• • • We do not use the following data for averages, fits, limits, etc. • • •				
−1.83±1.04±0.23	AUBERT	07BO	BABR	Repl. by AUBERT 09C
−1.75±1.78±0.22	[1] AUBERT,BE	05A	BABR	Repl. by AUBERT 07BO

[1] AUBERT,BE 05A reports a CP-odd fraction $R_\perp = 0.125 \pm 0.044 \pm 0.007$.

C ($B^0 \to D^*(2010)^+ D^*(2010)^- K^0_S$)

VALUE	DOCUMENT ID		TECN	COMMENT
0.01±0.28±0.09	[1] DALSENO	07	BELL	$e^+e^- \to \Upsilon(4S)$

[1] Reports value of A which is equal to $-C$.

S ($B^0 \to D^*(2010)^+ D^*(2010)^- K^0_S$)

VALUE	DOCUMENT ID		TECN	COMMENT
$0.06^{+0.45}_{-0.44}$**±0.06**	[1] DALSENO	07	BELL	$e^+e^- \to \Upsilon(4S)$

[1] This value includes an unknown CP dilution factor D due to possible contributions from intermediate resonances and different partial waves.

$C_{D^+D^-}$ ($B^0 \to D^+ D^-$)

VALUE	DOCUMENT ID		TECN	COMMENT
−0.22±0.24 OUR AVERAGE	Error includes scale factor of 2.5. See the ideogram below.			
$0.26^{+0.18}_{-0.17}$±0.02	AAIJ	16AN	LHCB	pp at 7, 8 TeV
−0.43±0.16±0.05	ROHRKEN	12	BELL	$e^+e^- \to \Upsilon(4S)$
−0.07±0.23±0.03	AUBERT	09C	BABR	$e^+e^- \to \Upsilon(4S)$
−0.91±0.23±0.06	[1] FRATINA	07	BELL	$e^+e^- \to \Upsilon(4S)$
• • • We do not use the following data for averages, fits, limits, etc. • • •				
0.11±0.22±0.07	AUBERT	07AI	BABR	Repl. by AUBERT 09C
0.11±0.35±0.06	AUBERT,B	05Z	BABR	Repl. by AUBERT 07AI

[1] The paper reports A, which is equal to $-C$.

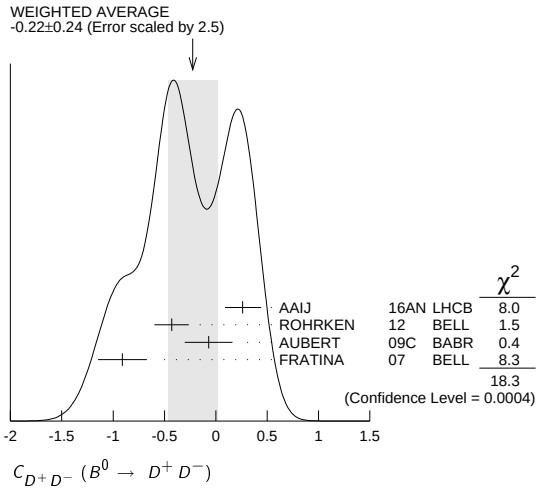

$C_{D^+D^-}$ ($B^0 \to D^+ D^-$)

$S_{D^+D^-}$ ($B^0 \to D^+ D^-$)

VALUE	DOCUMENT ID		TECN	COMMENT
$-0.76^{+0.15}_{-0.13}$ **OUR AVERAGE**	Error includes scale factor of 1.2.			
$-0.54^{+0.17}_{-0.16}$±0.05	AAIJ	16AN	LHCB	pp at 7, 8 TeV
$-1.06^{+0.21}_{-0.14}$±0.08	ROHRKEN	12	BELL	$e^+e^- \to \Upsilon(4S)$
−0.63±0.36±0.05	AUBERT	09C	BABR	$e^+e^- \to \Upsilon(4S)$
−1.13±0.37±0.09	FRATINA	07	BELL	$e^+e^- \to \Upsilon(4S)$
• • • We do not use the following data for averages, fits, limits, etc. • • •				
−0.54±0.34±0.06	AUBERT	07AI	BABR	Repl. by AUBERT 09C
−0.29±0.63±0.06	AUBERT,B	05Z	BABR	Repl. by AUBERT 07AI

$C_{J/\psi(1S)\pi^0}$ ($B^0 \to J/\psi(1S)\pi^0$)

VALUE	DOCUMENT ID		TECN	COMMENT
−0.13±0.13 OUR AVERAGE				
−0.20±0.19±0.03	AUBERT	08AU	BABR	$e^+e^- \to \Upsilon(4S)$
−0.08±0.16±0.05	[1] LEE	08A	BELL	$e^+e^- \to \Upsilon(4S)$
• • • We do not use the following data for averages, fits, limits, etc. • • •				
−0.21±0.26±0.06	AUBERT,B	06B	BABR	Repl. by AUBERT 08AU
0.01±0.29±0.03	[1] KATAOKA	04	BELL	Repl. by LEE 08A
0.38±0.41±0.09	AUBERT	03N	BABR	Repl. by AUBERT,B 06B

[1] BELLE Collab. quotes $A_{J/\psi\pi^0}$ which is equal to $-C_{J/\psi\pi^0}$.

$S_{J/\psi(1S)\pi^0}$ ($B^0 \to J/\psi(1S)\pi^0$)

VALUE	DOCUMENT ID		TECN	COMMENT
−0.94±0.29 OUR AVERAGE	Error includes scale factor of 1.9.			
−1.23±0.21±0.04	AUBERT	08AU	BABR	$e^+e^- \to \Upsilon(4S)$
−0.65±0.21±0.05	LEE	08A	BELL	$e^+e^- \to \Upsilon(4S)$
• • • We do not use the following data for averages, fits, limits, etc. • • •				
−0.68±0.30±0.04	AUBERT,B	06B	BABR	Repl. by AUBERT 08AU
−0.72±0.42±0.09	KATAOKA	04	BELL	Repl. by LEE 08A
0.05±0.49±0.16	AUBERT	03N	BABR	Repl. by AUBERT,B 06B

$C(B^0 \to J/\psi(1S)\rho^0)$

VALUE	DOCUMENT ID		TECN	COMMENT
$-0.063 \pm 0.056^{+0.019}_{-0.014}$	[1] AAIJ	15J	LHCB	pp at 7, 8 TeV

[1] Time-dependent CP violation is measured in the $B^0 \to J/\psi\rho^0$ and was used to limit the size of penguin amplitude contributions to ϕ_s in $B_s^0 \to J/\psi\phi$ decays to be between $[-1.05^\circ, 1.18^\circ]$ at 95% confidence level.

$S(B^0 \to J/\psi(1S)\rho^0)$

VALUE	DOCUMENT ID		TECN	COMMENT
$-0.66^{+0.13+0.09}_{-0.12-0.03}$	[1] AAIJ	15J	LHCB	pp at 7, 8 TeV

[1] Time-dependent CP violation is measured in the $B^0 \to J/\psi\rho^0$ and was used to limit the size of penguin amplitude contributions to ϕ_s in $B_s^0 \to J/\psi\phi$ decays to be between $[-1.05^\circ, 1.18^\circ]$ at 95% confidence level.

$C_{D_{CP}^{(*)}h^0}$ $(B^0 \to D_{CP}^{(*)}h^0)$

VALUE	DOCUMENT ID		TECN	COMMENT
$-0.02\pm0.07\pm0.03$	[1] ABDESSALAM	15		$e^+e^- \to \Upsilon(4S)$
• • • We do not use the following data for averages, fits, limits, etc. • • •				
$-0.23\pm0.16\pm0.04$	AUBERT	07AJ	BABR	Repl. by ABDESSALAM 15

[1] BABAR and BELLE combined analysis uses CP-eigenstate decay modes $D^0 \to K^+K^-$, $K_S^0\pi^0$, $K_S^0\omega$, and $h^0 = \pi^0, \eta, \omega$.

$S_{D_{CP}^{(*)}h^0}$ $(B^0 \to D_{CP}^{(*)}h^0)$

VALUE	DOCUMENT ID		TECN	COMMENT
$-0.66\pm0.10\pm0.06$	[1] ABDESSALAM	15		$e^+e^- \to \Upsilon(4S)$
• • • We do not use the following data for averages, fits, limits, etc. • • •				
$-0.56\pm0.23\pm0.05$	AUBERT	07AJ	BABR	Repl. by ABDESSALAM 15

[1] BABAR and BELLE combined analysis uses CP-eigenstate decay modes $D^0 \to K^+K^-$, $K_S^0\pi^0$, $K_S^0\omega$, and $h^0 = \pi^0, \eta, \omega$.

$C_{K^0\pi^0}$ $(B^0 \to K^0\pi^0)$

VALUE	DOCUMENT ID		TECN	COMMENT
0.00 ± 0.13 OUR AVERAGE	Error includes scale factor of 1.4.			
$-0.14\pm0.13\pm0.06$	[1] FUJIKAWA	10A	BELL	$e^+e^- \to \Upsilon(4S)$
$0.13\pm0.13\pm0.03$	AUBERT	09I	BABR	$e^+e^- \to \Upsilon(4S)$
• • • We do not use the following data for averages, fits, limits, etc. • • •				
$0.24\pm0.15\pm0.03$	AUBERT	08E	BABR	Repl. by AUBERT 09I
$0.05\pm0.14\pm0.05$	[1] CHAO	07	BELL	Repl. by FUJIKAWA 10A
$0.06\pm0.18\pm0.03$	AUBERT	05Y	BABR	Repl. by AUBERT 08E
$-0.16\pm0.29\pm0.05$	[1,2] CHAO	05A	BELL	Repl. by CHEN 05B
$0.11\pm0.20\pm0.09$	[1] CHEN	05B	BELL	Repl. by CHAO 07
$-0.03\pm0.36\pm0.11$	[1] AUBERT	04M	BABR	Repl. by AUBERT,B 04M
$0.40^{+0.27}_{-0.28}\pm0.09$	[3] AUBERT,B	04M	BABR	Repl. by AUBERT 05Y

[1] Reports A which is equal to $-C$.
[2] Corresponds to a 90% CL interval of $-0.33 < A_{CP} < 0.64$.
[3] Based on a total signal yield of 122 ± 16 events.

$S_{K^0\pi^0}$ $(B^0 \to K^0\pi^0)$

VALUE	DOCUMENT ID		TECN	COMMENT
0.58 ± 0.17 OUR AVERAGE				
$0.67\pm0.31\pm0.08$	FUJIKAWA	10A	BELL	$e^+e^- \to \Upsilon(4S)$
$0.55\pm0.20\pm0.03$	AUBERT	09I	BABR	$e^+e^- \to \Upsilon(4S)$
• • • We do not use the following data for averages, fits, limits, etc. • • •				
$0.40\pm0.23\pm0.03$	AUBERT	08E	BABR	Repl. by AUBERT 09I
$0.33\pm0.35\pm0.08$	CHAO	07	BELL	Repl. by FUJIKAWA 10A
$0.35^{+0.30}_{-0.33}\pm0.04$	AUBERT	05Y	BABR	Repl. by AUBERT 08E
$0.32\pm0.61\pm0.13$	CHEN	05B	BELL	Repl. by CHAO 07
$0.48^{+0.38}_{-0.47}\pm0.06$	[1] AUBERT,B	04M	BABR	Repl. by AUBERT 05Y

[1] Based on a total signal yield of 122 ± 16 events.

$C_{\eta'(958)K_S^0}$ $(B^0 \to \eta'(958)K_S^0)$

See updated measurements in $C_{\eta' K^0}$

VALUE	DOCUMENT ID		TECN	COMMENT
-0.04 ± 0.20 OUR AVERAGE	Error includes scale factor of 2.5.			
$-0.21\pm0.10\pm0.02$	AUBERT	05M	BABR	$e^+e^- \to \Upsilon(4S)$
$0.19\pm0.11\pm0.05$	[1] CHEN	05B	BELL	$e^+e^- \to \Upsilon(4S)$
• • • We do not use the following data for averages, fits, limits, etc. • • •				
$-0.26\pm0.22\pm0.03$	[1] ABE	03C	BELL	Repl. by ABE 03H
$0.01\pm0.16\pm0.04$	[1] ABE	03H	BELL	Repl. by CHEN 05B
$0.10\pm0.22\pm0.04$	AUBERT	03W	BABR	Repl. by AUBERT 05M
$-0.13\pm0.32^{+0.06}_{-0.09}$	[1] CHEN	02B	BELL	Repl. by ABE 03C

[1] BELLE Collab. quotes $A_{\eta'(958)K_S^0}$ which is equal to $-C_{\eta'(958)K_S^0}$.

$S_{\eta'(958)K_S^0}$ $(B^0 \to \eta'(958)K_S^0)$

See updated measurements in $S_{\eta' K^0}$

VALUE	DOCUMENT ID		TECN	COMMENT
0.43 ± 0.17 OUR AVERAGE	Error includes scale factor of 1.5.			
$0.30\pm0.14\pm0.02$	AUBERT	05M	BABR	$e^+e^- \to \Upsilon(4S)$
$0.65\pm0.18\pm0.04$	CHEN	05B	BELL	$e^+e^- \to \Upsilon(4S)$
• • • We do not use the following data for averages, fits, limits, etc. • • •				
$0.71\pm0.37^{+0.05}_{-0.06}$	ABE	03C	BELL	Repl. by ABE 03H
$0.43\pm0.27\pm0.05$	ABE	03H	BELL	Repl. by CHEN 05B
$0.02\pm0.34\pm0.03$	AUBERT	03W	BABR	Repl. by AUBERT 05M
$0.28\pm0.55^{+0.07}_{-0.08}$	CHEN	02B	BELL	Repl. by ABE 03C

$C_{\eta' K^0}$ $(B^0 \to \eta' K^0)$

VALUE	DOCUMENT ID		TECN	COMMENT
-0.06 ± 0.04 OUR AVERAGE				
$-0.03\pm0.05\pm0.04$	[1] SANTELJ	14	BELL	$e^+e^- \to \Upsilon(4S)$
$-0.08\pm0.06\pm0.02$	AUBERT	09I	BABR	$e^+e^- \to \Upsilon(4S)$
• • • We do not use the following data for averages, fits, limits, etc. • • •				
$-0.16\pm0.07\pm0.03$	[2] AUBERT	07A	BABR	Repl. by AUBERT 09I
$0.01\pm0.07\pm0.05$	[1,2] CHEN	07	BELL	Repl. by SANTELJ 14

[1] The paper reports A, which is equal to $-C$.
[2] The mixing-induced CP violation is reported with a significance of more than 5 standard deviations in this $b \to s$ penguin dominated mode.

$S_{\eta' K^0}$ $(B^0 \to \eta' K^0)$

VALUE	DOCUMENT ID		TECN	COMMENT
0.63 ± 0.06 OUR AVERAGE				
$0.68\pm0.07\pm0.03$	SANTELJ	14	BELL	$e^+e^- \to \Upsilon(4S)$
$0.57\pm0.08\pm0.02$	AUBERT	09I	BABR	$e^+e^- \to \Upsilon(4S)$
• • • We do not use the following data for averages, fits, limits, etc. • • •				
$0.58\pm0.10\pm0.03$	[1] AUBERT	07A	BABR	Repl. by AUBERT 09I
$0.64\pm0.10\pm0.04$	[1] CHEN	07	BELL	Repl. by SANTELJ 14

[1] The mixing-induced CP violation is reported with a significance of more than 5 standard deviations in this $b \to s$ penguin dominated mode.

$C_{\omega K_S^0}$ $(B^0 \to \omega K_S^0)$

VALUE	DOCUMENT ID		TECN	COMMENT
$0.0\ \pm0.4$ OUR AVERAGE	Error includes scale factor of 3.0.			
$0.36\pm0.19\pm0.05$	[1] CHOBANOVA	14	BELL	$e^+e^- \to \Upsilon(4S)$
$-0.52^{+0.22}_{-0.20}\pm0.03$	AUBERT	09I	BABR	$e^+e^- \to \Upsilon(4S)$
• • • We do not use the following data for averages, fits, limits, etc. • • •				
$0.09\pm0.29\pm0.06$	[1] CHAO	07	BELL	Repl. by CHOBANOVA 14
$-0.55^{+0.28}_{-0.26}\pm0.03$	AUBERT,B	06E	BABR	Repl. by AUBERT 09I
$-0.27\pm0.48\pm0.15$	[1] CHEN	05B	BELL	Repl. by CHAO 07

[1] Belle Collab. quotes $A_{\omega K_S^0}$ which is equal to $-C_{\omega K_S^0}$.

$S_{\omega K_S^0}$ $(B^0 \to \omega K_S^0)$

VALUE	DOCUMENT ID		TECN	COMMENT
0.70 ± 0.21 OUR AVERAGE				
$0.91\pm0.32\pm0.05$	CHOBANOVA	14	BELL	$e^+e^- \to \Upsilon(4S)$
$0.55^{+0.26}_{-0.29}\pm0.02$	AUBERT	09I	BABR	$e^+e^- \to \Upsilon(4S)$
• • • We do not use the following data for averages, fits, limits, etc. • • •				
$0.11\pm0.46\pm0.07$	CHAO	07	BELL	Repl. by CHOBANOVA 14
$0.51^{+0.35}_{-0.39}\pm0.02$	AUBERT,B	06E	BABR	Repl. by AUBERT 09I
$0.76\pm0.65^{+0.13}_{-0.16}$	CHEN	05B	BELL	Repl. by CHAO 07

C $(B^0 \to K_S^0\pi^0\pi^0)$

VALUE	DOCUMENT ID		TECN	COMMENT
$0.23\pm0.52\pm0.13$	AUBERT	07AQ	BABR	$e^+e^- \to \Upsilon(4S)$

S $(B^0 \to K_S^0\pi^0\pi^0)$

VALUE	DOCUMENT ID		TECN	COMMENT
$0.72\pm0.71\pm0.08$	AUBERT	07AQ	BABR	$e^+e^- \to \Upsilon(4S)$

$C_{\rho^0 K_S^0}$ $(B^0 \to \rho^0 K_S^0)$

VALUE	DOCUMENT ID		TECN	COMMENT
-0.04 ± 0.20 OUR AVERAGE				
$-0.05\pm0.26\pm0.10$	[1] AUBERT	09AU	BABR	$e^+e^- \to \Upsilon(4S)$
$-0.03^{+0.24}_{-0.23}\pm0.15$	[2,3] DALSENO	09	BELL	$e^+e^- \to \Upsilon(4S)$
• • • We do not use the following data for averages, fits, limits, etc. • • •				
$0.64\pm0.41\pm0.20$	AUBERT	07F	BABR	Repl. by AUBERT 09AU

[1] Uses Dalitz plot analysis of $B^0 \to K^0\pi^+\pi^-$ decays and the first of two equivalent solutions is used.
[2] Quotes $A_{\rho^0(KS)^0}$ which is equal to $-C_{\rho^0 K_S^0}$.
[3] Uses Dalitz plot analysis of $B^0 \to K^0\pi^+\pi^-$ decays and the first of two consistent solutions that may be preferred.

$S_{\rho^0 K_S^0}$ $(B^0 \to \rho^0 K_S^0)$

VALUE	DOCUMENT ID		TECN	COMMENT
$0.50^{+0.17}_{-0.21}$ OUR AVERAGE				
$0.35^{+0.26}_{-0.31}\pm0.07$	[1] AUBERT	09AU	BABR	$e^+e^- \to \Upsilon(4S)$

$0.64^{+0.19}_{-0.25}\pm0.13$	[2] DALSENO	09	BELL	$e^+e^-\to\Upsilon(4S)$	

• • • We do not use the following data for averages, fits, limits, etc. • • •

$0.20\pm0.52\pm0.24$	AUBERT	07F	BABR	Repl. by AUBERT 09AU	

[1] Uses Dalitz plot analysis of $B^0\to K^0\pi^+\pi^-$ decays and the first of two equivalent solutions is used.
[2] Uses Dalitz plot analysis of $B^0\to K^0\pi^+\pi^-$ decays and the first of two consistent solutions that may be preferred.

$C_{f_0(980)K^0_S}$ ($B^0\to f_0(980)K^0_S$)

VALUE	DOCUMENT ID		TECN	COMMENT
0.29±0.20 OUR AVERAGE				
$0.28\pm0.24\pm0.09$	[1] LEES	12O	BABR	$e^+e^-\to\Upsilon(4S)$
$0.30\pm0.29\pm0.14$	[2,3] NAKAHAMA	10	BELL	$e^+e^-\to\Upsilon(4S)$
• • • We do not use the following data for averages, fits, limits, etc. • • •				
$0.08\pm0.19\pm0.05$	[4] AUBERT	09AU	BABR	Repl. by LEES 12O
$0.06\pm0.17\pm0.11$	[2,5] DALSENO	09	BELL	Repl. by NAKAHAMA 10
$-0.41\pm0.23\pm0.07$	[2] AUBERT	07AX	BABR	Repl. by AUBERT 09AU
$0.15\pm0.15\pm0.07$	[2] CHAO	07	BELL	Repl. by DALSENO 09
$0.39\pm0.27\pm0.09$	[2] CHEN	05B	BELL	Repl. by CHAO 07

[1] Uses Dalitz plot analysis of the $B^0\to K^0_S K^+K^-$ decay.
[2] Quotes $A_{f_0(980)K^0_S}$ which is equal to $-C_{f_0(980)K^0_S}$.
[3] Uses Dalitz plot analysis of $B^0\to K^0_S K^+K^-$ decays and the first of four consistent solutions that may be preferred.
[4] Uses Dalitz plot analysis of $B^0\to K^0\pi^+\pi^-$ decays and the first of two equivalent solutions is used.
[5] Uses Dalitz plot analysis of $B^0\to K^0\pi^+\pi^-$ decays and the first of two consistent solutions that may be preferred.

$S_{f_0(980)K^0_S}$ ($B^0\to f_0(980)K^0_S$)

VALUE	DOCUMENT ID		TECN	COMMENT
−0.50±0.16 OUR AVERAGE				
$-0.55\pm0.18\pm0.12$	[1] LEES	12O	BABR	$e^+e^-\to\Upsilon(4S)$
$-0.43^{+0.22}_{-0.20}\pm0.14$	[2] DALSENO	09	BELL	$e^+e^-\to\Upsilon(4S)$
• • • We do not use the following data for averages, fits, limits, etc. • • •				
$-0.96^{+0.21}_{-0.04}\pm0.04$	[3] AUBERT	09AU	BABR	Repl. by LEES 12O
$-0.25\pm0.26\pm0.10$	[4] AUBERT	07AX	BABR	Repl. by AUBERT 09AU
$0.18\pm0.23\pm0.11$	CHAO	07	BELL	Repl. by DALSENO 09
$0.47\pm0.41\pm0.08$	CHEN	05B	BELL	Repl. by CHAO 07

[1] Uses Dalitz plot analysis of the $B^0\to K^0_S K^+K^-$ decay.
[2] Uses Dalitz plot analysis of $B^0\to K^0\pi^+\pi^-$ decays and the first of two consistent solutions that may be preferred.
[3] Uses Dalitz plot analysis of $B^0\to K^0\pi^+\pi^-$ decays and the first of two equivalent solutions is used.
[4] Reports β_{eff}. We quote S obtained from epaps: E-PRLTAO-99-076741.

$S_{f_2(1270)K^0_S}$ ($B^0\to f_2(1270)K^0_S$)

VALUE	DOCUMENT ID		TECN	COMMENT
−0.48±0.52±0.12	[1] AUBERT	09AU	BABR	$e^+e^-\to\Upsilon(4S)$

[1] Uses Dalitz plot analysis of $B^0\to K^0\pi^+\pi^-$ decays and the first of two equivalent solutions is used.

$C_{f_2(1270)K^0_S}$ ($B^0\to f_2(1270)K^0_S$)

VALUE	DOCUMENT ID		TECN	COMMENT
$\mathbf{0.28^{+0.35}_{-0.40}\pm0.11}$	[1] AUBERT	09AU	BABR	$e^+e^-\to\Upsilon(4S)$

[1] Uses Dalitz plot analysis of $B^0\to K^0\pi^+\pi^-$ decays and the first of two equivalent solutions is used.

$S_{f_x(1300)K^0_S}$ ($B^0\to f_x(1300)K^0_S$)

VALUE	DOCUMENT ID		TECN	COMMENT
−0.20±0.52±0.10	[1] AUBERT	09AU	BABR	$e^+e^-\to\Upsilon(4S)$

[1] Uses Dalitz plot analysis of $B^0\to K^0\pi^+\pi^-$ decays and the first of two equivalent solutions is used.

$C_{f_x(1300)K^0_S}$ ($B^0\to f_x(1300)K^0_S$)

VALUE	DOCUMENT ID		TECN	COMMENT
$\mathbf{0.13^{+0.33}_{-0.35}\pm0.10}$	[1] AUBERT	09AU	BABR	$e^+e^-\to\Upsilon(4S)$

[1] Uses Dalitz plot analysis of $B^0\to K^0\pi^+\pi^-$ decays and the first of two equivalent solutions is used.

$S_{K^0\pi^+\pi^-}$ ($B^0\to K^0\pi^+\pi^-$ nonresonant)

VALUE	DOCUMENT ID		TECN	COMMENT
−0.01±0.31±0.10	[1] AUBERT	09AU	BABR	$e^+e^-\to\Upsilon(4S)$

[1] Uses Dalitz plot analysis of $B^0\to K^0\pi^+\pi^-$ decays and the first of two equivalent solutions is used.

$C_{K^0\pi^+\pi^-}$ ($B^0\to K^0\pi^+\pi^-$ nonresonant)

VALUE	DOCUMENT ID		TECN	COMMENT
0.01±0.25±0.08	[1] AUBERT	09AU	BABR	$e^+e^-\to\Upsilon(4S)$

[1] Uses Dalitz plot analysis of $B^0\to K^0\pi^+\pi^-$ decays and the first of two equivalent solutions is used.

$C_{K^0_S K^0_S}$ ($B^0\to K^0_S K^0_S$)

VALUE	DOCUMENT ID		TECN	COMMENT
0.0 ±0.4 OUR AVERAGE	Error includes scale factor of 1.4.			
$0.38\pm0.38\pm0.05$	[1] NAKAHAMA	08	BELL	$e^+e^-\to\Upsilon(4S)$
$-0.40\pm0.41\pm0.06$	AUBERT,BE	06C	BABR	$e^+e^-\to\Upsilon(4S)$

[1] Reports $A_{K^0_S K^0_S}$ which equals to $-C_{K^0_S K^0_S}$.

$S_{K^0_S K^0_S}$ ($B^0\to K^0_S K^0_S$)

VALUE	DOCUMENT ID		TECN	COMMENT
−0.8 ±0.5 OUR AVERAGE				
$-0.38^{+0.69}_{-0.77}\pm0.09$	NAKAHAMA	08	BELL	$e^+e^-\to\Upsilon(4S)$
$-1.28^{+0.80+0.11}_{-0.73-0.16}$	AUBERT,BE	06C	BABR	$e^+e^-\to\Upsilon(4S)$

$C_{K^+K^-K^0_S}$ ($B^0\to K^+K^-K^0_S$ nonresonant)

VALUE	DOCUMENT ID		TECN	COMMENT
0.06 ±0.08 OUR AVERAGE				
$0.02\pm0.09\pm0.03$	[1,2] LEES	12O	BABR	$e^+e^-\to\Upsilon(4S)$
$0.14\pm0.11\pm0.09$	[3,4] NAKAHAMA	10	BELL	$e^+e^-\to\Upsilon(4S)$
• • • We do not use the following data for averages, fits, limits, etc. • • •				
$0.054\pm0.102\pm0.060$	[3,5] AUBERT	07AX	BABR	Repl. by LEES 12O
$0.09\pm0.10\pm0.05$	[3,5] CHAO	07	BELL	Repl. by NAKAHAMA 10
$0.10\pm0.14\pm0.04$	[5] AUBERT	05T	BABR	Repl. by AUBERT 07AX
$0.09\pm0.12\pm0.07$	[3] CHEN	05B	BELL	Repl. by CHAO 07
$-0.10\pm0.19\pm0.10$	[5] AUBERT,B	04V	BABR	Repl. by AUBERT 05T
$0.40\pm0.33^{+0.28}_{-0.10}$	[3] ABE	03C	BELL	Repl. by ABE 03H
$0.17\pm0.16\pm0.04$	[3,5] ABE	03H	BELL	Repl. by CHEN 05B

[1] Uses Dalitz plot analysis of the $B^0\to K^0_S K^+K^-$ decay.
[2] This measurement is performed on all the isobar components, excluding ϕK^0_S and $f_0(980)K^0_S$.
[3] Quotes $A_{K^+K^-K^0_S}$ which is equal to $-C_{K^+K^-K^0_S}$.
[4] Uses Dalitz plot analysis of $B^0\to K^0_S K^+K^-$ decays and the first of four consistent solutions that may be preferred.
[5] Excludes the events from $B^0\to\phi K^0_S$ decay. The results are derived from a combined sample of $K^+K^-K^0_S$ and $K^+K^-K^0_L$ decays.

$S_{K^+K^-K^0_S}$ ($B^0\to K^+K^-K^0_S$ nonresonant)

VALUE	DOCUMENT ID		TECN	COMMENT
−0.66 ±0.11 OUR AVERAGE				
$-0.65\pm0.12\pm0.03$	[1,2] LEES	12O	BABR	$e^+e^-\to\Upsilon(4S)$
$-0.68\pm0.15^{+0.21}_{-0.13}$	[3] CHAO	07	BELL	$e^+e^-\to\Upsilon(4S)$
• • • We do not use the following data for averages, fits, limits, etc. • • •				
$-0.764\pm0.111^{+0.071}_{-0.040}$	[3,4] AUBERT	07AX	BABR	Repl. by LEES 12O
$-0.42\pm0.17\pm0.03$	[3,5] AUBERT	05T	BABR	Repl. by AUBERT 07AX
$-0.49\pm0.18\pm0.04$	CHEN	05B	BELL	Repl. by CHAO 07
$-0.56\pm0.25\pm0.04$	[3,6] AUBERT,B	04V	BABR	Repl. by AUBERT 05T
$-0.49\pm0.43\pm0.11$	ABE	03C	BELL	Repl. by ABE 03H
$-0.51\pm0.26\pm0.05$	[3,7] ABE	03H	BELL	Repl. by CHEN 05B

[1] Uses Dalitz plot analysis of the $B^0\to K^0_S K^+K^-$ decay.
[2] This measurement is performed on all the isobar components, excluding ϕK^0_S and $f_0(980)K^0_S$. Note that the nonresonant component is not a CP eigenstate.
[3] Excludes events from $B^0\to\phi K^0_S$ decay. The results are derived from a combined sample of $K^+K^-K^0_S$ and $K^+K^-K^0_L$ decays.
[4] Reports β_{eff}. We quote S obtained from epaps: E-PRLTAO-99-076741.
[5] The measured CP-even final states fraction is $0.89\pm0.08\pm0.06$.
[6] The measured CP-even final states fraction is $0.98\pm0.15\pm0.04$.
[7] The measured CP-even final states fraction is $1.03\pm0.15\pm0.05$.

$C_{K^+K^-K^0_S}$ ($B^0\to K^+K^-K^0_S$ inclusive)

VALUE	DOCUMENT ID		TECN	COMMENT
0.015±0.077±0.053	[1,2] AUBERT	07AX	BABR	$e^+e^-\to\Upsilon(4S)$

[1] Measured using full Dalitz plot fit including ϕ component.
[2] The results are derived from a combined sample of $K^+K^-K^0_S$ and $K^+K^-K^0_L$ decays.

$S_{K^+K^-K^0_S}$ ($B^0\to K^+K^-K^0_S$ inclusive)

VALUE	DOCUMENT ID		TECN	COMMENT
−0.647±0.116±0.040	[1] AUBERT	07AX	BABR	$e^+e^-\to\Upsilon(4S)$

[1] Measured using full Dalitz plot fit including ϕ component.

$C_{\phi K^0_S}$ ($B^0\to\phi K^0_S$)

VALUE	DOCUMENT ID		TECN	COMMENT
0.01±0.14 OUR AVERAGE				
$0.05\pm0.18\pm0.05$	[1] LEES	12O	BABR	$e^+e^-\to\Upsilon(4S)$
$-0.04\pm0.20\pm0.10$	[2,3] NAKAHAMA	10	BELL	$e^+e^-\to\Upsilon(4S)$

• • • We do not use the following data for averages, fits, limits, etc. • • •

$0.08 \pm 0.18 \pm 0.04$	[2,4]	AUBERT	07AX	BABR	Repl. by LEES 12O
$-0.07 \pm 0.15 \pm 0.05$	[2,4]	CHEN	07	BELL	Repl. by NAKAHAMA 10
$0.00 \pm 0.23 \pm 0.05$	[4]	AUBERT	05T	BABR	Repl. by AUBERT 07AX
$-0.08 \pm 0.22 \pm 0.09$	[2,4]	CHEN	05B	BELL	Repl. by CHEN 07
$0.01 \pm 0.33 \pm 0.10$	[4]	AUBERT,B	04G	BABR	Repl. by AUBERT 05T
$0.56 \pm 0.41 \pm 0.16$	[2]	ABE	03C	BELL	Repl. by ABE 03H
$0.15 \pm 0.29 \pm 0.07$	[2]	ABE	03H	BELL	Repl. by CHEN 05B

[1] Uses Dalitz plot analysis of the $B^0 \to K^0_S K^+ K^-$ decay.
[2] Quotes $A_{\phi K^0_S}$ which is equal to $-C_{\phi K^0_S}$.
[3] Uses Dalitz plot analysis of $B^0 \to K^0_S K^+ K^-$ decays and the first of four consistent solutions that may be preferred.
[4] Result combines B-meson final states ϕK^0_S and ϕK^0_L by assuming $S_{\phi K^0_S} = -S_{\phi K^0_L}$

$S_{\phi K^0_S}$ ($B^0 \to \phi K^0_S$)

VALUE	DOCUMENT ID		TECN	COMMENT
0.59 ± 0.14 OUR AVERAGE				
$0.66 \pm 0.17 \pm 0.07$	[1] LEES	12O	BABR	$e^+e^- \to \Upsilon(4S)$
$0.50 \pm 0.21 \pm 0.06$	[2] CHEN	07	BELL	$e^+e^- \to \Upsilon(4S)$
• • • We do not use the following data for averages, fits, limits, etc. • • •				
$0.21 \pm 0.26 \pm 0.11$	[2,3] AUBERT	07AX	BABR	Repl. by LEES 12O
$0.50 \pm 0.25^{+0.07}_{-0.04}$	[2] AUBERT	05T	BABR	Repl. by AUBERT 07AX
$0.08 \pm 0.33 \pm 0.09$	[2] CHEN	05B	BELL	Repl. by CHEN 07
$0.47 \pm 0.34^{+0.08}_{-0.06}$	[2] AUBERT,B	04G	BABR	Repl. by AUBERT 05T
$-0.73 \pm 0.64 \pm 0.22$	ABE	03C	BELL	Repl. by ABE 03H
$-0.96 \pm 0.50^{+0.09}_{-0.11}$	ABE	03H	BELL	Repl. by CHEN 05B

[1] Uses Dalitz plot analysis of the $B^0 \to K^0_S K^+ K^-$ decay.
[2] Result combines B-meson final states ϕK^0_S and ϕK^0_L by assuming $S_{\phi K^0_S} = -S_{\phi K^0_L}$
[3] Reports β_{eff}. We quote S obtained from epaps: E-PRLTAO-99-076741.

$C_{K_S K_S K_S}$($B^0 \to K_S K_S K_S$)

VALUE	DOCUMENT ID		TECN	COMMENT
-0.23 ± 0.14 OUR AVERAGE				
$-0.17 \pm 0.18 \pm 0.04$	LEES	12I	BABR	$e^+e^- \to \Upsilon(4S)$
$-0.31 \pm 0.20 \pm 0.07$	[1] CHEN	07	BELL	$e^+e^- \to \Upsilon(4S)$
• • • We do not use the following data for averages, fits, limits, etc. • • •				
$0.02 \pm 0.21 \pm 0.05$	AUBERT	07AT	BABR	Repl. by LEES 12I
$-0.34^{+0.28}_{-0.25} \pm 0.05$	AUBERT,B	05	BABR	Repl. by AUBERT 07AT
$-0.54 \pm 0.34 \pm 0.09$	[1] SUMISAWA	05	BELL	Repl. by CHEN 07

[1] Belle Collab. quotes $A_{K_S K_S K_S}$ which is equal to $-C_{K_S K_S K_S}$.

$S_{K_S K_S K_S}$($B^0 \to K_S K_S K_S$)

VALUE	DOCUMENT ID		TECN	COMMENT
-0.5 ± 0.6 OUR AVERAGE	Error includes scale factor of 3.0.			
$-0.94^{+0.24}_{-0.21} \pm 0.06$	LEES	12I	BABR	$e^+e^- \to \Upsilon(4S)$
$0.30 \pm 0.32 \pm 0.08$	CHEN	07	BELL	$e^+e^- \to \Upsilon(4S)$
• • • We do not use the following data for averages, fits, limits, etc. • • •				
$-0.71 \pm 0.24 \pm 0.04$	AUBERT	07AT	BABR	Repl. by LEES 12I
$-0.71^{+0.38}_{-0.32} \pm 0.04$	AUBERT,B	05	BABR	Repl. by AUBERT 07AT
$1.26 \pm 0.68 \pm 0.20$	SUMISAWA	05	BELL	Repl. by CHEN 07.

$C_{K^0_S \pi^0 \gamma}$($B^0 \to K^0_S \pi^0 \gamma$)

VALUE	DOCUMENT ID		TECN	COMMENT
$0.36 \pm 0.33 \pm 0.04$	[1] AUBERT	08BA	BABR	$e^+e^- \to \Upsilon(4S)$
• • • We do not use the following data for averages, fits, limits, etc. • • •				
$0.20 \pm 0.20 \pm 0.06$	[2,3] USHIRODA	06	BELL	$e^+e^- \to \Upsilon(4S)$
$-1.0 \pm 0.5 \pm 0.2$	[1] AUBERT,B	05P	BABR	Repl. by AUBERT 08BA
$-0.03 \pm 0.34 \pm 0.11$	[3] USHIRODA	05	BELL	Repl. by USHIRODA 06

[1] Requires $1.1 < M_{K^0_S \pi^0} < 1.8$ GeV/c^2.
[2] Requires $M_{K^0_S \pi^0} < 1.8$ GeV/c^2.
[3] Reports $A_{K^0_S \pi^0 \gamma}$, which is $-C_{K^0_S \pi^0 \gamma}$.

$S_{K^0_S \pi^0 \gamma}$($B^0 \to K^0_S \pi^0 \gamma$)

VALUE	DOCUMENT ID		TECN	COMMENT
$-0.78 \pm 0.59 \pm 0.09$	[1] AUBERT	08BA	BABR	$e^+e^- \to \Upsilon(4S)$
• • • We do not use the following data for averages, fits, limits, etc. • • •				
$-0.10 \pm 0.31 \pm 0.07$	[2] USHIRODA	06	BELL	$e^+e^- \to \Upsilon(4S)$
$0.9 \pm 1.0 \pm 0.2$	[1] AUBERT,B	05P	BABR	Repl. by AUBERT 08BA
$-0.58^{+0.46}_{-0.38} \pm 0.11$	USHIRODA	05	BELL	Repl. by USHIRODA 06

[1] Requires $1.1 < M_{K^0_S \pi^0} < 1.8$ GeV/c^2.
[2] Requires $M_{K^0_S \pi^0} < 1.8$ GeV/c^2.

$C_{K^0_S \pi^+ \pi^- \gamma}$($B^0 \to K^0_S \pi^+ \pi^- \gamma$)

VALUE	DOCUMENT ID	TECN	COMMENT
$-0.39 \pm 0.20^{+0.03}_{-0.02}$	[1] DEL-AMO-SA...16	BABR	$e^+e^- \to \Upsilon(4S)$

[1] Requires $M_{K\pi\pi} < 1.8$ GeV/c^2, 0.6 GeV/c^2 $< m_{\pi^+\pi^-} < 0.9$ GeV/c^2, $m_{K\pi} <$ 0.845 GeV/c^2 or $m_{K\pi} > 0.945$ GeV/c^2.

$S_{K^0_S \pi^+ \pi^- \gamma}$($B^0 \to K^0_S \pi^+ \pi^- \gamma$)

VALUE	DOCUMENT ID	TECN	COMMENT
$0.14 \pm 0.25 \pm 0.03$	[1] DEL-AMO-SA...16	BABR	$e^+e^- \to \Upsilon(4S)$

[1] Requires $M_{K\pi\pi} < 1.8$ GeV/c^2, 0.6 GeV/c^2 $< m_{\pi^+\pi^-} < 0.9$ GeV/c^2, $m_{K\pi} <$ 0.845 GeV/c^2 or $m_{K\pi} > 0.945$ GeV/c^2.

$C_{K^*(892)^0 \gamma}$ ($B^0 \to K^*(892)^0 \gamma$)

VALUE	DOCUMENT ID		TECN	COMMENT
-0.04 ± 0.16 OUR AVERAGE	Error includes scale factor of 1.2.			
$-0.14 \pm 0.16 \pm 0.03$	[1] AUBERT	08BA	BABR	$e^+e^- \to \Upsilon(4S)$
$0.20 \pm 0.24 \pm 0.05$	[1,2] USHIRODA	06	BELL	$e^+e^- \to \Upsilon(4S)$
• • • We do not use the following data for averages, fits, limits, etc. • • •				
$-0.40 \pm 0.23 \pm 0.03$	AUBERT,B	05P	BABR	Repl. by AUBERT 08BA
$-0.57 \pm 0.32 \pm 0.09$	[3] AUBERT,B	04Z	BABR	Repl. by AUBERT,B 05P

[1] Requires $0.8 < M_{K^0_S \pi^0} < 1.0$ GeV/c^2.
[2] Reports value of A which is equal to $-C$.
[3] Based on a total signal of 105 ± 14 events with $K^*(892)^0 \to K^0_S \pi^0$ only.

$S_{K^*(892)^0 \gamma}$ ($B^0 \to K^*(892)^0 \gamma$)

VALUE	DOCUMENT ID		TECN	COMMENT
-0.15 ± 0.22 OUR AVERAGE				
$-0.03 \pm 0.29 \pm 0.03$	[1] AUBERT	08BA	BABR	$e^+e^- \to \Upsilon(4S)$
$-0.32^{+0.36}_{-0.33} \pm 0.05$	[1] USHIRODA	06	BELL	$e^+e^- \to \Upsilon(4S)$
• • • We do not use the following data for averages, fits, limits, etc. • • •				
$-0.21 \pm 0.40 \pm 0.05$	AUBERT,B	05P	BABR	Repl. by AUBERT 08BA
$-0.79^{+0.63}_{-0.50} \pm 0.10$	[2] USHIRODA	05	BELL	Repl. by USHIRODA 06
$0.25 \pm 0.63 \pm 0.14$	[3] AUBERT,B	04Z	BABR	Repl. by AUBERT,B 05P

[1] Requires $0.8 < M_{K^0_S \pi^0} < 1.0$ GeV/c^2.
[2] Assumes $C(B^0 \to K^*(892)^0 \gamma) = 0$.
[3] Based on a total signal of 105 ± 14 events with $K^*(892)^0 \to K^0_S \pi^0$ only.

$C_{\eta K^0 \gamma}$ ($B^0 \to \eta K^0 \gamma$)

VALUE	DOCUMENT ID		TECN	COMMENT
$-0.32^{+0.40}_{-0.39} \pm 0.07$	[1] AUBERT	09	BABR	$e^+e^- \to \Upsilon(4S)$

[1] $m_{\eta K} < 3.25$ GeV/c^2.

$S_{\eta K^0 \gamma}$ ($B^0 \to \eta K^0 \gamma$)

VALUE	DOCUMENT ID		TECN	COMMENT
$-0.18^{+0.49}_{-0.46} \pm 0.12$	[1] AUBERT	09	BABR	$e^+e^- \to \Upsilon(4S)$

[1] $m_{\eta K} < 3.25$ GeV/c^2.

$C_{K^0 \phi \gamma}$ ($B^0 \to K^0 \phi \gamma$)

VALUE	DOCUMENT ID		TECN	COMMENT
$-0.35 \pm 0.58^{+0.10}_{-0.23}$	[1] SAHOO	11A	BELL	$e^+e^- \to \Upsilon(4S)$

[1] Reports value of A, which is equal to $-C$.

$S_{K^0 \phi \gamma}$ ($B^0 \to K^0 \phi \gamma$)

VALUE	DOCUMENT ID		TECN	COMMENT
$0.74^{+0.72}_{-1.05} \pm 0.10_{-0.24}$	SAHOO	11A	BELL	$e^+e^- \to \Upsilon(4S)$

$C(B^0 \to K^0_S \rho^0 \gamma)$

VALUE	DOCUMENT ID		TECN	COMMENT
$-0.05 \pm 0.18 \pm 0.06$	[1,2] LI	08F	BELL	$e^+e^- \to \Upsilon(4S)$

[1] Requires $M_{K^0_S \pi^+ \pi^-} < 1.8$ GeV/c^2 and $0.6 < M_{\pi^+\pi^-} < 0.9$ GeV/c^2.
[2] Reports value of $A_{\rm eff}$ which is equal to $-C$, and includes the non-resonant $\pi^+\pi^-$ contribution in the ρ^0 region.

$S(B^0 \to K^0_S \rho^0 \gamma)$

VALUE	DOCUMENT ID		TECN	COMMENT
-0.04 ± 0.23 OUR AVERAGE				
$-0.18 \pm 0.32^{+0.06}_{-0.05}$	[1] DEL-AMO-SA...16		BABR	$e^+e^- \to \Upsilon(4S)$
$0.11 \pm 0.33^{+0.05}_{-0.09}$	[2] LI	08F	BELL	$e^+e^- \to \Upsilon(4S)$

[1] Requires $M_{K\pi\pi} < 1.8$ GeV/c^2, 0.6 GeV/c^2 $< m_{\pi^+\pi^-} < 0.9$ GeV/c^2, $m_{K\pi} <$ 0.845 GeV/c^2 or $m_{K\pi} > 0.945$ GeV/c^2.
[2] Requires $M_{K\pi\pi} < 1.8$ GeV/c^2.

C ($B^0 \to \rho^0\gamma$)

VALUE	DOCUMENT ID		TECN	COMMENT
0.44±0.49±0.14	[1] USHIRODA	08	BELL	$e^+e^- \to \Upsilon(4S)$

[1] Reports value of A which is equal to $-C$.

S ($B^0 \to \rho^0\gamma$)

VALUE	DOCUMENT ID		TECN	COMMENT
−0.83±0.65±0.18	USHIRODA	08	BELL	$e^+e^- \to \Upsilon(4S)$

$C_{\pi\pi}$ ($B^0 \to \pi^+\pi^-$)

$C_{\pi\pi}$ is defined as $(1-|\lambda|^2)/(1+|\lambda|^2)$, where the quantity $\lambda = q/p\,\overline{A}_f/A_f$ is a phase convention independent observable quantity for the final state f. For details, see the review on "CP Violation" in the Reviews section.

VALUE	DOCUMENT ID		TECN	COMMENT
−0.31±0.05 OUR AVERAGE				
−0.38±0.15±0.02	AAIJ	13BO	LHCB	pp at 7 TeV
−0.33±0.06±0.03	[1] DALSENO	13	BELL	$e^+e^- \to \Upsilon(4S)$
−0.25±0.08±0.02	LEES	13D	BABR	$e^+e^- \to \Upsilon(4S)$
• • • We do not use the following data for averages, fits, limits, etc. • • •				
−0.21±0.09±0.02	AUBERT	07AF	BABR	Repl. by LEES 13D
−0.55±0.08±0.05	[1] ISHINO	07	BELL	Repl. by DALSENO 13
−0.56±0.12±0.06	[1] ABE	05D	BELL	Repl. by ISHINO 07
−0.09±0.15±0.04	AUBERT,BE	05	BABR	Repl. by AUBERT 07AF
−0.58±0.15±0.07	[1] ABE	04E	BELL	Repl. by ABE 05D
−0.77±0.27±0.08	[1] ABE	03G	BELL	Repl. by ABE 04E.
$-0.94^{+0.31}_{-0.25}\pm0.09$	[1] ABE	02M	BELL	Repl. by ABE 03G
$-0.25^{+0.45}_{-0.47}\pm0.14$	[2] AUBERT	02D	BABR	Repl. by AUBERT 02Q
−0.30±0.25±0.04	[3] AUBERT	02Q	BABR	Repl. by AUBERT,BE 05

[1] Paper reports $A_{\pi\pi}$ which equals to $-C_{\pi\pi}$.
[2] Corresponds to 90% confidence range $-1.0 < C_{\pi\pi} < 0.47$.
[3] Corresponds to 90% confidence range $-0.72 < C_{\pi\pi} < 0.12$.

$S_{\pi\pi}$ ($B^0 \to \pi^+\pi^-$)

$S_{\pi\pi} = 2\mathrm{Im}\lambda/(1+|\lambda|^2)$, see the note in the $C_{\pi\pi}$ datablock above.

VALUE	DOCUMENT ID		TECN	COMMENT
−0.67±0.06 OUR AVERAGE				
−0.71±0.13±0.02	AAIJ	13BO	LHCB	pp at 7 TeV
−0.64±0.08±0.03	[1] DALSENO	13	BELL	$e^+e^- \to \Upsilon(4S)$
−0.68±0.10±0.03	LEES	13D	BABR	$e^+e^- \to \Upsilon(4S)$
• • • We do not use the following data for averages, fits, limits, etc. • • •				
−0.60±0.11±0.03	AUBERT	07AF	BABR	Repl. by LEES 13D
−0.61±0.10±0.04	ISHINO	07	BELL	Repl. by DALSENO 13
−0.67±0.16±0.06	[2] ABE	05D	BELL	Repl. by ISHINO 07
−0.30±0.17±0.03	AUBERT,BE	05	BABR	Repl. by AUBERT 07AF
−1.00±0.21±0.07	[3] ABE	04E	BELL	Repl. by ABE 05D
$-1.23\pm0.41^{+0.08}_{-0.07}$	ABE	03G	BELL	Repl. by ABE 04E.
$-1.21^{+0.38+0.16}_{-0.27-0.13}$	ABE	02M	BELL	Repl. by ABE 03G
$0.03^{+0.52}_{-0.56}\pm0.11$	[4] AUBERT	02D	BABR	Repl. by AUBERT 02Q
0.02±0.34±0.05	[5] AUBERT	02Q	BABR	Repl. by AUBERT,BE 05

[1] An isospin analysis using other BELLE measurements, disfavors the region of $23.8^\circ < \phi_2 < 66.8^\circ$ at 68% CL.
[2] Rule out the CP-conserving case, $C_{\pi\pi} = S_{\pi\pi} = 0$, at the 5.4 sigma level.
[3] Rule out the CP-conserving case, $C_{\pi\pi} = S_{\pi\pi} = 0$, at the 5.2 sigma level.
[4] Corresponds to 90% confidence range $-0.89 < S_{\pi\pi} < 0.85$.
[5] Corresponds to 90% confidence range $-0.54 < S_{\pi\pi} < 0.58$.

$C_{\pi^0\pi^0}$($B^0 \to \pi^0\pi^0$)

VALUE	DOCUMENT ID		TECN	COMMENT
−0.33±0.22 OUR AVERAGE				
−0.14±0.36±0.10	[1] JULIUS	17	BELL	$e^+e^- \to \Upsilon(4S)$
−0.43±0.26±0.05	LEES	13D	BABR	$e^+e^- \to \Upsilon(4S)$
• • • We do not use the following data for averages, fits, limits, etc. • • •				
−0.49±0.35±0.05	AUBERT	07BC	BABR	Repl. by LEES 13D
−0.12±0.56±0.06	[2] AUBERT	05L	BABR	Repl. by AUBERT 07BC
$-0.44^{+0.52}_{-0.53}\pm0.17$	[1] CHAO	05	BELL	Repl. by JULIUS 17

[1] BELLE Collab. quotes $A_{\pi^0\pi^0}$ which is equal to $-C_{\pi^0\pi^0}$.
[2] Corresponds to a 90% CL interval of $-0.88 < A_{CP} < 0.64$.

$C_{\rho\pi}$ ($B^0 \to \rho^+\pi^-$)

VALUE	DOCUMENT ID		TECN	COMMENT
−0.03 ±0.07 OUR AVERAGE	Error includes scale factor of 1.2.			
0.016±0.059±0.036	[1] LEES	13J	BABR	$e^+e^- \to \Upsilon(4S)$
−0.13 ±0.09 ±0.05	[1] KUSAKA	07	BELL	$e^+e^- \to \Upsilon(4S)$
• • • We do not use the following data for averages, fits, limits, etc. • • •				
0.15 ±0.09 ±0.05	AUBERT	07AA	BABR	Repl. by LEES 13J
$0.25\ \pm0.17\ ^{+0.02}_{-0.06}$	WANG	05	BELL	Repl. by KUSAKA 07
0.36 ±0.18 ±0.04	AUBERT	03T	BABR	Repl. by AUBERT 07AA

[1] Uses time-dependent Dalitz plot analysis of $B^0 \to \pi^+\pi^-\pi^0$ decays.

$S_{\rho\pi}$ ($B^0 \to \rho^+\pi^-$)

VALUE	DOCUMENT ID		TECN	COMMENT
0.05 ±0.07 OUR AVERAGE				
0.053±0.081±0.034	[1] LEES	13J	BABR	$e^+e^- \to \Upsilon(4S)$
0.06 ±0.13 ±0.05	[1] KUSAKA	07	BELL	$e^+e^- \to \Upsilon(4S)$
• • • We do not use the following data for averages, fits, limits, etc. • • •				
−0.03 ±0.11 ±0.04	AUBERT	07AA	BABR	Repl. by LEES 13J
$-0.28\ \pm0.23\ ^{+0.10}_{-0.08}$	WANG	05	BELL	Repl. by KUSAKA 07
0.19 ±0.24 ±0.03	AUBERT	03T	BABR	Repl. by AUBERT 07AA

[1] Uses time-dependent Dalitz plot analysis of $B^0 \to \pi^+\pi^-\pi^0$ decays.

$\Delta C_{\rho\pi}$ ($B^0 \to \rho^+\pi^-$)

$\Delta C_{\rho\pi}$ describes the asymmetry between the rates $\Gamma(B^0 \to \rho^+\pi^-) + \Gamma(\overline{B}^0 \to \rho^-\pi^+)$ and $\Gamma(B^0 \to \rho^-\pi^+) + \Gamma(\overline{B}^0 \to \rho^+\pi^-)$.

VALUE	DOCUMENT ID		TECN	COMMENT
0.27 ±0.06 OUR AVERAGE				
0.234±0.061±0.048	[1] LEES	13J	BABR	$e^+e^- \to \Upsilon(4S)$
0.36 ±0.10 ±0.05	[1] KUSAKA	07	BELL	$e^+e^- \to \Upsilon(4S)$
• • • We do not use the following data for averages, fits, limits, etc. • • •				
0.39 ±0.09 ±0.09	AUBERT	07AA	BABR	Repl. by LEES 13J
$0.38\ \pm0.18\ ^{+0.02}_{-0.04}$	WANG	05	BELL	Repl. by KUSAKA 07
$0.28\ ^{+0.18}_{-0.19}\ \pm0.04$	AUBERT	03T	BABR	Repl. by AUBERT 07AA

[1] Uses time-dependent Dalitz plot analysis of $B^0 \to \pi^+\pi^-\pi^0$ decays.

$\Delta S_{\rho\pi}$ ($B^0 \to \rho^+\pi^-$)

$\Delta S_{\rho\pi}$ is related to the strong phase difference between the amplitudes contributing to $B^0 \to \rho^+\pi^-$.

VALUE	DOCUMENT ID		TECN	COMMENT
0.01 ±0.08 OUR AVERAGE				
0.054±0.082±0.039	[1] LEES	13J	BABR	$e^+e^- \to \Upsilon(4S)$
−0.08 ±0.13 ±0.05	[1] KUSAKA	07	BELL	$e^+e^- \to \Upsilon(4S)$
• • • We do not use the following data for averages, fits, limits, etc. • • •				
−0.01 ±0.14 ±0.06	AUBERT	07AA	BABR	Repl. by LEES 13J
−0.30 ±0.24 ±0.09	WANG	05	BELL	Repl. by KUSAKA 07
0.15 ±0.25 ±0.03	AUBERT	03T	BABR	Repl. by AUBERT 07AA

[1] Uses time-dependent Dalitz plot analysis of $B^0 \to \pi^+\pi^-\pi^0$ decays.

$C_{\rho^0\pi^0}$ ($B^0 \to \rho^0\pi^0$)

VALUE	DOCUMENT ID		TECN	COMMENT
0.27±0.24 OUR AVERAGE				
0.19±0.23±0.15	[1] LEES	13J	BABR	$e^+e^- \to \Upsilon(4S)$
0.49±0.36±0.28	[1,2] KUSAKA	07	BELL	$e^+e^- \to \Upsilon(4S)$
• • • We do not use the following data for averages, fits, limits, etc. • • •				
−0.10±0.40±0.53	AUBERT	07AA	BABR	Repl. by LEES 13J
$0.53^{+0.67+0.10}_{-0.84-0.15}$	[2] DRAGIC	06	BELL	Repl. by KUSAKA 07

[1] Uses time-dependent Dalitz plot analysis of $B^0 \to \pi^+\pi^-\pi^0$ decays.
[2] Quotes $A_{\rho^0\pi^0}$ which is equal to $-C_{\rho^0\pi^0}$.

$S_{\rho^0\pi^0}$ ($B^0 \to \rho^0\pi^0$)

VALUE	DOCUMENT ID		TECN	COMMENT
−0.23±0.34 OUR AVERAGE				
−0.37±0.34±0.20	[1] LEES	13J	BABR	$e^+e^- \to \Upsilon(4S)$
0.17±0.57±0.35	[1] KUSAKA	07	BELL	$e^+e^- \to \Upsilon(4S)$
• • • We do not use the following data for averages, fits, limits, etc. • • •				
0.04±0.44±0.18	AUBERT	07AA	BABR	Repl. by LEES 13J

[1] Uses time-dependent Dalitz plot analysis of $B^0 \to \pi^+\pi^-\pi^0$ decays.

$C_{a_1\pi}$ ($B^0 \to a_1(1260)^+\pi^-$)

VALUE	DOCUMENT ID		TECN	COMMENT
−0.05±0.11 OUR AVERAGE				
−0.01±0.11±0.09	DALSENO	12	BELL	$e^+e^- \to \Upsilon(4S)$
−0.10±0.15±0.09	AUBERT	07O	BABR	$e^+e^- \to \Upsilon(4S)$

$S_{a_1\pi}$ ($B^0 \to a_1(1260)^+\pi^-$)

VALUE	DOCUMENT ID		TECN	COMMENT
−0.2 ±0.4 OUR AVERAGE	Error includes scale factor of 3.2.			
−0.51±0.14±0.08	DALSENO	12	BELL	$e^+e^- \to \Upsilon(4S)$
0.37±0.21±0.07	AUBERT	07O	BABR	$e^+e^- \to \Upsilon(4S)$

$\Delta C_{a_1\pi}$ ($B^0 \to a_1(1260)^+\pi^-$)

$\Delta C_{a_1\pi}$ describes the asymmetry between the rates $\Gamma(B^0 \to a_1^+\pi^-) + \Gamma(\overline{B}^0 \to a_1^-\pi^+)$ and $\Gamma(B^0 \to a_1^-\pi^+) + \Gamma(\overline{B}^0 \to a_1^+\pi^-)$.

VALUE	DOCUMENT ID		TECN	COMMENT
0.43±0.14 OUR AVERAGE	Error includes scale factor of 1.3.			
0.54±0.11±0.07	DALSENO	12	BELL	$e^+e^- \to \Upsilon(4S)$
0.26±0.15±0.07	AUBERT	07O	BABR	$e^+e^- \to \Upsilon(4S)$

Meson Particle Listings

B^0

$\Delta S_{a_1\pi}$ ($B^0 \to a_1(1260)^+\pi^-$)

$\Delta S_{a_1\pi}$ is related to the strong phase difference between the amplitudes contributing to $B^0 \to a_1\pi$ decays.

VALUE	DOCUMENT ID		TECN	COMMENT
-0.11 ± 0.12 OUR AVERAGE				
$-0.09\pm0.14\pm0.06$	DALSENO	12	BELL	$e^+e^- \to \Upsilon(4S)$
$-0.14\pm0.21\pm0.06$	AUBERT	07O	BABR	$e^+e^- \to \Upsilon(4S)$

C ($B^0 \to b_1^- K^+$)

VALUE	DOCUMENT ID		TECN	COMMENT
$-0.22\pm0.23\pm0.05$	AUBERT	07BI	BABR	$e^+e^- \to \Upsilon(4S)$

ΔC ($B^0 \to b_1^-\pi^+$)

VALUE	DOCUMENT ID		TECN	COMMENT
$-1.04\pm0.23\pm0.08$	AUBERT	07BI	BABR	$e^+e^- \to \Upsilon(4S)$

$C_{\rho^0\rho^0}$ ($B^0 \to \rho^0\rho^0$)

VALUE	DOCUMENT ID		TECN	COMMENT
$0.2\pm0.8\pm0.3$	AUBERT	08BB	BABR	$e^+e^- \to \Upsilon(4S)$

$S_{\rho^0\rho^0}$ ($B^0 \to \rho^0\rho^0$)

VALUE	DOCUMENT ID		TECN	COMMENT
$0.3\pm0.7\pm0.2$	AUBERT	08BB	BABR	$e^+e^- \to \Upsilon(4S)$

$C_{\rho\rho}$ ($B^0 \to \rho^+\rho^-$)

VALUE	DOCUMENT ID		TECN	COMMENT
0.00 ± 0.09 OUR AVERAGE				
$0.00\pm0.10\pm0.06$	[1] VANHOEFER	16	BELL	$e^+e^- \to \Upsilon(4S)$
$0.01\pm0.15\pm0.06$	AUBERT	07BF	BABR	$e^+e^- \to \Upsilon(4S)$
• • • We do not use the following data for averages, fits, limits, etc. • • •				
$-0.16\pm0.21\pm0.08$	[1] SOMOV	07	BELL	Repl. by VANHOEFER 16
$-0.00\pm0.30\pm0.09$	[1] SOMOV	06	BELL	Repl. by SOMOV 07
$-0.03\pm0.18\pm0.09$	AUBERT,B	05C	BABR	Repl. by AUBERT 07BF
$-0.17\pm0.27\pm0.14$	AUBERT,B	04R	BABR	Repl. by AUBERT,B 05C

[1] BELLE Collab. quotes A_{CP} which is equal to $-C$.

$S_{\rho\rho}$ ($B^0 \to \rho^+\rho^-$)

VALUE	DOCUMENT ID		TECN	COMMENT
-0.14 ± 0.13 OUR AVERAGE				
$-0.13\pm0.15\pm0.05$	VANHOEFER	16	BELL	$e^+e^- \to \Upsilon(4S)$
$-0.17\pm0.20^{+0.05}_{-0.06}$	AUBERT	07BF	BABR	$e^+e^- \to \Upsilon(4S)$
• • • We do not use the following data for averages, fits, limits, etc. • • •				
$0.19\pm0.30\pm0.08$	SOMOV	07	BELL	Repl. by VANHOEFER 16
$0.08\pm0.41\pm0.09$	SOMOV	06	BELL	Repl. by SOMOV 07
$-0.33\pm0.24^{+0.08}_{-0.14}$	AUBERT,B	05C	BABR	Repl. by AUBERT 07BF
$-0.42\pm0.42\pm0.14$	AUBERT,B	04R	BABR	Repl. by AUBERT,B 05C

$|\lambda|$ ($B^0 \to J/\psi K^*(892)^0$)

VALUE	CL%	DOCUMENT ID		TECN	COMMENT
<0.25	95	[1] AUBERT,B	04H	BABR	$e^+e^- \to \Upsilon(4S)$

[1] Uses the measured cosine coefficients C and $\overline{C}$ and assumes $|q/p| = 1$.

$\cos 2\beta$ ($B^0 \to J/\psi K^*(892)^0$)

$\beta(\phi_1)$ is one of the angles of CMK unitarity triangle, see the review on "*CP* Violation in the Reviews section.

VALUE	DOCUMENT ID		TECN	COMMENT
$1.7\ ^{+0.7}_{-0.9}$ OUR AVERAGE Error includes scale factor of 1.6.				
$2.72^{+0.50}_{-0.79}\pm0.27$	[1] AUBERT	05P	BABR	$e^+e^- \to \Upsilon(4S)$
$0.87\pm0.74\pm0.12$	[2] ITOH	05	BELL	$e^+e^- \to \Upsilon(4S)$

[1] The measurement is obtained when sin 2β is fixed to 0.726 and the sign of cos 2β is positive with 86% confidence level.
[2] The measurement is obtained with sin 2β fixed to 0.731.

$\cos 2\beta$ ($B^0 \to [K^0_S\pi^+\pi^-]_{D^{(*)}}\ h^0$)

VALUE	DOCUMENT ID		TECN	COMMENT
0.84 ± 0.31 OUR AVERAGE				
$1.06\pm0.33^{+0.21}_{-0.15}$	[1] VOROBYEV	16	BELL	$e^+e^- \to \Upsilon(4S)$
$0.42\pm0.49\pm0.16$	[2] AUBERT	07BH	BABR	$e^+e^- \to \Upsilon(4S)$
• • • We do not use the following data for averages, fits, limits, etc. • • •				
$1.87^{+0.40+0.22}_{-0.53-0.32}$	[3] KROKOVNY	06	BELL	Repl. by VOROBYEV 16

[1] A model-independent measurement uses the binned Dalitz plot technique.
[2] AUBERT 07BH evaluates the likelihoods for the positive and negative solutions assuming $\sin(2\beta_{eff}) = 0.678$. It quotes $L_+ / (L_+ + L_-) = 0.86$ corresponding to a likelihood ratio of $L_+/L_- = 6.14$ in favor of the positive solution.
[3] KROKOVNY 06 evaluates the likelihoods for the positive and negative solutions assuming $\sin(2\beta_{eff}) = 0.689$. It quotes $L_+ / (L_+ + L_-) = 0.983$ corresponding to a likelihood ratio of $L_+/L_- = 57.8$ in favor of the positive solution.

$(S_+ + S_-)/2$ ($B^0 \to D^{*-}\pi^+$)

$S_\pm = -\frac{2Im(\lambda_\pm)}{1+|\lambda_\pm|^2}$ where λ_+ and λ_- are defined in the $C_{\pi\pi}$ datablock above for $B^0 \to D^{*-}\pi^+$ and $\overline{B}^0 \to D^{*+}\pi^-$.

VALUE	DOCUMENT ID		TECN	COMMENT
-0.039 ± 0.011 OUR AVERAGE				
$-0.046\pm0.013\pm0.015$	[1] BAHINIPATI	11	BELL	$e^+e^- \to \Upsilon(4S)$
$-0.040\pm0.023\pm0.010$	[2] AUBERT	06Y	BABR	$e^+e^- \to \Upsilon(4S)$
$-0.034\pm0.014\pm0.009$	[1] AUBERT	05Z	BABR	$e^+e^- \to \Upsilon(4S)$
• • • We do not use the following data for averages, fits, limits, etc. • • •				
$-0.039\pm0.020\pm0.013$	[3] RONGA	06	BELL	Repl. by BAHINIPATI 11
$-0.030\pm0.028\pm0.018$	[1] GERSHON	05	BELL	Repl. by RONGA 06
$-0.068\pm0.038\pm0.020$	[2] AUBERT	04V	BABR	Repl. by AUBERT 06Y
$-0.063\pm0.024\pm0.014$	[1] AUBERT	04W	BABR	Repl. by AUBERT 05Z
$0.060\pm0.040\pm0.019$	[2] SARANGI	04	BELL	Repl. by RONGA 06

[1] Uses partially reconstructed $B^0 \to D^{*\pm}\pi^\mp$ decays.
[2] Uses fully reconstructed $B^0 \to D^{*\pm}\pi^\mp$ decays.
[3] Combines the results from fully reconstructed and partially reconstructed $D^*\pi$ events by taking weighted averages. Assumes that systematic errors from physics parameters and fit biases in the two measurements are 100% correlated.

$(S_- - S_+)/2$ ($B^0 \to D^{*-}\pi^+$)

VALUE	DOCUMENT ID		TECN	COMMENT
-0.009 ± 0.015 OUR AVERAGE				
$-0.015\pm0.013\pm0.015$	[1] BAHINIPATI	11	BELL	$e^+e^- \to \Upsilon(4S)$
$0.049\pm0.042\pm0.015$	[2] AUBERT	06Y	BABR	$e^+e^- \to \Upsilon(4S)$
$-0.019\pm0.022\pm0.013$	[1] AUBERT	05Z	BABR	$e^+e^- \to \Upsilon(4S)$
• • • We do not use the following data for averages, fits, limits, etc. • • •				
$-0.011\pm0.020\pm0.013$	[3] RONGA	06	BELL	Repl. by BAHINIPATI 11
$-0.005\pm0.028\pm0.018$	[1] GERSHON	05	BELL	Repl. by RONGA 06
$0.031\pm0.070\pm0.033$	[2] AUBERT	04V	BABR	Repl. by AUBERT 06Y
$-0.004\pm0.037\pm0.014$	[1] AUBERT	04W	BABR	Repl. by AUBERT 05Z
$0.049\pm0.040\pm0.019$	[2] SARANGI	04	BELL	Repl. by RONGA 06

[1] Uses partially reconstructed $B^0 \to D^{*\pm}\pi^\mp$ decays.
[2] Uses fully reconstructed $B^0 \to D^{*\pm}\pi^\mp$ decays.
[3] Combines the results from fully reconstructed and partially reconstructed $D^*\pi$ events by taking weighted averages. Assumes that systematic errors from physics parameters and fit biases in the two measurements are 100% correlated.

$(S_+ + S_-)/2$ ($B^0 \to D^-\pi^+$)

VALUE	DOCUMENT ID		TECN	COMMENT
-0.046 ± 0.023 OUR AVERAGE				
$-0.010\pm0.023\pm0.07$	[1] AUBERT	06Y	BABR	$e^+e^- \to \Upsilon(4S)$
$-0.050\pm0.021\pm0.012$	[2] RONGA	06	BELL	$e^+e^- \to \Upsilon(4S)$
• • • We do not use the following data for averages, fits, limits, etc. • • •				
$-0.022\pm0.038\pm0.020$	[1] AUBERT	04V	BABR	Repl. by AUBERT 06Y
$-0.062\pm0.037\pm0.018$	[1] SARANGI	04	BELL	Repl. by RONGA 06

[1] Uses fully reconstructed $B^0 \to D^\pm\pi^\mp$ decays.
[2] Combines the results from fully reconstructed and partially reconstructed $D\pi$ events by taking weighted averages. Assumes that systematic errors from physics parameters and fit biases in the two measurements are 100% correlated.

$(S_- - S_+)/2$ ($B^0 \to D^-\pi^+$)

VALUE	DOCUMENT ID		TECN	COMMENT
-0.022 ± 0.021 OUR AVERAGE				
$-0.033\pm0.042\pm0.012$	[1] AUBERT	06Y	BABR	$e^+e^- \to \Upsilon(4S)$
$-0.019\pm0.021\pm0.012$	[2] RONGA	06	BELL	$e^+e^- \to \Upsilon(4S)$
• • • We do not use the following data for averages, fits, limits, etc. • • •				
$0.025\pm0.068\pm0.033$	[1] AUBERT	04V	BABR	Repl. by AUBERT 06Y
$-0.025\pm0.037\pm0.018$	[1] SARANGI	04	BELL	Repl. by RONGA 06

[1] Uses fully reconstructed $B^0 \to D^\pm\pi^\mp$ decays.
[2] Combines the results from fully reconstructed and partially reconstructed $D\pi$ events by taking weighted averages. Assumes that systematic errors from physics parameters and fit biases in the two measurements are 100% correlated.

$(S_+ + S_-)/2$ ($B^0 \to D^-\rho^+$)

VALUE	DOCUMENT ID		TECN	COMMENT
$-0.024\pm0.031\pm0.009$	[1] AUBERT	06Y	BABR	$e^+e^- \to \Upsilon(4S)$

[1] Uses fully reconstructed $B^0 \to D^-\rho^+$ decays.

$(S_- - S_+)/2$ ($B^0 \to D^-\rho^+$)

VALUE	DOCUMENT ID		TECN	COMMENT
$-0.098\pm0.055\pm0.018$	[1] AUBERT	06Y	BABR	$e^+e^- \to \Upsilon(4S)$

[1] Uses fully reconstructed $B^0 \to D^-\rho^+$ decays.

$C_{\eta_c K^0_S}$ ($B^0 \to \eta_c K^0_S$)

VALUE	DOCUMENT ID		TECN	COMMENT
$0.080\pm0.124\pm0.029$	AUBERT	09K	BABR	$e^+e^- \to \Upsilon(4S)$

$S_{\eta_c K^0_S}$ ($B^0 \to \eta_c K^0_S$)

VALUE	DOCUMENT ID		TECN	COMMENT
$0.925\pm0.160\pm0.057$	AUBERT	09K	BABR	$e^+e^- \to \Upsilon(4S)$

$C_{c\overline{c}K^{(*)0}}$ ($B^0 \to c\overline{c}K^{(*)0}$)

"OUR EVALUATION" is an average using rescaled values of the data listed below. The average and rescaling were performed by the Heavy Flavor Averaging Group (HFLAV) and are described at http://www.slac.stanford.edu/xorg/hflav/. The averaging/rescaling procedure takes into account correlations between the measurements.

VALUE (units 10^{-2})	DOCUMENT ID		TECN	COMMENT
0.5 ± 1.7 OUR EVALUATION				
0.0 ± 1.4 OUR AVERAGE				
− 1.7 ± 2.9	[1,2] AAIJ	17BN	LHCB	pp at 7, 8 TeV
− 0.6 ± 1.6 ± 1.2	[3] ADACHI	12A	BELL	$e^+e^- \to \Upsilon(4S)$
−29 $^{+53}_{-44}$ ± 6	[4] AUBERT	09AU	BABR	$e^+e^- \to \Upsilon(4S)$
2.4 ± 2.0 ± 1.6	[5] AUBERT	09K	BABR	$e^+e^- \to \Upsilon(4S)$
• • • We do not use the following data for averages, fits, limits, etc. • • •				
− 4 ± 7 ± 5	[6] SAHOO	08	BELL	Repl. by ADACHI 12A
4.9 ± 2.3 ± 1.8	[5] AUBERT	07AY	BABR	Repl. by AUBERT 09K
− 1.8 ± 2.1 ± 1.4	[7] CHEN	07	BELL	Repl. by ADACHI 12A
− 0.7 ± 4.1 ± 3.3	[8] ABE	05B	BELL	Repl. by CHEN 07
5.1 ± 3.2 ± 1.4	[9] AUBERT	05F	BABR	Repl. by AUBERT 07AY
5.1 ± 5.1 ± 2.6	[10] ABE	02Z	BELL	Repl. by ABE 05B
5.3 ± 5.4 ± 3.2	[11] AUBERT	02P	BABR	Repl. by AUBERT 05F

[1] Measurement based on $B^0 \to J/\psi K^0_S$, $B^0 \to \psi(2S) K^0_S$ with $J/\psi \to \mu^+\mu^-$, $J/\psi \to e^+e^-$ and $\psi(2S) \to \mu^+\mu^-$.
[2] AAIJ 17BN provides the correlation coefficient ρ=0.42 between the uncertainties of $S_{B^0 \to c\overline{c}K^{(*)0}}(B^0 \to c\overline{c}K^{(*)0})$ and $C_{c\overline{c}K^{(*)0}}$ ($B^0 \to c\overline{c}K^{(*)0}$) measurements.
[3] Measurement based on $B^0 \to J/\psi K^0_S$, $B^0 \to \psi(2S) K^0_S$, $B^0 \to J/\psi K^0_L$, and $B^0 \to \chi_{c1}(1P) K^0_S$ decays.
[4] Uses Dalitz plot analysis of $B^0 \to K^0\pi^+\pi^-$ decays and the first of two equivalent solutions is used.
[5] Measurement based on $B^0 \to c\overline{c}K^{(*)0}$ decays.
[6] Reports value of A of $B^0 \to \psi(2S) K^0$ which is equal to $-C$.
[7] Reports value of A of $B^0 \to J/\psi K^0$ which is equal to $-C$.
[8] Measurement based on 152×10^6 $B\overline{B}$ pairs.
[9] Measurement based on 227×10^6 $B\overline{B}$ pairs.
[10] Measured with both $\eta_f = \pm 1$ samples.
[11] Measured with the high purity of $\eta_f = -1$ samples.

sin(2β)

For a discussion of CP violation, see the review on "CP Violation" in the Reviews section. sin(2β) is a measure of the CP-violating amplitude in the $B^0_d \to J/\psi(1S) K^0_S$.

"OUR EVALUATION" is an average using rescaled values of the data listed below. The average and rescaling were performed by the Heavy Flavor Averaging Group (HFLAV) and are described at http://www.slac.stanford.edu/xorg/hflav/. The averaging/rescaling procedure takes into account correlations between the measurements.

VALUE	DOCUMENT ID		TECN	COMMENT
0.699±0.017 OUR EVALUATION				
0.698±0.027 OUR AVERAGE	Error includes scale factor of 1.6. See the ideogram below.			
0.760±0.034	[1,2] AAIJ	17BN	LHCB	pp at 7, 8 TeV
0.667±0.023±0.012	[3] ADACHI	12A	BELL	$e^+e^- \to \Upsilon(4S)$
0.57 ±0.58 ±0.06	[4] SATO	12	BELL	$e^+e^- \to \Upsilon(5S)$
0.69 ±0.52 ±0.08	[5] AUBERT	09AU	BABR	$e^+e^- \to \Upsilon(4S)$
0.687±0.028±0.012	[6] AUBERT	09K	BABR	$e^+e^- \to \Upsilon(4S)$
1.56 ±0.42 ±0.21	[7] AUBERT	04R	BABR	$e^+e^- \to \Upsilon(4S)$
0.79 $^{+0.41}_{-0.44}$	[8] AFFOLDER	00C	CDF	$p\overline{p}$ at 1.8 TeV
0.84 $^{+0.82}_{-1.04}$ ±0.16	[9] BARATE	00Q	ALEP	$e^+e^- \to Z$
3.2 $^{+1.8}_{-2.0}$ ±0.5	[10] ACKERSTAFF	98Z	OPAL	$e^+e^- \to Z$
• • • We do not use the following data for averages, fits, limits, etc. • • •				
0.72 ±0.09 ±0.03	[11] SAHOO	08	BELL	Repl. by ADACHI 12A
0.714±0.032±0.018	[6] AUBERT	07AY	BABR	Repl. by AUBERT 09K
0.642±0.031±0.017	CHEN	07	BELL	Repl. by ADACHI 12A
0.728±0.056±0.023	[12] ABE	05B	BELL	Repl. by CHEN 07
0.722±0.040±0.023	[13] AUBERT	05F	BABR	Repl. by AUBERT 07AY
0.99 ±0.14 ±0.06	[14] ABE	02U	BELL	$e^+e^- \to \Upsilon(4S)$
0.719±0.074±0.035	[15] ABE	02Z	BELL	Repl. by ABE 05B
0.59 ±0.14 ±0.05	[16] AUBERT	02N	BABR	$e^+e^- \to \Upsilon(4S)$
0.741±0.067±0.034	[17] AUBERT	02P	BABR	Repl. by AUBERT 05F
0.58 $^{+0.32}_{-0.34}$ $^{+0.09}_{-0.10}$	ABASHIAN	01	BELL	Repl. by ABE 01G
0.99 ±0.14 ±0.06	[18] ABE	01G	BELL	Repl. by ABE 02Z
0.34 ±0.20 ±0.05	AUBERT	01	BABR	Repl. by AUBERT 01B
0.59 ±0.14 ±0.05	[18] AUBERT	01B	BABR	Repl. by AUBERT 02P
1.8 ±1.1 ±0.3	[19] ABE	98U	CDF	Repl. by AFFOLDER 00C

[1] Measurement based on $B^0 \to J/\psi K^0_S$, $B^0 \to \psi(2S) K^0_S$ with $J/\psi \to \mu^+\mu^-$, $J/\psi \to e^+e^-$ and $\psi(2S) \to \mu^+\mu^-$.
[2] AAIJ 17BN provides the correlation coefficient $\rho = 0.42$ between the uncertainties of sin(2β) and cos(2β) measurements.
[3] Measurement based on $B^0 \to J/\psi K^0_S$, $B^0 \to \psi(2S) K^0_S$, $B^0 \to J/\psi K^0_L$, and $B^0 \to \chi_{c1}(1P) K^0_S$ decays.
[4] SATO 12 uses 121 fb^{-1} data collected on $\Upsilon(5S)$ resonance. Uses the "$B-\pi$ tagging" where $B\pi^+$ and $B\pi^-$ tagged $J/\psi K^0_S$ events are compared.
[5] Uses Dalitz plot analysis of $B^0 \to K^0\pi^+\pi^-$ decays and the first of two equivalent solutions.
[6] Measurement based on $B^0 \to c\overline{c}K^{(*)0}$ decays.
[7] Measurement in which the J/ψ decays to hadrons or to muons that do not satisfy the standard identification criteria.
[8] AFFOLDER 00C uses about 400 $B^0 \to J/\psi(1S) K^0_S$ events. The production flavor of B^0 was determined using three tagging algorithms: a same-side tag, a jet-charge tag, and a soft-lepton tag.
[9] BARATE 00Q uses 23 candidates for $B^0 \to J/\psi(1S) K^0_S$ decays. A combination of jet-charge, vertex-charge, and same-side tagging techniques were used to determine the B^0 production flavor.
[10] ACKERSTAFF 98Z uses 24 candidates for $B^0_d \to J/\psi(1S) K^0_S$ decay. A combination of jet-charge and vertex-charge techniques were used to tag the B^0_d production flavor.
[11] Based on $B^0 \to \psi(2S) K^0_S$ decays.
[12] Measurement based on 152×10^6 $B\overline{B}$ pairs.
[13] Measurement based on 227×10^6 $B\overline{B}$ pairs.
[14] ABE 02U result is based on the same analysis and data sample reported in ABE 01G.
[15] ABE 02Z result is based on 85×10^6 $B\overline{B}$ pairs.
[16] AUBERT 02N result based on the same analysis and data sample reported in AUBERT 01B.
[17] AUBERT 02P result is based on 88×10^6 $B\overline{B}$ pairs.
[18] First observation of CP violation in B^0 meson system.
[19] ABE 98U uses 198 ± 17 $B^0_d \to J/\psi(1S) K^0$ events. The production flavor of B^0 was determined using the same side tagging technique.

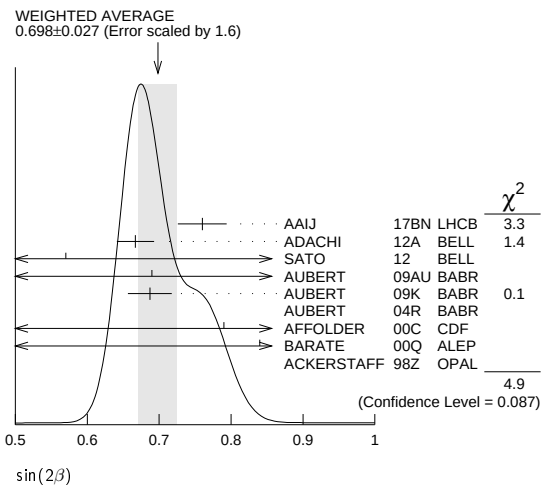

$C_{J/\psi(nS)K^0}$ ($B^0 \to J/\psi(nS)K^0$)

"OUR EVALUATION" is an average using rescaled values of the data listed below. The average and rescaling were performed by the Heavy Flavor Averaging Group (HFLAV) and are described at http://www.slac.stanford.edu/xorg/hflav/. The averaging/rescaling procedure takes into account correlations between the measurements.

VALUE (units 10^{-2})	DOCUMENT ID		TECN	COMMENT
0.5 ± 2.0 OUR EVALUATION				
− 0.5 ± 1.6 OUR AVERAGE				
− 1.7 ± 2.9	[1,2] AAIJ	17BN	LHCB	pp at 7, 8 TeV
1.5 ± 2.1 $^{+2.3}_{-4.5}$	[3,4] ADACHI	12A	BELL	$e^+e^- \to \Upsilon(4S)$
−10.4 ± 5.5 $^{+2.7}_{-4.7}$	[4,5] ADACHI	12A	BELL	$e^+e^- \to \Upsilon(4S)$
− 1.9 ± 2.6 $^{+4.1}_{-1.7}$	[4,6] ADACHI	12A	BELL	$e^+e^- \to \Upsilon(4S)$
8.9 ± 7.6 ± 2.0	[5] AUBERT	09K	BABR	$e^+e^- \to \Upsilon(4S)$
1.6 ± 2.3 ± 1.8	AUBERT	09K	BABR	$e^+e^- \to \Upsilon(4S)$
• • • We do not use the following data for averages, fits, limits, etc. • • •				
− 1.4 ± 3.0	[7] AAIJ	17BN	LHCB	pp at 7, 8 TeV
− 5 ±10 ±1	[8] AAIJ	17BN	LHCB	pp at 7, 8 TeV
− 3.8 ± 3.2 ± 0.5	[9] AAIJ	15N	LHCB	Repl. by AAIJ 17BN
3 ± 9 ±1	[10] AAIJ	13K	LHCB	Repl. by AAIJ 15N
− 4 ± 7 ± 5	[4,5] SAHOO	08	BELL	Repl. by ADACHI 12A
− 1.8 ± 2.1 ± 1.4	[4] CHEN	07	BELL	Repl. by ADACHI 12A

[1] Measurement based on $B^0 \to J/\psi K^0_S$, $B^0 \to \psi(2S) K^0_S$ with $J/\psi \to \mu^+\mu^-$, $J/\psi \to e^+e^-$ and $\psi(2S) \to \mu^+\mu^-$.
[2] AAIJ 17BN provides the correlation coefficient $\rho = 0.42$ between the uncertainties of $S_{J/\psi(nS)K^0}$ ($B^0 \to J/\psi(nS)K^0$) and $C_{J/\psi(nS)K^0}$ ($B^0 \to J/\psi(nS)K^0$) measurements.
[3] Uses $B^0 \to J/\psi K^0_S$ decays.
[4] The paper reports A, which is equal to $-C$.
[5] Uses $B^0 \to \psi(2S) K^0_S$ decays.
[6] Uses $B^0 \to J/\psi K^0_L$ decays.
[7] Measurement based on $B^0 \to J/\psi K^0_S$ with $J/\psi \to \mu^+\mu^-$ and $J/\psi \to e^+e^-$.
[8] Measurement based on $B^0 \to \psi(2S) K^0_S$ with $\psi(2S) \to \mu^+\mu^-$.
[9] AAIJ 15N uses 41,560 flavor-tagged $B_d \to J/\psi K^0_S$ events from 3 fb^{-1} of integrated luminosity. Provides the correlation coefficient $\rho = 0.483$ between the statistical uncertainties of and measurements.

[10] AAIJ 13K uses 8200 flavor-tagged $B_d \to J/\psi K^0_S$ events from 1 fb^{-1} of integrated luminosity. Provides the correlation coefficient $\rho = 0.42$ between the statistical uncertainties of $S_{J/\psi(nS)K^0}$ ($B^0 \to J/\psi(nS)K^0$) and $C_{J/\psi(nS)K^0}$ ($B^0 \to J/\psi(nS)K^0$) measurements.

$S_{J/\psi(nS)K^0}$ ($B^0 \to J/\psi(nS)K^0$)

"OUR EVALUATION" is an average using rescaled values of the data listed below. The average and rescaling were performed by the Heavy Flavor Averaging Group (HFLAV) and are described at http://www.slac.stanford.edu/xorg/hflav/. The averaging/rescaling procedure takes into account correlations between the measurements.

VALUE	DOCUMENT ID		TECN	COMMENT
0.701±0.017 OUR EVALUATION				
0.698±0.024 OUR AVERAGE	Error includes scale factor of 1.4. See the ideogram below.			
0.760±0.034	[1,2] AAIJ	17BN	LHCB	pp at 7, 8 TeV
0.670±0.029±0.013	[3] ADACHI	12A	BELL	$e^+e^- \to \Upsilon(4S)$
0.738±0.079±0.036	[4] ADACHI	12A	BELL	$e^+e^- \to \Upsilon(4S)$
0.642±0.047±0.021	[5] ADACHI	12A	BELL	$e^+e^- \to \Upsilon(4S)$
0.57 ±0.58 ±0.06	[6] SATO	12	BELL	$e^+e^- \to \Upsilon(5S)$
0.897±0.100±0.036	[4] AUBERT	09K	BABR	$e^+e^- \to \Upsilon(4S)$
0.666±0.031±0.013	AUBERT	09K	BABR	$e^+e^- \to \Upsilon(4S)$
0.79 $^{+0.41}_{-0.44}$	[7] AFFOLDER	00C	CDF	$p\overline{p}$ at 1.8 TeV
0.84 $^{+0.82}_{-1.04}$ ±0.16	[8] BARATE	00Q	ALEP	$e^+e^- \to Z$
3.2 $^{+1.8}_{-2.0}$ ±0.5	[9] ACKERSTAFF	98Z	OPAL	$e^+e^- \to Z$
• • • We do not use the following data for averages, fits, limits, etc. • • •				
0.75 ±0.04	[10] AAIJ	17BN	LHCB	pp at 7, 8 TeV
0.84 ±0.10 ±0.01	[11] AAIJ	17BN	LHCB	pp at 7, 8 TeV
0.731±0.035±0.020	[12] AAIJ	15N	LHCB	Repl. by AAIJ 17BN
0.73 ±0.07 ±0.04	[13] AAIJ	13K	LHCB	Repl. by AAIJ 15N
0.650±0.029±0.018	[14] SAHOO	08	BELL	Repl. by ADACHI 12A
0.72 ±0.09 ±0.03	[4] SAHOO	08	BELL	Repl. by ADACHI 12A
0.642±0.031±0.017	CHEN	07	BELL	Repl. by ADACHI 12A

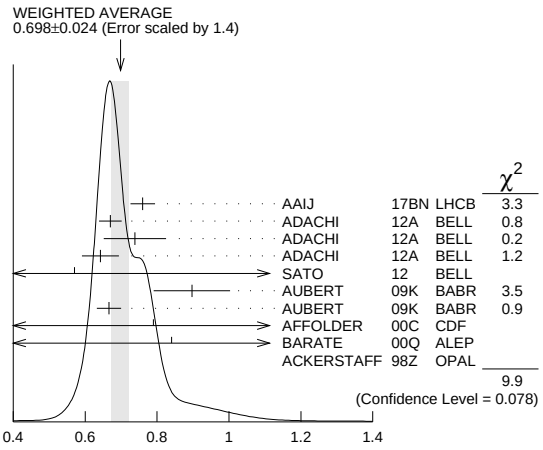

$S_{J/\psi(nS)K^0}$ ($B^0 \to J/\psi(nS)K^0$)

[1] Measurement based on $B^0 \to J/\psi K^0_S$, $B^0 \to \psi(2S)K^0_S$ with $J/\psi \to \mu^+\mu^-$, $J/\psi \to e^+e^-$ and $\psi(2S) \to \mu^+\mu^-$.

[2] AAIJ 17BN provides the correlation coefficient $\rho = 0.42$ between the uncertainties of $S_{J/\psi(nS)K^0}$ ($B^0 \to J/\psi(nS)K^0$) and $C_{J/\psi(nS)K^0}$ ($B^0 \to J/\psi(nS)K^0$) measurements.

[3] Uses $B^0 \to J/\psi K^0_S$ decays.

[4] Based on $B^0 \to \psi(2S)K^0_S$ decays.

[5] Uses $B^0 \to J/\psi K^0_L$ decays.

[6] SATO 12 uses 121 fb^{-1} data collected at $\Upsilon(5S)$ resonance. Uses the "$B-\pi$ tagging" where $B\pi^+$ and $B\pi^-$ tagged $J/\psi K^0_S$ events are compared.

[7] AFFOLDER 00C uses about 400 $B^0 \to J/\psi(1S)K^0_S$ events. The production flavor of B^0 was determined using three tagging algorithms: a same-side tag, a jet-charge tag, and a soft-lepton tag.

[8] BARATE 00Q uses 23 candidates for $B^0 \to J/\psi(1S)K^0_S$ decays. A combination of jet-charge, vertex-charge, and same-side tagging techniques were used to determine the B^0 production flavor.

[9] ACKERSTAFF 98Z uses 24 candidates for $B^0_d \to J/\psi(1S)K^0_S$ decay. A combination of jet-charge and vertex-charge techniques were used to tag the B^0_d production flavor.

[10] Measurement based on $B^0 \to J/\psi K^0_S$ with $J/\psi \to \mu^+\mu^-$ and $J/\psi \to e^+e^-$.

[11] Measurement based on $B^0 \to \psi(2S)K^0_S$ with $\psi(2S) \to \mu^+\mu^-$.

[12] AAIJ 15N uses 41,560 flavor-tagged $B_d \to J/\psi K^0_S$ events from 3 fb^{-1} of integrated luminosity. Provides the correlation coefficient $\rho = 0.483$ between the statistical uncertainties of and measurements.

[13] AAIJ 13K uses 8200 flavor-tagged $B_d \to J/\psi K^0_S$ events from 1 fb^{-1} of integrated luminosity. Provides the correlation coefficient $\rho = 0.42$ between the statistical uncertainties of $S_{J/\psi(nS)K^0}$ ($B^0 \to J/\psi(nS)K^0$) and $C_{J/\psi(nS)K^0}$ ($B^0 \to J/\psi(nS)K^0$) measurements.

[14] Combined result of CHEN 07 and SAHOO 08.

$C_{J/\psi K^{*0}}$ ($B^0 \to J/\psi K^{*0}$)

VALUE	DOCUMENT ID		TECN	COMMENT
0.025±0.083±0.054	[1] AUBERT	09K	BABR	$e^+e^- \to \Upsilon(4S)$

[1] Based on $B^0 \to J/\psi K^{*0}$, $K^{*0} \to K^0_S\pi^0$.

$S_{J/\psi K^{*0}}$ ($B^0 \to J/\psi K^{*0}$)

VALUE	DOCUMENT ID		TECN	COMMENT
0.601±0.239±0.087	[1,2] AUBERT	09K	BABR	$e^+e^- \to \Upsilon(4S)$

[1] Based on $B^0 \to J/\psi K^{*0}$, $K^{*0} \to K^0_S\pi^0$.

[2] This $S_{J/\psi K^{*0}}$ value has been corrected for the dilution of the sin(ΔM Δt) coefficient of the CP asymmetry by a factor of $1-R_\perp$, which arises from the mixture of CP-even and CP-odd B decay amplitudes.

$C_{\chi_{c0}K^0_S}$ ($B^0 \to \chi_{c0}K^0_S$)

VALUE	DOCUMENT ID		TECN	COMMENT
−0.29 $^{+0.53}_{-0.44}$ ±0.06	[1] AUBERT	09AU	BABR	$e^+e^- \to \Upsilon(4S)$

[1] Uses Dalitz plot analysis of $B^0 \to K^0\pi^+\pi^-$ decays and the first of two equivalent solutions is used.

$S_{\chi_{c0}K^0_S}$ ($B^0 \to \chi_{c0}K^0_S$)

VALUE	DOCUMENT ID		TECN	COMMENT
−0.69±0.52±0.08	[1] AUBERT	09AU	BABR	$e^+e^- \to \Upsilon(4S)$

[1] Uses Dalitz plot analysis of $B^0 \to K^0\pi^+\pi^-$ decays and the first of two equivalent solutions is used.

$C_{\chi_{c1}K^0_S}$ ($B^0 \to \chi_{c1}K^0_S$)

VALUE	DOCUMENT ID		TECN	COMMENT
0.06 ±0.07 OUR AVERAGE				
0.017±0.083 $^{+0.026}_{-0.046}$	ADACHI	12A	BELL	$e^+e^- \to \Upsilon(4S)$
0.129±0.109±0.025	AUBERT	09K	BABR	$e^+e^- \to \Upsilon(4S)$

$S_{\chi_{c1}K^0_S}$ ($B^0 \to \chi_{c1}K^0_S$)

VALUE	DOCUMENT ID		TECN	COMMENT
0.63 ±0.10 OUR AVERAGE				
0.640±0.117±0.040	ADACHI	12A	BELL	$e^+e^- \to \Upsilon(4S)$
0.614±0.160±0.040	AUBERT	09K	BABR	$e^+e^- \to \Upsilon(4S)$

$\sin(2\beta_{\rm eff})$ ($B^0 \to \phi K^0$)

VALUE	DOCUMENT ID		TECN	COMMENT
0.22±0.27±0.12	AUBERT	07AX	BABR	$e^+e^- \to \Upsilon(4S)$
• • • We do not use the following data for averages, fits, limits, etc. • • •				
0.50±0.25 $^{+0.07}_{-0.04}$	[1] AUBERT	05T	BABR	Repl. by AUBERT 07AX

[1] Obtained by constraining $C = 0$.

$\sin(2\beta_{\rm eff})$ ($B^0 \to \phi K^*_0(1430)^0$)

VALUE	DOCUMENT ID		TECN	COMMENT
0.97 $^{+0.03}_{-0.52}$	[1] AUBERT	08BG	BABR	$e^+e^- \to \Upsilon(4S)$

[1] Measured using the CP-violation phase difference $\Delta\phi_{00}$ between the B and $\overline{B}$ decay amplitude.

$\sin(2\beta_{\rm eff})$ ($B^0 \to K^+K^-K^0_S$)

VALUE	DOCUMENT ID		TECN	COMMENT
0.77±0.11 $^{+0.07}_{-0.04}$	AUBERT	07AX	BABR	$e^+e^- \to \Upsilon(4S)$
• • • We do not use the following data for averages, fits, limits, etc. • • •				
0.55±0.22±0.12	[1] AUBERT	05T	BABR	Repl. by AUBERT 07AX

[1] Obtained by constraining $C = 0$.

$\sin(2\beta_{\rm eff})$ ($B^0 \to [K^0_S\pi^+\pi^-]_{D^{(*)}}h^0$)

VALUE	DOCUMENT ID		TECN	COMMENT
0.37±0.22 OUR AVERAGE				
0.43±0.27±0.08	[1] VOROBYEV	16	BELL	$e^+e^- \to \Upsilon(4S)$
0.29±0.34±0.06	AUBERT	07BH	BABR	$e^+e^- \to \Upsilon(4S)$
• • • We do not use the following data for averages, fits, limits, etc. • • •				
0.78±0.44±0.22	KROKOVNY	06	BELL	Repl. by VOROBYEV 16

[1] A model-independent measurement uses the binned Dalitz plot technique.

$\beta_{\rm eff}$ ($B^0 \to [K^0_S\pi^+\pi^-]_{D^{(*)}}h^0$)

VALUE (°)	DOCUMENT ID		TECN	COMMENT
11.7±7.8±2.1	[1] VOROBYEV	16	BELL	$e^+e^- \to \Upsilon(4S)$

[1] A model-independent measurement uses the binned Dalitz plot technique.

$2\beta_{\rm eff}$ ($B^0 \to J/\psi\rho^0$)

VALUE (°)	DOCUMENT ID		TECN	COMMENT
41.7±9.6 $^{+2.8}_{-6.3}$	AAIJ	15J	LHCB	pp at 7, 8 TeV

$|\lambda|$ ($B^0 \to [K^0_S\pi^+\pi^-]_{D(*)}\, h^0$)

VALUE	DOCUMENT ID		TECN	COMMENT
1.01±0.08±0.02	AUBERT	07BH	BABR	$e^+e^- \to \Upsilon(4S)$

$|\sin(2\beta+\gamma)|$

β (ϕ_1) and γ (ϕ_3) are angles of CKM unitarity triangle, see the review on "*CP* Violation" in the Reviews section.

VALUE	CL%	DOCUMENT ID		TECN	COMMENT
>0.40	90	[1] AUBERT	06Y	BABR	$e^+e^- \to \Upsilon(4S)$
• • • We do not use the following data for averages, fits, limits, etc. • • •					
>0.13	95	[2] RONGA	06	BELL	$e^+e^- \to \Upsilon(4S)$
>0.07	95	[2] RONGA	06	BELL	$e^+e^- \to \Upsilon(4S)$
>0.35	90	[3] AUBERT	05Z	BABR	$e^+e^- \to \Upsilon(4S)$
>0.69	68	[4] AUBERT	04V	BABR	$e^+e^- \to \Upsilon(4S)$
>0.58	95	[5] AUBERT	04W	BABR	Repl. by AUBERT 05Z

[1] Uses fully reconstructed $B^0 \to D^{(*)\pm}\pi^\mp$ and $D^\pm\rho^\mp$ decays and some theoretical assumptions.
[2] Combines the results from fully reconstructed and partially reconstructed $D^{(*)}\pi$ events by taking weighted averages. Assumes that systematic errors from physics parameters and fit biases in the two measurements are 100% correlated.
[3] Uses partially reconstructed $B^0 \to D^{*\pm}\pi^\mp$ decays and some theoretical assumptions.
[4] Uses fully reconstructed $B^0 \to D^{(*)\pm}\pi^\mp$ decays and some theoretical assumptions, such as the SU(3) symmetry relation.
[5] Combining this measurement with the results from AUBERT 04V for fully reconstructed $B^0 \to D^{(*)\pm}\pi^\mp$ and some theoretical assumptions, such as the SU(3) symmetry relation.

$2\beta+\gamma$

VALUE (°)	DOCUMENT ID		TECN	COMMENT
83±53±20	[1] AUBERT	08AC	BABR	$e^+e^- \to \Upsilon(4S)$

[1] Used a time-dependent Dalitz-plot analysis of $B^0 \to D^\mp K^0\pi^\pm$ assuming the ratio of the $b \to u$ and $b \to c$ decay amplitudes to be 0.3.

α

For angle $\alpha(\phi_2)$ of the CKM unitarity triangle, see the review on "*CP* violation" in the reviews section.

VALUE (°)	DOCUMENT ID		TECN	COMMENT
93 ± 5 OUR AVERAGE				
93.7±10.6	[1] VANHOEFER	16	BELL	$e^+e^- \to \Upsilon(4S)$
$92.4^{+\ 6.0}_{-\ 6.5}$	[1] AUBERT	09G	BABR	$e^+e^- \to \Upsilon(4S)$
• • • We do not use the following data for averages, fits, limits, etc. • • •				
84.9±13.5	[1] VANHOEFER	14	BELL	Repl. by VANHOEFER 16
79 ± 7 ±11	[2] AUBERT	10D	BABR	$e^+e^- \to \Upsilon(4S)$
78.6± 7.3	[3] AUBERT	07O	BABR	$e^+e^- \to \Upsilon(4S)$
88 ±17	[4] SOMOV	06	BELL	Repl. by VANHOEFER 14
100 ±13	[5] AUBERT,B	05C	BABR	Repl. by AUBERT 09G
$102\ ^{+16}_{-12}$ ±14	[6] AUBERT,B	04R	BABR	Repl. by AUBERT,B 05C

[1] Based on an isospin analysis of the $B \to \rho\rho$ system.
[2] Obtained using the time dependent analysis of $B^0 \to a_1(1260)^\pm\pi^\mp$ and branching fraction measurements of $B \to a_1(1260)K$ and $B \to K_1\pi$. Uses SU(3) flavor relations.
[3] The angle $\alpha_{\rm eff}$ is obtained using the measured *CP* parameters of $B^0 \to a_1(1260)^\pm\pi^\mp$ and choosing one of the four solutions that is compatible with the result of SM-based fits.
[4] Obtained using isospin relation and selecting a solution closest to the CKM best fit average; the 90% CL allowed interval is $59^\circ < \phi_2\ (\equiv\alpha) < 115^\circ$.
[5] Obtained using isospin relation and selecting a solution closest to the CKM best fit average; 90% CL allowed interval is $79^\circ < \alpha < 123^\circ$.
[6] Obtained from the measured *CP* parameters of the longitudinal polarization by selecting the solution closest to the CKM best fit central value of $\alpha = 95^\circ - 98^\circ$.

CP VIOLATION PARAMETERS IN $B^0 \to D^0K^{*0}$ DECAY

The parameters r_{B^0} and δ_{B^0} are the magnitude ratio and strong phase difference between the amplitudes of $A(B^0 \to D^0K^{*0})$ and $A(B^0 \to \overline{D}{}^0K^{*0})$. The measured observables and are defined as $x_\pm = r_{B^0}\cos(\delta_{B^0} \pm \gamma)$ and $y_\pm = r_{B^0}\sin(\delta_{B^0} \pm \gamma)$ where γ is the CKM angle γ.

"OUR EVALUATION" is provided by the Heavy Flavor Averaging Group (HFLAV). The CKM angle γ is listed in the B^+ section for "*CP* VIOLATION PARAMETERS IN $B^+ \to DK^+$ AND SIMILAR DECAYS."

$x_+(B^0 \to DK^{*0})$

VALUE	DOCUMENT ID		TECN	COMMENT
0.04±0.17 OUR AVERAGE				
0.04±0.16±0.11	[1] AAIJ	16S	LHCB	pp at 7, 8 TeV
0.05±0.35±0.02	AAIJ	16Z	LHCB	pp at 7, 8 TeV
• • • We do not use the following data for averages, fits, limits, etc. • • •				
0.05±0.24±0.04	[2] AAIJ	16AA	LHCB	Repl. by AAIJ 16Z

[1] Uses Dalitz plof of $B^0 \to DK^+\pi^-$ with $D \to K^+K^-$, $\pi^+\pi^-$, or $K^+\pi^-$.
[2] Uses Dalitz plot analysis of $D \to K^0_S\pi^+\pi^-$ decays coming from $B^0 \to DK^*(892)^0$ modes.

$x_-(B^0 \to DK^{*0})$

VALUE	DOCUMENT ID		TECN	COMMENT
−0.16±0.14 OUR AVERAGE				
−0.02±0.13±0.14	[1] AAIJ	16S	LHCB	pp at 7, 8 TeV
−0.31±0.20±0.04	AAIJ	16Z	LHCB	pp at 7, 8 TeV
• • • We do not use the following data for averages, fits, limits, etc. • • •				
−0.15±0.14±0.03	[2] AAIJ	16AA	LHCB	Repl. by AAIJ 16Z

[1] Uses Dalitz plot of $B^0 \to DK^+\pi^-$ with $D \to K^+K^-$, $\pi^+\pi^-$, or $K^+\pi^-$.
[2] Uses Dalitz plot analysis of $D \to K^0_S\pi^+\pi^-$ decays coming from $B^0 \to DK^*(892)^0$ modes.

$y_+(B^0 \to DK^{*0})$

VALUE	DOCUMENT ID		TECN	COMMENT
−0.68±0.22 OUR AVERAGE				
−0.47±0.28±0.22	[1] AAIJ	16S	LHCB	pp at 7, 8 TeV
−0.81±0.28±0.06	AAIJ	16Z	LHCB	pp at 7, 8 TeV
• • • We do not use the following data for averages, fits, limits, etc. • • •				
$-0.65^{+0.24}_{-0.23}$±0.08	[2] AAIJ	16AA	LHCB	Repl. by AAIJ 16Z

[1] Uses Dalitz plof of $B^0 \to DK^+\pi^-$ with $D \to K^+K^-$, $\pi^+\pi^-$, or $K^+\pi^-$.
[2] Uses Dalitz plot analysis of $D \to K^0_S\pi^+\pi^-$ decays coming from $B^0 \to DK^*(892)^0$ modes.

$y_-(B^0 \to DK^{*0})$

VALUE	DOCUMENT ID		TECN	COMMENT
0.20±0.25 OUR AVERAGE Error includes scale factor of 1.2.				
−0.35±0.26±0.41	[1] AAIJ	16S	LHCB	pp at 7, 8 TeV
0.31±0.21±0.05	AAIJ	16Z	LHCB	pp at 7, 8 TeV
• • • We do not use the following data for averages, fits, limits, etc. • • •				
0.25±0.15±0.06	[2] AAIJ	16AA	LHCB	Repl. by AAIJ 16Z

[1] Uses Dalitz plof of $B^0 \to DK^+\pi^-$ with $D \to K^+K^-$, $\pi^+\pi^-$, or $K^+\pi^-$.
[2] Uses Dalitz plot analysis of $D \to K^0_S\pi^+\pi^-$ decays coming from $B^0 \to DK^*(892)^0$ modes.

$r_{B^0}(B^0 \to DK^{*0})$

VALUE	DOCUMENT ID		TECN	COMMENT
$0.223^{+0.041}_{-0.045}$ OUR EVALUATION				
0.56 ±0.17	[1] AAIJ	16Z	LHCB	pp at 7, 8 TeV
• • • We do not use the following data for averages, fits, limits, etc. • • •				
0.39 ±0.13	[2] AAIJ	16AA	LHCB	Repl. by AAIJ 16Z

[1] Measurement is performed with $K^+\pi^-$ masses within 50 MeV of the K^{*0} mass and an absolute value of the cosine of the K^{*0} helicity angle greater than 0.4. Angle γ is required to satisfy $0 < \gamma < 180$ degrees.
[2] Uses Dalitz plot analysis of $D \to K^0_S\pi^+\pi^-$ decays coming from $B^0 \to DK^*(892)^0$ modes.

$\delta_{B^0}(B^0 \to DK^{*0})$

VALUE (°)	DOCUMENT ID		TECN	COMMENT
193^{+27}_{-21} OUR EVALUATION				
204^{+21}_{-20}	[1] AAIJ	16Z	LHCB	pp at 7, 8 TeV
• • • We do not use the following data for averages, fits, limits, etc. • • •				
197^{+24}_{-20}	[2] AAIJ	16AA	LHCB	Repl. by AAIJ 16Z

[1] Measurement is performed with $K^+\pi^-$ masses within 50 MeV of the K^{*0} mass and an absolute value of the cosine of the K^{*0} helicity angle greater than 0.4. Angle γ is required to satisfy $0 < \gamma < 180$ degrees.
[2] Uses Dalitz plot analysis of $D \to K^0_S\pi^+\pi^-$ decays coming from $B^0 \to DK^*(892)^0$ modes.

T and *CPT* VIOLATION PARAMETERS

Measured values of the *T*-, *CP*-, and *CPT*-asymmetry parameters, defined as the differences in $S^\pm_{\alpha,\beta}$ and $C^\pm_{\alpha,\beta}$ between symmetry-transformed transitions. The indices $\alpha = \ell^+$, ℓ^- and $\beta = K^0_S$, K^0_L stand for reconstructed the flavor final state and the *CP* final states from $\Upsilon(4S)$ decay. The sign $\pm$ indicates whether the decay to the flavor final state α occurs before or after the decay to the *CP* final state.

Alternatively, violations of *CPT* symmetry and Lorentz invariance are searched for by studying interference effects in B^0 mixing. Results are expressed in terms of the standard model extension parameter Δa, which describes the difference between the couplings of the valence quarks within B^0 meson with the Lorentz-violating fields.

ΔS^+_T ($S^-_{\ell^-,K^0_S} - S^+_{\ell^+,K^0_S}$)

VALUE	DOCUMENT ID		TECN	COMMENT
−1.37±0.14±0.06	LEES	12W	BABR	$e^+e^- \to \Upsilon(4S)$

ΔS^-_T ($S^+_{\ell^-,K^0_S} - S^-_{\ell^+,K^0_S}$)

VALUE	DOCUMENT ID		TECN	COMMENT
1.17±0.18±0.11	LEES	12W	BABR	$e^+e^- \to \Upsilon(4S)$

ΔC_T^+ ($C_{\ell^-,K_S^0}^- - C_{\ell^+,K_S^0}^+$)

VALUE	DOCUMENT ID		TECN	COMMENT
0.10±0.14±0.08	LEES	12W	BABR	$e^+e^- \to \Upsilon(4S)$

ΔC_T^- ($C_{\ell^-,K_S^0}^+ - C_{\ell^+,K_S^0}^-$)

VALUE	DOCUMENT ID		TECN	COMMENT
0.04±0.14±0.08	LEES	12W	BABR	$e^+e^- \to \Upsilon(4S)$

ΔS_{CP}^+ ($S_{\ell^-,K_S^0}^+ - S_{\ell^+,K_S^0}^+$)

VALUE	DOCUMENT ID		TECN	COMMENT
−1.30±0.11±0.07	LEES	12W	BABR	$e^+e^- \to \Upsilon(4S)$

ΔS_{CP}^- ($S_{\ell^-,K_S^0}^- - S_{\ell^+,K_S^0}^-$)

VALUE	DOCUMENT ID		TECN	COMMENT
1.33±0.12±0.06	LEES	12W	BABR	$e^+e^- \to \Upsilon(4S)$

ΔC_{CP}^+ ($C_{\ell^-,K_S^0}^+ - C_{\ell^+,K_S^0}^+$)

VALUE	DOCUMENT ID		TECN	COMMENT
0.07±0.09±0.03	LEES	12W	BABR	$e^+e^- \to \Upsilon(4S)$

ΔC_{CP}^- ($C_{\ell^-,K_S^0}^- - C_{\ell^+,K_S^0}^-$)

VALUE	DOCUMENT ID		TECN	COMMENT
0.08±0.10±0.04	LEES	12W	BABR	$e^+e^- \to \Upsilon(4S)$

ΔS_{CPT}^+ ($S_{\ell^+,K_S^0}^- - S_{\ell^+,K_S^0}^+$)

VALUE	DOCUMENT ID		TECN	COMMENT
0.16±0.21±0.09	LEES	12W	BABR	$e^+e^- \to \Upsilon(4S)$

ΔS_{CPT}^- ($S_{\ell^+,K_S^0}^+ - S_{\ell^+,K_S^0}^-$)

VALUE	DOCUMENT ID		TECN	COMMENT
−0.03±0.13±0.06	LEES	12W	BABR	$e^+e^- \to \Upsilon(4S)$

ΔC_{CPT}^+ ($C_{\ell^+,K_S^0}^- - C_{\ell^+,K_S^0}^+$)

VALUE	DOCUMENT ID		TECN	COMMENT
0.14±0.15±0.07	LEES	12W	BABR	$e^+e^- \to \Upsilon(4S)$

ΔC_{CPT}^- ($C_{\ell^+,K_S^0}^+ - C_{\ell^+,K_S^0}^-$)

VALUE	DOCUMENT ID		TECN	COMMENT
0.03±0.12±0.08	LEES	12W	BABR	$e^+e^- \to \Upsilon(4S)$

$\Delta a_\parallel$ CPT parameter in B^0 mixing

VALUE (10^{-15} GeV)	DOCUMENT ID		TECN	COMMENT
−0.10±0.82±0.54	[1] AAIJ	16E	LHCB	pp at 7, 8 TeV

[1] Uses $B^0 \to J/\psi K_S^0$ decays.

$\Delta a_\perp$ CPT parameter in B^0 mixing

VALUE (10^{-13} GeV)	DOCUMENT ID		TECN	COMMENT
−0.20±0.22±0.04	[1] AAIJ	16E	LHCB	pp at 7, 8 TeV

[1] Uses $B^0 \to J/\psi K_S^0$ decays.

Δa_X CPT parameter in B^0 mixing

VALUE (10^{-15} GeV)	DOCUMENT ID		TECN	COMMENT
+1.97±1.30±0.29	[1] AAIJ	16E	LHCB	pp at 7, 8 TeV

[1] Uses $B^0 \to J/\psi K_S^0$ decays.

Δa_Y CPT parameter in B^0 mixing

VALUE (10^{-15} GeV)	DOCUMENT ID		TECN	COMMENT
+0.44±1.26±0.29	[1] AAIJ	16E	LHCB	pp at 7, 8 TeV

[1] Uses $B^0 \to J/\psi K_S^0$ decays.

$B^0 \to D^{*-}\ell^+\nu_\ell$ FORM FACTORS

R_1 (form factor ratio $\sim V/A_1$)

VALUE	DOCUMENT ID		TECN	COMMENT
1.41 ±0.04 OUR AVERAGE				
1.401±0.034±0.018	[1] DUNGEL	10	BELL	$e^+e^- \to \Upsilon(4S)$
1.56 ±0.07 ±0.15	AUBERT	09A	BABR	$e^+e^- \to \Upsilon(4S)$
1.18 ±0.30 ±0.12	DUBOSCQ	96	CLE2	$e^+e^- \to \Upsilon(4S)$
• • • We do not use the following data for averages, fits, limits, etc. • • •				
1.429±0.061±0.044	AUBERT	08R	BABR	Repl. by AUBERT 09A
1.396±0.060±0.044	AUBERT,B	06Z	BABR	Repl. by AUBERT 08R

[1] Uses fully reconstructed $D^{*-}\ell^+\nu$ events ($\ell = e$ or μ).

R_2 (form factor ratio $\sim A_2/A_1$)

VALUE	DOCUMENT ID		TECN	COMMENT
0.85 ±0.05 OUR AVERAGE	Error includes scale factor of 1.9.			
0.864±0.024±0.008	[1] DUNGEL	10	BELL	$e^+e^- \to \Upsilon(4S)$
0.66 ±0.05 ±0.09	AUBERT	09A	BABR	$e^+e^- \to \Upsilon(4S)$
0.71 ±0.22 ±0.07	DUBOSCQ	96	CLE2	$e^+e^- \to \Upsilon(4S)$
• • • We do not use the following data for averages, fits, limits, etc. • • •				
0.827±0.038±0.022	AUBERT	08R	BABR	Repl. by AUBERT 09A
0.885±0.040±0.026	AUBERT,B	06Z	BABR	Repl. by AUBERT 08R

[1] Uses fully reconstructed $D^{*-}\ell^+\nu$ events ($\ell = e$ or μ).

$\rho^2_{A_1}$ (form factor slope)

VALUE	DOCUMENT ID		TECN	COMMENT
1.204±0.031 OUR AVERAGE				
1.214±0.034±0.009	[1] DUNGEL	10	BELL	$e^+e^- \to \Upsilon(4S)$
1.22 ±0.02 ±0.07	AUBERT	09A	BABR	$e^+e^- \to \Upsilon(4S)$
0.91 ±0.15 ±0.06	DUBOSCQ	96	CLE2	$e^+e^- \to \Upsilon(4S)$
• • • We do not use the following data for averages, fits, limits, etc. • • •				
1.191±0.048±0.028	AUBERT	08R	BABR	Repl. by AUBERT 09A
1.145±0.059±0.046	AUBERT,B	06Z	BABR	Repl. by AUBERT 08R

[1] Uses fully reconstructed $D^{*-}\ell^+\nu$ events ($\ell = e$ or μ).

PARTIAL BRANCHING FRACTIONS IN $B^0 \to K^{(*)0}\ell^+\ell^-$

B($B^0 \to K^{*0}e^+e^-$) ($0.0009 < q^2 < 1.0$ GeV$^2/c^4$)

VALUE (units 10^{-7})	DOCUMENT ID		TECN	COMMENT
$3.1^{+0.9}_{-0.8}{}^{+0.2}_{-0.3}\pm0.2$	[1] AAIJ	13U	LHCB	pp at 7 TeV

[1] The last uncertainty is due to uncertainties of B($B^0 \to J/\psi K^{*0}$) and B($J/\psi \to e^+e^-$) branching fraction measurements.

B($B^0 \to K^{*0}\ell^+\ell^-$) ($0.1 < q^2 < 2.0$ GeV$^2/c^4$)

VALUE (units 10^{-7})	DOCUMENT ID		TECN	COMMENT
$1.24^{+0.23}_{-0.27}$ **OUR AVERAGE**	Error includes scale factor of 1.6.			
$1.14\pm0.11^{+0.11}_{-0.15}$	AAIJ	13Y	LHCB	pp at 7 TeV, $K^{*0}\mu^+\mu^-$
1.80±0.36±0.11	AALTONEN	11AI	CDF	$p\overline{p}$ at 1.96 TeV
• • • We do not use the following data for averages, fits, limits, etc. • • •				
$0.48^{+0.14}_{-0.12}\pm0.04$	[1] CHATRCHYAN	13BL	CMS	pp at 7 TeV
1.16±0.23±0.11	AAIJ	12U	LHCB	Repl. by AAIJ 13Y

[1] CHATRCHYAN 13BL uses, for this bin, $1.0 < q^2 < 2.0$ GeV$^2/c^4$.

B($B^0 \to K^{*0}\ell^+\ell^-$) ($2.0 < q^2 < 4.3$ GeV$^2/c^4$)

VALUE (units 10^{-7})	DOCUMENT ID		TECN	COMMENT
0.76 ±0.07 OUR AVERAGE				
0.759±0.115±0.046	KHACHATRY...16D		CMS	pp at 8 TeV
0.69 ±0.07 ±0.09	AAIJ	13Y	LHCB	pp at 7 TeV, $K^{*0}\mu^+\mu^-$
0.87 ±0.16 ±0.07	CHATRCHYAN	13BL	CMS	pp at 7 TeV
0.84 ±0.28 ±0.06	AALTONEN	11AI	CDF	$p\overline{p}$ at 1.96 TeV
• • • We do not use the following data for averages, fits, limits, etc. • • •				
0.78 ±0.21 ±0.05	AAIJ	12U	LHCB	Repl. by AAIJ 13Y

B($B^0 \to K^{*0}\ell^+\ell^-$) ($4.3 < q^2 < 8.68$ GeV$^2/c^4$)

VALUE (units 10^{-7})	DOCUMENT ID		TECN	COMMENT
1.87±0.21 OUR AVERAGE				
$2.15\pm0.18^{+0.22}_{-0.28}$	AAIJ	13Y	LHCB	pp at 7 TeV, $K^{*0}\mu^+\mu^-$
1.62±0.31±0.18	CHATRCHYAN	13BL	CMS	pp at 7 TeV
1.73±0.43±0.15	AALTONEN	11AI	CDF	$p\overline{p}$ at 1.96 TeV
• • • We do not use the following data for averages, fits, limits, etc. • • •				
3.02±0.35±0.22	AAIJ	12U	LHCB	Repl. by AAIJ 13Y

B($B^0 \to K^{*0}\ell^+\ell^-$) ($10.09 < q^2 < 12.86$ GeV$^2/c^4$)

VALUE (units 10^{-7})	DOCUMENT ID		TECN	COMMENT
1.49±0.15 OUR AVERAGE	Error includes scale factor of 1.3. See the ideogram below.			
1.72±0.11±0.14	KHACHATRY...16D		CMS	pp at 8 TeV
$1.19\pm0.11^{+0.14}_{-0.17}$	AAIJ	13Y	LHCB	pp at 7 TeV, $K^{*0}\mu^+\mu^-$
1.50±0.25±0.25	CHATRCHYAN	13BL	CMS	pp at 7 TeV
1.77±0.36±0.12	AALTONEN	11AI	CDF	$p\overline{p}$ at 1.96 TeV
• • • We do not use the following data for averages, fits, limits, etc. • • •				
1.52±0.25±0.19	AAIJ	12U	LHCB	Repl. by AAIJ 13Y

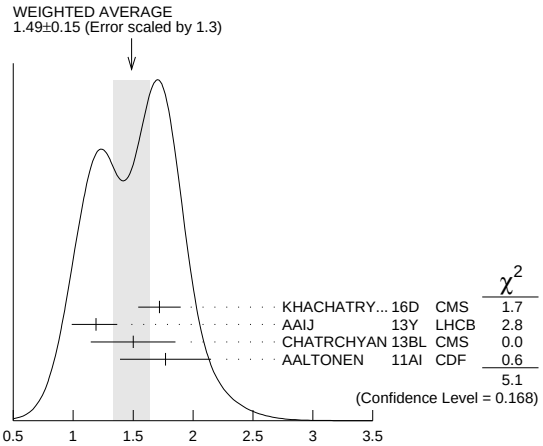

B($B^0 \to K^{*0}\ell^+\ell^-$) ($10.09 < q^2 < 12.86$ GeV$^2/c^4$) (units 10^{-7})

B($B^0 \to K^{*0}\ell^+\ell^-$) ($14.18 < q^2 < 16.0$ GeV$^2/c^4$)

VALUE (units 10^{-7})	DOCUMENT ID		TECN	COMMENT
1.09±0.10 OUR AVERAGE	Error includes scale factor of 1.1.			
1.22±0.11±0.09	KHACHATRY...16D		CMS	pp at 8 TeV
$1.02\pm0.11^{+0.11}_{-0.15}$	AAIJ	13Y	LHCB	pp at 7 TeV, $K^{*0}\mu^+\mu^-$
$0.84^{+0.16}_{-0.15}\pm0.09$	CHATRCHYAN	13BL	CMS	pp at 7 TeV
1.34±0.26±0.08	AALTONEN	11AI	CDF	$p\overline{p}$ at 1.96 TeV
• • • We do not use the following data for averages, fits, limits, etc. • • •				
1.15±0.20±0.09	AAIJ	12U	LHCB	Repl. by AAIJ 13Y

B($B^0 \to K^{*0}\ell^+\ell^-$) ($16.0 < q^2 < 19.0$ GeV$^2/c^4$)

VALUE (units 10^{-7})	DOCUMENT ID		TECN	COMMENT
1.27±0.09 OUR AVERAGE				
1.26±0.09±0.09	KHACHATRY...16D		CMS	pp at 8 TeV
$1.23\pm0.12^{+0.15}_{-0.18}$	AAIJ	13Y	LHCB	pp at 7 TeV, $K^{*0}\mu^+\mu^-$
1.56±0.18±0.15	CHATRCHYAN	13BL	CMS	pp at 7 TeV
0.97±0.26±0.07	AALTONEN	11AI	CDF	$p\overline{p}$ at 1.96 TeV
• • • We do not use the following data for averages, fits, limits, etc. • • •				
1.50±0.24±0.15	AAIJ	12U	LHCB	Repl. by AAIJ 13Y

B($B^0 \to K^*(892)^0\ell^+\ell^-$) ($15.0 < q^2 < 19.0$ GeV$^2/c^4$)

VALUE (units 10^{-7})	DOCUMENT ID		TECN	COMMENT
$\mathbf{1.744^{+0.072}_{-0.076}\pm0.123}$	AAIJ	17Q	LHCB	pp at 7, 8 TeV
• • • We do not use the following data for averages, fits, limits, etc. • • •				
$1.95\ ^{+0.08}_{-0.09}\pm0.13$	AAIJ	16AO	LHCB	Repl. by AAIJ 17Q

B($B^0 \to K^{*0}\ell^+\ell^-$) ($1.0 < q^2 < 6.0$ GeV$^2/c^4$)

VALUE (units 10^{-7})	DOCUMENT ID		TECN	COMMENT
1.73±0.11 OUR AVERAGE				
1.68±0.083±0.12	[1] AAIJ	17Q	LHCB	pp at 7, 8 TeV
1.90±0.20	KHACHATRY...16D		CMS	pp at 7, 8 TeV
1.42±0.41 ±0.12	AALTONEN	11AI	CDF	$p\overline{p}$ at 1.96 TeV
• • • We do not use the following data for averages, fits, limits, etc. • • •				
$1.92^{+0.10}_{-0.09}$ ±0.14	AAIJ	16AO	LHCB	Repl. by AAIJ 17Q
$1.70\pm0.15\ ^{+0.20}_{-0.25}$	AAIJ	13Y	LHCB	Repl. by AAIJ 16AO
2.20±0.30 ±0.20	CHATRCHYAN	13BL	CMS	Repl. by KHACHATRYAN 16D
2.10±0.30 ±0.15	AAIJ	12U	LHCB	Repl. by AAIJ 13Y

[1] AAIJ 17Q result is determined for the range $1.1 < q^2 < 6.0$ GeV$^4/c^2$.

B($B^0 \to K^{*0}\ell^+\ell^-$) ($0.0 < q^2 < 4.3$ GeV$^2/c^4$)

VALUE (units 10^{-7})	DOCUMENT ID		TECN	COMMENT
2.60±0.45±0.17	AALTONEN	11AI	CDF	$p\overline{p}$ at 1.96 TeV

B($B^0 \to K^{*0}\mu^+\mu^-$)/B($B^0 \to K^{*0}e^+e^-$) ($0.045 < q^2 < 1.1$ GeV$^2/c^4$)

VALUE	DOCUMENT ID		TECN	COMMENT
$\mathbf{0.66^{+0.11}_{-0.07}\pm0.03}$	AAIJ	17W	LHCB	pp at 7, 8 TeV

B($B^0 \to K^{*0}\mu^+\mu^-$)/B($B^0 \to K^{*0}e^+e^-$) ($1.1 < q^2 < 6.0$ GeV$^2/c^4$)

VALUE	DOCUMENT ID		TECN	COMMENT
$\mathbf{0.69^{+0.11}_{-0.07}\pm0.05}$	AAIJ	17W	LHCB	pp at 7, 8 TeV

B($B^0 \to K^0\ell^+\ell^-$) ($q^2 < 2.0$ GeV$^2/c^4$)

VALUE (units 10^{-7})	DOCUMENT ID		TECN	COMMENT
$\mathbf{0.24^{+0.22}_{-0.20}}$ **OUR AVERAGE**				
$0.21^{+0.27}_{-0.23}$	AAIJ	12AH	LHCB	pp at 7 TeV
0.31±0.37±0.02	AALTONEN	11AI	CDF	$p\overline{p}$ at 1.96 TeV

B($B^0 \to K^0\ell^+\ell^-$) ($2.0 < q^2 < 4.3$ GeV$^2/c^4$)

VALUE (units 10^{-7})	DOCUMENT ID		TECN	COMMENT
$\mathbf{0.24^{+0.35}_{-0.30}}$ **OUR AVERAGE**	Error includes scale factor of 1.6.			
$0.07^{+0.25}_{-0.21}$	AAIJ	12AH	LHCB	pp at 7 TeV
0.93±0.49±0.07	AALTONEN	11AI	CDF	$p\overline{p}$ at 1.96 TeV

B($B^0 \to K^0\ell^+\ell^-$) ($4.3 < q^2 < 8.68$ GeV$^2/c^4$)

VALUE (units 10^{-7})	DOCUMENT ID		TECN	COMMENT
1.08±0.27 OUR AVERAGE				
1.23±0.31	AAIJ	12AH	LHCB	pp at 7 TeV
0.66±0.51±0.05	AALTONEN	11AI	CDF	$p\overline{p}$ at 1.96 TeV

B($B^0 \to K^0\ell^+\ell^-$) ($10.09 < q^2 < 12.86$ GeV$^2/c^4$)

VALUE (units 10^{-7})	DOCUMENT ID		TECN	COMMENT
0.27±0.27 OUR AVERAGE	Error includes scale factor of 1.8.			
$0.50^{+0.22}_{-0.19}$	AAIJ	12AH	LHCB	pp at 7 TeV
−0.03±0.22±0.01	AALTONEN	11AI	CDF	$p\overline{p}$ at 1.96 TeV

B($B^0 \to K^0\ell^+\ell^-$) ($14.18 < q^2 < 16.0$ GeV$^2/c^4$)

VALUE (units 10^{-7})	DOCUMENT ID		TECN	COMMENT
$\mathbf{0.29^{+0.21}_{-0.15}}$ **OUR AVERAGE**	Error includes scale factor of 1.8.			
$0.20^{+0.13}_{-0.09}$	AAIJ	12AH	LHCB	pp at 7 TeV
0.73±0.26±0.06	AALTONEN	11AI	CDF	$p\overline{p}$ at 1.96 TeV

B($B^0 \to K^0\ell^+\ell^-$) ($q^2 > 16.0$ GeV$^2/c^4$)

VALUE (units 10^{-7})	DOCUMENT ID		TECN	COMMENT
$\mathbf{0.31^{+0.16}_{-0.12}}$ **OUR AVERAGE**				
$0.35^{+0.21}_{-0.14}$	AAIJ	12AH	LHCB	pp at 7 TeV
0.21±0.18±0.16	AALTONEN	11AI	CDF	$p\overline{p}$ at 1.96 TeV

B($B^0 \to K^0\ell^+\ell^-$) ($1.0 < q^2 < 6.0$ GeV$^2/c^4$)

VALUE (units 10^{-7})	DOCUMENT ID		TECN	COMMENT
0.92 ±0.16 OUR AVERAGE				
$0.916^{+0.172}_{-0.157}\pm0.004$	[1] AAIJ	14M	LHCB	pp at 7, 8 TeV
0.98 ±0.61 ±0.08	AALTONEN	11AI	CDF	$p\overline{p}$ at 1.96 TeV
• • • We do not use the following data for averages, fits, limits, etc. • • •				
$0.65\ ^{+0.45}_{-0.35}$	AAIJ	12AH	LHCB	Repl. by AAIJ 14M

[1] Uses B($B^0 \to J/\psi(1S)K^0$) = (0.928 ± 0.013 ± 0.037) × 10^{-3} for normalisation and $\mu^+\mu^-$ as a lepton pair. Measured in $1.1 < q^2 < 6.0$ GeV$^2/c^4$.

B($B^0 \to K^0\ell^+\ell^-$) ($0.0 < q^2 < 4.3$ GeV$^2/c^4$)

VALUE (units 10^{-7})	DOCUMENT ID		TECN	COMMENT
1.27±0.62±0.10	AALTONEN	11AI	CDF	$p\overline{p}$ at 1.96 TeV

B($B^0 \to K^0\ell^+\ell^-$) ($15.0 < q^2 < 22.0$ GeV$^2/c^4$)

VALUE (units 10^{-7})	DOCUMENT ID		TECN	COMMENT
$\mathbf{0.67^{+0.11}_{-0.11}\pm0.04}$	[1] AAIJ	14M	LHCB	pp at 7, 8 TeV

[1] Uses B($B^0 \to J/\psi(1S)K^0$) = (0.928 ± 0.013 ± 0.037) × 10^{-3} for normalisation and $\mu^+\mu^-$ as a lepton pair.

B($B^0 \to K^*_{0,2}(1430)^0\mu^+\mu^-$) ($1.10 < q^2 < 6.00$ GeV$^2/c^4$)

VALUE (units 10^{-8})	DOCUMENT ID		TECN	COMMENT
4.02±0.44±0.31	[1,2] AAIJ	16AP	LHCB	pp at 7, 8 TeV

[1] Measured the differential branching fraction and angular moments of the decay $B^0 \to K^+\pi^-\mu^+\mu^-$ in the $K^+\pi^-$ invariant mass range $1330 < m(K^+\pi^-) < 1530$ MeV/c^2.
[2] The reported value is converted from the measured $dB/dq^2 = (0.82 \pm 0.09 \pm 0.063) \times 10^{-8}$ (GeV$^2/c^4)^{-1}$ by multiplying by the $\Delta q^2 = 4.9$ GeV$^2/c^4$ range.

F_H($B^0 \to K^0\mu^+\mu^-$) ($1.1 < q^2 < 6.0$ GeV$^2/c^4$)

F_H is a fractional contribution of (pseudo) scalar and tensor amplitudes to the decay width in the massless muon approximation.

VALUE	DOCUMENT ID		TECN	COMMENT
0.78±0.46±0.09	[1] AAIJ	14O	LHCB	pp at 7, 8 TeV

[1] AAIJ 14O reports 68% C.L. interval, which we encode as midpoint with uncertainty as half of the width of interval.

Meson Particle Listings

B^0

$F_H(B^0 \to K^0\mu^+\mu^-)$ ($15.0 < q^2 < 22.0$ GeV$^2/c^4$)

VALUE	DOCUMENT ID		TECN	COMMENT
0.34±0.25±0.03	[1] AAIJ	14O	LHCB	pp at 7, 8 TeV

[1] AAIJ 14O reports 68% C.L. interval, which we encode as midpoint with uncertainty as half of the width of interval.

PRODUCTION ASYMMETRIES

$A_P(B^0)$

$A_P(B^0) = [\sigma(\overline{B}^0) - \sigma(B^0)] \,/\, [\sigma(\overline{B}^0) + \sigma(B^0)]$

VALUE (units 10^{-2})	DOCUMENT ID		TECN	COMMENT
−0.3 ±0.6 OUR AVERAGE	Error includes scale factor of 1.7. See the ideogram below.			
0.44±0.88±0.11	[1] AAIJ	17BF	LHCB	pp at 7 TeV
−1.40±0.55±0.10	[1] AAIJ	17BF	LHCB	pp at 8 TeV
0.25±0.48±0.05	[2] AABOUD	16G	ATLS	pp at 7, 8 TeV
• • • We do not use the following data for averages, fits, limits, etc. • • •				
−0.35±0.76±0.28	[3] AAIJ	14BP	LHCB	Repl. by AAIJ 17BF, pp at 7 TeV

[1] AAIJ 17BF uses $B^0 \to J/\psi K^{*0}$ decays with B^0 transverse momenta p_T and rapidities y in the region of $0 < p_T < 30$ GeV/c and $2.1 < y < 4.5$.

[2] Based on time-dependent analysis of $B^0 \to J/\psi K^{*0}$ decay in kinematic range $p_T > 10$ GeV/c and $|\eta| < 2.5$.

[3] Based on time-dependent analysis of $B^0 \to J/\psi K^{*0}$ and $B^0 \to D^-\pi^+$ in kinematic range $4 < p_T < 30$ GeV/c and $2.5 < \eta < 4.5$.

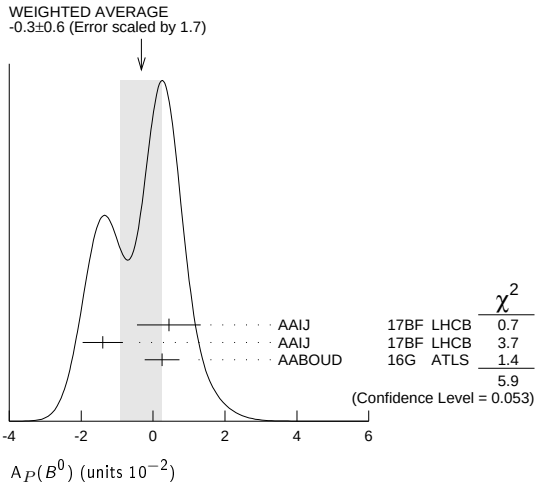

B^0 REFERENCES

AAIJ	17A	PR D95 012006	R. Aaij *et al.*	(LHCb Collab.)
AAIJ	17AI	PRL 118 191801	R. Aaij *et al.*	(LHCb Collab.)
AAIJ	17AJ	PRL 118 251802	R. Aaij *et al.*	(LHCb Collab.)
AAIJ	17BD	PR D96 051103	R. Aaij *et al.*	(LHCb Collab.)
AAIJ	17BF	PL B774 139	R. Aaij *et al.*	(LHCb Collab.)
AAIJ	17BJ	PRL 119 232001	R. Aaij *et al.*	(LHCb Collab.)
AAIJ	17BN	JHEP 1711 170	R. Aaij *et al.*	(LHCb Collab.)
AAIJ	17BP	JHEP 1711 027	R. Aaij *et al.*	(LHCb Collab.)
AAIJ	17G	PRL 118 081801	R. Aaij *et al.*	(LHCb Collab.)
AAIJ	17N	JHEP 1703 001	R. Aaij *et al.*	(LHCb Collab.)
AAIJ	17Q	JHEP 1704 142	R. Aaij *et al.*	(LHCb Collab.)
AAIJ	17W	JHEP 1708 055	R. Aaij *et al.*	(LHCb Collab.)
GRYGIER	17	PR D96 091101	J. Grygier *et al.*	(BELLE Collab.)
HORIGUCHI	17	PRL 119 191802	T. Horiguchi *et al.*	(BELLE Collab.)
JULIUS	17	PR D96 032007	T. Julius *et al.*	(BELLE Collab.)
AABOUD	16G	JHEP 1606 081	M. Aaboud *et al.*	(ATLAS Collab.)
AABOUD	16L	EPJ C76 513	M. Aaboud *et al.*	(ATLAS Collab.)
AAIJ	16	JHEP 1601 012	R. Aaij *et al.*	(LHCb Collab.)
AAIJ	16AA	JHEP 1608 137	R. Aaij *et al.*	(LHCb Collab.)
AAIJ	16AN	PRL 117 261801	R. Aaij *et al.*	(LHCb Collab.)
AAIJ	16AO	JHEP 1611 047	R. Aaij *et al.*	(LHCb Collab.)
AAIJ	16AP	JHEP 1612 065	R. Aaij *et al.*	(LHCb Collab.)
AAIJ	16AV	EPJ C76 412	R. Aaij *et al.*	(LHCb Collab.)
AAIJ	16E	PRL 116 241601	R. Aaij *et al.*	(LHCb Collab.)
AAIJ	16S	PR D93 112018	R. Aaij *et al.*	(LHCb Collab.)
AAIJ	16Z	JHEP 1606 131	R. Aaij *et al.*	(LHCb Collab.)
BHARDWAJ	16	PR D93 052016	V. Bhardwaj *et al.*	(BELLE Collab.)
CHOBANOVA	16	PR D93 031101	V. Chobanova *et al.*	(BELLE Collab.)
DEL-AMO-SA...	16	PR D93 052013	P. del Amo Sanchez *et al.*	(BABAR Collab.)
GLATTAUER	16	PR D93 032006	R. Glattauer *et al.*	(BELLE Collab.)
HAMER	16	PR D93 032007	P. Hamer *et al.*	(BELLE Collab.)
KHACHATRY...	16D	PL B753 424	V. Khachatryan *et al.*	(CMS Collab.)
KING	16	PR D93 111101	Z. King *et al.*	(BELLE Collab.)
LEES	16	PRL 116 041801	J.P. Lees *et al.*	(BABAR Collab.)
LEES	16E	PR D94 011101	J.P. Lees *et al.*	(BABAR Collab.)
LEES	16H	PR D94 091101	J.P. Lees *et al.*	(BABAR Collab.)
SATO	16B	PR D94 072007	Y. Sato *et al.*	(BELLE Collab.)
VANHOEFER	16	PR D93 032010	P. Vanhoefer *et al.*	(BELLE Collab.)
Also		PR D94 099903 (errat.)	P. Vanhoefer *et al.*	(BELLE Collab.)
VOROBYEV	16	PR D94 052004	V. Vorobyev *et al.*	(BELLE Collab.)
AAIJ	15AC	JHEP 1505 019	R. Aaij *et al.*	(LHCb Collab.)
AAIJ	15AS	JHEP 1510 053	R. Aaij *et al.*	(LHCb Collab.)
AAIJ	15AZ	PRL 115 161802	R. Aaij *et al.*	(LHCb Collab.)
AAIJ	15BB	PR D92 112002	R. Aaij *et al.*	(LHCb Collab.)
AAIJ	15D	JHEP 1501 024	R. Aaij *et al.*	(LHCb Collab.)
AAIJ	15F	PRL 114 041601	R. Aaij *et al.*	(LHCb Collab.)
AAIJ	15J	PL B742 38	R. Aaij *et al.*	(LHCb Collab.)
AAIJ	15N	PRL 115 031601	R. Aaji *et al.*	(LHCb Collab.)
AAIJ	15Q	PRL 115 111803	R. Aaij *et al.*	(LHCb Collab.)
AAIJ	15S	PL B743 46	R. Aaij *et al.*	(LHCb Collab.)
AAIJ	15T	PL B747 468	R. Aaij *et al.*	(LHCb Collab.)
AAIJ	15X	PR D92 012012	R. Aaij *et al.*	(LHCb Collab.)
AAIJ	15Y	PR D92 032002	R. Aaij *et al.*	(LHCb Collab.)
AAIJ	15Z	JHEP 1504 064	R. Aaij *et al.*	(LHCb Collab.)
ABAZOV	15A	PRL 114 062001	V.M. Abazov *et al.*	(D0 Collab.)
ABDESSALAM	15	PRL 115 121604	A. Abdessalam *et al.*	(BABAR and BELLE Collabs.)
BALA	15	PR D91 051101	A. Bala *et al.*	(BELLE Collab.)
CHANG	15	PRL 115 221803	Y.-Y. Chang *et al.*	(BELLE Collab.)
CHOI	15A	PR D91 092011	S.-K. Choi *et al.*	(BELLE Collab.)
KHACHATRY...	15BE	NAT 522 68	V. Khachatryan *et al.*	(CMS and LHCb Collab.)
LEES	15	PR D91 012003	J.P. Lees *et al.*	(BABAR Collab.)
LEES	15A	PRL 114 081801	J.P. Lees *et al.*	(BABAR Collab.)
LEES	15B	PR D91 031102	J.P. Lees *et al.*	(BABAR Collab.)
LEES	15C	PR D91 052002	J.P. Lees *et al.*	(BABAR Collab.)
MATVIENKO	15	PR D92 012013	D. Matvienko *et al.*	(BELLE Collab.)
PAL	15	PR D92 011101	B. Pal *et al.*	(BELLE Collab.)
WIECHCZYN...	15	PR D91 032008	J. Wiechczynski *et al.*	(BELLE Collab.)
AAIJ	14AA	PRL 112 202001	R. Aaij *et al.*	(LHCb Collab.)
AAIJ	14AM	JHEP 1405 069	R. Aaij *et al.*	(LHCb Collab.)
AAIJ	14AN	JHEP 1409 177	R. Aaij *et al.*	(LHCb Collab.)
AAIJ	14BM	NJP 16 123001	R. Aaij *et al.*	(LHCb Collab.)
AAIJ	14BN	PR D90 112002	R. Aaij *et al.*	(LHCb Collab.)
AAIJ	14BP	PL B739 218	R. Aaij *et al.*	(LHCb Collab.)
AAIJ	14E	JHEP 1404 114	R. Aaij *et al.*	(LHCb Collab.)
AAIJ	14L	JHEP 1407 140	R. Aaij *et al.*	(LHCb Collab.)
AAIJ	14M	JHEP 1406 133	R. Aaij *et al.*	(LHCb Collab.)
AAIJ	14O	JHEP 1405 082	R. Aaij *et al.*	(LHCb Collab.)
AAIJ	14R	PL B736 446	R. Aaij *et al.*	(LHCb Collab.)
AAIJ	14X	PR D90 012003	R. Aaij *et al.*	(LHCb Collab.)
AAIJ	14Y	PRL 112 091802	R. Aaij *et al.*	(LHCb Collab.)
AALTONEN	14P	PRL 113 242001	T. Aaltonen *et al.*	(CDF Collab.)
ABAZOV	14	PR D89 012002	V.M. Abazov *et al.*	(D0 Collab.)
CHILIKIN	14	PR D90 112009	K. Chilikin *et al.*	(BELLE Collab.)
CHOBANOVA	14	PR D90 012002	V. Chobanova *et al.*	(BELLE Collab.)
IWASHITA	14	PTEP 2014 043C01	T. Iwashita *et al.*	(BELLE Collab.)
LAI	14	PR D89 051103	Y.-T. Lai *et al.*	(BELLE Collab.)
LEES	14	PR D89 051101	J.P. Lees *et al.*	(BABAR Collab.)
LEES	14B	PR D89 112002	J.P. Lees *et al.*	(BABAR Collab.)
LEES	14C	PR D89 071102	J.P. Lees *et al.*	(BABAR Collab.)
PDG	14	CP C38 070001	K. Olive *et al.*	(PDG Collab.)
SANTELJ	14	JHEP 1410 165	L. Santelj *et al.*	(BELLE Collab.)
SATO	14	PR D90 072009	S. Sato *et al.*	(BELLE Collab.)
VANHOEFER	14	PR D89 072008	P. Vanhoefer *et al.*	(BELLE Collab.)
AAD	13U	PR D87 032002	G. Aad *et al.*	(ATLAS Collab.)
AAIJ	13	NP B867 1	R. Aaij *et al.*	(LHCb Collab.)
AAIJ	13A	NP B867 547	R. Aaij *et al.*	(LHCb Collab.)
AAIJ	13AA	NP B871 403	R. Aaij *et al.*	(LHCb Collab.)
AAIJ	13AC	NP B874 663	R. Aaij *et al.*	(LHCb Collab.)
AAIJ	13AO	PR D87 092001	R. Aaij *et al.*	(LHCb Collab.)
AAIJ	13AP	PR D87 092007	R. Aaij *et al.*	(LHCb Collab.)
AAIJ	13AQ	PR D87 112009	R. Aaij *et al.*	(LHCb Collab.)
AAIJ	13AT	PR D88 052002	R. Aaij *et al.*	(LHCb Collab.)
AAIJ	13AW	PRL 110 211801	R. Aaij *et al.*	(LHCb Collab.)
AAIJ	13AX	PRL 110 221601	R. Aaij *et al.*	(LHCb Collab.)
AAIJ	13B	PRL 110 021801	R. Aaij *et al.*	(LHCb Collab.)
AAIJ	13BA	PRL 111 101805	R. Aaij *et al.*	(LHCb Collab.)
AAIJ	13BM	PRL 111 141801	R. Aaij *et al.*	(LHCb Collab.)
AAIJ	13BO	JHEP 1310 183	R. Aaij *et al.*	(LHCb Collab.)
AAIJ	13BP	JHEP 1310 143	R. Aaij *et al.*	(LHCb Collab.)
AAIJ	13BQ	JHEP 1310 005	R. Aaij *et al.*	(LHCb Collab.)
AAIJ	13BT	PR D88 072005	R. Aaij *et al.*	(LHCb Collab.)
AAIJ	13CF	EPJ C73 2655	R. Aaij *et al.*	(LHCb Collab.)
AAIJ	13E	PRL 110 031801	R. Aaij *et al.*	(LHCb Collab.)
AAIJ	13F	PL B719 318	R. Aaij *et al.*	(LHCb Collab.)
AAIJ	13K	PL B721 24	R. Aaij *et al.*	(LHCb Collab.)
AAIJ	13L	JHEP 1303 067	R. Aaij *et al.*	(LHCb Collab.)
AAIJ	13M	PR D87 052001	R. Aaij *et al.*	(LHCb Collab.)
AAIJ	13P	JHEP 1304 001	R. Aaij *et al.*	(LHCb Collab.)
AAIJ	13U	JHEP 1305 159	R. Aaij *et al.*	(LHCb Collab.)
AAIJ	13Y	JHEP 1308 131	R. Aaij *et al.*	(LHCb Collab.)
AAIJ	13Z	JHEP 1309 006	R. Aaij *et al.*	(LHCb Collab.)
AALTONEN	13F	PR D87 072003	T. Aaltonen *et al.*	(CDF Collab.)
CHATRCHYAN	13AW	PRL 111 101804	S. Chatrchyan *et al.*	(CMS Collab.)
CHATRCHYAN	13BL	PL B727 77	S. Chatrchyan *et al.*	(CMS Collab.)
CHILIKIN	13	PR D88 074026	K. Chilikin *et al.*	(BELLE Collab.)
DALSENO	13	PR D88 092003	J. Dalseno *et al.*	(BELLE Collab.)
DUH	13	PR D87 031103	Y. T. Duh *et al.*	(BELLE Collab.)
GAUR	13	PR D87 091101	V. Gaur *et al.*	(BELLE Collab.)
LEES	13D	PR D87 052009	J.P. Lees *et al.*	(BABAR Collab.)
LEES	13H	PR D87 092004	J.P. Lees *et al.*	(BABAR Collab.)
LEES	13I	PR D87 112005	J.P. Lees *et al.*	(BABAR Collab.)
LEES	13J	PR D88 012003	J.P. Lees *et al.*	(BABAR Collab.)
LEES	13M	PR D88 032012	J.P. Lees *et al.*	(BABAR Collab.)
LEES	13N	PRL 111 101802	J.P. Lees *et al.*	(BABAR Collab.)
Also		PRL 111 159901(errat.)	J.P. Lees *et al.*	(BABAR Collab.)
Also		PR D93 032001	J.P. Lees *et al.*	(BABAR Collab.)
LUTZ	13	PR D87 111103	O. Lutz *et al.*	(BELLE Collab.)
PRIM	13	PR D88 072004	M. Prim *et al.*	(BELLE Collab.)
SIBIDANOV	13	PR D88 032005	A. Sibidanov *et al.*	(BELLE Collab.)
AAIJ	12A	PL B708 55	R. Aaij *et al.*	(LHCb Collab.)
AAIJ	12AH	JHEP 1207 133	R. Aaij *et al.*	(LHCb Collab.)
AAIJ	12AM	PRL 109 131801	R. Aaij *et al.*	(LHCb Collab.)
AAIJ	12AR	JHEP 1210 037	R. Aaij *et al.*	(LHCb Collab.)
AAIJ	12AX	PR D86 112005	R. Aaij *et al.*	(LHCb Collab.)
AAIJ	12E	PL B708 241	R. Aaij *et al.*	(LHCb Collab.)
AAIJ	12I	PL B709 177	R. Aaij *et al.*	(LHCb Collab.)
AAIJ	12L	EPJ C72 2118	R. Aaij *et al.*	(LHCb Collab.)
AAIJ	12T	PRL 108 161801	R. Aaij *et al.*	(LHCb Collab.)
AAIJ	12U	PRL 108 181806	R. Aaij *et al.*	(LHCb Collab.)
AAIJ	12V	PRL 108 201601	R. Aaij *et al.*	(LHCb Collab.)
AAIJ	12W	PRL 108 231801	R. Aaij *et al.*	(LHCb Collab.)
AALTONEN	12L	PRL 108 211803	T. Aaltonen *et al.*	(CDF Collab.)
ABAZOV	12AC	PR D86 072009	V.M. Abazov *et al.*	(D0 Collab.)
ABAZOV	12U	PR D85 112003	V.M. Abazov *et al.*	(D0 Collab.)
ADACHI	12A	PRL 108 171802	I. Adachi *et al.*	(BELLE Collab.)
CHANG	12	PR D85 091102	M.-C. Chang *et al.*	(BELLE Collab.)
CHATRCHYAN	12A	JHEP 1204 033	S. Chatrchyan *et al.*	(CMS Collab.)
DALSENO	12	PR D86 092012	J. Dalseno *et al.*	(BELLE Collab.)
DEL-AMO-SA...	12	PR D85 092017	P. del Amo Sanchez *et al.*	(BABAR Collab.)
HIGUCHI	12	PR D85 071105	T. Higuchi *et al.*	(BELLE Collab.)
HOI	12	PRL 108 031801	C.-T. Hoi *et al.*	(BELLE Collab.)
HSU	12	PR D86 032002	C.-L. Hsu *et al.*	(BELLE Collab.)
KIM	12A	PR D86 031101	J.H. Kim *et al.*	(BELLE Collab.)
KRONENBIT...	12	PR D86 071103	B. Kronenbitter *et al.*	(BELLE Collab.)
LEES	12AA	PR D86 092004	J.P. Lees *et al.*	(BABAR Collab.)
LEES	12AF	PR D86 112006	J.P. Lees *et al.*	(BABAR Collab.)
LEES	12B	PR D85 052003	J.P. Lees *et al.*	(BABAR Collab.)
LEES	12D	PRL 109 101802	J.P. Lees *et al.*	(BABAR Collab.)
Also		PR D88 072012	J.P. Lees *et al.*	(BABAR Collab.)
LEES	12I	PR D85 054023	J.P. Lees *et al.*	(BABAR Collab.)
LEES	12K	PR D85 072005	J.P. Lees *et al.*	(BABAR Collab.)

LEES	12O	PR D85 112010	J.P. Lees *et al.*	(BABAR Collab.)
LEES	12T	PR D86 051105	J.P. Lees *et al.*	(BABAR Collab.)
LEES	12W	PRL 109 211801	J.P. Lees *et al.*	(BABAR Collab.)
NEGISHI	12	PR D86 011101	K. Negishi *et al.*	(BELLE Collab.)
PDG	12	PR D86 010001	J. Beringer *et al.*	(PDG Collab.)
ROHRKEN	12	PR D85 091106	M. Rohrken *et al.*	(BELLE Collab.)
SATO	12	PRL 108 171801	Y. Sato *et al.*	(BELLE Collab.)
AAIJ	11B	PL B699 330	R. Aaij *et al.*	(LHCb Collab.)
AAIJ	11E	PR D84 092001	R. Aaij *et al.*	(LHCb Collab.)
Also		PR D85 039904 (errat.)	R. Aaij *et al.*	(LHCb Collab.)
AAIJ	11F	PRL 107 211801	R. Aaij *et al.*	(LHCb Collab.)
AALTONEN	11	PRL 106 121804	T. Aaltonen *et al.*	(CDF Collab.)
AALTONEN	11AG	PRL 107 191801	T. Aaltonen *et al.*	(CDF Collab.)
Also		PRL 107 239903 (errat.)	T. Aaltonen *et al.*	(CDF Collab.)
AALTONEN	11AI	PRL 107 201802	T. Aaltonen *et al.*	(CDF Collab.)
AALTONEN	11L	PRL 106 161801	T. Aaltonen *et al.*	(CDF Collab.)
AALTONEN	11N	PRL 106 181802	T. Aaltonen *et al.*	(CDF Collab.)
ABAZOV	11U	PR D84 052007	V.M. Abazov *et al.*	(D0 Collab.)
AUSHEV	11	PR D83 051102	T. Aushev *et al.*	(BELLE Collab.)
BAHINIPATI	11	PR D84 021101	S. Bahinipati *et al.*	(BELLE Collab.)
BHARDWAJ	11	PRL 107 091803	V. Bhardwaj *et al.*	(BELLE Collab.)
CHATRCHYAN	11T	PRL 107 191802	S. Chatrchyan *et al.*	(CMS Collab.)
CHOI	11	PR D84 052004	S.-K. Choi *et al.*	(BELLE Collab.)
DEL-AMO-SA...	11A	PR D83 032006	P. del Amo Sanchez *et al.*	(BABAR Collab.)
DEL-AMO-SA...	11B	PR D83 032004	P. del Amo Sanchez *et al.*	(BABAR Collab.)
DEL-AMO-SA...	11C	PR D83 032007	P. del Amo Sanchez *et al.*	(BABAR Collab.)
DEL-AMO-SA...	11F	PR D83 052011	P. del Amo Sanchez *et al.*	(BABAR Collab.)
DEL-AMO-SA...	11K	PR D83 091101	P. del Amo Sanchez *et al.*	(BABAR Collab.)
HA	11	PR D83 071101	H. Ha *et al.*	(BELLE Collab.)
LEES	11	PR D83 112010	J.P. Lees *et al.*	(BABAR Collab.)
LEES	11A	PR D84 012001	J.P. Lees *et al.*	(BABAR Collab.)
LEES	11F	PR D84 071102	J.P. Lees *et al.*	(BABAR Collab.)
LEES	11M	PR D84 112007	J.P. Lees *et al.*	(BABAR Collab.)
Also		PR D87 039901 (errat.)	J.P. Lees *et al.*	(BABAR Collab.)
SAHOO	11A	PR D84 071101	H. Sahoo *et al.*	(BELLE Collab.)
AUBERT	10	PRL 104 011802	B. Aubert *et al.*	(BABAR Collab.)
AUBERT	10D	PR D81 052009	B. Aubert *et al.*	(BABAR Collab.)
AUBERT	10H	PR D82 031102	B. Aubert *et al.*	(BABAR Collab.)
AUSHEV	10	PR D81 031103	T. Aushev *et al.*	(BELLE Collab.)
CHIANG	10	PR D81 071101	C.-C. Chiang *et al.*	(BELLE Collab.)
DAS	10	PR D82 051103	A. Das *et al.*	(BELLE Collab.)
DEL-AMO-SA...	10A	PR D82 011502	P. del Amo Sanchez *et al.*	(BABAR Collab.)
DEL-AMO-SA...	10B	PR D82 011101	P. del Amo Sanchez *et al.*	(BABAR Collab.)
DEL-AMO-SA...	10E	PR D82 031101	P. del Amo Sanchez *et al.*	(BABAR Collab.)
DEL-AMO-SA...	10Q	PR D82 112002	P. del Amo Sanchez *et al.*	(BABAR Collab.)
DUNGEL	10	PR D82 112007	W. Dungel *et al.*	(BELLE Collab.)
FUJIKAWA	10A	PR D81 011101	M. Fujikawa *et al.*	(BELLE Collab.)
HYUN	10	PRL 105 091801	H.J. Hyun *et al.*	(BELLE Collab.)
JOSHI	10	PR D81 031101	N.J. Joshi *et al.*	(BELLE Collab.)
NAKAHAMA	10	PR D82 073011	Y. Nakahama *et al.*	(BELLE Collab.)
WEDD	10	PR D81 111104	R. Wedd *et al.*	(BELLE Collab.)
AALTONEN	09B	PR D79 011104	T. Aaltonen *et al.*	(CDF Collab.)
AALTONEN	09C	PRL 103 031801	T. Aaltonen *et al.*	(CDF Collab.)
AALTONEN	09E	PR D79 032001	T. Aaltonen *et al.*	(CDF Collab.)
AALTONEN	09P	PRL 102 201801	T. Aaltonen *et al.*	(CDF Collab.)
ABAZOV	09E	PRL 102 032001	V.M. Abazov *et al.*	(D0 Collab.)
AUBERT	09	PR D79 011102	B. Aubert *et al.*	(BABAR Collab.)
AUBERT	09A	PR D79 012002	B. Aubert *et al.*	(BABAR Collab.)
AUBERT	09AA	PR D79 112001	B. Aubert *et al.*	(BABAR Collab.)
AUBERT	09AC	PR D79 112009	B. Aubert *et al.*	(BABAR Collab.)
AUBERT	09AD	PR D80 011101	B. Aubert *et al.*	(BABAR Collab.)
AUBERT	09AE	PR D80 031102	B. Aubert *et al.*	(BABAR Collab.)
AUBERT	09AF	PR D80 051101	B. Aubert *et al.*	(BABAR Collab.)
AUBERT	09AG	PR D80 051105	B. Aubert *et al.*	(BABAR Collab.)
AUBERT	09AL	PR D80 092007	B. Aubert *et al.*	(BABAR Collab.)
AUBERT	09AO	PRL 103 211802	B. Aubert *et al.*	(BABAR Collab.)
AUBERT	09AU	PR D80 112001	B. Aubert *et al.*	(BABAR Collab.)
AUBERT	09AV	PR D80 112002	B. Aubert *et al.*	(BABAR Collab.)
AUBERT	09B	PRL 102 132001	B. Aubert *et al.*	(BABAR Collab.)
AUBERT	09C	PR D79 032002	B. Aubert *et al.*	(BABAR Collab.)
AUBERT	09G	PRL 102 141802	B. Aubert *et al.*	(BABAR Collab.)
AUBERT	09H	PR D79 052005	B. Aubert *et al.*	(BABAR Collab.)
AUBERT	09I	PR D79 052003	B. Aubert *et al.*	(BABAR Collab.)
AUBERT	09K	PR D79 072009	B. Aubert *et al.*	(BABAR Collab.)
AUBERT	09S	PR D79 092002	B. Aubert *et al.*	(BABAR Collab.)
AUBERT	09T	PRL 102 091803	B. Aubert *et al.*	(BABAR Collab.)
Also		EPAPS Document No. E-PRLTAO-102-060910		(BABAR Collab.)
AUBERT	09Y	PRL 103 051803	B. Aubert *et al.*	(BABAR Collab.)
CHANG	09	PR D79 052006	Y.-W. Chang *et al.*	(BELLE Collab.)
DALSENO	09	PR D79 072004	J. Dalseno *et al.*	(BELLE Collab.)
KYEONG	09	PR D80 051103	S.-H. Kyeong *et al.*	(BELLE Collab.)
MIZUK	09	PR D80 031104	R. Mizuk *et al.*	(BELLE Collab.)
VERVINK	09	PR D80 111104	K. Vervink *et al.*	(BELLE Collab.)
WEI	09A	PRL 103 171801	J.-T. Wei *et al.*	(BELLE Collab.)
Also		EPAPS Supplement EPAPS_appendix.pdf		(BELLE Collab.)
ADACHI	08	PR D77 091101	I. Adachi *et al.*	(BELLE Collab.)
AUBERT	08AB	PR D78 012006	B. Aubert *et al.*	(BABAR Collab.)
AUBERT	08AC	PR D77 071102	B. Aubert *et al.*	(BABAR Collab.)
AUBERT	08AD	PR D77 091104	B. Aubert *et al.*	(BABAR Collab.)
AUBERT	08AF	PR D78 011103	B. Aubert *et al.*	(BABAR Collab.)
AUBERT	08AG	PR D78 011104	B. Aubert *et al.*	(BABAR Collab.)
AUBERT	08AH	PR D78 011107	B. Aubert *et al.*	(BABAR Collab.)
AUBERT	08AJ	PR D78 032005	B. Aubert *et al.*	(BABAR Collab.)
AUBERT	08AP	PR D78 051103	B. Aubert *et al.*	(BABAR Collab.)
AUBERT	08AQ	PR D78 052005	B. Aubert *et al.*	(BABAR Collab.)
AUBERT	08AU	PRL 101 021801	B. Aubert *et al.*	(BABAR Collab.)
AUBERT	08AV	PRL 101 081801	B. Aubert *et al.*	(BABAR Collab.)
AUBERT	08B	PR D77 011102	B. Aubert *et al.*	(BABAR Collab.)
AUBERT	08BA	PR D78 071102	B. Aubert *et al.*	(BABAR Collab.)
AUBERT	08BB	PR D78 071104	B. Aubert *et al.*	(BABAR Collab.)
AUBERT	08BC	PR D78 072007	B. Aubert *et al.*	(BABAR Collab.)
AUBERT	08BD	PR D78 091101	B. Aubert *et al.*	(BABAR Collab.)
AUBERT	08BG	PR D78 092008	B. Aubert *et al.*	(BABAR Collab.)
AUBERT	08BH	PR D78 112001	B. Aubert *et al.*	(BABAR Collab.)
AUBERT	08BK	PRL 101 201801	B. Aubert *et al.*	(BABAR Collab.)
AUBERT	08BL	PRL 101 261802	B. Aubert *et al.*	(BABAR Collab.)
AUBERT	08BN	PR D78 112003	B. Aubert *et al.*	(BABAR Collab.)
AUBERT	08C	PR D77 011104	B. Aubert *et al.*	(BABAR Collab.)
AUBERT	08E	PR D77 012003	B. Aubert *et al.*	(BABAR Collab.)
AUBERT	08F	PRL 100 051803	B. Aubert *et al.*	(BABAR Collab.)
AUBERT	08G	PRL 100 171803	B. Aubert *et al.*	(BABAR Collab.)
AUBERT	08H	PR D77 031101	B. Aubert *et al.*	(BABAR Collab.)
AUBERT	08I	PRL 100 081801	B. Aubert *et al.*	(BABAR Collab.)
AUBERT	08N	PRL 100 021801	B. Aubert *et al.*	(BABAR Collab.)
Also		PR D79 092002	B. Aubert *et al.*	(BABAR Collab.)
AUBERT	08P	PR D77 032007	B. Aubert *et al.*	(BABAR Collab.)
AUBERT	08Q	PRL 100 151802	B. Aubert *et al.*	(BABAR Collab.)
AUBERT	08R	PR D77 032002	B. Aubert *et al.*	(BABAR Collab.)
AUBERT	08W	PRL 101 082001	B. Aubert *et al.*	(BABAR Collab.)
AUBERT	08Y	PR D77 111101	B. Aubert *et al.*	(BABAR Collab.)
CHEN	08C	PRL 100 251801	J.-H. Chen *et al.*	(BELLE Collab.)
CHIANG	08	PR D78 111102	C.C. Chiang *et al.*	(BELLE Collab.)
CHOI	08	PRL 100 142001	S.-K. Choi *et al.*	(BELLE Collab.)
GOLDENZWE...	08	PRL 101 231801	P. Goldenzweig *et al.*	(BELLE Collab.)
KIM	08	PL B669 287	H.O. Kim *et al.*	(BELLE Collab.)
KUMAR	08	PR D78 091104	R. Kumar *et al.*	(BELLE Collab.)
KUSAKA	08	PR D77 072001	A. Kusaka *et al.*	(BELLE Collab.)
LEE	08A	PR D77 071101	S.E. Lee *et al.*	(BELLE Collab.)
LI	08F	PRL 101 251601	J. Li *et al.*	(BELLE Collab.)
LIN	08	NAT 452 332	S.-W. Lin *et al.*	(BELLE Collab.)
LIU	08I	PR D78 011106	Y. Liu *et al.*	(BELLE Collab.)
LIVENTSEV	08	PR D77 091503	D. Liventsev *et al.*	(BELLE Collab.)
MIZUK	08	PR D78 072004	R. Mizuk *et al.*	(BELLE Collab.)
NAKAHAMA	08	PRL 100 121601	Y. Nakahama *et al.*	(BELLE Collab.)
PDG	08	PL B667 1	C. Amsler *et al.*	(PDG Collab.)
SAHOO	08	PR D77 091103	H. Sahoo *et al.*	(BELLE Collab.)
TANIGUCHI	08	PRL 101 111801	N. Taniguchi *et al.*	(BELLE Collab.)
UCHIDA	08	PR D77 051101	Y. Uchida *et al.*	(BELLE Collab.)
USHIRODA	08	PRL 100 021602	Y. Ushiroda *et al.*	(BELLE Collab.)
WEI	08A	PR D78 011101	J.-T. Wei *et al.*	(BELLE Collab.)
ABAZOV	07S	PRL 99 142001	V.M. Abazov *et al.*	(D0 Collab.)
ABULENCIA	07A	PRL 98 122001	A. Abulencia *et al.*	(FNAL CDF Collab.)
ADAM	07	PRL 99 041802	N.E. Adam *et al.*	(CLEO Collab.)
Also		PR D76 012007	D.M. Asner *et al.*	(CLEO Collab.)
AUBERT	07A	PRL 98 031801	B. Aubert *et al.*	(BABAR Collab.)
AUBERT	07AA	PR D76 012004	B. Aubert *et al.*	(BABAR Collab.)
AUBERT	07AC	PR D76 031101	B. Aubert *et al.*	(BABAR Collab.)
AUBERT	07AD	PR D76 031102	B. Aubert *et al.*	(BABAR Collab.)
AUBERT	07AE	PR D76 031103	B. Aubert *et al.*	(BABAR Collab.)
AUBERT	07AF	PRL 99 021603	B. Aubert *et al.*	(BABAR Collab.)
AUBERT	07AG	PRL 99 051801	B. Aubert *et al.*	(BABAR Collab.)
AUBERT	07AI	PRL 99 071801	B. Aubert *et al.*	(BABAR Collab.)
AUBERT	07AJ	PRL 99 081801	B. Aubert *et al.*	(BABAR Collab.)
AUBERT	07AN	PR D76 051101	B. Aubert *et al.*	(BABAR Collab.)
AUBERT	07AO	PR D76 051103	B. Aubert *et al.*	(BABAR Collab.)
AUBERT	07AQ	PR D76 071101	B. Aubert *et al.*	(BABAR Collab.)
AUBERT	07AS	PR D76 071104	B. Aubert *et al.*	(BABAR Collab.)
AUBERT	07AT	PR D76 091101	B. Aubert *et al.*	(BABAR Collab.)
AUBERT	07AV	PR D76 092004	B. Aubert *et al.*	(BABAR Collab.)
AUBERT	07AX	PRL 99 161802	B. Aubert *et al.*	(BABAR Collab.)
AUBERT	07AY	PRL 99 171803	B. Aubert *et al.*	(BABAR Collab.)
AUBERT	07B	PR D75 012008	B. Aubert *et al.*	(BABAR Collab.)
AUBERT	07BC	PR D76 091102	B. Aubert *et al.*	(BABAR Collab.)
AUBERT	07BF	PR D76 052007	B. Aubert *et al.*	(BABAR Collab.)
AUBERT	07BH	PRL 99 231802	B. Aubert *et al.*	(BABAR Collab.)
AUBERT	07BI	PRL 99 241803	B. Aubert *et al.*	(BABAR Collab.)
AUBERT	07BO	PR D76 111102	B. Aubert *et al.*	(BABAR Collab.)
AUBERT	07D	PRL 98 051801	B. Aubert *et al.*	(BABAR Collab.)
AUBERT	07E	PRL 98 051802	B. Aubert *et al.*	(BABAR Collab.)
AUBERT	07F	PRL 98 051803	B. Aubert *et al.*	(BABAR Collab.)
AUBERT	07G	PRL 98 111801	B. Aubert *et al.*	(BABAR Collab.)
AUBERT	07H	PR D75 031101	B. Aubert *et al.*	(BABAR Collab.)
AUBERT	07J	PRL 98 091801	B. Aubert *et al.*	(BABAR Collab.)
AUBERT	07K	PRL 98 081801	B. Aubert *et al.*	(BABAR Collab.)
AUBERT	07L	PRL 98 151802	B. Aubert *et al.*	(BABAR Collab.)
AUBERT	07N	PR D75 072002	B. Aubert *et al.*	(BABAR Collab.)
AUBERT	07O	PRL 98 181803	B. Aubert *et al.*	(BABAR Collab.)
AUBERT	07Q	PR D75 051102	B. Aubert *et al.*	(BABAR Collab.)
AUBERT	07R	PRL 98 211804	B. Aubert *et al.*	(BABAR Collab.)
Also		PRL 100 189903E	B. Aubert *et al.*	(BABAR Collab.)
Also		PRL 100 199905E	B. Aubert *et al.*	(BABAR Collab.)
AUBERT	07Y	PR D75 111102	B. Aubert *et al.*	(BABAR Collab.)
CHANG	07A	PRL 98 131803	M.-C. Chang *et al.*	(BELLE Collab.)
CHANG	07B	PR D75 071104	P. Chang *et al.*	(BELLE Collab.)
CHAO	07	PR D76 091103	Y. Chao *et al.*	(BELLE Collab.)
CHEN	07	PRL 98 031802	K.-F. Chen *et al.*	(BELLE Collab.)
CHEN	07D	PRL 99 221802	K.-F. Chen *et al.*	(BELLE Collab.)
DALSENO	07	PR D76 072004	J. Dalseno *et al.*	(BELLE Collab.)
FRATINA	07	PRL 98 221802	S. Fratina *et al.*	(BELLE Collab.)
GARMASH	07	PR D75 012006	A. Garmash *et al.*	(BELLE Collab.)
HOKUUE	07	PL B648 139	T. Hokuue *et al.*	(BELLE Collab.)
ISHINO	07	PRL 98 211801	H. Ishino *et al.*	(BELLE Collab.)
KUSAKA	07	PRL 98 221602	A. Kusaka *et al.*	(BELLE Collab.)
Also		PR D77 072001	A. Kusaka *et al.*	(BELLE Collab.)
KUZMIN	07	PR D76 012006	A. Kuzmin *et al.*	(BELLE Collab.)
LIN	07	PRL 98 181804	S.-W. Lin *et al.*	(BELLE Collab.)
LIN	07A	PRL 99 121601	S.-W. Lin *et al.*	(BELLE Collab.)
MATYJA	07	PRL 99 191807	A. Matyja *et al.*	(BELLE Collab.)
MEDVEDEVA	07	PR D76 051102	T. Medvedeva *et al.*	(BELLE Collab.)
PARK	07	PR D75 011101	K.S. Park *et al.*	(BELLE Collab.)
SCHUEMANN	07	PR D75 092002	J. Schuemann *et al.*	(BELLE Collab.)
SOMOV	07	PR D76 011104	A. Somov *et al.*	(BELLE Collab.)
TSAI	07	PR D75 111101	Y.-T. Tsai *et al.*	(BELLE Collab.)
URQUIJO	07	PR D75 032001	P. Urquijo *et al.*	(BELLE Collab.)
WANG	07B	PR D75 092005	C.H. Wang *et al.*	(BELLE Collab.)
WANG	07C	PR D76 052004	M.-Z. Wang *et al.*	(BELLE Collab.)
XIE	07	PR D75 017101	Q.L. Xie *et al.*	(BELLE Collab.)
ZUPANC	07	PR D75 091102	A. Zupanc *et al.*	(BELLE Collab.)
ABAZOV	06S	PR D74 092001	V.M. Abazov *et al.*	(D0 Collab.)
ABAZOV	06W	PR D74 112002	V.M. Abazov *et al.*	(D0 Collab.)
ABULENCIA,A	06D	PRL 97 211802	A. Abulencia *et al.*	(CDF Collab.)
ACOSTA	06	PRL 96 202001	D. Acosta *et al.*	(CDF Collab.)
AUBERT	06	PR D73 011101	B. Aubert *et al.*	(BABAR Collab.)
AUBERT	06A	PRL 96 011803	B. Aubert *et al.*	(BABAR Collab.)
AUBERT	06E	PRL 96 052002	B. Aubert *et al.*	(BABAR Collab.)
AUBERT	06G	PR D73 012004	B. Aubert *et al.*	(BABAR Collab.)
AUBERT	06I	PR D73 031101	B. Aubert *et al.*	(BABAR Collab.)
AUBERT	06L	PR D74 012001	B. Aubert *et al.*	(BABAR Collab.)
AUBERT	06N	PR D74 031103	B. Aubert *et al.*	(BABAR Collab.)
AUBERT	06S	PRL 96 241802	B. Aubert *et al.*	(BABAR Collab.)
AUBERT	06T	PRL 96 251802	B. Aubert *et al.*	(BABAR Collab.)
AUBERT	06V	PRL 97 051802	B. Aubert *et al.*	(BABAR Collab.)
AUBERT	06W	PR D73 071102	B. Aubert *et al.*	(BABAR Collab.)
AUBERT	06X	PR D73 071103	B. Aubert *et al.*	(BABAR Collab.)
AUBERT	06Y	PR D73 111101	B. Aubert *et al.*	(BABAR Collab.)
AUBERT,B	06A	PR D73 112004	B. Aubert *et al.*	(BABAR Collab.)
AUBERT,B	06B	PR D74 011101	B. Aubert *et al.*	(BABAR Collab.)
AUBERT,B	06C	PR D74 011102	B. Aubert *et al.*	(BABAR Collab.)
AUBERT,B	06E	PR D74 011106	B. Aubert *et al.*	(BABAR Collab.)
AUBERT,B	06G	PRL 97 201801	B. Aubert *et al.*	(BABAR Collab.)
AUBERT,B	06H	PRL 97 201802	B. Aubert *et al.*	(BABAR Collab.)
AUBERT,B	06J	PR D73 092001	B. Aubert *et al.*	(BABAR Collab.)
AUBERT,B	06K	PRL 97 211801	B. Aubert *et al.*	(BABAR Collab.)
AUBERT,B	06L	PR D74 031101	B. Aubert *et al.*	(BABAR Collab.)
AUBERT,B	06M	PR D74 031102	B. Aubert *et al.*	(BABAR Collab.)
AUBERT,B	06O	PR D74 031104	B. Aubert *et al.*	(BABAR Collab.)
AUBERT,B	06P	PR D74 031105	B. Aubert *et al.*	(BABAR Collab.)
AUBERT,B	06Q	PR D74 091101	B. Aubert *et al.*	(BABAR Collab.)
AUBERT,B	06R	PR D74 032005	B. Aubert *et al.*	(BABAR Collab.)
AUBERT,B	06S	PR D74 051101	B. Aubert *et al.*	(BABAR Collab.)
AUBERT,B	06T	PR D74 051102	B. Aubert *et al.*	(BABAR Collab.)
AUBERT,B	06V	PR D74 051106	B. Aubert *et al.*	(BABAR Collab.)
AUBERT,B	06Y	PR D74 091105	B. Aubert *et al.*	(BABAR Collab.)
AUBERT,B	06Z	PR D74 092004	B. Aubert *et al.*	(BABAR Collab.)

Meson Particle Listings

B^0

AUBERT,BE 06C PRL 97 171805 B. Aubert *et al.* (BABAR Collab.)
AUBERT,BE 06H PRL 97 261803 B. Aubert *et al.* (BABAR Collab.)
AUBERT,BE 06J PR D74 111102 B. Aubert *et al.* (BABAR Collab.)
AUBERT,BE 06N PR D74 072008 B. Aubert *et al.* (BABAR Collab.)
BLYTH 06 PR D74 092002 S. Blyth *et al.* (BELLE Collab.)
CHISTOV 06A PR D74 111105 R. Chistov *et al.* (BELLE Collab.)
DRAGIC 06 PR D73 111105 J. Dragic *et al.* (BELLE Collab.)
GABYSHEV 06 PRL 97 202003 N. Gabyshev *et al.* (BELLE Collab.)
GOKHROO 06 PRL 97 162002 G. Gokhroo *et al.* (BELLE Collab.)
JEN 06 PR D74 111101 C.-M. Jen *et al.* (BELLE Collab.)
KROKOVNY 06 PRL 97 081801 P. Krokovny *et al.* (BELLE Collab.)
MOHAPATRA 06 PRL 96 221601 D. Mohapatra *et al.* (BELLE Collab.)
NAKANO 06 PR D73 112002 E. Nakano *et al.* (BELLE Collab.)
RONGA 06 PR D73 092003 F.J. Ronga *et al.* (BELLE Collab.)
SCHUEMANN 06 PRL 97 061802 J. Schuemann *et al.* (BELLE Collab.)
SOMOV 06 PRL 96 171801 A. Somov *et al.* (BELLE Collab.)
SONI 06 PL B634 155 N. Soni *et al.* (BELLE Collab.)
USHIRODA 06 PR D74 111104 Y. Ushiroda *et al.* (BELLE Collab.)
VILLA 06 PR D73 051107 S. Villa *et al.* (BELLE Collab.)
ABAZOV 05B PRL 94 042001 V.M. Abazov *et al.* (D0 Collab.)
ABAZOV 05C PRL 94 102001 V.M. Abazov *et al.* (D0 Collab.)
ABAZOV 05D PRL 94 182001 V.M. Abazov *et al.* (D0 Collab.)
ABAZOV 05W PRL 95 171801 V.M. Abazov *et al.* (D0 Collab.)
ABE 05A PRL 94 221805 K. Abe *et al.* (BELLE Collab.)
ABE 05B PR D71 072003 K. Abe *et al.* (BELLE Collab.)
Also PR D71 079903 (errat.) K. Abe *et al.* (BELLE Collab.)
ABE 05D PRL 95 101801 K. Abe *et al.* (BELLE Collab.)
ABE 05G PRL 95 231802 K. Abe *et al.* (BELLE Collab.)
ACOSTA 05 PRL 94 101803 D. Acosta *et al.* (CDF Collab.)
AUBERT 05 PRL 94 011801 B. Aubert *et al.* (BABAR Collab.)
AUBERT 05B PR D71 031501 B. Aubert *et al.* (BABAR Collab.)
AUBERT 05E PR D71 051502 B. Aubert *et al.* (BABAR Collab.)
AUBERT 05F PRL 94 161803 B. Aubert *et al.* (BABAR Collab.)
AUBERT 05I PRL 94 131801 B. Aubert *et al.* (BABAR Collab.)
AUBERT 05J PRL 94 141801 B. Aubert *et al.* (BABAR Collab.)
AUBERT 05K PRL 94 171801 B. Aubert *et al.* (BABAR Collab.)
AUBERT 05L PRL 94 181802 B. Aubert *et al.* (BABAR Collab.)
AUBERT 05M PRL 94 191802 B. Aubert *et al.* (BABAR Collab.)
AUBERT 05O PR D71 031103 B. Aubert *et al.* (BABAR Collab.)
AUBERT 05P PR D71 032005 B. Aubert *et al.* (BABAR Collab.)
AUBERT 05T PR D71 091102 B. Aubert *et al.* (BABAR Collab.)
AUBERT 05U PR D71 091103 B. Aubert *et al.* (BABAR Collab.)
AUBERT 05V PR D71 091104 B. Aubert *et al.* (BABAR Collab.)
AUBERT 05W PRL 94 221803 B. Aubert *et al.* (BABAR Collab.)
AUBERT 05Y PR D71 111102 B. Aubert *et al.* (BABAR Collab.)
AUBERT 05Z PR D71 112003 B. Aubert *et al.* (BABAR Collab.)
AUBERT,B 05 PRL 95 011801 B. Aubert *et al.* (BABAR Collab.)
AUBERT,B 05C PRL 95 041805 B. Aubert *et al.* (BABAR Collab.)
AUBERT,B 05K PRL 95 131803 B. Aubert *et al.* (BABAR Collab.)
AUBERT,B 05O PR D72 051102 B. Aubert *et al.* (BABAR Collab.)
AUBERT,B 05P PR D72 051103 B. Aubert *et al.* (BABAR Collab.)
AUBERT,B 05Q PR D72 051106 B. Aubert *et al.* (BABAR Collab.)
AUBERT,B 05Z PRL 95 131802 B. Aubert *et al.* (BABAR Collab.)
AUBERT,BE 05 PRL 95 151803 B. Aubert *et al.* (BABAR Collab.)
AUBERT,BE 05A PRL 95 151804 B. Aubert *et al.* (BABAR Collab.)
AUBERT,BE 05B PRL 95 171802 B. Aubert *et al.* (BABAR Collab.)
AUBERT,BE 05C PR D72 091103 B. Aubert *et al.* (BABAR Collab.)
AUBERT,BE 05E PRL 95 221801 B. Aubert *et al.* (BABAR Collab.)
AUBERT,BE 05F PR D72 111101 B. Aubert *et al.* (BABAR Collab.)
CHANG 05 PR D71 072007 M.-C. Chang *et al.* (BELLE Collab.)
CHANG 05A PR D71 091106 P. Chang *et al.* (BELLE Collab.)
CHAO 05 PRL 94 181803 Y. Chao *et al.* (BELLE Collab.)
CHAO 05A PR D71 031502 Y. Chao *et al.* (BELLE Collab.)
CHEN 05A PRL 94 221804 K.-F. Chen *et al.* (BELLE Collab.)
CHEN 05B PR D72 012004 K.-F. Chen *et al.* (BELLE Collab.)
DRUTSKOY 05 PRL 94 061802 A. Drutskoy *et al.* (BELLE Collab.)
GERSHON 05 PL B624 11 T. Gershon *et al.* (BELLE Collab.)
ITOH 05 PRL 95 091601 R. Itoh *et al.* (BELLE Collab.)
LIVENTSEV 05 PR D72 051109 D. Liventsev *et al.* (BELLE Collab.)
MAJUMDER 05 PRL 95 041803 G. Majumder *et al.* (BELLE Collab.)
MIYAKE 05 PL B618 34 H. Miyake *et al.* (BELLE Collab.)
MOHAPATRA 05 PR D72 011101 D. Mohapatra *et al.* (BELLE Collab.)
NISHIDA 05 PL B610 23 S. Nishida *et al.* (BELLE Collab.)
OKABE 05 PL B614 27 T. Okabe *et al.* (BELLE Collab.)
PARK 05 PRL 94 021801 H.K. Park *et al.* (FNAL HyperCP Collab.)
SCHUMANN 05 PR D72 011103 J. Schumann *et al.* (BELLE Collab.)
SUMISAWA 05 PRL 95 061801 K. Sumisawa *et al.* (BELLE Collab.)
USHIRODA 05 PRL 94 231601 Y. Ushiroda *et al.* (BELLE Collab.)
WANG 05 PRL 94 121801 C.C. Wang *et al.* (BELLE Collab.)
WANG 05A PL B617 141 M.-Z. Wang *et al.* (BELLE Collab.)
XIE 05 PR D72 051105 Q.L. Xie *et al.* (BELLE Collab.)
YANG 05 PRL 94 111802 H. Yang *et al.* (BELLE Collab.)
ZHANG 05B PR D71 091107 L.M. Zhang *et al.* (BELLE Collab.)
ABDALLAH 04D EPJ C33 213 J. Abdallah *et al.* (DELPHI Collab.)
ABDALLAH 04E EPJ C33 307 J. Abdallah *et al.* (DELPHI Collab.)
ABE 04E PRL 93 021601 K. Abe *et al.* (BELLE Collab.)
AUBERT 04A PR D69 011102 B. Aubert *et al.* (BABAR Collab.)
AUBERT 04B PR D69 032004 B. Aubert *et al.* (BABAR Collab.)
AUBERT 04C PRL 92 111801 B. Aubert *et al.* (BABAR Collab.)
AUBERT 04G PR D69 031102 B. Aubert *et al.* (BABAR Collab.)
AUBERT 04H PRL 92 061801 B. Aubert *et al.* (BABAR Collab.)
AUBERT 04M PRL 92 201802 B. Aubert *et al.* (BABAR Collab.)
AUBERT 04R PR D69 052001 B. Aubert *et al.* (BABAR Collab.)
AUBERT 04U PR D69 091503 B. Aubert *et al.* (BABAR Collab.)
AUBERT 04V PRL 92 251801 B. Aubert *et al.* (BABAR Collab.)
AUBERT 04W PRL 92 251802 B. Aubert *et al.* (BABAR Collab.)
AUBERT 04Y PRL 93 041801 B. Aubert *et al.* (BABAR Collab.)
AUBERT 04Z PRL 93 051802 B. Aubert *et al.* (BABAR Collab.)
AUBERT,B 04B PR D70 011101 B. Aubert *et al.* (BABAR Collab.)
AUBERT,B 04C PR D70 012007 B. Aubert *et al.* (BABAR Collab.)
Also PRL 92 181801 B. Aubert *et al.* (BABAR Collab.)
AUBERT,B 04D PR D70 032006 B. Aubert *et al.* (BABAR Collab.)
AUBERT,B 04G PRL 93 071801 B. Aubert *et al.* (BABAR Collab.)
AUBERT,B 04H PRL 93 081801 B. Aubert *et al.* (BABAR Collab.)
AUBERT,B 04J PRL 93 091802 B. Aubert *et al.* (BABAR Collab.)
AUBERT,B 04K PRL 93 131801 B. Aubert *et al.* (BABAR Collab.)
AUBERT,B 04M PRL 93 131805 B. Aubert (BABAR Collab.)
AUBERT,B 04O PR D70 091103 B. Aubert *et al.* (BABAR Collab.)
AUBERT,B 04R PRL 93 231801 B. Aubert *et al.* (BABAR Collab.)
AUBERT,B 04S PRL 93 181801 B. Aubert *et al.* (BABAR Collab.)
AUBERT,B 04T PR D70 091104 B. Aubert *et al.* (BABAR Collab.)
AUBERT,B 04U PR D70 091105 B. Aubert *et al.* (BABAR Collab.)
AUBERT,B 04V PRL 93 181805 B. Aubert *et al.* (BABAR Collab.)
AUBERT,B 04W PRL 93 231804 B. Aubert *et al.* (BABAR Collab.)
AUBERT,B 04X PRL 93 181806 B. Aubert *et al.* (BABAR Collab.)
AUBERT,B 04Z PRL 93 201801 B. Aubert *et al.* (BABAR Collab.)
AUBERT,BE 04 PR D70 111102 B. Aubert *et al.* (BABAR Collab.)
AUBERT,BE 04A PR D70 112006 B. Aubert *et al.* (BABAR Collab.)
AUBERT,BE 04B PR D70 091106 B. Aubert *et al.* (BABAR Collab.)
AUSHEV 04 PRL 93 201802 T. Aushev *et al.* (BELLE Collab.)
BORNHEIM 04 PRL 93 241802 A. Bornheim *et al.* (CLEO Collab.)
CHANG 04 PL B599 148 P. Chang *et al.* (BELLE Collab.)
CHAO 04 PR D69 111102 Y. Chao *et al.* (BELLE Collab.)
CHAO 04B PRL 93 191802 Y. Chao *et al.* (BELLE Collab.)
DRAGIC 04 PRL 93 131802 J. Dragic (BELLE Collab.)
DRUTSKOY 04 PRL 92 051801 A. Drutskoy *et al.* (BELLE Collab.)
GARMASH 04 PR D69 012001 A. Garmash *et al.* (BELLE Collab.)
KATAOKA 04 PRL 93 261801 S.U. Kataoka *et al.* (BELLE Collab.)
MAJUMDER 04 PR D70 111103 G. Majumder *et al.* (BELLE Collab.)
NAKAO 04 PR D69 112001 M. Nakao *et al.* (BELLE Collab.)
SARANGI 04 PRL 93 031802 T.R. Sarangi *et al.* (BELLE Collab.)
WANG 04 PRL 92 131801 M.Z. Wang *et al.* (BELLE Collab.)
WANG 04A PR D70 012001 C.H. Wang *et al.* (BELLE Collab.)
ABDALLAH 03B EPJ C28 155 J. Abdallah *et al.* (DELPHI Collab.)
ABE 03B PR D67 032003 K. Abe *et al.* (BELLE Collab.)
ABE 03C PR D67 031102 K. Abe *et al.* (BELLE Collab.)
ABE 03G PR D68 012001 K. Abe *et al.* (BELLE Collab.)
ABE 03H PRL 91 261602 K. Abe *et al.* (BELLE Collab.)
ADAM 03 PR D67 032001 N.E. Adam *et al.* (CLEO Collab.)
ATHAR 03 PR D68 072003 S.B. Athar *et al.* (CLEO Collab.)
AUBERT 03B PRL 90 091801 B. Aubert *et al.* (BABAR Collab.)
AUBERT 03C PR D67 072002 B. Aubert *et al.* (BABAR Collab.)
AUBERT 03D PRL 90 181803 B. Aubert *et al.* (BABAR Collab.)
AUBERT 03E PRL 90 181801 B. Aubert *et al.* (BABAR Collab.)
AUBERT 03H PR D67 091101 B. Aubert *et al.* (BABAR Collab.)
AUBERT 03I PR D67 092003 B. Aubert *et al.* (BABAR Collab.)
AUBERT 03J PRL 90 221801 B. Aubert *et al.* (BABAR Collab.)
AUBERT 03K PRL 90 231801 B. Aubert *et al.* (BABAR Collab.)
AUBERT 03L PRL 91 021801 B. Aubert *et al.* (BABAR Collab.)
AUBERT 03N PRL 91 061802 B. Aubert *et al.* (BABAR Collab.)
AUBERT 03O PRL 91 071801 B. Aubert *et al.* (BABAR Collab.)
AUBERT 03Q PRL 91 131801 B. Aubert *et al.* (BABAR Collab.)
AUBERT 03S PRL 91 241801 B. Aubert *et al.* (BABAR Collab.)
AUBERT 03T PRL 91 201802 B. Aubert *et al.* (BABAR Collab.)
AUBERT 03U PRL 91 221802 B. Aubert *et al.* (BABAR Collab.)
AUBERT 03V PRL 91 171802 B. Aubert *et al.* (BABAR Collab.)
AUBERT 03W PRL 91 161801 B. Aubert *et al.* (BABAR Collab.)
AUBERT 03X PR D68 092001 B. Aubert *et al.* (BABAR Collab.)
BORNHEIM 03 PR D68 052002 A. Bornheim *et al.* (CLEO Collab.)
CHANG 03 PR D68 111101 M.-C. Chang *et al.* (BELLE Collab.)
CHEN 03B PRL 91 201801 K.-F. Chen *et al.* (BELLE Collab.)
CSORNA 03 PR D67 112002 S.E. Csorna *et al.* (CLEO Collab.)
EISENSTEIN 03 PR D68 017101 B.I. Eisenstein *et al.* (CLEO Collab.)
FANG 03 PRL 90 071801 F. Fang *et al.* (BELLE Collab.)
GABYSHEV 03 PRL 90 121802 N. Gabyshev *et al.* (BELLE Collab.)
HASTINGS 03 PR D67 052004 N.C. Hastings *et al.* (BELLE Collab.)
ISHIKAWA 03 PRL 91 261601 A. Ishikawa *et al.* (BELLE Collab.)
KROKOVNY 03 PRL 90 141802 P. Krokovny *et al.* (BELLE Collab.)
KROKOVNY 03B PRL 91 262002 P. Krokovny *et al.* (BELLE Collab.)
LEE 03 PRL 91 261801 S.H. Lee *et al.* (BELLE Collab.)
SATPATHY 03 PL B553 159 A. Satpathy *et al.* (BELLE Collab.)
WANG 03 PRL 90 201802 M.-Z. Wang *et al.* (BELLE Collab.)
ZHENG 03 PR D67 092004 Y. Zheng *et al.* (BELLE Collab.)
ABE 02 PRL 88 021801 K. Abe *et al.* (BELLE Collab.)
ABE 02E PL B526 258 K. Abe *et al.* (BELLE Collab.)
ABE 02F PL B526 247 K. Abe *et al.* (BELLE Collab.)
ABE 02H PRL 88 171801 K. Abe *et al.* (BELLE Collab.)
ABE 02J PRL 88 052002 K. Abe *et al.* (BELLE Collab.)
ABE 02K PRL 88 181803 K. Abe *et al.* (BELLE Collab.)
ABE 02M PRL 89 071801 K. Abe *et al.* (BELLE Collab.)
ABE 02N PL B538 11 K. Abe *et al.* (BELLE Collab.)
ABE 02O PR D65 091103 K. Abe *et al.* (BELLE Collab.)
ABE 02Q PRL 89 122001 K. Abe *et al.* (BELLE Collab.)
ABE 02U PR D66 032007 K. Abe *et al.* (BELLE Collab.)
ABE 02W PRL 89 151802 K. Abe *et al.* (BELLE Collab.)
ABE 02Z PR D66 071102 K. Abe *et al.* (BELLE Collab.)
ACOSTA 02C PR D65 092009 D. Acosta *et al.* (CDF Collab.)
ACOSTA 02G PR D66 112002 D. Acosta *et al.* (CDF Collab.)
AFFOLDER 02B PRL 88 071801 T. Affolder *et al.* (CDF Collab.)
AHMED 02B PR D66 031101 S. Ahmed *et al.* (CLEO Collab.)
ASNER 02 PR D65 031103 D.M. Asner *et al.* (CLEO Collab.)
AUBERT 02 PR D65 032001 B. Aubert *et al.* (BABAR Collab.)
AUBERT 02C PRL 88 101805 B. Aubert *et al.* (BABAR Collab.)
AUBERT 02D PR D65 051502 B. Aubert *et al.* (BABAR Collab.)
AUBERT 02E PR D65 051101 B. Aubert *et al.* (BABAR Collab.)
AUBERT 02H PRL 89 011802 B. Aubert *et al.* (BABAR Collab.)
Also PRL 89 169903 (errat.) B. Aubert *et al.* (BABAR Collab.)
AUBERT 02I PRL 88 221802 B. Aubert *et al.* (BABAR Collab.)
AUBERT 02J PRL 88 221803 B. Aubert *et al.* (BABAR Collab.)
AUBERT 02K PRL 88 231801 B. Aubert *et al.* (BABAR Collab.)
AUBERT 02L PRL 88 241801 B. Aubert *et al.* (BABAR Collab.)
AUBERT 02M PRL 89 061801 B. Aubert *et al.* (BABAR Collab.)
AUBERT 02N PR D66 032003 B. Aubert *et al.* (BABAR Collab.)
AUBERT 02P PRL 89 201802 B. Aubert *et al.* (BABAR Collab.)
AUBERT 02Q PRL 89 281802 B. Aubert *et al.* (BABAR Collab.)
BRIERE 02 PRL 89 081803 R. Briere *et al.* (CLEO Collab.)
CASEY 02 PR D66 092002 B.C.K. Casey *et al.* (BELLE Collab.)
CHEN 02B PL B546 196 K.-F. Chen *et al.* (BELLE Collab.)
COAN 02 PRL 88 062001 T.E. Coan *et al.* (CLEO Collab.)
Also PRL 88 069902 (errat.) T.E. Coan *et al.* (CLEO Collab.)
DRUTSKOY 02 PL B542 171 A. Drutskoy *et al.* (BELLE Collab.)
DYTMAN 02 PR D66 091101 S.A. Dytman *et al.* (CLEO Collab.)
ECKHART 02 PRL 89 251801 E. Eckhart *et al.* (CLEO Collab.)
EDWARDS 02 PR D65 012002 K.W. Edwards *et al.* (CLEO Collab.)
GABYSHEV 02 PR D66 091102 N. Gabyshev *et al.* (BELLE Collab.)
GODANG 02 PRL 88 021802 R. Godang *et al.* (CLEO Collab.)
GORDON 02 PL B542 183 A. Gordon *et al.* (BELLE Collab.)
HARA 02 PRL 89 251803 K. Hara *et al.* (BELLE Collab.)
KROKOVNY 02 PRL 89 231804 P. Korkovny *et al.* (BELLE Collab.)
MAHAPATRA 02 PRL 88 101803 R. Mahapatra *et al.* (CLEO Collab.)
NISHIDA 02 PRL 89 231801 S. Nishida *et al.* (BELLE Collab.)
TOMURA 02 PL B542 207 T. Tomura *et al.* (BELLE Collab.)
ABASHIAN 01 PRL 86 2509 A. Abashian *et al.* (BELLE Collab.)
ABE 01D PRL 86 3228 K. Abe *et al.* (BELLE Collab.)
ABE 01G PRL 87 091802 K. Abe *et al.* (BELLE Collab.)
ABE 01H PRL 87 101801 K. Abe *et al.* (BELLE Collab.)
ABE 01I PRL 87 111801 K. Abe *et al.* (BELLE Collab.)
ABE 01K PR D64 071101 K. Abe *et al.* (BELLE Collab.)
ABE 01L PRL 87 161601 K. Abe *et al.* (BELLE Collab.)
ABE 01M PL B517 309 K. Abe *et al.* (BELLE Collab.)
ABREU 01H PL B510 55 P. Abreu *et al.* (DELPHI Collab.)
ALEXANDER 01B PR D64 092001 J.P. Alexander *et al.* (CLEO Collab.)
AMMAR 01B PRL 87 271801 R. Ammar *et al.* (CLEO Collab.)
ANDERSON 01 PRL 86 2732 S. Anderson *et al.* (CLEO Collab.)
ANDERSON 01B PRL 87 181803 S. Anderson *et al.* (CLEO Collab.)
AUBERT 01 PRL 86 2515 B. Aubert *et al.* (BABAR Collab.)
AUBERT 01B PRL 87 091801 B. Aubert *et al.* (BABAR Collab.)
AUBERT 01D PRL 87 151801 B. Aubert *et al.* (BABAR Collab.)
AUBERT 01E PRL 87 151802 B. Aubert *et al.* (BABAR Collab.)
AUBERT 01F PRL 87 201803 B. Aubert *et al.* (BABAR Collab.)
AUBERT 01G PRL 87 221802 B. Aubert *et al.* (BABAR Collab.)
AUBERT 01H PRL 87 241801 B. Aubert *et al.* (BABAR Collab.)
AUBERT 01I PRL 87 241803 B. Aubert *et al.* (BABAR Collab.)
BARATE 01D EPJ C20 431 R. Barate *et al.* (ALEPH Collab.)

BRIERE 01 PRL 86 3718 R.A. Biere *et al.* (CLEO Collab.)
EDWARDS 01 PRL 86 30 K.W. Edwards *et al.* (CLEO Collab.)
JAFFE 01 PRL 86 5000 D. Jaffe *et al.* (CLEO Collab.)
RICHICHI 01 PR D63 031103 S.J. Richichi *et al.* (CLEO Collab.)
ABBIENDI 00Q PL B482 15 G. Abbiendi *et al.* (OPAL Collab.)
ABBIENDI,G 00B PL B493 266 G. Abbiendi *et al.* (OPAL Collab.)
ABE 00C PR D62 071101 K. Abe *et al.* (SLD Collab.)
AFFOLDER 00C PR D61 072005 T. Affolder *et al.* (CDF Collab.)
AFFOLDER 00N PRL 85 4668 T. Affolder *et al.* (CDF Collab.)
AHMED 00B PR D62 112003 S. Ahmed *et al.* (CLEO Collab.)
ANASTASSOV 00 PRL 84 1393 A. Anastassov *et al.* (CLEO Collab.)
ARTUSO 00 PRL 84 4292 M. Artuso *et al.* (CLEO Collab.)
AVERY 00 PR D62 051101 P. Avery *et al.* (CLEO Collab.)
BARATE 00Q PL B492 259 R. Barate *et al.* (ALEPH Collab.)
BARATE 00R PL B492 275 R. Barate *et al.* (ALEPH Collab.)
BEHRENS 00 PR D61 052001 B.H. Behrens *et al.* (CLEO Collab.)
BEHRENS 00B PL B490 36 B.H. Behrens *et al.* (CLEO Collab.)
BERGFELD 00B PR D62 091102 T. Bergfeld *et al.* (CLEO Collab.)
CHEN 00 PRL 85 525 S. Chen *et al.* (CLEO Collab.)
COAN 00 PRL 84 5283 T.E. Coan *et al.* (CLEO Collab.)
CRONIN-HEN... 00 PRL 85 515 D. Cronin-Hennessy *et al.* (CLEO Collab.)
CSORNA 00 PR D61 111101 S.E. Csorna *et al.* (CLEO Collab.)
JESSOP 00 PRL 85 2881 C.P. Jessop *et al.* (CLEO Collab.)
LIPELES 00 PR D62 032005 E. Lipeles *et al.* (CLEO Collab.)
RICHICHI 00 PRL 85 520 S.J. Richichi *et al.* (CLEO Collab.)
ABBIENDI 99J EPJ C12 609 G. Abbiendi *et al.* (OPAL Collab.)
ABE 99K PR D60 051101 F. Abe *et al.* (CDF Collab.)
ABE 99Q PR D60 072003 F. Abe *et al.* (CDF Collab.)
AFFOLDER 99B PRL 83 3378 T. Affolder *et al.* (CDF Collab.)
AFFOLDER 99C PR D60 112004 T. Affolder *et al.* (CDF Collab.)
ARTUSO 99 PRL 82 3020 M. Artuso *et al.* (CLEO Collab.)
BARTELT 99 PRL 82 3746 J. Bartelt *et al.* (CLEO Collab.)
COAN 99 PR D59 111101 T.E. Coan *et al.* (CLEO Collab.)
ABE 98B PR D57 5382 F. Abe *et al.* (CDF Collab.)
ABE 98C PRL 80 2057 F. Abe *et al.* (CDF Collab.)
Also PR D59 032001 F. Abe *et al.* (CDF Collab.)
ABE 98O PR D58 072001 F. Abe *et al.* (CDF Collab.)
ABE 98Q PR D58 092002 F. Abe *et al.* (CDF Collab.)
ABE 98U PRL 81 5513 F. Abe *et al.* (CDF Collab.)
ABE 98V PRL 81 5742 F. Abe *et al.* (CDF Collab.)
ACCIARRI 98D EPJ C5 195 M. Acciarri *et al.* (L3 Collab.)
ACCIARRI 98S PL B438 417 M. Acciarri *et al.* (L3 Collab.)
ACKERSTAFF 98Z EPJ C5 379 K. Ackerstaff *et al.* (OPAL Collab.)
BARATE 98Q EPJ C4 387 R. Barate *et al.* (ALEPH Collab.)
BEHRENS 98 PRL 80 3710 B.H. Behrens *et al.* (CLEO Collab.)
BERGFELD 98 PRL 81 272 T. Bergfeld *et al.* (CLEO Collab.)
BRANDENB... 98 PRL 80 2762 G. Brandenbrug *et al.* (CLEO Collab.)
GODANG 98 PRL 80 3456 R. Godang *et al.* (CLEO Collab.)
NEMATI 98 PR D57 5363 B. Nemati *et al.* (CLEO Collab.)
ABE 97J PRL 79 590 K. Abe *et al.* (SLD Collab.)
ABREU 97F ZPHY C74 19 P. Abreu *et al.* (DELPHI Collab.)
Also ZPHY C75 579 (erratum) P. Abreu *et al.* (DELPHI Collab.)
ABREU 97N ZPHY C76 579 P. Abreu *et al.* (DELPHI Collab.)
ACCIARRI 97B PL B391 474 M. Acciarri *et al.* (L3 Collab.)
ACCIARRI 97C PL B391 481 M. Acciarri *et al.* (L3 Collab.)
ACKERSTAFF 97G PL B395 128 K. Ackerstaff *et al.* (OPAL Collab.)
ACKERSTAFF 97U ZPHY C76 401 K. Ackerstaff *et al.* (OPAL Collab.)
ACKERSTAFF 97V ZPHY C76 417 K. Ackerstaff *et al.* (OPAL Collab.)
ARTUSO 97 PL B399 321 M. Artuso *et al.* (CLEO Collab.)
ASNER 97 PRL 79 799 D. Asner *et al.* (CLEO Collab.)
ATHANAS 97 PRL 79 2208 M. Athanas *et al.* (CLEO Collab.)
BUSKULIC 97 PL B395 373 D. Buskulic *et al.* (ALEPH Collab.)
BUSKULIC 97D ZPHY C75 397 D. Buskulic *et al.* (ALEPH Collab.)
FU 97 PRL 79 3125 X. Fu *et al.* (CLEO Collab.)
JESSOP 97 PRL 79 4533 C.P. Jessop *et al.* (CLEO Collab.)
ABE 96B PR D53 3496 F. Abe *et al.* (CDF Collab.)
ABE 96C PRL 76 4462 F. Abe *et al.* (CDF Collab.)
ABE 96H PRL 76 2015 F. Abe *et al.* (CDF Collab.)
ABE 96Q PR D54 6596 F. Abe *et al.* (CDF Collab.)
ABREU 96P ZPHY C71 539 P. Abreu *et al.* (DELPHI Collab.)
ABREU 96Q ZPHY C72 17 P. Abreu *et al.* (DELPHI Collab.)
ACCIARRI 96E PL B383 487 M. Acciarri *et al.* (L3 Collab.)
ADAM 96D ZPHY C72 207 W. Adam *et al.* (DELPHI Collab.)
ALBRECHT 96D PL B374 256 H. Albrecht *et al.* (ARGUS Collab.)
ALEXANDER 96T PRL 77 5000 J.P. Alexander *et al.* (CLEO Collab.)
ALEXANDER 96V ZPHY C72 377 G. Alexander *et al.* (OPAL Collab.)
ASNER 96 PR D53 1039 D.M. Asner *et al.* (CLEO Collab.)
BARISH 96B PRL 76 1570 B.C. Barish *et al.* (CLEO Collab.)
BISHAI 96 PL B369 186 M. Bishai *et al.* (CLEO Collab.)
BUSKULIC 96J ZPHY C71 31 D. Buskulic *et al.* (ALEPH Collab.)
BUSKULIC 96V PL B384 471 D. Buskulic *et al.* (ALEPH Collab.)
DUBOSCQ 96 PRL 76 3898 J.E. Duboscq *et al.* (CLEO Collab.)
GIBAUT 96 PR D53 4734 D. Gibaut *et al.* (CLEO Collab.)
PDG 96 PR D54 1 R. M. Barnett *et al.* (PDG Collab.)
ABE 95Z PRL 75 3068 F. Abe *et al.* (CDF Collab.)
ABREU 95N PL B357 255 P. Abreu *et al.* (DELPHI Collab.)
ABREU 95Q ZPHY C68 13 P. Abreu *et al.* (DELPHI Collab.)
ACCIARRI 95H PL B363 127 M. Acciarri *et al.* (L3 Collab.)
ACCIARRI 95I PL B363 137 M. Acciarri *et al.* (L3 Collab.)
ADAM 95 ZPHY C68 363 W. Adam *et al.* (DELPHI Collab.)
AKERS 95J ZPHY C66 555 R. Akers *et al.* (OPAL Collab.)
AKERS 95T ZPHY C67 379 R. Akers *et al.* (OPAL Collab.)
ALEXANDER 95 PL B341 435 J. Alexander *et al.* (CLEO Collab.)
Also PL B347 469 (erratum) J. Alexander *et al.* (CLEO Collab.)
BARISH 95 PR D51 1014 B.C. Barish *et al.* (CLEO Collab.)
BUSKULIC 95N PL B359 236 D. Buskulic *et al.* (ALEPH Collab.)
ABE 94D PRL 72 3456 F. Abe *et al.* (CDF Collab.)
ABREU 94M PL B338 409 P. Abreu *et al.* (DELPHI Collab.)
AKERS 94C PL B327 411 R. Akers *et al.* (OPAL Collab.)
AKERS 94H PL B336 585 R. Akers *et al.* (OPAL Collab.)
AKERS 94J PL B337 196 R. Akers *et al.* (OPAL Collab.)
AKERS 94L PL B337 393 R. Akers *et al.* (OPAL Collab.)
ALAM 94 PR D50 43 M.S. Alam *et al.* (CLEO Collab.)
ALBRECHT 94 PL B324 249 H. Albrecht *et al.* (ARGUS Collab.)
ALBRECHT 94G PL B340 217 H. Albrecht *et al.* (ARGUS Collab.)
AMMAR 94 PR D49 5701 R. Ammar *et al.* (CLEO Collab.)
ATHANAS 94 PRL 73 3503 M. Athanas *et al.* (CLEO Collab.)
Also PRL 74 3090 (erratum) M. Athanas *et al.* (CLEO Collab.)
BUSKULIC 94B PL B322 441 D. Buskulic *et al.* (ALEPH Collab.)
PDG 94 PR D50 1173 L. Montanet *et al.* (CERN, LBL, BOST+)
PROCARIO 94 PRL 73 1472 M. Procario *et al.* (CLEO Collab.)
STONE 94 HEPSY 93-11 S. Stone
Published in B Decays, 2nd Edition, World Scientific, Singapore
ABREU 93D ZPHY C57 181 P. Abreu *et al.* (DELPHI Collab.)
ABREU 93G PL B312 253 P. Abreu *et al.* (DELPHI Collab.)
ACTON 93C PL B307 247 P.D. Acton *et al.* (OPAL Collab.)
ALBRECHT 93 ZPHY C57 533 H. Albrecht *et al.* (ARGUS Collab.)
ALBRECHT 93E ZPHY C60 11 H. Albrecht *et al.* (ARGUS Collab.)
ALEXANDER 93B PL B319 365 J. Alexander *et al.* (CLEO Collab.)
AMMAR 93 PRL 71 674 R. Ammar *et al.* (CLEO Collab.)
BARTELT 93 PRL 71 1680 J.E. Bartelt *et al.* (CLEO Collab.)
BATTLE 93 PRL 71 3922 M. Battle *et al.* (CLEO Collab.)
BEAN 93B PRL 70 2681 A. Bean *et al.* (CLEO Collab.)
BUSKULIC 93D PL B307 194 D. Buskulic *et al.* (ALEPH Collab.)
Also PL B325 537 (erratum) D. Buskulic *et al.* (ALEPH Collab.)
BUSKULIC 93K PL B313 498 D. Buskulic *et al.* (ALEPH Collab.)
SANGHERA 93 PR D47 791 S. Sanghera *et al.* (CLEO Collab.)
ALBRECHT 92C PL B275 195 H. Albrecht *et al.* (ARGUS Collab.)
ALBRECHT 92G ZPHY C54 1 H. Albrecht *et al.* (ARGUS Collab.)
ALBRECHT 92L ZPHY C55 357 H. Albrecht *et al.* (ARGUS Collab.)
BORTOLETTO 92 PR D45 21 D. Bortoletto *et al.* (CLEO Collab.)
HENDERSON 92 PR D45 2212 S. Henderson *et al.* (CLEO Collab.)
KRAMER 92 PL B279 181 G. Kramer, W.F. Palmer (HAMB, OSU)
ALBAJAR 91E PL B273 540 C. Albajar *et al.* (UA1 Collab.)
ALBRECHT 91B PL B254 288 H. Albrecht *et al.* (ARGUS Collab.)
ALBRECHT 91C PL B255 297 H. Albrecht *et al.* (ARGUS Collab.)
ALBRECHT 91E PL B262 148 H. Albrecht *et al.* (ARGUS Collab.)
BERKELMAN 91 ARNPS 41 1 K. Berkelman, S. Stone (CORN, SYRA)
"Decays of B Mesons"
FULTON 91 PR D43 651 R. Fulton *et al.* (CLEO Collab.)
ALBRECHT 90B PL B241 278 H. Albrecht *et al.* (ARGUS Collab.)
ALBRECHT 90J ZPHY C48 543 H. Albrecht *et al.* (ARGUS Collab.)
ANTREASYAN 90B ZPHY C48 553 D. Antreasyan *et al.* (Crystal Ball Collab.)
BORTOLETTO 90 PRL 64 2117 D. Bortoletto *et al.* (CLEO Collab.)
ELSEN 90 ZPHY C46 349 E. Elsen *et al.* (JADE Collab.)
ROSNER 90 PR D42 3732 J.L. Rosner
WAGNER 90 PRL 64 1095 S.R. Wagner *et al.* (Mark II Collab.)
ALBRECHT 89C PL B219 121 H. Albrecht *et al.* (ARGUS Collab.)
ALBRECHT 89G PL B229 304 H. Albrecht *et al.* (ARGUS Collab.)
ALBRECHT 89J PL B229 175 H. Albrecht *et al.* (ARGUS Collab.)
ALBRECHT 89L PL B232 554 H. Albrecht *et al.* (ARGUS Collab.)
ARTUSO 89 PRL 62 2233 M. Artuso *et al.* (CLEO Collab.)
AVERILL 89 PR D39 123 D.A. Averill *et al.* (HRS Collab.)
AVERY 89B PL B223 470 P. Avery *et al.* (CLEO Collab.)
BEBEK 89 PRL 62 8 C. Bebek *et al.* (CLEO Collab.)
BORTOLETTO 89 PRL 62 2436 D. Bortoletto *et al.* (CLEO Collab.)
BORTOLETTO 89B PRL 63 1667 D. Bortoletto *et al.* (CLEO Collab.)
ALBRECHT 88F PL B209 119 H. Albrecht *et al.* (ARGUS Collab.)
ALBRECHT 88K PL B215 424 H. Albrecht *et al.* (ARGUS Collab.)
ALBRECHT 87C PL B185 218 H. Albrecht *et al.* (ARGUS Collab.)
ALBRECHT 87D PL B199 451 H. Albrecht *et al.* (ARGUS Collab.)
ALBRECHT 87I PL B192 245 H. Albrecht *et al.* (ARGUS Collab.)
ALBRECHT 87J PL B197 452 H. Albrecht *et al.* (ARGUS Collab.)
AVERY 87 PL B183 429 P. Avery *et al.* (CLEO Collab.)
BEAN 87B PRL 58 183 A. Bean *et al.* (CLEO Collab.)
BEBEK 87 PR D36 1289 C. Bebek *et al.* (CLEO Collab.)
ALAM 86 PR D34 3279 M.S. Alam *et al.* (CLEO Collab.)
ALBRECHT 86F PL B182 95 H. Albrecht *et al.* (ARGUS Collab.)
PDG 86 PL 170B 1 M. Aguilar-Benitez *et al.* (CERN, CIT+)
CHEN 85 PR D31 2386 A. Chen *et al.* (CLEO Collab.)
HAAS 85 PRL 55 1248 J. Haas *et al.* (CLEO Collab.)
AVERY 84 PRL 53 1309 P. Avery *et al.* (CLEO Collab.)
GILES 84 PR D30 2279 R. Giles *et al.* (CLEO Collab.)
BEHRENDS 83 PRL 50 881 S. Behrends *et al.* (CLEO Collab.)

$B^\pm/B^0$ ADMIXTURE

B DECAY MODES

The branching fraction measurements are for an admixture of B mesons at the $\Upsilon(4S)$. The values quoted assume that $B(\Upsilon(4S) \to B\overline{B}) = 100\%$.

For inclusive branching fractions, *e.g.*, $B \to D^\pm$ *anything*, the treatment of multiple D's in the final state must be defined. One possibility would be to count the number of events with one-or-more D's and divide by the total number of B's. Another possibility would be to count the total number of D's and divide by the total number of B's, which is the definition of average multiplicity. The two definitions are identical if only one D is allowed in the final state. Even though the "one-or-more" definition seems sensible, for practical reasons inclusive branching fractions are almost always measured using the multiplicity definition. For heavy final state particles, authors call their results inclusive branching fractions while for light particles some authors call their results multiplicities. In the B sections, we list all results as inclusive branching fractions, adopting a multiplicity definition. This means that inclusive branching fractions can exceed 100% and that inclusive partial widths can exceed total widths, just as inclusive cross sections can exceed total cross section.

$\overline{B}$ modes are charge conjugates of the modes below. Reactions indicate the weak decay vertex and do not include mixing.

Mode	Fraction (Γ_i/Γ)	Scale factor/ Confidence level
Semileptonic and leptonic modes		
Γ_1 $e^+\nu_e$ anything	[a]	
Γ_2 $\mu^+\nu_\mu$ anything	[a]	
Γ_3 $\ell^+\nu_\ell$ anything	[a,b] (10.86 ± 0.16) %	
Γ_4 $D^-\ell^+\nu_\ell$ anything	[b] (2.8 ± 0.9) %	
Γ_5 $\overline{D}^0\ell^+\nu_\ell$ anything	[b] (7.3 ± 1.5) %	
Γ_6 $\overline{D}\ell^+\nu_\ell$	(2.42 ± 0.12) %	
Γ_7 $D^{*-}\ell^+\nu_\ell$ anything	[c] (6.7 ± 1.3) $\times 10^{-3}$	
Γ_8 $D^{*0}\ell^+\nu_\ell$ anything		
Γ_9 $D^*\ell^+\nu_\ell$	[d] (4.95 ± 0.11) %	
Γ_{10} $\overline{D}^{**}\ell^+\nu_\ell$	[b,e] (2.7 ± 0.7) %	
Γ_{11} $\overline{D}_1(2420)\ell^+\nu_\ell$ anything	(3.8 ± 1.3) $\times 10^{-3}$	S=2.4
Γ_{12} $D\pi\ell^+\nu_\ell$ anything + $D^*\pi\ell^+\nu_\ell$ anything	(2.6 ± 0.5) %	S=1.5
Γ_{13} $D\pi\ell^+\nu_\ell$ anything	(1.5 ± 0.6) %	
Γ_{14} $D^*\pi\ell^+\nu_\ell$ anything	(1.9 ± 0.4) %	
Γ_{15} $\overline{D}_2^*(2460)\ell^+\nu_\ell$ anything	(4.4 ± 1.6) $\times 10^{-3}$	

Meson Particle Listings

$B^{\pm}/B^{0}$ ADMIXTURE

Γ_{16}	$D^{*-}\pi^+\ell^+\nu_\ell$ anything		(	1.00	± 0.34	) %		
Γ_{17}	$\overline{D}\pi^+\pi^-\ell^+\nu_\ell$		(	1.62	± 0.32	) $\times 10^{-3}$		
Γ_{18}	$\overline{D}^*\pi^+\pi^-\ell^+\nu_\ell$		(	9.4	± 3.2	) $\times 10^{-4}$		
Γ_{19}	$D_s^-\ell^+\nu_\ell$ anything	[b]	<	7		$\times 10^{-3}$		CL=90%
Γ_{20}	$D_s^-\ell^+\nu_\ell K^+$ anything	[b]	<	5		$\times 10^{-3}$		CL=90%
Γ_{21}	$D_s^-\ell^+\nu_\ell K^0$ anything	[b]	<	7		$\times 10^{-3}$		CL=90%
Γ_{22}	$X_c\ell^+\nu_\ell$		(	10.65	± 0.16	) %		
Γ_{23}	$X_u\ell^+\nu_\ell$		(	2.13	± 0.31	) $\times 10^{-3}$		
Γ_{24}	$K^+\ell^+\nu_\ell$ anything	[b]	(	6.3	± 0.6	) %		
Γ_{25}	$K^-\ell^+\nu_\ell$ anything	[b]	(	10	± 4	) $\times 10^{-3}$		
Γ_{26}	$K^0/\overline{K}^0\ell^+\nu_\ell$ anything	[b]	(	4.6	± 0.5	) %		
Γ_{27}	$\overline{D}\tau^+\nu_\tau$		(	9.9	± 1.2	) $\times 10^{-3}$		
Γ_{28}	$D^*\tau^+\nu_\tau$		(	1.50	± 0.08	) %		

D, D^*, or D_s modes

Γ_{29}	$D^{\pm}$ anything		(	24.1	± 1.4	) %		
Γ_{30}	$D^0/\overline{D}^0$ anything		(	62.4	± 2.9	) %		S=1.3
Γ_{31}	$D^*(2010)^{\pm}$ anything		(	22.5	± 1.5	) %		
Γ_{32}	$D^*(2007)^0$ anything		(	26.0	± 2.7	) %		
Γ_{33}	$D_s^{\pm}$ anything	[f]	(	8.3	± 0.8	) %		
Γ_{34}	$D_s^{*\pm}$ anything		(	6.3	± 1.0	) %		
Γ_{35}	$D_s^{*\pm}\overline{D}^{(*)}$		(	3.4	± 0.6	) %		
Γ_{36}	$\overline{D}D_{s0}(2317)$			seen				
Γ_{37}	$\overline{D}D_{sJ}(2457)$			seen				
Γ_{38}	$D^{(*)}\overline{D}^{(*)}K^0 + D^{(*)}\overline{D}^{(*)}K^{\pm}$	[f,g]	(	7.1	$^{+\ 2.7}_{-\ 1.7}$	) %		
Γ_{39}	$b \to c\overline{c}s$		(	22	± 4	) %		
Γ_{40}	$D_s^{(*)}\overline{D}^{(*)}$	[f,g]	(	3.9	± 0.4	) %		
Γ_{41}	$D^*D^*(2010)^{\pm}$	[f]	<	5.9		$\times 10^{-3}$		CL=90%
Γ_{42}	$DD^*(2010)^{\pm} + D^*D^{\pm}$	[f]	<	5.5		$\times 10^{-3}$		CL=90%
Γ_{43}	$DD^{\pm}$	[f]	<	3.1		$\times 10^{-3}$		CL=90%
Γ_{44}	$D_s^{(*)\pm}\overline{D}^{(*)}X(n\pi^{\pm})$	[f,g]	(	9	$^{+\ 5}_{-\ 4}$	) %		
Γ_{45}	$D^*(2010)\gamma$		<	1.1		$\times 10^{-3}$		CL=90%
Γ_{46}	$D_s^+\pi^-$, $D_s^{*+}\pi^-$, $D_s^+\rho^-$, $D_s^{*+}\rho^-$, $D_s^+\pi^0$, $D_s^{*+}\pi^0$, $D_s^+\eta$, $D_s^{*+}\eta$, $D_s^+\rho^0$, $D_s^{*+}\rho^0$, $D_s^+\omega$, $D_s^{*+}\omega$	[f]	<	4		$\times 10^{-4}$		CL=90%
Γ_{47}	$D_{s1}(2536)^+$ anything		<	9.5		$\times 10^{-3}$		CL=90%

Charmonium modes

Γ_{48}	$J/\psi(1S)$ anything		(	1.094	± 0.032) %			S=1.1
Γ_{49}	$J/\psi(1S)$ (direct) anything		(	7.8	± 0.4	) $\times 10^{-3}$		S=1.1
Γ_{50}	$\psi(2S)$ anything		(	3.07	± 0.21	) $\times 10^{-3}$		
Γ_{51}	$\chi_{c1}(1P)$ anything		(	3.55	± 0.27	) $\times 10^{-3}$		S=1.3
Γ_{52}	$\chi_{c1}(1P)$ (direct) anything		(	3.08	± 0.19	) $\times 10^{-3}$		
Γ_{53}	$\chi_{c2}(1P)$ anything		(	10.0	± 1.7	) $\times 10^{-4}$		S=1.6
Γ_{54}	$\chi_{c2}(1P)$ (direct) anything		(	7.5	± 1.1	) $\times 10^{-4}$		
Γ_{55}	$\eta_c(1S)$ anything		<	9		$\times 10^{-3}$		CL=90%
Γ_{56}	$K\chi_{c1}(3872)$, $\chi_{c1} \to D^0\overline{D}^0\pi^0$		(	1.2	± 0.4	) $\times 10^{-4}$		
Γ_{57}	$K\chi_{c1}(3872)$, $\chi_{c1} \to D^{*0}D^0$		(	8.0	± 2.2	) $\times 10^{-5}$		
Γ_{58}	$KX(3940)$, $X \to D^{*0}D^0$		<	6.7		$\times 10^{-5}$		CL=90%
Γ_{59}	$KX(3915)$, $X \to \omega J/\psi$	[h]	(	7.1	± 3.4	) $\times 10^{-5}$		

K or K^* modes

Γ_{60}	$K^{\pm}$ anything	[f]	(	78.9	± 2.5	) %		
Γ_{61}	K^+ anything		(	66	± 5	) %		
Γ_{62}	K^- anything		(	13	± 4	) %		
Γ_{63}	$K^0/\overline{K}^0$ anything	[f]	(	64	± 4	) %		
Γ_{64}	$K^*(892)^{\pm}$ anything		(	18	± 6	) %		
Γ_{65}	$K^*(892)^0/\overline{K}^*(892)^0$ anything	[f]	(	14.6	± 2.6	) %		
Γ_{66}	$K^*(892)\gamma$		(	4.2	± 0.6	) $\times 10^{-5}$		
Γ_{67}	$\eta K\gamma$		(	8.5	$^{+\ 1.8}_{-\ 1.6}$	) $\times 10^{-6}$		
Γ_{68}	$K_1(1400)\gamma$		<	1.27		$\times 10^{-4}$		CL=90%
Γ_{69}	$K_2^*(1430)\gamma$		(	1.7	$^{+\ 0.6}_{-\ 0.5}$	) $\times 10^{-5}$		
Γ_{70}	$K_2(1770)\gamma$		<	1.2		$\times 10^{-3}$		CL=90%
Γ_{71}	$K_3^*(1780)\gamma$		<	3.7		$\times 10^{-5}$		CL=90%
Γ_{72}	$K_4^*(2045)\gamma$		<	1.0		$\times 10^{-3}$		CL=90%
Γ_{73}	$K\eta'(958)$		(	8.3	± 1.1	) $\times 10^{-5}$		
Γ_{74}	$K^*(892)\eta'(958)$		(	4.1	± 1.1	) $\times 10^{-6}$		
Γ_{75}	$K\eta$		<	5.2		$\times 10^{-6}$		CL=90%
Γ_{76}	$K^*(892)\eta$		(	1.8	± 0.5	) $\times 10^{-5}$		
Γ_{77}	$K\phi\phi$		(	2.3	± 0.9	) $\times 10^{-6}$		
Γ_{78}	$\overline{b} \to \overline{s}\gamma$		(	3.49	± 0.19	) $\times 10^{-4}$		
Γ_{79}	$\overline{b} \to \overline{d}\gamma$		(	9.2	± 3.0	) $\times 10^{-6}$		
Γ_{80}	$\overline{b} \to \overline{s}$ gluon		<	6.8		%		CL=90%
Γ_{81}	η anything		(	2.6	$^{+\ 0.5}_{-\ 0.8}$	) $\times 10^{-4}$		
Γ_{82}	η' anything		(	4.2	± 0.9	) $\times 10^{-4}$		
Γ_{83}	K^+ gluon (charmless)		<	1.87		$\times 10^{-4}$		CL=90%
Γ_{84}	K^0 gluon (charmless)		(	1.9	± 0.7	) $\times 10^{-4}$		

Light unflavored meson modes

Γ_{85}	$\rho\gamma$		(	1.39	± 0.25	) $\times 10^{-6}$		S=1.2
Γ_{86}	$\rho/\omega\gamma$		(	1.30	± 0.23	) $\times 10^{-6}$		S=1.2
Γ_{87}	$\pi^{\pm}$ anything	[f,i]	(	358	± 7	) %		
Γ_{88}	π^0 anything		(	235	±11	) %		
Γ_{89}	η anything		(	17.6	± 1.6	) %		
Γ_{90}	ρ^0 anything		(	21	± 5	) %		
Γ_{91}	ω anything		<	81		%		CL=90%
Γ_{92}	ϕ anything		(	3.43	± 0.12	) %		
Γ_{93}	$\phi K^*(892)$		<	2.2		$\times 10^{-5}$		CL=90%
Γ_{94}	$\overline{b} \to \overline{d}$ gluon							
Γ_{95}	π^+ gluon (charmless)		(	3.7	± 0.8	) $\times 10^{-4}$		

Baryon modes

Γ_{96}	$\Lambda_c^+ / \overline{\Lambda}_c^-$ anything		(	3.6	± 0.4	) %		
Γ_{97}	Λ_c^+ anything		<	1.3		%		CL=90%
Γ_{98}	$\overline{\Lambda}_c^-$ anything		<	7		%		CL=90%
Γ_{99}	$\overline{\Lambda}_c^-\ell^+$ anything		<	9		$\times 10^{-4}$		CL=90%
Γ_{100}	$\overline{\Lambda}_c^- e^+$ anything		<	1.8		$\times 10^{-3}$		CL=90%
Γ_{101}	$\overline{\Lambda}_c^- \mu^+$ anything		<	− 1.4		$\times 10^{-3}$		CL=90%
Γ_{102}	$\overline{\Lambda}_c^- p$ anything		(	2.06	± 0.33	) %		
Γ_{103}	$\overline{\Lambda}_c^- p e^+\nu_e$		<	8		$\times 10^{-4}$		CL=90%
Γ_{104}	$\overline{\Sigma}_c^{--}$ anything		(	3.4	± 1.7	) $\times 10^{-3}$		
Γ_{105}	$\overline{\Sigma}_c^-$ anything		<	8		$\times 10^{-3}$		CL=90%
Γ_{106}	$\overline{\Sigma}_c^0$ anything		(	3.7	± 1.7	) $\times 10^{-3}$		
Γ_{107}	$\overline{\Sigma}_c^0 N(N = p \text{ or } n)$		<	1.2		$\times 10^{-3}$		CL=90%
Γ_{108}	Ξ_c^0 anything, $\Xi_c^0 \to \Xi^-\pi^+$		(	1.93	± 0.30	) $\times 10^{-4}$		S=1.1
Γ_{109}	Ξ_c^+, $\Xi_c^+ \to \Xi^-\pi^+\pi^+$		(	4.5	$^{+\ 1.3}_{-\ 1.2}$	) $\times 10^{-4}$		
Γ_{110}	$p/\overline{p}$ anything	[f]	(	8.0	± 0.4	) %		
Γ_{111}	$p/\overline{p}$ (direct) anything	[f]	(	5.5	± 0.5	) %		
Γ_{112}	$\overline{p}e^+\nu_e$ anything		<	5.9		$\times 10^{-4}$		CL=90%
Γ_{113}	$\Lambda/\overline{\Lambda}$ anything	[f]	(	4.0	± 0.5	) %		
Γ_{114}	Λ anything			seen				
Γ_{115}	$\overline{\Lambda}$ anything			seen				
Γ_{116}	$\Xi^-/\overline{\Xi}^+$ anything	[f]	(	2.7	± 0.6	) $\times 10^{-3}$		
Γ_{117}	baryons anything		(	6.8	± 0.6	) %		
Γ_{118}	$p\overline{p}$ anything		(	2.47	± 0.23	) %		
Γ_{119}	$\Lambda\overline{p}/\overline{\Lambda}p$ anything	[f]	(	2.5	± 0.4	) %		
Γ_{120}	$\Lambda\overline{\Lambda}$ anything		<	5		$\times 10^{-3}$		CL=90%

Lepton Family number (LF) violating modes or $\Delta B = 1$ weak neutral current ($B1$) modes

Γ_{121}	se^+e^-	$B1$		(	6.7	± 1.7	) $\times 10^{-6}$		S=2.0
Γ_{122}	$s\mu^+\mu^-$	$B1$		(	4.3	± 1.0	) $\times 10^{-6}$		
Γ_{123}	$s\ell^+\ell^-$	$B1$	[b]	(	5.8	± 1.3	) $\times 10^{-6}$		S=1.8
Γ_{124}	$\pi\ell^+\ell^-$	$B1$		<	5.9		$\times 10^{-8}$		CL=90%
Γ_{125}	πe^+e^-	$B1$		<	1.10		$\times 10^{-7}$		CL=90%
Γ_{126}	$\pi\mu^+\mu^-$	$B1$		<	5.0		$\times 10^{-8}$		CL=90%
Γ_{127}	Ke^+e^-	$B1$		(	4.4	± 0.6	) $\times 10^{-7}$		
Γ_{128}	$K^*(892)e^+e^-$	$B1$		(	1.19	± 0.20	) $\times 10^{-6}$		S=1.2
Γ_{129}	$K\mu^+\mu^-$	$B1$		(	4.4	± 0.4	) $\times 10^{-7}$		
Γ_{130}	$K^*(892)\mu^+\mu^-$	$B1$		(	1.06	± 0.09	) $\times 10^{-6}$		
Γ_{131}	$K\ell^+\ell^-$	$B1$		(	4.8	± 0.4	) $\times 10^{-7}$		
Γ_{132}	$K^*(892)\ell^+\ell^-$	$B1$		(	1.05	± 0.10	) $\times 10^{-6}$		
Γ_{133}	$K\nu\overline{\nu}$	$B1$		<	1.6		$\times 10^{-5}$		CL=90%
Γ_{134}	$K^*\nu\overline{\nu}$	$B1$		<	2.7		$\times 10^{-5}$		CL=90%
Γ_{135}	$\pi\nu\overline{\nu}$	$B1$		<	8		$\times 10^{-6}$		CL=90%
Γ_{136}	$\rho\nu\overline{\nu}$	$B1$		<	2.8		$\times 10^{-5}$		CL=90%
Γ_{137}	$se^{\pm}\mu^{\mp}$	LF	[f]	<	2.2		$\times 10^{-5}$		CL=90%
Γ_{138}	$\pi e^{\pm}\mu^{\mp}$	LF		<	9.2		$\times 10^{-8}$		CL=90%
Γ_{139}	$\rho e^{\pm}\mu^{\mp}$	LF		<	3.2		$\times 10^{-6}$		CL=90%
Γ_{140}	$Ke^{\pm}\mu^{\mp}$	LF		<	3.8		$\times 10^{-8}$		CL=90%
Γ_{141}	$K^*(892)e^{\pm}\mu^{\mp}$	LF		<	5.1		$\times 10^{-7}$		CL=90%

[a] These values are model dependent.

[b] An ℓ indicates an e or a μ mode, not a sum over these modes.

[c] Here "anything" means at least one particle observed.

[d] This is a B($B^0 \rightarrow D^{*-}\ell^+\nu_\ell$) value.

[e] D^{**} stands for the sum of the $D(1\,^1P_1)$, $D(1\,^3P_0)$, $D(1\,^3P_1)$, $D(1\,^3P_2)$, $D(2\,^1S_0)$, and $D(2\,^1S_1)$ resonances.

[f] The value is for the sum of the charge states or particle/antiparticle states indicated.

[g] $D^{(*)}\overline{D}^{(*)}$ stands for the sum of $D^*\overline{D}^*$, $D^*\overline{D}$, $D\overline{D}^*$, and $D\overline{D}$.

[h] $X(3915)$ denotes a near-threshold enhancement in the $\omega J/\psi$ mass spectrum.

[i] Inclusive branching fractions have a multiplicity definition and can be greater than 100%.

$B^{\pm}/B^0$ ADMIXTURE BRANCHING RATIOS

$\Gamma(\ell^+\nu_\ell \text{anything})/\Gamma_{\text{total}}$ Γ_3/Γ

These branching fraction values are model dependent.

"OUR EVALUATION" assumes lepton universality and is an average using rescaled values of the data listed below. The average and rescaling were performed by the Heavy Flavor Averaging Group (HFLAV) and are described at http://www.slac.stanford.edu/xorg/hflav/. The averaging/rescaling procedure takes into account correlations between the measurements.

VALUE (%)	DOCUMENT ID		TECN	COMMENT
10.86±0.16 OUR EVALUATION				
10.49±0.20 OUR AVERAGE	Error includes scale factor of 1.3. See the ideogram below.			
10.34±0.04±0.26	[1] LEES	17B	BABR	$e^+e^- \rightarrow \Upsilon(4S)$
10.28±0.18±0.24	[2] URQUIJO	07	BELL	$e^+e^- \rightarrow \Upsilon(4S)$
10.91±0.09±0.24	[3] MAHMOOD	04	CLEO	$e^+e^- \rightarrow \Upsilon(4S)$
9.7 ±0.5 ±0.4	[4] ALBRECHT	93H	ARG	$e^+e^- \rightarrow \Upsilon(4S)$
• • • We do not use the following data for averages, fits, limits, etc. • • •				
9.96±0.19±0.32	[5] AUBERT,B	06Y	BABR	Repl. by LEES 17B
10.85±0.21±0.36	[6] OKABE	05	BELL	Repl. by URQUIJO 07
10.83±0.16±0.06	[7] AUBERT	04X	BABR	Repl. by AUBERT,B 06Y
10.36±0.06±0.23	[8] AUBERT,B	04A	BABR	$e^+e^- \rightarrow \Upsilon(4S)$
10.87±0.18±0.30	[9] AUBERT	03	BABR	Repl. by AUBERT 04X
10.90±0.12±0.49	[10] ABE	02Y	BELL	Repl. by OKABE 05
10.49±0.17±0.43	[11] BARISH	96B	CLE2	Repl. by MAHMOOD 04
10.80±0.20±0.56	[12] HENDERSON	92	CLEO	$e^+e^- \rightarrow \Upsilon(4S)$
10.0 ±0.4 ±0.3	[13] YANAGISAWA	91	CSB2	$e^+e^- \rightarrow \Upsilon(4S)$
10.3 ±0.6 ±0.2	[14] ALBRECHT	90H	ARG	Direct e at $\Upsilon(4S)$
10.0 ±0.6 ±0.2	[15] ALBRECHT	90H	ARG	Direct μ at $\Upsilon(4S)$
11.7 ±0.4 ±1.0	[16] WACHS	89	CBAL	Direct e at $\Upsilon(4S)$
12.0 ±0.7 ±0.5	CHEN	84	CLEO	Direct e at $\Upsilon(4S)$
10.8 ±0.6 ±1.0	CHEN	84	CLEO	Direct μ at $\Upsilon(4S)$
11.2 ±0.9 ±1.0	LEVMAN	84	CUSB	Direct μ at $\Upsilon(4S)$
13.2 ±0.8 ±1.4	[17] KLOPFEN...	83B	CUSB	Direct e at $\Upsilon(4S)$

[1] LEES 17B measurement is obtained from semileptonic decays to electrons. The result is averaged over $B^{\pm}$ and B^0 mesons, assuming lepton universality.

[2] URQUIJO 07 report a measurement of (10.07 ± 0.18 ± 0.21)% for the partial branching fraction of $B \rightarrow e\nu_e X_c$ decay with electron energy above 0.6 GeV. We converted the result to $B \rightarrow e\nu_e X$ branching fraction.

[3] Uses charge and angular correlations in $\Upsilon(4S)$ events with a high-momentum lepton and an additional electron.

[4] ALBRECHT 93H analysis performed using tagged semileptonic decays of the B. This technique is almost model independent for the lepton branching ratio.

[5] The measurements are obtained for charged and neutral B mesons partial rates of semileptonic decay to electrons with momentum above 0.6 GeV/c in the B rest frame. The best precision on the ratio is achieved for a momentum threshold of 1.0 GeV: B($B^+ \rightarrow e^+\nu_e X$) / B($B^0 \rightarrow e^+\nu_e X$) = 1.074 ± 0.041 ± 0.026.

[6] The measurements are obtained for charged and neutral B mesons partial rates of semileptonic decay to electrons with momentum above 0.6 GeV/c in the B rest frame, and their ratio of B($B^+ \rightarrow e^+\nu_e X$)/B($B^0 \rightarrow e^+\nu_e X$) = 1.08 ± 0.05 ± 0.02.

[7] The semileptonic branching ratio, $|V_{cb}|$ and other heavy-quark parameters are determined from a simultaneous fit to moments of the hadronic-mass and lepton-energy distribution.

[8] Uses the high-momentum lepton tag method and requires the electron energy above 0.6 GeV.

[9] Uses the high-momentum lepton tag method. They also report $|V_{cb}|$ = 0.0423 ± 0.0007(exp) ±0.0020(theo.).

[10] Uses the high-momentum lepton tag method. ABE 02Y also reports $|V_{cb}|$ = 0.0408 ± 0.0010(exp) ±0.0025(theo.). The second error is due to uncertainties of theoretical inputs.

[11] BARISH 96B analysis performed using tagged semileptonic decays of the B. This technique is almost model independent for the lepton branching ratio.

[12] HENDERSON 92 measurement employs e and μ. The systematic error contains 0.004 in quadrature from model dependence. The authors average a variation of the Isgur, Scora, Grinstein, and Wise model with that of the Altarelli-Cabibbo-Corbò-Maiani-Martinelli model for semileptonic decays to correct the acceptance.

[13] YANAGISAWA 91 also measures an average semileptonic branching ratio at the $\Upsilon(5S)$ of 9.6–10.5% depending on assumptions about the relative production of different B meson species.

[14] ALBRECHT 90H uses the model of ALTARELLI 82 to correct over all lepton momenta. 0.099 ± 0.006 is obtained using ISGUR 89B.

[15] ALBRECHT 90H uses the model of ALTARELLI 82 to correct over all lepton momenta. 0.097 ± 0.006 is obtained using ISGUR 89B.

[16] Using data above $p(e)$ = 2.4 GeV, WACHS 89 determine $\sigma(B \rightarrow e\nu\text{up})/\sigma(B \rightarrow e\nu\text{charm}) < 0.065$ at 90% CL.

[17] Ratio $\sigma(b \rightarrow e\nu\text{up})/\sigma(b \rightarrow e\nu\text{charm}) < 0.055$ at CL = 90%.

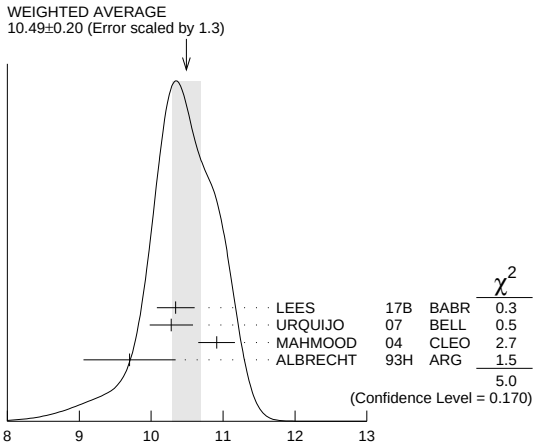

$\Gamma(D^-\ell^+\nu_\ell \text{anything})/\Gamma(\ell^+\nu_\ell \text{anything})$ Γ_4/Γ_3

$\ell = e$ or μ.

VALUE	DOCUMENT ID		TECN	COMMENT
0.26±0.07±0.04	[1] FULTON	91	CLEO	$e^+e^- \rightarrow \Upsilon(4S)$

[1] FULTON 91 uses B($D^+ \rightarrow K^-\pi^+\pi^+$) = (9.1 ±1.3 ±0.4)% as measured by MARK III.

$\Gamma(\overline{D}^0\ell^+\nu_\ell \text{anything})/\Gamma(\ell^+\nu_\ell \text{anything})$ Γ_5/Γ_3

$\ell = e$ or μ.

VALUE	DOCUMENT ID		TECN	COMMENT
0.67±0.09±0.10	[1] FULTON	91	CLEO	$e^+e^- \rightarrow \Upsilon(4S)$

[1] FULTON 91 uses B($D^0 \rightarrow K^-\pi^+$) = (4.2 ± 0.4 ± 0.4)% as measured by MARK III.

$\Gamma(\overline{D}\ell^+\nu_\ell)/\Gamma(\ell^+\nu_\ell \text{anything})$ Γ_6/Γ_3

VALUE	DOCUMENT ID		TECN	COMMENT
0.223±0.006±0.009	[1] AUBERT	10	BABR	$e^+e^- \rightarrow \Upsilon(4S)$

[1] Uses a fully reconstructed B meson as a tag on the recoil side.

$\Gamma(D^{*-}\ell^+\nu_\ell \text{anything})/\Gamma_{\text{total}}$ Γ_7/Γ

VALUE (units 10^{-2})	DOCUMENT ID		TECN	COMMENT
0.67±0.08±0.10	ABDALLAH	04D	DLPH	$e^+e^- \rightarrow Z^0$
• • • We do not use the following data for averages, fits, limits, etc. • • •				
0.6 ±0.3 ±0.1	[1] BARISH	95	CLE2	$e^+e^- \rightarrow \Upsilon(4S)$

[1] BARISH 95 use B($D^0 \rightarrow K^-\pi^+$) = (3.91 ± 0.08 ± 0.17)% and B($D^{*+} \rightarrow D^0\pi^+$) = (68.1 ± 1.0 ± 1.3)%.

$\Gamma(D^{*0}\ell^+\nu_\ell \text{anything})/\Gamma_{\text{total}}$ Γ_8/Γ

VALUE (units 10^{-2})	DOCUMENT ID		TECN	COMMENT
• • • We do not use the following data for averages, fits, limits, etc. • • •				
0.6±0.6±0.1	[1] BARISH	95	CLE2	$e^+e^- \rightarrow \Upsilon(4S)$

[1] BARISH 95 use B($D^0 \rightarrow K^-\pi^+$) = (3.91 ± 0.08 ± 0.17)%, B($D^{*+} \rightarrow D^0\pi^+$) = (68.1 ± 1.0 ± 1.3)%, B($D^{*0} \rightarrow D^0\pi^0$) = (63.6 ± 2.3 ± 3.3)%.

$\Gamma(\overline{D}^{**}\ell^+\nu_\ell)/\Gamma_{\text{total}}$ Γ_{10}/Γ

D^{**} stands for the sum of the $D(1\,^1P_1)$, $D(1\,^3P_0)$, $D(1\,^3P_1)$, $D(1\,^3P_2)$, $D(2\,^1S_0)$, and $D(2\,^1S_1)$ resonances. $\ell = e$ or μ, not sum over e and μ modes.

VALUE	CL%	EVTS	DOCUMENT ID		TECN	COMMENT
0.027±0.005±0.005		63	[1] ALBRECHT	93	ARG	$e^+e^- \rightarrow \Upsilon(4S)$
• • • We do not use the following data for averages, fits, limits, etc. • • •						
<0.028	95		[2] BARISH	95	CLE2	$e^+e^- \rightarrow \Upsilon(4S)$

[1] ALBRECHT 93 assumes the GISW model to correct for unseen modes. Using the BHKT model, the result becomes 0.023 ± 0.006 ± 0.004. Assumes B($D^{*+} \rightarrow D^0\pi^+$) = 68.1%, B($D^0 \rightarrow K^-\pi^+$) = 3.65%, B($D^0 \rightarrow K^-\pi^+\pi^-\pi^+$) = 7.5%. We have taken their average e and μ value.

[2] BARISH 95 use B($D^0 \rightarrow K^-\pi^+$) = (3.91 ± 0.08 ± 0.17)%, assume all nonresonant channels are zero, and use GISW model for relative abundances of D^{**} states.

$\Gamma(\overline{D}_1(2420)\ell^+\nu_\ell \text{anything})/\Gamma_{\text{total}}$ Γ_{11}/Γ

VALUE	DOCUMENT ID		TECN	COMMENT
0.0038±0.0013 OUR AVERAGE	Error includes scale factor of 2.4.			
0.0033±0.0006	[1] ABAZOV	05O	D0	$p\overline{p}$ at 1.96 TeV
0.0074±0.0016	[2] BUSKULIC	97B	ALEP	$e^+e^- \rightarrow Z$
• • • We do not use the following data for averages, fits, limits, etc. • • •				
seen	[3] BUSKULIC	95B	ALEP	Repl. by BUSKULIC 97B

[1] Assumes B($D_1 \rightarrow D^*\pi$) = 1, B($D_1 \rightarrow D^*\pi^{\pm}$) = 2/3, and B($b \rightarrow B$) =0.397.

[2] BUSKULIC 97B assumes B($D_1(2420) \rightarrow D^*\pi$) = 1, B($D_1(2420) \rightarrow D^*\pi^{\pm}$) = 2/3, and B($b \rightarrow B$) = 0.378 ± 0.022.

[3] BUSKULIC 95B reports $f_B \times B(B \to \overline{D}_1(2420)^0 \ell^+ \nu_\ell \text{anything}) \times B(\overline{D}_1(2420)^0 \to \overline{D}^*(2010)^- \pi^+) = (2.04 \pm 0.58 \pm 0.34)10^{-3}$, where f_B is the production fraction for a single B charge state.

$[\Gamma(D\pi\ell^+\nu_\ell \text{anything}) + \Gamma(D^*\pi\ell^+\nu_\ell \text{anything})]/\Gamma_{\text{total}}$ Γ_{12}/Γ

VALUE	DOCUMENT ID		TECN	COMMENT
0.026 ±0.005 OUR AVERAGE	Error includes scale factor of 1.5.			
0.0340±0.0052±0.0032	[1] ABREU	00R	DLPH	$e^+e^- \to Z$
0.0226±0.0029±0.0033	[2] BUSKULIC	97B	ALEP	$e^+e^- \to Z$

[1] Assumes no contribution from B_s and b baryons. Further assumes contributions from single pion ($D\pi$ and $D^*\pi$) states only, allowing isospin conservation to relate the relative π^0 and π^+ rates.

[2] BUSKULIC 97B assumes $B(b \to B) = 0.378 \pm 0.022$ and uses isospin invariance by assuming that all observed $D^0\pi^+$, $D^{*0}\pi^+$, $D^+\pi^-$, and $D^{*+}\pi^-$ are from D^{**} states. A correction has been applied to account for the production of B_s^0 and Λ_b^0.

$\Gamma(D\pi\ell^+\nu_\ell \text{anything})/\Gamma_{\text{total}}$ Γ_{13}/Γ

VALUE	DOCUMENT ID		TECN	COMMENT
0.0154±0.0061	ABREU	00R	DLPH	$e^+e^- \to Z$

$\Gamma(D^*\pi\ell^+\nu_\ell \text{anything})/\Gamma_{\text{total}}$ Γ_{14}/Γ

VALUE	DOCUMENT ID		TECN	COMMENT
0.0186±0.0038	ABREU	00R	DLPH	$e^+e^- \to Z$

$\Gamma(\overline{D}_2^*(2460)\ell^+\nu_\ell \text{anything})/\Gamma_{\text{total}}$ Γ_{15}/Γ

VALUE	CL%	DOCUMENT ID		TECN	COMMENT
0.0044±0.0016		[1] ABAZOV	05O	D0	$p\overline{p}$ at 1.96 TeV
• • • We do not use the following data for averages, fits, limits, etc. • • •					
<0.0065	95	[2] BUSKULIC	97B	ALEP	$e^+e^- \to Z$
not seen		[3] BUSKULIC	95B	ALEP	$e^+e^- \to Z$

[1] Assumes $B(D_2^* \to D^*\pi^\pm) = 0.30 \pm 0.06$ and $B(b \to B) = 0.397$.

[2] A revised number based on BUSKULIC 97B which assumes $B(D_2^*(2460) \to D^*\pi^\pm) = 0.20$ and $B(b \to B) = 0.378 \pm 0.022$.

[3] BUSKULIC 95B reports $f_B \times B(B \to \overline{D}_2^*(2460)^0 \ell^+ \nu_\ell \text{anything}) \times B(\overline{D}_2^*(2460)^0 \to \overline{D}^*(2010)^- \pi^+) \leq 0.81 \times 10^{-3}$ at CL=95%, where f_B is the production fraction for a single B charge state.

$\frac{\Gamma(B \to \overline{D}_2^*(2460)\ell^+\nu_\ell \text{anything}) \times B(D_2^*(2460) \to D^{*-}\pi^+)}{\Gamma(B \to \overline{D}_1(2420)\ell^+\nu_\ell \text{anything}) \times B(\overline{D}_1(2420) \to D^{*-}\pi^+)}$

VALUE	DOCUMENT ID		TECN	COMMENT
0.39±0.09±0.12	ABAZOV	05O	D0	$p\overline{p}$ at 1.96 TeV

$\Gamma(D^{*-}\pi^+\ell^+\nu_\ell \text{anything})/\Gamma_{\text{total}}$ Γ_{16}/Γ

Includes resonant and nonresonant contributions.

VALUE (units 10^{-3})	DOCUMENT ID		TECN	COMMENT
10.0±2.7±2.1	[1] BUSKULIC	95B	ALEP	$e^+e^- \to Z$

[1] BUSKULIC 95B reports $f_B \times B(B \to \overline{D}^*(2010)^- \pi^+ \ell^+ \nu_\ell \text{anything}) = (3.7 \pm 1.0 \pm 0.7)10^{-3}$. Above value assumes $f_B = 0.37 \pm 0.03$.

$\Gamma(\overline{D}\pi^+\pi^-\ell^+\nu_\ell)/\Gamma(\overline{D}\ell^+\nu_\ell)$ Γ_{17}/Γ_6

VALUE (units 10^{-2})	DOCUMENT ID		TECN	COMMENT
6.7±1.0±0.8	[1] LEES	16	BABR	$e^+e^- \to \Upsilon(4S)$

[1] Measurement used electrons and muons as leptons.

$\Gamma(\overline{D}^*\pi^+\pi^-\ell^+\nu_\ell)/\Gamma(D^*\ell^+\nu_\ell)$ Γ_{18}/Γ_9

VALUE (units 10^{-2})	DOCUMENT ID		TECN	COMMENT
1.9±0.5±0.4	[1] LEES	16	BABR	$e^+e^- \to \Upsilon(4S)$

[1] Measurement used electrons and muons as leptons.

$\Gamma(D_s^-\ell^+\nu_\ell \text{anything})/\Gamma_{\text{total}}$ Γ_{19}/Γ

VALUE	CL%	DOCUMENT ID		TECN	COMMENT
<7 × 10⁻³	90	[1] ALBRECHT	93E	ARG	$e^+e^- \to \Upsilon(4S)$

[1] ALBRECHT 93E reports < 0.012 from a measurement of $[\Gamma(B \to D_s^-\ell^+\nu_\ell \text{anything})/\Gamma_{\text{total}}] \times [B(D_s^+ \to \phi\pi^+)]$ assuming $B(D_s^+ \to \phi\pi^+) = 0.027$, which we rescale to our best value $B(D_s^+ \to \phi\pi^+) = 4.5 \times 10^{-2}$.

$\Gamma(D_s^-\ell^+\nu_\ell K^+ \text{anything})/\Gamma_{\text{total}}$ Γ_{20}/Γ

VALUE	CL%	DOCUMENT ID		TECN	COMMENT
<5 × 10⁻³	90	[1] ALBRECHT	93E	ARG	$e^+e^- \to \Upsilon(4S)$

[1] ALBRECHT 93E reports < 0.008 from a measurement of $[\Gamma(B \to D_s^-\ell^+\nu_\ell K^+ \text{anything})/\Gamma_{\text{total}}] \times [B(D_s^+ \to \phi\pi^+)]$ assuming $B(D_s^+ \to \phi\pi^+) = 0.027$, which we rescale to our best value $B(D_s^+ \to \phi\pi^+) = 4.5 \times 10^{-2}$.

$\Gamma(D_s^-\ell^+\nu_\ell K^0 \text{anything})/\Gamma_{\text{total}}$ Γ_{21}/Γ

VALUE	CL%	DOCUMENT ID		TECN	COMMENT
<7 × 10⁻³	90	[1] ALBRECHT	93E	ARG	$e^+e^- \to \Upsilon(4S)$

[1] ALBRECHT 93E reports < 0.012 from a measurement of $[\Gamma(B \to D_s^-\ell^+\nu_\ell K^0 \text{anything})/\Gamma_{\text{total}}] \times [B(D_s^+ \to \phi\pi^+)]$ assuming $B(D_s^+ \to \phi\pi^+) = 0.027$, which we rescale to our best value $B(D_s^+ \to \phi\pi^+) = 4.5 \times 10^{-2}$.

$\Gamma(X_c\ell^+\nu_\ell)/\Gamma_{\text{total}}$ Γ_{22}/Γ

"OUR EVALUATION" is an average using rescaled values of the data listed below. The average and rescaling were performed by the Heavy Flavor Averaging Group (HFLAV) and are described at http://www.slac.stanford.edu/xorg/hflav/. The averaging/rescaling procedure takes into account correlations between the measurements.

VALUE (%)	DOCUMENT ID		TECN	COMMENT
10.65±0.16 OUR EVALUATION				
10.29±0.19 OUR AVERAGE				
10.18±0.03±0.24	[1] LEES	17B	BABR	$e^+e^- \to \Upsilon(4S)$
10.44±0.19±0.22	[2] URQUIJO	07	BELL	$e^+e^- \to \Upsilon(4S)$
• • • We do not use the following data for averages, fits, limits, etc. • • •				
10.64±0.17±0.06	[3] AUBERT	10A	BABR	Repl. by LEES 17B
10.61±0.16±0.06	[4] AUBERT	04X	BABR	Repl. by AUBERT 10A

[1] The measurement is obtained from semileptonic decays to electrons $B \to X e\nu$, and using a theoretical model (GAMBINO 07, GAMBINO 11) to predict the contribution from $B \to X_u e\nu$. The result is averaged over $B^\pm$ and B^0 mesons, assuming lepton universality.

[2] Measured the independent B^+ and B^0 partial branching fractions with electron energy above 0.4 GeV.

[3] Obtained from a combined fit to the moments of observed spectra in inclusive $B \to X_c\ell^+\nu_\ell$ decay.

[4] The semileptonic branching ratio, $|V_{cb}|$ and other heavy-quark parameters are determined from a simultaneous fit to moments of the hadronic-mass and lepton-energy distribution.

$\Gamma(X_u\ell^+\nu_\ell)/\Gamma_{\text{total}}$ Γ_{23}/Γ

"OUR EVALUATION" is an average using rescaled values of the data listed below. The average and rescaling were performed by the Heavy Flavor Averaging Group (HFLAV) and are described at http://www.slac.stanford.edu/xorg/hflav/. The averaging/rescaling procedure takes into account correlations between the measurements.

VALUE (units 10^{-3})	DOCUMENT ID		TECN	COMMENT
2.13 ±0.31 OUR EVALUATION				
$1.665 \pm 0.087^{+0.103}_{-0.094}$	[1] LEES	17B	BABR	$e^+e^- \to \Upsilon(4S)$
2.01 ±0.15 ±0.25	[2] LEES	12R	BABR	$e^+e^- \to \Upsilon(4S)$
2.53 ±0.24 ±0.24	[3] AUBERT,B	05X	BABR	$e^+e^- \to \Upsilon(4S)$
2.80 ±0.52 ±0.41	[4] LIMOSANI	05	BELL	$e^+e^- \to \Upsilon(4S)$
1.77 ±0.29 ±0.38	[5] BORNHEIM	02	CLE2	$e^+e^- \to \Upsilon(4S)$
• • • We do not use the following data for averages, fits, limits, etc. • • •				
1.963±0.173±0.159	[6] URQUIJO	10	BELL	$e^+e^- \to \Upsilon(4S)$
1.18 ±0.09 ±0.07	[7] AUBERT	08AS	BABR	Repl. by LEES 12R
2.27 ±0.26 $^{+0.37}_{-0.33}$	[8] AUBERT	06H	BABR	Repl. by LEES 17B
2.24 ±0.27 ±0.47	[9,10] AUBERT	04I	BABR	Repl. by AUBERT,B 05X

[1] Obtained from the partial rate $\Delta B = (1.554 \pm 0.082^{+0.095}_{-0.086}) \times 10^{-3}$ for the electron momentum interval of 0.8–2.7 GeV/c based on GGOU1 method ($X_c\ell\nu$, m_c constraint fit of SF parameters).

[2] Measures several partial branching fractions in different phase space regions. The most precise result on the full branching fraction is obtained in the region for lepton momentum in B rest frame $p_\ell^* > 1$ GeV/c, where the measured partial branching fraction is $\Delta B = (1.80 \pm 0.13 \pm 0.15) \times 10^{-3}$. The acceptance in that region is reported in a private communication by the Authors to be 0.894. The corresponding $|V_{ub}|$ from the BLNP method is $(4.28 \pm 0.15 \pm 0.18 \pm 0.19) \times 10^{-3}$, where the last uncertainty comes from theoretical prediction.

[3] Determined from the partial rate $\Delta B = (4.41 \pm 0.42 \pm 0.42) \times 10^{-4}$ measured for electron energy > 2 GeV and hadronic mass squared < 3.5 GeV^2, and calculated acceptance 0.174 in that region. The V_{ub} is measured as $(4.41 \pm 0.30^{+0.65}_{-0.47} \pm 0.28) \times 10^{-3}$.

[4] Uses electrons in the momentum interval 1.9–2.6 GeV/c in the center-of-mass frame. The V_{ub} is found to be $(5.08 \pm 0.47^{+0.49}_{-0.48}) \times 10^{-3}$.

[5] BORNHEIM 02 uses the observed yield of leptons from semileptonic B decays in the end-point momentum interval 2.2–2.6 GeV/c with recent CLEO-2 data on $B \to X_s\gamma$. The V_{ub} is found to be $(4.08 \pm 0.34 \pm 0.53) \times 10^{-3}$.

[6] Uses a multivariate analysis method and requires lepton momentum in the B rest frame, $p_l^{*B} > 1.0$ GeV/c.

[7] Measures several partial branching fractions in different phase space regions. The most precise result is obtained in the region for hadronic mass $M_X < 1.55$ GeV/c^2, and is $\Delta B = (1.18 \pm 0.09 \pm 0.07) \times 10^{-3}$. The corresponding $|V_{ub}|$ from the BLNP method is $(4.27 \pm 0.16 \pm 0.13 \pm 0.30) \times 10^{-3}$, where the last uncertainty comes from the theoretical prediction of the partial rate in the given phase-space region.

[8] Obtained from the partial rate $\Delta B = (0.572 \pm 0.041 \pm 0.065) \times 10^{-3}$ for the electron momentum interval of 2.0–2.6 GeV/c based on BLNP method.

[9] Used BaBar measurement of Semileptonic branching fraction $B(B \to X\ell\nu_\ell) = (10.87 \pm 0.18 \pm 0.30)\%$ to convert the ratio of rates to branching fraction.

[10] The third error includes the systematics and theoretical errors summed in quadrature.

$\Gamma(X_u\ell^+\nu_\ell)/\Gamma(\ell^+\nu_\ell \text{anything})$ Γ_{23}/Γ_3

ℓ denotes e or μ, not the sum. These experiments measure this ratio in very limited momentum intervals.

VALUE (units 10^{-2})	CL%	EVTS	DOCUMENT ID		TECN	COMMENT
2.06±0.25±0.42			[1] AUBERT	04I	BABR	$e^+e^- \to \Upsilon(4S)$

• • • We do not use the following data for averages, fits, limits, etc. • • •

			[2] ALBRECHT	94C	ARG	$e^+e^- \to \Upsilon(4S)$
		107	[3] BARTELT	93B	CLE2	$e^+e^- \to \Upsilon(4S)$
		77	[4] ALBRECHT	91C	ARG	$e^+e^- \to \Upsilon(4S)$
		41	[5] ALBRECHT	90	ARG	$e^+e^- \to \Upsilon(4S)$
		76	[6] FULTON	90	CLEO	$e^+e^- \to \Upsilon(4S)$
<4.0	90		[7] BEHRENDS	87	CLEO	$e^+e^- \to \Upsilon(4S)$
<4.0	90		CHEN	84	CLEO	Direct e at $\Upsilon(4S)$
<5.5	90		KLOPFEN...	83B	CUSB	Direct e at $\Upsilon(4S)$

[1] The third error includes the systematics and theoretical errors summed in quadrature.

[2] ALBRECHT 94C find $\Gamma(b \to c)/\Gamma(b \to \text{all}) = 0.99 \pm 0.02 \pm 0.04$.

[3] BARTELT 93B (CLEO II) measures an excess of $107 \pm 15 \pm 11$ leptons in the lepton momentum interval 2.3–2.6 GeV/c which is attributed to $b \to u\ell\nu_\ell$. This corresponds to a model-dependent partial branching ratio ΔB_{ub} between $(1.15 \pm 0.16 \pm 0.15) \times 10^{-4}$, as evaluated using the KS model (KOERNER 88), and $(1.54 \pm 0.22 \pm 0.20) \times 10^{-4}$ using the ACCMM model (ARTUSO 93). The corresponding values of $|V_{ub}|/|V_{cb}|$ are 0.056 ± 0.006 and 0.076 ± 0.008, respectively.

[4] ALBRECHT 91C result supersedes ALBRECHT 90. Two events are fully reconstructed providing evidence for the $b \to u$ transition. Using the model of ALTARELLI 82, they obtain $|V_{ub}/V_{cb}| = 0.11 \pm 0.012$ from 77 leptons in the 2.3–2.6 GeV momentum range.

[5] ALBRECHT 90 observes 41 ± 10 excess e and μ (lepton) events in the momentum interval $p = 2.3$–2.6 GeV signaling the presence of the $b \to u$ transition. The events correspond to a model-dependent measurement of $|V_{ub}/V_{cb}| = 0.10 \pm 0.01$.

[6] FULTON 90 observe 76 ± 20 excess e and μ (lepton) events in the momentum interval $p = 2.4$–2.6 GeV signaling the presence of the $b \to u$ transition. The average branching ratio, $(1.8 \pm 0.4 \pm 0.3) \times 10^{-4}$, corresponds to a model-dependent measurement of approximately $|V_{ub}/V_{cb}| = 0.1$ using $B(b \to c\ell\nu) = 10.2 \pm 0.2 \pm 0.7\%$.

[7] The quoted possible limits range from 0.018 to 0.04 for the ratio, depending on which model or momentum range is chosen. We select the most conservative limit they have calculated. This corresponds to a limit on $|V_{ub}|/|V_{cb}| < 0.20$. While the endpoint technique employed is more robust than their previous results in CHEN 84, these results do not provide a numerical improvement in the limit.

$\Gamma(K^+\ell^+\nu_\ell \text{anything})/\Gamma(\ell^+\nu_\ell \text{anything})$ Γ_{24}/Γ_3

ℓ denotes e or μ, not the sum.

VALUE	DOCUMENT ID		TECN	COMMENT
0.58 ±0.05 OUR AVERAGE				
0.594±0.021±0.056	ALBRECHT	94C	ARG	$e^+e^- \to \Upsilon(4S)$
0.54 ±0.07 ±0.06	[1] ALAM	87B	CLEO	$e^+e^- \to \Upsilon(4S)$

[1] ALAM 87B measurement relies on lepton-kaon correlations.

$\Gamma(K^-\ell^+\nu_\ell \text{anything})/\Gamma(\ell^+\nu_\ell \text{anything})$ Γ_{25}/Γ_3

ℓ denotes e or μ, not the sum.

VALUE	DOCUMENT ID		TECN	COMMENT
0.092±0.035 OUR AVERAGE				
0.086±0.011±0.044	ALBRECHT	94C	ARG	$e^+e^- \to \Upsilon(4S)$
0.10 ±0.05 ±0.02	[1] ALAM	87B	CLEO	$e^+e^- \to \Upsilon(4S)$

[1] ALAM 87B measurement relies on lepton-kaon correlations.

$\Gamma(K^0/\overline{K}^0\ell^+\nu_\ell \text{anything})/\Gamma(\ell^+\nu_\ell \text{anything})$ Γ_{26}/Γ_3

ℓ denotes e or μ, not the sum. Sum over K^0 and $\overline{K}^0$ states.

VALUE	DOCUMENT ID		TECN	COMMENT
0.42 ±0.05 OUR AVERAGE				
0.452±0.038±0.056	[1] ALBRECHT	94C	ARG	$e^+e^- \to \Upsilon(4S)$
0.39 ±0.06 ±0.04	[2] ALAM	87B	CLEO	$e^+e^- \to \Upsilon(4S)$

[1] ALBRECHT 94C assume a $K^0/\overline{K}^0$ multiplicity twice that of K^0_S.

[2] ALAM 87B measurement relies on lepton-kaon correlations.

$\Gamma(\overline{D}\tau^+\nu_\tau)/\Gamma(\overline{D}\ell^+\nu_\ell)$ Γ_{27}/Γ_6

"OUR EVALUATION" is an average using rescaled values of the data listed below. The average and rescaling were performed by the Heavy Flavor Averaging Group (HFLAV) and are described at http://www.slac.stanford.edu/xorg/hflav/. The averaging/rescaling procedure takes into account correlations between the measurements.

VALUE (units 10^{-2})	DOCUMENT ID		TECN	COMMENT
40.7 ± 4.6 OUR EVALUATION				
41 ± 5 OUR AVERAGE				
37.5 ± 6.4±2.6	[1,2] HUSCHLE	15	BELL	$e^+e^- \to \Upsilon(4S)$
44.0 ± 5.8±4.2	[1,2] LEES	12D	BABR	$e^+e^- \to \Upsilon(4S)$
• • • We do not use the following data for averages, fits, limits, etc. • • •				
4.16±11.7±5.2	[1] AUBERT	08N	BABR	Repl. by LEES 12D

[1] Uses a fully reconstructed B meson as a tag on the recoil side.

[2] Uses $\tau^+ \to e^+\nu_e\overline{\nu}_\tau$ and $\tau^+ \to \mu^+\nu_\mu\overline{\nu}_\tau$ and e^+ or μ^+ as ℓ^+. Obtained from simultaneous fit to B+ and B0 assuming isospin symmetry.

$\Gamma(D^*\tau^+\nu_\tau)/\Gamma(D^*\ell^+\nu_\ell)$ Γ_{28}/Γ_9

"OUR EVALUATION" is an average using rescaled values of the data listed below. The average and rescaling were performed by the Heavy Flavor Averaging Group (HFLAV) and are described at http://www.slac.stanford.edu/xorg/hflav/. The averaging/rescaling procedure takes into account correlations between the measurements.

VALUE (units 10^{-2})	DOCUMENT ID		TECN	COMMENT
30.4±1.5 OUR EVALUATION				
30.7±2.1 OUR AVERAGE				
$27.0 \pm 3.5^{+2.8}_{-2.5}$	[1] HIROSE	17	BELL	$e^+e^- \to \Upsilon(4S)$
29.3±3.8±1.5	[2] HUSCHLE	15	BELL	$e^+e^- \to \Upsilon(4S)$
33.2±2.4±1.8	[2] LEES	12D	BABR	$e^+e^- \to \Upsilon(4S)$
• • • We do not use the following data for averages, fits, limits, etc. • • •				
29.7±5.6±1.8	[3] AUBERT	08N	BABR	Repl. by LEES 12D

[1] Uses a fully reconstructed B meson as a tag on the recoil side.

[2] Uses $\tau^+ \to e^+\nu_e\overline{\nu}_\tau$ and $\tau^+ \to \mu^+\nu_\mu\overline{\nu}_\tau$ and e^+ or μ^+ as ℓ^+. Obtained from simultaneous fit to B+ and B0 assuming isospin symmetry. Uses a fully reconstructed B meson as a tag on the recoil side.

[3] Uses a fully reconstructed B meson as a tag on the recoil side. The results are normalized to the B^+ decay rate.

$\langle n_c \rangle$

VALUE	DOCUMENT ID		TECN	COMMENT
1.10±0.05	[1] GIBBONS	97B	CLE2	$e^+e^- \to \Upsilon(4S)$
• • • We do not use the following data for averages, fits, limits, etc. • • •				
0.98±0.16±0.12	[2] ALAM	87B	CLEO	$e^+e^- \to \Upsilon(4S)$

[1] GIBBONS 97B from charm counting using $B(D_s^+ \to \phi\pi) = 0.036 \pm 0.009$ and $B(\Lambda_c^+ \to pK^-\pi^+) = 0.044 \pm 0.006$.

[2] From the difference between K^- and K^+ widths. ALAM 87B measurement relies on lepton-kaon correlations. It does not consider the possibility of $B\overline{B}$ mixing. We have thus removed it from the average.

$\Gamma(D^\pm \text{anything})/\Gamma_{\text{total}}$ Γ_{29}/Γ

VALUE	EVTS	DOCUMENT ID		TECN	COMMENT
0.241±0.014 OUR AVERAGE					
0.240±0.013±0.008		[1] GIBBONS	97B	CLE2	$e^+e^- \to \Upsilon(4S)$
0.25 ±0.04 ±0.01		[2] BORTOLETTO	92	CLEO	$e^+e^- \to \Upsilon(4S)$
0.23 ±0.05 ±0.01		[3] ALBRECHT	91H	ARG	$e^+e^- \to \Upsilon(4S)$
• • • We do not use the following data for averages, fits, limits, etc. • • •					
0.21 ±0.05 ±0.01	20k	[4] BORTOLETTO	87	CLEO	Sup. by BORTOLETTO 92

[1] GIBBONS 97B reports $[\Gamma(B \to D^\pm\text{anything})/\Gamma_{\text{total}}] \times [B(D^+ \to K^-2\pi^+)] = 0.0216 \pm 0.0008 \pm 0.00082$ which we divide by our best value $B(D^+ \to K^-2\pi^+) = (8.98 \pm 0.28) \times 10^{-2}$. Our first error is their experiment's error and our second error is the systematic error from using our best value.

[2] BORTOLETTO 92 reports $[\Gamma(B \to D^\pm\text{anything})/\Gamma_{\text{total}}] \times [B(D^+ \to K^-2\pi^+)] = 0.0226 \pm 0.0030 \pm 0.0018$ which we divide by our best value $B(D^+ \to K^-2\pi^+) = (8.98 \pm 0.28) \times 10^{-2}$. Our first error is their experiment's error and our second error is the systematic error from using our best value.

[3] ALBRECHT 91H reports $[\Gamma(B \to D^\pm\text{anything})/\Gamma_{\text{total}}] \times [B(D^+ \to K^-2\pi^+)] = 0.0209 \pm 0.0027 \pm 0.0040$ which we divide by our best value $B(D^+ \to K^-2\pi^+) = (8.98 \pm 0.28) \times 10^{-2}$. Our first error is their experiment's error and our second error is the systematic error from using our best value.

[4] BORTOLETTO 87 reports $[\Gamma(B \to D^\pm\text{anything})/\Gamma_{\text{total}}] \times [B(D^+ \to K^-2\pi^+)] = 0.019 \pm 0.004 \pm 0.002$ which we divide by our best value $B(D^+ \to K^-2\pi^+) = (8.98 \pm 0.28) \times 10^{-2}$. Our first error is their experiment's error and our second error is the systematic error from using our best value.

$\Gamma(D^0/\overline{D}^0\text{anything})/\Gamma_{\text{total}}$ Γ_{30}/Γ

VALUE	EVTS	DOCUMENT ID		TECN	COMMENT
0.624±0.029 OUR AVERAGE		Error includes scale factor of 1.3. See the ideogram below.			
0.645±0.025±0.006		[1] GIBBONS	97B	CLE2	$e^+e^- \to \Upsilon(4S)$
0.60 ±0.05 ±0.01		[2] BORTOLETTO	92	CLEO	$e^+e^- \to \Upsilon(4S)$
0.50 ±0.07 ±0.01		[3] ALBRECHT	91H	ARG	$e^+e^- \to \Upsilon(4S)$
• • • We do not use the following data for averages, fits, limits, etc. • • •					
0.54 ±0.07 ±0.01	21k	[4] BORTOLETTO	87	CLEO	$e^+e^- \to \Upsilon(4S)$
0.62 ±0.19 ±0.01		[5] GREEN	83	CLEO	Repl. by BORTOLETTO 87

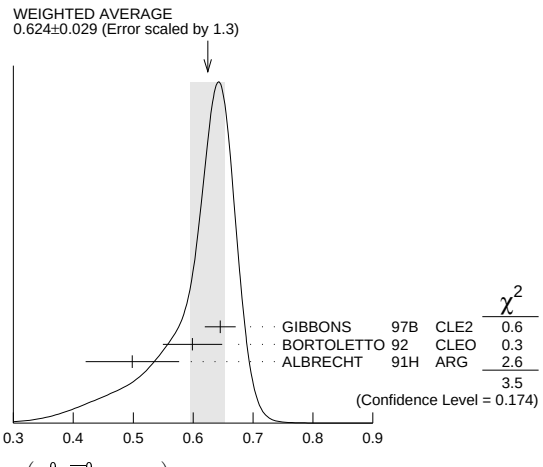

[1] GIBBONS 97B reports $[\Gamma(B \to D^0/\overline{D}^0\text{anything})/\Gamma_{\text{total}}] \times [B(D^0 \to K^-\pi^+)] = 0.0251 \pm 0.0006 \pm 0.00075$ which we divide by our best value $B(D^0 \to K^-\pi^+) = (3.89 \pm 0.04) \times 10^{-2}$. Our first error is their experiment's error and our second error is the systematic error from using our best value.

[2] BORTOLETTO 92 reports $[\Gamma(B \to D^0/\overline{D}^0 \text{anything})/\Gamma_{total}] \times [B(D^0 \to K^-\pi^+)] = 0.0233 \pm 0.0012 \pm 0.0014$ which we divide by our best value $B(D^0 \to K^-\pi^+) = (3.89 \pm 0.04) \times 10^{-2}$. Our first error is their experiment's error and our second error is the systematic error from using our best value.

[3] ALBRECHT 91H reports $[\Gamma(B \to D^0/\overline{D}^0 \text{anything})/\Gamma_{total}] \times [B(D^0 \to K^-\pi^+)] = 0.0194 \pm 0.0015 \pm 0.0025$ which we divide by our best value $B(D^0 \to K^-\pi^+) = (3.89 \pm 0.04) \times 10^{-2}$. Our first error is their experiment's error and our second error is the systematic error from using our best value.

[4] BORTOLETTO 87 reports $[\Gamma(B \to D^0/\overline{D}^0 \text{anything})/\Gamma_{total}] \times [B(D^0 \to K^-\pi^+)] = 0.0210 \pm 0.0015 \pm 0.0021$ which we divide by our best value $B(D^0 \to K^-\pi^+) = (3.89 \pm 0.04) \times 10^{-2}$. Our first error is their experiment's error and our second error is the systematic error from using our best value.

[5] GREEN 83 reports $[\Gamma(B \to D^0/\overline{D}^0 \text{anything})/\Gamma_{total}] \times [B(D^0 \to K^-\pi^+)] = 0.024 \pm 0.006 \pm 0.004$ which we divide by our best value $B(D^0 \to K^-\pi^+) = (3.89 \pm 0.04) \times 10^{-2}$. Our first error is their experiment's error and our second error is the systematic error from using our best value.

$\Gamma(D^*(2010)^{\pm} \text{anything})/\Gamma_{total}$ Γ_{31}/Γ

VALUE	EVTS	DOCUMENT ID		TECN	COMMENT
0.225±0.015 OUR AVERAGE					
0.247±0.019±0.01		[1] GIBBONS	97B	CLE2	$e^+e^- \to \Upsilon(4S)$
0.205±0.019±0.007		[2] ALBRECHT	96D	ARG	$e^+e^- \to \Upsilon(4S)$
0.230±0.028±0.009		[3] BORTOLETTO	92	CLEO	$e^+e^- \to \Upsilon(4S)$
• • • We do not use the following data for averages, fits, limits, etc. • • •					
0.283±0.053±0.002		[4] ALBRECHT	91H	ARG	Sup. by ALBRECHT 96D
0.22 ±0.04 $^{+0.07}_{-0.04}$	5200	[5] BORTOLETTO	87	CLEO	$e^+e^- \to \Upsilon(4S)$
0.27 ±0.06 $^{+0.08}_{-0.06}$	510	[6] CSORNA	85	CLEO	Repl. by BORTOLETTO 87

[1] GIBBONS 97B reports $B(B \to D^*(2010)^+ \text{anything}) = 0.239 \pm 0.015 \pm 0.014 \pm 0.009$ using CLEO measured D and D^* branching fractions. We rescale to our PDG 96 values of D and D^* branching ratios. Our first error is their experiment's error and our second error is the systematic error from using our best value.

[2] ALBRECHT 96D reports $B(B \to D^*(2010)^+ \text{anything})$ 0.196 ± 0.019 using CLEO measured $B(D^*(2010)^+ \to D^0\pi^+) = 0.681 \pm 0.01 \pm 0.013$, $B(D^0 \to K^-\pi^+) = 0.0401 \pm 0.0014$, $B(D^0 \to K^-\pi^+\pi^+\pi^-) = 0.081 \pm 0.005$., We rescale to our PDG 96 values of D and D^* branching ratios. Our first error is their experiment's error and our second error is the systematic error from using our best value.

[3] BORTOLETTO 92 reports $B(B \to D^*(2010)^+ \text{anything}) = 0.25 \pm 0.03 \pm 0.04$ using MARK II $B(D^*(2010)^+ \to D^0\pi^+) = 0.57 \pm 0.06$ and $B(D^0 \to K^-\pi^+) = 0.042 \pm 0.008$. We rescale to our PDG 96 values of D and D^* branching ratios. Our first error is their experiment's error and our second error is the systematic error from using our best value.

[4] ALBRECHT 91H reports 0.348 ± 0.060 ± 0.035 from a measurement of $[\Gamma(B \to D^*(2010)^{\pm} \text{anything})/\Gamma_{total}] \times [B(D^*(2010)^+ \to D^0\pi^+)]$ assuming $B(D^*(2010)^+ \to D^0\pi^+) = 0.55 \pm 0.04$, which we rescale to our best value $B(D^*(2010)^+ \to D^0\pi^+) = (67.7 \pm 0.5) \times 10^{-2}$. Our first error is their experiment's error and our second error is the systematic error from using our best value. Uses the PDG 90 $B(D^0 \to K^-\pi^+) = 0.0371 \pm 0.0025$.

[5] BORTOLETTO 87 uses old MARK III (BALTRUSAITIS 86E) branching ratios $B(D^0 \to K^-\pi^+) = 0.056 \pm 0.004 \pm 0.003$ and also assumes $B(D^*(2010)^+ \to D^0\pi^+) = 0.60^{+0.08}_{-0.15}$. The product branching ratio for $B(B \to D^*(2010)^+)\ B(D^*(2010)^+ \to D^0\pi^+)$ is 0.13 ± 0.02 ± 0.012. Superseded by BORTOLETTO 92.

[6] $V-A$ momentum spectrum used to extrapolate below $p = 1$ GeV. We correct the value assuming $B(D^0 \to K^-\pi^+) = 0.042 \pm 0.006$ and $B(D^{*+} \to D^0\pi^+) = 0.6^{+0.08}_{-0.15}$. The product branching fraction is $B(B \to D^{*+}X) \cdot B(D^{*+} \to \pi^+ D^0) \cdot B(D^0 \to K^-\pi^+) = (68 \pm 15 \pm 9) \times 10^{-4}$.

$\Gamma(D^*(2007)^0 \text{anything})/\Gamma_{total}$ Γ_{32}/Γ

VALUE	DOCUMENT ID		TECN	COMMENT
0.260±0.023±0.015	[1] GIBBONS	97B	CLE2	$e^+e^- \to \Upsilon(4S)$

[1] GIBBONS 97B reports $B(B \to D^*(2007)^0 \text{anything})$ 0.247 ± 0.012 ± 0.018 ± 0.018 using CLEO measured D and D^* branching fractions. We rescale to our PDG 96 values of D and D^* branching ratios. Our first error is their experiment's error and our second error is the systematic error from using our best value.

$\Gamma(D_s^{\pm} \text{anything})/\Gamma_{total}$ Γ_{33}/Γ

VALUE	EVTS	DOCUMENT ID		TECN	COMMENT
0.083±0.008 OUR AVERAGE					
0.089±0.010±0.008		[1] ARTUSO	05B	CLE2	$e^+e^- \to \Upsilon(5S)$
0.087±0.005±0.008		[2] AUBERT	02G	BABR	$e^+e^- \to \Upsilon(4S)$
0.065±0.011±0.006		[3] ALBRECHT	92G	ARG	$e^+e^- \to \Upsilon(4S)$
0.068±0.010±0.006	257	[4] BORTOLETTO	90	CLEO	$e^+e^- \to \Upsilon(4S)$
0.085±0.022±0.008		[5] HAAS	86	CLEO	$e^+e^- \to \Upsilon(4S)$
• • • We do not use the following data for averages, fits, limits, etc. • • •					
0.094±0.007±0.008		[6] GIBAUT	96	CLE2	Repl. by ARTUSO 05B
0.094±0.024±0.008		[7] ALBRECHT	87H	ARG	$e^+e^- \to \Upsilon(4S)$

[1] ARTUSO 05B reports 0.0905 ± 0.0025 ± 0.0140 from a measurement of $[\Gamma(B \to D_s^{\pm} \text{anything})/\Gamma_{total}] \times [B(D_s^+ \to \phi\pi^+)]$ assuming $B(D_s^+ \to \phi\pi^+) = (4.4 \pm 0.5) \times 10^{-2}$, which we rescale to our best value $B(D_s^+ \to \phi\pi^+) = (4.5 \pm 0.4) \times 10^{-2}$. Our first error is their experiment's error and our second error is the systematic error from using our best value.

[2] AUBERT 02G reports $[\Gamma(B \to D_s^{\pm} \text{anything})/\Gamma_{total}] \times [B(D_s^+ \to \phi\pi^+)] = 0.00393 \pm 0.00007 \pm 0.00021$ which we divide by our best value $B(D_s^+ \to \phi\pi^+) = (4.5 \pm 0.4) \times 10^{-2}$. Our first error is their experiment's error and our second error is the systematic error from using our best value.

[3] ALBRECHT 92G reports $[\Gamma(B \to D_s^{\pm} \text{anything})/\Gamma_{total}] \times [B(D_s^+ \to \phi\pi^+)] = 0.00292 \pm 0.00039 \pm 0.00031$ which we divide by our best value $B(D_s^+ \to \phi\pi^+) = (4.5 \pm 0.4) \times 10^{-2}$. Our first error is their experiment's error and our second error is the systematic error from using our best value.

[4] BORTOLETTO 90 reports $[\Gamma(B \to D_s^{\pm} \text{anything})/\Gamma_{total}] \times [B(D_s^+ \to \phi\pi^+)] = 0.00306 \pm 0.00047$ which we divide by our best value $B(D_s^+ \to \phi\pi^+) = (4.5 \pm 0.4) \times 10^{-2}$. Our first error is their experiment's error and our second error is the systematic error from using our best value.

[5] HAAS 86 reports $[\Gamma(B \to D_s^{\pm} \text{anything})/\Gamma_{total}] \times [B(D_s^+ \to \phi\pi^+)] = 0.0038 \pm 0.0010$ which we divide by our best value $B(D_s^+ \to \phi\pi^+) = (4.5 \pm 0.4) \times 10^{-2}$. Our first error is their experiment's error and our second error is the systematic error from using our best value. 64 ± 22% decays are 2-body.

[6] GIBAUT 96 reports 0.1211 ± 0.0039 ± 0.0088 from a measurement of $[\Gamma(B \to D_s^{\pm} \text{anything})/\Gamma_{total}] \times [B(D_s^+ \to \phi\pi^+)]$ assuming $B(D_s^+ \to \phi\pi^+) = 0.035$, which we rescale to our best value $B(D_s^+ \to \phi\pi^+) = (4.5 \pm 0.4) \times 10^{-2}$. Our first error is their experiment's error and our second error is the systematic error from using our best value.

[7] ALBRECHT 87H reports $[\Gamma(B \to D_s^{\pm} \text{anything})/\Gamma_{total}] \times [B(D_s^+ \to \phi\pi^+)] = 0.0042 \pm 0.0009 \pm 0.0006$ which we divide by our best value $B(D_s^+ \to \phi\pi^+) = (4.5 \pm 0.4) \times 10^{-2}$. Our first error is their experiment's error and our second error is the systematic error from using our best value. 46 ± 16% of $B \to D_s X$ decays are 2-body. Superseded by ALBRECHT 92G.

$\Gamma(D_s^{*\pm} \text{anything})/\Gamma_{total}$ Γ_{34}/Γ

VALUE	DOCUMENT ID		TECN	COMMENT
0.063±0.009±0.006	[1] AUBERT	02G	BABR	$e^+e^- \to \Upsilon(4S)$

[1] AUBERT 02G reports $[\Gamma(B \to D_s^{*\pm} \text{anything})/\Gamma_{total}] \times [B(D_s^+ \to \phi\pi^+)] = 0.00284 \pm 0.00029 \pm 0.00025$ which we divide by our best value $B(D_s^+ \to \phi\pi^+) = (4.5 \pm 0.4) \times 10^{-2}$. Our first error is their experiment's error and our second error is the systematic error from using our best value.

$\Gamma(D_s^{*\pm}\overline{D}^{(*)})/\Gamma(D_s^{*\pm} \text{anything})$ Γ_{35}/Γ_{34}

Sum over modes

VALUE	DOCUMENT ID	TECN	COMMENT
0.533±0.037±0.037	AUBERT 02G	BABR	$e^+e^- \to \Upsilon(4S)$

$\Gamma(\overline{D}D_{s0}(2317))/\Gamma_{total}$ Γ_{36}/Γ

VALUE	DOCUMENT ID		TECN	COMMENT
seen	[1] KROKOVNY	03B	BELL	$e^+e^- \to \Upsilon(4S)$

[1] The product branching ratio for $B(B \to \overline{D}D_{s0}(2317)^+) \times B(D_{s0}(2317)^+ \to D_s\pi^0)$ is measured to be $(8.5^{+2.1}_{-1.9} \pm 2.6) \times 10^{-4}$.

$\Gamma(\overline{D}D_{sJ}(2457))/\Gamma_{total}$ Γ_{37}/Γ

VALUE	DOCUMENT ID		TECN	COMMENT
seen	[1] KROKOVNY	03B	BELL	$e^+e^- \to \Upsilon(4S)$

[1] The product branching ratio for $B(B \to \overline{D}D_{sJ}(2457)^+) \times B(D_{sJ}(2457)^+ \to D_s^{*+}\pi^0, D_s^+\gamma)$ are measured to be $(17.8^{+4.5}_{-3.9} \pm 5.3) \times 10^{-4}$ and $(6.7^{+1.3}_{-1.2} \pm 2.0) \times 10^{-4}$, respectively.

$[\Gamma(D^{(*)}\overline{D}^{(*)}K^0) + \Gamma(D^{(*)}\overline{D}^{(*)}K^{\pm})]/\Gamma_{total}$ Γ_{38}/Γ

VALUE	DOCUMENT ID		TECN	COMMENT
$0.071^{+0.025}_{-0.015}{}^{+0.010}_{-0.009}$	[1] BARATE	98Q	ALEP	$e^+e^- \to Z$

[1] The systematic error includes the uncertainties due to the charm branching ratios.

$\Gamma(b \to c\overline{c}s)/\Gamma_{total}$ Γ_{39}/Γ

VALUE	DOCUMENT ID		TECN	COMMENT
0.219±0.037	[1] COAN	98	CLE2	$e^+e^- \to \Upsilon(4S)$

[1] COAN 98 uses D-ℓ correlation.

$\Gamma(D_s^{(*)}\overline{D}^{(*)})/\Gamma(D_s^{\pm} \text{anything})$ Γ_{40}/Γ_{33}

Sum over modes.

VALUE	DOCUMENT ID		TECN	COMMENT
0.469±0.017 OUR AVERAGE				
0.464±0.013±0.015	AUBERT	02G	BABR	$e^+e^- \to \Upsilon(4S)$
0.56 $^{+0.21}_{-0.15}$ $^{+0.09}_{-0.08}$	[1] BARATE	98Q	ALEP	$e^+e^- \to Z$
0.457±0.019±0.037	GIBAUT	96	CLE2	$e^+e^- \to \Upsilon(4S)$
0.58 ±0.07 ±0.09	ALBRECHT	92G	ARG	$e^+e^- \to \Upsilon(4S)$
0.56 ±0.10	BORTOLETTO	90	CLEO	$e^+e^- \to \Upsilon(4S)$

[1] BARATE 98Q measures $B(B \to D_s^{(*)}\overline{D}^{(*)}) = 0.056^{+0.021}_{-0.015}{}^{+0.009}_{-0.008}{}^{+0.019}_{-0.011}$, where the third error results from the uncertainty on the different D branching ratios and is dominated by the uncertainty on $B(D_s^+ \to \phi\pi^+)$. We divide $B(B \to D_s^{(*)}\overline{D}^{(*)})$ by our best value of $B(B \to D_s \text{anything}) = 0.1 \pm 0.025$.

$\Gamma(D^*D^*(2010)^{\pm})/\Gamma_{total}$ Γ_{41}/Γ

VALUE	CL%	DOCUMENT ID		TECN	COMMENT
$<5.9 \times 10^{-3}$	90	BARATE	98Q	ALEP	$e^+e^- \to Z$

$[\Gamma(DD^*(2010)^{\pm}) + \Gamma(D^*D^{\pm})]/\Gamma_{total}$ Γ_{42}/Γ

VALUE	CL%	DOCUMENT ID		TECN	COMMENT
$<5.5 \times 10^{-3}$	90	BARATE	98Q	ALEP	$e^+e^- \to Z$

$\Gamma(DD^{\pm})/\Gamma_{total}$ Γ_{43}/Γ

VALUE	CL%	DOCUMENT ID		TECN	COMMENT
$<3.1 \times 10^{-3}$	90	BARATE	98Q	ALEP	$e^+e^- \to Z$

$\Gamma(D_s^{(*)\pm}\overline{D}^{(*)}X(n\pi^{\pm}))/\Gamma_{total}$ Γ_{44}/Γ

VALUE	DOCUMENT ID		TECN	COMMENT
$0.094^{+0.040}_{-0.031}{}^{+0.034}_{-0.024}$	[1] BARATE	98Q	ALEP	$e^+e^- \to Z$

[1] The systematic error includes the uncertainties due to the charm branching ratios.

$\Gamma(D^*(2010)\gamma)/\Gamma_{total}$ Γ_{45}/Γ

VALUE	CL%	DOCUMENT ID		TECN	COMMENT
$<1.1 \times 10^{-3}$	90	[1] LESIAK	92	CBAL	$e^+e^- \to \Upsilon(4S)$

[1] LESIAK 92 set a limit on the inclusive process $B(b \to s\gamma) < 2.8 \times 10^{-3}$ at 90% CL for the range of masses of 892–2045 MeV, independent of assumptions about s-quark hadronization.

$\Gamma(D_s^+\pi^-, D_s^{*+}\pi^-, D_s^+\rho^-, D_s^{*+}\rho^-, D_s^+\pi^0, D_s^{*+}\pi^0, D_s^+\eta, D_s^{*+}\eta, D_s^+\rho^0, D_s^{*+}\rho^0, D_s^+\omega, D_s^{*+}\omega)/\Gamma_{total}$ Γ_{46}/Γ

Sum over modes.

VALUE	CL%	DOCUMENT ID		TECN	COMMENT
$<4 \times 10^{-4}$	90	[1] ALEXANDER	93B	CLE2	$e^+e^- \to \Upsilon(4S)$

[1] ALEXANDER 93B reports $< 4.8 \times 10^{-4}$ from a measurement of $[\Gamma(B \to D_s^+\pi^-, D_s^{*+}\pi^-, D_s^+\rho^-, D_s^{*+}\rho^-, D_s^+\pi^0, D_s^{*+}\pi^0, D_s^+\eta, D_s^{*+}\eta, D_s^+\rho^0, D_s^{*+}\rho^0, D_s^+\omega, D_s^{*+}\omega)/\Gamma_{total}] \times [B(D_s^+ \to \phi\pi^+)]$ assuming $B(D_s^+ \to \phi\pi^+) = 0.037$, which we rescale to our best value $B(D_s^+ \to \phi\pi^+) = 4.5 \times 10^{-2}$. This branching ratio limit provides a model-dependent upper limit $|V_{ub}|/|V_{cb}| < 0.16$ at CL=90%.

$\Gamma(D_{s1}(2536)^+ \text{anything})/\Gamma_{total}$ Γ_{47}/Γ

$D_{s1}(2536)^+$ is the narrow P-wave D_s^+ meson with $J^P = 1^+$.

VALUE	CL%	DOCUMENT ID		TECN	COMMENT
<0.0095	90	[1] BISHAI	98	CLE2	$e^+e^- \to \Upsilon(4S)$

[1] Assuming factorization, the decay constant $f_{D_{s1}^+}$ is at least a factor of 2.5 times smaller than $f_{D_s^+}$.

$\Gamma(J/\psi(1S) \text{anything})/\Gamma_{total}$ Γ_{48}/Γ

VALUE (units 10^{-2})	EVTS	DOCUMENT ID		TECN	COMMENT
1.094 ± 0.032 OUR AVERAGE		Error includes scale factor of 1.1.			
$1.057 \pm 0.012 \pm 0.040$		[1] AUBERT	03F	BABR	$e^+e^- \to \Upsilon(4S)$
$1.121 \pm 0.013 \pm 0.042$		ANDERSON	02	CLE2	$e^+e^- \to \Upsilon(4S)$
$1.29 \pm 0.45 \pm 0.01$	27	[2] MASCHMANN	90	CBAL	$e^+e^- \to \Upsilon(4S)$
$1.24 \pm 0.27 \pm 0.01$	120	[3] ALBRECHT	87D	ARG	$e^+e^- \to \Upsilon(4S)$
$1.35 \pm 0.24 \pm 0.01$	52	[4] ALAM	86	CLEO	$e^+e^- \to \Upsilon(4S)$
• • • We do not use the following data for averages, fits, limits, etc. • • •					
$1.12 \pm 0.06 \pm 0.01$	1489	[5] BALEST	95B	CLE2	$e^+e^- \to \Upsilon(4S)$
$1.4 \ ^{+0.6}_{-0.5}$	7	[6] ALBRECHT	85H	ARG	$e^+e^- \to \Upsilon(4S)$
$1.1 \pm 0.21 \pm 0.23$	46	[7] HAAS	85	CLEO	Repl. by ALAM 86

[1] AUBERT 03F also reports the momentum distribution and helicity of $J/\psi \to \ell^+\ell^-$ in the $\Upsilon(4S)$ center-of-mass frame.

[2] MASCHMANN 90 reports $(1.12 \pm 0.33 \pm 0.25) \times 10^{-2}$ from a measurement of $[\Gamma(B \to J/\psi(1S) \text{anything})/\Gamma_{total}] \times [B(J/\psi(1S) \to e^+e^-)]$ assuming $B(J/\psi(1S) \to e^+e^-) = 0.069 \pm 0.009$, which we rescale to our best value $B(J/\psi(1S) \to e^+e^-) = (5.971 \pm 0.032) \times 10^{-2}$. Our first error is their experiment's error and our second error is the systematic error from using our best value.

[3] ALBRECHT 87D reports $(1.07 \pm 0.16 \pm 0.22) \times 10^{-2}$ from a measurement of $[\Gamma(B \to J/\psi(1S) \text{anything})/\Gamma_{total}] \times [B(J/\psi(1S) \to e^+e^-)]$ assuming $B(J/\psi(1S) \to e^+e^-) = 0.069 \pm 0.009$, which we rescale to our best value $B(J/\psi(1S) \to e^+e^-) = (5.971 \pm 0.032) \times 10^{-2}$. Our first error is their experiment's error and our second error is the systematic error from using our best value. ALBRECHT 87D find the branching ratio for J/ψ not from $\psi(2S)$ to be 0.0081 ± 0.0023.

[4] ALAM 86 reports $(1.09 \pm 0.16 \pm 0.21) \times 10^{-2}$ from a measurement of $[\Gamma(B \to J/\psi(1S) \text{anything})/\Gamma_{total}] \times [B(J/\psi(1S) \to \mu^+\mu^-)]$ assuming $B(J/\psi(1S) \to \mu^+\mu^-) = 0.074 \pm 0.012$, which we rescale to our best value $B(J/\psi(1S) \to \mu^+\mu^-) = (5.961 \pm 0.033) \times 10^{-2}$. Our first error is their experiment's error and our second error is the systematic error from using our best value.

[5] BALEST 95B reports $(1.12 \pm 0.04 \pm 0.06) \times 10^{-2}$ from a measurement of $[\Gamma(B \to J/\psi(1S) \text{anything})/\Gamma_{total}] \times [B(J/\psi(1S) \to e^+e^-)]$ assuming $B(J/\psi(1S) \to e^+e^-) = 0.0599 \pm 0.0025$, which we rescale to our best value $B(J/\psi(1S) \to e^+e^-) = (5.971 \pm 0.032) \times 10^{-2}$. Our first error is their experiment's error and our second error is the systematic error from using our best value. They measure $J/\psi(1S) \to e^+e^-$ and $\mu^+\mu^-$ and use PDG 1994 values for the branching fractions. The rescaling is the same for either mode so we use e^+e^-.

[6] Statistical and systematic errors were added in quadrature. ALBRECHT 85H also report a CL = 90% limit of 0.007 for $B \to J/\psi(1S) + X$ where $m_X < 1$ GeV.

[7] Dimuon and dielectron events used.

$\Gamma(J/\psi(1S) \text{(direct) anything})/\Gamma_{total}$ Γ_{49}/Γ

VALUE	DOCUMENT ID		TECN	COMMENT
0.0078 ± 0.0004 OUR AVERAGE	Error includes scale factor of 1.1.			
$0.00740 \pm 0.00023 \pm 0.00043$	[1] AUBERT	03F	BABR	$e^+e^- \to \Upsilon(4S)$
$0.00813 \pm 0.00017 \pm 0.00037$	[2] ANDERSON	02	CLE2	$e^+e^- \to \Upsilon(4S)$
• • • We do not use the following data for averages, fits, limits, etc. • • •				
0.0080 ± 0.0008	[3] BALEST	95B	CLE2	$e^+e^- \to \Upsilon(4S)$

[1] AUBERT 03F also reports the helicity of $J/\psi \to \ell^+\ell^-$ produced directly in B decay.

[2] Also reports the measurement of $J/\psi \to \ell^+\ell^-$ polarization produced directly from B decay.

[3] BALEST 95B assume PDG 1994 values for sub mode branching ratios. $J/\psi(1S)$ mesons are reconstructed in $J/\psi(1S) \to e^+e^-$ and $J/\psi(1S) \to \mu^+\mu^-$. The $B \to J/\psi(1S)X$ branching ratio contains $J/\psi(1S)$ mesons directly from B decays and also from feeddown through $\psi(2S) \to J/\psi(1S)$, $\chi_{c1}(1P) \to J/\psi(1S)$, or $\chi_{c2}(1P) \to J/\psi(1S)$. Using the measured inclusive rates, BALEST 95B corrects for the feeddown and finds the $B \to J/\psi(1S)$ (direct) X branching ratio.

$\Gamma(\psi(2S) \text{anything})/\Gamma_{total}$ Γ_{50}/Γ

VALUE	EVTS	DOCUMENT ID		TECN	COMMENT
0.00307 ± 0.00021 OUR AVERAGE					
$0.00297 \pm 0.00020 \pm 0.00020$		AUBERT	03F	BABR	$e^+e^- \to \Upsilon(4S)$
$0.00316 \pm 0.00014 \pm 0.00028$		[1] ANDERSON	02	CLE2	$e^+e^- \to \Upsilon(4S)$
$0.0046 \pm 0.0017 \pm 0.0011$	8	ALBRECHT	87D	ARG	$e^+e^- \to \Upsilon(4S)$
• • • We do not use the following data for averages, fits, limits, etc. • • •					
$0.0034 \pm 0.0004 \pm 0.0003$	240	[2] BALEST	95B	CLE2	$e^+e^- \to \Upsilon(4S)$

[1] Also reports the measurement of $\psi(2S) \to \ell^+\ell^-$ polarization produced directly from B decay.

[2] BALEST 95B assume PDG 1994 values for sub mode branching ratios. They find $B(B \to \psi(2S)X, \psi(2S) \to \ell^+\ell^-) = 0.30 \pm 0.05 \pm 0.04$ and $B(B \to \psi(2S)X, \psi(2S) \to J/\psi(1S)\pi^+\pi^-) = 0.37 \pm 0.05 \pm 0.05$. Weighted average is quoted for $B(B \to \psi(2S)X)$.

$\Gamma(\chi_{c1}(1P) \text{anything})/\Gamma_{total}$ Γ_{51}/Γ

VALUE (units 10^{-3})	EVTS	DOCUMENT ID		TECN	COMMENT
3.55 ± 0.27 OUR AVERAGE	Error includes scale factor of 1.3. See the ideogram below.				
$3.33 \pm 0.05 \pm 0.24$		[1] BHARDWAJ	16	BELL	$e^+e^- \to \Upsilon(4S)$
$3.67 \pm 0.35 \pm 0.44$		AUBERT	03F	BABR	$e^+e^- \to \Upsilon(4S)$
$4.35 \pm 0.29 \pm 0.40$		ANDERSON	02	CLE2	$e^+e^- \to \Upsilon(4S)$
• • • We do not use the following data for averages, fits, limits, etc. • • •					
$3.63 \pm 0.22 \pm 0.34$		[2] ABE	02L	BELL	Repl. by BHARDWAJ 16
$3.30 \pm 0.35 \pm 0.09$		[3] CHEN	01	CLE2	$e^+e^- \to \Upsilon(4S)$
$4.0 \pm 0.6 \pm 0.4$	112	[4] BALEST	95B	CLE2	Repl. by CHEN 01
$10.5 \pm 3.5 \pm 2.5$		[5] ALBRECHT	92E	ARG	$e^+e^- \to \Upsilon(4S)$

[1] Assumes equal production of B^+ and B^0 at the $\Upsilon(4S)$.

[2] ABE 02L uses PDG 01 values for $B(J/\psi(1S) \to \ell^+\ell^-)$ and $B(\chi_{c1,c2} \to J/\psi(1S)\gamma)$.

[3] CHEN 01 reports $0.00414 \pm 0.00031 \pm 0.00040$ from a measurement of $[\Gamma(B \to \chi_{c1}(1P) \text{anything})/\Gamma_{total}] \times [B(\chi_{c1}(1P) \to \gamma J/\psi(1S))]$ assuming $B(\chi_{c1}(1P) \to \gamma J/\psi(1S)) = 0.273 \pm 0.016$, which we rescale to our best value $B(\chi_{c1}(1P) \to \gamma J/\psi(1S)) = (34.3 \pm 1.0) \times 10^{-2}$. Our first error is their experiment's error and our second error is the systematic error from using our best value. Assumes equal production of B^+ and B^0 at the $\Upsilon(4S)$.

[4] BALEST 95B assume $B(\chi_{c1}(1P) \to J/\psi(1S)\gamma) = (27.3 \pm 1.6) \times 10^{-2}$, the PDG 1994 value. Fit to ψ-photon invariant mass distribution allows for a $\chi_{c1}(1P)$ and a $\chi_{c2}(1P)$ component.

[5] ALBRECHT 92E assumes no $\chi_{c2}(1P)$ production.

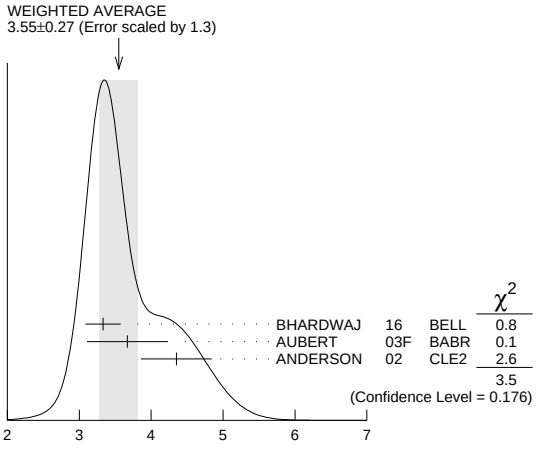

$\Gamma(\chi_{c1}(1P) \text{(direct) anything})/\Gamma_{total}$ Γ_{52}/Γ

VALUE (units 10^{-3})	DOCUMENT ID		TECN	COMMENT
3.08 ± 0.19 OUR AVERAGE				
$3.03 \pm 0.05 \pm 0.24$	[1] BHARDWAJ	16	BELL	$e^+e^- \to \Upsilon(4S)$
$3.41 \pm 0.35 \pm 0.42$	AUBERT	03F	BABR	$e^+e^- \to \Upsilon(4S)$
$3.1 \pm 0.4 \pm 0.1$	[2] CHEN	01	CLE2	$e^+e^- \to \Upsilon(4S)$

• • • We do not use the following data for averages, fits, limits, etc. • • •

3.32±0.22±0.34	[3] ABE	02L	BELL	Repl. by BHARDWAJ 16	
3.7 ±0.7	[4] BALEST	95B	CLE2	Repl. by CHEN 01	

[1] Assumes equal production of B^+ and B^0 at the $\Upsilon(4S)$.

[2] CHEN 01 reports 0.00383 ± 0.00031 ± 0.00040 from a measurement of $[\Gamma(B \to \chi_{c1}(1P)(\text{direct anything})/\Gamma_{\text{total}}] \times [\text{B}(\chi_{c1}(1P) \to \gamma J/\psi(1S))]$ assuming $\text{B}(\chi_{c1}(1P) \to \gamma J/\psi(1S)) = 0.273 \pm 0.016$, which we rescale to our best value $\text{B}(\chi_{c1}(1P) \to \gamma J/\psi(1S)) = (34.3 \pm 1.0) \times 10^{-2}$. Our first error is their experiment's error and our second error is the systematic error from using our best value. Assumes equal production of B^+ and B^0 at the $\Upsilon(4S)$.

[3] ABE 02L uses PDG 01 values for $\text{B}(J/\psi(1S) \to \ell^+\ell^-)$ and $\text{B}(\chi_{c1,c2} \to J/\psi(1S)\gamma)$.

[4] BALEST 95B assume PDG 1994 values. $J/\psi(1S)$ mesons are reconstructed in the e^+e^- and $\mu^+\mu^-$ modes. The $B \to \chi_{c1}(1P)$X branching ratio contains $\chi_{c1}(1P)$ mesons directly from B decays and also from feeddown through $\psi(2S) \to \chi_{c1}(1P)\gamma$. Using the measured inclusive rates, BALEST 95B corrects for the feeddown and finds the $B \to \chi_{c1}(1P)$(direct) X branching ratio.

$\Gamma(\chi_{c2}(1P)\text{anything})/\Gamma_{\text{total}}$ Γ_{53}/Γ

VALUE (units 10^{-4})	CL%	DOCUMENT ID		TECN	COMMENT
10.0±1.7 OUR AVERAGE		Error includes scale factor of 1.6. See the ideogram below.			
9.8±0.6±1.0		[1] BHARDWAJ	16	BELL	$e^+e^- \to \Upsilon(4S)$
21.0±4.5±3.1		AUBERT	03F	BABR	$e^+e^- \to \Upsilon(4S)$
7.0±3.5±0.2		[2] CHEN	01	CLE2	$e^+e^- \to \Upsilon(4S)$

• • • We do not use the following data for averages, fits, limits, etc. • • •

$18.0^{+2.3}_{-2.8}$±2.6		[3] ABE	02L	BELL	Repl. by BHARDWAJ 16
<38	90	[4] BALEST	95B	CLE2	Repl. by CHEN 01

[1] Assumes equal production of B^+ and B^0 at the $\Upsilon(4S)$.

[2] CHEN 01 reports $(9.8 \pm 4.8 \pm 1.5) \times 10^{-4}$ from a measurement of $[\Gamma(B \to \chi_{c2}(1P)\text{anything})/\Gamma_{\text{total}}] \times [\text{B}(\chi_{c2}(1P) \to \gamma J/\psi(1S))]$ assuming $\text{B}(\chi_{c2}(1P) \to \gamma J/\psi(1S)) = 0.135 \pm 0.011$, which we rescale to our best value $\text{B}(\chi_{c2}(1P) \to \gamma J/\psi(1S)) = (19.0 \pm 0.5) \times 10^{-2}$. Our first error is their experiment's error and our second error is the systematic error from using our best value. Assumes equal production of B^+ and B^0 at the $\Upsilon(4S)$.

[3] ABE 02L uses PDG 01 values for $\text{B}(J/\psi(1S) \to \ell^+\ell^-)$ and $\text{B}(\chi_{c1,c2} \to J/\psi(1S)\gamma)$.

[4] BALEST 95B assume $\text{B}(\chi_{c2}(1P) \to J/\psi(1S)\gamma) = (13.5 \pm 1.1) \times 10^{-2}$, the PDG 1994 value. $J/\psi(1S)$ mesons are reconstructed in the e^+e^- and $\mu^+\mu^-$ modes, and PDG 1994 branching fractions are used. If interpreted as signal, the 35 ± 13 events correspond to $\text{B}(B \to \chi_{c2}(1P)\text{X}) = (0.25 \pm 0.10 \pm 0.03) \times 10^{-2}$.

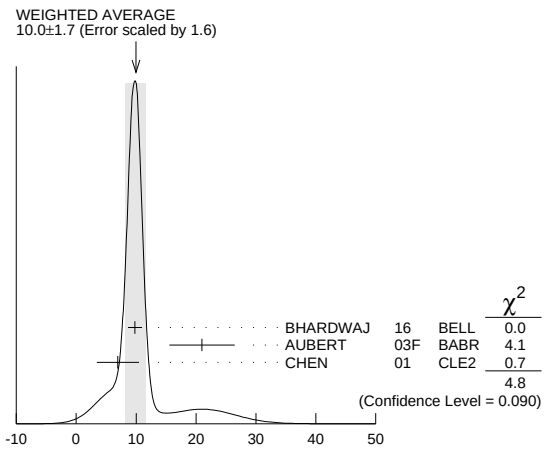

$\Gamma(\chi_{c2}(1P)(\text{direct anything})/\Gamma_{\text{total}}$ Γ_{54}/Γ

VALUE (units 10^{-3})	DOCUMENT ID		TECN	COMMENT
0.75±0.11 OUR AVERAGE				
0.70±0.06±0.10	[1] BHARDWAJ	16	BELL	$e^+e^- \to \Upsilon(4S)$
1.90±0.45±0.29	AUBERT	03F	BABR	$e^+e^- \to \Upsilon(4S)$

• • • We do not use the following data for averages, fits, limits, etc. • • •

$1.53^{+0.23}_{-0.28}$±0.27	[2] ABE	02L	BELL	Repl. by BHARDWAJ 16

[1] Assumes equal production of B^+ and B^0 at the $\Upsilon(4S)$.

[2] ABE 02L uses PDG 01 values for $\text{B}(J/\psi(1S) \to \ell^+\ell^-)$ and $\text{B}(\chi_{c1,c2} \to J/\psi(1S)\gamma)$.

$\Gamma(\eta_c(1S)\text{anything})/\Gamma_{\text{total}}$ Γ_{55}/Γ

VALUE	CL%	DOCUMENT ID		TECN	COMMENT
<0.009	90	[1] BALEST	95B	CLE2	$e^+e^- \to \Upsilon(4S)$

[1] BALEST 95B assume PDG 1994 values for sub mode branching ratios. $J/\psi(1S)$ mesons are reconstructed in $J/\psi(1S) \to e^+e^-$ and $J/\psi(1S) \to \mu^+\mu^-$. Search region $2960 < m_{\eta_c(1S)} < 3010$ MeV/c^2.

$\Gamma(K\chi_{c1}(3872),\ \chi_{c1} \to D^0\overline{D}{}^0\pi^0)/\Gamma_{\text{total}}$ Γ_{56}/Γ

VALUE (units 10^{-4})	DOCUMENT ID		TECN	COMMENT
$\mathbf{1.22 \pm 0.31^{+0.23}_{-0.30}}$	[1] GOKHROO	06	BELL	$e^+e^- \to \Upsilon(4S)$

[1] Measure the near-threshold enhancements in the $(D^0\overline{D}{}^0\pi^0)$ system at a mass 3875.2 ± $0.7^{+0.3}_{-1.6}$ ± 0.8 MeV/c^2.

$\Gamma(K\chi_{c1}(3872),\ \chi_{c1} \to D^{*0}D^0)/\Gamma_{\text{total}}$ Γ_{57}/Γ

VALUE (units 10^{-4})	DOCUMENT ID		TECN	COMMENT
0.80±0.20±0.10	AUSHEV	10	BELL	$e^+e^- \to \Upsilon(4S)$

$\Gamma(KX(3940),\ X \to D^{*0}D^0)/\Gamma_{\text{total}}$ Γ_{58}/Γ

VALUE (units 10^{-4})	CL%	DOCUMENT ID		TECN	COMMENT
<0.67	90	AUSHEV	10	BELL	$e^+e^- \to \Upsilon(4S)$

$\Gamma(KX(3915),\ X \to \omega J/\psi)/\Gamma_{\text{total}}$ Γ_{59}/Γ

VALUE (units 10^{-5})	DOCUMENT ID		TECN	COMMENT
7.1±1.3±3.1	[1] CHOI	05	BELL	$e^+e^- \to \Upsilon(4S)$

[1] CHOI 05 reports the observation of a near-threshold enhancement in the $\omega J/\psi$ mass spectrum in exclusive $B \to K\omega J/\psi$. The new state, denoted as $X(3915)$, is measured to have a mass of 3943 ± 11 ± 13 GeV/c^2 and a width Γ = 87 ± 22 ± 26 MeV.

$\Gamma(K^{\pm}\text{anything})/\Gamma_{\text{total}}$ Γ_{60}/Γ

VALUE	DOCUMENT ID		TECN	COMMENT
0.789±0.025 OUR AVERAGE				
0.82 ±0.01 ±0.05	ALBRECHT	94C	ARG	$e^+e^- \to \Upsilon(4S)$
0.775±0.015±0.025	[1] ALBRECHT	93I	ARG	$e^+e^- \to \Upsilon(4S)$
0.85 ±0.07 ±0.09	ALAM	87B	CLEO	$e^+e^- \to \Upsilon(4S)$

• • • We do not use the following data for averages, fits, limits, etc. • • •

seen	[2] BRODY	82	CLEO	$e^+e^- \to \Upsilon(4S)$
seen	[3] GIANNINI	82	CUSB	$e^+e^- \to \Upsilon(4S)$

[1] ALBRECHT 93I value is not independent of the sum of $B \to K^+$ anything and $B \to K^-$ anything ALBRECHT 94C values.

[2] Assuming $\Upsilon(4S) \to B\overline{B}$, a total of 3.38 ± 0.34 ± 0.68 kaons per $\Upsilon(4S)$ decay is found (the second error is systematic). In the context of the standard B-decay model, this leads to a value for (b-quark → c-quark)/(b-quark → all) of 1.09 ± 0.33 ± 0.13.

[3] GIANNINI 82 at CESR-CUSB observed 1.58 ± 0.35 K^0 per hadronic event much higher than 0.82 ± 0.10 below threshold. Consistent with predominant $b \to c$X decay.

$\Gamma(K^+\text{anything})/\Gamma_{\text{total}}$ Γ_{61}/Γ

VALUE	DOCUMENT ID		TECN	COMMENT
0.66 ±0.05	[1] ALBRECHT	94C	ARG	$e^+e^- \to \Upsilon(4S)$

• • • We do not use the following data for averages, fits, limits, etc. • • •

0.620±0.013±0.038	[2] ALBRECHT	94C	ARG	$e^+e^- \to \Upsilon(4S)$
0.66 ±0.05 ±0.07	[2] ALAM	87B	CLEO	$e^+e^- \to \Upsilon(4S)$

[1] Measurement relies on lepton-kaon correlations. It is for the weak decay vertex and does not include mixing of the neutral B meson. Mixing effects were corrected for by assuming a mixing parameter r of (18.1 ± 4.3)%.

[2] Measurement relies on lepton-kaon correlations. It includes production through mixing of the neutral B meson.

$\Gamma(K^-\text{anything})/\Gamma_{\text{total}}$ Γ_{62}/Γ

VALUE	DOCUMENT ID		TECN	COMMENT
0.13 ±0.04	[1] ALBRECHT	94C	ARG	$e^+e^- \to \Upsilon(4S)$

• • • We do not use the following data for averages, fits, limits, etc. • • •

0.165±0.011±0.036	[2] ALBRECHT	94C	ARG	$e^+e^- \to \Upsilon(4S)$
0.19 ±0.05 ±0.02	[2] ALAM	87B	CLEO	$e^+e^- \to \Upsilon(4S)$

[1] Measurement relies on lepton-kaon correlations. It is for the weak decay vertex and does not include mixing of the neutral B meson. Mixing effects were corrected for by assuming a mixing parameter r of (18.1 ± 4.3)%.

[2] Measurement relies on lepton-kaon correlations. It includes production through mixing of the neutral B meson.

$\Gamma(K^0/\overline{K}{}^0\text{anything})/\Gamma_{\text{total}}$ Γ_{63}/Γ

VALUE	DOCUMENT ID		TECN	COMMENT
0.64 ±0.04 OUR AVERAGE				
0.642±0.010±0.042	[1] ALBRECHT	94C	ARG	$e^+e^- \to \Upsilon(4S)$
0.63 ±0.06 ±0.06	ALAM	87B	CLEO	$e^+e^- \to \Upsilon(4S)$

[1] ALBRECHT 94C assume a $K^0/\overline{K}{}^0$ multiplicity twice that of K^0_S.

$\Gamma(K^*(892)^{\pm}\text{anything})/\Gamma_{\text{total}}$ Γ_{64}/Γ

VALUE	DOCUMENT ID		TECN	COMMENT
0.182±0.054±0.024	ALBRECHT	94J	ARG	$e^+e^- \to \Upsilon(4S)$

$\Gamma(K^*(892)^0/\overline{K}{}^*(892)^0\text{anything})/\Gamma_{\text{total}}$ Γ_{65}/Γ

VALUE	DOCUMENT ID		TECN	COMMENT
0.146±0.016±0.020	ALBRECHT	94J	ARG	$e^+e^- \to \Upsilon(4S)$

$\Gamma(K^*(892)\gamma)/\Gamma_{\text{total}}$ Γ_{66}/Γ

VALUE (units 10^{-5})	CL%	DOCUMENT ID		TECN	COMMENT
4.24±0.54±0.32		[1] COAN	00	CLE2	$e^+e^- \to \Upsilon(4S)$

• • • We do not use the following data for averages, fits, limits, etc. • • •

<150	90	[2] LESIAK	92	CBAL	$e^+e^- \to \Upsilon(4S)$
< 24	90	ALBRECHT	88H	ARG	$e^+e^- \to \Upsilon(4S)$

[1] An average of $B(B^+ \to K^*(892)^+\gamma)$ and $B(B^0 \to K^*(892)^0\gamma)$ measurements reported in COAN 00 by assuming full correlated systematic errors.
[2] LESIAK 92 set a limit on the inclusive process $B(b \to s\gamma) < 2.8 \times 10^{-3}$ at 90% CL for the range of masses of 892–2045 MeV, independent of assumptions about s-quark hadronization.

$\Gamma(\eta K\gamma)/\Gamma_{\text{total}}$ Γ_{67}/Γ

VALUE (units 10^{-6})	DOCUMENT ID		TECN	COMMENT
$8.5 \pm 1.3^{+1.2}_{-0.9}$	[1] NISHIDA	05	BELL	$e^+e^- \to \Upsilon(4S)$

[1] $m_{\eta K} < 2.4$ GeV/c^2

$\Gamma(K_1(1400)\gamma)/\Gamma_{\text{total}}$ Γ_{68}/Γ

VALUE	CL%	DOCUMENT ID		TECN	COMMENT
$<12.7 \times 10^{-5}$	90	[1] COAN	00	CLE2	$e^+e^- \to \Upsilon(4S)$

• • • We do not use the following data for averages, fits, limits, etc. • • •

$< 1.6 \times 10^{-3}$	90	[2] LESIAK	92	CBAL	$e^+e^- \to \Upsilon(4S)$
$< 4.1 \times 10^{-4}$	90	ALBRECHT	88H	ARG	$e^+e^- \to \Upsilon(4S)$

[1] Assumes equal production of B^+ and B^0 at the $\Upsilon(4S)$.
[2] LESIAK 92 set a limit on the inclusive process $B(b \to s\gamma) < 2.8 \times 10^{-3}$ at 90% CL for the range of masses of 892–2045 MeV, independent of assumptions about s-quark hadronization.

$\Gamma(K_2^*(1430)\gamma)/\Gamma_{\text{total}}$ Γ_{69}/Γ

VALUE (units 10^{-5})	CL%	DOCUMENT ID		TECN	COMMENT
$1.66^{+0.59}_{-0.53} \pm 0.13$		[1] COAN	00	CLE2	$e^+e^- \to \Upsilon(4S)$

• • • We do not use the following data for averages, fits, limits, etc. • • •

<83	90	ALBRECHT	88H	ARG	$e^+e^- \to \Upsilon(4S)$

[1] COAN 00 obtains a fitted signal yield of $15.9^{+5.7}_{-5.2}$ events. A search for contamination by $K^*(1410)$ yielded a rate consistent with 0; the central value assumes no contamination.

$\Gamma(K_2(1770)\gamma)/\Gamma_{\text{total}}$ Γ_{70}/Γ

VALUE	CL%	DOCUMENT ID		TECN	COMMENT
$<1.2 \times 10^{-3}$	90	[1] LESIAK	92	CBAL	$e^+e^- \to \Upsilon(4S)$

[1] LESIAK 92 set a limit on the inclusive process $B(b \to s\gamma) < 2.8 \times 10^{-3}$ at 90% CL for the range of masses of 892–2045 MeV, independent of assumptions about s-quark hadronization.

$\Gamma(K_3^*(1780)\gamma)/\Gamma_{\text{total}}$ Γ_{71}/Γ

VALUE	CL%	DOCUMENT ID		TECN	COMMENT
$<3.7 \times 10^{-5}$	90	[1] NISHIDA	05	BELL	$e^+e^- \to \Upsilon(4S)$

• • • We do not use the following data for averages, fits, limits, etc. • • •

$<3.0 \times 10^{-3}$	90	ALBRECHT	88H	ARG	$e^+e^- \to \Upsilon(4S)$

[1] Uses $B(K_3^*(1780) \to \eta K) = 0.11^{+0.05}_{-0.04}$.

$\Gamma(K_4^*(2045)\gamma)/\Gamma_{\text{total}}$ Γ_{72}/Γ

VALUE	CL%	DOCUMENT ID		TECN	COMMENT
$<1.0 \times 10^{-3}$	90	[1] LESIAK	92	CBAL	$e^+e^- \to \Upsilon(4S)$

[1] LESIAK 92 set a limit on the inclusive process $B(b \to s\gamma) < 2.8 \times 10^{-3}$ at 90% CL for the range of masses of 892–2045 MeV, independent of assumptions about s-quark hadronization.

$\Gamma(K\eta'(958))/\Gamma_{\text{total}}$ Γ_{73}/Γ

VALUE	DOCUMENT ID		TECN	COMMENT
$(8.3^{+0.9}_{-0.8} \pm 0.7) \times 10^{-5}$	[1] RICHICHI	00	CLE2	$e^+e^- \to \Upsilon(4S)$

[1] Assumes equal production of B^+ and B^0 at the $\Upsilon(4S)$.

$\Gamma(K^*(892)\eta'(958))/\Gamma_{\text{total}}$ Γ_{74}/Γ

VALUE (units 10^{-6})	CL%	DOCUMENT ID		TECN	COMMENT
$4.1^{+1.0}_{-0.9} \pm 0.5$		[1] AUBERT	07E	BABR	$e^+e^- \to \Upsilon(4S)$

• • • We do not use the following data for averages, fits, limits, etc. • • •

<22	90	[1] RICHICHI	00	CLE2	$e^+e^- \to \Upsilon(4S)$

[1] Assumes equal production of B^+ and B^0 at the $\Upsilon(4S)$.

$\Gamma(K\eta)/\Gamma_{\text{total}}$ Γ_{75}/Γ

VALUE	CL%	DOCUMENT ID		TECN	COMMENT
$<5.2 \times 10^{-6}$	90	[1] RICHICHI	00	CLE2	$e^+e^- \to \Upsilon(4S)$

[1] Assumes equal production of B^+ and B^0 at the $\Upsilon(4S)$.

$\Gamma(K^*(892)\eta)/\Gamma_{\text{total}}$ Γ_{76}/Γ

VALUE	DOCUMENT ID		TECN	COMMENT
$(1.80^{+0.49}_{-0.43} \pm 0.18) \times 10^{-5}$	[1] RICHICHI	00	CLE2	$e^+e^- \to \Upsilon(4S)$

[1] Assumes equal production of B^+ and B^0 at the $\Upsilon(4S)$.

$\Gamma(K\phi\phi)/\Gamma_{\text{total}}$ Γ_{77}/Γ

VALUE (units 10^{-6})	DOCUMENT ID		TECN	COMMENT
$2.3^{+0.9}_{-0.8} \pm 0.3$	[1] HUANG	03	BELL	$e^+e^- \to \Upsilon(4S)$

[1] Assumes equal production of charged and neutral B meson pairs and isospin symmetry.

$\Gamma(\bar{b} \to \bar{s}\gamma)/\Gamma_{\text{total}}$ Γ_{78}/Γ

VALUE (units 10^{-4})	DOCUMENT ID		TECN	COMMENT
3.49 ± 0.19 OUR AVERAGE				
$3.75 \pm 0.18 \pm 0.35$	[1,2] SAITO	15	BELL	$e^+e^- \to \Upsilon(4S)$
$3.52 \pm 0.20 \pm 0.51$	[1,3] LEES	12U	BABR	$e^+e^- \to \Upsilon(4S)$
$3.32 \pm 0.16 \pm 0.31$	[1,4] LEES	12V	BABR	$e^+e^- \to \Upsilon(4S)$
$3.47 \pm 0.15 \pm 0.40$	[1,5] LIMOSANI	09	BELL	$e^+e^- \to \Upsilon(4S)$
$3.90 \pm 0.91 \pm 0.64$	[1,6] AUBERT	08O	BABR	$e^+e^- \to \Upsilon(4S)$
$3.29 \pm 0.44 \pm 0.29$	[1,7] CHEN	01C	CLE2	$e^+e^- \to \Upsilon(4S)$

• • • We do not use the following data for averages, fits, limits, etc. • • •

$2.30 \pm 0.08 \pm 0.30$	[8] DEL-AMO-SA...10M	BABR	$e^+e^- \to \Upsilon(4S)$	
$4.3 \pm 0.3 \pm 0.7$	[9] AUBERT	09U	BABR	Repl. by DEL-AMO-SANCHEZ 10M
$3.92 \pm 0.31 \pm 0.47$	[1,10] AUBERT,BE	06B	BABR	Repl. by LEES 12V
$3.49 \pm 0.20^{+0.59}_{-0.46}$	[1,11] AUBERT,B	05R	BABR	Repl. by LEES 12U
$3.50 \pm 0.32 \pm 0.31$	[1,12] KOPPENBURG	04	BELL	Repl. by LIMOSANI 09
$3.36 \pm 0.53^{+0.65}_{-0.68}$	[13] ABE	01F	BELL	Repl. by SAITO 15
$2.32 \pm 0.57 \pm 0.35$	ALAM	95	CLE2	Repl. by CHEN 01C

[1] We extrapolate the measured value to $E_\gamma > 1.6$ GeV using the method of BUCHMUELLER 06 (average of three theoretical models).
[2] SAITO 15 measured $(3.51 \pm 0.17 \pm 0.33) \times 10^{-4}$ using a sum-of-exclusive approach in which 38 of the hadronic final states with $m_{X_s} < 2.8$ GeV/c^2 are reconstructed. The cut of minimum photon energy is $E_\gamma > 1.9$ GeV.
[3] Reports $(3.29 \pm 0.19 \pm 0.48) \times 10^{-4}$ for $E_\gamma > 1.9$ GeV.
[4] Reports $(3.21 \pm 0.15 \pm 0.29 \pm 0.08) \times 10^{-4}$ for $1.8 < E_\gamma < 2.8$ GeV, where the last systematic uncertainty is for model dependency. Results with other cutoffs are also reported.
[5] The measurement reported is $(3.45 \pm 0.15 \pm 0.40) \times 10^{-4}$ for $E_\gamma > 1.7$ GeV.
[6] Uses a fully reconstructed B meson as a tag on the recoil side. The measurement reported is $(3.66 \pm 0.85 \pm 0.60) \times 10^{-4}$ for $E_\gamma > 1.9$ GeV.
[7] The measurement reported is $(3.21 \pm 0.43^{+0.32}_{-0.29}) \times 10^{-4}$ for $E_\gamma > 2.0$ GeV.
[8] Measured using sums of seven exclusive final states $B \to X_{d(s)}\gamma$ where $X_{d(s)}$ is a nonstrange (strange) charmless hadronic system in mass range 0.5–2.0 GeV/c^2.
[9] Measured using sums of seven exclusive final states $B \to X_{d(s)}\gamma$ where $X_{d(s)}$ is a nonstrange (strange) charmless hadronic system in mass range 0.6–1.8 GeV/c^2.
[10] The measurement reported is $(3.67 \pm 0.29 \pm 0.45) \times 10^{-4}$ for $E_\gamma > 1.9$ GeV.
[11] The measurement reported is $(3.27 \pm 0.18^{+0.55}_{-0.42}) \times 10^{-4}$ for $E_\gamma > 1.9$ GeV.
[12] The measurement reported is $(3.55 \pm 0.32 \pm 0.32) \times 10^{-4}$ for $E_\gamma > 1.8$ GeV.
[13] ABE 01F reports their systematic errors $(\pm 0.42^{+0.50}_{-0.54}) \times 10^{-4}$, where the second error is due to the theoretical uncertainty. We combine them in quadrature.

$\Gamma(\bar{b} \to \bar{d}\gamma)/\Gamma_{\text{total}}$ Γ_{79}/Γ

VALUE (units 10^{-6})	DOCUMENT ID		TECN	COMMENT
$9.2 \pm 2.0 \pm 2.3$	[1] DEL-AMO-SA...10M	BABR	$e^+e^- \to \Upsilon(4S)$	

• • • We do not use the following data for averages, fits, limits, etc. • • •

$14 \pm 5 \pm 4$	[2] AUBERT	09U	BABR	Repl. by DEL-AMO-SANCHEZ 10M

[1] Measured using sums of seven exclusive final states $B \to X_{d(s)}\gamma$ where $X_{d(s)}$ is a nonstrange (strange) charmless hadronic system in mass range 0.5–2.0 GeV/c^2.
[2] Measured using sums of seven exclusive final states $B \to X_{d(s)}\gamma$ where $X_{d(s)}$ is a nonstrange (strange) charmless hadronic system in mass range 0.6–1.8 GeV/c^2.

$\Gamma(\bar{b} \to \bar{d}\gamma)/\Gamma(\bar{b} \to \bar{s}\gamma)$ Γ_{79}/Γ_{78}

VALUE	DOCUMENT ID		TECN	COMMENT
$0.040 \pm 0.009 \pm 0.010$	[1] DEL-AMO-SA...10M	BABR	$e^+e^- \to \Upsilon(4S)$	

• • • We do not use the following data for averages, fits, limits, etc. • • •

$0.033 \pm 0.013 \pm 0.009$	[2] AUBERT	09U	BABR	Repl. by DEL-AMO-SANCHEZ 10M

[1] Measured using sums of seven exclusive final states $B \to X_{d(s)}\gamma$ where $X_{d(s)}$ is a nonstrange (strange) charmless hadronic system in mass range 0.5–2.0 GeV/c^2.
[2] Measured using sums of seven exclusive final states $B \to X_{d(s)}\gamma$ where $X_{d(s)}$ is a nonstrange (strange) charmless hadronic system in mass range 0.6–1.8 GeV/c^2.

$\Gamma(\bar{b} \to \bar{s}\text{gluon})/\Gamma_{\text{total}}$ Γ_{80}/Γ

VALUE	CL%	EVTS	DOCUMENT ID		TECN	COMMENT
<0.068	90		[1] COAN	98	CLE2	$e^+e^- \to \Upsilon(4S)$

• • • We do not use the following data for averages, fits, limits, etc. • • •

<0.08		2	[2] ALBRECHT	95D	ARG	$e^+e^- \to \Upsilon(4S)$

[1] COAN 98 uses D-ℓ correlation.
[2] ALBRECHT 95D use full reconstruction of one B decay as tag. Two candidate events for charmless B decay can be interpreted as either $b \to s$gluon or $b \to u$ transition. If interpreted as $b \to s$gluon they find a branching ratio of ~ 0.026 or the upper limit quoted above. Result is highly model dependent.

Meson Particle Listings

$B^{\pm}/B^0$ ADMIXTURE

$\Gamma(\eta \text{ anything})/\Gamma_{\text{total}}$ Γ_{81}/Γ

VALUE (units 10^{-4})	CL%	DOCUMENT ID		TECN	COMMENT
$2.61 \pm 0.30^{+0.44}_{-0.74}$		[1] NISHIMURA	10	BELL	$e^+e^- \to \Upsilon(4S)$
• • • We do not use the following data for averages, fits, limits, etc. • • •					
$1.69 \pm 0.29^{+0.36}_{-0.62}$		[2] NISHIMURA	10	BELL	$e^+e^- \to \Upsilon(4S)$
<4.4	90	[3] BROWDER	98	CLE2	$e^+e^- \to \Upsilon(4S)$

[1] Uses $B \to \eta X_s$ with $0.4 < m_{X_s} < 2.6$ GeV/c^2.

[2] Uses $B \to \eta X_s$ with $1.8 < m_{X_s} < 2.6$ GeV/c^2.

[3] BROWDER 98 search for high momentum $B \to \eta X_s$ between 2.1 and 2.7 GeV/c.

$\Gamma(\eta' \text{ anything})/\Gamma_{\text{total}}$ Γ_{82}/Γ

VALUE (units 10^{-4})	DOCUMENT ID		TECN	COMMENT
4.2 ± 0.9 OUR AVERAGE				
$3.9 \pm 0.8 \pm 0.9$	[1] AUBERT,B	04F	BABR	$e^+e^- \to \Upsilon(4S)$
$4.6 \pm 1.1 \pm 0.6$	[2] BONVICINI	03	CLE2	$e^+e^- \to \Upsilon(4S)$
• • • We do not use the following data for averages, fits, limits, etc. • • •				
$6.2 \pm 1.6^{+1.3}_{-2.0}$	[3] BROWDER	98	CLE2	$e^+e^- \to \Upsilon(4S)$

[1] AUBERT,B 04F reports branching ratio $B \to \eta' X_s$ for high momentum η' between 2.0 and 2.7 GeV/c in the $\Upsilon(4S)$ center-of-mass frame. X_s represents a recoil system consisting of a kaon and zero to four pions.

[2] BONVICINI 03 observed a signal of 61.2 ± 13.9 events in $B \to \eta' X_{nc}$ production for high momentum η' between 2.0 and 2.7 GeV/c in the $\Upsilon(4S)$ center-of-mass frame. The X_{nc} denotes "charmless" hadronic states recoiling against η'. The second error combines systematic and background subtraction uncertainties in quadrature.

[3] BROWDER 98 observed a signal of 39.0 ± 11.6 events in high momentum $B \to \eta' X_s$ production between 2.0 and 2.7 GeV/c. The branching fraction is based on the interpretation of $b \to sg$, where the last error includes additional uncertainties due to the color-suppressed $b \to$ backgrounds.

$\Gamma(K^+ \text{gluon (charmless)})/\Gamma_{\text{total}}$ Γ_{83}/Γ

VALUE (units 10^{-4})	CL%	DOCUMENT ID		TECN	COMMENT
<1.87	90	[1] DEL-AMO-SA...11		BABR	$e^+e^- \to \Upsilon(4S)$

[1] $B \to K^+ X$ with $m_X < 1.69$ GeV/c^2.

$\Gamma(K^0 \text{gluon (charmless)})/\Gamma_{\text{total}}$ Γ_{84}/Γ

VALUE (units 10^{-4})	DOCUMENT ID		TECN	COMMENT
$1.95^{+0.51}_{-0.45} \pm 0.50$	[1] DEL-AMO-SA...11		BABR	$e^+e^- \to \Upsilon(4S)$

[1] $B \to K^0 X$ with $m_X < 1.69$ GeV/c^2.

$\Gamma(\rho\gamma)/\Gamma_{\text{total}}$ Γ_{85}/Γ

VALUE (units 10^{-6})	CL%	DOCUMENT ID		TECN	COMMENT
1.39 ± 0.25 OUR AVERAGE		Error includes scale factor of 1.2.			
$1.73^{+0.34}_{-0.32} \pm 0.17$		[1,2] AUBERT	08BH	BABR	$e^+e^- \to \Upsilon(4S)$
$1.21^{+0.24}_{-0.22} \pm 0.12$		[1,2] TANIGUCHI	08	BELL	$e^+e^- \to \Upsilon(4S)$
• • • We do not use the following data for averages, fits, limits, etc. • • •					
$1.36^{+0.29}_{-0.27} \pm 0.10$		[1,3] AUBERT	07L	BABR	Repl. by AUBERT 08BH
< 1.9	90	[1,3] AUBERT	04C	BABR	Repl. by AUBERT 07L
<14	90	[1,4] COAN	00	CLE2	$e^+e^- \to \Upsilon(4S)$

[1] Assumes equal production of B^+ and B^0 at the $\Upsilon(4S)$.

[2] Assumes $\Gamma(B \to \rho\gamma) = \Gamma(B^+ \to \rho^+\gamma) = 2\,\Gamma(B^0 \to \rho^0\gamma)$ and uses lifetime ratio of $\tau_{B^+}/\tau_{B^0} = 1.071 \pm 0.009$.

[3] Assumes $\Gamma(B \to \rho\gamma) = \Gamma(B^+ \to \rho^+\gamma) = 2\,\Gamma(B^0 \to \rho^0\gamma)$ and uses lifetime ratio of $\tau_{B^+}/\tau_{B^0} = 1.083 \pm 0.017$.

[4] COAN 00 reports $B(B \to \rho\gamma)/B(B \to K^*(892)\gamma) < 0.32$ at 90%CL and scaled by the central value of $B(B \to K^*(892)\gamma)=(4.24 \pm 0.54 \pm 0.32) \times 10^{-5}$.

$\Gamma(\rho\gamma)/\Gamma(K^*(892)\gamma)$ Γ_{85}/Γ_{66}

VALUE (units 10^{-2})	DOCUMENT ID		TECN	COMMENT
$3.02^{+0.60+0.26}_{-0.55-0.28}$	TANIGUCHI	08	BELL	$e^+e^- \to \Upsilon(4S)$

$\Gamma(\rho/\omega\gamma)/\Gamma_{\text{total}}$ Γ_{86}/Γ

VALUE (units 10^{-6})	CL%	DOCUMENT ID		TECN	COMMENT
1.30 ± 0.23 OUR AVERAGE		Error includes scale factor of 1.2.			
$1.63^{+0.30}_{-0.28} \pm 0.16$		[1,2,3] AUBERT	08BH	BABR	$e^+e^- \to \Upsilon(4S)$
$1.14 \pm 0.20^{+0.10}_{-0.12}$		[1,3] TANIGUCHI	08	BELL	$e^+e^- \to \Upsilon(4S)$
• • • We do not use the following data for averages, fits, limits, etc. • • •					
$1.25^{+0.25}_{-0.24} \pm 0.09$		[4] AUBERT	07L	BABR	Repl. by AUBERT 08BH
$1.32^{+0.34+0.10}_{-0.31-0.09}$		[4] MOHAPATRA	06	BELL	Repl. by TANIGUCHI 08
$0.6 \pm 0.3 \pm 0.1$		[4] AUBERT	05	BABR	Repl. by AUBERT 07L
<1.4	90	[4] MOHAPATRA	05	BELL	$e^+e^- \to \Upsilon(4S)$

[1] Assumes $\Gamma(B \to \rho\gamma) = \Gamma(B^+ \to \rho^+\gamma) = 2\,\Gamma(B^0 \to \rho^0\gamma)$ and uses lifetime ratio of $\tau_{B^+}/\tau_{B^0} = 1.071 \pm 0.009$.

[2] Also reports $|V_{td}/V_{ts}| = 0.233^{+0.025+0.022}_{-0.024-0.021}$.

[3] Assumes equal production of B^+ and B^0 at the $\Upsilon(4S)$.

[4] Assumes $\Gamma(B \to \rho\gamma) = \Gamma(B^+ \to \rho^+\gamma) = 2\,\Gamma(B^0 \to \rho^0\gamma)$ and uses lifetime ratio of $\tau_{B^+}/\tau_{B^0} = 1.083 \pm 0.017$.

$\Gamma(\rho/\omega\gamma)/\Gamma(K^*(892)\gamma)$ Γ_{86}/Γ_{66}

VALUE (units 10^{-2})	CL%	DOCUMENT ID		TECN	COMMENT
$2.84 \pm 0.50^{+0.27}_{-0.29}$		[1] TANIGUCHI	08	BELL	$e^+e^- \to \Upsilon(4S)$
• • • We do not use the following data for averages, fits, limits, etc. • • •					
<3.5	90	MOHAPATRA	05	BELL	Repl. by TANIGUCHI 08

[1] Also reports $|V_{td}/V_{ts}| = 0.195^{+0.020}_{-0.019} \pm 0.015$.

$\Gamma(\pi^{\pm} \text{ anything})/\Gamma_{\text{total}}$ Γ_{87}/Γ

VALUE	DOCUMENT ID		TECN	COMMENT
$3.585 \pm 0.025 \pm 0.070$	[1] ALBRECHT	93I	ARG	$e^+e^- \to \Upsilon(4S)$

[1] ALBRECHT 93 excludes $\pi^{\pm}$ from K^0_S and Λ decays. If included, they find $4.105 \pm 0.025 \pm 0.080$.

$\Gamma(\pi^0 \text{ anything})/\Gamma_{\text{total}}$ Γ_{88}/Γ

VALUE	DOCUMENT ID		TECN	COMMENT
$2.35 \pm 0.02 \pm 0.11$	[1] ABE	01J	BELL	$e^+e \to \Upsilon(4S)$

[1] From fully inclusive π^0 yield with no corrections from decays of K^0_S or other particles.

$\Gamma(\eta \text{ anything})/\Gamma_{\text{total}}$ Γ_{89}/Γ

VALUE	DOCUMENT ID		TECN	COMMENT
$0.176 \pm 0.011 \pm 0.012$	KUBOTA	96	CLE2	$e^+e^- \to \Upsilon(4S)$

$\Gamma(\rho^0 \text{ anything})/\Gamma_{\text{total}}$ Γ_{90}/Γ

VALUE	DOCUMENT ID		TECN	COMMENT
$0.208 \pm 0.042 \pm 0.032$	ALBRECHT	94J	ARG	$e^+e^- \to \Upsilon(4S)$

$\Gamma(\omega \text{ anything})/\Gamma_{\text{total}}$ Γ_{91}/Γ

VALUE	CL%	DOCUMENT ID		TECN	COMMENT
<0.81	90	ALBRECHT	94J	ARG	$e^+e^- \to \Upsilon(4S)$

$\Gamma(\phi \text{ anything})/\Gamma_{\text{total}}$ Γ_{92}/Γ

VALUE	DOCUMENT ID		TECN	COMMENT
0.0343 ± 0.0012 OUR AVERAGE				
$0.0353 \pm 0.0005 \pm 0.0030$	HUANG	07	CLEO	$e^+e^- \to \Upsilon(4S)$
$0.0341 \pm 0.0006 \pm 0.0012$	AUBERT	04S	BABR	$e^+e^- \to \Upsilon(4S)$
$0.0390 \pm 0.0030 \pm 0.0035$	ALBRECHT	94J	ARG	$e^+e^- \to \Upsilon(4S)$
$0.023 \pm 0.006 \pm 0.005$	BORTOLETTO	86	CLEO	$e^+e^- \to \Upsilon(4S)$

$\Gamma(\phi K^*(892))/\Gamma_{\text{total}}$ Γ_{93}/Γ

VALUE	CL%	DOCUMENT ID		TECN
$<2.2 \times 10^{-5}$	90	[1] BERGFELD	98	CLE2

[1] Assumes equal production of B^+ and B^0 at the $\Upsilon(4S)$.

$\Gamma(\pi^+ \text{ gluon (charmless)})/\Gamma_{\text{total}}$ Γ_{95}/Γ

VALUE (units 10^{-4})	DOCUMENT ID		TECN	COMMENT
$3.72^{+0.50}_{-0.47} \pm 0.59$	[1] DEL-AMO-SA...11		BABR	$e^+e^- \to \Upsilon(4S)$

[1] $B \to \pi^+ X$ with $m_X < 1.71$ GeV/c^2.

$\Gamma(\Lambda_c^+ / \overline{\Lambda}_c^- \text{ anything})/\Gamma_{\text{total}}$ Γ_{96}/Γ

VALUE (%)	CL%	DOCUMENT ID		TECN	COMMENT
$3.61 \pm 0.32^{+0.20}_{-0.19}$		[1] AUBERT	07C	BABR	$e^+e^- \to \Upsilon(4S)$
• • • We do not use the following data for averages, fits, limits, etc. • • •					
$6.4 \pm 0.8 \pm 0.8$		[2] CRAWFORD	92	CLEO	$e^+e^- \to \Upsilon(4S)$
14 ± 9		[3] ALBRECHT	88E	ARG	$e^+e^- \to \Upsilon(4S)$
<11.2	90	[4] ALAM	87	CLEO	$e^+e^- \to \Upsilon(4S)$

[1] AUBERT 07C reports $0.045 \pm 0.003 \pm 0.012$ from a measurement of $[\Gamma(B \to \Lambda_c^+ / \overline{\Lambda}_c^- \text{anything})/\Gamma_{\text{total}}] \times [B(\Lambda_c^+ \to pK^-\pi^+)]$ assuming $B(\Lambda_c^+ \to pK^-\pi^+) = (5.0 \pm 1.3) \times 10^{-2}$, which we rescale to our best value $B(\Lambda_c^+ \to pK^-\pi^+) = (6.23 \pm 0.33) \times 10^{-2}$. Our first error is their experiment's error and our second error is the systematic error from using our best value.

[2] CRAWFORD 92 result derived from lepton baryon correlations. Assumes all charmed baryons in B^0 and $B^{\pm}$ decay are Λ_C.

[3] ALBRECHT 88E measured $B(B \to \Lambda_c^+ X) \cdot B(\Lambda_c^+ \to pK^-\pi^+) = (0.30 \pm 0.12 \pm 0.06)\%$ and used $B(\Lambda_c^+ \to pK^-\pi^+) = (2.2 \pm 1.0)\%$ from ABRAMS 80 to obtain above number.

[4] Assuming all baryons result from charmed baryons, ALAM 86 conclude the branching fraction is $7.4 \pm 2.9\%$. The limit given above is model independent.

$\Gamma(\Lambda_c^+ \text{ anything})/\Gamma(\overline{\Lambda}_c^- \text{ anything})$ Γ_{97}/Γ_{98}

VALUE	DOCUMENT ID		TECN	COMMENT
$0.19 \pm 0.13 \pm 0.04$	[1] AMMAR	97	CLE2	$e^+e^- \to \Upsilon(4S)$

[1] AMMAR 97 uses a high-momentum lepton tag ($P_\ell > 1.4$ GeV/c^2).

$\Gamma(\overline{\Lambda}_c^- \mu^+ \text{anything})/\Gamma(\overline{\Lambda}_c^- \text{anything})$ Γ_{101}/Γ_{98}

VALUE (units 10^{-2})	DOCUMENT ID		TECN	COMMENT
$-2.0 \pm 2.0 \pm 1.9$	LEES	12	BABR	$e^+e^- \to \Upsilon(4S)$

$\Gamma(\overline{\Lambda}_c^- \ell^+ \text{anything})/\Gamma(\Lambda_c^+ \text{ / } \overline{\Lambda}_c^- \text{anything})$ Γ_{99}/Γ_{96}

VALUE	CL%	DOCUMENT ID		TECN	COMMENT
$< 2.5 \times 10^{-2}$	90	[1] LEES	12	BABR	$e^+e^- \to \Upsilon(4S)$

[1] LEES 12 quotes also the measurement $\Gamma(B \to \overline{\Lambda}_c^- \ell^+ \text{anything})/\Gamma(B \to \Lambda_c^+ \text{ / } \overline{\Lambda}_c^- \text{anything}) = (1.2 \pm 0.7 \pm 0.4) \times 10^{-2}$.

$\Gamma(\overline{\Lambda}_c^- e^+ \text{anything})/\Gamma(\Lambda_c^+ \text{ / } \overline{\Lambda}_c^- \text{anything})$ Γ_{100}/Γ_{96}

VALUE	CL%	DOCUMENT ID		TECN	COMMENT
< 0.05	90	[1] BONVICINI	98	CLE2	$e^+e^- \to \Upsilon(4S)$

[1] BONVICINI 98 uses the electron with momentum above 0.6 GeV/c.

$\Gamma(\overline{\Lambda}_c^- e^+ \text{anything})/\Gamma(\overline{\Lambda}_c^- \text{anything})$ Γ_{100}/Γ_{98}

VALUE (units 10^{-2})	DOCUMENT ID		TECN	COMMENT
$2.5 \pm 1.1 \pm 0.6$	[1] LEES	12	BABR	$e^+e^- \to \Upsilon(4S)$

[1] Uses the full reconstruction of the recoiling B in a hadronic decay as a tag.

$\Gamma(\overline{\Lambda}_c^- \ell^+ \text{anything})/\Gamma(\overline{\Lambda}_c^- \text{anything})$ Γ_{99}/Γ_{98}

VALUE	CL%	DOCUMENT ID		TECN	COMMENT
$< 3.5 \times 10^{-2}$	90	[1] LEES	12	BABR	$e^+e^- \to \Upsilon(4S)$

[1] LEES 12 quotes also the measurement $\Gamma(B \to \overline{\Lambda}_c^- \ell^+ \text{anything})/\Gamma(B \to \overline{\Lambda}_c^- \text{anything}) = (1.7 \pm 1.0 \pm 0.6) \times 10^{-2}$.

$\Gamma(\overline{\Lambda}_c^- p \text{ anything})/\Gamma(\Lambda_c^+ \text{ / } \overline{\Lambda}_c^- \text{anything})$ Γ_{102}/Γ_{96}

VALUE	DOCUMENT ID		TECN	COMMENT
$0.57 \pm 0.05 \pm 0.05$	BONVICINI	98	CLE2	$e^+e^- \to \Upsilon(4S)$

$\Gamma(\overline{\Lambda}_c^- p e^+ \nu_e)/\Gamma(\overline{\Lambda}_c^- p \text{ anything})$ $\Gamma_{103}/\Gamma_{102}$

VALUE	CL%	DOCUMENT ID		TECN	COMMENT
< 0.04	90	[1] BONVICINI	98	CLE2	$e^+e^- \to \Upsilon(4S)$

[1] BONVICINI 98 uses the electron with momentum above 0.6 GeV/c.

$\Gamma(\overline{\Sigma}_c^{--} \text{anything})/\Gamma_{\text{total}}$ Γ_{104}/Γ

VALUE	EVTS	DOCUMENT ID		TECN	COMMENT
$0.0034 \pm 0.0017 \pm 0.0002$	77	[1] PROCARIO	94	CLE2	$e^+e^- \to \Upsilon(4S)$

[1] PROCARIO 94 reports $[\Gamma(B \to \overline{\Sigma}_c^{--} \text{anything})/\Gamma_{\text{total}}] \times [\text{B}(\Lambda_c^+ \to p K^- \pi^+)] = 0.00021 \pm 0.00008 \pm 0.00007$ which we divide by our best value $\text{B}(\Lambda_c^+ \to p K^- \pi^+) = (6.23 \pm 0.33) \times 10^{-2}$. Our first error is their experiment's error and our second error is the systematic error from using our best value.

$\Gamma(\overline{\Sigma}_c^- \text{anything})/\Gamma_{\text{total}}$ Γ_{105}/Γ

VALUE	CL%	DOCUMENT ID		TECN	COMMENT
$< 8 \times 10^{-3}$	90	[1] PROCARIO	94	CLE2	$e^+e^- \to \Upsilon(4S)$

[1] PROCARIO 94 reports $[\Gamma(B \to \overline{\Sigma}_c^- \text{anything})/\Gamma_{\text{total}}] \times [\text{B}(\Lambda_c^+ \to p K^- \pi^+)] < 0.00048$ which we divide by our best value $\text{B}(\Lambda_c^+ \to p K^- \pi^+) = 6.23 \times 10^{-2}$.

$\Gamma(\overline{\Sigma}_c^0 \text{anything})/\Gamma_{\text{total}}$ Γ_{106}/Γ

VALUE	EVTS	DOCUMENT ID		TECN	COMMENT
$0.0037 \pm 0.0017 \pm 0.0002$	76	[1] PROCARIO	94	CLE2	$e^+e^- \to \Upsilon(4S)$

[1] PROCARIO 94 reports $[\Gamma(B \to \overline{\Sigma}_c^0 \text{anything})/\Gamma_{\text{total}}] \times [\text{B}(\Lambda_c^+ \to p K^- \pi^+)] = 0.00023 \pm 0.00008 \pm 0.00007$ which we divide by our best value $\text{B}(\Lambda_c^+ \to p K^- \pi^+) = (6.23 \pm 0.33) \times 10^{-2}$. Our first error is their experiment's error and our second error is the systematic error from using our best value.

$\Gamma(\overline{\Sigma}_c^0 N (N = p \text{ or } n))/\Gamma_{\text{total}}$ Γ_{107}/Γ

VALUE	CL%	DOCUMENT ID		TECN	COMMENT
$< 1.2 \times 10^{-3}$	90	[1] PROCARIO	94	CLE2	$e^+e^- \to \Upsilon(4S)$

[1] PROCARIO 94 reports < 0.0017 from a measurement of $[\Gamma(B \to \overline{\Sigma}_c^0 N(N = p \text{ or } n))/\Gamma_{\text{total}}] \times [\text{B}(\Lambda_c^+ \to p K^- \pi^+)]$ assuming $\text{B}(\Lambda_c^+ \to p K^- \pi^+) = 0.043$, which we rescale to our best value $\text{B}(\Lambda_c^+ \to p K^- \pi^+) = 6.23 \times 10^{-2}$.

$\Gamma(\Xi_c^0 \text{anything}, \Xi_c^0 \to \Xi^- \pi^+)/\Gamma_{\text{total}}$ Γ_{108}/Γ

VALUE (units 10^{-3})	DOCUMENT ID		TECN	COMMENT
0.193 ± 0.030 OUR AVERAGE	Error includes scale factor of 1.1.			
$0.211 \pm 0.019 \pm 0.025$	[1] AUBERT,B	05M	BABR	$e^+e^- \to \Upsilon(4S)$
$0.144 \pm 0.048 \pm 0.021$	[2] BARISH	97	CLE2	$e^+e^- \to \Upsilon(4S)$

[1] The yield is obtained by requiring the momentum $P < 2.15$ GeV/c.
[2] BARISH 97 find 79 ± 27 Ξ_c^0 events.

$\Gamma(\Xi_c^+, \Xi_c^+ \to \Xi^- \pi^+ \pi^+)/\Gamma_{\text{total}}$ Γ_{109}/Γ

VALUE (units 10^{-3})	DOCUMENT ID		TECN	COMMENT
$0.453 \pm 0.096^{+0.085}_{-0.065}$	[1] BARISH	97	CLE2	$e^+e^- \to \Upsilon(4S)$

[1] BARISH 97 find 125 ± 28 Ξ_c^+ events.

$\Gamma(p/\overline{p} \text{ anything})/\Gamma_{\text{total}}$ Γ_{110}/Γ

Includes p and $\overline{p}$ from Λ and $\overline{\Lambda}$ decay.

VALUE	EVTS	DOCUMENT ID		TECN	COMMENT
0.080 ± 0.004 OUR AVERAGE					
$0.080 \pm 0.005 \pm 0.005$		ALBRECHT	93I	ARG	$e^+e^- \to \Upsilon(4S)$
$0.080 \pm 0.005 \pm 0.003$		CRAWFORD	92	CLEO	$e^+e^- \to \Upsilon(4S)$
$0.082 \pm 0.005^{+0.013}_{-0.010}$	2163	[1] ALBRECHT	89K	ARG	$e^+e^- \to \Upsilon(4S)$
• • • We do not use the following data for averages, fits, limits, etc. • • •					
> 0.021		[2] ALAM	83B	CLEO	$e^+e^- \to \Upsilon(4S)$

[1] ALBRECHT 89K include direct and nondirect protons.
[2] ALAM 83B reported their result as $> 0.036 \pm 0.006 \pm 0.009$. Data are consistent with equal yields of p and $\overline{p}$. Using assumed yields below cut, $\text{B}(B \to p + \text{X}) = 0.03$ not including protons from Λ decays.

$\Gamma(p/\overline{p} \text{ (direct) anything})/\Gamma_{\text{total}}$ Γ_{111}/Γ

VALUE	EVTS	DOCUMENT ID		TECN	COMMENT
0.055 ± 0.005 OUR AVERAGE					
$0.055 \pm 0.005 \pm 0.0035$		ALBRECHT	93I	ARG	$e^+e^- \to \Upsilon(4S)$
$0.056 \pm 0.006 \pm 0.005$		CRAWFORD	92	CLEO	$e^+e^- \to \Upsilon(4S)$
0.055 ± 0.016	1220	[1] ALBRECHT	89K	ARG	$e^+e^- \to \Upsilon(4S)$

[1] ALBRECHT 89K subtract contribution of Λ decay from the inclusive proton yield.

$\Gamma(\overline{p} e^+ \nu_e \text{ anything})/\Gamma_{\text{total}}$ Γ_{112}/Γ

VALUE	CL%	DOCUMENT ID		TECN	COMMENT
$< 5.9 \times 10^{-4}$	90	[1] ADAM	03B	CLE2	$e^+e^- \to \Upsilon(4S)$
• • • We do not use the following data for averages, fits, limits, etc. • • •					
$< 16 \times 10^{-4}$	90	ALBRECHT	90H	ARG	$e^+e^- \to \Upsilon(4S)$

[1] Based on $V-A$ model.

$\Gamma(\Lambda/\overline{\Lambda} \text{ anything})/\Gamma_{\text{total}}$ Γ_{113}/Γ

VALUE	EVTS	DOCUMENT ID		TECN	COMMENT
0.040 ± 0.005 OUR AVERAGE					
$0.038 \pm 0.004 \pm 0.006$	2998	CRAWFORD	92	CLEO	$e^+e^- \to \Upsilon(4S)$
$0.042 \pm 0.005 \pm 0.006$	943	ALBRECHT	89K	ARG	$e^+e^- \to \Upsilon(4S)$
• • • We do not use the following data for averages, fits, limits, etc. • • •					
$0.022 \pm 0.003 \pm 0.0022$		[1] ACKERSTAFF	97N	OPAL	$e^+e^- \to Z$
> 0.011		[2] ALAM	83B	CLEO	$e^+e^- \to \Upsilon(4S)$

[1] ACKERSTAFF 97N assumes $\text{B}(b \to B) = 0.868 \pm 0.041$, *i.e.*, an admixture of B^0, $B^{\pm}$, and B_s.
[2] ALAM 83B reported their result as $> 0.022 \pm 0.007 \pm 0.004$. Values are for $(\text{B}(\Lambda\text{X}) + \text{B}(\overline{\Lambda}\text{X}))/2$. Data are consistent with equal yields of p and $\overline{p}$. Using assumed yields below cut, $\text{B}(B \to \Lambda\text{X}) = 0.03$.

$\Gamma(\Lambda \text{ anything})/\Gamma(\overline{\Lambda} \text{ anything})$ $\Gamma_{114}/\Gamma_{115}$

VALUE	DOCUMENT ID		TECN	COMMENT
$0.43 \pm 0.09 \pm 0.07$	[1] AMMAR	97	CLE2	$e^+e^- \to \Upsilon(4S)$

[1] AMMAR 97 uses a high-momentum lepton tag ($P_\ell > 1.4$ GeV/c^2).

$\Gamma(\Xi^-/\overline{\Xi}^+ \text{anything})/\Gamma_{\text{total}}$ Γ_{116}/Γ

VALUE	EVTS	DOCUMENT ID		TECN	COMMENT
0.0027 ± 0.0006 OUR AVERAGE					
$0.0027 \pm 0.0005 \pm 0.0004$	147	CRAWFORD	92	CLEO	$e^+e^- \to \Upsilon(4S)$
0.0028 ± 0.0014	54	ALBRECHT	89K	ARG	$e^+e^- \to \Upsilon(4S)$

$\Gamma(\text{baryons anything})/\Gamma_{\text{total}}$ Γ_{117}/Γ

VALUE	DOCUMENT ID		TECN	COMMENT
$0.068 \pm 0.005 \pm 0.003$	[1] ALBRECHT	92O	ARG	$e^+e^- \to \Upsilon(4S)$
• • • We do not use the following data for averages, fits, limits, etc. • • •				
0.076 ± 0.014	[2] ALBRECHT	89K	ARG	$e^+e^- \to \Upsilon(4S)$

[1] ALBRECHT 92O result is from simultaneous analysis of p and Λ yields, $p\overline{p}$ and $\Lambda\overline{p}$ correlations, and various lepton-baryon and lepton-baryon-antibaryon correlations. Supersedes ALBRECHT 89K.
[2] ALBRECHT 89K obtain this result by adding their their measurements $(5.5 \pm 1.6)\%$ for direct protons and $(4.2 \pm 0.5 \pm 0.6)\%$ for inclusive Λ production. They then assume $(5.5 \pm 1.6)\%$ for neutron production and add it in also. Since each B decay has two baryons, they divide by 2 to obtain $(7.6 \pm 1.4)\%$.

$\Gamma(p\overline{p} \text{ anything})/\Gamma_{\text{total}}$ Γ_{118}/Γ

Includes p and $\overline{p}$ from Λ and $\overline{\Lambda}$ decay.

VALUE	EVTS	DOCUMENT ID		TECN	COMMENT
0.0247 ± 0.0023 OUR AVERAGE					
$0.024 \pm 0.001 \pm 0.004$		CRAWFORD	92	CLEO	$e^+e^- \to \Upsilon(4S)$
$0.025 \pm 0.002 \pm 0.002$	918	ALBRECHT	89K	ARG	$e^+e^- \to \Upsilon(4S)$

$\Gamma(p\overline{p} \text{ anything})/\Gamma(p/\overline{p} \text{ anything})$ $\Gamma_{118}/\Gamma_{110}$

Includes p and $\overline{p}$ from Λ and $\overline{\Lambda}$ decay.

VALUE	DOCUMENT ID		TECN	COMMENT
• • • We do not use the following data for averages, fits, limits, etc. • • •				
$0.30 \pm 0.02 \pm 0.05$	[1] CRAWFORD	92	CLEO	$e^+e^- \to \Upsilon(4S)$

[1] CRAWFORD 92 value is not independent of their $\Gamma(p\overline{p} \text{ anything})/\Gamma_{\text{total}}$ value.

$\Gamma(\Lambda\overline{p}/\overline{\Lambda}p \text{ anything})/\Gamma_{\text{total}}$ Γ_{119}/Γ

Includes p and $\overline{p}$ from Λ and $\overline{\Lambda}$ decay.

VALUE	EVTS	DOCUMENT ID		TECN	COMMENT
0.025±0.004 OUR AVERAGE					
0.029±0.005±0.005		CRAWFORD	92	CLEO	$e^+e^- \to \Upsilon(4S)$
0.023±0.004±0.003	165	ALBRECHT	89K	ARG	$e^+e^- \to \Upsilon(4S)$

$\Gamma(\Lambda\overline{p}/\overline{\Lambda}p \text{ anything})/\Gamma(\Lambda/\overline{\Lambda} \text{ anything})$ $\Gamma_{119}/\Gamma_{113}$

Includes p and $\overline{p}$ from Λ and $\overline{\Lambda}$ decay.

VALUE	DOCUMENT ID		TECN	COMMENT
• • • We do not use the following data for averages, fits, limits, etc. • • •				
0.76±0.11±0.08	[1] CRAWFORD	92	CLEO	$e^+e^- \to \Upsilon(4S)$

[1] CRAWFORD 92 value is not independent of their $[\Gamma(\Lambda\overline{p}\text{anything})+\Gamma(\overline{\Lambda}p\text{anything})]/\Gamma_{\text{total}}$ value.

$\Gamma(\Lambda\overline{\Lambda} \text{ anything})/\Gamma_{\text{total}}$ Γ_{120}/Γ

VALUE	CL%	EVTS	DOCUMENT ID		TECN	COMMENT
<0.005	90		CRAWFORD	92	CLEO	$e^+e^- \to \Upsilon(4S)$
• • • We do not use the following data for averages, fits, limits, etc. • • •						
<0.0088	90	12	ALBRECHT	89K	ARG	$e^+e^- \to \Upsilon(4S)$

$\Gamma(\Lambda\overline{\Lambda} \text{ anything})/\Gamma(\Lambda/\overline{\Lambda} \text{ anything})$ $\Gamma_{120}/\Gamma_{113}$

VALUE	CL%	DOCUMENT ID		TECN	COMMENT
• • • We do not use the following data for averages, fits, limits, etc. • • •					
<0.13	90	[1] CRAWFORD	92	CLEO	$e^+e^- \to \Upsilon(4S)$

[1] CRAWFORD 92 value is not independent of their $\Gamma(\Lambda\overline{\Lambda}\text{anything})/\Gamma_{\text{total}}$ value.

$\Gamma(s e^+ e^-)/\Gamma_{\text{total}}$ Γ_{121}/Γ

Test for $\Delta B = 1$ weak neutral current. Allowed by higher-order electroweak interactions.

VALUE (units 10^{-6})	CL%	DOCUMENT ID		TECN	COMMENT
6.7 ±1.7 OUR AVERAGE		Error includes scale factor of 2.0.			
$7.69^{+0.82}_{-0.77}{}^{+0.71}_{-0.60}$		[1] LEES	14D	BABR	$e^+e^- \to \Upsilon(4S)$
$4.04\pm1.30^{+0.87}_{-0.83}$		[2] IWASAKI	05	BELL	$e^+e^- \to \Upsilon(4S)$
• • • We do not use the following data for averages, fits, limits, etc. • • •					
6.0 ±1.7 ±1.3		[2] AUBERT,B	04I	BABR	Repl. by LEES 14D
$5.0 \pm 2.3\ ^{+1.3}_{-1.1}$		[2] KANEKO	03	BELL	Repl. by IWASAKI 05
< 57	90	GLENN	98	CLEO	$e^+e^- \to \Upsilon(4S)$
<50000	90	BEBEK	81	CLEO	$e^+e^- \to \Upsilon(4S)$

[1] Measured from sum of exclusive modes through K^+, $K^+\pi^0$, $K^+\pi^-$, $K^+\pi^-\pi^0$, $K^+\pi^-\pi^+$, K^0_S, $K^0_S\pi^0$, $K^0_S\pi^+$, $K^0_S\pi^+\pi^0$, and $K^0_S\pi^+\pi^-$ corrected for unobserved modes.
[2] Requires $M_{\ell^+\ell^-} > 0.2$ GeV/c^2.

$\Gamma(s\mu^+\mu^-)/\Gamma_{\text{total}}$ Γ_{122}/Γ

Test for $\Delta B = 1$ weak neutral current. Allowed by higher-order electroweak interactions.

VALUE (units 10^{-6})	CL%	DOCUMENT ID		TECN	COMMENT
4.3 ±1.0 OUR AVERAGE					
$4.41^{+1.31}_{-1.17}{}^{+0.63}_{-0.50}$		[1] LEES	14D	BABR	$e^+e^- \to \Upsilon(4S)$
$4.13\pm1.05^{+0.85}_{-0.81}$		[2] IWASAKI	05	BELL	$e^+e^- \to \Upsilon(4S)$
• • • We do not use the following data for averages, fits, limits, etc. • • •					
5.0 ±2.8 ±1.2		AUBERT,B	04I	BABR	Repl. by LEES 14D
$7.9 \pm 2.1\ ^{+2.1}_{-1.5}$		KANEKO	03	BELL	Repl. by IWASAKI 05
< 58	90	GLENN	98	CLEO	$e^+e^- \to \Upsilon(4S)$
<17000	90	CHADWICK	81	CLEO	$e^+e^- \to \Upsilon(4S)$

[1] Measured from sum of exclusive modes through K^+, $K^+\pi^0$, $K^+\pi^-$, $K^+\pi^-\pi^0$, $K^+\pi^-\pi^+$, K^0_S, $K^0_S\pi^0$, $K^0_S\pi^+$, $K^0_S\pi^+\pi^0$, and $K^0_S\pi^+\pi^-$ corrected for unobserved modes.
[2] Requires $M_{\ell^+\ell^-} > 0.2$ GeV/c^2.

$[\Gamma(s e^+ e^-) + \Gamma(s\mu^+\mu^-)]/\Gamma_{\text{total}}$ $(\Gamma_{121}+\Gamma_{122})/\Gamma$

Test for $\Delta B = 1$ weak neutral current. Allowed by higher-order electroweak interactions.

VALUE	CL%	DOCUMENT ID		TECN	COMMENT
<4.2 ×10^{-5}	90	GLENN	98	CLEO	$e^+e^- \to \Upsilon(4S)$
• • • We do not use the following data for averages, fits, limits, etc. • • •					
<0.0024	90	[1] BEAN	87	CLEO	Repl. by GLENN 98
<0.0062	90	[2] AVERY	84	CLEO	Repl. by BEAN 87

[1] BEAN 87 reports $[(\mu^+\mu^-)+(e^+e^-)]/2$ and we converted it.
[2] Determine ratio of B^+ to B^0 semileptonic decays to be in the range 0.25–2.9.

$\Gamma(s\ell^+\ell^-)/\Gamma_{\text{total}}$ Γ_{123}/Γ

Test for $\Delta B = 1$ weak neutral current.

VALUE (units 10^{-6})	DOCUMENT ID		TECN	COMMENT
5.8 ±1.3 OUR AVERAGE	Error includes scale factor of 1.8.			
$6.73^{+0.70}_{-0.64}{}^{+0.60}_{-0.56}$	[1] LEES	14D	BABR	$e^+e^- \to \Upsilon(4S)$
$4.11\pm0.83^{+0.85}_{-0.81}$	[2] IWASAKI	05	BELL	$e^+e^- \to \Upsilon(4S)$
• • • We do not use the following data for averages, fits, limits, etc. • • •				
5.6 ±1.5 ±1.3	[3] AUBERT,B	04I	BABR	Repl. by LEES 14D
$6.1 \pm 1.4\ ^{+1.4}_{-1.1}$	[3] KANEKO	03	BELL	Repl. by IWASAKI 05

[1] Measured from sum of exclusive modes through K^+, $K^+\pi^0$, $K^+\pi^-$, $K^+\pi^-\pi^0$, $K^+\pi^-\pi^+$, K^0_S, $K^0_S\pi^0$, $K^0_S\pi^+$, $K^0_S\pi^+\pi^0$, and $K^0_S\pi^+\pi^-$ corrected for unobserved modes.
[2] Requires $M_{\ell^+\ell^-} > 0.2$ GeV/c^2.
[3] Requires $M_{e^+e^-} > 0.2$ GeV/c^2.

$\Gamma(\pi\ell^+\ell^-)/\Gamma_{\text{total}}$ Γ_{124}/Γ

VALUE	CL%	DOCUMENT ID		TECN	COMMENT
<5.9 × 10^{-8}	90	[1] LEES	13M	BABR	$e^+e^- \to \Upsilon(4S)$
• • • We do not use the following data for averages, fits, limits, etc. • • •					
<6.2 × 10^{-8}	90	[1] WEI	08A	BELL	$e^+e^- \to \Upsilon(4S)$
<9.1 × 10^{-8}	90	[1] AUBERT	07AG	BABR	$e^+e^- \to \Upsilon(4S)$

[1] Assumes equal production of B^+ and B^0 at the $\Upsilon(4S)$.

$\Gamma(\pi e^+ e^-)/\Gamma_{\text{total}}$ Γ_{125}/Γ

VALUE	CL%	DOCUMENT ID		TECN	COMMENT
<11.0 × 10^{-8}	90	[1] LEES	13M	BABR	$e^+e^- \to \Upsilon(4S)$

[1] Assumes equal production of B^+ and B^0 at the $\Upsilon(4S)$.

$\Gamma(\pi\mu^+\mu^-)/\Gamma_{\text{total}}$ Γ_{126}/Γ

VALUE	CL%	DOCUMENT ID		TECN	COMMENT
<5.0 × 10^{-8}	90	[1] LEES	13M	BABR	$e^+e^- \to \Upsilon(4S)$

[1] Assumes equal production of B^+ and B^0 at the $\Upsilon(4S)$.

$\Gamma(K e^+ e^-)/\Gamma_{\text{total}}$ Γ_{127}/Γ

Test for $\Delta B = 1$ weak neutral current. Allowed by higher-order electroweak interactions.

VALUE (units 10^{-7})	CL%	DOCUMENT ID		TECN	COMMENT
4.4±0.6 OUR AVERAGE					
$3.9^{+0.9}_{-0.8}\pm0.2$		[1] AUBERT	09T	BABR	$e^+e^- \to \Upsilon(4S)$
$4.8^{+0.8}_{-0.7}\pm0.3$		[1] WEI	09A	BELL	$e^+e^- \to \Upsilon(4S)$
• • • We do not use the following data for averages, fits, limits, etc. • • •					
$3.3^{+0.9}_{-0.8}\pm0.2$		[1] AUBERT,B	06J	BABR	Repl. by AUBERT 09T
$7.4^{+1.8}_{-1.6}\pm0.5$		[1] AUBERT	03U	BABR	Repl. by AUBERT,B 06J
$4.8^{+1.5}_{-1.3}\pm0.3$		[1,2] ISHIKAWA	03	BELL	Repl. by WEI 09A
<13	90	ABE	02	BELL	Repl. by ISHIKAWA 03

[1] Assumes equal production of B^+ and B^0 at the $\Upsilon(4S)$.
[2] The second error is a total of systematic uncertainties including model dependence.

$\Gamma(K^*(892)e^+e^-)/\Gamma_{\text{total}}$ Γ_{128}/Γ

Test for $\Delta B = 1$ weak neutral current. Allowed by higher-order electroweak interactions.

VALUE (units 10^{-7})	CL%	DOCUMENT ID		TECN	COMMENT
11.9±2.0 OUR AVERAGE		Error includes scale factor of 1.2.			
$9.9^{+2.3}_{-2.1}\pm0.6$		[1] AUBERT	09T	BABR	$e^+e^- \to \Upsilon(4S)$
$13.9^{+2.3}_{-2.0}\pm1.2$		[1] WEI	09A	BELL	$e^+e^- \to \Upsilon(4S)$
• • • We do not use the following data for averages, fits, limits, etc. • • •					
$9.7^{+3.0}_{-2.7}\pm1.4$		[1] AUBERT,B	06J	BABR	Repl. by AUBERT 09T
$9.8^{+5.0}_{-4.2}\pm1.1$		[1] AUBERT	03U	BABR	Repl. by AUBERT,B 06J
$14.9^{+5.2}_{-4.6}{}^{+1.2}_{-1.3}$		[2] ISHIKAWA	03	BELL	Repl. by WEI 09A
<56	90	ABE	02	BELL	Repl. by ISHIKAWA 03

[1] Assumes equal production of B^+ and B^0 at the $\Upsilon(4S)$.
[2] Assumes equal production of B^0 and B^+ at $\Upsilon(4S)$. The second error is a total of systematic uncertainties including model dependence.

$\Gamma(K\mu^+\mu^-)/\Gamma_{\text{total}}$ Γ_{129}/Γ

Test for $\Delta B = 1$ weak neutral current. Allowed by higher-order electroweak interactions.

VALUE (units 10^{-7})	DOCUMENT ID		TECN	COMMENT
4.4±0.4 OUR AVERAGE				
4.2±0.4±0.2	AALTONEN	11AI	CDF	$p\overline{p}$ at 1.96 TeV
$4.1^{+1.3}_{-1.2}\pm0.2$	[1] AUBERT	09T	BABR	$e^+e^- \to \Upsilon(4S)$
5.0±0.6±0.3	[1] WEI	09A	BELL	$e^+e^- \to \Upsilon(4S)$
• • • We do not use the following data for averages, fits, limits, etc. • • •				
$3.5^{+1.3}_{-1.1}\pm0.3$	[1] AUBERT,B	06J	BABR	Repl. by AUBERT 09T
$4.5^{+2.3}_{-1.9}\pm0.4$	[1] AUBERT	03U	BABR	Repl. by AUBERT,B 06J
$4.8^{+1.2}_{-1.1}\pm0.4$	[1,2] ISHIKAWA	03	BELL	Repl. by WEI 09A
$9.9^{+4.0}_{-3.2}{}^{+1.3}_{-1.0}$	ABE	02	BELL	Repl. by ISHIKAWA 03

[1] Assumes equal production of B^+ and B^0 at the $\Upsilon(4S)$.
[2] The second error is a total of systematic uncertainties including model dependence.

$\Gamma(K\mu^+\mu^-)/\Gamma(Ke^+e^-)$ $\Gamma_{129}/\Gamma_{127}$

VALUE	DOCUMENT ID		TECN	COMMENT
1.01±0.15 OUR AVERAGE				
$1.00^{+0.31}_{-0.25}\pm0.07$	[1] LEES	12S	BABR	$e^+e^-\to\Upsilon(4S)$
$0.96^{+0.44}_{-0.34}\pm0.05$	AUBERT	09T	BABR	$e^+e^-\to\Upsilon(4S)$
$1.03\pm0.19\pm0.06$	WEI	09A	BELL	$e^+e^-\to\Upsilon(4S)$
• • • We do not use the following data for averages, fits, limits, etc. • • •				
$1.06\pm0.48\pm0.08$	AUBERT,B	06J	BABR	Repl. by AUBERT 09T

[1] Measured in the union of $0.10 < q^2 < 8.12$ GeV$^2/c^4$ and $q^2 > 10.11$ GeV$^2/c^4$. LEES 12S reports also individual measurements $\Gamma(B\to K\mu^+\mu^-)/\Gamma(B\to Ke^+e^-) = 0.74^{+0.40}_{-0.31}\pm0.06$ for $0.10 < q^2 < 8.12$ GeV$^2/c^4$ and $\Gamma(B\to K\mu^+\mu^-)/\Gamma(B\to Ke^+e^-) = 1.43^{+0.65}_{-0.44}\pm0.12$ for $q^2 > 10.11$ GeV$^2/c^4$.

$\Gamma(K^*(892)\mu^+\mu^-)/\Gamma_{\rm total}$ Γ_{130}/Γ

Test for $\Delta B = 1$ weak neutral current. Allowed by higher-order electroweak interactions.

VALUE (units 10^{-7})	CL%	DOCUMENT ID		TECN	COMMENT
10.6±0.9 OUR AVERAGE					
$10.1\pm1.0\pm0.5$		AALTONEN	11AI	CDF	$p\overline{p}$ at 1.96 TeV
$13.5^{+3.5}_{-3.3}\pm1.0$		[1] AUBERT	09T	BABR	$e^+e^-\to\Upsilon(4S)$
$11.0^{+1.6}_{-1.4}\pm0.8$		[1] WEI	09A	BELL	$e^+e^-\to\Upsilon(4S)$
• • • We do not use the following data for averages, fits, limits, etc. • • •					
$8.8^{+3.5}_{-3.0}\pm1.2$		[1] AUBERT,B	06J	BABR	Repl. by AUBERT 09T
$12.7^{+7.6}_{-6.1}\pm1.6$		[1] AUBERT	03U	BABR	Repl. by AUBERT,B 06J
$11.7^{+3.6}_{-3.1}\pm1.0$		[2] ISHIKAWA	03	BELL	Repl. by WEI 09A
<31	90	ABE	02	BELL	Repl. by ISHIKAWA 03

[1] Assumes equal production of B^+ and B^0 at the $\Upsilon(4S)$.
[2] Assumes equal production of B^0 and B^+ at $\Upsilon(4S)$. The second error is a total of systematic uncertainties including model dependence.

$\Gamma(K^*(892)\mu^+\mu^-)/\Gamma(K^*(892)e^+e^-)$ $\Gamma_{130}/\Gamma_{128}$

VALUE	DOCUMENT ID		TECN	COMMENT
0.98±0.15 OUR AVERAGE				
$1.13^{+0.34}_{-0.26}\pm0.10$	[1] LEES	12S	BABR	$e^+e^-\to\Upsilon(4S)$
$1.37^{+0.53}_{-0.40}\pm0.09$	AUBERT	09T	BABR	$e^+e^-\to\Upsilon(4S)$
$0.83\pm0.17\pm0.08$	WEI	09A	BELL	$e^+e^-\to\Upsilon(4S)$
• • • We do not use the following data for averages, fits, limits, etc. • • •				
$0.91\pm0.45\pm0.06$	AUBERT,B	06J	BABR	Repl. by AUBERT 09T

[1] Measured in the union of $0.10 < q^2 < 8.12$ GeV$^2/c^4$ and $q^2 > 10.11$ GeV$^2/c^4$. LEES 12S reports also individual measurements $\Gamma(B\to K^*(892)\mu^+\mu^-)/\Gamma(B\to K^*(892)e^+e^-) = 1.06^{+0.48}_{-0.33}\pm0.08$ for $0.10 < q^2 < 8.12$ GeV$^2/c^4$ and $\Gamma(B\to K^*(892)\mu^+\mu^-)/\Gamma(B\to K^*(892)e^+e^-) = 1.18^{+0.55}_{-0.37}\pm0.11$ for $q^2 > 10.11$ GeV$^2/c^4$.

$\Gamma(K\ell^+\ell^-)/\Gamma_{\rm total}$ Γ_{131}/Γ

Test for $\Delta B = 1$ weak neutral current. Allowed by higher-order electroweak interactions.

VALUE (units 10^{-7})	CL%	DOCUMENT ID		TECN	COMMENT
4.8±0.4 OUR AVERAGE					
$4.7\pm0.6\pm0.2$		LEES	12S	BABR	$e^+e^-\to\Upsilon(4S)$
$4.8^{+0.5}_{-0.4}\pm0.3$		WEI	09A	BELL	$e^+e^-\to\Upsilon(4S)$
• • • We do not use the following data for averages, fits, limits, etc. • • •					
$3.9\pm0.7\pm0.2$		[1] AUBERT	09T	BABR	Repl. by LEES 12S
$3.4\pm0.7\pm0.2$		[1] AUBERT,B	06J	BABR	Repl. by AUBERT 09T
$6.5^{+1.4}_{-1.3}\pm0.4$		[2] AUBERT	03U	BABR	Repl. by AUBERT,B 06J
$4.8^{+1.0}_{-0.9}\pm0.3$		[3] ISHIKAWA	03	BELL	Repl. by WEI 09A
$7.5^{+2.5}_{-2.1}\pm0.6$		[4] ABE	02	BELL	Repl. by ISHIKAWA 03
< 5.1	90	[1] AUBERT	02L	BABR	$e^+e^-\to\Upsilon(4S)$
<17	90	[5] ANDERSON	01B	CLE2	$e^+e^-\to\Upsilon(4S)$

[1] Assumes equal production of B^+ and B^0 at the $\Upsilon(4S)$.
[2] Assumes all four $B\to K\ell^+\ell^-$ modes having equal partial widths in the fit.
[3] Assumes equal production rate for charge and neutral B meson pairs, isospin invariance, lepton universality for $B\to K\ell^+\ell^-$, and $B(B\to K^*(892)\mu^+\mu^-) = 1.33$. The second error is total systematic uncertainties including model dependence.
[4] Assumes lepton universality.
[5] The result is for di-lepton masses above 0.5 GeV.

$\Gamma(K^*(892)\ell^+\ell^-)/\Gamma_{\rm total}$ Γ_{132}/Γ

Test for $\Delta B = 1$ weak neutral current. Allowed by higher-order electroweak interactions.

VALUE (units 10^{-7})	CL%	DOCUMENT ID		TECN	COMMENT
10.5±1.0 OUR AVERAGE					
$10.2^{+1.4}_{-1.3}\pm0.5$		LEES	12S	BABR	$e^+e^-\to\Upsilon(4S)$
$10.7^{+1.1}_{-1.0}\pm0.9$		WEI	09A	BELL	$e^+e^-\to\Upsilon(4S)$
• • • We do not use the following data for averages, fits, limits, etc. • • •					
$11.1^{+1.9}_{-1.8}\pm0.7$		[1] AUBERT	09T	BABR	Repl. by LEES 12S
$7.8^{+1.9}_{-1.7}\pm1.1$		[1] AUBERT,B	06J	BABR	Repl. by AUBERT 09T
$8.8^{+3.3}_{-2.9}\pm1.0$		[2] AUBERT	03U	BABR	Repl. by AUBERT,B 06J
$11.5^{+2.6}_{-2.4}\pm0.8$		[3] ISHIKAWA	03	BELL	Repl. by WEI 09A
<31	90	[1,4] AUBERT	02L	BABR	Repl. by AUBERT 03U
<33	90	[5] ANDERSON	01B	CLE2	$e^+e^-\to\Upsilon(4S)$

[1] Assumes equal production of B^+ and B^0 at the $\Upsilon(4S)$.
[2] Assumes the partial width ratio of electron and muon modes to be $\Gamma(B\to K^*(892)e^+e^-)/\Gamma(B\to K^*(892)\mu^+\mu^-) = 1.33$.
[3] Assumes equal production rate for charge and neutral B meson pairs, isospin invariance, lepton universality for $B\to K\ell^+\ell^-$, and $B(B\to K^*(892)\mu^+\mu^-) = 1.33$. The second error is total systematic uncertainties including model dependence.
[4] For averaging $K^*(892)\mu^+\mu^-$ and $K^*(892)e^+e^-$ modes, AUBERT 02L assumed $B(B\to K^*(892)e^+e^-)/B(B\to K^*(892)\mu^+\mu^-) = 1.2$.
[5] The result is for di-lepton masses above 0.5 GeV.

$\Gamma(K\nu\overline{\nu})/\Gamma_{\rm total}$ Γ_{133}/Γ

Test for $\Delta B = 1$ weak neutral current.

VALUE	CL%	DOCUMENT ID		TECN	COMMENT
$<1.6\times10^{-5}$	90	[1] GRYGIER	17	BELL	$e^+e^-\to\Upsilon(4S)$
• • • We do not use the following data for averages, fits, limits, etc. • • •					
$<1.7\times10^{-5}$	90	[1,2] LEES	13I	BABR	$e^+e^-\to\Upsilon(4S)$
$<1.4\times10^{-5}$	90	[1] DEL-AMO-SA...10Q		BABR	Repl. by LEES 13I

[1] Assumes equal production of B^+ and B^0 at the $\Upsilon(4S)$.
[2] Also reported a limit $< 3.2\times10^{-5}$ at 90% CL obtained using a fully reconstructed hadronic B-tag evnets.

$\Gamma(K^*\nu\overline{\nu})/\Gamma_{\rm total}$ Γ_{134}/Γ

Test for $\Delta B = 1$ weak neutral current.

VALUE	CL%	DOCUMENT ID		TECN	COMMENT
$<2.7\times10^{-5}$	90	[1] GRYGIER	17	BELL	$e^+e^-\to\Upsilon(4S)$
• • • We do not use the following data for averages, fits, limits, etc. • • •					
$<7.6\times10^{-5}$	90	[1,2] LEES	13I	BABR	$e^+e^-\to\Upsilon(4S)$
$<8\times10^{-5}$	90	AUBERT	08BC	BABR	Repl. by LEES 13I

[1] Assumes equal production of B^+ and B^0 at the $\Upsilon(4S)$.
[2] Also reported a limit $< 7.9\times10^{-5}$ at 90% CL obtained using a fully reconstructed hadronic B-tag evnets.

$\Gamma(\pi\nu\overline{\nu})/\Gamma_{\rm total}$ Γ_{135}/Γ

VALUE	CL%	DOCUMENT ID		TECN	COMMENT
$<0.8\times10^{-5}$	90	[1] GRYGIER	17	BELL	$e^+e^-\to\Upsilon(4S)$

[1] Assumes equal production of B^+ and B^0 at the $\Upsilon(4S)$.

$\Gamma(\rho\nu\overline{\nu})/\Gamma_{\rm total}$ Γ_{136}/Γ

VALUE	CL%	DOCUMENT ID		TECN	COMMENT
$<2.8\times10^{-5}$	90	[1] GRYGIER	17	BELL	$e^+e^-\to\Upsilon(4S)$

[1] Assumes equal production of B^+ and B^0 at the $\Upsilon(4S)$.

$\Gamma(se^\pm\mu^\mp)/\Gamma_{\rm total}$ Γ_{137}/Γ

Test for lepton family number conservation. Allowed by higher-order electroweak interactions.

VALUE	CL%	DOCUMENT ID		TECN	COMMENT
$<2.2\times10^{-5}$	90	GLENN	98	CLEO	$e^+e^-\to\Upsilon(4S)$

$\Gamma(\pi e^\pm\mu^\mp)/\Gamma_{\rm total}$ Γ_{138}/Γ

Test of lepton family number conservation.

VALUE	CL%	DOCUMENT ID		TECN	COMMENT
$<9.2\times10^{-8}$	90	[1] AUBERT	07AG	BABR	$e^+e^-\to\Upsilon(4S)$
• • • We do not use the following data for averages, fits, limits, etc. • • •					
$<1.6\times10^{-6}$	90	[1] EDWARDS	02B	CLE2	$e^+e^-\to\Upsilon(4S)$

[1] Assumes equal production of B^+ and B^0 at the $\Upsilon(4S)$.

$\Gamma(\rho e^\pm\mu^\mp)/\Gamma_{\rm total}$ Γ_{139}/Γ

Test of lepton family number conservation.

VALUE	CL%	DOCUMENT ID		TECN	COMMENT
$<3.2\times10^{-6}$	90	[1] EDWARDS	02B	CLE2	$e^+e^-\to\Upsilon(4S)$

[1] Assumes equal production of B^+ and B^0 at the $\Upsilon(4S)$.

$\Gamma(Ke^\pm\mu^\mp)/\Gamma_{\rm total}$ Γ_{140}/Γ

Test of lepton family number conservation.

VALUE (units 10^{-7})	CL%	DOCUMENT ID		TECN	COMMENT
< 0.38	90	[1] AUBERT,B	06J	BABR	$e^+e^-\to\Upsilon(4S)$
• • • We do not use the following data for averages, fits, limits, etc. • • •					
<16	90	[1] EDWARDS	02B	CLE2	$e^+e^-\to\Upsilon(4S)$

[1] Assumes equal production of B^+ and B^0 at the $\Upsilon(4S)$.

$\Gamma(K^*(892)e^\pm\mu^\mp)/\Gamma_{\rm total}$ Γ_{141}/Γ

Test of lepton family number conservation.

VALUE (units 10^{-7})	CL%	DOCUMENT ID		TECN	COMMENT
< 5.1	90	[1] AUBERT,B	06J	BABR	$e^+e^-\to\Upsilon(4S)$

• • • We do not use the following data for averages, fits, limits, etc. • • •

<62	90	[1] EDWARDS	02B	CLE2	$e^+e^- \to \Upsilon(4S)$

[1] Assumes equal production of B^+ and B^0 at the $\Upsilon(4S)$.

CP VIOLATION

A_{CP} is defined as

$$\frac{B(\overline{B} \to \overline{f}) - B(B \to f)}{B(\overline{B} \to \overline{f}) + B(B \to f)},$$

the CP-violation charge asymmetry of inclusive $B^{\pm}$ and B^0 decay.

$A_{CP}(B \to K^*(892)\gamma)$

VALUE	DOCUMENT ID		TECN	COMMENT
−0.003±0.011 OUR AVERAGE				
−0.004±0.014±0.003	[1] HORIGUCHI	17	BELL	$e^+e^- \to \Upsilon(4S)$
−0.003±0.017±0.007	[2] AUBERT	09AO	BABR	$e^+e^- \to \Upsilon(4S)$
0.08 ±0.13 ±0.03	[3] COAN	00	CLE2	$e^+e^- \to \Upsilon(4S)$
• • • We do not use the following data for averages, fits, limits, etc. • • •				
−0.013±0.036±0.010	[4] AUBERT,BE	04A	BABR	Repl. by AUBERT 09AO
−0.015±0.044±0.012	[3] NAKAO	04	BELL	Repl. by HORIGUCHI 17
−0.044±0.076±0.012	[5] AUBERT	02C	BABR	Repl. by AUBERT,BE 04A

[1] Uses B($\Upsilon(4S) \to B^+B^-$) = (51.4±0.6)% and B($\Upsilon(4S) \to B^0\overline{B}^0$) = (48.6±0.6)%.
[2] Corresponds to a 90% CL interval $-0.033 < A_{CP} < 0.028$.
[3] Assumes equal production of B^+ and B^0 at the $\Upsilon(4S)$.
[4] Corresponds to a 90% CL allowed region, $-0.074 < A_{CP} < 0.049$.
[5] A 90% CL range is $-0.170 < A_{CP} < 0.082$.

$A_{CP}(b \to s\gamma)$

VALUE	DOCUMENT ID		TECN	COMMENT
0.015±0.020 OUR AVERAGE				
0.017±0.019±0.010	[1] LEES	14K	BABR	$e^+e^- \to \Upsilon(4S)$
0.002±0.050±0.030	[2] NISHIDA	04	BELL	$e^+e^- \to \Upsilon(4S)$
• • • We do not use the following data for averages, fits, limits, etc. • • •				
−0.011±0.030±0.014	[3] AUBERT	08BJ	BABR	Repl. by LEES 14K
0.025±0.050±0.015	[4] AUBERT,B	04E	BABR	Repl. by AUBERT 08BJ

[1] Measured with 16 exclusively reconstructed $B \to X_s\gamma$ decays with $0.6 < m_{X_s} < 2.0$ GeV/c^2 (ten charged and six neutral self-tagging B modes).
[2] This measurement is performed inclusively for recoil mass X_s less than 2.1 GeV, which corresponds to $-0.093 < A_{CP} < 0.096$ at 90% CL.
[3] Uses a sum of exclusively reconstructed $B \to X_s$ decay modes, with X_s mass between 0.6 and 2.8 GeV/c^2.
[4] Corresponds to $-0.06 < A_{CP} < 0.11$ at 90% CL.

$A_{CP}(b \to (s+d)\gamma)$

VALUE	DOCUMENT ID		TECN	COMMENT
0.010±0.031 OUR AVERAGE				
0.022±0.039±0.009	[1] PESANTEZ	15	BELL	$e^+e^- \to \Upsilon(4S)$
0.057±0.060±0.018	LEES	12V	BABR	$e^+e^- \to \Upsilon(4S)$
−0.10 ±0.18 ±0.05	[2] AUBERT	08O	BABR	$e^+e^- \to \Upsilon(4S)$
−0.110±0.115±0.017	AUBERT,BE	06B	BABR	$e^+e^- \to \Upsilon(4S)$
−0.079±0.108±0.022	[3] COAN	01	CLE2	$e^+e^- \to \Upsilon(4S)$

[1] Assumes equal production of B^+ and B^0 at the $\Upsilon(4S)$. Uses an opposite side lepton tag. Requires center-of-mass frame $E_\gamma > 2.1$ GeV.
[2] Uses a fully reconstructed B meson as a tag on the recoil side. Requires $E_\gamma > 2.2$ GeV.
[3] Corresponds to $-0.27 < A_{CP} < 0.10$ at 90% CL.

$A_{CP}(B \to X_s\ell^+\ell^-)$

VALUE	DOCUMENT ID		TECN	COMMENT
0.04±0.11±0.01	[1] LEES	14D	BABR	$e^+e^- \to \Upsilon(4S)$
• • • We do not use the following data for averages, fits, limits, etc. • • •				
−0.22±0.26±0.02	[2] AUBERT,B	04I	BABR	Repl. by LEES 14D

[1] Measured from sum of exclusive modes through K^+, $K^+\pi^0$, $K^+\pi^-$, $K^+\pi^-\pi^0$, $K^+\pi^-\pi^+$, $K^0_S\pi^+$, and $K^0_S\pi^+\pi^0$.
[2] The final state flavor is determined by the kaon and pion charges where modes with $X_s = K^0_S$, $K^0_S\pi^0$ or $K^0_S\pi^+\pi^-$ are not used.

$A_{CP}(B \to X_s\ell^+\ell^-)$ ($1.0 < q^2 < 6.0$ GeV$^2/c^4$)

VALUE	DOCUMENT ID		TECN	COMMENT
−0.06±0.22±0.01	[1] LEES	14D	BABR	$e^+e^- \to \Upsilon(4S)$

[1] Measured from sum of exclusive modes through K^+, $K^+\pi^0$, $K^+\pi^-$, $K^+\pi^-\pi^0$, $K^+\pi^-\pi^+$, $K^0_S\pi^+$, and $K^0_S\pi^+\pi^0$.

$A_{CP}(B \to X_s\ell^+\ell^-)$ ($10.1 < q^2 < 12.9$ or $q^2 > 14.2$ GeV$^2/c^4$)

VALUE	DOCUMENT ID		TECN	COMMENT
$0.19^{+0.18}_{-0.17}\pm0.01$	[1] LEES	14D	BABR	$e^+e^- \to \Upsilon(4S)$

[1] Measured from sum of exclusive modes through K^+, $K^+\pi^0$, $K^+\pi^-$, $K^+\pi^-\pi^0$, $K^+\pi^-\pi^+$, $K^0_S\pi^+$, and $K^0_S\pi^+ + (pi-)^0$.

$A_{CP}(B \to K^*e^+e^-)$

VALUE	DOCUMENT ID		TECN	COMMENT
−0.18±0.15±0.01	WEI	09A	BELL	$e^+e^- \to \Upsilon(4S)$

$A_{CP}(B \to K^*\mu^+\mu^-)$

VALUE	DOCUMENT ID		TECN	COMMENT
−0.03±0.13±0.02	WEI	09A	BELL	$e^+e^- \to \Upsilon(4S)$

$A_{CP}(B \to K^*\ell^+\ell^-)$

VALUE	DOCUMENT ID		TECN	COMMENT
−0.04±0.07 OUR AVERAGE				
0.03±0.13±0.01	[1] LEES	12S	BABR	$e^+e^- \to \Upsilon(4S)$
$+0.01^{+0.16}_{-0.15}\pm0.01$	AUBERT	09T	BABR	$e^+e^- \to \Upsilon(4S)$
−0.10±0.10±0.01	WEI	09A	BELL	$e^+e^- \to \Upsilon(4S)$

[1] Measured in the union of $0.10 < q^2 < 8.12$ GeV$^2/c^4$ and $q^2 > 10.11$ GeV$^2/c^4$. LEES 12S reports also individual measurements $A_{CP}(B \to K^*\ell^+\ell^-) = -0.13^{+0.18}_{-0.19}\pm 0.01$ for $0.10 < q^2 < 8.12$ GeV$^2/c^4$ and $A_{CP}(B \to K^*\ell^+\ell^-) = 0.16^{+0.18}_{-0.19}\pm 0.01$ for $q^2 > 10.11$ GeV$^2/c^4$.

$A_{CP}(B \to \eta$anything$)$

VALUE	DOCUMENT ID		TECN	COMMENT
$-0.13\pm0.04^{+0.02}_{-0.03}$	[1] NISHIMURA	10	BELL	$e^+e^- \to \Upsilon(4S)$

[1] Uses $B \to \eta X_s$ with $0.4 < m_{X_s} < 2.6$ GeV/c^2.

$\Delta A_{CP}(X_s\gamma) = A_{CP}(B^{\pm} \to X_s\gamma) - A_{CP}(B^0 \to X_s\gamma)$

This is the isospin difference of the CP asymmetries.

VALUE	DOCUMENT ID		TECN	COMMENT
0.050±0.039±0.015	[1] LEES	14K	BABR	$e^+e^- \to \Upsilon(4S)$

[1] Measured with 16 exclusively reconstructed $B \to X_s\gamma$ decays with $0.6 < m_{X_s} < 2.0$ GeV/c^2 (ten charged and six neutral self-tagging B modes).

$\Delta A_{CP}(B \to K^*\gamma) = A_{CP}(B^+ \to K^{*+}\gamma) - A_{CP}(B^0 \to K^{*0}\gamma)$

This is the isospin difference of the CP asymmetries.

VALUE	DOCUMENT ID		TECN	COMMENT
0.024±0.028±0.005	[1] HORIGUCHI	17	BELL	$e^+e^- \to \Upsilon(4S)$

[1] Uses B($\Upsilon(4S) \to B^+B^-$) = (51.4±0.6)% and B($\Upsilon(4S) \to B^0\overline{B}^0$) = (48.6±0.6)%.

$\overline{A}_{CP}(B \to K^*\gamma) = (A_{CP}(B^+ \to K^{*+}\gamma) + A_{CP}(B^0 \to K^{*0}\gamma))/2$

This is the average CP asymmetry.

VALUE	DOCUMENT ID		TECN	COMMENT
−0.001±0.014±0.003	[1] HORIGUCHI	17	BELL	$e^+e^- \to \Upsilon(4S)$

[1] Uses B($\Upsilon(4S) \to B^+B^-$) = (51.4±0.6)% and B($\Upsilon(4S) \to B^0\overline{B}^0$) = (48.6±0.6)%.

POLARIZATION IN B DECAY

In decays involving two vector mesons, one can distinguish among the states in which meson polarizations are both longitudinal (L) or both are transverse and parallel ($\|$) or perpendicular ($\perp$) to each other with the parameters Γ_L/Γ, $\Gamma_\perp/\Gamma$, and the relative phases $\phi_\|$ and $\phi_\perp$. See the definitions in the note on "Polarization in B Decays" review in the B^0 Particle Listings.

$F_L(B \to K^*\ell^+\ell^-)$ ($q^2 > 0.1$ GeV$^2/c^4$)

VALUE	DOCUMENT ID		TECN	COMMENT
$0.63^{+0.18}_{-0.19}\pm0.05$	[1] AUBERT,B	06J	BABR	$e^+e^- \to \Upsilon(4S)$

[1] Results with different q^2 cuts are also reported.

$F_L(B \to K^*\ell^+\ell^-)$ ($m_{\ell\ell} < 2.5$ GeV/c^2)

VALUE	DOCUMENT ID		TECN	COMMENT
0.35±0.16±0.04	AUBERT	09N	BABR	$e^+e^- \to \Upsilon(4S)$

$F_L(B \to K^*\ell^+\ell^-)$ ($m_{\ell\ell} > 3.2$ GeV/c^2)

VALUE	DOCUMENT ID		TECN	COMMENT
$0.71^{+0.20}_{-0.22}\pm0.04$	AUBERT	09N	BABR	$e^+e^- \to \Upsilon(4S)$

$F_L(B \to K^*\ell^+\ell^-)$ ($0.10 < q^2 < 0.98$ GeV$^2/c^4$)

VALUE	DOCUMENT ID		TECN	COMMENT
$0.263^{+0.045}_{-0.044}\pm0.017$	AAIJ	16B	LHCB	pp at 7, 8 TeV

$F_L(B \to K^*\ell^+\ell^-)$ ($1.1 < q^2 < 2.5$ GeV$^2/c^4$)

VALUE	DOCUMENT ID		TECN	COMMENT
$0.660^{+0.083}_{-0.077}\pm0.022$	AAIJ	16B	LHCB	pp at 7, 8 TeV

$F_L(B \to K^*\ell^+\ell^-)$ ($0.1 < q^2 < 2.0$ GeV$^2/c^4$)

VALUE	DOCUMENT ID		TECN	COMMENT
$0.34^{+0.08}_{-0.07}$ OUR AVERAGE				
$0.37^{+0.10+0.04}_{-0.09-0.03}$	AAIJ	13Y	LHCB	pp at 7 TeV, $K^{*0}\mu^+\mu^-$
0.30±0.16±0.02	AALTONEN	12I	CDF	$p\overline{p}$ at 1.96 TeV
$0.29^{+0.21}_{-0.18}\pm0.02$	WEI	09A	BELL	$e^+e^- \to \Upsilon(4S)$
• • • We do not use the following data for averages, fits, limits, etc. • • •				
$0.60^{+0.00}_{-0.28}\pm0.19$	[1] CHATRCHYAN	13BL	CMS	pp at 7 TeV

$0.00^{+0.13}_{-0.00}\pm0.02$	AAIJ	12U	LHCB	Repl. by AAIJ 13Y	
$0.53^{+0.32}_{-0.34}\pm0.07$	AALTONEN	11L	CDF	Repl. by AALTONEN 12I	

[1] CHATRCHYAN 13BL uses, for this bin, $1.0 < q^2 < 2.0$ GeV$^2/c^4$.

$F_L(B \to K^*\ell^+\ell^-)$ ($2.0 < q^2 < 4.3$ GeV$^2/c^4$)

VALUE	DOCUMENT ID		TECN	COMMENT
0.77 ±0.05 OUR AVERAGE				
$0.876^{+0.109}_{-0.097}\pm0.017$	[1] AAIJ	16B	LHCB	pp at 7, 8 TeV
0.80 ±0.08 ±0.06	KHACHATRY...16D		CMS	pp at 8 TeV
$0.74\ ^{+0.10}_{-0.09}\ ^{+0.02}_{-0.03}$	AAIJ	13Y	LHCB	pp at 7 TeV, $K^{*0}\mu^+\mu^-$
0.65 ±0.17 ±0.03	CHATRCHYAN 13BL		CMS	pp at 7 TeV
$0.37\ ^{+0.25}_{-0.24}$ ±0.10	AALTONEN	12I	CDF	$p\overline{p}$ at 1.96 TeV
0.71 ±0.24 ±0.05	WEI	09A	BELL	$e^+e^- \to \Upsilon(4S)$
• • • We do not use the following data for averages, fits, limits, etc. • • •				
0.77 ±0.15 ±0.03	AAIJ	12U	LHCB	Repl. by AAIJ 13Y
$0.40\ ^{+0.32}_{-0.33}$ ±0.08	AALTONEN	11L	CDF	Repl. by AALTONEN 12I

[1] Measured in $2.5 < q^2 < 4.0$ GeV$^2/c^4$.

$F_L(B \to K^*\ell^+\ell^-)$ ($4.0 < q^2 < 6.0$ GeV$^2/c^4$)

VALUE	DOCUMENT ID		TECN	COMMENT
$\mathbf{0.611^{+0.052}_{-0.053}\pm0.017}$	AAIJ	16B	LHCB	pp at 7, 8 TeV

$F_L(B \to K^*\ell^+\ell^-)$ ($6.0 < q^2 < 8.0$ GeV$^2/c^4$)

VALUE	DOCUMENT ID		TECN	COMMENT
0.579±0.046±0.015	AAIJ	16B	LHCB	pp at 7, 8 TeV

$F_L(B \to K^*\ell^+\ell^-)$ ($4.3 < q^2 < 8.6$ GeV$^2/c^4$)

VALUE	DOCUMENT ID		TECN	COMMENT
0.64±0.06 OUR AVERAGE				
0.57±0.07±0.03	AAIJ	13Y	LHCB	pp at 7 TeV, $K^{*0}\mu^+\mu^-$
$0.81^{+0.13}_{-0.12}\pm0.05$	CHATRCHYAN 13BL		CMS	pp at 7 TeV
$0.68^{+0.15}_{-0.17}\pm0.09$	AALTONEN	12I	CDF	$p\overline{p}$ at 1.96 TeV
$0.64^{+0.23}_{-0.24}\pm0.07$	WEI	09A	BELL	$e^+e^- \to \Upsilon(4S)$
• • • We do not use the following data for averages, fits, limits, etc. • • •				
$0.60^{+0.06}_{-0.07}\pm0.01$	AAIJ	12U	LHCB	Repl. by AAIJ 13Y
$0.82^{+0.19}_{-0.23}\pm0.07$	AALTONEN	11L	CDF	Repl. by AALTONEN 12I

$F_L(B \to K^*\ell^+\ell^-)$ ($10.09 < q^2 < 12.86$ GeV$^2/c^4$)

VALUE	DOCUMENT ID		TECN	COMMENT
0.448±0.033 OUR AVERAGE				
$0.493^{+0.049}_{-0.047}\pm0.013$	[1] AAIJ	16B	LHCB	pp at 7, 8 TeV
0.39 ±0.05 ±0.04	KHACHATRY...16D		CMS	pp at 8 TeV
$0.48\ ^{+0.08}_{-0.09}$ ±0.03	AAIJ	13Y	LHCB	pp at 7 TeV, $K^{*0}\mu^+\mu^-$
$0.45\ ^{+0.10}_{-0.11}$ ±0.04	CHATRCHYAN 13BL		CMS	pp at 7 TeV
0.47 ±0.14 ±0.03	AALTONEN	12I	CDF	$p\overline{p}$ at 1.96 TeV
$0.17\ ^{+0.17}_{-0.15}$ ±0.03	WEI	09A	BELL	$e^+e^- \to \Upsilon(4S)$
• • • We do not use the following data for averages, fits, limits, etc. • • •				
0.41 ±0.11 ±0.03	AAIJ	12U	LHCB	Repl. by AAIJ 13Y
$0.31\ ^{+0.19}_{-0.18}$ ±0.02	AALTONEN	11L	CDF	Repl. by AALTONEN 12I

[1] Measured in $11.0 < q^2 < 12.5$ GeV$^2/c^4$.

$F_L(B \to K^*\ell^+\ell^-)$ ($15.0 < q^2 < 17.0$ GeV$^2/c^4$)

VALUE	DOCUMENT ID		TECN	COMMENT
0.349±0.039±0.009	AAIJ	16B	LHCB	pp at 7, 8 TeV

$F_L(B \to K^*\ell^+\ell^-)$ ($17.0 < q^2 < 19.0$ GeV$^2/c^4$)

VALUE	DOCUMENT ID		TECN	COMMENT
$\mathbf{0.354^{+0.049}_{-0.048}\pm0.025}$	AAIJ	16B	LHCB	pp at 7, 8 TeV

$F_L(B \to K^*\ell^+\ell^-)$ ($14.18 < q^2 < 16.0$ GeV$^2/c^4$)

VALUE	DOCUMENT ID		TECN	COMMENT
0.40±0.06 OUR AVERAGE Error includes scale factor of 1.4. See the ideogram below.				
$0.48^{+0.05}_{-0.06}\pm0.04$	KHACHATRY...16D		CMS	pp at 8 TeV
$0.33^{+0.08}_{-0.07}\ ^{+0.02}_{-0.03}$	AAIJ	13Y	LHCB	pp at 7 TeV, $K^{*0}\mu^+\mu^-$
0.53±0.12±0.03	CHATRCHYAN 13BL		CMS	pp at 7 TeV
$0.29^{+0.14}_{-0.13}\pm0.05$	AALTONEN	12I	CDF	$p\overline{p}$ at 1.96 TeV
$-0.15^{+0.27}_{-0.23}\pm0.07$	WEI	09A	BELL	$e^+e^- \to \Upsilon(4S)$
• • • We do not use the following data for averages, fits, limits, etc. • • •				
0.37±0.09±0.05	AAIJ	12U	LHCB	Repl. by AAIJ 13Y
$0.55^{+0.17}_{-0.18}\pm0.02$	AALTONEN	11L	CDF	Repl. by AALTONEN 12I

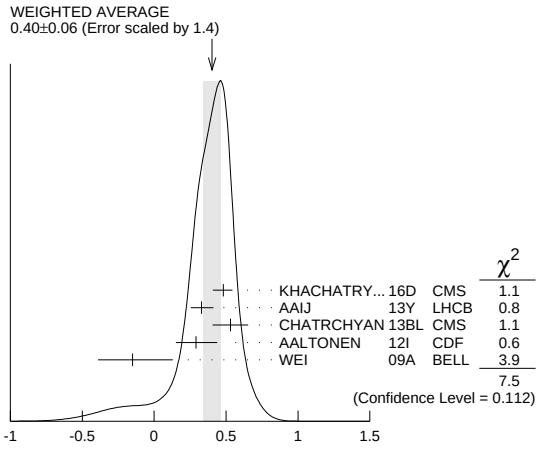

$F_L(B \to K^*\ell^+\ell^-)$ ($14.18 < q^2 < 16.0$ GeV$^2/c^4$)

$F_L(B \to K^*\ell^+\ell^-)$ ($16.0 < q^2 < 19.0$ GeV$^2/c^4$)

VALUE	DOCUMENT ID		TECN	COMMENT
0.353±0.024 OUR AVERAGE				
$0.344^{+0.028}_{-0.030}\pm0.008$	[1] AAIJ	16B	LHCB	pp at 7, 8 TeV
$0.38\ ^{+0.05}_{-0.06}$ ±0.04	KHACHATRY...16D		CMS	pp at 8 TeV
$0.38\ ^{+0.09}_{-0.07}$ ±0.03	AAIJ	13Y	LHCB	pp at 7 TeV, $K^{*0}\mu^+\mu^-$
0.44 ±0.07 ±0.03	CHATRCHYAN 13BL		CMS	pp at 7 TeV
$0.20\ ^{+0.19}_{-0.17}$ ±0.05	AALTONEN	12I	CDF	$p\overline{p}$ at 1.96 TeV
$0.12\ ^{+0.15}_{-0.13}$ ±0.02	WEI	09A	BELL	$e^+e^- \to \Upsilon(4S)$
• • • We do not use the following data for averages, fits, limits, etc. • • •				
$0.26\ ^{+0.10}_{-0.08}$ ±0.03	AAIJ	12U	LHCB	Repl. by AAIJ 13Y
$0.09\ ^{+0.18}_{-0.14}$ ±0.03	AALTONEN	11L	CDF	Repl. by AALTONEN 12I

[1] Measured in $15.0 < q^2 < 19.0$ GeV$^2/c^4$.

$F_L(B \to K^*\ell^+\ell^-)$ ($1.0 < q^2 < 6.0$ GeV$^2/c^4$)

VALUE	DOCUMENT ID		TECN	COMMENT
0.65 ±0.08 OUR AVERAGE Error includes scale factor of 2.7. See the ideogram below.				
$0.690^{+0.035}_{-0.036}\pm0.017$	[1] AAIJ	16B	LHCB	pp at 7, 8 TeV
0.72 ±0.06	KHACHATRY...16D		CMS	pp at 7, 8 TeV
$0.24\ ^{+0.09}_{-0.08}$ ±0.02	[2] LEES	16C	BABR	$e^+e^- \to \Upsilon(4S)$
$0.65\ ^{+0.08}_{-0.07}$ ±0.03	AAIJ	13Y	LHCB	pp at 7 TeV, $K^{*0}\mu^+\mu^-$
$0.69\ ^{+0.19}_{-0.21}$ ±0.08	AALTONEN	12I	CDF	$p\overline{p}$ at 1.96 TeV
0.67 ±0.23 ±0.05	WEI	09A	BELL	$e^+e^- \to \Upsilon(4S)$
• • • We do not use the following data for averages, fits, limits, etc. • • •				
0.68 ±0.10 ±0.02	CHATRCHYAN 13BL		CMS	Repl. by KHACHATRYAN 16D
0.55 ±0.10 ±0.03	AAIJ	12U	LHCB	Repl. by AAIJ 13Y
$0.50\ ^{+0.27}_{-0.30}$ ±0.03	AALTONEN	11L	CDF	Repl. by AALTONEN 12I

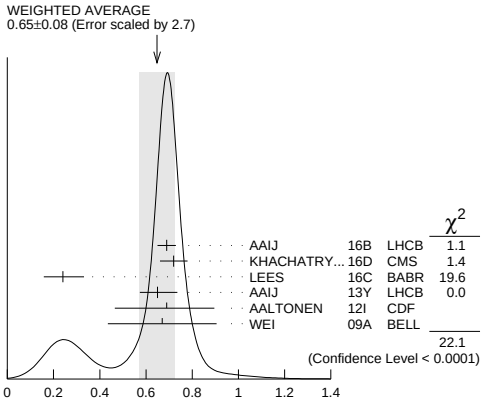

$F_L(B \to K^*\ell^+\ell^-)$ ($1.0 < q^2 < 6.0$ GeV$^2/c^4$)

[1] Measured in $1.1 < q^2 < 6.0$ GeV$^2/c^4$.

[2] Measured by combining B^0 and B^+ with e and μ as leptons. Results are also provided separately for B^0 and B^+.

$F_L(B \to K^* \ell^+ \ell^-)$ ($0.0 < q^2 < 4.3$ GeV$^2/c^4$)

VALUE	DOCUMENT ID		TECN	COMMENT
$0.33^{+0.14}_{-0.13} \pm 0.03$	AALTONEN	12I	CDF	$p\overline{p}$ at 1.96 TeV
• • • We do not use the following data for averages, fits, limits, etc. • • •				
$0.47^{+0.23}_{-0.24} \pm 0.03$	AALTONEN	11L	CDF	Repl. by AALTONEN 12I

$P_\tau(B \to D^* \tau^+ \nu_\tau)$

Measures difference in decay widths with positive and negative τ^+ helicities normalized to the sum of those decay widths.

VALUE	DOCUMENT ID		TECN	COMMENT
$-0.38 \pm 0.51^{+0.21}_{-0.16}$	[1] HIROSE	17	BELL	$e^+e^- \to \Upsilon(4S)$

[1] Uses a fully reconstructed B meson as a tag on the recoil side.

PARTIAL BRANCHING FRACTIONS IN $B \to K^{(*)} \ell^+ \ell^-$

$B(B \to K^* \ell^+ \ell^-)$ ($q^2 < 2.0$ GeV$^2/c^4$)

VALUE (units 10^{-7})	DOCUMENT ID		TECN	COMMENT
1.68 ± 0.23 OUR AVERAGE				
$1.89^{+0.52}_{-0.46} \pm 0.06$	[1] LEES	12S	BABR	$e^+e^- \to \Upsilon(4S)$
$1.73 \pm 0.33 \pm 0.10$	AALTONEN	11AI	CDF	$p\overline{p}$ at 1.96 TeV
$1.46^{+0.40}_{-0.35} \pm 0.11$	WEI	09A	BELL	$e^+e^- \to \Upsilon(4S)$
• • • We do not use the following data for averages, fits, limits, etc. • • •				
$0.98 \pm 0.40 \pm 0.09$	AALTONEN	11L	CDF	Repl. by AALTONEN 11AI

[1] The value reported here from LEES 12S refers to $0.1 < q^2 < 2.0$ GeV$^2/c^2$.

$B(B \to K^* \ell^+ \ell^-)$ ($2.0 < q^2 < 4.3$ GeV$^2/c^4$)

VALUE (units 10^{-7})	DOCUMENT ID		TECN	COMMENT
0.87 ± 0.17 OUR AVERAGE				
$0.95^{+0.35}_{-0.30} \pm 0.04$	LEES	12S	BABR	$e^+e^- \to \Upsilon(4S)$
$0.82 \pm 0.26 \pm 0.06$	AALTONEN	11AI	CDF	$p\overline{p}$ at 1.96 TeV
$0.86^{+0.31}_{-0.27} \pm 0.07$	WEI	09A	BELL	$e^+e^- \to \Upsilon(4S)$
• • • We do not use the following data for averages, fits, limits, etc. • • •				
$1.00 \pm 0.38 \pm 0.09$	AALTONEN	11L	CDF	Repl. by AALTONEN 11AI

$B(B \to K^* \ell^+ \ell^-)$ ($4.3 < q^2 < 8.68$ GeV$^2/c^4$)

VALUE (units 10^{-7})	DOCUMENT ID		TECN	COMMENT
1.67 ± 0.29 OUR AVERAGE				
$1.82^{+0.56}_{-0.52} \pm 0.09$	[1] LEES	12S	BABR	$e^+e^- \to \Upsilon(4S)$
$1.72 \pm 0.41 \pm 0.14$	AALTONEN	11AI	CDF	$p\overline{p}$ at 1.96 TeV
$1.37^{+0.47}_{-0.42} \pm 0.39$	WEI	09A	BELL	$e^+e^- \to \Upsilon(4S)$
• • • We do not use the following data for averages, fits, limits, etc. • • •				
$1.69 \pm 0.57 \pm 0.15$	AALTONEN	11L	CDF	Repl. by AALTONEN 11AI

[1] The value reported here from LEES 12S refers to $4.3 < q^2 < 8.12$ GeV$^2/c^2$.

$B(B \to K^* \ell^+ \ell^-)$ ($10.09 < q^2 < 12.86$ GeV$^2/c^4$)

VALUE (units 10^{-7})	DOCUMENT ID		TECN	COMMENT
1.93 ± 0.25 OUR AVERAGE				
$1.86^{+0.52}_{-0.48} \pm 0.10$	[1] LEES	12S	BABR	$e^+e^- \to \Upsilon(4S)$
$1.77 \pm 0.34 \pm 0.11$	AALTONEN	11AI	CDF	$p\overline{p}$ at 1.96 TeV
$2.24^{+0.44}_{-0.40} \pm 0.19$	WEI	09A	BELL	$e^+e^- \to \Upsilon(4S)$
• • • We do not use the following data for averages, fits, limits, etc. • • •				
$1.97 \pm 0.47 \pm 0.17$	AALTONEN	11L	CDF	Repl. by AALTONEN 11AI

[1] The value reported here from LEES 12S refers to $10.11 < q^2 < 12.89$ GeV$^2/c^2$.

$B(B \to K^* \ell^+ \ell^-)$ ($14.18 < q^2 < 16.0$ GeV$^2/c^4$)

VALUE (units 10^{-7})	DOCUMENT ID		TECN	COMMENT
1.21 ± 0.17 OUR AVERAGE				
$1.46^{+0.41}_{-0.36} \pm 0.06$	[1] LEES	12S	BABR	$e^+e^- \to \Upsilon(4S)$
$1.21 \pm 0.24 \pm 0.07$	AALTONEN	11AI	CDF	$p\overline{p}$ at 1.96 TeV
$1.05^{+0.29}_{-0.26} \pm 0.08$	WEI	09A	BELL	$e^+e^- \to \Upsilon(4S)$
• • • We do not use the following data for averages, fits, limits, etc. • • •				
$1.51 \pm 0.36 \pm 0.13$	AALTONEN	11L	CDF	Repl. by AALTONEN 11AI

[1] The value reported here from LEES 12S refers to $14.21 < q^2 < 16.0$ GeV$^2/c^2$.

$B(B \to K^* \ell^+ \ell^-)$ ($16.0 < q^2$ GeV$^2/c^4$)

VALUE (units 10^{-7})	DOCUMENT ID		TECN	COMMENT
1.3 ± 0.4 OUR AVERAGE	Error includes scale factor of 2.3. See the ideogram below.			
$1.02^{+0.47}_{-0.42} \pm 0.06$	LEES	12S	BABR	$e^+e^- \to \Upsilon(4S)$
$0.88 \pm 0.22 \pm 0.05$	AALTONEN	11AI	CDF	$p\overline{p}$ at 1.96 TeV
$2.04^{+0.27}_{-0.24} \pm 0.16$	WEI	09A	BELL	$e^+e^- \to \Upsilon(4S)$
• • • We do not use the following data for averages, fits, limits, etc. • • •				
$1.35 \pm 0.37 \pm 0.12$	AALTONEN	11L	CDF	Repl. by AALTONEN 11AI

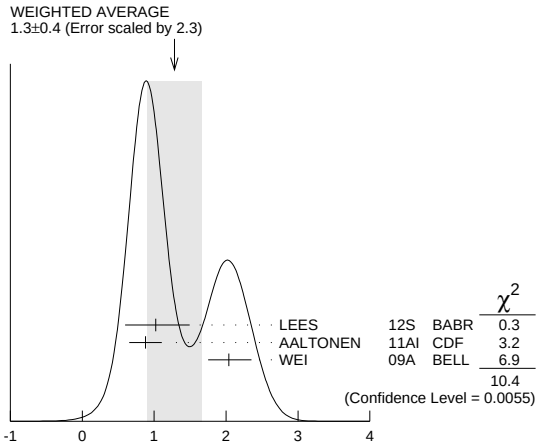

$B(B \to K^* \ell^+ \ell^-)$ ($16.0 < q^2$ GeV$^2/c^4$) (units 10^{-7})

$B(B \to K^* \ell^+ \ell^-)$ ($1.0 < q^2 < 6.0$ GeV$^2/c^4$)

VALUE (units 10^{-7})	DOCUMENT ID		TECN	COMMENT
1.64 ± 0.26 OUR AVERAGE				
$2.05^{+0.53}_{-0.48} \pm 0.07$	LEES	12S	BABR	$e^+e^- \to \Upsilon(4S)$
$1.48 \pm 0.39 \pm 0.12$	AALTONEN	11AI	CDF	$p\overline{p}$ at 1.96 TeV
$1.49^{+0.45}_{-0.40} \pm 0.12$	WEI	09A	BELL	$e^+e^- \to \Upsilon(4S)$
• • • We do not use the following data for averages, fits, limits, etc. • • •				
$1.60 \pm 0.54 \pm 0.14$	AALTONEN	11L	CDF	Repl. by AALTONEN 11AI

$B(B \to K^* \ell^+ \ell^-)$ ($0.0 < q^2 < 4.3$ GeV$^2/c^4$)

VALUE (units 10^{-7})	DOCUMENT ID		TECN	COMMENT
$2.53 \pm 0.43 \pm 0.15$	AALTONEN	11AI	CDF	$p\overline{p}$ at 1.96 TeV
• • • We do not use the following data for averages, fits, limits, etc. • • •				
$1.98 \pm 0.55 \pm 0.18$	AALTONEN	11L	CDF	Repl. by AALTONEN 11AI

$B(B \to K \ell^+ \ell^-)$ ($q^2 < 2.0$ GeV$^2/c^4$)

VALUE (units 10^{-7})	DOCUMENT ID		TECN	COMMENT
0.51 ± 0.16 OUR AVERAGE	Error includes scale factor of 1.9. See the ideogram below.			
$0.71^{+0.20}_{-0.18} \pm 0.02$	[1] LEES	12S	BABR	$e^+e^- \to \Upsilon(4S)$
$0.33 \pm 0.10 \pm 0.02$	AALTONEN	11AI	CDF	$p\overline{p}$ at 1.96 TeV
$0.81^{+0.18}_{-0.16} \pm 0.05$	WEI	09A	BELL	$e^+e^- \to \Upsilon(4S)$
• • • We do not use the following data for averages, fits, limits, etc. • • •				
$0.38 \pm 0.16 \pm 0.03$	AALTONEN	11L	CDF	Repl. by AALTONEN 11AI

[1] The value reported here from LEES 12S refers to $0.1 < q^2 < 2.0$ GeV$^2/c^2$.

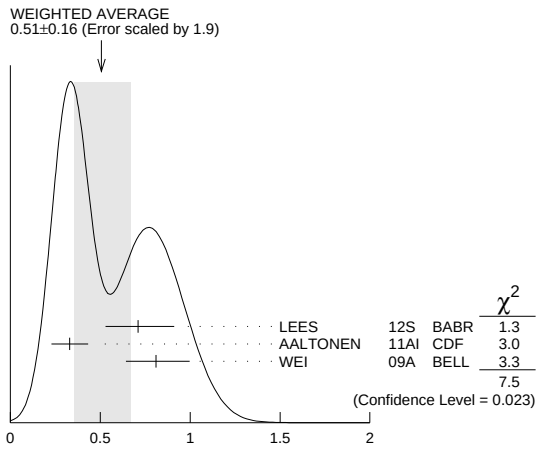

$B(B \to K \ell^+ \ell^-)$ ($q^2 < 2.0$ GeV$^2/c^4$) (units 10^{-7})

$B(B \to K \ell^+ \ell^-)$ ($2.0 < q^2 < 4.3$ GeV$^2/c^4$)

VALUE (units 10^{-7})	DOCUMENT ID		TECN	COMMENT
$0.57^{+0.10}_{-0.09}$ OUR AVERAGE	Error includes scale factor of 1.2.			
$0.49^{+0.15}_{-0.13} \pm 0.01$	LEES	12S	BABR	$e^+e^- \to \Upsilon(4S)$
$0.77 \pm 0.14 \pm 0.05$	AALTONEN	11AI	CDF	$p\overline{p}$ at 1.96 TeV
$0.46^{+0.14}_{-0.12} \pm 0.03$	WEI	09A	BELL	$e^+e^- \to \Upsilon(4S)$

• • • We do not use the following data for averages, fits, limits, etc. • • •

$0.58 \pm 0.19 \pm 0.04$	AALTONEN	11L	CDF	Repl. by AALTONEN 11AI

$B(B \to K\ell^+\ell^-)$ $(4.3 < q^2 < 8.68\ \text{GeV}^2/c^4)$

VALUE (units 10^{-7})	DOCUMENT ID		TECN	COMMENT
1.00 ± 0.11 OUR AVERAGE				
$0.94^{+0.20}_{-0.19} \pm 0.02$	[1] LEES	12S	BABR	$e^+e^- \to \Upsilon(4S)$
$1.05 \pm 0.17 \pm 0.07$	AALTONEN	11AI	CDF	$p\overline{p}$ at 1.96 TeV
$1.00^{+0.19}_{-0.18} \pm 0.06$	WEI	09A	BELL	$e^+e^- \to \Upsilon(4S)$
• • • We do not use the following data for averages, fits, limits, etc. • • •				
$0.93 \pm 0.25 \pm 0.06$	AALTONEN	11L	CDF	Repl. by AALTONEN 11AI

[1] The value reported here from LEES 12S refers to $4.3 < q^2 < 8.12\ \text{GeV}^2/c^2$.

$B(B \to K\ell^+\ell^-)$ $(10.09 < q^2 < 12.86\ \text{GeV}^2/c^4)$

VALUE (units 10^{-7})	DOCUMENT ID		TECN	COMMENT
0.57 ± 0.11 OUR AVERAGE	Error includes scale factor of 1.4. See the ideogram below.			
$0.90^{+0.20}_{-0.19} \pm 0.04$	[1] LEES	12S	BABR	$e^+e^- \to \Upsilon(4S)$
$0.48 \pm 0.10 \pm 0.03$	AALTONEN	11AI	CDF	$p\overline{p}$ at 1.96 TeV
$0.55^{+0.16}_{-0.14} \pm 0.03$	WEI	09A	BELL	$e^+e^- \to \Upsilon(4S)$
• • • We do not use the following data for averages, fits, limits, etc. • • •				
$0.72 \pm 0.17 \pm 0.05$	AALTONEN	11L	CDF	Repl. by AALTONEN 11AI

[1] The value reported here from LEES 12S refers to $10.11 < q^2 < 12.89\ \text{GeV}^2/c^2$.

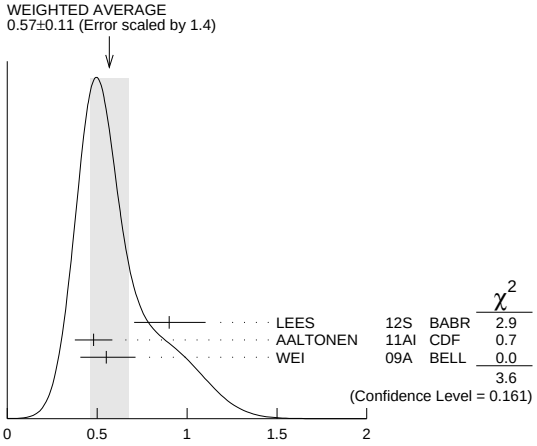

B($B \to K\ell^+\ell^-$) $(10.09 < q^2 < 12.86\ \text{GeV}^2/c^4)$ (units 10^{-7})

$B(B \to K\ell^+\ell^-)$ $(14.18 < q^2 < 16.0\ \text{GeV}^2/c^4)$

VALUE (units 10^{-7})	DOCUMENT ID		TECN	COMMENT
0.49 ± 0.07 OUR AVERAGE				
$0.49^{+0.15}_{-0.14} \pm 0.02$	[1] LEES	12S	BABR	$e^+e^- \to \Upsilon(4S)$
$0.52 \pm 0.09 \pm 0.03$	AALTONEN	11AI	CDF	$p\overline{p}$ at 1.96 TeV
$0.38^{+0.19}_{-0.12} \pm 0.02$	WEI	09A	BELL	$e^+e^- \to \Upsilon(4S)$
• • • We do not use the following data for averages, fits, limits, etc. • • •				
$0.38 \pm 0.12 \pm 0.03$	AALTONEN	11L	CDF	Repl. by AALTONEN 11AI

[1] The value reported here from LEES 12S refers to $14.21 < q^2 < 16.0\ \text{GeV}^2/c^2$.

$B(B \to K\ell^+\ell^-)$ $(16.0 < q^2\ \text{GeV}^2/c^4)$

VALUE (units 10^{-7})	DOCUMENT ID		TECN	COMMENT
0.52 ± 0.16 OUR AVERAGE	Error includes scale factor of 2.1. See the ideogram below.			
$0.67^{+0.23}_{-0.21} \pm 0.05$	LEES	12S	BABR	$e^+e^- \to \Upsilon(4S)$
$0.38 \pm 0.09 \pm 0.02$	AALTONEN	11AI	CDF	$p\overline{p}$ at 1.96 TeV
$0.98^{+0.20}_{-0.18} \pm 0.06$	WEI	09A	BELL	$e^+e^- \to \Upsilon(4S)$
• • • We do not use the following data for averages, fits, limits, etc. • • •				
$0.35 \pm 0.13 \pm 0.02$	AALTONEN	11L	CDF	Repl. by AALTONEN 11AI

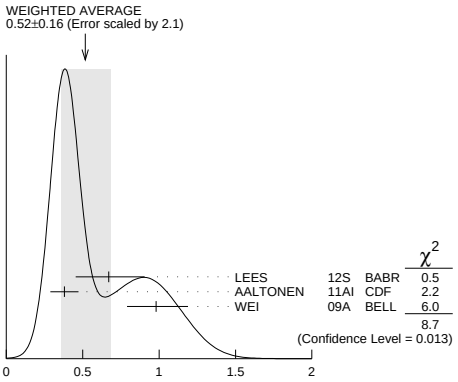

B($B \to K\ell^+\ell^-$) $(16.0 < q^2\ \text{GeV}^2/c^4)$ (units 10^{-7})

$B(B \to K\ell^+\ell^-)$ $(1.0 < q^2 < 6.0\ \text{GeV}^2/c^4)$

VALUE (units 10^{-7})	DOCUMENT ID		TECN	COMMENT
1.33 ± 0.13 OUR AVERAGE				
$1.36^{+0.27}_{-0.24} \pm 0.03$	LEES	12S	BABR	$e^+e^- \to \Upsilon(4S)$
$1.29 \pm 0.18 \pm 0.08$	AALTONEN	11AI	CDF	$p\overline{p}$ at 1.96 TeV
$1.36^{+0.23}_{-0.21} \pm 0.08$	WEI	09A	BELL	$e^+e^- \to \Upsilon(4S)$
• • • We do not use the following data for averages, fits, limits, etc. • • •				
$1.01 \pm 0.26 \pm 0.07$	AALTONEN	11L	CDF	Repl. by AALTONEN 11AI

$B(B \to K\ell^+\ell^-)$ $(0.0 < q^2 < 4.3\ \text{GeV}^2/c^4)$

VALUE (units 10^{-7})	DOCUMENT ID	TECN	COMMENT
$1.07 \pm 0.17 \pm 0.07$	AALTONEN 11AI	CDF	$p\overline{p}$ at 1.96 TeV
• • • We do not use the following data for averages, fits, limits, etc. • • •			
$0.96 \pm 0.25 \pm 0.06$	AALTONEN 11L	CDF	Repl. by AALTONEN 11AI

$B(B \to X_s\ell^+\ell^-)$ $(1.0 < q^2 < 6.0\ \text{GeV}^2/c^4)$

VALUE (units 10^{-6})	DOCUMENT ID		TECN	COMMENT
$\mathbf{1.60^{+0.41+0.25}_{-0.39-0.22}}$	[1] LEES	14D	BABR	$e^+e^- \to \Upsilon(4S)$

[1] Measured from sum of exclusive modes through K^+, $K^+\pi^0$, $K^+\pi^-$, $K^+\pi^-\pi^0$, $K^+\pi^-\pi^+$, K^0_S, $K^0_S\pi^0$, $K^0_S\pi^+$, $K^0_S\pi^+\pi^0$, and $K^0_S\pi^+ + \pi^-$ corrected for unobserved modes.

$B(B \to X_s e^+e^-)$ $(1.0 < q^2 < 6.0\ \text{GeV}^2/c^4)$

VALUE (units 10^{-6})	DOCUMENT ID		TECN	COMMENT
$\mathbf{1.93^{+0.47+0.28}_{-0.45-0.24}}$	[1] LEES	14D	BABR	$e^+e^- \to \Upsilon(4S)$

[1] Measured from sum of exclusive modes through K^+, $K^+\pi^0$, $K^+\pi^-$, $K^+\pi^-\pi^0$, $K^+\pi^-\pi^+$, K^0_S, $K^0_S\pi^0$, $K^0_S\pi^+$, $K^0_S\pi^+\pi^0$, and $K^0_S\pi^+ + \pi^-$ corrected for unobserved modes.

$B(B \to X_s\mu^+\mu^-)$ $(1.0 < q^2 < 6.0\ \text{GeV}^2/c^4)$

VALUE (units 10^{-6})	DOCUMENT ID		TECN	COMMENT
$\mathbf{0.66^{+0.82+0.31}_{-0.76-0.25}}$	[1] LEES	14D	BABR	$e^+e^- \to \Upsilon(4S)$

[1] Measured from sum of exclusive modes through K^+, $K^+\pi^0$, $K^+\pi^-$, $K^+\pi^-\pi^0$, $K^+\pi^-\pi^+$, K^0_S, $K^0_S\pi^0$, $K^0_S\pi^+$, $K^0_S\pi^+\pi^0$, and $K^0_S\pi^+ + \pi^-$ corrected for unobserved modes.

$B(B \to X_s\ell^+\ell^-)$ $(14.2 < q^2\ \text{GeV}^2/c^4)$

VALUE (units 10^{-6})	DOCUMENT ID		TECN	COMMENT
$\mathbf{0.57^{+0.16+0.03}_{-0.15-0.02}}$	[1] LEES	14D	BABR	$e^+e^- \to \Upsilon(4S)$

[1] Measured from sum of exclusive modes through K^+, $K^+\pi^0$, $K^+\pi^-$, $K^+\pi^-\pi^0$, $K^+\pi^-\pi^+$, K^0_S, $K^0_S\pi^0$, $K^0_S\pi^+$, $K^0_S\pi^+\pi^0$, and $K^0_S\pi^+ + \pi^-$ corrected for unobserved modes.

$B(B \to X_s e^+e^-)$ $(14.2 < q^2\ \text{GeV}^2/c^4)$

VALUE (units 10^{-6})	DOCUMENT ID		TECN	COMMENT
$\mathbf{0.56^{+0.19+0.03}_{-0.18-0.03}}$	[1] LEES	14D	BABR	$e^+e^- \to \Upsilon(4S)$

[1] Measured from sum of exclusive modes through K^+, $K^+\pi^0$, $K^+\pi^-$, $K^+\pi^-\pi^0$, $K^+\pi^-\pi^+$, K^0_S, $K^0_S\pi^0$, $K^0_S\pi^+$, $K^0_S\pi^+\pi^0$, and $K^0_S\pi^+ + \pi^-$ corrected for unobserved modes.

$B(B \to X_s\mu^+\mu^-)$ $(14.2 < q^2\ \text{GeV}^2/c^4)$

VALUE (units 10^{-6})	DOCUMENT ID		TECN	COMMENT
$\mathbf{0.60^{+0.31+0.05}_{-0.29-0.04}}$	[1] LEES	14D	BABR	$e^+e^- \to \Upsilon(4S)$

[1] Measured from sum of exclusive modes through K^+, $K^+\pi^0$, $K^+\pi^-$, $K^+\pi^-\pi^0$, $K^+\pi^-\pi^+$, K^0_S, $K^0_S\pi^0$, $K^0_S\pi^+$, $K^0_S\pi^+\pi^0$, and $K^0_S\pi^+ + \pi^-$ corrected for unobserved modes.

LEPTON (HADRON) FORWARD-BACKWARD ASYMMETRY IN $B \to K^{(*)}\ell^+\ell^-$ ($B \to K/\pi h^+ h^-$) DECAY

The forward-backward angular asymmetry of the lepton pair in $B \to K^{(*)}\ell^+\ell^-$ ($B \to K/\pi h^+ h^-$) decay is defined as

$$A_{FB}(s) = \frac{N(cos\theta>0)-N(cos\theta<0)}{N(cos\theta>0)+N(cos\theta<0)},$$

where $s=q^2/m_B^2$, and θ is the angle of the ℓ^- (h^-) with respect to the flight direction of the B meson, measured in the dilepton (dihadron) rest frame. In addition, the fraction of longitudinal polarization F_L of the K^* and F_S, the relative contribution from scalar and pseudoscalar penguin amplitudes in $B \to K\ell^+\ell^-$, can be measured from the angular distribution of its decay products.

$A_{FB}(B \to K^*\ell^+\ell^-)$ ($q^2 > 0.1$ GeV$^2/c^4$)

VALUE	CL%	DOCUMENT ID		TECN	COMMENT
0.50 ± 0.15 ± 0.02		[1] ISHIKAWA	06	BELL	$e^+e^- \to \Upsilon(4S)$
• • • We do not use the following data for averages, fits, limits, etc. • • •					
>0.55	95	[2] AUBERT,B	06J	BABR	$e^+e^- \to \Upsilon(4S)$

[1] Using an unbinned max. likelihood fits to the M_{bc} distribution in five q^2 bins for $\cos\theta > 0$ and $\cos\theta < 0$.
[2] Results with different q^2 cuts are also reported.

$A_{FB}(B \to K^*\ell^+\ell^-)$ ($0.1 < q^2 < 2.0$ GeV$^2/c^4$)

VALUE	DOCUMENT ID		TECN	COMMENT
−0.01 ± 0.14 OUR AVERAGE	Error includes scale factor of 1.4. See the ideogram below.			
−0.02 ± 0.12 ± 0.01	AAIJ	13Y	LHCB	pp at 7 TeV, $K^{*0}\mu^+\mu^-$
$-0.35^{+0.26}_{-0.23} \pm 0.10$	AALTONEN	12I	CDF	$p\overline{p}$ at 1.96 TeV
$0.47^{+0.26}_{-0.32} \pm 0.03$	WEI	09A	BELL	$e^+e^- \to \Upsilon(4S)$
• • • We do not use the following data for averages, fits, limits, etc. • • •				
$-0.29^{+0.37}_{-0.00} \pm 0.18$	[1] CHATRCHYAN	13BL	CMS	pp at 7 TeV
−0.15 ± 0.20 ± 0.06	AAIJ	12U	LHCB	Repl. by AAIJ 13Y
$0.13^{+1.65}_{-0.75} \pm 0.25$	AALTONEN	11L	CDF	Repl. by AALTONEN 12I

[1] CHATRCHYAN 13BL uses, for this bin, $1.0 < q^2 < 2.0$ GeV$^2/c^4$.

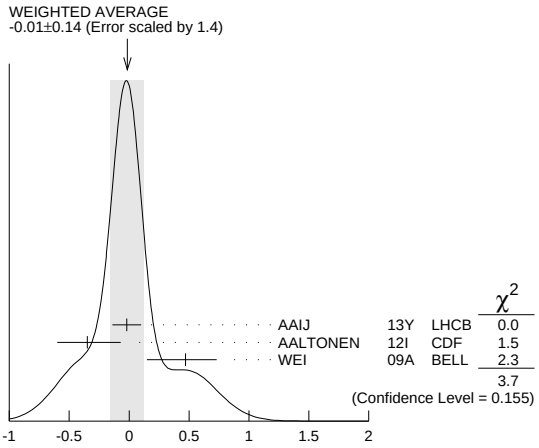

$A_{FB}(B \to K^*\ell^+\ell^-)$ ($0.1 < q^2 < 2.0$ GeV$^2/c^4$)

$A_{FB}(B \to K^*\ell^+\ell^-)$ ($m_{\ell\ell} < 2.5$ GeV/c^2)

VALUE	DOCUMENT ID		TECN	COMMENT
$\mathbf{0.24^{+0.18}_{-0.23} \pm 0.05}$	AUBERT	09N	BABR	$e^+e^- \to \Upsilon(4S)$

$A_{FB}(B \to K^*\ell^+\ell^-)$ ($m_{\ell\ell} > 3.2$ GeV/c^2)

VALUE	DOCUMENT ID		TECN	COMMENT
$\mathbf{0.76^{+0.52}_{-0.32} \pm 0.07}$	AUBERT	09N	BABR	$e^+e^- \to \Upsilon(4S)$

$A_{FB}(B \to K^*\ell^+\ell^-)$ ($0.10 < q^2 < 0.98$ GeV$^2/c^4$)

VALUE	DOCUMENT ID		TECN	COMMENT
$\mathbf{-0.003^{+0.058}_{-0.057} \pm 0.009}$	AAIJ	16B	LHCB	pp at 7, 8 TeV

$A_{FB}(B \to K^*\ell^+\ell^-)$ ($1.1 < q^2 < 2.5$ GeV$^2/c^4$)

VALUE	DOCUMENT ID		TECN	COMMENT
$\mathbf{-0.191^{+0.068}_{-0.080} \pm 0.012}$	AAIJ	16B	LHCB	pp at 7, 8 TeV

$A_{FB}(B \to K^*\ell^+\ell^-)$ ($2.0 < q^2 < 4.3$ GeV$^2/c^4$)

VALUE	DOCUMENT ID		TECN	COMMENT
−0.14 ± 0.05 OUR AVERAGE				
$-0.118^{+0.082}_{-0.090} \pm 0.007$	[1] AAIJ	16B	LHCB	pp at 7, 8 TeV
$-0.12\ ^{+0.15}_{-0.17} \pm 0.05$	KHACHATRY...	16D	CMS	pp at 8 TeV
−0.20 ± 0.08 ± 0.01	AAIJ	13Y	LHCB	pp at 7 TeV, $K^{*0}\mu^+\mu^-$
−0.07 ± 0.20 ± 0.02	CHATRCHYAN	13BL	CMS	pp at 7 TeV
$0.29\ ^{+0.32}_{-0.35} \pm 0.15$	AALTONEN	12I	CDF	$p\overline{p}$ at 1.96 TeV
$0.11\ ^{+0.31}_{-0.36} \pm 0.07$	WEI	09A	BELL	$e^+e^- \to \Upsilon(4S)$
• • • We do not use the following data for averages, fits, limits, etc. • • •				
$0.05\ ^{+0.16}_{-0.20} \pm 0.04$	AAIJ	12U	LHCB	Repl. by AAIJ 13Y
$0.19\ ^{+0.40}_{-0.41} \pm 0.14$	AALTONEN	11L	CDF	Repl. by AALTONEN 12I

[1] Measured in $2.5 < q^2 < 4.0$ GeV$^2/c^4$.

$A_{FB}(B \to K^*\ell^+\ell^-)$ ($0.0 < q^2 < 4.3$ GeV$^2/c^4$)

VALUE	DOCUMENT ID	TECN	COMMENT
$\mathbf{-0.08^{+0.21}_{-0.20} \pm 0.05}$	AALTONEN	12I	CDF	$p\overline{p}$ at 1.96 TeV
• • • We do not use the following data for averages, fits, limits, etc. • • •			
$0.21\ ^{+0.31}_{-0.33} \pm 0.05$	AALTONEN	11L	CDF	Repl. by AALTONEN 12I

$A_{FB}(B \to K^*\ell^+\ell^-)$ ($4.0 < q^2 < 6.0$ GeV$^2/c^4$)

VALUE	DOCUMENT ID	TECN	COMMENT
$\mathbf{0.025^{+0.051}_{-0.052} \pm 0.004}$	AAIJ	16B	LHCB	pp at 7, 8 TeV

$A_{FB}(B \to K^*\ell^+\ell^-)$ ($6.0 < q^2 < 8.0$ GeV$^2/c^4$)

VALUE	DOCUMENT ID	TECN	COMMENT
$\mathbf{0.152^{+0.041}_{-0.040} \pm 0.008}$	AAIJ	16B	LHCB	pp at 7, 8 TeV

$A_{FB}(B \to K^*\ell^+\ell^-)$ ($1.0 < q^2 < 6.0$ GeV$^2/c^4$)

VALUE	DOCUMENT ID		TECN	COMMENT
−0.085 ± 0.035 OUR AVERAGE	Error includes scale factor of 1.3. See the ideogram below.			
$-0.075^{+0.032}_{-0.034} \pm 0.007$	[1] AAIJ	16B	LHCB	pp at 7, 8 TeV
−0.12 ± 0.08	KHACHATRY...	16D	CMS	pp at 7, 8 TeV
$0.21\ ^{+0.10}_{-0.15}\ ^{+0.07}_{-0.09}$	[2] LEES	16C	BABR	$e^+e^- \to \Upsilon(4S)$
−0.17 ± 0.06 ± 0.01	AAIJ	13Y	LHCB	pp at 7 TeV, $K^{*0}\mu^+\mu^-$
$0.29\ ^{+0.20}_{-0.23} \pm 0.07$	AALTONEN	12I	CDF	$p\overline{p}$ at 1.96 TeV
$0.26\ ^{+0.27}_{-0.30} \pm 0.07$	WEI	09A	BELL	$e^+e^- \to \Upsilon(4S)$
• • • We do not use the following data for averages, fits, limits, etc. • • •				
0.55 ± 0.43	[3] SATO	16	BELL	$e^+e^- \to \Upsilon(4S)$
−0.07 ± 0.12 ± 0.01	CHATRCHYAN	13BL	CMS	Repl. by KHACHATRYAN 16D
$-0.06\ ^{+0.13}_{-0.14} \pm 0.07$	AAIJ	12U	LHCB	Repl. by AAIJ 13Y
$0.43\ ^{+0.36}_{-0.37} \pm 0.06$	AALTONEN	11L	CDF	Repl. by AALTONEN 12I

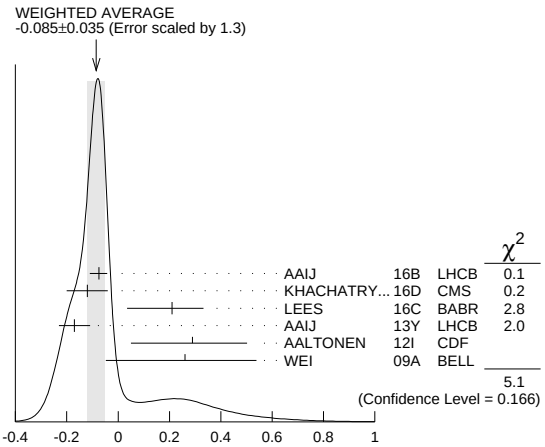

$A_{FB}(B \to K^*\ell^+\ell^-)$ ($1.0 < q^2 < 6.0$ GeV$^2/c^4$)

[1] Measured in $1.1 < q^2 < 6.0$ GeV$^2/c^4$.
[2] Measured by combining B^0 and B^+ with e and μ as leptons. Results are also provided separately for B^0 and B^+.
[3] Uses $K^* \to K^-\pi^+$, $K^-\pi^0$, $K^0_S\pi^-$ in the range $M(K\pi) < 1.1$ GeV/c^2. Uncertainty is statistical only.

$A_{FB}(B \to K^{*}\ell^{+}\ell^{-})$ $(4.3 < q^2 < 8.6\ \text{GeV}^2/c^4)$

VALUE	DOCUMENT ID		TECN	COMMENT
$0.13^{+0.06}_{-0.05}$ OUR AVERAGE	Error includes scale factor of 1.1.			
$0.16^{+0.06}_{-0.05}\pm0.01$	AAIJ	13Y	LHCB	pp at 7 TeV, $K^{*0}\mu^{+}\mu^{-}$
$-0.01\pm0.11\pm0.03$	CHATRCHYAN	13BL	CMS	pp at 7 TeV
$0.01\pm0.20\pm0.09$	AALTONEN	12I	CDF	$p\overline{p}$ at 1.96 TeV
$0.45^{+0.15}_{-0.21}\pm0.15$	WEI	09A	BELL	$e^{+}e^{-} \to \Upsilon(4S)$
• • • We do not use the following data for averages, fits, limits, etc. • • •				
$0.27^{+0.06}_{-0.08}\pm0.02$	AAIJ	12U	LHCB	Repl. by AAIJ 13Y
$-0.06^{+0.30}_{-0.28}\pm0.05$	AALTONEN	11L	CDF	Repl. by AALTONEN 12I

$A_{FB}(B \to K^{*}\ell^{+}\ell^{-})$ $(10.09 < q^2 < 12.86\ \text{GeV}^2/c^4)$

VALUE	DOCUMENT ID		TECN	COMMENT
0.02 ± 0.13 OUR AVERAGE	Error includes scale factor of 4.5. See the ideogram below.			
$-0.318^{+0.044}_{-0.040}\pm0.009$	[1] AAIJ	16B	LHCB	pp at 7, 8 TeV
$0.16\pm0.06\pm0.01$	KHACHATRY...	16D	CMS	pp at 8 TeV
$0.28^{+0.07}_{-0.06}\pm0.02$	AAIJ	13Y	LHCB	pp at 7 TeV, $K^{*0}\mu^{+}\mu^{-}$
$0.40\pm0.08\pm0.05$	CHATRCHYAN	13BL	CMS	pp at 7 TeV
$0.38^{+0.16}_{-0.19}\pm0.09$	AALTONEN	12I	CDF	$p\overline{p}$ at 1.96 TeV
$0.43^{+0.18}_{-0.20}\pm0.03$	WEI	09A	BELL	$e^{+}e^{-} \to \Upsilon(4S)$
• • • We do not use the following data for averages, fits, limits, etc. • • •				
$0.27^{+0.11}_{-0.13}\pm0.02$	AAIJ	12U	LHCB	Repl. by AAIJ 13Y
$0.66^{+0.23}_{-0.20}\pm0.07$	AALTONEN	11L	CDF	Repl. by AALTONEN 12I

[1] Measured in $11.0 < q^2 < 12.5\ \text{GeV}^2/c^4$.

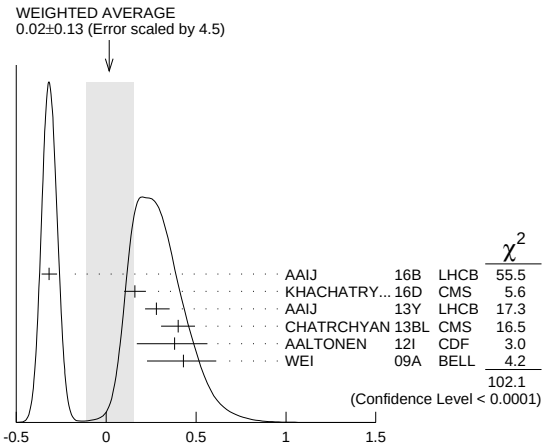

$A_{FB}(B \to K^{*}\ell^{+}\ell^{-})$ $(10.09 < q^2 < 12.86\ \text{GeV}^2/c^4)$

$A_{FB}(B \to K^{*}\ell^{+}\ell^{-})$ $(14.18 < q^2 < 16.0\ \text{GeV}^2/c^4)$

VALUE	DOCUMENT ID		TECN	COMMENT
$0.43^{+0.05}_{-0.06}$ OUR AVERAGE	Error includes scale factor of 1.6. See the ideogram below.			
$0.39^{+0.04}_{-0.06}\pm0.01$	KHACHATRY...	16D	CMS	pp at 8 TeV
$0.51^{+0.07}_{-0.05}\pm0.02$	AAIJ	13Y	LHCB	pp at 7 TeV, $K^{*0}\mu^{+}\mu^{-}$
$0.29\pm0.09\pm0.05$	CHATRCHYAN	13BL	CMS	pp at 7 TeV
$0.44^{+0.18}_{-0.21}\pm0.10$	AALTONEN	12I	CDF	$p\overline{p}$ at 1.96 TeV
$0.70^{+0.16}_{-0.22}\pm0.10$	WEI	09A	BELL	$e^{+}e^{-} \to \Upsilon(4S)$
• • • We do not use the following data for averages, fits, limits, etc. • • •				
$0.47^{+0.06}_{-0.08}\pm0.03$	AAIJ	12U	LHCB	Repl. by AAIJ 13Y
$0.42\pm0.16\pm0.09$	AALTONEN	11L	CDF	Repl. by AALTONEN 12I

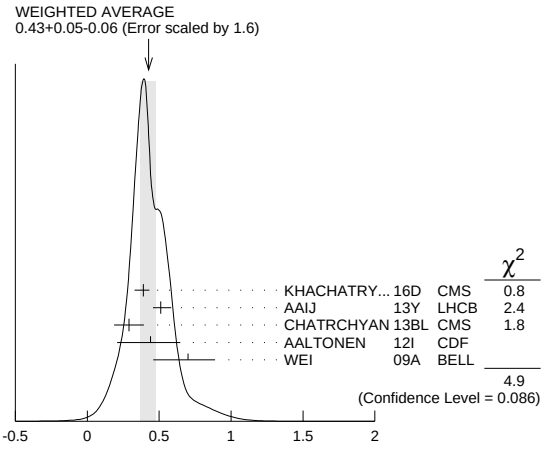

$A_{FB}(B \to K^{*}\ell^{+}\ell^{-})$ $(14.18 < q^2 < 16.0\ \text{GeV}^2/c^4)$

$A_{FB}(B \to K^{*}\ell^{+}\ell^{-})$ $(15.0 < q^2 < 17.0\ \text{GeV}^2/c^4)$

VALUE	DOCUMENT ID		TECN	COMMENT
$0.411^{+0.41}_{-0.037}\pm0.008$	AAIJ	16B	LHCB	pp at 7, 8 TeV

$A_{FB}(B \to K^{*}\ell^{+}\ell^{-})$ $(17.0 < q^2 < 19.0\ \text{GeV}^2/c^4)$

VALUE	DOCUMENT ID		TECN	COMMENT
$0.305^{+0.049}_{-0.048}\pm0.013$	AAIJ	16B	LHCB	pp at 7, 8 TeV

$A_{FB}(B \to K^{*}\ell^{+}\ell^{-})$ $(16.0 < q^2 < 19.0\ \text{GeV}^2/c^4)$

VALUE	DOCUMENT ID		TECN	COMMENT
0.367 ± 0.024 OUR AVERAGE	Error includes scale factor of 1.1.			
$0.355\pm0.027\pm0.009$	[1] AAIJ	16B	LHCB	pp at 7, 8 TeV
$0.35\pm0.07\pm0.01$	KHACHATRY...	16D	CMS	pp at 8 TeV
$0.30\pm0.08^{+0.01}_{-0.02}$	AAIJ	13Y	LHCB	pp at 7 TeV, $K^{*0}\mu^{+}\mu^{-}$
$0.41\pm0.05\pm0.03$	CHATRCHYAN	13BL	CMS	pp at 7 TeV
$0.65^{+0.17}_{-0.18}\pm0.16$	AALTONEN	12I	CDF	$p\overline{p}$ at 1.96 TeV
$0.66^{+0.11}_{-0.16}\pm0.04$	WEI	09A	BELL	$e^{+}e^{-} \to \Upsilon(4S)$
• • • We do not use the following data for averages, fits, limits, etc. • • •				
$0.16^{+0.11}_{-0.13}\pm0.06$	AAIJ	12U	LHCB	Repl. by AAIJ 13Y
$0.70^{+0.16}_{-0.25}\pm0.10$	AALTONEN	11L	CDF	Repl. by AALTONEN 12I

[1] Measured in $15.0 < q^2 < 19.0\ \text{GeV}^2/c^4$.

$A_{FB}(B \to K\ell^{+}\ell^{-})$ $(q^2 > 0.1\ \text{GeV}^2/c^4)$

VALUE	DOCUMENT ID		TECN	COMMENT
0.11 ± 0.12 OUR AVERAGE				
$0.15^{+0.21}_{-0.23}\pm0.08$	[1] AUBERT,B	06J	BABR	$e^{+}e^{-} \to \Upsilon(4S)$
$0.10\pm0.14\pm0.01$	[2] ISHIKAWA	06	BELL	$e^{+}e^{-} \to \Upsilon(4S)$

[1] Results with different q^2 cuts are also reported.

[2] Using an unbinned max. likelihood fits to the M_{bc} distribution in five q^2 bins for $\cos\theta > 0$ and $\cos\theta < 0$.

$A_{FB}(B \to K\ell^{+}\ell^{-})$ $(q^2 < 2.0\ \text{GeV}^2/c^4)$

VALUE	DOCUMENT ID		TECN	COMMENT
$0.00^{+0.06}_{-0.05}$ OUR AVERAGE				
$0.00^{+0.06+0.03}_{-0.05-0.01}$	AAIJ	13H	LHCB	pp at 7 TeV
$0.13^{+0.42}_{-0.43}\pm0.07$	AALTONEN	12I	CDF	$p\overline{p}$ at 1.96 TeV
$0.06^{+0.32}_{-0.35}\pm0.02$	WEI	09A	BELL	$e^{+}e^{-} \to \Upsilon(4S)$
• • • We do not use the following data for averages, fits, limits, etc. • • •				
$-0.15^{+0.46}_{-0.39}\pm0.08$	AALTONEN	11L	CDF	Repl. by AALTONEN 12I

$A_{FB}(B \to K\ell^{+}\ell^{-})$ $(2.0 < q^2 < 4.3\ \text{GeV}^2/c^4)$

VALUE	DOCUMENT ID		TECN	COMMENT
$0.09^{+0.10}_{-0.07}$ OUR AVERAGE	Error includes scale factor of 1.4.			
$0.07^{+0.08+0.02}_{-0.05-0.01}$	AAIJ	13H	LHCB	pp at 7 TeV
$0.32^{+0.15}_{-0.16}\pm0.05$	AALTONEN	12I	CDF	$p\overline{p}$ at 1.96 TeV
$-0.43^{+0.38}_{-0.40}\pm0.09$	WEI	09A	BELL	$e^{+}e^{-} \to \Upsilon(4S)$
• • • We do not use the following data for averages, fits, limits, etc. • • •				
$0.72^{+0.40}_{-0.35}\pm0.07$	AALTONEN	11L	CDF	Repl. by AALTONEN 12I

$A_{FB}(B \to K\ell^+\ell^-)$ $(0.0 < q^2 < 4.3\ \mathrm{GeV}^2/c^4)$

VALUE	DOCUMENT ID		TECN	COMMENT
$0.31 \pm 0.16 \pm 0.04$	AALTONEN	12I	CDF	$p\overline{p}$ at 1.96 TeV
• • • We do not use the following data for averages, fits, limits, etc. • • •				
$0.36^{+0.24}_{-0.26} \pm 0.06$	AALTONEN	11L	CDF	Repl. by AALTONEN 12I

$A_{FB}(B \to K\ell^+\ell^-)$ $(1.0 < q^2 < 6.0\ \mathrm{GeV}^2/c^4)$

VALUE	DOCUMENT ID		TECN	COMMENT
$0.034^{+0.040}_{-0.029}$ OUR AVERAGE				
$0.02\ ^{+0.05}_{-0.03}\ ^{+0.02}_{-0.01}$	AAIJ	13H	LHCB	pp at 7 TeV
$0.13 \pm 0.09 \pm 0.02$	AALTONEN	12I	CDF	$p\overline{p}$ at 1.96 TeV
$-0.04\ ^{+0.13}_{-0.16} \pm 0.05$	WEI	09A	BELL	$e^+e^- \to \Upsilon(4S)$
• • • We do not use the following data for averages, fits, limits, etc. • • •				
0.00 ± 0.13	[1] SATO	16	BELL	$e^+e^- \to \Upsilon(4S)$
$0.08\ ^{+0.27}_{-0.22} \pm 0.07$	AALTONEN	11L	CDF	Repl. by AALTONEN 12I

[1] Statistical uncertainty only.

$A_{FB}(B \to K\ell^+\ell^-)$ $(4.3 < q^2 < 8.6\ \mathrm{GeV}^2/c^4)$

VALUE	DOCUMENT ID		TECN	COMMENT
$-0.04^{+0.04}_{-0.05}$ OUR AVERAGE				
$-0.02^{+0.03}_{-0.05} \pm 0.03$	AAIJ	13H	LHCB	pp at 7 TeV
$0.01^{+0.13}_{-0.10} \pm 0.01$	AALTONEN	12I	CDF	$p\overline{p}$ at 1.96 TeV
$-0.20^{+0.12}_{-0.14} \pm 0.03$	WEI	09A	BELL	$e^+e^- \to \Upsilon(4S)$
• • • We do not use the following data for averages, fits, limits, etc. • • •				
$-0.20^{+0.17}_{-0.28} \pm 0.03$	AALTONEN	11L	CDF	Repl. by AALTONEN 12I

$A_{FB}(B \to K\ell^+\ell^-)$ $(10.09 < q^2 < 12.86\ \mathrm{GeV}^2/c^4)$

VALUE	DOCUMENT ID		TECN	COMMENT
-0.05 ± 0.06 OUR AVERAGE				
$-0.03 \pm 0.07 \pm 0.01$	AAIJ	13H	LHCB	pp at 7 TeV
$-0.03^{+0.11}_{-0.10} \pm 0.04$	AALTONEN	12I	CDF	$p\overline{p}$ at 1.96 TeV
$-0.21^{+0.17}_{-0.15} \pm 0.06$	WEI	09A	BELL	$e^+e^- \to \Upsilon(4S)$
• • • We do not use the following data for averages, fits, limits, etc. • • •				
$-0.10^{+0.17}_{-0.15} \pm 0.07$	AALTONEN	11L	CDF	Repl. by AALTONEN 12I

$A_{FB}(B \to K\ell^+\ell^-)$ $(14.18 < q^2 < 16.0\ \mathrm{GeV}^2/c^4)$

VALUE	DOCUMENT ID		TECN	COMMENT
$-0.02^{+0.07}_{-0.05}$ OUR AVERAGE				
$-0.01^{+0.12}_{-0.06} \pm 0.01$	AAIJ	13H	LHCB	pp at 7 TeV
$-0.05^{+0.09}_{-0.11} \pm 0.03$	AALTONEN	12I	CDF	$p\overline{p}$ at 1.96 TeV
$0.04^{+0.32}_{-0.26} \pm 0.05$	WEI	09A	BELL	$e^+e^- \to \Upsilon(4S)$
• • • We do not use the following data for averages, fits, limits, etc. • • •				
$0.03^{+0.49}_{-0.16} \pm 0.04$	AALTONEN	11L	CDF	Repl. by AALTONEN 12I

$A_{FB}(B \to K\ell^+\ell^-)$ $(16.0 < q^2 < 18.0\ \mathrm{GeV}^2/c^4)$

VALUE	DOCUMENT ID		TECN	COMMENT
$-0.09^{+0.07+0.02}_{-0.09-0.01}$	AAIJ	13H	LHCB	pp at 7 TeV

$A_{FB}(B \to K\ell^+\ell^-)$ $(18.0 < q^2 < 22.0\ \mathrm{GeV}^2/c^4)$

VALUE	DOCUMENT ID		TECN	COMMENT
$0.02 \pm 0.11 \pm 0.01$	AAIJ	13H	LHCB	pp at 7 TeV

$A_{FB}(B \to K\ell^+\ell^-)$ $(q^2 > 16.0\ \mathrm{GeV}^2/c^4)$

VALUE	DOCUMENT ID		TECN	COMMENT
$0.04^{+0.09}_{-0.07}$ OUR AVERAGE				
$0.09^{+0.17}_{-0.13} \pm 0.03$	AALTONEN	12I	CDF	$p\overline{p}$ at 1.96 TeV
$0.02^{+0.11}_{-0.08} \pm 0.02$	WEI	09A	BELL	$e^+e^- \to \Upsilon(4S)$
• • • We do not use the following data for averages, fits, limits, etc. • • •				
$0.07^{+0.30}_{-0.23} \pm 0.02$	AALTONEN	11L	CDF	Repl. by AALTONEN 12I

$A_{FB}(B \to X_s\ell^+\ell^-)$ $(1.0 < q^2 < 6.0\ \mathrm{GeV}^2/c^4)$

VALUE	DOCUMENT ID		TECN	COMMENT
• • • We do not use the following data for averages, fits, limits, etc. • • •				
0.74 ± 0.54	[1] SATO	16	BELL	$e^+e^- \to \Upsilon(4S)$

[1] Uses the sum of 10 exclusive X_s modes in the range $M(X_s) > 1.1\ \mathrm{GeV}/c^2$. Uncertainty is statistical only.

$F_S(B \to K\ell^+\ell^-)$ $(q^2 > 0.1\ \mathrm{GeV}^2/c^4)$

VALUE	DOCUMENT ID		TECN	COMMENT
$0.81^{+0.58}_{-0.61} \pm 0.46$	[1] AUBERT,B	06J	BABR	$e^+e^- \to \Upsilon(4S)$

[1] Results with different q^2 cuts are also reported.

$A_{FB}(B \to Kp\overline{p})$ $(m_{p\overline{p}} < 2.85\ \mathrm{GeV}/c^2)$

VALUE	DOCUMENT ID		TECN	COMMENT
$0.495 \pm 0.012 \pm 0.007$	[1] AAIJ	14AF	LHCB	pp at 7, 8 TeV

[1] Measured in $B^+ \to K^+p\overline{p}$ decays.

$A_{FB}(B \to \pi p\overline{p})$ $(m_{p\overline{p}} < 2.85\ \mathrm{GeV}/c^2)$

VALUE	DOCUMENT ID		TECN	COMMENT
$-0.409 \pm 0.033 \pm 0.006$	[1] AAIJ	14AF	LHCB	pp at 7, 8 TeV

[1] Measured in $B^+ \to \pi^+p\overline{p}$ decays.

ISOSPIN ASYMMETRY

Δ_{0-} is defined as

$$\frac{\Gamma(\overline{B}^0 \to f_d) - \Gamma(B^- \to f_u)}{\Gamma(\overline{B}^0 \to f_d) + \Gamma(B^- \to f_u)},$$

the isospin asymmetry of inclusive neutral and charged B decay.

$\Delta_{0-}(B(B \to X_s\gamma))$

VALUE	DOCUMENT ID		TECN	COMMENT
-0.01 ± 0.06 OUR AVERAGE				
$-0.06 \pm 0.15 \pm 0.07$	[1,2] AUBERT	08O	BABR	$e^+e^- \to \Upsilon(4S)$
$-0.006 \pm 0.058 \pm 0.026$	AUBERT,B	05R	BABR	$e^+e^- \to \Upsilon(4S)$

[1] The result is for $E_\gamma > 2.2$ GeV.

[2] Uses a fully reconstructed B meson as a tag on the recoil side.

$\Delta_{0+}(B \to K^*(892)\gamma)$

Δ_{0+} describes the isospin asymmetry between $\Gamma(B^0 \to K^*(892)^0\gamma)$ and $\Gamma(B^+ \to K^*(892)^+\gamma)$.

VALUE	DOCUMENT ID		TECN	COMMENT
0.063 ± 0.017 OUR AVERAGE				
$0.062 \pm 0.015 \pm 0.013$	[1] HORIGUCHI	17	BELL	$e^+e^- \to \Upsilon(4S)$
$0.066 \pm 0.021 \pm 0.022$	[2] AUBERT	09AO	BABR	$e^+e^- \to \Upsilon(4S)$
• • • We do not use the following data for averages, fits, limits, etc. • • •				
$0.050 \pm 0.045 \pm 0.037$	[3] AUBERT,BE	04A	BABR	Repl. by AUBERT 09AO
$0.012 \pm 0.044 \pm 0.026$	NAKAO	04	BELL	Repl. by HORIGUCHI 17

[1] Uses $B(\Upsilon(4S) \to B^+B^-) = (51.4 \pm 0.6)\%$ and $B(\Upsilon(4S) \to B^0\overline{B}^0) = (48.6 \pm 0.6)\%$.

[2] Uses the production ratio of charged and neutral B from $\Upsilon(4S)$ decays and the lifetime ratio $\tau_{B^+}/\tau_{B^0} = 1.071 \pm 0.009$. The 90% CL interval is $0.017 < \Delta_{0+} < 0.116$

[3] Uses the production ratio of charged and neutral B from $\Upsilon(4S)$ decays $R^{+/0} = 1.006 \pm 0.048$ and the lifetime ratio of $\tau_{B^+}\ /\ \tau_{B^0} = 1.083 \pm 0.017$. The 90% CL interval is $-0.046 < \Delta_{0+} < 0.146$.

$\Delta_{\rho\gamma} = \Gamma(B^+ \to \rho^+\gamma)\ /\ (2 \cdot \Gamma(B^0 \to \rho^0\gamma)\ ) - 1$

VALUE	DOCUMENT ID		TECN	COMMENT
-0.46 ± 0.17 OUR AVERAGE				
$-0.43^{+0.25}_{-0.22} \pm 0.10$	AUBERT	08BH	BABR	$e^+e^- \to \Upsilon(4S)$
$-0.48^{+0.21}_{-0.19}\ ^{+0.08}_{-0.09}$	TANIGUCHI	08	BELL	$e^+e^- \to \Upsilon(4S)$

$\Delta_{0-}(B(B \to K\ell^+\ell^-))$

VALUE	DOCUMENT ID		TECN	COMMENT
-0.13 ± 0.06 OUR AVERAGE	Error includes scale factor of 1.1.			
$-0.10^{+0.08}_{-0.09} \pm 0.02$	[1] AAIJ	14M	LHCB	pp at 7, 8 TeV
$-0.09^{+0.08}_{-0.08} \pm 0.02$	[2] AAIJ	14M	LHCB	pp at 7, 8 TeV
$-0.58^{+0.29}_{-0.37} \pm 0.02$	[3] LEES	12S	BABR	$e^+e^- \to \Upsilon(4S)$
$-0.31^{+0.17}_{-0.14} \pm 0.08$	[4] WEI	09A	BELL	$e^+e^- \to \Upsilon(4S)$
• • • We do not use the following data for averages, fits, limits, etc. • • •				
$-0.35^{+0.23}_{-0.27}$	[5] AAIJ	12AH	LHCB	Repl. by AAIJ 14M
$-1.43^{+0.56}_{-0.85} \pm 0.05$	[6,7] AUBERT	09T	BABR	Repl. by LEES 12S

[1] For $1.1 < q^2 < 6.0\ \mathrm{GeV}^2/c^4$ using $\mu^+\mu^-$ as a lepton pair and assuming isospin symmetry for the $B \to J/\psi(1S)K$. Measurements in other q^2 bins are also reported.

[2] For $15.0 < q^2 < 19.0\ \mathrm{GeV}^2/c^4$ using $\mu^+\mu^-$ as a lepton pair and assuming isospin symmetry for the $B \to J/\psi(1S)K$. Measurements in other q^2 bins are also reported.

[3] For $0.10 < q^2 < 8.12\ \mathrm{GeV}^2/c^4$. Measurements in other q^2 bins are also reported.

[4] For $q^2 < 8.68\ \mathrm{GeV}^2/c^4$.

[5] For $1 < q^2 < 6\ \mathrm{GeV}^2/c^4$.

[6] For $0.1 < m^2_{\ell^+\ell^-} < 7.02\ \mathrm{GeV}^2/c^4$.

[7] Assumes equal production of B^+ and B^0 at the $\Upsilon(4S)$.

$\Delta_{0-}(B(B \to K^* \ell^+ \ell^-))$

VALUE	DOCUMENT ID		TECN	COMMENT
$-0.03^{+0.08}_{-0.07}$ OUR AVERAGE	Error includes scale factor of 1.2.			
$0.00^{+0.12}_{-0.10}\pm0.02$	[1] AAIJ	14M	LHCB	pp at 7, 8 TeV
$0.06^{+0.10}_{-0.09}\pm0.02$	[2] AAIJ	14M	LHCB	pp at 7, 8 TeV
$-0.25^{+0.20}_{-0.17}\pm0.03$	[3] LEES	12S	BABR	$e^+e^- \to \Upsilon(4S)$
$-0.29\pm0.16\pm0.09$	[4] WEI	09A	BELL	$e^+e^- \to \Upsilon(4S)$
• • • We do not use the following data for averages, fits, limits, etc. • • •				
-0.15 ± 0.16	[5] AAIJ	12AH	LHCB	Repl. by AAIJ 14M
$-0.56^{+0.17}_{-0.15}\pm0.03$	[6,7] AUBERT	09T	BABR	Repl. by LEES 12S

[1] For $1.1 < q^2 < 6.0$ GeV$^2/c^4$ using $\mu^+\mu^-$ as a lepton pair and assuming isospin symmetry for the B($B \to J/\psi(1S)K^*(892)$). Measurements in other q^2 bins are also reported.
[2] For $15.0 < q^2 < 22.0$ GeV$^2/c^4$ using $\mu^+\mu^-$ as a lepton pair and assuming isospin symmetry for the B($B \to J/\psi(1S)K^*(892)$). Measurements in other q^2 bins are also reported.
[3] For $0.10 < q^2 < 8.12$ GeV$^2/c^4$. Measurements in other q^2 bins are also reported.
[4] For $q^2 < 8.68$ GeV$^2/c^4$.
[5] For $1 < q^2 < 6$ GeV$^2/c^4$.
[6] For $0.1 < m^2_{\ell^+\ell^-} < 7.02$ GeV$^2/c^4$.
[7] Assumes equal production of B^+ and B^0 at the $\Upsilon(4S)$.

$\Delta_{0-}(B(B \to K^{(*)} \ell^+ \ell^-))$

VALUE	DOCUMENT ID		TECN	COMMENT
-0.45 ± 0.17 OUR AVERAGE	Error includes scale factor of 1.7.			
$-0.64^{+0.15}_{-0.14}\pm0.03$	[1,2] AUBERT	09T	BABR	$e^+e^- \to \Upsilon(4S)$
$-0.30^{+0.12}_{-0.11}\pm0.08$	[3] WEI	09A	BELL	$e^+e^- \to \Upsilon(4S)$

[1] For $0.1 < m^2_{\ell^+\ell^-} < 7.02$ GeV$^2/c^4$.
[2] Assumes equal production of B^+ and B^0 at the $\Upsilon(4S)$.
[3] For $q^2 < 8.68$ GeV$^2/c^2$.

$B \to X_c \ell \nu$ HADRONIC MASS MOMENTS

$\langle M_X^2 - \overline{M}_D^2 \rangle$ (First Moments)

VALUE (GeV^2)	DOCUMENT ID		TECN	COMMENT
0.36 ±0.08 OUR AVERAGE	Error includes scale factor of 1.8.			
$0.467\pm0.038\pm0.068$	[1] ACOSTA	05F	CDF	$p\overline{p}$ at 1.96 TeV
$0.293\pm0.012\pm0.058$	[2] CSORNA	04	CLE2	$e^+e^- \to \Upsilon(4S)$
• • • We do not use the following data for averages, fits, limits, etc. • • •				
$0.251\pm0.023\pm0.062$	[3] CRONIN-HEN..	01B	CLE2	$e^+e^- \to \Upsilon(4S)$

[1] Moments are measured with a minimum lepton momentum of 0.7 GeV/c in the B rest frame;
[2] Uses minimum lepton energy of 1.5 GeV and also reports moments with $E_\ell > 1.0$ GeV.
[3] The leptons are required to have $P_\ell > 1.5$ GeV/c.

$\langle M_X^2 \rangle$ (First Moments)

VALUE (GeV^2)	DOCUMENT ID		TECN	COMMENT
4.156±0.029 OUR AVERAGE				
$4.144\pm0.028\pm0.022$	[1] SCHWANDA	07	BELL	$e^+e^- \to \Upsilon(4S)$
$4.18\ \pm0.04\ \pm0.03$	[1] AUBERT,B	04	BABR	$e^+e^- \to \Upsilon(4S)$

[1] The leptons are required to have $E_\ell > 1.5$ GeV/c.

$\langle (M_X^2 - \overline{M}_X^2)^2 \rangle$ (Second Moments)

VALUE (GeV^4)	DOCUMENT ID		TECN	COMMENT
0.55 ±0.08 OUR AVERAGE				
$0.515\pm0.061\pm0.064$	[1] SCHWANDA	07	BELL	$e^+e^- \to \Upsilon(4S)$
$0.629\pm0.031\pm0.143$	[2] CSORNA	04	CLE2	$e^+e^- \to \Upsilon(4S)$
• • • We do not use the following data for averages, fits, limits, etc. • • •				
$1.05\ \pm0.26\ \pm0.13$	[3] ACOSTA	05F	CDF	$p\overline{p}$ at 1.96 TeV
$0.576\pm0.048\pm0.168$	[1] CRONIN-HEN..	01B	CLE2	$e^+e^- \to \Upsilon(4S)$

[1] The leptons are required to have $E_\ell > 1.5$ GeV/c.
[2] Uses minimum lepton energy of 1.5 GeV and also reports moments with $E_\ell > 1.0$ GeV.
[3] Moments are measured with a minimum lepton momentum of 0.7 GeV/c in the B rest frame;

$\langle (M_X^2 - \overline{M}_D^2)^2 \rangle$ (Second Moments)

VALUE (GeV^4)	DOCUMENT ID		TECN	COMMENT
0.639±0.056±0.178	[1] CRONIN-HEN..	01B	CLE2	$e^+e^- \to \Upsilon(4S)$

[1] The leptons are required to have $E_\ell > 1.5$ GeV/c.

$B \to X_c \ell \nu$ LEPTON MOMENTUM MOMENTS

R_0 ($\Gamma_{E_l>1.7GeV}$ / $\Gamma_{E_l>1.5GeV}$)

VALUE	DOCUMENT ID		TECN	COMMENT
0.6187±0.0014±0.0016	[1] MAHMOOD	03	CLE2	$e^+e^- \to \Upsilon(4S)$

[1] The leptons are required to have $E_l > 1.5$ GeV in the B rest frame.

R_1 ($\langle E_l \rangle_{E_l>1.5GeV}$)

VALUE	DOCUMENT ID		TECN	COMMENT
1.7797±0.0018 OUR AVERAGE	Error includes scale factor of 1.8. See the ideogram below.			
$1.7743\pm0.0019\pm0.0014$	[1] AUBERT,B	04A	BABR	$e^+e^- \to \Upsilon(4S)$
$1.7792\pm0.0021\pm0.0027$	[2] MAHMOOD	04	CLEO	$e^+e^- \to \Upsilon(4S)$
$1.7810\pm0.0007\pm0.0009$	[3] MAHMOOD	03	CLE2	$e^+e^- \to \Upsilon(4S)$

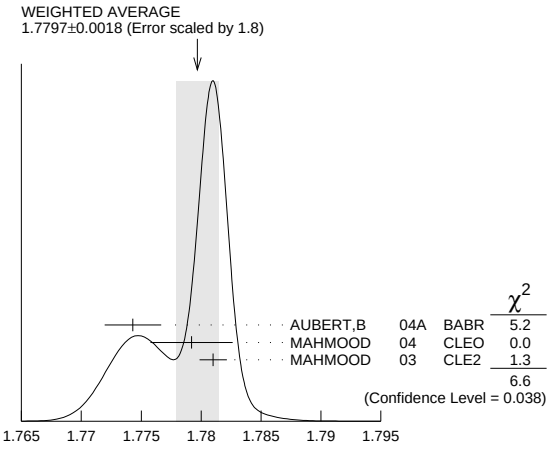

[1] The leptons are required to have $E_l > 1.5$ GeV in the B rest frame. The result with $E_l > 0.6$ GeV is also given.
[2] Uses $E_e > 1.5$ GeV and also reports moments with other minimum minimum E_e conditions, as low as $E_e > 0.6$ GeV.
[3] The leptons are required to have $E_l > 1.5$ GeV in the B rest frame.

R_2 ($\langle E_l^2 - \overline{E}_l^2 \rangle_{E_l>1.5GeV}$)

VALUE (10^{-3} GeV^2)	DOCUMENT ID		TECN	COMMENT
30.8±0.8 OUR AVERAGE				
$30.3\pm0.9\pm0.5$	[1] AUBERT,B	04A	BABR	$e^+e^- \to \Upsilon(4S)$
$31.6\pm0.8\pm1.0$	[2] MAHMOOD	04	CLEO	$e^+e^- \to \Upsilon(4S)$

[1] The leptons are required to have $E_l > 1.5$ GeV in the B rest frame. The result with $E_l > 0.6$ GeV is also given.
[2] Uses $E_e > 1.5$ GeV and also reports moments with other minimum minimum E_e conditions, as low as $E_e > 0.6$ GeV.

R_3 ($\langle E_l^3 - \overline{E}_l^3 \rangle_{E_l>1.5GeV}$)

VALUE (10^{-3} GeV^3)	DOCUMENT ID		TECN	COMMENT
2.12±0.47±0.20	[1] AUBERT,B	04A	BABR	$e^+e^- \to \Upsilon(4S)$

[1] The leptons are required to have $E_l > 1.5$ GeV in the B rest frame. The result with $E_l > 0.6$ GeV is also given.

$B \to X_s \gamma$ PHOTON ENERGY MOMENTS

$\langle E_\gamma \rangle$

VALUE (GeV)	DOCUMENT ID		TECN	COMMENT
2.314±0.011 OUR AVERAGE				
$2.346\pm0.018^{+0.027}_{-0.022}$	[1,2] LEES	12U	BABR	$e^+e^- \to \Upsilon(4S)$
$2.304\pm0.014\pm0.017$	[2,3] LEES	12V	BABR	$e^+e^- \to \Upsilon(4S)$
$2.311\pm0.009\pm0.015$	[3] LIMOSANI	09	BELL	$e^+e^- \to \Upsilon(4S)$
$2.289\pm0.058\pm0.027$	[3,4] AUBERT	08O	BABR	$e^+e^- \to \Upsilon(4S)$
$2.309\pm0.023\pm0.023$	[2,3] SCHWANDA	08	BELL	$e^+e^- \to \Upsilon(4S)$
• • • We do not use the following data for averages, fits, limits, etc. • • •				
$2.288\pm0.025\pm0.023$	[3] AUBERT,BE	06B	BABR	Repl. by LEES 12V

[1] LEES 12U uses $E_\gamma > 1.897$ GeV to calculate the moments; the moments are used to calculate the HQET parameters $m_b = 4.579^{+0.032}_{-0.029}$ GeV/c^2 and $\mu_\pi^2 = 0.257^{+0.034}_{-0.039}$ GeV^2 in the shape function model. The same HQET parameters are also determined in the kinetic model.
[2] Results for different E_γ threshold values are also measured.
[3] The result is for $E_\gamma > 1.9$ GeV.
[4] Uses a fully reconstructed B meson as a tag on the recoil side.

$\langle E_\gamma^2 \rangle - \langle E_\gamma \rangle^2$

VALUE (10^{-2} GeV^2)	DOCUMENT ID		TECN	COMMENT
3.03±0.25 OUR AVERAGE				
$2.11\pm0.57^{+0.55}_{-0.69}$	[1,2] LEES	12U	BABR	$e^+e^- \to \Upsilon(4S)$
$3.62\pm0.33\pm0.33$	[2,3] LEES	12V	BABR	$e^+e^- \to \Upsilon(4S)$
$3.02\pm0.19\pm0.30$	[3] LIMOSANI	09	BELL	$e^+e^- \to \Upsilon(4S)$
$3.34\pm1.24\pm0.62$	[3,4] AUBERT	08O	BABR	$e^+e^- \to \Upsilon(4S)$
$2.17\pm0.60\pm0.55$	[2,3] SCHWANDA	08	BELL	$e^+e^- \to \Upsilon(4S)$

Meson Particle Listings

$B^{\pm}/B^{0}$ ADMIXTURE

• • • We do not use the following data for averages, fits, limits, etc. • • •

$3.28 \pm 0.40 \pm 0.43$ [3] AUBERT,BE 06B BABR Repl. by LEES 12V

[1] LEES 12U uses $E_\gamma > 1.897$ GeV to calculate the moments; the moments are used to calculate the HQET parameters $m_b = 4.579^{+0.032}_{-0.029}$ GeV/c^2 and $\mu_\pi^2 = 0.257^{+0.034}_{-0.039}$ GeV^2 in the shape function model. The same HQET parameters are also determined in the kinetic model.

[2] Results for different E_γ threshold values are also measured.

[3] The result is for $E_\gamma > 1.9$ GeV.

[4] Uses a fully reconstructed B meson as a tag on the recoil side.

$B^{\pm}/B^{0}$ ADMIXTURE REFERENCES

GRYGIER	17	PR D96 091101	J. Grygier *et al.*	(BELLE Collab.)
HIROSE	17	PRL 118 211801	S. Hirose *et al.*	(BELLE Collab.)
HORIGUCHI	17	PRL 119 191802	T. Horiguchi *et al.*	(BELLE Collab.)
LEES	17B	PR D95 072001	J.P. Lees *et al.*	(BABAR Collab.)
AAIJ	16B	JHEP 1602 104	R. Aaij *et al.*	(LHCb Collab.)
BHARDWAJ	16	PR D93 052016	V. Bhardwaj *et al.*	(BELLE Collab.)
KHACHATRY...	16D	PL B753 424	V. Khachatryan *et al.*	(CMS Collab.)
LEES	16	PRL 116 041801	J.P. Lees *et al.*	(BABAR Collab.)
LEES	16C	PR D93 052015	J.P. Lees *et al.*	(BABAR Collab.)
SATO	16	PR D93 032008	Y. Sato *et al.*	(BELLE Collab.)
Also		PR D93 059901 (errat.)	Y. Sato *et al.*	(BELLE Collab.)
HUSCHLE	15	PR D92 072014	M. Huschle *et al.*	(BELLE Collab.)
PESANTEZ	15	PRL 114 151601	L. Pesantez *et al.*	(BELLE Collab.)
SAITO	15	PR D91 052004	T. Saito *et al.*	(BELLE Collab.)
AAIJ	14AF	PRL 113 141801	R. Aaij *et al.*	(LHCb Collab.)
AAIJ	14M	JHEP 1406 133	R. Aaij *et al.*	(LHCb Collab.)
LEES	14D	PRL 112 211802	J.P. Lees *et al.*	(BABAR Collab.)
LEES	14K	PR D90 092001	J.P. Lees *et al.*	(BABAR Collab.)
AAIJ	13H	JHEP 1302 105	R. Aaij *et al.*	(LHCb Collab.)
AAIJ	13Y	JHEP 1308 131	R. Aaij *et al.*	(LHCb Collab.)
CHATRCHYAN	13BL	PL B727 77	S. Chatrchyan *et al.*	(CMS Collab.)
LEES	13I	PR D87 112005	J.P. Lees *et al.*	(BABAR Collab.)
LEES	13M	PR D88 032012	J.P. Lees *et al.*	(BABAR Collab.)
AAIJ	12AH	JHEP 1207 133	R. Aaij *et al.*	(LHCb Collab.)
AAIJ	12U	PRL 108 181806	R. Aaij *et al.*	(LHCb Collab.)
AALTONEN	12I	PRL 108 081807	T. Aaltonen *et al.*	(CDF Collab.)
LEES	12	PR D85 011102	J.P. Lees *et al.*	(BABAR Collab.)
LEES	12D	PRL 109 101802	J.P. Lees *et al.*	(BABAR Collab.)
Also		PR D88 072012	J.P. Lees *et al.*	(BABAR Collab.)
LEES	12R	PR D86 032004	J.P. Lees *et al.*	(BABAR Collab.)
LEES	12S	PR D86 032012	J.P. Lees *et al.*	(BABAR Collab.)
LEES	12U	PR D86 052012	J.P. Lees *et al.*	(BABAR Collab.)
LEES	12V	PRL 109 191801	J.P. Lees	(BABAR Collab.)
Also		PR D86 112008	J.P. Lees *et al.*	(BABAR Collab.)
AALTONEN	11AI	PRL 107 201802	T. Aaltonen *et al.*	(CDF Collab.)
AALTONEN	11L	PRL 106 161801	T. Aaltonen *et al.*	(CDF Collab.)
DEL-AMO-SA...	11	PR D83 031103	P. del Amo Sanchez *et al.*	(BABAR Collab.)
GAMBINO	11	JHEP 1109 055	P. Gambino	(LCGT)
AUBERT	10	PRL 104 011802	B. Aubert *et al.*	(BABAR Collab.)
AUBERT	10A	PR D81 032003	B. Aubert *et al.*	(BABAR Collab.)
AUSHEV	10	PR D81 031103	T. Aushev *et al.*	(BELLE Collab.)
DEL-AMO-SA...	10M	PR D82 051101	P. del Amo Sanchez *et al.*	(BABAR Collab.)
DEL-AMO-SA...	10Q	PR D82 112002	P. del Amo Sanchez *et al.*	(BABAR Collab.)
NISHIMURA	10	PRL 105 191803	K. Nishimura *et al.*	(BELLE Collab.)
URQUIJO	10	PRL 104 021801	P. Urquijo *et al.*	(BELLE Collab.)
AUBERT	09AO	PRL 103 211802	B. Aubert *et al.*	(BABAR Collab.)
AUBERT	09N	PR D79 031102	B. Aubert *et al.*	(BABAR Collab.)
AUBERT	09T	PRL 102 091803	B. Aubert *et al.*	(BABAR Collab.)
Also		EPAPS Document No. E-PRLTAO-102-060910		(BABAR Collab.)
AUBERT	09U	PRL 102 161803	B. Aubert *et al.*	(BABAR Collab.)
LIMOSANI	09	PRL 103 241801	A. Limosani *et al.*	(BELLE Collab.)
WEI	09A	PRL 103 171801	J.-T. Wei *et al.*	(BELLE Collab.)
Also		EPAPS Supplement EPAPS_appendix.pdf		(BELLE Collab.)
AUBERT	08AS	PRL 100 171802	B. Aubert *et al.*	(BABAR Collab.)
AUBERT	08BC	PR D78 072007	B. Aubert *et al.*	(BABAR Collab.)
AUBERT	08BH	PR D78 112001	B. Aubert *et al.*	(BABAR Collab.)
AUBERT	08BJ	PRL 101 171804	B. Aubert *et al.*	(BABAR Collab.)
AUBERT	08N	PRL 100 021801	B. Aubert *et al.*	(BABAR Collab.)
Also		PR D79 092002	B. Aubert *et al.*	(BABAR Collab.)
AUBERT	08O	PR D77 051103	B. Aubert *et al.*	(BABAR Collab.)
SCHWANDA	08	PR D78 032016	C. Schwanda *et al.*	(BELLE Collab.)
TANIGUCHI	08	PRL 101 111801	N. Taniguchi *et al.*	(BELLE Collab.)
WEI	08A	PR D78 011101	J.-T. Wei *et al.*	(BELLE Collab.)
AUBERT	07AG	PRL 99 051801	B. Aubert *et al.*	(BABAR Collab.)
AUBERT	07C	PR D75 012003	B. Aubert *et al.*	(BABAR Collab.)
AUBERT	07E	PRL 98 051802	B. Aubert *et al.*	(BABAR Collab.)
AUBERT	07L	PRL 98 151802	B. Aubert *et al.*	(BABAR Collab.)
GAMBINO	07	JHEP 0710 058	P. Gambino *et al.*	
HUANG	07	PR D75 012002	G.S. Huang *et al.*	(CLEO Collab.)
SCHWANDA	07	PR D75 032005	C. Schwanda *et al.*	(BELLE Collab.)
URQUIJO	07	PR D75 032001	P. Urquijo *et al.*	(BELLE Collab.)
AUBERT	06H	PR D73 012006	B. Aubert *et al.*	(BABAR Collab.)
AUBERT,B	06J	PR D73 092001	B. Aubert *et al.*	(BABAR Collab.)
AUBERT,B	06Y	PR D74 091105	B. Aubert *et al.*	(BABAR Collab.)
AUBERT,BE	06B	PRL 97 171803	B. Aubert *et al.*	(BABAR Collab.)
BUCHMUEL...	06	PR D73 073008	O.L. Buchmueller, H.U. Flacher	(RHBL)
GOKHROO	06	PRL 97 162002	G. Gokhroo *et al.*	(BELLE Collab.)
ISHIKAWA	06	PRL 96 251801	A. Ishikawa *et al.*	(BELLE Collab.)
MOHAPATRA	06	PRL 96 221601	D. Mohapatra *et al.*	(BELLE Collab.)
ABAZOV	05O	PRL 95 171803	V.M. Abazov *et al.*	(D0 Collab.)
ACOSTA	05F	PR D71 051103	D. Acosta *et al.*	(CDF Collab.)
ARTUSO	05B	PRL 95 261801	M. Artuso *et al.*	(CLEO Collab.)
AUBERT	05	PRL 94 011801	B. Aubert *et al.*	(BABAR Collab.)
AUBERT,B	05M	PRL 95 142003	B. Aubert *et al.*	(BABAR Collab.)
AUBERT,B	05R	PR D72 052004	B. Aubert *et al.*	(BABAR Collab.)
AUBERT,B	05X	PRL 95 111801	B. Aubert *et al.*	(BABAR Collab.)
Also		PRL 97 019903 (errat.)	B. Aubert *et al.*	(BABAR Collab.)
CHOI	05	PRL 94 182002	S.-K. Choi *et al.*	(BELLE Collab.)
IWASAKI	05	PR D72 092005	M. Iwasaki *et al.*	(BELLE Collab.)
LIMOSANI	05	PL B621 28	A. Limosani *et al.*	(BELLE Collab.)
MOHAPATRA	05	PR D72 011101	D. Mohapatra *et al.*	(BELLE Collab.)
NISHIDA	05	PL B610 23	S. Nishida *et al.*	(BELLE Collab.)
OKABE	05	PL B614 27	T. Okabe *et al.*	(BELLE Collab.)
ABDALLAH	04D	EPJ C33 213	J. Abdallah *et al.*	(DELPHI Collab.)
AUBERT	04C	PRL 92 111801	B. Aubert *et al.*	(BABAR Collab.)
AUBERT	04I	PRL 92 071802	B. Aubert *et al.*	(BABAR Collab.)
AUBERT	04S	PR D69 052005	B. Aubert *et al.*	(BABAR Collab.)
AUBERT	04X	PRL 93 011803	B. Aubert *et al.*	(BABAR Collab.)
AUBERT,B	04	PR D69 111103	B. Aubert *et al.*	(BABAR Collab.)
AUBERT,B	04A	PR D69 111104	B. Aubert *et al.*	(BABAR Collab.)
AUBERT,B	04E	PRL 93 021804	B. Aubert *et al.*	(BABAR Collab.)
AUBERT,B	04F	PRL 93 061801	B. Aubert *et al.*	(BABAR Collab.)
AUBERT,B	04I	PRL 93 081802	B. Aubert *et al.*	(BABAR Collab.)
AUBERT,BE	04A	PR D70 112006	B. Aubert *et al.*	(BABAR Collab.)
CSORNA	04	PR D70 032002	S.E. Csorna *et al.*	(CLEO Collab.)
KOPPENBURG	04	PRL 93 061803	P. Koppenburg *et al.*	(BELLE Collab.)
MAHMOOD	04	PR D70 032003	A.H. Mahmood *et al.*	(CLEO Collab.)
NAKAO	04	PR D69 112001	M. Nakao *et al.*	(BELLE Collab.)
NISHIDA	04	PRL 93 031803	S. Nishida *et al.*	(BELLE Collab.)
ADAM	03B	PR D68 012004	N.E. Adam *et al.*	(CLEO Collab.)
AUBERT	03	PR D67 031101	B. Aubert *et al.*	(BABAR Collab.)
AUBERT	03F	PR D67 032002	B. Aubert *et al.*	(BABAR Collab.)
AUBERT	03U	PRL 91 221802	B. Aubert *et al.*	(BABAR Collab.)
BONVICINI	03	PR D68 011101	G. Bonvicini *et al.*	(CLEO Collab.)
HUANG	03	PRL 91 241802	H.-C. Huang *et al.*	(BELLE Collab.)
ISHIKAWA	03	PRL 91 261601	A. Ishikawa *et al.*	(BELLE Collab.)
KANEKO	03	PRL 90 021801	J. Kaneko *et al.*	(BELLE Collab.)
KROKOVNY	03B	PRL 91 262002	P. Krokovny *et al.*	(BELLE Collab.)
MAHMOOD	03	PR D67 072001	A.H. Mahmood *et al.*	(CLEO Collab.)
ABE	02	PRL 88 021801	K. Abe *et al.*	(BELLE Collab.)
ABE	02L	PRL 89 011803	K. Abe *et al.*	(BELLE Collab.)
ABE	02Y	PL B547 181	K. Abe *et al.*	(BELLE Collab.)
ANDERSON	02	PRL 89 282001	S. Anderson *et al.*	(CLEO Collab.)
AUBERT	02C	PRL 88 101805	B. Aubert *et al.*	(BABAR Collab.)
AUBERT	02G	PR D65 091104	B. Aubert *et al.*	(BABAR Collab.)
AUBERT	02L	PRL 88 241801	B. Aubert *et al.*	(BABAR Collab.)
BORNHEIM	02	PRL 88 231803	A. Bornheim *et al.*	(CLEO Collab.)
EDWARDS	02B	PR D65 111102	K.W. Edwards *et al.*	(CLEO Collab.)
ABE	01F	PL B511 151	K. Abe *et al.*	(BELLE Collab.)
ABE	01J	PR D64 072001	K. Abe *et al.*	(BELLE Collab.)
ANDERSON	01B	PRL 87 181803	S. Anderson *et al.*	(CLEO Collab.)
CHEN	01	PR D63 031102	S. Chen *et al.*	(CLEO Collab.)
CHEN	01C	PRL 87 251807	S. Chen *et al.*	(CLEO Collab.)
COAN	01	PRL 86 5661	T.E. Coan *et al.*	(CLEO Collab.)
CRONIN-HEN...	01B	PRL 87 251808	D. Cronin-Hennessy *et al.*	(CLEO Collab.)
PDG	01	Unofficial 2001 WWW edition		
ABREU	00R	PL B475 407	P. Abreu *et al.*	(DELPHI Collab.)
COAN	00	PRL 84 5283	T.E. Coan *et al.*	(CLEO Collab.)
RICHICHI	00	PRL 85 520	S.J. Richichi *et al.*	(CLEO Collab.)
BARATE	98Q	EPJ C4 387	R. Barate *et al.*	(ALEPH Collab.)
BERGFELD	98	PRL 81 272	T. Bergfeld *et al.*	(CLEO Collab.)
BISHAI	98	PR D57 3847	M. Bishai *et al.*	(CLEO Collab.)
BONVICINI	98	PR D57 6604	G. Bonvicini *et al.*	(CLEO Collab.)
BROWDER	98	PRL 81 1786	T.E. Browder *et al.*	(CLEO Collab.)
COAN	98	PRL 80 1150	T.E. Coan *et al.*	(CLEO Collab.)
GLENN	98	PRL 80 2289	S. Glenn *et al.*	(CLEO Collab.)
ACKERSTAFF	97N	ZPHY C74 423	K. Ackerstaff *et al.*	(OPAL Collab.)
AMMAR	97	PR D55 13	R. Ammar *et al.*	(CLEO Collab.)
BARISH	97	PRL 79 3599	B. Barish *et al.*	(CLEO Collab.)
BUSKULIC	97B	ZPHY C73 601	D. Buskulic *et al.*	(ALEPH Collab.)
GIBBONS	97B	PR D56 3783	L. Gibbons *et al.*	(CLEO Collab.)
ALBRECHT	96D	PL B374 256	H. Albrecht *et al.*	(ARGUS Collab.)
BARISH	96B	PRL 76 1570	B.C. Barish *et al.*	(CLEO Collab.)
GIBAUT	96	PR D53 4734	D. Gibaut *et al.*	(CLEO Collab.)
KUBOTA	96	PR D53 6033	Y. Kubota *et al.*	(CLEO Collab.)
PDG	96	PR D54 1	R. M. Barnett *et al.*	(PDG Collab.)
ALAM	95	PRL 74 2885	M.S. Alam *et al.*	(CLEO Collab.)
ALBRECHT	95D	PL B353 554	H. Albrecht *et al.*	(ARGUS Collab.)
BALEST	95B	PR D52 2661	R. Balest *et al.*	(CLEO Collab.)
BARISH	95	PR D51 1014	B.C. Barish *et al.*	(CLEO Collab.)
BUSKULIC	95B	PL B345 103	D. Buskulic *et al.*	(ALEPH Collab.)
ALBRECHT	94C	ZPHY C62 371	H. Albrecht *et al.*	(ARGUS Collab.)
ALBRECHT	94J	ZPHY C61 1	H. Albrecht *et al.*	(ARGUS Collab.)
PROCARIO	94	PRL 73 1472	M. Procario *et al.*	(CLEO Collab.)
ALBRECHT	93	ZPHY C57 533	H. Albrecht *et al.*	(ARGUS Collab.)
ALBRECHT	93E	ZPHY C60 11	H. Albrecht *et al.*	(ARGUS Collab.)
ALBRECHT	93H	PL B318 397	H. Albrecht *et al.*	(ARGUS Collab.)
ALBRECHT	93I	ZPHY C58 191	H. Albrecht *et al.*	(ARGUS Collab.)
ALEXANDER	93B	PL B319 365	J. Alexander *et al.*	(CLEO Collab.)
ARTUSO	93	PL B311 307	M. Artuso	(SYRA)
BARTELT	93B	PRL 71 4111	J.E. Bartelt *et al.*	(CLEO Collab.)
ALBRECHT	92E	PL B277 209	H. Albrecht *et al.*	(ARGUS Collab.)
ALBRECHT	92G	ZPHY C54 1	H. Albrecht *et al.*	(ARGUS Collab.)
ALBRECHT	92O	ZPHY C56 1	H. Albrecht *et al.*	(ARGUS Collab.)
BORTOLETTO	92	PR D45 21	D. Bortoletto *et al.*	(CLEO Collab.)
CRAWFORD	92	PR D45 752	G. Crawford *et al.*	(CLEO Collab.)
HENDERSON	92	PR D45 2212	S. Henderson *et al.*	(CLEO Collab.)
LESIAK	92	ZPHY C55 33	T. Lesiak *et al.*	(Crystal Ball Collab.)
ALBRECHT	91C	PL B255 297	H. Albrecht *et al.*	(ARGUS Collab.)
ALBRECHT	91H	ZPHY C52 353	H. Albrecht *et al.*	(ARGUS Collab.)
FULTON	91	PR D43 651	R. Fulton *et al.*	(CLEO Collab.)
YANAGISAWA	91	PRL 66 2436	C. Yanagisawa *et al.*	(CUSB II Collab.)
ALBRECHT	90	PL B234 409	H. Albrecht *et al.*	(ARGUS Collab.)
ALBRECHT	90H	PL B249 359	H. Albrecht *et al.*	(ARGUS Collab.)
BORTOLETTO	90	PRL 64 2117	D. Bortoletto *et al.*	(CLEO Collab.)
Also		PR D45 21	D. Bortoletto *et al.*	(CLEO Collab.)
FULTON	90	PRL 64 16	R. Fulton *et al.*	(CLEO Collab.)
MASCHMANN	90	ZPHY C46 555	W.S. Maschmann *et al.*	(Crystal Ball Collab.)
PDG	90	PL B239 1	J.J. Hernandez *et al.*	(IFIC, BOST, CIT+)
ALBRECHT	89K	ZPHY C42 519	H. Albrecht *et al.*	(ARGUS Collab.)
ISGUR	89B	PR D39 799	N. Isgur *et al.*	(TNTO, CIT)
WACHS	89	ZPHY C42 33	K. Wachs *et al.*	(Crystal Ball Collab.)
ALBRECHT	88E	PL B210 263	H. Albrecht *et al.*	(ARGUS Collab.)
ALBRECHT	88H	PL B210 258	H. Albrecht *et al.*	(ARGUS Collab.)
KOERNER	88	ZPHY C38 511	J.G. Korner, G.A. Schuler	(MANZ, DESY)
ALAM	87	PRL 59 22	M.S. Alam *et al.*	(CLEO Collab.)
ALAM	87B	PRL 58 1814	M.S. Alam *et al.*	(CLEO Collab.)
ALBRECHT	87D	PL B199 451	H. Albrecht *et al.*	(ARGUS Collab.)
ALBRECHT	87H	PL B187 425	H. Albrecht *et al.*	(ARGUS Collab.)
BEAN	87	PR D35 3533	A. Bean *et al.*	(CLEO Collab.)
BEHRENDS	87	PRL 59 407	S. Behrends *et al.*	(CLEO Collab.)
BORTOLETTO	87	PR D35 19	D. Bortoletto *et al.*	(CLEO Collab.)
ALAM	86	PR D34 3279	M.S. Alam *et al.*	(CLEO Collab.)
BALTRUSAIT...	86E	PRL 56 2140	R.M. Baltrusaitis *et al.*	(Mark III Collab.)
BORTOLETTO	86	PRL 56 800	D. Bortoletto *et al.*	(CLEO Collab.)
HAAS	86	PRL 56 2781	J. Haas *et al.*	(CLEO Collab.)
ALBRECHT	85H	PL 162B 395	H. Albrecht *et al.*	(ARGUS Collab.)
CSORNA	85	PRL 54 1894	S.E. Csorna *et al.*	(CLEO Collab.)
HAAS	85	PRL 55 1248	J. Haas *et al.*	(CLEO Collab.)
AVERY	84	PRL 53 1309	P. Avery *et al.*	(CLEO Collab.)
CHEN	84	PRL 52 1084	A. Chen *et al.*	(CLEO Collab.)
LEVMAN	84	PL 141B 271	G.M. Levman *et al.*	(CUSB Collab.)
ALAM	83B	PRL 51 1143	M.S. Alam *et al.*	(CLEO Collab.)
GREEN	83	PRL 51 347	J. Green *et al.*	(CLEO Collab.)
KLOPFEN...	83B	PL 130B 444	C. Klopfenstein *et al.*	(CUSB Collab.)
ALTARELLI	82	NP B208 365	G. Altarelli *et al.*	(ROMA, INFN, FRAS)
BRODY	82	PRL 48 1070	A.D. Brody *et al.*	(CLEO Collab.)
GIANNINI	82	NP B206 1	G. Giannini *et al.*	(CUSB Collab.)
BEBEK	81	PRL 46 84	C. Bebek *et al.*	(CLEO Collab.)
CHADWICK	81	PRL 46 88	K. Chadwick *et al.*	(CLEO Collab.)
ABRAMS	80	PRL 44 10	G.S. Abrams *et al.*	(SLAC, LBL)

$B^{\pm}/B^0/B^0_s$/b-baryon ADMIXTURE

$B^{\pm}/B^0/B^0_s$/b-baryon ADMIXTURE MEAN LIFE

Each measurement of the B mean life is an average over an admixture of various bottom mesons and baryons which decay weakly. Different techniques emphasize different admixtures of produced particles, which could result in a different B mean life.

"OUR EVALUATION" is an average using rescaled values of the data listed below. The average and rescaling were performed by the Heavy Flavor Averaging Group (HFLAV) and are described at http://www.slac.stanford.edu/xorg/hflav/. This is a weighted average of the lifetimes of the five main b-hadron species (B^+, B^0, B^0_{sH}, B^0_{sL}, and Λ_b) that assumes the production fractions in Z decays (given at the end of this section) and equal production fractions of B^0_{sH} and B^0_{sL} mesons.

VALUE (10^{-12} s)	EVTS	DOCUMENT ID		TECN	COMMENT
1.566±0.003 OUR EVALUATION					
• • • We do not use the following data for averages, fits, limits, etc. • • •					
1.570±0.005±0.008		[1] ABDALLAH	04E	DLPH	$e^+e^- \to Z$
$1.533\pm0.015^{+0.035}_{-0.031}$		[2] ABE	98B	CDF	$p\overline{p}$ at 1.8 TeV
1.549±0.009±0.015		[3] ACCIARRI	98	L3	$e^+e^- \to Z$
1.611±0.010±0.027		[4] ACKERSTAFF	97F	OPAL	$e^+e^- \to Z$
1.582±0.011±0.027		[4] ABREU	96E	DLPH	$e^+e^- \to Z$
1.575±0.010±0.026		[5] ABREU	96E	DLPH	$e^+e^- \to Z$
1.533±0.013±0.022	19.8k	[6] BUSKULIC	96F	ALEP	$e^+e^- \to Z$
1.564±0.030±0.036		[7] ABE,K	95B	SLD	$e^+e^- \to Z$
1.542±0.021±0.045		[8] ABREU	94L	DLPH	$e^+e^- \to Z$
$1.50\ ^{+0.24}_{-0.21}\ \pm0.03$		[9] ABREU	94P	DLPH	$e^+e^- \to Z$
1.46 ±0.06 ±0.06	5344	[10] ABE	93J	CDF	Repl. by ABE 98B
$1.23\ ^{+0.14}_{-0.13}\ \pm0.15$	188	[11] ABREU	93D	DLPH	Sup. by ABREU 94L
1.49 ±0.11 ±0.12	253	[12] ABREU	93G	DLPH	Sup. by ABREU 94L
$1.51\ ^{+0.16}_{-0.14}\ \pm0.11$	130	[13] ACTON	93C	OPAL	$e^+e^- \to Z$
1.523±0.034±0.038	5372	[14] ACTON	93L	OPAL	$e^+e^- \to Z$
1.535±0.035±0.028	7357	[14] ADRIANI	93K	L3	Repl. by ACCIARRI 98
1.511±0.022±0.078		[15] BUSKULIC	93O	ALEP	$e^+e^- \to Z$
1.28 ±0.10		[16] ABREU	92	DLPH	Sup. by ABREU 94L
1.37 ±0.07 ±0.06	1354	[17] ACTON	92	OPAL	Sup. by ACTON 93L
1.49 ±0.03 ±0.06		[18] BUSKULIC	92F	ALEP	Sup. by BUSKULIC 96F
$1.35\ ^{+0.19}_{-0.17}\ \pm0.05$		[19] BUSKULIC	92G	ALEP	$e^+e^- \to Z$
1.32 ±0.08 ±0.09	1386	[20] ADEVA	91H	L3	Sup. by ADRIANI 93K
$1.32\ ^{+0.31}_{-0.25}\ \pm0.15$	37	[21] ALEXANDER	91G	OPAL	$e^+e^- \to Z$
1.29 ±0.06 ±0.10	2973	[22] DECAMP	91C	ALEP	Sup. by BUSKULIC 92F
$1.36\ ^{+0.25}_{-0.23}$		[23] HAGEMANN	90	JADE	E^{ee}_{cm}= 35 GeV
1.13 ±0.15		[24] LYONS	90	RVUE	
1.35 ±0.10 ±0.24		BRAUNSCH...	89B	TASS	E^{ee}_{cm}= 35 GeV
0.98 ±0.12 ±0.13		ONG	89	MRK2	E^{ee}_{cm}= 29 GeV
$1.17\ ^{+0.27}_{-0.22}\ ^{+0.17}_{-0.16}$		KLEM	88	DLCO	E^{ee}_{cm}= 29 GeV
1.29 ±0.20 ±0.21		[25] ASH	87	MAC	E^{ee}_{cm}= 29 GeV
$1.02\ ^{+0.42}_{-0.39}$	301	[26] BROM	87	HRS	E^{ee}_{cm}= 29 GeV

[1] Measurement performed using an inclusive reconstruction and B flavor identification technique.
[2] Measured using inclusive $J/\psi(1S) \to \mu^+\mu^-$ vertex.
[3] ACCIARRI 98 uses inclusively reconstructed secondary vertex and lepton impact parameter.
[4] ACKERSTAFF 97F uses inclusively reconstructed secondary vertices.
[5] Combines ABREU 96E secondary vertex result with ABREU 94L impact parameter result.
[6] BUSKULIC 96F analyzed using 3D impact parameter.
[7] ABE,K 95B uses an inclusive topological technique.
[8] ABREU 94L uses charged particle impact parameters. Their result from inclusively reconstructed secondary vertices is superseded by ABREU 96E.
[9] From proper time distribution of $b \to J/\psi(1S)$ anything.
[10] ABE 93J analyzed using $J/\psi(1S) \to \mu\mu$ vertices.
[11] ABREU 93D data analyzed using $D/D^*\ell$anything event vertices.
[12] ABREU 93G data analyzed using charged and neutral vertices.
[13] ACTON 93C analysed using $D/D^*\ell$anything event vertices.
[14] ACTON 93L and ADRIANI 93K analyzed using lepton (e and μ) impact parameter at Z.
[15] BUSKULIC 93O analyzed using dipole method.
[16] ABREU 92 is combined result of muon and hadron impact parameter analyses. Hadron tracks gave $(12.7 \pm 0.4 \pm 1.2) \times 10^{-13}$ s for an admixture of B species weighted by production fraction and mean charge multiplicity, while muon tracks gave $(13.0 \pm 1.0 \pm 0.8) \times 10^{-13}$ s for an admixture weighted by production fraction and semileptonic branching fraction.
[17] ACTON 92 is combined result of muon and electron impact parameter analyses.
[18] BUSKULIC 92F uses the lepton impact parameter distribution for data from the 1991 run.
[19] BUSKULIC 92G use $J/\psi(1S)$ tags to measure the average b lifetime. This is comparable to other methods only if the $J/\psi(1S)$ branching fractions of the different b-flavored hadrons are in the same ratio.
[20] Using $Z \to e^+$X or μ^+X, ADEVA 91H determined the average lifetime for an admixture of B hadrons from the impact parameter distribution of the lepton.
[21] Using $Z \to J/\psi(1S)$X, $J/\psi(1S) \to \ell^+\ell^-$, ALEXANDER 91G determined the average lifetime for an admixture of B hadrons from the decay point of the $J/\psi(1S)$.
[22] Using $Z \to e$X or μX, DECAMP 91C determines the average lifetime for an admixture of B hadrons from the signed impact parameter distribution of the lepton.
[23] HAGEMANN 90 uses electrons and muons in an impact parameter analysis.
[24] LYONS 90 combine the results of the B lifetime measurements of ONG 89, BRAUNSCHWEIG 89B, KLEM 88, and ASH 87, and JADE data by private communication. They use statistical techniques which include variation of the error with the mean life, and possible correlations between the systematic errors. This result is not independent of the measured results used in our average.
[25] We have combined an overall scale error of 15% in quadrature with the systematic error of ±0.7 to obtain ±2.1 systematic error.
[26] Statistical and systematic errors were combined by BROM 87.

CHARGED b-HADRON ADMIXTURE MEAN LIFE

VALUE (10^{-12} s)	DOCUMENT ID		TECN	COMMENT
1.72±0.08±0.06	[1] ADAM	95	DLPH	$e^+e^- \to Z$

[1] ADAM 95 data analyzed using vertex-charge technique to tag b-hadron charge.

NEUTRAL b-HADRON ADMIXTURE MEAN LIFE

VALUE (10^{-12} s)	DOCUMENT ID		TECN	COMMENT
1.58±0.11±0.09	[1] ADAM	95	DLPH	$e^+e^- \to Z$

[1] ADAM 95 data analyzed using vertex-charge technique to tag b-hadron charge.

MEAN LIFE RATIO $\tau_{\text{charged } b\text{-hadron}}/\tau_{\text{neutral } b\text{-hadron}}$

VALUE	DOCUMENT ID		TECN	COMMENT
$\mathbf{1.09^{+0.11}_{-0.10}\pm0.08}$	[1] ADAM	95	DLPH	$e^+e^- \to Z$

[1] ADAM 95 data analyzed using vertex-charge technique to tag b-hadron charge.

$|\Delta\tau_b|/\tau_{b,\overline{b}}$

$\tau_{b,\overline{b}}$ and $|\Delta\tau_b|$ are the mean life average and difference between b and $\overline{b}$ hadrons.

VALUE	DOCUMENT ID		TECN	COMMENT
−0.001±0.012±0.008	[1] ABBIENDI	99J	OPAL	$e^+e^- \to Z$

[1] Data analyzed using both the jet charge and the charge of secondary vertex in the opposite hemisphere.

$\overline{b}$ PRODUCTION FRACTIONS AND DECAY MODES

The branching fraction measurements are for an admixture of B mesons and baryons at energies above the $\Upsilon(4S)$. Only the highest energy results (LHC, LEP, Tevatron, S$p\overline{p}$S) are used in the branching fraction averages. In the following, we assume that the production fractions are the same at the LHC, LEP, and at the Tevatron.

For inclusive branching fractions, *e.g.*, $B \to D^{\pm}$anything, the values usually are multiplicities, not branching fractions. They can be greater than one.

The modes below are listed for a $\overline{b}$ initial state. b modes are their charge conjugates. Reactions indicate the weak decay vertex and do not include mixing.

Mode	Fraction (Γ_i/Γ)	Scale factor/ Confidence level

PRODUCTION FRACTIONS

The production fractions for weakly decaying b-hadrons at high energy have been calculated from the best values of mean lives, mixing parameters, and branching fractions in this edition by the Heavy Flavor Averaging Group (HFLAV) as described in the note "B^0-$\overline{B}^0$ Mixing" in the B^0 Particle Listings. The production fractions in b-hadronic Z decay or $p\overline{p}$ collisions at the Tevatron are also listed at the end of the section. Values assume

$$\mathrm{B}(\overline{b} \to B^+) = \mathrm{B}(\overline{b} \to B^0)$$
$$\mathrm{B}(\overline{b} \to B^+) + \mathrm{B}(\overline{b} \to B^0) + \mathrm{B}(\overline{b} \to B^0_s) + \mathrm{B}(b \to b\text{-baryon}) = 100\%.$$

The correlation coefficients between production fractions are also reported:

$cor(B^0_s, b\text{-baryon}) = -0.259$
$cor(B^0_s, B^{\pm}{=}B^0) = -0.133$
$cor(b\text{-baryon}, B^{\pm}{=}B^0) = -0.923.$

The notation for production fractions varies in the literature (f_d, d_{B^0}, $f(b \to \overline{B}^0)$, $\mathrm{Br}(b \to \overline{B}^0)$). We use our own branching fraction notation here, $\mathrm{B}(\overline{b} \to B^0)$.

Meson Particle Listings

$B^{\pm}/B^0/B_s^0/b$-baryon ADMIXTURE

Note these production fractions are b-hadronization fractions, not the conventional branching fractions of b-quark to a B-hadron, which may have considerable dependence on the initial and final state kinematic and production environment.

Γ_1	B^+	(40.5 ± 0.6) %	
Γ_2	B^0	(40.5 ± 0.6) %	
Γ_3	B_s^0	(10.1 ± 0.4) %	
Γ_4	b-baryon	(8.9 ± 1.2) %	

DECAY MODES

Semileptonic and leptonic modes

Γ_5	ν anything	(23.1 ± 1.5) %		
Γ_6	$\ell^+ \nu_\ell$ anything	[a]	(10.69 ± 0.22) %	
Γ_7	$e^+ \nu_e$ anything		(10.86 ± 0.35) %	
Γ_8	$\mu^+ \nu_\mu$ anything		(10.95 $^{+0.29}_{-0.25}$) %	
Γ_9	$D^- \ell^+ \nu_\ell$ anything	[a]	(2.30 ± 0.34) %	S=1.6
Γ_{10}	$D^- \pi^+ \ell^+ \nu_\ell$ anything		(4.9 ± 1.9) × 10^{-3}	
Γ_{11}	$D^- \pi^- \ell^+ \nu_\ell$ anything		(2.6 ± 1.6) × 10^{-3}	
Γ_{12}	$\overline{D}^0 \ell^+ \nu_\ell$ anything	[a]	(6.83 ± 0.35) %	
Γ_{13}	$\overline{D}^0 \pi^- \ell^+ \nu_\ell$ anything		(1.07 ± 0.27) %	
Γ_{14}	$\overline{D}^0 \pi^+ \ell^+ \nu_\ell$ anything		(2.3 ± 1.6) × 10^{-3}	
Γ_{15}	$D^{*-} \ell^+ \nu_\ell$ anything	[a]	(2.75 ± 0.19) %	
Γ_{16}	$D^{*-} \pi^- \ell^+ \nu_\ell$ anything		(6 ± 7) × 10^{-4}	
Γ_{17}	$D^{*-} \pi^+ \ell^+ \nu_\ell$ anything		(4.8 ± 1.0) × 10^{-3}	
Γ_{18}	$\overline{D}_j^0 \ell^+ \nu_\ell$ anything × B($\overline{D}_j^0 \to D^{*+} \pi^-$)	[a,b]	(2.6 ± 0.9) × 10^{-3}	
Γ_{19}	$D_j^- \ell^+ \nu_\ell$ anything × B($D_j^- \to D^0 \pi^-$)	[a,b]	(7.0 ± 2.3) × 10^{-3}	
Γ_{20}	$\overline{D}_2^*(2460)^0 \ell^+ \nu_\ell$ anything × B($\overline{D}_2^*(2460)^0 \to D^{*-} \pi^+$)	<	1.4 × 10^{-3}	CL=90%
Γ_{21}	$D_2^*(2460)^- \ell^+ \nu_\ell$ anything × B($D_2^*(2460)^- \to D^0 \pi^-$)		(4.2 $^{+1.5}_{-1.8}$) × 10^{-3}	
Γ_{22}	$\overline{D}_2^*(2460)^0 \ell^+ \nu_\ell$ anything × B($\overline{D}_2^*(2460)^0 \to D^- \pi^+$)		(1.6 ± 0.8) × 10^{-3}	
Γ_{23}	charmless $\ell \overline{\nu}_\ell$	[a]	(1.7 ± 0.5) × 10^{-3}	
Γ_{24}	$\tau^+ \nu_\tau$ anything		(2.41 ± 0.23) %	
Γ_{25}	$D^{*-} \tau \nu_\tau$ anything		(9 ± 4) × 10^{-3}	
Γ_{26}	$\overline{c} \to \ell^- \overline{\nu}_\ell$ anything	[a]	(8.02 ± 0.19) %	
Γ_{27}	$c \to \ell^+ \nu$ anything		(1.6 $^{+0.4}_{-0.5}$) %	

Charmed meson and baryon modes

Γ_{28}	$\overline{D}^0$ anything	(59.5 ± 2.9) %		
Γ_{29}	$D^0 D_s^{\pm}$ anything	[c]	(9.1 $^{+4.0}_{-2.8}$) %	
Γ_{30}	$D^{\mp} D_s^{\pm}$ anything	[c]	(4.0 $^{+2.3}_{-1.8}$) %	
Γ_{31}	$\overline{D}^0 D^0$ anything	[c]	(5.1 $^{+2.0}_{-1.8}$) %	
Γ_{32}	$D^0 D^{\pm}$ anything	[c]	(2.7 $^{+1.8}_{-1.6}$) %	
Γ_{33}	$D^{\pm} D^{\mp}$ anything	[c] <	9 × 10^{-3}	CL=90%
Γ_{34}	D^0 anything			
Γ_{35}	D^+ anything			
Γ_{36}	D^- anything	(23.7 ± 1.8) %		
Γ_{37}	$D^*(2010)^+$ anything	(17.3 ± 2.0) %		
Γ_{38}	$D_1(2420)^0$ anything	(5.0 ± 1.5) %		
Γ_{39}	$D^*(2010)^{\mp} D_s^{\pm}$ anything	[c]	(3.3 $^{+1.6}_{-1.3}$) %	
Γ_{40}	$D^0 D^*(2010)^{\pm}$ anything	[c]	(3.0 $^{+1.1}_{-0.9}$) %	
Γ_{41}	$D^*(2010)^{\pm} D^{\mp}$ anything	[c]	(2.5 $^{+1.2}_{-1.0}$) %	
Γ_{42}	$D^*(2010)^{\pm} D^*(2010)^{\mp}$ anything	[c]	(1.2 ± 0.4) %	
Γ_{43}	$\overline{D} D$ anything	(10 $^{+11}_{-10}$) %		
Γ_{44}	$D_2^*(2460)^0$ anything	(4.7 ± 2.7) %		
Γ_{45}	D_s^- anything	(14.7 ± 2.1) %		
Γ_{46}	D_s^+ anything	(10.1 ± 3.1) %		
Γ_{47}	Λ_c^+ anything	(7.8 ± 1.2) %		
Γ_{48}	$\overline{c}/c$ anything	[d]	(116.2 ± 3.2) %	

Charmonium modes

Γ_{49}	$J/\psi(1S)$ anything	(1.16 ± 0.10) %		
Γ_{50}	$\psi(2S)$ anything	(2.86 ± 0.28) × 10^{-3}		
Γ_{51}	$\chi_{c0}(1P)$ anything	(1.5 ± 0.6) %		
Γ_{52}	$\chi_{c1}(1P)$ anything	(1.4 ± 0.4) %		
Γ_{53}	$\chi_{c2}(1P)$ anything	(6.2 ± 2.9) × 10^{-3}		
Γ_{54}	$\chi_c(2P)$ anything, $\chi_c \to \phi\phi$	<	2.8 × 10^{-7}	CL=95%
Γ_{55}	$\eta_c(1S)$ anything	(4.5 ± 1.9) %		
Γ_{56}	$\eta_c(2S)$ anything, $\eta_c \to \phi\phi$	(3.2 ± 1.7) × 10^{-6}		
Γ_{57}	$\chi_{c1}(3872)$ anything, $\chi_{c1} \to \phi\phi$	<	4.5 × 10^{-7}	CL=95%
Γ_{58}	$X(3915)$ anything, $X \to \phi\phi$	<	3.1 × 10^{-7}	CL=95%

K or K^* modes

Γ_{59}	$\overline{s}\gamma$		(3.1 ± 1.1) × 10^{-4}		
Γ_{60}	$\overline{s}\overline{\nu}\nu$	B1	<	6.4 × 10^{-4}	CL=90%
Γ_{61}	$K^{\pm}$ anything		(74 ± 6) %		
Γ_{62}	K_S^0 anything		(29.0 ± 2.9) %		

Pion modes

Γ_{63}	$\pi^{\pm}$ anything		(397 ±21) %	
Γ_{64}	π^0 anything	[d]	(278 ±60) %	
Γ_{65}	ϕ anything		(2.82 ± 0.23) %	

Baryon modes

Γ_{66}	$p/\overline{p}$ anything	(13.1 ± 1.1) %		
Γ_{67}	$\Lambda/\overline{\Lambda}$ anything	(5.9 ± 0.6) %		
Γ_{68}	b-baryon anything	(10.2 ± 2.8) %		

Other modes

Γ_{69}	charged anything	[d]	(497 ± 7) %	
Γ_{70}	hadron$^+$ hadron$^-$		(1.7 $^{+1.0}_{-0.7}$) × 10^{-5}	
Γ_{71}	charmless		(7 ±21) × 10^{-3}	

$\Delta B = 1$ weak neutral current ($B1$) modes

Γ_{72}	$e^+ e^-$ anything	B1			
Γ_{73}	$\mu^+ \mu^-$ anything	B1	<	3.2 × 10^{-4}	CL=90%
Γ_{74}	$\nu\overline{\nu}$ anything	B1			

[a] An ℓ indicates an e or a μ mode, not a sum over these modes.

[b] D_j represents an unresolved mixture of pseudoscalar and tensor D^{**} (P-wave) states.

[c] The value is for the sum of the charge states or particle/antiparticle states indicated.

[d] Inclusive branching fractions have a multiplicity definition and can be greater than 100%.

$B^{\pm}/B^0/B_s^0/b$-baryon ADMIXTURE BRANCHING RATIOS

$\Gamma(B^+)/\Gamma_{total}$ Γ_1/Γ

"OUR EVALUATION" is an average using rescaled values of the data listed below and from the best values of mean lives, mixing parameters, and branching fractions in this edition by the Heavy Flavor Averaging Group (HFLAV) as described at http://www.slac.stanford.edu/xorg/hflav/.

VALUE	DOCUMENT ID		TECN	COMMENT
0.405 ±0.006 OUR EVALUATION				
0.4099±0.0082±0.0111	[1] ABDALLAH	03K	DLPH	$e^+e^- \to Z$

[1] The analysis is based on a neural network, to estimate the charge of the weakly-decaying b hadron by distinguishing its decay products from particles produced at the primary vertex.

$\Gamma(B^+)/\Gamma(B^0)$ Γ_1/Γ_2

VALUE	DOCUMENT ID		TECN	COMMENT
1.054±0.018 $^{+0.062}_{-0.074}$	AALTONEN	08N	CDF	$p\overline{p}$ at 1.96 TeV

$\Gamma(B_s^0)/[\Gamma(B^+) + \Gamma(B^0)]$ $\Gamma_3/(\Gamma_1+\Gamma_2)$

VALUE	DOCUMENT ID		TECN	COMMENT
0.125 ±0.006 OUR EVALUATION				
0.134 ±0.008 OUR AVERAGE				
0.134 ±0.004 $^{+0.011}_{-0.010}$	[1] AAIJ	12J	LHCB	pp at 7 TeV
0.1265 ±0.0085 ±0.0131	[2] AAIJ	11F	LHCB	pp at 7 TeV
0.128 $^{+0.011}_{-0.010}$ ±0.011	[3] AALTONEN	08N	CDF	$p\overline{p}$ at 1.96 TeV
0.213 ±0.068	[4] AFFOLDER	00E	CDF	$p\overline{p}$ at 1.8 TeV
0.21 ±0.036 $^{+0.038}_{-0.030}$	[5] ABE	99P	CDF	$p\overline{p}$ at 1.8 TeV

[1] Measured using b-hadron semileptonic decays and assuming isospin symmetry.

[2] AAIJ 11F measured $f_s/f_d = 0.253 \pm 0.017 \pm 0.017 \pm 0.020$, where the errors are statistical, systematic, and theoretical. We divide their value by 2. Our second error combines systematic and theoretical uncertainties.

[3] AALTONEN 08N reports $[\Gamma(\overline{b} \to B^0_s)/[\Gamma(\overline{b} \to B^+) + \Gamma(\overline{b} \to B^0)]] \times [B(D^+_s \to \phi\pi^+)] = (5.76 \pm 0.18^{+0.45}_{-0.42}) \times 10^{-3}$ which we divide by our best value $B(D^+_s \to \phi\pi^+) = (4.5 \pm 0.4) \times 10^{-2}$. Our first error is their experiment's error and our second error is the systematic error from using our best value.

[4] AFFOLDER 00E uses several electron-charm final states in $b \to ce^-X$.

[5] ABE 99P uses the numbers of $K^*(892)^0$, $K^*(892)^+$, and $\phi(1020)$ events produced in association with the double semileptonic decays $b \to c\mu^-X$ with $c \to s\mu^+X$.

$\Gamma(B^0_s)/\Gamma(B^0)$ Γ_3/Γ_2

VALUE	DOCUMENT ID		TECN	COMMENT
0.250±0.012 OUR EVALUATION				
0.239±0.016 OUR AVERAGE				
0.240±0.004±0.020	[1] AAD	15CM	ATLS	pp at 7 TeV
0.238±0.004±0.015±0.021	[2] AAIJ	13P	LHCB	pp at 7 TeV

[1] The measurement is derived from the observed $B^0_s \to J/\psi\phi$ and $B^0_d \to J/\psi K^{*0}$ yields and a recent theory prediction of $B(B^0_s \to J/\psi\phi)/B(B^0_d \to J/\psi K^{*0})$. The second uncertainty combines in quadrature systematic and theoretical uncertainties.

[2] AAIJ 13P studies also separately the $p_T(B)$ and $\eta(B)$ dependency of $\Gamma(\overline{b} \to B^0_s)/\Gamma(\overline{b} \to B^0)$, finding $f_s/f_d(p_T) = (0.256 \pm 0.020) + (-2.0 \pm 0.6)\ 10^{-3}$ /GeV/c $(p_T - \langle p_T \rangle)$ and $f_s/f_d(\eta) = (0.256 \pm 0.020) + (0.005 \pm 0.006)\ (\eta - \langle\eta\rangle)$, where $\langle p_T \rangle = 10.4$ GeV/c and $\langle\eta\rangle = 3.28$.

$\Gamma(b\text{-baryon})/[\Gamma(B^+) + \Gamma(B^0)]$ $\Gamma_4/(\Gamma_1+\Gamma_2)$

VALUE	DOCUMENT ID		TECN	COMMENT
0.110±0.016 OUR EVALUATION				
0.27 $^{+0.06}_{-0.05}$ OUR AVERAGE				
0.305±0.010±0.081	[1] AAIJ	12J	LHCB	pp at 7 TeV
0.31 ±0.11 $^{+0.12}_{-0.08}$	[2] AALTONEN	09E	CDF	$p\overline{p}$ at 1.8 TeV
0.23 $^{+0.09}_{-0.07}$ ±0.01	[3] AALTONEN	08N	CDF	$p\overline{p}$ at 1.96 TeV
• • • We do not use the following data for averages, fits, limits, etc. • • •				
0.118±0.042	[4] AFFOLDER	00E	CDF	$p\overline{p}$ at 1.8 TeV

[1] Measured the ratio to be $(0.404 \pm 0.017 \pm 0.027 \pm 0.105) \times [1 - (0.031 \pm 0.004 \pm 0.003) \times P_T]$ using b-hadron semileptonic decays where the P_T is the momentum of charmed hadron-muon pair in GeV/c. We quote their weighted average value where the second error combines systematic and the error on $B(\Lambda^+_c \to pK^-\pi^+)$.

[2] Errata to the measurement reported in AFFOLDER 00E using the p_T spectra from fully reconstructed B^0 and Λ_b decays.

[3] AALTONEN 08N reports $[\Gamma(\overline{b} \to b\text{-baryon})/[\Gamma(\overline{b} \to B^+) + \Gamma(\overline{b} \to B^0)]] \times [B(\Lambda^+_c \to pK^-\pi^+)] = (14.1 \pm 0.6^{+5.3}_{-4.4}) \times 10^{-3}$ which we divide by our best value $B(\Lambda^+_c \to pK^-\pi^+) = (6.23 \pm 0.33) \times 10^{-2}$. Our first error is their experiment's error and our second error is the systematic error from using our best value.

[4] AFFOLDER 00E uses several electron-charm final states in $b \to ce^-X$.

$\Gamma(\nu\text{anything})/\Gamma_{\text{total}}$ Γ_5/Γ

VALUE	DOCUMENT ID		TECN	COMMENT
0.2308±0.0077±0.0124	[1,2] ACCIARRI	96C	L3	$e^+e^- \to Z$

[1] ACCIARRI 96C assumes relative b semileptonic decay rates $e{:}\mu{:}\tau$ of 1:1:0.25. Based on missing-energy spectrum.

[2] Assumes Standard Model value for R_B.

$\Gamma(\ell^+\nu_\ell\text{anything})/\Gamma_{\text{total}}$ Γ_6/Γ

"OUR EVALUATION" is an average of the data listed below, excluding all asymmetry measurements, performed by the LEP Electroweak Working Group as described in the "Note on the Z boson" in the Z Particle Listings.

VALUE	DOCUMENT ID		TECN	COMMENT
0.1069±0.0022 OUR EVALUATION				
0.1064±0.0016 OUR AVERAGE				
0.1070±0.0010±0.0035	[1] HEISTER	02G	ALEP	$e^+e^- \to Z$
0.1070±0.0008 $^{+0.0037}_{-0.0049}$	[2] ABREU	01L	DLPH	$e^+e^- \to Z$
0.1083±0.0010 $^{+0.0028}_{-0.0024}$	[3] ABBIENDI	00E	OPAL	$e^+e^- \to Z$
0.1016±0.0013±0.0030	[4] ACCIARRI	00	L3	$e^+e^- \to Z$
0.1085±0.0012±0.0047	[5,6] ACCIARRI	96C	L3	$e^+e^- \to Z$
• • • We do not use the following data for averages, fits, limits, etc. • • •				
0.1106±0.0039±0.0022	[7] ABREU	95D	DLPH	$e^+e^- \to Z$
0.114 ±0.003 ±0.004	[8] BUSKULIC	94G	ALEP	$e^+e^- \to Z$
0.100 ±0.007 ±0.007	[9] ABREU	93C	DLPH	$e^+e^- \to Z$
0.105 ±0.006 ±0.005	[10] AKERS	93B	OPAL	Repl. by ABBIENDI 00E

[1] Uses the combination of lepton transverse momentum spectrum and the correlation between the charge of the lepton and opposite jet charge. The first error is statistic and the second error is the total systematic error including the modeling.

[2] The experimental systematic and model uncertainties are combined in quadrature.

[3] ABBIENDI 00E result is determined by comparing the distribution of several kinematic variables of leptonic events in a lifetime tagged $Z \to b\overline{b}$ sample using artificial neural network techniques. The first error is statistic; the second error is the total systematic error.

[4] ACCIARRI 00 result obtained from a combined fit of $R_b = \Gamma(Z \to b\overline{b})/\Gamma(Z \to \text{hadrons})$ and $B(b \to \ell\nu X)$, using double-tagging method.

[5] ACCIARRI 96C result obtained by a fit to the single lepton spectrum.

[6] Assumes Standard Model value for R_B.

[7] ABREU 95D give systematic errors ±0.0019 (model) and 0.0012 (R_c). We combine these in quadrature.

[8] BUSKULIC 94G uses e and μ events. This value is from a global fit to the lepton p and p_T (relative to jet) spectra which also determines the b and c production fractions, the fragmentation functions, and the forward-backward asymmetries. This branching ratio depends primarily on the ratio of dileptons to single leptons at high p_T, but the lower p_T portion of the lepton spectrum is included in the global fit to reduce the model dependence. The model dependence is ±0.0026 and is included in the systematic error.

[9] ABREU 93C event count includes ee events. Combining ee, $\mu\mu$, and $e\mu$ events, they obtain 0.100 ± 0.007 ± 0.007.

[10] AKERS 93B analysis performed using single and dilepton events.

$\Gamma(e^+\nu_e\text{anything})/\Gamma_{\text{total}}$ Γ_7/Γ

VALUE	EVTS	DOCUMENT ID		TECN	COMMENT
0.1086±0.0035 OUR AVERAGE					
0.1078±0.0008 $^{+0.0050}_{-0.0046}$		[1] ABBIENDI	00E	OPAL	$e^+e^- \to Z$
0.1089±0.0020±0.0051		[2,3] ACCIARRI	96C	L3	$e^+e^- \to Z$
0.107 ±0.015 ±0.007	260	[4] ABREU	93C	DLPH	$e^+e^- \to Z$
0.138 ±0.032 ±0.008		[5] ADEVA	91C	L3	$e^+e^- \to Z$
• • • We do not use the following data for averages, fits, limits, etc. • • •					
0.086 ±0.027 ±0.008		[6] ABE	93E	VNS	$E^{ee}_{\text{cm}} = 58$ GeV
0.109 $^{+0.014}_{-0.013}$ ±0.0055	2719	[7] AKERS	93B	OPAL	Repl. by ABBIENDI 00E
0.111 ±0.028 ±0.026		BEHREND	90D	CELL	$E^{ee}_{\text{cm}} = 43$ GeV
0.150 ±0.011 ±0.022		BEHREND	90D	CELL	$E^{ee}_{\text{cm}} = 35$ GeV
0.112 ±0.009 ±0.011		ONG	88	MRK2	$E^{ee}_{\text{cm}} = 29$ GeV
0.149 $^{+0.022}_{-0.019}$		PAL	86	DLCO	$E^{ee}_{\text{cm}} = 29$ GeV
0.110 ±0.018 ±0.010		AIHARA	85	TPC	$E^{ee}_{\text{cm}} = 29$ GeV
0.111 ±0.034 ±0.040		ALTHOFF	84J	TASS	$E^{ee}_{\text{cm}} = 34.6$ GeV
0.146 ±0.028		KOOP	84	DLCO	Repl. by PAL 86
0.116 ±0.021 ±0.017		NELSON	83	MRK2	$E^{ee}_{\text{cm}} = 29$ GeV

[1] ABBIENDI 00E result is determined by comparing the distribution of several kinematic variables of leptonic events in a lifetime tagged $Z \to b\overline{b}$ sample using artificial neural network techniques. The first error is statistic; the second error is the total systematic error.

[2] ACCIARRI 96C result obtained by a fit to the single lepton spectrum.

[3] Assumes Standard Model value for R_B.

[4] ABREU 93C event count includes ee events. Combining ee, $\mu\mu$, and $e\mu$ events, they obtain 0.100 ± 0.007 ± 0.007.

[5] ADEVA 91C measure the average $B(b \to eX)$ branching ratio using single and double tagged b enhanced Z events. Combining e and μ results, they obtain 0.113 ± 0.010 ± 0.006. Constraining the initial number of b quarks by the Standard Model prediction (378 ± 3 MeV) for the decay of the Z into $b\overline{b}$, the electron result gives 0.112 ± 0.004 ± 0.008. They obtain 0.119 ± 0.003 ± 0.006 when e and μ results are combined. Used to measure the $b\overline{b}$ width itself, this electron result gives 370 ± 12 ± 24 MeV and combined with the muon result gives 385 ± 7 ± 22 MeV.

[6] ABE 93E experiment also measures forward-backward asymmetries and fragmentation functions for b and c.

[7] AKERS 93B analysis performed using single and dilepton events.

$\Gamma(\mu^+\nu_\mu\text{anything})/\Gamma_{\text{total}}$ Γ_8/Γ

VALUE	EVTS	DOCUMENT ID		TECN	COMMENT
0.1095 $^{+0.0029}_{-0.0025}$ OUR AVERAGE					
0.1096±0.0008 $^{+0.0034}_{-0.0027}$		[1] ABBIENDI	00E	OPAL	$e^+e^- \to Z$
0.1082±0.0015±0.0059		[2,3] ACCIARRI	96C	L3	$e^+e^- \to Z$
0.110 ±0.012 ±0.007	656	[4] ABREU	93C	DLPH	$e^+e^- \to Z$
0.113 ±0.012 ±0.006		[5] ADEVA	91C	L3	$e^+e^- \to Z$
• • • We do not use the following data for averages, fits, limits, etc. • • •					
0.122 ±0.006 ±0.007		[3] UENO	96	AMY	e^+e^- at 57.9 GeV
0.101 $^{+0.010}_{-0.009}$ ±0.0055	4248	[6] AKERS	93B	OPAL	Repl. by ABBIENDI 00E
0.104 ±0.023 ±0.016		BEHREND	90D	CELL	$E^{ee}_{\text{cm}} = 43$ GeV
0.148 ±0.010 ±0.016		BEHREND	90D	CELL	$E^{ee}_{\text{cm}} = 35$ GeV
0.118 ±0.012 ±0.010		ONG	88	MRK2	$E^{ee}_{\text{cm}} = 29$ GeV
0.117 ±0.016 ±0.015		BARTEL	87	JADE	$E^{ee}_{\text{cm}} = 34.6$ GeV
0.114 ±0.018 ±0.025		BARTEL	85J	JADE	Repl. by BARTEL 87
0.117 ±0.028 ±0.010		ALTHOFF	84G	TASS	$E^{ee}_{\text{cm}} = 34.5$ GeV
0.105 ±0.015 ±0.013		ADEVA	83B	MRKJ	$E^{ee}_{\text{cm}} = 33$–38.5 GeV
0.155 $^{+0.054}_{-0.029}$		FERNANDEZ	83D	MAC	$E^{ee}_{\text{cm}} = 29$ GeV

[1] ABBIENDI 00E result is determined by comparing the distribution of several kinematic variables of leptonic events in a lifetime tagged $Z \to b\overline{b}$ sample using artificial neural network techniques. The first error is statistic; the second error is the total systematic error.

[2] ACCIARRI 96C result obtained by a fit to the single lepton spectrum.

[3] Assumes Standard Model value for R_B.

[4] ABREU 93C event count includes $\mu\mu$ events. Combining ee, $\mu\mu$, and $e\mu$ events, they obtain 0.100 ± 0.007 ± 0.007.

[5] ADEVA 91C measure the average $B(b \to eX)$ branching ratio using single and double tagged b enhanced Z events. Combining e and μ results, they obtain 0.113 ± 0.010 ± 0.006. Constraining the initial number of b quarks by the Standard Model prediction (378±3 MeV) for the decay of the Z into $b\overline{b}$, the muon result gives 0.123±0.003±0.006. They obtain 0.119 ± 0.003 ± 0.006 when e and μ results are combined. Used to measure the $b\overline{b}$ width itself, this muon result gives 394 ± 9 ± 22 MeV and combined with the electron result gives 385 ± 7 ± 22 MeV.

[6] AKERS 93B analysis performed using single and dilepton events.

Meson Particle Listings

$B^{\pm}/B^0/B_s^0/b$-baryon ADMIXTURE

$\Gamma(D^-\ell^+\nu_\ell\text{anything})/\Gamma_{\text{total}}$ Γ_9/Γ

VALUE	DOCUMENT ID		TECN	COMMENT
0.0230±0.0034 OUR AVERAGE	Error includes scale factor of 1.6.			
0.0272±0.0028±0.0018	[1] ABREU	00R	DLPH	$e^+e^- \to Z$
0.0203±0.0026±0.0006	[2] AKERS	95Q	OPAL	$e^+e^- \to Z$

[1] ABREU 00R reports their experiment's uncertainties ±0.0019 ± 0.0016 ± 0.0018, where the first error is statistical, the second is systematic, and the third is the uncertainty due to the D branching fraction. We combine first two in quadrature.

[2] AKERS 95Q reports $[\Gamma(\overline{b} \to D^-\ell^+\nu_\ell\text{anything})/\Gamma_{\text{total}}] \times [\text{B}(D^+ \to K^-2\pi^+)] = (1.82 \pm 0.20 \pm 0.12) \times 10^{-3}$ which we divide by our best value $\text{B}(D^+ \to K^-2\pi^+) = (8.98 \pm 0.28) \times 10^{-2}$. Our first error is their experiment's error and our second error is the systematic error from using our best value.

$\Gamma(D^-\pi^+\ell^+\nu_\ell\text{anything})/\Gamma_{\text{total}}$ Γ_{10}/Γ

VALUE	DOCUMENT ID		TECN	COMMENT
0.0049±0.0018±0.0007	ABREU	00R	DLPH	$e^+e^- \to Z$

$\Gamma(D^-\pi^-\ell^+\nu_\ell\text{anything})/\Gamma_{\text{total}}$ Γ_{11}/Γ

VALUE	DOCUMENT ID		TECN	COMMENT
0.0026±0.0015±0.0004	ABREU	00R	DLPH	$e^+e^- \to Z$

$\Gamma(\overline{D}^0\ell^+\nu_\ell\text{anything})/\Gamma_{\text{total}}$ Γ_{12}/Γ

VALUE	DOCUMENT ID		TECN	COMMENT
0.0683±0.0035 OUR AVERAGE				
0.0704±0.0040±0.0017	[1] ABREU	00R	DLPH	$e^+e^- \to Z$
0.065 ±0.006 ±0.001	[2] AKERS	95Q	OPAL	$e^+e^- \to Z$

[1] ABREU 00R reports their experiment's uncertainties ±0.0034 ± 0.0036 ± 0.0017, where the first error is statistical, the second is systematic, and the third is the uncertainty due to the D branching fraction. We combine first two in quadrature.

[2] AKERS 95Q reports $[\Gamma(\overline{b} \to \overline{D}^0\ell^+\nu_\ell\text{anything})/\Gamma_{\text{total}}] \times [\text{B}(D^0 \to K^-\pi^+)] = (2.52 \pm 0.14 \pm 0.17) \times 10^{-3}$ which we divide by our best value $\text{B}(D^0 \to K^-\pi^+) = (3.89 \pm 0.04) \times 10^{-2}$. Our first error is their experiment's error and our second error is the systematic error from using our best value.

$\Gamma(\overline{D}^0\pi^-\ell^+\nu_\ell\text{anything})/\Gamma_{\text{total}}$ Γ_{13}/Γ

VALUE	DOCUMENT ID		TECN	COMMENT
0.0107±0.0025±0.0011	ABREU	00R	DLPH	$e^+e^- \to Z$

$\Gamma(\overline{D}^0\pi^+\ell^+\nu_\ell\text{anything})/\Gamma_{\text{total}}$ Γ_{14}/Γ

VALUE	DOCUMENT ID		TECN	COMMENT
0.0023±0.0015±0.0004	ABREU	00R	DLPH	$e^+e^- \to Z$

$\Gamma(D^{*-}\ell^+\nu_\ell\text{anything})/\Gamma_{\text{total}}$ Γ_{15}/Γ

VALUE	DOCUMENT ID		TECN	COMMENT
0.0275±0.0019 OUR AVERAGE				
0.0275±0.0021±0.0009	[1] ABREU	00R	DLPH	$e^+e^- \to Z$
0.0276±0.0027±0.0011	[2] AKERS	95Q	OPAL	$e^+e^- \to Z$

[1] ABREU 00R reports their experiment's uncertainties ±0.0017 ± 0.0013 ± 0.0009, where the first error is statistical, the second is systematic, and the third is the uncertainty due to the D branching fraction. We combine first two in quadrature.

[2] AKERS 95Q reports $[\text{B}(\overline{b} \to D^*\ell^+\nu_\ell\text{X}) \times \text{B}(D^{*+} \to D^0\pi^+) \times \text{B}(D^0 \to K^-\pi^+)] = ((7.53 \pm 0.47 \pm 0.56) \times 10^{-4})$ and uses $\text{B}(D^{*+} \to D^0\pi^+) = 0.681 \pm 0.013$ and $\text{B}(D^0 \to K^-\pi^+) = 0.0401 \pm 0.0014$ to obtain the above result. The first error is the experiments error and the second error is the systematic error from the D^{*+} and D^0 branching ratios.

$\Gamma(D^{*-}\pi^-\ell^+\nu_\ell\text{anything})/\Gamma_{\text{total}}$ Γ_{16}/Γ

VALUE	DOCUMENT ID		TECN	COMMENT
0.0006±0.0007±0.0002	ABREU	00R	DLPH	$e^+e^- \to Z$

$\Gamma(D^{*-}\pi^+\ell^+\nu_\ell\text{anything})/\Gamma_{\text{total}}$ Γ_{17}/Γ

VALUE	DOCUMENT ID		TECN	COMMENT
0.0048±0.0009±0.0005	ABREU	00R	DLPH	$e^+e^- \to Z$

$\Gamma(\overline{D}_j^0\ell^+\nu_\ell\text{anything} \times \text{B}(\overline{D}_j^0 \to D^{*+}\pi^-))/\Gamma_{\text{total}}$ Γ_{18}/Γ

D_j represents an unresolved mixture of pseudoscalar and tensor D^{**} (P-wave) states.

VALUE (units 10^{-3})	DOCUMENT ID		TECN	COMMENT
2.64±0.79±0.39	ABBIENDI	03M	OPAL	$e^+e^- \to Z$
• • • We do not use the following data for averages, fits, limits, etc. • • •				
6.1 ±1.3 ±1.3	AKERS	95Q	OPAL	Repl. by ABBIENDI 03M

$\Gamma(D_j^-\ell^+\nu_\ell\text{anything} \times \text{B}(D_j^- \to D^0\pi^-))/\Gamma_{\text{total}}$ Γ_{19}/Γ

D_j represents an unresolved mixture of pseudoscalar and tensor D^{**} (P-wave) states.

VALUE (units 10^{-3})	DOCUMENT ID		TECN	COMMENT
$7.0 \pm 1.9^{+1.2}_{-1.3}$	AKERS	95Q	OPAL	$e^+e^- \to Z$

$\Gamma(\overline{D}_2^*(2460)^0\ell^+\nu_\ell\text{anything} \times \text{B}(\overline{D}_2^*(2460)^0 \to D^{*-}\pi^+))/\Gamma_{\text{total}}$ Γ_{20}/Γ

VALUE (units 10^{-3})	CL%	DOCUMENT ID		TECN	COMMENT
<1.4	90	ABBIENDI	03M	OPAL	$e^+e^- \to Z$

$\Gamma(D_2^*(2460)^-\ell^+\nu_\ell\text{anything} \times \text{B}(D_2^*(2460)^- \to D^0\pi^-))/\Gamma_{\text{total}}$ Γ_{21}/Γ

VALUE (units 10^{-3})	DOCUMENT ID		TECN	COMMENT
$4.2 \pm 1.3^{+0.7}_{-1.2}$	AKERS	95Q	OPAL	$e^+e^- \to Z$

$\Gamma(\overline{D}_2^*(2460)^0\ell^+\nu_\ell\text{anything} \times \text{B}(\overline{D}_2^*(2460)^0 \to D^-\pi^+))/\Gamma_{\text{total}}$ Γ_{22}/Γ

VALUE (units 10^{-3})	DOCUMENT ID		TECN	COMMENT
1.6±0.7±0.3	AKERS	95Q	OPAL	$e^+e^- \to Z$

$\Gamma(\text{charmless } \ell\overline{\nu}_\ell)/\Gamma_{\text{total}}$ Γ_{23}/Γ

"OUR EVALUATION" is an average of the data listed below performed by the LEP Heavy Flavour Steering Group. The averaging procedure takes into account correlations between the measurements.

VALUE	DOCUMENT ID		TECN	COMMENT
0.00171±0.00052 OUR EVALUATION				
0.0017 ±0.0004 OUR AVERAGE				
$0.00163 \pm 0.00053^{+0.00055}_{-0.00062}$	[1] ABBIENDI	01R	OPAL	$e^+e^- \to Z$
0.00157±0.00035±0.00055	[2] ABREU	00D	DLPH	$e^+e^- \to Z$
0.00173±0.00055±0.00055	[3] BARATE	99G	ALEP	$e^+e^- \to Z$
0.0033 ±0.0010 ±0.0017	[4] ACCIARRI	98K	L3	$e^+e^- \to Z$

[1] Obtained from the best fit of the MC simulated events to the data based on the $b \to X_u\ell\nu$ neutral network output distributions.

[2] ABREU 00D result obtained from a fit to the numbers of decays in $b \to u$ enriched and depleted samples and their lepton spectra, and assuming $|V_{cb}| = 0.0384 \pm 0.0033$ and $\tau_b = 1.564 \pm 0.014$ ps.

[3] Uses lifetime tagged $b\overline{b}$ sample.

[4] ACCIARRI 98K assumes $R_b = 0.2174 \pm 0.0009$ at Z decay.

$\Gamma(\tau^+\nu_\tau\text{anything})/\Gamma_{\text{total}}$ Γ_{24}/Γ

VALUE (units 10^{-2})	EVTS	DOCUMENT ID		TECN	COMMENT
2.41±0.23 OUR AVERAGE					
2.78±0.18±0.51		[1] ABBIENDI	01Q	OPAL	$e^+e^- \to Z$
2.43±0.20±0.25		[2] BARATE	01E	ALEP	$e^+e^- \to Z$
2.19±0.24±0.39		[3] ABREU	00C	DLPH	$e^+e^- \to Z$
1.7 ±0.5 ±1.1		[4,5] ACCIARRI	96C	L3	$e^+e^- \to Z$
2.4 ±0.7 ±0.8	1032	[6] ACCIARRI	94C	L3	$e^+e^- \to Z$
• • • We do not use the following data for averages, fits, limits, etc. • • •					
2.75±0.30±0.37	405	[7] BUSKULIC	95	ALEP	Repl. by BARATE 01E
4.08±0.76±0.62		BUSKULIC	93B	ALEP	Repl. by BUSKULIC 95

[1] ABBIENDI 01Q uses a missing energy technique.

[2] The energy-flow and b-tagging algorithms were used.

[3] Uses the missing energy in $Z \to b\overline{b}$ decays without identifying leptons.

[4] ACCIARRI 96C result obtained from missing energy spectrum.

[5] Assumes Standard Model value for R_b.

[6] This is a direct result using tagged $b\overline{b}$ events at the Z, but species are not separated.

[7] BUSKULIC 95 uses missing-energy technique.

$\Gamma(D^{*-}\tau\nu_\tau\text{anything})/\Gamma_{\text{total}}$ Γ_{25}/Γ

VALUE	DOCUMENT ID		TECN	COMMENT
$(0.88 \pm 0.31 \pm 0.28) \times 10^{-2}$	[1] BARATE	01E	ALEP	$e^+e^- \to Z$

[1] The energy-flow and b-tagging algorithms were used.

$\Gamma(\overline{b} \to \overline{c} \to \ell^-\overline{\nu}_\ell\text{anything})/\Gamma_{\text{total}}$ Γ_{26}/Γ

"OUR EVALUATION" is an average of the data listed below, excluding all asymmetry measurements, performed by the LEP Electroweak Working Group as described in the "Note on the Z boson" in the Z Particle Listings.

VALUE	DOCUMENT ID		TECN	COMMENT
0.0802±0.0019 OUR EVALUATION				
0.0817±0.0020 OUR AVERAGE				
$0.0818 \pm 0.0015^{+0.0024}_{-0.0026}$	[1] HEISTER	02G	ALEP	$e^+e^- \to Z$
$0.0798 \pm 0.0022^{+0.0025}_{-0.0029}$	[2] ABREU	01L	DLPH	$e^+e^- \to Z$
$0.0840 \pm 0.0016^{+0.0039}_{-0.0036}$	[3] ABBIENDI	00E	OPAL	$e^+e^- \to Z$
• • • We do not use the following data for averages, fits, limits, etc. • • •				
0.0770±0.0097±0.0046	[4] ABREU	95D	DLPH	$e^+e^- \to Z$
0.082 ±0.003 ±0.012	[5] BUSKULIC	94G	ALEP	$e^+e^- \to Z$
0.077 ±0.004 ±0.007	[6] AKERS	93B	OPAL	Repl. by ABBIENDI 00E

[1] Uses the combination of lepton transverse momentum spectrum and the correlation between the charge of the lepton and opposite jet charge. The first error is statistic and the second error is the total systematic error including the modeling.

[2] The experimental systematic and model uncertainties are combined in quadrature.

[3] ABBIENDI 00E result is determined by comparing the distribution of several kinematic variables of leptonic events in a lifetime tagged $Z \to b\overline{b}$ sample using artificial neural network techniques. The first error is statistic; the second error is the total systematic error.

[4] ABREU 95D give systematic errors ±0.0033 (model) and 0.0032 (R_c). We combine these in quadrature. This result is from the same global fit as their $\Gamma(\overline{b} \to \ell^+\nu_\ell\text{X})$ data.

[5] BUSKULIC 94G uses e and μ events. This value is from the same global fit as their $\Gamma(\overline{b} \to \ell^+\nu_\ell\text{anything})/\Gamma_{\text{total}}$ data.

[6] AKERS 93B analysis performed using single and dilepton events.

$\Gamma(c \to \ell^+\nu\text{anything})/\Gamma_{\text{total}}$ Γ_{27}/Γ

VALUE	DOCUMENT ID		TECN	COMMENT
$0.0161 \pm 0.0020^{+0.0034}_{-0.0047}$	[1] ABREU	01L	DLPH	$e^+e^- \to Z$

[1] The experimental systematic and model uncertainties are combined in quadrature.

$\Gamma(\overline{D}^0 \text{ anything})/\Gamma_{\text{total}}$ Γ_{28}/Γ

VALUE	DOCUMENT ID		TECN	COMMENT
0.595 ± 0.028 ± 0.006	[1] BUSKULIC	96Y	ALEP	$e^+e^- \to Z$

[1] BUSKULIC 96Y reports 0.605 ± 0.024 ± 0.016 from a measurement of $[\Gamma(\overline{b} \to \overline{D}^0 \text{ anything})/\Gamma_{\text{total}}] \times [\text{B}(D^0 \to K^-\pi^+)]$ assuming $\text{B}(D^0 \to K^-\pi^+) = 0.0383$, which we rescale to our best value $\text{B}(D^0 \to K^-\pi^+) = (3.89 \pm 0.04) \times 10^{-2}$. Our first error is their experiment's error and our second error is the systematic error from using our best value.

$\Gamma(D^0 D_s^{\pm} \text{ anything})/\Gamma_{\text{total}}$ Γ_{29}/Γ

VALUE	DOCUMENT ID		TECN	COMMENT
$\mathbf{0.091^{+0.020}_{-0.018}{}^{+0.034}_{-0.022}}$	[1] BARATE	98Q	ALEP	$e^+e^- \to Z$

[1] The systematic error includes the uncertainties due to the charm branching ratios.

$\Gamma(D^{\mp} D_s^{\pm} \text{ anything})/\Gamma_{\text{total}}$ Γ_{30}/Γ

VALUE	DOCUMENT ID		TECN	COMMENT
$\mathbf{0.040^{+0.017}_{-0.014}{}^{+0.016}_{-0.011}}$	[1] BARATE	98Q	ALEP	$e^+e^- \to Z$

[1] The systematic error includes the uncertainties due to the charm branching ratios.

$[\Gamma(D^0 D_s^{\pm} \text{ anything}) + \Gamma(D^{\mp} D_s^{\pm} \text{ anything})]/\Gamma_{\text{total}}$ $(\Gamma_{29}+\Gamma_{30})/\Gamma$

VALUE	DOCUMENT ID		TECN	COMMENT
$\mathbf{0.131^{+0.026}_{-0.022}{}^{+0.048}_{-0.031}}$	[1] BARATE	98Q	ALEP	$e^+e^- \to Z$

[1] The systematic error includes the uncertainties due to the charm branching ratios.

$\Gamma(\overline{D}^0 D^0 \text{ anything})/\Gamma_{\text{total}}$ Γ_{31}/Γ

VALUE	DOCUMENT ID		TECN	COMMENT
$\mathbf{0.051^{+0.016}_{-0.014}{}^{+0.012}_{-0.011}}$	[1] BARATE	98Q	ALEP	$e^+e^- \to Z$

[1] The systematic error includes the uncertainties due to the charm branching ratios.

$\Gamma(D^0 D^{\pm} \text{ anything})/\Gamma_{\text{total}}$ Γ_{32}/Γ

VALUE	DOCUMENT ID		TECN	COMMENT
$\mathbf{0.027^{+0.015}_{-0.013}{}^{+0.010}_{-0.009}}$	[1] BARATE	98Q	ALEP	$e^+e^- \to Z$

[1] The systematic error includes the uncertainties due to the charm branching ratios.

$[\Gamma(\overline{D}^0 D^0 \text{ anything}) + \Gamma(D^0 D^{\pm} \text{ anything})]/\Gamma_{\text{total}}$ $(\Gamma_{31}+\Gamma_{32})/\Gamma$

VALUE	DOCUMENT ID		TECN	COMMENT
$\mathbf{0.078^{+0.020}_{-0.018}{}^{+0.018}_{-0.016}}$	[1] BARATE	98Q	ALEP	$e^+e^- \to Z$

[1] The systematic error includes the uncertainties due to the charm branching ratios.

$\Gamma(D^{\pm} D^{\mp} \text{ anything})/\Gamma_{\text{total}}$ Γ_{33}/Γ

VALUE	CL%	DOCUMENT ID		TECN	COMMENT
< 0.009	90	BARATE	98Q	ALEP	$e^+e^- \to Z$

$[\Gamma(D^0 \text{ anything}) + \Gamma(D^+ \text{ anything})]/\Gamma_{\text{total}}$ $(\Gamma_{34}+\Gamma_{35})/\Gamma$

VALUE	DOCUMENT ID		TECN	COMMENT
0.093 ± 0.017 ± 0.014	[1] ABDALLAH	03E	DLPH	$e^+e^- \to Z$

[1] The second error is the total of systematic uncertainties including the branching fractions used in the measurement.

$\Gamma(D^- \text{ anything})/\Gamma_{\text{total}}$ Γ_{36}/Γ

VALUE	DOCUMENT ID		TECN	COMMENT
0.237 ± 0.017 ± 0.008	[1] BUSKULIC	96Y	ALEP	$e^+e^- \to Z$

[1] BUSKULIC 96Y reports 0.234 ± 0.013 ± 0.010 from a measurement of $[\Gamma(\overline{b} \to D^- \text{ anything})/\Gamma_{\text{total}}] \times [\text{B}(D^+ \to K^-2\pi^+)]$ assuming $\text{B}(D^+ \to K^-2\pi^+) = 0.091$, which we rescale to our best value $\text{B}(D^+ \to K^-2\pi^+) = (8.98 \pm 0.28) \times 10^{-2}$. Our first error is their experiment's error and our second error is the systematic error from using our best value.

$\Gamma(D^*(2010)^+ \text{ anything})/\Gamma_{\text{total}}$ Γ_{37}/Γ

VALUE	DOCUMENT ID		TECN	COMMENT
0.173 ± 0.016 ± 0.012	[1] ACKERSTAFF	98E	OPAL	$e^+e^- \to Z$

[1] Uses lepton tags to select $Z \to b\overline{b}$ events.

$\Gamma(D_1(2420)^0 \text{ anything})/\Gamma_{\text{total}}$ Γ_{38}/Γ

VALUE	DOCUMENT ID		TECN	COMMENT
0.050 ± 0.014 ± 0.006	[1] ACKERSTAFF	97W	OPAL	$e^+e^- \to Z$

[1] ACKERSTAFF 97W assumes $\text{B}(D_2^*(2460)^0 \to D^{*+}\pi^-) = 0.21 \pm 0.04$ and $\Gamma_{b\overline{b}}/\Gamma_{\text{hadrons}} = 0.216$ at Z decay.

$\Gamma(D^*(2010)^{\mp} D_s^{\pm} \text{ anything})/\Gamma_{\text{total}}$ Γ_{39}/Γ

VALUE	DOCUMENT ID		TECN	COMMENT
$\mathbf{0.033^{+0.010}_{-0.009}{}^{+0.012}_{-0.009}}$	[1] BARATE	98Q	ALEP	$e^+e^- \to Z$

[1] The systematic error includes the uncertainties due to the charm branching ratios.

$\Gamma(D^0 D^*(2010)^{\pm} \text{ anything})/\Gamma_{\text{total}}$ Γ_{40}/Γ

VALUE	DOCUMENT ID		TECN	COMMENT
$\mathbf{0.030^{+0.009}_{-0.008}{}^{+0.007}_{-0.005}}$	[1] BARATE	98Q	ALEP	$e^+e^- \to Z$

[1] The systematic error includes the uncertainties due to the charm branching ratios.

$\Gamma(D^*(2010)^{\pm} D^{\mp} \text{ anything})/\Gamma_{\text{total}}$ Γ_{41}/Γ

VALUE	DOCUMENT ID		TECN	COMMENT
$\mathbf{0.025^{+0.010}_{-0.009}{}^{+0.006}_{-0.005}}$	[1] BARATE	98Q	ALEP	$e^+e^- \to Z$

[1] The systematic error includes the uncertainties due to the charm branching ratios.

$\Gamma(D^*(2010)^{\pm} D^*(2010)^{\mp} \text{ anything})/\Gamma_{\text{total}}$ Γ_{42}/Γ

VALUE	DOCUMENT ID		TECN	COMMENT
$\mathbf{0.012^{+0.004}_{-0.003} \pm 0.002}$	[1] BARATE	98Q	ALEP	$e^+e^- \to Z$

[1] The systematic error includes the uncertainties due to the charm branching ratios.

$\Gamma(\overline{D} D \text{ anything})/\Gamma_{\text{total}}$ Γ_{43}/Γ

VALUE	DOCUMENT ID		TECN	COMMENT
$\mathbf{0.10 \pm 0.032^{+0.107}_{-0.095}}$	[1] ABBIENDI	04I	OPAL	$e^+e^- \to Z$

[1] Measurement performed using an inclusive identification of B mesons and the D candidates.

$\Gamma(D_2^*(2460)^0 \text{ anything})/\Gamma_{\text{total}}$ Γ_{44}/Γ

VALUE	DOCUMENT ID		TECN	COMMENT
0.047 ± 0.024 ± 0.013	[1] ACKERSTAFF	97W	OPAL	$e^+e^- \to Z$

[1] ACKERSTAFF 97W assumes $\text{B}(D_2^*(2460)^0 \to D^{*+}\pi^-) = 0.21 \pm 0.04$ and $\Gamma_{b\overline{b}}/\Gamma_{\text{hadrons}} = 0.216$ at Z decay.

$\Gamma(D_s^- \text{ anything})/\Gamma_{\text{total}}$ Γ_{45}/Γ

VALUE	DOCUMENT ID		TECN	COMMENT
0.147 ± 0.017 ± 0.013	[1] BUSKULIC	96Y	ALEP	$e^+e^- \to Z$

[1] BUSKULIC 96Y reports 0.183 ± 0.019 ± 0.009 from a measurement of $[\Gamma(\overline{b} \to D_s^- \text{ anything})/\Gamma_{\text{total}}] \times [\text{B}(D_s^+ \to \phi\pi^+)]$ assuming $\text{B}(D_s^+ \to \phi\pi^+) = 0.036$, which we rescale to our best value $\text{B}(D_s^+ \to \phi\pi^+) = (4.5 \pm 0.4) \times 10^{-2}$. Our first error is their experiment's error and our second error is the systematic error from using our best value.

$\Gamma(D_s^+ \text{ anything})/\Gamma_{\text{total}}$ Γ_{46}/Γ

VALUE	DOCUMENT ID		TECN	COMMENT
0.101 ± 0.010 ± 0.029	[1] ABDALLAH	03E	DLPH	$e^+e^- \to Z$

[1] The second error is the total of systematic uncertainties including the branching fractions used in the measurement.

$\Gamma(b \to \Lambda_c^+ \text{ anything})/\Gamma_{\text{total}}$ Γ_{47}/Γ

VALUE	DOCUMENT ID		TECN	COMMENT
0.078 ± 0.011 ± 0.004	[1] BUSKULIC	96Y	ALEP	$e^+e^- \to Z$

[1] BUSKULIC 96Y reports 0.110 ± 0.014 ± 0.006 from a measurement of $[\Gamma(b \to \Lambda_c^+ \text{ anything})/\Gamma_{\text{total}}] \times [\text{B}(\Lambda_c^+ \to pK^-\pi^+)]$ assuming $\text{B}(\Lambda_c^+ \to pK^-\pi^+) = 0.044$, which we rescale to our best value $\text{B}(\Lambda_c^+ \to pK^-\pi^+) = (6.23 \pm 0.33) \times 10^{-2}$. Our first error is their experiment's error and our second error is the systematic error from using our best value.

$\Gamma(\overline{c}/c \text{ anything})/\Gamma_{\text{total}}$ Γ_{48}/Γ

VALUE	DOCUMENT ID		TECN	COMMENT
1.162 ± 0.032 OUR AVERAGE				
$1.12\ ^{+0.11}_{-0.10}$	[1] ABBIENDI	04I	OPAL	$e^+e^- \to Z$
1.166 ± 0.031 ± 0.080	[2] ABREU	00	DLPH	$e^+e^- \to Z$
1.147 ± 0.041	[3] ABREU	98D	DLPH	$e^+e^- \to Z$
1.230 ± 0.036 ± 0.065	[4] BUSKULIC	96Y	ALEP	$e^+e^- \to Z$

[1] Measurement performed using an inclusive identification of B mesons and the D candidates.
[2] Evaluated via summation of exclusive and inclusive channels.
[3] ABREU 98D results are extracted from a fit to the b-tagging probability distribution based on the impact parameter.
[4] BUSKULIC 96Y assumes PDG 96 production fractions for B^0, B^+, B_s, b baryons, and PDG 96 branching ratios for charm decays. This is sum of their inclusive $\overline{D}^0$, D^-, $\overline{D}_s$, and Λ_c branching ratios, corrected to include inclusive Ξ_c and charmonium.

$\Gamma(J/\psi(1S) \text{ anything})/\Gamma_{\text{total}}$ Γ_{49}/Γ

VALUE (units 10^{-2})	CL%	EVTS	DOCUMENT ID		TECN	COMMENT
1.16 ± 0.10 OUR AVERAGE						
1.12 ± 0.12 ± 0.10			[1] ABREU	94P	DLPH	$e^+e^- \to Z$
1.16 ± 0.16 ± 0.14		121	[2] ADRIANI	93J	L3	$e^+e^- \to Z$
1.21 ± 0.13 ± 0.08			BUSKULIC	92G	ALEP	$e^+e^- \to Z$
• • • We do not use the following data for averages, fits, limits, etc. • • •						
1.3 ± 0.2 ± 0.2			[3] ADRIANI	92	L3	$e^+e^- \to Z$
< 4.9	90		MATTEUZZI	83	MRK2	$E_{\text{cm}}^{ee} = 29$ GeV

[1] ABREU 94P is an inclusive measurement from b decays at the Z. Uses $J/\psi(1S) \to e^+e^-$ and $\mu^+\mu^-$ channels. Assumes $\Gamma(Z \to b\overline{b})/\Gamma_{\text{hadron}} = 0.22$.
[2] ADRIANI 93J is an inclusive measurement from b decays at the Z. Uses $J/\psi(1S) \to \mu^+\mu^-$ and $J/\psi(1S) \to e^+e^-$ channels.
[3] ADRIANI 92 measurement is an inclusive result for $\text{B}(Z \to J/\psi(1S)\,X) = (4.1 \pm 0.7 \pm 0.3) \times 10^{-3}$ which is used to extract the b-hadron contribution to $J/\psi(1S)$ production.

Meson Particle Listings

$B^{\pm}/B^0/B_s^0/b$-baryon ADMIXTURE

$\Gamma(\psi(2S)\,\text{anything})/\Gamma_{\text{total}}$ Γ_{50}/Γ

VALUE	DOCUMENT ID	TECN	COMMENT
• • • We do not use the following data for averages, fits, limits, etc. • • •			
$0.0048 \pm 0.0022 \pm 0.0010$	[1] ABREU 94P	DLPH	$e^+e^- \to Z$

[1] ABREU 94P is an inclusive measurement from b decays at the Z. Uses $\psi(2S) \to J/\psi(1S)\,\pi^+\pi^-$, $J/\psi(1S) \to \mu^+\mu^-$ channels. Assumes $\Gamma(Z \to b\overline{b})/\Gamma_{\text{hadron}} = 0.22$.

$\Gamma(\psi(2S)\,\text{anything})/\Gamma(J/\psi(1S)\,\text{anything})$ Γ_{50}/Γ_{49}

VALUE	DOCUMENT ID	TECN	COMMENT
0.245 ± 0.013 OUR AVERAGE			
$0.240 \pm 0.015 \pm 0.005$	[1,2] AAIJ 12BD	LHCB	pp at 7 TeV
$0.258 \pm 0.015 \pm 0.019$	[3,4] CHATRCHYAN 12AK	CMS	pp at 7 TeV

[1] AAIJ 12BD reports $0.235 \pm 0.005 \pm 0.015$ from a measurement of $[\Gamma(\overline{b} \to \psi(2S)\,\text{anything})/\Gamma(\overline{b} \to J/\psi(1S)\,\text{anything})] \times [B(J/\psi(1S) \to \mu^+\mu^-)] / [B(\psi(2S) \to e^+e^-)]$ assuming $B(J/\psi(1S) \to \mu^+\mu^-) = (5.93 \pm 0.06) \times 10^{-2}$, $B(\psi(2S) \to e^+e^-) = (7.72 \pm 0.17) \times 10^{-3}$, which we rescale to our best values $B(J/\psi(1S) \to \mu^+\mu^-) = (5.961 \pm 0.033) \times 10^{-2}$, $B(\psi(2S) \to e^+e^-) = (7.93 \pm 0.17) \times 10^{-3}$. Our first error is their experiment's error and our second error is the systematic error from using our best values.

[2] Assumes lepton universality imposing $B(\psi(2s) \to \mu^+\mu^-) = B(\psi(2s) \to e^+e^-)$.

[3] CHATRCHYAN 12AK really reports $\Gamma_{50}/\Gamma = (3.08 \pm 0.12 \pm 0.13 \pm 0.42) \times 10^{-3}$ assuming PDG 10 value of $\Gamma_{49}/\Gamma = (1.16 \pm 0.10) \times 10^{-2}$ which we present as a ratio of $\Gamma_{50}/\Gamma_{49} = (26.5 \pm 1.0 \pm 1.1 \pm 2.8) \times 10^{-2}$.

[4] CHATRCHYAN 12AK reports $(26.5 \pm 1.0 \pm 1.1 \pm 2.8) \times 10^{-2}$ from a measurement of $[\Gamma(\overline{b} \to \psi(2S)\,\text{anything})/\Gamma(\overline{b} \to J/\psi(1S)\,\text{anything})] \times [B(\psi(2S) \to \mu^+\mu^-)] / [B(J/\psi(1S) \to \mu^+\mu^-)]$ assuming $B(\psi(2S) \to \mu^+\mu^-) = (7.7 \pm 0.8) \times 10^{-3}$, $B(J/\psi(1S) \to \mu^+\mu^-) = (5.93 \pm 0.06) \times 10^{-2}$, which we rescale to our best values $B(\psi(2S) \to \mu^+\mu^-) = (8.0 \pm 0.6) \times 10^{-3}$, $B(J/\psi(1S) \to \mu^+\mu^-) = (5.961 \pm 0.033) \times 10^{-2}$. Our first error is their experiment's error and our second error is the systematic error from using our best values.

$\Gamma(\chi_{c0}(1P)\,\text{anything})/\Gamma(\eta_c(1S)\,\text{anything})$ Γ_{51}/Γ_{55}

VALUE	DOCUMENT ID	TECN	COMMENT
$0.33 \pm 0.06 \pm 0.05$	[1] AAIJ 17BB	LHCB	pp at 7, 8 TeV

[1] AAIJ 17BB reports $[\Gamma(\overline{b} \to \chi_{c0}(1P)\,\text{anything})/\Gamma(\overline{b} \to \eta_c(1S)\,\text{anything})] / [B(\eta_c(1S) \to \phi\phi)] \times [B(\chi_{c0}(1P) \to \phi\phi)] = 0.147 \pm 0.023 \pm 0.011$ which we multiply or divide by our best values $B(\eta_c(1S) \to \phi\phi) = (1.79 \pm 0.20) \times 10^{-3}$, $B(\chi_{c0}(1P) \to \phi\phi) = (8.0 \pm 0.7) \times 10^{-4}$. Our first error is their experiment's error and our second error is the systematic error from using our best values.

$\Gamma(\chi_{c1}(1P)\,\text{anything})/\Gamma_{\text{total}}$ Γ_{52}/Γ

VALUE	EVTS	DOCUMENT ID	TECN	COMMENT
0.014 ± 0.004 OUR AVERAGE				
$0.0112^{+0.0057}_{-0.0050} \pm 0.0003$		[1] ABREU 94P	DLPH	$e^+e^- \to Z$
$0.019 \pm 0.007 \pm 0.001$	19	[2] ADRIANI 93J	L3	$e^+e^- \to Z$

[1] ABREU 94P reports $0.014 \pm 0.006^{+0.004}_{-0.002}$ from a measurement of $[\Gamma(\overline{b} \to \chi_{c1}(1P)\,\text{anything})/\Gamma_{\text{total}}] \times [B(\chi_{c1}(1P) \to \gamma J/\psi(1S))]$ assuming $B(\chi_{c1}(1P) \to \gamma J/\psi(1S)) = 0.273 \pm 0.016$, which we rescale to our best value $B(\chi_{c1}(1P) \to \gamma J/\psi(1S)) = (34.3 \pm 1.0) \times 10^{-2}$. Our first error is their experiment's error and our second error is the systematic error from using our best value. Assumes no $\chi_{c2}(1P)$ and $\Gamma(Z \to b\overline{b})/\Gamma_{\text{hadron}} = 0.22$.

[2] ADRIANI 93J reports $0.024 \pm 0.009 \pm 0.002$ from a measurement of $[\Gamma(\overline{b} \to \chi_{c1}(1P)\,\text{anything})/\Gamma_{\text{total}}] \times [B(\chi_{c1}(1P) \to \gamma J/\psi(1S))]$ assuming $B(\chi_{c1}(1P) \to \gamma J/\psi(1S)) = 0.273 \pm 0.016$, which we rescale to our best value $B(\chi_{c1}(1P) \to \gamma J/\psi(1S)) = (34.3 \pm 1.0) \times 10^{-2}$. Our first error is their experiment's error and our second error is the systematic error from using our best value.

$\Gamma(\chi_{c1}(1P)\,\text{anything})/\Gamma(J/\psi(1S)\,\text{anything})$ Γ_{52}/Γ_{49}

VALUE	EVTS	DOCUMENT ID	TECN	COMMENT
• • • We do not use the following data for averages, fits, limits, etc. • • •				
1.92 ± 0.82	121	[1] ADRIANI 93J	L3	$e^+e^- \to Z$

[1] ADRIANI 93J is a ratio of inclusive measurements from b decays at the Z using only the $J/\psi(1S) \to \mu^+\mu^-$ channel since some systematics cancel.

$\Gamma(\chi_{c1}(1P)\,\text{anything})/\Gamma(\chi_{c0}(1P)\,\text{anything})$ Γ_{52}/Γ_{51}

VALUE	DOCUMENT ID	TECN	COMMENT
$0.96 \pm 0.21 \pm 0.15$	[1] AAIJ 17BB	LHCB	pp at 7, 8 TeV

[1] AAIJ 17BB reports $[\Gamma(\overline{b} \to \chi_{c1}(1P)\,\text{anything})/\Gamma(\overline{b} \to \chi_{c0}(1P)\,\text{anything})] / [B(\chi_{c0}(1P) \to \phi\phi)] \times [B(\chi_{c1}(1P) \to \phi\phi)] = 0.50 \pm 0.11 \pm 0.01$ which we multiply or divide by our best values $B(\chi_{c0}(1P) \to \phi\phi) = (8.0 \pm 0.7) \times 10^{-4}$, $B(\chi_{c1}(1P) \to \phi\phi) = (4.2 \pm 0.5) \times 10^{-4}$. Our first error is their experiment's error and our second error is the systematic error from using our best values.

$\Gamma(\chi_{c1}(1P)\,\text{anything})/\Gamma(\eta_c(1S)\,\text{anything})$ Γ_{52}/Γ_{55}

VALUE	DOCUMENT ID	TECN	COMMENT
$0.31 \pm 0.07 \pm 0.05$	[1] AAIJ 17BB	LHCB	pp at 7, 8 TeV

[1] AAIJ 17BB reports $[\Gamma(\overline{b} \to \chi_{c1}(1P)\,\text{anything})/\Gamma(\overline{b} \to \eta_c(1S)\,\text{anything})] / [B(\eta_c(1S) \to \phi\phi)] \times [B(\chi_{c1}(1P) \to \phi\phi)] = 0.073 \pm 0.016 \pm 0.006$ which we multiply or divide by our best values $B(\eta_c(1S) \to \phi\phi) = (1.79 \pm 0.20) \times 10^{-3}$, $B(\chi_{c1}(1P) \to \phi\phi) = (4.2 \pm 0.5) \times 10^{-4}$. Our first error is their experiment's error and our second error is the systematic error from using our best values.

$\Gamma(\chi_{c2}(1P)\,\text{anything})/\Gamma(\chi_{c0}(1P)\,\text{anything})$ Γ_{53}/Γ_{51}

VALUE	DOCUMENT ID	TECN	COMMENT
$0.42 \pm 0.08 \pm 0.05$	[1] AAIJ 17BB	LHCB	pp at 7, 8 TeV

[1] AAIJ 17BB reports $[\Gamma(\overline{b} \to \chi_{c2}(1P)\,\text{anything})/\Gamma(\overline{b} \to \chi_{c0}(1P)\,\text{anything})] / [B(\chi_{c0}(1P) \to \phi\phi)] \times [B(\chi_{c2}(1P) \to \phi\phi)] = 0.56 \pm 0.10 \pm 0.01$ which we multiply or divide by our best values $B(\chi_{c0}(1P) \to \phi\phi) = (8.0 \pm 0.7) \times 10^{-4}$, $B(\chi_{c2}(1P) \to \phi\phi) = (1.06 \pm 0.09) \times 10^{-3}$. Our first error is their experiment's error and our second error is the systematic error from using our best values.

$\Gamma(\chi_{c2}(1P)\,\text{anything})/\Gamma(\eta_c(1S)\,\text{anything})$ Γ_{53}/Γ_{55}

VALUE	DOCUMENT ID	TECN	COMMENT
$0.136 \pm 0.023 \pm 0.019$	[1] AAIJ 17BB	LHCB	pp at 7, 8 TeV

[1] AAIJ 17BB reports $[\Gamma(\overline{b} \to \chi_{c2}(1P)\,\text{anything})/\Gamma(\overline{b} \to \eta_c(1S)\,\text{anything})] / [B(\eta_c(1S) \to \phi\phi)] \times [B(\chi_{c2}(1P) \to \phi\phi)] = 0.081 \pm 0.013 \pm 0.005$ which we multiply or divide by our best values $B(\eta_c(1S) \to \phi\phi) = (1.79 \pm 0.20) \times 10^{-3}$, $B(\chi_{c2}(1P) \to \phi\phi) = (1.06 \pm 0.09) \times 10^{-3}$. Our first error is their experiment's error and our second error is the systematic error from using our best values.

$\Gamma(\chi_c(2P)\,\text{anything},\ \chi_c \to \phi\phi)/\Gamma_{\text{total}}$ Γ_{54}/Γ

VALUE	CL%	DOCUMENT ID	TECN	COMMENT
$< 2.8 \times 10^{-7}$	95	AAIJ 17BB	LHCB	pp at 7, 8 TeV

$\Gamma(\eta_c(2S)\,\text{anything},\ \eta_c \to \phi\phi)/\Gamma(\eta_c(1S)\,\text{anything})$ Γ_{56}/Γ_{55}

VALUE (units 10^{-5})	DOCUMENT ID	TECN	COMMENT
$7.2 \pm 2.1 \pm 0.8$	[1] AAIJ 17BB	LHCB	pp at 7, 8 TeV

[1] AAIJ 17BB reports $[\Gamma(\overline{b} \to \eta_c(2S)\,\text{anything},\ \eta_c \to \phi\phi)/\Gamma(\overline{b} \to \eta_c(1S)\,\text{anything})] / [B(\eta_c(1S) \to \phi\phi)] = 0.040 \pm 0.011 \pm 0.004$ which we multiply by our best value $B(\eta_c(1S) \to \phi\phi) = (1.79 \pm 0.20) \times 10^{-3}$. Our first error is their experiment's error and our second error is the systematic error from using our best value.

$\Gamma(\chi_{c1}(3872)\,\text{anything},\ \chi_{c1} \to \phi\phi)/\Gamma_{\text{total}}$ Γ_{57}/Γ

VALUE	CL%	DOCUMENT ID	TECN	COMMENT
$< 4.5 \times 10^{-7}$	95	AAIJ 17BB	LHCB	pp at 7, 8 TeV

$\Gamma(X(3915)\,\text{anything},\ X \to \phi\phi)/\Gamma_{\text{total}}$ Γ_{58}/Γ

VALUE	CL%	DOCUMENT ID	TECN	COMMENT
$< 3.1 \times 10^{-7}$	95	AAIJ 17BB	LHCB	pp at 7, 8 TeV

$\Gamma(\overline{s}\gamma)/\Gamma_{\text{total}}$ Γ_{59}/Γ

VALUE (units 10^{-4})	CL%	DOCUMENT ID	TECN	COMMENT
$3.11 \pm 0.80 \pm 0.72$		[1] BARATE 98I	ALEP	$e^+e^- \to Z$
• • • We do not use the following data for averages, fits, limits, etc. • • •				
< 5.4	90	[2] ADAM 96D	DLPH	$e^+e^- \to Z$
< 12	90	[3] ADRIANI 93L	L3	$e^+e^- \to Z$

[1] BARATE 98I uses lifetime tagged $Z \to b\overline{b}$ sample.

[2] ADAM 96D assumes $f_{B^0} = f_{B^-} = 0.39$ and $f_{B_s} = 0.12$.

[3] ADRIANI 93L result is for $\overline{b} \to \overline{s}\gamma$ is performed inclusively.

$\Gamma(\overline{s}\overline{\nu}\nu)/\Gamma_{\text{total}}$ Γ_{60}/Γ

VALUE	CL%	DOCUMENT ID	TECN	COMMENT
$< 6.4 \times 10^{-4}$	90	[1] BARATE 01E	ALEP	$e^+e^- \to Z$

[1] The energy-flow and b-tagging algorithms were used.

$\Gamma(K^{\pm}\,\text{anything})/\Gamma_{\text{total}}$ Γ_{61}/Γ

VALUE	DOCUMENT ID	TECN	COMMENT
0.74 ± 0.06 OUR AVERAGE			
$0.72 \pm 0.02 \pm 0.06$	BARATE 98V	ALEP	$e^+e^- \to Z$
$0.88 \pm 0.05 \pm 0.18$	ABREU 95C	DLPH	$e^+e^- \to Z$

$\Gamma(K_S^0\,\text{anything})/\Gamma_{\text{total}}$ Γ_{62}/Γ

VALUE	DOCUMENT ID	TECN	COMMENT
$0.290 \pm 0.011 \pm 0.027$	ABREU 95C	DLPH	$e^+e^- \to Z$

$\Gamma(\pi^{\pm}\,\text{anything})/\Gamma_{\text{total}}$ Γ_{63}/Γ

VALUE	DOCUMENT ID	TECN	COMMENT
$3.97 \pm 0.02 \pm 0.21$	BARATE 98V	ALEP	$e^+e^- \to Z$

$\Gamma(\pi^0\,\text{anything})/\Gamma_{\text{total}}$ Γ_{64}/Γ

VALUE	DOCUMENT ID	TECN	COMMENT
$2.78 \pm 0.15 \pm 0.60$	[1] ADAM 96	DLPH	$e^+e^- \to Z$

[1] ADAM 96 measurement obtained from a fit to the rapidity distribution of $\pi^{0\prime s}$ in $Z \to b\,b$ events.

$\Gamma(\phi\,\text{anything})/\Gamma_{\text{total}}$ Γ_{65}/Γ

VALUE	DOCUMENT ID	TECN	COMMENT
$0.0282 \pm 0.0013 \pm 0.0019$	ABBIENDI 00Z	OPAL	$e^+e^- \to Z$

$\Gamma(p/\overline{p}\,\text{anything})/\Gamma_{\text{total}}$ Γ_{66}/Γ

VALUE	DOCUMENT ID	TECN	COMMENT
0.131 ± 0.011 OUR AVERAGE			
$0.131 \pm 0.004 \pm 0.011$	BARATE 98V	ALEP	$e^+e^- \to Z$
$0.141 \pm 0.018 \pm 0.056$	ABREU 95C	DLPH	$e^+e^- \to Z$

$\Gamma(\Lambda/\overline{\Lambda}\text{anything})/\Gamma_{\text{total}}$ Γ_{67}/Γ

VALUE	DOCUMENT ID		TECN	COMMENT
0.059 ±0.006 OUR AVERAGE				
0.0587±0.0046±0.0048	ACKERSTAFF	97N	OPAL	$e^+e^- \to Z$
0.059 ±0.007 ±0.009	ABREU	95C	DLPH	$e^+e^- \to Z$

$\Gamma(b\text{-baryon anything})/\Gamma_{\text{total}}$ Γ_{68}/Γ

VALUE	DOCUMENT ID		TECN	COMMENT
0.102±0.007±0.027	[1] BARATE	98V	ALEP	$e^+e^- \to Z$

[1] BARATE 98V assumes B($B_s \to pX$) = 8 ± 4% and B(b-baryon $\to pX$) = 58 ± 6%.

$\Gamma(\text{charged anything})/\Gamma_{\text{total}}$ Γ_{69}/Γ

VALUE	DOCUMENT ID		TECN	COMMENT
4.97±0.03±0.06	[1] ABREU	98H	DLPH	$e^+e^- \to Z$
• • • We do not use the following data for averages, fits, limits, etc. • • •				
5.84±0.04±0.38	ABREU	95C	DLPH	Repl. by ABREU 98H

[1] ABREU 98H measurement excludes the contribution from K^0 and Λ decay.

$\Gamma(\text{hadron}^+\,\text{hadron}^-)/\Gamma_{\text{total}}$ Γ_{70}/Γ

VALUE (units 10^{-5})	DOCUMENT ID		TECN	COMMENT
$1.7^{+1.0}_{-0.7}$±0.2	[1,2] BUSKULIC	96V	ALEP	$e^+e^- \to Z$

[1] BUSKULIC 96V assumes PDG 96 production fractions for B^0, B^+, B_s, b baryons.
[2] Average branching fraction of weakly decaying B hadrons into two long-lived charged hadrons, weighted by their production cross section and lifetimes.

$\Gamma(\text{charmless})/\Gamma_{\text{total}}$ Γ_{71}/Γ

VALUE	DOCUMENT ID		TECN	COMMENT
0.007±0.021	[1] ABREU	98D	DLPH	$e^+e^- \to Z$

[1] ABREU 98D results are extracted from a fit to the b-tagging probability distribution based on the impact parameter. The expected hidden charm contribution of 0.026 ± 0.004 has been subtracted.

$\Gamma(\mu^+\mu^-\text{anything})/\Gamma_{\text{total}}$ Γ_{73}/Γ

Test for $\Delta B = 1$ weak neutral current.

VALUE	CL%	DOCUMENT ID		TECN	COMMENT
<3.2 $\times 10^{-4}$	90	ABBOTT	98B	D0	$p\overline{p}$ 1.8 TeV
• • • We do not use the following data for averages, fits, limits, etc. • • •					
<5.0 $\times 10^{-5}$	90	[1] ALBAJAR	91C	UA1	$E_{\text{cm}}^{p\overline{p}}$= 630 GeV
<0.02	95	ALTHOFF	84G	TASS	E_{cm}^{ee}= 34.5 GeV
<0.007	95	ADEVA	83	MRKJ	E_{cm}^{ee}= 30–38 GeV
<0.007	95	BARTEL	83B	JADE	E_{cm}^{ee}= 33–37 GeV

[1] Both ABBOTT 98B and GLENN 98 claim that the efficiency quoted in ALBAJAR 91C was overestimated by a large factor.

$[\Gamma(e^+e^-\text{anything}) + \Gamma(\mu^+\mu^-\text{anything})]/\Gamma_{\text{total}}$ $(\Gamma_{72}+\Gamma_{73})/\Gamma$

Test for $\Delta B = 1$ weak neutral current.

VALUE	CL%	DOCUMENT ID		TECN	COMMENT
• • • We do not use the following data for averages, fits, limits, etc. • • •					
<0.008	90	MATTEUZZI	83	MRK2	E_{cm}^{ee}= 29 GeV

$\Gamma(\nu\overline{\nu}\text{anything})/\Gamma_{\text{total}}$ Γ_{74}/Γ

VALUE	DOCUMENT ID		TECN	COMMENT
• • • We do not use the following data for averages, fits, limits, etc. • • •				
$<3.9 \times 10^{-4}$	[1] GROSSMAN	96	RVUE	$e^+e^- \to Z$

[1] GROSSMAN 96 limit is derived from the ALEPH BUSKULIC 95 limit B($B^+ \to \tau^+\nu_\tau$) $< 1.8 \times 10^{-3}$ at CL=90% using conservative simplifying assumptions.

χ_b AT HIGH ENERGY

For a discussion of B-$\overline{B}$ mixing, see the note on "B^0-$\overline{B}^0$ Mixing" in the B^0 Particle Listings.

χ_b is the average B-$\overline{B}$ mixing parameter at high-energy $\chi_b = f'_d\chi_d + f'_s\chi_s$ where f'_d and f'_s are the fractions of B^0 and B_s^0 hadrons in an unbiased sample of semileptonic b-hadron decays.

"OUR EVALUATION" is an average using rescaled values of the data listed below. The average and rescaling were performed by the Heavy Flavor Averaging Group (HFLAV) and are described at http://www.slac.stanford.edu/xorg/hflav/. The averaging/rescaling procedure takes into account correlations between the measurements.

VALUE	EVTS	DOCUMENT ID		TECN	COMMENT
0.1284±0.0069 OUR EVALUATION					
0.129 ±0.004 OUR AVERAGE					
0.132 ±0.001 ±0.024		[1] ABAZOV	06S	D0	$p\overline{p}$ at 1.96 TeV
0.152 ±0.007 ±0.011		[2] ACOSTA	04A	CDF	$p\overline{p}$ at 1.8 TeV
0.1312±0.0049±0.0042		[3] ABBIENDI	03P	OPAL	$e^+e^- \to Z$
0.127 ±0.013 ±0.006		[4] ABREU	01L	DLPH	$e^+e^- \to Z$
0.1192±0.0068±0.0051		[5] ACCIARRI	99D	L3	$e^+e^- \to Z$
0.121 ±0.016 ±0.006		[6] ABREU	94J	DLPH	$e^+e^- \to Z$
0.114 ±0.014 ±0.008		[7] BUSKULIC	94G	ALEP	$e^+e^- \to Z$
0.129 ±0.022		[8] BUSKULIC	92B	ALEP	$e^+e^- \to Z$
0.176 ±0.031 ±0.032	1112	[9] ABE	91G	CDF	$p\overline{p}$ 1.8 TeV
0.148 ±0.029 ±0.017		[10] ALBAJAR	91D	UA1	$p\overline{p}$ 630 GeV
• • • We do not use the following data for averages, fits, limits, etc. • • •					
0.131 ±0.020 ±0.016		[11] ABE	97I	CDF	Repl. by ACOSTA 04A
0.1107±0.0062±0.0055		[12] ALEXANDER	96	OPAL	Rep. by ABBIENDI 03P
0.136 ±0.037 ±0.040		[13] UENO	96	AMY	e^+e^- at 57.9 GeV
0.144 ±0.014 $^{+0.017}_{-0.011}$		[14] ABREU	94F	DLPH	Sup. by ABREU 94J
0.131 ±0.014		[15] ABREU	94J	DLPH	$e^+e^- \to Z$
0.123 ±0.012 ±0.008		ACCIARRI	94D	L3	Repl. by ACCIARRI 99D
0.157 ±0.020 ±0.032		[16] ALBAJAR	94	UA1	$\sqrt{s}$ = 630 GeV
0.121 $^{+0.044}_{-0.040}$ ±0.017	1665	[17] ABREU	93C	DLPH	Sup. by ABREU 94J
0.143 $^{+0.022}_{-0.021}$ ±0.007		[18] AKERS	93B	OPAL	Sup. by ALEXANDER 96
0.145 $^{+0.041}_{-0.035}$ ±0.018		[19] ACTON	92C	OPAL	$e^+e^- \to Z$
0.121 ±0.017 ±0.006		[20] ADEVA	92C	L3	Sup. by ACCIARRI 94D
0.132 ±0.22 $^{+0.015}_{-0.012}$	823	[21] DECAMP	91	ALEP	$e^+e^- \to Z$
0.178 $^{+0.049}_{-0.040}$ ±0.020		[22] ADEVA	90P	L3	$e^+e^- \to Z$
0.17 $^{+0.15}_{-0.08}$		[23,24] WEIR	90	MRK2	e^+e^- 29 GeV
0.21 $^{+0.29}_{-0.15}$		[23] BAND	88	MAC	E_{cm}^{ee}= 29 GeV
>0.02 at 90% CL		[23] BAND	88	MAC	E_{cm}^{ee}= 29 GeV
0.121 ±0.047		[23,25] ALBAJAR	87C	UA1	Repl. by ALBAJAR 91D
<0.12 at 90% CL		[23,26] SCHAAD	85	MRK2	E_{cm}^{ee}= 29 GeV

[1] Uses the dimuon charge asymmetry. Averaged over the mix of b-flavored hadrons.
[2] Measurement performed using events containing a dimuon or an e/μ pair.
[3] The average B mixing parameter is determined simultaneously with b and c forward-backward asymmetries in the fit.
[4] The experimental systematic and model uncertainties are combined in quadrature.
[5] ACCIARRI 99D uses maximum-likelihood fits to extract χ_b as well as the A_{FB}^b in $Z \to b\overline{b}$ events containing prompt leptons.
[6] This ABREU 94J result is from 5182 $\ell\ell$ and 279 $\Lambda\ell$ events. The systematic error includes 0.004 for model dependence.
[7] BUSKULIC 94G data analyzed using ee, $e\mu$, and $\mu\mu$ events.
[8] BUSKULIC 92B uses a jet charge technique combined with electrons and muons.
[9] ABE 91G measurement of χ is done with $e\mu$ and ee events.
[10] ALBAJAR 91D measurement of χ is done with dimuons.
[11] Uses di-muon events.
[12] ALEXANDER 96 uses a maximum likelihood fit to simultaneously extract χ as well as the forward-backward asymmetries in $e^+e^- \to Z \to b\overline{b}$ and $c\overline{c}$.
[13] UENO 96 extracted χ from the energy dependence of the forward-backward asymmetry.
[14] ABREU 94F uses the average electric charge sum of the jets recoiling against a b-quark jet tagged by a high p_T muon. The result is for $\overline{\chi} = f_d\chi_d + 0.9 f_s\chi_s$.
[15] This ABREU 94J result combines $\ell\ell$, $\Lambda\ell$, and jet-charge ℓ (ABREU 94F) analyses. It is for $\overline{\chi} = f_d\chi_d + 0.96 f_s\chi_s$.
[16] ALBAJAR 94 uses dimuon events. Not independent of ALBAJAR 91D.
[17] ABREU 93C data analyzed using ee, $e\mu$, and $\mu\mu$ events.
[18] AKERS 93B analysis performed using dilepton events.
[19] ACTON 92C uses electrons and muons. Superseded by AKERS 93B.
[20] ADEVA 92C uses electrons and muons.
[21] DECAMP 91 done with opposite and like-sign dileptons. Superseded by BUSKULIC 92B.
[22] ADEVA 90P measurement uses ee, $\mu\mu$, and $e\mu$ events from 118k events at the Z. Superseded by ADEVA 92C.
[23] These experiments are not in the average because the combination of B_s and B_d mesons which they see could differ from those at higher energy.
[24] The WEIR 90 measurement supersedes the limit obtained in SCHAAD 85. The 90% CL are 0.06 and 0.38.
[25] ALBAJAR 87C measured $\chi = (\overline{B}^0 \to B^0 \to \mu^+X)$ divided by the average production weighted semileptonic branching fraction for B hadrons at 546 and 630 GeV.
[26] Limit is average probability for hadron containing B quark to produce a positive lepton.

CP VIOLATION PARAMETERS in semileptonic b-hadron decays.

$\text{Re}(\epsilon_b) / (1 + |\epsilon_b|^2)$

CP impurity in semileptonic b-hadron decays.

VALUE (units 10^{-3})	DOCUMENT ID		TECN	COMMENT
−1.3 ±0.4 OUR AVERAGE				
−6.2 ±5.2 ±4.7	[1] AABOUD	17E	ATLS	pp at 8 TeV
−1.24±0.38±0.18	[2] ABAZOV	14	D0	$p\overline{p}$ at 1.96 TeV
• • • We do not use the following data for averages, fits, limits, etc. • • •				
−1.97±0.43±0.23	[3] ABAZOV	11U	D0	Repl. by ABAZOV 14
−2.39±0.63±0.37	[4] ABAZOV	10H	D0	Repl. by ABAZOV 11U

[1] AABOUD 17E reports a measurement of charge asymmetry of $A_{SL}^b = (-25 \pm 21 \pm 19) \times 10^{-3}$ in lepton + jets $t\overline{t}$ events in which a b-hadron decays semileptonically to a soft muon.
[2] ABAZOV 14 reports a measurement of like-sign dimuon charge asymmetry of $A_{SL}^b = (-4.96 \pm 1.53 \pm 0.72) \times 10^{-3}$ in semileptonic b-hadron decays.
[3] ABAZOV 11U reports a measurement of like-sign dimuon charge asymmetry of $A_{SL}^b = (-7.87 \pm 1.72 \pm 0.93) \times 10^{-3}$ in semileptonic b-hadron decays.
[4] ABAZOV 10H reports a measurement of like-sign dimuon charge asymmetry of $A_{SL}^b = (-9.57 \pm 2.51 \pm 1.46) \times 10^{-3}$ in semileptonic b-hadron decays. Using the measured production ratio of B_d^0 and B_s^0, and the asymmetry of B_d^0 $A_{SL}^d = (-4.7 \pm 4.6) \times$

Meson Particle Listings

$B^{\pm}/B^0/B^0_s/b$-baryon ADMIXTURE

10^{-3} measured from B-factories, they obtain the asymmetry for B^0_s as $A^s_{SL}=(-14.6\pm 7.5)\times 10^{-3}$.

B-HADRON PRODUCTION FRACTIONS IN HADRONIC Z DECAY

The production fractions of b-hadrons in hadronic Z decays have been calculated using the best values of mean lives, mixing parameters and branching fractions in this edition by the Heavy Flavor Averaging Group (HFLAV) (see http://www.slac.stanford.edu/xorg/hflav/).

The values reported below assume:

$f(\overline{b}\to B^+) = f(\overline{b}\to B^0)$

$f(\overline{b}\to B^+) + f(\overline{b}\to B^0) + f(\overline{b}\to B^0_s) + f(b\to b\text{-baryon}) = 1$

The values are:

$f(\overline{b}\to B^+) = f(\overline{b}\to B^0) = 0.407\pm 0.007$

$f(\overline{b}\to B^0_s) = 0.101\pm 0.008$

$f(b\to b\text{-baryon}) = 0.085\pm 0.011$

$f(\overline{b}\to B^0_s)\ /\ f(\overline{b}\to B^0_d) = 0.249\pm 0.023$

and their correlation coefficients are:

$cor(B^0_s,\ b\text{-baryon}) = +0.074$

$cor(B^0_s,\ B^+{=}B^0) = -0.625$

$cor(b\text{-baryon},\ B^+{=}B^0) = -0.825$

as obtained using a time-integrated mixing parameter $\overline{\chi} = 0.1259\pm 0.0042$ given by a fit to heavy quark quantities with asymmetries removed (see the note "The Z boson").

B-HADRON PRODUCTION FRACTIONS IN $p\overline{p}$ COLLISIONS AT Tevatron

The production fractions for b-hadrons in $p\overline{p}$ collisions at the Tevatron have been calculated from the best values of mean lifetimes, mixing parameters, and branching fractions in this edition by the Heavy Flavor Averaging Group (HFLAV) (see http://www.slac.stanford.edu/xorg/hflav/).

The values reported below assume:

$f(\overline{b}\to B^+) = f(\overline{b}\to B^0)$

$f(\overline{b}\to B^+) + f(\overline{b}\to B^0) + f(\overline{b}\to B^0_s) + f(b\to b\text{-baryon}) = 1$

The values are:

$f(\overline{b}\to B^+) = f(\overline{b}\to B^0) = 0.343\pm 0.021$

$f(\overline{b}\to B^0_s) = 0.115\pm 0.013$

$f(b\to b\text{-baryon}) = 0.199\pm 0.047$

$f(\overline{b}\to B^0_s)\ /\ f(\overline{b}\to B^0_d) = 0.334\pm 0.041$

and their correlation coefficients are:

$cor(B^0_s,\ b\text{-baryon}) = -0.431$

$cor(B^0_s,\ B^+{=}B^0) = +0.162$

$cor(b\text{-baryon},\ B^+{=}B^0) = -0.960$

as obtained with the Tevatron average of time-integrated mixing parameter $\overline{\chi} = 0.147\pm 0.011$.

PRODUCTION ASYMMETRIES

$\mathbf{A^{b\overline{b}}_C}$

$A^{b\overline{b}}_C = [N(\Delta y>0) - N(\Delta y<0)]\ /\ [N(\Delta y>0) + N(\Delta y<0)]$ with $\Delta y = |y_b| - |y_{\overline{b}}|$ where $y_{b/\overline{b}}$ is rapidity of b or $\overline{b}$ quarks.

VALUE (units 10^{-2})	DOCUMENT ID		TECN	COMMENT
Average is meaningless.				
$0.4\pm 0.4\pm 0.3$	[1] AAIJ	14AS	LHCB	pp at 7 TeV
$2.0\pm 0.9\pm 0.6$	[2] AAIJ	14AS	LHCB	pp at 7 TeV
$1.6\pm 1.7\pm 0.6$	[3] AAIJ	14AS	LHCB	pp at 7 TeV

[1] Measured for $40 < M(b\overline{b}) < 75$ GeV/c^2.

[2] Measured for $75 < M(b\overline{b}) < 105$ GeV/c^2.

[3] Measured for $M(b\overline{b}) > 105$ GeV/c^2.

$B^{\pm}/B^0/B^0_s/b$-baryon ADMIXTURE REFERENCES

AABOUD	17E	JHEP 1702 071	M. Aaboud *et al.*	(ATLAS Collab.)
AAIJ	17BB	EPJ C77 609	R. Aaij *et al.*	(LHCb Collab.)
AAD	15CM	PRL 115 262001	G. Aad *et al.*	(ATLAS Collab.)
AAIJ	14AS	PRL 113 082003	R. Aaij *et al.*	(LHCb Collab.)
ABAZOV	14	PR D89 012002	V.M. Abazov *et al.*	(D0 Collab.)
AAIJ	13P	JHEP 1304 001	R. Aaij *et al.*	(LHCb Collab.)
AAIJ	12BD	EPJ C72 2100	R. Aaij *et al.*	(LHCb Collab.)
AAIJ	12J	PR D85 032008	R. Aaji *et al.*	(LHCb Collab.)
CHATRCHYAN	12AK	JHEP 1202 011	S. Chatrchyan *et al.*	(CMS Collab.)
AAIJ	11F	PRL 107 211801	R. Aaij *et al.*	(LHCb Collab.)
ABAZOV	11U	PR D84 052007	V.M. Abazov *et al.*	(D0 Collab.)
ABAZOV	10H	PRL 105 081801	V.M. Abazov *et al.*	(D0 Collab.)
Also		PR D82 032001	V.M. Abazov *et al.*	(D0 Collab.)
PDG	10	JP G37 075021	K. Nakamura *et al.*	(PDG Collab.)
AALTONEN	09E	PR D79 032001	T. Aaltonen *et al.*	(CDF Collab.)
AALTONEN	08N	PR D77 072003	T. Aaltonen *et al.*	(CDF Collab.)
ABAZOV	06S	PR D74 092001	V.M. Abazov *et al.*	(D0 Collab.)
ABBIENDI	04I	EPJ C35 149	G. Abbiendi *et al.*	(OPAL Collab.)
ABDALLAH	04E	EPJ C33 307	J. Abdallah *et al.*	(DELPHI Collab.)
ACOSTA	04A	PR D69 012002	D. Acosta *et al.*	(CDF Collab.)
ABBIENDI	03M	EPJ C30 467	G. Abbiendi *et al.*	(OPAL Collab.)
ABBIENDI	03P	PL B577 18	G. Abbiendi *et al.*	(OPAL Collab.)
ABDALLAH	03E	PL B561 26	J. Abdallah *et al.*	(DELPHI Collab.)
ABDALLAH	03K	PL B576 29	J. Abdallah *et al.*	(DELPHI Collab.)
HEISTER	02G	EPJ C22 613	A. Heister *et al.*	(ALEPH Collab.)
ABBIENDI	01Q	PL B520 1	G. Abbiendi *et al.*	(OPAL Collab.)
ABBIENDI	01R	EPJ C21 399	G. Abbiendi *et al.*	(OPAL Collab.)
ABREU	01L	EPJ C20 455	P. Abreu *et al.*	(DELPHI Collab.)
BARATE	01E	EPJ C19 213	R. Barate *et al.*	(ALEPH Collab.)
ABBIENDI	00E	EPJ C13 225	G. Abbiendi *et al.*	(OPAL Collab.)
ABBIENDI	00Z	PL B492 13	G. Abbiendi *et al.*	(OPAL Collab.)
ABREU	00	EPJ C12 225	P. Abreu *et al.*	(DELPHI Collab.)
ABREU	00C	PL B496 43	P. Abreu *et al.*	(DELPHI Collab.)
ABREU	00D	PL B478 14	P. Abreu *et al.*	(DELPHI Collab.)
ABREU	00R	PL B475 407	P. Abreu *et al.*	(DELPHI Collab.)
ACCIARRI	00	EPJ C13 47	M. Acciarri *et al.*	(L3 Collab.)
AFFOLDER	00E	PRL 84 1663	T. Affolder *et al.*	(CDF Collab.)
ABBIENDI	99J	EPJ C12 609	G. Abbiendi *et al.*	(OPAL Collab.)
ABE	99P	PR D60 092005	F. Abe *et al.*	(CDF Collab.)
ACCIARRI	99D	PL B448 152	M. Acciarri *et al.*	(L3 Collab.)
BARATE	99G	EPJ C6 555	R. Barate *et al.*	(ALEPH Collab.)
ABBOTT	98B	PL B423 419	B. Abbott *et al.*	(D0 Collab.)
ABE	98B	PR D57 5382	F. Abe *et al.*	(CDF Collab.)
ABREU	98D	PL B426 193	P. Abreu *et al.*	(DELPHI Collab.)
ABREU	98H	PL B425 399	P. Abreu *et al.*	(DELPHI Collab.)
ACCIARRI	98	PL B416 220	M. Acciarri *et al.*	(L3 Collab.)
ACCIARRI	98K	PL B436 174	M. Acciarri *et al.*	(L3 Collab.)
ACKERSTAFF	98E	EPJ C1 439	K. Ackerstaff *et al.*	(OPAL Collab.)
BARATE	98I	PL B429 169	R. Barate *et al.*	(ALEPH Collab.)
BARATE	98Q	EPJ C4 387	R. Barate *et al.*	(ALEPH Collab.)
BARATE	98V	EPJ C5 205	R. Barate *et al.*	(ALEPH Collab.)
GLENN	98	PRL 80 2289	S. Glenn *et al.*	(CLEO Collab.)
ABE	97I	PR D55 2546	F. Abe *et al.*	(CDF Collab.)
ACKERSTAFF	97F	ZPHY C73 397	K. Ackerstaff *et al.*	(OPAL Collab.)
ACKERSTAFF	97N	ZPHY C74 423	K. Ackerstaff *et al.*	(OPAL Collab.)
ACKERSTAFF	97W	ZPHY C76 425	K. Ackerstaff *et al.*	(OPAL Collab.)
ABREU	96E	PL B377 195	P. Abreu *et al.*	(DELPHI Collab.)
ACCIARRI	96C	ZPHY C71 379	M. Acciarri *et al.*	(L3 Collab.)
ADAM	96	ZPHY C69 561	W. Adam *et al.*	(DELPHI Collab.)
ADAM	96D	ZPHY C72 207	W. Adam *et al.*	(DELPHI Collab.)
ALEXANDER	96	ZPHY C70 357	G. Alexander *et al.*	(OPAL Collab.)
BUSKULIC	96F	PL B369 151	D. Buskulic *et al.*	(ALEPH Collab.)
BUSKULIC	96V	PL B384 471	D. Buskulic *et al.*	(ALEPH Collab.)
BUSKULIC	96Y	PL B388 648	D. Buskulic *et al.*	(ALEPH Collab.)
GROSSMAN	96	NP B465 369	Y. Grossman, Z. Ligeti, E. Nardi	(REHO, CIT)
Also		NP B480 753 (erratum)	Y. Grossman, Z. Ligeti, E. Nardi	
PDG	96	PR D54 1	R. M. Barnett *et al.*	(PDG Collab.)
UENO	96	PL B381 365	K. Ueno *et al.*	(AMY Collab.)
ABE,K	95B	PRL 75 3624	K. Abe *et al.*	(SLD Collab.)
ABREU	95C	PL B347 447	P. Abreu *et al.*	(DELPHI Collab.)
ABREU	95D	ZPHY C66 323	P. Abreu *et al.*	(DELPHI Collab.)
ADAM	95	ZPHY C68 363	W. Adam *et al.*	(DELPHI Collab.)
AKERS	95Q	ZPHY C67 57	R. Akers *et al.*	(OPAL Collab.)
BUSKULIC	95	PL B343 444	D. Buskulic *et al.*	(ALEPH Collab.)
ABREU	94F	PL B322 459	P. Abreu *et al.*	(DELPHI Collab.)
ABREU	94J	PL B332 488	P. Abreu *et al.*	(DELPHI Collab.)
ABREU	94L	ZPHY C63 3	P. Abreu *et al.*	(DELPHI Collab.)
ABREU	94P	PL B341 109	P. Abreu *et al.*	(DELPHI Collab.)
ACCIARRI	94C	PL B332 201	M. Acciarri *et al.*	(L3 Collab.)
ACCIARRI	94D	PL B335 542	M. Acciarri *et al.*	(L3 Collab.)
ALBAJAR	94	ZPHY C61 41	C. Albajar *et al.*	(UA1 Collab.)
BUSKULIC	94G	ZPHY C62 179	D. Buskulic *et al.*	(ALEPH Collab.)
ABE	93E	PL B313 288	K. Abe *et al.*	(VENUS Collab.)
ABE	93J	PRL 71 3421	F. Abe *et al.*	(CDF Collab.)
ABREU	93C	PL B301 145	P. Abreu *et al.*	(DELPHI Collab.)
ABREU	93D	ZPHY C57 181	P. Abreu *et al.*	(DELPHI Collab.)
ABREU	93G	PL B312 253	P. Abreu *et al.*	(DELPHI Collab.)
ACTON	93C	PL B307 247	P.D. Acton *et al.*	(OPAL Collab.)
ACTON	93L	ZPHY C60 217	P.D. Acton *et al.*	(OPAL Collab.)
ADRIANI	93J	PL B317 467	O. Adriani *et al.*	(L3 Collab.)
ADRIANI	93K	PL B317 474	O. Adriani *et al.*	(L3 Collab.)
ADRIANI	93L	PL B317 637	O. Adriani *et al.*	(L3 Collab.)
AKERS	93B	ZPHY C60 199	R. Akers *et al.*	(OPAL Collab.)
BUSKULIC	93B	PL B298 479	D. Buskulic *et al.*	(ALEPH Collab.)
BUSKULIC	93O	PL B314 459	D. Buskulic *et al.*	(ALEPH Collab.)
ABREU	92	ZPHY C53 567	P. Abreu *et al.*	(DELPHI Collab.)
ACTON	92	PL B274 513	D.P. Acton *et al.*	(OPAL Collab.)
ACTON	92C	PL B276 379	D.P. Acton *et al.*	(OPAL Collab.)
ADEVA	92C	PL B288 395	B. Adeva *et al.*	(L3 Collab.)
ADRIANI	92	PL B288 412	O. Adriani *et al.*	(L3 Collab.)
BUSKULIC	92B	PL B284 177	D. Buskulic *et al.*	(ALEPH Collab.)
BUSKULIC	92F	PL B295 174	D. Buskulic *et al.*	(ALEPH Collab.)
BUSKULIC	92G	PL B295 396	D. Buskulic *et al.*	(ALEPH Collab.)
ABE	91G	PRL 67 3351	F. Abe *et al.*	(CDF Collab.)
ADEVA	91C	PL B261 177	B. Adeva *et al.*	(L3 Collab.)
ADEVA	91H	PL B270 111	B. Adeva *et al.*	(L3 Collab.)
ALBAJAR	91C	PL B262 163	C. Albajar *et al.*	(UA1 Collab.)
ALBAJAR	91D	PL B262 171	C. Albajar *et al.*	(UA1 Collab.)
ALEXANDER	91G	PL B266 485	G. Alexander *et al.*	(OPAL Collab.)
DECAMP	91	PL B258 236	D. Decamp *et al.*	(ALEPH Collab.)
DECAMP	91C	PL B257 492	D. Decamp *et al.*	(ALEPH Collab.)
ADEVA	90P	PL B252 703	B. Adeva *et al.*	(L3 Collab.)
BEHREND	90D	ZPHY C47 333	H.J. Behrend *et al.*	(CELLO Collab.)
HAGEMANN	90	ZPHY C48 401	J. Hagemann *et al.*	(JADE Collab.)
LYONS	90	PR D41 982	L. Lyons, A.J. Martin, D.H. Saxon	(OXF, BRIS+)
WEIR	90	PL B240 289	A.J. Weir *et al.*	(Mark II Collab.)
BRAUNSCH...	89B	ZPHY C44 1	R. Braunschweig *et al.*	(TASSO Collab.)
ONG	89	PRL 62 1236	R.A. Ong *et al.*	(Mark II Collab.)
BAND	88	PL B200 221	H.R. Band *et al.*	(MAC Collab.)
KLEM	88	PR D37 41	D.E. Klem *et al.*	(DELCO Collab.)
ONG	88	PRL 60 2587	R.A. Ong *et al.*	(Mark II Collab.)
ALBAJAR	87C	PL B186 247	C. Albajar *et al.*	(UA1 Collab.)
ASH	87	PRL 58 640	W.W. Ash *et al.*	(MAC Collab.)
BARTEL	87	ZPHY C33 339	W. Bartel *et al.*	(JADE Collab.)
BROM	87	PL B195 301	J.M. Brom *et al.*	(HRS Collab.)
PAL	86	PR D33 2708	T. Pal *et al.*	(DELCO Collab.)
AIHARA	85	ZPHY C27 39	H. Aihara *et al.*	(TPC Collab.)
BARTEL	85J	PL 163B 277	W. Bartel *et al.*	(JADE Collab.)
SCHAAD	85	PL 160B 188	T. Schaad *et al.*	(Mark II Collab.)
ALTHOFF	84G	ZPHY C22 219	M. Althoff *et al.*	(TASSO Collab.)
ALTHOFF	84J	PL 146B 443	M. Althoff *et al.*	(TASSO Collab.)
KOOP	84	PRL 52 970	D.E. Koop *et al.*	(DELCO Collab.)
ADEVA	83	PRL 50 799	B. Adeva *et al.*	(Mark-J Collab.)
ADEVA	83B	PRL 51 443	B. Adeva *et al.*	(Mark-J Collab.)
BARTEL	83B	PL 132B 241	W. Bartel *et al.*	(JADE Collab.)
FERNANDEZ	83D	PRL 50 2054	E. Fernandez *et al.*	(MAC Collab.)
MATTEUZZI	83	PL 129B 141	C. Matteuzzi *et al.*	(Mark II Collab.)
NELSON	83	PRL 50 1542	M.E. Nelson *et al.*	(Mark II Collab.)

V_{cb} and V_{ub} CKM Matrix Elements

OMITTED FROM SUMMARY TABLE

See the related review(s):

Semileptonic B Hadron Decays, Determination of V_{cb} and V_{ub}

V_{cb} MEASUREMENTS

For the discussion of V_{cb} measurements, which is not repeated here, see the review on "Determination of $|V_{cb}|$ and $|V_{ub}|$."

The CKM matrix element $|V_{cb}|$ can be determined by studying the rate of the semileptonic decay $B \to D^{(*)}\ell\nu$ as a function of the recoil kinematics of $D^{(*)}$ mesons. Taking advantage of theoretical constraints on the normalization and a linear ω dependence of the form factors ($F(\omega)$, $G(\omega)$) provided by Heavy Quark Effective Theory (HQET), the $|V_{cb}|\times F(\omega)$ and ρ^2 (a^2) can be simultaneously extracted from data, where ω is the scalar product of the two-meson four velocities, $F(1)$ is the form factor at zero recoil (ω=1) and ρ^2 is the slope, sometimes denoted as a^2. Using the theoretical input of $F(1)$, a value of $|V_{cb}|$ can be obtained.

"OUR EVALUATION" is an average using rescaled values of the data listed below. The average and rescaling were performed by the Heavy Flavor Averaging Group (HFLAV) and are described at http://www.slac.stanford.edu/xorg/hflav/. The averaging/rescaling procedure takes into account correlations between the measurements.

$|V_{cb}| \times F(1)$ (from $B^0 \to D^{*-}\ell^+\nu$)

VALUE	DOCUMENT ID		TECN	COMMENT
0.03561±0.00043 OUR EVALUATION	with ρ^2=1.205 ± 0.026 and a correlation 0.338. The fitted χ^2 is 30.2 for 23 degrees of freedom.			
0.0360 ±0.0009 OUR AVERAGE	Error includes scale factor of 1.5. See the ideogram below.			
0.0346 ±0.0002 ±0.0010	[1] DUNGEL	10	BELL	$e^+e^- \to \Upsilon(4S)$
0.0359 ±0.0002 ±0.0012	[2] AUBERT	09A	BABR	$e^+e^- \to \Upsilon(4S)$
0.0359 ±0.0006 ±0.0014	[3] AUBERT	08AT	BABR	$e^+e^- \to \Upsilon(4S)$
0.0392 ±0.0018 ±0.0023	[4] ABDALLAH	04D	DLPH	$e^+e^- \to Z^0$
0.0431 ±0.0013 ±0.0018	[5] ADAM	03	CLE2	$e^+e^- \to \Upsilon(4S)$
0.0355 ±0.0014 $^{+0.0023}_{-0.0024}$	[6] ABREU	01H	DLPH	$e^+e^- \to Z$
0.0371 ±0.0010 ±0.0020	[7] ABBIENDI	00Q	OPAL	$e^+e^- \to Z$
0.0319 ±0.0018 ±0.0019	[8] BUSKULIC	97	ALEP	$e^+e^- \to Z$
• • • We do not use the following data for averages, fits, limits, etc. • • •				
0.0344 ±0.0003 ±0.0011	[9] AUBERT	08R	BABR	Repl. by AUBERT 09A
0.0355 ±0.0003 ±0.0016	[10] AUBERT	05E	BABR	Repl. by AUBERT 08R
0.0377 ±0.0011 ±0.0019	[11] ABDALLAH	04D	DLPH	$e^+e^- \to Z^0$
0.0354 ±0.0019 ±0.0018	[12] ABE	02F	BELL	Repl. by DUNGEL 10
0.0431 ±0.0013 ±0.0018	[13] BRIERE	02	CLE2	$e^+e^- \to \Upsilon(4S)$
0.0328 ±0.0019 ±0.0022	ACKERSTAFF	97G	OPAL	Repl. by ABBIENDI 00Q
0.0350 ±0.0019 ±0.0023	[14] ABREU	96P	DLPH	Repl. by ABREU 01H
0.0351 ±0.0019 ±0.0020	[15] BARISH	95	CLE2	Repl. by ADAM 03
0.0314 ±0.0023 ±0.0025	BUSKULIC	95N	ALEP	Repl. by BUSKULIC 97

[1] Uses fully reconstructed $D^{*-}\ell^+\nu$ events ($\ell = e$ or μ).

[2] Obtained from a global fit to $B \to D^{(*)}\ell\nu_\ell$ events, with reconstructed $D^0\ell$ and $D^+\ell$ final states and $\rho^2 = 1.22 \pm 0.02 \pm 0.07$.

[3] Measured using the dependence of $B^- \to D^{*0}e^-\overline{\nu}_e$ decay differential rate and the form factor description by CAPRINI 98 with $\rho^2 = 1.16 \pm 0.06 \pm 0.08$.

[4] Measurement using fully reconstructed D^* sample with a $\rho^2 = 1.32 \pm 0.15 \pm 0.33$.

[5] Average of the $B^0 \to D^*(2010)^-\ell^+\nu$ and $B^+ \to \overline{D}^*(2007)\ell^+\nu$ modes with $\rho^2 = 1.61 \pm 0.09 \pm 0.21$ and $f_{+-} = 0.521 \pm 0.012$.

[6] ABREU 01H measured using about 5000 partial reconstructed D^* sample with a ρ^2=1.34 ± 0.14 $^{+0.24}_{-0.22}$.

[7] ABBIENDI 00Q: measured using both inclusively and exclusively reconstructed $D^{*\pm}$ samples with a ρ^2=1.21 ± 0.12 ± 0.20. The statistical and systematic correlations between $|V_{cb}|\times F(1)$ and ρ^2 are 0.90 and 0.54 respectively.

[8] BUSKULIC 97: measured using exclusively reconstructed $D^{*\pm}$ with a a^2=0.31 ± 0.17 ± 0.08. The statistical correlation is 0.92.

[9] Measured using fully reconstructed D^* sample and a simultaneous fit to the Caprini-Lellouch-Neubert form factor parameters: $\rho^2 = 1.191 \pm 0.048 \pm 0.028$, $R_1(1) = 1.429 \pm 0.061 \pm 0.044$, and $R_2(1) = 0.827 \pm 0.038 \pm 0.022$.

[10] Measurement using fully reconstructed D^* sample with a $\rho^2 = 1.29 \pm 0.03 \pm 0.27$.

[11] Combines with previous partial reconstructed D^* measurement with a $\rho^2 = 1.39 \pm 0.10 \pm 0.33$.

[12] Measured using exclusive $B^0 \to D^*(892)^-e^+\nu$ decays with ρ^2= 1.35 ± 0.17 ± 0.19 and a correlation of 0.91.

[13] BRIERE 02 result is based on the same analysis and data sample reported in ADAM 03.

[14] ABREU 96P: measured using both inclusively and exclusively reconstructed $D^{*\pm}$ samples.

[15] BARISH 95: measured using both exclusive reconstructed $B^0 \to D^{*-}\ell^+\nu$ and $B^+ \to D^{*0}\ell^+\nu$ samples. They report their experiment's uncertainties ±0.0019 ± 0.0018 ± 0.0008, where the first error is statistical, the second is systematic, and the third is the uncertainty in the lifetimes. We combine the last two in quadrature.

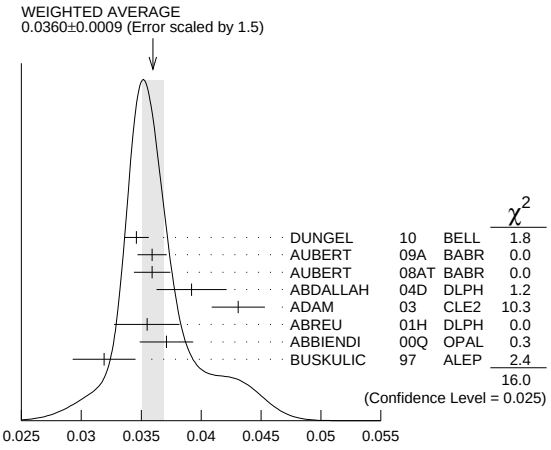

$|V_{cb}| \times G(1)$ (from $B \to D^-\ell^+\nu$)

VALUE	DOCUMENT ID		TECN	COMMENT
0.04157±0.00100 OUR EVALUATION	with ρ^2=1.128 ± 0.033 and a correlation 0.751. The fitted χ^2 is 4.7 for 8 degrees of freedom.			
0.0422 ±0.0010 OUR AVERAGE				
0.04229±0.00137	[1] GLATTAUER	16	BELL	$e^+e^- \to \Upsilon(4S)$
0.0423 ±0.0019 ±0.0014	[2] AUBERT	10	BABR	$e^+e^- \to \Upsilon(4S)$
0.0431 ±0.0008 ±0.0023	[3] AUBERT	09A	BABR	$e^+e^- \to \Upsilon(4S)$
0.0416 ±0.0047 ±0.0037	[4] BARTELT	99	CLE2	$e^+e^- \to \Upsilon(4S)$
0.0278 ±0.0068 ±0.0065	[5] BUSKULIC	97	ALEP	$e^+e^- \to Z$
• • • We do not use the following data for averages, fits, limits, etc. • • •				
0.0411 ±0.0044 ±0.0052	[6] ABE	02E	BELL	Repl. by GLATTAUER 16
0.0337 ±0.0044 $^{+0.0072}_{-0.0049}$	[7] ATHANAS	97	CLE2	Repl. by BARTELT 99

[1] Obtained from a fit to the combined partially reconstructed $B \to \overline{D}\ell\nu_\ell$ sample while tagged by the other fully reconstructed B meson in the event. Also reports fitted $\rho^2 = 1.09 \pm 0.05$.

[2] Obtained from a fit to the combined $B \to \overline{D}\ell^+\nu_\ell$ sample in which a hadronic decay of the second B meson is fully reconstructed and $\rho^2 = 1.20 \pm 0.09 \pm 0.04$.

[3] Obtained from a global fit to $B \to D^{(*)}\ell\nu_\ell$ events, with reconstructed $D^0\ell$ and $D^+\ell$ final states and $\rho^2 = 1.20 \pm 0.04 \pm 0.07$.

[4] BARTELT 99: measured using both exclusive reconstructed $B^0 \to D^-\ell^+\nu$ and $B^+ \to D^0\ell^+\nu$ samples.

[5] BUSKULIC 97: measured using exclusively reconstructed $D^{\pm}$ with a a^2=−0.05 ± 0.53 ± 0.38. The statistical correlation is 0.99.

[6] Using the missing energy and momentum to extract kinematic information about the undetected neutrino in the $B^0 \to D^-\ell^+\nu$ decay.

[7] ATHANAS 97: measured using both exclusive reconstructed $B^0 \to D^-\ell^+\nu$ and $B^+ \to D^0\ell^+\nu$ samples with a ρ^2=0.59 ± 0.22 ± 0.12 $^{+0.59}_{-0}$. They report their experiment's uncertainties ±0.0044 ± 0.0048 $^{+0.0053}_{-0.0012}$, where the first error is statistical, the second is systematic, and the third is the uncertainty due to the form factor model variations. We combine the last two in quadrature.

V_{ub} MEASUREMENTS

For the discussion of V_{ub} measurements, which is not repeated here, see the review on "Determination of $|V_{cb}|$ and $|V_{ub}|$."

The CKM matrix element $|V_{ub}|$ can be determined by studying the rate of the charmless semileptonic decay $b \to u\ell\nu$. The relevant branching ratio measurements based on exclusive and inclusive decays can be found in the B Listings, and are not repeated here.

V_{cb} and V_{ub} CKM Matrix Elements REFERENCES

GLATTAUER	16	PR D93 032006	R. Glattauer *et al.*	(BELLE Collab.)
AUBERT	10	PRL 104 011802	B. Aubert *et al.*	(BABAR Collab.)
DUNGEL	10	PR D82 112007	W. Dungel *et al.*	(BELLE Collab.)
AUBERT	09A	PR D79 012002	B. Aubert *et al.*	(BABAR Collab.)
AUBERT	08AT	PRL 100 231803	B. Aubert *et al.*	(BABAR Collab.)
AUBERT	08R	PR D77 032002	B. Aubert *et al.*	(BABAR Collab.)
AUBERT	05E	PR D71 051502	B. Aubert *et al.*	(BABAR Collab.)
ABDALLAH	04D	EPJ C33 213	J. Abdallah *et al.*	(DELPHI Collab.)
ADAM	03	PR D67 032001	N.E. Adam *et al.*	(CLEO Collab.)
ABE	02E	PL B526 258	K. Abe *et al.*	(BELLE Collab.)
ABE	02F	PL B526 247	K. Abe *et al.*	(BELLE Collab.)
BRIERE	02	PRL 89 081803	R. Briere *et al.*	(CLEO Collab.)
ABREU	01H	PL B510 55	P. Abreu *et al.*	(DELPHI Collab.)
ABBIENDI	00Q	PL B482 15	G. Abbiendi *et al.*	(OPAL Collab.)
BARTELT	99	PRL 82 3746	J. Bartelt *et al.*	(CLEO Collab.)
CAPRINI	98	NP B530 153	I. Caprini, L. Lellouch, M. Neubert	(BCIP, CERN)
ACKERSTAFF	97G	PL B395 128	K. Ackerstaff *et al.*	(OPAL Collab.)
ATHANAS	97	PRL 79 2208	M. Athanas *et al.*	(CLEO Collab.)
BUSKULIC	97	PL B395 373	D. Buskulic *et al.*	(ALEPH Collab.)
ABREU	96P	ZPHY C71 539	P. Abreu *et al.*	(DELPHI Collab.)

Meson Particle Listings

V_{cb} and V_{ub} CKM Matrix Elements, B^*, $B_1(5721)^+$, $B_1(5721)^0$

BARISH 95 PR D51 1014 B.C. Barish *et al.* (CLEO Collab.)
BUSKULIC 95N PL B359 236 D. Buskulic *et al.* (ALEPH Collab.)

B^*

$I(J^P) = \frac{1}{2}(1^-)$

I, *J*, *P* need confirmation. Quantum numbers shown are quark-model predictions.

B^* MASS

From mass difference below and the average of our B masses $(m_{B^\pm} + m_{B^0})/2$.

VALUE (MeV)	DOCUMENT ID
5324.65 ± 0.25 OUR FIT	

$m_{B^*} - m_B$

VALUE (MeV)	EVTS	DOCUMENT ID		TECN	COMMENT
45.18 ± 0.23 OUR FIT					
45.42 ± 0.26 OUR AVERAGE		Includes data from the datablock that follows this one.			
46.2 ± 0.3 ± 0.8		[1] ACKERSTAFF	97M	OPAL	$e^+e^- \to Z$
45.3 ± 0.35 ± 0.87	4227	[1] BUSKULIC	96D	ALEP	$E_{\rm cm}^{ee}$ = 88–94 GeV
45.5 ± 0.3 ± 0.8		[1] ABREU	95R	DLPH	$E_{\rm cm}^{ee}$ = 88–94 GeV
46.3 ± 1.9	1378	[1] ACCIARRI	95B	L3	$E_{\rm cm}^{ee}$ = 88–94 GeV
46.4 ± 0.3 ± 0.8		[2] AKERIB	91	CLE2	$e^+e^- \to \gamma X$
45.6 ± 0.8		[2] WU	91	CSB2	$e^+e^- \to \gamma X, \gamma \ell X$
45.4 ± 1.0		[3] LEE-FRANZINI	90	CSB2	$e^+e^- \to \Upsilon(5S)$
• • • We do not use the following data for averages, fits, limits, etc. • • •					
52 ± 2 ± 4	1400	[4] HAN	85	CUSB	$e^+e^- \to \gamma e X$

[1] *u*, *d*, *s* flavor averaged.
[2] These papers report E_γ in the B^* center of mass. The $m_{B^*} - m_B$ is 0.2 MeV higher. $E_{\rm cm}$ = 10.61–10.7 GeV. Admixture of B^0 and B^+ mesons, but not B_s.
[3] LEE-FRANZINI 90 value is for an admixture of B^0 and B^+. They measure 46.7 ± 0.4 ± 0.2 MeV for an admixture of B^0, B^+, and B_s, and use the shape of the photon line to separate the above value.
[4] HAN 85 is for $E_{\rm cm}$ = 10.6–11.2 GeV, giving an admixture of B^0, B^+, and B_s.

$m_{B^{*+}} - m_{B^+}$

VALUE (MeV)	DOCUMENT ID		TECN	COMMENT
The data in this block is included in the average printed for a previous datablock.				
45.34 ± 0.23 OUR FIT				
45.01 ± 0.30 ± 0.23	[5] AAIJ	13O	LHCB	pp at 7 TeV

[5] Obtained the mass difference between $B^{*+}K^-$ and B^+K^- from $B_{s2}^*(5840)^0$ decay.

$|(m_{B^{*+}} - m_{B^+}) - (m_{B^{*0}} - m_{B^0})|$

VALUE (MeV)	CL%	DOCUMENT ID		TECN	COMMENT
< 6	95	ABREU	95R	DLPH	$E_{\rm cm}^{ee}$ = 88–94 GeV

B^* DECAY MODES

	Mode	Fraction (Γ_i/Γ)
Γ_1	$B\gamma$	dominant

B^* REFERENCES

AAIJ 13O PRL 110 151803 R. Aaij *et al.* (LHCb Collab.)
ACKERSTAFF 97M ZPHY C74 413 K. Ackerstaff *et al.* (OPAL Collab.)
BUSKULIC 96D ZPHY C69 393 D. Buskulic *et al.* (ALEPH Collab.)
ABREU 95R ZPHY C68 353 P. Abreu *et al.* (DELPHI Collab.)
ACCIARRI 95B PL B345 589 M. Acciarri *et al.* (L3 Collab.)
AKERIB 91 PRL 67 1692 D.S. Akerib *et al.* (CLEO Collab.)
WU 91 PL B273 177 Q.W. Wu *et al.* (CUSB II Collab.)
LEE-FRANZINI 90 PRL 65 2947 J. Lee-Franzini *et al.* (CUSB II Collab.)
HAN 85 PRL 55 36 K. Han *et al.* (COLU, LSU, MPIM, STON)

$B_1(5721)^+$

$I(J^P) = \frac{1}{2}(1^+)$ Status: **

I, *J*, *P* need confirmation.

Quantum numbers shown are quark-model predictions.

$B_1(5721)^+$ MASS

OUR FIT uses $m_{B^{*0}}$ and $m_{B_1^+} - m_{B^{*0}}$ to determine $m_{B_1(5721)^+}$.

VALUE (MeV)	DOCUMENT ID
5725.9 $^{+2.5}_{-2.7}$ OUR FIT	

$m_{B_1^+} - m_{B^{*0}}$

VALUE (MeV)	EVTS	DOCUMENT ID		TECN	COMMENT
401.2 $^{+2.4}_{-2.7}$ OUR FIT					
401.2 $^{+2.4}_{-2.7}$ OUR AVERAGE					
400.5 ± 1.8 ± 3.1	8K	[1] AAIJ	15AB	LHCB	pp at 7, 8 TeV
402 ± 3 $^{+1}_{-3}$		[2] AALTONEN	14I	CDF	$p\overline{p}$ at 1.96 TeV

[1] AAIJ 15AB reports $[m_{B_1^+} - m_{B^0}] - (m_{B^{*0}} - m_{B^0}) - m_{\pi^+} = 260.9 \pm 1.8 \pm 3.1$ MeV which we adjust by the π^+ mass and assume $(m_{B^{*0}} - m_{B^0}) = (m_{B^{*+}} - m_{B^+})$ = 45.01 ± 0.30 ± 0.23 MeV. The masses inside the square brackets were measured for each candidate event.
[2] AALTONEN 14I reports $m_{B_1(5721)^+} - m_{B^{*0}} - m_{\pi^+} = 262 \pm 3^{+1}_{-3}$ MeV which we adjusted by the π^+ mass.

$B_1(5721)^+$ WIDTH

VALUE (MeV)	EVTS	DOCUMENT ID		TECN	COMMENT
31 ± 6 OUR AVERAGE		Error includes scale factor of 1.1.			
29.1 ± 3.6 ± 4.3	8K	AAIJ	15AB	LHCB	pp at 7, 8 TeV
49 $^{+12}_{-10}$ $^{+2}_{-13}$		AALTONEN	14I	CDF	$p\overline{p}$ at 1.96 TeV

$B_1(5721)^+$ DECAY MODES

	Mode	Fraction (Γ_i/Γ)
Γ_1	$B^{*0}\pi^+$	seen

$B_1(5721)^+$ BRANCHING RATIOS

$\Gamma(B^{*0}\pi^+)/\Gamma_{\rm total}$ Γ_1/Γ

VALUE	EVTS	DOCUMENT ID		TECN	COMMENT
seen	8K	AAIJ	15AB	LHCB	pp at 7, 8 TeV
seen		AALTONEN	14I	CDF	$p\overline{p}$ at 1.96 TeV

$B_1(5721)^+$ REFERENCES

AAIJ 15AB JHEP 1504 024 R. Aaij *et al.* (LHCb Collab.)
AALTONEN 14I PR D90 012013 T. Aaltonen *et al.* (CDF Collab.)

$B_1(5721)^0$

$I(J^P) = \frac{1}{2}(1^+)$ Status: ***

I, *J*, *P* need confirmation.

Quantum numbers shown are quark-model predictions.

$B_1(5721)^0$ MASS

OUR FIT uses mass differences measurements listed below to determine the mass $m_{B_1(5721)^0}$.

VALUE (MeV)	DOCUMENT ID
5726.0 ± 1.3 OUR FIT Error includes scale factor of 1.2.	

$m_{B_1^0} - m_{B^+}$

VALUE (MeV)	DOCUMENT ID		TECN	COMMENT
446.7 ± 1.3 OUR FIT Error includes scale factor of 1.2.				
441.5 ± 2.4 ± 1.3	[1] ABAZOV	07T	D0	$p\overline{p}$ at 1.96 TeV
• • • We do not use the following data for averages, fits, limits, etc. • • •				
446.2 $^{+1.9}_{-2.1}$ $^{+1.0}_{-1.2}$	[1] AALTONEN	09D	CDF	Repl. by AALTONEN 14I

[1] Observed in $B_1^0 \to B^{*+}\pi^-$.

$m_{B_1^0} - m_{B^{*+}}$

VALUE (MeV)	EVTS	DOCUMENT ID		TECN	COMMENT
401.4 ± 1.2 OUR FIT Error includes scale factor of 1.2.					
402.8 ± 1.1 OUR AVERAGE					
403.4 ± 0.7 ± 1.5	35K	[2] AAIJ	15AB	LHCB	pp at 7, 8 TeV
402.3 ± 0.9 $^{+1.1}_{-1.2}$		[3] AALTONEN	14I	CDF	$p\overline{p}$ at 1.96 TeV

[2] AAIJ 15AB reports $[m_{B_1^0} - m_{B^+}] - (m_{B^{*+}} - m_{B^+}) - m_{\pi^-} = 263.9 \pm 0.7 \pm 1.4$ MeV which we adjust by the π^- mass and $(m_{B^{*+}} - m_{B^+}) = 45.01 \pm 0.30 \pm 0.23$ MeV. The masses inside the square brackets were measured for each candidate event.
[3] AALTONEN 14I reports $m_{B_1(5721)^0} - m_{B^{*+}} - m_{\pi^-} = 262.7 \pm 0.9^{+1.1}_{-1.2}$ MeV which we adjusted by the π^- mass.

$B_1(5721)^0$ WIDTH

VALUE (MeV)	EVTS	DOCUMENT ID		TECN	COMMENT
27.5±3.4 OUR AVERAGE		Error includes scale factor of 1.1.			
30.1±1.5±3.5	35k	AAIJ	15AB	LHCB	pp at 7, 8 TeV
23 ±3 ±4		AALTONEN	14I	CDF	$p\overline{p}$ at 1.96 TeV

$B_1(5721)^0$ DECAY MODES

	Mode	Fraction (Γ_i/Γ)
Γ_1	$B^{*+}\pi^-$	dominant

$B_1(5721)^0$ BRANCHING RATIOS

$\Gamma(B^{*+}\pi^-)/\Gamma_{total}$ Γ_1/Γ

VALUE	EVTS	DOCUMENT ID		TECN	COMMENT
seen	35K	AAIJ	15AB	LHCB	pp at 7, 8 TeV
dominant		AALTONEN	09D	CDF	$p\overline{p}$ at 1.96 TeV
dominant		[4] ABAZOV	07T	D0	$p\overline{p}$ at 1.96 TeV

[4] Observed in $B_1^0 \to B^{*+}\pi^-$ with $B^{*+} \to B^+\gamma$ and $B^+ \to J/\psi\pi^+$.

$B_1(5721)^0$ REFERENCES

AAIJ	15AB	JHEP 1504 024	R. Aaij *et al.*	(LHCb Collab.)
AALTONEN	14I	PR D90 012013	T. Aaltonen *et al.*	(CDF Collab.)
AALTONEN	09D	PRL 102 102003	T. Aaltonen *et al.*	(CDF Collab.)
ABAZOV	07T	PRL 99 172001	V.M. Abazov *et al.*	(D0 Collab.)

$B_J^*(5732)$

$I(J^P) = ?(?^?)$
I, J, P need confirmation.

OMITTED FROM SUMMARY TABLE
also known as B^{**}

Signal can be interpreted as stemming from several narrow and broad resonances. Needs confirmation.

$B_J^*(5732)$ MASS

VALUE (MeV)	EVTS	DOCUMENT ID		TECN	COMMENT
5698± 8 OUR AVERAGE		Error includes scale factor of 1.2.			
5710±20		[1] AFFOLDER	01F	CDF	$p\overline{p}$ at 1.8 TeV
5695^{+17}_{-19}		[2] BARATE	98L	ALEP	$e^+e^- \to Z$
5704± 4±10	1944	[3] BUSKULIC	96D	ALEP	E_{cm}^{ee}= 88–94 GeV
5732± 5±20	2157	ABREU	95B	DLPH	E_{cm}^{ee}= 88–94 GeV
5681±11	1738	AKERS	95E	OPAL	E_{cm}^{ee}= 88–94 GeV
• • • We do not use the following data for averages, fits, limits, etc. • • •					
5713± 2		[4] ACCIARRI	99N	L3	$e^+e^- \to Z$

[1] AFFOLDER 01F uses the reconstructed B meson through semileptonic decay channels. The fraction of light B mesons that are produced at L=1 B^{**} states is measured to be 0.28 ± 0.06 ± 0.03.

[2] BARATE 98L uses fully reconstructed B mesons to search for B^{**} production in the $B\pi^\pm$ system. In the framework of heavy quark symmetry (HQS), they also measured the mass of B_2^* to be $5739^{+8}_{-11}{}^{+6}_{-4}$ MeV/c^2 and the relative production rate of B($b \to B_2^* \to B^{(*)}\pi$)/B($b \to B_{u,d}$) = $(31 \pm 9^{+6}_{-5})$%.

[3] Using $m_{B\pi} - m_B$ = 424 ± 4 ± 10 MeV.

[4] ACCIARRI 99N uses inclusive reconstructed B mesons to search for B^{**} production in the $B^{(*)}\pi^\pm$ system. In the framework of HQET, they measured the mass of B_1^* and B_2^* to be 5670±10±13 MeV and 5768±5±6 with the B($b \to B^{**}$)= (32±3±6)×10^{-2}. They also reported the evidence for the existence of an excited B-meson state or mixture of states in the region 5.9–6.0 GeV.

$B_J^*(5732)$ WIDTH

VALUE (MeV)	EVTS	DOCUMENT ID		TECN	COMMENT
128±18 OUR AVERAGE					
145±28	2157	ABREU	95B	DLPH	E_{cm}^{ee}= 88–94 GeV
116±24	1738	AKERS	95E	OPAL	E_{cm}^{ee}= 88–94 GeV

$B_J^*(5732)$ DECAY MODES

	Mode	Fraction (Γ_i/Γ)
Γ_1	$B^*\pi + B\pi$	dominant
Γ_2	$B^*\pi$(X)	[a] (85±29) %

[a] X refers to decay modes with or without additional accompanying decay particles.

$B_J^*(5732)$ BRANCHING RATIOS

X refers to decay modes with or without additional accompanying decay particles.

$\Gamma(B^*\pi(X))/\Gamma_{total}$ Γ_2/Γ

VALUE	DOCUMENT ID		TECN	COMMENT
$\mathbf{0.85^{+0.26}_{-0.27}\pm0.12}$	ABBIENDI	02E	OPAL	$e^+e^- \to Z$

$B_J^*(5732)$ REFERENCES

ABBIENDI	02E	EPJ C23 437	G. Abbiendi *et al.*	(OPAL Collab.)
AFFOLDER	01F	PR D64 072002	T. Affolder *et al.*	(CDF Collab.)
ACCIARRI	99N	PL B465 323	M. Acciarri *et al.*	(L3 Collab.)
BARATE	98L	PL B425 215	R. Barate *et al.*	(ALEPH Collab.)
BUSKULIC	96D	ZPHY C69 393	D. Buskulic *et al.*	(ALEPH Collab.)
ABREU	95B	PL B345 598	P. Abreu *et al.*	(DELPHI Collab.)
AKERS	95E	ZPHY C66 19	R. Akers *et al.*	(OPAL Collab.)

$B_2^*(5747)^+$

$I(J^P) = \frac{1}{2}(2^+)$ Status: **
I, J, P need confirmation.

Quantum numbers shown are quark-model predictions.

$B_2^*(5747)^+$ MASS

OUR FIT uses m_{B^0} and $m_{B_2^{*+}} - m_{B^0}$ to determine $m_{B_2^*(5747)^+}$.

VALUE (MeV)	DOCUMENT ID
5737.2±0.7 OUR FIT	

$m_{B_2^{*+}} - m_{B^0}$

VALUE (MeV)	EVTS	DOCUMENT ID		TECN	COMMENT
457.5 ±0.7 OUR FIT					
457.5 ±0.7 OUR AVERAGE					
457.62±0.72±0.40	4K	[1] AAIJ	15AB	LHCB	pp at 7, 8 TeV
457.3 ±1.3 $^{+0.3}_{-0.9}$		[2] AALTONEN	14I	CDF	$p\overline{p}$ at 1.96 TeV

[1] AAIJ 15AB reports $[m_{B_2^{*+}} - m_{B^0}] - m_{\pi^+}$ = 318.1 ± 0.7 ± 0.4 MeV which we adjust by the π^+ mass. The masses inside the square brackets were measured for each candidate event.

[2] AALTONEN 14I reports $m_{B_2^*(5747)^+} - m_{B^0} - m_{\pi^+}$ = 317.7 ± 1.2 $^{+0.3}_{-0.9}$ MeV which we adjusted by the π^+ mass.

$B_2^*(5747)^+$ WIDTH

VALUE (MeV)	EVTS	DOCUMENT ID		TECN	COMMENT
20 ±5 OUR AVERAGE		Error includes scale factor of 2.2.			
23.6±2.0±2.1	4K	AAIJ	15AB	LHCB	pp at 7, 8 TeV
11 $^{+4}_{-3}$ $^{+3}_{-4}$		AALTONEN	14I	CDF	$p\overline{p}$ at 1.96 TeV

$B_2^*(5747)^+$ DECAY MODES

	Mode	Fraction (Γ_i/Γ)
Γ_1	$B^0\pi^+$	seen
Γ_2	$B^{*0}\pi^+$	seen

$B_2^*(5747)^+$ BRANCHING RATIOS

$\Gamma(B^0\pi^+)/\Gamma_{total}$ Γ_1/Γ

VALUE	EVTS	DOCUMENT ID		TECN	COMMENT
seen	4K	AAIJ	15AB	LHCB	pp at 7, 8 TeV
seen		AALTONEN	14I	CDF	$p\overline{p}$ at 1.96 TeV

$\Gamma(B^{*0}\pi^+)/\Gamma_{total}$ Γ_2/Γ

VALUE	EVTS	DOCUMENT ID		TECN	COMMENT
seen	4k	AAIJ	15AB	LHCB	pp at 7, 8 TeV

$\Gamma(B^{*0}\pi^+)/\Gamma(B^0\pi^+)$ Γ_2/Γ_1

VALUE	EVTS	DOCUMENT ID		TECN	COMMENT
1.0±0.5±0.8	4k	AAIJ	15AB	LHCB	pp at 7, 8 TeV

$B_2^*(5747)^+$ REFERENCES

AAIJ	15AB	JHEP 1504 024	R. Aaij *et al.*	(LHCb Collab.)
AALTONEN	14I	PR D90 012013	T. Aaltonen *et al.*	(CDF Collab.)

Meson Particle Listings

$B_2^*(5747)^0$, $B_J(5840)^+$

$B_2^*(5747)^0$

$I(J^P) = \frac{1}{2}(2^+)$ Status: ***
I, *J*, *P* need confirmation.

Quantum numbers shown are quark-model predictions.

$B_2^*(5747)^0$ MASS

OUR FIT uses m_{B^+}, $m_{B_1^0} - m_{B^+}$, and $m_{B_2^{*0}} - m_{B_1^0}$ to determine $m_{B_2^*(5747)^0}$. The −0.659 correlation between statistical uncertainties of $m_{B_1^0} - m_{B^+}$ and $m_{B_2^{*0}} - m_{B_1^0}$ measurements reported by ABAZOV 07T is taken into account.

VALUE (MeV)	DOCUMENT ID
5739.5±0.7 OUR FIT	Error includes scale factor of 1.4.

$m_{B_2^{*0}} - m_{B_1^0}$

VALUE (MeV)	DOCUMENT ID	TECN	COMMENT
13.5±1.4 OUR FIT	Error includes scale factor of 1.3.		
26.2±3.1±0.9	[1] ABAZOV 07T	D0	$p\overline{p}$ at 1.96 TeV
• • • We do not use the following data for averages, fits, limits, etc. • • •			
$14.9^{+2.2}_{-2.5}{}^{+1.2}_{-1.4}$	[1] AALTONEN 09D	CDF	Repl. by AALTONEN 14I

[1] Observed in $B_2^{*0} \to B^{*+}\pi^-$ and $B_2^{*0} \to B^+\pi^-$.

$m_{B_2^{*0}} - m_{B^+}$

VALUE (MeV)	EVTS	DOCUMENT ID	TECN	COMMENT
460.2 ±0.6 OUR FIT		Error includes scale factor of 1.4.		
459.9 ±0.8 OUR AVERAGE		Error includes scale factor of 1.8.		
460.18±0.37±0.33	17K	[2] AAIJ 15AB	LHCB	pp at 7, 8 TeV
$457.5 \pm 1.2\ ^{+0.8}_{-0.9}$		[3] AALTONEN 14I	CDF	$p\overline{p}$ at 1.96 TeV

[2] AAIJ 15AB reports $[m_{B_2^{*0}} - m_{B^+}] - m_{\pi^-} = 320.6 \pm 0.4 \pm 0.3$ MeV which we adjust by the π^- mass. The masses inside the square brackets were measured for each candidate event.

[3] AALTONEN 14I reports $m_{B_2^*(5747)^0} - m_{B^+} - m_{\pi^-} = 317.9 \pm 1.2^{+0.8}_{-0.9}$ MeV which we adjusted by the π^- mass.

$B_2^*(5747)^0$ WIDTH

VALUE (MeV)	EVTS	DOCUMENT ID	TECN	COMMENT
24.2±1.7 OUR AVERAGE				
24.5±1.0± 1.5	17K	AAIJ 15AB	LHCB	pp at 7, 8 TeV
$22\ ^{+3}_{-2}\ ^{+4}_{-5}$		AALTONEN 14I	CDF	$p\overline{p}$ at 1.96 TeV
• • • We do not use the following data for averages, fits, limits, etc. • • •				
$22.7^{+3.8}_{-3.2}{}^{+3.2}_{-10.2}$		AALTONEN 09D	CDF	Repl. by AALTONEN 14I

$B_2^*(5747)^0$ DECAY MODES

	Mode	Fraction (Γ_i/Γ)
Γ_1	$B^+\pi^-$	dominant
Γ_2	$B^{*+}\pi^-$	dominant

$B_2^*(5747)^0$ BRANCHING RATIOS

$\Gamma(B^+\pi^-)/\Gamma_{total}$ Γ_1/Γ

VALUE	EVTS	DOCUMENT ID	TECN	COMMENT
seen	17K	AAIJ 15AB	LHCB	pp at 7, 8 TeV
dominant		AALTONEN 09D	CDF	$p\overline{p}$ at 1.96 TeV
dominant		ABAZOV 07T	D0	$p\overline{p}$ at 1.96 TeV

$\Gamma(B^{*+}\pi^-)/\Gamma_{total}$ Γ_2/Γ

VALUE	EVTS	DOCUMENT ID	TECN	COMMENT
seen	17K	AAIJ 15AB	LHCB	pp at 7, 8 TeV
dominant		AALTONEN 09D	CDF	$p\overline{p}$ at 1.96 TeV
dominant		ABAZOV 07T	D0	$p\overline{p}$ at 1.96 TeV

$\Gamma(B^{*+}\pi^-)/\Gamma(B^+\pi^-)$ Γ_2/Γ_1

VALUE	EVTS	DOCUMENT ID	TECN	COMMENT
0.82±0.28 OUR AVERAGE				
0.71±0.14±0.30	17K	AAIJ 15AB	LHCB	pp at 7, 8 TeV
1.10±0.42±0.31		[4] ABAZOV 07T	D0	$p\overline{p}$ at 1.96 TeV

[4] Converted from measured ratio of $R = B(B_2^{*0} \to B^{*+}\pi^-) / B(B_2^{*0} \to B^{(*)+}\pi^-) = 0.475 \pm 0.095 \pm 0.069$.

$B_2^*(5747)^0$ REFERENCES

AAIJ 15AB JHEP 1504 024 R. Aaij *et al.* (LHCb Collab.)
AALTONEN 14I PR D90 012013 T. Aaltonen *et al.* (CDF Collab.)
AALTONEN 09D PRL 102 102003 T. Aaltonen *et al.* (CDF Collab.)
ABAZOV 07T PRL 99 172001 V.M. Abazov *et al.* (D0 Collab.)

$B_J(5840)^+$

$I(J^P) = \frac{1}{2}(?^?)$ Status: **
I, *J*, *P* need confirmation.

OMITTED FROM SUMMARY TABLE

Quantum numbers shown are quark-model predictions.

$B_J(5840)^+$ MASS

OUR FIT uses m_{B^0} and $m_{B_J(5840)^+} - m_{B^0}$ to determine $m_{B_J(5840)^+}$.

VALUE (MeV)	DOCUMENT ID
5851±19 OUR FIT	

$m_{B_J(5840)^+} - m_{B^0}$

VALUE (MeV)	EVTS	DOCUMENT ID	TECN	COMMENT
571±19 OUR FIT				
571±13±14	7k	[1] AAIJ 15AB	LHCB	pp at 7, 8 TeV
• • • We do not use the following data for averages, fits, limits, etc. • • •				
595±26±14	7k	[2] AAIJ 15AB	LHCB	pp at 7, 8 TeV

[1] AAIJ 15AB reports $[m_{B_J^+} - m_{B^0}] - m_{\pi^+} = 431 \pm 13 \pm 14$ MeV which we adjust by the π^+ mass. The masses inside the square brackets were measured for each candidate event. The result assumes $P = (-1)^J$ and uses two relativistic Breit-Wigner functions in the fit for mass difference.

[2] AAIJ 15AB reports $[m_{B_J^+} - m_{B^0}] - m_{\pi^+} = 455 \pm 26 \pm 14$ MeV which we adjust by the π^+ mass. The masses inside the square brackets were measured for each candidate event. The result assumes $P = (-1)^J$ and uses three relativistic Breit-Wigner functions in the fit for mass difference.

$m_{B_J(5840)^+} - m_{B^{*0}}$

VALUE (MeV)	EVTS	DOCUMENT ID	TECN	COMMENT
• • • We do not use the following data for averages, fits, limits, etc. • • •				
565±15±14	7k	[3] AAIJ 15AB	LHCB	pp at 7, 8 TeV

[3] AAIJ 15AB reports $[m_{B_J^+} - m_{B^0}] - (m_{B^{*+}} - m_{B^+}) - m_{\pi^+} = 425 \pm 15 \pm 14$ MeV which we adjust by the π^+ mass. The masses inside the square brackets were measured for each candidate event. The result assumes $P = -(-1)^J$, $(m_{B^{*0}} - m_{B^0}) = (m_{B^{*+}} - m_{B^+}) = 45.01 \pm 0.30 \pm 0.23$ MeV, and uses three relativistic Breit-Wigner functions in the fit for mass difference.

$B_J(5840)^+$ WIDTH

VALUE (MeV)	EVTS	DOCUMENT ID	TECN	COMMENT
224±24±80	7k	[4] AAIJ 15AB	LHCB	pp at 7, 8 TeV
• • • We do not use the following data for averages, fits, limits, etc. • • •				
215±27±80	7k	[5] AAIJ 15AB	LHCB	pp at 7, 8 TeV
229±27±80	7k	[6] AAIJ 15AB	LHCB	pp at 7, 8 TeV

[4] Assuming $P = (-1)^J$ and using two relativistic Breit-Wigner functions in the fit for mass difference.

[5] Assuming $P = (-1)^J$ and using three relativistic Breit-Wigner functions in the fit for mass difference.

[6] Assuming $P = -(-1)^J$ and using three relativistic Breit-Wigner functions in the fit for mass difference.

$B_J(5840)^+$ DECAY MODES

	Mode	Fraction (Γ_i/Γ)
Γ_1	$B^{*0}\pi^+$	seen
Γ_2	$B^0\pi^+$	possibly seen

$B_J(5840)^+$ BRANCHING RATIOS

$\Gamma(B^{*0}\pi^+)/\Gamma_{total}$ Γ_1/Γ

VALUE	EVTS	DOCUMENT ID	TECN	COMMENT
seen	7k	AAIJ 15AB	LHCB	pp at 7, 8 TeV

$\Gamma(B^0\pi^+)/\Gamma_{total}$ Γ_2/Γ

VALUE	EVTS	DOCUMENT ID	TECN	COMMENT
possibly seen	7k	[7] AAIJ 15AB	LHCB	pp at 7, 8 TeV

[7] A $B\pi$ decay is forbidden from a $P = -(-1)^J$ parent, whereas $B^*\pi$ is allowed.

$B_J(5840)^+$ REFERENCES

AAIJ 15AB JHEP 1504 024 R. Aaij *et al.* (LHCb Collab.)

$B_J(5840)^0$

$I(J^P) = \frac{1}{2}(?^?)$ Status: **

I, *J*, *P* need confirmation.

OMITTED FROM SUMMARY TABLE

Quantum numbers shown are quark-model predictions.

$B_J(5840)^0$ MASS

OUR FIT uses m_{B^+} and $m_{B_J(5840)^0} - m_{B^+}$ to determine $m_{B_J(5840)^0}$.

VALUE (MeV)	DOCUMENT ID
5863±9 OUR FIT	

$m_{B_J(5840)^0} - m_{B^+}$

VALUE (MeV)	EVTS	DOCUMENT ID		TECN	COMMENT
584± 9 OUR FIT					
584± 5±7	12k	[1] AAIJ	15AB	LHCB	pp at 7, 8 TeV
• • • We do not use the following data for averages, fits, limits, etc. • • •					
610±22±7	12k	[2] AAIJ	15AB	LHCB	pp at 7, 8 TeV

[1] AAIJ 15AB reports $[m_{B_J^0} - m_{B^+}] - m_{\pi^-} = 444 \pm 5 \pm 7$ MeV which we adjust by the π^- mass. The masses inside the square brackets were measured for each candidate event. The result assumes $P = (-1)^J$ and uses two relativistic Breit-Wigner functions in the fit for mass difference.

[2] AAIJ 15AB reports $[m_{B_J^0} - m_{B^+}] - m_{\pi^-} = 471 \pm 22 \pm 7$ MeV which we adjust by the π^- mass. The masses inside the square brackets were measured for each candidate event. The result assumes $P = (-1)^J$ and uses three relativistic Breit-Wigner functions in the fit for mass difference.

$m_{B_J(5840)^0} - m_{B^{*+}}$

VALUE (MeV)	EVTS	DOCUMENT ID		TECN	COMMENT
• • • We do not use the following data for averages, fits, limits, etc. • • •					
584±5±7	12k	[3] AAIJ	15AB	LHCB	pp at 7, 8 TeV

[3] AAIJ 15AB reports $[m_{B_J^0} - m_{B^+}] - (m_{B^{*+}} - m_{B^+}) - m_{\pi^-} = 444 \pm 5 \pm 7$ MeV which we adjust by the π^- mass. The masses inside the square brackets were measured for each candidate event. The result assumes $P = -(-1)^J$, $(m_{B^{*+}} - m_{B^+}) = 45.01 \pm 0.30 \pm 0.23$ MeV, and uses three relativistic Breit-Wigner functions in the fit for mass difference.

$B_J(5840)^0$ WIDTH

VALUE (MeV)	EVTS	DOCUMENT ID		TECN	COMMENT
127±17±34	12k	[4] AAIJ	15AB	LHCB	pp at 7, 8 TeV
• • • We do not use the following data for averages, fits, limits, etc. • • •					
107±20±34	12k	[5] AAIJ	15AB	LHCB	pp at 7, 8 TeV
119±17±34	12k	[6] AAIJ	15AB	LHCB	pp at 7, 8 TeV

[4] Assuming $P = (-1)^J$ and using two relativistic Breit-Wigner functions in the fit for mass difference.

[5] Assuming $P = (-1)^J$ and using three relativistic Breit-Wigner functions in the fit for mass difference.

[6] Assuming $P = -(-1)^J$ and using three relativistic Breit-Wigner functions in the fit for mass difference.

$B_J(5840)^0$ DECAY MODES

	Mode	Fraction (Γ_i/Γ)
Γ_1	$B^{*+}\pi^-$	seen
Γ_2	$B^+\pi^-$	possibly seen

$B_J(5840)^0$ BRANCHING RATIOS

$\Gamma(B^{*+}\pi^-)/\Gamma_{total}$ Γ_1/Γ

VALUE	EVTS	DOCUMENT ID		TECN	COMMENT
seen	12k	AAIJ	15AB	LHCB	pp at 7, 8 TeV

$\Gamma(B^+\pi^-)/\Gamma_{total}$ Γ_2/Γ

VALUE	DOCUMENT ID		TECN	COMMENT
possibly seen	[7] AAIJ	15AB	LHCB	pp at 7, 8 TeV

[7] A $B\pi$ decay is forbidden from a $P = -(-1)^J$ parent, whereas $B^*\pi$ is allowed.

$B_J(5840)^0$ REFERENCES

AAIJ 15AB JHEP 1504 024 R. Aaij *et al.* (LHCb Collab.)

$B_J(5970)^+$

$I(J^P) = \frac{1}{2}(?^?)$ Status: **

I, *J*, *P* need confirmation.

Quantum numbers shown are quark-model predictions.

$B_J(5970)^+$ MASS

OUR FIT uses m_{B^0} and $m_{B_J(5970)^+} - m_{B^0}$ to determine $m_{B_J(5970)^+}$.

VALUE (MeV)	DOCUMENT ID
5964±5 OUR FIT	

$m_{B_J(5970)^+} - m_{B^0}$

VALUE (MeV)	EVTS	DOCUMENT ID		TECN	COMMENT
685 ±5 OUR FIT					
685 ±5 OUR AVERAGE					
685.3±4.1± 2.5	2K	[1] AAIJ	15AB	LHCB	pp at 7, 8 TeV
681 ±5 ±12	1.4k	[2] AALTONEN	14I	CDF	$p\overline{p}$ at 1.96 TeV
• • • We do not use the following data for averages, fits, limits, etc. • • •					
686.8±4.5± 2.5	2K	[3] AAIJ	15AB	LHCB	pp at 7, 8 TeV

[1] AAIJ 15AB reports $[m_{B_J^+} - m_{B^0}] - m_{\pi^+} = 545.8 \pm 4.1 \pm 2.5$ MeV which we adjust by the π^+ mass. The masses inside the square brackets were measured for each candidate event. The result assumes $P = (-1)^J$ and uses two relativistic Breit-Wigner functions in the fit for mass difference.

[2] AALTONEN 14I reports $m_{B_J(5970)^+} - m_{B^0} - m_{\pi^+} = 541 \pm 5 \pm 12$ MeV which we adjusted by the π^+ mass.

[3] AAIJ 15AB reports $[m_{B_J^+} - m_{B^0}] - m_{\pi^+} = 547 \pm 5 \pm 3$ MeV which we adjust by the π^+ mass. The masses inside the square brackets were measured for each candidate event. The result assumes $P = (-1)^J$ and uses three relativistic Breit-Wigner functions in the fit for mass difference.

$m_{B_J(5970)^+} - m_{B^{*0}}$

VALUE (MeV)	EVTS	DOCUMENT ID		TECN	COMMENT
• • • We do not use the following data for averages, fits, limits, etc. • • •					
686.0±4.0±2.5	2k	[4] AAIJ	15AB	LHCB	pp at 7, 8 TeV

[4] AAIJ 15AB reports $[m_{B_J^+} - m_{B^0}] - (m_{B^{*+}} - m_{B^+}) - m_{\pi^+} = 547 \pm 4 \pm 3$ MeV which we adjust by the π^+ mass. The masses inside the square brackets were measured for each candidate event. The result assumes $P = -(-1)^J$, $(m_{B^{*0}} - m_{B^0}) = (m_{B^{*+}} - m_{B^+}) = 45.01 \pm 0.30 \pm 0.23$ MeV, and uses three relativistic Breit-Wigner functions in the fit for mass difference.

$B_J(5970)^+$ WIDTH

VALUE (MeV)	EVTS	DOCUMENT ID		TECN	COMMENT
62±20 OUR AVERAGE					
63±15±17	2K	[5] AAIJ	15AB	LHCB	pp at 7, 8 TeV
60^{+30}_{-20}±40	1.4k	AALTONEN	14I	CDF	$p\overline{p}$ at 1.96 TeV
• • • We do not use the following data for averages, fits, limits, etc. • • •					
61±14±17	2K	[6] AAIJ	15AB	LHCB	pp at 7, 8 TeV
61±15±17	2K	[7] AAIJ	15AB	LHCB	pp at 7, 8 TeV

[5] Assuming $P = (-1)^J$ and using two relativistic Breit-Wigner functions in the fit for mass difference.

[6] Assuming $P = (-1)^J$ and using three relativistic Breit-Wigner functions in the fit for mass difference.

[7] Assuming $P = -(-1)^J$ and using three relativistic Breit-Wigner functions in the fit for mass difference.

$B_J(5970)^+$ DECAY MODES

	Mode	Fraction (Γ_i/Γ)
Γ_1	$B^0\pi^+$	possibly seen
Γ_2	$B^{*0}\pi^+$	seen

$B_J(5970)^+$ BRANCHING RATIOS

$\Gamma(B^0\pi^+)/\Gamma_{total}$ Γ_1/Γ

VALUE	EVTS	DOCUMENT ID		TECN	COMMENT
possibly seen	2K	[8] AAIJ	15AB	LHCB	pp at 7, 8 TeV
possibly seen	1.4k	AALTONEN	14I	CDF	$p\overline{p}$ at 1.96 TeV

[8] A $B\pi$ decay is forbidden from a $P = -(-1)^J$ parent, whereas $B^*\pi$ is allowed.

$\Gamma(B^{*0}\pi^+)/\Gamma_{total}$ Γ_2/Γ

VALUE	EVTS	DOCUMENT ID		TECN	COMMENT
seen	2k	AAIJ	15AB	LHCB	pp at 7, 8 TeV
seen	1.4k	AALTONEN	14I	CDF	$p\overline{p}$ at 1.96 TeV

Meson Particle Listings

$B_J(5970)^+$, $B_J(5970)^0$

$B_J(5970)^+$ REFERENCES

AAIJ	15AB	JHEP 1504 024	R. Aaij *et al.*	(LHCb Collab.)
AALTONEN	14I	PR D90 012013	T. Aaltonen *et al.*	(CDF Collab.)

$B_J(5970)^0$

$I(J^P) = \frac{1}{2}(?^?)$ Status: **

I, *J*, *P* need confirmation.

Quantum numbers shown are quark-model predictions.

$B_J(5970)^0$ MASS

OUR FIT uses m_{B^+} and $m_{B_J(5970)^0} - m_{B^+}$ to determine $m_{B_J(5970)^0}$.

VALUE (MeV)	*DOCUMENT ID*
5971±5 OUR FIT	

$m_{B_J(5970)^0} - m_{B^+}$

VALUE (MeV)	*EVTS*	*DOCUMENT ID*		*TECN*	*COMMENT*
691 ±5 OUR FIT					
691 ±5 OUR AVERAGE					
689.9±2.9± 5.1	10K	[1] AAIJ	15AB	LHCB	pp at 7, 8 TeV
698 ±5 ±12	2.6k	[2] AALTONEN	14I	CDF	$p\overline{p}$ at 1.96 TeV
• • • We do not use the following data for averages, fits, limits, etc. • • •					
714.3±6.4± 5.1	10K	[3] AAIJ	15AB	LHCB	pp at 7, 8 TeV

[1] AAIJ 15AB reports $[m_{B_J^0} - m_{B^+}] - m_{\pi^-} = 550.4 \pm 2.9 \pm 5.1$ MeV which we adjust by the π^- mass. The masses inside the square brackets were measured for each candidate event. The result assumes $P = (-1)^J$ and uses two relativistic Breit-Wigner functions in the fit for mass difference.

[2] AALTONEN 14I reports $m_{B_J(5970)^0} - m_{B^+} - m_{\pi^-} = 558 \pm 5 \pm 12$ MeV which we adjusted by the π^- mass.

[3] AAIJ 15AB reports $[m_{B_J^0} - m_{B^+}] - m_{\pi^-} = 575 \pm 6 \pm 5$ MeV which we adjust by the π^- mass. The masses inside the square brackets were measured for each candidate event. The result assumes $P = (-1)^J$ and uses three relativistic Breit-Wigner functions in the fit for mass difference.

$m_{B_J(5970)^0} - m_{B^{*+}}$

VALUE (MeV)	*EVTS*	*DOCUMENT ID*		*TECN*	*COMMENT*
• • • We do not use the following data for averages, fits, limits, etc. • • •					
691.6±3.7±5.1	10k	[4] AAIJ	15AB	LHCB	pp at 7, 8 TeV

[4] AAIJ 15AB reports $[m_{B_J^0} - m_{B^+}] - (m_{B^{*+}} - m_{B^+}) - m_{\pi^-} = 552 \pm 4 \pm 5$ MeV which we adjust by the π^- mass. The masses inside the square brackets were measured for each candidate event. The result assumes $P = -(-1)^J$, $(m_{B^{*+}} - m_{B^+}) = 45.01 \pm 0.30 \pm 0.23$ MeV, and uses three relativistic Breit-Wigner functions in the fit for mass difference.

$B_J(5970)^0$ WIDTH

VALUE (MeV)	*EVTS*	*DOCUMENT ID*		*TECN*	*COMMENT*
81±12 OUR AVERAGE					
82± 8± 9	10K	[5] AAIJ	15AB	LHCB	pp at 7, 8 TeV
$70^{+30}_{-20}\pm30$	2.6k	AALTONEN	14I	CDF	$p\overline{p}$ at 1.96 TeV
• • • We do not use the following data for averages, fits, limits, etc. • • •					
56± 7± 9	10K	[6] AAIJ	15AB	LHCB	pp at 7, 8 TeV
82±10± 9	10K	[7] AAIJ	15AB	LHCB	pp at 7, 8 TeV

[5] Assuming $P = (-1)^J$ and using two relativistic Breit-Wigner functions in the fit for mass difference.

[6] Assuming $P = (-1)^J$ and using three relativistic Breit-Wigner functions in the fit for mass difference.

[7] Assuming $P = -(-1)^J$ and using three relativistic Breit-Wigner functions in the fit for mass difference.

$B_J(5970)^0$ DECAY MODES

	Mode	Fraction (Γ_i/Γ)
Γ_1	$B^+\pi^-$	possibly seen
Γ_2	$B^{*+}\pi^-$	seen

$B_J(5970)^0$ BRANCHING RATIOS

$\Gamma(B^+\pi^-)/\Gamma_{total}$ Γ_1/Γ

VALUE	*EVTS*	*DOCUMENT ID*		*TECN*	*COMMENT*
possibly seen	10K	[8] AAIJ	15AB	LHCB	pp at 7, 8 TeV
possibly seen	2.6k	AALTONEN	14I	CDF	$p\overline{p}$ at 1.96 TeV

[8] A $B\pi$ decay is forbidden from a $P = -(-1)^J$ parent, whereas $B^*\pi$ is allowed.

$\Gamma(B^{*+}\pi^-)/\Gamma_{total}$ Γ_2/Γ

VALUE	*EVTS*	*DOCUMENT ID*		*TECN*	*COMMENT*
seen	10K	AAIJ	15AB	LHCB	pp at 7, 8 TeV
seen	2.6k	AALTONEN	14I	CDF	$p\overline{p}$ at 1.96 TeV

$B_J(5970)^0$ REFERENCES

AAIJ	15AB	JHEP 1504 024	R. Aaij *et al.*	(LHCb Collab.)
AALTONEN	14I	PR D90 012013	T. Aaltonen *et al.*	(CDF Collab.)

BOTTOM, STRANGE MESONS ($B = \pm 1$, $S = \mp 1$)

$B_s^0 = s\overline{b}$, $\overline{B}_s^0 = \overline{s}b$, similarly for B_s^*'s

B_s^0

$I(J^P) = 0(0^-)$

I, J, P need confirmation. Quantum numbers shown are quark-model predictions.

B_s^0 MASS

VALUE (MeV)	EVTS	DOCUMENT ID		TECN	COMMENT
5366.89± 0.19 OUR FIT					
5366.84± 0.30 OUR AVERAGE		Error includes scale factor of 1.2.			
5367.08± 0.38±0.15	128	[1] AAIJ	16U	LHCB	pp at 7, 8 TeV
5366.90± 0.28±0.23		[2] AAIJ	12E	LHCB	pp at 7 TeV
5364.4 ± 1.3 ±0.7		LOUVOT	09	BELL	$e^+e^- \to \Upsilon(5S)$
5366.01± 0.73±0.33		[3] ACOSTA	06	CDF	$p\overline{p}$ at 1.96 TeV
5369.9 ± 2.3 ±1.3	32	[4] ABE	96B	CDF	$p\overline{p}$ at 1.8 TeV
5374 ±16 ±2	3	ABREU	94D	DLPH	$e^+e^- \to Z$
5359 ±19 ±7	1	[4] AKERS	94J	OPAL	$e^+e^- \to Z$
5368.6 ± 5.6 ±1.5	2	BUSKULIC	93G	ALEP	$e^+e^- \to Z$
• • • We do not use the following data for averages, fits, limits, etc. • • •					
5370 ± 1 ±3		DRUTSKOY	07A	BELL	Repl. by LOUVOT 09
5370 ±40	6	[5] AKERS	94J	OPAL	$e^+e^- \to Z$
5383.3 ± 4.5 ±5.0	14	ABE	93F	CDF	Repl. by ABE 96B

[1] Uses $J/\psi \to \mu^+\mu^-$, $\phi \to K^+K^-$ decays, and observes 128 ± 13 events of $B_s^0 \to J/\psi\phi\phi$.
[2] Uses $B_s^0 \to J/\psi\phi$ fully reconstructed decays.
[3] Uses exclusively reconstructed final states containing a $J/\psi \to \mu^+\mu^-$ decays.
[4] From the decay $B_s \to J/\psi(1S)\phi$.
[5] From the decay $B_s \to D_s^-\pi^+$.

$m_{B_s^0} - m_B$

m_B is the average of our B masses $(m_{B^\pm} + m_{B^0})/2$.

VALUE (MeV)	CL%	DOCUMENT ID		TECN	COMMENT
87.42±0.19 OUR FIT					
87.42±0.24 OUR AVERAGE					
87.60±0.44±0.09		[1] AAIJ	15U	LHCB	pp at 7, 8 TeV
87.42±0.30±0.09		[2] AAIJ	12E	LHCB	pp at 7 TeV
86.64±0.80±0.08		[3] ACOSTA	06	CDF	$p\overline{p}$ at 1.96 TeV
• • • We use the following data for averages but not for fits. • • •					
89.7 ±2.7 ±1.2		ABE	96B	CDF	$p\overline{p}$ at 1.8 TeV
• • • We do not use the following data for averages, fits, limits, etc. • • •					
80 to 130	68	LEE-FRANZINI 90		CSB2	$e^+e^- \to \Upsilon(5S)$

[1] The reported result is $m_{B_s^0} - m_{B^0} = 87.45 \pm 0.44 \pm 0.09$ MeV. We convert it to the mass difference with respect to the average of $(m_{B^\pm} + m_{B^0})/2$. Uses the mode $B_s^0 \to \psi(2S)K^-\pi^+$.
[2] The reported result is $m_{B_s^0} - m_{B^+} = 87.52 \pm 0.30 \pm 0.12$ MeV. We convert it to the mass difference with respect to the average of $(m_{B^\pm} + m_{B^0})/2$.
[3] The reported result is $m_{B_s^0} - m_{B^0} = 86.38 \pm 0.90 \pm 0.06$ MeV. We convert it to the mass difference with respect to the average of $(m_{B^\pm} + m_{B^0})/2$.

$m_{B_{sH}^0} - m_{B_{sL}^0}$

See the B_s^0-$\overline{B}_s^0$ MIXING section near the end of these B_s^0 Listings.

B_s^0 MEAN LIFE

"OUR EVALUATION" is provided by the Heavy Flavor Averaging Group (HFLAV). It is derived from the average of $\Gamma_{B_s^0}$.

VALUE (10^{-12} s)	EVTS	DOCUMENT ID		TECN	COMMENT
1.509±0.004 OUR EVALUATION					
• • • We do not use the following data for averages, fits, limits, etc. • • •					
1.518±0.041±0.027		[1] AALTONEN	11AP	CDF	$p\overline{p}$ at 1.96 TeV
1.398±0.044 $^{+0.028}_{-0.025}$		[2] ABAZOV	06V	D0	$p\overline{p}$ at 1.96 TeV
1.42 $^{+0.14}_{-0.13}$ ±0.03		[3] ABREU	00Y	DLPH	$e^+e^- \to Z$
1.53 $^{+0.16}_{-0.15}$ ±0.07		[4] ABREU,P	00G	DLPH	$e^+e^- \to Z$
1.36 ±0.09 $^{+0.06}_{-0.05}$		[5] ABE	99D	CDF	$p\overline{p}$ at 1.8 TeV
1.72 $^{+0.20}_{-0.19}$ $^{+0.18}_{-0.17}$		[6] ACKERSTAFF	98F	OPAL	$e^+e^- \to Z$
1.50 $^{+0.16}_{-0.15}$ ±0.04		[5] ACKERSTAFF	98G	OPAL	$e^+e^- \to Z$
1.47 ±0.14 ±0.08		[4] BARATE	98C	ALEP	$e^+e^- \to Z$
1.51 ±0.11		[7] BARATE	98C	ALEP	$e^+e^- \to Z$
1.56 $^{+0.29}_{-0.26}$ $^{+0.08}_{-0.07}$		[5] ABREU	96F	DLPH	Repl. by ABREU 00Y
1.65 $^{+0.34}_{-0.31}$ ±0.12		[4] ABREU	96F	DLPH	Repl. by ABREU 00Y
1.76 ±0.20 $^{+0.15}_{-0.10}$		[8] ABREU	96F	DLPH	Repl. by ABREU 00Y
1.60 ±0.26 $^{+0.13}_{-0.15}$		[9] ABREU	96F	DLPH	Repl. by ABREU,P 00G
1.67 ±0.14		[10] ABREU	96F	DLPH	$e^+e^- \to Z$
1.61 $^{+0.30}_{-0.29}$ $^{+0.18}_{-0.16}$	90	[4] BUSKULIC	96E	ALEP	Repl. by BARATE 98C
1.54 $^{+0.14}_{-0.13}$ ±0.04		[5] BUSKULIC	96M	ALEP	$e^+e^- \to Z$
1.42 $^{+0.27}_{-0.23}$ ±0.11	76	[5] ABE	95R	CDF	Repl. by ABE 99D
1.74 $^{+1.08}_{-0.69}$ ±0.07	8	[11] ABE	95R	CDF	Sup. by ABE 96N
1.54 $^{+0.25}_{-0.21}$ ±0.06	79	[5] AKERS	95G	OPAL	Repl. by ACKERSTAFF 98G
1.59 $^{+0.17}_{-0.15}$ ±0.03	134	[5] BUSKULIC	95O	ALEP	Sup. by BUSKULIC 96M
0.96 ±0.37	41	[12] ABREU	94E	DLPH	Sup. by ABREU 96F
1.92 $^{+0.45}_{-0.35}$ ±0.04	31	[5] BUSKULIC	94C	ALEP	Sup. by BUSKULIC 95O
1.13 $^{+0.35}_{-0.26}$ ±0.09	22	[5] ACTON	93H	OPAL	Sup. by AKERS 95G

[1] AALTONEN 11AP combines the fully reconstrcuted $B_s^0 \to D_s^-\pi^+$ decays and partially reconstructed $B_s^0 \to D_s X$ decays.
[2] Measured using $D_s\mu^+$ vertices.
[3] Uses $D_s^-\ell^+$, and $\phi\ell^+$ vertices.
[4] Measured using D_s hadron vertices.
[5] Measured using $D_s^-\ell^+$ vertices.
[6] ACKERSTAFF 98F use fully reconstructed $D_s^- \to \phi\pi^-$ and $D_s^- \to K^{*0}K^-$ in the inclusive B_s^0 decay.
[7] Combined results from $D_s^-\ell^+$ and D_s hadron.
[8] Measured using $\phi\ell$ vertices.
[9] Measured using inclusive D_s vertices.
[10] Combined result for the four ABREU 96F methods.
[11] Exclusive reconstruction of $B_s \to \psi\phi$.
[12] ABREU 94E uses the flight-distance distribution of D_s vertices, ϕ-lepton vertices, and $D_s\mu$ vertices.

$\Gamma_{B_s^0}$

"OUR EVALUATION" is an average performed by the Heavy Flavor Averaging Group (HFLAV) as described in our "Review on B-$\overline{B}$ Mixing" in the B^0 section of these Listings. It includes the measurements of $\Gamma_{B_s^0}$ and $\Delta\Gamma_{B_s^0}$ listed in this section, as well as constraints from effective lifetimes with pure CP modes and flavor-specific modes.

VALUE (10^{12} s^{-1})	DOCUMENT ID		TECN	COMMENT
0.6629±0.0018 OUR EVALUATION				
0.664 ±0.004 OUR AVERAGE	Error includes scale factor of 1.7. See the ideogram below.			
0.650 ±0.006 ±0.004	[1] AAIJ	17V	LHCB	pp at 7, 8 TeV
0.675 ±0.003 ±0.003	[2] AAD	16AP	ATLS	pp at 7, 8 TeV
0.668 ±0.011 ±0.006	[3] AAIJ	16AK	LHCB	pp at 7, 8 TeV
0.6704±0.0043±0.0055	[2] KHACHATRY...	16S	CMS	pp at 8 TeV
0.6603±0.0027±0.0015	[4] AAIJ	15I	LHCB	pp at 7, 8 TeV
0.654 ±0.008 ±0.004	[2] AALTONEN	12AJ	CDF	$p\overline{p}$ at 1.96 TeV
0.693 $^{+0.018}_{-0.017}$	[2] ABAZOV	12D	D0	$p\overline{p}$ at 1.96 TeV
• • • We do not use the following data for averages, fits, limits, etc. • • •				
0.677 ±0.007 ±0.004	[2] AAD	14U	ATLS	Repl. by AAD 16AP
0.661 ±0.004 ±0.006	[5] AAIJ	13AR	LHCB	Repl. by AAIJ 15I
0.677 ±0.007 ±0.004	[2] AAD	12CV	ATLS	Repl. by AAD 14U
0.657 ±0.009 ±0.008	[2] AAIJ	12D	LHCB	Repl. by AAIJ 13AR
0.654 ±0.011 ±0.005	[2,6] AALTONEN	12D	CDF	Repl. by AALTONEN 12AJ
0.672 ±0.027 ±0.013	[2] ABAZOV	09E	D0	Repl. by ABAZOV 08AM
0.658 ±0.017 ±0.009	[2,7] AALTONEN	08J	CDF	Repl. by AALTONEN 12D
0.658 ±0.022 ±0.004	[2] ABAZOV	08AM	D0	Repl. by ABAZOV 12D
0.658 ±0.035 $^{+0.0130}_{-0.004}$	[2,7] ABAZOV	07	D0	Repl. by ABAZOV 09E
0.714 $^{+0.007}_{-0.008}$ ±0.010	[2,7] ACOSTA	05	CDF	Repl. by AALTONEN 08J

[1] Measured using time-dependent angular analysis of $B_s^0 \to J/\psi K^+K^-$ in the region m(KK) > 1.05 GeV.
[2] Measured using a time-dependent angular analysis of $B_s^0 \to J/\psi\phi$ decays.
[3] Measured using a time-dependent angular analysis of $B_s^0 \to \psi(2S)\phi$ decays.
[4] Measured using a time-dependent angular analysis of $B_s^0 \to J/\psi K^+K^-$ decays.

Meson Particle Listings

B_s^0

[5] Measured using a combined time-dependent angular analysis of $B_s^0 \to J/\psi K^+ K^-$ and $B_s^0 \to J/\psi \pi^+ \pi^-$ decays.
[6] Assuming CPV phase $\phi_s = -0.04$.
[7] Assuming CPV phase $\phi_s = 0$.

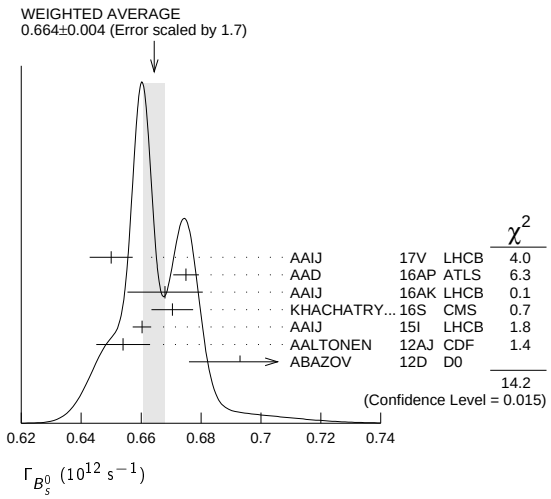

$\Delta\Gamma_{B_s^0}$

"OUR EVALUATION" is an average performed by the Heavy Flavor Averaging Group (HFLAV) as described in our "Review on B-$\overline{B}$ Mixing" in the B^0 section of these Listings. It includes the measurements of $\Gamma_{B_s^0}$ and $\Delta\Gamma_{B_s^0}$ listed in this section, as well as constraints from effective lifetimes with pure CP modes and flavor-specific modes.

VALUE (10^{12} s^{-1})			DOCUMENT ID		TECN	COMMENT
0.088 ±0.006		**OUR EVALUATION**				
0.083 ±0.006		**OUR AVERAGE**				
0.066	±0.018	±0.010	[1] AAIJ	17V	LHCB	pp at 7, 8 TeV
0.085	±0.011	±0.007	[2] AAD	16AP	ATLS	pp at 7, 8 TeV
0.066	$^{+0.041}_{-0.044}$	±0.007	[3] AAIJ	16AK	LHCB	pp at 7, 8 TeV
0.095	±0.013	±0.007	[2] KHACHATRY...	16S	CMS	pp at 8 TeV
0.0805	±0.0091	±0.0032	[4] AAIJ	15I	LHCB	pp at 7, 8 TeV
0.068	±0.026	±0.009	[2] AALTONEN	12AJ	CDF	$p\overline{p}$ at 1.96 TeV
0.163	$^{+0.065}_{-0.064}$		[2,5] ABAZOV	12D	D0	$p\overline{p}$ at 1.96 TeV
• • • We do not use the following data for averages, fits, limits, etc. • • •						
0.053	±0.021	±0.010	[2] AAD	14U	ATLS	Repl. by AAD 16AP
0.106	±0.011	±0.007	[6] AAIJ	13AR	LHCB	Repl. by AAIJ 15I
0.053	±0.021	±0.010	[2] AAD	12CV	ATLS	Repl. by AAD 14U
0.123	±0.029	±0.011	[2] AAIJ	12D	LHCB	Repl. by AAIJ 13AR
0.075	±0.035	±0.006	[7] AALTONEN	12D	CDF	Repl. by AALTONEN 12AJ
0.085	$^{+0.072}_{-0.078}$	±0.001	[8] ABAZOV	09E	D0	Repl. by ABAZOV 08AM
0.076	$^{+0.059}_{-0.063}$	±0.006	[9] AALTONEN	08J	CDF	Repl. by AALTONEN 12D
0.19	±0.07	$^{+0.02}_{-0.01}$	[2,10] ABAZOV	08AM	D0	Repl. by ABAZOV 12D
0.12	$^{+0.08}_{-0.10}$	±0.02	[9,11] ABAZOV	07	D0	Repl. by ABAZOV 07N
0.13	±0.09		[12] ABAZOV	07N	D0	Repl. by ABAZOV 09E
0.47	$^{+0.19}_{-0.24}$	±0.01	[9] ACOSTA	05	CDF	Repl. by AALTONEN 08J

[1] Measured using time-dependent angular analysis of $B_s^0 \to J/\psi K^+ K^-$ in the region $m(K\,K) > 1.05$ GeV.
[2] Measured using the time-dependent angular analysis of $B_s^0 \to J/\psi\phi$ decays.
[3] Measured using time-dependent angular analysis of $B_s^0 \to \psi(2S)\,\phi$ decays.
[4] Measured using time-dependent angular analysis of $B_s^0 \to J/\psi K^+ K^-$ decays.
[5] The error includes both statistical and systematic uncertainties.
[6] AAIJ 13AR result comes from a combined fit to $B_s^0 \to J/\psi K^+ K^-$ and $B_s^0 \to J/\psi\pi^+\pi^-$ data sets. Also reports $\Delta\Gamma_s = 0.100 \pm 0.016 \pm 0.003$ ps^{-1} from a fit to $B_s^0 \to J/\psi K^+ K^-$ decays.
[7] Uses the time-dependent angular analysis of $B_s^0 \to J/\psi\phi$ decays and assuming CP-violating angle $\beta_s(B^0 \to J/\psi\phi) = 0.02$.
[8] Measured the angular and lifetime parameters for the time-dependent angular untagged decays $B_d^0 \to J/\psi K^{*0}$ and $B_s^0 \to J/\psi\phi$.
[9] Measured using the time-dependent angular analysis of $B_s^0 \to J/\psi\phi$ decays and assuming CP-violating phase $\phi_s = 0$.
[10] Obtaines 90% CL interval $-0.06 < \Delta\Gamma_s < 0.30$.
[11] ABAZOV 07 reports $0.17 \pm 0.09 \pm 0.02$ with CP-violating phase ϕ_s as a free parameter.
[12] Combines D^0 measurements of time-dependent angular distributions in $B_s^0 \to J/\psi\phi$ and charge asymmetry in semileptonic decays. There is a 4-fold ambiguity in the solution.

$\Delta\Gamma_{B_s^0}/\Gamma_{B_s^0}$

$\Gamma_{B_s^0}$ and $\Delta\Gamma_{B_s^0}$ are the decay rate average and difference between two B_s^0 CP eigenstates (light − heavy).

"OUR EVALUATION" is provided by the Heavy Flavor Averaging Group (HFLAV). It is derived from the averages of $\Gamma_{B_s^0}$ and $\Delta\Gamma_{B_s^0}$ (and their correlation).

VALUE	CL%	DOCUMENT ID		TECN	COMMENT
0.132±0.008 OUR EVALUATION					
• • • We do not use the following data for averages, fits, limits, etc. • • •					
0.090±0.009±0.023		[1] ESEN	13	BELL	$e^+e^- \to \Upsilon(5S)$
		[2] AAIJ	12D	LHCB	pp at 7 TeV
		[3] AALTONEN	12D	CDF	$p\overline{p}$ at 1.96 TeV
		[4] ABAZOV	12D	D0	$p\overline{p}$ at 1.96 TeV
$0.147^{+0.036}_{-0.030}{}^{+0.042}_{-0.041}$		[1] ESEN	10	BELL	$e^+e^- \to \Upsilon(5S)$
0.072±0.021±0.022		[5] ABAZOV	09I	D0	$p\overline{p}$ at 1.96 TeV
>0.012	95	[5] AALTONEN	08F	CDF	$p\overline{p}$ at 1.96 TeV
$0.116^{+0.09}_{-0.10}$ ±0.010		[6] AALTONEN	08J	CDF	Repl. by AALTONEN 12D
$0.079^{+0.038}_{-0.035}{}^{+0.031}_{-0.030}$		[5] ABAZOV	07Y	D0	Repl. by ABAZOV 09I
$0.24\ ^{+0.28}_{-0.38}\ ^{+0.03}_{-0.04}$		[6,7] ABAZOV	05W	D0	Repl. by ABAZOV 08AM
$0.65\ ^{+0.25}_{-0.33}$ ±0.01		[6] ACOSTA	05	CDF	Repl. by AALTONEN 08J
<0.46	95	[8] ABREU	00Y	DLPH	$e^+e^- \to Z$
<0.69	95	[9] ABREU,P	00G	DLPH	$e^+e^- \to Z$
$0.25\ ^{+0.21}_{-0.14}$		[10] BARATE	00K	ALEP	$e^+e^- \to Z$
<0.83	95	[11] ABE	99D	CDF	$p\overline{p}$ at 1.8 TeV
<0.67	95	[12] ACCIARRI	98S	L3	$e^+e^- \to Z$

[1] Assumes CP violation is negligible.
[2] Measured using the time-dependent angular analysis of $B_s^0 \to J/\psi\phi$ decays.
[3] Uses the time-dependent angular analysis of $B_s^0 \to J/\psi\phi$ decays and assuming CP-violating angle $\beta_s(B^0 \to J/\psi\phi) = 0.02$.
[4] Measured using fully reconstructed $B_s \to J/\psi\phi$ decays.
[5] Assumes 2 $B(B_s^0 \to D_s^{(*)} D_s^{(*)}) \simeq \Delta\Gamma_s^{CP} / \Gamma_s$.
[6] Measured using the time-dependent angular analysis of $B_s^0 \to J/\psi\phi$ decays.
[7] Uses $|A_0|^2 - |A_\parallel|^2 = 0.355 \pm 0.066$ from ACOSTA 05.
[8] Uses $D_s^- \ell^+$, and $\phi\ell^+$ vertices.
[9] Measured using D_s hadron vertices.
[10] Uses $\phi\phi$ correlations from $B_s^0 \to D_s^{(*)+} D_s^{(*)-}$.
[11] ABE 99D assumes $\tau_{B_s^0} = 1.55 \pm 0.05$ ps.
[12] ACCIARRI 98S assumes $\tau_{B_s^0} = 1.49 \pm 0.06$ ps and PDG 98 values of b production fraction.

B_{sH}^0 MEAN LIFE

B_{sH}^0 is the heavy mass state of two B_s^0 CP eigenstates.

"OUR EVALUATION" is provided by the Heavy Flavor Averaging Group (HFLAV). It is derived from the averages of $\Gamma_{B_s^0}$ and $\Delta\Gamma_{B_s^0}$ (and their correlation).

VALUE (10^{-12} s)	DOCUMENT ID		TECN	COMMENT
1.615±0.009 OUR EVALUATION				
2.04 ±0.44 ±0.05	[1] AAIJ	17AI	LHCB	pp at 7, 8, 13 TeV
• • • We do not use the following data for averages, fits, limits, etc. • • •				
1.70 ±0.14 ±0.05	[2] ABAZOV	16C	D0	$p\overline{p}$ at 1.96 TeV
1.75 ±0.12 ±0.07	[3] AAIJ	13AB	LHCB	pp at 7 TeV
1.652±0.024±0.024	[4] AAIJ	13AR	LHCB	pp at 7 TeV
1.700±0.040±0.026	[5] AAIJ	12AN	LHCB	pp at 7 TeV
	[6] AALTONEN	12D	CDF	$p\overline{p}$ at 1.96 TeV
1.70 $^{+0.12}_{-0.11}$ ±0.03	[5] AALTONEN	11AB	CDF	$p\overline{p}$ at 1.96 TeV
$1.613^{+0.123}_{-0.113}$	[7,8] AALTONEN	08J	CDF	Repl. by AALTONEN 12D
1.58 $^{+0.39}_{-0.42}$ $^{+0.01}_{-0.02}$	[8] ABAZOV	05W	D0	Repl. by ABAZOV 08AM
2.07 $^{+0.58}_{-0.46}$ ±0.03	[8] ACOSTA	05	CDF	Repl. by AALTONEN 08J

[1] Measured using $B_s \to \mu^+\mu^-$ decays which, in the Standard Model, correspond to B_{sH}^0 decays. Assumes $-2\,\mathrm{Re}(\lambda)/(1+|\lambda|^2) = 1$.
[2] Measured using $J/\psi\pi^+\pi^-$ mode with $0.880 < m(\pi\pi) < 1.080$ GeV/c^2, which is mostly $J/\psi f(0)(980)$ mode, a pure CP-odd final state.
[3] Measured using a pure CP-odd final state $J/\psi K_S^0$ with the assumption that contributions from penguin diagrams are small.

[4] Measured using $B_s \to J/\psi\pi^+\pi^-$ decays which, in the limit of $\phi_s = 0$ and $|\lambda| = 1$, correspond to B^0_{sH} decays.
[5] Measured using a pure CP-odd final state $J/\psi f_0(980)$.
[6] Uses the time-dependent angular analysis of $B_s^0 \to J/\psi\phi$ decays assuming CP-violating angle $\beta_s(B^0 \to J/\psi\phi) = 0.02$.
[7] Obtained from $\Delta\Gamma_s$ and Γ_s fit with a correlation of 0.6.
[8] Measured using the time-dependent angular analysis of $B_s^0 \to J/\psi\phi$ decays.

B^0_{sL} MEAN LIFE

B^0_{sL} is the light mass state of two B_s^0 CP eigenstates.

"OUR EVALUATION" is provided by the Heavy Flavor Averaging Group (HFLAV). It is derived from the averages of $\Gamma_{B_s^0}$ and $\Delta\Gamma_{B_s^0}$ (and their correlation).

VALUE (10^{-12} s)	DOCUMENT ID		TECN	COMMENT
1.415±0.006 OUR EVALUATION				
• • • We do not use the following data for averages, fits, limits, etc. • • •				
1.479±0.034±0.011	[1] AAIJ	16AL	LHCB	pp at 7, 8 TeV
1.379±0.026±0.017	[2] AAIJ	14F	LHCB	pp at 7, 8 TeV
1.407±0.016±0.007	[3] AAIJ	14R	LHCB	pp at 7 TeV
1.440±0.096±0.009	[3] AAIJ	12	LHCB	Repl. by AAIJ 14R
1.455±0.046±0.006	[3] AAIJ	12R	LHCB	Repl. by AAIJ 14R
	[4] AALTONEN	12D	CDF	$p\overline{p}$ at 1.96 TeV
$1.437^{+0.054}_{-0.047}$	[5,6] AALTONEN	08J	CDF	Repl. by AALTONEN 12D
$1.24\ ^{+0.14}_{-0.11}\ ^{+0.01}_{-0.02}$	[6] ABAZOV	05W	D0	Repl. by ABAZOV 08AM
$1.05\ ^{+0.16}_{-0.13}\ \pm0.02$	[6] ACOSTA	05	CDF	Repl. by AALTONEN 08J
1.27 ±0.33 ±0.08	[7] BARATE	00K	ALEP	$e^+e^- \to Z$

[1] Measured using $B_s^0 \to J/\psi\eta$ decays.
[2] Measured using $B_s^0 \to D_s^- D_s^+$. The effective lifetime is translated into a decay width of $\Gamma_L = 0.725 \pm 0.014 \pm 0.009$ ps^{-1}.
[3] Measured using $B_s^0 \to K^+K^-$ decays. There may still be CPV in the decay.
[4] Uses the time-dependent angular analysis of $B_s^0 \to J/\psi\phi$ decays and assuming CP-violating angle $\beta_s(B^0 \to J/\psi\phi) = 0.02$.
[5] Obtained from $\Delta\Gamma_s$ and Γ_s fit with a correlation of 0.6.
[6] Measured using the time-dependent angular analysis of $B_s^0 \to J/\psi\phi$ decays.
[7] Uses $\phi\phi$ correlations from $B_s^0 \to D_s^{(*)+} D_s^{(*)-}$.

B_s^0 MEAN LIFE (Flavor specific)

VALUE (10^{-12} s)	DOCUMENT ID		TECN	COMMENT
1.527±0.011 OUR EVALUATION				
1.526±0.015 OUR AVERAGE Error includes scale factor of 1.3. See the ideogram below.				
1.547±0.013±0.011	[1] AAIJ	17AN	LHCB	pp at 7, 8 TeV
1.479±0.010±0.021	[2] ABAZOV	15A	D0	$p\overline{p}$ at 1.96 TeV
1.535±0.015±0.014	[3] AAIJ	14AX	LHCB	pp at 7 TeV
1.52 ±0.15 ±0.01	[4] AAIJ	14F	LHCB	pp at 7, 8 TeV
1.60 ±0.06 ±0.01	[5] AAIJ	14R	LHCB	pp at 7 TeV
1.518±0.041±0.027	[6] AALTONEN	11AP	CDF	$p\overline{p}$ at 1.96 TeV
$1.42\ ^{+0.14}_{-0.13}\ \pm0.03$	[7] ABREU	00Y	DLPH	$e^+e^- \to Z$
$1.36\ \pm0.09\ ^{+0.06}_{-0.05}$	[8] ABE	99D	CDF	$p\overline{p}$ at 1.8 TeV
$1.50\ ^{+0.16}_{-0.15}\ \pm0.04$	[8] ACKERSTAFF	98G	OPAL	$e^+e^- \to Z$
$1.54\ ^{+0.14}_{-0.13}\ \pm0.04$	[8] BUSKULIC	96M	ALEP	$e^+e^- \to Z$
• • • We do not use the following data for averages, fits, limits, etc. • • •				
$1.398\pm0.044^{+0.028}_{-0.025}$	[9] ABAZOV	06V	D0	Repl. by ABAZOV 15A

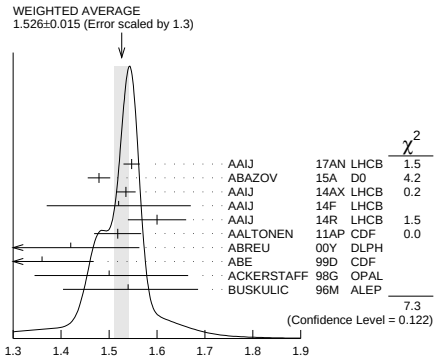

B_s^0 MEAN LIFE (Flavor specific) (10^{-12} s)

[1] AAIJ 17AN value was measured using $B_s^0 \to D_s^{(*)-}\mu^+\nu_\mu$ decays relative to $B^0 \to D^{(*)-}\mu^+\nu_\mu$ decays.
[2] Measured using $B_s^0 \to D_s^-\mu^+\nu_\mu X$ decays.
[3] Measured using the $B_s^0 \to D_s^-\pi^+$ decays.
[4] Measured using $B_s^0 \to D^+D_s^-$.
[5] Measured using $B_s^0 \to \pi^+K^-$ decays.
[6] AALTONEN 11AP combines the fully reconstrcuted $B_s^0 \to D_s^-\pi^+$ decays and partially reconstructed $B_s^0 \to D_s X$ decays.
[7] Uses $D_s^-\ell^+$, and $\phi\ell^+$ vertices.
[8] Measured using $D_s^-\ell^+$ vertices.
[9] Measured using $D_s^-\mu^+$ vertices.

B_s^0 MEAN LIFE ($B_S \to J/\psi\phi$)

VALUE (10^{-12} s)	DOCUMENT ID		TECN	COMMENT
1.479±0.012 OUR EVALUATION				
1.479±0.012 OUR AVERAGE				
1.480±0.011±0.005	[1] AAIJ	14E	LHCB	pp at 7 TeV
$1.444^{+0.098}_{-0.090}\pm0.020$	[1] ABAZOV	05B	D0	$p\overline{p}$ at 1.96 TeV
$1.34\ ^{+0.23}_{-0.19}\ \pm0.05$	[2] ABE	98B	CDF	$p\overline{p}$ at 1.8 TeV
• • • We do not use the following data for averages, fits, limits, etc. • • •				
$1.39\ ^{+0.13}_{-0.16}\ ^{+0.01}_{-0.02}$	[2] ABAZOV	05W	D0	$p\overline{p}$ at 1.96 TeV
$1.34\ ^{+0.23}_{-0.19}\ \pm0.05$	[3] ABE	96N	CDF	Repl. by ABE 98B

[1] Measured using fully reconstructed $B_s \to J/\psi\phi$ decays.
[2] Measured using the time-dependent angular analysis of $B_s^0 \to J/\psi\phi$ decays.
[3] ABE 96N uses 58 ± 12 exclusive $B_s \to J/\psi\phi$ events.

B_s^0 DECAY MODES

These branching fractions all scale with B($\overline{b} \to B_s^0$).

The branching fraction B($B_s^0 \to D_s^-\ell^+\nu_\ell$anything) is not a pure measurement since the measured product branching fraction B($\overline{b} \to B_s^0$) × B($B_s^0 \to D_s^-\ell^+\nu_\ell$anything) was used to determine B($\overline{b} \to B_s^0$), as described in the note on "B^0-$\overline{B}^0$ Mixing"

For inclusive branching fractions, *e.g.*, $B \to D^\pm$anything, the values usually are multiplicities, not branching fractions. They can be greater than one.

	Mode		Fraction (Γ_i/Γ)	Scale factor/ Confidence level
Γ_1	D_s^- anything		(93 ±25) %	
Γ_2	$\ell\nu_\ell X$		(9.6 ± 0.8) %	
Γ_3	$e^+\nu X^-$		(9.1 ± 0.8) %	
Γ_4	$\mu^+\nu X^-$		(10.2 ± 1.0) %	
Γ_5	$D_s^-\ell^+\nu_\ell$anything	[a]	(8.1 ± 1.3) %	
Γ_6	$D_s^{*-}\ell^+\nu_\ell$anything		(5.4 ± 1.1) %	
Γ_7	$D_{s1}(2536)^-\mu^+\nu_\mu$, $D_{s1}^- \to D^{*-}K_S^0$		(2.6 ± 0.7) $\times 10^{-3}$	
Γ_8	$D_{s1}(2536)^- X\,\mu^+\nu$, $D_{s1}^- \to \overline{D}^0K^+$		(4.4 ± 1.3) $\times 10^{-3}$	
Γ_9	$D_{s2}(2573)^- X\,\mu^+\nu$, $D_{s2}^- \to \overline{D}^0K^+$		(2.7 ± 1.0) $\times 10^{-3}$	
Γ_{10}	$D_s^-\pi^+$		(3.00± 0.23) $\times 10^{-3}$	
Γ_{11}	$D_s^-\rho^+$		(6.9 ± 1.4) $\times 10^{-3}$	
Γ_{12}	$D_s^-\pi^+\pi^+\pi^-$		(6.1 ± 1.0) $\times 10^{-3}$	
Γ_{13}	$D_{s1}(2536)^-\pi^+$, $D_{s1}^- \to D_s^-\pi^+\pi^-$		(2.5 ± 0.8) $\times 10^{-5}$	
Γ_{14}	$D_s^\mp K^\pm$		(2.27± 0.19) $\times 10^{-4}$	
Γ_{15}	$D_s^-K^+\pi^+\pi^-$		(3.2 ± 0.6) $\times 10^{-4}$	
Γ_{16}	$D_s^+D_s^-$		(4.4 ± 0.5) $\times 10^{-3}$	
Γ_{17}	$D_s^-D^+$		(2.8 ± 0.5) $\times 10^{-4}$	
Γ_{18}	D^+D^-		(2.2 ± 0.6) $\times 10^{-4}$	
Γ_{19}	$D^0\overline{D}^0$		(1.9 ± 0.5) $\times 10^{-4}$	
Γ_{20}	$D_s^{*-}\pi^+$		(2.0 ± 0.5) $\times 10^{-3}$	
Γ_{21}	$D_s^{*\mp}K^\pm$		(1.33± 0.35) $\times 10^{-4}$	
Γ_{22}	$D_s^{*-}\rho^+$		(9.6 ± 2.1) $\times 10^{-3}$	
Γ_{23}	$D_s^{*+}D_s^- + D_s^{*-}D_s^+$		(1.38± 0.16) %	
Γ_{24}	$D_s^{*+}D_s^{*-}$		(1.44± 0.20) %	S=1.1
Γ_{25}	$D_s^{(*)+}D_s^{(*)-}$		(4.5 ± 1.4) %	
Γ_{26}	$\overline{D}^{*0}\overline{K}^0$		(2.8 ± 1.1) $\times 10^{-4}$	
Γ_{27}	$\overline{D}^0\overline{K}^0$		(4.3 ± 0.9) $\times 10^{-4}$	

Meson Particle Listings

B_s^0

Γ_{28}	$\overline{D}^0 K^- \pi^+$	$(1.04 \pm 0.13) \times 10^{-3}$		
Γ_{29}	$\overline{D}^0 \overline{K}^*(892)^0$	$(4.4 \pm 0.6) \times 10^{-4}$		
Γ_{30}	$\overline{D}^0 \overline{K}^*(1410)$	$(3.9 \pm 3.5) \times 10^{-4}$		
Γ_{31}	$\overline{D}^0 \overline{K}_0^*(1430)$	$(3.0 \pm 0.7) \times 10^{-4}$		
Γ_{32}	$\overline{D}^0 \overline{K}_2^*(1430)$	$(1.1 \pm 0.4) \times 10^{-4}$		
Γ_{33}	$\overline{D}^0 \overline{K}^*(1680)$	$< 7.8 \times 10^{-5}$		CL=90%
Γ_{34}	$\overline{D}^0 \overline{K}_0^*(1950)$	$< 1.1 \times 10^{-4}$		CL=90%
Γ_{35}	$\overline{D}^0 \overline{K}_2^*(1780)$	$< 2.6 \times 10^{-5}$		CL=90%
Γ_{36}	$\overline{D}^0 \overline{K}_4^*(2045)$	$< 3.1 \times 10^{-5}$		CL=90%
Γ_{37}	$\overline{D}^0 K^- \pi^+$ (non-resonant)	$(2.1 \pm 0.8) \times 10^{-4}$		
Γ_{38}	$D_{s2}^*(2573)^- \pi^+$, $D_{s2}^* \to \overline{D}^0 K^-$	$(2.6 \pm 0.4) \times 10^{-4}$		
Γ_{39}	$D_{s1}^*(2700)^- \pi^+$, $D_{s1}^* \to \overline{D}^0 K^-$	$(1.6 \pm 0.8) \times 10^{-5}$		
Γ_{40}	$D_{s1}^*(2860)^- \pi^+$, $D_{s1}^* \to \overline{D}^0 K^-$	$(5 \pm 4) \times 10^{-5}$		
Γ_{41}	$D_{s3}^*(2860)^- \pi^+$, $D_{s3}^* \to \overline{D}^0 K^-$	$(2.2 \pm 0.6) \times 10^{-5}$		
Γ_{42}	$\overline{D}^0 K^+ K^-$	$(4.4 \pm 2.0) \times 10^{-5}$		
Γ_{43}	$\overline{D}^0 f_0(980)$	$< 3.1 \times 10^{-6}$		CL=90%
Γ_{44}	$\overline{D}^0 \phi$	$(3.0 \pm 0.8) \times 10^{-5}$		
Γ_{45}	$D^{*\mp} \pi^\pm$	$< 6.1 \times 10^{-6}$		CL=90%
Γ_{46}	$\eta_c \phi$	$(5.0 \pm 0.9) \times 10^{-4}$		
Γ_{47}	$\eta_c \pi^+ \pi^-$	$(1.8 \pm 0.7) \times 10^{-4}$		
Γ_{48}	$J/\psi(1S) \phi$	$(1.08 \pm 0.08) \times 10^{-3}$		
Γ_{49}	$J/\psi(1S) \phi\phi$	$(1.24^{+0.17}_{-0.19}) \times 10^{-5}$		
Γ_{50}	$J/\psi(1S) \pi^0$	$< 1.2 \times 10^{-3}$		CL=90%
Γ_{51}	$J/\psi(1S) \eta$	$(4.0 \pm 0.7) \times 10^{-4}$		S=1.4
Γ_{52}	$J/\psi(1S) K_S^0$	$(1.88 \pm 0.15) \times 10^{-5}$		
Γ_{53}	$J/\psi(1S) \overline{K}^*(892)^0$	$(4.1 \pm 0.4) \times 10^{-5}$		
Γ_{54}	$J/\psi(1S) \eta'$	$(3.3 \pm 0.4) \times 10^{-4}$		
Γ_{55}	$J/\psi(1S) \pi^+ \pi^-$	$(2.09 \pm 0.23) \times 10^{-4}$		S=1.3
Γ_{56}	$J/\psi(1S) f_0(500)$, $f_0 \to \pi^+ \pi^-$	$< 4 \times 10^{-6}$		CL=90%
Γ_{57}	$J/\psi(1S) \rho$, $\rho \to \pi^+ \pi^-$	$< 4 \times 10^{-6}$		CL=90%
Γ_{58}	$J/\psi(1S) f_0(980)$, $f_0 \to \pi^+ \pi^-$	$(1.28 \pm 0.18) \times 10^{-4}$		S=1.7
Γ_{59}	$J/\psi(1S) f_2(1270)$, $f_2 \to \pi^+ \pi^-$	$(1.1 \pm 0.4) \times 10^{-6}$		
Γ_{60}	$J/\psi(1S) f_2(1270)_0$, $f_2 \to \pi^+ \pi^-$	$(7.5 \pm 1.8) \times 10^{-7}$		
Γ_{61}	$J/\psi(1S) f_2(1270)_\parallel$, $f_2 \to \pi^+ \pi^-$	$(1.09 \pm 0.34) \times 10^{-6}$		
Γ_{62}	$J/\psi(1S) f_2(1270)_\perp$, $f_2 \to \pi^+ \pi^-$	$(1.3 \pm 0.8) \times 10^{-6}$		
Γ_{63}	$J/\psi(1S) f_0(1370)$, $f_0 \to \pi^+ \pi^-$	$(4.5^{+0.7}_{-4.0}) \times 10^{-5}$		
Γ_{64}	$J/\psi(1S) f_0(1500)$, $f_0 \to \pi^+ \pi^-$	$(2.11^{+0.40}_{-0.29}) \times 10^{-5}$		
Γ_{65}	$J/\psi(1S) f_2'(1525)_0$, $f_2' \to \pi^+ \pi^-$	$(1.07 \pm 0.24) \times 10^{-6}$		
Γ_{66}	$J/\psi(1S) f_2'(1525)_\parallel$, $f_2' \to \pi^+ \pi^-$	$(1.3^{+2.7}_{-0.9}) \times 10^{-7}$		
Γ_{67}	$J/\psi(1S) f_2'(1525)_\perp$, $f_2' \to \pi^+ \pi^-$	$(5 \pm 4) \times 10^{-7}$		
Γ_{68}	$J/\psi(1S) f_0(1790)$, $f_0 \to \pi^+ \pi^-$	$(5.0^{+11.0}_{-1.1}) \times 10^{-6}$		
Γ_{69}	$J/\psi(1S) \pi^+ \pi^-$ (nonresonant)	$(1.8^{+1.1}_{-0.4}) \times 10^{-5}$		
Γ_{70}	$J/\psi(1S) \overline{K}^0 \pi^+ \pi^-$	$< 4.4 \times 10^{-5}$		CL=90%
Γ_{71}	$J/\psi(1S) K^+ K^-$	$(7.9 \pm 0.7) \times 10^{-4}$		
Γ_{72}	$J/\psi(1S) K^0 K^- \pi^+ +$ c.c.	$(9.3 \pm 1.3) \times 10^{-4}$		
Γ_{73}	$J/\psi(1S) \overline{K}^0 K^+ K^-$	$< 1.2 \times 10^{-5}$		CL=90%
Γ_{74}	$J/\psi(1S) f_2'(1525)$	$(2.6 \pm 0.6) \times 10^{-4}$		
Γ_{75}	$J/\psi(1S) p\overline{p}$	$< 4.8 \times 10^{-6}$		CL=90%
Γ_{76}	$J/\psi(1S) \gamma$	$< 7.3 \times 10^{-6}$		CL=90%
Γ_{77}	$J/\psi(1S) \pi^+ \pi^- \pi^+ \pi^-$	$(7.8 \pm 1.0) \times 10^{-5}$		
Γ_{78}	$J/\psi(1S) f_1(1285)$	$(7.0 \pm 1.4) \times 10^{-5}$		
Γ_{79}	$\psi(2S) \eta$	$(3.3 \pm 0.9) \times 10^{-4}$		
Γ_{80}	$\psi(2S) \eta'$	$(1.29 \pm 0.35) \times 10^{-4}$		
Γ_{81}	$\psi(2S) \pi^+ \pi^-$	$(7.1 \pm 1.3) \times 10^{-5}$		
Γ_{82}	$\psi(2S) \phi$	$(5.4 \pm 0.6) \times 10^{-4}$		
Γ_{83}	$\psi(2S) K^- \pi^+$	$(3.12 \pm 0.30) \times 10^{-5}$		
Γ_{84}	$\psi(2S) \overline{K}^*(892)^0$	$(3.3 \pm 0.5) \times 10^{-5}$		
Γ_{85}	$\chi_{c1} \phi$	$(2.04 \pm 0.30) \times 10^{-4}$		
Γ_{86}	$\pi^+ \pi^-$	$(7.0 \pm 0.8) \times 10^{-7}$		
Γ_{87}	$\pi^0 \pi^0$	$< 2.1 \times 10^{-4}$		CL=90%
Γ_{88}	$\eta \pi^0$	$< 1.0 \times 10^{-3}$		CL=90%
Γ_{89}	$\eta\eta$	$< 1.5 \times 10^{-3}$		CL=90%
Γ_{90}	$\rho^0 \rho^0$	$< 3.20 \times 10^{-4}$		CL=90%
Γ_{91}	$\eta' \eta'$	$(3.3 \pm 0.7) \times 10^{-5}$		
Γ_{92}	$\eta' \phi$	$< 8.2 \times 10^{-7}$		CL=90%
Γ_{93}	$\phi f_0(980)$, $f_0(980) \to \pi^+ \pi^-$	$(1.12 \pm 0.21) \times 10^{-6}$		
Γ_{94}	$\phi f_2(1270)$, $f_2(1270) \to \pi^+ \pi^-$	$(6.1^{+1.8}_{-1.5}) \times 10^{-7}$		
Γ_{95}	$\phi \rho^0$	$(2.7 \pm 0.8) \times 10^{-7}$		
Γ_{96}	$\phi \pi^+ \pi^-$	$(3.5 \pm 0.5) \times 10^{-6}$		
Γ_{97}	$\phi\phi$	$(1.87 \pm 0.15) \times 10^{-5}$		
Γ_{98}	$\phi\phi\phi$	$(2.2 \pm 0.7) \times 10^{-6}$		
Γ_{99}	$\pi^+ K^-$	$(5.7 \pm 0.6) \times 10^{-6}$		
Γ_{100}	$K^+ K^-$	$(2.59 \pm 0.17) \times 10^{-5}$		
Γ_{101}	$K^0 \overline{K}^0$	$(2.0 \pm 0.6) \times 10^{-5}$		
Γ_{102}	$K^0 \pi^+ \pi^-$	$(9.4 \pm 2.1) \times 10^{-6}$		
Γ_{103}	$K^0 K^\pm \pi^\mp$	$(8.4 \pm 0.9) \times 10^{-5}$		
Γ_{104}	$K^*(892)^- \pi^+$	$(3.3 \pm 1.2) \times 10^{-6}$		
Γ_{105}	$K^*(892)^\pm K^\mp$	$(1.25 \pm 0.26) \times 10^{-5}$		
Γ_{106}	$K_S^0 \overline{K}^*(892)^0 +$ c.c.	$(1.6 \pm 0.4) \times 10^{-5}$		
Γ_{107}	$K^0 K^+ K^-$	$(1.3 \pm 0.6) \times 10^{-6}$		
Γ_{108}	$\overline{K}^*(892)^0 \rho^0$	$< 7.67 \times 10^{-4}$		CL=90%
Γ_{109}	$\overline{K}^*(892)^0 K^*(892)^0$	$(1.11 \pm 0.27) \times 10^{-5}$		
Γ_{110}	$\phi K^*(892)^0$	$(1.14 \pm 0.30) \times 10^{-6}$		
Γ_{111}	$p\overline{p}$	$< 1.5 \times 10^{-8}$		CL=90%
Γ_{112}	$p\overline{p} K^+ K^-$	$(4.5 \pm 0.5) \times 10^{-6}$		
Γ_{113}	$p\overline{p} K^+ \pi^-$	$(1.39 \pm 0.26) \times 10^{-6}$		
Γ_{114}	$p\overline{p} \pi^+ \pi^-$	$(4.3 \pm 2.0) \times 10^{-7}$		
Γ_{115}	$p\overline{\Lambda} K^- +$ c.c.	$(5.5 \pm 1.0) \times 10^{-6}$		
Γ_{116}	$\Lambda_c^- \Lambda \pi^+$	$(3.6 \pm 1.6) \times 10^{-4}$		
Γ_{117}	$\Lambda_c^- \Lambda_c^+$	$< 8.0 \times 10^{-5}$		CL=95%

Lepton Family number (LF) violating modes or $\Delta B = 1$ weak neutral current ($B1$) modes

Γ_{118}	$\gamma\gamma$	$B1$	$< 3.1 \times 10^{-6}$		CL=90%
Γ_{119}	$\phi\gamma$	$B1$	$(3.4 \pm 0.4) \times 10^{-5}$		
Γ_{120}	$\mu^+ \mu^-$	$B1$	$(2.7^{+0.6}_{-0.5}) \times 10^{-9}$		S=1.2
Γ_{121}	$e^+ e^-$	$B1$	$< 2.8 \times 10^{-7}$		CL=90%
Γ_{122}	$\tau^+ \tau^-$	$B1$	$< 6.8 \times 10^{-3}$		CL=95%
Γ_{123}	$\mu^+ \mu^- \mu^+ \mu^-$	$B1$	$< 2.5 \times 10^{-9}$		CL=95%
Γ_{124}	SP, $S \to \mu^+ \mu^-$, $P \to \mu^+ \mu^-$	$B1$	[b] $< 2.2 \times 10^{-9}$		CL=95%
Γ_{125}	$\phi(1020) \mu^+ \mu^-$	$B1$	$(8.2 \pm 1.2) \times 10^{-7}$		
Γ_{126}	$\pi^+ \pi^- \mu^+ \mu^-$	$B1$	$(8.4 \pm 1.7) \times 10^{-8}$		
Γ_{127}	$\phi\nu\overline{\nu}$	$B1$	$< 5.4 \times 10^{-3}$		CL=90%
Γ_{128}	$e^\pm \mu^\mp$	LF	[c] $< 1.1 \times 10^{-8}$		CL=90%

[a] Not a pure measurement. See note at head of B_s^0 Decay Modes.

[b] Here S and P are the hypothetical scalar and pseudoscalar particles with masses of 2.5 GeV/c^2 and 214.3 MeV/c^2, respectively.

[c] The value is for the sum of the charge states or particle/antiparticle states indicated.

CONSTRAINED FIT INFORMATION

An overall fit to 12 branching ratios uses 20 measurements and one constraint to determine 8 parameters. The overall fit has a $\chi^2 = 26.7$ for 13 degrees of freedom.

The following *off-diagonal* array elements are the correlation coefficients $\langle \delta x_i \delta x_j \rangle / (\delta x_i \cdot \delta x_j)$, in percent, from the fit to the branching fractions, $x_i \equiv \Gamma_i / \Gamma_{\text{total}}$. The fit constrains the x_i whose labels appear in this array to sum to one.

x_{12}	28					
x_{14}	92	26				
x_{48}	0	0	0			
x_{55}	0	0	0	72		
x_{58}	0	0	0	57	67	
x_{97}	0	0	0	29	21	17
	x_{10}	x_{12}	x_{14}	x_{48}	x_{55}	x_{58}

B_s^0 BRANCHING RATIOS

$\Gamma(D_s^- \text{anything})/\Gamma_{\text{total}}$ Γ_1/Γ

VALUE	EVTS	DOCUMENT ID		TECN	COMMENT
0.93±0.25 OUR AVERAGE					
0.91±0.18±0.41		[1] DRUTSKOY	07	BELL	$e^+e^- \to \Upsilon(4S)$
0.81±0.24±0.22	90	[2] BUSKULIC	96E	ALEP	$e^+e^- \to Z$
1.56±0.58±0.44	147	[3] ACTON	92N	OPAL	$e^+e^- \to Z$

[1] The extraction of this result takes into account the correlation between the measurements of $B(\Upsilon(5S) \to D_s X)$ and $B(\Upsilon(5S) \to D^0 X)$.

[2] BUSKULIC 96E separate $c\overline{c}$ and $b\overline{b}$ sources of D_s^+ mesons using a lifetime tag, subtract generic $\overline{b} \to W^+ \to D_s^+$ events, and obtain $B(\overline{b} \to B_s^0) \times B(B_s^0 \to D_s^- \text{anything}) = 0.088 \pm 0.020 \pm 0.020$ assuming $B(D_s \to \phi\pi) = (3.5 \pm 0.4) \times 10^{-2}$ and PDG 1994 values for the relative partial widths to other D_s channels. We evaluate using our current values $B(\overline{b} \to B_s^0) = 0.107 \pm 0.014$ and $B(D_s \to \phi\pi) = 0.036 \pm 0.009$. Our first error is their experiment's and our second error is that due to $B(\overline{b} \to B_s^0)$ and $B(D_s \to \phi\pi)$.

[3] ACTON 92N assume that excess of 147 ± 48 D_s^0 events over that expected from B^0, B^+, and $c\overline{c}$ is all from B_s^0 decay. The product branching fraction is measured to be $B(\overline{b} \to B_s^0) B(B_s^0 \to D_s^- \text{anything}) \times B(D_s^- \to \phi\pi^-) = (5.9 \pm 1.9 \pm 1.1) \times 10^{-3}$. We evaluate using our current values $B(\overline{b} \to B_s^0) = 0.107 \pm 0.014$ and $B(D_s \to \phi\pi) = 0.036 \pm 0.009$. Our first error is their experiment's and our second error is that due to $B(\overline{b} \to B_s^0)$ and $B(D_s \to \phi\pi)$.

$\Gamma(\ell\nu_\ell X)/\Gamma_{\text{total}}$ Γ_2/Γ

VALUE (units 10^{-2})	DOCUMENT ID		TECN	COMMENT
9.6±0.8 OUR AVERAGE				
9.6±0.4±0.7	[1] OSWALD	13	BELL	$e^+e^- \to \Upsilon(5S)$
$9.5^{+2.5}_{-2.0}{}^{+1.1}_{-1.9}$	[2] LEES	12A	BABR	e^+e^-

[1] The measurement corresponds to the average of the electron and muon branching fractions.

[2] The measurement corresponds to a branching fraction where the lepton originates from bottom decay and is the average between the electron and muon branching fractions. LEES 12A uses the correlation of the production of ϕ mesons in association with a lepton in e^+e^- data taken at center-of-mass energies between 10.54 and 11.2 GeV.

$\Gamma(e^+\nu X^-)/\Gamma_{\text{total}}$ Γ_3/Γ

VALUE (units 10^{-2})	DOCUMENT ID		TECN	COMMENT
9.1±0.5±0.6	OSWALD	13	BELL	$e^+e^- \to \Upsilon(5S)$

$\Gamma(\mu^+\nu X^-)/\Gamma_{\text{total}}$ Γ_4/Γ

VALUE (units 10^{-2})	DOCUMENT ID		TECN	COMMENT
10.2±0.6±0.8	OSWALD	13	BELL	$e^+e^- \to \Upsilon(5S)$

$\Gamma(D_s^- \ell^+ \nu_\ell \text{anything})/\Gamma_{\text{total}}$ Γ_5/Γ

The values and averages in this section serve only to show what values result if one assumes our $B(\overline{b} \to B_s^0)$. They cannot be thought of as measurements since the underlying product branching fractions were also used to determine $B(\overline{b} \to B_s^0)$ as described in the note on "Production and Decay of b-Flavored Hadrons."

VALUE (units 10^{-2})	EVTS	DOCUMENT ID		TECN	COMMENT
8.1±1.3 OUR AVERAGE					
8.2±0.2±1.5		[1] OSWALD	15	BELL	$e^+e^- \to \Upsilon(5S)$
7.6±1.2±2.1	134	[2] BUSKULIC	95O	ALEP	$e^+e^- \to Z$
10.7±4.3±2.9		[3] ABREU	92M	DLPH	$e^+e^- \to Z$
10.3±3.6±2.8	18	[4] ACTON	92N	OPAL	$e^+e^- \to Z$
• • • We do not use the following data for averages, fits, limits, etc. • • •					
13 ±4 ±4	27	[5] BUSKULIC	92E	ALEP	$e^+e^- \to Z$

[1] Obtains $B_s \to D_s X e\nu$, and $D_s X \mu\nu$ separately, then combines them by assuming systematic uncertainties are fully correlated, except for the one on lepton identification. The third uncertainty adds in quadrature systematic uncertainties from external sources (number of B_s events, and $D_s^{(*)}$ branching fractions). OSWALD 15 also measures the cross-section $\sigma(e^+e^- \to B_s^{(*)}\overline{B}_s^{(*)}) = 53.8 \pm 1.4 \pm 5.3$ pb at $\sqrt{s} = 10.86$ GeV.

[2] BUSKULIC 95O use $D_s\ell$ correlations. The measured product branching ratio is $B(\overline{b} \to B_s) \times B(B_s \to D_s^- \ell^+ \nu_\ell \text{anything}) = (0.82 \pm 0.09^{+0.13}_{-0.14})\%$ assuming $B(D_s \to \phi\pi) = (3.5 \pm 0.4) \times 10^{-2}$ and PDG 1994 values for the relative partial widths to the six other D_s channels used in this analysis. Combined with results from $\Upsilon(4S)$ experiments this can be used to extract $B(\overline{b} \to B_s) = (11.0 \pm 1.2^{+2.5}_{-2.6})\%$. We evaluate using our current values $B(\overline{b} \to B_s^0) = 0.107 \pm 0.014$ and $B(D_s \to \phi\pi) = 0.036 \pm 0.009$. Our first error is their experiment's and our second error is that due to $B(\overline{b} \to B_s^0)$ and $B(D_s \to \phi\pi)$.

[3] ABREU 92M measured muons only and obtained product branching ratio $B(Z \to b\text{or } \overline{b}) \times B(\overline{b} \to B_s) \times B(B_s \to D_s \mu^+ \nu_\mu \text{anything}) \times B(D_s \to \phi\pi) = (18 \pm 8) \times 10^{-5}$. We evaluate using our current values $B(\overline{b} \to B_s^0) = 0.107 \pm 0.014$ and $B(D_s \to \phi\pi) = 0.036 \pm 0.009$. Our first error is their experiment's and our second error is that due to $B(\overline{b} \to B_s^0)$ and $B(D_s \to \phi\pi)$. We use $B(Z \to b\text{or } \overline{b}) = 2B(Z \to b\overline{b}) = 2 \times (0.2212 \pm 0.0019)$.

[4] ACTON 92N is measured using $D_s \to \phi\pi^+$ and $K^*(892)^0 K^+$ events. The product branching fraction measured is measured to be $B(\overline{b} \to B_s^0) B(B_s^0 \to D_s^- \ell^+ \nu_\ell \text{anything}) \times B(D_s^- \to \phi\pi^-) = (3.9 \pm 1.1 \pm 0.8) \times 10^{-4}$. We evaluate using our current values $B(\overline{b} \to B_s^0) = 0.107 \pm 0.014$ and $B(D_s \to \phi\pi) = 0.036 \pm 0.009$. Our first error is their experiment's and our second error is that due to $B(\overline{b} \to B_s^0)$ and $B(D_s \to \phi\pi)$.

[5] BUSKULIC 92E is measured using $D_s \to \phi\pi^+$ and $K^*(892)^0 K^+$ events. They use 2.7 ± 0.7% for the $\phi\pi^+$ branching fraction. The average product branching fraction is measured to be $B(\overline{b} \to B_s^0) B(B_s^0 \to D_s^- \ell^+ \nu_\ell \text{anything}) = 0.020 \pm 0.0055^{+0.005}_{-0.006}$. We evaluate using our current values $B(\overline{b} \to B_s^0) = 0.107 \pm 0.014$ and $B(D_s \to \phi\pi) = 0.036 \pm 0.009$. Our first error is their experiment's and our second error is that due to $B(\overline{b} \to B_s^0)$ and $B(D_s \to \phi\pi)$. Superseded by BUSKULIC 95O.

$\Gamma(D_s^{*-} \ell^+ \nu_\ell \text{anything})/\Gamma_{\text{total}}$ Γ_6/Γ

VALUE (units 10^{-2})	DOCUMENT ID		TECN	COMMENT
5.4±0.4±1.0	[1] OSWALD	15	BELL	$e^+e^- \to \Upsilon(5S)$

[1] Obtains $B_s \to D_s^* X e\nu$, and $D_s^* X \mu\nu$ separately, then combines them by assuming systematic uncertainties are fully correlated, except for the one on lepton identification. The third uncertainty adds in quadrature systematic uncertainties from external sources (number of B_s events, and $D_s^{(*)}$ branching fractions). OSWALD 15 also measures the cross-section $\sigma(e^+e^- \to B_s^{(*)}\overline{B}_s^{(*)}) = 53.8 \pm 1.4 \pm 5.3$ pb at $\sqrt{s} = 10.86$ GeV.

$\Gamma(D_{s1}(2536)^- \mu^+ \nu_\mu,\ D_{s1}^- \to D^{*-} K_S^0)/\Gamma_{\text{total}}$ Γ_7/Γ

VALUE (units 10^{-3})	DOCUMENT ID		TECN	COMMENT
2.6±0.7±0.1	[1] ABAZOV	09G	D0	$p\overline{p}$ at 1.96 TeV

[1] ABAZOV 09G reports $[\Gamma(B_s^0 \to D_{s1}(2536)^- \mu^+ \nu_\mu,\ D_{s1}^- \to D^{*-} K_S^0)/\Gamma_{\text{total}}] \times [B(\overline{b} \to B_s^0)] = (2.66 \pm 0.52 \pm 0.45) \times 10^{-4}$ which we divide by our best value $B(\overline{b} \to B_s^0) = (10.1 \pm 0.4) \times 10^{-2}$. Our first error is their experiment's error and our second error is the systematic error from using our best value.

$\Gamma(D_{s1}(2536)^- X \mu^+ \nu,\ D_{s1}^- \to \overline{D}{}^0 K^+)/\Gamma(D_s^- \ell^+ \nu_\ell \text{anything})$ Γ_8/Γ_5

VALUE (units 10^{-2})	DOCUMENT ID		TECN	COMMENT
5.4±1.2±0.5	AAIJ	11A	LHCB	pp at 7 TeV

$\Gamma(D_{s2}(2573)^- X \mu^+ \nu,\ D_{s2}^- \to \overline{D}{}^0 K^+)/\Gamma(D_s^- \ell^+ \nu_\ell \text{anything})$ Γ_9/Γ_5

VALUE (units 10^{-2})	DOCUMENT ID		TECN	COMMENT
3.3±1.0±0.4	AAIJ	11A	LHCB	pp at 7 TeV

$\Gamma(D_{s1}(2536)^- X \mu^+ \nu,\ D_{s1}^- \to \overline{D}{}^0 K^+)/\Gamma(D_{s2}(2573)^- X \mu^+ \nu,\ D_{s2}^- \to \overline{D}{}^0 K^+)$ Γ_8/Γ_9

VALUE	DOCUMENT ID		TECN	COMMENT
• • • We do not use the following data for averages, fits, limits, etc. • • •				
0.61±0.14±0.05	[1] AAIJ	11A	LHCB	pp at 7 TeV

[1] Not independent of other AAIJ 11A measurements.

$\Gamma(D_s^- \pi^+)/\Gamma_{\text{total}}$ Γ_{10}/Γ

VALUE (units 10^{-3})	EVTS	DOCUMENT ID		TECN	COMMENT
3.00±0.23 OUR FIT					
2.99±0.24 OUR AVERAGE					
$2.95 \pm 0.05^{+0.25}_{-0.28}$		[1] AAIJ	12AG	LHCB	pp at 7 TeV
3.6 ±0.5 ±0.5		[2] LOUVOT	09	BELL	$e^+e^- \to \Upsilon(5S)$
2.8 ±0.6 ±0.1		[3] ABULENCIA	07C	CDF	$p\overline{p}$ at 1.96 TeV
• • • We do not use the following data for averages, fits, limits, etc. • • •					
6.8 ±2.2 ±1.6		DRUTSKOY	07A	BELL	Repl. by LOUVOT 09
3.3 ±1.1 ±0.2		[4] ABULENCIA	06J	CDF	Repl. by ABULENCIA 07C
<130	6	[5] AKERS	94J	OPAL	$e^+e^- \to Z$
seen	1	BUSKULIC	93G	ALEP	$e^+e^- \to Z$

[1] AAIJ 12AG reports $(2.95 \pm 0.05 \pm 0.17^{+0.18}_{-0.22}) \times 10^{-3}$ where the last uncertainty comes from the semileptonic f_s/f_d measurement. We combined the systematics in quadrature.

[2] LOUVOT 09 reports $(3.67^{+0.35+0.65}_{-0.33-0.645}) \times 10^{-3}$ from a measurement of $[\Gamma(B_s^0 \to D_s^- \pi^+)/\Gamma_{\text{total}}] \times [B(\Upsilon(10860) \to B_s^{(*)}\overline{B}_s^{(*)})]$ assuming $B(\Upsilon(10860) \to B_s^{(*)}\overline{B}_s^{(*)}) = (19.5 \pm 2.6) \times 10^{-2}$, which we rescale to our best value $B(\Upsilon(10860) \to B_s^{(*)}\overline{B}_s^{(*)}) = (20.1 \pm 3.1) \times 10^{-2}$. Our first error is their experiment's error and our second error is the systematic error from using our best value.

[3] ABULENCIA 07C reports $[\Gamma(B_s^0 \to D_s^- \pi^+)/\Gamma_{\text{total}}] / [B(B^0 \to D^- \pi^+)] = 1.13 \pm 0.08 \pm 0.23$ which we multiply by our best value $B(B^0 \to D^- \pi^+) = (2.52 \pm 0.13) \times 10^{-3}$. Our first error is their experiment's error and our second error is the systematic error from using our best value.

[4] ABULENCIA 06J reports $[\Gamma(B_s^0 \to D_s^- \pi^+)/\Gamma_{\text{total}}] / [B(B^0 \to D^- \pi^+)] = 1.32 \pm 0.18 \pm 0.38$ which we multiply by our best value $B(B^0 \to D^- \pi^+) = (2.52 \pm 0.13) \times 10^{-3}$. Our first error is their experiment's error and our second error is the systematic error from using our best value.

[5] AKERS 94J sees ≤ 6 events and measures the limit on the product branching fraction $f(\overline{b} \to B_s^0) \cdot B(B_s^0 \to D_s^- \pi^+) < 1.3\%$ at CL = 90%. We divide by our current value $B(\overline{b} \to B_s^0) = 0.105$.

$\Gamma(D_s^- \rho^+)/\Gamma_{\text{total}}$ Γ_{11}/Γ

VALUE (units 10^{-3})	DOCUMENT ID		TECN	COMMENT
6.9±1.3±0.5	[1] LOUVOT	10	BELL	$e^+e^- \to \Upsilon(5S)$

Meson Particle Listings

B_s^0

[1] LOUVOT 10 reports $[\Gamma(B_s^0 \to D_s^- \rho^+)/\Gamma_{\text{total}}] / [B(B_s^0 \to D_s^- \pi^+)] = 2.3 \pm 0.4 \pm 0.2$ which we multiply by our best value $B(B_s^0 \to D_s^- \pi^+) = (3.00 \pm 0.23) \times 10^{-3}$. Our first error is their experiment's error and our second error is the systematic error from using our best value.

$\Gamma(D_s^- \pi^+ \pi^+ \pi^-)/\Gamma_{\text{total}}$ Γ_{12}/Γ

VALUE (units 10^{-3})	DOCUMENT ID		TECN	COMMENT
6.1±1.0 OUR FIT				
6.3±1.5±0.7	[1] ABULENCIA	07C	CDF	$p\overline{p}$ at 1.96 TeV

[1] ABULENCIA 07C reports $[\Gamma(B_s^0 \to D_s^- \pi^+ \pi^+ \pi^-)/\Gamma_{\text{total}}] / [B(B^0 \to D^- \pi^+ \pi^+ \pi^-)] = 1.05 \pm 0.10 \pm 0.22$ which we multiply by our best value $B(B^0 \to D^- \pi^+ \pi^+ \pi^-) = (6.0 \pm 0.7) \times 10^{-3}$. Our first error is their experiment's error and our second error is the systematic error from using our best value.

$\Gamma(D_s^- \pi^+ \pi^+ \pi^-)/\Gamma(D_s^- \pi^+)$ Γ_{12}/Γ_{10}

VALUE	DOCUMENT ID		TECN	COMMENT
2.05±0.34 OUR FIT				
2.01±0.37±0.20	AAIJ	11E	LHCB	pp at 7 TeV

$\Gamma(D_{s1}(2536)^- \pi^+,\ D_{s1}^- \to D_s^- \pi^+ \pi^-)/\Gamma(D_s^- \pi^+ \pi^+ \pi^-)$ Γ_{13}/Γ_{12}

VALUE (units 10^{-3})	DOCUMENT ID		TECN	COMMENT
4.0±1.0±0.4	AAIJ	12AX	LHCB	pp at 7 TeV

$\Gamma(D_s^{\mp} K^{\pm})/\Gamma_{\text{total}}$ Γ_{14}/Γ

VALUE (units 10^{-4})	DOCUMENT ID		TECN	COMMENT
2.27±0.19 OUR FIT				
$2.3\ ^{+1.2}_{-1.0}\ ^{+0.4}_{-0.3}$	[1] LOUVOT	09	BELL	$e^+e^- \to \Upsilon(5S)$

[1] LOUVOT 09 reports $(2.4\ ^{+1.2}_{-1.0} \pm 0.42) \times 10^{-4}$ from a measurement of $[\Gamma(B_s^0 \to D_s^{\mp} K^{\pm})/\Gamma_{\text{total}}] \times [B(\Upsilon(10860) \to B_s^{(*)} \overline{B}_s^{(*)})]$ assuming $B(\Upsilon(10860) \to B_s^{(*)} \overline{B}_s^{(*)}) = (19.5 \pm 2.6) \times 10^{-2}$, which we rescale to our best value $B(\Upsilon(10860) \to B_s^{(*)} \overline{B}_s^{(*)}) = (20.1 \pm 3.1) \times 10^{-2}$. Our first error is their experiment's error and our second error is the systematic error from using our best value.

$\Gamma(D_s^{\mp} K^{\pm})/\Gamma(D_s^- \pi^+)$ Γ_{14}/Γ_{10}

VALUE (units 10^{-2})	DOCUMENT ID		TECN	COMMENT
7.55±0.24 OUR FIT				
7.55±0.24 OUR AVERAGE				
7.52±0.15±0.19	AAIJ	15AC	LHCB	pp at 7, 8 TeV
9.7 ±1.8 ±0.9	AALTONEN	09AQ	CDF	$p\overline{p}$ at 1.96 TeV
• • • We do not use the following data for averages, fits, limits, etc. • • •				
6.46±0.43±0.25	AAIJ	12AG	LHCB	Repl. by AAIJ 15AC

$\Gamma(D_s^- K^+ \pi^+ \pi^-)/\Gamma(D_s^- \pi^+ \pi^+ \pi^-)$ Γ_{15}/Γ_{12}

VALUE (units 10^{-2})	DOCUMENT ID		TECN	COMMENT
5.2±0.5±0.3	AAIJ	12AX	LHCB	pp at 7 TeV

$\Gamma(D_s^+ D_s^-)/\Gamma_{\text{total}}$ Γ_{16}/Γ

VALUE (units 10^{-3})	CL%	DOCUMENT ID		TECN	COMMENT
4.4±0.5 OUR AVERAGE					
4.0±0.2±0.5		[1] AAIJ	13AP	LHCB	pp at 7 TeV
$5.8\ ^{+1.1}_{-0.9}$±1.3		[2] ESEN	13	BELL	$e^+e^- \to \Upsilon(5S)$
5.3±0.8±0.6		[3] AALTONEN	12C	CDF	$p\overline{p}$ at 1.96 TeV
• • • We do not use the following data for averages, fits, limits, etc. • • •					
$10.3\ ^{+3.9}_{-3.2}\ ^{+2.6}_{-2.5}$		[4] ESEN	10	BELL	Repl. by ESEN 13
$10.4\ ^{+3.5}_{-3.2}$±1.1		[5] AALTONEN	08F	CDF	Repl. by AALTONEN 12C
<67	90	DRUTSKOY	07A	BELL	Repl. by ESEN 10

[1] Uses $B(B^0 \to D^- D_s^+) = (7.2 \pm 0.8) \times 10^{-3}$.

[2] Use $\Upsilon(5S) \to B_s^* \overline{B}_s^*$ decays assuming $B(\Upsilon(5S) \to B_s^* \overline{B}_s^*) = (17.1 \pm 3.0)\%$ and $\Gamma(\Upsilon(5S) \to B_s^* \overline{B}_s^*) / \Gamma(\Upsilon(5S) \to B_s^{(*)} \overline{B}_s^{(*)}) = (87.0 \pm 1.7)\%$.

[3] AALTONEN 12C reports $(f_s/f_d)\ (B(B_s^0 \to D_s^+ D_s^-) / B(B^0 \to D^- D_s^+)) = 0.183 \pm 0.021 \pm 0.017$. We multiply this result by our best value of $B(B^0 \to D^- D_s^+) = (7.2 \pm 0.8) \times 10^{-3}$ and divide by our best value of f_s/f_d, where $1/2\ f_s/f_d = 0.125 \pm 0.006$. Our first quoted uncertainty is the combined experiment's uncertainty and our second is the systematic uncertainty from using out best values.

[4] Uses $\Upsilon(10860) \to B_s^* \overline{B}_s^*$ assuming $B(\Upsilon(10860) \to B_s^{(*)} \overline{B}_s^{(*)}) = (19.3 \pm 2.9)\%$ and $\Gamma(\Upsilon(10860) \to B_s^* \overline{B}_s^*) / \Gamma(\Upsilon(10860) \to B_s^{(*)} \overline{B}_s^{(*)}) = (90.1\ ^{+3.8}_{-4.0})\%$.

[5] AALTONEN 08F reports $[\Gamma(B_s^0 \to D_s^+ D_s^-)/\Gamma_{\text{total}}] / [B(B^0 \to D^- D_s^+)] = 1.44\ ^{+0.48}_{-0.44}$ which we multiply by our best value $B(B^0 \to D^- D_s^+) = (7.2 \pm 0.8) \times 10^{-3}$. Our first error is their experiment's error and our second error is the systematic error from using our best value.

$\Gamma(D_s^- D^+)/\Gamma_{\text{total}}$ Γ_{17}/Γ

VALUE (units 10^{-4})	DOCUMENT ID		TECN	COMMENT
2.8±0.4±0.3	[1] AAIJ	14AA	LHCB	pp at 7 TeV
• • • We do not use the following data for averages, fits, limits, etc. • • •				
3.6±0.6±0.5	[2] AAIJ	13AP	LHCB	Repl. by AAIJ 14AA

[1] AAIJ 14AA reports $[\Gamma(B_s^0 \to D_s^- D^+)/\Gamma_{\text{total}}] / [B(B^0 \to D^- D_s^+)] = 0.038 \pm 0.004 \pm 0.003$ which we multiply by our best value $B(B^0 \to D^- D_s^+) = (7.2 \pm 0.8) \times 10^{-3}$. Our first error is their experiment's error and our second error is the systematic error from using our best value..

[2] Uses $B(B^0 \to D^- D_s^+) = (7.2 \pm 0.8) \times 10^{-3}$.

$\Gamma(D^+ D^-)/\Gamma_{\text{total}}$ Γ_{18}/Γ

VALUE (units 10^{-4})	DOCUMENT ID		TECN	COMMENT
2.2±0.4±0.4	[1] AAIJ	13AP	LHCB	pp at 7 TeV

[1] Uses $B(B^0 \to D^- D^+) = (2.11 \pm 0.31) \times 10^{-4}$ and $B(B^+ \to \overline{D}^0 D_s^+) = (10.1 \pm 1.7) \times 10^{-3}$.

$\Gamma(D^0 \overline{D}^0)/\Gamma_{\text{total}}$ Γ_{19}/Γ

VALUE (units 10^{-4})	DOCUMENT ID		TECN	COMMENT
1.9±0.3±0.4	[1] AAIJ	13AP	LHCB	pp at 7 TeV

[1] Uses $B(B^0 \to D^- D^+) = (2.11 \pm 0.31) \times 10^{-4}$ and $B(B^+ \to \overline{D}^0 D_s^+) = (10.1 \pm 1.7) \times 10^{-3}$.

$\Gamma(D_s^{*-} \pi^+)/\Gamma_{\text{total}}$ Γ_{20}/Γ

VALUE (units 10^{-3})	DOCUMENT ID		TECN	COMMENT
$2.0\ ^{+0.5}_{-0.4}\ ^{+0.1}_{-0.2}$	[1] LOUVOT	10	BELL	$e^+e^- \to \Upsilon(5S)$

[1] LOUVOT 10 reports $[\Gamma(B_s^0 \to D_s^{*-} \pi^+)/\Gamma_{\text{total}}] / [B(B_s^0 \to D_s^- \pi^+)] = 0.65\ ^{+0.15}_{-0.13} \pm 0.07$ which we multiply by our best value $B(B_s^0 \to D_s^- \pi^+) = (3.00 \pm 0.23) \times 10^{-3}$. Our first error is their experiment's error and our second error is the systematic error from using our best value.

$\Gamma(D_s^{*\mp} K^{\pm})/\Gamma(D_s^{*-} \pi^+)$ Γ_{21}/Γ_{20}

VALUE	DOCUMENT ID		TECN	COMMENT
$0.068 \pm 0.005\ ^{+0.003}_{-0.002}$	AAIJ	15AD	LHCB	pp at 7, 8 TeV

$\Gamma(D_s^{*-} \rho^+)/\Gamma_{\text{total}}$ Γ_{22}/Γ

VALUE (units 10^{-3})	DOCUMENT ID		TECN	COMMENT
$9.6 \pm 2.0\ ^{+0.7}_{-0.8}$	[1] LOUVOT	10	BELL	$e^+e^- \to \Upsilon(5S)$

[1] LOUVOT 10 reports $[\Gamma(B_s^0 \to D_s^{*-} \rho^+)/\Gamma_{\text{total}}] / [B(B_s^0 \to D_s^- \pi^+)] = 3.2 \pm 0.6 \pm 0.3$ which we multiply by our best value $B(B_s^0 \to D_s^- \pi^+) = (3.00 \pm 0.23) \times 10^{-3}$. Our first error is their experiment's error and our second error is the systematic error from using our best value.

$\Gamma(D_s^{*-} \rho^+)/\Gamma(D_s^- \rho^+)$ Γ_{22}/Γ_{11}

VALUE	DOCUMENT ID		TECN	COMMENT
• • • We do not use the following data for averages, fits, limits, etc. • • •				
1.4±0.3±0.1	LOUVOT	10	BELL	$e^+e^- \to \Upsilon(5S)$

$[\Gamma(D_s^{*+} D_s^-) + \Gamma(D_s^{*-} D_s^+)]/\Gamma_{\text{total}}$ Γ_{23}/Γ

VALUE (units 10^{-3})	CL%	DOCUMENT ID		TECN	COMMENT
13.8±1.6 OUR AVERAGE					
13.6±1.0±1.4		[1] AAIJ	16P	LHCB	pp at 7 TeV
$17.6\ ^{+2.3}_{-2.2}$±4.0		[2] ESEN	13	BELL	$e^+e^- \to \Upsilon(5S)$
12.3±1.7±1.4		[3] AALTONEN	12C	CDF	$p\overline{p}$ at 1.96 TeV
• • • We do not use the following data for averages, fits, limits, etc. • • •					
$27.5\ ^{+8.3}_{-7.1}$±6.9		[4] ESEN	10	BELL	Repl. by ESEN 13
<121	90	DRUTSKOY	07A	BELL	Repl. by ESEN 10

[1] AAIJ 16P reports $[\left[\Gamma(B_s^0 \to D_s^{*+} D_s^-) + \Gamma(D_s^{*-} D_s^+)\right]/\Gamma_{\text{total}}] / [B(B^0 \to D^- D_s^+)] = 1.88 \pm 0.08 \pm 0.12$ which we multiply by our best value $B(B^0 \to D^- D_s^+) = (7.2 \pm 0.8) \times 10^{-3}$. Our first error is their experiment's error and our second error is the systematic error from using our best value.

[2] Use $\Upsilon(5S) \to B_s^* \overline{B}_s^*$ decays assuming $B(\Upsilon(5S) \to B_s^* \overline{B}_s^*) = (17.1 \pm 3.0)\%$ and $\Gamma(\Upsilon(5S) \to B_s^* \overline{B}_s^*) / \Gamma(\Upsilon(5S) \to B_s^{(*)} \overline{B}_s^{(*)}) = (87.0 \pm 1.7)\%$.

[3] AALTONEN 12C reports $(f_s/f_d)\ (B(B_s^0 \to D_s^{*+} D_s^- + D_s^{*-} D_s^+) / B(B^0 \to D^- D_s^+)) = 0.424 \pm 0.046 \pm 0.035$. We multiply this result by our best value of $B(B^0 \to D^- D_s^+) = (7.2 \pm 0.8) \times 10^{-3}$ and divide by our best value of f_s/f_d, where $1/2\ f_s/f_d = 0.125 \pm 0.006$. Our first quoted uncertainty is the combined experiment's uncertainty and our second is the systematic uncertainty from using out best values.

[4] Uses $\Upsilon(10860) \to B_s^* \overline{B}_s^*$ assuming $B(\Upsilon(10860) \to B_s^{(*)} \overline{B}_s^{(*)}) = (19.3 \pm 2.9)\%$ and $\Gamma(\Upsilon(10860) \to B_s^* \overline{B}_s^*) / \Gamma(\Upsilon(10860) \to B_s^{(*)} \overline{B}_s^{(*)}) = (90.1\ ^{+3.8}_{-4.0})\%$.

$\Gamma(D_s^{*+} D_s^{*-})/\Gamma_{\text{total}}$ Γ_{24}/Γ

VALUE (units 10^{-3})	CL%	DOCUMENT ID		TECN	COMMENT
14.4± 2.0 OUR AVERAGE		Error includes scale factor of 1.1.			
12.7± 1.3±1.4		[1] AAIJ	16P	LHCB	pp at 7 TeV
$19.8^{+\ 3.3+5.2}_{-\ 3.1-5.0}$		[2] ESEN	13	BELL	$e^+e^- \to \Upsilon(5S)$
18.9± 2.8±2.2		[3] AALTONEN	12C	CDF	$p\overline{p}$ at 1.96 TeV
• • • We do not use the following data for averages, fits, limits, etc. • • •					

$30.8^{+12.2}_{-10.4}\pm8.5$		[4] ESEN	10	BELL	Repl. by ESEN 13
<257	90	DRUTSKOY	07A	BELL	Repl. by ESEN 10

[1] AAIJ 16P reports $[\Gamma(B_s^0 \to D_s^{*+}D_s^{*-})/\Gamma_{\rm total}] / [{\rm B}(B^0 \to D^-D_s^+)] = 1.76 \pm 0.11 \pm 0.14$ which we multiply by our best value ${\rm B}(B^0 \to D^-D_s^+) = (7.2 \pm 0.8) \times 10^{-3}$. Our first error is their experiment's error and our second error is the systematic error from using our best value.

[2] Use $\Upsilon(5S) \to B_s^*\overline{B}_s^*$ decays assuming ${\rm B}(\Upsilon(5S) \to B_s^*\overline{B}_s^*) = (17.1 \pm 3.0)\%$ and $\Gamma(\Upsilon(5S) \to B_s^*\overline{B}_s^*) / \Gamma(\Upsilon(5S) \to B_s^{(*)}\overline{B}_s^{(*)}) = (87.0 \pm 1.7)\%$.

[3] AALTONEN 12C reports $(f_s/f_d)\,({\rm B}(B_s^0 \to D_s^{*+}D_s^{*-}) / {\rm B}(B^0 \to D^-D_s^+)) = 0.654 \pm 0.072 \pm 0.065$. We multiply this result by our best value ${\rm B}(B^0 \to D^-D_s^+) = (7.2 \pm 0.8) \times 10^{-3}$ and divide by our best value of f_s/f_d, where $1/2\ f_s/f_d = 0.125 \pm 0.006$. Our first quoted uncertainty is the combined experiment's uncertainty and our second is the systematic uncertainty from using out best values.

[4] Uses $\Upsilon(10860) \to B_s^*\overline{B}_s^*$ assuming ${\rm B}(\Upsilon(10860) \to B_s^{(*)}\overline{B}_s^{(*)}) = (19.3 \pm 2.9)\%$ and $\Gamma(\Upsilon(10860) \to B_s^*\overline{B}_s^*) / \Gamma(\Upsilon(10860) \to B_s^{(*)}\overline{B}_s^{(*)}) = (90.1^{+3.8}_{-4.0})\%$.

$\Gamma(D_s^{(*)+}D_s^{(*)-})/\Gamma_{\rm total}$ Γ_{25}/Γ

"OUR EVALUATION" is an average using rescaled values of the data listed below. The average and rescaling were performed by the Heavy Flavor Averaging Group (HFLAV) and are described at http://www.slac.stanford.edu/xorg/hflav/. The averaging/rescaling procedure takes into account correlations between the measurements.

VALUE (%)	CL%	DOCUMENT ID		TECN	COMMENT
4.5 ±1.4 OUR EVALUATION					
3.4 ±0.4 OUR AVERAGE					
$3.07\pm0.22\pm0.33$		[1] AAIJ	16P	LHCB	pp at 7 TeV
$4.32^{+0.42}_{-0.39}{}^{+1.04}_{-1.03}$		[2] ESEN	13	BELL	$e^+e^- \to \Upsilon(5S)$
3.7 ±0.4 ±0.4		[3] AALTONEN	12C	CDF	$p\overline{p}$ at 1.96 TeV
3.5 ±1.0 ±1.1		[4] ABAZOV	09I	D0	$p\overline{p}$ at 1.96 TeV
14 ±6 ±3		[5,6] BARATE	00K	ALEP	$e^+e^- \to Z$
• • • We do not use the following data for averages, fits, limits, etc. • • •					
$6.85^{+1.53}_{-1.30}{}^{+1.79}_{-1.80}$		[7,8] ESEN	10	BELL	Repl. by ESEN 13
$3.9\ ^{+1.9}_{-1.7}\ ^{+1.6}_{-1.5}$		[4] ABAZOV	07Y	D0	Repl. by ABAZOV 09I
<0.218	90	BARATE	98Q	ALEP	$e^+e^- \to Z$

[1] AAIJ 16P reports $[\Gamma(B_s^0 \to D_s^{(*)+}D_s^{(*)-})/\Gamma_{\rm total}] / [{\rm B}(B^0 \to D^-D_s^+)] = 4.24 \pm 0.14 \pm 0.27$ which we multiply by our best value ${\rm B}(B^0 \to D^-D_s^+) = (7.2 \pm 0.8) \times 10^{-3}$. Our first error is their experiment's error and our second error is the systematic error from using our best value.

[2] Use $\Upsilon(5S) \to B_s^*\overline{B}_s^*$ decays assuming ${\rm B}(\Upsilon(5S) \to B_s^*\overline{B}_s^*) = (17.1 \pm 3.0)\%$ and $\Gamma(\Upsilon(5S) \to B_s^*\overline{B}_s^*) / \Gamma(\Upsilon(5S) \to B_s^{(*)}\overline{B}_s^{(*)}) = (87.0 \pm 1.7)\%$.

[3] AALTONEN 12C reports $(f_s/f_d)\,({\rm B}(B_s^0 \to D_s^{(*)+}D_s^{(*)-}) / {\rm B}(B^0 \to D^-D_s^+)) = 1.261 \pm 0.095 \pm 0.112$. We multiply this result by our best value of ${\rm B}(B^0 \to D^-D_s^+) = (7.2 \pm 0.8) \times 10^{-3}$ and divide by our best value of f_s/f_d, where $1/2\ f_s/f_d = 0.125 \pm 0.006$. Our first quoted uncertainty is the combined experiment's uncertainty and our second is the systematic uncertainty from using out best values.

[4] Uses the final states where $D_s^+ \to \phi\pi^+$ and $D_s^- \to \phi\mu^-\overline{\nu}_\mu$.

[5] Reports ${\rm B}(B_s^0({\rm short}) \to D_s^{(*)}D_s^{(*)}) = (0.23 \pm 0.10 \pm 0.05) \cdot [0.17/{\rm B}(D_s \to \phi\chi)]^2$ assuming ${\rm B}(B_s^0 \to B_s^0({\rm short})) = 50\%$. We use our best value of ${\rm B}(D_s \to \phi\chi) = 15.7 \pm 1.0\%$ to obtain the quoted result.

[6] Uses $\phi\phi$ correlations from $B_s^0({\rm short}) \to D_s^{(*)+}D_s^{(*)-}$.

[7] Sum of exclusive $B_s \to D_s^+D_s^-$, $B_s \to D_s^{*\pm}D_s^{\mp}$ and $B_s \to D_s^{*+}D_s^{*-}$.

[8] Uses $\Upsilon(10860) \to B_s^*\overline{B}_s^*$ assuming ${\rm B}(\Upsilon(10860) \to B_s^{(*)}\overline{B}_s^{(*)}) = (19.3 \pm 2.9)\%$ and $\Gamma(\Upsilon(10860) \to B_s^*\overline{B}_s^*) / \Gamma(\Upsilon(10860) \to B_s^{(*)}\overline{B}_s^{(*)}) = (90.1^{+3.8}_{-4.0})\%$.

$\Gamma(\overline{D}^{*0}\overline{K}^0)/\Gamma_{\rm total}$ Γ_{26}/Γ

VALUE (units 10^{-4})	DOCUMENT ID		TECN	COMMENT
2.8±1.0±0.5	[1] AAIJ	16C	LHCB	pp at 7, 8 TeV

[1] Measured and normalized to the $B_s^0 \to \overline{D}^{*0}K_S^0$ decay with $f_s/f_d = 0.259 \pm 0.015$. Signal significance is 4.4 standard deviations.

$\Gamma(\overline{D}^0\overline{K}^0)/\Gamma_{\rm total}$ Γ_{27}/Γ

VALUE (units 10^{-4})	DOCUMENT ID		TECN	COMMENT
4.3±0.5±0.7	[1] AAIJ	16C	LHCB	pp at 7, 8 TeV

[1] Measured and normalized to the $B^0 \to \overline{D}^0K_S^0$ decay with $f_s/f_d = 0.259 \pm 0.015$.

$\Gamma(\overline{D}^0K^-\pi^+)/\Gamma_{\rm total}$ Γ_{28}/Γ

VALUE (units 10^{-4})	DOCUMENT ID		TECN	COMMENT
10.4±1.1±0.5	[1] AAIJ	13AQ	LHCB	pp at 7 TeV

[1] AAIJ 13AQ reports $[\Gamma(B_s^0 \to \overline{D}^0K^-\pi^+)/\Gamma_{\rm total}] / [{\rm B}(B^0 \to \overline{D}^0\pi^+\pi^-)] = 1.18 \pm 0.05 \pm 0.12$ which we multiply by our best value ${\rm B}(B^0 \to \overline{D}^0\pi^+\pi^-) = (8.8 \pm 0.5) \times 10^{-4}$. Our first error is their experiment's error and our second error is the systematic error from using our best value.

$\Gamma(\overline{D}^0\overline{K}^*(892)^0)/\Gamma_{\rm total}$ Γ_{29}/Γ

VALUE (units 10^{-4})	DOCUMENT ID		TECN	COMMENT
4.4 ±0.6 OUR AVERAGE				
$4.29\pm0.09\pm0.65$	[1] AAIJ	14BH	LHCB	pp at 7, 8 TeV
4.7 ±1.2 ±0.3	[2] AAIJ	11D	LHCB	pp at 7 TeV
• • • We do not use the following data for averages, fits, limits, etc. • • •				
3.5 ±0.4 ±0.4	[3] AAIJ	13BX	LHCB	Repl. by AAIJ 14BH

[1] Uses Dalitz plot analysis of $B_s^0 \to \overline{D}^0K^-\pi^+$ decays.

[2] AAIJ 11D reports $[\Gamma(B_s^0 \to \overline{D}^0\overline{K}^*(892)^0)/\Gamma_{\rm total}] / [{\rm B}(B^0 \to \overline{D}^0\rho^0)] = 1.48 \pm 0.34 \pm 0.19$ which we multiply by our best value ${\rm B}(B^0 \to \overline{D}^0\rho^0) = (3.21 \pm 0.21) \times 10^{-4}$. Our first error is their experiment's error and our second error is the systematic error from using our best value.

[3] AAIJ 13BX reports $[\Gamma(B_s^0 \to \overline{D}^0\overline{K}^*(892)^0)/\Gamma_{\rm total}] / [{\rm B}(B^0 \to \overline{D}^0K^*(892)^0)] = 7.8 \pm 0.7 \pm 0.3 \pm 0.6$ which we multiply by our best value ${\rm B}(B^0 \to \overline{D}^0K^*(892)^0) = (4.5 \pm 0.6) \times 10^{-5}$. Our first error is their experiment's error and our second error is the systematic error from using our best value.

$\Gamma(\overline{D}^0\overline{K}^*(1410))/\Gamma_{\rm total}$ Γ_{30}/Γ

VALUE (units 10^{-5})	DOCUMENT ID		TECN	COMMENT
38.6±11.4±33.3	[1] AAIJ	14BH	LHCB	pp at 7, 8 TeV

[1] Uses Dalitz plot analysis of $B_s^0 \to \overline{D}^0K^-\pi^+$ decays.

$\Gamma(\overline{D}^0\overline{K}_0^*(1430))/\Gamma_{\rm total}$ Γ_{31}/Γ

VALUE (units 10^{-5})	DOCUMENT ID		TECN	COMMENT
30.0±2.4±6.8	[1] AAIJ	14BH	LHCB	pp at 7, 8 TeV

[1] Uses Dalitz plot analysis of $B_s^0 \to \overline{D}^0K^-\pi^+$ decays. Corresponds to the resonant $K_0^*(1430)$ part of LASS parametrization.

$\Gamma(\overline{D}^0\overline{K}_2^*(1430))/\Gamma_{\rm total}$ Γ_{32}/Γ

VALUE (units 10^{-5})	DOCUMENT ID		TECN	COMMENT
11.1±1.8±3.8	[1] AAIJ	14BH	LHCB	pp at 7, 8 TeV

[1] Uses Dalitz plot analysis of $B_s^0 \to \overline{D}^0K^-\pi^+$ decays.

$\Gamma(\overline{D}^0\overline{K}^*(1680))/\Gamma_{\rm total}$ Γ_{33}/Γ

VALUE (units 10^{-5})	CL%	DOCUMENT ID		TECN	COMMENT
<7.8	90	[1] AAIJ	14BH	LHCB	pp at 7, 8 TeV

[1] Uses Dalitz plot analysis of $B_s^0 \to \overline{D}^0K^-\pi^+$ decays.

$\Gamma(\overline{D}^0\overline{K}_0^*(1950))/\Gamma_{\rm total}$ Γ_{34}/Γ

VALUE (units 10^{-5})	CL%	DOCUMENT ID		TECN	COMMENT
<11	90	[1] AAIJ	14BH	LHCB	pp at 7, 8 TeV

[1] Uses Dalitz plot analysis of $B_s^0 \to \overline{D}^0K^-\pi^+$ decays.

$\Gamma(\overline{D}^0\overline{K}_3^*(1780))/\Gamma_{\rm total}$ Γ_{35}/Γ

VALUE (units 10^{-5})	CL%	DOCUMENT ID		TECN	COMMENT
<2.6	90	[1] AAIJ	14BH	LHCB	pp at 7, 8 TeV

[1] Uses Dalitz plot analysis of $B_s^0 \to \overline{D}^0K^-\pi^+$ decays.

$\Gamma(\overline{D}^0\overline{K}_4^*(2045))/\Gamma_{\rm total}$ Γ_{36}/Γ

VALUE (units 10^{-5})	CL%	DOCUMENT ID		TECN	COMMENT
<3.1	90	[1] AAIJ	14BH	LHCB	pp at 7, 8 TeV

[1] Uses Dalitz plot analysis of $B_s^0 \to \overline{D}^0K^-\pi^+$ decays.

$\Gamma(\overline{D}^0K^-\pi^+\,({\rm non\text{-}resonant}))/\Gamma_{\rm total}$ Γ_{37}/Γ

VALUE (units 10^{-5})	DOCUMENT ID		TECN	COMMENT
20.6±3.8±7.3	[1] AAIJ	14BH	LHCB	pp at 7, 8 TeV

[1] Uses Dalitz plot analysis of $B_s^0 \to \overline{D}^0K^-\pi^+$ decays. Corresponds to the non-resonant part of the LASS parametrization.

$\Gamma(D_{s2}^*(2573)^-\pi^+,\ D_{s2}^* \to \overline{D}^0K^-)/\Gamma_{\rm total}$ Γ_{38}/Γ

VALUE (units 10^{-5})	DOCUMENT ID		TECN	COMMENT
25.7±0.7±4.0	[1] AAIJ	14BH	LHCB	pp at 7, 8 TeV

[1] Uses Dalitz plot analysis of $B_s^0 \to \overline{D}^0K^-\pi^+$ decays.

$\Gamma(D_{s1}^*(2700)^-\pi^+,\ D_{s1}^* \to \overline{D}^0K^-)/\Gamma_{\rm total}$ Γ_{39}/Γ

VALUE (units 10^{-5})	DOCUMENT ID		TECN	COMMENT
1.6±0.4±0.7	[1] AAIJ	14BH	LHCB	pp at 7, 8 TeV

[1] Uses Dalitz plot analysis of $B_s^0 \to \overline{D}^0K^-\pi^+$ decays.

$\Gamma(D_{s1}^*(2860)^-\pi^+,\ D_{s1}^* \to \overline{D}^0K^-)/\Gamma_{\rm total}$ Γ_{40}/Γ

VALUE (units 10^{-5})	DOCUMENT ID		TECN	COMMENT
5.0±1.2±3.4	[1] AAIJ	14BH	LHCB	pp at 7, 8 TeV

[1] Uses Dalitz plot analysis of $B_s^0 \to \overline{D}^0K^-\pi^+$ decays.

$\Gamma(D_{s3}^*(2860)^-\pi^+,\ D_{s3}^* \to \overline{D}^0K^-)/\Gamma_{\rm total}$ Γ_{41}/Γ

VALUE (units 10^{-5})	DOCUMENT ID		TECN	COMMENT
2.2±0.1±0.6	[1] AAIJ	14BH	LHCB	pp at 7, 8 TeV

[1] Uses Dalitz plot analysis of $B_s^0 \to \overline{D}^0 K^- \pi^+$ decays.

$\Gamma(\overline{D}^0 K^+ K^-)/\Gamma_{total}$ Γ_{42}/Γ

VALUE (units 10^{-5})		DOCUMENT ID		TECN	COMMENT
4.4±1.7±1.1	[1,2]	AAIJ	12AM	LHCB	pp at 7 TeV

[1] AAIJ 12AM reports $[\Gamma(B_s^0 \to \overline{D}^0 K^+ K^-)/\Gamma_{total}] / [B(B^0 \to \overline{D}^0 K^+ K^-)] = 0.90 \pm 0.27 \pm 0.20$ which we multiply by our best value $B(B^0 \to \overline{D}^0 K^+ K^-) = (4.9 \pm 1.2) \times 10^{-5}$. Our first error is their experiment's error and our second error is the systematic error from using our best value.
[2] Uses $B(b \to B_s^0)/B(b \to B^0) = 0.267^{+0.023}_{-0.020}$ measured by the same authors.

$\Gamma(\overline{D}^0 f_0(980))/\Gamma_{total}$ Γ_{43}/Γ

VALUE	CL%	DOCUMENT ID		TECN	COMMENT
<3.1 × 10⁻⁶	90	AAIJ	15AG	LHCB	pp at 7, 8 TeV

$\Gamma(\overline{D}^0 \phi)/\Gamma(\overline{D}^0 K^*(892)^0)$ Γ_{44}/Γ_{29}

VALUE	DOCUMENT ID		TECN	COMMENT
0.069±0.013±0.007	AAIJ	13BX	LHCB	pp at 7 TeV

$\Gamma(D^{*\mp}\pi^{\pm})/\Gamma_{total}$ Γ_{45}/Γ

VALUE	CL%	DOCUMENT ID		TECN	COMMENT
<6.1 × 10⁻⁶	90	[1] AAIJ	13AL	LHCB	pp at 7 TeV

[1] Uses $f_s/f_d = 0.256 \pm 0.020$ and $B(B^0 \to D^{*-}\pi^+) = (2.76 \pm 0.13) \times 10^{-3}$.

$\Gamma(\eta_c \phi)/\Gamma_{total}$ Γ_{46}/Γ

VALUE (units 10^{-4})	DOCUMENT ID		TECN	COMMENT
5.01±0.53±0.68	[1] AAIJ	17U	LHCB	pp at 7, 8 TeV

[1] The last uncertainty includes the limited knowledge of the external branching fractions where the η_c is reconstructed in the $p\overline{p}$, $K^+K^-\pi^+\pi^-$, $\pi^+\pi^-\pi^+\pi^-$, and $K^+K^-K^+K^-$ decays and $\phi(1020) \to K^+K^-$.

$\Gamma(\eta_c \pi^+\pi^-)/\Gamma_{total}$ Γ_{47}/Γ

VALUE (units 10^{-4})	DOCUMENT ID		TECN	COMMENT
1.76±0.59±0.31	[1] AAIJ	17U	LHCB	pp at 7, 8 TeV

[1] The last uncertainty includes the limited knowledge of the external branching fractions where the η_c is reconstructed in the $p\overline{p}$, $K^+K^-\pi^+\pi^-$, $\pi^+\pi^-\pi^+\pi^-$, and $K^+K^-K^+K^-$ decays. The significance of the signal, including systematic uncertainties, is 4.6 standard deviations.

$\Gamma(J/\psi(1S)\phi)/\Gamma_{total}$ Γ_{48}/Γ

VALUE (units 10^{-3})	EVTS	DOCUMENT ID		TECN	COMMENT
1.08 ±0.08 OUR FIT					
1.10 ±0.09 OUR AVERAGE					
1.050±0.013±0.104		[1] AAIJ	13AN	LHCB	pp at 7 TeV
1.25 ±0.07 ±0.23		[2] THORNE	13	BELL	$e^+e^- \to \Upsilon(5S)$
1.5 ±0.5 ±0.1		[3] ABE	96Q	CDF	$p\overline{p}$
• • • We do not use the following data for averages, fits, limits, etc. • • •					
<6	1	[4] AKERS	94J	OPAL	$e^+e^- \to Z$
seen	14	[5] ABE	93F	CDF	$p\overline{p}$ at 1.8 TeV
seen	1	[6] ACTON	92N	OPAL	Sup. by AKERS 94J

[1] Uses $f_s/f_d = 0.256 \pm 0.020$ and $B(B^+ \to J/\psi K^+) = (10.18 \pm 0.42) \times 10^{-4}$.
[2] Uses $f_s = (17.2 \pm 3.0)\%$ as the fraction of $\Upsilon(5S)$ decaying to $B_s^{(*)}\overline{B}_s^{(*)}$.
[3] ABE 96Q reports $[\Gamma(B_s^0 \to J/\psi(1S)\phi)/\Gamma_{total}] \times [\Gamma(\overline{b} \to B_s^0)/\left[\Gamma(\overline{b} \to B^+) + \Gamma(\overline{b} \to B^0)\right]] = (0.185 \pm 0.055 \pm 0.020) \times 10^{-3}$ which we divide by our best value $\Gamma(\overline{b} \to B_s^0)/\left[\Gamma(\overline{b} \to B^+) + \Gamma(\overline{b} \to B^0)\right] = 0.125 \pm 0.006$. Our first error is their experiment's error and our second error is the systematic error from using our best value.
[4] AKERS 94J sees one event and measures the limit on the product branching fraction $f(\overline{b} \to B_s^0)\cdot B(B_s^0 \to J/\psi(1S)\phi) < 7 \times 10^{-4}$ at CL = 90%. We divide by $B(\overline{b} \to B_s^0) = 0.112$.
[5] ABE 93F measured using $J/\psi(1S) \to \mu^+\mu^-$ and $\phi \to K^+K^-$.
[6] In ACTON 92N a limit on the product branching fraction is measured to be $f(\overline{b} \to B_s^0)\cdot B(B_s^0 \to J/\psi(1S)\phi) \leq 0.22 \times 10^{-2}$.

$\Gamma(J/\psi(1S)\phi\phi)/\Gamma(J/\psi(1S)\phi)$ Γ_{49}/Γ_{48}

VALUE (units 10^{-2})	EVTS	DOCUMENT ID		TECN	COMMENT
1.15±0.12$^{+0.05}_{-0.09}$	128	[1] AAIJ	16U	LHCB	pp at 7, 8 TeV

[1] Uses $J/\psi \to \mu^+\mu^-$, $\phi \to K^+K^-$ decays, and observes 128 ± 13 events of $B_s^0 \to J/\psi\phi\phi$.

$\Gamma(J/\psi(1S)\pi^0)/\Gamma_{total}$ Γ_{50}/Γ

VALUE	CL%	DOCUMENT ID		TECN
<1.2 × 10⁻³	90	[1] ACCIARRI	97C	L3

[1] ACCIARRI 97C assumes B^0 production fraction (39.5 ± 4.0%) and B_s (12.0 ± 3.0%).

$\Gamma(J/\psi(1S)\eta)/\Gamma_{total}$ Γ_{51}/Γ

VALUE (units 10^{-4})	CL%	DOCUMENT ID		TECN	COMMENT
4.0 ±0.7 OUR AVERAGE		Error includes scale factor of 1.4.			
3.6 $^{+0.5}_{-0.6}$ $^{+0.3}_{-0.2}$		[1] AAIJ	13A	LHCB	pp at 7 TeV
5.10±0.50$^{+1.17}_{-0.83}$		[2] LI	12	BELL	$e^+e^- \to \Upsilon(4S)$
• • • We do not use the following data for averages, fits, limits, etc. • • •					
<38	90	[3] ACCIARRI	97C	L3	

[1] AAIJ 13A reports $[\Gamma(B_s^0 \to J/\psi(1S)\eta)/\Gamma_{total}] / [B(B^0 \to J/\psi(1S)\rho^0)] = 14.0 \pm 1.2^{+1.1}_{-1.5}{}^{+1.1}_{-1.0}$ which we multiply by our best value $B(B^0 \to J/\psi(1S)\rho^0) = (2.55^{+0.18}_{-0.16}) \times 10^{-5}$. Our first error is their experiment's error and our second error is the systematic error from using our best value.
[2] Observed for the first time with significances over 10 σ. The second error are total systematic uncertainties including the error on $N(B_s^{(*)}\overline{B}_s^{(*)})$.
[3] ACCIARRI 97C assumes B^0 production fraction (39.5 ± 4.0%) and B_s (12.0 ± 3.0%).

$\Gamma(J/\psi(1S)K_S^0)/\Gamma_{total}$ Γ_{52}/Γ

VALUE (units 10^{-5})	DOCUMENT ID		TECN	COMMENT
1.88±0.15 OUR AVERAGE				
1.88±0.14±0.07	[1] AAIJ	15AL	LHCB	pp at 7, 8 TeV
1.9 ±0.4 ±0.1	[2] AALTONEN	11A	CDF	$p\overline{p}$ at 1.96 TeV
• • • We do not use the following data for averages, fits, limits, etc. • • •				
1.96±0.15±0.12	[3] AAIJ	13AB	LHCB	Repl. by AAIJ 15AL
1.96±0.25±0.12	[4] AAIJ	12O	LHCB	Repl. by AAIJ 13AB

[1] AAIJ 15AL reports $[\Gamma(B_s^0 \to J/\psi(1S)K_S^0)/\Gamma_{total}] / [B(B^0 \to J/\psi(1S)K_S^0)] = (4.31 \pm 0.17 \pm 0.12 \pm 0.25) \times 10^{-2}$ which we multiply by our best value $B(B^0 \to J/\psi(1S)K_S^0) = (4.36 \pm 0.16) \times 10^{-4}$. Our first error is their experiment's error and our second error is the systematic error from using our best value.
[2] AALTONEN 11A reports $[\Gamma(B_s^0 \to J/\psi(1S)K_S^0)/\Gamma_{total}] \times [B(\overline{b} \to B_s^0)] / [B(\overline{b} \to B^0)] / [B(B^0 \to J/\psi(1S)K_S^0)] = (1.09 \pm 0.19 \pm 0.11) \times 10^{-2}$ which we multiply or divide by our best values $B(\overline{b} \to B_s^0) = (10.1 \pm 0.4) \times 10^{-2}$, $B(\overline{b} \to B^0) = (40.5 \pm 0.6) \times 10^{-2}$, $B(B^0 \to J/\psi(1S)K_S^0) = 1/2 \times B(B^0 \to J/\psi(1S)K^0) = 1/2 \times (8.73 \pm 0.32) \times 10^{-4}$. Our firs t error is their experiment's error and our second error is the systematic error from using our best values.
[3] AAIJ 13AB reports $(1.97 \pm 0.14 \pm 0.07 \pm 0.15 \pm 0.08) \times 10^{-5}$ from a measurement of $[\Gamma(B_s^0 \to J/\psi(1S)K_S^0)/\Gamma_{total}] / [B(B^0 \to J/\psi(1S)K^0)] \times [\Gamma(\overline{b} \to B_s^0)/\Gamma(\overline{b} \to B^0)]$ assuming $B(B^0 \to J/\psi(1S)K^0) = (8.98 \pm 0.35) \times 10^{-4}$, $\Gamma(\overline{b} \to B_s^0)/\Gamma(\overline{b} \to B^0) = 0.256 \pm 0.020$, which we rescale to our best values $B(B^0 \to J/\psi(1S)K^0) = (8.73 \pm 0.32) \times 10^{-4}$, $\Gamma(\overline{b} \to B_s^0)/\Gamma(\overline{b} \to B^0) = 0.250 \pm 0.012$. Our first error is their experiment's error and our second error is the systematic error from using our best values.
[4] AAIJ 12O reports $(1.83 \pm 0.21 \pm 0.10 \pm 0.14 \pm 0.07) \times 10^{-5}$ from a measurement of $[\Gamma(B_s^0 \to J/\psi(1S)K_S^0)/\Gamma_{total}] / [B(B^0 \to J/\psi(1S)K^0)] \times [\Gamma(\overline{b} \to B_s^0)/\Gamma(\overline{b} \to B^0)]$ assuming $B(B^0 \to J/\psi(1S)K^0) = (8.71 \pm 0.32) \times 10^{-4}$, $\Gamma(\overline{b} \to B_s^0)/\Gamma(\overline{b} \to B^0) = 0.267^{+0.021}_{-0.02}$, which we rescale to our best values $B(B^0 \to J/\psi(1S)K^0) = (8.73 \pm 0.32) \times 10^{-4}$, $\Gamma(\overline{b} \to B_s^0)/\Gamma(\overline{b} \to B^0) = 0.250 \pm 0.012$. Our first error is their experiment's error and our second error is the systematic error from using our best values.

$\Gamma(J/\psi(1S)\overline{K}^*(892)^0)/\Gamma_{total}$ Γ_{53}/Γ

VALUE (units 10^{-5})	DOCUMENT ID		TECN	COMMENT
4.14±0.18±0.35	[1] AAIJ	15AV	LHCB	pp at 7, 8 TeV
• • • We do not use the following data for averages, fits, limits, etc. • • •				
4.4 $^{+0.5}_{-0.4}$ ±0.8	[2] AAIJ	12AP	LHCB	Repl. by AAIJ 15AV
8.5 ±3.7 ±0.5	[3] AALTONEN	11A	CDF	$p\overline{p}$ at 1.96 TeV

[1] AAIJ 15AV result combines two measurements with different normalizing modes of $B^0 \to J/\psi K^*(892)^0$ and $B_s^0 \to J/\psi\phi$.
[2] AAIJ 12AP reports $B(B_s^0 \to J/\psi(1S)\overline{K}^*(892)^0)/B(B^0 \to J/\psi(1S)K^*(892)^0) = (3.43^{+0.34}_{-0.36} \pm 0.50) \times 10^{-2}$ and $B(B^0 \to J/\psi(1S)K^*(892)^0) = (1.29 \pm 0.05 \pm 0.13) \times 10^{-3}$ after correcting for the contribution from $K\pi$ S-wave beneath the K^* peak.
[3] AALTONEN 11A reports $[\Gamma(B_s^0 \to J/\psi(1S)\overline{K}^*(892)^0)/\Gamma_{total}] \times [B(\overline{b} \to B_s^0)] / [B(\overline{b} \to B^0)] / [B(B^0 \to J/\psi(1S)K^*(892)^0)] = 0.0168 \pm 0.0024 \pm 0.0068$ which we multiply or divide by our best values $B(\overline{b} \to B_s^0) = (10.1 \pm 0.4) \times 10^{-2}$, $B(\overline{b} \to B^0) = (40.5 \pm 0.6) \times 10^{-2}$, $B(B^0 \to J/\psi(1S)K^*(892)^0) = (1.27 \pm 0.05) \times 10^{-3}$. Our first error is their experiment's error and our second error is the systematic error from using our best values.

$\Gamma(J/\psi(1S)\eta')/\Gamma_{total}$ Γ_{54}/Γ

VALUE (units 10^{-4})	DOCUMENT ID		TECN	COMMENT
3.3 ±0.4 OUR AVERAGE				
3.2 $^{+0.4}_{-0.5}$ ±0.2	[1] AAIJ	13A	LHCB	pp at 7 TeV
3.71±0.61$^{+0.85}_{-0.60}$	[2] LI	12	BELL	$e^+e^- \to \Upsilon(4S)$

[1] AAIJ 13A reports $[\Gamma(B_s^0 \to J/\psi(1S)\eta')/\Gamma_{total}] / [B(B^0 \to J/\psi(1S)\rho^0)] = 12.7 \pm 1.1^{+0.5}_{-1.3}{}^{+1.0}_{-0.9}$ which we multiply by our best value $B(B^0 \to J/\psi(1S)\rho^0) =$

$(2.55^{+0.18}_{-0.16}) \times 10^{-5}$. Our first error is their experiment's error and our second error is the systematic error from using our best value.

[2] Observed for the first time with significances over 10 σ. The second error are total systematic uncertainties including the error on $N(B_s^{(*)}\overline{B}_s^{(*)})$.

$\Gamma(J/\psi(1S)\eta')/\Gamma(J/\psi(1S)\eta)$ Γ_{54}/Γ_{51}

VALUE	DOCUMENT ID		TECN	COMMENT
0.87 ±0.06 OUR AVERAGE				
0.902±0.072±0.045	[1] AAIJ	15D	LHCB	pp at 7, 8 TeV
0.90 $\pm 0.09\ ^{+0.06}_{-0.02}$	[2] AAIJ	13A	LHCB	pp at 7 TeV
0.73 ±0.14 ±0.02	[2] LI	12	BELL	$e^+e^- \to \Upsilon(4S)$

[1] Uses $J/\psi \to \mu^+\mu^-$, $\eta' \to \rho^0\gamma$, and $\eta' \to \eta\pi^+\pi^-$ decays.

[2] Strongly correlated with measurements of $\Gamma(J/\psi(1S)\eta)/\Gamma$ and $\Gamma(J/\psi(1S)\eta')/\Gamma$ reported in the same reference.

$\Gamma(J/\psi(1S)\pi^+\pi^-)/\Gamma(J/\psi(1S)\phi)$ Γ_{55}/Γ_{48}

VALUE (units 10^{-2})	DOCUMENT ID		TECN	COMMENT
19.4±1.5 OUR FIT Error includes scale factor of 2.2.				
19.9±0.7±0.2	[1] AAIJ	12AO	LHCB	pp at 7 TeV

[1] AAIJ 12AO reports $(19.79 \pm 0.47 \pm 0.52) \times 10^{-2}$ from a measurement of $[\Gamma(B_s^0 \to J/\psi(1S)\pi^+\pi^-)/\Gamma(B_s^0 \to J/\psi(1S)\phi)]$ / $[B(\phi(1020) \to K^+K^-)]$ assuming $B(\phi(1020) \to K^+K^-) = (48.9 \pm 0.5) \times 10^{-2}$, which we rescale to our best value $B(\phi(1020) \to K^+K^-) = (49.2 \pm 0.5) \times 10^{-2}$. Our first error is their experiment's error and our second error is the systematic error from using our best value.

$\Gamma(J/\psi(1S)f_0(980),\ f_0 \to \pi^+\pi^-)/\Gamma_{\text{total}}$ Γ_{58}/Γ

VALUE (units 10^{-4})	DOCUMENT ID		TECN	COMMENT
1.28±0.18 OUR FIT Error includes scale factor of 1.7.				
$1.16^{+0.31}_{-0.19}{}^{+0.30}_{-0.25}$	[1] LI	11	BELL	$e^+e^- \to \Upsilon(5S)$

[1] The second error includes both the detector systematic and the uncertainty in the number of produced $Y(5S) \to B_s^{(*)}\overline{B}_s^{(*)}$ pairs.

$\Gamma(J/\psi(1S)f_0(500),\ f_0 \to \pi^+\pi^-)/\Gamma(J/\psi(1S)f_0(980),\ f_0 \to \pi^+\pi^-)$ Γ_{56}/Γ_{58}

VALUE	CL%	DOCUMENT ID		TECN	COMMENT
<0.034	90	[1] AAIJ	14BR	LHCB	pp at 7, 8 TeV

[1] Reported first of two solutions using the full Dalitz analysis.

$\Gamma(J/\psi(1S)\rho,\ \rho \to \pi^+\pi^-)/\Gamma(J/\psi(1S)\pi^+\pi^-)$ Γ_{57}/Γ_{55}

VALUE	CL%	DOCUMENT ID		TECN	COMMENT
<0.017	90	[1] AAIJ	14BR	LHCB	pp at 7, 8 TeV

[1] Reported first of two solutions using the full Dalitz analysis.

$\Gamma(J/\psi(1S)f_0(980),\ f_0 \to \pi^+\pi^-)/\Gamma(J/\psi(1S)\pi^+\pi^-)$ Γ_{58}/Γ_{55}

VALUE	DOCUMENT ID		TECN	COMMENT
0.61 $^{+0.06}_{-0.07}$ OUR FIT Error includes scale factor of 2.1.				
$\mathbf{0.703 \pm 0.015\ ^{+0.004}_{-0.051}}$	[1] AAIJ	14BR	LHCB	pp at 7, 8 TeV

[1] Reported first of two solutions using the full Dalitz analysis.

$\Gamma(J/\psi(1S)f_2(1270)_0,\ f_2 \to \pi^+\pi^-)/\Gamma(J/\psi(1S)\pi^+\pi^-)$ Γ_{60}/Γ_{55}

VALUE (%)	DOCUMENT ID		TECN	COMMENT
0.36±0.07±0.03	[1] AAIJ	14BR	LHCB	pp at 7, 8 TeV

[1] Reported first of two solutions using the full Dalitz analysis.

$\Gamma(J/\psi(1S)f_2(1270)_\parallel,\ f_2 \to \pi^+\pi^-)/\Gamma(J/\psi(1S)\pi^+\pi^-)$ Γ_{61}/Γ_{55}

VALUE (%)	DOCUMENT ID		TECN	COMMENT
$\mathbf{0.52 \pm 0.15\ ^{+0.05}_{-0.02}}$	[1] AAIJ	14BR	LHCB	pp at 7, 8 TeV

[1] Reported first of two solutions using the full Dalitz analysis.

$\Gamma(J/\psi(1S)f_2(1270)_\perp,\ f_2 \to \pi^+\pi^-)/\Gamma(J/\psi(1S)\pi^+\pi^-)$ Γ_{62}/Γ_{55}

VALUE (%)	DOCUMENT ID		TECN	COMMENT
$\mathbf{0.63 \pm 0.34\ ^{+0.16}_{-0.08}}$	[1] AAIJ	14BR	LHCB	pp at 7, 8 TeV

[1] Reported first of two solutions using the full Dalitz analysis.

$\Gamma(J/\psi(1S)f_0(1500),\ f_0 \to \pi^+\pi^-)/\Gamma(J/\psi(1S)\pi^+\pi^-)$ Γ_{64}/Γ_{55}

VALUE	DOCUMENT ID		TECN	COMMENT
$\mathbf{0.101 \pm 0.008\ ^{+0.011}_{-0.003}}$	[1] AAIJ	14BR	LHCB	pp at 7, 8 TeV

[1] Reported first of two solutions using the full Dalitz analysis.

$\Gamma(J/\psi(1S)f_2'(1525)_0,\ f_2' \to \pi^+\pi^-)/\Gamma(J/\psi(1S)\pi^+\pi^-)$ Γ_{65}/Γ_{55}

VALUE (%)	DOCUMENT ID		TECN	COMMENT
$\mathbf{0.51 \pm 0.09\ ^{+0.05}_{-0.04}}$	[1] AAIJ	14BR	LHCB	pp at 7, 8 TeV

[1] Reported first of two solutions using the full Dalitz analysis.

$\Gamma(J/\psi(1S)f_2'(1525)_\parallel,\ f_2' \to \pi^+\pi^-)/\Gamma(J/\psi(1S)\pi^+\pi^-)$ Γ_{66}/Γ_{55}

VALUE (%)	DOCUMENT ID		TECN	COMMENT
$\mathbf{0.06\ ^{+0.13}_{-0.04} \pm 0.01}$	[1] AAIJ	14BR	LHCB	pp at 7, 8 TeV

[1] Reported first of two solutions using the full Dalitz analysis.

$\Gamma(J/\psi(1S)f_2'(1525)_\perp,\ f_2' \to \pi^+\pi^-)/\Gamma(J/\psi(1S)\pi^+\pi^-)$ Γ_{67}/Γ_{55}

VALUE (%)	DOCUMENT ID		TECN	COMMENT
$\mathbf{0.26 \pm 0.18\ ^{+0.06}_{-0.04}}$	[1] AAIJ	14BR	LHCB	pp at 7, 8 TeV

[1] Reported first of two solutions using the full Dalitz analysis.

$\Gamma(J/\psi(1S)f_0(1790),\ f_0 \to \pi^+\pi^-)/\Gamma(J/\psi(1S)\pi^+\pi^-)$ Γ_{68}/Γ_{55}

VALUE	DOCUMENT ID		TECN	COMMENT
$\mathbf{0.024 \pm 0.004\ ^{+0.050}_{-0.002}}$	[1] AAIJ	14BR	LHCB	pp at 7, 8 TeV

[1] Reported first of two solutions using the full Dalitz analysis.

$\Gamma(J/\psi(1S)f_0(980),\ f_0 \to \pi^+\pi^-)/\Gamma(J/\psi(1S)\phi)$ Γ_{58}/Γ_{48}

VALUE	DOCUMENT ID		TECN	COMMENT
$\mathbf{0.119\ ^{+0.013}_{-0.014}}$ **OUR FIT** Error includes scale factor of 2.4.				
$\mathbf{0.111\ ^{+0.020}_{-0.018}}$ **OUR AVERAGE** Error includes scale factor of 2.5. See the ideogram below.				
0.069±0.012±0.001	[1] KHACHATRY...16Q		CMS	pp at 7 TeV
$0.140\ ^{+0.026}_{-0.013} \pm 0.002$	[2,3] AAIJ	12AO	LHCB	pp at 7 TeV
0.135±0.036±0.001	[4] ABAZOV	12C	D0	$p\overline{p}$ at 1.96 TeV
0.126±0.012±0.001	[5] AALTONEN	11AB	CDF	$p\overline{p}$ at 1.96 TeV
• • • We do not use the following data for averages, fits, limits, etc. • • •				
$0.124\ ^{+0.026}_{-0.023} \pm 0.001$	[6] AAIJ	11	LHCB	Repl. by AAIJ 12AO

[1] KHACHATRYAN 16Q reports $[\Gamma(B_s^0 \to J/\psi(1S)f_0(980),\ f_0 \to \pi^+\pi^-)/\Gamma(B_s^0 \to J/\psi(1S)\phi)]$ / $[B(\phi(1020) \to K^+K^-)] = 0.140 \pm 0.008 \pm 0.023$ which we multiply by our best value $B(\phi(1020) \to K^+K^-) = (49.2 \pm 0.5) \times 10^{-2}$. Our first error is their experiment's error and our second error is the systematic error from using our best value.

[2] AAIJ 12AO reports $(13.9 \pm 0.6^{+2.5}_{-1.2}) \times 10^{-2}$ from a measurement of $[\Gamma(B_s^0 \to J/\psi(1S)f_0(980),\ f_0 \to \pi^+\pi^-)/\Gamma(B_s^0 \to J/\psi(1S)\phi)]$ / $[B(\phi(1020) \to K^+K^-)]$ assuming $B(\phi(1020) \to K^+K^-) = (48.9 \pm 0.5) \times 10^{-2}$, which we rescale to our best value $B(\phi(1020) \to K^+K^-) = (49.2 \pm 0.5) \times 10^{-2}$. Our first error is their experiment's error and our second error is the systematic error from using our best value.

[3] Measured in Dalitz plot like analysis of $B_s \to J/\psi\pi^+\pi^-$ decays.

[4] ABAZOV 12C reports $[\Gamma(B_s^0 \to J/\psi(1S)f_0(980),\ f_0 \to \pi^+\pi^-)/\Gamma(B_s^0 \to J/\psi(1S)\phi)]$ / $[B(\phi(1020) \to K^+K^-)] = 0.275 \pm 0.041 \pm 0.061$ which we multiply by our best value $B(\phi(1020) \to K^+K^-) = (49.2 \pm 0.5) \times 10^{-2}$. Our first error is their experiment's error and our second error is the systematic error from using our best value.

[5] AALTONEN 11AB reports $[\Gamma(B_s^0 \to J/\psi(1S)f_0(980),\ f_0 \to \pi^+\pi^-)/\Gamma(B_s^0 \to J/\psi(1S)\phi)]$ / $[B(\phi(1020) \to K^+K^-)] = 0.257 \pm 0.020 \pm 0.014$ which we multiply by our best value $B(\phi(1020) \to K^+K^-) = (49.2 \pm 0.5) \times 10^{-2}$. Our first error is their experiment's error and our second error is the systematic error from using our best value.

[6] AAIJ 11 reports $[\Gamma(B_s^0 \to J/\psi(1S)f_0(980),\ f_0 \to \pi^+\pi^-)/\Gamma(B_s^0 \to J/\psi(1S)\phi)]$ / $[B(\phi(1020) \to K^+K^-)] = 0.252^{+0.046+0.027}_{-0.032-0.033}$ which we multiply by our best value $B(\phi(1020) \to K^+K^-) = (49.2 \pm 0.5) \times 10^{-2}$. Our first error is their experiment's error and our second error is the systematic error from using our best value.

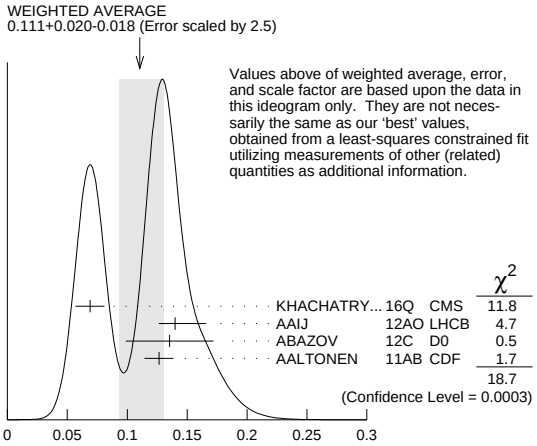

$\Gamma(J/\psi(1S)f_0(1370),\ f_0 \to \pi^+\pi^-)/\Gamma_{\text{total}}$ Γ_{63}/Γ

VALUE (units 10^{-4})	DOCUMENT ID		TECN	COMMENT
• • • We do not use the following data for averages, fits, limits, etc. • • •				
$0.34\ ^{+0.11+0.085}_{-0.14-0.054}$	[1] LI	11	BELL	$e^+e^- \to \Upsilon(5S)$

[1] The second error includes both the detector systematic and the uncertainty in the number of produced $Y(5S) \to B_s^{(*)}\overline{B}_s^{(*)}$ pairs.

$\Gamma(J/\psi(1S)f_0(1370),\ f_0\to\pi^+\pi^-)/\Gamma(J/\psi(1S)\phi)$ Γ_{63}/Γ_{48}

VALUE (units 10^{-2})	DOCUMENT ID		TECN	COMMENT
$4.22^{+0.55}_{-3.76}\pm0.05$	[1,2] AAIJ	12AO	LHCB	pp at 7 TeV

[1] AAIJ 12AO reports $(4.19\pm0.53^{+0.12}_{-3.7})\times10^{-2}$ from a measurement of $[\Gamma(B_s^0\to J/\psi(1S)f_0(1370),\ f_0\to\pi^+\pi^-)/\Gamma(B_s^0\to J/\psi(1S)\phi)]$ / $[B(\phi(1020)\to K^+K^-)]$ assuming $B(\phi(1020)\to K^+K^-)=(48.9\pm0.5)\times10^{-2}$, which we rescale to our best value $B(\phi(1020)\to K^+K^-)=(49.2\pm0.5)\times10^{-2}$. Our first error is their experiment's error and our second error is the systematic error from using our best value.
[2] Measured in Dalitz plot like analysis of $B_s\to J/\psi\pi^+\pi^-$ decays.

$\Gamma(J/\psi(1S)f_2(1270),\ f_2\to\pi^+\pi^-)/\Gamma(J/\psi(1S)\phi)$ Γ_{59}/Γ_{48}

VALUE (units 10^{-4})	DOCUMENT ID		TECN	COMMENT
$9.9^{+3.4}_{-3.6}\pm1.0$	[1,2] AAIJ	12AO	LHCB	pp at 7 TeV

[1] AAIJ 12AO reports $(0.098\pm0.033^{+0.006}_{-0.015})\times10^{-2}$ from a measurement of $[\Gamma(B_s^0\to J/\psi(1S)f_2(1270),\ f_2\to\pi^+\pi^-)/\Gamma(B_s^0\to J/\psi(1S)\phi)]$ / $[B(\phi(1020)\to K^+K^-)]$ assuming $B(\phi(1020)\to K^+K^-)=(48.9\pm0.5)\times10^{-2}$, which we rescale to our best value $B(\phi(1020)\to K^+K^-)=(49.2\pm0.5)\times10^{-2}$. Our first error is their experiment's error and our second error is the systematic error from using our best value.
[2] Measured in Dalitz plot like analysis of $B_s\to J/\psi\pi^+\pi^-$ decays for the f_2 helicity state $\lambda=0$.

$\Gamma(J/\psi(1S)\pi^+\pi^-\text{(nonresonant)})/\Gamma(J/\psi(1S)\phi)$ Γ_{69}/Γ_{48}

VALUE (units 10^{-2})	DOCUMENT ID		TECN	COMMENT
$1.67^{+1.02}_{-0.32}\pm0.02$	[1,2] AAIJ	12AO	LHCB	pp at 7 TeV

[1] AAIJ 12AO reports $(1.66\pm0.31^{+0.96}_{-0.08})\times10^{-2}$ from a measurement of $[\Gamma(B_s^0\to J/\psi(1S)\pi^+\pi^-\text{(nonresonant)})/\Gamma(B_s^0\to J/\psi(1S)\phi)]$ / $[B(\phi(1020)\to K^+K^-)]$ assuming $B(\phi(1020)\to K^+K^-)=(48.9\pm0.5)\times10^{-2}$, which we rescale to our best value $B(\phi(1020)\to K^+K^-)=(49.2\pm0.5)\times10^{-2}$. Our first error is their experiment's error and our second error is the systematic error from using our best value.
[2] Measured in Dalitz plot like analysis of $B_s\to J/\psi\pi^+\pi^-$ decays.

$\Gamma(J/\psi(1S)\overline{K}^0\pi^+\pi^-)/\Gamma_{\text{total}}$ Γ_{70}/Γ

VALUE	CL%	DOCUMENT ID		TECN	COMMENT
$<4.4\times10^{-5}$	90	[1] AAIJ	14L	LHCB	pp at 7 TeV

[1] Measured with $B(B_s^0\to J/\psi K_S^0\pi^+\pi^-)$ / $B(B^0\to J/\psi K_S^0\pi^+\pi^-)$ using PDG 12 values for the involved branching fractions.

$\Gamma(J/\psi(1S)K^+K^-)/\Gamma_{\text{total}}$ Γ_{71}/Γ

VALUE (units 10^{-4})	DOCUMENT ID		TECN	COMMENT
7.9 ±0.7 OUR AVERAGE				
$7.70\pm0.08\pm0.72$	[1] AAIJ	13AN	LHCB	pp at 7 TeV
10.1 ±0.9 ±2.1	[2] THORNE	13	BELL	$e^+e^-\to\Upsilon(5S)$

[1] Uses $f_s/f_d=0.256\pm0.020$ and $B(B^+\to J/\psi K^+)=(10.18\pm0.42)\times10^{-4}$.
[2] Uses $f_s=(17.2\pm3.0)\%$ as the fraction of $\Upsilon(5S)$ decaying to $B_s^{(*)}\overline{B}_s^{(*)}$.

$\Gamma(J/\psi(1S)K^0K^-\pi^+ + \text{c.c.})/\Gamma_{\text{total}}$ Γ_{72}/Γ

VALUE (units 10^{-4})	DOCUMENT ID		TECN	COMMENT
$9.3\pm1.0\pm0.9$	[1] AAIJ	14L	LHCB	pp at 7 TeV

[1] AAIJ 14L reports $[\Gamma(B_s^0\to J/\psi(1S)K^0K^-\pi^+ + \text{c.c.})/\Gamma_{\text{total}}]$ / $[B(B^0\to J/\psi(1S)K^0\pi^+\pi^-)]=2.12\pm0.15\pm0.18$ which we multiply by our best value $B(B^0\to J/\psi(1S)K^0\pi^+\pi^-)=(4.4\pm0.4)\times10^{-4}$. Our first error is their experiment's error and our second error is the systematic error from using our best value. This is an observation of $B_s^0\to J/\psi K_S^0K^\pm\pi^\mp$ with more than 10 standard deviations.

$\Gamma(J/\psi(1S)\overline{K}^0K^+K^-)/\Gamma_{\text{total}}$ Γ_{73}/Γ

VALUE	CL%	DOCUMENT ID		TECN	COMMENT
$<12\times10^{-6}$	90	[1] AAIJ	14L	LHCB	pp at 7 TeV

[1] Measured with $B(B_s^0\to J/\psi K_S^0K^+K^-)/B(B^0\to J/\psi K_S^0\pi^+\pi^-)$ using PDG 12 values for the involved branching fractions.

$\Gamma(J/\psi(1S)f_2'(1525))/\Gamma(J/\psi(1S)\phi)$ Γ_{74}/Γ_{48}

VALUE (units 10^{-2})	DOCUMENT ID		TECN	COMMENT
21 ±4 OUR AVERAGE				
$21.5\pm4.9\pm2.6$	[1] THORNE	13	BELL	$e^+e^-\to\Upsilon(5S)$
21 ±7 ±1	[2,3] ABAZOV	12AF	D0	$p\overline{p}$ at 1.96 TeV
• • • We do not use the following data for averages, fits, limits, etc. • • •				
27 ±4 ±1	[4] AAIJ	12S	LHCB	Repl. by AAIJ 13AN

[1] Uses $B(f_2'(1525)\to K^+K^-)=(44.4\pm1.1)\%$.
[2] ABAZOV 12AF reports $[\Gamma(B_s^0\to J/\psi(1S)f_2'(1525))/\Gamma(B_s^0\to J/\psi(1S)\phi)]\times B(f_2'(1525)\to K^+K^-)$ / $B(\phi(1020)\to K^+K^-)=0.19\pm0.05\pm0.04$ which we divide and multiply by our best values $B(f_2'(1525)\to K^+K^-)=\frac{1}{2}(88.7\pm2.2)\times10^{-2}$, $B(\phi(1020)\to K^+K^-)=(49.2\pm0.5)\times10^{-2}$. Our first error is their experiment's error and our second error is the systematic error from using our best values.
[3] ABAZOV 12AF fits the invariant masses of the K^+K^- pair in the range $1.35<M(K^+K^-)<2$ GeV.
[4] AAIJ 12S reports $[(26.4\pm2.7\pm2.4)\times10^{-2}$ from a measurement of $\Gamma(B_s^0\to J/\psi(1S)f_2'(1525))/\Gamma(B_s^0\to J/\psi(1S)\phi)]\times B(f_2'(1525)\to K^+K^-)$ / $B(\phi(1020)\to K^+K^-)$ assuming $B(f_2'(1525)\to K^+K^-)=(44.4\pm1.1)\times10^{-2}$, $B(\phi(1020)\to K^+K^-)=(48.9\pm0.5)\times10^{-2}$, which we rescale to our best values $B(f_2'(1525)\to K^+K^-)=\frac{1}{2}(88.7\pm2.2)\times10^{-2}$, $B(\phi(1020)\to K^+K^-)=(49.2\pm0.5)\times10^{-2}$. Our first error is their experiment's error and our second error is the systematic error from using our best values.

$\Gamma(J/\psi(1S)f_2'(1525))/\Gamma_{\text{total}}$ Γ_{74}/Γ

VALUE (units 10^{-4})	DOCUMENT ID		TECN	COMMENT
$2.61\pm0.20^{+0.56}_{-0.50}$	[1] AAIJ	13AN	LHCB	pp at 7 TeV

[1] Uses $f_s/f_d=0.256\pm0.020$ and $B(B^+\to J/\psi K^+)=(10.18\pm0.42)\times10^{-4}$.

$\Gamma(\psi(2S)\eta)/\Gamma(J/\psi(1S)\eta)$ Γ_{79}/Γ_{51}

VALUE	DOCUMENT ID		TECN	COMMENT
$0.83\pm0.14\pm0.12$	[1] AAIJ	13AA	LHCB	pp at 7 TeV

[1] Assuming lepton universality for dimuon decay modes of J/ψ and $\psi(2S)$ mesons, the ratio $B(J/\psi\to\mu^+\mu^-)/B(\psi(2S)\to\mu^+\mu^-)=B(J/\psi\to e^+e^-)/B(\psi(2S)\to e^+e^-)=7.69\pm0.19$ was used.

$\Gamma(\psi(2S)\eta')/\Gamma(J/\psi(1S)\eta')$ Γ_{80}/Γ_{54}

VALUE (units 10^{-2})	DOCUMENT ID		TECN	COMMENT
$38.7\pm9.0\pm1.6$	[1] AAIJ	15D	LHCB	pp at 7, 8 TeV

[1] Uses $J/\psi\to\mu^+\mu^-$, $\eta'\to\rho^0\gamma$, and $\eta'\to\eta\pi^+\pi^-$ decays.

$\Gamma(J/\psi(1S)p\overline{p})/\Gamma_{\text{total}}$ Γ_{75}/Γ

VALUE	CL%	DOCUMENT ID		TECN	COMMENT
$<4.8\times10^{-6}$	90	[1] AAIJ	13Z	LHCB	pp at 7 TeV

[1] Uses $B(B_s^0\to J/\psi(1S)\pi^+\pi^-)=(1.98\pm0.20)\times10^{-4}$.

$\Gamma(J/\psi(1S)\gamma)/\Gamma_{\text{total}}$ Γ_{76}/Γ

VALUE	CL%	DOCUMENT ID		TECN	COMMENT
$<7.3\times10^{-6}$	90	[1] AAIJ	15BB	LHCB	pp at 7, 8 TeV

[1] Branching fractions of normalization modes $B_s^0\to J/\psi\gamma X$ taken from PDG 14. Uses $f_s/f_d=0.259\pm0.015$.

$\Gamma(J/\psi(1S)\pi^+\pi^-\pi^+\pi^-)/\Gamma(J/\psi(1S)\pi^+\pi^-)$ Γ_{77}/Γ_{55}

VALUE	DOCUMENT ID		TECN	COMMENT
$0.371\pm0.015\pm0.022$	[1] AAIJ	14Y	LHCB	pp at 7,8 TeV

[1] Excludes contributions from $\psi(2S)$ and $\chi_{c1}(3872)$ decaying to $J/\psi(1S)\pi^+\pi^-$.

$\Gamma(J/\psi(1S)f_1(1285))/\Gamma_{\text{total}}$ Γ_{78}/Γ

VALUE (units 10^{-5})	DOCUMENT ID		TECN	COMMENT
$7.0\pm1.3\pm0.4$	[1] AAIJ	14Y	LHCB	pp at 7, 8 TeV

[1] AAIJ 14Y reports $(7.14\pm0.99^{+0.83}_{-0.91}\pm0.41)\times10^{-5}$ from a measurement of $[\Gamma(B_s^0\to J/\psi(1S)f_1(1285))/\Gamma_{\text{total}}]\times[B(f_1(1285)\to 2\pi^+2\pi^-)]$ assuming $B(f_1(1285)\to 2\pi^+2\pi^-)=0.11^{+0.007}_{-0.006}$, which we rescale to our best value $B(f_1(1285)\to 2\pi^+2\pi^-)=(11.2^{+0.7}_{-0.6})\times10^{-2}$. Our first error is their experiment's error and our second error is the systematic error from using our best value.

$\Gamma(\psi(2S)\phi)/\Gamma_{\text{total}}$ Γ_{82}/Γ

VALUE (units 10^{-4})	EVTS	DOCUMENT ID		TECN	COMMENT
• • • We do not use the following data for averages, fits, limits, etc. • • •					
seen	1	BUSKULIC	93G	ALEP	$e^+e^-\to Z$

$\Gamma(\psi(2S)\phi)/\Gamma(J/\psi(1S)\phi)$ Γ_{82}/Γ_{48}

VALUE	DOCUMENT ID		TECN	COMMENT
0.503±0.034 OUR AVERAGE				
$0.500\pm0.034\pm0.011$	[1,2] AAIJ	12L	LHCB	pp at 7 TeV
0.53 ±0.10 ±0.09	ABAZOV	09Y	D0	$p\overline{p}$ at 1.96 TeV
0.52 ±0.13 ±0.07	ABULENCIA	06N	CDF	$p\overline{p}$ at 1.96 TeV

[1] AAIJ 12L reports $0.489\pm0.026\pm0.021\pm0.012$ from a measurement of $[\Gamma(B_s^0\to\psi(2S)\phi)/\Gamma(B_s^0\to J/\psi(1S)\phi)]\times[B(J/\psi(1S)\to e^+e^-)]$ / $[B(\psi(2S)\to e^+e^-)]$ assuming $B(J/\psi(1S)\to e^+e^-)=(5.94\pm0.06)\times10^{-2}$, $B(\psi(2S)\to e^+e^-)=(7.72\pm0.17)\times10^{-3}$, which we rescale to our best values $B(J/\psi(1S)\to e^+e^-)=(5.971\pm0.032)\times10^{-2}$, $B(\psi(2S)\to e^+e^-)=(7.93\pm0.17)\times10^{-3}$. Our first error is their experiment's error and our second error is the systematic error from using our best values.
[2] Assumes $B(J/\psi\to\mu^+\mu^-)$ / $B(\psi(2S)\to\mu^+\mu^-)=B(J/\psi\to e^+e^-)$ / $B(\psi(2S)\to e^+e^-)=7.69\pm0.19$.

$\Gamma(\psi(2S)K^-\pi^+)/\Gamma_{\text{total}}$ Γ_{83}/Γ

VALUE (units 10^{-5})	DOCUMENT ID		TECN	COMMENT
$3.12\pm0.30\pm0.21$	[1] AAIJ	15U	LHCB	pp at 7, 8 TeV

[1] AAIJ 15U reports $[\Gamma(B_s^0\to\psi(2S)K^-\pi^+)/\Gamma_{\text{total}}]$ / $[B(B^0\to\psi(2S)K^+\pi^-)]=(5.38\pm0.36\pm0.22\pm0.31)\times10^{-2}$ which we multiply by our best value $B(B^0\to\psi(2S)K^+\pi^-)=(5.8\pm0.4)\times10^{-4}$. Our first error is their experiment's error and our second error is the systematic error from using our best value.

$\Gamma(\psi(2S)\overline{K}^*(892)^0)/\Gamma_{total}$ Γ_{84}/Γ

VALUE (units 10^{-5})	DOCUMENT ID		TECN	COMMENT
$3.3\pm0.5^{+0.2}_{-0.3}$	[1] AAIJ	15U	LHCB	pp at 7, 8 TeV

[1] AAIJ 15U reports $[\Gamma(B_s^0 \to \psi(2S)\overline{K}^*(892)^0)/\Gamma_{total}]$ / $[B(B^0 \to \psi(2S)K^*(892)^0)]$ $= (5.58 \pm 0.57 \pm 0.40 \pm 0.32) \times 10^{-2}$ which we multiply by our best value $B(B^0 \to \psi(2S)K^*(892)^0) = (5.9 \pm 0.4) \times 10^{-4}$. Our first error is their experiment's error and our second error is the systematic error from using our best value.

$\Gamma(\chi_{c1}\phi)/\Gamma(J/\psi(1S)\phi)$ Γ_{85}/Γ_{48}

VALUE (units 10^{-2})	DOCUMENT ID		TECN	COMMENT
$18.9\pm1.8\pm1.5$	[1] AAIJ	13AC	LHCB	pp at 7 TeV

[1] Uses $B(\chi_{c1} \to J/\psi\gamma) = (34.4 \pm 1.5)\%$.

$\Gamma(\psi(2S)\pi^+\pi^-)/\Gamma(J/\psi(1S)\pi^+\pi^-)$ Γ_{81}/Γ_{55}

VALUE	DOCUMENT ID		TECN	COMMENT
$0.34\pm0.04\pm0.03$	[1] AAIJ	13AA	LHCB	pp at 7 TeV

[1] Assuming lepton universality for dimuon decay modes of J/ψ and $\psi(2S)$ mesons, the ratio $B(J/\psi \to \mu^+\mu^-)/B(\psi(2S) \to \mu^+\mu^-) = B(J/\psi \to e^+e^-)/B(\psi(2S) \to e^+e^-) = 7.69 \pm 0.19$ was used.

$\Gamma(\pi^+\pi^-)/\Gamma_{total}$ Γ_{86}/Γ

VALUE (units 10^{-7})	CL%	DOCUMENT ID		TECN	COMMENT
7.0±0.8 OUR AVERAGE					
$7.2\pm0.9\pm0.4$		[1] AAIJ	17G	LHCB	pp at 7 and 8 TeV
$6.3\pm1.8\pm0.3$		[2] AALTONEN	12L	CDF	$p\overline{p}$ at 1.96 TeV
• • • We do not use the following data for averages, fits, limits, etc. • • •					
$10.2^{+2.4}_{-2.0}\pm0.6$		[3] AAIJ	12AR	LHCB	Repl. by AAIJ 17G
< 120	90	[4] PENG	10	BELL	$e^+e^- \to \Upsilon(5S)$
< 12	90	[5] AALTONEN	09C	CDF	Repl. by AALTONEN 12L
< 17	90	[6] ABULENCIA,A	06D	CDF	Repl. by AALTONEN 09C
<2320	90	[7] ABE	00C	SLD	$e^+e^- \to Z$
<1700	90	[8] BUSKULIC	96V	ALEP	$e^+e^- \to Z$

[1] AAIJ 17G reports $[\Gamma(B_s^0 \to \pi^+\pi^-)/\Gamma_{total}]$ / $[B(B^0 \to K^+\pi^-)] \times [\Gamma(\overline{b} \to B_s^0)/\Gamma(\overline{b} \to B^0)] = (9.15 \pm 0.71 \pm 0.83) \times 10^{-3}$ which we multiply or divide by our best values $B(B^0 \to K^+\pi^-) = (1.96 \pm 0.05) \times 10^{-5}$, $\Gamma(\overline{b} \to B_s^0)/\Gamma(\overline{b} \to B^0) = 0.250 \pm 0.012$. Our first error is their experiment's error and our second error is the systematic error from using our best values.

[2] AALTONEN 12L reports $[\Gamma(B_s^0 \to \pi^+\pi^-)/\Gamma_{total}]$ / $[B(B^0 \to K^+\pi^-)] \times [\Gamma(\overline{b} \to B_s^0)/\Gamma(\overline{b} \to B^0)] = 0.008 \pm 0.002 \pm 0.001$ which we multiply or divide by our best values $B(B^0 \to K^+\pi^-) = (1.96 \pm 0.05) \times 10^{-5}$, $\Gamma(\overline{b} \to B_s^0)/\Gamma(\overline{b} \to B^0) = 0.250 \pm 0.012$. Our first error is their experiment's error and our second error is the systematic error from using our best values.

[3] AAIJ 12AR reports $[\Gamma(B_s^0 \to \pi^+\pi^-)/\Gamma_{total}]$ / $[B(B^0 \to \pi^+\pi^-)] \times [\Gamma(\overline{b} \to B_s^0)/\Gamma(\overline{b} \to B^0)] = 0.050^{+0.011}_{-0.009} \pm 0.004$ which we multiply or divide by our best values $B(B^0 \to \pi^+\pi^-) = (5.12 \pm 0.19) \times 10^{-6}$, $\Gamma(\overline{b} \to B_s^0)/\Gamma(\overline{b} \to B^0) = 0.250 \pm 0.012$. Our first error is their experiment's error and our second error is the systematic error from using our best values.

[4] Uses $\Upsilon(10860) \to B_s^* \overline{B}_s^*$ and assumes $B(\Upsilon(10860) \to B_s^{(*)}\overline{B}_s^{(*)}) = (19.3 \pm 2.9)\%$ and $\Gamma(\Upsilon(10860) \to B_s^* \overline{B}_s^*)$ / $\Gamma(\Upsilon(10860) \to B_s^{(*)}\overline{B}_s^{(*)}) = (90.1^{+3.8}_{-4.0})\%$.

[5] Obtains this result from $(f_s/f_d) \cdot B(B_s \to \pi^+\pi^-)/B(B^0 \to K^+\pi^-) = 0.007 \pm 0.004 \pm 0.005$, assuming $f_s/f_d = 0.276 \pm 0.034$ and $B(B^0 \to K^+\pi^-) = (19.4 \pm 0.6) \times 10^{-6}$.

[6] ABULENCIA,A 06D obtains this from $B(B_s \to \pi^+\pi^-)$ / $B(B_s \to K^+K^-) < 0.05$ at 90% CL, assuming $B(B_s \to K^+K^-) = (33 \pm 6 \pm 7) \times 10^{-6}$.

[7] ABE 00C assumes $B(Z \to b\overline{b})=(21.7 \pm 0.1)\%$ and the B fractions $f_{B^0}=f_{B^+}=(39.7^{+1.8}_{-2.2})\%$ and $f_{B_s}=(10.5^{+1.8}_{-2.2})\%$.

[8] BUSKULIC 96V assumes PDG 96 production fractions for B^0, B^+, B_s, b baryons.

$\Gamma(\pi^0\pi^0)/\Gamma_{total}$ Γ_{87}/Γ

VALUE	CL%	DOCUMENT ID		TECN	COMMENT
$<2.1 \times 10^{-4}$	90	[1] ACCIARRI	95H	L3	$e^+e^- \to Z$

[1] ACCIARRI 95H assumes $f_{B^0} = 39.5 \pm 4.0$ and $f_{B_s} = 12.0 \pm 3.0\%$.

$\Gamma(\eta\pi^0)/\Gamma_{total}$ Γ_{88}/Γ

VALUE	CL%	DOCUMENT ID		TECN	COMMENT
$<1.0 \times 10^{-3}$	90	[1] ACCIARRI	95H	L3	$e^+e^- \to Z$

[1] ACCIARRI 95H assumes $f_{B^0} = 39.5 \pm 4.0$ and $f_{B_s} = 12.0 \pm 3.0\%$.

$\Gamma(\eta\eta)/\Gamma_{total}$ Γ_{89}/Γ

VALUE	CL%	DOCUMENT ID		TECN	COMMENT
$<1.5 \times 10^{-3}$	90	[1] ACCIARRI	95H	L3	$e^+e^- \to Z$

[1] ACCIARRI 95H assumes $f_{B^0} = 39.5 \pm 4.0$ and $f_{B_s} = 12.0 \pm 3.0\%$.

$\Gamma(\rho^0\rho^0)/\Gamma_{total}$ Γ_{90}/Γ

VALUE	CL%	DOCUMENT ID		TECN	COMMENT
$<3.20 \times 10^{-4}$	90	[1] ABE	00C	SLD	$e^+e^- \to Z$

[1] ABE 00C assumes $B(Z \to b\overline{b})=(21.7 \pm 0.1)\%$ and the B fractions $f_{B^0}=f_{B^+}=(39.7^{+1.8}_{-2.2})\%$ and $f_{B_s}=(10.5^{+1.8}_{-2.2})\%$.

$\Gamma(\eta'\eta')/\Gamma_{total}$ Γ_{91}/Γ

VALUE (units 10^{-5})	DOCUMENT ID		TECN	COMMENT
$3.3\pm0.7\pm0.1$	[1] AAIJ	15O	LHCB	pp at 7, 8 TeV

[1] AAIJ 15O reports $[\Gamma(B_s^0 \to \eta'\eta')/\Gamma_{total}]$ / $[B(B^+ \to \eta' K^+)] = 0.47 \pm 0.09 \pm 0.04$ which we multiply by our best value $B(B^+ \to \eta' K^+) = (7.06 \pm 0.25) \times 10^{-5}$. Our first error is their experiment's error and our second error is the systematic error from using our best value.

$\Gamma(\eta'\phi)/\Gamma_{total}$ Γ_{92}/Γ

VALUE	CL%	DOCUMENT ID		TECN	COMMENT
$<0.82 \times 10^{-6}$	90	[1] AAIJ	17BA	LHCB	pp at 7, 8 TeV

[1] Corresponds to the 95% CL upper limit 1.01×10^{-6}. Uses the normalization mode $B^+ \to \eta' K^+$ with branching fraction $(70.6 \pm 2.5) \times 10^{-6}$ and the ratio of hadronisation fractions $f_s/f_d = 0.259 \pm 0.015$, which is assumed equal to f_s/f_u.

$\Gamma(\phi\pi^+\pi^-)/\Gamma_{total}$ Γ_{96}/Γ

VALUE (units 10^{-6})	DOCUMENT ID		TECN	COMMENT
$3.48\pm0.23\pm0.39$	[1] AAIJ	17A	LHCB	pp at 7, 8 TeV

[1] Inclusive decays in mass range $400 < m(\pi^+\pi^-) < 1600$ MeV/c^2.

$\Gamma(\phi\rho^0)/\Gamma_{total}$ Γ_{95}/Γ

VALUE (units 10^{-7})	CL%	DOCUMENT ID		TECN	COMMENT
$2.7\pm0.7\pm0.3$		[1] AAIJ	17A	LHCB	pp at 7, 8 TeV
• • • We do not use the following data for averages, fits, limits, etc. • • •					
<6170	90	[2] ABE	00C	SLD	$e^+e^- \to Z$

[1] Signal evidence is 4 standard deviations.

[2] ABE 00C assumes $B(Z \to b\overline{b})=(21.7 \pm 0.1)\%$ and the B fractions $f_{B^0}=f_{B^+}=(39.7^{+1.8}_{-2.2})\%$ and $f_{B_s}=(10.5^{+1.8}_{-2.2})\%$.

$\Gamma(\phi f_0(980),\ f_0(980) \to \pi^+\pi^-)/\Gamma_{total}$ Γ_{93}/Γ

VALUE (units 10^{-6})	DOCUMENT ID		TECN	COMMENT
$1.12\pm0.16\pm0.14$	[1] AAIJ	17A	LHCB	pp at 7, 8 TeV

[1] Signal is observed with 8 standard deviations significance.

$\Gamma(\phi f_2(1270),\ f_2(1270) \to \pi^+\pi^-)/\Gamma_{total}$ Γ_{94}/Γ

VALUE (units 10^{-6})	DOCUMENT ID		TECN	COMMENT
$0.61\pm0.13^{+0.13}_{-0.08}$	[1] AAIJ	17A	LHCB	pp at 7, 8 TeV

[1] Signal is observed with 5 standard deviations significance.

$\Gamma(\phi\phi)/\Gamma_{total}$ Γ_{97}/Γ

VALUE (units 10^{-6})	CL%	DOCUMENT ID		TECN	COMMENT
18.7±1.5 OUR FIT					
18.5±1.4±1.0		[1] AAIJ	15AS	LHCB	pp at 7, 8 TeV
• • • We do not use the following data for averages, fits, limits, etc. • • •					
$14\ ^{+6}_{-5}\ \pm6$		[2] ACOSTA	05J	CDF	Repl. by AALTONEN 11AN
<1183	90	[3] ABE	00C	SLD	$e^+e^- \to Z$

[1] AAIJ 15AS reports $[\Gamma(B_s^0 \to \phi\phi)/\Gamma_{total}]$ / $[B(B^0 \to K^*(892)^0\phi)] = 1.84 \pm 0.05 \pm 0.13$ which we multiply by our best value $B(B^0 \to K^*(892)^0\phi) = (1.00 \pm 0.05) \times 10^{-5}$. Our first error is their experiment's error and our second error is the systematic error from using our best value.

[2] Uses $B(B^0 \to J/\psi\phi) = (1.38 \pm 0.49) \times 10^{-3}$ and production cross-section ratio of $\sigma(B_s)/\sigma(B^0) = 0.26 \pm 0.04$.

[3] ABE 00C assumes $B(Z \to b\overline{b})=(21.7 \pm 0.1)\%$ and the B fractions $f_{B^0}=f_{B^+}=(39.7^{+1.8}_{-2.2})\%$ and $f_{B_s}=(10.5^{+1.8}_{-2.2})\%$.

$\Gamma(\phi\phi)/\Gamma(J/\psi(1S)\phi)$ Γ_{97}/Γ_{48}

VALUE (units 10^{-2})	DOCUMENT ID		TECN	COMMENT
1.73±0.16 OUR FIT				
1.78±0.14±0.20	AALTONEN	11AN	CDF	$p\overline{p}$ at 1.96 TeV

$\Gamma(\phi\phi\phi)/\Gamma(\phi\phi)$ Γ_{98}/Γ_{97}

VALUE	DOCUMENT ID		TECN	COMMENT
$0.117\pm0.030\pm0.015$	AAIJ	17BB	LHCB	pp at 7, 8 TeV

$\Gamma(\pi^+K^-)/\Gamma_{total}$ Γ_{99}/Γ

VALUE (units 10^{-6})	CL%	DOCUMENT ID		TECN	COMMENT
5.7±0.6 OUR AVERAGE					
$5.8\pm0.7\pm0.3$		[1] AAIJ	12AR	LHCB	pp at 7 TeV
$5.6\pm1.0\pm0.3$		[2] AALTONEN	09C	CDF	$p\overline{p}$ at 1.96 TeV
• • • We do not use the following data for averages, fits, limits, etc. • • •					
< 26	90	[3] PENG	10	BELL	$e^+e^- \to \Upsilon(5S)$
< 5.6	90	[4] ABULENCIA,A	06D	CDF	Repl. by AALTONEN 09C
<261	90	[5] ABE	00C	SLD	$e^+e^- \to Z$
<210	90	[6] BUSKULIC	96V	ALEP	$e^+e^- \to Z$
<260	90	[7] AKERS	94L	OPAL	$e^+e^- \to Z$

Meson Particle Listings

B_s^0

[1] AAIJ 12AR reports $[\Gamma(B_s^0 \to \pi^+K^-)/\Gamma_{total}]$ / $[B(B^0 \to K^+\pi^-)] \times [\Gamma(\overline{b} \to B_s^0)/\Gamma(\overline{b} \to B^0)] = 0.074 \pm 0.006 \pm 0.006$ which we multiply or divide by our best values $B(B^0 \to K^+\pi^-) = (1.96 \pm 0.05) \times 10^{-5}$, $\Gamma(\overline{b} \to B_s^0)/\Gamma(\overline{b} \to B^0) = 0.250 \pm 0.012$. Our first error is their experiment's error and our second error is the systematic error from using our best values.

[2] AALTONEN 09C reports $[\Gamma(B_s^0 \to \pi^+K^-)/\Gamma_{total}]$ / $[B(B^0 \to K^+\pi^-)] \times [B(\overline{b} \to B_s^0)]$ / $[B(\overline{b} \to B^0)] = 0.071 \pm 0.010 \pm 0.007$ which we multiply or divide by our best values $B(B^0 \to K^+\pi^-) = (1.96 \pm 0.05) \times 10^{-5}$, $B(\overline{b} \to B_s^0) = (10.1 \pm 0.4) \times 10^{-2}$, $B(\overline{b} \to B^0) = (40.5 \pm 0.6) \times 10^{-2}$. Our first error is their experiment's error and our second error is the systematic error from using our best values.

[3] Uses $\Upsilon(10860) \to B_s^* \overline{B}_s^*$ and assumes $B(\Upsilon(10860) \to B_s^{(*)}\overline{B}_s^{(*)}) = (19.3 \pm 2.9)\%$ and $\Gamma(\Upsilon(10860) \to B_s^*\overline{B}_s^*)$ / $\Gamma(\Upsilon(10860) \to B_s^{(*)}\overline{B}_s^{(*)}) = (90.1^{+3.8}_{-4.0})\%$.

[4] ABULENCIA,A 06D obtains this from (f_s/f_d) $(B(B_s \to \pi^+K^-)$ / $B(B^0 \to K^+\pi^-))$ < 0.08 at 90% CL, assuming $f_s/f_d = 0.260 \pm 0.039$ and $B(B^0 \to K^+\pi^-) = (18.9 \pm 0.7) \times 10^{-6}$.

[5] ABE 00C assumes $B(Z \to b\overline{b})$=(21.7 ± 0.1)% and the B fractions $f_{B^0} = f_{B^+} = (39.7^{+1.8}_{-2.2})\%$ and $f_{B_s} = (10.5^{+1.8}_{-2.2})\%$.

[6] BUSKULIC 96V assumes PDG 96 production fractions for B^0, B^+, B_s, b baryons.

[7] Assumes $B(Z \to b\overline{b}) = 0.217$ and B_d^0 (B_s^0) fraction 39.5% (12%).

$\Gamma(K^+K^-)/\Gamma_{total}$ Γ_{100}/Γ

VALUE (units 10^{-6})	CL%	DOCUMENT ID		TECN	COMMENT
25.9± 1.7 OUR AVERAGE					
24.8± 1.6±1.3		[1] AAIJ	12AR	LHCB	pp at 7 TeV
27.2± 2.3±1.5		[2] AALTONEN	11N	CDF	$p\overline{p}$ at 1.96 TeV
38 $^{+10}_{-9}$ ±7		[3] PENG	10	BELL	$e^+e^- \to \Upsilon(5S)$
• • • We do not use the following data for averages, fits, limits, etc. • • •					
<310	90	DRUTSKOY	07A	BELL	$e^+e^- \to \Upsilon(5S)$
33 ± 6 ±7		[4] ABULENCIA,A	06D	CDF	Repl. by AALTONEN 11N
<283	90	[5] ABE	00C	SLD	$e^+e^- \to Z$
< 59	90	[6] BUSKULIC	96V	ALEP	$e^+e^- \to Z$
<140	90	[7] AKERS	94L	OPAL	$e^+e^- \to Z$

[1] AAIJ 12AR reports $[\Gamma(B_s^0 \to K^+K^-)/\Gamma_{total}]$ / $[B(B^0 \to K^+\pi^-)] \times [\Gamma(\overline{b} \to B_s^0)/\Gamma(\overline{b} \to B^0)] = 0.316 \pm 0.009 \pm 0.019$ which we multiply or divide by our best values $B(B^0 \to K^+\pi^-) = (1.96 \pm 0.05) \times 10^{-5}$, $\Gamma(\overline{b} \to B_s^0)/\Gamma(\overline{b} \to B^0) = 0.250 \pm 0.012$. Our first error is their experiment's error and our second error is the systematic error from using our best values.

[2] AALTONEN 11N reports (f_s/f_d) $(B(B_s^0 \to K^+K^-)$ / $B(B^0 \to K^+\pi^-)) = 0.347 \pm 0.020 \pm 0.021$. We multiply this result by our best value of $B(B^0 \to K^+\pi^-) = (1.96 \pm 0.05) \times 10^{-5}$ and divide by our best value of f_s/f_d, where $1/2\ f_s/f_d = 0.125 \pm 0.006$. Our first quoted uncertainty is the combined experiment's uncertainty and our second is the systematic uncertainty from using out best values.

[3] Uses $\Upsilon(10860) \to B_s^*\overline{B}_s^*$ and assumes $B(\Upsilon(10860) \to B_s^{(*)}\overline{B}_s^{(*)}) = (19.3 \pm 2.9)\%$ and $\Gamma(\Upsilon(10860) \to B_s^*\overline{B}_s^*)$ / $\Gamma(\Upsilon(10860) \to B_s^{(*)}\overline{B}_s^{(*)}) = (90.1^{+3.8}_{-4.0})\%$.

[4] ABULENCIA,A 06D obtains this from (f_s/f_d) $(B(B_s \to K^+K^-)$ / $B(B^0 \to K^+\pi^-))$ $= 0.46 \pm 0.08 \pm 0.07$, assuming $f_s/f_d = 0.260 \pm 0.039$ and $B(B^0 \to K^+\pi^-) = (18.9 \pm 0.7) \times 10^{-6}$.

[5] ABE 00C assumes $B(Z \to b\overline{b})$=(21.7 ± 0.1)% and the B fractions $f_{B^0} = f_{B^+} = (39.7^{+1.8}_{-2.2})\%$ and $f_{B_s} = (10.5^{+1.8}_{-2.2})\%$.

[6] BUSKULIC 96V assumes PDG 96 production fractions for B^0, B^+, B_s, b baryons.

[7] Assumes $B(Z \to b\overline{b}) = 0.217$ and B_d^0 (B_s^0) fraction 39.5% (12%).

$\Gamma(K^0\overline{K}^0)/\Gamma_{total}$ Γ_{101}/Γ

VALUE (units 10^{-5})	CL%	DOCUMENT ID		TECN	COMMENT
1.96$^{+0.58}_{-0.51}$±0.10±0.20		[1] PAL	16	BELL	$e^+e^- \to \Upsilon(5S)$
• • • We do not use the following data for averages, fits, limits, etc. • • •					
<6.6	90	[2] PENG	10	BELL	Repl. by PAL 16

[1] Observed in $B_s^0 \to K_S^0K_S^0$ with significance of 5.1 σ. The last uncertainty is due to the uncertainty of the total number of $B_s^0\overline{B}_s^0$ pairs.

[2] Uses $\Upsilon(10860) \to B_s^*\overline{B}_s^*$ and assumes $B(\Upsilon(10860) \to B_s^{(*)}\overline{B}_s^{(*)}) = (19.3 \pm 2.9)\%$ and $\Gamma(\Upsilon(10860) \to B_s^*\overline{B}_s^*)$ / $\Gamma(\Upsilon(10860) \to B_s^{(*)}\overline{B}_s^{(*)}) = (90.1^{+3.8}_{-4.0})\%$.

$\Gamma(K^0\pi^+\pi^-)/\Gamma_{total}$ Γ_{102}/Γ

VALUE (units 10^{-6})	DOCUMENT ID		TECN	COMMENT
9.4±2.1±0.3	[1,2] AAIJ	17BP	LHCB	pp at 7, 8 TeV
• • • We do not use the following data for averages, fits, limits, etc. • • •				
14 ±4 ±1	[3] AAIJ	13BP	LHCB	Repl. by AAIJ 17BP

[1] AAIJ 17BP reports $[\Gamma(B_s^0 \to K^0\pi^+\pi^-)/\Gamma_{total}]$ / $[B(B^0 \to K^0\pi^+\pi^-)] = 0.191 \pm 0.027 \pm 0.033$ which we multiply by our best value $B(B^0 \to K^0\pi^+\pi^-) = (4.94 \pm 0.18) \times 10^{-5}$. Our first error is their experiment's error and our second error is the systematic error from using our best value.

[2] Used $f_s/f_d = 0.259 \pm 0.015$.

[3] AAIJ 13BP reports $[\Gamma(B_s^0 \to K^0\pi^+\pi^-)/\Gamma_{total}]$ / $[B(B^0 \to K^0\pi^+\pi^-)] = 0.29 \pm 0.06 \pm 0.04$ which we multiply by our best value $B(B^0 \to K^0\pi^+\pi^-) = (4.94 \pm 0.18) \times 10^{-5}$. Our first error is their experiment's error and our second error is the systematic error from using our best value.

$\Gamma(K^*(892)^-\pi^+)/\Gamma_{total}$ Γ_{104}/Γ

VALUE (units 10^{-6})	DOCUMENT ID		TECN	COMMENT
3.3±1.2±0.3	[1,2] AAIJ	14BM	LHCB	pp at 7 TeV

[1] AAIJ 14BM reports $[\Gamma(B_s^0 \to K^*(892)^-\pi^+)/\Gamma_{total}]$ / $[B(B^0 \to K^*(892)^+\pi^-)] = 0.39 \pm 0.13 \pm 0.05$ which we multiply by our best value $B(B^0 \to K^*(892)^+\pi^-) = (8.4 \pm 0.8) \times 10^{-6}$. Our first error is their experiment's error and our second error is the systematic error from using our best value.

[2] Uses $f_s/f_d = 0.259 \pm 0.015$.

$\Gamma(K^0K^\pm\pi^\mp)/\Gamma_{total}$ Γ_{103}/Γ

VALUE (units 10^{-5})	DOCUMENT ID		TECN	COMMENT
8.4±0.8±0.3	[1,2] AAIJ	17BP	LHCB	pp at 7, 8 TeV
• • • We do not use the following data for averages, fits, limits, etc. • • •				
7.3±0.9±0.3	[3] AAIJ	13BP	LHCB	Repl. by AAIJ 17BP

[1] AAIJ 17BP reports $[\Gamma(B_s^0 \to K^0K^\pm\pi^\mp)/\Gamma_{total}]$ / $[B(B^0 \to K^0\pi^+\pi^-)] = 1.70 \pm 0.07 \pm 0.15$ which we multiply by our best value $B(B^0 \to K^0\pi^+\pi^-) = (4.94 \pm 0.18) \times 10^{-5}$. Our first error is their experiment's error and our second error is the systematic error from using our best value.

[2] Used $f_s/f_d = 0.259 \pm 0.015$.

[3] AAIJ 13BP reports $[\Gamma(B_s^0 \to K^0K^\pm\pi^\mp)/\Gamma_{total}]$ / $[B(B^0 \to K^0\pi^+\pi^-)] = 1.48 \pm 0.12 \pm 0.14$ which we multiply by our best value $B(B^0 \to K^0\pi^+\pi^-) = (4.94 \pm 0.18) \times 10^{-5}$. Our first error is their experiment's error and our second error is the systematic error from using our best value.

$\Gamma(K^*(892)^\pm K^\mp)/\Gamma_{total}$ Γ_{105}/Γ

VALUE (units 10^{-5})	DOCUMENT ID		TECN	COMMENT
1.25±0.24±0.11	[1,2] AAIJ	14BM	LHCB	pp at 7 TeV

[1] AAIJ 14BM reports $[\Gamma(B_s^0 \to K^*(892)^\pm K^\mp)/\Gamma_{total}]$ / $[B(B^0 \to K^*(892)^+\pi^-)] = 1.49 \pm 0.22 \pm 0.18$ which we multiply by our best value $B(B^0 \to K^*(892)^+\pi^-) = (8.4 \pm 0.8) \times 10^{-6}$. Our first error is their experiment's error and our second error is the systematic error from using our best value.

[2] Uses $f_s/f_d = 0.259 \pm 0.015$.

$\Gamma(K_S^0\overline{K}^*(892)^0 + c.c.)/\Gamma_{total}$ Γ_{106}/Γ

VALUE (units 10^{-6})	DOCUMENT ID		TECN	COMMENT
16.4±3.4±2.3	[1] AAIJ	16	LHCB	pp at 7 TeV

[1] Measured relative to $B^0 \to K_S^0\pi^+\pi^-$ using the value of $B(B^0 \to K^0\pi^+\pi^-) = (4.96 \pm 0.2) \times 10^{-5}$.

$\Gamma(K^0K^+K^-)/\Gamma_{total}$ Γ_{107}/Γ

VALUE (units 10^{-7})	CL%	DOCUMENT ID		TECN	COMMENT
12.9±6.4±0.5		[1,2,3] AAIJ	17BP	LHCB	pp at 7, 8 TeV
• • • We do not use the following data for averages, fits, limits, etc. • • •					
<34	90	[4] AAIJ	13BP	LHCB	Repl. by AAIJ 17BP

[1] AAIJ 17BP reports $[\Gamma(B_s^0 \to K^0K^+K^-)/\Gamma_{total}]$ / $[B(B^0 \to K^0\pi^+\pi^-)] = 0.026 \pm 0.011 \pm 0.007$ which we multiply by our best value $B(B^0 \to K^0\pi^+\pi^-) = (4.94 \pm 0.18) \times 10^{-5}$. Our first error is their experiment's error and our second error is the systematic error from using our best value.

[2] AAIJ 17BP also set the limit range $4\text{–}25 \times 10^{-7}$ at 90% CL using the world average value $B(B^0 \to K^0\pi^+\pi^-) = (4.96 \pm 0.20) \times 10^{-5}$.

[3] Used $f_s/f_d = 0.259 \pm 0.015$.

[4] AAIJ 13BP reports $[\Gamma(B_s^0 \to K^0K^+K^-)/\Gamma_{total}]$ / $[B(B^0 \to K^0\pi^+\pi^-)] < 0.068$ which we multiply by our best value $B(B^0 \to K^0\pi^+\pi^-) = 4.94 \times 10^{-5}$.

$\Gamma(\overline{K}^*(892)^0\rho^0)/\Gamma_{total}$ Γ_{108}/Γ

VALUE	CL%	DOCUMENT ID		TECN	COMMENT
<7.67 × 10^{-4}	90	[1] ABE	00C	SLD	$e^+e^- \to Z$

[1] ABE 00C assumes $B(Z \to b\overline{b})$=(21.7 ± 0.1)% and the B fractions $f_{B^0} = f_{B^+} = (39.7^{+1.8}_{-2.2})\%$ and $f_{B_s} = (10.5^{+1.8}_{-2.2})\%$.

$\Gamma(\overline{K}^*(892)^0K^*(892)^0)/\Gamma_{total}$ Γ_{109}/Γ

VALUE (units 10^{-5})	CL%	DOCUMENT ID		TECN	COMMENT
1.11±0.26±0.06		[1] AAIJ	15AF	LHCB	pp at 7 TeV
• • • We do not use the following data for averages, fits, limits, etc. • • •					
2.81±0.46±0.56		[2] AAIJ	12F	LHCB	Repl. by AAIJ 15AF
<168.1	90	[3] ABE	00C	SLD	$e^+e^- \to Z$

[1] AAIJ 15AF reports $[\Gamma(B_s^0 \to \overline{K}^*(892)^0K^*(892)^0)/\Gamma_{total}]$ / $[B(B^0 \to K^*(892)^0\phi)] = 1.11 \pm 0.22 \pm 0.12 \pm 0.06$ which we multiply by our best value $B(B^0 \to K^*(892)^0\phi) = (1.00 \pm 0.05) \times 10^{-5}$. Our first error is their experiment's error and our second error is the systematic error from using our best value.

[2] Uses $B^0 \to J/\psi K^{*0}$ for normalization and assumes $B(B^0 \to J/\psi K^{*0})$ $B(J/\psi \to \mu^+\mu^-)$ $B(K^{*0} \to K^+\pi^-) = (1.33 \pm 0.06) \times 10^{-3}$ and $f_s/f_d = 0.253 \pm 0.031$. The second quoted error is total uncertainty including the error of 0.34 on f_s/f_d.

[3] ABE 00C assumes $B(Z \to b\overline{b})$=(21.7 ± 0.1)% and the B fractions $f_{B^0} = f_{B^+} = (39.7^{+1.8}_{-2.2})\%$ and $f_{B_s} = (10.5^{+1.8}_{-2.2})\%$.

$\Gamma(\phi K^*(892)^0)/\Gamma_{total}$ Γ_{110}/Γ

VALUE (units 10^{-6})	CL%	DOCUMENT ID		TECN	COMMENT
1.14±0.29±0.06		[1] AAIJ	13BW	LHCB	pp at 7 TeV
• • • We do not use the following data for averages, fits, limits, etc. • • •					
<1013	90	[2] ABE	00C	SLD	$e^+e^- \to Z$

[1] AAIJ 13BW reports $[\Gamma(B_s^0 \to \phi K^*(892)^0)/\Gamma_{total}] / [B(B^0 \to K^*(892)^0\phi)] = 0.113 \pm 0.024 \pm 0.016$ which we multiply by our best value $B(B^0 \to K^*(892)^0\phi) = (1.00 \pm 0.05) \times 10^{-5}$. Our first error is their experiment's error and our second error is the systematic error from using our best value.

[2] ABE 00C assumes $B(Z \to b\overline{b})$=(21.7 ± 0.1)% and the B fractions $f_{B^0}=f_{B^+}=(39.7^{+1.8}_{-2.2})$% and $f_{B_s}=(10.5^{+1.8}_{-2.2})$%.

$\Gamma(p\overline{p})/\Gamma_{total}$ Γ_{111}/Γ

Test for ΔB=1 weak neutral current. Allowed by higher-order electroweak interactions.

VALUE (units 10^{-8})	CL%	DOCUMENT ID		TECN	COMMENT
< 1.5	90	[1] AAIJ	17BJ	LHCB	pp at 7 and 8 TeV
• • • We do not use the following data for averages, fits, limits, etc. • • •					
$2.84^{+2.03+0.85}_{-1.68-0.18}$		[2] AAIJ	13BQ	LHCB	Repl. by AAIJ 17BJ
<5900	90	[3] BUSKULIC	96V	ALEP	$e^+e^- \to Z$

[1] Uses normalization mode $B(B^0 \to K^+\pi^-) = (19.6 \pm 0.5) \times 10^{-6}$ and B production ratio $f(\overline{b} \to B_s^0)/f(\overline{b} \to B_d^0) = 0.259 \pm 0.015$.

[2] Uses normalization mode $B(B^0 \to K^+\pi^-) = (19.55 \pm 0.54) \times 10^{-6}$ and B production ratio $f(\overline{b} \to B_s^0)/f(\overline{b} \to B_d^0) = 0.256 \pm 0.020$.

[3] BUSKULIC 96V assumes PDG 96 production fractions for B^0, B^+, B_s, b baryons.

$\Gamma(p\overline{p}K^+K^-)/\Gamma_{total}$ Γ_{112}/Γ

VALUE (units 10^{-6})	DOCUMENT ID		TECN	COMMENT
4.5±0.4±0.2	[1,2] AAIJ	17BD	LHCB	pp at 7, 8 TeV

[1] AAIJ 17BD reports $[\Gamma(B_s^0 \to p\overline{p}K^+K^-)/\Gamma_{total}] / [B(B^0 \to J/\psi(1S)K^*(892)^0)] / [B(J/\psi(1S) \to p\overline{p})] / [B(K^*(892) \to (K\pi)^\pm)] = 1.67 \pm 0.12 \pm 0.11$ which we multiply by our best values $B(B^0 \to J/\psi(1S)K^*(892)^0) = (1.27 \pm 0.05) \times 10^{-3}$, $B(J/\psi(1S) \to p\overline{p}) = (2.121 \pm 0.029) \times 10^{-3}$, $B(K^*(892) \to (K\pi)^\pm) = (99.900 \pm 0.009) \times 10^{-2}$. Our first error is their experiment's error and our second error is the systematic error from using our best values. Reported value assumes $f_s/f_d = 0.259 \pm 0.015$.

[2] The branching ratio is given for $m_{p\overline{p}}$ <2.85 GeV.

$\Gamma(p\overline{p}K^+\pi^-)/\Gamma_{total}$ Γ_{113}/Γ

VALUE (units 10^{-7})	DOCUMENT ID		TECN	COMMENT
13.9±2.5±0.5	[1,2] AAIJ	17BD	LHCB	pp at 7, 8 TeV

[1] AAIJ 17BD reports $[\Gamma(B_s^0 \to p\overline{p}K^+\pi^-)/\Gamma_{total}] / [B(B^0 \to J/\psi(1S)K^*(892)^0)] / [B(J/\psi(1S) \to p\overline{p})] / [B(K^*(892) \to (K\pi)^\pm)] = 0.52 \pm 0.08 \pm 0.05$ which we multiply by our best values $B(B^0 \to J/\psi(1S)K^*(892)^0) = (1.27 \pm 0.05) \times 10^{-3}$, $B(J/\psi(1S) \to p\overline{p}) = (2.121 \pm 0.029) \times 10^{-3}$, $B(K^*(892) \to (K\pi)^\pm) = (99.900 \pm 0.009) \times 10^{-2}$. Our first error is their experiment's error and our second error is the systematic error from using our best values. Reported value assumes $f_s/f_d = 0.259 \pm 0.015$.

[2] The branching ratio is given for $m_{p\overline{p}}$ <2.85 GeV.

$\Gamma(p\overline{p}K^+\pi^-)/\Gamma(p\overline{p}K^+K^-)$ $\Gamma_{113}/\Gamma_{112}$

VALUE	DOCUMENT ID		TECN	COMMENT
0.31±0.05±0.02	[1,2] AAIJ	17BD	LHCB	pp at 7, 8 TeV

[1] Reports $B(B_s^0 \to p\overline{p}K^+\pi^-) / B(B^0 \to p\overline{p}K^+\pi^-) = 0.22 \pm 0.04 \pm 0.02 \pm 0.01$, where the third error is due to f_s/f_d.

[2] The ratio is given for $m_{p\overline{p}}$ <2.85 GeV and assuming $f_s/f_d = 0.259 \pm 0.015$.

$\Gamma(p\overline{p}\pi^+\pi^-)/\Gamma_{total}$ Γ_{114}/Γ

VALUE (units 10^{-7})	DOCUMENT ID		TECN	COMMENT
4.3±2.0±0.2	[1,2] AAIJ	17BD	LHCB	pp at 7, 8 TeV

[1] AAIJ 17BD reports $[\Gamma(B_s^0 \to p\overline{p}\pi^+\pi^-)/\Gamma_{total}] / [B(B^0 \to J/\psi(1S)K^*(892)^0)] / [B(J/\psi(1S) \to p\overline{p})] / [B(K^*(892) \to (K\pi)^\pm)] = 0.16 \pm 0.07 \pm 0.02$ which we multiply by our best values $B(B^0 \to J/\psi(1S)K^*(892)^0) = (1.27 \pm 0.05) \times 10^{-3}$, $B(J/\psi(1S) \to p\overline{p}) = (2.121 \pm 0.029) \times 10^{-3}$, $B(K^*(892) \to (K\pi)^\pm) = (99.900 \pm 0.009) \times 10^{-2}$. Our first error is their experiment's error and our second error is the systematic error from using our best values. Reported value assumes $f_s/f_d = 0.259 \pm 0.015$.

[2] The branching ratio is given for $m_{p\overline{p}}$ <2.85 GeV.

$\Gamma(p\overline{\Lambda}K^- + \text{c.c.})/\Gamma_{total}$ Γ_{115}/Γ

VALUE (units 10^{-6})	DOCUMENT ID		TECN	COMMENT
5.5±0.6±0.8	[1,2] AAIJ	17AL	LHCB	pp at 7, 8 TeV

[1] AAIJ 17AL reports $(5.46 \pm 0.61 \pm 0.82) \times 10^{-6}$ from a measurement of $[\Gamma(B_s^0 \to p\overline{\Lambda}K^- + \text{c.c.})/\Gamma_{total}] / [B(B^0 \to p\overline{\Lambda}\pi^-)]$ assuming $B(B^0 \to p\overline{\Lambda}\pi^-) = (3.14 \pm 0.29) \times 10^{-6}$.

[2] AAIJ 17AL value represents the sum of $B_s^0 \to p\overline{\Lambda}K^-$ and $B_s^0 \to \overline{p}\Lambda K^+$ and assumes the fraction $f_s/f_d = 0.259 \pm 0.015$.

$\Gamma(\Lambda_c^-\Lambda\pi^+)/\Gamma_{total}$ Γ_{116}/Γ

VALUE (units 10^{-4})	DOCUMENT ID		TECN	COMMENT
3.6±1.1±1.2	[1] SOLOVIEVA	13	BELL	$e^+e^- \to \Upsilon(4S)$

[1] The second error is the total systematic uncertainty including the Λ_c absolute branching fractions and the normalizion number of B_s events.

$\Gamma(\Lambda_c^-\Lambda_c^+)/\Gamma_{total}$ Γ_{117}/Γ

VALUE	CL%	DOCUMENT ID		TECN	COMMENT
<8.0 × 10^{-5}	95	[1] AAIJ	14AA	LHCB	pp at 7 TeV

[1] Uses $B(\overline{B}^0 \to D^+D_s^-) = (7.2 \pm 0.8) \times 10^{-3}$.

$\Gamma(\gamma\gamma)/\Gamma_{total}$ Γ_{118}/Γ

Test for ΔB=1 weak neutral current.

VALUE (units 10^{-6})	CL%	DOCUMENT ID		TECN	COMMENT
< 3.1	90	[1] DUTTA	15	BELL	$e^+e^- \to \Upsilon(5S)$
• • • We do not use the following data for averages, fits, limits, etc. • • •					
< 8.7	90	[2] WICHT	08A	BELL	Repl. by DUTTA 15
< 53	90	DRUTSKOY	07A	BELL	Repl. by WICHT 08A
<148	90	[3] ACCIARRI	95I	L3	$e^+e^- \to Z$

[1] Assumes the fraction of $B_s^{(*)}\overline{B}_s^{(*)}$ in $b\overline{b}$ events is $f_s = (17.2 \pm 3.0)$%.

[2] Assumes $\Upsilon(5S) \to B_s^*\overline{B}_s^*$ = $(19.5^{+3.0}_{-2.3})$%.

[3] ACCIARRI 95I assumes $f_{B^0} = 39.5 \pm 4.0$ and $f_{B_s} = (12.0 \pm 3.0)$%.

$\Gamma(\phi\gamma)/\Gamma_{total}$ Γ_{119}/Γ

VALUE (units 10^{-6})	CL%	DOCUMENT ID		TECN	COMMENT
34 ± 4 OUR AVERAGE					
36 ± 5 ± 7		[1] DUTTA	15	BELL	$e^+e^- \to \Upsilon(5S)$
33.8± 3.4± 2.0		[2] AAIJ	13	LHCB	pp at 7 TeV
• • • We do not use the following data for averages, fits, limits, etc. • • •					
39 ± 5		[3] AAIJ	12AE	LHCB	Repl. by AAIJ 13
$57^{+18}_{-15}{}^{+12}_{-11}$		[4] WICHT	08A	BELL	Repl. by DUTTA 15
<390	90	DRUTSKOY	07A	BELL	$e^+e^- \to \Upsilon(5S)$
<120	90	ACOSTA	02G	CDF	$p\overline{p}$ at 1.8 TeV
<700	90	[5] ADAM	96D	DLPH	$e^+e^- \to Z$

[1] Assumes the fraction of $B_s^{(*)}\overline{B}_s^{(*)}$ in $b\overline{b}$ events is $f_s = (17.2 \pm 3.0)$%. The systematic uncertainty from f_s is 0.6×10^{-5}.

[2] AAIJ 13 reports $[\Gamma(B_s^0 \to \phi\gamma)/\Gamma_{total}] / [B(B^0 \to K^*(892)^0\gamma)] = 0.81 \pm 0.04 \pm 0.07$ which we multiply by our best value $B(B^0 \to K^*(892)^0\gamma) = (4.18 \pm 0.25) \times 10^{-5}$. Our first error is their experiment's error and our second error is the systematic error from using our best value.

[3] Measures $B(B^0 \to K^{*0}\gamma)/B(B_s \to \phi\gamma) = 1.12 \pm 0.08(\text{stat})^{+0.06}_{-0.04}(\text{sys})^{+0.09}_{-0.08}(f_s/f_d)$ and uses current world-average value of $B(B^0 \to K^{*0}\gamma) = (4.33 \pm 0.15) \times 10^{-5}$.

[4] Assumes $\Upsilon(5S) \to B_s^*\overline{B}_s^*$ = $(19.5^{+3.0}_{-2.3})$%.

[5] ADAM 96D assumes $f_{B^0} = f_{B^-} = 0.39$ and $f_{B_s} = 0.12$.

$\Gamma(\mu^+\mu^-)/\Gamma_{total}$ Γ_{120}/Γ

Test for $\Delta B = 1$ weak neutral current.

VALUE (units 10^{-9})	CL%	DOCUMENT ID		TECN	COMMENT
$2.7^{+0.6}_{-0.5}$ OUR AVERAGE		Error includes scale factor of 1.2.			
$3.0 \pm 0.6^{+0.3}_{-0.2}$		AAIJ	17AI	LHCB	pp at 7, 8, 13 TeV
$0.9^{+1.1}_{-0.8}$		[1] AABOUD	16L	ATLS	pp at 7, 8 TeV
13^{+9}_{-7}		[2] AALTONEN	13F	CDF	$p\overline{p}$ at 1.96 TeV
$3.0^{+1.0}_{-0.9}$		[3] CHATRCHYAN	13AW	CMS	pp at 7, 8 TeV
• • • We do not use the following data for averages, fits, limits, etc. • • •					
$2.8^{+0.7}_{-0.6}$		[4] KHACHATRY...	15BE	LHC	pp at 7, 8 TeV
$3.2^{+1.4+0.5}_{-1.2-0.3}$		[5] AAIJ	13B	LHCB	Repl. by AAIJ 13BA
$2.9^{+1.1+0.3}_{-1.0-0.1}$		[6] AAIJ	13BA	LHCB	Repl. by KHACHA-TRYAN 15BE
<12	90	[7] ABAZOV	13C	D0	$p\overline{p}$ at 1.96 TeV
<19	90	[8] AAD	12AE	ATLS	pp at 7 TeV
<12	90	[9] AAIJ	12A	LHCB	Repl. by AAIJ 12W
< 3.8	90	[10] AAIJ	12W	LHCB	Repl. by AAIJ 13B
< 6.4	90	[11] CHATRCHYAN	12A	CMS	pp at 7 TeV
<43	90	[12] AAIJ	11B	LHCB	Repl. by AAIJ 12A
<35	90	[13] AALTONEN	11AG	CDF	$p\overline{p}$ at 1.96 TeV
<16	90	[14] CHATRCHYAN	11T	CMS	Repl. by CHATRCHYAN 12A
<42	90	[15] ABAZOV	10S	D0	$p\overline{p}$ at 1.96 TeV

[1] This value corresponds to an upper limit of $< 3.0 \times 10^{-9}$ at 95% C.L. It uses $f_s/f_d = 0.24 \pm 0.02$.

[2] Uses normalization mode $B(B^+ \to J/\psi K^+) = (10.22 \pm 0.35) \times 10^{-4}$ and B production ratio $f(\overline{b} \to B_s^0)/f(\overline{b} \to B_d^0) = 0.28 \pm 0.04$.

[3] Uses B production ratio $f(\overline{b} \to B_s^0)/f(\overline{b} \to B_d^0) = 0.256 \pm 0.020$ and $B(B^+ \to J/\psi K^+ \to \mu^+\mu^- K^+) = (6.0 \pm 0.2) \times 10^{-5}$ for normalization.

[4] Determined from the joint fit to CMS and LHCb data. Uncertainty includes both statistical and systematic component.

[5] Uses B production ratio $f(\overline{b} \to B_s^0)/f(\overline{b} \to B_d^0) = 0.256 \pm 0.020$ and two normalization modes: $B(B^+ \to J/\psi K^+ \to \mu^+\mu^- K^+) = (6.01 \pm 0.21) \times 10^{-5}$ and $B(B^0 \to K^+\pi^-) = (1.94 \pm 0.06) \times 10^{-5}$.

Meson Particle Listings

B_s^0

[6] Uses B production ratio $f(\overline{b} \to B_s^0)/f(\overline{b} \to B_d^0) = 0.259 \pm 0.015$ and normalization modes $B^+ \to J/\psi K^+ \to \mu^+\mu^- K^+$ and $B^0 \to K^+\pi^-$.

[7] Uses normalization mode $B(B^+ \to J/\psi K^+ \to \mu^+\mu^- K^+) = (6.01 \pm 0.21) \times 10^{-5}$ and B production ratio $f(\overline{b} \to B_s^0)/f(\overline{b} \to B_d^0) = 0.263 \pm 0.017$.

[8] Uses B production ratio $f(\overline{b} \to B^+)/f(\overline{b} \to B_s^0) = 3.75 \pm 0.29$ and $B(B^+ \to J/\psi K^+ \to \mu^+\mu^- K^+) = (6.0 \pm 0.2) \times 10^{-5}$.

[9] Uses B production ratio $f(\overline{b} \to B_s^0)/f(\overline{b} \to B_d^0) = 0.267^{+0.021}_{-0.020}$ and three normalization modes $B(B^+ \to J/\psi K^+ \to \mu^+\mu^- K^+) = (6.01 \pm 0.21) \times 10^{-5}$, $B(B^0 \to K^+\pi^-) = (1.94 \pm 0.06) \times 10^{-5}$, and $B(B_s^0 \to J/\psi\phi \to \mu^+\mu^- K^+ K^-) = (3.4 \pm 0.9) \times 10^{-5}$.

[10] Uses B production ratio $f(\overline{b} \to B_s^0)/f(\overline{b} \to B_d^0) = 0.267^{+0.021}_{-0.020}$ and three normalization modes of $B^+ \to J/\psi K^+$, $B^0 \to K^+\pi^-$, and $B_s^0 \to J/\psi\phi$.

[11] Uses $f_s/f_u = 0.267 \pm 0.021$ and $B(B^+ \to J/\psi K^+ \to \mu^+\mu^- K^+) = (6.0 \pm 0.2) \times 10^{-5}$.

[12] Uses B production ratio $f(\overline{b} \to B^+)/f(\overline{b} \to B_s^0) = 3.71 \pm 0.47$ and three normalization modes.

[13] Uses B production ratio $f(\overline{b} \to B^+)/f(\overline{b} \to B_s^0) = 3.55 \pm 0.47$ and $B(B^+ \to J/\psi K^+ \to \mu^+\mu^- K^+) = (6.01 \pm 0.21) \times 10^{-5}$.

[14] Uses B production ratio $f(\overline{b} \to B^+)/f(\overline{b} \to B_s^0) = 3.55 \pm 0.42$ and $B(B^+ \to J/\psi K^+ \to \mu^+\mu^- K^+) = (6.0 \pm 0.2) \times 10^{-5}$.

[15] Uses B production ratio $f(\overline{b} \to B^+)/f(\overline{b} \to B_s^0) = 3.86 \pm 0.59$, and the number of $B^+ \to J/\psi K^+$ decays.

$\Gamma(e^+e^-)/\Gamma_{total}$ Γ_{121}/Γ

Test for $\Delta B = 1$ weak neutral current.

VALUE	CL%	DOCUMENT ID		TECN	COMMENT
$< 2.8 \times 10^{-7}$	90	AALTONEN	09P	CDF	$p\overline{p}$ at 1.96 TeV
• • • We do not use the following data for averages, fits, limits, etc. • • •					
$< 5.4 \times 10^{-5}$	90	[1] ACCIARRI	97B	L3	$e^+e^- \to Z$

[1] ACCIARRI 97B assume PDG 96 production fractions for B^+, B^0, B_s, and Λ_b.

$\Gamma(\tau^+\tau^-)/\Gamma_{total}$ Γ_{122}/Γ

VALUE	CL%	DOCUMENT ID		TECN	COMMENT
$< 6.8 \times 10^{-3}$	95	[1] AAIJ	17AJ	LHCB	pp at 7, 8 TeV

[1] Assuming no contribution from $B^0 \to \tau^+\tau^-$.

$\Gamma(\mu^+\mu^-\mu^+\mu^-)/\Gamma_{total}$ Γ_{123}/Γ

VALUE	CL%	DOCUMENT ID		TECN	COMMENT
$< 2.5 \times 10^{-9}$	95	AAIJ	17N	LHCB	pp at 7, 8 TeV
• • • We do not use the following data for averages, fits, limits, etc. • • •					
$< 1.2 \times 10^{-8}$	90	[1] AAIJ	13AW	LHCB	Repl. by AAIJ 17N

[1] Also reports a limit of $< 1.6 \times 10^{-8}$ at 95% CL.

$\Gamma(SP, S \to \mu^+\mu^-, P \to \mu^+\mu^-)/\Gamma_{total}$ Γ_{124}/Γ

Here S and P are the hypothetical scalar and pseudoscalar particles with masses of 2.5 GeV/c^2 and 214.3 MeV/c^2, respectively.

VALUE	CL%	DOCUMENT ID		TECN	COMMENT
$< 2.2 \times 10^{-9}$	95	AAIJ	17N	LHCB	pp at 7, 8 TeV
• • • We do not use the following data for averages, fits, limits, etc. • • •					
$< 1.2 \times 10^{-8}$	90	[1] AAIJ	13AW	LHCB	Repl. by AAIJ 17N

[1] Also reports a limit of $< 1.6 \times 10^{-8}$ at 95% CL.

$\Gamma(\phi(1020)\mu^+\mu^-)/\Gamma_{total}$ Γ_{125}/Γ

Test for $\Delta B = 1$ weak neutral current.

VALUE (units 10^{-7})	CL%	DOCUMENT ID		TECN	COMMENT
• • • We do not use the following data for averages, fits, limits, etc. • • •					
< 32	90	[1] ABAZOV	06G	D0	$p\overline{p}$ at 1.96 TeV
$< 4.7 \times 10^2$	90	ACOSTA	02D	CDF	$p\overline{p}$ at 1.8 TeV

[1] Uses $B(B_s^0 \to J/\psi\phi) = 9.3 \times 10^{-4}$.

$\Gamma(\phi(1020)\mu^+\mu^-)/\Gamma(J/\psi(1S)\phi)$ Γ_{125}/Γ_{48}

VALUE (units 10^{-3})	CL%	DOCUMENT ID		TECN	COMMENT
0.76 ±0.09 OUR AVERAGE		Error includes scale factor of 1.9.			
$0.741^{+0.042}_{-0.040} \pm 0.029$		AAIJ	15AQ	LHCB	pp at 7, 8 TeV
1.13 ±0.19 ±0.07		AALTONEN	11AI	CDF	$p\overline{p}$ at 1.96 TeV
• • • We do not use the following data for averages, fits, limits, etc. • • •					
$0.674^{+0.061}_{-0.056} \pm 0.016$		[1] AAIJ	13X	LHCB	Repl. by AAIJ 15AQ
1.11 ±0.25 ±0.09		AALTONEN	11L	CDF	Repl. by AALTONEN 11AI
< 2.3	90	AALTONEN	09B	CDF	Repl. by AALTONEN 11L

[1] Replaced by AAIJ 15AQ.

$\Gamma(\pi^+\pi^-\mu^+\mu^-)/\Gamma_{total}$ Γ_{126}/Γ

VALUE (units 10^{-8})	DOCUMENT ID		TECN	COMMENT
8.4±1.6±0.3	[1] AAIJ	15S	LHCB	pp at 7, 8 TeV

[1] AAIJ 15S reports $(8.6 \pm 1.5 \pm 0.7 \pm 0.7) \times 10^{-8}$ from a measurement of $[\Gamma(B_s^0 \to \pi^+\pi^-\mu^+\mu^-)/\Gamma_{total}] / [B(B^0 \to J/\psi(1S) K^*(892)^0)]$ assuming $B(B^0 \to J/\psi(1S) K^*(892)^0) = (1.3 \pm 0.1) \times 10^{-3}$, which we rescale to our best value $B(B^0 \to J/\psi(1S) K^*(892)^0) = (1.27 \pm 0.05) \times 10^{-3}$. Our first error is their experiment's error and our second error is the systematic error from using our best value.

$\Gamma(\phi\nu\overline{\nu})/\Gamma_{total}$ Γ_{127}/Γ

Test for $\Delta B = 1$ weak neutral current.

VALUE	CL%	DOCUMENT ID		TECN	COMMENT
$< 5.4 \times 10^{-3}$	90	[1] ADAM	96D	DLPH	$e^+e^- \to Z$

[1] ADAM 96D assumes $f_{B^0} = f_{B^-} = 0.39$ and $f_{B_s} = 0.12$.

$\Gamma(e^\pm\mu^\mp)/\Gamma_{total}$ Γ_{128}/Γ

Test of lepton family number conservation.

VALUE	CL%	DOCUMENT ID		TECN	COMMENT
$< 1.1 \times 10^{-8}$	90	[1] AAIJ	13BM	LHCB	pp at 7 TeV
• • • We do not use the following data for averages, fits, limits, etc. • • •					
$< 2.0 \times 10^{-7}$	90	AALTONEN	09P	CDF	$p\overline{p}$ at 1.96 TeV
$< 6.1 \times 10^{-6}$	90	ABE	98V	CDF	Repl. by AALTONEN 09P
$< 4.1 \times 10^{-5}$	90	[2] ACCIARRI	97B	L3	$e^+e^- \to Z$

[1] Uses normalization mode $B(B^0 \to K^+\pi^-) = (19.4 \pm 0.6) \times 10^{-6}$ and B production ratio $f(\overline{b} \to B_s^0)/f(\overline{b} \to B_d^0) = 0.256 \pm 0.020$.

[2] ACCIARRI 97B assume PDG 96 production fractions for B^+, B^0, B_s, and Λ_b.

POLARIZATION IN B_s^0 DECAY

In decays involving two vector mesons, one can distinguish among the states in which meson polarizations are both longitudinal (L), or both are transverse and parallel ($\|$), or perpendicular ($\perp$) to each other with the parameters Γ_L/Γ, $\Gamma_\perp/\Gamma$, and the relative phases $\phi_\|$ and $\phi_\perp$. See the definitions in the note on "Polarization in B Decays" review in the B^0 Particle Listings.

Γ_L/Γ in $B_s^0 \to D_s^{*}\rho^+$

VALUE	DOCUMENT ID		TECN	COMMENT
$1.05^{+0.08}_{-0.10} \pm 0.03$	LOUVOT	10	BELL	$e^+e^- \to \Upsilon(5S)$

Γ_L/Γ in $B_s^0 \to J/\psi(1S)\phi$

VALUE	DOCUMENT ID		TECN	COMMENT
0.523 ±0.005 OUR AVERAGE	Error includes scale factor of 1.1.			
0.522 ±0.003 ±0.007	[1] AAD	16AP	ATLS	pp at 7, 8 TeV
0.510 ±0.005 ±0.011	KHACHATRY...16S		CMS	pp at 8 TeV
0.5241 ±0.0034 ±0.0067	AAIJ	15I	LHCB	pp at 7, 8 TeV
0.524 ±0.013 ±0.015	[2] AALTONEN	12D	CDF	$p\overline{p}$ at 1.96 TeV
$0.558^{+0.017}_{-0.019}$	[2,3] ABAZOV	12D	D0	$p\overline{p}$ at 1.96 TeV
0.61 ±0.14 ±0.02	[4] AFFOLDER	00N	CDF	$p\overline{p}$ at 1.8 TeV
0.56 ±0.21 $^{+0.02}_{-0.04}$	ABE	95Z	CDF	$p\overline{p}$ at 1.8 TeV
• • • We do not use the following data for averages, fits, limits, etc. • • •				
0.529 ±0.006 ±0.012	[1] AAD	14U	ATLS	Repl. by AAD 16AP
0.539 ±0.014 ±0.016	[2] AAD	12CV	ATLS	Repl. by AAD 14U
0.555 ±0.027 ±0.006	[5] ABAZOV	09E	D0	Repl. by ABAZOV 12D
0.531 ±0.020 ±0.007	[2] AALTONEN	08J	CDF	Repl. by AALTONEN 12D
0.62 ±0.06 ±0.01	ACOSTA	05	CDF	Repl. by AALTONEN 08J

[1] Measured using the flavor tagged, time-dependent angular analysis of $B_s^0 \to J/\psi\phi$ decays.

[2] Measured using the time-dependent angular analysis of $B_s^0 \to J/\psi\phi$ decays.

[3] The error includes both statistical and systematic uncertainties.

[4] AFFOLDER 00N measurements are based on 40 B_s^0 candidates obtained from a data sample of 89 pb^{-1}. The P-wave fraction is found to be $0.23 \pm 0.19 \pm 0.04$.

[5] Measured the angular and lifetime parameters for the time-dependent angular untagged decays $B_d^0 \to J/\psi K^{*0}$ and $B_s^0 \to J/\psi\phi$.

Γ_L/Γ in $B_s^0 \to D_s^{*+} D_s^{*-}$

VALUE	DOCUMENT ID		TECN	COMMENT
$0.06^{+0.18}_{-0.17} \pm 0.03$	ESEN	13	BELL	$e^+e^- \to \Upsilon(5S)$

$\Gamma_\|/\Gamma$ in $B_s^0 \to J/\psi(1S)\phi$

VALUE	DOCUMENT ID		TECN	COMMENT
0.228±0.007 OUR AVERAGE				
0.227±0.004±0.006	[1] AAD	16AP	ATLS	pp at 7, 8 TeV
0.231±0.014±0.015	[2] AALTONEN	12D	CDF	$p\overline{p}$ at 1.96 TeV
$0.231^{+0.024}_{-0.030}$	[2,3] ABAZOV	12D	D0	$p\overline{p}$ at 1.96 TeV
• • • We do not use the following data for averages, fits, limits, etc. • • •				
0.220±0.008±0.009	[1] AAD	14U	ATLS	Repl. by AAD 16AP
0.224±0.010±0.009	[2] AAD	12CV	ATLS	Repl. by AAD 14U
0.244±0.032±0.014	[4] ABAZOV	09E	D0	Repl. by ABAZOV 12D
0.230±0.029±0.011	[2] AALTONEN	08J	CDF	Repl. by AALTONEN 12D
0.260±0.084±0.013	ACOSTA	05	CDF	Repl. by AALTONEN 08J

[1] Measured using a tagged, time-dependent angular analysis of $B_s^0 \to J/\psi\phi$ decays.

[2] Measured using the time-dependent angular analysis of $B_s^0 \to J/\psi\phi$ decays.

[3] The error includes both statistical and systematic uncertainties.

[4] Measured the angular and lifetime parameters for the time-dependent angular untagged decays $B_d^0 \to J/\psi K^{*0}$ and $B_s^0 \to J/\psi\phi$.

$\Gamma_\perp/\Gamma$ in $B_s^0 \to J/\psi(1S)\phi$

VALUE	DOCUMENT ID		TECN	COMMENT
0.249 ±0.006 OUR AVERAGE				
0.243 ±0.008 ±0.012	KHACHATRY...16S		CMS	pp at 8 TeV
0.2504±0.0049±0.0036	AAIJ	15I	LHCB	pp at 7, 8 TeV

$\phi_\parallel$ in $B_s^0 \to J/\psi(1S)\phi$

VALUE (rad)	DOCUMENT ID		TECN	COMMENT
$3.19^{+0.08}_{-0.09}$ OUR AVERAGE				
3.15±0.10±0.05	AAD	16AP	ATLS	pp at 7, 8 TeV
$3.48^{+0.07}_{-0.09}$±0.68	KHACHATRY...16S		CMS	pp at 8 TeV
$3.26^{+0.10}_{-0.17}{}^{+0.06}_{-0.07}$	AAIJ	15I	LHCB	pp at 7, 8 TeV
3.15±0.22	[1] ABAZOV	12D	D0	$p\overline{p}$ at 1.96 TeV
• • • We do not use the following data for averages, fits, limits, etc. • • •				
$2.72^{+1.12}_{-0.27}$±0.26	ABAZOV	09E	D0	Repl. by ABAZOV 12D

[1] The error includes both statistical and systematic uncertainties.

$\phi_\perp$ in $B_s^0 \to J/\psi(1S)\phi$

VALUE (rad)	DOCUMENT ID		TECN	COMMENT
3.2 ±0.4 OUR AVERAGE Error includes scale factor of 2.8.				
4.15±0.32±0.16	[1] AAD	16AP	ATLS	pp at 7, 8 TeV
2.98±0.36±0.66	KHACHATRY...16S		CMS	pp at 8 TeV
$3.08^{+0.14}_{-0.15}$±0.06	AAIJ	15I	LHCB	pp at 7, 8 TeV
• • • We do not use the following data for averages, fits, limits, etc. • • •				
3.89±0.47±0.11	[1] AAD	14U	ATLS	Repl. by AAD 16AP

[1] Measured using a tagged, time-dependent angular analysis of $B_s^0 \to J/\psi\phi$ decays.

$\Gamma_\perp/\Gamma$ in $B_s^0 \to \psi(2S)\phi$

VALUE	DOCUMENT ID		TECN	COMMENT
$0.264^{+0.024}_{-0.023}$±0.002	[1] AAIJ	16AK	LHCB	pp at 7, 8 TeV

[1] Measured using time-dependent angular analysis of $B_s^0 \to \psi(2S)\phi$ decays.

$\phi_\parallel$ in $B_s^0 \to \psi(2S)\phi$

VALUE (rad)	DOCUMENT ID		TECN	COMMENT
$3.67^{+0.13}_{-0.18}$±0.03	[1] AAIJ	16AK	LHCB	pp at 7, 8 TeV

[1] Measured using time-dependent angular analysis of $B_s^0 \to \psi(2S)\phi$ decays.

$\phi_\perp$ in $B_s^0 \to \psi(2S)\phi$

VALUE (rad)	DOCUMENT ID		TECN	COMMENT
$3.29^{+0.43}_{-0.39}$±0.04	[1] AAIJ	16AK	LHCB	pp at 7, 8 TeV

[1] Measured using time-dependent angular analysis of $B_s^0 \to \psi(2S)\phi$ decays.

Γ_L/Γ for $B_s^0 \to J/\psi(1S)\overline{K}^*(892)^0$

Longitudinal polarization fraction, equals to f_L using notation of "Polarization in B decays" review.

VALUE	DOCUMENT ID		TECN	COMMENT
0.497±0.025±0.025	AAIJ	15AV	LHCB	pp at 7, 8 TeV
• • • We do not use the following data for averages, fits, limits, etc. • • •				
0.50 ±0.08 ±0.02	[1] AAIJ	12AP	LHCB	Repl. by AAIJ 15AV

[1] The non-resonant $K\pi$ background contributions are subtracted. Also reports an S-wave amplitude $|A_S|^2 = 0.07^{+0.15}_{-0.07}$.

$\Gamma_\parallel/\Gamma$ for $B_s^0 \to J/\psi(1S)\overline{K}^*(892)^0$

Parallel polarization fraction, equals to $1 - f_L - f_\perp$ using notation of "Polarization in B decays" review.

VALUE	DOCUMENT ID		TECN	COMMENT
0.179±0.027±0.013	AAIJ	15AV	LHCB	pp at 7, 8 TeV
• • • We do not use the following data for averages, fits, limits, etc. • • •				
0.19 $^{+0.10}_{-0.08}$ ±0.02	[1] AAIJ	12AP	LHCB	Repl. by AAIJ 15AV

[1] The non-resonant $K\pi$ background contributions are subtracted. Also reports an S-wave amplitude $|A_S|^2 = 0.07^{+0.15}_{-0.07}$.

$\Gamma_\parallel/\Gamma$ of $K^*(892)^0$ in $B_s^0 \to \psi(2S)\overline{K}^*(892)^0$

VALUE	DOCUMENT ID		TECN	COMMENT
0.524±0.056±0.029	AAIJ	15U	LHCB	pp at 7, 8 TeV

Γ_L/Γ in $B_s^0 \to \phi\phi$

VALUE	DOCUMENT ID		TECN	COMMENT
0.362±0.014 OUR AVERAGE				
0.364±0.012±0.009	AAIJ	14AE	LHCB	pp at 7, 8 TeV
0.348±0.041±0.021	AALTONEN	11AN	CDF	$p\overline{p}$ at 1.96 TeV
• • • We do not use the following data for averages, fits, limits, etc. • • •				
0.365±0.022±0.012	AAIJ	12P	LHCB	Repl. by AAIJ 14AE

$\Gamma_\perp/\Gamma$ in $B_s^0 \to \phi\phi$

VALUE	DOCUMENT ID		TECN	COMMENT
0.309±0.015 OUR AVERAGE Error includes scale factor of 1.1.				
0.305±0.013±0.005	AAIJ	14AE	LHCB	pp at 7, 8 TeV
0.365±0.044±0.027	AALTONEN	11AN	CDF	$p\overline{p}$ at 1.96 TeV
• • • We do not use the following data for averages, fits, limits, etc. • • •				
0.291±0.024±0.010	AAIJ	12P	LHCB	Repl. by AAIJ 14AE

$\phi_\parallel$ in $B_s^0 \to \phi\phi$

VALUE (rad)	DOCUMENT ID		TECN	COMMENT
2.55±0.11 OUR AVERAGE				
2.54±0.07±0.09	[1] AAIJ	14AE	LHCB	pp at 7, 8 TeV
$2.71^{+0.31}_{-0.36}$±0.22	[2] AALTONEN	11AN	CDF	$p\overline{p}$ at 1.96 TeV
• • • We do not use the following data for averages, fits, limits, etc. • • •				
2.57±0.15±0.06	[3] AAIJ	12P	LHCB	Repl. by AAIJ 14AE

[1] AAIJ 14AE reports measurement of $\phi_\perp$ and $\phi_\perp - \phi_\parallel$, which we convert into $\phi_\parallel$. Statistical uncertainty includes correlation between measured parameters, while systematic uncertainties are assumed uncorrelated.

[2] AALTONEN 11AN quotes $\cos\phi_\parallel = -0.91^{+0.15}_{-0.13} \pm 0.09$ which we convert to $\phi_\parallel$ taking the smaller solution.

[3] AAIJ 12P quotes $\cos\phi_\parallel = -0.844 \pm 0.068 \pm 0.029$ which we convert to $\phi_\parallel$, taking the smaller solution.

$\phi_\perp$ in $B_s^0 \to \phi\phi$

VALUE (rad)	DOCUMENT ID		TECN	COMMENT
2.67±0.23±0.07	AAIJ	14AE	LHCB	pp at 7, 8 TeV

Γ_L/Γ in $B_s^0 \to K^{*0}\overline{K}^{*0}$

VALUE	DOCUMENT ID		TECN	COMMENT
0.201±0.057±0.040	[1] AAIJ	15AF	LHCB	pp at 7 TeV
• • • We do not use the following data for averages, fits, limits, etc. • • •				
0.31 ±0.12 ±0.04	AAIJ	12F	LHCB	Repl. by AAIJ 15AF

[1] Measured in angular analysis, which takes into account S-wave contributions.

$\Gamma_\perp/\Gamma$ in $B_s^0 \to K^{*0}\overline{K}^{*0}$

VALUE	DOCUMENT ID		TECN	COMMENT
0.38±0.11±0.04	AAIJ	12F	LHCB	pp at 7 TeV

$\Gamma_\parallel/\Gamma$ in $B_s^0 \to K^*(892)^0\overline{K}^*(892)^0$

VALUE	DOCUMENT ID		TECN	COMMENT
0.215±0.046±0.015	AAIJ	15AF	LHCB	pp at 7 TeV

$\Phi_\parallel$ in $B_s^0 \to K^*(892)^0\overline{K}^*(892)^0$

VALUE	DOCUMENT ID		TECN	COMMENT
5.31±0.24±0.14	AAIJ	15AF	LHCB	pp at 7 TeV

Γ_L/Γ in $B_s^0 \to \phi\overline{K}^{*0}$

VALUE	DOCUMENT ID		TECN	COMMENT
0.51±0.15±0.07	AAIJ	13BW	LHCB	pp at 7 TeV

$\Gamma_\parallel/\Gamma$ in $B_s^0 \to \phi\overline{K}^{*0}$

VALUE	DOCUMENT ID		TECN	COMMENT
0.21±0.11±0.02	AAIJ	13BW	LHCB	pp at 7 TeV

$\phi_\parallel$ in $B_s^0 \to \phi\overline{K}^{*0}$

VALUE (rad)	DOCUMENT ID		TECN	COMMENT
1.75±0.53±0.29	[1] AAIJ	13BW	LHCB	pp at 7 TeV

[1] Measures $\cos(\phi_\parallel) = -0.18 \pm 0.52 \pm 0.29$, which we convert to $\phi_\parallel$ by taking the smaller solution.

$F_L(B_s^0 \to \phi\mu^+\mu^-)$ $(0.10 < q^2 < 2.00\ \text{GeV}^2/c^4)$

VALUE	DOCUMENT ID		TECN	COMMENT
$0.20^{+0.08}_{-0.09}$±0.02	AAIJ	15AQ	LHCB	pp at 7, 8 TeV
• • • We do not use the following data for averages, fits, limits, etc. • • •				
$0.37^{+0.19}_{-0.17}$±0.07	AAIJ	13X	LHCB	Repl. by AAIJ 15AQ

$F_L(B_s^0 \to \phi\mu^+\mu^-)$ $(2.00 < q^2 < 5.0\ \text{GeV}^2/c^4)$

VALUE	DOCUMENT ID		TECN	COMMENT
$0.68^{+0.16}_{-0.13}$±0.03	AAIJ	15AQ	LHCB	pp at 7, 8 TeV
• • • We do not use the following data for averages, fits, limits, etc. • • •				
$0.53^{+0.25}_{-0.23}$±0.10	[1] AAIJ	13X	LHCB	Repl. by AAIJ 15AQ

[1] Measured in $2.0 < q^2 < 4.3\ \text{GeV}^2/c^4$.

$F_L(B_s^0 \to \phi\mu^+\mu^-)$ $(5.0 < q^2 < 8.0\ \text{GeV}^2/c^4)$

VALUE	DOCUMENT ID		TECN	COMMENT
$0.54^{+0.10}_{-0.09}$±0.02	AAIJ	15AQ	LHCB	pp at 7, 8 TeV
• • • We do not use the following data for averages, fits, limits, etc. • • •				
$0.81^{+0.11}_{-0.13}$±0.05	[1] AAIJ	13X	LHCB	Repl. by AAIJ 15AQ

[1] Measured in $4.3 < q^2 < 8.68$ GeV$^2/c^4$.

$F_L(B_s^0 \to \phi\mu^+\mu^-)$ ($11.0 < q^2 < 12.5$ GeV$^2/c^4$)

VALUE	DOCUMENT ID		TECN	COMMENT
$0.29 \pm 0.11 \pm 0.04$	AAIJ	15AQ	LHCB	pp at 7, 8 TeV
• • • We do not use the following data for averages, fits, limits, etc. • • •				
$0.33^{+0.14}_{-0.12} \pm 0.06$	[1] AAIJ	13X	LHCB	Repl. by AAIJ 15AQ

[1] Measured in $10.09 < q^2 < 12.90$ GeV$^2/c^4$.

$F_L(B_s^0 \to \phi\mu^+\mu^-)$ ($15.0 < q^2 < 17.0$ GeV$^2/c^4$)

VALUE	DOCUMENT ID		TECN	COMMENT
$0.23^{+0.09}_{-0.08} \pm 0.02$	AAIJ	15AQ	LHCB	pp at 7, 8 TeV
• • • We do not use the following data for averages, fits, limits, etc. • • •				
$0.34^{+0.18}_{-0.17} \pm 0.07$	[1] AAIJ	13X	LHCB	Repl. by AAIJ 15AQ

[1] Measured in $14.18 < q^2 < 16$ GeV$^2/c^4$.

$F_L(B_s^0 \to \phi\mu^+\mu^-)$ ($17.0 < q^2 < 19.0$ GeV$^2/c^4$)

VALUE	DOCUMENT ID		TECN	COMMENT
$0.40^{+0.13}_{-0.15} \pm 0.02$	AAIJ	15AQ	LHCB	pp at 7, 8 TeV
• • • We do not use the following data for averages, fits, limits, etc. • • •				
$0.16^{+0.17}_{-0.10} \pm 0.07$	[1] AAIJ	13X	LHCB	Repl. by AAIJ 15AQ

[1] Measured in $16.0 < q^2 < 19.0$ GeV$^2/c^4$.

$F_L(B_s^0 \to \phi\mu^+\mu^-)$ ($1.00 < q^2 < 6.00$ GeV$^2/c^4$)

VALUE	DOCUMENT ID		TECN	COMMENT
$0.63^{+0.09}_{-0.09} \pm 0.03$	AAIJ	15AQ	LHCB	pp at 7, 8 TeV
• • • We do not use the following data for averages, fits, limits, etc. • • •				
$0.56^{+0.17}_{-0.16} \pm 0.09$	AAIJ	13X	LHCB	Repl. by AAIJ 15AQ

B_s^0-$\overline{B}_s^0$ MIXING

For a discussion of B_s^0-$\overline{B}_s^0$ mixing see the note on "B^0-$\overline{B}^0$ Mixing" in the B^0 Particle Listings above.

χ_s is a measure of the time-integrated B_s^0-$\overline{B}_s^0$ mixing probability that produced $B_s^0(\overline{B}_s^0)$ decays as a $\overline{B}_s^0(B_s^0)$. Mixing violates $\Delta B \neq 2$ rule.

$$\chi_s = \frac{x_s^2}{2(1+x_s^2)}$$

$$x_s = \frac{\Delta m_{B_s^0}}{\Gamma_{B_s^0}} = (m_{B_{sH}^0} - m_{B_{sL}^0})\,\tau_{B_s^0},$$

where H, L stand for heavy and light states of two B_s^0 CP eigenstates and $\tau_{B_s^0} = \frac{1}{0.5(\Gamma_{B_{sH}^0} + \Gamma_{B_{sL}^0})}$.

$\Delta m_{B_s^0} = m_{B_{sH}^0} - m_{B_{sL}^0}$

$\Delta m_{B_s^0}$ is a measure of 2π times the B_s^0-$\overline{B}_s^0$ oscillation frequency in time-dependent mixing experiments.

"OUR EVALUATION" is provided by the Heavy Flavor Averaging Group (HFLAV) by taking into account correlations between measurements.

VALUE ($10^{12}\ \hbar\,s^{-1}$)	CL%	DOCUMENT ID		TECN	COMMENT
17.757 ± 0.021 OUR EVALUATION					
17.756 ± 0.021 OUR AVERAGE					
$17.711^{+0.055}_{-0.057} \pm 0.011$		[1] AAIJ	15I	LHCB	pp at 7, 8 TeV
$17.768 \pm 0.023 \pm 0.006$		[2] AAIJ	13BI	LHCB	pp at 7 TeV
$17.93 \pm 0.22 \pm 0.15$		[3] AAIJ	13CF	LHCB	pp at 7 TeV
$17.63 \pm 0.11 \pm 0.02$		[4] AAIJ	12I	LHCB	pp at 7 TeV
$17.77 \pm 0.10 \pm 0.07$		[5] ABULENCIA,A	06G	CDF	$p\overline{p}$ at 1.96 TeV
• • • We do not use the following data for averages, fits, limits, etc. • • •					
17–21	90	[6] ABAZOV	06B	D0	$p\overline{p}$ at 1.96 TeV
$17.31^{+0.33}_{-0.18} \pm 0.07$		[7] ABULENCIA	06Q	CDF	Repl. by ABULENCIA,A 06G
> 8.0	95	[8] ABDALLAH	04J	DLPH	$e^+e^- \to Z^0$
> 4.9	95	[9] ABDALLAH	04J	DLPH	$e^+e^- \to Z^0$
> 8.5	95	[10] ABDALLAH	04J	DLPH	$e^+e^- \to Z^0$
> 5.0	95	[11] ABDALLAH	03B	DLPH	$e^+e^- \to Z$
>10.3	95	[12] ABE	03	SLD	$e^+e^- \to Z$
>10.9	95	[13] HEISTER	03E	ALEP	$e^+e^- \to Z$
> 5.3	95	[14] ABE	02V	SLD	$e^+e^- \to Z$
> 1.0	95	[15] ABBIENDI	01D	OPAL	$e^+e^- \to Z$
> 7.4	95	[16] ABREU	00Y	DLPH	Repl. by ABDALLAH 04J
> 4.0	95	[17] ABREU,P	00G	DLPH	$e^+e^- \to Z$
> 5.2	95	[18] ABBIENDI	99S	OPAL	$e^+e^- \to Z$
<96	95	[19] ABE	99D	CDF	$p\overline{p}$ at 1.8 TeV
> 5.8	95	[20] ABE	99J	CDF	$p\overline{p}$ at 1.8 TeV
> 9.6	95	[21] BARATE	99J	ALEP	$e^+e^- \to Z$
> 7.9	95	[22] BARATE	98C	ALEP	Repl. by BARATE 99J
> 3.1	95	[23] ACKERSTAFF	97U	OPAL	Repl. by ABBIENDI 99S
> 2.2	95	[24] ACKERSTAFF	97V	OPAL	Repl. by ABBIENDI 99S
> 6.5	95	[25] ADAM	97	DLPH	Repl. by ABREU 00Y
> 6.6	95	[26] BUSKULIC	96M	ALEP	Repl. by BARATE 98C
> 2.2	95	[24] AKERS	95J	OPAL	Sup. by ACKERSTAFF 97V
> 5.7	95	[27] BUSKULIC	95J	ALEP	$e^+e^- \to Z$
> 1.8	95	[24] BUSKULIC	94B	ALEP	$e^+e^- \to Z$

[1] Measured using time-dependent angular analysis of $B_s^0 \to J/\psi K^+K^-$ decays.
[2] Measured using $B_s^0 \to D_s^-\pi^+$ decays.
[3] Measured using $B_s^0 \to D_s^-\mu^+\nu_\mu X$ decays.
[4] Measured using $B_s^0 \to D_s^-\pi^+$ and $D_s^-\pi^+\pi^-\pi^+$ decays.
[5] Significance of oscillation signal is 5.4 σ. Also reports $|V_{td}\ /\ V_{ts}| = 0.2060 \pm 0.0007^{+0.0081}_{-0.0060}$.
[6] A likelihood scan over the oscillation frequency, Δm_s, gives a most probable value of 19 ps^{-1} and a range of $17 < \Delta m_s < 21$ (ps^{-1}) at 90% C.L. assuming Gaussian uncertainties. Also excludes $\Delta m_s < 14.8$ ps^{-1} at 95% C.L
[7] Significance of oscillation signal is 0.2%. Also reported the value $|V_{td}\ /\ V_{ts}| = 0.208^{+0.001+0.008}_{-0.002-0.006}$.
[8] Uses leptons emitted with large momentum transverse to a jet and improved techniques for vertexing and flavor-tagging.
[9] Updates of D_s-lepton analysis.
[10] Combined results from all Delphi analyses.
[11] Events with a high transverse momentum lepton were removed and an inclusively reconstructed vertex was required.
[12] ABE 03 uses the novel "charge dipole" technique to reconstruct separate secondary and tertiary vertices originating from the $B \to D$ decay chain. The analysis excludes $\Delta m_s < 4.9$ ps^{-1} and $7.9 < \Delta m_s < 10.3$ ps^{-1}.
[13] Three analyses based on complementary event selections: (1) fully-reconstructed hadronic decays; (2) semileptonic decays with D_s exclusively reconstructed; (3) inclusive semileptonic decays.
[14] ABE 02V uses exclusively reconstructed D_s^- mesons and excludes $\Delta m_s < 1.4$ ps^{-1} and $2.4 < \Delta m_s < 5.3$ ps^{-1} at 95%CL.
[15] Uses fully or partially reconstructed $D_s\ell$ vertices and a mixing tag as a flavor tagging.
[16] Replaced by ABDALLAH 04A. Uses $D_s^-\ell^+$, and $\phi\ell^+$ vertices, and a multi-variable discriminant as a flavor tagging.
[17] Uses inclusive D_s vertices and fully reconstructed B_s decays and a multi-variable discriminant as a flavor tagging.
[18] Uses ℓ-$Q_{\rm hem}$ and ℓ-ℓ.
[19] ABE 99D assumes $\tau_{B_s^0} = 1.55 \pm 0.05$ ps and $\Delta\Gamma/\Delta m = (5.6 \pm 2.6) \times 10^{-3}$.
[20] ABE 99J uses ϕ ℓ-ℓ correlation.
[21] BARATE 99J uses combination of an inclusive lepton and D_s^--based analyses.
[22] BARATE 98C combines results from $D_s h$-$\ell/Q_{\rm hem}$, $D_s h$-K in the same side, $D_s\ell$-$\ell/Q_{\rm hem}$ and $D_s\ell$-K in the same side.
[23] Uses ℓ-$Q_{\rm hem}$.
[24] Uses ℓ-ℓ.
[25] ADAM 97 combines results from $D_s\ell$-$Q_{\rm hem}$, ℓ-$Q_{\rm hem}$, and ℓ-ℓ.
[26] BUSKULIC 96M uses D_s lepton correlations and lepton, kaon, and jet charge tags.
[27] BUSKULIC 95J uses ℓ-$Q_{\rm hem}$. They find $\Delta m_s > 5.6$ [> 6.1] for f_s=10% [12%]. We interpolate to our central value f_s=10.5%.

$x_s = \Delta m_{B_s^0}/\Gamma_{B_s^0}$

This is derived by the Heavy Flavor Averaging Group (HFLAV) from the results on $\Delta m_{B_s^0}$ and "OUR EVALUATION" of the B_s^0 mean lifetime.

VALUE	DOCUMENT ID
26.79 ± 0.08 OUR EVALUATION	

χ_s

This is a B_s^0-$\overline{B}_s^0$ integrated mixing parameter derived from x_s above and OUR EVALUATION of $\Delta\Gamma_{B_s^0}/\Gamma_{B_s^0}$.

VALUE	DOCUMENT ID
0.499307 ± 0.000004 OUR EVALUATION	

CP VIOLATION PARAMETERS in B_s^0

$\mathrm{Re}(\epsilon_{B_s^0})\ /\ (1 + |\epsilon_{B_s^0}|^2)$

CP impurity in B_s^0 system.

"OUR EVALUATION" is an average obtained by the Heavy Flavor Averaging Group (HFLAV) and described at http://www.slac.stanford.edu/xorg/hflav/. It is the result of a fit to B_d and B_s CP asymmetries, which includes the B_s measurements listed below and the B_d measurements listed in the B_d section, and takes into account correlations between those measurements.

VALUE (units 10^{-3})	DOCUMENT ID		TECN	COMMENT
-0.15 ± 0.70 OUR EVALUATION				
0.0 ± 1.1 OUR AVERAGE Error includes scale factor of 1.6. See the ideogram below.				
$0.98 \pm 0.65 \pm 0.5$	[1] AAIJ	16G	LHCB	pp at 7, 8 TeV
-2.15 ± 1.85	[2] ABAZOV	14	D0	$p\overline{p}$ at 1.96 TeV
$-2.8 \pm 1.9 \pm 0.4$	[3] ABAZOV	13	D0	$p\overline{p}$ at 1.96 TeV

• • • We do not use the following data for averages, fits, limits, etc. • • •

−0.15 ±1.25 ±0.90	[4] AAIJ	14D	LHCB	Repl. by AAIJ 16G	
−4.5 ±2.7	[5] ABAZOV	11U	D0	Repl. by ABAZOV 14	
−0.4 ±2.3 ±0.4	[6] ABAZOV	10E	D0	Repl. by ABAZOV 13	
−3.6 ±1.9	[7] ABAZOV	10H	D0	Repl. by ABAZOV 11U	
6.1 ±4.8 ±0.9	[8] ABAZOV	07A	D0	Repl. by ABAZOV 10E	

[1] AAIJ 16G reports a measurement of time-integrated flavor-specific asymmetry in $B_s^0 \to \mu^+ D_s^- X$ decays, $A_{SL}^s = (0.39 \pm 0.26 \pm 0.20)\%$, which is approximately equal to $4 \times \mathrm{Re}(\epsilon_{B_s^0}) / (1 + |\epsilon_{B_s^0}|^2)$.

[2] ABAZOV 14 uses the dimuon charge asymmetry with different impact parameters from which it reports $A_{SL}^s = (-0.86 \pm 0.74) \times 10^{-2}$.

[3] ABAZOV 13 reports a measurement of time-integrated flavor-specific asymmetry in mixed semileptonic $B_s^0 \to \mu^+ D_s^- X$ decays $A_{SL}^s = (-1.12 \pm 0.74 \pm 0.17)\%$ which is approximately equal to $4 \times \mathrm{Re}(\epsilon_{B_s^0}) / (1 + |\epsilon_{B_s^0}|^2)$.

[4] AAIJ 14D reports a measurement of time-integrated flavor-specific asymmetry in $B_s^0 \to \mu^+ D_s^- X$ decays, $A_{SL}^s = (-0.06 \pm 0.50 \pm 0.36)\%$, which is approximately equal to $4 \times \mathrm{Re}(\epsilon_{B_s^0}) / (1 + |\epsilon_{B_s^0}|^2)$.

[5] ABAZOV 11U uses the dimuon charge asymmetry with different impact parameters from which it reports $A_{SL}^s = (-18.1 \pm 10.6) \times 10^{-3}$.

[6] ABAZOV 10E reports a measurement of flavor-specific asymmetry in $B_{(s)}^0 \to \mu^+ D_{(s)}^{*-} X$ decays with a decay-time analysis including initial-state flavor tagging, $A_{SL}^s = (-1.7 \pm 9.1^{+1.4}_{-1.5}) \times 10^{-3}$ which is approximately equal to $4 \times \mathrm{Re}(\epsilon_{B_s^0}) / (1 + |\epsilon_{B_s^0}|^2)$.

[7] ABAZOV 10H reports a measurement of like-sign dimuon charge asymmetry of $A_{SL}^s = (-9.57 \pm 2.51 \pm 1.46) \times 10^{-3}$ in semileptonic b-hadron decays. Using the measured production ratio of B_d^0 and B_s^0, and the asymmetry of B_d^0 $A_{SL}^s = (-4.7 \pm 4.6) \times 10^{-3}$ measured from B-factories, they obtain the asymmetry for B_s^0.

[8] The first direct measurement of the time integrated flavor untagged charge asymmetry in semileptonic B_s^0 decays is reported as $2 \times A_{SL}^s(\text{untagged}) = A_{SL}^s = (2.45 \pm 1.93 \pm 0.35) \times 10^{-2}$.

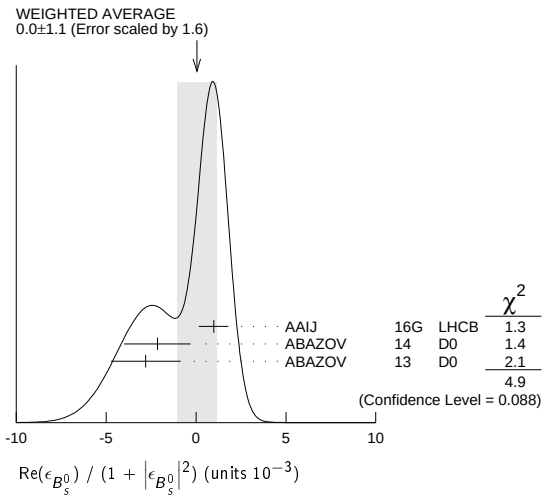

$C_{KK}(B_s^0 \to K^+K^-)$

VALUE	DOCUMENT ID	TECN	COMMENT
0.14±0.11±0.03	AAIJ 13BO	LHCB	pp at 7 TeV

$S_{KK}(B_s^0 \to K^+K^-)$

VALUE	DOCUMENT ID	TECN	COMMENT
0.30±0.12±0.04	AAIJ 13BO	LHCB	pp at 7 TeV

$r_B(B_s^0 \to D_s^\mp K^\pm)$

r_B and δ_B are the amplitude ratio and relative strong phase between the amplitudes of $A(B_s^0 \to D_s^+ K^-)$ and $A(B_s^0 \to D_s^- K^+)$,

VALUE	DOCUMENT ID	TECN	COMMENT
$\mathbf{0.53^{+0.17}_{-0.16}}$	[1] AAIJ 14BF	LHCB	pp at 7 TeV

[1] Measured in $B_s^0 \to D_s^\mp K^\pm$ decays, constraining $-2\beta_s$ by the measurement of $\phi_s = 0.01 \pm 0.07 \pm 0.0$ from AAIJ 13AR. At 68% CL.

$\delta_B(B_s^0 \to D_s^\pm K^\mp)$

VALUE (°)	DOCUMENT ID	TECN	COMMENT
$\mathbf{3^{+19}_{-20}}$	[1] AAIJ 14BF	LHCB	pp at 7 TeV

[1] Measured in $B_s^0 \to D_s^\mp K^\pm$ decays, constraining $-2\beta_s$ by the measurement of $\phi_s = 0.01 \pm 0.07 \pm 0.0$ from AAIJ 13AR. The value is modulo 180° at 68% CL.

CP Violation phase β_s

$-2\beta_s$ is the weak phase difference between B_s^0 mixing amplitude and the $B_s^0 \to J/\psi\phi$ decay amplitude driven by the $b \to c\overline{c}s$ transition (such as $B_s \to J/\psi\phi$, $J/\psi K^+K^-$, $J/\psi\pi^+\pi^-$, and $D_s^+ D_s^-$). The Standard Model value of β_s is $\arg(-\frac{V_{ts}V_{tb}^*}{V_{cs}V_{cb}^*})$ if penguin contributions are neglected.

"OUR EVALUATION" is an average using rescaled values of the data listed below. The average and rescaling were performed by the Heavy Flavor Averaging Group (HFLAV) and are described at http://www.slac.stanford.edu/xorg/hflav/. The averaging/scaling procedure takes into account correlation between the measurements.

VALUE (10^{-2} rad)	DOCUMENT ID	TECN	COMMENT
1.1 ± 1.6 OUR EVALUATION			
1.8 ± 1.7 OUR AVERAGE			
11.9 ±10.7 ±3.4	[1] AAIJ 17V	LHCB	pp at 7, 8 TeV
4.5 ± 3.9 ±2.1	[2] AAD 16AP	ATLS	pp at 7, 8 TeV
$-11.5\ ^{+14}_{-14.5}$ ±1	[3] AAIJ 16AK	LHCB	pp at 7, 8 TeV
3.75± 4.85±1.55	[4] KHACHATRY...16S	CMS	pp at 8 TeV
2.9 ± 2.5 ±0.3	[5] AAIJ 15I	LHCB	pp at 7, 8 TeV
− 1 ± 9 ±1	[6] AAIJ 14AY	LHCB	pp at 7, 8 TeV
− 3.5 ± 3.4 ±0.4	[7] AAIJ 14S	LHCB	pp at 7, 8 TeV
	[8] AALTONEN 12AJ	CDF	$p\overline{p}$ at 1.96 TeV
$28\ ^{+18}_{-19}$	[9] ABAZOV 12D	D0	$p\overline{p}$ at 1.96 TeV

• • • We do not use the following data for averages, fits, limits, etc. • • •

$6\ ^{+\ 8}_{-\ 7}$	[10,11] AAIJ 15K	LHCB	pp at 7, 8 TeV	
− 6 ±13 ±3	[12] AAD 14U	ATLS	Repl. by AAD 16AP	
−17 ±15 ±3	[13] AAIJ 14AE	LHCB	pp at 7, 8 TeV	
− 0.5 ± 3.5 ±0.5	[14] AAIJ 13AR	LHCB	Repl. by AAIJ 15I	
	[15] AAIJ 13AY	LHCB	pp at 7 TeV	
−11.0 ±20.5 ±5.0	[16] AAD 12CV	ATLS	Repl. by AAD 14U	
22 ±22 ±1	[17] AAIJ 12B	LHCB	Repl. by AAIJ 12Q	
− 8 ± 9 ±3	[18] AAIJ 12D	LHCB	Repl. by AAIJ 13AR	
$0.95\pm\ 8.70^{+0.15}_{-\ 8.65-0.20}$	[19] AAIJ 12Q	LHCB	Repl. by AAIJ 13AR	
	[20] AALTONEN 12D	CDF	Repl. by AALTONEN 12AJ	
	[21] AALTONEN 08G	CDF	Repl. by AALTONEN 12D	
$28\ ^{+12}_{-15}\ ^{+4}_{-1}$	[9,22] ABAZOV 08AM	D0	Repl. by ABAZOV 12D	
$39.5\ \pm 28.0\ ^{+0.5}_{-7.0}$	[23,24] ABAZOV 07	D0	Repl. by ABAZOV 07N	
$35\ ^{+20}_{-24}$	[24,25] ABAZOV 07N	D0	Repl. by ABAZOV 08AM	

[1] Measured using time-dependent angular analysis of $B_s^0 \to J/\psi K^+K^-$ in the region $m(KK) > 1.05$ GeV.

[2] AAD 16AP reports $\phi_s = -2\,\beta_s = -0.090 \pm 0.078 \pm 0.041$ rad. that was measured using a time-dependent angular analysis of $B_s^0 \to J/\psi\phi$ decays.

[3] AAIJ 16AK reports $\phi_s = -2\,\beta_s = 0.23^{+0.29}_{-0.28} \pm 0.02$ rad. that was measured using a time-dependent angular analysis of $B_s^0 \to \psi(2S)\,\phi$ decays.

[4] KHACHATRYAN 16S reports $\phi_s = -2\,\beta_s = -0.075 \pm 0.097 \pm 0.031$ rad. that was measured using a time-dependent angular analysis of $B_s^0 \to J/\psi\phi$ decays.

[5] AAIJ 15I reports $\phi_s = -2\,\beta_s = -0.058 \pm 0.049 \pm 0.006$ rad. that was measured using a time-dependent angular analysis of $B_s^0 \to J/\psi K^+K^-$ decays. It also combines this result with that of AAIJ 14S and quotes $\phi_s = -2\,\beta_s = -0.010 \pm 0.039$ rad.

[6] AAIJ 14AY reports $\phi_s = -2\,\beta_s = 0.02 \pm 0.17 \pm 0.02$ rad. in a time-dependent fit to $B_s^0 \to D_s^+ D_s^-$, while allowing *CP* violation in decay.

[7] AAIJ 14S reports $\phi_s = -2\,\beta_s = 0.070 \pm 0.068 \pm 0.008$ rad. and $|\lambda| = 0.89 \pm 0.05 \pm 0.01$, when direct *CP* violation is allowed. Measured using a time-dependent fit to $B_s^0 \to J/\psi\pi^+\pi^-$ decays.

[8] AALTONEN 12AJ reports $-\pi/2 < \beta_s < -1.51$ or $-0.06 < \beta_s < 0.30$, or $1.26 < \beta_s < \pi/2$ rad. at 68% CL. Measured using the time-dependent angular analysis of $B_s^0 \to J/\psi\phi$ decays.

[9] ABAZOV 12D reports $\phi_s = -2\,\beta_s = -0.55^{+0.38}_{-0.36}$ rad. that was measured using a time-dependent angular analysis of $B_s^0 \to J/\psi\phi$ decays. A single error includes both statistical and systematic uncertainties.

[10] AAIJ 15K reports $-2\beta_s = -0.12^{+0.14}_{-0.16}$ rad. The value was obtained by measuring time-dependent *CP* asymmetry in $B_s^0 \to K^+K^-$ and using a U-spin relation between $B_s^0 \to K^+K^-$ and $B^0 \to \pi^+\pi^-$.

[11] Results are also presented using additional inputs on $B^0 \to \pi^0\pi^0$ and $B^+ \to \pi^+\pi^0$ decays from other experiments and isospin symmetry assumptions. The dependence of the results on the maximum allowed amount of U-spin breaking up to 50% is also included.

[12] AAD 14U reports $\phi_s = -2\,\beta_s = 0.12 \pm 0.25 \pm 0.05$ rad. that was measured using a time-dependent angular analysis of $B_s^0 \to J/\psi\phi$ decays.

[13] Measured in $B_s^0 \to \phi\phi$ decays. This is a $b \to s\overline{s}s$ transition with a decay amplitude phase different from that of $b \to c\overline{c}s$ transition.

[14] AAIJ 13AR reports $\phi_s = -2\beta_s = 0.01 \pm 0.07 \pm 0.01$ rad. obtained from combined fit to $B_s^0 \to J/\psi K^+K^-$ and $B_s^0 \to J/\psi\pi^+\pi^-$ data sets. Also reports separate results of $\phi_s = 0.07 \pm 0.09 \pm 0.01$ rad. from $B_s^0 \to J/\psi K^+K^-$ decays and $\phi_s = -0.14^{+0.17}_{-0.16} \pm 0.01$ rad. from $B_s^0 \to J/\psi\pi^+\pi^-$ decays.

[15] AAIJ 13AY uses $B_s^0 \to \phi\phi$ mode, and reports the 68% CL interval of $\phi_s = -2\,\beta_s$ as $[-2.46, -0.76]$ rad.

Meson Particle Listings

B_s^0

[16] AAD 12CV reports $\phi_s = -2\,\beta_s = 0.22 \pm 0.41 \pm 0.10$ rad. that was measured using a time-dependent angular analysis of $B_s^0 \to J/\psi\phi$ decays.

[17] Reports $\phi_s = -2\,\beta_s = -0.44 \pm 0.44 \pm 0.02$ rad. that was measured using a time-dependent fit to $B_s^0 \to J/\psi f_0(980)$ decays.

[18] Reports $\phi_s = -2\,\beta_s = 0.15 \pm 0.18 \pm 0.06$ rad. that was measured using a time-dependent angular analysis of $B_s^0 \to J/\psi\phi$ decays.

[19] Reports $\phi_s = -2\,\beta_s = -0.019^{+0.173}_{-0.174} \pm 0.004_{-0.003}$ rad. which was measured using a time-dependent fit to $B_s^0 \to J/\psi\pi^+\pi^-$ decays, with the $\pi^+\pi^-$ mass within 775–1550 MeV. Searches for, but finds no evidence, for direct CP violation in $B_s^0 \to J/\psi\pi\pi$ decays.

[20] Reports $0.02 < \phi_s < 0.52$ or $1.08 < \phi_s < 1.55$ rad. at 68% C.L. confidence regions in the two-dimensional space of ϕ_s and $\Delta\Gamma_{B_s^0}$ from $B_s^0 \to J/\psi\phi$ decays.

[21] Reports $0.32 < 2\beta_s < 2.82$ rad. at 68% C.L. and confidence regions in the two-dimensional space of $2\beta_s$ and $\Delta\Gamma$ from the first measurement of $B_s^0 \to J/\psi\phi$ decays using flavor tagging. The probability of a deviation from SM prediction as large as the level of observed data is 15%.

[22] Reports $\phi_s = -2\,\beta_s$ and obtains 90% CL interval $-0.03 < \beta_s < 0.60$ rad.

[23] The first direct measurement of the CP-violating mixing phase is reported from the time-dependent analysis of flavor untagged $B_s^0 \to J/\psi\phi$ decays.

[24] Reports ϕ_s which equals to $-2\beta_s$.

[25] Combines D0 collaboration measurements of time-dependent angular distributions in $B_s^0 \to J/\psi\phi$ and charge asymmetry in semileptonic decays. There is a 4-fold ambiguity in the solution.

$|\lambda|$ ($B_s^0 \to J/\psi(1S)\phi$)

VALUE	DOCUMENT ID		TECN	COMMENT
0.964±0.019±0.007	AAIJ	15I	LHCB	pp at 7, 8 TeV

$|\lambda|$

VALUE	DOCUMENT ID		TECN	COMMENT
1.001±0.017 OUR AVERAGE				
0.994±0.018±0.006	[1] AAIJ	17V	LHCB	pp at 7, 8 TeV
$1.045^{+0.069}_{-0.050}\pm0.007$	[2] AAIJ	16AK	LHCB	pp at 7, 8 TeV
1.04 ±0.07 ±0.03	[3] AAIJ	14AE	LHCB	pp at 7, 8 TeV
$0.91\ ^{+0.18}_{-0.15}$ ±0.02	[4] AAIJ	14AY	LHCB	pp at 7, 8 TeV

[1] Measured using time-dependent angular analysis of $B_s^0 \to J/\psi K^+K^-$ in the region $m(KK) > 1.05$ GeV.

[2] Measured using time-dependent angular analysis of $B_s^0 \to \psi(2S)\phi$ decays.

[3] Measured in $B_s^0 \to \phi\phi$ decays.

[4] Measured in $B_s^0 \to D_s^+ D_s^-$ decays.

A, CP violation parameter

$A = -2\,\mathrm{Re}(\lambda) / (1 + |\lambda|^2)$

VALUE	DOCUMENT ID		TECN	COMMENT
$\mathbf{0.49^{+0.77}_{-0.65}\pm0.06}$	[1] AAIJ	15AL	LHCB	pp at 7, 8 TeV

[1] Measured in $B_s^0 \to J/\psi K_S^0$ decays.

C, CP violation parameter

$C = (1 - |\lambda|^2) / (1 + |\lambda|^2)$

VALUE	DOCUMENT ID		TECN	COMMENT
−0.28±0.41±0.08	[1] AAIJ	15AL	LHCB	pp at 7, 8 TeV

[1] Measured in $B_s^0 \to J/\psi K_S^0$ decays.

S, CP violation parameter

$S = -2\,\mathrm{Im}(\lambda) / (1 + |\lambda|^2)$

VALUE	DOCUMENT ID		TECN	COMMENT
−0.08±0.40±0.08	[1] AAIJ	15AL	LHCB	pp at 7, 8 TeV

[1] Measured in $B_s^0 \to J/\psi K_S^0$ decays.

$A_{CP}^{L}(B_s \to J/\psi\overline{K}^*(892)^0)$

VALUE	DOCUMENT ID		TECN	COMMENT
−0.048±0.057±0.020	AAIJ	15AV	LHCB	pp at 7, 8 TeV

$A_{CP}^{\parallel}(B_s \to J/\psi\overline{K}^*(892)^0)$

VALUE	DOCUMENT ID		TECN	COMMENT
0.171±0.152±0.028	AAIJ	15AV	LHCB	pp at 7, 8 TeV

$A_{CP}^{\perp}(B_s \to J/\psi\overline{K}^*(892)^0)$

VALUE	DOCUMENT ID		TECN	COMMENT
−0.049±0.096±0.025	AAIJ	15AV	LHCB	pp at 7, 8 TeV

$A_{CP}(B_s \to \pi^+K^-)$

A_{CP} is defined as

$$\frac{B(\overline{B}_s^0 \to f) - B(B_s^0 \to \overline{f})}{B(\overline{B}_s^0 \to f) + B(B_s^0 \to \overline{f})},$$

the CP-violation asymmetry of exclusive B_s^0 and $\overline{B}_s^0$ decay.

VALUE	DOCUMENT ID		TECN	COMMENT
0.26±0.04 OUR AVERAGE				
0.22±0.07±0.02	AALTONEN	14P	CDF	$p\overline{p}$ at 1.96 TeV
0.27±0.04±0.01	AAIJ	13AX	LHCB	pp at 7 TeV

• • • We do not use the following data for averages, fits, limits, etc. • • •

0.27±0.08±0.02	AAIJ	12V	LHCB	Repl. by AAIJ 13AX
0.39±0.15±0.08	AALTONEN	11N	CDF	Repl. by AALTONEN 14P

$A_{CP}(B_s^0 \to [K^+K^-]_D\overline{K}^*(892)^0)$

VALUE	DOCUMENT ID		TECN	COMMENT
−0.04±0.07±0.02	AAIJ	14BN	LHCB	pp at 7, 8 TeV

• • • We do not use the following data for averages, fits, limits, etc. • • •

0.04±0.16±0.01	AAIJ	13L	LHCB	Repl. by AAIJ 14BN

$A_{CP}(B_s^0 \to [\pi^+K^-]_D K^*(892)^0)$

VALUE	DOCUMENT ID		TECN	COMMENT
−0.01±0.03±0.02	AAIJ	14BN	LHCB	pp at 7, 8 TeV

$A_{CP}(B_s^0 \to [\pi^+\pi^-]_D K^*(892)^0)$

VALUE	DOCUMENT ID		TECN	COMMENT
0.06±0.13±0.02	AAIJ	14BN	LHCB	pp at 7, 8 TeV

$A^{\Delta}(B_s \to \phi\gamma)$

$A^{\Delta}(B_s \to \phi\gamma)$ is the multiplicative coefficient of the $\sinh(\Delta\Gamma t/2)$ term in the $B_s \to \phi\gamma$ decay rate time dependence.

VALUE	DOCUMENT ID		TECN	COMMENT
$\mathbf{-0.98^{+0.46}_{-0.52}\pm0.23_{-0.20}}$	[1] AAIJ	17B	LHCB	pp at 7, 8 TeV

[1] Measured in time dependent analysis without initial flavor tagging.

CPT VIOLATION PARAMETERS

In the B_s^0 mixing, propagating mass eigenstates can be written as

$$|B_{sL}\rangle \propto p\sqrt{1-\xi}\,|B_s^0\rangle + q\sqrt{1+\xi}\,|\overline{B}_s^0\rangle$$
$$|B_{sH}\rangle \propto p\sqrt{1+\xi}\,|B_s^0\rangle - q\sqrt{1-\xi}\,|\overline{B}_s^0\rangle$$

where parameter ξ controls CPT violation. If ξ is zero, then CPT is conserved. The parameter ξ can be written as

$$\xi = \frac{2(M_{11}-M_{22}) - i(\Gamma_{11}-\Gamma_{22})}{-2\Delta m_s + i\Delta\Gamma_s} \approx \frac{-2\beta^\mu \Delta a_\mu}{2\Delta m_s - i\Delta\Gamma_s},$$

where M_{ii}, Γ_{ii}, Δm_s, and $\Delta\Gamma_s$ are parameters of Hamiltonian governing B_s oscillations, β^μ is the B_s^0 meson velocity and Δa_μ characterizes Lorentz-invariance violation.

$\Delta a_\perp$

VALUE (10^{-12} GeV)	CL%	DOCUMENT ID		TECN	COMMENT
−0.47±0.39±0.08		[1] AAIJ	16E	LHCB	pp at 7, 8 TeV
< 1.2	95	[2] ABAZOV	15L	D0	$p\overline{p}$ at 1.96 TeV

[1] Uses $B_s^0 \to J/\psi K^+K^-$ decays.

[2] Measured in semileptonic $B_s^0 \to D_s^-\mu^+X$ decays. Also extracts limit on time and longitudinal components ($-0.8 < \Delta a_T - 0.396\,\Delta a_Z < 3.9$) 10^{-13} GeV.

$\Delta a_\parallel$

VALUE (10^{-14} GeV)	DOCUMENT ID		TECN	COMMENT
−0.89±1.41±0.36	[1] AAIJ	16E	LHCB	pp at 7, 8 TeV

[1] Uses $B_s^0 \to J/\psi K^+K^-$ decays.

Δa_X

VALUE (10^{-14} GeV)	DOCUMENT ID		TECN	COMMENT
+1.01±2.08±0.71	[1] AAIJ	16E	LHCB	pp at 7, 8 TeV

[1] Uses $B_s^0 \to J/\psi K^+K^-$ decays.

Δa_Y

VALUE (10^{-14} GeV)	DOCUMENT ID		TECN	COMMENT
−3.83±2.09±0.71	[1] AAIJ	16E	LHCB	pp at 7, 8 TeV

[1] Uses $B_s^0 \to J/\psi K^+K^-$ decays.

Re(ξ)

VALUE	DOCUMENT ID		TECN	COMMENT
−0.022±0.033±0.003	[1] AAIJ	16E	LHCB	pp at 7, 8 TeV

[1] Uses $B_s^0 \to J/\psi K^+K^-$ decays.

Im(ξ)

VALUE	DOCUMENT ID		TECN	COMMENT
0.004±0.011±0.002	[1] AAIJ	16E	LHCB	pp at 7, 8 TeV

[1] Uses $B_s^0 \to J/\psi K^+K^-$ decays.

PARTIAL BRANCHING FRACTIONS IN $B_s \to \phi\ell^+\ell^-$

B($B_s \to \phi\ell^+\ell^-$) ($0.1 < q^2 < 2.0$ GeV$^2/c^4$)

VALUE (units 10^{-7})	DOCUMENT ID		TECN	COMMENT
1.14 ±0.16 OUR AVERAGE				
$1.11\ ^{+0.14}_{-0.13} \pm 0.09$	[1] AAIJ	15AQ	LHCB	pp at 7, 8 TeV
2.78 ±0.95 ±0.89	AALTONEN	11AI	CDF	$p\overline{p}$ at 1.96 TeV
• • • We do not use the following data for averages, fits, limits, etc. • • •				
$0.897^{+0.207}_{-0.186} \pm 0.097$	[1] AAIJ	13X	LHCB	Repl. by AAIJ 15AQ

[1] Measured in $B_s^0 \to \phi\mu^+\mu^-$ decays.

B($B_s \to \phi\ell^+\ell^-$) ($2.0 < q^2 < 5.0$ GeV$^2/c^4$)

VALUE (units 10^{-7})	DOCUMENT ID		TECN	COMMENT
0.77 ±0.12 ±0.06	[1] AAIJ	15AQ	LHCB	pp at 7, 8 TeV
• • • We do not use the following data for averages, fits, limits, etc. • • •				
$0.529^{+0.182}_{-0.159} \pm 0.057$	[1,2] AAIJ	13X	LHCB	Repl. by AAIJ 15AQ
0.58 ±0.55 ±0.19	[2] AALTONEN	11AI	CDF	$p\overline{p}$ at 1.96 TeV

[1] Measured in $B_s^0 \to \phi\mu^+\mu^-$ decays.
[2] Measured in $2 < q^2 < 4.3$ GeV$^2/c^4$.

B($B_s \to \phi\ell^+\ell^-$) ($5.0 < q^2 < 8.0$ GeV$^2/c^4$)

VALUE (units 10^{-7})	DOCUMENT ID		TECN	COMMENT
0.96±0.13±0.08	[1] AAIJ	15AQ	LHCB	pp at 7, 8 TeV
• • • We do not use the following data for averages, fits, limits, etc. • • •				
$1.38^{+0.25}_{-0.23} \pm 0.14$	[1,2] AAIJ	13X	LHCB	Repl. by AAIJ 15AQ
1.34±0.83±0.43	[2] AALTONEN	11AI	CDF	$p\overline{p}$ at 1.96 TeV

[1] Measured in $B_s^0 \to \phi\mu^+\mu^-$ decays.
[2] Measured in $4.3 < q^2 < 8.68$ GeV$^2/c^4$.

B($B_s \to \phi\ell^+\ell^-$) ($11.0 < q^2 < 12.5$ GeV$^2/c^4$)

VALUE (units 10^{-7})	DOCUMENT ID		TECN	COMMENT
0.71±0.10±0.06	[1] AAIJ	15AQ	LHCB	pp at 7, 8 TeV
• • • We do not use the following data for averages, fits, limits, etc. • • •				
$1.18^{+0.22}_{-0.21} \pm 0.14$	[1,2] AAIJ	13X	LHCB	Repl. by AAIJ 15AQ
2.98±0.95±0.95	[2] AALTONEN	11AI	CDF	$p\overline{p}$ at 1.96 TeV

[1] Measured in $B_s^0 \to \phi\mu^+\mu^-$ decays.
[2] Measured in $10.9 < q^2 < 12.86$ GeV$^2/c^4$.

B($B_s \to \phi\ell^+\ell^-$) ($15.0 < q^2 < 17.0$ GeV$^2/c^4$)

VALUE (units 10^{-7})	DOCUMENT ID		TECN	COMMENT
0.90 ±0.11 ±0.07	[1] AAIJ	15AQ	LHCB	pp at 7, 8 TeV
• • • We do not use the following data for averages, fits, limits, etc. • • •				
$0.760^{+0.189}_{-0.169} \pm 0.087$	[1,2] AAIJ	13X	LHCB	Repl. by AAIJ 15AQ
1.86 ±0.66 ±0.59	[2] AALTONEN	11AI	CDF	$p\overline{p}$ at 1.96 TeV

[1] Measured in $B_s^0 \to \phi\mu^+\mu^-$ decays.
[2] Measured in $14.18 < q^2 < 16$ GeV$^2/c^4$.

B($B_s \to \phi\ell^+\ell^-$) ($17.0 < q^2 < 19.0$ GeV$^2/c^4$)

VALUE (units 10^{-7})	DOCUMENT ID		TECN	COMMENT
0.79±0.11±0.07	[1] AAIJ	15AQ	LHCB	pp at 7, 8 TeV
• • • We do not use the following data for averages, fits, limits, etc. • • •				
$1.06^{+0.23}_{-0.21} \pm 0.12$	[1,2] AAIJ	13X	LHCB	Repl. by AAIJ 15AQ
2.32±0.76±0.74	[2] AALTONEN	11AI	CDF	$p\overline{p}$ at 1.96 TeV

[1] Measured in $B_s^0 \to \phi\mu^+\mu^-$ decays.
[2] Measured in $16 < q^2 < 19$ GeV$^2/c^4$.

B($B_s \to \phi\ell^+\ell^-$) ($1.0 < q^2 < 6.0$ GeV$^2/c^4$)

VALUE (units 10^{-7})	DOCUMENT ID		TECN	COMMENT
1.28±0.18 OUR AVERAGE				
1.29±0.16±0.10	[1] AAIJ	15AQ	LHCB	pp at 7, 8 TeV
1.14±0.79±0.36	AALTONEN	11AI	CDF	$p\overline{p}$ at 1.96 TeV
• • • We do not use the following data for averages, fits, limits, etc. • • •				
$1.14^{+0.25}_{-0.23} \pm 0.13$	[1] AAIJ	13X	LHCB	Repl. by AAIJ 15AQ

[1] Measured in $B_s^0 \to \phi\mu^+\mu^-$ decays.

B($B_s \to \phi\ell^+\ell^-$) ($0.0 < q^2 < 4.3$ GeV$^2/c^4$)

VALUE (units 10^{-7})	DOCUMENT ID		TECN	COMMENT
3.30±1.09±1.05	AALTONEN	11AI	CDF	$p\overline{p}$ at 1.96 TeV

PRODUCTION ASYMMETRIES

$A_P(B_s^0)$

$A_P(B_s^0) = [\sigma(\overline{B}_s^0) - \sigma(B_s^0)] \ / \ [\sigma(\overline{B}_s^0) + \sigma(B_s^0)]$

VALUE (units 10^{-2})	DOCUMENT ID		TECN	COMMENT
1.2 ±1.6 OUR AVERAGE				
−0.65±2.88±0.59	[1] AAIJ	17BF	LHCB	pp at 7 TeV
1.98±1.90±0.59	[1] AAIJ	17BF	LHCB	pp at 8 TeV
• • • We do not use the following data for averages, fits, limits, etc. • • •				
1.09±2.61±0.66	[2] AAIJ	14BP	LHCB	Repl. by AAIJ 17BF, pp at 7 TeV

[1] Based on time-dependent analysis of $B_s^0 \to D_s^-\pi^+$ in kinematic range $2 < p_T < 30$ GeV/c and $2.1 < \eta < 4.5$.
[2] Based on time-dependent analysis of $B_s^0 \to D_s^-\pi^+$ in kinematic range $4 < p_T < 30$ GeV/c and $2.5 < \eta < 4.5$.

B_s^0 REFERENCES

AAIJ	17A	PR D95 012006	R. Aaij *et al.*	(LHCb Collab.)
AAIJ	17AI	PRL 118 191801	R. Aaij *et al.*	(LHCb Collab.)
AAIJ	17AJ	PRL 118 251802	R. Aaij *et al.*	(LHCb Collab.)
AAIJ	17AL	PRL 119 041802	R. Aaij *et al.*	(LHCb Collab.)
AAIJ	17AN	PRL 119 101801	R. Aaij *et al.*	(LHCb Collab.)
AAIJ	17B	PRL 118 021801	R. Aaij *et al.*	(LHCb Collab.)
AAIJ	17BA	JHEP 1705 158	R. Aaij *et al.*	(LHCb Collab.)
AAIJ	17BB	EPJ C77 609	R. Aaij *et al.*	(LHCb Collab.)
AAIJ	17BD	PR D96 051103	R. Aaij *et al.*	(LHCb Collab.)
AAIJ	17BF	PL B774 139	R. Aaij *et al.*	(LHCb Collab.)
AAIJ	17BJ	PRL 119 232001	R. Aaij *et al.*	(LHCb Collab.)
AAIJ	17BP	JHEP 1711 027	R. Aaij *et al.*	(LHCb Collab.)
AAIJ	17G	PRL 118 081801	R. Aaij *et al.*	(LHCb Collab.)
AAIJ	17N	JHEP 1703 001	R. Aaij *et al.*	(LHCb Collab.)
AAIJ	17U	JHEP 1707 021	R. Aaij *et al.*	(LHCb Collab.)
AAIJ	17V	JHEP 1708 037	R. Aaij *et al.*	(LHCb Collab.)
AABOUD	16L	EPJ C76 513	M. Aaboud *et al.*	(ATLAS Collab.)
AAD	16AP	JHEP 1608 147	G. Aad *et al.*	(ATLAS Collab.)
AAIJ	16	JHEP 1601 012	R. Aaij *et al.*	(LHCb Collab.)
AAIJ	16AK	PL B762 253	R. Aaij *et al.*	(LHCb Collab.)
AAIJ	16AL	PL B762 484	R. Aaij *et al.*	(LHCb Collab.)
AAIJ	16C	PRL 116 161802	R. Aaij *et al.*	(LHCb Collab.)
AAIJ	16E	PRL 116 241601	R. Aaij *et al.*	(LHCb Collab.)
AAIJ	16G	PRL 117 061803	R. Aaij *et al.*	(LHCb Collab.)
AAIJ	16P	PR D93 092008	R. Aaij *et al.*	(LHCb Collab.)
AAIJ	16U	JHEP 1603 040	R. Aaij *et al.*	(LHCb Collab.)
ABAZOV	16C	PR D94 012001	V.M. Abazov *et al.*	(D0 Collab.)
KHACHATRY...	16Q	PL B756 84	V. Khachatryan *et al.*	(CMS Collab.)
KHACHATRY...	16S	PL B757 97	V. Khachatryan *et al.*	(CMS Collab.)
PAL	16	PRL 116 161801	B. Pal *et al.*	(BELLE Collab.)
AAIJ	15AC	JHEP 1505 019	R. Aaij *et al.*	(LHCb Collab.)
AAIJ	15AD	JHEP 1506 130	R. Aaij *et al.*	(LHCb Collab.)
AAIJ	15AF	JHEP 1507 166	R. Aaij *et al.*	(LHCb Collab.)
AAIJ	15AG	JHEP 1508 005	R. Aaij *et al.*	(LHCb Collab.)
AAIJ	15AL	JHEP 1506 131	R. Aaji *et al.*	(LHCb Collab.)
AAIJ	15AQ	JHEP 1509 179	R. Aaij *et al.*	(LHCb Collab.)
AAIJ	15AS	JHEP 1510 053	R. Aaij *et al.*	(LHCb Collab.)
AAIJ	15AV	JHEP 1511 082	R. Aaij *et al.*	(LHCb Collab.)
AAIJ	15BB	PR D92 112002	R. Aaij *et al.*	(LHCb Collab.)
AAIJ	15D	JHEP 1501 024	R. Aaij *et al.*	(LHCb Collab.)
AAIJ	15I	PRL 114 041801	R. Aaij *et al.*	(LHCb Collab.)
AAIJ	15K	PL B741 1	R. Aaij *et al.*	(LHCb Collab.)
AAIJ	15O	PRL 115 051801	R. Aaij *et al.*	(LHCb Collab.)
AAIJ	15S	PL B743 46	R. Aaij *et al.*	(LHCb Collab.)
AAIJ	15U	PL B747 484	R. Aaij *et al.*	(LHCb Collab.)
ABAZOV	15A	PRL 114 062001	V.M. Abazov *et al.*	(D0 Collab.)
ABAZOV	15L	PRL 115 161601	V.M. Abazov *et al.*	(D0 Collab.)
DUTTA	15	PR D91 011101	D. Dutta *et al.*	(BELLE Collab.)
KHACHATRY...	15BE	NAT 522 68	V. Khachatryan *et al.*	(CMS and LHCb Collab.)
OSWALD	15	PR D92 072013	C. Oswald *et al.*	(BELLE Collab.)
AAD	14U	PR D90 052007	G. Aad *et al.*	(ATLAS Collab.)
AAIJ	14AA	PRL 112 202001	R. Aaij *et al.*	(LHCb Collab.)
AAIJ	14AE	PR D90 052011	R. Aaij *et al.*	(LHCb Collab.)
AAIJ	14AX	PRL 113 172001	R. Aaij *et al.*	(LHCb Collab.)
AAIJ	14AY	PRL 113 211801	R. Aaij *et al.*	(LHCb Collab.)
AAIJ	14BF	JHEP 1411 060	R. Aaij *et al.*	(LHCb Collab.)
AAIJ	14BH	PR D90 072003	R. Aaij *et al.*	(LHCb Collab.)
AAIJ	14BM	NJP 16 123001	R. Aaij *et al.*	(LHCb Collab.)
AAIJ	14BN	PR D90 112002	R. Aaij *et al.*	(LHCb Collab.)
AAIJ	14BP	PL B739 218	R. Aaij *et al.*	(LHCb Collab.)
AAIJ	14BR	PR D89 092006	R. Aaij *et al.*	(LHCb Collab.)
AAIJ	14D	PL B728 607	R. Aaij *et al.*	(LHCb Collab.)
AAIJ	14E	JHEP 1404 114	R. Aaij *et al.*	(LHCb Collab.)
AAIJ	14F	PRL 112 111802	R. Aaij *et al.*	(LHCb Collab.)
AAIJ	14L	JHEP 1407 140	R. Aaij *et al.*	(LHCb Collab.)
AAIJ	14R	PL B736 446	R. Aaij *et al.*	(LHCb Collab.)
AAIJ	14S	PL B736 186	R. Aaij *et al.*	(LHCb Collab.)
AAIJ	14Y	PRL 112 091802	R. Aaij *et al.*	(LHCb Collab.)
AALTONEN	14P	PRL 113 242001	T. Aaltonen *et al.*	(CDF Collab.)
ABAZOV	14	PR D89 012002	V.M. Abazov *et al.*	(D0 Collab.)
PDG	14	CP C38 070001	K. Olive *et al.*	(PDG Collab.)
AAIJ	13	NP B867 1	R. Aaij *et al.*	(LHCb Collab.)
AAIJ	13A	NP B867 547	R. Aaij *et al.*	(LHCb Collab.)
AAIJ	13AA	NP B871 403	R. Aaij *et al.*	(LHCb Collab.)
AAIJ	13AB	NP B873 275	R. Aaij *et al.*	(LHCb Collab.)
AAIJ	13AC	NP B874 663	R. Aaij *et al.*	(LHCb Collab.)
AAIJ	13AL	PR D87 071101	R. Aaij *et al.*	(LHCb Collab.)
AAIJ	13AN	PR D87 072004	R. Aaij *et al.*	(LHCb Collab.)
AAIJ	13AP	PR D87 092007	R. Aaij *et al.*	(LHCb Collab.)
AAIJ	13AQ	PR D87 112009	R. Aaij *et al.*	(LHCb Collab.)
AAIJ	13AR	PR D87 112010	R. Aaij *et al.*	(LHCb Collab.)
AAIJ	13AW	PRL 110 211801	R. Aaij *et al.*	(LHCb Collab.)
AAIJ	13AX	PRL 110 221601	R. Aaij *et al.*	(LHCb Collab.)
AAIJ	13AY	PRL 110 241802	R. Aaij *et al.*	(LHCb Collab.)
AAIJ	13B	PRL 110 021801	R. Aaij *et al.*	(LHCb Collab.)
AAIJ	13BA	PRL 111 101805	R. Aaij *et al.*	(LHCb Collab.)
AAIJ	13BI	NJP 15 053021	R. Aaij *et al.*	(LHCb Collab.)
AAIJ	13BM	PRL 111 141801	R. Aaij *et al.*	(LHCb Collab.)
AAIJ	13BO	JHEP 1310 183	R. Aaij *et al.*	(LHCb Collab.)
AAIJ	13BP	JHEP 1310 143	R. Aaij *et al.*	(LHCb Collab.)
AAIJ	13BQ	JHEP 1310 005	R. Aaij *et al.*	(LHCb Collab.)
AAIJ	13BW	JHEP 1311 092	R. Aaij *et al.*	(LHCb Collab.)
AAIJ	13BX	PL B727 403	R. Aaij *et al.*	(LHCb Collab.)
AAIJ	13CF	EPJ C73 2655	R. Aaij *et al.*	(LHCb Collab.)
AAIJ	13L	JHEP 1303 067	R. Aaij *et al.*	(LHCb Collab.)
AAIJ	13X	JHEP 1307 084	R. Aaij *et al.*	(LHCb Collab.)
AAIJ	13Z	JHEP 1309 006	R. Aaij *et al.*	(LHCb Collab.)
AALTONEN	13F	PR D87 072003	T. Aaltonen *et al.*	(CDF Collab.)
ABAZOV	13	PRL 110 011801	V.M. Abazov *et al.*	(D0 Collab.)
ABAZOV	13C	PR D87 072006	V.M. Abazov *et al.*	(D0 Collab.)
CHATRCHYAN	13AW	PRL 111 101804	S. Chatrchyan *et al.*	(CMS Collab.)
ESEN	13	PR D87 031101	S. Esen *et al.*	(BELLE Collab.)
OSWALD	13	PR D87 072008	C. Oswald *et al.*	(BELLE Collab.)
Also		PR D90 119901 (errat.)	C. Oswald *et al.*	(BELLE Collab.)

SOLOVIEVA	13	PL B726 206	E. Solovieva *et al.*	(BELLE Collab.)
THORNE	13	PR D88 114006	F. Thorne *et al.*	(BELLE Collab.)
AAD	12AE	PL B713 387	G. Aad *et al.*	(ATLAS Collab.)
AAD	12CV	JHEP 1212 072	G. Aad *et al.*	(ATLAS Collab.)
AAIJ	12	PL B707 349	R. Aaij *et al.*	(LHCb Collab.)
AAIJ	12A	PL B708 55	R. Aaij *et al.*	(LHCb Collab.)
AAIJ	12AE	PR D85 112013	R. Aaij *et al.*	(LHCb Collab.)
AAIJ	12AG	JHEP 1206 115	R. Aaij *et al.*	(LHCb Collab.)
AAIJ	12AM	PRL 109 131801	R. Aaij *et al.*	(LHCb Collab.)
AAIJ	12AN	PRL 109 152002	R. Aaij *et al.*	(LHCb Collab.)
AAIJ	12AO	PR D86 052006	R. Aaij *et al.*	(LHCb Collab.)
AAIJ	12AP	PR D86 071102	R. Aaij *et al.*	(LHCb Collab.)
AAIJ	12AR	JHEP 1210 037	R. Aaij *et al.*	(LHCb Collab.)
AAIJ	12AX	PR D86 112005	R. Aaij *et al.*	(LHCb Collab.)
AAIJ	12B	PL B707 497	R. Aaij *et al.*	(LHCb Collab.)
AAIJ	12D	PRL 108 101803	R. Aaij *et al.*	(LHCb Collab.)
AAIJ	12E	PL B708 241	R. Aaij *et al.*	(LHCb Collab.)
AAIJ	12F	PL B709 50	R. Aaij *et al.*	(LHCb Collab.)
AAIJ	12I	PL B709 177	R. Aaij *et al.*	(LHCb Collab.)
AAIJ	12L	EPJ C72 2118	R. Aaij *et al.*	(LHCb Collab.)
AAIJ	12O	PL B713 172	R. Aaij *et al.*	(LHCb Collab.)
AAIJ	12P	PL B713 369	R. Aaij *et al.*	(LHCb Collab.)
AAIJ	12Q	PL B713 378	R. Aaij *et al.*	(LHCb Collab.)
AAIJ	12R	PL B716 393	R. Aaij *et al.*	(LHCb Collab.)
AAIJ	12S	PRL 108 151801	R. Aaij *et al.*	(LHCb Collab.)
AAIJ	12V	PRL 108 201601	R. Aaij *et al.*	(LHCb Collab.)
AAIJ	12W	PRL 108 231801	R. Aaij *et al.*	(LHCb Collab.)
AALTONEN	12AJ	PRL 109 171802	T. Aaltonen *et al.*	(CDF Collab.)
AALTONEN	12C	PRL 108 201801	T. Aaltonen *et al.*	(CDF Collab.)
AALTONEN	12D	PR D85 072002	T. Aaltonen *et al.*	(CDF Collab.)
AALTONEN	12L	PRL 108 211803	T. Aaltonen *et al.*	(CDF Collab.)
ABAZOV	12AF	PR D86 092011	V.M. Abazov *et al.*	(D0 Collab.)
ABAZOV	12C	PR D85 011103	V.M. Abazov *et al.*	(D0 Collab.)
ABAZOV	12D	PR D85 032006	V.M. Abazov *et al.*	(D0 Collab.)
CHATRCHYAN	12A	JHEP 1204 033	S. Chatrchyan *et al.*	(CMS Collab.)
LEES	12A	PR D85 011101	J.P. Lees *et al.*	(BABAR Collab.)
LI	12	PRL 108 181808	J. Li *et al.*	(BELLE Collab.)
PDG	12	PR D86 010001	J. Beringer *et al.*	(PDG Collab.)
AAIJ	11	PL B698 115	R. Aaij *et al.*	(LHCb Collab.)
AAIJ	11A	PL B698 14	R. Aaij *et al.*	(LHCb Collab.)
AAIJ	11B	PL B699 330	R. Aaij *et al.*	(LHCb Collab.)
AAIJ	11D	PL B706 32	R. Aaij	(LHCb Collab.)
AAIJ	11E	PR D84 092001	R. Aaij *et al.*	(LHCb Collab.)
Also		PR D85 039904 (errat.)	R. Aaij *et al.*	(LHCb Collab.)
AALTONEN	11A	PR D83 052012	T. Aaltonen *et al.*	(CDF Collab.)
AALTONEN	11AB	PR D84 052012	T. Aaltonen *et al.*	(CDF Collab.)
AALTONEN	11AG	PRL 107 191801	T. Aaltonen *et al.*	(CDF Collab.)
Also		PRL 107 239903 (errat.)	T. Aaltonen *et al.*	(CDF Collab.)
AALTONEN	11AI	PRL 107 201802	T. Aaltonen *et al.*	(CDF Collab.)
AALTONEN	11AN	PRL 107 261802	T. Aaltonen *et al.*	(CDF Collab.)
AALTONEN	11AP	PRL 107 272001	T. Aaltonen *et al.*	(CDF Collab.)
AALTONEN	11L	PRL 106 161801	T. Aaltonen *et al.*	(CDF Collab.)
AALTONEN	11N	PRL 106 181802	T. Aaltonen *et al.*	(CDF Collab.)
ABAZOV	11U	PR D84 052007	V.M. Abazov *et al.*	(D0 Collab.)
CHATRCHYAN	11T	PRL 107 191802	S. Chatrchyan *et al.*	(CMS Collab.)
LI	11	PRL 106 121802	J. Li *et al.*	(BELLE Collab.)
ABAZOV	10E	PR D82 012003	V.M. Abazov *et al.*	(D0 Collab.)
ABAZOV	10H	PRL 105 081801	V.M. Abazov *et al.*	(D0 Collab.)
Also		PR D82 032001	V.M. Abazov *et al.*	(D0 Collab.)
ABAZOV	10S	PL B693 539	V.M. Abazov *et al.*	(D0 Collab.)
ESEN	10	PRL 105 201802	S. Esen *et al.*	(BELLE Collab.)
LOUVOT	10	PRL 104 231801	R. LOUVOT *et al.*	(BELLE Collab.)
PENG	10	PR D82 072007	C.-C. Peng *et al.*	(BELLE Collab.)
AALTONEN	09AQ	PRL 103 191802	T. Aaltonen *et al.*	(CDF Collab.)
AALTONEN	09B	PR D79 011104	T. Aaltonen *et al.*	(CDF Collab.)
AALTONEN	09C	PRL 103 031801	T. Aaltonen *et al.*	(CDF Collab.)
AALTONEN	09P	PRL 102 201801	T. Aaltonen *et al.*	(CDF Collab.)
ABAZOV	09E	PRL 102 032001	V.M. Abazov *et al.*	(D0 Collab.)
ABAZOV	09G	PRL 102 051801	V.M. Abazov *et al.*	(D0 Collab.)
ABAZOV	09I	PRL 102 091801	V.M. Abazov *et al.*	(D0 Collab.)
ABAZOV	09Y	PR D79 111102	V.M. Abazov *et al.*	(D0 Collab.)
LOUVOT	09	PRL 102 021801	R. Louvot *et al.*	(BELLE Collab.)
AALTONEN	08F	PRL 100 021803	T. Aaltonen *et al.*	(CDF Collab.)
AALTONEN	08G	PRL 100 161802	T. Aaltonen *et al.*	(CDF Collab.)
AALTONEN	08J	PRL 100 121803	T. Aaltonen *et al.*	(CDF Collab.)
ABAZOV	08AM	PRL 101 241801	V.M. Abazov *et al.*	(D0 Collab.)
WICHT	08A	PRL 100 121801	J. Wicht *et al.*	(BELLE Collab.)
ABAZOV	07	PRL 98 121801	V.M. Abazov *et al.*	(D0 Collab.)
ABAZOV	07A	PRL 98 151801	V.M. Abazov *et al.*	(D0 Collab.)
ABAZOV	07N	PR D76 057101	V.M. Abazov *et al.*	(D0 Collab.)
ABAZOV	07Y	PRL 99 241801	V.M. Abazov *et al.*	(D0 Collab.)
ABULENCIA	07C	PRL 98 061802	A. Abulencia *et al.*	(CDF Collab.)
DRUTSKOY	07	PRL 98 052001	A. Drutskoy *et al.*	(BELLE Collab.)
DRUTSKOY	07A	PR D76 012002	A. Drutskoy *et al.*	(BELLE Collab.)
ABAZOV	06B	PRL 97 021802	V.M. Abazov *et al.*	(D0 Collab.)
ABAZOV	06G	PR D74 031107	V.M. Abazov *et al.*	(D0 Collab.)
ABAZOV	06V	PRL 97 241801	V.M. Abazov *et al.*	(D0 Collab.)
ABULENCIA	06J	PRL 96 191801	A. Abulencia *et al.*	(CDF Collab.)
ABULENCIA	06N	PRL 96 231801	A. Abulencia *et al.*	(CDF Collab.)
ABULENCIA	06Q	PRL 97 062003	A. Abulencia *et al.*	(CDF Collab.)
ABULENCIA,A	06D	PRL 97 211802	A. Abulencia *et al.*	(CDF Collab.)
ABULENCIA,A	06G	PRL 97 242003	A. Abulencia *et al.*	(CDF Collab.)
ACOSTA	06	PRL 96 202001	D. Acosta *et al.*	(CDF Collab.)
ABAZOV	05B	PRL 94 042001	V.M. Abazov *et al.*	(D0 Collab.)
ABAZOV	05W	PRL 95 171801	V.M. Abazov *et al.*	(D0 Collab.)
ACOSTA	05	PRL 94 101803	D. Acosta *et al.*	(CDF Collab.)
ACOSTA	05J	PRL 95 031801	D. Acosta *et al.*	(CDF Collab.)
ABDALLAH	04A	PL B585 63	J. Abdallah *et al.*	(DELPHI Collab.)
ABDALLAH	04J	EPJ C35 35	J. Abdallah *et al.*	(DELPHI Collab.)
ABDALLAH	03B	EPJ C28 155	J. Abdallah *et al.*	(DELPHI Collab.)
ABE	03	PR D67 012006	K. Abe *et al.*	(SLD Collab.)
HEISTER	03E	EPJ C29 143	A. Heister *et al.*	(ALEPH Collab.)
ABE	02V	PR D66 032009	K. Abe *et al.*	(SLD Collab.)
ACOSTA	02D	PR D65 111101	D. Acosta *et al.*	(CDF Collab.)
ACOSTA	02G	PR D66 112002	D. Acosta *et al.*	(CDF Collab.)
ABBIENDI	01D	EPJ C19 241	G. Abbiendi *et al.*	(OPAL Collab.)
ABE	00C	PR D62 071101	K. Abe *et al.*	(SLD Collab.)
ABREU	00Y	EPJ C16 555	P. Abreu *et al.*	(DELPHI Collab.)
ABREU,P	00G	EPJ C18 229	P. Abreu *et al.*	(DELPHI Collab.)
AFFOLDER	00N	PRL 85 4668	T. Affolder *et al.*	(CDF Collab.)
BARATE	00K	PL B486 286	R. Barate *et al.*	(ALEPH Collab.)
ABBIENDI	99S	EPJ C11 587	G. Abbiendi *et al.*	(OPAL Collab.)
ABE	99D	PR D59 032004	F. Abe *et al.*	(CDF Collab.)
ABE	99J	PRL 82 3576	F. Abe *et al.*	(CDF Collab.)
BARATE	99J	EPJ C7 553	R. Barate *et al.*	(ALEPH Collab.)
Also		EPJ C12 181 (errat.)	R. Barate *et al.*	(ALEPH Collab.)
ABE	98B	PR D57 5382	F. Abe *et al.*	(CDF Collab.)
ABE	98V	PRL 81 5742	F. Abe *et al.*	(CDF Collab.)
ACCIARRI	98S	PL B438 417	M. Acciarri *et al.*	(L3 Collab.)
ACKERSTAFF	98F	EPJ C2 407	K. Ackerstaff *et al.*	(OPAL Collab.)
ACKERSTAFF	98G	PL B426 161	K. Ackerstaff *et al.*	(OPAL Collab.)
BARATE	98C	EPJ C4 367	R. Barate *et al.*	(ALEPH Collab.)
BARATE	98Q	EPJ C4 387	R. Barate *et al.*	(ALEPH Collab.)
PDG	98	EPJ C3 1	C. Caso *et al.*	(PDG Collab.)
ACCIARRI	97B	PL B391 474	M. Acciarri *et al.*	(L3 Collab.)
ACCIARRI	97C	PL B391 481	M. Acciarri *et al.*	(L3 Collab.)
ACKERSTAFF	97U	ZPHY C76 401	K. Ackerstaff *et al.*	(OPAL Collab.)
ACKERSTAFF	97V	ZPHY C76 417	K. Ackerstaff *et al.*	(OPAL Collab.)
ADAM	97	PL B414 382	W. Adam *et al.*	(DELPHI Collab.)
ABE	96B	PR D53 3496	F. Abe *et al.*	(CDF Collab.)
ABE	96N	PRL 77 1945	F. Abe *et al.*	(CDF Collab.)
ABE	96Q	PR D54 6596	F. Abe *et al.*	(CDF Collab.)
ABREU	96F	ZPHY C71 11	P. Abreu *et al.*	(DELPHI Collab.)
ADAM	96D	ZPHY C72 207	W. Adam *et al.*	(DELPHI Collab.)
BUSKULIC	96E	ZPHY C69 585	D. Buskulic *et al.*	(ALEPH Collab.)
BUSKULIC	96M	PL B377 205	D. Buskulic *et al.*	(ALEPH Collab.)
BUSKULIC	96V	PL B384 471	D. Buskulic *et al.*	(ALEPH Collab.)
PDG	96	PR D54 1	R. M. Barnett *et al.*	(PDG Collab.)
ABE	95R	PRL 74 4988	F. Abe *et al.*	(CDF Collab.)
ABE	95Z	PRL 75 3068	F. Abe *et al.*	(CDF Collab.)
ACCIARRI	95H	PL B363 127	M. Acciarri *et al.*	(L3 Collab.)
ACCIARRI	95I	PL B363 137	M. Acciarri *et al.*	(L3 Collab.)
AKERS	95G	PL B350 273	R. Akers *et al.*	(OPAL Collab.)
AKERS	95J	ZPHY C66 555	R. Akers *et al.*	(OPAL Collab.)
BUSKULIC	95J	PL B356 409	D. Buskulic *et al.*	(ALEPH Collab.)
BUSKULIC	95O	PL B361 221	D. Buskulic *et al.*	(ALEPH Collab.)
ABREU	94D	PL B324 500	P. Abreu *et al.*	(DELPHI Collab.)
ABREU	94E	ZPHY C61 407	P. Abreu *et al.*	(DELPHI Collab.)
Also		PL B289 199	P. Abreu *et al.*	(DELPHI Collab.)
AKERS	94J	PL B337 196	R. Akers *et al.*	(OPAL Collab.)
AKERS	94L	PL B337 393	R. Akers *et al.*	(OPAL Collab.)
BUSKULIC	94B	PL B322 441	D. Buskulic *et al.*	(ALEPH Collab.)
BUSKULIC	94C	PL B322 275	D. Buskulic *et al.*	(ALEPH Collab.)
ABE	93F	PRL 71 1685	F. Abe *et al.*	(CDF Collab.)
ACTON	93H	PL B312 501	P.D. Acton *et al.*	(OPAL Collab.)
BUSKULIC	93G	PL B311 425	D. Buskulic *et al.*	(ALEPH Collab.)
ABREU	92M	PL B289 199	P. Abreu *et al.*	(DELPHI Collab.)
ACTON	92N	PL B295 357	P.D. Acton *et al.*	(OPAL Collab.)
BUSKULIC	92E	PL B294 145	D. Buskulic *et al.*	(ALEPH Collab.)
LEE-FRANZINI	90	PRL 65 2947	J. Lee-Franzini *et al.*	(CUSB II Collab.)

B_s^*

$I(J^P) = 0(1^-)$

I, *J*, *P* need confirmation. Quantum numbers shown are quark-model predictions.

B_s^* MASS

From mass difference below and the B_s^0 mass.

VALUE (MeV)	*DOCUMENT ID*		*TECN*	*COMMENT*
$5415.4^{+1.8}_{-1.5}$ OUR FIT Error includes scale factor of 2.9.				
5415.8±1.5 OUR AVERAGE Error includes scale factor of 2.6.				
5416.4±0.4±0.5	LOUVOT	09	BELL	$e^+e^- \to \Upsilon(5S)$
5411.7±1.6±0.6	[1] AQUINES	06	CLEO	$e^+e^- \to \Upsilon(5S)$
• • • We do not use the following data for averages, fits, limits, etc. • • •				
5418 ±1 ±3	DRUTSKOY	07A	BELL	Repl. by LOUVOT 09
5414 ±1 ±3	[2] BONVICINI	06	CLEO	$e^+e^- \to \Upsilon(5S)$

[1] Utilized the beam constrained invariant mass peak positions for B^* and B_s^* to extract the measurement.

[2] Uses 14 candidates consistent with B_S decays into final states with a J/ψ and a $D_s^{(*)-}$.

$m_{B_s^*} - m_{B_s}$

VALUE (MeV)	*DOCUMENT ID*		*TECN*	*COMMENT*
$48.5^{+1.8}_{-1.5}$ OUR FIT Error includes scale factor of 2.8.				
46.1±1.5 OUR AVERAGE				
45.7±1.7±0.7	[3] AQUINES	06	CLEO	$e^+e^- \to \Upsilon(5S)$
47.0±2.6	[4] LEE-FRANZINI	90	CSB2	$e^+e^- \to \Upsilon(5S)$
• • • We do not use the following data for averages, fits, limits, etc. • • •				
48 ±1 ±3	[5] BONVICINI	06	CLEO	Repl. by AQUINES 06

[3] Utilized the beam constrained invariant mass peak positions for B^* and B_s^* to extract the measurement.

[4] LEE-FRANZINI 90 measure 46.7 ± 0.4 ± 0.2 MeV for an admixture of B^0, B^+, and B_S. They use the shape of the photon line to separate the above value for B_S.

[5] Uses 14 candidates consistent with B_S decays into final states with a J/ψ and a $D_s^{(*)-}$.

$|(m_{B_s^*} - m_{B_s}) - (m_{B^*} - m_B)|$

VALUE (MeV)	*CL%*	*DOCUMENT ID*		*TECN*	*COMMENT*
<6	95	ABREU	95R	DLPH	$E_{\rm cm}^{ee}$= 88–94 GeV

B_s^* DECAY MODES

	Mode	Fraction (Γ_j/Γ)
Γ_1	$B_s\gamma$	dominant

B_s^* REFERENCES

LOUVOT	09	PRL 102 021801	R. Louvot *et al.*	(BELLE Collab.)
DRUTSKOY	07A	PR D76 012002	A. Drutskoy *et al.*	(BELLE Collab.)
AQUINES	06	PRL 96 152001	O. Aquines *et al.*	(CLEO Collab.)

BONVICINI 06 PRL 96 022002 G. Bonvicini *et al.* (CLEO Collab.)
ABREU 95R ZPHY C68 353 P. Abreu *et al.* (DELPHI Collab.)
LEE-FRANZINI 90 PRL 65 2947 J. Lee-Franzini *et al.* (CUSB II Collab.)

$X(5568)^{\pm}$

$I(J^P) = ?(?^?)$

OMITTED FROM SUMMARY TABLE

Seen as a peak in the $B_s\pi^{\pm}$ mass spectrum with a significance of more than 3σ by ABAZOV 16E in inclusive $p\overline{p}$ collisions at 1.96 TeV. Not seen by AAIJ 16AI. Needs confirmation.

$X(5568)^{\pm}$ MASS

VALUE (MeV)	EVTS	DOCUMENT ID		TECN	COMMENT
$5567.8 \pm 2.9^{+0.9}_{-1.9}$	133	[1] ABAZOV	16E	D0	$p\overline{p} \to B_s\pi^{\pm}X$

[1] Assumes $X(5568)^{\pm} \to B_s\pi^{\pm}$ decay. If $X(5568)^{\pm} \to B_s^*\pi^{\pm}$ decay is assumed, the mass shifts upward by 49 MeV.

$X(5568)^{\pm}$ WIDTH

VALUE (MeV)	EVTS	DOCUMENT ID		TECN	COMMENT
$21.9 \pm 6.4^{+5.0}_{-2.5}$	133	ABAZOV	16E	D0	$p\overline{p} \to B_s\pi^{\pm}X$

$X(5568)^{\pm}$ DECAY MODES

	Mode	Fraction (Γ_i/Γ)
Γ_1	$B_s\pi^{\pm}$	seen

$X(5568)^{\pm}$ BRANCHING RATIOS

$\Gamma(B_s\pi^{\pm})/\Gamma_{total}$ **Γ_1/Γ**

VALUE	EVTS	DOCUMENT ID		TECN	COMMENT
not seen		[1] AAIJ	16AI	LHCB	$pp \to B_s^0\pi^{\pm}X$
seen	133	[2] ABAZOV	16E	D0	$p\overline{p} \to B_s\pi^{\pm}X$

[1] Not seen in 3 fb^{-1} of pp collision data at $\sqrt{s} = 7$ and 8 TeV in a scan over the $X(5568)$ mass and width, with B_s mesons reconstructed in decays to $D_s^-\pi^+$ or $J/\psi\phi$. An upper limit on a rate of X production relative to inclusive B_s production at $p_T(B_s) > 10$ GeV/c is less than 2.1% at 90% CL.

[2] Seen in $p\overline{p}$ collisions at 1.96 TeV at a rate of $(8.6 \pm 1.9 \pm 1.4)\%$ relative to inclusive B_s production in the kinematic region $10 < p_T(B_s) < 30$ GeV/c, with B_s mesons reconstructed in decays to $J/\psi\phi$. An alternative possibility, $X(5568)^{\pm} \to B_s^*\pi^{\pm}$ with a missing γ, could not be ruled out.

$X(5568)^{\pm}$ REFERENCES

AAIJ 16AI PRL 117 152003 R. Aaij *et al.* (LHCb Collab.)
ABAZOV 16E PRL 117 022003 V.M. Abazov *et al.* (D0 Collab.)

$B_{s1}(5830)^0$

$I(J^P) = 0(1^+)$ Status: ***

I, J, P need confirmation.

Quantum numbers shown are quark-model predictions.

$B_{s1}(5830)^0$ MASS

VALUE (MeV)	DOCUMENT ID		TECN	COMMENT
5828.63 ± 0.27 OUR FIT				
$5828.40 \pm 0.04 \pm 0.41$	[1] AAIJ	13O	LHCB	pp at 7 TeV
• • • We do not use the following data for averages, fits, limits, etc. • • •				
5829.4 ± 0.7	[2] AALTONEN	08K	CDF	Repl. by AALTONEN 14I

[1] Uses $B_{s1}(5830)^0 \to B^{*+}K^-$ decay.

[2] Uses two-body decays into K^- and B^+ mesons reconstructed as $B^+ \to J/\psi K^+$, $J/\psi \to \mu^+\mu^-$ or $B^+ \to \overline{D}^0\pi^+$, $\overline{D}^0 \to K^+\pi^-$.

$m_{B_{s1}^0} - m_{B^{*+}}$

VALUE (MeV)	DOCUMENT ID		TECN	COMMENT
503.98 ± 0.18 OUR FIT				
$504.03 \pm 0.12 \pm 0.15$	[3] AALTONEN	14I	CDF	$p\overline{p}$ at 1.96 TeV
• • • We do not use the following data for averages, fits, limits, etc. • • •				
$504.41 \pm 0.21 \pm 0.14$	[4] AALTONEN	08K	CDF	Repl. by AALTONEN 14I

[3] AALTONEN 14I reports $m_{B_{s1}(5830)^0} - m_{B^{*+}} - m_{K^-} = 10.35 \pm 0.12 \pm 0.15$ MeV which we adjusted by the K^- mass.

[4] Uses two-body decays into K^- and B^+ mesons reconstructed as $B^+ \to J/\psi K^+$, $J/\psi \to \mu^+\mu^-$ or $B^+ \to \overline{D}^0\pi^+$, $\overline{D}^0 \to K^+\pi^-$.

$B_{s1}(5830)^0$ WIDTH

VALUE (MeV)	DOCUMENT ID		TECN	COMMENT
$0.5 \pm 0.3 \pm 0.3$	AALTONEN	14I	CDF	$p\overline{p}$ at 1.96 TeV

$B_{s1}(5830)^0$ DECAY MODES

	Mode	Fraction (Γ_i/Γ)
Γ_1	$B^{*+}K^-$	dominant

$B_{s1}(5830)^0$ BRANCHING RATIOS

$\Gamma(B^{*+}K^-)/\Gamma_{total}$ **Γ_1/Γ**

VALUE	DOCUMENT ID		TECN	COMMENT
dominant	AALTONEN	08K	CDF	$p\overline{p}$ at 1.96 TeV

$B_{s1}(5830)^0$ REFERENCES

AALTONEN 14I PR D90 012013 T. Aaltonen *et al.* (CDF Collab.)
AAIJ 13O PRL 110 151803 R. Aaij *et al.* (LHCb Collab.)
AALTONEN 08K PRL 100 082001 T. Aaltonen *et al.* (CDF Collab.)

$B_{s2}^*(5840)^0$

$I(J^P) = 0(2^+)$ Status: ***

I, J, P need confirmation.

Quantum numbers shown are quark-model predictions.

$B_{s2}^*(5840)^0$ MASS

VALUE (MeV)	DOCUMENT ID		TECN	COMMENT
5839.85 ± 0.17 OUR FIT Error includes scale factor of 1.1.				
5839.98 ± 0.20 OUR AVERAGE				
$5839.99 \pm 0.05 \pm 0.20$	AAIJ	13O	LHCB	pp at 7 TeV
$5839.6 \pm 1.1 \pm 0.7$	[1] ABAZOV	08E	D0	$p\overline{p}$ at 1.96 TeV
• • • We do not use the following data for averages, fits, limits, etc. • • •				
5839.7 ± 0.7	[2] AALTONEN	08K	CDF	Repl. by AALTONEN 14I

[1] Observed in $B_{s2}^{*0} \to B^+K^-$. Measured production rate of B_{s2}^{*0} relative to B^+ to be $(1.15 \pm 0.23 \pm 0.13)\%$.

[2] Uses two-body decays into K^- and B^+ mesons reconstructed as $B^+ \to J/\psi K^+$, $J/\psi \to \mu^+\mu^-$ or $B^+ \to \overline{D}^0\pi^+$, $\overline{D}^0 \to K^+\pi^-$.

$m_{B_{s2}^{*0}} - m_{B_{s1}^0}$

VALUE (MeV)	DOCUMENT ID		TECN	COMMENT
• • • We do not use the following data for averages, fits, limits, etc. • • •				
10.5 ± 0.6	[3] AALTONEN	08K	CDF	Repl. by AALTONEN 14I

[3] Uses two-body decays into K^- and B^+ mesons reconstructed as $B^+ \to J/\psi K^+$, $J/\psi \to \mu^+\mu^-$ or $B^+ \to \overline{D}^0\pi^+$, $\overline{D}^0 \to K^+\pi^-$.

$m_{B_{s2}^{*0}} - m_{B^+}$

VALUE (MeV)	DOCUMENT ID		TECN	COMMENT
560.53 ± 0.17 OUR FIT Error includes scale factor of 1.1.				
$560.41 \pm 0.13 \pm 0.14$	[4] AALTONEN	14I	CDF	$p\overline{p}$ at 1.96 TeV

[4] AALTONEN 14I reports $m_{B_{s2}(5840)^0} - m_{B^+} - m_{K^-} = 66.73 \pm 0.13 \pm 0.14$ MeV which we adjusted by the K^- mass.

$B_{s2}^*(5840)^0$ WIDTH

VALUE (MeV)	DOCUMENT ID		TECN	COMMENT
1.47 ± 0.33 OUR AVERAGE				
$1.4 \pm 0.4 \pm 0.2$	AALTONEN	14I	CDF	$p\overline{p}$ at 1.96 TeV
$1.56 \pm 0.13 \pm 0.47$	[5] AAIJ	13O	LHCB	pp at 7 TeV

[5] Uses $B_{s2}^*(5840)^0 \to B^{*+}K^-$ decays.

$B_{s2}^*(5840)^0$ DECAY MODES

	Mode	Fraction (Γ_i/Γ)
Γ_1	B^+K^-	dominant
Γ_2	$B^{*+}K^-$	

$B_{s2}^*(5840)^0$ BRANCHING RATIOS

$\Gamma(B^+K^-)/\Gamma_{total}$ **Γ_1/Γ**

VALUE	DOCUMENT ID		TECN	COMMENT
dominant	AALTONEN	08K	CDF	$p\overline{p}$ at 1.96 TeV
dominant	[6] ABAZOV	08E	D0	$p\overline{p}$ at 1.96 TeV

[6] Measured production rate of B_{s2}^{*0} relative to B^+ to be $(1.15 \pm 0.23 \pm 0.13)\%$.

Meson Particle Listings

$B^*_{s2}(5840)^0$, $B^*_{sJ}(5850)$

$\Gamma(B^{*+}K^-)/\Gamma(B^+K^-)$ Γ_2/Γ_1

VALUE	DOCUMENT ID		TECN	COMMENT
0.093±0.013±0.012	AAIJ	13O	LHCB	pp at 7 TeV

$B^*_{s2}(5840)^0$ REFERENCES

AALTONEN	14I	PR D90 012013	T. Aaltonen *et al.*	(CDF Collab.)
AAIJ	13O	PRL 110 151803	R. Aaij *et al.*	(LHCb Collab.)
AALTONEN	08K	PRL 100 082001	T. Aaltonen *et al.*	(CDF Collab.)
ABAZOV	08E	PRL 100 082002	V.M. Abazov *et al.*	(D0 Collab.)

$B^*_{sJ}(5850)$

$I(J^P) = ?(?^?)$
I, J, P need confirmation.

OMITTED FROM SUMMARY TABLE

Signal can be interpreted as coming from $\overline{b}s$ states. Needs confirmation.

$B^*_{sJ}(5850)$ MASS

VALUE (MeV)	EVTS	DOCUMENT ID		TECN	COMMENT
5853±15	141	AKERS	95E	OPAL	$E^{ee}_{\rm cm}$ = 88–94 GeV

$B^*_{sJ}(5850)$ WIDTH

VALUE (MeV)	EVTS	DOCUMENT ID		TECN	COMMENT
47±22	141	AKERS	95E	OPAL	$E^{ee}_{\rm cm}$ = 88–94 GeV

$B^*_{sJ}(5850)$ REFERENCES

AKERS	95E	ZPHY C66 19	R. Akers *et al.*	(OPAL Collab.)

BOTTOM, CHARMED MESONS ($B = C = \pm 1$)

$B_c^+ = c\overline{b}$, $B_c^- = \overline{c}b$, similarly for B_c^*'s

B_c^+

$I(J^P) = 0(0^-)$
I, J, P need confirmation.

Quantum numbers shown are quark-model predictions.

B_c^+ MASS

VALUE (MeV)			DOCUMENT ID		TECN	COMMENT
6274.9 ± 0.8 OUR AVERAGE						
6274.28 ± 1.40 ± 0.32			[1] AAIJ	17L	LHCB	pp at 7, 8 TeV
6274.0 ± 1.8 ± 0.4			[2] AAIJ	14AQ	LHCB	pp at 7, 8 TeV
6276.28 ± 1.44 ± 0.36			[3] AAIJ	13AS	LHCB	pp at 7, 8 TeV
6273.7 ± 1.3 ± 1.6			[4] AAIJ	12AV	LHCB	pp at 7 TeV
6275.6 ± 2.9 ± 2.5			[5] AALTONEN	08M	CDF	$p\overline{p}$ at 1.96 TeV
6300 ± 14 ± 5			[5] ABAZOV	08T	D0	$p\overline{p}$ at 1.96 TeV
6400 ±390 ±130			[6] ABE	98M	CDF	$p\overline{p}$ at 1.8 TeV
• • • We do not use the following data for averages, fits, limits, etc. • • •						
6285.7 ± 5.3 ± 1.2			[5] ABULENCIA	06C	CDF	Repl. by AALTONEN 08M
6320 ± 60			[7] ACKERSTAFF	98O	OPAL	$e^+e^- \to Z$

[1] Measured using $B_c^+ \to J/\psi D^0 K^+$ decays.
[2] Uses $B_c^+ \to J/\psi p\overline{p}\pi^+$ decays.
[3] AAIJ 13AS uses the $B_c^+ \to J/\psi D_s^+$.
[4] AAIJ 12AV uses the $B_c^+ \to J/\psi\pi^+$ mode and also measures the mass difference $M(B_c^+) - M(B^+) = 994.6 \pm 1.3 \pm 0.6$ MeV/c^2.
[5] Measured using a fully reconstructed decay mode of $B_c \to J/\psi\pi$.
[6] ABE 98M observed $20.4^{+6.2}_{-5.5}$ events in the $B_c^+ \to J/\psi(1s)\ell\nu_\ell$ with a significance of > 4.8 standard deviations. The mass value is estimated from $m(J/\psi(1S)\ell)$.
[7] ACKERSTAFF 98O observed 2 candidate events in the $B_c^+ \to J/\psi(1S)\pi^+$ channel with an estimated background of 0.63 ± 0.20 events.

B_c^+ MEAN LIFE

"OUR EVALUATION" is an average using rescaled values of the data listed below. The average and rescaling were performed by the Heavy Flavor Averaging Group (HFLAV) and are described at http://www.slac.stanford.edu/xorg/hflav/. The averaging/rescaling procedure takes into account correlations between the measurements.

VALUE (10^{-12} s)		DOCUMENT ID		TECN	COMMENT
0.507 ±0.009 OUR EVALUATION					
0.507 ±0.009 OUR AVERAGE					
0.5134 ± 0.0110 ± 0.0057		[1,2] AAIJ	15G	LHCB	pp at 7, 8 TeV
0.509 ± 0.008 ± 0.012		[3] AAIJ	14G	LHCB	pp at 8 TeV
0.452 ± 0.048 ± 0.027		[2] AALTONEN	13	CDF	$p\overline{p}$ at 1.96 TeV
0.448 $^{+0.038}_{-0.036}$ ± 0.032		[4] ABAZOV	09H	D0	$p\overline{p}$ at 1.96 TeV
0.463 $^{+0.073}_{-0.065}$ ± 0.036		[4] ABULENCIA	06O	CDF	$p\overline{p}$ at 1.96 TeV
0.46 $^{+0.18}_{-0.16}$ ± 0.03		[4] ABE	98M	CDF	$p\overline{p}$ 1.8 TeV

[1] Also measures the width difference $\Delta\Gamma = \Gamma_{B_c^+} - \Gamma_{B^+} = 4.46 \pm 0.14 \pm 0.07$ mm^{-1} c.
[2] Uses fully reconstructed $B_c^+ \to J/\psi\pi^+$ decays.
[3] Measured using $B_c^+ \to J/\psi\mu^+\nu_\mu X$ decays.
[4] The lifetime is measured from the $J/\psi e$ decay vertices.

B_c^+ DECAY MODES × B($\overline{b} \to B_c$)

B_c^- modes are charge conjugates of the modes below.

	Mode	Fraction (Γ_i/Γ)	Confidence level
	The following quantities are not pure branching ratios; rather the fraction $\Gamma_i/\Gamma \times$ B($\overline{b} \to B_c$).		
Γ_1	$J/\psi(1S)\ell^+\nu_\ell$ anything	$(8.1 \pm 1.2) \times 10^{-5}$	
Γ_2	$J/\psi(1S)\mu^+\nu_\mu$		
Γ_3	$J/\psi(1S)\pi^+$	seen	
Γ_4	$J/\psi(1S)K^+$	seen	
Γ_5	$J/\psi(1S)\pi^+\pi^+\pi^-$	seen	
Γ_6	$J/\psi(1S)a_1(1260)$	$< 1.2 \times 10^{-3}$	90%
Γ_7	$J/\psi(1S)K^+K^-\pi^+$	seen	
Γ_8	$J/\psi(1S)\pi^+\pi^+\pi^+\pi^-\pi^-$	seen	
Γ_9	$\psi(2S)\pi^+$	seen	
Γ_{10}	$J/\psi(1S)D^0K^+$	seen	
Γ_{11}	$J/\psi(1S)D^*(2007)^0K^+$	seen	
Γ_{12}	$J/\psi(1S)D^*(2010)^+K^{*0}$	seen	
Γ_{13}	$J/\psi(1S)D^+K^{*0}$	seen	
Γ_{14}	$J/\psi(1S)D_s^+$	seen	
Γ_{15}	$J/\psi(1S)D_s^{*+}$	seen	
Γ_{16}	$J/\psi(1S)p\overline{p}\pi^+$	seen	
Γ_{17}	$\chi_c^0\pi^+$	$(2.4\ ^{+0.9}_{-0.8}) \times 10^{-5}$	
Γ_{18}	$p\overline{p}\pi^+$	not seen	
Γ_{19}	D^0K^+	$(3.8\ ^{+1.2}_{-1.0}) \times 10^{-7}$	
Γ_{20}	$D^0\pi^+$	$< 1.6 \times 10^{-7}$	95%
Γ_{21}	$D^{*0}\pi^+$	$< 4 \times 10^{-7}$	95%
Γ_{22}	$D^{*0}K^+$	$< 4 \times 10^{-7}$	95%
Γ_{23}	$D^*(2010)^+\overline{D}^0$	$< 6.2 \times 10^{-3}$	90%
Γ_{24}	D^+K^{*0}	$< 0.20 \times 10^{-6}$	90%
Γ_{25}	$D^+\overline{K}^{*0}$	$< 0.16 \times 10^{-6}$	90%
Γ_{26}	$D_s^+K^{*0}$	$< 0.28 \times 10^{-6}$	90%
Γ_{27}	$D_s^+\overline{K}^{*0}$	$< 0.4 \times 10^{-6}$	90%
Γ_{28}	$D_s^+\phi$	$< 0.32 \times 10^{-6}$	90%
Γ_{29}	K^+K^0	$< 4.6 \times 10^{-7}$	90%
Γ_{30}	$B_s^0\pi^+$ / B($\overline{b} \to B_s$)	$(2.37^{+0.37}_{-0.35}) \times 10^{-3}$	

B_c^+ BRANCHING RATIOS

$\Gamma(J/\psi(1S)\ell^+\nu_\ell \text{anything})/\Gamma_{\text{total}} \times$ B($\overline{b} \to B_c$) $\quad \Gamma_1/\Gamma \times$ B

VALUE (units 10^{-5})	CL%	DOCUMENT ID		TECN	COMMENT
8.1 ±1.2 OUR AVERAGE Error includes scale factor of 1.3.					
8.6 ± 1.0 ± 0.3		[1,2] AALTONEN	16A	CDF	$p\overline{p}$ at 1.96 TeV
$5.2^{+2.4}_{-2.1}$		[3] ABE	98M	CDF	$p\overline{p}$ 1.8 TeV
• • • We do not use the following data for averages, fits, limits, etc. • • •					
<16	90	[4] ACKERSTAFF	98O	OPAL	$e^+e^- \to Z$
<19	90	[5] ABREU	97E	DLPH	$e^+e^- \to Z$
<12	90	[6] BARATE	97H	ALEP	$e^+e^- \to Z$

[1] AALTONEN 16A reports $[\Gamma(B_c^+ \to J/\psi(1S)\ell^+\nu_\ell \text{anything})/\Gamma_{\text{total}} \times$ B($\overline{b} \to B_c$)$]$ / $[$B($\overline{b} \to B^+$)$]$ / $[$B($B^+ \to J/\psi(1S)K^+$)$] = 0.211 \pm 0.012^{+0.021}_{-0.020}$ which we multiply by our best values B($\overline{b} \to B^+$) $= (40.5 \pm 0.6) \times 10^{-2}$, B($B^+ \to J/\psi(1S)K^+$) $= (1.010 \pm 0.029) \times 10^{-3}$. Our first error is their experiment's error and our second error is the systematic error from using our best values.
[2] AALTONEN 16A also measures the cross-section $\sigma(B_C) \times$B($B_C \to J/\psi\mu\nu_\mu$) $= 0.60 \pm 0.09$ nb and estimates the total cross-section $\sigma(B_C)$ to be in the range 25 ± 4 to 52 ± 8 nb for $p_T(B_C) > 6$ GeV/c and $|y(B_C)| < 1$.
[3] ABE 98M result is derived from the measurement of $[\sigma(B_C) \times$B($B_C \to J/\psi(1S)\ell\nu_\ell$)$]$ / $[\sigma(B^+) \times$B($B^+ \to J/\psi(1S)K^+$)$] = 0.132^{+0.041}_{-0.037}$(stat)$\pm 0.031(sys)^{+0.032}_{-0.020}$(lifetime) by using PDG 98 values of B($b \to B^+$) and B($B^+ \to J/\psi(1S)K^+$).
[4] ACKERSTAFF 98O reports B($Z \to B_C$X)/B($Z \to q\overline{q}$)×B($B_C \to J/\psi(1S)\ell\nu_\ell$) $< 6.95 \times 10^{-5}$ at 90%CL. We rescale to our PDG 98 values of B($Z \to b\overline{b}$).
[5] ABREU 97E value listed is for an assumed $\tau_{B_C} = 0.4$ ps and improves to 1.6×10^{-4} for $\tau_{B_C} = 1.4$ ps.
[6] BARATE 97H reports B($Z \to B_C$X)/B($Z \to q\overline{q}$)·B($B_C \to J/\psi(1S)\ell\nu_\ell$) $< 5.2 \times 10^{-5}$ at 90%CL. We rescale to our PDG 96 values of B($Z \to b\overline{b}$). A $B_c^+ \to J/\psi(1S)\mu^+\nu_\mu$ candidate event is found, compared to all the known background sources 2×10^{-3}, which gives $m_{B_c} = 5.96^{+0.25}_{-0.19}$ GeV and $\tau_{B_c} = 1.77 \pm 0.17$ ps.

$\Gamma(J/\psi(1S)\pi^+)/\Gamma_{\text{total}} \times$ B($\overline{b} \to B_c$) $\quad \Gamma_3/\Gamma \times$ B

VALUE	CL%	DOCUMENT ID		TECN	COMMENT
seen		[1] AAIJ	15M	LHCB	pp at 8 TeV
seen		[2] KHACHATRY...15AA		CMS	pp at 7 TeV
seen		AALTONEN	13	CDF	$p\overline{p}$ at 1.96 TeV
seen		[3] AAIJ	12AV	LHCB	pp at 7 TeV
seen		AALTONEN	08M	CDF	$p\overline{p}$ at 1.96 TeV
seen		ABAZOV	08T	D0	$p\overline{p}$ at 1.96 TeV
• • • We do not use the following data for averages, fits, limits, etc. • • •					
$< 2.4 \times 10^{-4}$	90	[4] ACKERSTAFF	98O	OPAL	$e^+e^- \to Z$
$< 3.4 \times 10^{-4}$	90	[5] ABREU	97E	DLPH	$e^+e^- \to Z$
$< 8.2 \times 10^{-5}$	90	[6] BARATE	97H	ALEP	$e^+e^- \to Z$
$< 2.0 \times 10^{-5}$	95	[7] ABE	96R	CDF	$p\overline{p}$ 1.8 TeV

[1] AAIJ 15M reports a measurement of B($B_c^+ \to J/\psi\pi^+$) / B($B^+ \to J/\psi K^+$) $\cdot f_c/f_u = (0.683 \pm 0.018 \pm 0.009)\%$ at $p_T(B) < 20$ GeV and $2.0 < y(B) < 4.5$.
[2] KHACHATRYAN 15AA reports a measurement of B($B_c^+ \to J/\psi\pi^+$) / B($B^+ \to J/\psi K^+$) $\cdot f_c/f_u = (0.48 \pm 0.05 \pm 0.03 \pm 0.05)\%$, at $p_T > 15$ GeV and $|\eta(B)| < 1.6$.
[3] AAIJ 12AV reports a measurement of B($B_c^+ \to J/\psi\pi^+$)/B($B^+ \to J/\psi K^+$) $f_c/f_u = (0.68 \pm 0.10 \pm 0.03 \pm 0.05)\%$ at $p_T(B) > 4$ GeV and $2.5 < \eta(B) < 4.5$.
[4] ACKERSTAFF 98O reports B($Z \to B_C$X)/B($Z \to q\overline{q}$)×B($B_C \to J/\psi(1S)\pi^+$) $< 1.06 \times 10^{-4}$ at 90%CL. We rescale to our PDG 98 values of B($Z \to b\overline{b}$).

Meson Particle Listings

B_c^+

[5] ABREU 97E value listed is for an assumed $\tau_{B_c} = 0.4$ ps and improves to 2.7×10^{-4} for $\tau_{B_c} = 1.4$ ps.

[6] BARATE 97H reports $B(Z \to B_c X)/B(Z \to q\overline{q}) \cdot B(B_c \to J/\psi(1S)\pi) < 3.6 \times 10^{-5}$ at 90%CL. We rescale to our PDG 96 values of $B(Z \to b\overline{b})$.

[7] ABE 96R reports $B(b \to B_c X)/B(b \to B^+ X) \cdot B(B_c^+ \to J/\psi(1S)\pi^+)/B(B^+ \to J/\psi(1S)K^+) < 0.053$ at 95%CL for $\tau_{B_c} = 0.8$ ps. It changes from 0.15 to 0.04 for 0.17 ps $< \tau_{B_c} < 1.6$ ps. We rescale to our PDG 96 values of $B(b \to B^+) = 0.378 \pm 0.022$ and $B(B^+ \to J/\psi(1S)K^+) = 0.00101 \pm 0.00014$.

$\Gamma(J/\psi(1S)\pi^+)/\Gamma(J/\psi(1S)\mu^+\nu_\mu)$ Γ_3/Γ_2

VALUE	DOCUMENT ID		TECN	COMMENT
(4.69±0.28±0.46) × 10⁻²	[1] AAIJ	14W	LHCB	pp at 7 TeV

[1] AAIJ 14W reports also a measurement $B(B_c^+ \to J/\psi\pi^+) / B(B_c^+ \to J/\psi\mu^+\nu_\mu) = 0.271 \pm 0.016 \pm 0.016$ in the region $m_{J/\psi\mu^+} > 5.3$ GeV.

$\Gamma(J/\psi(1S)K^+)/\Gamma(J/\psi(1S)\pi^+)$ Γ_4/Γ_3

VALUE	EVTS	DOCUMENT ID		TECN	COMMENT
0.079±0.007±0.003		AAIJ	16AF	LHCB	pp at 7, 8 TeV
• • • We do not use the following data for averages, fits, limits, etc. • • •					
0.069±0.019±0.005	50	AAIJ	13BY	LHCB	Repl. by AAIJ 16AF

$\Gamma(J/\psi(1S)\pi^+\pi^+\pi^-)/\Gamma_{\text{total}} \times B(\overline{b} \to B_c)$ $\Gamma_5/\Gamma \times B$

VALUE	CL%	DOCUMENT ID		TECN	COMMENT
seen		AAIJ	12Y	LHCB	pp at 7 TeV
• • • We do not use the following data for averages, fits, limits, etc. • • •					
$< 5.7 \times 10^{-4}$	90	[1] ABREU	97E	DLPH	$e^+e^- \to Z$

[1] ABREU 97E value listed is independent of 0.4 ps $< \tau_{B_c} <$ 1.4 ps.

$\Gamma(J/\psi(1S)\pi^+\pi^+\pi^-)/\Gamma(J/\psi(1S)\pi^+)$ Γ_5/Γ_3

VALUE	DOCUMENT ID		TECN	COMMENT
2.4 ±0.4 OUR AVERAGE				
$2.55 \pm 0.80 \pm 0.33^{+0.04}_{-0.01}$	KHACHATRY...15AA		CMS	pp at 7 TeV
2.41±0.30±0.33	AAIJ	12Y	LHCB	pp at 7 TeV

$\Gamma(J/\psi(1S)a_1(1260))/\Gamma_{\text{total}} \times B(\overline{b} \to B_c)$ $\Gamma_6/\Gamma \times B$

VALUE	CL%	DOCUMENT ID		TECN	COMMENT
< 1.2 × 10⁻³	90	[1] ACKERSTAFF	98O	OPAL	$e^+e^- \to Z$

[1] ACKERSTAFF 98O reports $B(Z \to B_c X)/B(Z \to q\overline{q}) \times B(B_c \to J/\psi(1S)a_1(1260)) < 5.29 \times 10^{-4}$ at 90%CL. We rescale to our PDG 98 values of $B(Z \to b\overline{b})$.

$\Gamma(J/\psi(1S)K^+K^-\pi^+)/\Gamma_{\text{total}} \times B(\overline{b} \to B_c)$ $\Gamma_7/\Gamma \times B$

VALUE	DOCUMENT ID		TECN	COMMENT
seen	[1] AAIJ	13CA	LHCB	pp at 7, 8 TeV

[1] A signal yield of 78 ± 14 decays is reported with a significance of 6.2 standard deviations using an integrated luminosity of 3 fb^{-1} data.

$\Gamma(J/\psi(1S)K^+K^-\pi^+)/\Gamma(J/\psi(1S)\pi^+)$ Γ_7/Γ_3

VALUE	DOCUMENT ID		TECN	COMMENT
0.53±0.10±0.05	[1] AAIJ	13CA	LHCB	pp at 7, 8 TeV

[1] A signal yield of 78 ± 14 decays is reported with a significance of 6.2 standard deviations using an integrated luminosity of 3 fb^{-1} data.

$\Gamma(J/\psi(1S)\pi^+\pi^+\pi^+\pi^-\pi^-)/\Gamma(J/\psi(1S)\pi^+)$ Γ_8/Γ_3

VALUE	DOCUMENT ID		TECN	COMMENT
1.74±0.44±0.24	[1] AAIJ	14P	LHCB	pp at 7, 8 TeV

[1] A signal yield of 32 ± 8 decays is reported with a significance of 4.5 standard deviations.

$\Gamma(\psi(2S)\pi^+)/\Gamma(J/\psi(1S)\pi^+)$ Γ_9/Γ_3

VALUE	DOCUMENT ID		TECN	COMMENT
0.268±0.032±0.007±0.006	[1] AAIJ	15AY	LHCB	pp at 7, 8 TeV
• • • We do not use the following data for averages, fits, limits, etc. • • •				
0.250±0.068±0.014±0.006	[1] AAIJ	13AM	LHCB	Repl. by AAIJ 15AY

[1] The last uncertainty is due to the uncertainty of the $B(\psi(2S) \to \mu^+\mu^-)/B(J/\psi \to \mu^+\mu^-)$ ratio measurement.

$\Gamma(J/\psi(1S)D^0K^+)/\Gamma(J/\psi(1S)\pi^+)$ Γ_{10}/Γ_3

VALUE	DOCUMENT ID		TECN	COMMENT
0.432±0.136±0.028	AAIJ	17L	LHCB	pp at 7, 8 TeV

$\Gamma(J/\psi(1S)D^*(2007)^0K^+)/\Gamma(J/\psi(1S)D^0K^+)$ Γ_{11}/Γ_{10}

VALUE	DOCUMENT ID		TECN	COMMENT
5.1±1.8±0.4	AAIJ	17L	LHCB	pp at 7, 8 TeV

$\Gamma(J/\psi(1S)D^*(2010)^+K^{*0})/\Gamma(J/\psi(1S)D^0K^+)$ Γ_{12}/Γ_{10}

VALUE	DOCUMENT ID		TECN	COMMENT
2.10±1.08±0.34	AAIJ	17L	LHCB	pp at 7, 8 TeV

$\Gamma(J/\psi(1S)D^+K^{*0})/\Gamma(J/\psi(1S)D^0K^+)$ Γ_{13}/Γ_{10}

VALUE	DOCUMENT ID		TECN	COMMENT
0.63±0.39±0.08	AAIJ	17L	LHCB	pp at 7, 8 TeV

$\Gamma(J/\psi(1S)D_s^+)/\Gamma(J/\psi(1S)\pi^+)$ Γ_{14}/Γ_3

VALUE	DOCUMENT ID		TECN	COMMENT
3.1 ±0.5 OUR AVERAGE				
3.8 ±1.1 ±0.4	AAD	16H	ATLS	pp at 7, 8 TeV
2.90±0.57±0.24	AAIJ	13AS	LHCB	pp at 7, 8 TeV

$\Gamma(J/\psi(1S)D_s^{*+})/\Gamma(J/\psi(1S)\pi^+)$ Γ_{15}/Γ_3

VALUE	DOCUMENT ID		TECN	COMMENT
10.4±3.1±1.6	AAD	16H	ATLS	pp at 7, 8 TeV

$\Gamma(J/\psi(1S)D_s^{*+})/\Gamma(J/\psi(1S)D_s^+)$ Γ_{15}/Γ_{14}

VALUE	DOCUMENT ID		TECN	COMMENT
2.5 ±0.5 OUR AVERAGE				
$2.8\ ^{+1.2}_{-0.8}$ ±0.3	AAD	16H	ATLS	pp at 7, 8 TeV
2.37±0.56±0.10	AAIJ	13AS	LHCB	pp at 7, 8 TeV

$\Gamma(J/\psi(1S)p\overline{p}\pi^+)/\Gamma(J/\psi(1S)\pi^+)$ Γ_{16}/Γ_3

VALUE	DOCUMENT ID		TECN	COMMENT
$0.143^{+0.041}_{-0.036}$	AAIJ	14AQ	LHCB	pp at 7, 8 TeV

$\Gamma(\chi_c^0\pi^+)/\Gamma_{\text{total}}$ Γ_{17}/Γ

VALUE (units 10^{-6})	DOCUMENT ID		TECN	COMMENT
$24.2^{+8.6}_{-7.7}$±0.4	[1,2] AAIJ	16AT	LHCB	pp at 7 and 8 TeV

[1] AAIJ 16AT reports $[\Gamma(B_c^+ \to \chi_c^0\pi^+)/\Gamma_{\text{total}}] \times [\Gamma(\overline{b} \to B^+)/\Gamma_{\text{total}}] = (9.8^{+3.4}_{-3.0} \pm 0.8) \times 10^{-6}$ which we divide by our best value $\Gamma(\overline{b} \to B^+)/\Gamma_{\text{total}} = 0.405 \pm 0.006$. Our first error is their experiment's error and our second error is the systematic error from using our best value.

[2] The significance of the observed signal is 4.0 standard deviations.

$\Gamma(p\overline{p}\pi^+)/\Gamma_{\text{total}}$ Γ_{18}/Γ

VALUE	DOCUMENT ID		TECN	COMMENT
not seen	[1] AAIJ	16K	LHCB	pp at 7, 8 TeV

[1] Measures the ratio $(f_c/f_u) \times B(B_c^+ \to p\overline{p}\pi^+) < 3.6 \times 10^{-8}$ at 95% CL, in the region $m(p\overline{p}) < 2.85$ GeV/c^2, where f_c (f_u) represents the fragmentation fraction of the b-quark into the B_c^+ (B_u^+) meson.

$\Gamma(D^0K^+)/\Gamma_{\text{total}} \times B(\overline{b} \to B_c)$ $\Gamma_{19}/\Gamma \times B$

VALUE (units 10^{-7})	DOCUMENT ID		TECN	COMMENT
$3.8^{+1.2}_{-1.0}$±0.1	[1] AAIJ	17AG	LHCB	pp at 7, 8 TeV

[1] AAIJ 17AG reports $[\Gamma(B_c^+ \to D^0K^+)/\Gamma_{\text{total}} \times B(\overline{b} \to B_c)] / [B(\overline{b} \to B^+)] = (9.3^{+2.8}_{-2.5} \pm 0.6) \times 10^{-7}$ which we multiply by our best value $B(\overline{b} \to B^+) = (40.5 \pm 0.6) \times 10^{-2}$. Our first error is their experiment's error and our second error is the systematic error from using our best value.

$\Gamma(D^0\pi^+)/\Gamma_{\text{total}} \times B(\overline{b} \to B_c)$ $\Gamma_{20}/\Gamma \times B$

VALUE	CL%	DOCUMENT ID		TECN	COMMENT
< 1.6 × 10⁻⁷	95	[1] AAIJ	17AG	LHCB	pp at 7, 8 TeV

[1] AAIJ 17AG reports $[\Gamma(B_c^+ \to D^0\pi^+)/\Gamma_{\text{total}} \times B(\overline{b} \to B_c)] / [B(\overline{b} \to B^+)] < 3.9 \times 10^{-7}$ which we multiply by our best value $B(\overline{b} \to B^+) = 40.5 \times 10^{-2}$.

$\Gamma(D^{*0}\pi^+)/\Gamma_{\text{total}} \times B(\overline{b} \to B_c)$ $\Gamma_{21}/\Gamma \times B$

VALUE	CL%	DOCUMENT ID		TECN	COMMENT
< 4 × 10⁻⁷	95	[1] AAIJ	17AG	LHCB	pp at 7, 8 TeV

[1] AAIJ 17AG reports $[\Gamma(B_c^+ \to D^{*0}\pi^+)/\Gamma_{\text{total}} \times B(\overline{b} \to B_c)] / [B(\overline{b} \to B^+)] < 1.1 \times 10^{-6}$ which we multiply by our best value $B(\overline{b} \to B^+) = 40.5 \times 10^{-2}$.

$\Gamma(D^{*0}K^+)/\Gamma_{\text{total}} \times B(\overline{b} \to B_c)$ $\Gamma_{22}/\Gamma \times B$

VALUE	CL%	DOCUMENT ID		TECN	COMMENT
< 4 × 10⁻⁷	95	[1] AAIJ	17AG	LHCB	pp at 7, 8 TeV

[1] AAIJ 17AG reports $[\Gamma(B_c^+ \to D^{*0}K^+)/\Gamma_{\text{total}} \times B(\overline{b} \to B_c)] / [B(\overline{b} \to B^+)] < 1.1 \times 10^{-6}$ which we multiply by our best value $B(\overline{b} \to B^+) = 40.5 \times 10^{-2}$.

$\Gamma(D^*(2010)^+\overline{D}^0)/\Gamma_{\text{total}} \times B(\overline{b} \to B_c)$ $\Gamma_{23}/\Gamma \times B$

VALUE	CL%	DOCUMENT ID		TECN	COMMENT
< 6.2 × 10⁻³	90	[1] BARATE	98Q	ALEP	$e^+e^- \to Z$

[1] BARATE 98Q reports $B(Z \to B_c X) \times B(B_c \to D^*(2010)^+\overline{D}^0) < 1.9 \times 10^{-3}$ at 90%CL. We rescale to our PDG 98 values of $B(Z \to b\overline{b})$.

$\Gamma(D^+K^{*0})/\Gamma_{\text{total}} \times B(\overline{b} \to B_c)$ $\Gamma_{24}/\Gamma \times B$

VALUE (units 10^{-6})	CL%	DOCUMENT ID		TECN	COMMENT
< 0.20	90	[1] AAIJ	13R	LHCB	pp at 7 TeV

[1] AAIJ 13R reports $[\Gamma(B_c^+ \to D^+K^{*0})/\Gamma_{\text{total}} \times B(\overline{b} \to B_c)] / [B(\overline{b} \to B^+)] < 0.5 \times 10^{-6}$ which we multiply by our best value $B(\overline{b} \to B^+) = 40.5 \times 10^{-2}$.

$\Gamma(D^+\overline{K}^{*0})/\Gamma_{total} \times B(\overline{b} \to B_c)$ $\Gamma_{25}/\Gamma \times B$

VALUE (units 10^{-6})	CL%	DOCUMENT ID		TECN	COMMENT
<0.16	90	[1] AAIJ	13R	LHCB	pp at 7 TeV

[1] AAIJ 13R reports $[\Gamma(B_c^+ \to D^+\overline{K}^{*0})/\Gamma_{total} \times B(\overline{b} \to B_c)] / [B(\overline{b} \to B^+)] < 0.4 \times 10^{-6}$ which we multiply by our best value $B(\overline{b} \to B^+) = 40.5 \times 10^{-2}$.

$\Gamma(D_s^+ K^{*0})/\Gamma_{total} \times B(\overline{b} \to B_c)$ $\Gamma_{26}/\Gamma \times B$

VALUE (units 10^{-6})	CL%	DOCUMENT ID		TECN	COMMENT
<0.28	90	[1] AAIJ	13R	LHCB	pp at 7 TeV

[1] AAIJ 13R reports $[\Gamma(B_c^+ \to D_s^+ K^{*0})/\Gamma_{total} \times B(\overline{b} \to B_c)] / [B(\overline{b} \to B^+)] < 0.7 \times 10^{-6}$ which we multiply by our best value $B(\overline{b} \to B^+) = 40.5 \times 10^{-2}$.

$\Gamma(D_s^+ \overline{K}^{*0})/\Gamma_{total} \times B(\overline{b} \to B_c)$ $\Gamma_{27}/\Gamma \times B$

VALUE (units 10^{-6})	CL%	DOCUMENT ID		TECN	COMMENT
<0.4	90	[1] AAIJ	13R	LHCB	pp at 7 TeV

[1] AAIJ 13R reports $[\Gamma(B_c^+ \to D_s^+ \overline{K}^{*0})/\Gamma_{total} \times B(\overline{b} \to B_c)] / [B(\overline{b} \to B^+)] < 1.1 \times 10^{-6}$ which we multiply by our best value $B(\overline{b} \to B^+) = 40.5 \times 10^{-2}$.

$\Gamma(D_s^+ \phi)/\Gamma_{total} \times B(\overline{b} \to B_c)$ $\Gamma_{28}/\Gamma \times B$

VALUE (units 10^{-6})	CL%	DOCUMENT ID		TECN	COMMENT
<0.32	90	[1] AAIJ	13R	LHCB	pp at 7 TeV

[1] AAIJ 13R reports $[\Gamma(B_c^+ \to D_s^+ \phi)/\Gamma_{total} \times B(\overline{b} \to B_c)] / [B(\overline{b} \to B^+)] < 0.8 \times 10^{-6}$ which we multiply by our best value $B(\overline{b} \to B^+) = 40.5 \times 10^{-2}$.

$\Gamma(K^+ K^0)/\Gamma_{total} \times B(\overline{b} \to B_c)$ $\Gamma_{29}/\Gamma \times B$

VALUE	CL%	DOCUMENT ID		TECN	COMMENT
$<4.6 \times 10^{-7}$	90	[1] AAIJ	13BS	LHCB	pp at 7 TeV

[1] Derived from $\Gamma(K^+ K^0)/\Gamma \times B(\overline{b} \to B_c) / (B(B^+ \to K^0\pi^+)\, B(\overline{b} \to B^+)) < 5.8\%$ at 90% CL using normalization mode $B(B^+ \to K^0\pi^+) = (23.97 \pm 0.53 \pm 0.71) \times 10^{-6}$ and assuming a B production ratio $f(\overline{b} \to B_u^+) = 0.33$.

$\Gamma(B_s^0\pi^+ / B(\overline{b} \to B_s))/\Gamma_{total} \times B(\overline{b} \to B_c)$ $\Gamma_{30}/\Gamma \times B$

VALUE (units 10^{-3})	DOCUMENT ID		TECN	COMMENT
$2.37 \pm 0.31 \pm 0.11 {}^{+0.17}_{-0.13}$	[1] AAIJ	13BU	LHCB	pp at 7, 8 TeV

[1] The last uncertainty is due to the uncertainty of the B_c^+ lifetime measurement.

POLARIZATION IN B_c^+ DECAY

In decays involving two vector mesons, one can distinguish among the states in which meson polarizations are both longitudinal (L) or both are transverse and parallel ($\|$) or perpendicular ($\perp$) to each other with the parameters Γ_L/Γ, $\Gamma_\perp/\Gamma$, and the relative phases $\phi_\|$ and $\phi_\perp$. See the definitions in the note on "Polarization in B Decays" review in the B^0 Particle Listings.

Γ_L/Γ in $B_c^+ \to J/\psi D_s^{*+}$

VALUE	DOCUMENT ID		TECN	COMMENT
0.54±0.15 OUR AVERAGE				
0.62±0.24	[1] AAD	16H	ATLS	pp at 7, 8 TeV
0.48±0.20	[2] AAIJ	13AS	LHCB	pp at 7, 8 TeV

[1] AAD 16H measures $1 - \Gamma_L/\Gamma = 0.38 \pm 0.24$.
[2] AAIJ 13AS measures $1 - \Gamma_L/\Gamma = 0.52 \pm 0.20$.

B_c^+ REFERENCES

AAIJ	17AG	PRL 118 111803	R. Aaij *et al.*	(LHCb Collab.)
AAIJ	17L	PR D95 032005	R. Aaij *et al.*	(LHCb Collab.)
AAD	16H	EPJ C76 4	G. Aad *et al.*	(ATLAS Collab.)
AAIJ	16AF	JHEP 1609 153	R. Aaij *et al.*	(LHCb Collab.)
AAIJ	16AT	PR D94 091102	R. Aaij *et al.*	(LHCb Collab.)
AAIJ	16K	PL B759 313	R. Aaij *et al.*	(LHCb Collab.)
AALTONEN	16A	PR D93 052001	T. Aaltonen *et al.*	(CDF Collab.)
AAIJ	15AY	PR D92 072007	R. Aaij *et al.*	(LHCb Collab.)
AAIJ	15G	PL B742 29	R. Aaij *et al.*	(LHCb Collab.)
AAIJ	15M	PRL 114 132001	R. Aaij *et al.*	(LHCb Collab.)
KHACHATRY...	15AA	JHEP 1501 063	V. Khachatryan *et al.*	(CMS Collab.)
AAIJ	14AQ	PRL 113 152003	R. Aaij *et al.*	(LHCb Collab.)
AAIJ	14G	EPJ C74 2839	R. Aaij *et al.*	(LHCb Collab.)
AAIJ	14P	JHEP 1405 148	R. Aaij *et al.*	(LHCb Collab.)
AAIJ	14W	PR D90 032009	R. Aaij *et al.*	(LHCb Collab.)
AAIJ	13AM	PR D87 071103	R. Aaij *et al.*	(LHCb Collab.)
AAIJ	13AS	PR D87 112012	R. Aaij *et al.*	(LHCb Collab.)
Also		PR D89 019901 (errat.)	R. Aaij *et al.*	(LHCb Collab.)
AAIJ	13BS	PL B726 646	R. Aaij *et al.*	(LHCb Collab.)
AAIJ	13BU	PRL 111 181801	R. Aaij *et al.*	(LHCb Collab.)
AAIJ	13BY	JHEP 1309 075	R. Aaij *et al.*	(LHCb Collab.)
AAIJ	13CA	JHEP 1311 094	R. Aaij *et al.*	(LHCb Collab.)
AAIJ	13R	JHEP 1302 043	R. Aaij *et al.*	(LHCb Collab.)
AALTONEN	13	PR D87 011101	T. Aaltonen *et al.*	(CDF Collab.)
AAIJ	12AV	PRL 109 232001	R. Aaij *et al.*	(LHCb Collab.)
AAIJ	12Y	PRL 108 251802	R. Aaij *et al.*	(LHCb Collab.)
ABAZOV	09H	PRL 102 092001	V.M. Abazov *et al.*	(D0 Collab.)
AALTONEN	08M	PRL 100 182002	T. Aaltonen *et al.*	(CDF Collab.)
ABAZOV	08T	PRL 101 012001	V.M. Abazov *et al.*	(D0 Collab.)
ABULENCIA	06C	PRL 96 082002	A. Abulencia *et al.*	(CDF Collab.)
ABULENCIA	06O	PRL 97 012002	A. Abulencia *et al.*	(CDF Collab.)
ABE	98M	PRL 81 2432	F. Abe *et al.*	(CDF Collab.)
Also		PR D58 112004	F. Abe *et al.*	(CDF Collab.)
ACKERSTAFF	98O	PL B420 157	K. Ackerstaff *et al.*	(OPAL Collab.)
BARATE	98Q	EPJ C4 387	R. Barate *et al.*	(ALEPH Collab.)
PDG	98	EPJ C3 1	C. Caso *et al.*	(PDG Collab.)
ABREU	97E	PL B398 207	P. Abreu *et al.*	(DELPHI Collab.)
BARATE	97H	PL B402 213	R. Barate *et al.*	(ALEPH Collab.)
ABE	96R	PRL 77 5176	F. Abe *et al.*	(CDF Collab.)
PDG	96	PR D54 1	R. M. Barnett *et al.*	(PDG Collab.)

$B_c(2S)^\pm$ $I(J^P) = 0(0^-)$

OMITTED FROM SUMMARY TABLE
Quantum numbers neither measured nor confirmed.

$B_c(2S)^\pm$ MASS

VALUE (MeV)	EVTS	DOCUMENT ID		TECN	COMMENT
6842±4±5	57	[1] AAD	14AQ	ATLS	pp at 7, 8 TeV

[1] Observed in the decay mode $B_c(2S)^+ \to B_c^+\pi^+\pi^-$ ($B_c^+ \to J/\psi\pi^+$) with 5.2 standard deviations significance.

$B_c(2S)^\pm$ DECAY MODES

	Mode	Fraction (Γ_i/Γ)
Γ_1	$B_c^+\pi^+\pi^-$	seen

$B_c(2S)^\pm$ BRANCHING RATIOS

$\Gamma(B_c^+\pi^+\pi^-)/\Gamma_{total}$ Γ_1/Γ

VALUE	EVTS	DOCUMENT ID		TECN	COMMENT
seen	57	[1] AAD	14AQ	ATLS	pp at 7, 8 TeV

[1] Observed with 5.2 standard deviations significance.

$B_c(2S)^\pm$ REFERENCES

AAD	14AQ	PRL 113 212004	G. Aad *et al.*	(ATLAS Collab.)

See the related review(s):
Spectroscopy of Mesons Containing Two Heavy Quarks

$c\overline{c}$ MESONS (including possibly non-$q\overline{q}$ states)

See the related review(s):
Charmonium System

$\eta_c(1S)$

$I^G(J^{PC}) = 0^+(0^{-+})$

$\eta_c(1S)$ MASS

VALUE (MeV)	EVTS	DOCUMENT ID		TECN	COMMENT
2983.9 ± 0.5 OUR AVERAGE		Error includes scale factor of 1.3. See the ideogram below.			
2986.7 ± 0.5 ± 0.9	11K	[1] AAIJ	17AD	LHCB	$pp \to B^+X \to p\overline{p}K^+X$
2982.8 ± 1.0 ± 0.5	6.4k	[2] AAIJ	17BB	LHCB	$pp \to b\overline{b}X \to 2(K^+K^-)X$
2982.2 ± 1.5 ± 0.1	2.0k	[3] AAIJ	15BI	LHCB	$pp \to \eta_c(1S)X$
2983.5 ± 1.4 $^{+1.6}_{-3.6}$		[4] ANASHIN	14	KEDR	$J/\psi \to \gamma\eta_c$
2979.8 ± 0.8 ± 3.5	4.5k	[5,6] LEES	14E	BABR	$\gamma\gamma \to K^+K^-\pi^0$
2984.1 ± 1.1 ± 2.1	900	[5,6,7] LEES	14E	BABR	$\gamma\gamma \to K^+K^-\eta$
2984.3 ± 0.6 ± 0.6		[8,9] ABLIKIM	12F	BES3	$\psi(2S) \to \gamma\eta_c$
2984.49 ± 1.16 ± 0.52	832	[5] ABLIKIM	12N	BES3	$\psi(2S) \to \pi^0\gamma$ hadrons
2982.7 ± 1.8 ± 2.2	486	ZHANG	12A	BELL	$e^+e^- \to e^+e^-\eta'\pi^+\pi^-$
2984.5 ± 0.8 ± 3.1	11k	DEL-AMO-SA...	11M	BABR	$\gamma\gamma \to K^+K^-\pi^+\pi^-\pi^0$
2985.4 ± 1.5 $^{+0.5}_{-2.0}$	920	[9] VINOKUROVA	11	BELL	$B^\pm \to K^\pm(K^0_S K^\pm\pi^\mp)$
2982.2 ± 0.4 ± 1.6	14k	[10] LEES	10	BABR	10.6 $e^+e^- \to e^+e^- K^0_S K^\pm\pi^\mp$
2985.8 ± 1.5 ± 3.1	0.9k	AUBERT	08AB	BABR	$B \to \eta_c(1S)K^{(*)} \to K\overline{K}\pi K^{(*)}$
2986.1 ± 1.0 ± 2.5	7.5k	UEHARA	08	BELL	$\gamma\gamma \to \eta_c \to$ hadrons
2970 ± 5 ± 6	501	[11] ABE	07	BELL	$e^+e^- \to J/\psi(c\overline{c})$
2971 ± 3 $^{+2}_{-1}$	195	WU	06	BELL	$B^+ \to p\overline{p}K^+$
2974 ± 7 $^{+2}_{-1}$	20	WU	06	BELL	$B^+ \to \Lambda\overline{\Lambda}K^+$
2981.8 ± 1.3 ± 1.5	592	ASNER	04	CLEO	$\gamma\gamma \to \eta_c \to K^0_S K^\pm\pi^\mp$
2984.1 ± 2.1 ± 1.0	190	[12] AMBROGIANI	03	E835	$\overline{p}p \to \eta_c \to \gamma\gamma$
• • • We do not use the following data for averages, fits, limits, etc. • • •					
2982.5 ± 0.4 ± 1.4	12k	[13] DEL-AMO-SA...	11M	BABR	$\gamma\gamma \to K^0_S K^\pm\pi^\mp$
2982.2 ± 0.6		[14] MITCHELL	09	CLEO	$e^+e^- \to \gamma X$
2982 ± 5	270	[15] AUBERT	06E	BABR	$B^\pm \to K^\pm X_{c\overline{c}}$
2982.5 ± 1.1 ± 0.9	2.5k	[16] AUBERT	04D	BABR	$\gamma\gamma \to \eta_c(1S) \to K\overline{K}\pi$
2977.5 ± 1.0 ± 1.2		[14,17] BAI	03	BES	$J/\psi \to \gamma\eta_c$
2979.6 ± 2.3 ± 1.6	180	[18] FANG	03	BELL	$B \to \eta_c K$
2976.3 ± 2.3 ± 1.2		[14,19] BAI	00F	BES	$J/\psi,\ \psi(2S) \to \gamma\eta_c$
2976.6 ± 2.9 ± 1.3	140	[14,20] BAI	00F	BES	$J/\psi \to \gamma\eta_c$
2980.4 ± 2.3 ± 0.6		[21] BRANDENB...	00B	CLE2	$\gamma\gamma \to \eta_c \to K^\pm K^0_S\pi^\mp$
2975.8 ± 3.9 ± 1.2		[20] BAI	99B	BES	Sup. by BAI 00F
2999 ± 8	25	ABREU	98O	DLPH	$e^+e^- \to e^+e^-$ +hadrons
2988.3 $^{+3.3}_{-3.1}$		ARMSTRONG	95F	E760	$\overline{p}p \to \gamma\gamma$
2974.4 ± 1.9		[14,22] BISELLO	91	DM2	$J/\psi \to \eta_c\gamma$
2969 ± 4 ± 4	80	[14] BAI	90B	MRK3	$J/\psi \to \gamma K^+K^-K^+K^-$
2956 ±12 ±12		[14] BAI	90B	MRK3	$J/\psi \to \gamma K^+K^-K^0_S K^0_L$
2982.6 $^{+2.7}_{-2.3}$	12	BAGLIN	87B	SPEC	$\overline{p}p \to \gamma\gamma$
2980.2 ± 1.6		[14,22] BALTRUSAIT...	86	MRK3	$J/\psi \to \eta_c\gamma$
2984 ± 2.3 ± 4.0		[14] GAISER	86	CBAL	$J/\psi \to \gamma X,\ \psi(2S) \to \gamma X$
2976 ± 8		[14,23] BALTRUSAIT...	84	MRK3	$J/\psi \to 2\phi\gamma$
2982 ± 8	18	[24] HIMEL	80B	MRK2	e^+e^-
2980 ± 9		[24] PARTRIDGE	80B	CBAL	e^+e^-

[1] AAIJ 17AD report $m_{J/\psi} - m_{\eta_c(1S)} = 110.2 \pm 0.5 \pm 0.9$ MeV. We use the current value $m_{J/\psi} = 3096.900 \pm 0.006$ MeV to obtain the quoted mass.
[2] From a fit of the $\phi\phi$ invariant mass with the mass and width of $\eta_c(1S)$ as free parameters.
[3] AAIJ 15BI reports $m_{J/\psi} - m_{\eta_c(1S)} = 114.7 \pm 1.5 \pm 0.1$ MeV from a sample of $\eta_c(1S)$ and J/ψ produced in b-hadron decays. We have used current value of $m_{J/\psi} = 3096.900 \pm 0.006$ MeV to arrive at the quoted $m_{\eta_c(1S)}$ result.
[4] Taking into account an asymmetric photon lineshape.
[5] With floating width.
[6] Ignoring possible interference with the non-resonant 0^- amplitude.
[7] Using both, $\eta \to \gamma\gamma$ and $\eta \to \pi^+\pi^-\pi^0$ decays.
[8] From a simultaneous fit to six decay modes of the η_c.
[9] Accounts for interference with non-resonant continuum.
[10] Taking into account interference with the non-resonant $J^P = 0^-$ amplitude.
[11] From a fit of the J/ψ recoil mass spectrum. Supersedes ABE,K 02 and ABE 04G.
[12] Using mass of $\psi(2S) = 3686.00$ MeV.
[13] Not independent from the measurements reported by LEES 10.
[14] MITCHELL 09 observes a significant asymmetry in the lineshapes of $\psi(2S) \to \gamma\eta_c$ and $J/\psi \to \gamma\eta_c$ transitions. If ignored, this asymmetry could lead to significant bias whenever the mass and width are measured in $\psi(2S)$ or J/ψ radiative decays.
[15] From the fit of the kaon momentum spectrum. Systematic errors not evaluated.
[16] Superseded by LEES 10.
[17] From a simultaneous fit of five decay modes of the η_c.
[18] Superseded by VINOKUROVA 11.
[19] Weighted average of the $\psi(2S)$ and $J/\psi(1S)$ samples. Using an η_c width of 13.2 MeV.
[20] Average of several decay modes. Using an η_c width of 13.2 MeV.
[21] Superseded by ASNER 04.
[22] Average of several decay modes.
[23] $\eta_c \to \phi\phi$.
[24] Mass adjusted by us to correspond to $J/\psi(1S)$ mass = 3097 MeV.

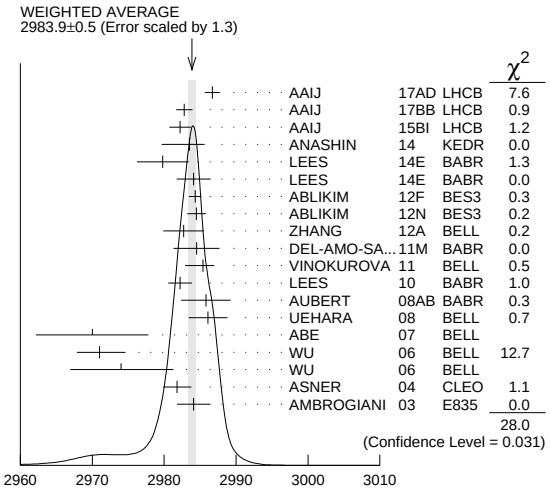

$\eta_c(1S)$ WIDTH

VALUE (MeV)	EVTS	DOCUMENT ID		TECN	COMMENT
32.0± 0.8 OUR FIT					
32.1± 0.9 OUR AVERAGE		Error includes scale factor of 1.1.			
34.0± 1.9±1.3	11K	AAIJ	17AD	LHCB	$pp \to B^+X \to p\overline{p}K^+X$
31.4± 3.5±2.0	6.4k	[1] AAIJ	17BB	LHCB	$pp \to b\overline{b}X \to 2(K^+K^-)X$
27.2± 3.1 $^{+5.4}_{-2.6}$		[2] ANASHIN	14	KEDR	$J/\psi \to \gamma\eta_c$
25.2± 2.6±2.4	4.5k	[3,4] LEES	14E	BABR	$\gamma\gamma \to K^+K^-\pi^0$
34.8± 3.1±4.0	900	[3,4,5] LEES	14E	BABR	$\gamma\gamma \to K^+K^-\eta$
32.0± 1.2±1.0		[6,7] ABLIKIM	12F	BES3	$\psi(2S) \to \gamma\eta_c$
36.4± 3.2±1.7	832	[3] ABLIKIM	12N	BES3	$\psi(2S) \to \pi^0\gamma$ hadrons
37.8 $^{+5.8}_{-5.3}$ ±3.1	486	ZHANG	12A	BELL	$e^+e^- \to e^+e^-\eta'\pi^+\pi^-$
36.2± 2.8±3.0	11k	DEL-AMO-SA...	11M	BABR	$\gamma\gamma \to K^+K^-\pi^+\pi^-\pi^0$
35.1± 3.1 $^{+1.0}_{-1.6}$	920	[7] VINOKUROVA	11	BELL	$B^\pm \to K^\pm(K^0_S K^\pm\pi^\mp)$
31.7± 1.2±0.8	14k	[8] LEES	10	BABR	10.6 $e^+e^- \to e^+e^- K^0_S K^\pm\pi^\mp$
36.3 $^{+3.7}_{-3.6}$ ±4.4	0.9k	AUBERT	08AB	BABR	$B \to \eta_c(1S)K^{(*)} \to K\overline{K}\pi K^{(*)}$
28.1± 3.2±2.2	7.5k	UEHARA	08	BELL	$\gamma\gamma \to \eta_c \to$ hadrons
48 $^{+8}_{-7}$ ±5	195	WU	06	BELL	$B^+ \to p\overline{p}K^+$
40 ±19 ±5	20	WU	06	BELL	$B^+ \to \Lambda\overline{\Lambda}K^+$
24.8± 3.4±3.5	592	ASNER	04	CLEO	$\gamma\gamma \to \eta_c \to K^0_S K^\pm\pi^\mp$
20.4 $^{+7.7}_{-6.7}$ ±2.0	190	AMBROGIANI	03	E835	$\overline{p}p \to \eta_c \to \gamma\gamma$
23.9 $^{+12.6}_{-7.1}$		ARMSTRONG	95F	E760	$\overline{p}p \to \gamma\gamma$
• • • We do not use the following data for averages, fits, limits, etc. • • •					
32.1± 1.1±1.3	12k	[9] DEL-AMO-SA...	11M	BABR	$\gamma\gamma \to K^0_S K^\pm\pi^\mp$
34.3± 2.3±0.9	2.5k	[10] AUBERT	04D	BABR	$\gamma\gamma \to \eta_c(1S) \to K\overline{K}\pi$
17.0± 3.7±7.4		[11] BAI	03	BES	$J/\psi \to \gamma\eta_c$

29 ± 8 ±6	180	[12] FANG	03	BELL	$B \to \eta_c K$
11.0± 8.1±4.1		[13] BAI	00F	BES	$J/\psi \to \gamma\eta_c$ and $\psi(2S) \to \gamma\eta_c$
27.0± 5.8±1.4		[14] BRANDENB...	00B	CLE2	$\gamma\gamma \to \eta_c \to K^\pm K^0_S \pi^\mp$
$7.0^{+7.5}_{-7.0}$	12	BAGLIN	87B	SPEC	$\overline{p}p \to \gamma\gamma$
$10.1^{+33.0}_{-8.2}$	23	[15] BALTRUSAIT...	86	MRK3	$J/\psi \to \gamma p\overline{p}$
11.5± 4.5		GAISER	86	CBAL	$J/\psi \to \gamma$X, $\psi(2S) \to \gamma$X
< 40 90% CL	18	HIMEL	80B	MRK2	e^+e^-
< 20 90% CL		PARTRIDGE	80B	CBAL	e^+e^-

[1] From a fit of the $\phi\phi$ invariant mass with the mass and width of $\eta_c(1S)$ as free parameters.
[2] Taking into account an asymmetric photon lineshape.
[3] With floating mass.
[4] Ignoring possible interference with the non-resonant 0^- amplitude.
[5] Using both, $\eta \to \gamma\gamma$ and $\eta \to \pi^+\pi^-\pi^0$ decays.
[6] From a simultaneous fit to six decay modes of the η_c.
[7] Accounts for interference with non-resonant continuum.
[8] Taking into account interference with the non-resonant $J^P = 0^-$ amplitude.
[9] Not independent from the measurements reported by LEES 10.
[10] Superseded by LEES 10.
[11] From a simultaneous fit of five decay modes of the η_c.
[12] Superseded by VINOKUROVA 11.
[13] From a fit to the 4-prong invariant mass in $\psi(2S) \to \gamma\eta_c$ and $J/\psi(1S) \to \gamma\eta_c$ decays.
[14] Superseded by ASNER 04.
[15] Positive and negative errors correspond to 90% confidence level.

$\eta_c(1S)$ DECAY MODES

	Mode	Fraction (Γ_i/Γ)	Confidence level
	Decays involving hadronic resonances		
Γ_1	$\eta'(958)\pi\pi$	(4.1 ±1.7) %	
Γ_2	$\rho\rho$	(1.8 ±0.5) %	
Γ_3	$K^*(892)^0 K^-\pi^+$ + c.c.	(2.0 ±0.7) %	
Γ_4	$K^*(892)\overline{K}^*(892)$	(7.1 ±1.3) $\times 10^{-3}$	
Γ_5	$K^*(892)^0\overline{K}^*(892)^0\pi^+\pi^-$	(1.1 ±0.5) %	
Γ_6	ϕK^+K^-	(2.9 ±1.4) $\times 10^{-3}$	
Γ_7	$\phi\phi$	(1.79±0.20) $\times 10^{-3}$	
Γ_8	$\phi 2(\pi^+\pi^-)$	< 4 $\times 10^{-3}$	90%
Γ_9	$a_0(980)\pi$	< 2 %	90%
Γ_{10}	$a_2(1320)\pi$	< 2 %	90%
Γ_{11}	$K^*(892)\overline{K}$ + c.c.	< 1.28 %	90%
Γ_{12}	$f_2(1270)\eta$	< 1.1 %	90%
Γ_{13}	$\omega\omega$	< 3.1 $\times 10^{-3}$	90%
Γ_{14}	$\omega\phi$	< 2.5 $\times 10^{-4}$	90%
Γ_{15}	$f_2(1270)f_2(1270)$	(9.8 ±2.5) $\times 10^{-3}$	
Γ_{16}	$f_2(1270)f_2'(1525)$	(9.8 ±3.2) $\times 10^{-3}$	
Γ_{17}	$f_0(980)\eta$	seen	
Γ_{18}	$f_0(1500)\eta$	seen	
Γ_{19}	$f_0(2200)\eta$	seen	
Γ_{20}	$a_0(980)\pi$	seen	
Γ_{21}	$a_0(1320)\pi$	seen	
Γ_{22}	$a_0(1450)\pi$	seen	
Γ_{23}	$a_0(1950)\pi$	seen	
Γ_{24}	$a_2(1950)\pi$	not seen	
Γ_{25}	$K_0^*(1430)\overline{K}$	seen	
Γ_{26}	$K_2^*(1430)\overline{K}$	seen	
Γ_{27}	$K_0^*(1950)\overline{K}$	seen	
	Decays into stable hadrons		
Γ_{28}	$K\overline{K}\pi$	(7.3 ±0.5) %	
Γ_{29}	$K\overline{K}\eta$	(1.36±0.16) %	
Γ_{30}	$\eta\pi^+\pi^-$	(1.7 ±0.5) %	
Γ_{31}	$\eta 2(\pi^+\pi^-)$	(4.4 ±1.3) %	
Γ_{32}	$K^+K^-\pi^+\pi^-$	(6.9 ±1.1) $\times 10^{-3}$	
Γ_{33}	$K^+K^-\pi^+\pi^-\pi^0$	(3.5 ±0.6) %	
Γ_{34}	$K^0K^-\pi^+\pi^-\pi^+$ + c.c.	(5.6 ±1.5) %	
Γ_{35}	$K^+K^-2(\pi^+\pi^-)$	(7.5 ±2.4) $\times 10^{-3}$	
Γ_{36}	$2(K^+K^-)$	(1.47±0.31) $\times 10^{-3}$	
Γ_{37}	$\pi^+\pi^-\pi^0$	< 5 $\times 10^{-4}$	90%
Γ_{38}	$\pi^+\pi^-\pi^0\pi^0$	(4.7 ±1.0) %	
Γ_{39}	$2(\pi^+\pi^-)$	(9.7 ±1.2) $\times 10^{-3}$	
Γ_{40}	$2(\pi^+\pi^-\pi^0)$	(17.4 ±3.3) %	
Γ_{41}	$3(\pi^+\pi^-)$	(1.8 ±0.4) %	
Γ_{42}	$p\overline{p}$	(1.52±0.16) $\times 10^{-3}$	
Γ_{43}	$p\overline{p}\pi^0$	(3.6 ±1.3) $\times 10^{-3}$	
Γ_{44}	$\Lambda\overline{\Lambda}$	(1.09±0.24) $\times 10^{-3}$	
Γ_{45}	$\Sigma^+\overline{\Sigma}^-$	(2.1 ±0.6) $\times 10^{-3}$	
Γ_{46}	$\Xi^-\overline{\Xi}^+$	(9.0 ±2.6) $\times 10^{-4}$	
Γ_{47}	$\pi^+\pi^- p\overline{p}$	(5.3 ±1.8) $\times 10^{-3}$	

Radiative decays

Γ_{48}	$\gamma\gamma$	(1.57±0.12) $\times 10^{-4}$		

Charge conjugation (C), Parity (P), Lepton family number (LF) violating modes

Γ_{49}	$\pi^+\pi^-$	P,CP	< 1.1	$\times 10^{-4}$	90%
Γ_{50}	$\pi^0\pi^0$	P,CP	< 4	$\times 10^{-5}$	90%
Γ_{51}	K^+K^-	P,CP	< 6	$\times 10^{-4}$	90%
Γ_{52}	$K^0_S K^0_S$	P,CP	< 3.1	$\times 10^{-4}$	90%

CONSTRAINED FIT INFORMATION

An overall fit to the total width, 8 combinations of partial widths obtained from integrated cross section, and 19 branching ratios uses 88 measurements and one constraint to determine 13 parameters. The overall fit has a $\chi^2 = 119.9$ for 76 degrees of freedom.

The following *off-diagonal* array elements are the correlation coefficients $\langle \delta p_i \delta p_j \rangle / (\delta p_i \cdot \delta p_j)$, in percent, from the fit to parameters p_i, including the branching fractions, $x_i \equiv \Gamma_i/\Gamma_{\rm total}$. The fit constrains the x_i whose labels appear in this array to sum to one.

x_7	18									
x_{15}	3	6								
x_{28}	21	41	7							
x_{29}	11	22	4	54						
x_{32}	11	20	4	24	13					
x_{36}	9	16	3	25	13	10				
x_{39}	13	25	5	30	16	15	12			
x_{42}	14	25	5	35	19	16	13	19		
x_{44}	3	6	1	9	5	4	3	5	25	
x_{48}	−29	−54	−10	−65	−35	−34	−26	−41	−45	−11
Γ	−1	−3	−1	−3	−2	−2	−1	−2	6	2
	x_4	x_7	x_{15}	x_{28}	x_{29}	x_{32}	x_{36}	x_{39}	x_{42}	x_{44}

Γ	−26	
	x_{48}	

	Mode	Rate (MeV)
Γ_4	$K^*(892)\overline{K}^*(892)$	0.23 ±0.04
Γ_7	$\phi\phi$	0.057 ±0.006
Γ_{15}	$f_2(1270)f_2(1270)$	0.31 ±0.08
Γ_{28}	$K\overline{K}\pi$	2.34 ±0.16
Γ_{29}	$K\overline{K}\eta$	0.43 ±0.05
Γ_{32}	$K^+K^-\pi^+\pi^-$	0.222 ±0.034
Γ_{36}	$2(K^+K^-)$	0.047 ±0.010
Γ_{39}	$2(\pi^+\pi^-)$	0.31 ±0.04
Γ_{42}	$p\overline{p}$	0.048 ±0.005
Γ_{44}	$\Lambda\overline{\Lambda}$	0.035 ±0.008
Γ_{48}	$\gamma\gamma$	0.0050±0.0004

$\eta_c(1S)$ PARTIAL WIDTHS

$\Gamma(\gamma\gamma)$ Γ_{48}

VALUE (keV)	EVTS	DOCUMENT ID		TECN	COMMENT
5.0± 0.4 OUR FIT					
• • • We do not use the following data for averages, fits, limits, etc. • • •					
5.8± 1.1	486	[1] ZHANG	12A	BELL	$e^+e^- \to e^+e^-\eta'\pi^+\pi^-$
5.2± 1.2	273 ± 43	[2,3] AUBERT	06E	BABR	$B^\pm \to K^\pm X_{c\overline{c}}$
5.5± 1.2± 1.8	157 ± 33	[4] KUO	05	BELL	$\gamma\gamma \to p\overline{p}$
7.4± 0.4± 2.3		[5] ASNER	04	CLEO	$\gamma\gamma \to \eta_c \to K^0_S K^\pm\pi^\mp$
13.9± 2.0± 3.0	41	[6] ABDALLAH	03J	DLPH	$\gamma\gamma \to \eta_c$
$3.8^{+1.1}_{-1.0} \pm 1.9$	190	[7] AMBROGIANI	03	E835	$\overline{p}p \to \eta_c \to \gamma\gamma$
7.6± 0.8± 2.3		[5,8] BRANDENB...	00B	CLE2	$\gamma\gamma \to \eta_c \to K^\pm K^0_S \pi^\mp$
6.9± 1.7± 2.1	76	[9] ACCIARRI	99T	L3	$e^+e^- \to e^+e^-\eta_c$
27 ±16 ±10	5	[5] SHIRAI	98	AMY	58 e^+e^-
$6.7^{+2.4}_{-1.7} \pm 2.3$		[4] ARMSTRONG	95F	E760	$\overline{p}p \to \gamma\gamma$
11.3± 4.2		[10] ALBRECHT	94H	ARG	$e^+e^- \to e^+e^-\eta_c$
8.0± 2.3± 2.4	17	[11] ADRIANI	93N	L3	$e^+e^- \to e^+e^-\eta_c$
$5.9^{+2.1}_{-1.8} \pm 1.9$		[7] CHEN	90B	CLEO	$e^+e^- \to e^+e^-\eta_c$
$6.4^{+5.0}_{-3.4}$		[12] AIHARA	88D	TPC	$e^+e^- \to e^+e^-$X
$4.3^{+3.4}_{-3.7} \pm 2.4$		[4] BAGLIN	87B	SPEC	$\overline{p}p \to \gamma\gamma$
28 ±15		[5,13] BERGER	86	PLUT	$\gamma\gamma \to K\overline{K}\pi$

[1] Assuming there is no interference with the non-resonant background.

[2] Calculated by us using $\Gamma(\eta_c \to K\overline{K}\pi) \times \Gamma(\eta_c \to \gamma\gamma) / \Gamma = 0.44 \pm 0.05$ keV from PDG 06 and $B(\eta_c \to K\overline{K}\pi) = (8.5 \pm 1.8)\%$ from AUBERT 06E.
[3] Systematic errors not evaluated.
[4] Normalized to $B(\eta_c \to p\overline{p}) = (1.3 \pm 0.4) \times 10^{-3}$.
[5] Normalized to $B(\eta_c \to K^\pm K^0_S \pi^\mp)$.
[6] Average of $K^0_S K^\pm \pi^\mp$, $\pi^+\pi^- K^+ K^-$, and $2(K^+K^-)$ decay modes.
[7] Normalized to the sum of $B(\eta_c \to K^\pm K^0_S \pi^\mp)$, $B(\eta_c \to K^+K^-\pi^+\pi^-)$, and $B(\eta_c \to 2\pi^+2\pi^-)$.
[8] Superseded by ASNER 04.
[9] Normalized to the sum of 9 branching ratios.
[10] Normalized to the sum of $B(\eta_c \to K^\pm K^0_S \pi^\mp)$, $B(\eta_c \to \phi\phi)$, $B(\eta_c \to K^+K^-\pi^+\pi^-)$, and $B(\eta_c \to 2\pi^+2\pi^-)$.
[11] Superseded by ACCIARRI 99T.
[12] Normalized to the sum of $B(\eta_c \to K^\pm K^0_S \pi^\mp)$, $B(\eta_c \to 2K^+2K^-)$, $B(\eta_c \to K^+K^-\pi^+\pi^-)$, and $B(\eta_c \to 2\pi^+2\pi^-)$.
[13] Re-evaluated by AIHARA 88D.

$\eta_c(1S)$ Γ(i)$\Gamma(\gamma\gamma)/\Gamma$(total)

$\Gamma(\eta'(958)\pi\pi) \times \Gamma(\gamma\gamma)/\Gamma_{total}$ — $\Gamma_1\Gamma_{48}/\Gamma$

VALUE (keV)	EVTS	DOCUMENT ID		TECN	COMMENT
$75.8^{+6.3}_{-6.2} \pm 8.4$	486	[1] ZHANG	12A	BELL	$e^+e^- \to e^+e^-\eta'\pi^+\pi^-$

[1] Assuming there is no interference with the non-resonant background.

$\Gamma(\rho\rho) \times \Gamma(\gamma\gamma)/\Gamma_{total}$ — $\Gamma_2\Gamma_{48}/\Gamma$

VALUE (eV)	CL%	EVTS	DOCUMENT ID		TECN	COMMENT
• • • We do not use the following data for averages, fits, limits, etc. • • •						
<39	90	<1556	UEHARA	08	BELL	$\gamma\gamma \to 2(\pi^+\pi^-)$

$\Gamma(K^*(892)\overline{K}^*(892)) \times \Gamma(\gamma\gamma)/\Gamma_{total}$ — $\Gamma_4\Gamma_{48}/\Gamma$

VALUE (eV)	EVTS	DOCUMENT ID		TECN	COMMENT
35 ±6 OUR FIT					
$32.4 \pm 4.2 \pm 5.8$	882 ± 115	UEHARA	08	BELL	$\gamma\gamma \to \pi^+\pi^- K^+K^-$

$\Gamma(\phi\phi) \times \Gamma(\gamma\gamma)/\Gamma_{total}$ — $\Gamma_7\Gamma_{48}/\Gamma$

VALUE (eV)	EVTS	DOCUMENT ID		TECN	COMMENT
9.0 ±0.8 OUR FIT					
$7.75 \pm 0.66 \pm 0.62$	386 ± 31	[1] LIU	12B	BELL	$\gamma\gamma \to 2(K^+K^-)$
• • • We do not use the following data for averages, fits, limits, etc. • • •					
$6.8 \pm 1.2 \pm 1.3$	132 ± 23	UEHARA	08	BELL	$\gamma\gamma \to 2(K^+K^-)$

[1] Supersedes UEHARA 08. Using $B(\phi \to K^+K^-) = (48.9 \pm 0.5)\%$.

$\Gamma(\omega\omega) \times \Gamma(\gamma\gamma)/\Gamma_{total}$ — $\Gamma_{13}\Gamma_{48}/\Gamma$

VALUE (eV)	EVTS	DOCUMENT ID		TECN	COMMENT
$8.67 \pm 2.86 \pm 0.96$	85 ± 29	[1] LIU	12B	BELL	$\gamma\gamma \to 2(\pi^+\pi^-\pi^0)$

[1] Using $B(\omega \to \pi^+\pi^-\pi^0) = (89.2 \pm 0.7)\%$.

$\Gamma(\omega\phi) \times \Gamma(\gamma\gamma)/\Gamma_{total}$ — $\Gamma_{14}\Gamma_{48}/\Gamma$

VALUE (eV)	CL%	DOCUMENT ID		TECN	COMMENT
• • • We do not use the following data for averages, fits, limits, etc. • • •					
<0.49	90	[1] LIU	12B	BELL	$\gamma\gamma \to K^+K^-\pi^+\pi^-\pi^0$

[1] Using $B(\phi \to K^+K^-) = (48.9 \pm 0.5)\%$ and $B(\omega \to \pi^+\pi^-\pi^0) = (89.2 \pm 0.7)\%$.

$\Gamma(f_2(1270)f_2(1270)) \times \Gamma(\gamma\gamma)/\Gamma_{total}$ — $\Gamma_{15}\Gamma_{48}/\Gamma$

VALUE (eV)	EVTS	DOCUMENT ID		TECN	COMMENT
49±13 OUR FIT					
$69 \pm 17 \pm 12$	3182 ± 766	UEHARA	08	BELL	$\gamma\gamma \to 2(\pi^+\pi^-)$

$\Gamma(f_2(1270)f_2'(1525)) \times \Gamma(\gamma\gamma)/\Gamma_{total}$ — $\Gamma_{16}\Gamma_{48}/\Gamma$

VALUE (eV)	EVTS	DOCUMENT ID		TECN	COMMENT
49±9±13	1128 ± 206	UEHARA	08	BELL	$\gamma\gamma \to \pi^+\pi^- K^+K^-$

$\Gamma(K\overline{K}\pi) \times \Gamma(\gamma\gamma)/\Gamma_{total}$ — $\Gamma_{28}\Gamma_{48}/\Gamma$

VALUE (keV)	CL%	EVTS	DOCUMENT ID		TECN	COMMENT
0.367±0.021 OUR FIT						
0.407±0.027 OUR AVERAGE Error includes scale factor of 1.2.						
$0.374 \pm 0.009 \pm 0.031$		14k	[1] LEES	10	BABR	$10.6\ e^+e^- \to e^+e^- K^0_S K^\pm\pi^\mp$
$0.407 \pm 0.022 \pm 0.028$			[2,3] ASNER	04	CLEO	$\gamma\gamma \to \eta_c \to K^0_S K^\pm\pi^\mp$
$0.60 \pm 0.12 \pm 0.09$		41	[3,4] ABDALLAH	03J	DLPH	$\gamma\gamma \to K^0_S K^\pm\pi^\mp$
$1.47 \pm 0.87 \pm 0.27$			[3] SHIRAI	98	AMY	$\gamma\gamma \to \eta_c \to K^\pm K^0_S\pi^\mp$
0.84 ± 0.21			[3] ALBRECHT	94H	ARG	$\gamma\gamma \to K^\pm K^0_S\pi^\mp$
$0.60\ ^{+0.23}_{-0.20}$			[3] CHEN	90B	CLEO	$\gamma\gamma \to \eta_c K^\pm K^0_S\pi^\mp$
$1.06 \pm 0.41 \pm 0.27$		11	[3] BRAUNSCH...	89	TASS	$\gamma\gamma \to K\overline{K}\pi$
$1.5\ ^{+0.60}_{-0.45} \pm 0.3$		7	[3] BERGER	86	PLUT	$\gamma\gamma \to K\overline{K}\pi$
• • • We do not use the following data for averages, fits, limits, etc. • • •						
$0.386 \pm 0.008 \pm 0.021$		12k	[5] DEL-AMO-SA...11M		BABR	$\gamma\gamma \to K^0_S K^\pm\pi^\mp$
$0.418 \pm 0.044 \pm 0.022$			[3,6] BRANDENB...	00B	CLE2	$\gamma\gamma \to \eta_c \to K^\pm K^0_S\pi^\mp$
<0.63	95		[3] BEHREND	89	CELL	$\gamma\gamma \to K^0_S K^\pm\pi^\mp$
<4.4	95		ALTHOFF	85B	TASS	$\gamma\gamma \to K\overline{K}\pi$

[1] From the corrected and unfolded mass spectrum.
[2] Calculated by us from the value reported in ASNER 04 that assumes $B(\eta_c \to K\overline{K}\pi) = 5.5 \pm 1.7\%$
[3] We have multiplied $K^\pm K^0_S\pi^\mp$ measurement by 3 to obtain $K\overline{K}\pi$.
[4] Calculated by us from the value reported in ABDALLAH 03J, which uses $B(\eta_c \to K^0_S K^\pm\pi^\mp) = (1.5 \pm 0.4)\%$.
[5] Not independent from the measurements reported by LEES 10.
[6] Superseded by ASNER 04.

$\Gamma(K^+K^-\pi^+\pi^-) \times \Gamma(\gamma\gamma)/\Gamma_{total}$ — $\Gamma_{32}\Gamma_{48}/\Gamma$

VALUE (eV)	EVTS	DOCUMENT ID		TECN	COMMENT
35 ± 5 OUR FIT					
27 ± 6 OUR AVERAGE					
$25.7 \pm 3.2 \pm 4.9$	2019 ± 248	UEHARA	08	BELL	$\gamma\gamma \to \pi^+\pi^- K^+K^-$
$280 \pm 100 \pm 60$	42	[1] ABDALLAH	03J	DLPH	$\gamma\gamma \to \pi^+\pi^- K^+K^-$
$170 \pm 80 \pm 20$	13.9 ± 6.6	ALBRECHT	94H	ARG	$\gamma\gamma \to \pi^+\pi^- K^+K^-$

[1] Calculated by us from the value reported in ABDALLAH 03J, which uses $B(\eta_c \to \pi^+\pi^- K^+K^-) = (2.0 \pm 0.7)\%$.

$\Gamma(K^+K^-\pi^+\pi^-\pi^0) \times \Gamma(\gamma\gamma)/\Gamma_{total}$ — $\Gamma_{33}\Gamma_{48}/\Gamma$

VALUE (keV)	EVTS	DOCUMENT ID		TECN	COMMENT
• • • We do not use the following data for averages, fits, limits, etc. • • •					
$0.190 \pm 0.006 \pm 0.028$	11k	[1] DEL-AMO-SA...11M		BABR	$\gamma\gamma \to K^+K^-\pi^+\pi^-\pi^0$

[1] Not independent from other measurements reported in DEL-AMO-SANCHEZ 11M.

$\Gamma(2(K^+K^-)) \times \Gamma(\gamma\gamma)/\Gamma_{total}$ — $\Gamma_{36}\Gamma_{48}/\Gamma$

VALUE (eV)	EVTS	DOCUMENT ID		TECN	COMMENT
7.4± 1.5 OUR FIT					
5.8± 1.9 OUR AVERAGE					
$5.6 \pm 1.1 \pm 1.6$	216 ± 42	UEHARA	08	BELL	$\gamma\gamma \to 2(K^+K^-)$
$350 \pm 90 \pm 60$	46	[1] ABDALLAH	03J	DLPH	$\gamma\gamma \to 2(K^+K^-)$
$231 \pm 90 \pm 23$	9.1 ± 3.3	[2] ALBRECHT	94H	ARG	$\gamma\gamma \to 2(K^+K^-)$

[1] Calculated by us from the value reported in ABDALLAH 03J, which uses $B(\eta_c \to 2(K^+K^-)) = (2.1 \pm 1.2)\%$.
[2] Includes all topological modes except $\eta_c \to \phi\phi$.

$\Gamma(2(\pi^+\pi^-)) \times \Gamma(\gamma\gamma)/\Gamma_{total}$ — $\Gamma_{39}\Gamma_{48}/\Gamma$

VALUE (eV)	EVTS	DOCUMENT ID		TECN	COMMENT
49 ± 6 OUR FIT					
42 ± 6 OUR AVERAGE					
$40.7 \pm 3.7 \pm 5.3$	5381 ± 492	UEHARA	08	BELL	$\gamma\gamma \to 2(\pi^+\pi^-)$
$180 \pm 70 \pm 20$	21.4 ± 8.6	ALBRECHT	94H	ARG	$\gamma\gamma \to 2(\pi^+\pi^-)$

$\Gamma(p\overline{p}) \times \Gamma(\gamma\gamma)/\Gamma_{total}$ — $\Gamma_{42}\Gamma_{48}/\Gamma$

VALUE (eV)	EVTS	DOCUMENT ID		TECN	COMMENT
7.6 ±0.7 OUR FIT					
$7.20 \pm 1.53^{+0.67}_{-0.75}$	157 ± 33	[1] KUO	05	BELL	$\gamma\gamma \to p\overline{p}$
• • • We do not use the following data for averages, fits, limits, etc. • • •					
$4.6\ ^{+1.3}_{-1.1} \pm 0.4$	190	[1] AMBROGIANI	03	E835	$\overline{p}p \to \gamma\gamma$
$8.1\ ^{+2.9}_{-2.0}$		[1] ARMSTRONG	95F	E760	$\overline{p}p \to \gamma\gamma$

[1] Not independent from the $\Gamma_{\gamma\gamma}$ reported by the same experiment.

$\Gamma(K^0_S K^0_S) \times \Gamma(\gamma\gamma)/\Gamma_{total}$ — $\Gamma_{52}\Gamma_{48}/\Gamma$

VALUE (eV)	CL%	DOCUMENT ID		TECN	COMMENT
<1.6	90	[1] UEHARA	13	BELL	$\gamma\gamma \to K^0_S K^0_S$
• • • We do not use the following data for averages, fits, limits, etc. • • •					
<0.29	90	[2] UEHARA	13	BELL	$\gamma\gamma \to K^0_S K^0_S$

[1] Taking into account interference with the non-resonant continuum.
[2] Neglecting interference with the non-resonant continuum.

$\eta_c(1S)$ BRANCHING RATIOS

HADRONIC DECAYS

$\Gamma(\eta'(958)\pi\pi)/\Gamma_{total}$ — Γ_1/Γ

VALUE	EVTS	DOCUMENT ID		TECN	COMMENT
0.041±0.017	14	[1] BALTRUSAIT...86		MRK3	$J/\psi \to \eta_c\gamma$

[1] The quoted branching ratios use $B(J/\psi(1S) \to \gamma\eta_c(1S)) = 0.0127 \pm 0.0036$.

$\Gamma(\rho\rho)/\Gamma_{\text{total}}$ Γ_2/Γ

VALUE (units 10^{-3})	CL%	EVTS	DOCUMENT ID		TECN	COMMENT
18 ± 5 OUR AVERAGE						
12.6± 3.8±5.1		72	[1] ABLIKIM	05L	BES2	$J/\psi \to \pi^+\pi^-\pi^+\pi^-\gamma$
26.0± 2.4±8.8		113	[1] BISELLO	91	DM2	$J/\psi \to \gamma\rho^0\rho^0$
23.6±10.6±8.2		32	[1] BISELLO	91	DM2	$J/\psi \to \gamma\rho^+\rho^-$
• • • We do not use the following data for averages, fits, limits, etc. • • •						
<14	90		[1] BALTRUSAIT...86		MRK3	$J/\psi \to \eta_c\gamma$

[1] The quoted branching ratios use $B(J/\psi(1S) \to \gamma\eta_c(1S)) = 0.0127 \pm 0.0036$. Where relevant, the error in this branching ratio is treated as a common systematic in computing averages.

$\Gamma(K^*(892)^0 K^-\pi^+ + \text{c.c.})/\Gamma_{\text{total}}$ Γ_3/Γ

VALUE	EVTS	DOCUMENT ID		TECN	COMMENT
0.02±0.007	63	[1,2] BALTRUSAIT...86		MRK3	$J/\psi \to \eta_c\gamma$

[1] BALTRUSAITIS 86 has an error according to Partridge.
[2] The quoted branching ratios use $B(J/\psi(1S) \to \gamma\eta_c(1S)) = 0.0127 \pm 0.0036$.

$\Gamma(K^*(892)\overline{K}^*(892))/\Gamma_{\text{total}}$ Γ_4/Γ

VALUE (units 10^{-4})	EVTS	DOCUMENT ID		TECN	COMMENT
71±13 OUR FIT					
91±26 OUR AVERAGE					
108±25±44	60	[1] ABLIKIM	05L	BES2	$J/\psi \to K^+K^-\pi^+\pi^-\gamma$
82±28±27	14	[1] BISELLO	91	DM2	$e^+e^- \to \gamma K^+K^-\pi^+\pi^-$
90±50	9	[1] BALTRUSAIT...86		MRK3	$J/\psi \to \eta_c\gamma$

[1] The quoted branching ratios use $B(J/\psi(1S) \to \gamma\eta_c(1S)) = 0.0127 \pm 0.0036$. Where relevant, the error in this branching ratio is treated as a common systematic in computing averages.

$\Gamma(K^*(892)^0\overline{K}^*(892)^0\pi^+\pi^-)/\Gamma_{\text{total}}$ Γ_5/Γ

VALUE (units 10^{-4})	EVTS	DOCUMENT ID		TECN	COMMENT
113±47±24	45	[1] ABLIKIM	06A	BES2	$J/\psi \to K^{*0}\overline{K}^{*0}\pi^+\pi^-\gamma$

[1] ABLIKIM 06A reports $[\Gamma(\eta_c(1S) \to K^*(892)^0\overline{K}^*(892)^0\pi^+\pi^-)/\Gamma_{\text{total}}] \times [B(J/\psi(1S) \to \gamma\eta_c(1S))] = (1.91 \pm 0.64 \pm 0.48) \times 10^{-4}$ which we divide by our best value $B(J/\psi(1S) \to \gamma\eta_c(1S)) = (1.7 \pm 0.4) \times 10^{-2}$. Our first error is their experiment's error and our second error is the systematic error from using our best value.

$\Gamma(\phi K^+K^-)/\Gamma_{\text{total}}$ Γ_6/Γ

VALUE (units 10^{-3})	EVTS	DOCUMENT ID		TECN	COMMENT
$2.9^{+0.9}_{-0.8}\pm1.1$	$14.1^{+4.4}_{-3.7}$	[1] HUANG	03	BELL	$B^+ \to (\phi K^+K^-)\,K^+$

[1] Using $B(B^+ \to \eta_c K^+) = (1.25 \pm 0.12^{+0.10}_{-0.12}) \times 10^{-3}$ from FANG 03 and $B(\eta_c \to K\overline{K}\pi) = (5.5 \pm 1.7) \times 10^{-2}$.

$\Gamma(\phi\phi)/\Gamma_{\text{total}}$ Γ_7/Γ

VALUE (units 10^{-4})	EVTS	DOCUMENT ID		TECN	COMMENT
17.9± 2.0 OUR FIT					
28 ± 4 OUR AVERAGE					
$26\ ^{+\ 4}_{-\ 8}\ \pm 5$	1.2k	[1] ABLIKIM	17P	BES3	$J/\psi \to K^+K^-K^+K^-\gamma$
25.3± 5.1± 9.1	72	[2] ABLIKIM	05L	BES2	$J/\psi \to K^+K^-K^+K^-\gamma$
26 ± 9	357	[2] BAI	04	BES	$J/\psi \to \gamma K^+K^-K^+K^-$
31 ± 7 ±10	19	[2] BISELLO	91	DM2	$J/\psi \to \gamma K^+K^-K^+K^-$
$30\ ^{+18}_{-12}$ ±10	5	[2] BISELLO	91	DM2	$J/\psi \to \gamma K^+K^-K^0_SK^0_L$
74 ±18 ±24	80	[2] BAI	90B	MRK3	$J/\psi \to \gamma K^+K^-K^+K^-$
67 ±21 ±24		[2] BAI	90B	MRK3	$J/\psi \to \gamma K^+K^-K^0_SK^0_L$
• • • We do not use the following data for averages, fits, limits, etc. • • •					
$18\ ^{+\ 8}_{-\ 6}\ \pm 7$	7	[3] HUANG	03	BELL	$B^+ \to (\phi\phi)\,K^+$

[1] ABLIKIM 17P reports $[\Gamma(\eta_c(1S) \to \phi\phi)/\Gamma_{\text{total}}] \times [B(J/\psi(1S) \to \gamma\eta_c(1S))] = (4.3 \pm 0.5^{+0.5}_{-1.2}) \times 10^{-5}$ which we divide by our best value $B(J/\psi(1S) \to \gamma\eta_c(1S)) = (1.7 \pm 0.4) \times 10^{-2}$. Our first error is their experiment's error and our second error is the systematic error from using our best value.
[2] The quoted branching ratios use $B(J/\psi(1S) \to \gamma\eta_c(1S)) = 0.0127 \pm 0.0036$. Where relevant, the error in this branching ratio is treated as a common systematic in computing averages.
[3] Using $B(B^+ \to \eta_c K^+) = (1.25 \pm 0.12^{+0.10}_{-0.12}) \times 10^{-3}$ from FANG 03 and $B(\eta_c \to K\overline{K}\pi) = (5.5 \pm 1.7) \times 10^{-2}$.

$\Gamma(\phi\phi)/\Gamma(K\overline{K}\pi)$ Γ_7/Γ_{28}

VALUE	EVTS	DOCUMENT ID		TECN	COMMENT
0.0245±0.0025 OUR FIT					
0.044 $^{+0.012}_{-0.010}$ OUR AVERAGE					
0.055 ±0.014 ±0.005		AUBERT,B	04B	BABR	$B^\pm \to K^\pm\eta_c$
0.032 $^{+0.014}_{-0.010}$ ±0.009	7	[1] HUANG	03	BELL	$B^\pm \to K^\pm\phi\phi$

[1] Using $B(B^+ \to \eta_c K^+) = (1.25 \pm 0.12^{+0.10}_{-0.12}) \times 10^{-3}$ from FANG 03 and $B(\eta_c \to K\overline{K}\pi) = (5.5 \pm 1.7) \times 10^{-2}$.

$\Gamma(\phi\phi)/\Gamma(p\overline{p})$ Γ_7/Γ_{42}

VALUE	EVTS	DOCUMENT ID		TECN	COMMENT
1.79±0.14±0.32	6.4k	[1] AAIJ	17BB	LHCB	$pp \to b\overline{b}X \to 2(K^+K^-)X$

[1] Using inputs from AAIJ 15AS and AAIJ 15BI and $\Gamma(b \to J/\psi(1S)\,\text{anything}))/\Gamma_{\text{total}} = (1.16 \pm 0.10)\%$ and $\Gamma(J/\psi(1S) \to p\overline{p})/\Gamma_{\text{total}} = (2.120 \pm 0.029) \times 10^{-3}$ from PDG 16.

$\Gamma(\phi 2(\pi^+\pi^-))/\Gamma_{\text{total}}$ Γ_8/Γ

VALUE (units 10^{-4})	CL%	DOCUMENT ID		TECN	COMMENT
<40	90	[1] ABLIKIM	06A	BES2	$J/\psi \to \phi 2(\pi^+\pi^-)\gamma$

[1] ABLIKIM 06A reports $[\Gamma(\eta_c(1S) \to \phi 2(\pi^+\pi^-))/\Gamma_{\text{total}}] \times [B(J/\psi(1S) \to \gamma\eta_c(1S))] < 0.603 \times 10^{-4}$ which we divide by our best value $B(J/\psi(1S) \to \gamma\eta_c(1S)) = 1.7 \times 10^{-2}$.

$\Gamma(a_0(980)\pi)/\Gamma_{\text{total}}$ Γ_9/Γ

VALUE	CL%	DOCUMENT ID		TECN	COMMENT
<0.02	90	[1,2] BALTRUSAIT...86		MRK3	$J/\psi \to \eta_c\gamma$

[1] The quoted branching ratios use $B(J/\psi(1S) \to \gamma\eta_c(1S)) = 0.0127 \pm 0.0036$.
[2] We are assuming $B(a_0(980) \to \eta\pi) > 0.5$.

$\Gamma(a_2(1320)\pi)/\Gamma_{\text{total}}$ Γ_{10}/Γ

VALUE	CL%	DOCUMENT ID		TECN	COMMENT
<0.02	90	[1] BALTRUSAIT...86		MRK3	$J/\psi \to \eta_c\gamma$

[1] The quoted branching ratios use $B(J/\psi(1S) \to \gamma\eta_c(1S)) = 0.0127 \pm 0.0036$.

$\Gamma(K^*(892)\overline{K} + \text{c.c.})/\Gamma_{\text{total}}$ Γ_{11}/Γ

VALUE	CL%	DOCUMENT ID		TECN	COMMENT
<0.0128	90	BISELLO	91	DM2	$J/\psi \to \gamma K^0_S K^\pm\pi^\mp$
<0.0132	90	[1] BISELLO	91	DM2	$J/\psi \to \gamma K^+K^-\pi^0$

[1] The quoted branching ratios use $B(J/\psi(1S) \to \gamma\eta_c(1S)) = 0.0127 \pm 0.0036$.

$\Gamma(f_2(1270)\eta)/\Gamma_{\text{total}}$ Γ_{12}/Γ

VALUE	CL%	DOCUMENT ID		TECN	COMMENT
<0.011	90	[1] BALTRUSAIT...86		MRK3	$J/\psi \to \eta_c\gamma$

[1] The quoted branching ratios use $B(J/\psi(1S) \to \gamma\eta_c(1S)) = 0.0127 \pm 0.0036$.

$\Gamma(\omega\omega)/\Gamma_{\text{total}}$ Γ_{13}/Γ

VALUE	CL%	DOCUMENT ID		TECN	COMMENT
<0.0031	90	[1] BALTRUSAIT...86		MRK3	$J/\psi \to \eta_c\gamma$
• • • We do not use the following data for averages, fits, limits, etc. • • •					
<0.0063	90	[1] ABLIKIM	05L	BES2	$J/\psi \to \pi^+\pi^-\pi^0\pi^+\pi^-\pi^0\gamma$
<0.0063		[1] BISELLO	91	DM2	$J/\psi \to \gamma\omega\omega$

[1] The quoted branching ratios use $B(J/\psi(1S) \to \gamma\eta_c(1S)) = 0.0127 \pm 0.0036$. Where relevant, the error in this branching ratio is treated as a common systematic in computing averages.

$\Gamma(\omega\phi)/\Gamma_{\text{total}}$ Γ_{14}/Γ

VALUE	CL%	DOCUMENT ID		TECN	COMMENT
< 2.5 × 10^{-4}	90	[1] ABLIKIM	17P	BES3	$J/\psi \to \pi^+\pi^-\pi^0K^+K^-\gamma$
• • • We do not use the following data for averages, fits, limits, etc. • • •					
<17 × 10^{-4}	90	[2] ABLIKIM	05L	BES2	$J/\psi \to \pi^+\pi^-\pi^0K^+K^-\gamma$

[1] Using $B(J/\psi \to \gamma\eta_c) = 0.017 \pm 0.004$.
[2] The quoted branching ratios use $B(J/\psi(1S) \to \gamma\eta_c(1S)) = 0.0127 \pm 0.0036$.

$\Gamma(f_2(1270)f_2(1270))/\Gamma_{\text{total}}$ Γ_{15}/Γ

VALUE (units 10^{-2})	EVTS	DOCUMENT ID		TECN	COMMENT
0.98±0.25 OUR FIT					
0.77 $^{+0.25}_{-0.30}$ ±0.17	91.2 ± 19.8	[1] ABLIKIM	04M	BES	$J/\psi \to \gamma 2\pi^+ 2\pi^-$

[1] ABLIKIM 04M reports $[\Gamma(\eta_c(1S) \to f_2(1270)f_2(1270))/\Gamma_{\text{total}}] \times [B(J/\psi(1S) \to \gamma\eta_c(1S))] = (1.3 \pm 0.3^{+0.3}_{-0.4}) \times 10^{-4}$ which we divide by our best value $B(J/\psi(1S) \to \gamma\eta_c(1S)) = (1.7 \pm 0.4) \times 10^{-2}$. Our first error is their experiment's error and our second error is the systematic error from using our best value.

$\Gamma(f_0(980)\eta)/\Gamma_{\text{total}}$ Γ_{17}/Γ

VALUE	DOCUMENT ID		TECN	COMMENT
seen	LEES	14E	BABR	Dalitz anal. of $\eta_c \to K^+K^-\eta$

$\Gamma(f_0(1500)\eta)/\Gamma_{\text{total}}$ Γ_{18}/Γ

VALUE	DOCUMENT ID		TECN	COMMENT
seen	LEES	14E	BABR	Dalitz anal. of $\eta_c \to K^+K^-\eta$

$\Gamma(f_0(2200)\eta)/\Gamma_{\text{total}}$ Γ_{19}/Γ

VALUE	DOCUMENT ID		TECN	COMMENT
seen	LEES	14E	BABR	Dalitz anal. of $\eta_c \to K^+K^-\eta$

$\Gamma(a_0(980)\pi)/\Gamma_{\text{total}}$ Γ_{20}/Γ

VALUE	DOCUMENT ID		TECN	COMMENT
seen	LEES	14E	BABR	Dalitz anal. of $\eta_c \to K^+K^-\pi^0$

$\Gamma(a_0(1320)\pi)/\Gamma_{\text{total}}$ Γ_{21}/Γ

VALUE	DOCUMENT ID		TECN	COMMENT
seen	LEES	14E	BABR	Dalitz anal. of $\eta_c \to K^+K^-\pi^0$

Meson Particle Listings

$\eta_c(1S)$

$\Gamma(a_0(1450)\pi)/\Gamma_{\text{total}}$ Γ_{22}/Γ

VALUE	DOCUMENT ID		TECN	COMMENT
seen	LEES	14E	BABR	Dalitz anal. of $\eta_c \to K^+K^-\pi^0$

$\Gamma(a_0(1950)\pi)/\Gamma_{\text{total}}$ Γ_{23}/Γ

VALUE	EVTS	DOCUMENT ID		TECN	COMMENT
seen	12k	[1] LEES	16A	BABR	$\gamma\gamma \to \eta_c(1S) \to K\overline{K}\pi$

[1] From a model-independant partial wave analysis.

$\Gamma(a_2(1950)\pi)/\Gamma_{\text{total}}$ Γ_{24}/Γ

VALUE	EVTS	DOCUMENT ID		TECN	COMMENT
not seen	12k	[1] LEES	16A	BABR	$\gamma\gamma \to \eta_c(1S) \to K\overline{K}\pi$

[1] From a model-independent partial wave analysis assuming the existence of a hypothetical tensor isovector $a_2(1950)$.

$\Gamma(K_0^*(1430)\overline{K})/\Gamma_{\text{total}}$ Γ_{25}/Γ

VALUE	EVTS	DOCUMENT ID		TECN	COMMENT
seen	12k	[1] LEES	16A	BABR	$\gamma\gamma \to \eta_c(1S) \to K\overline{K}\pi$
seen		LEES	14E	BABR	Dalitz anal. of $\eta_c \to K^+K^-\eta/\pi^0$

[1] From a model-independant partial wave analysis.

$\Gamma(K_2^*(1430)\overline{K})/\Gamma_{\text{total}}$ Γ_{26}/Γ

VALUE	DOCUMENT ID		TECN	COMMENT
seen	LEES	14E	BABR	Dalitz anal. of $\eta_c \to K^+K^-\pi^0$

$\Gamma(K_0^*(1950)\overline{K})/\Gamma_{\text{total}}$ Γ_{27}/Γ

VALUE	EVTS	DOCUMENT ID		TECN	COMMENT
seen	12K	[1] LEES	16A	BABR	$\gamma\gamma \to \eta_c(1S) \to K\overline{K}\pi$
seen		LEES	14E	BABR	Dalitz anal. of $\eta_c \to K^+K^-\eta/\pi^0$

[1] From a Dalitz plot analysis using an isobar model.

$\Gamma(K\overline{K}\pi)/\Gamma_{\text{total}}$ Γ_{28}/Γ

VALUE (units 10^{-2})	EVTS	DOCUMENT ID		TECN	COMMENT
7.3 ±0.5 OUR FIT					
6.5 ±0.6 OUR AVERAGE					
6.3 ±1.3 ±0.6	55	[1,2] ABLIKIM	12N	BES3	$\psi(2S) \to \pi^0\gamma K^+K^-\pi^0$
7.9 ±1.4 ±0.7	107	[3,4] ABLIKIM	12N	BES3	$\psi(2S) \to \pi^0\gamma K_S^0 K^\mp\pi^\pm$
8.5 ±1.8		[5] AUBERT	06E	BABR	$B^\pm \to K^\pm X_{c\overline{c}}$
5.1 ±2.1	0.6k	[6] BAI	04	BES	$J/\psi \to \gamma K^\pm\pi^\mp K_S^0$
6.90±1.42±1.32	33	[6] BISELLO	91	DM2	$J/\psi \to \gamma K^+K^-\pi^0$
5.43±0.94±0.94	68	[6] BISELLO	91	DM2	$J/\psi \to \gamma K^\pm\pi^\mp K_S^0$
4.8 ±1.7	95	[6,7] BALTRUSAIT...86		MRK3	$J/\psi \to \eta_c\gamma$
16.1 $^{+9.2}_{-7.3}$		[8,9] HIMEL	80B	MRK2	$\psi(2S) \to \eta_c\gamma$
• • • We do not use the following data for averages, fits, limits, etc. • • •					
< 10.7 90% CL		[6,10] PARTRIDGE	80B	CBAL	$J/\psi \to \eta_c\gamma$

[1] ABLIKIM 12N quotes $B(\psi(2S) \to \pi^0 h_c) \cdot B(h_c \to \gamma\eta_c) \cdot B(\eta_c \to K^+K^-\pi^0) = (4.54 \pm 0.76 \pm 0.48) \times 10^{-6}$ which we multiply by 6 to account for isospin symmetry.

[2] ABLIKIM 12N reports $[\Gamma(\eta_c(1S) \to K\overline{K}\pi)/\Gamma_{\text{total}}] \times [\Gamma(h_c(1P) \to \gamma\eta_c(1S))/\Gamma_{\text{total}} \times \Gamma(\psi(2S) \to \pi^0 h_c(1P))/\Gamma_{\text{total}}] = (27.24 \pm 4.56 \pm 2.88) \times 10^{-6}$ which we divide by our best value $\Gamma(h_c(1P) \to \gamma\eta_c(1S))/\Gamma_{\text{total}} \times \Gamma(\psi(2S) \to \pi^0 h_c(1P))/\Gamma_{\text{total}} = (4.3 \pm 0.4) \times 10^{-4}$. Our first error is their experiment's error and our second error is the systematic error from using our best value.

[3] ABLIKIM 12N quotes $B(\psi(2S) \to \pi^0 h_c) \cdot B(h_c \to \gamma\eta_c) \cdot B(\eta_c \to K_S^0 K^\pm\pi^\mp) = (11.35 \pm 1.25 \pm 1.50) \times 10^{-6}$ which we multiply by 3 to account for isospin symmetry.

[4] ABLIKIM 12N reports $[\Gamma(\eta_c(1S) \to K\overline{K}\pi)/\Gamma_{\text{total}}] \times [\Gamma(h_c(1P) \to \gamma\eta_c(1S))/\Gamma_{\text{total}} \times \Gamma(\psi(2S) \to \pi^0 h_c(1P))/\Gamma_{\text{total}}] = (34.05 \pm 3.75 \pm 4.50) \times 10^{-6}$ which we divide by our best value $\Gamma(h_c(1P) \to \gamma\eta_c(1S))/\Gamma_{\text{total}} \times \Gamma(\psi(2S) \to \pi^0 h_c(1P))/\Gamma_{\text{total}} = (4.3 \pm 0.4) \times 10^{-4}$. Our first error is their experiment's error and our second error is the systematic error from using our best value.

[5] Determined from the ratio of $B(B^\pm \to K^\pm\eta_c)\, B(\eta_c \to K\overline{K}\pi) = (7.4 \pm 0.5 \pm 0.7) \times 10^{-5}$ reported in AUBERT,B 04B and $B(B^\pm \to K^\pm\eta_c) = (8.7 \pm 1.5) \times 10^{-3}$ reported in AUBERT 06E.

[6] The quoted branching ratios use $B(J/\psi(1S) \to \gamma\eta_c(1S)) = 0.0127 \pm 0.0036$. Where relevant, the error in this branching ratio is treated as a common systematic in computing averages.

[7] Average from $K^+K^-\pi^0$ and $K^\pm K_S^0\pi^\mp$ decay channels.

[8] $K^\pm K_S^0\pi^\mp$ corrected to $K\overline{K}\pi$ by factor 3. KS, MR.

[9] Estimated using $B(\psi(2S) \to \gamma\eta_c(1S)) = 0.0028 \pm 0.0006$.

[10] $K^+K^-\pi^0$ corrected to $K\overline{K}\pi$ by factor 6. KS, MR

$\Gamma(\phi K^+K^-)/\Gamma(K\overline{K}\pi)$ Γ_6/Γ_{28}

VALUE	EVTS	DOCUMENT ID		TECN	COMMENT
0.052 $^{+0.016}_{-0.014}$ ±0.014	7	[1] HUANG	03	BELL	$B^\pm \to K^\pm\phi\phi$

[1] Using $B(B^+ \to \eta_c K^+) = (1.25 \pm 0.12^{+0.10}_{-0.12}) \times 10^{-3}$ from FANG 03 and $B(\eta_c \to K\overline{K}\pi) = (5.5 \pm 1.7) \times 10^{-2}$.

$\Gamma(K\overline{K}\eta)/\Gamma_{\text{total}}$ Γ_{29}/Γ

VALUE (units 10^{-2})	CL%	EVTS	DOCUMENT ID		TECN	COMMENT
1.36±0.16 OUR FIT						
1.0 ±0.5 ±0.2		7	[1,2] ABLIKIM	12N	BES3	$\psi(2S) \to \pi^0\gamma\eta K^+K^-$
• • • We do not use the following data for averages, fits, limits, etc. • • •						
<3.1	90		[3] BALTRUSAIT...86		MRK3	$J/\psi \to \eta_c\gamma$

[1] ABLIKIM 12N quotes $B(\psi(2S) \to \pi^0 h_c) \cdot B(h_c \to \gamma\eta_c) \cdot B(\eta_c \to K^+K^-\eta) = (2.11 \pm 1.01 \pm 0.32) \times 10^{-6}$ which we multiply by 2 to account for isospin symmetry.

[2] ABLIKIM 12N reports $[\Gamma(\eta_c(1S) \to K\overline{K}\eta)/\Gamma_{\text{total}}] \times [B(\psi(2S) \to \pi^0 h_c(1P))] \times [B(h_c(1P) \to \gamma\eta_c(1S))] = (4.22 \pm 2.02 \pm 0.64) \times 10^{-6}$ which we divide by our best values $B(\psi(2S) \to \pi^0 h_c(1P)) = (8.6 \pm 1.3) \times 10^{-4}$, $B(h_c(1P) \to \gamma\eta_c(1S)) = (51 \pm 6) \times 10^{-2}$. Our first error is their experiment's error and our second error is the systematic error from using our best values.

[3] The quoted branching ratios use $B(J/\psi(1S) \to \gamma\eta_c(1S)) = 0.0127 \pm 0.0036$.

$\Gamma(K\overline{K}\eta)/\Gamma(K\overline{K}\pi)$ Γ_{29}/Γ_{28}

VALUE	EVTS	DOCUMENT ID		TECN	COMMENT
0.186±0.018 OUR FIT					
0.190±0.008±0.017	5.4k	[1] LEES	14E	BABR	$\gamma\gamma \to K^+K^-\eta/\pi^0$

[1] LEES 14E reports $B(\eta_c(1S) \to K^+K^-\eta)/B(\eta_c(1S) \to K^+K^-\pi^0) = 0.571 \pm 0.025 \pm 0.051$, which we divide by 3 to account for isospin symmetry. It uses both $\eta \to \gamma\gamma$ and $\eta \to \pi^+\pi^-\pi^0$ decays.

$\Gamma(\eta\pi^+\pi^-)/\Gamma_{\text{total}}$ Γ_{30}/Γ

VALUE (units 10^{-2})	EVTS	DOCUMENT ID		TECN	COMMENT
1.7±0.4±0.1	33	[1] ABLIKIM	12N	BES3	$\psi(2S) \to \pi^0\gamma\eta\pi^+\pi^-$
• • • We do not use the following data for averages, fits, limits, etc. • • •					
5.4±2.0	75	[2] BALTRUSAIT...86		MRK3	$J/\psi \to \eta_c\gamma$
3.7±1.3±2.0	18	[2] PARTRIDGE	80B	CBAL	$J/\psi \to \eta\pi^+\pi^-\gamma$

[1] ABLIKIM 12N reports $[\Gamma(\eta_c(1S) \to \eta\pi^+\pi^-)/\Gamma_{\text{total}}] \times [\Gamma(h_c(1P) \to \gamma\eta_c(1S))/\Gamma_{\text{total}} \times \Gamma(\psi(2S) \to \pi^0 h_c(1P))/\Gamma_{\text{total}}] = (7.22 \pm 1.47 \pm 1.11) \times 10^{-6}$ which we divide by our best value $\Gamma(h_c(1P) \to \gamma\eta_c(1S))/\Gamma_{\text{total}} \times \Gamma(\psi(2S) \to \pi^0 h_c(1P))/\Gamma_{\text{total}} = (4.3 \pm 0.4) \times 10^{-4}$. Our first error is their experiment's error and our second error is the systematic error from using our best value.

[2] The quoted branching ratios use $B(J/\psi(1S) \to \gamma\eta_c(1S)) = 0.0127 \pm 0.0036$. Where relevant, the error in this branching ratio is treated as a common systematic in computing averages.

$\Gamma(\eta 2(\pi^+\pi^-))/\Gamma_{\text{total}}$ Γ_{31}/Γ

VALUE (units 10^{-2})	EVTS	DOCUMENT ID		TECN	COMMENT
4.4±1.2±0.4	39	[1] ABLIKIM	12N	BES3	$\psi(2S) \to \pi^0\gamma\eta 2(\pi^+\pi^-)$

[1] ABLIKIM 12N reports $[\Gamma(\eta_c(1S) \to \eta 2(\pi^+\pi^-))/\Gamma_{\text{total}}] \times [\Gamma(h_c(1P) \to \gamma\eta_c(1S))/\Gamma_{\text{total}} \times \Gamma(\psi(2S) \to \pi^0 h_c(1P))/\Gamma_{\text{total}}] = (19.17 \pm 3.77 \pm 3.72) \times 10^{-6}$ which we divide by our best value $\Gamma(h_c(1P) \to \gamma\eta_c(1S))/\Gamma_{\text{total}} \times \Gamma(\psi(2S) \to \pi^0 h_c(1P))/\Gamma_{\text{total}} = (4.3 \pm 0.4) \times 10^{-4}$. Our first error is their experiment's error and our second error is the systematic error from using our best value.

$\Gamma(K^+K^-\pi^+\pi^-)/\Gamma_{\text{total}}$ Γ_{32}/Γ

VALUE (units 10^{-3})	EVTS	DOCUMENT ID		TECN	COMMENT
6.9± 1.1 OUR FIT					
11.2± 1.9 OUR AVERAGE					
9.7± 2.2±0.9	38	[1] ABLIKIM	12N	BES3	$\psi(2S) \to \pi^0\gamma K^+K^-\pi^+\pi^-$
12 ± 4	0.4k	[2] BAI	04	BES	$J/\psi \to \gamma K^+K^-\pi^+\pi^-$
21 ± 7	110	[2] BALTRUSAIT...86		MRK3	$J/\psi \to \eta_c\gamma$
14 $^{+22}_{-9}$		[3] HIMEL	80B	MRK2	$\psi(2S) \to \eta_c\gamma$

[1] ABLIKIM 12N reports $[\Gamma(\eta_c(1S) \to K^+K^-\pi^+\pi^-)/\Gamma_{\text{total}}] \times [\Gamma(h_c(1P) \to \gamma\eta_c(1S))/\Gamma_{\text{total}} \times \Gamma(\psi(2S) \to \pi^0 h_c(1P))/\Gamma_{\text{total}}] = (4.16 \pm 0.76 \pm 0.59) \times 10^{-6}$ which we divide by our best value $\Gamma(h_c(1P) \to \gamma\eta_c(1S))/\Gamma_{\text{total}} \times \Gamma(\psi(2S) \to \pi^0 h_c(1P))/\Gamma_{\text{total}} = (4.3 \pm 0.4) \times 10^{-4}$. Our first error is their experiment's error and our second error is the systematic error from using our best value.

[2] The quoted branching ratios use $B(J/\psi(1S) \to \gamma\eta_c(1S)) = 0.0127 \pm 0.0036$. Where relevant, the error in this branching ratio is treated as a common systematic in computing averages.

[3] Estimated using $B(\psi(2S) \to \gamma\eta_c(1S)) = 0.0028 \pm 0.0006$.

$\Gamma(K^+K^-\pi^+\pi^-\pi^0)/\Gamma(K\overline{K}\pi)$ Γ_{33}/Γ_{28}

VALUE	EVTS	DOCUMENT ID		TECN	COMMENT
0.477±0.017±0.070	11k	[1] DEL-AMO-SA...11M		BABR	$\gamma\gamma \to K^+K^-\pi^+\pi^-\pi^0$

[1] We have multiplied the value of $\Gamma(K^+K^-\pi^+\pi^-\pi^0)/\Gamma(K_S^0 K^\pm\pi^\mp)$ reported in DEL-AMO-SANCHEZ 11M by a factor 1/3 to obtain $\Gamma(K^+K^-\pi^+\pi^-\pi^0)/\Gamma(K\overline{K}\pi)$. Not independent from other measurements reported in DEL-AMO-SANCHEZ 11M.

$\Gamma(K^0K^-\pi^+\pi^-\pi^+ + \text{c.c.})/\Gamma_{\text{total}}$ Γ_{34}/Γ

VALUE (units 10^{-2})	EVTS	DOCUMENT ID		TECN	COMMENT
5.6±1.4±0.5	43	[1,2] ABLIKIM	12N	BES3	$\psi(2S) \to \pi^0\gamma K_S^0 K^\mp\pi^\mp 2\pi^\pm$

[1] ABLIKIM 12N quotes $B(\psi(2S) \to \pi^0 h_c) \cdot B(h_c \to \gamma\eta_c) \cdot B(\eta_c \to K_S^0 K^-\pi^- 2\pi^+) = (12.01 \pm 2.22 \pm 2.04) \times 10^{-6}$ which we multiply by 2 to take c.c. into account.

[2] ABLIKIM 12N reports $[\Gamma(\eta_c(1S) \to K^0K^-\pi^+\pi^-\pi^+ + \text{c.c.})/\Gamma_{\text{total}}] \times [\Gamma(h_c(1P) \to \gamma\eta_c(1S))/\Gamma_{\text{total}} \times \Gamma(\psi(2S) \to \pi^0 h_c(1P))/\Gamma_{\text{total}}] = (24.02 \pm 4.44 \pm 4.08) \times 10^{-6}$ which we divide by our best value $\Gamma(h_c(1P) \to \gamma\eta_c(1S))/\Gamma_{\text{total}} \times \Gamma(\psi(2S) \to$

$\pi^0 h_c(1P))/\Gamma_{total} = (4.3 \pm 0.4) \times 10^{-4}$. Our first error is their experiment's error and our second error is the systematic error from using our best value.

$\Gamma(K^+K^-2(\pi^+\pi^-))/\Gamma_{total}$ Γ_{35}/Γ

VALUE (units 10^{-3})	EVTS	DOCUMENT ID		TECN	COMMENT
7.5±2.4 OUR AVERAGE					
8 ±4 ±1	10	[1] ABLIKIM	12N	BES3	$\psi(2S) \to \pi^0\gamma K^+K^-2(\pi^+\pi^-)$
7.2±2.4±1.5	100	[2] ABLIKIM	06A	BES2	$J/\psi \to K^+K^-2(\pi^+\pi^-)\gamma$

[1] ABLIKIM 12N reports $[\Gamma(\eta_c(1S) \to K^+K^-2(\pi^+\pi^-))/\Gamma_{total}] \times [\Gamma(h_c(1P) \to \gamma\eta_c(1S))/\Gamma_{total} \times \Gamma(\psi(2S) \to \pi^0 h_c(1P))/\Gamma_{total}] = (3.60 \pm 1.71 \pm 0.64) \times 10^{-6}$ which we divide by our best value $\Gamma(h_c(1P) \to \gamma\eta_c(1S))/\Gamma_{total} \times \Gamma(\psi(2S) \to \pi^0 h_c(1P))/\Gamma_{total} = (4.3 \pm 0.4) \times 10^{-4}$. Our first error is their experiment's error and our second error is the systematic error from using our best value.

[2] ABLIKIM 06A reports $[\Gamma(\eta_c(1S) \to K^+K^-2(\pi^+\pi^-))/\Gamma_{total}] \times [B(J/\psi(1S) \to \gamma\eta_c(1S))] = (1.21 \pm 0.32 \pm 0.24) \times 10^{-4}$ which we divide by our best value $B(J/\psi(1S) \to \gamma\eta_c(1S)) = (1.7 \pm 0.4) \times 10^{-2}$. Our first error is their experiment's error and our second error is the systematic error from using our best value.

$\Gamma(2(K^+K^-))/\Gamma_{total}$ Γ_{36}/Γ

VALUE (units 10^{-3})	EVTS	DOCUMENT ID		TECN	COMMENT
1.47± 0.31 OUR FIT					
2.2 ± 0.9 ±0.2	7	[1] ABLIKIM	12N	BES3	$\psi(2S) \to \pi^0\gamma 2(K^+K^-)$
• • • We do not use the following data for averages, fits, limits, etc. • • •					
$1.4 \pm 0.5 \pm 0.6$	$14.5 \pm 4.6 - 3.0$	[2] HUANG	03	BELL	$B^+ \to 2(K^+K^-)\ K^+$
21 ±10 ±6		[3] ALBRECHT	94H	ARG	$\gamma\gamma \to K^+K^-K^+K^-$

[1] ABLIKIM 12N reports $[\Gamma(\eta_c(1S) \to 2(K^+K^-))/\Gamma_{total}] \times [\Gamma(h_c(1P) \to \gamma\eta_c(1S))/\Gamma_{total} \times \Gamma(\psi(2S) \to \pi^0 h_c(1P))/\Gamma_{total}] = (0.94 \pm 0.37 \pm 0.14) \times 10^{-6}$ which we divide by our best value $\Gamma(h_c(1P) \to \gamma\eta_c(1S))/\Gamma_{total} \times \Gamma(\psi(2S) \to \pi^0 h_c(1P))/\Gamma_{total} = (4.3 \pm 0.4) \times 10^{-4}$. Our first error is their experiment's error and our second error is the systematic error from using our best value.

[2] Using $B(B^+ \to \eta_c K^+) = (1.25 \pm 0.12^{+0.10}_{-0.12}) \times 10^{-3}$ from FANG 03 and $B(\eta_c \to K\overline{K}\pi) = (5.5 \pm 1.7) \times 10^{-2}$.

[3] Normalized to the sum of $B(\eta_c \to K^\pm K^0_S \pi^\mp)$, $B(\eta_c \to \phi\phi)$, $B(\eta_c \to K^+K^-\pi^+\pi^-)$, and $B(\eta_c \to 2\pi^+2\pi^-)$.

$\Gamma(2(K^+K^-))/\Gamma(K\overline{K}\pi)$ Γ_{36}/Γ_{28}

VALUE	EVTS	DOCUMENT ID		TECN	COMMENT
0.020±0.004 OUR FIT					
0.024±0.007 OUR AVERAGE					
0.023±0.007±0.006		AUBERT,B	04B	BABR	$B^\pm \to K^\pm\eta_c$
$0.026^{+0.009}_{-0.007} \pm 0.007$	15	[1] HUANG	03	BELL	$B^\pm \to K^\pm(2K^+2K^-)$

[1] Using $B(B^+ \to \eta_c K^+) = (1.25 \pm 0.12^{+0.10}_{-0.12}) \times 10^{-3}$ from FANG 03 and $B(\eta_c \to K\overline{K}\pi) = (5.5 \pm 1.7) \times 10^{-2}$.

$\Gamma(\pi^+\pi^-\pi^0)/\Gamma_{total}$ Γ_{37}/Γ

VALUE	CL%	DOCUMENT ID		TECN	COMMENT
$<5 \times 10^{-4}$	90	[1] ABLIKIM	17AJ	BES3	$\psi(2S) \to \gamma\pi^+\pi^-\pi^0$

[1] ABLIKIM 17AJ reports $[\Gamma(\eta_c(1S) \to \pi^+\pi^-\pi^0)/\Gamma_{total}] \times [B(\psi(2S) \to \gamma\eta_c(1S))] < 1.6 \times 10^{-6}$ which we divide by our best value $B(\psi(2S) \to \gamma\eta_c(1S)) = 3.4 \times 10^{-3}$.

$\Gamma(\pi^+\pi^-\pi^0\pi^0)/\Gamma_{total}$ Γ_{38}/Γ

VALUE (units 10^{-2})	EVTS	DOCUMENT ID		TECN	COMMENT
4.7±0.9±0.4	118	[1] ABLIKIM	12N	BES3	$\psi(2S) \to \pi^0\gamma\pi^+\pi^-2\pi^0$

[1] ABLIKIM 12N reports $[\Gamma(\eta_c(1S) \to \pi^+\pi^-\pi^0\pi^0)/\Gamma_{total}] \times [\Gamma(h_c(1P) \to \gamma\eta_c(1S))/\Gamma_{total} \times \Gamma(\psi(2S) \to \pi^0 h_c(1P))/\Gamma_{total}] = (20.31 \pm 2.20 \pm 3.33) \times 10^{-6}$ which we divide by our best value $\Gamma(h_c(1P) \to \gamma\eta_c(1S))/\Gamma_{total} \times \Gamma(\psi(2S) \to \pi^0 h_c(1P))/\Gamma_{total} = (4.3 \pm 0.4) \times 10^{-4}$. Our first error is their experiment's error and our second error is the systematic error from using our best value.

$\Gamma(2(\pi^+\pi^-))/\Gamma_{total}$ Γ_{39}/Γ

VALUE (units 10^{-2})	EVTS	DOCUMENT ID		TECN	COMMENT
0.97±0.12 OUR FIT					
1.35±0.21 OUR AVERAGE					
1.74±0.32±0.15	100	[1] ABLIKIM	12N	BES3	$\psi(2S) \to \pi^0\gamma 2(\pi^+\pi^-)$
1.0 ±0.5	542 ± 75	[2] BAI	04	BES	$J/\psi \to \gamma\ 2(\pi^+\pi^-)$
1.05±0.17±0.34	137	[2] BISELLO	91	DM2	$J/\psi \to \gamma 2\pi^+2\pi^-$
1.3 ±0.6	25	[2] BALTRUSAIT...86		MRK3	$J/\psi \to \eta_c\gamma$
$2.0 \pm 1.5 - 1.0$		[3] HIMEL	80B	MRK2	$\psi(2S) \to \eta_c\gamma$

[1] ABLIKIM 12N reports $[\Gamma(\eta_c(1S) \to 2(\pi^+\pi^-))/\Gamma_{total}] \times [\Gamma(h_c(1P) \to \gamma\eta_c(1S))/\Gamma_{total} \times \Gamma(\psi(2S) \to \pi^0 h_c(1P))/\Gamma_{total}] = (7.51 \pm 0.85 \pm 1.11) \times 10^{-6}$ which we divide by our best value $\Gamma(h_c(1P) \to \gamma\eta_c(1S))/\Gamma_{total} \times \Gamma(\psi(2S) \to \pi^0 h_c(1P))/\Gamma_{total} = (4.3 \pm 0.4) \times 10^{-4}$. Our first error is their experiment's error and our second error is the systematic error from using our best value.

[2] The quoted branching ratios use $B(J/\psi(1S) \to \gamma\eta_c(1S)) = 0.0127 \pm 0.0036$. Where relevant, the error in this branching ratio is treated as a common systematic in computing averages.

[3] Estimated using $B(\psi(2S) \to \gamma\eta_c(1S)) = 0.0028 \pm 0.0006$.

$\Gamma(2(\pi^+\pi^-\pi^0))/\Gamma_{total}$ Γ_{40}/Γ

VALUE (units 10^{-2})	EVTS	DOCUMENT ID		TECN	COMMENT
17.4±2.9±1.5	175	[1] ABLIKIM	12N	BES3	$\psi(2S) \to \pi^0\gamma 2(\pi^+\pi^-2\pi^0)$

[1] ABLIKIM 12N reports $[\Gamma(\eta_c(1S) \to 2(\pi^+\pi^-\pi^0))/\Gamma_{total}] \times [\Gamma(h_c(1P) \to \gamma\eta_c(1S))/\Gamma_{total} \times \Gamma(\psi(2S) \to \pi^0 h_c(1P))/\Gamma_{total}] = (75.13 \pm 7.42 \pm 9.99) \times 10^{-6}$ which we divide by our best value $\Gamma(h_c(1P) \to \gamma\eta_c(1S))/\Gamma_{total} \times \Gamma(\psi(2S) \to \pi^0 h_c(1P))/\Gamma_{total} = (4.3 \pm 0.4) \times 10^{-4}$. Our first error is their experiment's error and our second error is the systematic error from using our best value.

$\Gamma(3(\pi^+\pi^-))/\Gamma_{total}$ Γ_{41}/Γ

VALUE (units 10^{-3})	EVTS	DOCUMENT ID		TECN	COMMENT
18 ±4 OUR AVERAGE					
20 ±5 ±2	51	[1] ABLIKIM	12N	BES3	$\psi(2S) \to \pi^0\gamma 3(\pi^+\pi^-)$
15.4±3.4±3.3	479	[2] ABLIKIM	06A	BES2	$J/\psi \to 3(\pi^+\pi^-)\gamma$

[1] ABLIKIM 12N reports $[\Gamma(\eta_c(1S) \to 3(\pi^+\pi^-))/\Gamma_{total}] \times [\Gamma(h_c(1P) \to \gamma\eta_c(1S))/\Gamma_{total} \times \Gamma(\psi(2S) \to \pi^0 h_c(1P))/\Gamma_{total}] = (8.82 \pm 1.57 \pm 1.59) \times 10^{-6}$ which we divide by our best value $\Gamma(h_c(1P) \to \gamma\eta_c(1S))/\Gamma_{total} \times \Gamma(\psi(2S) \to \pi^0 h_c(1P))/\Gamma_{total} = (4.3 \pm 0.4) \times 10^{-4}$. Our first error is their experiment's error and our second error is the systematic error from using our best value.

[2] ABLIKIM 06A reports $[\Gamma(\eta_c(1S) \to 3(\pi^+\pi^-))/\Gamma_{total}] \times [B(J/\psi(1S) \to \gamma\eta_c(1S))] = (2.59 \pm 0.32 \pm 0.47) \times 10^{-4}$ which we divide by our best value $B(J/\psi(1S) \to \gamma\eta_c(1S)) = (1.7 \pm 0.4) \times 10^{-2}$. Our first error is their experiment's error and our second error is the systematic error from using our best value.

$\Gamma(p\overline{p})/\Gamma_{total}$ Γ_{42}/Γ

VALUE (units 10^{-4})	EVTS	DOCUMENT ID		TECN	COMMENT
15.2± 1.6 OUR FIT					
13.2± 2.7 OUR AVERAGE					
15 ± 5 ±1	15	[1] ABLIKIM	12N	BES3	$\psi(2S) \to \pi^0\gamma p\overline{p}$
15 ± 6	213 ± 33	[2] BAI	04	BES	$J/\psi \to \gamma p\overline{p}$
10 ± 3 ±4	18	[2] BISELLO	91	DM2	$J/\psi \to \gamma p\overline{p}$
11 ± 6	23	[2] BALTRUSAIT...86		MRK3	$J/\psi \to \eta_c\gamma$
$29 \pm 29 - 15$		[3] HIMEL	80B	MRK2	$\psi(2S) \to \eta_c\gamma$
• • • We do not use the following data for averages, fits, limits, etc. • • •					
$13.1 \pm 1.8 \pm 1.0 - 2.1 - 1.1$	195	[4] WU	06	BELL	$B^+ \to p\overline{p}K^+$

[1] ABLIKIM 12N reports $[\Gamma(\eta_c(1S) \to p\overline{p})/\Gamma_{total}] \times [\Gamma(h_c(1P) \to \gamma\eta_c(1S))/\Gamma_{total} \times \Gamma(\psi(2S) \to \pi^0 h_c(1P))/\Gamma_{total}] = (0.65 \pm 0.19 \pm 0.10) \times 10^{-6}$ which we divide by our best value $\Gamma(h_c(1P) \to \gamma\eta_c(1S))/\Gamma_{total} \times \Gamma(\psi(2S) \to \pi^0 h_c(1P))/\Gamma_{total} = (4.3 \pm 0.4) \times 10^{-4}$. Our first error is their experiment's error and our second error is the systematic error from using our best value.

[2] The quoted branching ratios use $B(J/\psi(1S) \to \gamma\eta_c(1S)) = 0.0127 \pm 0.0036$. Where relevant, the error in this branching ratio is treated as a common systematic in computing averages.

[3] Estimated using $B(\psi(2S) \to \gamma\eta_c(1S)) = 0.0028 \pm 0.0006$.

[4] WU 06 reports $[\Gamma(\eta_c(1S) \to p\overline{p})/\Gamma_{total}] \times [B(B^+ \to \eta_c K^+)] = (1.42 \pm 0.11^{+0.16}_{-0.20}) \times 10^{-6}$ which we divide by our best value $B(B^+ \to \eta_c K^+) = (1.09 \pm 0.09) \times 10^{-3}$. Our first error is their experiment's error and our second error is the systematic error from using our best value.

$\Gamma(p\overline{p})/\Gamma(K\overline{K}\pi)$ Γ_{42}/Γ_{28}

VALUE	EVTS	DOCUMENT ID		TECN	COMMENT
0.0207±0.0021 OUR FIT					
0.021 ±0.002 $^{+0.004}_{-0.006}$	195	[1] WU	06	BELL	$B^\pm \to K^\pm p\overline{p}$

[1] Using $B(B^+ \to \eta_c K^+) = (1.25 \pm 0.12^{+0.10}_{-0.12}) \times 10^{-3}$ from FANG 03 and $B(\eta_c \to K\overline{K}\pi) = (5.5 \pm 1.7) \times 10^{-2}$.

$\Gamma(p\overline{p})/\Gamma_{total} \times \Gamma(\phi\phi)/\Gamma_{total}$ $\Gamma_{42}/\Gamma \times \Gamma_7/\Gamma$

VALUE (units 10^{-5})	DOCUMENT ID		TECN	COMMENT
0.27±0.05 OUR FIT				
4.0 $^{+3.5}_{-3.2}$	BAGLIN	89	SPEC	$\overline{p}p \to K^+K^-K^+K^-$

$\Gamma(p\overline{p}\pi^0)/\Gamma_{total}$ Γ_{43}/Γ

VALUE (units 10^{-2})	EVTS	DOCUMENT ID		TECN	COMMENT
0.36±0.13±0.03	14	[1] ABLIKIM	12N	BES3	$\psi(2S) \to \pi^0\gamma p\overline{p}\pi^0$

[1] ABLIKIM 12N reports $[\Gamma(\eta_c(1S) \to p\overline{p}\pi^0)/\Gamma_{total}] \times [\Gamma(h_c(1P) \to \gamma\eta_c(1S))/\Gamma_{total} \times \Gamma(\psi(2S) \to \pi^0 h_c(1P))/\Gamma_{total}] = (1.53 \pm 0.49 \pm 0.23) \times 10^{-6}$ which we divide by our best value $\Gamma(h_c(1P) \to \gamma\eta_c(1S))/\Gamma_{total} \times \Gamma(\psi(2S) \to \pi^0 h_c(1P))/\Gamma_{total} = (4.3 \pm 0.4) \times 10^{-4}$. Our first error is their experiment's error and our second error is the systematic error from using our best value.

$\Gamma(\Lambda\overline{\Lambda})/\Gamma_{total}$ Γ_{44}/Γ

VALUE (units 10^{-4})	CL%	EVTS	DOCUMENT ID		TECN	COMMENT
10.9±2.4 OUR FIT						
11.7±2.3±2.5			[1] ABLIKIM	12B	BES3	
• • • We do not use the following data for averages, fits, limits, etc. • • •						
$8.8 \pm 2.4 \pm 0.7 - 2.3$		20	[2] WU	06	BELL	$B^+ \to \Lambda\overline{\Lambda}K^+$
<20	90		[3] BISELLO	91	DM2	$e^+e^- \to \gamma\Lambda\overline{\Lambda}$

[1] ABLIKIM 12B reports $[\Gamma(\eta_c(1S) \to \Lambda\overline{\Lambda})/\Gamma_{\rm total}] \times [{\rm B}(J/\psi(1S) \to \gamma\eta_c(1S))] = (0.198 \pm 0.021 \pm 0.032) \times 10^{-4}$ which we divide by our best value ${\rm B}(J/\psi(1S) \to \gamma\eta_c(1S)) = (1.7 \pm 0.4) \times 10^{-2}$. Our first error is their experiment's error and our second error is the systematic error from using our best value.
[2] WU 06 reports $[\Gamma(\eta_c(1S) \to \Lambda\overline{\Lambda})/\Gamma_{\rm total}] \times [{\rm B}(B^+ \to \eta_c K^+)] = (0.95^{+0.25}_{-0.22}{}^{+0.08}_{-0.11}) \times 10^{-6}$ which we divide by our best value ${\rm B}(B^+ \to \eta_c K^+) = (1.09 \pm 0.09) \times 10^{-3}$. Our first error is their experiment's error and our second error is the systematic error from using our best value.
[3] The quoted branching ratios use ${\rm B}(J/\psi(1S) \to \gamma\eta_c(1S)) = 0.0127 \pm 0.0036$.

$\Gamma(\Lambda\overline{\Lambda})/\Gamma(p\overline{p})$ Γ_{44}/Γ_{42}

VALUE	DOCUMENT ID		TECN	COMMENT
0.72±0.16 OUR FIT				
$0.67^{+0.19}_{-0.16}\pm0.12$	[1] WU	06	BELL	$B^+ \to p\overline{p}K^+$, $\Lambda\overline{\Lambda}K^+$

[1] Not independent from other $\eta_c \to \Lambda\overline{\Lambda}$, $p\overline{p}$ branching ratios reported by WU 06.

$\Gamma(\Sigma^+\overline{\Sigma}^-)/\Gamma_{\rm total}$ Γ_{45}/Γ

VALUE (units 10^{-3})	EVTS	DOCUMENT ID		TECN	COMMENT
2.1±0.3±0.5	112	[1] ABLIKIM	13C	BES3	$J/\psi \to \gamma p\overline{p}\pi^0\pi^0$

[1] ABLIKIM 13C reports $[\Gamma(\eta_c(1S) \to \Sigma^+\overline{\Sigma}^-)/\Gamma_{\rm total}] \times [{\rm B}(J/\psi(1S) \to \gamma\eta_c(1S))] = (3.60 \pm 0.48 \pm 0.31) \times 10^{-5}$ which we divide by our best value ${\rm B}(J/\psi(1S) \to \gamma\eta_c(1S)) = (1.7 \pm 0.4) \times 10^{-2}$. Our first error is their experiment's error and our second error is the systematic error from using our best value.

$\Gamma(\Xi^-\overline{\Xi}^+)/\Gamma_{\rm total}$ Γ_{46}/Γ

VALUE (units 10^{-3})	EVTS	DOCUMENT ID		TECN	COMMENT
0.90±0.18±0.19	78	[1] ABLIKIM	13C	BES3	$J/\psi \to \gamma\Lambda\overline{\Lambda}\pi^+\pi^-$

[1] ABLIKIM 13C reports $[\Gamma(\eta_c(1S) \to \Xi^-\overline{\Xi}^+)/\Gamma_{\rm total}] \times [{\rm B}(J/\psi(1S) \to \gamma\eta_c(1S))] = (1.51 \pm 0.27 \pm 0.14) \times 10^{-5}$ which we divide by our best value ${\rm B}(J/\psi(1S) \to \gamma\eta_c(1S)) = (1.7 \pm 0.4) \times 10^{-2}$. Our first error is their experiment's error and our second error is the systematic error from using our best value.

$\Gamma(\pi^+\pi^-p\overline{p})/\Gamma_{\rm total}$ Γ_{47}/Γ

VALUE (units 10^{-3})	CL%	EVTS	DOCUMENT ID		TECN	COMMENT
5.3±1.7±0.5		19	[1] ABLIKIM	12N	BES3	$\psi(2S) \to \pi^0\gamma p\overline{p}\pi^+\pi^-$
• • • We do not use the following data for averages, fits, limits, etc. • • •						
<12	90		HIMEL	80B	MRK2	$\psi(2S) \to \eta_c\gamma$

[1] ABLIKIM 12N reports $[\Gamma(\eta_c(1S) \to \pi^+\pi^-p\overline{p})/\Gamma_{\rm total}] \times [\Gamma(h_c(1P) \to \gamma\eta_c(1S))/\Gamma_{\rm total} \times \Gamma(\psi(2S) \to \pi^0 h_c(1P))/\Gamma_{\rm total}] = (2.30 \pm 0.65 \pm 0.36) \times 10^{-6}$ which we divide by our best value $\Gamma(h_c(1P) \to \gamma\eta_c(1S))/\Gamma_{\rm total} \times \Gamma(\psi(2S) \to \pi^0 h_c(1P))/\Gamma_{\rm total} = (4.3 \pm 0.4) \times 10^{-4}$. Our first error is their experiment's error and our second error is the systematic error from using our best value.

RADIATIVE DECAYS

$\Gamma(\gamma\gamma)/\Gamma_{\rm total}$ Γ_{48}/Γ

VALUE (units 10^{-4})	CL%	EVTS	DOCUMENT ID		TECN	COMMENT
1.57±0.12 OUR FIT						
$1.9\ ^{+0.7}_{-0.6}$ OUR AVERAGE						
2.7 ±0.8 ±0.6			[1] ABLIKIM	13I	BES3	
$1.4\ ^{+0.7}_{-0.5}$ ±0.3		$1.2^{+2.8}_{-1.1}$	[2] ADAMS	08	CLEO	$\psi(2S) \to \pi^+\pi^- J/\psi$
• • • We do not use the following data for averages, fits, limits, etc. • • •						
$2.0\ ^{+0.9}_{-0.7}$ ±0.2		13	[3] WICHT	08	BELL	$B^\pm \to K^\pm\gamma\gamma$
$2.80^{+0.67}_{-0.58}\pm1.0$			[4] ARMSTRONG	95F	E760	$\overline{p}p \to \gamma\gamma$
< 9	90		[5] BISELLO	91	DM2	$J/\psi \to \gamma\gamma\gamma$
$6\ ^{+4}_{-3}$ ±4			[4] BAGLIN	87B	SPEC	$\overline{p}p \to \gamma\gamma$
< 18	90		[6] BLOOM	83	CBAL	$J/\psi \to \eta_c\gamma$

[1] ABLIKIM 13I reports $[\Gamma(\eta_c(1S) \to \gamma\gamma)/\Gamma_{\rm total}] \times [{\rm B}(J/\psi(1S) \to \gamma\eta_c(1S))] = (4.5 \pm 1.2 \pm 0.6) \times 10^{-6}$ which we divide by our best value ${\rm B}(J/\psi(1S) \to \gamma\eta_c(1S)) = (1.7 \pm 0.4) \times 10^{-2}$. Our first error is their experiment's error and our second error is the systematic error from using our best value.
[2] ADAMS 08 reports $[\Gamma(\eta_c(1S) \to \gamma\gamma)/\Gamma_{\rm total}] \times [{\rm B}(J/\psi(1S) \to \gamma\eta_c(1S))] = (2.4^{+1.1}_{-0.8} \pm 0.3) \times 10^{-6}$ which we divide by our best value ${\rm B}(J/\psi(1S) \to \gamma\eta_c(1S)) = (1.7 \pm 0.4) \times 10^{-2}$. Our first error is their experiment's error and our second error is the systematic error from using our best value.
[3] WICHT 08 reports $[\Gamma(\eta_c(1S) \to \gamma\gamma)/\Gamma_{\rm total}] \times [{\rm B}(B^+ \to \eta_c K^+)] = (2.2^{+0.9}_{-0.7}{}^{+0.4}_{-0.2}) \times 10^{-7}$ which we divide by our best value ${\rm B}(B^+ \to \eta_c K^+) = (1.09 \pm 0.09) \times 10^{-3}$. Our first error is their experiment's error and our second error is the systematic error from using our best value.
[4] Not independent from the values of the total and two-photon width quoted by the same experiment.
[5] The quoted branching ratios use ${\rm B}(J/\psi(1S) \to \gamma\eta_c(1S)) = 0.0127 \pm 0.0036$.
[6] Using ${\rm B}(J/\psi(1S) \to \gamma\eta_c(1S)) = 0.0127 \pm 0.0036$.

$\Gamma(\gamma\gamma)/\Gamma(K\overline{K}\pi)$ Γ_{48}/Γ_{28}

VALUE (units 10^{-3})	EVTS	DOCUMENT ID		TECN	COMMENT
2.15±0.28 OUR FIT					
$3.2\ ^{+1.3}_{-1.0}\ ^{+0.8}_{-0.6}$	13	[1] WICHT	08	BELL	$B^\pm \to K^\pm\gamma\gamma$

[1] Using ${\rm B}(B^+ \to \eta_c K^+) = (1.25 \pm 0.12^{+0.10}_{-0.12}) \times 10^{-3}$ from FANG 03 and ${\rm B}(\eta_c \to K\overline{K}\pi) = (5.5 \pm 1.7) \times 10^{-2}$.

$\Gamma(p\overline{p})/\Gamma_{\rm total} \times \Gamma(\gamma\gamma)/\Gamma_{\rm total}$ $\Gamma_{42}/\Gamma \times \Gamma_{48}/\Gamma$

VALUE (units 10^{-6})	EVTS	DOCUMENT ID		TECN	COMMENT
0.238±0.023 OUR FIT					
0.26 ±0.05 OUR AVERAGE	Error includes scale factor of 1.4.				
$0.224^{+0.038}_{-0.037}\pm0.020$	190	AMBROGIANI	03	E835	$\overline{p}p \to \eta_c \to \gamma\gamma$
$0.336^{+0.080}_{-0.070}$		ARMSTRONG	95F	E760	$\overline{p}p \to \gamma\gamma$
$0.68\ ^{+0.42}_{-0.31}$	12	BAGLIN	87B	SPEC	$\overline{p}p \to \gamma\gamma$

Charge conjugation (C), Parity (P), Lepton family number (LF) violating modes

$\Gamma(\pi^+\pi^-)/\Gamma_{\rm total}$ Γ_{49}/Γ

VALUE (units 10^{-5})	CL%	DOCUMENT ID		TECN	COMMENT
<11	90	[1] ABLIKIM	11G	BES3	$J/\psi \to \gamma\pi^+\pi^-$
• • • We do not use the following data for averages, fits, limits, etc. • • •					
<70	90	[2] ABLIKIM	06B	BES2	$J/\psi \to \pi^+\pi^-\gamma$

[1] ABLIKIM 11G reports $[\Gamma(\eta_c(1S) \to \pi^+\pi^-)/\Gamma_{\rm total}] \times [{\rm B}(J/\psi(1S) \to \gamma\eta_c(1S))] < 1.82\times10^{-6}$ which we divide by our best value ${\rm B}(J/\psi(1S) \to \gamma\eta_c(1S)) = 1.7\times10^{-2}$.
[2] ABLIKIM 06B reports $[\Gamma(\eta_c(1S) \to \pi^+\pi^-)/\Gamma_{\rm total}] \times [{\rm B}(J/\psi(1S) \to \gamma\eta_c(1S))] < 1.1\times10^{-5}$ which we divide by our best value ${\rm B}(J/\psi(1S) \to \gamma\eta_c(1S)) = 1.7\times10^{-2}$.

$\Gamma(\pi^0\pi^0)/\Gamma_{\rm total}$ Γ_{50}/Γ

VALUE (units 10^{-5})	CL%	DOCUMENT ID		TECN	COMMENT
< 4	90	[1] ABLIKIM	11G	BES3	$J/\psi \to \gamma\pi^0\pi^0$
• • • We do not use the following data for averages, fits, limits, etc. • • •					
<40	90	[2] ABLIKIM	06B	BES2	$J/\psi \to \pi^0\pi^0\gamma$

[1] ABLIKIM 11G reports $[\Gamma(\eta_c(1S) \to \pi^0\pi^0)/\Gamma_{\rm total}] \times [{\rm B}(J/\psi(1S) \to \gamma\eta_c(1S))] < 6.0\times10^{-7}$ which we divide by our best value ${\rm B}(J/\psi(1S) \to \gamma\eta_c(1S)) = 1.7\times10^{-2}$.
[2] ABLIKIM 06B reports $[\Gamma(\eta_c(1S) \to \pi^0\pi^0)/\Gamma_{\rm total}] \times [{\rm B}(J/\psi(1S) \to \gamma\eta_c(1S))] < 0.71\times10^{-5}$ which we divide by our best value ${\rm B}(J/\psi(1S) \to \gamma\eta_c(1S)) = 1.7\times10^{-2}$.

$\Gamma(K^+K^-)/\Gamma_{\rm total}$ Γ_{51}/Γ

VALUE (units 10^{-5})	CL%	DOCUMENT ID		TECN	COMMENT
<60	90	[1] ABLIKIM	06B	BES2	$J/\psi \to K^+K^-\gamma$

[1] ABLIKIM 06B reports $[\Gamma(\eta_c(1S) \to K^+K^-)/\Gamma_{\rm total}] \times [{\rm B}(J/\psi(1S) \to \gamma\eta_c(1S))] < 0.96\times10^{-5}$ which we divide by our best value ${\rm B}(J/\psi(1S) \to \gamma\eta_c(1S)) = 1.7\times10^{-2}$.

$\Gamma(K^0_SK^0_S)/\Gamma_{\rm total}$ Γ_{52}/Γ

VALUE (units 10^{-5})	CL%	DOCUMENT ID		TECN	COMMENT
<31	90	[1] ABLIKIM	06B	BES2	$J/\psi \to K^0_SK^0_S\gamma$
• • • We do not use the following data for averages, fits, limits, etc. • • •					
<32	90	[2] UEHARA	13	BELL	$\gamma\gamma \to K^0_SK^0_S$
< 5.6	90	[3] UEHARA	13	BELL	$\gamma\gamma \to K^0_SK^0_S$

[1] ABLIKIM 06B reports $[\Gamma(\eta_c(1S) \to K^0_SK^0_S)/\Gamma_{\rm total}] \times [{\rm B}(J/\psi(1S) \to \gamma\eta_c(1S))] < 0.53\times10^{-5}$ which we divide by our best value ${\rm B}(J/\psi(1S) \to \gamma\eta_c(1S)) = 1.7\times10^{-2}$.
[2] Taking into account interference with the non-resonant continuum.
[3] Neglecting interference with the non-resonant continuum.

$\eta_c(1S)$ REFERENCES

AAIJ	17AD	PL B769 305	R. Aaij *et al.*	(LHCb Collab.)
AAIJ	17BB	EPJ C77 609	R. Aaij *et al.*	(LHCb Collab.)
ABLIKIM	17AJ	PR D96 112008	M. Ablikim *et al.*	(BES III Collab.)
ABLIKIM	17P	PR D95 092004	M. Ablikim *et al.*	(BES III Collab.)
LEES	16A	PR D93 012005	J.P. Lees *et al.*	(BABAR Collab.)
PDG	16	CP C40 100001	C. Patrignani *et al.*	(PDG Collab.)
AAIJ	15AS	JHEP 1510 053	R. Aaij *et al.*	(LHCb Collab.)
AAIJ	15BI	EPJ C75 311	R. Aaij *et al.*	(LHCb Collab.)
ANASHIN	14	PL B738 391	V.V. Anashin *et al.*	(KEDR Collab.)
LEES	14E	PR D89 112004	J.P. Lees *et al.*	(BABAR Collab.)
ABLIKIM	13C	PR D87 012003	M. Ablikim *et al.*	(BES III Collab.)
ABLIKIM	13I	PR D87 032003	M. Ablikim *et al.*	(BES III Collab.)
UEHARA	13	PTEP 2013 123C01	S. Uehara *et al.*	(BELLE Collab.)
ABLIKIM	12B	PR D86 032008	M. Ablikim *et al.*	(BES III Collab.)
ABLIKIM	12F	PRL 108 222002	M. Ablikim *et al.*	(BES III Collab.)
ABLIKIM	12N	PR D86 092009	M. Ablikim *et al.*	(BES III Collab.)
LIU	12B	PRL 108 232001	Z.Q. Liu *et al.*	(BELLE Collab.)
ZHANG	12A	PR D86 052002	C.C. Zhang *et al.*	(BELLE Collab.)
ABLIKIM	11G	PR D84 032006	M. Ablikim *et al.*	(BES III Collab.)
DEL-AMO-SA...	11M	PR D84 012004	P. del Amo Sanchez *et al.*	(BABAR Collab.)
VINOKUROVA	11	PL B706 139	A. Vinokurova *et al.*	(BELLE Collab.)
LEES	10	PR D81 052010	J.P. Lees *et al.*	(BABAR Collab.)
MITCHELL	09	PRL 102 011801	R.E. Mitchell *et al.*	(CLEO Collab.)
ADAMS	08	PRL 101 101801	G.S. Adams *et al.*	(CLEO Collab.)
AUBERT	08AB	PR D78 012006	B. Aubert *et al.*	(BABAR Collab.)
UEHARA	08	EPJ C53 1	S. Uehara *et al.*	(BELLE Collab.)
WICHT	08	PL B662 323	J. Wicht *et al.*	(BELLE Collab.)
ABE	07	PRL 98 082001	K. Abe *et al.*	(BELLE Collab.)
ABLIKIM	06A	PL B633 19	M. Ablikim *et al.*	(BES Collab.)
ABLIKIM	06B	EPJ C45 337	M. Ablikim *et al.*	(BES Collab.)
AUBERT	06E	PRL 96 052002	B. Aubert *et al.*	(BABAR Collab.)
PDG	06	JP G33 1	W.-M. Yao *et al.*	(PDG Collab.)
WU	06	PRL 97 162003	C.-H. Wu *et al.*	(BELLE Collab.)
ABLIKIM	05L	PR D72 072005	M. Ablikim *et al.*	(BES Collab.)
KUO	05	PL B621 41	C.C. Kuo *et al.*	(BELLE Collab.)
ABE	04G	PR D70 071102	K. Abe *et al.*	(BELLE Collab.)

ABLIKIM	04M	PR D70 112008	M. Ablikim *et al.*	(BES Collab.)
ASNER	04	PRL 92 142001	D.M. Asner *et al.*	(CLEO Collab.)
AUBERT	04D	PRL 92 142002	B. Aubert *et al.*	(BABAR Collab.)
AUBERT,B	04B	PR D70 011101	B. Aubert *et al.*	(BABAR Collab.)
BAI	04	PL B578 16	J.Z. Bai *et al.*	(BES Collab.)
ABDALLAH	03J	EPJ C31 481	J. Abdallah *et al.*	(DELPHI Collab.)
AMBROGIANI	03	PL B566 45	M. Ambrogiani *et al.*	(FNAL E835 Collab.)
BAI	03	PL B555 174	J.Z. Bai *et al.*	(BES Collab.)
FANG	03	PRL 90 071801	F. Fang *et al.*	(BELLE Collab.)
HUANG	03	PRL 91 241802	H.-C. Huang *et al.*	(BELLE Collab.)
ABE,K	02	PRL 89 142001	K. Abe *et al.*	(BELLE Collab.)
BAI	00F	PR D62 072001	J.Z. Bai *et al.*	(BES Collab.)
BRANDENB...	00B	PRL 85 3095	G. Brandenburg *et al.*	(CLEO Collab.)
ACCIARRI	99T	PL B461 155	M. Acciarri *et al.*	(L3 Collab.)
BAI	99B	PR D60 072001	J.Z. Bai *et al.*	(BES Collab.)
ABREU	98O	PL B441 479	P. Abreu *et al.*	(DELPHI Collab.)
SHIRAI	98	PL B424 405	M. Shirai *et al.*	(AMY Collab.)
ARMSTRONG	95F	PR D52 4839	T.A. Armstrong *et al.*	(FNAL, FERR, GENO+)
ALBRECHT	94H	PL B338 390	H. Albrecht *et al.*	(ARGUS Collab.)
ADRIANI	93N	PL B318 575	O. Adriani *et al.*	(L3 Collab.)
BISELLO	91	NP B350 1	D. Bisello *et al.*	(DM2 Collab.)
BAI	90B	PRL 65 1309	Z. Bai *et al.*	(Mark III Collab.)
CHEN	90B	PL B243 169	W.Y. Chen *et al.*	(CLEO Collab.)
BAGLIN	89	PL B231 557	C. Baglin, S. Baird, G. Bassompierre	(R704 Collab.)
BEHREND	89	ZPHY C42 367	H.J. Behrend *et al.*	(CELLO Collab.)
BRAUNSCH...	89	ZPHY C41 533	W. Braunschweig *et al.*	(TASSO Collab.)
AIHARA	88D	PRL 60 2355	H. Aihara *et al.*	(TPC Collab.)
BAGLIN	87B	PL B187 191	C. Baglin *et al.*	(R704 Collab.)
BALTRUSAIT...	86	PR D33 629	R.M. Baltrusaitis *et al.*	(Mark III Collab.)
BERGER	86	PL 167B 120	C. Berger *et al.*	(PLUTO Collab.)
GAISER	86	PR D34 711	J. Gaiser *et al.*	(Crystal Ball Collab.)
ALTHOFF	85B	ZPHY C29 189	M. Althoff *et al.*	(TASSO Collab.)
BALTRUSAIT...	84	PRL 52 2126	R.M. Baltrusaitis *et al.*	(CIT, UCSC+) JP
BLOOM	83	ARNS 33 143	E.D. Bloom, C. Peck	(SLAC, CIT)
HIMEL	80B	PRL 45 1146	T.M. Himel *et al.*	(SLAC, LBL, UCB)
PARTRIDGE	80B	PRL 45 1150	R. Partridge *et al.*	(CIT, HARV, PRIN+)

$J/\psi(1S)$

$I^G(J^{PC}) = 0^-(1^{--})$

$J/\psi(1S)$ MASS

VALUE (MeV)	EVTS	DOCUMENT ID		TECN	COMMENT
3096.900±0.006 OUR AVERAGE					
3096.900±0.002±0.006		[1] ANASHIN	15	KEDR	$e^+e^- \to$ hadrons
3096.89 ±0.09	502	[2] ARTAMONOV	00	OLYA	$e^+e^- \to$ hadrons
3096.91 ±0.03 ±0.01		[3] ARMSTRONG	93B	E760	$\overline{p}p \to e^+e^-$
3096.95 ±0.1 ±0.3	193	BAGLIN	87	SPEC	$\overline{p}p \to e^+e^-$X
• • • We do not use the following data for averages, fits, limits, etc. • • •					
3096.66 ±0.19 ±0.02	6.1k	[4] AAIJ	15BI	LHCB	$pp \to J/\psi X$
3096.917±0.010±0.007		AULCHENKO	03	KEDR	$e^+e^- \to$ hadrons
3097.5 ±0.3		GRIBUSHIN	96	FMPS	515 π^-Be $\to 2\mu X$
3098.4 ±2.0	38k	LEMOIGNE	82	GOLI	185 π^-Be $\to \gamma\mu^+\mu^-$A
3096.93 ±0.09	502	[5] ZHOLENTZ	80	REDE	e^+e^-
3097.0 ±1		[6] BRANDELIK	79C	DASP	e^+e^-

[1] Supersedes AULCHENKO 03.

[2] Reanalysis of ZHOLENTZ 80 using new electron mass (COHEN 87) and radiative corrections (KURAEV 85).

[3] Mass central value and systematic error recalculated by us according to Eq. (16) in ARMSTRONG 93B, using the value for the $\psi(2S)$ mass from AULCHENKO 03.

[4] From a sample of $\eta_c(1S)$ and J/ψ produced in b-hadron decays. Systematic uncertainties not estimated.

[5] Superseded by ARTAMONOV 00.

[6] From a simultaneous fit to e^+e^-, $\mu^+\mu^-$ and hadronic channels assuming $\Gamma(e^+e^-) = \Gamma(\mu^+\mu^-)$.

$J/\psi(1S)$ WIDTH

VALUE (keV)	EVTS	DOCUMENT ID		TECN	COMMENT
92.9± 2.8 OUR AVERAGE Error includes scale factor of 1.1.					
96.1± 3.2	13k	[1] ADAMS	06A	CLEO	$e^+e^- \to \mu^+\mu^-\gamma$
84.4± 8.9		BAI	95B	BES	e^+e^-
91 ±11 ±6		[2] ARMSTRONG	93B	E760	$\overline{p}p \to e^+e^-$
$85.5^{+\ 6.1}_{-\ 5.8}$		[3] HSUEH	92	RVUE	See Υ mini-review
• • • We do not use the following data for averages, fits, limits, etc. • • •					
94.1± 2.7		[4] ANASHIN	10	KEDR	3.097 $e^+e^- \to e^+e^-$, $\mu^+\mu^-$
93.7± 3.5	7.8k	[1] AUBERT	04	BABR	$e^+e^- \to \mu^+\mu^-\gamma$

[1] Calculated by us from the reported values of $\Gamma(e^+e^-)\times B(\mu^+\mu^-)$ using $B(e^+e^-) = (5.94 \pm 0.06)\%$ and $B(\mu^+\mu^-) = (5.93 \pm 0.06)\%$.

[2] The initial-state radiation correction reevaluated by ANDREOTTI 07 in its Ref. [4].

[3] Using data from COFFMAN 92, BALDINI-CELIO 75, BOYARSKI 75, ESPOSITO 75B, BRANDELIK 79C.

[4] Assuming $\Gamma(e^+e^-) = \Gamma(\mu^+\mu^-)$ and using $\Gamma(e^+e^-)/\Gamma_{total} = (5.94 \pm 0.06)\%$.

$J/\psi(1S)$ DECAY MODES

	Mode	Fraction (Γ_i/Γ)	Scale factor/ Confidence level
Γ_1	hadrons	(87.7 ± 0.5) %	
Γ_2	virtual$\gamma \to$ hadrons	(13.50 ± 0.30) %	
Γ_3	ggg	(64.1 ± 1.0) %	
Γ_4	γgg	(8.8 ± 1.1) %	
Γ_5	e^+e^-	(5.971± 0.032) %	
Γ_6	$e^+e^-\gamma$	[a] (8.8 ± 1.4) $\times 10^{-3}$	
Γ_7	$\mu^+\mu^-$	(5.961± 0.033) %	

Decays involving hadronic resonances

Γ_8	$\rho\pi$	(1.69 ± 0.15) %		S=2.4
Γ_9	$\rho^0\pi^0$	(5.6 ± 0.7) $\times 10^{-3}$		
Γ_{10}	$\rho(770)^\mp K^\pm K^0_S$	(1.9 ± 0.4) $\times 10^{-3}$		
Γ_{11}	$\rho(1450)\pi$			
Γ_{12}	$\rho(1450)\pi \to \pi^+\pi^-\pi^0$	(2.3 ± 0.7) $\times 10^{-3}$		
Γ_{13}	$\rho(1450)^\pm\pi^\mp \to K^0_S K^\pm\pi^\mp$	(3.5 ± 0.6) $\times 10^{-4}$		
Γ_{14}	$\rho(1450)^0\pi^0 \to K^+K^-\pi^0$	(2.0 ± 0.5) $\times 10^{-4}$		
Γ_{15}	$\rho(1450)\eta'(958) \to \pi^+\pi^-\eta'(958)$	(3.3 ± 0.7) $\times 10^{-6}$		
Γ_{16}	$\rho(1700)\pi$			
Γ_{17}	$\rho(1700)\pi \to \pi^+\pi^-\pi^0$	(1.7 ± 1.1) $\times 10^{-4}$		
Γ_{18}	$\rho(2150)\pi$			
Γ_{19}	$\rho(2150)\pi \to \pi^+\pi^-\pi^0$	(8 ±40) $\times 10^{-6}$		
Γ_{20}	$\rho_3(1690)\pi \to \pi^+\pi^-\pi^0$			
Γ_{21}	$a_2(1320)\rho$	(1.09 ± 0.22) %		
Γ_{22}	$\omega\pi^+\pi^+\pi^-\pi^-$	(8.5 ± 3.4) $\times 10^{-3}$		
Γ_{23}	$\omega\pi^+\pi^-\pi^0$	(4.0 ± 0.7) $\times 10^{-3}$		
Γ_{24}	$\omega\pi^+\pi^-$	(8.6 ± 0.7) $\times 10^{-3}$		S=1.1
Γ_{25}	$\omega f_2(1270)$	(4.3 ± 0.6) $\times 10^{-3}$		
Γ_{26}	$K^*(892)^0\overline{K}^*(892)^0$	(2.3 ± 0.6) $\times 10^{-4}$		
Γ_{27}	$K^*(892)^\pm K^*(892)^\mp$	(1.00 $^{+\ 0.22}_{-\ 0.40}$) $\times 10^{-3}$		
Γ_{28}	$K^*(892)^\pm K^*(700)^\mp$	(1.1 $^{+\ 1.0}_{-\ 0.6}$) $\times 10^{-3}$		
Γ_{29}	$K^0_S\pi^- K^*(892)^+$ + c.c.	(2.0 ± 0.5) $\times 10^{-3}$		
Γ_{30}	$K^0_S\pi^- K^*(892)^+$ + c.c. $\to K^0_S K^0_S\pi^+\pi^-$	(6.7 ± 2.2) $\times 10^{-4}$		
Γ_{31}	$\eta K^*(892)^0\overline{K}^*(892)^0$	(1.15 ± 0.26) $\times 10^{-3}$		
Γ_{32}	$K^*(1410)\overline{K}$+c.c.			
Γ_{33}	$K^*(1410)\overline{K}$+c.c $\to K^\pm K^\mp\pi^0$	(4.9 ± 2.8) $\times 10^{-5}$		
Γ_{34}	$K^*(1410)\overline{K}$+ c.c. $\to K^0_S K^\pm\pi^\mp$	(8 ± 6) $\times 10^{-5}$		
Γ_{35}	$K^*_2(1430)\overline{K}$+c.c.			
Γ_{36}	$K^*_2(1430)\overline{K}$+c.c. $\to K^\pm K^\mp\pi^0$	(7.5 ± 3.5) $\times 10^{-5}$		
Γ_{37}	$K^*_2(1430)\overline{K}$+ c.c. $\to K^0_S K^\pm\pi^\mp$	(4.0 ± 1.0) $\times 10^{-4}$		
Γ_{38}	$K^*(892)^0\overline{K}^*_2(1430)^0$ + c.c.	(4.66 ± 0.31) $\times 10^{-3}$		
Γ_{39}	$K^*(892)^+K^*_2(1430)^-$ + c.c.	(3.4 ± 2.9) $\times 10^{-3}$		
Γ_{40}	$K^*(892)^+K^*_2(1430)^-$ + c.c. $\to K^*(892)^+K^0_S\pi^-$ + c.c.	(4 ± 4) $\times 10^{-4}$		
Γ_{41}	$K^*(892)^0\overline{K}_2(1770)^0$ + c.c. $\to K^*(892)^0K^-\pi^+$ + c.c.	(6.9 ± 0.9) $\times 10^{-4}$		
Γ_{42}	$\omega K^*(892)\overline{K}$+ c.c.	(6.1 ± 0.9) $\times 10^{-3}$		
Γ_{43}	$\overline{K}K^*(892)$+c.c.			
Γ_{44}	$\overline{K}K^*(892)$+c.c. $\to K^0_S K^\pm\pi^\mp$	(5.1 ± 0.5) $\times 10^{-3}$		
Γ_{45}	$K^+K^*(892)^-$ + c.c.	(5.12 ± 0.30) $\times 10^{-3}$		
Γ_{46}	$K^+K^*(892)^-$ + c.c. $\to K^+K^-\pi^0$	(1.97 ± 0.20) $\times 10^{-3}$		
Γ_{47}	$K^+K^*(892)^-$ + c.c. $\to K^0K^\pm\pi^\mp$ + c.c.	(3.0 ± 0.4) $\times 10^{-3}$		
Γ_{48}	$K^0\overline{K}^*(892)^0$ + c.c.	(4.39 ± 0.31) $\times 10^{-3}$		
Γ_{49}	$K^0\overline{K}^*(892)^0$ + c.c. $\to K^0K^\pm\pi^\mp$ + c.c.	(3.2 ± 0.4) $\times 10^{-3}$		
Γ_{50}	$K_1(1400)^\pm K^\mp$	(3.8 ± 1.4) $\times 10^{-3}$		
Γ_{51}	$\overline{K}^*(892)^0K^+\pi^-$ + c.c.	seen		
Γ_{52}	$K^*(892)^\pm K^\mp\pi^0$	(4.1 ± 1.3) $\times 10^{-3}$		
Γ_{53}	$K^*(892)^0K^0_S\pi^0$	(6 ± 4) $\times 10^{-4}$		
Γ_{54}	$\omega\pi^0\pi^0$	(3.4 ± 0.8) $\times 10^{-3}$		
Γ_{55}	$b_1(1235)^\pm\pi^\mp$	[b] (3.0 ± 0.5) $\times 10^{-3}$		
Γ_{56}	$\omega K^\pm K^0_S\pi^\mp$	[b] (3.4 ± 0.5) $\times 10^{-3}$		
Γ_{57}	$b_1(1235)^0\pi^0$	(2.3 ± 0.6) $\times 10^{-3}$		
Γ_{58}	$\eta K^\pm K^0_S\pi^\mp$	[b] (2.2 ± 0.4) $\times 10^{-3}$		
Γ_{59}	$\phi K^*(892)\overline{K}$+ c.c.	(2.18 ± 0.23) $\times 10^{-3}$		
Γ_{60}	$\omega K\overline{K}$	(1.70 ± 0.32) $\times 10^{-3}$		
Γ_{61}	$\omega f_0(1710) \to \omega K\overline{K}$	(4.8 ± 1.1) $\times 10^{-4}$		
Γ_{62}	$\phi 2(\pi^+\pi^-)$	(1.66 ± 0.23) $\times 10^{-3}$		
Γ_{63}	$\Delta(1232)^{++}\overline{p}\pi^-$	(1.6 ± 0.5) $\times 10^{-3}$		

Meson Particle Listings

$J/\psi(1S)$

Γ_{64}	$\omega\eta$		(1.74 ± 0.20)	$\times 10^{-3}$		S=1.6
Γ_{65}	$\phi K\overline{K}$		(1.77 ± 0.16)	$\times 10^{-3}$		S=1.3
Γ_{66}	$\phi K_S^0 K_S^0$		(5.9 ± 1.5)	$\times 10^{-4}$		
Γ_{67}	$\phi f_0(1710) \rightarrow \phi K\overline{K}$		(3.6 ± 0.6)	$\times 10^{-4}$		
Γ_{68}	$\phi K^+ K^-$		(8.3 ± 1.2)	$\times 10^{-4}$		
Γ_{69}	$\phi f_2(1270)$		(3.2 ± 0.6)	$\times 10^{-4}$		
Γ_{70}	$\Delta(1232)^{++}\overline{\Delta}(1232)^{--}$		(1.10 ± 0.29)	$\times 10^{-3}$		
Γ_{71}	$\Sigma(1385)^-\overline{\Sigma}(1385)^+$ (or c.c.)	[b]	(1.16 ± 0.05)	$\times 10^{-3}$		
Γ_{72}	$\Sigma(1385)^0\overline{\Sigma}(1385)^0$		(1.07 ± 0.08)	$\times 10^{-3}$		
Γ_{73}	$K^+K^-f_2'(1525)$		(1.04 ± 0.35)	$\times 10^{-3}$		
Γ_{74}	$\phi f_2'(1525)$		(8 ± 4)	$\times 10^{-4}$		S=2.7
Γ_{75}	$\phi\pi^+\pi^-$		(8.7 ± 0.9)	$\times 10^{-4}$		S=1.4
Γ_{76}	$\phi\pi^0\pi^0$		(5.0 ± 1.0)	$\times 10^{-4}$		
Γ_{77}	$\phi K^\pm K_S^0\pi^\mp$	[b]	(7.2 ± 0.8)	$\times 10^{-4}$		
Γ_{78}	$\omega f_1(1420)$		(6.8 ± 2.4)	$\times 10^{-4}$		
Γ_{79}	$\phi\eta$		(7.5 ± 0.8)	$\times 10^{-4}$		S=1.5
Γ_{80}	$\Xi^0\overline{\Xi}^0$		(1.17 ± 0.04)	$\times 10^{-3}$		
Γ_{81}	$\Xi(1530)^-\overline{\Xi}^+$		(5.9 ± 1.5)	$\times 10^{-4}$		
Γ_{82}	$pK^-\overline{\Sigma}(1385)^0$		(5.1 ± 3.2)	$\times 10^{-4}$		
Γ_{83}	$\omega\pi^0$		(4.5 ± 0.5)	$\times 10^{-4}$		S=1.4
Γ_{84}	$\omega\pi^0 \rightarrow \pi^+\pi^-\pi^0$		(1.7 ± 0.8)	$\times 10^{-5}$		
Γ_{85}	$\phi\eta'(958)$		(4.6 ± 0.5)	$\times 10^{-4}$		S=2.2
Γ_{86}	$\phi f_0(980)$		(3.2 ± 0.9)	$\times 10^{-4}$		S=1.9
Γ_{87}	$\phi f_0(980) \rightarrow \phi\pi^+\pi^-$		(2.59 ± 0.34)	$\times 10^{-4}$		
Γ_{88}	$\phi f_0(980) \rightarrow \phi\pi^0\pi^0$		(1.8 ± 0.5)	$\times 10^{-4}$		
Γ_{89}	$\phi\pi^0 f_0(980) \rightarrow \phi\pi^0\pi^+\pi^-$		(4.5 ± 1.0)	$\times 10^{-6}$		
Γ_{90}	$\phi\pi^0 f_0(980) \rightarrow \phi\pi^0 p^0\pi^0$		(1.7 ± 0.6)	$\times 10^{-6}$		
Γ_{91}	$\eta\phi f_0(980) \rightarrow \eta\phi\pi^+\pi^-$		(3.2 ± 1.0)	$\times 10^{-4}$		
Γ_{92}	$\phi a_0(980)^0 \rightarrow \phi\eta\pi^0$		(5 ± 4)	$\times 10^{-6}$		
Γ_{93}	$\Xi(1530)^0\overline{\Xi}^0$		(3.2 ± 1.4)	$\times 10^{-4}$		
Γ_{94}	$\Sigma(1385)^-\overline{\Sigma}^+$ (or c.c.)	[b]	(3.1 ± 0.5)	$\times 10^{-4}$		
Γ_{95}	$\phi f_1(1285)$		(2.6 ± 0.5)	$\times 10^{-4}$		
Γ_{96}	$\phi f_1(1285) \rightarrow \phi\pi^0 f_0(980) \rightarrow \phi\pi^0\pi^+\pi^-$		(9.4 ± 2.8)	$\times 10^{-7}$		
Γ_{97}	$\phi f_1(1285) \rightarrow \phi\pi^0 f_0(980) \rightarrow \phi\pi^0\pi^0\pi^0$		(2.1 ± 2.2)	$\times 10^{-7}$		
Γ_{98}	$\eta\pi^+\pi^-$		(4.0 ± 1.7)	$\times 10^{-4}$		
Γ_{99}	$\eta\rho$		(1.93 ± 0.23)	$\times 10^{-4}$		
Γ_{100}	$\omega\eta'(958)$		(1.89 ± 0.18)	$\times 10^{-4}$		
Γ_{101}	$\omega f_0(980)$		(1.4 ± 0.5)	$\times 10^{-4}$		
Γ_{102}	$\rho\eta'(958)$		(8.1 ± 0.8)	$\times 10^{-5}$		S=1.6
Γ_{103}	$a_2(1320)^\pm\pi^\mp$	[b]	< 4.3	$\times 10^{-3}$		CL=90%
Γ_{104}	$K\overline{K}_2^*(1430)+$ c.c.		< 4.0	$\times 10^{-3}$		CL=90%
Γ_{105}	$K_1(1270)^\pm K^\mp$		< 3.0	$\times 10^{-3}$		CL=90%
Γ_{106}	$K_S^0\pi^- K_2^*(1430)^+ +$ c.c.		(3.6 ± 1.8)	$\times 10^{-3}$		
Γ_{107}	$K_S^0\pi^- K_2^*(1430)^+ +$ c.c. $\rightarrow K_S^0 K_S^0\pi^+\pi^-$		(4.5 ± 2.2)	$\times 10^{-4}$		
Γ_{108}	$K_2^*(1430)^0\overline{K}_2^*(1430)^0$		< 2.9	$\times 10^{-3}$		CL=90%
Γ_{109}	$\phi\pi^0$		3×10^{-6} or 1×10^{-7}			
Γ_{110}	$\phi\eta(1405) \rightarrow \phi\eta\pi^+\pi^-$		(2.0 ± 1.0)	$\times 10^{-5}$		
Γ_{111}	$\omega f_2'(1525)$		< 2.2	$\times 10^{-4}$		CL=90%
Γ_{112}	$\omega X(1835) \rightarrow \omega p\overline{p}$		< 3.9	$\times 10^{-6}$		CL=95%
Γ_{113}	$\phi X(1835) \rightarrow \phi p\overline{p}$		< 2.1	$\times 10^{-7}$		CL=90%
Γ_{114}	$\phi X(1835) \rightarrow \phi\eta\pi^+\pi^-$		< 2.8	$\times 10^{-4}$		CL=90%
Γ_{115}	$\phi X(1870) \rightarrow \phi\eta\pi^+\pi^-$		< 6.13	$\times 10^{-5}$		CL=90%
Γ_{116}	$\eta\phi(2170) \rightarrow \eta\phi f_0(980) \rightarrow \eta\phi\pi^+\pi^-$		(1.2 ± 0.4)	$\times 10^{-4}$		
Γ_{117}	$\eta\phi(2170) \rightarrow \eta K^*(892)^0\overline{K}^*(892)^0$		< 2.52	$\times 10^{-4}$		CL=90%
Γ_{118}	$\Sigma(1385)^0\overline{\Lambda}+$ c.c.		< 8.2	$\times 10^{-6}$		CL=90%
Γ_{119}	$\Delta(1232)^+\overline{p}$		< 1	$\times 10^{-4}$		CL=90%
Γ_{120}	$\Lambda(1520)\overline{\Lambda}+$ c.c. $\rightarrow \gamma\Lambda\overline{\Lambda}$		< 4.1	$\times 10^{-6}$		CL=90%
Γ_{121}	$\Theta(1540)\overline{\Theta}(1540) \rightarrow K_S^0 pK^-\overline{n}+$ c.c.		< 1.1	$\times 10^{-5}$		CL=90%
Γ_{122}	$\Theta(1540)K^-\overline{n} \rightarrow K_S^0 pK^-\overline{n}$		< 2.1	$\times 10^{-5}$		CL=90%
Γ_{123}	$\Theta(1540)K_S^0\overline{p} \rightarrow K_S^0\overline{p}K^+n$		< 1.6	$\times 10^{-5}$		CL=90%
Γ_{124}	$\overline{\Theta}(1540)K^+n \rightarrow K_S^0\overline{p}K^+n$		< 5.6	$\times 10^{-5}$		CL=90%
Γ_{125}	$\overline{\Theta}(1540)K_S^0 p \rightarrow K_S^0 pK^-\overline{n}$		< 1.1	$\times 10^{-5}$		CL=90%
Γ_{126}	$\Sigma^0\overline{\Lambda}$		< 9	$\times 10^{-5}$		CL=90%

Decays into stable hadrons

Γ_{127}	$2(\pi^+\pi^-)\pi^0$		(4.1 ± 0.5)	%		S=2.4
Γ_{128}	$3(\pi^+\pi^-)\pi^0$		(2.9 ± 0.6)	%		
Γ_{129}	$\pi^+\pi^-\pi^0$		(2.11 ± 0.07)	%		S=1.5
Γ_{130}	$\pi^+\pi^-\pi^0 K^+K^-$		(1.79 ± 0.29)	%		S=2.2
Γ_{131}	$4(\pi^+\pi^-)\pi^0$		(9.0 ± 3.0)	$\times 10^{-3}$		
Γ_{132}	$\pi^+\pi^- K^+K^-$		(6.84 ± 0.32)	$\times 10^{-3}$		
Γ_{133}	$\pi^+\pi^- K_S^0 K_L^0$		(3.8 ± 0.6)	$\times 10^{-3}$		
Γ_{134}	$\pi^+\pi^- K_S^0 K_S^0$		(1.68 ± 0.19)	$\times 10^{-3}$		
Γ_{135}	$\pi^\pm\pi^0 K^\mp K_S^0$		(5.7 ± 0.5)	$\times 10^{-3}$		
Γ_{136}	$K^+K^- K_S^0 K_S^0$		(4.1 ± 0.8)	$\times 10^{-4}$		
Γ_{137}	$\pi^+\pi^- K^+K^-\eta$		(1.84 ± 0.28)	$\times 10^{-3}$		
Γ_{138}	$\pi^0\pi^0 K^+K^-$		(2.12 ± 0.23)	$\times 10^{-3}$		
Γ_{139}	$\pi^0\pi^0 K_S^0 K_L^0$		(1.9 ± 0.4)	$\times 10^{-3}$		
Γ_{140}	$K\overline{K}\pi$		(6.1 ± 1.0)	$\times 10^{-3}$		
Γ_{141}	$K^+K^-\pi^0$		(2.14 ± 0.24)	$\times 10^{-3}$		
Γ_{142}	$K_S^0 K^\pm\pi^\mp$		(5.6 ± 0.5)	$\times 10^{-3}$		
Γ_{143}	$K_S^0 K_L^0\pi^0$		(2.06 ± 0.27)	$\times 10^{-3}$		
Γ_{144}	$K^*(892)^0\overline{K}^0+$ c.c. $\rightarrow K_S^0 K_L^0\pi^0$		(1.21 ± 0.18)	$\times 10^{-3}$		
Γ_{145}	$K_2^*(1430)^0\overline{K}^0+$ c.c. $\rightarrow K_S^0 K_L^0\pi^0$		(4.3 ± 1.3)	$\times 10^{-4}$		
Γ_{146}	$K_S^0 K_L^0\eta$		(1.44 ± 0.34)	$\times 10^{-3}$		
Γ_{147}	$2(\pi^+\pi^-)$		(3.57 ± 0.30)	$\times 10^{-3}$		
Γ_{148}	$3(\pi^+\pi^-)$		(4.3 ± 0.4)	$\times 10^{-3}$		
Γ_{149}	$2(\pi^+\pi^-\pi^0)$		(1.62 ± 0.21)	%		
Γ_{150}	$2(\pi^+\pi^-)\eta$		(2.29 ± 0.24)	$\times 10^{-3}$		
Γ_{151}	$3(\pi^+\pi^-)\eta$		(7.2 ± 1.5)	$\times 10^{-4}$		
Γ_{152}	$p\overline{p}$		(2.121 ± 0.029)	$\times 10^{-3}$		
Γ_{153}	$p\overline{p}\pi^0$		(1.19 ± 0.08)	$\times 10^{-3}$		S=1.1
Γ_{154}	$p\overline{p}\pi^+\pi^-$		(6.0 ± 0.5)	$\times 10^{-3}$		S=1.3
Γ_{155}	$p\overline{p}\pi^+\pi^-\pi^0$	[c]	(2.3 ± 0.9)	$\times 10^{-3}$		S=1.9
Γ_{156}	$p\overline{p}\eta$		(2.00 ± 0.12)	$\times 10^{-3}$		
Γ_{157}	$p\overline{p}\rho$		< 3.1	$\times 10^{-4}$		CL=90%
Γ_{158}	$p\overline{p}\omega$		(9.8 ± 1.0)	$\times 10^{-4}$		S=1.3
Γ_{159}	$p\overline{p}\eta'(958)$		(2.1 ± 0.4)	$\times 10^{-4}$		
Γ_{160}	$p\overline{p}a_0(980) \rightarrow p\overline{p}\pi^0\eta$		(6.8 ± 1.8)	$\times 10^{-5}$		
Γ_{161}	$p\overline{p}\phi$		(5.19 ± 0.33)	$\times 10^{-5}$		
Γ_{162}	$n\overline{n}$		(2.09 ± 0.16)	$\times 10^{-3}$		
Γ_{163}	$n\overline{n}\pi^+\pi^-$		(4 ± 4)	$\times 10^{-3}$		
Γ_{164}	$\Sigma^+\overline{\Sigma}^-$		(1.50 ± 0.24)	$\times 10^{-3}$		
Γ_{165}	$\Sigma^0\overline{\Sigma}^0$		(1.172 ± 0.031)	$\times 10^{-3}$		S=1.4
Γ_{166}	$2(\pi^+\pi^-)K^+K^-$		(4.7 ± 0.7)	$\times 10^{-3}$		S=1.3
Γ_{167}	$p\overline{n}\pi^-$		(2.12 ± 0.09)	$\times 10^{-3}$		
Γ_{168}	$nN(1440)$		seen			
Γ_{169}	$nN(1520)$		seen			
Γ_{170}	$nN(1535)$		seen			
Γ_{171}	$\Xi^-\overline{\Xi}^+$		(9.7 ± 0.8)	$\times 10^{-4}$		S=1.4
Γ_{172}	$\Lambda\overline{\Lambda}$		(1.89 ± 0.08)	$\times 10^{-3}$		S=2.5
Γ_{173}	$\Lambda\overline{\Sigma}^-\pi^+$ (or c.c.)	[b]	(8.3 ± 0.7)	$\times 10^{-4}$		S=1.2
Γ_{174}	$pK^-\overline{\Lambda}$		(8.9 ± 1.6)	$\times 10^{-4}$		
Γ_{175}	$2(K^+K^-)$		(7.4 ± 0.7)	$\times 10^{-4}$		
Γ_{176}	$pK^-\overline{\Sigma}^0$		(2.9 ± 0.8)	$\times 10^{-4}$		
Γ_{177}	K^+K^-		(2.86 ± 0.21)	$\times 10^{-4}$		
Γ_{178}	$K_S^0 K_L^0$		(1.95 ± 0.11)	$\times 10^{-4}$		S=2.4
Γ_{179}	$\Lambda\overline{\Lambda}\pi^+\pi^-$		(4.3 ± 1.0)	$\times 10^{-3}$		
Γ_{180}	$\Lambda\overline{\Lambda}\eta$		(1.62 ± 0.17)	$\times 10^{-4}$		
Γ_{181}	$\Lambda\overline{\Lambda}\pi^0$		(3.8 ± 0.4)	$\times 10^{-5}$		
Γ_{182}	$\overline{\Lambda}nK_S^0+$ c.c.		(6.5 ± 1.1)	$\times 10^{-4}$		
Γ_{183}	$\pi^+\pi^-$		(1.47 ± 0.14)	$\times 10^{-4}$		
Γ_{184}	$\Lambda\overline{\Sigma}+$ c.c.		(2.83 ± 0.23)	$\times 10^{-5}$		
Γ_{185}	$K_S^0 K_S^0$		< 1.4	$\times 10^{-8}$		CL=95%

Radiative decays

Γ_{186}	3γ		(1.16 ± 0.22)	$\times 10^{-5}$		
Γ_{187}	4γ		< 9	$\times 10^{-6}$		CL=90%
Γ_{188}	5γ		< 1.5	$\times 10^{-5}$		CL=90%
Γ_{189}	$\gamma\pi^0\pi^0$		(1.15 ± 0.05)	$\times 10^{-3}$		
Γ_{190}	$\gamma\eta\pi^0$		(2.14 ± 0.31)	$\times 10^{-5}$		
Γ_{191}	$\gamma a_0(980)^0 \rightarrow \gamma\eta\pi^0$		< 2.5	$\times 10^{-6}$		CL=95%
Γ_{192}	$\gamma a_2(1320)^0 \rightarrow \gamma\eta\pi^0$		< 6.6	$\times 10^{-6}$		CL=95%
Γ_{193}	$\gamma\eta_c(1S)$		(1.7 ± 0.4)	%		S=1.5
Γ_{194}	$\gamma\eta_c(1S) \rightarrow 3\gamma$		(3.8 $^{+1.3}_{-1.0}$)	$\times 10^{-6}$		S=1.1
Γ_{195}	$\gamma\pi^+\pi^-2\pi^0$		(8.3 ± 3.1)	$\times 10^{-3}$		
Γ_{196}	$\gamma\eta\pi\pi$		(6.1 ± 1.0)	$\times 10^{-3}$		
Γ_{197}	$\gamma\eta_2(1870) \rightarrow \gamma\eta\pi^+\pi^-$		(6.2 ± 2.4)	$\times 10^{-4}$		
Γ_{198}	$\gamma\eta(1405/1475) \rightarrow \gamma K\overline{K}\pi$	[d]	(2.8 ± 0.6)	$\times 10^{-3}$		S=1.6
Γ_{199}	$\gamma\eta(1405/1475) \rightarrow \gamma\gamma\rho^0$		(7.8 ± 2.0)	$\times 10^{-5}$		S=1.8
Γ_{200}	$\gamma\eta(1405/1475) \rightarrow \gamma\eta\pi^+\pi^-$		(3.0 ± 0.5)	$\times 10^{-4}$		

Γ_{201}	$\gamma\eta(1405/1475) \rightarrow \gamma\gamma\phi$	$<$ 8.2		$\times 10^{-5}$	CL=95%
Γ_{202}	$\gamma\rho\rho$	(4.5	$\pm$ 0.8)	$\times 10^{-3}$	
Γ_{203}	$\gamma\rho\omega$	$<$ 5.4		$\times 10^{-4}$	CL=90%
Γ_{204}	$\gamma\rho\phi$	$<$ 8.8		$\times 10^{-5}$	CL=90%
Γ_{205}	$\gamma\eta'(958)$	(5.13	$\pm$ 0.17)	$\times 10^{-3}$	S=1.3
Γ_{206}	$\gamma 2\pi^+ 2\pi^-$	(2.8	$\pm$ 0.5)	$\times 10^{-3}$	S=1.9
Γ_{207}	$\gamma f_2(1270) f_2(1270)$	(9.5	$\pm$ 1.7)	$\times 10^{-4}$	
Γ_{208}	$\gamma f_2(1270) f_2(1270)$(non resonant)	(8.2	$\pm$ 1.9)	$\times 10^{-4}$	
Γ_{209}	$\gamma K^+ K^- \pi^+ \pi^-$	(2.1	$\pm$ 0.6)	$\times 10^{-3}$	
Γ_{210}	$\gamma f_4(2050)$	(2.7	$\pm$ 0.7)	$\times 10^{-3}$	
Γ_{211}	$\gamma\omega\omega$	(1.61	$\pm$ 0.33)	$\times 10^{-3}$	
Γ_{212}	$\gamma\eta(1405/1475) \rightarrow \gamma\rho^0\rho^0$	(1.7	$\pm$ 0.4)	$\times 10^{-3}$	S=1.3
Γ_{213}	$\gamma f_2(1270)$	(1.64	$\pm$ 0.12)	$\times 10^{-3}$	S=1.3
Γ_{214}	$\gamma f_0(1370) \rightarrow \gamma K\overline{K}$	(4.2	$\pm$ 1.5)	$\times 10^{-4}$	
Γ_{215}	$\gamma f_0(1710) \rightarrow \gamma K\overline{K}$	(1.00	$^{+\ 0.11}_{-\ 0.09}$)	$\times 10^{-3}$	S=1.5
Γ_{216}	$\gamma f_0(1710) \rightarrow \gamma\pi\pi$	(3.8	$\pm$ 0.5)	$\times 10^{-4}$	
Γ_{217}	$\gamma f_0(1710) \rightarrow \gamma\omega\omega$	(3.1	$\pm$ 1.0)	$\times 10^{-4}$	
Γ_{218}	$\gamma f_0(1710) \rightarrow \gamma\eta\eta$	(2.4	$^{+\ 1.2}_{-\ 0.7}$)	$\times 10^{-4}$	
Γ_{219}	$\gamma\eta$	(1.104	$\pm$ 0.034)	$\times 10^{-3}$	
Γ_{220}	$\gamma f_1(1420) \rightarrow \gamma K\overline{K}\pi$	(7.9	$\pm$ 1.3)	$\times 10^{-4}$	
Γ_{221}	$\gamma f_1(1285)$	(6.1	$\pm$ 0.8)	$\times 10^{-4}$	
Γ_{222}	$\gamma f_1(1510) \rightarrow \gamma\eta\pi^+\pi^-$	(4.5	$\pm$ 1.2)	$\times 10^{-4}$	
Γ_{223}	$\gamma f_2'(1525)$	(5.7	$^{+\ 0.8}_{-\ 0.5}$)	$\times 10^{-4}$	S=1.5
Γ_{224}	$\gamma f_2'(1525) \rightarrow \gamma\eta\eta$	(3.4	$\pm$ 1.4)	$\times 10^{-5}$	
Γ_{225}	$\gamma f_2(1640) \rightarrow \gamma\omega\omega$	(2.8	$\pm$ 1.8)	$\times 10^{-4}$	
Γ_{226}	$\gamma f_2(1910) \rightarrow \gamma\omega\omega$	(2.0	$\pm$ 1.4)	$\times 10^{-4}$	
Γ_{227}	$\gamma f_0(1800) \rightarrow \gamma\omega\phi$	(2.5	$\pm$ 0.6)	$\times 10^{-4}$	
Γ_{228}	$\gamma f_2(1810) \rightarrow \gamma\eta\eta$	(5.4	$^{+\ 3.5}_{-\ 2.4}$)	$\times 10^{-5}$	
Γ_{229}	$\gamma f_2(1950) \rightarrow \gamma K^*(892)\overline{K}^*(892)$	(7.0	$\pm$ 2.2)	$\times 10^{-4}$	
Γ_{230}	$\gamma K^*(892)\overline{K}^*(892)$	(4.0	$\pm$ 1.3)	$\times 10^{-3}$	
Γ_{231}	$\gamma\phi\phi$	(4.0	$\pm$ 1.2)	$\times 10^{-4}$	S=2.1
Γ_{232}	$\gamma p\overline{p}$	(3.8	$\pm$ 1.0)	$\times 10^{-4}$	
Γ_{233}	$\gamma\eta(2225)$	(3.14	$^{+\ 0.50}_{-\ 0.19}$)	$\times 10^{-4}$	
Γ_{234}	$\gamma\eta(1760) \rightarrow \gamma\rho^0\rho^0$	(1.3	$\pm$ 0.9)	$\times 10^{-4}$	
Γ_{235}	$\gamma\eta(1760) \rightarrow \gamma\omega\omega$	(1.98	$\pm$ 0.33)	$\times 10^{-3}$	
Γ_{236}	$\gamma X(1835) \rightarrow \gamma\pi^+\pi^-\eta'$	(2.77	$^{+\ 0.34}_{-\ 0.40}$)	$\times 10^{-4}$	S=1.1
Γ_{237}	$\gamma X(1835) \rightarrow \gamma p\overline{p}$	(7.7	$^{+\ 1.5}_{-\ 0.9}$)	$\times 10^{-5}$	
Γ_{238}	$\gamma X(1835) \rightarrow \gamma K_S^0 K_S^0\eta$	(3.3	$^{+\ 2.0}_{-\ 1.3}$)	$\times 10^{-5}$	
Γ_{239}	$\gamma X(1840) \rightarrow \gamma 3(\pi^+\pi^-)$	(2.4	$^{+\ 0.7}_{-\ 0.8}$)	$\times 10^{-5}$	
Γ_{240}	$\gamma(K\overline{K}\pi)$ $[J^{PC} = 0^{-+}]$	(7	$\pm$ 4)	$\times 10^{-4}$	S=2.1
Γ_{241}	$\gamma\pi^0$	(3.49	$^{+\ 0.33}_{-\ 0.30}$)	$\times 10^{-5}$	
Γ_{242}	$\gamma p\overline{p}\pi^+\pi^-$	$<$ 7.9		$\times 10^{-4}$	CL=90%
Γ_{243}	$\gamma\Lambda\overline{\Lambda}$	$<$ 1.3		$\times 10^{-4}$	CL=90%
Γ_{244}	$\gamma f_0(2100) \rightarrow \gamma\eta\eta$	(1.13	$^{+\ 0.60}_{-\ 0.30}$)	$\times 10^{-4}$	
Γ_{245}	$\gamma f_0(2100) \rightarrow \gamma\pi\pi$	(6.2	$\pm$ 1.0)	$\times 10^{-4}$	
Γ_{246}	$\gamma f_0(2200)$				
Γ_{247}	$\gamma f_0(2200) \rightarrow \gamma K\overline{K}$	(5.9	$\pm$ 1.3)	$\times 10^{-4}$	
Γ_{248}	$\gamma f_J(2220)$				
Γ_{249}	$\gamma f_J(2220) \rightarrow \gamma\pi\pi$	$<$ 3.9		$\times 10^{-5}$	CL=90%
Γ_{250}	$\gamma f_J(2220) \rightarrow \gamma K\overline{K}$	$<$ 4.1		$\times 10^{-5}$	CL=90%
Γ_{251}	$\gamma f_J(2220) \rightarrow \gamma p\overline{p}$	(1.5	$\pm$ 0.8)	$\times 10^{-5}$	
Γ_{252}	$\gamma f_2(2340) \rightarrow \gamma\eta\eta$	(5.6	$^{+\ 2.4}_{-\ 2.2}$)	$\times 10^{-5}$	
Γ_{253}	$\gamma f_0(1500) \rightarrow \gamma\pi\pi$	(1.09	$\pm$ 0.24)	$\times 10^{-4}$	
Γ_{254}	$\gamma f_0(1500) \rightarrow \gamma\eta\eta$	(1.7	$^{+\ 0.6}_{-\ 1.4}$)	$\times 10^{-5}$	
Γ_{255}	$\gamma A \rightarrow \gamma$ invisible	[e] $<$ 6.3		$\times 10^{-6}$	CL=90%
Γ_{256}	$\gamma A^0 \rightarrow \gamma\mu^+\mu^-$	[f] $<$ 5		$\times 10^{-6}$	CL=90%

Dalitz decays

Γ_{257}	$\pi^0 e^+ e^-$	(7.6	$\pm$ 1.4)	$\times 10^{-7}$	
Γ_{258}	$\eta e^+ e^-$	(1.16	$\pm$ 0.09)	$\times 10^{-5}$	
Γ_{259}	$\eta'(958) e^+ e^-$	(5.81	$\pm$ 0.35)	$\times 10^{-5}$	

Weak decays

Γ_{260}	$D^- e^+ \nu_e$ + c.c.	$<$ 1.2		$\times 10^{-5}$	CL=90%
Γ_{261}	$\overline{D}^0 e^+ e^-$ + c.c.	$<$ 8.5		$\times 10^{-8}$	CL=90%
Γ_{262}	$D_s^- e^+ \nu_e$ + c.c.	$<$ 1.3		$\times 10^{-6}$	CL=90%
Γ_{263}	$D_s^{*-} e^+ \nu_e$ + c.c.	$<$ 1.8		$\times 10^{-6}$	CL=90%
Γ_{264}	$D^-\pi^+$ + c.c.	$<$ 7.5		$\times 10^{-5}$	CL=90%
Γ_{265}	$\overline{D}^0 K^0$ + c.c.	$<$ 1.7		$\times 10^{-4}$	CL=90%
Γ_{266}	$\overline{D}^0 K^{*0}$ + c.c.	$<$ 2.5		$\times 10^{-6}$	CL=90%
Γ_{267}	$D_s^-\pi^+$ + c.c.	$<$ 1.3		$\times 10^{-4}$	CL=90%
Γ_{268}	$D_s^-\rho^+$ + c.c.	$<$ 1.3		$\times 10^{-5}$	CL=90%

Charge conjugation (C), Parity (P), Lepton Family number (LF) violating modes

Γ_{269}	$\gamma\gamma$	C	$<$ 2.7	$\times 10^{-7}$	CL=90%
Γ_{270}	$\gamma\phi$	C	$<$ 1.4	$\times 10^{-6}$	CL=90%
Γ_{271}	$e^\pm\mu^\mp$	LF	$<$ 1.6	$\times 10^{-7}$	CL=90%
Γ_{272}	$e^\pm\tau^\mp$	LF	$<$ 8.3	$\times 10^{-6}$	CL=90%
Γ_{273}	$\mu^\pm\tau^\mp$	LF	$<$ 2.0	$\times 10^{-6}$	CL=90%

Other decays

Γ_{274}	invisible		$<$ 7	$\times 10^{-4}$	CL=90%

[a] For $E_\gamma > 100$ MeV.

[b] The value is for the sum of the charge states or particle/antiparticle states indicated.

[c] Includes $p\overline{p}\pi^+\pi^-\gamma$ and excludes $p\overline{p}\eta$, $p\overline{p}\omega$, $p\overline{p}\eta'$.

[d] See the "Note on the $\eta(1405)$" in the $\eta(1405)$ Particle Listings.

[e] For a narrow state A with mass less than 960 MeV.

[f] For a narrow scalar or pseudoscalar A^0 with mass 0.21–3.0 GeV.

$J/\psi(1S)$ PARTIAL WIDTHS

Γ(hadrons) Γ_1

VALUE (keV)	DOCUMENT ID		TECN	COMMENT
• • • We do not use the following data for averages, fits, limits, etc. • • •				
74.1 $\pm$ 8.1	BAI	95B	BES	e^+e^-
59 $\pm$24	BALDINI-...	75	FRAG	e^+e^-
59 $\pm$14	BOYARSKI	75	MRK1	e^+e^-
50 $\pm$25	ESPOSITO	75B	FRAM	e^+e^-

$\Gamma(e^+e^-)$ Γ_5

VALUE (keV)	EVTS	DOCUMENT ID		TECN	COMMENT
5.55 $\pm$ 0.14 $\pm$ 0.02 OUR EVALUATION					
• • • We do not use the following data for averages, fits, limits, etc. • • •					
5.58 $\pm$ 0.05 $\pm$ 0.08		[1] ABLIKIM	16Q	BES3	3.773 $e^+e^- \rightarrow \mu^+\mu^-\gamma$
5.71 $\pm$ 0.16	13k	[2] ADAMS	06A	CLEO	$e^+e^- \rightarrow \mu^+\mu^-\gamma$
5.57 $\pm$ 0.19	7.8k	[2] AUBERT	04	BABR	$e^+e^- \rightarrow \mu^+\mu^-\gamma$
5.14 $\pm$ 0.39		BAI	95B	BES	e^+e^-
$5.36^{+0.29}_{-0.28}$		[3] HSUEH	92	RVUE	See Υ mini-review
4.72 $\pm$ 0.35		ALEXANDER	89	RVUE	See Υ mini-review
4.4 $\pm$0.6		[3] BRANDELIK	79C	DASP	e^+e^-
4.6 $\pm$0.8		[4] BALDINI-...	75	FRAG	e^+e^-
4.8 $\pm$0.6		BOYARSKI	75	MRK1	e^+e^-
4.6 $\pm$1.0		ESPOSITO	75B	FRAM	e^+e^-

[1] Using B($J/\psi \rightarrow \mu^+\mu^-$) = (5.973 $\pm$ 0.007 $\pm$ 0.037)% from ABLIKIM 13R.

[2] Calculated by us from the reported values of $\Gamma(e^+e^-)\times$B($\mu^+\mu^-$) using B($\mu^+\mu^-$) = (5.93 $\pm$ 0.06)%.

[3] From a simultaneous fit to e^+e^-, $\mu^+\mu^-$, and hadronic channels assuming $\Gamma(e^+e^-) = \Gamma(\mu^+\mu^-)$.

[4] Assuming equal partial widths for e^+e^- and $\mu^+\mu^-$.

$\Gamma(\mu^+\mu^-)$ Γ_7

VALUE (keV)	DOCUMENT ID		TECN	COMMENT
• • • We do not use the following data for averages, fits, limits, etc. • • •				
5.13 $\pm$ 0.52	BAI	95B	BES	e^+e^-
4.8 $\pm$0.6	BOYARSKI	75	MRK1	e^+e^-
5 $\pm$1	ESPOSITO	75B	FRAM	e^+e^-

$\Gamma(\gamma\gamma)$ Γ_{269}

VALUE (eV)	CL%	DOCUMENT ID	TECN	COMMENT
<5.4	90	BRANDELIK 79C	DASP	e^+e^-

$J/\psi(1S)$ Γ(i)$\Gamma(e^+e^-)/\Gamma$(total)

This combination of a partial width with the partial width into e^+e^- and with the total width is obtained from the integrated cross section into channel$_i$ in the e^+e^- annihilation.

Γ(hadrons) $\times$ $\Gamma(e^+e^-)/\Gamma_{\text{total}}$ $\Gamma_1\Gamma_5/\Gamma$

VALUE (keV)	DOCUMENT ID		TECN	COMMENT
• • • We do not use the following data for averages, fits, limits, etc. • • •				
4 $\pm$0.8	[1] BALDINI-...	75	FRAG	e^+e^-

3.9±0.8 [1] ESPOSITO 75B FRAM e^+e^-

[1] Data redundant with branching ratios or partial widths above.

$\Gamma(e^+e^-) \times \Gamma(e^+e^-)/\Gamma_{total}$ $\Gamma_5\Gamma_5/\Gamma$

VALUE (eV)	DOCUMENT ID		TECN	COMMENT
332.3± 6.4±4.8	ANASHIN	10	KEDR	3.097 $e^+e^- \to e^+e^-$
• • • We do not use the following data for averages, fits, limits, etc. • • •				
350 ± 20	BRANDELIK	79C	DASP	e^+e^-
320 ± 70	[1] BALDINI-...	75	FRAG	e^+e^-
340 ± 90	[1] ESPOSITO	75B	FRAM	e^+e^-
360 ±100	[1] FORD	75	SPEC	e^+e^-

[1] Data redundant with branching ratios or partial widths above.

$\Gamma(\mu^+\mu^-) \times \Gamma(e^+e^-)/\Gamma_{total}$ $\Gamma_7\Gamma_5/\Gamma$

VALUE (eV)	EVTS	DOCUMENT ID		TECN	COMMENT
333 ± 4 OUR AVERAGE					
333.4± 2.5±4.4		ABLIKIM	16Q	BES3	3.773 $e^+e^- \to \mu^+\mu^-\gamma$
331.8± 5.2±6.3		ANASHIN	10	KEDR	3.097 $e^+e^- \to \mu^+\mu^-$
338.4± 5.8±7.1	13k	ADAMS	06A	CLEO	$e^+e^- \to \mu^+\mu^-\gamma$
330.1± 7.7±7.3	7.8k	AUBERT	04	BABR	$e^+e^- \to \mu^+\mu^-\gamma$
• • • We do not use the following data for averages, fits, limits, etc. • • •					
510 ±90		DASP	75	DASP	e^+e^-
380 ±50		[1] ESPOSITO	75B	FRAM	e^+e^-

[1] Data redundant with branching ratios or partial widths above.

$\Gamma(\rho(770)^\mp K^\pm K^0_S) \times \Gamma(e^+e^-)/\Gamma_{total}$ $\Gamma_{10}\Gamma_5/\Gamma$

VALUE (eV)	EVTS	DOCUMENT ID		TECN	COMMENT
10.4±1.0±1.9	130	LEES	17D	BABR	$e^+e^- \to K^0_S K^\pm\pi^\mp\pi^0\gamma$

$\Gamma(\omega\pi^+\pi^-\pi^0) \times \Gamma(e^+e^-)/\Gamma_{total}$ $\Gamma_{23}\Gamma_5/\Gamma$

VALUE (10^{-2} keV)	EVTS	DOCUMENT ID		TECN	COMMENT
2.2±0.3±0.2	170	AUBERT	06D	BABR	10.6 $e^+e^- \to \omega\pi^+\pi^-\pi^0\gamma$

$\Gamma(\omega\pi^+\pi^-) \times \Gamma(e^+e^-)/\Gamma_{total}$ $\Gamma_{24}\Gamma_5/\Gamma$

VALUE (eV)	EVTS	DOCUMENT ID		TECN	COMMENT
53.6±5.0±0.4	788	[1] AUBERT	07AU	BABR	10.6 $e^+e^- \to \omega\pi^+\pi^-\gamma$

[1] AUBERT 07AU reports $[\Gamma(J/\psi(1S) \to \omega\pi^+\pi^-) \times \Gamma(J/\psi(1S) \to e^+e^-)/\Gamma_{total}] \times [B(\omega(782) \to \pi^+\pi^-\pi^0)] = 47.8 \pm 3.1 \pm 3.2$ eV which we divide by our best value $B(\omega(782) \to \pi^+\pi^-\pi^0) = (89.2 \pm 0.7) \times 10^{-2}$. Our first error is their experiment's error and our second error is the systematic error from using our best value.

$\Gamma(K^*(892)^0\overline{K}^*(892)^0) \times \Gamma(e^+e^-)/\Gamma_{total}$ $\Gamma_{26}\Gamma_5/\Gamma$

VALUE (eV)	EVTS	DOCUMENT ID		TECN	COMMENT
1.28±0.34±0.07	47±12	[1] LEES	12F	BABR	10.6 $e^+e^- \to \pi^+\pi^- K^+K^-\gamma$
• • • We do not use the following data for averages, fits, limits, etc. • • •					
1.28±0.40±0.11	25 ± 8	[1,2] AUBERT	07AK	BABR	10.6 $e^+e^- \to \pi^+\pi^- K^+K^-\gamma$

[1] Dividing by $(2/3)^2$ to take twice into account that $B(K^{*0} \to K^+\pi^-) = 2/3\, B(K^{*0} \to K\pi)$.

[2] Superseded by LEES 12F.

$\Gamma(K^*(892)^0\overline{K}^*_2(1430)^0 + \text{c.c.}) \times \Gamma(e^+e^-)/\Gamma_{total}$ $\Gamma_{38}\Gamma_5/\Gamma$

VALUE (eV)	EVTS	DOCUMENT ID		TECN	COMMENT
25.8±1.4±0.6	710	[1,2,3] LEES	12F	BABR	10.6 $e^+e^- \to \pi^+\pi^- K^+K^-\gamma$
• • • We do not use the following data for averages, fits, limits, etc. • • •					
33 ±4 ±1	317	[2,4] AUBERT	07AK	BABR	10.6 $e^+e^- \to \pi^+\pi^- K^+K^-\gamma$

[1] LEES 12F reports $[\Gamma(J/\psi(1S) \to K^*(892)^0\overline{K}^*_2(1430)^0 + \text{c.c.}) \times \Gamma(J/\psi(1S) \to e^+e^-)/\Gamma_{total}] \times [B(K^*_2(1430) \to K\pi)] = 12.89 \pm 0.54 \pm 0.41$ eV which we divide by our best value $B(K^*_2(1430) \to K\pi) = (49.9 \pm 1.2) \times 10^{-2}$. Our first error is their experiment's error and our second error is the systematic error from using our best value.

[2] Dividing by 2/3 to take into account that $B(K^{*0} \to K^+\pi^-) = 2/3\ B(K^{*0} \to K\pi)$.

[3] The $K^*_2(1430)$ cannot be distinguished from the $K^*_0(1430)$.

[4] Superseded by LEES 12F. AUBERT 07AK reports $[\Gamma(J/\psi(1S) \to K^*(892)^0\overline{K}^*_2(1430)^0 + \text{c.c.}) \times \Gamma(J/\psi(1S) \to e^+e^-)/\Gamma_{total}] \times [B(K^*_2(1430) \to K\pi)] = 16.4 \pm 1.1 \pm 1.4$ eV which we divide by our best value $B(K^*_2(1430) \to K\pi) = (49.9 \pm 1.2) \times 10^{-2}$. Our first error is their experiment's error and our second error is the systematic error from using our best value.

$\Gamma(K^*(892)^0\overline{K}_2(1770)^0 + \text{c.c.} \to K^*(892)^0 K^-\pi^+ + \text{c.c.}) \times \Gamma(e^+e^-)/\Gamma_{total}$ $\Gamma_{41}\Gamma_5/\Gamma$

VALUE (eV)	EVTS	DOCUMENT ID		TECN	COMMENT
3.8±0.4±0.3	110 ± 14	[1] AUBERT	07AK	BABR	10.6 $e^+e^- \to \pi^+\pi^- K^+K^-\gamma$

[1] Dividing by 2/3 to take into account that $B(K^{*0} \to K^+\pi^-) = 2/3$.

$\Gamma(K^+K^*(892)^- + \text{c.c.}) \times \Gamma(e^+e^-)/\Gamma_{total}$ $\Gamma_{45}\Gamma_5/\Gamma$

VALUE (eV)	DOCUMENT ID		TECN	COMMENT
29.0±1.7±1.3	AUBERT	08S	BABR	10.6 $e^+e^- \to K^+K^*(892)^-\gamma$

$\Gamma(K^+K^*(892)^- + \text{c.c.} \to K^+K^-\pi^0) \times \Gamma(e^+e^-)/\Gamma_{total}$ $\Gamma_{46}\Gamma_5/\Gamma$

VALUE (eV)	EVTS	DOCUMENT ID		TECN	COMMENT
10.96±0.85±0.70	155	AUBERT	08S	BABR	10.6 $e^+e^- \to K^+K^-\pi^0\gamma$

$\Gamma(K^+K^*(892)^- + \text{c.c.} \to K^0K^\pm\pi^\mp + \text{c.c.}) \times \Gamma(e^+e^-)/\Gamma_{total}$ $\Gamma_{47}\Gamma_5/\Gamma$

VALUE (eV)	EVTS	DOCUMENT ID		TECN	COMMENT
16.76±1.70±1.00	89	AUBERT	08S	BABR	10.6 $e^+e^- \to K^0_S K^\pm\pi^\mp\gamma$

$\Gamma(K^0\overline{K}^*(892)^0 + \text{c.c.}) \times \Gamma(e^+e^-)/\Gamma_{total}$ $\Gamma_{48}\Gamma_5/\Gamma$

VALUE (eV)	DOCUMENT ID		TECN	COMMENT
26.6±2.5±1.5	AUBERT	08S	BABR	10.6 $e^+e^- \to K^0\overline{K}^*(892)^0\gamma$

$\Gamma(K^0\overline{K}^*(892)^0 + \text{c.c.} \to K^0K^\pm\pi^\mp + \text{c.c.}) \times \Gamma(e^+e^-)/\Gamma_{total}$ $\Gamma_{49}\Gamma_5/\Gamma$

VALUE (eV)	EVTS	DOCUMENT ID		TECN	COMMENT
17.70±1.70±1.00	94	AUBERT	08S	BABR	10.6 $e^+e^- \to K^0_S K^\pm\pi^\mp\gamma$

$\Gamma(K^*(892)^\pm K^\mp\pi^0) \times \Gamma(e^+e^-)/\Gamma_{total}$ $\Gamma_{52}\Gamma_5/\Gamma$

VALUE (eV)	EVTS	DOCUMENT ID		TECN	COMMENT
22.8±2.8±6.8	80	[1] LEES	17D	BABR	$e^+e^- \to K^0_S K^\pm\pi^\mp\pi^0\gamma$

[1] Dividing by 1/4 to account for $B(K^*(892)^\pm \to K^0_S\pi^\pm) = 1/4$.

$\Gamma(K^*(892)^0 K^0_S\pi^0) \times \Gamma(e^+e^-)/\Gamma_{total}$ $\Gamma_{53}\Gamma_5/\Gamma$

VALUE (eV)	EVTS	DOCUMENT ID		TECN	COMMENT
3.60±0.75±2.25	34	[1] LEES	17D	BABR	$e^+e^- \to K^0_S K^\pm\pi^\mp\pi^0\gamma$

[1] Dividing by 2/3 to account for $B(K^*(892)^0 \to K^+\pi^-) = 2/3$.

$\Gamma(\omega K\overline{K}) \times \Gamma(e^+e^-)/\Gamma_{total}$ $\Gamma_{60}\Gamma_5/\Gamma$

VALUE (eV)	EVTS	DOCUMENT ID		TECN	COMMENT
3.70±1.98±0.03	24	[1] AUBERT	07AU	BABR	10.6 $e^+e^- \to \omega K^+K^-\gamma$

[1] AUBERT 07AU reports $[\Gamma(J/\psi(1S) \to \omega K\overline{K}) \times \Gamma(J/\psi(1S) \to e^+e^-)/\Gamma_{total}] \times [B(\omega(782) \to \pi^+\pi^-\pi^0)] = 3.3 \pm 1.3 \pm 1.2$ eV which we divide by our best value $B(\omega(782) \to \pi^+\pi^-\pi^0) = (89.2 \pm 0.7) \times 10^{-2}$. Our first error is their experiment's error and our second error is the systematic error from using our best value.

$\Gamma(\phi 2(\pi^+\pi^-)) \times \Gamma(e^+e^-)/\Gamma_{total}$ $\Gamma_{62}\Gamma_5/\Gamma$

VALUE (10^{-2} keV)	EVTS	DOCUMENT ID		TECN	COMMENT
0.95±0.19±0.01	35	[1] AUBERT	06D	BABR	10.6 $e^+e^- \to \phi 2(\pi^+\pi^-)\gamma$

[1] AUBERT 06D reports $[\Gamma(J/\psi(1S) \to \phi 2(\pi^+\pi^-)) \times \Gamma(J/\psi(1S) \to e^+e^-)/\Gamma_{total}] \times [B(\phi(1020) \to K^+K^-)] = (0.47 \pm 0.09 \pm 0.03) \times 10^{-2}$ keV which we divide by our best value $B(\phi(1020) \to K^+K^-) = (49.2 \pm 0.5) \times 10^{-2}$. Our first error is their experiment's error and our second error is the systematic error from using our best value.

$\Gamma(\phi K^+K^-) \times \Gamma(e^+e^-)/\Gamma_{total}$ $\Gamma_{68}\Gamma_5/\Gamma$

VALUE (eV)	EVTS	DOCUMENT ID		TECN	COMMENT
4.59±0.62±0.05	163	[1] LEES	12F	BABR	10.6 $e^+e^- \to K^+K^-K^+K^-\gamma$

[1] LEES 12F reports $[\Gamma(J/\psi(1S) \to \phi K^+K^-) \times \Gamma(J/\psi(1S) \to e^+e^-)/\Gamma_{total}] \times [B(\phi(1020) \to K^+K^-)] = 2.26 \pm 0.26 \pm 0.16$ eV which we divide by our best value $B(\phi(1020) \to K^+K^-) = (49.2 \pm 0.5) \times 10^{-2}$. Our first error is their experiment's error and our second error is the systematic error from using our best value.

$\Gamma(\phi f_2(1270)) \times \Gamma(e^+e^-)/\Gamma_{total}$ $\Gamma_{69}\Gamma_5/\Gamma$

VALUE (eV)	EVTS	DOCUMENT ID		TECN	COMMENT
$1.79\pm0.32^{+0.02}_{-0.06}$	61 ± 10	[1,2,3] LEES	12F	BABR	10.6 $e^+e^- \to \pi^+\pi^- K^+K^-\gamma$
• • • We do not use the following data for averages, fits, limits, etc. • • •					
$4.08\pm0.73^{+0.04}_{-0.14}$	44 ± 7	[2,4] AUBERT	07AK	BABR	10.6 $e^+e^- \to \pi^+\pi^- K^+K^-\gamma$

[1] LEES 12F reports $[\Gamma(J/\psi(1S) \to \phi f_2(1270)) \times \Gamma(J/\psi(1S) \to e^+e^-)/\Gamma_{total}] \times [B(f_2(1270) \to \pi\pi)] = 1.51 \pm 0.25 \pm 0.10$ eV which we divide by our best value $B(f_2(1270) \to \pi\pi) = (84.2^{+2.9}_{-0.9}) \times 10^{-2}$. Our first error is their experiment's error and our second error is the systematic error from using our best value.

[2] Using $B(\phi \to K^+K^-) = (48.9 \pm 0.5)\%$.

[3] Using $\pi^+\pi^-$ invariant mass between 1.1 and 1.5 GeV. May include other sources such as $f_0(1370)$.

[4] Superseded by LEES 12F. AUBERT 07AK reports $[\Gamma(J/\psi(1S) \to \phi f_2(1270)) \times \Gamma(J/\psi(1S) \to e^+e^-)/\Gamma_{total}] \times [B(f_2(1270) \to \pi\pi)] = 3.44 \pm 0.55 \pm 0.28$ eV which we divide by our best value $B(f_2(1270) \to \pi\pi) = (84.2^{+2.9}_{-0.9}) \times 10^{-2}$. Our first error is their experiment's error and our second error is the systematic error from using our best value.

$\Gamma(\phi\pi^+\pi^-) \times \Gamma(e^+e^-)/\Gamma_{total}$ $\Gamma_{75}\Gamma_5/\Gamma$

VALUE (eV)	EVTS	DOCUMENT ID		TECN	COMMENT
4.47±0.35 OUR AVERAGE					
4.45±0.49±0.05	181	[1] LEES	12F	BABR	10.6 $e^+e^- \to K^+K^-\pi^+\pi^-\gamma$
4.50±0.48±0.05	254 ± 23	[2] SHEN	09	BELL	10.6 $e^+e^- \to K^+K^-\pi^+\pi^-\gamma$
• • • We do not use the following data for averages, fits, limits, etc. • • •					
5.3 ±0.7 ±0.1	103	[3] AUBERT,BE	06D	BABR	10.6 $e^+e^- \to K^+K^-\pi^+\pi^-\gamma$

[1] LEES 12F reports $[\Gamma(J/\psi(1S) \to \phi\pi^+\pi^-) \times \Gamma(J/\psi(1S) \to e^+e^-)/\Gamma_{total}] \times [B(\phi(1020) \to K^+K^-)] = 2.19 \pm 0.23 \pm 0.07$ eV which we divide by our best value $B(\phi(1020) \to K^+K^-) = (49.2 \pm 0.5) \times 10^{-2}$. Our first error is their experiment's error and our second error is the systematic error from using our best value.

[2] SHEN 09 reports 4.50 ± 0.41 ± 0.26 eV from a measurement of $[\Gamma(J/\psi(1S) \to \phi\pi^+\pi^-) \times \Gamma(J/\psi(1S) \to e^+e^-)/\Gamma_{\text{total}}] \times [B(\phi(1020) \to K^+K^-)]$ assuming $B(\phi(1020) \to K^+K^-) = (49.2 \pm 0.6) \times 10^{-2}$, which we rescale to our best value $B(\phi(1020) \to K^+K^-) = (49.2 \pm 0.5) \times 10^{-2}$. Our first error is their experiment's error and our second error is the systematic error from using our best value.

[3] Superseded by LEES 12F. AUBERT,BE 06D reports $[\Gamma(J/\psi(1S) \to \phi\pi^+\pi^-) \times \Gamma(J/\psi(1S) \to e^+e^-)/\Gamma_{\text{total}}] \times [B(\phi(1020) \to K^+K^-)] = 2.61 \pm 0.30 \pm 0.18$ eV which we divide by our best value $B(\phi(1020) \to K^+K^-) = (49.2 \pm 0.5) \times 10^{-2}$. Our first error is their experiment's error and our second error is the systematic error from using our best value.

$\Gamma(\phi\pi^0\pi^0) \times \Gamma(e^+e^-)/\Gamma_{\text{total}}$ $\Gamma_{76}\Gamma_5/\Gamma$

VALUE (eV)	EVTS	DOCUMENT ID		TECN	COMMENT
2.76±0.57±0.03	45	[1] LEES	12F	BABR	10.6 $e^+e^- \to K^+K^-\pi^0\pi^0\gamma$
• • • We do not use the following data for averages, fits, limits, etc. • • •					
3.13±0.88±0.03	23	[2] AUBERT,BE	06D	BABR	10.6 $e^+e^- \to K^+K^-\pi^0\pi^0\gamma$

[1] LEES 12F reports $[\Gamma(J/\psi(1S) \to \phi\pi^0\pi^0) \times \Gamma(J/\psi(1S) \to e^+e^-)/\Gamma_{\text{total}}] \times [B(\phi(1020) \to K^+K^-)] = 1.36 \pm 0.27 \pm 0.07$ eV which we divide by our best value $B(\phi(1020) \to K^+K^-) = (49.2 \pm 0.5) \times 10^{-2}$. Our first error is their experiment's error and our second error is the systematic error from using our best value.

[2] Superseded by LEES 12F. AUBERT,BE 06D reports $[\Gamma(J/\psi(1S) \to \phi\pi^0\pi^0) \times \Gamma(J/\psi(1S) \to e^+e^-)/\Gamma_{\text{total}}] \times [B(\phi(1020) \to K^+K^-)] = 1.54 \pm 0.40 \pm 0.16$ eV which we divide by our best value $B(\phi(1020) \to K^+K^-) = (49.2 \pm 0.5) \times 10^{-2}$. Our first error is their experiment's error and our second error is the systematic error from using our best value.

$\Gamma(\phi\eta) \times \Gamma(e^+e^-)/\Gamma_{\text{total}}$ $\Gamma_{79}\Gamma_5/\Gamma$

VALUE (eV)	EVTS	DOCUMENT ID		TECN	COMMENT
6.1±2.7±0.4	6	[1] AUBERT	07AU	BABR	10.6 $e^+e^- \to \phi\eta\gamma$

[1] AUBERT 07AU quotes $\Gamma_{ee}^{J/\psi} \cdot B(J/\psi \to \phi\eta) \cdot B(\phi \to K^+K^-) \cdot B(\eta \to 3\pi) = 0.84 \pm 0.37 \pm 0.05$ eV.

$\Gamma(\phi f_0(980) \to \phi\pi^+\pi^-) \times \Gamma(e^+e^-)/\Gamma_{\text{total}}$ $\Gamma_{87}\Gamma_5/\Gamma$

VALUE (eV)	EVTS	DOCUMENT ID		TECN	COMMENT
1.44±0.19 OUR AVERAGE					
1.40±0.25±0.02	57 ± 9	[1] LEES	12F	BABR	10.6 $e^+e^- \to \pi^+\pi^-K^+K^-\gamma$
1.48±0.27±0.09	60±11	[2] SHEN	09	BELL	10.6 $e^+e^- \to K^+K^-\pi^+\pi^-\gamma$
• • • We do not use the following data for averages, fits, limits, etc. • • •					
1.02±0.24±0.01	20 ± 5	[3] AUBERT	07AK	BABR	10.6 $e^+e^- \to \pi^+\pi^-K^+K^-\gamma$

[1] LEES 12F reports $[\Gamma(J/\psi(1S) \to \phi f_0(980) \to \phi\pi^+\pi^-) \times \Gamma(J/\psi(1S) \to e^+e^-)/\Gamma_{\text{total}}] \times [B(\phi(1020) \to K^+K^-)] = 0.69 \pm 0.11 \pm 0.05$ eV which we divide by our best value $B(\phi(1020) \to K^+K^-) = (49.2 \pm 0.5) \times 10^{-2}$. Our first error is their experiment's error and our second error is the systematic error from using our best value.

[2] Multiplied by 2/3 to take into account the $\phi\pi^+\pi^-$ mode only. Using $B(\phi \to K^+K^-) = (49.2 \pm 0.6)\%$.

[3] Superseded by LEES 12F. AUBERT 07AK reports $[\Gamma(J/\psi(1S) \to \phi f_0(980) \to \phi\pi^+\pi^-) \times \Gamma(J/\psi(1S) \to e^+e^-)/\Gamma_{\text{total}}] \times [B(\phi(1020) \to K^+K^-)] = 0.50 \pm 0.11 \pm 0.04$ eV which we divide by our best value $B(\phi(1020) \to K^+K^-) = (49.2 \pm 0.5) \times 10^{-2}$. Our first error is their experiment's error and our second error is the systematic error from using our best value.

$\Gamma(\phi f_0(980) \to \phi\pi^0\pi^0) \times \Gamma(e^+e^-)/\Gamma_{\text{total}}$ $\Gamma_{88}\Gamma_5/\Gamma$

VALUE (eV)	EVTS	DOCUMENT ID		TECN	COMMENT
0.98±0.26±0.01	16 ± 4	[1] LEES	12F	BABR	10.6 $e^+e^- \to \pi^0\pi^0K^+K^-\gamma$
• • • We do not use the following data for averages, fits, limits, etc. • • •					
0.95±0.40±0.01	7.0 ± 2.8	[2] AUBERT	07AK	BABR	10.6 $e^+e^- \to \pi^0\pi^0K^+K^-\gamma$

[1] LEES 12F reports $[\Gamma(J/\psi(1S) \to \phi f_0(980) \to \phi\pi^0\pi^0) \times \Gamma(J/\psi(1S) \to e^+e^-)/\Gamma_{\text{total}}] \times [B(\phi(1020) \to K^+K^-)] = 0.48 \pm 0.12 \pm 0.05$ eV which we divide by our best value $B(\phi(1020) \to K^+K^-) = (49.2 \pm 0.5) \times 10^{-2}$. Our first error is their experiment's error and our second error is the systematic error from using our best value.

[2] Superseded by LEES 12F. AUBERT 07AK reports $[\Gamma(J/\psi(1S) \to \phi f_0(980) \to \phi\pi^0\pi^0) \times \Gamma(J/\psi(1S) \to e^+e^-)/\Gamma_{\text{total}}] \times [B(\phi(1020) \to K^+K^-)] = 0.47 \pm 0.19 \pm 0.05$ eV which we divide by our best value $B(\phi(1020) \to K^+K^-) = (49.2 \pm 0.5) \times 10^{-2}$. Our first error is their experiment's error and our second error is the systematic error from using our best value.

$\Gamma(\eta\pi^+\pi^-) \times \Gamma(e^+e^-)/\Gamma_{\text{total}}$ $\Gamma_{98}\Gamma_5/\Gamma$

VALUE (eV)	EVTS	DOCUMENT ID		TECN	COMMENT
2.23±0.97±0.03	9	[1] AUBERT	07AU	BABR	10.6 $e^+e^- \to \eta\pi^+\pi^-\gamma$

[1] AUBERT 07AU reports $[\Gamma(J/\psi(1S) \to \eta\pi^+\pi^-) \times \Gamma(J/\psi(1S) \to e^+e^-)/\Gamma_{\text{total}}] \times [B(\eta \to \pi^+\pi^-\pi^0)] = 0.51 \pm 0.22 \pm 0.03$ eV which we divide by our best value $B(\eta \to \pi^+\pi^-\pi^0) = (22.92 \pm 0.28) \times 10^{-2}$. Our first error is their experiment's error and our second error is the systematic error from using our best value.

$\Gamma(2(\pi^+\pi^-)\pi^0) \times \Gamma(e^+e^-)/\Gamma_{\text{total}}$ $\Gamma_{127}\Gamma_5/\Gamma$

VALUE (eV)	EVTS	DOCUMENT ID		TECN	COMMENT
303±5±18	4990	AUBERT	07AU	BABR	10.6 $e^+e^- \to 2(\pi^+\pi^-)\pi^0\gamma$

$\Gamma(\pi^+\pi^-\pi^0) \times \Gamma(e^+e^-)/\Gamma_{\text{total}}$ $\Gamma_{129}\Gamma_5/\Gamma$

VALUE (keV)	DOCUMENT ID		TECN	COMMENT
0.122±0.005±0.008	AUBERT,B	04N	BABR	10.6 $e^+e^- \to \pi^+\pi^-\pi^0\gamma$

$\Gamma(\pi^+\pi^-\pi^0K^+K^-) \times \Gamma(e^+e^-)/\Gamma_{\text{total}}$ $\Gamma_{130}\Gamma_5/\Gamma$

VALUE (eV)	EVTS	DOCUMENT ID		TECN	COMMENT
107.0±4.3±6.4	768	AUBERT	07AU	BABR	10.6 $e^+e^- \to K^+K^-\pi^+\pi^-\pi^0\gamma$

$\Gamma(\pi^+\pi^-K^+K^-) \times \Gamma(e^+e^-)/\Gamma_{\text{total}}$ $\Gamma_{132}\Gamma_5/\Gamma$

VALUE (eV)	EVTS	DOCUMENT ID		TECN	COMMENT
37.94±0.81±1.10	3.1k	LEES	12F	BABR	10.6 $e^+e^- \to \pi^+\pi^-K^+K^-\gamma$
• • • We do not use the following data for averages, fits, limits, etc. • • •					
36.3 ±1.3 ±2.1	1.5k	[1] AUBERT	07AK	BABR	10.6 $e^+e^- \to \pi^+\pi^-K^+K^-\gamma$
33.6 ±2.7 ±2.7	233	[2] AUBERT	05D	BABR	10.6 $e^+e^- \to K^+K^-\pi^+\pi^-\gamma$

[1] Superseded by LEES 12F.

[2] Superseded by AUBERT 07AK.

$\Gamma(\pi^\pm\pi^0K^\mp K^0_S) \times \Gamma(e^+e^-)/\Gamma_{\text{total}}$ $\Gamma_{135}\Gamma_5/\Gamma$

VALUE (eV)	EVTS	DOCUMENT ID		TECN	COMMENT
31.7±1.9±1.8	393	LEES	17D	BABR	$e^+e^- \to K^0_S K^\pm\pi^\mp\pi^0\gamma$

$\Gamma(\pi^+\pi^-K^+K^-\eta) \times \Gamma(e^+e^-)/\Gamma_{\text{total}}$ $\Gamma_{137}\Gamma_5/\Gamma$

VALUE (eV)	EVTS	DOCUMENT ID		TECN	COMMENT
25.9±3.9±0.1	73	[1] AUBERT	07AU	BABR	10.6 $e^+e^- \to K^+K^-\pi^+\pi^-\eta\gamma$

[1] AUBERT 07AU reports $[\Gamma(J/\psi(1S) \to \pi^+\pi^-K^+K^-\eta) \times \Gamma(J/\psi(1S) \to e^+e^-)/\Gamma_{\text{total}}] \times [B(\eta \to 2\gamma)] = 10.2 \pm 1.3 \pm 0.8$ eV which we divide by our best value $B(\eta \to 2\gamma) = (39.41 \pm 0.20) \times 10^{-2}$. Our first error is their experiment's error and our second error is the systematic error from using our best value.

$\Gamma(\pi^0\pi^0K^+K^-) \times \Gamma(e^+e^-)/\Gamma_{\text{total}}$ $\Gamma_{138}\Gamma_5/\Gamma$

VALUE (eV)	EVTS	DOCUMENT ID		TECN	COMMENT
11.75±0.81±0.90	388	LEES	12F	BABR	10.6 $e^+e^- \to \pi^0\pi^0K^+K^-\gamma$
• • • We do not use the following data for averages, fits, limits, etc. • • •					
13.6 ±1.1 ±1.3	203	[1] AUBERT	07AK	BABR	10.6 $e^+e^- \to \pi^0\pi^0K^+K^-\gamma$

[1] Superseded by LEES 12F.

$\Gamma(\pi^+\pi^-K^0_LK^0_L) \times \Gamma(e^+e^-)/\Gamma_{\text{total}}$ $\Gamma_{133}\Gamma_5/\Gamma$

VALUE (eV)	EVTS	DOCUMENT ID		TECN	COMMENT
20.8±2.3±2.1	248	LEES	14H	BABR	$e^+e^- \to \pi^+\pi^-K^0_SK^0_L\gamma$

$\Gamma(\pi^+\pi^-K^0_SK^0_S) \times \Gamma(e^+e^-)/\Gamma_{\text{total}}$ $\Gamma_{134}\Gamma_5/\Gamma$

VALUE (eV)	EVTS	DOCUMENT ID		TECN	COMMENT
9.3±0.9±0.5	133	LEES	14H	BABR	$e^+e^- \to \pi^+\pi^-K^0_SK^0_S\gamma$

$\Gamma(K^+K^-K^0_SK^0_S) \times \Gamma(e^+e^-)/\Gamma_{\text{total}}$ $\Gamma_{136}\Gamma_5/\Gamma$

VALUE (eV)	EVTS	DOCUMENT ID		TECN	COMMENT
2.3±0.4±0.1	29	LEES	14H	BABR	$e^+e^- \to K^0_SK^0_SK^+K^-\gamma$

$\Gamma(K^0_S\pi^-K^*(892)^+ + \text{c.c.}) \times \Gamma(e^+e^-)/\Gamma_{\text{total}}$ $\Gamma_{29}\Gamma_5/\Gamma$

VALUE (eV)	EVTS	DOCUMENT ID		TECN	COMMENT
11.0±2.8 OUR AVERAGE					
9.2±1.2±3.2	64	[1] LEES	17D	BABR	$e^+e^- \to K^0_S K^\pm\pi^\mp\pi^0\gamma$
14.8±4.8±1.2	53	[2] LEES	14H	BABR	$e^+e^- \to \pi^+\pi^-K^0_SK^0_S\gamma$

[1] Dividing by 1/2 to take into account $B(K^*(892)^\pm \to K^\pm\pi^\mp) = 1/2$.

[2] Dividing by 1/4 to take into account $B(K^*(892) \to K^0_S\pi) = 1/4$.

$\Gamma(K^0_S\pi^-K^*(892)^+ + \text{c.c.} \to K^0_SK^0_S\pi^+\pi^-) \times \Gamma(e^+e^-)/\Gamma_{\text{total}}$ $\Gamma_{30}\Gamma_5/\Gamma$

VALUE (eV)	EVTS	DOCUMENT ID		TECN	COMMENT
3.7±1.2±0.3	53	LEES	14H	BABR	$e^+e^- \to \pi^+\pi^-K^0_SK^0_S\gamma$

$\Gamma(K^0_S\pi^-K^*_2(1430)^+ + \text{c.c.}) \times \Gamma(e^+e^-)/\Gamma_{\text{total}}$ $\Gamma_{106}\Gamma_5/\Gamma$

VALUE (eV)	EVTS	DOCUMENT ID		TECN	COMMENT
20.1±9.8±0.5	35	[1,2] LEES	14H	BABR	$e^+e^- \to \pi^+\pi^-K^0_SK^0_S\gamma$

[1] Dividing by 1/4 to take into account $B(K^*(1430) \to K^0_S\pi) = 1/4$ $B(K^*(1430) \to K\pi)$.

[2] LEES 14H reports $[\Gamma(J/\psi(1S) \to K^0_S\pi^-K^*_2(1430)^+ + \text{c.c.}) \times \Gamma(J/\psi(1S) \to e^+e^-)/\Gamma_{\text{total}}] \times [B(K^*_2(1430) \to K\pi)] = 10.0 \pm 4.8 \pm 0.8$ eV which we divide by our best value $B(K^*_2(1430) \to K\pi) = (49.9 \pm 1.2) \times 10^{-2}$. Our first error is their experiment's error and our second error is the systematic error from using our best value.

$\Gamma(K^0_S\pi^-K^*_2(1430)^+ + \text{c.c.} \to K^0_SK^0_S\pi^+\pi^-) \times \Gamma(e^+e^-)/\Gamma_{\text{total}}$ $\Gamma_{107}\Gamma_5/\Gamma$

VALUE (eV)	EVTS	DOCUMENT ID		TECN	COMMENT
2.5±1.2±0.2	35	LEES	14H	BABR	$e^+e^- \to \pi^+\pi^-K^0_SK^0_S\gamma$

$\Gamma(K^*(892)^\pm K^*(892)^\mp) \times \Gamma(e^+e^-)/\Gamma_{\text{total}}$ $\Gamma_{27}\Gamma_5/\Gamma$

VALUE (eV)	EVTS	DOCUMENT ID		TECN	COMMENT
0.80±0.48±0.32	1 ± 5	[1] LEES	14H	BABR	$e^+e^- \to \pi^+\pi^-K^0_SK^0_S\gamma$

[1] Dividing by $(1/4)^2$ to take twice into account $B(K^*(892) \to K^0_S\pi) = 1/4$.

$\Gamma(K^*(892)^+ K_2^*(1430)^- + \text{c.c.}) \times \Gamma(e^+e^-)/\Gamma_{\text{total}}$ $\Gamma_{39}\Gamma_5/\Gamma$

VALUE (eV)	EVTS	DOCUMENT ID		TECN	COMMENT
18.6±16.1±0.4	8 ± 8	[1,2] LEES	14H	BABR	$e^+e^- \to \pi^+\pi^- K_S^0 K_S^0 \gamma$

[1] Dividing by $(1/4)^2$ to take into account $B(K^*(892) \to K_S^0\pi) = 1/4$ and $B(K^*(1430) \to K_S^0\pi) = 1/4$ $B(K^*(1430) \to K\pi)$.
[2] LEES 14H reports $[\Gamma(J/\psi(1S) \to K^*(892)^+ K_2^*(1430)^- + \text{c.c.}) \times \Gamma(J/\psi(1S) \to e^+e^-)/\Gamma_{\text{total}}] \times [B(K_2^*(1430) \to K\pi)] = 9.28 \pm 8.0 \pm 0.32$ eV which we divide by our best value $B(K_2^*(1430) \to K\pi) = (49.9 \pm 1.2) \times 10^{-2}$. Our first error is their experiment's error and our second error is the systematic error from using our best value.

$\Gamma(K^*(892)^+ K_2^*(1430)^- + \text{c.c.} \to K^*(892)^+ K_S^0\pi^- + \text{c.c.}) \times \Gamma(e^+e^-)/\Gamma_{\text{total}}$ $\Gamma_{40}\Gamma_5/\Gamma$

VALUE (eV)	EVTS	DOCUMENT ID		TECN	COMMENT
2.32±2.00±0.08	8 ± 8	[1] LEES	14H	BABR	$e^+e^- \to \pi^+\pi^- K_S^0 K_S^0 \gamma$

[1] Dividing by 1/4 to take into account $B(K^*(892) \to K_S^0\pi) = 1/4$.

$\Gamma(\phi K_S^0 K_S^0) \times \Gamma(e^+e^-)/\Gamma_{\text{total}}$ $\Gamma_{66}\Gamma_5/\Gamma$

VALUE (eV)	EVTS	DOCUMENT ID		TECN	COMMENT
3.25±0.84±0.03	29	[1] LEES	14H	BABR	$e^+e^- \to K_S^0 K_S^0 K^+ K^- \gamma$

[1] LEES 14H reports $[\Gamma(J/\psi(1S) \to \phi K_S^0 K_S^0) \times \Gamma(J/\psi(1S) \to e^+e^-)/\Gamma_{\text{total}}] \times [B(\phi(1020) \to K^+K^-)] = 1.6 \pm 0.4 \pm 0.1$ eV which we divide by our best value $B(\phi(1020) \to K^+K^-) = (49.2 \pm 0.5) \times 10^{-2}$. Our first error is their experiment's error and our second error is the systematic error from using our best value.

$\Gamma(\phi f_2'(1525)) \times \Gamma(e^+e^-)/\Gamma_{\text{total}}$ $\Gamma_{74}\Gamma_5/\Gamma$

VALUE (eV)	EVTS	DOCUMENT ID		TECN	COMMENT
8.1±3.2±0.2	11	[1,2] LEES	14H	BABR	$e^+e^- \to K_S^0 K_S^0 K^+ K^- \gamma$

[1] Dividing by 1/4 to take into account $B(f_2'(1525) \to K_S^0 K_S^0) = 1/4$ $B(f_2'(1525) \to K\overline{K})$ and using $B(\phi \to K^+K^-) = (48.9 \pm 0.5)\%$.
[2] LEES 14H reports $[\Gamma(J/\psi(1S) \to \phi f_2'(1525)) \times \Gamma(J/\psi(1S) \to e^+e^-)/\Gamma_{\text{total}}] \times [B(f_2'(1525) \to K\overline{K})] = 7.2 \pm 2.8 \pm 0.3$ eV which we divide by our best value $B(f_2'(1525) \to K\overline{K}) = (88.7 \pm 2.2) \times 10^{-2}$. Our first error is their experiment's error and our second error is the systematic error from using our best value.

$\Gamma(K^+K^- f_2'(1525)) \times \Gamma(e^+e^-)/\Gamma_{\text{total}}$ $\Gamma_{73}\Gamma_5/\Gamma$

VALUE (eV)	EVTS	DOCUMENT ID		TECN	COMMENT
5.8±1.9±0.1	16	[1,2] LEES	14H	BABR	$e^+e^- \to K_S^0 K_S^0 K^+ K^- \gamma$

[1] Dividing by 1/4 to take into account $B(f_2'(1525) \to K_S^0 K_S^0) = 1/4$ $B(f_2'(1525) \to K\overline{K})$.
[2] LEES 14H reports $[\Gamma(J/\psi(1S) \to K^+K^- f_2'(1525)) \times \Gamma(J/\psi(1S) \to e^+e^-)/\Gamma_{\text{total}}] \times [B(f_2'(1525) \to K\overline{K})] = 5.12 \pm 1.68 \pm 0.20$ eV which we divide by our best value $B(f_2'(1525) \to K\overline{K}) = (88.7 \pm 2.2) \times 10^{-2}$. Our first error is their experiment's error and our second error is the systematic error from using our best value.

$\Gamma(K_S^0 K_L^0 \eta) \times \Gamma(e^+e^-)/\Gamma_{\text{total}}$ $\Gamma_{146}\Gamma_5/\Gamma$

VALUE (eV)	EVTS	DOCUMENT ID		TECN	COMMENT
8.0±1.8±0.4	45	LEES	17A	BABR	$e^+e^- \to K_S^0 K_L^0 \eta\gamma$

$\Gamma(\eta K^\pm K_S^0 \pi^\mp) \times \Gamma(e^+e^-)/\Gamma_{\text{total}}$ $\Gamma_{58}\Gamma_5/\Gamma$

VALUE (eV)	EVTS	DOCUMENT ID		TECN	COMMENT
7.3±1.4±0.4	44	LEES	17D	BABR	$e^+e^- \to K_S^0 K^\pm\pi^\mp\pi^0\gamma$

$\Gamma(\overline{K}^*(892)^0 K^+\pi^- + \text{c.c.}) \times \Gamma(e^+e^-)/\Gamma_{\text{total}}$ $\Gamma_{51}\Gamma_5/\Gamma$

VALUE (eV)	EVTS	DOCUMENT ID		TECN	COMMENT
42.6±4.8±7.2	99	[1] LEES	17D	BABR	$e^+e^- \to K_S^0 K^\pm\pi^\mp\pi^0\gamma$

[1] Dividing by 1/6 to account for $B(K^*(892)^0 \to K_S^0\pi^0) = 1/6$.

$\Gamma(\pi^0\pi^0 K_S^0 K_L^0) \times \Gamma(e^+e^-)/\Gamma_{\text{total}}$ $\Gamma_{139}\Gamma_5/\Gamma$

VALUE (eV)	EVTS	DOCUMENT ID		TECN	COMMENT
10.3±2.3±0.5	47	LEES	17A	BABR	$e^+e^- \to K_S^0 K_L^0 \pi^0\pi^0\gamma$

$\Gamma(K_S^0 K_L^0 \pi^0) \times \Gamma(e^+e^-)/\Gamma_{\text{total}}$ $\Gamma_{143}\Gamma_5/\Gamma$

VALUE (eV)	EVTS	DOCUMENT ID		TECN	COMMENT
11.4±1.3±0.6	182	LEES	17A	BABR	$e^+e^- \to K_S^0 K_L^0 \pi^0\gamma$

$\Gamma(K^*(892)^0\overline{K}^0 + \text{c.c.} \to K_S^0 K_L^0 \pi^0) \times \Gamma(e^+e^-)/\Gamma_{\text{total}}$ $\Gamma_{144}\Gamma_5/\Gamma$

VALUE (eV)	EVTS	DOCUMENT ID		TECN	COMMENT
6.7±0.9±0.4	106	LEES	17A	BABR	$e^+e^- \to K_S^0 K_L^0 \pi^0\gamma$

$\Gamma(K_2^*(1430)^0\overline{K}^0 + \text{c.c.} \to K_S^0 K_L^0 \pi^0) \times \Gamma(e^+e^-)/\Gamma_{\text{total}}$ $\Gamma_{145}\Gamma_5/\Gamma$

VALUE (eV)	EVTS	DOCUMENT ID		TECN	COMMENT
2.4±0.7±0.1	37	LEES	17A	BABR	$e^+e^- \to K_S^0 K_L^0 \pi^0\gamma$

$\Gamma(2(\pi^+\pi^-)) \times \Gamma(e^+e^-)/\Gamma_{\text{total}}$ $\Gamma_{147}\Gamma_5/\Gamma$

VALUE (eV)	EVTS	DOCUMENT ID		TECN	COMMENT
20.4±0.9±0.4		LEES	12E	BABR	$10.6\ e^+e^- \to 2\pi^+2\pi^-\gamma$
• • • We do not use the following data for averages, fits, limits, etc. • • •					
19.5±1.4±1.3	270	[1] AUBERT	05D	BABR	$10.6\ e^+e^- \to 2(\pi^+\pi^-)\gamma$

[1] Superseded by LEES 12E.

$\Gamma(3(\pi^+\pi^-)) \times \Gamma(e^+e^-)/\Gamma_{\text{total}}$ $\Gamma_{148}\Gamma_5/\Gamma$

VALUE (10^{-2} keV)	EVTS	DOCUMENT ID		TECN	COMMENT
2.37±0.16±0.14	496	AUBERT	06D	BABR	$10.6\ e^+e^- \to 3(\pi^+\pi^-)\gamma$

$\Gamma(2(\pi^+\pi^-\pi^0)) \times \Gamma(e^+e^-)/\Gamma_{\text{total}}$ $\Gamma_{149}\Gamma_5/\Gamma$

VALUE (10^{-2} keV)	EVTS	DOCUMENT ID		TECN	COMMENT
8.9±0.5±1.0	761	AUBERT	06D	BABR	$10.6\ e^+e^- \to 2(\pi^+\pi^-\pi^0)\gamma$

$\Gamma(2(\pi^+\pi^-)\eta) \times \Gamma(e^+e^-)/\Gamma_{\text{total}}$ $\Gamma_{150}\Gamma_5/\Gamma$

VALUE (eV)	EVTS	DOCUMENT ID		TECN	COMMENT
13.1±2.4±0.1	85	[1] AUBERT	07AU	BABR	$10.6\ e^+e^- \to 2(\pi^+\pi^-)\eta\gamma$

[1] AUBERT 07AU reports $[\Gamma(J/\psi(1S) \to 2(\pi^+\pi^-)\eta) \times \Gamma(J/\psi(1S) \to e^+e^-)/\Gamma_{\text{total}}] \times [B(\eta \to 2\gamma)] = 5.16 \pm 0.85 \pm 0.39$ eV which we divide by our best value $B(\eta \to 2\gamma) = (39.41 \pm 0.20) \times 10^{-2}$. Our first error is their experiment's error and our second error is the systematic error from using our best value.

$\Gamma(p\overline{p}) \times \Gamma(e^+e^-)/\Gamma_{\text{total}}$ $\Gamma_{152}\Gamma_5/\Gamma$

VALUE (eV)	EVTS	DOCUMENT ID		TECN	COMMENT
11.9±0.6 OUR AVERAGE	Error includes scale factor of 1.8. See the ideogram below.				
11.3±0.4±0.3	821	[1] LEES	13O	BABR	$e^+e^- \to p\overline{p}\gamma$
12.9±0.4±0.4	918	[2] LEES	13Y	BABR	$e^+e^- \to p\overline{p}\gamma$
9.7±1.7		[3] ARMSTRONG	93B	E760	$\overline{p}p \to e^+e^-$
• • • We do not use the following data for averages, fits, limits, etc. • • •					
12.0±0.6±0.5	438	[4] AUBERT	06B	BABR	$e^+e^- \to p\overline{p}\gamma$

[1] ISR photon reconstructed in the detector
[2] ISR photon undetected
[3] Using $\Gamma_{\text{total}} = 85.5^{+6.1}_{-5.8}$ MeV.
[4] Superseded by LEES 13O

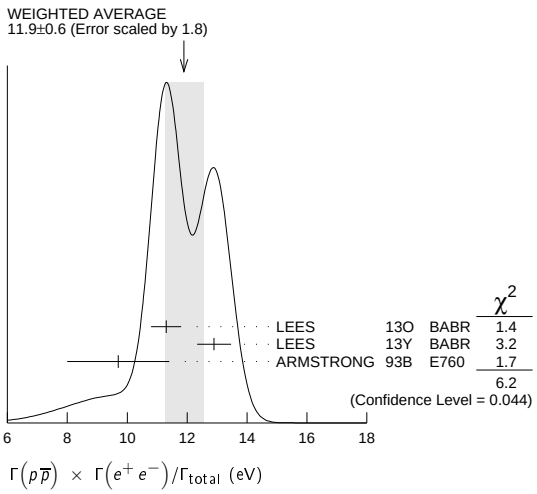

$\Gamma(\Sigma^0\overline{\Sigma}^0) \times \Gamma(e^+e^-)/\Gamma_{\text{total}}$ $\Gamma_{165}\Gamma_5/\Gamma$

VALUE (eV)	DOCUMENT ID		TECN	COMMENT
6.4±1.2±0.6	AUBERT	07BD	BABR	$10.6\ e^+e^- \to \Sigma^0\overline{\Sigma}^0\gamma$

$\Gamma(2(\pi^+\pi^-)K^+K^-) \times \Gamma(e^+e^-)/\Gamma_{\text{total}}$ $\Gamma_{166}\Gamma_5/\Gamma$

VALUE (10^{-2} keV)	EVTS	DOCUMENT ID		TECN	COMMENT
2.75±0.23±0.17	205	AUBERT	06D	BABR	$10.6\ e^+e^- \to K^+K^-2(\pi^+\pi^-)\gamma$

$\Gamma(\Lambda\overline{\Lambda}) \times \Gamma(e^+e^-)/\Gamma_{\text{total}}$ $\Gamma_{172}\Gamma_5/\Gamma$

VALUE (eV)	DOCUMENT ID		TECN	COMMENT
10.7±0.9±0.7	AUBERT	07BD	BABR	$10.6\ e^+e^- \to \Lambda\overline{\Lambda}\gamma$

$\Gamma(2(K^+K^-)) \times \Gamma(e^+e^-)/\Gamma_{\text{total}}$ $\Gamma_{175}\Gamma_5/\Gamma$

VALUE (eV)	EVTS	DOCUMENT ID		TECN	COMMENT
4.00±0.33±0.29	287 ± 24	LEES	12F	BABR	$10.6\ e^+e^- \to 2(K^+K^-)\gamma$
• • • We do not use the following data for averages, fits, limits, etc. • • •					
4.11±0.39±0.30	156 ± 15	[1] AUBERT	07AK	BABR	$10.6\ e^+e^- \to 2(K^+K^-)\gamma$
4.0 ±0.7 ±0.6	38	[2] AUBERT	05D	BABR	$10.6\ e^+e^- \to 2(K^+K^-)\gamma$

[1] Superseded by LEES 12F.
[2] Superseded by AUBERT 07AK.

$\Gamma(K^+K^-) \times \Gamma(e^+e^-)/\Gamma_{total}$ $\Gamma_{177}\Gamma_5/\Gamma$

VALUE (eV)	EVTS	DOCUMENT ID		TECN	COMMENT
• • • We do not use the following data for averages, fits, limits, etc. • • •					
1.78±0.11±0.05	462	[1] LEES	15J	BABR	$e^+e^- \to K^+K^-\gamma$
1.94±0.11±0.05	462	[2] LEES	15J	BABR	$e^+e^- \to K^+K^-\gamma$
1.42±0.23±0.08	51	[3] LEES	13Q	BABR	$e^+e^- \to K^+K^-\gamma$

[1] $\sin\phi > 0$.
[2] $\sin\phi < 0$.
[3] Interference with non-resonant K^+K^- production not taken into account.

$J/\psi(1S)$ BRANCHING RATIOS

For the first four branching ratios, see also the partial widths, and (partial widths) $\times \Gamma(e^+e^-)/\Gamma_{total}$ above.

$\Gamma(\text{hadrons})/\Gamma_{total}$ Γ_1/Γ

VALUE	DOCUMENT ID		TECN	COMMENT
0.877±0.005 OUR AVERAGE				
0.878±0.005	BAI	95B	BES	e^+e^-
0.86 ±0.02	BOYARSKI	75	MRK1	e^+e^-

$\Gamma(\text{virtual}\,\gamma \to \text{hadrons})/\Gamma_{total}$ Γ_2/Γ

VALUE	DOCUMENT ID		TECN	COMMENT
0.135±0.003	[1,2] SETH	04	RVUE	e^+e^-
• • • We do not use the following data for averages, fits, limits, etc. • • •				
0.17 ±0.02	[1] BOYARSKI	75	MRK1	e^+e^-

[1] Included in $\Gamma(\text{hadrons})/\Gamma_{total}$.
[2] Using $B(J/\psi \to \ell^+\ell^-) = (5.90 \pm 0.09)\%$ from RPP-2002 and $R = 2.28 \pm 0.04$ determined by a fit to data from BAI 00 and BAI 02c.

$\Gamma(ggg)/\Gamma_{total}$ Γ_3/Γ

VALUE (units 10^{-2})	EVTS	DOCUMENT ID		TECN	COMMENT
64.1±1.0	6 M	[1] BESSON	08	CLEO	$\psi(2S) \to \pi^+\pi^-$ + hadrons

[1] Calculated using the value $\Gamma(\gamma gg)/\Gamma(ggg) = 0.137 \pm 0.001 \pm 0.016 \pm 0.004$ from BESSON 08 and the PDG 08 values of $B(\ell^+\ell^-)$, B(virtual $\gamma \to$ hadrons), and $B(\gamma\eta_c)$. The statistical error is negligible and the systematic error is partially correlated with that of $\Gamma(\gamma gg)/\Gamma_{total}$ measurement of BESSON 08.

$\Gamma(\gamma gg)/\Gamma_{total}$ Γ_4/Γ

VALUE (units 10^{-2})	EVTS	DOCUMENT ID		TECN	COMMENT
8.79±1.05	200 k	[1] BESSON	08	CLEO	$\psi(2S) \to \pi^+\pi^-\gamma$ + hadrons

[1] Calculated using the value $\Gamma(\gamma gg)/\Gamma(ggg) = 0.137 \pm 0.001 \pm 0.016 \pm 0.004$ from BESSON 08 and the value of $\Gamma(ggg)/\Gamma_{total}$. The statistical error is negligible and the systematic error is partially correlated with that of $\Gamma(ggg)/\Gamma_{total}$ measurement of BESSON 08.

$\Gamma(\gamma gg)/\Gamma(ggg)$ Γ_4/Γ_3

VALUE (units 10^{-2})	EVTS	DOCUMENT ID		TECN	COMMENT
13.7±0.1±0.7	6 M	BESSON	08	CLEO	$\psi(2S) \to \pi^+\pi^- J/\psi$

$\Gamma(e^+e^-)/\Gamma_{total}$ Γ_5/Γ

VALUE (units 10^{-2})	EVTS	DOCUMENT ID		TECN	COMMENT
5.971±0.032 OUR AVERAGE					
5.983±0.007±0.037	720k	ABLIKIM	13R	BES3	$\psi(2S) \to J/\psi\pi^+\pi^-$
5.945±0.067±0.042	15k	LI	05C	CLEO	$\psi(2S) \to J/\psi\pi^+\pi^-$
5.90 ±0.05 ±0.10		BAI	98D	BES	$\psi(2S) \to J/\psi\pi^+\pi^-$
6.09 ±0.33		BAI	95B	BES	e^+e^-
5.92 ±0.15 ±0.20		COFFMAN	92	MRK3	$\psi(2S) \to J/\psi\pi^+\pi^-$
6.9 ±0.9		BOYARSKI	75	MRK1	e^+e^-

$\Gamma(e^+e^-\gamma)/\Gamma_{total}$ Γ_6/Γ

VALUE (units 10^{-3})	DOCUMENT ID		TECN	COMMENT
8.8±1.3±0.4	[1] ARMSTRONG	96	E760	$\overline{p}p \to e^+e^-\gamma$

[1] For $E_\gamma > 100$ MeV.

$\Gamma(\mu^+\mu^-)/\Gamma_{total}$ Γ_7/Γ

VALUE (units 10^{-2})	EVTS	DOCUMENT ID		TECN	COMMENT
5.961±0.033 OUR AVERAGE					
5.973±0.007±0.038	770k	ABLIKIM	13R	BES3	$\psi(2S) \to J/\psi\pi^+\pi^-$
5.960±0.065±0.050	17k	LI	05C	CLEO	$\psi(2S) \to J/\psi\pi^+\pi^-$
5.84 ±0.06 ±0.10		BAI	98D	BES	$\psi(2S) \to J/\psi\pi^+\pi^-$
6.08 ±0.33		BAI	95B	BES	e^+e^-
5.90 ±0.15 ±0.19		COFFMAN	92	MRK3	$\psi(2S) \to J/\psi\pi^+\pi^-$
6.9 ±0.9		BOYARSKI	75	MRK1	e^+e^-

$\Gamma(e^+e^-)/\Gamma(\mu^+\mu^-)$ Γ_5/Γ_7

VALUE	DOCUMENT ID		TECN	COMMENT
1.0016±0.0031 OUR AVERAGE				
1.0022±0.0044±0.0048	[1] AULCHENKO	14	KEDR	3.097 $e^+e^- \to e^+e^-,\mu^+\mu^-$
1.0017±0.0017±0.0033	[2] ABLIKIM	13R	BES3	$\psi(2S) \to J/\psi\pi^+\pi^-$
1.002 ±0.021 ±0.013	[3] ANASHIN	10	KEDR	3.097 $e^+e^- \to e^+e^-,\mu^+\mu^-$
0.997 ±0.012 ±0.006	LI	05C	CLEO	$\psi(2S) \to J/\psi\pi^+\pi^-$
• • • We do not use the following data for averages, fits, limits, etc. • • •				
1.011 ±0.013 ±0.016	BAI	98D	BES	$\psi(2S) \to J/\psi\pi^+\pi^-$
1.00 ±0.07	BAI	95B	BES	e^+e^-
1.00 ±0.05	BOYARSKI	75	MRK1	e^+e^-
0.91 ±0.15	ESPOSITO	75B	FRAM	e^+e^-
0.93 ±0.10	FORD	75	SPEC	e^+e^-

[1] From 235.3k $J/\psi \to e^+e^-$ and 156.6k $J/\psi \to \mu^+\mu^-$ observed events.
[2] Not independent of the corresponding measurements of $\Gamma(e^+e^-)/\Gamma_{total}$ and $\Gamma(\mu^+\mu^-)/\Gamma_{total}$.
[3] Not independent of the corresponding measurements of $\Gamma(e^+e^-) \times \Gamma(e^+e^-)/\Gamma_{total}$ and $\Gamma(\mu^+\mu^-) \times \Gamma(e^+e^-)/\Gamma_{total}$.

HADRONIC DECAYS

$\Gamma(\rho\pi)/\Gamma_{total}$ Γ_8/Γ

VALUE (units 10^{-2})	EVTS	DOCUMENT ID		TECN	COMMENT
1.69 ±0.15 OUR AVERAGE		Error includes scale factor of 2.4. See the ideogram below.			
2.18 ±0.19		[1,2] AUBERT,B	04N	BABR	10.6 $e^+e^- \to \pi^+\pi^-\pi^0\gamma$
2.184±0.005±0.201	220k	[2,3] BAI	04H	BES	$e^+e^- \to J/\psi \to \pi^+\pi^-\pi^0$
2.091±0.021±0.116		[2,4] BAI	04H	BES	$\psi(2S) \to \pi^+\pi^- J/\psi$
1.21 ±0.20		BAI	96D	BES	$e^+e^- \to \rho\pi$
1.42 ±0.01 ±0.19		COFFMAN	88	MRK3	e^+e^-
1.3 ±0.3	150	FRANKLIN	83	MRK2	e^+e^-
1.6 ±0.4	183	ALEXANDER	78	PLUT	e^+e^-
1.33 ±0.21		BRANDELIK	78B	DASP	e^+e^-
1.0 ±0.2	543	BARTEL	76	CNTR	e^+e^-
1.3 ±0.3	153	JEAN-MARIE	76	MRK1	e^+e^-

[1] From the ratio of $\Gamma(e^+e^-)\,B(\pi^+\pi^-\pi^0)$ and $\Gamma(e^+e^-)\,B(\mu^+\mu^-)$ (AUBERT 04).
[2] Not independent of their $B(\pi^+\pi^-\pi^0)$.
[3] From $J/\psi \to \pi^+\pi^-\pi^0$ events directly.
[4] Obtained comparing the rates for $\pi^+\pi^-\pi^0$ and $\mu^+\mu^-$, using J/ψ events produced via $\psi(2S) \to \pi^+\pi^- J/\psi$ and with $B(J/\psi \to \mu^+\mu^-) = 5.88 \pm 0.10\%$.

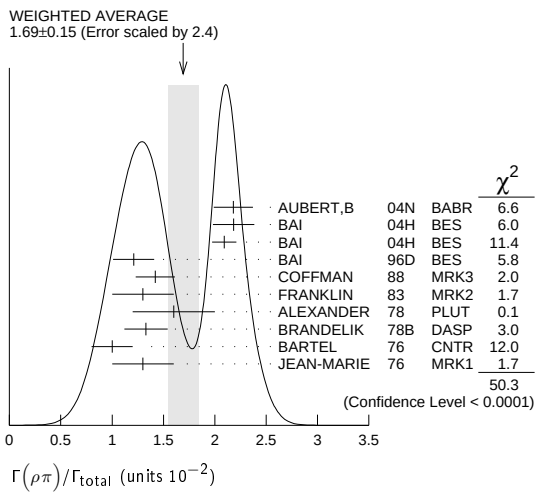

$\Gamma(\rho^0\pi^0)/\Gamma(\rho\pi)$ Γ_9/Γ_8

VALUE	DOCUMENT ID		TECN	COMMENT
0.328±0.005±0.027	COFFMAN	88	MRK3	e^+e^-
• • • We do not use the following data for averages, fits, limits, etc. • • •				
0.35 ±0.08	ALEXANDER	78	PLUT	e^+e^-
0.32 ±0.08	BRANDELIK	78B	DASP	e^+e^-
0.39 ±0.11	BARTEL	76	CNTR	e^+e^-
0.37 ±0.09	JEAN-MARIE	76	MRK1	e^+e^-

$\Gamma(\rho\pi)/\Gamma(\pi^+\pi^-\pi^0)$ Γ_8/Γ_{129}

VALUE	EVTS	DOCUMENT ID		TECN	COMMENT
1.142±0.011±0.026	20K	[1] LEES	17C	BABR	$J/\psi \to \pi^+\pi^-\pi^0$
• • • We do not use the following data for averages, fits, limits, etc. • • •					
1.331±0.033	20K	[2] LEES	17C	BABR	$J/\psi \to \pi^+\pi^-\pi^0$

[1] From a Dalitz plot analysis in an isobar model.
[2] From a Dalitz plot analysis in a Veneziano model.

$\Gamma(\rho(1450)\pi \to \pi^+\pi^-\pi^0)/\Gamma(\pi^+\pi^-\pi^0)$ Γ_{12}/Γ_{129}

VALUE (%)	EVTS	DOCUMENT ID		TECN	COMMENT
10.9 ±1.7 ±2.7	20K	[1] LEES	17C	BABR	$J/\psi \to \pi^+\pi^-\pi^0$
• • • We do not use the following data for averages, fits, limits, etc. • • •					
0.80±0.27	20K	[2] LEES	17C	BABR	$J/\psi \to \pi^+\pi^-\pi^0$

[1] From a Dalitz plot analysis in an isobar model.
[2] From a Dalitz plot analysis in a Veneziano model.

$\Gamma(\rho(1450)^0\pi^0 \to K^+K^-\pi^0)/\Gamma(K^+K^-\pi^0)$ Γ_{14}/Γ_{141}

VALUE (%)	EVTS	DOCUMENT ID		TECN	COMMENT
9.3±2.0±0.6	2K	[1] LEES	17C	BABR	$J/\psi \to K^+K^-\pi^0$

[1] From a Dalitz plot analysis in an isobar model.

$\Gamma(\rho(1450)^\pm\pi^\mp \to K^0_S K^\pm\pi^\mp)/\Gamma(K^0_S K^\pm\pi^\mp)$ Γ_{13}/Γ_{142}

VALUE (%)	EVTS	DOCUMENT ID		TECN	COMMENT
6.3±0.8±0.6	4K	[1] LEES	17C	BABR	$J/\psi \to K^0_S K^\pm\pi^\mp$

[1] From a Dalitz plot analysis in an isobar model.

$\Gamma(\rho(1450)\eta'(958) \to \pi^+\pi^-\eta'(958))/\Gamma_{\text{total}}$ Γ_{15}/Γ

VALUE (units 10^{-6})	EVTS	DOCUMENT ID		TECN	COMMENT
3.28±0.55±0.44	119	[1] ABLIKIM	17AK	BES3	$J/\psi \to \pi^+\pi^-\eta'$

[1] From a partial wave analysis of the decay $J/\psi \to \pi^+\pi^-\eta'$.

$\Gamma(\rho_3(1690)\pi \to \pi^+\pi^-\pi^0)/\Gamma(\pi^+\pi^-\pi^0)$ Γ_{20}/Γ_{129}

VALUE (units 10^{-3})	EVTS	DOCUMENT ID		TECN	COMMENT
• • • We do not use the following data for averages, fits, limits, etc. • • •					
4.0±0.8	20K	[1] LEES	17C	BABR	$J/\psi \to \pi^+\pi^-\pi^0$

[1] From a Dalitz plot analysis in a Veneziano model.

$\Gamma(\rho(1700)\pi \to \pi^+\pi^-\pi^0)/\Gamma(\pi^+\pi^-\pi^0)$ Γ_{17}/Γ_{129}

VALUE (units 10^{-3})	EVTS	DOCUMENT ID		TECN	COMMENT
8±2±5	20K	[1] LEES	17C	BABR	$J/\psi \to \pi^+\pi^-\pi^0$
• • • We do not use the following data for averages, fits, limits, etc. • • •					
22±6	20K	[2] LEES	17C	BABR	$J/\psi \to \pi^+\pi^-\pi^0$

[1] From a Dalitz plot analysis in an isobar model.
[2] From a Dalitz plot analysis in a Veneziano model.

$\Gamma(\rho(2150)\pi \to \pi^+\pi^-\pi^0)/\Gamma(\pi^+\pi^-\pi^0)$ Γ_{19}/Γ_{129}

VALUE (units 10^{-4})	EVTS	DOCUMENT ID		TECN	COMMENT
4± 1±20	20K	[1] LEES	17C	BABR	$J/\psi \to \pi^+\pi^-\pi^0$
• • • We do not use the following data for averages, fits, limits, etc. • • •					
600±250	20K	[2] LEES	17C	BABR	$J/\psi \to \pi^+\pi^-\pi^0$

[1] From a Dalitz plot analysis in an isobar model.
[2] From a Dalitz plot analysis in a Veneziano model.

$\Gamma(a_2(1320)\rho)/\Gamma_{\text{total}}$ Γ_{21}/Γ

VALUE (units 10^{-3})	EVTS	DOCUMENT ID		TECN	COMMENT
10.9±2.2 OUR AVERAGE					
11.7±0.7±2.5	7584	AUGUSTIN	89	DM2	$J/\psi \to \rho^0\rho^\pm\pi^\mp$
8.4±4.5	36	VANNUCCI	77	MRK1	$e^+e^- \to 2(\pi^+\pi^-)\pi^0$

$\Gamma(\omega\pi^+\pi^+\pi^-\pi^-)/\Gamma_{\text{total}}$ Γ_{22}/Γ

VALUE (units 10^{-4})	EVTS	DOCUMENT ID		TECN	COMMENT
85±34	140	VANNUCCI	77	MRK1	$e^+e^- \to 3(\pi^+\pi^-)\pi^0$

$\Gamma(\omega\pi^+\pi^-\pi^0)/\Gamma_{\text{total}}$ Γ_{23}/Γ

VALUE (units 10^{-2})	EVTS	DOCUMENT ID		TECN	COMMENT
0.40±0.06±0.04	170	[1] AUBERT	06D	BABR	10.6 $e^+e^- \to \omega\pi^+\pi^-\pi^0\gamma$

[1] Using $\Gamma(J/\psi \to e^+e^-) = 5.52 \pm 0.14 \pm 0.04$ keV.

$\Gamma(\omega\pi^+\pi^-)/\Gamma_{\text{total}}$ Γ_{24}/Γ

VALUE (units 10^{-3})	EVTS	DOCUMENT ID		TECN	COMMENT
8.6±0.7 OUR AVERAGE Error includes scale factor of 1.1.					
9.7±0.6±0.6	788	[1] AUBERT	07AU	BABR	10.6 $e^+e^- \to \omega\pi^+\pi^-\gamma$
7.0±1.6	18058	AUGUSTIN	89	DM2	$J/\psi \to 2(\pi^+\pi^-)\pi^0$
7.8±1.6	215	BURMESTER	77D	PLUT	e^+e^-
6.8±1.9	348	VANNUCCI	77	MRK1	$e^+e^- \to 2(\pi^+\pi^-)\pi^0$

[1] AUBERT 07AU quotes $\Gamma^{J/\psi}_{ee}\cdot B(J/\psi \to \omega\pi^+\pi^-)\cdot B(\omega \to 3\pi) = 47.8 \pm 3.1 \pm 3.2$ eV.

$\Gamma(\omega f_2(1270))/\Gamma_{\text{total}}$ Γ_{25}/Γ

VALUE (units 10^{-3})	EVTS	DOCUMENT ID		TECN	COMMENT
4.3±0.6 OUR AVERAGE					
4.3±0.2±0.6	5860	AUGUSTIN	89	DM2	e^+e^-
4.0±1.6	70	BURMESTER	77D	PLUT	e^+e^-
• • • We do not use the following data for averages, fits, limits, etc. • • •					
1.9±0.8	81	VANNUCCI	77	MRK1	$e^+e^- \to 2(\pi^+\pi^-)\pi^0$

$\Gamma(K^*(892)^0\overline{K}^*(892)^0)/\Gamma_{\text{total}}$ Γ_{26}/Γ

VALUE (units 10^{-4})	CL%	EVTS	DOCUMENT ID		TECN	COMMENT
• • • We do not use the following data for averages, fits, limits, etc. • • •						
2.3±0.7±0.1		25 ± 8	[1] AUBERT	07AK	BABR	10.6 $e^+e^- \to \pi^+\pi^-K^+K^-\gamma$
<5	90		VANNUCCI	77	MRK1	$e^+e^- \to \pi^+\pi^-K^+K^-$

[1] Superseded by LEES 12F. AUBERT 07AK reports $[\Gamma(J/\psi(1S) \to K^*(892)^0\overline{K}^*(892)^0)/\Gamma_{\text{total}}] \times [\Gamma(J/\psi(1S) \to e^+e^-)] = (1.28 \pm 0.40 \pm 0.11)\times10^{-3}$ keV which we divide by our best value $\Gamma(J/\psi(1S) \to e^+e^-) = 5.55 \pm 0.14 \pm 0.02$ keV. Our first error is their experiment's error and our second error is the systematic error from using our best value.

$\Gamma(K^*(892)^\pm K^*(892)^\mp)/\Gamma_{\text{total}}$ Γ_{27}/Γ

VALUE (units 10^{-3})	EVTS	DOCUMENT ID		TECN	COMMENT
1.00±0.19$^{+0.11}_{-0.32}$	323	ABLIKIM	10E	BES2	$J/\psi \to K^\pm K^0_S\pi^\mp\pi^0$

$\Gamma(K^*(892)^\pm K^*(700)^\mp)/\Gamma_{\text{total}}$ Γ_{28}/Γ

VALUE (units 10^{-3})	EVTS	DOCUMENT ID		TECN	COMMENT
1.09±0.18$^{+0.94}_{-0.54}$	655	ABLIKIM	10E	BES2	$J/\psi \to K^\pm K^0_S\pi^\mp\pi^0$

$\Gamma(\eta K^*(892)^0\overline{K}^*(892)^0)/\Gamma_{\text{total}}$ Γ_{31}/Γ

VALUE (units 10^{-3})	EVTS	DOCUMENT ID		TECN	COMMENT
1.15±0.13±0.22	209	ABLIKIM	10C	BES2	$J/\psi \to \eta K^+\pi^-K^-\pi^+$

$\Gamma(K^*(892)^0\overline{K}^*_2(1430)^0 + \text{c.c.})/\Gamma_{\text{total}}$ Γ_{38}/Γ

VALUE (units 10^{-3})	EVTS	DOCUMENT ID		TECN	COMMENT
• • • We do not use the following data for averages, fits, limits, etc. • • •					
5.9±0.6±0.2	317 ± 23	[1,2] AUBERT	07AK	BABR	10.6 $e^+e^- \to \pi^+\pi^-K^+K^-\gamma$
6.7±2.6	40	VANNUCCI	77	MRK1	$e^+e^- \to \pi^+\pi^-K^+K^-$

[1] Using $B(K^*_2(1430)^0 \to K\pi) = (49.9 \pm 1.2)\%$.
[2] Superseded by LEES 12F. AUBERT 07AK reports $[\Gamma(J/\psi(1S) \to K^*(892)^0\overline{K}^*_2(1430)^0 + \text{c.c.})/\Gamma_{\text{total}}] \times [\Gamma(J/\psi(1S) \to e^+e^-)] = (32.9 \pm 2.3 \pm 2.7)\times10^{-3}$ keV which we divide by our best value $\Gamma(J/\psi(1S) \to e^+e^-) = 5.55 \pm 0.14 \pm 0.02$ keV. Our first error is their experiment's error and our second error is the systematic error from using our best value.

$\Gamma(\omega K^*(892)\overline{K} + \text{c.c.})/\Gamma_{\text{total}}$ Γ_{42}/Γ

VALUE (units 10^{-4})	EVTS	DOCUMENT ID		TECN	COMMENT
61 ± 9 OUR AVERAGE					
62.0± 6.8±10.6	899 ± 98	ABLIKIM	08E	BES2	$J/\psi \to \omega K^0_S K^\pm\pi^\mp$
65.3±10.2±13.5	176 ± 28	ABLIKIM	08E	BES2	$J/\psi \to \omega K^+K^-\pi^0$
53 ±14 ±14	530±140	BECKER	87	MRK3	e^+e^- → hadrons

$\Gamma(K^+K^*(892)^- + \text{c.c.})/\Gamma_{\text{total}}$ Γ_{45}/Γ

VALUE (units 10^{-3})	EVTS	DOCUMENT ID		TECN	COMMENT
5.12±0.30 OUR AVERAGE					
5.2 ±0.4 ±0.1		[1] AUBERT	08S	BABR	10.6 $e^+e^- \to K^+K^*(892)^-\gamma$
4.57±0.17±0.70	2285	JOUSSET	90	DM2	$J/\psi \to$ hadrons
5.26±0.13±0.53		COFFMAN	88	MRK3	$J/\psi \to K^\pm K^0_S\pi^\mp$, $K^+K^-\pi^0$
• • • We do not use the following data for averages, fits, limits, etc. • • •					
2.6 ±0.6	24	FRANKLIN	83	MRK2	$J/\psi \to K^+K^-\pi^0$
3.2 ±0.6	48	VANNUCCI	77	MRK1	$J/\psi \to K^\pm K^0_S\pi^\mp$
4.1 ±1.2	39	BRAUNSCH...	76	DASP	$J/\psi \to K^\pm X$

[1] AUBERT 08S reports $[\Gamma(J/\psi(1S) \to K^+K^*(892)^- + \text{c.c.})/\Gamma_{\text{total}}] \times [\Gamma(J/\psi(1S) \to e^+e^-)] = (29.0\pm1.7\pm1.3)\times10^{-3}$ keV which we divide by our best value $\Gamma(J/\psi(1S) \to e^+e^-) = 5.55 \pm 0.14 \pm 0.02$ keV. Our first error is their experiment's error and our second error is the systematic error from using our best value.

$\Gamma(K^+K^*(892)^- + \text{c.c.} \to K^+K^-\pi^0)/\Gamma_{\text{total}}$ Γ_{46}/Γ

VALUE (units 10^{-3})	EVTS	DOCUMENT ID		TECN	COMMENT
1.97±0.20±0.05	155	[1] AUBERT	08S	BABR	10.6 $e^+e^- \to K^+K^-\pi^0\gamma$

[1] AUBERT 08S reports $[\Gamma(J/\psi(1S) \to K^+K^*(892)^- + \text{c.c.} \to K^+K^-\pi^0)/\Gamma_{\text{total}}] \times [\Gamma(J/\psi(1S) \to e^+e^-)] = (10.96 \pm 0.85 \pm 0.70)\times10^{-3}$ keV which we divide by our best value $\Gamma(J/\psi(1S) \to e^+e^-) = 5.55 \pm 0.14 \pm 0.02$ keV. Our first error is their experiment's error and our second error is the systematic error from using our best value.

$\Gamma(K^+K^*(892)^- + \text{c.c.} \to K^+K^-\pi^0)/\Gamma(K^+K^-\pi^0)$ Γ_{46}/Γ_{141}

VALUE (%)	EVTS	DOCUMENT ID		TECN	COMMENT
92.4±1.5±3.4	2K	[1] LEES	17C	BABR	$J/\psi \to K^+K^-\pi^0$

[1] From a Dalitz plot analysis in an isobar model.

$\Gamma(\overline{K}K^*(892) + \text{c.c.} \to K^0_S K^\pm\pi^\mp)/\Gamma(K^0_S K^\pm\pi^\mp)$ Γ_{44}/Γ_{142}

VALUE (%)	EVTS	DOCUMENT ID		TECN	COMMENT
90.5±0.9±3.8	4K	[1] LEES	17C	BABR	$J/\psi \to K^0_S K^\pm\pi^\mp$

[1] From a Dalitz plot analysis in an isobar model.

$\Gamma(K^+K^*(892)^- + \text{c.c.} \to K^0K^\pm\pi^\mp + \text{c.c.})/\Gamma_{\text{total}}$ Γ_{47}/Γ

VALUE (units 10^{-3})	EVTS	DOCUMENT ID		TECN	COMMENT
3.0±0.4±0.1	89	[1] AUBERT	08S	BABR	10.6 $e^+e^- \to K^0_S K^\pm\pi^\mp\gamma$

[1] AUBERT 08S reports $[\Gamma(J/\psi(1S) \to K^+K^*(892)^- + \text{c.c.} \to K^0K^\pm\pi^\mp + \text{c.c.})/\Gamma_{\text{total}}] \times [\Gamma(J/\psi(1S) \to e^+e^-)] = (16.76 \pm 1.70 \pm 1.00)\times10^{-3}$ keV which we divide by our best value $\Gamma(J/\psi(1S) \to e^+e^-) = 5.55 \pm 0.14 \pm 0.02$ keV. Our first error is their experiment's error and our second error is the systematic error from using our best value.

$\Gamma(K^0\overline{K}^*(892)^0+\text{c.c.})/\Gamma_{\text{total}}$ Γ_{48}/Γ

VALUE (units 10^{-3})	EVTS	DOCUMENT ID		TECN	COMMENT
4.39±0.31 OUR AVERAGE					
4.8 ±0.5 ±0.1		[1] AUBERT	08S	BABR	10.6 $e^+e^- \to K^0\overline{K}^*(892)^0\gamma$
3.96±0.15±0.60	1192	JOUSSET	90	DM2	$J/\psi \to$ hadrons
4.33±0.12±0.45		COFFMAN	88	MRK3	$J/\psi \to K^\pm K^0_S\pi^\mp$
• • • We do not use the following data for averages, fits, limits, etc. • • •					
2.7 ±0.6	45	VANNUCCI	77	MRK1	$J/\psi \to K^\pm K^0_S\pi^\mp$

[1] AUBERT 08S reports $[\Gamma(J/\psi(1S) \to K^0\overline{K}^*(892)^0+\text{c.c.})/\Gamma_{\text{total}}] \times [\Gamma(J/\psi(1S) \to e^+e^-)] = (26.6\pm2.5\pm1.5)\times10^{-3}$ keV which we divide by our best value $\Gamma(J/\psi(1S) \to e^+e^-) = 5.55 \pm 0.14 \pm 0.02$ keV. Our first error is their experiment's error and our second error is the systematic error from using our best value.

$\Gamma(K^0\overline{K}^*(892)^0+\text{c.c.})/\Gamma(K^+K^*(892)^-+\text{c.c.})$ Γ_{48}/Γ_{45}

VALUE	DOCUMENT ID		TECN	COMMENT
0.82±0.05±0.09	COFFMAN	88	MRK3	$J/\psi \to K\overline{K}^*(892)+\text{c.c.}$

$\Gamma(K^0\overline{K}^*(892)^0+\text{c.c.} \to K^0K^\pm\pi^\mp+\text{c.c.})/\Gamma_{\text{total}}$ Γ_{49}/Γ

VALUE (units 10^{-3})	EVTS	DOCUMENT ID		TECN	COMMENT
3.2±0.4±0.1	94	[1] AUBERT	08S	BABR	10.6 $e^+e^- \to K^0_S K^\pm\pi^\mp\gamma$

[1] AUBERT 08S reports $[\Gamma(J/\psi(1S) \to K^0\overline{K}^*(892)^0+\text{c.c.} \to K^0K^\pm\pi^\mp+\text{c.c.})/\Gamma_{\text{total}}] \times [\Gamma(J/\psi(1S) \to e^+e^-)] = (17.70 \pm 1.70 \pm 1.00) \times 10^{-3}$ keV which we divide by our best value $\Gamma(J/\psi(1S) \to e^+e^-) = 5.55 \pm 0.14 \pm 0.02$ keV. Our first error is their experiment's error and our second error is the systematic error from using our best value.

$\Gamma(K_1(1400)^\pm K^\mp)/\Gamma_{\text{total}}$ Γ_{50}/Γ

VALUE (units 10^{-3})	DOCUMENT ID		TECN	COMMENT
3.8±0.8±1.2	[1] BAI	99C	BES	e^+e^-

[1] Assuming $B(K_1(1400) \to K^*\pi)$=0.94 ± 0.06

$\Gamma(\overline{K}^*(892)^0K^+\pi^-+\text{c.c.})/\Gamma_{\text{total}}$ Γ_{51}/Γ

VALUE	DOCUMENT ID		TECN	COMMENT
seen	[1] ABLIKIM	06C	BES2	$J/\psi \to \overline{K}^*(892)^0K^+\pi^-$

[1] A $K_0^*(700)$ is observed by ABLIKIM 06C in the $K^+\pi^-$ mass spectrum of the $\overline{K}^*(892)^0K^+\pi^-$ final state against the $\overline{K}^*(892)$. A corresponding branching fraction of the $J/\psi(1S)$ is not presented.

$\Gamma(K^*(1410)\overline{K}+\text{c.c.} \to K^\pm K^\mp\pi^0)/\Gamma(K^+K^-\pi^0)$ Γ_{33}/Γ_{141}

VALUE (%)	EVTS	DOCUMENT ID		TECN	COMMENT
2.3±1.1±0.7	2K	[1] LEES	17C	BABR	$J/\psi \to K^+K^-\pi^0$

[1] From a Dalitz plot analysis in an isobar model.

$\Gamma(K^*(1410)\overline{K}+\text{c.c.} \to K^0_SK^\pm\pi^\mp)/\Gamma(K^0_SK^\pm\pi^\mp)$ Γ_{34}/Γ_{142}

VALUE (%)	EVTS	DOCUMENT ID		TECN	COMMENT
1.5±0.5±0.9	4K	[1] LEES	17C	BABR	$J/\psi \to K^0_SK^\pm\pi^\mp$

[1] From a Dalitz plot analysis in an isobar model.

$\Gamma(K_2^*(1430)\overline{K}+\text{c.c.} \to K^\pm K^\mp\pi^0)/\Gamma(K^+K^-\pi^0)$ Γ_{36}/Γ_{141}

VALUE (%)	EVTS	DOCUMENT ID		TECN	COMMENT
3.5±1.3±0.9	2K	[1] LEES	17C	BABR	$J/\psi \to K^+K^-\pi^0$

[1] From a Dalitz plot analysis in an isobar model.

$\Gamma(K_2^*(1430)\overline{K}+\text{c.c.} \to K^0_SK^\pm\pi^\mp)/\Gamma(K^0_SK^\pm\pi^\mp)$ Γ_{37}/Γ_{142}

VALUE (%)	EVTS	DOCUMENT ID		TECN	COMMENT
7.1±1.3±1.2	4K	[1] LEES	17C	BABR	$J/\psi \to K^0_SK^\pm\pi^\mp$

[1] From a Dalitz plot analysis in an isobar model.

$\Gamma(\omega\pi^0\pi^0)/\Gamma_{\text{total}}$ Γ_{54}/Γ

VALUE (units 10^{-3})	EVTS	DOCUMENT ID		TECN	COMMENT
3.4±0.3±0.7	509	AUGUSTIN	89	DM2	$J/\psi \to \pi^+\pi^-3\pi^0$

$\Gamma(b_1(1235)^\pm\pi^\mp)/\Gamma_{\text{total}}$ Γ_{55}/Γ

VALUE (10^{-4})	EVTS	DOCUMENT ID		TECN	COMMENT
30±5 OUR AVERAGE					
31±6	4600	AUGUSTIN	89	DM2	$J/\psi \to 2(\pi^+\pi^-)\pi^0$
29±7	87	BURMESTER	77D	PLUT	e^+e^-

$\Gamma(\omega K^\pm K^0_S\pi^\mp)/\Gamma_{\text{total}}$ Γ_{56}/Γ

VALUE (units 10^{-4})	EVTS	DOCUMENT ID		TECN	COMMENT
34 ±5 OUR AVERAGE					
37.7±0.8±5.8	1972±41	ABLIKIM	08E	BES2	$e^+e^- \to J/\psi$
29.5±1.4±7.0	879 ± 41	BECKER	87	MRK3	$e^+e^- \to$ hadrons

$\Gamma(b_1(1235)^0\pi^0)/\Gamma_{\text{total}}$ Γ_{57}/Γ

VALUE (units 10^{-4})	EVTS	DOCUMENT ID		TECN	COMMENT
23±3±5	229	AUGUSTIN	89	DM2	e^+e^-

$\Gamma(\eta K^\pm K^0_S\pi^\mp)/\Gamma_{\text{total}}$ Γ_{58}/Γ

VALUE (units 10^{-4})	EVTS	DOCUMENT ID		TECN	COMMENT
21.8±2.2±3.4	232 ± 23	ABLIKIM	08E	BES2	$e^+e^- \to J/\psi$

$\Gamma(\phi K^*(892)\overline{K}+\text{c.c.})/\Gamma_{\text{total}}$ Γ_{59}/Γ

VALUE (units 10^{-4})	EVTS	DOCUMENT ID		TECN	COMMENT
21.8±2.3 OUR AVERAGE					
20.8±2.7±3.9	195 ± 25	ABLIKIM	08E	BES2	$J/\psi \to \phi K^0_S K^\pm\pi^\mp$
29.6±3.7±4.7	238 ± 30	ABLIKIM	08E	BES2	$J/\psi \to \phi K^+K^-\pi^0$
20.7±2.4±3.0		FALVARD	88	DM2	$J/\psi \to$ hadrons
20 ±3 ±3	155 ± 20	BECKER	87	MRK3	$e^+e^- \to$ hadrons

$\Gamma(\omega K\overline{K})/\Gamma_{\text{total}}$ Γ_{60}/Γ

VALUE (units 10^{-4})	EVTS	DOCUMENT ID		TECN	COMMENT
17.0± 3.2 OUR AVERAGE					
13.6± 5.0±1.0	24	[1] AUBERT	07AU	BABR	10.6 $e^+e^- \to \omega K^+K^-\gamma$
19.8± 2.1±3.9		[2] FALVARD	88	DM2	$J/\psi \to$ hadrons
16 ±10	22	FELDMAN	77	MRK1	e^+e^-

[1] AUBERT 07AU quotes $\Gamma^{J/\psi}_{ee}\cdot B(J/\psi \to \omega K^+K^-)\cdot B(\eta \to 3\pi) = 3.3 \pm 1.3 \pm 0.2$ eV.
[2] Addition of ωK^+K^- and $\omega K^0\overline{K}^0$ branching ratios.

$\Gamma(\omega f_0(1710) \to \omega K\overline{K})/\Gamma_{\text{total}}$ Γ_{61}/Γ

VALUE (10^{-4})	DOCUMENT ID		TECN	COMMENT
4.8±1.1±0.3	[1,2] FALVARD	88	DM2	$J/\psi \to$ hadrons

[1] Includes unknown branching fraction $f_0(1710) \to K\overline{K}$.
[2] Addition of $f_0(1710) \to K^+K^-$ and $f_0(1710) \to K^0\overline{K}^0$ branching ratios.

$\Gamma(\phi 2(\pi^+\pi^-))/\Gamma_{\text{total}}$ Γ_{62}/Γ

VALUE (units 10^{-4})	EVTS	DOCUMENT ID		TECN	COMMENT
16.6±2.3 OUR AVERAGE					
17.3±3.3±1.2	35	[1] AUBERT	06D	BABR	10.6 $e^+e^- \to \phi 2(\pi^+\pi^-)\gamma$
16.0±1.0±3.0		FALVARD	88	DM2	$J/\psi \to$ hadrons

[1] Using $\Gamma(J/\psi \to e^+e^-) = 5.52 \pm 0.14 \pm 0.04$ keV.

$\Gamma(\Delta(1232)^{++}\overline{p}\pi^-)/\Gamma_{\text{total}}$ Γ_{63}/Γ

VALUE (units 10^{-3})	EVTS	DOCUMENT ID		TECN	COMMENT
1.58±0.23±0.40	332	EATON	84	MRK2	e^+e^-

$\Gamma(\omega\eta)/\Gamma_{\text{total}}$ Γ_{64}/Γ

VALUE (units 10^{-3})	EVTS	DOCUMENT ID		TECN	COMMENT
1.74 ±0.20 OUR AVERAGE		Error includes scale factor of 1.6. See the ideogram below.			
2.352±0.273	5k	[1] ABLIKIM	06F	BES2	$J/\psi \to \omega\eta$
1.44 ±0.40 ±0.14	13	[2] AUBERT	06D	BABR	10.6 $e^+e^- \to \omega\eta\gamma$
1.43 ±0.10 ±0.21	378	JOUSSET	90	DM2	$J/\psi \to$ hadrons
1.71 ±0.08 ±0.20		COFFMAN	88	MRK3	$e^+e^- \to 3\pi\eta$

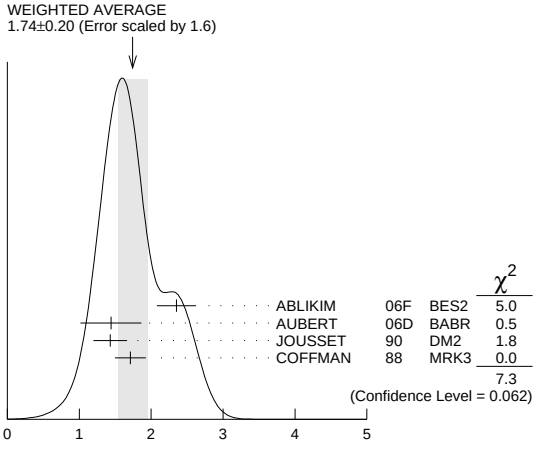

[1] Using $B(\eta \to 2\gamma) = (39.43 \pm 0.26)\%$, $B(\eta \to \pi^+\pi^-\pi^0) = 22.6 \pm 0.4\%$, $B(\eta \to \pi^+\pi^-\gamma) = 4.68 \pm 0.11\%$, and $B(\omega \to \pi^+\pi^-\pi^0) = (89.1 \pm 0.7)\%$.
[2] Using $\Gamma(J/\psi \to e^+e^-) = 5.52 \pm 0.14 \pm 0.04$ keV.

$\Gamma(\phi K\overline{K})/\Gamma_{\text{total}}$ Γ_{65}/Γ

VALUE (units 10^{-4})	EVTS	DOCUMENT ID		TECN	COMMENT
17.7± 1.6 OUR AVERAGE	Error includes scale factor of 1.3. See the ideogram below.				
16.6± 1.9±1.2	163 ± 19	LEES	12F	BABR	10.6 $e^+e^- \to 2(K^+K^-)\gamma$
21.4± 0.4±2.2		ABLIKIM	05	BES2	$J/\psi \to \phi\pi^+\pi^-$
48 $^{+20}_{-16}$ ±6	$9.0^{+3.7}_{-3.0}$	[1,2] HUANG	03	BELL	$B^+ \to (\phi K^+K^-)\ K^+$
14.6± 0.8±2.1		[3] FALVARD	88	DM2	$J/\psi \to$ hadrons
18 ± 8	14	FELDMAN	77	MRK1	e^+e^-

[1] We have multiplied K^+K^- measurement by 2 to obtain $K\overline{K}$.
[2] Using $B(B^+ \to J/\psi K^+) = (1.01 \pm 0.05) \times 10^{-3}$.
[3] Addition of ϕK^+K^- and $\phi K^0\overline{K}^0$ branching ratios.

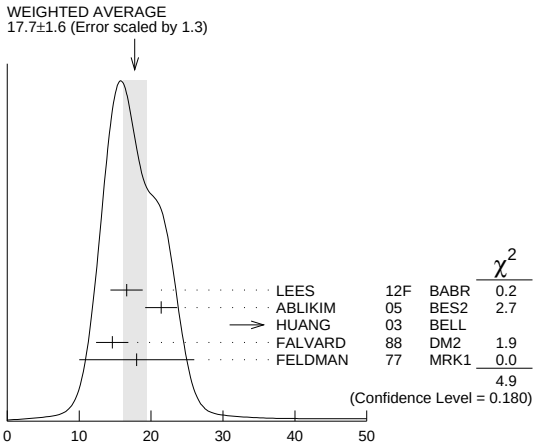

$\Gamma(\phi f_0(1710) \to \phi K\overline{K})/\Gamma_{total}$ Γ_{67}/Γ

VALUE (units 10^{-4})		DOCUMENT ID		TECN	COMMENT
3.6±0.2±0.6	[1,2]	FALVARD	88	DM2	$J/\psi \to$ hadrons

[1] Including interference with $f_2'(1525)$.
[2] Includes unknown branching fraction $f_0(1710) \to K\overline{K}$.

$\Gamma(\phi f_2(1270))/\Gamma_{total}$ Γ_{69}/Γ

VALUE (units 10^{-3})	CL%	EVTS	DOCUMENT ID		TECN	COMMENT
• • • We do not use the following data for averages, fits, limits, etc. • • •						
0.72±0.13±0.02		44 ± 7	[1,2] AUBERT	07AK	BABR	10.6 $e^+e^- \to \pi^+\pi^-K^+K^-\gamma$
< 0.45	90		FALVARD	88	DM2	$J/\psi \to$ hadrons
< 0.37	90		VANNUCCI	77	MRK1	$e^+e^- \to \pi^+\pi^-K^+K^-$

[1] Using $B(f_2(1270) \to \pi\pi) = (84.8^{+2.4}_{-1.2})\%$
[2] Superseded by LEES 12F. AUBERT 07AK reports $[\Gamma(J/\psi(1S) \to \phi f_2(1270))/\Gamma_{total}] \times [\Gamma(J/\psi(1S) \to e^+e^-)] = (4.02 \pm 0.65 \pm 0.33) \times 10^{-3}$ keV which we divide by our best value $\Gamma(J/\psi(1S) \to e^+e^-) = 5.55 \pm 0.14 \pm 0.02$ keV. Our first error is their experiment's error and our second error is the systematic error from using our best value.

$\Gamma(\Delta(1232)^{++}\overline{\Delta}(1232)^{--})/\Gamma_{total}$ Γ_{70}/Γ

VALUE (units 10^{-3})	EVTS	DOCUMENT ID		TECN	COMMENT
1.10±0.09±0.28	233	EATON	84	MRK2	e^+e^-

$\Gamma(\Sigma(1385)^-\overline{\Sigma}(1385)^+ \text{(or c.c.)})/\Gamma_{total}$ Γ_{71}/Γ

VALUE (units 10^{-3})	EVTS	DOCUMENT ID		TECN	COMMENT
1.16 ±0.05 OUR AVERAGE					
1.096±0.012±0.071	43K	ABLIKIM	16L	BES3	$J/\psi \to \Sigma(1385)^-\overline{\Sigma}(1385)^+$
1.258±0.014±0.078	53k	ABLIKIM	16L	BES3	$J/\psi \to \Sigma(1385)^+\overline{\Sigma}(1385)^-$
1.23 ±0.07 ±0.30	0.8k	ABLIKIM	12P	BES2	$J/\psi \to \Sigma(1385)^-\overline{\Sigma}(1385)^+$
1.50 ±0.08 ±0.38	1k	ABLIKIM	12P	BES2	$J/\psi \to \Sigma(1385)^+\overline{\Sigma}(1385)^-$
1.00 ±0.04 ±0.21	0.6k	HENRARD	87	DM2	$e^+e^- \to \Sigma^{*-}$
1.19 ±0.04 ±0.25	0.7k	HENRARD	87	DM2	$e^+e^- \to \Sigma^{*+}$
0.86 ±0.18 ±0.22	56	EATON	84	MRK2	$e^+e^- \to \Sigma^{*-}$
1.03 ±0.24 ±0.25	68	EATON	84	MRK2	$e^+e^- \to \Sigma^{*+}$

$\Gamma(\Sigma(1385)^0\overline{\Sigma}(1385)^0)/\Gamma_{total}$ Γ_{72}/Γ

VALUE (units 10^{-3})	EVTS	DOCUMENT ID		TECN	COMMENT
1.071±0.009±0.082	103k	ABLIKIM	17E	BES3	$e^+e^- \to J/\psi \to$ hadrons

$\Gamma(\phi f_2'(1525))/\Gamma_{total}$ Γ_{74}/Γ

VALUE (units 10^{-4})	EVTS	DOCUMENT ID		TECN	COMMENT
8 ±4 OUR AVERAGE Error includes scale factor of 2.7.					
12.3±0.6±2.0		[1,2] FALVARD	88	DM2	$J/\psi \to$ hadrons
4.8±1.8	46	[1] GIDAL	81	MRK2	$J/\psi \to K^+K^-K^+K^-$

[1] Re-evaluated using $B(f_2'(1525) \to K\overline{K}) = 0.713$.
[2] Including interference with $f_0(1710)$.

$\Gamma(\phi\pi^+\pi^-)/\Gamma_{total}$ Γ_{75}/Γ

VALUE (units 10^{-3})	EVTS	DOCUMENT ID		TECN	COMMENT
0.87±0.09 OUR AVERAGE Error includes scale factor of 1.4. See the ideogram below.					
0.81±0.08±0.03	181	LEES	12F	BABR	10.6 $e^+e^- \to K^+K^-\pi^+\pi^-\gamma$
1.09±0.02±0.13		ABLIKIM	05	BES2	$J/\psi \to \phi\pi^+\pi^-$
0.78±0.03±0.12		FALVARD	88	DM2	$J/\psi \to$ hadrons
2.1 ±0.9	23	FELDMAN	77	MRK1	e^+e^-
• • • We do not use the following data for averages, fits, limits, etc. • • •					
0.96±0.13	103	[1] AUBERT,BE	06D	BABR	10.6 $e^+e^- \to K^+K^-\pi^+\pi^-\gamma$

[1] Superseded by LEES 12F. Derived by us. AUBERT,BE 06D measures $\Gamma(J/\psi \to e^+e^-) \times B(J/\psi \to \phi\pi^+\pi^-) \times B(\phi \to K^+K^-) = (2.61 \pm 0.30 \pm 0.18)$ eV

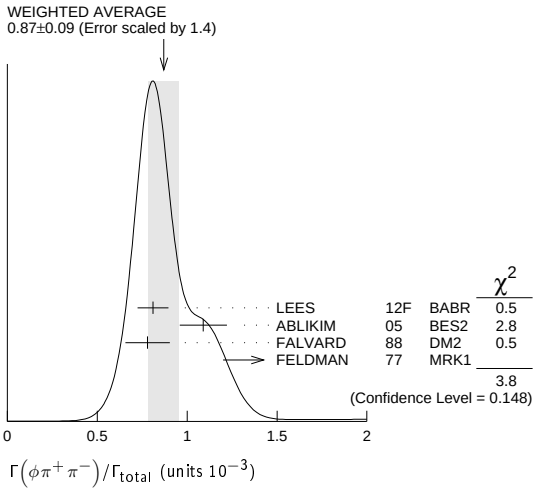

$\Gamma(\phi\pi^0\pi^0)/\Gamma_{total}$ Γ_{76}/Γ

VALUE (units 10^{-3})	EVTS	DOCUMENT ID		TECN	COMMENT
• • • We do not use the following data for averages, fits, limits, etc. • • •					
0.56±0.16	23	[1] AUBERT,BE	06D	BABR	10.6 $e^+e^- \to K^+K^-\pi^0\pi^0\gamma$

[1] Superseded by LEES 12F. Derived by us. AUBERT,BE 06D measures $\Gamma(J/\psi \to e^+e^-) \times B(J/\psi \to \phi\pi^0\pi^0) \times B(\phi \to K^+K^-) = (1.54 \pm 0.40 \pm 0.16)$ eV

$\Gamma(\phi K^\pm K_S^0\pi^\mp)/\Gamma_{total}$ Γ_{77}/Γ

VALUE (units 10^{-4})	EVTS	DOCUMENT ID		TECN	COMMENT
7.2±0.8 OUR AVERAGE					
7.4±0.6±1.4	227 ± 19	ABLIKIM	08E	BES2	$e^+e^- \to J/\psi$
7.4±0.9±1.1		FALVARD	88	DM2	$J/\psi \to$ hadrons
7 ±0.6±1.0	163 ± 15	BECKER	87	MRK3	$e^+e^- \to$ hadrons

$\Gamma(\omega f_1(1420))/\Gamma_{total}$ Γ_{78}/Γ

VALUE (units 10^{-4})	EVTS	DOCUMENT ID	TECN	COMMENT
$\mathbf{6.8^{+1.9}_{-1.6}\pm1.7}$	111^{+31}_{-26}	BECKER 87	MRK3	$e^+e^- \to$ hadrons

$\Gamma(\phi\eta)/\Gamma_{total}$ Γ_{79}/Γ

VALUE (units 10^{-3})	EVTS	DOCUMENT ID		TECN	COMMENT
0.75 ±0.08 OUR AVERAGE Error includes scale factor of 1.5. See the ideogram below.					
1.4 ±0.6 ±0.1	6	[1] AUBERT	07AU	BABR	10.6 $e^+e^- \to \phi\eta\gamma$
0.898±0.024±0.089		ABLIKIM	05B	BES2	$e^+e^- \to J/\psi \to$ hadr
0.64 ±0.04 ±0.11	346	JOUSSET	90	DM2	$J/\psi \to$ hadrons
0.661±0.045±0.078		COFFMAN	88	MRK3	$e^+e^- \to K^+K^-\eta$

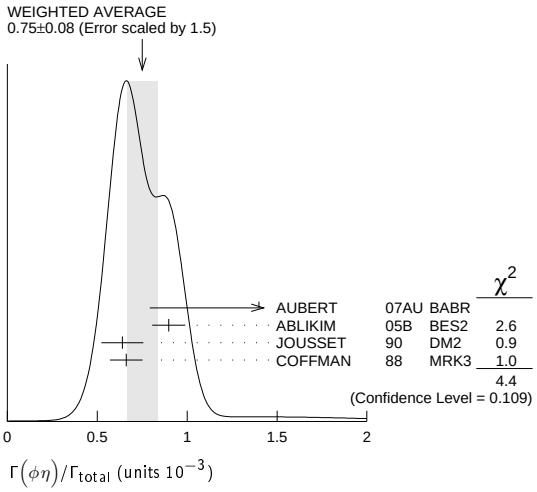

[1] AUBERT 07AU quotes $\Gamma_{ee}^{J/\psi} \cdot B(J/\psi \to \phi\eta) \cdot B(\phi \to K^+K^-) \cdot B(\eta \to \gamma\gamma) = 0.84 \pm 0.37 \pm 0.05$ eV.

$\Gamma(\Xi^0\overline{\Xi}^0)/\Gamma_{total}$ Γ_{80}/Γ

VALUE (units 10^{-3})	EVTS	DOCUMENT ID		TECN	COMMENT
1.17 ±0.04 OUR AVERAGE					
1.165±0.004±0.043	135K	ABLIKIM	17E	BES3	$e^+e^- \to J/\psi \to$ hadrons
1.20 ±0.12 ±0.21	206	ABLIKIM	08O	BES2	$e^+e^- \to J/\psi$

$\Gamma(\Xi(1530)^-\overline{\Xi}^+)/\Gamma_{total}$ Γ_{81}/Γ

VALUE (units 10^{-3})	EVTS	DOCUMENT ID		TECN	COMMENT
0.59±0.09±0.12	75 ± 11	HENRARD	87	DM2	e^+e^-

$\Gamma(pK^-\overline{\Sigma}(1385)^0)/\Gamma_{total}$ Γ_{82}/Γ

VALUE (units 10^{-3})	EVTS	DOCUMENT ID		TECN	COMMENT
0.51±0.26±0.18	89	EATON	84	MRK2	e^+e^-

$\Gamma(\omega\pi^0)/\Gamma_{total}$ Γ_{83}/Γ

VALUE (units 10^{-3})	EVTS	DOCUMENT ID		TECN	COMMENT
0.45 ±0.05 OUR AVERAGE		Error includes scale factor of 1.4. See the ideogram below.			
0.538±0.012±0.065	2090	[1] ABLIKIM	06F	BES2	$J/\psi \to \omega\pi^0$
0.360±0.028±0.054	222	JOUSSET	90	DM2	$J/\psi \to$ hadrons
0.482±0.019±0.064		COFFMAN	88	MRK3	$e^+e^- \to \pi^0\pi^+\pi^-\pi^0$

[1] Using B($\omega \to \pi^+\pi^-\pi^0$) = (89.1 ± 0.7)%.

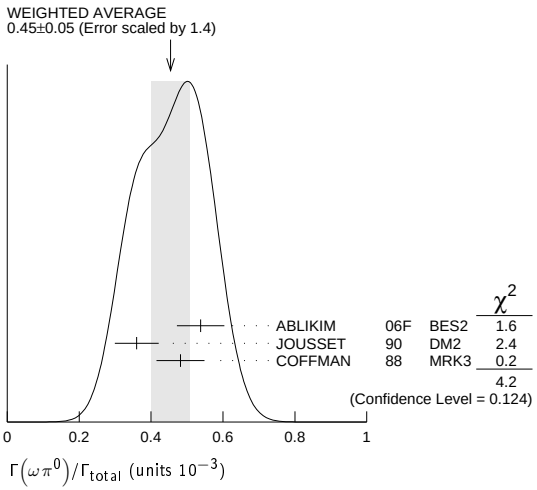

$\Gamma(\omega\pi^0 \to \pi^+\pi^-\pi^0)/\Gamma(\pi^+\pi^-\pi^0)$ Γ_{84}/Γ_{129}

VALUE (units 10^{-4})	EVTS	DOCUMENT ID		TECN	COMMENT
8±3±2	20K	[1] LEES	17C	BABR	$J/\psi \to \pi^+\pi^-\pi^0$

[1] From a Dalitz plot analysis in an isobar model and significance 4.9 σ.

$\Gamma(\phi\eta'(958))/\Gamma_{total}$ Γ_{85}/Γ

VALUE (units 10^{-4})	CL%	EVTS	DOCUMENT ID		TECN	COMMENT
4.6 ±0.5 OUR AVERAGE			Error includes scale factor of 2.2. See the ideogram below.			
5.10±0.03±0.32		31k	ABLIKIM	16M	BES3	$e^+e^- \to J/\psi \to$ hadrons
5.46±0.31±0.56			ABLIKIM	05B	BES2	$e^+e^- \to J/\psi \to$ hadrons
4.1 ±0.3 ±0.8		167	JOUSSET	90	DM2	$J/\psi \to$ hadrons
3.08±0.34±0.36			COFFMAN	88	MRK3	$e^+e^- \to K^+K^-\eta'$
• • • We do not use the following data for averages, fits, limits, etc. • • •						
< 13	90		VANNUCCI	77	MRK1	e^+e^-

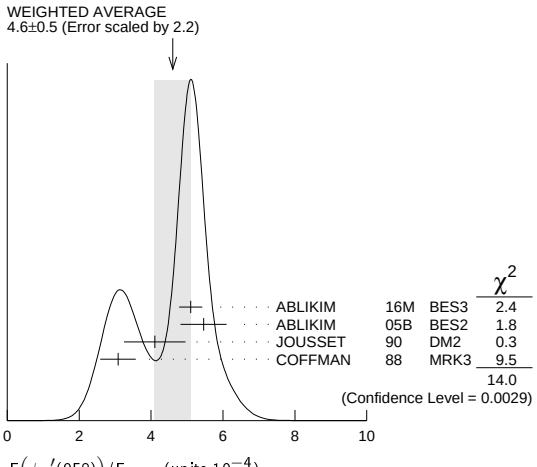

$\Gamma(\phi f_0(980))/\Gamma_{total}$ Γ_{86}/Γ

VALUE (units 10^{-4})	EVTS	DOCUMENT ID		TECN	COMMENT
3.2±0.9 OUR AVERAGE		Error includes scale factor of 1.9.			
4.6±0.4±0.8		[1] FALVARD	88	DM2	$J/\psi \to$ hadrons
2.6±0.6	50	[1] GIDAL	81	MRK2	$J/\psi \to K^+K^-K^+K^-$

[1] Assuming B($f_0(980) \to \pi\pi$) = 0.78.

$\Gamma(\phi f_0(980) \to \phi\pi^+\pi^-)/\Gamma_{total}$ Γ_{87}/Γ

VALUE (units 10^{-3})	EVTS	DOCUMENT ID		TECN	COMMENT
• • • We do not use the following data for averages, fits, limits, etc. • • •					
0.182±0.042±0.005	19.5 ±4.5	[1,2] AUBERT	07AK	BABR	10.6 $e^+e^- \to \pi^+\pi^-K^+K^-\gamma$

[1] Using B($\phi \to K^+K^-$) = (49.3 ± 0.6)%.

[2] Superseded by LEES 12F. AUBERT 07AK reports $[\Gamma(J/\psi(1S) \to \phi f_0(980) \to \phi\pi^+\pi^-)/\Gamma_{total}] \times [\Gamma(J/\psi(1S) \to e^+e^-)] = (1.01 \pm 0.22 \pm 0.08) \times 10^{-3}$ keV which we divide by our best value $\Gamma(J/\psi(1S) \to e^+e^-) = 5.55 \pm 0.14 \pm 0.02$ keV. Our first error is their experiment's error and our second error is the systematic error from using our best value.

$\Gamma(\phi f_0(980) \to \phi\pi^0\pi^0)/\Gamma_{total}$ Γ_{88}/Γ

VALUE (units 10^{-3})	EVTS	DOCUMENT ID		TECN	COMMENT
• • • We do not use the following data for averages, fits, limits, etc. • • •					
0.171±0.073±0.004	7.0 ± 2.8	[1,2] AUBERT	07AK	BABR	10.6 $e^+e^- \to \pi^0\pi^0K^+K^-\gamma$

[1] Using B($\phi \to K^+K^-$) = (49.3 ± 0.6)%.

[2] Superseded by LEES 12F. AUBERT 07AK reports $[\Gamma(J/\psi(1S) \to \phi f_0(980) \to \phi\pi^0\pi^0)/\Gamma_{total}] \times [\Gamma(J/\psi(1S) \to e^+e^-)] = (0.95 \pm 0.39 \pm 0.10) \times 10^{-3}$ keV which we divide by our best value $\Gamma(J/\psi(1S) \to e^+e^-) = 5.55 \pm 0.14 \pm 0.02$ keV. Our first error is their experiment's error and our second error is the systematic error from using our best value.

$\Gamma(\phi\pi^0 f_0(980) \to \phi\pi^0\pi^+\pi^-)/\Gamma_{total}$ Γ_{89}/Γ

VALUE (units 10^{-6})	EVTS	DOCUMENT ID		TECN	COMMENT
4.50±0.80±0.61	355	ABLIKIM	15P	BES3	$J/\psi \to K^+K^-3\pi$

$\Gamma(\phi\pi^0 f_0(980) \to \phi\pi^0 p^0\pi^0)/\Gamma_{total}$ Γ_{90}/Γ

VALUE (units 10^{-6})	EVTS	DOCUMENT ID		TECN	COMMENT
1.67±0.50±0.24	70	ABLIKIM	15P	BES3	$J/\psi \to K^+K^-3\pi$

$\Gamma(\eta\phi f_0(980) \to \eta\phi\pi^+\pi^-)/\Gamma_{total}$ Γ_{91}/Γ

VALUE (units 10^{-4})	EVTS	DOCUMENT ID		TECN	COMMENT
3.23±0.75±0.73	52	ABLIKIM	08F	BES	$J/\psi \to \eta\phi f_0(980)$

$\Gamma(\phi a_0(980)^0 \to \phi\eta\pi^0)/\Gamma_{total}$ Γ_{92}/Γ

VALUE (units 10^{-6})	DOCUMENT ID		TECN	COMMENT
5.0±2.7±2.5	[1] ABLIKIM	11D	BES3	$J/\psi \to \phi\eta\pi^0$

[1] Assuming $a_0(980) - f_0(980)$ mixing and isospin breaking via γ^* and K^*K loops.

$\Gamma(\Xi(1530)^0\overline{\Xi}^0)/\Gamma_{total}$ Γ_{93}/Γ

VALUE (units 10^{-3})	EVTS	DOCUMENT ID		TECN	COMMENT
0.32±0.12±0.07	24 ± 9	HENRARD	87	DM2	e^+e^-

$\Gamma(\Sigma(1385)^-\overline{\Sigma}^+ \text{(or c.c.)})/\Gamma_{total}$ Γ_{94}/Γ

VALUE (units 10^{-3})	EVTS	DOCUMENT ID		TECN	COMMENT
0.31±0.05 OUR AVERAGE					
0.30±0.03±0.07	74 ± 8	HENRARD	87	DM2	$e^+e^- \to \Sigma^{*-}$
0.34±0.04±0.07	77 ± 9	HENRARD	87	DM2	$e^+e^- \to \Sigma^{*+}$
0.29±0.11±0.10	26	EATON	84	MRK2	$e^+e^- \to \Sigma^{*-}$
0.31±0.11±0.11	28	EATON	84	MRK2	$e^+e^- \to \Sigma^{*+}$

$\Gamma(\phi f_1(1285))/\Gamma_{total}$ Γ_{95}/Γ

VALUE (units 10^{-4})	EVTS	DOCUMENT ID		TECN	COMMENT
2.6±0.5 OUR AVERAGE					
3.4±1.8±1.5	1.1k	[1] ABLIKIM	15H	BES3	$e^+e^- \to J/\psi \to \phi\eta\pi^+\pi^-$
3.2±0.6±0.4		JOUSSET	90	DM2	$J/\psi \to \phi 2(\pi^+\pi^-)$
2.1±0.5±0.4	25	[2] JOUSSET	90	DM2	$J/\psi \to \phi\eta\pi^+\pi^-$
• • • We do not use the following data for averages, fits, limits, etc. • • •					
0.6±0.2±0.1	16	BECKER	87	MRK3	$J/\psi \to \phi K\overline{K}\pi$

[1] ABLIKIM 15H reports $[\Gamma(J/\psi(1S) \to \phi f_1(1285))/\Gamma_{total}] \times [B(f_1(1285) \to \eta\pi^+\pi^-)] = (1.20 \pm 0.6 \pm 0.14) \times 10^{-4}$ which we divide by our best value $B(f_1(1285) \to \eta\pi^+\pi^-) = (35 \pm 15) \times 10^{-2}$. Our first error is their experiment's error and our second error is the systematic error from using our best value.

[2] We attribute to the $f_1(1285)$ the signal observed in the $\pi^+\pi^-\eta$ invariant mass distribution at 1297 MeV.

$\Gamma(\phi f_1(1285) \to \phi\pi^0 f_0(980) \to \phi\pi^0\pi^+\pi^-)/\Gamma_{total}$ Γ_{96}/Γ

VALUE (units 10^{-7})	EVTS	DOCUMENT ID		TECN	COMMENT
9.36±2.31±1.54	78	ABLIKIM	15P	BES3	$J/\psi \to K^+K^-3\pi$

Meson Particle Listings

$J/\psi(1S)$

$\Gamma(\phi f_1(1285) \to \phi\pi^0 f_0(980) \to \phi\pi^0\pi^0\pi^0)/\Gamma_{total}$ Γ_{97}/Γ

VALUE (units 10^{-7})	EVTS	DOCUMENT ID		TECN	COMMENT
2.08±1.63±1.47	9	ABLIKIM	15P	BES3	$J/\psi \to K^+K^-3\pi$

$\Gamma(\eta\pi^+\pi^-)/\Gamma_{total}$ Γ_{98}/Γ

VALUE (units 10^{-3})	EVTS	DOCUMENT ID		TECN	COMMENT
0.40±0.17±0.03	9	[1] AUBERT	07AU	BABR	$10.6\ e^+e^- \to \eta\pi^+\pi^-\gamma$

[1] AUBERT 07AU quotes $\Gamma_{ee}^{J/\psi}\cdot B(J/\psi \to \eta\pi^+\pi^-)\cdot B(\eta \to 3\pi) = 0.51 \pm 0.22 \pm 0.03$ eV.

$\Gamma(\eta\rho)/\Gamma_{total}$ Γ_{99}/Γ

VALUE (units 10^{-3})	EVTS	DOCUMENT ID		TECN	COMMENT
0.193±0.023 OUR AVERAGE					
0.194±0.017±0.029	299	JOUSSET	90	DM2	$J/\psi \to$ hadrons
0.193±0.013±0.029		COFFMAN	88	MRK3	$e^+e^- \to \pi^+\pi^-\eta$

$\Gamma(\omega\eta'(958))/\Gamma_{total}$ Γ_{100}/Γ

VALUE (units 10^{-4})	EVTS	DOCUMENT ID		TECN	COMMENT
1.89±0.18 OUR AVERAGE					
2.08±0.30±0.14	137	[1] ABLIKIM	17AK	BES3	$J/\psi \to \pi^+\pi^-\eta'$
2.26±0.43	218	[2] ABLIKIM	06F	BES2	$J/\psi \to \omega\eta'$
$1.8\ ^{+1.0}_{-0.8}\ \pm 0.3$	6	JOUSSET	90	DM2	$J/\psi \to$ hadrons
1.66±0.17±0.19		COFFMAN	88	MRK3	$e^+e^- \to 3\pi\eta'$

[1] From a partial wave analysis of the decay $J/\psi \to \pi^+\pi^-\eta'$.
[2] Using $B(\eta' \to \pi^+\pi^-\eta) = (44.3 \pm 1.5)\%$, $B(\eta' \to \pi^+\pi^-\gamma) = 29.5 \pm 1.0\%$, $B(\eta \to 2\gamma) = 39.43 \pm 0.26\%$, and $B(\omega \to \pi^+\pi^-\pi^0) = (89.1 \pm 0.7)\%$.

$\Gamma(\omega f_0(980))/\Gamma_{total}$ Γ_{101}/Γ

VALUE (units 10^{-4})	DOCUMENT ID		TECN	COMMENT
1.41±0.27±0.47	[1] AUGUSTIN	89	DM2	$J/\psi \to 2(\pi^+\pi^-)\pi^0$

[1] Assuming $B(f_0(980) \to \pi\pi) = 0.78$.

$\Gamma(\rho\eta'(958))/\Gamma_{total}$ Γ_{102}/Γ

VALUE (units 10^{-5})	EVTS	DOCUMENT ID		TECN	COMMENT
8.1 ±0.8 OUR AVERAGE		Error includes scale factor of 1.6.			
7.90±0.19±0.49	3476	[1] ABLIKIM	17AK	BES3	$J/\psi \to \pi^+\pi^-\eta'$
8.3 ±3.0 ±1.2	19	JOUSSET	90	DM2	$J/\psi \to$ hadrons
11.4 ±1.4 ±1.6		COFFMAN	88	MRK3	$J/\psi \to \pi^+\pi^-\eta'$

[1] From a partial wave analysis of the decay $J/\psi \to \pi^+\pi^-\eta'$.

$\Gamma(a_2(1320)^\pm\pi^\mp)/\Gamma_{total}$ Γ_{103}/Γ

VALUE (units 10^{-4})	CL%	DOCUMENT ID		TECN	COMMENT
<43	90	BRAUNSCH...	76	DASP	e^+e^-

$\Gamma(K\overline{K}_2^*(1430) + \text{c.c.})/\Gamma_{total}$ Γ_{104}/Γ

VALUE (units 10^{-4})	CL%	DOCUMENT ID		TECN	COMMENT
<40	90	VANNUCCI	77	MRK1	$e^+e^- \to K^0\overline{K}_2^{*0}$
• • • We do not use the following data for averages, fits, limits, etc. • • •					
<66	90	BRAUNSCH...	76	DASP	$e^+e^- \to K^\pm\overline{K}_2^{*\mp}$

$\Gamma(K_1(1270)^\pm K^\mp)/\Gamma_{total}$ Γ_{105}/Γ

VALUE (units 10^{-3})	CL%	DOCUMENT ID		TECN	COMMENT
<3.0	90	[1] BAI	99C	BES	e^+e^-

[1] Assuming $B(K_1(1270) \to K\rho) = 0.42 \pm 0.06$

$\Gamma(K_2^*(1430)^0\overline{K}_2^*(1430)^0)/\Gamma_{total}$ Γ_{108}/Γ

VALUE (units 10^{-4})	CL%	DOCUMENT ID		TECN	COMMENT
<29	90	VANNUCCI	77	MRK1	$e^+e^- \to \pi^+\pi^- K^+K^-$

$\Gamma(\phi\pi^0)/\Gamma_{total}$ Γ_{109}/Γ

The two different fit values of ABLIKIM 15K below have the same statistical significance of 6.4 σ and cannot be distinguished at this moment.

VALUE (units 10^{-6})	CL%	EVTS	DOCUMENT ID		TECN	COMMENT
2.94 ±0.16 ±0.16		0.8k	[1] ABLIKIM	15K	BES3	$e^+e^- \to J/\psi \to K^+K^-\gamma\gamma$
0.124±0.033±0.030		35 ± 9	[2] ABLIKIM	15K	BES3	$e^+e^- \to J/\psi \to K^+K^-\gamma\gamma$
• • • We do not use the following data for averages, fits, limits, etc. • • •						
<6.4	90		[3] ABLIKIM	05B	BES2	$e^+e^- \to J/\psi \to \phi\gamma\gamma$
<6.8	90		COFFMAN	88	MRK3	$e^+e^- \to K^+K^-\pi^0$

[1] Corresponding to one of the two fit solutions with $\delta = (-95.9 \pm 1.5)^\circ$ for the phase angle between the resonant $J/\psi \to \phi\pi^0$ and non-phi $J/\psi \to K^+K^-\pi^0$ contributions.
[2] Corresponding to one of the two fit solutions with $\delta = (-152.1 \pm 7.7)^\circ$ for the phase angle between the resonant $J/\psi \to \phi\pi^0$ and non-phi $J/\psi \to K^+K^-\pi^0$ contributions.
[3] Superseded by ABLIKIM 15K.

$\Gamma(\phi\eta(1405) \to \phi\eta\pi^+\pi^-)/\Gamma_{total}$ Γ_{110}/Γ

VALUE (units 10^{-5})	CL%	EVTS	DOCUMENT ID		TECN	COMMENT
2.01±0.58±0.82		172	[1] ABLIKIM	15H	BES3	$e^+e^- \to J/\psi \to \phi\eta\pi^+\pi^-$
• • • We do not use the following data for averages, fits, limits, etc. • • •						
< 17	90		[2] FALVARD	88	DM2	$J/\psi \to$ hadrons

[1] With 3.6 σ significance.
[2] Includes unknown branching fraction $\eta(1405) \to \eta\pi\pi$.

$\Gamma(\omega f_2'(1525))/\Gamma_{total}$ Γ_{111}/Γ

VALUE (units 10^{-4})	CL%	DOCUMENT ID		TECN	COMMENT
<2.2	90	[1] VANNUCCI	77	MRK1	$e^+e^- \to \pi^+\pi^-\pi^0 K^+K^-$
• • • We do not use the following data for averages, fits, limits, etc. • • •					
<2.8	90	[1] FALVARD	88	DM2	$J/\psi \to$ hadrons

[1] Re-evaluated assuming $B(f_2'(1525) \to K\overline{K}) = 0.713$.

$\Gamma(\omega X(1835) \to \omega p\overline{p})/\Gamma_{total}$ Γ_{112}/Γ

VALUE (units 10^{-6})	CL%	DOCUMENT ID		TECN	COMMENT
<3.9	95	ABLIKIM	13P	BES3	$J/\psi \to \gamma\pi^0 p\overline{p}$

$\Gamma(\phi X(1835) \to \phi p\overline{p})/\Gamma_{total}$ Γ_{113}/Γ

VALUE	CL%	DOCUMENT ID		TECN	COMMENT
<2.1 × 10^{-7}	90	[1] ABLIKIM	16K	BES3	$J/\psi \to p\overline{p}K_S^0K_L^0$, $p\overline{p}K^+K^-$

[1] Upper limit applies to any $p\overline{p}$ mass enhancement near threshold.

$\Gamma(\phi X(1835) \to \phi\eta\pi^+\pi^-)/\Gamma_{total}$ Γ_{114}/Γ

VALUE	CL%	DOCUMENT ID		TECN	COMMENT
<2.8 × 10^{-4}	90	ABLIKIM	15H	BES3	$e^+e^- \to J/\psi \to \phi\eta\pi^+\pi^-$

$\Gamma(\phi X(1870) \to \phi\eta\pi^+\pi^-)/\Gamma_{total}$ Γ_{115}/Γ

VALUE	CL%	DOCUMENT ID		TECN	COMMENT
<6.13 × 10^{-5}	90	ABLIKIM	15H	BES3	$e^+e^- \to J/\psi \to \phi\eta\pi^+\pi^-$

$\Gamma(\eta\phi(2170) \to \eta\phi f_0(980) \to \eta\phi\pi^+\pi^-)/\Gamma_{total}$ Γ_{116}/Γ

VALUE (units 10^{-4})	EVTS	DOCUMENT ID		TECN	COMMENT
1.20±0.14±0.37	471	ABLIKIM	15H	BES3	$e^+e^- \to J/\psi \to \phi\eta\pi^+\pi^-$

$\Gamma(\eta\phi(2170) \to \eta K^*(892)^0\overline{K}^*(892)^0)/\Gamma_{total}$ Γ_{117}/Γ

VALUE (units 10^{-4})	CL%	DOCUMENT ID		TECN	COMMENT
<2.52	90	ABLIKIM	10C	BES2	$J/\psi \to \eta K^+\pi^- K^-\pi^+$

$\Gamma(\Sigma(1385)^0\overline{\Lambda} + \text{c.c.})/\Gamma_{total}$ Γ_{118}/Γ

VALUE (units 10^{-5})	CL%	DOCUMENT ID		TECN	COMMENT
< 0.82	90	ABLIKIM	13F	BES3	$J/\psi \to p\overline{p}\pi^+\pi^-\gamma\gamma$
• • • We do not use the following data for averages, fits, limits, etc. • • •					
<20	90	HENRARD	87	DM2	e^+e^-

$\Gamma(\Delta(1232)^+\overline{p})/\Gamma_{total}$ Γ_{119}/Γ

VALUE (units 10^{-3})	CL%	DOCUMENT ID		TECN	COMMENT
<0.1	90	HENRARD	87	DM2	e^+e^-

$\Gamma(\Lambda(1520)\overline{\Lambda} + \text{c.c.} \to \gamma\Lambda\overline{\Lambda})/\Gamma_{total}$ Γ_{120}/Γ

VALUE (units 10^{-6})	CL%	DOCUMENT ID		TECN	COMMENT
<4.1	90	ABLIKIM	12B	BES3	$J/\psi \to \Lambda\overline{\Lambda}\gamma$

$\Gamma(\Theta(1540)\overline{\Theta}(1540) \to K_S^0 pK^-\overline{n} + \text{c.c.})/\Gamma_{total}$ Γ_{121}/Γ

VALUE (units 10^{-5})	CL%	DOCUMENT ID		TECN	COMMENT
<1.1	90	BAI	04G	BES2	e^+e^-

$\Gamma(\Theta(1540)K^-\overline{n} \to K_S^0 pK^-\overline{n})/\Gamma_{total}$ Γ_{122}/Γ

VALUE (units 10^{-5})	CL%	DOCUMENT ID		TECN	COMMENT
<2.1	90	BAI	04G	BES2	e^+e^-

$\Gamma(\Theta(1540)K_S^0\overline{p} \to K_S^0\overline{p}K^+n)/\Gamma_{total}$ Γ_{123}/Γ

VALUE (units 10^{-5})	CL%	DOCUMENT ID		TECN	COMMENT
<1.6	90	BAI	04G	BES2	e^+e^-

$\Gamma(\overline{\Theta}(1540)K^+n \to K_S^0\overline{p}K^+n)/\Gamma_{total}$ Γ_{124}/Γ

VALUE (units 10^{-5})	CL%	DOCUMENT ID		TECN	COMMENT
<5.6	90	BAI	04G	BES2	e^+e^-

$\Gamma(\overline{\Theta}(1540)K_S^0 p \to K_S^0 pK^-\overline{n})/\Gamma_{total}$ Γ_{125}/Γ

VALUE (units 10^{-5})	CL%	DOCUMENT ID		TECN	COMMENT
<1.1	90	BAI	04G	BES2	e^+e^-

$\Gamma(\Sigma^0\overline{\Lambda})/\Gamma_{total}$ Γ_{126}/Γ

VALUE (units 10^{-4})	CL%	DOCUMENT ID		TECN	COMMENT
<0.9	90	HENRARD	87	DM2	e^+e^-

STABLE HADRONS

$\Gamma(2(\pi^+\pi^-)\pi^0)/\Gamma_{total}$ Γ_{127}/Γ

VALUE (units 10^{-2})	EVTS	DOCUMENT ID		TECN	COMMENT
4.1 ±0.5 OUR AVERAGE		Error includes scale factor of 2.4. See the ideogram below.			
5.46±0.34±0.14	4990	[1] AUBERT	07AU	BABR	10.6 $e^+e^- \to 2(\pi^+\pi^-)\pi^0\gamma$
3.25±0.49	46055	AUGUSTIN	89	DM2	$J/\psi \to 2(\pi^+\pi^-)\pi^0$
3.17±0.42	147	FRANKLIN	83	MRK2	$e^+e^- \to$ hadrons
3.64±0.52	1500	BURMESTER	77D	PLUT	e^+e^-
4 ±1	675	JEAN-MARIE	76	MRK1	e^+e^-

[1] AUBERT 07AU reports $[\Gamma(J/\psi(1S) \to 2(\pi^+\pi^-)\pi^0)/\Gamma_{total}] \times [\Gamma(J/\psi(1S) \to e^+e^-)] = 0.303 \pm 0.005 \pm 0.018$ keV which we divide by our best value $\Gamma(J/\psi(1S) \to e^+e^-) = 5.55 \pm 0.14 \pm 0.02$ keV. Our first error is their experiment's error and our second error is the systematic error from using our best value.

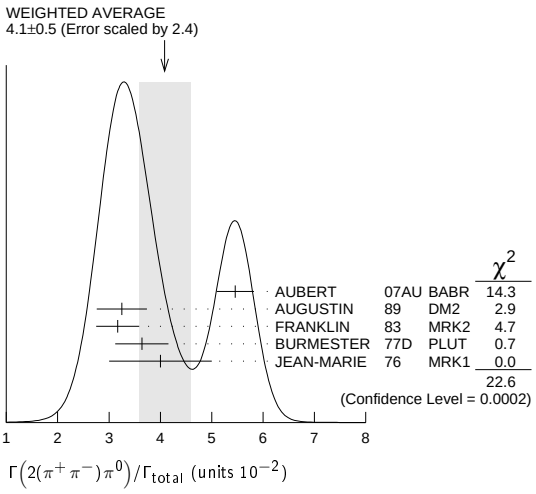

$\Gamma(\omega\pi^+\pi^-)/\Gamma(2(\pi^+\pi^-)\pi^0)$ Γ_{24}/Γ_{127}

VALUE	DOCUMENT ID		TECN	COMMENT
• • • We do not use the following data for averages, fits, limits, etc. • • •				
0.3	[1] JEAN-MARIE	76	MRK1	e^+e^-

[1] Final state $(\pi^+\pi^-)\pi^0$ under the assumption that $\pi\pi$ is isospin 0.

$\Gamma(3(\pi^+\pi^-)\pi^0)/\Gamma_{total}$ Γ_{128}/Γ

VALUE	EVTS	DOCUMENT ID		TECN	COMMENT
0.029±0.006 OUR AVERAGE					
0.028±0.009	11	FRANKLIN	83	MRK2	$e^+e^- \to$ hadrons
0.029±0.007	181	JEAN-MARIE	76	MRK1	e^+e^-

$\Gamma(\pi^+\pi^-\pi^0)/\Gamma_{total}$ Γ_{129}/Γ

VALUE (units 10^{-3})	EVTS	DOCUMENT ID		TECN	COMMENT
21.1 ±0.7 OUR AVERAGE		Error includes scale factor of 1.5. See the ideogram below.			
$21.37 \pm 0.04 \pm^{0.64}_{0.62}$	1.8M	[1,2] ABLIKIM	12H	BES3	$e^+e^- \to J/\psi$
23.0 ±2.0 ±0.4	256	[3] AUBERT	07AU	BABR	10.6 $e^+e^- \to J/\psi\pi^+\pi^-\gamma$
21.8 ±1.9		[4,5] AUBERT,B	04N	BABR	10.6 $e^+e^- \to \pi^+\pi^-\pi^0\gamma$
21.84±0.05±2.01	220k	[1,5] BAI	04H	BES	e^+e^-
20.91±0.21±1.16		[5,6] BAI	04H	BES	e^+e^-
15 ±2	168	FRANKLIN	83	MRK2	e^+e^-

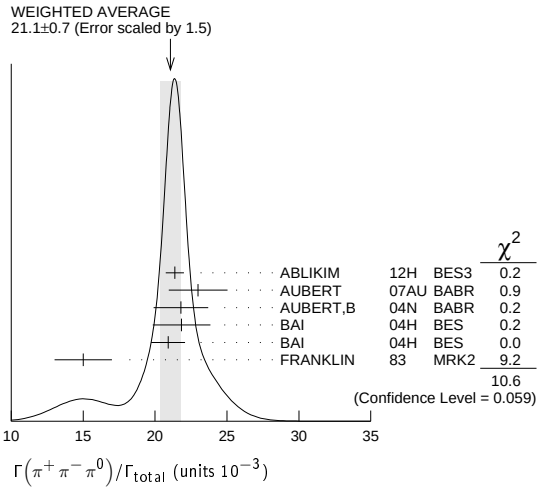

[1] From $J/\psi \to \pi^+\pi^-\pi^0$ events directly.

[2] The quoted systematic error includes a contribution of 1.23% (added in quadrature) from the uncertainty on the number of J/ψ events.

[3] AUBERT 07AU reports $[\Gamma(J/\psi(1S) \to \pi^+\pi^-\pi^0)/\Gamma_{total}] \times [\Gamma(\psi(2S) \to J/\psi(1S)\pi^+\pi^-) \times \Gamma(\psi(2S) \to e^+e^-)/\Gamma_{total}] = (18.6 \pm 1.2 \pm 1.1) \times 10^{-3}$ keV which we divide by our best value $\Gamma(\psi(2S) \to J/\psi(1S)\pi^+\pi^-) \times \Gamma(\psi(2S) \to e^+e^-)/\Gamma_{total} = 0.809 \pm 0.013$ keV. Our first error is their experiment's error and our second error is the systematic error from using our best value.

[4] From the ratio of $\Gamma(e^+e^-)\,B(\pi^+\pi^-\pi^0)$ and $\Gamma(e^+e^-)\,B(\mu^+\mu^-)$ (AUBERT 04).

[5] Mostly $\rho\pi$, see also $\rho\pi$ subsection.

[6] Obtained comparing the rates for $\pi^+\pi^-\pi^0$ and $\mu^+\mu^-$, using J/ψ events produced via $\psi(2S) \to \pi^+\pi^- J/\psi$ and with $B(J/\psi \to \mu^+\mu^-) = 5.88 \pm 0.10\%$.

$\Gamma(K^+K^-\pi^0)/\Gamma(\pi^+\pi^-\pi^0)$ $\Gamma_{141}/\Gamma_{129}$

VALUE (%)	EVTS	DOCUMENT ID		TECN	COMMENT
12.0±0.3±0.9	23K	LEES	17C	BABR	$J/\psi \to h^+h^-\pi^0$

$\Gamma(K^0_S K^\pm\pi^\mp)/\Gamma(\pi^+\pi^-\pi^0)$ $\Gamma_{142}/\Gamma_{129}$

VALUE (%)	EVTS	DOCUMENT ID		TECN	COMMENT
26.5±0.5±2.1	24K	LEES	17C	BABR	$J/\psi \to h^0h^+h^-$

$\Gamma(\pi^+\pi^-\pi^0K^+K^-)/\Gamma_{total}$ Γ_{130}/Γ

VALUE (units 10^{-2})	EVTS	DOCUMENT ID		TECN	COMMENT
1.79±0.29 OUR AVERAGE		Error includes scale factor of 2.2.			
1.93±0.14±0.05	768	[1] AUBERT	07AU	BABR	10.6 $e^+e^- \to K^+K^-\pi^+\pi^-\pi^0\gamma$
1.2 ±0.3	309	VANNUCCI	77	MRK1	e^+e^-

[1] AUBERT 07AU reports $[\Gamma(J/\psi(1S) \to \pi^+\pi^-\pi^0K^+K^-)/\Gamma_{total}] \times [\Gamma(J/\psi(1S) \to e^+e^-)] = 0.1070 \pm 0.0043 \pm 0.0064$ keV which we divide by our best value $\Gamma(J/\psi(1S) \to e^+e^-) = 5.55 \pm 0.14 \pm 0.02$ keV. Our first error is their experiment's error and our second error is the systematic error from using our best value.

$\Gamma(4(\pi^+\pi^-)\pi^0)/\Gamma_{total}$ Γ_{131}/Γ

VALUE (units 10^{-4})	EVTS	DOCUMENT ID		TECN	COMMENT
90±30	13	JEAN-MARIE	76	MRK1	e^+e^-

$\Gamma(\pi^+\pi^-K^+K^-)/\Gamma_{total}$ Γ_{132}/Γ

VALUE (units 10^{-3})	EVTS	DOCUMENT ID		TECN	COMMENT
• • • We do not use the following data for averages, fits, limits, etc. • • •					
6.5±0.4±0.2	1.6k	[1] AUBERT	07AK	BABR	10.6 $e^+e^- \to \pi^+\pi^-K^+K^-\gamma$
6.1±0.7±0.2	233	[2] AUBERT	05D	BABR	10.6 $e^+e^- \to K^+K^-\pi^+\pi^-\gamma$
7.2±2.3	205	VANNUCCI	77	MRK1	e^+e^-

[1] Superseded by LEES 12F. AUBERT 07AK reports $[\Gamma(J/\psi(1S) \to \pi^+\pi^-K^+K^-)/\Gamma_{total}] \times [\Gamma(J/\psi(1S) \to e^+e^-)] = (36.3 \pm 1.3 \pm 2.1) \times 10^{-3}$ keV which we divide by our best value $\Gamma(J/\psi(1S) \to e^+e^-) = 5.55 \pm 0.14 \pm 0.02$ keV. Our first error is their experiment's error and our second error is the systematic error from using our best value.

[2] Superseded by AUBERT 07AK. AUBERT 05D reports $[\Gamma(J/\psi(1S) \to \pi^+\pi^-K^+K^-)/\Gamma_{total}] \times [\Gamma(J/\psi(1S) \to e^+e^-)] = (33.6 \pm 2.7 \pm 2.7) \times 10^{-3}$ keV which we divide by our best value $\Gamma(J/\psi(1S) \to e^+e^-) = 5.55 \pm 0.14 \pm 0.02$ keV. Our first error is their experiment's error and our second error is the systematic error from using our best value.

$\Gamma(\pi^+\pi^-K^+K^-\eta)/\Gamma_{total}$ Γ_{137}/Γ

VALUE (units 10^{-3})	EVTS	DOCUMENT ID		TECN	COMMENT
1.84±0.28±0.05	73	[1] AUBERT	07AU	BABR	10.6 $e^+e^- \to K^+K^-\pi^+\pi^-\eta\gamma$

[1] AUBERT 07AU reports $[\Gamma(J/\psi(1S) \to \pi^+\pi^-K^+K^-\eta)/\Gamma_{total}] \times [\Gamma(J/\psi(1S) \to e^+e^-)] = (10.2 \pm 1.3 \pm 0.8) \times 10^{-3}$ keV which we divide by our best value $\Gamma(J/\psi(1S) \to e^+e^-) = 5.55 \pm 0.14 \pm 0.02$ keV. Our first error is their experiment's error and our second error is the systematic error from using our best value.

$\Gamma(\pi^0\pi^0K^+K^-)/\Gamma_{total}$ Γ_{138}/Γ

VALUE (units 10^{-3})	EVTS	DOCUMENT ID		TECN	COMMENT
• • • We do not use the following data for averages, fits, limits, etc. • • •					
2.45±0.31±0.06	203 ±16	[1] AUBERT	07AK	BABR	10.6 $e^+e^- \to \pi^0\pi^0K^+K^-\gamma$

[1] Superseded by LEES 12F. AUBERT 07AK reports $[\Gamma(J/\psi(1S) \to \pi^0\pi^0K^+K^-)/\Gamma_{total}] \times [\Gamma(J/\psi(1S) \to e^+e^-)] = (13.6 \pm 1.1 \pm 1.3) \times 10^{-3}$ keV which we divide by our best value $\Gamma(J/\psi(1S) \to e^+e^-) = 5.55 \pm 0.14 \pm 0.02$ keV. Our first error is their experiment's error and our second error is the systematic error from using our best value.

$\Gamma(K\overline{K}\pi)/\Gamma_{total}$ Γ_{140}/Γ

VALUE (units 10^{-4})	EVTS	DOCUMENT ID		TECN	COMMENT
61 ±10 OUR AVERAGE					
55.2±12.0	25	FRANKLIN	83	MRK2	$e^+e^- \to K^+K^-\pi^0$
78.0±21.0	126	VANNUCCI	77	MRK1	$e^+e^- \to K^0_S K^\pm\pi^\mp$

Meson Particle Listings

$J/\psi(1S)$

$\Gamma(2(\pi^+\pi^-))/\Gamma_{total}$ Γ_{147}/Γ

VALUE (units 10^{-3})	EVTS	DOCUMENT ID		TECN	COMMENT
3.57±0.30 OUR AVERAGE					
3.53±0.12±0.29	1107	[1] ABLIKIM	05H	BES2	$e^+e^- \to \psi(2S) \to J/\psi\pi^+\pi^-$, $J/\psi \to 2(\pi^+\pi^-)$
4.0 ±1.0	76	JEAN-MARIE	76	MRK1	e^+e^-
• • • We do not use the following data for averages, fits, limits, etc. • • •					
3.51±0.34±0.09	270	[2] AUBERT	05D	BABR	10.6 $e^+e^- \to 2(\pi^+\pi^-)\gamma$

[1] Computed using $B(J/\psi \to \mu^+\mu^-) = 0.0588 \pm 0.0010$.

[2] AUBERT 05D reports $[\Gamma(J/\psi(1S) \to 2(\pi^+\pi^-))/\Gamma_{total}] \times [\Gamma(J/\psi(1S) \to e^+e^-)] = (19.5 \pm 1.4 \pm 1.3) \times 10^{-3}$ keV which we divide by our best value $\Gamma(J/\psi(1S) \to e^+e^-) = 5.55 \pm 0.14 \pm 0.02$ keV. Our first error is their experiment's error and our second error is the systematic error from using our best value. Superseded by LEES 12E.

$\Gamma(3(\pi^+\pi^-))/\Gamma_{total}$ Γ_{148}/Γ

VALUE (units 10^{-4})	EVTS	DOCUMENT ID		TECN	COMMENT
43 ± 4 OUR AVERAGE					
43.0± 2.9±2.8	496	[1] AUBERT	06D	BABR	10.6 $e^+e^- \to 3(\pi^+\pi^-)\gamma$
40 ±20	32	JEAN-MARIE	76	MRK1	e^+e^-

[1] Using $\Gamma(J/\psi \to e^+e^-) = 5.52 \pm 0.14 \pm 0.04$ keV.

$\Gamma(2(\pi^+\pi^-\pi^0))/\Gamma_{total}$ Γ_{149}/Γ

VALUE (units 10^{-2})	EVTS	DOCUMENT ID		TECN	COMMENT
1.62±0.09±0.19	761	[1] AUBERT	06D	BABR	10.6 $e^+e^- \to 2(\pi^+\pi^-\pi^0)\gamma$

[1] Using $\Gamma(J/\psi \to e^+e^-) = 5.52 \pm 0.14 \pm 0.04$ keV.

$\Gamma(2(\pi^+\pi^-)\eta)/\Gamma_{total}$ Γ_{150}/Γ

VALUE (units 10^{-3})	EVTS	DOCUMENT ID		TECN	COMMENT
2.29±0.24 OUR AVERAGE					
2.35±0.39±0.20	85	[1] AUBERT	07AU	BABR	10.6 $e^+e^- \to 2(\pi^+\pi^-)\eta\gamma$
2.26±0.08±0.27	4839	ABLIKIM	05C	BES2	$e^+e^- \to 2(\pi^+\pi^-)\eta$

[1] AUBERT 07AU quotes $\Gamma_{ee}^{J/\psi} \cdot B(J/\psi \to 2(\pi^+\pi^-)\eta) \cdot B(\eta \to \gamma\gamma) = 5.16 \pm 0.85 \pm 0.39$ eV.

$\Gamma(3(\pi^+\pi^-)\eta)/\Gamma_{total}$ Γ_{151}/Γ

VALUE (units 10^{-4})	EVTS	DOCUMENT ID		TECN	COMMENT
7.24±0.96±1.11	616	ABLIKIM	05C	BES2	$e^+e^- \to 3(\pi^+\pi^-)\eta$

$\Gamma(p\overline{p})/\Gamma_{total}$ Γ_{152}/Γ

VALUE (units 10^{-3})	EVTS	DOCUMENT ID		TECN	COMMENT
2.121±0.029 OUR AVERAGE					
2.112±0.004±0.031	314k	ABLIKIM	12C	BES3	e^+e^-
2.19 ±0.16 ±0.06	317	[1] WU	06	BELL	$B^+ \to p\overline{p}K^+$
2.26 ±0.01 ±0.14	63316	BAI	04E	BES2	$e^+e^- \to J/\psi$
1.97 ±0.22	99	BALDINI	98	FENI	e^+e^-
1.91 ±0.04 ±0.30		PALLIN	87	DM2	e^+e^-
2.16 ±0.07 ±0.15	1420	EATON	84	MRK2	e^+e^-
2.5 ±0.4	133	BRANDELIK	79C	DASP	e^+e^-
2.0 ±0.5		BESCH	78	BONA	e^+e^-
2.2 ±0.2	331	[2] PERUZZI	78	MRK1	e^+e^-
• • • We do not use the following data for averages, fits, limits, etc. • • •					
2.0 ±0.3	48	ANTONELLI	93	SPEC	e^+e^-

[1] WU 06 reports $[\Gamma(J/\psi(1S) \to p\overline{p})/\Gamma_{total}] \times [B(B^+ \to J/\psi(1S)K^+)] = (2.21 \pm 0.13 \pm 0.10) \times 10^{-6}$ which we divide by our best value $B(B^+ \to J/\psi(1S)K^+) = (1.010 \pm 0.029) \times 10^{-3}$. Our first error is their experiment's error and our second error is the systematic error from using our best value.

[2] Assuming angular distribution $(1+\cos^2\theta)$.

$\Gamma(p\overline{p}\pi^0)/\Gamma_{total}$ Γ_{153}/Γ

VALUE (units 10^{-3})	EVTS	DOCUMENT ID		TECN	COMMENT
1.19±0.08 OUR AVERAGE Error includes scale factor of 1.1.					
1.33±0.02±0.11	11k	ABLIKIM	09B	BES2	e^+e^-
1.13±0.09±0.09	685	EATON	84	MRK2	e^+e^-
1.4 ±0.4		BRANDELIK	79C	DASP	e^+e^-
1.00±0.15	109	PERUZZI	78	MRK1	e^+e^-

$\Gamma(p\overline{p}\pi^+\pi^-)/\Gamma_{total}$ Γ_{154}/Γ

VALUE (units 10^{-3})	EVTS	DOCUMENT ID		TECN	COMMENT
6.0 ±0.5 OUR AVERAGE Error includes scale factor of 1.3. See the ideogram below.					
6.46±0.17±0.43	1435	EATON	84	MRK2	e^+e^-
3.8 ±1.6	48	BESCH	81	BONA	e^+e^-
5.5 ±0.6	533	PERUZZI	78	MRK1	e^+e^-

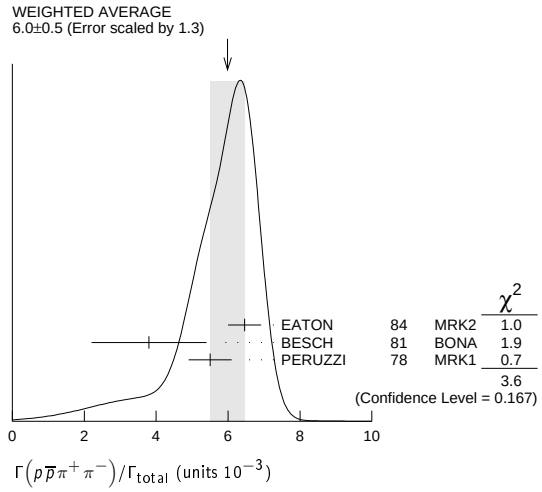

$\Gamma(p\overline{p}\pi^+\pi^-\pi^0)/\Gamma_{total}$ Γ_{155}/Γ

Including $p\overline{p}\pi^+\pi^-\gamma$ and excluding ω, η, η'

VALUE (units 10^{-3})	EVTS	DOCUMENT ID		TECN	COMMENT
2.3 ±0.9 OUR AVERAGE Error includes scale factor of 1.9.					
3.36±0.65±0.28	364	EATON	84	MRK2	e^+e^-
1.6 ±0.6	39	PERUZZI	78	MRK1	e^+e^-

$\Gamma(p\overline{p}\eta)/\Gamma_{total}$ Γ_{156}/Γ

VALUE (units 10^{-3})	EVTS	DOCUMENT ID		TECN	COMMENT
2.00±0.12 OUR AVERAGE					
1.91±0.02±0.17	13k	[1] ABLIKIM	09	BES2	e^+e^-
2.03±0.13±0.15	826	EATON	84	MRK2	e^+e^-
2.5 ±1.2		BRANDELIK	79C	DASP	e^+e^-
2.3 ±0.4	197	PERUZZI	78	MRK1	e^+e^-

[1] From the combination of $p\overline{p}\eta \to p\overline{p}\gamma\gamma$ and $p\overline{p}\eta \to p\overline{p}\pi^+\pi^-\pi^0$ channels.

$\Gamma(p\overline{p}\rho)/\Gamma_{total}$ Γ_{157}/Γ

VALUE (units 10^{-3})	CL%	DOCUMENT ID		TECN	COMMENT
<0.31	90	EATON	84	MRK2	$e^+e^- \to$ hadronsγ

$\Gamma(p\overline{p}\omega)/\Gamma_{total}$ Γ_{158}/Γ

VALUE (units 10^{-3})	EVTS	DOCUMENT ID		TECN	COMMENT
0.98±0.10 OUR AVERAGE Error includes scale factor of 1.3. See the ideogram below.					
0.90±0.02±0.09	2670	ABLIKIM	13P	BES3	e^+e^-
0.98±0.03±0.14	2449	ABLIKIM	08	BES2	e^+e^-
1.10±0.17±0.18	486	EATON	84	MRK2	e^+e^-
1.6 ±0.3	77	PERUZZI	78	MRK1	e^+e^-

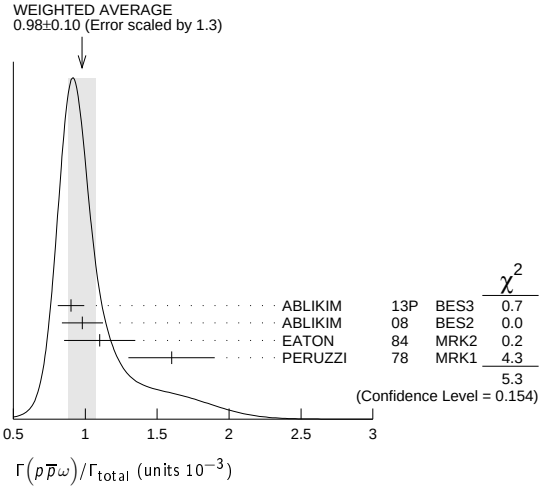

$\Gamma(p\overline{p}\eta'(958))/\Gamma_{total}$ Γ_{159}/Γ

VALUE (units 10^{-3})	EVTS	DOCUMENT ID		TECN	COMMENT
0.21 ±0.04 OUR AVERAGE					
0.200±0.023±0.028	265 ± 31	[1] ABLIKIM	09	BES2	e^+e^-
0.68 ±0.23 ±0.17	19	EATON	84	MRK2	e^+e^-
1.8 ±0.6	19	PERUZZI	78	MRK1	e^+e^-

[1] From the combination of $p\overline{p}\eta' \to p\overline{p}\pi^+\pi^-\eta$ and $p\overline{p}\eta' \to p\overline{p}\gamma\rho^0$ channels.

$\Gamma(p\overline{p}a_0(980) \to p\overline{p}\pi^0\eta)/\Gamma_{total}$ Γ_{160}/Γ

VALUE (units 10^{-5})	DOCUMENT ID		TECN	COMMENT
6.8±1.2±1.3	ABLIKIM	14N	BES3	$e^+e^- \to J/\psi$

$\Gamma(p\overline{p}\phi)/\Gamma_{total}$ Γ_{161}/Γ

VALUE (units 10^{-4})	EVTS	DOCUMENT ID		TECN	COMMENT
0.519±0.033 OUR AVERAGE					
0.523±0.006±0.033	14K	ABLIKIM	16K	BES3	$J/\psi \to p\overline{p}K^0_S K^0_L$, $p\overline{p}K^+K^-$
0.45 ±0.13 ±0.07		FALVARD	88	DM2	$J/\psi \to$ hadrons

$\Gamma(n\overline{n})/\Gamma_{total}$ Γ_{162}/Γ

VALUE (units 10^{-3})	EVTS	DOCUMENT ID		TECN	COMMENT
2.09±0.16 OUR AVERAGE					
2.07±0.01±0.17	36k	ABLIKIM	12C	BES3	e^+e^-
2.31±0.49	79	BALDINI	98	FENI	e^+e^-
1.8 ±0.9		BESCH	78	BONA	e^+e^-
• • • We do not use the following data for averages, fits, limits, etc. • • •					
1.90±0.55	40	ANTONELLI	93	SPEC	e^+e^-

$\Gamma(n\overline{n}\pi^+\pi^-)/\Gamma_{total}$ Γ_{163}/Γ

VALUE (units 10^{-3})	EVTS	DOCUMENT ID		TECN	COMMENT
3.8±3.6	5	BESCH	81	BONA	e^+e^-

$\Gamma(\Sigma^+\overline{\Sigma}^-)/\Gamma_{total}$ Γ_{164}/Γ

VALUE (units 10^{-3})	EVTS	DOCUMENT ID		TECN	COMMENT
1.50±0.10±0.22	399	ABLIKIM	08O	BES2	$e^+e^- \to J/\psi$

$\Gamma(\Sigma^0\overline{\Sigma}^0)/\Gamma_{total}$ Γ_{165}/Γ

VALUE (units 10^{-3})	EVTS	DOCUMENT ID		TECN	COMMENT
1.172±0.031 OUR AVERAGE		Error includes scale factor of 1.4.			
1.164±0.004±0.023	111k	ABLIKIM	17L	BES3	$J/\psi \to \Sigma^0\overline{\Sigma}^0$
1.15 ±0.24 ±0.03		[1] AUBERT	07BD	BABR	$10.6\ e^+e^- \to \Sigma^0\overline{\Sigma}^0\gamma$
1.33 ±0.04 ±0.11	1.7k	ABLIKIM	06	BES2	$J/\psi \to \Sigma^0\overline{\Sigma}^0$
1.06 ±0.04 ±0.23	884	PALLIN	87	DM2	$e^+e^- \to \Sigma^0\overline{\Sigma}^0$
1.58 ±0.16 ±0.25	90	EATON	84	MRK2	$e^+e^- \to \Sigma^0\overline{\Sigma}^0$
1.3 ±0.4	52	PERUZZI	78	MRK1	$e^+e^- \to \Sigma^0\overline{\Sigma}^0$
• • • We do not use the following data for averages, fits, limits, etc. • • •					
2.4 ±2.6	3	BESCH	81	BONA	$e^+e^- \to \Sigma^+\overline{\Sigma}^-$

[1] AUBERT 07BD reports $[\Gamma(J/\psi(1S) \to \Sigma^0\overline{\Sigma}^0)/\Gamma_{total}] \times [\Gamma(J/\psi(1S) \to e^+e^-)] = (6.4 \pm 1.2 \pm 0.6) \times 10^{-3}$ keV which we divide by our best value $\Gamma(J/\psi(1S) \to e^+e^-) = 5.55 \pm 0.14 \pm 0.02$ keV. Our first error is their experiment's error and our second error is the systematic error from using our best value.

$\Gamma(2(\pi^+\pi^-)K^+K^-)/\Gamma_{total}$ Γ_{166}/Γ

VALUE (units 10^{-4})	EVTS	DOCUMENT ID		TECN	COMMENT
47 ± 7 OUR AVERAGE		Error includes scale factor of 1.3.			
49.8± 4.2±3.4	205	[1] AUBERT	06D	BABR	$10.6\ e^+e^- \to \omega K^+K^-2(\pi^+\pi^-)\gamma$
31 ±13	30	VANNUCCI	77	MRK1	e^+e^-

[1] Using $\Gamma(J/\psi \to e^+e^-) = 5.52 \pm 0.14 \pm 0.04$ keV.

$\Gamma(p\overline{n}\pi^-)/\Gamma_{total}$ Γ_{167}/Γ

VALUE (units 10^{-3})	EVTS	DOCUMENT ID		TECN	COMMENT
2.12±0.09 OUR AVERAGE					
2.36±0.02±0.21	59k	ABLIKIM	06K	BES2	$J/\psi \to p\pi^-\overline{n}$
2.47±0.02±0.24	55k	ABLIKIM	06K	BES2	$J/\psi \to \overline{p}\pi^+n$
2.02±0.07±0.16	1288	EATON	84	MRK2	$e^+e^- \to p\pi^-$
1.93±0.07±0.16	1191	EATON	84	MRK2	$e^+e^- \to \overline{p}\pi^+$
1.7 ±0.7	32	BESCH	81	BONA	$e^+e^- \to p\pi^-$
1.6 ±1.2	5	BESCH	81	BONA	$e^+e^- \to \overline{p}\pi^+$
2.16±0.29	194	PERUZZI	78	MRK1	$e^+e^- \to p\pi^-$
2.04±0.27	204	PERUZZI	78	MRK1	$e^+e^- \to \overline{p}\pi^+$

$\Gamma(\Xi^-\overline{\Xi}^+)/\Gamma_{total}$ Γ_{171}/Γ

VALUE (units 10^{-3})	EVTS	DOCUMENT ID		TECN	COMMENT
0.97 ±0.08 OUR AVERAGE		Error includes scale factor of 1.4.			See the ideogram below.
1.040±0.006±0.074	43k	ABLIKIM	16L	BES3	$J/\psi \to \Xi^-\overline{\Xi}^+$
0.90 ±0.03 ±0.18	961	ABLIKIM	12P	BES2	$J/\psi \to \Xi^-\overline{\Xi}^+$
0.70 ±0.06 ±0.12	132	HENRARD	87	DM2	$e^+e^- \to \Xi^-\overline{\Xi}^+$
1.14 ±0.08 ±0.20	194	EATON	84	MRK2	$e^+e^- \to \Xi^-\overline{\Xi}^+$
1.4 ±0.5	51	PERUZZI	78	MRK1	$e^+e^- \to \Xi^-\overline{\Xi}^+$

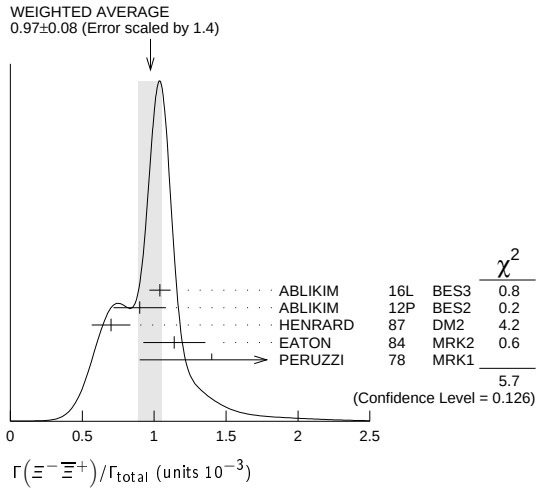

$\Gamma(\Lambda\overline{\Lambda})/\Gamma_{total}$ Γ_{172}/Γ

VALUE (units 10^{-3})	EVTS	DOCUMENT ID		TECN	COMMENT
1.89 ±0.08 OUR AVERAGE		Error includes scale factor of 2.5.			See the ideogram below.
1.943±0.003±0.033	441k	ABLIKIM	17L	BES3	e^+e^-
1.93 ±0.21 ±0.05		[1] AUBERT	07BD	BABR	$10.6\ e^+e^- \to \Lambda\overline{\Lambda}\gamma$
2.03 ±0.03 ±0.15	8887	ABLIKIM	06	BES2	$J/\psi \to \Lambda\overline{\Lambda}$
2.0 $^{+0.5}_{-0.4}$ ±0.1	46	[2] WU	06	BELL	$B^+ \to \Lambda\overline{\Lambda}K^+$
1.08 ±0.06 ±0.24	631	BAI	98G	BES	e^+e^-
1.38 ±0.05 ±0.20	1847	PALLIN	87	DM2	e^+e^-
1.58 ±0.08 ±0.19	365	EATON	84	MRK2	e^+e^-
2.6 ±1.6	5	BESCH	81	BONA	e^+e^-
1.1 ±0.2	196	PERUZZI	78	MRK1	e^+e^-

[1] AUBERT 07BD reports $[\Gamma(J/\psi(1S) \to \Lambda\overline{\Lambda})/\Gamma_{total}] \times [\Gamma(J/\psi(1S) \to e^+e^-)] = (10.7 \pm 0.9 \pm 0.7) \times 10^{-3}$ keV which we divide by our best value $\Gamma(J/\psi(1S) \to e^+e^-) = 5.55 \pm 0.14 \pm 0.02$ keV. Our first error is their experiment's error and our second error is the systematic error from using our best value.

[2] WU 06 reports $[\Gamma(J/\psi(1S) \to \Lambda\overline{\Lambda})/\Gamma_{total}] \times [B(B^+ \to J/\psi(1S)K^+)] = (2.00^{+0.34}_{-0.29} \pm 0.34) \times 10^{-6}$ which we divide by our best value $B(B^+ \to J/\psi(1S)K^+) = (1.010 \pm 0.029) \times 10^{-3}$. Our first error is their experiment's error and our second error is the systematic error from using our best value.

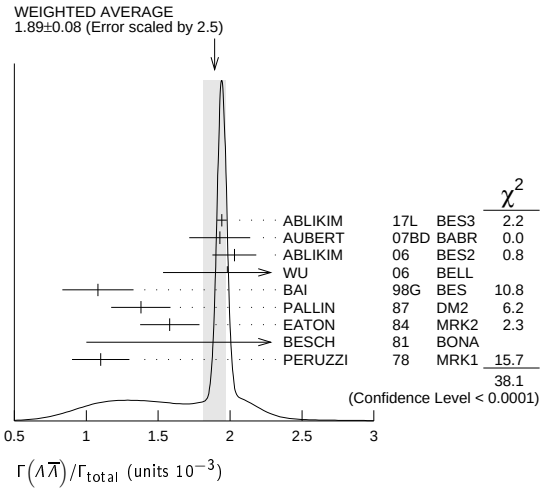

$\Gamma(\Lambda\overline{\Lambda})/\Gamma(p\overline{p})$ $\Gamma_{172}/\Gamma_{152}$

VALUE	DOCUMENT ID		TECN	COMMENT
0.90 $^{+0.15}_{-0.14}$ ±0.10	[1] WU	06	BELL	$B^+ \to p\overline{p}K^+$, $\Lambda\overline{\Lambda}K^+$

[1] Not independent of other $J/\psi \to \Lambda\overline{\Lambda}$, $p\overline{p}$ branching ratios reported by WU 06.

$\Gamma(\Lambda\overline{\Sigma}^-\pi^+ \text{(or c.c.)})/\Gamma_{total}$ Γ_{173}/Γ

VALUE (units 10^{-3})	EVTS	DOCUMENT ID		TECN	COMMENT
0.83 ±0.07 OUR AVERAGE		Error includes scale factor of 1.2.			
0.770±0.051±0.083	335	[1] ABLIKIM	07H	BES2	$e^+e^- \to \overline{\Lambda}\Sigma^+\pi^-$
0.747±0.056±0.076	254	[1] ABLIKIM	07H	BES2	$e^+e^- \to \Lambda\overline{\Sigma}^-\pi^+$
0.90 ±0.06 ±0.16	225 ± 15	HENRARD	87	DM2	$e^+e^- \to \overline{\Lambda}\Sigma^+\pi^-$
1.11 ±0.06 ±0.20	342 ± 18	HENRARD	87	DM2	$e^+e^- \to \Lambda\overline{\Sigma}^-\pi^+$
1.53 ±0.17 ±0.38	135	EATON	84	MRK2	$e^+e^- \to \overline{\Lambda}\Sigma^+\pi^-$
1.38 ±0.21 ±0.35	118	EATON	84	MRK2	$e^+e^- \to \Lambda\overline{\Sigma}^-\pi^+$

[1] Using $B(\Lambda \to \pi^- p) = 63.9\%$ and $B(\Sigma^+ \to \pi^0 p) = 51.6\%$.

$\Gamma(pK^-\overline{\Lambda})/\Gamma_{total}$ Γ_{174}/Γ

VALUE (units 10^{-3})	EVTS	DOCUMENT ID		TECN	COMMENT
0.89±0.07±0.14	307	EATON	84	MRK2	e^+e^-

$\Gamma(2(K^+K^-))/\Gamma_{total}$ Γ_{175}/Γ

VALUE (units 10^{-3})	EVTS	DOCUMENT ID		TECN	COMMENT
0.74±0.07 OUR AVERAGE					
0.72±0.06±0.05	287 ± 24	LEES	12F	BABR	10.6 $e^+e^- \to 2(K^+K^-)\gamma$
1.4 $^{+0.5}_{-0.4}$ ±0.2	11.0 $^{+4.3}_{-3.5}$	[1] HUANG	03	BELL	$B^+ \to 2(K^+K^-)\,K^+$
0.7 ±0.3		VANNUCCI	77	MRK1	e^+e^-
• • • We do not use the following data for averages, fits, limits, etc. • • •					
0.74±0.09±0.02	156 ± 15	[2] AUBERT	07AK	BABR	10.6 $e^+e^- \to 2(K^+K^-)\gamma$
0.72±0.17±0.02	38	[3] AUBERT	05D	BABR	10.6 $e^+e^- \to 2(K^+K^-)\gamma$

[1] Using $B(B^+ \to J/\psi K^+) = (1.01 \pm 0.05) \times 10^{-3}$.
[2] Superseded by LEES 12F. AUBERT 07AK reports $[\Gamma(J/\psi(1S) \to 2(K^+K^-))/\Gamma_{total}] \times [\Gamma(J/\psi(1S) \to e^+e^-)] = (4.11 \pm 0.39 \pm 0.30) \times 10^{-3}$ keV which we divide by our best value $\Gamma(J/\psi(1S) \to e^+e^-) = 5.55 \pm 0.14 \pm 0.02$ keV. Our first error is their experiment's error and our second error is the systematic error from using our best value.
[3] Superseded by AUBERT 07AK. AUBERT 05D reports $[\Gamma(J/\psi(1S) \to 2(K^+K^-))/\Gamma_{total}] \times [\Gamma(J/\psi(1S) \to e^+e^-)] = (4.0 \pm 0.7 \pm 0.6) \times 10^{-3}$ keV which we divide by our best value $\Gamma(J/\psi(1S) \to e^+e^-) = 5.55 \pm 0.14 \pm 0.02$ keV. Our first error is their experiment's error and our second error is the systematic error from using our best value.

$\Gamma(pK^-\overline{\Sigma}^0)/\Gamma_{total}$ Γ_{176}/Γ

VALUE (units 10^{-3})	EVTS	DOCUMENT ID		TECN	COMMENT
0.29±0.06±0.05	90	EATON	84	MRK2	e^+e^-

$\Gamma(K^+K^-)/\Gamma_{total}$ Γ_{177}/Γ

VALUE (units 10^{-4})	EVTS	DOCUMENT ID		TECN	COMMENT
2.86±0.09±0.19	1k	[1] METREVELI	12		$\psi(2S) \to \pi^+\pi^- K^+K^-$
• • • We do not use the following data for averages, fits, limits, etc. • • •					
3.22±0.20±0.12	462	[2,3] LEES	15J	BABR	$e^+e^- \to K^+K^-\gamma$
3.50±0.20±0.12	462	[3,4] LEES	15J	BABR	$e^+e^- \to K^+K^-\gamma$
2.39±0.24±0.22	107	[5] BALTRUSAIT...85D		MRK3	e^+e^-
2.2 ±0.9	6	[5] BRANDELIK	79C	DASP	e^+e^-

[1] Obtained by analyzing CLEO-c data but not authored by the CLEO Collaboration.
[2] $\sin\phi > 0$.
[3] Using $\Gamma(J/\psi \to e^+e^-) = (5.55 \pm 0.14)$ keV.
[4] $\sin\phi < 0$.
[5] Interference with non-resonant K^+K^- production not taken into account.

$\Gamma(K^0_S K^0_L)/\Gamma_{total}$ Γ_{178}/Γ

VALUE (units 10^{-4})	EVTS	DOCUMENT ID		TECN	COMMENT
1.95±0.11 OUR AVERAGE		Error includes scale factor of 2.4. See the ideogram below.			
1.93±0.01±0.05	110K	ABLIKIM	17AH	BES3	$J/\psi \to K^0_S K^0_L \to \pi^+\pi^- X$
2.62±0.15±0.14	0.3k	[1] METREVELI	12		$\psi(2S) \to \pi^+\pi^- K^0_S K^0_L$
1.82±0.04±0.13	2.1k	[2] BAI	04A	BES2	$J/\psi \to K^0_S K^0_L \to \pi^+\pi^- X$
• • • We do not use the following data for averages, fits, limits, etc. • • •					
1.18±0.12±0.18		JOUSSET	90	DM2	$J/\psi \to$ hadrons
1.01±0.16±0.09	74	BALTRUSAIT...85D		MRK3	e^+e^-

[1] Obtained by analyzing CLEO-c data but not authored by the CLEO Collaboration.
[2] Using $B(K^0_S \to \pi^+\pi^-) = 0.6868 \pm 0.0027$.

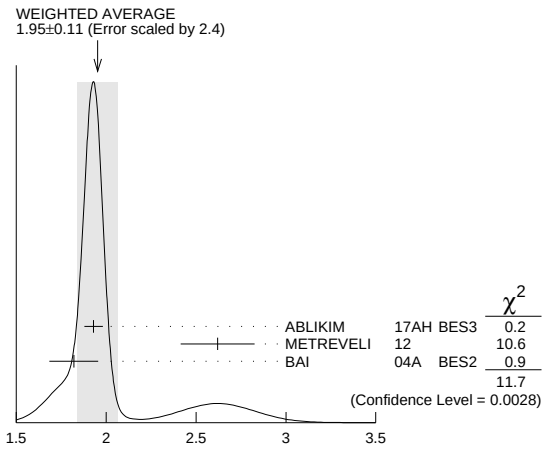

$\Gamma(K^0_S K^0_L)/\Gamma_{total}$ Γ_{178}/Γ

$\Gamma(\Lambda\overline{\Lambda}\pi^+\pi^-)/\Gamma_{total}$ Γ_{179}/Γ

VALUE (units 10^{-3})	EVTS	DOCUMENT ID		TECN	COMMENT
4.30±0.13±0.99	2.4k	ABLIKIM	12P	BES2	J/ψ

$\Gamma(\Lambda\overline{\Lambda}\eta)/\Gamma_{total}$ Γ_{180}/Γ

VALUE (units 10^{-5})	EVTS	DOCUMENT ID		TECN	COMMENT
16.2±1.7 OUR AVERAGE					
15.7±0.80±1.54	454	[1] ABLIKIM	13F	BES3	$J/\psi \to p\overline{p}\pi^+\pi^-\gamma\gamma$
26.2±6.0 ±4.4	44	[2] ABLIKIM	07H	BES2	$e^+e^- \to \psi(2S)$

[1] Using $B(\Lambda \to \pi^- p) = 63.9\%$ and $B(\eta \to \gamma\gamma) = 39.31\%$.
[2] Using $B(\Lambda \to \pi^- p) = 63.9\%$ and $B(\eta \to \gamma\gamma) = 39.4\%$.

$\Gamma(\Lambda\overline{\Lambda}\pi^0)/\Gamma_{total}$ Γ_{181}/Γ

VALUE (units 10^{-5})	CL%	EVTS	DOCUMENT ID		TECN	COMMENT
3.78±0.27±0.30		323	[1] ABLIKIM	13F	BES3	$J/\psi \to p\overline{p}\pi^+\pi^-\gamma\gamma$
• • • We do not use the following data for averages, fits, limits, etc. • • •						
< 6.4	90		[2] ABLIKIM	07H	BES2	$e^+e^- \to \psi(2S)$
23 ±7 ±8		11	BAI	98G	BES	e^+e^-
22 ±5 ±5		19	HENRARD	87	DM2	e^+e^-

[1] Using $B(\Lambda \to \pi^- p) = 63.9\%$ and $B(\pi^0 \to \gamma\gamma) = 98.8\%$.
[2] Using $B(\Lambda \to \pi^- p) = 63.9\%$.

$\Gamma(\overline{\Lambda}nK^0_S + \text{c.c.})/\Gamma_{total}$ Γ_{182}/Γ

VALUE (units 10^{-4})	EVTS	DOCUMENT ID		TECN	COMMENT
6.46±0.20±1.07	1058	[1] ABLIKIM	08C	BES2	$e^+e^- \to J/\psi$

[1] Using $B(\overline{\Lambda} \to \overline{p}\pi^+) = 63.9\%$ and $B(K^0_S \to \pi^+\pi^-) = 69.2\%$.

$\Gamma(\pi^+\pi^-)/\Gamma_{total}$ Γ_{183}/Γ

VALUE (units 10^{-4})	EVTS	DOCUMENT ID		TECN	COMMENT
1.47±0.14 OUR AVERAGE					
1.47±0.13±0.13	140	[1] METREVELI	12		$\psi(2S) \to 2(\pi^+\pi^-)$
1.58±0.20±0.15	84	BALTRUSAIT...85D		MRK3	e^+e^-
1.0 ±0.5	5	BRANDELIK	78B	DASP	e^+e^-
1.6 ±1.6	1	VANNUCCI	77	MRK1	e^+e^-

[1] Obtained by analyzing CLEO-c data but not authored by the CLEO Collaboration.

$\Gamma(\Lambda\overline{\Sigma}^- + \text{c.c.})/\Gamma_{total}$ Γ_{184}/Γ

VALUE (units 10^{-5})	CL%	EVTS	DOCUMENT ID		TECN	COMMENT
2.83±0.23 OUR AVERAGE						
2.74±0.24±0.22		234 ± 21	[1] ABLIKIM	12B	BES3	$J/\psi \to \Lambda\overline{\Sigma}^0$
2.92±0.22±0.24		308 ± 24	[2] ABLIKIM	12B	BES3	$J/\psi \to \overline{\Lambda}\Sigma^0$
• • • We do not use the following data for averages, fits, limits, etc. • • •						
<15	90		PERUZZI	78	MRK1	$e^+e^- \to \Lambda X$

[1] ABLIKIM 12B quotes $B(J/\psi \to \Lambda\overline{\Sigma}^0)$ which we multiply by 2.
[2] ABLIKIM 12B quotes $B(J/\psi \to \overline{\Lambda}\Sigma^0)$ which we multiply by 2.

$\Gamma(K^0_S K^0_S)/\Gamma_{total}$ Γ_{185}/Γ

VALUE	CL%	DOCUMENT ID		TECN	COMMENT
<1.4 × 10⁻⁸	95	[1] ABLIKIM	17AH	BES3	$J/\psi \to K^0_S K^0_S \to \pi^+\pi^-\pi^+\pi^-$
• • • We do not use the following data for averages, fits, limits, etc. • • •					
<1 × 10⁻⁶	95	[1] BAI	04D	BES	e^+e^-
<5.2 × 10⁻⁶	90	[1] BALTRUSAIT...85C		MRK3	e^+e^-

[1] Forbidden by CP.

RADIATIVE DECAYS

$\Gamma(3\gamma)/\Gamma_{total}$ Γ_{186}/Γ

VALUE (units 10^{-6})	CL%	EVTS	DOCUMENT ID		TECN	COMMENT
11.6±2.2 OUR AVERAGE						
11.3±1.8±2.0		113 ± 18	ABLIKIM	13I	BES3	$\psi(2S) \to \pi^+\pi^- J/\psi$
12 ±3 ±2		24.2 $^{+7.2}_{-6.0}$	ADAMS	08	CLEO	$\psi(2S) \to \pi^+\pi^- J/\psi$
• • • We do not use the following data for averages, fits, limits, etc. • • •						
<55	90		PARTRIDGE	80	CBAL	e^+e^-

$\Gamma(4\gamma)/\Gamma_{total}$ Γ_{187}/Γ

VALUE (units 10^{-6})	CL%	DOCUMENT ID		TECN	COMMENT
<9	90	ADAMS	08	CLEO	$\psi(2S) \to \pi^+\pi^- J/\psi$

$\Gamma(5\gamma)/\Gamma_{total}$ Γ_{188}/Γ

VALUE (units 10^{-6})	CL%	DOCUMENT ID		TECN	COMMENT
<15	90	ADAMS	08	CLEO	$\psi(2S) \to \pi^+\pi^- J/\psi$

$\Gamma(\gamma\pi^0\pi^0)/\Gamma_{total}$ Γ_{189}/Γ

VALUE (units 10^{-3})	DOCUMENT ID		TECN	COMMENT
1.15±0.05	[1] ABLIKIM	15AE	BES3	$J/\psi \to \gamma\pi^0\pi^0$

[1] The uncertainty is systematic as statistical is netligible.

$\Gamma(\gamma\eta\pi^0)/\Gamma_{total}$ Γ_{190}/Γ

VALUE (units 10^{-6})	EVTS	DOCUMENT ID		TECN	COMMENT
21.4±1.8±2.5	596	ABLIKIM	16P	BES3	$J/\psi \to 5\gamma$

$\Gamma(\gamma a_0(980)^0 \to \gamma\eta\pi^0)/\Gamma_{total}$ Γ_{191}/Γ

VALUE	CL%	DOCUMENT ID		TECN	COMMENT
$<2.5\times10^{-6}$	95	ABLIKIM	16P	BES3	$J/\psi \to 5\gamma$

$\Gamma(\gamma a_2(1320)^0 \to \gamma\eta\pi^0)/\Gamma_{total}$ Γ_{192}/Γ

VALUE	CL%	DOCUMENT ID		TECN	COMMENT
$<6.6\times10^{-6}$	95	ABLIKIM	16P	BES3	$J/\psi \to 5\gamma$

$\Gamma(\gamma\eta_c(1S))/\Gamma_{total}$ Γ_{193}/Γ

VALUE (units 10^{-2})	EVTS	DOCUMENT ID		TECN	COMMENT
1.7 ±0.4 OUR AVERAGE		Error includes scale factor of 1.5.			
$2.00\pm0.31\pm0.02$		[1] MITCHELL	09	CLEO	$e^+e^- \to \gamma X$
1.27 ± 0.36		GAISER	86	CBAL	$J/\psi \to \gamma X$
• • • We do not use the following data for averages, fits, limits, etc. • • •					
seen		ANASHIN	14	KEDR	$J/\psi \to \gamma\eta_c$
0.79 ± 0.20	273 ± 43	[2] AUBERT	06E	BABR	$B^\pm \to K^\pm X_{c\overline{c}}$
seen	16	BALTRUSAIT...84		MRK3	$J/\psi \to 2\phi\gamma$

[1] MITCHELL 09 reports $(1.98 \pm 0.09 \pm 0.30)\times10^{-2}$ from a measurement of $[\Gamma(J/\psi(1S) \to \gamma\eta_c(1S))/\Gamma_{total}] \times [B(\psi(2S) \to J/\psi(1S)\pi^+\pi^-)]$ assuming $B(\psi(2S) \to J/\psi(1S)\pi^+\pi^-) = (35.04 \pm 0.07 \pm 0.77)\times10^{-2}$, which we rescale to our best value $B(\psi(2S) \to J/\psi(1S)\pi^+\pi^-) = (34.67 \pm 0.30)\times10^{-2}$. Our first error is their experiment's error and our second error is the systematic error from using our best value.

[2] Calculated by the authors using an average of $B(J/\psi \to \gamma\eta_c) \times B(\eta_c \to K\overline{K}\pi)$ from BALTRUSAITIS 86, BISELLO 91, BAI 04 and $B(\eta_c \to K\overline{K}\pi) = (8.5 \pm 1.8)\%$ from AUBERT 06E.

$\Gamma(\gamma\eta_c(1S) \to 3\gamma)/\Gamma_{total}$ Γ_{194}/Γ

VALUE (units 10^{-6})	EVTS	DOCUMENT ID	TECN	COMMENT
$3.8^{+1.3}_{-1.0}$ OUR AVERAGE	Error includes scale factor of 1.1.			
$4.5\pm1.2\pm0.6$	33 ± 9	ABLIKIM 13I	BES3	$\psi(2S) \to \pi^+\pi^- J/\psi$
$1.2^{+2.7}_{-1.1}\pm0.3$	$1.2^{+2.8}_{-1.1}$	ADAMS 08	CLEO	$\psi(2S) \to \pi^+\pi^- J/\psi$

$\Gamma(\gamma\pi^+\pi^-2\pi^0)/\Gamma_{total}$ Γ_{195}/Γ

VALUE (units 10^{-3})	DOCUMENT ID	TECN	COMMENT
8.3±0.2±3.1	[1] BALTRUSAIT...86B	MRK3	$J/\psi \to 4\pi\gamma$

[1] 4π mass less than 2.0 GeV.

$\Gamma(\gamma\eta\pi\pi)/\Gamma_{total}$ Γ_{196}/Γ

VALUE (units 10^{-3})	DOCUMENT ID		TECN	COMMENT
6.1 ±1.0 OUR AVERAGE				
$5.85\pm0.3\pm1.05$	[1] EDWARDS	83B	CBAL	$J/\psi \to \eta\pi^+\pi^-$
$7.8\ \pm1.2\pm2.4$	[1] EDWARDS	83B	CBAL	$J/\psi \to \eta 2\pi^0$

[1] Broad enhancement at 1700 MeV.

$\Gamma(\gamma\eta_2(1870) \to \gamma\eta\pi^+\pi^-)/\Gamma_{total}$ Γ_{197}/Γ

VALUE (units 10^{-4})	DOCUMENT ID		TECN	COMMENT
6.2±2.2±0.9	BAI	99	BES	$J/\psi \to \gamma\eta\pi^+\pi^-$

$\Gamma(\gamma\eta(1405/1475) \to \gamma K\overline{K}\pi)/\Gamma_{total}$ Γ_{198}/Γ

VALUE (units 10^{-3})	DOCUMENT ID		TECN	COMMENT
2.8 ±0.6 OUR AVERAGE	Error includes scale factor of 1.6. See the ideogram below.			
$1.66\pm0.1\ \pm0.58$	[1,2] BAI	00D	BES	$J/\psi \to \gamma K^\pm K^0_S \pi^\mp$
$3.8\ \pm0.3\ \pm0.6$	[3] AUGUSTIN	90	DM2	$J/\psi \to \gamma K\overline{K}\pi$
$4.0\ \pm0.7\ \pm1.0$	[3] EDWARDS	82E	CBAL	$J/\psi \to K^+K^-\pi^0\gamma$
$4.3\ \pm1.7$	[3,4] SCHARRE	80	MRK2	e^+e^-
• • • We do not use the following data for averages, fits, limits, etc. • • •				
$1.78\pm0.21\pm0.33$	[3,5,6] AUGUSTIN	92	DM2	$J/\psi \to \gamma K\overline{K}\pi$
$0.83\pm0.13\pm0.18$	[3,7,8] AUGUSTIN	92	DM2	$J/\psi \to \gamma K\overline{K}\pi$
$0.66^{+0.17+0.24}_{-0.16-0.15}$	[3,6,9] BAI	90C	MRK3	$J/\psi \to \gamma K^0_S K^\pm\pi^\mp$
$1.03^{+0.21+0.26}_{-0.18-0.19}$	[3,8,10] BAI	90C	MRK3	$J/\psi \to \gamma K^0_S K^\pm\pi^\mp$

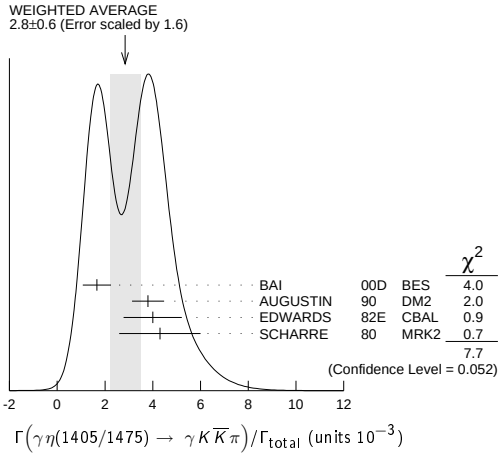

[1] Interference with the $J/\psi(1S)$ radiative transition to the broad $K\overline{K}\pi$ pseudoscalar state around 1800 is $(0.15 \pm 0.01 \pm 0.05)\times10^{-3}$.
[2] Interference with $J/\psi \to \gamma f_1(1420)$ is $(-0.03 \pm 0.01 \pm 0.01)\times10^{-3}$.
[3] Includes unknown branching fraction $\eta(1405) \to K\overline{K}\pi$.
[4] Corrected for spin-zero hypothesis for $\eta(1405)$.
[5] From fit to the $a_0(980)\pi\ 0^{-+}$ partial wave.
[6] $a_0(980)\pi$ mode.
[7] From fit to the $K^*(892)K\ 0^{-+}$ partial wave.
[8] K^*K mode.
[9] From $a_0(980)\pi$ final state.
[10] From $K^*(890)K$ final state.

$\Gamma(\gamma\eta(1405/1475) \to \gamma\gamma\rho^0)/\Gamma_{total}$ Γ_{199}/Γ

VALUE (units 10^{-4})	DOCUMENT ID		TECN	COMMENT
0.78±0.20 OUR AVERAGE	Error includes scale factor of 1.8.			
$1.07\pm0.17\pm0.11$	[1] BAI	04J	BES2	$J/\psi \to \gamma\gamma\pi^+\pi^-$
$0.64\pm0.12\pm0.07$	[1] COFFMAN	90	MRK3	$J/\psi \to \gamma\gamma\pi^+\pi^-$

[1] Includes unknown branching fraction $\eta(1405) \to \gamma\rho^0$.

$\Gamma(\gamma\eta(1405/1475) \to \gamma\eta\pi^+\pi^-)/\Gamma_{total}$ Γ_{200}/Γ

VALUE (units 10^{-4})	EVTS	DOCUMENT ID		TECN	COMMENT
3.0 ±0.5 OUR AVERAGE					
$2.6\ \pm0.7\ \pm0.4$		BAI	99	BES	$J/\psi \to \gamma\eta\pi^+\pi^-$
$3.38\pm0.33\pm0.64$		[1] BOLTON	92B	MRK3	$J/\psi \to \gamma\eta\pi^+\pi^-$
• • • We do not use the following data for averages, fits, limits, etc. • • •					
$7.0\ \pm0.6\ \pm1.1$	261	[2] AUGUSTIN	90	DM2	$J/\psi \to \gamma\eta\pi^+\pi^-$

[1] Via $a_0(980)\pi$.
[2] Includes unknown branching fraction to $\eta\pi^+\pi^-$.

$\Gamma(\gamma\eta(1405/1475) \to \gamma\gamma\phi)/\Gamma_{total}$ Γ_{201}/Γ

VALUE (units 10^{-4})	CL%	DOCUMENT ID		TECN	COMMENT
<0.82	95	BAI	04J	BES2	$J/\psi \to \gamma\gamma K^+K^-$

$\Gamma(\gamma\rho\rho)/\Gamma_{total}$ Γ_{202}/Γ

VALUE (units 10^{-3})	CL%	DOCUMENT ID		TECN	COMMENT
4.5 ±0.8 OUR AVERAGE					
$4.7\ \pm0.3\ \pm0.9$		[1] BALTRUSAIT...86B		MRK3	$J/\psi \to 4\pi\gamma$
$3.75\pm1.05\pm1.20$		[2] BURKE	82	MRK2	$J/\psi \to 4\pi\gamma$
• • • We do not use the following data for averages, fits, limits, etc. • • •					
<0.09	90	[3] BISELLO	89B		$J/\psi \to 4\pi\gamma$

[1] 4π mass less than 2.0 GeV.
[2] 4π mass less than 2.0 GeV. We have multiplied $2\rho^0$ measurement by 3 to obtain 2ρ.
[3] 4π mass in the range 2.0–25 GeV.

$\Gamma(\gamma\rho\omega)/\Gamma_{total}$ Γ_{203}/Γ

VALUE (units 10^{-4})	CL%	DOCUMENT ID		TECN	COMMENT
<5.4	90	ABLIKIM	08A	BES2	$e^+e^- \to J/\psi$

$\Gamma(\gamma\rho\phi)/\Gamma_{total}$ Γ_{204}/Γ

VALUE (units 10^{-5})	CL%	DOCUMENT ID		TECN	COMMENT
<8.8	90	ABLIKIM	08A	BES2	$e^+e^- \to J/\psi$

$\Gamma(\gamma\eta'(958))/\Gamma_{total}$ Γ_{205}/Γ

VALUE (units 10^{-3})	EVTS	DOCUMENT ID		TECN	COMMENT
5.13±0.17 OUR AVERAGE	Error includes scale factor of 1.3. See the ideogram below.				
$4.78\pm0.22\pm0.08$		[1] ABLIKIM	11	BES3	$J/\psi \to \eta'\gamma$
$5.24\pm0.12\pm0.11$		PEDLAR	09	CLE3	$J/\psi \to \eta'\gamma$
5.55 ± 0.44	35k	ABLIKIM	06E	BES2	$J/\psi \to \eta'\gamma$
• • • We do not use the following data for averages, fits, limits, etc. • • •					
$4.50\pm0.14\pm0.53$		BOLTON	92B	MRK3	$J/\psi \to \gamma\pi^+\pi^-\eta,\ \eta \to \gamma\gamma$
$4.30\pm0.31\pm0.71$		BOLTON	92B	MRK3	$J/\psi \to \gamma\pi^+\pi^-\eta,\ \eta \to \pi^+\pi^-\pi^0$
$4.04\pm0.16\pm0.85$	622	AUGUSTIN	90	DM2	$J/\psi \to \gamma\eta\pi^+\pi^-$
$4.39\pm0.09\pm0.66$	2420	AUGUSTIN	90	DM2	$J/\psi \to \gamma\gamma\pi^+\pi^-$
$4.1\ \pm0.3\ \pm0.6$		BLOOM	83	CBAL	$e^+e^- \to 3\gamma +$ hadrons
$2.9\ \pm1.1$	6	BRANDELIK	79C	DASP	$e^+e^- \to 3\gamma$
$2.4\ \pm0.7$	57	BARTEL	76	CNTR	$e^+e^- \to 2\gamma\rho$

[1] ABLIKIM 11 reports $(4.84 \pm 0.03 \pm 0.24)\times10^{-3}$ from a measurement of $[\Gamma(J/\psi(1S) \to \gamma\eta'(958))/\Gamma_{total}]$ / $[B(\eta'(958) \to \pi^+\pi^-\eta)]$ / $[B(\eta \to 2\gamma)]$ assuming $B(\eta'(958) \to \pi^+\pi^-\eta) = (43.2 \pm 0.7)\times10^{-2}$, $B(\eta \to 2\gamma) = (39.31 \pm 0.20)\times10^{-2}$, which we rescale to our best values $B(\eta'(958) \to \pi^+\pi^-\eta) = (42.6 \pm 0.7)\times10^{-2}$, $B(\eta \to 2\gamma) = (39.41 \pm 0.20)\times10^{-2}$. Our first error is their experiment's error and our second error is the systematic error from using our best values.

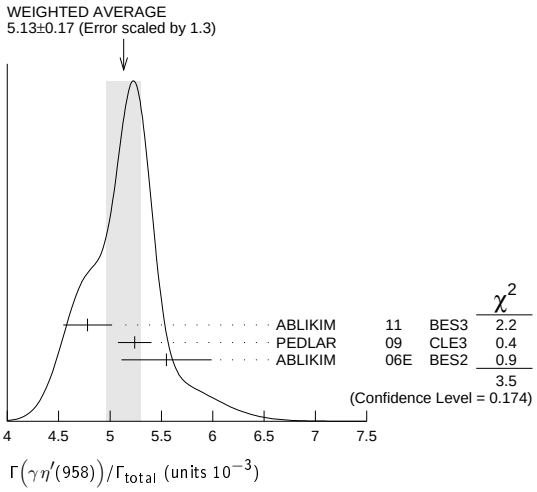

$\Gamma(\gamma 2\pi^+ 2\pi^-)/\Gamma_{total}$ Γ_{206}/Γ

VALUE (units 10^{-3})	DOCUMENT ID		TECN	COMMENT
2.8 ±0.5 OUR AVERAGE	Error includes scale factor of 1.9. See the ideogram below.			
4.32±0.14±0.73	[1] BISELLO	89B	DM2	$J/\psi \to 4\pi\gamma$
2.08±0.13±0.35	[2] BISELLO	89B	DM2	$J/\psi \to 4\pi\gamma$
3.05±0.08±0.45	[2] BALTRUSAIT...	86B	MRK3	$J/\psi \to 4\pi\gamma$
4.85±0.45±1.20	[3] BURKE	82	MRK2	e^+e^-

[1] 4π mass less than 3.0 GeV.
[2] 4π mass less than 2.0 GeV.
[3] 4π mass less than 2.5 GeV.

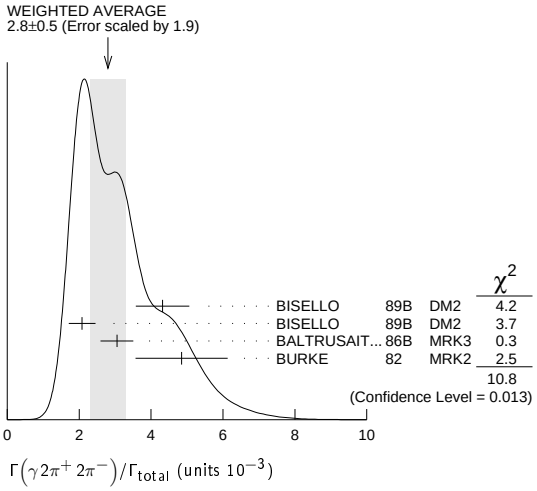

$\Gamma(\gamma f_2(1270) f_2(1270))/\Gamma_{total}$ Γ_{207}/Γ

VALUE (units 10^{-4})	EVTS	DOCUMENT ID		TECN	COMMENT
9.5±0.7±1.6	646 ± 45	ABLIKIM	04M	BES	$J/\psi \to \gamma 2\pi^+ 2\pi^-$

$\Gamma(\gamma f_2(1270) f_2(1270)\,(\text{non resonant}))/\Gamma_{total}$ Γ_{208}/Γ

VALUE (units 10^{-4})	DOCUMENT ID		TECN	COMMENT
8.2±0.8±1.7	[1] ABLIKIM	04M	BES	$J/\psi \to \gamma 2\pi^+ 2\pi^-$

[1] Subtracting contribution from intermediate $\eta_c(1S)$ decays.

$\Gamma(\gamma K^+ K^- \pi^+ \pi^-)/\Gamma_{total}$ Γ_{209}/Γ

VALUE (units 10^{-3})	EVTS	DOCUMENT ID		TECN	COMMENT
2.1±0.1±0.6	1516	BAI	00B	BES	$J/\psi \to \gamma K^+ K^0 \pi^+ \pi^-$

$\Gamma(\gamma f_4(2050))/\Gamma_{total}$ Γ_{210}/Γ

VALUE (units 10^{-3})	DOCUMENT ID		TECN	COMMENT
2.7±0.5±0.5	[1] BALTRUSAIT...87		MRK3	$J/\psi \to \gamma\pi^+\pi^-$

[1] Assuming branching fraction $f_4(2050) \to \pi\pi/$ total = 0.167.

$\Gamma(\gamma\omega\omega)/\Gamma_{total}$ Γ_{211}/Γ

VALUE (units 10^{-3})	EVTS	DOCUMENT ID		TECN	COMMENT
1.61±0.33 OUR AVERAGE					
6.0 ±4.8 ±1.8		ABLIKIM	08A	BES2	$J/\psi \to \gamma\omega\pi^+\pi^-$
1.41±0.2 ±0.42	120 ± 17	BISELLO	87	SPEC	e^+e^-, hadronsγ
1.76±0.09±0.45		BALTRUSAIT...85C		MRK3	$e^+e^- \to$ hadronsγ

$\Gamma(\gamma\eta(1405/1475) \to \gamma\rho^0\rho^0)/\Gamma_{total}$ Γ_{212}/Γ

VALUE (units 10^{-3})	DOCUMENT ID		TECN	COMMENT
1.7 ±0.4 OUR AVERAGE	Error includes scale factor of 1.3.			
2.1 ±0.4	BUGG	95	MRK3	$J/\psi \to \gamma\pi^+\pi^-\pi^+\pi^-$
1.36±0.38	[1,2] BISELLO	89B	DM2	$J/\psi \to 4\pi\gamma$

[1] Estimated by us from various fits.
[2] Includes unknown branching fraction to $\rho^0\rho^0$.

$\Gamma(\gamma f_2(1270))/\Gamma_{total}$ Γ_{213}/Γ

VALUE (units 10^{-3})	EVTS	DOCUMENT ID		TECN	COMMENT
1.64±0.12 OUR AVERAGE		Error includes scale factor of 1.3. See the ideogram below.			
$2.07\pm0.16^{+0.02}_{-0.07}$	2.4k	[1,2] DOBBS	15		$J/\psi \to \gamma\pi\pi$
$1.63\pm0.26^{+0.02}_{-0.06}$		[3] ABLIKIM	06V	BES2	$e^+e^- \to J/\psi \to \gamma\pi^+\pi^-$
$1.42\pm0.21^{+0.01}_{-0.05}$		[4] ABLIKIM	06V	BES2	$e^+e^- \to J/\psi \to \gamma\pi^0\pi^0$
1.33±0.05±0.20		[5] AUGUSTIN	87	DM2	$J/\psi \to \gamma\pi^+\pi^-$
1.36±0.09±0.23		[5] BALTRUSAIT...87		MRK3	$J/\psi \to \gamma\pi^+\pi^-$
1.48±0.25±0.30	178	EDWARDS	82B	CBAL	$e^+e^- \to 2\pi^0\gamma$
2.0 ±0.7	35	ALEXANDER	78	PLUT	e^+e^-
1.2 ±0.6	30	[6] BRANDELIK	78B	DASP	$e^+e^- \to \pi^+\pi^-\gamma$

[1] Using CLEO-c data but not authored by the CLEO Collaboration.
[2] DOBBS 15 reports $[\Gamma(J/\psi(1S) \to \gamma f_2(1270))/\Gamma_{total}] \times [B(f_2(1270) \to \pi\pi)] = (1.744 \pm 0.052 \pm 0.122) \times 10^{-3}$ which we divide by our best value $B(f_2(1270) \to \pi\pi) = (84.2^{+2.9}_{-0.9}) \times 10^{-2}$. Our first error is their experiment's error and our second error is the systematic error from using our best value.
[3] ABLIKIM 06V reports $[\Gamma(J/\psi(1S) \to \gamma f_2(1270))/\Gamma_{total}] \times [B(f_2(1270) \to \pi\pi)] = (1.371 \pm 0.010 \pm 0.222) \times 10^{-3}$ which we divide by our best value $B(f_2(1270) \to \pi\pi) = (84.2^{+2.9}_{-0.9}) \times 10^{-2}$. Our first error is their experiment's error and our second error is the systematic error from using our best value.
[4] ABLIKIM 06V reports $[\Gamma(J/\psi(1S) \to \gamma f_2(1270))/\Gamma_{total}] \times [B(f_2(1270) \to \pi\pi)] = (1.200 \pm 0.027 \pm 0.174) \times 10^{-3}$ which we divide by our best value $B(f_2(1270) \to \pi\pi) = (84.2^{+2.9}_{-0.9}) \times 10^{-2}$. Our first error is their experiment's error and our second error is the systematic error from using our best value.
[5] Estimated using $B(f_2(1270) \to \pi\pi)$=0.843 ± 0.012. The errors do not contain the uncertainty in the $f_2(1270)$ decay.
[6] Restated by us to take account of spread of E1, M2, E3 transitions.

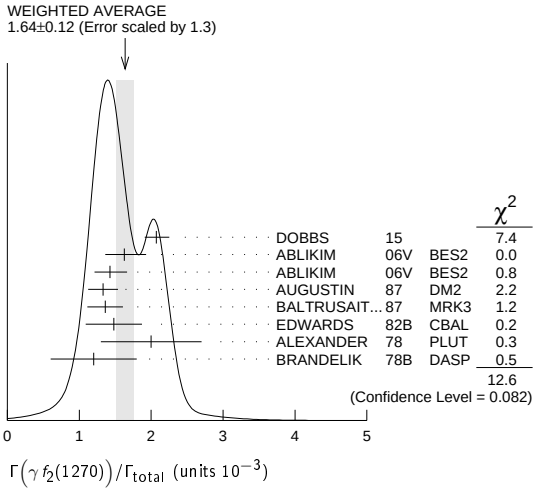

$\Gamma(\gamma f_0(1370) \to \gamma K\overline{K})/\Gamma_{total}$ Γ_{214}/Γ

VALUE (units 10^{-4})	EVTS	DOCUMENT ID		COMMENT
4.19±0.73±1.34	478	[1] DOBBS	15	$J/\psi \to \gamma K\overline{K}$

[1] Using CLEO-c data but not authored by the CLEO Collaboration.

$\Gamma(\gamma f_0(1710) \to \gamma K\overline{K})/\Gamma_{total}$ Γ_{215}/Γ

VALUE (units 10^{-4})	CL%	EVTS	DOCUMENT ID		TECN	COMMENT
$10.0 \pm {}^{1.1}_{0.9}$ OUR AVERAGE	Error includes scale factor of 1.5. See the ideogram below.					
11.76± 0.54±0.94		1.2k	[1] DOBBS	15		$J/\psi \to \gamma K\overline{K}$
$9.62\pm029\ {}^{+3.51}_{-1.86}$			[2] BAI	03G	BES	$J/\psi \to \gamma K\overline{K}$
5.0 ± 0.8 $^{+1.8}_{-0.4}$			[3,4] BAI	96C	BES	$J/\psi \to \gamma K^+K^-$
9.2 ± 1.4 ±1.4			[4] AUGUSTIN	88	DM2	$J/\psi \to \gamma K^+K^-$
10.4 ± 1.2 ±1.6			[4] AUGUSTIN	88	DM2	$J/\psi \to \gamma K^0_S K^0_S$
9.6 ± 1.2 ±1.8			[4] BALTRUSAIT...87		MRK3	$J/\psi \to \gamma K^+K^-$
• • • We do not use the following data for averages, fits, limits, etc. • • •						
1.6 ± 0.2 $^{+0.6}_{-0.2}$			[4,5] BAI	96C	BES	$J/\psi \to \gamma K^+K^-$
< 0.8	90		[6] BISELLO	89B		$J/\psi \to 4\pi\gamma$

1.6 ± 0.4 ±0.3 [7] BALTRUSAIT...87 MRK3 $J/\psi \to \gamma\pi^+\pi^-$

3.8 ± 1.6 [8] EDWARDS 82D CBAL $e^+e^- \to \eta\eta\gamma$

[1] Using CLEO-c data but not authored by the CLEO Collaboration.

[2] Includes unknown branching ratio to K^+K^- or $K^0_S K^0_S$.

[3] Assuming $J^P = 2^+$ for $f_0(1710)$.

[4] Includes unknown branching fraction to K^+K^- or $K^0_S K^0_S$. We have multiplied K^+K^- measurement by 2, and $K^0_S K^0_S$ by 4 to obtain $K\overline{K}$ result.

[5] Assuming $J^P = 0^+$ for $f_0(1710)$.

[6] Includes unknown branching fraction to $\rho^0\rho^0$.

[7] Includes unknown branching fraction to $\pi^+\pi^-$.

[8] Includes unknown branching fraction to $\eta\eta$.

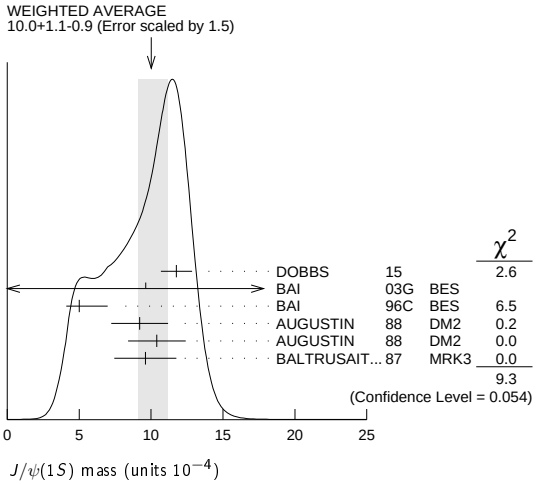

$\Gamma(\gamma f_0(1710) \to \gamma\pi\pi)/\Gamma_{total}$ Γ_{216}/Γ

VALUE (units 10^{-4})	EVTS	DOCUMENT ID		TECN	COMMENT
3.8 ±0.5 OUR AVERAGE					
3.72±0.30±0.43	483	[1] DOBBS	15		$J/\psi \to \gamma\pi\pi$
3.96±0.06±1.12		[2] ABLIKIM	06V	BES2	$e^+e^- \to J/\psi \to \gamma\pi^+\pi^-$
3.99±0.15±2.64		[2] ABLIKIM	06V	BES2	$e^+e^- \to J/\psi \to \gamma\pi^0\pi^0$
• • • We do not use the following data for averages, fits, limits, etc. • • •					
2.5 ±1.6 ±0.8		BAI	98H	BES	$J/\psi \to \gamma\pi^0\pi^0$

[1] Using CLEO-c data but not authored by the CLEO Collaboration.

[2] Including unknown branching fraction to $\pi\pi$.

$\Gamma(\gamma f_0(1710) \to \gamma\omega\omega)/\Gamma_{total}$ Γ_{217}/Γ

VALUE (units 10^{-3})	EVTS	DOCUMENT ID		TECN	COMMENT
0.31±0.06±0.08	180	ABLIKIM	06H	BES	$J/\psi \to \gamma\omega\omega$

$\Gamma(\gamma f_0(1710) \to \gamma\eta\eta)/\Gamma_{total}$ Γ_{218}/Γ

VALUE (units 10^{-4})	EVTS	DOCUMENT ID		TECN	COMMENT
$2.35^{+0.13+1.24}_{-0.11-0.74}$	5.5k	[1] ABLIKIM	13N	BES3	$J/\psi \to \gamma\eta\eta$

[1] From partial wave analysis including all possible combinations of 0^{++}, 2^{++}, and 4^{++} resonances.

$\Gamma(\gamma\eta)/\Gamma_{total}$ Γ_{219}/Γ

VALUE (units 10^{-3})	EVTS	DOCUMENT ID		TECN	COMMENT
1.104±0.034 OUR AVERAGE					
1.101±0.029±0.022		PEDLAR	09	CLE3	$J/\psi \to \eta\gamma$
1.123±0.089	11k	ABLIKIM	06E	BES2	$J/\psi \to \eta\gamma$
• • • We do not use the following data for averages, fits, limits, etc. • • •					
0.88 ±0.08 ±0.11		BLOOM	83	CBAL	e^+e^-
0.82 ±0.10		BRANDELIK	79C	DASP	e^+e^-
1.3 ±0.4	21	BARTEL	77	CNTR	e^+e^-

$\Gamma(\gamma f_1(1420) \to \gamma K\overline{K}\pi)/\Gamma_{total}$ Γ_{220}/Γ

VALUE (units 10^{-3})	DOCUMENT ID		TECN	COMMENT
0.79±0.13 OUR AVERAGE				
0.68±0.04±0.24	BAI	00D	BES	$J/\psi \to \gamma K^\pm K^0_S \pi^\mp$
0.76±0.15±0.21	[1,2] AUGUSTIN	92	DM2	$J/\psi \to \gamma K\overline{K}\pi$
$0.87\pm0.14^{+0.14}_{-0.11}$	[1] BAI	90C	MRK3	$J/\psi \to \gamma K^0_S K^\pm\pi^\mp$

[1] Included unknown branching fraction $f_1(1420) \to K\overline{K}\pi$.

[2] From fit to the $K^*(892)K$ 1^{++} partial wave.

$\Gamma(\gamma f_1(1285))/\Gamma_{total}$ Γ_{221}/Γ

VALUE (units 10^{-3})	DOCUMENT ID		TECN	COMMENT
0.61 ±0.08 OUR AVERAGE				
0.69 ±0.16 ±0.20	[1] BAI	04J	BES2	$J/\psi \to \gamma\gamma\rho^0$
0.61 ±0.04 ±0.21	[2] BAI	00D	BES	$J/\psi \to \gamma K^\pm K^0_S \pi^\mp$
0.45 ±0.09 ±0.17	[3] BAI	99	BES	$J/\psi \to \gamma\eta\pi^+\pi^-$
0.625±0.063±0.103	[4] BOLTON	92	MRK3	$J/\psi \to \gamma f_1(1285)$
0.70 ±0.08 ±0.16	[5] BOLTON	92B	MRK3	$J/\psi \to \gamma\eta\pi^+\pi^-$

[1] Assuming $B(f_1(1285) \to \rho^0\gamma) = 0.055 \pm 0.013$.

[2] Assuming $\Gamma(f_1(1285) \to K\overline{K}\pi)/\Gamma_{total} = 0.090 \pm 0.004$.

[3] Assuming $\Gamma(f_1(1285) \to \eta\pi\pi)/\Gamma_{total} = 0.5 \pm 0.18$.

[4] Obtained summing the sequential decay channels
$B(J/\psi \to \gamma f_1(1285), f_1(1285) \to \pi\pi\pi\pi) = (1.44 \pm 0.39 \pm 0.27) \times 10^{-4}$;
$B(J/\psi \to \gamma f_1(1285), f_1(1285) \to a_0(980)\pi, a_0(980) \to \eta\pi) = (3.90 \pm 0.42 \pm 0.87) \times 10^{-4}$;
$B(J/\psi \to \gamma f_1(1285), f_1(1285) \to a_0(980)\pi, a_0(980) \to K\overline{K}) = (0.66 \pm 0.26 \pm 0.29) \times 10^{-4}$;
$B(J/\psi \to \gamma f_1(1285), f_1(1285) \to \gamma\rho^0) = (0.25 \pm 0.07 \pm 0.03) \times 10^{-4}$.

[5] Using $B(f_1(1285) \to a_0(980)\pi) = 0.37$, and including unknown branching ratio for $a_0(980) \to \eta\pi$.

$\Gamma(\gamma f_1(1510) \to \gamma\eta\pi^+\pi^-)/\Gamma_{total}$ Γ_{222}/Γ

VALUE (units 10^{-4})	DOCUMENT ID		TECN	COMMENT
4.5±1.0±0.7	BAI	99	BES	$J/\psi \to \gamma\eta\pi^+\pi^-$

$\Gamma(\gamma f_2'(1525))/\Gamma_{total}$ Γ_{223}/Γ

VALUE (units 10^{-4})	CL%	EVTS	DOCUMENT ID		TECN	COMMENT
$5.7\ ^{+0.8}_{-0.5}$ OUR AVERAGE Error includes scale factor of 1.5. See the ideogram below.						
8.0 ±0.9 ±0.2		750	[1,2] DOBBS	15		$J/\psi \to \gamma K\overline{K}$
$3.85\pm0.17^{+1.91}_{-0.73}$			[3] BAI	03G	BES	$J/\psi \to \gamma K\overline{K}$
$3.6\ \pm0.4\ ^{+1.4}_{-0.4}$			[3] BAI	96C	BES	$J/\psi \to \gamma K^+K^-$
5.6 ±1.4 ±0.9			[3] AUGUSTIN	88	DM2	$J/\psi \to \gamma K^+K^-$
4.5 ±0.4 ±0.9			[3] AUGUSTIN	88	DM2	$J/\psi \to \gamma K^0_S K^0_S$
6.8 ±1.6 ±1.4			[3] BALTRUSAIT...87		MRK3	$J/\psi \to \gamma K^+K^-$
• • • We do not use the following data for averages, fits, limits, etc. • • •						
<3.4	90	4	[4] BRANDELIK	79C	DASP	$e^+e^- \to \pi^+\pi^-\gamma$
<2.3	90	3	ALEXANDER	78	PLUT	$e^+e^- \to K^+K^-\gamma$

[1] Using CLEO-c data but not authored by the CLEO Collaboration.

[2] DOBBS 15 reports $[\Gamma(J/\psi(1S) \to \gamma f_2'(1525))/\Gamma_{total}] \times [B(f_2'(1525) \to K\overline{K})] = (7.09 \pm 0.46 \pm 0.67) \times 10^{-4}$ which we divide by our best value $B(f_2'(1525) \to K\overline{K}) = (88.7 \pm 2.2) \times 10^{-2}$. Our first error is their experiment's error and our second error is the systematic error from using our best value.

[3] Using $B(f_2'(1525) \to K\overline{K}) = 0.888$.

[4] Assuming isotropic production and decay of the $f_2'(1525)$ and isospin.

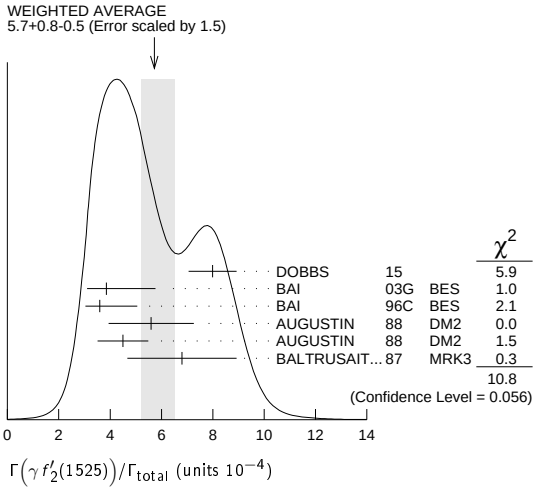

$\Gamma(\gamma f_2'(1525) \to \gamma\eta\eta)/\Gamma_{total}$ Γ_{224}/Γ

VALUE (units 10^{-5})	EVTS	DOCUMENT ID		TECN	COMMENT
$3.42^{+0.43+1.37}_{-0.51-1.30}$	5.5k	[1] ABLIKIM	13N	BES3	$J/\psi \to \gamma\eta\eta$

[1] From partial wave analysis including all possible combinations of 0^{++}, 2^{++}, and 4^{++} resonances.

$\Gamma(\gamma f_2(1640) \to \gamma\omega\omega)/\Gamma_{total}$ Γ_{225}/Γ

VALUE (units 10^{-3})	EVTS	DOCUMENT ID		TECN	COMMENT
0.28±0.05±0.17	141	ABLIKIM	06H	BES	$J/\psi \to \gamma\omega\omega$

$\Gamma(\gamma f_2(1910) \to \gamma\omega\omega)/\Gamma_{total}$ Γ_{226}/Γ

VALUE (units 10^{-3})	EVTS	DOCUMENT ID		TECN	COMMENT
0.20±0.04±0.13	151	ABLIKIM	06H	BES	$J/\psi \to \gamma\omega\omega$

$\Gamma(\gamma f_0(1800) \to \gamma\omega\phi)/\Gamma_{total}$ Γ_{227}/Γ

VALUE (units 10^{-4})	EVTS	DOCUMENT ID		TECN	COMMENT
2.5 ±0.6 OUR AVERAGE					
$2.00\pm0.08^{+1.38}_{-1.64}$	1.3k	ABLIKIM	13J	BES3	$J/\psi \to \gamma\omega\phi$
2.61±0.27±0.65	95	ABLIKIM	06J	BES2	$J/\psi \to \gamma\omega\phi$

$\Gamma(\gamma f_2(1810) \to \gamma\eta\eta)/\Gamma_{total}$ Γ_{228}/Γ

VALUE (units 10^{-5})	EVTS	DOCUMENT ID		TECN	COMMENT
$\mathbf{5.40^{+0.60+3.42}_{-0.67-2.35}}$	5.5k	[1] ABLIKIM	13N		$J/\psi \to \gamma\eta\eta$

[1] From partial wave analysis including all possible combinations of 0^{++}, 2^{++}, and 4^{++} resonances.

$\Gamma(\gamma f_2(1950) \to \gamma K^*(892)\overline{K}^*(892))/\Gamma_{total}$ Γ_{229}/Γ

VALUE (units 10^{-3})	DOCUMENT ID		TECN	COMMENT
0.7±0.1±0.2	BAI	00B	BES	$J/\psi \to \gamma K^+ K^0 \pi^+ \pi^-$

$\Gamma(\gamma K^*(892)\overline{K}^*(892))/\Gamma_{total}$ Γ_{230}/Γ

VALUE (units 10^{-3})	EVTS	DOCUMENT ID		TECN	COMMENT
4.0±0.3±1.3	320	[1] BAI	00B	BES	$J/\psi \to \gamma K^+ K^0 \pi^+ \pi^-$

[1] Summed over all charges.

$\Gamma(\gamma\phi\phi)/\Gamma_{total}$ Γ_{231}/Γ

VALUE (units 10^{-4})	EVTS	DOCUMENT ID		TECN	COMMENT
4.0±1.2 OUR AVERAGE Error includes scale factor of 2.1. See the ideogram below.					
7.5±0.6±1.2	168	BAI	90B	MRK3	$J/\psi \to \gamma 4K$
3.4±0.8±0.6	33 ± 7	[1] BISELLO	90	DM2	$J/\psi \to \gamma K^+ K^- K^0_S K^0_L$
3.1±0.7±0.4		[1] BISELLO	86B	DM2	$J/\psi \to \gamma K^+ K^- K^+ K^-$

[1] $\phi\phi$ mass less than 2.9 GeV, η_C excluded.

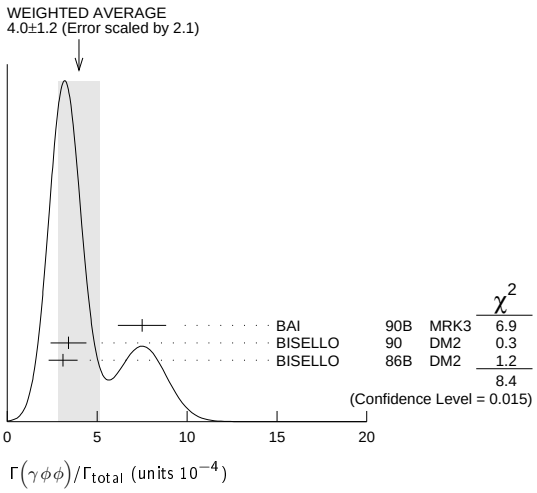

$\Gamma(\gamma p\overline{p})/\Gamma_{total}$ Γ_{232}/Γ

VALUE (units 10^{-3})	CL%	EVTS	DOCUMENT ID		TECN	COMMENT
0.38±0.07±0.07		49	EATON	84	MRK2	e^+e^-
• • • We do not use the following data for averages, fits, limits, etc. • • •						
<0.11	90		PERUZZI	78	MRK1	e^+e^-

$\Gamma(\gamma\eta(2225))/\Gamma_{total}$ Γ_{233}/Γ

VALUE (units 10^{-4})	EVTS	DOCUMENT ID		TECN	COMMENT
$\mathbf{3.14^{+0.50}_{-0.19}}$ **OUR AVERAGE**					
$2.40\pm0.10^{+2.47}_{-0.18}$		[1,2] ABLIKIM	16N	BES3	$J/\psi \to \gamma K^+ K^- K^+ K^-$
4.4 ±0.4 ±0.8	196	[2] ABLIKIM	08I	BES	$J/\psi \to \gamma K^+ K^- K^0_S K^0_L$
3.3 ±0.8 ±0.5		[2] BAI	90B	MRK3	$J/\psi \to \gamma K^+ K^- K^+ K^-$
2.7 ±0.6 ±0.6		[2] BAI	90B	MRK3	$J/\psi \to \gamma K^+ K^- K^0_S K^0_L$
$2.4\ ^{+1.5}_{-1.0}$		[3,4] BISELLO	89B	DM2	$J/\psi \to 4\pi\gamma$

[1] From a partial wave analysis of $J/\psi \to \gamma\phi\phi$ that also finds significant signals for for $\eta(2100)$, 0^{-+} phase space, $f_0(2100)$, $f_2(2010)$, $f_2(2300)$, $f_2(2340)$, and a previously unseen 0^{-+} state $X(2500)$ ($M = 2470^{+15+101}_{-19-23}$ MeV, $\Gamma = 230^{+64+56}_{-35-33}$ MeV).

[2] Includes unknown branching fraction to $\phi\phi$.

[3] Estimated by us from various fits.

[4] Includes unknown branching fraction to $\rho^0\rho^0$.

$\Gamma(\gamma\eta(1760) \to \gamma\rho^0\rho^0)/\Gamma_{total}$ Γ_{234}/Γ

VALUE (units 10^{-3})	DOCUMENT ID		TECN	COMMENT
0.13±0.09	[1,2] BISELLO	89B	DM2	$J/\psi \to 4\pi\gamma$

[1] Estimated by us from various fits.

[2] Includes unknown branching fraction to $\rho^0\rho^0$.

$\Gamma(\gamma\eta(1760) \to \gamma\omega\omega)/\Gamma_{total}$ Γ_{235}/Γ

VALUE (units 10^{-3})	EVTS	DOCUMENT ID		TECN	COMMENT
1.98±0.08±0.32	1045	ABLIKIM	06H	BES	$J/\psi \to \gamma\omega\omega$

$\Gamma(\gamma X(1835) \to \gamma\pi^+\pi^-\eta')/\Gamma_{total}$ Γ_{236}/Γ

VALUE (units 10^{-4})	EVTS	DOCUMENT ID		TECN	COMMENT
$\mathbf{2.77^{+0.34}_{-0.40}}$ **OUR AVERAGE** Error includes scale factor of 1.1.					
$3.93\pm0.38^{+0.31}_{-0.84}$		[1] ABLIKIM	16J	BES3	$J/\psi \to \gamma\pi^+\pi^-\eta'$
$2.87\pm0.09^{+0.49}_{-0.52}$	4265	[2] ABLIKIM	11C	BES3	$J/\psi \to \gamma\pi^+\pi^-\eta'$
2.2 ±0.4 ±0.4	264	ABLIKIM	05R	BES2	$J/\psi \to \gamma\pi^+\pi^-\eta'$

[1] From a fit of the measured $\pi^+\pi^-\eta'$ lineshape that accounts for the abrupt distortion observed at the $p\overline{p}$ threshold with a Flatte formula in addition to known backgrounds and contributors, as well as an *ad hoc* Breit-Wigner ($M \approx 1919$ MeV; $\Gamma \approx 51$ MeV) that is required for a good fit. Another explanation for the distortion provided by ABLIKIM 16J is that a second resonance near 1870 MeV interferes with the $X(1835)$; fits to this possibility yield product branching fraction values compatible with that shown within the respective systematic uncertainties.

[2] From a fit of the $\pi^+\pi^-\eta'$ mass distribution to a combination of $\gamma f_1(1510)$, $\gamma X(1835)$, and two unconfirmed states $\gamma X(2120)$, and $\gamma X(2370)$, for $M(p\overline{p}) < 2.8$ GeV, and accounting for backgrounds from non-η' events and $J/\psi \to \pi^0\pi^+\pi^-\eta'$.

$\Gamma(\gamma X(1835) \to \gamma p\overline{p})/\Gamma_{total}$ Γ_{237}/Γ

VALUE (units 10^{-4})	EVTS	DOCUMENT ID		TECN	COMMENT
$\mathbf{0.77^{+0.15}_{-0.09}}$ **OUR AVERAGE**					
$0.90^{+0.04+0.27}_{-0.11-0.55}$		[1] ABLIKIM	12D	BES3	$J/\psi \to \gamma p\overline{p}$
$1.14^{+0.43+0.42}_{-0.30-0.26}$	231	[2] ALEXANDER	10	CLEO	$J/\psi \to \gamma p\overline{p}$
$0.70\pm0.04^{+0.19}_{-0.08}$		BAI	03F	BES2	$J/\psi \to \gamma p\overline{p}$

[1] From the fit including final state interaction effects in isospin 0 S-wave according to SIBIRTSEV 05A.

[2] From a fit of the $p\overline{p}$ mass distribution to a combination of $\gamma X(1835)$, γR with $M(R) = 2100$ MeV and $\Gamma(R) = 160$ MeV, and $\gamma p\overline{p}$ phase space, for $M(p\overline{p}) < 2.85$ GeV.

$\Gamma(\gamma X(1835) \to \gamma K^0_S K^0_S \eta)/\Gamma_{total}$ Γ_{238}/Γ

VALUE (units 10^{-5})	DOCUMENT ID		TECN	COMMENT
$\mathbf{3.31^{+0.33+1.96}_{-0.30-1.29}}$	ABLIKIM	15T	BES3	$J/\psi \to \gamma K^0_S K^0_S \eta$

$\Gamma(\gamma X(1840) \to \gamma 3(\pi^+\pi^-))/\Gamma_{total}$ Γ_{239}/Γ

VALUE (units 10^{-5})	EVTS	DOCUMENT ID		TECN	COMMENT
$\mathbf{2.44\pm0.36^{+0.60}_{-0.74}}$	0.6k	ABLIKIM	13U	BES3	$J/\psi \to \gamma 3(\pi^+\pi^-)$

$\Gamma(\gamma(K\overline{K}\pi)\,[J^{PC} = 0^{-+}])/\Gamma_{total}$ Γ_{240}/Γ

VALUE (units 10^{-3})	DOCUMENT ID		TECN	COMMENT
0.7 ±0.4 OUR AVERAGE Error includes scale factor of 2.1.				
0.58±0.03±0.20	[1] BAI	00D	BES	$J/\psi \to \gamma K^\pm K^0_S \pi^\mp$
2.1 ±0.1 ±0.7	[2] BAI	00D	BES	$J/\psi \to \gamma K^\pm K^0_S \pi^\mp$

[1] For a broad structure around 1800 MeV.

[2] For a broad structure around 2040 MeV.

$\Gamma(\gamma\pi^0)/\Gamma_{total}$ Γ_{241}/Γ

VALUE (units 10^{-5})	EVTS	DOCUMENT ID		TECN	COMMENT
$\mathbf{3.49^{+0.33}_{-0.30}}$ **OUR AVERAGE**					
3.63±0.36±0.13		PEDLAR	09	CLE3	$J/\psi \to \pi^0\gamma$
$3.13^{+0.65}_{-0.47}$	586	ABLIKIM	06E	BES2	$J/\psi \to \pi^0\gamma$
• • • We do not use the following data for averages, fits, limits, etc. • • •					
3.6 ±1.1 ±0.7		BLOOM	83	CBAL	e^+e^-
7.3 ±4.7	10	BRANDELIK	79C	DASP	e^+e^-

$\Gamma(\gamma p\overline{p}\pi^+\pi^-)/\Gamma_{total}$ Γ_{242}/Γ

VALUE (units 10^{-3})	CL%	DOCUMENT ID		TECN	COMMENT
<0.79	90	EATON	84	MRK2	e^+e^-

$\Gamma(\gamma\Lambda\overline{\Lambda})/\Gamma_{total}$ Γ_{243}/Γ

VALUE (units 10^{-3})	CL%	DOCUMENT ID		TECN	COMMENT
<0.13	90	HENRARD	87	DM2	e^+e^-
• • • We do not use the following data for averages, fits, limits, etc. • • •					
<0.16	90	BAI	98G	BES	e^+e^-

$\Gamma(\gamma f_0(2100) \to \gamma\eta\eta)/\Gamma_{\text{total}}$ Γ_{244}/Γ

VALUE (units 10^{-4})	EVTS	DOCUMENT ID		TECN	COMMENT
$1.13^{+0.09}_{-0.10}{}^{+0.64}_{-0.28}$	5.5k	[1] ABLIKIM	13N	BES3	$J/\psi \to \gamma\eta\eta$

[1] From partial wave analysis including all possible combinations of 0^{++}, 2^{++}, and 4^{++} resonances.

$\Gamma(\gamma f_0(2100) \to \gamma\pi\pi)/\Gamma_{\text{total}}$ Γ_{245}/Γ

VALUE (units 10^{-4})	EVTS	DOCUMENT ID		COMMENT
$6.24 \pm 0.48 \pm 0.87$	744	[1] DOBBS	15	$J/\psi \to \gamma\pi\pi$

[1] Using CLEO-c data but not authored by the CLEO Collaboration.

$\Gamma(\gamma f_0(2200))/\Gamma_{\text{total}}$ Γ_{246}/Γ

VALUE (units 10^{-4})	DOCUMENT ID		TECN	COMMENT
• • • We do not use the following data for averages, fits, limits, etc. • • •				
1.5	[1] AUGUSTIN	88	DM2	$J/\psi \to \gamma K^0_S K^0_S$

[1] Includes unknown branching fraction to $K^0_S K^0_S$.

$\Gamma(\gamma f_0(2200) \to \gamma K\overline{K})/\Gamma_{\text{total}}$ Γ_{247}/Γ

VALUE (units 10^{-4})	EVTS	DOCUMENT ID		COMMENT
$5.86 \pm 0.49 \pm 1.20$	490	[1] DOBBS	15	$J/\psi \to \gamma K\overline{K}$

[1] Using CLEO-c data but not authored by the CLEO Collaboration.

$\Gamma(\gamma f_J(2220))/\Gamma_{\text{total}}$ Γ_{248}/Γ

VALUE (units 10^{-5})	CL%	EVTS	DOCUMENT ID		TECN	COMMENT
• • • We do not use the following data for averages, fits, limits, etc. • • •						
>300			[1] BAI	96B	BES	$e^+e^- \to \gamma\overline{p}p$, $K\overline{K}$
>250	99.9		[2] HASAN	96	SPEC	$\overline{p}p \to \pi^+\pi^-$
< 2.3	95		[3] AUGUSTIN	88	DM2	$J/\psi \to \gamma K^+K^-$
< 1.6	95		[3] AUGUSTIN	88	DM2	$J/\psi \to \gamma K^0_S K^0_S$
$12.4^{+6.4}_{-5.2} \pm 2.8$		23	[3] BALTRUSAIT...	86D	MRK3	$J/\psi \to \gamma K^0_S K^0_S$
$8.4^{+3.4}_{-2.8} \pm 1.6$		93	[3] BALTRUSAIT...	86D	MRK3	$J/\psi \to \gamma K^+K^-$

[1] Using BARNES 93.
[2] Using BAI 96B.
[3] Includes unknown branching fraction to K^+K^- or $K^0_S K^0_S$.

$\Gamma(\gamma f_J(2220) \to \gamma\pi\pi)/\Gamma_{\text{total}}$ Γ_{249}/Γ

VALUE (units 10^{-5})	CL%	DOCUMENT ID		TECN	COMMENT
< 3.9	90	[1,2] DOBBS	15		$J/\psi \to \gamma\pi\pi$
• • • We do not use the following data for averages, fits, limits, etc. • • •					
14 ±8 ±4		BAI	98H	BES	$J/\psi \to \gamma\pi^0\pi^0$
$8.4 \pm 2.6 \pm 3.0$		BAI	96B	BES	$e^+e^- \to J/\psi \to \gamma\pi^+\pi^-$

[1] Using CLEO-c data but not authored by the CLEO Collaboration.
[2] For $\Gamma = 20/50$ MeV, the 90% CL upper limits for $\pi^+\pi^-$ and $\pi^0\pi^0$ are $2.6/5.2 \times 10^{-5}$ and $1.3/1.9 \times 10^{-5}$, respectively.

$\Gamma(\gamma f_J(2220) \to \gamma K\overline{K})/\Gamma_{\text{total}}$ Γ_{250}/Γ

VALUE (units 10^{-5})	CL%	DOCUMENT ID		TECN	COMMENT
< 4.1	90	[1,2] DOBBS	15		$J/\psi \to \gamma K\overline{K}$
• • • We do not use the following data for averages, fits, limits, etc. • • •					
< 3.6		[3] DEL-AMO-SA...10O		BABR	$e^+e^- \to J/\psi \to \gamma K^+K^-$
< 2.9		[3] DEL-AMO-SA...10O		BABR	$e^+e^- \to J/\psi \to \gamma K^0_S K^0_S$
$6.6 \pm 2.9 \pm 2.4$		BAI	96B	BES	$e^+e^- \to J/\psi \to \gamma K^+K^-$
$10.8 \pm 4.0 \pm 3.2$		BAI	96B	BES	$e^+e^- \to J/\psi \to \gamma K^0_S K^0_S$

[1] Using CLEO-c data but not authored by the CLEO Collaboration.
[2] For $\Gamma = 20/50$ MeV, the 90% CL upper limits for K^+K^- and $K^0_S K^0_S$ are $1.7/3.1 \times 10^{-5}$ and $1.2/2.0 \times 10^{-5}$, respectively.
[3] For spin 2 and helicity 0; other combinations lead to more stringent upper limits.

$\Gamma(\gamma f_J(2220) \to \gamma p\overline{p})/\Gamma_{\text{total}}$ Γ_{251}/Γ

VALUE (units 10^{-5})	DOCUMENT ID		TECN	COMMENT
$1.5 \pm 0.6 \pm 0.5$	BAI	96B	BES	$e^+e^- \to J/\psi \to \gamma p\overline{p}$

$\Gamma(\gamma f_2(2340) \to \gamma\eta\eta)/\Gamma_{\text{total}}$ Γ_{252}/Γ

VALUE (units 10^{-5})	EVTS	DOCUMENT ID		TECN	COMMENT
$5.60^{+0.62}_{-0.65}{}^{+2.37}_{-2.07}$	5.5k	[1] ABLIKIM	13N	BES3	$J/\psi \to \gamma\eta\eta$

[1] From partial wave analysis including all possible combinations of 0^{++}, 2^{++}, and 4^{++} resonances.

$\Gamma(\gamma f_0(1500) \to \gamma\pi\pi)/\Gamma_{\text{total}}$ Γ_{253}/Γ

VALUE (units 10^{-4})	EVTS	DOCUMENT ID		TECN	COMMENT
1.09 ± 0.24 OUR AVERAGE					
$1.21 \pm 0.29 \pm 0.24$	174	[1] DOBBS	15		$J/\psi \to \gamma\pi\pi$
$1.00 \pm 0.03 \pm 0.45$		[2] ABLIKIM	06V	BES2	$e^+e^- \to J/\psi \to \gamma\pi^+\pi^-$
$1.02 \pm 0.09 \pm 0.45$		[2] ABLIKIM	06V	BES2	$e^+e^- \to J/\psi \to \gamma\pi^0\pi^0$
• • • We do not use the following data for averages, fits, limits, etc. • • •					
5.7 ±0.8		[3,4] BUGG	95	MRK3	$J/\psi \to \gamma\pi^+\pi^-\pi^+\pi^-$

[1] Using CLEO-c data but not authored by the CLEO Collaboration.
[2] Including unknown branching fraction to $\pi\pi$.
[3] Including unknown branching ratio for $f_0(1500) \to \pi^+\pi^-\pi^+\pi^-$.
[4] Assuming that $f_0(1500)$ decays only to two S-wave dipions.

$\Gamma(\gamma f_0(1500) \to \gamma\eta\eta)/\Gamma_{\text{total}}$ Γ_{254}/Γ

VALUE (units 10^{-5})	EVTS	DOCUMENT ID		TECN	COMMENT
$1.65^{+0.26}_{-0.31}{}^{+0.51}_{-1.40}$	5.5k	[1] ABLIKIM	13N	BES3	$J/\psi \to \gamma\eta\eta$

[1] From partial wave analysis including all possible combinations of 0^{++}, 2^{++}, and 4^{++} resonances.

$\Gamma(\gamma A \to \gamma\text{invisible})/\Gamma_{\text{total}}$ Γ_{255}/Γ
(narrow state A with m_A < 960 MeV)

VALUE (units 10^{-6})	CL%	DOCUMENT ID		TECN	COMMENT
<6.3	90	[1] INSLER	10	CLEO	$e^+e^- \to \pi^+\pi^- J/\psi$

[1] The limit varies with mass m_A of a narrow state A and is 4.3×10^{-6} for $m_A = 0$ MeV, reaches its largest value of 6.3×10^{-6} at $m_A = 500$ MeV, and is 3.6×10^{-6} at $m_A = 960$ MeV.

$\Gamma(\gamma A^0 \to \gamma\mu^+\mu^-)/\Gamma_{\text{total}}$ Γ_{256}/Γ
(narrow state A^0 with 0.2 GeV $< m_{A^0} <$ 3 GeV)

VALUE (units 10^{-5})	CL%	DOCUMENT ID		TECN	COMMENT
<0.5	90	[1] ABLIKIM	16E	BES3	$J/\psi \to \gamma\mu^+\mu^-$
• • • We do not use the following data for averages, fits, limits, etc. • • •					
<2.1	90	[2] ABLIKIM	12	BES3	$J/\psi \to \gamma\mu^+\mu^-$

[1] For a narrow scalar or pseudoscalar, A^0, with a mass in the range 0.212–3 GeV. The measured 90% CL limit as a function of m_{A^0} is in the range $(2.8\text{–}495.3) \times 10^{-8}$.
[2] For a narrow scalar or pseudoscalar, A^0, with a mass in the range 0.21–3.00 GeV. The measured 90% CL limit as a function of m_{A^0} ranges from 4×10^{-7} to 2.1×10^{-5}.

DALITZ DECAYS

$\Gamma(\pi^0 e^+ e^-)/\Gamma_{\text{total}}$ Γ_{257}/Γ

VALUE (units 10^{-7})	EVTS	DOCUMENT ID		TECN	COMMENT
$7.56 \pm 1.32 \pm 0.50$	39	ABLIKIM	14I	BES3	$J/\psi \to \pi^0 e^+ e^-$

$\Gamma(\eta e^+ e^-)/\Gamma_{\text{total}}$ Γ_{258}/Γ

VALUE (units 10^{-5})	EVTS	DOCUMENT ID		TECN	COMMENT
$1.16 \pm 0.07 \pm 0.06$	320	[1] ABLIKIM	14I	BES3	$J/\psi \to \eta e^+ e^-$

[1] Using both $\eta \to \gamma\gamma$ and $\eta \to \pi^+\pi^-\pi^0$ decays.

$\Gamma(\eta'(958) e^+ e^-)/\Gamma_{\text{total}}$ Γ_{259}/Γ

VALUE (units 10^{-5})	EVTS	DOCUMENT ID		TECN	COMMENT
$5.81 \pm 0.16 \pm 0.31$	1.4k	[1] ABLIKIM	14I	BES3	$J/\psi \to \eta' e^+ e^-$

[1] Using both $\eta' \to \gamma\pi^+\pi^-$ and $\eta' \to \pi^+\pi^-\eta$ decays.

WEAK DECAYS

$\Gamma(D^- e^+ \nu_e + \text{c.c.})/\Gamma_{\text{total}}$ Γ_{260}/Γ

VALUE (units 10^{-5})	CL%	DOCUMENT ID		TECN	COMMENT
<1.2	90	ABLIKIM	06M	BES2	$e^+e^- \to J/\psi$

$\Gamma(\overline{D}{}^0 e^+ e^- + \text{c.c.})/\Gamma_{\text{total}}$ Γ_{261}/Γ

VALUE	CL%	DOCUMENT ID		TECN	COMMENT
$<8.5 \times 10^{-8}$	90	[1] ABLIKIM	17AF	BES3	$e^+e^- \to J/\psi$
• • • We do not use the following data for averages, fits, limits, etc. • • •					
$<1.1 \times 10^{-5}$	90	ABLIKIM	06M	BES2	$e^+e^- \to J/\psi$

[1] Using D^0 decays to $K^-\pi^+$, $K^-\pi^+\pi^0$, and $K^-\pi^+\pi^+\pi^-$.

$\Gamma(D_s^- e^+ \nu_e + \text{c.c.})/\Gamma_{\text{total}}$ Γ_{262}/Γ

VALUE (units 10^{-6})	CL%	DOCUMENT ID		TECN	COMMENT
< 1.3	90	ABLIKIM	14R	BES3	$e^+e^- \to J/\psi$
• • • We do not use the following data for averages, fits, limits, etc. • • •					
<36	90	[1] ABLIKIM	06M	BES2	$e^+e^- \to J/\psi$

[1] Using $B(D_s^- \to \phi\pi^-) = 4.4 \pm 0.5$ %.

$\Gamma(D_s^{*-} e^+ \nu_e + \text{c.c.})/\Gamma_{\text{total}}$ Γ_{263}/Γ

VALUE	CL%	DOCUMENT ID		TECN	COMMENT
$<1.8 \times 10^{-6}$	90	ABLIKIM	14R	BES3	$e^+e^- \to J/\psi$

$\Gamma(D^- \pi^+ + \text{c.c.})/\Gamma_{\text{total}}$ Γ_{264}/Γ

VALUE	CL%	DOCUMENT ID		TECN	COMMENT
$<7.5 \times 10^{-5}$	90	ABLIKIM	08J	BES2	$e^+e^- \to J/\psi$

$\Gamma(\overline{D}{}^0 \overline{K}{}^0 + \text{c.c.})/\Gamma_{\text{total}}$ Γ_{265}/Γ

VALUE	CL%	DOCUMENT ID		TECN	COMMENT
$<1.7 \times 10^{-4}$	90	ABLIKIM	08J	BES2	$e^+e^- \to J/\psi$

Meson Particle Listings

$J/\psi(1S)$

$\Gamma(\overline{D}^0 K^{*0} + \text{c.c.})/\Gamma_{\text{total}}$ Γ_{266}/Γ

VALUE	CL%	DOCUMENT ID		TECN	COMMENT
$<2.5 \times 10^{-6}$	90	ABLIKIM	14K	BES3	$e^+ e^- \to J/\psi$

$\Gamma(D_s^- \pi^+ + \text{c.c.})/\Gamma_{\text{total}}$ Γ_{267}/Γ

VALUE	CL%	DOCUMENT ID		TECN	COMMENT
$<1.3 \times 10^{-4}$	90	ABLIKIM	08J	BES2	$e^+ e^- \to J/\psi$

$\Gamma(D_s^- \rho^+ + \text{c.c.})/\Gamma_{\text{total}}$ Γ_{268}/Γ

VALUE	CL%	DOCUMENT ID		TECN	COMMENT
$<1.3 \times 10^{-5}$	90	ABLIKIM	14K	BES3	$e^+ e^- \to J/\psi$

CHARGE CONJUGATION (C), PARITY (P), LEPTON FAMILY NUMBER (LF) VIOLATING MODES

$\Gamma(\gamma\gamma)/\Gamma_{\text{total}}$ Γ_{269}/Γ

VALUE (units 10^{-7})	CL%	DOCUMENT ID		TECN	COMMENT
< 2.7	90	ABLIKIM	14Q	BES3	$\psi(2S) \to \pi^+ \pi^- J/\psi$
• • • We do not use the following data for averages, fits, limits, etc. • • •					
< 50	90	ADAMS	08	CLEO	$\psi(2S) \to \pi^+ \pi^- J/\psi$
<1600	90	[1] WICHT	08	BELL	$B^\pm \to K^\pm \gamma\gamma$
< 220	90	ABLIKIM	07J	BES2	$\psi(2S) \to J/\psi \pi^+ \pi^-$
<5000	90	BARTEL	77	CNTR	$e^+ e^-$

[1] WICHT 08 reports $[\Gamma(J/\psi(1S) \to \gamma\gamma)/\Gamma_{\text{total}}] \times [\text{B}(B^+ \to J/\psi(1S) K^+)] < 0.16 \times 10^{-6}$ which we divide by our best value $\text{B}(B^+ \to J/\psi(1S) K^+) = 1.010 \times 10^{-3}$.

$\Gamma(\gamma\phi)/\Gamma_{\text{total}}$ Γ_{270}/Γ

VALUE	CL%	DOCUMENT ID		TECN	COMMENT
$<1.4 \times 10^{-6}$	90	ABLIKIM	14Q	BES3	$\psi(2S) \to \pi^+ \pi^- J/\psi$

$\Gamma(e^\pm \mu^\mp)/\Gamma_{\text{total}}$ Γ_{271}/Γ

VALUE (units 10^{-7})	CL%	DOCUMENT ID		TECN	COMMENT
< 1.6	90	ABLIKIM	13L	BES3	$e^+ e^- \to J/\psi$
• • • We do not use the following data for averages, fits, limits, etc. • • •					
<11	90	BAI	03D	BES	$e^+ e^- \to J/\psi$

$\Gamma(e^\pm \tau^\mp)/\Gamma_{\text{total}}$ Γ_{272}/Γ

VALUE (units 10^{-6})	CL%	DOCUMENT ID		TECN	COMMENT
<8.3	90	ABLIKIM	04	BES	$e^+ e^- \to J/\psi$

$\Gamma(\mu^\pm \tau^\mp)/\Gamma_{\text{total}}$ Γ_{273}/Γ

VALUE (units 10^{-6})	CL%	DOCUMENT ID		TECN	COMMENT
<2.0	90	ABLIKIM	04	BES	$e^+ e^- \to J/\psi$

OTHER DECAYS

$\Gamma(\text{invisible})/\Gamma(e^+ e^-)$ Γ_{274}/Γ_5

VALUE	CL%	DOCUMENT ID		TECN	COMMENT
$<6.6 \times 10^{-2}$	90	LEES	13I	BABR	$B \to K^{(*)} J/\psi$

$\Gamma(\text{invisible})/\Gamma(\mu^+ \mu^-)$ Γ_{274}/Γ_7

VALUE	CL%	DOCUMENT ID		TECN	COMMENT
$<1.2 \times 10^{-2}$	90	ABLIKIM	08G	BES2	$\psi(2S) \to \pi^+ \pi^- J/\psi$

$J/\psi(1S)$ REFERENCES

ABLIKIM 17AF PR D96 111101 M. Ablikim *et al.* (BES III Collab.)
ABLIKIM 17AH PR D96 112001 M. Ablikim *et al.* (BES III Collab.)
ABLIKIM 17AK PR D96 112012 M. Ablikim *et al.* (BES III Collab.)
ABLIKIM 17E PL B770 217 M. Ablikim *et al.* (BES III Collab.)
ABLIKIM 17L PR D95 052003 M. Ablikim *et al.* (BES III Collab.)
LEES 17A PR D95 052001 J.P. Lees *et al.* (BABAR Collab.)
LEES 17C PR D95 072007 J.P. Lees *et al.* (BABAR Collab)
LEES 17D PR D95 092005 J.P. Lees *et al.* (BABAR Collab.)
ABLIKIM 16E PR D93 052005 M. Ablikim *et al.* (BES III Collab.)
ABLIKIM 16J PRL 117 042002 M. Ablikim *et al.* (BES III Collab.)
ABLIKIM 16K PR D93 052010 M. Ablikim *et al.* (BES III Collab.)
ABLIKIM 16L PR D93 072003 M. Ablikim *et al.* (BES III Collab.)
ABLIKIM 16M PR D93 072008 M. Ablikim *et al.* (BES III Collab.)
ABLIKIM 16N PR D93 112011 M. Ablikim (BES III Collab.)
ABLIKIM 16P PR D94 072005 M. Ablikim *et al.* (BES III Collab.)
ABLIKIM 16Q PL B761 98 M. Ablikim *et al.* (BES III Collab.)
AAIJ 15BI EPJ C75 311 R. Aaij *et al.* (LHCb Collab.)
ABLIKIM 15AE PR D92 052003 M. Ablikim *et al.* (BES III Collab.)
ABLIKIM 15H PR D91 052017 M. Ablikim *et al.* (BES III Collab.)
ABLIKIM 15K PR D91 112001 M. Ablikim *et al.* (BES III Collab.)
ABLIKIM 15P PR D92 012007 M. Ablikim *et al.* (BES III Collab.)
ABLIKIM 15T PRL 115 091803 M. Ablikim *et al.* (BES III Collab.)
ANASHIN 15 PL B749 50 V.V. Anashin *et al.* (KEDR Collab.)
DOBBS 15 PR D91 052006 S. Dobbs *et al.* (NWES)
LEES 15J PR D92 072008 J.P. Lees *et al.* (BABAR Collab.)
ABLIKIM 14I PR D89 092008 M. Ablikim *et al.* (BES III Collab.)
ABLIKIM 14K PR D89 071101 M. Ablikim *et al.* (BES III Collab.)
ABLIKIM 14N PR D90 052009 M. Ablikim *et al.* (BES III Collab.)
ABLIKIM 14Q PR D90 092002 M. Ablikim *et al.* (BES III Collab.)
ABLIKIM 14R PR D90 112014 M. Ablikim *et al.* (BES III Collab.)
ANASHIN 14 PL B738 391 V.V. Anashin *et al.* (KEDR Collab.)
AULCHENKO 14 PL B731 227 V.M. Aulchenko *et al.* (KEDR Collab.)
LEES 14H PR D89 092002 J.P. Lees *et al.* (BABAR Collab)
ABLIKIM 13F PR D87 052007 M. Ablikim *et al.* (BES III Collab.)
ABLIKIM 13I PR D87 032003 M. Ablikim *et al.* (BES III Collab.)
ABLIKIM 13J PR D87 032008 M. Ablikim *et al.* (BES III Collab.)
ABLIKIM 13L PR D87 112007 Ablikim M. *et al.* (BES III Collab.)
ABLIKIM 13N PR D87 092009 Ablikim M. *et al.* (BES III Collab.)
ABLIKIM 13P PR D87 112004 M. Ablikim *et al.* (BES III Collab.)
ABLIKIM 13R PR D88 032007 M. Ablikim *et al.* (BES III Collab.)
ABLIKIM 13U PR D88 091502 M. Ablikim *et al.* (BES III Collab.)
LEES 13I PR D87 112005 J.P. Lees *et al.* (BABAR Collab.)
LEES 13O PR D87 092005 J.P. Lees *et al.* (BABAR Collab.)
LEES 13Q PR D88 032013 J.P. Lees *et al.* (BABAR Collab.)
LEES 13Y PR D88 072009 J.P. Lees *et al.* (BABAR Collab.)
ABLIKIM 12 PR D85 092012 M. Ablikim *et al.* (BES III Collab.)
ABLIKIM 12B PR D86 032008 M. Ablikim *et al.* (BES III Collab.)
ABLIKIM 12C PR D86 032014 M. Ablikim *et al.* (BES III Collab.)
ABLIKIM 12D PRL 108 112003 M. Ablikim *et al.* (BES III Collab.)
ABLIKIM 12H PL B710 594 M. Ablikim *et al.* (BES III Collab.)
ABLIKIM 12P CP C36 1031 M. Ablikim *et al.* (BES II Collab.)
LEES 12E PR D85 112009 J.P. Lees *et al.* (BABAR Collab.)
LEES 12F PR D86 012008 J.P. Lees *et al.* (BABAR Collab.)
METREVELI 12 PR D85 092007 Z. Metreveli *et al.* (NWES, FLOR, WAYN+)
ABLIKIM 11 PR D83 012003 M. Ablikim *et al.* (BES III Collab.)
ABLIKIM 11C PRL 106 072002 M. Ablikim *et al.* (BES III Collab.)
ABLIKIM 11D PR D83 032003 M. Ablikim *et al.* (BES III Collab.)
ABLIKIM 10C PL B685 27 M. Ablikim *et al.* (BES II Collab.)
ABLIKIM 10E PL B693 88 M. Ablikim *et al.* (BES II Collab.)
ALEXANDER 10 PR D82 092002 J.P. Alexander *et al.* (CLEO Collab.)
ANASHIN 10 PL B685 134 V.V. Anashin *et al.* (KEDR Collab.)
DEL-AMO-SA... 10O PRL 105 172001 P. del Amo Sanchez *et al.* (BABAR Collab.)
INSLER 10 PR D81 091101 J. Insler *et al.* (CLEO Collab.)
ABLIKIM 09 PL B676 25 M. Ablikim *et al.* (BES Collab.)
ABLIKIM 09B PR D80 052004 M. Ablikim *et al.* (BES II Collab.)
MITCHELL 09 PRL 102 011801 R.E. Mitchell *et al.* (CLEO Collab.)
PEDLAR 09 PR D79 111101 T.K. Pedlar *et al.* (CLEO Collab.)
SHEN 09 PR D80 031101 C.P. Shen *et al.* (BELLE Collab.)
ABLIKIM 08 EPJ C53 15 M. Ablikim *et al.* (BES Collab.)
ABLIKIM 08A PR D77 012001 M. Ablikim *et al.* (BES Collab.)
ABLIKIM 08C PL B659 789 M. Ablikim *et al.* (BES Collab.)
ABLIKIM 08E PR D77 032005 M. Ablikim *et al.* (BES Collab.)
ABLIKIM 08F PRL 100 102003 M. Ablikim *et al.* (BES Collab.)
ABLIKIM 08G PRL 100 192001 M. Ablikim *et al.* (BES Collab.)
ABLIKIM 08I PL B662 330 M. Ablikim *et al.* (BES Collab.)
ABLIKIM 08J PL B663 297 M. Ablikim *et al.* (BES Collab.)
ABLIKIM 08O PR D78 092005 M. Ablikim *et al.* (BES Collab.)
ADAMS 08 PRL 101 101801 G.S. Adams *et al.* (CLEO Collab.)
AUBERT 08S PR D77 092002 B. Aubert *et al.* (BABAR Collab.)
BESSON 08 PR D78 032012 D. Besson *et al.* (CLEO Collab.)
PDG 08 PL B667 1 C. Amsler *et al.* (PDG Collab.)
WICHT 08 PL B662 323 J. Wicht *et al.* (BELLE Collab.)
ABLIKIM 07H PR D76 092003 M. Ablikim *et al.* (BES Collab.)
ABLIKIM 07J PR D76 117101 M. Ablikim *et al.* (BES Collab.)
ANDREOTTI 07 PL B654 74 M. Andreotti *et al.* (Fermilab E835 Collab.)
AUBERT 07AK PR D76 012008 B. Aubert *et al.* (BABAR Collab.)
AUBERT 07AU PR D76 092005 B. Aubert *et al.* (BABAR Collab.)
Also PR D77 119902E (errat.) B. Aubert *et al.* (BABAR Collab.)
AUBERT 07BD PR D76 092006 B. Aubert *et al.* (BABAR Collab.)
ABLIKIM 06 PL B632 181 M. Ablikim *et al.* (BES Collab.)
ABLIKIM 06C PL B633 681 M. Ablikim *et al.* (BES Collab.)
ABLIKIM 06E PR D73 052008 M. Ablikim *et al.* (BES Collab.)
ABLIKIM 06F PR D73 052007 M. Ablikim *et al.* (BES Collab.)
ABLIKIM 06H PR D73 112007 M. Ablikim *et al.* (BES Collab.)
ABLIKIM 06J PRL 96 162002 M. Ablikim *et al.* (BES Collab.)
ABLIKIM 06K PRL 97 062001 M. Ablikim *et al.* (BES II Collab.)
ABLIKIM 06M PL B639 418 M. Ablikim *et al.* (BES Collab.)
ABLIKIM 06V PL B642 441 M. Ablikim *et al.* (BES Collab.)
ADAMS 06A PR D73 051103 G.S. Adams *et al.* (CLEO Collab.)
AUBERT 06B PR D73 012005 B. Aubert *et al.* (BABAR Collab.)
AUBERT 06D PR D73 052003 B. Aubert *et al.* (BABAR Collab.)
AUBERT 06E PRL 96 052002 B. Aubert *et al.* (BABAR Collab.)
AUBERT,BE 06D PR D74 091103 B. Aubert *et al.* (BABAR Collab.)
WU 06 PRL 97 162003 C.-H. Wu *et al.* (BELLE Collab.)
ABLIKIM 05 PL B607 243 M. Ablikim *et al.* (BES Collab.)
ABLIKIM 05B PR D71 032003 M. Ablikim *et al.* (BES Collab.)
ABLIKIM 05C PL B610 192 M. Ablikim *et al.* (BES Collab.)
ABLIKIM 05H PR D72 012002 M. Ablikim *et al.* (BES Collab.)
ABLIKIM 05R PRL 95 262001 M. Ablikim *et al.* (BES Collab.)
AUBERT 05D PR D71 052001 B. Aubert *et al.* (BABAR Collab.)
LI 05C PR D71 111103 Z. Li *et al.* (CLEO Collab.)
SIBIRTSEV 05A PR D71 054010 A. Sibirtsev, J. Haidenbauer
ABLIKIM 04 PL B598 172 M. Ablikim *et al.* (BES Collab.)
ABLIKIM 04M PR D70 112008 M. Ablikim *et al.* (BES Collab.)
AUBERT 04 PR D69 011103 B. Aubert *et al.* (BABAR Collab.)
AUBERT,B 04N PR D70 072004 B. Aubert *et al.* (BABAR Collab.)
BAI 04 PL B578 16 J.Z. Bai *et al.* (BES Collab.)
BAI 04A PR D69 012003 J.Z. Bai *et al.* (BES Collab.)
BAI 04D PL B589 7 J.Z. Bai *et al.* (BES Collab.)
BAI 04E PL B591 42 J.Z. Bai *et al.* (BES Collab.)
BAI 04G PR D70 012004 J.Z. Bai *et al.* (BES Collab.)
BAI 04H PR D70 012005 J.Z. Bai *et al.* (BES Collab.)
BAI 04J PL B594 47 J.Z. Bai *et al.* (BES Collab.)
SETH 04 PR D69 097503 K.K. Seth
AULCHENKO 03 PL B573 63 V.M. Aulchenko *et al.* (KEDR Collab.)
BAI 03D PL B561 49 J.Z. Bai *et al.* (BES Collab.)
BAI 03F PRL 91 022001 J.Z. Bai *et al.* (BES II Collab.)
BAI 03G PR D68 052003 J.Z. Bai *et al.* (BES Collab.)
HUANG 03 PRL 91 241802 H.-C. Huang *et al.* (BELLE Collab.)
BAI 02C PRL 88 101802 J.Z. Bai *et al.* (BES Collab.)
ARTAMONOV 00 PL B474 427 A.S. Artamonov *et al.*
BAI 00 PRL 84 594 J.Z. Bai *et al.* (BES Collab.)
BAI 00B PL B472 200 J.Z. Bai *et al.* (BES Collab.)
BAI 00D PL B476 25 J.Z. Bai *et al.* (BES Collab.)
BAI 99 PL B446 356 J.Z. Bai *et al.* (BES Collab.)
BAI 99C PRL 83 1918 J.Z. Bai *et al.* (BES Collab.)
BAI 98D PR D58 092006 J.Z. Bai *et al.* (BES Collab.)
BAI 98G PL B424 213 J.Z. Bai *et al.* (BES Collab.)
BAI 98H PRL 81 1179 J.Z. Bai *et al.* (BES Collab.)
BALDINI 98 PL B444 111 R. Baldini *et al.* (FENICE Collab.)
ARMSTRONG 96 PR D54 7067 T.A. Armstrong *et al.* (E760 Collab.)
BAI 96B PRL 76 3502 J.Z. Bai *et al.* (BES Collab.)
BAI 96C PRL 77 3959 J.Z. Bai *et al.* (BES Collab.)
BAI 96D PR D54 1221 J.Z. Bai *et al.* (BES Collab.)
GRIBUSHIN 96 PR D53 4723 A. Gribushin *et al.* (E672 Collab., E706 Collab.)
HASAN 96 PL B388 376 A. Hasan, D.V. Bugg (BRUN, LOQM)
BAI 95B PL B355 374 J.Z. Bai *et al.* (BES Collab.)
BUGG 95 PL B353 378 D.V. Bugg *et al.* (LOQM, PNPI, WASH)
ANTONELLI 93 PL B301 317 A. Antonelli *et al.* (FENICE Collab.)
ARMSTRONG 93B PR D47 772 T.A. Armstrong *et al.* (FNAL E760 Collab.)
BARNES 93 PL B309 469 P.D. Barnes *et al.* (PS185 Collab.)
AUGUSTIN 92 PR D46 1951 J.E. Augustin, G. Cosme (DM2 Collab.)
BOLTON 92 PL B278 495 T. Bolton *et al.* (Mark III Collab.)
BOLTON 92B PRL 69 1328 T. Bolton *et al.* (Mark III Collab.)
COFFMAN 92 PRL 68 282 D.M. Coffman *et al.* (Mark III Collab.)
HSUEH 92 PR D45 2181 S. Hsueh, S. Palestini (FNAL, TORI)
BISELLO 91 NP B350 1 D. Bisello *et al.* (DM2 Collab.)
AUGUSTIN 90 PR D42 10 J.E. Augustin *et al.* (DM2 Collab.)
BAI 90B PRL 65 1309 Z. Bai *et al.* (Mark III Collab.)

BAI	90C	PRL 65 2507	Z. Bai *et al.*	(Mark III Collab.)
BISELLO	90	PL B241 617	D. Bisello *et al.*	(DM2 Collab.)
COFFMAN	90	PR D41 1410	D.M. Coffman *et al.*	(Mark III Collab.)
JOUSSET	90	PR D41 1389	J. Jousset *et al.*	(DM2 Collab.)
ALEXANDER	89	NP B320 45	J.P. Alexander *et al.*	(LBL, MICH, SLAC)
AUGUSTIN	89	NP B320 1	J.E. Augustin, G. Cosme	(DM2 Collab.)
BISELLO	89B	PR D39 701	G. Busetto *et al.*	(DM2 Collab.)
AUGUSTIN	88	PRL 60 2238	J.E. Augustin *et al.*	(DM2 Collab.)
COFFMAN	88	PR D38 2695	D.M. Coffman *et al.*	(Mark III Collab.)
FALVARD	88	PR D38 2706	A. Falvard *et al.*	(CLER, FRAS, LALO+)
AUGUSTIN	87	ZPHY C36 369	J.E. Augustin *et al.*	(LALO, CLER, FRAS+)
BAGLIN	87	NP B286 592	C. Baglin *et al.*	(LAPP, CERN, GENO, LYON+)
BALTRUSAIT...	87	PR D35 2077	R.M. Baltrusaitis *et al.*	(Mark III Collab.)
BECKER	87	PRL 59 186	J.J. Becker *et al.*	(Mark III Collab.)
BISELLO	87	PL B192 239	D. Bisello *et al.*	(PADO, CLER, FRAS+)
COHEN	87	RMP 59 1121	E.R. Cohen, B.N. Taylor	(RISC, NBS)
HENRARD	87	NP B292 670	P. Henrard *et al.*	(CLER, FRAS, LALO+)
PALLIN	87	NP B292 653	D. Pallin *et al.*	(CLER, FRAS, LALO, PADO)
BALTRUSAIT...	86	PR D33 629	R.M. Baltrusaitis *et al.*	(Mark III Collab.)
BALTRUSAIT...	86B	PR D33 1222	R.M. Baltrusaitis *et al.*	(Mark III Collab.)
BALTRUSAIT...	86D	PRL 56 107	R.M. Baltrusaitis	(CIT, UCSC, ILL, SLAC+)
BISELLO	86B	PL B179 294	D. Bisello *et al.*	(DM2 Collab.)
GAISER	86	PR D34 711	J. Gaiser *et al.*	(Crystal Ball Collab.)
BALTRUSAIT...	85C	PRL 55 1723	R.M. Baltrusaitis *et al.*	(CIT, UCSC+)
BALTRUSAIT...	85D	PR D32 566	R.M. Baltrusaitis *et al.*	(CIT, UCSC+)
KURAEV	85	SJNP 41 466 Translated from YAF 41 733.	E.A. Kuraev, V.S. Fadin	(NOVO)
BALTRUSAIT...	84	PRL 52 2126	R.M. Baltrusaitis *et al.*	(CIT, UCSC+)
EATON	84	PR D29 804	M.W. Eaton *et al.*	(LBL, SLAC)
BLOOM	83	ARNS 33 143	E.D. Bloom, C. Peck	(SLAC, CIT)
EDWARDS	83B	PRL 51 859	C. Edwards *et al.*	(CIT, HARV, PRIN+)
FRANKLIN	83	PRL 51 963	M.E.B. Franklin *et al.*	(LBL, SLAC)
BURKE	82	PRL 49 632	D.L. Burke *et al.*	(LBL, SLAC)
EDWARDS	82B	PR D25 3065	C. Edwards *et al.*	(CIT, HARV, PRIN+)
EDWARDS	82D	PRL 48 458	C. Edwards *et al.*	(CIT, HARV, PRIN+)
Also		ARNS 33 143	E.D. Bloom, C. Peck	(SLAC, CIT)
EDWARDS	82E	PRL 49 259	C. Edwards *et al.*	(CIT, HARV, PRIN+)
LEMOIGNE	82	PL 113B 509	Y. Lemoigne *et al.*	(SACL, LOIC, SHMP+)
BESCH	81	ZPHY C8 1	H.J. Besch *et al.*	(BONN, DESY, MANZ)
GIDAL	81	PL 107B 153	G. Gidal *et al.*	(SLAC, LBL)
PARTRIDGE	80	PRL 44 712	R. Partridge *et al.*	(CIT, HARV, PRIN+)
SCHARRE	80	PL 97B 329	D.L. Scharre *et al.*	(SLAC, LBL)
ZHOLENTZ	80	PL 96B 214	A.A. Zholents *et al.*	(NOVO)
Also		SJNP 34 814 Translated from YAF 34 1471.	A.A. Zholents *et al.*	(NOVO)
BRANDELIK	79C	ZPHY C1 233	R. Brandelik *et al.*	(DASP Collab.)
ALEXANDER	78	PL 72B 493	G. Alexander *et al.*	(DESY, HAMB, SIEG+)
BESCH	78	PL 78B 347	H.J. Besch *et al.*	(BONN, DESY, MANZ)
BRANDELIK	78B	PL 74B 292	R. Brandelik *et al.*	(DASP Collab.)
PERUZZI	78	PR D17 2901	I. Peruzzi *et al.*	(SLAC, LBL)
BARTEL	77	PL 66B 489	W. Bartel *et al.*	(DESY, HEIDP)
BURMESTER	77D	PL 72B 135	J. Burmester *et al.*	(DESY, HAMB, SIEG+)
FELDMAN	77	PRPL 33C 285	G.J. Feldman, M.L. Perl	(LBL, SLAC)
VANNUCCI	77	PR D15 1814	F. Vannucci *et al.*	(SLAC, LBL)
BARTEL	76	PL 64B 483	W. Bartel *et al.*	(DESY, HEIDP)
BRAUNSCH...	76	PL 63B 487	W. Braunschweig *et al.*	(DASP Collab.)
JEAN-MARIE	76	PRL 36 291	B. Jean-Marie *et al.*	(SLAC, LBL) IG
BALDINI-...	75	PL 58B 471	R. Baldini-Celio *et al.*	(FRAS, ROMA)
BOYARSKI	75	PRL 34 1357	A.M. Boyarski *et al.*	(SLAC, LBL) JPC
DASP	75	PL 56B 491	W. Braunschweig *et al.*	(DASP Collab.)
ESPOSITO	75B	LNC 14 73	B. Esposito *et al.*	(FRAS, NAPL, PADO+)
FORD	75	PRL 34 604	R.L. Ford *et al.*	(SLAC, PENN)

See the related review(s):

Branching Ratios of $\psi(2S)$ and $\chi^0_{c,1,2}$

$\chi_{c0}(1P)$

$I^G(J^{PC}) = 0^+(0^{++})$

$\chi_{c0}(1P)$ MASS

VALUE (MeV)	*EVTS*	*DOCUMENT ID*		*TECN*	*COMMENT*
3414.71± 0.30 OUR AVERAGE					
3413.0 ± 1.9 ±0.6	933	[1] AAIJ	17BB	LHCB	$pp \to b\overline{b}X \to 2(K^+K^-)X$
3414.2 ± 0.5 ±2.3	5.4k	UEHARA	08	BELL	$\gamma\gamma \to \chi_{c0} \to$ hadrons
3406 ± 7 ±6	230	[2] ABE	07	BELL	$e^+e^- \to J/\psi(c\overline{c})$
3414.21± 0.39±0.27		ABLIKIM	05G	BES2	$\psi(2S) \to \gamma\chi_{c0}$
3414.7 $^{+\ 0.7}_{-\ 0.6}$ ±0.2		[3] ANDREOTTI	03	E835	$\overline{p}p \to \chi_{c0} \to \pi^0\pi^0$
3415.5 ± 0.4 ±0.4	392	[4] BAGNASCO	02	E835	$\overline{p}p \to \chi_{c0} \to J/\psi\gamma$
3417.4 $^{+\ 1.8}_{-\ 1.9}$ ±0.2		[3] AMBROGIANI	99B	E835	$\overline{p}p \to e^+e^-\gamma$
3414.1 ± 0.6 ±0.8		BAI	99B	BES	$\psi(2S) \to \gamma$X
3417.8 ± 0.4 ±4		[3] GAISER	86	CBAL	$\psi(2S) \to \gamma$X
3416 ± 3 ±4		[5] TANENBAUM	78	MRK1	e^+e^-
• • • We do not use the following data for averages, fits, limits, etc. • • •					
3414.6 ± 1.1	266	UEHARA	13	BELL	$\gamma\gamma \to K^0_S K^0_S$
3416.5 ± 3.0		EISENSTEIN	01	CLE2	$e^+e^- \to e^+e^-\chi_{c0}$
3422 ±10		[5] BARTEL	78B	CNTR	$e^+e^- \to J/\psi 2\gamma$
3415 ± 9		[5] BIDDICK	77	CNTR	$e^+e^- \to \gamma$X

[1] From a fit of the $\phi\phi$ invariant mass with the width of $\chi_{c0}(1P)$ fixed to the PDG 16 value.
[2] From a fit of the J/ψ recoil mass spectrum. Supersedes ABE,K 02 and ABE 04G.
[3] Using mass of $\psi(2S) = 3686.0$ MeV.
[4] Recalculated by ANDREOTTI 05A, using the value of $\psi(2S)$ mass from AULCHENKO 03.
[5] Mass value shifted by us by amount appropriate for $\psi(2S)$ mass = 3686 MeV and $J/\psi(1S)$ mass = 3097 MeV.

$\chi_{c0}(1P)$ WIDTH

VALUE (MeV)	*EVTS*	*DOCUMENT ID*		*TECN*	*COMMENT*
10.8±0.6 OUR FIT					
10.5±0.8 OUR AVERAGE Error includes scale factor of 1.1.					
10.6±1.9±2.6	5.4k	UEHARA	08	BELL	$\gamma\gamma \to \chi_{c0} \to$ hadrons
12.6$^{+1.5\ +0.9}_{-1.6\ -1.1}$		ABLIKIM	05G	BES2	$\psi(2S) \to \gamma\chi_{c0}$
8.6$^{+1.7}_{-1.3}$±0.1		ANDREOTTI	03	E835	$\overline{p}p \to \chi_{c0} \to \pi^0\pi^0$
9.7±1.0	392	[1] BAGNASCO	02	E835	$\overline{p}p \to \chi_{c0} \to J/\psi\gamma$
16.6$^{+5.2}_{-3.7}$±0.1		AMBROGIANI	99B	E835	$\overline{p}p \to e^+e^-\gamma$
14.3±2.0±3.0		BAI	98I	BES	$\psi(2S) \to \gamma\pi^+\pi^-$
13.5±3.3±4.2		GAISER	86	CBAL	$\psi(2S) \to \gamma$X, $\gamma\pi^0\pi^0$
• • • We do not use the following data for averages, fits, limits, etc. • • •					
13.2±2.1	266	UEHARA	13	BELL	$\gamma\gamma \to K^0_S K^0_S$

[1] Recalculated by ANDREOTTI 05A.

$\chi_{c0}(1P)$ DECAY MODES

Mode	Fraction (Γ_i/Γ)	Scale factor/ Confidence level
Hadronic decays		
Γ_1 $2(\pi^+\pi^-)$	(2.34±0.18) %	
Γ_2 $\rho^0\pi^+\pi^-$	(9.1 ±2.9) $\times 10^{-3}$	
Γ_3 $\rho^0\rho^0$		
Γ_4 $f_0(980)f_0(980)$	(6.6 ±2.1) $\times 10^{-4}$	
Γ_5 $\pi^+\pi^-\pi^0\pi^0$	(3.3 ±0.4) %	
Γ_6 $\rho^+\pi^-\pi^0$ + c.c.	(2.9 ±0.4) %	
Γ_7 $4\pi^0$	(3.3 ±0.4) $\times 10^{-3}$	
Γ_8 $\pi^+\pi^-K^+K^-$	(1.81±0.14) %	
Γ_9 $K_0^*(1430)^0\overline{K}_0^*(1430)^0 \to \pi^+\pi^-K^+K^-$	(9.8 $^{+4.0}_{-2.8}$) $\times 10^{-4}$	
Γ_{10} $K_0^*(1430)^0\overline{K}_2^*(1430)^0$ + c.c. $\to \pi^+\pi^-K^+K^-$	(8.0 $^{+2.0}_{-2.4}$) $\times 10^{-4}$	
Γ_{11} $K_1(1270)^+K^-$ + c.c. $\to \pi^+\pi^-K^+K^-$	(6.3 ±1.9) $\times 10^{-3}$	
Γ_{12} $K_1(1400)^+K^-$ + c.c. $\to \pi^+\pi^-K^+K^-$	< 2.7 $\times 10^{-3}$	CL=90%
Γ_{13} $f_0(980)f_0(980)$	(1.6 $^{+1.0}_{-0.9}$) $\times 10^{-4}$	
Γ_{14} $f_0(980)f_0(2200)$	(7.9 $^{+2.0}_{-2.5}$) $\times 10^{-4}$	
Γ_{15} $f_0(1370)f_0(1370)$	< 2.7 $\times 10^{-4}$	CL=90%
Γ_{16} $f_0(1370)f_0(1500)$	< 1.7 $\times 10^{-4}$	CL=90%
Γ_{17} $f_0(1370)f_0(1710)$	(6.7 $^{+3.5}_{-2.3}$) $\times 10^{-4}$	
Γ_{18} $f_0(1500)f_0(1370)$	< 1.3 $\times 10^{-4}$	CL=90%
Γ_{19} $f_0(1500)f_0(1500)$	< 5 $\times 10^{-5}$	CL=90%
Γ_{20} $f_0(1500)f_0(1710)$	< 7 $\times 10^{-5}$	CL=90%
Γ_{21} $K^+K^-\pi^+\pi^-\pi^0$	(8.6 ±0.9) $\times 10^{-3}$	
Γ_{22} $K^0_S K^\pm\pi^\mp\pi^+\pi^-$	(4.2 ±0.4) $\times 10^{-3}$	
Γ_{23} $K^+K^-\pi^0\pi^0$	(5.6 ±0.9) $\times 10^{-3}$	
Γ_{24} $K^+\pi^-\overline{K}^0\pi^0$ + c.c.	(2.49±0.33) %	
Γ_{25} $\rho^+K^-K^0$ + c.c.	(1.21±0.21) %	
Γ_{26} $K^*(892)^-K^+\pi^0 \to K^+\pi^-\overline{K}^0\pi^0$ + c.c.	(4.6 ±1.2) $\times 10^{-3}$	
Γ_{27} $K^0_S K^0_S\pi^+\pi^-$	(5.7 ±1.1) $\times 10^{-3}$	
Γ_{28} $K^+K^-\eta\pi^0$	(3.0 ±0.7) $\times 10^{-3}$	
Γ_{29} $3(\pi^+\pi^-)$	(1.20±0.18) %	
Γ_{30} $K^+\overline{K}^*(892)^0\pi^-$ + c.c.	(7.5 ±1.6) $\times 10^{-3}$	
Γ_{31} $K^*(892)^0\overline{K}^*(892)^0$	(1.7 ±0.6) $\times 10^{-3}$	
Γ_{32} $\pi\pi$	(8.51±0.33) $\times 10^{-3}$	
Γ_{33} $\pi^0\eta$	< 1.8 $\times 10^{-4}$	
Γ_{34} $\pi^0\eta'$	< 1.1 $\times 10^{-3}$	
Γ_{35} $\pi^0\eta_c$	< 1.6 $\times 10^{-3}$	CL=90%
Γ_{36} $\eta\eta$	(3.01±0.19) $\times 10^{-3}$	
Γ_{37} $\eta\eta'$	(9.1 ±1.1) $\times 10^{-5}$	
Γ_{38} $\eta'\eta'$	(2.17±0.12) $\times 10^{-3}$	
Γ_{39} $\omega\omega$	(9.7 ±1.1) $\times 10^{-4}$	
Γ_{40} $\omega\phi$	(1.18±0.22) $\times 10^{-4}$	
Γ_{41} ωK^+K^-	(1.94±0.21) $\times 10^{-3}$	
Γ_{42} K^+K^-	(6.05±0.31) $\times 10^{-3}$	
Γ_{43} $K^0_S K^0_S$	(3.16±0.17) $\times 10^{-3}$	
Γ_{44} $\pi^+\pi^-\eta$	< 2.0 $\times 10^{-4}$	CL=90%
Γ_{45} $\pi^+\pi^-\eta'$	< 4 $\times 10^{-4}$	CL=90%
Γ_{46} $\overline{K}^0K^+\pi^-$ + c.c.	< 9 $\times 10^{-5}$	CL=90%
Γ_{47} $K^+K^-\pi^0$	< 6 $\times 10^{-5}$	CL=90%

Meson Particle Listings

$\chi_{c0}(1P)$

Γ_{48}	$K^+K^-\eta$	< 2.3	$\times 10^{-4}$	CL=90%
Γ_{49}	$K^+K^-K^0_SK^0_S$	$(1.4 \pm 0.5) \times 10^{-3}$		
Γ_{50}	$K^+K^-K^+K^-$	$(2.82 \pm 0.29) \times 10^{-3}$		
Γ_{51}	$K^+K^-\phi$	$(9.7 \pm 2.5) \times 10^{-4}$		
Γ_{52}	$\overline{K}^0K^+\pi^-\phi$ + c.c.	$(3.7 \pm 0.6) \times 10^{-3}$		
Γ_{53}	$K^+K^-\pi^0\phi$	$(1.90 \pm 0.35) \times 10^{-3}$		
Γ_{54}	$\phi\pi^+\pi^-\pi^0$	$(1.18 \pm 0.15) \times 10^{-3}$		
Γ_{55}	$\phi\phi$	$(8.0 \pm 0.7) \times 10^{-4}$		
Γ_{56}	$p\overline{p}$	$(2.21 \pm 0.08) \times 10^{-4}$		
Γ_{57}	$p\overline{p}\pi^0$	$(7.0 \pm 0.7) \times 10^{-4}$		S=1.3
Γ_{58}	$p\overline{p}\eta$	$(3.5 \pm 0.4) \times 10^{-4}$		
Γ_{59}	$p\overline{p}\omega$	$(5.2 \pm 0.6) \times 10^{-4}$		
Γ_{60}	$p\overline{p}\phi$	$(6.0 \pm 1.4) \times 10^{-5}$		
Γ_{61}	$p\overline{p}\pi^+\pi^-$	$(2.1 \pm 0.7) \times 10^{-3}$		S=1.4
Γ_{62}	$p\overline{p}\pi^0\pi^0$	$(1.04 \pm 0.28) \times 10^{-3}$		
Γ_{63}	$p\overline{p}K^+K^-$ (non-resonant)	$(1.22 \pm 0.26) \times 10^{-4}$		
Γ_{64}	$p\overline{p}K^0_SK^0_S$	< 8.8	$\times 10^{-4}$	CL=90%
Γ_{65}	$p\overline{n}\pi^-$	$(1.27 \pm 0.11) \times 10^{-3}$		
Γ_{66}	$\overline{p}n\pi^+$	$(1.37 \pm 0.12) \times 10^{-3}$		
Γ_{67}	$p\overline{n}\pi^-\pi^0$	$(2.34 \pm 0.21) \times 10^{-3}$		
Γ_{68}	$\overline{p}n\pi^+\pi^0$	$(2.21 \pm 0.18) \times 10^{-3}$		
Γ_{69}	$\Lambda\overline{\Lambda}$	$(3.27 \pm 0.24) \times 10^{-4}$		
Γ_{70}	$\Lambda\overline{\Lambda}\pi^+\pi^-$	$(1.18 \pm 0.13) \times 10^{-3}$		
Γ_{71}	$\Lambda\overline{\Lambda}\pi^+\pi^-$ (non-resonant)	< 5	$\times 10^{-4}$	CL=90%
Γ_{72}	$\Sigma(1385)^+\overline{\Lambda}\pi^-$ + c.c.	< 5	$\times 10^{-4}$	CL=90%
Γ_{73}	$\Sigma(1385)^-\overline{\Lambda}\pi^+$ + c.c.	< 5	$\times 10^{-4}$	CL=90%
Γ_{74}	$K^+\overline{p}\Lambda$ + c.c.	$(1.25 \pm 0.12) \times 10^{-3}$		S=1.3
Γ_{75}	$K^+\overline{p}\Lambda(1520)$ + c.c.	$(2.9 \pm 0.7) \times 10^{-4}$		
Γ_{76}	$\Lambda(1520)\overline{\Lambda}(1520)$	$(3.1 \pm 1.2) \times 10^{-4}$		
Γ_{77}	$\Sigma^0\overline{\Sigma}^0$	$(4.5 \pm 0.4) \times 10^{-4}$		
Γ_{78}	$\Sigma^+\overline{\Sigma}^-$	$(4.0 \pm 0.7) \times 10^{-4}$		S=1.7
Γ_{79}	$\Sigma(1385)^+\overline{\Sigma}(1385)^-$	$(1.6 \pm 0.6) \times 10^{-4}$		
Γ_{80}	$\Sigma(1385)^-\overline{\Sigma}(1385)^+$	$(2.3 \pm 0.7) \times 10^{-4}$		
Γ_{81}	$K^-\Lambda\overline{\Xi}^+$ + c.c.	$(1.94 \pm 0.35) \times 10^{-4}$		
Γ_{82}	$\Xi^0\overline{\Xi}^0$	$(3.1 \pm 0.8) \times 10^{-4}$		
Γ_{83}	$\Xi^-\overline{\Xi}^+$	$(4.8 \pm 0.7) \times 10^{-4}$		
Γ_{84}	$\eta_c\pi^+\pi^-$	< 7	$\times 10^{-4}$	CL=90%

Radiative decays

Γ_{85}	$\gamma J/\psi(1S)$	(1.40 ± 0.05) %		
Γ_{86}	$\gamma\rho^0$	< 9	$\times 10^{-6}$	CL=90%
Γ_{87}	$\gamma\omega$	< 8	$\times 10^{-6}$	CL=90%
Γ_{88}	$\gamma\phi$	< 6	$\times 10^{-6}$	CL=90%
Γ_{89}	$\gamma\gamma$	$(2.04 \pm 0.09) \times 10^{-4}$		
Γ_{90}	$e^+e^-J/\psi(1S)$	$(1.54 \pm 0.33) \times 10^{-4}$		

CONSTRAINED FIT INFORMATION

A multiparticle fit to $\chi_{c1}(1P)$, $\chi_{c0}(1P)$, $\chi_{c2}(1P)$, and $\psi(2S)$ with 4 total widths, a partial width, 25 combinations of partial widths obtained from integrated cross section, and 84 branching ratios uses 247 measurements to determine 49 parameters. The overall fit has a $\chi^2 = 376.9$ for 198 degrees of freedom.

The following *off-diagonal* array elements are the correlation coefficients $\langle \delta p_i \delta p_j \rangle / (\delta p_i \cdot \delta p_j)$, in percent, from the fit to parameters p_i, including the branching fractions, $x_i \equiv \Gamma_i/\Gamma_{\rm total}$.

	x_1	x_2	x_8	x_{30}	x_{32}	x_{36}	x_{42}	x_{43}	x_{50}	x_{55}
x_2	24									
x_8	9	2								
x_{30}	5	1	28							
x_{32}	8	2	10	3						
x_{36}	4	1	5	1	14					
x_{42}	8	2	8	3	18	11				
x_{43}	7	2	8	2	18	10	14			
x_{50}	5	1	5	2	9	5	7	7		
x_{55}	7	2	6	2	9	5	7	7	4	
x_{56}	3	1	4	1	3	−1	7	7	3	3
x_{69}	4	1	5	1	13	8	10	10	5	5
x_{85}	5	1	6	2	17	11	13	12	6	6
x_{89}	−8	−2	−2	−3	14	9	10	10	3	1
Γ	−26	−6	−19	−10	−15	−7	−14	−12	−10	−13

	x_{56}	x_{69}	x_{85}	x_{89}
x_{69}	5			
x_{85}	−19	9		
x_{89}	6	9	13	
Γ	−4	−7	−9	−38

$\chi_{c0}(1P)$ PARTIAL WIDTHS

$\chi_{c0}(1P)$ Γ(i)$\Gamma(\gamma J/\psi(1S))/\Gamma$(total)

$\Gamma(p\overline{p}) \times \Gamma(\gamma J/\psi(1S))/\Gamma_{\rm total}$ $\Gamma_{56}\Gamma_{85}/\Gamma$

VALUE (eV)	EVTS	DOCUMENT ID		TECN	COMMENT
33.6± 2.3 OUR FIT					
• • • We do not use the following data for averages, fits, limits, etc. • • •					
26.6± 2.6±1.4	392	[1,2] BAGNASCO	02	E835	$\overline{p}p \to \chi_{c0} \to J/\psi\gamma$
$48.7^{+11.3}_{-\ 8.9}$±2.4		[1,2] AMBROGIANI	99B	E835	$\overline{p}p \to \gamma J/\psi$

[1] Calculated by us using $B(J/\psi(1S) \to e^+e^-) = 0.0593 \pm 0.0010$.
[2] Values in $(\Gamma(p\overline{p}) \times \Gamma(\gamma J/\psi(1S))/\Gamma_{\rm total})$ and $(\Gamma(p\overline{p})/\Gamma_{\rm total} \times \Gamma(\gamma J/\psi(1S))/\Gamma_{\rm total})$ are not independent. The latter is used in the fit since it is less correlated to the total width.

$\chi_{c0}(1P)$ Γ(i)$\Gamma(\gamma\gamma)/\Gamma$(total)

$\Gamma(2(\pi^+\pi^-)) \times \Gamma(\gamma\gamma)/\Gamma_{\rm total}$ $\Gamma_1\Gamma_{89}/\Gamma$

VALUE (eV)	EVTS	DOCUMENT ID		TECN	COMMENT
52 ± 4 OUR FIT					
49 ±10 OUR AVERAGE Error includes scale factor of 1.8.					
44.7± 3.6±4.9	3.6k	UEHARA	08	BELL	$\gamma\gamma \to \chi_{c0} \to 2(\pi^+\pi^-)$
75 ±13 ±8		EISENSTEIN	01	CLE2	$e^+e^- \to e^+e^-\chi_{c0}$

$\Gamma(\rho^0\rho^0) \times \Gamma(\gamma\gamma)/\Gamma_{\rm total}$ $\Gamma_3\Gamma_{89}/\Gamma$

VALUE (eV)	CL%	EVTS	DOCUMENT ID		TECN	COMMENT
• • • We do not use the following data for averages, fits, limits, etc. • • •						
<12	90	<252	UEHARA	08	BELL	$\gamma\gamma \to \chi_{c0} \to 2(\pi^+\pi^-)$

$\Gamma(\pi^+\pi^-K^+K^-) \times \Gamma(\gamma\gamma)/\Gamma_{\rm total}$ $\Gamma_8\Gamma_{89}/\Gamma$

VALUE (eV)	EVTS	DOCUMENT ID		TECN	COMMENT
40.0±3.5 OUR FIT					
38.8±3.7±4.7	1.7k	UEHARA	08	BELL	$\gamma\gamma \to \chi_{c0} \to K^+K^-\pi^+\pi^-$

$\Gamma(K^+K^-\pi^+\pi^-\pi^0) \times \Gamma(\gamma\gamma)/\Gamma_{\rm total}$ $\Gamma_{21}\Gamma_{89}/\Gamma$

VALUE (eV)	EVTS	DOCUMENT ID		TECN	COMMENT
26±4±4	1094	DEL-AMO-SA...11M		BABR	$\gamma\gamma \to K^+K^-\pi^+\pi^-\pi^0$

$\Gamma(K^+\overline{K}^*(892)^0\pi^- + \text{c.c.}) \times \Gamma(\gamma\gamma)/\Gamma_{\rm total}$ $\Gamma_{30}\Gamma_{89}/\Gamma$

VALUE (eV)	EVTS	DOCUMENT ID		TECN	COMMENT
16 ±4 OUR FIT					
16.7±6.1±3.0	495 ± 182	UEHARA	08	BELL	$\gamma\gamma \to \chi_{c0} \to K^+K^-\pi^+\pi^-$

$\Gamma(K^*(892)^0\overline{K}^*(892)^0) \times \Gamma(\gamma\gamma)/\Gamma_{\rm total}$ $\Gamma_{31}\Gamma_{89}/\Gamma$

VALUE (eV)	CL%	EVTS	DOCUMENT ID		TECN	COMMENT
• • • We do not use the following data for averages, fits, limits, etc. • • •						
<6	90	<148	UEHARA	08	BELL	$\gamma\gamma \to \chi_{c0} \to K^+K^-\pi^+\pi^-$

$\Gamma(\pi\pi) \times \Gamma(\gamma\gamma)/\Gamma_{\rm total}$ $\Gamma_{32}\Gamma_{89}/\Gamma$

VALUE (eV)	EVTS	DOCUMENT ID		TECN	COMMENT
18.8± 1.3 OUR FIT					
23 ± 5 OUR AVERAGE					
$29.7^{+17.4}_{-12.0}$±4.8	103^{+60}_{-42}	[1] UEHARA	09	BELL	10.6 $e^+e^- \to e^+e^-\pi^0\pi^0$
22.7± 3.2±3.5	129 ± 18	[2] NAKAZAWA	05	BELL	10.6 $e^+e^- \to e^+e^-\pi^+\pi^-$

[1] We multiplied the measurement by 3 to convert from $\pi^0\pi^0$ to $\pi\pi$. Interference with the continuum included.
[2] We have multiplied $\pi^+\pi^-$ measurement by 3/2 to obtain $\pi\pi$.

$\Gamma(\eta\eta) \times \Gamma(\gamma\gamma)/\Gamma_{\rm total}$ $\Gamma_{36}\Gamma_{89}/\Gamma$

VALUE (eV)	EVTS	DOCUMENT ID		TECN	COMMENT
9.4±2.3±1.2	22	[1] UEHARA	10A	BELL	10.6 $e^+e^- \to e^+e^-\eta\eta$

[1] Interference with the continuum not included.

$\Gamma(\omega\omega) \times \Gamma(\gamma\gamma)/\Gamma_{\rm total}$ $\Gamma_{39}\Gamma_{89}/\Gamma$

VALUE (eV)	CL%	DOCUMENT ID		TECN	COMMENT
• • • We do not use the following data for averages, fits, limits, etc. • • •					
<3.9	90	[1] LIU	12B	BELL	$\gamma\gamma \to 2(\pi^+\pi^-\pi^0)$

[1] Using $B(\omega \to \pi^+\pi^-\pi^0) = (89.2 \pm 0.7)\%$.

$\Gamma(\omega\phi) \times \Gamma(\gamma\gamma)/\Gamma_{\rm total}$ $\Gamma_{40}\Gamma_{89}/\Gamma$

VALUE (eV)	CL%	DOCUMENT ID		TECN	COMMENT
• • • We do not use the following data for averages, fits, limits, etc. • • •					
<0.34	90	[1] LIU	12B	BELL	$\gamma\gamma \to K^+K^-\pi^+\pi^-\pi^0$

[1] Using $B(\phi \to K^+K^-) = (48.9 \pm 0.5)\%$ and $B(\omega \to \pi^+\pi^-\pi^0) = (89.2 \pm 0.7)\%$.

$\Gamma(K^+K^-) \times \Gamma(\gamma\gamma)/\Gamma_{total}$ $\Gamma_{42}\Gamma_{89}/\Gamma$

VALUE (eV)	EVTS	DOCUMENT ID	TECN	COMMENT
13.4±1.0 OUR FIT				
14.3±1.6±2.3	153 ± 17	NAKAZAWA 05	BELL	10.6 $e^+e^- \to e^+e^-K^+K^-$

$\Gamma(K^0_S K^0_S) \times \Gamma(\gamma\gamma)/\Gamma_{total}$ $\Gamma_{43}\Gamma_{89}/\Gamma$

VALUE (eV)	EVTS	DOCUMENT ID	TECN	COMMENT
7.0 ±0.5 OUR FIT				
8.7 ±1.7 ±0.9	266	[1] UEHARA 13	BELL	$\gamma\gamma \to K^0_S K^0_S$
• • • We do not use the following data for averages, fits, limits, etc. • • •				
7.00±0.65±0.71	134 ± 12	CHEN 07B	BELL	$e^+e^- \to e^+e^-\chi_{c0}$

[1] Supersedes CHEN 07B.

$\Gamma(K^+K^-K^+K^-) \times \Gamma(\gamma\gamma)/\Gamma_{total}$ $\Gamma_{50}\Gamma_{89}/\Gamma$

VALUE (eV)	EVTS	DOCUMENT ID	TECN	COMMENT
6.2±0.7 OUR FIT				
7.9±1.3±1.1	215 ± 36	UEHARA 08	BELL	$\gamma\gamma \to \chi_{c0} \to 2(K^+K^-)$

$\Gamma(\phi\phi) \times \Gamma(\gamma\gamma)/\Gamma_{total}$ $\Gamma_{55}\Gamma_{89}/\Gamma$

VALUE (eV)	EVTS	DOCUMENT ID	TECN	COMMENT
1.76±0.18 OUR FIT				
1.72±0.33±0.14	56 ± 11	[1] LIU 12B	BELL	$\gamma\gamma \to 2(K^+K^-)$
• • • We do not use the following data for averages, fits, limits, etc. • • •				
2.3 ±0.9 ±0.4	23.6 ± 9.6	UEHARA 08	BELL	$\gamma\gamma \to \chi_{c0} \to 2(K^+K^-)$

[1] Supersedes UEHARA 08. Using $B(\phi \to K^+K^-) = (48.9 \pm 0.5)\%$.

$\chi_{c0}(1P)$ BRANCHING RATIOS

HADRONIC DECAYS

$\Gamma(2(\pi^+\pi^-))/\Gamma_{total}$ Γ_1/Γ

VALUE	DOCUMENT ID
0.0234±0.0018 OUR FIT	

$\Gamma(\rho^0\pi^+\pi^-)/\Gamma(2(\pi^+\pi^-))$ Γ_2/Γ_1

VALUE	DOCUMENT ID	TECN	COMMENT
0.39±0.12 OUR FIT			
0.39±0.12	TANENBAUM 78	MRK1	$\psi(2S) \to \gamma\chi_{c0}$

$\Gamma(\rho^0\pi^+\pi^-)/\Gamma_{total}$ Γ_2/Γ

VALUE	DOCUMENT ID
0.0091±0.0029 OUR FIT	

$\Gamma(f_0(980)f_0(980))/\Gamma_{total}$ Γ_4/Γ

VALUE (units 10^{-4})	EVTS	DOCUMENT ID	TECN	COMMENT
6.6±2.1±0.1	36 ± 9	[1] ABLIKIM 04G	BES	$\psi(2S) \to \gamma 2\pi^+ 2\pi^-$

[1] ABLIKIM 04G reports $[\Gamma(\chi_{c0}(1P) \to f_0(980)f_0(980))/\Gamma_{total}] \times [B(\psi(2S) \to \gamma\chi_{c0}(1P))] = (6.5 \pm 1.6 \pm 1.3) \times 10^{-5}$ which we divide by our best value $B(\psi(2S) \to \gamma\chi_{c0}(1P)) = (9.79 \pm 0.20) \times 10^{-2}$. Our first error is their experiment's error and our second error is the systematic error from using our best value.

$\Gamma(\pi^+\pi^-\pi^0\pi^0)/\Gamma_{total}$ Γ_5/Γ

VALUE (%)	EVTS	DOCUMENT ID	TECN	COMMENT
3.3±0.4±0.1	1751.4	[1] HE 08B	CLEO	$e^+e^- \to \gamma h^+h^-h^0h^0$

[1] HE 08B reports 3.54 ± 0.10 ± 0.43 ± 0.18 % from a measurement of $[\Gamma(\chi_{c0}(1P) \to \pi^+\pi^-\pi^0\pi^0)/\Gamma_{total}] \times [B(\psi(2S) \to \gamma\chi_{c0}(1P))]$ assuming $B(\psi(2S) \to \gamma\chi_{c0}(1P)) = (9.22 \pm 0.11 \pm 0.46) \times 10^{-2}$, which we rescale to our best value $B(\psi(2S) \to \gamma\chi_{c0}(1P)) = (9.79 \pm 0.20) \times 10^{-2}$. Our first error is their experiment's error and our second error is the systematic error from using our best value.

$\Gamma(\rho^+\pi^-\pi^0 + \text{c.c.})/\Gamma_{total}$ Γ_6/Γ

VALUE (%)	EVTS	DOCUMENT ID	TECN	COMMENT
2.9±0.4±0.1	1358.5	[1,2] HE 08B	CLEO	$e^+e^- \to \gamma h^+h^-h^0h^0$

[1] HE 08B reports 3.04 ± 0.18 ± 0.42 ± 0.16 % from a measurement of $[\Gamma(\chi_{c0}(1P) \to \rho^+\pi^-\pi^0 + \text{c.c.})/\Gamma_{total}] \times [B(\psi(2S) \to \gamma\chi_{c0}(1P))]$ assuming $B(\psi(2S) \to \gamma\chi_{c0}(1P)) = (9.22 \pm 0.11 \pm 0.46) \times 10^{-2}$, which we rescale to our best value $B(\psi(2S) \to \gamma\chi_{c0}(1P)) = (9.79 \pm 0.20) \times 10^{-2}$. Our first error is their experiment's error and our second error is the systematic error from using our best value.

[2] Calculated by us. We have added the values from HE 08B for $\rho^+\pi^-\pi^0$ and $\rho^-\pi^+\pi^0$ decays assuming uncorrelated statistical and fully correlated systematic uncertainties.

$\Gamma(4\pi^0)/\Gamma_{total}$ Γ_7/Γ

VALUE (units 10^{-3})	EVTS	DOCUMENT ID	TECN	COMMENT
3.3±0.4±0.1	3296	[1] ABLIKIM 11A	BES3	$e^+e^- \to \psi(2S) \to \gamma\chi_{c0}$

[1] ABLIKIM 11A reports $(3.34 \pm 0.06 \pm 0.44) \times 10^{-3}$ from a measurement of $[\Gamma(\chi_{c0}(1P) \to 4\pi^0)/\Gamma_{total}] \times [B(\psi(2S) \to \gamma\chi_{c0}(1P))]$ assuming $B(\psi(2S) \to \gamma\chi_{c0}(1P)) = (9.62 \pm 0.31) \times 10^{-2}$, which we rescale to our best value $B(\psi(2S) \to \gamma\chi_{c0}(1P)) = (9.79 \pm 0.20) \times 10^{-2}$. Our first error is their experiment's error and our second error is the systematic error from using our best value.

$\Gamma(\pi^+\pi^-K^+K^-)/\Gamma_{total}$ Γ_8/Γ

VALUE (units 10^{-3})	DOCUMENT ID
18.1±1.4 OUR FIT	

$\Gamma(K^+\overline{K}^*(892)^0\pi^- + \text{c.c.})/\Gamma(\pi^+\pi^-K^+K^-)$ Γ_{30}/Γ_8

VALUE	DOCUMENT ID	TECN	COMMENT
0.41±0.09 OUR FIT			
0.41±0.10	TANENBAUM 78	MRK1	$\psi(2S) \to \gamma\chi_{c0}$

$\Gamma(K^*_0(1430)^0\overline{K}^*_0(1430)^0 \to \pi^+\pi^-K^+K^-)/\Gamma_{total}$ Γ_9/Γ

VALUE (units 10^{-4})	EVTS	DOCUMENT ID	TECN	COMMENT
$9.8^{+3.6}_{-2.6}$±0.2	83	[1] ABLIKIM 05Q	BES2	$\psi(2S) \to \gamma\pi^+\pi^-K^+K^-$

[1] ABLIKIM 05Q reports $(10.44 \pm 2.37^{+3.05}_{-1.90}) \times 10^{-4}$ from a measurement of $[\Gamma(\chi_{c0}(1P) \to K^*_0(1430)^0\overline{K}^*_0(1430)^0 \to \pi^+\pi^-K^+K^-)/\Gamma_{total}] \times [B(\psi(2S) \to \gamma\chi_{c0}(1P))]$ assuming $B(\psi(2S) \to \gamma\chi_{c0}(1P)) = (9.22 \pm 0.11 \pm 0.46) \times 10^{-2}$, which we rescale to our best value $B(\psi(2S) \to \gamma\chi_{c0}(1P)) = (9.79 \pm 0.20) \times 10^{-2}$. Our first error is their experiment's error and our second error is the systematic error from using our best value.

$\Gamma(K^*_0(1430)^0\overline{K}^*_2(1430)^0 + \text{c.c.} \to \pi^+\pi^-K^+K^-)/\Gamma_{total}$ Γ_{10}/Γ

VALUE (units 10^{-4})	EVTS	DOCUMENT ID	TECN	COMMENT
$8.0^{+2.0}_{-2.4}$±0.2	62	[1] ABLIKIM 05Q	BES2	$\psi(2S) \to \gamma\pi^+\pi^-K^+K^-$

[1] ABLIKIM 05Q reports $(8.49 \pm 1.66^{+1.32}_{-1.99}) \times 10^{-4}$ from a measurement of $[\Gamma(\chi_{c0}(1P) \to K^*_0(1430)^0\overline{K}^*_2(1430)^0 + \text{c.c.} \to \pi^+\pi^-K^+K^-)/\Gamma_{total}] \times [B(\psi(2S) \to \gamma\chi_{c0}(1P))]$ assuming $B(\psi(2S) \to \gamma\chi_{c0}(1P)) = (9.22 \pm 0.11 \pm 0.46) \times 10^{-2}$, which we rescale to our best value $B(\psi(2S) \to \gamma\chi_{c0}(1P)) = (9.79 \pm 0.20) \times 10^{-2}$. Our first error is their experiment's error and our second error is the systematic error from using our best value.

$\Gamma(K_1(1270)^+K^- + \text{c.c.} \to \pi^+\pi^-K^+K^-)/\Gamma_{total}$ Γ_{11}/Γ

VALUE (units 10^{-3})	EVTS	DOCUMENT ID	TECN	COMMENT
6.3±1.9±0.1	68	[1] ABLIKIM 05Q	BES2	$\psi(2S) \to \gamma\pi^+\pi^-K^+K^-$

[1] ABLIKIM 05Q reports $(6.66 \pm 1.31^{+1.60}_{-1.51}) \times 10^{-3}$ from a measurement of $[\Gamma(\chi_{c0}(1P) \to K_1(1270)^+K^- + \text{c.c.} \to \pi^+\pi^-K^+K^-)/\Gamma_{total}] \times [B(\psi(2S) \to \gamma\chi_{c0}(1P))]$ assuming $B(\psi(2S) \to \gamma\chi_{c0}(1P)) = (9.22 \pm 0.11 \pm 0.46) \times 10^{-2}$, which we rescale to our best value $B(\psi(2S) \to \gamma\chi_{c0}(1P)) = (9.79 \pm 0.20) \times 10^{-2}$. Our first error is their experiment's error and our second error is the systematic error from using our best value. The measurement assumes $B(K_1(1270) \to K\rho(770)) = 42 \pm 6\%$.

$\Gamma(K_1(1400)^+K^- + \text{c.c.} \to \pi^+\pi^-K^+K^-)/\Gamma_{total}$ Γ_{12}/Γ

VALUE (units 10^{-3})	CL%	DOCUMENT ID	TECN	COMMENT
<2.7	90	[1] ABLIKIM 05Q	BES2	$\psi(2S) \to \gamma\pi^+\pi^-K^+K^-$

[1] ABLIKIM 05Q reports $< 2.85 \times 10^{-3}$ from a measurement of $[\Gamma(\chi_{c0}(1P) \to K_1(1400)^+K^- + \text{c.c.} \to \pi^+\pi^-K^+K^-)/\Gamma_{total}] \times [B(\psi(2S) \to \gamma\chi_{c0}(1P))]$ assuming $B(\psi(2S) \to \gamma\chi_{c0}(1P)) = (9.22 \pm 0.11 \pm 0.46) \times 10^{-2}$, which we rescale to our best value $B(\psi(2S) \to \gamma\chi_{c0}(1P)) = 9.79 \times 10^{-2}$. The measurement assumes $B(K_1(1400) \to K^*(892)\pi) = 94 \pm 6\%$.

$\Gamma(f_0(980)f_0(980))/\Gamma_{total}$ Γ_{13}/Γ

VALUE (units 10^{-5})	EVTS	DOCUMENT ID	TECN	COMMENT
$16.2^{+10.4}_{-9.0}$±0.3	28	[1] ABLIKIM 05Q	BES2	$\psi(2S) \to \gamma\pi^+\pi^-K^+K^-$

[1] ABLIKIM 05Q reports $[\Gamma(\chi_{c0}(1P) \to f_0(980)f_0(980))/\Gamma_{total}] \times [B(\psi(2S) \to \gamma\chi_{c0}(1P))] = (1.59 \pm 0.50^{+0.89}_{-0.72}) \times 10^{-5}$ which we divide by our best value $B(\psi(2S) \to \gamma\chi_{c0}(1P)) = (9.79 \pm 0.20) \times 10^{-2}$. Our first error is their experiment's error and our second error is the systematic error from using our best value. One of the $f_0(980)$ mesons is identified via decay to $\pi^+\pi^-$ while the other via K^+K^- decay.

$\Gamma(f_0(980)f_0(2200))/\Gamma_{total}$ Γ_{14}/Γ

VALUE (units 10^{-4})	EVTS	DOCUMENT ID	TECN	COMMENT
$7.9^{+2.0}_{-2.5}$±0.2	77	[1] ABLIKIM 05Q	BES2	$\psi(2S) \to \gamma\pi^+\pi^-K^+K^-$

[1] ABLIKIM 05Q reports $(8.42 \pm 1.42^{+1.65}_{-2.29}) \times 10^{-4}$ from a measurement of $[\Gamma(\chi_{c0}(1P) \to f_0(980)f_0(2200))/\Gamma_{total}] \times [B(\psi(2S) \to \gamma\chi_{c0}(1P))]$ assuming $B(\psi(2S) \to \gamma\chi_{c0}(1P)) = (9.22 \pm 0.11 \pm 0.46) \times 10^{-2}$, which we rescale to our best value $B(\psi(2S) \to \gamma\chi_{c0}(1P)) = (9.79 \pm 0.20) \times 10^{-2}$. Our first error is their experiment's error and our second error is the systematic error from using our best value. The f_0 mesons are identified via $f_0(980) \to \pi^+\pi^-$ and $f_0(2200) \to K^+K^-$ decays.

$\Gamma(f_0(1370)f_0(1370))/\Gamma_{total}$ Γ_{15}/Γ

VALUE (units 10^{-4})	CL%	DOCUMENT ID	TECN	COMMENT
<2.7	90	[1] ABLIKIM 05Q	BES2	$\psi(2S) \to \gamma\pi^+\pi^-K^+K^-$

[1] ABLIKIM 05Q reports $< 2.9 \times 10^{-4}$ from a measurement of $[\Gamma(\chi_{c0}(1P) \to f_0(1370)f_0(1370))/\Gamma_{total}] \times [B(\psi(2S) \to \gamma\chi_{c0}(1P))]$ assuming $B(\psi(2S) \to \gamma\chi_{c0}(1P)) = (9.22 \pm 0.11 \pm 0.46) \times 10^{-2}$, which we rescale to our best value $B(\psi(2S) \to \gamma\chi_{c0}(1P)) = 9.79 \times 10^{-2}$. One of the $f_0(1370)$ mesons is identified via decay to $\pi^+\pi^-$ while the other via K^+K^- decay. Both branching fractions for these f_0 decays are implicitly included in the quoted result.

$\Gamma(f_0(1370)f_0(1500))/\Gamma_{total}$ Γ_{16}/Γ

VALUE (units 10^{-4})	CL%	DOCUMENT ID		TECN	COMMENT
<1.7	90	[1] ABLIKIM	05Q	BES2	$\psi(2S) \to \gamma\pi^+\pi^- K^+K^-$

[1] ABLIKIM 05Q reports $< 1.8 \times 10^{-4}$ from a measurement of $[\Gamma(\chi_{c0}(1P) \to f_0(1370)\, f_0(1500))/\Gamma_{total}] \times [B(\psi(2S) \to \gamma\chi_{c0}(1P))]$ assuming $B(\psi(2S) \to \gamma\chi_{c0}(1P)) = (9.22\pm0.11\pm0.46)\times10^{-2}$, which we rescale to our best value $B(\psi(2S) \to \gamma\chi_{c0}(1P)) = 9.79 \times 10^{-2}$. The f_0 mesons are identified via $f_0(1370) \to \pi^+\pi^-$ and $f_0(1500) \to K^+K^-$ decays. Both branching fractions for these f_0 decays are implicitly included in the quoted result.

$\Gamma(f_0(1370)f_0(1710))/\Gamma_{total}$ Γ_{17}/Γ

VALUE (units 10^{-4})	EVTS	DOCUMENT ID		TECN	COMMENT
$6.7^{+3.5}_{-2.3}\pm0.1$	61	[1] ABLIKIM	05Q	BES2	$\psi(2S) \to \gamma\pi^+\pi^- K^+K^-$

[1] ABLIKIM 05Q reports $(7.12\pm1.85^{+3.28}_{-1.68})\times10^{-4}$ from a measurement of $[\Gamma(\chi_{c0}(1P) \to f_0(1370)\, f_0(1710))/\Gamma_{total}] \times [B(\psi(2S) \to \gamma\chi_{c0}(1P))]$ assuming $B(\psi(2S) \to \gamma\chi_{c0}(1P)) = (9.22\pm0.11\pm0.46)\times10^{-2}$, which we rescale to our best value $B(\psi(2S) \to \gamma\chi_{c0}(1P)) = (9.79 \pm 0.20) \times 10^{-2}$. Our first error is their experiment's error and our second error is the systematic error from using our best value. The f_0 mesons are identified via $f_0(1370) \to \pi^+\pi^-$ and $f_0(1710) \to K^+K^-$ decays. Both branching fractions for these f_0 decays are implicitly included in the quoted result.

$\Gamma(f_0(1500)f_0(1370))/\Gamma_{total}$ Γ_{18}/Γ

VALUE (units 10^{-4})	CL%	DOCUMENT ID		TECN	COMMENT
<1.3	90	[1] ABLIKIM	05Q	BES2	$\psi(2S) \to \gamma\pi^+\pi^- K^+K^-$

[1] ABLIKIM 05Q reports $< 1.4 \times 10^{-4}$ from a measurement of $[\Gamma(\chi_{c0}(1P) \to f_0(1500)\, f_0(1370))/\Gamma_{total}] \times [B(\psi(2S) \to \gamma\chi_{c0}(1P))]$ assuming $B(\psi(2S) \to \gamma\chi_{c0}(1P)) = (9.22\pm0.11\pm0.46)\times10^{-2}$, which we rescale to our best value $B(\psi(2S) \to \gamma\chi_{c0}(1P)) = 9.79 \times 10^{-2}$. The f_0 mesons are identified via $f_0(1500) \to \pi^+\pi^-$ and $f_0(1370) \to K^+K^-$ decays. Both branching fractions for these f_0 decays are implicitly included in the quoted result.

$\Gamma(f_0(1500)f_0(1500))/\Gamma_{total}$ Γ_{19}/Γ

VALUE (units 10^{-4})	CL%	DOCUMENT ID		TECN	COMMENT
<0.5	90	[1] ABLIKIM	05Q	BES2	$\psi(2S) \to \gamma\pi^+\pi^- K^+K^-$

[1] ABLIKIM 05Q reports $< 0.55 \times 10^{-4}$ from a measurement of $[\Gamma(\chi_{c0}(1P) \to f_0(1500)\, f_0(1500))/\Gamma_{total}] \times [B(\psi(2S) \to \gamma\chi_{c0}(1P))]$ assuming $B(\psi(2S) \to \gamma\chi_{c0}(1P)) = (9.22\pm0.11\pm0.46)\times10^{-2}$, which we rescale to our best value $B(\psi(2S) \to \gamma\chi_{c0}(1P)) = 9.79 \times 10^{-2}$. One of the $f_0(1500)$ is identified via decay to $\pi^+\pi^-$ while the other via K^+K^- decay. Both branching fractions for these f_0 decays are implicitly included in the quoted result.

$\Gamma(f_0(1500)f_0(1710))/\Gamma_{total}$ Γ_{20}/Γ

VALUE (units 10^{-4})	CL%	DOCUMENT ID		TECN	COMMENT
<0.7	90	[1] ABLIKIM	05Q	BES2	$\psi(2S) \to \gamma\pi^+\pi^- K^+K^-$

[1] ABLIKIM 05Q reports $< 0.73 \times 10^{-4}$ from a measurement of $[\Gamma(\chi_{c0}(1P) \to f_0(1500)\, f_0(1710))/\Gamma_{total}] \times [B(\psi(2S) \to \gamma\chi_{c0}(1P))]$ assuming $B(\psi(2S) \to \gamma\chi_{c0}(1P)) = (9.22\pm0.11\pm0.46)\times10^{-2}$, which we rescale to our best value $B(\psi(2S) \to \gamma\chi_{c0}(1P)) = 9.79 \times 10^{-2}$. The f_0 mesons are identified via $f_0(1500) \to \pi^+\pi^-$ and $f_0(1710) \to K^+K^-$ decays. Both branching fractions for these f_0 decays are implicitly included in the quoted result.

$\Gamma(K^+K^-\pi^+\pi^-\pi^0)/\Gamma_{total}$ Γ_{21}/Γ

VALUE (units 10^{-3})	EVTS	DOCUMENT ID		TECN	COMMENT
$8.61\pm0.13\pm0.94$	9.0k	[1] ABLIKIM	13B	BES3	$e^+e^- \to \psi(2S) \to \gamma\chi_{c0}$

[1] Using 1.06×10^8 $\psi(2S)$ mesons and $B(\psi(2S) \to \chi_{c0}\gamma) = (9.68 \pm 0.31)\%$.

$\Gamma(K^0_S K^\pm\pi^\mp\pi^+\pi^-)/\Gamma_{total}$ Γ_{22}/Γ

VALUE (units 10^{-3})	EVTS	DOCUMENT ID		TECN	COMMENT
$4.22\pm0.10\pm0.43$	2.7k	[1] ABLIKIM	13B	BES3	$e^+e^- \to \psi(2S) \to \gamma\chi_{c0}$

[1] Using 1.06×10^8 $\psi(2S)$ mesons and $B(\psi(2S) \to \chi_{c0}\gamma) = (9.68 \pm 0.31)\%$.

$\Gamma(K^+K^-\pi^0\pi^0)/\Gamma_{total}$ Γ_{23}/Γ

VALUE (%)	EVTS	DOCUMENT ID		TECN	COMMENT
$0.56\pm0.09\pm0.01$	213.5	[1] HE	08B	CLEO	$e^+e^- \to \gamma h^+h^-h^0h^0$

[1] HE 08B reports $0.59 \pm 0.05 \pm 0.08 \pm 0.03$ % from a measurement of $[\Gamma(\chi_{c0}(1P) \to K^+K^-\pi^0\pi^0)/\Gamma_{total}] \times [B(\psi(2S) \to \gamma\chi_{c0}(1P))]$ assuming $B(\psi(2S) \to \gamma\chi_{c0}(1P)) = (9.22 \pm 0.11 \pm 0.46) \times 10^{-2}$, which we rescale to our best value $B(\psi(2S) \to \gamma\chi_{c0}(1P)) = (9.79 \pm 0.20) \times 10^{-2}$. Our first error is their experiment's error and our second error is the systematic error from using our best value.

$\Gamma(K^+\pi^-\overline{K}^0\pi^0 + \text{c.c.})/\Gamma_{total}$ Γ_{24}/Γ

VALUE (%)	EVTS	DOCUMENT ID		TECN	COMMENT
$2.49\pm0.33\pm0.05$	401.7	[1] HE	08B	CLEO	$e^+e^- \to \gamma h^+h^-h^0h^0$

[1] HE 08B reports $2.64 \pm 0.15 \pm 0.31 \pm 0.14$ % from a measurement of $[\Gamma(\chi_{c0}(1P) \to K^+\pi^-\overline{K}^0\pi^0 + \text{c.c.})/\Gamma_{total}] \times [B(\psi(2S) \to \gamma\chi_{c0}(1P))]$ assuming $B(\psi(2S) \to \gamma\chi_{c0}(1P)) = (9.22\pm0.11\pm0.46)\times10^{-2}$, which we rescale to our best value $B(\psi(2S) \to \gamma\chi_{c0}(1P)) = (9.79 \pm 0.20) \times 10^{-2}$. Our first error is their experiment's error and our second error is the systematic error from using our best value.

$\Gamma(\rho^+K^-K^0 + \text{c.c.})/\Gamma_{total}$ Γ_{25}/Γ

VALUE (%)	EVTS	DOCUMENT ID		TECN	COMMENT
$1.21\pm0.21\pm0.02$	179.7	[1] HE	08B	CLEO	$e^+e^- \to \gamma h^+h^-h^0h^0$

[1] HE 08B reports $1.28 \pm 0.16 \pm 0.15 \pm 0.07$ % from a measurement of $[\Gamma(\chi_{c0}(1P) \to \rho^+K^-K^0 + \text{c.c.})/\Gamma_{total}] \times [B(\psi(2S) \to \gamma\chi_{c0}(1P))]$ assuming $B(\psi(2S) \to \gamma\chi_{c0}(1P)) = (9.22\pm0.11\pm0.46)\times10^{-2}$, which we rescale to our best value $B(\psi(2S) \to \gamma\chi_{c0}(1P)) = (9.79 \pm 0.20) \times 10^{-2}$. Our first error is their experiment's error and our second error is the systematic error from using our best value.

$\Gamma(K^*(892)^-K^+\pi^0 \to K^+\pi^-\overline{K}^0\pi^0 + \text{c.c.})/\Gamma_{total}$ Γ_{26}/Γ

VALUE (%)	EVTS	DOCUMENT ID		TECN	COMMENT
$0.46\pm0.12\pm0.01$	64.1	[1] HE	08B	CLEO	$e^+e^- \to \gamma h^+h^-h^0h^0$

[1] HE 08B reports $0.49 \pm 0.10 \pm 0.07 \pm 0.03$ % from a measurement of $[\Gamma(\chi_{c0}(1P) \to K^*(892)^-K^+\pi^0 \to K^+\pi^-\overline{K}^0\pi^0 + \text{c.c.})/\Gamma_{total}] \times [B(\psi(2S) \to \gamma\chi_{c0}(1P))]$ assuming $B(\psi(2S) \to \gamma\chi_{c0}(1P)) = (9.22 \pm 0.11 \pm 0.46) \times 10^{-2}$, which we rescale to our best value $B(\psi(2S) \to \gamma\chi_{c0}(1P)) = (9.79 \pm 0.20) \times 10^{-2}$. Our first error is their experiment's error and our second error is the systematic error from using our best value.

$\Gamma(K^0_S K^0_S \pi^+\pi^-)/\Gamma_{total}$ Γ_{27}/Γ

VALUE (units 10^{-3})	EVTS	DOCUMENT ID		TECN	COMMENT
$5.7\pm1.0\pm0.1$	152 ± 14	[1] ABLIKIM	05O	BES2	$\psi(2S) \to \gamma\chi_{c0}$

[1] ABLIKIM 05O reports $[\Gamma(\chi_{c0}(1P) \to K^0_S K^0_S \pi^+\pi^-)/\Gamma_{total}] \times [B(\psi(2S) \to \gamma\chi_{c0}(1P))] = (0.558 \pm 0.051 \pm 0.089) \times 10^{-3}$ which we divide by our best value $B(\psi(2S) \to \gamma\chi_{c0}(1P)) = (9.79 \pm 0.20) \times 10^{-2}$. Our first error is their experiment's error and our second error is the systematic error from using our best value.

$\Gamma(K^+K^-\eta\pi^0)/\Gamma_{total}$ Γ_{28}/Γ

VALUE (%)	EVTS	DOCUMENT ID		TECN	COMMENT
$0.30\pm0.07\pm0.01$	56.4	[1] HE	08B	CLEO	$e^+e^- \to \gamma h^+h^-h^0h^0$

[1] HE 08B reports $0.32 \pm 0.05 \pm 0.05 \pm 0.02$ % from a measurement of $[\Gamma(\chi_{c0}(1P) \to K^+K^-\eta\pi^0)/\Gamma_{total}] \times [B(\psi(2S) \to \gamma\chi_{c0}(1P))]$ assuming $B(\psi(2S) \to \gamma\chi_{c0}(1P)) = (9.22 \pm 0.11 \pm 0.46) \times 10^{-2}$, which we rescale to our best value $B(\psi(2S) \to \gamma\chi_{c0}(1P)) = (9.79 \pm 0.20) \times 10^{-2}$. Our first error is their experiment's error and our second error is the systematic error from using our best value.

$\Gamma(3(\pi^+\pi^-))/\Gamma_{total}$ Γ_{29}/Γ

VALUE (units 10^{-3})	DOCUMENT ID		TECN	COMMENT
12.0 ± 1.8 OUR EVALUATION	Treating systematic error as correlated.			
12.0 ± 1.7 OUR AVERAGE				
$11.7\pm1.0\pm1.9$	[1] BAI	99B	BES	$\psi(2S) \to \gamma\chi_{c0}$
$12.5\pm2.9\pm0.5$	[1] TANENBAUM	78	MRK1	$\psi(2S) \to \gamma\chi_{c0}$

[1] Rescaled by us using $B(\psi(2S) \to \gamma\chi_{c0}) = (9.4 \pm 0.4)\%$ and $B(\psi(2S) \to J/\psi(1S)\pi^+\pi^-) = (32.6 \pm 0.5)\%$.

$\Gamma(K^+\overline{K}^*(892)^0\pi^- + \text{c.c.})/\Gamma_{total}$ Γ_{30}/Γ

VALUE	DOCUMENT ID
0.0075 ± 0.0016 OUR FIT	

$\Gamma(K^*(892)^0\overline{K}^*(892)^0)/\Gamma_{total}$ Γ_{31}/Γ

VALUE (units 10^{-3})	EVTS	DOCUMENT ID		TECN	COMMENT
$1.72^{+0.60}_{-0.54}\pm0.04$	64	[1] ABLIKIM	05Q	BES2	$\psi(2S) \to \gamma\pi^+\pi^- K^+K^-$
• • • We do not use the following data for averages, fits, limits, etc. • • •					
$1.56\pm0.40\pm0.03$	30 ± 6	[2,3] ABLIKIM	04H	BES	Repl. by ABLIKIM 05Q

[1] ABLIKIM 05Q reports $[\Gamma(\chi_{c0}(1P) \to K^*(892)^0\overline{K}^*(892)^0)/\Gamma_{total}] \times [B(\psi(2S) \to \gamma\chi_{c0}(1P))] = (0.168 \pm 0.035^{+0.047}_{-0.040}) \times 10^{-3}$ which we divide by our best value $B(\psi(2S) \to \gamma\chi_{c0}(1P)) = (9.79 \pm 0.20) \times 10^{-2}$. Our first error is their experiment's error and our second error is the systematic error from using our best value.

[2] Assumes $B(K^*(892)^0 \to K^-\pi^+) = 2/3$.

[3] ABLIKIM 04H reports $[\Gamma(\chi_{c0}(1P) \to K^*(892)^0\overline{K}^*(892)^0)/\Gamma_{total}] \times [B(\psi(2S) \to \gamma\chi_{c0}(1P))] = (1.53\pm0.29\pm0.26)\times10^{-4}$ which we divide by our best value $B(\psi(2S) \to \gamma\chi_{c0}(1P)) = (9.79 \pm 0.20) \times 10^{-2}$. Our first error is their experiment's error and our second error is the systematic error from using our best value.

$\Gamma(\pi\pi)/\Gamma_{total}$ Γ_{32}/Γ

VALUE (units 10^{-3})	DOCUMENT ID
8.51 ± 0.33 OUR FIT	

$\Gamma(\pi^0\eta_c)/\Gamma_{total}$ Γ_{35}/Γ

VALUE	CL%	DOCUMENT ID		TECN	COMMENT
$<1.6 \times 10^{-3}$	90	[1] ABLIKIM	15N	BES3	$\psi(2s)\, e^+e^- \to \gamma\pi^0\eta_C$

[1] Using $B(\eta_C \to K^0_S K^\pm\pi^\mp) \times B(K^0_S \to \pi^+\pi^-) \times B(\pi^0 \to \gamma\gamma) = (1.66\pm0.11)\times10^{-2}$.

$\Gamma(\eta\eta)/\Gamma_{total}$ Γ_{36}/Γ

VALUE (units 10^{-3})	DOCUMENT ID
3.01 ± 0.19 OUR FIT	

$\Gamma(\eta\eta)/\Gamma(\pi\pi)$ Γ_{36}/Γ_{32}

VALUE	DOCUMENT ID		TECN	COMMENT
0.353 ± 0.025 OUR FIT				

• • • We do not use the following data for averages, fits, limits, etc. • • •

$0.26 \pm 0.09 \ {}^{+0.03}_{-0.02}$	[1] ANDREOTTI	05C	E835	$\overline{p}p \rightarrow$	2 mesons	
$0.24 \pm 0.10 \pm 0.08$	[1] BAI	03C	BES	$\psi(2S) \rightarrow$	5γ	

[1] We have multiplied $\pi^0\pi^0$ measurement by 3 to obtain $\pi\pi$.

$\Gamma(\eta\eta')/\Gamma_{\text{total}}$ Γ_{37}/Γ

VALUE (units 10^{-5})	CL%	EVTS	DOCUMENT ID		TECN	COMMENT
$9.1 \pm 1.1 \pm 0.2$		85	[1] ABLIKIM	17AI	BES3	$\psi(2S) \rightarrow \gamma\eta'\eta$
• • • We do not use the following data for averages, fits, limits, etc. • • •						
<24	90	35 ± 13	[2] ASNER	09	CLEO	$\psi(2S) \rightarrow \gamma\eta'\eta$
<50	90		[3] ADAMS	07	CLEO	$\psi(2S) \rightarrow \gamma\chi_{c0}$

[1] ABLIKIM 17AI reports $(8.92 \pm 0.84 \pm 0.65) \times 10^{-5}$ from a measurement of $[\Gamma(\chi_{c0}(1P) \rightarrow \eta\eta')/\Gamma_{\text{total}}] \times [B(\psi(2S) \rightarrow \gamma\chi_{c0}(1P))]$ assuming $B(\psi(2S) \rightarrow \gamma\chi_{c0}(1P)) = (9.99 \pm 0.27) \times 10^{-2}$, which we rescale to our best value $B(\psi(2S) \rightarrow \gamma\chi_{c0}(1P)) = (9.79 \pm 0.20) \times 10^{-2}$. Our first error is their experiment's error and our second error is the systematic error from using our best value.

[2] ASNER 09 reports $< 0.25 \times 10^{-3}$ from a measurement of $[\Gamma(\chi_{c0}(1P) \rightarrow \eta\eta')/\Gamma_{\text{total}}] \times [B(\psi(2S) \rightarrow \gamma\chi_{c0}(1P))]$ assuming $B(\psi(2S) \rightarrow \gamma\chi_{c0}(1P)) = (9.22 \pm 0.11 \pm 0.46) \times 10^{-2}$, which we rescale to our best value $B(\psi(2S) \rightarrow \gamma\chi_{c0}(1P)) = 9.79 \times 10^{-2}$.

[3] Superseded by ASNER 09. ADAMS 07 reports $< 0.5 \times 10^{-3}$ from a measurement of $[\Gamma(\chi_{c0}(1P) \rightarrow \eta\eta')/\Gamma_{\text{total}}] \times [B(\psi(2S) \rightarrow \gamma\chi_{c0}(1P))]$ assuming $B(\psi(2S) \rightarrow \gamma\chi_{c0}(1P)) = (9.22 \pm 0.11 \pm 0.46) \times 10^{-2}$, which we rescale to our best value $B(\psi(2S) \rightarrow \gamma\chi_{c0}(1P)) = 9.79 \times 10^{-2}$.

$\Gamma(\eta'\eta')/\Gamma_{\text{total}}$ Γ_{38}/Γ

VALUE (units 10^{-3})	EVTS	DOCUMENT ID		TECN	COMMENT
2.17 ± 0.12 OUR AVERAGE					
$2.23 \pm 0.13 \pm 0.05$	2.5k	[1] ABLIKIM	17AI	BES3	$\psi(2S) \rightarrow \gamma\eta'\eta'$
$2.00 \pm 0.21 \pm 0.04$	0.4k	[2] ASNER	09	CLEO	$\psi(2S) \rightarrow \gamma\eta'\eta'$
• • • We do not use the following data for averages, fits, limits, etc. • • •					
$1.60 \pm 0.41 \pm 0.03$	23	[3] ADAMS	07	CLEO	$\psi(2S) \rightarrow \gamma\chi_{c0}$

[1] ABLIKIM 17AI reports $(2.19 \pm 0.03 \pm 0.14) \times 10^{-3}$ from a measurement of $[\Gamma(\chi_{c0}(1P) \rightarrow \eta'\eta')/\Gamma_{\text{total}}] \times [B(\psi(2S) \rightarrow \gamma\chi_{c0}(1P))]$ assuming $B(\psi(2S) \rightarrow \gamma\chi_{c0}(1P)) = (9.99 \pm 0.27) \times 10^{-2}$, which we rescale to our best value $B(\psi(2S) \rightarrow \gamma\chi_{c0}(1P)) = (9.79 \pm 0.20) \times 10^{-2}$. Our first error is their experiment's error and our second error is the systematic error from using our best value.

[2] ASNER 09 reports $(2.12 \pm 0.13 \pm 0.21) \times 10^{-3}$ from a measurement of $[\Gamma(\chi_{c0}(1P) \rightarrow \eta'\eta')/\Gamma_{\text{total}}] \times [B(\psi(2S) \rightarrow \gamma\chi_{c0}(1P))]$ assuming $B(\psi(2S) \rightarrow \gamma\chi_{c0}(1P)) = (9.22 \pm 0.11 \pm 0.46) \times 10^{-2}$, which we rescale to our best value $B(\psi(2S) \rightarrow \gamma\chi_{c0}(1P)) = (9.79 \pm 0.20) \times 10^{-2}$. Our first error is their experiment's error and our second error is the systematic error from using our best value.

[3] Superseded by ASNER 09. ADAMS 07 reports $(1.7 \pm 0.4 \pm 0.2) \times 10^{-3}$ from a measurement of $[\Gamma(\chi_{c0}(1P) \rightarrow \eta'\eta')/\Gamma_{\text{total}}] \times [B(\psi(2S) \rightarrow \gamma\chi_{c0}(1P))]$ assuming $B(\psi(2S) \rightarrow \gamma\chi_{c0}(1P)) = 0.0922 \pm 0.0011 \pm 0.0046$, which we rescale to our best value $B(\psi(2S) \rightarrow \gamma\chi_{c0}(1P)) = (9.79 \pm 0.20) \times 10^{-2}$. Our first error is their experiment's error and our second error is the systematic error from using our best value.

$\Gamma(\omega\omega)/\Gamma_{\text{total}}$ Γ_{39}/Γ

VALUE (units 10^{-3})	EVTS	DOCUMENT ID		TECN	COMMENT
0.97 ± 0.11 OUR AVERAGE					
$0.93 \pm 0.11 \pm 0.02$	991	[1] ABLIKIM	11K	BES3	$\psi(2S) \rightarrow \gamma$ hadrons
$2.16 \pm 0.66 \pm 0.04$	38.1 ± 9.6	[2] ABLIKIM	05N	BES2	$\psi(2S) \rightarrow \gamma\chi_{c0} \rightarrow \gamma 6\pi$

[1] ABLIKIM 11K reports $(0.95 \pm 0.03 \pm 0.11) \times 10^{-3}$ from a measurement of $[\Gamma(\chi_{c0}(1P) \rightarrow \omega\omega)/\Gamma_{\text{total}}] \times [B(\psi(2S) \rightarrow \gamma\chi_{c0}(1P))]$ assuming $B(\psi(2S) \rightarrow \gamma\chi_{c0}(1P)) = (9.62 \pm 0.31) \times 10^{-2}$, which we rescale to our best value $B(\psi(2S) \rightarrow \gamma\chi_{c0}(1P)) = (9.79 \pm 0.20) \times 10^{-2}$. Our first error is their experiment's error and our second error is the systematic error from using our best value.

[2] ABLIKIM 05N reports $[\Gamma(\chi_{c0}(1P) \rightarrow \omega\omega)/\Gamma_{\text{total}}] \times [B(\psi(2S) \rightarrow \gamma\chi_{c0}(1P))] = (0.212 \pm 0.053 \pm 0.037) \times 10^{-3}$ which we divide by our best value $B(\psi(2S) \rightarrow \gamma\chi_{c0}(1P)) = (9.79 \pm 0.20) \times 10^{-2}$. Our first error is their experiment's error and our second error is the systematic error from using our best value.

$\Gamma(\omega\phi)/\Gamma_{\text{total}}$ Γ_{40}/Γ

VALUE (units 10^{-4})	EVTS	DOCUMENT ID		TECN	COMMENT
$1.18 \pm 0.22 \pm 0.02$	76	[1] ABLIKIM	11K	BES3	$\psi(2S) \rightarrow \gamma$ hadrons

[1] ABLIKIM 11K reports $(1.2 \pm 0.1 \pm 0.2) \times 10^{-4}$ from a measurement of $[\Gamma(\chi_{c0}(1P) \rightarrow \omega\phi)/\Gamma_{\text{total}}] \times [B(\psi(2S) \rightarrow \gamma\chi_{c0}(1P))]$ assuming $B(\psi(2S) \rightarrow \gamma\chi_{c0}(1P)) = (9.62 \pm 0.31) \times 10^{-2}$, which we rescale to our best value $B(\psi(2S) \rightarrow \gamma\chi_{c0}(1P)) = (9.79 \pm 0.20) \times 10^{-2}$. Our first error is their experiment's error and our second error is the systematic error from using our best value.

$\Gamma(\omega K^+ K^-)/\Gamma_{\text{total}}$ Γ_{41}/Γ

VALUE (units 10^{-3})	EVTS	DOCUMENT ID		TECN	COMMENT
$1.94 \pm 0.06 \pm 0.20$	1.4k	[1] ABLIKIM	13B	BES3	$e^+e^- \rightarrow \psi(2S) \rightarrow \gamma\chi_{c0}$

[1] Using 1.06×10^8 $\psi(2S)$ mesons and $B(\psi(2S) \rightarrow \chi_{c0}\gamma) = (9.68 \pm 0.31)\%$.

$\Gamma(K^+ K^-)/\Gamma_{\text{total}}$ Γ_{42}/Γ

VALUE (units 10^{-3})	DOCUMENT ID
6.05 ± 0.31 OUR FIT	

$\Gamma(K^0_S K^0_S)/\Gamma_{\text{total}}$ Γ_{43}/Γ

VALUE (units 10^{-3})	DOCUMENT ID
3.16 ± 0.17 OUR FIT	

$\Gamma(K^0_S K^0_S)/\Gamma(\pi\pi)$ Γ_{43}/Γ_{32}

VALUE	DOCUMENT ID		TECN	COMMENT
0.372 ± 0.023 OUR FIT				
• • • We do not use the following data for averages, fits, limits, etc. • • •				
$0.31 \pm 0.05 \pm 0.05$	[1,2] CHEN	07B	BELL	$e^+e^- \rightarrow e^+e^-\chi_{c0}$

[1] Using $\Gamma(\pi\pi) \times \Gamma(\gamma\gamma)/\Gamma_{\text{total}}$ from the $\pi^+\pi^-$ measurement of NAKAZAWA 05 rescaled by 3/2 to convert to $\pi\pi$.

[2] Not independent from other measurements.

$\Gamma(K^0_S K^0_S)/\Gamma(K^+ K^-)$ Γ_{43}/Γ_{42}

VALUE	DOCUMENT ID		TECN	COMMENT
0.52 ± 0.04 OUR FIT				
• • • We do not use the following data for averages, fits, limits, etc. • • •				
$0.49 \pm 0.07 \pm 0.08$	[1,2] CHEN	07B	BELL	$e^+e^- \rightarrow e^+e^-\chi_{c0}$

[1] Using $\Gamma(K^+K^-) \times \Gamma(\gamma\gamma)/\Gamma_{\text{total}}$ from NAKAZAWA 05.

[2] Not independent from other measurements.

$\Gamma(\pi^+\pi^-\eta)/\Gamma_{\text{total}}$ Γ_{44}/Γ

VALUE (units 10^{-3})	CL%	DOCUMENT ID		TECN	COMMENT
<0.20	90	[1] ATHAR	07	CLEO	$\psi(2S) \rightarrow \gamma h^+ h^- h^0$
• • • We do not use the following data for averages, fits, limits, etc. • • •					
<1.0	90	[2] ABLIKIM	06R	BES2	$\psi(2S) \rightarrow \gamma\chi_{c0}$

[1] ATHAR 07 reports $< 0.21 \times 10^{-3}$ from a measurement of $[\Gamma(\chi_{c0}(1P) \rightarrow \pi^+\pi^-\eta)/\Gamma_{\text{total}}] \times [B(\psi(2S) \rightarrow \gamma\chi_{c0}(1P))]$ assuming $B(\psi(2S) \rightarrow \gamma\chi_{c0}(1P)) = (9.22 \pm 0.11 \pm 0.46) \times 10^{-2}$, which we rescale to our best value $B(\psi(2S) \rightarrow \gamma\chi_{c0}(1P)) = 9.79 \times 10^{-2}$.

[2] ABLIKIM 06R reports $< 1.1 \times 10^{-3}$ from a measurement of $[\Gamma(\chi_{c0}(1P) \rightarrow \pi^+\pi^-\eta)/\Gamma_{\text{total}}] \times [B(\psi(2S) \rightarrow \gamma\chi_{c0}(1P))]$ assuming $B(\psi(2S) \rightarrow \gamma\chi_{c0}(1P)) = (9.2 \pm 0.4) \times 10^{-2}$, which we rescale to our best value $B(\psi(2S) \rightarrow \gamma\chi_{c0}(1P)) = 9.79 \times 10^{-2}$.

$\Gamma(\pi^+\pi^-\eta')/\Gamma_{\text{total}}$ Γ_{45}/Γ

VALUE (units 10^{-3})	CL%	DOCUMENT ID		TECN	COMMENT
<0.4	90	[1] ATHAR	07	CLEO	$\psi(2S) \rightarrow \gamma h^+ h^- h^0$

[1] ATHAR 07 reports $< 0.38 \times 10^{-3}$ from a measurement of $[\Gamma(\chi_{c0}(1P) \rightarrow \pi^+\pi^-\eta')/\Gamma_{\text{total}}] \times [B(\psi(2S) \rightarrow \gamma\chi_{c0}(1P))]$ assuming $B(\psi(2S) \rightarrow \gamma\chi_{c0}(1P)) = (9.22 \pm 0.11 \pm 0.46) \times 10^{-2}$, which we rescale to our best value $B(\psi(2S) \rightarrow \gamma\chi_{c0}(1P)) = 9.79 \times 10^{-2}$.

$\Gamma(\overline{K}^0 K^+\pi^- + \text{c.c.})/\Gamma_{\text{total}}$ Γ_{46}/Γ

VALUE (units 10^{-3})	CL%	DOCUMENT ID		TECN	COMMENT
<0.09	90	[1] ATHAR	07	CLEO	$\psi(2S) \rightarrow \gamma h^+ h^- h^0$
• • • We do not use the following data for averages, fits, limits, etc. • • •					
<0.7	90	[2,3] ABLIKIM	06R	BES2	$\psi(2S) \rightarrow \gamma\chi_{c0}$
<0.7	90	[3,4] BAI	99B	BES	$\psi(2S) \rightarrow \gamma\chi_{c0}$

[1] ATHAR 07 reports $< 0.10 \times 10^{-3}$ from a measurement of $[\Gamma(\chi_{c0}(1P) \rightarrow \overline{K}^0 K^+\pi^- + \text{c.c.})/\Gamma_{\text{total}}] \times [B(\psi(2S) \rightarrow \gamma\chi_{c0}(1P))]$ assuming $B(\psi(2S) \rightarrow \gamma\chi_{c0}(1P)) = (9.22 \pm 0.11 \pm 0.46) \times 10^{-2}$, which we rescale to our best value $B(\psi(2S) \rightarrow \gamma\chi_{c0}(1P)) = 9.79 \times 10^{-2}$.

[2] ABLIKIM 06R reports $< 0.70 \times 10^{-3}$ from a measurement of $[\Gamma(\chi_{c0}(1P) \rightarrow \overline{K}^0 K^+\pi^- + \text{c.c.})/\Gamma_{\text{total}}] \times [B(\psi(2S) \rightarrow \gamma\chi_{c0}(1P))]$ assuming $B(\psi(2S) \rightarrow \gamma\chi_{c0}(1P)) = (9.2 \pm 0.4) \times 10^{-2}$, which we rescale to our best value $B(\psi(2S) \rightarrow \gamma\chi_{c0}(1P)) = 9.79 \times 10^{-2}$.

[3] We have multiplied the $K^0_S K^+\pi^-$ measurement by a factor of 2 to convert to $K^0 K^+\pi^-$.

[4] Rescaled by us using $B(\psi(2S) \rightarrow \gamma\chi_{c0}) = (9.4 \pm 0.4)\%$ and $B(\psi(2S) \rightarrow J/\psi(1S)\pi^+\pi^-) = (32.6 \pm 0.5)\%$.

$\Gamma(K^+ K^-\pi^0)/\Gamma_{\text{total}}$ Γ_{47}/Γ

VALUE (units 10^{-3})	CL%	DOCUMENT ID		TECN	COMMENT
<0.06	90	[1] ATHAR	07	CLEO	$\psi(2S) \rightarrow \gamma h^+ h^- h^0$

[1] ATHAR 07 reports $< 0.06 \times 10^{-3}$ from a measurement of $[\Gamma(\chi_{c0}(1P) \rightarrow K^+K^-\pi^0)/\Gamma_{\text{total}}] \times [B(\psi(2S) \rightarrow \gamma\chi_{c0}(1P))]$ assuming $B(\psi(2S) \rightarrow \gamma\chi_{c0}(1P)) = (9.22 \pm 0.11 \pm 0.46) \times 10^{-2}$, which we rescale to our best value $B(\psi(2S) \rightarrow \gamma\chi_{c0}(1P)) = 9.79 \times 10^{-2}$.

$\Gamma(K^+ K^-\eta)/\Gamma_{\text{total}}$ Γ_{48}/Γ

VALUE (units 10^{-3})	CL%	DOCUMENT ID		TECN	COMMENT
<0.23	90	[1] ATHAR	07	CLEO	$\psi(2S) \rightarrow \gamma h^+ h^- h^0$

[1] ATHAR 07 reports $< 0.24 \times 10^{-3}$ from a measurement of $[\Gamma(\chi_{c0}(1P) \rightarrow K^+K^-\eta)/\Gamma_{\text{total}}] \times [B(\psi(2S) \rightarrow \gamma\chi_{c0}(1P))]$ assuming $B(\psi(2S) \rightarrow \gamma\chi_{c0}(1P)) = (9.22 \pm 0.11 \pm 0.46) \times 10^{-2}$, which we rescale to our best value $B(\psi(2S) \rightarrow \gamma\chi_{c0}(1P)) = 9.79 \times 10^{-2}$.

$\Gamma(K^+ K^- K^0_S K^0_S)/\Gamma_{\text{total}}$ Γ_{49}/Γ

VALUE (units 10^{-3})	EVTS	DOCUMENT ID		TECN	COMMENT
$1.41 \pm 0.47 \pm 0.03$	16.8 ± 4.8	[1] ABLIKIM	05O	BES2	$\psi(2S) \rightarrow \gamma\chi_{c0}$

[1] ABLIKIM 05O reports $[\Gamma(\chi_{c0}(1P) \to K^+K^-K^0_SK^0_S)/\Gamma_{\rm total}] \times [B(\psi(2S) \to \gamma\chi_{c0}(1P))] = (0.138 \pm 0.039 \pm 0.025) \times 10^{-3}$ which we divide by our best value $B(\psi(2S) \to \gamma\chi_{c0}(1P)) = (9.79 \pm 0.20) \times 10^{-2}$. Our first error is their experiment's error and our second error is the systematic error from using our best value.

$\Gamma(K^+K^-K^+K^-)/\Gamma_{\rm total}$ Γ_{50}/Γ

VALUE (units 10^{-3})	DOCUMENT ID
2.82±0.29 OUR FIT	

$\Gamma(K^+K^-\phi)/\Gamma_{\rm total}$ Γ_{51}/Γ

VALUE (units 10^{-3})	EVTS	DOCUMENT ID		TECN	COMMENT
0.97±0.25±0.02	38	[1] ABLIKIM	06T	BES2	$\psi(2S) \to \gamma 2K^+2K^-$

[1] ABLIKIM 06T reports $(1.03 \pm 0.22 \pm 0.15) \times 10^{-3}$ from a measurement of $[\Gamma(\chi_{c0}(1P) \to K^+K^-\phi)/\Gamma_{\rm total}] \times [B(\psi(2S) \to \gamma\chi_{c0}(1P))]$ assuming $B(\psi(2S) \to \gamma\chi_{c0}(1P)) = (9.2 \pm 0.4) \times 10^{-2}$, which we rescale to our best value $B(\psi(2S) \to \gamma\chi_{c0}(1P)) = (9.79 \pm 0.20) \times 10^{-2}$. Our first error is their experiment's error and our second error is the systematic error from using our best value.

$\Gamma(\overline{K}^0K^+\pi^-\phi + \text{c.c.})/\Gamma_{\rm total}$ Γ_{52}/Γ

VALUE (units 10^{-3})	DOCUMENT ID		TECN	COMMENT
3.68±0.30±0.50	ABLIKIM	15M	BES3	$\psi(2S) \to \gamma\chi_{c0}$

$\Gamma(K^+K^-\pi^0\phi)/\Gamma_{\rm total}$ Γ_{53}/Γ

VALUE (units 10^{-3})	DOCUMENT ID		TECN	COMMENT
1.90±0.14±0.32	ABLIKIM	15M	BES3	$\psi(2S) \to \gamma\chi_{c0}$

$\Gamma(\phi\pi^+\pi^-\pi^0)/\Gamma_{\rm total}$ Γ_{54}/Γ

VALUE (units 10^{-3})	EVTS	DOCUMENT ID		TECN	COMMENT
1.18±0.07±0.13	538	[1] ABLIKIM	13B	BES3	$e^+e^- \to \psi(2S) \to \gamma\chi_{c0}$

[1] Using 1.06×10^8 $\psi(2S)$ mesons and $B(\psi(2S) \to \chi_{c0}\gamma) = (9.68 \pm 0.31)\%$.

$\Gamma(\phi\phi)/\Gamma_{\rm total}$ Γ_{55}/Γ

VALUE (units 10^{-3})	DOCUMENT ID
0.80±0.07 OUR FIT	

$\Gamma(p\overline{p})/\Gamma_{\rm total}$ Γ_{56}/Γ

VALUE (units 10^{-4})	DOCUMENT ID
2.21±0.08 OUR FIT	

$\Gamma(p\overline{p}\pi^0)/\Gamma_{\rm total}$ Γ_{57}/Γ

VALUE (units 10^{-3})	DOCUMENT ID		TECN	COMMENT
0.70±0.07 OUR AVERAGE Error includes scale factor of 1.3.				
0.73±0.06±0.01	[1] ONYISI	10	CLE3	$\psi(2S) \to \gamma p\overline{p}X$
0.56±0.12±0.01	[2] ATHAR	07	CLEO	$\psi(2S) \to \gamma h^+h^-h^0$

[1] ONYISI 10 reports $(7.76 \pm 0.37 \pm 0.51 \pm 0.39) \times 10^{-4}$ from a measurement of $[\Gamma(\chi_{c0}(1P) \to p\overline{p}\pi^0)/\Gamma_{\rm total}] \times [B(\psi(2S) \to \gamma\chi_{c0}(1P))]$ assuming $B(\psi(2S) \to \gamma\chi_{c0}(1P)) = (9.22 \pm 0.11 \pm 0.46) \times 10^{-2}$, which we rescale to our best value $B(\psi(2S) \to \gamma\chi_{c0}(1P)) = (9.79 \pm 0.20) \times 10^{-2}$. Our first error is their experiment's error and our second error is the systematic error from using our best value.

[2] ATHAR 07 reports $(0.59 \pm 0.10 \pm 0.08) \times 10^{-3}$ from a measurement of $[\Gamma(\chi_{c0}(1P) \to p\overline{p}\pi^0)/\Gamma_{\rm total}] \times [B(\psi(2S) \to \gamma\chi_{c0}(1P))]$ assuming $B(\psi(2S) \to \gamma\chi_{c0}(1P)) = (9.22 \pm 0.11 \pm 0.46) \times 10^{-2}$, which we rescale to our best value $B(\psi(2S) \to \gamma\chi_{c0}(1P)) = (9.79 \pm 0.20) \times 10^{-2}$. Our first error is their experiment's error and our second error is the systematic error from using our best value.

$\Gamma(p\overline{p}\eta)/\Gamma_{\rm total}$ Γ_{58}/Γ

VALUE (units 10^{-3})	DOCUMENT ID		TECN	COMMENT
0.35±0.04 OUR AVERAGE				
0.35±0.04±0.01	[1] ONYISI	10	CLE3	$\psi(2S) \to \gamma p\overline{p}X$
0.37±0.11±0.01	[2] ATHAR	07	CLEO	$\psi(2S) \to \gamma h^+h^-h^0$

[1] ONYISI 10 reports $(3.73 \pm 0.38 \pm 0.28 \pm 0.19) \times 10^{-4}$ from a measurement of $[\Gamma(\chi_{c0}(1P) \to p\overline{p}\eta)/\Gamma_{\rm total}] \times [B(\psi(2S) \to \gamma\chi_{c0}(1P))]$ assuming $B(\psi(2S) \to \gamma\chi_{c0}(1P)) = (9.22 \pm 0.11 \pm 0.46) \times 10^{-2}$, which we rescale to our best value $B(\psi(2S) \to \gamma\chi_{c0}(1P)) = (9.79 \pm 0.20) \times 10^{-2}$. Our first error is their experiment's error and our second error is the systematic error from using our best value.

[2] ATHAR 07 reports $(0.39 \pm 0.11 \pm 0.04) \times 10^{-3}$ from a measurement of $[\Gamma(\chi_{c0}(1P) \to p\overline{p}\eta)/\Gamma_{\rm total}] \times [B(\psi(2S) \to \gamma\chi_{c0}(1P))]$ assuming $B(\psi(2S) \to \gamma\chi_{c0}(1P)) = (9.22 \pm 0.11 \pm 0.46) \times 10^{-2}$, which we rescale to our best value $B(\psi(2S) \to \gamma\chi_{c0}(1P)) = (9.79 \pm 0.20) \times 10^{-2}$. Our first error is their experiment's error and our second error is the systematic error from using our best value.

$\Gamma(p\overline{p}\omega)/\Gamma_{\rm total}$ Γ_{59}/Γ

VALUE (units 10^{-3})	DOCUMENT ID		TECN	COMMENT
0.52±0.06±0.01	[1] ONYISI	10	CLE3	$\psi(2S) \to \gamma p\overline{p}X$

[1] ONYISI 10 reports $(5.57 \pm 0.48 \pm 0.42 \pm 0.14) \times 10^{-4}$ from a measurement of $[\Gamma(\chi_{c0}(1P) \to p\overline{p}\omega)/\Gamma_{\rm total}] \times [B(\psi(2S) \to \gamma\chi_{c0}(1P))]$ assuming $B(\psi(2S) \to \gamma\chi_{c0}(1P)) = (9.22 \pm 0.11 \pm 0.46) \times 10^{-2}$, which we rescale to our best value $B(\psi(2S) \to \gamma\chi_{c0}(1P)) = (9.79 \pm 0.20) \times 10^{-2}$. Our first error is their experiment's error and our second error is the systematic error from using our best value.

$\Gamma(p\overline{p}\phi)/\Gamma_{\rm total}$ Γ_{60}/Γ

VALUE (units 10^{-5})	EVTS	DOCUMENT ID		TECN	COMMENT
6.0±1.4±0.1	42 ± 8	[1] ABLIKIM	11F	BES3	$\psi(2S) \to \gamma p\overline{p}K^+K^-$

[1] ABLIKIM 11F reports $(6.12 \pm 1.18 \pm 0.86) \times 10^{-5}$ from a measurement of $[\Gamma(\chi_{c0}(1P) \to p\overline{p}\phi)/\Gamma_{\rm total}] \times [B(\psi(2S) \to \gamma\chi_{c0}(1P))]$ assuming $B(\psi(2S) \to \gamma\chi_{c0}(1P)) = (9.62 \pm 0.31) \times 10^{-2}$, which we rescale to our best value $B(\psi(2S) \to \gamma\chi_{c0}(1P)) = (9.79 \pm 0.20) \times 10^{-2}$. Our first error is their experiment's error and our second error is the systematic error from using our best value.

$\Gamma(p\overline{p}\pi^+\pi^-)/\Gamma_{\rm total}$ Γ_{61}/Γ

VALUE (units 10^{-3})	DOCUMENT ID		TECN	COMMENT
2.1 ±0.7 OUR EVALUATION Error includes scale factor of 1.4. Treating systematic error as correlated.				
2.1 ±1.0 OUR AVERAGE Error includes scale factor of 2.0.				
1.57±0.21±0.53	[1] BAI	99B	BES	$\psi(2S) \to \gamma\chi_{c0}$
4.20±1.15±0.18	[1] TANENBAUM	78	MRK1	$\psi(2S) \to \gamma\chi_{c0}$

[1] Rescaled by us using $B(\psi(2S) \to \gamma\chi_{c0}) = (9.4 \pm 0.4)\%$ and $B(\psi(2S) \to J/\psi(1S)\pi^+\pi^-) = (32.6 \pm 0.5)\%$.

$\Gamma(p\overline{p}\pi^0\pi^0)/\Gamma_{\rm total}$ Γ_{62}/Γ

VALUE (%)	EVTS	DOCUMENT ID		TECN	COMMENT
0.104±0.028±0.002	39.5	[1] HE	08B	CLEO	$e^+e^- \to \gamma h^+h^-h^0h^0$

[1] HE 08B reports $0.11 \pm 0.02 \pm 0.02 \pm 0.01$ % from a measurement of $[\Gamma(\chi_{c0}(1P) \to p\overline{p}\pi^0\pi^0)/\Gamma_{\rm total}] \times [B(\psi(2S) \to \gamma\chi_{c0}(1P))]$ assuming $B(\psi(2S) \to \gamma\chi_{c0}(1P)) = (9.22 \pm 0.11 \pm 0.46) \times 10^{-2}$, which we rescale to our best value $B(\psi(2S) \to \gamma\chi_{c0}(1P)) = (9.79 \pm 0.20) \times 10^{-2}$. Our first error is their experiment's error and our second error is the systematic error from using our best value.

$\Gamma(p\overline{p}K^+K^-(\text{non-resonant}))/\Gamma_{\rm total}$ Γ_{63}/Γ

VALUE (units 10^{-4})	EVTS	DOCUMENT ID		TECN	COMMENT
1.22±0.26±0.02	48 ± 8	[1] ABLIKIM	11F	BES3	$\psi(2S) \to \gamma p\overline{p}K^+K^-$

[1] ABLIKIM 11F reports $(1.24 \pm 0.20 \pm 0.18) \times 10^{-4}$ from a measurement of $[\Gamma(\chi_{c0}(1P) \to p\overline{p}K^+K^-(\text{non-resonant}))/\Gamma_{\rm total}] \times [B(\psi(2S) \to \gamma\chi_{c0}(1P))]$ assuming $B(\psi(2S) \to \gamma\chi_{c0}(1P)) = (9.62 \pm 0.31) \times 10^{-2}$, which we rescale to our best value $B(\psi(2S) \to \gamma\chi_{c0}(1P)) = (9.79 \pm 0.20) \times 10^{-2}$. Our first error is their experiment's error and our second error is the systematic error from using our best value.

$\Gamma(p\overline{p}K^0_SK^0_S)/\Gamma_{\rm total}$ Γ_{64}/Γ

VALUE (units 10^{-4})	CL%	DOCUMENT ID		TECN	COMMENT
<8.8	90	[1] ABLIKIM	06D	BES2	$\psi(2S) \to \chi_{c0}\gamma$

[1] Using $B(\psi(2S) \to \chi_{c0}\gamma) = (9.2 \pm 0.5)\%$

$\Gamma(p\overline{n}\pi^-)/\Gamma_{\rm total}$ Γ_{65}/Γ

VALUE (units 10^{-4})	EVTS	DOCUMENT ID		TECN	COMMENT
12.7±1.1 OUR AVERAGE					
12.9±1.1±0.3	5150	[1] ABLIKIM	12J	BES3	$\psi(2S) \to \gamma p\overline{n}\pi^-$
11.2±3.1±0.2		[2] ABLIKIM	06I	BES2	$\psi(2S) \to \gamma p\pi^-X$

[1] ABLIKIM 12J reports $[\Gamma(\chi_{c0}(1P) \to p\overline{n}\pi^-)/\Gamma_{\rm total}] \times [B(\psi(2S) \to \gamma\chi_{c0}(1P))] = (1.26 \pm 0.02 \pm 0.11) \times 10^{-4}$ which we divide by our best value $B(\psi(2S) \to \gamma\chi_{c0}(1P)) = (9.79 \pm 0.20) \times 10^{-2}$. Our first error is their experiment's error and our second error is the systematic error from using our best value.

[2] ABLIKIM 06I reports $[\Gamma(\chi_{c0}(1P) \to p\overline{n}\pi^-)/\Gamma_{\rm total}] \times [B(\psi(2S) \to \gamma\chi_{c0}(1P))] = (1.10 \pm 0.24 \pm 0.18) \times 10^{-4}$ which we divide by our best value $B(\psi(2S) \to \gamma\chi_{c0}(1P)) = (9.79 \pm 0.20) \times 10^{-2}$. Our first error is their experiment's error and our second error is the systematic error from using our best value.

$\Gamma(\overline{p}n\pi^+)/\Gamma_{\rm total}$ Γ_{66}/Γ

VALUE (units 10^{-4})	EVTS	DOCUMENT ID		TECN	COMMENT
13.7±1.2±0.3	5808	[1] ABLIKIM	12J	BES3	$\psi(2S) \to \gamma\overline{p}n\pi^+$

[1] ABLIKIM 12J reports $[\Gamma(\chi_{c0}(1P) \to \overline{p}n\pi^+)/\Gamma_{\rm total}] \times [B(\psi(2S) \to \gamma\chi_{c0}(1P))] = (1.34 \pm 0.03 \pm 0.11) \times 10^{-4}$ which we divide by our best value $B(\psi(2S) \to \gamma\chi_{c0}(1P)) = (9.79 \pm 0.20) \times 10^{-2}$. Our first error is their experiment's error and our second error is the systematic error from using our best value.

$\Gamma(p\overline{n}\pi^-\pi^0)/\Gamma_{\rm total}$ Γ_{67}/Γ

VALUE (units 10^{-4})	EVTS	DOCUMENT ID		TECN	COMMENT
23.4±2.0±0.5	2480	[1] ABLIKIM	12J	BES3	$\psi(2S) \to \gamma p\overline{n}\pi^-\pi^0$

[1] ABLIKIM 12J reports $[\Gamma(\chi_{c0}(1P) \to p\overline{n}\pi^-\pi^0)/\Gamma_{\rm total}] \times [B(\psi(2S) \to \gamma\chi_{c0}(1P))] = (2.29 \pm 0.08 \pm 0.18) \times 10^{-4}$ which we divide by our best value $B(\psi(2S) \to \gamma\chi_{c0}(1P)) = (9.79 \pm 0.20) \times 10^{-2}$. Our first error is their experiment's error and our second error is the systematic error from using our best value.

$\Gamma(\overline{p}n\pi^+\pi^0)/\Gamma_{\rm total}$ Γ_{68}/Γ

VALUE (units 10^{-4})	EVTS	DOCUMENT ID		TECN	COMMENT
22.1±1.8±0.5	2757	[1] ABLIKIM	12J	BES3	$\psi(2S) \to \gamma\overline{p}n\pi^+\pi^0$

[1] ABLIKIM 12J reports $[\Gamma(\chi_{c0}(1P) \to \overline{p}n\pi^+\pi^0)/\Gamma_{\rm total}] \times [B(\psi(2S) \to \gamma\chi_{c0}(1P))] = (2.16 \pm 0.07 \pm 0.16) \times 10^{-4}$ which we divide by our best value $B(\psi(2S) \to \gamma\chi_{c0}(1P)) = (9.79 \pm 0.20) \times 10^{-2}$. Our first error is their experiment's error and our second error is the systematic error from using our best value.

$\Gamma(\Lambda\overline{\Lambda})/\Gamma_{total}$ Γ_{69}/Γ

VALUE (units 10^{-4})	DOCUMENT ID
3.27±0.24 OUR FIT	

$\Gamma(\Lambda\overline{\Lambda}\pi^+\pi^-)/\Gamma_{total}$ Γ_{70}/Γ

VALUE (units 10^{-5})	CL%	EVTS	DOCUMENT ID		TECN	COMMENT
118±12±2		426	[1] ABLIKIM	12I	BES3	$\psi(2S)\to\gamma\Lambda\overline{\Lambda}\pi^+\pi^-$
• • • We do not use the following data for averages, fits, limits, etc. • • •						
<400	90		[2] ABLIKIM	06D	BES2	$\psi(2S)\to\chi_{c0}\gamma$

[1] ABLIKIM 12I reports $(119.0\pm6.4\pm11.4)\times10^{-5}$ from a measurement of $[\Gamma(\chi_{c0}(1P)\to\Lambda\overline{\Lambda}\pi^+\pi^-)/\Gamma_{total}]\times[B(\psi(2S)\to\gamma\chi_{c0}(1P))]$ assuming $B(\psi(2S)\to\gamma\chi_{c0}(1P))=(9.68\pm0.31)\times10^{-2}$, which we rescale to our best value $B(\psi(2S)\to\gamma\chi_{c0}(1P))=(9.79\pm0.20)\times10^{-2}$. Our first error is their experiment's error and our second error is the systematic error from using our best value.

[2] Using $B(\psi(2S)\to\chi_{c0}\gamma)=(9.2\pm0.5)\%$

$\Gamma(\Lambda\overline{\Lambda}\pi^+\pi^-(\text{non-resonant}))/\Gamma_{total}$ Γ_{71}/Γ

VALUE (units 10^{-5})	CL%	DOCUMENT ID		TECN	COMMENT
<50	90	[1] ABLIKIM	12I	BES3	$\psi(2S)\to\gamma\Lambda\overline{\Lambda}\pi^+\pi^-$

[1] ABLIKIM 12I reports $<54\times10^{-5}$ from a measurement of $[\Gamma(\chi_{c0}(1P)\to\Lambda\overline{\Lambda}\pi^+\pi^-(\text{non-resonant}))/\Gamma_{total}]\times[B(\psi(2S)\to\gamma\chi_{c0}(1P))]$ assuming $B(\psi(2S)\to\gamma\chi_{c0}(1P))=(9.68\pm0.31)\times10^{-2}$, which we rescale to our best value $B(\psi(2S)\to\gamma\chi_{c0}(1P))=9.79\times10^{-2}$.

$\Gamma(\Sigma(1385)^+\overline{\Lambda}\pi^-+\text{c.c.})/\Gamma_{total}$ Γ_{72}/Γ

VALUE (units 10^{-5})	CL%	DOCUMENT ID		TECN	COMMENT
<50	90	[1] ABLIKIM	12I	BES3	$\psi(2S)\to\gamma\Sigma(1385)^+\overline{\Lambda}\pi^-$

[1] ABLIKIM 12I reports $<55\times10^{-5}$ from a measurement of $[\Gamma(\chi_{c0}(1P)\to\Sigma(1385)^+\overline{\Lambda}\pi^-+\text{c.c.})/\Gamma_{total}]\times[B(\psi(2S)\to\gamma\chi_{c0}(1P))]$ assuming $B(\psi(2S)\to\gamma\chi_{c0}(1P))=(9.68\pm0.31)\times10^{-2}$, which we rescale to our best value $B(\psi(2S)\to\gamma\chi_{c0}(1P))=9.79\times10^{-2}$.

$\Gamma(\Sigma(1385)^-\overline{\Lambda}\pi^++\text{c.c.})/\Gamma_{total}$ Γ_{73}/Γ

VALUE (units 10^{-5})	CL%	DOCUMENT ID		TECN	COMMENT
<50	90	[1] ABLIKIM	12I	BES3	$\psi(2S)\to\gamma\Sigma(1385)^-\overline{\Lambda}\pi^+$

[1] ABLIKIM 12I reports $<50\times10^{-5}$ from a measurement of $[\Gamma(\chi_{c0}(1P)\to\Sigma(1385)^-\overline{\Lambda}\pi^++\text{c.c.})/\Gamma_{total}]\times[B(\psi(2S)\to\gamma\chi_{c0}(1P))]$ assuming $B(\psi(2S)\to\gamma\chi_{c0}(1P))=(9.68\pm0.31)\times10^{-2}$, which we rescale to our best value $B(\psi(2S)\to\gamma\chi_{c0}(1P))=9.79\times10^{-2}$.

$\Gamma(K^+\overline{p}\Lambda+\text{c.c.})/\Gamma_{total}$ Γ_{74}/Γ

VALUE (units 10^{-3})	EVTS	DOCUMENT ID		TECN	COMMENT
1.25±0.12 OUR AVERAGE	Error includes scale factor of 1.3.				
1.30±0.09±0.03	9k	[1,2] ABLIKIM	13D	BES3	$\psi(2S)\to\gamma\Lambda\overline{p}K^+$
1.01±0.19±0.02		[3] ATHAR	07	CLEO	$\psi(2S)\to\gamma h^+h^-h^0$

[1] ABLIKIM 13D reports $(1.32\pm0.03\pm0.10)\times10^{-3}$ from a measurement of $[\Gamma(\chi_{c0}(1P)\to K^+\overline{p}\Lambda+\text{c.c.})/\Gamma_{total}]\times[B(\psi(2S)\to\gamma\chi_{c0}(1P))]$ assuming $B(\psi(2S)\to\gamma\chi_{c0}(1P))=(9.68\pm0.31)\times10^{-2}$, which we rescale to our best value $B(\psi(2S)\to\gamma\chi_{c0}(1P))=(9.79\pm0.20)\times10^{-2}$. Our first error is their experiment's error and our second error is the systematic error from using our best value.

[2] Using $B(\Lambda\to p\pi^-)=63.9\%$.

[3] ATHAR 07 reports $(1.07\pm0.17\pm0.12)\times10^{-3}$ from a measurement of $[\Gamma(\chi_{c0}(1P)\to K^+\overline{p}\Lambda+\text{c.c.})/\Gamma_{total}]\times[B(\psi(2S)\to\gamma\chi_{c0}(1P))]$ assuming $B(\psi(2S)\to\gamma\chi_{c0}(1P))=(9.22\pm0.11\pm0.46)\times10^{-2}$, which we rescale to our best value $B(\psi(2S)\to\gamma\chi_{c0}(1P))=(9.79\pm0.20)\times10^{-2}$. Our first error is their experiment's error and our second error is the systematic error from using our best value.

$\Gamma(K^+\overline{p}\Lambda(1520)+\text{c.c.})/\Gamma_{total}$ Γ_{75}/Γ

VALUE (units 10^{-4})	EVTS	DOCUMENT ID		TECN	COMMENT
2.9±0.7±0.1	62 ± 12	[1] ABLIKIM	11F	BES3	$\psi(2S)\to\gamma p\overline{p}K^+K^-$

[1] ABLIKIM 11F reports $(3.00\pm0.58\pm0.50)\times10^{-4}$ from a measurement of $[\Gamma(\chi_{c0}(1P)\to K^+\overline{p}\Lambda(1520)+\text{c.c.})/\Gamma_{total}]\times[B(\psi(2S)\to\gamma\chi_{c0}(1P))]$ assuming $B(\psi(2S)\to\gamma\chi_{c0}(1P))=(9.62\pm0.31)\times10^{-2}$, which we rescale to our best value $B(\psi(2S)\to\gamma\chi_{c0}(1P))=(9.79\pm0.20)\times10^{-2}$. Our first error is their experiment's error and our second error is the systematic error from using our best value.

$\Gamma(\Lambda(1520)\overline{\Lambda}(1520))/\Gamma_{total}$ Γ_{76}/Γ

VALUE (units 10^{-4})	EVTS	DOCUMENT ID		TECN	COMMENT
3.1±1.2±0.1	28 ± 10	[1] ABLIKIM	11F	BES3	$\psi(2S)\to\gamma p\overline{p}K^+K^-$

[1] ABLIKIM 11F reports $(3.18\pm1.11\pm0.53)\times10^{-4}$ from a measurement of $[\Gamma(\chi_{c0}(1P)\to\Lambda(1520)\overline{\Lambda}(1520))/\Gamma_{total}]\times[B(\psi(2S)\to\gamma\chi_{c0}(1P))]$ assuming $B(\psi(2S)\to\gamma\chi_{c0}(1P))=(9.62\pm0.31)\times10^{-2}$, which we rescale to our best value $B(\psi(2S)\to\gamma\chi_{c0}(1P))=(9.79\pm0.20)\times10^{-2}$. Our first error is their experiment's error and our second error is the systematic error from using our best value.

$\Gamma(\Sigma^0\overline{\Sigma}^0)/\Gamma_{total}$ Γ_{77}/Γ

VALUE (units 10^{-4})	EVTS	DOCUMENT ID		TECN	COMMENT
4.5±0.4 OUR AVERAGE					
4.7±0.5±0.1	243	[1] ABLIKIM	13H	BES3	$\psi(2S)\to\gamma\Sigma^0\overline{\Sigma}^0$
4.2±0.7±0.1	78 ± 10	[2] NAIK	08	CLEO	$\psi(2S)\to\gamma\Sigma^0\overline{\Sigma}^0$

[1] ABLIKIM 13H reports $(4.78\pm0.34\pm0.39)\times10^{-4}$ from a measurement of $[\Gamma(\chi_{c0}(1P)\to\Sigma^0\overline{\Sigma}^0)/\Gamma_{total}]\times[B(\psi(2S)\to\gamma\chi_{c0}(1P))]$ assuming $B(\psi(2S)\to\gamma\chi_{c0}(1P))=(9.62\pm0.31)\times10^{-2}$, which we rescale to our best value $B(\psi(2S)\to\gamma\chi_{c0}(1P))=(9.79\pm0.20)\times10^{-2}$. Our first error is their experiment's error and our second error is the systematic error from using our best value.

[2] NAIK 08 reports $(4.41\pm0.56\pm0.47)\times10^{-4}$ from a measurement of $[\Gamma(\chi_{c0}(1P)\to\Sigma^0\overline{\Sigma}^0)/\Gamma_{total}]\times[B(\psi(2S)\to\gamma\chi_{c0}(1P))]$ assuming $B(\psi(2S)\to\gamma\chi_{c0}(1P))=(9.22\pm0.11\pm0.46)\times10^{-2}$, which we rescale to our best value $B(\psi(2S)\to\gamma\chi_{c0}(1P))=(9.79\pm0.20)\times10^{-2}$. Our first error is their experiment's error and our second error is the systematic error from using our best value.

$\Gamma(\Sigma^+\overline{\Sigma}^-)/\Gamma_{total}$ Γ_{78}/Γ

VALUE (units 10^{-4})	EVTS	DOCUMENT ID		TECN	COMMENT
4.0±0.7 OUR AVERAGE	Error includes scale factor of 1.7.				
4.5±0.5±0.1	148	[1] ABLIKIM	13H	BES3	$\psi(2S)\to\gamma\Sigma^+\overline{\Sigma}^-$
3.1±0.7±0.1	39 ± 7	[2] NAIK	08	CLEO	$\psi(2S)\to\gamma\Sigma^+\overline{\Sigma}^-$

[1] ABLIKIM 13H reports $(4.54\pm0.42\pm0.30)\times10^{-4}$ from a measurement of $[\Gamma(\chi_{c0}(1P)\to\Sigma^+\overline{\Sigma}^-)/\Gamma_{total}]\times[B(\psi(2S)\to\gamma\chi_{c0}(1P))]$ assuming $B(\psi(2S)\to\gamma\chi_{c0}(1P))=(9.62\pm0.31)\times10^{-2}$, which we rescale to our best value $B(\psi(2S)\to\gamma\chi_{c0}(1P))=(9.79\pm0.20)\times10^{-2}$. Our first error is their experiment's error and our second error is the systematic error from using our best value.

[2] NAIK 08 reports $(3.25\pm0.57\pm0.43)\times10^{-4}$ from a measurement of $[\Gamma(\chi_{c0}(1P)\to\Sigma^+\overline{\Sigma}^-)/\Gamma_{total}]\times[B(\psi(2S)\to\gamma\chi_{c0}(1P))]$ assuming $B(\psi(2S)\to\gamma\chi_{c0}(1P))=(9.22\pm0.11\pm0.46)\times10^{-2}$, which we rescale to our best value $B(\psi(2S)\to\gamma\chi_{c0}(1P))=(9.79\pm0.20)\times10^{-2}$. Our first error is their experiment's error and our second error is the systematic error from using our best value.

$\Gamma(\Sigma(1385)^+\overline{\Sigma}(1385)^-)/\Gamma_{total}$ Γ_{79}/Γ

VALUE (units 10^{-5})	EVTS	DOCUMENT ID		TECN	COMMENT
16.2±5.8±0.3	27	[1] ABLIKIM	12I	BES3	$\psi(2S)\to\gamma\Lambda\overline{\Lambda}\pi^+\pi^-$

[1] ABLIKIM 12I reports $(16.4\pm5.7\pm1.6)\times10^{-5}$ from a measurement of $[\Gamma(\chi_{c0}(1P)\to\Sigma(1385)^+\overline{\Sigma}(1385)^-)/\Gamma_{total}]\times[B(\psi(2S)\to\gamma\chi_{c0}(1P))]$ assuming $B(\psi(2S)\to\gamma\chi_{c0}(1P))=(9.68\pm0.31)\times10^{-2}$, which we rescale to our best value $B(\psi(2S)\to\gamma\chi_{c0}(1P))=(9.79\pm0.20)\times10^{-2}$. Our first error is their experiment's error and our second error is the systematic error from using our best value.

$\Gamma(\Sigma(1385)^-\overline{\Sigma}(1385)^+)/\Gamma_{total}$ Γ_{80}/Γ

VALUE (units 10^{-5})	EVTS	DOCUMENT ID		TECN	COMMENT
23.2±6.5±0.5	33	[1] ABLIKIM	12I	BES3	$\psi(2S)\to\gamma\Lambda\overline{\Lambda}\pi^+\pi^-$

[1] ABLIKIM 12I reports $(23.5\pm6.2\pm2.3)\times10^{-5}$ from a measurement of $[\Gamma(\chi_{c0}(1P)\to\Sigma(1385)^-\overline{\Sigma}(1385)^+)/\Gamma_{total}]\times[B(\psi(2S)\to\gamma\chi_{c0}(1P))]$ assuming $B(\psi(2S)\to\gamma\chi_{c0}(1P))=(9.68\pm0.31)\times10^{-2}$, which we rescale to our best value $B(\psi(2S)\to\gamma\chi_{c0}(1P))=(9.79\pm0.20)\times10^{-2}$. Our first error is their experiment's error and our second error is the systematic error from using our best value.

$\Gamma(K^-\Lambda\overline{\Xi}^++\text{c.c.})/\Gamma_{total}$ Γ_{81}/Γ

VALUE (units 10^{-4})	EVTS	DOCUMENT ID		TECN	COMMENT
1.94±0.35±0.04	57	[1] ABLIKIM	15I	BES3	$\psi(2S)\to\gamma K^-\Lambda\overline{\Xi}^++\text{c.c.}$

[1] ABLIKIM 15I reports $[\Gamma(\chi_{c0}(1P)\to K^-\Lambda\overline{\Xi}^++\text{c.c.})/\Gamma_{total}]\times[B(\psi(2S)\to\gamma\chi_{c0}(1P))]=(1.90\pm0.30\pm0.16)\times10^{-5}$ which we divide by our best value $B(\psi(2S)\to\gamma\chi_{c0}(1P))=(9.79\pm0.20)\times10^{-2}$. Our first error is their experiment's error and our second error is the systematic error from using our best value.

$\Gamma(\Xi^0\overline{\Xi}^0)/\Gamma_{total}$ Γ_{82}/Γ

VALUE (units 10^{-4})	EVTS	DOCUMENT ID		TECN	COMMENT
3.1±0.8±0.1	23.3±4.9	[1] NAIK	08	CLEO	$\psi(2S)\to\gamma\Xi^0\overline{\Xi}^0$

[1] NAIK 08 reports $(3.34\pm0.70\pm0.48)\times10^{-4}$ from a measurement of $[\Gamma(\chi_{c0}(1P)\to\Xi^0\overline{\Xi}^0)/\Gamma_{total}]\times[B(\psi(2S)\to\gamma\chi_{c0}(1P))]$ assuming $B(\psi(2S)\to\gamma\chi_{c0}(1P))=(9.22\pm0.11\pm0.46)\times10^{-2}$, which we rescale to our best value $B(\psi(2S)\to\gamma\chi_{c0}(1P))=(9.79\pm0.20)\times10^{-2}$. Our first error is their experiment's error and our second error is the systematic error from using our best value.

$\Gamma(\Xi^-\overline{\Xi}^+)/\Gamma_{total}$ Γ_{83}/Γ

VALUE (units 10^{-4})	CL%	EVTS	DOCUMENT ID		TECN	COMMENT
4.8±0.7±0.1		95 ± 11	[1] NAIK	08	CLEO	$\psi(2S)\to\gamma\Xi^-\overline{\Xi}^-$
• • • We do not use the following data for averages, fits, limits, etc. • • •						
<10.3	90		[2] ABLIKIM	06D	BES2	$\psi(2S)\to\chi_{c0}\gamma$

[1] NAIK 08 reports $(5.14\pm0.60\pm0.47)\times10^{-4}$ from a measurement of $[\Gamma(\chi_{c0}(1P)\to\Xi^-\overline{\Xi}^+)/\Gamma_{total}]\times[B(\psi(2S)\to\gamma\chi_{c0}(1P))]$ assuming $B(\psi(2S)\to\gamma\chi_{c0}(1P))=(9.22\pm0.11\pm0.46)\times10^{-2}$, which we rescale to our best value $B(\psi(2S)\to\gamma\chi_{c0}(1P))=(9.79\pm0.20)\times10^{-2}$. Our first error is their experiment's error and our second error is the systematic error from using our best value.

[2] Using $B(\psi(2S)\to\chi_{c0}\gamma)=(9.2\pm0.5)\%$

$\Gamma(\eta_c\pi^+\pi^-)/\Gamma_{total}$ Γ_{84}/Γ

VALUE	CL%	DOCUMENT ID		TECN	COMMENT
< 7 × 10⁻⁴	90	[1,2] ABLIKIM	13B	BES3	$e^+e^-\to\psi(2S)\to\gamma\chi_{c0}$
• • • We do not use the following data for averages, fits, limits, etc. • • •					
<41 × 10⁻⁴	90	[1,3] ABLIKIM	13B	BES3	$e^+e^-\to\psi(2S)\to\gamma\chi_{c0}$

[1] Using 1.06×10^8 $\psi(2S)$ mesons and $B(\psi(2S)\to\chi_{c0}\gamma)=(9.68\pm0.31)\%$.

Meson Particle Listings

$\chi_{c0}(1P)$

[2] From the $\eta_c \to K^0_S K^\pm \pi^\mp$ decays.
[3] From the $\eta_c \to K^+ K^- \pi^0$ decays.

$\Gamma(p\overline{p})/\Gamma_{total} \times \Gamma(\pi\pi)/\Gamma_{total}$ $\Gamma_{56}/\Gamma \times \Gamma_{32}/\Gamma$

VALUE (units 10^{-7})	DOCUMENT ID		TECN	COMMENT
18.8±1.0 OUR FIT				
15.3±2.4±0.8	[1] ANDREOTTI	03	E835	$\overline{p}p \to \chi_{c0} \to \pi^0\pi^0$

[1] We have multiplied $B(p\overline{p})\cdot B(\pi^0\pi^0)$ measurement by 3 to obtain $B(p\overline{p})\cdot B(\pi\pi)$.

$\Gamma(p\overline{p})/\Gamma_{total} \times \Gamma(\pi^0\eta)/\Gamma_{total}$ $\Gamma_{56}/\Gamma \times \Gamma_{33}/\Gamma$

VALUE (units 10^{-7})	DOCUMENT ID		TECN	COMMENT
<0.4	ANDREOTTI	05C	E835	$\overline{p}p \to \pi^0\eta$

$\Gamma(p\overline{p})/\Gamma_{total} \times \Gamma(\pi^0\eta')/\Gamma_{total}$ $\Gamma_{56}/\Gamma \times \Gamma_{34}/\Gamma$

VALUE (units 10^{-7})	DOCUMENT ID		TECN	COMMENT
<2.5	ANDREOTTI	05C	E835	$\overline{p}p \to \pi^0\eta$

$\Gamma(p\overline{p})/\Gamma_{total} \times \Gamma(\eta\eta)/\Gamma_{total}$ $\Gamma_{56}/\Gamma \times \Gamma_{36}/\Gamma$

VALUE (units 10^{-7})	DOCUMENT ID		TECN	COMMENT
6.7±0.5 OUR FIT				
$4.0\pm1.2^{+0.5}_{-0.3}$	ANDREOTTI	05C	E835	$\overline{p}p \to \eta\eta$

$\Gamma(p\overline{p})/\Gamma_{total} \times \Gamma(\eta\eta')/\Gamma_{total}$ $\Gamma_{56}/\Gamma \times \Gamma_{37}/\Gamma$

VALUE (units 10^{-6})	DOCUMENT ID		TECN	COMMENT
• • • We do not use the following data for averages, fits, limits, etc. • • •				
$2.1^{+2.3}_{-1.5}$	ANDREOTTI	05C	E835	$\overline{p}p \to \pi^0\eta$

RADIATIVE DECAYS

$\Gamma(\gamma J/\psi(1S))/\Gamma_{total}$ Γ_{85}/Γ

VALUE (units 10^{-2})	EVTS	DOCUMENT ID		TECN	COMMENT
1.40±0.05 OUR FIT					
• • • We do not use the following data for averages, fits, limits, etc. • • •					
0.25±0.16±2.15	12k	[1] ABLIKIM	17U	BES3	$e^+e^- \to \gamma X$
2.0 ±0.2 ±0.2		[2] ADAM	05A	CLEO	$e^+e^- \to \psi(2S) \to \gamma\chi_{c0}$

[1] Not independent from $B(\psi(2S) \to \gamma\chi_{c0}(1P))$ and the product $B(\psi(2S) \to \gamma\chi_{c0}(1P)) \times B(\chi_{c0}(1P) \to \gamma J/\psi(1S))$ also measured in ABLIKIM 17U.
[2] Uses $B(\psi(2S) \to \gamma\chi_{c0} \to \gamma\gamma J/\psi)$ from ADAM 05A and $B(\psi(2S) \to \gamma\chi_{c0})$ from ATHAR 04.

$\Gamma(\gamma\rho^0)/\Gamma_{total}$ Γ_{86}/Γ

VALUE (units 10^{-6})	CL%	EVTS	DOCUMENT ID		TECN	COMMENT
< 9	90	1.2 ± 4.5	[1] BENNETT	08A	CLEO	$\psi(2S) \to \gamma\gamma\rho^0$
• • • We do not use the following data for averages, fits, limits, etc. • • •						
<10	90	6 ± 12	[2] ABLIKIM	11E	BES3	$\psi(2S) \to \gamma\gamma\rho^0$

[1] BENNETT 08A reports $< 9.6 \times 10^{-6}$ from a measurement of $[\Gamma(\chi_{c0}(1P) \to \gamma\rho^0)/\Gamma_{total}] \times [B(\psi(2S) \to \gamma\chi_{c0}(1P))]$ assuming $B(\psi(2S) \to \gamma\chi_{c0}(1P)) = (9.2 \pm 0.4) \times 10^{-2}$, which we rescale to our best value $B(\psi(2S) \to \gamma\chi_{c0}(1P)) = 9.79 \times 10^{-2}$.
[2] ABLIKIM 11E reports $< 10.5 \times 10^{-6}$ from a measurement of $[\Gamma(\chi_{c0}(1P) \to \gamma\rho^0)/\Gamma_{total}] \times [B(\psi(2S) \to \gamma\chi_{c0}(1P))]$ assuming $B(\psi(2S) \to \gamma\chi_{c0}(1P)) = (9.62 \pm 0.31) \times 10^{-2}$, which we rescale to our best value $B(\psi(2S) \to \gamma\chi_{c0}(1P)) = 9.79 \times 10^{-2}$.

$\Gamma(\gamma\omega)/\Gamma_{total}$ Γ_{87}/Γ

VALUE (units 10^{-6})	CL%	EVTS	DOCUMENT ID		TECN	COMMENT
< 8	90	0.0 ± 2.8	[1] BENNETT	08A	CLEO	$\psi(2S) \to \gamma\gamma\omega$
• • • We do not use the following data for averages, fits, limits, etc. • • •						
<13	90	5 ± 11	[2] ABLIKIM	11E	BES3	$\psi(2S) \to \gamma\gamma\omega$

[1] BENNETT 08A reports $< 8.8 \times 10^{-6}$ from a measurement of $[\Gamma(\chi_{c0}(1P) \to \gamma\omega)/\Gamma_{total}] \times [B(\psi(2S) \to \gamma\chi_{c0}(1P))]$ assuming $B(\psi(2S) \to \gamma\chi_{c0}(1P)) = (9.2 \pm 0.4) \times 10^{-2}$, which we rescale to our best value $B(\psi(2S) \to \gamma\chi_{c0}(1P)) = 9.79 \times 10^{-2}$.
[2] ABLIKIM 11E reports $< 12.9 \times 10^{-6}$ from a measurement of $[\Gamma(\chi_{c0}(1P) \to \gamma\omega)/\Gamma_{total}] \times [B(\psi(2S) \to \gamma\chi_{c0}(1P))]$ assuming $B(\psi(2S) \to \gamma\chi_{c0}(1P)) = (9.62 \pm 0.31) \times 10^{-2}$, which we rescale to our best value $B(\psi(2S) \to \gamma\chi_{c0}(1P)) = 9.79 \times 10^{-2}$.

$\Gamma(\gamma\phi)/\Gamma_{total}$ Γ_{88}/Γ

VALUE (units 10^{-6})	CL%	EVTS	DOCUMENT ID		TECN	COMMENT
< 6	90	0.1 ± 1.6	[1] BENNETT	08A	CLEO	$\psi(2S) \to \gamma\gamma\phi$
• • • We do not use the following data for averages, fits, limits, etc. • • •						
<16	90	15 ± 7	[2] ABLIKIM	11E	BES3	$\psi(2S) \to \gamma\gamma\phi$

[1] BENNETT 08A reports $< 6.4 \times 10^{-6}$ from a measurement of $[\Gamma(\chi_{c0}(1P) \to \gamma\phi)/\Gamma_{total}] \times [B(\psi(2S) \to \gamma\chi_{c0}(1P))]$ assuming $B(\psi(2S) \to \gamma\chi_{c0}(1P)) = (9.2 \pm 0.4) \times 10^{-2}$, which we rescale to our best value $B(\psi(2S) \to \gamma\chi_{c0}(1P)) = 9.79 \times 10^{-2}$.
[2] ABLIKIM 11E reports $< 16.2 \times 10^{-6}$ from a measurement of $[\Gamma(\chi_{c0}(1P) \to \gamma\phi)/\Gamma_{total}] \times [B(\psi(2S) \to \gamma\chi_{c0}(1P))]$ assuming $B(\psi(2S) \to \gamma\chi_{c0}(1P)) = (9.62 \pm 0.31) \times 10^{-2}$, which we rescale to our best value $B(\psi(2S) \to \gamma\chi_{c0}(1P)) = 9.79 \times 10^{-2}$.

$\Gamma(\gamma\gamma)/\Gamma_{total}$ Γ_{89}/Γ

VALUE (units 10^{-4})	CL%	DOCUMENT ID		TECN	COMMENT
2.04±0.09 OUR FIT					
• • • We do not use the following data for averages, fits, limits, etc. • • •					
<7	90	[1] WICHT	08	BELL	$B^\pm \to K^\pm\gamma\gamma$

[1] WICHT 08 reports $[\Gamma(\chi_{c0}(1P) \to \gamma\gamma)/\Gamma_{total}] \times [B(B^+ \to \chi_{c0}K^+)] < 0.11 \times 10^{-6}$ which we divide by our best value $B(B^+ \to \chi_{c0}K^+) = 1.49 \times 10^{-4}$.

$\Gamma(e^+e^- J/\psi(1S))/\Gamma_{total}$ Γ_{90}/Γ

VALUE (units 10^{-4})	EVTS	DOCUMENT ID		TECN	COMMENT
1.54±0.33±0.03	56	[1] ABLIKIM	17I	BES3	$\psi(2S) \to \gamma e^+e^- J/\psi$

[1] ABLIKIM 17I reports $(1.51 \pm 0.30 \pm 0.13) \times 10^{-4}$ from a measurement of $[\Gamma(\chi_{c0}(1P) \to e^+e^- J/\psi(1S))/\Gamma_{total}] \times [B(\psi(2S) \to \gamma\chi_{c0}(1P))]$ assuming $B(\psi(2S) \to \gamma\chi_{c0}(1P)) = (9.99 \pm 0.27) \times 10^{-2}$, which we rescale to our best value $B(\psi(2S) \to \gamma\chi_{c0}(1P)) = (9.79 \pm 0.20) \times 10^{-2}$. Our first error is their experiment's error and our second error is the systematic error from using our best value.

$\Gamma(e^+e^- J/\psi(1S))/\Gamma(\gamma J/\psi(1S))$ Γ_{90}/Γ_{85}

VALUE (units 10^{-3})	EVTS	DOCUMENT ID		TECN	COMMENT
9.5±1.9±0.7	56	[1] ABLIKIM	17I	BES3	$\psi(2S) \to e^+e^-\gamma J/\psi$

[1] Uses $B(\psi(2S) \to \gamma\chi_{c0}(1P)) \times B(\chi_{c0}(1P) \to \gamma J/\psi(1S)) = (15.8 \pm 0.3 \pm 0.6) \times 10^{-4}$ from ABLIKIM 17N and accounts for common systematic errors.

$\Gamma(\gamma\gamma)/\Gamma(\gamma J/\psi(1S))$ Γ_{89}/Γ_{85}

VALUE (units 10^{-2})	DOCUMENT ID		TECN	COMMENT
1.45±0.08 OUR FIT				
2.0 ±0.4 OUR AVERAGE				
$2.2 \pm 0.4\ ^{+0.1}_{-0.2}$	[1] ANDREOTTI	04	E835	$p\overline{p} \to \chi_{c0} \to \gamma\gamma$
1.45±0.74	[2] AMBROGIANI	00B	E835	$\overline{p}p \to \chi_{c2} \to \gamma\gamma, \gamma J/\psi$

[1] The values of $B(p\overline{p})B(\gamma\gamma)$ and $B(\gamma\gamma)B(\gamma J/\psi)$ measured by ANDREOTTI 04 are not independent. The latter is used in the fit because of smaller systematics.
[2] Calculated by us using $B(J/\psi(1S) \to e^+e^-) = 0.0593 \pm 0.0010$.

$\Gamma(p\overline{p})/\Gamma_{total} \times \Gamma(\gamma J/\psi(1S))/\Gamma_{total}$ $\Gamma_{56}/\Gamma \times \Gamma_{85}/\Gamma$

VALUE (units 10^{-7})	EVTS	DOCUMENT ID		TECN	COMMENT
31.1±1.5 OUR FIT					
28.2±2.1 OUR AVERAGE					
28.0±1.9±1.3	392	[1,2,3] BAGNASCO	02	E835	$\overline{p}p \to \chi_{c0} \to J/\psi\gamma$
$29.3^{+5.7}_{-4.7}$±1.5	89	[1,2] AMBROGIANI	99B		$\overline{p}p \to \chi_{c0} \to J/\psi\gamma$

[1] Values in $(\Gamma(p\overline{p}) \times \Gamma(\gamma J/\psi(1S))/\Gamma_{total})$ and $(\Gamma(p\overline{p})/\Gamma_{total} \times \Gamma(\gamma J/\psi(1S))/\Gamma_{total})$ are not independent. The latter is used in the fit since it is less correlated to the total width.
[2] Calculated by us using $B(J/\psi(1S) \to e^+e^-) = 0.0593 \pm 0.0010$.
[3] Recalculated by ANDREOTTI 05A.

$\Gamma(p\overline{p})/\Gamma_{total} \times \Gamma(\gamma\gamma)/\Gamma_{total}$ $\Gamma_{56}/\Gamma \times \Gamma_{89}/\Gamma$

VALUE (units 10^{-8})	DOCUMENT ID		TECN	COMMENT
4.52±0.27 OUR FIT				
• • • We do not use the following data for averages, fits, limits, etc. • • •				
$6.52 \pm 1.18^{+0.48}_{-0.72}$	[1] ANDREOTTI	04	E835	$p\overline{p} \to \chi_{c0} \to \gamma\gamma$

[1] The values of $B(p\overline{p})B(\gamma\gamma)$ and $B(\gamma\gamma)B(\gamma J/\psi)$ measured by ANDREOTTI 04 are not independent. The latter is used in the fit because of smaller systematics.

$\chi_{c0}(1P)$ CROSS-PARTICLE BRANCHING RATIOS

$\Gamma(\chi_{c0}(1P) \to p\overline{p})/\Gamma_{total} \times \Gamma(\psi(2S) \to \gamma\chi_{c0}(1P))/\Gamma_{total}$ $\Gamma_{56}/\Gamma \times \Gamma^{\psi(2S)}_{139}/\Gamma^{\psi(2S)}$

VALUE (units 10^{-6})	EVTS	DOCUMENT ID		TECN	COMMENT
21.7±0.9 OUR FIT					
23.7±1.0 OUR AVERAGE					
23.7±0.8±0.9	1222	ABLIKIM	13V	BES3	$\psi(2S) \to \gamma p\overline{p}$
23.7±1.4±1.4	383 ± 22	[1] NAIK	08	CLEO	$\psi(2S) \to \gamma p\overline{p}$
$23.6^{+3.7}_{-3.4}$±3.4	89.5^{+14}_{-13}	BAI	04F	BES	$\psi(2S) \to \gamma\chi_{c0}(1P) \to \gamma\overline{p}p$

[1] Calculated by us. NAIK 08 reports $B(\chi_{c0} \to p\overline{p}) = (25.7 \pm 1.5 \pm 1.3) \times 10^{-5}$ using $B(\psi(2S) \to \gamma\chi_{c0}) = (9.22 \pm 0.11 \pm 0.46)\%$.

$\Gamma(\chi_{c0}(1P) \to p\overline{p})/\Gamma_{total} \times \Gamma(\psi(2S) \to \gamma\chi_{c0}(1P))/\Gamma(\psi(2S) \to J/\psi(1S)\pi^+\pi^-)$ $\Gamma_{56}/\Gamma \times \Gamma^{\psi(2S)}_{139}/\Gamma^{\psi(2S)}_{11}$

VALUE (units 10^{-5})	DOCUMENT ID		TECN	COMMENT
6.25±0.26 OUR FIT				
4.6 ±1.9	[1] BAI	98I	BES	$\psi(2S) \to \gamma\chi_{c0} \to \gamma\overline{p}p$

[1] Calculated by us. The value for $B(\chi_{c0} \to p\overline{p})$ reported in BAI 98I is derived using $B(\psi(2S) \to \gamma\chi_{c0}) = (9.3 \pm 0.8)\%$ and $B(\psi(2S) \to J/\psi(1S)\pi^+\pi^-) = (32.4 \pm 2.6)\%$ [BAI 98D].

$\Gamma(\chi_{c0}(1P) \to \Lambda\overline{\Lambda})/\Gamma_{total} \times \Gamma(\psi(2S) \to \gamma\chi_{c0}(1P))/\Gamma_{total}$ $\Gamma_{69}/\Gamma \times \Gamma^{\psi(2S)}_{139}/\Gamma^{\psi(2S)}$

VALUE (units 10^{-6})	EVTS	DOCUMENT ID		TECN	COMMENT
32.0±2.3 OUR FIT					
31.7±2.3 OUR AVERAGE					
32.0±1.9±2.2	369	[1] ABLIKIM	13H	BES3	$\psi(2S) \to \gamma\Lambda\overline{\Lambda}$
31.2±3.3±2.0	131 ± 12	[2] NAIK	08	CLEO	$\psi(2S) \to \gamma\Lambda\overline{\Lambda}$

[1] Calculated by us. ABLIKIM 13H reports $B(\chi_{c0} \to \Lambda\overline{\Lambda}) = (33.3 \pm 2.0 \pm 2.6) \times 10^{-5}$ from a measurement of $B(\chi_{c0} \to \Lambda\overline{\Lambda}) \times B(\psi(2S) \to \gamma\chi_{c0})$ assuming $B(\psi(2S) \to \gamma\chi_{c0}) = (9.62 \pm 0.31)\%$.
[2] Calculated by us. NAIK 08 reports $B(\chi_{c0} \to \Lambda\overline{\Lambda}) = (33.8 \pm 3.6 \pm 2.2 \pm 1.7) \times 10^{-5}$ using $B(\psi(2S) \to \gamma\chi_{c0}) = (9.22 \pm 0.11 \pm 0.46)\%$.

$\Gamma(\chi_{c0}(1P) \to \Lambda\overline{\Lambda})/\Gamma_{total} \times \Gamma(\psi(2S) \to \gamma\chi_{c0}(1P))/\Gamma(\psi(2S) \to J/\psi(1S)\pi^+\pi^-)$ $\Gamma_{69}/\Gamma \times \Gamma_{139}^{\psi(2S)}/\Gamma_{11}^{\psi(2S)}$

VALUE (units 10^{-5})	EVTS	DOCUMENT ID	TECN	COMMENT
9.2±0.7 OUR FIT				
$13.0^{+3.6}_{-3.5}\pm2.5$	$15.2^{+4.2}_{-4.0}$	[1] BAI	03E BES	$\psi(2S) \to \gamma\Lambda\overline{\Lambda}$

[1] BAI 03E reports [$B(\chi_{c0} \to \Lambda\overline{\Lambda})$ $B(\psi(2S) \to \gamma\chi_{c0})$ / $B(\psi(2S) \to J/\psi\pi^+\pi^-)$] × [$B^2(\Lambda \to \pi^- p)$ / $B(J/\psi \to p\overline{p})$] = $(2.45^{+0.68}_{-0.65} \pm 0.46)\%$. We calculate from this measurement the presented value using $B(\Lambda \to \pi^- p) = (63.9 \pm 0.5)\%$ and $B(J/\psi \to p\overline{p}) = (2.17 \pm 0.07) \times 10^{-3}$.

$\Gamma(\chi_{c0}(1P) \to \gamma J/\psi(1S))/\Gamma_{total} \times \Gamma(\psi(2S) \to \gamma\chi_{c0}(1P))/\Gamma_{total}$ $\Gamma_{85}/\Gamma \times \Gamma_{139}^{\psi(2S)}/\Gamma^{\psi(2S)}$

VALUE (units 10^{-2})	EVTS	DOCUMENT ID	TECN	COMMENT
0.138±0.005 OUR FIT				
0.147±0.029 OUR AVERAGE		Error includes scale factor of 4.6.		
0.158±0.003±0.006	4.8k	[1] ABLIKIM 17N	BES3	$\psi(2S) \to \gamma\gamma J/\psi$
0.024±0.015±0.205	12k	ABLIKIM 17U	BES3	$e^+e^- \to \gamma X$
0.069±0.018		[2] OREGLIA 82	CBAL	$\psi(2S) \to \gamma\chi_{c0}$
0.4 ±0.3		[3] BRANDELIK 79B	DASP	$\psi(2S) \to \gamma\chi_{c0}$
0.16 ±0.11		[3] BARTEL 78B	CNTR	$\psi(2S) \to \gamma\chi_{c0}$
3.3 ±1.7		[4] BIDDICK 77	CNTR	$e^+e^- \to \gamma X$
• • • We do not use the following data for averages, fits, limits, etc. • • •				
0.151±0.003±0.010	4.3k	[5] ABLIKIM 12O	BES3	$\psi(2S) \to \gamma\chi_{c0}$
0.125±0.007±0.013	560	[6] MENDEZ 08	CLEO	$\psi(2S) \to \gamma\chi_{c0}$
0.18 ±0.01 ±0.02	172	[7] ADAM 05A	CLEO	Repl. by MENDEZ 08

[1] Uses B($J/\psi \to e^+e^-$) = (5.971 ± 0.032)% and B($J/\psi \to \mu^+\mu^-$) = (5.961 ± 0.033)%.
[2] Recalculated by us using $B(J/\psi(1S) \to \ell^+\ell^-) = 0.1181 \pm 0.0020$.
[3] Recalculated by us using $B(J/\psi(1S) \to \mu^+\mu^-) = 0.0588 \pm 0.0010$.
[4] Assumes isotropic gamma distribution.
[5] Superseded by ABLIKIM 17N.
[6] Not independent from other measurements of MENDEZ 08.
[7] Not independent from other values reported by ADAM 05A.

$\Gamma(\chi_{c0}(1P) \to \gamma J/\psi(1S))/\Gamma_{total} \times \Gamma(\psi(2S) \to \gamma\chi_{c0}(1P))/\Gamma(\psi(2S) \to J/\psi(1S)\text{anything})$ $\Gamma_{85}/\Gamma \times \Gamma_{139}^{\psi(2S)}/\Gamma_{9}^{\psi(2S)}$

$\Gamma_{85}/\Gamma \times \Gamma_{139}^{\psi(2S)}/\Gamma_{9}^{\psi(2S)} = \Gamma_{85}/\Gamma \times \Gamma_{139}^{\psi(2S)}/(\Gamma_{11}^{\psi(2S)} + \Gamma_{12}^{\psi(2S)} + \Gamma_{13}^{\psi(2S)} + 0.343\Gamma_{140}^{\psi(2S)} + 0.190\Gamma_{141}^{\psi(2S)})$

VALUE (units 10^{-2})	EVTS	DOCUMENT ID	TECN	COMMENT
0.224±0.009 OUR FIT				
• • • We do not use the following data for averages, fits, limits, etc. • • •				
0.201±0.011±0.021	560	[1] MENDEZ 08	CLEO	$\psi(2S) \to \gamma\chi_{c0}$
0.31 ±0.02 ±0.03	172	ADAM 05A	CLEO	Repl. by MENDEZ 08

[1] Not independent from other measurements of MENDEZ 08.

$\Gamma(\chi_{c0}(1P) \to \gamma J/\psi(1S))/\Gamma_{total} \times \Gamma(\psi(2S) \to \gamma\chi_{c0}(1P))/\Gamma(\psi(2S) \to J/\psi(1S)\pi^+\pi^-)$ $\Gamma_{85}/\Gamma \times \Gamma_{139}^{\psi(2S)}/\Gamma_{11}^{\psi(2S)}$

VALUE (units 10^{-2})	EVTS	DOCUMENT ID	TECN	COMMENT
0.397±0.015 OUR FIT				
0.358±0.020±0.037	560	MENDEZ 08	CLEO	$\psi(2S) \to \gamma\chi_{c0}$
• • • We do not use the following data for averages, fits, limits, etc. • • •				
0.55 ±0.04 ±0.06	172	[1] ADAM 05A	CLEO	Repl. by MENDEZ 08

[1] Not independent from other values reported by ADAM 05A.

$\Gamma(\chi_{c0}(1P) \to \gamma\gamma)/\Gamma_{total} \times \Gamma(\psi(2S) \to \gamma\chi_{c0}(1P))/\Gamma_{total}$ $\Gamma_{89}/\Gamma \times \Gamma_{139}^{\psi(2S)}/\Gamma^{\psi(2S)}$

VALUE (units 10^{-5})	EVTS	DOCUMENT ID	TECN	COMMENT
2.00±0.08 OUR FIT				
1.95±0.09 OUR AVERAGE				
1.93±0.08±0.05	3.5k	ABLIKIM 17AE	BES3	$\psi(2S) \to \gamma\chi_{c0} \to 3\gamma$
2.17±0.32±0.10	0.2k	ECKLUND 08A	CLEO	$\psi(2S) \to \gamma\chi_{c0} \to 3\gamma$
3.7 ±1.8 ±1.0		LEE 85	CBAL	$\psi(2S) \to \gamma\chi_{c0}$
• • • We do not use the following data for averages, fits, limits, etc. • • •				
2.17±0.17±0.12	0.8k	[1] ABLIKIM 12A	BES3	$\psi(2S) \to \gamma\chi_{c0} \to 3\gamma$

[1] Superseded by ABLIKIM 17AE.

$\Gamma(\chi_{c0}(1P) \to \pi\pi)/\Gamma_{total} \times \Gamma(\psi(2S) \to \gamma\chi_{c0}(1P))/\Gamma_{total}$ $\Gamma_{32}/\Gamma \times \Gamma_{139}^{\psi(2S)}/\Gamma^{\psi(2S)}$

VALUE (units 10^{-4})	EVTS	DOCUMENT ID	TECN	COMMENT
8.34±0.29 OUR FIT				
8.80±0.34 OUR AVERAGE				
9.11±0.08±0.65	17k	[1] ABLIKIM 10A	BES3	$e^+e^- \to \psi(2S) \to \gamma\chi_{c0}$
8.81±0.11±0.43	8.9k	[2] ASNER 09	CLEO	$\psi(2S) \to \gamma\pi^+\pi^-$
8.13±0.19±0.89	2.8k	[3] ASNER 09	CLEO	$\psi(2S) \to \gamma\pi^0\pi^0$

[1] Calculated by us. ABLIKIM 10A reports $B(\chi_{c0} \to \pi^0\pi^0) = (3.23 \pm 0.03 \pm 0.23 \pm 0.14) \times 10^{-3}$ using $B(\psi(2S) \to \gamma\chi_{c0}) = (9.4 \pm 0.4)\%$. We have multiplied the $\pi^0\pi^0$ measurement by 3 to obtain $\pi\pi$.
[2] Calculated by us. ASNER 09 reports $B(\chi_{c0} \to \pi^+\pi^-) = (6.37 \pm 0.08 \pm 0.31 \pm 0.32) \times 10^{-3}$ using $B(\psi(2S) \to \gamma\chi_{c0}) = (9.22 \pm 0.11 \pm 0.46)\%$. We have multiplied the $\pi^+\pi^-$ measurement by 3/2 to obtain $\pi\pi$.
[3] Calculated by us. ASNER 09 reports $B(\chi_{c0} \to \pi^0\pi^0) = (2.94 \pm 0.07 \pm 0.32 \pm 0.15) \times 10^{-3}$ using $B(\psi(2S) \to \gamma\chi_{c0}) = (9.22 \pm 0.11 \pm 0.46)\%$. We have multiplied the $\pi^0\pi^0$ measurement by 3 to obtain $\pi\pi$.

$\Gamma(\chi_{c0}(1P) \to \pi\pi)/\Gamma_{total} \times \Gamma(\psi(2S) \to \gamma\chi_{c0}(1P))/\Gamma(\psi(2S) \to J/\psi(1S)\pi^+\pi^-)$ $\Gamma_{32}/\Gamma \times \Gamma_{139}^{\psi(2S)}/\Gamma_{11}^{\psi(2S)}$

VALUE (units 10^{-4})	EVTS	DOCUMENT ID	TECN	COMMENT
24.0±0.8 OUR FIT				
20.7±1.7 OUR AVERAGE				
23.9±2.7±4.1	97 ± 11	[1] BAI 03C	BES	$\psi(2S) \to \gamma\chi_{c0} \to \gamma\pi^0\pi^0$
20.2±1.1±1.5	720 ± 32	[2] BAI 98I	BES	$\psi(2S) \to \gamma\chi_{c0} \to \gamma\pi^+\pi^-$

[1] We have multiplied $\pi^0\pi^0$ measurement by 3 to obtain $\pi\pi$.
[2] Calculated by us. The value for $B(\chi_{c0} \to \pi^+\pi^-)$ reported in BAI 98I is derived using $B(\psi' \to \gamma\chi_{c0}) = (9.3 \pm 0.8)\%$ and $B(\psi' \to J/\psi\pi^+\pi^-) = (32.4 \pm 2.6)\%$ [BAI 98D]. We have multiplied $\pi^+\pi^-$ measurement by 3/2 to obtain $\pi\pi$.

$\Gamma(\chi_{c0}(1P) \to \eta\eta)/\Gamma_{total} \times \Gamma(\psi(2S) \to \gamma\chi_{c0}(1P))/\Gamma_{total}$ $\Gamma_{36}/\Gamma \times \Gamma_{139}^{\psi(2S)}/\Gamma^{\psi(2S)}$

VALUE (units 10^{-4})	EVTS	DOCUMENT ID	TECN	COMMENT
2.95±0.18 OUR FIT				
3.12±0.19 OUR AVERAGE				
3.23±0.09±0.23	2132	[1] ABLIKIM 10A	BES3	$e^+e^- \to \psi(2S) \to \gamma\chi_{c0}$
2.93±0.12±0.29	0.9k	[2] ASNER 09	CLEO	$\psi(2S) \to \gamma\eta\eta$
• • • We do not use the following data for averages, fits, limits, etc. • • •				
2.86±0.46±0.37	48	[3] ADAMS 07	CLEO	$\psi(2S) \to \gamma\chi_{c0}$

[1] Calculated by us. ABLIKIM 10A reports $B(\chi_{c0} \to \eta\eta) = (3.44 \pm 0.10 \pm 0.24 \pm 0.13) \times 10^{-3}$ using $B(\psi(2S) \to \gamma\chi_{c0}) = (9.4 \pm 0.4)\%$.
[2] Calculated by us. ASNER 09 reports $B(\chi_{c0} \to \eta\eta) = (3.18 \pm 0.13 \pm 0.31 \pm 0.16) \times 10^{-3}$ using $B(\psi(2S) \to \gamma\chi_{c0}) = (9.22 \pm 0.11 \pm 0.46)\%$.
[3] Superseded by ASNER 09. Calculated by us. The value of $B(\chi_{c0}(1P) \to \eta\eta)$ reported by ADAMS 07 was derived using $B(\psi(2S) \to \gamma\chi_{c0}(1P)) = (9.22 \pm 0.11 \pm 0.46)\%$ (ATHAR 04).

$\Gamma(\chi_{c0}(1P) \to \eta\eta)/\Gamma_{total} \times \Gamma(\psi(2S) \to \gamma\chi_{c0}(1P))/\Gamma(\psi(2S) \to J/\psi(1S)\pi^+\pi^-)$ $\Gamma_{36}/\Gamma \times \Gamma_{139}^{\psi(2S)}/\Gamma_{11}^{\psi(2S)}$

VALUE (units 10^{-3})	DOCUMENT ID	TECN	COMMENT
0.85 ±0.05 OUR FIT			
0.578±0.241±0.158	BAI 03C	BES	$\psi(2S) \to \gamma\eta\eta$

$\Gamma(\chi_{c0}(1P) \to K^+K^-)/\Gamma_{total} \times \Gamma(\psi(2S) \to \gamma\chi_{c0}(1P))/\Gamma_{total}$ $\Gamma_{42}/\Gamma \times \Gamma_{139}^{\psi(2S)}/\Gamma^{\psi(2S)}$

VALUE (units 10^{-4})	EVTS	DOCUMENT ID	TECN	COMMENT
5.92±0.28 OUR FIT				
5.97±0.07±0.32	8.1k	[1] ASNER 09	CLEO	$\psi(2S) \to \gamma K^+K^-$

[1] Calculated by us. ASNER 09 reports $B(\chi_{c0} \to K^+K^-) = (6.47 \pm 0.08 \pm 0.35 \pm 0.32) \times 10^{-3}$ using $B(\psi(2S) \to \gamma\chi_{c0}) = (9.22 \pm 0.11 \pm 0.46)\%$.

$\Gamma(\chi_{c0}(1P) \to K^+K^-)/\Gamma_{total} \times \Gamma(\psi(2S) \to \gamma\chi_{c0}(1P))/\Gamma(\psi(2S) \to J/\psi(1S)\pi^+\pi^-)$ $\Gamma_{42}/\Gamma \times \Gamma_{139}^{\psi(2S)}/\Gamma_{11}^{\psi(2S)}$

VALUE (units 10^{-3})	EVTS	DOCUMENT ID	TECN	COMMENT
1.71±0.08 OUR FIT				
1.63±0.10±0.15	774 ± 38	[1] BAI 98I	BES	$\psi(2S) \to \gamma K^+K^-$

[1] Calculated by us. The value for $B(\chi_{c0} \to K^+K^-)$ reported by BAI 98I is derived using $B(\psi(2S) \to \gamma\chi_{c0}) = (9.3 \pm 0.8)\%$ and $B(\psi(2S) \to J/\psi\pi^+\pi^-) = (32.4 \pm 2.6)\%$ [BAI 98D].

$\Gamma(\chi_{c0}(1P) \to K^0_S K^0_S)/\Gamma_{total} \times \Gamma(\psi(2S) \to \gamma\chi_{c0}(1P))/\Gamma_{total}$ $\Gamma_{43}/\Gamma \times \Gamma_{139}^{\psi(2S)}/\Gamma^{\psi(2S)}$

VALUE (units 10^{-4})	EVTS	DOCUMENT ID	TECN	COMMENT
3.10±0.16 OUR FIT				
3.18±0.17 OUR AVERAGE				
3.22±0.07±0.17	2.1k	[1] ASNER 09	CLEO	$\psi(2S) \to \gamma K^0_S K^0_S$
3.02±0.19±0.33	322	ABLIKIM 05O	BES2	$\psi(2S) \to \gamma K^0_S K^0_S$

[1] Calculated by us. ASNER 09 reports $B(\chi_{c0} \to K^0_S K^0_S) = (3.49 \pm 0.08 \pm 0.18 \pm 0.17) \times 10^{-3}$ using $B(\psi(2S) \to \gamma\chi_{c0}) = (9.22 \pm 0.11 \pm 0.46)\%$.

$\Gamma(\chi_{c0}(1P) \to K^0_S K^0_S)/\Gamma_{total} \times \Gamma(\psi(2S) \to \gamma\chi_{c0}(1P))/\Gamma(\psi(2S) \to J/\psi(1S)\pi^+\pi^-)$ $\Gamma_{43}/\Gamma \times \Gamma_{139}^{\psi(2S)}/\Gamma_{11}^{\psi(2S)}$

VALUE (units 10^{-4})	DOCUMENT ID	TECN	COMMENT
8.9±0.5 OUR FIT			
5.6±0.8±1.3	[1] BAI 99B	BES	$\psi(2S) \to \gamma K^0_S K^0_S$

[1] Calculated by us. The value of $B(\chi_{c0} \to K^0_S K^0_S)$ reported by BAI 99B was derived using $B(\psi(2S) \to \gamma\chi_{c0}(1P)) = (9.3 \pm 0.8)\%$ and $B(\psi(2S) \to J/\psi\pi^+\pi^-) = (32.4 \pm 2.6)\%$ [BAI 98D].

$\Gamma(\chi_{c0}(1P) \to 2(\pi^+\pi^-))/\Gamma_{total} \times \Gamma(\psi(2S) \to \gamma\chi_{c0}(1P))/\Gamma(\psi(2S) \to J/\psi(1S)\pi^+\pi^-)$ $\Gamma_1/\Gamma \times \Gamma^{\psi(2S)}_{139}/\Gamma^{\psi(2S)}_{11}$

VALUE (units 10^{-3})	DOCUMENT ID		TECN	COMMENT
6.6±0.5 OUR FIT				
6.9±2.4 OUR AVERAGE	Error includes scale factor of 3.8.			
4.4±0.1±0.9	[1] BAI	99B	BES	$\psi(2S) \to \gamma\chi_{c0}$
9.3±0.9	[2] TANENBAUM	78	MRK1	$\psi(2S) \to \gamma\chi_{c0}$

[1] Calculated by us. The value for $B(\chi_{c0} \to 2\pi^+2\pi^-)$ reported in BAI 99B is derived using $B(\psi(2S) \to \gamma\chi_{c0}) = (9.3 \pm 0.8)\%$ and $B(\psi(2S) \to J/\psi(1S)\pi^+\pi^-) = (32.4 \pm 2.6)\%$ [BAI 98D].

[2] The value $B(\psi(1S) \to \gamma\chi_{c0}) \times B(\chi_{c0} \to 2\pi^+2\pi^-)$ reported in TANENBAUM 78 is derived using $B(\psi(2S) \to J/\psi(1S)\pi^+\pi^-) \times B(J/\psi(1S) \to \ell^+\ell^-) = (4.6 \pm 0.7)\%$. Calculated by us using $B(J/\psi(1S) \to \ell^+\ell^-) = 0.1181 \pm 0.0020$.

$\Gamma(\chi_{c0}(1P) \to \pi^+\pi^-K^+K^-)/\Gamma_{total} \times \Gamma(\psi(2S) \to \gamma\chi_{c0}(1P))/\Gamma_{total}$ $\Gamma_8/\Gamma \times \Gamma^{\psi(2S)}_{139}/\Gamma^{\psi(2S)}$

VALUE (units 10^{-3})	DOCUMENT ID		TECN	COMMENT
1.78±0.14 OUR FIT				
1.64±0.05±0.2	ABLIKIM	05Q	BES2	$\psi(2S) \to \gamma\chi_{c0}$

$\Gamma(\chi_{c0}(1P) \to \pi^+\pi^-K^+K^-)/\Gamma_{total} \times \Gamma(\psi(2S) \to \gamma\chi_{c0}(1P))/\Gamma(\psi(2S) \to J/\psi(1S)\pi^+\pi^-)$ $\Gamma_8/\Gamma \times \Gamma^{\psi(2S)}_{139}/\Gamma^{\psi(2S)}_{11}$

VALUE (units 10^{-3})	DOCUMENT ID		TECN	COMMENT
5.1 ±0.4 OUR FIT				
5.8 ±1.6 OUR AVERAGE	Error includes scale factor of 2.3.			
4.22±0.20±0.97	BAI	99B	BES	$\psi(2S) \to \gamma\chi_{c0}$
7.4 ±1.0	[1] TANENBAUM	78	MRK1	$\psi(2S) \to \gamma\chi_{c0}$

[1] The reported value is derived using $B(\psi(2S) \to \pi^+\pi^- J/\psi) \times B(J/\psi \to \ell^+\ell^-) = (4.6 \pm 0.7)\%$. Calculated by us using $B(J/\psi \to \ell^+\ell^-) = 0.1181 \pm 0.0020$.

$\Gamma(\chi_{c0}(1P) \to K^+K^-K^+K^-)/\Gamma_{total} \times \Gamma(\psi(2S) \to \gamma\chi_{c0}(1P))/\Gamma_{total}$ $\Gamma_{50}/\Gamma \times \Gamma^{\psi(2S)}_{139}/\Gamma^{\psi(2S)}$

VALUE (units 10^{-4})	EVTS	DOCUMENT ID		TECN	COMMENT
2.76±0.28 OUR FIT					
3.20±0.11±0.41	278	[1] ABLIKIM	06T	BES2	$\psi(2S) \to \gamma 2K^+2K^-$

[1] Calculated by us. The value of $B(\chi_{c0} \to 2K^+2K^-)$ reported by ABLIKIM 06T was derived using $B(\psi(2S) \to \gamma\chi_{c0}(1P)) = (9.2 \pm 0.4)\%$.

$\Gamma(\chi_{c0}(1P) \to K^+K^-K^+K^-)/\Gamma_{total} \times \Gamma(\psi(2S) \to \gamma\chi_{c0}(1P))/\Gamma(\psi(2S) \to J/\psi(1S)\pi^+\pi^-)$ $\Gamma_{50}/\Gamma \times \Gamma^{\psi(2S)}_{139}/\Gamma^{\psi(2S)}_{11}$

VALUE (units 10^{-4})	DOCUMENT ID		TECN	COMMENT
8.0±0.8 OUR FIT				
6.1±0.8±0.9	[1] BAI	99B	BES	$\psi(2S) \to \gamma 2K^+2K^-$

[1] Calculated by us. The value of $B(\chi_{c0} \to 2K^+2K^-)$ reported by BAI 99B was derived using $B(\psi(2S) \to \gamma\chi_{c0}(1P)) = (9.3 \pm 0.8)\%$ and $B(\psi(2S) \to J/\psi\pi^+\pi^-) = (32.4 \pm 2.6)\%$ [BAI 98D].

$\Gamma(\chi_{c0}(1P) \to \phi\phi)/\Gamma_{total} \times \Gamma(\psi(2S) \to \gamma\chi_{c0}(1P))/\Gamma_{total}$ $\Gamma_{55}/\Gamma \times \Gamma^{\psi(2S)}_{139}/\Gamma^{\psi(2S)}$

VALUE (units 10^{-4})	EVTS	DOCUMENT ID		TECN	COMMENT
0.78±0.07 OUR FIT					
0.78±0.08 OUR AVERAGE					
0.77±0.03±0.08	612	[1] ABLIKIM	11K	BES3	$\psi(2S) \to \gamma$ hadrons
0.86±0.19±0.12	26	[2] ABLIKIM	06T	BES2	$\psi(2S) \to \gamma 2K^+2K^-$

[1] Calculated by us. The value of $B(\chi_{c0} \to \phi\phi)$ reported by ABLIKIM 11K was derived using $B(\psi(2S) \to \gamma\chi_{c0}(1P)) = (9.62 \pm 0.31)\%$.

[2] Calculated by us. The value of $B(\chi_{c0} \to \phi\phi)$ reported by ABLIKIM 06T was derived using $B(\psi(2S) \to \gamma\chi_{c0}(1P)) = (9.2 \pm 0.4)\%$.

$\Gamma(\chi_{c0}(1P) \to \phi\phi)/\Gamma_{total} \times \Gamma(\psi(2S) \to \gamma\chi_{c0}(1P))/\Gamma(\psi(2S) \to J/\psi(1S)\pi^+\pi^-)$ $\Gamma_{55}/\Gamma \times \Gamma^{\psi(2S)}_{139}/\Gamma^{\psi(2S)}_{11}$

VALUE (units 10^{-4})	DOCUMENT ID		TECN	COMMENT
2.25±0.21 OUR FIT				
2.6 ±1.0 ±1.1	[1] BAI	99B	BES	$\psi(2S) \to \gamma 2K^+2K^-$

[1] Calculated by us. The value of $B(\chi_{c0} \to \phi\phi)$ reported by BAI 99B was derived using $B(\psi(2S) \to \gamma\chi_{c0}(1P)) = (9.3 \pm 0.8)\%$ and $B(\psi(2S) \to J/\psi\pi^+\pi^-) = (32.4 \pm 2.6)\%$ [BAI 98D].

$\chi_{c0}(1P)$ REFERENCES

AAIJ	17BB	EPJ C77 609	R. Aaij *et al.*	(LHCb Collab.)
ABLIKIM	17AE	PR D96 092007	M. Ablikim *et al.*	(BES III Collab.)
ABLIKIM	17AI	PR D96 112006	M. Ablikim *et al.*	(BES III Collab.)
ABLIKIM	17I	PRL 118 221802	M. Ablikim *et al.*	(BES III Collab.)
ABLIKIM	17N	PR D95 072004	M. Ablikim *et al.*	(BES III Collab.)
ABLIKIM	17U	PR D96 032001	M. Ablikim *et al.*	(BES III Collab.)
PDG	16	CP C40 100001	C. Patrignani *et al.*	(PDG Collab.)
ABLIKIM	15I	PR D91 092006	M. Ablikim *et al.*	(BES III Collab.)
ABLIKIM	15M	PR D91 112008	M. Ablikim *et al.*	(BES III Collab.)
ABLIKIM	15N	PR D91 112018	M. Ablikim *et al.*	(BES III Collab.)
ABLIKIM	13B	PR D87 012002	M. Ablikim *et al.*	(BES III Collab.)
ABLIKIM	13D	PR D87 012007	M. Ablikim *et al.*	(BES III Collab.)
ABLIKIM	13H	PR D87 032007	M. Ablikim *et al.*	(BES III Collab.)
ABLIKIM	13V	PR D88 112001	M. Ablikim *et al.*	(BES III Collab.)
UEHARA	13	PTEP 2013 123C01	S. Uehara *et al.*	(BELLE Collab.)
ABLIKIM	12A	PR D85 112008	M. Ablikim *et al.*	(BES III Collab.)
ABLIKIM	12I	PR D86 052004	M. Ablikim *et al.*	(BES III Collab.)
ABLIKIM	12J	PR D86 052011	M. Ablikim *et al.*	(BES III Collab.)
ABLIKIM	12O	PRL 109 172002	M. Ablikim *et al.*	(BES III Collab.)
LIU	12B	PRL 108 232001	Z.Q. Liu *et al.*	(BELLE Collab.)
ABLIKIM	11A	PR D83 012006	M. Ablikim *et al.*	(BES III Collab.)
ABLIKIM	11E	PR D83 112005	M. Ablikim *et al.*	(BES III Collab.)
ABLIKIM	11F	PR D83 112009	M. Ablikim *et al.*	(BES III Collab.)
ABLIKIM	11K	PRL 107 092001	M. Ablikim *et al.*	(BES III Collab.)
DEL-AMO-SA...	11M	PR D84 012004	P. del Amo Sanchez *et al.*	(BABAR Collab.)
ABLIKIM	10A	PR D81 052005	M. Ablikim *et al.*	(BES III Collab.)
ONYISI	10	PR D82 011103	P.U.E. Onyisi *et al.*	(CLEO Collab.)
UEHARA	10A	PR D82 114031	S. Uehara *et al.*	(BELLE Collab.)
ASNER	09	PR D79 072007	D.M. Asner *et al.*	(CLEO Collab.)
UEHARA	09	PR D79 052009	S. Uehara *et al.*	(BELLE Collab.)
BENNETT	08A	PRL 101 151801	J.V. Bennett *et al.*	(CLEO Collab.)
ECKLUND	08A	PR D78 091501	K.M. Ecklund *et al.*	(CLEO Collab.)
HE	08B	PR D78 092004	Q. He *et al.*	(CLEO Collab.)
MENDEZ	08	PR D78 011102	H. Mendez *et al.*	(CLEO Collab.)
NAIK	08	PR D78 031101	P. Naik *et al.*	(CLEO Collab.)
UEHARA	08	EPJ C53 1	S. Uehara *et al.*	(BELLE Collab.)
WICHT	08	PL B662 323	J. Wicht *et al.*	(BELLE Collab.)
ABE	07	PRL 98 082001	K. Abe *et al.*	(BELLE Collab.)
ADAMS	07	PR D75 071101	G.S. Adams *et al.*	(CLEO Collab.)
ATHAR	07	PR D75 032002	S.B. Athar *et al.*	(CLEO Collab.)
CHEN	07B	PL B651 15	W.T. Chen *et al.*	(BELLE Collab.)
ABLIKIM	06D	PR D73 052006	M. Ablikim *et al.*	(BES Collab.)
ABLIKIM	06I	PR D74 012004	M. Ablikim *et al.*	(BES Collab.)
ABLIKIM	06R	PR D74 072001	M. Ablikim *et al.*	(BES Collab.)
ABLIKIM	06T	PL B642 197	M. Ablikim *et al.*	(BES Collab.)
ABLIKIM	05G	PR D71 092002	M. Ablikim *et al.*	(BES Collab.)
ABLIKIM	05N	PL B630 7	M. Ablikim *et al.*	(BES Collab.)
ABLIKIM	05O	PL B630 21	M. Ablikim *et al.*	(BES Collab.)
ABLIKIM	05Q	PR D72 092002	M. Ablikim *et al.*	(BES Collab.)
ADAM	05A	PRL 94 232002	N.E. Adam *et al.*	(CLEO Collab.)
ANDREOTTI	05A	NP B717 34	M. Andreotti *et al.*	(FNAL E835 Collab.)
ANDREOTTI	05C	PR D72 112002	M. Andreotti *et al.*	(FNAL E835 Collab.)
NAKAZAWA	05	PL B615 39	H. Nakazawa *et al.*	(BELLE Collab.)
ABE	04G	PR D70 071102	K. Abe *et al.*	(BELLE Collab.)
ABLIKIM	04G	PR D70 092002	M. Ablikim *et al.*	(BES Collab.)
ABLIKIM	04H	PR D70 092003	M. Ablikim *et al.*	(BES Collab.)
ANDREOTTI	04	PL B584 16	M. Andreotti *et al.*	(E835 Collab.)
ATHAR	04	PR D70 112002	S.B. Athar *et al.*	(CLEO Collab.)
BAI	04F	PR D69 092001	J.Z. Bai *et al.*	(BES Collab.)
ANDREOTTI	03	PRL 91 091801	M. Andreotti *et al.*	(FNAL E835 Collab.)
AULCHENKO	03	PL B573 63	V.M. Aulchenko *et al.*	(KEDR Collab.)
BAI	03C	PR D67 032004	J.Z. Bai *et al.*	(BES Collab.)
BAI	03E	PR D67 112001	J.Z. Bai *et al.*	(BES Collab.)
ABE,K	02	PRL 89 142001	K. Abe *et al.*	(BELLE Collab.)
BAGNASCO	02	PL B533 237	S. Bagnasco *et al.*	(FNAL E835 Collab.)
EISENSTEIN	01	PRL 87 061801	B.I. Eisenstein *et al.*	(CLEO Collab.)
AMBROGIANI	00B	PR D62 052002	M. Ambrogiani *et al.*	(FNAL E835 Collab.)
AMBROGIANI	99B	PRL 83 2902	M. Ambrogiani *et al.*	(FNAL E835 Collab.)
BAI	99B	PR D60 072001	J.Z. Bai *et al.*	(BES Collab.)
BAI	98D	PR D58 092006	J.Z. Bai *et al.*	(BES Collab.)
BAI	98I	PRL 81 3091	J.Z. Bai *et al.*	(BES Collab.)
GAISER	86	PR D34 711	J. Gaiser *et al.*	(Crystal Ball Collab.)
LEE	85	SLAC 282	R.A. Lee	(SLAC)
OREGLIA	82	PR D25 2259	M.J. Oreglia *et al.*	(SLAC, CIT, HARV+)
BRANDELIK	79B	NP B160 426	R. Brandelik *et al.*	(DASP Collab.)
BARTEL	78B	PL 79B 492	W. Bartel *et al.*	(DESY, HEIDP)
TANENBAUM	78	PR D17 1731	W.M. Tanenbaum *et al.*	(SLAC, LBL)
Also		Private Comm.	G. Trilling	(LBL, UCB)
BIDDICK	77	PRL 38 1324	C.J. Biddick *et al.*	(UCSD, UMD, PAVI+)

$\chi_{c1}(1P)$

$I^G(J^{PC}) = 0^+(1^{++})$

See the Review on "$\psi(2S)$ and χ_c branching ratios" before the $\chi_{c0}(1P)$ Listings.

$\chi_{c1}(1P)$ MASS

VALUE (MeV)			EVTS	DOCUMENT ID		TECN	COMMENT
3510.67 ± 0.05 OUR AVERAGE				Error includes scale factor of 1.2.			
3508.4	± 1.9	±0.7	460	[1] AAIJ	17BB	LHCB	$pp \to b\overline{b}X \to 2(K^+K^-)X$
3510.71	± 0.04	±0.09	4.8k	[2] AAIJ	17BI	LHCB	$\chi_{c1} \to J/\psi\mu^+\mu^-$
3510.30	± 0.14	±0.16		ABLIKIM	05G	BES2	$\psi(2S) \to \gamma\chi_{c1}$
3510.719	± 0.051	±0.019		ANDREOTTI	05A	E835	$p\overline{p} \to e^+e^-\gamma$
3509.4	± 0.9			BAI	99B	BES	$\psi(2S) \to \gamma X$
3510.60	± 0.087	±0.019	513	[3] ARMSTRONG	92	E760	$\overline{p}p \to e^+e^-\gamma$
3511.3	± 0.4	±0.4	30	BAGLIN	86B	SPEC	$\overline{p}p \to e^+e^-X$
3512.3	± 0.3	±4.0		[4] GAISER	86	CBAL	$\psi(2S) \to \gamma X$
3507.4	± 1.7		91	[5] LEMOIGNE	82	GOLI	185 π^-Be $\to \gamma\mu^+\mu^-$A
3510.4	± 0.6			OREGLIA	82	CBAL	$e^+e^- \to J/\psi 2\gamma$
3510.1	± 1.1		254	[6] HIMEL	80	MRK2	$e^+e^- \to J/\psi 2\gamma$
3509	±11		21	BRANDELIK	79B	DASP	$e^+e^- \to J/\psi 2\gamma$
3507	± 3			[6] BARTEL	78B	CNTR	$e^+e^- \to J/\psi 2\gamma$
3505.0	± 4	±4		[6,7] TANENBAUM	78	MRK1	e^+e^-
3513	± 7		367	[6] BIDDICK	77	CNTR	$\psi(2S) \to \gamma X$
• • • We do not use the following data for averages, fits, limits, etc. • • •							
3500	±10		40	TANENBAUM	75	MRK1	Hadrons γ

[1] From a fit of the $\phi\phi$ invariant mass with the width of $\chi_{c1}(1P)$ fixed to the PDG 16 value.

[2] AAIJ 17BI reports also $m(\chi_{c2}) - m(\chi_{c1}) = 45.39 \pm 0.07 \pm 0.03$ MeV.

[3] Recalculated by ANDREOTTI 05A, using the value of $\psi(2S)$ mass from AULCHENKO 03.

[4] Using mass of $\psi(2S) = 3686.0$ MeV.

[5] $J/\psi(1S)$ mass constrained to 3097 MeV.
[6] Mass value shifted by us by amount appropriate for $\psi(2S)$ mass = 3686 MeV and $J/\psi(1S)$ mass = 3097 MeV.
[7] From a simultaneous fit to radiative and hadronic decay channels.

$\chi_{c1}(1P)$ WIDTH

VALUE (MeV)	CL%	EVTS	DOCUMENT ID		TECN	COMMENT
0.84 ±0.04 OUR FIT						
0.88 ±0.05 OUR AVERAGE						
$1.39\ ^{+0.40}_{-0.38}\ ^{+0.26}_{-0.77}$			ABLIKIM	05G	BES2	$\psi(2S) \to \gamma\chi_{c1}$
0.876±0.045±0.026			ANDREOTTI	05A	E835	$p\overline{p} \to e^+e^-\gamma$
0.87 ±0.11 ±0.08		513	[1] ARMSTRONG	92	E760	$\overline{p}p \to e^+e^-\gamma$
• • • We do not use the following data for averages, fits, limits, etc. • • •						
<1.3	95		BAGLIN	86B	SPEC	$\overline{p}p \to e^+e^-X$
<3.8	90		GAISER	86	CBAL	$\psi(2S) \to \gamma X$

[1] Recalculated by ANDREOTTI 05A.

$\chi_{c1}(1P)$ DECAY MODES

	Mode	Fraction (Γ_i/Γ)	Scale factor/ Confidence level
	Hadronic decays		
Γ_1	$3(\pi^+\pi^-)$	$(5.8 \pm 1.4) \times 10^{-3}$	S=1.2
Γ_2	$2(\pi^+\pi^-)$	$(7.6 \pm 2.6) \times 10^{-3}$	
Γ_3	$\pi^+\pi^-\pi^0\pi^0$	(1.19±0.15) %	
Γ_4	$\rho^+\pi^-\pi^0$ + c.c.	(1.45±0.24) %	
Γ_5	$\rho^0\pi^+\pi^-$	$(3.9 \pm 3.5) \times 10^{-3}$	
Γ_6	$4\pi^0$	$(5.4 \pm 0.8) \times 10^{-4}$	
Γ_7	$\pi^+\pi^-K^+K^-$	$(4.5 \pm 1.0) \times 10^{-3}$	
Γ_8	$K^+K^-\pi^0\pi^0$	(1.12±0.27) $\times 10^{-3}$	
Γ_9	$K^+K^-\pi^+\pi^-\pi^0$	(1.15±0.13) %	
Γ_{10}	$K^0_S K^\pm\pi^\mp\pi^+\pi^-$	$(7.5 \pm 0.8) \times 10^{-3}$	
Γ_{11}	$K^+\pi^-\overline{K}{}^0\pi^0$ + c.c.	$(8.6 \pm 1.4) \times 10^{-3}$	
Γ_{12}	$\rho^-K^+\overline{K}{}^0$ + c.c.	$(5.0 \pm 1.2) \times 10^{-3}$	
Γ_{13}	$K^*(892)^0\overline{K}{}^0\pi^0 \to K^+\pi^-\overline{K}{}^0\pi^0$ + c.c.	$(2.3 \pm 0.6) \times 10^{-3}$	
Γ_{14}	$K^+K^-\eta\pi^0$	(1.12±0.34) $\times 10^{-3}$	
Γ_{15}	$\pi^+\pi^-K^0_S K^0_S$	$(6.9 \pm 2.9) \times 10^{-4}$	
Γ_{16}	$K^+K^-\eta$	$(3.2 \pm 1.0) \times 10^{-4}$	
Γ_{17}	$\overline{K}{}^0K^+\pi^-$ + c.c.	$(7.0 \pm 0.6) \times 10^{-3}$	
Γ_{18}	$K^*(892)^0\overline{K}{}^0$ + c.c.	$(10 \pm 4) \times 10^{-4}$	
Γ_{19}	$K^*(892)^+K^-$ + c.c.	$(1.4 \pm 0.6) \times 10^{-3}$	
Γ_{20}	$K^*_J(1430)^0\overline{K}{}^0$ + c.c. $\to K^0_S K^+\pi^-$ + c.c.	$< 8 \times 10^{-4}$	CL=90%
Γ_{21}	$K^*_J(1430)^+K^-$ + c.c. $\to K^0_S K^+\pi^-$ + c.c.	$< 2.1 \times 10^{-3}$	CL=90%
Γ_{22}	$K^+K^-\pi^0$	(1.81±0.24) $\times 10^{-3}$	
Γ_{23}	$\eta\pi^+\pi^-$	(4.62±0.23) $\times 10^{-3}$	
Γ_{24}	$a_0(980)^+\pi^-$ + c.c. $\to \eta\pi^+\pi^-$	$(3.2 \pm 0.4) \times 10^{-3}$	S=2.2
Γ_{25}	$a_2(1320)^+\pi^-$ + c.c. $\to \eta\pi^+\pi^-$	(1.76±0.24) $\times 10^{-4}$	
Γ_{26}	$a_2(1700)^+\pi^-$ + c.c. $\to \eta\pi^+\pi^-$	$(4.6 \pm 0.7) \times 10^{-5}$	
Γ_{27}	$f_2(1270)\eta \to \eta\pi^+\pi^-$	$(3.5 \pm 0.6) \times 10^{-4}$	
Γ_{28}	$f_4(2050)\eta \to \eta\pi^+\pi^-$	$(2.5 \pm 0.9) \times 10^{-5}$	
Γ_{29}	$\pi_1(1400)^+\pi^-$ + c.c. $\to \eta\pi^+\pi^-$	$< 5 \times 10^{-5}$	CL=90%
Γ_{30}	$\pi_1(1600)^+\pi^-$ + c.c. $\to \eta\pi^+\pi^-$	$< 1.5 \times 10^{-5}$	CL=90%
Γ_{31}	$\pi_1(2015)^+\pi^-$ + c.c. $\to \eta\pi^+\pi^-$	$< 8 \times 10^{-6}$	CL=90%
Γ_{32}	$f_2(1270)\eta$	$(6.7 \pm 1.1) \times 10^{-4}$	
Γ_{33}	$\pi^+\pi^-\eta'$	$(2.2 \pm 0.4) \times 10^{-3}$	
Γ_{34}	$K^+K^-\eta'(958)$	$(8.8 \pm 0.9) \times 10^{-4}$	
Γ_{35}	$K^*_0(1430)^+K^-$ + c.c.	$(6.4\ ^{+2.2}_{-2.8}) \times 10^{-4}$	
Γ_{36}	$f_0(980)\eta'(958)$	$(1.6\ ^{+1.4}_{-0.7}) \times 10^{-4}$	
Γ_{37}	$f_0(1710)\eta'(958)$	$(7\ ^{+7}_{-5}) \times 10^{-5}$	
Γ_{38}	$f'_2(1525)\eta'(958)$	$(9 \pm 6) \times 10^{-5}$	
Γ_{39}	$\pi^0 f_0(980) \to \pi^0\pi^+\pi^-$	$< 6 \times 10^{-6}$	CL=90%
Γ_{40}	$K^+\overline{K}{}^*(892)^0\pi^-$ + c.c.	$(3.2 \pm 2.1) \times 10^{-3}$	
Γ_{41}	$K^*(892)^0\overline{K}{}^*(892)^0$	$(1.4 \pm 0.4) \times 10^{-3}$	
Γ_{42}	$K^+K^-K^0_S K^0_S$	$< 4 \times 10^{-4}$	CL=90%
Γ_{43}	$K^+K^-K^+K^-$	$(5.4 \pm 1.1) \times 10^{-4}$	
Γ_{44}	$K^+K^-\phi$	$(4.1 \pm 1.5) \times 10^{-4}$	
Γ_{45}	$\overline{K}{}^0K^+\pi^-\phi$ + c.c.	$(3.3 \pm 0.5) \times 10^{-3}$	
Γ_{46}	$K^+K^-\pi^0\phi$	(1.62±0.30) $\times 10^{-3}$	
Γ_{47}	$\phi\pi^+\pi^-\pi^0$	$(7.5 \pm 1.0) \times 10^{-4}$	
Γ_{48}	$\omega\omega$	$(5.7 \pm 0.7) \times 10^{-4}$	
Γ_{49}	ωK^+K^-	$(7.8 \pm 0.9) \times 10^{-4}$	
Γ_{50}	$\omega\phi$	$(2.1 \pm 0.6) \times 10^{-5}$	
Γ_{51}	$\phi\phi$	$(4.2 \pm 0.5) \times 10^{-4}$	
Γ_{52}	$p\overline{p}$	(7.60±0.34) $\times 10^{-5}$	
Γ_{53}	$p\overline{p}\pi^0$	(1.55±0.18) $\times 10^{-4}$	
Γ_{54}	$p\overline{p}\eta$	(1.45±0.25) $\times 10^{-4}$	
Γ_{55}	$p\overline{p}\omega$	(2.12±0.31) $\times 10^{-4}$	
Γ_{56}	$p\overline{p}\phi$	$< 1.7 \times 10^{-5}$	CL=90%
Γ_{57}	$p\overline{p}\pi^+\pi^-$	$(5.0 \pm 1.9) \times 10^{-4}$	
Γ_{58}	$p\overline{p}\pi^0\pi^0$		
Γ_{59}	$p\overline{p}K^+K^-$ (non-resonant)	(1.27±0.22) $\times 10^{-4}$	
Γ_{60}	$p\overline{p}K^0_S K^0_S$	$< 4.5 \times 10^{-4}$	CL=90%
Γ_{61}	$p\overline{n}\pi^-$	$(3.8 \pm 0.5) \times 10^{-4}$	
Γ_{62}	$\overline{p}n\pi^+$	$(3.9 \pm 0.5) \times 10^{-4}$	
Γ_{63}	$p\overline{n}\pi^-\pi^0$	(1.03±0.12) $\times 10^{-3}$	
Γ_{64}	$\overline{p}n\pi^+\pi^0$	(1.01±0.12) $\times 10^{-3}$	
Γ_{65}	$\Lambda\overline{\Lambda}$	(1.14±0.11) $\times 10^{-4}$	
Γ_{66}	$\Lambda\overline{\Lambda}\pi^+\pi^-$	$(2.9 \pm 0.5) \times 10^{-4}$	
Γ_{67}	$\Lambda\overline{\Lambda}\pi^+\pi^-$ (non-resonant)	$(2.5 \pm 0.6) \times 10^{-4}$	
Γ_{68}	$\Sigma(1385)^+\overline{\Lambda}\pi^-$ + c.c.	$< 1.3 \times 10^{-4}$	CL=90%
Γ_{69}	$\Sigma(1385)^-\overline{\Lambda}\pi^+$ + c.c.	$< 1.3 \times 10^{-4}$	CL=90%
Γ_{70}	$K^+\overline{p}\Lambda$	$(4.1 \pm 0.4) \times 10^{-4}$	S=1.2
Γ_{71}	$K^+\overline{p}\Lambda(1520)$ + c.c.	$(1.7 \pm 0.4) \times 10^{-4}$	
Γ_{72}	$\Lambda(1520)\overline{\Lambda}(1520)$	$< 9 \times 10^{-5}$	CL=90%
Γ_{73}	$\Sigma^0\overline{\Sigma}{}^0$	$< 4 \times 10^{-5}$	CL=90%
Γ_{74}	$\Sigma^+\overline{\Sigma}{}^-$	$< 6 \times 10^{-5}$	CL=90%
Γ_{75}	$\Sigma(1385)^+\overline{\Sigma}(1385)^-$	$< 9 \times 10^{-5}$	CL=90%
Γ_{76}	$\Sigma(1385)^-\overline{\Sigma}(1385)^+$	$< 5 \times 10^{-5}$	CL=90%
Γ_{77}	$K^-\Lambda\overline{\Xi}{}^+$ + c.c.	(1.35±0.24) $\times 10^{-4}$	
Γ_{78}	$\Xi^0\overline{\Xi}{}^0$	$< 6 \times 10^{-5}$	CL=90%
Γ_{79}	$\Xi^-\overline{\Xi}{}^+$	$(8.0 \pm 2.1) \times 10^{-5}$	
Γ_{80}	$\pi^+\pi^- + K^+K^-$	$< 2.1 \times 10^{-3}$	
Γ_{81}	$K^0_S K^0_S$	$< 6 \times 10^{-5}$	CL=90%
Γ_{82}	$\eta_c\pi^+\pi^-$	$< 3.2 \times 10^{-3}$	CL=90%
	Radiative decays		
Γ_{83}	$\gamma J/\psi(1S)$	(34.3 ±1.0) %	
Γ_{84}	$\gamma\rho^0$	(2.16±0.17) $\times 10^{-4}$	
Γ_{85}	$\gamma\omega$	$(6.8 \pm 0.8) \times 10^{-5}$	
Γ_{86}	$\gamma\phi$	$(2.4 \pm 0.5) \times 10^{-5}$	
Γ_{87}	$\gamma\gamma$	$< 6.3 \times 10^{-6}$	CL=90%
Γ_{88}	$e^+e^- J/\psi(1S)$	$(3.65 \pm 0.25) \times 10^{-3}$	

CONSTRAINED FIT INFORMATION

A multiparticle fit to $\chi_{c1}(1P)$, $\chi_{c0}(1P)$, $\chi_{c2}(1P)$, and $\psi(2S)$ with 4 total widths, a partial width, 25 combinations of partial widths obtained from integrated cross section, and 84 branching ratios uses 247 measurements to determine 49 parameters. The overall fit has a $\chi^2 = 376.9$ for 198 degrees of freedom.

The following *off-diagonal* array elements are the correlation coefficients $\langle \delta p_i \delta p_j \rangle / (\delta p_i \cdot \delta p_j)$, in percent, from the fit to parameters p_i, including the branching fractions, $x_i \equiv \Gamma_i/\Gamma_{\rm total}$.

	x_{17}	x_{43}	x_{52}	x_{65}	x_{83}
x_{43}	3				
x_{52}	4	2			
x_{65}	7	3	4		
x_{83}	23	9	2	20	
Γ	−12	−5	−63	−10	−41

$\chi_{c1}(1P)$ PARTIAL WIDTHS

$\chi_{c1}(1P)$ Γ(i)$\Gamma(\gamma J/\psi(1S))/\Gamma$(total)

$\Gamma(p\overline{p}) \times \Gamma(\gamma J/\psi(1S))/\Gamma_{\rm total}$ $\Gamma_{52}\Gamma_{83}/\Gamma$

VALUE (eV)	DOCUMENT ID		TECN	COMMENT
21.9±0.8 OUR FIT				
21.4±0.9 OUR AVERAGE				
21.5±0.5±0.8	[1] ANDREOTTI	05A	E835	$p\overline{p} \to e^+e^-\gamma$
21.4±1.5±2.2	[1,2] ARMSTRONG	92	E760	$\overline{p}p \to e^+e^-\gamma$
$19.9^{+4.4}_{-4.0}$	[1] BAGLIN	86B	SPEC	$\overline{p}p \to e^+e^-X$

[1] Calculated by us using $B(J/\psi(1S) \to e^+e^-) = 0.0593 \pm 0.0010$.
[2] Recalculated by ANDREOTTI 05A.

Meson Particle Listings

$\chi_{c1}(1P)$

$\chi_{c1}(1P)$ BRANCHING RATIOS

HADRONIC DECAYS

$\Gamma(3(\pi^+\pi^-))/\Gamma_{total}$ Γ_1/Γ

VALUE (units 10^{-3})	DOCUMENT ID		TECN	COMMENT
5.8±1.4 OUR EVALUATION	Error includes scale factor of 1.2.			Treating systematic error as correlated.
5.8±1.1 OUR AVERAGE				
5.4±0.7±0.9	[1] BAI	99B	BES	$\psi(2S) \to \gamma\chi_{c1}$
16.0±5.9±0.8	[1] TANENBAUM	78	MRK1	$\psi(2S) \to \gamma\chi_{c1}$

[1] Rescaled by us using $B(\psi(2S) \to \gamma\chi_{c1}) = (8.8 \pm 0.4)\%$ and $B(\psi(2S) \to J/\psi(1S)\pi^+\pi^-) = (32.6 \pm 0.5)\%$.

$\Gamma(2(\pi^+\pi^-))/\Gamma_{total}$ Γ_2/Γ

VALUE (units 10^{-3})	DOCUMENT ID		TECN	COMMENT
7.6±2.6 OUR EVALUATION	Treating systematic error as correlated.			
8 ±4 OUR AVERAGE	Error includes scale factor of 1.5.			
4.6±2.1±2.6	[1] BAI	99B	BES	$\psi(2S) \to \gamma\chi_{c1}$
12.5±4.2±0.6	[1] TANENBAUM	78	MRK1	$\psi(2S) \to \gamma\chi_{c1}$

[1] Rescaled by us using $B(\psi(2S) \to \gamma\chi_{c1}) = (8.8 \pm 0.4)\%$ and $B(\psi(2S) \to J/\psi(1S)\pi^+\pi^-) = (32.6 \pm 0.5)\%$.

$\Gamma(\pi^+\pi^-\pi^0\pi^0)/\Gamma_{total}$ Γ_3/Γ

VALUE (%)	EVTS	DOCUMENT ID		TECN	COMMENT
1.19±0.15±0.03	604.7	[1] HE	08B	CLEO	$e^+e^- \to \gamma h^+ h^- h^0 h^0$

[1] HE 08B reports $1.28 \pm 0.06 \pm 0.15 \pm 0.08$ % from a measurement of $[\Gamma(\chi_{c1}(1P) \to \pi^+\pi^-\pi^0\pi^0)/\Gamma_{total}] \times [B(\psi(2S) \to \gamma\chi_{c1}(1P))]$ assuming $B(\psi(2S) \to \gamma\chi_{c1}(1P)) = (9.07 \pm 0.11 \pm 0.54) \times 10^{-2}$, which we rescale to our best value $B(\psi(2S) \to \gamma\chi_{c1}(1P)) = (9.75 \pm 0.24) \times 10^{-2}$. Our first error is their experiment's error and our second error is the systematic error from using our best value.

$\Gamma(\rho^+\pi^-\pi^0 + \text{c.c.})/\Gamma_{total}$ Γ_4/Γ

VALUE (%)	EVTS	DOCUMENT ID		TECN	COMMENT
1.45±0.24±0.04	712.3	[1,2] HE	08B	CLEO	$e^+e^- \to \gamma h^+ h^- h^0 h^0$

[1] HE 08B reports $1.56 \pm 0.13 \pm 0.22 \pm 0.10$ % from a measurement of $[\Gamma(\chi_{c1}(1P) \to \rho^+\pi^-\pi^0 + \text{c.c.})/\Gamma_{total}] \times [B(\psi(2S) \to \gamma\chi_{c1}(1P))]$ assuming $B(\psi(2S) \to \gamma\chi_{c1}(1P)) = (9.07 \pm 0.11 \pm 0.54) \times 10^{-2}$, which we rescale to our best value $B(\psi(2S) \to \gamma\chi_{c1}(1P)) = (9.75 \pm 0.24) \times 10^{-2}$. Our first error is their experiment's error and our second error is the systematic error from using our best value.

[2] Calculated by us. We have added the values from HE 08B for $\rho^+\pi^-\pi^0$ and $\rho^-\pi^+\pi^0$ decays assuming uncorrelated statistical and fully correlated systematic uncertainties.

$\Gamma(\rho^0\pi^+\pi^-)/\Gamma_{total}$ Γ_5/Γ

VALUE (units 10^{-4})	DOCUMENT ID		TECN	COMMENT
39±35	[1] TANENBAUM	78	MRK1	$\psi(2S) \to \gamma\chi_{c1}$

[1] Estimated using $B(\psi(2S) \to \gamma\chi_{c1}(1P)) = 0.087$. The errors do not contain the uncertainty in the $\psi(2S)$ decay.

$\Gamma(4\pi^0)/\Gamma_{total}$ Γ_6/Γ

VALUE (units 10^{-3})	EVTS	DOCUMENT ID		TECN	COMMENT
0.54±0.08±0.01	608	[1] ABLIKIM	11A	BES3	$e^+e^- \to \psi(2S) \to \gamma\chi_{c1}$

[1] ABLIKIM 11A reports $(0.57 \pm 0.03 \pm 0.08) \times 10^{-3}$ from a measurement of $[\Gamma(\chi_{c1}(1P) \to 4\pi^0)/\Gamma_{total}] \times [B(\psi(2S) \to \gamma\chi_{c1}(1P))]$ assuming $B(\psi(2S) \to \gamma\chi_{c1}(1P)) = (9.2 \pm 0.4) \times 10^{-2}$, which we rescale to our best value $B(\psi(2S) \to \gamma\chi_{c1}(1P)) = (9.75 \pm 0.24) \times 10^{-2}$. Our first error is their experiment's error and our second error is the systematic error from using our best value.

$\Gamma(\pi^+\pi^-K^+K^-)/\Gamma_{total}$ Γ_7/Γ

VALUE (units 10^{-3})	DOCUMENT ID		TECN	COMMENT
4.5±1.0 OUR EVALUATION	Treating systematic error as correlated.			
4.5±0.9 OUR AVERAGE				
4.2±0.4±0.9	[1] BAI	99B	BES	$\psi(2S) \to \gamma\chi_{c1}$
7.3±3.0±0.4	[1] TANENBAUM	78	MRK1	$\psi(2S) \to \gamma\chi_{c1}$

[1] Rescaled by us using $B(\psi(2S) \to \gamma\chi_{c1}) = (8.8 \pm 0.4)\%$ and $B(\psi(2S) \to J/\psi(1S)\pi^+\pi^-) = (32.6 \pm 0.5)\%$.

$\Gamma(K^+K^-\pi^0\pi^0)/\Gamma_{total}$ Γ_8/Γ

VALUE (%)	EVTS	DOCUMENT ID		TECN	COMMENT
0.112±0.027±0.003	45.1	[1] HE	08B	CLEO	$e^+e^- \to \gamma h^+ h^- h^0 h^0$

[1] HE 08B reports $0.12 \pm 0.02 \pm 0.02 \pm 0.01$ % from a measurement of $[\Gamma(\chi_{c1}(1P) \to K^+K^-\pi^0\pi^0)/\Gamma_{total}] \times [B(\psi(2S) \to \gamma\chi_{c1}(1P))]$ assuming $B(\psi(2S) \to \gamma\chi_{c1}(1P)) = (9.07 \pm 0.11 \pm 0.54) \times 10^{-2}$, which we rescale to our best value $B(\psi(2S) \to \gamma\chi_{c1}(1P)) = (9.75 \pm 0.24) \times 10^{-2}$. Our first error is their experiment's error and our second error is the systematic error from using our best value.

$\Gamma(K^+K^-\pi^+\pi^-\pi^0)/\Gamma_{total}$ Γ_9/Γ

VALUE (units 10^{-3})	EVTS	DOCUMENT ID		TECN	COMMENT
11.46±0.12±1.29	12k	[1] ABLIKIM	13B	BES3	$e^+e^- \to \psi(2S) \to \gamma\chi_{c1}$

[1] Using 1.06×10^8 $\psi(2S)$ mesons and $B(\psi(2S) \to \chi_{c1}\gamma) = (9.2 \pm 0.4)\%$.

$\Gamma(K_S^0K^\pm\pi^\mp\pi^+\pi^-)/\Gamma_{total}$ Γ_{10}/Γ

VALUE (units 10^{-3})	EVTS	DOCUMENT ID		TECN	COMMENT
7.52±0.11±0.79	5.1k	[1] ABLIKIM	13B	BES3	$e^+e^- \to \psi(2S) \to \gamma\chi_{c1}$

[1] Using 1.06×10^8 $\psi(2S)$ mesons and $B(\psi(2S) \to \chi_{c1}\gamma) = (9.2 \pm 0.4)\%$.

$\Gamma(K^+\pi^-\overline{K}^0\pi^0 + \text{c.c.})/\Gamma_{total}$ Γ_{11}/Γ

VALUE (%)	EVTS	DOCUMENT ID		TECN	COMMENT
0.86±0.13±0.02	141.3	[1] HE	08B	CLEO	$e^+e^- \to \gamma h^+ h^- h^0 h^0$

[1] HE 08B reports $0.92 \pm 0.09 \pm 0.11 \pm 0.06$ % from a measurement of $[\Gamma(\chi_{c1}(1P) \to K^+\pi^-\overline{K}^0\pi^0 + \text{c.c.})/\Gamma_{total}] \times [B(\psi(2S) \to \gamma\chi_{c1}(1P))]$ assuming $B(\psi(2S) \to \gamma\chi_{c1}(1P)) = (9.07 \pm 0.11 \pm 0.54) \times 10^{-2}$, which we rescale to our best value $B(\psi(2S) \to \gamma\chi_{c1}(1P)) = (9.75 \pm 0.24) \times 10^{-2}$. Our first error is their experiment's error and our second error is the systematic error from using our best value.

$\Gamma(\rho^-K^+\overline{K}^0 + \text{c.c.})/\Gamma_{total}$ Γ_{12}/Γ

VALUE (%)	EVTS	DOCUMENT ID		TECN	COMMENT
0.50±0.12±0.01	141.3	[1] HE	08B	CLEO	$e^+e^- \to \gamma h^+ h^- h^0 h^0$

[1] HE 08B reports $0.54 \pm 0.11 \pm 0.07 \pm 0.03$ % from a measurement of $[\Gamma(\chi_{c1}(1P) \to \rho^-K^+\overline{K}^0 + \text{c.c.})/\Gamma_{total}] \times [B(\psi(2S) \to \gamma\chi_{c1}(1P))]$ assuming $B(\psi(2S) \to \gamma\chi_{c1}(1P)) = (9.07 \pm 0.11 \pm 0.54) \times 10^{-2}$, which we rescale to our best value $B(\psi(2S) \to \gamma\chi_{c1}(1P)) = (9.75 \pm 0.24) \times 10^{-2}$. Our first error is their experiment's error and our second error is the systematic error from using our best value.

$\Gamma(K^*(892)^0\overline{K}^0\pi^0 \to K^+\pi^-\overline{K}^0\pi^0 + \text{c.c.})/\Gamma_{total}$ Γ_{13}/Γ

VALUE (%)	EVTS	DOCUMENT ID		TECN	COMMENT
0.23±0.06±0.01	141.3	[1] HE	08B	CLEO	$e^+e^- \to \gamma h^+ h^- h^0 h^0$

[1] HE 08B reports $0.25 \pm 0.06 \pm 0.03 \pm 0.02$ % from a measurement of $[\Gamma(\chi_{c1}(1P) \to K^*(892)^0\overline{K}^0\pi^0 \to K^+\pi^-\overline{K}^0\pi^0 + \text{c.c.})/\Gamma_{total}] \times [B(\psi(2S) \to \gamma\chi_{c1}(1P))]$ assuming $B(\psi(2S) \to \gamma\chi_{c1}(1P)) = (9.07 \pm 0.11 \pm 0.54) \times 10^{-2}$, which we rescale to our best value $B(\psi(2S) \to \gamma\chi_{c1}(1P)) = (9.75 \pm 0.24) \times 10^{-2}$. Our first error is their experiment's error and our second error is the systematic error from using our best value.

$\Gamma(K^+K^-\eta\pi^0)/\Gamma_{total}$ Γ_{14}/Γ

VALUE (%)	EVTS	DOCUMENT ID		TECN	COMMENT
0.112±0.034±0.003	141.3	[1] HE	08B	CLEO	$e^+e^- \to \gamma h^+ h^- h^0 h^0$

[1] HE 08B reports $0.12 \pm 0.03 \pm 0.02 \pm 0.01$ % from a measurement of $[\Gamma(\chi_{c1}(1P) \to K^+K^-\eta\pi^0)/\Gamma_{total}] \times [B(\psi(2S) \to \gamma\chi_{c1}(1P))]$ assuming $B(\psi(2S) \to \gamma\chi_{c1}(1P)) = (9.07 \pm 0.11 \pm 0.54) \times 10^{-2}$, which we rescale to our best value $B(\psi(2S) \to \gamma\chi_{c1}(1P)) = (9.75 \pm 0.24) \times 10^{-2}$. Our first error is their experiment's error and our second error is the systematic error from using our best value.

$\Gamma(\pi^+\pi^-K_S^0K_S^0)/\Gamma_{total}$ Γ_{15}/Γ

VALUE (units 10^{-4})	EVTS	DOCUMENT ID		TECN	COMMENT
6.9±2.9±0.2	19.8±7.7	[1] ABLIKIM	05O	BES2	$\psi(2S) \to \chi_{c1}\gamma$

[1] ABLIKIM 05O reports $[\Gamma(\chi_{c1}(1P) \to \pi^+\pi^-K_S^0K_S^0)/\Gamma_{total}] \times [B(\psi(2S) \to \gamma\chi_{c1}(1P))] = (0.67 \pm 0.26 \pm 0.11) \times 10^{-4}$ which we divide by our best value $B(\psi(2S) \to \gamma\chi_{c1}(1P)) = (9.75 \pm 0.24) \times 10^{-2}$. Our first error is their experiment's error and our second error is the systematic error from using our best value.

$\Gamma(K^+K^-\eta)/\Gamma_{total}$ Γ_{16}/Γ

VALUE (units 10^{-3})	DOCUMENT ID		TECN	COMMENT
0.32±0.10±0.01	[1] ATHAR	07	CLEO	$\psi(2S) \to \gamma h^+ h^- h^0$

[1] ATHAR 07 reports $(0.34 \pm 0.10 \pm 0.04) \times 10^{-3}$ from a measurement of $[\Gamma(\chi_{c1}(1P) \to K^+K^-\eta)/\Gamma_{total}] \times [B(\psi(2S) \to \gamma\chi_{c1}(1P))]$ assuming $B(\psi(2S) \to \gamma\chi_{c1}(1P)) = 0.0907 \pm 0.0011 \pm 0.0054$, which we rescale to our best value $B(\psi(2S) \to \gamma\chi_{c1}(1P)) = (9.75 \pm 0.24) \times 10^{-2}$. Our first error is their experiment's error and our second error is the systematic error from using our best value.

$\Gamma(\overline{K}^0K^+\pi^- + \text{c.c.})/\Gamma_{total}$ Γ_{17}/Γ

VALUE (units 10^{-3})	DOCUMENT ID
7.0±0.6 OUR FIT	

$\Gamma(K^*(892)^0\overline{K}^0 + \text{c.c.})/\Gamma_{total}$ Γ_{18}/Γ

VALUE (units 10^{-3})	EVTS	DOCUMENT ID		TECN	COMMENT
0.98±0.37±0.02	22	[1] ABLIKIM	06R	BES2	$\psi(2S) \to \gamma\chi_{c1}$

[1] ABLIKIM 06R reports $(1.1 \pm 0.4 \pm 0.1) \times 10^{-3}$ from a measurement of $[\Gamma(\chi_{c1}(1P) \to K^*(892)^0\overline{K}^0 + \text{c.c.})/\Gamma_{total}] \times [B(\psi(2S) \to \gamma\chi_{c1}(1P))]$ assuming $B(\psi(2S) \to \gamma\chi_{c1}(1P)) = (8.7 \pm 0.4) \times 10^{-2}$, which we rescale to our best value $B(\psi(2S) \to \gamma\chi_{c1}(1P)) = (9.75 \pm 0.24) \times 10^{-2}$. Our first error is their experiment's error and our second error is the systematic error from using our best value.

$\Gamma(K^*(892)^+K^- + \text{c.c.})/\Gamma_{total}$ Γ_{19}/Γ

VALUE (units 10^{-3})	EVTS	DOCUMENT ID		TECN	COMMENT
1.43±0.65±0.03	27	[1] ABLIKIM	06R	BES2	$\psi(2S) \to \gamma\chi_{c1}$

[1] ABLIKIM 06R reports $(1.6 \pm 0.7 \pm 0.2) \times 10^{-3}$ from a measurement of $[\Gamma(\chi_{c1}(1P) \to K^*(892)^+K^- + \text{c.c.})/\Gamma_{total}] \times [B(\psi(2S) \to \gamma\chi_{c1}(1P))]$ assuming $B(\psi(2S) \to \gamma\chi_{c1}(1P)) = (8.7 \pm 0.4) \times 10^{-2}$, which we rescale to our best value $B(\psi(2S) \to \gamma\chi_{c1}(1P)) = (9.75 \pm 0.24) \times 10^{-2}$. Our first error is their experiment's error and our second error is the systematic error from using our best value.

$\Gamma(K_J^*(1430)^0\overline{K}^0 + \text{c.c.} \to K_S^0 K^+\pi^- + \text{c.c.})/\Gamma_{\text{total}}$ Γ_{20}/Γ

VALUE (units 10^{-3})	CL%	DOCUMENT ID		TECN	COMMENT
<0.8	90	[1] ABLIKIM	06R	BES2	$\psi(2S) \to \gamma\chi_{c1}$

[1] ABLIKIM 06R reports $< 0.9 \times 10^{-3}$ from a measurement of $[\Gamma(\chi_{c1}(1P) \to K_J^*(1430)^0\overline{K}^0 + \text{c.c.} \to K_S^0 K^+\pi^- + \text{c.c.})/\Gamma_{\text{total}}] \times [B(\psi(2S) \to \gamma\chi_{c1}(1P))]$ assuming $B(\psi(2S) \to \gamma\chi_{c1}(1P)) = (8.7 \pm 0.4) \times 10^{-2}$, which we rescale to our best value $B(\psi(2S) \to \gamma\chi_{c1}(1P)) = 9.75 \times 10^{-2}$.

$\Gamma(K_J^*(1430)^+ K^- + \text{c.c.} \to K_S^0 K^+\pi^- + \text{c.c.})/\Gamma_{\text{total}}$ Γ_{21}/Γ

VALUE (units 10^{-3})	CL%	DOCUMENT ID		TECN	COMMENT
<2.1	90	[1] ABLIKIM	06R	BES2	$\psi(2S) \to \gamma\chi_{c1}$

[1] ABLIKIM 06R reports $< 2.4 \times 10^{-3}$ from a measurement of $[\Gamma(\chi_{c1}(1P) \to K_J^*(1430)^+ K^- + \text{c.c.} \to K_S^0 K^+\pi^- + \text{c.c.})/\Gamma_{\text{total}}] \times [B(\psi(2S) \to \gamma\chi_{c1}(1P))]$ assuming $B(\psi(2S) \to \gamma\chi_{c1}(1P)) = (8.7 \pm 0.4) \times 10^{-2}$, which we rescale to our best value $B(\psi(2S) \to \gamma\chi_{c1}(1P)) = 9.75 \times 10^{-2}$.

$\Gamma(K^+K^-\pi^0)/\Gamma_{\text{total}}$ Γ_{22}/Γ

VALUE (units 10^{-3})	DOCUMENT ID		TECN	COMMENT
1.81±0.24±0.04	[1] ATHAR	07	CLEO	$\psi(2S) \to \gamma h^+ h^- h^0$

[1] ATHAR 07 reports $(1.95 \pm 0.16 \pm 0.23) \times 10^{-3}$ from a measurement of $[\Gamma(\chi_{c1}(1P) \to K^+K^-\pi^0)/\Gamma_{\text{total}}] \times [B(\psi(2S) \to \gamma\chi_{c1}(1P))]$ assuming $B(\psi(2S) \to \gamma\chi_{c1}(1P)) = 0.0907 \pm 0.0011 \pm 0.0054$, which we rescale to our best value $B(\psi(2S) \to \gamma\chi_{c1}(1P)) = (9.75 \pm 0.24) \times 10^{-2}$. Our first error is their experiment's error and our second error is the systematic error from using our best value.

$\Gamma(\eta\pi^+\pi^-)/\Gamma_{\text{total}}$ Γ_{23}/Γ

VALUE (units 10^{-3})	EVTS	DOCUMENT ID		TECN	COMMENT
4.62±0.23 OUR AVERAGE					
4.58±0.23±0.11		[1,2] ABLIKIM	17K	BES3	$\psi(2S) \to \gamma\eta\pi^+\pi^-$
4.7 ±0.5 ±0.1		[3] ATHAR	07	CLEO	$\psi(2S) \to \gamma h^+ h^- h^0$
5.3 ±0.9 ±0.1	222	[4] ABLIKIM	06R	BES2	$\psi(2S) \to \gamma\chi_{c1}$

[1] From an amplitude analysis using an isobar model.

[2] ABLIKIM 17K reports $(4.67 \pm 0.03 \pm 0.23 \pm 0.16) \times 10^{-3}$ from a measurement of $[\Gamma(\chi_{c1}(1P) \to \eta\pi^+\pi^-)/\Gamma_{\text{total}}] \times [B(\psi(2S) \to \gamma\chi_{c1}(1P))]$ assuming $B(\psi(2S) \to \gamma\chi_{c1}(1P)) = (9.55 \pm 0.31) \times 10^{-2}$, which we rescale to our best value $B(\psi(2S) \to \gamma\chi_{c1}(1P)) = (9.75 \pm 0.24) \times 10^{-2}$. Our first error is their experiment's error and our second error is the systematic error from using our best value.

[3] ATHAR 07 reports $(5.0 \pm 0.3 \pm 0.5) \times 10^{-3}$ from a measurement of $[\Gamma(\chi_{c1}(1P) \to \eta\pi^+\pi^-)/\Gamma_{\text{total}}] \times [B(\psi(2S) \to \gamma\chi_{c1}(1P))]$ assuming $B(\psi(2S) \to \gamma\chi_{c1}(1P)) = 0.0907 \pm 0.0011 \pm 0.0054$, which we rescale to our best value $B(\psi(2S) \to \gamma\chi_{c1}(1P)) = (9.75 \pm 0.24) \times 10^{-2}$. Our first error is their experiment's error and our second error is the systematic error from using our best value.

[4] ABLIKIM 06R reports $(5.9 \pm 0.7 \pm 0.8) \times 10^{-3}$ from a measurement of $[\Gamma(\chi_{c1}(1P) \to \eta\pi^+\pi^-)/\Gamma_{\text{total}}] \times [B(\psi(2S) \to \gamma\chi_{c1}(1P))]$ assuming $B(\psi(2S) \to \gamma\chi_{c1}(1P)) = (8.7 \pm 0.4) \times 10^{-2}$, which we rescale to our best value $B(\psi(2S) \to \gamma\chi_{c1}(1P)) = (9.75 \pm 0.24) \times 10^{-2}$. Our first error is their experiment's error and our second error is the systematic error from using our best value.

$\Gamma(a_0(980)^+\pi^- + \text{c.c.} \to \eta\pi^+\pi^-)/\Gamma_{\text{total}}$ Γ_{24}/Γ

VALUE (units 10^{-3})	EVTS	DOCUMENT ID		TECN	COMMENT
3.2 ±0.4 OUR AVERAGE Error includes scale factor of 2.2.					
3.33±0.19±0.08		[1,2] ABLIKIM	17K	BES3	$\psi(2S) \to \gamma\eta\pi^+\pi^-$
1.79±0.63±0.04	58	[3] ABLIKIM	06R	BES2	$\psi(2S) \to \gamma\chi_{c1}$

[1] From an amplitude analysis using an isobar model.

[2] ABLIKIM 17K reports $(3.40 \pm 0.03 \pm 0.19 \pm 0.11) \times 10^{-3}$ from a measurement of $[\Gamma(\chi_{c1}(1P) \to a_0(980)^+\pi^- + \text{c.c.} \to \eta\pi^+\pi^-)/\Gamma_{\text{total}}] \times [B(\psi(2S) \to \gamma\chi_{c1}(1P))]$ assuming $B(\psi(2S) \to \gamma\chi_{c1}(1P)) = (9.55 \pm 0.31) \times 10^{-2}$, which we rescale to our best value $B(\psi(2S) \to \gamma\chi_{c1}(1P)) = (9.75 \pm 0.24) \times 10^{-2}$. Our first error is their experiment's error and our second error is the systematic error from using our best value.

[3] ABLIKIM 06R reports $(2.0 \pm 0.5 \pm 0.5) \times 10^{-3}$ from a measurement of $[\Gamma(\chi_{c1}(1P) \to a_0(980)^+\pi^- + \text{c.c.} \to \eta\pi^+\pi^-)/\Gamma_{\text{total}}] \times [B(\psi(2S) \to \gamma\chi_{c1}(1P))]$ assuming $B(\psi(2S) \to \gamma\chi_{c1}(1P)) = (8.7 \pm 0.4) \times 10^{-2}$, which we rescale to our best value $B(\psi(2S) \to \gamma\chi_{c1}(1P)) = (9.75 \pm 0.24) \times 10^{-2}$. Our first error is their experiment's error and our second error is the systematic error from using our best value.

$\Gamma(a_2(1320)^+\pi^- + \text{c.c.} \to \eta\pi^+\pi^-)/\Gamma_{\text{total}}$ Γ_{25}/Γ

VALUE (units 10^{-3})	DOCUMENT ID		TECN	COMMENT
0.176±0.023±0.004	[1,2] ABLIKIM	17K	BES3	$\psi(2S) \to \gamma\eta\pi^+\pi^-$

[1] From an amplitude analysis using an isobar model.

[2] ABLIKIM 17K reports $(0.18 \pm 0.01 \pm 0.02 \pm 0.01) \times 10^{-3}$ from a measurement of $[\Gamma(\chi_{c1}(1P) \to a_2(1320)^+\pi^- + \text{c.c.} \to \eta\pi^+\pi^-)/\Gamma_{\text{total}}] \times [B(\psi(2S) \to \gamma\chi_{c1}(1P))]$ assuming $B(\psi(2S) \to \gamma\chi_{c1}(1P)) = (9.55 \pm 0.31) \times 10^{-2}$, which we rescale to our best value $B(\psi(2S) \to \gamma\chi_{c1}(1P)) = (9.75 \pm 0.24) \times 10^{-2}$. Our first error is their experiment's error and our second error is the systematic error from using our best value.

$\Gamma(a_2(1700)^+\pi^- + \text{c.c.} \to \eta\pi^+\pi^-)/\Gamma_{\text{total}}$ Γ_{26}/Γ

VALUE (units 10^{-5})	DOCUMENT ID		TECN	COMMENT
4.6±0.7±0.1	[1,2] ABLIKIM	17K	BES3	$\psi(2S) \to \gamma\eta\pi^+\pi^-$

[1] From an amplitude analysis using an isobar model.

[2] ABLIKIM 17K reports $(4.7 \pm 0.4 \pm 0.6 \pm 0.2) \times 10^{-5}$ from a measurement of $[\Gamma(\chi_{c1}(1P) \to a_2(1700)^+\pi^- + \text{c.c.} \to \eta\pi^+\pi^-)/\Gamma_{\text{total}}] \times [B(\psi(2S) \to \gamma\chi_{c1}(1P))]$ assuming $B(\psi(2S) \to \gamma\chi_{c1}(1P)) = (9.55 \pm 0.31) \times 10^{-2}$, which we rescale to our best value $B(\psi(2S) \to \gamma\chi_{c1}(1P)) = (9.75 \pm 0.24) \times 10^{-2}$. Our first error is their experiment's error and our second error is the systematic error from using our best value.

$\Gamma(f_2(1270)\eta \to \eta\pi^+\pi^-)/\Gamma_{\text{total}}$ Γ_{27}/Γ

VALUE (units 10^{-4})	DOCUMENT ID		TECN	COMMENT
3.5±0.6±0.1	[1,2] ABLIKIM	17K	BES3	$\psi(2S) \to \gamma\eta\pi^+\pi^-$

[1] From an amplitude analysis using an isobar model.

[2] ABLIKIM 17K reports $(0.36 \pm 0.01 \pm 0.06 \pm 0.01) \times 10^{-3}$ from a measurement of $[\Gamma(\chi_{c1}(1P) \to f_2(1270)\eta \to \eta\pi^+\pi^-)/\Gamma_{\text{total}}] \times [B(\psi(2S) \to \gamma\chi_{c1}(1P))]$ assuming $B(\psi(2S) \to \gamma\chi_{c1}(1P)) = (9.55 \pm 0.31) \times 10^{-2}$, which we rescale to our best value $B(\psi(2S) \to \gamma\chi_{c1}(1P)) = (9.75 \pm 0.24) \times 10^{-2}$. Our first error is their experiment's error and our second error is the systematic error from using our best value.

$\Gamma(f_4(2050)\eta \to \eta\pi^+\pi^-)/\Gamma_{\text{total}}$ Γ_{28}/Γ

VALUE (units 10^{-5})	DOCUMENT ID		TECN	COMMENT
2.5±0.9±0.1	[1,2] ABLIKIM	17K	BES3	$\psi(2S) \to \gamma\eta\pi^+\pi^-$

[1] From an amplitude analysis using an isobar model.

[2] ABLIKIM 17K reports $(2.6 \pm 0.4 \pm 0.8 \pm 0.1) \times 10^{-5}$ from a measurement of $[\Gamma(\chi_{c1}(1P) \to f_4(2050)\eta \to \eta\pi^+\pi^-)/\Gamma_{\text{total}}] \times [B(\psi(2S) \to \gamma\chi_{c1}(1P))]$ assuming $B(\psi(2S) \to \gamma\chi_{c1}(1P)) = (9.55 \pm 0.31) \times 10^{-2}$, which we rescale to our best value $B(\psi(2S) \to \gamma\chi_{c1}(1P)) = (9.75 \pm 0.24) \times 10^{-2}$. Our first error is their experiment's error and our second error is the systematic error from using our best value.

$\Gamma(\pi_1(1400)^+\pi^- + \text{c.c.} \to \eta\pi^+\pi^-)/\Gamma_{\text{total}}$ Γ_{29}/Γ

VALUE	CL%	DOCUMENT ID		TECN	COMMENT
$< 5 \times 10^{-5}$	90	[1,2] ABLIKIM	17K	BES3	$\psi(2S) \to \gamma\eta\pi^+\pi^-$

[1] From an amplitude analysis using an isobar model.

[2] ABLIKIM 17K reports $< 4.6 \times 10^{-5}$ from a measurement of $[\Gamma(\chi_{c1}(1P) \to \pi_1(1400)^+\pi^- + \text{c.c.} \to \eta\pi^+\pi^-)/\Gamma_{\text{total}}] \times [B(\psi(2S) \to \gamma\chi_{c1}(1P))]$ assuming $B(\psi(2S) \to \gamma\chi_{c1}(1P)) = (9.55 \pm 0.31) \times 10^{-2}$, which we rescale to our best value $B(\psi(2S) \to \gamma\chi_{c1}(1P)) = 9.75 \times 10^{-2}$.

$\Gamma(\pi_1(1600)^+\pi^- + \text{c.c.} \to \eta\pi^+\pi^-)/\Gamma_{\text{total}}$ Γ_{30}/Γ

VALUE	CL%	DOCUMENT ID		TECN	COMMENT
$< 1.5 \times 10^{-5}$	90	[1,2] ABLIKIM	17K	BES3	$\psi(2S) \to \gamma\eta\pi^+\pi^-$

[1] From an amplitude analysis using an isobar model.

[2] ABLIKIM 17K reports $< 1.5 \times 10^{-5}$ from a measurement of $[\Gamma(\chi_{c1}(1P) \to \pi_1(1600)^+\pi^- + \text{c.c.} \to \eta\pi^+\pi^-)/\Gamma_{\text{total}}] \times [B(\psi(2S) \to \gamma\chi_{c1}(1P))]$ assuming $B(\psi(2S) \to \gamma\chi_{c1}(1P)) = (9.55 \pm 0.31) \times 10^{-2}$, which we rescale to our best value $B(\psi(2S) \to \gamma\chi_{c1}(1P)) = 9.75 \times 10^{-2}$.

$\Gamma(\pi_1(2015)^+\pi^- + \text{c.c.} \to \eta\pi^+\pi^-)/\Gamma_{\text{total}}$ Γ_{31}/Γ

VALUE	CL%	DOCUMENT ID		TECN	COMMENT
$< 8 \times 10^{-6}$	90	[1,2] ABLIKIM	17K	BES3	$\psi(2S) \to \gamma\eta\pi^+\pi^-$

[1] From an amplitude analysis using an isobar model.

[2] ABLIKIM 17K reports $< 8 \times 10^{-6}$ from a measurement of $[\Gamma(\chi_{c1}(1P) \to \pi_1(2015)^+\pi^- + \text{c.c.} \to \eta\pi^+\pi^-)/\Gamma_{\text{total}}] \times [B(\psi(2S) \to \gamma\chi_{c1}(1P))]$ assuming $B(\psi(2S) \to \gamma\chi_{c1}(1P)) = (9.55 \pm 0.31) \times 10^{-2}$, which we rescale to our best value $B(\psi(2S) \to \gamma\chi_{c1}(1P)) = 9.75 \times 10^{-2}$.

$\Gamma(f_2(1270)\eta)/\Gamma_{\text{total}}$ Γ_{32}/Γ

VALUE (units 10^{-3})	EVTS	DOCUMENT ID		TECN	COMMENT
0.67±0.11 OUR AVERAGE					
0.63±0.11±0.02		[1,2] ABLIKIM	17K	BES3	$\psi(2S) \to \gamma\eta\pi^+\pi^-$
2.7 ±0.8 ±0.1	53	[3] ABLIKIM	06R	BES2	$\psi(2S) \to \gamma\chi_{c1}$

[1] ABLIKIM 17K reports $(6.4 \pm 1.1) \times 10^{-4}$ from a measurement of $[\Gamma(\chi_{c1}(1P) \to f_2(1270)\eta)/\Gamma_{\text{total}}] \times [B(\psi(2S) \to \gamma\chi_{c1}(1P))]$ assuming $B(\psi(2S) \to \gamma\chi_{c1}(1P)) = (9.55 \pm 0.31) \times 10^{-2}$, which we rescale to our best value $B(\psi(2S) \to \gamma\chi_{c1}(1P)) = (9.75 \pm 0.24) \times 10^{-2}$. Our first error is their experiment's error and our second error is the systematic error from using our best value.

[2] From an amplitude analysis using an isobar model.

[3] ABLIKIM 06R reports $(3.0 \pm 0.7 \pm 0.5) \times 10^{-3}$ from a measurement of $[\Gamma(\chi_{c1}(1P) \to f_2(1270)\eta)/\Gamma_{\text{total}}] \times [B(\psi(2S) \to \gamma\chi_{c1}(1P))]$ assuming $B(\psi(2S) \to \gamma\chi_{c1}(1P)) = (8.7 \pm 0.4) \times 10^{-2}$, which we rescale to our best value $B(\psi(2S) \to \gamma\chi_{c1}(1P)) = (9.75 \pm 0.24) \times 10^{-2}$. Our first error is their experiment's error and our second error is the systematic error from using our best value.

$\Gamma(\pi^+\pi^-\eta')/\Gamma_{\text{total}}$ Γ_{33}/Γ

VALUE (units 10^{-3})	DOCUMENT ID		TECN	COMMENT
2.2±0.4±0.1	[1] ATHAR	07	CLEO	$\psi(2S) \to \gamma h^+ h^- h^0$

[1] ATHAR 07 reports $(2.4 \pm 0.4 \pm 0.3) \times 10^{-3}$ from a measurement of $[\Gamma(\chi_{c1}(1P) \to \pi^+\pi^-\eta')/\Gamma_{\text{total}}] \times [B(\psi(2S) \to \gamma\chi_{c1}(1P))]$ assuming $B(\psi(2S) \to \gamma\chi_{c1}(1P)) = 0.0907 \pm 0.0011 \pm 0.0054$, which we rescale to our best value $B(\psi(2S) \to \gamma\chi_{c1}(1P)) = (9.75 \pm 0.24) \times 10^{-2}$. Our first error is their experiment's error and our second error is the systematic error from using our best value.

$\Gamma(K^+K^-\eta'(958))/\Gamma_{total}$ Γ_{34}/Γ

VALUE (units 10^{-4})	EVTS	DOCUMENT ID		TECN	COMMENT
8.75±0.87	310	[1] ABLIKIM	14J	BES3	$\psi(2S)\to\gamma K^+K^-\eta'(958)$

[1] Derived using $B(\psi(2S)\to\gamma\chi_{c1})=(9.2\pm0.4)\%$. Uncertainty includes both statistical and systematic contributions combined in quadrature.

$\Gamma(K_0^*(1430)^+K^-+\text{c.c.})/\Gamma_{total}$ Γ_{35}/Γ

VALUE (units 10^{-4})	DOCUMENT ID		TECN	COMMENT
$6.41\pm0.57^{+2.09}_{-2.71}$	[1] ABLIKIM	14J	BES3	$\psi(2S)\to\gamma K^+K^-\eta'(958)$

[1] Normalized to $B(\chi_{c1}\to K^+K^-\eta'(958))$ branching fraction.

$\Gamma(f_0(980)\eta'(958))/\Gamma_{total}$ Γ_{36}/Γ

VALUE (units 10^{-4})	DOCUMENT ID		TECN	COMMENT
$1.65\pm0.47^{+1.32}_{-0.56}$	[1] ABLIKIM	14J	BES3	$\psi(2S)\to\gamma K^+K^-\eta'(958)$

[1] Normalized to $B(\chi_{c1}\to K^+K^-\eta'(958))$ branching fraction.

$\Gamma(f_0(1710)\eta'(958))/\Gamma_{total}$ Γ_{37}/Γ

VALUE (units 10^{-4})	DOCUMENT ID		TECN	COMMENT
$0.71\pm0.22^{+0.68}_{-0.48}$	[1] ABLIKIM	14J	BES3	$\psi(2S)\to\gamma K^+K^-\eta'(958)$

[1] Normalized to $B(\chi_{c1}\to K^+K^-\eta'(958))$ branching fraction.

$\Gamma(f_2'(1525)\eta'(958))/\Gamma_{total}$ Γ_{38}/Γ

VALUE (units 10^{-4})	DOCUMENT ID		TECN	COMMENT
$0.92\pm0.23^{+0.55}_{-0.51}$	[1] ABLIKIM	14J	BES3	$\psi(2S)\to\gamma K^+K^-\eta'(958)$

[1] Normalized to $B(\chi_{c1}\to K^+K^-\eta'(958))$ branching fraction.

$\Gamma(\pi^0 f_0(980)\to\pi^0\pi^+\pi^-)/\Gamma_{total}$ Γ_{39}/Γ

VALUE	CL%	DOCUMENT ID		TECN	COMMENT
$<6\times10^{-6}$	90	[1] ABLIKIM	11D	BES3	$\psi(2S)\to\gamma\pi^0\pi^+\pi^-$

[1] ABLIKIM 11D reports $[\Gamma(\chi_{c1}(1P)\to\pi^0 f_0(980)\to\pi^0\pi^+\pi^-)/\Gamma_{total}]\times[B(\psi(2S)\to\gamma\chi_{c1}(1P))]<6.0\times10^{-7}$ which we divide by our best value $B(\psi(2S)\to\gamma\chi_{c1}(1P))=9.75\times10^{-2}$.

$\Gamma(K^+\overline{K}^*(892)^0\pi^-+\text{c.c.})/\Gamma_{total}$ Γ_{40}/Γ

VALUE (units 10^{-4})	DOCUMENT ID		TECN	COMMENT
32±21	[1] TANENBAUM	78	MRK1	$\psi(2S)\to\gamma\chi_{c1}$

[1] Estimated using $B(\psi(2S)\to\gamma\chi_{c1}(1P))=0.087$. The errors do not contain the uncertainty in the $\psi(2S)$ decay.

$\Gamma(K^*(892)^0\overline{K}^*(892)^0)/\Gamma_{total}$ Γ_{41}/Γ

VALUE (units 10^{-3})	EVTS	DOCUMENT ID		TECN	COMMENT
$1.44\pm0.36\pm0.03$	28.4 ± 5.5	[1,2] ABLIKIM	04H	BES	$\psi(2S)\to\gamma K^+K^-\pi^+\pi^-$

[1] ABLIKIM 04H reports $[\Gamma(\chi_{c1}(1P)\to K^*(892)^0\overline{K}^*(892)^0)/\Gamma_{total}]\times[B(\psi(2S)\to\gamma\chi_{c1}(1P))]=(1.40\pm0.27\pm0.22)\times10^{-4}$ which we divide by our best value $B(\psi(2S)\to\gamma\chi_{c1}(1P))=(9.75\pm0.24)\times10^{-2}$. Our first error is their experiment's error and our second error is the systematic error from using our best value.

[2] Assumes $B(K^*(892)^0\to K^-\pi^+)=2/3$.

$\Gamma(K^+K^-K_S^0K_S^0)/\Gamma_{total}$ Γ_{42}/Γ

VALUE (units 10^{-4})	CL%	EVTS	DOCUMENT ID		TECN	COMMENT
<4	90	3.2 ± 2.4	[1] ABLIKIM	05O	BES2	$\psi(2S)\to\chi_{c1}\gamma$

[1] ABLIKIM 05O reports $[\Gamma(\chi_{c1}(1P)\to K^+K^-K_S^0K_S^0)/\Gamma_{total}]\times[B(\psi(2S)\to\gamma\chi_{c1}(1P))]<4.2\times10^{-5}$ which we divide by our best value $B(\psi(2S)\to\gamma\chi_{c1}(1P))=9.75\times10^{-2}$.

$\Gamma(K^+K^-K^+K^-)/\Gamma_{total}$ Γ_{43}/Γ

VALUE (units 10^{-3})	DOCUMENT ID
0.54±0.11 OUR FIT	

$\Gamma(K^+K^-\phi)/\Gamma_{total}$ Γ_{44}/Γ

VALUE (units 10^{-3})	EVTS	DOCUMENT ID		TECN	COMMENT
$0.41\pm0.15\pm0.01$	17	[1] ABLIKIM	06T	BES2	$\psi(2S)\to\gamma2K^+2K^-$

[1] ABLIKIM 06T reports $(0.46\pm0.16\pm0.06)\times10^{-3}$ from a measurement of $[\Gamma(\chi_{c1}(1P)\to K^+K^-\phi)/\Gamma_{total}]\times[B(\psi(2S)\to\gamma\chi_{c1}(1P))]$ assuming $B(\psi(2S)\to\gamma\chi_{c1}(1P))=(8.7\pm0.4)\times10^{-2}$, which we rescale to our best value $B(\psi(2S)\to\gamma\chi_{c1}(1P))=(9.75\pm0.24)\times10^{-2}$. Our first error is their experiment's error and our second error is the systematic error from using our best value.

$\Gamma(\overline{K}^0K^+\pi^-\phi+\text{c.c.})/\Gamma_{total}$ Γ_{45}/Γ

VALUE (units 10^{-3})	DOCUMENT ID		TECN	COMMENT
$3.27\pm0.28\pm0.46$	ABLIKIM	15M	BES3	$\psi(2S)\to\gamma\chi_{c1}$

$\Gamma(K^+K^-\pi^0\phi)/\Gamma_{total}$ Γ_{46}/Γ

VALUE (units 10^{-3})	DOCUMENT ID		TECN	COMMENT
$1.62\pm0.12\pm0.28$	ABLIKIM	15M	BES3	$\psi(2S)\to\gamma\chi_{c1}$

$\Gamma(\phi\pi^+\pi^-\pi^0)/\Gamma_{total}$ Γ_{47}/Γ

VALUE (units 10^{-3})	EVTS	DOCUMENT ID		TECN	COMMENT
$0.75\pm0.06\pm0.08$	373	[1] ABLIKIM	13B	BES3	$e^+e^-\to\psi(2S)\to\gamma\chi_{c1}$

[1] Using 1.06×10^8 $\psi(2S)$ mesons and $B(\psi(2S)\to\chi_{c1}\gamma)=(9.2\pm0.4)\%$.

$\Gamma(\omega\omega)/\Gamma_{total}$ Γ_{48}/Γ

VALUE (units 10^{-4})	EVTS	DOCUMENT ID		TECN	COMMENT
$5.7\pm0.7\pm0.1$	597	[1] ABLIKIM	11K	BES3	$\psi(2S)\to\gamma$ hadrons

[1] ABLIKIM 11K reports $(6.0\pm0.3\pm0.7)\times10^{-4}$ from a measurement of $[\Gamma(\chi_{c1}(1P)\to\omega\omega)/\Gamma_{total}]\times[B(\psi(2S)\to\gamma\chi_{c1}(1P))]$ assuming $B(\psi(2S)\to\gamma\chi_{c1}(1P))=(9.2\pm0.4)\times10^{-2}$, which we rescale to our best value $B(\psi(2S)\to\gamma\chi_{c1}(1P))=(9.75\pm0.24)\times10^{-2}$. Our first error is their experiment's error and our second error is the systematic error from using our best value.

$\Gamma(\omega K^+K^-)/\Gamma_{total}$ Γ_{49}/Γ

VALUE (units 10^{-3})	EVTS	DOCUMENT ID		TECN	COMMENT
0.78±0.04±0.08	628	[1] ABLIKIM	13B	BES3	$e^+e^-\to\psi(2S)\to\gamma\chi_{c1}$

[1] Using 1.06×10^8 $\psi(2S)$ mesons and $B(\psi(2S)\to\chi_{c1}\gamma)=(9.2\pm0.4)\%$.

$\Gamma(\omega\phi)/\Gamma_{total}$ Γ_{50}/Γ

VALUE (units 10^{-4})	EVTS	DOCUMENT ID		TECN	COMMENT
$0.21\pm0.06\pm0.01$	15	[1] ABLIKIM	11K	BES3	$\psi(2S)\to\gamma$ hadrons

[1] ABLIKIM 11K reports $(0.22\pm0.06\pm0.02)\times10^{-4}$ from a measurement of $[\Gamma(\chi_{c1}(1P)\to\omega\phi)/\Gamma_{total}]\times[B(\psi(2S)\to\gamma\chi_{c1}(1P))]$ assuming $B(\psi(2S)\to\gamma\chi_{c1}(1P))=(9.2\pm0.4)\times10^{-2}$, which we rescale to our best value $B(\psi(2S)\to\gamma\chi_{c1}(1P))=(9.75\pm0.24)\times10^{-2}$. Our first error is their experiment's error and our second error is the systematic error from using our best value.

$\Gamma(\phi\phi)/\Gamma_{total}$ Γ_{51}/Γ

VALUE (units 10^{-4})	EVTS	DOCUMENT ID		TECN	COMMENT
$4.2\pm0.5\pm0.1$	366	[1] ABLIKIM	11K	BES3	$\psi(2S)\to\gamma$ hadrons

[1] ABLIKIM 11K reports $(4.4\pm0.3\pm0.5)\times10^{-4}$ from a measurement of $[\Gamma(\chi_{c1}(1P)\to\phi\phi)/\Gamma_{total}]\times[B(\psi(2S)\to\gamma\chi_{c1}(1P))]$ assuming $B(\psi(2S)\to\gamma\chi_{c1}(1P))=(9.2\pm0.4)\times10^{-2}$, which we rescale to our best value $B(\psi(2S)\to\gamma\chi_{c1}(1P))=(9.75\pm0.24)\times10^{-2}$. Our first error is their experiment's error and our second error is the systematic error from using our best value.

$\Gamma(p\overline{p})/\Gamma_{total}$ Γ_{52}/Γ

VALUE (units 10^{-4})	DOCUMENT ID
0.760±0.034 OUR FIT	

$\Gamma(p\overline{p}\pi^0)/\Gamma_{total}$ Γ_{53}/Γ

VALUE (units 10^{-3})	DOCUMENT ID		TECN	COMMENT
0.155±0.018 OUR AVERAGE				
$0.163\pm0.019\pm0.004$	[1] ONYISI	10	CLE3	$\psi(2S)\to\gamma p\overline{p}X$
$0.112\pm0.047\pm0.003$	[2] ATHAR	07	CLEO	$\psi(2S)\to\gamma h^+h^-h^0$

[1] ONYISI 10 reports $(1.75\pm0.16\pm0.13\pm0.11)\times10^{-4}$ from a measurement of $[\Gamma(\chi_{c1}(1P)\to p\overline{p}\pi^0)/\Gamma_{total}]\times[B(\psi(2S)\to\gamma\chi_{c1}(1P))]$ assuming $B(\psi(2S)\to\gamma\chi_{c1}(1P))=(9.07\pm0.11\pm0.54)\times10^{-2}$, which we rescale to our best value $B(\psi(2S)\to\gamma\chi_{c1}(1P))=(9.75\pm0.24)\times10^{-2}$. Our first error is their experiment's error and our second error is the systematic error from using our best value.

[2] ATHAR 07 reports $(1.2\pm0.5\pm0.1)\times10^{-4}$ from a measurement of $[\Gamma(\chi_{c1}(1P)\to p\overline{p}\pi^0)/\Gamma_{total}]\times[B(\psi(2S)\to\gamma\chi_{c1}(1P))]$ assuming $B(\psi(2S)\to\gamma\chi_{c1}(1P))=(9.07\pm0.11\pm0.54)\times10^{-2}$, which we rescale to our best value $B(\psi(2S)\to\gamma\chi_{c1}(1P))=(9.75\pm0.24)\times10^{-2}$. Our first error is their experiment's error and our second error is the systematic error from using our best value.

$\Gamma(p\overline{p}\eta)/\Gamma_{total}$ Γ_{54}/Γ

VALUE (units 10^{-3})	CL%	DOCUMENT ID		TECN	COMMENT
0.145±0.024±0.004		[1] ONYISI	10	CLE3	$\psi(2S)\to\gamma p\overline{p}X$
• • • We do not use the following data for averages, fits, limits, etc. • • •					
<0.15	90	[2] ATHAR	07	CLEO	$\psi(2S)\to\gamma h^+h^-h^0$

[1] ONYISI 10 reports $(1.56\pm0.22\pm0.14\pm0.10)\times10^{-4}$ from a measurement of $[\Gamma(\chi_{c1}(1P)\to p\overline{p}\eta)/\Gamma_{total}]\times[B(\psi(2S)\to\gamma\chi_{c1}(1P))]$ assuming $B(\psi(2S)\to\gamma\chi_{c1}(1P))=(9.07\pm0.11\pm0.54)\times10^{-2}$, which we rescale to our best value $B(\psi(2S)\to\gamma\chi_{c1}(1P))=(9.75\pm0.24)\times10^{-2}$. Our first error is their experiment's error and our second error is the systematic error from using our best value.

[2] ATHAR 07 reports $<0.16\times10^{-3}$ from a measurement of $[\Gamma(\chi_{c1}(1P)\to p\overline{p}\eta)/\Gamma_{total}]\times[B(\psi(2S)\to\gamma\chi_{c1}(1P))]$ assuming $B(\psi(2S)\to\gamma\chi_{c1}(1P))=(9.07\pm0.11\pm0.54)\times10^{-2}$, which we rescale to our best value $B(\psi(2S)\to\gamma\chi_{c1}(1P))=9.75\times10^{-2}$.

$\Gamma(p\overline{p}\omega)/\Gamma_{total}$ Γ_{55}/Γ

VALUE (units 10^{-3})	DOCUMENT ID		TECN	COMMENT
0.212±0.030±0.005	[1] ONYISI	10	CLE3	$\psi(2S)\to\gamma p\overline{p}X$

[1] ONYISI 10 reports $(2.28\pm0.28\pm0.16\pm0.14)\times10^{-4}$ from a measurement of $[\Gamma(\chi_{c1}(1P)\to p\overline{p}\omega)/\Gamma_{total}]\times[B(\psi(2S)\to\gamma\chi_{c1}(1P))]$ assuming $B(\psi(2S)\to\gamma\chi_{c1}(1P))=(9.07\pm0.11\pm0.54)\times10^{-2}$, which we rescale to our best value $B(\psi(2S)\to\gamma\chi_{c1}(1P))=(9.75\pm0.24)\times10^{-2}$. Our first error is their experiment's error and our second error is the systematic error from using our best value.

$\Gamma(p\overline{p}\phi)/\Gamma_{total}$ Γ_{56}/Γ

VALUE (units 10^{-5})	CL%	DOCUMENT ID		TECN	COMMENT
<1.7	90	[1] ABLIKIM	11F	BES3	$\psi(2S) \to \gamma p\overline{p}K^+K^-$

[1] ABLIKIM 11F reports $< 1.82 \times 10^{-5}$ from a measurement of $[\Gamma(\chi_{c1}(1P) \to p\overline{p}\phi)/\Gamma_{total}] \times [B(\psi(2S) \to \gamma\chi_{c1}(1P))]$ assuming $B(\psi(2S) \to \gamma\chi_{c1}(1P)) = (9.2 \pm 0.4) \times 10^{-2}$, which we rescale to our best value $B(\psi(2S) \to \gamma\chi_{c1}(1P)) = 9.75 \times 10^{-2}$.

$\Gamma(p\overline{p}\pi^+\pi^-)/\Gamma_{total}$ Γ_{57}/Γ

VALUE (units 10^{-3})		DOCUMENT ID		TECN	COMMENT
0.50±0.19 OUR EVALUATION		Treating systematic error as correlated.			
0.50±0.19 OUR AVERAGE					
0.46±0.12±0.15		[1] BAI	99B	BES	$\psi(2S) \to \gamma\chi_{c1}$
1.08±0.77±0.05		[1] TANENBAUM	78	MRK1	$\psi(2S) \to \gamma\chi_{c1}$

[1] Rescaled by us using $B(\psi(2S) \to \gamma\chi_{c1}) = (8.8 \pm 0.4)\%$ and $B(\psi(2S) \to J/\psi(1S)\pi^+\pi^-) = (32.6 \pm 0.5)\%$.

$\Gamma(p\overline{p}\pi^0\pi^0)/\Gamma_{total}$ Γ_{58}/Γ

VALUE (%)	CL%	DOCUMENT ID		TECN	COMMENT
<0.05	90	[1] HE	08B	CLEO	$e^+e^- \to \gamma h^+h^-h^0h^0$

[1] HE 08B reports < 0.05 % from a measurement of $[\Gamma(\chi_{c1}(1P) \to p\overline{p}\pi^0\pi^0)/\Gamma_{total}] \times [B(\psi(2S) \to \gamma\chi_{c1}(1P))]$ assuming $B(\psi(2S) \to \gamma\chi_{c1}(1P)) = (9.07 \pm 0.11 \pm 0.54) \times 10^{-2}$, which we rescale to our best value $B(\psi(2S) \to \gamma\chi_{c1}(1P)) = 9.75 \times 10^{-2}$.

$\Gamma(p\overline{p}K^+K^-(\text{non-resonant}))/\Gamma_{total}$ Γ_{59}/Γ

VALUE (units 10^{-4})	EVTS	DOCUMENT ID		TECN	COMMENT
1.27±0.22±0.03	82 ± 9	[1] ABLIKIM	11F	BES3	$\psi(2S) \to \gamma p\overline{p}K^+K^-$

[1] ABLIKIM 11F reports $(1.35 \pm 0.15 \pm 0.19) \times 10^{-4}$ from a measurement of $[\Gamma(\chi_{c1}(1P) \to p\overline{p}K^+K^-(\text{non-resonant}))/\Gamma_{total}] \times [B(\psi(2S) \to \gamma\chi_{c1}(1P))]$ assuming $B(\psi(2S) \to \gamma\chi_{c1}(1P)) = (9.2 \pm 0.4) \times 10^{-2}$, which we rescale to our best value $B(\psi(2S) \to \gamma\chi_{c1}(1P)) = (9.75 \pm 0.24) \times 10^{-2}$. Our first error is their experiment's error and our second error is the systematic error from using our best value.

$\Gamma(p\overline{p}K^0_SK^0_S)/\Gamma_{total}$ Γ_{60}/Γ

VALUE (units 10^{-4})	CL%	DOCUMENT ID		TECN	COMMENT
<4.5	90	[1] ABLIKIM	06D	BES2	$\psi(2S) \to \gamma\chi_{c1}$

[1] Using $B(\psi(2S) \to \chi_{c1}\gamma)$ (9.1 ± 0.6)%.

$\Gamma(p\overline{n}\pi^-)/\Gamma_{total}$ Γ_{61}/Γ

VALUE (units 10^{-4})	EVTS	DOCUMENT ID		TECN	COMMENT
3.8±0.5±0.1	1412	[1] ABLIKIM	12J	BES3	$\psi(2S) \to \gamma p\overline{n}\pi^-$

[1] ABLIKIM 12J reports $[\Gamma(\chi_{c1}(1P) \to p\overline{n}\pi^-)/\Gamma_{total}] \times [B(\psi(2S) \to \gamma\chi_{c1}(1P))] = (0.37 \pm 0.02 \pm 0.04) \times 10^{-4}$ which we divide by our best value $B(\psi(2S) \to \gamma\chi_{c1}(1P)) = (9.75 \pm 0.24) \times 10^{-2}$. Our first error is their experiment's error and our second error is the systematic error from using our best value.

$\Gamma(\overline{p}n\pi^+)/\Gamma_{total}$ Γ_{62}/Γ

VALUE (units 10^{-4})	EVTS	DOCUMENT ID		TECN	COMMENT
3.9±0.5±0.1	1625	[1] ABLIKIM	12J	BES3	$\psi(2S) \to \gamma\overline{p}n\pi^+$

[1] ABLIKIM 12J reports $[\Gamma(\chi_{c1}(1P) \to \overline{p}n\pi^+)/\Gamma_{total}] \times [B(\psi(2S) \to \gamma\chi_{c1}(1P))] = (0.38 \pm 0.02 \pm 0.04) \times 10^{-4}$ which we divide by our best value $B(\psi(2S) \to \gamma\chi_{c1}(1P)) = (9.75 \pm 0.24) \times 10^{-2}$. Our first error is their experiment's error and our second error is the systematic error from using our best value.

$\Gamma(p\overline{n}\pi^-\pi^0)/\Gamma_{total}$ Γ_{63}/Γ

VALUE (units 10^{-4})	EVTS	DOCUMENT ID		TECN	COMMENT
10.3±1.1±0.2	1082	[1] ABLIKIM	12J	BES3	$\psi(2S) \to \gamma p\overline{n}\pi^-\pi^0$

[1] ABLIKIM 12J reports $[\Gamma(\chi_{c1}(1P) \to p\overline{n}\pi^-\pi^0)/\Gamma_{total}] \times [B(\psi(2S) \to \gamma\chi_{c1}(1P))] = (1.00 \pm 0.05 \pm 0.10) \times 10^{-4}$ which we divide by our best value $B(\psi(2S) \to \gamma\chi_{c1}(1P)) = (9.75 \pm 0.24) \times 10^{-2}$. Our first error is their experiment's error and our second error is the systematic error from using our best value.

$\Gamma(\overline{p}n\pi^+\pi^0)/\Gamma_{total}$ Γ_{64}/Γ

VALUE (units 10^{-4})	EVTS	DOCUMENT ID		TECN	COMMENT
10.1±1.1±0.2	1261	[1] ABLIKIM	12J	BES3	$\psi(2S) \to \gamma\overline{p}n\pi^+\pi^0$

[1] ABLIKIM 12J reports $[\Gamma(\chi_{c1}(1P) \to \overline{p}n\pi^+\pi^0)/\Gamma_{total}] \times [B(\psi(2S) \to \gamma\chi_{c1}(1P))] = (0.98 \pm 0.05 \pm 0.10) \times 10^{-4}$ which we divide by our best value $B(\psi(2S) \to \gamma\chi_{c1}(1P)) = (9.75 \pm 0.24) \times 10^{-2}$. Our first error is their experiment's error and our second error is the systematic error from using our best value.

$\Gamma(\Lambda\overline{\Lambda})/\Gamma_{total}$ Γ_{65}/Γ

VALUE (units 10^{-4})	DOCUMENT ID
1.14±0.11 OUR FIT	

$\Gamma(\Lambda\overline{\Lambda}\pi^+\pi^-)/\Gamma_{total}$ Γ_{66}/Γ

VALUE (units 10^{-5})	CL%	EVTS	DOCUMENT ID		TECN	COMMENT
29±5±1		105	[1] ABLIKIM	12I	BES3	$\psi(2S) \to \gamma\Lambda\overline{\Lambda}\pi^+\pi^-$
• • • We do not use the following data for averages, fits, limits, etc. • • •						
<150	90		[2] ABLIKIM	06D	BES2	$\psi(2S) \to \gamma\chi_{c1}$

[1] ABLIKIM 12I reports $(31.1 \pm 3.4 \pm 3.9) \times 10^{-5}$ from a measurement of $[\Gamma(\chi_{c1}(1P) \to \Lambda\overline{\Lambda}\pi^+\pi^-)/\Gamma_{total}] \times [B(\psi(2S) \to \gamma\chi_{c1}(1P))]$ assuming $B(\psi(2S) \to \gamma\chi_{c1}(1P)) = (9.2 \pm 0.4) \times 10^{-2}$, which we rescale to our best value $B(\psi(2S) \to \gamma\chi_{c1}(1P)) = (9.75 \pm 0.24) \times 10^{-2}$. Our first error is their experiment's error and our second error is the systematic error from using our best value.

[2] Using $B(\psi(2S) \to \chi_{c1}\gamma)$ (9.1 ± 0.6)%.

$\Gamma(\Lambda\overline{\Lambda}\pi^+\pi^-(\text{non-resonant}))/\Gamma_{total}$ Γ_{67}/Γ

VALUE (units 10^{-5})	EVTS	DOCUMENT ID		TECN	COMMENT
25±6±1	13	[1] ABLIKIM	12I	BES3	$\psi(2S) \to \gamma\Lambda\overline{\Lambda}\pi^+\pi^-$

[1] ABLIKIM 12I reports $(26.2 \pm 5.5 \pm 3.3) \times 10^{-5}$ from a measurement of $[\Gamma(\chi_{c1}(1P) \to \Lambda\overline{\Lambda}\pi^+\pi^-(\text{non-resonant}))/\Gamma_{total}] \times [B(\psi(2S) \to \gamma\chi_{c1}(1P))]$ assuming $B(\psi(2S) \to \gamma\chi_{c1}(1P)) = (9.2 \pm 0.4) \times 10^{-2}$, which we rescale to our best value $B(\psi(2S) \to \gamma\chi_{c1}(1P)) = (9.75 \pm 0.24) \times 10^{-2}$. Our first error is their experiment's error and our second error is the systematic error from using our best value.

$\Gamma(\Sigma(1385)^+\overline{\Lambda}\pi^- + \text{c.c.})/\Gamma_{total}$ Γ_{68}/Γ

VALUE (units 10^{-5})	CL%	DOCUMENT ID		TECN	COMMENT
<13	90	[1] ABLIKIM	12I	BES3	$\psi(2S) \to \gamma\Sigma(1385)^+\overline{\Lambda}\pi^-$

[1] ABLIKIM 12I reports $< 14 \times 10^{-5}$ from a measurement of $[\Gamma(\chi_{c1}(1P) \to \Sigma(1385)^+\overline{\Lambda}\pi^- + \text{c.c.})/\Gamma_{total}] \times [B(\psi(2S) \to \gamma\chi_{c1}(1P))]$ assuming $B(\psi(2S) \to \gamma\chi_{c1}(1P)) = (9.2 \pm 0.4) \times 10^{-2}$, which we rescale to our best value $B(\psi(2S) \to \gamma\chi_{c1}(1P)) = 9.75 \times 10^{-2}$.

$\Gamma(\Sigma(1385)^-\overline{\Lambda}\pi^+ + \text{c.c.})/\Gamma_{total}$ Γ_{69}/Γ

VALUE (units 10^{-5})	CL%	DOCUMENT ID		TECN	COMMENT
<13	90	[1] ABLIKIM	12I	BES3	$\psi(2S) \to \gamma\Sigma(1385)^-\overline{\Lambda}\pi^+$

[1] ABLIKIM 12I reports $< 14 \times 10^{-5}$ from a measurement of $[\Gamma(\chi_{c1}(1P) \to \Sigma(1385)^-\overline{\Lambda}\pi^+ + \text{c.c.})/\Gamma_{total}] \times [B(\psi(2S) \to \gamma\chi_{c1}(1P))]$ assuming $B(\psi(2S) \to \gamma\chi_{c1}(1P)) = (9.2 \pm 0.4) \times 10^{-2}$, which we rescale to our best value $B(\psi(2S) \to \gamma\chi_{c1}(1P)) = 9.75 \times 10^{-2}$.

$\Gamma(K^+\overline{p}\Lambda)/\Gamma_{total}$ Γ_{70}/Γ

VALUE (units 10^{-4})	EVTS	DOCUMENT ID		TECN	COMMENT
4.1±0.4 OUR AVERAGE		Error includes scale factor of 1.2.			
4.2±0.4±0.1	3k	[1,2] ABLIKIM	13D	BES3	$\psi(2S) \to \gamma\Lambda\overline{p}K^+$
3.1±0.9±0.1		[3] ATHAR	07	CLEO	$\psi(2S) \to \gamma h^+h^-h^0$

[1] ABLIKIM 13D reports $(4.5 \pm 0.2 \pm 0.4) \times 10^{-4}$ from a measurement of $[\Gamma(\chi_{c1}(1P) \to K^+\overline{p}\Lambda)/\Gamma_{total}] \times [B(\psi(2S) \to \gamma\chi_{c1}(1P))]$ assuming $B(\psi(2S) \to \gamma\chi_{c1}(1P)) = (9.2 \pm 0.4) \times 10^{-2}$, which we rescale to our best value $B(\psi(2S) \to \gamma\chi_{c1}(1P)) = (9.75 \pm 0.24) \times 10^{-2}$. Our first error is their experiment's error and our second error is the systematic error from using our best value.

[2] Using $B(\Lambda \to p\pi^-) = 63.9\%$.

[3] ATHAR 07 reports $(3.3 \pm 0.9 \pm 0.4) \times 10^{-4}$ from a measurement of $[\Gamma(\chi_{c1}(1P) \to K^+\overline{p}\Lambda)/\Gamma_{total}] \times [B(\psi(2S) \to \gamma\chi_{c1}(1P))]$ assuming $B(\psi(2S) \to \gamma\chi_{c1}(1P)) = (9.07 \pm 0.11 \pm 0.54) \times 10^{-2}$, which we rescale to our best value $B(\psi(2S) \to \gamma\chi_{c1}(1P)) = (9.75 \pm 0.24) \times 10^{-2}$. Our first error is their experiment's error and our second error is the systematic error from using our best value.

$\Gamma(K^+\overline{p}\Lambda(1520) + \text{c.c.})/\Gamma_{total}$ Γ_{71}/Γ

VALUE (units 10^{-4})	EVTS	DOCUMENT ID		TECN	COMMENT
1.71±0.44±0.04	48 ± 10	[1] ABLIKIM	11F	BES3	$\psi(2S) \to \gamma p\overline{p}K^+K^-$

[1] ABLIKIM 11F reports $(1.81 \pm 0.38 \pm 0.28) \times 10^{-4}$ from a measurement of $[\Gamma(\chi_{c1}(1P) \to K^+\overline{p}\Lambda(1520) + \text{c.c.})/\Gamma_{total}] \times [B(\psi(2S) \to \gamma\chi_{c1}(1P))]$ assuming $B(\psi(2S) \to \gamma\chi_{c1}(1P)) = (9.2 \pm 0.4) \times 10^{-2}$, which we rescale to our best value $B(\psi(2S) \to \gamma\chi_{c1}(1P)) = (9.75 \pm 0.24) \times 10^{-2}$. Our first error is their experiment's error and our second error is the systematic error from using our best value.

$\Gamma(\Lambda(1520)\overline{\Lambda}(1520))/\Gamma_{total}$ Γ_{72}/Γ

VALUE (units 10^{-4})	CL%	DOCUMENT ID		TECN	COMMENT
<0.9	90	[1] ABLIKIM	11F	BES3	$\psi(2S) \to \gamma p\overline{p}K^+K^-$

[1] ABLIKIM 11F reports $< 1.00 \times 10^{-4}$ from a measurement of $[\Gamma(\chi_{c1}(1P) \to \Lambda(1520)\overline{\Lambda}(1520))/\Gamma_{total}] \times [B(\psi(2S) \to \gamma\chi_{c1}(1P))]$ assuming $B(\psi(2S) \to \gamma\chi_{c1}(1P)) = (9.2 \pm 0.4) \times 10^{-2}$, which we rescale to our best value $B(\psi(2S) \to \gamma\chi_{c1}(1P)) = 9.75 \times 10^{-2}$.

$\Gamma(\Sigma^0\overline{\Sigma}^0)/\Gamma_{total}$ Γ_{73}/Γ

VALUE (units 10^{-4})	CL%	EVTS	DOCUMENT ID		TECN	COMMENT
<0.4	90	3.8 ± 2.5	[1] NAIK	08	CLEO	$\psi(2S) \to \gamma\Sigma^0\overline{\Sigma}^0$
• • • We do not use the following data for averages, fits, limits, etc. • • •						
<0.6	90		[2] ABLIKIM	13H	BES3	$\psi(2S) \to \gamma\Sigma^0\overline{\Sigma}^0$

[1] NAIK 08 reports $< 0.44 \times 10^{-4}$ from a measurement of $[\Gamma(\chi_{c1}(1P) \to \Sigma^0\overline{\Sigma}^0)/\Gamma_{total}] \times [B(\psi(2S) \to \gamma\chi_{c1}(1P))]$ assuming $B(\psi(2S) \to \gamma\chi_{c1}(1P)) = (9.07 \pm 0.11 \pm 0.54) \times 10^{-2}$, which we rescale to our best value $B(\psi(2S) \to \gamma\chi_{c1}(1P)) = 9.75 \times 10^{-2}$.

[2] ABLIKIM 13H reports $< 0.62 \times 10^{-4}$ from a measurement of $[\Gamma(\chi_{c1}(1P) \to \Sigma^0\overline{\Sigma}^0)/\Gamma_{total}] \times [B(\psi(2S) \to \gamma\chi_{c1}(1P))]$ assuming $B(\psi(2S) \to \gamma\chi_{c1}(1P)) = (9.2 \pm 0.4) \times 10^{-2}$, which we rescale to our best value $B(\psi(2S) \to \gamma\chi_{c1}(1P)) = 9.75 \times 10^{-2}$.

Meson Particle Listings

$\chi_{c1}(1P)$

$\Gamma(\Sigma^+\overline{\Sigma}^-)/\Gamma_{total}$ Γ_{74}/Γ

VALUE (units 10^{-4})	CL%	EVTS	DOCUMENT ID		TECN	COMMENT
<0.6	90	4.3 ± 2.3	[1] NAIK	08	CLEO	$\psi(2S) \to \gamma\Sigma^+\overline{\Sigma}^-$

• • • We do not use the following data for averages, fits, limits, etc. • • •

<0.8	90	[2] ABLIKIM	13H	BES3	$\psi(2S) \to \gamma\Sigma^+\overline{\Sigma}^-$	

[1] NAIK 08 reports $< 0.65 \times 10^{-4}$ from a measurement of $[\Gamma(\chi_{c1}(1P) \to \Sigma^+\overline{\Sigma}^-)/\Gamma_{total}] \times [B(\psi(2S) \to \gamma\chi_{c1}(1P))]$ assuming $B(\psi(2S) \to \gamma\chi_{c1}(1P)) = (9.07 \pm 0.11 \pm 0.54) \times 10^{-2}$, which we rescale to our best value $B(\psi(2S) \to \gamma\chi_{c1}(1P)) = 9.75 \times 10^{-2}$.

[2] ABLIKIM 13H reports $< 0.87 \times 10^{-4}$ from a measurement of $[\Gamma(\chi_{c1}(1P) \to \Sigma^+\overline{\Sigma}^-)/\Gamma_{total}] \times [B(\psi(2S) \to \gamma\chi_{c1}(1P))]$ assuming $B(\psi(2S) \to \gamma\chi_{c1}(1P)) = (9.2 \pm 0.4) \times 10^{-2}$, which we rescale to our best value $B(\psi(2S) \to \gamma\chi_{c1}(1P)) = 9.75 \times 10^{-2}$.

$\Gamma(\Sigma(1385)^+\overline{\Sigma}(1385)^-)/\Gamma_{total}$ Γ_{75}/Γ

VALUE (units 10^{-5})	CL%	DOCUMENT ID		TECN	COMMENT
<9	90	[1] ABLIKIM	12I	BES3	$\psi(2S) \to \gamma\Lambda\overline{\Lambda}\pi^+\pi^-$

[1] ABLIKIM 12I reports $< 10 \times 10^{-5}$ from a measurement of $[\Gamma(\chi_{c1}(1P) \to \Sigma(1385)^+\overline{\Sigma}(1385)^-)/\Gamma_{total}] \times [B(\psi(2S) \to \gamma\chi_{c1}(1P))]$ assuming $B(\psi(2S) \to \gamma\chi_{c1}(1P)) = (9.2 \pm 0.4) \times 10^{-2}$, which we rescale to our best value $B(\psi(2S) \to \gamma\chi_{c1}(1P)) = 9.75 \times 10^{-2}$.

$\Gamma(\Sigma(1385)^-\overline{\Sigma}(1385)^+)/\Gamma_{total}$ Γ_{76}/Γ

VALUE (units 10^{-5})	CL%	DOCUMENT ID		TECN	COMMENT
<5	90	[1] ABLIKIM	12I	BES3	$\psi(2S) \to \gamma\Lambda\overline{\Lambda}\pi^+\pi^-$

[1] ABLIKIM 12I reports $< 5.7 \times 10^{-5}$ from a measurement of $[\Gamma(\chi_{c1}(1P) \to \Sigma(1385)^-\overline{\Sigma}(1385)^+)/\Gamma_{total}] \times [B(\psi(2S) \to \gamma\chi_{c1}(1P))]$ assuming $B(\psi(2S) \to \gamma\chi_{c1}(1P)) = (9.2 \pm 0.4) \times 10^{-2}$, which we rescale to our best value $B(\psi(2S) \to \gamma\chi_{c1}(1P)) = 9.75 \times 10^{-2}$.

$\Gamma(K^-\Lambda\overline{\Xi}^+ + \text{c.c.})/\Gamma_{total}$ Γ_{77}/Γ

VALUE (units 10^{-4})	EVTS	DOCUMENT ID		TECN	COMMENT
$1.35 \pm 0.24 \pm 0.03$	49	[1] ABLIKIM	15I	BES3	$\psi(2S) \to \gamma K^-\Lambda\overline{\Xi}^+ + \text{c.c.}$

[1] ABLIKIM 15I reports $[\Gamma(\chi_{c1}(1P) \to K^-\Lambda\overline{\Xi}^+ + \text{c.c.})/\Gamma_{total}] \times [B(\psi(2S) \to \gamma\chi_{c1}(1P))] = (1.32 \pm 0.20 \pm 0.12) \times 10^{-5}$ which we divide by our best value $B(\psi(2S) \to \gamma\chi_{c1}(1P)) = (9.75 \pm 0.24) \times 10^{-2}$. Our first error is their experiment's error and our second error is the systematic error from using our best value.

$\Gamma(\Xi^0\overline{\Xi}^0)/\Gamma_{total}$ Γ_{78}/Γ

VALUE (units 10^{-4})	CL%	EVTS	DOCUMENT ID		TECN	COMMENT
<0.6	90	1.7 ± 2.4	[1] NAIK	08	CLEO	$\psi(2S) \to \gamma\Xi^0\overline{\Xi}^0$

[1] NAIK 08 reports $< 0.60 \times 10^{-4}$ from a measurement of $[\Gamma(\chi_{c1}(1P) \to \Xi^0\overline{\Xi}^0)/\Gamma_{total}] \times [B(\psi(2S) \to \gamma\chi_{c1}(1P))]$ assuming $B(\psi(2S) \to \gamma\chi_{c1}(1P)) = (9.07 \pm 0.11 \pm 0.54) \times 10^{-2}$, which we rescale to our best value $B(\psi(2S) \to \gamma\chi_{c1}(1P)) = 9.75 \times 10^{-2}$.

$\Gamma(\Xi^-\overline{\Xi}^+)/\Gamma_{total}$ Γ_{79}/Γ

VALUE (units 10^{-4})	CL%	EVTS	DOCUMENT ID		TECN	COMMENT
$0.80 \pm 0.21 \pm 0.02$		16.4 ± 4.3	[1] NAIK	08	CLEO	$\psi(2S) \to \gamma\Xi^+\overline{\Xi}^-$

• • • We do not use the following data for averages, fits, limits, etc. • • •

< 3.4	90	[2] ABLIKIM	06D	BES2	$\psi(2S) \to \gamma\chi_{c1}$	

[1] NAIK 08 reports $(0.86 \pm 0.22 \pm 0.08) \times 10^{-4}$ from a measurement of $[\Gamma(\chi_{c1}(1P) \to \Xi^-\overline{\Xi}^+)/\Gamma_{total}] \times [B(\psi(2S) \to \gamma\chi_{c1}(1P))]$ assuming $B(\psi(2S) \to \gamma\chi_{c1}(1P)) = (9.07 \pm 0.11 \pm 0.54) \times 10^{-2}$, which we rescale to our best value $B(\psi(2S) \to \gamma\chi_{c1}(1P)) = (9.75 \pm 0.24) \times 10^{-2}$. Our first error is their experiment's error and our second error is the systematic error from using our best value.

[2] Using $B(\psi(2S) \to \chi_{c1}\gamma)$ $(9.1 \pm 0.6)\%$.

$[\Gamma(\pi^+\pi^-) + \Gamma(K^+K^-)]/\Gamma_{total}$ Γ_{80}/Γ

VALUE (units 10^{-4})	CL%	DOCUMENT ID		TECN	COMMENT
<21		[1] FELDMAN	77	MRK1	$\psi(2S) \to \gamma\chi_{c1}$

• • • We do not use the following data for averages, fits, limits, etc. • • •

<38	90	[1] BRANDELIK	79B	DASP	$\psi(2S) \to \gamma\chi_{c1}$	

[1] Estimated using $B(\psi(2S) \to \gamma\chi_{c1}(1P)) = 0.087$. The errors do not contain the uncertainty in the $\psi(2S)$ decay.

$\Gamma(K^0_S K^0_S)/\Gamma_{total}$ Γ_{81}/Γ

VALUE (units 10^{-4})	CL%	DOCUMENT ID		TECN	COMMENT
<0.6	90	[1] ABLIKIM	05O	BES2	$\psi(2S) \to \chi_{c1}\gamma$

[1] ABLIKIM 05O reports $[\Gamma(\chi_{c1}(1P) \to K^0_S K^0_S)/\Gamma_{total}] \times [B(\psi(2S) \to \gamma\chi_{c1}(1P))] < 0.6 \times 10^{-5}$ which we divide by our best value $B(\psi(2S) \to \gamma\chi_{c1}(1P)) = 9.75 \times 10^{-2}$.

$\Gamma(\eta_c\pi^+\pi^-)/\Gamma_{total}$ Γ_{82}/Γ

VALUE	CL%	DOCUMENT ID		TECN	COMMENT
$< 3.2 \times 10^{-3}$	90	[1,2] ABLIKIM	13B	BES3	$e^+e^- \to \psi(2S) \to \gamma\chi_{c1}$

• • • We do not use the following data for averages, fits, limits, etc. • • •

$< 4.4 \times 10^{-3}$	90	[1,3] ABLIKIM	13B	BES3	$e^+e^- \to \psi(2S) \to \gamma\chi_{c1}$	

[1] Using 1.06×10^8 $\psi(2S)$ mesons and $B(\psi(2S) \to \chi_{c1}\gamma) = (9.2 \pm 0.4)\%$.

[2] Using the $\eta_c \to K^0_S K^\pm\pi^\mp$ decays.

[3] Using the $\eta_c \to K^+K^-\pi^0$ decays.

RADIATIVE DECAYS

$\Gamma(\gamma J/\psi(1S))/\Gamma_{total}$ Γ_{83}/Γ

VALUE (units 10^{-2})	EVTS	DOCUMENT ID		TECN	COMMENT
34.3 ± 1.0 OUR FIT					

• • • We do not use the following data for averages, fits, limits, etc. • • •

$34.75 \pm 0.11 \pm 1.70$	1.9M	[1] ABLIKIM	17U	BES3	$e^+e^- \to \gamma X$	
$37.9 \pm 0.8 \pm 2.1$		[2] ADAM	05A	CLEO	$e^+e^- \to \psi(2S) \to \gamma\chi_{c1}$	

[1] Not independent from $B(\psi(2S) \to \gamma\chi_{c1}(1P))$ and the product $B(\psi(2S) \to \gamma\chi_{c1}(1P)) \times B(\chi_{c1}(1P) \to \gamma J/\psi(1S))$ also measured in ABLIKIM 17U.

[2] Uses $B(\psi(2S) \to \gamma\chi_{c1} \to \gamma\gamma J/\psi)$ from ADAM 05A and $B(\psi(2S) \to \gamma\chi_{c1})$ from ATHAR 04.

$\Gamma(\gamma\rho^0)/\Gamma_{total}$ Γ_{84}/Γ

VALUE (units 10^{-6})	EVTS	DOCUMENT ID		TECN	COMMENT
216 ± 17 OUR AVERAGE					
$215 \pm 22 \pm 5$	432 ± 25	[1] ABLIKIM	11E	BES3	$\psi(2S) \to \gamma\gamma\rho^0$
$217 \pm 24 \pm 5$	186 ± 15	[2] BENNETT	08A	CLEO	$\psi(2S) \to \gamma\gamma\rho^0$

[1] ABLIKIM 11E reports $(228 \pm 13 \pm 22) \times 10^{-6}$ from a measurement of $[\Gamma(\chi_{c1}(1P) \to \gamma\rho^0)/\Gamma_{total}] \times [B(\psi(2S) \to \gamma\chi_{c1}(1P))]$ assuming $B(\psi(2S) \to \gamma\chi_{c1}(1P)) = (9.2 \pm 0.4) \times 10^{-2}$, which we rescale to our best value $B(\psi(2S) \to \gamma\chi_{c1}(1P)) = (9.75 \pm 0.24) \times 10^{-2}$. Our first error is their experiment's error and our second error is the systematic error from using our best value.

[2] BENNETT 08A reports $(243 \pm 19 \pm 22) \times 10^{-6}$ from a measurement of $[\Gamma(\chi_{c1}(1P) \to \gamma\rho^0)/\Gamma_{total}] \times [B(\psi(2S) \to \gamma\chi_{c1}(1P))]$ assuming $B(\psi(2S) \to \gamma\chi_{c1}(1P)) = (8.7 \pm 0.4) \times 10^{-2}$, which we rescale to our best value $B(\psi(2S) \to \gamma\chi_{c1}(1P)) = (9.75 \pm 0.24) \times 10^{-2}$. Our first error is their experiment's error and our second error is the systematic error from using our best value.

$\Gamma(\gamma\omega)/\Gamma_{total}$ Γ_{85}/Γ

VALUE (units 10^{-6})	EVTS	DOCUMENT ID		TECN	COMMENT
68 ± 8 OUR AVERAGE					
$66 \pm 9 \pm 2$	136 ± 14	[1] ABLIKIM	11E	BES3	$\psi(2S) \to \gamma\gamma\omega$
$74 \pm 17 \pm 2$	39 ± 7	[2] BENNETT	08A	CLEO	$\psi(2S) \to \gamma\gamma\omega$

[1] ABLIKIM 11E reports $(69.7 \pm 7.2 \pm 6.6) \times 10^{-6}$ from a measurement of $[\Gamma(\chi_{c1}(1P) \to \gamma\omega)/\Gamma_{total}] \times [B(\psi(2S) \to \gamma\chi_{c1}(1P))]$ assuming $B(\psi(2S) \to \gamma\chi_{c1}(1P)) = (9.2 \pm 0.4) \times 10^{-2}$, which we rescale to our best value $B(\psi(2S) \to \gamma\chi_{c1}(1P)) = (9.75 \pm 0.24) \times 10^{-2}$. Our first error is their experiment's error and our second error is the systematic error from using our best value.

[2] BENNETT 08A reports $(83 \pm 15 \pm 12) \times 10^{-6}$ from a measurement of $[\Gamma(\chi_{c1}(1P) \to \gamma\omega)/\Gamma_{total}] \times [B(\psi(2S) \to \gamma\chi_{c1}(1P))]$ assuming $B(\psi(2S) \to \gamma\chi_{c1}(1P)) = (8.7 \pm 0.4) \times 10^{-2}$, which we rescale to our best value $B(\psi(2S) \to \gamma\chi_{c1}(1P)) = (9.75 \pm 0.24) \times 10^{-2}$. Our first error is their experiment's error and our second error is the systematic error from using our best value.

$\Gamma(\gamma\phi)/\Gamma_{total}$ Γ_{86}/Γ

VALUE (units 10^{-6})	CL%	EVTS	DOCUMENT ID		TECN	COMMENT
$24 \pm 5 \pm 1$		43 ± 9	[1] ABLIKIM	11E	BES3	$\psi(2S) \to \gamma\gamma\phi$

• • • We do not use the following data for averages, fits, limits, etc. • • •

<23	90	5.2 ± 3.1	[2] BENNETT	08A	CLEO	$\psi(2S) \to \gamma\gamma\phi$	

[1] ABLIKIM 11E reports $(25.8 \pm 5.2 \pm 2.3) \times 10^{-6}$ from a measurement of $[\Gamma(\chi_{c1}(1P) \to \gamma\phi)/\Gamma_{total}] \times [B(\psi(2S) \to \gamma\chi_{c1}(1P))]$ assuming $B(\psi(2S) \to \gamma\chi_{c1}(1P)) = (9.2 \pm 0.4) \times 10^{-2}$, which we rescale to our best value $B(\psi(2S) \to \gamma\chi_{c1}(1P)) = (9.75 \pm 0.24) \times 10^{-2}$. Our first error is their experiment's error and our second error is the systematic error from using our best value.

[2] BENNETT 08A reports $< 26 \times 10^{-6}$ from a measurement of $[\Gamma(\chi_{c1}(1P) \to \gamma\phi)/\Gamma_{total}] \times [B(\psi(2S) \to \gamma\chi_{c1}(1P))]$ assuming $B(\psi(2S) \to \gamma\chi_{c1}(1P)) = (8.7 \pm 0.4) \times 10^{-2}$, which we rescale to our best value $B(\psi(2S) \to \gamma\chi_{c1}(1P)) = 9.75 \times 10^{-2}$.

$\Gamma(\gamma\gamma)/\Gamma_{total}$ Γ_{87}/Γ

VALUE	CL%	DOCUMENT ID		TECN	COMMENT
$< 6.3 \times 10^{-6}$	90	ABLIKIM	17AE	BES3	$\psi(2S) \to \gamma\chi_{c1} \to 3\gamma$

• • • We do not use the following data for averages, fits, limits, etc. • • •

$< 3.5 \times 10^{-5}$	90	ECKLUND	08A	CLEO	$\psi(2S) \to \gamma\chi_{c1} \to 3\gamma$	
$< 150 \times 10^{-5}$	90	[1] YAMADA	77	DASP	$e^+e^- \to 3\gamma$	

[1] Estimated using $B(\psi(2S) \to \gamma\chi_{c1}(1P)) = 0.087$. The errors do not contain the uncertainty in the $\psi(2S)$ decay.

$\Gamma(e^+e^- J/\psi(1S))/\Gamma_{total}$ Γ_{88}/Γ

VALUE (units 10^{-3})	EVTS	DOCUMENT ID		TECN	COMMENT
$3.65 \pm 0.23 \pm 0.09$	1.9k	[1] ABLIKIM	17I	BES3	$\psi(2S) \to \gamma e^+e^- J/\psi$

[1] ABLIKIM 17I reports $(3.73 \pm 0.09 \pm 0.25) \times 10^{-3}$ from a measurement of $[\Gamma(\chi_{c1}(1P) \to e^+e^- J/\psi(1S))/\Gamma_{total}] \times [B(\psi(2S) \to \gamma\chi_{c1}(1P))]$ assuming $B(\psi(2S) \to \gamma\chi_{c1}(1P)) = (9.55 \pm 0.31) \times 10^{-2}$, which we rescale to our best value $B(\psi(2S) \to \gamma\chi_{c1}(1P)) = (9.75 \pm 0.24) \times 10^{-2}$. Our first error is their experiment's error and our second error is the systematic error from using our best value.

$\Gamma(e^+e^- J/\psi(1S))/\Gamma(\gamma J/\psi(1S))$ Γ_{88}/Γ_{83}

VALUE (units 10^{-3})	EVTS	DOCUMENT ID		TECN	COMMENT
$10.1 \pm 0.3 \pm 0.5$	1.9k	[1] ABLIKIM	17I	BES3	$\psi(2S) \to e^+e^-\gamma J/\psi$

[1] Uses B($\psi(2S) \to \gamma\chi_{c1}(1P)$) × B($\chi_{c1}(1P) \to \gamma J/\psi(1S)$) = (351.8 ± 1.0 ± 12.0) × 10^{-4} from ABLIKIM 17N and accounts for common systematic errors.

$\chi_{c1}(1P)$ CROSS-PARTICLE BRANCHING RATIOS

$\Gamma(\chi_{c1}(1P) \to p\overline{p})/\Gamma_{\text{total}} \times \Gamma(\psi(2S) \to \gamma\chi_{c1}(1P))/\Gamma(\psi(2S) \to J/\psi(1S)\pi^+\pi^-)$ $\Gamma_{52}/\Gamma \times \Gamma_{140}^{\psi(2S)}/\Gamma_{11}^{\psi(2S)}$

VALUE (units 10^{-5})	DOCUMENT ID		TECN	COMMENT
2.14±0.10 OUR FIT				
1.1 ±1.0	[1] BAI	98I	BES	$\psi(2S) \to \gamma\chi_{c1} \to \gamma\overline{p}p$

[1] Calculated by us. The value for B($\chi_{c1} \to p\overline{p}$) reported in BAI 98I is derived using B($\psi(2S) \to \gamma\chi_{c1}$) = (8.7 ± 0.8)% and B($\psi(2S) \to J/\psi(1S)\pi^+\pi^-$) = (32.4 ± 2.6)% [BAI 98D].

$\Gamma(\chi_{c1}(1P) \to \Lambda\overline{\Lambda})/\Gamma_{\text{total}} \times \Gamma(\psi(2S) \to \gamma\chi_{c1}(1P))/\Gamma_{\text{total}}$ $\Gamma_{65}/\Gamma \times \Gamma_{140}^{\psi(2S)}/\Gamma^{\psi(2S)}$

VALUE (units 10^{-6})	EVTS	DOCUMENT ID		TECN	COMMENT
11.1±1.1 OUR FIT					
10.9±1.1 OUR AVERAGE					
11.2±1.0±0.9	136	[1] ABLIKIM	13H	BES3	$\psi(2S) \to \gamma\Lambda\overline{\Lambda}$
10.5±1.6±0.6	46 ± 7	[2] NAIK	08	CLEO	$\psi(2S) \to \gamma\Lambda\overline{\Lambda}$

[1] Calculated by us. ABLIKIM 13H reports B($\chi_{c1} \to \Lambda\overline{\Lambda}$) = (12.2 ± 1.1 ± 1.1) × 10^{-5} from a measurement of B($\chi_{c1} \to \Lambda\overline{\Lambda}$) × B($\psi(2S) \to \gamma\chi_{c1}$) assuming B($\psi(2S) \to \gamma\chi_{c1}$) = (9.2 ± 0.4)%.
[2] Calculated by us. NAIK 08 reports B($\chi_{c1} \to \Lambda\overline{\Lambda}$) = (11.6 ± 1.8 ± 0.7 ± 0.7) × 10^{-5} using B($\psi(2S) \to \gamma\chi_{c1}$) = (9.07 ± 0.11 ± 0.54)%.

$\Gamma(\chi_{c1}(1P) \to \Lambda\overline{\Lambda})/\Gamma_{\text{total}} \times \Gamma(\psi(2S) \to \gamma\chi_{c1}(1P))/\Gamma(\psi(2S) \to J/\psi(1S)\pi^+\pi^-)$ $\Gamma_{65}/\Gamma \times \Gamma_{140}^{\psi(2S)}/\Gamma_{11}^{\psi(2S)}$

VALUE (units 10^{-5})	EVTS	DOCUMENT ID		TECN	COMMENT
3.20±0.30 OUR FIT					
7.1 $^{+2.8}_{-2.4}$ ±1.3	$9.0^{+3.5}_{-3.1}$	[1] BAI	03E	BES	$\psi(2S) \to \gamma\Lambda\overline{\Lambda}$

[1] BAI 03E reports [B($\chi_{c1} \to \Lambda\overline{\Lambda}$) B($\psi(2S) \to \gamma\chi_{c1}$) / B($\psi(2S) \to J/\psi\pi^+\pi^-$)] × [$B^2(\Lambda \to \pi^-p)$ / B($J/\psi \to p\overline{p}$)] = ($1.33^{+0.52}_{-0.46}$ ± 0.25)%. We calculate from this measurement the presented value using B($\Lambda \to \pi^-p$) = (63.9 ± 0.5)% and B($J/\psi \to p\overline{p}$) = (2.17 ± 0.07) × 10^{-3}.

$\Gamma(\chi_{c1}(1P) \to \gamma J/\psi(1S))/\Gamma_{\text{total}} \times \Gamma(\psi(2S) \to \gamma\chi_{c1}(1P))/\Gamma_{\text{total}}$ $\Gamma_{83}/\Gamma \times \Gamma_{140}^{\psi(2S)}/\Gamma^{\psi(2S)}$

VALUE (units 10^{-2})	EVTS	DOCUMENT ID		TECN	COMMENT
3.34 ±0.06 OUR FIT					
3.24 ±0.16 OUR AVERAGE		Error includes scale factor of 2.1. See the ideogram below.			
3.518±0.010±0.120	143k	[1] ABLIKIM	17N	BES3	$\psi(2S) \to \gamma\gamma J/\psi$
3.442±0.010±0.132	1.9M	ABLIKIM	17U	BES3	$e^+e^- \to \gamma X$
2.81 ±0.05 ±0.23	13k	BAI	04I	BES2	$\psi(2S) \to J/\psi\gamma\gamma$
2.56 ±0.12 ±0.20		GAISER	86	CBAL	$\psi(2S) \to \gamma X$
2.78 ±0.30		[2] OREGLIA	82	CBAL	$\psi(2S) \to \gamma\chi_{c1}$
2.2 ±0.5		[3] BRANDELIK	79B	DASP	$\psi(2S) \to \gamma\chi_{c1}$
2.9 ±0.5		[3] BARTEL	78B	CNTR	$\psi(2S) \to \gamma\chi_{c1}$
5.0 ±1.5		[4] BIDDICK	77	CNTR	$e^+e^- \to \gamma X$
2.8 ±0.9		[2] WHITAKER	76	MRK1	e^+e^-
• • • We do not use the following data for averages, fits, limits, etc. • • •					
3.377±0.009±0.183	142k	[5] ABLIKIM	12O	BES3	$\psi(2S) \to \gamma\chi_{c1}$
3.56 ±0.03 ±0.12	24.9k	[6] MENDEZ	08	CLEO	$\psi(2S) \to \gamma\chi_{c1}$
3.44 ±0.06 ±0.13	3.7k	[7] ADAM	05A	CLEO	Repl. by MENDEZ 08

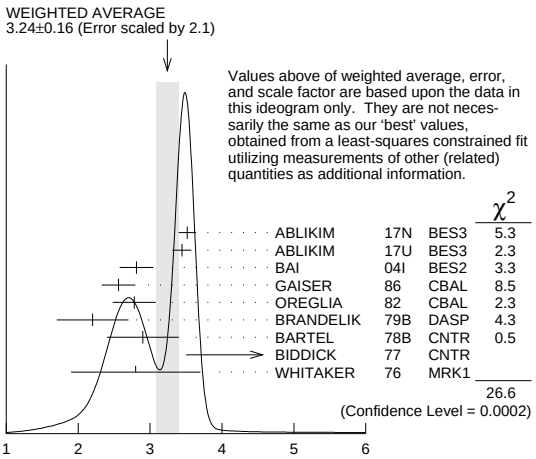

$\Gamma(\chi_{c1}(1P) \to \gamma J/\psi(1S))/\Gamma_{\text{total}} \times \Gamma(\psi(2S) \to \gamma\chi_{c1}(1P))/\Gamma_{\text{total}}$ (units 10^{-2})

[1] Uses B($J/\psi \to e^+e^-$) = (5.971 ± 0.032)% and B($J/\psi \to \mu^+\mu^-$) = (5.961 ± 0.033)%.
[2] Recalculated by us using B($J/\psi(1S) \to \ell^+\ell^-$) = 0.1181 ± 0.0020.
[3] Recalculated by us using B($J/\psi(1S) \to \mu^+\mu^-$) = 0.0588 ± 0.0010.
[4] Assumes isotropic gamma distribution.
[5] Superseded by ABLIKIM 17N.
[6] Not independent from other measurements of MENDEZ 08.
[7] Not independent from other values reported by ADAM 05A.

$\Gamma(\chi_{c1}(1P) \to \gamma J/\psi(1S))/\Gamma_{\text{total}} \times \Gamma(\psi(2S) \to \gamma\chi_{c1}(1P))/\Gamma(\psi(2S) \to J/\psi(1S)\text{anything})$ $\Gamma_{83}/\Gamma \times \Gamma_{140}^{\psi(2S)}/\Gamma_{9}^{\psi(2S)}$

$\Gamma_{83}/\Gamma \times \Gamma_{140}^{\psi(2S)}/\Gamma_{9}^{\psi(2S)} = \Gamma_{83}/\Gamma \times \Gamma_{140}^{\psi(2S)}/(\Gamma_{11}^{\psi(2S)} + \Gamma_{12}^{\psi(2S)} + \Gamma_{13}^{\psi(2S)} + 0.343\Gamma_{140}^{\psi(2S)} + 0.190\Gamma_{141}^{\psi(2S)})$

VALUE (units 10^{-2})	EVTS	DOCUMENT ID		TECN	COMMENT
5.44±0.10 OUR FIT					
• • • We do not use the following data for averages, fits, limits, etc. • • •					
5.70±0.04±0.15	24.9k	[1] MENDEZ	08	CLEO	$\psi(2S) \to \gamma\chi_{c1}$
5.77±0.10±0.12	3.7k	ADAM	05A	CLEO	Repl. by MENDEZ 08

[1] Not independent from other measurements of MENDEZ 08.

$\Gamma(\chi_{c1}(1P) \to \gamma J/\psi(1S))/\Gamma_{\text{total}} \times \Gamma(\psi(2S) \to \gamma\chi_{c1}(1P))/\Gamma(\psi(2S) \to J/\psi(1S)\pi^+\pi^-)$ $\Gamma_{83}/\Gamma \times \Gamma_{140}^{\psi(2S)}/\Gamma_{11}^{\psi(2S)}$

VALUE (units 10^{-2})	EVTS	DOCUMENT ID		TECN	COMMENT
9.63±0.17 OUR FIT					
10.15±0.28 OUR AVERAGE					
10.17±0.07±0.27	24.9k	MENDEZ	08	CLEO	$\psi(2S) \to \gamma\chi_{c1}$
12.6 ±0.3 ±3.8	3k	[1] ABLIKIM	04B	BES	$\psi(2S) \to J/\psi X$
8.5 ±2.1		[2] HIMEL	80	MRK2	$\psi(2S) \to \gamma\chi_{c1}$
• • • We do not use the following data for averages, fits, limits, etc. • • •					
10.24±0.17±0.23	3.7k	[3] ADAM	05A	CLEO	Repl. by MENDEZ 08

[1] From a fit to the J/ψ recoil mass spectra.
[2] The value for B($\psi(2S) \to \gamma\chi_{c1}$)×B($\chi_{c1} \to \gamma J/\psi(1S)$) quoted in HIMEL 80 is derived using B($\psi(2S) \to J/\psi(1S)\pi^+\pi^-$) = (33 ± 3)% and B($J/\psi(1S) \to \ell^+\ell^-$) = 0.138 ± 0.018. Calculated by us using B($J/\psi(1S) \to \ell^+\ell^-$) = 0.1181 ± 0.0020.
[3] Not independent from other values reported by ADAM 05A.

$\Gamma(\chi_{c1}(1P) \to \overline{K}^0K^+\pi^- + \text{c.c.})/\Gamma_{\text{total}} \times \Gamma(\psi(2S) \to \gamma\chi_{c1}(1P))/\Gamma_{\text{total}}$ $\Gamma_{17}/\Gamma \times \Gamma_{140}^{\psi(2S)}/\Gamma^{\psi(2S)}$

VALUE (units 10^{-4})	DOCUMENT ID		TECN	COMMENT
6.8±0.5 OUR FIT				
7.2±0.6 OUR AVERAGE				
7.3±0.5±0.5	[1] ATHAR	07	CLEO	$\psi(2S) \to \gamma K^0_S K^+\pi^-$
7.0±0.5±0.9	[2] ABLIKIM	06R	BES2	$\psi(2S) \to \gamma\chi_{c1}$

[1] Calculated by us. The value of B($\chi_{c1} \to K^0K^+\pi^-$ + c.c.) reported by ATHAR 07 was derived using B($\psi(2S) \to \gamma\chi_{c1}(1P)$) = (9.07 ± 0.11 ± 0.54)%.
[2] Calculated by us. ABLIKIM 06R reports B($\chi_{c1} \to K^0_S K^+\pi^-$) = (4.0 ± 0.3 ± 0.5) × 10^{-3}. We use B($\psi(2S) \to \gamma\chi_{c1}$) = (8.7 ± 0.4) × 10^{-2}.

$\Gamma(\chi_{c1}(1P) \to \overline{K}^0K^+\pi^- + \text{c.c.})/\Gamma_{\text{total}} \times \Gamma(\psi(2S) \to \gamma\chi_{c1}(1P))/\Gamma(\psi(2S) \to J/\psi(1S)\pi^+\pi^-)$ $\Gamma_{17}/\Gamma \times \Gamma_{140}^{\psi(2S)}/\Gamma_{11}^{\psi(2S)}$

VALUE (units 10^{-4})	DOCUMENT ID		TECN	COMMENT
19.6±1.6 OUR FIT				
13.2±2.4±3.2	[1] BAI	99B	BES	$\psi(2S) \to \gamma K^0_S K^+\pi^-$

[1] Calculated by us. The value of B($\chi_{c1} \to K^0_S K^+\pi^-$) reported by BAI 99B was derived using B($\psi(2S) \to \gamma\chi_{c1}(1P)$) = (8.7 ± 0.8)% and B($\psi(2S) \to J/\psi\pi^+\pi^-$) = (32.4 ± 2.6)% [BAI 98D].

$\Gamma(\chi_{c1}(1P) \to K^+K^-K^+K^-)/\Gamma_{\text{total}} \times \Gamma(\psi(2S) \to \gamma\chi_{c1}(1P))/\Gamma_{\text{total}}$ $\Gamma_{43}/\Gamma \times \Gamma_{140}^{\psi(2S)}/\Gamma^{\psi(2S)}$

VALUE (units 10^{-4})	EVTS	DOCUMENT ID		TECN	COMMENT
0.53±0.11 OUR FIT					
0.61±0.11±0.08	54	[1] ABLIKIM	06T	BES2	$\psi(2S) \to \gamma K^+K^+K^-K^-$

[1] Calculated by us. The value of B($\chi_{c1} \to 2K^+2K^-$) reported by ABLIKIM 06T was derived using B($\psi(2S) \to \gamma\chi_{c1}(1P)$) = (8.7 ± 0.8)%.

$\Gamma(\chi_{c1}(1P) \to K^+K^-K^+K^-)/\Gamma_{\text{total}} \times \Gamma(\psi(2S) \to \gamma\chi_{c1}(1P))/\Gamma(\psi(2S) \to J/\psi(1S)\pi^+\pi^-)$ $\Gamma_{43}/\Gamma \times \Gamma_{140}^{\psi(2S)}/\Gamma_{11}^{\psi(2S)}$

VALUE (units 10^{-4})	DOCUMENT ID		TECN	COMMENT
1.52±0.31 OUR FIT				
1.13±0.40±0.29	[1] BAI	99B	BES	$\psi(2S) \to \gamma K^+K^+K^-K^-$

[1] Calculated by us. The value of B($\chi_{c1} \to 2K^+2K^-$) reported by BAI 99B was derived using B($\psi(2S) \to \gamma\chi_{c1}(1P)$) = (8.7 ± 0.8)% and B($\psi(2S) \to J/\psi\pi^+\pi^-$) = (32.4 ± 2.6)% [BAI 98D].

Meson Particle Listings

$\chi_{c1}(1P)$, $h_c(1P)$

$\Gamma(\chi_{c1}(1P) \to p\overline{p})/\Gamma_{\text{total}} \times \Gamma(\psi(2S) \to \gamma\chi_{c1}(1P))/\Gamma_{\text{total}}$
$\Gamma_{52}/\Gamma \times \Gamma_{140}^{\psi(2S)}/\Gamma^{\psi(2S)}$

VALUE (units 10^{-6})	EVTS	DOCUMENT ID		TECN	COMMENT
7.41±0.35 OUR FIT					
7.8 ±0.6 OUR AVERAGE		Error includes scale factor of 1.4. See the ideogram below.			
7.9 ±0.4 ±0.3	453	ABLIKIM	13V	BES3	$\psi(2S) \to \gamma p\overline{p}$
8.2 ±0.7 ±0.4	141 ± 13	[1] NAIK	08	CLEO	$\psi(2S) \to \gamma p\overline{p}$
4.8 $^{+1.4}_{-1.3}$ ±0.6	$18.2^{+5.5}_{-4.9}$	BAI	04F	BES	$\psi(2S) \to \gamma\chi_{c1}(1P) \to \gamma p\overline{p}$

[1] Calculated by us. NAIK 08 reports $B(\chi_{c1} \to p\overline{p}) = (9.0 \pm 0.8 \pm 0.4 \pm 0.5) \times 10^{-5}$ using $B(\psi(2S) \to \gamma\chi_{c1}) = (9.07 \pm 0.11 \pm 0.54)\%$.

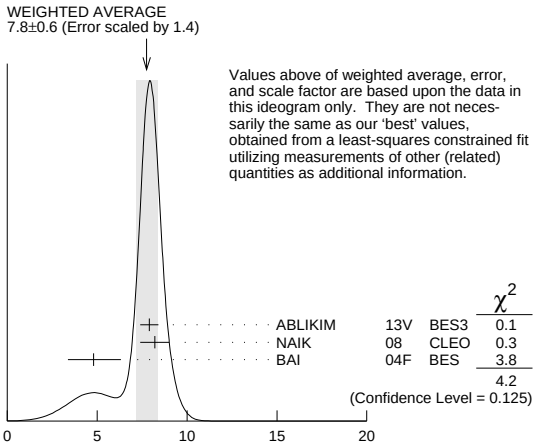

$\Gamma(\chi_{c1}(1P) \to p\overline{p})/\Gamma_{\text{total}} \times \Gamma(\psi(2S) \to \gamma\chi_{c1}(1P))/\Gamma_{\text{total}}$ (units 10^{-6})

MULTIPOLE AMPLITUDES IN $\chi_{c1}(1P) \to \gamma J/\psi(1S)$

$a_2 = M2/\sqrt{E1^2 + M2^2}$ Magnetic quadrupole fractional transition amplitude

VALUE (units 10^{-2})	EVTS	DOCUMENT ID		TECN	COMMENT
−6.7 ±0.9 OUR AVERAGE		Error includes scale factor of 2.6. See the ideogram below.			
−7.40±0.33±0.34	164k	[1] ABLIKIM	17N	BES3	$\psi(2S) \to \gamma\gamma\ell^+\ell^-$
−6.26±0.63±0.24	39k	ARTUSO	09	CLEO	$\psi(2S) \to \gamma\gamma\ell^+\ell^-$
0.2 ±3.2 ±0.4	2090	AMBROGIANI	02	E835	$p\overline{p} \to \chi_{c1} \to J/\psi\gamma$
−0.2 $^{+0.8}_{-2.0}$	921	OREGLIA	82	CBAL	$\psi(2S) \to \chi_{c1}\gamma \to J/\psi\gamma\gamma$

[1] Correlated with b_2 with correlation coefficient $\rho_{a_2 b_2} = 0.133$.

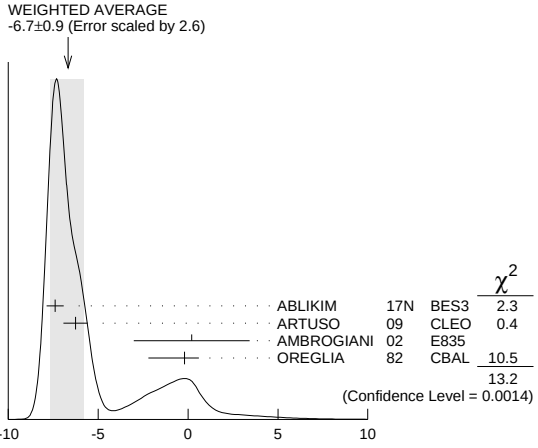

$a_2 = M2/\sqrt{E1^2 + M2^2}$ (units 10^{-2})

MULTIPOLE AMPLITUDES IN $\psi(2S) \to \gamma\chi_{c1}(1S)$ RADIATIVE DECAY

$b_2 = M2/\sqrt{E1^2 + M2^2}$ Magnetic quadrupole fractional transition amplitude

VALUE (units 10^{-2})	EVTS	DOCUMENT ID		TECN	COMMENT
2.5 ±0.4 OUR AVERAGE					
2.29±0.39±0.27	164k	[1] ABLIKIM	17N	BES3	$\psi(2S) \to \gamma\gamma\ell^+\ell^-$
2.76±0.73±0.23	39k	ARTUSO	09	CLEO	$\psi(2S) \to \gamma\gamma\ell^+\ell^-$
7.7 $^{+5.0}_{-4.5}$	921	OREGLIA	82	CBAL	$\psi(2S) \to \gamma\gamma\ell^+\ell^-$

[1] Correlated with a_2 with correlation coefficient $\rho_{a_2 b_2} = 0.133$.

MULTIPOLE AMPLITUDE RATIOS IN RADIATIVE DECAYS $\psi(2S) \to \gamma\chi_{c1}(1S)$ and $\chi_{c1} \to \gamma J/\psi(1S)$

a_2/b_2 Magnetic quadrupole transition amplitude ratio

VALUE	EVTS	DOCUMENT ID		TECN	COMMENT
$-2.27^{+0.57}_{-0.99}$	39k	[1] ARTUSO	09	CLEO	$\psi(2S) \to \gamma\gamma\ell^+\ell^-$

[1] Statistical and systematic errors combined. Not independent of $a_2(\chi_{c1})$ and $b_2(\chi_{c1})$ values from ARTUSO 09.

$\chi_{c1}(1P)$ REFERENCES

AAIJ	17BB	EPJ C77 609	R. Aaij *et al.*	(LHCb Collab.)
AAIJ	17BI	PRL 119 221801	R. Aaij *et al.*	(LHCb Collab.)
ABLIKIM	17AE	PR D96 092007	M. Ablikim *et al.*	(BES III Collab.)
ABLIKIM	17I	PRL 118 221802	M. Ablikim *et al.*	(BES III Collab.)
ABLIKIM	17K	PR D95 032002	M. Ablikim *et al.*	(BES III Collab.)
ABLIKIM	17N	PR D95 072004	M. Ablikim *et al.*	(BES III Collab.)
ABLIKIM	17U	PR D96 032001	M. Ablikim *et al.*	(BES III Collab.)
PDG	16	CP C40 100001	C. Patrignani *et al.*	(PDG Collab.)
ABLIKIM	15I	PR D91 092006	M. Ablikim *et al.*	(BES III Collab.)
ABLIKIM	15M	PR D91 112008	M. Ablikim *et al.*	(BES III Collab.)
ABLIKIM	14J	PR D89 074030	M. Ablikim *et al.*	(BES III Collab.)
ABLIKIM	13B	PR D87 012002	M. Ablikim *et al.*	(BES III Collab.)
ABLIKIM	13D	PR D87 012007	M. Ablikim *et al.*	(BES III Collab.)
ABLIKIM	13H	PR D87 032007	M. Ablikim *et al.*	(BES III Collab.)
ABLIKIM	13V	PR D88 112001	M. Ablikim *et al.*	(BES III Collab.)
ABLIKIM	12I	PR D86 052004	M. Ablikim *et al.*	(BES III Collab.)
ABLIKIM	12J	PR D86 052011	M. Ablikim *et al.*	(BES III Collab.)
ABLIKIM	12O	PRL 109 172002	M. Ablikim *et al.*	(BES III Collab.)
ABLIKIM	11A	PR D83 012006	M. Ablikim *et al.*	(BES III Collab.)
ABLIKIM	11D	PR D83 032003	M. Ablikim *et al.*	(BES III Collab.)
ABLIKIM	11E	PR D83 112005	M. Ablikim *et al.*	(BES III Collab.)
ABLIKIM	11F	PR D83 112009	M. Ablikim *et al.*	(BES III Collab.)
ABLIKIM	11K	PRL 107 092001	M. Ablikim *et al.*	(BES III Collab.)
ONYISI	10	PR D82 011103	P.U.E. Onyisi *et al.*	(CLEO Collab.)
ARTUSO	09	PR D80 112003	M. Artuso *et al.*	(CLEO Collab.)
BENNETT	08A	PRL 101 151801	J.V. Bennett *et al.*	(CLEO Collab.)
ECKLUND	08A	PR D78 091501	K.M. Ecklund *et al.*	(CLEO Collab.)
HE	08B	PR D78 092004	Q. He *et al.*	(CLEO Collab.)
MENDEZ	08	PR D78 011102	H. Mendez *et al.*	(CLEO Collab.)
NAIK	08	PR D78 031101	P. Naik *et al.*	(CLEO Collab.)
ATHAR	07	PR D75 032002	S.B. Athar *et al.*	(CLEO Collab.)
ABLIKIM	06D	PR D73 052006	M. Ablikim *et al.*	(BES Collab.)
ABLIKIM	06R	PR D74 072001	M. Ablikim *et al.*	(BES Collab.)
ABLIKIM	06T	PL B642 197	M. Ablikim *et al.*	(BES Collab.)
ABLIKIM	05G	PR D71 092002	M. Ablikim *et al.*	(BES Collab.)
ABLIKIM	05O	PL B630 21	M. Ablikim *et al.*	(BES Collab.)
ADAM	05A	PRL 94 232002	N.E. Adam *et al.*	(CLEO Collab.)
ANDREOTTI	05A	NP B717 34	M. Andreotti *et al.*	(FNAL E835 Collab.)
ABLIKIM	04B	PR D70 012003	M. Ablikim *et al.*	(BES Collab.)
ABLIKIM	04H	PR D70 092003	M. Ablikim *et al.*	(BES Collab.)
ATHAR	04	PR D70 112002	S.B. Athar *et al.*	(CLEO Collab.)
BAI	04F	PR D69 092001	J.Z. Bai *et al.*	(BES Collab.)
BAI	04I	PR D70 012006	J.Z. Bai *et al.*	(BES Collab.)
AULCHENKO	03	PL B573 63	V.M. Aulchenko *et al.*	(KEDR Collab.)
BAI	03E	PR D67 112001	J.Z. Bai *et al.*	(BES Collab.)
AMBROGIANI	02	PR D65 052002	M. Ambrogiani *et al.*	(FNAL E835 Collab.)
BAI	99B	PR D60 072001	J.Z. Bai *et al.*	(BES Collab.)
BAI	98D	PR D58 092006	J.Z. Bai *et al.*	(BES Collab.)
BAI	98I	PRL 81 3091	J.Z. Bai *et al.*	(BES Collab.)
ARMSTRONG	92	NP B373 35	T.A. Armstrong *et al.*	(FNAL, FERR, GENO+)
Also		PRL 68 1468	T.A. Armstrong *et al.*	(FNAL, FERR, GENO+)
BAGLIN	86B	PL B172 455	C. Baglin	(LAPP, CERN, GENO, LYON, OSLO+)
GAISER	86	PR D34 711	J. Gaiser *et al.*	(Crystal Ball Collab.)
LEMOIGNE	82	PL 113B 509	Y. Lemoigne *et al.*	(SACL, LOIC, SHMP+)
OREGLIA	82	PR D25 2259	M.J. Oreglia *et al.*	(SLAC, CIT, HARV+)
Also		Private Comm.	M.J. Oreglia	(EFI)
HIMEL	80	PRL 44 920	T. Himel *et al.*	(LBL, SLAC)
Also		Private Comm.	G. Trilling	(LBL, UCB)
BRANDELIK	79B	NP B160 426	R. Brandelik *et al.*	(DASP Collab.)
BARTEL	78B	PL 79B 492	W. Bartel *et al.*	(DESY, HEIDP)
TANENBAUM	78	PR D17 1731	W.M. Tanenbaum *et al.*	(SLAC, LBL)
Also		Private Comm.	G. Trilling	(LBL, UCB)
BIDDICK	77	PRL 38 1324	C.J. Biddick *et al.*	(UCSD, UMD, PAVI+)
FELDMAN	77	PRPL 33C 285	G.J. Feldman, M.L. Perl	(LBL, SLAC)
YAMADA	77	Hamburg Conf. 69	S. Yamada	(DASP Collab.)
WHITAKER	76	PRL 37 1596	J.S. Whitaker *et al.*	(SLAC, LBL)
TANENBAUM	75	PRL 35 1323	W.M. Tanenbaum *et al.*	(LBL, SLAC)

$h_c(1P)$

$I^G(J^{PC}) = ?^?(1^{+-})$

Quantum numbers are quark model prediction, $C = -$ established by $\eta_c\gamma$ decay.

$h_c(1P)$ MASS

VALUE (MeV)	EVTS	DOCUMENT ID		TECN	COMMENT
3525.38±0.11 OUR AVERAGE					
3525.31±0.11±0.14	832	[1] ABLIKIM	12N	BES3	$\psi(2S) \to \pi^0\gamma$ hadrons
3525.40±0.13±0.18	3679	ABLIKIM	10B	BES3	$\psi(2S) \to \pi^0\gamma\eta_c$
3525.20±0.18±0.12	1282	[2] DOBBS	08A	CLEO	$\psi(2S) \to \pi^0\eta_c\gamma$
3525.8 ±0.2 ±0.2	13	ANDREOTTI	05B	E835	$\overline{p}p \to \eta_c\gamma$
• • • We do not use the following data for averages, fits, limits, etc. • • •					
3525.6 ±0.5	92^{+23}_{-22}	ADAMS	09	CLEO	$\psi(2S) \to 2(\pi^+\pi^-\pi^0)$
3524.4 ±0.6 ±0.4	168 ± 40	[3] ROSNER	05	CLEO	$\psi(2S) \to \pi^0\eta_c\gamma$
3527 ±8	42	ANTONIAZZI	94	E705	300 $\pi^\pm$, pLi $\to$ $J/\psi\pi^0$X
3526.28±0.18±0.19	59	[4] ARMSTRONG	92D	E760	$\overline{p}p \to J/\psi\pi^0$
3525.4 ±0.8 ±0.4	5	BAGLIN	86	SPEC	$\overline{p}p \to J/\psi$X

[1] With floating width.

[2] Combination of exclusive and inclusive analyses for the reaction $\psi(2S) \to \pi^0 h_c \to \pi^0\eta_c\gamma$. This result is the average of DOBBS 08A and ROSNER 05.

[3] Superseded by DOBBS 08A.
[4] Mass central value and systematic error recalculated by us according to Eq. (16) in ARMSTRONG 93B, using the value for the $\psi(2S)$ mass from AULCHENKO 03.

$h_c(1P)$ WIDTH

VALUE (MeV)	CL%	EVTS	DOCUMENT ID		TECN	COMMENT
0.70±0.28±0.22		832	[1] ABLIKIM	12N	BES3	$\psi(2S) \to \pi^0\gamma$ hadrons
• • • We do not use the following data for averages, fits, limits, etc. • • •						
< 1.44	90	3679	[2] ABLIKIM	10B	BES3	$\psi(2S) \to \pi^0\gamma\eta_c$
< 1		13	ANDREOTTI	05B	E835	$\overline{p}p \to \eta_c\gamma$
< 1.1	90	59	ARMSTRONG	92D	E760	$\overline{p}p \to J/\psi\pi^0$

[1] With floating mass.
[2] The central value is $\Gamma = 0.73 \pm 0.45 \pm 0.28$ MeV.

$h_c(1P)$ DECAY MODES

	Mode	Fraction (Γ_i/Γ)	Confidence level
Γ_1	$J/\psi(1S)\pi^0$		
Γ_2	$J/\psi(1S)\pi\pi$	not seen	
Γ_3	$p\overline{p}$	$< 1.5 \times 10^{-4}$	90%
Γ_4	$\pi^+\pi^-\pi^0$	$< 2.2 \times 10^{-3}$	
Γ_5	$2\pi^+2\pi^-\pi^0$	$(2.2^{+0.8}_{-0.7})$ %	
Γ_6	$3\pi^+3\pi^-\pi^0$	< 2.9 %	
	Radiative decays		
Γ_7	$\gamma\eta$	$(4.7\pm2.1)\times10^{-4}$	
Γ_8	$\gamma\eta'(958)$	$(1.5\pm0.4)\times10^{-3}$	
Γ_9	$\gamma\eta_c(1S)$	(51 ±6) %	

$h_c(1P)$ PARTIAL WIDTHS

$h_c(1P)$ Γ(i)$\Gamma(\overline{p}p)/\Gamma$(total)

$\Gamma(\gamma\eta_c(1S)) \times \Gamma(p\overline{p})/\Gamma_{\text{total}}$ $\Gamma_9\Gamma_3/\Gamma$

VALUE (eV)	EVTS	DOCUMENT ID		TECN	COMMENT
• • • We do not use the following data for averages, fits, limits, etc. • • •					
12.0±4.5	13	[1] ANDREOTTI	05B	E835	$\overline{p}p \to \eta_c\gamma$

[1] Assuming $\Gamma = 1$ MeV.

$h_c(1P)$ BRANCHING RATIOS

$\Gamma(J/\psi(1S)\pi\pi)/\Gamma(J/\psi(1S)\pi^0)$ Γ_2/Γ_1

VALUE	CL%	DOCUMENT ID		TECN	COMMENT
<0.18	90	ARMSTRONG	92D	E760	$\overline{p}p \to J/\psi\pi^0$

$\Gamma(\pi^+\pi^-\pi^0)/\Gamma_{\text{total}}$ Γ_4/Γ

VALUE (units 10^{-3})	DOCUMENT ID		TECN	COMMENT
<2.2	[1] ADAMS	09	CLEO	$\psi(2S) \to \pi^0\gamma\eta_c$

[1] ADAMS 09 reports $[\Gamma(h_c(1P) \to \pi^+\pi^-\pi^0)/\Gamma_{\text{total}}] \times [B(\psi(2S) \to \pi^0 h_c(1P))] < 0.19\times10^{-5}$ which we divide by our best value $B(\psi(2S) \to \pi^0 h_c(1P)) = 8.6\times10^{-4}$.

$\Gamma(2\pi^+2\pi^-\pi^0)/\Gamma_{\text{total}}$ Γ_5/Γ

VALUE (units 10^{-2})	EVTS	DOCUMENT ID		TECN	COMMENT
$2.2^{+0.8}_{-0.6}\pm0.3$	92	[1] ADAMS	09	CLEO	$\psi(2S) \to \pi^0\gamma\eta_c$

[1] ADAMS 09 reports $[\Gamma(h_c(1P) \to 2\pi^+2\pi^-\pi^0)/\Gamma_{\text{total}}] \times [B(\psi(2S) \to \pi^0 h_c(1P))] = (1.88^{+0.48+0.47}_{-0.45-0.30})\times10^{-5}$ which we divide by our best value $B(\psi(2S) \to \pi^0 h_c(1P)) = (8.6\pm1.3)\times10^{-4}$. Our first error is their experiment's error and our second error is the systematic error from using our best value.

$\Gamma(3\pi^+3\pi^-\pi^0)/\Gamma_{\text{total}}$ Γ_6/Γ

VALUE (units 10^{-2})	DOCUMENT ID		TECN	COMMENT
<2.9	[1] ADAMS	09	CLEO	$\psi(2S) \to \pi^0\gamma\eta_c$

[1] ADAMS 09 reports $[\Gamma(h_c(1P) \to 3\pi^+3\pi^-\pi^0)/\Gamma_{\text{total}}] \times [B(\psi(2S) \to \pi^0 h_c(1P))] < 2.5\times10^{-5}$ which we divide by our best value $B(\psi(2S) \to \pi^0 h_c(1P)) = 8.6\times10^{-4}$.

RADIATIVE DECAYS

$\Gamma(\gamma\eta)/\Gamma_{\text{total}}$ Γ_7/Γ

VALUE (units 10^{-4})	EVTS	DOCUMENT ID		TECN	COMMENT
4.7±1.5±1.4	18	ABLIKIM	16I	BES3	$\psi(2S) \to \pi^0\gamma\eta$

$\Gamma(\gamma\eta'(958))/\Gamma_{\text{total}}$ Γ_8/Γ

VALUE (units 10^{-3})	EVTS	DOCUMENT ID		TECN	COMMENT
1.52±0.27±0.29	44	ABLIKIM	16I	BES3	$\psi(2S) \to \pi^0\gamma\eta'(958)$

$\Gamma(\gamma\eta_c(1S))/\Gamma_{\text{total}}$ Γ_9/Γ

VALUE (units 10^{-2})	EVTS	DOCUMENT ID		TECN	COMMENT
51 ± 6 OUR AVERAGE					
54.3± 6.7±5.2	3679	ABLIKIM	10B	BES3	$\psi(2S) \to \pi^0\gamma\eta_c$
48 ± 6 ±7		[1] DOBBS	08A	CLEO	$\psi(2S) \to \pi^0\eta_c\gamma$
• • • We do not use the following data for averages, fits, limits, etc. • • •					
48 ± 6 ±7	1282	[2] DOBBS	08A	CLEO	$\psi(2S) \to \pi^0\eta_c\gamma$
46 ±12 ±7	168	[3] ROSNER	05	CLEO	$\psi(2S) \to \pi^0\eta_c\gamma$

[1] Average of DOBBS 08A and ROSNER 05. DOBBS 08A reports $[\Gamma(h_c(1P) \to \gamma\eta_c(1S))/\Gamma_{\text{total}}] \times [B(\psi(2S) \to \pi^0 h_c(1P))] = (4.16\pm0.30\pm0.37)\times10^{-4}$ which we divide by our best value $B(\psi(2S) \to \pi^0 h_c(1P)) = (8.6\pm1.3)\times10^{-4}$. Our first error is their experiment's error and our second error is the systematic error from using our best value.
[2] DOBBS 08A reports $[\Gamma(h_c(1P) \to \gamma\eta_c(1S))/\Gamma_{\text{total}}] \times [B(\psi(2S) \to \pi^0 h_c(1P))] = (4.19\pm0.32\pm0.45)\times10^{-4}$ which we divide by our best value $B(\psi(2S) \to \pi^0 h_c(1P)) = (8.6\pm1.3)\times10^{-4}$. Our first error is their experiment's error and our second error is the systematic error from using our best value.
[3] ROSNER 05 reports $[\Gamma(h_c(1P) \to \gamma\eta_c(1S))/\Gamma_{\text{total}}] \times [B(\psi(2S) \to \pi^0 h_c(1P))] = (4.0\pm0.8\pm0.7)\times10^{-4}$ which we divide by our best value $B(\psi(2S) \to \pi^0 h_c(1P)) = (8.6\pm1.3)\times10^{-4}$. Our first error is their experiment's error and our second error is the systematic error from using our best value.

CROSS-PARTICLE BRANCHING RATIOS

$\Gamma(h_c(1P) \to p\overline{p})/\Gamma_{\text{total}} \times \Gamma(\psi(2S) \to \pi^0 h_c(1P))/\Gamma_{\text{total}}$ $\Gamma_3/\Gamma \times \Gamma_{15}^{\psi(2S)}/\Gamma^{\psi(2S)}$

VALUE	CL%	DOCUMENT ID		TECN	COMMENT
$<1.3\times10^{-7}$	90	ABLIKIM	13V	BES3	$\psi(2S) \to \gamma p\overline{p}$

$\Gamma(h_c(1P) \to \gamma\eta_c(1S))/\Gamma_{\text{total}} \times \Gamma(\psi(2S) \to \pi^0 h_c(1P))/\Gamma_{\text{total}}$ $\Gamma_9/\Gamma \times \Gamma_{15}^{\psi(2S)}/\Gamma^{\psi(2S)}$

VALUE (units 10^{-4})	EVTS	DOCUMENT ID		TECN	COMMENT
4.3 ±0.4 OUR AVERAGE					
4.58±0.40±0.50	3679	[1] ABLIKIM	10B	BES3	$\psi(2S) \to \pi^0\gamma X$
4.16±0.30±0.37	1430	[2] DOBBS	08A	CLEO	$\psi(2S) \to \pi^0\gamma\eta_c$

[1] Not independent of other branching fractions in ABLIKIM 10B.
[2] Not independent of other branching fractions in DOBBS 08A.

$h_c(1P)$ REFERENCES

ABLIKIM	16I	PRL 116 251802	M. Ablikim *et al.*	(BES III Collab.)
ABLIKIM	13V	PR D88 112001	M. Ablikim *et al.*	(BES III Collab.)
ABLIKIM	12N	PR D86 092009	M. Ablikim *et al.*	(BES III Collab.)
ABLIKIM	10B	PRL 104 132002	M. Ablikim *et al.*	(BES III Collab.)
ADAMS	09	PR D80 051106	G.S. Adams *et al.*	(CLEO Collab.)
DOBBS	08A	PRL 101 182003	S. Dobbs *et al.*	(CLEO Collab.)
ANDREOTTI	05B	PR D72 032001	M. Andreotti *et al.*	(FNAL E835 Collab.)
ROSNER	05	PRL 95 102003	J.L. Rosner *et al.*	(CLEO Collab.)
AULCHENKO	03	PL B573 63	V.M. Aulchenko *et al.*	(KEDR Collab.)
ANTONIAZZI	94	PR D50 4258	L. Antoniazzi *et al.*	(E705 Collab.)
ARMSTRONG	93B	PR D47 772	T.A. Armstrong *et al.*	(FNAL E760 Collab.)
ARMSTRONG	92D	PRL 69 2337	T.A. Armstrong *et al.*	(FNAL, FERR, GENO+)
BAGLIN	86	PL B171 135	C. Baglin *et al.*	(LAPP, CERN, TORI, STRB+)

$\chi_{c2}(1P)$

$I^G(J^{PC}) = 0^+(2^{++})$

See the Review on "$\psi(2S)$ and χ_c branching ratios" before the $\chi_{c0}(1P)$ Listings.

$\chi_{c2}(1P)$ MASS

VALUE (MeV)	EVTS	DOCUMENT ID		TECN	COMMENT
3556.17 ± 0.07 OUR AVERAGE					
3557.3 ± 1.7 ±0.7	611	[1] AAIJ	17BB	LHCB	$pp \to b\overline{b}X \to 2(K^+K^-)X$
3556.10 ± 0.06 ±0.11	4.0k	[2] AAIJ	17BI	LHCB	$\chi_{c2} \to J/\psi\mu^+\mu^-$
3555.3 ± 0.6 ±2.2	2.5k	UEHARA	08	BELL	$\gamma\gamma \to$ hadrons
3555.70 ± 0.59 ±0.39		ABLIKIM	05G	BES2	$\psi(2S) \to \gamma\chi_{c2}$
3556.173± 0.123±0.020		ANDREOTTI	05A	E835	$p\overline{p} \to e^+e^-\gamma$
3559.9 ± 2.9		EISENSTEIN	01	CLE2	$e^+e^- \to e^+e^-\chi_{c2}$
3556.4 ± 0.7		BAI	99B	BES	$\psi(2S) \to \gamma$X
3556.22 ± 0.131±0.020	585	[3] ARMSTRONG	92	E760	$\overline{p}p \to e^+e^-\gamma$
3556.9 ± 0.4 ±0.5	50	BAGLIN	86B	SPEC	$\overline{p}p \to e^+e^-$X
3557.8 ± 0.2 ±4		[4] GAISER	86	CBAL	$\psi(2S) \to \gamma$X
3553.4 ± 2.2	66	[5] LEMOIGNE	82	GOLI	185 π^-Be $\to \gamma\mu^+\mu^-$A
3555.9 ± 0.7		[6] OREGLIA	82	CBAL	$e^+e^- \to J/\psi 2\gamma$
3557 ± 1.5	69	[7] HIMEL	80	MRK2	$e^+e^- \to J/\psi 2\gamma$
3551 ±11	15	BRANDELIK	79B	DASP	$e^+e^- \to J/\psi 2\gamma$
3553 ± 4		[7] BARTEL	78B	CNTR	$e^+e^- \to J/\psi 2\gamma$
3553 ± 4 ±4		[7,8] TANENBAUM	78	MRK1	e^+e^-
3563 ± 7	360	[7] BIDDICK	77	CNTR	$e^+e^- \to \gamma$X
• • • We do not use the following data for averages, fits, limits, etc. • • •					
3555.4 ± 1.3	53	UEHARA	13	BELL	$\gamma\gamma \to K^0_S K^0_S$
3543 ±10	4	WHITAKER	76	MRK1	$e^+e^- \to J/\psi 2\gamma$

Meson Particle Listings

$\chi_{c2}(1P)$

[1] From a fit of the $\phi\phi$ invariant mass with the width of $\chi_{c2}(1P)$ fixed to the PDG 16 value.
[2] AAIJ 17BI reports also $m(\chi_{c2}) - m(\chi_{c1}) = 45.39 \pm 0.07 \pm 0.03$ MeV.
[3] Recalculated by ANDREOTTI 05A, using the value of $\psi(2S)$ mass from AULCHENKO 03.
[4] Using mass of $\psi(2S) = 3686.0$ MeV.
[5] $J/\psi(1S)$ mass constrained to 3097 MeV.
[6] Assuming $\psi(2S)$ mass = 3686 MeV and $J/\psi(1S)$ mass = 3097 MeV.
[7] Mass value shifted by us by amount appropriate for $\psi(2S)$ mass = 3686 MeV and $J/\psi(1S)$ mass = 3097 MeV.
[8] From a simultaneous fit to radiative and hadronic decay channels.

$\chi_{c2}(1P)$ WIDTH

VALUE (MeV)	EVTS	DOCUMENT ID		TECN	COMMENT
1.97 ±0.09 OUR FIT					
2.00 ±0.11 OUR AVERAGE					
2.10 ±0.20 ±0.02	4.0k	AAIJ	17BI	LHCB	$\chi_{c2} \to J/\psi\mu^+\mu^-$
1.915±0.188±0.013		ANDREOTTI	05A	E835	$p\overline{p} \to e^+e^-\gamma$
1.96 ±0.17 ±0.07	585	[1] ARMSTRONG	92	E760	$\overline{p}p \to e^+e^-\gamma$
2.6 $^{+1.4}_{-1.0}$	50	BAGLIN	86B	SPEC	$\overline{p}p \to e^+e^-$X
2.8 $^{+2.1}_{-2.0}$		[2] GAISER	86	CBAL	$\psi(2S) \to \gamma$X

[1] Recalculated by ANDREOTTI 05A.
[2] Errors correspond to 90% confidence level; authors give only width range.

$\chi_{c2}(1P)$ DECAY MODES

	Mode	Fraction (Γ_i/Γ)	Confidence level
	Hadronic decays		
Γ_1	$2(\pi^+\pi^-)$	(1.02±0.09) %	
Γ_2	$\rho\rho$		
Γ_3	$\pi^+\pi^-\pi^0\pi^0$	(1.83±0.23) %	
Γ_4	$\rho^+\pi^-\pi^0$ + c.c.	(2.19±0.34) %	
Γ_5	$4\pi^0$	(1.11±0.15) $\times 10^{-3}$	
Γ_6	$K^+K^-\pi^0\pi^0$	(2.1 ±0.4) $\times 10^{-3}$	
Γ_7	$K^+\pi^-\overline{K}^0\pi^0$ + c.c.	(1.38±0.20) %	
Γ_8	$\rho^- K^+\overline{K}^0$ + c.c.	(4.1 ±1.2) $\times 10^{-3}$	
Γ_9	$K^*(892)^0 K^-\pi^+ \to K^-\pi^+ K^0\pi^0$ + c.c.	(2.9 ±0.8) $\times 10^{-3}$	
Γ_{10}	$K^*(892)^0\overline{K}^0\pi^0 \to K^+\pi^-\overline{K}^0\pi^0$ + c.c.	(3.8 ±0.9) $\times 10^{-3}$	
Γ_{11}	$K^*(892)^- K^+\pi^0 \to K^+\pi^-\overline{K}^0\pi^0$ + c.c.	(3.7 ±0.8) $\times 10^{-3}$	
Γ_{12}	$K^*(892)^+\overline{K}^0\pi^- \to K^+\pi^-\overline{K}^0\pi^0$ + c.c.	(2.9 ±0.8) $\times 10^{-3}$	
Γ_{13}	$K^+K^-\eta\pi^0$	(1.3 ±0.4) $\times 10^{-3}$	
Γ_{14}	$K^+K^-\pi^+\pi^-$	(8.4 ±0.9) $\times 10^{-3}$	
Γ_{15}	$K^+K^-\pi^+\pi^-\pi^0$	(1.17±0.13) %	
Γ_{16}	$K^0_S K^\pm\pi^\mp\pi^+\pi^-$	(7.3 ±0.8) $\times 10^{-3}$	
Γ_{17}	$K^+\overline{K}^*(892)^0\pi^-$ + c.c.	(2.1 ±1.1) $\times 10^{-3}$	
Γ_{18}	$K^*(892)^0\overline{K}^*(892)^0$	(2.3 ±0.4) $\times 10^{-3}$	
Γ_{19}	$3(\pi^+\pi^-)$	(8.6 ±1.8) $\times 10^{-3}$	
Γ_{20}	$\phi\phi$	(1.06±0.09) $\times 10^{-3}$	
Γ_{21}	$\omega\omega$	(8.4 ±1.0) $\times 10^{-4}$	
Γ_{22}	ωK^+K^-	(7.3 ±0.9) $\times 10^{-4}$	
Γ_{23}	$\omega\phi$		
Γ_{24}	$\pi\pi$	(2.23±0.09) $\times 10^{-3}$	
Γ_{25}	$\rho^0\pi^+\pi^-$	(3.7 ±1.6) $\times 10^{-3}$	
Γ_{26}	$\pi^+\pi^-\pi^0$ (non-resonant)	(2.0 ±0.4) $\times 10^{-5}$	
Γ_{27}	$\rho(770)^\pm\pi^\mp$	(6 ±4) $\times 10^{-6}$	
Γ_{28}	$\pi^+\pi^-\eta$	(4.8 ±1.3) $\times 10^{-4}$	
Γ_{29}	$\pi^+\pi^-\eta'$	(5.0 ±1.8) $\times 10^{-4}$	
Γ_{30}	$\eta\eta$	(5.4 ±0.4) $\times 10^{-4}$	
Γ_{31}	K^+K^-	(1.01±0.06) $\times 10^{-3}$	
Γ_{32}	$K^0_S K^0_S$	(5.2 ±0.4) $\times 10^{-4}$	
Γ_{33}	$K^*(892)^\pm K^\mp$	(1.44±0.21) $\times 10^{-4}$	
Γ_{34}	$K^*(892)^0\overline{K}^0$ + c.c.	(1.24±0.27) $\times 10^{-4}$	
Γ_{35}	$K^*_2(1430)^\pm K^\mp$	(1.48±0.12) $\times 10^{-3}$	
Γ_{36}	$K^*_2(1430)^0\overline{K}^0$ + c.c.	(1.24±0.17) $\times 10^{-3}$	
Γ_{37}	$K^*_3(1780)^\pm K^\mp$	(5.2 ±0.8) $\times 10^{-4}$	
Γ_{38}	$K^*_3(1780)^0\overline{K}^0$ + c.c.	(5.6 ±2.1) $\times 10^{-4}$	
Γ_{39}	$a_2(1320)^0\pi^0$	(1.29±0.34) $\times 10^{-3}$	
Γ_{40}	$a_2(1320)^\pm\pi^\mp$	(1.8 ±0.6) $\times 10^{-3}$	
Γ_{41}	$\overline{K}^0 K^+\pi^-$ + c.c.	(1.28±0.18) $\times 10^{-3}$	
Γ_{42}	$K^+K^-\pi^0$	(3.0 ±0.8) $\times 10^{-4}$	
Γ_{43}	$K^+K^-\eta$	< 3.2 $\times 10^{-4}$	90%
Γ_{44}	$K^+K^-\eta'(958)$	(1.94±0.34) $\times 10^{-4}$	
Γ_{45}	$\eta\eta'$	(2.2 ±0.5) $\times 10^{-5}$	
Γ_{46}	$\eta'\eta'$	(4.6 ±0.6) $\times 10^{-5}$	
Γ_{47}	$\pi^+\pi^- K^0_S K^0_S$	(2.2 ±0.5) $\times 10^{-3}$	
Γ_{48}	$K^+K^- K^0_S K^0_S$	< 4 $\times 10^{-4}$	90%
Γ_{49}	$K^+K^-K^+K^-$	(1.65±0.20) $\times 10^{-3}$	
Γ_{50}	$K^+K^-\phi$	(1.42±0.29) $\times 10^{-3}$	
Γ_{51}	$\overline{K}^0 K^+\pi^-\phi$ + c.c.	(4.8 ±0.7) $\times 10^{-3}$	
Γ_{52}	$K^+K^-\pi^0\phi$	(2.7 ±0.5) $\times 10^{-3}$	
Γ_{53}	$\phi\pi^+\pi^-\pi^0$	(9.3 ±1.2) $\times 10^{-4}$	
Γ_{54}	$p\overline{p}$	(7.33±0.33) $\times 10^{-5}$	
Γ_{55}	$p\overline{p}\pi^0$	(4.7 ±0.4) $\times 10^{-4}$	
Γ_{56}	$p\overline{p}\eta$	(1.74±0.25) $\times 10^{-4}$	
Γ_{57}	$p\overline{p}\omega$	(3.6 ±0.4) $\times 10^{-4}$	
Γ_{58}	$p\overline{p}\phi$	(2.8 ±0.9) $\times 10^{-5}$	
Γ_{59}	$p\overline{p}\pi^+\pi^-$	(1.32±0.34) $\times 10^{-3}$	
Γ_{60}	$p\overline{p}\pi^0\pi^0$	(7.8 ±2.3) $\times 10^{-4}$	
Γ_{61}	$p\overline{p}K^+K^-$ (non-resonant)	(1.91±0.32) $\times 10^{-4}$	
Γ_{62}	$p\overline{p}K^0_S K^0_S$	< 7.9 $\times 10^{-4}$	90%
Γ_{63}	$p\overline{n}\pi^-$	(8.5 ±0.9) $\times 10^{-4}$	
Γ_{64}	$\overline{p}n\pi^+$	(8.9 ±0.8) $\times 10^{-4}$	
Γ_{65}	$p\overline{n}\pi^-\pi^0$	(2.17±0.18) $\times 10^{-3}$	
Γ_{66}	$\overline{p}n\pi^+\pi^0$	(2.11±0.18) $\times 10^{-3}$	
Γ_{67}	$\Lambda\overline{\Lambda}$	(1.84±0.15) $\times 10^{-4}$	
Γ_{68}	$\Lambda\overline{\Lambda}\pi^+\pi^-$	(1.25±0.15) $\times 10^{-3}$	
Γ_{69}	$\Lambda\overline{\Lambda}\pi^+\pi^-$ (non-resonant)	(6.6 ±1.5) $\times 10^{-4}$	
Γ_{70}	$\Sigma(1385)^+\overline{\Lambda}\pi^-$ + c.c.	< 4 $\times 10^{-4}$	90%
Γ_{71}	$\Sigma(1385)^-\overline{\Lambda}\pi^+$ + c.c.	< 6 $\times 10^{-4}$	90%
Γ_{72}	$K^+\overline{p}\Lambda$ + c.c.	(7.8 ±0.5) $\times 10^{-4}$	
Γ_{73}	$K^+\overline{p}\Lambda(1520)$ + c.c.	(2.8 ±0.7) $\times 10^{-4}$	
Γ_{74}	$\Lambda(1520)\overline{\Lambda}(1520)$	(4.6 ±1.5) $\times 10^{-4}$	
Γ_{75}	$\Sigma^0\overline{\Sigma}^0$	< 6 $\times 10^{-5}$	90%
Γ_{76}	$\Sigma^+\overline{\Sigma}^-$	< 7 $\times 10^{-5}$	90%
Γ_{77}	$\Sigma(1385)^+\overline{\Sigma}(1385)^-$	< 1.6 $\times 10^{-4}$	90%
Γ_{78}	$\Sigma(1385)^-\overline{\Sigma}(1385)^+$	< 8 $\times 10^{-5}$	90%
Γ_{79}	$K^-\Lambda\overline{\Xi}^+$ + c.c.	(1.76±0.32) $\times 10^{-4}$	
Γ_{80}	$\Xi^0\overline{\Xi}^0$	< 1.0 $\times 10^{-4}$	90%
Γ_{81}	$\Xi^-\overline{\Xi}^+$	(1.42±0.32) $\times 10^{-4}$	
Γ_{82}	$J/\psi(1S)\pi^+\pi^-\pi^0$	< 1.5 %	90%
Γ_{83}	$\pi^0\eta_c$	< 3.2 $\times 10^{-3}$	90%
Γ_{84}	$\eta_c(1S)\pi^+\pi^-$	< 5.4 $\times 10^{-3}$	90%
	Radiative decays		
Γ_{85}	$\gamma J/\psi(1S)$	(19.0 ±0.5) %	
Γ_{86}	$\gamma\rho^0$	< 1.9 $\times 10^{-5}$	90%
Γ_{87}	$\gamma\omega$	< 6 $\times 10^{-6}$	90%
Γ_{88}	$\gamma\phi$	< 7 $\times 10^{-6}$	90%
Γ_{89}	$\gamma\gamma$	(2.85±0.10) $\times 10^{-4}$	
Γ_{90}	$e^+e^- J/\psi(1S)$	(2.37±0.16) $\times 10^{-3}$	

CONSTRAINED FIT INFORMATION

A multiparticle fit to $\chi_{c1}(1P)$, $\chi_{c0}(1P)$, $\chi_{c2}(1P)$, and $\psi(2S)$ with 4 total widths, a partial width, 25 combinations of partial widths obtained from integrated cross section, and 84 branching ratios uses 247 measurements to determine 49 parameters. The overall fit has a $\chi^2 = 376.9$ for 198 degrees of freedom.

The following *off-diagonal* array elements are the correlation coefficients $\langle \delta p_i \delta p_j \rangle / (\delta p_i \cdot \delta p_j)$, in percent, from the fit to parameters p_i, including the branching fractions, $x_i \equiv \Gamma_i/\Gamma_{\text{total}}$.

x_{14}	7									
x_{17}	2	21								
x_{18}	4	3	1							
x_{20}	7	5	1	3						
x_{24}	7	6	1	4	10					
x_{25}	18	2	0	1	1	1				
x_{30}	3	3	1	2	5	12	1			
x_{31}	5	4	1	3	7	15	1	8		
x_{32}	5	4	1	2	6	13	1	7	8	
x_{41}	2	2	0	1	3	7	0	3	4	4
x_{49}	4	3	1	2	4	7	1	4	5	4
x_{54}	10	9	2	5	9	11	2	5	8	7
x_{67}	3	3	1	2	5	13	1	7	8	7
x_{85}	12	10	2	6	15	34	2	18	22	18
x_{89}	−6	−4	−1	−2	2	20	−2	12	12	10
Γ	−23	−19	−4	−11	−19	−25	−5	−12	−18	−15
	x_1	x_{14}	x_{17}	x_{18}	x_{20}	x_{24}	x_{25}	x_{30}	x_{31}	x_{32}

x_{49}	2					
x_{54}	4	5				
x_{67}	4	4	6			
x_{85}	10	11	4	18		
x_{89}	5	4	18	12	34	
Γ	−8	−11	−45	−12	−46	−43
	x_{41}	x_{49}	x_{54}	x_{67}	x_{85}	x_{89}

$\chi_{c2}(1P)$ PARTIAL WIDTHS

$\chi_{c2}(1P)$ Γ(i)$\Gamma(\gamma J/\psi(1S))/\Gamma$(total)

$\Gamma(p\overline{p}) \times \Gamma(\gamma J/\psi(1S))/\Gamma_{\text{total}}$ $\Gamma_{54}\Gamma_{85}/\Gamma$

VALUE (eV)	DOCUMENT ID		TECN	COMMENT
27.5±1.2 OUR FIT				
27.5±1.5 OUR AVERAGE				
27.0±1.5±1.1	[1] ANDREOTTI	05A	E835	$p\overline{p} \to e^+e^-\gamma$
27.7±1.5±2.0	[1,2] ARMSTRONG	92	E760	$\overline{p}p \to e^+e^-\gamma$
36 ±8	[1] BAGLIN	86B	SPEC	$\overline{p}p \to e^+e^-$X

[1] Calculated by us using B($J/\psi(1S) \to e^+e^-$) = 0.0593 ± 0.0010.
[2] Recalculated by ANDREOTTI 05A.

$\Gamma(\gamma\gamma) \times \Gamma(\gamma J/\psi(1S))/\Gamma_{\text{total}}$ $\Gamma_{89}\Gamma_{85}/\Gamma$

VALUE (eV)	EVTS	DOCUMENT ID		TECN	COMMENT
107± 5 OUR FIT					
117± 10 OUR AVERAGE					
111± 12± 9	147 ± 15	[1] DOBBS	06	CLE3	10.4 $e^+e^- \to e^+e^-\chi_{c2}$
114± 11± 9	136 ± 13.3	[1,2] ABE	02T	BELL	$e^+e^- \to e^+e^-\chi_{c2}$
139± 55± 21		[1,3] ACCIARRI	99E	L3	$e^+e^- \to e^+e^-\chi_{c2}$
242± 65± 51		[1,4] ACKER...,K...	98	OPAL	$e^+e^- \to e^+e^-\chi_{c2}$
150± 42± 36		[1,5] DOMINICK	94	CLE2	$e^+e^- \to e^+e^-\chi_{c2}$
470±240±120		[1,6] BAUER	93	TPC	$e^+e^- \to e^+e^-\chi_{c2}$

[1] Calculated by us using B($J/\psi \to \ell^+\ell^-$) = 0.1187 ± 0.0008.
[2] All systematic errors added in quadrature.
[3] The value for $\Gamma(\chi_{c2} \to \gamma\gamma)$ reported in ACCIARRI 99E is derived using B($\chi_{c2} \to \gamma J/\psi(1S)$)×B($J/\psi(1S) \to \ell^+\ell^-$) = 0.0162 ± 0.0014.
[4] The value for $\Gamma(\chi_{c2} \to \gamma\gamma)$ reported in ACKERSTAFF,K 98 is derived using B($\chi_{c2} \to \gamma J/\psi(1S)$) = 0.135 ± 0.011 and B($J/\psi(1S) \to \ell^+\ell^-$) = 0.1203 ± 0.0038.
[5] The value for $\Gamma(\chi_{c2} \to \gamma\gamma)$ reported in DOMINICK 94 is derived using B($\chi_{c2} \to \gamma J/\psi(1S)$)= 0.135 ± 0.011, B($J/\psi(1S) \to e^+e^-$) = 0.0627 ± 0.0020, and B($J/\psi(1S) \to \mu^+\mu^-$) = 0.0597 ± 0.0025.
[6] The value for $\Gamma(\chi_{c2} \to \gamma\gamma)$ reported in BAUER 93 is derived using B($\chi_{c2} \to \gamma J/\psi(1S)$)= 0.135 ± 0.011, B($J/\psi(1S) \to e^+e^-$) = 0.0627 ± 0.0020, and B($J/\psi(1S) \to \mu^+\mu^-$) = 0.0597 ± 0.0025.

$\chi_{c2}(1P)$ Γ(i)$\Gamma(\gamma\gamma)/\Gamma$(total)

$\Gamma(2(\pi^+\pi^-)) \times \Gamma(\gamma\gamma)/\Gamma_{\text{total}}$ $\Gamma_1\Gamma_{89}/\Gamma$

VALUE (eV)	EVTS	DOCUMENT ID		TECN	COMMENT
5.7 ±0.5 OUR FIT					
5.2 ±0.7 OUR AVERAGE					
5.01±0.44±0.55	1597±138	UEHARA	08	BELL	$\gamma\gamma \to \chi_{c2} \to 2(\pi^+\pi^-)$
6.4 ±1.8 ±0.8		EISENSTEIN	01	CLE2	$e^+e^- \to e^+e^-\chi_{c2}$

$\Gamma(\rho\rho) \times \Gamma(\gamma\gamma)/\Gamma_{\text{total}}$ $\Gamma_2\Gamma_{89}/\Gamma$

VALUE (eV)	CL%	EVTS	DOCUMENT ID	TECN	COMMENT
• • • We do not use the following data for averages, fits, limits, etc. • • •					
<7.8	90	<598	UEHARA 08	BELL	$\gamma\gamma \to \chi_{c2} \to 2(\pi^+\pi^-)$

$\Gamma(K^+K^-\pi^+\pi^-) \times \Gamma(\gamma\gamma)/\Gamma_{\text{total}}$ $\Gamma_{14}\Gamma_{89}/\Gamma$

VALUE (eV)	EVTS	DOCUMENT ID		TECN	COMMENT
4.7 ±0.5 OUR FIT					
4.42±0.42±0.53	780 ± 74	UEHARA	08	BELL	$\gamma\gamma \to \chi_{c2} \to K^+K^-\pi^+\pi^-$

$\Gamma(K^+K^-\pi^+\pi^-\pi^0) \times \Gamma(\gamma\gamma)/\Gamma_{\text{total}}$ $\Gamma_{15}\Gamma_{89}/\Gamma$

VALUE (eV)	EVTS	DOCUMENT ID		TECN	COMMENT
6.5±0.9±1.5	1250	DEL-AMO-SA...11M		BABR	$\gamma\gamma \to K^+K^-\pi^+\pi^-\pi^0$

$\Gamma(K^*(892)^0\overline{K}^*(892)^0) \times \Gamma(\gamma\gamma)/\Gamma_{\text{total}}$ $\Gamma_{18}\Gamma_{89}/\Gamma$

VALUE (eV)	EVTS	DOCUMENT ID		TECN	COMMENT
1.26±0.24 OUR FIT					
0.8 ±0.17±0.27	151 ± 30	UEHARA	08	BELL	$\gamma\gamma \to \chi_{c2} \to K^+K^-\pi^+\pi^-$

$\Gamma(\phi\phi) \times \Gamma(\gamma\gamma)/\Gamma_{\text{total}}$ $\Gamma_{20}\Gamma_{89}/\Gamma$

VALUE (eV)	EVTS	DOCUMENT ID		TECN	COMMENT
0.60±0.05 OUR FIT					
0.62±0.07±0.05	89 ± 11	[1] LIU	12B	BELL	$\gamma\gamma \to 2(K^+K^-)$
• • • We do not use the following data for averages, fits, limits, etc. • • •					
0.58±0.18±0.16	26.5 ± 8.1	UEHARA	08	BELL	$\gamma\gamma \to \chi_{c2} \to 2(K^+K^-)$

[1] Supersedes UEHARA 08. Using B($\phi \to K^+K^-$) = (48.9 ± 0.5)%.

$\Gamma(\omega\omega) \times \Gamma(\gamma\gamma)/\Gamma_{\text{total}}$ $\Gamma_{21}\Gamma_{89}/\Gamma$

VALUE (eV)	CL%	DOCUMENT ID		TECN	COMMENT
• • • We do not use the following data for averages, fits, limits, etc. • • •					
<0.64	90	[1] LIU	12B	BELL	$\gamma\gamma \to 2(\pi^+\pi^-\pi^0)$

[1] Using B($\omega \to \pi^+\pi^-\pi^0$) = (89.2 ± 0.7)%.

$\Gamma(\omega\phi) \times \Gamma(\gamma\gamma)/\Gamma_{\text{total}}$ $\Gamma_{23}\Gamma_{89}/\Gamma$

VALUE (eV)	CL%	DOCUMENT ID		TECN	COMMENT
• • • We do not use the following data for averages, fits, limits, etc. • • •					
<0.04	90	[1] LIU	12B	BELL	$\gamma\gamma \to K^+K^-\pi^+\pi^-\pi^0$

[1] Using B($\phi \to K^+K^-$) = (48.9 ± 0.5)% and B($\omega \to \pi^+\pi^-\pi^0$) = (89.2 ± 0.7)%.

$\Gamma(\pi\pi) \times \Gamma(\gamma\gamma)/\Gamma_{\text{total}}$ $\Gamma_{24}\Gamma_{89}/\Gamma$

VALUE (eV)	EVTS	DOCUMENT ID		TECN	COMMENT
1.25±0.07 OUR FIT					
1.18±0.25 OUR AVERAGE					
1.44±0.54±0.47	34 ± 13	[1] UEHARA	09	BELL	10.6 $e^+e^- \to e^+e^-\pi^0\pi^0$
1.14±0.21±0.17	54 ± 10	[2] NAKAZAWA	05	BELL	10.6 $e^+e^- \to e^+e^-\pi^+\pi^-$

[1] We multiplied the measurement by 3 to convert from $\pi^0\pi^0$ to $\pi\pi$. Interference with the continuum included.
[2] We have multiplied $\pi^+\pi^-$ measurement by 3/2 to obtain $\pi\pi$.

$\Gamma(\rho^0\pi^+\pi^-) \times \Gamma(\gamma\gamma)/\Gamma_{\text{total}}$ $\Gamma_{25}\Gamma_{89}/\Gamma$

VALUE (eV)	EVTS	DOCUMENT ID		TECN	COMMENT
2.1±0.9 OUR FIT					
3.2±1.9±0.5	986 ± 578	UEHARA	08	BELL	$\gamma\gamma \to \chi_{c2} \to 2(\pi^+\pi^-)$

$\Gamma(\eta\eta) \times \Gamma(\gamma\gamma)/\Gamma_{\text{total}}$ $\Gamma_{30}\Gamma_{89}/\Gamma$

VALUE (eV)	EVTS	DOCUMENT ID		TECN	COMMENT
0.53±0.22±0.09	8	[1] UEHARA	10A	BELL	10.6 $e^+e^- \to e^+e^-\eta\eta$

[1] Interference with the continuum not included.

$\Gamma(K^+K^-) \times \Gamma(\gamma\gamma)/\Gamma_{\text{total}}$ $\Gamma_{31}\Gamma_{89}/\Gamma$

VALUE (eV)	EVTS	DOCUMENT ID		TECN	COMMENT
0.56±0.04 OUR FIT					
0.44±0.11±0.07	33 ± 8	NAKAZAWA	05	BELL	10.6 $e^+e^- \to e^+e^-K^+K^-$

$\Gamma(K^0_SK^0_S) \times \Gamma(\gamma\gamma)/\Gamma_{\text{total}}$ $\Gamma_{32}\Gamma_{89}/\Gamma$

VALUE (eV)	EVTS	DOCUMENT ID		TECN	COMMENT
0.294±0.025 OUR FIT					
0.27 $^{+0.07}_{-0.06}$ ±0.03	53	[1] UEHARA	13	BELL	$\gamma\gamma \to K^0_SK^0_S$
• • • We do not use the following data for averages, fits, limits, etc. • • •					
0.31 ±0.05 ±0.03	38 ± 7	CHEN	07B	BELL	$e^+e^- \to e^+e^-\chi_{c2}$

[1] Supersedes CHEN 07B.

$\Gamma(\overline{K}^0K^+\pi^-$ + c.c.) $\times \Gamma(\gamma\gamma)/\Gamma_{\text{total}}$ $\Gamma_{41}\Gamma_{89}/\Gamma$

VALUE (eV)	EVTS	DOCUMENT ID		TECN	COMMENT
0.72±0.11 OUR FIT					
1.20±0.33±0.13	126	[1] DEL-AMO-SA...11M		BABR	$\gamma\gamma \to K^0_S K^\pm\pi^\mp$

[1] We have multiplied $\overline{K}K\pi$ by 2/3 to obtain $\overline{K}^0K^+\pi^-$ + c.c.

$\Gamma(K^+K^-K^+K^-) \times \Gamma(\gamma\gamma)/\Gamma_{\text{total}}$ $\Gamma_{49}\Gamma_{89}/\Gamma$

VALUE (eV)	EVTS	DOCUMENT ID		TECN	COMMENT
0.93±0.11 OUR FIT					
1.10±0.21±0.15	126 ± 24	UEHARA	08	BELL	$\gamma\gamma \to \chi_{c2} \to 2(K^+K^-)$

$\Gamma(\eta_c(1S)\pi^+\pi^-) \times \Gamma(\gamma\gamma)/\Gamma_{\text{total}}$ $\Gamma_{84}\Gamma_{89}/\Gamma$

VALUE (eV)	CL%	DOCUMENT ID		TECN	COMMENT
<15.7	90	LEES	12AE	BABR	$e^+e^- \to e^+e^-\pi^+\pi^-\eta_c$

$\chi_{c2}(1P)$ BRANCHING RATIOS

HADRONIC DECAYS

$\Gamma(2(\pi^+\pi^-))/\Gamma_{\text{total}}$ Γ_1/Γ

VALUE	DOCUMENT ID
0.0102±0.0009 OUR FIT	

$\Gamma(\rho^0\pi^+\pi^-)/\Gamma(2(\pi^+\pi^-))$ Γ_{25}/Γ_1

VALUE	DOCUMENT ID		TECN	COMMENT
0.36±0.15 OUR FIT				
0.31±0.17	TANENBAUM	78	MRK1	$\psi(2S) \to \gamma\chi_{c2}$

$\Gamma(\pi^+\pi^-\pi^0\pi^0)/\Gamma_{\text{total}}$ Γ_3/Γ

VALUE (%)	EVTS	DOCUMENT ID		TECN	COMMENT
1.83±0.23±0.04	903.5	[1] HE	08B	CLEO	$e^+e^- \to \gamma h^+h^-h^0h^0$

[1] HE 08B reports 1.87 ± 0.07 ± 0.22 ± 0.13 % from a measurement of [$\Gamma(\chi_{c2}(1P) \to \pi^+\pi^-\pi^0\pi^0)/\Gamma_{\text{total}}$] × [B($\psi(2S) \to \gamma\chi_{c2}(1P)$)] assuming B($\psi(2S) \to \gamma\chi_{c2}(1P)$) = (9.33 ± 0.14 ± 0.61)×10^{-2}, which we rescale to our best value B($\psi(2S) \to \gamma\chi_{c2}(1P)$)

$= (9.52 \pm 0.20) \times 10^{-2}$. Our first error is their experiment's error and our second error is the systematic error from using our best value.

$\Gamma(\rho^+\pi^-\pi^0 + \text{c.c.})/\Gamma_{\text{total}}$ Γ_4/Γ

VALUE (%)	EVTS	DOCUMENT ID		TECN	COMMENT
2.19±0.34±0.05	1031.9	[1,2] HE	08B	CLEO	$e^+e^- \to \gamma h^+ h^- h^0 h^0$

[1] HE 08B reports $2.23 \pm 0.11 \pm 0.32 \pm 0.16$ % from a measurement of $[\Gamma(\chi_{c2}(1P) \to \rho^+\pi^-\pi^0 + \text{c.c.})/\Gamma_{\text{total}}] \times [B(\psi(2S) \to \gamma\chi_{c2}(1P))]$ assuming $B(\psi(2S) \to \gamma\chi_{c2}(1P)) = (9.33 \pm 0.14 \pm 0.61) \times 10^{-2}$, which we rescale to our best value $B(\psi(2S) \to \gamma\chi_{c2}(1P)) = (9.52 \pm 0.20) \times 10^{-2}$. Our first error is their experiment's error and our second error is the systematic error from using our best value.

[2] Calculated by us. We have added the values from HE 08B for $\rho^+\pi^-\pi^0$ and $\rho^-\pi^+\pi^0$ decays assuming uncorrelated statistical and fully correlated systematic uncertainties.

$\Gamma(4\pi^0)/\Gamma_{\text{total}}$ Γ_5/Γ

VALUE (units 10^{-3})	EVTS	DOCUMENT ID		TECN	COMMENT
1.11±0.15±0.02	1164	[1] ABLIKIM	11A	BES3	$e^+e^- \to \psi(2S) \to \gamma\chi_{c2}$

[1] ABLIKIM 11A reports $(1.21 \pm 0.05 \pm 0.16) \times 10^{-3}$ from a measurement of $[\Gamma(\chi_{c2}(1P) \to 4\pi^0)/\Gamma_{\text{total}}] \times [B(\psi(2S) \to \gamma\chi_{c2}(1P))]$ assuming $B(\psi(2S) \to \gamma\chi_{c2}(1P)) = (8.74 \pm 0.35) \times 10^{-2}$, which we rescale to our best value $B(\psi(2S) \to \gamma\chi_{c2}(1P)) = (9.52 \pm 0.20) \times 10^{-2}$. Our first error is their experiment's error and our second error is the systematic error from using our best value.

$\Gamma(K^+K^-\pi^0\pi^0)/\Gamma_{\text{total}}$ Γ_6/Γ

VALUE (%)	EVTS	DOCUMENT ID		TECN	COMMENT
0.206±0.040±0.004	76.9	[1] HE	08B	CLEO	$e^+e^- \to \gamma h^+ h^- h^0 h^0$

[1] HE 08B reports $0.21 \pm 0.03 \pm 0.03 \pm 0.01$ % from a measurement of $[\Gamma(\chi_{c2}(1P) \to K^+K^-\pi^0\pi^0)/\Gamma_{\text{total}}] \times [B(\psi(2S) \to \gamma\chi_{c2}(1P))]$ assuming $B(\psi(2S) \to \gamma\chi_{c2}(1P)) = (9.33 \pm 0.14 \pm 0.61) \times 10^{-2}$, which we rescale to our best value $B(\psi(2S) \to \gamma\chi_{c2}(1P)) = (9.52 \pm 0.20) \times 10^{-2}$. Our first error is their experiment's error and our second error is the systematic error from using our best value.

$\Gamma(K^+\pi^-\overline{K}^0\pi^0 + \text{c.c.})/\Gamma_{\text{total}}$ Γ_7/Γ

VALUE (%)	EVTS	DOCUMENT ID		TECN	COMMENT
1.38±0.19±0.03	211.6	[1] HE	08B	CLEO	$e^+e^- \to \gamma h^+ h^- h^0 h^0$

[1] HE 08B reports $1.41 \pm 0.11 \pm 0.16 \pm 0.10$ % from a measurement of $[\Gamma(\chi_{c2}(1P) \to K^+\pi^-\overline{K}^0\pi^0 + \text{c.c.})/\Gamma_{\text{total}}] \times [B(\psi(2S) \to \gamma\chi_{c2}(1P))]$ assuming $B(\psi(2S) \to \gamma\chi_{c2}(1P)) = (9.33 \pm 0.14 \pm 0.61) \times 10^{-2}$, which we rescale to our best value $B(\psi(2S) \to \gamma\chi_{c2}(1P)) = (9.52 \pm 0.20) \times 10^{-2}$. Our first error is their experiment's error and our second error is the systematic error from using our best value.

$\Gamma(\rho^- K^+\overline{K}^0 + \text{c.c.})/\Gamma_{\text{total}}$ Γ_8/Γ

VALUE (%)	EVTS	DOCUMENT ID		TECN	COMMENT
0.41±0.12±0.01	62.9	[1] HE	08B	CLEO	$e^+e^- \to \gamma h^+ h^- h^0 h^0$

[1] HE 08B reports $0.42 \pm 0.11 \pm 0.06 \pm 0.03$ % from a measurement of $[\Gamma(\chi_{c2}(1P) \to \rho^- K^+\overline{K}^0 + \text{c.c.})/\Gamma_{\text{total}}] \times [B(\psi(2S) \to \gamma\chi_{c2}(1P))]$ assuming $B(\psi(2S) \to \gamma\chi_{c2}(1P)) = (9.33 \pm 0.14 \pm 0.61) \times 10^{-2}$, which we rescale to our best value $B(\psi(2S) \to \gamma\chi_{c2}(1P)) = (9.52 \pm 0.20) \times 10^{-2}$. Our first error is their experiment's error and our second error is the systematic error from using our best value.

$\Gamma(K^*(892)^0 K^-\pi^+ \to K^-\pi^+ K^0\pi^0 + \text{c.c.})/\Gamma_{\text{total}}$ Γ_9/Γ

VALUE (%)	EVTS	DOCUMENT ID		TECN	COMMENT
0.29±0.08±0.01	38.7	[1] HE	08B	CLEO	$e^+e^- \to \gamma h^+ h^- h^0 h^0$

[1] HE 08B reports $0.30 \pm 0.07 \pm 0.04 \pm 0.02$ % from a measurement of $[\Gamma(\chi_{c2}(1P) \to K^*(892)^0 K^-\pi^+ \to K^-\pi^+ K^0\pi^0 + \text{c.c.})/\Gamma_{\text{total}}] \times [B(\psi(2S) \to \gamma\chi_{c2}(1P))]$ assuming $B(\psi(2S) \to \gamma\chi_{c2}(1P)) = (9.33 \pm 0.14 \pm 0.61) \times 10^{-2}$, which we rescale to our best value $B(\psi(2S) \to \gamma\chi_{c2}(1P)) = (9.52 \pm 0.20) \times 10^{-2}$. Our first error is their experiment's error and our second error is the systematic error from using our best value.

$\Gamma(K^*(892)^0\overline{K}^0\pi^0 \to K^+\pi^-\overline{K}^0\pi^0 + \text{c.c.})/\Gamma_{\text{total}}$ Γ_{10}/Γ

VALUE (%)	EVTS	DOCUMENT ID		TECN	COMMENT
0.38±0.09±0.01	63.0	[1] HE	08B	CLEO	$e^+e^- \to \gamma h^+ h^- h^0 h^0$

[1] HE 08B reports $0.39 \pm 0.07 \pm 0.05 \pm 0.03$ % from a measurement of $[\Gamma(\chi_{c2}(1P) \to K^*(892)^0\overline{K}^0\pi^0 \to K^+\pi^-\overline{K}^0\pi^0 + \text{c.c.})/\Gamma_{\text{total}}] \times [B(\psi(2S) \to \gamma\chi_{c2}(1P))]$ assuming $B(\psi(2S) \to \gamma\chi_{c2}(1P)) = (9.33 \pm 0.14 \pm 0.61) \times 10^{-2}$, which we rescale to our best value $B(\psi(2S) \to \gamma\chi_{c2}(1P)) = (9.52 \pm 0.20) \times 10^{-2}$. Our first error is their experiment's error and our second error is the systematic error from using our best value.

$\Gamma(K^*(892)^- K^+\pi^0 \to K^+\pi^-\overline{K}^0\pi^0 + \text{c.c.})/\Gamma_{\text{total}}$ Γ_{11}/Γ

VALUE (%)	EVTS	DOCUMENT ID		TECN	COMMENT
0.37±0.08±0.01	51.1	[1] HE	08B	CLEO	$e^+e^- \to \gamma h^+ h^- h^0 h^0$

[1] HE 08B reports $0.38 \pm 0.07 \pm 0.04 \pm 0.03$ % from a measurement of $[\Gamma(\chi_{c2}(1P) \to K^*(892)^- K^+\pi^0 \to K^+\pi^-\overline{K}^0\pi^0 + \text{c.c.})/\Gamma_{\text{total}}] \times [B(\psi(2S) \to \gamma\chi_{c2}(1P))]$ assuming $B(\psi(2S) \to \gamma\chi_{c2}(1P)) = (9.33 \pm 0.14 \pm 0.61) \times 10^{-2}$, which we rescale to our best value $B(\psi(2S) \to \gamma\chi_{c2}(1P)) = (9.52 \pm 0.20) \times 10^{-2}$. Our first error is their experiment's error and our second error is the systematic error from using our best value.

$\Gamma(K^*(892)^+\overline{K}^0\pi^- \to K^+\pi^-\overline{K}^0\pi^0 + \text{c.c.})/\Gamma_{\text{total}}$ Γ_{12}/Γ

VALUE (%)	EVTS	DOCUMENT ID		TECN	COMMENT
0.29±0.08±0.01	39.3	[1] HE	08B	CLEO	$e^+e^- \to \gamma h^+ h^- h^0 h^0$

[1] HE 08B reports $0.30 \pm 0.07 \pm 0.04 \pm 0.02$ % from a measurement of $[\Gamma(\chi_{c2}(1P) \to K^*(892)^+\overline{K}^0\pi^- \to K^+\pi^-\overline{K}^0\pi^0 + \text{c.c.})/\Gamma_{\text{total}}] \times [B(\psi(2S) \to \gamma\chi_{c2}(1P))]$ assuming $B(\psi(2S) \to \gamma\chi_{c2}(1P)) = (9.33 \pm 0.14 \pm 0.61) \times 10^{-2}$, which we rescale to our best value $B(\psi(2S) \to \gamma\chi_{c2}(1P)) = (9.52 \pm 0.20) \times 10^{-2}$. Our first error is their experiment's error and our second error is the systematic error from using our best value.

$\Gamma(K^+K^-\eta\pi^0)/\Gamma_{\text{total}}$ Γ_{13}/Γ

VALUE (%)	EVTS	DOCUMENT ID		TECN	COMMENT
0.127±0.044±0.003	22.9	[1] HE	08B	CLEO	$e^+e^- \to \gamma h^+ h^- h^0 h^0$

[1] HE 08B reports $0.13 \pm 0.04 \pm 0.02 \pm 0.01$ % from a measurement of $[\Gamma(\chi_{c2}(1P) \to K^+K^-\eta\pi^0)/\Gamma_{\text{total}}] \times [B(\psi(2S) \to \gamma\chi_{c2}(1P))]$ assuming $B(\psi(2S) \to \gamma\chi_{c2}(1P)) = (9.33 \pm 0.14 \pm 0.61) \times 10^{-2}$, which we rescale to our best value $B(\psi(2S) \to \gamma\chi_{c2}(1P)) = (9.52 \pm 0.20) \times 10^{-2}$. Our first error is their experiment's error and our second error is the systematic error from using our best value.

$\Gamma(K^+K^-\pi^+\pi^-)/\Gamma_{\text{total}}$ Γ_{14}/Γ

VALUE (units 10^{-3})	DOCUMENT ID
8.4±0.9 OUR FIT	

$\Gamma(K^+K^-\pi^+\pi^-\pi^0)/\Gamma_{\text{total}}$ Γ_{15}/Γ

VALUE (units 10^{-3})	EVTS	DOCUMENT ID		TECN	COMMENT
11.69±0.13±1.31	11k	[1] ABLIKIM	13B	BES3	$e^+e^- \to \psi(2S) \to \gamma\chi_{c2}$

[1] Using 1.06×10^8 $\psi(2S)$ mesons and $B(\psi(2S) \to \chi_{c2}\gamma) = (8.72 \pm 0.34)\%$.

$\Gamma(K^0_S K^\pm\pi^\mp\pi^+\pi^-)/\Gamma_{\text{total}}$ Γ_{16}/Γ

VALUE (units 10^{-3})	EVTS	DOCUMENT ID		TECN	COMMENT
7.30±0.11±0.75	4.5k	[1] ABLIKIM	13B	BES3	$e^+e^- \to \psi(2S) \to \gamma\chi_{c2}$

[1] Using 1.06×10^8 $\psi(2S)$ mesons and $B(\psi(2S) \to \chi_{c2}\gamma) = (8.72 \pm 0.34)\%$.

$\Gamma(K^+\overline{K}^*(892)^0\pi^- + \text{c.c.})/\Gamma(K^+K^-\pi^+\pi^-)$ Γ_{17}/Γ_{14}

VALUE	DOCUMENT ID		TECN	COMMENT
0.25±0.13 OUR FIT				
0.25±0.13	TANENBAUM	78	MRK1	$\psi(2S) \to \gamma\chi_{c2}$

$\Gamma(K^+\overline{K}^*(892)^0\pi^- + \text{c.c.})/\Gamma_{\text{total}}$ Γ_{17}/Γ

VALUE (units 10^{-4})	DOCUMENT ID
21±11 OUR FIT	

$\Gamma(K^*(892)^0\overline{K}^*(892)^0)/\Gamma_{\text{total}}$ Γ_{18}/Γ

VALUE (units 10^{-3})	DOCUMENT ID
2.3±0.4 OUR FIT	

$\Gamma(3(\pi^+\pi^-))/\Gamma_{\text{total}}$ Γ_{19}/Γ

VALUE (units 10^{-3})	DOCUMENT ID		TECN	COMMENT
8.6±1.8 OUR EVALUATION	Treating systematic error as correlated.			
8.6±1.8 OUR AVERAGE				
8.6±0.9±1.6	[1] BAI	99B	BES	$\psi(2S) \to \gamma\chi_{c2}$
8.7±5.9±0.4	[1] TANENBAUM	78	MRK1	$\psi(2S) \to \gamma\chi_{c2}$

[1] Rescaled by us using $B(\psi(2S) \to \gamma\chi_{c2}) = (8.3 \pm 0.4)\%$ and $B(\psi(2S) \to J/\psi(1S)\pi^+\pi^-) = (32.6 \pm 0.5)\%$. Multiplied by a factor of 2 to convert from $K^0_S K^+\pi^-$ to $K^0 K^+\pi^-$ decay.

$\Gamma(\phi\phi)/\Gamma_{\text{total}}$ Γ_{20}/Γ

VALUE (units 10^{-3})	DOCUMENT ID
1.06±0.09 OUR FIT	

$\Gamma(\omega\omega)/\Gamma_{\text{total}}$ Γ_{21}/Γ

VALUE (units 10^{-3})	EVTS	DOCUMENT ID		TECN	COMMENT
0.84±0.10 OUR AVERAGE					
0.82±0.10±0.02	762	[1] ABLIKIM	11K	BES3	$\psi(2S) \to \gamma$ hadrons
1.73±0.57±0.04	27.7±7.4	[2] ABLIKIM	05N	BES2	$\psi(2S) \to \gamma\chi_{c2} \to \gamma 6\pi$

[1] ABLIKIM 11K reports $(8.9 \pm 0.3 \pm 1.1) \times 10^{-4}$ from a measurement of $[\Gamma(\chi_{c2}(1P) \to \omega\omega)/\Gamma_{\text{total}}] \times [B(\psi(2S) \to \gamma\chi_{c2}(1P))]$ assuming $B(\psi(2S) \to \gamma\chi_{c2}(1P)) = (8.74 \pm 0.35) \times 10^{-2}$, which we rescale to our best value $B(\psi(2S) \to \gamma\chi_{c2}(1P)) = (9.52 \pm 0.20) \times 10^{-2}$. Our first error is their experiment's error and our second error is the systematic error from using our best value.

[2] ABLIKIM 05N reports $[\Gamma(\chi_{c2}(1P) \to \omega\omega)/\Gamma_{\text{total}}] \times [B(\psi(2S) \to \gamma\chi_{c2}(1P))] = (0.165 \pm 0.044 \pm 0.032) \times 10^{-3}$ which we divide by our best value $B(\psi(2S) \to \gamma\chi_{c2}(1P)) = (9.52 \pm 0.20) \times 10^{-2}$. Our first error is their experiment's error and our second error is the systematic error from using our best value.

$\Gamma(\omega K^+K^-)/\Gamma_{\text{total}}$ Γ_{22}/Γ

VALUE (units 10^{-3})	EVTS	DOCUMENT ID		TECN	COMMENT
0.73±0.04±0.08	512	[1] ABLIKIM	13B	BES3	$e^+e^- \to \psi(2S) \to \gamma\chi_{c2}$

[1] Using 1.06×10^8 $\psi(2S)$ mesons and $B(\psi(2S) \to \chi_{c2}\gamma) = (8.72 \pm 0.34)\%$.

$\Gamma(\omega\phi)/\Gamma_{\text{total}}$ Γ_{23}/Γ

VALUE (units 10^{-5})	CL%	DOCUMENT ID		TECN	COMMENT
<1.8	90	[1] ABLIKIM	11K	BES3	$\psi(2S) \to \gamma$ hadrons

[1] ABLIKIM 11K reports $< 2 \times 10^{-5}$ from a measurement of $[\Gamma(\chi_{c2}(1P) \to \omega\phi)/\Gamma_{\text{total}}] \times [B(\psi(2S) \to \gamma\chi_{c2}(1P))]$ assuming $B(\psi(2S) \to \gamma\chi_{c2}(1P)) = (8.74 \pm 0.35) \times 10^{-2}$, which we rescale to our best value $B(\psi(2S) \to \gamma\chi_{c2}(1P)) = 9.52 \times 10^{-2}$.

$\Gamma(\pi\pi)/\Gamma_{\text{total}}$ Γ_{24}/Γ

VALUE (units 10^{-3})	DOCUMENT ID
2.23±0.09 OUR FIT	

$\Gamma(\rho^0\pi^+\pi^-)/\Gamma_{\text{total}}$ Γ_{25}/Γ

VALUE (units 10^{-4})	DOCUMENT ID
37±16 OUR FIT	

$\Gamma(\pi^+\pi^-\pi^0(\text{non-resonant}))/\Gamma_{\text{total}}$ Γ_{26}/Γ

VALUE (units 10^{-5})	EVTS	DOCUMENT ID		TECN	COMMENT
2.01±0.42±0.04	64	[1] ABLIKIM	17AG	BES3	$\psi(2S) \to \gamma\pi^+\pi^-\pi^0$

[1] ABLIKIM 17AG reports $(2.1 \pm 0.4 \pm 0.2) \times 10^{-5}$ from a measurement of $[\Gamma(\chi_{c2}(1P) \to \pi^+\pi^-\pi^0(\text{non-resonant}))/\Gamma_{\text{total}}] \times [B(\psi(2S) \to \gamma\chi_{c2}(1P))]$ assuming $B(\psi(2S) \to \gamma\chi_{c2}(1P)) = (9.11 \pm 0.31) \times 10^{-2}$, which we rescale to our best value $B(\psi(2S) \to \gamma\chi_{c2}(1P)) = (9.52 \pm 0.20) \times 10^{-2}$. Our first error is their experiment's error and our second error is the systematic error from using our best value.

$\Gamma(\rho(770)^\pm\pi^\mp)/\Gamma_{\text{total}}$ Γ_{27}/Γ

VALUE (units 10^{-5})	EVTS	DOCUMENT ID		TECN	COMMENT
0.61±0.38±0.01	15	[1] ABLIKIM	17AG	BES3	$\psi(2S) \to \gamma\pi^+\pi^-\pi^0$

[1] ABLIKIM 17AG reports $(0.64 \pm 0.39 \pm 0.07) \times 10^{-5}$ from a measurement of $[\Gamma(\chi_{c2}(1P) \to \rho(770)^\pm\pi^\mp)/\Gamma_{\text{total}}] \times [B(\psi(2S) \to \gamma\chi_{c2}(1P))]$ assuming $B(\psi(2S) \to \gamma\chi_{c2}(1P)) = (9.11 \pm 0.31) \times 10^{-2}$, which we rescale to our best value $B(\psi(2S) \to \gamma\chi_{c2}(1P)) = (9.52 \pm 0.20) \times 10^{-2}$. Our first error is their experiment's error and our second error is the systematic error from using our best value.

$\Gamma(\pi^+\pi^-\eta)/\Gamma_{\text{total}}$ Γ_{28}/Γ

VALUE (units 10^{-3})	CL%	DOCUMENT ID		TECN	COMMENT
0.48±0.13±0.01		[1] ATHAR	07	CLEO	$\psi(2S) \to \gamma h^+ h^- h^0$
• • • We do not use the following data for averages, fits, limits, etc. • • •					
<1.4	90	[2] ABLIKIM	06R	BES2	$\psi(2S) \to \gamma\chi_{c2}$

[1] ATHAR 07 reports $(0.49 \pm 0.12 \pm 0.06) \times 10^{-3}$ from a measurement of $[\Gamma(\chi_{c2}(1P) \to \pi^+\pi^-\eta)/\Gamma_{\text{total}}] \times [B(\psi(2S) \to \gamma\chi_{c2}(1P))]$ assuming $B(\psi(2S) \to \gamma\chi_{c2}(1P)) = (9.33 \pm 0.14 \pm 0.61) \times 10^{-2}$, which we rescale to our best value $B(\psi(2S) \to \gamma\chi_{c2}(1P)) = (9.52 \pm 0.20) \times 10^{-2}$. Our first error is their experiment's error and our second error is the systematic error from using our best value.

[2] ABLIKIM 06R reports $< 1.7 \times 10^{-3}$ from a measurement of $[\Gamma(\chi_{c2}(1P) \to \pi^+\pi^-\eta)/\Gamma_{\text{total}}] \times [B(\psi(2S) \to \gamma\chi_{c2}(1P))]$ assuming $B(\psi(2S) \to \gamma\chi_{c2}(1P)) = (8.1 \pm 0.4) \times 10^{-2}$, which we rescale to our best value $B(\psi(2S) \to \gamma\chi_{c2}(1P)) = 9.52 \times 10^{-2}$.

$\Gamma(\pi^+\pi^-\eta')/\Gamma_{\text{total}}$ Γ_{29}/Γ

VALUE (units 10^{-3})	DOCUMENT ID		TECN	COMMENT
0.50±0.18±0.01	[1] ATHAR	07	CLEO	$\psi(2S) \to \gamma h^+ h^- h^0$

[1] ATHAR 07 reports $(0.51 \pm 0.18 \pm 0.06) \times 10^{-3}$ from a measurement of $[\Gamma(\chi_{c2}(1P) \to \pi^+\pi^-\eta')/\Gamma_{\text{total}}] \times [B(\psi(2S) \to \gamma\chi_{c2}(1P))]$ assuming $B(\psi(2S) \to \gamma\chi_{c2}(1P)) = (9.33 \pm 0.14 \pm 0.61) \times 10^{-2}$, which we rescale to our best value $B(\psi(2S) \to \gamma\chi_{c2}(1P)) = (9.52 \pm 0.20) \times 10^{-2}$. Our first error is their experiment's error and our second error is the systematic error from using our best value.

$\Gamma(\eta\eta)/\Gamma_{\text{total}}$ Γ_{30}/Γ

VALUE (units 10^{-4})	DOCUMENT ID
5.4±0.4 OUR FIT	

$\Gamma(K^+K^-)/\Gamma_{\text{total}}$ Γ_{31}/Γ

VALUE (units 10^{-3})	DOCUMENT ID
1.01±0.06 OUR FIT	

$\Gamma(K_S^0K_S^0)/\Gamma_{\text{total}}$ Γ_{32}/Γ

VALUE (units 10^{-3})	DOCUMENT ID
0.52±0.04 OUR FIT	

$\Gamma(K_S^0K_S^0)/\Gamma(\pi\pi)$ Γ_{32}/Γ_{24}

VALUE	DOCUMENT ID		TECN	COMMENT
0.235±0.019 OUR FIT				
• • • We do not use the following data for averages, fits, limits, etc. • • •				
0.27 ±0.07 ±0.04	[1,2] CHEN	07B	BELL	$e^+e^- \to e^+e^-\chi_{c2}$

[1] Using $\Gamma(\pi\pi) \times \Gamma(\gamma\gamma)/\Gamma_{\text{total}}$ from the $\pi^+\pi^-$ measurement of NAKAZAWA 05 rescaled by 3/2 to convert to $\pi\pi$.

[2] Not independent from other measurements.

$\Gamma(K_S^0K_S^0)/\Gamma(K^+K^-)$ Γ_{32}/Γ_{31}

VALUE	DOCUMENT ID		TECN	COMMENT
0.52±0.05 OUR FIT				
• • • We do not use the following data for averages, fits, limits, etc. • • •				
0.70±0.21±0.12	[1,2] CHEN	07B	BELL	$e^+e^- \to e^+e^-\chi_{c2}$

[1] Using $\Gamma(K^+K^-) \times \Gamma(\gamma\gamma)/\Gamma_{\text{total}}$ from NAKAZAWA 05.

[2] Not independent from other measurements.

$\Gamma(K^*(892)^\pm K^\mp)/\Gamma_{\text{total}}$ Γ_{33}/Γ

VALUE (units 10^{-4})	DOCUMENT ID		TECN	COMMENT
1.44±0.21±0.03	[1] ABLIKIM	17AG	BES3	$\psi(2S) \to \gamma K\overline{K}\pi$
• • • We do not use the following data for averages, fits, limits, etc. • • •				
1.72±0.26±0.04	[2] ABLIKIM	17AG	BES3	$\psi(2S) \to \gamma K^+K^-\pi^0$
1.34±0.27±0.03	[3] ABLIKIM	17AG	BES3	$\psi(2S) \to \gamma K_S^0K^\pm\pi^\mp$

[1] ABLIKIM 17AG reports $(1.5 \pm 0.1 \pm 0.2) \times 10^{-4}$ from a measurement of $[\Gamma(\chi_{c2}(1P) \to K^*(892)^\pm K^\mp)/\Gamma_{\text{total}}] \times [B(\psi(2S) \to \gamma\chi_{c2}(1P))]$ assuming $B(\psi(2S) \to \gamma\chi_{c2}(1P)) = (9.11 \pm 0.31) \times 10^{-2}$, which we rescale to our best value $B(\psi(2S) \to \gamma\chi_{c2}(1P)) = (9.52 \pm 0.20) \times 10^{-2}$. Our first error is their experiment's error and our second error is the systematic error from using our best value.

[2] ABLIKIM 17AG reports $(1.8 \pm 0.2 \pm 0.2) \times 10^{-4}$ from a measurement of $[\Gamma(\chi_{c2}(1P) \to K^*(892)^\pm K^\mp)/\Gamma_{\text{total}}] \times [B(\psi(2S) \to \gamma\chi_{c2}(1P))]$ assuming $B(\psi(2S) \to \gamma\chi_{c2}(1P)) = (9.11 \pm 0.31) \times 10^{-2}$, which we rescale to our best value $B(\psi(2S) \to \gamma\chi_{c2}(1P)) = (9.52 \pm 0.20) \times 10^{-2}$. Our first error is their experiment's error and our second error is the systematic error from using our best value.

[3] ABLIKIM 17AG reports $(1.4 \pm 0.2 \pm 0.2) \times 10^{-4}$ from a measurement of $[\Gamma(\chi_{c2}(1P) \to K^*(892)^\pm K^\mp)/\Gamma_{\text{total}}] \times [B(\psi(2S) \to \gamma\chi_{c2}(1P))]$ assuming $B(\psi(2S) \to \gamma\chi_{c2}(1P)) = (9.11 \pm 0.31) \times 10^{-2}$, which we rescale to our best value $B(\psi(2S) \to \gamma\chi_{c2}(1P)) = (9.52 \pm 0.20) \times 10^{-2}$. Our first error is their experiment's error and our second error is the systematic error from using our best value.

$\Gamma(K^*(892)^0\overline{K}^0 + \text{c.c.})/\Gamma_{\text{total}}$ Γ_{34}/Γ

VALUE (units 10^{-4})	DOCUMENT ID		TECN	COMMENT
1.24±0.27±0.03	[1] ABLIKIM	17AG	BES3	$\psi(2S) \to \gamma K_S^0K^\pm\pi^\mp$

[1] ABLIKIM 17AG reports $(1.3 \pm 0.2 \pm 0.2) \times 10^{-4}$ from a measurement of $[\Gamma(\chi_{c2}(1P) \to K^*(892)^0\overline{K}^0 + \text{c.c.})/\Gamma_{\text{total}}] \times [B(\psi(2S) \to \gamma\chi_{c2}(1P))]$ assuming $B(\psi(2S) \to \gamma\chi_{c2}(1P)) = (9.11 \pm 0.31) \times 10^{-2}$, which we rescale to our best value $B(\psi(2S) \to \gamma\chi_{c2}(1P)) = (9.52 \pm 0.20) \times 10^{-2}$. Our first error is their experiment's error and our second error is the systematic error from using our best value.

$\Gamma(K_2^*(1430)^\pm K^\mp)/\Gamma_{\text{total}}$ Γ_{35}/Γ

VALUE (units 10^{-4})	DOCUMENT ID		TECN	COMMENT
14.8±1.2±0.3	[1] ABLIKIM	17AG	BES3	$\psi(2S) \to \gamma K\overline{K}\pi$
• • • We do not use the following data for averages, fits, limits, etc. • • •				
17.4±1.6±0.4	[2] ABLIKIM	17AG	BES3	$\psi(2S) \to \gamma K^+K^-\pi^0$
13.0±1.5±0.3	[3] ABLIKIM	17AG	BES3	$\psi(2S) \to \gamma K_S^0K^\pm\pi^\mp$

[1] ABLIKIM 17AG reports $(15.5 \pm 0.6 \pm 1.2) \times 10^{-4}$ from a measurement of $[\Gamma(\chi_{c2}(1P) \to K_2^*(1430)^\pm K^\mp)/\Gamma_{\text{total}}] \times [B(\psi(2S) \to \gamma\chi_{c2}(1P))]$ assuming $B(\psi(2S) \to \gamma\chi_{c2}(1P)) = (9.11 \pm 0.31) \times 10^{-2}$, which we rescale to our best value $B(\psi(2S) \to \gamma\chi_{c2}(1P)) = (9.52 \pm 0.20) \times 10^{-2}$. Our first error is their experiment's error and our second error is the systematic error from using our best value.

[2] ABLIKIM 17AG reports $(18.2 \pm 0.8 \pm 1.6) \times 10^{-4}$ from a measurement of $[\Gamma(\chi_{c2}(1P) \to K_2^*(1430)^\pm K^\mp)/\Gamma_{\text{total}}] \times [B(\psi(2S) \to \gamma\chi_{c2}(1P))]$ assuming $B(\psi(2S) \to \gamma\chi_{c2}(1P)) = (9.11 \pm 0.31) \times 10^{-2}$, which we rescale to our best value $B(\psi(2S) \to \gamma\chi_{c2}(1P)) = (9.52 \pm 0.20) \times 10^{-2}$. Our first error is their experiment's error and our second error is the systematic error from using our best value.

[3] ABLIKIM 17AG reports $(13.6 \pm 0.8 \pm 1.4) \times 10^{-4}$ from a measurement of $[\Gamma(\chi_{c2}(1P) \to K_2^*(1430)^\pm K^\mp)/\Gamma_{\text{total}}] \times [B(\psi(2S) \to \gamma\chi_{c2}(1P))]$ assuming $B(\psi(2S) \to \gamma\chi_{c2}(1P)) = (9.11 \pm 0.31) \times 10^{-2}$, which we rescale to our best value $B(\psi(2S) \to \gamma\chi_{c2}(1P)) = (9.52 \pm 0.20) \times 10^{-2}$. Our first error is their experiment's error and our second error is the systematic error from using our best value.

$\Gamma(K_2^*(1430)^0\overline{K}^0 + \text{c.c.})/\Gamma_{\text{total}}$ Γ_{36}/Γ

VALUE (units 10^{-4})	DOCUMENT ID		TECN	COMMENT
12.4±1.7±0.3	[1] ABLIKIM	17AG	BES3	$\psi(2S) \to \gamma K_S^0K^\pm\pi^\mp$

[1] ABLIKIM 17AG reports $(13.0 \pm 1.0 \pm 1.5) \times 10^{-4}$ from a measurement of $[\Gamma(\chi_{c2}(1P) \to K_2^*(1430)^0\overline{K}^0 + \text{c.c.})/\Gamma_{\text{total}}] \times [B(\psi(2S) \to \gamma\chi_{c2}(1P))]$ assuming $B(\psi(2S) \to \gamma\chi_{c2}(1P)) = (9.11 \pm 0.31) \times 10^{-2}$, which we rescale to our best value $B(\psi(2S) \to \gamma\chi_{c2}(1P)) = (9.52 \pm 0.20) \times 10^{-2}$. Our first error is their experiment's error and our second error is the systematic error from using our best value.

$\Gamma(K_3^*(1780)^\pm K^\mp)/\Gamma_{\text{total}}$ Γ_{37}/Γ

VALUE (units 10^{-4})	DOCUMENT ID		TECN	COMMENT
5.2±0.8±0.1	[1] ABLIKIM	17AG	BES3	$\psi(2S) \to \gamma K\overline{K}\pi$
• • • We do not use the following data for averages, fits, limits, etc. • • •				
5.1±1.0±0.1	[2] ABLIKIM	17AG	BES3	$\psi(2S) \to \gamma K^+K^-\pi^0$
5.6±1.8±0.1	[3] ABLIKIM	17AG	BES3	$\psi(2S) \to \gamma K_S^0K^\pm\pi^\mp$

[1] ABLIKIM 17AG reports $(5.4 \pm 0.5 \pm 0.7) \times 10^{-4}$ from a measurement of $[\Gamma(\chi_{c2}(1P) \to K_3^*(1780)^\pm K^\mp)/\Gamma_{\text{total}}] \times [B(\psi(2S) \to \gamma\chi_{c2}(1P))]$ assuming $B(\psi(2S) \to \gamma\chi_{c2}(1P)) = (9.11 \pm 0.31) \times 10^{-2}$, which we rescale to our best value $B(\psi(2S) \to \gamma\chi_{c2}(1P)) = (9.52 \pm 0.20) \times 10^{-2}$. Our first error is their experiment's error and our second error is the systematic error from using our best value.

[2] ABLIKIM 17AG reports $(5.3 \pm 0.5 \pm 0.9) \times 10^{-4}$ from a measurement of $[\Gamma(\chi_{c2}(1P) \to K_3^*(1780)^\pm K^\mp)/\Gamma_{\text{total}}] \times [B(\psi(2S) \to \gamma\chi_{c2}(1P))]$ assuming $B(\psi(2S) \to \gamma\chi_{c2}(1P)) = (9.11 \pm 0.31) \times 10^{-2}$, which we rescale to our best value $B(\psi(2S) \to \gamma\chi_{c2}(1P)) = (9.52 \pm 0.20) \times 10^{-2}$. Our first error is their experiment's error and our second error is the systematic error from using our best value.

[3] ABLIKIM 17AG reports $(5.9 \pm 1.1 \pm 1.5) \times 10^{-4}$ from a measurement of $[\Gamma(\chi_{c2}(1P) \to K_3^*(1780)^{\pm} K^{\mp})/\Gamma_{\text{total}}] \times [B(\psi(2S) \to \gamma\chi_{c2}(1P))]$ assuming $B(\psi(2S) \to \gamma\chi_{c2}(1P)) = (9.11 \pm 0.31) \times 10^{-2}$, which we rescale to our best value $B(\psi(2S) \to \gamma\chi_{c2}(1P)) = (9.52 \pm 0.20) \times 10^{-2}$. Our first error is their experiment's error and our second error is the systematic error from using our best value.

$\Gamma(K_3^*(1780)^0 \overline{K}{}^0 + \text{c.c.})/\Gamma_{\text{total}}$ Γ_{38}/Γ

VALUE (units 10^{-4})	DOCUMENT ID		TECN	COMMENT
5.6±2.1±0.1	[1] ABLIKIM	17AG	BES3	$\psi(2S) \to \gamma K_S^0 K^{\pm}\pi^{\mp}$

[1] ABLIKIM 17AG reports $(5.9 \pm 1.6 \pm 1.5) \times 10^{-4}$ from a measurement of $[\Gamma(\chi_{c2}(1P) \to K_3^*(1780)^0 \overline{K}{}^0 + \text{c.c.})/\Gamma_{\text{total}}] \times [B(\psi(2S) \to \gamma\chi_{c2}(1P))]$ assuming $B(\psi(2S) \to \gamma\chi_{c2}(1P)) = (9.11 \pm 0.31) \times 10^{-2}$, which we rescale to our best value $B(\psi(2S) \to \gamma\chi_{c2}(1P)) = (9.52 \pm 0.20) \times 10^{-2}$. Our first error is their experiment's error and our second error is the systematic error from using our best value.

$\Gamma(a_2(1320)^0\pi^0)/\Gamma_{\text{total}}$ Γ_{39}/Γ

VALUE (units 10^{-4})	DOCUMENT ID		TECN	COMMENT
12.9±3.4±0.3	[1] ABLIKIM	17AG	BES3	$\psi(2S) \to \gamma K^+ K^- \pi^0$

[1] ABLIKIM 17AG reports $(13.5 \pm 1.6 \pm 3.2) \times 10^{-4}$ from a measurement of $[\Gamma(\chi_{c2}(1P) \to a_2(1320)^0\pi^0)/\Gamma_{\text{total}}] \times [B(\psi(2S) \to \gamma\chi_{c2}(1P))]$ assuming $B(\psi(2S) \to \gamma\chi_{c2}(1P)) = (9.11 \pm 0.31) \times 10^{-2}$, which we rescale to our best value $B(\psi(2S) \to \gamma\chi_{c2}(1P)) = (9.52 \pm 0.20) \times 10^{-2}$. Our first error is their experiment's error and our second error is the systematic error from using our best value.

$\Gamma(a_2(1320)^{\pm}\pi^{\mp})/\Gamma_{\text{total}}$ Γ_{40}/Γ

VALUE (units 10^{-4})	DOCUMENT ID		TECN	COMMENT
17.6±6.1±0.4	[1] ABLIKIM	17AG	BES3	$\psi(2S) \to \gamma K_S^0 K^{\pm}\pi^{\mp}$

[1] ABLIKIM 17AG reports $(18.4 \pm 3.3 \pm 5.5) \times 10^{-4}$ from a measurement of $[\Gamma(\chi_{c2}(1P) \to a_2(1320)^{\pm}\pi^{\mp})/\Gamma_{\text{total}}] \times [B(\psi(2S) \to \gamma\chi_{c2}(1P))]$ assuming $B(\psi(2S) \to \gamma\chi_{c2}(1P)) = (9.11 \pm 0.31) \times 10^{-2}$, which we rescale to our best value $B(\psi(2S) \to \gamma\chi_{c2}(1P)) = (9.52 \pm 0.20) \times 10^{-2}$. Our first error is their experiment's error and our second error is the systematic error from using our best value.

$\Gamma(K^+ K^- \pi^0)/\Gamma_{\text{total}}$ Γ_{42}/Γ

VALUE (units 10^{-3})	DOCUMENT ID		TECN	COMMENT
0.30±0.08±0.01	[1] ATHAR	07	CLEO	$\psi(2S) \to \gamma h^+ h^- h^0$

[1] ATHAR 07 reports $(0.31 \pm 0.07 \pm 0.04) \times 10^{-3}$ from a measurement of $[\Gamma(\chi_{c2}(1P) \to K^+ K^- \pi^0)/\Gamma_{\text{total}}] \times [B(\psi(2S) \to \gamma\chi_{c2}(1P))]$ assuming $B(\psi(2S) \to \gamma\chi_{c2}(1P)) = (9.33 \pm 0.14 \pm 0.61) \times 10^{-2}$, which we rescale to our best value $B(\psi(2S) \to \gamma\chi_{c2}(1P)) = (9.52 \pm 0.20) \times 10^{-2}$. Our first error is their experiment's error and our second error is the systematic error from using our best value.

$\Gamma(K^+ K^- \eta)/\Gamma_{\text{total}}$ Γ_{43}/Γ

VALUE (units 10^{-3})	CL%	DOCUMENT ID		TECN	COMMENT
<0.32	90	[1] ATHAR	07	CLEO	$\psi(2S) \to \gamma h^+ h^- h^0$

[1] ATHAR 07 reports $< 0.33 \times 10^{-3}$ from a measurement of $[\Gamma(\chi_{c2}(1P) \to K^+ K^- \eta)/\Gamma_{\text{total}}] \times [B(\psi(2S) \to \gamma\chi_{c2}(1P))]$ assuming $B(\psi(2S) \to \gamma\chi_{c2}(1P)) = (9.33 \pm 0.14 \pm 0.61) \times 10^{-2}$, which we rescale to our best value $B(\psi(2S) \to \gamma\chi_{c2}(1P)) = 9.52 \times 10^{-2}$.

$\Gamma(K^+ K^- \eta'(958))/\Gamma_{\text{total}}$ Γ_{44}/Γ

VALUE (units 10^{-4})	EVTS	DOCUMENT ID		TECN	COMMENT
1.94±0.34	107	[1] ABLIKIM	14J	BES3	$\psi(2S) \to \gamma K^+ K^- \eta'(958)$

[1] Derived using $B(\psi(2S) \to \gamma\chi_{c2}) = (8.72 \pm 0.34)\%$. Uncertainty includes both statistical and systematic contributions combined in quadrature.

$\Gamma(\eta\eta')/\Gamma_{\text{total}}$ Γ_{45}/Γ

VALUE (units 10^{-5})	CL%	EVTS	DOCUMENT ID		TECN	COMMENT
2.17±0.47±0.05		20	[1] ABLIKIM	17AI	BES3	$\psi(2S) \to \gamma\eta'\eta$
• • • We do not use the following data for averages, fits, limits, etc. • • •						
< 6	90	3.3 ± 8.0	[2] ASNER	09	CLEO	$\psi(2S) \to \gamma\eta\eta'$
<23	90		[3] ADAMS	07	CLEO	$\psi(2S) \to \gamma\chi_{c2}$

[1] ABLIKIM 17AI reports $(2.27 \pm 0.43 \pm 0.25) \times 10^{-5}$ from a measurement of $[\Gamma(\chi_{c2}(1P) \to \eta\eta')/\Gamma_{\text{total}}] \times [B(\psi(2S) \to \gamma\chi_{c2}(1P))]$ assuming $B(\psi(2S) \to \gamma\chi_{c2}(1P)) = (9.11 \pm 0.31) \times 10^{-2}$, which we rescale to our best value $B(\psi(2S) \to \gamma\chi_{c2}(1P)) = (9.52 \pm 0.20) \times 10^{-2}$. Our first error is their experiment's error and our second error is the systematic error from using our best value.

[2] ASNER 09 reports $< 0.6 \times 10^{-4}$ from a measurement of $[\Gamma(\chi_{c2}(1P) \to \eta\eta')/\Gamma_{\text{total}}] \times [B(\psi(2S) \to \gamma\chi_{c2}(1P))]$ assuming $B(\psi(2S) \to \gamma\chi_{c2}(1P)) = (9.33 \pm 0.14 \pm 0.61) \times 10^{-2}$, which we rescale to our best value $B(\psi(2S) \to \gamma\chi_{c2}(1P)) = 9.52 \times 10^{-2}$.

[3] Superseded by ASNER 09. ADAMS 07 reports $< 2.3 \times 10^{-4}$ from a measurement of $[\Gamma(\chi_{c2}(1P) \to \eta\eta')/\Gamma_{\text{total}}] \times [B(\psi(2S) \to \gamma\chi_{c2}(1P))]$ assuming $B(\psi(2S) \to \gamma\chi_{c2}(1P)) = 0.0933 \pm 0.0014 \pm 0.0061$, which we rescale to our best value $B(\psi(2S) \to \gamma\chi_{c2}(1P)) = 9.52 \times 10^{-2}$.

$\Gamma(\eta'\eta')/\Gamma_{\text{total}}$ Γ_{46}/Γ

VALUE (units 10^{-5})	CL%	EVTS	DOCUMENT ID		TECN	COMMENT
4.6±0.6±0.1		60	[1] ABLIKIM	17AI	BES3	$\psi(2S) \to \gamma\eta'\eta'$
• • • We do not use the following data for averages, fits, limits, etc. • • •						
<10	90	12 ± 7	[2] ASNER	09	CLEO	$\psi(2S) \to \gamma\eta'\eta'$
<30	90		[3] ADAMS	07	CLEO	$\psi(2S) \to \gamma\chi_{c2}$

[1] ABLIKIM 17AI reports $(4.76 \pm 0.56 \pm 0.38) \times 10^{-5}$ from a measurement of $[\Gamma(\chi_{c2}(1P) \to \eta'\eta')/\Gamma_{\text{total}}] \times [B(\psi(2S) \to \gamma\chi_{c2}(1P))]$ assuming $B(\psi(2S) \to \gamma\chi_{c2}(1P)) = (9.11 \pm 0.31) \times 10^{-2}$, which we rescale to our best value $B(\psi(2S) \to \gamma\chi_{c2}(1P)) = (9.52 \pm 0.20) \times 10^{-2}$. Our first error is their experiment's error and our second error is the systematic error from using our best value.

[2] ASNER 09 reports $< 1.0 \times 10^{-4}$ from a measurement of $[\Gamma(\chi_{c2}(1P) \to \eta'\eta')/\Gamma_{\text{total}}] \times [B(\psi(2S) \to \gamma\chi_{c2}(1P))]$ assuming $B(\psi(2S) \to \gamma\chi_{c2}(1P)) = (9.33 \pm 0.14 \pm 0.61) \times 10^{-2}$, which we rescale to our best value $B(\psi(2S) \to \gamma\chi_{c2}(1P)) = 9.52 \times 10^{-2}$.

[3] Superseded by ASNER 09. ADAMS 07 reports $< 3.1 \times 10^{-4}$ from a measurement of $[\Gamma(\chi_{c2}(1P) \to \eta'\eta')/\Gamma_{\text{total}}] \times [B(\psi(2S) \to \gamma\chi_{c2}(1P))]$ assuming $B(\psi(2S) \to \gamma\chi_{c2}(1P)) = 0.0933 \pm 0.0014 \pm 0.0061$, which we rescale to our best value $B(\psi(2S) \to \gamma\chi_{c2}(1P)) = 9.52 \times 10^{-2}$.

$\Gamma(\pi^+\pi^- K_S^0 K_S^0)/\Gamma_{\text{total}}$ Γ_{47}/Γ

VALUE (units 10^{-3})	EVTS	DOCUMENT ID		TECN	COMMENT
2.17±0.54±0.05	57 ± 11	[1] ABLIKIM	05O	BES2	$\psi(2S) \to \gamma\chi_{c2}$

[1] ABLIKIM 05O reports $[\Gamma(\chi_{c2}(1P) \to \pi^+\pi^- K_S^0 K_S^0)/\Gamma_{\text{total}}] \times [B(\psi(2S) \to \gamma\chi_{c2}(1P))] = (0.207 \pm 0.039 \pm 0.033) \times 10^{-3}$ which we divide by our best value $B(\psi(2S) \to \gamma\chi_{c2}(1P)) = (9.52 \pm 0.20) \times 10^{-2}$. Our first error is their experiment's error and our second error is the systematic error from using our best value.

$\Gamma(K^+ K^- K_S^0 K_S^0)/\Gamma_{\text{total}}$ Γ_{48}/Γ

VALUE (units 10^{-4})	CL%	EVTS	DOCUMENT ID		TECN	COMMENT
<4	90	2.3 ± 2.2	[1] ABLIKIM	05O	BES2	$e^+e^- \to \chi_{c2}\gamma$

[1] ABLIKIM 05O reports $[\Gamma(\chi_{c2}(1P) \to K^+ K^- K_S^0 K_S^0)/\Gamma_{\text{total}}] \times [B(\psi(2S) \to \gamma\chi_{c2}(1P))] < 3.5 \times 10^{-5}$ which we divide by our best value $B(\psi(2S) \to \gamma\chi_{c2}(1P)) = 9.52 \times 10^{-2}$.

$\Gamma(K^+ K^- K^+ K^-)/\Gamma_{\text{total}}$ Γ_{49}/Γ

VALUE (units 10^{-3})	DOCUMENT ID
1.65±0.20 OUR FIT	

$\Gamma(K^+ K^- \phi)/\Gamma_{\text{total}}$ Γ_{50}/Γ

VALUE (units 10^{-3})	EVTS	DOCUMENT ID		TECN	COMMENT
1.42±0.29±0.03	52	[1] ABLIKIM	06T	BES2	$\psi(2S) \to \gamma 2K^+ 2K^-$

[1] ABLIKIM 06T reports $(1.67 \pm 0.26 \pm 0.24) \times 10^{-3}$ from a measurement of $[\Gamma(\chi_{c2}(1P) \to K^+ K^- \phi)/\Gamma_{\text{total}}] \times [B(\psi(2S) \to \gamma\chi_{c2}(1P))]$ assuming $B(\psi(2S) \to \gamma\chi_{c2}(1P)) = (8.1 \pm 0.4) \times 10^{-2}$, which we rescale to our best value $B(\psi(2S) \to \gamma\chi_{c2}(1P)) = (9.52 \pm 0.20) \times 10^{-2}$. Our first error is their experiment's error and our second error is the systematic error from using our best value.

$\Gamma(\overline{K}{}^0 K^+\pi^- \phi + \text{c.c.})/\Gamma_{\text{total}}$ Γ_{51}/Γ

VALUE (units 10^{-3})	DOCUMENT ID		TECN	COMMENT
4.83±0.32±0.66	ABLIKIM	15M	BES3	$\psi(2S) \to \gamma\chi_{c2}$

$\Gamma(K^+ K^- \pi^0 \phi)/\Gamma_{\text{total}}$ Γ_{52}/Γ

VALUE (units 10^{-3})	DOCUMENT ID		TECN	COMMENT
2.74±0.16±0.44	ABLIKIM	15M	BES3	$\psi(2S) \to \gamma\chi_{c2}$

$\Gamma(\phi\pi^+\pi^-\pi^0)/\Gamma_{\text{total}}$ Γ_{53}/Γ

VALUE (units 10^{-3})	EVTS	DOCUMENT ID		TECN	COMMENT
0.93±0.06±0.10	408	[1] ABLIKIM	13B	BES3	$e^+e^- \to \psi(2S) \to \gamma\chi_{c2}$

[1] Using 1.06×10^8 $\psi(2S)$ mesons and $B(\psi(2S) \to \chi_{c2}\gamma) = (8.72 \pm 0.34)\%$.

$\Gamma(p\overline{p})/\Gamma_{\text{total}}$ Γ_{54}/Γ

VALUE (units 10^{-4})	DOCUMENT ID
0.733±0.033 OUR FIT	

$\Gamma(p\overline{p}\pi^0)/\Gamma_{\text{total}}$ Γ_{55}/Γ

VALUE (units 10^{-3})	DOCUMENT ID		TECN	COMMENT
0.47±0.04 OUR AVERAGE				
0.47±0.04±0.01	[1] ONYISI	10	CLE3	$\psi(2S) \to \gamma p\overline{p}X$
0.43±0.09±0.01	[2] ATHAR	07	CLEO	$\psi(2S) \to \gamma h^+ h^- h^0$

[1] ONYISI 10 reports $(4.83 \pm 0.25 \pm 0.35 \pm 0.31) \times 10^{-4}$ from a measurement of $[\Gamma(\chi_{c2}(1P) \to p\overline{p}\pi^0)/\Gamma_{\text{total}}] \times [B(\psi(2S) \to \gamma\chi_{c2}(1P))]$ assuming $B(\psi(2S) \to \gamma\chi_{c2}(1P)) = (9.33 \pm 0.14 \pm 0.61) \times 10^{-2}$, which we rescale to our best value $B(\psi(2S) \to \gamma\chi_{c2}(1P)) = (9.52 \pm 0.20) \times 10^{-2}$. Our first error is their experiment's error and our second error is the systematic error from using our best value.

[2] ATHAR 07 reports $(0.44 \pm 0.08 \pm 0.05) \times 10^{-3}$ from a measurement of $[\Gamma(\chi_{c2}(1P) \to p\overline{p}\pi^0)/\Gamma_{\text{total}}] \times [B(\psi(2S) \to \gamma\chi_{c2}(1P))]$ assuming $B(\psi(2S) \to \gamma\chi_{c2}(1P)) = (9.33 \pm 0.14 \pm 0.61) \times 10^{-2}$, which we rescale to our best value $B(\psi(2S) \to \gamma\chi_{c2}(1P)) = (9.52 \pm 0.20) \times 10^{-2}$. Our first error is their experiment's error and our second error is the systematic error from using our best value.

$\Gamma(p\overline{p}\eta)/\Gamma_{total}$ Γ_{56}/Γ

VALUE (units 10^{-3})	DOCUMENT ID		TECN	COMMENT
0.174±0.025 OUR AVERAGE				
0.172±0.026±0.004	[1] ONYISI	10	CLE3	$\psi(2S) \to \gamma p\overline{p}X$
0.186±0.070±0.004	[2] ATHAR	07	CLEO	$\psi(2S) \to \gamma h^+h^-h^0$

[1] ONYISI 10 reports $(1.76 \pm 0.23 \pm 0.14 \pm 0.11) \times 10^{-4}$ from a measurement of $[\Gamma(\chi_{c2}(1P) \to p\overline{p}\eta)/\Gamma_{total}] \times [B(\psi(2S) \to \gamma\chi_{c2}(1P))]$ assuming $B(\psi(2S) \to \gamma\chi_{c2}(1P)) = (9.33\pm0.14\pm0.61)\times10^{-2}$, which we rescale to our best value $B(\psi(2S) \to \gamma\chi_{c2}(1P)) = (9.52 \pm 0.20) \times 10^{-2}$. Our first error is their experiment's error and our second error is the systematic error from using our best value.

[2] ATHAR 07 reports $(0.19 \pm 0.07 \pm 0.02) \times 10^{-3}$ from a measurement of $[\Gamma(\chi_{c2}(1P) \to p\overline{p}\eta)/\Gamma_{total}] \times [B(\psi(2S) \to \gamma\chi_{c2}(1P))]$ assuming $B(\psi(2S) \to \gamma\chi_{c2}(1P)) = (9.33 \pm 0.14 \pm 0.61) \times 10^{-2}$, which we rescale to our best value $B(\psi(2S) \to \gamma\chi_{c2}(1P)) = (9.52 \pm 0.20) \times 10^{-2}$. Our first error is their experiment's error and our second error is the systematic error from using our best value.

$\Gamma(p\overline{p}\omega)/\Gamma_{total}$ Γ_{57}/Γ

VALUE (units 10^{-3})	DOCUMENT ID		TECN	COMMENT
0.36±0.04±0.01	[1] ONYISI	10	CLE3	$\psi(2S) \to \gamma p\overline{p}X$

[1] ONYISI 10 reports $(3.68 \pm 0.35 \pm 0.26 \pm 0.24) \times 10^{-4}$ from a measurement of $[\Gamma(\chi_{c2}(1P) \to p\overline{p}\omega)/\Gamma_{total}] \times [B(\psi(2S) \to \gamma\chi_{c2}(1P))]$ assuming $B(\psi(2S) \to \gamma\chi_{c2}(1P)) = (9.33\pm0.14\pm0.61)\times10^{-2}$, which we rescale to our best value $B(\psi(2S) \to \gamma\chi_{c2}(1P)) = (9.52 \pm 0.20) \times 10^{-2}$. Our first error is their experiment's error and our second error is the systematic error from using our best value.

$\Gamma(p\overline{p}\phi)/\Gamma_{total}$ Γ_{58}/Γ

VALUE (units 10^{-5})	EVTS	DOCUMENT ID		TECN	COMMENT
2.8±0.9±0.1	24 ± 7	[1] ABLIKIM	11F	BES3	$\psi(2S) \to \gamma p\overline{p}K^+K^-$

[1] ABLIKIM 11F reports $(3.04\pm0.85\pm0.43)\times10^{-5}$ from a measurement of $[\Gamma(\chi_{c2}(1P) \to p\overline{p}\phi)/\Gamma_{total}] \times [B(\psi(2S) \to \gamma\chi_{c2}(1P))]$ assuming $B(\psi(2S) \to \gamma\chi_{c2}(1P)) = (8.74 \pm 0.35) \times 10^{-2}$, which we rescale to our best value $B(\psi(2S) \to \gamma\chi_{c2}(1P)) = (9.52 \pm 0.20) \times 10^{-2}$. Our first error is their experiment's error and our second error is the systematic error from using our best value.

$\Gamma(p\overline{p}\pi^+\pi^-)/\Gamma_{total}$ Γ_{59}/Γ

VALUE (units 10^{-3})	DOCUMENT ID		TECN	COMMENT
1.32±0.34 OUR EVALUATION Treating systematic error as correlated.				
1.3 ±0.4 OUR AVERAGE Error includes scale factor of 1.3.				
1.17±0.19±0.30	[1] BAI	99B	BES	$\psi(2S) \to \gamma\chi_{c2}$
2.64±1.03±0.14	[1] TANENBAUM	78	MRK1	$\psi(2S) \to \gamma\chi_{c2}$

[1] Rescaled by us using $B(\psi(2S) \to \gamma\chi_{c2}) = (8.3 \pm 0.4)\%$ and $B(\psi(2S) \to J/\psi(1S)\pi^+\pi^-) = (32.6 \pm 0.5)\%$. Multiplied by a factor of 2 to convert from $K^0_S K^+\pi^-$ to $K^0 K^+\pi^-$ decay.

$\Gamma(p\overline{p}\pi^0\pi^0)/\Gamma_{total}$ Γ_{60}/Γ

VALUE (%)	EVTS	DOCUMENT ID		TECN	COMMENT
0.078±0.023±0.002	29.2	[1] HE	08B	CLEO	$e^+e^- \to \gamma h^+h^-h^0h^0$

[1] HE 08B reports $0.08 \pm 0.02 \pm 0.01 \pm 0.01$ % from a measurement of $[\Gamma(\chi_{c2}(1P) \to p\overline{p}\pi^0\pi^0)/\Gamma_{total}] \times [B(\psi(2S) \to \gamma\chi_{c2}(1P))]$ assuming $B(\psi(2S) \to \gamma\chi_{c2}(1P)) = (9.33\pm0.14\pm0.61)\times10^{-2}$, which we rescale to our best value $B(\psi(2S) \to \gamma\chi_{c2}(1P)) = (9.52 \pm 0.20) \times 10^{-2}$. Our first error is their experiment's error and our second error is the systematic error from using our best value.

$\Gamma(p\overline{p}K^+K^-(\text{non-resonant}))/\Gamma_{total}$ Γ_{61}/Γ

VALUE (units 10^{-4})	EVTS	DOCUMENT ID		TECN	COMMENT
1.91±0.32±0.04	131 ± 12	[1] ABLIKIM	11F	BES3	$\psi(2S) \to \gamma p\overline{p}K^+K^-$

[1] ABLIKIM 11F reports $(2.08\pm0.19\pm0.30)\times10^{-4}$ from a measurement of $[\Gamma(\chi_{c2}(1P) \to p\overline{p}K^+K^-(\text{non-resonant}))/\Gamma_{total}] \times [B(\psi(2S) \to \gamma\chi_{c2}(1P))]$ assuming $B(\psi(2S) \to \gamma\chi_{c2}(1P)) = (8.74 \pm 0.35) \times 10^{-2}$, which we rescale to our best value $B(\psi(2S) \to \gamma\chi_{c2}(1P)) = (9.52 \pm 0.20) \times 10^{-2}$. Our first error is their experiment's error and our second error is the systematic error from using our best value.

$\Gamma(p\overline{p}K^0_S K^0_S)/\Gamma_{total}$ Γ_{62}/Γ

VALUE (units 10^{-4})	CL%	DOCUMENT ID		TECN	COMMENT
<7.9	90	[1] ABLIKIM	06D	BES2	$\psi(2S) \to \chi_{c2}\gamma$

[1] Using $B(\psi(2S) \to \chi_{c2}\gamma) = (9.3 \pm 0.6)\%$.

$\Gamma(p\overline{n}\pi^-)/\Gamma_{total}$ Γ_{63}/Γ

VALUE (units 10^{-4})	EVTS	DOCUMENT ID		TECN	COMMENT
8.5±0.9 OUR AVERAGE					
8.4±1.0±0.2	3309	[1] ABLIKIM	12J	BES3	$\psi(2S) \to \gamma p\overline{n}\pi^-$
10.2±3.4±0.2		[2] ABLIKIM	06I	BES2	$\psi(2S) \to \gamma p\pi^- X$

[1] ABLIKIM 12J reports $[\Gamma(\chi_{c2}(1P) \to p\overline{n}\pi^-)/\Gamma_{total}] \times [B(\psi(2S) \to \gamma\chi_{c2}(1P))] = (0.80 \pm 0.02 \pm 0.09) \times 10^{-4}$ which we divide by our best value $B(\psi(2S) \to \gamma\chi_{c2}(1P)) = (9.52 \pm 0.20) \times 10^{-2}$. Our first error is their experiment's error and our second error is the systematic error from using our best value.

[2] ABLIKIM 06I reports $[\Gamma(\chi_{c2}(1P) \to p\overline{n}\pi^-)/\Gamma_{total}] \times [B(\psi(2S) \to \gamma\chi_{c2}(1P))] = (0.97 \pm 0.20 \pm 0.26) \times 10^{-4}$ which we divide by our best value $B(\psi(2S) \to \gamma\chi_{c2}(1P)) = (9.52 \pm 0.20) \times 10^{-2}$. Our first error is their experiment's error and our second error is the systematic error from using our best value.

$\Gamma(\overline{p}n\pi^+)/\Gamma_{total}$ Γ_{64}/Γ

VALUE (units 10^{-4})	EVTS	DOCUMENT ID		TECN	COMMENT
8.9±0.8±0.2	3732	[1] ABLIKIM	12J	BES3	$\psi(2S) \to \gamma\overline{p}n\pi^+$

[1] ABLIKIM 12J reports $[\Gamma(\chi_{c2}(1P) \to \overline{p}n\pi^+)/\Gamma_{total}] \times [B(\psi(2S) \to \gamma\chi_{c2}(1P))] = (0.85 \pm 0.02 \pm 0.07) \times 10^{-4}$ which we divide by our best value $B(\psi(2S) \to \gamma\chi_{c2}(1P)) = (9.52 \pm 0.20) \times 10^{-2}$. Our first error is their experiment's error and our second error is the systematic error from using our best value.

$\Gamma(p\overline{n}\pi^-\pi^0)/\Gamma_{total}$ Γ_{65}/Γ

VALUE (units 10^{-4})	EVTS	DOCUMENT ID		TECN	COMMENT
21.7±1.7±0.5	2128	[1] ABLIKIM	12J	BES3	$\psi(2S) \to \gamma p\overline{n}\pi^-\pi^0$

[1] ABLIKIM 12J reports $[\Gamma(\chi_{c2}(1P) \to p\overline{n}\pi^-\pi^0)/\Gamma_{total}] \times [B(\psi(2S) \to \gamma\chi_{c2}(1P))] = (2.07 \pm 0.06 \pm 0.15) \times 10^{-4}$ which we divide by our best value $B(\psi(2S) \to \gamma\chi_{c2}(1P)) = (9.52 \pm 0.20) \times 10^{-2}$. Our first error is their experiment's error and our second error is the systematic error from using our best value.

$\Gamma(\overline{p}n\pi^+\pi^0)/\Gamma_{total}$ Γ_{66}/Γ

VALUE (units 10^{-4})	EVTS	DOCUMENT ID		TECN	COMMENT
21.1±1.8±0.4	2352	[1] ABLIKIM	12J	BES3	$\psi(2S) \to \gamma\overline{p}n\pi^+\pi^0$

[1] ABLIKIM 12J reports $[\Gamma(\chi_{c2}(1P) \to \overline{p}n\pi^+\pi^0)/\Gamma_{total}] \times [B(\psi(2S) \to \gamma\chi_{c2}(1P))] = (2.01 \pm 0.06 \pm 0.16) \times 10^{-4}$ which we divide by our best value $B(\psi(2S) \to \gamma\chi_{c2}(1P)) = (9.52 \pm 0.20) \times 10^{-2}$. Our first error is their experiment's error and our second error is the systematic error from using our best value.

$\Gamma(\Lambda\overline{\Lambda})/\Gamma_{total}$ Γ_{67}/Γ

VALUE (units 10^{-4})	DOCUMENT ID
1.84±0.15 OUR FIT	

$\Gamma(\Lambda\overline{\Lambda}\pi^+\pi^-)/\Gamma_{total}$ Γ_{68}/Γ

VALUE (units 10^{-5})	CL%	EVTS	DOCUMENT ID		TECN	COMMENT
125±15±3		371	[1] ABLIKIM	12I	BES3	$\psi(2S) \to \gamma\Lambda\overline{\Lambda}\pi^+\pi^-$
• • • We do not use the following data for averages, fits, limits, etc. • • •						
<350	90		[2] ABLIKIM	06D	BES2	$\psi(2S) \to \chi_{c2}\gamma$

[1] ABLIKIM 12I reports $(137.0\pm7.6\pm15.7)\times10^{-5}$ from a measurement of $[\Gamma(\chi_{c2}(1P) \to \Lambda\overline{\Lambda}\pi^+\pi^-)/\Gamma_{total}] \times [B(\psi(2S) \to \gamma\chi_{c2}(1P))]$ assuming $B(\psi(2S) \to \gamma\chi_{c2}(1P)) = (8.72 \pm 0.34) \times 10^{-2}$, which we rescale to our best value $B(\psi(2S) \to \gamma\chi_{c2}(1P)) = (9.52 \pm 0.20) \times 10^{-2}$. Our first error is their experiment's error and our second error is the systematic error from using our best value.

[2] Using $B(\psi(2S) \to \chi_{c2}\gamma) = (9.3 \pm 0.6)\%$.

$\Gamma(\Lambda\overline{\Lambda}\pi^+\pi^-(\text{non-resonant}))/\Gamma_{total}$ Γ_{69}/Γ

VALUE (units 10^{-5})	EVTS	DOCUMENT ID		TECN	COMMENT
66±15±1	36	[1] ABLIKIM	12I	BES3	$\psi(2S) \to \gamma\Lambda\overline{\Lambda}\pi^+\pi^-$

[1] ABLIKIM 12I reports $(71.8 \pm 14.5 \pm 8.2) \times 10^{-5}$ from a measurement of $[\Gamma(\chi_{c2}(1P) \to \Lambda\overline{\Lambda}\pi^+\pi^-(\text{non-resonant}))/\Gamma_{total}] \times [B(\psi(2S) \to \gamma\chi_{c2}(1P))]$ assuming $B(\psi(2S) \to \gamma\chi_{c2}(1P)) = (8.72 \pm 0.34) \times 10^{-2}$, which we rescale to our best value $B(\psi(2S) \to \gamma\chi_{c2}(1P)) = (9.52 \pm 0.20) \times 10^{-2}$. Our first error is their experiment's error and our second error is the systematic error from using our best value.

$\Gamma(\Sigma(1385)^+\overline{\Lambda}\pi^- + \text{c.c.})/\Gamma_{total}$ Γ_{70}/Γ

VALUE (units 10^{-5})	CL%	DOCUMENT ID		TECN	COMMENT
<40	90	[1] ABLIKIM	12I	BES3	$\psi(2S) \to \gamma\Sigma(1385)^+\overline{\Lambda}\pi^-$

[1] ABLIKIM 12I reports $< 42 \times 10^{-5}$ from a measurement of $[\Gamma(\chi_{c2}(1P) \to \Sigma(1385)^+\overline{\Lambda}\pi^- + \text{c.c.})/\Gamma_{total}] \times [B(\psi(2S) \to \gamma\chi_{c2}(1P))]$ assuming $B(\psi(2S) \to \gamma\chi_{c2}(1P)) = (8.72 \pm 0.34) \times 10^{-2}$, which we rescale to our best value $B(\psi(2S) \to \gamma\chi_{c2}(1P)) = 9.52 \times 10^{-2}$.

$\Gamma(\Sigma(1385)^-\overline{\Lambda}\pi^+ + \text{c.c.})/\Gamma_{total}$ Γ_{71}/Γ

VALUE (units 10^{-5})	CL%	DOCUMENT ID		TECN	COMMENT
<60	90	[1] ABLIKIM	12I	BES3	$\psi(2S) \to \gamma\Sigma(1385)^-\overline{\Lambda}\pi^+$

[1] ABLIKIM 12I reports $< 61 \times 10^{-5}$ from a measurement of $[\Gamma(\chi_{c2}(1P) \to \Sigma(1385)^-\overline{\Lambda}\pi^+ + \text{c.c.})/\Gamma_{total}] \times [B(\psi(2S) \to \gamma\chi_{c2}(1P))]$ assuming $B(\psi(2S) \to \gamma\chi_{c2}(1P)) = (8.72 \pm 0.34) \times 10^{-2}$, which we rescale to our best value $B(\psi(2S) \to \gamma\chi_{c2}(1P)) = 9.52 \times 10^{-2}$.

$\Gamma(K^+\overline{p}\Lambda + \text{c.c.})/\Gamma_{total}$ Γ_{72}/Γ

VALUE (units 10^{-4})	EVTS	DOCUMENT ID		TECN	COMMENT
7.8±0.5 OUR AVERAGE					
7.7±0.5±0.2	5k	[1,2] ABLIKIM	13D	BES3	$\psi(2S) \to \gamma\Lambda\overline{p}K^+$
8.3±1.6±0.2		[3] ATHAR	07	CLEO	$\psi(2S) \to \gamma h^+h^-h^0$

[1] ABLIKIM 13D reports $(8.4 \pm 0.3 \pm 0.6) \times 10^{-4}$ from a measurement of $[\Gamma(\chi_{c2}(1P) \to K^+\overline{p}\Lambda + \text{c.c.})/\Gamma_{total}] \times [B(\psi(2S) \to \gamma\chi_{c2}(1P))]$ assuming $B(\psi(2S) \to \gamma\chi_{c2}(1P)) = (8.72 \pm 0.34) \times 10^{-2}$, which we rescale to our best value $B(\psi(2S) \to \gamma\chi_{c2}(1P)) = (9.52 \pm 0.20) \times 10^{-2}$. Our first error is their experiment's error and our second error is the systematic error from using our best value.

[2] Using $B(\Lambda \to p\pi^-) = 63.9\%$.

[3] ATHAR 07 reports $(8.5 \pm 1.4 \pm 1.0) \times 10^{-4}$ from a measurement of $[\Gamma(\chi_{c2}(1P) \to K^+\overline{p}\Lambda + \text{c.c.})/\Gamma_{total}] \times [B(\psi(2S) \to \gamma\chi_{c2}(1P))]$ assuming $B(\psi(2S) \to \gamma\chi_{c2}(1P)) = (9.33 \pm 0.14 \pm 0.61) \times 10^{-2}$, which we rescale to our best value $B(\psi(2S) \to$

$\gamma\chi_{c2}(1P)) = (9.52 \pm 0.20) \times 10^{-2}$. Our first error is their experiment's error and our second error is the systematic error from using our best value.

$\Gamma(K^+\overline{p}\Lambda(1520)+\text{c.c.})/\Gamma_{\text{total}}$ Γ_{73}/Γ

VALUE (units 10^{-4})	EVTS	DOCUMENT ID		TECN	COMMENT
2.8±0.7±0.1	79 ± 13	[1] ABLIKIM	11F	BES3	$\psi(2S) \to \gamma p\overline{p}K^+K^-$

[1] ABLIKIM 11F reports $(3.06\pm0.50\pm0.54)\times10^{-4}$ from a measurement of $[\Gamma(\chi_{c2}(1P) \to K^+\overline{p}\Lambda(1520)+\text{ c.c.})/\Gamma_{\text{total}}] \times [B(\psi(2S) \to \gamma\chi_{c2}(1P))]$ assuming $B(\psi(2S) \to \gamma\chi_{c2}(1P)) = (8.74 \pm 0.35) \times 10^{-2}$, which we rescale to our best value $B(\psi(2S) \to \gamma\chi_{c2}(1P)) = (9.52 \pm 0.20) \times 10^{-2}$. Our first error is their experiment's error and our second error is the systematic error from using our best value.

$\Gamma(\Lambda(1520)\overline{\Lambda}(1520))/\Gamma_{\text{total}}$ Γ_{74}/Γ

VALUE (units 10^{-4})	EVTS	DOCUMENT ID		TECN	COMMENT
4.6±1.4±0.1	29 ± 7	[1] ABLIKIM	11F	BES3	$\psi(2S) \to \gamma p\overline{p}K^+K^-$

[1] ABLIKIM 11F reports $(5.05 \pm 1.29 \pm 0.93) \times 10^{-4}$ from a measurement of $[\Gamma(\chi_{c2}(1P) \to \Lambda(1520)\overline{\Lambda}(1520))/\Gamma_{\text{total}}] \times [B(\psi(2S) \to \gamma\chi_{c2}(1P))]$ assuming $B(\psi(2S) \to \gamma\chi_{c2}(1P)) = (8.74 \pm 0.35) \times 10^{-2}$, which we rescale to our best value $B(\psi(2S) \to \gamma\chi_{c2}(1P)) = (9.52 \pm 0.20) \times 10^{-2}$. Our first error is their experiment's error and our second error is the systematic error from using our best value.

$\Gamma(\Sigma^0\overline{\Sigma}^0)/\Gamma_{\text{total}}$ Γ_{75}/Γ

VALUE (units 10^{-4})	CL%	EVTS	DOCUMENT ID		TECN	COMMENT
<0.6	90		[1] ABLIKIM	13H	BES3	$\psi(2S) \to \gamma\Sigma^0\overline{\Sigma}^0$
• • • We do not use the following data for averages, fits, limits, etc. • • •						
<0.7	90	7.5 ± 3.4	[2] NAIK	08	CLEO	$\psi(2S) \to \gamma\Sigma^0\overline{\Sigma}^0$

[1] ABLIKIM 13H reports $< 0.65\times10^{-4}$ from a measurement of $[\Gamma(\chi_{c2}(1P) \to \Sigma^0\overline{\Sigma}^0)/\Gamma_{\text{total}}] \times [B(\psi(2S) \to \gamma\chi_{c2}(1P))]$ assuming $B(\psi(2S) \to \gamma\chi_{c2}(1P)) = (8.74\pm0.35)\times10^{-2}$, which we rescale to our best value $B(\psi(2S) \to \gamma\chi_{c2}(1P)) = 9.52\times10^{-2}$.

[2] NAIK 08 reports $< 0.75\times10^{-4}$ from a measurement of $[\Gamma(\chi_{c2}(1P) \to \Sigma^0\overline{\Sigma}^0)/\Gamma_{\text{total}}] \times [B(\psi(2S) \to \gamma\chi_{c2}(1P))]$ assuming $B(\psi(2S) \to \gamma\chi_{c2}(1P)) = (9.33\pm0.14\pm0.61)\times10^{-2}$, which we rescale to our best value $B(\psi(2S) \to \gamma\chi_{c2}(1P)) = 9.52\times10^{-2}$.

$\Gamma(\Sigma^+\overline{\Sigma}^-)/\Gamma_{\text{total}}$ Γ_{76}/Γ

VALUE (units 10^{-4})	CL%	EVTS	DOCUMENT ID		TECN	COMMENT
<0.7	90	4.0 ± 3.5	[1] NAIK	08	CLEO	$\psi(2S) \to \gamma\Sigma^+\overline{\Sigma}^-$
• • • We do not use the following data for averages, fits, limits, etc. • • •						
<0.8	90		[2] ABLIKIM	13H	BES3	$\psi(2S) \to \gamma\Sigma^+\overline{\Sigma}^-$

[1] NAIK 08 reports $< 0.67 \times 10^{-4}$ from a measurement of $[\Gamma(\chi_{c2}(1P) \to \Sigma^+\overline{\Sigma}^-)/\Gamma_{\text{total}}] \times [B(\psi(2S) \to \gamma\chi_{c2}(1P))]$ assuming $B(\psi(2S) \to \gamma\chi_{c2}(1P)) = (9.33 \pm 0.14 \pm 0.61) \times 10^{-2}$, which we rescale to our best value $B(\psi(2S) \to \gamma\chi_{c2}(1P)) = 9.52 \times 10^{-2}$.

[2] ABLIKIM 13H reports $< 0.88\times10^{-4}$ from a measurement of $[\Gamma(\chi_{c2}(1P) \to \Sigma^+\overline{\Sigma}^-)/\Gamma_{\text{total}}] \times [B(\psi(2S) \to \gamma\chi_{c2}(1P))]$ assuming $B(\psi(2S) \to \gamma\chi_{c2}(1P)) = (8.74\pm0.35)\times10^{-2}$, which we rescale to our best value $B(\psi(2S) \to \gamma\chi_{c2}(1P)) = 9.52\times10^{-2}$.

$\Gamma(\Sigma(1385)^+\overline{\Sigma}(1385)^-)/\Gamma_{\text{total}}$ Γ_{77}/Γ

VALUE (units 10^{-5})	CL%	DOCUMENT ID		TECN	COMMENT
<16	90	[1] ABLIKIM	12I	BES3	$\psi(2S) \to \gamma\Sigma(1385)^+\overline{\Sigma}(1385)^-$

[1] ABLIKIM 12I reports $< 17 \times 10^{-5}$ from a measurement of $[\Gamma(\chi_{c2}(1P) \to \Sigma(1385)^+\overline{\Sigma}(1385)^-)/\Gamma_{\text{total}}] \times [B(\psi(2S) \to \gamma\chi_{c2}(1P))]$ assuming $B(\psi(2S) \to \gamma\chi_{c2}(1P)) = (8.72 \pm 0.34) \times 10^{-2}$, which we rescale to our best value $B(\psi(2S) \to \gamma\chi_{c2}(1P)) = 9.52 \times 10^{-2}$.

$\Gamma(\Sigma(1385)^-\overline{\Sigma}(1385)^+)/\Gamma_{\text{total}}$ Γ_{78}/Γ

VALUE (units 10^{-5})	CL%	DOCUMENT ID		TECN	COMMENT
<8	90	[1] ABLIKIM	12I	BES3	$\psi(2S) \to \gamma\Sigma(1385)^-\overline{\Sigma}(1385)^+$

[1] ABLIKIM 12I reports $< 8.5 \times 10^{-5}$ from a measurement of $[\Gamma(\chi_{c2}(1P) \to \Sigma(1385)^-\overline{\Sigma}(1385)^+)/\Gamma_{\text{total}}] \times [B(\psi(2S) \to \gamma\chi_{c2}(1P))]$ assuming $B(\psi(2S) \to \gamma\chi_{c2}(1P)) = (8.72 \pm 0.34) \times 10^{-2}$, which we rescale to our best value $B(\psi(2S) \to \gamma\chi_{c2}(1P)) = 9.52 \times 10^{-2}$.

$\Gamma(K^-\Lambda\overline{\Xi}^+ + \text{c.c.})/\Gamma_{\text{total}}$ Γ_{79}/Γ

VALUE (units 10^{-4})	EVTS	DOCUMENT ID		TECN	COMMENT
1.76±0.32±0.04	51	[1] ABLIKIM	15I	BES3	$\psi(2S) \to \gamma K^-\Lambda\overline{\Xi}^+ + \text{c.c.}$

[1] ABLIKIM 15I reports $[\Gamma(\chi_{c2}(1P) \to K^-\Lambda\overline{\Xi}^+ + \text{ c.c.})/\Gamma_{\text{total}}] \times [B(\psi(2S) \to \gamma\chi_{c2}(1P))] = (1.68\pm0.26\pm0.15)\times10^{-5}$ which we divide by our best value $B(\psi(2S) \to \gamma\chi_{c2}(1P)) = (9.52 \pm 0.20) \times 10^{-2}$. Our first error is their experiment's error and our second error is the systematic error from using our best value.

$\Gamma(\Xi^0\overline{\Xi}^0)/\Gamma_{\text{total}}$ Γ_{80}/Γ

VALUE (units 10^{-4})	CL%	EVTS	DOCUMENT ID		TECN	COMMENT
<1.0	90	2.9 ± 1.7	[1] NAIK	08	CLEO	$\psi(2S) \to \gamma\Xi^0\overline{\Xi}^0$

[1] NAIK 08 reports $< 1.06\times10^{-4}$ from a measurement of $[\Gamma(\chi_{c2}(1P) \to \Xi^0\overline{\Xi}^0)/\Gamma_{\text{total}}] \times [B(\psi(2S) \to \gamma\chi_{c2}(1P))]$ assuming $B(\psi(2S) \to \gamma\chi_{c2}(1P)) = (9.33\pm0.14\pm0.61)\times10^{-2}$, which we rescale to our best value $B(\psi(2S) \to \gamma\chi_{c2}(1P)) = 9.52\times10^{-2}$.

$\Gamma(\Xi^-\overline{\Xi}^+)/\Gamma_{\text{total}}$ Γ_{81}/Γ

VALUE (units 10^{-4})	CL%	EVTS	DOCUMENT ID		TECN	COMMENT
1.42±0.31±0.03		29 ± 5	[1] NAIK	08	CLEO	$\psi(2S) \to \gamma\Xi^+\overline{\Xi}^-$
• • • We do not use the following data for averages, fits, limits, etc. • • •						
< 3.7	90		[2] ABLIKIM	06D	BES2	$\psi(2S) \to \chi_{c2}\gamma$

[1] NAIK 08 reports $(1.45 \pm 0.30 \pm 0.15) \times 10^{-4}$ from a measurement of $[\Gamma(\chi_{c2}(1P) \to \Xi^-\overline{\Xi}^+)/\Gamma_{\text{total}}] \times [B(\psi(2S) \to \gamma\chi_{c2}(1P))]$ assuming $B(\psi(2S) \to \gamma\chi_{c2}(1P)) = (9.33 \pm 0.14 \pm 0.61) \times 10^{-2}$, which we rescale to our best value $B(\psi(2S) \to \gamma\chi_{c2}(1P)) = (9.52 \pm 0.20) \times 10^{-2}$. Our first error is their experiment's error and our second error is the systematic error from using our best value.

[2] Using $B(\psi(2S) \to \chi_{c2}\gamma) = (9.3 \pm 0.6)\%$.

$\Gamma(J/\psi(1S)\pi^+\pi^-\pi^0)/\Gamma_{\text{total}}$ Γ_{82}/Γ

VALUE	CL%	DOCUMENT ID		TECN	COMMENT
<0.015	90	BARATE	81	SPEC	190 GeV π^-Be $\to 2\pi 2\mu$

$\Gamma(\pi^0\eta_c)/\Gamma_{\text{total}}$ Γ_{83}/Γ

VALUE	CL%	DOCUMENT ID		TECN	COMMENT
<3.2 × 10⁻³	90	[1] ABLIKIM	15N	BES3	$\psi(2S)e^+e^- \to \gamma\pi^0\eta_c$

[1] Using $B(\eta_c \to K^0_S K^\pm\pi^\mp)\times B(K^0_S \to \pi^+\pi^-)\times B(\pi^0 \to \gamma\gamma) = (1.66\pm0.11)\times10^{-2}$.

$\Gamma(\eta_c(1S)\pi^+\pi^-)/\Gamma_{\text{total}}$ Γ_{84}/Γ

VALUE	CL%	DOCUMENT ID		TECN	COMMENT
<0.54 × 10⁻²	90	[1,2] ABLIKIM	13B	BES3	$e^+e^- \to \psi(2S) \to \gamma\chi_{c2}$
• • • We do not use the following data for averages, fits, limits, etc. • • •					
<1.2 × 10⁻²	90	[1,3] ABLIKIM	13B	BES3	$e^+e^- \to \psi(2S) \to \gamma\chi_{c2}$

[1] Using 1.06×10^8 $\psi(2S)$ mesons and $B(\psi(2S) \to \chi_{c2}\gamma) = (8.72 \pm 0.34)\%$.

[2] From the $\eta_c \to K^0_S K^\pm\pi^\mp$ decays.

[3] From the $\eta_c \to K^+K^-\pi^0$ decays.

$\Gamma(\eta_c(1S)\pi^+\pi^-)/\Gamma(\overline{K}^0K^+\pi^- + \text{c.c.})$ Γ_{84}/Γ_{41}

VALUE	CL%	DOCUMENT ID		TECN	COMMENT
<16.4	90	[1] LEES	12AE	BABR	$e^+e^- \to e^+e^-\pi^+\pi^-\eta_c$

[1] We divided the reported limit by 2 to take into account the $K^0_L K^+\pi^-$ mode.

RADIATIVE DECAYS

$\Gamma(\gamma J/\psi(1S))/\Gamma_{\text{total}}$ Γ_{85}/Γ

VALUE (units 10^{-2})	EVTS	DOCUMENT ID		TECN	COMMENT
19.0 ±0.5 OUR FIT					
• • • We do not use the following data for averages, fits, limits, etc. • • •					
18.64±0.08±1.69	1.0M	[1] ABLIKIM	17U	BES3	$e^+e^- \to \gamma X$
19.9 ±0.5 ±1.2		[2] ADAM	05A	CLEO	$e^+e^- \to \psi(2S) \to \gamma\chi_{c2}$

[1] Not independent from B($\psi(2S) \to \gamma\chi_{c2}(1P)$) and the product B($\psi(2S) \to \gamma\chi_{c2}(1P)$) × B($\chi_{c2}(1P) \to \gamma J/\psi(1S)$) also measured in ABLIKIM 17U.

[2] Uses B($\psi(2S) \to \gamma\chi_{c2} \to \gamma\gamma J/\psi$) from ADAM 05A and B($\psi(2S) \to \gamma\chi_{c2}$) from ATHAR 04.

$\Gamma(\gamma\rho^0)/\Gamma_{\text{total}}$ Γ_{86}/Γ

VALUE (units 10^{-6})	CL%	EVTS	DOCUMENT ID		TECN	COMMENT
<19	90	13 ± 11	[1] ABLIKIM	11E	BES3	$\psi(2S) \to \gamma\gamma\rho^0$
• • • We do not use the following data for averages, fits, limits, etc. • • •						
<40	90	17.2 ± 6.8	[2] BENNETT	08A	CLEO	$\psi(2S) \to \gamma\gamma\rho^0$

[1] ABLIKIM 11E reports $< 20.8 \times 10^{-6}$ from a measurement of $[\Gamma(\chi_{c2}(1P) \to \gamma\rho^0)/\Gamma_{\text{total}}] \times [B(\psi(2S) \to \gamma\chi_{c2}(1P))]$ assuming $B(\psi(2S) \to \gamma\chi_{c2}(1P)) = (8.74\pm0.35)\times10^{-2}$, which we rescale to our best value $B(\psi(2S) \to \gamma\chi_{c2}(1P)) = 9.52\times10^{-2}$.

[2] BENNETT 08A reports $< 50 \times 10^{-6}$ from a measurement of $[\Gamma(\chi_{c2}(1P) \to \gamma\rho^0)/\Gamma_{\text{total}}] \times [B(\psi(2S) \to \gamma\chi_{c2}(1P))]$ assuming $B(\psi(2S) \to \gamma\chi_{c2}(1P)) = (8.1 \pm 0.4) \times 10^{-2}$, which we rescale to our best value $B(\psi(2S) \to \gamma\chi_{c2}(1P)) = 9.52 \times 10^{-2}$.

$\Gamma(\gamma\omega)/\Gamma_{\text{total}}$ Γ_{87}/Γ

VALUE (units 10^{-6})	CL%	EVTS	DOCUMENT ID		TECN	COMMENT
<6	90	1 ± 6	[1] ABLIKIM	11E	BES3	$\psi(2S) \to \gamma\gamma\omega$
• • • We do not use the following data for averages, fits, limits, etc. • • •						
<6	90	0.0 ± 1.8	[2] BENNETT	08A	CLEO	$\psi(2S) \to \gamma\gamma\omega$

[1] ABLIKIM 11E reports $< 6.1\times10^{-6}$ from a measurement of $[\Gamma(\chi_{c2}(1P) \to \gamma\omega)/\Gamma_{\text{total}}] \times [B(\psi(2S) \to \gamma\chi_{c2}(1P))]$ assuming $B(\psi(2S) \to \gamma\chi_{c2}(1P)) = (8.74 \pm 0.35)\times10^{-2}$, which we rescale to our best value $B(\psi(2S) \to \gamma\chi_{c2}(1P)) = 9.52 \times 10^{-2}$.

[2] BENNETT 08A reports $< 7.0 \times 10^{-6}$ from a measurement of $[\Gamma(\chi_{c2}(1P) \to \gamma\omega)/\Gamma_{\text{total}}] \times [B(\psi(2S) \to \gamma\chi_{c2}(1P))]$ assuming $B(\psi(2S) \to \gamma\chi_{c2}(1P)) = (8.1 \pm 0.4) \times 10^{-2}$, which we rescale to our best value $B(\psi(2S) \to \gamma\chi_{c2}(1P)) = 9.52 \times 10^{-2}$.

$\Gamma(\gamma\phi)/\Gamma_{\text{total}}$ Γ_{88}/Γ

VALUE (units 10^{-6})	CL%	EVTS	DOCUMENT ID		TECN	COMMENT
< 7	90	5 ± 5	[1] ABLIKIM	11E	BES3	$\psi(2S) \to \gamma\gamma\phi$
• • • We do not use the following data for averages, fits, limits, etc. • • •						
<11	90	1.3 ± 2.5	[2] BENNETT	08A	CLEO	$\psi(2S) \to \gamma\gamma\phi$

[1] ABLIKIM 11E reports $< 8.1\times10^{-6}$ from a measurement of $[\Gamma(\chi_{c2}(1P)\to\gamma\phi)/\Gamma_{\rm total}]\times[B(\psi(2S)\to\gamma\chi_{c2}(1P))]$ assuming $B(\psi(2S)\to\gamma\chi_{c2}(1P)) = (8.74\pm0.35)\times10^{-2}$, which we rescale to our best value $B(\psi(2S)\to\gamma\chi_{c2}(1P)) = 9.52\times10^{-2}$.

[2] BENNETT 08A reports $< 13\times10^{-6}$ from a measurement of $[\Gamma(\chi_{c2}(1P)\to\gamma\phi)/\Gamma_{\rm total}]\times[B(\psi(2S)\to\gamma\chi_{c2}(1P))]$ assuming $B(\psi(2S)\to\gamma\chi_{c2}(1P)) = (8.1\pm0.4)\times10^{-2}$, which we rescale to our best value $B(\psi(2S)\to\gamma\chi_{c2}(1P)) = 9.52\times10^{-2}$.

$\Gamma(\gamma\gamma)/\Gamma_{\rm total}$ Γ_{89}/Γ

VALUE (units 10^{-4})	DOCUMENT ID
2.85±0.10 OUR FIT	

$\Gamma(e^+e^-J/\psi(1S))/\Gamma_{\rm total}$ Γ_{90}/Γ

VALUE (units 10^{-3})	EVTS	DOCUMENT ID		TECN	COMMENT
2.37±0.15±0.05	1.3k	[1] ABLIKIM	17I	BES3	$\psi(2S)\to\gamma e^+e^-J/\psi$

[1] ABLIKIM 17I reports $(2.48\pm0.08\pm0.16)\times10^{-3}$ from a measurement of $[\Gamma(\chi_{c2}(1P)\to e^+e^-J/\psi(1S))/\Gamma_{\rm total}]\times[B(\psi(2S)\to\gamma\chi_{c2}(1P))]$ assuming $B(\psi(2S)\to\gamma\chi_{c2}(1P)) = (9.11\pm0.31)\times10^{-2}$, which we rescale to our best value $B(\psi(2S)\to\gamma\chi_{c2}(1P)) = (9.52\pm0.20)\times10^{-2}$. Our first error is their experiment's error and our second error is the systematic error from using our best value.

$\Gamma(e^+e^-J/\psi(1S))/\Gamma(\gamma J/\psi(1S))$ Γ_{90}/Γ_{85}

VALUE (units 10^{-3})	EVTS	DOCUMENT ID		TECN	COMMENT
11.3±0.4±0.5	1.3k	[1] ABLIKIM	17I	BES3	$\psi(2S)\to e^+e^-\gamma J/\psi$

[1] Uses $B(\psi(2S)\to\gamma\chi_{c2}(1P))\times B(\chi_{c2}(1P)\to\gamma J/\psi(1S)) = (199.6\pm0.8\pm7.0)\times10^{-4}$ from ABLIKIM 17N and accounts for common systematic errors.

$\Gamma(\gamma\gamma)/\Gamma(\gamma J/\psi(1S))$ Γ_{89}/Γ_{85}

VALUE (units 10^{-3})	DOCUMENT ID		TECN	COMMENT
1.50±0.05 OUR FIT				
0.99±0.18	[1] AMBROGIANI	00B	E835	$\overline{p}p\to\chi_{c2}\to\gamma\gamma,\gamma J/\psi$

[1] Calculated by us using $B(J/\psi(1S)\to e^+e^-) = 0.0593\pm0.0010$.

$\Gamma(\gamma\gamma)/\Gamma_{\rm total}\times\Gamma(p\overline{p})/\Gamma_{\rm total}$ $\Gamma_{89}/\Gamma\times\Gamma_{54}/\Gamma$

VALUE (units 10^{-8})	DOCUMENT ID		TECN	COMMENT
2.09±0.13 OUR FIT				
1.7 ±0.4 OUR AVERAGE				
1.60±0.42	ARMSTRONG	93	E760	$\overline{p}p\to\gamma\gamma X$
9.9 ±4.5	BAGLIN	87B	SPEC	$\overline{p}p\to\gamma\gamma X$

$\chi_{c2}(1P)$ CROSS-PARTICLE BRANCHING RATIOS

$\Gamma(\chi_{c2}(1P)\to K^+K^-\pi^+\pi^-)/\Gamma_{\rm total}\times\Gamma(\psi(2S)\to\gamma\chi_{c2}(1P))/\Gamma(\psi(2S)\to J/\psi(1S)\pi^+\pi^-)$ $\Gamma_{14}/\Gamma\times\Gamma_{141}^{\psi(2S)}/\Gamma_{11}^{\psi(2S)}$

VALUE (units 10^{-3})	DOCUMENT ID		TECN	COMMENT
2.31±0.26 OUR FIT				
2.5 ±0.9 OUR AVERAGE Error includes scale factor of 2.3.				
1.90±0.14±0.44	BAI	99B	BES	$\psi(2S)\to\gamma\chi_{c2}$
3.8 ±0.67	[1] TANENBAUM	78	MRK1	$\psi(2S)\to\gamma\chi_{c2}$

[1] The reported value is derived using $B(\psi(2S)\to\pi^+\pi^-J/\psi)\times B(J/\psi\to\ell^+\ell^-) = (4.6\pm0.7)\%$. Calculated by us using $B(J/\psi\to\ell^+\ell^-) = 0.1181\pm0.0020$.

$\Gamma(\chi_{c2}(1P)\to K^*(892)^0\overline{K}^*(892)^0)/\Gamma_{\rm total}\times\Gamma(\psi(2S)\to\gamma\chi_{c2}(1P))/\Gamma_{\rm total}$ $\Gamma_{18}/\Gamma\times\Gamma_{141}^{\psi(2S)}/\Gamma^{\psi(2S)}$

VALUE (units 10^{-4})	DOCUMENT ID		TECN	COMMENT
2.1 ±0.4 OUR FIT				
3.11±0.36±0.48	ABLIKIM	04H	BES2	$\psi(2S)\to\gamma\chi_{c2}$

$\Gamma(\chi_{c2}(1P)\to p\overline{p})/\Gamma_{\rm total}\times\Gamma(\psi(2S)\to\gamma\chi_{c2}(1P))/\Gamma(\psi(2S)\to J/\psi(1S)\pi^+\pi^-)$ $\Gamma_{54}/\Gamma\times\Gamma_{141}^{\psi(2S)}/\Gamma_{11}^{\psi(2S)}$

VALUE (units 10^{-5})	DOCUMENT ID		TECN	COMMENT
2.01±0.09 OUR FIT				
1.4 ±1.1	[1] BAI	98I	BES	$\psi(2S)\to\gamma\chi_{c2}\to\gamma\overline{p}p$

[1] Calculated by us. The value for $B(\chi_{c2}\to p\overline{p})$ reported in BAI 98I is derived using $B(\psi(2S)\to\gamma\chi_{c2}) = (7.8\pm0.8)\%$ and $B(\psi(2S)\to J/\psi(1S)\pi^+\pi^-) = (32.4\pm2.6)\%$ [BAI 98D].

$\Gamma(\chi_{c2}(1P)\to p\overline{p})/\Gamma_{\rm total}\times\Gamma(\psi(2S)\to\gamma\chi_{c2}(1P))/\Gamma_{\rm total}$ $\Gamma_{54}/\Gamma\times\Gamma_{141}^{\psi(2S)}/\Gamma^{\psi(2S)}$

VALUE (units 10^{-6})	EVTS	DOCUMENT ID		TECN	COMMENT
6.98±0.32 OUR FIT					
7.1 ±0.5 OUR AVERAGE Error includes scale factor of 1.2.					
7.3 ±0.4 ±0.3	405	ABLIKIM	13V	BES3	$\psi(2S)\to\gamma p\overline{p}$
7.2 ±0.7 ±0.4	121 ± 12	[1] NAIK	08	CLEO	$\psi(2S)\to\gamma p\overline{p}$
$4.4\ ^{+1.6}_{-1.4}$ ±0.6	$14.3^{+5.2}_{-4.7}$	BAI	04F	BES	$\psi(2S)\to\gamma\chi_{c2}(1P)\to\gamma\overline{p}p$

[1] Calculated by us. NAIK 08 reports $B(\chi_{c2}\to p\overline{p}) = (7.7\pm0.8\pm0.4\pm0.5)\times10^{-5}$ using $B(\psi(2S)\to\gamma\chi_{c2}) = (9.33\pm0.14\pm0.61)\%$.

$\Gamma(\chi_{c2}(1P)\to\Lambda\overline{\Lambda})/\Gamma_{\rm total}\times\Gamma(\psi(2S)\to\gamma\chi_{c2}(1P))/\Gamma_{\rm total}$ $\Gamma_{67}/\Gamma\times\Gamma_{141}^{\psi(2S)}/\Gamma^{\psi(2S)}$

VALUE (units 10^{-6})	EVTS	DOCUMENT ID		TECN	COMMENT
17.5±1.3 OUR FIT					
17.4±1.4 OUR AVERAGE					
18.2±1.4±0.9	207	[1] ABLIKIM	13H	BES3	$\psi(2S)\to\gamma\Lambda\overline{\Lambda}$
15.9±2.1±1.0	71 ± 9	[2] NAIK	08	CLEO	$\psi(2S)\to\gamma\Lambda\overline{\Lambda}$

[1] Calculated by us. ABLIKIM 13H reports $B(\chi_{c2}\to\Lambda\overline{\Lambda}) = (20.8\pm1.6\pm2.3)\times10^{-5}$ from a measurement of $B(\chi_{c2}\to\Lambda\overline{\Lambda})\times B(\psi(2S)\to\gamma\chi_{c2})$ assuming $B(\psi(2S)\to\gamma\chi_{c2}) = (8.74\pm0.35)\%$.

[2] Calculated by us. NAIK 08 reports $B(\chi_{c2}\to\Lambda\overline{\Lambda}) = (17.0\pm2.2\pm1.1\pm1.1)\times10^{-5}$ using $B(\psi(2S)\to\gamma\chi_{c2}) = (9.33\pm0.14\pm0.61)\%$.

$\Gamma(\chi_{c2}(1P)\to\Lambda\overline{\Lambda})/\Gamma_{\rm total}\times\Gamma(\psi(2S)\to\gamma\chi_{c2}(1P))/\Gamma(\psi(2S)\to J/\psi(1S)\pi^+\pi^-)$ $\Gamma_{67}/\Gamma\times\Gamma_{141}^{\psi(2S)}/\Gamma_{11}^{\psi(2S)}$

VALUE (units 10^{-5})	EVTS	DOCUMENT ID		TECN	COMMENT
5.1±0.4 OUR FIT					
$\mathbf{7.1^{+3.1}_{-2.9}\pm1.3}$	$8.3^{+3.7}_{-3.4}$	[1] BAI	03E	BES	$\psi(2S)\to\gamma\Lambda\overline{\Lambda}$

[1] BAI 03E reports $[B(\chi_{c2}\to\Lambda\overline{\Lambda})\,B(\psi(2S)\to\gamma\chi_{c2})\,/\,B(\psi(2S)\to J/\psi\pi^+\pi^-)]\times[B^2(\Lambda\to\pi^-p)\,/\,B(J/\psi\to p\overline{p})] = (1.33^{+0.59}_{-0.55}\pm0.25)\%$. We calculate from this measurement the presented value using $B(\Lambda\to\pi^-p) = (63.9\pm0.5)\%$ and $B(J/\psi\to p\overline{p}) = (2.17\pm0.07)\times10^{-3}$.

$\Gamma(\chi_{c2}(1P)\to\pi\pi)/\Gamma_{\rm total}\times\Gamma(\psi(2S)\to\gamma\chi_{c2}(1P))/\Gamma_{\rm total}$ $\Gamma_{24}/\Gamma\times\Gamma_{141}^{\psi(2S)}/\Gamma^{\psi(2S)}$

VALUE (units 10^{-4})	EVTS	DOCUMENT ID		TECN	COMMENT
2.12±0.08 OUR FIT					
2.17±0.09 OUR AVERAGE					
2.19±0.05±0.15	4.5k	[1] ABLIKIM	10A	BES3	$e^+e^-\to\psi(2S)\to\gamma\chi_{c2}$
2.23±0.06±0.10	2.5k	[2] ASNER	09	CLEO	$\psi(2S)\to\gamma\pi^+\pi^-$
1.90±0.08±0.20	0.8k	[3] ASNER	09	CLEO	$\psi(2S)\to\gamma\pi^0\pi^0$

[1] Calculated by us. ABLIKIM 10A reports $B(\chi_{c2}\to\pi^0\pi^0) = (0.88\pm0.02\pm0.06\pm0.04)\times10^{-3}$ using $B(\psi(2S)\to\gamma\chi_{c2}) = (8.3\pm0.4)\%$. We have multiplied the $\pi^0\pi^0$ measurement by 3 to obtain $\pi\pi$.

[2] Calculated by us. ASNER 09 reports $B(\chi_{c2}\to\pi^+\pi^-) = (1.59\pm0.04\pm0.07\pm0.10)\times10^{-3}$ using $B(\psi(2S)\to\gamma\chi_{c2}) = (9.33\pm0.14\pm0.61)\%$. We have multiplied the $\pi^+\pi^-$ measurement by 3/2 to obtain $\pi\pi$.

[3] Calculated by us. ASNER 09 reports $B(\chi_{c2}\to\pi^0\pi^0) = (0.68\pm0.03\pm0.07\pm0.04)\times10^{-3}$ using $B(\psi(2S)\to\gamma\chi_{c2}) = (9.33\pm0.14\pm0.61)\%$. We have multiplied the $\pi^0\pi^0$ measurement by 3 to obtain $\pi\pi$.

$\Gamma(\chi_{c2}(1P)\to\pi\pi)/\Gamma_{\rm total}\times\Gamma(\psi(2S)\to\gamma\chi_{c2}(1P))/\Gamma(\psi(2S)\to J/\psi(1S)\pi^+\pi^-)$ $\Gamma_{24}/\Gamma\times\Gamma_{141}^{\psi(2S)}/\Gamma_{11}^{\psi(2S)}$

VALUE (units 10^{-3})	EVTS	DOCUMENT ID		TECN	COMMENT
0.612±0.023 OUR FIT					
0.54 ±0.06 OUR AVERAGE					
0.66 ±0.18 ±0.37	21 ± 6	[1] BAI	03C	BES	$\psi(2S)\to\gamma\pi^0\pi^0$
0.54 ±0.05 ±0.04	185 ± 16	[2] BAI	98I	BES	$\psi(2S)\to\gamma\pi^+\pi^-$

[1] We have multiplied $\pi^0\pi^0$ measurement by 3 to obtain $\pi\pi$.

[2] Calculated by us. The value for $B(\chi_{c2}\to\pi^+\pi^-)$ reported by BAI 98I is derived using $B(\psi(2S)\to\gamma\chi_{c2}) = (7.8\pm0.8)\%$ and $B(\psi(2S)\to J/\psi\pi^+\pi^-) = (32.4\pm2.6)\%$ [BAI 98D]. We have multiplied $\pi^+\pi^-$ measurement by 3/2 to obtain $\pi\pi$.

$\Gamma(\chi_{c2}(1P)\to\eta\eta)/\Gamma_{\rm total}\times\Gamma(\psi(2S)\to\gamma\chi_{c2}(1P))/\Gamma_{\rm total}$ $\Gamma_{30}/\Gamma\times\Gamma_{141}^{\psi(2S)}/\Gamma^{\psi(2S)}$

VALUE (units 10^{-4})	CL%	EVTS	DOCUMENT ID		TECN	COMMENT
0.52±0.04 OUR FIT						
0.52±0.04 OUR AVERAGE						
0.54±0.03±0.04		386	[1] ABLIKIM	10A	BES3	$e^+e^-\to\psi(2S)\to\gamma\chi_{c2}$
0.47±0.05±0.05		156	ASNER	09	CLEO	$\psi(2S)\to\gamma\eta\eta$
• • • We do not use the following data for averages, fits, limits, etc. • • •						
< 0.44	90		[2] ADAMS	07	CLEO	$\psi(2S)\to\gamma\chi_{c2}$
< 3	90		BAI	03C	BES	$\psi(2S)\to\gamma\eta\eta\to5\gamma$
0.62±0.31±0.19			LEE	85	CBAL	$\psi(2S)\to$ photons

[1] Calculated by us. ABLIKIM 10A reports $B(\chi_{c2}\to\eta\eta) = (0.65\pm0.04\pm0.05\pm0.03)\times10^{-3}$ using $B(\psi(2S)\to\gamma\chi_{c2}) = (8.3\pm0.4)\%$.

[2] Superseded by ASNER 09.

$\Gamma(\chi_{c2}(1P)\to K^+K^-)/\Gamma_{\rm total}\times\Gamma(\psi(2S)\to\gamma\chi_{c2}(1P))/\Gamma_{\rm total}$ $\Gamma_{31}/\Gamma\times\Gamma_{141}^{\psi(2S)}/\Gamma^{\psi(2S)}$

VALUE (units 10^{-5})	EVTS	DOCUMENT ID		TECN	COMMENT
9.6±0.6 OUR FIT					
10.5±0.3±0.6	1.6k	[1] ASNER	09	CLEO	$\psi(2S)\to\gamma K^+K^-$

[1] Calculated by us. ASNER 09 reports $B(\chi_{c2}\to K^+K^-) = (1.13\pm0.03\pm0.06\pm0.07)\times10^{-3}$ using $B(\psi(2S)\to\gamma\chi_{c2}) = (9.33\pm0.14\pm0.61)\%$.

$\Gamma(\chi_{c2}(1P) \to K^+K^-)/\Gamma_{total} \times \Gamma(\psi(2S) \to \gamma\chi_{c2}(1P))/\Gamma(\psi(2S) \to J/\psi(1S)\pi^+\pi^-)$ $\Gamma_{31}/\Gamma \times \Gamma^{\psi(2S)}_{141}/\Gamma^{\psi(2S)}_{11}$

VALUE (units 10^{-3})	EVTS	DOCUMENT ID		TECN	COMMENT
0.276±0.017 OUR FIT					
0.190±0.034±0.019	115 ± 13	[1] BAI	98I	BES	$\psi(2S) \to \gamma K^+K^-$

[1] Calculated by us. The value for $B(\chi_{c2} \to K^+K^-)$ reported by BAI 98I is derived using $B(\psi(2S) \to \gamma\chi_{c2}) = (7.8 \pm 0.8)\%$ and $B(\psi(2S) \to J/\psi\pi^+\pi^-) = (32.4 \pm 2.6)\%$ [BAI 98D].

$\Gamma(\chi_{c2}(1P) \to K^0_S K^0_S)/\Gamma_{total} \times \Gamma(\psi(2S) \to \gamma\chi_{c2}(1P))/\Gamma_{total}$ $\Gamma_{32}/\Gamma \times \Gamma^{\psi(2S)}_{141}/\Gamma^{\psi(2S)}$

VALUE (units 10^{-5})	EVTS	DOCUMENT ID		TECN	COMMENT
5.0 ±0.4 OUR FIT					
5.0 ±0.4 OUR AVERAGE					
4.9 ±0.3 ±0.3	373 ± 20	[1] ASNER	09	CLEO	$\psi(2S) \to \gamma K^0_S K^0_S$
5.72±0.76±0.63	65	ABLIKIM	05O	BES2	$\psi(2S) \to \gamma K^0_S K^0_S$

[1] Calculated by us. ASNER 09 reports $B(\chi_{c2} \to K^0_S K^0_S) = (0.53 \pm 0.03 \pm 0.03 \pm 0.03) \times 10^{-3}$ using $B(\psi(2S) \to \gamma\chi_{c2}) = (9.33 \pm 0.14 \pm 0.61)\%$.

$\Gamma(\chi_{c2}(1P) \to K^0_S K^0_S)/\Gamma_{total} \times \Gamma(\psi(2S) \to \gamma\chi_{c2}(1P))/\Gamma(\psi(2S) \to J/\psi(1S)\pi^+\pi^-)$ $\Gamma_{32}/\Gamma \times \Gamma^{\psi(2S)}_{141}/\Gamma^{\psi(2S)}_{11}$

VALUE (units 10^{-5})	DOCUMENT ID		TECN	COMMENT
14.4±1.1 OUR FIT				
14.7±4.1±3.3	[1] BAI	99B	BES	$\psi(2S) \to \gamma K^0_S K^0_S$

[1] Calculated by us. The value of $B(\chi_{c2} \to K^0_S K^0_S)$ reported by BAI 99B was derived using $B(\psi(2S) \to \gamma\chi_{c2}(1P)) = (7.8 \pm 0.8)\%$ and $B(\psi(2S) \to J/\psi\pi^+\pi^-) = (32.4 \pm 2.6)\%$ [BAI 98D].

$\Gamma(\chi_{c2}(1P) \to \overline{K}^0 K^+\pi^- + \text{c.c.})/\Gamma_{total} \times \Gamma(\psi(2S) \to \gamma\chi_{c2}(1P))/\Gamma_{total}$ $\Gamma_{41}/\Gamma \times \Gamma^{\psi(2S)}_{141}/\Gamma^{\psi(2S)}$

VALUE (units 10^{-4})	EVTS	DOCUMENT ID		TECN	COMMENT
1.22±0.17 OUR FIT					
1.15±0.18 OUR AVERAGE					
1.21±0.19±0.09	37	[1] ATHAR	07	CLEO	$\psi(2S) \to \gamma K^0_S K^\pm\pi^\mp$
0.97±0.32±0.13	28	[2] ABLIKIM	06R	BES2	$\psi(2S) \to \gamma K^0_S K^\pm\pi^\mp$

[1] Calculated by us. ATHAR 07 reports $B(\chi_{c2} \to \overline{K}^0 K^+\pi^- + \text{c.c.}) = (1.3 \pm 0.2 \pm 0.1 \pm 0.1) \times 10^{-3}$ using $B(\psi(2S) \to \gamma\chi_{c2}) = (9.33 \pm 0.14 \pm 0.61)\%$.

[2] Calculated by us. ABLIKIM 06R reports $B(\chi_{c2} \to K^0_S K^\pm\pi^\mp) = (0.6 \pm 0.2 \pm 0.1) \times 10^{-3}$ using $B(\psi(2S) \to \gamma\chi_{c2}) = (8.1 \pm 0.6)\%$. We have multiplied by 2 to obtain $\overline{K}^0 K^+\pi^-$ + c.c. from $K^0_S K^\pm\pi^\mp$.

$\Gamma(\chi_{c2}(1P) \to 2(\pi^+\pi^-))/\Gamma_{total} \times \Gamma(\psi(2S) \to \gamma\chi_{c2}(1P))/\Gamma(\psi(2S) \to J/\psi(1S)\pi^+\pi^-)$ $\Gamma_1/\Gamma \times \Gamma^{\psi(2S)}_{141}/\Gamma^{\psi(2S)}_{11}$

VALUE (units 10^{-3})	DOCUMENT ID		TECN	COMMENT
2.79±0.26 OUR FIT				
3.1 ±1.0 OUR AVERAGE Error includes scale factor of 2.5.				
2.3 ±0.1 ±0.5	[1] BAI	99B	BES	$\psi(2S) \to \gamma\chi_{c2}$
4.3 ±0.6	[2] TANENBAUM	78	MRK1	$\psi(2S) \to \gamma\chi_{c2}$

[1] Calculated by us. The value for $B(\chi_{c2} \to 2\pi^+2\pi^-)$ reported in BAI 99B is derived using $B(\psi(2S) \to \gamma\chi_{c2}) = (7.8 \pm 0.8)\%$ and $B(\psi(2S) \to J/\psi(1S)\pi^+\pi^-) = (32.4 \pm 2.6)\%$ [BAI 98D].

[2] The value for $B(\psi(2S) \to \gamma\chi_{c2}) \times B(\chi_{c2} \to 2\pi^+\pi^-)$ reported in TANENBAUM 78 is derived using $B(\psi(2S) \to J/\psi(1S)\pi^+\pi^-) \times B(J/\psi(1S)\ell^+\ell^-) = (4.6 \pm 0.7)\%$. Calculated by us using $B(J/\psi(1S) \to \ell^+\ell^-) = 0.1181 \pm 0.0020$.

$\Gamma(\chi_{c2}(1P) \to K^+K^-K^+K^-)/\Gamma_{total} \times \Gamma(\psi(2S) \to \gamma\chi_{c2}(1P))/\Gamma_{total}$ $\Gamma_{49}/\Gamma \times \Gamma^{\psi(2S)}_{141}/\Gamma^{\psi(2S)}$

VALUE (units 10^{-4})	EVTS	DOCUMENT ID		TECN	COMMENT
1.57±0.19 OUR FIT					
1.76±0.16±0.24	160	[1] ABLIKIM	06T	BES2	$\psi(2S) \to \gamma 2K^+2K^-$

[1] Calculated by us. The value of $B(\chi_{c2} \to 2K^+2K^-)$ reported by ABLIKIM 06T was derived using $B(\psi(2S) \to \gamma\chi_{c2}(1P)) = (8.1 \pm 0.4)\%$.

$\Gamma(\chi_{c2}(1P) \to K^+K^-K^+K^-)/\Gamma_{total} \times \Gamma(\psi(2S) \to \gamma\chi_{c2}(1P))/\Gamma(\psi(2S) \to J/\psi(1S)\pi^+\pi^-)$ $\Gamma_{49}/\Gamma \times \Gamma^{\psi(2S)}_{141}/\Gamma^{\psi(2S)}_{11}$

VALUE (units 10^{-4})	DOCUMENT ID		TECN	COMMENT
4.5±0.5 OUR FIT				
3.6±0.6±0.6	[1] BAI	99B	BES	$\psi(2S) \to \gamma 2K^+2K^-$

[1] Calculated by us. The value of $B(\chi_{c2} \to 2K^+2K^-)$ reported by BAI 99B was derived using $B(\psi(2S) \to \gamma\chi_{c2}(1P)) = (7.8 \pm 0.8)\%$ and $B(\psi(2S) \to J/\psi\pi^+\pi^-) = (32.4 \pm 2.6)\%$ [BAI 98D].

$\Gamma(\chi_{c2}(1P) \to \phi\phi)/\Gamma_{total} \times \Gamma(\psi(2S) \to \gamma\chi_{c2}(1P))/\Gamma_{total}$ $\Gamma_{20}/\Gamma \times \Gamma^{\psi(2S)}_{141}/\Gamma^{\psi(2S)}$

VALUE (units 10^{-4})	EVTS	DOCUMENT ID		TECN	COMMENT
1.01±0.08 OUR FIT					
0.98±0.13 OUR AVERAGE Error includes scale factor of 1.3.					
0.94±0.03±0.10	849	[1] ABLIKIM	11K	BES3	$\psi(2S) \to \gamma$ hadrons
1.38±0.24±0.23	41	[2] ABLIKIM	06T	BES2	$\psi(2S) \to \gamma 2K^+2K^-$

[1] Calculated by us. The value of $B(\chi_{c2} \to \phi\phi)$ reported by ABLIKIM 11K was derived using $B(\psi(2S) \to \gamma\chi_{c2}(1P)) = (8.74 \pm 0.35)\%$.

[2] Calculated by us. The value of $B(\chi_{c2} \to \phi\phi)$ reported by ABLIKIM 06T was derived using $B(\psi(2S) \to \gamma\chi_{c2}(1P)) = (8.1 \pm 0.4)\%$.

$\Gamma(\chi_{c2}(1P) \to \phi\phi)/\Gamma_{total} \times \Gamma(\psi(2S) \to \gamma\chi_{c2}(1P))/\Gamma(\psi(2S) \to J/\psi(1S)\pi^+\pi^-)$ $\Gamma_{20}/\Gamma \times \Gamma^{\psi(2S)}_{141}/\Gamma^{\psi(2S)}_{11}$

VALUE (units 10^{-4})	DOCUMENT ID		TECN	COMMENT
2.92±0.24 OUR FIT				
4.8 ±1.3 ±1.3	[1] BAI	99B	BES	$\psi(2S) \to \gamma 2K^+2K^-$

[1] Calculated by us. The value of $B(\chi_{c2} \to \phi\phi)$ reported by BAI 99B was derived using $B(\psi(2S) \to \gamma\chi_{c2}(1P)) = (7.8 \pm 0.8)\%$ and $B(\psi(2S) \to J/\psi\pi^+\pi^-) = (32.4 \pm 2.6)\%$ [BAI 98D].

$\Gamma(\chi_{c2}(1P) \to \gamma J/\psi(1S))/\Gamma_{total} \times \Gamma(\psi(2S) \to \gamma\chi_{c2}(1P))/\Gamma_{total}$ $\Gamma_{85}/\Gamma \times \Gamma^{\psi(2S)}_{141}/\Gamma^{\psi(2S)}$

VALUE (units 10^{-2})	EVTS	DOCUMENT ID		TECN	COMMENT
1.81 ±0.04 OUR FIT					
1.69 ±0.16 OUR AVERAGE		Error includes scale factor of 3.4. See the ideogram below.			
1.996±0.008±0.070	81k	[1] ABLIKIM	17N	BES3	$\psi(2S) \to \gamma\gamma J/\psi$
1.793±0.008±0.163	1.0M	ABLIKIM	17U	BES3	$e^+e^- \to \gamma X$
1.62 ±0.04 ±0.12	5.8k	BAI	04I	BES2	$\psi(2S) \to J/\psi\gamma\gamma$
0.99 ±0.10 ±0.08		GAISER	86	CBAL	$\psi(2S) \to \gamma X$
1.47 ±0.17		[2] OREGLIA	82	CBAL	$\psi(2S) \to \gamma\chi_{c2}$
1.8 ±0.5		[3] BRANDELIK	79B	DASP	$\psi(2S) \to \gamma\chi_{c2}$
1.2 ±0.2		[3] BARTEL	78B	CNTR	$\psi(2S) \to \gamma\chi_{c2}$
2.2 ±1.2		[4] BIDDICK	77	CNTR	$e^+e^- \to \gamma X$
1.2 ±0.7		[2] WHITAKER	76	MRK1	e^+e^-
• • • We do not use the following data for averages, fits, limits, etc. • • •					
1.874±0.007±0.102	76k	[5] ABLIKIM	12O	BES3	$\psi(2S) \to \gamma\chi_{c2}$
1.95 ±0.02 ±0.07	12.4k	[6] MENDEZ	08	CLEO	$\psi(2S) \to \gamma\chi_{c2}$
1.85 ±0.04 ±0.07	1.9k	[7] ADAM	05A	CLEO	Repl. by MENDEZ 08

[1] Uses B($J/\psi \to e^+e^-$) = (5.971 ± 0.032)% and B($J/\psi \to \mu^+\mu^-$) = (5.961 ± 0.033)%.

[2] Recalculated by us using $B(J/\psi(1S) \to \ell^+\ell^-) = 0.1181 \pm 0.0020$.

[3] Recalculated by us using $B(J/\psi(1S) \to \mu^+\mu^-) = 0.0588 \pm 0.0010$.

[4] Assumes isotropic gamma distribution.

[5] Superseded by ABLIKIM 17N.

[6] Not independent from other measurements of MENDEZ 08.

[7] Not independent from other values reported by ADAM 05A.

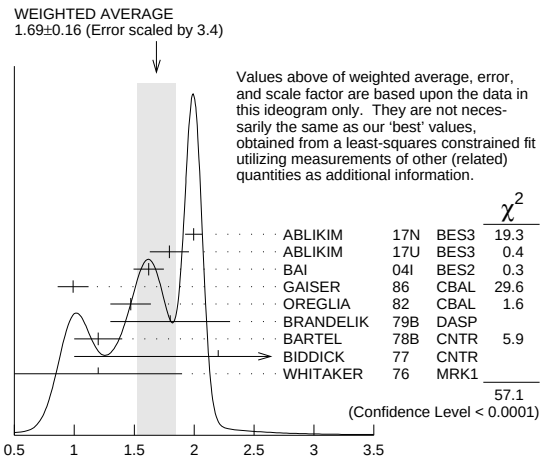

$\Gamma(\chi_{c2}(1P) \to \gamma J/\psi(1S))/\Gamma_{total} \times \Gamma(\psi(2S) \to \gamma\chi_{c2}(1P))/\Gamma_{total}$ (units 10^{-2})

$\Gamma(\chi_{c2}(1P) \to \gamma J/\psi(1S))/\Gamma_{total} \times \Gamma(\psi(2S) \to \gamma\chi_{c2}(1P))/\Gamma(\psi(2S) \to J/\psi(1S)\text{anything})$ $\Gamma_{85}/\Gamma \times \Gamma^{\psi(2S)}_{141}/\Gamma^{\psi(2S)}_{9}$

$\Gamma_{85}/\Gamma \times \Gamma^{\psi(2S)}_{141}/\Gamma^{\psi(2S)}_{9} = \Gamma_{85}/\Gamma \times \Gamma^{\psi(2S)}_{141}/(\Gamma^{\psi(2S)}_{11} + \Gamma^{\psi(2S)}_{12} + \Gamma^{\psi(2S)}_{13} + 0.343\Gamma^{\psi(2S)}_{140} + 0.190\Gamma^{\psi(2S)}_{141})$

VALUE (units 10^{-2})	EVTS	DOCUMENT ID		TECN	COMMENT
2.95±0.06 OUR FIT					
• • • We do not use the following data for averages, fits, limits, etc. • • •					
3.12±0.03±0.09	12.4k	[1] MENDEZ	08	CLEO	$\psi(2S) \to \gamma\chi_{c2}$
3.11±0.07±0.07	1.9k	ADAM	05A	CLEO	Repl. by MENDEZ 08

[1] Not independent from other measurements of MENDEZ 08.

$\Gamma(\chi_{c2}(1P) \to \gamma J/\psi(1S))/\Gamma_{total} \times \Gamma(\psi(2S) \to \gamma\chi_{c2}(1P))/\Gamma(\psi(2S) \to J/\psi(1S)\pi^+\pi^-)$ $\Gamma_{85}/\Gamma \times \Gamma_{141}^{\psi(2S)}/\Gamma_{11}^{\psi(2S)}$

VALUE (units 10^{-2})	EVTS	DOCUMENT ID		TECN	COMMENT
5.22±0.11 OUR FIT					
5.53±0.17 OUR AVERAGE					
5.56±0.05±0.16	12.4k	MENDEZ	08	CLEO	$\psi(2S) \to \gamma\chi_{c2}$
6.0 ±2.8	1.3k	[1] ABLIKIM	04B	BES	$\psi(2S) \to J/\psi X$
3.9 ±1.2		[2] HIMEL	80	MRK2	$\psi(2S) \to \gamma\chi_{c2}$
• • • We do not use the following data for averages, fits, limits, etc. • • •					
5.52±0.13±0.13	1.9k	[3] ADAM	05A	CLEO	Repl. by MENDEZ 08

[1] From a fit to the J/ψ recoil mass spectra.

[2] The value for $B(\psi(2S) \to \gamma\chi_{c2}) \times B(\chi_{c2} \to \gamma J/\psi(1S))$ reported in HIMEL 80 is derived using $B(\psi(2S) \to J/\psi(1S)\pi^+\pi^-) = (33 \pm 3)\%$ and $B(J/\psi(1S) \to \ell^+\ell^-) = 0.138 \pm 0.018$. Calculated by us using $B(J/\psi(1S) \to \ell^+\ell^-) = (0.1181 \pm 0.0020)$.

[3] Not independent from other values reported by ADAM 05A.

$\Gamma(\chi_{c2}(1P) \to \gamma\gamma)/\Gamma_{total} \times \Gamma(\psi(2S) \to \gamma\chi_{c2}(1P))/\Gamma_{total}$ $\Gamma_{89}/\Gamma \times \Gamma_{141}^{\psi(2S)}/\Gamma^{\psi(2S)}$

VALUE (units 10^{-5})	EVTS	DOCUMENT ID		TECN	COMMENT
2.71±0.08 OUR FIT					
2.82±0.10 OUR AVERAGE					
2.83±0.08±0.06	5k	[1] ABLIKIM	17AE	BES3	$\psi(2S) \to \gamma\chi_{c2} \to 3\gamma$
2.68±0.28±0.15	0.3k	ECKLUND	08A	CLEO	$\psi(2S) \to \gamma\chi_{c2} \to 3\gamma$
7.0 ±2.1 ±2.0		LEE	85	CBAL	$\psi(2S) \to \gamma\chi_{c2}$
• • • We do not use the following data for averages, fits, limits, etc. • • •					
2.81±0.17±0.15	1.1k	[2] ABLIKIM	12A	BES3	$\psi(2S) \to \gamma\chi_{c2} \to 3\gamma$

[1] ABLIKIM 17AE measures the ratio of two-photon partial widths for the helicity $\lambda = 0$ and helicity $\lambda = 2$ components to be $f_{0/2} = \Gamma_{\gamma\gamma}^{\lambda=0} / \Gamma_{\gamma\gamma}^{\lambda=2} = 0.000 \pm 0.006 \pm 0.012$.

[2] ABLIKIM 12A measures the ratio of two-photon partial widths for the helicity $\lambda = 0$ and helicity $\lambda = 2$ components to be $f_{0/2} = \Gamma_{\gamma\gamma}^{\lambda=0}/\Gamma_{\gamma\gamma}^{\lambda=2} = 0.00 \pm 0.02 \pm 0.02$. Superseded by ABLIKIM 17AE.

$\Gamma(\chi_{c2}(1P) \to \gamma\gamma)/\Gamma(\chi_{c0}(1P) \to \gamma\gamma)$ $\Gamma_{89}/\Gamma_{89}^{\chi_{c0}(1P)}$

VALUE	EVTS	DOCUMENT ID		TECN	COMMENT
0.292±0.028 OUR AVERAGE					
0.295±0.014±0.028	8k	[1] ABLIKIM	17AE	BES3	$\psi(2S) \to \gamma\chi_{cJ} \to 3\gamma$
0.278±0.050±0.036	0.5k	[1] ECKLUND	08A	CLEO	$\psi(2S) \to \gamma\chi_{cJ} \to 3\gamma$
• • • We do not use the following data for averages, fits, limits, etc. • • •					
0.271±0.029±0.030	1.9k	[1,2] ABLIKIM	12A	BES3	$\psi(2S) \to \gamma\chi_{cJ} \to 3\gamma$

[1] Not independent from the values of $\Gamma(\chi_{c0}, \chi_{c2})$ and $B(\psi(2S) \to \chi_{c0}, \chi_{c2})$.

[2] Superseded by ABLIKIM 17AE.

MULTIPOLE AMPLITUDES IN $\chi_{c2}(1P) \to \gamma J/\psi(1S)$ RADIATIVE DECAY

$a_2 = M2/\sqrt{E1^2 + M2^2 + E3^2}$ Magnetic quadrupole fractional transition amplitude

VALUE (units 10^{-2})	EVTS	DOCUMENT ID		TECN	COMMENT
−11.0± 1.0 OUR AVERAGE					
−12.0± 1.3±0.4	89k	[1] ABLIKIM	17N	BES3	$\psi(2S) \to \gamma\gamma\ell^+\ell^-$
− 9.3± 1.6±0.3	19.8k	[2] ARTUSO	09	CLEO	$\psi(2S) \to \gamma\gamma\ell^+\ell^-$
$-\ 9.3^{+\ 3.9}_{-\ 4.1}\pm 0.6$	5.9k	[3] AMBROGIANI	02	E835	$p\overline{p} \to \chi_{c2} \to J/\psi\gamma$
−14 ± 6	1.9k	[3] ARMSTRONG	93E	E760	$p\overline{p} \to \chi_{c2} \to J/\psi\gamma$
$-33.3^{+11.6}_{-29.2}$	441	[3] OREGLIA	82	CBAL	$\psi(2S) \to \chi_{c1}\gamma \to J/\psi\gamma\gamma$
• • • We do not use the following data for averages, fits, limits, etc. • • •					
− 7.9± 1.9±0.3	19.8k	[4] ARTUSO	09	CLEO	$\psi(2S) \to \gamma\gamma\ell^+\ell^-$

[1] Correlated with a_3, b_2, and b_3 with correlation coefficients $\rho_{a_2 a_3} = 0.733$, $\rho_{a_2 b_2} = -0.605$, and $\rho_{a_2 b_3} = -0.095$.

[2] From a fit with floating $M2$ amplitudes a_2 and b_2, and fixed $E3$ amplitudes $a_3 = b_3 = 0$.

[3] Assuming $a_3 = 0$.

[4] From a fit with floating $M2$ and $E3$ amplitudes a_2, b_2, and a_3, and b_3.

$a_3 = E3/\sqrt{E1^2 + M2^2 + E3^2}$ Electric octupole fractional transition amplitude

VALUE (units 10^{-2})	EVTS	DOCUMENT ID		TECN	COMMENT
−0.3±1.0 OUR AVERAGE	Error includes scale factor of 1.3. See the ideogram below.				
−1.3±0.9±0.4	89k	[1] ABLIKIM	17N	BES3	$\psi(2S) \to \gamma\gamma\ell^+\ell^-$
1.7±1.4±0.3	19.8k	[2] ARTUSO	09	CLEO	$\psi(2S) \to \gamma\gamma\ell^+\ell^-$
$2.0^{+5.5}_{-4.4}\pm 0.9$	5908	AMBROGIANI	02	E835	$p\overline{p} \to \chi_{c2} \to J/\psi\gamma$
$0\ ^{+6}_{-5}$	1904	ARMSTRONG	93E	E760	$p\overline{p} \to \chi_{c2} \to J/\psi\gamma$

[1] Correlated with a_2, b_2, and b_3 with correlation coefficients $\rho_{a_2 a_3} = 0.733$, $\rho_{a_3 b_2} = -0.422$, and $\rho_{a_3 b_3} = -0.024$.

[2] From a fit with floating $M2$ and $E3$ amplitudes a_2, b_2, and a_3, and b_3.

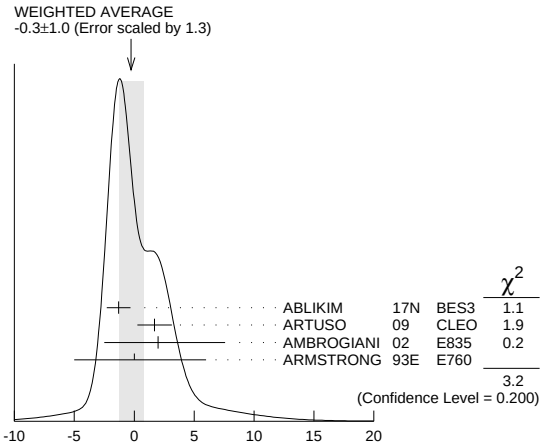

$a_3 = E3/\sqrt{E1^2 + M2^2 + E3^2}$ Electric octupole fractional transition amplitude (units 10^{-2})

MULTIPOLE AMPLITUDES IN $\psi(2S) \to \gamma\chi_{c2}(1P)$ RADIATIVE DECAY

$b_2 = M2/\sqrt{E1^2 + M2^2 + E3^2}$ Magnetic quadrupole fractional transition amplitude

VALUE (units 10^{-2})	EVTS	DOCUMENT ID		TECN	COMMENT
1.9±0.9 OUR AVERAGE	Error includes scale factor of 1.4. See the ideogram below.				
1.7±0.8±0.2	89k	[1] ABLIKIM	17N	BES3	$\psi(2S) \to \gamma\gamma\ell^+\ell^-$
4.6±1.0±1.3	13.8k	[2] ABLIKIM	11I	BES3	$\psi(2S) \to \gamma\pi^+\pi^-, \gamma K^+K^-$
0.2±1.5±0.4	19.8k	[3] ARTUSO	09	CLEO	$\psi(2S) \to \gamma\gamma\ell^+\ell^-$
$-\ 5.1^{+5.4}_{-3.6}$	721	[2] ABLIKIM	04I	BES2	$\psi(2S) \to \gamma\pi^+\pi^-, \gamma K^+K^-$
$13.2^{+9.8}_{-7.5}$	441	[4] OREGLIA	82	CBAL	$\psi(2S) \to \gamma\gamma\ell^+\ell^-$
• • • We do not use the following data for averages, fits, limits, etc. • • •					
1.0±1.3±0.3	19.8k	[4] ARTUSO	09	CLEO	$\psi(2S) \to \gamma\gamma\ell^+\ell^-$

[1] Correlated with a_2, a_3, and b_3 with correlation coefficients $\rho_{a_2 b_2} = -0.605$, $\rho_{a_3 b_2} = -0.422$, and $\rho_{b_2 b_3} = 0.384$.

[2] From a fit with floating $M2$ and $E3$ amplitudes b_2 and b_3.

[3] From a fit with floating $M2$ and $E3$ amplitudes a_2, b_2, and a_3, and b_3.

[4] From a fit with floating $M2$ amplitudes a_2 and b_2, and fixed $E3$ amplitudes $a_3 = b_3 = 0$.

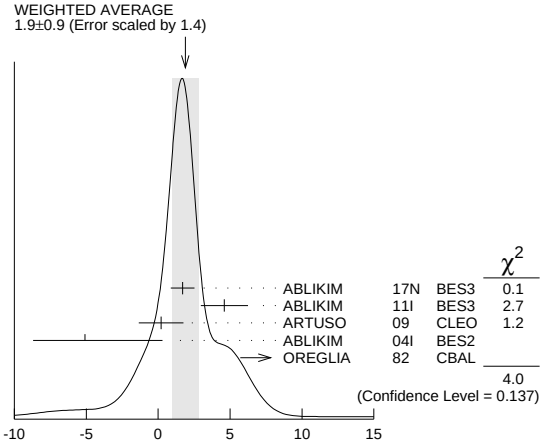

$b_2 = M2/\sqrt{E1^2 + M2^2 + E3^2}$ Magnetic quadrupole fractional transition amplitude (units 10^{-2})

$b_3 = E3/\sqrt{E1^2 + M2^2 + E3^2}$ Electric octupole fractional transition amplitude

VALUE (units 10^{-2})	EVTS	DOCUMENT ID		TECN	COMMENT
−1.0±0.6 OUR AVERAGE					
−1.4±0.7±0.4	89k	[1] ABLIKIM	17N	BES3	$\psi(2S) \to \gamma\gamma\ell^+\ell^-$
1.5±0.8±1.8	13.8k	[2] ABLIKIM	11I	BES3	$\psi(2S) \to \gamma\pi^+\pi^-, \gamma K^+K^-$
−0.8±1.2±0.2	19.8k	ARTUSO	09	CLEO	$\psi(2S) \to \gamma\gamma\ell^+\ell^-$
$-2.7^{+4.3}_{-2.9}$	721	[2] ABLIKIM	04I	BES2	$\psi(2S) \to \gamma\pi^+\pi^-, \gamma K^+K^-$

[1] Correlated with a_2, a_3, and b_2 with correlation coefficients $\rho_{a_2 b_3} = -0.095$, $\rho_{a_3 b_3} = -0.024$, and $\rho_{b_2 b_3} = 0.384$.

[2] From a fit with floating $M2$ and $E3$ amplitudes b_2 and b_3.

MULTIPOLE AMPLITUDE RATIOS IN RADIATIVE DECAYS $\psi(2S) \to \gamma\chi_{c2}(1P)$ and $\chi_{c2} \to \gamma J/\psi(1S)$

b_2/a_2 Magnetic quadrupole transition amplitude ratio

VALUE (units 10^{-2})	EVTS	DOCUMENT ID		TECN	COMMENT
-11^{+14}_{-15}	19.8k	[1] ARTUSO	09	CLEO	$\psi(2S) \to \gamma\gamma\ell^+\ell^-$

[1] Statistical and systematic errors combined. From a fit with floating $M2$ amplitudes a_2 and b_2, and fixed $E3$ amplitudes $a_3=b_3=0$. Not independent of values for $a_2(\chi_{c2}(1P))$ and $b_2(\chi_{c2}(1P))$ from ARTUSO 09.

$\chi_{c2}(1P)$ REFERENCES

AAIJ	17BB	EPJ C77 609	R. Aaij *et al.*	(LHCb Collab.)
AAIJ	17BI	PRL 119 221801	R. Aaij *et al.*	(LHCb Collab.)
ABLIKIM	17AE	PR D96 092007	M. Ablikim *et al.*	(BES III Collab.)
ABLIKIM	17AG	PR D96 111102	M. Ablikim *et al.*	(BES III Collab.)
ABLIKIM	17AI	PR D96 112006	M. Ablikim *et al.*	(BES III Collab.)
ABLIKIM	17I	PRL 118 221802	M. Ablikim *et al.*	(BES III Collab.)
ABLIKIM	17N	PR D95 072004	M. Ablikim *et al.*	(BES III Collab.)
ABLIKIM	17U	PR D96 032001	M. Ablikim *et al.*	(BES III Collab.)
PDG	16	CP C40 100001	C. Patrignani *et al.*	(PDG Collab.)
ABLIKIM	15I	PR D91 092006	M. Ablikim *et al.*	(BES III Collab.)
ABLIKIM	15M	PR D91 112008	M. Ablikim *et al.*	(BES III Collab.)
ABLIKIM	15N	PR D91 112018	M. Ablikim *et al.*	(BES III Collab.)
ABLIKIM	14J	PR D89 074030	M. Ablikim *et al.*	(BES III Collab.)
ABLIKIM	13B	PR D87 012002	M. Ablikim *et al.*	(BES III Collab.)
ABLIKIM	13D	PR D87 012007	M. Ablikim *et al.*	(BES III Collab.)
ABLIKIM	13H	PR D87 032007	M. Ablikim *et al.*	(BES III Collab.)
ABLIKIM	13V	PR D88 112001	M. Ablikim *et al.*	(BES III Collab.)
UEHARA	13	PTEP 2013 123C01	S. Uehara *et al.*	(BELLE Collab.)
ABLIKIM	12A	PR D85 112008	M. Ablikim *et al.*	(BES III Collab.)
ABLIKIM	12I	PR D86 052004	M. Ablikim *et al.*	(BES III Collab.)
ABLIKIM	12J	PR D86 052011	M. Ablikim *et al.*	(BES III Collab.)
ABLIKIM	12O	PRL 109 172002	M. Ablikim *et al.*	(BES III Collab.)
LEES	12AE	PR D86 092005	J.P. Lees *et al.*	(BABAR Collab.)
LIU	12B	PRL 108 232001	Z.Q. Liu *et al.*	(BELLE Collab.)
ABLIKIM	11A	PR D83 012006	M. Ablikim *et al.*	(BES III Collab.)
ABLIKIM	11E	PR D83 112005	M. Ablikim *et al.*	(BES III Collab.)
ABLIKIM	11F	PR D83 112009	M. Ablikim *et al.*	(BES III Collab.)
ABLIKIM	11I	PR D84 092006	M. Ablikim *et al.*	(BES III Collab.)
ABLIKIM	11K	PRL 107 092001	M. Ablikim *et al.*	(BES III Collab.)
DEL-AMO-SA...	11M	PR D84 012004	P. del Amo Sanchez *et al.*	(BABAR Collab.)
ABLIKIM	10A	PR D81 052005	M. Ablikim *et al.*	(BES III Collab.)
ONYISI	10	PR D82 011103	P.U.E. Onyisi *et al.*	(CLEO Collab.)
UEHARA	10A	PR D82 114031	S. Uehara *et al.*	(BELLE Collab.)
ARTUSO	09	PR D80 112003	M. Artuso *et al.*	(CLEO Collab.)
ASNER	09	PR D79 072007	D.M. Asner *et al.*	(CLEO Collab.)
UEHARA	09	PR D79 052009	S. Uehara *et al.*	(BELLE Collab.)
BENNETT	08A	PRL 101 151801	J.V. Bennett *et al.*	(CLEO Collab.)
ECKLUND	08A	PR D78 091501	K.M. Ecklund *et al.*	(CLEO Collab.)
HE	08B	PR D78 092004	Q. He *et al.*	(CLEO Collab.)
MENDEZ	08	PR D78 011102	H. Mendez *et al.*	(CLEO Collab.)
NAIK	08	PR D78 031101	P. Naik *et al.*	(CLEO Collab.)
UEHARA	08	EPJ C53 1	S. Uehara *et al.*	(BELLE Collab.)
ADAMS	07	PR D75 071101	G.S. Adams *et al.*	(CLEO Collab.)
ATHAR	07	PR D75 032002	S.B. Athar *et al.*	(CLEO Collab.)
CHEN	07B	PL B651 15	W.T. Chen *et al.*	(BELLE Collab.)
ABLIKIM	06D	PR D73 052006	M. Ablikim *et al.*	(BES Collab.)
ABLIKIM	06I	PR D74 012004	M. Ablikim *et al.*	(BES Collab.)
ABLIKIM	06R	PR D74 072001	M. Ablikim *et al.*	(BES Collab.)
ABLIKIM	06T	PL B642 197	M. Ablikim *et al.*	(BES Collab.)
DOBBS	06	PR D73 071101	S. Dobbs *et al.*	(CLEO Collab.)
ABLIKIM	05G	PR D71 092002	M. Ablikim *et al.*	(BES Collab.)
ABLIKIM	05N	PL B630 7	M. Ablikim *et al.*	(BES Collab.)
ABLIKIM	05O	PL B630 21	M. Ablikim *et al.*	(BES Collab.)
ADAM	05A	PRL 94 232002	N.E. Adam *et al.*	(CLEO Collab.)
ANDREOTTI	05A	NP B717 34	M. Andreotti *et al.*	(FNAL E835 Collab.)
NAKAZAWA	05	PL B615 39	H. Nakazawa *et al.*	(BELLE Collab.)
ABLIKIM	04B	PR D70 012003	M. Ablikim *et al.*	(BES Collab.)
ABLIKIM	04H	PR D70 092003	M. Ablikim *et al.*	(BES Collab.)
ABLIKIM	04I	PR D70 092004	M. Ablikim *et al.*	(BES Collab.)
ATHAR	04	PR D70 112002	S.B. Athar *et al.*	(CLEO Collab.)
BAI	04F	PR D69 092001	J.Z. Bai *et al.*	(BES Collab.)
BAI	04I	PR D70 012006	J.Z. Bai *et al.*	(BES Collab.)
AULCHENKO	03	PL B573 63	V.M. Aulchenko *et al.*	(KEDR Collab.)
BAI	03C	PR D67 032004	J.Z. Bai *et al.*	(BES Collab.)
BAI	03E	PR D67 112001	J.Z. Bai *et al.*	(BES Collab.)
ABE	02T	PL B540 33	K. Abe *et al.*	(BELLE Collab.)
AMBROGIANI	02	PR D65 052002	M. Ambrogiani *et al.*	(FNAL E835 Collab.)
EISENSTEIN	01	PRL 87 061801	B.I. Eisenstein *et al.*	(CLEO Collab.)
AMBROGIANI	00B	PR D62 052002	M. Ambrogiani *et al.*	(FNAL E835 Collab.)
ACCIARRI	99E	PL B453 73	M. Acciarri *et al.*	(L3 Collab.)
BAI	99B	PR D60 072001	J.Z. Bai *et al.*	(BES Collab.)
ACKER..,K...	98	PL B439 197	K. Ackerstaff *et al.*	(OPAL Collab.)
BAI	98D	PR D58 092006	J.Z. Bai *et al.*	(BES Collab.)
BAI	98I	PRL 81 3091	J.Z. Bai *et al.*	(BES Collab.)
DOMINICK	94	PR D50 4265	J. Dominick *et al.*	(CLEO Collab.)
ARMSTRONG	93	PRL 70 2988	T.A. Armstrong *et al.*	(FNAL E760 Collab.)
ARMSTRONG	93E	PR D48 3037	T.A. Armstrong *et al.*	(FNAL-E760 Collab.)
BAUER	93	PL B302 345	D.A. Bauer *et al.*	(TPC Collab.)
ARMSTRONG	92	NP B373 35	T.A. Armstrong *et al.*	(FNAL, FERR, GENO+)
Also		PRL 68 1468	T.A. Armstrong *et al.*	(FNAL, FERR, GENO+)
BAGLIN	87B	PL B187 191	C. Baglin *et al.*	(R704 Collab.)
BAGLIN	86B	PL B172 455	C. Baglin	(LAPP, CERN, GENO, LYON, OSLO+)
GAISER	86	PR D34 711	J. Gaiser *et al.*	(Crystal Ball Collab.)
LEE	85	SLAC 282	R.A. Lee	(SLAC)
LEMOIGNE	82	PL 113B 509	Y. Lemoigne *et al.*	(SACL, LOIC, SHMP+)
OREGLIA	82	PR D25 2259	M.J. Oreglia *et al.*	(SLAC, CIT, HARV+)
Also		Private Comm.	M.J. Oreglia	(EFI)
BARATE	81	PR D24 2994	R. Barate *et al.*	(SACL, LOIC, SHMP, CERN+)
HIMEL	80	PRL 44 920	T. Himel *et al.*	(LBL, SLAC)
Also		Private Comm.	G. Trilling	(LBL, UCB)
BRANDELIK	79B	NP B160 426	R. Brandelik *et al.*	(DASP Collab.)
BARTEL	78B	PL 79B 492	W. Bartel *et al.*	(DESY, HEIDP)
TANENBAUM	78	PR D17 1731	W.M. Tanenbaum *et al.*	(SLAC, LBL)
Also		Private Comm.	G. Trilling	(LBL, UCB)
BIDDICK	77	PRL 38 1324	C.J. Biddick *et al.*	(UCSD, UMD, PAVI+)
WHITAKER	76	PRL 37 1596	J.S. Whitaker *et al.*	(SLAC, LBL)

$\eta_c(2S)$ $I^G(J^{PC}) = 0^+(0^{-+})$

Quantum numbers are quark model predictions.

$\eta_c(2S)$ MASS

VALUE (MeV)	EVTS	DOCUMENT ID		TECN	COMMENT
3637.6±1.2 OUR AVERAGE		Error includes scale factor of 1.2.			
3633.6±1.7±0.6	106	[1] AAIJ	17AD	LHCB	$pp \to B^+X \to p\overline{p}K^+X$
3636.4±4.1±0.7	365	[2] AAIJ	17BB	LHCB	$pp \to b\overline{b}X \to 2(K^+K^-)X$
3637.0±5.7±3.4	178	[3,4] LEES	14E	BABR	$\gamma\gamma \to K^+K^-\pi^0$
3635.1±5.8±2.1	47	[3,5] LEES	14E	BABR	$\gamma\gamma \to K^+K^-\eta$
3646.9±1.6±3.6	57 ± 17	ABLIKIM	13K	BES3	$\psi(2S) \to \gamma K^0_S K^\pm\pi^\mp\pi^+\pi^-$
3637.6±2.9±1.6	127 ± 18	[6] ABLIKIM	12G	BES3	$\psi(2S) \to \gamma K^0 K\pi$, $KK\pi^0$
3638.5±1.5±0.8	624	[3] DEL-AMO-SA...	11M	BABR	$\gamma\gamma \to K^0_S K^\pm\pi^\mp$
3640.5±3.2±2.5	1201	[3] DEL-AMO-SA...	11M	BABR	$\gamma\gamma \to K^+K^-\pi^+\pi^-\pi^0$
$3636.1^{+3.9+0.7}_{-4.2-2.0}$	128	[7] VINOKUROVA	11	BELL	$B^\pm \to K^\pm(K^0_S K^\pm\pi^\mp)$
3626 ±5 ±6	311	[8] ABE	07	BELL	$e^+e^- \to J/\psi(c\overline{c})$
$3645.0\pm5.5^{+4.9}_{-7.8}$	121 ± 27	AUBERT	05C	BABR	$e^+e^- \to J/\psi c\overline{c}$
3642.9±3.1±1.5	61	ASNER	04	CLEO	$\gamma\gamma \to \eta_c \to K^0_S K^\pm\pi^\mp$
• • • We do not use the following data for averages, fits, limits, etc. • • •					
3639 ±7	98 ± 52	[9] AUBERT	06E	BABR	$B^\pm \to K^\pm X_{c\overline{c}}$
3630.8±3.4±1.0	112 ± 24	[10] AUBERT	04D	BABR	$\gamma\gamma \to \eta_c(2S) \to K\overline{K}\pi$
3654 ±6 ±8	39 ± 11	[11] CHOI	02	BELL	$B \to KK_SK^-\pi^+$
3594 ±5		[12] EDWARDS	82C	CBAL	$e^+e^- \to \gamma X$

[1] AAIJ 17AD report $m_{\psi(2S)} - m_{\eta_c(2S)} = 52.5 \pm 1.7 \pm 0.6$ MeV. We use the current value $m_{\psi(2S)} = 3686.097 \pm 0.025$ MeV to obtain the quoted mass.
[2] From a fit of the $\phi\phi$ invariant mass with the width of $\eta_c(2S)$ fixed to the PDG 16 value.
[3] Ignoring possible interference with continuum.
[4] With a width fixed to 11.3 MeV.
[5] With a width fixed to 11.3 MeV. Using both $\eta \to \gamma\gamma$ and $\eta \to \pi^+\pi^-\pi^0$ decays.
[6] From a simultaneous fit to $K^0_S K^\pm\pi^\mp$ and $K^+K^-\pi^0$ decay modes.
[7] Accounts for interference with non-resonant continuum.
[8] From a fit of the J/ψ recoil mass spectrum. Supersedes ABE,K 02 and ABE 04G.
[9] From the fit of the kaon momentum spectrum. Systematic errors not evaluated.
[10] Superseded by DEL-AMO-SANCHEZ 11M.
[11] Superseded by VINOKUROVA 11.
[12] Assuming mass of $\psi(2S) = 3686$ MeV.

$\eta_c(2S)$ WIDTH

VALUE (MeV)	CL%	EVTS	DOCUMENT ID		TECN	COMMENT
$11.3^{+3.2}_{-2.9}$ OUR AVERAGE						
9.9± 4.8±2.9		57 ± 17	ABLIKIM	13K	BES3	$\psi(2S) \to \gamma K^0_S K^\pm\pi^\mp\pi^+\pi^-$
16.9± 6.4±4.8		127 ± 18	[13] ABLIKIM	12G	BES3	$\psi(2S) \to \gamma K^0 K\pi$, $KK\pi^0$
13.4± 4.6±3.2		624	[14] DEL-AMO-SA...	11M	BABR	$\gamma\gamma \to K^0_S K^\pm\pi^\mp$
$6.6^{+\ 8.4+2.6}_{-\ 5.1-0.9}$		128	[15] VINOKUROVA	11	BELL	$B^\pm \to K^\pm(K^0_S K^\pm\pi^\mp)$
6.3±12.4±4.0		61	ASNER	04	CLEO	$\gamma\gamma \to \eta_c \to K^0_S K^\pm\pi^\mp$
• • • We do not use the following data for averages, fits, limits, etc. • • •						
< 23	90	98 ± 52	[16] AUBERT	06E	BABR	$B^\pm \to K^\pm X_{c\overline{c}}$
22 ±14		121 ± 27	AUBERT	05C	BABR	$e^+e^- \to J/\psi c\overline{c}$
17.0± 8.3±2.5		112 ± 24	[17] AUBERT	04D	BABR	$\gamma\gamma \to \eta_c(2S) \to K\overline{K}\pi$
<55	90	39 ± 11	[18] CHOI	02	BELL	$B \to KK_SK^-\pi^+$
<8.0	95		[19] EDWARDS	82C	CBAL	$e^+e^- \to \gamma X$

[13] From a simultaneous fit to $K^0_S K^\pm\pi^\mp$ and $K^+K^-\pi^0$ decay modes.
[14] Ignoring possible interference with continuum.
[15] Accounts for interference with non-resonant continuum.
[16] From the fit of the kaon momentum spectrum. Systematic errors not evaluated.
[17] Superseded by DEL-AMO-SANCHEZ 11M.
[18] For a mass value of 3654 ± 6 MeV. Superseded by VINOKUROVA 11.
[19] For a mass value of 3594 ± 5 MeV

$\eta_c(2S)$ DECAY MODES

	Mode	Fraction (Γ_i/Γ)	Confidence level
Γ_1	hadrons	not seen	
Γ_2	$K\overline{K}\pi$	(1.9±1.2) %	
Γ_3	$K\overline{K}\eta$	(5 ±4) $\times 10^{-3}$	
Γ_4	$2\pi^+2\pi^-$	not seen	
Γ_5	$\rho^0\rho^0$	not seen	
Γ_6	$3\pi^+3\pi^-$	not seen	

Γ_7	$K^+K^-\pi^+\pi^-$	not seen		
Γ_8	$K^{*0}\overline{K}^{*0}$	not seen		
Γ_9	$K^+K^-\pi^+\pi^-\pi^0$	(1.4±1.0)	%	
Γ_{10}	$K^+K^-2\pi^+2\pi^-$	not seen		
Γ_{11}	$K^0_S K^-2\pi^+\pi^-$ + c.c.	seen		
Γ_{12}	$2K^+2K^-$	not seen		
Γ_{13}	$\phi\phi$	not seen		
Γ_{14}	$p\overline{p}$	seen		
Γ_{15}	$\gamma\gamma$	(1.9±1.3) × 10^{-4}		
Γ_{16}	$\gamma J/\psi(1S)$	< 1.4	%	90%
Γ_{17}	$\pi^+\pi^-\eta$	not seen		
Γ_{18}	$\pi^+\pi^-\eta'$	not seen		
Γ_{19}	$\pi^+\pi^-\eta_c(1S)$	< 25	%	90%

$\eta_c(2S)$ PARTIAL WIDTHS

$\Gamma(\gamma\gamma)$ Γ_{15}

VALUE (keV)	DOCUMENT ID		TECN	COMMENT
• • • We do not use the following data for averages, fits, limits, etc. • • •				
1.3±0.6	[20] ASNER	04	CLEO	$\gamma\gamma \to \eta_c \to K^0_S K^\pm\pi^\mp$

[20] They measure $\Gamma(\eta_c(2S)\gamma\gamma)$ B$(\eta_c(2S) \to K\overline{K}\pi) = (0.18 \pm 0.05 \pm 0.02)\ \Gamma(\eta_c(1S)\gamma\gamma)$ B$(\eta_c(1S) \to K\overline{K}\pi)$. The value for $\Gamma(\eta_c(2S) \to \gamma\gamma)$ is derived assuming that the branching fractions for $\eta_c(2S)$ and $\eta_c(1S)$ decays to $K_S K\pi$ are equal and using $\Gamma(\eta_c(1S) \to \gamma\gamma) = 7.4 \pm 0.4 \pm 2.3$ keV.

$\eta_c(2S)$ Γ(i)$\Gamma(\gamma\gamma)/\Gamma$(total)

$\Gamma(2\pi^+2\pi^-) \times \Gamma(\gamma\gamma)/\Gamma_{\rm total}$ $\Gamma_4\Gamma_{15}/\Gamma$

VALUE (eV)	CL%	DOCUMENT ID		TECN	COMMENT
<6.5	90	UEHARA	08	BELL	$\gamma\gamma \to \eta_c(2S) \to 2(\pi^+\pi^-)$

$\Gamma(K\overline{K}\pi) \times \Gamma(\gamma\gamma)/\Gamma_{\rm total}$ $\Gamma_2\Gamma_{15}/\Gamma$

VALUE (eV)	EVTS	DOCUMENT ID		TECN	COMMENT
41±4±6	624	[21] DEL-AMO-SA...11M		BABR	$\gamma\gamma \to K^0_S K^\pm\pi^\mp$

[21] Not independent from other measurements reported in DEL-AMO-SANCHEZ 11M.

$\Gamma(K^+K^-\pi^+\pi^-) \times \Gamma(\gamma\gamma)/\Gamma_{\rm total}$ $\Gamma_7\Gamma_{15}/\Gamma$

VALUE (eV)	CL%	DOCUMENT ID		TECN	COMMENT
<5.0	90	UEHARA	08	BELL	$\gamma\gamma \to \eta_c(2S) \to K^+K^-\pi^+\pi^-$

$\Gamma(K^+K^-\pi^+\pi^-\pi^0) \times \Gamma(\gamma\gamma)/\Gamma_{\rm total}$ $\Gamma_9\Gamma_{15}/\Gamma$

VALUE (eV)	EVTS	DOCUMENT ID		TECN	COMMENT
30±6±5	1201	[22] DEL-AMO-SA...11M		BABR	$\gamma\gamma \to K^+K^-\pi^+\pi^-\pi^0$

[22] Not independent from other measurements reported in DEL-AMO-SANCHEZ 11M.

$\Gamma(2K^+2K^-) \times \Gamma(\gamma\gamma)/\Gamma_{\rm total}$ $\Gamma_{12}\Gamma_{15}/\Gamma$

VALUE (eV)	CL%	DOCUMENT ID		TECN	COMMENT
<2.9	90	UEHARA	08	BELL	$\gamma\gamma \to \eta_c(2S) \to 2(K^+K^-)$

$\Gamma(\pi^+\pi^-\eta_c(1S)) \times \Gamma(\gamma\gamma)/\Gamma_{\rm total}$ $\Gamma_{19}\Gamma_{15}/\Gamma$

VALUE (eV)	CL%	DOCUMENT ID		TECN	COMMENT
<133	90	LEES	12AE	BABR	$e^+e^- \to e^+e^-\pi^+\pi^-\eta_c$

$\eta_c(2S)$ Γ(i)$\Gamma(\gamma\gamma)/\Gamma^2$(total)

$\Gamma(p\overline{p})/\Gamma_{\rm total} \times \Gamma(\gamma\gamma)/\Gamma_{\rm total}$ $\Gamma_{14}/\Gamma \times \Gamma_{15}/\Gamma$

VALUE ($\times 10^{-8}$)	CL%	DOCUMENT ID		TECN	COMMENT
< 5.6	90	[23,24,25] AMBROGIANI	01	E835	$\overline{p}p \to \gamma\gamma$
• • • We do not use the following data for averages, fits, limits, etc. • • •					
< 8.0	90	[23,24,26] AMBROGIANI	01	E835	$\overline{p}p \to \gamma\gamma$
<12.0	90	[24,26] AMBROGIANI	01	E835	$\overline{p}p \to \gamma\gamma$

[23] Including the measurements of of ARMSTRONG 95F in the AMBROGIANI 01 analysis.
[24] For a total width Γ=5 MeV.
[25] For the resonance mass region 3589–3599 MeV/c^2.
[26] For the resonance mass region 3575–3660 MeV/c^2.

$\eta_c(2S)$ BRANCHING RATIOS

Γ(hadrons)/$\Gamma_{\rm total}$ Γ_1/Γ

VALUE	DOCUMENT ID		TECN	COMMENT
not seen	ABREU	98O	DLPH	$e^+e^- \to e^+e^-$ + hadrons
• • • We do not use the following data for averages, fits, limits, etc. • • •				
seen	[27] EDWARDS	82C	CBAL	$e^+e^- \to \gamma$X

[27] For a mass value of 3594 ± 5 MeV

$\Gamma(K\overline{K}\pi)/\Gamma_{\rm total}$ Γ_2/Γ

VALUE ($\times 10^{-2}$)	EVTS	DOCUMENT ID		TECN	COMMENT
1.9±0.4±1.1	59 ± 12	[28] AUBERT	08AB	BABR	$B \to \eta_c(2S)K \to K\overline{K}\pi K$
• • • We do not use the following data for averages, fits, limits, etc. • • •					
seen	127 ± 18	ABLIKIM	13K	BES3	$\psi(2S) \to \gamma K\overline{K}\pi$
seen	39 ± 11	[29] CHOI	02	BELL	$B \to K K_S K^-\pi^+$

[28] Derived from a measurement of [B$(B^+ \to \eta_c(2S)K^+) \times$ B$(\eta_c(2S) \to K\overline{K}\pi)$] / [B$(B^+ \to \eta_c K^+) \times$ B$(\eta_c \to K\overline{K}\pi)$] = $(9.6^{+2.0}_{-1.9} \pm 2.5)$% and using B$(B^+ \to \eta_c(2S)K^+) = (3.4 \pm 1.8) \times 10^{-4}$, and [B$(B^+ \to \eta_c K^+) \times$ B$(\eta_c \to K\overline{K}\pi)$] = $(6.88 \pm 0.77^{+0.55}_{-0.66}) \times 10^{-5}$.
[29] For a mass value of 3654 ± 6 MeV

$\Gamma(K\overline{K}\eta)/\Gamma(K\overline{K}\pi)$ Γ_3/Γ_2

VALUE (units 10^{-2})	EVTS	DOCUMENT ID		TECN	COMMENT
27.3±7.0±9.0	225	[30] LEES	14E	BABR	$\gamma\gamma \to K^+K^-\gamma\gamma$

[30] LEES 14E reports B$(\eta_c(2S) \to K^+K^-\eta)$/B$(\eta_c(2S) \to K^+K^-\pi^0) = 0.82 \pm 0.21 \pm 0.27$, which we divide by 3 to account for isospin symmetry.

$\Gamma(2\pi^+2\pi^-)/\Gamma_{\rm total}$ Γ_4/Γ

VALUE	DOCUMENT ID		TECN	COMMENT
not seen	UEHARA	08	BELL	$\gamma\gamma \to \eta_c(2S)$

$\Gamma(\rho^0\rho^0)/\Gamma_{\rm total}$ Γ_5/Γ

VALUE	DOCUMENT ID		TECN	COMMENT
not seen	ABLIKIM	11H	BES3	$\psi(2S) \to \gamma 2\pi^+2\pi^-$

$\Gamma(K^+K^-\pi^+\pi^-)/\Gamma_{\rm total}$ Γ_7/Γ

VALUE	DOCUMENT ID		TECN	COMMENT
not seen	UEHARA	08	BELL	$\gamma\gamma \to \eta_c(2S)$

$\Gamma(K^+K^-\pi^+\pi^-\pi^0)/\Gamma(K\overline{K}\pi)$ Γ_9/Γ_2

VALUE	EVTS	DOCUMENT ID		TECN	COMMENT
0.73±0.17±0.17	1201	[31] DEL-AMO-SA...11M		BABR	$\gamma\gamma \to K^+K^-\pi^+\pi^-\pi^0$

[31] We have multiplied the value of $\Gamma(K^+K^-\pi^+\pi^-\pi^0)/\Gamma(K^0_S K^\pm\pi^\mp)$ reported in DEL-AMO-SANCHEZ 11M by a factor 1/3 to obtain $\Gamma(K^+K^-\pi^+\pi^-\pi^0)/\Gamma(K\overline{K}\pi)$. Not independent from other measurements reported in DEL-AMO-SANCHEZ 11M.

$\Gamma(K^{*0}\overline{K}^{*0})/\Gamma_{\rm total}$ Γ_8/Γ

VALUE	DOCUMENT ID		TECN	COMMENT
not seen	ABLIKIM	11H	BES3	$\psi(2S) \to \gamma K^+K^-\pi^+\pi^-$

$\Gamma(K^0_S K^-2\pi^+\pi^-$ + c.c.)/$\Gamma_{\rm total}$ Γ_{11}/Γ

VALUE	EVTS	DOCUMENT ID		TECN	COMMENT
seen	57±17	ABLIKIM	13K	BES3	$\psi(2S) \to \gamma K^0_S K^\pm\pi^\mp\pi^+\pi^-$

$\Gamma(2K^+2K^-)/\Gamma_{\rm total}$ Γ_{12}/Γ

VALUE	DOCUMENT ID		TECN	COMMENT
not seen	UEHARA	08	BELL	$\gamma\gamma \to \eta_c(2S)$

$\Gamma(\phi\phi)/\Gamma_{\rm total}$ Γ_{13}/Γ

VALUE	DOCUMENT ID		TECN	COMMENT
not seen	ABLIKIM	11H	BES3	$\psi(2S) \to \gamma K^+K^-K^+K^-$

$\Gamma(p\overline{p})/\Gamma_{\rm total}$ Γ_{14}/Γ

VALUE	EVTS	DOCUMENT ID		TECN	COMMENT
seen	106	[32] AAIJ	17AD	LHCB	$pp \to B^+X \to p\overline{p}K^+X$

[32] AAIJ 17AD report a 6.4 standard deviation signal, with B$(B^+ \to \eta_c(2S)K^+ \to p\overline{p}K^+)$/B$(B^+ \to J/\psi K^+ \to p\overline{p}K^+) = (1.58 \pm 0.33 \pm 0.09) \times 10^{-2}$.

$\Gamma(\gamma\gamma)/\Gamma_{\rm total}$ Γ_{15}/Γ

VALUE	CL%	DOCUMENT ID		TECN	COMMENT
• • • We do not use the following data for averages, fits, limits, etc. • • •					
<4 × 10^{-4}	90	[33] WICHT	08	BELL	$B^\pm \to K^\pm\gamma\gamma$
not seen		AMBROGIANI	01	E835	$\overline{p}p \to \gamma\gamma$
<0.01	90	LEE	85	CBAL	$\psi' \to$ photons

[33] WICHT 08 reports $[\Gamma(\eta_c(2S) \to \gamma\gamma)/\Gamma_{\rm total}] \times$ [B$(B^+ \to \eta_c(2S)K^+)] < 0.18 \times 10^{-6}$ which we divide by our best value B$(B^+ \to \eta_c(2S)K^+) = 4.4 \times 10^{-4}$.

$\Gamma(\pi^+\pi^-\eta_c(1S))/\Gamma(K\overline{K}\pi)$ Γ_{19}/Γ_2

VALUE	CL%	DOCUMENT ID		TECN	COMMENT
<3.33	90	[34] LEES	12AE	BABR	$e^+e^- \to e^+e^-\pi^+\pi^-\eta_c$

[34] We divided the reported limit by 3 to take into account isospin relations.

$\eta_c(2S)$ CROSS-PARTICLE BRANCHING RATIOS

$\Gamma(\eta_c(2S) \to K\overline{K}\eta)/\Gamma_{\rm total} \times \Gamma(\psi(2S) \to \gamma\eta_c(2S))/\Gamma_{\rm total}$ $\Gamma_3/\Gamma \times \Gamma^{\psi(2S)}_{143}/\Gamma^{\psi(2S)}$

VALUE	CL%	DOCUMENT ID		TECN	COMMENT
• • • We do not use the following data for averages, fits, limits, etc. • • •					
<11.8 × 10^{-6}	90	[35] CRONIN-HEN...10		CLEO	$\psi(2S) \to \gamma K^+K^-\eta$

[35] CRONIN-HENNESSY 10 reports a limit of $< 5.9 \times 10^{-6}$ for the decay $\eta_c(2S) \to K^+ K^- \eta$ which we multiply by 2 account for isospin symmetry. It assumes $\Gamma(\eta_c(2S)) = 14$ MeV. It also gives the analytic dependence of limits on width.

$\Gamma(\eta_c(2S) \to 2\pi^+ 2\pi^-)/\Gamma_{\text{total}} \times \Gamma(\psi(2S) \to \gamma\eta_c(2S))/\Gamma_{\text{total}}$
$\Gamma_4/\Gamma \times \Gamma^{\psi(2S)}_{143}/\Gamma^{\psi(2S)}$

VALUE	CL%	DOCUMENT ID	TECN	COMMENT
$< 14.6 \times 10^{-6}$	90	[36] CRONIN-HEN..10	CLEO	$\psi(2S) \to \gamma 2\pi^+ 2\pi^-$

[36] Assuming $\Gamma(\eta_c(2S)) = 14$ MeV. CRONIN-HENNESSY 10 gives the analytic dependence of limits on width.

$\Gamma(\eta_c(2S) \to \rho^0 \rho^0)/\Gamma_{\text{total}} \times \Gamma(\psi(2S) \to \gamma\eta_c(2S))/\Gamma_{\text{total}}$
$\Gamma_5/\Gamma \times \Gamma^{\psi(2S)}_{143}/\Gamma^{\psi(2S)}$

VALUE	CL%	DOCUMENT ID	TECN	COMMENT
$< 12.7 \times 10^{-7}$	90	ABLIKIM 11H	BES3	$\psi(2S) \to \gamma 2\pi^+ 2\pi^-$

$\Gamma(\eta_c(2S) \to 3\pi^+ 3\pi^-)/\Gamma_{\text{total}} \times \Gamma(\psi(2S) \to \gamma\eta_c(2S))/\Gamma_{\text{total}}$
$\Gamma_6/\Gamma \times \Gamma^{\psi(2S)}_{143}/\Gamma^{\psi(2S)}$

VALUE	CL%	DOCUMENT ID	TECN	COMMENT
$< 13.2 \times 10^{-6}$	90	[37] CRONIN-HEN..10	CLEO	$\psi(2S) \to \gamma 3\pi^+ 3\pi^-$

[37] Assuming $\Gamma(\eta_c(2S)) = 14$ MeV. CRONIN-HENNESSY 10 gives the analytic dependence of limits on width.

$\Gamma(\eta_c(2S) \to K^+ K^- \pi^+ \pi^-)/\Gamma_{\text{total}} \times \Gamma(\psi(2S) \to \gamma\eta_c(2S))/\Gamma_{\text{total}}$
$\Gamma_7/\Gamma \times \Gamma^{\psi(2S)}_{143}/\Gamma^{\psi(2S)}$

VALUE	CL%	DOCUMENT ID	TECN	COMMENT
$< 9.6 \times 10^{-6}$	90	[38] CRONIN-HEN..10	CLEO	$\psi(2S) \to \gamma K^+ K^- \pi^+ \pi^-$

[38] Assuming $\Gamma(\eta_c(2S)) = 14$ MeV. CRONIN-HENNESSY 10 gives the analytic dependence of limits on width.

$\Gamma(\eta_c(2S) \to K^{*0}\overline{K}^{*0})/\Gamma_{\text{total}} \times \Gamma(\psi(2S) \to \gamma\eta_c(2S))/\Gamma_{\text{total}}$
$\Gamma_8/\Gamma \times \Gamma^{\psi(2S)}_{143}/\Gamma^{\psi(2S)}$

VALUE	CL%	DOCUMENT ID	TECN	COMMENT
$< 19.6 \times 10^{-7}$	90	ABLIKIM 11H	BES3	$\psi(2S) \to \gamma K^+ K^- \pi^+ \pi^-$

$\Gamma(\eta_c(2S) \to K^+ K^- \pi^+ \pi^- \pi^0)/\Gamma_{\text{total}} \times \Gamma(\psi(2S) \to \gamma\eta_c(2S))/\Gamma_{\text{total}}$
$\Gamma_9/\Gamma \times \Gamma^{\psi(2S)}_{143}/\Gamma^{\psi(2S)}$

VALUE	CL%	DOCUMENT ID	TECN	COMMENT
$< 43.0 \times 10^{-6}$	90	[39] CRONIN-HEN..10	CLEO	$\psi(2S) \to \gamma K^+ K^- \pi^+ \pi^- \pi^0$

[39] Assuming $\Gamma(\eta_c(2S)) = 14$ MeV. CRONIN-HENNESSY 10 gives the analytic dependence of limits on width.

$\Gamma(\eta_c(2S) \to K^+ K^- 2\pi^+ 2\pi^-)/\Gamma_{\text{total}} \times \Gamma(\psi(2S) \to \gamma\eta_c(2S))/\Gamma_{\text{total}}$
$\Gamma_{10}/\Gamma \times \Gamma^{\psi(2S)}_{143}/\Gamma^{\psi(2S)}$

VALUE	CL%	DOCUMENT ID	TECN	COMMENT
$< 9.7 \times 10^{-6}$	90	[40] CRONIN-HEN..10	CLEO	$\psi(2S) \to \gamma K^+ K^- 2\pi^+ 2\pi^-$

[40] Assuming $\Gamma(\eta_c(2S)) = 14$ MeV. CRONIN-HENNESSY 10 gives the analytic dependence of limits on width.

$\Gamma(\eta_c(2S) \to K^0_S K^- 2\pi^+ \pi^- + \text{c.c.})/\Gamma_{\text{total}} \times \Gamma(\psi(2S) \to \gamma\eta_c(2S))/\Gamma_{\text{total}}$
$\Gamma_{11}/\Gamma \times \Gamma^{\psi(2S)}_{143}/\Gamma^{\psi(2S)}$

VALUE (units 10^{-6})	CL%	EVTS	DOCUMENT ID	TECN	COMMENT
$7.03 \pm 2.10 \pm 0.7$		60	ABLIKIM 13K	BES3	$\psi(2S) \to \gamma K^0_S K^- 2\pi^+ \pi^- +$c.c.
• • • We do not use the following data for averages, fits, limits, etc. • • •					
< 15.2	90		[41] CRONIN-HEN..10	CLEO	$\psi(2S) \to \gamma K^0_S K^- 2\pi^+ \pi^- +$c.c.

[41] Assuming $\Gamma(\eta_c(2S)) = 14$ MeV. CRONIN-HENNESSY 10 gives the analytic dependence of limits on width.

$\Gamma(\eta_c(2S) \to \phi\phi)/\Gamma_{\text{total}} \times \Gamma(\psi(2S) \to \gamma\eta_c(2S))/\Gamma_{\text{total}}$
$\Gamma_{13}/\Gamma \times \Gamma^{\psi(2S)}_{143}/\Gamma^{\psi(2S)}$

VALUE	CL%	DOCUMENT ID	TECN	COMMENT
$< 7.8 \times 10^{-7}$	90	ABLIKIM 11H	BES3	$\psi(2S) \to \gamma K^+ K^- K^+ K^-$

$\Gamma(\eta_c(2S) \to p\overline{p})/\Gamma_{\text{total}} \times \Gamma(\psi(2S) \to \gamma\eta_c(2S))/\Gamma_{\text{total}}$
$\Gamma_{14}/\Gamma \times \Gamma^{\psi(2S)}_{143}/\Gamma^{\psi(2S)}$

VALUE	CL%	DOCUMENT ID	TECN	COMMENT
$< 1.4 \times 10^{-6}$	90	ABLIKIM 13V	BES3	$\psi(2S) \to \gamma p\overline{p}$

$\Gamma(\eta_c(2S) \to \gamma J/\psi(1S))/\Gamma_{\text{total}} \times \Gamma(\psi(2S) \to \gamma\eta_c(2S))/\Gamma_{\text{total}}$
$\Gamma_{16}/\Gamma \times \Gamma^{\psi(2S)}_{143}/\Gamma^{\psi(2S)}$

VALUE	CL%	EVTS	DOCUMENT ID	TECN	COMMENT
$< 9.7 \times 10^{-6}$	90	33	[42] ABLIKIM 17N	BES3	$\psi(2S) \to \gamma\gamma J/\psi$

[42] Uses B($J/\psi \to e^+ e^-$) = (5.971 ± 0.032)% and B($J/\psi \to \mu^+ \mu^-$) = (5.961 ± 0.033)%.

$\Gamma(\eta_c(2S) \to \pi^+ \pi^- \eta)/\Gamma_{\text{total}} \times \Gamma(\psi(2S) \to \gamma\eta_c(2S))/\Gamma_{\text{total}}$
$\Gamma_{17}/\Gamma \times \Gamma^{\psi(2S)}_{143}/\Gamma^{\psi(2S)}$

VALUE	CL%	DOCUMENT ID	TECN	COMMENT
$< 4.3 \times 10^{-6}$	90	[43] CRONIN-HEN..10	CLEO	$\psi(2S) \to \gamma\pi^+ \pi^- \eta$

[43] Assuming $\Gamma(\eta_c(2S)) = 14$ MeV. CRONIN-HENNESSY 10 gives the analytic dependence of limits on width.

$\Gamma(\eta_c(2S) \to \pi^+ \pi^- \eta')/\Gamma_{\text{total}} \times \Gamma(\psi(2S) \to \gamma\eta_c(2S))/\Gamma_{\text{total}}$
$\Gamma_{18}/\Gamma \times \Gamma^{\psi(2S)}_{143}/\Gamma^{\psi(2S)}$

VALUE	CL%	DOCUMENT ID	TECN	COMMENT
$< 14.2 \times 10^{-6}$	90	[44] CRONIN-HEN..10	CLEO	$\psi(2S) \to \gamma\pi^+ \pi^- \eta'$

[44] Assuming $\Gamma(\eta_c(2S)) = 14$ MeV. CRONIN-HENNESSY 10 gives the analytic dependence of limits on width.

$\Gamma(\eta_c(2S) \to \pi^+ \pi^- \eta_c(1S))/\Gamma_{\text{total}} \times \Gamma(\psi(2S) \to \gamma\eta_c(2S))/\Gamma_{\text{total}}$
$\Gamma_{19}/\Gamma \times \Gamma^{\psi(2S)}_{143}/\Gamma^{\psi(2S)}$

VALUE	CL%	DOCUMENT ID	TECN	COMMENT
$< 1.7 \times 10^{-4}$	90	[45] CRONIN-HEN..10	CLEO	$\psi(2S) \to \gamma\pi^+ \pi^- \eta_c(1S)$

[45] Assuming $\Gamma(\eta_c(2S)) = 14$ MeV. CRONIN-HENNESSY 10 gives the analytic dependence of limits on width.

$\eta_c(2S)$ REFERENCES

AAIJ	17AD	PL B769 305	R. Aaij *et al.*	(LHCb Collab.)
AAIJ	17BB	EPJ C77 609	R. Aaij *et al.*	(LHCb Collab.)
ABLIKIM	17N	PR D95 072004	M. Ablikim *et al.*	(BES III Collab.)
PDG	16	CP C40 100001	C. Patrignani *et al.*	(PDG Collab.)
LEES	14E	PR D89 112004	J.P. Lees *et al.*	(BABAR Collab.)
ABLIKIM	13K	PR D87 052005	M. Ablikim *et al.*	(BES III Collab.)
ABLIKIM	13V	PR D88 112001	M. Ablikim *et al.*	(BES III Collab.)
ABLIKIM	12G	PRL 109 042003	M. Ablikim *et al.*	(BES III Collab.)
LEES	12AE	PR D86 092005	J.P. Lees *et al.*	(BABAR Collab.)
ABLIKIM	11H	PR D84 091102	M. Ablikim *et al.*	(BES III Collab.)
DEL-AMO-SA...	11M	PR D84 012004	P. del Amo Sanchez *et al.*	(BABAR Collab.)
VINOKUROVA	11	PL B706 139	A. Vinokurova *et al.*	(BELLE Collab.)
CRONIN-HEN...	10	PR D81 052002	D. Cronin-Hennessey *et al.*	(CLEO Collab.)
AUBERT	08AB	PR D78 012006	B. Aubert *et al.*	(BABAR Collab.)
UEHARA	08	EPJ C53 1	S. Uehara *et al.*	(BELLE Collab.)
WICHT	08	PL B662 323	J. Wicht *et al.*	(BELLE Collab.)
ABE	07	PRL 98 082001	K. Abe *et al.*	(BELLE Collab.)
AUBERT	06E	PRL 96 052002	B. Aubert *et al.*	(BABAR Collab.)
AUBERT	05C	PR D72 031101	B. Aubert *et al.*	(BABAR Collab.)
ABE	04G	PR D70 071102	K. Abe *et al.*	(BELLE Collab.)
ASNER	04	PRL 92 142001	D.M. Asner *et al.*	(CLEO Collab.)
AUBERT	04D	PRL 92 142002	B. Aubert *et al.*	(BABAR Collab.)
ABE,K	02	PRL 89 142001	K. Abe *et al.*	(BELLE Collab.)
CHOI	02	PRL 89 102001	S.-K. Choi *et al.*	(BELLE Collab.)
AMBROGIANI	01	PR D64 052003	M. Ambrogiani *et al.*	(FNAL E835 Collab.)
ABREU	98O	PL B441 479	P. Abreu *et al.*	(DELPHI Collab.)
ARMSTRONG	95F	PR D52 4839	T.A. Armstrong *et al.*	(FNAL, FERR, GENO+)
LEE	85	SLAC 282	R.A. Lee	(SLAC)
EDWARDS	82C	PRL 48 70	C. Edwards *et al.*	(CIT, HARV, PRIN+)

$\psi(2S)$

$I^G(J^{PC}) = 0^-(1^{--})$

See the Review on "$\psi(2S)$ and χ_c branching ratios" before the $\chi_{c0}(1P)$ Listings.

$\psi(2S)$ MASS

OUR FIT includes measurements of $m_{\psi(2S)}$, $m_{\psi(3770)}$, and $m_{\psi(3770)} - m_{\psi(2S)}$.

VALUE (MeV)	EVTS	DOCUMENT ID	TECN	COMMENT
3686.097±0.025 OUR FIT Error includes scale factor of 2.6.				
3686.097±0.010 OUR AVERAGE				
3686.099±0.004±0.009		[1] ANASHIN 15	KEDR	$e^+ e^- \to$ hadrons
3686.12 ±0.06 ±0.10	4k	AAIJ 12H	LHCB	$pp \to J/\psi\pi^+ \pi^- X$
3685.95 ±0.10	413	[2] ARTAMONOV 00	OLYA	$e^+ e^- \to$ hadrons
3685.98 ±0.09 ±0.04		[3] ARMSTRONG 93B	E760	$\overline{p}p \to e^+ e^-$
• • • We do not use the following data for averages, fits, limits, etc. • • •				
3686.114±0.007 $^{+0.011}_{-0.016}$		[4] ANASHIN 12	KEDR	$e^+ e^- \to$ hadrons
3686.111±0.025±0.009		AULCHENKO 03	KEDR	$e^+ e^- \to$ hadrons
3686.00 ±0.10	413	[5] ZHOLENTZ 80	OLYA	$e^+ e^-$

[1] Supersedes AULCHENKO 03 and ANASHIN 12.
[2] Reanalysis of ZHOLENTZ 80 using new electron mass (COHEN 87) and radiative corrections (KURAEV 85).
[3] Mass central value and systematic error recalculated by us according to Eq. (16) in ARMSTRONG 93B, using the value for the $J/\psi(1S)$ mass from AULCHENKO 03.
[4] From the scans in 2004 and 2006. ANASHIN 12 reports the value 3686.114 ± 0.007 ± 0.011 $^{+0.002}_{-0.012}$ MeV, where the third uncertainty is due to assumptions on the interference between the resonance and hadronic continuum. We combined the two systematic uncertainties.
[5] Superseded by ARTAMONOV 00.

$m_{\psi(2S)} - m_{J/\psi(1S)}$

VALUE (MeV)	DOCUMENT ID		TECN	COMMENT
589.188±0.028 OUR AVERAGE				
589.194±0.027±0.011	[1] AULCHENKO	03	KEDR	e^+e^- → hadrons
589.7 ±1.2	LEMOIGNE	82	GOLI	185 π^- Be → $\gamma\mu^+\mu^-$ A
589.07 ±0.13	[1] ZHOLENTZ	80	OLYA	e^+e^-
588.7 ±0.8	LUTH	75	MRK1	
• • • We do not use the following data for averages, fits, limits, etc. • • •				
588 ±1	[2] BAI	98E	BES	e^+e^-

[1] Redundant with data in mass above.
[2] Systematic errors not evaluated.

$\psi(2S)$ WIDTH

VALUE (keV)	EVTS	DOCUMENT ID		TECN	COMMENT
294± 8 OUR FIT					
286±16 OUR AVERAGE					
358±88± 4		ABLIKIM	08B	BES2	e^+e^- → hadrons
290±25± 4	2.7k	ANDREOTTI	07	E835	$p\overline{p}$ → e^+e^-, $J/\psi X$
331±58± 2		ABLIKIM	06L	BES2	e^+e^- → hadrons
264±27		[1] BAI	02B	BES2	e^+e^-
287±37±16		[2] ARMSTRONG	93B	E760	$\overline{p}p$ → e^+e^-

[1] From a simultaneous fit to the hadronic and $\mu^+\mu^-$ cross section, assuming $\Gamma = \Gamma_h + \Gamma_e + \Gamma_\mu + \Gamma_\tau$ and lepton universality. Does not include vacuum polarization correction.
[2] The initial-state radiation correction reevaluated by ANDREOTTI 07 in its Ref. [4].

$\psi(2S)$ DECAY MODES

	Mode	Fraction (Γ_i/Γ)	Scale factor / Confidence level
Γ_1	hadrons	(97.85 ±0.13) %	
Γ_2	virtualγ → hadrons	(1.73 ±0.14) %	S=1.5
Γ_3	ggg	(10.6 ±1.6) %	
Γ_4	γgg	(1.03 ±0.29) %	
Γ_5	light hadrons	(15.4 ±1.5) %	
Γ_6	e^+e^-	(7.93 ±0.17) × 10^{-3}	
Γ_7	$\mu^+\mu^-$	(8.0 ±0.6) × 10^{-3}	
Γ_8	$\tau^+\tau^-$	(3.1 ±0.4) × 10^{-3}	
	Decays into $J/\psi(1S)$ and anything		
Γ_9	$J/\psi(1S)$ anything	(61.4 ±0.6) %	
Γ_{10}	$J/\psi(1S)$ neutrals	(25.37 ±0.32) %	
Γ_{11}	$J/\psi(1S)\pi^+\pi^-$	(34.67 ±0.30) %	
Γ_{12}	$J/\psi(1S)\pi^0\pi^0$	(18.23 ±0.31) %	
Γ_{13}	$J/\psi(1S)\eta$	(3.37 ±0.05) %	
Γ_{14}	$J/\psi(1S)\pi^0$	(1.268±0.032) × 10^{-3}	
	Hadronic decays		
Γ_{15}	$\pi^0 h_c(1P)$	(8.6 ±1.3) × 10^{-4}	
Γ_{16}	$3(\pi^+\pi^-)\pi^0$	(3.5 ±1.6) × 10^{-3}	
Γ_{17}	$2(\pi^+\pi^-)\pi^0$	(2.9 ±1.0) × 10^{-3}	S=4.7
Γ_{18}	$\rho a_2(1320)$	(2.6 ±0.9) × 10^{-4}	
Γ_{19}	$p\overline{p}$	(2.88 ±0.10) × 10^{-4}	
Γ_{20}	$\Delta^{++}\overline{\Delta}^{--}$	(1.28 ±0.35) × 10^{-4}	
Γ_{21}	$\Lambda\overline{\Lambda}\pi^0$	< 2.9 × 10^{-6}	CL=90%
Γ_{22}	$\Lambda\overline{\Lambda}\eta$	(2.5 ±0.4) × 10^{-5}	
Γ_{23}	$\Lambda\overline{p}K^+$	(1.00 ±0.14) × 10^{-4}	
Γ_{24}	$\Lambda\overline{p}K^+\pi^+\pi^-$	(1.8 ±0.4) × 10^{-4}	
Γ_{25}	$\Lambda\overline{\Lambda}\pi^+\pi^-$	(2.8 ±0.6) × 10^{-4}	
Γ_{26}	$\Lambda\overline{\Lambda}$	(3.81 ±0.13) × 10^{-4}	S=1.4
Γ_{27}	$\Lambda\overline{\Sigma}^+\pi^-$ + c.c.	(1.40 ±0.13) × 10^{-4}	
Γ_{28}	$\Lambda\overline{\Sigma}^-\pi^+$ + c.c.	(1.54 ±0.14) × 10^{-4}	
Γ_{29}	$\Lambda\overline{\Sigma}^0$	(1.23 ±0.24) × 10^{-5}	
Γ_{30}	$\Sigma^0\overline{p}K^+$ + c.c.	(1.67 ±0.18) × 10^{-5}	
Γ_{31}	$\Sigma^+\overline{\Sigma}^-$	(2.32 ±0.12) × 10^{-4}	
Γ_{32}	$\Sigma^0\overline{\Sigma}^0$	(2.35 ±0.09) × 10^{-4}	S=1.1
Γ_{33}	$\Sigma(1385)^+\overline{\Sigma}(1385)^-$	(8.5 ±0.7) × 10^{-5}	
Γ_{34}	$\Sigma(1385)^-\overline{\Sigma}(1385)^+$	(8.5 ±0.8) × 10^{-5}	
Γ_{35}	$\Sigma(1385)^0\overline{\Sigma}(1385)^0$	(6.9 ±0.7) × 10^{-5}	
Γ_{36}	$\Xi^-\overline{\Xi}^+$	(2.87 ±0.11) × 10^{-4}	S=1.1
Γ_{37}	$\Xi^0\overline{\Xi}^0$	(2.3 ±0.4) × 10^{-4}	S=4.2
Γ_{38}	$\Xi(1530)^0\overline{\Xi}(1530)^0$	(5.2 $^{+3.2}_{-1.2}$) × 10^{-5}	
Γ_{39}	$K^-\Lambda\overline{\Xi}^+$ + c.c.	(3.9 ±0.4) × 10^{-5}	
Γ_{40}	$\Xi(1690)^-\overline{\Xi}^+$ → $K^-\Lambda\overline{\Xi}^+$ + c.c.	(5.2 ±1.6) × 10^{-6}	
Γ_{41}	$\Xi(1820)^-\overline{\Xi}^+$ → $K^-\Lambda\overline{\Xi}^+$ + c.c.	(1.20 ±0.32) × 10^{-5}	
Γ_{42}	$K^-\Sigma^0\overline{\Xi}^+$ + c.c.	(3.7 ±0.4) × 10^{-5}	
Γ_{43}	$\Omega^-\overline{\Omega}^+$	(5.2 ±0.4) × 10^{-5}	
Γ_{44}	$\pi^0 p\overline{p}$	(1.53 ±0.07) × 10^{-4}	
Γ_{45}	$N(940)\overline{p}$ + c.c. → $\pi^0 p\overline{p}$	(6.4 $^{+1.8}_{-1.3}$) × 10^{-5}	
Γ_{46}	$N(1440)\overline{p}$ + c.c. → $\pi^0 p\overline{p}$	(7.3 $^{+1.7}_{-1.5}$) × 10^{-5}	S=2.5
Γ_{47}	$N(1520)\overline{p}$ + c.c. → $\pi^0 p\overline{p}$	(6.4 $^{+2.3}_{-1.8}$) × 10^{-6}	
Γ_{48}	$N(1535)\overline{p}$ + c.c. → $\pi^0 p\overline{p}$	(2.5 ±1.0) × 10^{-5}	
Γ_{49}	$N(1650)\overline{p}$ + c.c. → $\pi^0 p\overline{p}$	(3.8 $^{+1.4}_{-1.7}$) × 10^{-5}	
Γ_{50}	$N(1720)\overline{p}$ + c.c. → $\pi^0 p\overline{p}$	(1.79 $^{+0.26}_{-0.70}$) × 10^{-5}	
Γ_{51}	$N(2300)\overline{p}$ + c.c. → $\pi^0 p\overline{p}$	(2.6 $^{+1.2}_{-0.7}$) × 10^{-5}	
Γ_{52}	$N(2570)\overline{p}$ + c.c. → $\pi^0 p\overline{p}$	(2.13 $^{+0.40}_{-0.31}$) × 10^{-5}	
Γ_{53}	$\pi^0 f_0(2100)$ → $\pi^0 p\overline{p}$	(1.1 ±0.4) × 10^{-5}	
Γ_{54}	$\eta p\overline{p}$	(6.0 ±0.4) × 10^{-5}	
Γ_{55}	$\eta f_0(2100)$ → $\eta p\overline{p}$	(1.2 ±0.4) × 10^{-5}	
Γ_{56}	$N(1535)\overline{p}$ → $\eta p\overline{p}$	(4.4 ±0.7) × 10^{-5}	
Γ_{57}	$\omega p\overline{p}$	(6.9 ±2.1) × 10^{-5}	
Γ_{58}	$\phi p\overline{p}$	< 2.4 × 10^{-5}	CL=90%
Γ_{59}	$\pi^+\pi^- p\overline{p}$	(6.0 ±0.4) × 10^{-4}	
Γ_{60}	$p\overline{n}\pi^-$ or c.c.	(2.48 ±0.17) × 10^{-4}	
Γ_{61}	$p\overline{n}\pi^-\pi^0$	(3.2 ±0.7) × 10^{-4}	
Γ_{62}	$2(\pi^+\pi^-\pi^0)$	(4.8 ±1.5) × 10^{-3}	
Γ_{63}	$\eta\pi^+\pi^-$	< 1.6 × 10^{-4}	CL=90%
Γ_{64}	$\eta\pi^+\pi^-\pi^0$	(9.5 ±1.7) × 10^{-4}	
Γ_{65}	$2(\pi^+\pi^-)\eta$	(1.2 ±0.6) × 10^{-3}	
Γ_{66}	$\eta'\pi^+\pi^-\pi^0$	(4.5 ±2.1) × 10^{-4}	
Γ_{67}	$\omega\pi^+\pi^-$	(7.3 ±1.2) × 10^{-4}	S=2.1
Γ_{68}	$b_1^\pm\pi^\mp$	(4.0 ±0.6) × 10^{-4}	S=1.1
Γ_{69}	$b_1^0\pi^0$	(2.4 ±0.6) × 10^{-4}	
Γ_{70}	$\omega f_2(1270)$	(2.2 ±0.4) × 10^{-4}	
Γ_{71}	$\pi^0\pi^0 K^+K^-$	(2.6 ±1.3) × 10^{-4}	
Γ_{72}	$\pi^+\pi^- K^+K^-$	(7.3 ±0.5) × 10^{-4}	
Γ_{73}	$\pi^0\pi^0 K_S^0 K_L^0$	(1.3 ±0.5) × 10^{-3}	
Γ_{74}	$\rho^0 K^+K^-$	(2.2 ±0.4) × 10^{-4}	
Γ_{75}	$K^*(892)^0\overline{K}_2^*(1430)^0$	(1.9 ±0.5) × 10^{-4}	
Γ_{76}	$K^+K^-\pi^+\pi^-\eta$	(1.3 ±0.7) × 10^{-3}	
Γ_{77}	$K^+K^-2(\pi^+\pi^-)\pi^0$	(1.00 ±0.31) × 10^{-3}	
Γ_{78}	$K^+K^-2(\pi^+\pi^-)$	(1.9 ±0.9) × 10^{-3}	
Γ_{79}	$K_1(1270)^\pm K^\mp$	(1.00 ±0.28) × 10^{-3}	
Γ_{80}	$K_S^0 K_S^0\pi^+\pi^-$	(2.2 ±0.4) × 10^{-4}	
Γ_{81}	$\rho^0 p\overline{p}$	(5.0 ±2.2) × 10^{-5}	
Γ_{82}	$K^+\overline{K}^*(892)^0\pi^-$ + c.c.	(6.7 ±2.5) × 10^{-4}	
Γ_{83}	$2(\pi^+\pi^-)$	(2.4 ±0.6) × 10^{-4}	S=2.2
Γ_{84}	$\rho^0\pi^+\pi^-$	(2.2 ±0.6) × 10^{-4}	S=1.4
Γ_{85}	$K^+K^-\pi^+\pi^-\pi^0$	(1.26 ±0.09) × 10^{-3}	
Γ_{86}	$\omega f_0(1710)$ → ωK^+K^-	(5.9 ±2.2) × 10^{-5}	
Γ_{87}	$K^*(892)^0 K^-\pi^+\pi^0$ + c.c.	(8.6 ±2.2) × 10^{-4}	
Γ_{88}	$K^*(892)^+ K^-\pi^+\pi^-$ + c.c.	(9.6 ±2.8) × 10^{-4}	
Γ_{89}	$K^*(892)^+ K^-\rho^0$ + c.c.	(7.3 ±2.6) × 10^{-4}	
Γ_{90}	$K^*(892)^0 K^-\rho^+$ + c.c.	(6.1 ±1.8) × 10^{-4}	
Γ_{91}	ηK^+K^-, no $\eta\phi$	(3.1 ±0.4) × 10^{-5}	
Γ_{92}	ωK^+K^-	(1.62 ±0.11) × 10^{-4}	S=1.1
Γ_{93}	$\omega K^*(892)^+ K^-$ + c.c.	(2.07 ±0.26) × 10^{-4}	
Γ_{94}	$\omega K_2^*(1430)^+ K^-$ + c.c.	(6.1 ±1.2) × 10^{-5}	
Γ_{95}	$\omega\overline{K}^*(892)^0 K^0$	(1.68 ±0.30) × 10^{-4}	
Γ_{96}	$\omega\overline{K}_2^*(1430)^0 K^0$	(5.8 ±2.2) × 10^{-5}	
Γ_{97}	$\omega X(1440)$ → $\omega K_S^0 K^-\pi^+$ + c.c.	(1.6 ±0.4) × 10^{-5}	
Γ_{98}	$\omega X(1440)$ → $\omega K^+K^-\pi^0$	(1.09 ±0.26) × 10^{-5}	
Γ_{99}	$\omega f_1(1285)$ → $\omega K_S^0 K^-\pi^+$ + c.c.	(3.0 ±1.0) × 10^{-6}	
Γ_{100}	$\omega f_1(1285)$ → $\omega K^+K^-\pi^0$	(1.2 ±0.7) × 10^{-6}	
Γ_{101}	$3(\pi^+\pi^-)$	(3.5 ±2.0) × 10^{-4}	S=2.8
Γ_{102}	$p\overline{p}\pi^+\pi^-\pi^0$	(7.3 ±0.7) × 10^{-4}	
Γ_{103}	K^+K^-	(7.5 ±0.5) × 10^{-5}	
Γ_{104}	$K_S^0 K_L^0$	(5.34 ±0.33) × 10^{-5}	
Γ_{105}	$\pi^+\pi^-\pi^0$	(2.01 ±0.17) × 10^{-4}	S=1.7
Γ_{106}	$\rho(2150)\pi$ → $\pi^+\pi^-\pi^0$	(1.9 $^{+1.2}_{-0.4}$) × 10^{-4}	
Γ_{107}	$\rho(770)\pi$ → $\pi^+\pi^-\pi^0$	(3.2 ±1.2) × 10^{-5}	S=1.8
Γ_{108}	$\pi^+\pi^-$	(7.8 ±2.6) × 10^{-6}	
Γ_{109}	$K_1(1400)^\pm K^\mp$	< 3.1 × 10^{-4}	CL=90%
Γ_{110}	$K_2^*(1430)^\pm K^\mp$	(7.1 $^{+1.3}_{-0.9}$) × 10^{-5}	

Γ_{111}	$K^+K^-\pi^0$	$(\ 4.07\ \pm0.31\ )\times10^{-5}$		
Γ_{112}	$K^0_S K^0_L\pi^0$	$<\ 3.0\ \times10^{-4}$		CL=90%
Γ_{113}	$K^0_S K^0_L\eta$	$(\ 1.3\ \pm0.5\ )\times10^{-3}$		
Γ_{114}	$K^+K^*(892)^- +$ c.c.	$(\ 2.9\ \pm0.4\ )\times10^{-5}$		S=1.2
Γ_{115}	$K^*(892)^0\overline{K}^0 +$ c.c.	$(\ 1.09\ \pm0.20\ )\times10^{-4}$		
Γ_{116}	$\phi\pi^+\pi^-$	$(\ 1.18\ \pm0.26\ )\times10^{-4}$		S=1.5
Γ_{117}	$\phi f_0(980)\ \to\ \pi^+\pi^-$	$(\ 7.5\ \pm3.3\ )\times10^{-5}$		S=1.6
Γ_{118}	$2(K^+K^-)$	$(\ 6.3\ \pm1.3\ )\times10^{-5}$		
Γ_{119}	ϕK^+K^-	$(\ 7.0\ \pm1.6\ )\times10^{-5}$		
Γ_{120}	$2(K^+K^-)\pi^0$	$(\ 1.10\ \pm0.28\ )\times10^{-4}$		
Γ_{121}	$\phi\eta$	$(\ 3.10\ \pm0.31\ )\times10^{-5}$		
Γ_{122}	$\phi\eta'$	$(\ 3.1\ \pm1.6\ )\times10^{-5}$		
Γ_{123}	$\omega\eta'$	$(\ 3.2\ {}^{+2.5}_{-2.1}\ )\times10^{-5}$		
Γ_{124}	$\omega\pi^0$	$(\ 2.1\ \pm0.6\ )\times10^{-5}$		
Γ_{125}	$\rho\eta'$	$(\ 1.9\ {}^{+1.7}_{-1.2}\ )\times10^{-5}$		
Γ_{126}	$\rho\eta$	$(\ 2.2\ \pm0.6\ )\times10^{-5}$		S=1.1
Γ_{127}	$\omega\eta$	$<\ 1.1\ \times10^{-5}$		CL=90%
Γ_{128}	$\phi\pi^0$	$<\ 4\ \times10^{-7}$		CL=90%
Γ_{129}	$\eta_c\pi^+\pi^-\pi^0$	$<\ 1.0\ \times10^{-3}$		CL=90%
Γ_{130}	$p\overline{p}K^+K^-$	$(\ 2.7\ \pm0.7\ )\times10^{-5}$		
Γ_{131}	$\overline{\Lambda}nK^0_S +$ c.c.	$(\ 8.1\ \pm1.8\ )\times10^{-5}$		
Γ_{132}	$\phi f'_2(1525)$	$(\ 4.4\ \pm1.6\ )\times10^{-5}$		
Γ_{133}	$\Theta(1540)\overline{\Theta}(1540)\ \to\ K^0_S pK^-\overline{n} +$ c.c.	$<\ 8.8\ \times10^{-6}$		CL=90%
Γ_{134}	$\Theta(1540)K^-\overline{n}\ \to\ K^0_S pK^-\overline{n}$	$<\ 1.0\ \times10^{-5}$		CL=90%
Γ_{135}	$\Theta(1540)K^0_S\overline{p}\ \to\ K^0_S\overline{p}K^+n$	$<\ 7.0\ \times10^{-6}$		CL=90%
Γ_{136}	$\overline{\Theta}(1540)K^+n\ \to\ K^0_S\overline{p}K^+n$	$<\ 2.6\ \times10^{-5}$		CL=90%
Γ_{137}	$\overline{\Theta}(1540)K^0_S p\ \to\ K^0_S pK^-\overline{n}$	$<\ 6.0\ \times10^{-6}$		CL=90%
Γ_{138}	$K^0_S K^0_S$	$<\ 4.6\ \times10^{-6}$		

Radiative decays

Γ_{139}	$\gamma\chi_{c0}(1P)$	$(\ 9.79\ \pm0.20\ )\ \%$		
Γ_{140}	$\gamma\chi_{c1}(1P)$	$(\ 9.75\ \pm0.24\ )\ \%$		
Γ_{141}	$\gamma\chi_{c2}(1P)$	$(\ 9.52\ \pm0.20\ )\ \%$		
Γ_{142}	$\gamma\eta_c(1S)$	$(\ 3.4\ \pm0.5\ )\times10^{-3}$		S=1.3
Γ_{143}	$\gamma\eta_c(2S)$	$(\ 7\ \pm5\ )\times10^{-4}$		
Γ_{144}	$\gamma\pi^0$	$(\ 1.04\ \pm0.22\ )\times10^{-6}$		S=1.4
Γ_{145}	$\gamma\eta'(958)$	$(\ 1.24\ \pm0.04\ )\times10^{-4}$		
Γ_{146}	$\gamma f_2(1270)$	$(\ 2.73\ {}^{+0.29}_{-0.25}\ )\times10^{-4}$		S=1.8
Γ_{147}	$\gamma f_0(1370)\ \to\ \gamma K\overline{K}$	$(\ 3.1\ \pm1.7\ )\times10^{-5}$		
Γ_{148}	$\gamma f_0(1500)$	$(\ 9.2\ \pm1.9\ )\times10^{-5}$		
Γ_{149}	$\gamma f'_2(1525)$	$(\ 3.3\ \pm0.8\ )\times10^{-5}$		
Γ_{150}	$\gamma f_0(1710)$			
Γ_{151}	$\gamma f_0(1710)\ \to\ \gamma\pi\pi$	$(\ 3.5\ \pm0.6\ )\times10^{-5}$		
Γ_{152}	$\gamma f_0(1710)\ \to\ \gamma K\overline{K}$	$(\ 6.6\ \pm0.7\ )\times10^{-5}$		
Γ_{153}	$\gamma f_0(2100)\ \to\ \gamma\pi\pi$	$(\ 4.8\ \pm1.0\ )\times10^{-6}$		
Γ_{154}	$\gamma f_0(2200)\ \to\ \gamma K\overline{K}$	$(\ 3.2\ \pm1.0\ )\times10^{-6}$		
Γ_{155}	$\gamma f_J(2220)\ \to\ \gamma\pi\pi$	$<\ 5.8\ \times10^{-6}$		CL=90%
Γ_{156}	$\gamma f_J(2220)\ \to\ \gamma K\overline{K}$	$<\ 9.5\ \times10^{-6}$		CL=90%
Γ_{157}	$\gamma\gamma$	$<\ 1.5\ \times10^{-4}$		CL=90%
Γ_{158}	$\gamma\eta$	$(\ 9.2\ \pm1.8\ )\times10^{-7}$		
Γ_{159}	$\gamma\eta\pi^+\pi^-$	$(\ 8.7\ \pm2.1\ )\times10^{-4}$		
Γ_{160}	$\gamma\eta(1405)$			
Γ_{161}	$\gamma\eta(1405)\ \to\ \gamma K\overline{K}\pi$	$<\ 9\ \times10^{-5}$		CL=90%
Γ_{162}	$\gamma\eta(1405)\ \to\ \eta\pi^+\pi^-$	$(\ 3.6\ \pm2.5\ )\times10^{-5}$		
Γ_{163}	$\gamma\eta(1405)\ \to\ \gamma f_0(980)\pi^0\ \to\ \gamma\pi^+\pi^-\pi^0$	$<\ 5.0\ \times10^{-7}$		CL=90%
Γ_{164}	$\gamma\eta(1475)$			
Γ_{165}	$\gamma\eta(1475)\ \to\ K\overline{K}\pi$	$<\ 1.4\ \times10^{-4}$		CL=90%
Γ_{166}	$\gamma\eta(1475)\ \to\ \eta\pi^+\pi^-$	$<\ 8.8\ \times10^{-5}$		CL=90%
Γ_{167}	$\gamma 2(\pi^+\pi^-)$	$(\ 4.0\ \pm0.6\ )\times10^{-4}$		
Γ_{168}	$\gamma K^{*0}K^+\pi^- +$ c.c.	$(\ 3.7\ \pm0.9\ )\times10^{-4}$		
Γ_{169}	$\gamma K^{*0}\overline{K}^{*0}$	$(\ 2.4\ \pm0.7\ )\times10^{-4}$		
Γ_{170}	$\gamma K^0_S K^+\pi^- +$ c.c.	$(\ 2.6\ \pm0.5\ )\times10^{-4}$		
Γ_{171}	$\gamma K^+K^-\pi^+\pi^-$	$(\ 1.9\ \pm0.5\ )\times10^{-4}$		
Γ_{172}	$\gamma p\overline{p}$	$(\ 3.9\ \pm0.5\ )\times10^{-5}$		S=2.0
Γ_{173}	$\gamma f_2(1950)\ \to\ \gamma p\overline{p}$	$(\ 1.20\ \pm0.22\ )\times10^{-5}$		
Γ_{174}	$\gamma f_2(2150)\ \to\ \gamma p\overline{p}$	$(\ 7.2\ \pm1.8\ )\times10^{-6}$		
Γ_{175}	$\gamma X(1835)\ \to\ \gamma p\overline{p}$	$(\ 4.6\ {}^{+1.8}_{-4.0}\ )\times10^{-6}$		
Γ_{176}	$\gamma X\ \to\ \gamma p\overline{p}$	[a] $<\ 2\ \times10^{-6}$		CL=90%
Γ_{177}	$\gamma\pi^+\pi^- p\overline{p}$	$(\ 2.8\ \pm1.4\ )\times10^{-5}$		
Γ_{178}	$\gamma 2(\pi^+\pi^-)K^+K^-$	$<\ 2.2\ \times10^{-4}$		CL=90%
Γ_{179}	$\gamma 3(\pi^+\pi^-)$	$<\ 1.7\ \times10^{-4}$		CL=90%
Γ_{180}	$\gamma K^+K^-K^+K^-$	$<\ 4\ \times10^{-5}$		CL=90%
Γ_{181}	$\gamma\gamma J/\psi$	$(\ 3.1\ {}^{+1.0}_{-1.2}\ )\times10^{-4}$		
Γ_{182}	$e^+e^-\chi_{c0}(1P)$	$(\ 1.06\ \pm0.24\ )\times10^{-3}$		
Γ_{183}	$e^+e^-\chi_{c1}(1P)$	$(\ 8.5\ \pm0.6\ )\times10^{-4}$		
Γ_{184}	$e^+e^-\chi_{c2}(1P)$	$(\ 7.0\ \pm0.8\ )\times10^{-4}$		

Weak decays

Γ_{185}	$D^0e^+e^- +$ c.c.	$<\ 1.4\ \times10^{-7}$		CL=90%

Other decays

Γ_{186}	invisible	$<\ 1.6$	%	CL=90%

[a] For a narrow resonance in the range $2.2 < M(X) < 2.8$ GeV.

CONSTRAINED FIT INFORMATION

A multiparticle fit to $\chi_{c1}(1P)$, $\chi_{c0}(1P)$, $\chi_{c2}(1P)$, and $\psi(2S)$ with 4 total widths, a partial width, 25 combinations of partial widths obtained from integrated cross section, and 84 branching ratios uses 247 measurements to determine 49 parameters. The overall fit has a $\chi^2 = 376.9$ for 198 degrees of freedom.

The following *off-diagonal* array elements are the correlation coefficients $\langle\delta p_i\delta p_j\rangle/(\delta p_i\cdot\delta p_j)$, in percent, from the fit to parameters p_i, including the branching fractions, $x_i \equiv \Gamma_i/\Gamma_{\rm total}$.

x_7	3									
x_8	1	0								
x_{11}	29	11	2							
x_{12}	28	6	1	48						
x_{13}	13	4	1	36	15					
x_{19}	0	1	0	5	3	2				
x_{139}	1	0	0	2	1	1	0			
x_{140}	1	0	0	2	1	1	0	0		
x_{141}	1	0	0	3	1	1	0	0	0	
Γ	−81	−4	−1	−38	−34	−16	−8	−1	−1	−1
	x_6	x_7	x_8	x_{11}	x_{12}	x_{13}	x_{19}	x_{139}	x_{140}	x_{141}

$\psi(2S)$ PARTIAL WIDTHS

Γ(hadrons) Γ_1

VALUE (keV)	DOCUMENT ID		TECN	COMMENT
• • • We do not use the following data for averages, fits, limits, etc. • • •				
258±26	BAI	02B	BES2	e^+e^-
224±56	LUTH	75	MRK1	e^+e^-

$\Gamma(e^+e^-)$ Γ_6

VALUE (keV)	DOCUMENT ID		TECN	COMMENT
2.33 ±0.04 OUR FIT				
2.29 ±0.06 OUR AVERAGE				
2.23 ±0.10 ±0.02	[1] ABLIKIM	15V	BES3	4.0–4.4 $e^+e^-\to\pi^+\pi^- J/\psi$
2.338±0.037±0.096	ABLIKIM	08B	BES2	$e^+e^-\to$ hadrons
2.330±0.036±0.110	ABLIKIM	06L	BES2	$e^+e^-\to$ hadrons
2.44 ±0.21	[2] BAI	02B	BES2	e^+e^-
2.14 ±0.21	ALEXANDER	89	RVUE	See Υ mini-review
• • • We do not use the following data for averages, fits, limits, etc. • • •				
2.0 ±0.3	BRANDELIK	79C	DASP	e^+e^-
2.1 ±0.3	[3] LUTH	75	MRK1	e^+e^-

[1] ABLIKIM 15V reports $2.213 \pm 0.018 \pm 0.099$ keV from a measurement of $[\Gamma(\psi(2S)\to e^+e^-)]\times[B(\psi(2S)\to J/\psi(1S)\pi^+\pi^-)]$ assuming $B(\psi(2S)\to J/\psi(1S)\pi^+\pi^-) = (34.95\pm0.45)\times10^{-2}$, which we rescale to our best value $B(\psi(2S)\to J/\psi(1S)\pi^+\pi^-) = (34.67\pm0.30)\times10^{-2}$. Our first error is their experiment's error and our second error is the systematic error from using our best value.

[2] From a simultaneous fit to e^+e^-, $\mu^+\mu^-$, and hadronic channel, assuming $\Gamma_e = \Gamma_\mu = \Gamma_\tau/0.38847$.

[3] From a simultaneous fit to e^+e^-, $\mu^+\mu^-$, and hadronic channels assuming $\Gamma(e^+e^-) = \Gamma(\mu^+\mu^-)$.

$\Gamma(\gamma\gamma)$ Γ_{157}

VALUE (eV)	CL%	DOCUMENT ID		TECN	COMMENT
<43	90	BRANDELIK	79C	DASP	e^+e^-

$\psi(2S)\ \Gamma(i)\Gamma(e^+e^-)/\Gamma(\text{total})$

This combination of a partial width with the partial width into e^+e^- and with the total width is obtained from the integrated cross section into channel(i) in the e^+e^- annihilation. We list only data that have not been used to determine the partial width $\Gamma(i)$ or the branching ratio $\Gamma(i)$/total.

$\Gamma(\text{hadrons}) \times \Gamma(e^+e^-)/\Gamma_{\text{total}}$ $\Gamma_1\Gamma_6/\Gamma$

VALUE (keV)	DOCUMENT ID		TECN	COMMENT
2.233±0.015±0.042	[1] ANASHIN	12	KEDR	$e^+e^- \to$ hadrons
• • • We do not use the following data for averages, fits, limits, etc. • • •				
2.2 ±0.4	ABRAMS	75	MRK1	e^+e^-

[1] ANASHIN 12 reports the value 2.233 ± 0.015 ± 0.037 ± 0.020 keV, where the third uncertainty is due to assumptions on the interference between the resonance and hadronic continuum. We combined the two systematic uncertainties.

$\Gamma(\tau^+\tau^-) \times \Gamma(e^+e^-)/\Gamma_{\text{total}}$ $\Gamma_8\Gamma_6/\Gamma$

VALUE (eV)	EVTS	DOCUMENT ID		TECN	COMMENT
• • • We do not use the following data for averages, fits, limits, etc. • • •					
9.0±2.6	79	[1] ANASHIN	07	KEDR	$e^+e^- \to \psi(2S) \to \tau^+\tau^-$

[1] Using $\psi(2S)$ total width of 337 ± 13 keV. Systematic errors not evaluated.

$\Gamma(J/\psi(1S)\pi^+\pi^-) \times \Gamma(e^+e^-)/\Gamma_{\text{total}}$ $\Gamma_{11}\Gamma_6/\Gamma$

VALUE (keV)	EVTS	DOCUMENT ID		TECN	COMMENT
0.809±0.013 OUR FIT					
0.837±0.025 OUR AVERAGE	Error includes scale factor of 1.3. See the ideogram below.				
0.837±0.028±0.005		[1] LEES	12E	BABR	10.6 $e^+e^- \to 2\pi^+2\pi^-\gamma$
0.852±0.010±0.026	19.5k	ADAM	06	CLEO	3.773 $e^+e^- \to \gamma\psi(2S)$
0.68 ±0.09		[2] BAI	98E	BES	e^+e^-
• • • We do not use the following data for averages, fits, limits, etc. • • •					
0.88 ±0.08 ±0.03	256	[3] AUBERT	07AU	BABR	10.6 $e^+e^- \to J/\psi\pi^+\pi^-\gamma$
0.755±0.048±0.004	544	[4] AUBERT	05D	BABR	10.6 $e^+e^- \to \pi^+\pi^-\mu^+\mu^-\gamma$

[1] LEES 12E reports $[\Gamma(\psi(2S) \to J/\psi(1S)\pi^+\pi^-) \times \Gamma(\psi(2S) \to e^+e^-)/\Gamma_{\text{total}}] \times [B(J/\psi(1S) \to \mu^+\mu^-)] = (49.9 \pm 1.3 \pm 1.0) \times 10^{-3}$ keV which we divide by our best value $B(J/\psi(1S) \to \mu^+\mu^-) = (5.961 \pm 0.033) \times 10^{-2}$. Our first error is their experiment's error and our second error is the systematic error from using our best value.

[2] The value of $\Gamma(e^+e^-)$ quoted in BAI 98E is derived using $B(\psi(2S) \to J/\psi(1S)\pi^+\pi^-) = (32.4 \pm 2.6) \times 10^{-2}$ and $B(J/\psi(1S) \to \ell^+\ell^-) = 0.1203 \pm 0.0038$. Recalculated by us using $B(J/\psi(1S) \to \ell^+\ell^-) = 0.1181 \pm 0.0020$.

[3] AUBERT 07AU reports $[\Gamma(\psi(2S) \to J/\psi(1S)\pi^+\pi^-) \times \Gamma(\psi(2S) \to e^+e^-)/\Gamma_{\text{total}}] \times [B(J/\psi(1S) \to \pi^+\pi^-\pi^0)] = 0.0186 \pm 0.0012 \pm 0.0011$ keV which we divide by our best value $B(J/\psi(1S) \to \pi^+\pi^-\pi^0) = (2.11 \pm 0.07) \times 10^{-2}$. Our first error is their experiment's error and our second error is the systematic error from using our best value.

[4] AUBERT 05D reports $[\Gamma(\psi(2S) \to J/\psi(1S)\pi^+\pi^-) \times \Gamma(\psi(2S) \to e^+e^-)/\Gamma_{\text{total}}] \times [B(J/\psi(1S) \to \mu^+\mu^-)] = 0.0450 \pm 0.0018 \pm 0.0022$ keV which we divide by our best value $B(J/\psi(1S) \to \mu^+\mu^-) = (5.961 \pm 0.033) \times 10^{-2}$. Our first error is their experiment's error and our second error is the systematic error from using our best value. Superseded by LEES 12E.

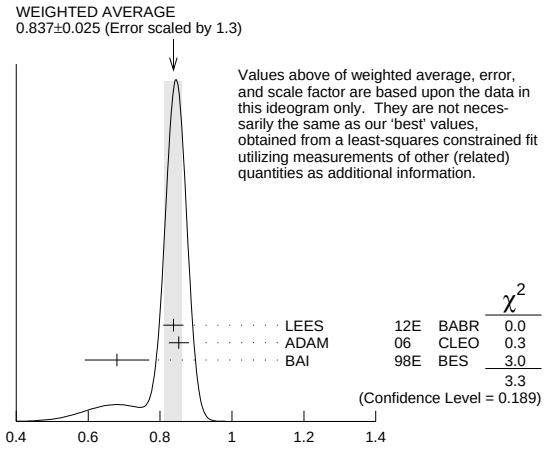

$\Gamma(J/\psi(1S)\pi^0\pi^0) \times \Gamma(e^+e^-)/\Gamma_{\text{total}}$ $\Gamma_{12}\Gamma_6/\Gamma$

VALUE (keV)	EVTS	DOCUMENT ID		TECN	COMMENT
0.425±0.009 OUR FIT					
0.411±0.008±0.018	3.6k±96	ADAM	06	CLEO	3.773 $e^+e^- \to \gamma\psi(2S)$

$\Gamma(J/\psi(1S)\eta) \times \Gamma(e^+e^-)/\Gamma_{\text{total}}$ $\Gamma_{13}\Gamma_6/\Gamma$

VALUE (eV)	EVTS	DOCUMENT ID		TECN	COMMENT
78.7± 1.6 OUR FIT					
87 ± 9 OUR AVERAGE					
83 ±25 ±5	14	[1] AUBERT	07AU	BABR	10.6 $e^+e^- \to J/\psi\pi^+\pi^-\pi^0\gamma$
88 ± 6 ±7	291 ± 24	ADAM	06	CLEO	3.773 $e^+e^- \to \gamma\psi(2S)$

[1] AUBERT 07AU quotes $\Gamma_{ee}^{\psi(2S)} \cdot B(\psi(2S) \to J/\psi\eta) \cdot B(J/\psi \to \mu^+\mu^-) \cdot B(\eta \to \pi^+\pi^-\pi^0) = 1.11 \pm 0.33 \pm 0.07$ eV.

$\Gamma(J/\psi(1S)\pi^0) \times \Gamma(e^+e^-)/\Gamma_{\text{total}}$ $\Gamma_{14}\Gamma_6/\Gamma$

VALUE (eV)	CL%	EVTS	DOCUMENT ID		TECN	COMMENT
<8	90	<37	ADAM	06	CLEO	3.773 $e^+e^- \to \gamma\psi(2S)$

$\Gamma(p\overline{p}) \times \Gamma(e^+e^-)/\Gamma_{\text{total}}$ $\Gamma_{19}\Gamma_6/\Gamma$

VALUE (eV)	EVTS	DOCUMENT ID		TECN	COMMENT
0.672±0.023 OUR FIT					
0.63 ±0.05 OUR AVERAGE	Error includes scale factor of 1.2.				
0.67 ±0.12 ±0.02	43	[1] LEES	13O	BABR	$e^+e^- \to p\overline{p}\gamma$
0.74 ±0.07 ±0.04	142	[2] LEES	13Y	BABR	$e^+e^- \to p\overline{p}\gamma$
0.579±0.038±0.036	2.7k	ANDREOTTI	07	E835	$p\overline{p} \to e^+e^-$, $J/\psi X$
• • • We do not use the following data for averages, fits, limits, etc. • • •					
0.70 ±0.17 ±0.03	22	[3] AUBERT	06B	BABR	$e^+e^- \to p\overline{p}\gamma$

[1] ISR photon reconstructed in the detector

[2] ISR photon undetected

[3] Superseded by LEES 13O

$\Gamma(\Lambda\overline{\Lambda}) \times \Gamma(e^+e^-)/\Gamma_{\text{total}}$ $\Gamma_{26}\Gamma_6/\Gamma$

VALUE (eV)	DOCUMENT ID		TECN	COMMENT
1.5±0.4±0.1	AUBERT	07BD	BABR	10.6 $e^+e^- \to \Lambda\overline{\Lambda}\gamma$

$\Gamma(2(\pi^+\pi^-\pi^0)) \times \Gamma(e^+e^-)/\Gamma_{\text{total}}$ $\Gamma_{62}\Gamma_6/\Gamma$

VALUE (eV)	EVTS	DOCUMENT ID		TECN	COMMENT
11.2±3.3±1.3	43	AUBERT	06D	BABR	10.6 $e^+e^- \to 2(\pi^+\pi^-\pi^0)\gamma$

$\Gamma(\pi^0\pi^0K^+K^-) \times \Gamma(e^+e^-)/\Gamma_{\text{total}}$ $\Gamma_{71}\Gamma_6/\Gamma$

VALUE (eV)	EVTS	DOCUMENT ID		TECN	COMMENT
0.60±0.31±0.03	17	LEES	12F	BABR	10.6 $e^+e^- \to \pi^0\pi^0K^+K^-\gamma$

$\Gamma(K^+K^-2(\pi^+\pi^-)) \times \Gamma(e^+e^-)/\Gamma_{\text{total}}$ $\Gamma_{78}\Gamma_6/\Gamma$

VALUE (eV)	EVTS	DOCUMENT ID		TECN	COMMENT
4.4±2.1±0.3	26	AUBERT	06D	BABR	10.6 $e^+e^- \to K^+K^-2(\pi^+\pi^-)\gamma$

$\Gamma(\pi^+\pi^-K^+K^-) \times \Gamma(e^+e^-)/\Gamma_{\text{total}}$ $\Gamma_{72}\Gamma_6/\Gamma$

VALUE (eV)	EVTS	DOCUMENT ID		TECN	COMMENT
1.92±0.30±0.06	133	LEES	12F	BABR	10.6 $e^+e^- \to \pi^+\pi^-K^+K^-\gamma$
• • • We do not use the following data for averages, fits, limits, etc. • • •					
2.56±0.42±0.16	85	[1] AUBERT	07AK	BABR	10.6 $e^+e^- \to \pi^+\pi^-K^+K^-\gamma$

[1] Superseded by LEES 12F.

$\Gamma(\pi^0\pi^0K_S^0K_L^0) \times \Gamma(e^+e^-)/\Gamma_{\text{total}}$ $\Gamma_{73}\Gamma_6/\Gamma$

VALUE (eV)	EVTS	DOCUMENT ID		TECN	COMMENT
2.92±1.27±0.15	14	LEES	17A	BABR	$e^+e^- \to K_S^0K_L^0\pi^0\pi^0\gamma$

$\Gamma(K_S^0K_L^0\pi^0) \times \Gamma(e^+e^-)/\Gamma_{\text{total}}$ $\Gamma_{112}\Gamma_6/\Gamma$

VALUE (eV)	CL%	EVTS	DOCUMENT ID		TECN	COMMENT
<0.7	90	8	LEES	17A	BABR	$e^+e^- \to K_S^0K_L^0\pi^0\gamma$

$\Gamma(K_S^0K_L^0\eta) \times \Gamma(e^+e^-)/\Gamma_{\text{total}}$ $\Gamma_{113}\Gamma_6/\Gamma$

VALUE (eV)	EVTS	DOCUMENT ID		TECN	COMMENT
3.14±1.08±0.16	16	LEES	17A	BABR	$e^+e^- \to K_S^0K_L^0\eta\gamma$

$\Gamma(\phi f_0(980) \to \pi^+\pi^-) \times \Gamma(e^+e^-)/\Gamma_{\text{total}}$ $\Gamma_{117}\Gamma_6/\Gamma$

VALUE (eV)	EVTS	DOCUMENT ID		TECN	COMMENT
0.345±0.128±0.004	12	[1] LEES	12F	BABR	10.6 $e^+e^- \to \pi^+\pi^-K^+K^-\gamma$
• • • We do not use the following data for averages, fits, limits, etc. • • •					
0.345±0.168±0.004	6 ± 3	[2] AUBERT	07AK	BABR	10.6 $e^+e^- \to \pi^+\pi^-K^+K^-\gamma$

[1] LEES 12F reports $[\Gamma(\psi(2S) \to \phi f_0(980) \to \pi^+\pi^-) \times \Gamma(\psi(2S) \to e^+e^-)/\Gamma_{\text{total}}] \times [B(\phi(1020) \to K^+K^-)] = 0.17 \pm 0.06 \pm 0.02$ eV which we divide by our best value $B(\phi(1020) \to K^+K^-) = (49.2 \pm 0.5) \times 10^{-2}$. Our first error is their experiment's error and our second error is the systematic error from using our best value.

[2] Superseded by LEES 12F. AUBERT 07AK reports $[\Gamma(\psi(2S) \to \phi f_0(980) \to \pi^+\pi^-) \times \Gamma(\psi(2S) \to e^+e^-)/\Gamma_{\text{total}}] \times [B(\phi(1020) \to K^+K^-)] = 0.17 \pm 0.08 \pm 0.02$ eV which we divide by our best value $B(\phi(1020) \to K^+K^-) = (49.2 \pm 0.5) \times 10^{-2}$. Our first error is their experiment's error and our second error is the systematic error from using our best value.

$\Gamma(2(K^+K^-)) \times \Gamma(e^+e^-)/\Gamma_{\text{total}}$ $\Gamma_{118}\Gamma_6/\Gamma$

VALUE (eV)	EVTS	DOCUMENT ID		TECN	COMMENT
0.22±0.10±0.02	13	LEES	12F	BABR	10.6 $e^+e^- \to K^+K^-K^+K^-\gamma$

$\Gamma(\phi\pi^+\pi^-) \times \Gamma(e^+e^-)/\Gamma_{\text{total}}$ $\Gamma_{116}\Gamma_6/\Gamma$

VALUE (eV)	EVTS	DOCUMENT ID		TECN	COMMENT
0.55±0.19±0.01	19	[1] LEES	12F	BABR	10.6 $e^+e^- \to K^+K^-\pi^+\pi^-\gamma$
• • • We do not use the following data for averages, fits, limits, etc. • • •					
0.57±0.23±0.01	10	[2] AUBERT,BE	06D	BABR	10.6 $e^+e^- \to K^+K^-\pi^+\pi^-\gamma$

[1] LEES 12F reports $[\Gamma(\psi(2S) \to \phi\pi^+\pi^-) \times \Gamma(\psi(2S) \to e^+e^-)/\Gamma_{total}] \times [B(\phi(1020) \to K^+K^-)] = 0.27 \pm 0.09 \pm 0.02$ eV which we divide by our best value $B(\phi(1020) \to K^+K^-) = (49.2 \pm 0.5) \times 10^{-2}$. Our first error is their experiment's error and our second error is the systematic error from using our best value.

[2] Superseded by LEES 12F. AUBERT,BE 06D reports $[\Gamma(\psi(2S) \to \phi\pi^+\pi^-) \times \Gamma(\psi(2S) \to e^+e^-)/\Gamma_{total}] \times [B(\phi(1020) \to K^+K^-)] = 0.28 \pm 0.11 \pm 0.02$ eV which we divide by our best value $B(\phi(1020) \to K^+K^-) = (49.2 \pm 0.5) \times 10^{-2}$. Our first error is their experiment's error and our second error is the systematic error from using our best value.

$\Gamma(2(\pi^+\pi^-)\pi^0) \times \Gamma(e^+e^-)/\Gamma_{total}$ $\Gamma_{17}\Gamma_6/\Gamma$

VALUE (eV)	EVTS	DOCUMENT ID		TECN	COMMENT
29.7±2.2±1.8	410	AUBERT	07AU	BABR	10.6 $e^+e^- \to 2(\pi^+\pi^-)\pi^0\gamma$

$\Gamma(\omega\pi^+\pi^-) \times \Gamma(e^+e^-)/\Gamma_{total}$ $\Gamma_{67}\Gamma_6/\Gamma$

VALUE (eV)	EVTS	DOCUMENT ID		TECN	COMMENT
3.01±0.84±0.02	37	[1] AUBERT	07AU	BABR	10.6 $e^+e^- \to \omega\pi^+\pi^-\gamma$

[1] AUBERT 07AU reports $[\Gamma(\psi(2S) \to \omega\pi^+\pi^-) \times \Gamma(\psi(2S) \to e^+e^-)/\Gamma_{total}] \times [B(\omega(782) \to \pi^+\pi^-\pi^0)] = 2.69 \pm 0.73 \pm 0.16$ eV which we divide by our best value $B(\omega(782) \to \pi^+\pi^-\pi^0) = (89.2 \pm 0.7) \times 10^{-2}$. Our first error is their experiment's error and our second error is the systematic error from using our best value.

$\Gamma(2(\pi^+\pi^-)\eta) \times \Gamma(e^+e^-)/\Gamma_{total}$ $\Gamma_{65}\Gamma_6/\Gamma$

VALUE (eV)	EVTS	DOCUMENT ID		TECN	COMMENT
2.87±1.41±0.01	16	[1] AUBERT	07AU	BABR	10.6 $e^+e^- \to 2(\pi^+\pi^-)\eta\gamma$

[1] AUBERT 07AU reports $[\Gamma(\psi(2S) \to 2(\pi^+\pi^-)\eta) \times \Gamma(\psi(2S) \to e^+e^-)/\Gamma_{total}] \times [B(\eta \to 2\gamma)] = 1.13 \pm 0.55 \pm 0.08$ eV which we divide by our best value $B(\eta \to 2\gamma) = (39.41 \pm 0.20) \times 10^{-2}$. Our first error is their experiment's error and our second error is the systematic error from using our best value.

$\Gamma(K^+K^-\pi^+\pi^-\pi^0) \times \Gamma(e^+e^-)/\Gamma_{total}$ $\Gamma_{85}\Gamma_6/\Gamma$

VALUE (eV)	EVTS	DOCUMENT ID		TECN	COMMENT
4.4±1.3±0.3	32	AUBERT	07AU	BABR	10.6 $e^+e^- \to K^+K^-\pi^+\pi^-\pi^0\gamma$

$\Gamma(K^+K^-\pi^+\pi^-\eta) \times \Gamma(e^+e^-)/\Gamma_{total}$ $\Gamma_{76}\Gamma_6/\Gamma$

VALUE (eV)	EVTS	DOCUMENT ID		TECN	COMMENT
3.04±1.79±0.02	7	[1] AUBERT	07AU	BABR	10.6 $e^+e^- \to K^+K^-\pi^+\pi^-\eta\gamma$

[1] AUBERT 07AU reports $[\Gamma(\psi(2S) \to K^+K^-\pi^+\pi^-\eta) \times \Gamma(\psi(2S) \to e^+e^-)/\Gamma_{total}] \times [B(\eta \to 2\gamma)] = 1.2 \pm 0.7 \pm 0.1$ eV which we divide by our best value $B(\eta \to 2\gamma) = (39.41 \pm 0.20) \times 10^{-2}$. Our first error is their experiment's error and our second error is the systematic error from using our best value.

$\Gamma(K^+K^-) \times \Gamma(e^+e^-)/\Gamma_{total}$ $\Gamma_{103}\Gamma_6/\Gamma$

VALUE (eV)	EVTS	DOCUMENT ID		TECN	COMMENT
• • • We do not use the following data for averages, fits, limits, etc. • • •					
0.147±0.035±0.005	66	[1] LEES	15J	BABR	$e^+e^- \to K^+K^-\gamma$
0.197±0.035±0.005	66	[2] LEES	15J	BABR	$e^+e^- \to K^+K^-\gamma$
0.35 ±0.14 ±0.03	11	[3] LEES	13Q	BABR	$e^+e^- \to K^+K^-\gamma$

[1] $\sin\phi > 0$.

[2] $\sin\phi < 0$.

[3] Interference with non-resonant K^+K^- production not taken into account.

$\psi(2S)$ BRANCHING RATIOS

$\Gamma(\text{hadrons})/\Gamma_{total}$ Γ_1/Γ

VALUE	DOCUMENT ID		TECN	COMMENT
0.9785±0.0013 OUR AVERAGE				
0.9779±0.0015	[1] BAI	02B	BES2	e^+e^-
0.981 ±0.003	[1] LUTH	75	MRK1	e^+e^-

[1] Includes cascade decay into $J/\psi(1S)$.

$\Gamma(\text{virtual}\,\gamma \to \text{hadrons})/\Gamma_{total}$ Γ_2/Γ

VALUE	DOCUMENT ID		TECN	COMMENT
0.0173±0.0014 OUR AVERAGE Error includes scale factor of 1.5.				
0.0166±0.0010	[1,2] SETH	04	RVUE	e^+e^-
0.0199±0.0019	[1] BAI	02B	BES2	e^+e^-
• • • We do not use the following data for averages, fits, limits, etc. • • •				
0.029 ±0.004	[1] LUTH	75	MRK1	e^+e^-

[1] Included in $\Gamma(\text{hadrons})/\Gamma_{total}$.

[2] Using $B(\psi(2S) \to \ell^+\ell^-) = (0.73 \pm 0.04)\%$ from RPP-2002 and $R = 2.28 \pm 0.04$ determined by a fit to data from BAI 00 and BAI 02C.

$\Gamma(ggg)/\Gamma_{total}$ Γ_3/Γ

VALUE (units 10^{-2})	EVTS	DOCUMENT ID		TECN	COMMENT
10.58±1.62	2.9 M	[1] LIBBY	09	CLEO	$\psi(2S) \to$ hadrons

[1] Calculated using $\Gamma(\gamma gg)/\Gamma(ggg) = 0.097 \pm 0.026 \pm 0.016$ from LIBBY 09, $B(\psi(2S) \to X\,J/\psi)$ relative and absolute branching fractions from MENDEZ 08, $B(\psi(2S) \to \gamma\eta_C)$ from MITCHELL 09, and $B(\psi(2S) \to$ virtual $\gamma \to$ hadrons), $B(\psi(2S) \to \gamma\chi_{cJ})$, and $B(\psi(2S) \to \ell^+\ell^-)$ from PDG 08. The statistical error is negligible and the systematic error is largely uncorrelated with that of $\Gamma(\gamma gg)/\Gamma_{total}$ LIBBY 09 measurement.

$\Gamma(\gamma gg)/\Gamma_{total}$ Γ_4/Γ

VALUE (units 10^{-2})	EVTS	DOCUMENT ID		TECN	COMMENT
1.025±0.288	200 k	[1] LIBBY	09	CLEO	$\psi(2S) \to \gamma +$ hadrons

[1] Calculated using $\Gamma(\gamma gg)/\Gamma(ggg) = 0.097 \pm 0.026 \pm 0.016$ from LIBBY 09. The statistical error is negligible and the systematic error is largely uncorrelated with that of $\Gamma(ggg)/\Gamma_{total}$ LIBBY 09 measurement.

$\Gamma(\gamma gg)/\Gamma(ggg)$ Γ_4/Γ_3

VALUE (units 10^{-2})	EVTS	DOCUMENT ID		TECN	COMMENT
9.7±2.6±1.6	2.9 M	LIBBY	09	CLEO	$\psi(2S) \to (\gamma +)$ hadrons

$\Gamma(\text{light hadrons})/\Gamma_{total}$ Γ_5/Γ

VALUE	DOCUMENT ID		TECN	COMMENT
0.154±0.015	[1] MENDEZ	08	CLEO	$e^+e^- \to \psi(2S)$
• • • We do not use the following data for averages, fits, limits, etc. • • •				
0.169±0.026	[2] ADAM	05A	CLEO	$e^+e^- \to \psi(2S)$

[1] Uses $B(\psi(2S) \to J/\psi X)$ from MENDEZ 08 and other branching fractions from PDG 07.

[2] Uses $B(J/\psi X)$ from ADAM 05A, $B(\chi_{cJ}\gamma)$, $B(\eta_C\gamma)$ from ATHAR 04 and $B(\ell^+\ell^-)$ from PDG 04. Superseded by MENDEZ 08.

$\Gamma(e^+e^-)/\Gamma_{total}$ Γ_6/Γ

VALUE (units 10^{-4})	DOCUMENT ID		TECN	COMMENT
79.3± 1.7 OUR FIT				
• • • We do not use the following data for averages, fits, limits, etc. • • •				
88 ±13	[1] FELDMAN	77	RVUE	e^+e^-

[1] From an overall fit assuming equal partial widths for e^+e^- and $\mu^+\mu^-$. For a measurement of the ratio see the entry $\Gamma(\mu^+\mu^-)/\Gamma(e^+e^-)$ below. Includes LUTH 75, HILGER 75, BURMESTER 77.

$\Gamma(\mu^+\mu^-)/\Gamma_{total}$ Γ_7/Γ

VALUE (units 10^{-4})	DOCUMENT ID
80±6 OUR FIT	

$\Gamma(\mu^+\mu^-)/\Gamma(e^+e^-)$ Γ_7/Γ_6

VALUE	DOCUMENT ID		TECN	COMMENT
1.00±0.08 OUR FIT				
• • • We do not use the following data for averages, fits, limits, etc. • • •				
0.89±0.16	BOYARSKI	75C	MRK1	e^+e^-

$\Gamma(\tau^+\tau^-)/\Gamma_{total}$ Γ_8/Γ

VALUE (units 10^{-4})	DOCUMENT ID		TECN	COMMENT
31 ±4 OUR FIT				
30.8±2.1±3.8	[1] ABLIKIM	06W	BES	$e^+e^- \to \psi(2S)$

[1] Computed using PDG 02 value of $B(\psi(2S) \to \text{hadrons}) = 0.9810 \pm 0.0030$ to estimate the total number of $\psi(2S)$ events.

DECAYS INTO $J/\psi(1S)$ AND ANYTHING

$\Gamma(J/\psi(1S)\,\text{anything})/\Gamma_{total}$ Γ_9/Γ

VALUE	EVTS	DOCUMENT ID		TECN	COMMENT
0.614 ±0.006 OUR FIT					
0.55 ±0.07 OUR AVERAGE					
0.51 ±0.12		BRANDELIK	79C	DASP	$e^+e^- \to \mu^+\mu^-X$
0.57 ±0.08		ABRAMS	75B	MRK1	$e^+e^- \to \mu^+\mu^-X$
• • • We do not use the following data for averages, fits, limits, etc. • • •					
0.6254±0.0016±0.0155	1.1M	[1] MENDEZ	08	CLEO	$\psi(2S) \to \ell^+\ell^-X$
0.5950±0.0015±0.0190	151k	ADAM	05A	CLEO	Repl. by MENDEZ 08

[1] Not independent from other measurements of MENDEZ 08.

$\Gamma(e^+e^-)/\Gamma(J/\psi(1S)\,\text{anything})$ $\Gamma_6/\Gamma_9 = \Gamma_6/(\Gamma_{11}+\Gamma_{12}+\Gamma_{13}+0.343\Gamma_{140}+0.190\Gamma_{141})$

VALUE (units 10^{-2})	EVTS	DOCUMENT ID		TECN	COMMENT
1.292±0.026 OUR FIT					
1.28 ±0.04 OUR AVERAGE Error includes scale factor of 1.6. See the ideogram below.					
1.22 ±0.02 ±0.05	5097 ± 73	[1] ANDREOTTI	05	E835	$p\overline{p} \to \psi(2S) \to e^+e^-$
1.28 ±0.03 ±0.02		[1] AMBROGIANI	00A	E835	$p\overline{p} \to \psi(2S)$
1.44 ±0.08 ±0.02		[1] ARMSTRONG	97	E760	$\overline{p}p \to \psi(2S)$

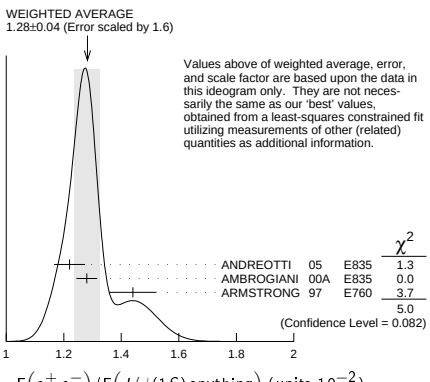

[1] Using B($J/\psi(1S) \to e^+e^-$) = 0.0593 ± 0.0010.

$\Gamma(\mu^+\mu^-)/\Gamma(J/\psi(1S)\text{anything})$ $\Gamma_7/\Gamma_9 = \Gamma_7/(\Gamma_{11}+\Gamma_{12}+\Gamma_{13}+0.343\Gamma_{140}+0.190\Gamma_{141})$

VALUE	DOCUMENT ID		TECN	COMMENT
0.0130±0.0010 OUR FIT				
0.014 ±0.003	HILGER	75	SPEC	e^+e^-

$\Gamma(J/\psi(1S)\text{neutrals})/\Gamma_{\text{total}}$ Γ_{10}/Γ

VALUE	DOCUMENT ID
0.2537±0.0032 OUR FIT	

$\Gamma(J/\psi(1S)\pi^+\pi^-)/\Gamma_{\text{total}}$ Γ_{11}/Γ

VALUE	EVTS	DOCUMENT ID		TECN	COMMENT
0.3467±0.0030 OUR FIT					
0.348 ±0.005 OUR AVERAGE		Error includes scale factor of 1.3. See the ideogram below.			
0.3498±0.0002±0.0045	20M	ABLIKIM	13R	BES3	$\psi(2S) \to J/\psi\pi^+\pi^-$
0.3504±0.0007±0.0077	565k	MENDEZ	08	CLEO	$\psi(2S) \to \ell^+\ell^-\pi^+\pi^-$
0.323 ±0.014		BAI	02B	BES2	e^+e^-
0.32 ±0.04		ABRAMS	75B	MRK1	$e^+e^- \to J/\psi\pi^+\pi^-$
• • • We do not use the following data for averages, fits, limits, etc. • • •					
0.3354±0.0014±0.0110	60k	[1] ADAM	05A	CLEO	Repl. by MENDEZ 08

[1] Not independent from other values reported by ADAM 05A.

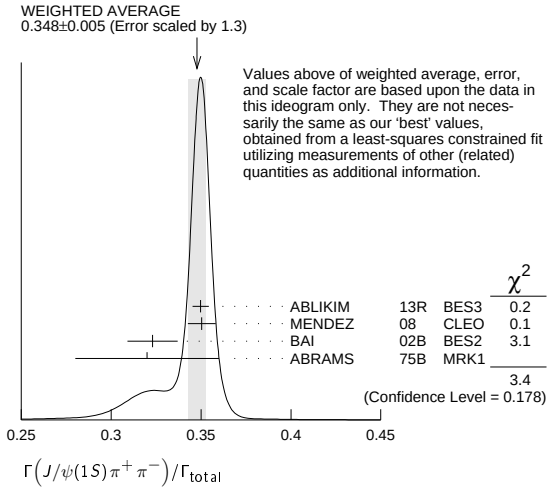

$\Gamma(e^+e^-)/\Gamma(J/\psi(1S)\pi^+\pi^-)$ Γ_6/Γ_{11}

VALUE	DOCUMENT ID		TECN	COMMENT
0.0229±0.0005 OUR FIT				
0.0252±0.0028±0.0011	[1] AUBERT	02B	BABR	e^+e^-

[1] Using B($J/\psi(1S) \to e^+e^-$) = 0.0593 ± 0.0010.

$\Gamma(\mu^+\mu^-)/\Gamma(J/\psi(1S)\pi^+\pi^-)$ Γ_7/Γ_{11}

VALUE	DOCUMENT ID		TECN	COMMENT
0.0230±0.0017 OUR FIT				
0.0228±0.0018 OUR AVERAGE				
0.0230±0.0020±0.0012	[1] AAIJ	16Y	LHCB	$\Lambda_b^0 \to \psi(2S)X$
0.0216±0.0026±0.0014	[2] AUBERT	02B	BABR	e^+e^-
0.0327±0.0077±0.0072	[2] GRIBUSHIN	96	FMPS	515 π^-Be $\to 2\mu X$

[1] Using B($J/\psi(1S) \to \mu^+\mu^-$) = (5.961 ± 0.033) × 10^{-2}.
[2] Using B($J/\psi(1S) \to \mu^+\mu^-$) = (5.88 ± 0.10) × 10^{-2}.

$\Gamma(\tau^+\tau^-)/\Gamma(J/\psi(1S)\pi^+\pi^-)$ Γ_8/Γ_{11}

VALUE (units 10^{-3})	DOCUMENT ID		TECN	COMMENT
8.8 ±1.1 OUR FIT				
8.73±1.39±1.57	BAI	02	BES	e^+e^-

$\Gamma(J/\psi(1S)\pi^+\pi^-)/\Gamma(J/\psi(1S)\text{anything})$ Γ_{11}/Γ_9

VALUE	EVTS	DOCUMENT ID		TECN	COMMENT
0.5645±0.0026 OUR FIT					
0.554 ±0.008 OUR AVERAGE		Error includes scale factor of 1.3. See the ideogram below.			
0.5604±0.0009±0.0062	565k	MENDEZ	08	CLEO	$\psi(2S) \to \ell^+\ell^-\pi^+\pi^-$
0.525 ±0.009 ±0.022	4k	ANDREOTTI	05	E835	$\psi(2S) \to J/\psi X$
0.536 ±0.007 ±0.016	20k	[1,2] ABLIKIM	04B	BES	$\psi(2S) \to J/\psi X$
0.496 ±0.037		ARMSTRONG	97	E760	$\overline{p}p \to \psi(2S)$
• • • We do not use the following data for averages, fits, limits, etc. • • •					
0.5637±0.0027±0.0046	60k	ADAM	05A	CLEO	Repl. by MENDEZ 08

[1] From a fit to the J/ψ recoil mass spectra.
[2] ABLIKIM 04B quotes B($\psi(2S) \to J/\psi X$) / B($\psi(2S) \to J/\psi\pi^+\pi^-$).

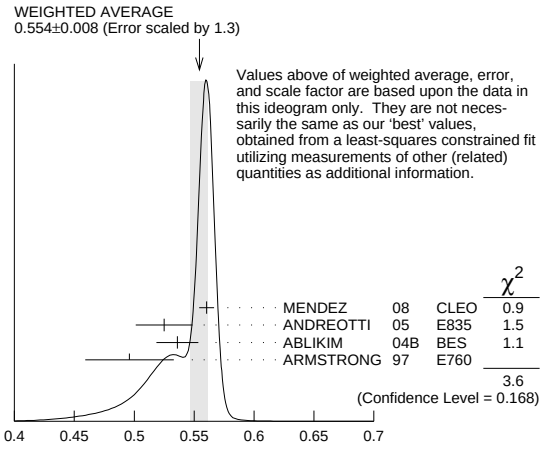

$\Gamma(J/\psi(1S)\text{neutrals})/\Gamma(J/\psi(1S)\pi^+\pi^-)$ $\Gamma_{10}/\Gamma_{11} = (0.9761\Gamma_{12}+0.719\Gamma_{13}+0.343\Gamma_{140}+0.190\Gamma_{141})/\Gamma_{11}$

VALUE	DOCUMENT ID		TECN	COMMENT
0.732±0.008 OUR FIT				
0.73 ±0.09	TANENBAUM	76	MRK1	e^+e^-

$\Gamma(J/\psi(1S)\pi^0\pi^0)/\Gamma_{\text{total}}$ Γ_{12}/Γ

VALUE	EVTS	DOCUMENT ID		TECN	COMMENT
0.1823±0.0031 OUR FIT					
• • • We do not use the following data for averages, fits, limits, etc. • • •					
0.1769±0.0008±0.0053	61k	[1] MENDEZ	08	CLEO	$\psi(2S) \to \ell^+\ell^- 2\pi^0$
0.1652±0.0014±0.0058	13.4k	[2] ADAM	05A	CLEO	Repl. by MENDEZ 08

[1] Not independent from other measurements of MENDEZ 08.
[2] Not independent from other values reported by ADAM 05A.

$\Gamma(J/\psi(1S)\pi^0\pi^0)/\Gamma(J/\psi(1S)\text{anything})$ Γ_{12}/Γ_9

VALUE	EVTS	DOCUMENT ID		TECN	COMMENT
0.2968±0.0031 OUR FIT					
0.320 ±0.012 OUR AVERAGE					
0.300 ±0.008 ±0.022	1655 ± 44	ANDREOTTI	05	E835	$\psi(2S) \to J/\psi X$
0.328 ±0.013 ±0.008		AMBROGIANI	00A	E835	$p\overline{p} \to \psi(2S)$
0.323 ±0.033		ARMSTRONG	97	E760	$\overline{p}p \to \psi(2S)$
• • • We do not use the following data for averages, fits, limits, etc. • • •					
0.2829±0.0012±0.0056	61k	MENDEZ	08	CLEO	$\psi(2S) \to \ell^+\ell^- 2\pi^0$
0.2776±0.0025±0.0043	13.4k	ADAM	05A	CLEO	Repl. by MENDEZ 08

$\Gamma(J/\psi(1S)\pi^0\pi^0)/\Gamma(J/\psi(1S)\pi^+\pi^-)$ Γ_{12}/Γ_{11}

VALUE	EVTS	DOCUMENT ID		TECN	COMMENT
0.526 ±0.008 OUR FIT					
0.513 ±0.022 OUR AVERAGE		Error includes scale factor of 2.2.			
0.5047±0.0022±0.0102	61k	MENDEZ	08	CLEO	$\psi(2S) \to \ell^+\ell^- 2\pi^0$
0.570 ±0.009 ±0.026	14k	[1] ABLIKIM	04B	BES	$\psi(2S) \to J/\psi X$
• • • We do not use the following data for averages, fits, limits, etc. • • •					
0.4924±0.0047±0.0086	73k	[2,3] ADAM	05A	CLEO	Repl. by MENDEZ 08
0.571 ±0.018 ±0.044		[4] ANDREOTTI	05	E835	$\psi(2S) \to J/\psi X$
0.53 ±0.06		TANENBAUM	76	MRK1	e^+e^-
0.64 ±0.15		[5] HILGER	75	SPEC	e^+e^-

[1] From a fit to the J/ψ recoil mass spectra.
[2] Not independent from other values reported by ADAM 05A.
[3] Using 13,217 $J/\psi\pi^0\pi^0$ and 60,010 $J/\psi\pi^+\pi^-$ events.
[4] Not independent from other values reported by ANDREOTTI 05.
[5] Ignoring the $J/\psi(1S)\eta$ and $J/\psi(1S)\gamma\gamma$ decays.

$\Gamma(J/\psi(1S)\eta)/\Gamma_{\text{total}}$ Γ_{13}/Γ

VALUE (units 10^{-3})	EVTS	DOCUMENT ID		TECN	COMMENT
33.7 ± 0.5 OUR FIT					
32.9 ± 1.7 OUR AVERAGE		Error includes scale factor of 2.1. See the ideogram below.			
33.75± 0.17±0.86	68.2k	ABLIKIM	12M	BES3	$e^+e^- \to \ell^+\ell^- 2\gamma$
29.8 ± 0.9 ±2.3	5.7k	BAI	04I	BES2	$\psi(2S) \to J/\psi\gamma\gamma$
25.5 ± 2.9	386	[1] OREGLIA	80	CBAL	$e^+e^- \to J/\psi 2\gamma$
45 ±12	17	[2] BRANDELIK	79B	DASP	$e^+e^- \to J/\psi 2\gamma$
42 ± 6	164	[2] BARTEL	78B	CNTR	e^+e^-
• • • We do not use the following data for averages, fits, limits, etc. • • •					
34.3 ± 0.4 ±0.9	18.4k	[3] MENDEZ	08	CLEO	$\psi(2S) \to \ell^+\ell^-\eta$
32.5 ± 0.6 ±1.1	2.8k	[4] ADAM	05A	CLEO	Repl. by MENDEZ 08
43 ± 8	44	TANENBAUM	76	MRK1	e^+e^-

[1] Recalculated by us using B($J/\psi(1S) \to \ell^+\ell^-$) = 0.1181 ± 0.0020.
[2] Recalculated by us using B($J/\psi(1S) \to \mu^+\mu^-$) = 0.0588 ± 0.0010.
[3] Not independent from other measurements of MENDEZ 08.
[4] Not independent from other values reported by ADAM 05A.

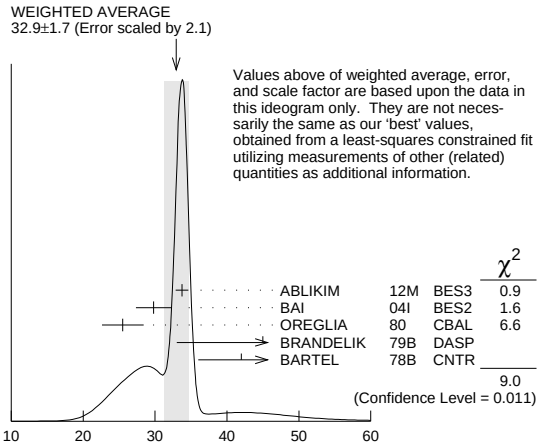

$\Gamma(J/\psi(1S)\eta)/\Gamma(J/\psi(1S)\text{anything})$ Γ_{13}/Γ_9

VALUE	EVTS	DOCUMENT ID		TECN	COMMENT
0.0549±0.0008 OUR FIT					
0.058 ±0.007 OUR AVERAGE Error includes scale factor of 1.4. See the ideogram below.					
0.050 ±0.006 ±0.003	298 ± 20	ANDREOTTI	05	E835	$\psi(2S) \to J/\psi X$
0.072 ±0.009		AMBROGIANI	00A	E835	$p\overline{p} \to \psi(2S)$
0.061 ±0.015		ARMSTRONG	97	E760	$\overline{p}p \to \psi(2S)$
• • • We do not use the following data for averages, fits, limits, etc. • • •					
0.0549±0.0006±0.0009	18.4k	[1] MENDEZ	08	CLEO	$\psi(2S) \to \ell^+\ell^-\eta$
0.0546±0.0010±0.0007	2.8k	ADAM	05A	CLEO	Repl. by MENDEZ 08

[1] Not independent from other measurements of MENDEZ 08.

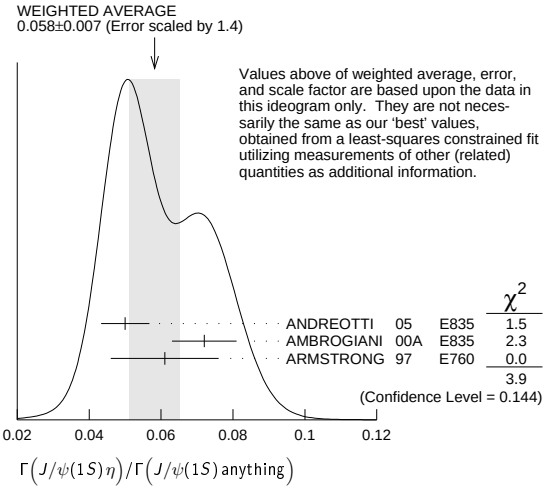

$\Gamma(J/\psi(1S)\eta)/\Gamma(J/\psi(1S)\pi^+\pi^-)$ Γ_{13}/Γ_{11}

VALUE	EVTS	DOCUMENT ID		TECN	COMMENT
0.0972±0.0014 OUR FIT					
0.0979±0.0018 OUR AVERAGE					
0.0979±0.0010±0.0015	18.4k	MENDEZ	08	CLEO	$\psi(2S) \to \ell^+\ell^-\eta$
0.098 ±0.005 ±0.010	2k	[1] ABLIKIM	04B	BES	$\psi(2S) \to J/\psi X$
0.091 ±0.021		[2] HIMEL	80	MRK2	$e^+e^- \to \psi(2S)X$
• • • We do not use the following data for averages, fits, limits, etc. • • •					
0.0968±0.0019±0.0013	2.8k	[3] ADAM	05A	CLEO	Repl. by MENDEZ 08
0.095 ±0.007 ±0.007		[4] ANDREOTTI	05	E835	$\psi(2S) \to J/\psi X$

[1] From a fit to the J/ψ recoil mass spectra.
[2] The value for $B(\psi(2S) \to J/\psi(1s)\eta)$ reported in HIMEL 80 is derived using $B(\psi(2S)) \to J/\psi(1S)\pi^+\pi^-) = (33\pm3))\%$ and $B(J/\psi(1S) \to \ell^+\ell^-) = 0.138\pm0.018$. Calculated by us using $B(J/\psi(1S) \to \ell^+\ell^-) = (0.1181 \pm 0.0020)$.
[3] Not independent from other values reported by ADAM 05A.
[4] Not independent from other values reported by ANDREOTTI 05.

$\Gamma(J/\psi(1S)\pi^0)/\Gamma_{\text{total}}$ Γ_{14}/Γ

VALUE (units 10^{-4})	EVTS	DOCUMENT ID		TECN	COMMENT
12.68±0.32 OUR AVERAGE					
12.6 ±0.2 ±0.3	4.1k	ABLIKIM	12M	BES3	$e^+e^- \to \ell^+\ell^-2\gamma$
13.3 ±0.8 ±0.3	530	MENDEZ	08	CLEO	$\psi(2S) \to \ell^+\ell^-2\gamma$
14.3 ±1.4 ±1.2	280	BAI	04I	BES2	$\psi(2S) \to J/\psi\gamma\gamma$
14 ±6	7	HIMEL	80	MRK2	e^+e^-
9 ±2 ±1	23	[1] OREGLIA	80	CBAL	$\psi(2S) \to J/\psi 2\gamma$
• • • We do not use the following data for averages, fits, limits, etc. • • •					
13 ±1 ±1	88	ADAM	05A	CLEO	Repl. by MENDEZ 08

[1] Recalculated by us using $B(J/\psi(1S) \to \ell^+\ell^-) = 0.1181 \pm 0.0020$.

$\Gamma(J/\psi(1S)\pi^0)/\Gamma(J/\psi(1S)\text{anything})$ $\Gamma_{14}/\Gamma_9 = \Gamma_{14}/(\Gamma_{11}+\Gamma_{12}+\Gamma_{13}+0.343\Gamma_{140}+0.190\Gamma_{141})$

VALUE (units 10^{-2})	EVTS	DOCUMENT ID		TECN	COMMENT
• • • We do not use the following data for averages, fits, limits, etc. • • •					
0.213±0.012±0.003	527	[1] MENDEZ	08	CLEO	$e^+e^- \to J/\psi\gamma\gamma$
0.22 ±0.02 ±0.01		[2] ADAM	05A	CLEO	$e^+e^- \to \psi(2S) \to J/\psi\gamma\gamma$

[1] Not independent from other values reported by MENDEZ 08. Supersedes ADAM 05A.
[2] Not independent from other values reported by ADAM 05A.

$\Gamma(J/\psi(1S)\pi^0)/\Gamma(J/\psi(1S)\pi^+\pi^-)$ Γ_{14}/Γ_{11}

VALUE (units 10^{-2})	EVTS	DOCUMENT ID		TECN	COMMENT
• • • We do not use the following data for averages, fits, limits, etc. • • •					
0.380±0.022±0.005	527	[1] MENDEZ	08	CLEO	$e^+e^- \to J/\psi\gamma\gamma$
0.39 ±0.04 ±0.01		[2] ADAM	05A	CLEO	$e^+e^- \to \psi(2S) \to J/\psi\gamma\gamma$

[1] Not independent from other values reported by MENDEZ 08. Supersedes ADAM 05A.
[2] Not independent from other values reported by ADAM 05A.

HADRONIC DECAYS

$\Gamma(\pi^0 h_c(1P))/\Gamma_{\text{total}}$ Γ_{15}/Γ

VALUE (units 10^{-4})	EVTS	DOCUMENT ID		TECN	COMMENT
8.6±1.3 OUR AVERAGE					
9.0±1.5±1.3	3k	[1] GE	11	CLEO	$\psi(2S) \to \pi^0$ anything
8.4±1.3±1.0	11k	ABLIKIM	10B	BES3	$\psi(2S) \to \pi^0 h_c$
• • • We do not use the following data for averages, fits, limits, etc. • • •					
seen	92^{+23}_{-22}	ADAMS	09	CLEO	$\psi(2S) \to 2\pi^+2\pi^-2\pi^0$
seen	1282	DOBBS	08A	CLEO	$\psi(2S) \to \pi^0\eta_c\gamma$
seen	168 ± 40	ROSNER	05	CLEO	$\psi(2S) \to \pi^0\eta_c\gamma$

[1] Assuming a width $\Gamma(h_c(1P)) = 0.86$ MeV $\equiv \Gamma_0$, a measured dependence of the central value of $B = (7.6 +1.4 \times \Gamma(h_c(1P)/\Gamma_0) \times 10^{-4}$, and with a systematic error that accounts for the width variation range 0.43–1.29 MeV.

$\Gamma(3(\pi^+\pi^-)\pi^0)/\Gamma_{\text{total}}$ Γ_{16}/Γ

VALUE (units 10^{-4})	EVTS	DOCUMENT ID		TECN	COMMENT
35±16	6	FRANKLIN	83	MRK2	$e^+e^- \to$ hadrons

$\Gamma(2(\pi^+\pi^-)\pi^0)/\Gamma_{\text{total}}$ Γ_{17}/Γ

VALUE (units 10^{-4})	EVTS	DOCUMENT ID		TECN	COMMENT
29 ±10 OUR AVERAGE Error includes scale factor of 4.7. See the ideogram below.					
24.9± 0.7±3.6	2173	ABLIKIM	07D	BES2	$e^+e^- \to \psi(2S)$
127 ±12 ±2	410	[1] AUBERT	07AU	BABR	$10.6\ e^+e^- \to 2(\pi^+\pi^-)\pi^0\gamma$
26.1± 0.7±3.0	1703	BRIERE	05	CLEO	$e^+e^- \to \psi(2S) \to 2(\pi^+\pi^-)\pi^0$
30 ± 8	42	FRANKLIN	83	MRK2	e^+e^-

[1] AUBERT 07AU reports $[\Gamma(\psi(2S) \to 2(\pi^+\pi^-)\pi^0)/\Gamma_{\text{total}}] \times [\Gamma(\psi(2S) \to e^+e^-)] = (297 \pm 22 \pm 18) \times 10^{-4}$ keV which we divide by our best value $\Gamma(\psi(2S) \to e^+e^-) = 2.33 \pm 0.04$ keV. Our first error is their experiment's error and our second error is the systematic error from using our best value.

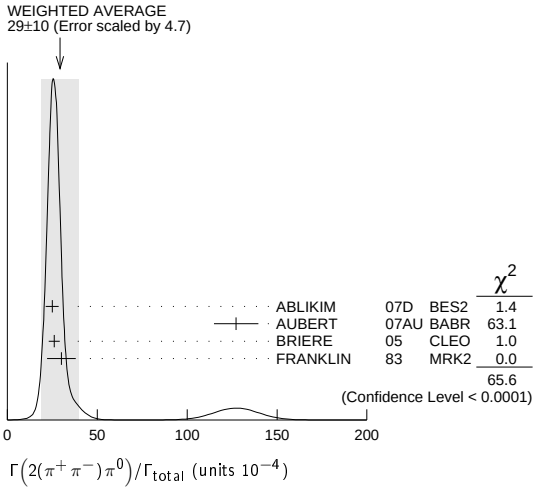

$\Gamma(\rho a_2(1320))/\Gamma_{\text{total}}$ Γ_{18}/Γ

VALUE (units 10^{-4})	CL%	EVTS	DOCUMENT ID		TECN	COMMENT
2.55±0.73±0.47		112 ± 31	BAI	04C	BES2	$\psi(2S) \to 2(\pi^+\pi^-)\pi^0$

• • • We do not use the following data for averages, fits, limits, etc. • • •

<2.3	90		BAI	98J BES	e^+e^-

$\Gamma(p\overline{p})/\Gamma_{total}$ Γ_{19}/Γ

VALUE (units 10^{-4})	EVTS	DOCUMENT ID		TECN	COMMENT
2.88±0.10 OUR FIT					
3.00±0.13 OUR AVERAGE	Error includes scale factor of 1.1.				
3.08±0.05±0.18	4.5k	[1] DOBBS	14		$e^+e^- \to \psi(2S) \to p\overline{p}$
3.36±0.09±0.25	1.6k	ABLIKIM	07C	BES	$e^+e^- \to \psi(2S) \to p\overline{p}$
2.87±0.12±0.15	557	PEDLAR	05	CLEO	$e^+e^- \to \psi(2S) \to p\overline{p}$
1.4 ±0.8	4	BRANDELIK	79C	DASP	$e^+e^- \to \psi(2S) \to p\overline{p}$
2.3 ±0.7		FELDMAN	77	MRK1	$e^+e^- \to \psi(2S) \to p\overline{p}$

[1] Using CLEO-c data but not authored by the CLEO Collaboration.

$\Gamma(p\overline{p})/\Gamma(J/\psi(1S)\pi^+\pi^-)$ Γ_{19}/Γ_{11}

VALUE (units 10^{-4})	DOCUMENT ID		TECN	COMMENT
8.31±0.28 OUR FIT				
6.98±0.49±0.97	BAI	01	BES	$e^+e^- \to \psi(2S) \to p\overline{p}$

$\Gamma(\Delta^{++}\overline{\Delta}^{--})/\Gamma_{total}$ Γ_{20}/Γ

VALUE (units 10^{-5})	EVTS	DOCUMENT ID		TECN	COMMENT
12.8±1.0±3.4	157	[1] BAI	01	BES	$e^+e^- \to \psi(2S) \to$ hadrons

[1] Estimated using $B(\psi(2S) \to J/\psi\pi^+\pi^-) = 0.310 \pm 0.028$.

$\Gamma(\Lambda\overline{\Lambda}\pi^0)/\Gamma_{total}$ Γ_{21}/Γ

VALUE (units 10^{-5})	CL%	DOCUMENT ID		TECN	COMMENT
< 0.29	90	[1] ABLIKIM	13F	BES3	$\psi(2S) \to p\overline{p}\pi^+\pi^-\gamma\gamma$

• • • We do not use the following data for averages, fits, limits, etc. • • •

<12	90	[2] ABLIKIM	07H	BES2	$e^+e^- \to \psi(2S)$

[1] Using $B(\Lambda \to \pi^-p) = 63.9\%$ and $B(\pi^0 \to \gamma\gamma) = 98.8\%$.
[2] Using $B(\Lambda \to \pi^-p) = 63.9\%$ and $B(\eta \to \gamma\gamma) = 39.4\%$.

$\Gamma(\Lambda\overline{\Lambda}\eta)/\Gamma_{total}$ Γ_{22}/Γ

VALUE (units 10^{-5})	CL%	EVTS	DOCUMENT ID		TECN	COMMENT
2.48±0.34±0.19		60	[1] ABLIKIM	13F	BES3	$\psi(2S) \to p\overline{p}\pi^+\pi^-\gamma\gamma$

• • • We do not use the following data for averages, fits, limits, etc. • • •

<4.9	90	[2] ABLIKIM	07H	BES2	$e^+e^- \to \psi(2S)$

[1] Using $B(\Lambda \to \pi^-p) = 63.9\%$ and $B(\eta \to \gamma\gamma) = 39.31\%$.
[2] Using $B(\Lambda \to \pi^-p) = 63.9\%$.

$\Gamma(\Lambda\overline{p}K^+)/\Gamma_{total}$ Γ_{23}/Γ

VALUE (units 10^{-4})	EVTS	DOCUMENT ID		TECN	COMMENT
1.0±0.1±0.1	74.0	BRIERE	05	CLEO	$e^+e^- \to \psi(2S) \to p\overline{p}K^+\pi^-$

$\Gamma(\Lambda\overline{p}K^+\pi^+\pi^-)/\Gamma_{total}$ Γ_{24}/Γ

VALUE (units 10^{-4})	EVTS	DOCUMENT ID		TECN	COMMENT
1.8±0.3±0.3	45.8	BRIERE	05	CLEO	$e^+e^- \to \psi(2S) \to p\overline{p}K^+\pi^+\pi^-\pi^-$

$\Gamma(\Lambda\overline{\Lambda}\pi^+\pi^-)/\Gamma_{total}$ Γ_{25}/Γ

VALUE (units 10^{-4})	EVTS	DOCUMENT ID		TECN	COMMENT
2.8±0.4±0.5	73.4	BRIERE	05	CLEO	$e^+e^- \to \psi(2S) \to p\overline{p}2(\pi^+\pi^-)$

$\Gamma(\Lambda\overline{\Lambda})/\Gamma_{total}$ Γ_{26}/Γ

VALUE (units 10^{-4})	CL%	EVTS	DOCUMENT ID		TECN	COMMENT
3.81±0.13 OUR AVERAGE		Error includes scale factor of 1.4. See the ideogram below.				
3.97±0.02±0.12		31k	ABLIKIM	17L	BES3	$e^+e^- \to \Lambda\overline{\Lambda}$
3.71±0.05±0.15		6.5k	[1] DOBBS	17		$e^+e^- \to \Lambda\overline{\Lambda}$
3.39±0.20±0.32		337	ABLIKIM	07C	BES	$e^+e^- \to \psi(2S) \to$ hadrons
6.4 ±1.8 ±0.1			[2] AUBERT	07BD	BABR	10.6 $e^+e^- \to \Lambda\overline{\Lambda}\gamma$
3.28±0.23±0.25		208	PEDLAR	05	CLEO	$e^+e^- \to \psi(2S) \to$ hadrons

• • • We do not use the following data for averages, fits, limits, etc. • • •

3.75±0.09±0.23		1.9k	[1,3] DOBBS	14		$e^+e^- \to \Lambda\overline{\Lambda}$
1.81±0.20±0.27		80	[4] BAI	01	BES	$e^+e^- \to \psi(2S) \to$ hadrons
< 4	90		FELDMAN	77	MRK1	$e^+e^- \to \psi(2S) \to$ hadrons

[1] Using CLEO-c data but not authored by the CLEO Collaboration.
[2] AUBERT 07BD reports $[\Gamma(\psi(2S) \to \Lambda\overline{\Lambda})/\Gamma_{total}] \times [\Gamma(\psi(2S) \to e^+e^-)] = (15 \pm 4 \pm 1) \times 10^{-4}$ keV which we divide by our best value $\Gamma(\psi(2S) \to e^+e^-) = 2.33 \pm 0.04$ keV. Our first error is their experiment's error and our second error is the systematic error from using our best value.
[3] Superseded by DOBBS 17.
[4] Estimated using $B(\psi(2S) \to J/\psi\pi^+\pi^-) = 0.310 \pm 0.028$.

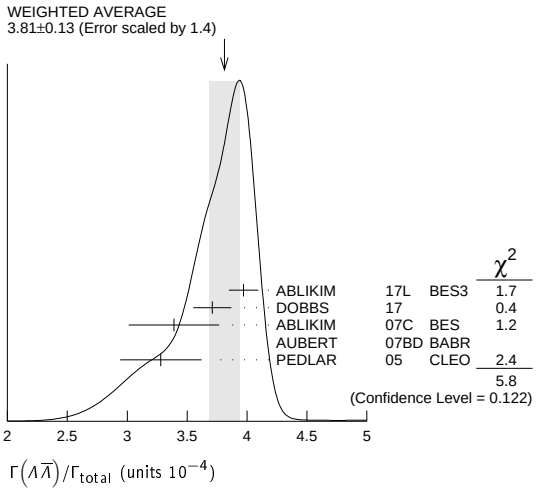

$\Gamma(\Lambda\overline{\Sigma}^+\pi^- + c.c.)/\Gamma_{total}$ Γ_{27}/Γ

VALUE (units 10^{-4})	EVTS	DOCUMENT ID		TECN	COMMENT
1.40±0.03±0.13	2.8k	ABLIKIM	13W	BES3	$\psi(2S) \to$ hadrons

$\Gamma(\Lambda\overline{\Sigma}^-\pi^+ + c.c.)/\Gamma_{total}$ Γ_{28}/Γ

VALUE (units 10^{-4})	EVTS	DOCUMENT ID		TECN	COMMENT
1.54±0.04±0.13	2.8k	ABLIKIM	13W	BES3	$\psi(2S) \to$ hadrons

$\Gamma(\Lambda\overline{\Sigma}^0)/\Gamma_{total}$ Γ_{29}/Γ

VALUE (units 10^{-5})	EVTS	DOCUMENT ID		TECN	COMMENT
1.23±0.23±0.08	30	[1] DOBBS	17		$e^+e^- \to \psi(2S) \to$ hadrons

[1] Using CLEO-c data but not authored by the CLEO Collaboration.

$\Gamma(\Sigma^0\overline{p}K^+ + c.c.)/\Gamma_{total}$ Γ_{30}/Γ

VALUE (units 10^{-5})	EVTS	DOCUMENT ID		TECN	COMMENT
1.67±0.13±0.12	276	[1] ABLIKIM	13D	BES3	$\psi(2S) \to \gamma\Lambda\overline{p}K^+$

[1] Using $B(\Lambda \to p\pi^-) = 63.9\%$, and $B(\Sigma^0 \to \Lambda\gamma) = 100\%$.

$\Gamma(\Sigma^+\overline{\Sigma}^-)/\Gamma_{total}$ Γ_{31}/Γ

VALUE (units 10^{-4})	EVTS	DOCUMENT ID		TECN	COMMENT
2.32±0.12 OUR AVERAGE					
2.31±0.06±0.10	1.9k	[1] DOBBS	17		$e^+e^- \to \psi(2S) \to$ hadrons
2.57±0.44±0.68	35	PEDLAR	05	CLEO	$e^+e^- \to \psi(2S) \to$ hadrons

• • • We do not use the following data for averages, fits, limits, etc. • • •

2.51±0.15±0.16	281	[1,2] DOBBS	14		$e^+e^- \to \psi(2S) \to$ hadrons

[1] Using CLEO-c data but not authored by the CLEO Collaboration.
[2] Superseded by DOBBS 17.

$\Gamma(\Sigma^0\overline{\Sigma}^0)/\Gamma_{total}$ Γ_{32}/Γ

VALUE (units 10^{-4})	EVTS	DOCUMENT ID		TECN	COMMENT
2.35±0.09 OUR AVERAGE	Error includes scale factor of 1.1.				
2.44±0.03±0.11	7k	ABLIKIM	17L	BES3	$e^+e^- \to \psi(2S) \to$ hadrons
2.22±0.05±0.11	2.6k	[1] DOBBS	17		$e^+e^- \to \psi(2S) \to$ hadrons
2.35±0.36±0.32	59	ABLIKIM	07C	BES	$e^+e^- \to \psi(2S) \to$ hadrons
2.63±0.35±0.21	58	PEDLAR	05	CLEO	$e^+e^- \to \psi(2S) \to$ hadrons

• • • We do not use the following data for averages, fits, limits, etc. • • •

2.25±0.11±0.16	439	[1,2] DOBBS	14			$e^+e^- \to \psi(2S) \to$ hadrons
1.2 ±0.4 ±0.4	8	[3] BAI	01	BES		$e^+e^- \to \psi(2S) \to$ hadrons

[1] Using CLEO-c data but not authored by the CLEO Collaboration.
[2] Superseded by DOBBS 17.
[3] Estimated using $B(\psi(2S) \to J/\psi\pi^+\pi^-) = 0.310 \pm 0.028$.

$\Gamma(\Sigma(1385)^+\overline{\Sigma}(1385)^-)/\Gamma_{total}$ Γ_{33}/Γ

VALUE (units 10^{-5})	EVTS	DOCUMENT ID		TECN	COMMENT
8.5±0.7 OUR AVERAGE					
8.4±0.5±0.5	1.5k	ABLIKIM	16L	BES3	$\psi(2S) \to \Sigma(1385)^+\overline{\Sigma}(1385)^-$
11 ±3 ±3	14	[1] BAI	01	BES	$e^+e^- \to \psi(2S) \to$ hadrons

[1] Estimated using $B(\psi(2S) \to J/\psi\pi^+\pi^-) = 0.310 \pm 0.028$.

$\Gamma(\Sigma(1385)^-\overline{\Sigma}(1385)^+)/\Gamma_{total}$ Γ_{34}/Γ

VALUE (units 10^{-5})	EVTS	DOCUMENT ID		TECN	COMMENT
8.5±0.6±0.6	1.4K	ABLIKIM	16L	BES3	$\psi(2S) \to \Sigma(1385)^-\overline{\Sigma}(1385)^+$

$\Gamma(\Sigma(1385)^0\overline{\Sigma}(1385)^0)/\Gamma_{total}$ Γ_{35}/Γ

VALUE (units 10^{-4})	EVTS	DOCUMENT ID		TECN	COMMENT
0.69±0.05±0.05	2.2k	ABLIKIM	17E	BES3	$e^+e^- \to \psi(2S) \to$ hadrons

$\Gamma(\Xi^-\overline{\Xi}^+)/\Gamma_{total}$ Γ_{36}/Γ

VALUE (units 10^{-4})	CL%	EVTS	DOCUMENT ID		TECN	COMMENT
2.87±0.11 OUR AVERAGE			Error includes scale factor of 1.1.			
3.03±0.05±0.14		3.6k	[1] DOBBS	17		$e^+e^- \to \psi(2S) \to$ hadrons
2.78±0.05±0.14		5k	ABLIKIM	16L	BES3	$\psi(2S) \to \Xi^-\overline{\Xi}^+$
3.03±0.40±0.32		67	ABLIKIM	07C	BES	$e^+e^- \to \psi(2S) \to$ hadrons
2.38±0.30±0.21		63	PEDLAR	05	CLEO	$e^+e^- \to \psi(2S) \to$ hadrons
• • • We do not use the following data for averages, fits, limits, etc. • • •						
2.66±0.12±0.20		548	[1,2] DOBBS	14		$e^+e^- \to \psi(2S) \to$ hadrons
0.94±0.27±0.15		12	[3] BAI	01	BES	$e^+e^- \to \psi(2S) \to$ hadrons
<2	90		FELDMAN	77	MRK1	$e^+e^- \to \psi(2S) \to$ hadrons

[1] Using CLEO-c data but not authored by the CLEO Collaboration.
[2] Superseded by DOBBS 17.
[3] Estimated using B($\psi(2S) \to J/\psi\pi^+\pi^-$)= 0.310 ± 0.028.

$\Gamma(\Xi^0\overline{\Xi}^0)/\Gamma_{total}$ Γ_{37}/Γ

VALUE (units 10^{-4})	EVTS	DOCUMENT ID		TECN	COMMENT
2.3 ±0.4 OUR AVERAGE		Error includes scale factor of 4.2.			
2.73±0.03±0.13	11k	ABLIKIM	17E	BES3	$e^+e^- \to \psi(2S) \to$ hadrons
1.97±0.06±0.11	1.2k	[1] DOBBS	17		$e^+e^- \to \psi(2S) \to$ hadrons
2.75±0.64±0.61	19	PEDLAR	05	CLEO	$e^+e^- \to \psi(2S) \to$ hadrons
• • • We do not use the following data for averages, fits, limits, etc. • • •					
2.02±0.19±0.15	112	[1,2] DOBBS	14		$e^+e^- \to \psi(2S) \to$ hadrons

[1] Using CLEO-c data but not authored by the CLEO Collaboration.
[2] Superseded by DOBBS 17.

$\Gamma(\Xi(1530)^0\overline{\Xi}(1530)^0)/\Gamma_{total}$ Γ_{38}/Γ

VALUE (units 10^{-5})	CL%	EVTS	DOCUMENT ID		TECN	COMMENT
$\mathbf{5.2\pm0.3^{+3.2}_{-1.2}}$		527	[1] ABLIKIM	13S	BES3	$\psi(2S) \to \eta p\overline{p}$
• • • We do not use the following data for averages, fits, limits, etc. • • •						
<32	90		PEDLAR	05	CLEO	$e^+e^- \to \psi(2S) \to$ hadrons
< 8.1	90		[2] BAI	01	BES	$e^+e^- \to \psi(2S) \to$ hadrons

[1] With $N(1535)$ decaying to $p\eta$.
[2] Estimated using B($\psi(2S) \to J/\psi\pi^+\pi^-$)= 0.310 ± 0.028.

$\Gamma(K^-\Lambda\overline{\Xi}^+ + \text{c.c.})/\Gamma_{total}$ Γ_{39}/Γ

VALUE (units 10^{-5})	EVTS	DOCUMENT ID		TECN	COMMENT
3.86±0.27±0.32	236	ABLIKIM	15I	BES3	$e^+e^- \to \psi(2S) \to K^-\Lambda\overline{\Xi}^+ +$ c.c.

$\Gamma(\Xi(1690)^-\overline{\Xi}^+ \to K^-\Lambda\overline{\Xi}^+ + \text{c.c.})/\Gamma_{total}$ Γ_{40}/Γ

VALUE (units 10^{-6})	EVTS	DOCUMENT ID		TECN	COMMENT
5.21±1.48±0.57	74	ABLIKIM	15I	BES3	$e^+e^- \to \psi(2S) \to K^-\Lambda\overline{\Xi}^+ +$ c.c.

$\Gamma(\Xi(1820)^-\overline{\Xi}^+ \to K^-\Lambda\overline{\Xi}^+ + \text{c.c.})/\Gamma_{total}$ Γ_{41}/Γ

VALUE (units 10^{-6})	EVTS	DOCUMENT ID		TECN	COMMENT
12.03±2.94±1.22	136	ABLIKIM	15I	BES3	$e^+e^- \to \psi(2S) \to K^-\Lambda\overline{\Xi}^+ +$ c.c.

$\Gamma(K^-\Sigma^0\overline{\Xi}^+ + \text{c.c.})/\Gamma_{total}$ Γ_{42}/Γ

VALUE (units 10^{-5})	EVTS	DOCUMENT ID		TECN	COMMENT
3.67±0.33±0.28	142	ABLIKIM	15I	BES3	$e^+e^- \to \psi(2S) \to K^-\Sigma^0\overline{\Xi}^+ +$ c.c.

$\Gamma(\Omega^-\overline{\Omega}^+)/\Gamma_{total}$ Γ_{43}/Γ

VALUE (units 10^{-4})	CL%	EVTS	DOCUMENT ID		TECN	COMMENT
0.52±0.03±0.03		326	[1] DOBBS	17		$e^+e^- \to \psi(2S) \to$ hadrons
• • • We do not use the following data for averages, fits, limits, etc. • • •						
0.47±0.09±0.05		27	[1,2] DOBBS	14		$e^+e^- \to \psi(2S) \to$ hadrons
<1.5	90		ABLIKIM	12Q	BES2	$e^+e^- \to \psi(2S) \to$ hadrons
<1.6	90		PEDLAR	05	CLEO	$e^+e^- \to \psi(2S) \to$ hadrons
<0.73	90		[3] BAI	01	BES	$e^+e^- \to \psi(2S) \to$ hadrons

[1] Using CLEO-c data but not authored by the CLEO Collaboration.
[2] Superseded by DOBBS 17.
[3] Estimated using B($\psi(2S) \to J/\psi\pi^+\pi^-$)= 0.310 ± 0.028.

$\Gamma(\pi^0 p\overline{p})/\Gamma_{total}$ Γ_{44}/Γ

VALUE (units 10^{-4})	EVTS	DOCUMENT ID		TECN	COMMENT
1.53±0.07 OUR AVERAGE					
1.65±0.03±0.15	4.5k	ABLIKIM	13A	BES3	$\psi(2S) \to p\overline{p}\pi^0$
1.54±0.06±0.06	948	ALEXANDER	10	CLEO	$\psi(2S) \to \pi^0 p\overline{p}$
1.32±0.10±0.15	256	[1] ABLIKIM	05E	BES2	$e^+e^- \to \psi(2S) \to p\overline{p}\gamma\gamma$
1.4 ±0.5	9	FRANKLIN	83	MRK2	e^+e^-

[1] Computed using B($\pi^0 \to \gamma\gamma$) = (98.80 ± 0.03)%.

$\Gamma(N(940)\overline{p}+ \text{c.c.} \to \pi^0 p\overline{p})/\Gamma_{total}$ Γ_{45}/Γ

VALUE (units 10^{-5})	EVTS	DOCUMENT ID		TECN	COMMENT
$\mathbf{6.42\pm0.20^{+1.78}_{-1.28}}$	1.9k	[1] ABLIKIM	13A	BES3	$\psi(2S) \to p\overline{p}\pi^0$

[1] From a fit of $\pi^0 p\overline{p}$ data to eight distinct intermediate $N\overline{p}$ resonant states.

$\Gamma(N(1440)\overline{p}+ \text{c.c.} \to \pi^0 p\overline{p})/\Gamma_{total}$ Γ_{46}/Γ

VALUE (units 10^{-5})	EVTS	DOCUMENT ID		TECN	COMMENT
$\mathbf{7.3\ ^{+1.7}_{-1.5}}$ **OUR AVERAGE**		Error includes scale factor of 2.5.			
$3.58\pm0.25^{+1.59}_{-0.84}$	1.1k	[1] ABLIKIM	13A	BES3	$\psi(2S) \to p\overline{p}\pi^0$
8.1 ±0.7 ±0.3	474	[2] ALEXANDER	10	CLEO	$\psi(2S) \to \pi^0 p\overline{p}$

[1] From a fit of $\pi^0 p\overline{p}$ data to eight distinct intermediate $N\overline{p}$ resonant states.
[2] From a fit of the $p\overline{p}$ and $p\pi^0$ mass distributions to a combination of $N(1440)\overline{p}$, $\pi^0 f_0(2100)$, and two other broad, unestablished resonances.

$\Gamma(N(1520)\overline{p}+ \text{c.c.} \to \pi^0 p\overline{p})/\Gamma_{total}$ Γ_{47}/Γ

VALUE (units 10^{-5})	EVTS	DOCUMENT ID		TECN	COMMENT
$\mathbf{0.64\pm0.05^{+0.22}_{-0.17}}$	0.2k	[1] ABLIKIM	13A	BES3	$\psi(2S) \to p\overline{p}\pi^0$

[1] From a fit of $\pi^0 p\overline{p}$ data to eight distinct intermediate $N\overline{p}$ resonant states.

$\Gamma(N(1535)\overline{p}+ \text{c.c.} \to \pi^0 p\overline{p})/\Gamma_{total}$ Γ_{48}/Γ

VALUE (units 10^{-5})	EVTS	DOCUMENT ID		TECN	COMMENT
$\mathbf{2.47\pm0.28^{+0.99}_{-0.97}}$	0.7k	[1] ABLIKIM	13A	BES3	$\psi(2S) \to p\overline{p}\pi^0$

[1] From a fit of $\pi^0 p\overline{p}$ data to eight distinct intermediate $N\overline{p}$ resonant states.

$\Gamma(N(1650)\overline{p}+ \text{c.c.} \to \pi^0 p\overline{p})/\Gamma_{total}$ Γ_{49}/Γ

VALUE (units 10^{-5})	EVTS	DOCUMENT ID		TECN	COMMENT
$\mathbf{3.76\pm0.28^{+1.37}_{-1.66}}$	1.1k	[1] ABLIKIM	13A	BES3	$\psi(2S) \to p\overline{p}\pi^0$

[1] From a fit of $\pi^0 p\overline{p}$ data to eight distinct intermediate $N\overline{p}$ resonant states.

$\Gamma(N(1720)\overline{p}+ \text{c.c.} \to \pi^0 p\overline{p})/\Gamma_{total}$ Γ_{50}/Γ

VALUE (units 10^{-5})	EVTS	DOCUMENT ID		TECN	COMMENT
$\mathbf{1.79\pm0.10^{+0.24}_{-0.71}}$	0.5k	[1] ABLIKIM	13A	BES3	$\psi(2S) \to p\overline{p}\pi^0$

[1] From a fit of $\pi^0 p\overline{p}$ data to eight distinct intermediate $N\overline{p}$ resonant states.

$\Gamma(N(2300)\overline{p}+ \text{c.c.} \to \pi^0 p\overline{p})/\Gamma_{total}$ Γ_{51}/Γ

VALUE (units 10^{-5})	EVTS	DOCUMENT ID		TECN	COMMENT
$\mathbf{2.62\pm0.28^{+1.12}_{-0.64}}$	0.9k	[1] ABLIKIM	13A	BES3	$\psi(2S) \to p\overline{p}\pi^0$

[1] From a fit of $\pi^0 p\overline{p}$ data to eight distinct intermediate $N\overline{p}$ resonant states.

$\Gamma(N(2570)\overline{p}+ \text{c.c.} \to \pi^0 p\overline{p})/\Gamma_{total}$ Γ_{52}/Γ

VALUE (units 10^{-5})	EVTS	DOCUMENT ID		TECN	COMMENT
$\mathbf{2.13\pm0.08^{+0.40}_{-0.30}}$	0.8k	[1] ABLIKIM	13A	BES3	$\psi(2S) \to p\overline{p}\pi^0$

[1] From a fit of $\pi^0 p\overline{p}$ data to eight distinct intermediate $N\overline{p}$ resonant states.

$\Gamma(\pi^0 f_0(2100) \to \pi^0 p\overline{p})/\Gamma_{total}$ Γ_{53}/Γ

VALUE (units 10^{-5})	EVTS	DOCUMENT ID		TECN	COMMENT
1.1±0.4±0.1	76	[1] ALEXANDER	10	CLEO	$\psi(2S) \to \pi^0 p\overline{p}$

[1] From a fit of the $p\overline{p}$ and $p\pi^0$ mass distributions to a combination of $N_1^*(1440)\overline{p}$, $\pi^0 f_0(2100)$, and two other broad, unestablished resonances.

$\Gamma(\eta p\overline{p})/\Gamma_{total}$ Γ_{54}/Γ

VALUE (units 10^{-5})	EVTS	DOCUMENT ID		TECN	COMMENT
6.0±0.4 OUR AVERAGE					
6.4±0.2±0.6	679	[1] ABLIKIM	13S	BES3	$\psi(2S) \to \eta p\overline{p}$
5.6±0.6±0.3	154	[1] ALEXANDER	10	CLEO	$\psi(2S) \to \eta p\overline{p}$
5.8±1.1±0.7	44.8 ± 8.5	[2] ABLIKIM	05E	BES2	$e^+e^- \to \psi(2S) \to p\overline{p}\gamma\gamma$
8 ±3 ±3	9.8	BRIERE	05	CLEO	$e^+e^- \to \psi(2S) \to p\overline{p}\pi^+\pi^-\pi^0$

[1] With $N(1535)$ decaying to $p\eta$.
[2] Computed using B($\eta \to \gamma\gamma$) = (39.43 ± 0.26)%.

$\Gamma(\eta f_0(2100) \to \eta p\overline{p})/\Gamma_{total}$ Γ_{55}/Γ

VALUE (units 10^{-5})	EVTS	DOCUMENT ID		TECN	COMMENT
1.2±0.4±0.1	31	[1] ALEXANDER	10	CLEO	$\psi(2S) \to \eta p\overline{p}$

[1] From a fit of the $p\overline{p}$ and $p\eta$ distributions to a combination of $N^*(1535)\overline{p}$ and $\eta f_0(2100)$.

$\Gamma(N(1535)\overline{p} \to \eta p\overline{p})/\Gamma_{total}$ Γ_{56}/Γ

VALUE (units 10^{-5})	EVTS	DOCUMENT ID		TECN	COMMENT
4.4±0.6±0.3	123	[1] ALEXANDER	10	CLEO	$\psi(2S) \to \eta p\overline{p}$

[1] From a fit of the $p\overline{p}$ and $p\eta$ distributions to a combination of $N^*(1535)\overline{p}$ and $\eta f_0(2100)$.

$\Gamma(\omega p\overline{p})/\Gamma_{total}$ Γ_{57}/Γ

VALUE (units 10^{-4})	EVTS	DOCUMENT ID		TECN	COMMENT
0.69±0.21 OUR AVERAGE					
0.6 ±0.2 ±0.2	21.2	BRIERE	05	CLEO	$e^+e^- \to \psi(2S) \to p\overline{p}\pi^+\pi^-\pi^0$
0.8 ±0.3 ±0.1	14.9 ± 0.1	[1] BAI	03B	BES	$\psi(2S) \to p\overline{p}\pi^+\pi^-\pi^0$

[1] Normalized to $B(\psi(2S) \to J/\psi\pi^+\pi^-) = 0.305 \pm 0.016$.

$\Gamma(\phi p\overline{p})/\Gamma_{total}$ Γ_{58}/Γ

VALUE (units 10^{-4})	CL%	DOCUMENT ID		TECN	COMMENT
<0.24	90	BRIERE	05	CLEO	$e^+e^- \to \psi(2S) \to p\overline{p}K^+K^-$
• • • We do not use the following data for averages, fits, limits, etc. • • •					
<0.26	90	[1] BAI	03B	BES	$\psi(2S) \to K^+K^-p\overline{p}$

[1] Normalized to $B(\psi(2S) \to J/\psi\pi^+\pi^-) = 0.305 \pm 0.016$.

$\Gamma(\pi^+\pi^-p\overline{p})/\Gamma_{total}$ Γ_{59}/Γ

VALUE (units 10^{-4})	EVTS	DOCUMENT ID		TECN	COMMENT
6.0±0.4 OUR AVERAGE					
5.9±0.2±0.4	904.5	BRIERE	05	CLEO	$e^+e^- \to \psi(2S) \to p\overline{p}\pi^+\pi^-$
8 ±2		[1] TANENBAUM	78	MRK1	e^+e^-

[1] Assuming entirely strong decay.

$\Gamma(p\overline{n}\pi^-$ or c.c.$)/\Gamma_{total}$ Γ_{60}/Γ

VALUE (units 10^{-4})	EVTS	DOCUMENT ID		TECN	COMMENT
2.48±0.17 OUR AVERAGE					
2.45±0.11±0.21	851	ABLIKIM	06I	BES2	$e^+e^- \to p\pi^-X$
2.52±0.12±0.22	849	ABLIKIM	06I	BES2	$e^+e^- \to \overline{p}\pi^+X$

$\Gamma(p\overline{n}\pi^-\pi^0)/\Gamma_{total}$ Γ_{61}/Γ

VALUE (units 10^{-4})	EVTS	DOCUMENT ID		TECN	COMMENT
3.18±0.50±0.50	135 ± 21	ABLIKIM	06I	BES2	$e^+e^- \to p\pi^-\pi^0X$

$\Gamma(\eta\pi^+\pi^-)/\Gamma_{total}$ Γ_{63}/Γ

VALUE (units 10^{-4})	CL%	DOCUMENT ID		TECN	COMMENT
<1.6	90	BRIERE	05	CLEO	$e^+e^- \to \psi(2S) \to 2(\pi^+\pi^-)\pi^0$

$\Gamma(\eta\pi^+\pi^-\pi^0)/\Gamma_{total}$ Γ_{64}/Γ

VALUE (units 10^{-4})	EVTS	DOCUMENT ID		TECN	COMMENT
9.5±0.7±1.5		[1] BRIERE	05	CLEO	$e^+e^- \to \psi(2S) \to$ hadr
• • • We do not use the following data for averages, fits, limits, etc. • • •					
10.3±0.8±1.4	201.7	[2] BRIERE	05	CLEO	$e^+e^- \to \psi(2S) \to \eta 3\pi(\eta \to \gamma\gamma)$
8.1±1.4±1.6	50.0	[2] BRIERE	05	CLEO	$e^+e^- \to \psi(2S) \to \eta 3\pi(\eta \to 3\pi)$

[1] Average of $\eta \to \gamma\gamma$ and $\eta \to 3\pi$.
[2] Not independent from other values reported by BRIERE 05.

$\Gamma(2(\pi^+\pi^-)\eta)/\Gamma_{total}$ Γ_{65}/Γ

VALUE (units 10^{-3})	EVTS	DOCUMENT ID		TECN	COMMENT
1.2±0.6±0.1	16	[1] AUBERT	07AU	BABR	10.6 $e^+e^- \to 2(\pi^+\pi^-)\eta\gamma$

[1] AUBERT 07AU quotes $\Gamma_{ee}^{\psi(2S)} \cdot B(\psi(2S) \to 2(\pi^+\pi)\eta) \cdot B(\eta \to \gamma\gamma) = 1.2 \pm 0.7 \pm 0.1$ eV.

$\Gamma(\eta'\pi^+\pi^-\pi^0)/\Gamma_{total}$ Γ_{66}/Γ

VALUE (units 10^{-4})	EVTS	DOCUMENT ID		TECN	COMMENT
4.5±1.6±1.3	12.8	BRIERE	05	CLEO	$e^+e^- \to \psi(2S) \to$ hadr

$\Gamma(\omega\pi^+\pi^-)/\Gamma_{total}$ Γ_{67}/Γ

VALUE (units 10^{-4})	EVTS	DOCUMENT ID		TECN	COMMENT
7.3±1.2 OUR AVERAGE		Error includes scale factor of 2.1. See the ideogram below.			
8.4±0.5±1.2	386	ABLIKIM	07D	BES2	$e^+e^- \to \psi(2S)$
12.2±2.2±0.7	37	[1] AUBERT	07AU	BABR	10.6 $e^+e^- \to \omega\pi^+\pi^-\gamma$
8.2±0.5±0.7	391	BRIERE	05	CLEO	$e^+e^- \to \psi(2S) \to 2(\pi^+\pi^-)\pi^0$
4.8±0.6±0.7	100 ± 22	[2] BAI	03B	BES	$\psi(2S) \to 2(\pi^+\pi^-)\pi^0$

[1] AUBERT 07AU quotes $\Gamma_{ee}^{\psi(2S)} \cdot B(\psi(2S) \to \omega\pi^+\pi^-) \cdot B(\omega \to 3\pi) = 2.69 \pm 0.73 \pm 0.16$ eV.
[2] Normalized to $B(\psi(2S) \to J/\psi\pi^+\pi^-) = 0.305 \pm 0.016$.

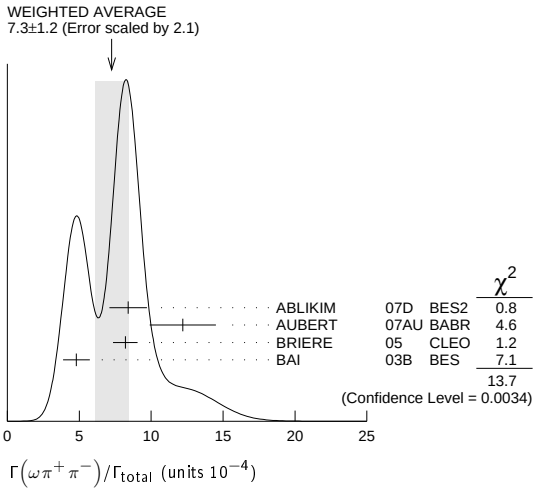

$\Gamma(b_1^\pm\pi^\mp)/\Gamma_{total}$ Γ_{68}/Γ

VALUE (units 10^{-4})	EVTS	DOCUMENT ID		TECN	COMMENT
4.0 ±0.6 OUR AVERAGE		Error includes scale factor of 1.1.			
5.1 ±0.6 ±0.8	202	ABLIKIM	07D	BES2	$e^+e^- \to \psi(2S)$
$4.18^{+0.43}_{-0.42}\pm0.92$	170	ADAM	05	CLEO	$e^+e^- \to \psi(2S)$
3.2 ±0.6 ±0.5	61 ± 11	[1,2] BAI	03B	BES	$\psi(2S) \to 2(\pi^+\pi^-)\pi^0$
• • • We do not use the following data for averages, fits, limits, etc. • • •					
5.2 ±0.8 ±1.0		[1] BAI	99C	BES	Repl. by BAI 03B

[1] Assuming $B(b_1 \to \omega\pi)=1$.
[2] Normalized to $B(\psi(2S) \to J/\psi\pi^+\pi^-) = 0.305 \pm 0.016$.

$\Gamma(b_1^0\pi^0)/\Gamma_{total}$ Γ_{69}/Γ

VALUE (units 10^{-4})	EVTS	DOCUMENT ID		TECN	COMMENT
$\mathbf{2.35^{+0.47}_{-0.42}\pm0.40}$	45	ADAM	05	CLEO	$e^+e^- \to \psi(2S)$

$\Gamma(\omega f_2(1270))/\Gamma_{total}$ Γ_{70}/Γ

VALUE (units 10^{-4})	CL%	EVTS	DOCUMENT ID		TECN	COMMENT
2.2 ±0.4 OUR AVERAGE						
2.3 ±0.5 ±0.4		57	ABLIKIM	07D	BES2	$e^+e^- \to \psi(2S)$
2.05±0.41±0.38		62±12	BAI	04C	BES2	$\psi(2S) \to 2(\pi^+\pi^-)\pi^0$
• • • We do not use the following data for averages, fits, limits, etc. • • •						
<1.5	90		[1] BAI	03B	BES	$\psi(2S) \to 2(\pi^+\pi^-)\pi^0$
<1.7	90		BAI	98J	BES	Repl. by BAI 03B

[1] Normalized to $B(\psi(2S) \to J/\psi\pi^+\pi^-) = 0.305 \pm 0.016$.

$\Gamma(\pi^+\pi^-K^+K^-)/\Gamma_{total}$ Γ_{72}/Γ

VALUE (units 10^{-4})	EVTS	DOCUMENT ID		TECN	COMMENT
7.3±0.5 OUR AVERAGE					
8.1±1.3±0.3	133	LEES	12F	BABR	10.6 $e^+e^- \to \pi^+\pi^-K^+K^-\gamma$
7.1±0.3±0.4	817.2	BRIERE	05	CLEO	$e^+e^- \to \psi(2S) \to K^+K^-\pi^+\pi^-$
16 ±4		[1] TANENBAUM	78	MRK1	e^+e^-
• • • We do not use the following data for averages, fits, limits, etc. • • •					
11.0±1.9±0.2	85	[2] AUBERT	07AK	BABR	10.6 $e^+e^- \to \pi^+\pi^-K^+K^-\gamma$

[1] Assuming entirely strong decay.
[2] Superseded by LEES 12F. AUBERT 07AK reports $[\Gamma(\psi(2S) \to \pi^+\pi^-K^+K^-)/\Gamma_{total}] \times [\Gamma(\psi(2S) \to e^+e^-)] = (2.56 \pm 0.42 \pm 0.16) \times 10^{-3}$ keV which we divide by our best value $\Gamma(\psi(2S) \to e^+e^-) = 2.33 \pm 0.04$ keV. Our first error is their experiment's error and our second error is the systematic error from using our best value.

$\Gamma(\rho^0K^+K^-)/\Gamma_{total}$ Γ_{74}/Γ

VALUE (units 10^{-4})	EVTS	DOCUMENT ID		TECN	COMMENT
2.2±0.2±0.4	223.8	BRIERE	05	CLEO	$e^+e^- \to \psi(2S) \to K^+K^-\pi^+\pi^-$

$\Gamma(K^*(892)^0\overline{K}_2^*(1430)^0)/\Gamma_{total}$ Γ_{75}/Γ

VALUE (units 10^{-4})	CL%	EVTS	DOCUMENT ID		TECN	COMMENT
1.86±0.32±0.43		93 ± 16	BAI	04C		$\psi(2S) \to K^+K^-\pi^+\pi^-$
• • • We do not use the following data for averages, fits, limits, etc. • • •						
<1.2	90		BAI	98J	BES	e^+e^-

$\Gamma(K^+K^-\pi^+\pi^-\eta)/\Gamma_{total}$ Γ_{76}/Γ

VALUE (units 10^{-3})	EVTS	DOCUMENT ID		TECN	COMMENT
1.3±0.7±0.1	7	[1] AUBERT	07AU	BABR	10.6 $e^+e^- \to K^+K^-\pi^+\pi^-\eta\gamma$

[1] AUBERT 07AU quotes $\Gamma_{ee}^{\psi(2S)} \cdot B(\psi(2S) \to 2(\pi^+\pi)\eta) \cdot B(\eta \to \gamma\gamma) = 1.2 \pm 0.7 \pm 0.1$ eV.

$\Gamma(K^+K^-2(\pi^+\pi^-)\pi^0)/\Gamma_{total}$ Γ_{77}/Γ

VALUE (units 10^{-4})	EVTS	DOCUMENT ID		TECN	COMMENT
10.0±2.5±1.8	65	ABLIKIM	07D	BES2	$e^+e^- \to \psi(2S)$

$\Gamma((K_1(1270)^\pm K^\mp)/\Gamma_{total}$ Γ_{79}/Γ

VALUE (units 10^{-4})	DOCUMENT ID		TECN	COMMENT
10.0±1.8±2.1	[1] BAI	99C	BES	e^+e^-

[1] Assuming $B(K_1(1270) \to K\rho)$=0.42 ± 0.06

$\Gamma(K^0_S K^0_S \pi^+\pi^-)/\Gamma_{total}$ Γ_{80}/Γ

VALUE (units 10^{-4})	EVTS	DOCUMENT ID		TECN	COMMENT
2.20±0.25±0.37	83 ± 9	ABLIKIM	05O	BES2	$e^+e^- \to \psi(2S)$

$\Gamma(\rho^0 p\overline{p})/\Gamma_{total}$ Γ_{81}/Γ

VALUE (units 10^{-4})	EVTS	DOCUMENT ID		TECN	COMMENT
0.5±0.1±0.2	61.1	BRIERE	05	CLEO	$e^+e^- \to \psi(2S) \to p\overline{p}\pi^+\pi^-$

$\Gamma(K^+\overline{K}^*(892)^0\pi^- + c.c.)/\Gamma_{total}$ Γ_{82}/Γ

VALUE (units 10^{-4})	DOCUMENT ID		TECN	COMMENT
6.7±2.5	TANENBAUM	78	MRK1	e^+e^-

$\Gamma(2(\pi^+\pi^-))/\Gamma_{total}$ Γ_{83}/Γ

VALUE (units 10^{-4})	EVTS	DOCUMENT ID		TECN	COMMENT
2.4±0.6 OUR AVERAGE Error includes scale factor of 2.2.					
2.2±0.2±0.2	308	BRIERE	05	CLEO	$e^+e^- \to \psi(2S) \to 2(\pi^+\pi^-)$
4.5±1.0		TANENBAUM	78	MRK1	e^+e^-

$\Gamma(\rho^0\pi^+\pi^-)/\Gamma_{total}$ Γ_{84}/Γ

VALUE (units 10^{-4})	EVTS	DOCUMENT ID		TECN	COMMENT
2.2±0.6 OUR AVERAGE Error includes scale factor of 1.4.					
2.0±0.2±0.4	285.5	BRIERE	05	CLEO	$e^+e^- \to \psi(2S) \to 2(\pi^+\pi^-)$
4.2±1.5		TANENBAUM	78	MRK1	e^+e^-

$\Gamma(K^+K^-\pi^+\pi^-\pi^0)/\Gamma_{total}$ Γ_{85}/Γ

VALUE (units 10^{-4})	EVTS	DOCUMENT ID		TECN	COMMENT
12.6±0.9 OUR AVERAGE					
18.9±5.7±0.3	32	[1] AUBERT	07AU	BABR	10.6 $e^+e^- \to K^+K^-\pi^+\pi^-\pi^0\gamma$
11.7±1.0±1.5	597	ABLIKIM	06G	BES2	$\psi(2S) \to K^+K^-\pi^+\pi^-\pi^0$
12.7±0.5±1.0	711.6	BRIERE	05	CLEO	$e^+e^- \to \psi(2S) \to K^+K^-\pi^+\pi^-\pi^0$

[1] AUBERT 07AU reports $[\Gamma(\psi(2S) \to K^+K^-\pi^+\pi^-\pi^0)/\Gamma_{total}] \times [\Gamma(\psi(2S) \to e^+e^-)] = (44 \pm 13 \pm 3)\times10^{-4}$ keV which we divide by our best value $\Gamma(\psi(2S) \to e^+e^-) = 2.33 \pm 0.04$ keV. Our first error is their experiment's error and our second error is the systematic error from using our best value.

$\Gamma(\omega f_0(1710) \to \omega K^+K^-)/\Gamma_{total}$ Γ_{86}/Γ

VALUE (units 10^{-5})	EVTS	DOCUMENT ID		TECN	COMMENT
5.9±2.0±0.9	19	ABLIKIM	06G	BES2	$\psi(2S) \to K^+K^-\pi^+\pi^-\pi^0$

$\Gamma(K^*(892)^0K^-\pi^+\pi^0 + c.c.)/\Gamma_{total}$ Γ_{87}/Γ

VALUE (units 10^{-4})	EVTS	DOCUMENT ID		TECN	COMMENT
8.6±1.3±1.8	238	ABLIKIM	06G	BES2	$\psi(2S) \to K^+K^-\pi^+\pi^-\pi^0$

$\Gamma(K^*(892)^+K^-\pi^+\pi^- + c.c.)/\Gamma_{total}$ Γ_{88}/Γ

VALUE (units 10^{-4})	EVTS	DOCUMENT ID		TECN	COMMENT
9.6±2.2±1.7	133	ABLIKIM	06G	BES2	$\psi(2S) \to K^+K^-\pi^+\pi^-\pi^0$

$\Gamma(K^*(892)^+K^-\rho^0 + c.c.)/\Gamma_{total}$ Γ_{89}/Γ

VALUE (units 10^{-4})	EVTS	DOCUMENT ID		TECN	COMMENT
7.3±2.2±1.4	78	ABLIKIM	06G	BES2	$\psi(2S) \to K^+K^-\pi^+\pi^-\pi^0$

$\Gamma(K^*(892)^0K^-\rho^+ + c.c.)/\Gamma_{total}$ Γ_{90}/Γ

VALUE (units 10^{-4})	EVTS	DOCUMENT ID		TECN	COMMENT
6.1±1.3±1.2	125	ABLIKIM	06G	BES2	$\psi(2S) \to K^+K^-\pi^+\pi^-\pi^0$

$\Gamma(\eta K^+K^-, \text{no } \eta\phi)/\Gamma_{total}$ Γ_{91}/Γ

VALUE (units 10^{-5})	CL%	EVTS	DOCUMENT ID		TECN	COMMENT
3.08±0.29±0.25		0.3k	[1] ABLIKIM	12L	BES3	$\psi(2S) \to K^+K^-\gamma\gamma$
• • • We do not use the following data for averages, fits, limits, etc. • • •						
<13	90		BRIERE	05	CLEO	$e^+e^- \to \psi(2S) \to K^+K^-\pi^+\pi^-\pi^0$

[1] Excluding $\eta\phi$.

$\Gamma(\omega K^+K^-)/\Gamma_{total}$ Γ_{92}/Γ

VALUE (units 10^{-4})	EVTS	DOCUMENT ID		TECN	COMMENT
1.62±0.11 OUR AVERAGE Error includes scale factor of 1.1.					
1.56±0.04±0.11	2.8k	ABLIKIM	14G	BES3	$\psi(2S) \to K^+K^-\pi^+\pi^-\pi^0$
2.38±0.37±0.29	78	ABLIKIM	06G	BES2	$\psi(2S) \to K^+K^-\pi^+\pi^-\pi^0$
1.9 ±0.3 ±0.3	76.8	BRIERE	05	CLEO	$e^+e^- \to \psi(2S) \to K^+K^-\pi^+\pi^-\pi^0$
1.5 ±0.3 ±0.2	23	[1] BAI	03B	BES	$\psi(2S) \to K^+K^-\pi^+\pi^-\pi^0$

[1] Normalized to $B(\psi(2S) \to J/\psi\pi^+\pi^-) = 0.305 \pm 0.016$.

$\Gamma(\omega K^*(892)^+K^- + c.c.)/\Gamma_{total}$ Γ_{93}/Γ

VALUE (units 10^{-5})	EVTS	DOCUMENT ID		TECN	COMMENT
20.7±2.6 OUR AVERAGE					
18.9±2.9±2.2	396	ABLIKIM	13M	BES3	$\psi(2S) \to \omega K^0_S K^-\pi^+$
22.6±3.0±2.4	535	ABLIKIM	13M	BES3	$\psi(2S) \to \omega K^+K^-\pi^0$

$\Gamma(\omega K^*_2(1430)^+K^- + c.c.)/\Gamma_{total}$ Γ_{94}/Γ

VALUE (units 10^{-5})	EVTS	DOCUMENT ID		TECN	COMMENT
6.1 ±1.2 OUR AVERAGE					
6.39±1.50±0.78	128	ABLIKIM	13M	BES3	$\psi(2S) \to \omega K^0_S K^-\pi^+$
5.86±1.61±0.83	143	ABLIKIM	13M	BES3	$\psi(2S) \to \omega K^+K^-\pi^0$

$\Gamma(\omega\overline{K}^*(892)^0K^0)/\Gamma_{total}$ Γ_{95}/Γ

VALUE (units 10^{-5})	EVTS	DOCUMENT ID		TECN	COMMENT
16.8±2.5±1.6	356	ABLIKIM	13M	BES3	$\psi(2S) \to \omega K^0_S K^-\pi^+$

$\Gamma(\omega\overline{K}^*_2(1430)^0K^0)/\Gamma_{total}$ Γ_{96}/Γ

VALUE (units 10^{-5})	EVTS	DOCUMENT ID		TECN	COMMENT
5.82±2.08±0.72	116	ABLIKIM	13M	BES3	$\psi(2S) \to \omega K^0_S K^-\pi^+$

$\Gamma(\omega X(1440) \to \omega K^0_S K^-\pi^+ + c.c.)/\Gamma_{total}$ Γ_{97}/Γ

VALUE (units 10^{-5})	EVTS	DOCUMENT ID		TECN	COMMENT
1.60±0.27±0.24	109	[1] ABLIKIM	13M	BES3	$\psi(2S) \to \omega K^0_S K^-\pi^+$

[1] $X(1440)$ compatible with $\eta(1405)$ and $\eta(1475)$. A $f_1(1420)$ is also possible.

$\Gamma(\omega X(1440) \to \omega K^+K^-\pi^0)/\Gamma_{total}$ Γ_{98}/Γ

VALUE (units 10^{-5})	EVTS	DOCUMENT ID		TECN	COMMENT
1.09±0.20±0.16	82	[1] ABLIKIM	13M	BES3	$\psi(2S) \to \omega K^+K^-\pi^0$

[1] $X(1440)$ compatible with $\eta(1405)$ and $\eta(1475)$. A $f_1(1420)$ is also possible.

$\Gamma(\omega f_1(1285) \to \omega K^0_S K^-\pi^+ + c.c.)/\Gamma_{total}$ Γ_{99}/Γ

VALUE (units 10^{-5})	EVTS	DOCUMENT ID		TECN	COMMENT
0.302±0.098±0.027	22	[1] ABLIKIM	13M	BES3	$\psi(2S) \to \omega K^0_S K^-\pi^+$

[1] Statistical signficance 4.5 σ. This measurement is equivalent to a limit of $< 0.478\times10^{-5}$ at 90% C.L.

$\Gamma(\omega f_1(1285) \to \omega K^+K^-\pi^0)/\Gamma_{total}$ Γ_{100}/Γ

VALUE (units 10^{-5})	EVTS	DOCUMENT ID		TECN	COMMENT
0.125±0.070±0.013	10	[1] ABLIKIM	13M	BES3	$\psi(2S) \to \omega K^+K^-\pi^0$

[1] Statistical signficance 3.2 σ. This measurement is equivalent to a limit of $< 0.221\times10^{-5}$ at 90% C.L.

$\Gamma(3(\pi^+\pi^-))/\Gamma_{total}$ Γ_{101}/Γ

VALUE (units 10^{-4})	EVTS	DOCUMENT ID		TECN	COMMENT
3.5 ±2.0 OUR AVERAGE Error includes scale factor of 2.8.					
5.45±0.42±0.87	671	ABLIKIM	05H	BES2	$e^+e^- \to \psi(2S) \to 3(\pi^+\pi^-)$
1.5 ±1.0		[1] TANENBAUM	78	MRK1	e^+e^-

[1] Assuming entirely strong decay.

$\Gamma(p\overline{p}\pi^+\pi^-\pi^0)/\Gamma_{total}$ Γ_{102}/Γ

VALUE (units 10^{-4})	EVTS	DOCUMENT ID		TECN	COMMENT
7.3±0.4±0.6	434.9	BRIERE	05	CLEO	$e^+e^- \to \psi(2S) \to p\overline{p}\pi^+\pi^-\pi^0$

$\Gamma(K^+K^-)/\Gamma_{total}$ Γ_{103}/Γ

VALUE (units 10^{-5})	CL%	EVTS	DOCUMENT ID		TECN	COMMENT
7.48±0.23±0.39		1.3k	[1] METREVELI	12		$\psi(2S) \to K^+K^-$
• • • We do not use the following data for averages, fits, limits, etc. • • •						
6.2 ±1.5 ±0.2		66	[2,3] LEES	15J	BABR	$e^+e^- \to K^+K^-\gamma$
8.3 ±1.5 ±0.2		66	[3,4] LEES	15J	BABR	$e^+e^- \to K^+K^-\gamma$
6.3 ±0.6 ±0.3			[5] DOBBS	06A	CLEO	e^+e^-
10 ±7			[5] BRANDELIK	79C	DASP	e^+e^-
< 5	90		FELDMAN	77	MRK1	e^+e^-

[1] Obtained by analyzing CLEO-c data but not authored by the CLEO Collaboration.
[2] $\sin\phi > 0$.
[3] Using $\Gamma(\psi(2S) \to e^+e^-) = (2.37 \pm 0.04)$ keV.
[4] $\sin\phi < 0$.
[5] Interference with non-resonant K^+K^- production not taken into account.

$\Gamma(K_S^0 K_L^0)/\Gamma_{total}$ Γ_{104}/Γ

VALUE (units 10^{-5})	EVTS	DOCUMENT ID		TECN	COMMENT
5.34±0.33 OUR AVERAGE					
5.28±0.25±0.34	478 ± 23	[1] METREVELI	12		$\psi(2S) \to K_S^0 K_L^0$
5.8 ±0.8 ±0.4		DOBBS	06A	CLEO	e^+e^-
5.24±0.47±0.48	156 ± 14	[2] BAI	04B	BES2	$\psi(2S) \to K_S^0 K_L^0 \to \pi^+\pi^- X$

[1] Obtained by analyzing CLEO-c data but not authored by the CLEO Collaboration.
[2] Using $B(K_S^0 \to \pi^+\pi^-) = 0.6860 \pm 0.0027$.

$\Gamma(\pi^+\pi^-\pi^0)/\Gamma_{total}$ Γ_{105}/Γ

VALUE (units 10^{-4})	EVTS	DOCUMENT ID		TECN	COMMENT
2.01±0.17 OUR AVERAGE Error includes scale factor of 1.7. See the ideogram below.					
$2.14\pm0.03^{+0.12}_{-0.11}$	7k	[1] ABLIKIM	12H	BES3	$e^+e^- \to \psi(2S)$
1.81±0.18±0.19	260 ± 19	[2] ABLIKIM	05J	BES2	$e^+e^- \to \psi(2S)$
$1.88^{+0.16}_{-0.15}\pm0.28$	194	ADAM	05	CLEO	$e^+e^- \to \psi(2S)$
0.85±0.46	4	FRANKLIN	83	MRK2	$e^+e^- \to$ hadrons

[1] From $\psi(2S) \to \pi^+\pi^-\pi^0$ events directly. The quoted systematic error includes a contribution of 4% (added in quadrature) from the uncertainty on the number of $\psi(2S)$ events.
[2] From a PW analysis of $\psi(2S) \to \pi^+\pi^-\pi^0$.

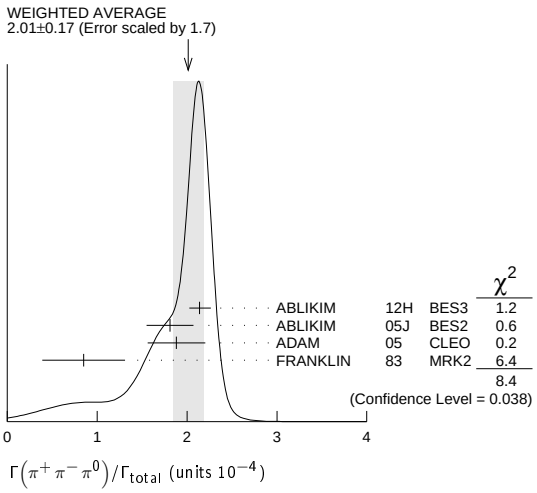

$\Gamma(\rho(2150)\pi \to \pi^+\pi^-\pi^0)/\Gamma_{total}$ Γ_{106}/Γ

VALUE (units 10^{-4})	DOCUMENT ID		TECN	COMMENT
$\mathbf{1.94\pm0.25^{+1.15}_{-0.34}}$	[1] ABLIKIM	05J	BES2	$\psi(2S) \to \rho(2150)\pi \to \pi^+\pi^-\pi^0$

[1] From a PW analysis of $\psi(2S) \to \pi^+\pi^-\pi^0$.

$\Gamma(\rho(770)\pi \to \pi^+\pi^-\pi^0)/\Gamma_{total}$ Γ_{107}/Γ

VALUE (units 10^{-4})	CL%	EVTS	DOCUMENT ID		TECN	COMMENT
0.32±0.12 OUR AVERAGE Error includes scale factor of 1.8.						
0.51±0.07±0.11			[1] ABLIKIM	05J	BES2	$\psi(2S) \to \rho(770)\pi \to \pi^+\pi^-\pi^0$
$0.24^{+0.08}_{-0.07}\pm0.02$		22	ADAM	05	CLEO	$e^+e^- \to \psi(2S)$
• • • We do not use the following data for averages, fits, limits, etc. • • •						
<0.83	90	1	FRANKLIN	83	MRK2	e^+e^-
<10	90		BARTEL	76	CNTR	e^+e^-
<10	90		[2] ABRAMS	75	MRK1	e^+e^-

[1] From a PW analysis of $\psi(2S) \to \pi^+\pi^-\pi^0$.
[2] Final state $\rho^0\pi^0$.

$\Gamma(\pi^+\pi^-)/\Gamma_{total}$ Γ_{108}/Γ

VALUE (units 10^{-5})	CL%	EVTS	DOCUMENT ID		TECN	COMMENT
0.78±0.26 OUR AVERAGE						
0.76±0.25±0.06		30	[1] METREVELI	12		$\psi(2S) \to \pi^+\pi^-$
8 ±5			BRANDELIK	79C	DASP	e^+e^-
• • • We do not use the following data for averages, fits, limits, etc. • • •						
<2.1	90		DOBBS	06A	CLEO	$e^+e^- \to \psi(2S)$
<5	90		FELDMAN	77	MRK1	e^+e^-

[1] Obtained by analyzing CLEO-c data but not authored by the CLEO Collaboration. Using $\psi(3770) \to \pi^+\pi^-$ for continuum subtraction.

$\Gamma(K_1(1400)^\pm K^\mp)/\Gamma_{total}$ Γ_{109}/Γ

VALUE (units 10^{-4})	CL%	DOCUMENT ID		TECN	COMMENT
<3.1	90	[1] BAI	99C	BES	e^+e^-

[1] Assuming $B(K_1(1400) \to K^*\pi)$=0.94 ± 0.06

$\Gamma(K_2^*(1430)^\pm K^\mp)/\Gamma_{total}$ Γ_{110}/Γ

VALUE (units 10^{-5})	EVTS	DOCUMENT ID		TECN	COMMENT
$\mathbf{7.12\pm0.62^{+1.13}_{-0.61}}$	251 ± 22	ABLIKIM	12L	BES3	$e^+e^- \to \psi(2S)$

$\Gamma(K^+K^-\pi^0)/\Gamma_{total}$ Γ_{111}/Γ

VALUE (units 10^{-5})	CL%	EVTS	DOCUMENT ID		TECN	COMMENT
4.07±0.16±0.26		0.9k	ABLIKIM	12L	BES3	$e^+e^- \to \psi(2S)$
• • • We do not use the following data for averages, fits, limits, etc. • • •						
<8.9	90	1	FRANKLIN	83	MRK2	$e^+e^- \to$ hadrons

$\Gamma(K^+K^*(892)^- + \text{c.c.})/\Gamma_{total}$ Γ_{114}/Γ

VALUE (units 10^{-5})	CL%	EVTS	DOCUMENT ID		TECN	COMMENT
2.9 ±0.4 OUR AVERAGE Error includes scale factor of 1.2.						
$3.18\pm0.30^{+0.26}_{-0.31}$		0.2k	ABLIKIM	12L	BES3	$e^+e^- \to \psi(2S)$
$2.9\ ^{+1.3}_{-1.7}\ \pm0.4$		9.6 ± 4.2	ABLIKIM	05I	BES2	$e^+e^- \to \psi(2S)$
$1.3\ ^{+1.0}_{-0.7}\ \pm0.3$		7	ADAM	05	CLEO	$e^+e^- \to \psi(2S)$
• • • We do not use the following data for averages, fits, limits, etc. • • •						
<5.4	90		FRANKLIN	83	MRK2	$e^+e^- \to$ hadrons

$\Gamma(K^*(892)^0\overline{K}{}^0 + \text{c.c.})/\Gamma_{total}$ Γ_{115}/Γ

VALUE (units 10^{-5})	EVTS	DOCUMENT ID		TECN	COMMENT
10.9±2.0 OUR AVERAGE					
$13.3^{+2.4}_{-2.8}\pm1.7$	65.6 ± 9.0	ABLIKIM	05I	BES2	$e^+e^- \to \psi(2S)$
$9.2^{+2.7}_{-2.2}\pm0.9$	25	ADAM	05	CLEO	$e^+e^- \to \psi(2S)$

$\Gamma(K^+K^*(892)^- + \text{c.c.})/\Gamma(K^*(892)^0\overline{K}{}^0 + \text{c.c.})$ $\Gamma_{114}/\Gamma_{115}$

VALUE	DOCUMENT ID		TECN	COMMENT
0.16±0.06 OUR AVERAGE				
$0.22^{+0.10}_{-0.14}$	ABLIKIM	05I	BES2	$e^+e^- \to \psi(2S)$
$0.14^{+0.08}_{-0.06}$	ADAM	05	CLEO	$e^+e^- \to \psi(2S)$

$\Gamma(\phi\pi^+\pi^-)/\Gamma_{total}$ Γ_{116}/Γ

VALUE (units 10^{-4})	EVTS	DOCUMENT ID		TECN	COMMENT
1.18±0.26 OUR AVERAGE Error includes scale factor of 1.5. See the ideogram below.					
2.3 ±0.8 ±0.1	19 ± 6	LEES	12F	BABR	10.6 $e^+e^- \to \pi^+\pi^- K^+K^-\gamma$
0.9 ±0.2 ±0.1	47.6	BRIERE	05	CLEO	$e^+e^- \to \psi(2S) \to K^+K^-\pi^+\pi^-$
1.5 ±0.2 ±0.2	51.5 ± 8.3	[1] BAI	03B	BES	$\psi(2S) \to K^+K^-\pi^+\pi^-$
• • • We do not use the following data for averages, fits, limits, etc. • • •					
2.44±0.96±0.04	10 ± 4	[2,3] AUBERT	07AK	BABR	10.6 $e^+e^- \to \pi^+\pi^- K^+K^-\gamma$

[1] Normalized to $B(\psi(2S) \to J/\psi\pi^+\pi^-) = 0.305 \pm 0.016$.
[2] Superseded by LEES 12F. AUBERT 07AK reports $[\Gamma(\psi(2S) \to \phi\pi^+\pi^-)/\Gamma_{total}] \times [\Gamma(\psi(2S) \to e^+e^-)] = (0.57 \pm 0.22 \pm 0.04) \times 10^{-3}$ keV which we divide by our best value $\Gamma(\psi(2S) \to e^+e^-) = 2.33 \pm 0.04$ keV. Our first error is their experiment's error and our second error is the systematic error from using our best value.
[3] Using $B(\phi \to K^+K^-) = (49.3 \pm 0.6)\%$.

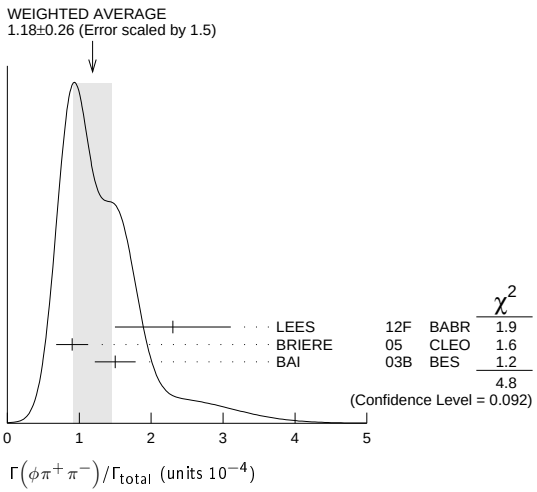

$\Gamma(\phi f_0(980) \to \pi^+\pi^-)/\Gamma_{total}$ Γ_{117}/Γ

VALUE (units 10^{-4})	EVTS	DOCUMENT ID		TECN	COMMENT
0.75±0.33 OUR AVERAGE Error includes scale factor of 1.6.					
1.5 ±0.5 ±0.1	12 ± 4	LEES	12F	BABR	10.6 $e^+e^- \to \pi^+\pi^- K^+K^-\gamma$
0.6 ±0.2 ±0.1	18.4 ± 6.4	[1] BAI	03B	BES	$\psi(2S) \to K^+K^-\pi^+\pi^-$

• • • We do not use the following data for averages, fits, limits, etc. • • •

1.46±0.71±0.02	6 ± 3	[2,3] AUBERT	07AK	BABR	10.6 $e^+e^- \to \pi^+\pi^- K^+ K^- \gamma$

[1] Normalized to B($\psi(2S) \to J/\psi\pi^+\pi^-$) = 0.305 ± 0.016.
[2] Superseded by LEES 12F. AUBERT 07AK reports [$\Gamma(\psi(2S) \to \phi f_0(980) \to \pi^+\pi^-)/\Gamma_{total}$] × [$\Gamma(\psi(2S) \to e^+e^-)$] = (0.34 ± 0.16 ± 0.04) × 10^{-3} keV which we divide by our best value $\Gamma(\psi(2S) \to e^+e^-)$ = 2.33 ± 0.04 keV. Our first error is their experiment's error and our second error is the systematic error from using our best value.
[3] Using B($\phi \to K^+K^-$) = (49.3 ± 0.6)%.

$\Gamma(2(K^+K^-))/\Gamma_{total}$ Γ_{118}/Γ

VALUE (units 10^{-4})	EVTS	DOCUMENT ID		TECN	COMMENT
0.63±0.13 OUR AVERAGE					
0.9 ±0.4 ±0.1	13	LEES	12F	BABR	10.6 $e^+e^- \to 2(K^+K^-)\gamma$
0.6 ±0.1 ±0.1	59.2	BRIERE	05	CLEO	$e^+e^- \to \psi(2S) \to 2(K^+K^-)$

$\Gamma(\phi K^+K^-)/\Gamma_{total}$ Γ_{119}/Γ

VALUE (units 10^{-4})	EVTS	DOCUMENT ID		TECN	COMMENT
0.70±0.16 OUR AVERAGE					
0.8 ±0.2 ±0.1	36.8	BRIERE	05	CLEO	$e^+e^- \to \psi(2S) \to 2(K^+K^-)$
0.6 ±0.2 ±0.1	16.1 ± 5.0	[1] BAI	03B	BES	$\psi(2S) \to 2(K^+K^-)$

[1] Normalized to B($\psi(2S) \to J/\psi\pi^+\pi^-$) = 0.305 ± 0.016.

$\Gamma(2(K^+K^-)\pi^0)/\Gamma_{total}$ Γ_{120}/Γ

VALUE (units 10^{-4})	EVTS	DOCUMENT ID	TECN	COMMENT
1.1±0.2±0.2	44.7	BRIERE 05	CLEO	$e^+e^- \to \psi(2S) \to 2(K^+K^-)\pi^0$

$\Gamma(\phi\eta)/\Gamma_{total}$ Γ_{121}/Γ

VALUE (units 10^{-5})	EVTS	DOCUMENT ID		TECN	COMMENT
3.10±0.31 OUR AVERAGE					
3.14±0.23±0.23	0.2k	ABLIKIM	12L	BES3	$e^+e^- \to \psi(2S)$
2.0 $^{+1.5}_{-1.1}$ ±0.4	6	ADAM	05	CLEO	$e^+e^- \to \psi(2S)$
3.3 ±1.1 ±0.5	17	ABLIKIM	04K	BES	$e^+e^- \to \psi(2S)$

$\Gamma(\phi\eta')/\Gamma_{total}$ Γ_{122}/Γ

VALUE (units 10^{-5})	EVTS	DOCUMENT ID		TECN	COMMENT
3.1±1.4±0.7	8	[1] ABLIKIM	04K	BES	$e^+e^- \to \psi(2S)$

[1] Calculated combining $\eta' \to \gamma\rho$ and $\eta\pi^+\pi^-$ channels.

$\Gamma(\omega\eta')/\Gamma_{total}$ Γ_{123}/Γ

VALUE (units 10^{-5})	EVTS	DOCUMENT ID		TECN	COMMENT
3.2 $^{+2.4}_{-2.0}$ ±0.7	4	[1] ABLIKIM	04K	BES	$e^+e^- \to \psi(2S)$

[1] Calculated combining $\eta' \to \gamma\rho$ and $\eta\pi^+\pi^-$ channels.

$\Gamma(\omega\pi^0)/\Gamma_{total}$ Γ_{124}/Γ

VALUE (units 10^{-5})	EVTS	DOCUMENT ID		TECN	COMMENT
2.1 ±0.6 OUR AVERAGE					
2.5 $^{+1.2}_{-1.0}$ ±0.2	14	ADAM	05	CLEO	$e^+e^- \to \psi(2S)$
1.87 $^{+0.68}_{-0.62}$ ±0.28	14	ABLIKIM	04L	BES	$e^+e^- \to \psi(2S)$

$\Gamma(\rho\eta')/\Gamma_{total}$ Γ_{125}/Γ

VALUE (units 10^{-5})	EVTS	DOCUMENT ID		TECN	COMMENT
1.87 $^{+1.64}_{-1.11}$ ±0.33	2	ABLIKIM	04L	BES	$e^+e^- \to \psi(2S)$

• • • We do not use the following data for averages, fits, limits, etc. • • •

1.02 ±0.11 ±0.24	143	[1] ABLIKIM	17AK	BES3	$e^+e^- \to \psi(2S)$
0.569±0.128±0.236	80	[2] ABLIKIM	17AK	BES3	$e^+e^- \to \psi(2S)$

[1] Destructive-interference solution of a partial wave analysis of the decay $\psi(2S) \to \pi^+\pi^-\eta'$.
[2] Constructive-interference solution of a partial wave analysis of the decay $\psi(2S) \to \pi^+\pi^-\eta'$.

$\Gamma(\rho\eta)/\Gamma_{total}$ Γ_{126}/Γ

VALUE (units 10^{-5})	EVTS	DOCUMENT ID		TECN	COMMENT
2.2 ±0.6 OUR AVERAGE Error includes scale factor of 1.1.					
3.0 $^{+1.1}_{-0.9}$ ±0.2	18	ADAM	05	CLEO	$e^+e^- \to \psi(2S)$
1.78 $^{+0.67}_{-0.62}$ ±0.17	13	ABLIKIM	04L	BES	$e^+e^- \to \psi(2S)$

$\Gamma(\omega\eta)/\Gamma_{total}$ Γ_{127}/Γ

VALUE (units 10^{-5})	CL%	DOCUMENT ID		TECN	COMMENT
<1.1	90	ADAM	05	CLEO	$e^+e^- \to \psi(2S)$

• • • We do not use the following data for averages, fits, limits, etc. • • •

<3.1	90	ABLIKIM	04K	BES	$e^+e^- \to \psi(2S)$

$\Gamma(\phi\pi^0)/\Gamma_{total}$ Γ_{128}/Γ

VALUE (units 10^{-5})	CL%	DOCUMENT ID		TECN	COMMENT
<0.04	90	ABLIKIM	12L	BES3	$e^+e^- \to \psi(2S)$

• • • We do not use the following data for averages, fits, limits, etc. • • •

<0.7	90	ADAM	05	CLEO	$e^+e^- \to \psi(2S)$
<0.4	90	ABLIKIM	04K	BES	$e^+e^- \to \psi(2S)$

$\Gamma(\eta_c\pi^+\pi^-\pi^0)/\Gamma_{total}$ Γ_{129}/Γ

VALUE (units 10^{-3})	CL%	DOCUMENT ID		TECN	COMMENT
<1.0	90	PEDLAR	07	CLEO	$e^+e^- \to \psi(2S)$

$\Gamma(p\overline{p}K^+K^-)/\Gamma_{total}$ Γ_{130}/Γ

VALUE (units 10^{-5})	EVTS	DOCUMENT ID		TECN	COMMENT
2.7±0.6±0.4	30.1	BRIERE	05	CLEO	$e^+e^- \to \psi(2S) \to p\overline{p}K^+K^-$

$\Gamma(\overline{\Lambda}nK^0_S + \text{c.c.})/\Gamma_{total}$ Γ_{131}/Γ

VALUE (units 10^{-4})	EVTS	DOCUMENT ID		TECN	COMMENT
0.81±0.11±0.14	50	[1] ABLIKIM	08C	BES2	$e^+e^- \to J/\psi$

[1] Using B($\overline{\Lambda} \to \overline{p}\pi^+$) = 63.9% and B($K^0_S \to \pi^+\pi^-$) = 69.2%.

$\Gamma(\phi f'_2(1525))/\Gamma_{total}$ Γ_{132}/Γ

VALUE (units 10^{-4})	CL%	EVTS	DOCUMENT ID		TECN	COMMENT
0.44±0.12±0.11		20 ± 6	BAI	04C		$\psi(2S) \to 2(K^+K^-)$

• • • We do not use the following data for averages, fits, limits, etc. • • •

<0.45	90		BAI	98J	BES	$e^+e^- \to 2(K^+K^-)$

$\Gamma(\Theta(1540)\overline{\Theta}(1540) \to K^0_S pK^-\overline{n} + \text{c.c.})/\Gamma_{total}$ Γ_{133}/Γ

VALUE (units 10^{-5})	CL%	DOCUMENT ID		TECN	COMMENT
<0.88	90	BAI	04G	BES2	e^+e^-

$\Gamma(\Theta(1540)K^-\overline{n} \to K^0_S pK^-\overline{n})/\Gamma_{total}$ Γ_{134}/Γ

VALUE (units 10^{-5})	CL%	DOCUMENT ID		TECN	COMMENT
<1.0	90	BAI	04G	BES2	e^+e^-

$\Gamma(\Theta(1540)K^0_S\overline{p} \to K^0_S\overline{p}K^+n)/\Gamma_{total}$ Γ_{135}/Γ

VALUE (units 10^{-5})	CL%	DOCUMENT ID		TECN	COMMENT
<0.70	90	BAI	04G	BES2	e^+e^-

$\Gamma(\overline{\Theta}(1540)K^+n \to K^0_S\overline{p}K^+n)/\Gamma_{total}$ Γ_{136}/Γ

VALUE (units 10^{-5})	CL%	DOCUMENT ID		TECN	COMMENT
<2.6	90	BAI	04G	BES2	e^+e^-

$\Gamma(\overline{\Theta}(1540)K^0_S p \to K^0_S pK^-\overline{n})/\Gamma_{total}$ Γ_{137}/Γ

VALUE (units 10^{-5})	CL%	DOCUMENT ID		TECN	COMMENT
<0.60	90	BAI	04G	BES2	e^+e^-

$\Gamma(K^0_S K^0_S)/\Gamma_{total}$ Γ_{138}/Γ

VALUE (units 10^{-4})	DOCUMENT ID		TECN	COMMENT
<0.046	[1] BAI	04D	BES	e^+e^-

[1] Forbidden by *CP*.

RADIATIVE DECAYS

$\Gamma(\gamma\chi_{c0}(1P))/\Gamma_{total}$ Γ_{139}/Γ

VALUE (units 10^{-2})	EVTS	DOCUMENT ID		TECN	COMMENT
9.79 ±0.20 OUR FIT					
9.33 ±0.26 OUR AVERAGE					
9.389±0.014±0.332	4.7M	ABLIKIM	17U	BES3	$e^+e^- \to \gamma X$
9.22 ±0.11 ±0.46	72k	ATHAR	04	CLEO	$e^+e^- \to \gamma X$
9.9 ±0.5 ±0.8		[1] GAISER	86	CBAL	$e^+e^- \to \gamma X$
7.2 ±2.3		[1] BIDDICK	77	CNTR	$e^+e^- \to \gamma X$
7.5 ±2.6		[1] WHITAKER	76	MRK1	e^+e^-

[1] Angular distribution (1+$\cos^2\theta$) assumed.

$\Gamma(\gamma\chi_{c1}(1P))/\Gamma_{total}$ Γ_{140}/Γ

VALUE (units 10^{-2})	EVTS	DOCUMENT ID		TECN	COMMENT
9.75 ±0.24 OUR FIT					
9.54 ±0.29 OUR AVERAGE					
9.905±0.011±0.353	5.0M	ABLIKIM	17U	BES3	$e^+e^- \to \gamma X$
9.07 ±0.11 ±0.54	76k	ATHAR	04	CLEO	$e^+e^- \to \gamma X$
9.0 ±0.5 ±0.7		[1] GAISER	86	CBAL	$e^+e^- \to \gamma X$
7.1 ±1.9		[2] BIDDICK	77	CNTR	$e^+e^- \to \gamma X$

[1] Angular distribution (1−0.189 $\cos^2\theta$) assumed.
[2] Valid for isotropic distribution of the photon.

$\Gamma(\gamma\chi_{c2}(1P))/\Gamma_{total}$ Γ_{141}/Γ

VALUE (units 10^{-2})	EVTS	DOCUMENT ID		TECN	COMMENT
9.52 ±0.20 OUR FIT					
9.42 ±0.31 OUR AVERAGE		Error includes scale factor of 1.3. See the ideogram below.			
9.621±0.013±0.272	4.2M	ABLIKIM	17U	BES3	$e^+e^- \to \gamma X$
9.33 ±0.14 ±0.61	79k	ATHAR	04	CLEO	$e^+e^- \to \gamma X$
8.0 ±0.5 ±0.7		[1] GAISER	86	CBAL	$e^+e^- \to \gamma X$
7.0 ±2.0		[2] BIDDICK	77	CNTR	$e^+e^- \to \gamma X$

[1] Angular distribution $(1-0.052\cos^2\theta)$ assumed.
[2] Valid for isotropic distribution of the photon.

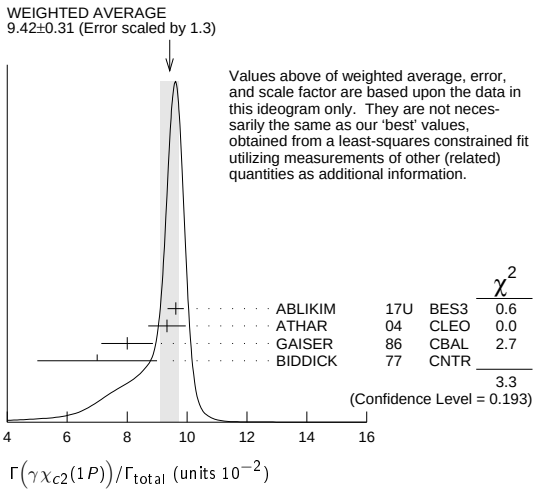

$[\Gamma(\gamma\chi_{c0}(1P)) + \Gamma(\gamma\chi_{c1}(1P)) + \Gamma(\gamma\chi_{c2}(1P))]/\Gamma_{total}$ $(\Gamma_{139}+\Gamma_{140}+\Gamma_{141})/\Gamma$

VALUE	DOCUMENT ID		TECN	COMMENT
• • • We do not use the following data for averages, fits, limits, etc. • • •				
27.6±0.3±2.0	[1] ATHAR	04	CLEO	$e^+e^- \to \gamma X$

[1] Not independent from ATHAR 04 measurements of $B(\gamma\chi_{cJ})$.

$\Gamma(\gamma\chi_{c0}(1P))/\Gamma(\gamma\chi_{c1}(1P))$ $\Gamma_{139}/\Gamma_{140}$

VALUE	DOCUMENT ID		TECN	COMMENT
• • • We do not use the following data for averages, fits, limits, etc. • • •				
1.02±0.01±0.07	[1] ATHAR	04	CLEO	$e^+e^- \to \gamma X$

[1] Not independent from ATHAR 04 measurements of $B(\gamma\chi_{cJ})$.

$\Gamma(\gamma\chi_{c2}(1P))/\Gamma(\gamma\chi_{c1}(1P))$ $\Gamma_{141}/\Gamma_{140}$

VALUE	DOCUMENT ID		TECN	COMMENT
• • • We do not use the following data for averages, fits, limits, etc. • • •				
1.03±0.02±0.03	[1] ATHAR	04	CLEO	$e^+e^- \to \gamma X$

[1] Not independent from ATHAR 04 measurements of $B(\gamma\chi_{cJ})$.

$\Gamma(\gamma\chi_{c0}(1P))/\Gamma(\gamma\chi_{c2}(1P))$ $\Gamma_{139}/\Gamma_{141}$

VALUE	DOCUMENT ID		TECN	COMMENT
• • • We do not use the following data for averages, fits, limits, etc. • • •				
0.99±0.02±0.08	[1] ATHAR	04	CLEO	$e^+e^- \to \gamma X$

[1] Not independent from ATHAR 04 measurements of $B(\gamma\chi_{cJ})$.

$\Gamma(\gamma\eta_c(1S))/\Gamma_{total}$ Γ_{142}/Γ

VALUE (units 10^{-2})	EVTS	DOCUMENT ID		TECN	COMMENT
0.34 ±0.05 OUR AVERAGE		Error includes scale factor of 1.3. See the ideogram below.			
0.432±0.016±0.060		MITCHELL	09	CLEO	$e^+e^- \to \gamma X$
0.32 ±0.04 ±0.06	2.5k	[1] ATHAR	04	CLEO	$e^+e^- \to \gamma X$
0.28 ±0.06		[2] GAISER	86	CBAL	$e^+e^- \to \gamma X$

[1] ATHAR 04 used $\Gamma_{\eta_c(1S)} = 24.8 \pm 4.9$ MeV to obtain this result.
[2] GAISER 86 used $\Gamma_{\eta_c(1S)} = 11.5 \pm 4.5$ MeV to obtain this result.

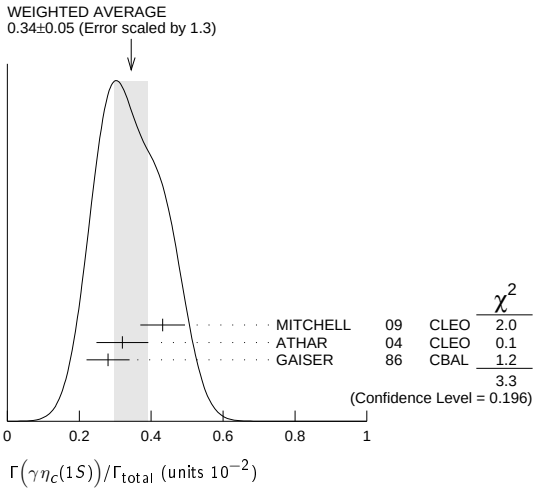

$\Gamma(\gamma\eta_c(2S))/\Gamma_{total}$ Γ_{143}/Γ

VALUE (units 10^{-4})	CL%	DOCUMENT ID		TECN	COMMENT
7±2±4		[1] ABLIKIM	12G	BES3	$\psi(2S) \to \gamma K^0 K\pi,\ KK\pi^0$
• • • We do not use the following data for averages, fits, limits, etc. • • •					
< 8	90	[2] CRONIN-HEN..10		CLEO	$\psi(2S) \to \gamma K\overline{K}\pi$
<20	90	ATHAR	04	CLEO	$e^+e^- \to \gamma X$
20–130	95	EDWARDS	82C	CBAL	$e^+e^- \to \gamma X$

[1] ABLIKIM 12G reports $[\Gamma(\psi(2S) \to \gamma\eta_c(2S))/\Gamma_{total}] \times [B(\eta_c(2S) \to K\overline{K}\pi)] = (1.30 \pm 0.20 \pm 0.30) \times 10^{-5}$ which we divide by our best value $B(\eta_c(2S) \to K\overline{K}\pi) = (1.9 \pm 1.2) \times 10^{-2}$. Our first error is their experiment's error and our second error is the systematic error from using our best value.
[2] CRONIN-HENNESSY 10 reports $[\Gamma(\psi(2S) \to \gamma\eta_c(2S))/\Gamma_{total}] \times [B(\eta_c(2S) \to K\overline{K}\pi)] < 14.5 \times 10^{-6}$ which we divide by our best value $B(\eta_c(2S) \to K\overline{K}\pi) = 1.9 \times 10^{-2}$. This measurement assumes $\Gamma(\eta_c(2S)) = 14$ MeV. CRONIN-HENNESSY 10 gives the analytic dependence of limits on width.

$\Gamma(\gamma\pi^0)/\Gamma_{total}$ Γ_{144}/Γ

VALUE (units 10^{-6})	CL%	EVTS	DOCUMENT ID		TECN	COMMENT
1.04±0.22 OUR AVERAGE			Error includes scale factor of 1.4.			
0.95±0.16±0.05		423	ABLIKIM	17X	BES3	$\psi(2S) \to \gamma\pi^0$
1.58±0.40±0.13		37	ABLIKIM	10F	BES3	$\psi(2S) \to \gamma\pi^0$
• • • We do not use the following data for averages, fits, limits, etc. • • •						
< 5	90		PEDLAR	09	CLE3	$\psi(2S) \to \gamma X$
<5400	95		[1] LIBERMAN	75	SPEC	e^+e^-
$< 1 \times 10^4$	90		WIIK	75	DASP	e^+e^-

[1] Restated by us using $B(\psi(2S) \to \mu^+\mu^-) = 0.0077$.

$\Gamma(\gamma\eta'(958))/\Gamma_{total}$ Γ_{145}/Γ

VALUE (units 10^{-4})	CL%	EVTS	DOCUMENT ID		TECN	COMMENT
1.24 ±0.04 OUR AVERAGE						
1.251±0.022±0.062		56K	ABLIKIM	17X	BES3	$\psi(2S) \to \gamma\pi^+\pi^-\eta,\ \gamma\pi^0\pi^0\eta$
1.26 ±0.03 ±0.08		2226	[1] ABLIKIM	10F	BES3	$\psi(2S) \to 3\gamma\pi^+\pi^-,\ 2\gamma\pi^+\pi^-$
1.19 ±0.08 ±0.03			PEDLAR	09	CLE3	$\psi(2S) \to \gamma X$
1.24 ±0.27 ±0.15		23	ABLIKIM	06R	BES2	$e^+e^- \to \psi(2S)$
1.54 ±0.31 ±0.20		~ 43	BAI	98F	BES	$\psi(2S) \to \pi^+\pi^-2\gamma,\ \pi^+\pi^-3\gamma$
• • • We do not use the following data for averages, fits, limits, etc. • • •						
< 60	90		[2] BRAUNSCH...	77	DASP	e^+e^-
< 11	90		[3] BARTEL	76	CNTR	e^+e^-

[1] Combining the results from $\eta' \to \pi^+\pi^-\eta$ and $\eta' \to \pi^+\pi^-\gamma$ decay modes.
[2] Restated by us using total decay width 228 keV.
[3] The value is normalized to the branching ratio for $\Gamma(J/\psi(1S)\eta)/\Gamma_{total}$.

$\Gamma(\gamma f_2(1270))/\Gamma_{total}$ Γ_{146}/Γ

VALUE (units 10^{-4})	EVTS	DOCUMENT ID		TECN	COMMENT
$2.73^{+0.29}_{-0.25}$ OUR AVERAGE		Error includes scale factor of 1.8.			
$2.84\pm0.15^{+0.03}_{-0.10}$	1.9k	[1,2] DOBBS	15		$\psi(2S) \to \gamma\pi\pi$
2.12±0.19±0.32		[3,4] BAI	03C	BES	$\psi(2S) \to \gamma\pi\pi$
• • • We do not use the following data for averages, fits, limits, etc. • • •					
2.08±0.19±0.33	200.6 ± 18.8	[3] BAI	03C	BES	$\psi(2S) \to \gamma\pi^+\pi^-$
2.90±1.08±1.07	29.9 ± 11.1	[3] BAI	03C	BES	$\psi(2S) \to \gamma\pi^0\pi^0$

[1] Using CLEO-c data but not authored by the CLEO Collaboration.
[2] DOBBS 15 reports $[\Gamma(\psi(2S) \to \gamma f_2(1270))/\Gamma_{total}] \times [B(f_2(1270) \to \pi\pi)] = (2.39 \pm 0.09 \pm 0.09) \times 10^{-4}$ which we divide by our best value $B(f_2(1270) \to \pi\pi) =$

$(84.2^{+2.9}_{-0.9}) \times 10^{-2}$. Our first error is their experiment's error and our second error is the systematic error from using our best value.
[3] Normalized to B($\psi(2S) \to J/\psi\pi^+\pi^-$) = 0.305 ± 0.016.
[4] Combining the results from $\pi^+\pi^-$ and $\pi^0\pi^0$ decay modes.

$\Gamma(\gamma f_0(1370) \to \gamma K\overline{K})/\Gamma_{total}$ Γ_{147}/Γ

VALUE (units 10^{-5})	EVTS	DOCUMENT ID		COMMENT
3.1±1.0±1.4	175	[1] DOBBS	15	$\psi(2S) \to \gamma K\overline{K}$

[1] Using CLEO-c data but not authored by the CLEO Collaboration.

$\Gamma(\gamma f_0(1500))/\Gamma_{total}$ Γ_{148}/Γ

VALUE (units 10^{-5})	EVTS	DOCUMENT ID		COMMENT
9.2±1.8±0.6	274	[1,2] DOBBS	15	$\psi(2S) \to \gamma\pi\pi$

[1] DOBBS 15 reports $[\Gamma(\psi(2S) \to \gamma f_0(1500))/\Gamma_{total}] \times [B(f_0(1500) \to \pi\pi)] = (3.2 \pm 0.6 \pm 0.2) \times 10^{-5}$ which we divide by our best value $B(f_0(1500) \to \pi\pi) = (34.9 \pm 2.3) \times 10^{-2}$. Our first error is their experiment's error and our second error is the systematic error from using our best value.
[2] Using CLEO-c data but not authored by the CLEO Collaboration.

$\Gamma(\gamma f_2'(1525))/\Gamma_{total}$ Γ_{149}/Γ

VALUE (units 10^{-5})	EVTS	DOCUMENT ID		COMMENT
3.3±0.8±0.1	136	[1,2] DOBBS	15	$\psi(2S) \to \gamma K\overline{K}$

[1] DOBBS 15 reports $[\Gamma(\psi(2S) \to \gamma f_2'(1525))/\Gamma_{total}] \times [B(f_2'(1525) \to K\overline{K})] = (2.9 \pm 0.6 \pm 0.3) \times 10^{-5}$ which we divide by our best value $B(f_2'(1525) \to K\overline{K}) = (88.7 \pm 2.2) \times 10^{-2}$. Our first error is their experiment's error and our second error is the systematic error from using our best value.
[2] Using CLEO-c data but not authored by the CLEO Collaboration.

$\Gamma(\gamma f_0(1710) \to \gamma\pi\pi)/\Gamma_{total}$ Γ_{151}/Γ

VALUE (units 10^{-5})	EVTS	DOCUMENT ID		TECN	COMMENT
3.5 ±0.6 OUR AVERAGE					
3.6 ±0.4 ±0.5	290	[1] DOBBS	15		$\psi(2S) \to \gamma\pi\pi$
3.01±0.41±1.24	35.6 ± 4.8	[2] BAI	03C	BES	$\psi(2S) \to \gamma\pi^+\pi^-$

[1] Using CLEO-c data but not authored by the CLEO Collaboration.
[2] Normalized to B($\psi(2S) \to J/\psi\pi^+\pi^-$) = 0.305 ± 0.016.

$\Gamma(\gamma f_0(1710) \to \gamma K\overline{K})/\Gamma_{total}$ Γ_{152}/Γ

VALUE (units 10^{-5})	CL%	EVTS	DOCUMENT ID		TECN	COMMENT
6.6 ±0.7 OUR AVERAGE						
6.7 ±0.6 ±0.6		375	[1] DOBBS	15		$\psi(2S) \to \gamma K\overline{K}$
6.04±0.90±1.32		39.6±5.9	[2,3] BAI	03C	BES	$\psi(2S) \to \gamma K^+K^-$
• • • We do not use the following data for averages, fits, limits, etc. • • •						
< 15.6	90	6.8 ± 3.1	[2,3] BAI	03C	BES	$\psi(2S) \to \gamma K^0_S K^0_S$

[1] Using CLEO-c data but not authored by the CLEO Collaboration.
[2] Includes unknown branching fractions to K^+K^- or $K^0_S K^0_S$. We have multiplied the K^+K^- result by a factor of 2 and the $K^0_S K^0_S$ result by a factor of 4 to obtain the $K\overline{K}$ result.
[3] Normalized to B($\psi(2S) \to J/\psi\pi^+\pi^-$) = 0.305 ± 0.016.

$\Gamma(\gamma f_0(2100) \to \gamma\pi\pi)/\Gamma_{total}$ Γ_{153}/Γ

VALUE (units 10^{-6})	EVTS	DOCUMENT ID		COMMENT
4.8±0.5±0.9	373	[1] DOBBS	15	$\psi(2S) \to \gamma\pi\pi$

[1] Using CLEO-c data but not authored by the CLEO Collaboration.

$\Gamma(\gamma f_0(2200) \to \gamma K\overline{K})/\Gamma_{total}$ Γ_{154}/Γ

VALUE (units 10^{-6})	EVTS	DOCUMENT ID		COMMENT
3.2±0.6±0.8	207	[1] DOBBS	15	$\psi(2S) \to \gamma K\overline{K}$

[1] Using CLEO-c data but not authored by the CLEO Collaboration.

$\Gamma(\gamma f_J(2220) \to \gamma\pi\pi)/\Gamma_{total}$ Γ_{155}/Γ

VALUE	CL%	DOCUMENT ID		COMMENT
<5.8 × 10^{-6}	90	[1,2] DOBBS	15	$\psi(2S) \to \gamma\pi\pi$

[1] Using CLEO-c data but not authored by the CLEO Collaboration.
[2] For Γ = 20/50 MeV, the 90% CL upper limits for $\pi^+\pi^-$ and $\pi^0\pi^0$ are $3.2/4.3 \times 10^{-6}$ and $2.6/4.0 \times 10^{-6}$, respectively.

$\Gamma(\gamma f_J(2220) \to \gamma K\overline{K})/\Gamma_{total}$ Γ_{156}/Γ

VALUE	CL%	DOCUMENT ID		COMMENT
<9.5 × 10^{-6}	90	[1,2] DOBBS	15	$\psi(2S) \to \gamma K\overline{K}$

[1] Using CLEO-c data but not authored by the CLEO Collaboration.
[2] For Γ = 20/50 MeV, the 90% CL upper limits for K^+K^- and $K^0_S K^0_S$ are $2.1/4.3 \times 10^{-6}$ and $3.7/5.5 \times 10^{-6}$, respectively.

$\Gamma(\gamma\eta)/\Gamma_{total}$ Γ_{158}/Γ

VALUE (units 10^{-6})	CL%	EVTS	DOCUMENT ID		TECN	COMMENT
0.92±0.18 OUR AVERAGE						
0.85±0.18±0.04		382	[1] ABLIKIM	17X	BES3	$\psi(2S) \to \gamma\pi^+\pi^-\pi^0$, $\gamma 3\pi^0$
1.38±0.48±0.09		13	[1] ABLIKIM	10F	BES3	$\psi(2S) \to \gamma\pi^+\pi^-\pi^0$, $\gamma 3\pi^0$
• • • We do not use the following data for averages, fits, limits, etc. • • •						
< 2	90		PEDLAR	09	CLE3	$\psi(2S) \to \gamma X$
< 90	90		BAI	98F	BES	$\psi(2S) \to \pi^+\pi^- 3\gamma$
<200	90		YAMADA	77	DASP	$e^+e^- \to 3\gamma$

[1] Combining the results from $\eta \to \pi^+\pi^-\pi^0$ and $\eta \to 3\pi^0$ decay modes.

$\Gamma(\gamma\eta\pi^+\pi^-)/\Gamma_{total}$ Γ_{159}/Γ

VALUE (units 10^{-4})	EVTS	DOCUMENT ID		TECN	COMMENT
8.71±1.25±1.64	418	ABLIKIM	06R	BES2	$\psi(2S) \to \gamma\eta\pi^+\pi^-$

$\Gamma(\gamma\eta(1405) \to \gamma K\overline{K}\pi)/\Gamma_{total}$ Γ_{161}/Γ

VALUE (units 10^{-4})	CL%	DOCUMENT ID		TECN	COMMENT
<0.9	90	ABLIKIM	06R	BES2	$\psi(2S) \to \gamma K^0_S K^+\pi^- +$ c.c.
• • • We do not use the following data for averages, fits, limits, etc. • • •					
<1.3	90	ABLIKIM	06R	BES2	$\psi(2S) \to \gamma K^+K^-\pi^0$
<1.2	90	[1] SCHARRE	80	MRK1	e^+e^-

[1] Includes unknown branching fraction $\eta(1405) \to K\overline{K}\pi$.

$\Gamma(\gamma\eta(1405) \to \eta\pi^+\pi^-)/\Gamma_{total}$ Γ_{162}/Γ

VALUE (units 10^{-4})	EVTS	DOCUMENT ID		TECN	COMMENT
0.36±0.25±0.05	10	ABLIKIM	06R	BES2	$\psi(2S) \to \gamma\eta\pi^+\pi^-$

$\Gamma(\gamma\eta(1405) \to \gamma f_0(980)\pi^0 \to \gamma\pi^+\pi^-\pi^0)/\Gamma_{total}$ Γ_{163}/Γ

VALUE	CL%	DOCUMENT ID		TECN	COMMENT
<5.0 × 10^{-7}	90	ABLIKIM	17AJ	BES3	$\psi(2S) \to \gamma\pi^+\pi^-\pi^0$

$\Gamma(\gamma\eta(1475) \to K\overline{K}\pi)/\Gamma_{total}$ Γ_{165}/Γ

VALUE (units 10^{-4})	CL%	DOCUMENT ID		TECN	COMMENT
<1.4	90	ABLIKIM	06R	BES2	$\psi(2S) \to \gamma K^+K^-\pi^0$
• • • We do not use the following data for averages, fits, limits, etc. • • •					
<1.5	90	ABLIKIM	06R	BES2	$\psi(2S) \to \gamma K^0_S K^+\pi^- +$ c.c.

$\Gamma(\gamma\eta(1475) \to \eta\pi^+\pi^-)/\Gamma_{total}$ Γ_{166}/Γ

VALUE (units 10^{-4})	CL%	DOCUMENT ID		TECN	COMMENT
<0.88	90	ABLIKIM	06R	BES2	$\psi(2S) \to \gamma\eta\pi^+\pi^-$

$\Gamma(\gamma 2(\pi^+\pi^-))/\Gamma_{total}$ Γ_{167}/Γ

VALUE (units 10^{-5})	EVTS	DOCUMENT ID		TECN	COMMENT
39.6±2.8±5.0	583	ABLIKIM	07D	BES2	$e^+e^- \to \psi(2S)$

$\Gamma(\gamma K^{*0}K^+\pi^- +$ c.c.$)/\Gamma_{total}$ Γ_{168}/Γ

VALUE (units 10^{-5})	EVTS	DOCUMENT ID		TECN	COMMENT
37.0±6.1±7.2	237	ABLIKIM	07D	BES2	$e^+e^- \to \psi(2S)$

$\Gamma(\gamma K^{*0}\overline{K}^{*0})/\Gamma_{total}$ Γ_{169}/Γ

VALUE (units 10^{-5})	EVTS	DOCUMENT ID		TECN	COMMENT
24.0±4.5±5.0	41	ABLIKIM	07D	BES2	$e^+e^- \to \psi(2S)$

$\Gamma(\gamma K^0_S K^+\pi^-$ + c.c.$)/\Gamma_{total}$ Γ_{170}/Γ

VALUE (units 10^{-5})	EVTS	DOCUMENT ID		TECN	COMMENT
25.6±3.6±3.6	115	ABLIKIM	07D	BES2	$e^+e^- \to \psi(2S)$

$\Gamma(\gamma K^+K^-\pi^+\pi^-)/\Gamma_{total}$ Γ_{171}/Γ

VALUE (units 10^{-5})	EVTS	DOCUMENT ID		TECN	COMMENT
19.1±2.7±4.3	132	ABLIKIM	07D	BES2	$e^+e^- \to \psi(2S)$

$\Gamma(\gamma p\overline{p})/\Gamma_{total}$ Γ_{172}/Γ

VALUE (units 10^{-5})	EVTS	DOCUMENT ID		TECN	COMMENT
3.9 ±0.5 OUR AVERAGE Error includes scale factor of 2.0.					
4.18±0.26±0.18	348	[1] ALEXANDER	10	CLEO	$\psi(2S) \to \gamma p\overline{p}$
2.9 ±0.4 ±0.4	142	ABLIKIM	07D	BES2	$e^+e^- \to \psi(2S)$

[1] From a fit of the $p\overline{p}$ mass distribution to a combination of $\gamma f_2(1950)$, $\gamma f_2(2150)$, and $\gamma p\overline{p}$ phase space, for $M(p\overline{p}) < 2.85$ GeV, and accounting for backgrounds from $\psi(2S) \to \pi^0 p\overline{p}$ and continuum.

$\Gamma(\gamma f_2(1950) \to \gamma p\overline{p})/\Gamma_{total}$ Γ_{173}/Γ

VALUE (units 10^{-5})	EVTS	DOCUMENT ID		TECN	COMMENT
1.2±0.2±0.1	111	[1] ALEXANDER	10	CLEO	$\psi(2S) \to \gamma p\overline{p}$

[1] From a fit of the $p\overline{p}$ mass distribution to a combination of $\gamma f_2(1950)$, $\gamma f_2(2150)$, and $\gamma p\overline{p}$ phase space, for $M(p\overline{p}) < 2.85$ GeV, and accounting for backgrounds from $\psi(2S) \to \pi^0 p\overline{p}$ and continuum.

$\Gamma(\gamma f_2(2150) \to \gamma p\overline{p})/\Gamma_{total}$ Γ_{174}/Γ

VALUE (units 10^{-5})	EVTS	DOCUMENT ID		TECN	COMMENT
0.72±0.18±0.03	73	[1] ALEXANDER	10	CLEO	$\psi(2S) \to \gamma p\overline{p}$

[1] From a fit of the $p\overline{p}$ mass distribution to a combination of $\gamma f_2(1950)$, $\gamma f_2(2150)$, and $\gamma p\overline{p}$ phase space, for $M(p\overline{p}) < 2.85$ GeV, and accounting for backgrounds from $\psi(2S) \to \pi^0 p\overline{p}$ and continuum.

$\Gamma(\gamma X(1835) \to \gamma p\overline{p})/\Gamma_{total}$ Γ_{175}/Γ

VALUE (units 10^{-6})	CL%	DOCUMENT ID		TECN	COMMENT
$4.57 \pm 0.36^{+1.77}_{-4.26}$		ABLIKIM	12D	BES3	$J/\psi \to \gamma p\overline{p}$
• • • We do not use the following data for averages, fits, limits, etc. • • •					
<1.6	90	ALEXANDER	10	CLEO	$\psi(2S) \to \gamma p\overline{p}$
<5.4	90	ABLIKIM	07D	BES	$\psi(2S) \to \gamma p\overline{p}$

$\Gamma(\gamma X \to \gamma p\overline{p})/\Gamma_{total}$ Γ_{176}/Γ

For a narrow resonance in the range $2.2 < M(X) < 2.8$ GeV.

VALUE (units 10^{-6})	CL%	DOCUMENT ID		TECN	COMMENT
<2	90	ALEXANDER	10	CLEO	$\psi(2S) \to \gamma p\overline{p}$

$\Gamma(\gamma \pi^+\pi^- p\overline{p})/\Gamma_{total}$ Γ_{177}/Γ

VALUE (units 10^{-5})	EVTS	DOCUMENT ID		TECN	COMMENT
$2.8 \pm 1.2 \pm 0.7$	17	ABLIKIM	07D	BES2	$e^+e^- \to \psi(2S)$

$\Gamma(\gamma 2(\pi^+\pi^-)K^+K^-)/\Gamma_{total}$ Γ_{178}/Γ

VALUE (units 10^{-5})	CL%	DOCUMENT ID		TECN	COMMENT
<22	90	ABLIKIM	07D	BES2	$e^+e^- \to \psi(2S)$

$\Gamma(\gamma 3(\pi^+\pi^-))/\Gamma_{total}$ Γ_{179}/Γ

VALUE (units 10^{-5})	CL%	DOCUMENT ID		TECN	COMMENT
<17	90	ABLIKIM	07D	BES2	$e^+e^- \to \psi(2S)$

$\Gamma(\gamma K^+K^-K^+K^-)/\Gamma_{total}$ Γ_{180}/Γ

VALUE (units 10^{-5})	CL%	DOCUMENT ID		TECN	COMMENT
<4	90	ABLIKIM	07D	BES2	$e^+e^- \to \psi(2S)$

$\Gamma(\gamma\gamma J/\psi)/\Gamma_{total}$ Γ_{181}/Γ

VALUE (units 10^{-4})	EVTS	DOCUMENT ID		TECN	COMMENT
$3.1 \pm 0.6^{+0.8}_{-1.0}$	1.1k	ABLIKIM	12O	BES3	$e^+e^- \to \psi(2S)$
• • • We do not use the following data for averages, fits, limits, etc. • • •					
3.2 ± 0.6	1.1k	[1] ABLIKIM	17N	BES3	$\psi(2S) \to \gamma\gamma J/\psi$

[1] Uses B($J/\psi \to e^+e^-$) = (5.971 ± 0.032)% and B($J/\psi \to \mu^+\mu^-$) = (5.961 ± 0.033)%. No systematic error estimation.

$\Gamma(e^+e^-\chi_{c0}(1P))/\Gamma_{total}$ Γ_{182}/Γ

VALUE (units 10^{-4})	EVTS	DOCUMENT ID		TECN	COMMENT
$10.6 \pm 2.4 \pm 0.4$	48	[1] ABLIKIM	17I	BES3	$\psi(2S) \to e^+e^-\gamma J/\psi$

[1] ABLIKIM 17I reports $(11.7 \pm 2.5 \pm 1.0) \times 10^{-4}$ from a measurement of $[\Gamma(\psi(2S) \to e^+e^-\chi_{c0}(1P))/\Gamma_{total}] \times [B(\chi_{c0}(1P) \to \gamma J/\psi(1S))]$ assuming $B(\chi_{c0}(1P) \to \gamma J/\psi(1S)) = (1.27 \pm 0.06) \times 10^{-2}$, which we rescale to our best value $B(\chi_{c0}(1P) \to \gamma J/\psi(1S)) = (1.40 \pm 0.05) \times 10^{-2}$. Our first error is their experiment's error and our second error is the systematic error from using our best value.

$\Gamma(e^+e^-\chi_{c1}(1P))/\Gamma_{total}$ Γ_{183}/Γ

VALUE (units 10^{-4})	EVTS	DOCUMENT ID		TECN	COMMENT
$8.5 \pm 0.6 \pm 0.2$	873	[1] ABLIKIM	17I	BES3	$\psi(2S) \to e^+e^-\gamma J/\psi$

[1] ABLIKIM 17I reports $(8.6 \pm 0.3 \pm 0.6) \times 10^{-4}$ from a measurement of $[\Gamma(\psi(2S) \to e^+e^-\chi_{c1}(1P))/\Gamma_{total}] \times [B(\chi_{c1}(1P) \to \gamma J/\psi(1S))]$ assuming $B(\chi_{c1}(1P) \to \gamma J/\psi(1S)) = (33.9 \pm 1.2) \times 10^{-2}$, which we rescale to our best value $B(\chi_{c1}(1P) \to \gamma J/\psi(1S)) = (34.3 \pm 1.0) \times 10^{-2}$. Our first error is their experiment's error and our second error is the systematic error from using our best value.

$\Gamma(e^+e^-\chi_{c2}(1P))/\Gamma_{total}$ Γ_{184}/Γ

VALUE (units 10^{-4})	EVTS	DOCUMENT ID		TECN	COMMENT
$7.0 \pm 0.7 \pm 0.2$	227	[1] ABLIKIM	17I	BES3	$\psi(2S) \to e^+e^-\gamma J/\psi$

[1] ABLIKIM 17I reports $(6.9 \pm 0.5 \pm 0.6) \times 10^{-4}$ from a measurement of $[\Gamma(\psi(2S) \to e^+e^-\chi_{c2}(1P))/\Gamma_{total}] \times [B(\chi_{c2}(1P) \to \gamma J/\psi(1S))]$ assuming $B(\chi_{c2}(1P) \to \gamma J/\psi(1S)) = (19.2 \pm 0.7) \times 10^{-2}$, which we rescale to our best value $B(\chi_{c2}(1P) \to \gamma J/\psi(1S)) = (19.0 \pm 0.5) \times 10^{-2}$. Our first error is their experiment's error and our second error is the systematic error from using our best value.

$\Gamma(e^+e^-\chi_{c0}(1P))/\Gamma(\gamma\chi_{c0}(1P))$ $\Gamma_{182}/\Gamma_{139}$

VALUE (units 10^{-3})	EVTS	DOCUMENT ID		TECN	COMMENT
$9.4 \pm 1.9 \pm 0.6$	48	[1] ABLIKIM	17I	BES3	$\psi(2S) \to e^+e^-\gamma J/\psi$

[1] Uses B($\psi(2S) \to \gamma\chi_{c0}(1P)$) × B($\chi_{c0}(1P) \to \gamma J/\psi(1S)$) = $(15.8 \pm 0.3 \pm 0.6) \times 10^{-4}$ from ABLIKIM 17N and accounts for common systematic errors.

$\Gamma(e^+e^-\chi_{c1}(1P))/\Gamma(\gamma\chi_{c1}(1P))$ $\Gamma_{183}/\Gamma_{140}$

VALUE (units 10^{-3})	EVTS	DOCUMENT ID		TECN	COMMENT
$8.3 \pm 0.3 \pm 0.4$	873	[1] ABLIKIM	17I	BES3	$\psi(2S) \to e^+e^-\gamma J/\psi$

[1] Uses B($\psi(2S) \to \gamma\chi_{c1}(1P)$) × B($\chi_{c1}(1P) \to \gamma J/\psi(1S)$) = $(351.8 \pm 1.0 \pm 12.0) \times 10^{-4}$ from ABLIKIM 17N and accounts for common systematic errors.

$\Gamma(e^+e^-\chi_{c2}(1P))/\Gamma(\gamma\chi_{c2}(1P))$ $\Gamma_{184}/\Gamma_{141}$

VALUE (units 10^{-3})	EVTS	DOCUMENT ID		TECN	COMMENT
$6.6 \pm 0.5 \pm 0.4$	227	[1] ABLIKIM	17I	BES3	$\psi(2S) \to e^+e^-\gamma J/\psi$

[1] Uses B($\psi(2S) \to \gamma\chi_{c2}(1P)$) × B($\chi_{c2}(1P) \to \gamma J/\psi(1S)$) = $(199.6 \pm 0.8 \pm 7.0) \times 10^{-4}$ from ABLIKIM 17N and accounts for common systematic errors.

WEAK DECAYS

$\Gamma(D^0 e^+ e^- + \text{c.c.})/\Gamma_{total}$ Γ_{185}/Γ

VALUE	CL%	DOCUMENT ID		TECN	COMMENT
$<1.4 \times 10^{-7}$	90	[1] ABLIKIM	17AF	BES3	$e^+e^- \to \psi(2S)$

[1] Using D^0 decays to $K^-\pi^+$, $K^-\pi^+\pi^0$, and $K^-\pi^+\pi^+\pi^-$.

OTHER DECAYS

$\Gamma(\text{invisible})/\Gamma(e^+e^-)$ Γ_{186}/Γ_6

VALUE	CL%	DOCUMENT ID		TECN	COMMENT
<2.0	90	LEES	13I	BABR	$B \to K^{(*)}\psi(2S)$

$\psi(2S)$ CROSS-PARTICLE BRANCHING RATIOS

For measurements involving $B(\psi(2S) \to \gamma\chi_{cJ}(1P)) \times B(\chi_{cJ}(1P) \to X)$ see the corresponding entries in the $\chi_{cJ}(1P)$ sections.

MULTIPOLE AMPLITUDE RATIOS IN RADIATIVE DECAYS $\psi(2S) \to \gamma\chi_{cJ}(1P)$ and $\chi_{cJ} \to \gamma J/\psi(1S)$

$a_2(\chi_{c1})/a_2(\chi_{c2})$ Magnetic quadrupole transition amplitude ratio

VALUE (units 10^{-2})	EVTS	DOCUMENT ID		TECN	COMMENT
63 ± 7 OUR AVERAGE					
61.7 ± 8.3	253k	[1] ABLIKIM	17N	BES3	$\psi(2S) \to \gamma\gamma\ell^+\ell^-$
$67\ ^{+19}_{-13}$	59k	[2] ARTUSO	09	CLEO	$\psi(2S) \to \gamma\gamma\ell^+\ell^-$

[1] Statistical and systematic errors combined.

[2] Statistical and systematic errors combined. Using values from fits with floating $M2$ amplitudes $a_2(\chi_{c1})$, $a_2(\chi_{c2})$, $b_2(\chi_{c1})$, $b_2(\chi_{c2})$ and fixed $E3$ amplitudes of $a_3(\chi_{c2}) = b_3(\chi_{c2}) = 0$. Not independent of values for $a_2(\chi_{c1}(1P))$ and $a_2(\chi_{c2}(1P))$ from ARTUSO 09.

$b_2(\chi_{c2})/b_2(\chi_{c1})$ Magnetic quadrupole transition amplitude ratio

VALUE (units 10^{-2})	EVTS	DOCUMENT ID		TECN	COMMENT
60±31 OUR AVERAGE					
74 ± 40	253k	[1] ABLIKIM	17N	BES3	$\psi(2S) \to \gamma\gamma\ell^+\ell^-$
37^{+53}_{-47}	59k	[2] ARTUSO	09	CLEO	$\psi(2S) \to \gamma\gamma\ell^+\ell^-$

[1] Statistical and systematic errors combined. Derived from the reported measurement of $b_2(\chi_{c1})/b_2(\chi_{c2}) = 1.35 \pm 0.72$.

[2] Statistical and systematic errors combined. Using values from fits with floating $M2$ amplitudes $a_2(\chi_{c1})$, $a_2(\chi_{c2})$, $b_2(\chi_{c1})$, $b_2(\chi_{c2})$ and fixed $E3$ amplitudes of $a_3(\chi_{c2}) = b_3(\chi_{c2}) = 0$. Not independent of values for $b_2(\chi_{c1}(1P))$ and $b_2(\chi_{c2}(1P))$ from ARTUSO 09.

$\psi(2S)$ REFERENCES

ABLIKIM	17AF	PR D96 111101	M. Ablikim *et al.*	(BES III Collab.)
ABLIKIM	17AJ	PR D96 112008	M. Ablikim *et al.*	(BES III Collab.)
ABLIKIM	17AK	PR D96 112012	M. Ablikim *et al.*	(BES III Collab.)
ABLIKIM	17E	PL B770 217	M. Ablikim *et al.*	(BES III Collab.)
ABLIKIM	17I	PRL 118 221802	M. Ablikim *et al.*	(BES III Collab.)
ABLIKIM	17L	PR D95 052003	M. Ablikim *et al.*	(BES III Collab.)
ABLIKIM	17N	PR D95 072004	M. Ablikim *et al.*	(BES III Collab.)
ABLIKIM	17U	PR D96 032001	M. Ablikim *et al.*	(BES III Collab.)
ABLIKIM	17X	PR D96 052003	M. Ablikim *et al.*	(BES III Collab.)
DOBBS	17	PR D96 092004	S. Dobbs *et al.*	(NWES, WAYN)
LEES	17A	PR D95 052001	J.P. Lees *et al.*	(BABAR Collab.)
AAIJ	16Y	JHEP 1605 132	R. Aaij *et al.*	(LHCb Collab.)
ABLIKIM	16L	PR D93 072003	M. Ablikim *et al.*	(BES III Collab.)
ABLIKIM	15I	PR D91 092006	M. Ablikim *et al.*	(BES III Collab.)
ABLIKIM	15V	PL B749 414	M. Ablikim *et al.*	(BES III Collab.)
ANASHIN	15	PL B749 50	V.V. Anashin *et al.*	(KEDR Collab.)
DOBBS	15	PR D91 052006	S. Dobbs *et al.*	(NWES)
LEES	15J	PR D92 072008	J.P. Lees *et al.*	(BABAR Collab.)
ABLIKIM	14G	PR D89 112006	M. Ablikim *et al.*	(BES III Collab.)
DOBBS	14	PL B739 90	S. Dobbs *et al.*	(NWES, WAYN)
ABLIKIM	13A	PRL 110 022001	M. Ablikim *et al.*	(BES III Collab.)
ABLIKIM	13D	PR D87 012007	M. Ablikim *et al.*	(BES III Collab.)
ABLIKIM	13F	PR D87 052007	M. Ablikim *et al.*	(BES III Collab.)
ABLIKIM	13M	PR D87 092006	M. Ablikim *et al.*	(BES III Collab.)
ABLIKIM	13R	PR D88 032007	M. Ablikim *et al.*	(BES III Collab.)
ABLIKIM	13S	PR D88 032010	M. Ablikim *et al.*	(BES III Collab.)
ABLIKIM	13W	PR D88 112007	M. Ablikim *et al.*	(BES III Collab.)
LEES	13I	PR D87 112005	J.P. Lees *et al.*	(BABAR Collab.)
LEES	13O	PR D87 092005	J.P. Lees *et al.*	(BABAR Collab.)
LEES	13Q	PR D88 032013	J.P. Lees *et al.*	(BABAR Collab.)
LEES	13Y	PR D88 072009	J.P. Lees *et al.*	(BABAR Collab.)
AAIJ	12H	EPJ C72 1972	R. Aaij *et al.*	(LHCb Collab.)
ABLIKIM	12D	PRL 108 112003	M. Ablikim *et al.*	(BES III Collab.)
ABLIKIM	12G	PR D85 092008	M. Ablikim *et al.*	(BES III Collab.)
ABLIKIM	12H	PL B710 594	M. Ablikim *et al.*	(BES III Collab.)
ABLIKIM	12L	PR D86 072011	M. Ablikim *et al.*	(BES III Collab.)
ABLIKIM	12M	PR D86 092008	M. Ablikim *et al.*	(BES III Collab.)
ABLIKIM	12O	PRL 109 172002	M. Ablikim *et al.*	(BES III Collab.)
ABLIKIM	12Q	CP C36 1040	M. Ablikim *et al.*	(BES II Collab.)
ANASHIN	12	PL B711 280	V.V. Anashin *et al.*	(KEDR Collab.)
LEES	12E	PR D85 112009	J.P. Lees *et al.*	(BABAR Collab.)
LEES	12F	PR D86 012008	J.P. Lees *et al.*	(BABAR Collab.)
METREVELI	12	PR D85 092007	Z. Metreveli *et al.*	(NWES, FLOR, WAYN+)
GE	11	PR D84 032008	J.Y. Ge *et al.*	(CLEO Collab.)
ABLIKIM	10B	PRL 104 132002	M. Ablikim *et al.*	(BES III Collab.)
ABLIKIM	10F	PRL 105 261801	M. Ablikim *et al.*	(BES III Collab.)
ALEXANDER	10	PR D82 092002	J.P. Alexander *et al.*	(CLEO Collab.)
CRONIN-HEN...	10	PR D81 052002	D. Cronin-Hennessey *et al.*	(CLEO Collab.)
ADAMS	09	PR D80 051106	G.S. Adams *et al.*	(CLEO Collab.)
ARTUSO	09	PR D80 112003	M. Artuso *et al.*	(CLEO Collab.)

Meson Particle Listings

$\psi(2S)$, $\psi(3770)$

LIBBY	09	PR D80 072002	J. Libby *et al.*	(CLEO Collab.)
MITCHELL	09	PRL 102 011801	R.E. Mitchell *et al.*	(CLEO Collab.)
PEDLAR	09	PR D79 111101	T.K. Pedlar *et al.*	(CLEO Collab.)
ABLIKIM	08B	PL B659 74	M. Ablikim *et al.*	(BES Collab.)
ABLIKIM	08C	PL B659 789	M. Ablikim *et al.*	(BES Collab.)
DOBBS	08A	PRL 101 182003	S. Dobbs *et al.*	(CLEO Collab.)
MENDEZ	08	PR D78 011102	H. Mendez *et al.*	(CLEO Collab.)
PDG	08	PL B667 1	C. Amsler *et al.*	(PDG Collab.)
ABLIKIM	07C	PL B648 149	M. Ablikim *et al.*	(BES Collab.)
ABLIKIM	07D	PRL 99 011802	M. Ablikim *et al.*	(BES II Collab.)
ABLIKIM	07H	PR D76 092003	M. Ablikim *et al.*	(BES Collab.)
ANASHIN	07	JETPL 85 347	V.V. Anashin *et al.*	(KEDR Collab.)
		Translated from ZETFP 85 429.		
ANDREOTTI	07	PL B654 74	M. Andreotti *et al.*	(Fermilab E835 Collab.)
AUBERT	07AK	PR D76 012008	B. Aubert *et al.*	(BABAR Collab.)
AUBERT	07AU	PR D76 092005	B. Aubert *et al.*	(BABAR Collab.)
Also		PR D77 119902E (errat.)	B. Aubert *et al.*	(BABAR Collab.)
AUBERT	07BD	PR D76 092006	B. Aubert *et al.*	(BABAR Collab.)
PDG	07	Unofficial 2007 WWW edition		(PDG Collab.)
PEDLAR	07	PR D75 011102	T.K. Pedlar *et al.*	(CLEO Collab.)
ABLIKIM	06G	PR D73 052004	M. Ablikim *et al.*	(BES Collab.)
ABLIKIM	06I	PR D74 012004	M. Ablikim *et al.*	(BES Collab.)
ABLIKIM	06L	PRL 97 121801	M. Ablikim *et al.*	(BES Collab.)
ABLIKIM	06R	PR D74 072001	M. Ablikim *et al.*	(BES Collab.)
ABLIKIM	06W	PR D74 112003	M. Ablikim *et al.*	(BES Collab.)
ADAM	06	PRL 96 082004	N.E. Adam *et al.*	(CLEO Collab.)
AUBERT	06B	PR D73 012005	B. Aubert *et al.*	(BABAR Collab.)
AUBERT	06D	PR D73 052003	B. Aubert *et al.*	(BABAR Collab.)
AUBERT,BE	06D	PR D74 091103	B. Aubert *et al.*	(BABAR Collab.)
DOBBS	06A	PR D74 011105	S. Dobbs *et al.*	(CLEO Collab.)
ABLIKIM	05E	PR D71 072006	M. Ablikim *et al.*	(BES Collab.)
ABLIKIM	05H	PR D72 012002	M. Ablikim *et al.*	(BES Collab.)
ABLIKIM	05I	PL B614 37	M. Ablikim *et al.*	(BES Collab.)
ABLIKIM	05J	PL B619 247	M. Ablikim *et al.*	(BES Collab.)
ABLIKIM	05O	PL B630 21	M. Ablikim *et al.*	(BES Collab.)
ADAM	05	PRL 94 012005	N.E. Adam *et al.*	(CLEO Collab.)
ADAM	05A	PRL 94 232002	N.E. Adam *et al.*	(CLEO Collab.)
ANDREOTTI	05	PR D71 032006	M. Andreotti *et al.*	(FNAL E835 Collab.)
AUBERT	05D	PR D71 052001	B. Aubert *et al.*	(BABAR Collab.)
BRIERE	05	PRL 95 062001	R.A. Briere *et al.*	(CLEO Collab.)
PEDLAR	05	PR D72 051108	T.K. Pedlar *et al.*	(CLEO Collab.)
ROSNER	05	PRL 95 102003	J.L. Rosner *et al.*	(CLEO Collab.)
ABLIKIM	04B	PR D70 012003	M. Ablikim *et al.*	(BES Collab.)
ABLIKIM	04K	PR D70 112003	M. Ablikim *et al.*	(BES Collab.)
ABLIKIM	04L	PR D70 112007	M. Ablikim *et al.*	(BES Collab.)
ATHAR	04	PR D70 112002	S.B. Athar *et al.*	(CLEO Collab.)
BAI	04B	PRL 92 052001	J.Z. Bai *et al.*	(BES Collab.)
BAI	04C	PR D69 072001	J.Z. Bai *et al.*	(BES Collab.)
BAI	04D	PL B589 7	J.Z. Bai *et al.*	(BES Collab.)
BAI	04G	PR D70 012004	J.Z. Bai *et al.*	(BES Collab.)
BAI	04I	PR D70 012006	J.Z. Bai *et al.*	(BES Collab.)
PDG	04	PL B592 1	S. Eidelman *et al.*	(PDG Collab.)
SETH	04	PR D69 097503	K.K. Seth	
AULCHENKO	03	PL B573 63	V.M. Aulchenko *et al.*	(KEDR Collab.)
BAI	03B	PR D67 052002	J.Z. Bai *et al.*	(BES Collab.)
BAI	03C	PR D67 032004	J.Z. Bai *et al.*	(BES Collab.)
AUBERT	02B	PR D65 031101	B. Aubert *et al.*	(BABAR Collab.)
BAI	02	PR D65 052004	J.Z. Bai *et al.*	(BES Collab.)
BAI	02B	PL B550 24	J.Z. Bai *et al.*	(BES Collab.)
BAI	02C	PRL 88 101802	J.Z. Bai *et al.*	(BES Collab.)
PDG	02	PR D66 010001	K. Hagiwara *et al.*	(PDG Collab.)
BAI	01	PR D63 032002	J.Z. Bai *et al.*	(BES Collab.)
AMBROGIANI	00A	PR D62 032004	M. Ambrogiani *et al.*	(FNAL E835 Collab.)
ARTAMONOV	00	PL B474 427	A.S. Artamonov *et al.*	
BAI	00	PRL 84 594	J.Z. Bai *et al.*	(BES Collab.)
BAI	99C	PRL 83 1918	J.Z. Bai *et al.*	(BES Collab.)
BAI	98E	PR D57 3854	J.Z. Bai *et al.*	(BES Collab.)
BAI	98F	PR D58 097101	J.Z. Bai *et al.*	(BES Collab.)
BAI	98J	PRL 81 5080	J.Z. Bai *et al.*	(BES Collab.)
ARMSTRONG	97	PR D55 1153	T.A. Armstrong *et al.*	(E760 Collab.)
GRIBUSHIN	96	PR D53 4723	A. Gribushin *et al.*	(E672 Collab., E706 Collab.)
ARMSTRONG	93B	PR D47 772	T.A. Armstrong *et al.*	(FNAL E760 Collab.)
ALEXANDER	89	NP B320 45	J.P. Alexander *et al.*	(LBL, MICH, SLAC)
COHEN	87	RMP 59 1121	E.R. Cohen, B.N. Taylor	(RISC, NBS)
GAISER	86	PR D34 711	J. Gaiser *et al.*	(Crystal Ball Collab.)
KURAEV	85	SJNP 41 466	E.A. Kuraev, V.S. Fadin	(NOVO)
		Translated from YAF 41 733.		
FRANKLIN	83	PRL 51 963	M.E.B. Franklin *et al.*	(LBL, SLAC)
EDWARDS	82C	PRL 48 70	C. Edwards *et al.*	(CIT, HARV, PRIN+)
LEMOIGNE	82	PL 113B 509	Y. Lemoigne *et al.*	(SACL, LOIC, SHMP+)
HIMEL	80	PRL 44 920	T. Himel *et al.*	(LBL, SLAC)
OREGLIA	80	PRL 45 959	M.J. Oreglia *et al.*	(SLAC, CIT, HARV+)
SCHARRE	80	PL 97B 329	D.L. Scharre *et al.*	(SLAC, LBL)
ZHOLENTZ	80	PL 96B 214	A.A. Zholents *et al.*	(NOVO)
Also		SJNP 34 814	A.A. Zholents *et al.*	(NOVO)
		Translated from YAF 34 1471.		
BRANDELIK	79B	NP B160 426	R. Brandelik *et al.*	(DASP Collab.)
BRANDELIK	79C	ZPHY C1 233	R. Brandelik *et al.*	(DASP Collab.)
BARTEL	78B	PL 79B 492	W. Bartel *et al.*	(DESY, HEIDP)
TANENBAUM	78	PR D17 1731	W.M. Tanenbaum *et al.*	(SLAC, LBL)
BIDDICK	77	PRL 38 1324	C.J. Biddick *et al.*	(UCSD, UMD, PAVI+)
BRAUNSCH...	77	PL 67B 249	W. Braunschweig *et al.*	(DASP Collab.)
BURMESTER	77	PL 66B 395	J. Burmester *et al.*	(DESY, HAMB, SIEG+)
FELDMAN	77	PRPL 33C 285	G.J. Feldman, M.L. Perl	(LBL, SLAC)
YAMADA	77	Hamburg Conf. 69	S. Yamada	(DASP Collab.)
BARTEL	76	PL 64B 483	W. Bartel *et al.*	(DESY, HEIDP)
TANENBAUM	76	PRL 36 402	W.M. Tanenbaum *et al.*	(SLAC, LBL) IG
WHITAKER	76	PRL 37 1596	J.S. Whitaker *et al.*	(SLAC, LBL)
ABRAMS	75	Stanford Symp. 25	G.S. Abrams	(LBL)
ABRAMS	75B	PRL 34 1181	G.S. Abrams *et al.*	(LBL, SLAC)
BOYARSKI	75C	Palermo Conf. 54	A.M. Boyarski *et al.*	(SLAC, LBL)
HILGER	75	PRL 35 625	E. Hilger *et al.*	(STAN, PENN)
LIBERMAN	75	Stanford Symp. 55	A.D. Liberman	(STAN)
LUTH	75	PRL 35 1124	V. Luth *et al.*	(SLAC, LBL) JPC
WIIK	75	Stanford Symp. 69	B.H. Wiik	(DESY)

$\psi(3770)$

$I^G(J^{PC}) = 0^-(1^{--})$

$\psi(3770)$ MASS (MeV)

OUR FIT includes measurements of $m_{\psi(2S)}$, $m_{\psi(3770)}$, and $m_{\psi(3770)} - m_{\psi(2S)}$.

VALUE (MeV)	EVTS	DOCUMENT ID		TECN	COMMENT
3773.13±0.35 OUR FIT Error includes scale factor of 1.1.					
3778.1 ±1.2 OUR AVERAGE					
3779.2 $^{+1.8}_{-1.7}$ $^{+0.6}_{-0.8}$		[1] ANASHIN	12A	KEDR	$e^+e^- \to D\overline{D}$
3775.5 ±2.4 ±0.5	57	AUBERT	08B	BABR	$B \to D\overline{D}K$
3776 ±5 ±4	68	BRODZICKA	08	BELL	$B^+ \to D^0\overline{D}^0K^+$
3778.8 ±1.9 ±0.9		AUBERT	07BE	BABR	$e^+e^- \to D\overline{D}\gamma$
• • • We do not use the following data for averages, fits, limits, etc. • • •					
3779.8 ±0.6		[2] SHAMOV	17	RVUE	$e^+e^- \to D\overline{D}$, hadrons
3772.0 ±1.9		[3,4] ABLIKIM	08D	BES2	$e^+e^- \to$ hadrons
3778.4 ±3.0 ±1.3	34	CHISTOV	04	BELL	Sup. by BRODZICKA 08

[1] Taking into account interference between the resonant and non-resonant $D\overline{D}$ production.
[2] From the joint analysis of the data on the $D\overline{D}$ and inclusive hadronic cross sections in the $\psi(3770)$ region from BaBar, Belle, BES-II, CLEO and KEDR.
[3] Reanalysis of data presented in BAI 02C. From a global fit over the center-of-mass energy region 3.7–5.0 GeV covering the $\psi(3770)$, $\psi(4040)$, $\psi(4160)$, and $\psi(4415)$ resonances. Phase angle fixed in the fit to $\delta = 0°$.
[4] Interference between the resonant and non-resonant $D\overline{D}$ production not taken into account.

$m_{\psi(3770)} - m_{\psi(2S)}$

OUR FIT includes measurements of $m_{\psi(2S)}$, $m_{\psi(3770)}$, and $m_{\psi(3770)} - m_{\psi(2S)}$.

VALUE (MeV)	DOCUMENT ID		TECN	COMMENT
87.04±0.35 OUR FIT Error includes scale factor of 1.1.				
86.6 ±0.7 OUR AVERAGE Error includes scale factor of 2.0. See the ideogram below.				
86.9 ±0.4	[1] ABLIKIM	07E	BES2	$e^+e^- \to$ hadrons
86.7 ±0.7	ABLIKIM	06L	BES2	$e^+e^- \to$ hadrons
80 ±2	SCHINDLER	80	MRK2	e^+e^-
86 ±2	[2] BACINO	78	DLCO	e^+e^-
88 ±3	RAPIDIS	77	LGW	e^+e^-

[1] BES-II $\psi(2S)$ mass subtracted (see ABLIKIM 06L).
[2] SPEAR $\psi(2S)$ mass subtracted (see SCHINDLER 80).

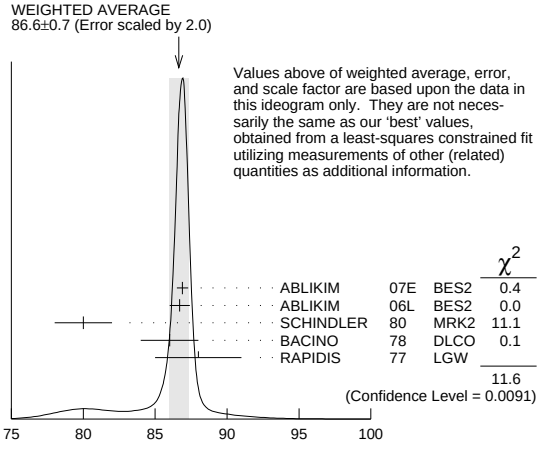

$\psi(3770)$ WIDTH

VALUE (MeV)	EVTS	DOCUMENT ID		TECN	COMMENT
27.2± 1.0 OUR FIT					
27.5± 0.9 OUR AVERAGE					
24.9 $^{+\ 4.6\ +0.5}_{-\ 4.0\ -1.1}$		[1] ANASHIN	12A	KEDR	$e^+e^- \to D\overline{D}$
30.4± 8.5		[2,3] ABLIKIM	08D	BES2	$e^+e^- \to$ hadrons
27 ±10 ±5	68	BRODZICKA	08	BELL	$B^+ \to D^0\overline{D}^0K^+$
28.5± 1.2±0.2		[3] ABLIKIM	07E	BES2	$e^+e^- \to$ hadrons
23.5± 3.7±0.9		AUBERT	07BE	BABR	$e^+e^- \to D\overline{D}\gamma$
26.9± 2.4±0.3		[3] ABLIKIM	06L	BES2	$e^+e^- \to$ hadrons
24 ± 5		[3] SCHINDLER	80	MRK2	e^+e^-
24 ± 5		[3] BACINO	78	DLCO	e^+e^-
28 ± 5		[3] RAPIDIS	77	LGW	e^+e^-
• • • We do not use the following data for averages, fits, limits, etc. • • •					
25.8± 1.3		[4] SHAMOV	17	RVUE	$e^+e^- \to D\overline{D}$, hadrons

[1] Taking into account interference between the resonant and non-resonant $D\overline{D}$ production.
[2] Reanalysis of data presented in BAI 02C. From a global fit over the center-of-mass energy region 3.7–5.0 GeV covering the $\psi(3770)$, $\psi(4040)$, $\psi(4160)$, and $\psi(4415)$ resonances. Phase angle fixed in the fit to $\delta = 0^{\circ}$.
[3] Interference between the resonant and non-resonant $D\overline{D}$ production not taken into account.
[4] From the joint analysis of the data on the $D\overline{D}$ and inclusive hadronic cross sections in the $\psi(3770)$ region from BaBar, Belle, BES-II, CLEO and KEDR.

$\psi(3770)$ DECAY MODES

In addition to the dominant decay mode to $D\overline{D}$, $\psi(3770)$ was found to decay into the final states containing the J/ψ (BAI 05, ADAM 06). ADAMS 06 and HUANG 06A searched for various decay modes with light hadrons and found a statistically significant signal for the decay to $\phi\eta$ only (ADAMS 06).

	Mode	Fraction (Γ_i/Γ)	Scale factor/ Confidence level
Γ_1	$D\overline{D}$	$(93\ ^{+8}_{-9})\%$	S=2.0
Γ_2	$D^0\overline{D}^0$	$(52\ ^{+4}_{-5})\%$	S=2.0
Γ_3	D^+D^-	$(41\ \pm4)\%$	S=2.0
Γ_4	$J/\psi\pi^+\pi^-$	$(1.93\pm0.28)\times10^{-3}$	
Γ_5	$J/\psi\pi^0\pi^0$	$(8.0\ \pm3.0)\times10^{-4}$	
Γ_6	$J/\psi\eta$	$(9\ \pm4)\times10^{-4}$	
Γ_7	$J/\psi\pi^0$	$<2.8\times10^{-4}$	CL=90%
Γ_8	e^+e^-	$(9.6\ \pm0.7)\times10^{-6}$	S=1.3
	Decays to light hadrons		
Γ_9	$b_1(1235)\pi$	$<1.4\times10^{-5}$	CL=90%
Γ_{10}	$\phi\eta'$	$<7\times10^{-4}$	CL=90%
Γ_{11}	$\omega\eta'$	$<4\times10^{-4}$	CL=90%
Γ_{12}	$\rho^0\eta'$	$<6\times10^{-4}$	CL=90%
Γ_{13}	$\phi\eta$	$(3.1\ \pm0.7)\times10^{-4}$	
Γ_{14}	$\omega\eta$	$<1.4\times10^{-5}$	CL=90%
Γ_{15}	$\rho^0\eta$	$<5\times10^{-4}$	CL=90%
Γ_{16}	$\phi\pi^0$	$<3\times10^{-5}$	CL=90%
Γ_{17}	$\omega\pi^0$	$<6\times10^{-4}$	CL=90%
Γ_{18}	$\pi^+\pi^-\pi^0$	$<5\times10^{-6}$	CL=90%
Γ_{19}	$\rho\pi$	$<5\times10^{-6}$	CL=90%
Γ_{20}	K^+K^-		
Γ_{21}	$K^*(892)^+K^-$ + c.c.	$<1.4\times10^{-5}$	CL=90%
Γ_{22}	$K^*(892)^0\overline{K}^0$ + c.c.	$<1.2\times10^{-3}$	CL=90%
Γ_{23}	$K^0_SK^0_L$	$<1.2\times10^{-5}$	CL=90%
Γ_{24}	$2(\pi^+\pi^-)$	$<1.12\times10^{-3}$	CL=90%
Γ_{25}	$2(\pi^+\pi^-)\pi^0$	$<1.06\times10^{-3}$	CL=90%
Γ_{26}	$2(\pi^+\pi^-\pi^0)$	$<5.85\%$	CL=90%
Γ_{27}	$\omega\pi^+\pi^-$	$<6.0\times10^{-4}$	CL=90%
Γ_{28}	$3(\pi^+\pi^-)$	$<9.1\times10^{-3}$	CL=90%
Γ_{29}	$3(\pi^+\pi^-)\pi^0$	$<1.37\%$	CL=90%
Γ_{30}	$3(\pi^+\pi^-)2\pi^0$	$<11.74\%$	CL=90%
Γ_{31}	$\eta\pi^+\pi^-$	$<1.24\times10^{-3}$	CL=90%
Γ_{32}	$\pi^+\pi^-2\pi^0$	$<8.9\times10^{-3}$	CL=90%
Γ_{33}	$\rho^0\pi^+\pi^-$	$<6.9\times10^{-3}$	CL=90%
Γ_{34}	$\eta3\pi$	$<1.34\times10^{-3}$	CL=90%
Γ_{35}	$\eta2(\pi^+\pi^-)$	$<2.43\%$	CL=90%
Γ_{36}	$\eta\rho^0\pi^+\pi^-$	$<1.45\%$	CL=90%
Γ_{37}	$\eta'3\pi$	$<2.44\times10^{-3}$	CL=90%
Γ_{38}	$K^+K^-\pi^+\pi^-$	$<9.0\times10^{-4}$	CL=90%
Γ_{39}	$\phi\pi^+\pi^-$	$<4.1\times10^{-4}$	CL=90%
Γ_{40}	$K^+K^-2\pi^0$	$<4.2\times10^{-3}$	CL=90%
Γ_{41}	$4(\pi^+\pi^-)$	$<1.67\%$	CL=90%
Γ_{42}	$4(\pi^+\pi^-)\pi^0$	$<3.06\%$	CL=90%
Γ_{43}	$\phi f_0(980)$	$<4.5\times10^{-4}$	CL=90%
Γ_{44}	$K^+K^-\pi^+\pi^-\pi^0$	$<2.36\times10^{-3}$	CL=90%
Γ_{45}	$K^+K^-\rho^0\pi^0$	$<8\times10^{-4}$	CL=90%
Γ_{46}	$K^+K^-\rho^+\pi^-$	$<1.46\%$	CL=90%
Γ_{47}	ωK^+K^-	$<3.4\times10^{-4}$	CL=90%
Γ_{48}	$\phi\pi^+\pi^-\pi^0$	$<3.8\times10^{-3}$	CL=90%
Γ_{49}	$K^{*0}K^-\pi^+\pi^0$ + c.c.	$<1.62\%$	CL=90%
Γ_{50}	$K^{*+}K^-\pi^+\pi^-$ + c.c.	$<3.23\%$	CL=90%
Γ_{51}	$K^+K^-\pi^+\pi^-2\pi^0$	$<2.67\%$	CL=90%
Γ_{52}	$K^+K^-2(\pi^+\pi^-)$	$<1.03\%$	CL=90%
Γ_{53}	$K^+K^-2(\pi^+\pi^-)\pi^0$	$<3.60\%$	CL=90%
Γ_{54}	ηK^+K^-	$<4.1\times10^{-4}$	CL=90%
Γ_{55}	$\eta K^+K^-\pi^+\pi^-$	$<1.24\%$	CL=90%
Γ_{56}	$\rho^0K^+K^-$	$<5.0\times10^{-3}$	CL=90%
Γ_{57}	$2(K^+K^-)$	$<6.0\times10^{-4}$	CL=90%
Γ_{58}	ϕK^+K^-	$<7.5\times10^{-4}$	CL=90%
Γ_{59}	$2(K^+K^-)\pi^0$	$<2.9\times10^{-4}$	CL=90%
Γ_{60}	$2(K^+K^-)\pi^+\pi^-$	$<3.2\times10^{-3}$	CL=90%
Γ_{61}	$K^0_SK^-\pi^+$	$<3.2\times10^{-3}$	CL=90%
Γ_{62}	$K^0_SK^-\pi^+\pi^0$	$<1.33\%$	CL=90%
Γ_{63}	$K^0_SK^-\rho^+$	$<6.6\times10^{-3}$	CL=90%
Γ_{64}	$K^0_SK^-2\pi^+\pi^-$	$<8.7\times10^{-3}$	CL=90%
Γ_{65}	$K^0_SK^-\pi^+\rho^0$	$<1.6\%$	CL=90%
Γ_{66}	$K^0_SK^-\pi^+\eta$	$<1.3\%$	CL=90%
Γ_{67}	$K^0_SK^-2\pi^+\pi^-\pi^0$	$<4.18\%$	CL=90%
Γ_{68}	$K^0_SK^-2\pi^+\pi^-\eta$	$<4.8\%$	CL=90%
Γ_{69}	$K^0_SK^-\pi^+2(\pi^+\pi^-)$	$<1.22\%$	CL=90%
Γ_{70}	$K^0_SK^-\pi^+2\pi^0$	$<2.65\%$	CL=90%
Γ_{71}	$K^0_SK^-K^+K^-\pi^+$	$<4.9\times10^{-3}$	CL=90%
Γ_{72}	$K^0_SK^-K^+K^-\pi^+\pi^0$	$<3.0\%$	CL=90%
Γ_{73}	$K^0_SK^-K^+K^-\pi^+\eta$	$<2.2\%$	CL=90%
Γ_{74}	$K^{*0}K^-\pi^+$ + c.c.	$<9.7\times10^{-3}$	CL=90%
Γ_{75}	$p\overline{p}$		
Γ_{76}	$p\overline{p}\pi^0$	$<4\times10^{-5}$	CL=90%
Γ_{77}	$p\overline{p}\pi^+\pi^-$	$<5.8\times10^{-4}$	CL=90%
Γ_{78}	$\Lambda\overline{\Lambda}$	$<1.2\times10^{-4}$	CL=90%
Γ_{79}	$p\overline{p}\pi^+\pi^-\pi^0$	$<1.85\times10^{-3}$	CL=90%
Γ_{80}	$\omega p\overline{p}$	$<2.9\times10^{-4}$	CL=90%
Γ_{81}	$\Lambda\overline{\Lambda}\pi^0$	$<7\times10^{-5}$	CL=90%
Γ_{82}	$p\overline{p}2(\pi^+\pi^-)$	$<2.6\times10^{-3}$	CL=90%
Γ_{83}	$\eta p\overline{p}$	$<5.4\times10^{-4}$	CL=90%
Γ_{84}	$\eta p\overline{p}\pi^+\pi^-$	$<3.3\times10^{-3}$	CL=90%
Γ_{85}	$\rho^0p\overline{p}$	$<1.7\times10^{-3}$	CL=90%
Γ_{86}	$p\overline{p}K^+K^-$	$<3.2\times10^{-4}$	CL=90%
Γ_{87}	$\eta p\overline{p}K^+K^-$	$<6.9\times10^{-3}$	CL=90%
Γ_{88}	$\pi^0p\overline{p}K^+K^-$	$<1.2\times10^{-3}$	CL=90%
Γ_{89}	$\phi p\overline{p}$	$<1.3\times10^{-4}$	CL=90%
Γ_{90}	$\Lambda\overline{\Lambda}\pi^+\pi^-$	$<2.5\times10^{-4}$	CL=90%
Γ_{91}	$\Lambda\overline{p}K^+$	$<2.8\times10^{-4}$	CL=90%
Γ_{92}	$\Lambda\overline{p}K^+\pi^+\pi^-$	$<6.3\times10^{-4}$	CL=90%
Γ_{93}	$\Lambda\overline{\Lambda}\eta$	$<1.9\times10^{-4}$	CL=90%
Γ_{94}	$\Sigma^+\overline{\Sigma}^-$	$<1.0\times10^{-4}$	CL=90%
Γ_{95}	$\Sigma^0\overline{\Sigma}^0$	$<4\times10^{-5}$	CL=90%
Γ_{96}	$\Xi^+\overline{\Xi}^-$	$<1.5\times10^{-4}$	CL=90%
Γ_{97}	$\Xi^0\overline{\Xi}^0$	$<1.4\times10^{-4}$	CL=90%
	Radiative decays		
Γ_{98}	$\gamma\chi_{c2}$	$<6.4\times10^{-4}$	CL=90%
Γ_{99}	$\gamma\chi_{c1}$	$(2.49\pm0.23)\times10^{-3}$	
Γ_{100}	$\gamma\chi_{c0}$	$(6.9\ \pm0.6)\times10^{-3}$	
Γ_{101}	$\gamma\eta_c$	$<7\times10^{-4}$	CL=90%
Γ_{102}	$\gamma\eta_c(2S)$	$<9\times10^{-4}$	CL=90%
Γ_{103}	$\gamma\eta'$	$<1.8\times10^{-4}$	CL=90%
Γ_{104}	$\gamma\eta$	$<1.5\times10^{-4}$	CL=90%
Γ_{105}	$\gamma\pi^0$	$<2\times10^{-4}$	CL=90%

CONSTRAINED FIT INFORMATION

An overall fit to the total width, a partial width, and 3 branching ratios uses 23 measurements and one constraint to determine 5 parameters. The overall fit has a $\chi^2 = 20.1$ for 19 degrees of freedom.

The following *off-diagonal* array elements are the correlation coefficients $\langle\delta p_i\delta p_j\rangle/(\delta p_i\cdot\delta p_j)$, in percent, from the fit to parameters p_i, including the branching fractions, $x_i \equiv \Gamma_i/\Gamma_{\rm total}$. The fit constrains the x_i whose labels appear in this array to sum to one.

x_3	99		
x_8	0	0	
Γ	0	0	−44
	x_2	x_3	x_8

	Mode	Rate (MeV)	Scale factor
Γ_2	$D^0\overline{D}^0$	$14.0\ \pm1.4$	1.8
Γ_3	D^+D^-	$11.2\ \pm1.1$	1.7
Γ_8	e^+e^-	$(2.62\pm0.18)\times10^{-4}$	1.4

Meson Particle Listings

$\psi(3770)$

$\psi(3770)$ PARTIAL WIDTHS

$\Gamma(e^+e^-)$ Γ_8

VALUE (keV)	EVTS	DOCUMENT ID		TECN	COMMENT
0.262±0.018 OUR FIT	Error includes scale factor of 1.4.				
0.256±0.016 OUR AVERAGE	Error includes scale factor of 1.2.				
$0.154^{+0.079}_{-0.058}{}^{+0.021}_{-0.027}$		[1,2] ANASHIN	12A	KEDR	$e^+e^- \to D\overline{D}$
0.22 ±0.05		[3,4] ABLIKIM	08D	BES2	$e^+e^- \to$ hadrons
0.277±0.011±0.013		[4] ABLIKIM	07E	BES2	$e^+e^- \to$ hadrons
$0.203\pm0.003^{+0.041}_{-0.027}$	1.4M	[4,5] BESSON	06	CLEO	$e^+e^- \to$ hadrons
0.276±0.050		[4] SCHINDLER	80	MRK2	e^+e^-
0.18 ±0.06		[4] BACINO	78	DLCO	e^+e^-
• • • We do not use the following data for averages, fits, limits, etc. • • •					
0.196±0.018		[6] SHAMOV	17	RVUE	$e^+e^- \to D\overline{D}$, hadrons
$0.414^{+0.072}_{-0.080}{}^{+0.093}_{-0.028}$		[2,7] ANASHIN	12A	KEDR	$e^+e^- \to D\overline{D}$
0.37 ±0.09		[8] RAPIDIS	77	LGW	e^+e^-

[1] Solution I of the two solutions.
[2] Taking into account interference between the resonant and non-resonant $D\overline{D}$ production.
[3] Reanalysis of data presented in BAI 02C. From a global fit over the center-of-mass energy region 3.7–5.0 GeV covering the $\psi(3770)$, $\psi(4040)$, $\psi(4160)$, and $\psi(4415)$ resonances. Phase angle fixed in the fit to $\delta = 0^\circ$.
[4] Interference between the resonant and non-resonant $D\overline{D}$ production not taken into account.
[5] BESSON 06 (as corrected in BESSON 10) measure $\sigma(e^+e^- \to \psi(3770) \to \text{hadrons}) = 6.36 \pm 0.08^{+0.41}_{-0.30}$ nb at $\sqrt{s} = 3773 \pm 1$ MeV, and obtain Γ_{ee} from the Born-level cross section calculated using $\psi(3770)$ mass and width from our 2004 edition, PDG 04.
[6] From the joint analysis of the data on the $D\overline{D}$ and inclusive hadronic cross sections in the $\psi(3770)$ region from BaBar, Belle, BES-II, CLEO and KEDR.
[7] Solution II of the two solutions.
[8] See also $\Gamma(e^+e^-)/\Gamma_{\text{total}}$ below.

$\psi(3770)$ BRANCHING RATIOS

$\Gamma(D\overline{D})/\Gamma_{\text{total}}$ $\Gamma_1/\Gamma = (\Gamma_2+\Gamma_3)/\Gamma$

VALUE	EVTS	DOCUMENT ID		TECN	COMMENT
$0.93\ ^{+0.08}_{-0.09}$ OUR FIT	Error includes scale factor of 2.0.				
$0.93\ ^{+0.08}_{-0.09}$ OUR AVERAGE	Error includes scale factor of 2.1.				
0.849±0.056±0.018		[1] ABLIKIM	08B	BES2	$e^+e^- \to$ non-$D\overline{D}$
$1.033\pm0.014^{+0.048}_{-0.066}$	1.427M	[2] BESSON	06	CLEO	$e^+e^- \to$ hadrons
• • • We do not use the following data for averages, fits, limits, etc. • • •					
0.836±0.049		[3] SHAMOV	17	RVUE	$e^+e^- \to D\overline{D}$, hadrons
0.866±0.050±0.036		[4,5] ABLIKIM	07K	BES2	$e^+e^- \to$ non-$D\overline{D}$
0.836±0.073±0.042		[5] ABLIKIM	06L	BES2	$e^+e^- \to D\overline{D}$
0.855±0.017±0.058		[5,6] ABLIKIM	06N	BES2	$e^+e^- \to D\overline{D}$

[1] Neglecting interference.
[2] Obtained by comparing a measurement of the total cross section (corrected in BESSON 10) with that of $D\overline{D}$ reported by CLEO in DOBBS 07.
[3] From the joint analysis of the data on the $D\overline{D}$ and inclusive hadronic cross sections in the $\psi(3770)$ region from BaBar, Belle, BES-II, CLEO and KEDR.
[4] Using $\sigma^{obs} = 7.07 \pm 0.58$ nb and neglecting interference.
[5] Not independent of ABLIKIM 08B.
[6] From a measurement of $\sigma(e^+e^- \to D\overline{D})$ at $\sqrt{s} = 3773$ MeV, using the $\psi(3770)$ resonance parameters measured by ABLIKIM 06L.

$\Gamma(D^0\overline{D}^0)/\Gamma_{\text{total}}$ Γ_2/Γ

VALUE	DOCUMENT ID		TECN	COMMENT
$0.52\ ^{+0.04}_{-0.05}$ OUR FIT	Error includes scale factor of 2.0.			
• • • We do not use the following data for averages, fits, limits, etc. • • •				
0.467±0.047±0.023	ABLIKIM	06L	BES2	$e^+e^- \to D^0\overline{D}^0$
0.499±0.013±0.038	[1] ABLIKIM	06N	BES2	$e^+e^- \to D^0\overline{D}^0$

[1] From a measurement of $\sigma(e^+e^- \to D\overline{D})$ at $\sqrt{s} = 3773$ MeV, using the $\psi(3770)$ resonance parameters measured by ABLIKIM 06L.

$\Gamma(D^+D^-)/\Gamma_{\text{total}}$ Γ_3/Γ

VALUE	DOCUMENT ID		TECN	COMMENT
0.41 ±0.04 OUR FIT	Error includes scale factor of 2.0.			
• • • We do not use the following data for averages, fits, limits, etc. • • •				
0.369±0.037±0.028	ABLIKIM	06L	BES2	$e^+e^- \to D^+D^-$
0.357±0.011±0.034	[1] ABLIKIM	06N	BES2	$e^+e^- \to D^+D^-$

[1] From a measurement of $\sigma(e^+e^- \to D\overline{D})$ at $\sqrt{s} = 3773$ MeV, using the $\psi(3770)$ resonance parameters measured by ABLIKIM 06L.

$\Gamma(D^0\overline{D}^0)/\Gamma(D^+D^-)$ Γ_2/Γ_3

VALUE	EVTS	DOCUMENT ID		TECN	COMMENT
1.253±0.016 OUR FIT					
1.253±0.016 OUR AVERAGE					
1.252±0.009±0.013	5.3M	BONVICINI	14	CLEO	$e^+e^- \to D\overline{D}$
1.39 ±0.31 ±0.12		PAKHLOVA	08	BELL	10.6 $e^+e^- \to D\overline{D}\gamma$
1.78 ±0.33 ±0.24		AUBERT	07BE	BABR	$e^+e^- \to D\overline{D}\gamma$
1.27 ±0.12 ±0.08		ABLIKIM	06L	BES2	$e^+e^- \to D\overline{D}$
2.43 ±1.50 ±0.43	34	[1] CHISTOV	04	BELL	$B^+ \to \psi(3770)K^+$
• • • We do not use the following data for averages, fits, limits, etc. • • •					
1.258±0.016±0.014		[2] DOBBS	07	CLEO	$e^+e^- \to D\overline{D}$

[1] See ADLER 88C for older measurements of this quantity.
[2] Superseded by BONVICINI 14.

$\Gamma(J/\psi\pi^+\pi^-)/\Gamma_{\text{total}}$ Γ_4/Γ

VALUE (units 10^{-3})	EVTS	DOCUMENT ID		TECN	COMMENT
1.93±0.28 OUR AVERAGE					
1.89±0.20±0.20	231 ± 33	ADAM	06	CLEO	$e^+e^- \to \psi(3770)$
3.4 ±1.4 ±0.9	17.8 ± 4.8	BAI	05	BES2	$e^+e^- \to \psi(3770)$

$\Gamma(J/\psi\pi^0\pi^0)/\Gamma_{\text{total}}$ Γ_5/Γ

VALUE (units 10^{-2})	EVTS	DOCUMENT ID		TECN	COMMENT
0.080±0.025±0.016	39 ± 14	ADAM	06	CLEO	$e^+e^- \to \psi(3770)$

$\Gamma(J/\psi\eta)/\Gamma_{\text{total}}$ Γ_6/Γ

VALUE (units 10^{-5})	EVTS	DOCUMENT ID		TECN	COMMENT
87±33±22	22 ± 10	ADAM	06	CLEO	$e^+e^- \to \psi(3770)$

$\Gamma(J/\psi\pi^0)/\Gamma_{\text{total}}$ Γ_7/Γ

VALUE (units 10^{-5})	CL%	EVTS	DOCUMENT ID		TECN	COMMENT
<28	90	<10	ADAM	06	CLEO	$e^+e^- \to \psi(3770)$

$\Gamma(e^+e^-)/\Gamma_{\text{total}}$ Γ_8/Γ

VALUE (units 10^{-5})	DOCUMENT ID		TECN	COMMENT
0.96±0.07 OUR FIT	Error includes scale factor of 1.3.			
1.3 ±0.2	RAPIDIS	77	LGW	e^+e^-

DECAYS TO LIGHT HADRONS

$\Gamma(b_1(1235)\pi)/\Gamma_{\text{total}}$ Γ_9/Γ

VALUE (units 10^{-5})	CL%	DOCUMENT ID		TECN	COMMENT
<1.4	90	[1] ADAMS	06	CLEO	$e^+e^- \to \psi(3770)$

[1] Comparing cross sections at $\sqrt{s} = 3.773$ GeV and $\sqrt{s} = 3.671$ GeV, neglecting interference, and using $\sigma(\psi(3770) \to D\overline{D}) = 6.39 \pm 0.20$ nb.

$\Gamma(\phi\eta')/\Gamma_{\text{total}}$ Γ_{10}/Γ

VALUE (units 10^{-4})	CL%	DOCUMENT ID		TECN	COMMENT
<7	90	[1] ADAMS	06	CLEO	$e^+e^- \to \psi(3770)$

[1] Comparing cross sections at $\sqrt{s} = 3.773$ GeV and $\sqrt{s} = 3.671$ GeV, neglecting interference, and using $\sigma(\psi(3770) \to D\overline{D}) = 6.39 \pm 0.20$ nb.

$\Gamma(\omega\eta')/\Gamma_{\text{total}}$ Γ_{11}/Γ

VALUE (units 10^{-4})	CL%	DOCUMENT ID		TECN	COMMENT
<4	90	[1] ADAMS	06	CLEO	$e^+e^- \to \psi(3770)$

[1] Comparing cross sections at $\sqrt{s} = 3.773$ GeV and $\sqrt{s} = 3.671$ GeV, neglecting interference, and using $\sigma(\psi(3770) \to D\overline{D}) = 6.39 \pm 0.20$ nb.

$\Gamma(\rho^0\eta')/\Gamma_{\text{total}}$ Γ_{12}/Γ

VALUE (units 10^{-4})	CL%	DOCUMENT ID		TECN	COMMENT
<6	90	[1] ADAMS	06	CLEO	$e^+e^- \to \psi(3770)$

[1] Comparing cross sections at $\sqrt{s} = 3.773$ GeV and $\sqrt{s} = 3.671$ GeV, neglecting interference, and using $\sigma(\psi(3770) \to D\overline{D}) = 6.39 \pm 0.20$ nb.

$\Gamma(\phi\eta)/\Gamma_{\text{total}}$ Γ_{13}/Γ

VALUE (units 10^{-4})	CL%	DOCUMENT ID		TECN	COMMENT
3.1±0.6±0.3		[1] ADAMS	06	CLEO	3.773 $e^+e^- \to \phi\eta$
• • • We do not use the following data for averages, fits, limits, etc. • • •					
<19	90	[2] ABLIKIM	07B	BES2	$e^+e^- \to \psi(3770)$

[1] Comparing cross sections at $\sqrt{s} = 3.773$ GeV and $\sqrt{s} = 3.671$ GeV, neglecting interference, and using $\sigma(\psi(3770) \to D\overline{D}) = 6.39 \pm 0.20$ nb.
[2] Assuming that interference effects between resonance and continuum can be neglected and using $\sigma^{obs}(e^+e^- \to \psi(3770)) = 7.15 \pm 0.38$ nb.

$\Gamma(\omega\eta)/\Gamma_{\text{total}}$ Γ_{14}/Γ

VALUE (units 10^{-5})	CL%	DOCUMENT ID		TECN	COMMENT
<1.4	90	[1] ADAMS	06	CLEO	$e^+e^- \to \psi(3770)$

[1] Comparing cross sections at $\sqrt{s} = 3.773$ GeV and $\sqrt{s} = 3.671$ GeV, neglecting interference, and using $\sigma(\psi(3770) \to D\overline{D}) = 6.39 \pm 0.20$ nb.

$\Gamma(\rho^0\eta)/\Gamma_{\text{total}}$ Γ_{15}/Γ

VALUE (units 10^{-4})	CL%	DOCUMENT ID		TECN	COMMENT
<5	90	[1] ADAMS	06	CLEO	$e^+e^- \to \psi(3770)$

[1] Comparing cross sections at $\sqrt{s} = 3.773$ GeV and $\sqrt{s} = 3.671$ GeV, neglecting interference, and using $\sigma(\psi(3770) \to D\overline{D}) = 6.39 \pm 0.20$ nb.

$\Gamma(\phi\pi^0)/\Gamma_{\text{total}}$ Γ_{16}/Γ

VALUE (units 10^{-5})	CL%	DOCUMENT ID		TECN	COMMENT
< 3	90	[1] ADAMS	06	CLEO	$e^+e^- \to \psi(3770)$

See key on page 885

• • • We do not use the following data for averages, fits, limits, etc. • • •

<50	90	[2]	ABLIKIM	07B	BES2	$e^+e^- \to \psi(3770)$

[1] Comparing cross sections at $\sqrt{s} = 3.773$ GeV and $\sqrt{s} = 3.671$ GeV, neglecting interference, and using $\sigma(\psi(3770) \to D\overline{D}) = 6.39 \pm 0.20$ nb.
[2] Assuming that interference effects between resonance and continuum can be neglected and using $\sigma^{obs}(e^+e^- \to \psi(3770)) = 7.15 \pm 0.38$ nb.

$\Gamma(\omega\pi^0)/\Gamma_{total}$ Γ_{17}/Γ

VALUE (units 10^{-4})	CL%	DOCUMENT ID		TECN	COMMENT
<6	90	[1] ADAMS	06	CLEO	$e^+e^- \to \psi(3770)$

[1] Comparing cross sections at $\sqrt{s} = 3.773$ GeV and $\sqrt{s} = 3.671$ GeV, neglecting interference, and using $\sigma(\psi(3770) \to D\overline{D}) = 6.39 \pm 0.20$ nb.

$\Gamma(\pi^+\pi^-\pi^0)/\Gamma_{total}$ Γ_{18}/Γ

VALUE (units 10^{-6})	CL%	DOCUMENT ID		TECN	COMMENT
<5	90	[1,2] ADAMS	06	CLEO	$e^+e^- \to \psi(3770)$

[1] Data suggest possible destructive interference with continuum.
[2] Comparing cross sections at $\sqrt{s} = 3.773$ GeV and $\sqrt{s} = 3.671$ GeV, neglecting interference, and using $\sigma(\psi(3770) \to D\overline{D}) = 6.39 \pm 0.20$ nb.

$\Gamma(\rho\pi)/\Gamma_{total}$ Γ_{19}/Γ

VALUE (units 10^{-6})	CL%	DOCUMENT ID		TECN	COMMENT
<5	90	[1,2] ADAMS	06	CLEO	$e^+e^- \to \psi(3770)$

[1] Comparing cross sections at $\sqrt{s} = 3.773$ GeV and $\sqrt{s} = 3.671$ GeV, neglecting interference, and using $\sigma(\psi(3770) \to D\overline{D}) = 6.39 \pm 0.20$ nb.
[2] Data suggest possible destructive interference with continuum.

$\Gamma(K^+K^-)/\Gamma_{total}$ Γ_{20}/Γ

VALUE	DOCUMENT ID			TECN	COMMENT
• • • We do not use the following data for averages, fits, limits, etc. • • •					
$\sim 10^{-5}$	[1] DRUZHININ	15		RVUE	$e^+e^- \to \psi(3770)$

[1] DRUZHININ 15 uses BABAR and CLEO data takitaking into account interference of the processes $e^+e^- \to K^+K^-$ and $e^+e^- \to K^0_S K^0_L$.

$\Gamma(K^*(892)^+K^- + \text{c.c.})/\Gamma_{total}$ Γ_{21}/Γ

VALUE (units 10^{-5})	CL%	DOCUMENT ID		TECN	COMMENT
<1.4	90	[1] ADAMS	06	CLEO	$e^+e^- \to \psi(3770)$

[1] Comparing cross sections at $\sqrt{s} = 3.773$ GeV and $\sqrt{s} = 3.671$ GeV, neglecting interference, and using $\sigma(\psi(3770) \to D\overline{D}) = 6.39 \pm 0.20$ nb.

$\Gamma(K^*(892)^0\overline{K}^0 + \text{c.c.})/\Gamma_{total}$ Γ_{22}/Γ

VALUE (units 10^{-3})	CL%	DOCUMENT ID		TECN	COMMENT
<1.2	90	[1] ADAMS	06	CLEO	$e^+e^- \to \psi(3770)$

[1] Comparing cross sections at $\sqrt{s} = 3.773$ GeV and $\sqrt{s} = 3.671$ GeV, neglecting interference, and using $\sigma(\psi(3770) \to D\overline{D}) = 6.39 \pm 0.20$ nb.

$\Gamma(K^0_S K^0_L)/\Gamma_{total}$ Γ_{23}/Γ

VALUE (units 10^{-5})	CL%	DOCUMENT ID		TECN	COMMENT
< 1.2	90	[1] CRONIN-HEN..06		CLEO	$e^+e^- \to \psi(3770)$
• • • We do not use the following data for averages, fits, limits, etc. • • •					
<21	90	[2] ABLIKIM	04F	BES	$e^+e^- \to \psi(3770)$

[1] Using $\sigma(e^+e^- \to \psi(3770) \to \text{hadrons}) = (6.38 \pm 0.08^{+0.41}_{-0.30})$ nb from BESSON 06 and $B(K^0_S \to \pi^+\pi^-) = 0.6895 \pm 0.0014$.
[2] Using $B(K^0_S \to \pi^+\pi^-) = 0.6860 \pm 0.0027$.

$\Gamma(2(\pi^+\pi^-))/\Gamma_{total}$ Γ_{24}/Γ

VALUE (units 10^{-4})	CL%	DOCUMENT ID		TECN	COMMENT
<11.2	90	[1] HUANG	06A	CLEO	$e^+e^- \to \psi(3770)$
• • • We do not use the following data for averages, fits, limits, etc. • • •					
<48	90	[2] ABLIKIM	07B	BES2	$e^+e^- \to \psi(3770)$

[1] Using $\sigma_{tot}(e^+e^- \to \psi(3770)) = 7.9 \pm 0.6$ nb at the resonance.
[2] Assuming that interference effects between resonance and continuum can be neglected and using $\sigma^{obs}(e^+e^- \to \psi(3770)) = 7.15 \pm 0.38$ nb.

$\Gamma(2(\pi^+\pi^-)\pi^0)/\Gamma_{total}$ Γ_{25}/Γ

VALUE (units 10^{-4})	CL%	DOCUMENT ID		TECN	COMMENT
<10.6	90	[1] HUANG	06A	CLEO	$e^+e^- \to \psi(3770)$
• • • We do not use the following data for averages, fits, limits, etc. • • •					
<62	90	[2] ABLIKIM	07B	BES2	$e^+e^- \to \psi(3770)$

[1] Using $\sigma_{tot}(e^+e^- \to \psi(3770)) = 7.9 \pm 0.6$ nb at the resonance.
[2] Assuming that interference effects between resonance and continuum can be neglected and using $\sigma^{obs}(e^+e^- \to \psi(3770)) = 7.15 \pm 0.38$ nb.

$\Gamma(2(\pi^+\pi^-\pi^0))/\Gamma_{total}$ Γ_{26}/Γ

VALUE (units 10^{-3})	CL%	EVTS	DOCUMENT ID		TECN	COMMENT
<58.5	90	305	ABLIKIM	08N	BES2	$e^+e^- \to \psi(3770)$

$\Gamma(\omega\pi^+\pi^-)/\Gamma_{total}$ Γ_{27}/Γ

VALUE (units 10^{-4})	CL%	DOCUMENT ID		TECN	COMMENT
< 6.0	90	[1] HUANG	06A	CLEO	$e^+e^- \to \psi(3770)$
• • • We do not use the following data for averages, fits, limits, etc. • • •					
<55	90	[2] ABLIKIM	07I	BES2	3.77 e^+e^-

[1] Using $\sigma_{tot}(e^+e^- \to \psi(3770)) = 7.9 \pm 0.6$ nb at the resonance.
[2] Assuming that interference effects between resonance and continuum can be neglected and using $\sigma^{obs}(e^+e^- \to \psi(3770)) = 7.15 \pm 0.38$ nb.

$\Gamma(3(\pi^+\pi^-))/\Gamma_{total}$ Γ_{28}/Γ

VALUE (units 10^{-4})	CL%	DOCUMENT ID		TECN	COMMENT
<91	90	[1] ABLIKIM	07B	BES2	$e^+e^- \to \psi(3770)$

[1] Assuming that interference effects between resonance and continuum can be neglected and using $\sigma^{obs}(e^+e^- \to \psi(3770)) = 7.15 \pm 0.38$ nb.

$\Gamma(3(\pi^+\pi^-)\pi^0)/\Gamma_{total}$ Γ_{29}/Γ

VALUE (units 10^{-4})	CL%	DOCUMENT ID		TECN	COMMENT
<137	90	[1] ABLIKIM	07B	BES2	$e^+e^- \to \psi(3770)$

[1] Assuming that interference effects between resonance and continuum can be neglected and using $\sigma^{obs}(e^+e^- \to \psi(3770)) = 7.15 \pm 0.38$ nb.

$\Gamma(3(\pi^+\pi^-)2\pi^0)/\Gamma_{total}$ Γ_{30}/Γ

VALUE (units 10^{-3})	CL%	EVTS	DOCUMENT ID		TECN	COMMENT
<117.4	90	59	ABLIKIM	08N	BES2	$e^+e^- \to \psi(3770)$

$\Gamma(\eta\pi^+\pi^-)/\Gamma_{total}$ Γ_{31}/Γ

VALUE (units 10^{-3})	CL%	DOCUMENT ID		TECN	COMMENT
<1.24	90	[1] HUANG	06A	CLEO	$e^+e^- \to \psi(3770)$
• • • We do not use the following data for averages, fits, limits, etc. • • •					
<2.3	90	[2] ABLIKIM	10D	BES2	$e^+e^- \to \psi(3770)$

[1] Using $\sigma_{tot}(e^+e^- \to \psi(3770)) = 7.9 \pm 0.6$ nb at the resonance.
[2] Assuming that interference effects between resonance and continuum can be neglected and using $\sigma^{obs}(e^+e^- \to \psi(3770)) = 7.15 \pm 0.38$ nb.

$\Gamma(\pi^+\pi^-2\pi^0)/\Gamma_{total}$ Γ_{32}/Γ

VALUE (units 10^{-3})	CL%	EVTS	DOCUMENT ID		TECN	COMMENT
<8.9	90	218	ABLIKIM	08N	BES2	$e^+e^- \to \psi(3770)$

$\Gamma(\rho^0\pi^+\pi^-)/\Gamma_{total}$ Γ_{33}/Γ

VALUE (units 10^{-3})	CL%	DOCUMENT ID		TECN	COMMENT
<6.9	90	[1] ABLIKIM	07F	BES2	$e^+e^- \to \psi(3770)$

[1] Assuming that interference effects between resonance and continuum can be neglected and using $\sigma^{obs}(e^+e^- \to \psi(3770)) = 7.15 \pm 0.38$ nb.

$\Gamma(\eta 3\pi)/\Gamma_{total}$ Γ_{34}/Γ

VALUE (units 10^{-4})	CL%	DOCUMENT ID		TECN	COMMENT
<13.4	90	[1] HUANG	06A	CLEO	$e^+e^- \to \psi(3770)$

[1] Using $\sigma_{tot}(e^+e^- \to \psi(3770)) = 7.9 \pm 0.6$ nb at the resonance.

$\Gamma(\eta 2(\pi^+\pi^-))/\Gamma_{total}$ Γ_{35}/Γ

VALUE (units 10^{-4})	CL%	DOCUMENT ID		TECN	COMMENT
<243	90	[1] ABLIKIM	07B	BES2	$e^+e^- \to \psi(3770)$

[1] Assuming that interference effects between resonance and continuum can be neglected and using $\sigma^{obs}(e^+e^- \to \psi(3770)) = 7.15 \pm 0.38$ nb.

$\Gamma(\eta\rho^0\pi^+\pi^-)/\Gamma_{total}$ Γ_{36}/Γ

VALUE (units 10^{-2})	CL%	DOCUMENT ID		TECN	COMMENT
<1.45	90	[1] ABLIKIM	10D	BES2	$e^+e^- \to \psi(3770)$

[1] Assuming that interference effects between resonance and continuum can be neglected and using $\sigma^{obs}(e^+e^- \to \psi(3770)) = 7.15 \pm 0.38$ nb.

$\Gamma(\eta' 3\pi)/\Gamma_{total}$ Γ_{37}/Γ

VALUE (units 10^{-4})	CL%	DOCUMENT ID		TECN	COMMENT
<24.4	90	[1] HUANG	06A	CLEO	$e^+e^- \to \psi(3770)$

[1] Using $\sigma_{tot}(e^+e^- \to \psi(3770)) = 7.9 \pm 0.6$ nb at the resonance.

$\Gamma(K^+K^-\pi^+\pi^-)/\Gamma_{total}$ Γ_{38}/Γ

VALUE (units 10^{-4})	CL%	DOCUMENT ID		TECN	COMMENT
< 9.0	90	[1] HUANG	06A	CLEO	$e^+e^- \to \psi(3770)$
• • • We do not use the following data for averages, fits, limits, etc. • • •					
<48	90	[2] ABLIKIM	07B	BES2	$e^+e^- \to \psi(3770)$

[1] Using $\sigma_{tot}(e^+e^- \to \psi(3770)) = 7.9 \pm 0.6$ nb at the resonance.
[2] Assuming that interference effects between resonance and continuum can be neglected and using $\sigma^{obs}(e^+e^- \to \psi(3770)) = 7.15 \pm 0.38$ nb.

$\Gamma(\phi\pi^+\pi^-)/\Gamma_{total}$ Γ_{39}/Γ

VALUE (units 10^{-4})	CL%	DOCUMENT ID		TECN	COMMENT
< 4.1	90	[1] HUANG	06A	CLEO	$e^+e^- \to \psi(3770)$

• • • We do not use the following data for averages, fits, limits, etc. • • •

<16		90	[2] ABLIKIM	07B	BES2	$e^+e^- \to \psi(3770)$

[1] Using $\sigma_{tot}(e^+e^- \to \psi(3770)) = 7.9 \pm 0.6$ nb at the resonance.
[2] Assuming that interference effects between resonance and continuum can be neglected and using $\sigma^{obs}(e^+e^- \to \psi(3770)) = 7.15 \pm 0.38$ nb.

$\Gamma(K^+K^-2\pi^0)/\Gamma_{total}$ Γ_{40}/Γ

VALUE (units 10^{-3})	CL%	EVTS	DOCUMENT ID		TECN	COMMENT
<4.2	90	14	ABLIKIM	08N	BES2	$e^+e^- \to \psi(3770)$

$\Gamma(4(\pi^+\pi^-))/\Gamma_{total}$ Γ_{41}/Γ

VALUE (units 10^{-3})	CL%	DOCUMENT ID		TECN	COMMENT
<16.7	90	[1] ABLIKIM	07F	BES2	$e^+e^- \to \psi(3770)$

[1] Assuming that interference effects between resonance and continuum can be neglected and using $\sigma^{obs}(e^+e^- \to \psi(3770)) = 7.15 \pm 0.38$ nb.

$\Gamma(4(\pi^+\pi^-)\pi^0)/\Gamma_{total}$ Γ_{42}/Γ

VALUE (units 10^{-3})	CL%	DOCUMENT ID		TECN	COMMENT
<30.6	90	[1] ABLIKIM	07F	BES2	$e^+e^- \to \psi(3770)$

[1] Assuming that interference effects between resonance and continuum can be neglected and using $\sigma^{obs}(e^+e^- \to \psi(3770)) = 7.15 \pm 0.38$ nb.

$\Gamma(\phi f_0(980))/\Gamma_{total}$ Γ_{43}/Γ

VALUE (units 10^{-4})	CL%	DOCUMENT ID		TECN	COMMENT
<4.5	90	[1] HUANG	06A	CLEO	$e^+e^- \to \psi(3770)$

[1] Using $\sigma_{tot}(e^+e^- \to \psi(3770)) = 7.9 \pm 0.6$ nb at the resonance.

$\Gamma(K^+K^-\pi^+\pi^-\pi^0)/\Gamma_{total}$ Γ_{44}/Γ

VALUE (units 10^{-4})	CL%	DOCUMENT ID		TECN	COMMENT
< 23.6	90	[1] HUANG	06A	CLEO	$e^+e^- \to \psi(3770)$

• • • We do not use the following data for averages, fits, limits, etc. • • •

<111	90	[2] ABLIKIM	07B	BES2	$e^+e^- \to \psi(3770)$

[1] Using $\sigma_{tot}(e^+e^- \to \psi(3770)) = 7.9 \pm 0.6$ nb at the resonance.
[2] Assuming that interference effects between resonance and continuum can be neglected and using $\sigma^{obs}(e^+e^- \to \psi(3770)) = 7.15 \pm 0.38$ nb.

$\Gamma(K^+K^-\rho^0\pi^0)/\Gamma_{total}$ Γ_{45}/Γ

VALUE (units 10^{-4})	CL%	DOCUMENT ID		TECN	COMMENT
<8	90	[1] ABLIKIM	07I	BES2	3.77 e^+e^-

[1] Assuming that interference effects between resonance and continuum can be neglected and using $\sigma^{obs}(e^+e^- \to \psi(3770)) = 7.15 \pm 0.38$ nb.

$\Gamma(K^+K^-\rho^+\pi^-)/\Gamma_{total}$ Γ_{46}/Γ

VALUE (units 10^{-4})	CL%	DOCUMENT ID		TECN	COMMENT
<146	90	[1] ABLIKIM	07I	BES2	3.77 e^+e^-

[1] Assuming that interference effects between resonance and continuum can be neglected and using $\sigma^{obs}(e^+e^- \to \psi(3770)) = 7.15 \pm 0.38$ nb.

$\Gamma(\omega K^+K^-)/\Gamma_{total}$ Γ_{47}/Γ

VALUE (units 10^{-4})	CL%	DOCUMENT ID		TECN	COMMENT
< 3.4	90	[1] HUANG	06A	CLEO	$e^+e^- \to \psi(3770)$

• • • We do not use the following data for averages, fits, limits, etc. • • •

<66	90	[2] ABLIKIM	07I	BES2	3.77 e^+e^-

[1] Using $\sigma_{tot}(e^+e^- \to \psi(3770)) = 7.9 \pm 0.6$ nb at the resonance.
[2] Assuming that interference effects between resonance and continuum can be neglected and using $\sigma^{obs}(e^+e^- \to \psi(3770)) = 7.15 \pm 0.38$ nb.

$\Gamma(\phi\pi^+\pi^-\pi^0)/\Gamma_{total}$ Γ_{48}/Γ

VALUE (units 10^{-4})	CL%	DOCUMENT ID		TECN	COMMENT
<38	90	[1] ABLIKIM	07I	BES2	3.77 e^+e^-

[1] Assuming that interference effects between resonance and continuum can be neglected and using $\sigma^{obs}(e^+e^- \to \psi(3770)) = 7.15 \pm 0.38$ nb.

$\Gamma(K^{*0}K^-\pi^+\pi^0 + \text{c.c.})/\Gamma_{total}$ Γ_{49}/Γ

VALUE (units 10^{-4})	CL%	DOCUMENT ID		TECN	COMMENT
<162	90	[1] ABLIKIM	07I	BES2	3.77 e^+e^-

[1] Assuming that interference effects between resonance and continuum can be neglected and using $\sigma^{obs}(e^+e^- \to \psi(3770)) = 7.15 \pm 0.38$ nb.

$\Gamma(K^{*+}K^-\pi^+\pi^- + \text{c.c.})/\Gamma_{total}$ Γ_{50}/Γ

VALUE (units 10^{-4})	CL%	DOCUMENT ID		TECN	COMMENT
<323	90	[1] ABLIKIM	07I	BES2	3.77 e^+e^-

[1] Assuming that interference effects between resonance and continuum can be neglected and using $\sigma^{obs}(e^+e^- \to \psi(3770)) = 7.15 \pm 0.38$ nb.

$\Gamma(K^+K^-\pi^+\pi^-2\pi^0)/\Gamma_{total}$ Γ_{51}/Γ

VALUE (units 10^{-3})	CL%	EVTS	DOCUMENT ID		TECN	COMMENT
<26.7	90	24	ABLIKIM	08N	BES2	$e^+e^- \to \psi(3770)$

$\Gamma(K^+K^-2(\pi^+\pi^-))/\Gamma_{total}$ Γ_{52}/Γ

VALUE (units 10^{-3})	CL%	DOCUMENT ID		TECN	COMMENT
<10.3	90	[1] ABLIKIM	07F	BES2	$e^+e^- \to \psi(3770)$

[1] Assuming that interference effects between resonance and continuum can be neglected and using $\sigma^{obs}(e^+e^- \to \psi(3770)) = 7.15 \pm 0.38$ nb.

$\Gamma(K^+K^-2(\pi^+\pi^-)\pi^0)/\Gamma_{total}$ Γ_{53}/Γ

VALUE (units 10^{-3})	CL%	DOCUMENT ID		TECN	COMMENT
<36.0	90	[1] ABLIKIM	07F	BES2	$e^+e^- \to \psi(3770)$

[1] Assuming that interference effects between resonance and continuum can be neglected and using $\sigma^{obs}(e^+e^- \to \psi(3770)) = 7.15 \pm 0.38$ nb.

$\Gamma(\eta K^+K^-)/\Gamma_{total}$ Γ_{54}/Γ

VALUE (units 10^{-4})	CL%	DOCUMENT ID		TECN	COMMENT
< 4.1	90	[1] HUANG	06A	CLEO	$e^+e^- \to \psi(3770)$

• • • We do not use the following data for averages, fits, limits, etc. • • •

<31	90	[2] ABLIKIM	10D	BES2	$e^+e^- \to \psi(3770)$

[1] Using $\sigma_{tot}(e^+e^- \to \psi(3770)) = 7.9 \pm 0.6$ nb at the resonance.
[2] Assuming that interference effects between resonance and continuum can be neglected and using $\sigma^{obs}(e^+e^- \to \psi(3770)) = 7.15 \pm 0.38$ nb.

$\Gamma(\eta K^+K^-\pi^+\pi^-)/\Gamma_{total}$ Γ_{55}/Γ

VALUE (units 10^{-2})	CL%	DOCUMENT ID		TECN	COMMENT
<1.24	90	[1] ABLIKIM	10D	BES2	$e^+e^- \to \psi(3770)$

[1] Assuming that interference effects between resonance and continuum can be neglected and using $\sigma^{obs}(e^+e^- \to \psi(3770)) = 7.15 \pm 0.38$ nb.

$\Gamma(\rho^0K^+K^-)/\Gamma_{total}$ Γ_{56}/Γ

VALUE (units 10^{-3})	CL%	DOCUMENT ID		TECN	COMMENT
<5.0	90	[1] ABLIKIM	07F	BES2	$e^+e^- \to \psi(3770)$

[1] Assuming that interference effects between resonance and continuum can be neglected and using $\sigma^{obs}(e^+e^- \to \psi(3770)) = 7.15 \pm 0.38$ nb.

$\Gamma(2(K^+K^-))/\Gamma_{total}$ Γ_{57}/Γ

VALUE (units 10^{-4})	CL%	DOCUMENT ID		TECN	COMMENT
< 6.0	90	[1] HUANG	06A	CLEO	$e^+e^- \to \psi(3770)$

• • • We do not use the following data for averages, fits, limits, etc. • • •

<17	90	[2] ABLIKIM	07B	BES2	$e^+e^- \to \psi(3770)$

[1] Using $\sigma_{tot}(e^+e^- \to \psi(3770)) = 7.9 \pm 0.6$ nb at the resonance.
[2] Assuming that interference effects between resonance and continuum can be neglected and using $\sigma^{obs}(e^+e^- \to \psi(3770)) = 7.15 \pm 0.38$ nb.

$\Gamma(\phi K^+K^-)/\Gamma_{total}$ Γ_{58}/Γ

VALUE (units 10^{-4})	CL%	DOCUMENT ID		TECN	COMMENT
< 7.5	90	[1] HUANG	06A	CLEO	$e^+e^- \to \psi(3770)$

• • • We do not use the following data for averages, fits, limits, etc. • • •

<24	90	[2] ABLIKIM	07B	BES2	$e^+e^- \to \psi(3770)$

[1] Using $\sigma_{tot}(e^+e^- \to \psi(3770)) = 7.9 \pm 0.6$ nb at the resonance.
[2] Assuming that interference effects between resonance and continuum can be neglected and using $\sigma^{obs}(e^+e^- \to \psi(3770)) = 7.15 \pm 0.38$ nb.

$\Gamma(2(K^+K^-)\pi^0)/\Gamma_{total}$ Γ_{59}/Γ

VALUE (units 10^{-4})	CL%	DOCUMENT ID		TECN	COMMENT
< 2.9	90	[1] HUANG	06A	CLEO	$e^+e^- \to \psi(3770)$

• • • We do not use the following data for averages, fits, limits, etc. • • •

<46	90	[2] ABLIKIM	07B	BES2	$e^+e^- \to \psi(3770)$

[1] Using $\sigma_{tot}(e^+e^- \to \psi(3770)) = 7.9 \pm 0.6$ nb at the resonance.
[2] Assuming that interference effects between resonance and continuum can be neglected and using $\sigma^{obs}(e^+e^- \to \psi(3770)) = 7.15 \pm 0.38$ nb.

$\Gamma(2(K^+K^-)\pi^+\pi^-)/\Gamma_{total}$ Γ_{60}/Γ

VALUE (units 10^{-3})	CL%	DOCUMENT ID		TECN	COMMENT
<3.2	90	[1] ABLIKIM	07F	BES2	$e^+e^- \to \psi(3770)$

[1] Assuming that interference effects between resonance and continuum can be neglected and using $\sigma^{obs}(e^+e^- \to \psi(3770)) = 7.15 \pm 0.38$ nb.

$\Gamma(K^0_S K^-\pi^+)/\Gamma_{total}$ Γ_{61}/Γ

VALUE (units 10^{-3})	CL%	EVTS	DOCUMENT ID		TECN	COMMENT
<3.2	90	18	ABLIKIM	08M	BES2	$e^+e^- \to \psi(3770)$

$\Gamma(K^0_S K^-\pi^+\pi^0)/\Gamma_{total}$ Γ_{62}/Γ

VALUE (units 10^{-3})	CL%	EVTS	DOCUMENT ID		TECN	COMMENT
<13.3	90	40	ABLIKIM	08M	BES2	$e^+e^- \to \psi(3770)$

$\Gamma(K^0_S K^-\rho^+)/\Gamma_{total}$ Γ_{63}/Γ

VALUE (units 10^{-3})	CL%	DOCUMENT ID		TECN	COMMENT
<6.6	90	ABLIKIM	09C	BES2	$e^+e^- \to \psi(3770)$

$\Gamma(K_S^0 K^- 2\pi^+\pi^-)/\Gamma_{total}$ Γ_{64}/Γ

VALUE (units 10^{-3})	CL%	EVTS	DOCUMENT ID		TECN	COMMENT
<8.7	90	39	ABLIKIM	08M	BES2	$e^+e^- \to \psi(3770)$

$\Gamma(K_S^0 K^-\pi^+\rho^0)/\Gamma_{total}$ Γ_{65}/Γ

VALUE (units 10^{-2})	CL%	DOCUMENT ID		TECN	COMMENT
<1.6	90	ABLIKIM	09C	BES2	$e^+e^- \to \psi(3770)$

$\Gamma(K_S^0 K^-\pi^+\eta)/\Gamma_{total}$ Γ_{66}/Γ

VALUE (units 10^{-2})	CL%	DOCUMENT ID		TECN	COMMENT
<1.3	90	ABLIKIM	09C	BES2	$e^+e^- \to \psi(3770)$

$\Gamma(K_S^0 K^- 2\pi^+\pi^-\pi^0)/\Gamma_{total}$ Γ_{67}/Γ

VALUE (units 10^{-3})	CL%	EVTS	DOCUMENT ID		TECN	COMMENT
<41.8	90	23	ABLIKIM	08M	BES2	$e^+e^- \to \psi(3770)$

$\Gamma(K_S^0 K^- 2\pi^+\pi^-\eta)/\Gamma_{total}$ Γ_{68}/Γ

VALUE (units 10^{-2})	CL%	DOCUMENT ID		TECN	COMMENT
<4.8	90	ABLIKIM	09C	BES2	$e^+e^- \to \psi(3770)$

$\Gamma(K_S^0 K^-\pi^+ 2(\pi^+\pi^-))/\Gamma_{total}$ Γ_{69}/Γ

VALUE (units 10^{-3})	CL%	EVTS	DOCUMENT ID		TECN	COMMENT
<12.2	90	4	ABLIKIM	08M	BES2	$e^+e^- \to \psi(3770)$

$\Gamma(K_S^0 K^-\pi^+ 2\pi^0)/\Gamma_{total}$ Γ_{70}/Γ

VALUE (units 10^{-3})	CL%	EVTS	DOCUMENT ID		TECN	COMMENT
<26.5	90	17	ABLIKIM	08M	BES2	$e^+e^- \to \psi(3770)$

$\Gamma(K_S^0 K^- K^+ K^-\pi^+)/\Gamma_{total}$ Γ_{71}/Γ

VALUE (units 10^{-3})	CL%	DOCUMENT ID		TECN	COMMENT
<4.9	90	ABLIKIM	09C	BES2	$e^+e^- \to \psi(3770)$

$\Gamma(K_S^0 K^- K^+ K^-\pi^+\pi^0)/\Gamma_{total}$ Γ_{72}/Γ

VALUE (units 10^{-2})	CL%	DOCUMENT ID		TECN	COMMENT
<3.0	90	ABLIKIM	09C	BES2	$e^+e^- \to \psi(3770)$

$\Gamma(K_S^0 K^- K^+ K^-\pi^+\eta)/\Gamma_{total}$ Γ_{73}/Γ

VALUE (units 10^{-2})	CL%	DOCUMENT ID		TECN	COMMENT
<2.2	90	ABLIKIM	09C	BES2	$e^+e^- \to \psi(3770)$

$\Gamma(K^{*0} K^-\pi^+ + \text{c.c.})/\Gamma_{total}$ Γ_{74}/Γ

VALUE (units 10^{-3})	CL%	DOCUMENT ID		TECN	COMMENT
<9.7	90	[1] ABLIKIM	07F	BES2	$e^+e^- \to \psi(3770)$

[1] Assuming that interference effects between resonance and continuum can be neglected and using $\sigma^{obs}(e^+e^- \to \psi(3770)) = 7.15 \pm 0.38$ nb.

$\Gamma(p\overline{p})/\Gamma_{total}$ Γ_{75}/Γ

VALUE (units 10^{-6})	EVTS	DOCUMENT ID		TECN	COMMENT
• • • We do not use the following data for averages, fits, limits, etc. • • •					
not seen		[1] AAIJ	17AD	LHCB	$pp \to B^+X \to p\overline{p}K^+X$
$7.1^{+\ 8.6}_{-\ 2.9}$	684	[2] ABLIKIM	14L	BES3	$e^+e^- \to \psi(3770)$
310 ± 30	684	[3] ABLIKIM	14L	BES3	$e^+e^- \to \psi(3770)$

[1] AAIJ 17AD reports $B(B^+ \to \psi(3770)\,K^+ \to p\overline{p}K^+)/B(B^+ \to J/\psi K^+ \to p\overline{p}K^+) < 0.09\ (0.10)$ at 90% (95%) CL.
[2] Solution I of two equivalent solutions in a fit with a resonance interfering with continuum.
[3] Solution II of two equivalent solutions in a fit with a resonance interfering with continuum.

$\Gamma(p\overline{p}\pi^0)/\Gamma_{total}$ Γ_{76}/Γ

VALUE (units 10^{-4})	CL%	DOCUMENT ID		TECN	COMMENT
< 0.4	90	[1,2] ABLIKIM	14O	BES3	$e^+e^- \to \psi(3770)$
• • • We do not use the following data for averages, fits, limits, etc. • • •					
$59\ ^{+3}_{-2}\pm 5$		[1,3] ABLIKIM	14O	BES3	$e^+e^- \to \psi(3770)$
<12	90	[4] ABLIKIM	07B	BES2	$e^+e^- \to \psi(3770)$

[1] Calculated by the authors using $\sigma(e^+e^- \to \psi(3770) \to \text{hadrons}) = 6.36 \pm 0.08^{+0.41}_{-0.30}$ nb from BESSON 10.
[2] Solution I of two equivalent solutions in a fit with a resonance interfering with continuum.
[3] Solution II of two equivalent solutions in a fit with a resonance interfering with continuum.
[4] Assuming that interference effects between resonance and continuum can be neglected and using $\sigma^{obs}(e^+e^- \to \psi(3770)) = 7.15 \pm 0.38$ nb.

$\Gamma(p\overline{p}\pi^+\pi^-)/\Gamma_{total}$ Γ_{77}/Γ

VALUE (units 10^{-4})	CL%	DOCUMENT ID		TECN	COMMENT
< 5.8	90	[1] HUANG	06A	CLEO	$e^+e^- \to \psi(3770)$
• • • We do not use the following data for averages, fits, limits, etc. • • •					
<16	90	[2] ABLIKIM	07B	BES2	$e^+e^- \to \psi(3770)$

[1] Using $\sigma_{tot}(e^+e^- \to \psi(3770)) = 7.9 \pm 0.6$ nb at the resonance.
[2] Assuming that interference effects between resonance and continuum can be neglected and using $\sigma^{obs}(e^+e^- \to \psi(3770)) = 7.15 \pm 0.38$ nb.

$\Gamma(\lambda\overline{\lambda})/\Gamma_{total}$ Γ_{78}/Γ

VALUE (units 10^{-4})	CL%	DOCUMENT ID		TECN	COMMENT
<1.2	90	[1] HUANG	06A	CLEO	$e^+e^- \to \psi(3770)$
• • • We do not use the following data for averages, fits, limits, etc. • • •					
<4	90	[2] ABLIKIM	07F	BES2	$e^+e^- \to \psi(3770)$

[1] Using $\sigma_{tot}(e^+e^- \to \psi(3770)) = 7.9 \pm 0.6$ nb at the resonance.
[2] Assuming that interference effects between resonance and continuum can be neglected and using $\sigma^{obs}(e^+e^- \to \psi(3770)) = 7.15 \pm 0.38$ nb.

$\Gamma(p\overline{p}\pi^+\pi^-\pi^0)/\Gamma_{total}$ Γ_{79}/Γ

VALUE (units 10^{-4})	CL%	DOCUMENT ID		TECN	COMMENT
<18.5	90	[1] HUANG	06A	CLEO	$e^+e^- \to \psi(3770)$
• • • We do not use the following data for averages, fits, limits, etc. • • •					
<73	90	[2] ABLIKIM	07B	BES2	$e^+e^- \to \psi(3770)$

[1] Using $\sigma_{tot}(e^+e^- \to \psi(3770)) = 7.9 \pm 0.6$ nb at the resonance.
[2] Assuming that interference effects between resonance and continuum can be neglected and using $\sigma^{obs}(e^+e^- \to \psi(3770)) = 7.15 \pm 0.38$ nb.

$\Gamma(\omega p\overline{p})/\Gamma_{total}$ Γ_{80}/Γ

VALUE (units 10^{-4})	CL%	DOCUMENT ID		TECN	COMMENT
< 2.9	90	[1] HUANG	06A	CLEO	$e^+e^- \to \psi(3770)$
• • • We do not use the following data for averages, fits, limits, etc. • • •					
<30	90	[2] ABLIKIM	07I	BES2	3.77 e^+e^-

[1] Using $\sigma_{tot}(e^+e^- \to \psi(3770)) = 7.9 \pm 0.6$ nb at the resonance.
[2] Using $\sigma^{obs} = 7.15 \pm 0.27 \pm 0.27$ nb and neglecting interference.

$\Gamma(\lambda\overline{\lambda}\pi^0)/\Gamma_{total}$ Γ_{81}/Γ

VALUE (units 10^{-4})	CL%	DOCUMENT ID		TECN	COMMENT
< 0.7	90	[1] ABLIKIM	13Q	BES3	$e^+e^- \to \psi(3770)$
• • • We do not use the following data for averages, fits, limits, etc. • • •					
<12	90	[2] ABLIKIM	07I	BES2	3.77 e^+e^-

[1] Assuming that interference effects between resonance and continuum can be neglected.
[2] Assuming that interference effects between resonance and continuum can be neglected and using $\sigma^{obs}(e^+e^- \to \psi(3770)) = 7.15 \pm 0.38$ nb.

$\Gamma(p\overline{p}2(\pi^+\pi^-))/\Gamma_{total}$ Γ_{82}/Γ

VALUE (units 10^{-3})	CL%	DOCUMENT ID		TECN	COMMENT
<2.6	90	[1] ABLIKIM	07F	BES2	$e^+e^- \to \psi(3770)$

[1] Assuming that interference effects between resonance and continuum can be neglected and using $\sigma^{obs}(e^+e^- \to \psi(3770)) = 7.15 \pm 0.38$ nb.

$\Gamma(\eta p\overline{p})/\Gamma_{total}$ Γ_{83}/Γ

VALUE (units 10^{-4})	CL%	DOCUMENT ID		TECN	COMMENT
< 5.4	90	[1] HUANG	06A	CLEO	$e^+e^- \to \psi(3770)$
• • • We do not use the following data for averages, fits, limits, etc. • • •					
<11	90	[2] ABLIKIM	10D	BES2	$e^+e^- \to \psi(3770)$

[1] Using $\sigma_{tot}(e^+e^- \to \psi(3770)) = 7.9 \pm 0.6$ nb at the resonance.
[2] Assuming that interference effects between resonance and continuum can be neglected and using $\sigma^{obs}(e^+e^- \to \psi(3770)) = 7.15 \pm 0.38$ nb.

$\Gamma(\eta p\overline{p}\pi^+\pi^-)/\Gamma_{total}$ Γ_{84}/Γ

VALUE (units 10^{-3})	CL%	DOCUMENT ID		TECN	COMMENT
<3.3	90	[1] ABLIKIM	10D	BES2	$e^+e^- \to \psi(3770)$

[1] Assuming that interference effects between resonance and continuum can be neglected and using $\sigma^{obs}(e^+e^- \to \psi(3770)) = 7.15 \pm 0.38$ nb.

$\Gamma(\rho^0 p\overline{p})/\Gamma_{total}$ Γ_{85}/Γ

VALUE (units 10^{-3})	CL%	DOCUMENT ID		TECN	COMMENT
<1.7	90	[1] ABLIKIM	07F	BES2	$e^+e^- \to \psi(3770)$

[1] Assuming that interference effects between resonance and continuum can be neglected and using $\sigma^{obs}(e^+e^- \to \psi(3770)) = 7.15 \pm 0.38$ nb.

$\Gamma(p\overline{p}K^+K^-)/\Gamma_{total}$ Γ_{86}/Γ

VALUE (units 10^{-4})	CL%	DOCUMENT ID		TECN	COMMENT
< 3.2	90	[1] HUANG	06A	CLEO	$e^+e^- \to \psi(3770)$
• • • We do not use the following data for averages, fits, limits, etc. • • •					
<11	90	[2] ABLIKIM	07B	BES2	$e^+e^- \to \psi(3770)$

[1] Using $\sigma_{tot}(e^+e^- \to \psi(3770)) = 7.9 \pm 0.6$ nb at the resonance.
[2] Assuming that interference effects between resonance and continuum can be neglected and using $\sigma^{obs}(e^+e^- \to \psi(3770)) = 7.15 \pm 0.38$ nb.

$\Gamma(\eta p\overline{p}K^+K^-)/\Gamma_{total}$ Γ_{87}/Γ

VALUE (units 10^{-3})	CL%	DOCUMENT ID		TECN	COMMENT
<6.9	90	[1] ABLIKIM	10D	BES2	$e^+e^- \to \psi(3770)$

[1] Assuming that interference effects between resonance and continuum can be neglected and using $\sigma^{obs}(e^+e^- \to \psi(3770)) = 7.15 \pm 0.38$ nb.

$\Gamma(\pi^0 p\overline{p}K^+K^-)/\Gamma_{total}$ Γ_{88}/Γ

VALUE (units 10^{-3})	CL%	DOCUMENT ID		TECN	COMMENT
<1.2	90	[1] ABLIKIM	10D	BES2	$e^+e^- \to \psi(3770)$

[1] Assuming that interference effects between resonance and continuum can be neglected and using $\sigma^{obs}(e^+e^- \to \psi(3770)) = 7.15 \pm 0.38$ nb.

$\Gamma(\phi p\overline{p})/\Gamma_{total}$ Γ_{89}/Γ

VALUE (units 10^{-4})	CL%	DOCUMENT ID		TECN	COMMENT
<1.3	90	[1] HUANG	06A	CLEO	$e^+e^- \to \psi(3770)$
• • • We do not use the following data for averages, fits, limits, etc. • • •					
<9	90	[2] ABLIKIM	07B	BES2	$e^+e^- \to \psi(3770)$

[1] Using $\sigma_{tot}(e^+e^- \to \psi(3770)) = 7.9 \pm 0.6$ nb at the resonance.
[2] Assuming that interference effects between resonance and continuum can be neglected and using $\sigma^{obs}(e^+e^- \to \psi(3770)) = 7.15 \pm 0.38$ nb.

$\Gamma(\Lambda\overline{\Lambda}\pi^+\pi^-)/\Gamma_{total}$ Γ_{90}/Γ

VALUE (units 10^{-4})	CL%	DOCUMENT ID		TECN	COMMENT
< 2.5	90	[1] HUANG	06A	CLEO	$e^+e^- \to \psi(3770)$
• • • We do not use the following data for averages, fits, limits, etc. • • •					
< 4.7	90	[2] ABLIKIM	13Q	BES3	$e^+e^- \to \psi(3770)$
<39	90	[3] ABLIKIM	07F	BES2	$e^+e^- \to \psi(3770)$

[1] Using $\sigma_{tot}(e^+e^- \to \psi(3770)) = 7.9 \pm 0.6$ nb at the resonance.
[2] Assuming that interference effects between resonance and continuum can be neglected.
[3] Assuming that interference effects between resonance and continuum can be neglected and using $\sigma^{obs}(e^+e^- \to \psi(3770)) = 7.15 \pm 0.38$ nb.

$\Gamma(\Lambda\overline{p}K^+)/\Gamma_{total}$ Γ_{91}/Γ

VALUE (units 10^{-4})	CL%	DOCUMENT ID		TECN	COMMENT
<2.8	90	[1] HUANG	06A	CLEO	$e^+e^- \to \psi(3770)$

[1] Using $\sigma_{tot}(e^+e^- \to \psi(3770)) = 7.9 \pm 0.6$ nb at the resonance.

$\Gamma(\Lambda\overline{p}K^+\pi^+\pi^-)/\Gamma_{total}$ Γ_{92}/Γ

VALUE (units 10^{-4})	CL%	DOCUMENT ID		TECN	COMMENT
<6.3	90	[1] HUANG	06A	CLEO	$e^+e^- \to \psi(3770)$

[1] Using $\sigma_{tot}(e^+e^- \to \psi(3770)) = 7.9 \pm 0.6$ nb at the resonance.

$\Gamma(\Lambda\overline{\Lambda}\eta)/\Gamma_{total}$ Γ_{93}/Γ

VALUE (units 10^{-4})	CL%	DOCUMENT ID		TECN	COMMENT
<1.9	90	[1] ABLIKIM	13Q	BES3	$e^+e^- \to \psi(3770)$

[1] Assuming that interference effects between resonance and continuum can be neglected.

$\Gamma(\Sigma^+\overline{\Sigma}^-)/\Gamma_{total}$ Γ_{94}/Γ

VALUE (units 10^{-4})	CL%	DOCUMENT ID		TECN	COMMENT
<1.0	90	[1] ABLIKIM	13Q	BES3	$e^+e^- \to \psi(3770)$

[1] Assuming that interference effects between resonance and continuum can be neglected.

$\Gamma(\Sigma^0\overline{\Sigma}^0)/\Gamma_{total}$ Γ_{95}/Γ

VALUE (units 10^{-4})	CL%	DOCUMENT ID		TECN	COMMENT
<0.4	90	[1] ABLIKIM	13Q	BES3	$e^+e^- \to \psi(3770)$

[1] Assuming that interference effects between resonance and continuum can be neglected.

$\Gamma(\Xi^+\overline{\Xi}^-)/\Gamma_{total}$ Γ_{96}/Γ

VALUE (units 10^{-4})	CL%	DOCUMENT ID		TECN	COMMENT
<1.5	90	[1] ABLIKIM	13Q	BES3	$e^+e^- \to \psi(3770)$

[1] Assuming that interference effects between resonance and continuum can be neglected.

$\Gamma(\Xi^0\overline{\Xi}^0)/\Gamma_{total}$ Γ_{97}/Γ

VALUE (units 10^{-4})	CL%	DOCUMENT ID		TECN	COMMENT
<1.4	90	[1] ABLIKIM	13Q	BES3	$e^+e^- \to \psi(3770)$

[1] Assuming that interference effects between resonance and continuum can be neglected.

RADIATIVE DECAYS

$\Gamma(\gamma\chi_{c2})/\Gamma_{total}$ Γ_{98}/Γ

VALUE (units 10^{-3})	CL%	DOCUMENT ID		TECN	COMMENT
<0.64	90	[1] ABLIKIM	15J	BES3	$e^+e^- \to \psi(3770) \to \gamma\gamma J/\psi$
• • • We do not use the following data for averages, fits, limits, etc. • • •					
<2.0	90	[2] BRIERE	06	CLEO	$e^+e^- \to \psi(3770) \to \gamma +$ hadrons
<0.9	90	[3] COAN	06A	CLEO	$e^+e^- \to \psi(3770) \to \gamma\gamma J/\psi$

[1] This limit is equivalent to $(0.25 \pm 0.21 \pm 0.18) \times 10^{-3}$ branching fraction value.
[2] Uses $B(\psi(2S) \to \gamma\chi_{c2}) = 9.22 \pm 0.11 \pm 0.46$ % from ATHAR 04, $\psi(2S)$ mass and width from PDG 04, and $\Gamma_{ee}(\psi(2S)) = 2.54 \pm 0.03 \pm 0.11$ keV from ADAM 06.
[3] Using $\Gamma_{ee}(\psi(2S)) = (2.54 \pm 0.03 \pm 0.11)$ keV from ADAM 06 and taking $\sigma(e^+e^- \to D\overline{D})$ from HE 05 for $\sigma(e^+e^- \to \psi(3770))$.

$\Gamma(\gamma\chi_{c1})/\Gamma_{total}$ Γ_{99}/Γ

VALUE (units 10^{-3})	EVTS	DOCUMENT ID		TECN	COMMENT
2.49±0.23 OUR AVERAGE					
1.98±0.78±0.05	202	[1] ABLIKIM	16B	BES3	$e^+e^- \to \psi(3770) \to \gamma +$ hadrons
2.48±0.15±0.23	0.6k	ABLIKIM	15J	BES3	$e^+e^- \to \psi(3770) \to \gamma\gamma J/\psi$
2.4 ±0.8 ±0.2		[2] ABLIKIM	14H	BES3	$e^+e^- \to \psi(3770) \to K^0_S K^\pm\pi^\mp$
2.9 ±0.5 ±0.4		[3] BRIERE	06	CLEO	$e^+e^- \to \psi(3770) \to \gamma +$ hadrons, $\gamma\gamma J/\psi$
• • • We do not use the following data for averages, fits, limits, etc. • • •					
3.9 ±1.4 ±0.6	54	[4] BRIERE	06	CLEO	$e^+e^- \to \psi(3770) \to \gamma +$ hadrons
2.8 ±0.5 ±0.4	53	[5] COAN	06A	CLEO	$e^+e^- \to \psi(3770) \to \gamma\gamma J/\psi$

[1] ABLIKIM 16B reports $(1.94 \pm 0.42 \pm 0.64) \times 10^{-3}$ from a measurement of $[\Gamma(\psi(3770) \to \gamma\chi_{c1})/\Gamma_{total}]$ / $[B(\psi(2S) \to \gamma\chi_{c1}(1P))]$ assuming $B(\psi(2S) \to \gamma\chi_{c1}(1P)) = (9.55 \pm 0.31) \times 10^{-2}$, which we rescale to our best value $B(\psi(2S) \to \gamma\chi_{c1}(1P)) = (9.75 \pm 0.24) \times 10^{-2}$. Our first error is their experiment's error and our second error is the systematic error from using our best value.
[2] ABLIKIM 14H reports $[\Gamma(\psi(3770) \to \gamma\chi_{c1})/\Gamma_{total}] \times [B(\chi_{c1}(1P) \to K^0_S K^\pm\pi^\mp)] = (8.51 \pm 2.39 \pm 1.42) \times 10^{-6}$ which we divide by our best value $B(\chi_{c1}(1P) \to K^0_S K^\pm\pi^\mp) = 0.00349 \pm 0.00029$. Our first error is their experiment's error and our second error is the systematic error from using our best value. We have calculated the best value of $B(\chi_{c1}(1P) \to K^0_S K^\pm\pi^\mp)$ as 1/2 of $B(\chi_{c1}(1P) \to \overline{K}^0 K^+\pi^-$ + c.c.) $= (7.0 \pm 0.6) \times 10^{-3}$.
[3] Averages the two measurements from COAN 06A and BRIERE 06.
[4] Uses $B(\psi(2S) \to \gamma\chi_{c1}) = 9.07 \pm 0.11 \pm 0.54$ % from ATHAR 04, $\psi(2S)$ mass and width from PDG 04, and $\Gamma_{ee}(\psi(2S)) = 2.54 \pm 0.03 \pm 0.11$ keV from ADAM 06.
[5] Using $\Gamma_{ee}(\psi(2S)) = (2.54 \pm 0.03 \pm 0.11)$ keV from ADAM 06 and taking $\sigma(e^+e^- \to D\overline{D})$ from HE 05 for $\sigma(e^+e^- \to \psi(3770))$.

$\Gamma(\gamma\chi_{c1})/\Gamma(J/\psi\pi^+\pi^-)$ Γ_{99}/Γ_4

VALUE	EVTS	DOCUMENT ID		TECN	COMMENT
1.49±0.31±0.26	53 ± 10	[1] COAN	06A	CLEO	$e^+e^- \to \psi(3770) \to \gamma\gamma J/\psi$

[1] Using $B(\psi(3770) \to J/\psi\pi^+\pi^-) = (1.89 \pm 0.20 \pm 0.20) \times 10^{-3}$ from ADAM 06.

$\Gamma(\gamma\chi_{c0})/\Gamma_{total}$ Γ_{100}/Γ

VALUE (units 10^{-3})	CL%	EVTS	DOCUMENT ID		TECN	COMMENT
6.9±0.6 OUR AVERAGE						
6.7±0.7±0.1		2.2K	[1] ABLIKIM	16B	BES3	$e^+e^- \to \psi(3770) \to \gamma +$ hadrons
7.3±0.7±0.6		274	BRIERE	06	CLEO	$e^+e^- \to \psi(3770) \to \gamma +$ hadrons
• • • We do not use the following data for averages, fits, limits, etc. • • •						
< 44	90		[2] COAN	06A	CLEO	$e^+e^- \to \psi(3770) \to \gamma\gamma J/\psi$

[1] ABLIKIM 16B reports $(6.88 \pm 0.28 \pm 0.67) \times 10^{-3}$ from a measurement of $[\Gamma(\psi(3770) \to \gamma\chi_{c0})/\Gamma_{total}]$ / $[B(\psi(2S) \to \gamma\chi_{c0}(1P))]$ assuming $B(\psi(2S) \to \gamma\chi_{c0}(1P)) = (9.99 \pm 0.27) \times 10^{-2}$, which we rescale to our best value $B(\psi(2S) \to \gamma\chi_{c0}(1P)) = (9.79 \pm 0.20) \times 10^{-2}$. Our first error is their experiment's error and our second error is the systematic error from using our best value.
[2] Using $\Gamma_{ee}(\psi(2S)) = (2.54 \pm 0.03 \pm 0.11)$ keV from ADAM 06 and taking $\sigma(e^+e^- \to D\overline{D})$ from HE 05 for $\sigma(e^+e^- \to \psi(3770))$.

$\Gamma(\gamma\chi_{c0})/\Gamma(\gamma\chi_{c2})$ Γ_{100}/Γ_{98}

VALUE	CL%	DOCUMENT ID		TECN	COMMENT
• • • We do not use the following data for averages, fits, limits, etc. • • •					
>8	90	[1] BRIERE	06	CLEO	$e^+e^- \to \psi(3770)$

[1] Not independent of other results in BRIERE 06.

$\Gamma(\gamma\chi_{c0})/\Gamma(\gamma\chi_{c1})$ Γ_{100}/Γ_{99}

VALUE	DOCUMENT ID		TECN	COMMENT
• • • We do not use the following data for averages, fits, limits, etc. • • •				
2.5±0.6	[1] BRIERE	06	CLEO	$e^+e^- \to \psi(3770)$

[1] Not independent of other results in BRIERE 06.

$\Gamma(\gamma\eta_c)/\Gamma_{total}$ Γ_{101}/Γ

VALUE	CL%	DOCUMENT ID		TECN
<7 × 10⁻⁴	90	[1] ABLIKIM	14H	BES3

[1] ABLIKIM 14H reports $[\Gamma(\psi(3770) \to \gamma\eta_c)/\Gamma_{total}] \times [B(\eta_c(1S) \to K^0_S K^\pm\pi^\mp)] < 16 \times 10^{-6}$ which we divide by our best value $B(\eta_c(1S) \to K^0_S K^\pm\pi^\mp) = 2.44 \times 10^{-2}$. We have calculated the best value of $B(\eta_c(1S) \to K^0_S K^\pm\pi^\mp)$ as 1/3 of $B(\eta_c(1S) \to K\overline{K}\pi) = 7.3 \times 10^{-2}$.

$\Gamma(\gamma\eta_c(2S))/\Gamma_{total}$ Γ_{102}/Γ

VALUE	CL%	DOCUMENT ID		TECN
<9 × 10⁻⁴	90	[1] ABLIKIM	14H	BES3

[1] ABLIKIM 14H reports $[\Gamma(\psi(3770) \to \gamma\eta_c(2S))/\Gamma_{total}] \times [B(\eta_c(2S) \to K^0_S K^\pm\pi^\mp)] < 5.6 \times 10^{-6}$ which we divide by our best value $B(\eta_c(2S) \to K^0_S K^\pm\pi^\mp) = 6 \times 10^{-3}$.

We have calculated the best value of $B(\eta_c(2S) \to K^0_S K^\pm \pi^\mp)$ as 1/3 of $B(\eta_c(2S) \to K\overline{K}\pi) = 1.9 \times 10^{-2}$.

$\Gamma(\gamma\eta')/\Gamma_{total}$ Γ_{103}/Γ

VALUE (units 10^{-4})	CL%	DOCUMENT ID		TECN	COMMENT
<1.8	90	[1] PEDLAR	09	CLE3	$\psi(2S) \to \gamma X$

[1] Assuming maximal destructive interference between $\psi(3770)$ and continuum sources.

$\Gamma(\gamma\eta)/\Gamma_{total}$ Γ_{104}/Γ

VALUE (units 10^{-4})	CL%	DOCUMENT ID		TECN	COMMENT
<1.5	90	[1] PEDLAR	09	CLE3	$\psi(2S) \to \gamma X$

[1] Assuming maximal destructive interference between $\psi(3770)$ and continuum sources.

$\Gamma(\gamma\pi^0)/\Gamma_{total}$ Γ_{105}/Γ

VALUE (units 10^{-4})	CL%	DOCUMENT ID		TECN	COMMENT
<2	90	PEDLAR	09	CLE3	$\psi(2S) \to \gamma X$

$\psi(3770)$ REFERENCES

AAIJ	17AD	PL B769 305	R. Aaij *et al.*	(LHCb Collab.)
SHAMOV	17	PL B769 187	A.G. Shamov, K.Yu. Todyshev	
ABLIKIM	16B	PL B753 103	M. Ablikim *et al.*	(BES III Collab.)
ABLIKIM	15J	PR D91 092009	M. Ablikim *et al.*	(BES III Collab.)
DRUZHININ	15	PR D92 054024	V.P. Druzhinin	(NOVO)
ABLIKIM	14H	PR D89 112005	M. Ablikim *et al.*	(BES III Collab.)
ABLIKIM	14L	PL B735 101	M. Ablikim *et al.*	(BES III Collab.)
ABLIKIM	14O	PR D90 032007	M. Ablikim *et al.*	(BES III Collab.)
BONVICINI	14	PR D89 072002	G. Bonvicini *et al.*	(CLEO Collab.)
ABLIKIM	13Q	PR D87 112011	Ablikim M. *et al.*	(BES III Collab.)
ANASHIN	12A	PL B711 292	V.V. Anashin *et al.*	(KEDR Collab.)
ABLIKIM	10D	EPJ C66 11	M. Ablikim *et al.*	(BES II Collab.)
BESSON	10	PRL 104 159901 (errat.)	D. Besson *et al.*	(CLEO Collab.)
ABLIKIM	09C	EPJ C64 243	M. Ablikim *et al.*	(BES Collab.)
PEDLAR	09	PR D79 111101	T.K. Pedlar *et al.*	(CLEO Collab.)
ABLIKIM	08B	PL B659 74	M. Ablikim *et al.*	(BES Collab.)
ABLIKIM	08D	PL B660 315	M. Ablikim *et al.*	(BES Collab.)
ABLIKIM	08M	PL B670 179	M. Ablikim *et al.*	(BES Collab.)
ABLIKIM	08N	PL B670 184	M. Ablikim *et al.*	(BES Collab.)
AUBERT	08B	PR D77 011102	B. Aubert *et al.*	(BABAR Collab.)
BRODZICKA	08	PRL 100 092001	J. Brodzicka *et al.*	(BELLE Collab.)
PAKHLOVA	08	PR D77 011103	G. Pakhlova *et al.*	(BELLE Collab.)
ABLIKIM	07B	PL B650 111	M. Ablikim *et al.*	(BES Collab.)
ABLIKIM	07E	PL B652 238	M. Ablikim *et al.*	(BES Collab.)
ABLIKIM	07F	PL B656 30	M. Ablikim *et al.*	(BES Collab.)
ABLIKIM	07I	EPJ C52 805	M. Ablikim *et al.*	(BES Collab.)
ABLIKIM	07K	PR D76 122002	M. Ablikim *et al.*	(BES Collab.)
AUBERT	07BE	PR D76 111105	B. Aubert *et al.*	(BABAR Collab.)
DOBBS	07	PR D76 112001	S. Dobbs *et al.*	(CLEO Collab.)
ABLIKIM	06L	PRL 97 121801	M. Ablikim *et al.*	(BES Collab.)
ABLIKIM	06N	PL B641 145	M. Ablikim *et al.*	(BES Collab.)
ADAM	06	PRL 96 082004	N.E. Adam *et al.*	(CLEO Collab.)
ADAMS	06	PR D73 012002	G.S. Adams *et al.*	(CLEO Collab.)
BESSON	06	PRL 96 092002	D. Besson *et al.*	(CLEO Collab.)
Also		PRL 104 159901 (errat.)	D. Besson *et al.*	(CLEO Collab.)
BRIERE	06	PR D74 031106	R.A. Briere *et al.*	(CLEO Collab.)
COAN	06A	PRL 96 182002	T.E. Coan *et al.*	(CLEO Collab.)
CRONIN-HEN...	06	PR D74 012005	D. Cronin-Hennessy *et al.*	(CLEO Collab.)
HUANG	06A	PRL 96 032003	G.S. Huang *et al.*	(CLEO Collab.)
BAI	05	PL B605 63	J.Z. Bai *et al.*	(BES Collab.)
HE	05	PRL 95 121801	Q. He *et al.*	(CLEO Collab.)
Also		PRL 96 199903 (errat.)	Q. He *et al.*	(CLEO Collab.)
ABLIKIM	04F	PR D70 077101	M. Ablikim *et al.*	(BES Collab.)
ATHAR	04	PR D70 112002	S.B. Athar *et al.*	(CLEO Collab.)
CHISTOV	04	PRL 93 051803	R. Chistov *et al.*	(BELLE Collab.)
PDG	04	PL B592 1	S. Eidelman *et al.*	(PDG Collab.)
BAI	02C	PRL 88 101802	J.Z. Bai *et al.*	(BES Collab.)
ADLER	88C	PRL 60 89	J. Adler *et al.*	(Mark III Collab.)
SCHINDLER	80	PR D21 2716	R.H. Schindler *et al.*	(Mark II Collab.)
BACINO	78	PRL 40 671	W.J. Bacino *et al.*	(SLAC, UCLA, UCI)
RAPIDIS	77	PRL 39 526	P.A. Rapidis *et al.*	(LGW Collab.)

$\psi_2(3823)$

$I^G(J^{PC}) = 0^-(2^{--})$
I, J, P need confirmation.

was $\psi(3823)$, $X(3823)$

Seen by BHARDWAJ 13 in $B \to \chi_{c1}\gamma K$ and ABLIKIM 15S in $e^+e^- \to \pi^+\pi^-\gamma\chi_{c1}$ decays as a narrow peak in the invariant mass distribution of the $\chi_{c1}\gamma$ system. Properties consistent with the $\psi_2(1^3D_2)$ $c\overline{c}$ state.

$\psi_2(3823)$ MASS

VALUE (MeV)	EVTS	DOCUMENT ID		TECN	COMMENT
3822.2±1.2 OUR AVERAGE					
3821.7±1.3±0.7	19 ± 5	[1] ABLIKIM	15S	BES3	$e^+e^- \to \pi^+\pi^-\chi_{c1}\gamma$
3823.1±1.8±0.7	33 ± 10	[2] BHARDWAJ	13	BELL	$B \to \chi_{c1}\gamma K$

[1] From a simultaneous unbinned maximum likelihood fit of $e^+e^- \to \pi^+\pi^-\chi_{c1}\gamma$ data (the $\pi^+\pi^-$ recoil mass) taken at $\sqrt{s}$ values of 4.23, 4.26, 4.36, 4.42, and 4.60 GeV to simulated events including both $\psi(2S) \to \chi_{c1}\gamma$ and $\psi_2(3823) \to \chi_{c1}\gamma$ together, with floating mass scale offset for $\psi(2S)$, floating $\psi_2(3823)$ mass, and zero $\psi_2(3823)$ width, resulting in a significance of 5.9σ when including systematic uncertainties.

[2] From a simultaneous fit to $B^\pm \to (\chi_{c1}\gamma)K^\pm$ and $B^0 \to (\chi_{c1}\gamma)K^0_S$ with significance 4.0σ including systematics. Corrected for the measured $\psi(2S)$ mass using $B \to \psi(2S)K \to (\gamma\chi_{c1})K$ decays.

$\psi_2(3823)$ WIDTH

VALUE (MeV)	CL%	DOCUMENT ID		TECN	COMMENT
<16	90	[1] ABLIKIM	15S	BES3	$e^+e^- \to \pi^+\pi^-\chi_{c1}\gamma$
• • • We do not use the following data for averages, fits, limits, etc. • • •					
<24	90	[2] BHARDWAJ	13	BELL	$B \to \chi_{c1}\gamma K$

[1] From a fit of $e^+e^- \to \pi^+\pi^-\chi_{c1}\gamma$ data (the $\pi^+\pi^-$ recoil mass) taken at $\sqrt{s}$ values of 4.23, 4.26, 4.36, 4.42, and 4.60 GeV to a Breit-Wigner function with the mass fixed from the likelihood fit above, Gaussian resolution smearing, and floating width.

[2] From a simultaneous fit to $B^\pm \to (\chi_{c1}\gamma)K^\pm$ and $B^0 \to (\chi_{c1}\gamma)K^0_S$ with significance 4.0σ including systematics.

$\psi_2(3823)$ DECAY MODES

	Mode	Fraction (Γ_i/Γ)
Γ_1	$\chi_{c1}\gamma$	seen
Γ_2	$\chi_{c2}\gamma$	not seen

$\psi_2(3823)$ BRANCHING RATIOS

$\Gamma(\chi_{c1}\gamma)/\Gamma_{total}$ Γ_1/Γ

VALUE	EVTS	DOCUMENT ID		TECN	COMMENT
seen	33 ± 10	[1] BHARDWAJ	13	BELL	$B^+ \to \chi_{c1}\gamma K^+$

[1] Reported $B(B^\pm \to \psi_2(3823)K^\pm) \times B(\psi_2(3823) \to \gamma\chi_{c1}) = (9.7 \pm 2.8 \pm 1.1) \times 10^{-6}$ with statistical significance 3.8σ.

$\Gamma(\chi_{c2}\gamma)/\Gamma_{total}$ Γ_2/Γ

VALUE	DOCUMENT ID		TECN	COMMENT
not seen	[1] ABLIKIM	15S	BES3	$e^+e^- \to \pi^+\pi^-\chi_{c2}\gamma$
not seen	[2] BHARDWAJ	13	BELL	$B^+ \to \chi_{c2}\gamma K^+$

[1] From a simultaneous unbinned maximum likelihood fit of $e^+e^- \to \pi^+\pi^-\chi_{c2}\gamma$ data (the $\pi^+\pi^-$ recoil mass) taken at $\sqrt{s}$ values of 4.23, 4.26, 4.36, 4.42, and 4.60 GeV to simulated events including both $\psi(2S) \to \chi_{c2}\gamma$ and $\psi_2(3823) \to \chi_{c2}\gamma$ together, with floating mass scale offset for $\psi(2S)$, $\psi_2(3823)$ mass floating (fixed to that above), and zero $\psi_2(3823)$ width.

[2] Reported $B(B^\pm \to \psi_2(3823)K^\pm) \times B(\psi_2(3823) \to \gamma\chi_{c2}) < 3.6 \times 10^{-6}$ at 90% CL.

$\Gamma(\chi_{c2}\gamma)/\Gamma(\chi_{c1}\gamma)$ Γ_2/Γ_1

VALUE	CL%	DOCUMENT ID		TECN	COMMENT
<0.41	90	BHARDWAJ	13	BELL	$B^+ \to \chi_{c1/c2}\gamma K^+$
• • • We do not use the following data for averages, fits, limits, etc. • • •					
<0.42	90	[1] ABLIKIM	15S	BES3	$e^+e^- \to \pi^+\pi^-\chi_{c1}\gamma$

[1] From a simultaneous unbinned maximum likelihood fit of $e^+e^- \to \pi^+\pi^-\chi_{c1(2)}\gamma$ data (the $\pi^+\pi^-$ recoil mass) taken at $\sqrt{s}$ values of 4.23, 4.26, 4.36, 4.42, and 4.60 GeV to simulated events including both $\psi(2S) \to \chi_{c1(2)}\gamma$ and $\psi_2(3823) \to \chi_{c1(2)}\gamma$ together, with floating mass scale offset for $\psi(2S)$, $\psi_2(3823)$ mass floating (fixed to that above), and zero $\psi_2(3823)$ width.

$\psi_2(3823)$ REFERENCES

ABLIKIM	15S	PRL 115 011803	M. Ablikim *et al.*	(BES III Collab.)
BHARDWAJ	13	PRL 111 032001	V. Bhardwaj *et al.*	(BELLE Collab.)

$\chi_{c0}(3860)$

$I^G(J^{PC}) = 0^+(0^{++})$

OMITTED FROM SUMMARY TABLE

Observed by CHILIKIN 17 using full amplitude analysis of the process $e^+e^- \to J/\psi D\overline{D}$, where $D = D^0, D^+$.

$\chi_{c0}(3860)$ MASS

VALUE (MeV)	DOCUMENT ID		TECN	COMMENT
3862^{+26+40}_{-32-13}	CHILIKIN	17	BELL	$e^+e^- \to J/\psi D\overline{D}$

$\chi_{c0}(3860)$ WIDTH

VALUE (MeV)	DOCUMENT ID		TECN	COMMENT
$201^{+154+88}_{-67-82}$	CHILIKIN	17	BELL	$e^+e^- \to J/\psi D\overline{D}$

$\chi_{c0}(3860)$ DECAY MODES

	Mode	Fraction (Γ_i/Γ)
Γ_1	$D^0\overline{D}^0$	seen
Γ_2	D^+D^-	seen

$\chi_{c0}(3860)$ BRANCHING RATIOS

$\Gamma(D^0\overline{D}^0)/\Gamma_{total}$ — Γ_1/Γ

VALUE	DOCUMENT ID		TECN	COMMENT
seen	CHILIKIN	17	BELL	$e^+e^- \to J/\psi D^0\overline{D}^0$

$\Gamma(D^+D^-)/\Gamma_{total}$ — Γ_2/Γ

VALUE	DOCUMENT ID		TECN	COMMENT
seen	CHILIKIN	17	BELL	$e^+e^- \to J/\psi D^+D^-$

$\chi_{c0}(3860)$ REFERENCES

CHILIKIN 17 PR D95 112003 K. Chilikin *et al.* (BELLE Collab.) JPC

$\chi_{c1}(3872)$

$I^G(J^{PC}) = 0^+(1^{++})$

also known as $X(3872)$

This state shows properties different from a conventional $q\overline{q}$ state. A candidate for an exotic structure. See the review on non-$q\overline{q}$ states.

First observed by CHOI 03 in $B \to K\pi^+\pi^- J/\psi(1S)$ decays as a narrow peak in the invariant mass distribution of the $\pi^+\pi^- J/\psi(1S)$ final state. Isovector hypothesis excluded by AUBERT 05B and CHOI 11.

AAIJ 13Q perform a full five-dimensional amplitude analysis of the angular correlations between the decay products in $B^+ \to \chi_{c1}(3872)K^+$ decays, where $\chi_{c1}(3872) \to J/\psi\pi^+\pi^-$ and $J/\psi \to \mu^+\mu^-$, which unambiguously gives the $J^{PC} = 1^{++}$ assignment under the assumption that the $\pi^+\pi^-$ and J/ψ are in an S-wave. AAIJ 15AO extend this analysis with more data to limit D-wave contributions to $< 4\%$ at 95% CL.

See our note on "Developments in Heavy Quarkonium Spectroscopy".

$\chi_{c1}(3872)$ MASS FROM $J/\psi X$ MODE

VALUE (MeV)	EVTS	DOCUMENT ID		TECN	COMMENT
3871.69± 0.17 OUR AVERAGE					
3871.9 ± 0.7 ±0.2	20 ± 5	ABLIKIM	14	BES3	$e^+e^- \to J/\psi\pi^+\pi^-\gamma$
3871.95± 0.48±0.12	0.6k	AAIJ	12H	LHCB	$pp \to J/\psi\pi^+\pi^- X$
3871.85± 0.27±0.19	~ 170	[1] CHOI	11	BELL	$B \to K\pi^+\pi^- J/\psi$
3873 $^{+1.8}_{-1.6}$ ±1.3	27 ± 8	[2] DEL-AMO-SA.	10B	BABR	$B \to \omega J/\psi K$
3871.61± 0.16±0.19	6k	[2,3] AALTONEN	09AU	CDF2	$p\overline{p} \to J/\psi\pi^+\pi^- X$
3871.4 ± 0.6 ±0.1	93.4	AUBERT	08Y	BABR	$B^+ \to K^+ J/\psi\pi^+\pi^-$
3868.7 ± 1.5 ±0.4	9.4	AUBERT	08Y	BABR	$B^0 \to K^0_S J/\psi\pi^+\pi^-$
3871.8 ± 3.1 ±3.0	522	[2,4] ABAZOV	04F	D0	$p\overline{p} \to J/\psi\pi^+\pi^- X$
• • • We do not use the following data for averages, fits, limits, etc. • • •					
3868.6 ± 1.2 ±0.2	8	[5] AUBERT	06	BABR	$B^0 \to K^0_S J/\psi\pi^+\pi^-$
3871.3 ± 0.6 ±0.1	61	[5] AUBERT	06	BABR	$B^- \to K^- J/\psi\pi^+\pi^-$
3873.4 ± 1.4	25	[6] AUBERT	05R	BABR	$B^+ \to K^+ J/\psi\pi^+\pi^-$
3871.3 ± 0.7 ±0.4	730	[2,7] ACOSTA	04	CDF2	$p\overline{p} \to J/\psi\pi^+\pi^- X$
3872.0 ± 0.6 ±0.5	36	[8] CHOI	03	BELL	$B \to K\pi^+\pi^- J/\psi$
3836 ±13	58	[2,9] ANTONIAZZI	94	E705	300 $\pi^\pm$Li $\to J/\psi\pi^+\pi^- X$

[1] The mass difference for the $\chi_{c1}(3872)$ produced in B^+ and B^0 decays is $(-0.71 \pm 0.96 \pm 0.19)$ MeV.
[2] Width consistent with detector resolution.
[3] A possible equal mixture of two states with a mass difference greater than 3.6 MeV/c^2 is excluded at 95% CL.
[4] Calculated from the corresponding $m_{\chi_{c1}(3872)} - m_{J/\psi}$ using $m_{J/\psi}$=3096.916 MeV.
[5] Calculated from the corresponding $m_{\chi_{c1}(3872)} - m_{\psi(2S)}$ using $m_{\psi(2S)}$ = 3686.093 MeV. Superseded by AUBERT 08Y.
[6] Calculated from the corresponding $m_{\chi_{c1}(3872)} - m_{\psi(2S)}$ using $m_{\psi(2S)}$ = 3685.96MeV. Superseded by AUBERT 06.
[7] Superseded by AALTONEN 09AU.
[8] Superseded by CHOI 11.
[9] A lower mass value can be due to an incorrect momentum scale for soft pions.

$\chi_{c1}(3872)$ MASS FROM $\overline{D}^{*0}D^0$ MODE

VALUE (MeV)	EVTS	DOCUMENT ID		TECN	COMMENT
• • • We do not use the following data for averages, fits, limits, etc. • • •					
3872.9 $^{+0.6}_{-0.4}$ $^{+0.4}_{-0.5}$	50	[1,2] AUSHEV	10	BELL	$B \to \overline{D}^{*0}D^0 K$
3875.1 $^{+0.7}_{-0.5}$ ±0.5	33 ± 6	[2] AUBERT	08B	BABR	$B \to \overline{D}^{*0}D^0 K$
3875.2±0.7 $^{+0.9}_{-1.8}$	24 ± 6	[2,3] GOKHROO	06	BELL	$B \to D^0\overline{D}^0\pi^0 K$

[1] Calculated from the measured $m_{\chi_{c1}(3872)} - m_{D^{*0}} - m_{\overline{D}^0} = 1.1^{+0.6}_{-0.4}{}^{+0.1}_{-0.3}$ MeV.
[2] Experiments report $D^{*0}\overline{D}^0$ invariant mass above $D^{*0}\overline{D}^0$ threshold because D^{*0} decay products are kinematically constrained to the D^{*0} mass, even though the D^{*0} may decay off-shell.
[3] Superseded by AUSHEV 10.

$m_{\chi_{c1}(3872)} - m_{J/\psi}$

VALUE (MeV)	EVTS	DOCUMENT ID		TECN	COMMENT
774.9±3.1±3.0	522	ABAZOV	04F	D0	$p\overline{p} \to J/\psi\pi^+\pi^- X$

$m_{\chi_{c1}(3872)} - m_{\psi(2S)}$

VALUE (MeV)	EVTS	DOCUMENT ID		TECN	COMMENT
• • • We do not use the following data for averages, fits, limits, etc. • • •					
187.4±1.4	25	[1] AUBERT	05R	BABR	$B^+ \to K^+ J/\psi\pi^+\pi^-$

[1] Superseded by AUBERT 06.

$\chi_{c1}(3872)$ WIDTH

VALUE (MeV)	CL%	EVTS	DOCUMENT ID		TECN	COMMENT
<1.2	90		CHOI	11	BELL	$B \to K\pi^+\pi^- J/\psi$
• • • We do not use the following data for averages, fits, limits, etc. • • •						
<2.4	90		ABLIKIM	14	BES3	$e^+e^- \to J/\psi\pi^+\pi^-\gamma$
<3.3	90		AUBERT	08Y	BABR	$B^+ \to K^+ J/\psi\pi^+\pi^-$
<4.1	90	69	AUBERT	06	BABR	$B \to K\pi^+\pi^- J/\psi$
<2.3	90	36	[1] CHOI	03	BELL	$B \to K\pi^+\pi^- J/\psi$

[1] Superseded by CHOI 11.

$\chi_{c1}(3872)$ WIDTH FROM $\overline{D}^{*0}D^0$ MODE

VALUE (MeV)	EVTS	DOCUMENT ID		TECN	COMMENT
• • • We do not use the following data for averages, fits, limits, etc. • • •					
3.9 $^{+2.8}_{-1.4}$ $^{+0.2}_{-1.1}$	50	[1] AUSHEV	10	BELL	$B \to \overline{D}^{*0}D^0 K$
3.0 $^{+1.9}_{-1.4}$ ±0.9	33 ± 6	AUBERT	08B	BABR	$B \to \overline{D}^{*0}D^0 K$

[1] With a measured value of $B(B \to \chi_{c1}(3872)K) \times B(\chi_{c1}(3872) \to D^{*0}\overline{D}^0) = (0.80 \pm 0.20 \pm 0.10) \times 10^{-4}$, assumed to be equal for both charged and neutral modes.

$\chi_{c1}(3872)$ DECAY MODES

	Mode	Fraction (Γ_i/Γ)
Γ_1	e^+e^-	
Γ_2	$\pi^+\pi^- J/\psi(1S)$	> 3.2 %
Γ_3	$\rho^0 J/\psi(1S)$	
Γ_4	$\omega J/\psi(1S)$	> 2.3 %
Γ_5	$D^0\overline{D}^0\pi^0$	>40 %
Γ_6	$\overline{D}^{*0}D^0$	>30 %
Γ_7	$\gamma\gamma$	
Γ_8	$D^0\overline{D}^0$	
Γ_9	D^+D^-	
Γ_{10}	$\gamma\chi_{c1}$	
Γ_{11}	$\gamma\chi_{c2}$	
Γ_{12}	$\gamma J/\psi$	$> 7 \times 10^{-3}$
Γ_{13}	$\gamma\psi(2S)$	> 4 %
Γ_{14}	$\pi^+\pi^-\eta_c(1S)$	not seen
Γ_{15}	$\pi^+\pi^-\chi_{c1}$	not seen
Γ_{16}	$p\overline{p}$	not seen
	***C*-violating decays**	
Γ_{17}	$\eta J/\psi$	

$\chi_{c1}(3872)$ PARTIAL WIDTHS

$\Gamma(e^+e^-)$ — Γ_1

VALUE (eV)	CL%	DOCUMENT ID		TECN	COMMENT
• • • We do not use the following data for averages, fits, limits, etc. • • •					
< 4.3	90	[1] ABLIKIM	15V	BES3	4.0–4.4 $e^+e^- \to \pi^+\pi^- J/\psi$
<280	90	[2] YUAN	04	RVUE	$e^+e^- \to \pi^+\pi^- J/\psi$

[1] ABLIKIM 15V reports this limit from the measurement of $\Gamma(\chi_{c1}(3872) \to \pi^+\pi^- J/\psi(1S)) \times \Gamma(\chi_{c1}(3872) \to e^+e^-)/\Gamma < 0.13$ eV using $\Gamma(\chi_{c1}(3872) \to \pi^+\pi^- J/\psi(1S))/\Gamma = 3\%$.
[2] Using BAI 98E data on $e^+e^- \to \pi^+\pi^-\ell^+\ell^-$. Assuming that $\Gamma(\pi^+\pi^- J/\psi)$ of $\chi_{c1}(3872)$ is the same as that of $\psi(2S)$ (85.4 keV).

$\chi_{c1}(3872)$ Γ(i)$\Gamma(e^+e^-)/\Gamma$(total)

$\Gamma(\pi^+\pi^- J/\psi(1S)) \times \Gamma(e^+e^-)/\Gamma_{total}$ — $\Gamma_2\Gamma_1/\Gamma$

VALUE (eV)	CL%	DOCUMENT ID		TECN	COMMENT
< 0.13	90	ABLIKIM	15V	BES3	4.0–4.4 $e^+e^- \to \pi^+\pi^- J/\psi$

• • • We do not use the following data for averages, fits, limits, etc. • • •

< 6.2	90	1,2 AUBERT	05D	BABR	10.6 e^+e^- → $K^+K^-\pi^+\pi^-\gamma$	
< 8.3	90	2 DOBBS	05	CLE3	e^+e^- → $\pi^+\pi^- J/\psi$	
<10	90	3 YUAN	04	RVUE	e^+e^- → $\pi^+\pi^- J/\psi$	

[1] Using $B(\chi_{c1}(3872) \to J/\psi\pi^+\pi^-) \cdot B(J/\psi \to \mu^+\mu^-) \cdot \Gamma(\chi_{c1}(3872) \to e^+e^-) < 0.37$ eV from AUBERT 05D and $B(J/\psi \to \mu^+\mu^-) = 0.0588 \pm 0.0010$ from the PDG 04.

[2] Assuming $\chi_{c1}(3872)$ has $J^{PC} = 1^{--}$.

[3] Using BAI 98E data on $e^+e^- \to \pi^+\pi^-\ell^+\ell^-$. From theoretical calculation of the production cross section and using $B(J/\psi \to \mu^+\mu^-) = (5.88 \pm 0.10)\%$.

$\chi_{c1}(3872)$ Γ(i)Γ(γγ)/Γ(total)

$\Gamma(\pi^+\pi^- J/\psi(1S)) \times \Gamma(\gamma\gamma)/\Gamma_{total}$ $\Gamma_2\Gamma_7/\Gamma$

VALUE (eV)	CL%	DOCUMENT ID	TECN	COMMENT
• • • We do not use the following data for averages, fits, limits, etc. • • •				
<12.9	90	1 DOBBS 05	CLE3	$e^+e^- \to \pi^+\pi^- J/\psi\gamma$

[1] Assuming $\chi_{c1}(3872)$ has positive C parity and spin 0.

$\Gamma(\omega J/\psi(1S)) \times \Gamma(\gamma\gamma)/\Gamma_{total}$ $\Gamma_4\Gamma_7/\Gamma$

VALUE (eV)	CL%	DOCUMENT ID	TECN	COMMENT
• • • We do not use the following data for averages, fits, limits, etc. • • •				
<1.7	90	1 LEES 12AD	BABR	$e^+e^- \to e^+e^-\omega J/\psi$

[1] Assuming $\chi_{c1}(3872)$ has spin 2.

$\Gamma(\pi^+\pi^-\eta_c(1S)) \times \Gamma(\gamma\gamma)/\Gamma_{total}$ $\Gamma_{14}\Gamma_7/\Gamma$

VALUE (eV)	CL%	DOCUMENT ID	TECN	COMMENT
<11.1	90	LEES 12AE	BABR	$e^+e^- \to e^+e^-\pi^+\pi^-\eta_c$

$\chi_{c1}(3872)$ BRANCHING RATIOS

$\Gamma(\pi^+\pi^- J/\psi(1S))/\Gamma_{total}$ Γ_2/Γ

VALUE	EVTS	DOCUMENT ID	TECN	COMMENT
>0.032	93 ± 17	1 AUBERT 08Y	BABR	$B \to \chi_{c1}(3872) K$
• • • We do not use the following data for averages, fits, limits, etc. • • •				
seen	151	2 BALA 15	BELL	$B \to \chi_{c1}(3872) K\pi$
>0.05	30	3 AUBERT 05R	BABR	$B^+ \to K^+\pi^+\pi^- J/\psi$
>0.05	36 ± 7	4 CHOI 03	BELL	$B^+ \to K^+\pi^+\pi^- J/\psi$

[1] AUBERT 08Y reports $[\Gamma(\chi_{c1}(3872) \to \pi^+\pi^- J/\psi(1S))/\Gamma_{total}] \times [B(B^+ \to \chi_{c1}(3872) K^+)] = (8.4 \pm 1.5 \pm 0.7) \times 10^{-6}$ which we divide by our best value $B(B^+ \to \chi_{c1}(3872) K^+) < 2.6 \times 10^{-4}$.

[2] BALA 15 reports $B(\chi_{c1}(3872) \to \pi^+\pi^- J/\psi) \times B(B^0 \to \chi_{c1}(3872) K^+\pi^-) = (7.9 \pm 1.3 \pm 0.4) \times 10^{-6}$ and $B(\chi_{c1}(3872) \to \pi^+\pi^- J/\psi) \times B(B^+ \to \chi_{c1}(3872) K^0\pi^+) = (10.6 \pm 3.0 \pm 0.9) \times 10^{-6}$.

[3] Superseded by AUBERT 08Y. AUBERT 05R reports $[\Gamma(\chi_{c1}(3872) \to \pi^+\pi^- J/\psi(1S))/\Gamma_{total}] \times [B(B^+ \to \chi_{c1}(3872) K^+)] = (1.28 \pm 0.41) \times 10^{-5}$ which we divide by our best value $B(B^+ \to \chi_{c1}(3872) K^+) < 2.6 \times 10^{-4}$.

[4] CHOI 03 reports $[\Gamma(\chi_{c1}(3872) \to \pi^+\pi^- J/\psi(1S))/\Gamma_{total}] \times [B(B^+ \to \chi_{c1}(3872) K^+)] / [B(B^+ \to \psi(2S) K^+)] / [B(\psi(2S) \to J/\psi(1S)\pi^+\pi^-)] = 0.063 \pm 0.012 \pm 0.007$ which we multiply or divide by our best values $B(B^+ \to \chi_{c1}(3872) K^+) < 2.6 \times 10^{-4}$, $B(B^+ \to \psi(2S) K^+) = (6.21 \pm 0.23) \times 10^{-4}$, $B(\psi(2S) \to J/\psi(1S)\pi^+\pi^-) = (34.67 \pm 0.30) \times 10^{-2}$.

$\Gamma(\omega J/\psi(1S))/\Gamma_{total}$ Γ_4/Γ

VALUE	EVTS	DOCUMENT ID	TECN	COMMENT
>0.023	21 ± 7	1 DEL-AMO-SA...10B	BABR	$B^+ \to \omega J/\psi K^+$

[1] DEL-AMO-SANCHEZ 10B reports $[\Gamma(\chi_{c1}(3872) \to \omega J/\psi(1S))/\Gamma_{total}] \times [B(B^+ \to \chi_{c1}(3872) K^+)] = (6 \pm 2 \pm 1) \times 10^{-6}$ which we divide by our best value $B(B^+ \to \chi_{c1}(3872) K^+) < 2.6 \times 10^{-4}$. DEL-AMO-SANCHEZ 10B also reports $B(B^0 \to \chi_{c1}(3872) K^0) \times B(\chi_{c1}(3872) \to J/\psi\omega) = (6 \pm 3 \pm 1) \times 10^{-6}$.

$\Gamma(\omega J/\psi(1S))/\Gamma(\pi^+\pi^- J/\psi(1S))$ Γ_4/Γ_2

VALUE	DOCUMENT ID	TECN	COMMENT
0.8±0.3	1 DEL-AMO-SA...10B	BABR	$B \to \omega J/\psi K$

[1] Statistical and systematic errors added in quadrature. Uses the values of $B(B \to \chi_{c1}(3872) K) \times B(\chi_{c1}(3872) \to J/\psi\pi^+\pi^-)$ reported in AUBERT 08Y, taking into account the common systematics.

$\Gamma(D^0\overline{D}{}^0\pi^0)/\Gamma_{total}$ Γ_5/Γ

VALUE	EVTS	DOCUMENT ID	TECN	COMMENT
>0.4	17 ± 5	1 GOKHROO 06	BELL	$B^+ \to D^0\overline{D}{}^0\pi^0 K^+$

[1] GOKHROO 06 reports $[\Gamma(\chi_{c1}(3872) \to D^0\overline{D}{}^0\pi^0)/\Gamma_{total}] \times [B(B^+ \to \chi_{c1}(3872) K^+)] = (1.02 \pm 0.31^{+0.21}_{-0.29}) \times 10^{-4}$ which we divide by our best value $B(B^+ \to \chi_{c1}(3872) K^+) < 2.6 \times 10^{-4}$.

$\Gamma(D^0\overline{D}{}^0\pi^0)/\Gamma(\pi^+\pi^- J/\psi(1S))$ Γ_5/Γ_2

VALUE	DOCUMENT ID	TECN	COMMENT
seen	1 GOKHROO 06	BELL	$B \to D^0\overline{D}{}^0\pi^0 K$
• • • We do not use the following data for averages, fits, limits, etc. • • •			
seen	AUSHEV 10	BELL	$B \to D^0\overline{D}{}^0\pi^0 K$

[1] May not necessarily be the same state as that observed in the $J/\psi\pi^+\pi^-$ mode. Supersedes CHISTOV 04.

$\Gamma(\overline{D}{}^{*0} D^0)/\Gamma_{total}$ Γ_6/Γ

VALUE	EVTS	DOCUMENT ID	TECN	COMMENT
>0.30	41^{+9}_{-8}	1 AUSHEV 10	BELL	$B^+ \to D^{*0}\overline{D}{}^0 K^+$
• • • We do not use the following data for averages, fits, limits, etc. • • •				
>0.6	27 ± 6	2 AUBERT 08B	BABR	$B^+ \to \overline{D}{}^{*0} D^0 K^+$

[1] AUSHEV 10 reports $[\Gamma(\chi_{c1}(3872) \to \overline{D}{}^{*0} D^0)/\Gamma_{total}] \times [B(B^+ \to \chi_{c1}(3872) K^+)] = (0.77 \pm 0.16 \pm 0.10) \times 10^{-4}$ which we divide by our best value $B(B^+ \to \chi_{c1}(3872) K^+) < 2.6 \times 10^{-4}$.

[2] AUBERT 08B reports $[\Gamma(\chi_{c1}(3872) \to \overline{D}{}^{*0} D^0)/\Gamma_{total}] \times [B(B^+ \to \chi_{c1}(3872) K^+)] = (1.67 \pm 0.36 \pm 0.47) \times 10^{-4}$ which we divide by our best value $B(B^+ \to \chi_{c1}(3872) K^+) < 2.6 \times 10^{-4}$.

$\Gamma(D^0\overline{D}{}^0)/\Gamma(\pi^+\pi^- J/\psi(1S))$ Γ_8/Γ_2

VALUE	DOCUMENT ID	TECN	COMMENT
• • • We do not use the following data for averages, fits, limits, etc. • • •			
not seen	CHISTOV 04	BELL	$B \to K D^0\overline{D}{}^0$

$\Gamma(D^+ D^-)/\Gamma(\pi^+\pi^- J/\psi(1S))$ Γ_9/Γ_2

VALUE	DOCUMENT ID	TECN	COMMENT
• • • We do not use the following data for averages, fits, limits, etc. • • •			
not seen	CHISTOV 04	BELL	$B \to K D^+ D^-$

$\Gamma(\gamma\chi_{c1})/\Gamma(\pi^+\pi^- J/\psi(1S))$ Γ_{10}/Γ_2

VALUE	CL%	DOCUMENT ID	TECN	COMMENT
not seen		1 BHARDWAJ 13	BELL	$B^+ \to \chi_{c1}\gamma K^+$
<0.89	90	CHOI 03	BELL	$B \to K\pi^+\pi^- J/\psi$

[1] Reported $B(B^\pm \to \chi_{c1}(3872) K^\pm) \times B(\chi_{c1}(3872) \to \gamma\chi_{c1}) < 1.9 \times 10^{-6}$ at 90% CL.

$\Gamma(\gamma\chi_{c2})/\Gamma(\pi^+\pi^- J/\psi(1S))$ Γ_{11}/Γ_2

VALUE	DOCUMENT ID	TECN	COMMENT
not seen	1 BHARDWAJ 13	BELL	$B^\pm \to \chi_{c2}\gamma K^+$

[1] Reported $B(B^\pm \to \chi_{c1}(3872) K^\pm) \times B(\chi_{c1}(3872) \to \gamma\chi_{c2}) < 6.7 \times 10^{-6}$ at 90% CL.

$\Gamma(\gamma J/\psi)/\Gamma_{total}$ Γ_{12}/Γ

VALUE	EVTS	DOCUMENT ID	TECN	COMMENT
>7 $\times 10^{-3}$		1 BHARDWAJ 11	BELL	$B^\pm \to \gamma J/\psi K^\pm$
• • • We do not use the following data for averages, fits, limits, etc. • • •				
>0.011	20	2 AUBERT 09B	BABR	$B^+ \to \gamma J/\psi K^+$
>0.013	19	3 AUBERT,BE 06M	BABR	$B^+ \to \gamma J/\psi K^+$

[1] BHARDWAJ 11 reports $[\Gamma(\chi_{c1}(3872) \to \gamma J/\psi)/\Gamma_{total}] \times [B(B^+ \to \chi_{c1}(3872) K^+)] = (1.78^{+0.48}_{-0.44} \pm 0.12) \times 10^{-6}$ which we divide by our best value $B(B^+ \to \chi_{c1}(3872) K^+) < 2.6 \times 10^{-4}$.

[2] AUBERT 09B reports $[\Gamma(\chi_{c1}(3872) \to \gamma J/\psi)/\Gamma_{total}] \times [B(B^+ \to \chi_{c1}(3872) K^+)] = (2.8 \pm 0.8 \pm 0.1) \times 10^{-6}$ which we divide by our best value $B(B^+ \to \chi_{c1}(3872) K^+) < 2.6 \times 10^{-4}$.

[3] Superseded by AUBERT 09B. AUBERT,BE 06M reports $[\Gamma(\chi_{c1}(3872) \to \gamma J/\psi)/\Gamma_{total}] \times [B(B^+ \to \chi_{c1}(3872) K^+)] = (3.3 \pm 1.0 \pm 0.3) \times 10^{-6}$ which we divide by our best value $B(B^+ \to \chi_{c1}(3872) K^+) < 2.6 \times 10^{-4}$.

$\Gamma(\gamma\psi(2S))/\Gamma_{total}$ Γ_{13}/Γ

VALUE	EVTS	DOCUMENT ID	TECN	COMMENT
seen	36 ± 9	1 AAIJ 14AH	LHCB	$B^+ \to \gamma\psi(2S) K^+$
>0.04	25 ± 7	2 AUBERT 09B	BABR	$B^+ \to \gamma\psi(2S) K^+$
• • • We do not use the following data for averages, fits, limits, etc. • • •				
not seen		3 BHARDWAJ 11	BELL	$B^+ \to \gamma\psi(2S) K^+$

[1] From 36.4 ± 9.0 events of $\chi_{c1}(3872) \to J/\psi\gamma$ decays with a statistical significance of 4.4σ.

[2] AUBERT 09B reports $[\Gamma(\chi_{c1}(3872) \to \gamma\psi(2S))/\Gamma_{total}] \times [B(B^+ \to \chi_{c1}(3872) K^+)] = (9.5 \pm 2.7 \pm 0.6) \times 10^{-6}$ which we divide by our best value $B(B^+ \to \chi_{c1}(3872) K^+) < 2.6 \times 10^{-4}$.

[3] BHARDWAJ 11 reports $B(B^+ \to K^+\chi_{c1}(3872)) \times B(\chi_{c1} \to \gamma\psi(2S)) < 3.45 \times 10^{-6}$ at 90% CL.

$\Gamma(\gamma\psi(2S))/\Gamma(\gamma J/\psi)$ Γ_{13}/Γ_{12}

VALUE	CL%	EVTS	DOCUMENT ID	TECN	COMMENT
2.6 ±0.6 OUR AVERAGE					
$2.46 \pm 0.64 \pm 0.29$		36 ± 9	1 AAIJ 14AH	LHCB	$B^+ \to \gamma\psi(2S) K^+$
3.4 ±1.4			AUBERT 09B	BABR	$B^+ \to \gamma c\bar{c} K'$
• • • We do not use the following data for averages, fits, limits, etc. • • •					
<2.1	90		BHARDWAJ 11	BELL	$B^+ \to \gamma\psi(2S) K^+$

[1] From 36.4 ± 9.0 events of $\chi_{c1}(3872) \to J/\psi\gamma$ decays with a statistical significance of 4.4σ.

$\Gamma(\pi^+\pi^-\chi_{c1})/\Gamma_{total}$ Γ_{15}/Γ

VALUE	DOCUMENT ID		TECN	COMMENT
not seen	[1] BHARDWAJ	16	BELL	$B^+ \to \pi^+\pi^-\chi_{c1}K^+$

[1] BHARDWAJ 16 quotes $B(B^+ \to \chi_{c1}(3872)K^+)\cdot B(\chi_{c1}(3872) \to \pi^+\pi^-\chi_{c1}) < 1.5\times10^{-6}$ at 90% CL.

$\Gamma(p\overline{p})/\Gamma_{total}$ Γ_{16}/Γ

VALUE	DOCUMENT ID		TECN	COMMENT
not seen	[1] AAIJ	17AD	LHCB	$pp \to B^+X \to p\overline{p}K^+X$

[1] AAIJ 17AD reports $B(B^+ \to \chi_{c1}(3872)K^+ \to p\overline{p}K^+)/B(B^+ \to J/\psi K^+ \to p\overline{p}K^+) < 2.0\ (2.5)\times10^{-3}$ at 90% (95%) CL.

$\Gamma(p\overline{p})/\Gamma(\pi^+\pi^- J/\psi(1S))$ Γ_{16}/Γ_2

VALUE	CL%	DOCUMENT ID		TECN	COMMENT
<2.0 × 10⁻³	95	[1] AAIJ	13S	LHCB	$B^+ \to p\overline{p}K^+$

[1] AAIJ 13S reports $[\Gamma(\chi_{c1}(3872) \to p\overline{p})/\Gamma(\chi_{c1}(3872) \to \pi^+\pi^- J/\psi(1S))] \times [B(B^+ \to \chi_{c1}(3872)K^+,\ \chi_{c1} \to J/\psi\pi^+\pi^-)] < 1.7\times10^{-8}$ which we divide by our best value $B(B^+ \to \chi_{c1}(3872)K^+,\ \chi_{c1} \to J/\psi\pi^+\pi^-) = 8.6\times10^{-6}$.

C-violating decays

$\Gamma(\eta J/\psi)/\Gamma(\pi^+\pi^- J/\psi(1S))$ Γ_{17}/Γ_2

VALUE	CL%	DOCUMENT ID		TECN	COMMENT
<0.4	90	[1,2] IWASHITA	14	BELL	$B \to K\eta J/\psi$
• • • We do not use the following data for averages, fits, limits, etc. • • •					
<0.6	90	AUBERT	04Y	BABR	$B \to K\eta J/\psi$

[1] IWASHITA 14 reports $[\Gamma(\chi_{c1}(3872) \to \eta J/\psi)/\Gamma(\chi_{c1}(3872) \to \pi^+\pi^- J/\psi(1S))] \times [B(B^+ \to \chi_{c1}(3872)K^+,\ \chi_{c1} \to J/\psi\pi^+\pi^-)] < 3.8\times10^{-6}$ which we divide by our best value $B(B^+ \to \chi_{c1}(3872)K^+,\ \chi_{c1} \to J/\psi\pi^+\pi^-) = 8.6\times10^{-6}$.

[2] IWASHITA 14 also scans the $\eta J/\psi$ mass range 3.8–4.75 GeV and sets upper limits for $B(B^\pm \to \chi_{c1}(3872)K^\pm)\times B(\chi_{c1}(3872) \to \eta J/\psi)$ in 5 MeV intervals.

$\chi_{c1}(3872)$ REFERENCES

AAIJ	17AD	PL B769 305	R. Aaij *et al.*	(LHCb Collab.)
BHARDWAJ	16	PR D93 052016	V. Bhardwaj *et al.*	(BELLE Collab.)
AAIJ	15AO	PR D92 011102	R. Aaij *et al.*	(LHCb Collab.)
ABLIKIM	15V	PL B749 414	M. Ablikim *et al.*	(BES III Collab.)
BALA	15	PR D91 051101	A. Bala *et al.*	(BELLE Collab.)
AAIJ	14AH	NP B886 665	R. Aaij *et al.*	(LHCb Collab.)
ABLIKIM	14	PRL 112 092001	M. Ablikim *et al.*	(BES III Collab.)
IWASHITA	14	PTEP 2014 043C01	T. Iwashita *et al.*	(BELLE Collab.)
AAIJ	13Q	PRL 110 222001	R. Aaij *et al.*	(LHCb Collab.) JP
AAIJ	13S	EPJ C73 2462	R. Aaij *et al.*	(LHCb Collab.)
BHARDWAJ	13	PRL 111 032001	V. Bhardwaj *et al.*	(BELLE Collab.)
AAIJ	12H	EPJ C72 1972	R. Aaij *et al.*	(LHCb Collab.)
LEES	12AD	PR D86 072002	J.P. Lees *et al.*	(BABAR Collab.)
LEES	12AE	PR D86 092005	J.P. Lees *et al.*	(BABAR Collab.)
BHARDWAJ	11	PRL 107 091803	V. Bhardwaj *et al.*	(BELLE Collab.)
CHOI	11	PR D84 052004	S.-K. Choi *et al.*	(BELLE Collab.)
AUSHEV	10	PR D81 031103	T. Aushev *et al.*	(BELLE Collab.)
DEL-AMO-SA...	10B	PR D82 011101	P. del Amo Sanchez *et al.*	(BABAR Collab.)
AALTONEN	09AU	PRL 103 152001	T. Aaltonen *et al.*	(CDF Collab.)
AUBERT	09B	PRL 102 132001	B. Aubert *et al.*	(BABAR Collab.)
AUBERT	08B	PR D77 011102	B. Aubert *et al.*	(BABAR Collab.)
AUBERT	08Y	PR D77 111101	B. Aubert *et al.*	(BABAR Collab.)
AUBERT	06	PR D73 011101	B. Aubert *et al.*	(BABAR Collab.)
AUBERT,BE	06M	PR D74 071101	B. Aubert *et al.*	(BABAR Collab.)
GOKHROO	06	PRL 97 162002	G. Gokhroo *et al.*	(BELLE Collab.)
AUBERT	05B	PR D71 031501	B. Aubert *et al.*	(BABAR Collab.)
AUBERT	05D	PR D71 052001	B. Aubert *et al.*	(BABAR Collab.)
AUBERT	05R	PR D71 071103	B. Aubert *et al.*	(BABAR Collab.)
DOBBS	05	PRL 94 032004	S. Dobbs *et al.*	(CLEO Collab.)
ABAZOV	04F	PRL 93 162002	V.M. Abazov *et al.*	(D0 Collab.)
ACOSTA	04	PRL 93 072001	D. Acosta *et al.*	(CDF Collab.)
AUBERT	04Y	PRL 93 041801	B. Aubert *et al.*	(BABAR Collab.)
CHISTOV	04	PRL 93 051803	R. Chistov *et al.*	(BELLE Collab.)
PDG	04	PL B592 1	S. Eidelman *et al.*	(PDG Collab.)
YUAN	04	PL B579 74	C.Z. Yuan *et al.*	
CHOI	03	PRL 91 262001	S.-K. Choi *et al.*	(BELLE Collab.)
BAI	98E	PR D57 3854	J.Z. Bai *et al.*	(BES Collab.)
ANTONIAZZI	94	PR D50 4258	L. Antoniazzi *et al.*	(E705 Collab.)

$Z_c(3900)$

$I^G(J^{PC}) = 1^+(1^{+-})$

was $X(3900)$

Properties incompatible with a $q\overline{q}$ structure (exotic state). See the review on non-$q\overline{q}$ states.

Charged $Z_c(3900)$ seen as a peak in the invariant mass distribution of the $J/\psi\pi^\pm$ system by BES III (ABLIKIM 13T) in $e^+e^- \to \pi^+\pi^- J/\psi$ at c.m. energy of 4.26 GeV and by radiative return from e^+e^- collisions at $\sqrt{s}$ from 9.46 to 10.86 GeV at Belle (LIU 13B). Partial wave analysis of ABLIKIM 17J determines $J^P = 1^+$ with more than 7σ significance. Neutral $Z_c(3900)$ seen in the $J/\psi\pi^0$ invariant mass distribution in $e^+e^- \to \pi^0\pi^0 J/\psi$ at c.m. energies of 4.23, 4.26, and 4.36 GeV by BES III (ABLIKIM 15U) and at 4.17 GeV by XIAO 13A. Peaks in $(D\overline{D}^*)^{0,\pm}$ reported by BES III (ABLIKIM 14A, ABLIKIM 15AB) are assumed to be related.

$Z_c(3900)$ MASS

VALUE (MeV)	EVTS	DOCUMENT ID		TECN	CHG	COMMENT
3886.6±2.4 OUR AVERAGE		Error includes scale factor of 1.6. See the ideogram below.				
$3885.7^{+4.3}_{-5.7}\pm 8.4$		[1] ABLIKIM	15AB	BES3	0	$e^+e^- \to \pi^0(D\overline{D}^*)^0$
3881.7±1.6± 1.6	1.2k	[1] ABLIKIM	15AC	BES3	±	$e^+e^- \to \pi^\pm(D\overline{D}^*)^\mp$
3894.8±2.3± 3.2	356	[1] ABLIKIM	15U	BES3	0	$e^+e^- \to \pi^0\pi^0 J/\psi$
3883.9±1.5± 4.2	1.2k	[1] ABLIKIM	14A	BES3	±	$e^+e^- \to \pi^\pm(D\overline{D}^*)^\mp$
3899.0±3.6± 4.9	307	[1] ABLIKIM	13T	BES3	±	$e^+e^- \to \pi^+\pi^- J/\psi$
3894.5±6.6± 4.5	159	[1] LIU	13B	BELL	±	$e^+e^- \to \gamma\pi^+\pi^- J/\psi$
3886 ±4 ± 2	81	[1,2] XIAO	13A		±	4.17 $e^+e^- \to \pi^+\pi^- J/\psi$
3904 ±9 ± 5	25	[1,2] XIAO	13A		0	4.17 $e^+e^- \to \pi^0\pi^0 J/\psi$
• • • We do not use the following data for averages, fits, limits, etc. • • •						
3881.2±4.2±52.7	6k	[3] ABLIKIM	17J	BES3	±	$e^+e^- \to \pi^+\pi^- J/\psi$

[1] Neglecting interference between the $Z_c(3900)$ and non-resonant continuum.

[2] For $M^2(\pi^+\pi^-) < 0.65\ \text{GeV}^2$. Obtained by analyzing CLEO-c data but not authored by the CLEO Collaboration.

[3] Pole mass obtained from a fit to a Flatte-like formula.

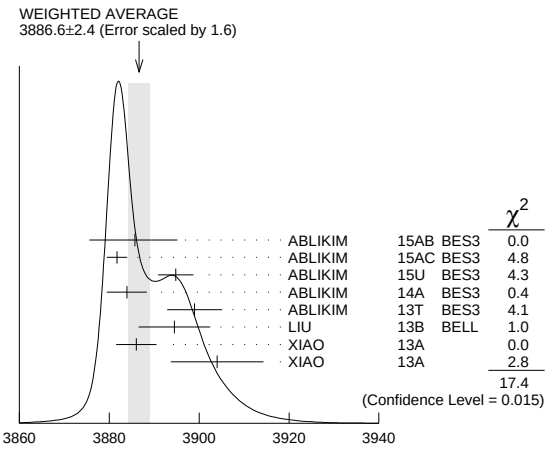

$Z_c(3900)$ WIDTH

VALUE (MeV)	EVTS	DOCUMENT ID		TECN	CHG	COMMENT
28.2± 2.6 OUR AVERAGE						
51.8± 4.6±36.0	6 k	[1] ABLIKIM	17J	BES3	±	$e^+e^- \to \pi^+\pi^- J/\psi$
$35\ ^{+11}_{-12}\ \pm 15$		[2] ABLIKIM	15AB	BES3	0	$e^+e^- \to \pi^0(D\overline{D}^*)^0$
26.6± 2.0± 2.1	1248	[2] ABLIKIM	15AC	BES3	±	$e^+e^- \to \pi^\pm(D\overline{D}^*)^\mp$
29.6± 8.2± 8.2	356	[2] ABLIKIM	15U	BES3	0	$e^+e^- \to \pi^0\pi^0 J/\psi$
24.8± 3.3±11.0	1212	[2] ABLIKIM	14A	BES3	±	$e^+e^- \to \pi^\pm(D\overline{D}^*)^\mp$
46 ±10 ±20	307	[2] ABLIKIM	13T	BES3	±	$e^+e^- \to \pi^+\pi^- J/\psi$
63 ±24 ±26	159	[2] LIU	13B	BELL	±	$e^+e^- \to \gamma\pi^+\pi^- J/\psi$
37 ± 4 ± 8	81	[2,3] XIAO	13A		±	4.17 $e^+e^- \to \pi^+\pi^- J/\psi$

[1] Pole width obtained from a fit to a Flatte-like formula.

[2] Neglecting interference between the $Z_c(3900)$ and non-resonant continuum.

[3] For $M^2(\pi^+\pi^-) < 0.65\ \text{GeV}^2$. Obtained by analyzing CLEO-c data but not authored by the CLEO Collaboration.

$Z_c(3900)$ DECAY MODES

	Mode	Fraction (Γ_i/Γ)
Γ_1	$J/\psi\pi$	seen
Γ_2	$h_c\pi^\pm$	not seen
Γ_3	$\eta_c\pi^+\pi^-$	not seen
Γ_4	$(D\overline{D}^*)^\pm$	seen
Γ_5	D^0D^{*-} + c.c.	seen
Γ_6	D^-D^{*0} + c.c.	seen
Γ_7	$\omega\pi^\pm$	not seen
Γ_8	$J/\psi\eta$	not seen
Γ_9	D^+D^{*-} + c.c	seen
Γ_{10}	$D^0\overline{D}^{*0}$ + c.c	seen

$Z_c(3900)$ BRANCHING RATIOS

$\Gamma(J/\psi\pi)/\Gamma_{total}$ Γ_1/Γ

VALUE	CL%	EVTS	DOCUMENT ID		TECN	CHG	COMMENT
seen		356	ABLIKIM	15U	BES3	0	$e^+e^- \to \pi^0\pi^0 J/\psi$
seen		307	ABLIKIM	13T	BES3	$\pm$	$e^+e^- \to \pi^+\pi^- J/\psi$
seen		25	[1] XIAO	13A		0	4.17 $e^+e^- \to \pi^0\pi^0 J/\psi$

• • • We do not use the following data for averages, fits, limits, etc. • • •

not seen	90	[2] ADOLPH	15D	COMP	$\pm$		$\gamma N \to J/\psi\pi^\pm N$

[1] Obtained by analyzing CLEO-c data but not authored by the CLEO Collaboration.
[2] ADOLPH 15D measure $B(Z_c(3900)^\pm \to J/\psi\pi^\pm)\ \sigma(\gamma N \to Z_c(3900)^\pm N)/\sigma(\gamma N \to J/\psi N) < 3.7\times10^{-3}$ at 90% CL.

$\Gamma(h_c\pi^\pm)/\Gamma_{total}$ Γ_2/Γ

VALUE	DOCUMENT ID		TECN	CHG	COMMENT
not seen	ABLIKIM	13X	BES3	$\pm$	$e^+e^- \to h_c\pi^+\pi^-$

$\Gamma(\eta_c\pi^+\pi^-)/\Gamma_{total}$ Γ_3/Γ

VALUE	DOCUMENT ID		TECN	CHG	COMMENT
not seen	[1] VINOKUROVA 15		BELL	0	$B^+ \to K^+\eta_c\pi^+\pi^-$

[1] VINOKUROVA 15 reports $B(B^+ \to K^+ Z_c(3900)^0) \times B(X \to \eta_c\pi^+\pi^-) < 4.7\times10^{-5}$ at 90% CL.

$\Gamma((D\overline{D}^*)^\pm)/\Gamma(J/\psi\pi)$ Γ_4/Γ_1

VALUE	DOCUMENT ID		TECN	CHG	COMMENT
6.2±1.1±2.7	[1] ABLIKIM	14A	BES3	$\pm$	$e^+e^- \to \pi^\pm (D\overline{D}^*)^\mp$

[1] Assuming the same origin of the $(D\overline{D}^*)^\pm$ and $\pi^\pm J/\psi$ decay modes.

$\Gamma(D^0D^{*-}+\text{c.c.})/\Gamma_{total}$ Γ_5/Γ

VALUE	DOCUMENT ID		TECN	CHG	COMMENT
seen	ABLIKIM	15AC	BES3	$\pm$	$e^+e^- \to \pi^+ D^0 D^{*-}+$ c.c.
seen	ABLIKIM	14A	BES3	$\pm$	$e^+e^- \to \pi^+ D^0 D^{*-}+$ c.c.

$\Gamma(D^-D^{*0}+\text{c.c.})/\Gamma_{total}$ Γ_6/Γ

VALUE	DOCUMENT ID		TECN	CHG	COMMENT
seen	ABLIKIM	15AC	BES3	$\pm$	$e^+e^- \to \pi^+ D^- D^{*0}+$ c.c.
seen	ABLIKIM	14A	BES3	$\pm$	$e^+e^- \to \pi^+ D^- D^{*0}+$ c.c.

$\Gamma(\omega\pi^\pm)/\Gamma_{total}$ Γ_7/Γ

VALUE	DOCUMENT ID		TECN	CHG	COMMENT
not seen	ABLIKIM	15R	BES3	$\pm$	$e^+e^- \to \omega\pi^+\pi^-$

$\Gamma(J/\psi\eta)/\Gamma_{total}$ Γ_8/Γ

VALUE	DOCUMENT ID		TECN	CHG	COMMENT
not seen	ABLIKIM	15Q	BES3	0	4.0–4.6 $e^+e^- \to J/\psi\eta\pi^0$

$\Gamma(J/\psi\eta)/\Gamma(J/\psi\pi)$ Γ_8/Γ_1

VALUE	CL%	DOCUMENT ID		TECN	CHG	COMMENT
<0.15	90	ABLIKIM	15Q	BES3	0	4.226 $e^+e^- \to J/\psi\eta\pi^0$

• • • We do not use the following data for averages, fits, limits, etc. • • •

<0.65	90	ABLIKIM	15Q	BES3	0	4.257 $e^+e^- \to J/\psi\eta\pi^0$

$\Gamma(D^+D^{*-}+\text{c.c})/\Gamma_{total}$ Γ_9/Γ

VALUE	DOCUMENT ID		TECN	CHG	COMMENT
seen	ABLIKIM	15AB	BES3	0	$e^+e^- \to \pi^0(D\overline{D}^*)^0$

$\Gamma(D^0\overline{D}^{*0}+\text{c.c})/\Gamma_{total}$ Γ_{10}/Γ

VALUE	DOCUMENT ID		TECN	CHG	COMMENT
seen	ABLIKIM	15AB	BES3	0	$e^+e^- \to \pi^0(D\overline{D}^*)^0$

$\Gamma(D^+D^{*-}+\text{c.c})/\Gamma(D^0\overline{D}^{*0}+\text{c.c})$ Γ_9/Γ_{10}

VALUE	DOCUMENT ID		TECN	CHG	COMMENT
0.96±0.18±0.12	ABLIKIM	15AB	BES3	0	$e^+e^- \to \pi^0(D\overline{D}^*)^0$

$Z_c(3900)$ REFERENCES

ABLIKIM	17J	PRL 119 072001	M. Ablikim *et al.*	(BES III Collab.)
ABLIKIM	15AB	PRL 115 222002	M. Ablikim *et al.*	(BES III Collab.)
ABLIKIM	15AC	PR D92 092006	M. Ablikim *et al.*	(BES III Collab.) JP
ABLIKIM	15Q	PR D92 012008	M. Ablikim *et al.*	(BES III Collab.)
ABLIKIM	15R	PR D92 032009	M. Ablikim *et al.*	(BES III Collab.)
ABLIKIM	15U	PRL 115 112003	M. Ablikim *et al.*	(BES III Collab.)
ADOLPH	15D	PL B742 330	C. Adolph *et al.*	(COMPASS Collab.)
VINOKUROVA	15	JHEP 1506 132	A. Vinokurova *et al.*	(BELLE Collab.)
Also		JHEP 1702 088 (errat.)	A. Vinokurava *et al.*	(BELLE Collab.)
ABLIKIM	14A	PRL 112 022001	M. Ablikim *et al.*	(BES III Collab.) JP
ABLIKIM	13T	PRL 110 252001	M. Ablikim *et al.*	(BES III Collab.)
ABLIKIM	13X	PRL 111 242001	M. Ablikim *et al.*	(BES III Collab.)
LIU	13B	PRL 110 252002	Z.Q. Liu *et al.*	(BELLE Collab.)
XIAO	13A	PL B727 366	T. Xiao *et al.*	(NWES)

$X(3915)$

$I^G(J^{PC}) = 0^+(0 \text{ or } 2^{++})$

was $\chi_{c0}(3915)$

The experimental analysis prefers $J^{PC} = 0^{++}$. However, a re-analysis presented in ZHOU 15C shows that if helicity-2 dominance assumption is abandoned and a sizable helicity-0 component is allowed, a $J^{PC} = 2^{++}$ assignment is possible.

$X(3915)$ MASS

VALUE (MeV)	EVTS	DOCUMENT ID		TECN	COMMENT
3918.4± 1.9 OUR AVERAGE					
$3919.4\pm 2.2\pm 1.6$	59 ± 10	LEES	12AD	BABR	$e^+e^- \to e^+e^-\omega J/\psi$
$3919.1^{+3.8}_{-3.4}\pm 2.0$		DEL-AMO-SA...10B		BABR	$B \to \omega J/\psi K$
$3915 \pm 3 \pm 2$	49 ± 15	UEHARA	10	BELL	10.6 $e^+e^- \to e^+e^-\omega J/\psi$
$3943 \pm11 \pm13$	58 ± 11	[1] CHOI	05	BELL	$B \to \omega J/\psi K$

• • • We do not use the following data for averages, fits, limits, etc. • • •

$3914.6^{+3.8}_{-3.4}\pm 2.0$	[1] AUBERT	08W	BABR	Superseded by DEL-AMO-SANCHEZ 10B	

[1] $\omega J/\psi$ threshold enhancement fitted as an S-wave Breit-Wigner resonance.

$X(3915)$ WIDTH

VALUE (MeV)	EVTS	DOCUMENT ID		TECN	COMMENT
20± 5 OUR AVERAGE Error includes scale factor of 1.1.					
$13\pm 6\pm 3$	59 ± 10	LEES	12AD	BABR	$e^+e^- \to e^+e^-\omega J/\psi$
$31^{+10}_{-8}\pm 5$		DEL-AMO-SA...10B		BABR	$B \to \omega J/\psi K$
$17\pm10\pm 3$	49 ± 15	UEHARA	10	BELL	10.6 $e^+e^- \to e^+e^-\omega J/\psi$
$87\pm22\pm26$	58 ± 11	[2] CHOI	05	BELL	$B \to \omega J/\psi K$

• • • We do not use the following data for averages, fits, limits, etc. • • •

$34^{+12}_{-8}\pm 5$	[2] AUBERT	08W	BABR	Superseded by DEL-AMO-SANCHEZ 10B	

[2] $\omega J/\psi$ threshold enhancement fitted as an S-wave Breit-Wigner resonance.

$X(3915)$ DECAY MODES

	Mode	Fraction (Γ_i/Γ)
Γ_1	$\omega J/\psi$	seen
Γ_2	$\overline{D}^{*0}D^0$	
Γ_3	$\pi^+\pi^-\eta_c(1S)$	not seen
Γ_4	$\eta_c\eta$	not seen
Γ_5	$\eta_c\pi^0$	not seen
Γ_6	$K\overline{K}$	not seen
Γ_7	$\gamma\gamma$	seen

$X(3915)$ $\Gamma(i)\Gamma(\gamma\gamma)/\Gamma(\text{total})$

$\Gamma(\omega J/\psi) \times \Gamma(\gamma\gamma)/\Gamma_{total}$ $\Gamma_1\Gamma_7/\Gamma$

VALUE (eV)	EVTS	DOCUMENT ID		TECN	COMMENT
54± 9 OUR AVERAGE					
$52\pm10\pm3$	59 ± 10	[3] LEES	12AD	BABR	$e^+e^- \to e^+e^-\omega J/\psi$
$61\pm17\pm8$	49 ± 15	UEHARA	10	BELL	10.6 $e^+e^- \to e^+e^-\omega J/\psi$

• • • We do not use the following data for averages, fits, limits, etc. • • •

$18\pm 5\pm2$	49 ± 15	[4] UEHARA	10	BELL	10.6 $e^+e^- \to e^+e^-\omega J/\psi$

[3] For $J^P = 0^+$.
[4] For $J^P = 2^+$, helicity-2.

$\Gamma(\pi^+\pi^-\eta_c(1S)) \times \Gamma(\gamma\gamma)/\Gamma_{total}$ $\Gamma_3\Gamma_7/\Gamma$

VALUE (eV)	CL%	DOCUMENT ID		TECN	COMMENT
<16	90	LEES	12AE	BABR	$e^+e^- \to e^+e^-\pi^+\pi^-\eta_c$

$\Gamma(K\overline{K}) \times \Gamma(\gamma\gamma)/\Gamma_{total}$ $\Gamma_6\Gamma_7/\Gamma$

VALUE (eV)	CL%	DOCUMENT ID		TECN	COMMENT
<1.96	90	UEHARA	13	BELL	$\gamma\gamma \to K^0_S K^0_S$

$X(3915)$ BRANCHING RATIOS

$\Gamma(\omega J/\psi)/\Gamma_{total}$ Γ_1/Γ

VALUE	DOCUMENT ID		TECN	COMMENT
seen	[5] DEL-AMO-SA...10B		BABR	$B \to \omega J/\psi K$
seen	[6] CHOI	05	BELL	$B \to \omega J/\psi K$

[5] DEL-AMO-SANCHEZ 10B reports $B(B^\pm \to X(3915)K^\pm) \times B(X(3915) \to J/\psi\omega) = (3.0^{+0.7}_{-0.6}{}^{+0.5}_{-0.3}) \times 10^{-5}$ and $B(B^0 \to X(3915)K^0) \times B(X(3915) \to J/\psi\omega) = (2.1 \pm 0.9 \pm 0.3) \times 10^{-5}$.
[6] CHOI 05 reports $B(B \to X(3915)K) \times B(X(3915) \to J/\psi\omega) = (7.1 \pm 1.3 \pm 3.1) \times 10^{-5}$.

Meson Particle Listings

$X(3915)$, $\chi_{c2}(3930)$, $X(3940)$

$\Gamma(\omega J/\psi)/\Gamma(\overline{D}^{*0}D^0)$ Γ_1/Γ_2

VALUE	CL%	DOCUMENT ID		TECN	COMMENT
>0.71	90	[7] AUSHEV	10	BELL	$B \to \overline{D}^{*0} D^0 K$

[7] By combining the upper limit $B(B \to X(3915) K) \times B(X(3915) \to D^{*0}\overline{D}^0) < 0.67 \times 10^{-4}$ from AUSHEV 10 with the average of CHOI 05 and AUBERT 08W measurements $B(B \to X(3915) K) \times B(X(3915) \to \omega J/\psi) = (0.51 \pm 0.11) \times 10^{-4}$.

$\Gamma(\eta_c\eta)/\Gamma_{total}$ Γ_4/Γ

VALUE	DOCUMENT ID		TECN	COMMENT
not seen	[8] VINOKUROVA 15		BELL	$B^+ \to K^+ \eta_c \eta$

[8] VINOKUROVA 15 reports $B(B^+ \to K^+ X(3915)^0) \times B(X \to \eta_c \eta) < 3.3 \times 10^{-5}$ at 90% CL.

$\Gamma(\eta_c\pi^0)/\Gamma_{total}$ Γ_5/Γ

VALUE	DOCUMENT ID		TECN	COMMENT
not seen	[9] VINOKUROVA 15		BELL	$B^+ \to K^+ \eta_c \pi^0$

[9] VINOKUROVA 15 reports $B(B^+ \to K^+ X(3915)^0) \times B(X \to \eta_c \pi^0) < 1.8 \times 10^{-5}$ at 90% CL.

$\Gamma(\gamma\gamma)/\Gamma_{total}$ Γ_7/Γ

VALUE	EVTS	DOCUMENT ID		TECN	COMMENT
seen	59 ± 10	LEES	12AD	BABR	$e^+e^- \to e^+e^- \omega J/\psi$
seen		UEHARA	10	BELL	$10.6\ e^+e^- \to e^+e^- \omega J/\psi$

$X(3915)$ REFERENCES

VINOKUROVA	15	JHEP 1506 132	A. Vinokurova *et al.*	(BELLE Collab.)
Also		JHEP 1702 088 (errat.)	A. Vinokurava *et al.*	(BELLE Collab.)
ZHOU	15C	PRL 115 022001	Z.-Y. Zhou, Z. Xiao, H.-Q. Zhou	(BEIJT, NANJ)
UEHARA	13	PTEP 2013 123C01	S. Uehara *et al.*	(BELLE Collab.)
LEES	12AD	PR D86 072002	J.P. Lees *et al.*	(BABAR Collab.)
LEES	12AE	PR D86 092005	J.P. Lees *et al.*	(BABAR Collab.)
AUSHEV	10	PR D81 031103	T. Aushev *et al.*	(BELLE Collab.)
DEL-AMO-SA...	10B	PR D82 011101	P. del Amo Sanchez *et al.*	(BABAR Collab.)
UEHARA	10	PRL 104 092001	S. Uehara *et al.*	(BELLE Collab.)
AUBERT	08W	PRL 101 082001	B. Aubert *et al.*	(BABAR Collab.)
CHOI	05	PRL 94 182002	S.-K. Choi *et al.*	(BELLE Collab.)

$\chi_{c2}(3930)$

$I^G(J^{PC}) = 0^+(2^{++})$

was $\chi_{c2}(2P)$

$\chi_{c2}(3930)$ MASS

VALUE (MeV)	EVTS	DOCUMENT ID		TECN	COMMENT
3927.2±2.6 OUR AVERAGE					
3926.7±2.7±1.1	76 ± 17	AUBERT	10G	BABR	$10.6\ e^+e^- \to e^+e^- D\overline{D}$
3929 ±5 ±2	64	UEHARA	06	BELL	$10.6\ e^+e^- \to e^+e^- D\overline{D}$

$\chi_{c2}(3930)$ WIDTH

VALUE (MeV)	EVTS	DOCUMENT ID		TECN	COMMENT
24 ± 6 OUR AVERAGE					
21.3± 6.8±3.6	76 ± 17	AUBERT	10G	BABR	$10.6\ e^+e^- \to e^+e^- D\overline{D}$
29 ±10 ±2	64	UEHARA	06	BELL	$10.6\ e^+e^- \to e^+e^- D\overline{D}$

$\chi_{c2}(3930)$ DECAY MODES

	Mode	Fraction (Γ_i/Γ)
Γ_1	$\gamma\gamma$	seen
Γ_2	$K\overline{K}\pi$	
Γ_3	$K^+K^-\pi^+\pi^-\pi^0$	
Γ_4	$D\overline{D}$	seen
Γ_5	D^+D^-	seen
Γ_6	$D^0\overline{D}^0$	seen
Γ_7	$\pi^+\pi^-\eta_c(1S)$	not seen
Γ_8	$K\overline{K}$	not seen

$\chi_{c2}(3930)$ PARTIAL WIDTHS

$\chi_{c2}(3930)$ $\Gamma(i)\Gamma(\gamma\gamma)/\Gamma(total)$

$\Gamma(K\overline{K}\pi) \times \Gamma(\gamma\gamma)/\Gamma_{total}$ $\Gamma_2\Gamma_1/\Gamma$

VALUE (eV)	CL%	DOCUMENT ID	TECN	COMMENT
<2.1	90	DEL-AMO-SA...11M	BABR	$\gamma\gamma \to K^0_S K^\pm\pi^\mp$

$\Gamma(K^+K^-\pi^+\pi^-\pi^0) \times \Gamma(\gamma\gamma)/\Gamma_{total}$ $\Gamma_3\Gamma_1/\Gamma$

VALUE (eV)	CL%	DOCUMENT ID	TECN	COMMENT
<3.4	90	DEL-AMO-SA...11M	BABR	$\gamma\gamma \to K^+K^-\pi^+\pi^-\pi^0$

$\Gamma(D\overline{D}) \times \Gamma(\gamma\gamma)/\Gamma_{total}$ $\Gamma_4\Gamma_1/\Gamma$

VALUE (keV)	EVTS	DOCUMENT ID		TECN	COMMENT
0.21±0.04 OUR AVERAGE					
0.24±0.05±0.04	76 ± 17	AUBERT	10G	BABR	$10.6\ e^+e^- \to e^+e^- D\overline{D}$
0.18±0.05±0.03	64	[1] UEHARA	06	BELL	$10.6\ e^+e^- \to e^+e^- D\overline{D}$

[1] Assuming $B(D^+D^-) = 0.89\ B(D^0\overline{D}^0)$.

$\Gamma(\pi^+\pi^-\eta_c(1S)) \times \Gamma(\gamma\gamma)/\Gamma_{total}$ $\Gamma_7\Gamma_1/\Gamma$

VALUE (eV)	CL%	DOCUMENT ID	TECN	COMMENT
<18	90	LEES	12AE BABR	$e^+e^- \to e^+e^-\pi^+\pi^-\eta_c$

$\Gamma(K\overline{K}) \times \Gamma(\gamma\gamma)/\Gamma_{total}$ $\Gamma_8\Gamma_1/\Gamma$

VALUE (eV)	CL%	DOCUMENT ID		TECN	COMMENT
<0.256	90	UEHARA	13	BELL	$\gamma\gamma \to K^0_S K^0_S$

$\chi_{c2}(3930)$ BRANCHING RATIOS

$\Gamma(D^+D^-)/\Gamma(D^0\overline{D}^0)$ Γ_5/Γ_6

VALUE	EVTS	DOCUMENT ID		TECN	COMMENT
0.74±0.43±0.16	64	UEHARA	06	BELL	$10.6\ e^+e^- \to e^+e^- D\overline{D}$

$\chi_{c2}(3930)$ REFERENCES

UEHARA	13	PTEP 2013 123C01	S. Uehara *et al.*	(BELLE Collab.)
LEES	12AE	PR D86 092005	J.P. Lees *et al.*	(BABAR Collab.)
DEL-AMO-SA...	11M	PR D84 012004	P. del Amo Sanchez *et al.*	(BABAR Collab.)
AUBERT	10G	PR D81 092003	B. Aubert *et al.*	(BABAR Collab.)
UEHARA	06	PRL 96 082003	S. Uehara *et al.*	(BELLE Collab.)

$X(3940)$

$I^G(J^{PC}) = ?^?(?^{??})$

OMITTED FROM SUMMARY TABLE

Reported by ABE 07, observed in $e^+e^- \to J/\psi X$.

$X(3940)$ MASS

VALUE (MeV)	EVTS	DOCUMENT ID		TECN	COMMENT
$3942^{+\ 7}_{-\ 6}\pm 6$	52	PAKHLOV	08	BELL	$e^+e^- \to J/\psi X$
• • • We do not use the following data for averages, fits, limits, etc. • • •					
3943± 6±6	25	[1] ABE	07	BELL	$e^+e^- \to J/\psi X$
3936±14	266	[2] ABE	07	BELL	$e^+e^- \to J/\psi(c\overline{c})$

[1] From a fit to $D^{*+}D^-$ and $D^{*0}\overline{D}^0$ events.
[2] From the inclusive fit. Not independent of the exclusive measurement by ABE 07.

$X(3940)$ WIDTH

VALUE (MeV)	CL%	EVTS	DOCUMENT ID		TECN	COMMENT
$37^{+26}_{-15}\pm 8$		52	PAKHLOV	08	BELL	$e^+e^- \to J/\psi X$
• • • We do not use the following data for averages, fits, limits, etc. • • •						
<52	90	25	ABE	07	BELL	$e^+e^- \to J/\psi X$

$X(3940)$ DECAY MODES

	Mode	Fraction (Γ_i/Γ)
Γ_1	$D\overline{D}^*$ + c.c.	seen
Γ_2	$D\overline{D}$	not seen
Γ_3	$J/\psi\omega$	not seen

$X(3940)$ BRANCHING RATIOS

$\Gamma(D\overline{D}^* + c.c.)/\Gamma_{total}$ Γ_1/Γ

VALUE	CL%	EVTS	DOCUMENT ID		TECN	COMMENT
• • • We do not use the following data for averages, fits, limits, etc. • • •						
>0.45	90	25	[1,2] ABE		07	BELL $e^+e^- \to J/\psi X$

[1] For $X(3940)$ decaying to final states with more than two tracks.
[2] PAKHLOV 08 finds that the inclusive peak near 3940 MeV/c^2 may consist of several states.

$\Gamma(D\overline{D})/\Gamma_{total}$ Γ_2/Γ

VALUE	CL%	DOCUMENT ID		TECN	COMMENT
• • • We do not use the following data for averages, fits, limits, etc. • • •					
<0.41	90	[1,2] ABE		07	BELL $e^+e^- \to J/\psi X$

[1] For $X(3940)$ decaying to final states with more than two tracks.
[2] PAKHLOV 08 finds that the inclusive peak near 3940 MeV/c^2 may consist of several states.

$\Gamma(J/\psi\omega)/\Gamma_{total}$ Γ_3/Γ

VALUE	CL%	DOCUMENT ID	TECN	COMMENT
• • • We do not use the following data for averages, fits, limits, etc. • • •				
<0.26	90	[1,2] ABE	07 BELL	$e^+e^- \to J/\psi X$

[1] For $X(3940)$ decaying to final states with more than two tracks.
[2] PAKHLOV 08 finds that the inclusive peak near 3940 MeV/c^2 may consist of several states.

$X(3940)$ REFERENCES

PAKHLOV	08	PRL 100 202001	P. Pakhlov *et al.*	(BELLE Collab.)
ABE	07	PRL 98 082001	K. Abe *et al.*	(BELLE Collab.)

$X(4020)$

$I^G(J^{PC}) = 1^+(?^{?-})$

Properties incompatible with a $q\overline{q}$ structure (exotic state). See the review on non-$q\overline{q}$ states.

Charged X(4020) seen by ABLIKIM 13X from $e^+e^- \to \pi^+\pi^- h_c(1P)$ at c.m. energy from 3.90 to 4.42 GeV as a peak in the invariant mass distribution of the $\pi^\pm h_c(1P)$ system, and by ABLIKIM 14B from $e^+e^- \to (D^*\overline{D}^*)^\pm\pi^\mp$ events in $(D^*\overline{D}^*)^\pm$ mass. A neutral X(4020) seen by ABLIKIM 14P at three c.m. energies in the same range in $e^+e^- \to \pi^0\pi^0 h_c(1P)$ as a peak in the larger of the two masses recoiling against a π^0. ABLIKIM 15AA observes a 5.9 σ signal in $(D^*\overline{D}^*)^0$ in $e^+e^- \to (D^*\overline{D}^*)^0\pi^0$ events using collisions at two c.m. energies. Production rates and mass values support grouping neutral and charged X(4020) together as manifestations of a single $I = 1$ particle.

$X(4020)$ MASS

VALUE (MeV)	EVTS	DOCUMENT ID	TECN	CHG	COMMENT
4024.1±1.9 OUR AVERAGE					
$4025.5^{+2.0}_{-4.7}\pm3.1$	116	[1] ABLIKIM 15AA	BES3	0	$e^+e^- \to (D^*\overline{D}^*)^0\pi^0$
$4026.3\pm2.6\pm3.7$	401	[1] ABLIKIM 14B	BES3	±	$e^+e^- \to (D^*\overline{D}^*)^\pm\pi^\mp$
$4023.9\pm2.2\pm3.8$	61	[1,2] ABLIKIM 14P	BES3	0	$e^+e^- \to \pi^0\pi^0 h_c$
$4022.9\pm0.8\pm2.7$	253	[1] ABLIKIM 13X	BES3	±	$e^+e^- \to \pi^+\pi^- h_c$

[1] Neglecting interference between the $X(4020)$ and non-resonant continuum.
[2] Assuming $J^P = 1^+$ and width of 7.9 ± 2.6 MeV.

$X(4020)$ WIDTH

VALUE (MeV)	EVTS	DOCUMENT ID	TECN	CHG	COMMENT
13 ±5 OUR AVERAGE		Error includes scale factor of 1.7. See the ideogram below.			
$23.0\pm6.0\pm1.0$	116	[1] ABLIKIM 15AA	BES3	0	$e^+e^- \to (D^*\overline{D}^*)^0\pi^0$
$24.8\pm5.6\pm7.7$	401	[1] ABLIKIM 14B	BES3	±	$e^+e^- \to (D^*\overline{D}^*)^\pm\pi^\mp$
$7.9\pm2.7\pm2.6$	253	[1] ABLIKIM 13X	BES3	±	$e^+e^- \to \pi^+\pi^- h_c$

[1] Neglecting interference between the $X(4020)$ and non-resonant continuum.

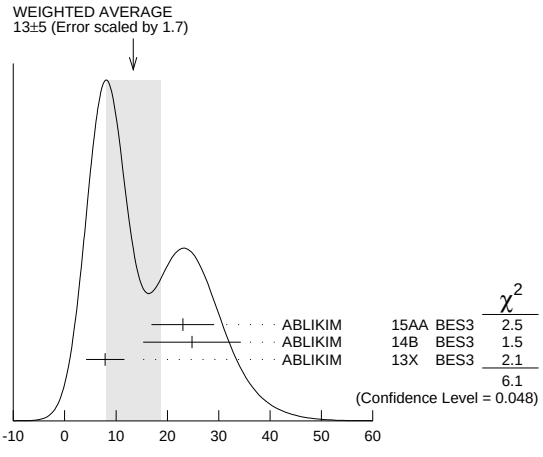

$X(4020)$ DECAY MODES

	Mode	Fraction (Γ_i/Γ)
Γ_1	$h_c(1P)\pi$	seen
Γ_2	$D^*\overline{D}^*$	seen
Γ_3	$D\overline{D}^*$ + c.c.	not seen
Γ_4	$\eta_c\pi^+\pi^-$	not seen
Γ_5	$J/\psi(1S)\pi^\pm$	not seen

$X(4020)$ BRANCHING RATIOS

$\Gamma(h_c(1P)\pi)/\Gamma_{total}$ Γ_1/Γ

VALUE	EVTS	DOCUMENT ID	TECN	CHG	COMMENT
seen	61	ABLIKIM 14P	BES3	0	$e^+e^- \to \pi^0\pi^0 h_c$
seen	253	ABLIKIM 13X	BES3	±	$e^+e^- \to \pi^+\pi^- h_c$

$\Gamma(D^*\overline{D}^*)/\Gamma_{total}$ Γ_2/Γ

VALUE	EVTS	DOCUMENT ID	TECN	CHG	COMMENT
seen	116	[1] ABLIKIM 15AA	BES3	0	$e^+e^- \to (D^*\overline{D}^*)^0\pi^0$
seen	401	[1] ABLIKIM 14B	BES3	±	$e^+e^- \to (D^*\overline{D}^*)^\pm\pi^\mp$

[1] Neglecting interference between the $X(4020)$ and non-resonant continuum.

$\Gamma(D\overline{D}^*$ + c.c.$)/\Gamma_{total}$ Γ_3/Γ

VALUE	DOCUMENT ID	TECN	CHG	COMMENT
not seen	ABLIKIM 15AC	BES3	±	$e^+e^- \to \pi^\pm(D\overline{D}^*)^\mp$

$\Gamma(\eta_c\pi^+\pi^-)/\Gamma_{total}$ Γ_4/Γ

VALUE	DOCUMENT ID	TECN	COMMENT
not seen	[1] VINOKUROVA 15	BELL	$B^+ \to K^+\eta_c\pi^+\pi^-$

[1] VINOKUROVA 15 reports $B(B^+ \to K^+X(4020)^0) \times B(X \to \eta_c\pi^+\pi^-) < 1.6 \times 10^{-5}$ at 90% CL.

$\Gamma(J/\psi(1S)\pi^\pm)/\Gamma_{total}$ Γ_5/Γ

VALUE	DOCUMENT ID	TECN	COMMENT
not seen	[1] ABLIKIM 17J	BES3	$e^+e^- \to \pi^+\pi^- J/\psi$

[1] From Partial Wave Analysis assuming $J^P = 1^+$.

$X(4020)$ REFERENCES

ABLIKIM	17J	PRL 119 072001	M. Ablikim *et al.*	(BES III Collab.)
ABLIKIM	15AA	PRL 115 182002	M. Ablikim *et al.*	(BES III Collab.)
ABLIKIM	15AC	PR D92 092006	M. Ablikim *et al.*	(BES III Collab.)
VINOKUROVA	15	JHEP 1506 132	A. Vinokurova *et al.*	(BELLE Collab.)
Also		JHEP 1702 088 (errat.)	A. Vinokurava *et al.*	(BELLE Collab.)
ABLIKIM	14B	PRL 112 132001	M. Ablikim *et al.*	(BES III Collab.)
ABLIKIM	14P	PRL 113 212002	M. Ablikim *et al.*	(BES III Collab.)
ABLIKIM	13X	PRL 111 242001	M. Ablikim *et al.*	(BES III Collab.)

$\psi(4040)$

$I^G(J^{PC}) = 0^-(1^{--})$

$\psi(4040)$ MASS

VALUE (MeV)	DOCUMENT ID	TECN	COMMENT
4039 ± 1 OUR ESTIMATE			
4039.6± 4.3	[1] ABLIKIM 08D	BES2	$e^+e^- \to$ hadrons
• • • We do not use the following data for averages, fits, limits, etc. • • •			
4034 ± 6	[2] MO 10	RVUE	$e^+e^- \to$ hadrons
4037 ± 2	[3] SETH 05A	RVUE	$e^+e^- \to$ hadrons
4040 ± 1	[4] SETH 05A	RVUE	$e^+e^- \to$ hadrons
4040 ±10	BRANDELIK 78C	DASP	e^+e^-

[1] Reanalysis of data presented in BAI 02C. From a global fit over the center-of-mass energy region 3.7–5.0 GeV covering the $\psi(3770)$, $\psi(4040)$, $\psi(4160)$, and $\psi(4415)$ resonances. Phase angle fixed in the fit to $\delta = (130 \pm 46)^\circ$.
[2] Reanalysis of data presented in BAI 00 and BAI 02C. From a global fit over the center-of-mass energy 3.8–4.8 GeV covering the $\psi(4040)$, $\psi(4160)$ and $\psi(4415)$ resonances and including interference effects.
[3] From a fit to Crystal Ball (OSTERHELD 86) data.
[4] From a fit to BES (BAI 02C) data.

$\psi(4040)$ WIDTH

VALUE (MeV)	DOCUMENT ID	TECN	COMMENT
80 ±10 OUR ESTIMATE			
84.5±12.3	[5] ABLIKIM 08D	BES2	$e^+e^- \to$ hadrons
• • • We do not use the following data for averages, fits, limits, etc. • • •			
87 ±11	[6] MO 10	RVUE	$e^+e^- \to$ hadrons
85 ±10	[7] SETH 05A	RVUE	$e^+e^- \to$ hadrons
89 ± 6	[8] SETH 05A	RVUE	$e^+e^- \to$ hadrons
52 ±10	BRANDELIK 78C	DASP	e^+e^-

[5] Reanalysis of data presented in BAI 02C. From a global fit over the center-of-mass energy region 3.7–5.0 GeV covering the $\psi(3770)$, $\psi(4040)$, $\psi(4160)$, and $\psi(4415)$ resonances. Phase angle fixed in the fit to $\delta = (130 \pm 46)^\circ$.

[6] Reanalysis of data presented in BAI 00 and BAI 02C. From a global fit over the center-of-mass energy 3.8-4.8 GeV covering the $\psi(4040)$, $\psi(4160)$ and $\psi(4415)$ resonances and including interference effects.

[7] From a fit to Crystal Ball (OSTERHELD 86) data.

[8] From a fit to BES (BAI 02C) data.

$\psi(4040)$ DECAY MODES

Due to the complexity of the $c\overline{c}$ threshold region, in this listing, "seen" ("not seen") means that a cross section for the mode in question has been measured at effective $\sqrt{s}$ near this particle's central mass value, more (less) than 2σ above zero, without regard to any peaking behavior in $\sqrt{s}$ or absence thereof. See mode listing(s) for details and references.

	Mode	Fraction (Γ_j/Γ)	Confidence level
Γ_1	e^+e^-	$(1.07\pm0.16)\times10^{-5}$	
Γ_2	$D\overline{D}$	seen	
Γ_3	$D^0\overline{D}^0$	seen	
Γ_4	D^+D^-	seen	
Γ_5	$D^*\overline{D}$ + c.c.	seen	
Γ_6	$D^*(2007)^0\overline{D}^0$ + c.c.	seen	
Γ_7	$D^*(2010)^+D^-$ + c.c.	seen	
Γ_8	$D^*\overline{D}^*$	seen	
Γ_9	$D^*(2007)^0\overline{D}^*(2007)^0$	seen	
Γ_{10}	$D^*(2010)^+D^*(2010)^-$	seen	
Γ_{11}	$D\overline{D}\pi$ (excl. $D^*\overline{D}$)		
Γ_{12}	$D^0D^-\pi^+$ +c.c. (excl. $D^*(2007)^0\overline{D}^0$ +c.c., $D^*(2010)^+D^-$ +c.c.)	not seen	
Γ_{13}	$D\overline{D}^*\pi$ (excl. $D^*\overline{D}^*$)	not seen	
Γ_{14}	$D^0\overline{D}^{*-}\pi^+$ +c.c. (excl. $D^*(2010)^+D^*(2010)^-$)	seen	
Γ_{15}	$D_s^+D_s^-$	seen	
Γ_{16}	$J/\psi(1S)$ hadrons		
Γ_{17}	$J/\psi\pi^+\pi^-$	$<4\times10^{-3}$	90%
Γ_{18}	$J/\psi\pi^0\pi^0$	$<2\times10^{-3}$	90%
Γ_{19}	$J/\psi\eta$	$(5.2\pm0.7)\times10^{-3}$	
Γ_{20}	$J/\psi\pi^0$	$<2.8\times10^{-4}$	90%
Γ_{21}	$J/\psi\pi^+\pi^-\pi^0$	$<2\times10^{-3}$	90%
Γ_{22}	$\chi_{c1}\gamma$	$<3.4\times10^{-3}$	90%
Γ_{23}	$\chi_{c2}\gamma$	$<5\times10^{-3}$	90%
Γ_{24}	$\chi_{c1}\pi^+\pi^-\pi^0$	<1.1 %	90%
Γ_{25}	$\chi_{c2}\pi^+\pi^-\pi^0$	<3.2 %	90%
Γ_{26}	$h_c(1P)\pi^+\pi^-$	$<3\times10^{-3}$	90%
Γ_{27}	$\phi\pi^+\pi^-$	$<3\times10^{-3}$	90%
Γ_{28}	$\Lambda\overline{\Lambda}\pi^+\pi^-$	$<2.9\times10^{-4}$	90%
Γ_{29}	$\Lambda\overline{\Lambda}\pi^0$	$<9\times10^{-5}$	90%
Γ_{30}	$\Lambda\overline{\Lambda}\eta$	$<3.0\times10^{-4}$	90%
Γ_{31}	$\Sigma^+\overline{\Sigma}^-$	$<1.3\times10^{-4}$	90%
Γ_{32}	$\Sigma^0\overline{\Sigma}^0$	$<7\times10^{-5}$	90%
Γ_{33}	$\Xi^+\overline{\Xi}^-$	$<1.6\times10^{-4}$	90%
Γ_{34}	$\Xi^0\overline{\Xi}^0$	$<1.8\times10^{-4}$	90%
Γ_{35}	$\mu^+\mu^-$		

$\psi(4040)$ PARTIAL WIDTHS

$\Gamma(e^+e^-)$ Γ_1

VALUE (keV)	DOCUMENT ID		TECN	COMMENT
0.86±0.07 OUR ESTIMATE				
0.83±0.20	[9] ABLIKIM	08D	BES2	$e^+e^-\to$ hadrons
• • • We do not use the following data for averages, fits, limits, etc. • • •				
0.6 to 1.4	[10] MO	10	RVUE	$e^+e^-\to$ hadrons
0.88±0.11	[11] SETH	05A	RVUE	$e^+e^-\to$ hadrons
0.91±0.13	[12] SETH	05A	RVUE	$e^+e^-\to$ hadrons
0.75±0.15	BRANDELIK	78C	DASP	e^+e^-

[9] Reanalysis of data presented in BAI 02C. From a global fit over the center-of-mass energy region 3.7–5.0 GeV covering the $\psi(3770)$, $\psi(4040)$, $\psi(4160)$, and $\psi(4415)$ resonances. Phase angle fixed in the fit to $\delta = (130 \pm 46)^\circ$.

[10] Reanalysis of data presented in BAI 00 and BAI 02C. From a global fit over the center-of-mass energy 3.8-4.8 GeV covering the $\psi(4040)$, $\psi(4160)$ and $\psi(4415)$ resonances and including interference effects. Four sets of solutions are obtained with the same fit quality, mass and total width, but with different e^+e^- partial widths. We quote only the range of values.

[11] From a fit to Crystal Ball (OSTERHELD 86) data.

[12] From a fit to BES (BAI 02C) data.

$\psi(4040)$ Γ(i) × $\Gamma(e^+e^-)/\Gamma$(total)

$\Gamma(\chi_{c1}\gamma)$ × $\Gamma(e^+e^-)/\Gamma_{total}$ $\Gamma_{22}\Gamma_1/\Gamma$

VALUE (eV)	CL%	DOCUMENT ID		TECN	COMMENT
<2.9	90	[13] HAN	15	BELL	$10.58\ e^+e^-\to\chi_{c1}\gamma$

[13] Using $B(\eta\to\gamma\gamma) = (39.41\pm0.21)\%$.

$\Gamma(\chi_{c2}\gamma)$ × $\Gamma(e^+e^-)/\Gamma_{total}$ $\Gamma_{23}\Gamma_1/\Gamma$

VALUE (eV)	CL%	DOCUMENT ID		TECN	COMMENT
<4.6	90	[14] HAN	15	BELL	$10.58\ e^+e^-\to\chi_{c2}\gamma$

[14] Using $B(\eta\to\gamma\gamma) = (39.41\pm0.21)\%$.

$\psi(4040)$ Γ(i) × $\Gamma(e^+e^-)/\Gamma^2$(total)

$\Gamma(J/\psi\eta)/\Gamma_{total}$ × $\Gamma(e^+e^-)/\Gamma_{total}$ $\Gamma_{19}/\Gamma\times\Gamma_1/\Gamma$

VALUE (units 10^{-8})	DOCUMENT ID		TECN	COMMENT
• • • We do not use the following data for averages, fits, limits, etc. • • •				
5.1±1.4±1.5	[15] WANG	13B	BELL	$e^+e^-\to J/\psi\eta\gamma$
12.8±2.1±1.9	[16] WANG	13B	BELL	$e^+e^-\to J/\psi\eta\gamma$

[15] Solution I of two equivalent solutions in a fit using two interfering resonances. Mass and width fixed at 4039 MeV and 80 MeV, respectively.

[16] Solution II of two equivalent solutions in a fit using two interfering resonances. Mass and width fixed at 4039 MeV and 80 MeV, respectively.

$\psi(4040)$ BRANCHING RATIOS

$\Gamma(e^+e^-)/\Gamma_{total}$ Γ_1/Γ

VALUE (units 10^{-5})	DOCUMENT ID		TECN	COMMENT
• • • We do not use the following data for averages, fits, limits, etc. • • •				
~ 1.0	FELDMAN	77	MRK1	e^+e^-

$\Gamma(D^0\overline{D}^0)/\Gamma_{total}$ Γ_3/Γ

VALUE	DOCUMENT ID		TECN	COMMENT
seen	AUBERT	09M	BABR	$e^+e^-\to D^0\overline{D}^0\gamma$
seen	CRONIN-HEN..	09	CLEO	$e^+e^-\to D^0\overline{D}^0$
seen	PAKHLOVA	08	BELL	$e^+e^-\to D^0\overline{D}^0\gamma$

$\Gamma(D^+D^-)/\Gamma_{total}$ Γ_4/Γ

VALUE	DOCUMENT ID		TECN	COMMENT
seen	AUBERT	09M	BABR	$e^+e^-\to D^+D^-\gamma$
seen	CRONIN-HEN..	09	CLEO	$e^+e^-\to D^+D^-$
seen	PAKHLOVA	08	BELL	$e^+e^-\to D^+D^-\gamma$

$\Gamma(D\overline{D})/\Gamma(D^*\overline{D}+\text{c.c.})$ Γ_2/Γ_5

VALUE	DOCUMENT ID		TECN	COMMENT
0.24±0.05±0.12	AUBERT	09M	BABR	$e^+e^-\to\gamma D^{(*)}\overline{D}$

$\Gamma(D^0\overline{D}^0)/\Gamma(D^*(2007)^0\overline{D}^0+\text{c.c.})$ Γ_3/Γ_6

VALUE	DOCUMENT ID		TECN	COMMENT
0.05±0.03	[17] GOLDHABER	77	MRK1	e^+e^-

[17] Phase-space factor (p^3) explicitly removed.

$\Gamma(D^*(2007)^0\overline{D}^0+\text{c.c.})/\Gamma_{total}$ Γ_6/Γ

VALUE	DOCUMENT ID		TECN	COMMENT
seen	AUBERT	09M	BABR	$e^+e^-\to D^{*0}\overline{D}^0\gamma$
seen	CRONIN-HEN..	09	CLEO	$e^+e^-\to D^{*0}\overline{D}^0$

$\Gamma(D^*(2010)^+D^-+\text{c.c.})/\Gamma_{total}$ Γ_7/Γ

VALUE	DOCUMENT ID		TECN	COMMENT
seen	[18] ZHUKOVA	18	BELL	$e^+e^-\to D^{*+}D^-\gamma$
seen	AUBERT	09M	BABR	$e^+e^-\to D^{*+}D^-\gamma$
seen	CRONIN-HEN..	09	CLEO	$e^+e^-\to D^{*+}D^-$
• • • We do not use the following data for averages, fits, limits, etc. • • •				
seen	PAKHLOVA	07	BELL	$e^+e^-\to D^{*+}D^-\gamma$

[18] Supersedes PAKHLOVA 07.

$\Gamma(D^*(2010)^+D^-+\text{c.c.})/\Gamma(D^*(2007)^0\overline{D}^0+\text{c.c.})$ Γ_7/Γ_6

VALUE	DOCUMENT ID		TECN	COMMENT
0.95±0.09±0.10	AUBERT	09M	BABR	$e^+e^-\to\gamma D^*\overline{D}$

$\Gamma(D^*\overline{D}^*)/\Gamma(D^*\overline{D}+\text{c.c.})$ Γ_8/Γ_5

VALUE	DOCUMENT ID		TECN	COMMENT
0.18±0.14±0.03	AUBERT	09M	BABR	$e^+e^-\to\gamma D^{(*)}\overline{D}^{(*)}$

$\Gamma(D^*(2007)^0\overline{D}^*(2007)^0)/\Gamma_{total}$ Γ_9/Γ

VALUE	DOCUMENT ID		TECN	COMMENT
seen	AUBERT	09M	BABR	$e^+e^-\to D^{*0}\overline{D}^{*0}\gamma$
seen	CRONIN-HEN..	09	CLEO	$e^+e^-\to D^{*0}\overline{D}^{*0}$

See key on page 885

$\Gamma(D^*(2007)^0\overline{D}^*(2007)^0)/\Gamma(D^*(2007)^0\overline{D}^0+\text{c.c.})$ Γ_9/Γ_6

VALUE	DOCUMENT ID		TECN	COMMENT
32.0±12.0	[19] GOLDHABER	77	MRK1	e^+e^-

[19] Phase-space factor (p^3) explicitly removed.

$\Gamma(D^*(2010)^+D^*(2010)^-)/\Gamma_{\text{total}}$ Γ_{10}/Γ

VALUE	DOCUMENT ID		TECN	COMMENT
seen	[20] ZHUKOVA	18	BELL	$e^+e^- \to D^{*+}D^{*-}\gamma$
seen	AUBERT	09M	BABR	$e^+e^- \to D^{*+}D^{*-}\gamma$
seen	CRONIN-HEN...	09	CLEO	$e^+e^- \to D^{*+}D^{*-}$
• • • We do not use the following data for averages, fits, limits, etc. • • •				
seen	PAKHLOVA	07	BELL	$e^+e^- \to D^{*+}D^{*-}\gamma$

[20] Supersedes PAKHLOVA 07.

$\Gamma(D^0D^-\pi^+ + \text{c.c. (excl. } D^*(2007)^0\overline{D}^0 + \text{c.c., } D^*(2010)^+D^- + \text{c.c.}))/\Gamma_{\text{total}}$ Γ_{12}/Γ

VALUE	DOCUMENT ID		TECN	COMMENT
not seen	PAKHLOVA	08A	BELL	$e^+e^- \to D^0D^-\pi^+\gamma$

$\Gamma(D\overline{D}^*\pi(\text{excl. } D^*\overline{D}^*))/\Gamma_{\text{total}}$ Γ_{13}/Γ

VALUE	DOCUMENT ID		TECN	COMMENT
not seen	CRONIN-HEN...	09	CLEO	$e^+e^- \to D\overline{D}^*\pi$

$\Gamma(D^0\overline{D}^{*-}\pi^+ + \text{c.c. (excl. } D^*(2010)^+D^*(2010)^-))/\Gamma_{\text{total}}$ Γ_{14}/Γ

VALUE	DOCUMENT ID		TECN	COMMENT
seen	PAKHLOVA	09	BELL	$e^+e^- \to D^0D^{*-}\pi^+\gamma$

$\Gamma(D_s^+D_s^-)/\Gamma_{\text{total}}$ Γ_{15}/Γ

VALUE	DOCUMENT ID		TECN	COMMENT
seen	PAKHLOVA	11	BELL	$e^+e^- \to D_s^+D_s^-\gamma$
seen	DEL-AMO-SA...	10N	BABR	$e^+e^- \to D_s^+D_s^-\gamma$
seen	CRONIN-HEN...	09	CLEO	$e^+e^- \to D_s^+D_s^-$

$\Gamma(J/\psi\pi^+\pi^-)/\Gamma_{\text{total}}$ Γ_{17}/Γ

VALUE (units 10^{-3})	CL%	DOCUMENT ID		TECN	COMMENT
<4	90	COAN	06	CLEO	3.97–4.06 $e^+e^- \to$ hadrons

$\Gamma(J/\psi\pi^0\pi^0)/\Gamma_{\text{total}}$ Γ_{18}/Γ

VALUE (units 10^{-3})	CL%	DOCUMENT ID		TECN	COMMENT
<2	90	COAN	06	CLEO	3.97–4.06 $e^+e^- \to$ hadrons

$\Gamma(J/\psi\eta)/\Gamma_{\text{total}}$ Γ_{19}/Γ

VALUE (units 10^{-3})	CL%	DOCUMENT ID		TECN	COMMENT
5.2±0.5±0.5		[21] ABLIKIM	12K	BES3	$e^+e^- \to \ell^+\ell^-2\gamma$
• • • We do not use the following data for averages, fits, limits, etc. • • •					
<7	90	COAN	06	CLEO	3.97–4.06 $e^+e^- \to$ hadrons

[21] ABLIKIM 12K measure $\sigma(e^+e^- \to J/\psi\eta) = 32.1 \pm 2.8 \pm 1.3$ pb. They assume the $\eta J/\psi$ fully originates from $\psi(4040)$ decays.

$\Gamma(J/\psi\pi^0)/\Gamma_{\text{total}}$ Γ_{20}/Γ

VALUE (units 10^{-3})	CL%	DOCUMENT ID		TECN	COMMENT
<0.28	90	[22] ABLIKIM	12K	BES3	$e^+e^- \to \ell^+\ell^-2\gamma$
• • • We do not use the following data for averages, fits, limits, etc. • • •					
<2	90	COAN	06	CLEO	3.97–4.06 $e^+e^- \to$ hadrons

[22] ABLIKIM 12K measure $\sigma(e^+e^- \to J/\psi\pi^0) < 1.6$ pb. They assume the $\eta J/\psi$ fully originates from $\psi(4040)$ decays.

$\Gamma(J/\psi\pi^+\pi^-\pi^0)/\Gamma_{\text{total}}$ Γ_{21}/Γ

VALUE (units 10^{-3})	CL%	DOCUMENT ID		TECN	COMMENT
<2	90	COAN	06	CLEO	3.97–4.06 $e^+e^- \to$ hadrons

$\Gamma(\chi_{c1}\gamma)/\Gamma_{\text{total}}$ Γ_{22}/Γ

VALUE (units 10^{-3})	CL%	DOCUMENT ID		TECN	COMMENT
• • • We do not use the following data for averages, fits, limits, etc. • • •					
<11	90	COAN	06	CLEO	3.97–4.06 $e^+e^- \to$ hadrons

$\Gamma(\chi_{c2}\gamma)/\Gamma_{\text{total}}$ Γ_{23}/Γ

VALUE (units 10^{-3})	CL%	DOCUMENT ID		TECN	COMMENT
• • • We do not use the following data for averages, fits, limits, etc. • • •					
<17	90	COAN	06	CLEO	3.97–4.06 $e^+e^- \to$ hadrons

$\Gamma(\chi_{c1}\pi^+\pi^-\pi^0)/\Gamma_{\text{total}}$ Γ_{24}/Γ

VALUE (units 10^{-3})	CL%	DOCUMENT ID		TECN	COMMENT
<11	90	COAN	06	CLEO	3.97–4.06 $e^+e^- \to$ hadrons

$\Gamma(\chi_{c2}\pi^+\pi^-\pi^0)/\Gamma_{\text{total}}$ Γ_{25}/Γ

VALUE (units 10^{-3})	CL%	DOCUMENT ID		TECN	COMMENT
<32	90	COAN	06	CLEO	3.97–4.06 $e^+e^- \to$ hadrons

$\Gamma(h_c(1P)\pi^+\pi^-)/\Gamma_{\text{total}}$ Γ_{26}/Γ

VALUE (units 10^{-3})	CL%	DOCUMENT ID		TECN	COMMENT
<3	90	[23] PEDLAR	11	CLEO	$e^+e^- \to h_c(1P)\pi^+\pi^-$

[23] From several values of $\sqrt{s}$ near the peak of the $\psi(4040)$, PEDLAR 11 measures $\sigma(e^+e^- \to h_c(1P)\pi^+\pi^-) = 1.0 \pm 8.0 \pm 5.4 \pm 0.2$ pb, where the errors are statistical, systematic, and due to uncertainty in $B(\psi(2S) \to \pi^0 h_c(1P))$, respectively.

$\Gamma(\phi\pi^+\pi^-)/\Gamma_{\text{total}}$ Γ_{27}/Γ

VALUE (units 10^{-3})	CL%	DOCUMENT ID		TECN	COMMENT
<3	90	COAN	06	CLEO	3.97–4.06 e^+e^- → hadrons

$\Gamma(\Lambda\overline{\Lambda}\pi^+\pi^-)/\Gamma_{\text{total}}$ Γ_{28}/Γ

VALUE (units 10^{-4})	CL%	DOCUMENT ID		TECN	COMMENT
<2.9	90	[24] ABLIKIM	13Q	BES3	$e^+e^- \to \psi(4040)$

[24] Assuming that interference effects between resonance and continuum can be neglected.

$\Gamma(\Lambda\overline{\Lambda}\pi^0)/\Gamma_{\text{total}}$ Γ_{29}/Γ

VALUE (units 10^{-4})	CL%	DOCUMENT ID		TECN	COMMENT
<0.9	90	[25] ABLIKIM	13Q	BES3	$e^+e^- \to \psi(4040)$

[25] Assuming that interference effects between resonance and continuum can be neglected.

$\Gamma(\Lambda\overline{\Lambda}\eta)/\Gamma_{\text{total}}$ Γ_{30}/Γ

VALUE (units 10^{-4})	CL%	DOCUMENT ID		TECN	COMMENT
<3.0	90	[26] ABLIKIM	13Q	BES3	$e^+e^- \to \psi(4040)$

[26] Assuming that interference effects between resonance and continuum can be neglected.

$\Gamma(\Sigma^+\overline{\Sigma}^-)/\Gamma_{\text{total}}$ Γ_{31}/Γ

VALUE (units 10^{-4})	CL%	DOCUMENT ID		TECN	COMMENT
<1.3	90	[27] ABLIKIM	13Q	BES3	$e^+e^- \to \psi(4040)$

[27] Assuming that interference effects between resonance and continuum can be neglected.

$\Gamma(\Sigma^0\overline{\Sigma}^0)/\Gamma_{\text{total}}$ Γ_{32}/Γ

VALUE (units 10^{-4})	CL%	DOCUMENT ID		TECN	COMMENT
<0.7	90	[28] ABLIKIM	13Q	BES3	$e^+e^- \to \psi(4040)$

[28] Assuming that interference effects between resonance and continuum can be neglected.

$\Gamma(\Xi^+\overline{\Xi}^-)/\Gamma_{\text{total}}$ Γ_{33}/Γ

VALUE (units 10^{-4})	CL%	DOCUMENT ID		TECN	COMMENT
<1.6	90	[29] ABLIKIM	13Q	BES3	$e^+e^- \to \psi(4040)$

[29] Assuming that interference effects between resonance and continuum can be neglected.

$\Gamma(\Xi^0\overline{\Xi}^0)/\Gamma_{\text{total}}$ Γ_{34}/Γ

VALUE (units 10^{-4})	CL%	DOCUMENT ID		TECN	COMMENT
<1.8	90	[30] ABLIKIM	13Q	BES3	$e^+e^- \to \psi(4040)$

[30] Assuming that interference effects between resonance and continuum can be neglected.

$\psi(4040)$ REFERENCES

ZHUKOVA	18	PR D97 012002	V. Zhukova *et al.*	(BELLE Collab.)
HAN	15	PR D92 012011	Y.L. Han *et al.*	(BELLE Collab.)
ABLIKIM	13Q	PR D87 112011	Ablikim M. *et al.*	(BES III Collab.)
WANG	13B	PR D87 051101	X.L. Wang *et al.*	(BELLE Collab.)
ABLIKIM	12K	PR D86 071101	M. Ablikim *et al.*	(BES III Collab.)
PAKHLOVA	11	PR D83 011101	G. Pakhlova *et al.*	(BELLE Collab.)
PEDLAR	11	PRL 107 041803	T. Pedlar *et al.*	(CLEO Collab.)
DEL-AMO-SA...	10N	PR D82 052004	P. del Amo Sanchez *et al.*	(BABAR Collab.)
MO	10	PR D82 077501	X.H. Mo, C.Z. Yuan, P. Wang	(BHEP)
AUBERT	09M	PR D79 092001	B. Aubert *et al.*	(BABAR Collab.)
CRONIN-HEN...	09	PR D80 072001	D. Cronin-Hennessy *et al.*	(CLEO Collab.)
PAKHLOVA	09	PR D80 091101	G. Pakhlova *et al.*	(BELLE Collab.)
ABLIKIM	08D	PL B660 315	M. Ablikim *et al.*	(BES Collab.)
PAKHLOVA	08	PR D77 011103	G. Pakhlova *et al.*	(BELLE Collab.)
PAKHLOVA	08A	PRL 100 062001	G. Pakhlova *et al.*	(BELLE Collab.)
PAKHLOVA	07	PRL 98 092001	G. Pakhlova *et al.*	(BELLE Collab.)
COAN	06	PRL 96 162003	T.E. Coan *et al.*	(CLEO Collab.)
SETH	05A	PR D72 017501	K.K. Seth	
BAI	02C	PRL 88 101802	J.Z. Bai *et al.*	(BES Collab.)
BAI	00	PRL 84 594	J.Z. Bai *et al.*	(BES Collab.)
OSTERHELD	86	SLAC-PUB-4160	A. Osterheld *et al.*	(SLAC Crystal Ball Collab.)
BRANDELIK	78C	PL 76B 361	R. Brandelik *et al.*	(DASP Collab.)
Also		ZPHY C1 233	R. Brandelik *et al.*	(DASP Collab.)
FELDMAN	77	PRPL 33C 285	G.J. Feldman, M.L. Perl	(LBL, SLAC)
GOLDHABER	77	PL 69B 503	G. Goldhaber *et al.*	(Mark I Collab.)

Meson Particle Listings

$X(4050)^{\pm}$, $X(4055)^{\pm}$, $\chi_{c1}(4140)$

$X(4050)^{\pm}$

$I^G(J^{PC}) = 1^-(?^{?+})$
I, *G*, *C* need confirmation.

OMITTED FROM SUMMARY TABLE

Properties incompatible with a $q\overline{q}$ structure (exotic state). See the review on non-$q\overline{q}$ states.

Observed by MIZUK 08 in the $\pi^+\chi_{c1}(1P)$ invariant mass distribution in $\overline{B}^0 \to K^-\pi^+\chi_{c1}(1P)$ decays. Not seen by LEES 12B in this same mode after accounting for $K\pi$ resonant mass and angular structure.

$X(4050)^{\pm}$ MASS

VALUE (MeV)	DOCUMENT ID		TECN	COMMENT
$4051 \pm 14^{+20}_{-41}$	[1] MIZUK	08	BELL	$\overline{B}^0 \to K^-\pi^+\chi_{c1}(1P)$

[1] From a Dalitz plot analysis with two Breit-Wigner amplitudes.

$X(4050)^{\pm}$ WIDTH

VALUE (MeV)	DOCUMENT ID		TECN	COMMENT
$82^{+21}_{-17}{}^{+47}_{-22}$	[1] MIZUK	08	BELL	$\overline{B}^0 \to K^-\pi^+\chi_{c1}(1P)$

[1] From a Dalitz plot analysis with two Breit-Wigner amplitudes.

$X(4050)^{\pm}$ DECAY MODES

	Mode	Fraction (Γ_i/Γ)
Γ_1	$\pi^+\chi_{c1}(1P)$	seen

$X(4050)^{\pm}$ BRANCHING RATIOS

$\Gamma(\pi^+\chi_{c1}(1P))/\Gamma_{total}$ Γ_1/Γ

VALUE	DOCUMENT ID		TECN	COMMENT
seen	[1] MIZUK	08	BELL	$\overline{B}^0 \to K^-\pi^+\chi_{c1}(1P)$
• • • We do not use the following data for averages, fits, limits, etc. • • •				
not seen	[2] LEES	12B	BABR	$B \to K\pi\chi_{c1}(1P)$

[1] With a product branching fraction measurement of $B(\overline{B}^0 \to K^- X(4050)^+) \times B(X(4050)^+ \to \pi^+\chi_{c1}(1P)) = (3.0^{+1.5}_{-0.8}{}^{+3.7}_{-1.6}) \times 10^{-5}$.

[2] With a product branching fraction limit of $B(\overline{B}^0 \to X(4050)^+ K^-) \times B(X(4050)^+ \to \chi_{c1}\pi^+) < 1.8 \times 10^{-5}$ at 90% CL.

$X(4050)^{\pm}$ REFERENCES

LEES	12B	PR D85 052003	J.P. Lees *et al.*		(BABAR Collab.)
MIZUK	08	PR D78 072004	R. Mizuk *et al.*		(BELLE Collab.)

$X(4055)^{\pm}$

$I^G(J^{PC}) = 1^+(?^{?-})$
I, *G*, *C* need confirmation.

OMITTED FROM SUMMARY TABLE

Properties incompatible with a $q\overline{q}$ structure (exotic state). See the review on non-$q\overline{q}$ states.

Needs confirmation. Seen by WANG 15A in the $\psi(2S)\pi^+$ invariant mass distribution in $\psi(4360) \to \psi(2S)\pi^+\pi^-$ decay.

$X(4055)^{\pm}$ MASS

VALUE (MeV)	DOCUMENT ID		TECN	COMMENT
4054 ±3 ±1	[1] WANG	15A	BELL	10.58 $e^+e^- \to \gamma\pi^+\pi^-\psi(2S)$
• • • We do not use the following data for averages, fits, limits, etc. • • •				
4032.1 ± 2.4	[2] ABLIKIM	17V	BES3	$e^+e^- \to \pi^+\pi^-\psi(2S)$

[1] Statistical significance of 3.5 σ.

[2] Statistical error only, with significance of 9.2 σ. From an unbinned maximum likelihood fit of the $\pi^+\pi^-\psi(2S)$ Dalitz plot from data collected at $\sqrt{s} = 4.416$ GeV for a $J^C = 1^+$ state. The fit does not match the detailed structure of the data, having a C.L. of only 8%.

$X(4055)^{\pm}$ WIDTH

VALUE (MeV)	DOCUMENT ID		TECN	COMMENT
45 ±11 ±6	[1] WANG	15A	BELL	10.58 $e^+e^- \to \gamma\pi^+\pi^-\psi(2S)$
• • • We do not use the following data for averages, fits, limits, etc. • • •				
26.1 ± 5.3	[2] ABLIKIM	17V	BES3	$e^+e^- \to \pi^+\pi^-\psi(2S)$

[1] Statistical significance of 3.5 σ.

[2] Statistical error only, with significance of 9.2 σ. From an unbinned maximum likelihood fit of the $\pi^+\pi^-\psi(2S)$ Dalitz plot from data collected at $\sqrt{s} = 4.416$ GeV for a $J^C = 1^+$ state. The fit does not match the detailed structure of the data, having a C.L. of only 8%.

$X(4055)^{\pm}$ DECAY MODES

	Mode	Fraction (Γ_i/Γ)
Γ_1	$\pi^+\psi(2S)$	seen

$X(4055)^{\pm}$ BRANCHING RATIOS

$\Gamma(\pi^+\psi(2S))/\Gamma_{total}$ Γ_1/Γ

VALUE	DOCUMENT ID		TECN	COMMENT
seen	[1] WANG	15A	BELL	10.58 $e^+e^- \to \gamma\pi^+\pi^-\psi(2S)$

[1] Statistical significance of 3.5 σ.

$X(4055)^{\pm}$ REFERENCES

ABLIKIM	17V	PR D96 032004	M. Ablikim *et al.*	(BES III Collab.)
WANG	15A	PR D91 112007	X.L. Wang *et al.*	(BELLE Collab.)

$\chi_{c1}(4140)$

$I^G(J^{PC}) = 0^+(1^{++})$

was $X(4140)$

This state shows properties different from a conventional $q\overline{q}$ state. A candidate for an exotic structure. See the review on non-$q\overline{q}$ states.

Seen by AALTONEN 09AH, ABAZOV 14A, CHATRCHYAN 14M, AAIJ 17C in $B^+ \to \chi_{c1}K^+$, $\chi_{c1} \to J/\psi\phi$, and by ABAZOV 15M separately in both prompt (4.7 σ) and non-prompt (5.6 σ) production in $p\overline{p} \to J/\psi\phi +$ anything. Not seen by SHEN 10 in $\gamma\gamma \to J/\psi\phi$ and ABLIKIM 15 in $e^+e^- \to \gamma J/\psi\phi$ at $\sqrt{s} = 4.23$, 4.26, 4.36 GeV.

$\chi_{c1}(4140)$ MASS

VALUE (MeV)	EVTS	DOCUMENT ID		TECN	COMMENT
4146.8±2.4 OUR AVERAGE		Error includes scale factor of 1.1.			
$4146.5 \pm 4.5^{+4.6}_{-2.8}$	4289	[1] AAIJ	17C	LHCB	$B^+ \to J/\psi\phi K^+$
$4143.4^{+2.9}_{-3.0} \pm 0.6$	19	[2] AALTONEN	17	CDF	$B^+ \to J/\psi\phi K^+$
$4152.5 \pm 1.7^{+6.2}_{-5.4}$	616	[3] ABAZOV	15M	D0	$p\overline{p} \to J/\psi\phi +$ anything
4159.0 ± 4.3 ± 6.6	52	[4] ABAZOV	14A	D0	$B^+ \to J/\psi\phi K^+$
4148.0 ± 2.4 ± 6.3	0.3k	[5] CHATRCHYAN	14M	CMS	$B^+ \to J/\psi\phi K^+$
• • • We do not use the following data for averages, fits, limits, etc. • • •					
4143.0 ± 2.9 ± 1.2	14	[6,7] AALTONEN	09AH	CDF	$B^+ \to J/\psi\phi K^+$

[1] From an amplitude analysis of the decay $B^+ \to J/\psi\phi K^+$ with a significance of 8.4 σ.
[2] Statistical significance of more than 5 σ.
[3] Statistical significance of more than 6 σ.
[4] Statistical significance of 3.1 σ.
[5] From a fit assuming an *S*-wave relativistic Breit-Wigner shape above a three-body phase-space non-resonant component with statistical significance of more than 5 σ.
[6] Statistical significance of 3.8 σ.
[7] Superseded by AALTONEN 17.

$\chi_{c1}(4140)$ WIDTH

VALUE (MeV)	EVTS	DOCUMENT ID		TECN	COMMENT
22 $^{+\ 8}_{-\ 7}$ OUR AVERAGE		Error includes scale factor of 1.3. See the ideogram below.			
$83 \pm 21\ ^{+21}_{-14}$	4289	[1] AAIJ	17C	LHCB	$B^+ \to J/\psi\phi K^+$
$15.3^{+10.4}_{-\ 6.1} \pm 2.5$	19	[2] AALTONEN	17	CDF	$B^+ \to J/\psi\phi K^+$
16.3 ± 5.6 ± 11.4	616	[3] ABAZOV	15M	D0	$p\overline{p} \to J/\psi\phi +$ anything
$20 \pm 13\ ^{+\ 3}_{-\ 8}$	52	[4] ABAZOV	14A	D0	$B^+ \to J/\psi\phi K^+$
$28\ ^{+15}_{-11} \pm 19$	0.3k	[5] CHATRCHYAN	14M	CMS	$B^+ \to J/\psi\phi K^+$
• • • We do not use the following data for averages, fits, limits, etc. • • •					
$11.7^{+\ 8.3}_{-\ 5.0} \pm 3.7$	14	[6,7] AALTONEN	09AH	CDF	$B^+ \to J/\psi\phi K^+$

[1] From an amplitude analysis of the decay $B^+ \to J/\psi\phi K^+$ with a significance of 8.4 σ.
[2] Statistical significance of more than 5 σ.
[3] Statistical significance of more than 6 σ.
[4] Statistical significance of 3.1 σ.
[5] From a fit assuming an *S*-wave relativistic Breit-Wigner shape above a three-body phase-space non-resonant component with statistical significance of more than 5 σ.
[6] Statistical significance of 3.8 σ.
[7] Superseded by AALTONEN 17.

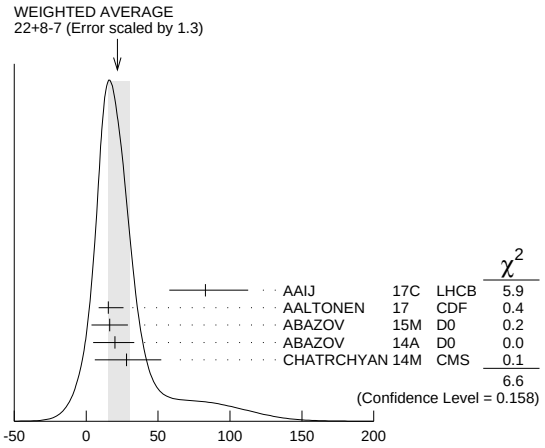

$\chi_{c1}(4140)$ DECAY MODES

	Mode	Fraction (Γ_i/Γ)
Γ_1	$J/\psi\phi$	seen
Γ_2	$\gamma\gamma$	not seen

$\chi_{c1}(4140)$ Γ(i)$\Gamma(\gamma\gamma)/\Gamma$(total)

$\Gamma(\gamma\gamma) \times \Gamma(J/\psi\phi)/\Gamma_{total}$ **$\Gamma_2\Gamma_1/\Gamma$**

VALUE (eV)	CL%	DOCUMENT ID		TECN	COMMENT
<41	90	[1] SHEN	10	BELL	10.6 $e^+e^- \to e^+e^- J/\psi\phi$
• • • We do not use the following data for averages, fits, limits, etc. • • •					
< 6	90	[2] SHEN	10	BELL	10.6 $e^+e^- \to e^+e^- J/\psi\phi$

[1] For $J^P = 0^+$.
[2] For $J^P = 2^+$.

$\chi_{c1}(4140)$ BRANCHING RATIOS

$\Gamma(J/\psi\phi)/\Gamma_{total}$ **Γ_1/Γ**

VALUE	EVTS	DOCUMENT ID		TECN	COMMENT
seen	4289	[1] AAIJ	17C	LHCB	$B^+ \to J/\psi\phi K^+$
seen	616	[2] ABAZOV	15M	D0	$p\overline{p} \to J/\psi\phi$ + anything
seen	52	[3] ABAZOV	14A	D0	$B^+ \to J/\psi\phi K^+$
seen	0.3k	[4] CHATRCHYAN	14M	CMS	$B^+ \to J/\psi\phi K^+$
seen	14	[5] AALTONEN	09AH	CDF	$B^+ \to J/\psi\phi K^+$
• • • We do not use the following data for averages, fits, limits, etc. • • •					
not seen		[6] ABLIKIM	15	BES3	$e^+e^- \to \gamma\phi J/\psi$
not seen		[7] AAIJ	12AA	LHCB	$pp \to B^+X$ at 7 TeV

[1] From an amplitude analysis of the decay $B^+ \to J/\psi\phi K^+$ with a significance of 8.4 σ.
[2] Statistical significance of more than 6 σ.
[3] ABAZOV 14A reports $B(B^+ \to \chi_{c1}(4140)K^+ \to J/\psi\phi K^+)/B(B^+ \to J/\psi\phi K^+) = (19 \pm 7 \pm 4)\%$ with 3.1 σ signficance.
[4] From a fit assuming an S-wave relativistic Breit-Wigner shape above a three-body phase-space non-resonant component with statistical significance of more than 5 σ.
[5] Statistical significance of 3.8 σ.
[6] Reported $\sigma(e^+e^- \to \gamma\chi_{c1}(4140))\cdot B(\chi_{c1}(4140) \to J/\psi\phi) < 0.35$, 0.28, and 0.33 pb at 4.23, 4.26, and 4.36 GeV, respectively, at 90% CL.
[7] Reported $B(B^+ \to \chi_{c1}(4140)K^+)\cdot B(\chi_{c1}(4140) \to J/\psi\phi)/B(B^+ \to J/\psi\phi K^+) < 0.07$ at 90% CL.

$\Gamma(\gamma\gamma)/\Gamma_{total}$ **Γ_2/Γ**

VALUE	DOCUMENT ID		TECN	COMMENT
not seen	SHEN	10	BELL	10.6 $e^+e^- \to e^+e^- J/\psi\phi$

$\chi_{c1}(4140)$ REFERENCES

AAIJ	17C	PRL 118 022003	R. Aaij *et al.*	(LHCb Collab.) JP
Also		PR D95 012002	R. Aaij *et al.*	(LHCb Collab.)
AALTONEN	17	MPL A32 1750139	T. Altonen *et al.*	(CDF Collab.)
ABAZOV	15M	PRL 115 232001	V.M. Abazov *et al.*	(D0 Collab.)
ABLIKIM	15	PR D91 032002	M. Ablikim *et al.*	(BES III Collab.)
ABAZOV	14A	PR D89 012004	V.M. Abazov *et al.*	(D0 Collab.)
CHATRCHYAN	14M	PL B734 261	S. Chatrchyan *et al.*	(CMS Collab.)
AAIJ	12AA	PR D85 091103	R. Aaij *et al.*	(LHCb Collab.)
SHEN	10	PRL 104 112004	C.P. Shen *et al.*	(BELLE Collab.)
AALTONEN	09AH	PRL 102 242002	T. Aaltonen *et al.*	(CDF Collab.)

$\psi(4160)$

$I^G(J^{PC}) = 0^-(1^{--})$

$\psi(4160)$ MASS

VALUE (MeV)		DOCUMENT ID		TECN	COMMENT
4191 ± 5 OUR AVERAGE					
4191	$^{+9}_{-8}$	AAIJ	13BC	LHCB	$B^+ \to K^+\mu^+\mu^-$
4191.7	± 6.5	[1] ABLIKIM	08D	BES2	$e^+e^- \to$ hadrons
• • • We do not use the following data for averages, fits, limits, etc. • • •					
4193	± 7	[2] MO	10	RVUE	$e^+e^- \to$ hadrons
4151	± 4	[3] SETH	05A	RVUE	$e^+e^- \to$ hadrons
4155	± 5	[4] SETH	05A	RVUE	$e^+e^- \to$ hadrons
4159	±20	BRANDELIK	78C	DASP	e^+e^-

[1] Reanalysis of data presented in BAI 02C. From a global fit over the center-of-mass energy region 3.7–5.0 GeV covering the $\psi(3770)$, $\psi(4040)$, $\psi(4160)$, and $\psi(4415)$ resonances. Phase angle fixed in the fit to $\delta = (293 \pm 57)^\circ$.
[2] Reanalysis of data presented in BAI 00 and BAI 02C. From a global fit over the center-of-mass energy 3.8–4.8 GeV covering the $\psi(4040)$, $\psi(4160)$ and $\psi(4415)$ resonances and including interference effects.
[3] From a fit to Crystal Ball (OSTERHELD 86) data.
[4] From a fit to BES (BAI 02C) data.

$\psi(4160)$ WIDTH

VALUE (MeV)		DOCUMENT ID		TECN	COMMENT
70 ±10 OUR AVERAGE					
65	$^{+22}_{-16}$	AAIJ	13BC	LHCB	$B^+ \to K^+\mu^+\mu^-$
71.8	±12.3	[1] ABLIKIM	08D	BES2	$e^+e^- \to$ hadrons
• • • We do not use the following data for averages, fits, limits, etc. • • •					
79	±14	[2] MO	10	RVUE	$e^+e^- \to$ hadrons
107	±10	[3] SETH	05A	RVUE	$e^+e^- \to$ hadrons
107	±16	[4] SETH	05A	RVUE	$e^+e^- \to$ hadrons
78	±20	BRANDELIK	78C	DASP	e^+e^-

[1] Reanalysis of data presented in BAI 02C. From a global fit over the center-of-mass energy region 3.7–5.0 GeV covering the $\psi(3770)$, $\psi(4040)$, $\psi(4160)$, and $\psi(4415)$ resonances. Phase angle fixed in the fit to $\delta = (293 \pm 57)^\circ$.
[2] Reanalysis of data presented in BAI 00 and BAI 02C. From a global fit over the center-of-mass energy 3.8–4.8 GeV covering the $\psi(4040)$, $\psi(4160)$ and $\psi(4415)$ resonances and including interference effects.
[3] From a fit to Crystal Ball (OSTERHELD 86) data.
[4] From a fit to BES (BAI 02C) data.

$\psi(4160)$ DECAY MODES

Due to the complexity of the $c\overline{c}$ threshold region, in this listing, "seen" ("not seen") means that a cross section for the mode in question has been measured at effective $\sqrt{s}$ near this particle's central mass value, more (less) than 2σ above zero, without regard to any peaking behavior in $\sqrt{s}$ or absence thereof. See mode listing(s) for details and references.

	Mode	Fraction (Γ_i/Γ)	Confidence level
Γ_1	e^+e^-	$(6.9 \pm 3.3) \times 10^{-6}$	
Γ_2	$\mu^+\mu^-$	seen	
Γ_3	$D\overline{D}$	seen	
Γ_4	$D^0\overline{D}^0$	seen	
Γ_5	D^+D^-	seen	
Γ_6	$D^*\overline{D}$ + c.c.	seen	
Γ_7	$D^*(2007)^0\overline{D}^0$ + c.c.	seen	
Γ_8	$D^*(2010)^+D^-$ + c.c.	seen	
Γ_9	$D^*\overline{D}^*$	seen	
Γ_{10}	$D^*(2007)^0\overline{D}^*(2007)^0$	seen	
Γ_{11}	$D^*(2010)^+D^*(2010)^-$	seen	
Γ_{12}	$D^0D^-\pi^+$ + c.c. (excl. $D^*(2007)^0\overline{D}^0$ + c.c., $D^*(2010)^+D^-$ + c.c.)	not seen	
Γ_{13}	$D\overline{D}^*\pi$ + c.c. (excl. $D^*\overline{D}^*$)	seen	
Γ_{14}	$D^0D^{*-}\pi^+$ + c.c. (excl. $D^*(2010)^+D^*(2010)^-$)	not seen	
Γ_{15}	$D_s^+D_s^-$	not seen	
Γ_{16}	$D_s^{*+}D_s^-$ + c.c.	seen	
Γ_{17}	$J/\psi\pi^+\pi^-$	$< 3 \times 10^{-3}$	90%
Γ_{18}	$J/\psi\pi^0\pi^0$	$< 3 \times 10^{-3}$	90%
Γ_{19}	$J/\psi K^+K^-$	$< 2 \times 10^{-3}$	90%
Γ_{20}	$J/\psi\eta$	$< 8 \times 10^{-3}$	90%
Γ_{21}	$J/\psi\pi^0$	$< 1 \times 10^{-3}$	90%
Γ_{22}	$J/\psi\eta'$	$< 5 \times 10^{-3}$	90%

Γ_{23}	$J/\psi\pi^+\pi^-\pi^0$	< 1	$\times 10^{-3}$	90%
Γ_{24}	$\psi(2S)\pi^+\pi^-$	< 4	$\times 10^{-3}$	90%
Γ_{25}	$\chi_{c1}\gamma$	< 5	$\times 10^{-3}$	90%
Γ_{26}	$\chi_{c2}\gamma$	< 1.3	%	90%
Γ_{27}	$\chi_{c1}\pi^+\pi^-\pi^0$	< 2	$\times 10^{-3}$	90%
Γ_{28}	$\chi_{c2}\pi^+\pi^-\pi^0$	< 8	$\times 10^{-3}$	90%
Γ_{29}	$h_c(1P)\pi^+\pi^-$	< 5	$\times 10^{-3}$	90%
Γ_{30}	$h_c(1P)\pi^0\pi^0$	< 2	$\times 10^{-3}$	90%
Γ_{31}	$h_c(1P)\eta$	< 2	$\times 10^{-3}$	90%
Γ_{32}	$h_c(1P)\pi^0$	< 4	$\times 10^{-4}$	90%
Γ_{33}	$\phi\pi^+\pi^-$	< 2	$\times 10^{-3}$	90%
Γ_{34}	$\gamma\chi_{c1}(3872) \rightarrow \gamma J/\psi\pi^+\pi^-$	< 6.8	$\times 10^{-5}$	90%
Γ_{35}	$\gamma X(3915) \rightarrow \gamma J/\psi\pi^+\pi^-$	< 1.36	$\times 10^{-4}$	90%
Γ_{36}	$\gamma X(3930) \rightarrow \gamma J/\psi\pi^+\pi^-$	< 1.18	$\times 10^{-4}$	90%
Γ_{37}	$\gamma X(3940) \rightarrow \gamma J/\psi\pi^+\pi^-$	< 1.47	$\times 10^{-4}$	90%
Γ_{38}	$\gamma\chi_{c1}(3872) \rightarrow \gamma\gamma J/\psi$	< 1.05	$\times 10^{-4}$	90%
Γ_{39}	$\gamma X(3915) \rightarrow \gamma\gamma J/\psi$	< 1.26	$\times 10^{-4}$	90%
Γ_{40}	$\gamma X(3930) \rightarrow \gamma\gamma J/\psi$	< 8.8	$\times 10^{-5}$	90%
Γ_{41}	$\gamma X(3940) \rightarrow \gamma\gamma J/\psi$	< 1.79	$\times 10^{-4}$	90%
Γ_{42}	K^+K^-			

$\psi(4160)$ PARTIAL WIDTHS

$\Gamma(e^+e^-)$ Γ_1

VALUE (keV)	DOCUMENT ID		TECN	COMMENT
0.48±0.22	[1] ABLIKIM	08D	BES2	$e^+e^- \rightarrow$ hadrons
• • • We do not use the following data for averages, fits, limits, etc. • • •				
0.4 to 1.1	[2] MO	10	RVUE	$e^+e^- \rightarrow$ hadrons
0.83±0.08	[3] SETH	05A	RVUE	$e^+e^- \rightarrow$ hadrons
0.84±0.13	[4] SETH	05A	RVUE	$e^+e^- \rightarrow$ hadrons
0.77±0.23	BRANDELIK	78C	DASP	e^+e^-

[1] Reanalysis of data presented in BAI 02C. From a global fit over the center-of-mass energy region 3.7–5.0 GeV covering the $\psi(3770)$, $\psi(4040)$, $\psi(4160)$, and $\psi(4415)$ resonances. Phase angle fixed in the fit to $\delta = (293 \pm 57)^\circ$.
[2] Reanalysis of data presented in BAI 00 and BAI 02C. From a global fit over the center-of-mass energy 3.8–4.8 GeV covering the $\psi(4040)$, $\psi(4160)$ and $\psi(4415)$ resonances and including interference effects. Four sets of solutions are obtained with the same fit quality, mass and total width, but with different e^+e^- partial widths. We quote only the range of values.
[3] From a fit to Crystal Ball (OSTERHELD 86) data.
[4] From a fit to BES (BAI 02C) data.

$\psi(4160)$ $\Gamma(i) \times \Gamma(e^+e^-)/\Gamma(\text{total})$

$\Gamma(\chi_{c1}\gamma) \times \Gamma(e^+e^-)/\Gamma_{\text{total}}$ $\Gamma_{25}\Gamma_1/\Gamma$

VALUE (eV)	CL%	DOCUMENT ID		TECN	COMMENT
<2.2	90	[1] HAN	15	BELL	10.58 $e^+e^- \rightarrow \chi_{c1}\gamma$

[1] Using B($\eta \rightarrow \gamma\gamma$) = (39.41 ± 0.21)%.

$\Gamma(\chi_{c2}\gamma) \times \Gamma(e^+e^-)/\Gamma_{\text{total}}$ $\Gamma_{26}\Gamma_1/\Gamma$

VALUE (eV)	CL%	DOCUMENT ID		TECN	COMMENT
• • • We do not use the following data for averages, fits, limits, etc. • • •					
<6.1	90	[1] HAN	15	BELL	10.58 $e^+e^- \rightarrow \chi_{c2}\gamma$

[1] Using B($\eta \rightarrow \gamma\gamma$) = (39.41 ± 0.21)%.

$\psi(4160)$ $\Gamma(i) \times \Gamma(e^+e^-)/\Gamma^2(\text{total})$

$\Gamma(J/\psi\eta)/\Gamma_{\text{total}} \times \Gamma(e^+e^-)/\Gamma_{\text{total}}$ $\Gamma_{20}/\Gamma \times \Gamma_1/\Gamma$

VALUE (units 10^{-8})	DOCUMENT ID		TECN	COMMENT
• • • We do not use the following data for averages, fits, limits, etc. • • •				
2.8±0.9±0.9	[1] WANG	13B	BELL	$e^+e^- \rightarrow J/\psi\eta\gamma$
12.8±1.7±2.0	[2] WANG	13B	BELL	$e^+e^- \rightarrow J/\psi\eta\gamma$

[1] Solution I of two equivalent solutions in a fit using two interfering resonances. Mass and width fixed at 4153 MeV and 103 MeV, respectively.
[2] Solution II of two equivalent solutions in a fit using two interfering resonances. Mass and width fixed at 4153 MeV and 103 MeV, respectively.

$\psi(4160)$ BRANCHING RATIOS

$\Gamma(\mu^+\mu^-)/\Gamma_{\text{total}}$ Γ_2/Γ

VALUE	DOCUMENT ID		TECN	COMMENT
seen	[1] AAIJ	13BC	LHCB	$B^+ \rightarrow K^+\mu^+\mu^-$

[1] AAIJ 13BC report $B(B^+ \rightarrow K^+\psi(4160)) B(\psi(4160) \rightarrow \mu^+\mu^-) = (3.5^{+0.9}_{-0.8}) \times 10^{-9}$.

$\Gamma(D\overline{D})/\Gamma(D^*\overline{D}^*)$ Γ_3/Γ_9

VALUE	DOCUMENT ID		TECN	COMMENT
0.02±0.03±0.02	AUBERT	09M	BABR	$e^+e^- \rightarrow \gamma D^{(*)}\overline{D}^{(*)}$

$\Gamma(D^0\overline{D}^0)/\Gamma_{\text{total}}$ Γ_4/Γ

VALUE	DOCUMENT ID		TECN	COMMENT
seen	CRONIN-HEN...	09	CLEO	$e^+e^- \rightarrow D^0\overline{D}^0$
seen	PAKHLOVA	08	BELL	$e^+e^- \rightarrow D^0\overline{D}^0\gamma$
• • • We do not use the following data for averages, fits, limits, etc. • • •				
not seen	AUBERT	09M	BABR	$e^+e^- \rightarrow D^0\overline{D}^0\gamma$

$\Gamma(D^+D^-)/\Gamma_{\text{total}}$ Γ_5/Γ

VALUE	DOCUMENT ID		TECN	COMMENT
seen	CRONIN-HEN...	09	CLEO	$e^+e^- \rightarrow D^+D^-$
seen	PAKHLOVA	08	BELL	$e^+e^- \rightarrow D^+D^-\gamma$
• • • We do not use the following data for averages, fits, limits, etc. • • •				
not seen	AUBERT	09M	BABR	$e^+e^- \rightarrow D^+D^-\gamma$

$\Gamma(D^*(2007)^0\overline{D}^0 + \text{c.c.})/\Gamma_{\text{total}}$ Γ_7/Γ

VALUE	DOCUMENT ID		TECN	COMMENT
seen	AUBERT	09M	BABR	$e^+e^- \rightarrow D^{*0}\overline{D}^0\gamma$
seen	CRONIN-HEN...	09	CLEO	$e^+e^- \rightarrow D^{*0}\overline{D}^0$

$\Gamma(D^*(2010)^+D^- + \text{c.c.})/\Gamma_{\text{total}}$ Γ_8/Γ

VALUE	DOCUMENT ID		TECN	COMMENT
seen	[1] ZHUKOVA	18	BELL	$e^+e^- \rightarrow D^{*+}D^-\gamma$
seen	AUBERT	09M	BABR	$e^+e^- \rightarrow D^{*+}D^-\gamma$
seen	CRONIN-HEN...	09	CLEO	$e^+e^- \rightarrow D^{*+}D^-$
• • • We do not use the following data for averages, fits, limits, etc. • • •				
seen	PAKHLOVA	07	BELL	$e^+e^- \rightarrow D^{*+}D^-\gamma$

[1] Supersedes PAKHLOVA 07.

$\Gamma(D^*\overline{D} + \text{c.c.})/\Gamma(D^*\overline{D}^*)$ Γ_6/Γ_9

VALUE	DOCUMENT ID		TECN	COMMENT
0.34±0.14±0.05	AUBERT	09M	BABR	$e^+e^- \rightarrow \gamma D^{(*)}\overline{D}^{(*)}$

$\Gamma(D^*(2007)^0\overline{D}^*(2007)^0)/\Gamma_{\text{total}}$ Γ_{10}/Γ

VALUE	DOCUMENT ID		TECN	COMMENT
seen	AUBERT	09M	BABR	$e^+e^- \rightarrow D^{*0}\overline{D}^{*0}\gamma$
seen	CRONIN-HEN...	09	CLEO	$e^+e^- \rightarrow D^{*0}\overline{D}^{*0}$

$\Gamma(D^*(2010)^+D^*(2010)^-)/\Gamma_{\text{total}}$ Γ_{11}/Γ

VALUE	DOCUMENT ID		TECN	COMMENT
seen	[1] ZHUKOVA	18	BELL	$e^+e^- \rightarrow D^{*+}D^{*-}\gamma$
seen	AUBERT	09M	BABR	$e^+e^- \rightarrow D^{*+}D^{*-}\gamma$
seen	CRONIN-HEN...	09	CLEO	$e^+e^- \rightarrow D^{*+}D^{*-}$
• • • We do not use the following data for averages, fits, limits, etc. • • •				
seen	PAKHLOVA	07	BELL	$e^+e^- \rightarrow D^{*+}D^{*-}\gamma$

[1] Supersedes PAKHLOVA 07.

$\Gamma(D^0D^-\pi^+ + \text{c.c. (excl. } D^*(2007)^0\overline{D}^0 + \text{c.c., } D^*(2010)^+D^- + \text{c.c.}))/\Gamma_{\text{total}}$ Γ_{12}/Γ

VALUE	DOCUMENT ID		TECN	COMMENT
not seen	PAKHLOVA	08A	BELL	$e^+e^- \rightarrow D^0D^-\pi^+\gamma$

$\Gamma(D\overline{D}^*\pi + \text{c.c. (excl. } D^*\overline{D}^*))/\Gamma_{\text{total}}$ Γ_{13}/Γ

VALUE	DOCUMENT ID		TECN	COMMENT
seen	CRONIN-HEN...	09	CLEO	$e^+e^- \rightarrow D\overline{D}^*\pi$

$\Gamma(D^0D^{*-}\pi^+ + \text{c.c. (excl. } D^*(2010)^+D^*(2010)^-))/\Gamma_{\text{total}}$ Γ_{14}/Γ

VALUE	DOCUMENT ID		TECN	COMMENT
not seen	PAKHLOVA	09	BELL	$e^+e^- \rightarrow D^0D^{*-}\pi^+\gamma$

$\Gamma(D_s^+D_s^-)/\Gamma_{\text{total}}$ Γ_{15}/Γ

VALUE	DOCUMENT ID		TECN	COMMENT
not seen	PAKHLOVA	11	BELL	$e^+e^- \rightarrow D_s^+D_s^-\gamma$
not seen	DEL-AMO-SA...	10N	BABR	$e^+e^- \rightarrow D_s^+D_s^-\gamma$
not seen	CRONIN-HEN...	09	CLEO	$e^+e^- \rightarrow D_s^+D_s^-$

$\Gamma(D_s^{*+}D_s^- + \text{c.c.})/\Gamma_{\text{total}}$ Γ_{16}/Γ

VALUE	DOCUMENT ID		TECN	COMMENT
seen	PAKHLOVA	11	BELL	$e^+e^- \rightarrow D_s^{*+}D_s^-\gamma$
seen	DEL-AMO-SA...	10N	BABR	$e^+e^- \rightarrow D_s^{*+}D_s^-\gamma$
seen	CRONIN-HEN...	09	CLEO	$e^+e^- \rightarrow D_s^{*+}D_s^-$

$\Gamma(J/\psi\pi^+\pi^-)/\Gamma_{\text{total}}$ Γ_{17}/Γ

VALUE (units 10^{-3})	CL%	DOCUMENT ID		TECN	COMMENT
<3	90	COAN	06	CLEO	4.12–4.2 $e^+e^- \rightarrow$ hadrons

$\Gamma(J/\psi\pi^0\pi^0)/\Gamma_{\text{total}}$ Γ_{18}/Γ

VALUE (units 10^{-3})	CL%	DOCUMENT ID		TECN	COMMENT
<3	90	COAN	06	CLEO	4.12–4.2 $e^+e^- \rightarrow$ hadrons

$\Gamma(J/\psi K^+ K^-)/\Gamma_{total}$ Γ_{19}/Γ

VALUE (units 10^{-3})	CL%	DOCUMENT ID		TECN	COMMENT
<2	90	COAN	06	CLEO	4.12–4.2 e^+e^- → hadrons

$\Gamma(J/\psi\eta)/\Gamma_{total}$ Γ_{20}/Γ

VALUE (units 10^{-3})	CL%	DOCUMENT ID		TECN	COMMENT
<8	90	COAN	06	CLEO	4.12–4.2 e^+e^- → hadrons
• • • We do not use the following data for averages, fits, limits, etc. • • •					
possibly seen		[1] ABLIKIM	15L	BES3	e^+e^- → $J/\psi\eta$
seen		WANG	13B	BELL	e^+e^- → $J/\psi\eta\gamma$

[1] An enhancement around 4.2 GeV is observed.

$\Gamma(J/\psi\pi^0)/\Gamma_{total}$ Γ_{21}/Γ

VALUE (units 10^{-3})	CL%	DOCUMENT ID		TECN	COMMENT
<1	90	COAN	06	CLEO	4.12–4.2 e^+e^- → hadrons

$\Gamma(J/\psi\eta')/\Gamma_{total}$ Γ_{22}/Γ

VALUE (units 10^{-3})	CL%	DOCUMENT ID		TECN	COMMENT
<5	90	COAN	06	CLEO	4.12–4.2 e^+e^- → hadrons

$\Gamma(J/\psi\pi^+\pi^-\pi^0)/\Gamma_{total}$ Γ_{23}/Γ

VALUE (units 10^{-3})	CL%	DOCUMENT ID		TECN	COMMENT
<1	90	COAN	06	CLEO	4.12–4.2 e^+e^- → hadrons

$\Gamma(\psi(2S)\pi^+\pi^-)/\Gamma_{total}$ Γ_{24}/Γ

VALUE (units 10^{-3})	CL%	DOCUMENT ID		TECN	COMMENT
<4	90	COAN	06	CLEO	4.12–4.2 e^+e^- → hadrons

$\Gamma(\chi_{c1}\gamma)/\Gamma_{total}$ Γ_{25}/Γ

VALUE (units 10^{-3})	CL%	DOCUMENT ID		TECN	COMMENT
• • • We do not use the following data for averages, fits, limits, etc. • • •					
<7	90	COAN	06	CLEO	4.12–4.2 e^+e^- → hadrons

$\Gamma(\chi_{c2}\gamma)/\Gamma_{total}$ Γ_{26}/Γ

VALUE (units 10^{-3})	CL%	DOCUMENT ID		TECN	COMMENT
<13	90	COAN	06	CLEO	4.12–4.2 e^+e^- → hadrons

$\Gamma(\chi_{c1}\pi^+\pi^-\pi^0)/\Gamma_{total}$ Γ_{27}/Γ

VALUE (units 10^{-3})	CL%	DOCUMENT ID		TECN	COMMENT
<2	90	COAN	06	CLEO	4.12–4.2 e^+e^- → hadrons

$\Gamma(\chi_{c2}\pi^+\pi^-\pi^0)/\Gamma_{total}$ Γ_{28}/Γ

VALUE (units 10^{-3})	CL%	DOCUMENT ID		TECN	COMMENT
<8	90	COAN	06	CLEO	4.12–4.2 e^+e^- → hadrons

$\Gamma(h_c(1P)\pi^+\pi^-)/\Gamma_{total}$ Γ_{29}/Γ

VALUE (units 10^{-3})	CL%	DOCUMENT ID		TECN	COMMENT
<5	90	[1] PEDLAR	11	CLEO	e^+e^- → $h_c(1P)\pi^+\pi^-$

[1] At $\sqrt{s}$ = 4170 MeV, PEDLAR 11 measures $\sigma(e^+e^- \to h_c(1P)\pi^+\pi^-) = 15.6 \pm 2.3 \pm 1.9 \pm 3.0$ pb, where the errors are statistical, systematic, and due to uncertainty in $B(\psi(2S) \to \pi^0 h_c(1P))$, respectively.

$\Gamma(h_c(1P)\pi^0\pi^0)/\Gamma_{total}$ Γ_{30}/Γ

VALUE (units 10^{-3})	CL%	DOCUMENT ID		TECN	COMMENT
<2	90	[1] PEDLAR	11	CLEO	e^+e^- → $h_c(1P)\pi^0\pi^0$

[1] At $\sqrt{s}$ = 4170 MeV, PEDLAR 11 measures $\sigma(e^+e^- \to h_c(1P)\pi^0\pi^0) = 3.0 \pm 3.3 \pm 1.1 \pm 0.6$ pb, where the errors are statistical, systematic, and due to uncertainty in $B(\psi(2S) \to \pi^0 h_c(1P))$, respectively.

$\Gamma(h_c(1P)\eta)/\Gamma_{total}$ Γ_{31}/Γ

VALUE (units 10^{-3})	CL%	EVTS	DOCUMENT ID		TECN	COMMENT
<2	90		[1] PEDLAR	11	CLEO	e^+e^- → $h_c(1P)\eta$
• • • We do not use the following data for averages, fits, limits, etc. • • •						
possibly seen		41	[2] ABLIKIM	17R	BES3	e^+e^- → $h_c(1P)\eta$

[1] At $\sqrt{s}$ = 4170 MeV, PEDLAR 11 measures $\sigma(e^+e^- \to h_c(1P)\eta) = 4.7 \pm 1.7 \pm 1.0 \pm 0.9$ pb, where the errors are statistical, systematic, and due to uncertainty in $B(\psi(2S) \to \pi^0 h_c(1P))$, respectively.

[2] An enhancement around 4.2 GeV is observed.

$\Gamma(h_c(1P)\pi^0)/\Gamma_{total}$ Γ_{32}/Γ

VALUE (units 10^{-3})	CL%	DOCUMENT ID		TECN	COMMENT
<0.4	90	[1] PEDLAR	11	CLEO	e^+e^- → $h_c(1P)\pi^0$

[1] At $\sqrt{s}$ = 4170 MeV, PEDLAR 11 measures $\sigma(e^+e^- \to h_c(1P)\pi^0) = -0.7 \pm 1.8 \pm 0.7 \pm 0.1$ pb, where the errors are statistical, systematic, and due to uncertainty in $B(\psi(2S) \to \pi^0 h_c(1P))$, respectively.

$\Gamma(\phi\pi^+\pi^-)/\Gamma_{total}$ Γ_{33}/Γ

VALUE (units 10^{-3})	CL%	DOCUMENT ID		TECN	COMMENT
<2	90	COAN	06	CLEO	4.12–4.2 e^+e^- → hadrons

$\Gamma(\gamma\chi_{c1}(3872) \to \gamma J/\psi\pi^+\pi^-)/\Gamma_{total}$ Γ_{34}/Γ

VALUE	CL%	DOCUMENT ID		COMMENT
$<0.68 \times 10^{-4}$	90	[1] XIAO	13	$\psi(4160) \to \gamma J/\psi\pi^+\pi^-$

[1] Obtained by analyzing CLEO data but not authored by the CLEO Collaboration.

$\Gamma(\gamma X(3915) \to \gamma J/\psi\pi^+\pi^-)/\Gamma_{total}$ Γ_{35}/Γ

VALUE	CL%	DOCUMENT ID		COMMENT
$<1.36 \times 10^{-4}$	90	[1] XIAO	13	$\psi(4160) \to \gamma J/\psi\pi^+\pi^-$

[1] Obtained by analyzing CLEO data but not authored by the CLEO Collaboration.

$\Gamma(\gamma X(3930) \to \gamma J/\psi\pi^+\pi^-)/\Gamma_{total}$ Γ_{36}/Γ

VALUE	CL%	DOCUMENT ID		COMMENT
$<1.18 \times 10^{-4}$	90	[1] XIAO	13	$\psi(4160) \to \gamma J/\psi\pi^+\pi^-$

[1] Obtained by analyzing CLEO data but not authored by the CLEO Collaboration.

$\Gamma(\gamma X(3940) \to \gamma J/\psi\pi^+\pi^-)/\Gamma_{total}$ Γ_{37}/Γ

VALUE	CL%	DOCUMENT ID		COMMENT
$<1.47 \times 10^{-4}$	90	[1] XIAO	13	$\psi(4160) \to \gamma J/\psi\pi^+\pi^-$

[1] Obtained by analyzing CLEO data but not authored by the CLEO Collaboration.

$\Gamma(\gamma\chi_{c1}(3872) \to \gamma\gamma J/\psi)/\Gamma_{total}$ Γ_{38}/Γ

VALUE	CL%	DOCUMENT ID		COMMENT
$<1.05 \times 10^{-4}$	90	[1] XIAO	13	$\psi(4160) \to \gamma\gamma J/\psi$

[1] Obtained by analyzing CLEO data but not authored by the CLEO Collaboration.

$\Gamma(\gamma X(3915) \to \gamma\gamma J/\psi)/\Gamma_{total}$ Γ_{39}/Γ

VALUE	CL%	DOCUMENT ID		COMMENT
$<1.26 \times 10^{-4}$	90	[1] XIAO	13	$\psi(4160) \to \gamma\gamma J/\psi$

[1] Obtained by analyzing CLEO data but not authored by the CLEO Collaboration.

$\Gamma(\gamma X(3930) \to \gamma\gamma J/\psi)/\Gamma_{total}$ Γ_{40}/Γ

VALUE	CL%	DOCUMENT ID		COMMENT
$<0.88 \times 10^{-4}$	90	[1] XIAO	13	$\psi(4160) \to \gamma\gamma J/\psi$

[1] Obtained by analyzing CLEO data but not authored by the CLEO Collaboration.

$\Gamma(\gamma X(3940) \to \gamma\gamma J/\psi)/\Gamma_{total}$ Γ_{41}/Γ

VALUE	CL%	DOCUMENT ID		COMMENT
$<1.79 \times 10^{-4}$	90	[1] XIAO	13	$\psi(4160) \to \gamma\gamma J/\psi$

[1] Obtained by analyzing CLEO data but not authored by the CLEO Collaboration.

$\Gamma(K^+K^-)/\Gamma_{total}$ Γ_{42}/Γ

VALUE	CL%	DOCUMENT ID		TECN	COMMENT
• • • We do not use the following data for averages, fits, limits, etc. • • •					
$<2 \times 10^{-5}$	90	[1] DRUZHININ	15	RVUE	e^+e^- → $\psi(3770)$

[1] DRUZHININ 15 uses BABAR and CLEO data takitaking into account interference of the processes $e^+e^- \to K^+K^-$ and $e^+e^- \to K^0_S K^0_L$.

$\psi(4160)$ REFERENCES

ZHUKOVA	18	PR D97 012002	V. Zhukova *et al.*	(BELLE Collab.)
ABLIKIM	17R	PR D96 012001	M. Ablikim *et al.*	(BES III Collab.)
ABLIKIM	15L	PR D91 112005	M. Ablikim *et al.*	(BES III Collab.)
DRUZHININ	15	PR D92 054024	V.P. Druzhinin	(NOVO)
HAN	15	PR D92 012011	Y.L. Han *et al.*	(BELLE Collab.)
AAIJ	13BC	PRL 111 112003	R. Aaij *et al.*	(LHCb Collab.)
WANG	13B	PR D87 051101	X.L. Wang *et al.*	(BELLE Collab.)
XIAO	13	PR D87 057501	T. Xiao *et al.*	(NWES, WAYN)
PAKHLOVA	11	PR D83 011101	G. Pakhlova *et al.*	(BELLE Collab.)
PEDLAR	11	PRL 107 041803	T. Pedlar *et al.*	(CLEO Collab.)
DEL-AMO-SA...	10N	PR D82 052004	P. del Amo Sanchez *et al.*	(BABAR Collab.)
MO	10	PR D82 077501	X.H. Mo, C.Z. Yuan, P. Wang	(BHEP)
AUBERT	09M	PR D79 092001	B. Aubert *et al.*	(BABAR Collab.)
CRONIN-HEN...	09	PR D80 072001	D. Cronin-Hennessy *et al.*	(CLEO Collab.)
PAKHLOVA	09	PR D80 091101	G. Pakhlova *et al.*	(BELLE Collab.)
ABLIKIM	08D	PL B660 315	M. Ablikim *et al.*	(BES Collab.)
PAKHLOVA	08	PR D77 011103	G. Pakhlova *et al.*	(BELLE Collab.)
PAKHLOVA	08A	PRL 100 062001	G. Pakhlova *et al.*	(BELLE Collab.)
PAKHLOVA	07	PRL 98 092001	G. Pakhlova *et al.*	(BELLE Collab.)
COAN	06	PRL 96 162003	T.E. Coan *et al.*	(CLEO Collab.)
SETH	05A	PR D72 017501	K.K. Seth	
BAI	02C	PRL 88 101802	J.Z. Bai *et al.*	(BES Collab.)
BAI	00	PRL 84 594	J.Z. Bai *et al.*	(BES Collab.)
OSTERHELD	86	SLAC-PUB-4160	A. Osterheld *et al.*	(SLAC Crystal Ball Collab.)
BRANDELIK	78C	PL 76B 361	R. Brandelik *et al.*	(DASP Collab.)

$X(4160)$ $I^G(J^{PC}) = ?^?(?^{??})$

OMITTED FROM SUMMARY TABLE

Seen by PAKHLOV 08 in $e^+e^- \to J/\psi X$, $X \to D^*\overline{D}^*$

$X(4160)$ MASS

VALUE (MeV)	EVTS	DOCUMENT ID		TECN	COMMENT
$4156^{+25}_{-20} \pm 15$	24	PAKHLOV	08	BELL	e^+e^- → $J/\psi X$

Meson Particle Listings

$X(4160)$, $Z_c(4200)$, $\psi(4230)$

$X(4160)$ WIDTH

VALUE (MeV)	EVTS	DOCUMENT ID		TECN	COMMENT
$139^{+111}_{61}\pm21$	24	PAKHLOV	08	BELL	$e^+e^- \to J/\psi X$

$X(4160)$ DECAY MODES

	Mode	Fraction (Γ_i/Γ)
Γ_1	$D\overline{D}$	not seen
Γ_2	$D^*\overline{D}$ + c.c.	not seen
Γ_3	$D^*\overline{D}^*$	seen

$X(4160)$ BRANCHING RATIOS

$\Gamma(D\overline{D})/\Gamma(D^*\overline{D}^*)$ Γ_1/Γ_3

VALUE	CL%	DOCUMENT ID		TECN	COMMENT
<0.09	90	PAKHLOV	08	BELL	$e^+e^- \to J/\psi X$

$\Gamma(D^*\overline{D}+\text{c.c.})/\Gamma(D^*\overline{D}^*)$ Γ_2/Γ_3

VALUE	CL%	DOCUMENT ID		TECN	COMMENT
<0.22	90	PAKHLOV	08	BELL	$e^+e^- \to J/\psi X$

$X(4160)$ REFERENCES

PAKHLOV 08 PRL 100 202001 P. Pakhlov *et al.* (BELLE Collab.)

$Z_c(4200)$

$I^G(J^{PC}) = 1^+(1^{+-})$
I, *G*, *C* need confirmation.

OMITTED FROM SUMMARY TABLE
was $X(4200)^{\pm}$

This state shows properties different from a conventional $q\overline{q}$ state. A candidate for an exotic structure. See the review on non-$q\overline{q}$ states.

Reported by CHILIKIN 14 in $J/\psi\pi^+$ at a significance of 6.2σ. Assignments of 0^-, 1^-, 2^-, and 2^+ excluded at 6.1σ, 7.4σ, 4.4σ, and 7.0σ level, respectively. Needs confirmation.

$Z_c(4200)$ MASS

VALUE (MeV)	DOCUMENT ID		TECN	COMMENT
$4196^{+31}_{-29}{}^{+17}_{-13}$	CHILIKIN	14	BELL	$\overline{B}^0 \to J/\psi K^-\pi^+$

$Z_c(4200)$ WIDTH

VALUE (MeV)	DOCUMENT ID		TECN	COMMENT
$370\pm70^{+70}_{-132}$	CHILIKIN	14	BELL	$\overline{B}^0 \to J/\psi K^-\pi^+$

$Z_c(4200)$ DECAY MODES

	Mode	Fraction (Γ_i/Γ)
Γ_1	$J/\psi\pi^+$	seen

$Z_c(4200)$ BRANCHING RATIOS

$\Gamma(J/\psi\pi^+)/\Gamma_{\text{total}}$ Γ_1/Γ

VALUE	DOCUMENT ID		TECN	COMMENT
seen	CHILIKIN	14	BELL	$\overline{B}^0 \to J/\psi K^-\pi^+$

$Z_c(4200)$ REFERENCES

CHILIKIN 14 PR D90 112009 K. Chilikin *et al.* (BELLE Collab.)

$\psi(4230)$

$I^G(J^{PC}) = 0^-(1^{--})$

OMITTED FROM SUMMARY TABLE
was $X(4230)$

This state shows properties different from a conventional $q\overline{q}$ state. A candidate for an exotic structure. See the review on non-$q\overline{q}$ states.

Enhancement reported by ABLIKIM 15C in $e^+e^- \to \omega\chi_{c0}$ at $\sqrt{s}$ = 4.23–4.26 GeV at 9σ significance. Lineshape found to be inconsistent with origination from $\psi(4260)$. Needs confirmation.

$\psi(4230)$ MASS

VALUE (MeV)	EVTS	DOCUMENT ID		TECN	COMMENT
$4218\ ^{+5}_{-4}$ OUR AVERAGE Error includes scale factor of 1.2.					
$4218\ ^{+5.5}_{-4.5}\pm0.9$		ABLIKIM	17G	BES3	$e^+e^- \to \pi^+\pi^- h_c$
$4209.5\pm7.4\pm1.4$		[1] ABLIKIM	17V	BES3	$e^+e^- \to \pi^+\pi^-\psi(2S)$
$4230\ \pm8\ \pm6$	180	[2] ABLIKIM	15C	BES3	$e^+e^- \to \omega\chi_{c0}$

[1] From a fit to the cross section for $e^+e^- \to \pi^+\pi^-\psi(2S) \to 2(\pi^+\pi^-)\ell^+\ell^-$ obtained from 16 center-of-mass energies between 4.008 and 4.600 GeV and comprising 5.1 fb^{-1}.
[2] From a 3-parameter fit of measured cross sections from $\sqrt{s}$ = 4.21–4.42 GeV to a phase-space modified Breit-Wigner function, using the decays $\chi_{c0} \to \pi^+\pi^-$, $\chi_{c0} \to K^+K^-$, and $\omega \to \pi^+\pi^-\pi^0$.

$\psi(4230)$ WIDTH

VALUE (MeV)	EVTS	DOCUMENT ID		TECN	COMMENT
$59\ ^{+12}_{-10}$ OUR AVERAGE Error includes scale factor of 1.5. See the ideogram below.					
$66.0^{+12.3}_{-\ 8.3}\pm0.4$		ABLIKIM	17G	BES3	$e^+e^- \to \pi^+\pi^- h_c$
$80.1\pm24.6\pm2.9$		[1] ABLIKIM	17V	BES3	$e^+e^- \to \pi^+\pi^-\psi(2S)$
$38\ \pm12\ \pm2$	180	[2] ABLIKIM	15C	BES3	$e^+e^- \to \omega\chi_{c0}$

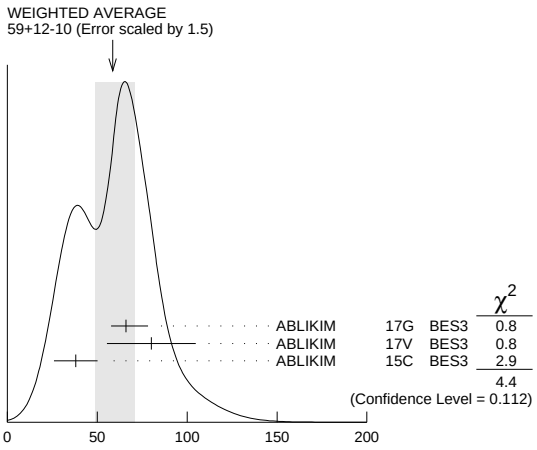

[1] From a fit to the cross section for $e^+e^- \to \pi^+\pi^-\psi(2S) \to 2(\pi^+\pi^-)\ell^+\ell^-$ obtained from 16 center-of-mass energies between 4.008 and 4.600 GeV and comprising 5.1 fb^{-1}.
[2] From a 3-parameter fit of measured cross sections from $\sqrt{s}$ = 4.21–4.42 GeV to a phase-space modified Breit-Wigner function, using the decays $\chi_{c0} \to \pi^+\pi^-$, $\chi_{c0} \to K^+K^-$, and $\omega \to \pi^+\pi^-\pi^0$.

$\psi(4230)$ DECAY MODES

	Mode	Fraction (Γ_i/Γ)
Γ_1	e^+e^-	
Γ_2	$\omega\chi_{c0}$	seen
Γ_3	$\pi^+\pi^- h_c$	seen
Γ_4	$\pi^+\pi^-\psi(2S)$	seen

$\psi(4230)$ Γ(i)$\Gamma(e^+e^-)/\Gamma$(total)

$\Gamma(\omega\chi_{c0}) \times \Gamma(e^+e^-)/\Gamma_{\text{total}}$ $\Gamma_2\Gamma_1/\Gamma$

VALUE (eV)	EVTS	DOCUMENT ID		TECN	COMMENT
$2.7\pm0.5\pm0.4$	180	[1] ABLIKIM	15C	BES3	$e^+e^- \to \omega\chi_{c0}$

[1] From a 3-parameter fit of measured cross sections from $\sqrt{s}$ = 4.21–4.42 GeV to a phase-space modified Breit-Wigner function, using the decays $\chi_{c0} \to \pi^+\pi^-$, $\chi_{c0} \to K^+K^-$, and $\omega \to \pi^+\pi^-\pi^0$.

$\psi(4230)$ BRANCHING RATIOS

$\Gamma(\omega\chi_{c0})/\Gamma_{\text{total}}$ Γ_2/Γ

VALUE	EVTS	DOCUMENT ID		TECN	COMMENT
seen	180	[1] ABLIKIM	15C	BES3	$e^+e^- \to \omega\chi_{c0}$

[1] From a 3-parameter fit of measured cross sections from $\sqrt{s}$ = 4.21–4.42 GeV to a phase-space modified Breit-Wigner function, using the decays $\chi_{c0} \to \pi^+\pi^-$, $\chi_{c0} \to K^+K^-$, and $\omega \to \pi^+\pi^-\pi^0$.

$\Gamma(\pi^+\pi^- h_c)/\Gamma_{total}$ Γ_3/Γ

VALUE	DOCUMENT ID		TECN	COMMENT
seen	ABLIKIM	17G	BES3	$e^+e^- \to \pi^+\pi^- h_c$

$\Gamma(\pi^+\pi^-\psi(2S))/\Gamma_{total}$ Γ_4/Γ

VALUE	DOCUMENT ID		TECN	COMMENT
seen	[1] ABLIKIM	17V	BES3	$e^+e^- \to \pi^+\pi^-\psi(2S)$

[1] From a fit to the cross section for $e^+e^- \to \pi^+\pi^-\psi(2S) \to 2(\pi^+\pi^-)\ell^+\ell^-$ obtained from 16 center-of-mass energies between 4.008 and 4.600 GeV and comprising 5.1 fb^{-1}.

$\psi(4230)$ REFERENCES

ABLIKIM	17G	PRL 118 092002	M. Ablikim *et al.*	(BES III Collab.)
ABLIKIM	17V	PR D96 032004	M. Ablikim *et al.*	(BES III Collab.)
ABLIKIM	15C	PRL 114 092003	M. Ablikim *et al.*	(BES III Collab.)

$R_{c0}(4240)$

$I^G(J^{PC}) = 1^+(0^{--})$
I, *G*, *C* need confirmation.

OMITTED FROM SUMMARY TABLE
was $X(4240)^{\pm}$

Properties incompatible with a $q\overline{q}$ structure (exotic state). See the review on non-$q\overline{q}$ states.

Spin and parity assigment $J^P = 0^-$ is favored over 1^-, 2^-, and 2^+ by 8 σ and over 1^+ by 1 σ, according to the four-dimensional amplitude analysis of AAIJ 14AG.

$R_{c0}(4240)$ MASS

VALUE (MeV)	DOCUMENT ID		TECN	COMMENT
$4239 \pm 18^{+45}_{-10}$	[1] AAIJ	14AG	LHCB	$B^0 \to K^+\pi^-\psi(2S)$

[1] From a 4-dimensional analysis when a second, lower mass resonance is allowed in the $Z_c(4430)$ fit, with significance 6 σ including systematic variations.

$R_{c0}(4240)$ WIDTH

VALUE (MeV)	DOCUMENT ID		TECN	COMMENT
$220 \pm 47^{+108}_{-74}$	[1] AAIJ	14AG	LHCB	$B^0 \to K^+\pi^-\psi(2S)$

[1] From a 4-dimensional analysis when a second, lower mass resonance is allowed in the $Z_c(4430)$ fit, with significance 6 σ including systematic variations.

$R_{c0}(4240)$ DECAY MODES

	Mode	Fraction (Γ_i/Γ)
Γ_1	$\pi^-\psi(2S)$	seen

$R_{c0}(4240)$ BRANCHING RATIOS

$\Gamma(\pi^-\psi(2S))/\Gamma_{total}$ Γ_1/Γ

VALUE	DOCUMENT ID		TECN	COMMENT
seen	[1] AAIJ	14AG	LHCB	$B^0 \to K^+\pi^-\psi(2S)$

[1] From a 4-dimensional analysis when a second, lower mass resonance is allowed in the $Z_c(4430)$ fit. No partial branching fraction quoted.

$R_{c0}(4240)$ REFERENCES

AAIJ	14AG	PRL 112 222002	R. Aaij *et al.*	(LHCb Collab.)

$X(4250)^{\pm}$

$I^G(J^{PC}) = 1^-(?^{?+})$
I, *G*, *C* need confirmation.

OMITTED FROM SUMMARY TABLE

Properties incompatible with a $q\overline{q}$ structure (exotic state). See the review on non-$q\overline{q}$ states.

Observed by MIZUK 08 in the $\pi^+\chi_{c1}(1P)$ invariant mass distribution in $\overline{B}^0 \to K^-\pi^+\chi_{c1}(1P)$ decays. Not seen by LEES 12B in this same mode after accounting for $K\pi$ resonant mass and angular structure.

$X(4250)^{\pm}$ MASS

VALUE (MeV)	DOCUMENT ID		TECN	COMMENT
$4248^{+44}_{-29}{}^{+180}_{-35}$	[1] MIZUK	08	BELL	$\overline{B}^0 \to K^-\pi^+\chi_{c1}(1P)$

[1] From a Dalitz plot analysis with two Breit-Wigner amplitudes.

$X(4250)^{\pm}$ WIDTH

VALUE (MeV)	DOCUMENT ID		TECN	COMMENT
$177^{+54}_{-39}{}^{+316}_{-61}$	[1] MIZUK	08	BELL	$\overline{B}^0 \to K^-\pi^+\chi_{c1}(1P)$

[1] From a Dalitz plot analysis with two Breit-Wigner amplitudes.

$X(4250)^{\pm}$ DECAY MODES

	Mode	Fraction (Γ_i/Γ)
Γ_1	$\pi^+\chi_{c1}(1P)$	seen

$X(4250)^{\pm}$ BRANCHING RATIOS

$\Gamma(\pi^+\chi_{c1}(1P))/\Gamma_{total}$ Γ_1/Γ

VALUE	DOCUMENT ID		TECN	COMMENT
seen	[1] MIZUK	08	BELL	$\overline{B}^0 \to K^-\pi^+\chi_{c1}(1P)$
• • • We do not use the following data for averages, fits, limits, etc. • • •				
not seen	[2] LEES	12B	BABR	$B \to K\pi\chi_{c1}(1P)$

[1] With a product branching fraction measurement of $B(\overline{B}^0 \to K^- X(4250)^+) \times B(X(4250)^+ \to \pi^+\chi_{c1}(1P)) = (4.0^{+2.3}_{-0.9}{}^{+19.7}_{-0.5}) \times 10^{-5}$.

[2] With a product branching fraction limit of $B(\overline{B}^0 \to X(4250)^+ K^-) \times B(X(4250)^+ \to \chi_{c1}\pi^+) < 4.0 \times 10^{-5}$ at 90% CL.

$X(4250)^{\pm}$ REFERENCES

LEES	12B	PR D85 052003	J.P. Lees *et al.*	(BABAR Collab.)
MIZUK	08	PR D78 072004	R. Mizuk *et al.*	(BELLE Collab.)

$\psi(4260)$

$I^G(J^{PC}) = 0^-(1^{--})$

also known as $Y(4260)$; was $X(4260)$

This state shows properties different from a conventional $q\overline{q}$ state. A candidate for an exotic structure. See the review on non-$q\overline{q}$ states.

Seen in radiative return from e^+e^- collisions at $\sqrt{s} = 9.54$–10.58 GeV by AUBERT,B 05I, HE 06B, and YUAN 07, and in e^+e^- collisions at $\sqrt{s} \approx 4.26$ GeV by COAN 06. Possibly seen by AUBERT 06 in $B^- \to K^-\pi^+\pi^- J/\psi$. See also the review on "Spectroscopy of mesons containing two heavy quarks."

$\psi(4260)$ MASS

VALUE (MeV)	EVTS	DOCUMENT ID		TECN	COMMENT
4230 ± 8 OUR AVERAGE Error includes scale factor of 2.9. See the ideogram below.					
4222.0 ± 3.1 ± 1.4		[1] ABLIKIM	17B	BES3	$e^+e^- \to \pi^+\pi^- J/\psi$
4258.6 ± 8.3 ± 12.1		[2] LIU	13B	BELL	$e^+e^- \to \gamma\pi^+\pi^- J/\psi$
4245 ± 5 ± 4		[3] LEES	12AC	BABR	10.58 $e^+e^- \to \gamma\pi^+\pi^- J/\psi$
4284 $^{+17}_{-16}$ ± 4	13.6	HE	06B	CLEO	9.4–10.6 $e^+e^- \to \gamma\pi^+\pi^- J/\psi$
• • • We do not use the following data for averages, fits, limits, etc. • • •					
4209.1 ± 6.8 ± 7.0		[4] ZHANG	17B	RVUE	$e^+e^- \to \pi^+\pi^-\psi(2S)$
4223.3 ± 1.6 ± 2.5		[5] ZHANG	17C	RVUE	$e^+e^- \to \pi^+\pi^- J/\psi$ or $\psi(2S)$
4247 ± 12 $^{+17}_{-32}$		[2,6] YUAN	07	BELL	10.58 $e^+e^- \to \gamma\pi^+\pi^- J/\psi$
4259 ± 8 $^{+2}_{-6}$	125	[7] AUBERT,B	05I	BABR	10.58 $e^+e^- \to \gamma\pi^+\pi^- J/\psi$

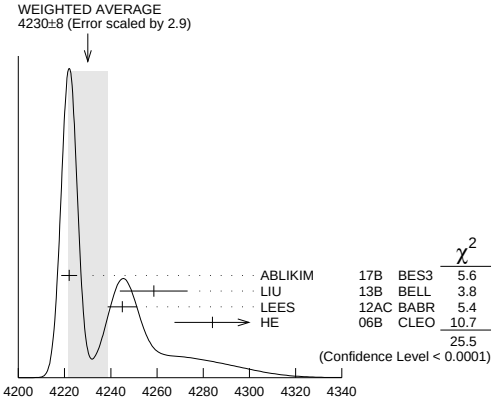

[1] From a three-resonance fit.
[2] From a two-resonance fit.
[3] From a single-resonance fit. Supersedes AUBERT,B 05I.

[4] From a three-resonance fit.
[5] From a combined fit of BELLE, BABAR and BES3 $e^+e^- \to \pi^+\pi^- J/\psi$ and $e^+e^- \to \pi^+\pi^-\psi(2S)$ data.
[6] Superseded by LIU 13B.
[7] From a single-resonance fit. Two interfering resonances are not excluded. Superseded by LEES 12AC.

$\psi(4260)$ WIDTH

VALUE (MeV)	EVTS	DOCUMENT ID		TECN	COMMENT
55 ±19 OUR AVERAGE		Error includes scale factor of 4.4. See the ideogram below.			
44.1± 4.3± 2.0		[1] ABLIKIM	17B	BES3	$e^+e^- \to \pi^+\pi^- J/\psi$
134.1±16.4± 5.5		[2] LIU	13B	BELL	$e^+e^- \to \gamma\pi^+\pi^- J/\psi$
114 $^{+16}_{-15}$ ± 7		[3] LEES	12AC	BABR	10.58 $e^+e^- \to \gamma\pi^+\pi^- J/\psi$
73 $^{+39}_{-25}$ ± 5 13.6		HE	06B	CLEO	9.4–10.6 $e^+e^- \to \gamma\pi^+\pi^- J/\psi$
• • • We do not use the following data for averages, fits, limits, etc. • • •					
76.6±14.2± 2.4		[4] ZHANG	17B	RVUE	$e^+e^- \to \pi^+\pi^-\psi(2S)$
54.2± 2.6± 1.0		[5] ZHANG	17C	RVUE	$e^+e^- \to \pi^+\pi^- J/\psi$ or $\psi(2S)$
108 ±19 ±10		[2,6] YUAN	07	BELL	10.58 $e^+e^- \to \gamma\pi^+\pi^- J/\psi$
88 ±23 $^{+6}_{-4}$ 125		[7] AUBERT,B	05I	BABR	10.58 $e^+e^- \to \gamma\pi^+\pi^- J/\psi$

[1] From a three-resonance fit.
[2] From a two-resonance fit.
[3] From a single-resonance fit. Supersedes AUBERT,B 05I.
[4] From a three-resonance fit.
[5] From a combined fit of BELLE, BABAR and BES3 $e^+e^- \to \pi^+\pi^- J/\psi$ and $e^+e^- \to \pi^+\pi^-\psi(2S)$ data.
[6] Superseded by LIU 13B.
[7] From a single-resonance fit. Two interfering resonances are not excluded. Superseded by LEES 12AC.

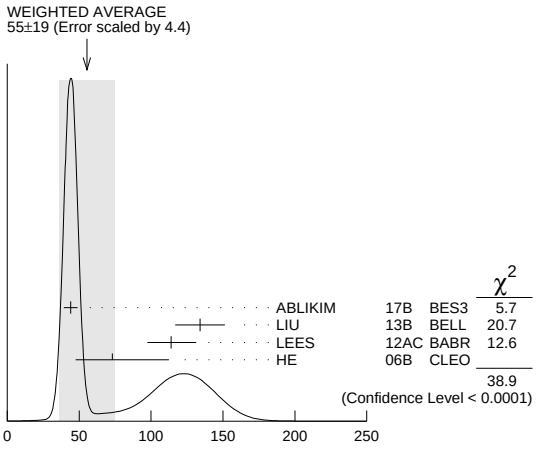

$\psi(4260)$ DECAY MODES

	Mode	Fraction (Γ_i/Γ)
Γ_1	e^+e^-	
Γ_2	$J/\psi\pi^+\pi^-$	seen
Γ_3	$J/\psi f_0(980)$, $f_0(980) \to \pi^+\pi^-$	seen
Γ_4	$Z_c(3900)^\pm\pi^\mp$, $Z_c^\pm \to J/\psi\pi^\pm$	seen
Γ_5	$J/\psi\pi^0\pi^0$	seen
Γ_6	$J/\psi K^+K^-$	seen
Γ_7	$J/\psi K^0_S K^0_S$	not seen
Γ_8	$J/\psi\eta$	not seen
Γ_9	$J/\psi\pi^0$	not seen
Γ_{10}	$J/\psi\eta'$	not seen
Γ_{11}	$J/\psi\pi^+\pi^-\pi^0$	not seen
Γ_{12}	$J/\psi\eta\pi^0$	not seen
Γ_{13}	$J/\psi\eta\eta$	not seen
Γ_{14}	$\psi(2S)\pi^+\pi^-$	not seen
Γ_{15}	$\psi(2S)\eta$	not seen
Γ_{16}	$\chi_{c0}\omega$	not seen
Γ_{17}	$\chi_{c1}\pi^+\pi^-\pi^0$	not seen
Γ_{18}	$\chi_{c2}\pi^+\pi^-\pi^0$	not seen
Γ_{19}	$h_c(1P)\pi^+\pi^-$	not seen
Γ_{20}	$\phi\pi^+\pi^-$	not seen
Γ_{21}	$\phi f_0(980) \to \phi\pi^+\pi^-$	not seen
Γ_{22}	$D\overline{D}$	not seen
Γ_{23}	$D^0\overline{D}^0$	not seen
Γ_{24}	D^+D^-	not seen
Γ_{25}	$D^*\overline{D}$ + c.c.	not seen
Γ_{26}	$D^*(2007)^0\overline{D}^0$ + c.c.	not seen
Γ_{27}	$D^*(2010)^+D^-$ + c.c.	not seen
Γ_{28}	$D^*\overline{D}^*$	not seen
Γ_{29}	$D^*(2007)^0\overline{D}^*(2007)^0$	not seen
Γ_{30}	$D^*(2010)^+D^*(2010)^-$	not seen
Γ_{31}	$D\overline{D}\pi$ + c.c.	
Γ_{32}	$D^0D^-\pi^+$ + c.c. (excl. $D^*(2007)^0\overline{D}^{*0}$ + c.c., $D^*(2010)^+D^-$ + c.c.)	not seen
Γ_{33}	$D\overline{D}^*\pi$ + c.c. (excl. $D^*\overline{D}^*$)	not seen
Γ_{34}	$D^0D^{*-}\pi^+$ + c.c. (excl. $D^*(2010)^+D^*(2010)^-$)	not seen
Γ_{35}	$D^0D^*(2010)^-\pi^+$ + c.c.	not seen
Γ_{36}	$D^*\overline{D}^*\pi$	not seen
Γ_{37}	$D_s^+D_s^-$	not seen
Γ_{38}	$D_s^{*+}D_s^-$ + c.c.	not seen
Γ_{39}	$D_s^{*+}D_s^{*-}$	not seen
Γ_{40}	$p\overline{p}$	not seen
Γ_{41}	$p\overline{p}\pi^0$	not seen
Γ_{42}	$K^0_S K^\pm\pi^\mp$	not seen
Γ_{43}	$K^+K^-\pi^0$	not seen
	Radiative decays	
Γ_{44}	$\eta_c(1S)\gamma$	possibly seen
Γ_{45}	$\chi_{c1}\gamma$	not seen
Γ_{46}	$\chi_{c2}\gamma$	not seen
Γ_{47}	$\chi_{c1}(3872)\gamma$	seen

$\psi(4260)$ $\Gamma(i) \times \Gamma(e^+e^-)/\Gamma(\text{total})$

$\Gamma(J/\psi\pi^+\pi^-) \times \Gamma(e^+e^-)/\Gamma_{\text{total}}$ $\quad \Gamma_2\Gamma_1/\Gamma$

VALUE (eV)	EVTS	DOCUMENT ID		TECN	COMMENT
9.2±1.0 OUR AVERAGE					
9.2±0.8±0.7		[1] LEES	12AC	BABR	10.58 $e^+e^- \to \gamma\pi^+\pi^- J/\psi$
8.9 $^{+3.9}_{-3.1}$ ±1.8	8.1	HE	06B	CLEO	9.4–10.6 $e^+e^- \to \gamma\pi^+\pi^- J/\psi$
• • • We do not use the following data for averages, fits, limits, etc. • • •					
6.4±0.8±0.6		[2] LIU	13B	BELL	$e^+e^- \to \gamma\pi^+\pi^- J/\psi$
20.5±1.4±2.0		[3] LIU	13B	BELL	$e^+e^- \to \gamma\pi^+\pi^- J/\psi$
6.0±1.2 $^{+4.7}_{-0.5}$		[2,4] YUAN	07	BELL	10.58 $e^+e^- \to \gamma\pi^+\pi^- J/\psi$
20.6±2.3 $^{+9.1}_{-1.7}$		[3,4] YUAN	07	BELL	10.58 $e^+e^- \to \gamma\pi^+\pi^- J/\psi$
5.5±1.0 $^{+0.8}_{-0.7}$	125	[5] AUBERT,B	05I	BABR	10.58 $e^+e^- \to \gamma\pi^+\pi^- J/\psi$

[1] From a single-resonance fit. Supersedes AUBERT,B 05I.
[2] Solution I of two equivalent solutions in a fit using two interfering resonances.
[3] Solution II of two equivalent solutions in a fit using two interfering resonances.
[4] Superseded by LIU 13B.
[5] From a single-resonance fit. Two interfering resonances are not excluded. Superseded by LEES 12AC.

$\Gamma(J/\psi K^+K^-) \times \Gamma(e^+e^-)/\Gamma_{\text{total}}$ $\quad \Gamma_6\Gamma_1/\Gamma$

VALUE (eV)	CL%	DOCUMENT ID		TECN	COMMENT
<1.7	90	[1] SHEN	14	BELL	9.4–10.9 $e^+e^- \to \gamma K^+K^- J/\psi$
• • • We do not use the following data for averages, fits, limits, etc. • • •					
<1.2	90	[2] YUAN	08	BELL	$e^+e^- \to \gamma K^+K^- J/\psi$

[1] From a fit of the broad $K^+K^- J/\psi$ enhancement including a coherent $\psi(4260)$ amplitude with mass and width from LIU 13B. Supersedes YUAN 08.
[2] From a fit of the broad $K^+K^- J/\psi$ enhancement including a coherent $\psi(4260)$ amplitude with mass and width from YUAN 07.

$\Gamma(J/\psi K^0_S K^0_S) \times \Gamma(e^+e^-)/\Gamma_{\text{total}}$ $\quad \Gamma_7\Gamma_1/\Gamma$

VALUE (eV)	CL%	DOCUMENT ID		TECN	COMMENT
<0.85	90	[1] SHEN	14	BELL	9.4–10.9 $e^+e^- \to \gamma K^0_S K^0_S J/\psi$

[1] From a fit of the $K^0_S K^0_S J/\psi$ mass range from 4.4 to 5.5 GeV including a coherent $\psi(4260)$ amplitude with mass and width from LIU 13B.

$\Gamma(J/\psi\eta) \times \Gamma(e^+e^-)/\Gamma_{\text{total}}$ $\quad \Gamma_8\Gamma_1/\Gamma$

VALUE (eV)	CL%	DOCUMENT ID	TECN	COMMENT
• • • We do not use the following data for averages, fits, limits, etc. • • •				
<14.2	90	WANG	13B BELL	$e^+e^- \to J/\psi\eta\gamma$

$\Gamma(\psi(2S)\pi^+\pi^-) \times \Gamma(e^+e^-)/\Gamma_{\text{total}}$ $\quad \Gamma_{14}\Gamma_1/\Gamma$

VALUE (eV)	CL%	DOCUMENT ID		TECN	COMMENT
• • • We do not use the following data for averages, fits, limits, etc. • • •					
<4.3	90	[1] LIU	08H	RVUE	10.58 $e^+e^- \to \psi(2S)\pi^+\pi^-\gamma$
7.4 $^{+2.1}_{-1.7}$		[2] LIU	08H	RVUE	10.58 $e^+e^- \to \psi(2S)\pi^+\pi^-\gamma$

[1] For constructive interference with the $\psi(4360)$ in a combined fit of AUBERT 07S and WANG 07D data with three resonances.
[2] For destructive interference with the $\psi(4360)$ in a combined fit of AUBERT 07S and WANG 07D data with three resonances.

$\Gamma(\phi\pi^+\pi^-) \times \Gamma(e^+e^-)/\Gamma_{total}$ $\Gamma_{20}\Gamma_1/\Gamma$

VALUE (eV)	CL%	DOCUMENT ID		TECN	COMMENT
<0.4	90	AUBERT,BE	06D	BABR	10.6 $e^+e^- \to K^+K^-\pi^+\pi^-\gamma$

$\Gamma(\phi f_0(980) \to \phi\pi^+\pi^-) \times \Gamma(e^+e^-)/\Gamma_{total}$ $\Gamma_{21}\Gamma_1/\Gamma$

VALUE (eV)	CL%	DOCUMENT ID		TECN	COMMENT
<0.28	90	[1] AUBERT	07AK	BABR	10.6 $e^+e^- \to \pi^+\pi^- K^+K^-\gamma$

[1] AUBERT 07AK reports $[\Gamma(\psi(4260) \to \phi f_0(980) \to \phi\pi^+\pi^-) \times \Gamma(\psi(4260) \to e^+e^-)/\Gamma_{total}] \times [B(\phi(1020) \to K^+K^-)] < 0.14$ eV which we divide by our best value $B(\phi(1020) \to K^+K^-) = 49.2 \times 10^{-2}$.

$\Gamma(K^0_S K^\pm\pi^\mp) \times \Gamma(e^+e^-)/\Gamma_{total}$ $\Gamma_{42}\Gamma_1/\Gamma$

VALUE (eV)	CL%	DOCUMENT ID		TECN	COMMENT
• • • We do not use the following data for averages, fits, limits, etc. • • •					
<0.5	90	AUBERT	08S	BABR	10.6 $e^+e^- \to K^0_S K^\pm\pi^\mp\gamma$

$\Gamma(K^+K^-\pi^0) \times \Gamma(e^+e^-)/\Gamma_{total}$ $\Gamma_{43}\Gamma_1/\Gamma$

VALUE (eV)	CL%	DOCUMENT ID		TECN	COMMENT
• • • We do not use the following data for averages, fits, limits, etc. • • •					
<0.6	90	AUBERT	08S	BABR	10.6 $e^+e^- \to K^+K^-\pi^0\gamma$

$\Gamma(\chi_{c1}\gamma) \times \Gamma(e^+e^-)/\Gamma_{total}$ $\Gamma_{45}\Gamma_1/\Gamma$

VALUE (eV)	CL%	DOCUMENT ID		TECN	COMMENT
<1.4	90	[1] HAN	15	BELL	10.58 $e^+e^- \to \chi_{c1}\gamma$

[1] Using $B(\eta \to \gamma\gamma) = (39.41 \pm 0.21)\%$.

$\Gamma(\chi_{c2}\gamma) \times \Gamma(e^+e^-)/\Gamma_{total}$ $\Gamma_{46}\Gamma_1/\Gamma$

VALUE (eV)	CL%	DOCUMENT ID		TECN	COMMENT
<4.0	90	[1] HAN	15	BELL	10.58 $e^+e^- \to \chi_{c2}\gamma$

[1] Using $B(\eta \to \gamma\gamma) = (39.41 \pm 0.21)\%$.

$\psi(4260)$ BRANCHING RATIOS

$\Gamma(J/\psi f_0(980), f_0(980) \to \pi^+\pi^-)/\Gamma(J/\psi\pi^+\pi^-)$ Γ_3/Γ_2

VALUE	DOCUMENT ID		TECN	COMMENT
• • • We do not use the following data for averages, fits, limits, etc. • • •				
0.17±0.13	[1] LEES	12AC	BABR	10.58 $e^+e^- \to \gamma\pi^+\pi^- J/\psi$

[1] Systematic uncertainties not estimated.

$\Gamma(Z_c(3900)^\pm\pi^\mp, Z_c^\pm \to J/\psi\pi^\pm)/\Gamma(J/\psi\pi^+\pi^-)$ Γ_4/Γ_2

VALUE	DOCUMENT ID		TECN	COMMENT
0.215±0.033±0.075	[1] ABLIKIM	13T	BES3	$e^+e^- \to \pi^+\pi^- J/\psi$
• • • We do not use the following data for averages, fits, limits, etc. • • •				
0.29 ±0.08	[2] LIU	13B	BELL	$e^+e^- \to \gamma\pi^+\pi^- J/\psi$

[1] Assuming that the cross section of $e^+e^- \to \pi^+\pi^- J/\psi$ is fully due to the $\psi(4260)$.
[2] Systematic error not evaluated.

$\Gamma(J/\psi K^0_S K^0_S)/\Gamma_{total}$ Γ_7/Γ

VALUE	DOCUMENT ID		TECN	COMMENT
not seen	SHEN	14	BELL	9.4–10.9 $e^+e^- \to \gamma K^0_S K^0_S J/\psi$

$\Gamma(J/\psi\eta\pi^0)/\Gamma_{total}$ Γ_{12}/Γ

VALUE	DOCUMENT ID		TECN	COMMENT
not seen	ABLIKIM	15Q	BES3	4.0–4.6 $e^+e^- \to J/\psi\eta\pi^0$

$\Gamma(\psi(2S)\pi^+\pi^-)/\Gamma(J/\psi\pi^+\pi^-)$ Γ_{14}/Γ_2

VALUE	DOCUMENT ID		TECN	COMMENT
• • • We do not use the following data for averages, fits, limits, etc. • • •				
(0.11±0.03±0.03) to (0.55±0.18±0.19)	[1] ZHANG	17C	RVUE	$e^+e^- \to \pi^+\pi^- J/\psi$ or $\psi(2S)$

[1] From a combined fit of BELLE, BABAR and BES3 $e^+e^- \to \pi^+\pi^- J/\psi$ and $e^+e^- \to \pi^+\pi^-\psi(2S)$ data.

$\Gamma(h_c(1P)\pi^+\pi^-)/\Gamma(J/\psi\pi^+\pi^-)$ Γ_{19}/Γ_2

VALUE	CL%	DOCUMENT ID		TECN	COMMENT
<1.0	90	[1] PEDLAR	11	CLEO	$e^+e^- \to h_c(1P)\pi^+\pi^-$

[1] At $\sqrt{s} = 4260$ MeV, PEDLAR 11 measures $\sigma(e^+e^- \to h_c(1P)\pi^+\pi^-) = 32 \pm 17 \pm 6 \pm 6$ pb, where the errors are statistical, systematic, and due to uncertainty in $B(\psi(2S) \to \pi^0 h_c(1P))$, respectively.

$\Gamma(D\overline{D})/\Gamma(J/\psi\pi^+\pi^-)$ Γ_{22}/Γ_2

VALUE	CL%	DOCUMENT ID		TECN	COMMENT
<1.0	90	[1] AUBERT	07BE	BABR	$e^+e^- \to D\overline{D}\gamma$
• • • We do not use the following data for averages, fits, limits, etc. • • •					
<4.0	90	CRONIN-HEN..09		CLEO	e^+e^-

[1] Using 4259 ± 10 MeV for the mass and 88 ± 24 MeV for the width of $\psi(4260)$.

$\Gamma(D^0\overline{D}^0)/\Gamma_{total}$ Γ_{23}/Γ

VALUE	DOCUMENT ID		TECN	COMMENT
not seen	CRONIN-HEN..09		CLEO	$e^+e^- \to D^0\overline{D}^0$
• • • We do not use the following data for averages, fits, limits, etc. • • •				
not seen	AUBERT	09M	BABR	$e^+e^- \to D^0\overline{D}^0\gamma$
not seen	PAKHLOVA	08	BELL	$e^+e^- \to D^0\overline{D}^0\gamma$

$\Gamma(D^+D^-)/\Gamma_{total}$ Γ_{24}/Γ

VALUE	DOCUMENT ID		TECN	COMMENT
not seen	CRONIN-HEN..09		CLEO	$e^+e^- \to D^+D^-$
• • • We do not use the following data for averages, fits, limits, etc. • • •				
not seen	AUBERT	09M	BABR	$e^+e^- \to D^+D^-\gamma$
not seen	PAKHLOVA	08	BELL	$e^+e^- \to D^+D^-\gamma$

$\Gamma(D^*\overline{D}+\text{c.c.})/\Gamma(J/\psi\pi^+\pi^-)$ Γ_{25}/Γ_2

VALUE	CL%	DOCUMENT ID		TECN	COMMENT
<34	90	AUBERT	09M	BABR	$e^+e^- \to \gamma D^*\overline{D}$
• • • We do not use the following data for averages, fits, limits, etc. • • •					
<45	90	CRONIN-HEN..09		CLEO	e^+e^-

$\Gamma(D^*(2007)^0\overline{D}^0+\text{c.c.})/\Gamma_{total}$ Γ_{26}/Γ

VALUE	DOCUMENT ID		TECN	COMMENT
not seen	CRONIN-HEN..09		CLEO	$e^+e^- \to D^{*0}\overline{D}^0$
• • • We do not use the following data for averages, fits, limits, etc. • • •				
not seen	AUBERT	09M	BABR	$e^+e^- \to D^{*0}\overline{D}^0\gamma$

$\Gamma(D^*(2010)^+D^-+\text{c.c.})/\Gamma_{total}$ Γ_{27}/Γ

VALUE	DOCUMENT ID		TECN	COMMENT
not seen	CRONIN-HEN..09		CLEO	$e^+e^- \to D^{*+}D^-$
not seen	PAKHLOVA	07	BELL	$e^+e^- \to D^{*+}D^-\gamma$
• • • We do not use the following data for averages, fits, limits, etc. • • •				
not seen	AUBERT	09M	BABR	$e^+e^- \to D^{*+}D^-\gamma$

$\Gamma(D^*\overline{D}^*)/\Gamma(J/\psi\pi^+\pi^-)$ Γ_{28}/Γ_2

VALUE	CL%	DOCUMENT ID		TECN	COMMENT
<11	90	CRONIN-HEN..09		CLEO	e^+e^-
• • • We do not use the following data for averages, fits, limits, etc. • • •					
<40	90	AUBERT	09M	BABR	$e^+e^- \to \gamma D^*\overline{D}^*$

$\Gamma(D^*(2007)^0\overline{D}^*(2007)^0)/\Gamma_{total}$ Γ_{29}/Γ

VALUE	DOCUMENT ID		TECN	COMMENT
not seen	CRONIN-HEN..09		CLEO	$e^+e^- \to D^{*0}\overline{D}^{*0}$
• • • We do not use the following data for averages, fits, limits, etc. • • •				
not seen	AUBERT	09M	BABR	$e^+e^- \to D^{*0}\overline{D}^{*0}\gamma$

$\Gamma(D^*(2010)^+D^*(2010)^-)/\Gamma_{total}$ Γ_{30}/Γ

VALUE	DOCUMENT ID		TECN	COMMENT
not seen	CRONIN-HEN..09		CLEO	$e^+e^- \to D^{*+}D^{*-}$
not seen	PAKHLOVA	07	BELL	$e^+e^- \to D^{*+}D^{*-}\gamma$
• • • We do not use the following data for averages, fits, limits, etc. • • •				
not seen	AUBERT	09M	BABR	$e^+e^- \to D^{*+}D^{*-}\gamma$

$\Gamma(D^0D^-\pi^+ + \text{c.c. (excl. } D^*(2007)^0\overline{D}^{*0} + \text{c.c., } D^*(2010)^+D^- + \text{c.c.}))/\Gamma_{total}$ Γ_{32}/Γ

VALUE	DOCUMENT ID		TECN	COMMENT
not seen	PAKHLOVA	08A	BELL	10.6 $e^+e^- \to D^0D^-\pi^+\gamma$

$\Gamma(D\overline{D}^*\pi + \text{c.c. (excl. } D^*\overline{D}^*))/\Gamma_{total}$ Γ_{33}/Γ

VALUE	DOCUMENT ID		TECN	COMMENT
not seen	CRONIN-HEN..09		CLEO	$e^+e^- \to D^*\overline{D}\pi$

$\Gamma(D\overline{D}^*\pi + \text{c.c. (excl. } D^*\overline{D}^*))/\Gamma(J/\psi\pi^+\pi^-)$ Γ_{33}/Γ_2

VALUE	CL%	DOCUMENT ID		TECN	COMMENT
<15	90	CRONIN-HEN..09		CLEO	e^+e^-

$\Gamma(D^0D^{*-}\pi^+ + \text{c.c. (excl. } D^*(2010)^+D^*(2010)^-))/\Gamma_{total}$ Γ_{34}/Γ

VALUE	DOCUMENT ID		TECN	COMMENT
not seen	PAKHLOVA	09	BELL	$e^+e^- \to D^0D^{*-}\pi^+\gamma$

$\Gamma(D^0D^*(2010)^-\pi^+ + \text{c.c.})/\Gamma(J/\psi\pi^+\pi^-)$ Γ_{35}/Γ_2

VALUE	CL%	DOCUMENT ID		TECN	COMMENT
<9	90	PAKHLOVA	09	BELL	$e^+e^- \to D^0D^{*-}\pi^+$

$\Gamma(D^0D^*(2010)^-\pi^+ + \text{c.c.})/\Gamma_{total} \times \Gamma(e^+e^-)/\Gamma_{total}$ $\Gamma_{35}/\Gamma \times \Gamma_1/\Gamma$

VALUE	CL%	DOCUMENT ID		TECN	COMMENT
<0.42 × 10⁻⁶	90	[1] PAKHLOVA	09	BELL	$e^+e^- \to D^0D^{*-}\pi^+$

[1] Using 4263^{+8}_{-9} MeV for the mass of $\psi(4260)$.

$\Gamma(D^*\overline{D}^*\pi)/\Gamma_{total}$ **Γ_{36}/Γ**

VALUE	DOCUMENT ID	TECN	COMMENT
not seen	CRONIN-HEN..09	CLEO	$e^+e^- \to D^*\overline{D}^*\pi$

$\Gamma(D^*\overline{D}^*\pi)/\Gamma(J/\psi\pi^+\pi^-)$ **Γ_{36}/Γ_2**

VALUE	CL%	DOCUMENT ID	TECN	COMMENT
<8.2	90	CRONIN-HEN..09	CLEO	e^+e^-

$\Gamma(D_s^+D_s^-)/\Gamma_{total}$ **Γ_{37}/Γ**

VALUE	DOCUMENT ID	TECN	COMMENT
not seen	DEL-AMO-SA..10N	BABR	$e^+e^- \to D_s^+D_s^-\gamma$
not seen	CRONIN-HEN..09	CLEO	$e^+e^- \to D_s^+D_s^-$
• • • We do not use the following data for averages, fits, limits, etc. • • •			
not seen	PAKHLOVA 11	BELL	$e^+e^- \to D_s^+D_s^-\gamma$

$\Gamma(D_s^+D_s^-)/\Gamma(J/\psi\pi^+\pi^-)$ **Γ_{37}/Γ_2**

VALUE	CL%	DOCUMENT ID	TECN	COMMENT
<0.7	95	DEL-AMO-SA..10N	BABR	10.6 e^+e^-
• • • We do not use the following data for averages, fits, limits, etc. • • •				
<1.3	90	CRONIN-HEN..09	CLEO	e^+e^-

$\Gamma(D_s^{*+}D_s^- + \text{c.c.})/\Gamma_{total}$ **Γ_{38}/Γ**

VALUE	DOCUMENT ID	TECN	COMMENT
not seen	DEL-AMO-SA..10N	BABR	$e^+e^- \to D_s^{*+}D_s^-\gamma$
not seen	CRONIN-HEN..09	CLEO	$e^+e^- \to D_s^{*+}D_s^-$
• • • We do not use the following data for averages, fits, limits, etc. • • •			
not seen	PAKHLOVA 11	BELL	$e^+e^- \to D_s^{*+}D_s^-\gamma$

$\Gamma(D_s^{*+}D_s^- + \text{c.c.})/\Gamma(J/\psi\pi^+\pi^-)$ **Γ_{38}/Γ_2**

VALUE	CL%	DOCUMENT ID	TECN	COMMENT
< 0.8	90	CRONIN-HEN..09	CLEO	e^+e^-
• • • We do not use the following data for averages, fits, limits, etc. • • •				
<44	95	DEL-AMO-SA..10N	BABR	10.6 e^+e^-

$\Gamma(D_s^{*+}D_s^{*-})/\Gamma_{total}$ **Γ_{39}/Γ**

VALUE	DOCUMENT ID	TECN	COMMENT
not seen	CRONIN-HEN..09	CLEO	$e^+e^- \to D_s^{*+}D_s^{*-}$
• • • We do not use the following data for averages, fits, limits, etc. • • •			
not seen	PAKHLOVA 11	BELL	$e^+e^- \to D_s^{*+}D_s^{*-}\gamma$
not seen	DEL-AMO-SA..10N	BABR	$e^+e^- \to D_s^{*+}D_s^{*-}\gamma$

$\Gamma(D_s^{*+}D_s^{*-})/\Gamma(J/\psi\pi^+\pi^-)$ **Γ_{39}/Γ_2**

VALUE	CL%	DOCUMENT ID	TECN	COMMENT
< 9.5	90	CRONIN-HEN..09	CLEO	e^+e^-
• • • We do not use the following data for averages, fits, limits, etc. • • •				
<30	95	DEL-AMO-SA..10N	BABR	10.6 e^+e^-

$\Gamma(p\overline{p})/\Gamma(J/\psi\pi^+\pi^-)$ **Γ_{40}/Γ_2**

VALUE	CL%	DOCUMENT ID	TECN	COMMENT
<0.13	90	[1] AUBERT 06B	BABR	$e^+e^- \to p\overline{p}\gamma$

[1] Using 4259 ± 10 MeV for the mass and 88 ± 24 MeV for the width of $\psi(4260)$.

$\Gamma(p\overline{p}\pi^0)/\Gamma(J/\psi\pi^+\pi^-)$ **Γ_{41}/Γ_2**

VALUE	CL%	DOCUMENT ID	TECN	COMMENT
$<2\times10^{-4}$	90	ABLIKIM 17F	BES3	$e^+e^- \to \psi(4260) \to$ hadrons

Radiative decays

$\Gamma(\eta_c(1S)\gamma)/\Gamma_{total}$ **Γ_{44}/Γ**

VALUE	DOCUMENT ID	COMMENT
possibly seen	[1] ABLIKIM 17W	$e^+e^- \to \gamma\eta_c(1S)$

[1] Significance ranges from 4.2 σ to as low as 1.5 σ for a flat component plus $\psi(4260)$ spectrum. Needs confirmation.

$\Gamma(\chi_{c1}(3872)\gamma)/\Gamma_{total}$ **Γ_{47}/Γ**

VALUE	EVTS	DOCUMENT ID	TECN	COMMENT
seen	20 ± 5	ABLIKIM 14	BES3	$e^+e^- \to J/\psi\pi^+\pi^-\gamma$

$\psi(4260)$ REFERENCES

ABLIKIM	17B	PRL 118 092001	M. Ablikim *et al.*	(BES III Collab.)
ABLIKIM	17F	PL B771 45	M. Ablikim *et al.*	(BES III Collab.)
ABLIKIM	17W	PR D96 051101	M. Ablikim *et al.*	(BES III Collab.)
ZHANG	17B	PR D96 054008	J. Zhang, J. Zhang	
ZHANG	17C	EPJ C77 727	J. Zhang, L. Yuan	
ABLIKIM	15Q	PR D92 012008	M. Ablikim *et al.*	(BES III Collab.)
HAN	15	PR D92 012011	Y.L. Han *et al.*	(BELLE Collab.)
ABLIKIM	14	PRL 112 092001	M. Ablikim *et al.*	(BES III Collab.)
SHEN	14	PR D89 072015	C.P. Shen *et al.*	(BELLE Collab.)
ABLIKIM	13T	PRL 110 252001	M. Ablikim *et al.*	(BES III Collab.)
LIU	13B	PRL 110 252002	Z.Q. Liu *et al.*	(BELLE Collab.)
WANG	13B	PR D87 051101	X.L. Wang *et al.*	(BELLE Collab.)
LEES	12AC	PR D86 051102	J.P. Lees *et al.*	(BABAR Collab.)
PAKHLOVA	11	PR D83 011101	G. Pakhlova *et al.*	(BELLE Collab.)
PEDLAR	11	PRL 107 041803	T. Pedlar *et al.*	(CLEO Collab.)
DEL-AMO-SA...	10N	PR D82 052004	P. del Amo Sanchez *et al.*	(BABAR Collab.)
AUBERT	09M	PR D79 092001	B. Aubert *et al.*	(BABAR Collab.)
CRONIN-HEN...	09	PR D80 072001	D. Cronin-Hennessy *et al.*	(CLEO Collab.)
PAKHLOVA	09	PR D80 091101	G. Pakhlova *et al.*	(BELLE Collab.)
AUBERT	08S	PR D77 092002	B. Aubert *et al.*	(BABAR Collab.)
LIU	08H	PR D78 014032	Z.Q. Liu, X.S. Qin, C.Z. Yuan	
PAKHLOVA	08	PR D77 011103	G. Pakhlova *et al.*	(BELLE Collab.)
PAKHLOVA	08A	PRL 100 062001	G. Pakhlova *et al.*	(BELLE Collab.)
YUAN	08	PR D77 011105	C.Z. Yuan *et al.*	(BELLE Collab.)
AUBERT	07AK	PR D76 012008	B. Aubert *et al.*	(BABAR Collab.)
AUBERT	07BE	PR D76 111105	B. Aubert *et al.*	(BABAR Collab.)
AUBERT	07S	PRL 98 212001	B. Aubert *et al.*	(BABAR Collab.)
PAKHLOVA	07	PRL 98 092001	G. Pakhlova *et al.*	(BELLE Collab.)
WANG	07D	PRL 99 142002	X.L. Wang *et al.*	(BELLE Collab.)
YUAN	07	PRL 99 182004	C.Z. Yuan *et al.*	(BELLE Collab.)
AUBERT	06	PR D73 011101	B. Aubert *et al.*	(BABAR Collab.)
AUBERT	06B	PR D73 012005	B. Aubert *et al.*	(BABAR Collab.)
AUBERT,BE	06D	PR D74 091103	B. Aubert *et al.*	(BABAR Collab.)
COAN	06	PRL 96 162003	T.E. Coan *et al.*	(CLEO Collab.)
HE	06B	PR D74 091104	Q. He *et al.*	(CLEO Collab.)
AUBERT,B	05I	PRL 95 142001	B. Aubert *et al.*	(BABAR Collab.)

$\chi_{c1}(4274)$ $I^G(J^{PC}) = 0^+(1^{++})$

was $X(4274)$

This state shows properties different from a conventional $q\overline{q}$ state. A candidate for an exotic structure. See the review on non-$q\overline{q}$ states.

Seen by AAIJ 17C in $B^+ \to \chi_{c1}K^+$, $\chi_{c1} \to J/\psi\phi$ using an amplitude analysis of $B^+ \to J/\psi\phi K^+$ with a significance (accounting for systematic uncertainties) of 6.0 σ.

$\chi_{c1}(4274)$ MASS

VALUE (MeV)	EVTS	DOCUMENT ID	TECN	COMMENT
$4274\ ^{+8}_{-6}$ OUR AVERAGE				
$4273.3 \pm 8.3^{+17.2}_{-3.6}$	4289	[1] AAIJ 17C	LHCB	$B^+ \to J/\psi\phi K^+$
$4274.4^{+8.4}_{-6.7} \pm 1.9$	22	[2] AALTONEN 17	CDF	$B^+ \to J/\psi\phi K^+$

[1] From an amplitude analysis of the decay $B^+ \to J/\psi\phi K^+$ with a significance of 6.0 σ.
[2] From a fit to the invariant mass spectrum with a significance of 3.1 σ.

$\chi_{c1}(4274)$ WIDTH

VALUE (MeV)	EVTS	DOCUMENT ID	TECN	COMMENT
49 ±12 OUR AVERAGE				
56 ±11 $^{+8}_{-11}$	4289	[1] AAIJ 17C	LHCB	$B^+ \to J/\psi\phi K^+$
$32.3^{+21.9}_{-15.3} \pm 7.6$	22	[2] AALTONEN 17	CDF	$B^+ \to J/\psi\phi K^+$

[1] From an amplitude analysis of the decay $B^+ \to J/\psi\phi K^+$ with a significance of 6.0 σ.
[2] From a fit to the invariant mass spectrum with a significance of 3.1 σ.

$\chi_{c1}(4274)$ DECAY MODES

	Mode	Fraction (Γ_i/Γ)
Γ_1	$J/\psi\phi$	seen

$\chi_{c1}(4274)$ BRANCHING RATIOS

$\Gamma(J/\psi\phi)/\Gamma_{total}$ **Γ_1/Γ**

VALUE	EVTS	DOCUMENT ID	TECN	COMMENT
seen	4289	[1] AAIJ 17C	LHCB	$B^+ \to J/\psi\phi K^+$

[1] From an amplitude analysis of the decay $B^+ \to J/\psi\phi K^+$ with a significance of 6.0 σ.

$\chi_{c1}(4274)$ REFERENCES

AAIJ	17C	PRL 118 022003	R. Aaij *et al.*	(LHCb Collab.) JP
Also		PR D95 012002	R. Aaij *et al.*	(LHCb Collab.)
AALTONEN	17	MPL A32 1750139	T. Altonen *et al.*	(CDF Collab.)

$X(4350)$ $I^G(J^{PC}) = 0^+(?^{?+})$

OMITTED FROM SUMMARY TABLE

Seen by SHEN 10 in the $\gamma\gamma \to J/\psi\phi$. Needs confirmation.

$X(4350)$ MASS

VALUE (MeV)	EVTS	DOCUMENT ID	TECN	COMMENT
$4350.6^{+4.6}_{-5.1} \pm 0.7$	$8.8^{+4.2}_{-3.2}$	[1] SHEN 10	BELL	10.6 $e^+e^- \to e^+e^- J/\psi\phi$

[1] Statistical significance of 3.2 σ.

$X(4350)$ WIDTH

VALUE (MeV)	EVTS	DOCUMENT ID		TECN	COMMENT
$13^{+18}_{-9}\pm4$	$8.8^{+4.2}_{-3.2}$	[1] SHEN	10	BELL	10.6 $e^+e^- \to e^+e^- J/\psi\phi$

[1] Statistical significance of 3.2 σ.

$X(4350)$ DECAY MODES

	Mode	Fraction (Γ_i/Γ)
Γ_1	$J/\psi\phi$	seen
Γ_2	$\gamma\gamma$	seen

$X(4350)$ $\Gamma(i)\Gamma(\gamma\gamma)/\Gamma(\text{total})$

$\Gamma(\gamma\gamma) \times \Gamma(J/\psi\phi)/\Gamma_{\text{total}}$ $\Gamma_2\Gamma_1/\Gamma$

VALUE (eV)	EVTS	DOCUMENT ID		TECN	COMMENT
$6.7^{+3.2}_{-2.4}\pm1.1$	$8.8^{+4.2}_{-3.2}$	[1] SHEN	10	BELL	10.6 $e^+e^- \to e^+e^- J/\psi\phi$
• • • We do not use the following data for averages, fits, limits, etc. • • •					
$1.5^{+0.7}_{-0.6}\pm0.3$	$8.8^{+4.2}_{-3.2}$	[2] SHEN	10	BELL	10.6 $e^+e^- \to e^+e^- J/\psi\phi$

[1] For $J^P = 0^+$. Statistical significance of 3.2 σ.
[2] For $J^P = 2^+$. Statistical significance of 3.2 σ.

$X(4350)$ BRANCHING RATIOS

$\Gamma(J/\psi\phi)/\Gamma_{\text{total}}$ Γ_1/Γ

VALUE	DOCUMENT ID		TECN	COMMENT
seen	[1] SHEN	10	BELL	10.6 $e^+e^- \to e^+e^- J/\psi\phi$

[1] Statistical significance of 3.2 σ.

$\Gamma(\gamma\gamma)/\Gamma_{\text{total}}$ Γ_2/Γ

VALUE	DOCUMENT ID		TECN	COMMENT
seen	[1] SHEN	10	BELL	10.6 $e^+e^- \to e^+e^- J/\psi\phi$

[1] Statistical significance of 3.2 σ.

$X(4350)$ REFERENCES

SHEN 10 PRL 104 112004 C.P. Shen *et al.* (BELLE Collab.)

$\psi(4360)$

$I^G(J^{PC}) = 0^-(1^{--})$
I needs confirmation.

also known as $Y(4360)$; was $X(4360)$

This state shows properties different from a conventional $q\overline{q}$ state. A candidate for an exotic structure. See the review on non-$q\overline{q}$ states.

Seen in radiative return from e^+e^- collisions at $\sqrt{s} = 9.54$–10.58 GeV by AUBERT 07S, WANG 07D, and LEES 14F. See also the review on "Spectroscopy of mesons containing two heavy quarks."

$\psi(4360)$ MASS

VALUE (MeV)	EVTS	DOCUMENT ID		TECN	COMMENT
4368 ±13 OUR AVERAGE		Error includes scale factor of 3.7. See the ideogram below.			
$4320.0\pm10.4\pm7.0$		[1] ABLIKIM	17B	BES3	$e^+e^- \to \pi^+\pi^- J/\psi$
$4383.8\pm4.2\pm0.8$		[2] ABLIKIM	17V	BES3	$e^+e^- \to \pi^+\pi^-\psi(2S)$
$4347 \pm 6 \pm3$	279	[3] WANG	15A	BELL	10.58 $e^+e^- \to \gamma\pi^+\pi^-\psi(2S)$
$4340 \pm16 \pm9$	37	[4] LEES	14F	BABR	10.58 $e^+e^- \to \gamma\pi^+\pi^-\psi(2S)$
• • • We do not use the following data for averages, fits, limits, etc. • • •					
$4383.7\pm2.9\pm6.2$		[5] ZHANG	17B	RVUE	$e^+e^- \to \pi^+\pi^-\psi(2S)$
$4386.4\pm2.1\pm6.4$		[6] ZHANG	17C	RVUE	$e^+e^- \to \pi^+\pi^- J/\psi$ or $\psi(2S)$
$4355 \pm^{9}_{10} \pm9$	74	[7] LIU	08H	RVUE	10.58 $e^+e^- \to \gamma\pi^+\pi^-\psi(2S)$
4324 ± 24		[8] AUBERT	07S	BABR	10.58 $e^+e^- \to \gamma\pi^+\pi^-\psi(2S)$
$4361 \pm 9 \pm9$	47	[4] WANG	07D	BELL	10.58 $e^+e^- \to \gamma\pi^+\pi^-\psi(2S)$

[1] From a three-resonance fit.
[2] From a fit to the cross section for $e^+e^- \to \pi^+\pi^-\psi(2S) \to 2(\pi^+\pi^-)\ell^+\ell^-$ obtained from 16 center-of-mass energies between 4.008 and 4.600 GeV and comprising 5.1 fb^{-1}.
[3] From a two-resonance fit. Supersedes WANG 07D.
[4] From a two-resonance fit.
[5] From a three-resonance fit.
[6] From a combined fit of BELLE, BABAR and BES3 $e^+e^- \to \pi^+\pi^- J/\psi$ and $e^+e^- \to \pi^+\pi^-\psi(2S)$ data.
[7] From a combined fit of AUBERT 07S and WANG 07D data with two resonances.
[8] From a single-resonance fit. Systematic errors not estimated.

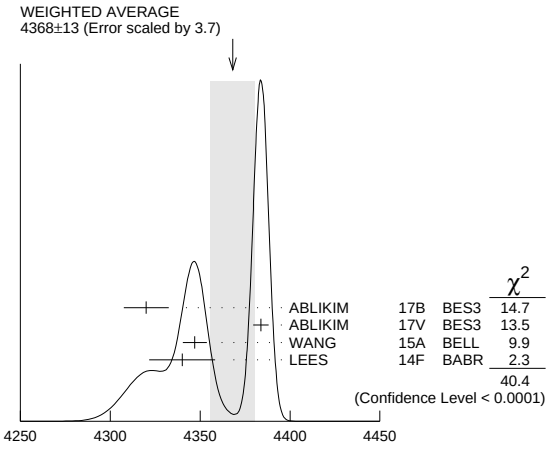

$\psi(4360)$ WIDTH

VALUE (MeV)	EVTS	DOCUMENT ID		TECN	COMMENT
96 ± 7 OUR AVERAGE					
$101.4^{+25.3}_{-19.7}\pm10.2$		[1] ABLIKIM	17B	BES3	$e^+e^- \to \pi^+\pi^- J/\psi$
$84.2\pm12.5\pm2.1$		[2] ABLIKIM	17V	BES3	$e^+e^- \to \pi^+\pi^-\psi(2S)$
$103 \pm 9 \pm5$	279	[3] WANG	15A	BELL	10.58 $e^+e^- \to \gamma\pi^+\pi^-\psi(2S)$
$94 \pm32 \pm13$	37	[4] LEES	14F	BABR	10.58 $e^+e^- \to \gamma\pi^+\pi^-\psi(2S)$
• • • We do not use the following data for averages, fits, limits, etc. • • •					
$94.2\pm7.3\pm2.0$		[5] ZHANG	17B	RVUE	$e^+e^- \to \pi^+\pi^-\psi(2S)$
$96.0\pm6.7\pm2.7$		[6] ZHANG	17C	RVUE	$e^+e^- \to \pi^+\pi^- J/\psi$ or $\psi(2S)$
$103 \pm^{17}_{15} \pm11$	74	[7] LIU	08H	RVUE	10.58 $e^+e^- \to \gamma\pi^+\pi^-\psi(2S)$
172 ± 33		[8] AUBERT	07S	BABR	10.58 $e^+e^- \to \gamma\pi^+\pi^-\psi(2S)$
$74 \pm15 \pm10$	47	[4] WANG	07D	BELL	10.58 $e^+e^- \to \gamma\pi^+\pi^-\psi(2S)$

[1] From a three-resonance fit.
[2] From a fit to the cross section for $e^+e^- \to \pi^+\pi^-\psi(2S) \to 2(\pi^+\pi^-)\ell^+\ell^-$ obtained from 16 center-of-mass energies between 4.008 and 4.600 GeV and comprising 5.1 fb^{-1}.
[3] From a two-resonance fit. Supersedes WANG 07D.
[4] From a two-resonance fit.
[5] From a three-resonance fit.
[6] From a combined fit of BELLE, BABAR and BES3 $e^+e^- \to \pi^+\pi^- J/\psi$ and $e^+e^- \to \pi^+\pi^-\psi(2S)$ data.
[7] From a combined fit of AUBERT 07S and WANG 07D data with two resonances.
[8] From a single-resonance fit. Systematic errors not estimated.

$\psi(4360)$ DECAY MODES

	Mode	Fraction (Γ_i/Γ)
Γ_1	e^+e^-	
Γ_2	$J/\psi\pi^+\pi^-$	
Γ_3	$\psi(2S)\pi^+\pi^-$	seen
Γ_4	$\psi_2(3823)\pi^+\pi^-$	possibly seen
Γ_5	$J/\psi\eta$	
Γ_6	$D^0D^{*-}\pi^+$	
Γ_7	$\chi_{c1}\gamma$	
Γ_8	$\chi_{c2}\gamma$	

$\psi(4360)$ $\Gamma(i) \times \Gamma(e^+e^-)/\Gamma(\text{total})$

$\Gamma(\psi(2S)\pi^+\pi^-) \times \Gamma(e^+e^-)/\Gamma_{\text{total}}$ $\Gamma_3\Gamma_1/\Gamma$

VALUE (eV)	EVTS	DOCUMENT ID		TECN	COMMENT
• • • We do not use the following data for averages, fits, limits, etc. • • •					
$9.2\pm0.6\pm0.6$	279	[1] WANG	15A	BELL	10.58 $e^+e^- \to \gamma\pi^+\pi^-\psi(2S)$
$10.9\pm0.6\pm0.7$	279	[2] WANG	15A	BELL	10.58 $e^+e^- \to \gamma\pi^+\pi^-\psi(2S)$
$6.0\pm1.0\pm0.5$	37	[3] LEES	14F	BABR	10.58 $e^+e^- \to \gamma\pi^+\pi^-\psi(2S)$
$7.2\pm1.0\pm0.6$	37	[4] LEES	14F	BABR	10.58 $e^+e^- \to \gamma\pi^+\pi^-\psi(2S)$
$11.1^{+1.3}_{-1.2}$	74	[5] LIU	08H	RVUE	10.58 $e^+e^- \to \gamma\pi^+\pi^-\psi(2S)$
12.3 ± 1.2	74	[6] LIU	08H	RVUE	10.58 $e^+e^- \to \gamma\pi^+\pi^-\psi(2S)$
$10.4\pm1.7\pm1.5$	47	[3] WANG	07D	BELL	10.58 $e^+e^- \to \gamma\pi^+\pi^-\psi(2S)$
$11.8\pm1.8\pm1.4$	47	[4] WANG	07D	BELL	10.58 $e^+e^- \to \gamma\pi^+\pi^-\psi(2S)$

[1] Solution I of two equivalent solutions from a fit using two interfering resonances. Supersedes WANG 07D.
[2] Solution II of two equivalent solutions from a fit using two interfering resonances. Supersedes WANG 07D.
[3] Solution I of two equivalent solutions in a fit using two interfering resonances.
[4] Solution II of two equivalent solutions in a fit using two interfering resonances.
[5] Solution I in a combined fit of AUBERT 07S and WANG 07D data with two resonances.
[6] Solution II in a combined fit of AUBERT 07S and WANG 07D data with two resonances.

$\Gamma(J/\psi\eta) \times \Gamma(e^+e^-)/\Gamma_{total}$ **$\Gamma_5\Gamma_1/\Gamma$**

VALUE (eV)	CL%	DOCUMENT ID		TECN	COMMENT
• • • We do not use the following data for averages, fits, limits, etc. • • •					
<6.8	90	WANG	13B	BELL	$e^+e^- \to J/\psi\eta\gamma$

$\Gamma(\chi_{c1}\gamma) \times \Gamma(e^+e^-)/\Gamma_{total}$ **$\Gamma_7\Gamma_1/\Gamma$**

VALUE (eV)	CL%	DOCUMENT ID		TECN	COMMENT
<0.57	90	[1] HAN	15	BELL	10.58 $e^+e^- \to \chi_{c1}\gamma$

[1] Using B($\eta \to \gamma\gamma$) = (39.41 ± 0.21)%.

$\Gamma(\chi_{c2}\gamma) \times \Gamma(e^+e^-)/\Gamma_{total}$ **$\Gamma_8\Gamma_1/\Gamma$**

VALUE (eV)	CL%	DOCUMENT ID		TECN	COMMENT
<1.9	90	[1] HAN	15	BELL	10.58 $e^+e^- \to \chi_{c2}\gamma$

[1] Using B($\eta \to \gamma\gamma$) = (39.41 ± 0.21)%.

$\psi(4360)$ BRANCHING RATIOS

$\Gamma(D^0D^{*-}\pi^+)/\Gamma(\psi(2S)\pi^+\pi^-)$ **Γ_6/Γ_3**

VALUE	CL%	DOCUMENT ID		TECN	COMMENT
<8	90	PAKHLOVA	09	BELL	$e^+e^- \to \psi(4360) \to D^0D^{*-}\pi^+$

$\Gamma(\psi(2S)\pi^+\pi^-)/\Gamma_{total}$ **Γ_3/Γ**

VALUE	DOCUMENT ID		TECN	COMMENT
seen	[1] ABLIKIM	17V	BES3	$e^+e^- \to \pi^+\pi^-\psi(2S)$

[1] From a fit to the cross section for $e^+e^- \to \pi^+\pi^-\psi(2S) \to 2(\pi^+\pi^-)\ell^+\ell^-$ obtained from 16 center-of-mass energies between 4.008 and 4.600 GeV and comprising 5.1 fb^{-1}.

$\Gamma(\psi(2S)\pi^+\pi^-)/\Gamma(J/\psi\pi^+\pi^-)$ **Γ_3/Γ_2**

VALUE	DOCUMENT ID		TECN	COMMENT
• • • We do not use the following data for averages, fits, limits, etc. • • •				
(0.81 ± 0.12 ± 0.13) to (42 ± 15 ± 15)	[1] ZHANG	17C	RVUE	$e^+e^- \to \pi^+\pi^- J/\psi$ or $\psi(2S)$

[1] From a combined fit of BELLE, BABAR and BES3 $e^+e^- \to \pi^+\pi^- J/\psi$ and $e^+e^- \to \pi^+\pi^-\psi(2S)$ data.

$\Gamma(\psi_2(3823)\pi^+\pi^-)/\Gamma_{total}$ **Γ_4/Γ**

VALUE	EVTS	DOCUMENT ID		TECN	COMMENT
possibly seen	19	[1] ABLIKIM	15S	BES3	$e^+e^- \to \pi^+\pi^-\chi_{c1}\gamma$

[1] From a fit of $e^+e^- \to \pi^+\pi^-\psi_2(3823)$, $\psi_2(3823) \to \chi_{c1}\gamma$ cross sections taken at $\sqrt{s}$ values of 4.23, 4.26, 4.36, 4.42, and 4.60 GeV to the $\psi(4360)$ line shape.

$\Gamma(D^0D^{*-}\pi^+)/\Gamma_{total} \times \Gamma(e^+e^-)/\Gamma_{total}$ **$\Gamma_6/\Gamma \times \Gamma_1/\Gamma$**

VALUE	CL%	DOCUMENT ID		TECN	COMMENT
<0.72 × 10^{-6}	90	[1] PAKHLOVA	09	BELL	$e^+e^- \to \psi(4360) \to D^0D^{*-}\pi^+$

[1] Using 4355^{+9}_{-10} ± 9 MeV for the mass of $\psi(4360)$.

$\psi(4360)$ REFERENCES

ABLIKIM	17B	PRL 118 092001	M. Ablikim *et al.*	(BES III Collab.)
ABLIKIM	17V	PR D96 032004	M. Ablikim *et al.*	(BES III Collab.)
ZHANG	17B	PR D96 054008	J. Zhang, J. Zhang	
ZHANG	17C	EPJ C77 727	J. Zhang, L. Yuan	
ABLIKIM	15S	PRL 115 011803	M. Ablikim *et al.*	(BES III Collab.)
HAN	15	PR D92 012011	Y.L. Han *et al.*	(BELLE Collab.)
WANG	15A	PR D91 112007	X.L. Wang *et al.*	(BELLE Collab.)
LEES	14F	PR D89 111103	J.P. Lees *et al.*	(BABAR Collab.)
WANG	13B	PR D87 051101	X.L. Wang *et al.*	(BELLE Collab.)
PAKHLOVA	09	PR D80 091101	G. Pakhlova *et al.*	(BELLE Collab.)
LIU	08H	PR D78 014032	Z.Q. Liu, X.S. Qin, C.Z. Yuan	
AUBERT	07S	PRL 98 212001	B. Aubert *et al.*	(BABAR Collab.)
WANG	07D	PRL 99 142002	X.L. Wang *et al.*	(BELLE Collab.)

$\psi(4390)$

$I^G(J^{PC}) = 0^-(1^{--})$
I needs confirmation.

OMITTED FROM SUMMARY TABLE
was $X(4390)$
This state shows properties different from a conventional $q\overline{q}$ state.
A candidate for an exotic structure. See the review on non-$q\overline{q}$ states.

$\psi(4390)$ MASS

VALUE (MeV)	DOCUMENT ID		TECN	COMMENT
4391.5$^{+6.3}_{-6.8}$±1.0	ABLIKIM	17G	BES3	$e^+e^- \to \pi^+\pi^- h_c$

$\psi(4390)$ WIDTH

VALUE (MeV)	DOCUMENT ID		TECN	COMMENT
139.5$^{+16.2}_{-20.6}$±0.6	ABLIKIM	17G	BES3	$e^+e^- \to \pi^+\pi^- h_c$

$\psi(4390)$ DECAY MODES

	Mode	Fraction (Γ_i/Γ)
Γ_1	$\pi^+\pi^- h_c$	seen

$\psi(4390)$ BRANCHING RATIOS

$\Gamma(\pi^+\pi^- h_c)/\Gamma_{total}$ **Γ_1/Γ**

VALUE	DOCUMENT ID		TECN	COMMENT
seen	ABLIKIM	17G	BES3	$e^+e^- \to \pi^+\pi^- h_c$

$\psi(4390)$ REFERENCES

ABLIKIM	17G	PRL 118 092002	M. Ablikim *et al.*	(BES III Collab.)

$\psi(4415)$

$I^G(J^{PC}) = 0^-(1^{--})$

$\psi(4415)$ MASS

VALUE (MeV)		DOCUMENT ID		TECN	COMMENT
4421 ± 4 OUR ESTIMATE					
4415.1± 7.9		[1] ABLIKIM	08D	BES2	$e^+e^- \to$ hadrons
• • • We do not use the following data for averages, fits, limits, etc. • • •					
4412	±15	[2] MO	10	RVUE	$e^+e^- \to$ hadrons
4411	± 7	[3] PAKHLOVA	08A	BELL	10.6 $e^+e^- \to D^0D^-\pi^+\gamma$
4425	± 6	[4] SETH	05A	RVUE	$e^+e^- \to$ hadrons
4429	± 9	[5] SETH	05A	RVUE	$e^+e^- \to$ hadrons
4417	±10	BRANDELIK	78C	DASP	e^+e^-
4414	± 7	SIEGRIST	76	MRK1	e^+e^-

[1] Reanalysis of data presented in BAI 02C. From a global fit over the center-of-mass energy region 3.7–5.0 GeV covering the $\psi(3770)$, $\psi(4040)$, $\psi(4160)$, and $\psi(4415)$ resonances. Phase angle fixed in the fit to $\delta = (234 \pm 88)^\circ$.
[2] Reanalysis of data presented in BAI 00 and BAI 02C. From a global fit over the center-of-mass energy 3.8-4.8 GeV covering the $\psi(4040)$, $\psi(4160)$ and $\psi(4415)$ resonances and including interference effects.
[3] Systematic uncertainties not estimated.
[4] From a fit to Crystal Ball (OSTERHELD 86) data.
[5] From a fit to BES (BAI 02C) data.

$\psi(4415)$ WIDTH

VALUE (MeV)		DOCUMENT ID		TECN	COMMENT
62 ±20 OUR ESTIMATE					
71.5±19.0		[6] ABLIKIM	08D	BES2	$e^+e^- \to$ hadrons
• • • We do not use the following data for averages, fits, limits, etc. • • •					
118	±32	[7] MO	10	RVUE	$e^+e^- \to$ hadrons
77	±20	[8] PAKHLOVA	08A	BELL	10.6 $e^+e^- \to D^0D^-\pi^+\gamma$
119	±16	[9] SETH	05A	RVUE	$e^+e^- \to$ hadrons
118	±35	[10] SETH	05A	RVUE	$e^+e^- \to$ hadrons
66	±15	BRANDELIK	78C	DASP	e^+e^-
33	±10	SIEGRIST	76	MRK1	e^+e^-

[6] Reanalysis of data presented in BAI 02C. From a global fit over the center-of-mass energy region 3.7–5.0 GeV covering the $\psi(3770)$, $\psi(4040)$, $\psi(4160)$, and $\psi(4415)$ resonances. Phase angle fixed in the fit to $\delta = (234 \pm 88)^\circ$.
[7] Reanalysis of data presented in BAI 00 and BAI 02C. From a global fit over the center-of-mass energy 3.8-4.8 GeV covering the $\psi(4040)$, $\psi(4160)$ and $\psi(4415)$ resonances and including interference effects.
[8] Systematic uncertainties not estimated.
[9] From a fit to Crystal Ball (OSTERHELD 86) data.
[10] From a fit to BES (BAI 02C) data.

$\psi(4415)$ DECAY MODES

Due to the complexity of the $c\overline{c}$ threshold region, in this listing, "seen" ("not seen") means that a cross section for the mode in question has been measured at effective $\sqrt{s}$ near this particle's central mass value, more (less) than 2σ above zero, without regard to any peaking behavior in $\sqrt{s}$ or absence thereof. See mode listing(s) for details and references.

	Mode	Fraction (Γ_i/Γ)	Confidence level
Γ_1	$D\overline{D}$	seen	
Γ_2	$D^0\overline{D}^0$	seen	
Γ_3	D^+D^-	seen	
Γ_4	$D^*\overline{D}$ + c.c.	seen	
Γ_5	$D^*(2007)^0\overline{D}^0$ + c.c.	seen	
Γ_6	$D^*(2010)^+D^-$ + c.c.	seen	
Γ_7	$D^*\overline{D}^*$	seen	
Γ_8	$D^*(2007)^0\overline{D}^*(2007)^0$ + c.c.	seen	
Γ_9	$D^*(2010)^+D^*(2010)^-$ + c.c.	seen	
Γ_{10}	$D^0D^-\pi^+$ (excl. $D^*(2007)^0\overline{D}^0$ +c.c., $D^*(2010)^+D^-$ +c.c.	< 2.3 %	90%
Γ_{11}	$D\overline{D}_2^*(2460) \to D^0D^-\pi^+$+c.c.	(10 ± 4) %	
Γ_{12}	$D^0D^{*-}\pi^+$+c.c.	< 11 %	90%
Γ_{13}	$D_s^+D_s^-$	not seen	
Γ_{14}	$\omega\chi_{c2}$	possibly seen	
Γ_{15}	$D_s^{*+}D_s^-$ +c.c.	seen	
Γ_{16}	$D_s^{*+}D_s^{*-}$	not seen	
Γ_{17}	$\psi_2(3823)\pi^+\pi^-$	possibly seen	
Γ_{18}	$J/\psi\eta$	$< 6 \times 10^{-3}$	90%
Γ_{19}	$\chi_{c1}\gamma$	$< 8 \times 10^{-4}$	90%
Γ_{20}	$\chi_{c2}\gamma$	$< 4 \times 10^{-3}$	90%
Γ_{21}	e^+e^-	$(9.4 \pm 3.2) \times 10^{-6}$	

$\psi(4415)$ PARTIAL WIDTHS

$\Gamma(e^+e^-)$ Γ_{21}

VALUE (keV)	DOCUMENT ID		TECN	COMMENT
0.58±0.07 OUR ESTIMATE				
0.35±0.12	[11] ABLIKIM	08D	BES2	$e^+e^- \to$ hadrons
• • • We do not use the following data for averages, fits, limits, etc. • • •				
0.4 to 0.8	[12] MO	10	RVUE	$e^+e^- \to$ hadrons
0.72±0.11	[13] SETH	05A	RVUE	$e^+e^- \to$ hadrons
0.64±0.23	[14] SETH	05A	RVUE	$e^+e^- \to$ hadrons
0.49±0.13	BRANDELIK	78C	DASP	e^+e^-
0.44±0.14	SIEGRIST	76	MRK1	e^+e^-

[11] Reanalysis of data presented in BAI 02C. From a global fit over the center-of-mass energy region 3.7–5.0 GeV covering the $\psi(3770)$, $\psi(4040)$, $\psi(4160)$, and $\psi(4415)$ resonances. Phase angle fixed in the fit to $\delta = (234 \pm 88)^\circ$.

[12] Reanalysis of data presented in BAI 00 and BAI 02C. From a global fit over the center-of-mass energy 3.8-4.8 GeV covering the $\psi(4040)$, $\psi(4160)$ and $\psi(4415)$ resonances and including interference effects. Four sets of solutions are obtained with the same fit quality, mass and total width, but with different e^+e^- partial widths. We quote only the range of values.

[13] From a fit to Crystal Ball (OSTERHELD 86) data.

[14] From a fit to BES (BAI 02C) data.

$\psi(4415)$ $\Gamma(i) \times \Gamma(e^+e^-)/\Gamma(\text{total})$

$\Gamma(J/\psi\eta) \times \Gamma(e^+e^-)/\Gamma_{\text{total}}$ $\Gamma_{18}\Gamma_{21}/\Gamma$

VALUE (eV)	CL%	DOCUMENT ID		TECN	COMMENT
<3.6	90	WANG	13B	BELL	$e^+e^- \to J/\psi\eta\gamma$

$\Gamma(\chi_{c1}\gamma) \times \Gamma(e^+e^-)/\Gamma_{\text{total}}$ $\Gamma_{19}\Gamma_{21}/\Gamma$

VALUE (eV)	CL%	DOCUMENT ID		TECN	COMMENT
<0.47	90	[15] HAN	15	BELL	10.58 $e^+e^- \to \chi_{c1}\gamma$

[15] Using $B(\eta \to \gamma\gamma) = (39.41 \pm 0.21)\%$.

$\Gamma(\chi_{c2}\gamma) \times \Gamma(e^+e^-)/\Gamma_{\text{total}}$ $\Gamma_{20}\Gamma_{21}/\Gamma$

VALUE (eV)	CL%	DOCUMENT ID		TECN	COMMENT
<2.3	90	[16] HAN	15	BELL	10.58 $e^+e^- \to \chi_{c2}\gamma$

[16] Using $B(\eta \to \gamma\gamma) = (39.41 \pm 0.21)\%$.

$\psi(4415)$ BRANCHING RATIOS

$\Gamma(D^0\overline{D}^0)/\Gamma_{\text{total}}$ Γ_2/Γ

VALUE	DOCUMENT ID		TECN	COMMENT
seen	PAKHLOVA	08	BELL	$e^+e^- \to D^0\overline{D}^0\gamma$
• • • We do not use the following data for averages, fits, limits, etc. • • •				
not seen	AUBERT	09M	BABR	$e^+e^- \to D^0\overline{D}^0\gamma$

$\Gamma(D^+D^-)/\Gamma_{\text{total}}$ Γ_3/Γ

VALUE	DOCUMENT ID		TECN	COMMENT
seen	PAKHLOVA	08	BELL	$e^+e^- \to D^+D^-\gamma$
• • • We do not use the following data for averages, fits, limits, etc. • • •				
not seen	AUBERT	09M	BABR	$e^+e^- \to D^+D^-\gamma$

$\Gamma(D\overline{D})/\Gamma(D^*\overline{D}^*)$ Γ_1/Γ_7

VALUE	DOCUMENT ID		TECN	COMMENT
0.14±0.12±0.03	AUBERT	09M	BABR	$e^+e^- \to \gamma D^{(*)}\overline{D}^{(*)}$

$\Gamma(D^*(2007)^0\overline{D}^0 + \text{c.c.})/\Gamma_{\text{total}}$ Γ_5/Γ

VALUE	DOCUMENT ID		TECN	COMMENT
seen	AUBERT	09M	BABR	$e^+e^- \to D^{*0}\overline{D}^0\gamma$

$\Gamma(D^*(2010)^+D^- + \text{c.c.})/\Gamma_{\text{total}}$ Γ_6/Γ

VALUE	DOCUMENT ID		TECN	COMMENT
seen	[17] ZHUKOVA	18	BELL	$e^+e^- \to D^{*+}D^-\gamma$
seen	AUBERT	09M	BABR	$e^+e^- \to D^{*+}D^-\gamma$
• • • We do not use the following data for averages, fits, limits, etc. • • •				
seen	PAKHLOVA	07	BELL	$e^+e^- \to D^{*+}D^-\gamma$

[17] Supersedes PAKHLOVA 07.

$\Gamma(D^*\overline{D} + \text{c.c.})/\Gamma(D^*\overline{D}^*)$ Γ_4/Γ_7

VALUE	DOCUMENT ID		TECN	COMMENT
0.17±0.25±0.03	AUBERT	09M	BABR	$e^+e^- \to \gamma D^{(*)}\overline{D}^{(*)}$

$\Gamma(D^*(2007)^0\overline{D}^*(2007)^0 + \text{c.c.})/\Gamma_{\text{total}}$ Γ_8/Γ

VALUE	DOCUMENT ID		TECN	COMMENT
seen	AUBERT	09M	BABR	$e^+e^- \to D^{*0}\overline{D}^{*0}\gamma$

$\Gamma(D^*(2010)^+D^*(2010)^- + \text{c.c.})/\Gamma_{\text{total}}$ Γ_9/Γ

VALUE	DOCUMENT ID		TECN	COMMENT
seen	[18] ZHUKOVA	18	BELL	$e^+e^- \to D^{*+}D^{*-}\gamma$
seen	AUBERT	09M	BABR	$e^+e^- \to D^{*+}D^{*-}\gamma$
• • • We do not use the following data for averages, fits, limits, etc. • • •				
seen	PAKHLOVA	07	BELL	$e^+e^- \to D^{*+}D^{*-}\gamma$

[18] Supersedes PAKHLOVA 07.

$\Gamma(D\overline{D}_2^*(2460) \to D^0D^-\pi^+ + \text{c.c.})/\Gamma_{\text{total}}$ Γ_{11}/Γ

VALUE (units 10^{-2})	DOCUMENT ID		TECN	COMMENT
10.5±2.4±3.8	[19] PAKHLOVA	08A	BELL	10.6 $e^+e^- \to D^0D^-\pi^+\gamma$

[19] Using 4421 ± 4 MeV for the mass and 62 ± 20 MeV for the width of $\psi(4415)$.

$\Gamma(D^0D^-\pi^+ (\text{excl. } D^*(2007)^0\overline{D}^0 + \text{c.c.}, D^*(2010)^+D^- + \text{c.c.}))/\Gamma(D\overline{D}_2^*(2460) \to D^0D^-\pi^+ + \text{c.c.})$ Γ_{10}/Γ_{11}

VALUE	CL%	DOCUMENT ID		TECN	COMMENT
<0.22	90	[20] PAKHLOVA	08A	BELL	10.6 $e^+e^- \to D^0D^-\pi^+\gamma$

[20] Using 4421 ± 4 MeV for the mass and 62 ± 20 MeV for the width of $\psi(4415)$.

$\Gamma(D^0D^{*-}\pi^+ + \text{c.c.})/\Gamma_{\text{total}} \times \Gamma(e^+e^-)/\Gamma_{\text{total}}$ $\Gamma_{12}/\Gamma \times \Gamma_{21}/\Gamma$

VALUE	CL%	DOCUMENT ID		TECN	COMMENT
<0.99 × 10^{-6}	90	[21] PAKHLOVA	09	BELL	$e^+e^- \to D^0D^{*-}\pi^+$

[21] Using 4421 ± 4 MeV for the mass of $\psi(4415)$.

$\Gamma(D_s^+D_s^-)/\Gamma_{\text{total}}$ Γ_{13}/Γ

VALUE	DOCUMENT ID		TECN	COMMENT
not seen	PAKHLOVA	11	BELL	$e^+e^- \to D_s^+D_s^-\gamma$
not seen	DEL-AMO-SA...10N		BABR	$e^+e^- \to D_s^+D_s^-\gamma$

$\Gamma(\omega\chi_{c2})/\Gamma_{\text{total}}$ Γ_{14}/Γ

VALUE	DOCUMENT ID		TECN	COMMENT
possibly seen	ABLIKIM	16A	BES3	$e^+e^- \to \gamma\pi^+\pi^-\pi^0\ell^+\ell^-$

$\Gamma(D_s^{*+}D_s^- + \text{c.c.})/\Gamma_{\text{total}}$ Γ_{15}/Γ

VALUE	DOCUMENT ID		TECN	COMMENT
seen	PAKHLOVA	11	BELL	$e^+e^- \to D_s^{*+}D_s^-\gamma$
seen	DEL-AMO-SA...10N		BABR	$e^+e^- \to D_s^{*+}D_s^-\gamma$

$\Gamma(D_s^{*+}D_s^{*-})/\Gamma_{\text{total}}$ Γ_{16}/Γ

VALUE	DOCUMENT ID		TECN	COMMENT
not seen	PAKHLOVA	11	BELL	$e^+e^- \to D_s^{*+}D_s^{*-}\gamma$
not seen	DEL-AMO-SA...10N		BABR	$e^+e^- \to D_s^{*+}D_s^{*-}\gamma$

$\Gamma(\psi_2(3823)\pi^+\pi^-)/\Gamma_{\text{total}}$ Γ_{17}/Γ

VALUE	EVTS	DOCUMENT ID		TECN	COMMENT
possibly seen	19	[22] ABLIKIM	15S	BES3	$e^+e^- \to \pi^+\pi^-\chi_{c1}\gamma$

[22] From a fit of $e^+e^- \to \pi^+\pi^-\psi_2(3823)$, $\psi_2(3823) \to \chi_{c1}\gamma$ cross sections taken at $\sqrt{s}$ values of 4.23, 4.26, 4.36, 4.42, and 4.60 GeV to the $\psi(4415)$ line shape.

$\psi(4415)$ REFERENCES

ZHUKOVA	18	PR D97 012002	V. Zhukova *et al.*	(BELLE Collab.)
ABLIKIM	16A	PR D93 011102	M. Ablikim *et al.*	(BES III Collab.)
ABLIKIM	15S	PRL 115 011803	M. Ablikim *et al.*	(BES III Collab.)
HAN	15	PR D92 012011	Y.L. Han *et al.*	(BELLE Collab.)
WANG	13B	PR D87 051101	X.L. Wang *et al.*	(BELLE Collab.)
PAKHLOVA	11	PR D83 011101	G. Pakhlova *et al.*	(BELLE Collab.)
DEL-AMO-SA...	10N	PR D82 052004	P. del Amo Sanchez *et al.*	(BABAR Collab.)
MO	10	PR D82 077501	X.H. Mo, C.Z. Yuan, P. Wang	(BHEP)
AUBERT	09M	PR D79 092001	B. Aubert *et al.*	(BABAR Collab.)
PAKHLOVA	09	PR D80 091101	G. Pakhlova *et al.*	(BELLE Collab.)
ABLIKIM	08D	PL B660 315	M. Ablikim *et al.*	(BES Collab.)
PAKHLOVA	08	PR D77 011103	G. Pakhlova *et al.*	(BELLE Collab.)
PAKHLOVA	08A	PRL 100 062001	G. Pakhlova *et al.*	(BELLE Collab.)
PAKHLOVA	07	PRL 98 092001	G. Pakhlova *et al.*	(BELLE Collab.)
SETH	05A	PR D72 017501	K.K. Seth	
BAI	02C	PRL 88 101802	J.Z. Bai *et al.*	(BES Collab.)
BAI	00	PRL 84 594	J.Z. Bai *et al.*	(BES Collab.)
OSTERHELD	86	SLAC-PUB-4160	A. Osterheld *et al.*	(SLAC Crystal Ball Collab.)
BRANDELIK	78C	PL 76B 361	R. Brandelik *et al.*	(DASP Collab.)
SIEGRIST	76	PRL 36 700	J.L. Siegrist *et al.*	(LBL, SLAC)

$Z_c(4430)$

$I^G(J^{PC}) = 1^+(1^{+-})$
I, *G*, *C* need confirmation.

was $X(4430)^\pm$

Properties incompatible with a $q\overline{q}$ structure (exotic state). See the review on non-$q\overline{q}$ states.

First seen by CHOI 08 in $B \to K\pi^+\psi(2S)$ decays, confirmed by AAIJ 14AG, and confirmed in a model-independent way by AAIJ 15BH. Also seen by CHILIKIN 14 in $B \to K^+\pi J/\psi$ decays. J^P was determined by CHILIKIN 13 and AAIJ 14AG.

$Z_c(4430)$ MASS

VALUE (MeV)	DOCUMENT ID		TECN	COMMENT
4478^{+15}_{-18} OUR AVERAGE				
$4475 \pm 7^{+15}_{-25}$	[1] AAIJ	14AG	LHCB	$B^0 \to K^+\pi^-\psi(2S)$
$4485 \pm 22^{+28}_{-11}$	[1] CHILIKIN	13	BELL	$B^0 \to K^+\pi^-\psi(2S)$
• • • We do not use the following data for averages, fits, limits, etc. • • •				
4443^{+15+19}_{-12-13}	[2] MIZUK	09	BELL	$B \to K\pi^+\psi(2S)$
$4433 \pm 4 \pm 2$	[3] CHOI	08	BELL	$B \to K\pi^+\psi(2S)$

[1] From a four-dimensional amplitude analysis.
[2] From a Dalitz plot analysis. Superseded by CHILIKIN 13.
[3] Superseded by MIZUK 09 and CHILIKIN 13.

$Z_c(4430)$ WIDTH

VALUE (MeV)	DOCUMENT ID		TECN	COMMENT
181 ± 31 OUR AVERAGE				
$172 \pm 13^{+37}_{-34}$	[1] AAIJ	14AG	LHCB	$B^0 \to K^+\pi^-\psi(2S)$
200^{+41+26}_{-46-35}	[1] CHILIKIN	13	BELL	$B^0 \to K^+\pi^-\psi(2S)$
• • • We do not use the following data for averages, fits, limits, etc. • • •				
107^{+86+74}_{-43-56}	[2] MIZUK	09	BELL	$B \to K\pi^+\psi(2S)$
45^{+18+30}_{-13-13}	[3] CHOI	08	BELL	$B \to K\pi^+\psi(2S)$

[1] From a four-dimensional amplitude analysis.
[2] From a Dalitz plot analysis. Superseded by CHILIKIN 13.
[3] Superseded by MIZUK 09 and CHILIKIN 13.

$Z_c(4430)$ DECAY MODES

	Mode	Fraction (Γ_i/Γ)
Γ_1	$\pi^+\psi(2S)$	seen
Γ_2	$\pi^+ J/\psi$	seen

$Z_c(4430)$ BRANCHING RATIOS

$\Gamma(\pi^+\psi(2S))/\Gamma_{\text{total}}$ Γ_1/Γ

VALUE	DOCUMENT ID		TECN	COMMENT
seen	[1] AAIJ	14AG	LHCB	$B^0 \to K^+\pi^-\psi(2S)$
seen	[2] CHILIKIN	13	BELL	$B^0 \to K^+\pi^-\psi(2S)$
• • • We do not use the following data for averages, fits, limits, etc. • • •				
not seen	[3] AUBERT	09AA	BABR	$B \to K\pi^+\psi(2S)$
seen	[4] MIZUK	09	BELL	$B \to K\pi^+\psi(2S)$

[1] From a four-dimensional amplitude analysis. No product of branching fractions quoted.
[2] From a four-dimensional amplitude analysis. Measured a product of branching fractions $B(B^0 \to Z_c(4430)^- K^+) \times B(Z_c(4430)^- \to \psi(2S)\pi^-) = (6.0^{+1.7+2.5}_{-2.0-1.4}) \times 10^{-5}$.
[3] AUBERT 09AA quotes $B(B^+ \to \overline{K}^0 Z_c(4430)^+) \times B(Z_c(4430)^+ \to \pi^+\psi(2S)) < 4.7\times10^{-5}$ and $B(\overline{B}^0 \to K^- Z_c(4430)^+) \times B(Z_c(4430)^+ \to \pi^+\psi(2S)) < 3.1\times10^{-5}$ at 95% CL.
[4] Measured a product of branching fractions $B(\overline{B}^0 \to K^- Z_c(4430)^+) \times B(Z_c(4430)^+ \to \pi^+\psi(2S)) = (3.2^{+1.8+5.3}_{-0.9-1.6}) \times 10^{-5}$. Superseded by CHILIKIN 13.

$\Gamma(\pi^+ J/\psi)/\Gamma_{\text{total}}$ Γ_2/Γ

VALUE	DOCUMENT ID		TECN	COMMENT
seen	[1] CHILIKIN	14	BELL	$\overline{B}^0 \to K^-\pi^+ J/\psi$
• • • We do not use the following data for averages, fits, limits, etc. • • •				
not seen	[2] AUBERT	09AA	BABR	$B \to K\pi^+ J/\psi$

[1] CHILIKIN 14 reports $B(\overline{B}^0 \to Z_c(4430)^+ K^-) \times B(Z_c(4430)^+ \to J/\psi\pi^+) = (5.4^{+4.0+1.1}_{-1.0-0.9}) \times 10^{-6}$.
[2] AUBERT 09AA quotes $B(B^+ \to \overline{K}^0 Z_c(4430)^+) \times B(Z_c(4430)^+ \to \pi^+ J/\psi) < 1.5\times10^{-5}$ and $B(\overline{B}^0 \to K^- Z_c(4430)^+) \times B(Z_c(4430)^+ \to \pi^+ J/\psi) < 0.4\times10^{-5}$ at 95% CL.

$Z_c(4430)$ REFERENCES

AAIJ	15BH	PR D92 112009	R. Aaij *et al.*	(LHCb Collab.)
AAIJ	14AG	PRL 112 222002	R. Aaij *et al.*	(LHCb Collab.) JP
CHILIKIN	14	PR D90 112009	K. Chilikin *et al.*	(BELLE Collab.)
CHILIKIN	13	PR D88 074026	K. Chilikin *et al.*	(BELLE Collab.) JP
AUBERT	09AA	PR D79 112001	B. Aubert *et al.*	(BABAR Collab.)
MIZUK	09	PR D80 031104	R. Mizuk *et al.*	(BELLE Collab.)
CHOI	08	PRL 100 142001	S.-K. Choi *et al.*	(BELLE Collab.)

$\chi_{c0}(4500)$

$I^G(J^{PC}) = 0^+(0^{++})$

OMITTED FROM SUMMARY TABLE
was $X(4500)$

This state shows properties different from a conventional $q\overline{q}$ state. A candidate for an exotic structure. See the review on non-$q\overline{q}$ states.

Seen by AAIJ 17C in $B^+ \to \chi_{c0} K^+$, $\chi_{c0} \to J/\psi\phi$ using an amplitude analysis of $B^+ \to J/\psi\phi K^+$ with a significance (accounting for systematic uncertainties) of 6.1 σ.

$\chi_{c0}(4500)$ MASS

VALUE (MeV)	EVTS	DOCUMENT ID		TECN	COMMENT
$4506 \pm 11^{+12}_{-15}$	4289	[1] AAIJ	17C	LHCB	$B^+ \to J/\psi\phi K^+$

[1] From an amplitude analysis of the decay $B^+ \to J/\psi\phi K^+$ with a significance of 6.1 σ.

$\chi_{c0}(4500)$ WIDTH

VALUE (MeV)	EVTS	DOCUMENT ID		TECN	COMMENT
$92 \pm 21^{+21}_{-20}$	4289	[1] AAIJ	17C	LHCB	$B^+ \to J/\psi\phi K^+$

[1] From an amplitude analysis of the decay $B^+ \to J/\psi\phi K^+$ with a significance of 6.1 σ.

$\chi_{c0}(4500)$ DECAY MODES

	Mode
Γ_1	$J/\psi\phi$

$\chi_{c0}(4500)$ BRANCHING RATIOS

$\Gamma(J/\psi\phi)/\Gamma_{\text{total}}$ Γ_1/Γ

VALUE	EVTS	DOCUMENT ID		TECN	COMMENT
seen	4289	[1] AAIJ	17C	LHCB	$B^+ \to J/\psi\phi K^+$

[1] From an amplitude analysis of the decay $B^+ \to J/\psi\phi K^+$ with a significance of 6.1 σ.

$\chi_{c0}(4500)$ REFERENCES

AAIJ	17C	PRL 118 022003	R. Aaij *et al.*	(LHCb Collab.) JP
Also		PR D95 012002	R. Aaij *et al.*	(LHCb Collab.)

$\psi(4660)$

$I^G(J^{PC}) = 0^-(1^{--})$
I needs confirmation.

also known as $Y(4660)$; was $X(4660)$

This state shows properties different from a conventional $q\overline{q}$ state. A candidate for an exotic structure. See the review on non-$q\overline{q}$ states.

Seen in radiative return from e^+e^- collisions at $\sqrt{s} = 9.54$–10.58 GeV by WANG 07D. Also obtained in a combined fit of WANG 07D, AUBERT 07S, and LEES 14F. See also the review on "Spectroscopy of mesons containing two heavy quarks."

$\psi(4660)$ MASS

VALUE (MeV)			EVTS	DOCUMENT ID		TECN	COMMENT
4643	**± 9**	**OUR AVERAGE**		Error includes scale factor of 1.2.			
4652	±10	±11	279	[1] WANG	15A	BELL	10.58 $e^+e^- \to \gamma\pi^+\pi^-\psi(2S)$
4669	±21	± 3	37	[2] LEES	14F	BABR	10.58 $e^+e^- \to \gamma\pi^+\pi^-\psi(2S)$
4634	$^{+\ 8}_{-\ 7}$	$^{+\ 5}_{-\ 8}$	142	[3] PAKHLOVA	08B	BELL	$e^+e^- \to \Lambda_c^+\Lambda_c^-$
• • • We do not use the following data for averages, fits, limits, etc. • • •							
4652.5	± 3.4	± 1.1		[4] DAI	17	RVUE	$e^+e^- \to \Lambda_c^+\Lambda_c^-$
4645.2	± 9.5	± 6.0		[5] ZHANG	17B	RVUE	$e^+e^- \to \pi^+\pi^-\psi(2S)$
4646.4	± 9.7	± 4.8		[6] ZHANG	17C	RVUE	$e^+e^- \to \pi^+\pi^- J/\psi$ or $\psi(2S)$
4661	$^{+\ 9}_{-\ 8}$	± 6	44	[7] LIU	08H	RVUE	10.58 $e^+e^- \to \gamma\pi^+\pi^-\psi(2S)$
4664	±11	± 5	44	WANG	07D	BELL	10.58 $e^+e^- \to \gamma\pi^+\pi^-\psi(2S)$

[1] From a two-resonance fit. Supersedes WANG 07D.
[2] From a two-resonance fit.
[3] The $\pi^+\pi^-\psi(2S)$ and $\Lambda_c^+\Lambda_c^-$ states are not necessarily the same.
[4] The pole parameters are extracted from the speed plot.
[5] From a three-resonance fit.
[6] From a combined fit of BELLE, BABAR and BES3 $e^+e^- \to \pi^+\pi^- J/\psi$ and $e^+e^- \to \pi^+\pi^-\psi(2S)$ data.
[7] From a combined fit of AUBERT 07S and WANG 07D data with two resonances.

$\psi(4660)$ WIDTH

VALUE (MeV)			EVTS	DOCUMENT ID		TECN	COMMENT
72	**±11**	**OUR AVERAGE**					
68	±11	± 5	279	[1] WANG	15A	BELL	10.58 $e^+e^- \to \gamma\pi^+\pi^-\psi(2S)$
104	±48	±10	37	[2] LEES	14F	BABR	10.58 $e^+e^- \to \gamma\pi^+\pi^-\psi(2S)$
92	$^{+40}_{-24}$	$^{+10}_{-21}$	142	[3] PAKHLOVA	08B	BELL	$e^+e^- \to \Lambda_c^+\Lambda_c^-$
• • • We do not use the following data for averages, fits, limits, etc. • • •							
62.6	± 5.6	± 4.3		[4] DAI	17	RVUE	$e^+e^- \to \Lambda_c^+\Lambda_c^-$
113.8	±18.1	± 3.4		[5] ZHANG	17B	RVUE	$e^+e^- \to \pi^+\pi^-\psi(2S)$
103.5	±15.6	± 4.0		[6] ZHANG	17C	RVUE	$e^+e^- \to \pi^+\pi^- J/\psi$ or $\psi(2S)$
42	$^{+17}_{-12}$	± 6	44	[7] LIU	08H	RVUE	10.58 $e^+e^- \to \gamma\pi^+\pi^-\psi(2S)$
48	±15	± 3	44	WANG	07D	BELL	10.58 $e^+e^- \to \gamma\pi^+\pi^-\psi(2S)$

[1] From a two-resonance fit. Supersedes WANG 07D.
[2] From a two-resonance fit.
[3] The $\pi^+\pi^-\psi(2S)$ and $\Lambda_c^+\Lambda_c^-$ states are not necessarily the same.
[4] The pole parameters are extracted from the speed plot.
[5] From a three-resonance fit.
[6] From a combined fit of BELLE, BABAR and BES3 $e^+e^- \to \pi^+\pi^- J/\psi$ and $e^+e^- \to \pi^+\pi^-\psi(2S)$ data.
[7] From a combined fit of AUBERT 07S and WANG 07D data with two resonances.

$\psi(4660)$ DECAY MODES

	Mode	Fraction (Γ_i/Γ)
Γ_1	e^+e^-	
Γ_2	$\psi(2S)\pi^+\pi^-$	seen
Γ_3	$J/\psi\eta$	
Γ_4	$D^0D^{*-}\pi^+$	
Γ_5	$\chi_{c1}\gamma$	
Γ_6	$\chi_{c2}\gamma$	
Γ_7	$\Lambda_c^+\Lambda_c^-$	

$\psi(4660)$ $\Gamma(i) \times \Gamma(e^+e^-)/\Gamma(\text{total})$

$\Gamma(\psi(2S)\pi^+\pi^-) \times \Gamma(e^+e^-)/\Gamma_{\text{total}}$ $\quad \Gamma_2\Gamma_1/\Gamma$

VALUE (eV)	EVTS	DOCUMENT ID		TECN	COMMENT
• • • We do not use the following data for averages, fits, limits, etc. • • •					
2.0±0.3±0.2	279	[1] WANG	15A	BELL	10.58 $e^+e^- \to \gamma\pi^+\pi^-\psi(2S)$
8.1±1.1±1.0	279	[2] WANG	15A	BELL	10.58 $e^+e^- \to \gamma\pi^+\pi^-\psi(2S)$
2.7±1.3±0.5	37	[3] LEES	14F	BABR	10.58 $e^+e^- \to \gamma\pi^+\pi^-\psi(2S)$
7.5±1.7±0.7	37	[4] LEES	14F	BABR	10.58 $e^+e^- \to \gamma\pi^+\pi^-\psi(2S)$
$2.2^{+0.7}_{-0.6}$	44	[5] LIU	08H	RVUE	10.58 $e^+e^- \to \gamma\pi^+\pi^-\psi(2S)$
5.9±1.6	44	[6] LIU	08H	RVUE	10.58 $e^+e^- \to \gamma\pi^+\pi^-\psi(2S)$
3.0±0.9±0.3	44	[3] WANG	07D	BELL	10.58 $e^+e^- \to \gamma\pi^+\pi^-\psi(2S)$
7.6±1.8±0.8	44	[4] WANG	07D	BELL	10.58 $e^+e^- \to \gamma\pi^+\pi^-\psi(2S)$

[1] Solution I of two equivalent solutions from a fit using two interfering resonances. Supersedes WANG 07D.
[2] Solution II of two equivalent solutions from a fit using two interfering resonances. Supersedes WANG 07D.
[3] Solution I of two equivalent solutions in a fit using two interfering resonances.
[4] Solution II of two equivalent solutions in a fit using two interfering resonances.
[5] Solution I in a combined fit of AUBERT 07S and WANG 07D data with two resonances.
[6] Solution II in a combined fit of AUBERT 07S and WANG 07D data with two resonances.

$\Gamma(J/\psi\eta) \times \Gamma(e^+e^-)/\Gamma_{\text{total}}$ $\quad \Gamma_3\Gamma_1/\Gamma$

VALUE (eV)	CL%	DOCUMENT ID		TECN	COMMENT
• • • We do not use the following data for averages, fits, limits, etc. • • •					
<0.94	90	WANG	13B	BELL	$e^+e^- \to J/\psi\eta\gamma$

$\Gamma(\chi_{c1}\gamma) \times \Gamma(e^+e^-)/\Gamma_{\text{total}}$ $\quad \Gamma_5\Gamma_1/\Gamma$

VALUE (eV)	CL%	DOCUMENT ID		TECN	COMMENT
<0.45	90	[1] HAN	15	BELL	10.58 $e^+e^- \to \chi_{c1}\gamma$

[1] Using B($\eta \to \gamma\gamma$) = (39.41 ± 0.21)%.

$\Gamma(\chi_{c2}\gamma) \times \Gamma(e^+e^-)/\Gamma_{\text{total}}$ $\quad \Gamma_6\Gamma_1/\Gamma$

VALUE (eV)	CL%	DOCUMENT ID		TECN	COMMENT
<2.1	90	[1] HAN	15	BELL	10.58 $e^+e^- \to \chi_{c2}\gamma$

[1] Using B($\eta \to \gamma\gamma$) = (39.41 ± 0.21)%.

$\psi(4660)$ BRANCHING RATIOS

$\Gamma(D^0D^{*-}\pi^+)/\Gamma(\psi(2S)\pi^+\pi^-)$ $\quad \Gamma_4/\Gamma_2$

VALUE	CL%	DOCUMENT ID		TECN	COMMENT
<10	90	PAKHLOVA	09	BELL	$e^+e^- \to D^0D^{*-}\pi^+$

$\Gamma(D^0D^{*-}\pi^+)/\Gamma_{\text{total}} \times \Gamma(e^+e^-)/\Gamma_{\text{total}}$ $\quad \Gamma_4/\Gamma \times \Gamma_1/\Gamma$

VALUE	CL%	DOCUMENT ID		TECN	COMMENT
$<0.37 \times 10^{-6}$	90	[1] PAKHLOVA	09	BELL	$e^+e^- \to D^0D^{*-}\pi^+$

[1] Using 4664 ± 11 ± 5 MeV for the mass of $\psi(4660)$.

$\Gamma(\Lambda_c^+\Lambda_c^-)/\Gamma_{\text{total}} \times \Gamma(e^+e^-)/\Gamma_{\text{total}}$ $\quad \Gamma_7/\Gamma \times \Gamma_1/\Gamma$

VALUE (units 10^{-6})	EVTS	DOCUMENT ID		TECN	COMMENT
$\mathbf{0.68^{+0.16+0.29}_{-0.15-0.30}}$	142	[1] PAKHLOVA	08B	BELL	$e^+e^- \to \Lambda_c^+\Lambda_c^-$

[1] The $\pi^+\pi^-\psi(2S)$ and $\Lambda_c^+\Lambda_c^-$ states are not necessarily the same.

$\psi(4660)$ REFERENCES

DAI	17	PR D96 116001	L.-Y. Dai, J. Haidenbauer, U.-G. Meissner	(JULI+)
ZHANG	17B	PR D96 054008	J. Zhang, J. Zhang	
ZHANG	17C	EPJ C77 727	J. Zhang, L. Yuan	
HAN	15	PR D92 012011	Y.L. Han *et al.*	(BELLE Collab.)
WANG	15A	PR D91 112007	X.L. Wang *et al.*	(BELLE Collab.)
LEES	14F	PR D89 111103	J.P. Lees *et al.*	(BABAR Collab.)
WANG	13B	PR D87 051101	X.L. Wang *et al.*	(BELLE Collab.)
PAKHLOVA	09	PR D80 091101	G. Pakhlova *et al.*	(BELLE Collab.)
LIU	08H	PR D78 014032	Z.Q. Liu, X.S. Qin, C.Z. Yuan	
PAKHLOVA	08B	PRL 101 172001	G. Pakhlova *et al.*	(BELLE Collab.)
AUBERT	07S	PRL 98 212001	B. Aubert *et al.*	(BABAR Collab.)
WANG	07D	PRL 99 142002	X.L. Wang *et al.*	(BELLE Collab.)

Meson Particle Listings

$\chi_{c0}(4700)$

$\chi_{c0}(4700)$

$I^G(J^{PC}) = 0^+(0^{++})$

OMITTED FROM SUMMARY TABLE
was $X(4700)$

This state shows properties different from a conventional $q\overline{q}$ state. A candidate for an exotic structure. See the review on non-$q\overline{q}$ states.

Seen by AAIJ 17C in $B^+ \to \chi_{c0} K^+$, $\chi_{c0} \to J/\psi\phi$ using an amplitude analysis of $B^+ \to J/\psi\phi K^+$ with a significance (accounting for systematic uncertainties) of 5.6 σ.

$\chi_{c0}(4700)$ MASS

VALUE (MeV)	EVTS	DOCUMENT ID		TECN	COMMENT
$4704 \pm 10^{+14}_{-24}$	4289	[1] AAIJ	17C	LHCB	$B^+ \to J/\psi\phi K^+$

[1] From an amplitude analysis of the decay $B^+ \to J/\psi\phi K^+$ with a significance of 5.6 σ.

$\chi_{c0}(4700)$ WIDTH

VALUE (MeV)	EVTS	DOCUMENT ID		TECN	COMMENT
$120 \pm 31^{+42}_{-33}$	4289	[1] AAIJ	17C	LHCB	$B^+ \to J/\psi\phi K^+$

[1] From an amplitude analysis of the decay $B^+ \to J/\psi\phi K^+$ with a significance of 5.6 σ.

$\chi_{c0}(4700)$ DECAY MODES

	Mode	Fraction (Γ_i/Γ)
Γ_1	$J/\psi\phi$	seen

$\chi_{c0}(4700)$ BRANCHING RATIOS

$\Gamma(J/\psi\phi)/\Gamma_{total}$ Γ_1/Γ

VALUE	EVTS	DOCUMENT ID		TECN	COMMENT
seen	4289	[1] AAIJ	17C	LHCB	$B^+ \to J/\psi\phi K^+$

[1] From an amplitude analysis of the decay $B^+ \to J/\psi\phi K^+$ with a significance of 5.6 σ.

$\chi_{c0}(4700)$ REFERENCES

AAIJ	17C	PRL 118 022003	R. Aaij *et al.*	(LHCb Collab.) JP
Also		PR D95 012002	R. Aaij *et al.*	(LHCb Collab.)

$b\bar{b}$ MESONS (including possibly non-$q\bar{q}$ states)

See the related review(s):

Bottomonium System

Width Determination of the Υ States

$\eta_b(1S)$

$I^G(J^{PC}) = 0^+(0^{-+})$

Quantum numbers shown are quark-model predictions. Observed in radiative decay of the $\Upsilon(3S)$, therefore $C = +$.

$\eta_b(1S)$ MASS

VALUE (MeV)	EVTS	DOCUMENT ID		TECN	COMMENT
9399.0± 2.3 OUR AVERAGE		Error includes scale factor of 1.6. See the ideogram below.			
9400.7± 1.7± 1.6	33.1k	TAMPONI	15	BELL	$e^+e^- \to \gamma\eta +$ hadrons
9402.4± 1.5± 1.8	34k	[1] MIZUK	12	BELL	$e^+e^- \to \gamma\pi^+\pi^- +$ hadrons
9391.8± 6.6± 2.0	2.3k	[2] BONVICINI	10	CLEO	$\Upsilon(3S) \to \gamma X$
$9394.2^{+4.8}_{-}$ $^{}_{4.9}\pm$ 2.0	13k	[2] AUBERT	09AQ	BABR	$\Upsilon(2S) \to \gamma X$
$9388.9^{+3.1}_{-}$ $^{}_{2.3}\pm$ 2.7	19k	[2] AUBERT	08V	BABR	$\Upsilon(3S) \to \gamma X$
• • • We do not use the following data for averages, fits, limits, etc. • • •					
9393.2± 3.4± 2.3	10	[2,3] DOBBS	12		$\Upsilon(2S) \to \gamma$ hadrons
9300 ±20 ±20		HEISTER	02D	ALEP	181–209 e^+e^-

[1] With floating width. Not independent of the corresponding mass difference measurement.
[2] Assuming $\Gamma_{\eta_b(1S)} = 10$ MeV. Not independent of the corresponding γ energy or mass difference measurements.
[3] Obtained by analyzing CLEO III data but not authored by the CLEO Collaboration.

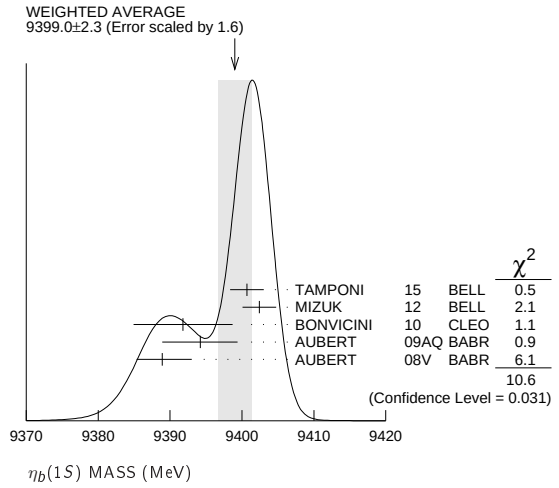

$m_{\Upsilon(1S)} - m_{\eta_b}$

VALUE (MeV)	EVTS	DOCUMENT ID		TECN	COMMENT
62.3±3.2 OUR AVERAGE		Error includes scale factor of 1.8. See the ideogram below.			
57.9±1.5±1.8	34k	[4] MIZUK	12	BELL	$e^+e^- \to \gamma\pi^+\pi^-$ + hadrons
68.5±6.6±2.0	2.3 ± 0.5k	[5] BONVICINI	10	CLEO	$\Upsilon(3S) \to \gamma X$
$66.1^{+4.8}_{-4.9}\pm$2.0	13 ± 5k	[5] AUBERT	09AQ	BABR	$\Upsilon(2S) \to \gamma X$
$71.4^{+2.3}_{-3.1}\pm$2.7	19 ± 3k	[5] AUBERT	08V	BABR	$\Upsilon(3S) \to \gamma X$
• • • We do not use the following data for averages, fits, limits, etc. • • •					
67.1±3.4±2.3	10^{+5}_{-4}	[5,6] DOBBS	12		$\Upsilon(2S) \to \gamma$ hadrons

[4] With floating width. Not independent of the corresponding mass measurement.
[5] Assuming $\Gamma_{\eta_b(1S)} = 10$ MeV. Not independent of the corresponding γ energy or mass measurements.
[6] Obtained by analyzing CLEO III data but not authored by the CLEO Collaboration.

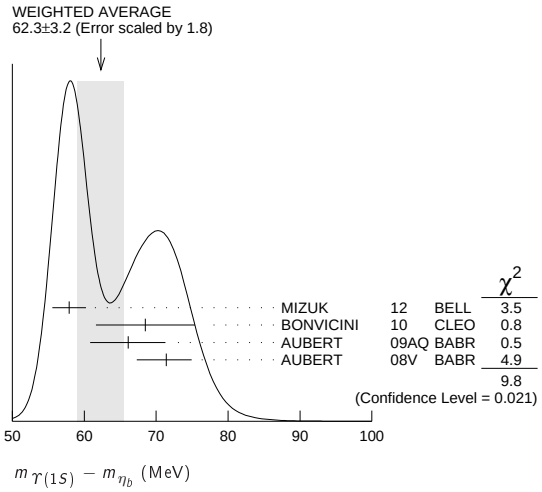

γ ENERGY IN $\Upsilon(3S)$ DECAY

VALUE (MeV)	EVTS	DOCUMENT ID		TECN	COMMENT
$920.6^{+2.8}_{-3.2}$ OUR AVERAGE					
918.6±6.0±1.9	2.3 ± 0.5k	[7] BONVICINI	10	CLEO	$\Upsilon(3S) \to \gamma X$
$921.2^{+2.1}_{-2.8}\pm$2.4	19 ± 3k	[7] AUBERT	08V	BABR	$\Upsilon(3S) \to \gamma X$

[7] Assuming $\Gamma_{\eta_b(1S)} = 10$ MeV. Not independent of the corresponding mass or mass difference measurements.

γ ENERGY IN $\Upsilon(2S)$ DECAY

VALUE (MeV)	EVTS	DOCUMENT ID		TECN	COMMENT
$609.3^{+4.6}_{-4.5}\pm1.9$	13 ± 5k	[8] AUBERT	09AQ	BABR	$\Upsilon(2S) \to \gamma X$

[8] Assuming $\Gamma_{\eta_b(1S)} = 10$ MeV. Not independent of the corresponding mass or mass difference measurements.

$\eta_b(1S)$ WIDTH

VALUE (MeV)	EVTS	DOCUMENT ID		TECN	COMMENT
10 $^{+5}_{-4}$ OUR AVERAGE					
8 $^{+6}_{-5}$ ±5	33.1k	[9] TAMPONI	15	BELL	$e^+e^- \to \gamma\eta +$ hadrons
$10.8^{+4.0}_{-3.7}{}^{+4.5}_{-2.0}$	34k	[9] MIZUK	12	BELL	$e^+e^- \to \gamma\pi^+\pi^- +$ hadrons

[9] With floating mass.

$\eta_b(1S)$ DECAY MODES

	Mode	Fraction (Γ_i/Γ)	Confidence level
Γ_1	hadrons	seen	
Γ_2	$3h^+3h^-$	not seen	
Γ_3	$2h^+2h^-$	not seen	
Γ_4	$4h^+4h^-$		
Γ_5	$\gamma\gamma$	not seen	
Γ_6	$\mu^+\mu^-$	$<9\times10^{-3}$	90%
Γ_7	$\tau^+\tau^-$	<8 %	90%

$\eta_b(1S)$ Γ(i)$\Gamma(\gamma\gamma)/\Gamma$(total)

$\Gamma(3h^+3h^-) \times \Gamma(\gamma\gamma)/\Gamma_{\text{total}}$ **$\Gamma_2\Gamma_5/\Gamma$**

VALUE (eV)	CL%	DOCUMENT ID		TECN	COMMENT
• • • We do not use the following data for averages, fits, limits, etc. • • •					
<470	95	ABDALLAH	06	DLPH	161–209 e^+e^-
<132	95	HEISTER	02D	ALEP	181–209 e^+e^-

$\Gamma(2h^+2h^-) \times \Gamma(\gamma\gamma)/\Gamma_{\text{total}}$ **$\Gamma_3\Gamma_5/\Gamma$**

VALUE (eV)	CL%	DOCUMENT ID		TECN	COMMENT
• • • We do not use the following data for averages, fits, limits, etc. • • •					
<190	95	ABDALLAH	06	DLPH	161–209 e^+e^-
< 48	95	HEISTER	02D	ALEP	181–209 e^+e^-

Meson Particle Listings

$\eta_b(1S)$, $\Upsilon(1S)$

$\Gamma(4h^+4h^-) \times \Gamma(\gamma\gamma)/\Gamma_{total}$ **$\Gamma_4\Gamma_5/\Gamma$**

VALUE (eV)	CL%	DOCUMENT ID		TECN	COMMENT
• • • We do not use the following data for averages, fits, limits, etc. • • •					
<660	95	ABDALLAH	06	DLPH	161–209 e^+e^-

$\eta_b(1S)$ BRANCHING RATIOS

$\Gamma(\text{hadrons})/\Gamma_{total}$ **Γ_1/Γ**

VALUE	EVTS	DOCUMENT ID		TECN	COMMENT
seen	34k	MIZUK	12	BELL	$e^+e^- \to \gamma\pi^+\pi^-$ + hadrons

$\Gamma(\mu^+\mu^-)/\Gamma_{total}$ **Γ_6/Γ**

VALUE	CL%	DOCUMENT ID		TECN	COMMENT
$<9\times10^{-3}$	90	[10] AUBERT	09Z	BABR	$e^+e^- \to \Upsilon(2S,3S) \to \gamma\eta_b$

[10] Obtained using $B(\Upsilon(2S) \to \gamma\eta_b) = (4.2^{+1.1}_{-1.0} \pm 0.9)\times10^{-4}$ and $B(\Upsilon(3S) \to \gamma\eta_b) = (4.8 \pm 0.5 \pm 0.6)\times10^{-4}$. This limit is equivalent to $B(\eta_b \to \mu^+\mu^-) = (-0.25 \pm 0.51 \pm 0.33)\%$ measurement.

$\Gamma(\tau^+\tau^-)/\Gamma_{total}$ **Γ_7/Γ**

VALUE	CL%	DOCUMENT ID		TECN	COMMENT
$<8\times10^{-2}$	90	AUBERT	09P	BABR	$e^+e^- \to \gamma\tau^+\tau^-$

$\eta_b(1S)$ REFERENCES

TAMPONI	15	PRL 115 142001	U. Tamponi *et al.*	(BELLE Collab.)
DOBBS	12	PRL 109 082001	S. Dobbs *et al.*	
MIZUK	12	PRL 109 232002	R. Mizuk *et al.*	(BELLE Collab.)
BONVICINI	10	PR D81 031104	G. Bonvicini *et al.*	(CLEO Collab.)
AUBERT	09AQ	PRL 103 161801	B. Aubert *et al.*	(BABAR Collab.)
AUBERT	09P	PRL 103 181801	B. Aubert *et al.*	(BABAR Collab.)
AUBERT	09Z	PRL 103 081803	B. Aubert *et al.*	(BABAR Collab.)
AUBERT	08V	PRL 101 071801	B. Aubert *et al.*	(BABAR Collab.)
ABDALLAH	06	PL B634 340	J.M. Abdallah *et al.*	(DELPHI Collab.)
HEISTER	02D	PL B530 56	A. Heister *et al.*	(ALEPH Collab.)

$\Upsilon(1S)$

$I^G(J^{PC}) = 0^-(1^{--})$

$\Upsilon(1S)$ MASS

VALUE (MeV)	DOCUMENT ID		TECN	COMMENT
9460.30±0.26 OUR AVERAGE	Error includes scale factor of 3.3.			
9460.51±0.09±0.05	[1] ARTAMONOV	00	MD1	$e^+e^- \to$ hadrons
9459.97±0.11±0.07	MACKAY	84	REDE	$e^+e^- \to$ hadrons
• • • We do not use the following data for averages, fits, limits, etc. • • •				
9460.60±0.09±0.05	[2,3] BARU	92B	REDE	$e^+e^- \to$ hadrons
9460.59±0.12	BARU	86	REDE	$e^+e^- \to$ hadrons
9460.6 ±0.4	[3,4] ARTAMONOV	84	REDE	$e^+e^- \to$ hadrons

[1] Reanalysis of BARU 92B and ARTAMONOV 84 using new electron mass (COHEN 87).
[2] Superseding BARU 86.
[3] Superseded by ARTAMONOV 00.
[4] Value includes data of ARTAMONOV 82.

$\Upsilon(1S)$ WIDTH

VALUE (keV)	DOCUMENT ID
54.02±1.25 OUR EVALUATION	See the Note on "Width Determinations of the Υ States"

$\Upsilon(1S)$ DECAY MODES

	Mode	Fraction (Γ_i/Γ)	Scale factor/ Confidence level
Γ_1	$\tau^+\tau^-$	(2.60 ±0.10) %	
Γ_2	e^+e^-	(2.38 ±0.11) %	
Γ_3	$\mu^+\mu^-$	(2.48 ±0.05) %	
	Hadronic decays		
Γ_4	ggg	(81.7 ±0.7) %	
Γ_5	γgg	(2.2 ±0.6) %	
Γ_6	$\eta'(958)$ anything	(2.94 ±0.24) %	
Γ_7	$J/\psi(1S)$ anything	(5.4 ±0.4) $\times10^{-4}$	S=1.4
Γ_8	$J/\psi(1S)\eta_c$	< 2.2 $\times10^{-6}$	CL=90%
Γ_9	$J/\psi(1S)\chi_{c0}$	< 3.4 $\times10^{-6}$	CL=90%
Γ_{10}	$J/\psi(1S)\chi_{c1}$	(3.9 ±1.2) $\times10^{-6}$	
Γ_{11}	$J/\psi(1S)\chi_{c2}$	< 1.4 $\times10^{-6}$	CL=90%
Γ_{12}	$J/\psi(1S)\eta_c(2S)$	< 2.2 $\times10^{-6}$	CL=90%
Γ_{13}	$J/\psi(1S)X(3940)$	< 5.4 $\times10^{-6}$	CL=90%
Γ_{14}	$J/\psi(1S)X(4160)$	< 5.4 $\times10^{-6}$	CL=90%
Γ_{15}	$X(4350)$ anything, $X \to J/\psi(1S)\phi$	< 8.1 $\times10^{-6}$	CL=90%
Γ_{16}	$Z_c(3900)^\pm$ anything, $Z_c \to J/\psi(1S)\pi^\pm$	< 1.3 $\times10^{-5}$	CL=90%
Γ_{17}	$Z_c(4200)^\pm$ anything, $Z_c \to J/\psi(1S)\pi^\pm$	< 6.0 $\times10^{-5}$	CL=90%
Γ_{18}	$Z_c(4430)^\pm$ anything, $Z_c \to J/\psi(1S)\pi^\pm$	< 4.9 $\times10^{-5}$	CL=90%
Γ_{19}	$X^\pm_{cs}$ anything, $X \to J/\psi K^\pm$	< 5.7 $\times10^{-6}$	CL=90%
Γ_{20}	$\chi_{c1}(3872)$ anything, $\chi_{c1} \to J/\psi(1S)\pi^+\pi^-$	< 9.5 $\times10^{-6}$	CL=90%
Γ_{21}	$\psi(4260)$ anything, $\psi \to J/\psi(1S)\pi^+\pi^-$	< 3.8 $\times10^{-5}$	CL=90%
Γ_{22}	$\psi(4260)$ anything, $\psi \to J/\psi(1S)K^+K^-$	< 7.5 $\times10^{-6}$	CL=90%
Γ_{23}	$\chi_{c1}(4140)$ anything, $\chi_{c1} \to J/\psi(1S)\phi$	< 5.2 $\times10^{-6}$	CL=90%
Γ_{24}	χ_{c0} anything	< 4 $\times10^{-3}$	CL=90%
Γ_{25}	χ_{c1} anything	(1.90 ±0.35) $\times10^{-4}$	
Γ_{26}	$\chi_{c1}(1P)X_{tetra}$	< 3.78 $\times10^{-5}$	CL=90%
Γ_{27}	χ_{c2} anything	(2.8 ±0.8) $\times10^{-4}$	
Γ_{28}	$\psi(2S)$ anything	(1.23 ±0.20) $\times10^{-4}$	
Γ_{29}	$\psi(2S)\eta_c$	< 3.6 $\times10^{-6}$	CL=90%
Γ_{30}	$\psi(2S)\chi_{c0}$	< 6.5 $\times10^{-6}$	CL=90%
Γ_{31}	$\psi(2S)\chi_{c1}$	< 4.5 $\times10^{-6}$	CL=90%
Γ_{32}	$\psi(2S)\chi_{c2}$	< 2.1 $\times10^{-6}$	CL=90%
Γ_{33}	$\psi(2S)\eta_c(2S)$	< 3.2 $\times10^{-6}$	CL=90%
Γ_{34}	$\psi(2S)X(3940)$	< 2.9 $\times10^{-6}$	CL=90%
Γ_{35}	$\psi(2S)X(4160)$	< 2.9 $\times10^{-6}$	CL=90%
Γ_{36}	$\psi(4260)$ anything, $\psi \to \psi(2S)\pi^+\pi^-$	< 7.9 $\times10^{-5}$	CL=90%
Γ_{37}	$\psi(4360)$ anything, $\psi \to \psi(2S)\pi^+\pi^-$	< 5.2 $\times10^{-5}$	CL=90%
Γ_{38}	$\psi(4660)$ anything, $\psi \to \psi(2S)\pi^+\pi^-$	< 2.2 $\times10^{-5}$	CL=90%
Γ_{39}	$X(4050)^\pm$ anything, $X \to \psi(2S)\pi^\pm$	< 8.8 $\times10^{-5}$	CL=90%
Γ_{40}	$Z_c(4430)^\pm$ anything, $Z_c \to \psi(2S)\pi^\pm$	< 6.7 $\times10^{-5}$	CL=90%
Γ_{41}	$\rho\pi$	< 3.68 $\times10^{-6}$	CL=90%
Γ_{42}	$\omega\pi^0$	< 3.90 $\times10^{-6}$	CL=90%
Γ_{43}	$\pi^+\pi^-$	< 5 $\times10^{-4}$	CL=90%
Γ_{44}	K^+K^-	< 5 $\times10^{-4}$	CL=90%
Γ_{45}	$p\overline{p}$	< 5 $\times10^{-4}$	CL=90%
Γ_{46}	$\pi^+\pi^-\pi^0$	(2.1 ±0.8) $\times10^{-6}$	
Γ_{47}	ϕK^+K^-	(2.4 ±0.5) $\times10^{-6}$	
Γ_{48}	$\omega\pi^+\pi^-$	(4.5 ±1.0) $\times10^{-6}$	
Γ_{49}	$K^*(892)^0K^-\pi^+$ + c.c.	(4.4 ±0.8) $\times10^{-6}$	
Γ_{50}	$\phi f_2'(1525)$	< 1.63 $\times10^{-6}$	CL=90%
Γ_{51}	$\omega f_2(1270)$	< 1.79 $\times10^{-6}$	CL=90%
Γ_{52}	$\rho(770)a_2(1320)$	< 2.24 $\times10^{-6}$	CL=90%
Γ_{53}	$K^*(892)^0\overline{K}_2^*(1430)^0$ + c.c.	(3.0 ±0.8) $\times10^{-6}$	
Γ_{54}	$K_1(1270)^\pm K^\mp$	< 2.41 $\times10^{-6}$	CL=90%
Γ_{55}	$K_1(1400)^\pm K^\mp$	(1.0 ±0.4) $\times10^{-6}$	
Γ_{56}	$b_1(1235)^\pm\pi^\mp$	< 1.25 $\times10^{-6}$	CL=90%
Γ_{57}	$\pi^+\pi^-\pi^0\pi^0$	(1.28 ±0.30) $\times10^{-5}$	
Γ_{58}	$K^0_SK^+\pi^-$ + c.c.	(1.6 ±0.4) $\times10^{-6}$	
Γ_{59}	$K^*(892)^0\overline{K}^0$ + c.c.	(2.9 ±0.9) $\times10^{-6}$	
Γ_{60}	$K^*(892)^-K^+$ + c.c.	< 1.11 $\times10^{-6}$	CL=90%
Γ_{61}	$f_1(1285)$ anything	(4.6 ±3.1) $\times10^{-3}$	
Γ_{62}	$D^*(2010)^\pm$ anything	(2.52 ±0.20) %	
Γ_{63}	$f_1(1285)X_{tetra}$	< 6.24 $\times10^{-5}$	CL=90%
Γ_{64}	^2H anything	(2.85 ±0.25) $\times10^{-5}$	
Γ_{65}	Sum of 100 exclusive modes	(1.200±0.017) %	
	Radiative decays		
Γ_{66}	$\gamma\pi^+\pi^-$	(6.3 ±1.8) $\times10^{-5}$	
Γ_{67}	$\gamma\pi^0\pi^0$	(1.7 ±0.7) $\times10^{-5}$	
Γ_{68}	$\gamma\pi^0\eta$	< 2.4 $\times10^{-6}$	CL=90%
Γ_{69}	γK^+K^-	[a] (1.14 ±0.13) $\times10^{-5}$	
Γ_{70}	$\gamma p\overline{p}$	[b] < 6 $\times10^{-6}$	CL=90%
Γ_{71}	$\gamma 2h^+2h^-$	(7.0 ±1.5) $\times10^{-4}$	
Γ_{72}	$\gamma 3h^+3h^-$	(5.4 ±2.0) $\times10^{-4}$	
Γ_{73}	$\gamma 4h^+4h^-$	(7.4 ±3.5) $\times10^{-4}$	
Γ_{74}	$\gamma\pi^+\pi^-K^+K^-$	(2.9 ±0.9) $\times10^{-4}$	
Γ_{75}	$\gamma 2\pi^+2\pi^-$	(2.5 ±0.9) $\times10^{-4}$	
Γ_{76}	$\gamma 3\pi^+3\pi^-$	(2.5 ±1.2) $\times10^{-4}$	
Γ_{77}	$\gamma 2\pi^+2\pi^-K^+K^-$	(2.4 ±1.2) $\times10^{-4}$	

Γ_{78}	$\gamma\pi^+\pi^- p\overline{p}$	(1.5	± 0.6)	$\times 10^{-4}$	
Γ_{79}	$\gamma 2\pi^+ 2\pi^- p\overline{p}$	(4	± 6)	$\times 10^{-5}$	
Γ_{80}	$\gamma 2K^+ 2K^-$	(2.0	± 2.0)	$\times 10^{-5}$	
Γ_{81}	$\gamma\eta'(958)$	$<$ 1.9		$\times 10^{-6}$	CL=90%
Γ_{82}	$\gamma\eta$	$<$ 1.0		$\times 10^{-6}$	CL=90%
Γ_{83}	$\gamma f_0(980)$	$<$ 3		$\times 10^{-5}$	CL=90%
Γ_{84}	$\gamma f_2'(1525)$	(3.8	± 0.9)	$\times 10^{-5}$	
Γ_{85}	$\gamma f_2(1270)$	(1.01	± 0.09)	$\times 10^{-4}$	
Γ_{86}	$\gamma\eta(1405)$	$<$ 8.2		$\times 10^{-5}$	CL=90%
Γ_{87}	$\gamma f_0(1500)$	$<$ 1.5		$\times 10^{-5}$	CL=90%
Γ_{88}	$\gamma f_0(1710)$	$<$ 2.6		$\times 10^{-4}$	CL=90%
Γ_{89}	$\gamma f_0(1710) \to \gamma K^+ K^-$	$<$ 7		$\times 10^{-6}$	CL=90%
Γ_{90}	$\gamma f_0(1710) \to \gamma\pi^0\pi^0$	$<$ 1.4		$\times 10^{-6}$	CL=90%
Γ_{91}	$\gamma f_0(1710) \to \gamma\eta\eta$	$<$ 1.8		$\times 10^{-6}$	CL=90%
Γ_{92}	$\gamma f_4(2050)$	$<$ 5.3		$\times 10^{-5}$	CL=90%
Γ_{93}	$\gamma f_0(2200) \to \gamma K^+ K^-$	$<$ 2		$\times 10^{-4}$	CL=90%
Γ_{94}	$\gamma f_J(2220) \to \gamma K^+ K^-$	$<$ 8		$\times 10^{-7}$	CL=90%
Γ_{95}	$\gamma f_J(2220) \to \gamma\pi^+\pi^-$	$<$ 6		$\times 10^{-7}$	CL=90%
Γ_{96}	$\gamma f_J(2220) \to \gamma p\overline{p}$	$<$ 1.1		$\times 10^{-6}$	CL=90%
Γ_{97}	$\gamma\eta(2225) \to \gamma\phi\phi$	$<$ 3		$\times 10^{-3}$	CL=90%
Γ_{98}	$\gamma\eta_c(1S)$	$<$ 5.7		$\times 10^{-5}$	CL=90%
Γ_{99}	$\gamma\chi_{c0}$	$<$ 6.5		$\times 10^{-4}$	CL=90%
Γ_{100}	$\gamma\chi_{c1}$	$<$ 2.3		$\times 10^{-5}$	CL=90%
Γ_{101}	$\gamma\chi_{c2}$	$<$ 7.6		$\times 10^{-6}$	CL=90%
Γ_{102}	$\gamma\chi_{c1}(3872) \to \pi^+\pi^- J/\psi$	$<$ 1.6		$\times 10^{-6}$	CL=90%
Γ_{103}	$\gamma\chi_{c1}(3872) \to \pi^+\pi^-\pi^0 J/\psi$	$<$ 2.8		$\times 10^{-6}$	CL=90%
Γ_{104}	$\gamma X(3915) \to \omega J/\psi$	$<$ 3.0		$\times 10^{-6}$	CL=90%
Γ_{105}	$\gamma\chi_{c1}(4140) \to \phi J/\psi$	$<$ 2.2		$\times 10^{-6}$	CL=90%
Γ_{106}	γX	[c] $<$ 4.5		$\times 10^{-6}$	CL=90%
Γ_{107}	$\gamma X\overline{X}(m_X < 3.1$ GeV)	[d] $<$ 1		$\times 10^{-3}$	CL=90%
Γ_{108}	$\gamma X\overline{X}(m_X < 4.5$ GeV)	[e] $<$ 2.4		$\times 10^{-4}$	CL=90%
Γ_{109}	$\gamma X \to \gamma +\geq 4$ prongs	[f] $<$ 1.78		$\times 10^{-4}$	CL=95%
Γ_{110}	$\gamma a_1^0 \to \gamma\mu^+\mu^-$	[g] $<$ 9		$\times 10^{-6}$	CL=90%
Γ_{111}	$\gamma a_1^0 \to \gamma\tau^+\tau^-$	[a] $<$ 1.30		$\times 10^{-4}$	CL=90%
Γ_{112}	$\gamma a_1^0 \to \gamma gg$	[h] $<$ 1		%	CL=90%
Γ_{113}	$\gamma a_1^0 \to \gamma s\overline{s}$	[h] $<$ 1		$\times 10^{-3}$	CL=90%

Lepton Family number (LF) violating modes

Γ_{114}	$\mu^\pm\tau^\mp$	LF $<$ 6.0		$\times 10^{-6}$	CL=95%

Other decays

Γ_{115}	invisible	$<$ 3.0		$\times 10^{-4}$	CL=90%

[a] $2m_\tau < M(\tau^+\tau^-) < 9.2$ GeV

[b] 2 GeV $< m_{K^+K^-} <$ 3 GeV

[c] X = scalar with $m < 8.0$ GeV

[d] $X\overline{X}$ = vectors with $m < 3.1$ GeV

[e] X and $\overline{X}$ = zero spin with $m < 4.5$ GeV

[f] 1.5 GeV $< m_X <$ 5.0 GeV

[g] 201 MeV $< M(\mu^+\mu^-) <$ 3565 MeV

[h] 0.5 GeV $< m_X <$ 9.0 GeV, where m_X is the invariant mass of the hadronic final state.

$\Upsilon(1S)$ Γ(i)$\Gamma(e^+e^-)/\Gamma$(total)

$\Gamma(e^+e^-) \times \Gamma(\mu^+\mu^-)/\Gamma_{total}$ $\quad \Gamma_2\Gamma_3/\Gamma$

VALUE (eV)	DOCUMENT ID		TECN	COMMENT
31.2±1.6±1.7	KOBEL	92	CBAL	$e^+e^- \to \mu^+\mu^-$

Γ(hadrons) $\times \Gamma(e^+e^-)/\Gamma_{total}$ $\quad \Gamma_0\Gamma_2/\Gamma$

VALUE (keV)	DOCUMENT ID		TECN	COMMENT
1.240±0.016 OUR AVERAGE				
1.252±0.004±0.019	[5] ROSNER	06	CLEO	9.5 $e^+e^- \to$ hadrons
1.187±0.023±0.031	[5] BARU	92B	MD1	$e^+e^- \to$ hadrons
1.23 ±0.02 ±0.05	[5] JAKUBOWSKI	88	CBAL	$e^+e^- \to$ hadrons
1.37 ±0.06 ±0.09	[6] GILES	84B	CLEO	$e^+e^- \to$ hadrons
1.23 ±0.08 ±0.04	[6] ALBRECHT	82	DASP	$e^+e^- \to$ hadrons
1.13 ±0.07 ±0.11	[6] NICZYPORUK	82	LENA	$e^+e^- \to$ hadrons
1.09 ±0.25	[6] BOCK	80	CNTR	$e^+e^- \to$ hadrons
1.35 ±0.14	[7] BERGER	79	PLUT	$e^+e^- \to$ hadrons

[5] Radiative corrections evaluated following KURAEV 85.

[6] Radiative corrections reevaluated by BUCHMUELLER 88 following KURAEV 85.

[7] Radiative corrections reevaluated by ALEXANDER 89 using $B(\mu\mu) = 0.026$.

$\Upsilon(1S)$ PARTIAL WIDTHS

$\Gamma(e^+e^-)$ $\quad \Gamma_2$

VALUE (keV)	DOCUMENT ID
1.340±0.018 OUR EVALUATION	

$\Upsilon(1S)$ BRANCHING RATIOS

$\Gamma(\tau^+\tau^-)/\Gamma_{total}$ $\quad \Gamma_1/\Gamma$

VALUE (units 10^{-2})	EVTS	DOCUMENT ID		TECN	COMMENT
2.60±0.10 OUR AVERAGE					
2.53±0.13±0.05	60k	[8] BESSON	07	CLEO	$e^+e^- \to \Upsilon(1S) \to \tau^+\tau^-$
$2.61\pm0.12^{+0.09}_{-0.13}$	25k	CINABRO	94B	CLE2	$e^+e^- \to \tau^+\tau^-$
2.7 ±0.4 ±0.2		[9] ALBRECHT	85C	ARG	$\Upsilon(2S) \to \pi^+\pi^-\tau^+\tau^-$
3.4 ±0.4 ±0.4		GILES	83	CLEO	$e^+e^- \to \tau^+\tau^-$

[8] BESSON 07 reports $[\Gamma(\Upsilon(1S) \to \tau^+\tau^-)/\Gamma_{total}] / [B(\Upsilon(1S) \to \mu^+\mu^-)] = 1.02 \pm 0.02 \pm 0.05$ which we multiply by our best value $B(\Upsilon(1S) \to \mu^+\mu^-) = (2.48 \pm 0.05) \times 10^{-2}$. Our first error is their experiment's error and our second error is the systematic error from using our best value.

[9] Using $B(\Upsilon(1S) \to ee) = B(\Upsilon(1S) \to \mu\mu) = 0.0256$; not used for width evaluations.

$\Gamma(e^+e^-)/\Gamma_{total}$ $\quad \Gamma_2/\Gamma$

VALUE (units 10^{-2})	EVTS	DOCUMENT ID		TECN	COMMENT
2.38±0.11 OUR AVERAGE					
2.29±0.08±0.11		ALEXANDER	98	CLE2	$\Upsilon(2S) \to \pi^+\pi^- e^+e^-$
2.42±0.14±0.14	307	ALBRECHT	87	ARG	$\Upsilon(2S) \to \pi^+\pi^- e^+e^-$
2.8 ±0.3 ±0.2	826	BESSON	84	CLEO	$\Upsilon(2S) \to \pi^+\pi^- e^+e^-$
5.1 ±3.0		BERGER	80C	PLUT	$e^+e^- \to e^+e^-$

$\Gamma(\mu^+\mu^-)/\Gamma_{total}$ $\quad \Gamma_3/\Gamma$

VALUE	EVTS	DOCUMENT ID		TECN	COMMENT
0.0248±0.0005 OUR AVERAGE					
0.0249±0.0002±0.0007	345k	ADAMS	05	CLEO	$e^+e^- \to \mu^+\mu^-$
0.0249±0.0008±0.0013		ALEXANDER	98	CLE2	$\Upsilon(2S) \to \pi^+\pi^-\mu^+\mu^-$
0.0212±0.0020±0.0010		[10] BARU	92	MD1	$e^+e^- \to \mu^+\mu^-$
0.0231±0.0012±0.0010		[10] KOBEL	92	CBAL	$e^+e^- \to \mu^+\mu^-$
0.0252±0.0007±0.0007		CHEN	89B	CLEO	$e^+e^- \to \mu^+\mu^-$
0.0261±0.0009±0.0011		KAARSBERG	89	CSB2	$e^+e^- \to \mu^+\mu^-$
0.0230±0.0025±0.0013	86	ALBRECHT	87	ARG	$\Upsilon(2S) \to \pi^+\pi^-\mu^+\mu^-$
0.029 ±0.003 ±0.002	864	BESSON	84	CLEO	$\Upsilon(2S) \to \pi^+\pi^-\mu^+\mu^-$
0.027 ±0.003 ±0.003		ANDREWS	83	CLEO	$e^+e^- \to \mu^+\mu^-$
0.032 ±0.013 ±0.003		ALBRECHT	82	DASP	$e^+e^- \to \mu^+\mu^-$
0.038 ±0.015 ±0.002		NICZYPORUK	82	LENA	$e^+e^- \to \mu^+\mu^-$
$0.014\ ^{+0.034}_{-0.014}$		BOCK	80	CNTR	$e^+e^- \to \mu^+\mu^-$
0.022 ±0.020		BERGER	79	PLUT	$e^+e^- \to \mu^+\mu^-$

[10] Taking into account interference between the resonance and continuum.

$\Gamma(\tau^+\tau^-)/\Gamma(\mu^+\mu^-)$ $\quad \Gamma_1/\Gamma_3$

VALUE	EVTS	DOCUMENT ID		TECN	COMMENT
1.008±0.023 OUR AVERAGE					
1.005±0.013±0.022	0.7M	[11] DEL-AMO-SA..10C		BABR	$\Upsilon(3S) \to \pi^+\pi^-\Upsilon(1S)$
1.02 ±0.02 ±0.05	60k	BESSON	07	CLEO	$e^+e^- \to \Upsilon(1S)$

[11] Allows any number of extra photons with total energy < 500 MeV.

$\Gamma(ggg)/\Gamma_{total}$ $\quad \Gamma_4/\Gamma$

VALUE (units 10^{-2})	EVTS	DOCUMENT ID		TECN	COMMENT
81.7±0.7	20M	[12] BESSON	06A	CLEO	$\Upsilon(1S) \to$ hadrons

[12] Calculated using the value $\Gamma(\gamma gg)/\Gamma(ggg) = (2.70 \pm 0.01 \pm 0.13 \pm 0.24)\%$ from BESSON 06A and PDG 08 values of $B(\mu^+\mu^-) = (2.48 \pm 0.05)\%$ and $R_{hadrons} = 3.51$. The statistical error is negligible and the systematic error is partially correlated with that of $\Gamma(\gamma gg)/\Gamma_{total}$ measurement of BESSON 06A.

$\Gamma(\gamma gg)/\Gamma_{total}$ $\quad \Gamma_5/\Gamma$

VALUE (units 10^{-2})	EVTS	DOCUMENT ID		TECN	COMMENT
2.20±0.60	400k	[13] BESSON	06A	CLEO	$\Upsilon(1S) \to \gamma +$ hadrons

[13] Calculated using BESSON 06A values of $\Gamma(\gamma gg)/\Gamma(ggg) = (2.70 \pm 0.01 \pm 0.13 \pm 0.24)\%$ and $\Gamma(ggg)/\Gamma_{total}$. The statistical error is negligible and the systematic error is partially correlated with that of $\Gamma(ggg)/\Gamma_{total}$ measurement of BESSON 06A.

$\Gamma(\gamma gg)/\Gamma(ggg)$ $\quad \Gamma_5/\Gamma_4$

VALUE (units 10^{-2})	EVTS	DOCUMENT ID		TECN	COMMENT
2.70±0.01±0.27	20M	BESSON	06A	CLEO	$\Upsilon(1S) \to (\gamma +)$ hadrons

$\Gamma(\eta'(958)$ anything$)/\Gamma_{total}$ $\quad \Gamma_6/\Gamma$

VALUE	DOCUMENT ID		TECN	COMMENT
0.0294±0.0024 OUR AVERAGE				
0.030 ±0.002 ±0.002	AQUINES	06A	CLE3	$\Upsilon(1S) \to \eta'$ anything
0.028 ±0.004 ±0.002	ARTUSO	03	CLE2	$\Upsilon(1S) \to \eta'$ anything

Meson Particle Listings

$\Upsilon(1S)$

$\Gamma(J/\psi(1S)\text{ anything})/\Gamma_{\text{total}}$ Γ_7/Γ

VALUE (units 10^{-4})	CL%	EVTS	DOCUMENT ID		TECN	COMMENT
5.4 ±0.4 OUR FIT Error includes scale factor of 1.4.						
5.4 ±0.4 OUR AVERAGE Error includes scale factor of 1.5.						
5.25±0.13±0.25		3k	SHEN	16	BELL	$e^+e^- \to J/\psi X$
6.4 ±0.4 ±0.6		730	BRIERE	04	CLEO	$e^+e^- \to J/\psi X$
11 ±4 ±2			[14] FULTON	89	CLEO	$e^+e^- \to \mu^+\mu^- X$
• • • We do not use the following data for averages, fits, limits, etc. • • •						
<6.8	90		ALBRECHT	92J	ARG	$e^+e^- \to e^+e^- X$, $\mu^+\mu^- X$
<17	90		MASCHMANN	90	CBAL	$e^+e^- \to$ hadrons
<200	90		NICZYPORUK	83	LENA	

[14] Using B($(J/\psi) \to \mu^+\mu^-$) = (6.9 ± 0.9)%.

$\Gamma(J/\psi(1S)\eta_c)/\Gamma_{\text{total}}$ Γ_8/Γ

VALUE	CL%	DOCUMENT ID		TECN	COMMENT
<2.2 × 10⁻⁶	90	YANG	14	BELL	$e^+e^- \to J/\psi X$

$\Gamma(J/\psi(1S)\chi_{c0})/\Gamma_{\text{total}}$ Γ_9/Γ

VALUE	CL%	DOCUMENT ID		TECN	COMMENT
<3.4 × 10⁻⁶	90	YANG	14	BELL	$e^+e^- \to J/\psi X$

$\Gamma(J/\psi(1S)\chi_{c1})/\Gamma_{\text{total}}$ Γ_{10}/Γ

VALUE (units 10^{-6})	EVTS	DOCUMENT ID		TECN	COMMENT
3.90±1.21±0.23	20	YANG	14	BELL	$e^+e^- \to J/\psi X$

$\Gamma(J/\psi(1S)\chi_{c2})/\Gamma_{\text{total}}$ Γ_{11}/Γ

VALUE	CL%	DOCUMENT ID		TECN	COMMENT
<1.4 × 10⁻⁶	90	YANG	14	BELL	$e^+e^- \to J/\psi X$

$\Gamma(J/\psi(1S)\eta_c(2S))/\Gamma_{\text{total}}$ Γ_{12}/Γ

VALUE	CL%	DOCUMENT ID		TECN	COMMENT
<2.2 × 10⁻⁶	90	YANG	14	BELL	$e^+e^- \to J/\psi X$

$\Gamma(J/\psi(1S)X(3940))/\Gamma_{\text{total}}$ Γ_{13}/Γ

VALUE	CL%	DOCUMENT ID		TECN	COMMENT
<5.4 × 10⁻⁶	90	YANG	14	BELL	$e^+e^- \to J/\psi X$

$\Gamma(J/\psi(1S)X(4160))/\Gamma_{\text{total}}$ Γ_{14}/Γ

VALUE	CL%	DOCUMENT ID		TECN	COMMENT
<5.4 × 10⁻⁶	90	YANG	14	BELL	$e^+e^- \to J/\psi X$

$\Gamma(X(4350)\text{ anything}, X \to J/\psi(1S)\phi)/\Gamma_{\text{total}}$ Γ_{15}/Γ

VALUE	CL%	DOCUMENT ID		TECN	COMMENT
<8.1 × 10⁻⁶	90	SHEN	16	BELL	$\Upsilon(1S) \to J/\psi K^+K^- X$

$\Gamma(Z_c(3900)^\pm\text{ anything}, Z_c \to J/\psi(1S)\pi^\pm)/\Gamma_{\text{total}}$ Γ_{16}/Γ

VALUE	CL%	DOCUMENT ID		TECN	COMMENT
<1.3 × 10⁻⁵	90	SHEN	16	BELL	$\Upsilon(1S) \to J/\psi\pi^\pm X$

$\Gamma(Z_c(4200)^\pm\text{ anything}, Z_c \to J/\psi(1S)\pi^\pm)/\Gamma_{\text{total}}$ Γ_{17}/Γ

VALUE	CL%	DOCUMENT ID		TECN	COMMENT
<6.0 × 10⁻⁵	90	SHEN	16	BELL	$\Upsilon(1S) \to J/\psi\pi^\pm X$

$\Gamma(Z_c(4430)^\pm\text{ anything}, Z_c \to J/\psi(1S)\pi^\pm)/\Gamma_{\text{total}}$ Γ_{18}/Γ

VALUE	CL%	DOCUMENT ID		TECN	COMMENT
<4.9 × 10⁻⁵	90	SHEN	16	BELL	$\Upsilon(1S) \to J/\psi\pi^\pm X$

$\Gamma(X_{cs}^\pm\text{ anything}, X \to J/\psi K^\pm)/\Gamma_{\text{total}}$ Γ_{19}/Γ

VALUE	CL%	DOCUMENT ID		TECN	COMMENT
<5.7 × 10⁻⁶	90	SHEN	16	BELL	$\Upsilon(1S) \to J/\psi K^- X$

$\Gamma(\chi_{c1}(3872)\text{ anything}, \chi_{c1} \to J/\psi(1S)\pi^+\pi^-)/\Gamma_{\text{total}}$ Γ_{20}/Γ

VALUE	CL%	DOCUMENT ID		TECN	COMMENT
<9.5 × 10⁻⁶	90	SHEN	16	BELL	$\Upsilon(1S) \to J/\psi\pi^+\pi^- X$

$\Gamma(\psi(4260)\text{ anything}, \psi \to J/\psi(1S)\pi^+\pi^-)/\Gamma_{\text{total}}$ Γ_{21}/Γ

VALUE	CL%	DOCUMENT ID		TECN	COMMENT
<3.8 × 10⁻⁵	90	SHEN	16	BELL	$\Upsilon(1S) \to J/\psi\pi^+\pi^- X$

$\Gamma(\psi(4260)\text{ anything}, \psi \to J/\psi(1S)K^+K^-)/\Gamma_{\text{total}}$ Γ_{22}/Γ

VALUE	CL%	DOCUMENT ID		TECN	COMMENT
<7.5 × 10⁻⁶	90	SHEN	16	BELL	$\Upsilon(1S) \to J/\psi K^+K^- X$

$\Gamma(\chi_{c1}(4140)\text{ anything}, \chi_{c1} \to J/\psi(1S)\phi)/\Gamma_{\text{total}}$ Γ_{23}/Γ

VALUE	CL%	DOCUMENT ID		TECN	COMMENT
<5.2 × 10⁻⁶	90	SHEN	16	BELL	$\Upsilon(1S) \to J/\psi K^+K^- X$

$\Gamma(\chi_{c0}\text{ anything})/\Gamma(J/\psi(1S)\text{ anything})$ Γ_{24}/Γ_7

VALUE	CL%	DOCUMENT ID		TECN	COMMENT
<7.4	90	BRIERE	04	CLEO	$e^+e^- \to J/\psi X$

$\Gamma(\chi_{c1}\text{ anything})/\Gamma_{\text{total}}$ Γ_{25}/Γ

VALUE (units 10^{-4})	EVTS	DOCUMENT ID		TECN	COMMENT
1.90±0.35 OUR FIT					
1.90±0.43±0.14	215	JIA	17	BELL	$\Upsilon(1S) \to \gamma J/\psi(1S)$

$\Gamma(\chi_{c1}\text{ anything})/\Gamma(J/\psi(1S)\text{ anything})$ Γ_{25}/Γ_7

VALUE	EVTS	DOCUMENT ID		TECN	COMMENT
0.35±0.07 OUR FIT					
0.35±0.08±0.06	52 ± 12	BRIERE	04	CLEO	$e^+e^- \to J/\psi X$

$\Gamma(\chi_{c1}(1P)X_{tetra})/\Gamma_{\text{total}}$ Γ_{26}/Γ

VALUE	CL%	DOCUMENT ID		TECN	COMMENT
<37.8 × 10⁻⁶	90	[15] JIA	17A	BELL	$e^+e^- \to$ hadrons

[15] For a tetraquark state X_{tetra}, with mass in the range 1.16–2.46 GeV and width in the range 0–0.3 GeV. Measured 90% CL limits as a function of X_{tetra} mass and width range from 4.4×10^{-6} to 37.8×10^{-6}.

$\Gamma(\chi_{c2}\text{ anything})/\Gamma(J/\psi(1S)\text{ anything})$ Γ_{27}/Γ_7

VALUE	EVTS	DOCUMENT ID		TECN	COMMENT
0.52±0.12±0.09	47 ± 11	BRIERE	04	CLEO	$e^+e^- \to J/\psi X$

$\Gamma(\psi(2S)\text{ anything})/\Gamma_{\text{total}}$ Γ_{28}/Γ

VALUE (units 10^{-4})	EVTS	DOCUMENT ID		TECN	COMMENT
1.23±0.17±0.11	215	SHEN	16	BELL	$e^+e^- \to \psi(2S) X$

$\Gamma(\psi(2S)\text{ anything})/\Gamma(J/\psi(1S)\text{ anything})$ Γ_{28}/Γ_7

VALUE	EVTS	DOCUMENT ID		TECN	COMMENT
0.41±0.11±0.08	42 ± 11	BRIERE	04	CLEO	$e^+e^- \to J/\psi\pi^+\pi^- X$

$\Gamma(\psi(2S)\eta_c)/\Gamma_{\text{total}}$ Γ_{29}/Γ

VALUE	CL%	DOCUMENT ID		TECN	COMMENT
<3.6 × 10⁻⁶	90	YANG	14	BELL	$e^+e^- \to \psi(2S) X$

$\Gamma(\psi(2S)\chi_{c0})/\Gamma_{\text{total}}$ Γ_{30}/Γ

VALUE	CL%	DOCUMENT ID		TECN	COMMENT
<6.5 × 10⁻⁶	90	YANG	14	BELL	$e^+e^- \to \psi(2S) X$

$\Gamma(\psi(2S)\chi_{c1})/\Gamma_{\text{total}}$ Γ_{31}/Γ

VALUE	CL%	DOCUMENT ID		TECN	COMMENT
<4.5 × 10⁻⁶	90	YANG	14	BELL	$e^+e^- \to \psi(2S) X$

$\Gamma(\psi(2S)\chi_{c2})/\Gamma_{\text{total}}$ Γ_{32}/Γ

VALUE	CL%	DOCUMENT ID		TECN	COMMENT
<2.1 × 10⁻⁶	90	YANG	14	BELL	$e^+e^- \to \psi(2S) X$

$\Gamma(\psi(2S)\eta_c(2S))/\Gamma_{\text{total}}$ Γ_{33}/Γ

VALUE	CL%	DOCUMENT ID		TECN	COMMENT
<3.2 × 10⁻⁶	90	YANG	14	BELL	$e^+e^- \to \psi(2S) X$

$\Gamma(\psi(2S)X(3940))/\Gamma_{\text{total}}$ Γ_{34}/Γ

VALUE	CL%	DOCUMENT ID		TECN	COMMENT
<2.9 × 10⁻⁶	90	YANG	14	BELL	$e^+e^- \to \psi(2S) X$

$\Gamma(\psi(2S)X(4160))/\Gamma_{\text{total}}$ Γ_{35}/Γ

VALUE	CL%	DOCUMENT ID		TECN	COMMENT
<2.9 × 10⁻⁶	90	YANG	14	BELL	$e^+e^- \to \psi(2S) X$

$\Gamma(\psi(4260)\text{ anything}, \psi \to \psi(2S)\pi^+\pi^-)/\Gamma_{\text{total}}$ Γ_{36}/Γ

VALUE	CL%	DOCUMENT ID		TECN	COMMENT
<7.9 × 10⁻⁵	90	SHEN	16	BELL	$\Upsilon(1S) \to \psi(2S)\pi^+\pi^- X$

$\Gamma(\psi(4360)\text{ anything}, \psi \to \psi(2S)\pi^+\pi^-)/\Gamma_{\text{total}}$ Γ_{37}/Γ

VALUE	CL%	DOCUMENT ID		TECN	COMMENT
<5.2 × 10⁻⁵	90	SHEN	16	BELL	$\Upsilon(1S) \to \psi(2S)\pi^+\pi^- X$

$\Gamma(\psi(4660)\text{ anything}, \psi \to \psi(2S)\pi^+\pi^-)/\Gamma_{\text{total}}$ Γ_{38}/Γ

VALUE	CL%	DOCUMENT ID		TECN	COMMENT
<2.2 × 10⁻⁵	90	SHEN	16	BELL	$\Upsilon(1S) \to \psi(2S)\pi^+\pi^- X$

$\Gamma(X(4050)^\pm\text{ anything}, X \to \psi(2S)\pi^\pm)/\Gamma_{\text{total}}$ Γ_{39}/Γ

VALUE	CL%	DOCUMENT ID		TECN	COMMENT
<8.8 × 10⁻⁵	90	SHEN	16	BELL	$\Upsilon(1S) \to \psi(2S)\pi^\pm X$

$\Gamma(Z_c(4430)^\pm\text{ anything}, Z_c \to \psi(2S)\pi^\pm)/\Gamma_{\text{total}}$ Γ_{40}/Γ

VALUE	CL%	DOCUMENT ID		TECN	COMMENT
<6.7 × 10⁻⁵	90	SHEN	16	BELL	$\Upsilon(1S) \to \psi(2S)\pi^\pm X$

$\Gamma(\rho\pi)/\Gamma_{\text{total}}$ Γ_{41}/Γ

VALUE (units 10^{-6})	CL%	DOCUMENT ID		TECN	COMMENT
<3.68	90	SHEN	13	BELL	$\Upsilon(1S) \to \pi^+\pi^-\pi^0$

• • • We do not use the following data for averages, fits, limits, etc. • • •

<1	$\times 10^3$	90	BLINOV	90	MD1	$\Upsilon(1S) \to \rho^0\pi^0$
<2	$\times 10^2$	90	FULTON	90B		$\Upsilon(1S) \to \rho^0\pi^0$
<2.1	$\times 10^3$	90	NICZYPORUK	83	LENA	$\Upsilon(1S) \to \rho^0\pi^0$

$\Gamma(\omega\pi^0)/\Gamma_{total}$ Γ_{42}/Γ

VALUE (units 10^{-6})	CL%	DOCUMENT ID		TECN	COMMENT
<3.90	90	SHEN	13	BELL	$\Upsilon(1S) \to \pi^+\pi^-\pi^0\pi^0$

$\Gamma(\pi^+\pi^-)/\Gamma_{total}$ Γ_{43}/Γ

VALUE (units 10^{-4})	CL%	DOCUMENT ID		TECN	COMMENT
<5	90	BARU	92	MD1	$\Upsilon(1S) \to \pi^+\pi^-$

$\Gamma(K^+K^-)/\Gamma_{total}$ Γ_{44}/Γ

VALUE (units 10^{-4})	CL%	DOCUMENT ID		TECN	COMMENT
<5	90	BARU	92	MD1	$\Upsilon(1S) \to K^+K^-$

$\Gamma(p\overline{p})/\Gamma_{total}$ Γ_{45}/Γ

VALUE (units 10^{-4})	CL%	DOCUMENT ID		TECN	COMMENT
<5	90	[16] BARU	96	MD1	$\Upsilon(1S) \to p\overline{p}$

[16] Supersedes BARU 92 in this node.

$\Gamma(\pi^+\pi^-\pi^0)/\Gamma_{total}$ Γ_{46}/Γ

VALUE (units 10^{-6})	CL%	EVTS	DOCUMENT ID		TECN	COMMENT
2.14±0.72±0.34		26 ± 9	SHEN	13	BELL	$\Upsilon(1S) \to \pi^+\pi^-\pi^0$

• • • We do not use the following data for averages, fits, limits, etc. • • •

<18.4	90		ANASTASSOV	99	CLE2	$e^+e^- \to$ hadrons

$\Gamma(\phi K^+K^-)/\Gamma_{total}$ Γ_{47}/Γ

VALUE (units 10^{-6})	EVTS	DOCUMENT ID		TECN	COMMENT
2.36±0.37±0.29	56	SHEN	12A	BELL	$\Upsilon(1S) \to 2(K^+K^-)$

$\Gamma(\omega\pi^+\pi^-)/\Gamma_{total}$ Γ_{48}/Γ

VALUE (units 10^{-6})	EVTS	DOCUMENT ID		TECN	COMMENT
4.46±0.67±0.72	64	SHEN	12A	BELL	$\Upsilon(1S) \to 2(\pi^+\pi^-)\pi^0$

$\Gamma(K^*(892)^0K^-\pi^+ + \text{c.c.})/\Gamma_{total}$ Γ_{49}/Γ

VALUE (units 10^{-6})	EVTS	DOCUMENT ID		TECN	COMMENT
4.42±0.50±0.58	173	SHEN	12A	BELL	$\Upsilon(1S) \to K^+K^-\pi^+\pi^-$

$\Gamma(\phi f_2'(1525))/\Gamma_{total}$ Γ_{50}/Γ

VALUE (units 10^{-6})	CL%	DOCUMENT ID		TECN	COMMENT
<1.63	90	SHEN	12A	BELL	$\Upsilon(1S) \to 2(K^+K^-)$

$\Gamma(\omega f_2(1270))/\Gamma_{total}$ Γ_{51}/Γ

VALUE (units 10^{-6})	CL%	DOCUMENT ID		TECN	COMMENT
<1.79	90	SHEN	12A	BELL	$\Upsilon(1S) \to 2(\pi^+\pi^-)\pi^0$

$\Gamma(\rho(770)a_2(1320))/\Gamma_{total}$ Γ_{52}/Γ

VALUE (units 10^{-6})	CL%	DOCUMENT ID		TECN	COMMENT
<2.24	90	SHEN	12A	BELL	$\Upsilon(1S) \to 2(\pi^+\pi^-)\pi^0$

$\Gamma(K^*(892)^0\overline{K}{}^*_2(1430)^0 + \text{c.c.})/\Gamma_{total}$ Γ_{53}/Γ

VALUE (units 10^{-6})	EVTS	DOCUMENT ID		TECN	COMMENT
3.02±0.68±0.34	42	SHEN	12A	BELL	$\Upsilon(1S) \to K^+K^-\pi^+\pi^-$

$\Gamma(K_1(1270)^\pm K^\mp)/\Gamma_{total}$ Γ_{54}/Γ

VALUE (units 10^{-6})	CL%	DOCUMENT ID		TECN	COMMENT
<2.41	90	SHEN	12A	BELL	$\Upsilon(1S) \to K^+K^-\pi^+\pi^-$

$\Gamma(K_1(1400)^\pm K^\mp)/\Gamma_{total}$ Γ_{55}/Γ

VALUE (units 10^{-6})	EVTS	DOCUMENT ID		TECN	COMMENT
1.02±0.35±0.22	24	SHEN	12A	BELL	$\Upsilon(1S) \to K^+K^-\pi^+\pi^-$

$\Gamma(b_1(1235)^\pm\pi^\mp)/\Gamma_{total}$ Γ_{56}/Γ

VALUE (units 10^{-6})	CL%	DOCUMENT ID		TECN	COMMENT
<1.25	90	SHEN	12A	BELL	$\Upsilon(1S) \to 2(\pi^+\pi^-)\pi^0$

$\Gamma(\pi^+\pi^-\pi^0\pi^0)/\Gamma_{total}$ Γ_{57}/Γ

VALUE (units 10^{-6})	EVTS	DOCUMENT ID		TECN	COMMENT
12.8±2.0±2.3	143 ± 22	SHEN	13	BELL	$\Upsilon(1S) \to \pi^+\pi^-\pi^0\pi^0$

$\Gamma(K^0_S K^+\pi^- + \text{c.c.})/\Gamma_{total}$ Γ_{58}/Γ

VALUE (units 10^{-6})	CL%	EVTS	DOCUMENT ID		TECN	COMMENT
1.59±0.33±0.18		37 ± 8	SHEN	13	BELL	$\Upsilon(1S) \to K^0_S K^-\pi^+$

• • • We do not use the following data for averages, fits, limits, etc. • • •

<3.4	90	[17]	DOBBS	12A		$\Upsilon(1S) \to K^0_S K^-\pi^+$

[17] Obtained by analyzing CLEO III data but not authored by the CLEO Collaboration.

$\Gamma(K^*(892)^0\overline{K}{}^0 + \text{c.c.})/\Gamma_{total}$ Γ_{59}/Γ

VALUE (units 10^{-6})	EVTS	DOCUMENT ID		TECN	COMMENT
2.92±0.85±0.37	16 ± 5	SHEN	13	BELL	$\Upsilon(1S) \to K^0_S K^-\pi^+$

$\Gamma(K^*(892)^- K^+ + \text{c.c.})/\Gamma_{total}$ Γ_{60}/Γ

VALUE (units 10^{-6})	CL%	DOCUMENT ID		TECN	COMMENT
<1.11	90	SHEN	13	BELL	$\Upsilon(1S) \to K^0_S K^-\pi^+$

$\Gamma(f_1(1285)\text{ anything})/\Gamma_{total}$ Γ_{61}/Γ

VALUE (units 10^{-3})	EVTS	DOCUMENT ID		TECN	COMMENT
4.6±2.8±1.3	3.1k	JIA	17A	BELL	$e^+e^- \to$ hadrons

$\Gamma(D^*(2010)^\pm\text{ anything})/\Gamma_{total}$ Γ_{62}/Γ

VALUE (units 10^{-3})	CL%	EVTS	DOCUMENT ID		TECN	COMMENT
25.2±1.3±1.5		≈ 2k	[18] AUBERT	10C	BABR	$\Upsilon(2S) \to \pi^+\pi^-\Upsilon(1S)$

• • • We do not use the following data for averages, fits, limits, etc. • • •

<19	90	[19]	ALBRECHT	92J	ARG	$e^+e^- \to D^0\pi^\pm$X

[18] For $x_p > 0.1$.

[19] For $x_p > 0.2$.

$\Gamma(f_1(1285)X_{tetra})/\Gamma_{total}$ Γ_{63}/Γ

VALUE	CL%	DOCUMENT ID		TECN	COMMENT
<62.4 × 10⁻⁶	90	[20] JIA	17A	BELL	$e^+e^- \to$ hadrons

[20] For a tetraquark state X_{tetra}, with mass in the range 1.16–2.46 GeV and width in the range 0–0.3 GeV. Measured 90% CL limits as a function of X_{tetra} mass and width range from 4.6×10^{-6} to 62.4×10^{-6}.

$\Gamma(\overline{^2H}\text{ anything})/\Gamma_{total}$ Γ_{64}/Γ

VALUE (units 10^{-5})	EVTS	DOCUMENT ID		TECN	COMMENT
2.85±0.25 OUR AVERAGE					
$2.81 \pm 0.49^{+0.20}_{-0.24}$		LEES	14G	BABR	$e^+e^- \to \overline{^2H}X$
2.86±0.19±0.21	455	ASNER	07	CLEO	$e^+e^- \to \overline{^2H}X$

$\Gamma(\text{Sum of 100 exclusive modes})/\Gamma_{total}$ Γ_{65}/Γ

VALUE (units 10^{-2})	DOCUMENT ID		COMMENT
1.200±0.017	[21,22] DOBBS	12A	$\Upsilon(1S) \to$ hadrons

[21] DOBBS 12A presents individual exclusive branching fractions or upper limits for 100 modes of four to ten pions, kaons, or protons.

[22] Obtained by analyzing CLEO III data but not authored by the CLEO Collaboration.

$\Gamma(ggg, \gamma gg \to \overline{d}\text{ anything})/\Gamma(ggg, \gamma gg \to \text{anything})$

VALUE (units 10^{-5})	EVTS	DOCUMENT ID		TECN	COMMENT
3.36±0.23±0.25	455	ASNER	07	CLEO	$e^+e^- \to \overline{d}X$

$\Gamma(\gamma\pi^+\pi^-)/\Gamma_{total}$ Γ_{66}/Γ

VALUE (units 10^{-5})	DOCUMENT ID		TECN	COMMENT
6.3±1.2±1.3	[23] ANASTASSOV	99	CLE2	$e^+e^- \to$ hadrons

[23] For $m_{\pi\pi} > 1$ GeV.

$\Gamma(\gamma\pi^0\pi^0)/\Gamma_{total}$ Γ_{67}/Γ

VALUE (units 10^{-5})	DOCUMENT ID		TECN	COMMENT
1.7±0.6±0.3	[24] ANASTASSOV	99	CLE2	$e^+e^- \to$ hadrons

[24] For $m_{\pi\pi} > 1$ GeV.

$\Gamma(\gamma\pi^0\eta)/\Gamma_{total}$ Γ_{68}/Γ

VALUE (units 10^{-6})	CL%	DOCUMENT ID		TECN	COMMENT
<2.4	90	[25] BESSON	07A	CLEO	$e^+e^- \to \Upsilon(1S)$

[25] BESSON 07A obtained this limit for $0.7 < m_{\pi^0\eta} < 3$ GeV.

$\Gamma(\gamma K^+K^-)/\Gamma_{total}$ Γ_{69}/Γ

($2 < m_{K^+K^-} < 3$ GeV)

VALUE (units 10^{-5})	CL%	DOCUMENT ID		TECN	COMMENT
1.14±0.08±0.10	90	ATHAR	06	CLE3	$\Upsilon(1S) \to \gamma K^+K^-$

$\Gamma(\gamma p\overline{p})/\Gamma_{total}$ Γ_{70}/Γ

($2 < m_{p\overline{p}} < 3$ GeV)

VALUE (units 10^{-5})	CL%	DOCUMENT ID		TECN	COMMENT
<0.6	90	ATHAR	06	CLE3	$\Upsilon(1S) \to \gamma p\overline{p}$

$\Gamma(\gamma 2h^+2h^-)/\Gamma_{total}$ Γ_{71}/Γ

VALUE (units 10^{-4})	EVTS	DOCUMENT ID		TECN	COMMENT
7.0±1.1±1.0	80 ± 12	FULTON	90B	CLEO	$e^+e^- \to$ hadrons

$\Gamma(\gamma 3h^+3h^-)/\Gamma_{total}$ Γ_{72}/Γ

VALUE (units 10^{-4})	EVTS	DOCUMENT ID		TECN	COMMENT
5.4±1.5±1.3	39 ± 11	FULTON	90B	CLEO	$e^+e^- \to$ hadrons

$\Gamma(\gamma 4h^+4h^-)/\Gamma_{total}$ Γ_{73}/Γ

VALUE (units 10^{-4})	EVTS	DOCUMENT ID		TECN	COMMENT
7.4±2.5±2.5	36 ± 12	FULTON	90B	CLEO	$e^+e^- \to$ hadrons

$\Gamma(\gamma\pi^+\pi^-K^+K^-)/\Gamma_{total}$ Γ_{74}/Γ

VALUE (units 10^{-4})	EVTS	DOCUMENT ID		TECN	COMMENT
2.9±0.7±0.6	29 ± 8	FULTON	90B	CLEO	$e^+e^- \to$ hadrons

$\Gamma(\gamma 2\pi^+2\pi^-)/\Gamma_{total}$ Γ_{75}/Γ

VALUE (units 10^{-4})	EVTS	DOCUMENT ID		TECN	COMMENT
2.5±0.7±0.5	26 ± 7	FULTON	90B	CLEO	$e^+e^- \to$ hadrons

$\Gamma(\gamma 3\pi^+3\pi^-)/\Gamma_{total}$ Γ_{76}/Γ

VALUE (units 10^{-4})	EVTS	DOCUMENT ID		TECN	COMMENT
2.5±0.9±0.8	17 ± 5	FULTON	90B	CLEO	$e^+e^- \to$ hadrons

$\Gamma(\gamma 2\pi^+2\pi^-K^+K^-)/\Gamma_{total}$ Γ_{77}/Γ

VALUE (units 10^{-4})	EVTS	DOCUMENT ID		TECN	COMMENT
2.4±0.9±0.8	18 ± 7	FULTON	90B	CLEO	$e^+e^- \to$ hadrons

$\Gamma(\gamma\pi^+\pi^-p\overline{p})/\Gamma_{total}$ Γ_{78}/Γ

VALUE (units 10^{-4})	EVTS	DOCUMENT ID		TECN	COMMENT
1.5±0.5±0.3	22 ± 6	FULTON	90B	CLEO	$e^+e^- \to$ hadrons

$\Gamma(\gamma 2\pi^+2\pi^-p\overline{p})/\Gamma_{total}$ Γ_{79}/Γ

VALUE (units 10^{-4})	EVTS	DOCUMENT ID		TECN	COMMENT
0.4±0.4±0.4	7 ± 6	FULTON	90B	CLEO	$e^+e^- \to$ hadrons

$\Gamma(\gamma 2K^+2K^-)/\Gamma_{total}$ Γ_{80}/Γ

VALUE (units 10^{-4})	EVTS	DOCUMENT ID		TECN	COMMENT
0.2±0.2	2 ± 2	FULTON	90B	CLEO	$e^+e^- \to$ hadrons

$\Gamma(\gamma\eta'(958))/\Gamma_{total}$ Γ_{81}/Γ

VALUE (units 10^{-6})	CL%	DOCUMENT ID		TECN	COMMENT
< 1.9	90	ATHAR	07A	CLEO	$\Upsilon(1S) \to \gamma\eta' \to \gamma\pi^+\pi^-\eta, \gamma\rho$
• • • We do not use the following data for averages, fits, limits, etc. • • •					
<16	90	RICHICHI	01B	CLE2	$\Upsilon(1S) \to \gamma\eta' \to \gamma\eta\pi^+\pi^-$

$\Gamma(\gamma\eta)/\Gamma_{total}$ Γ_{82}/Γ

VALUE (units 10^{-6})	CL%	DOCUMENT ID		TECN	COMMENT
< 1.0	90	ATHAR	07A	CLEO	$\Upsilon(1S) \to \gamma\eta \to \gamma\gamma\gamma$, $\gamma\pi^+\pi^-\pi^0$, $\gamma 3\pi^0$
• • • We do not use the following data for averages, fits, limits, etc. • • •					
<21	90	MASEK	02	CLEO	$\Upsilon(1S) \to \gamma\eta$

$\Gamma(\gamma f_0(980))/\Gamma_{total}$ Γ_{83}/Γ

VALUE (units 10^{-5})	CL%	DOCUMENT ID		TECN	COMMENT
<3	90	[26] ATHAR	06	CLE3	$\Upsilon(1S) \to \gamma\pi^+\pi^-$

[26] Assuming $B(f_0(980) \to \pi\pi) = 1$.

$\Gamma(\gamma f_2'(1525))/\Gamma_{total}$ Γ_{84}/Γ

VALUE (units 10^{-5})	CL%	EVTS	DOCUMENT ID		TECN	COMMENT
3.8±0.9 OUR AVERAGE						
$4.0\pm1.4\pm0.1$		17 ± 5	[27] BESSON	11	CLEO	$\Upsilon(1S) \to K^0_S K^0_S$
$3.7^{+0.9}_{-0.7}\pm0.8$			ATHAR	06	CLE3	$\Upsilon(1S) \to \gamma K^+K^-$
• • • We do not use the following data for averages, fits, limits, etc. • • •						
<14	90		[28] FULTON	90B	CLEO	$\Upsilon(1S) \to \gamma K^+K^-$
<19.4	90		[28] ALBRECHT	89	ARG	$\Upsilon(1S) \to \gamma K^+K^-$

[27] BESSON 11 reports $(4.0 \pm 1.3 \pm 0.6) \times 10^{-5}$ from a measurement of $[\Gamma(\Upsilon(1S) \to \gamma f_2'(1525))/\Gamma_{total}] \times [B(f_2'(1525) \to K\overline{K})]$ assuming $B(f_2'(1525) \to K\overline{K}) = (88.8 \pm 3.1) \times 10^{-2}$, which we rescale to our best value $B(f_2'(1525) \to K\overline{K}) = (88.7 \pm 2.2) \times 10^{-2}$. Our first error is their experiment's error and our second error is the systematic error from using our best value. The result also assumes $B(K^0_S \to \pi^+\pi^-) = (69.20 \pm 0.05)\%$ and $B(f_2'(1525) \to K\overline{K}) = 4\, B(f_2'(1525) \to K^0_S K^0_S)$.

[28] Assuming $B(f_2'(1525) \to K\overline{K}) = 0.71$.

$\Gamma(\gamma f_2(1270))/\Gamma_{total}$ Γ_{85}/Γ

VALUE (units 10^{-5})	CL%	DOCUMENT ID		TECN	COMMENT
10.1±0.9 OUR AVERAGE					
$10.5\pm1.6^{+1.9}_{-1.8}$		[29] BESSON	07A	CLE3	$\Upsilon(1S) \to \gamma\pi^0\pi^0$
$10.2\pm0.8\pm0.7$		ATHAR	06	CLE3	$\Upsilon(1S) \to \gamma\pi^+\pi^-$
$8.1\pm2.3^{+2.9}_{-2.7}$		[30] ANASTASSOV	99	CLE2	$e^+e^- \to$ hadrons
• • • We do not use the following data for averages, fits, limits, etc. • • •					
<21	90	[30] FULTON	90B	CLEO	$\Upsilon(1S) \to \gamma\pi^+\pi^-$
<13	90	[30] ALBRECHT	89	ARG	$\Upsilon(1S) \to \gamma\pi^+\pi^-$
<81	90	SCHMITT	88	CBAL	$\Upsilon(1S) \to \gamma X$

[29] Using $B(f_2(1270) \to \pi^0\pi^0) = B(f_2(1270) \to \pi\pi)/3$ and $B(f_2(1270) \to \pi\pi) = (0.845^{+0.025}_{-0.012})\%$.

[30] Using $B(f_2(1270) \to \pi\pi) = 0.84$.

$\Gamma(\gamma\eta(1405))/\Gamma_{total}$ Γ_{86}/Γ

VALUE (units 10^{-5})	CL%	DOCUMENT ID		TECN	COMMENT
<8.2	90	[31] FULTON	90B	CLEO	$\Upsilon(1S) \to \gamma K^\pm\pi^\mp K^0_S$

[31] Includes unknown branching ratio of $\eta(1405) \to K^\pm\pi^\mp K^0_S$.

$\Gamma(\gamma f_0(1500))/\Gamma_{total}$ Γ_{87}/Γ

VALUE (units 10^{-5})	CL%	DOCUMENT ID		TECN	COMMENT
<1.5	90	[32] BESSON	07A	CLEO	$e^+e^- \to \Upsilon(1S) \to \gamma\pi^0\pi^0$
• • • We do not use the following data for averages, fits, limits, etc. • • •					
<6.1	90	[33] BESSON	07A	CLEO	$e^+e^- \to \Upsilon(1S) \to \gamma\eta\eta$

[32] Using $B(f_0(1500) \to \pi^0\pi^0) = B(f_0(1500) \to \pi\pi)/3$ and $B(f_0(1500) \to \pi\pi) = (0.349 \pm 0.023)\%$.

[33] Calculated by us using $B(f_0(1500) \to \eta\eta) = (5.1 \pm 0.9)\%$.

$\Gamma(\gamma f_0(1710))/\Gamma_{total}$ Γ_{88}/Γ

VALUE (units 10^{-4})	CL%	DOCUMENT ID		TECN	COMMENT
< 2.6	90	[34] ALBRECHT	89	ARG	$\Upsilon(1S) \to \gamma K^+K^-$
• • • We do not use the following data for averages, fits, limits, etc. • • •					
< 6.3	90	[34] FULTON	90B	CLEO	$\Upsilon(1S) \to \gamma K^+K^-$
<19	90	[34] FULTON	90B	CLEO	$\Upsilon(1S) \to \gamma K^0_S K^0_S$
< 8	90	[35] ALBRECHT	89	ARG	$\Upsilon(1S) \to \gamma\pi^+\pi^-$
<24	90	[36] SCHMITT	88	CBAL	$\Upsilon(1S) \to \gamma X$

[34] Assuming $B(f_0(1710) \to K\overline{K}) = 0.38$.

[35] Assuming $B(f_0(1710) \to \pi\pi) = 0.04$.

[36] Assuming $B(f_0(1710) \to \eta\eta) = 0.18$.

$\Gamma(\gamma f_0(1710) \to \gamma K^+K^-)/\Gamma_{total}$ Γ_{89}/Γ

VALUE (units 10^{-5})	CL%	DOCUMENT ID		TECN	COMMENT
<0.7	90	ATHAR	06	CLEO	$e^+e^- \to \Upsilon(1S) \to \gamma K^+K^-$

$\Gamma(\gamma f_0(1710) \to \gamma\pi^0\pi^0)/\Gamma_{total}$ Γ_{90}/Γ

VALUE (units 10^{-6})	CL%	DOCUMENT ID		TECN	COMMENT
<1.4	90	BESSON	07A	CLEO	$e^+e^- \to \Upsilon(1S) \to \gamma\pi^0\pi^0$

$\Gamma(\gamma f_0(1710) \to \gamma\eta\eta)/\Gamma_{total}$ Γ_{91}/Γ

VALUE (units 10^{-6})	CL%	DOCUMENT ID		TECN	COMMENT
<1.8	90	BESSON	07A	CLEO	$e^+e^- \to \Upsilon(1S) \to \gamma\eta\eta$

$\Gamma(\gamma f_4(2050))/\Gamma_{total}$ Γ_{92}/Γ

VALUE (units 10^{-5})	CL%	DOCUMENT ID		TECN	COMMENT
<5.3	90	[37] ATHAR	06	CLE3	$\Upsilon(1S) \to \gamma\pi^+\pi^-$

[37] Assuming $B(f_4(2050) \to \pi\pi) = 0.17$.

$\Gamma(\gamma f_0(2200) \to \gamma K^+K^-)/\Gamma_{total}$ Γ_{93}/Γ

VALUE	CL%	DOCUMENT ID		TECN	COMMENT
<0.0002	90	BARU	89	MD1	$\Upsilon(1S) \to \gamma K^+K^-$

$\Gamma(\gamma f_J(2220) \to \gamma K^+K^-)/\Gamma_{total}$ Γ_{94}/Γ

VALUE (units 10^{-7})	CL%	DOCUMENT ID		TECN	COMMENT
< 8	90	ATHAR	06	CLE3	$\Upsilon(1S) \to \gamma K^+K^-$
• • • We do not use the following data for averages, fits, limits, etc. • • •					
< 160	90	MASEK	02	CLEO	$\Upsilon(1S) \to \gamma K^+K^-$
< 150	90	FULTON	90B	CLEO	$\Upsilon(1S) \to \gamma K^+K^-$
< 290	90	ALBRECHT	89	ARG	$\Upsilon(1S) \to \gamma K^+K^-$
<2000	90	BARU	89	MD1	$\Upsilon(1S) \to \gamma K^+K^-$

$\Gamma(\gamma f_J(2220) \to \gamma\pi^+\pi^-)/\Gamma_{total}$ Γ_{95}/Γ

VALUE (units 10^{-7})	CL%	DOCUMENT ID		TECN	COMMENT
< 6	90	ATHAR	06	CLE3	$\Upsilon(1S) \to \gamma\pi^+\pi^-$
• • • We do not use the following data for averages, fits, limits, etc. • • •					
<120	90	MASEK	02	CLEO	$\Upsilon(1S) \to \gamma\pi^+\pi^-$

$\Gamma(\gamma f_J(2220) \to \gamma p\overline{p})/\Gamma_{total}$ Γ_{96}/Γ

VALUE (units 10^{-7})	CL%	DOCUMENT ID		TECN	COMMENT
< 11	90	ATHAR	06	CLE3	$\Upsilon(1S) \to \gamma p\overline{p}$
• • • We do not use the following data for averages, fits, limits, etc. • • •					
<160	90	MASEK	02	CLEO	$\Upsilon(1S) \to \gamma p\overline{p}$

$\Gamma(\gamma\eta(2225) \to \gamma\phi\phi)/\Gamma_{total}$ Γ_{97}/Γ

VALUE	CL%	DOCUMENT ID		TECN	COMMENT
<0.003	90	BARU	89	MD1	$\Upsilon(1S) \to \gamma K^+K^-K^+K^-$

$\Gamma(\gamma\eta_c(1S))/\Gamma_{total}$ Γ_{98}/Γ

VALUE (units 10^{-5})	CL%	DOCUMENT ID		TECN	COMMENT
<5.7	90	SHEN	10A	BELL	$\Upsilon(1S) \to \gamma X$

$\Gamma(\gamma\chi_{c0})/\Gamma_{total}$ Γ_{99}/Γ

VALUE (units 10^{-4})	CL%	DOCUMENT ID		TECN	COMMENT
<6.5	90	SHEN	10A	BELL	$\Upsilon(1S) \to \gamma X$

$\Gamma(\gamma\chi_{c1})/\Gamma_{total}$ Γ_{100}/Γ

VALUE (units 10^{-5})	CL%	DOCUMENT ID		TECN	COMMENT
<2.3	90	SHEN	10A	BELL	$\Upsilon(1S) \to \gamma X$

$\Gamma(\gamma\chi_{c2})/\Gamma_{total}$ Γ_{101}/Γ

VALUE (units 10^{-6})	CL%	DOCUMENT ID		TECN	COMMENT
<7.6	90	SHEN	10A	BELL	$\Upsilon(1S) \to \gamma X$

$\Gamma(\gamma\chi_{c1}(3872) \to \pi^+\pi^- J/\psi)/\Gamma_{total}$ Γ_{102}/Γ

VALUE (units 10^{-6})	CL%	DOCUMENT ID		TECN	COMMENT
<1.6	90	SHEN	10A	BELL	$\Upsilon(1S) \to \gamma X$

$\Gamma(\gamma\chi_{c1}(3872) \to \pi^+\pi^-\pi^0 J/\psi)/\Gamma_{total}$ Γ_{103}/Γ

VALUE (units 10^{-6})	CL%	DOCUMENT ID		TECN	COMMENT
<2.8	90	SHEN	10A	BELL	$\Upsilon(1S) \to \gamma X$

$\Gamma(\gamma X(3915) \to \omega J/\psi)/\Gamma_{total}$ Γ_{104}/Γ

VALUE (units 10^{-6})	CL%	DOCUMENT ID		TECN	COMMENT
<3.0	90	SHEN	10A	BELL	$\Upsilon(1S) \to \gamma X$

$\Gamma(\gamma\chi_{c1}(4140) \to \phi J/\psi)/\Gamma_{total}$ Γ_{105}/Γ

VALUE (units 10^{-6})	CL%	DOCUMENT ID		TECN	COMMENT
<2.2	90	SHEN	10A	BELL	$\Upsilon(1S) \to \gamma X$

$\Gamma(\gamma X)/\Gamma_{total}$ Γ_{106}/Γ

(X = scalar with $m < 8.0$ GeV)

VALUE (units 10^{-6})	CL%	DOCUMENT ID		TECN	COMMENT
< 4.5	90	[38] DEL-AMO-SA...11J		BABR	$e^+e^- \to \gamma +$ X
• • • We do not use the following data for averages, fits, limits, etc. • • •					
<30	90	[39] BALEST	95	CLEO	$e^+e^- \to \gamma +$ X

[38] For a noninteracting scalar X with mass $m < 8.0$ GeV.
[39] For a noninteracting pseudoscalar X with mass < 7.2 GeV.

$\Gamma(\gamma X\overline{X}(m_X < 3.1\ \text{GeV}))/\Gamma_{total}$ Γ_{107}/Γ

($X\overline{X}$ = vectors with m< 3.1 GeV)

VALUE (units 10^{-3})	CL%	DOCUMENT ID		TECN	COMMENT
<1	90	[40] BALEST	95	CLEO	$e^+e^- \to \gamma +$ $X\overline{X}$

[40] For a noninteracting vector X with mass < 3.1 GeV.

$\Gamma(\gamma X\overline{X}(m_X < 4.5\ \text{GeV}))/\Gamma_{total}$ Γ_{108}/Γ

X and $\overline{X}$ = zero spin with $m < 4.5$ GeV

VALUE (units 10^{-5})	CL%	DOCUMENT ID		TECN	COMMENT
<24	90	[41] DEL-AMO-SA...11J		BABR	$e^+e^- \to \gamma +$ $X\overline{X}$

[41] For a noninteracting scalar X with mass $m < 4.5$ GeV.

$\Gamma(\gamma X \to \gamma + \geq 4\ \text{prongs})/\Gamma_{total}$ Γ_{109}/Γ

(1.5 GeV $< m_X <$ 5.0 GeV)

VALUE (units 10^{-4})	CL%	DOCUMENT ID		TECN	COMMENT
<1.78	95	ROSNER	07A	CLEO	$e^+e^- \to \gamma X$

$\Gamma(\gamma a_1^0 \to \gamma\mu^+\mu^-)/\Gamma_{total}$ Γ_{110}/Γ

(201 < M($\mu^+\mu^-$) < 3565 MeV)

VALUE (units 10^{-6})	CL%	DOCUMENT ID		TECN	COMMENT
<9	90	[42] LOVE	08	CLEO	$e^+e^- \to \gamma a_1^0 \to \gamma\mu^+\mu^-$
• • • We do not use the following data for averages, fits, limits, etc. • • •					
<9.7	90	[43] LEES	13C	BABR	$e^+e^- \to \gamma a_1^0 \to \gamma\mu^+\mu^-$

[42] For a narrow scalar or pseudoscalar a_1^0 with 201 < M($\mu^+\mu^-$) < 3565 MeV, excluding J/ψ. Measured 90% CL limits as a function of M($\mu^+\mu^-$) range from 1–9 $\times 10^{-6}$.
[43] For a narrow scalar or pseudoscalar a_1^0 with mass in the range 212–9200 MeV, excluding J/ψ and $\psi(2S)$. Measured 90% CL limits as a function of $m_{a_1^0}$ range from 0.28–9.7 $\times$ 10^{-6}.

$\Gamma(\gamma a_1^0 \to \gamma\tau^+\tau^-)/\Gamma_{total}$ Γ_{111}/Γ

($2m_\tau <$ M($\tau^+\tau^-$) < 9.2 GeV)

VALUE (units 10^{-6})	CL%	DOCUMENT ID		TECN	COMMENT
<130	90	[44] LEES	13R	BABR	$\Upsilon(2S) \to \gamma\tau^+\tau^-\pi^+\pi^-$
• • • We do not use the following data for averages, fits, limits, etc. • • •					
< 50	90	[45] LOVE	08	CLEO	$e^+e^- \to \gamma a_1^0 \to \gamma\tau^+\tau^-$

[44] For a narrow scalar a_1^0 with $2m_\tau <$ M(a_1^0) < 9.2 GeV, which result in a 90% CL upper limits of 0.9×10^{-5} at M(a_1^0) = $2m_\tau$, $\approx 1.5\times10^{-5}$ at M(a_1^0) = 7.5 GeV, and 13×10^{-5} at M(a_1^0) = 9.2 GeV.
[45] For a narrow scalar or pseudoscalar a_1^0 with $2m_\tau <$ M(a_1^0) < 7.5 GeV, which result in a 90% CL limits ranging from 1×10^{-5} at M(a_1^0)=$2m_\tau$ to 5×10^{-5} at M(a_1^0)=7.5 GeV.

$\Gamma(\gamma a_1^0 \to \gamma g g)/\Gamma_{total}$ Γ_{112}/Γ

(0.5 GeV < m < 9.0 GeV)

VALUE	CL%	DOCUMENT ID		TECN	COMMENT
<1 × 10^{-2}	90	[46] LEES	13L	BABR	$\Upsilon(1S) \to \gamma X$

[46] For a narrow, CP-odd pseudoscalar a_1^0 searched for in 26 hadronic decay modes with invariant mass 0.5 GeV < m_X < 9.0 GeV. Measured 90% CL limit as a function of m_X range from 10^{-6} to 10^{-2}.

$\Gamma(\gamma a_1^0 \to \gamma s\overline{s})/\Gamma_{total}$ Γ_{113}/Γ

(0.5 GeV < m < 9.0 GeV)

VALUE	CL%	DOCUMENT ID		TECN	COMMENT
<1 × 10^{-3}	90	[47] LEES	13L	BABR	$\Upsilon(1S) \to \gamma X$

[47] For a narrow, CP-odd pseudoscalar a_1^0 searched for in 14 hadronic decay modes with invariant mass 1.5 GeV < m_X < 9.0 GeV. Measured 90% CL limit as a function of m_X range from 10^{-5} to 10^{-3}.

LEPTON FAMILY NUMBER (LF) VIOLATING MODES

$\Gamma(\mu^\pm\tau^\mp)/\Gamma_{total}$ Γ_{114}/Γ

VALUE (units 10^{-6})	CL%	DOCUMENT ID		TECN	COMMENT
<6.0	95	LOVE	08A	CLEO	$e^+e^- \to \mu^\pm\tau^\mp$

OTHER DECAYS

$\Gamma(\text{invisible})/\Gamma_{total}$ Γ_{115}/Γ

VALUE (units 10^{-4})	CL%	DOCUMENT ID		TECN	COMMENT
< 3.0	90	AUBERT	09AX	BABR	$\Upsilon(3S) \to \pi^+\pi^-\Upsilon(1S)$
• • • We do not use the following data for averages, fits, limits, etc. • • •					
<39	90	RUBIN	07	CLEO	$\Upsilon(2S) \to \pi^+\pi^-\Upsilon(1S)$
<25	90	TAJIMA	07	BELL	$\Upsilon(3S) \to \pi^+\pi^-\Upsilon(1S)$

$\Upsilon(1S)$ REFERENCES

JIA	17	PR D95 012001	S. Jia *et al.*	(BELLE Collab.)
JIA	17A	PR D96 112002	S. Jia *et al.*	(BELLE Collab.)
SHEN	16	PR D93 112013	C.P. Shen *et al.*	(BELLE Collab.)
LEES	14G	PR D89 111102	J.P. Lees *et al.*	(BABAR Collab.)
YANG	14	PR D90 112008	S.D. Yang *et al.*	(BELLE Collab.)
LEES	13C	PR D87 031102	J.P. Lees *et al.*	(BABAR Collab.)
LEES	13L	PR D88 031701	J.P. Lees *et al.*	(BABAR Collab.)
LEES	13R	PR D88 071102	J.P. Lees *et al.*	(BABAR Collab.)
SHEN	13	PR D88 011102	C.P. Shen *et al.*	(BELLE Collab.)
DOBBS	12A	PR D86 052003	S. Dobbs *et al.*	
SHEN	12A	PR D86 031102	C.P. Shen *et al.*	(BELLE Collab.)
BESSON	11	PR D83 037101	D. Besson *et al.*	(CLEO Collab.)
DEL-AMO-SA...	11J	PRL 107 021804	P. del Amo Sanchez *et al.*	(BABAR Collab.)
AUBERT	10C	PR D81 011102	B. Aubert *et al.*	(BABAR Collab.)
DEL-AMO-SA...	10C	PRL 104 191801	P. del Amo Sanchez *et al.*	(BABAR Collab.)
SHEN	10A	PR D82 051504	C.P. Shen *et al.*	(BELLE Collab.)
AUBERT	09AX	PRL 103 251801	B. Aubert *et al.*	(BABAR Collab.)
LOVE	08	PRL 101 151802	W. Love *et al.*	(CLEO Collab.)
LOVE	08A	PRL 101 201601	W. Love *et al.*	(CLEO Collab.)
PDG	08	PL B667 1	C. Amsler *et al.*	(PDG Collab.)
ASNER	07	PR D75 012009	D.M. Asner *et al.*	(CLEO Collab.)
ATHAR	07A	PR D76 072003	S.B. Athar *et al.*	(CLEO Collab.)
BESSON	07	PRL 98 052002	D. Besson *et al.*	(CLEO Collab.)
BESSON	07A	PR D75 072001	D. Besson *et al.*	(CLEO Collab.)
ROSNER	07A	PR D76 117102	J.L. Rosner *et al.*	(CLEO Collab.)
RUBIN	07	PR D75 031104	P. Rubin *et al.*	(CLEO Collab.)
TAJIMA	07	PRL 98 132001	O. Tajima *et al.*	(BELLE Collab.)
AQUINES	06A	PR D74 092006	O. Aquines *et al.*	(CLEO Collab.)
ATHAR	06	PR D73 032001	S.B. Athar *et al.*	(CLEO Collab.)
BESSON	06A	PR D74 012003	D. Besson *et al.*	(CLEO Collab.)
ROSNER	06	PRL 96 092003	J.L. Rosner *et al.*	(CLEO Collab.)
ADAMS	05	PRL 94 012001	G.S. Adams *et al.*	(CLEO Collab.)
BRIERE	04	PR D70 072001	R.A. Briere *et al.*	(CLEO Collab.)
ARTUSO	03	PR D67 052003	M. Artuso *et al.*	(CLEO Collab.)
MASEK	02	PR D65 072002	G. Masek *et al.*	(CLEO Collab.)
RICHICHI	01B	PRL 87 141801	S.J. Richichi *et al.*	(CLEO Collab.)
ARTAMONOV	00	PL B474 427	A.S. Artamonov *et al.*	
ANASTASSOV	99	PRL 82 286	A. Anastassov *et al.*	(CLEO Collab.)
ALEXANDER	98	PR D58 052004	J.P. Alexander *et al.*	(CLEO Collab.)
BARU	96	PRPL 267 71	S.E. Baru *et al.*	(NOVO)
BALEST	95	PR D51 2053	R. Balest *et al.*	(CLEO Collab.)
CINABRO	94B	PL B340 129	D. Cinabro *et al.*	(CLEO Collab.)
ALBRECHT	92J	ZPHY C55 25	H. Albrecht *et al.*	(ARGUS Collab.)
BARU	92	ZPHY C54 229	S.E. Baru *et al.*	(NOVO)
BARU	92B	ZPHY C56 547	S.E. Baru *et al.*	(NOVO)
KOBEL	92	ZPHY C53 193	M. Kobel *et al.*	(Crystal Ball Collab.)
BLINOV	90	PL B245 311	A.E. Blinov *et al.*	(NOVO)
FULTON	90B	PR D41 1401	R. Fulton *et al.*	(CLEO Collab.)
MASCHMANN	90	ZPHY C46 555	W.S. Maschmann *et al.*	(Crystal Ball Collab.)
ALBRECHT	89	ZPHY C42 349	H. Albrecht *et al.*	(ARGUS Collab.)
ALEXANDER	89	NP B320 45	J.P. Alexander *et al.*	(LBL, MICH, SLAC)
BARU	89	ZPHY C42 505	S.E. Baru *et al.*	(NOVO)
CHEN	89B	PR D39 3528	W.Y. Chen *et al.*	(CLEO Collab.)
FULTON	89	PL B224 445	R. Fulton *et al.*	(CLEO Collab.)
KAARSBERG	89	PRL 62 2077	T.M. Kaarsberg *et al.*	(CUSB Collab.)
BUCHMUEL...	88	HE e^+e^- Physics 412	W. Buchmueller, S. Cooper	(HANN, DESY, MIT)
		Editors: A. Ali and P. Soeding, World Scientific, Singapore		
JAKUBOWSKI	88	ZPHY C40 49	Z. Jakubowski *et al.*	(Crystal Ball Collab.) IGJPC
SCHMITT	88	ZPHY C40 199	P. Schmitt *et al.*	(Crystal Ball Collab.)
ALBRECHT	87	ZPHY C35 283	H. Albrecht *et al.*	(ARGUS Collab.)
COHEN	87	RMP 59 1121	E.R. Cohen, B.N. Taylor	(RISC, NBS)
BARU	86	ZPHY C30 551	S.E. Baru *et al.*	(NOVO)
ALBRECHT	85C	PL 154B 452	H. Albrecht *et al.*	(ARGUS Collab.)
KURAEV	85	SJNP 41 466	E.A. Kuraev, V.S. Fadin	(NOVO)
		Translated from YAF 41 733.		
ARTAMONOV	84	PL 137B 272	A.S. Artamonov *et al.*	(NOVO)
BESSON	84	PR D30 1433	D. Besson *et al.*	(CLEO Collab.)
GILES	84B	PR D29 1285	R. Giles *et al.*	(CLEO Collab.)
MACKAY	84	PR D29 2483	W.W. MacKay *et al.*	(CUSB Collab.)
ANDREWS	83	PRL 50 807	D.E. Andrews *et al.*	(CLEO Collab.)
GILES	83	PRL 50 877	R. Giles *et al.*	(HARV, OSU, ROCH, RUTG+)
NICZYPORUK	83	ZPHY C17 197	B. Niczyporuk *et al.*	(LENA Collab.)
ALBRECHT	82	PL 116B 383	H. Albrecht *et al.*	(DESY, DORT, HEIDH+)

Meson Particle Listings

$\Upsilon(1S)$, $\chi_{b0}(1P)$

ARTAMONOV	82	PL 118B 225	A.S. Artamonov *et al.*	(NOVO)
NICZYPORUK	82	ZPHY C15 299	B. Niczyporuk *et al.*	(LENA Collab.)
BERGER	80C	PL 93B 497	C. Berger *et al.*	(PLUTO Collab.)
BOCK	80	ZPHY C6 125	P. Bock *et al.*	(HEIDP, MPIM, DESY, HAMB)
BERGER	79	ZPHY C1 343	C. Berger *et al.*	(PLUTO Collab.)

$\chi_{b0}(1P)$

$I^G(J^{PC}) = 0^+(0^{++})$
J needs confirmation.

Observed in radiative decay of the $\Upsilon(2S)$, therefore $C = +$. Branching ratio requires E1 transition, M1 is strongly disfavored, therefore $P = +$.

$\chi_{b0}(1P)$ MASS

VALUE (MeV)	DOCUMENT ID
9859.44±0.42±0.31 OUR EVALUATION	From average γ energy below, using $\Upsilon(2S)$ mass = 10023.26 ± 0.31 MeV

$m_{\chi_{b1}(1P)} - m_{\chi_{b0}(1P)}$

VALUE (MeV)	DOCUMENT ID		TECN	COMMENT
32.49±0.93	LEES	14M	BABR	$\Upsilon(2S) \to \gamma\gamma\mu^+\mu^-$

γ ENERGY IN $\Upsilon(2S)$ DECAY

VALUE (MeV)	DOCUMENT ID		TECN	COMMENT
162.5 ±0.4 OUR AVERAGE				
162.56±0.19±0.42	ARTUSO	05	CLEO	$\Upsilon(2S) \to \gamma X$
162.0 ±0.8 ±1.2	EDWARDS	99	CLE2	$\Upsilon(2S) \to \gamma\chi(1P)$
162.1 ±0.5 ±1.4	ALBRECHT	85E	ARG	$\Upsilon(2S) \to$ conv.γX
163.8 ±1.6 ±2.7	NERNST	85	CBAL	$\Upsilon(2S) \to \gamma$X
158.0 ±7 ±1	HAAS	84	CLEO	$\Upsilon(2S) \to$ conv.γX
• • • We do not use the following data for averages, fits, limits, etc. • • •				
149.4 ±0.7 ±5.0	KLOPFEN...	83	CUSB	$\Upsilon(2S) \to \gamma$X

$\chi_{b0}(1P)$ DECAY MODES

	Mode	Fraction (Γ_i/Γ)	Confidence level
Γ_1	$\gamma\Upsilon(1S)$	(1.94±0.27) %	
Γ_2	D^0X	< 10.4 %	90%
Γ_3	$\pi^+\pi^-K^+K^-\pi^0$	< 1.6 $\times 10^{-4}$	90%
Γ_4	$2\pi^+\pi^-K^-K^0_S$	< 5 $\times 10^{-5}$	90%
Γ_5	$2\pi^+\pi^-K^-K^0_S2\pi^0$	< 5 $\times 10^{-4}$	90%
Γ_6	$2\pi^+2\pi^-2\pi^0$	< 2.1 $\times 10^{-4}$	90%
Γ_7	$2\pi^+2\pi^-K^+K^-$	(1.1 ±0.6) $\times 10^{-4}$	
Γ_8	$2\pi^+2\pi^-K^+K^-\pi^0$	< 2.7 $\times 10^{-4}$	90%
Γ_9	$2\pi^+2\pi^-K^+K^-2\pi^0$	< 5 $\times 10^{-4}$	90%
Γ_{10}	$3\pi^+2\pi^-K^-K^0_S\pi^0$	< 1.6 $\times 10^{-4}$	90%
Γ_{11}	$3\pi^+3\pi^-$	< 8 $\times 10^{-5}$	90%
Γ_{12}	$3\pi^+3\pi^-2\pi^0$	< 6 $\times 10^{-4}$	90%
Γ_{13}	$3\pi^+3\pi^-K^+K^-$	(2.4 ±1.2) $\times 10^{-4}$	
Γ_{14}	$3\pi^+3\pi^-K^+K^-\pi^0$	< 1.0 $\times 10^{-3}$	90%
Γ_{15}	$4\pi^+4\pi^-$	< 8 $\times 10^{-5}$	90%
Γ_{16}	$4\pi^+4\pi^-2\pi^0$	< 2.1 $\times 10^{-3}$	90%
Γ_{17}	$J/\psi J/\psi$	< 7 $\times 10^{-5}$	90%
Γ_{18}	$J/\psi\psi(2S)$	< 1.2 $\times 10^{-4}$	90%
Γ_{19}	$\psi(2S)\psi(2S)$	< 3.1 $\times 10^{-5}$	90%
Γ_{20}	$J/\psi(1S)$ anything	< 2.3 $\times 10^{-3}$	90%

$\chi_{b0}(1P)$ BRANCHING RATIOS

$\Gamma(\gamma\Upsilon(1S))/\Gamma_{total}$ — Γ_1/Γ

VALUE (%)	CL%	EVTS	DOCUMENT ID		TECN	COMMENT
1.94±0.27 OUR AVERAGE						
2.07±0.24±0.21			[1,2] LEES	14M	BABR	$\Upsilon(2S) \to \gamma\gamma\mu^+\mu^-$
1.76±0.30±0.18		87	[3,4] KORNICER	11	CLEO	$e^+e^- \to \gamma\gamma\ell^+\ell^-$
• • • We do not use the following data for averages, fits, limits, etc. • • •						
< 4.6	90		[5] LEES	11J	BABR	$\Upsilon(2S) \to X\gamma$
< 6	90		WALK	86	CBAL	$\Upsilon(2S) \to \gamma\gamma\ell^+\ell^-$
<11	90		PAUSS	83	CUSB	$\Upsilon(2S) \to \gamma\gamma\ell^+\ell^-$

[1] LEES 14M quotes $\Gamma(\chi_{b0}(1P) \to \gamma\Upsilon(1S))/\Gamma_{total} \times \Gamma(\Upsilon(2S) \to \gamma\chi_{b0}(1P))/\Gamma_{total}$ = (7.75 ± 0.91) × 10^{-4} combining the results from samples of $\Upsilon(2S) \to \gamma\gamma\mu^+\mu^-$ with and without converted photons. Assumes B($\Upsilon(1S) \to \mu^+\mu^-$) = (2.48 ± 0.05)%.

[2] LEES 14M reports $[\Gamma(\chi_{b0}(1P) \to \gamma\Upsilon(1S))/\Gamma_{total}] \times [B(\Upsilon(2S) \to \gamma\chi_{b0}(1P))]$ = (7.75 ± 0.91) × 10^{-4} which we divide by our best value B($\Upsilon(2S) \to \gamma\chi_{b0}(1P)$) = (3.8 ± 0.4) × 10^{-2}. Our first error is their experiment's error and our second error is the systematic error from using our best value.

[3] Assuming B($\Upsilon(1S) \to \ell^+\ell^-$) = (2.48 ± 0.05)%.

[4] KORNICER 11 reports $[\Gamma(\chi_{b0}(1P) \to \gamma\Upsilon(1S))/\Gamma_{total}] \times [B(\Upsilon(2S) \to \gamma\chi_{b0}(1P))]$ = (6.59 ± 0.96 ± 0.60) × 10^{-4} which we divide by our best value B($\Upsilon(2S) \to \gamma\chi_{b0}(1P)$) = (3.8 ± 0.4) × 10^{-2}. Our first error is their experiment's error and our second error is the systematic error from using our best value.

[5] LEES 11J quotes a central value of $\Gamma(\chi_{b0}(1P) \to \gamma\Upsilon(1S))/\Gamma_{total} \times \Gamma(\Upsilon(2S) \to \gamma\chi_{b0}(1P))/\Gamma_{total} = (8.3 \pm 5.6^{+3.7}_{-2.6}) \times 10^{-4}$.

$\Gamma(D^0X)/\Gamma_{total}$ — Γ_2/Γ

VALUE	CL%	DOCUMENT ID		TECN	COMMENT
<10.4 × 10^{-2}	90	[6,7] BRIERE	08	CLEO	$\Upsilon(2S) \to \gamma D^0X$

[6] For $p_{D^0} > 2.5$ GeV/c.

[7] The authors also present their result as (5.6 ± 3.6 ± 0.5) × 10^{-2}.

$\Gamma(\pi^+\pi^-K^+K^-\pi^0)/\Gamma_{total}$ — Γ_3/Γ

VALUE (units 10^{-4})	CL%	DOCUMENT ID		TECN	COMMENT
<1.6	90	[8] ASNER	08A	CLEO	$\Upsilon(2S) \to \gamma\pi^+\pi^-K^+K^-\pi^0$

[8] ASNER 08A reports $[\Gamma(\chi_{b0}(1P) \to \pi^+\pi^-K^+K^-\pi^0)/\Gamma_{total}] \times [B(\Upsilon(2S) \to \gamma\chi_{b0}(1P))] < 6 \times 10^{-6}$ which we divide by our best value B($\Upsilon(2S) \to \gamma\chi_{b0}(1P)$) = 3.8×10^{-2}.

$\Gamma(2\pi^+\pi^-K^-K^0_S)/\Gamma_{total}$ — Γ_4/Γ

VALUE (units 10^{-4})	CL%	DOCUMENT ID		TECN	COMMENT
<0.5	90	[9] ASNER	08A	CLEO	$\Upsilon(2S) \to \gamma 2\pi^+\pi^-K^-K^0_S$

[9] ASNER 08A reports $[\Gamma(\chi_{b0}(1P) \to 2\pi^+\pi^-K^0_S)/\Gamma_{total}] \times [B(\Upsilon(2S) \to \gamma\chi_{b0}(1P))] < 2 \times 10^{-6}$ which we divide by our best value B($\Upsilon(2S) \to \gamma\chi_{b0}(1P)$) = 3.8×10^{-2}.

$\Gamma(2\pi^+\pi^-K^-K^0_S2\pi^0)/\Gamma_{total}$ — Γ_5/Γ

VALUE (units 10^{-4})	CL%	DOCUMENT ID		TECN	COMMENT
<5	90	[10] ASNER	08A	CLEO	$\Upsilon(2S) \to \gamma 2\pi^+\pi^-K^-2\pi^0$

[10] ASNER 08A reports $[\Gamma(\chi_{b0}(1P) \to 2\pi^+\pi^-K^0_S2\pi^0)/\Gamma_{total}] \times [B(\Upsilon(2S) \to \gamma\chi_{b0}(1P))] < 18 \times 10^{-6}$ which we divide by our best value B($\Upsilon(2S) \to \gamma\chi_{b0}(1P)$) = 3.8×10^{-2}.

$\Gamma(2\pi^+2\pi^-2\pi^0)/\Gamma_{total}$ — Γ_6/Γ

VALUE (units 10^{-4})	CL%	DOCUMENT ID		TECN	COMMENT
<2.1	90	[11] ASNER	08A	CLEO	$\Upsilon(2S) \to \gamma 2\pi^+2\pi^-2\pi^0$

[11] ASNER 08A reports $[\Gamma(\chi_{b0}(1P) \to 2\pi^+2\pi^-2\pi^0)/\Gamma_{total}] \times [B(\Upsilon(2S) \to \gamma\chi_{b0}(1P))] < 8 \times 10^{-6}$ which we divide by our best value B($\Upsilon(2S) \to \gamma\chi_{b0}(1P)$) = 3.8×10^{-2}.

$\Gamma(2\pi^+2\pi^-K^+K^-)/\Gamma_{total}$ — Γ_7/Γ

VALUE (units 10^{-4})	EVTS	DOCUMENT ID		TECN	COMMENT
1.1±0.6±0.1	7	[12] ASNER	08A	CLEO	$\Upsilon(2S) \to \gamma 2\pi^+2\pi^-K^+K^-$

[12] ASNER 08A reports $[\Gamma(\chi_{b0}(1P) \to 2\pi^+2\pi^-K^+K^-)/\Gamma_{total}] \times [B(\Upsilon(2S) \to \gamma\chi_{b0}(1P))] = (4 \pm 2 \pm 1) \times 10^{-6}$ which we divide by our best value B($\Upsilon(2S) \to \gamma\chi_{b0}(1P)$) = (3.8 ± 0.4) × 10^{-2}. Our first error is their experiment's error and our second error is the systematic error from using our best value.

$\Gamma(2\pi^+2\pi^-K^+K^-\pi^0)/\Gamma_{total}$ — Γ_8/Γ

VALUE (units 10^{-4})	CL%	DOCUMENT ID		TECN	COMMENT
<2.7	90	[13] ASNER	08A	CLEO	$\Upsilon(2S) \to \gamma 2\pi^+2\pi^-K^+K^-\pi^0$

[13] ASNER 08A reports $[\Gamma(\chi_{b0}(1P) \to 2\pi^+2\pi^-K^+K^-\pi^0)/\Gamma_{total}] \times [B(\Upsilon(2S) \to \gamma\chi_{b0}(1P))] < 10 \times 10^{-6}$ which we divide by our best value B($\Upsilon(2S) \to \gamma\chi_{b0}(1P)$) = 3.8×10^{-2}.

$\Gamma(2\pi^+2\pi^-K^+K^-2\pi^0)/\Gamma_{total}$ — Γ_9/Γ

VALUE (units 10^{-4})	CL%	DOCUMENT ID		TECN	COMMENT
<5	90	[14] ASNER	08A	CLEO	$\Upsilon(2S) \to \gamma 2\pi^+2\pi^-K^+K^-2\pi^0$

[14] ASNER 08A reports $[\Gamma(\chi_{b0}(1P) \to 2\pi^+2\pi^-K^+K^-2\pi^0)/\Gamma_{total}] \times [B(\Upsilon(2S) \to \gamma\chi_{b0}(1P))] < 20 \times 10^{-6}$ which we divide by our best value B($\Upsilon(2S) \to \gamma\chi_{b0}(1P)$) = 3.8×10^{-2}.

$\Gamma(3\pi^+2\pi^-K^-K^0_S\pi^0)/\Gamma_{total}$ — Γ_{10}/Γ

VALUE (units 10^{-4})	CL%	DOCUMENT ID		TECN	COMMENT
<1.6	90	[15] ASNER	08A	CLEO	$\Upsilon(2S) \to \gamma 3\pi^+2\pi^-K^-K^0_S\pi^0$

[15] ASNER 08A reports $[\Gamma(\chi_{b0}(1P) \to 3\pi^+2\pi^-K^-K^0_S\pi^0)/\Gamma_{total}] \times [B(\Upsilon(2S) \to \gamma\chi_{b0}(1P))] < 6 \times 10^{-6}$ which we divide by our best value B($\Upsilon(2S) \to \gamma\chi_{b0}(1P)$) = 3.8×10^{-2}.

$\Gamma(3\pi^+3\pi^-)/\Gamma_{total}$ — Γ_{11}/Γ

VALUE (units 10^{-4})	CL%	DOCUMENT ID		TECN	COMMENT
<0.8	90	[16] ASNER	08A	CLEO	$\Upsilon(2S) \to \gamma 3\pi^+3\pi^-$

[16] ASNER 08A reports $[\Gamma(\chi_{b0}(1P) \to 3\pi^+3\pi^-)/\Gamma_{total}] \times [B(\Upsilon(2S) \to \gamma\chi_{b0}(1P))] < 3 \times 10^{-6}$ which we divide by our best value B($\Upsilon(2S) \to \gamma\chi_{b0}(1P)$) = 3.8×10^{-2}.

$\Gamma(3\pi^+3\pi^-2\pi^0)/\Gamma_{total}$ — Γ_{12}/Γ

VALUE (units 10^{-4})	CL%	DOCUMENT ID		TECN	COMMENT
<6	90	[17] ASNER	08A	CLEO	$\Upsilon(2S) \to \gamma 3\pi^+3\pi^-2\pi^0$

[17] ASNER 08A reports $[\Gamma(\chi_{b0}(1P) \to 3\pi^+3\pi^-2\pi^0)/\Gamma_{total}] \times [B(\Upsilon(2S) \to \gamma\chi_{b0}(1P))] < 22 \times 10^{-6}$ which we divide by our best value B($\Upsilon(2S) \to \gamma\chi_{b0}(1P)$) = 3.8×10^{-2}.

$\Gamma(3\pi^+3\pi^-K^+K^-)/\Gamma_{total}$ Γ_{13}/Γ

VALUE (units 10^{-4})	EVTS	DOCUMENT ID		TECN	COMMENT
2.4±1.2±0.2	9	[18] ASNER	08A	CLEO	$\Upsilon(2S) \to \gamma 3\pi^+3\pi^-K^+K^-$

[18] ASNER 08A reports $[\Gamma(\chi_{b0}(1P) \to 3\pi^+3\pi^-K^+K^-)/\Gamma_{total}] \times [B(\Upsilon(2S) \to \gamma\chi_{b0}(1P))] = (9 \pm 4 \pm 2) \times 10^{-6}$ which we divide by our best value $B(\Upsilon(2S) \to \gamma\chi_{b0}(1P)) = (3.8 \pm 0.4) \times 10^{-2}$. Our first error is their experiment's error and our second error is the systematic error from using our best value.

$\Gamma(3\pi^+3\pi^-K^+K^-\pi^0)/\Gamma_{total}$ Γ_{14}/Γ

VALUE (units 10^{-4})	CL%	DOCUMENT ID		TECN	COMMENT
<10	90	[19] ASNER	08A	CLEO	$\Upsilon(2S) \to \gamma 3\pi^+3\pi^-K^+K^-\pi^0$

[19] ASNER 08A reports $[\Gamma(\chi_{b0}(1P) \to 3\pi^+3\pi^-K^+K^-\pi^0)/\Gamma_{total}] \times [B(\Upsilon(2S) \to \gamma\chi_{b0}(1P))] < 37 \times 10^{-6}$ which we divide by our best value $B(\Upsilon(2S) \to \gamma\chi_{b0}(1P)) = 3.8 \times 10^{-2}$.

$\Gamma(4\pi^+4\pi^-)/\Gamma_{total}$ Γ_{15}/Γ

VALUE (units 10^{-4})	CL%	DOCUMENT ID		TECN	COMMENT
<0.8	90	[20] ASNER	08A	CLEO	$\Upsilon(2S) \to \gamma 4\pi^+4\pi^-$

[20] ASNER 08A reports $[\Gamma(\chi_{b0}(1P) \to 4\pi^+4\pi^-)/\Gamma_{total}] \times [B(\Upsilon(2S) \to \gamma\chi_{b0}(1P))] < 3 \times 10^{-6}$ which we divide by our best value $B(\Upsilon(2S) \to \gamma\chi_{b0}(1P)) = 3.8 \times 10^{-2}$.

$\Gamma(4\pi^+4\pi^-2\pi^0)/\Gamma_{total}$ Γ_{16}/Γ

VALUE (units 10^{-4})	CL%	DOCUMENT ID		TECN	COMMENT
<21	90	[21] ASNER	08A	CLEO	$\Upsilon(2S) \to \gamma 4\pi^+4\pi^-2\pi^0$

[21] ASNER 08A reports $[\Gamma(\chi_{b0}(1P) \to 4\pi^+4\pi^-2\pi^0)/\Gamma_{total}] \times [B(\Upsilon(2S) \to \gamma\chi_{b0}(1P))] < 77 \times 10^{-6}$ which we divide by our best value $B(\Upsilon(2S) \to \gamma\chi_{b0}(1P)) = 3.8 \times 10^{-2}$.

$\Gamma(J/\psi J/\psi)/\Gamma_{total}$ Γ_{17}/Γ

VALUE (units 10^{-5})	CL%	DOCUMENT ID		TECN	COMMENT
<7	90	[22] SHEN	12	BELL	$\Upsilon(2S) \to \gamma\psi X$

[22] SHEN 12 reports $< 7.1 \times 10^{-5}$ from a measurement of $[\Gamma(\chi_{b0}(1P) \to J/\psi J/\psi)/\Gamma_{total}] \times [B(\Upsilon(2S) \to \gamma\chi_{b0}(1P))]$ assuming $B(\Upsilon(2S) \to \gamma\chi_{b0}(1P)) = (3.8 \pm 0.4) \times 10^{-2}$.

$\Gamma(J/\psi\psi(2S))/\Gamma_{total}$ Γ_{18}/Γ

VALUE (units 10^{-5})	CL%	DOCUMENT ID		TECN	COMMENT
<12	90	[23] SHEN	12	BELL	$\Upsilon(2S) \to \gamma\psi X$

[23] SHEN 12 reports $< 12 \times 10^{-5}$ from a measurement of $[\Gamma(\chi_{b0}(1P) \to J/\psi\psi(2S))/\Gamma_{total}] \times [B(\Upsilon(2S) \to \gamma\chi_{b0}(1P))]$ assuming $B(\Upsilon(2S) \to \gamma\chi_{b0}(1P)) = (3.8 \pm 0.4) \times 10^{-2}$.

$\Gamma(\psi(2S)\psi(2S))/\Gamma_{total}$ Γ_{19}/Γ

VALUE (units 10^{-5})	CL%	DOCUMENT ID		TECN	COMMENT
<3.1	90	[24] SHEN	12	BELL	$\Upsilon(2S) \to \gamma\psi X$

[24] SHEN 12 reports $< 3.1 \times 10^{-5}$ from a measurement of $[\Gamma(\chi_{b0}(1P) \to \psi(2S)\psi(2S))/\Gamma_{total}] \times [B(\Upsilon(2S) \to \gamma\chi_{b0}(1P))]$ assuming $B(\Upsilon(2S) \to \gamma\chi_{b0}(1P)) = (3.8 \pm 0.4) \times 10^{-2}$.

$\Gamma(J/\psi(1S)\,\text{anything})/\Gamma_{total}$ Γ_{20}/Γ

VALUE	CL%	DOCUMENT ID		TECN	COMMENT
<2.3 × 10⁻³	90	JIA	17A	BELL	$e^+e^- \to$ hadrons

$\chi_{b0}(1P)$ CROSS-PARTICLE BRANCHING RATIOS

$\Gamma(\chi_{b0}(1P) \to \gamma\Upsilon(1S))/\Gamma_{total} \times \Gamma(\Upsilon(2S) \to \gamma\chi_{b0}(1P))/\Gamma_{total}$ $\Gamma_1/\Gamma \times \Gamma_{52}^{\Upsilon(2S)}/\Gamma^{\Upsilon(2S)}$

VALUE	CL%	DOCUMENT ID		TECN	COMMENT
<1.7 × 10⁻³	90	[25] LEES	11J	BABR	$\Upsilon(2S) \to X\gamma$

[25] LEES 11J quotes a central value of $\Gamma(\chi_{b0}(1P) \to \gamma\Upsilon(1S))/\Gamma_{total} \times \Gamma(\Upsilon(2S) \to \gamma\chi_{b0}(1P))/\Gamma_{total} = (8.3 \pm 5.6^{+3.7}_{-2.6}) \times 10^{-4}$ and derives a 90% CL upper limit of $\Gamma(\gamma\Upsilon(1S))/\Gamma_{total} < 4.6\%$ using $B(\Upsilon(2S) \to \gamma\chi_{b0}(1P)) = (3.8 \pm 0.4)\%$.

$B(\chi_{b0}(1P) \to \gamma\Upsilon(1S)) \times B(\Upsilon(2S) \to \gamma\chi_{b0}(1P)) \times B(\Upsilon(1S) \to \ell^+\ell^-)$

VALUE (units 10^{-5})	EVTS	DOCUMENT ID		TECN	COMMENT
1.67±0.28 OUR AVERAGE					
$2.9\ ^{+1.7}_{-1.4}\ \pm 0.1 \pm 0.8$		[26] LEES	14M	BABR	$\Upsilon(2S) \to \gamma\gamma\mu^+\mu^-$
1.63±0.24±0.15	87	KORNICER	11	CLEO	$e^+e^- \to \gamma\gamma\ell^+\ell^-$

[26] From a sample of $\Upsilon(2S) \to \gamma\gamma\mu^+\mu^-$ with one converted photon.

$[B(\chi_{b0}(1P) \to \gamma\Upsilon(1S)) \times B(\Upsilon(2S) \to \gamma\chi_{b0}(1P))]$ / $[B(\chi_{b1}(1P) \to \gamma\Upsilon(1S)) \times B(\Upsilon(2S) \to \gamma\chi_{b1}(1P))]$

VALUE (%)	DOCUMENT ID		TECN	COMMENT
3.28±0.37	[27] LEES	14M	BABR	$\Upsilon(2S) \to \gamma\gamma\mu^+\mu^-$

[27] From a sample of $\Upsilon(2S) \to \gamma\gamma\mu^+\mu^-$ without converted photons.

$\chi_{b0}(1P)$ REFERENCES

JIA	17A	PR D96 112002	S. Jia *et al.*	(BELLE Collab.)
LEES	14M	PR D90 112010	J.P. Lees *et al.*	(BABAR Collab.)
SHEN	12	PR D85 071102	C.P. Shen *et al.*	(BELLE Collab.)
KORNICER	11	PR D83 054003	M. Kornicer *et al.*	(CLEO Collab.)
LEES	11J	PR D84 072002	J.P. Lees *et al.*	(BABAR Collab.)
ASNER	08A	PR D78 091103	D.M. Asner *et al.*	(CLEO Collab.)
BRIERE	08	PR D78 092007	R.A. Briere *et al.*	(CLEO Collab.)
ARTUSO	05	PRL 94 032001	M. Artuso *et al.*	(CLEO Collab.)
EDWARDS	99	PR D59 032003	K.W. Edwards *et al.*	(CLEO Collab.)
WALK	86	PR D34 2611	W.S. Walk *et al.*	(Crystal Ball Collab.)
ALBRECHT	85E	PL 160B 331	H. Albrecht *et al.*	(ARGUS Collab.)
NERNST	85	PRL 54 2195	R. Nernst *et al.*	(Crystal Ball Collab.)
HAAS	84	PRL 52 799	J. Haas *et al.*	(CLEO Collab.)
KLOPFEN...	83	PRL 51 160	C. Klopfenstein *et al.*	(CUSB Collab.)
PAUSS	83	PL 130B 439	F. Pauss *et al.*	(MPIM, COLU, CORN, LSU+)

$\chi_{b1}(1P)$

$I^G(J^{PC}) = 0^+(1^{++})$

J needs confirmation.

Observed in radiative decay of the $\Upsilon(2S)$, therefore $C = +$. Branching ratio requires E1 transition, M1 is strongly disfavored, therefore $P = +$. $J = 1$ from SKWARNICKI 87.

$\chi_{b1}(1P)$ MASS

VALUE (MeV)	DOCUMENT ID
9892.78±0.26±0.31 OUR EVALUATION	From average γ energy below, using $\Upsilon(2S)$ mass = 10023.26 ± 0.31 MeV

γ ENERGY IN $\Upsilon(2S)$ DECAY

VALUE (MeV)	DOCUMENT ID		TECN	COMMENT
129.63±0.33 OUR AVERAGE	Error includes scale factor of 1.3.			See the ideogram below.
129.58±0.09±0.29	ARTUSO	05	CLEO	$\Upsilon(2S) \to \gamma X$
128.8 ±0.4 ±0.6	EDWARDS	99	CLE2	$\Upsilon(2S) \to \gamma\chi(1P)$
131.7 ±0.9 ±1.3	WALK	86	CBAL	$\Upsilon(2S) \to \gamma\gamma\ell^+\ell^-$
131.7 ±0.3 ±1.1	ALBRECHT	85E	ARG	$\Upsilon(2S) \to$ conv.γX
130.6 ±0.8 ±2.4	NERNST	85	CBAL	$\Upsilon(2S) \to \gamma$X
129 ±0.8 ±1	HAAS	84	CLEO	$\Upsilon(2S) \to$ conv.γX
128.1 ±0.4 ±3.0	KLOPFEN...	83	CUSB	$\Upsilon(2S) \to \gamma$X
130.6 ±3.0	PAUSS	83	CUSB	$\Upsilon(2S) \to \gamma\gamma\ell^+\ell^-$

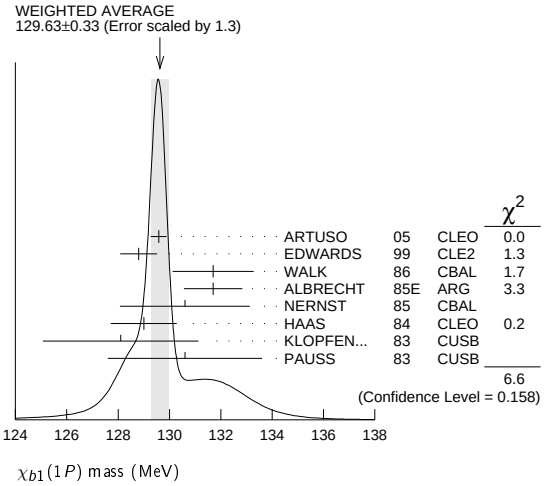

$\chi_{b1}(1P)$ DECAY MODES

	Mode	Fraction (Γ_j/Γ)	Confidence level
Γ_1	$\gamma\Upsilon(1S)$	(35.0 ±2.1) %	
Γ_2	D^0X	(12.6 ±2.2) %	
Γ_3	$\pi^+\pi^-K^+K^-\pi^0$	(2.0 ±0.6) × 10^{-4}	
Γ_4	$2\pi^+\pi^-K^-K^0_S$	(1.3 ±0.5) × 10^{-4}	
Γ_5	$2\pi^+\pi^-K^-K^0_S2\pi^0$	< 6 × 10^{-4}	90%
Γ_6	$2\pi^+2\pi^-2\pi^0$	(8.0 ±2.5) × 10^{-4}	
Γ_7	$2\pi^+2\pi^-K^+K^-$	(1.5 ±0.5) × 10^{-4}	
Γ_8	$2\pi^+2\pi^-K^+K^-\pi^0$	(3.5 ±1.2) × 10^{-4}	
Γ_9	$2\pi^+2\pi^-K^+K^-2\pi^0$	(8.6 ±3.2) × 10^{-4}	
Γ_{10}	$3\pi^+2\pi^-K^-K^0_S\pi^0$	(9.3 ±3.3) × 10^{-4}	
Γ_{11}	$3\pi^+3\pi^-$	(1.9 ±0.6) × 10^{-4}	
Γ_{12}	$3\pi^+3\pi^-2\pi^0$	(1.7 ±0.5) × 10^{-3}	
Γ_{13}	$3\pi^+3\pi^-K^+K^-$	(2.6 ±0.8) × 10^{-4}	
Γ_{14}	$3\pi^+3\pi^-K^+K^-\pi^0$	(7.5 ±2.6) × 10^{-4}	
Γ_{15}	$4\pi^+4\pi^-$	(2.6 ±0.9) × 10^{-4}	

Meson Particle Listings

$\chi_{b1}(1P)$

Γ_{16}	$4\pi^+4\pi^-2\pi^0$	(1.4 ±0.6) × 10^{-3}		
Γ_{17}	ω anything	(4.9 ±1.4) %		
Γ_{18}	ωX_{tetra}	< 4.44	× 10^{-4}	90%
Γ_{19}	$J/\psi J/\psi$	< 2.7	× 10^{-5}	90%
Γ_{20}	$J/\psi\psi(2S)$	< 1.7	× 10^{-5}	90%
Γ_{21}	$\psi(2S)\psi(2S)$	< 6	× 10^{-5}	90%
Γ_{22}	$J/\psi(1S)$ anything	< 1.1	× 10^{-3}	90%
Γ_{23}	$J/\psi(1S)X_{tetra}$	< 2.27	× 10^{-4}	90%

$\chi_{b1}(1P)$ BRANCHING RATIOS

$\Gamma(\gamma\Upsilon(1S))/\Gamma_{total}$ Γ_1/Γ

VALUE	EVTS	DOCUMENT ID		TECN	COMMENT
0.350±0.021 OUR AVERAGE					
0.364±0.017±0.019		1,2,3 LEES	14M	BABR	$\Upsilon(2S) \to \gamma\gamma\mu^+\mu^-$
0.331±0.018±0.017	3222	3,4 KORNICER	11	CLEO	$e^+e^- \to \gamma\gamma\ell^+\ell^-$
0.350±0.023±0.018	13k	5 LEES	11J	BABR	$\Upsilon(2S) \to X\gamma$
0.34 ±0.07 ±0.02	53	3,6,7 WALK	86	CBAL	$\Upsilon(2S) \to \gamma\gamma\ell^+\ell^-$
0.47 ±0.18		KLOPFEN...	83	CUSB	$\Upsilon(2S) \to \gamma\gamma\ell^+\ell^-$

[1] LEES 14M quotes $\Gamma(\chi_{b1}(1P) \to \gamma\Upsilon(1S))/\Gamma_{total} \times \Gamma(\Upsilon(2S) \to \gamma\chi_{b1}(1P))/\Gamma_{total}$ = (2.51 ± 0.12) % combining the results from samples of $\Upsilon(2S) \to \gamma\gamma\mu^+\mu^-$ with and without converted photons.

[2] LEES 14M reports $[\Gamma(\chi_{b1}(1P) \to \gamma\Upsilon(1S))/\Gamma_{total}] \times [B(\Upsilon(2S) \to \gamma\chi_{b1}(1P))]$ = (2.51 ± 0.12) × 10^{-2} which we divide by our best value $B(\Upsilon(2S) \to \gamma\chi_{b1}(1P))$ = (6.9 ± 0.4) × 10^{-2}. Our first error is their experiment's error and our second error is the systematic error from using our best value.

[3] Assuming $B(\Upsilon(1S) \to \mu^+\mu^-)$ = (2.48 ± 0.05)%.

[4] KORNICER 11 reports $[\Gamma(\chi_{b1}(1P) \to \gamma\Upsilon(1S))/\Gamma_{total}] \times [B(\Upsilon(2S) \to \gamma\chi_{b1}(1P))]$ = (22.8 ± 0.4 ± 1.2) × 10^{-3} which we divide by our best value $B(\Upsilon(2S) \to \gamma\chi_{b1}(1P))$ = (6.9 ± 0.4) × 10^{-2}. Our first error is their experiment's error and our second error is the systematic error from using our best value.

[5] LEES 11J reports $[\Gamma(\chi_{b1}(1P) \to \gamma\Upsilon(1S))/\Gamma_{total}] \times [B(\Upsilon(2S) \to \gamma\chi_{b1}(1P))]$ = (24.1 ± 0.6 ± 1.5) × 10^{-3} which we divide by our best value $B(\Upsilon(2S) \to \gamma\chi_{b1}(1P))$ = (6.9 ± 0.4) × 10^{-2}. Our first error is their experiment's error and our second error is the systematic error from using our best value.

[6] WALK 86 quotes $B(\Upsilon(2S) \to \gamma\chi_{b1}(1P)) \times B(\chi_{b1}(1P) \to \gamma\Upsilon(1S)) \times B(\Upsilon(1S) \to \ell^+\ell^-)$ = (5.8 ± 0.9 ± 0.7) %.

[7] WALK 86 reports $[\Gamma(\chi_{b1}(1P) \to \gamma\Upsilon(1S))/\Gamma_{total}] \times [B(\Upsilon(2S) \to \gamma\chi_{b1}(1P))]$ = (23.4 ± 3.63 ± 2.82) × 10^{-3} which we divide by our best value $B(\Upsilon(2S) \to \gamma\chi_{b1}(1P))$ = (6.9 ± 0.4) × 10^{-2}. Our first error is their experiment's error and our second error is the systematic error from using our best value.

$\Gamma(D^0X)/\Gamma_{total}$ Γ_2/Γ

VALUE (units 10^{-2})	EVTS	DOCUMENT ID		TECN	COMMENT
12.6±1.9±1.1	2310	8 BRIERE	08	CLEO	$\Upsilon(2S) \to \gamma D^0X$

[8] For $p_{D^0} > 2.5$ GeV/c.

$\Gamma(\pi^+\pi^-K^+K^-\pi^0)/\Gamma_{total}$ Γ_3/Γ

VALUE (units 10^{-4})	EVTS	DOCUMENT ID		TECN	COMMENT
2.0±0.6±0.1	18	9 ASNER	08A	CLEO	$\Upsilon(2S) \to \gamma\pi^+\pi^-K^+K^-\pi^0$

[9] ASNER 08A reports $[\Gamma(\chi_{b1}(1P) \to \pi^+\pi^-K^+K^-\pi^0)/\Gamma_{total}] \times [B(\Upsilon(2S) \to \gamma\chi_{b1}(1P))]$ = (14 ± 3 ± 3) × 10^{-6} which we divide by our best value $B(\Upsilon(2S) \to \gamma\chi_{b1}(1P))$ = (6.9 ± 0.4) × 10^{-2}. Our first error is their experiment's error and our second error is the systematic error from using our best value.

$\Gamma(2\pi^+\pi^-K^-K^0_S)/\Gamma_{total}$ Γ_4/Γ

VALUE (units 10^{-4})	EVTS	DOCUMENT ID		TECN	COMMENT
1.3±0.5±0.1	11	10 ASNER	08A	CLEO	$\Upsilon(2S) \to \gamma 2\pi^+\pi^-K^-K^0_S$

[10] ASNER 08A reports $[\Gamma(\chi_{b1}(1P) \to 2\pi^+\pi^-K^-K^0_S)/\Gamma_{total}] \times [B(\Upsilon(2S) \to \gamma\chi_{b1}(1P))]$ = (9 ± 3 ± 2) × 10^{-6} which we divide by our best value $B(\Upsilon(2S) \to \gamma\chi_{b1}(1P))$ = (6.9 ± 0.4) × 10^{-2}. Our first error is their experiment's error and our second error is the systematic error from using our best value.

$\Gamma(2\pi^+\pi^-K^-K^0_S2\pi^0)/\Gamma_{total}$ Γ_5/Γ

VALUE (units 10^{-4})	CL%	DOCUMENT ID		TECN	COMMENT
<6	90	11 ASNER	08A	CLEO	$\Upsilon(2S) \to \gamma 2\pi^+\pi^-K^-2\pi^0$

[11] ASNER 08A reports $[\Gamma(\chi_{b1}(1P) \to 2\pi^+\pi^-K^-K^0_S2\pi^0)/\Gamma_{total}] \times [B(\Upsilon(2S) \to \gamma\chi_{b1}(1P))] < 42 \times 10^{-6}$ which we divide by our best value $B(\Upsilon(2S) \to \gamma\chi_{b1}(1P))$ = 6.9 × 10^{-2}.

$\Gamma(2\pi^+2\pi^-2\pi^0)/\Gamma_{total}$ Γ_6/Γ

VALUE (units 10^{-4})	EVTS	DOCUMENT ID		TECN	COMMENT
8.0±2.4±0.4	46	12 ASNER	08A	CLEO	$\Upsilon(2S) \to \gamma 2\pi^+2\pi^-2\pi^0$

[12] ASNER 08A reports $[\Gamma(\chi_{b1}(1P) \to 2\pi^+2\pi^-2\pi^0)/\Gamma_{total}] \times [B(\Upsilon(2S) \to \gamma\chi_{b1}(1P))]$ = (55 ± 9 ± 14) × 10^{-6} which we divide by our best value $B(\Upsilon(2S) \to \gamma\chi_{b1}(1P))$ = (6.9 ± 0.4) × 10^{-2}. Our first error is their experiment's error and our second error is the systematic error from using our best value.

$\Gamma(2\pi^+2\pi^-K^+K^-)/\Gamma_{total}$ Γ_7/Γ

VALUE (units 10^{-4})	EVTS	DOCUMENT ID		TECN	COMMENT
1.5±0.5±0.1	18	13 ASNER	08A	CLEO	$\Upsilon(2S) \to \gamma 2\pi^+2\pi^-K^+K^-$

[13] ASNER 08A reports $[\Gamma(\chi_{b1}(1P) \to 2\pi^+2\pi^-K^+K^-)/\Gamma_{total}] \times [B(\Upsilon(2S) \to \gamma\chi_{b1}(1P))]$ = (10 ± 3 ± 2) × 10^{-6} which we divide by our best value $B(\Upsilon(2S) \to \gamma\chi_{b1}(1P))$ = (6.9 ± 0.4) × 10^{-2}. Our first error is their experiment's error and our second error is the systematic error from using our best value.

$\Gamma(2\pi^+2\pi^-K^+K^-\pi^0)/\Gamma_{total}$ Γ_8/Γ

VALUE (units 10^{-4})	EVTS	DOCUMENT ID		TECN	COMMENT
3.5±1.2±0.2	22	14 ASNER	08A	CLEO	$\Upsilon(2S) \to \gamma 2\pi^+2\pi^-K^+K^-\pi^0$

[14] ASNER 08A reports $[\Gamma(\chi_{b1}(1P) \to 2\pi^+2\pi^-K^+K^-\pi^0)/\Gamma_{total}] \times [B(\Upsilon(2S) \to \gamma\chi_{b1}(1P))]$ = (24 ± 6 ± 6) × 10^{-6} which we divide by our best value $B(\Upsilon(2S) \to \gamma\chi_{b1}(1P))$ = (6.9 ± 0.4) × 10^{-2}. Our first error is their experiment's error and our second error is the systematic error from using our best value.

$\Gamma(2\pi^+2\pi^-K^+K^-2\pi^0)/\Gamma_{total}$ Γ_9/Γ

VALUE (units 10^{-4})	EVTS	DOCUMENT ID		TECN	COMMENT
8.6±3.2±0.4	26	15 ASNER	08A	CLEO	$\Upsilon(2S) \to \gamma 2\pi^+2\pi^-K^+K^-2\pi^0$

[15] ASNER 08A reports $[\Gamma(\chi_{b1}(1P) \to 2\pi^+2\pi^-K^+K^-2\pi^0)/\Gamma_{total}] \times [B(\Upsilon(2S) \to \gamma\chi_{b1}(1P))]$ = (59 ± 14 ± 17) × 10^{-6} which we divide by our best value $B(\Upsilon(2S) \to \gamma\chi_{b1}(1P))$ = (6.9 ± 0.4) × 10^{-2}. Our first error is their experiment's error and our second error is the systematic error from using our best value.

$\Gamma(3\pi^+2\pi^-K^-K^0_S\pi^0)/\Gamma_{total}$ Γ_{10}/Γ

VALUE (units 10^{-4})	EVTS	DOCUMENT ID		TECN	COMMENT
9.3±3.3±0.5	21	16 ASNER	08A	CLEO	$\Upsilon(2S) \to \gamma 3\pi^+2\pi^-K^-K^0_S\pi^0$

[16] ASNER 08A reports $[\Gamma(\chi_{b1}(1P) \to 3\pi^+2\pi^-K^-K^0_S\pi^0)/\Gamma_{total}] \times [B(\Upsilon(2S) \to \gamma\chi_{b1}(1P))]$ = (64 ± 16 ± 16) × 10^{-6} which we divide by our best value $B(\Upsilon(2S) \to \gamma\chi_{b1}(1P))$ = (6.9 ± 0.4) × 10^{-2}. Our first error is their experiment's error and our second error is the systematic error from using our best value.

$\Gamma(3\pi^+3\pi^-)/\Gamma_{total}$ Γ_{11}/Γ

VALUE (units 10^{-4})	EVTS	DOCUMENT ID		TECN	COMMENT
1.9±0.6±0.1	25	17 ASNER	08A	CLEO	$\Upsilon(2S) \to \gamma 3\pi^+3\pi^-$

[17] ASNER 08A reports $[\Gamma(\chi_{b1}(1P) \to 3\pi^+3\pi^-)/\Gamma_{total}] \times [B(\Upsilon(2S) \to \gamma\chi_{b1}(1P))]$ = (13 ± 3 ± 3) × 10^{-6} which we divide by our best value $B(\Upsilon(2S) \to \gamma\chi_{b1}(1P))$ = (6.9 ± 0.4) × 10^{-2}. Our first error is their experiment's error and our second error is the systematic error from using our best value.

$\Gamma(3\pi^+3\pi^-2\pi^0)/\Gamma_{total}$ Γ_{12}/Γ

VALUE (units 10^{-4})	EVTS	DOCUMENT ID		TECN	COMMENT
17±5±1	56	18 ASNER	08A	CLEO	$\Upsilon(2S) \to \gamma 3\pi^+3\pi^-2\pi^0$

[18] ASNER 08A reports $[\Gamma(\chi_{b1}(1P) \to 3\pi^+3\pi^-2\pi^0)/\Gamma_{total}] \times [B(\Upsilon(2S) \to \gamma\chi_{b1}(1P))]$ = (119 ± 18 ± 32) × 10^{-6} which we divide by our best value $B(\Upsilon(2S) \to \gamma\chi_{b1}(1P))$ = (6.9 ± 0.4) × 10^{-2}. Our first error is their experiment's error and our second error is the systematic error from using our best value.

$\Gamma(3\pi^+3\pi^-K^+K^-)/\Gamma_{total}$ Γ_{13}/Γ

VALUE (units 10^{-4})	EVTS	DOCUMENT ID		TECN	COMMENT
2.6±0.8±0.1	21	19 ASNER	08A	CLEO	$\Upsilon(2S) \to \gamma 3\pi^+3\pi^-K^+K^-$

[19] ASNER 08A reports $[\Gamma(\chi_{b1}(1P) \to 3\pi^+3\pi^-K^+K^-)/\Gamma_{total}] \times [B(\Upsilon(2S) \to \gamma\chi_{b1}(1P))]$ = (18 ± 4 ± 4) × 10^{-6} which we divide by our best value $B(\Upsilon(2S) \to \gamma\chi_{b1}(1P))$ = (6.9 ± 0.4) × 10^{-2}. Our first error is their experiment's error and our second error is the systematic error from using our best value.

$\Gamma(3\pi^+3\pi^-K^+K^-\pi^0)/\Gamma_{total}$ Γ_{14}/Γ

VALUE (units 10^{-4})	EVTS	DOCUMENT ID		TECN	COMMENT
7.5±2.6±0.4	28	20 ASNER	08A	CLEO	$\Upsilon(2S) \to \gamma 3\pi^+3\pi^-K^+K^-\pi^0$

[20] ASNER 08A reports $[\Gamma(\chi_{b1}(1P) \to 3\pi^+3\pi^-K^+K^-\pi^0)/\Gamma_{total}] \times [B(\Upsilon(2S) \to \gamma\chi_{b1}(1P))]$ = (52 ± 11 ± 14) × 10^{-6} which we divide by our best value $B(\Upsilon(2S) \to \gamma\chi_{b1}(1P))$ = (6.9 ± 0.4) × 10^{-2}. Our first error is their experiment's error and our second error is the systematic error from using our best value.

$\Gamma(4\pi^+4\pi^-)/\Gamma_{total}$ Γ_{15}/Γ

VALUE (units 10^{-4})	EVTS	DOCUMENT ID		TECN	COMMENT
2.6±0.9±0.1	24	21 ASNER	08A	CLEO	$\Upsilon(2S) \to \gamma 4\pi^+4\pi^-$

[21] ASNER 08A reports $[\Gamma(\chi_{b1}(1P) \to 4\pi^+4\pi^-)/\Gamma_{total}] \times [B(\Upsilon(2S) \to \gamma\chi_{b1}(1P))]$ = (18 ± 4 ± 5) × 10^{-6} which we divide by our best value $B(\Upsilon(2S) \to \gamma\chi_{b1}(1P))$ = (6.9 ± 0.4) × 10^{-2}. Our first error is their experiment's error and our second error is the systematic error from using our best value.

$\Gamma(4\pi^+4\pi^-2\pi^0)/\Gamma_{total}$ Γ_{16}/Γ

VALUE (units 10^{-4})	EVTS	DOCUMENT ID		TECN	COMMENT
14±5±1	26	22 ASNER	08A	CLEO	$\Upsilon(2S) \to \gamma 4\pi^+4\pi^-2\pi^0$

[22] ASNER 08A reports $[\Gamma(\chi_{b1}(1P) \to 4\pi^+4\pi^-2\pi^0)/\Gamma_{total}] \times [B(\Upsilon(2S) \to \gamma\chi_{b1}(1P))]$ = (96 ± 24 ± 29) × 10^{-6} which we divide by our best value $B(\Upsilon(2S) \to \gamma\chi_{b1}(1P))$ = (6.9 ± 0.4) × 10^{-2}. Our first error is their experiment's error and our second error is the systematic error from using our best value.

$\Gamma(\omega\,\text{anything})/\Gamma_{\text{total}}$ Γ_{17}/Γ

VALUE (units 10^{-2})	EVTS	DOCUMENT ID		TECN	COMMENT
4.9±1.3±0.6	51k	JIA	17A	BELL	$e^+e^- \to$ hadrons

$\Gamma(\omega X_{tetra})/\Gamma_{\text{total}}$ Γ_{18}/Γ

VALUE	CL%	DOCUMENT ID		TECN	COMMENT
$<44.4\times10^{-5}$	90	[23] JIA	17A	BELL	$e^+e^- \to$ hadrons

[23] For a tetraquark state X_{tetra}, with mass in the range 1.16–2.46 GeV and width in the range 0–0.3 GeV. Measured 90% CL limits as a function of X_{tetra} mass and width range from 3.3×10^{-5} to 44.4×10^{-5}.

$\Gamma(J/\psi J/\psi)/\Gamma_{\text{total}}$ Γ_{19}/Γ

VALUE (units 10^{-5})	CL%	DOCUMENT ID		TECN	COMMENT
<2.7	90	[24] SHEN	12	BELL	$\Upsilon(2S) \to \gamma\psi X$

[24] SHEN 12 reports $<2.7\times10^{-5}$ from a measurement of $[\Gamma(\chi_{b1}(1P) \to J/\psi J/\psi)/\Gamma_{\text{total}}] \times [\text{B}(\Upsilon(2S) \to \gamma\chi_{b1}(1P))]$ assuming $\text{B}(\Upsilon(2S) \to \gamma\chi_{b1}(1P)) = (6.9\pm0.4)\times10^{-2}$.

$\Gamma(J/\psi\psi(2S))/\Gamma_{\text{total}}$ Γ_{20}/Γ

VALUE (units 10^{-5})	CL%	DOCUMENT ID		TECN	COMMENT
<1.7	90	[25] SHEN	12	BELL	$\Upsilon(2S) \to \gamma\psi X$

[25] SHEN 12 reports $<1.7\times10^{-5}$ from a measurement of $[\Gamma(\chi_{b1}(1P) \to J/\psi\psi(2S))/\Gamma_{\text{total}}] \times [\text{B}(\Upsilon(2S) \to \gamma\chi_{b1}(1P))]$ assuming $\text{B}(\Upsilon(2S) \to \gamma\chi_{b1}(1P)) = (6.9\pm0.4)\times10^{-2}$.

$\Gamma(\psi(2S)\psi(2S))/\Gamma_{\text{total}}$ Γ_{21}/Γ

VALUE (units 10^{-5})	CL%	DOCUMENT ID		TECN	COMMENT
<6	90	[26] SHEN	12	BELL	$\Upsilon(2S) \to \gamma\psi X$

[26] SHEN 12 reports $<6.2\times10^{-5}$ from a measurement of $[\Gamma(\chi_{b1}(1P) \to \psi(2S)\psi(2S))/\Gamma_{\text{total}}] \times [\text{B}(\Upsilon(2S) \to \gamma\chi_{b1}(1P))]$ assuming $\text{B}(\Upsilon(2S) \to \gamma\chi_{b1}(1P)) = (6.9\pm0.4)\times10^{-2}$.

$\Gamma(J/\psi(1S)\,\text{anything})/\Gamma_{\text{total}}$ Γ_{22}/Γ

VALUE	CL%	DOCUMENT ID		TECN	COMMENT
$<1.1\times10^{-3}$	90	JIA	17A	BELL	$e^+e^- \to$ hadrons

$\Gamma(J/\psi(1S)X_{tetra})/\Gamma_{\text{total}}$ Γ_{23}/Γ

VALUE	CL%	DOCUMENT ID		TECN	COMMENT
$<22.7\times10^{-5}$	90	[27] JIA	17A	BELL	$e^+e^- \to$ hadrons

[27] For a tetraquark state X_{tetra}, with mass in the range 1.16–2.46 GeV and width in the range 0–0.3 GeV. Measured 90% CL limits as a function of X_{tetra} mass and width range from 1.8×10^{-5} to 22.7×10^{-5}.

$\chi_{b1}(1P)$ Cross-Particle Branching Ratios

$\Gamma(\chi_{b1}(1P) \to \gamma\Upsilon(1S))/\Gamma_{\text{total}} \times \Gamma(\Upsilon(2S) \to \gamma\chi_{b1}(1P))/\Gamma_{\text{total}}$ $\Gamma_1/\Gamma \times \Gamma_{50}^{\Upsilon(2S)}/\Gamma^{\Upsilon(2S)}$

VALUE (units 10^{-3})	EVTS	DOCUMENT ID		TECN	COMMENT
24.1±0.6±1.5	13k	LEES	11J	BABR	$\Upsilon(2S) \to X\gamma$

$\text{B}(\chi_{b1}(1P) \to \gamma\Upsilon(1S)) \times \text{B}(\Upsilon(2S) \to \gamma\chi_{b1}(1P)) \times \text{B}(\Upsilon(1S) \to \ell^+\ell^-)$

VALUE (units 10^{-4})	EVTS	DOCUMENT ID		TECN	COMMENT
5.90±0.34 OUR AVERAGE Error includes scale factor of 1.3. See the ideogram below.					
$6.86^{+0.47}_{-0.45}{}^{+0.44}_{-0.35}$		[28] LEES	14M	BABR	$\Upsilon(2S) \to \gamma\gamma\mu^+\mu^-$
$5.65\pm0.11\pm0.27$	3222	KORNICER	11	CLEO	$e^+e^- \to \gamma\gamma\ell^+\ell^-$
$5.8\ \pm0.9\ \pm0.7$	53	WALK	86	CBAL	$\Upsilon(2S) \to \gamma\gamma\ell^+\ell^-$

[28] From a sample of $\Upsilon(2S) \to \gamma\gamma\mu^+\mu^-$ with one converted photon.

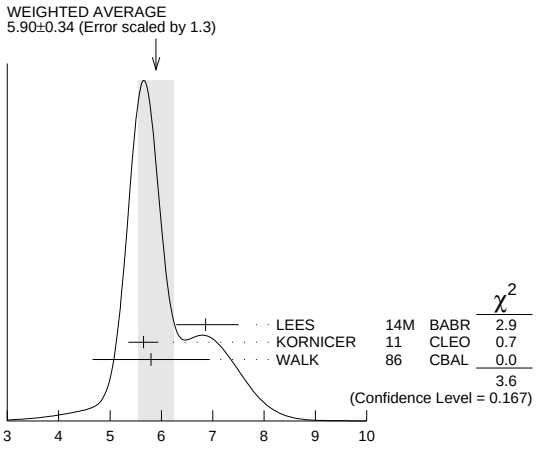

$\text{B}(\chi_{b1}(1P) \to \gamma\Upsilon(1S)) \times \text{B}(\Upsilon(3S) \to \gamma\chi_{b1}(1P)) \times \text{B}(\Upsilon(1S) \to \ell^+\ell^-)$

VALUE (units 10^{-5})	EVTS	DOCUMENT ID		TECN	COMMENT
1.30±0.34 OUR AVERAGE					
$1.16^{+0.78}_{-0.67}{}^{+0.14}_{-0.16}$		[29] LEES	14M	BABR	$\Upsilon(3S) \to \gamma\gamma\mu^+\mu^-$
$1.33\pm0.30\pm0.23$	50	KORNICER	11	CLEO	$e^+e^- \to \gamma\gamma\ell^+\ell^-$

[29] From a sample of $\Upsilon(3S) \to \gamma\gamma\mu^+\mu^-$ with converted photons.

$\text{B}(\chi_{b2}(1P) \to pX + \bar{p}X)/\text{B}(\chi_{b1}(1P) \to pX + \bar{p}X)$

VALUE	DOCUMENT ID		TECN	COMMENT
1.068±0.010±0.040	BRIERE	07	CLEO	$\Upsilon(2S) \to \gamma\chi_{bJ}(1P)$

$\text{B}(\chi_{b0}(1P) \to pX + \bar{p}X)/\text{B}(\chi_{b1}(1P) \to pX + \bar{p}X)$

VALUE	DOCUMENT ID		TECN	COMMENT
1.11±0.15±0.20	BRIERE	07	CLEO	$\Upsilon(2S) \to \gamma\chi_{bJ}(1P)$

$\chi_{b1}(1P)$ REFERENCES

JIA	17A	PR D96 112002	S. Jia *et al.*	(BELLE Collab.)
LEES	14M	PR D90 112010	J.P. Lees *et al.*	(BABAR Collab.)
SHEN	12	PR D85 071102	C.P. Shen *et al.*	(BELLE Collab.)
KORNICER	11	PR D83 054003	M. Kornicer *et al.*	(CLEO Collab.)
LEES	11J	PR D84 072002	J.P. Lees *et al.*	(BABAR Collab.)
ASNER	08A	PR D78 091103	D.M. Asner *et al.*	(CLEO Collab.)
BRIERE	08	PR D78 092007	R.A. Briere *et al.*	(CLEO Collab.)
BRIERE	07	PR D76 012005	R.A. Briere *et al.*	(CLEO Collab.)
ARTUSO	05	PRL 94 032001	M. Artuso *et al.*	(CLEO Collab.)
EDWARDS	99	PR D59 032003	K.W. Edwards *et al.*	(CLEO Collab.)
SKWARNICKI	87	PRL 58 972	T. Skwarnicki *et al.*	(Crystal Ball Collab.) J
WALK	86	PR D34 2611	W.S. Walk *et al.*	(Crystal Ball Collab.)
ALBRECHT	85E	PL 160B 331	H. Albrecht *et al.*	(ARGUS Collab.)
NERNST	85	PRL 54 2195	R. Nernst *et al.*	(Crystal Ball Collab.)
HAAS	84	PRL 52 799	J. Haas *et al.*	(CLEO Collab.)
KLOPFEN...	83	PRL 51 160	C. Klopfenstein *et al.*	(CUSB Collab.)
PAUSS	83	PL 130B 439	F. Pauss *et al.*	(MPIM, COLU, CORN, LSU+)

$h_b(1P)$

$I^G(J^{PC}) = ?^?(1^{+-})$

Quantum numbers are quark model predictions, $C = -$ established by $\eta_b\gamma$ decay.

$h_b(1P)$ MASS

VALUE (MeV)	EVTS	DOCUMENT ID		TECN	COMMENT
9899.3±0.8 OUR AVERAGE					
$9899.3\pm0.4\pm1.0$	112k	TAMPONI	15	BELL	$e^+e^- \to \gamma\eta+$ hadrons
$9899.1\pm0.4\pm1.0$	70k	MIZUK	12	BELL	$e^+e^- \to \pi^+\pi^-$ hadrons
$9902\ \pm4\ \pm2$	10.8k	LEES	11K	BABR	$\Upsilon(3S) \to \eta_b\gamma\pi^0$
• • • We do not use the following data for averages, fits, limits, etc. • • •					
$9898.2^{+1.1}_{-1.0}{}^{+1.0}_{-1.1}$	50.0k	[1] ADACHI	12	BELL	10.86 $e^+e^- \to \pi^+\pi^-$ MM

[1] Superseded by MIZUK 12.

$h_b(1P)$ DECAY MODES

	Mode	Fraction (Γ_i/Γ)
Γ_1	$\eta_b(1S)\gamma$	(52^{+6}_{-5}) %

$h_b(1P)$ BRANCHING RATIOS

$\Gamma(\eta_b(1S)\gamma)/\Gamma_{\text{total}}$ Γ_1/Γ

VALUE (units 10^{-2})	EVTS	DOCUMENT ID		TECN	COMMENT
$52\ ^{+6}_{-5}$ OUR AVERAGE					
$56\ \pm8\ \pm4$	33.1k	[1] TAMPONI	15	BELL	$e^+e^- \to \gamma\eta+$ hadrons
$49.2\pm5.7^{+5.6}_{-3.3}$	24k	MIZUK	12	BELL	$e^+e^- \to (\gamma)\pi^+\pi^-$ hadrons
• • • We do not use the following data for averages, fits, limits, etc. • • •					
seen	10.8k	LEES	11K	BABR	$\Upsilon(3S) \to \eta_b\gamma\pi^0$

[1] Using $\text{B}(\eta \to 2\gamma) = (39.41\pm0.20)\%$.

$h_b(1P)$ REFERENCES

TAMPONI	15	PRL 115 142001	U. Tamponi *et al.*	(BELLE Collab.)
ADACHI	12	PRL 108 032001	I. Adachi *et al.*	(BELLE Collab.)
MIZUK	12	PRL 109 232002	R. Mizuk *et al.*	(BELLE Collab.)
LEES	11K	PR D84 091101	J.P. Lees *et al.*	(BABAR Collab.)

$\chi_{b2}(1P)$

$I^G(J^{PC}) = 0^+(2^{++})$

J needs confirmation.

Observed in radiative decay of the $\Upsilon(2S)$, therefore $C = +$. Branching ratio requires E1 transition, M1 is strongly disfavored, therefore $P = +$. $J = 2$ from SKWARNICKI 87.

$\chi_{b2}(1P)$ MASS

VALUE (MeV)	DOCUMENT ID
9912.21±0.26±0.31 OUR EVALUATION	From average γ energy below, using $\Upsilon(2S)$ mass = 10023.26 ± 0.31 MeV

$m_{\chi_{b2}(1P)} - m_{\chi_{b1}(1P)}$

VALUE (MeV)	DOCUMENT ID		TECN	COMMENT
19.10±0.25 OUR AVERAGE	Error includes scale factor of 1.1.			
19.81±0.65±0.20	[1] AAIJ	14BG	LHCB	$pp \to \gamma\mu^+\mu^- X$
19.01±0.24	LEES	14M	BABR	$\Upsilon(2S) \to \gamma\gamma\mu^+\mu^-$

[1] From the $\chi_{bJ}(1P) \to \Upsilon(1S)\gamma$ transition.

γ ENERGY IN $\Upsilon(2S)$ DECAY

VALUE (MeV)	DOCUMENT ID		TECN	COMMENT
110.44±0.29 OUR AVERAGE	Error includes scale factor of 1.1.			
110.58±0.08±0.30	ARTUSO	05	CLEO	$\Upsilon(2S) \to \gamma X$
110.8 ±0.3 ±0.6	EDWARDS	99	CLE2	$\Upsilon(2S) \to \gamma\chi(1P)$
107.0 ±1.1 ±1.3	WALK	86	CBAL	$\Upsilon(2S) \to \gamma\gamma\ell^+\ell^-$
110.6 ±0.3 ±0.9	ALBRECHT	85E	ARG	$\Upsilon(2S) \to$ conv.γX
110.4 ±0.8 ±2.2	NERNST	85	CBAL	$\Upsilon(2S) \to \gamma$X
109.5 ±0.7 ±1.0	HAAS	84	CLEO	$\Upsilon(2S) \to$ conv.γX
108.2 ±0.3 ±2.0	KLOPFEN...	83	CUSB	$\Upsilon(2S) \to \gamma$X
108.8 ±4.0	PAUSS	83	CUSB	$\Upsilon(2S) \to \gamma\gamma\ell^+\ell^-$

$\chi_{b2}(1P)$ DECAY MODES

	Mode	Fraction (Γ_i/Γ)	Confidence level
Γ_1	$\gamma\Upsilon(1S)$	(18.8±1.1) %	
Γ_2	D^0X	< 7.9 %	90%
Γ_3	$\pi^+\pi^-K^+K^-\pi^0$	(8 ±5) × 10^{-5}	
Γ_4	$2\pi^+\pi^-K^-K^0_S$	< 1.0 × 10^{-4}	90%
Γ_5	$2\pi^+\pi^-K^-K^0_S2\pi^0$	(5.3±2.4) × 10^{-4}	
Γ_6	$2\pi^+2\pi^-2\pi^0$	(3.5±1.4) × 10^{-4}	
Γ_7	$2\pi^+2\pi^-K^+K^-$	(1.1±0.4) × 10^{-4}	
Γ_8	$2\pi^+2\pi^-K^+K^-\pi^0$	(2.1±0.9) × 10^{-4}	
Γ_9	$2\pi^+2\pi^-K^+K^-2\pi^0$	(3.9±1.8) × 10^{-4}	
Γ_{10}	$3\pi^+2\pi^-K^-K^0_S\pi^0$	< 5 × 10^{-4}	90%
Γ_{11}	$3\pi^+3\pi^-$	(7.0±3.1) × 10^{-5}	
Γ_{12}	$3\pi^+3\pi^-2\pi^0$	(1.0±0.4) × 10^{-3}	
Γ_{13}	$3\pi^+3\pi^-K^+K^-$	< 8 × 10^{-5}	90%
Γ_{14}	$3\pi^+3\pi^-K^+K^-\pi^0$	(3.6±1.5) × 10^{-4}	
Γ_{15}	$4\pi^+4\pi^-$	(8 ±4) × 10^{-5}	
Γ_{16}	$4\pi^+4\pi^-2\pi^0$	(1.8±0.7) × 10^{-3}	
Γ_{17}	$J/\psi J/\psi$	< 4 × 10^{-5}	90%
Γ_{18}	$J/\psi\psi(2S)$	< 5 × 10^{-5}	90%
Γ_{19}	$\psi(2S)\psi(2S)$	< 1.6 × 10^{-5}	90%
Γ_{20}	$J/\psi(1S)$ anything	(1.5±0.4) × 10^{-3}	

$\chi_{b2}(1P)$ BRANCHING RATIOS

$\Gamma(\gamma\Upsilon(1S))/\Gamma_{total}$ Γ_1/Γ

VALUE	EVTS		DOCUMENT ID		TECN	COMMENT
0.188±0.011 OUR AVERAGE						
0.185±0.008±0.009		[2,3,4]	LEES	14M	BABR	$\Upsilon(2S) \to \gamma\gamma\mu^+\mu^-$
0.186±0.011±0.009	1770	[4,5]	KORNICER	11	CLEO	$e^+e^- \to \gamma\gamma\ell^+\ell^-$
$0.194^{+0.014}_{-0.017}$±0.009	8k	[6]	LEES	11J	BABR	$\Upsilon(2S) \to X\gamma$
0.25 ±0.06 ±0.01	35	[4,7,8]	WALK	86	CBAL	$\Upsilon(2S) \to \gamma\gamma\ell^+\ell^-$
0.20 ±0.05			KLOPFEN...	83	CUSB	$\Upsilon(2S) \to \gamma\gamma\ell^+\ell^-$

[2] LEES 14M quotes $\Gamma(\chi_{b2}(1P) \to \gamma\Upsilon(1S))/\Gamma_{total} \times \Gamma(\Upsilon(2S) \to \gamma\chi_{b2}(1P))/\Gamma_{total}$ = (1.32 ± 0.06)% combining the results from samples of $\Upsilon(2S) \to \gamma\gamma\mu^+\mu^-$ with and without converted photons.

[3] LEES 14M reports $[\Gamma(\chi_{b2}(1P) \to \gamma\Upsilon(1S))/\Gamma_{total}] \times [B(\Upsilon(2S) \to \gamma\chi_{b2}(1P))]$ = (1.32 ± 0.06) × 10^{-2} which we divide by our best value $B(\Upsilon(2S) \to \gamma\chi_{b2}(1P))$ = (7.15 ± 0.35) × 10^{-2}. Our first error is their experiment's error and our second error is the systematic error from using our best value.

[4] Assuming $B(\Upsilon(1S) \to \mu^+\mu^-)$ = (2.48 ± 0.05)%.

[5] KORNICER 11 reports $[\Gamma(\chi_{b2}(1P) \to \gamma\Upsilon(1S))/\Gamma_{total}] \times [B(\Upsilon(2S) \to \gamma\chi_{b2}(1P))]$ = (1.33 ± 0.04 ± 0.07) × 10^{-2} which we divide by our best value $B(\Upsilon(2S) \to \gamma\chi_{b2}(1P))$ = (7.15 ± 0.35) × 10^{-2}. Our first error is their experiment's error and our second error is the systematic error from using our best value.

[6] LEES 11J reports $[\Gamma(\chi_{b2}(1P) \to \gamma\Upsilon(1S))/\Gamma_{total}] \times [B(\Upsilon(2S) \to \gamma\chi_{b2}(1P))]$ = $(13.9 \pm 0.5^{+0.9}_{-1.1}) \times 10^{-3}$ which we divide by our best value $B(\Upsilon(2S) \to \gamma\chi_{b2}(1P))$ = (7.15 ± 0.35) × 10^{-2}. Our first error is their experiment's error and our second error is the systematic error from using our best value.

[7] WALK 86 quotes $B(\Upsilon(2S) \to \gamma\chi_{b2}(1P)) \times B(\chi_{b2}(1P) \to \gamma\Upsilon(1S)) \times B(\Upsilon(1S) \to \ell^+\ell^-)$ = (4.4 ± 0.9 ± 0.5) %.

[8] WALK 86 reports $[\Gamma(\chi_{b2}(1P) \to \gamma\Upsilon(1S))/\Gamma_{total}] \times [B(\Upsilon(2S) \to \gamma\chi_{b2}(1P))]$ = (17.7 ± 3.6 ± 2.0) × 10^{-3} which we divide by our best value $B(\Upsilon(2S) \to \gamma\chi_{b2}(1P))$ = (7.15 ± 0.35) × 10^{-2}. Our first error is their experiment's error and our second error is the systematic error from using our best value.

$\Gamma(D^0X)/\Gamma_{total}$ Γ_2/Γ

VALUE	CL%		DOCUMENT ID		TECN	COMMENT
<7.9 × 10^{-2}	90	[9,10]	BRIERE	08	CLEO	$\Upsilon(2S) \to \gamma D^0X$

[9] For $p_{D^0} > 2.5$ GeV/c.

[10] The authors also present their result as (5.4 ± 1.9 ± 0.5) × 10^{-2}.

$\Gamma(\pi^+\pi^-K^+K^-\pi^0)/\Gamma_{total}$ Γ_3/Γ

VALUE (units 10^{-4})	EVTS		DOCUMENT ID		TECN	COMMENT
0.84±0.50±0.04	8	[11]	ASNER	08A	CLEO	$\Upsilon(2S) \to \gamma\pi^+\pi^-K^+K^-\pi^0$

[11] ASNER 08A reports $[\Gamma(\chi_{b2}(1P) \to \pi^+\pi^-K^+K^-\pi^0)/\Gamma_{total}] \times [B(\Upsilon(2S) \to \gamma\chi_{b2}(1P))]$ = (6 ± 3 ± 2) × 10^{-6} which we divide by our best value $B(\Upsilon(2S) \to \gamma\chi_{b2}(1P))$ = (7.15 ± 0.35) × 10^{-2}. Our first error is their experiment's error and our second error is the systematic error from using our best value.

$\Gamma(2\pi^+\pi^-K^-K^0_S)/\Gamma_{total}$ Γ_4/Γ

VALUE (units 10^{-4})	CL%		DOCUMENT ID		TECN	COMMENT
<1.0	90	[12]	ASNER	08A	CLEO	$\Upsilon(2S) \to \gamma 2\pi^+\pi^-K^-K^0_S$

[12] ASNER 08A reports $[\Gamma(\chi_{b2}(1P) \to 2\pi^+\pi^-K^-K^0_S)/\Gamma_{total}] \times [B(\Upsilon(2S) \to \gamma\chi_{b2}(1P))]$ < 7 × 10^{-6} which we divide by our best value $B(\Upsilon(2S) \to \gamma\chi_{b2}(1P))$ = 7.15 × 10^{-2}.

$\Gamma(2\pi^+\pi^-K^-K^0_S2\pi^0)/\Gamma_{total}$ Γ_5/Γ

VALUE (units 10^{-4})	EVTS		DOCUMENT ID		TECN	COMMENT
5.3±2.4±0.3	11	[13]	ASNER	08A	CLEO	$\Upsilon(2S) \to \gamma 2\pi^+\pi^-K^-2\pi^0$

[13] ASNER 08A reports $[\Gamma(\chi_{b2}(1P) \to 2\pi^+\pi^-K^-K^0_S2\pi^0)/\Gamma_{total}] \times [B(\Upsilon(2S) \to \gamma\chi_{b2}(1P))]$ = (38 ± 14 ± 10) × 10^{-6} which we divide by our best value $B(\Upsilon(2S) \to \gamma\chi_{b2}(1P))$ = (7.15 ± 0.35) × 10^{-2}. Our first error is their experiment's error and our second error is the systematic error from using our best value.

$\Gamma(2\pi^+2\pi^-2\pi^0)/\Gamma_{total}$ Γ_6/Γ

VALUE (units 10^{-4})	EVTS		DOCUMENT ID		TECN	COMMENT
3.5±1.4±0.2	19	[14]	ASNER	08A	CLEO	$\Upsilon(2S) \to \gamma 2\pi^+2\pi^-2\pi^0$

[14] ASNER 08A reports $[\Gamma(\chi_{b2}(1P) \to 2\pi^+2\pi^-2\pi^0)/\Gamma_{total}] \times [B(\Upsilon(2S) \to \gamma\chi_{b2}(1P))]$ = (25 ± 8 ± 6) × 10^{-6} which we divide by our best value $B(\Upsilon(2S) \to \gamma\chi_{b2}(1P))$ = (7.15 ± 0.35) × 10^{-2}. Our first error is their experiment's error and our second error is the systematic error from using our best value.

$\Gamma(2\pi^+2\pi^-K^+K^-)/\Gamma_{total}$ Γ_7/Γ

VALUE (units 10^{-4})	EVTS		DOCUMENT ID		TECN	COMMENT
1.1±0.4±0.1	14	[15]	ASNER	08A	CLEO	$\Upsilon(2S) \to \gamma 2\pi^+2\pi^-K^+K^-$

[15] ASNER 08A reports $[\Gamma(\chi_{b2}(1P) \to 2\pi^+2\pi^-K^+K^-)/\Gamma_{total}] \times [B(\Upsilon(2S) \to \gamma\chi_{b2}(1P))]$ = (8 ± 2 ± 2) × 10^{-6} which we divide by our best value $B(\Upsilon(2S) \to \gamma\chi_{b2}(1P))$ = (7.15 ± 0.35) × 10^{-2}. Our first error is their experiment's error and our second error is the systematic error from using our best value.

$\Gamma(2\pi^+2\pi^-K^+K^-\pi^0)/\Gamma_{total}$ Γ_8/Γ

VALUE (units 10^{-4})	EVTS		DOCUMENT ID		TECN	COMMENT
2.1±0.9±0.1	13	[16]	ASNER	08A	CLEO	$\Upsilon(2S) \to \gamma 2\pi^+2\pi^-K^+K^-\pi^0$

[16] ASNER 08A reports $[\Gamma(\chi_{b2}(1P) \to 2\pi^+2\pi^-K^+K^-\pi^0)/\Gamma_{total}] \times [B(\Upsilon(2S) \to \gamma\chi_{b2}(1P))]$ = (15 ± 5 ± 4) × 10^{-6} which we divide by our best value $B(\Upsilon(2S) \to \gamma\chi_{b2}(1P))$ = (7.15 ± 0.35) × 10^{-2}. Our first error is their experiment's error and our second error is the systematic error from using our best value.

$\Gamma(2\pi^+2\pi^-K^+K^-2\pi^0)/\Gamma_{total}$ Γ_9/Γ

VALUE (units 10^{-4})	EVTS		DOCUMENT ID		TECN	COMMENT
3.9±1.8±0.2	11	[17]	ASNER	08A	CLEO	$\Upsilon(2S) \to \gamma 2\pi^+2\pi^-K^+K^-2\pi^0$

[17] ASNER 08A reports $[\Gamma(\chi_{b2}(1P) \to 2\pi^+2\pi^-K^+K^-2\pi^0)/\Gamma_{total}] \times [B(\Upsilon(2S) \to \gamma\chi_{b2}(1P))]$ = (28 ± 11 ± 7) × 10^{-6} which we divide by our best value $B(\Upsilon(2S) \to \gamma\chi_{b2}(1P))$ = (7.15 ± 0.35) × 10^{-2}. Our first error is their experiment's error and our second error is the systematic error from using our best value.

$\Gamma(3\pi^+2\pi^-K^-K^0_S\pi^0)/\Gamma_{total}$ Γ_{10}/Γ

VALUE (units 10^{-4})	CL%		DOCUMENT ID		TECN	COMMENT
<5	90	[18]	ASNER	08A	CLEO	$\Upsilon(2S) \to \gamma 3\pi^+2\pi^-K^-K^0_S\pi^0$

[18] ASNER 08A reports $[\Gamma(\chi_{b2}(1P) \to 3\pi^+2\pi^-K^-K^0_S\pi^0)/\Gamma_{total}] \times [B(\Upsilon(2S) \to \gamma\chi_{b2}(1P))]$ < 36 × 10^{-6} which we divide by our best value $B(\Upsilon(2S) \to \gamma\chi_{b2}(1P))$ = 7.15 × 10^{-2}.

$\Gamma(3\pi^+3\pi^-)/\Gamma_{total}$ Γ_{11}/Γ

VALUE (units 10^{-4})	EVTS		DOCUMENT ID		TECN	COMMENT
0.70±0.31±0.03	9	[19]	ASNER	08A	CLEO	$\Upsilon(2S) \to \gamma 3\pi^+3\pi^-$

[19] ASNER 08A reports $[\Gamma(\chi_{b2}(1P) \to 3\pi^+3\pi^-)/\Gamma_{total}] \times [B(\Upsilon(2S) \to \gamma\chi_{b2}(1P))]$ = (5 ± 2 ± 1) × 10^{-6} which we divide by our best value $B(\Upsilon(2S) \to \gamma\chi_{b2}(1P))$ = (7.15 ± 0.35) × 10^{-2}. Our first error is their experiment's error and our second error is the systematic error from using our best value.

$\Gamma(3\pi^+3\pi^-2\pi^0)/\Gamma_{total}$ Γ_{12}/Γ

VALUE (units 10^{-4})	EVTS	DOCUMENT ID		TECN	COMMENT
10.2±3.6±0.5	34	[20] ASNER	08A	CLEO	$\Upsilon(2S) \to \gamma 3\pi^+ 3\pi^- 2\pi^0$

[20] ASNER 08A reports $[\Gamma(\chi_{b2}(1P) \to 3\pi^+3\pi^-2\pi^0)/\Gamma_{total}] \times [B(\Upsilon(2S) \to \gamma\chi_{b2}(1P))] = (73 \pm 16 \pm 20) \times 10^{-6}$ which we divide by our best value $B(\Upsilon(2S) \to \gamma\chi_{b2}(1P)) = (7.15 \pm 0.35) \times 10^{-2}$. Our first error is their experiment's error and our second error is the systematic error from using our best value.

$\Gamma(3\pi^+3\pi^-K^+K^-)/\Gamma_{total}$ Γ_{13}/Γ

VALUE (units 10^{-4})	CL%	DOCUMENT ID		TECN	COMMENT
<0.8	90	[21] ASNER	08A	CLEO	$\Upsilon(2S) \to \gamma 3\pi^+ 3\pi^- K^+ K^-$

[21] ASNER 08A reports $[\Gamma(\chi_{b2}(1P) \to 3\pi^+3\pi^-K^+K^-)/\Gamma_{total}] \times [B(\Upsilon(2S) \to \gamma\chi_{b2}(1P))] < 6 \times 10^{-6}$ which we divide by our best value $B(\Upsilon(2S) \to \gamma\chi_{b2}(1P)) = 7.15 \times 10^{-2}$.

$\Gamma(3\pi^+3\pi^-K^+K^-\pi^0)/\Gamma_{total}$ Γ_{14}/Γ

VALUE (units 10^{-4})	EVTS	DOCUMENT ID		TECN	COMMENT
3.6±1.5±0.2	14	[22] ASNER	08A	CLEO	$\Upsilon(2S) \to \gamma 3\pi^+ 3\pi^- K^+ K^- \pi^0$

[22] ASNER 08A reports $[\Gamma(\chi_{b2}(1P) \to 3\pi^+3\pi^-K^+K^-\pi^0)/\Gamma_{total}] \times [B(\Upsilon(2S) \to \gamma\chi_{b2}(1P))] = (26 \pm 8 \pm 7) \times 10^{-6}$ which we divide by our best value $B(\Upsilon(2S) \to \gamma\chi_{b2}(1P)) = (7.15 \pm 0.35) \times 10^{-2}$. Our first error is their experiment's error and our second error is the systematic error from using our best value.

$\Gamma(4\pi^+4\pi^-)/\Gamma_{total}$ Γ_{15}/Γ

VALUE (units 10^{-4})	EVTS	DOCUMENT ID		TECN	COMMENT
0.84±0.40±0.04	7	[23] ASNER	08A	CLEO	$\Upsilon(2S) \to \gamma 4\pi^+ 4\pi^-$

[23] ASNER 08A reports $[\Gamma(\chi_{b2}(1P) \to 4\pi^+4\pi^-)/\Gamma_{total}] \times [B(\Upsilon(2S) \to \gamma\chi_{b2}(1P))] = (6 \pm 2 \pm 2) \times 10^{-6}$ which we divide by our best value $B(\Upsilon(2S) \to \gamma\chi_{b2}(1P)) = (7.15 \pm 0.35) \times 10^{-2}$. Our first error is their experiment's error and our second error is the systematic error from using our best value.

$\Gamma(4\pi^+4\pi^-2\pi^0)/\Gamma_{total}$ Γ_{16}/Γ

VALUE (units 10^{-4})	EVTS	DOCUMENT ID		TECN	COMMENT
18±7±1	29	[24] ASNER	08A	CLEO	$\Upsilon(2S) \to \gamma 4\pi^+ 4\pi^- 2\pi^0$

[24] ASNER 08A reports $[\Gamma(\chi_{b2}(1P) \to 4\pi^+4\pi^-2\pi^0)/\Gamma_{total}] \times [B(\Upsilon(2S) \to \gamma\chi_{b2}(1P))] = (132 \pm 31 \pm 40) \times 10^{-6}$ which we divide by our best value $B(\Upsilon(2S) \to \gamma\chi_{b2}(1P)) = (7.15 \pm 0.35) \times 10^{-2}$. Our first error is their experiment's error and our second error is the systematic error from using our best value.

$\Gamma(J/\psi J/\psi)/\Gamma_{total}$ Γ_{17}/Γ

VALUE (units 10^{-5})	CL%	DOCUMENT ID		TECN	COMMENT
<5	90	[25] SHEN	12	BELL	$\Upsilon(2S) \to \gamma\psi X$

[25] SHEN 12 reports $< 4.5 \times 10^{-5}$ from a measurement of $[\Gamma(\chi_{b2}(1P) \to J/\psi J/\psi)/\Gamma_{total}] \times [B(\Upsilon(2S) \to \gamma\chi_{b2}(1P))]$ assuming $B(\Upsilon(2S) \to \gamma\chi_{b2}(1P)) = (7.15 \pm 0.35) \times 10^{-2}$.

$\Gamma(J/\psi\psi(2S))/\Gamma_{total}$ Γ_{18}/Γ

VALUE (units 10^{-5})	CL%	DOCUMENT ID		TECN	COMMENT
<5	90	[26] SHEN	12	BELL	$\Upsilon(2S) \to \gamma\psi X$

[26] SHEN 12 reports $< 4.9 \times 10^{-5}$ from a measurement of $[\Gamma(\chi_{b2}(1P) \to J/\psi\psi(2S))/\Gamma_{total}] \times [B(\Upsilon(2S) \to \gamma\chi_{b2}(1P))]$ assuming $B(\Upsilon(2S) \to \gamma\chi_{b2}(1P)) = (7.15 \pm 0.35) \times 10^{-2}$.

$\Gamma(\psi(2S)\psi(2S))/\Gamma_{total}$ Γ_{19}/Γ

VALUE (units 10^{-5})	CL%	DOCUMENT ID		TECN	COMMENT
<1.6	90	[27] SHEN	12	BELL	$\Upsilon(2S) \to \gamma\psi X$

[27] SHEN 12 reports $< 1.6 \times 10^{-5}$ from a measurement of $[\Gamma(\chi_{b2}(1P) \to \psi(2S)\psi(2S))/\Gamma_{total}] \times [B(\Upsilon(2S) \to \gamma\chi_{b2}(1P))]$ assuming $B(\Upsilon(2S) \to \gamma\chi_{b2}(1P)) = (7.15 \pm 0.35) \times 10^{-2}$.

$\Gamma(J/\psi(1S)\,\text{anything})/\Gamma_{total}$ Γ_{20}/Γ

VALUE (units 10^{-3})	EVTS	DOCUMENT ID		TECN	COMMENT
1.50±0.34±0.22	462	JIA	17A	BELL	$e^+e^- \to$ hadrons

$\chi_{b2}(1P)$ Cross-Particle Branching Ratios

$\Gamma(\chi_{b2}(1P) \to \gamma\Upsilon(1S))/\Gamma_{total} \times \Gamma(\Upsilon(2S) \to \gamma\chi_{b2}(1P))/\Gamma_{total}$ $\Gamma_1/\Gamma \times \Gamma_{51}^{\Upsilon(2S)}/\Gamma^{\Upsilon(2S)}$

VALUE (units 10^{-3})	EVTS	DOCUMENT ID		TECN	COMMENT
13.9±0.5$^{+0.9}_{-1.1}$	8k	LEES	11J	BABR	$\Upsilon(2S) \to X\gamma$

$B(\chi_{b2}(1P) \to \gamma\Upsilon(1S)) \times B(\Upsilon(2S) \to \gamma\chi_{b2}(1P)) \times B(\Upsilon(1S) \to \ell^+\ell^-)$

VALUE (units 10^{-4})	EVTS	DOCUMENT ID		TECN	COMMENT
3.38±0.16 OUR AVERAGE					
3.63$^{+0.36+0.18}_{-0.34-0.19}$		[28] LEES	14M	BABR	$\Upsilon(2S) \to \gamma\gamma\mu^+\mu^-$
3.29±0.09±0.16	1770	KORNICER	11	CLEO	$e^+e^- \to \gamma\gamma\ell^+\ell^-$
4.4 ±0.9 ±0.5	35	WALK	86	CBAL	$\Upsilon(2S) \to \gamma\gamma\ell^+\ell^-$

[28] From a sample of $\Upsilon(2S) \to \gamma\gamma\mu^+\mu^-$ with converted photons.

$[B(\chi_{b2}(1P) \to \gamma\Upsilon(1S)) \times B(\Upsilon(2S) \to \gamma\chi_{b2}(1P))]$ / $[B(\chi_{b1}(1P) \to \gamma\Upsilon(1S)) \times B(\Upsilon(2S) \to \gamma\chi_{b1}(1P))]$

VALUE (%)	DOCUMENT ID		TECN	COMMENT
55.6±1.6	[29] LEES	14M	BABR	$\Upsilon(2S) \to \gamma\gamma\mu^+\mu^-$

[29] From a sample of $\Upsilon(2S) \to \gamma\gamma\mu^+\mu^-$ events without converted photons.

$B(\chi_{b2}(1P) \to \gamma\Upsilon(1S)) \times B(\Upsilon(3S) \to \gamma\chi_{b2}(1P)) \times B(\Upsilon(1S) \to \ell^+\ell^-)$

VALUE (units 10^{-5})	EVTS	DOCUMENT ID		TECN	COMMENT
3.8 ±0.5 OUR AVERAGE					
4.68$^{+0.99}_{-0.92}$±0.37		[30] LEES	14M	BABR	$\Upsilon(3S) \to \gamma\gamma\mu^+\mu^-$
3.56±0.40±0.41	126	KORNICER	11	CLEO	$e^+e^- \to \gamma\gamma\ell^+\ell^-$

[30] From a sample of $\Upsilon(3S) \to \gamma\gamma\mu^+\mu^-$ with converted photons.

$\chi_{b2}(1P)$ REFERENCES

JIA	17A	PR D96 112002	S. Jia *et al.*	(BELLE Collab.)
AAIJ	14BG	JHEP 1410 088	R. Aaij *et al.*	(LHCb Collab.)
LEES	14M	PR D90 112010	J.P. Lees *et al.*	(BABAR Collab.)
SHEN	12	PR D85 071102	C.P. Shen *et al.*	(BELLE Collab.)
KORNICER	11	PR D83 054003	M. Kornicer *et al.*	(CLEO Collab.)
LEES	11J	PR D84 072002	J.P. Lees *et al.*	(BABAR Collab.)
ASNER	08A	PR D78 091103	D.M. Asner *et al.*	(CLEO Collab.)
BRIERE	08	PR D78 092007	R.A. Briere *et al.*	(CLEO Collab.)
ARTUSO	05	PRL 94 032001	M. Artuso *et al.*	(CLEO Collab.)
EDWARDS	99	PR D59 032003	K.W. Edwards *et al.*	(CLEO Collab.)
SKWARNICKI	87	PRL 58 972	T. Skwarnicki *et al.*	(Crystal Ball Collab.) J
WALK	86	PR D34 2611	W.S. Walk *et al.*	(Crystal Ball Collab.)
ALBRECHT	85E	PL 160B 331	H. Albrecht *et al.*	(ARGUS Collab.)
NERNST	85	PRL 54 2195	R. Nernst *et al.*	(Crystal Ball Collab.)
HAAS	84	PRL 52 799	J. Haas *et al.*	(CLEO Collab.)
KLOPFEN...	83	PRL 51 160	C. Klopfenstein *et al.*	(CUSB Collab.)
PAUSS	83	PL 130B 439	F. Pauss *et al.*	(MPIM, COLU, CORN, LSU+)

$\eta_b(2S)$

$I^G(J^{PC}) = 0^+(0^{-+})$

OMITTED FROM SUMMARY TABLE

Quantum numbers shown are quark-model predictions.

$\eta_b(2S)$ MASS

VALUE (MeV)	EVTS	DOCUMENT ID		TECN	COMMENT
9999.0±3.5$^{+2.8}_{-1.9}$	26k	[1] MIZUK	12	BELL	$e^+e^- \to \gamma\pi^+\pi^-$ + hadrons
• • • We do not use the following data for averages, fits, limits, etc. • • •					
9974.6±2.3±2.1	11 ± 4	[2,3] DOBBS	12		$\Upsilon(2S) \to \gamma$ hadrons

[1] Assuming $\Gamma_{\eta_b(2S)} = 4.9$ MeV. Not independent of the corresponding mass difference measurement.
[2] Obtained by analyzing CLEO III data but not authored by the CLEO Collaboration.
[3] Assuming $\Gamma_{\eta_b(2S)} = 5$ MeV. Not independent of the corresponding mass difference measurement.

$m_{\Upsilon(2S)} - m_{\eta_b(2S)}$

VALUE (MeV)	EVTS	DOCUMENT ID		TECN	COMMENT
24.3±3.5$^{+2.8}_{-1.9}$	26k	[4] MIZUK	12	BELL	$e^+e^- \to \gamma\pi^+\pi^-$ + hadrons
• • • We do not use the following data for averages, fits, limits, etc. • • •					
48.7±2.3±2.1	11 ± 4	[5,6] DOBBS	12		$\Upsilon(2S) \to \gamma$ hadrons

[4] Assuming $\Gamma_{\eta_b(2S)} = 4.9$ MeV. Not independent of the corresponding mass measurement.
[5] Obtained by analyzing CLEO III data but not authored by the CLEO Collaboration.
[6] Assuming $\Gamma_{\eta_b(2S)} = 5$ MeV. Not independent of the corresponding mass measurement.

$\eta_b(2S)$ WIDTH

VALUE (MeV)	CL%	DOCUMENT ID		TECN	COMMENT
<24	90	MIZUK	12	BELL	$e^+e^- \to \gamma\pi^+\pi^-$ hadrons

$\eta_b(2S)$ DECAY MODES

	Mode	Fraction (Γ_i/Γ)
Γ_1	hadrons	seen

$\eta_b(2S)$ BRANCHING RATIOS

$\Gamma(\text{hadrons})/\Gamma_{total}$ Γ_1/Γ

VALUE	EVTS	DOCUMENT ID		TECN	COMMENT
seen	26k	MIZUK	12	BELL	$e^+e^- \to \gamma\pi^+\pi^-$ hadrons
• • • We do not use the following data for averages, fits, limits, etc. • • •					
seen		[7] DOBBS	12		$\Upsilon(2S) \to \gamma$ hadrons

[7] Obtained by analyzing CLEO III data but not authored by the CLEO Collaboration.

Meson Particle Listings

$\eta_b(2S)$, $\Upsilon(2S)$

$\eta_b(2S)$ REFERENCES

DOBBS	12	PRL 109 082001	S. Dobbs *et al.*	
MIZUK	12	PRL 109 232002	R. Mizuk *et al.*	(BELLE Collab.)

$\Upsilon(2S)$

$I^G(J^{PC}) = 0^-(1^{--})$

$\Upsilon(2S)$ MASS

VALUE (MeV)	DOCUMENT ID		TECN	COMMENT
10023.26±0.31 OUR AVERAGE				
10023.5 ±0.5	[1] ARTAMONOV	00	MD1	$e^+e^- \to$ hadrons
10023.1 ±0.4	BARBER	84	REDE	$e^+e^- \to$ hadrons
• • • We do not use the following data for averages, fits, limits, etc. • • •				
10023.6 ±0.5	[2,3] BARU	86B	REDE	$e^+e^- \to$ hadrons

[1] Reanalysis of BARU 86B using new electron mass (COHEN 87).
[2] Reanalysis of ARTAMONOV 84.
[3] Superseded by ARTAMONOV 00.

$m_{\Upsilon(3S)} - m_{\Upsilon(2S)}$

VALUE (MeV)	DOCUMENT ID		TECN	COMMENT
331.50±0.02±0.13	LEES	11C	BABR	$e^+e^- \to \pi^+\pi^- X$

$\Upsilon(2S)$ WIDTH

VALUE (keV)	DOCUMENT ID
31.98±2.63 OUR EVALUATION	See the Note on "Width Determinations of the Υ States"

$\Upsilon(2S)$ DECAY MODES

	Mode	Fraction (Γ_i/Γ)	Scale factor/ Confidence level
Γ_1	$\Upsilon(1S)\pi^+\pi^-$	(17.85± 0.26) %	
Γ_2	$\Upsilon(1S)\pi^0\pi^0$	(8.6 ± 0.4) %	
Γ_3	$\tau^+\tau^-$	(2.00± 0.21) %	
Γ_4	$\mu^+\mu^-$	(1.93± 0.17) %	S=2.2
Γ_5	e^+e^-	(1.91± 0.16) %	
Γ_6	$\Upsilon(1S)\pi^0$	$< 4 \times 10^{-5}$	CL=90%
Γ_7	$\Upsilon(1S)\eta$	$(2.9 \pm 0.4) \times 10^{-4}$	S=2.0
Γ_8	$J/\psi(1S)$ anything	$< 6 \times 10^{-3}$	CL=90%
Γ_9	$J/\psi(1S)\eta_c$	$< 5.4 \times 10^{-6}$	CL=90%
Γ_{10}	$J/\psi(1S)\chi_{c0}$	$< 3.4 \times 10^{-6}$	CL=90%
Γ_{11}	$J/\psi(1S)\chi_{c1}$	$< 1.2 \times 10^{-6}$	CL=90%
Γ_{12}	$J/\psi(1S)\chi_{c2}$	$< 2.0 \times 10^{-6}$	CL=90%
Γ_{13}	$J/\psi(1S)\eta_c(2S)$	$< 2.5 \times 10^{-6}$	CL=90%
Γ_{14}	$J/\psi(1S)X(3940)$	$< 2.0 \times 10^{-6}$	CL=90%
Γ_{15}	$J/\psi(1S)X(4160)$	$< 2.0 \times 10^{-6}$	CL=90%
Γ_{16}	χ_{c1} anything	$(2.2 \pm 0.5) \times 10^{-4}$	
Γ_{17}	$\chi_{c1}(1P)^0 X_{tetra}$	$< 3.67 \times 10^{-5}$	CL=90%
Γ_{18}	χ_{c2} anything	$(2.3 \pm 0.8) \times 10^{-4}$	
Γ_{19}	$\psi(2S)\eta_c$	$< 5.1 \times 10^{-6}$	CL=90%
Γ_{20}	$\psi(2S)\chi_{c0}$	$< 4.7 \times 10^{-6}$	CL=90%
Γ_{21}	$\psi(2S)\chi_{c1}$	$< 2.5 \times 10^{-6}$	CL=90%
Γ_{22}	$\psi(2S)\chi_{c2}$	$< 1.9 \times 10^{-6}$	CL=90%
Γ_{23}	$\psi(2S)\eta_c(2S)$	$< 3.3 \times 10^{-6}$	CL=90%
Γ_{24}	$\psi(2S)X(3940)$	$< 3.9 \times 10^{-6}$	CL=90%
Γ_{25}	$\psi(2S)X(4160)$	$< 3.9 \times 10^{-6}$	CL=90%
Γ_{26}	$\overline{2H}$ anything	$(2.78^{+\ 0.30}_{-\ 0.26}) \times 10^{-5}$	S=1.2
Γ_{27}	hadrons	(94 ±11) %	
Γ_{28}	ggg	(58.8 ± 1.2) %	
Γ_{29}	γgg	(1.87± 0.28) %	
Γ_{30}	ϕK^+K^-	$(1.6 \pm 0.4) \times 10^{-6}$	
Γ_{31}	$\omega\pi^+\pi^-$	$< 2.58 \times 10^{-6}$	CL=90%
Γ_{32}	$K^*(892)^0 K^-\pi^+ +$ c.c.	$(2.3 \pm 0.7) \times 10^{-6}$	
Γ_{33}	$\phi f_2'(1525)$	$< 1.33 \times 10^{-6}$	CL=90%
Γ_{34}	$\omega f_2(1270)$	$< 5.7 \times 10^{-7}$	CL=90%
Γ_{35}	$\rho(770)a_2(1320)$	$< 8.8 \times 10^{-7}$	CL=90%
Γ_{36}	$K^*(892)^0\overline{K}_2^*(1430)^0 +$ c.c.	$(1.5 \pm 0.6) \times 10^{-6}$	
Γ_{37}	$K_1(1270)^\pm K^\mp$	$< 3.22 \times 10^{-6}$	CL=90%
Γ_{38}	$K_1(1400)^\pm K^\mp$	$< 8.3 \times 10^{-7}$	CL=90%
Γ_{39}	$b_1(1235)^\pm\pi^\mp$	$< 4.0 \times 10^{-7}$	CL=90%
Γ_{40}	$\rho\pi$	$< 1.16 \times 10^{-6}$	CL=90%
Γ_{41}	$\pi^+\pi^-\pi^0$	$< 8.0 \times 10^{-7}$	CL=90%
Γ_{42}	$\omega\pi^0$	$< 1.63 \times 10^{-6}$	CL=90%
Γ_{43}	$\pi^+\pi^-\pi^0\pi^0$	$(1.30\pm 0.28) \times 10^{-5}$	
Γ_{44}	$K_S^0 K^+\pi^- +$ c.c.	$(1.14\pm 0.33) \times 10^{-6}$	
Γ_{45}	$K^*(892)^0\overline{K}^0 +$ c.c.	$< 4.22 \times 10^{-6}$	CL=90%
Γ_{46}	$K^*(892)^- K^+ +$ c.c.	$< 1.45 \times 10^{-6}$	CL=90%
Γ_{47}	$f_1(1285)$ anything	$(2.2 \pm 1.6) \times 10^{-3}$	
Γ_{48}	$f_1(1285)X_{tetra}$	$< 6.47 \times 10^{-5}$	CL=90%
Γ_{49}	Sum of 100 exclusive modes	$(2.90\pm 0.30) \times 10^{-3}$	

Radiative decays

Γ_{50}	$\gamma\chi_{b1}(1P)$	(6.9 ± 0.4) %	
Γ_{51}	$\gamma\chi_{b2}(1P)$	(7.15± 0.35) %	
Γ_{52}	$\gamma\chi_{b0}(1P)$	(3.8 ± 0.4) %	
Γ_{53}	$\gamma f_0(1710)$	$< 5.9 \times 10^{-4}$	CL=90%
Γ_{54}	$\gamma f_2'(1525)$	$< 5.3 \times 10^{-4}$	CL=90%
Γ_{55}	$\gamma f_2(1270)$	$< 2.41 \times 10^{-4}$	CL=90%
Γ_{56}	$\gamma f_J(2220)$		
Γ_{57}	$\gamma\eta_c(1S)$	$< 2.7 \times 10^{-5}$	CL=90%
Γ_{58}	$\gamma\chi_{c0}$	$< 1.0 \times 10^{-4}$	CL=90%
Γ_{59}	$\gamma\chi_{c1}$	$< 3.6 \times 10^{-6}$	CL=90%
Γ_{60}	$\gamma\chi_{c2}$	$< 1.5 \times 10^{-5}$	CL=90%
Γ_{61}	$\gamma\chi_{c1}(3872) \to \pi^+\pi^- J/\psi$	$< 8 \times 10^{-7}$	CL=90%
Γ_{62}	$\gamma\chi_{c1}(3872) \to \pi^+\pi^-\pi^0 J/\psi$	$< 2.4 \times 10^{-6}$	CL=90%
Γ_{63}	$\gamma X(3915) \to \omega J/\psi$	$< 2.8 \times 10^{-6}$	CL=90%
Γ_{64}	$\gamma\chi_{c1}(4140) \to \phi J/\psi$	$< 1.2 \times 10^{-6}$	CL=90%
Γ_{65}	$\gamma X(4350) \to \phi J/\psi$	$< 1.3 \times 10^{-6}$	CL=90%
Γ_{66}	$\gamma\eta_b(1S)$	$(3.9 \pm 1.5) \times 10^{-4}$	
Γ_{67}	$\gamma\eta_b(1S) \to \gamma$Sum of 26 exclusive modes	$< 3.7 \times 10^{-6}$	CL=90%
Γ_{68}	$\gamma X_{b\overline{b}} \to \gamma$Sum of 26 exclusive modes	$< 4.9 \times 10^{-6}$	CL=90%
Γ_{69}	$\gamma X \to \gamma + \geq 4$ prongs	[a] $< 1.95 \times 10^{-4}$	CL=95%
Γ_{70}	$\gamma A^0 \to \gamma$hadrons	$< 8 \times 10^{-5}$	CL=90%
Γ_{71}	$\gamma a_1^0 \to \gamma\mu^+\mu^-$	$< 8.3 \times 10^{-6}$	CL=90%

Lepton Family number (LF) violating modes

Γ_{72}	$e^\pm\tau^\mp$	LF	$< 3.2 \times 10^{-6}$	CL=90%
Γ_{73}	$\mu^\pm\tau^\mp$	LF	$< 3.3 \times 10^{-6}$	CL=90%

[a] 1.5 GeV $< m_X <$ 5.0 GeV

CONSTRAINED FIT INFORMATION

An overall fit to 3 branching ratios uses 13 measurements and one constraint to determine 3 parameters. The overall fit has a $\chi^2 = 11.8$ for 11 degrees of freedom.

The following *off-diagonal* array elements are the correlation coefficients $\langle \delta x_i \delta x_j \rangle / (\delta x_i \cdot \delta x_j)$, in percent, from the fit to the branching fractions, $x_i \equiv \Gamma_i/\Gamma_{\rm total}$. The fit constrains the x_i whose labels appear in this array to sum to one.

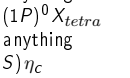

$\Upsilon(2S)$ $\Gamma(i)\Gamma(e^+e^-)/\Gamma(\text{total})$

$\Gamma(\mu^+\mu^-) \times \Gamma(e^+e^-)/\Gamma_{\rm total}$ $\quad \Gamma_4\Gamma_5/\Gamma$

VALUE (eV)	DOCUMENT ID		TECN	COMMENT
6.5±1.5±1.0	KOBEL	92	CBAL	$e^+e^- \to \mu^+\mu^-$

$\Gamma(\Upsilon(1S)\pi^+\pi^-) \times \Gamma(e^+e^-)/\Gamma_{\rm total}$ $\quad \Gamma_1\Gamma_5/\Gamma$

VALUE (eV)	EVTS	DOCUMENT ID		TECN	COMMENT
105.4±1.0±4.2	11.8K	[1] AUBERT	08BP	BABR	10.58 $e^+e^- \to \gamma\pi^+\pi^-\ell^+\ell^-$

[1] Using B($\Upsilon(1S) \to e^+e^-$) = (2.38 ± 0.11)% and B($\Upsilon(1S) \to \mu^+\mu^-$) = (2.48 ± 0.05)%.

$\Gamma(\text{hadrons}) \times \Gamma(e^+e^-)/\Gamma_{\rm total}$ $\quad \Gamma_{27}\Gamma_5/\Gamma$

VALUE (keV)	DOCUMENT ID		TECN	COMMENT
0.577±0.009 OUR AVERAGE				
0.581±0.004±0.009	[1] ROSNER	06	CLEO	10.0 $e^+e^- \to$ hadrons
0.552±0.031±0.017	[1] BARU	96	MD1	$e^+e^- \to$ hadrons
0.54 ±0.04 ±0.02	[1] JAKUBOWSKI	88	CBAL	$e^+e^- \to$ hadrons
0.58 ±0.03 ±0.04	[2] GILES	84B	CLEO	$e^+e^- \to$ hadrons
0.60 ±0.12 ±0.07	[2] ALBRECHT	82	DASP	$e^+e^- \to$ hadrons
0.54 ±0.07 $^{+0.09}_{-0.05}$	[2] NICZYPORUK	81C	LENA	$e^+e^- \to$ hadrons
0.41 ±0.18	[2] BOCK	80	CNTR	$e^+e^- \to$ hadrons

[1] Radiative corrections evaluated following KURAEV 85.
[2] Radiative corrections reevaluated by BUCHMUELLER 88 following KURAEV 85.

$\Upsilon(2S)$ PARTIAL WIDTHS

$\Gamma(e^+e^-)$ Γ_5

VALUE (keV)	DOCUMENT ID
0.612±0.011 OUR EVALUATION	

$\Upsilon(2S)$ BRANCHING RATIOS

$\Gamma(\Upsilon(1S)\pi^+\pi^-)/\Gamma_{total}$ Γ_1/Γ

Abbreviation MM in the *COMMENT* field below stands for missing mass.

VALUE (units 10^{-2})	EVTS	DOCUMENT ID		TECN	COMMENT
17.85±0.26 OUR FIT					
17.92±0.26 OUR AVERAGE					
16.8 ±1.1 ±1.3	906k	[1] LEES	11C	BABR	$e^+e^- \to \pi^+\pi^- X$
17.80±0.05±0.37	170k	[2] LEES	11L	BABR	$\Upsilon(2S) \to \pi^+\pi^-\mu^+\mu^-$
18.02±0.02±0.61	851k	[3] BHARI	09	CLEO	$e^+e^- \to \pi^+\pi^-$ MM
17.22±0.17±0.75	11.8K	[4] AUBERT	08BP	BABR	$e^+e^- \to \gamma\pi^+\pi^-\ell^+\ell^-$
19.2 ±0.2 ±1.0	52.6k	[5] ALEXANDER	98	CLE2	$\pi^+\pi^-\ell^+\ell^-$, $\pi^+\pi^-$ MM
18.1 ±0.5 ±1.0	11.6k	ALBRECHT	87	ARG	$e^+e^- \to \pi^+\pi^-$ MM
16.9 ±4.0		GELPHMAN	85	CBAL	$e^+e^- \to e^+e^-\pi^+\pi^-$
19.1 ±1.2 ±0.6		BESSON	84	CLEO	$\pi^+\pi^-$ MM
18.9 ±2.6		FONSECA	84	CUSB	$e^+e^- \to \ell^+\ell^-\pi^+\pi^-$
21 ±7	7	NICZYPORUK	81B	LENA	$e^+e^- \to \ell^+\ell^-\pi^+\pi^-$

[1] LEES 11C reports $[\Gamma(\Upsilon(2S) \to \Upsilon(1S)\pi^+\pi^-)/\Gamma_{total}] \times [B(\Upsilon(3S) \to \Upsilon(2S)\text{anything})] = (1.78 \pm 0.02 \pm 0.11) \times 10^{-2}$ which we divide by our best value $B(\Upsilon(3S) \to \Upsilon(2S)\text{anything}) = (10.6 \pm 0.8) \times 10^{-2}$. Our first error is their experiment's error and our second error is the systematic error from using our best value.

[2] Using $B(\Upsilon(1S) \to \mu^+\mu^-) = (2.48 \pm 0.05)\%$.

[3] A weighted average of the inclusive and exclusive results.

[4] Using $B(\Upsilon(2S) \to e^+e^-) = (1.91 \pm 0.16)\%$, $B(\Upsilon(2S) \to \mu^+\mu^-) = (1.93 \pm 0.17)\%$ and, $\Gamma_{ee}(\Upsilon(2S)) = 0.612 \pm 0.011$ keV.

[5] Using $B(\Upsilon(1S) \to e^+e^-) = (2.52 \pm 0.17)\%$ and $B(\Upsilon(1S) \to \mu^+\mu^-) = (2.48 \pm 0.07)\%$.

$\Gamma(\Upsilon(1S)\pi^0\pi^0)/\Gamma_{total}$ Γ_2/Γ

VALUE (units 10^{-2})	EVTS	DOCUMENT ID		TECN	COMMENT
8.6 ±0.4 OUR AVERAGE					
8.43±0.16±0.42	38k	[1] BHARI	09	CLEO	$e^+e^- \to \pi^0\pi^0\ell^+\ell^-$
9.2 ±0.6 ±0.8	275	[2] ALEXANDER	98	CLE2	$e^+e^- \to \pi^0\pi^0\ell^+\ell^-$
9.5 ±1.9 ±1.9	25	ALBRECHT	87	ARG	$e^+e^- \to \pi^0\pi^0\ell^+\ell^-$
8.0 ±1.5		GELPHMAN	85	CBAL	$e^+e^- \to \pi^0\pi^0\ell^+\ell^-$
10.3 ±2.3		FONSECA	84	CUSB	$e^+e^- \to \pi^0\pi^0\ell^+\ell^-$

[1] Authors assume $B(\Upsilon(1S) \to e^+e^-) + B(\Upsilon(1S) \to \mu^+\mu^-) = 4.96\%$.

[2] Using $B(\Upsilon(1S) \to e^+e^-) = (2.52 \pm 0.17)\%$ and $B(\Upsilon(1S) \to \mu^+\mu^-) = (2.48 \pm 0.07)\%$.

$\Gamma(\Upsilon(1S)\pi^0\pi^0)/\Gamma(\Upsilon(1S)\pi^+\pi^-)$ Γ_2/Γ_1

VALUE	DOCUMENT ID		TECN	COMMENT
• • • We do not use the following data for averages, fits, limits, etc. • • •				
0.462±0.037	[1] BHARI	09	CLEO	$e^+e^- \to \Upsilon(2S)$

[1] Not independent of other values reported by BHARI 09.

$\Gamma(\tau^+\tau^-)/\Gamma_{total}$ Γ_3/Γ

VALUE (units 10^{-2})	EVTS	DOCUMENT ID		TECN	COMMENT
2.00±0.21 OUR AVERAGE					
2.00±0.12±0.18	22k	[1] BESSON	07	CLEO	$e^+e^- \to \Upsilon(2S) \to \tau^+\tau^-$
1.7 ±1.5 ±0.6		HAAS	84B	CLEO	$e^+e^- \to \tau^+\tau^-$

[1] BESSON 07 reports $[\Gamma(\Upsilon(2S) \to \tau^+\tau^-)/\Gamma_{total}] / [B(\Upsilon(2S) \to \mu^+\mu^-)] = 1.04 \pm 0.04 \pm 0.05$ which we multiply by our best value $B(\Upsilon(2S) \to \mu^+\mu^-) = (1.93 \pm 0.17) \times 10^{-2}$. Our first error is their experiment's error and our second error is the systematic error from using our best value.

$\Gamma(\mu^+\mu^-)/\Gamma_{total}$ Γ_4/Γ

VALUE	CL%	EVTS	DOCUMENT ID		TECN	COMMENT
0.0193±0.0017 OUR AVERAGE Error includes scale factor of 2.2. See the ideogram below.						
0.0203±0.0003±0.0008		120k	ADAMS	05	CLEO	$e^+e^- \to \mu^+\mu^-$
0.0122±0.0028±0.0019			[1] KOBEL	92	CBAL	$e^+e^- \to \mu^+\mu^-$
0.0138±0.0025±0.0015			KAARSBERG	89	CSB2	$e^+e^- \to \mu^+\mu^-$
0.009 ±0.006 ±0.006			[2] ALBRECHT	85	ARG	$e^+e^- \to \mu^+\mu^-$
0.018 ±0.008 ±0.005			HAAS	84B	CLEO	$e^+e^- \to \mu^+\mu^-$
• • • We do not use the following data for averages, fits, limits, etc. • • •						
<0.038	90		NICZYPORUK	81C	LENA	$e^+e^- \to \mu^+\mu^-$

[1] Taking into account interference between the resonance and continuum.

[2] Re-evaluated using $B(\Upsilon(1S) \to \mu^+\mu^-) = 0.026$.

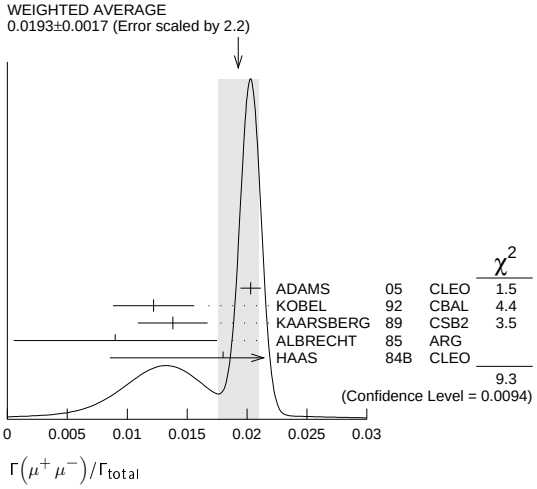

$\Gamma(\tau^+\tau^-)/\Gamma(\mu^+\mu^-)$ Γ_3/Γ_4

VALUE	EVTS	DOCUMENT ID		TECN	COMMENT
1.04±0.04±0.05	22k	BESSON	07	CLEO	$e^+e^- \to \Upsilon(2S)$

$\Gamma(\Upsilon(1S)\pi^0)/\Gamma_{total}$ Γ_6/Γ

VALUE (units 10^{-5})	CL%	DOCUMENT ID		TECN	COMMENT
• • • We do not use the following data for averages, fits, limits, etc. • • •					
< 4	90	[1] TAMPONI	13	BELL	$e^+e^- \to \Upsilon(1S)\pi^0$
< 18	90	[2] HE	08A	CLEO	$e^+e^- \to \ell^+\ell^-\gamma\gamma$
<110	90	ALEXANDER	98	CLE2	$e^+e^- \to \ell^+\ell^-\gamma\gamma$
<800	90	LURZ	87	CBAL	$e^+e^- \to \ell^+\ell^-\gamma\gamma$

[1] TAMPONI 13 reports $[\Gamma(\Upsilon(2S) \to \Upsilon(1S)\pi^0)/\Gamma_{total}] / [B(\Upsilon(2S) \to \Upsilon(1S)\pi^+\pi^-)] < 2.3 \times 10^{-4}$ which we multiply by our best value $B(\Upsilon(2S) \to \Upsilon(1S)\pi^+\pi^-) = 17.85 \times 10^{-2}$.

[2] Authors assume $B(\Upsilon(1S) \to e^+e^-) + B(\Upsilon(1S) \to \mu^+\mu^-) = 4.96\%$.

$\Gamma(\Upsilon(1S)\pi^0)/\Gamma(\Upsilon(1S)\pi^+\pi^-)$ Γ_6/Γ_1

VALUE (units 10^{-4})	CL%	DOCUMENT ID		TECN	COMMENT
<2.3	90	TAMPONI	13	BELL	$e^+e^- \to \Upsilon(1S)\pi^0$

$\Gamma(\Upsilon(1S)\eta)/\Gamma_{total}$ Γ_7/Γ

VALUE (units 10^{-4})	CL%	EVTS	DOCUMENT ID		TECN	COMMENT
2.9 ±0.4 OUR FIT Error includes scale factor of 2.0.						
2.9 ±0.4 OUR AVERAGE Error includes scale factor of 1.9. See the ideogram below.						
2.39±0.31±0.14		112	[1] LEES	11L	BABR	$\Upsilon(2S) \to \ell^+\ell^-\eta$
2.1 $^{+0.7}_{-0.6}$ ±0.3		14	[2] HE	08A	CLEO	$e^+e^- \to \ell^+\ell^-\eta$
• • • We use the following data for averages but not for fits. • • •						
3.55±0.32±0.05		241	[3] TAMPONI	13	BELL	$e^+e^- \to \Upsilon(1S)\eta$
• • • We do not use the following data for averages, fits, limits, etc. • • •						
< 9	90		[1,4] AUBERT	08BP	BABR	$e^+e^- \to \gamma\pi^+\pi^-\pi^0\ell^+\ell^-$
< 28	90		ALEXANDER	98	CLE2	$e^+e^- \to \ell^+\ell^-\eta$
< 50	90		ALBRECHT	87	ARG	$e^+e^- \to \pi^+\pi^-\ell^+\ell^-$ MM
< 70	90		LURZ	87	CBAL	$e^+e^- \to \ell^+\ell^-(\gamma\gamma,\ 3\pi^0)$
< 100	90		BESSON	84	CLEO	$e^+e^- \to \pi^+\pi^-\ell^+\ell^-$ MM
< 20	90		FONSECA	84	CUSB	$e^+e^- \to \ell^+\ell^-(\gamma\gamma, \pi^+\pi^-\pi^0)$

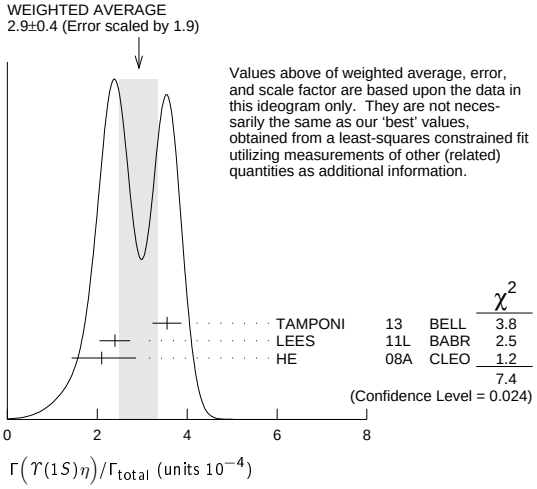

[1] Using B($\Upsilon(1S) \to e^+e^-$) = (2.38 ± 0.11)% and B($\Upsilon(1S) \to \mu^+\mu^-$) = (2.48 ± 0.05)%.
[2] Authors assume B($\Upsilon(1S) \to e^+e^-$) + B($\Upsilon(1S) \to \mu^+\mu^-$) = 4.96%.
[3] TAMPONI 13 reports [$\Gamma(\Upsilon(2S) \to \Upsilon(1S)\eta)/\Gamma_{total}$] / [B($\Upsilon(2S) \to \Upsilon(1S)\pi^+\pi^-$)] = (1.99 ± 0.14 ± 0.11) × 10^{-3} which we multiply by our best value B($\Upsilon(2S) \to \Upsilon(1S)\pi^+\pi^-$) = (17.85 ± 0.26) × 10^{-2}. Our first error is their experiment's error and our second error is the systematic error from using our best value.
[4] Using $\Gamma_{ee}(\Upsilon(2S))$ = 0.612 ± 0.011 keV.

$\Gamma(\Upsilon(1S)\eta)/\Gamma(\Upsilon(1S)\pi^+\pi^-)$ Γ_7/Γ_1

VALUE (units 10^{-3})	CL%	EVTS	DOCUMENT ID		TECN	COMMENT
1.64±0.25 OUR FIT			Error includes scale factor of 2.0.			
1.99±0.14±0.11		241	TAMPONI	13	BELL	$e^+e^- \to \Upsilon(1S)\eta$
• • • We do not use the following data for averages, fits, limits, etc. • • •						
1.35±0.17±0.08			[1] LEES	11L	BABR	$\Upsilon(2S) \to (\pi^+\pi^-)(\gamma\gamma)\mu^+\mu^-$
< 5.2	90		[2] AUBERT	08BP	BABR	$e^+e^- \to \gamma\pi^+\pi^-(\pi^0)\ell^+\ell^-$

[1] Not independent of other values reported by LEES 11L.
[2] Not independent of other values reported by AUBERT 08BP.

$\Gamma(\Upsilon(1S)\pi^0)/\Gamma(\Upsilon(1S)\eta)$ Γ_6/Γ_7

VALUE	CL%	DOCUMENT ID		TECN	COMMENT
• • • We do not use the following data for averages, fits, limits, etc. • • •					
<0.13	90	TAMPONI	13	BELL	$e^+e^- \to \Upsilon(1S)\pi^0$

$\Gamma(J/\psi(1S)\text{ anything})/\Gamma_{total}$ Γ_8/Γ

VALUE	CL%	DOCUMENT ID		TECN	COMMENT
<0.006	90	MASCHMANN	90	CBAL	$e^+e^- \to$ hadrons

$\Gamma(J/\psi(1S)\eta_c)/\Gamma_{total}$ Γ_9/Γ

VALUE	CL%	DOCUMENT ID		TECN	COMMENT
<5.4 × 10^{-6}	90	YANG	14	BELL	$e^+e^- \to J/\psi X$

$\Gamma(J/\psi(1S)\chi_{c0})/\Gamma_{total}$ Γ_{10}/Γ

VALUE	CL%	DOCUMENT ID		TECN	COMMENT
<3.4 × 10^{-6}	90	YANG	14	BELL	$e^+e^- \to J/\psi X$

$\Gamma(J/\psi(1S)\chi_{c1})/\Gamma_{total}$ Γ_{11}/Γ

VALUE	CL%	DOCUMENT ID		TECN	COMMENT
<1.2 × 10^{-6}	90	YANG	14	BELL	$e^+e^- \to J/\psi X$

$\Gamma(J/\psi(1S)\chi_{c2})/\Gamma_{total}$ Γ_{12}/Γ

VALUE	CL%	DOCUMENT ID		TECN	COMMENT
<2.0 × 10^{-6}	90	YANG	14	BELL	$e^+e^- \to J/\psi X$

$\Gamma(J/\psi(1S)\eta_c(2S))/\Gamma_{total}$ Γ_{13}/Γ

VALUE	CL%	DOCUMENT ID		TECN	COMMENT
<2.5 × 10^{-6}	90	YANG	14	BELL	$e^+e^- \to J/\psi X$

$\Gamma(J/\psi(1S)X(3940))/\Gamma_{total}$ Γ_{14}/Γ

VALUE	CL%	DOCUMENT ID		TECN	COMMENT
<2.0 × 10^{-6}	90	YANG	14	BELL	$e^+e^- \to J/\psi X$

$\Gamma(J/\psi(1S)X(4160))/\Gamma_{total}$ Γ_{15}/Γ

VALUE	CL%	DOCUMENT ID		TECN	COMMENT
<2.0 × 10^{-6}	90	YANG	14	BELL	$e^+e^- \to J/\psi X$

$\Gamma(\chi_{c1}\text{ anything})/\Gamma_{total}$ Γ_{16}/Γ

VALUE (units 10^{-4})	EVTS	DOCUMENT ID		TECN	COMMENT
2.24±0.44±0.20	376	JIA	17	BELL	$\Upsilon(2S) \to \gamma J/\psi(1S)$

$\Gamma(\chi_{c1}(1P)^0 X_{tetra})/\Gamma_{total}$ Γ_{17}/Γ

VALUE	CL%	DOCUMENT ID		TECN	COMMENT
<36.7 × 10^{-6}	90	[1] JIA	17A	BELL	$e^+e^- \to$ hadrons

[1] For a tetraquark state X_{tetra}, with mass in the range 1.16–2.46 GeV and width in the range 0–0.3 GeV. Measured 90% CL limits as a function of X_{tetra} mass and width range from 4.4 × 10^{-6} to 36.7 × 10^{-6}.

$\Gamma(\chi_{c2}\text{ anything})/\Gamma_{total}$ Γ_{18}/Γ

VALUE (units 10^{-4})	DOCUMENT ID		TECN	COMMENT
2.28±0.73±0.34	JIA	17	BELL	$\Upsilon(2S) \to \gamma J/\psi(1S)$

$\Gamma(\psi(2S)\eta_c)/\Gamma_{total}$ Γ_{19}/Γ

VALUE	CL%	DOCUMENT ID		TECN	COMMENT
<5.1 × 10^{-6}	90	YANG	14	BELL	$e^+e^- \to \psi(2S)X$

$\Gamma(\psi(2S)\chi_{c0})/\Gamma_{total}$ Γ_{20}/Γ

VALUE	CL%	DOCUMENT ID		TECN	COMMENT
<4.7 × 10^{-6}	90	YANG	14	BELL	$e^+e^- \to \psi(2S)X$

$\Gamma(\psi(2S)\chi_{c1})/\Gamma_{total}$ Γ_{21}/Γ

VALUE	CL%	DOCUMENT ID		TECN	COMMENT
<2.5 × 10^{-6}	90	YANG	14	BELL	$e^+e^- \to \psi(2S)X$

$\Gamma(\psi(2S)\chi_{c2})/\Gamma_{total}$ Γ_{22}/Γ

VALUE	CL%	DOCUMENT ID		TECN	COMMENT
<1.9 × 10^{-6}	90	YANG	14	BELL	$e^+e^- \to \psi(2S)X$

$\Gamma(\psi(2S)\eta_c(2S))/\Gamma_{total}$ Γ_{23}/Γ

VALUE	CL%	DOCUMENT ID		TECN	COMMENT
<3.3 × 10^{-6}	90	YANG	14	BELL	$e^+e^- \to \psi(2S)X$

$\Gamma(\psi(2S)X(3940))/\Gamma_{total}$ Γ_{24}/Γ

VALUE	CL%	DOCUMENT ID		TECN	COMMENT
<3.9 × 10^{-6}	90	YANG	14	BELL	$e^+e^- \to \psi(2S)X$

$\Gamma(\psi(2S)X(4160))/\Gamma_{total}$ Γ_{25}/Γ

VALUE	CL%	DOCUMENT ID		TECN	COMMENT
<3.9 × 10^{-6}	90	YANG	14	BELL	$e^+e^- \to \psi(2S)X$

$\Gamma(\overline{2H}\text{ anything})/\Gamma_{total}$ Γ_{26}/Γ

VALUE (units 10^{-5})	EVTS	DOCUMENT ID		TECN	COMMENT
$2.78^{+0.30}_{-0.26}$ OUR AVERAGE		Error includes scale factor of 1.2.			
$2.64 \pm 0.11^{+0.26}_{-0.21}$		LEES	14G	BABR	$e^+e^- \to \overline{2H}X$
3.37±0.50±0.25	58	ASNER	07	CLEO	$e^+e^- \to \overline{2H}X$

$\Gamma(ggg)/\Gamma_{total}$ Γ_{28}/Γ

VALUE (units 10^{-2})	EVTS	DOCUMENT ID		TECN	COMMENT
58.8±1.2	6M	[1] BESSON	06A	CLEO	$\Upsilon(2S) \to$ hadrons

[1] Calculated using the value $\Gamma(\gamma gg)/\Gamma(ggg)$ = (3.18 ± 0.04 ± 0.22 ± 0.41)% from BESSON 06A and PDG 08 values of B($\pi^+\pi^-\Upsilon(1S)$) = (18.1±0.4)%, B($\pi^0\pi^0\Upsilon(1S)$) = (8.6±0.4)%, B($\mu^+\mu^-$) = (1.93±0.17)%, and $R_{hadrons}$ = 3.51. The statistical error is negligible and the systematic error is partially correlated with that of $\Gamma(\gamma gg)/\Gamma_{total}$ measurement of BESSON 06A.

$\Gamma(\gamma gg)/\Gamma(ggg)$ Γ_{29}/Γ_{28}

VALUE (units 10^{-2})	EVTS	DOCUMENT ID		TECN	COMMENT
3.18±0.04±0.47	6M	BESSON	06A	CLEO	$\Upsilon(2S) \to (\gamma\ +)$ hadrons

$\Gamma(\phi K^+K^-)/\Gamma_{total}$ Γ_{30}/Γ

VALUE (units 10^{-6})	EVTS	DOCUMENT ID		TECN	COMMENT
1.58±0.33±0.18	58	SHEN	12A	BELL	$\Upsilon(1S) \to 2(K^+K^-)$

$\Gamma(\omega\pi^+\pi^-)/\Gamma_{total}$ Γ_{31}/Γ

VALUE (units 10^{-6})	CL%	DOCUMENT ID		TECN	COMMENT
<2.58	90	SHEN	12A	BELL	$\Upsilon(1S) \to 2(\pi^+\pi^-)\pi^0$

$\Gamma(K^*(892)^0K^-\pi^+ + \text{c.c.})/\Gamma_{total}$ Γ_{32}/Γ

VALUE (units 10^{-6})	EVTS	DOCUMENT ID		TECN	COMMENT
2.32±0.40±0.54	135	SHEN	12A	BELL	$\Upsilon(1S) \to K^+K^-\pi^+\pi^-$

$\Gamma(\phi f_2'(1525))/\Gamma_{total}$ Γ_{33}/Γ

VALUE (units 10^{-6})	CL%	DOCUMENT ID		TECN	COMMENT
<1.33	90	SHEN	12A	BELL	$\Upsilon(1S) \to 2(K^+K^-)$

$\Gamma(\omega f_2(1270))/\Gamma_{total}$ Γ_{34}/Γ

VALUE (units 10^{-6})	CL%	DOCUMENT ID		TECN	COMMENT
<0.57	90	SHEN	12A	BELL	$\Upsilon(1S) \to 2(\pi^+\pi^-)\pi^0$

$\Gamma(\rho(770)a_2(1320))/\Gamma_{total}$ Γ_{35}/Γ

VALUE (units 10^{-6})	CL%	DOCUMENT ID		TECN	COMMENT
<0.88	90	SHEN	12A	BELL	$\Upsilon(1S) \to 2(\pi^+\pi^-)\pi^0$

$\Gamma(K^*(892)^0\overline{K}_2^*(1430)^0 + \text{c.c.})/\Gamma_{total}$ Γ_{36}/Γ

VALUE (units 10^{-6})	EVTS	DOCUMENT ID		TECN	COMMENT
1.53±0.52±0.19	32	SHEN	12A	BELL	$\Upsilon(1S) \to K^+K^-\pi^+\pi^-$

$\Gamma(K_1(1270)^\pm K^\mp)/\Gamma_{total}$ Γ_{37}/Γ

VALUE (units 10^{-6})	CL%	DOCUMENT ID		TECN	COMMENT
<3.22	90	SHEN	12A	BELL	$\Upsilon(1S) \to K^+K^-\pi^+\pi^-$

$\Gamma(K_1(1400)^\pm K^\mp)/\Gamma_{total}$ Γ_{38}/Γ

VALUE (units 10^{-6})	CL%	DOCUMENT ID		TECN	COMMENT
<0.83	90	SHEN	12A	BELL	$\Upsilon(1S) \to K^+K^-\pi^+\pi^-$

$\Gamma(b_1(1235)^\pm\pi^\mp)/\Gamma_{total}$ Γ_{39}/Γ

VALUE (units 10^{-6})	CL%	DOCUMENT ID		TECN	COMMENT
<0.40	90	SHEN	12A	BELL	$\Upsilon(1S) \to 2(\pi^+\pi^-)\pi^0$

$\Gamma(\rho\pi)/\Gamma_{total}$ Γ_{40}/Γ

VALUE (units 10^{-6})	CL%	DOCUMENT ID		TECN	COMMENT
<1.16	90	SHEN	13	BELL	$\Upsilon(2S) \to \pi^+\pi^-\pi^0$

$\Gamma(\pi^+\pi^-\pi^0)/\Gamma_{total}$ Γ_{41}/Γ

VALUE (units 10^{-6})	CL%	DOCUMENT ID		TECN	COMMENT
<0.80	90	SHEN	13	BELL	$\Upsilon(2S) \to \pi^+\pi^-\pi^0$

$\Gamma(\omega\pi^0)/\Gamma_{total}$ Γ_{42}/Γ

VALUE (units 10^{-6})	CL%	DOCUMENT ID		TECN	COMMENT
<1.63	90	SHEN	13	BELL	$\Upsilon(2S) \to \pi^+\pi^-\pi^0\pi^0$

$\Gamma(\pi^+\pi^-\pi^0\pi^0)/\Gamma_{total}$ Γ_{43}/Γ

VALUE (units 10^{-6})	EVTS	DOCUMENT ID		TECN	COMMENT
13.0±1.9±2.1	261 ± 37	SHEN	13	BELL	$\Upsilon(2S) \to \pi^+\pi^-\pi^0\pi^0$

$\Gamma(K^0_S K^+\pi^- + c.c.)/\Gamma_{total}$ Γ_{44}/Γ

VALUE (units 10^{-6})	CL%	EVTS	DOCUMENT ID		TECN	COMMENT
1.14±0.30±0.13		40 ± 10	SHEN	13	BELL	$\Upsilon(2S) \to K^0_S K^-\pi^+$
• • • We do not use the following data for averages, fits, limits, etc. • • •						
<3.2	90		[1] DOBBS	12A		$\Upsilon(2S) \to K^0_S K^-\pi^+$

[1] Obtained by analyzing CLEO III data but not authored by the CLEO Collaboration.

$\Gamma(K^*(892)^0\overline{K}{}^0 + c.c.)/\Gamma_{total}$ Γ_{45}/Γ

VALUE (units 10^{-6})	CL%	DOCUMENT ID		TECN	COMMENT
<4.22	90	SHEN	13	BELL	$\Upsilon(2S) \to K^0_S K^-\pi^+$

$\Gamma(K^*(892)^- K^+ + c.c.)/\Gamma_{total}$ Γ_{46}/Γ

VALUE (units 10^{-6})	CL%	DOCUMENT ID		TECN	COMMENT
<1.45	90	SHEN	13	BELL	$\Upsilon(2S) \to K^0_S K^-\pi^+$

$\Gamma(f_1(1285)\,\text{anything})/\Gamma_{total}$ Γ_{47}/Γ

VALUE (units 10^{-3})	EVTS	DOCUMENT ID		TECN	COMMENT
2.20±1.50±0.63	2.9k	JIA	17A	BELL	$e^+e^- \to$ hadrons

$\Gamma(f_1(1285)X_{tetra})/\Gamma_{total}$ Γ_{48}/Γ

VALUE	CL%	DOCUMENT ID		TECN	COMMENT
<64.7 × 10^{-6}	90	[1] JIA	17A	BELL	$e^+e^- \to$ hadrons

[1] For a tetraquark state X_{tetra}, with mass in the range 1.16–2.46 GeV and width in the range 0–0.3 GeV. Measured 90% CL limits as a function of X_{tetra} mass and width range from 7.8×10^{-6} to 64.7×10^{-6}.

$\Gamma(\text{Sum of 100 exclusive modes})/\Gamma_{total}$ Γ_{49}/Γ

VALUE (units 10^{-2})	DOCUMENT ID		COMMENT
0.29±0.03	[1,2] DOBBS	12A	$\Upsilon(2S) \to$ hadrons

[1] DOBBS 12A presents individual exclusive branching fractions or upper limits for 100 modes of four to ten pions, kaons, or protons.

[2] Obtained by analyzing CLEO III data but not authored by the CLEO Collaboration.

$\Gamma(\gamma\chi_{b1}(1P))/\Gamma_{total}$ Γ_{50}/Γ

VALUE	EVTS	DOCUMENT ID		TECN	COMMENT
0.069 ±0.004 OUR AVERAGE					
0.0693±0.0012±0.0041	407k	ARTUSO	05	CLEO	$e^+e^- \to \gamma X$
0.069 ±0.005 ±0.009		EDWARDS	99	CLE2	$\Upsilon(2S) \to \gamma\chi(1P)$
0.091 ±0.018 ±0.022		ALBRECHT	85E	ARG	$e^+e^- \to \gamma$conv. X
0.065 ±0.007 ±0.012		NERNST	85	CBAL	$e^+e^- \to \gamma X$
0.080 ±0.017 ±0.016		HAAS	84	CLEO	$e^+e^- \to \gamma$conv. X
0.059 ±0.014		KLOPFEN...	83	CUSB	$e^+e^- \to \gamma X$

$\Gamma(\gamma\chi_{b2}(1P))/\Gamma_{total}$ Γ_{51}/Γ

VALUE	EVTS	DOCUMENT ID		TECN	COMMENT
0.0715±0.0035 OUR AVERAGE					
0.0724±0.0011±0.0040	410k	ARTUSO	05	CLEO	$e^+e^- \to \gamma X$
0.074 ±0.005 ±0.008		EDWARDS	99	CLE2	$\Upsilon(2S) \to \gamma\chi(1P)$
0.098 ±0.021 ±0.024		ALBRECHT	85E	ARG	$e^+e^- \to \gamma$conv. X
0.058 ±0.007 ±0.010		NERNST	85	CBAL	$e^+e^- \to \gamma X$
0.102 ±0.018 ±0.021		HAAS	84	CLEO	$e^+e^- \to \gamma$conv. X
0.061 ±0.014		KLOPFEN...	83	CUSB	$e^+e^- \to \gamma X$

$\Gamma(\gamma\chi_{b0}(1P))/\Gamma_{total}$ Γ_{52}/Γ

VALUE	EVTS	DOCUMENT ID		TECN	COMMENT
0.038 ±0.004 OUR AVERAGE					
0.0375±0.0012±0.0047	198k	ARTUSO	05	CLEO	$e^+e^- \to \gamma X$
0.034 ±0.005 ±0.006		EDWARDS	99	CLE2	$\Upsilon(2S) \to \gamma\chi(1P)$
0.064 ±0.014 ±0.016		ALBRECHT	85E	ARG	$e^+e^- \to \gamma$conv. X
0.036 ±0.008 ±0.009		NERNST	85	CBAL	$e^+e^- \to \gamma X$
0.044 ±0.023 ±0.009		HAAS	84	CLEO	$e^+e^- \to \gamma$conv. X
• • • We do not use the following data for averages, fits, limits, etc. • • •					
0.035 ±0.014		KLOPFEN...	83	CUSB	$e^+e^- \to \gamma X$

$\Gamma(\gamma f_0(1710))/\Gamma_{total}$ Γ_{53}/Γ

VALUE (units 10^{-5})	CL%	DOCUMENT ID		TECN	COMMENT
<59	90	[1] ALBRECHT	89	ARG	$\Upsilon(2S) \to \gamma K^+K^-$
• • • We do not use the following data for averages, fits, limits, etc. • • •					
< 5.9	90	[2] ALBRECHT	89	ARG	$\Upsilon(2S) \to \gamma\pi^+\pi^-$

[1] Re-evaluated assuming $B(f_0(1710) \to K^+K^-) = 0.19$.

[2] Includes unknown branching ratio of $f_0(1710) \to \pi^+\pi^-$.

$\Gamma(\gamma f_2'(1525))/\Gamma_{total}$ Γ_{54}/Γ

VALUE (units 10^{-5})	CL%	DOCUMENT ID		TECN	COMMENT
<53	90	[1] ALBRECHT	89	ARG	$\Upsilon(2S) \to \gamma K^+K^-$

[1] Re-evaluated assuming $B(f_2'(1525) \to K\overline{K}) = 0.71$.

$\Gamma(\gamma f_2(1270))/\Gamma_{total}$ Γ_{55}/Γ

VALUE (units 10^{-5})	CL%	DOCUMENT ID		TECN	COMMENT
<24.1	90	[1] ALBRECHT	89	ARG	$\Upsilon(2S) \to \gamma\pi^+\pi^-$

[1] Using $B(f_2(1270) \to \pi\pi) = 0.84$.

$\Gamma(\gamma f_J(2220))/\Gamma_{total}$ Γ_{56}/Γ

VALUE (units 10^{-5})	CL%	DOCUMENT ID		TECN	COMMENT
• • • We do not use the following data for averages, fits, limits, etc. • • •					
<6.8	90	[1] ALBRECHT	89	ARG	$\Upsilon(2S) \to \gamma K^+K^-$

[1] Includes unknown branching ratio of $f_J(2220) \to K^+K^-$.

$\Gamma(\gamma\eta_c(1S))/\Gamma_{total}$ Γ_{57}/Γ

VALUE	CL%	DOCUMENT ID		TECN	COMMENT
<2.7 × 10^{-5}	90	WANG	11B	BELL	$\Upsilon(2S) \to \gamma X$

$\Gamma(\gamma\chi_{c0})/\Gamma_{total}$ Γ_{58}/Γ

VALUE	CL%	DOCUMENT ID		TECN	COMMENT
<1.0 × 10^{-4}	90	WANG	11B	BELL	$\Upsilon(2S) \to \gamma X$

$\Gamma(\gamma\chi_{c1})/\Gamma_{total}$ Γ_{59}/Γ

VALUE	CL%	DOCUMENT ID		TECN	COMMENT
<3.6 × 10^{-6}	90	WANG	11B	BELL	$\Upsilon(2S) \to \gamma X$

$\Gamma(\gamma\chi_{c2})/\Gamma_{total}$ Γ_{60}/Γ

VALUE	CL%	DOCUMENT ID		TECN	COMMENT
<1.5 × 10^{-5}	90	WANG	11B	BELL	$\Upsilon(2S) \to \gamma X$

$\Gamma(\gamma\chi_{c1}(3872) \to \pi^+\pi^- J/\psi)/\Gamma_{total}$ Γ_{61}/Γ

VALUE	CL%	DOCUMENT ID		TECN	COMMENT
<0.8 × 10^{-6}	90	WANG	11B	BELL	$\Upsilon(2S) \to \gamma X$

$\Gamma(\gamma\chi_{c1}(3872) \to \pi^+\pi^-\pi^0 J/\psi)/\Gamma_{total}$ Γ_{62}/Γ

VALUE	CL%	DOCUMENT ID		TECN	COMMENT
<2.4 × 10^{-6}	90	WANG	11B	BELL	$\Upsilon(2S) \to \gamma X$

$\Gamma(\gamma X(3915) \to \omega J/\psi)/\Gamma_{total}$ Γ_{63}/Γ

VALUE	CL%	DOCUMENT ID		TECN	COMMENT
<2.8 × 10^{-6}	90	WANG	11B	BELL	$\Upsilon(2S) \to \gamma X$

$\Gamma(\gamma\chi_{c1}(4140) \to \phi J/\psi)/\Gamma_{total}$ Γ_{64}/Γ

VALUE	CL%	DOCUMENT ID		TECN	COMMENT
<1.2 × 10^{-6}	90	WANG	11B	BELL	$\Upsilon(2S) \to \gamma X$

$\Gamma(\gamma X(4350) \to \phi J/\psi)/\Gamma_{total}$ Γ_{65}/Γ

VALUE	CL%	DOCUMENT ID		TECN	COMMENT
<1.3 × 10^{-6}	90	WANG	11B	BELL	$\Upsilon(2S) \to \gamma X$

$\Gamma(\gamma\eta_b(1S))/\Gamma_{total}$ Γ_{66}/Γ

VALUE (units 10^{-4})	CL%	EVTS	DOCUMENT ID		TECN	COMMENT
$3.9\pm1.1^{+1.1}_{-0.9}$		13 ± 5k	[1] AUBERT	09AQ	BABR	$\Upsilon(2S) \to \gamma X$
• • • We do not use the following data for averages, fits, limits, etc. • • •						
<21	90		LEES	11J	BABR	$\Upsilon(2S) \to X\gamma$
< 8.4	90		[1] BONVICINI	10	CLEO	$\Upsilon(2S) \to \gamma X$
< 5.1	90		[2] ARTUSO	05	CLEO	$e^+e^- \to \gamma X$

[1] Assuming $\Gamma_{\eta_b(1S)} = 10$ MeV.

[2] Superseded by BONVICINI 10.

$\Gamma(\gamma\eta_b(1S) \to \gamma\,\text{Sum of 26 exclusive modes})/\Gamma_{total}$ Γ_{67}/Γ

VALUE	CL%	DOCUMENT ID		TECN	COMMENT
<3.7 × 10^{-6}	90	SANDILYA	13	BELL	$\Upsilon(2S) \to \gamma$ hadrons

Meson Particle Listings

$\Upsilon(2S)$, $\Upsilon_2(1D)$, $\chi_{b0}(2P)$

$\Gamma(\gamma X_{b\overline{b}} \to \gamma$Sum of 26 exclusive modes$)/\Gamma_{total}$ Γ_{68}/Γ

VALUE (units 10^{-6})	CL%	EVTS	DOCUMENT ID		TECN	COMMENT
< 4.9	90		SANDILYA	13	BELL	$\Upsilon(2S) \to \gamma$ hadrons
• • • We do not use the following data for averages, fits, limits, etc. • • •						
$46.2^{+29.7}_{-14.2} \pm 10.6$	10		[1] DOBBS	12		$\Upsilon(2S) \to \gamma$ hadrons

[1] Obtained by analyzing CLEO III data but not authored by the CLEO Collaboration.

$\Gamma(\gamma X \to \gamma + \geq 4$ prongs$)/\Gamma_{total}$ Γ_{69}/Γ

(1.5 GeV $< m_X <$ 5.0 GeV)

VALUE (units 10^{-4})	CL%	DOCUMENT ID		TECN	COMMENT
<1.95	95	ROSNER	07A	CLEO	$e^+e^- \to \gamma X$

$\Gamma(\gamma A^0 \to \gamma$hadrons$)/\Gamma_{total}$ Γ_{70}/Γ

(0.3 GeV $< m_{A^0} <$ 7 GeV)

VALUE	CL%	DOCUMENT ID		TECN	COMMENT
$<8 \times 10^{-5}$	90	[1] LEES	11H	BABR	$\Upsilon(2S) \to \gamma$ hadrons

[1] For a narrow scalar or pseudoscalar A^0, excluding known resonances, with mass in the range 0.3–7 GeV. Measured 90% CL limits as a function of m_{A^0} range from 1×10^{-6} to 8×10^{-5}.

$\Gamma(\gamma a_1^0 \to \gamma\mu^+\mu^-)/\Gamma_{total}$ Γ_{71}/Γ

VALUE (units 10^{-6})	CL%	DOCUMENT ID		TECN	COMMENT
<8.3	90	[1] AUBERT	09Z	BABR	$e^+e^- \to \gamma a_1^0 \to \gamma\mu^+\mu^-$

[1] For a narrow scalar or pseudoscalar a_1^0 with mass in the range 212–9300 MeV, excluding J/ψ and $\psi(2S)$. Measured 90% CL limits as a function of $m_{a_1^0}$ range from 0.26–8.3 $\times$ 10^{-6}.

LEPTON FAMILY NUMBER (LF) VIOLATING MODES

$\Gamma(e^\pm\tau^\mp)/\Gamma_{total}$ Γ_{72}/Γ

VALUE (units 10^{-6})	CL%	DOCUMENT ID		TECN	COMMENT
<3.2	90	LEES	10B	BABR	$e^+e^- \to e^\pm\tau^\mp$

$\Gamma(\mu^\pm\tau^\mp)/\Gamma_{total}$ Γ_{73}/Γ

VALUE (units 10^{-6})	CL%	DOCUMENT ID		TECN	COMMENT
< 3.3	90	LEES	10B	BABR	$e^+e^- \to \mu^\pm\tau^\mp$
• • • We do not use the following data for averages, fits, limits, etc. • • •					
<14.4	95	LOVE	08A	CLEO	$e^+e^- \to \mu^\pm\tau^\mp$

$\Upsilon(2S)$ Cross-Particle Branching Ratios

B($\Upsilon(2S) \to \pi^+\pi^-$) $\times$ B($\Upsilon(3S) \to \Upsilon(2S)X$)

VALUE (units 10^{-2})	EVTS	DOCUMENT ID		TECN	COMMENT
1.78±0.02±0.11	906k	LEES	11C	BABR	$e^+e^- \to \pi^+\pi^- X$

$\Upsilon(2S)$ REFERENCES

JIA	17	PR D95 012001	S. Jia *et al.*	(BELLE Collab.)
JIA	17A	PR D96 112002	S. Jia *et al.*	(BELLE Collab.)
LEES	14G	PR D89 111102	J.P. Lees *et al.*	(BABAR Collab.)
YANG	14	PR D90 112008	S.D. Yang *et al.*	(BELLE Collab.)
SANDILYA	13	PRL 111 112001	S. Sandilya *et al.*	(BELLE Collab.)
SHEN	13	PR D88 011102	C.P. Shen *et al.*	(BELLE Collab.)
TAMPONI	13	PR D87 011104	U. Tamponi *et al.*	(BELLE Collab.)
DOBBS	12	PRL 109 082001	S. Dobbs *et al.*	
DOBBS	12A	PR D86 052003	S. Dobbs *et al.*	
SHEN	12A	PR D86 031102	C.P. Shen *et al.*	(BELLE Collab.)
LEES	11C	PR D84 011104	J.P. Lees *et al.*	(BABAR Collab.)
LEES	11H	PRL 107 221803	J.P. Lees *et al.*	(BABAR Collab.)
LEES	11J	PR D84 072002	J.P. Lees *et al.*	(BABAR Collab.)
LEES	11L	PR D84 092003	J.P. Lees *et al.*	(BABAR Collab.)
WANG	11B	PR D84 071107	X.L. Wang *et al.*	(BELLE Collab.)
BONVICINI	10	PR D81 031104	G. Bonvicini *et al.*	(CLEO Collab.)
LEES	10B	PRL 104 151802	J.P. Lees *et al.*	(BABAR Collab.)
AUBERT	09AQ	PRL 103 161801	B. Aubert *et al.*	(BABAR Collab.)
AUBERT	09Z	PRL 103 081803	B. Aubert *et al.*	(BABAR Collab.)
BHARI	09	PR D79 011103	S.R. Bhari *et al.*	(CLEO Collab.)
AUBERT	08BP	PR D78 112002	B. Aubert *et al.*	(BABAR Collab.)
HE	08A	PRL 101 192001	Q. He *et al.*	(CLEO Collab.)
LOVE	08A	PRL 101 201601	W. Love *et al.*	(CLEO Collab.)
PDG	08	PL B667 1	C. Amsler *et al.*	(PDG Collab.)
ASNER	07	PR D75 012009	D.M. Asner *et al.*	(CLEO Collab.)
BESSON	07	PRL 98 052002	D. Besson *et al.*	(CLEO Collab.)
ROSNER	07A	PR D76 117102	J.L. Rosner *et al.*	(CLEO Collab.)
BESSON	06A	PR D74 012003	D. Besson *et al.*	(CLEO Collab.)
ROSNER	06	PRL 96 092003	J.L. Rosner *et al.*	(CLEO Collab.)
ADAMS	05	PRL 94 012001	G.S. Adams *et al.*	(CLEO Collab.)
ARTUSO	05	PRL 94 032001	M. Artuso *et al.*	(CLEO Collab.)
ARTAMONOV	00	PL B474 427	A.S. Artamonov *et al.*	
EDWARDS	99	PR D59 032003	K.W. Edwards *et al.*	(CLEO Collab.)
ALEXANDER	98	PR D58 052004	J.P. Alexander *et al.*	(CLEO Collab.)
BARU	96	PRPL 267 71	S.E. Baru *et al.*	(NOVO)
KOBEL	92	ZPHY C53 193	M. Kobel *et al.*	(Crystal Ball Collab.)
MASCHMANN	90	ZPHY C46 555	W.S. Maschmann *et al.*	(Crystal Ball Collab.)
ALBRECHT	89	ZPHY C42 349	H. Albrecht *et al.*	(ARGUS Collab.)
KAARSBERG	89	PRL 62 2077	T.M. Kaarsberg *et al.*	(CUSB Collab.)
BUCHMUEL...	88	HE e^+e^- Physics 412 Editors: A. Ali and P. Soeding, World Scientific, Singapore	W. Buchmueller, S. Cooper	(HANN, DESY, MIT)
JAKUBOWSKI	88	ZPHY C40 49	Z. Jakubowski *et al.*	(Crystal Ball Collab.) IGJPC
ALBRECHT	87	ZPHY C35 283	H. Albrecht *et al.*	(ARGUS Collab.)
COHEN	87	RMP 59 1121	E.R. Cohen, B.N. Taylor	(RISC, NBS)
LURZ	87	ZPHY C36 383	B. Lurz *et al.*	(Crystal Ball Collab.)
BARU	86B	ZPHY C32 622 (erratum)	S.E. Baru *et al.*	(NOVO)
ALBRECHT	85	ZPHY C28 45	H. Albrecht *et al.*	(ARGUS Collab.)
ALBRECHT	85E	PL 160B 331	H. Albrecht *et al.*	(ARGUS Collab.)
GELPHMAN	85	PR D32 2893	D. Gelphman *et al.*	(Crystal Ball Collab.)
KURAEV	85	SJNP 41 466 Translated from YAF 41 733.	E.A. Kuraev, V.S. Fadin	(NOVO)
NERNST	85	PRL 54 2195	R. Nernst *et al.*	(Crystal Ball Collab.)
ARTAMONOV	84	PL 137B 272	A.S. Artamonov *et al.*	(NOVO)
BARBER	84	PL 135B 498	D.P. Barber *et al.*	(DESY, ARGUS Collab.+)
BESSON	84	PR D30 1433	D. Besson *et al.*	(CLEO Collab.)
FONSECA	84	NP B242 31	V. Fonseca *et al.*	(CUSB Collab.)
GILES	84B	PR D29 1285	R. Giles *et al.*	(CLEO Collab.)
HAAS	84	PRL 52 799	J. Haas *et al.*	(CLEO Collab.)
HAAS	84B	PR D30 1996	J. Haas *et al.*	(CLEO Collab.)
KLOPFEN...	83	PRL 51 160	C. Klopfenstein *et al.*	(CUSB Collab.)
ALBRECHT	82	PL 116B 383	H. Albrecht *et al.*	(DESY, DORT, HEIDH+)
NICZYPORUK	81B	PL 100B 95	B. Niczyporuk *et al.*	(LENA Collab.)
NICZYPORUK	81C	PL 99B 169	B. Niczyporuk *et al.*	(LENA Collab.)
BOCK	80	ZPHY C6 125	P. Bock *et al.*	(HEIDP, MPIM, DESY, HAMB)

$\Upsilon_2(1D)$

$I^G(J^{PC}) = 0^-(2^{--})$

was $\Upsilon(1D)$

First observed by BONVICINI 04 in the decay to $\gamma\gamma\,\Upsilon(1S)$ and confirmed by DEL-AMO-SANCHEZ 10R in the decay to $\pi^+\pi^-\,\Upsilon(1S)$. Data consistent with $J^P = 2^-$. The states with $J = 1$ and 3 also possibly seen, but need confirmation.

$\Upsilon_2(1D)$ MASS

VALUE (MeV)	EVTS	DOCUMENT ID		TECN	COMMENT
10163.7±1.4 OUR AVERAGE		Error includes scale factor of 1.7.			
10164.5 ± 0.8 ± 0.5		DEL-AMO-SA...10R		BABR	$\Upsilon(3S) \to \gamma\gamma\pi^+\pi^-\ell^+\ell^-$
10161.1 ± 0.6 ± 1.6	38	BONVICINI	04	CLE3	$\Upsilon(3S) \to 4\gamma\ell^+\ell^-$

$\Upsilon_2(1D)$ DECAY MODES

	Mode	Fraction (Γ_i/Γ)
Γ_1	$\gamma\gamma\,\Upsilon(1S)$	seen
Γ_2	$\gamma\chi_{bJ}(1P)$	seen
Γ_3	$\eta\,\Upsilon(1S)$	not seen
Γ_4	$\pi^+\pi^-\,\Upsilon(1S)$	$(6.6\pm1.6) \times 10^{-3}$

$\Upsilon_2(1D)$ BRANCHING RATIOS

$\Gamma(\eta\,\Upsilon(1S))/\Gamma(\gamma\gamma\,\Upsilon(1S))$ Γ_3/Γ_1

VALUE	CL%	DOCUMENT ID		TECN	COMMENT
<0.25	90	BONVICINI	04	CLE3	$\Upsilon(3S) \to 4\gamma\ell^+\ell^-$

$\Gamma(\pi^+\pi^-\,\Upsilon(1S))/\Gamma_{total}$ Γ_4/Γ

VALUE (units 10^{-2})	DOCUMENT ID		TECN	COMMENT
$0.66^{+0.15}_{-0.14} \pm 0.06$	[1] DEL-AMO-SA...10R		BABR	$\Upsilon(3S) \to \gamma\gamma\pi^+\pi^-\ell^+\ell^-$

[1] Using theoretical predictions for B($\chi_{bJ}(2P) \to \gamma\,\Upsilon_2(1D)$).

$\Gamma(\pi^+\pi^-\,\Upsilon(1S))/\Gamma(\gamma\gamma\,\Upsilon(1S))$ Γ_4/Γ_1

VALUE	CL%	DOCUMENT ID		TECN	COMMENT
<1.2	90	[2] BONVICINI	04	CLE3	$\Upsilon(3S) \to 4\gamma\ell^+\ell^-$

[2] Assuming $J = 2$.

$\Upsilon_2(1D)$ REFERENCES

DEL-AMO-SA...	10R	PR D82 111102	P. del Amo Sanchez *et al.*	(BABAR Collab.)
BONVICINI	04	PR D70 032001	G. Bonvicini *et al.*	(CLEO Collab.)

$\chi_{b0}(2P)$

$I^G(J^{PC}) = 0^+(0^{++})$

J needs confirmation.

Observed in radiative decay of the $\Upsilon(3S)$, therefore $C = +$. Branching ratio requires E1 transition, M1 is strongly disfavored, therefore $P = +$.

$\chi_{b0}(2P)$ MASS

VALUE (MeV)	DOCUMENT ID
10232.5±0.4±0.5 OUR EVALUATION	From γ energy below, using $\Upsilon(3S)$ mass = 10355.2 ± 0.5 MeV

$m_{\chi_{b1}(2P)} - m_{\chi_{b0}(2P)}$

VALUE (MeV)	DOCUMENT ID		TECN	COMMENT
23.8±1.7	LEES	14M	BABR	$\Upsilon(3S) \to \gamma\gamma\mu^+\mu^-$

γ ENERGY IN $\Upsilon(3S)$ DECAY

VALUE (MeV)	EVTS	DOCUMENT ID		TECN	COMMENT
121.9 ±0.4 OUR EVALUATION		Treating systematic errors as correlated			
122.2 ±0.5 OUR AVERAGE		Error includes scale factor of 1.4. See the ideogram below.			
121.55±0.16±0.46		ARTUSO	05	CLEO	$\Upsilon(3S) \to \gamma X$
123.0 ±0.8	4959	[1] HEINTZ	92	CSB2	$e^+e^- \to \gamma X$
124.6 ±1.4	17	[2] HEINTZ	92	CSB2	$e^+e^- \to \ell^+\ell^-\gamma\gamma$
122.3 ±0.3 ±0.6	9903	MORRISON	91	CLE2	$e^+e^- \to \gamma X$

[1] A systematic uncertainty on the energy scale of 0.9% not included. Supersedes NARAIN 91.
[2] A systematic uncertainty on the energy scale of 0.9% not included. Supersedes HEINTZ 91.

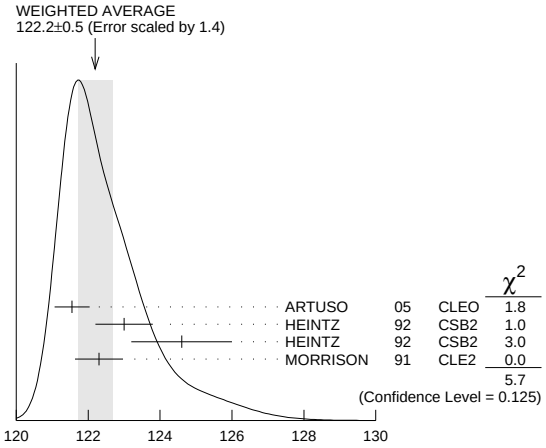

$\chi_{b0}(2P)$ DECAY MODES

	Mode	Fraction (Γ_i/Γ)		Confidence level
Γ_1	$\gamma\Upsilon(2S)$	(1.38±0.30) %		
Γ_2	$\gamma\Upsilon(1S)$	(3.8 ±1.7) × 10^{-3}		
Γ_3	D^0X	< 8.2	%	90%
Γ_4	$\pi^+\pi^-K^+K^-\pi^0$	< 3.4	× 10^{-5}	90%
Γ_5	$2\pi^+\pi^-K^-K^0_S$	< 5	× 10^{-5}	90%
Γ_6	$2\pi^+\pi^-K^-K^0_S2\pi^0$	< 2.2	× 10^{-4}	90%
Γ_7	$2\pi^+2\pi^-2\pi^0$	< 2.4	× 10^{-4}	90%
Γ_8	$2\pi^+2\pi^-K^+K^-$	< 1.5	× 10^{-4}	90%
Γ_9	$2\pi^+2\pi^-K^+K^-\pi^0$	< 2.2	× 10^{-4}	90%
Γ_{10}	$2\pi^+2\pi^-K^+K^-2\pi^0$	< 1.1	× 10^{-3}	90%
Γ_{11}	$3\pi^+2\pi^-K^-K^0_S\pi^0$	< 7	× 10^{-4}	90%
Γ_{12}	$3\pi^+3\pi^-$	< 7	× 10^{-5}	90%
Γ_{13}	$3\pi^+3\pi^-2\pi^0$	< 1.2	× 10^{-3}	90%
Γ_{14}	$3\pi^+3\pi^-K^+K^-$	< 1.5	× 10^{-4}	90%
Γ_{15}	$3\pi^+3\pi^-K^+K^-\pi^0$	< 7	× 10^{-4}	90%
Γ_{16}	$4\pi^+4\pi^-$	< 1.7	× 10^{-4}	90%
Γ_{17}	$4\pi^+4\pi^-2\pi^0$	< 6	× 10^{-4}	90%

$\chi_{b0}(2P)$ BRANCHING RATIOS

$\Gamma(\gamma\Upsilon(2S))/\Gamma_{total}$ Γ_1/Γ

VALUE (%)	CL%	DOCUMENT ID		TECN	COMMENT
1.38±0.30 OUR AVERAGE					
$1.31\pm0.27^{+0.13}_{-0.12}$		[3,4] LEES	14M	BABR	$\Upsilon(3S) \to \gamma\gamma\mu^+\mu^-$
3.6 ±1.6 ±0.3		[3,5] HEINTZ	92	CSB2	$e^+e^- \to \ell^+\ell^-\gamma\gamma$
• • • We do not use the following data for averages, fits, limits, etc. • • •					
<2.8	90	[6] LEES	11J	BABR	$\Upsilon(3S) \to X\gamma$
<8.9	90	[7] CRAWFORD	92B	CLE2	$e^+e^- \to \ell^+\ell^-\gamma\gamma$

[3] Assuming B($\Upsilon(2S) \to \mu^+\mu^-$) = (1.93 ± 0.17)%.
[4] LEES 14M reports [$\Gamma(\chi_{b0}(2P) \to \gamma\Upsilon(2S))/\Gamma_{total}$] × [B($\Upsilon(3S) \to \gamma\chi_{b0}(2P)$)] = (7.7 ± 1.6) × 10^{-4} which we divide by our best value B($\Upsilon(3S) \to \gamma\chi_{b0}(2P)$) = (5.9 ± 0.6) × 10^{-2}. Our first error is their experiment's error and our second error is the systematic error from using our best value.
[5] Recalculated by us. HEINTZ 92 quotes B($\Upsilon(3S) \to \gamma\chi_{b0}(2P)$) × B($\chi_{b0}(2P) \to \gamma\Upsilon(2S)$) = (0.28 ± 0.12 ± 0.03)% using B($\Upsilon(2S) \to \mu^+\mu^-$) = (1.44 ± 0.10)%. Supersedes HEINTZ 91.
[6] LEES 11J quotes a central value of $\Gamma(\chi_{b0}(2P) \to \gamma\Upsilon(2S))/\Gamma_{total}$ × $\Gamma(\Upsilon(3S) \to \gamma\chi_{b0}(2P))/\Gamma_{total}$ = $(-0.3 \pm 0.2^{+0.5}_{-0.4})$%.
[7] Using B($\Upsilon(2S) \to \mu^+\mu^-$) = (1.37±0.26)%, B($\Upsilon(3S) \to \gamma\gamma\Upsilon(2S)$)×2 B($\Upsilon(2S) \to \mu^+\mu^-$) < 1.19 × 10^{-4}, and B($\Upsilon(3S) \to \chi_{b0}(2P)\gamma$) = 0.049.

$\Gamma(\gamma\Upsilon(1S))/\Gamma_{total}$ Γ_2/Γ

VALUE (%)	CL%	DOCUMENT ID		TECN	COMMENT
0.38±0.17 OUR AVERAGE					
0.36±0.17±0.03		[8,9,10] LEES	14M	BABR	$\Upsilon(3S) \to \gamma\gamma\mu^+\mu^-$
0.9 ±0.7 ±0.1		[9,11] HEINTZ	92	CSB2	$e^+e^- \to \ell^+\ell^-\gamma\gamma$
• • • We do not use the following data for averages, fits, limits, etc. • • •					
<1.2	90	[12] LEES	11J	BABR	$\Upsilon(3S) \to X\gamma$
<2.5	90	[13] CRAWFORD	92B	CLE2	$e^+e^- \to \ell^+\ell^-\gamma\gamma$

[8] LEES 14M quotes $\Gamma(\chi_{b0}(2P) \to \gamma\Upsilon(1S))/\Gamma_{total}$ × $\Gamma(\Upsilon(3S) \to \gamma\chi_{b0}(2P))/\Gamma_{total}$ = (2.1 ± 1.0) × 10^{-4} combining the results from $\Upsilon(3S) \to \gamma\gamma\mu^+\mu^-$ samples with and without photon conversions.
[9] Assuming B($\Upsilon(1S) \to \mu^+\mu^-$) = (2.48 ± 0.05)%.
[10] LEES 14M reports [$\Gamma(\chi_{b0}(2P) \to \gamma\Upsilon(1S))/\Gamma_{total}$] × [B($\Upsilon(3S) \to \gamma\chi_{b0}(2P)$)] = (2.1 ± 1.0) × 10^{-4} which we divide by our best value B($\Upsilon(3S) \to \gamma\chi_{b0}(2P)$) = (5.9 ± 0.6) × 10^{-2}. Our first error is their experiment's error and our second error is the systematic error from using our best value.
[11] Recalculated by us. HEINTZ 92 quotes B($\Upsilon(3S) \to \gamma\chi_{b0}(2P)$) × B($\chi_{b0}(2P) \to \gamma\Upsilon(1S)$) = (0.05 ± 0.04 ± 0.01)% using B($\Upsilon(1S) \to \mu^+\mu^-$) = (2.57 ± 0.05)%. Supersedes HEINTZ 91.
[12] LEES 11J quotes a central value of $\Gamma(\chi_{b0}(2P) \to \gamma\Upsilon(1S))/\Gamma_{total}$ × $\Gamma(\Upsilon(3S) \to \gamma\chi_{b0}(2P))/\Gamma_{total}$ = $(3.9 \pm 2.2^{+1.2}_{-0.6}) \times 10^{-4}$.
[13] Using B($\Upsilon(1S) \to \mu^+\mu^-$) = (2.57±0.07)%, B($\Upsilon(3S) \to \gamma\gamma\Upsilon(1S)$)×2 B($\Upsilon(1S) \to \mu^+\mu^-$) < 0.63 × 10^{-4}, and B($\Upsilon(3S) \to \chi_{b0}(2P)\gamma$) = 0.049.

$\Gamma(D^0X)/\Gamma_{total}$ Γ_3/Γ

VALUE	CL%	DOCUMENT ID		TECN	COMMENT
<8.2 × 10^{-2}	90	[14,15] BRIERE	08	CLEO	$\Upsilon(3S) \to \gamma D^0X$

[14] For p_{D^0} > 2.5 GeV/c.
[15] The authors also present their result as (4.1 ± 3.0 ± 0.4) × 10^{-2}.

$\Gamma(\pi^+\pi^-K^+K^-\pi^0)/\Gamma_{total}$ Γ_4/Γ

VALUE (units 10^{-4})	CL%	DOCUMENT ID		TECN	COMMENT
<0.34	90	[16] ASNER	08A	CLEO	$\Upsilon(3S) \to \gamma\pi^+\pi^-K^+K^-\pi^0$

[16] ASNER 08A reports [$\Gamma(\chi_{b0}(2P) \to \pi^+\pi^-K^+K^-\pi^0)/\Gamma_{total}$] × [B($\Upsilon(3S) \to \gamma\chi_{b0}(2P)$)] < 2 × 10^{-6} which we divide by our best value B($\Upsilon(3S) \to \gamma\chi_{b0}(2P)$) = 5.9 × 10^{-2}.

$\Gamma(2\pi^+\pi^-K^-K^0_S)/\Gamma_{total}$ Γ_5/Γ

VALUE (units 10^{-4})	CL%	DOCUMENT ID		TECN	COMMENT
<0.5	90	[17] ASNER	08A	CLEO	$\Upsilon(3S) \to \gamma 2\pi^+\pi^-K^-K^0_S$

[17] ASNER 08A reports [$\Gamma(\chi_{b0}(2P) \to 2\pi^+\pi^-K^-K^0_S)/\Gamma_{total}$] × [B($\Upsilon(3S) \to \gamma\chi_{b0}(2P)$)] < 3 × 10^{-6} which we divide by our best value B($\Upsilon(3S) \to \gamma\chi_{b0}(2P)$) = 5.9 × 10^{-2}.

$\Gamma(2\pi^+\pi^-K^-K^0_S2\pi^0)/\Gamma_{total}$ Γ_6/Γ

VALUE (units 10^{-4})	CL%	DOCUMENT ID		TECN	COMMENT
<2.2	90	[18] ASNER	08A	CLEO	$\Upsilon(3S) \to \gamma 2\pi^+\pi^-K^-2\pi^0$

[18] ASNER 08A reports [$\Gamma(\chi_{b0}(2P) \to 2\pi^+\pi^-K^-K^0_S2\pi^0)/\Gamma_{total}$] × [B($\Upsilon(3S) \to \gamma\chi_{b0}(2P)$)] < 13 × 10^{-6} which we divide by our best value B($\Upsilon(3S) \to \gamma\chi_{b0}(2P)$) = 5.9 × 10^{-2}.

$\Gamma(2\pi^+2\pi^-2\pi^0)/\Gamma_{total}$ Γ_7/Γ

VALUE (units 10^{-4})	CL%	DOCUMENT ID		TECN	COMMENT
<2.4	90	[19] ASNER	08A	CLEO	$\Upsilon(3S) \to \gamma 2\pi^+2\pi^-2\pi^0$

[19] ASNER 08A reports [$\Gamma(\chi_{b0}(2P) \to 2\pi^+2\pi^-2\pi^0)/\Gamma_{total}$] × [B($\Upsilon(3S) \to \gamma\chi_{b0}(2P)$)] < 14 × 10^{-6} which we divide by our best value B($\Upsilon(3S) \to \gamma\chi_{b0}(2P)$) = 5.9 × 10^{-2}.

$\Gamma(2\pi^+2\pi^-K^+K^-)/\Gamma_{total}$ Γ_8/Γ

VALUE (units 10^{-4})	CL%	DOCUMENT ID		TECN	COMMENT
<1.5	90	[20] ASNER	08A	CLEO	$\Upsilon(3S) \to \gamma 2\pi^+2\pi^-K^+K^-$

[20] ASNER 08A reports [$\Gamma(\chi_{b0}(2P) \to 2\pi^+2\pi^-K^+K^-)/\Gamma_{total}$] × [B($\Upsilon(3S) \to \gamma\chi_{b0}(2P)$)] < 9 × 10^{-6} which we divide by our best value B($\Upsilon(3S) \to \gamma\chi_{b0}(2P)$) = 5.9 × 10^{-2}.

$\Gamma(2\pi^+2\pi^-K^+K^-\pi^0)/\Gamma_{total}$ Γ_9/Γ

VALUE (units 10^{-4})	CL%	DOCUMENT ID		TECN	COMMENT
<2.2	90	[21] ASNER	08A	CLEO	$\Upsilon(3S) \to \gamma 2\pi^+2\pi^-K^+K^-\pi^0$

[21] ASNER 08A reports [$\Gamma(\chi_{b0}(2P) \to 2\pi^+2\pi^-K^+K^-\pi^0)/\Gamma_{total}$] × [B($\Upsilon(3S) \to \gamma\chi_{b0}(2P)$)] < 13 × 10^{-6} which we divide by our best value B($\Upsilon(3S) \to \gamma\chi_{b0}(2P)$) = 5.9 × 10^{-2}.

$\Gamma(2\pi^+2\pi^-K^+K^-2\pi^0)/\Gamma_{total}$ Γ_{10}/Γ

VALUE (units 10^{-4})	CL%	DOCUMENT ID		TECN	COMMENT
<11	90	[22] ASNER	08A	CLEO	$\Upsilon(3S) \to \gamma 2\pi^+2\pi^-K^+K^-2\pi^0$

[22] ASNER 08A reports [$\Gamma(\chi_{b0}(2P) \to 2\pi^+2\pi^-K^+K^-2\pi^0)/\Gamma_{total}$] × [B($\Upsilon(3S) \to \gamma\chi_{b0}(2P)$)] < 63 × 10^{-6} which we divide by our best value B($\Upsilon(3S) \to \gamma\chi_{b0}(2P)$) = 5.9 × 10^{-2}.

$\Gamma(3\pi^+2\pi^-K^-K^0_S\pi^0)/\Gamma_{total}$ Γ_{11}/Γ

VALUE (units 10^{-4})	CL%	DOCUMENT ID		TECN	COMMENT
<7	90	[23] ASNER	08A	CLEO	$\Upsilon(3S) \to \gamma 3\pi^+2\pi^-K^-K^0_S\pi^0$

[23] ASNER 08A reports $[\Gamma(\chi_{b0}(2P) \to 3\pi^+2\pi^-K^-K^0_S\pi^0)/\Gamma_{total}] \times [B(\Upsilon(3S) \to \gamma\chi_{b0}(2P))] < 39\times10^{-6}$ which we divide by our best value $B(\Upsilon(3S) \to \gamma\chi_{b0}(2P)) = 5.9\times10^{-2}$.

$\Gamma(3\pi^+3\pi^-)/\Gamma_{total}$ Γ_{12}/Γ

VALUE (units 10^{-4})	CL%	DOCUMENT ID		TECN	COMMENT
<0.7	90	[24] ASNER	08A	CLEO	$\Upsilon(3S) \to \gamma 3\pi^+3\pi^-$

[24] ASNER 08A reports $[\Gamma(\chi_{b0}(2P) \to 3\pi^+3\pi^-)/\Gamma_{total}] \times [B(\Upsilon(3S) \to \gamma\chi_{b0}(2P))] < 4\times10^{-6}$ which we divide by our best value $B(\Upsilon(3S) \to \gamma\chi_{b0}(2P)) = 5.9\times10^{-2}$.

$\Gamma(3\pi^+3\pi^-2\pi^0)/\Gamma_{total}$ Γ_{13}/Γ

VALUE (units 10^{-4})	CL%	DOCUMENT ID		TECN	COMMENT
<12	90	[25] ASNER	08A	CLEO	$\Upsilon(3S) \to \gamma 3\pi^+3\pi^-2\pi^0$

[25] ASNER 08A reports $[\Gamma(\chi_{b0}(2P) \to 3\pi^+3\pi^-2\pi^0)/\Gamma_{total}] \times [B(\Upsilon(3S) \to \gamma\chi_{b0}(2P))] < 72\times10^{-6}$ which we divide by our best value $B(\Upsilon(3S) \to \gamma\chi_{b0}(2P)) = 5.9\times10^{-2}$.

$\Gamma(3\pi^+3\pi^-K^+K^-)/\Gamma_{total}$ Γ_{14}/Γ

VALUE (units 10^{-4})	CL%	DOCUMENT ID		TECN	COMMENT
<1.5	90	[26] ASNER	08A	CLEO	$\Upsilon(3S) \to \gamma 3\pi^+3\pi^-K^+K^-$

[26] ASNER 08A reports $[\Gamma(\chi_{b0}(2P) \to 3\pi^+3\pi^-K^+K^-)/\Gamma_{total}] \times [B(\Upsilon(3S) \to \gamma\chi_{b0}(2P))] < 9\times10^{-6}$ which we divide by our best value $B(\Upsilon(3S) \to \gamma\chi_{b0}(2P)) = 5.9\times10^{-2}$.

$\Gamma(3\pi^+3\pi^-K^+K^-\pi^0)/\Gamma_{total}$ Γ_{15}/Γ

VALUE (units 10^{-4})	CL%	DOCUMENT ID		TECN	COMMENT
<7	90	[27] ASNER	08A	CLEO	$\Upsilon(3S) \to \gamma 3\pi^+3\pi^-K^+K^-\pi^0$

[27] ASNER 08A reports $[\Gamma(\chi_{b0}(2P) \to 3\pi^+3\pi^-K^+K^-\pi^0)/\Gamma_{total}] \times [B(\Upsilon(3S) \to \gamma\chi_{b0}(2P))] < 43\times10^{-6}$ which we divide by our best value $B(\Upsilon(3S) \to \gamma\chi_{b0}(2P)) = 5.9\times10^{-2}$.

$\Gamma(4\pi^+4\pi^-)/\Gamma_{total}$ Γ_{16}/Γ

VALUE (units 10^{-4})	CL%	DOCUMENT ID		TECN	COMMENT
<1.7	90	[28] ASNER	08A	CLEO	$\Upsilon(3S) \to \gamma 4\pi^+4\pi^-$

[28] ASNER 08A reports $[\Gamma(\chi_{b0}(2P) \to 4\pi^+4\pi^-)/\Gamma_{total}] \times [B(\Upsilon(3S) \to \gamma\chi_{b0}(2P))] < 10\times10^{-6}$ which we divide by our best value $B(\Upsilon(3S) \to \gamma\chi_{b0}(2P)) = 5.9\times10^{-2}$.

$\Gamma(4\pi^+4\pi^-2\pi^0)/\Gamma_{total}$ Γ_{17}/Γ

VALUE (units 10^{-4})	CL%	DOCUMENT ID		TECN	COMMENT
<6	90	[29] ASNER	08A	CLEO	$\Upsilon(3S) \to \gamma 4\pi^+4\pi^-2\pi^0$

[29] ASNER 08A reports $[\Gamma(\chi_{b0}(2P) \to 4\pi^+4\pi^-2\pi^0)/\Gamma_{total}] \times [B(\Upsilon(3S) \to \gamma\chi_{b0}(2P))] < 38\times10^{-6}$ which we divide by our best value $B(\Upsilon(3S) \to \gamma\chi_{b0}(2P)) = 5.9\times10^{-2}$.

$\Gamma(\chi_{b0}(2P) \to \gamma\Upsilon(1S))/\Gamma_{total} \times \Gamma(\Upsilon(3S) \to \gamma\chi_{b0}(2P))/\Gamma_{total}$ $\Gamma_2/\Gamma \times \Gamma_{22}^{\Upsilon(3S)}/\Gamma^{\Upsilon(3S)}$

VALUE (units 10^{-4})	CL%	DOCUMENT ID		TECN	COMMENT
<8.2	90	[30] LEES	11J	BABR	$\Upsilon(3S) \to X\gamma$

[30] LEES 11J quotes a central value of $\Gamma(\chi_{b0}(2P) \to \gamma\Upsilon(1S))/\Gamma_{total} \times \Gamma(\Upsilon(3S) \to \gamma\chi_{b0}(2P))/\Gamma_{total} = (3.9 \pm 2.2^{+1.2}_{-0.6}) \times 10^{-4}$ and derives a 90% CL upper limit of $B(\chi_{b0}(2P) \to \gamma\Upsilon(1S)) < 1.2\%$ using $B(\Upsilon(3S) \to \gamma\chi_{b0}(2P)) = (5.9 \pm 0.6)\%$.

$B(\chi_{b0}(2P) \to \gamma\Upsilon(1S)) \times B(\Upsilon(3S) \to \gamma\chi_{b0}(2P)) \times B(\Upsilon(1S) \to \ell^+\ell^-)$

VALUE (units 10^{-5})	DOCUMENT ID		TECN	COMMENT
1.4±0.9 OUR AVERAGE				
$1.7^{+1.5}_{-1.4}{}^{+0.1}_{-1.2}$	[31] LEES	14M	BABR	$\Upsilon(3S) \to \gamma\gamma\mu^+\mu^-$
1.3±1.0±0.3	[32] HEINTZ	92	CSB2	$\Upsilon(3S) \to \gamma\gamma\ell^+\ell^-$

[31] From a sample of $\Upsilon(3S) \to \gamma\gamma\mu^+\mu^-$ with one converted photon.
[32] Calculated by us. HEINTZ 92 quotes $B(\Upsilon(3S) \to \gamma\chi_{b0}(2P)) \times B(\chi_{b0}(2P) \to \gamma\Upsilon(1S)) = (0.05 \pm 0.04 \pm 0.01)\%$ using $B(\Upsilon(1S) \to \mu^+\mu^-) = (2.57 \pm 0.05)\%$.

$[B(\chi_{b0}(2P) \to \gamma\Upsilon(1S)) \times B(\Upsilon(3S) \to \gamma\chi_{b0}(2P))] / [B(\chi_{b1}(2P) \to \gamma\Upsilon(1S)) \times B(\Upsilon(3S) \to \gamma\chi_{b1}(2P))]$

VALUE (%)	DOCUMENT ID		TECN	COMMENT
1.71±0.80	[33] LEES	14M	BABR	$\Upsilon(3S) \to \gamma\gamma\mu^+\mu^-$

[33] From a sample of $\Upsilon(3S) \to \gamma\gamma\mu^+\mu^-$ without converted photons.

$\Gamma(\chi_{b0}(2P) \to \gamma\Upsilon(2S))/\Gamma_{total} \times \Gamma(\Upsilon(3S) \to \gamma\chi_{b0}(2P))/\Gamma_{total}$ $\Gamma_1/\Gamma \times \Gamma_{22}^{\Upsilon(3S)}/\Gamma^{\Upsilon(3S)}$

VALUE (units 10^{-3})	CL%	DOCUMENT ID		TECN	COMMENT
<1.6	90	[34] LEES	11J	BABR	$\Upsilon(3S) \to X\gamma$

[34] LEES 11J quotes a central value of $\Gamma(\chi_{b0}(2P) \to \gamma\Upsilon(2S))/\Gamma_{total} \times \Gamma(\Upsilon(3S) \to \gamma\chi_{b0}(2P))/\Gamma_{total} = (-0.3 \pm 0.2^{+0.5}_{-0.4})\%$ and derives a 90% CL upper limit of $B(\chi_{b0}(2P) \to \gamma\Upsilon(2S)) < 2.8\%$ using $B(\Upsilon(3S) \to \gamma\chi_{b0}(2P)) = (5.9 \pm 0.6)\%$.

$B(\chi_{b0}(2P) \to \gamma\Upsilon(2S)) \times B(\Upsilon(3S) \to \gamma\chi_{b0}(2P)) \times B(\Upsilon(2S) \to \ell^+\ell^-)$

VALUE (units 10^{-5})	DOCUMENT ID		TECN	COMMENT
4.4±1.6 OUR AVERAGE				
$6.6^{+4.9}_{-4.0}{}^{+2.0}_{-0.3}$	[35] LEES	14M	BABR	$\Upsilon(3S) \to \gamma\gamma\mu^+\mu^-$
4.0±1.7±0.3	[36] HEINTZ	92	CSB2	$\Upsilon(3S) \to \gamma\gamma\ell^+\ell^-$

[35] From a sample of $\Upsilon(3S) \to \gamma\gamma\mu^+\mu^-$ with one converted photon.
[36] Calculated by us. HEINTZ 92 quotes $B(\Upsilon(3S) \to \gamma\chi_{b0}(2P)) \times B(\chi_{b0}(2P) \to \gamma\Upsilon(2S)) = (0.28 \pm 0.12 \pm 0.03)\%$ using $B(\Upsilon(2S) \to \mu^+\mu^-) = (1.44 \pm 0.10)\%$.

$[B(\chi_{b0}(2P) \to \gamma\Upsilon(2S)) \times B(\Upsilon(3S) \to \gamma\chi_{b0}(2P))] / [B(\chi_{b1}(2P) \to \gamma\Upsilon(2S)) \times B(\Upsilon(3S) \to \gamma\chi_{b1}(2P))]$

VALUE (%)	DOCUMENT ID		TECN	COMMENT
3.31±0.56	[37] LEES	14M	BABR	$\Upsilon(3S) \to \gamma\gamma\mu^+\mu^-$

[37] From a sample of $\Upsilon(3S) \to \gamma\gamma\mu^+\mu^-$ without converted photons.

$\chi_{b0}(2P)$ REFERENCES

LEES	14M	PR D90 112010	J.P. Lees *et al.*	(BABAR Collab.)
LEES	11J	PR D84 072002	J.P. Lees *et al.*	(BABAR Collab.)
ASNER	08A	PR D78 091103	D.M. Asner *et al.*	(CLEO Collab.)
BRIERE	08	PR D78 092007	R.A. Briere *et al.*	(CLEO Collab.)
ARTUSO	05	PRL 94 032001	M. Artuso *et al.*	(CLEO Collab.)
CRAWFORD	92B	PL B294 139	G. Crawford *et al.*	(CLEO Collab.)
HEINTZ	92	PR D46 1928	U. Heintz *et al.*	(CUSB II Collab.)
HEINTZ	91	PRL 66 1563	U. Heintz *et al.*	(CUSB Collab.)
MORRISON	91	PRL 67 1696	R.J. Morrison *et al.*	(CLEO Collab.)
NARAIN	91	PRL 66 3113	M. Narain *et al.*	(CUSB Collab.)

$\chi_{b1}(2P)$

$I^G(J^{PC}) = 0^+(1^{++})$
J needs confirmation.

Observed in radiative decay of the $\Upsilon(3S)$, therefore $C = +$. Branching ratio requires E1 transition, M1 is strongly disfavored, therefore $P = +$.

$\chi_{b1}(2P)$ MASS

VALUE (MeV)	DOCUMENT ID
10255.46±0.22±0.50 OUR EVALUATION	From γ energy below, using $\Upsilon(3S)$ mass = 10355.2 ± 0.5 MeV

$m_{\chi_{b1}(2P)} - m_{\chi_{b0}(2P)}$

VALUE (MeV)	DOCUMENT ID		TECN	COMMENT
23.5±0.7±0.7	[1] HEINTZ	92	CSB2	$e^+e^- \to \gamma X, \ell^+\ell^-\gamma\gamma$

[1] From the average photon energy for inclusive and exclusive events. Supersedes NARAIN 91.

γ ENERGY IN $\Upsilon(3S)$ DECAY

VALUE (MeV)	EVTS	DOCUMENT ID		TECN	COMMENT
99.26±0.22 OUR EVALUATION		Treating systematic errors as correlated			
99.53±0.23 OUR AVERAGE		Error includes scale factor of 1.3. See the ideogram below.			
99.15±0.07±0.25		ARTUSO	05	CLEO	$\Upsilon(3S) \to \gamma X$
99 ±1	169	CRAWFORD	92B	CLE2	$e^+e^- \to \ell^+\ell^-\gamma\gamma$
100.1 ±0.4	11147	[2] HEINTZ	92	CSB2	$e^+e^- \to \gamma X$
100.2 ±0.5	223	[3] HEINTZ	92	CSB2	$e^+e^- \to \ell^+\ell^-\gamma\gamma$
99.5 ±0.1 ±0.5	25759	MORRISON	91	CLE2	$e^+e^- \to \gamma X$

[2] A systematic uncertainty on the energy scale of 0.9% not included. Supersedes NARAIN 91.
[3] A systematic uncertainty on the energy scale of 0.9% not included. Supersedes HEINTZ 91.

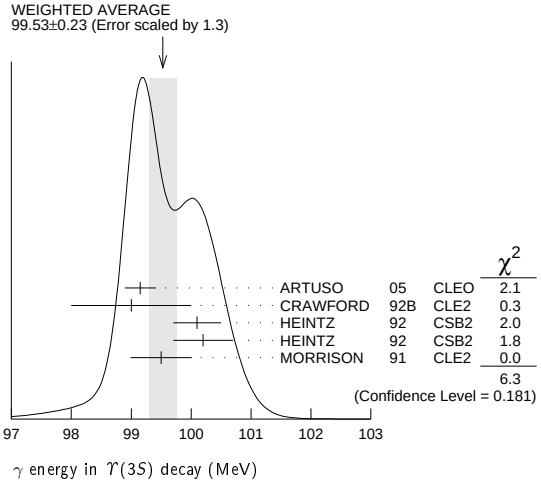

$\chi_{b1}(2P)$ DECAY MODES

	Mode	Fraction (Γ_i/Γ)
Γ_1	$\omega\,\Upsilon(1S)$	$(\ 1.63^{+0.40}_{-0.34}\ )$ %
Γ_2	$\gamma\,\Upsilon(2S)$	$(18.1\ \pm1.9\ )$ %
Γ_3	$\gamma\,\Upsilon(1S)$	$(\ 9.9\ \pm1.0\ )$ %
Γ_4	$\pi\pi\chi_{b1}(1P)$	$(\ 9.1\ \pm1.3\ )\times10^{-3}$
Γ_5	D^0X	$(\ 8.8\ \pm1.7\ )$ %
Γ_6	$\pi^+\pi^-K^+K^-\pi^0$	$(\ 3.1\ \pm1.0\ )\times10^{-4}$
Γ_7	$2\pi^+\pi^-K^-K^0_S$	$(\ 1.1\ \pm0.5\ )\times10^{-4}$
Γ_8	$2\pi^+\pi^-K^-K^0_S2\pi^0$	$(\ 7.7\ \pm3.2\ )\times10^{-4}$
Γ_9	$2\pi^+2\pi^-2\pi^0$	$(\ 5.9\ \pm2.0\ )\times10^{-4}$
Γ_{10}	$2\pi^+2\pi^-K^+K^-$	$(10\ \ \pm4\ \ )\times10^{-5}$
Γ_{11}	$2\pi^+2\pi^-K^+K^-\pi^0$	$(\ 5.5\ \pm1.8\ )\times10^{-4}$
Γ_{12}	$2\pi^+2\pi^-K^+K^-2\pi^0$	$(10\ \ \pm4\ \ )\times10^{-4}$
Γ_{13}	$3\pi^+2\pi^-K^-K^0_S\pi^0$	$(\ 6.7\ \pm2.6\ )\times10^{-4}$
Γ_{14}	$3\pi^+3\pi^-$	$(\ 1.2\ \pm0.4\ )\times10^{-4}$
Γ_{15}	$3\pi^+3\pi^-2\pi^0$	$(\ 1.2\ \pm0.4\ )\times10^{-3}$
Γ_{16}	$3\pi^+3\pi^-K^+K^-$	$(\ 2.0\ \pm0.8\ )\times10^{-4}$
Γ_{17}	$3\pi^+3\pi^-K^+K^-\pi^0$	$(\ 6.1\ \pm2.2\ )\times10^{-4}$
Γ_{18}	$4\pi^+4\pi^-$	$(\ 1.7\ \pm0.6\ )\times10^{-4}$
Γ_{19}	$4\pi^+4\pi^-2\pi^0$	$(\ 1.9\ \pm0.7\ )\times10^{-3}$

$\chi_{b1}(2P)$ BRANCHING RATIOS

$\Gamma(\omega\,\Upsilon(1S))/\Gamma_{\rm total}$ Γ_1/Γ

VALUE (units 10^{-2})	EVTS	DOCUMENT ID		TECN	COMMENT
$\mathbf{1.63^{+0.35+0.16}_{-0.31-0.15}}$	$32.6^{+6.9}_{-6.1}$	[4] CRONIN-HEN...04		CLE3	$\Upsilon(3S)\to\gamma\omega\,\Upsilon(1S)$

[4] Using $B(\Upsilon(3S)\to\gamma\chi_{b1}(2P))=(11.3\pm0.6)\%$ and $B(\Upsilon(1S)\to\ell^+\ell^-)=2$ $B(\Upsilon(1S)\to\mu^+\mu^-)=2\,(2.48\pm0.06)\%$.

$\Gamma(\gamma\,\Upsilon(2S))/\Gamma_{\rm total}$ Γ_2/Γ

VALUE	EVTS	DOCUMENT ID		TECN	COMMENT
0.181±0.019 OUR AVERAGE					
0.211±0.017±0.019		[5,6,7] LEES	14M	BABR	$\Upsilon(3S)\to\gamma\gamma\mu^+\mu^-$
0.190±0.018±0.017	4.3k	[8] LEES	11J	BABR	$\Upsilon(3S)\to X\gamma$
0.206±0.035±0.019		[5,9] CRAWFORD	92B	CLE2	$e^+e^-\to\ell^+\ell^-\gamma\gamma$
0.132±0.018±0.012		[5,10] HEINTZ	92	CSB2	$e^+e^-\to\ell^+\ell^-\gamma\gamma$

[5] Assuming $B(\Upsilon(2S)\to\mu^+\mu^-)=(1.93\pm0.17)\%$.

[6] LEES 14M quotes $\Gamma(\chi_{b1}(2P)\to\gamma\,\Upsilon(2S))/\Gamma_{\rm total}\times\Gamma(\Upsilon(3S)\to\gamma\chi_{b1}(2P))/\Gamma_{\rm total}$ $=(2.66\pm0.22)\%$ combining the results from $\Upsilon(3S)\to\gamma\gamma\mu^+\mu^-$ samples with and without photon conversions.

[7] LEES 14M reports $[\Gamma(\chi_{b1}(2P)\to\gamma\,\Upsilon(2S))/\Gamma_{\rm total}]\times[B(\Upsilon(3S)\to\gamma\chi_{b1}(2P))]=(2.66\pm0.22)\times10^{-2}$ which we divide by our best value $B(\Upsilon(3S)\to\gamma\chi_{b1}(2P))=(12.6\pm1.2)\times10^{-2}$. Our first error is their experiment's error and our second error is the systematic error from using our best value.

[8] LEES 11J reports $[\Gamma(\chi_{b1}(2P)\to\gamma\,\Upsilon(2S))/\Gamma_{\rm total}]\times[B(\Upsilon(3S)\to\gamma\chi_{b1}(2P))]=(2.4\pm0.1\pm0.2)\times10^{-2}$ which we divide by our best value $B(\Upsilon(3S)\to\gamma\chi_{b1}(2P))=(12.6\pm1.2)\times10^{-2}$. Our first error is their experiment's error and our second error is the systematic error from using our best value.

[9] CRAWFORD 92B quotes $B(\Upsilon(3S)\to\gamma\chi_{b1}(2P))\times B(\chi_{b1}(2P)\to\gamma\,\Upsilon(2S))\times2$ $B(\Upsilon(2S)\to\ell^+\ell^-)=(10.23\pm1.20\pm1.26)\,10^{-4}$.

[10] Recalculated by us. HEINTZ 92 quotes $B(\Upsilon(3S)\to\gamma\chi_{b1}(2P))\times B(\chi_{b1}(2P)\to\gamma\,\Upsilon(2S))=(2.29\pm0.23\pm0.21)$ % using $B(\Upsilon(2S)\to\mu^+\mu^-)=(1.44\pm0.10)\%$. Supersedes HEINTZ 91.

$\Gamma(\gamma\,\Upsilon(1S))/\Gamma_{\rm total}$ Γ_3/Γ

VALUE	EVTS	DOCUMENT ID		TECN	COMMENT
0.099±0.010 OUR AVERAGE					
0.107±0.006±0.010		[11,12,13] LEES	14M	BABR	$\Upsilon(3S)\to\gamma\gamma\mu^+\mu^-$
0.098±0.005±0.009	15k	[14] LEES	11J	BABR	$\Upsilon(3S)\to X\gamma$
0.103±0.023±0.009		[11,15] CRAWFORD	92B	CLE2	$e^+e^-\to\ell^+\ell^-\gamma\gamma$
0.075±0.010±0.007		[11,16] HEINTZ	92	CSB2	$e^+e^-\to\ell^+\ell^-\gamma\gamma$

[11] Assuming $B(\Upsilon(1S)\to\mu^+\mu^-)=(2.48\pm0.05)\%$.

[12] LEES 14M quotes $\Gamma(\chi_{b1}(2P)\to\gamma\,\Upsilon(1S))/\Gamma_{\rm total}\times\Gamma(\Upsilon(3S)\to\gamma\chi_{b1}(2P))/\Gamma_{\rm total}$ $=(13.48\pm0.72)\times10^{-3}$ combining the results from samples of $\Upsilon(3S)\to\gamma\gamma\mu^+\mu^-$ with and without converted photons.

[13] LEES 14M reports $[\Gamma(\chi_{b1}(2P)\to\gamma\,\Upsilon(1S))/\Gamma_{\rm total}]\times[B(\Upsilon(3S)\to\gamma\chi_{b1}(2P))]=(13.48\pm0.72)\times10^{-3}$ which we divide by our best value $B(\Upsilon(3S)\to\gamma\chi_{b1}(2P))=(12.6\pm1.2)\times10^{-2}$. Our first error is their experiment's error and our second error is the systematic error from using our best value.

[14] LEES 11J reports $[\Gamma(\chi_{b1}(2P)\to\gamma\,\Upsilon(1S))/\Gamma_{\rm total}]\times[B(\Upsilon(3S)\to\gamma\chi_{b1}(2P))]=(12.4\pm0.3\pm0.6)\times10^{-3}$ which we divide by our best value $B(\Upsilon(3S)\to\gamma\chi_{b1}(2P))=(12.6\pm1.2)\times10^{-2}$. Our first error is their experiment's error and our second error is the systematic error from using our best value.

[15] CRAWFORD 92B quotes $B(\Upsilon(3S)\to\gamma\chi_{b1}(2P))\times B(\chi_{b1}(2P)\to\gamma\,\Upsilon(1S))\times2$ $B(\Upsilon(1S)\to\ell^+\ell^-)=(6.47\pm1.12\pm0.82)\,10^{-4}$.

[16] Recalculated by us. HEINTZ 92 quotes $B(\Upsilon(3S)\to\gamma\chi_{b1}(2P))\times B(\chi_{b1}(2P)\to\gamma\,\Upsilon(1S))=(0.91\pm0.11\pm0.06)\%$ using $B(\Upsilon(1S)\to\mu^+\mu^-)=(2.57\pm0.05)\%$. Supersedes HEINTZ 91.

$\Gamma(\pi\pi\chi_{b1}(1P))/\Gamma_{\rm total}$ Γ_4/Γ

VALUE (units 10^{-3})	EVTS	DOCUMENT ID		TECN	COMMENT
9.1±1.3 OUR AVERAGE					
9.2±1.1±0.8	31k	[17] LEES	11C	BABR	$e^+e^-\to\pi^+\pi^-X$
8.6±2.3±2.1		[18] CAWLFIELD	06	CLE3	$\Upsilon(3S)\to2(\gamma\pi\ell)$

[17] LEES 11C measures $B(\Upsilon(3S)\to\chi_{b1}(2P)X)\times B(\chi_{b1}(2P)\to\chi_{b1}(1P)\pi^+\pi^-)=(1.16\pm0.07\pm0.12)\times10^{-3}$. We derive the value assuming $B(\Upsilon(3S)\to\chi_{b1}(2P)X)=B(\Upsilon(3S)\to\chi_{b1}(2P)\gamma)=(12.6\pm1.2)\times10^{-2}$.

[18] CAWLFIELD 06 quote $\Gamma(\chi_b(2P)\to\pi\pi\chi_b(1P))=0.83\pm0.22\pm0.08\pm0.19$ keV assuming l-spin conservation, no D-wave contribution, $\Gamma(\chi_{b1}(2P))=96\pm16$keV, and $\Gamma(\chi_{b2}(2P))=138\pm19$ keV.

$\Gamma(D^0X)/\Gamma_{\rm total}$ Γ_5/Γ

VALUE (units 10^{-2})	EVTS	DOCUMENT ID		TECN	COMMENT
8.8±1.5±0.8	2243	[19] BRIERE	08	CLEO	$\Upsilon(3S)\to\gamma D^0X$

[19] For $p_{D^0}>2.5$ GeV/c.

$\Gamma(\pi^+\pi^-K^+K^-\pi^0)/\Gamma_{\rm total}$ Γ_6/Γ

VALUE (units 10^{-4})	EVTS	DOCUMENT ID		TECN	COMMENT
3.1±1.0±0.3	30	[20] ASNER	08A	CLEO	$\Upsilon(3S)\to\gamma\pi^+\pi^-K^+K^-\pi^0$

[20] ASNER 08A reports $[\Gamma(\chi_{b1}(2P)\to\pi^+\pi^-K^+K^-\pi^0)/\Gamma_{\rm total}]\times[B(\Upsilon(3S)\to\gamma\chi_{b1}(2P))]=(39\pm8\pm9)\times10^{-6}$ which we divide by our best value $B(\Upsilon(3S)\to\gamma\chi_{b1}(2P))=(12.6\pm1.2)\times10^{-2}$. Our first error is their experiment's error and our second error is the systematic error from using our best value.

$\Gamma(2\pi^+\pi^-K^-K^0_S)/\Gamma_{\rm total}$ Γ_7/Γ

VALUE (units 10^{-4})	EVTS	DOCUMENT ID		TECN	COMMENT
1.1±0.5±0.1	10	[21] ASNER	08A	CLEO	$\Upsilon(3S)\to\gamma2\pi^+\pi^-K^-K^0_S$

[21] ASNER 08A reports $[\Gamma(\chi_{b1}(2P)\to2\pi^+\pi^-K^-K^0_S)/\Gamma_{\rm total}]\times[B(\Upsilon(3S)\to\gamma\chi_{b1}(2P))]=(14\pm5\pm3)\times10^{-6}$ which we divide by our best value $B(\Upsilon(3S)\to\gamma\chi_{b1}(2P))=(12.6\pm1.2)\times10^{-2}$. Our first error is their experiment's error and our second error is the systematic error from using our best value.

$\Gamma(2\pi^+\pi^-K^-K^0_S2\pi^0)/\Gamma_{\rm total}$ Γ_8/Γ

VALUE (units 10^{-4})	EVTS	DOCUMENT ID		TECN	COMMENT
7.7±3.1±0.7	15	[22] ASNER	08A	CLEO	$\Upsilon(3S)\to\gamma2\pi^+\pi^-K^-2\pi^0$

[22] ASNER 08A reports $[\Gamma(\chi_{b1}(2P)\to2\pi^+\pi^-K^-K^0_S2\pi^0)/\Gamma_{\rm total}]\times[B(\Upsilon(3S)\to\gamma\chi_{b1}(2P))]=(97\pm30\pm26)\times10^{-6}$ which we divide by our best value $B(\Upsilon(3S)\to\gamma\chi_{b1}(2P))=(12.6\pm1.2)\times10^{-2}$. Our first error is their experiment's error and our second error is the systematic error from using our best value.

$\Gamma(2\pi^+2\pi^-2\pi^0)/\Gamma_{\rm total}$ Γ_9/Γ

VALUE (units 10^{-4})	EVTS	DOCUMENT ID		TECN	COMMENT
5.9±2.0±0.5	36	[23] ASNER	08A	CLEO	$\Upsilon(3S)\to\gamma2\pi^+2\pi^-2\pi^0$

[23] ASNER 08A reports $[\Gamma(\chi_{b1}(2P)\to2\pi^+2\pi^-2\pi^0)/\Gamma_{\rm total}]\times[B(\Upsilon(3S)\to\gamma\chi_{b1}(2P))]=(74\pm16\pm19)\times10^{-6}$ which we divide by our best value $B(\Upsilon(3S)\to\gamma\chi_{b1}(2P))=(12.6\pm1.2)\times10^{-2}$. Our first error is their experiment's error and our second error is the systematic error from using our best value.

$\Gamma(2\pi^+2\pi^-K^+K^-)/\Gamma_{\rm total}$ Γ_{10}/Γ

VALUE (units 10^{-4})	EVTS	DOCUMENT ID		TECN	COMMENT
1.0±0.4±0.1	12	[24] ASNER	08A	CLEO	$\Upsilon(3S)\to\gamma2\pi^+2\pi^-K^+K^-$

[24] ASNER 08A reports $[\Gamma(\chi_{b1}(2P)\to2\pi^+2\pi^-K^+K^-)/\Gamma_{\rm total}]\times[B(\Upsilon(3S)\to\gamma\chi_{b1}(2P))]=(12\pm4\pm3)\times10^{-6}$ which we divide by our best value $B(\Upsilon(3S)\to\gamma\chi_{b1}(2P))=(12.6\pm1.2)\times10^{-2}$. Our first error is their experiment's error and our second error is the systematic error from using our best value.

$\Gamma(2\pi^+2\pi^-K^+K^-\pi^0)/\Gamma_{\rm total}$ Γ_{11}/Γ

VALUE (units 10^{-4})	EVTS	DOCUMENT ID		TECN	COMMENT
5.5±1.7±0.5	38	[25] ASNER	08A	CLEO	$\Upsilon(3S)\to\gamma2\pi^+2\pi^-K^+K^-\pi^0$

[25] ASNER 08A reports $[\Gamma(\chi_{b1}(2P)\to2\pi^+2\pi^-K^+K^-\pi^0)/\Gamma_{\rm total}]\times[B(\Upsilon(3S)\to\gamma\chi_{b1}(2P))]=(69\pm13\pm17)\times10^{-6}$ which we divide by our best value $B(\Upsilon(3S)\to\gamma\chi_{b1}(2P))=(12.6\pm1.2)\times10^{-2}$. Our first error is their experiment's error and our second error is the systematic error from using our best value.

$\Gamma(2\pi^+2\pi^-K^+K^-2\pi^0)/\Gamma_{\rm total}$ Γ_{12}/Γ

VALUE (units 10^{-4})	EVTS	DOCUMENT ID		TECN	COMMENT
9.6±3.5±0.9	27	[26] ASNER	08A	CLEO	$\Upsilon(3S)\to\gamma2\pi^+2\pi^-K^+K^-2\pi^0$

[26] ASNER 08A reports $[\Gamma(\chi_{b1}(2P)\to2\pi^+2\pi^-K^+K^-2\pi^0)/\Gamma_{\rm total}]\times[B(\Upsilon(3S)\to\gamma\chi_{b1}(2P))]=(121\pm29\pm33)\times10^{-6}$ which we divide by our best value $B(\Upsilon(3S)\to\gamma\chi_{b1}(2P))=(12.6\pm1.2)\times10^{-2}$. Our first error is their experiment's error and our second error is the systematic error from using our best value.

$\Gamma(3\pi^+2\pi^-K^-K^0_S\pi^0)/\Gamma_{\rm total}$ Γ_{13}/Γ

VALUE (units 10^{-4})	EVTS	DOCUMENT ID		TECN	COMMENT
6.7±2.5±0.6	17	[27] ASNER	08A	CLEO	$\Upsilon(3S)\to\gamma3\pi^+2\pi^-K^-K^0_S\pi^0$

[27] ASNER 08A reports $[\Gamma(\chi_{b1}(2P)\to3\pi^+2\pi^-K^-K^0_S\pi^0)/\Gamma_{\rm total}]\times[B(\Upsilon(3S)\to\gamma\chi_{b1}(2P))]=(85\pm23\pm22)\times10^{-6}$ which we divide by our best value $B(\Upsilon(3S)\to\gamma\chi_{b1}(2P))=(12.6\pm1.2)\times10^{-2}$. Our first error is their experiment's error and our second error is the systematic error from using our best value.

Meson Particle Listings

$\chi_{b1}(2P)$

$\Gamma(3\pi^+3\pi^-)/\Gamma_{total}$ Γ_{14}/Γ

VALUE (units 10^{-4})	EVTS	DOCUMENT ID		TECN	COMMENT
1.2±0.4±0.1	18	[28] ASNER	08A	CLEO	$\Upsilon(3S) \to \gamma 3\pi^+ 3\pi^-$

[28] ASNER 08A reports $[\Gamma(\chi_{b1}(2P) \to 3\pi^+3\pi^-)/\Gamma_{total}] \times [B(\Upsilon(3S) \to \gamma\chi_{b1}(2P))] = (15 \pm 4 \pm 3) \times 10^{-6}$ which we divide by our best value $B(\Upsilon(3S) \to \gamma\chi_{b1}(2P)) = (12.6 \pm 1.2) \times 10^{-2}$. Our first error is their experiment's error and our second error is the systematic error from using our best value.

$\Gamma(3\pi^+3\pi^-2\pi^0)/\Gamma_{total}$ Γ_{15}/Γ

VALUE (units 10^{-4})	EVTS	DOCUMENT ID		TECN	COMMENT
12±4±1	44	[29] ASNER	08A	CLEO	$\Upsilon(3S) \to \gamma 3\pi^+ 3\pi^- 2\pi^0$

[29] ASNER 08A reports $[\Gamma(\chi_{b1}(2P) \to 3\pi^+3\pi^-2\pi^0)/\Gamma_{total}] \times [B(\Upsilon(3S) \to \gamma\chi_{b1}(2P))] = (150 \pm 30 \pm 40) \times 10^{-6}$ which we divide by our best value $B(\Upsilon(3S) \to \gamma\chi_{b1}(2P)) = (12.6 \pm 1.2) \times 10^{-2}$. Our first error is their experiment's error and our second error is the systematic error from using our best value.

$\Gamma(3\pi^+3\pi^-K^+K^-)/\Gamma_{total}$ Γ_{16}/Γ

VALUE (units 10^{-4})	EVTS	DOCUMENT ID		TECN	COMMENT
2.0±0.7±0.2	16	[30] ASNER	08A	CLEO	$\Upsilon(3S) \to \gamma 3\pi^+ 3\pi^- K^+ K^-$

[30] ASNER 08A reports $[\Gamma(\chi_{b1}(2P) \to 3\pi^+3\pi^-K^+K^-)/\Gamma_{total}] \times [B(\Upsilon(3S) \to \gamma\chi_{b1}(2P))] = (25 \pm 7 \pm 6) \times 10^{-6}$ which we divide by our best value $B(\Upsilon(3S) \to \gamma\chi_{b1}(2P)) = (12.6 \pm 1.2) \times 10^{-2}$. Our first error is their experiment's error and our second error is the systematic error from using our best value.

$\Gamma(3\pi^+3\pi^-K^+K^-\pi^0)/\Gamma_{total}$ Γ_{17}/Γ

VALUE (units 10^{-4})	EVTS	DOCUMENT ID		TECN	COMMENT
6.1±2.1±0.6	25	[31] ASNER	08A	CLEO	$\Upsilon(3S) \to \gamma 3\pi^+ 3\pi^- K^+ K^- \pi^0$

[31] ASNER 08A reports $[\Gamma(\chi_{b1}(2P) \to 3\pi^+3\pi^-K^+K^-\pi^0)/\Gamma_{total}] \times [B(\Upsilon(3S) \to \gamma\chi_{b1}(2P))] = (77 \pm 17 \pm 21) \times 10^{-6}$ which we divide by our best value $B(\Upsilon(3S) \to \gamma\chi_{b1}(2P)) = (12.6 \pm 1.2) \times 10^{-2}$. Our first error is their experiment's error and our second error is the systematic error from using our best value.

$\Gamma(4\pi^+4\pi^-)/\Gamma_{total}$ Γ_{18}/Γ

VALUE (units 10^{-4})	EVTS	DOCUMENT ID		TECN	COMMENT
1.7±0.6±0.2	16	[32] ASNER	08A	CLEO	$\Upsilon(3S) \to \gamma 4\pi^+ 4\pi^-$

[32] ASNER 08A reports $[\Gamma(\chi_{b1}(2P) \to 4\pi^+4\pi^-)/\Gamma_{total}] \times [B(\Upsilon(3S) \to \gamma\chi_{b1}(2P))] = (22 \pm 6 \pm 5) \times 10^{-6}$ which we divide by our best value $B(\Upsilon(3S) \to \gamma\chi_{b1}(2P)) = (12.6 \pm 1.2) \times 10^{-2}$. Our first error is their experiment's error and our second error is the systematic error from using our best value.

$\Gamma(4\pi^+4\pi^-2\pi^0)/\Gamma_{total}$ Γ_{19}/Γ

VALUE (units 10^{-4})	EVTS	DOCUMENT ID		TECN	COMMENT
19±7±2	41	[33] ASNER	08A	CLEO	$\Upsilon(3S) \to \gamma 4\pi^+ 4\pi^- 2\pi^0$

[33] ASNER 08A reports $[\Gamma(\chi_{b1}(2P) \to 4\pi^+4\pi^-2\pi^0)/\Gamma_{total}] \times [B(\Upsilon(3S) \to \gamma\chi_{b1}(2P))] = (241 \pm 47 \pm 72) \times 10^{-6}$ which we divide by our best value $B(\Upsilon(3S) \to \gamma\chi_{b1}(2P)) = (12.6 \pm 1.2) \times 10^{-2}$. Our first error is their experiment's error and our second error is the systematic error from using our best value.

$\chi_{b1}(2P)$ Cross-Particle Branching Ratios

$\Gamma(\chi_{b1}(2P) \to \gamma\Upsilon(1S))/\Gamma_{total} \times \Gamma(\Upsilon(3S) \to \gamma\chi_{b1}(2P))/\Gamma_{total}$ $\Gamma_3/\Gamma \times \Gamma_{21}^{\Upsilon(3S)}/\Gamma^{\Upsilon(3S)}$

VALUE (units 10^{-3})	EVTS	DOCUMENT ID		TECN	COMMENT
12.4±0.3±0.6	15k	LEES	11J	BABR	$\Upsilon(3S) \to X\gamma$

$B(\chi_{b1}(2P) \to \gamma\Upsilon(1S)) \times B(\Upsilon(3S) \to \gamma\chi_{b1}(2P)) \times B(\Upsilon(1S) \to \ell^+\ell^-)$

VALUE (units 10^{-4})	EVTS	DOCUMENT ID		TECN	COMMENT
2.9 ±0.4 OUR AVERAGE		Error includes scale factor of 1.9. See the ideogram below.			
$3.52^{+0.28}_{-0.27}\pm0.17$		[34] LEES	14M	BABR	$\Upsilon(3S) \to \gamma\gamma\mu^+\mu^-$
3.24±0.56±0.41	58	[35] CRAWFORD	92B	CLE2	$\Upsilon(3S) \to \gamma\gamma\ell^+\ell^-$
2.34±0.28±0.15		[36] HEINTZ	92	CSB2	$\Upsilon(3S) \to \gamma\gamma\ell^+\ell^-$

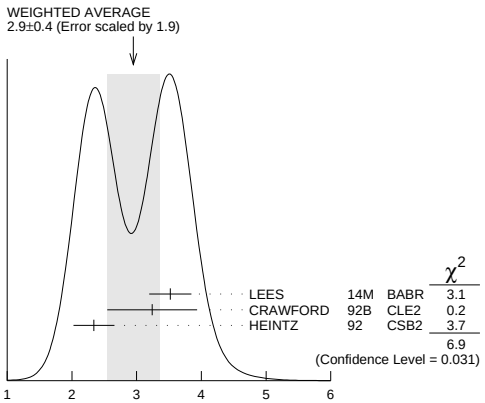

$B(\chi_{b1}(2P) \to \gamma\Upsilon(1S)) \times B(\Upsilon(3S) \to \gamma\chi_{b1}(2P)) \times B(\Upsilon(1S) \to \ell^+\ell^-)$ (units 10^{-4})

[34] From a sample of $\Upsilon(3S) \to \gamma\gamma\mu^+\mu^-$ with one converted photon.

[35] CRAWFORD 92B quotes $2\times B(\Upsilon(3S) \to \gamma\chi_{bJ}(2P))\ B(\chi_{bJ}(2P) \to \gamma\Upsilon(nS))\ B(\Upsilon(nS) \to \ell^+\ell^-)$.

[36] Calculated by us. HEINTZ 92 quotes $B(\Upsilon(3S) \to \gamma\chi_{b1}(2P)) \times B(\chi_{b1}(2P) \to \gamma\Upsilon(1S)) = (0.91 \pm 0.11 \pm 0.06)\%$ using $B(\Upsilon(1S) \to \mu^+\mu^-) = (2.57 \pm 0.05)\%$.

$\Gamma(\chi_{b1}(2P) \to \gamma\Upsilon(2S))/\Gamma_{total} \times \Gamma(\Upsilon(3S) \to \gamma\chi_{b1}(2P))/\Gamma_{total}$ $\Gamma_2/\Gamma \times \Gamma_{21}^{\Upsilon(3S)}/\Gamma^{\Upsilon(3S)}$

VALUE (units 10^{-2})	EVTS	DOCUMENT ID		TECN	COMMENT
2.4±0.1±0.2	4.3k	LEES	11J	BABR	$\Upsilon(3S) \to X\gamma$

$B(\chi_{b1}(2P) \to \gamma\Upsilon(2S)) \times B(\Upsilon(3S) \to \gamma\chi_{b1}(2P)) \times B(\Upsilon(2S) \to \ell^+\ell^-)$

VALUE (units 10^{-4})	EVTS	DOCUMENT ID		TECN	COMMENT
3.8 ±0.6 OUR AVERAGE		Error includes scale factor of 1.8. See the ideogram below.			
$4.95^{+0.75}_{-0.70}\pm1.01\pm0.24$		[37] LEES	14M	BABR	$\Upsilon(3S) \to \gamma\gamma\mu^+\mu^-$
5.12±0.60±0.63	111	[38] CRAWFORD	92B	CLE2	$\Upsilon(3S) \to \gamma\gamma\ell^+\ell^-$
3.30±0.33±0.20		[39] HEINTZ	92	CSB2	$\Upsilon(3S) \to \gamma\gamma\ell^+\ell^-$

[37] From a sample of $\Upsilon(3S) \to \gamma\gamma\mu^+\mu^-$ with one converted photon.

[38] CRAWFORD 92B quotes $2\times B(\Upsilon(3S) \to \gamma\chi_{bJ}(2P))\ B(\chi_{bJ}(2P) \to \gamma\Upsilon(nS))\ B(\Upsilon(nS) \to \ell^+\ell^-)$.

[39] Calculated by us. HEINTZ 92 quotes $B(\Upsilon(3S) \to \gamma\chi_{b1}(2P)) \times B(\chi_{b1}(2P) \to \gamma\Upsilon(2S)) = (2.29 \pm 0.23 \pm 0.21)$ % using $B(\Upsilon(2S) \to \mu^+\mu^-) = (1.44 \pm 0.10)\%$.

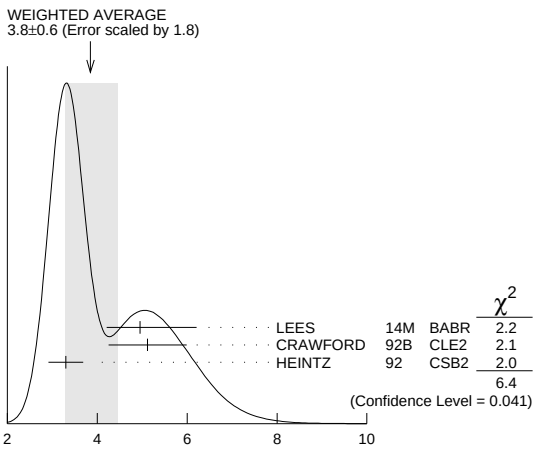

$B(\chi_{b1}(2P) \to \gamma\Upsilon(2S)) \times B(\Upsilon(3S) \to \gamma\chi_{b1}(2P)) \times B(\Upsilon(2S) \to \ell^+\ell^-)$ (units 10^{-4})

$B(\chi_{b1}(2P) \to \chi_{b1}(1P)\pi^+\pi^-) \times B(\Upsilon(3S) \to \chi_{b1}(2P)X)$

VALUE (units 10^{-3})	EVTS	DOCUMENT ID		TECN	COMMENT
1.16±0.07±0.12	31k	LEES	11C	BABR	$e^+e^- \to \pi^+\pi^- X$

$B(\chi_{b2}(2P) \to pX + \bar{p}X)/B(\chi_{b1}(2P) \to pX + \bar{p}X)$

VALUE	DOCUMENT ID		TECN	COMMENT
1.109±0.007±0.040	BRIERE	07	CLEO	$\Upsilon(3S) \to \gamma\chi_{bJ}(2P)$

$B(\chi_{b0}(2P) \to pX + \bar{p}X)/B(\chi_{b1}(2P) \to pX + \bar{p}X)$

VALUE	DOCUMENT ID		TECN	COMMENT
1.082±0.025±0.060	BRIERE	07	CLEO	$\Upsilon(3S) \to \gamma\chi_{bJ}(2P)$

$\chi_{b1}(2P)$ REFERENCES

LEES	14M	PR D90 112010	J.P. Lees *et al.*	(BABAR Collab.)
LEES	11C	PR D84 011104	J.P. Lees *et al.*	(BABAR Collab.)
LEES	11J	PR D84 072002	J.P. Lees *et al.*	(BABAR Collab.)
ASNER	08A	PR D78 091103	D.M. Asner *et al.*	(CLEO Collab.)
BRIERE	08	PR D78 092007	R.A. Briere *et al.*	(CLEO Collab.)
BRIERE	07	PR D76 012005	R.A. Briere *et al.*	(CLEO Collab.)
CAWLFIELD	06	PR D73 012003	C. Cawlfield *et al.*	(CLEO Collab.)
ARTUSO	05	PRL 94 032001	M. Artuso *et al.*	(CLEO Collab.)
CRONIN-HEN...	04	PRL 92 222002	D. Cronin-Hennessy *et al.*	(CLEO Collab.)
CRAWFORD	92B	PL B294 139	G. Crawford *et al.*	(CLEO Collab.)
HEINTZ	92	PR D46 1928	U. Heintz *et al.*	(CUSB II Collab.)
HEINTZ	91	PRL 66 1563	U. Heintz *et al.*	(CUSB Collab.)
MORRISON	91	PRL 67 1696	R.J. Morrison *et al.*	(CLEO Collab.)
NARAIN	91	PRL 66 3113	M. Narain *et al.*	(CUSB Collab.)

$h_b(2P)$

$I^G(J^{PC}) = ?^?(1^{+-})$

OMITTED FROM SUMMARY TABLE

Quantum numbers are quark model predictions.

$h_b(2P)$ MASS

VALUE (MeV)	EVTS	DOCUMENT ID		TECN	COMMENT
10259.8±0.5±1.1	90k	MIZUK	12	BELL	$e^+e^- \to \pi^+\pi^-$ hadrons
• • • We do not use the following data for averages, fits, limits, etc. • • •					
$10259.8 \pm 0.6^{+1.4}_{-1.0}$	83.9k	[1] ADACHI	12	BELL	10.86 $e^+e^- \to \pi^+\pi^-$ MM

[1] Superseded by MIZUK 12.

$h_b(2P)$ DECAY MODES

	Mode	Fraction (Γ_i/Γ)
Γ_1	hadrons	not seen
Γ_2	$\eta_b(1S)\gamma$	(22± 5) %
Γ_3	$\eta_b(2S)\gamma$	(48±13) %

$h_b(2P)$ BRANCHING RATIOS

$\Gamma(\text{hadrons})/\Gamma_{\text{total}}$ Γ_1/Γ

VALUE	EVTS	DOCUMENT ID		TECN	COMMENT
not seen	83.9k	ADACHI	12	BELL	10.86 $e^+e^- \to \pi^+\pi^-$ MM

$\Gamma(\eta_b(1S)\gamma)/\Gamma_{\text{total}}$ Γ_2/Γ

VALUE (units 10^{-2})	EVTS	DOCUMENT ID		TECN	COMMENT
$22.3 \pm 3.8^{+3.1}_{-3.3}$	10k	MIZUK	12	BELL	$e^+e^- \to (\gamma)\pi^+\pi^-$ hadrons

$\Gamma(\eta_b(2S)\gamma)/\Gamma_{\text{total}}$ Γ_3/Γ

VALUE (units 10^{-2})	EVTS	DOCUMENT ID		TECN	COMMENT
$47.5 \pm 10.5^{+6.8}_{-7.7}$	26k	MIZUK	12	BELL	$e^+e^- \to (\gamma)\pi^+\pi^-$ hadrons

$h_b(2P)$ REFERENCES

ADACHI	12	PRL 108 032001	I. Adachi *et al.*	(BELLE Collab.)
MIZUK	12	PRL 109 232002	R. Mizuk *et al.*	(BELLE Collab.)

$\chi_{b2}(2P)$

$I^G(J^{PC}) = 0^+(2^{++})$

J needs confirmation.

Observed in radiative decay of the $\Upsilon(3S)$, therefore $C = +$. Branching ratio requires E1 transition, M1 is strongly disfavored, therefore $P = +$.

$\chi_{b2}(2P)$ MASS

VALUE (MeV)	DOCUMENT ID
10268.65±0.22±0.50 OUR EVALUATION	From γ energy below, using $\Upsilon(3S)$ mass = 10355.2 ± 0.5 MeV

$m_{\chi_{b2}(2P)} - m_{\chi_{b1}(2P)}$

VALUE (MeV)	DOCUMENT ID		TECN	COMMENT
13.10±0.24 OUR AVERAGE				
12.3 ±2.6 ±0.6	[1] AAIJ	14BG	LHCB	$pp \to \gamma\mu^+\mu^- X$
13.04±0.26	LEES	14M	BABR	$\Upsilon(3S) \to \gamma\gamma\mu^+\mu^-$
13.5 ±0.4 ±0.5	[2] HEINTZ	92	CSB2	$e^+e^- \to \gamma X, \ell^+\ell^-\gamma\gamma$

[1] From the $\chi_{bJ}(2P) \to \Upsilon(1S)\gamma$ transition.

[2] From the average photon energy for inclusive and exclusive events. Supersedes NARAIN 91.

γ ENERGY IN $\Upsilon(3S)$ DECAY

VALUE (MeV)	EVTS	DOCUMENT ID		TECN	COMMENT
86.19±0.22 OUR EVALUATION		Treating systematic errors as correlated			
86.40±0.18 OUR AVERAGE					
86.04±0.06±0.27		ARTUSO	05	CLEO	$\Upsilon(3S) \to \gamma X$
86 ±1	101	CRAWFORD	92B	CLE2	$e^+e^- \to \ell^+\ell^-\gamma\gamma$
86.7 ±0.4	10319	[3] HEINTZ	92	CSB2	$e^+e^- \to \gamma X$
86.9 ±0.4	157	[4] HEINTZ	92	CSB2	$e^+e^- \to \ell^+\ell^-\gamma\gamma$
86.4 ±0.1 ±0.4	30741	MORRISON	91	CLE2	$e^+e^- \to \gamma X$

[3] A systematic uncertainty on the energy scale of 0.9% not included. Supersedes NARAIN 91.

[4] A systematic uncertainty on the energy scale of 0.9% not included. Supersedes HEINTZ 91.

$\chi_{b2}(2P)$ DECAY MODES

	Mode	Fraction (Γ_i/Γ)	Confidence level
Γ_1	$\omega\,\Upsilon(1S)$	$(1.10^{+0.34}_{-0.30})$ %	
Γ_2	$\gamma\,\Upsilon(2S)$	(8.9 ±1.2) %	
Γ_3	$\gamma\,\Upsilon(1S)$	(6.6 ±0.8) %	
Γ_4	$\pi\pi\chi_{b2}(1P)$	(5.1 ±0.9) $\times 10^{-3}$	
Γ_5	D^0X	< 2.4 %	90%
Γ_6	$\pi^+\pi^-K^+K^-\pi^0$	< 1.1 $\times 10^{-4}$	90%
Γ_7	$2\pi^+\pi^-K^-K^0_S$	< 9 $\times 10^{-5}$	90%
Γ_8	$2\pi^+\pi^-K^-K^0_S 2\pi^0$	< 7 $\times 10^{-4}$	90%
Γ_9	$2\pi^+2\pi^-2\pi^0$	(3.9 ±1.6) $\times 10^{-4}$	
Γ_{10}	$2\pi^+2\pi^-K^+K^-$	(9 ±4) $\times 10^{-5}$	
Γ_{11}	$2\pi^+2\pi^-K^+K^-\pi^0$	(2.4 ±1.1) $\times 10^{-4}$	
Γ_{12}	$2\pi^+2\pi^-K^+K^-2\pi^0$	(4.7 ±2.3) $\times 10^{-4}$	
Γ_{13}	$3\pi^+2\pi^-K^-K^0_S\pi^0$	< 4 $\times 10^{-4}$	90%
Γ_{14}	$3\pi^+3\pi^-$	(9 ±4) $\times 10^{-5}$	
Γ_{15}	$3\pi^+3\pi^-2\pi^0$	(1.2 ±0.4) $\times 10^{-3}$	
Γ_{16}	$3\pi^+3\pi^-K^+K^-$	(1.4 ±0.7) $\times 10^{-4}$	
Γ_{17}	$3\pi^+3\pi^-K^+K^-\pi^0$	(4.2 ±1.7) $\times 10^{-4}$	
Γ_{18}	$4\pi^+4\pi^-$	(9 ±5) $\times 10^{-5}$	
Γ_{19}	$4\pi^+4\pi^-2\pi^0$	(1.3 ±0.5) $\times 10^{-3}$	

$\chi_{b2}(2P)$ BRANCHING RATIOS

$\Gamma(\omega\,\Upsilon(1S))/\Gamma_{\text{total}}$ Γ_1/Γ

VALUE (units 10^{-2})	EVTS	DOCUMENT ID		TECN	COMMENT
$1.10^{+0.32+0.11}_{-0.28-0.10}$	$20.1^{+5.8}_{-5.1}$	[5] CRONIN-HEN..04		CLE3	$\Upsilon(3S) \to \gamma\omega\,\Upsilon(1S)$

[5] Using B($\Upsilon(3S) \to \gamma\chi_{b2}(2P)$) = (11.4 ± 0.8)% and B($\Upsilon(1S) \to \ell^+\ell^-$) = 2 B($\Upsilon(1S) \to \mu^+\mu^-$) = 2 (2.48 ± 0.06)%.

$\Gamma(\gamma\,\Upsilon(2S))/\Gamma_{\text{total}}$ Γ_2/Γ

VALUE	EVTS	DOCUMENT ID		TECN	COMMENT
0.089±0.012 OUR AVERAGE					
0.085±0.010±0.010		[6,7,8] LEES	14M	BABR	$\Upsilon(3S) \to \gamma\gamma\mu^+\mu^-$
0.084±0.011±0.010	2.5k	[9] LEES	11J	BABR	$\Upsilon(3S) \to X\gamma$
0.096±0.022±0.012		[7,10] CRAWFORD	92B	CLE2	$e^+e^- \to \ell^+\ell^-\gamma\gamma$
0.106±0.016±0.013		[7,11] HEINTZ	92	CSB2	$e^+e^- \to \ell^+\ell^-\gamma\gamma$

[6] LEES 14M quotes $\Gamma(\chi_{b2}(2P) \to \gamma\,\Upsilon(2S))/\Gamma_{\text{total}} \times \Gamma(\Upsilon(3S) \to \gamma\chi_{b2}(2P))/\Gamma_{\text{total}}$ = (1.12 ± 0.13)% combining the results from samples of $\Upsilon(3S) \to \gamma\gamma\mu^+\mu^-$ with and without converted photons.

[7] Assuming B($\Upsilon(2S) \to \mu^+\mu^-$) = (1.93 ± 0.17)%.

[8] LEES 14M reports $[\Gamma(\chi_{b2}(2P) \to \gamma\,\Upsilon(2S))/\Gamma_{\text{total}}] \times [\text{B}(\Upsilon(3S) \to \gamma\chi_{b2}(2P))]$ = (1.12 ± 0.13) $\times 10^{-2}$ which we divide by our best value B($\Upsilon(3S) \to \gamma\chi_{b2}(2P)$) = (13.1 ± 1.6) $\times 10^{-2}$. Our first error is their experiment's error and our second error is the systematic error from using our best value.

[9] LEES 11J reports $[\Gamma(\chi_{b2}(2P) \to \gamma\,\Upsilon(2S))/\Gamma_{\text{total}}] \times [\text{B}(\Upsilon(3S) \to \gamma\chi_{b2}(2P))]$ = (1.1 ± 0.1 ± 0.1) $\times 10^{-2}$ which we divide by our best value B($\Upsilon(3S) \to \gamma\chi_{b2}(2P)$) = (13.1 ± 1.6) $\times 10^{-2}$. Our first error is their experiment's error and our second error is the systematic error from using our best value.

[10] CRAWFORD 92B quotes B($\Upsilon(3S) \to \gamma\chi_{b1}(2P)$) ×B($\chi_{b2}(2P) \to \gamma\,\Upsilon(2S)$) × 2 B($\Upsilon(2S) \to \ell^+\ell^-$) = (4.98 ± 0.94 ± 0.62) 10^{-4}.

[11] Recalculated by us. HEINTZ 92 quotes B($\Upsilon(3S) \to \gamma\chi_{b2}(2P)$) ×B($\chi_{b2}(2P) \to \gamma\,\Upsilon(2S)$) = (1.90 ± 0.23 ± 0.18) % using B($\Upsilon(2S) \to \mu^+\mu^-$) = (1.44 ± 0.10)%. Supersedes HEINTZ 91.

$\Gamma(\gamma\,\Upsilon(1S))/\Gamma_{\text{total}}$ Γ_3/Γ

VALUE	EVTS	DOCUMENT ID		TECN	COMMENT
0.066±0.008 OUR AVERAGE					
0.061±0.004±0.007		[12,13,14] LEES	14M	BABR	$\Upsilon(3S) \to \gamma\gamma\mu^+\mu^-$
0.070±0.004±0.008	11k	[15] LEES	11J	BABR	$\Upsilon(3S) \to X\gamma$
0.077±0.018±0.009		[13,16] CRAWFORD	92B	CLE2	$e^+e^- \to \ell^+\ell^-\gamma\gamma$
0.061±0.009±0.007		[13,17] HEINTZ	92	CSB2	$e^+e^- \to \ell^+\ell^-\gamma\gamma$

[12] LEES 14M quotes $\Gamma(\chi_{b2}(2P) \to \gamma\,\Upsilon(1S))/\Gamma_{\text{total}} \times \Gamma(\Upsilon(3S) \to \gamma\chi_{b2}(2P))/\Gamma_{\text{total}}$ = (8.03 ± 0.50) $\times 10^{-3}$ combining the results from samples of $\Upsilon(3S) \to \gamma\gamma\mu^+\mu^-$ with and without converted photons.

[13] Assuming B($\Upsilon(1S) \to \mu^+\mu^-$) = (2.48 ± 0.05)%.

[14] LEES 14M reports $[\Gamma(\chi_{b2}(2P) \to \gamma\,\Upsilon(1S))/\Gamma_{\text{total}}] \times [\text{B}(\Upsilon(3S) \to \gamma\chi_{b2}(2P))]$ = (8.03 ± 0.50) $\times 10^{-3}$ which we divide by our best value B($\Upsilon(3S) \to \gamma\chi_{b2}(2P)$) = (13.1 ± 1.6) $\times 10^{-2}$. Our first error is their experiment's error and our second error is the systematic error from using our best value.

[15] LEES 11J reports $[\Gamma(\chi_{b2}(2P) \to \gamma\,\Upsilon(1S))/\Gamma_{\text{total}}] \times [\text{B}(\Upsilon(3S) \to \gamma\chi_{b2}(2P))]$ = (9.2 ± 0.3 ± 0.4) $\times 10^{-3}$ which we divide by our best value B($\Upsilon(3S) \to \gamma\chi_{b2}(2P)$) = (13.1 ± 1.6) $\times 10^{-2}$. Our first error is their experiment's error and our second error is the systematic error from using our best value.

[16] CRAWFORD 92B quotes B($\Upsilon(3S) \to \gamma\chi_{b2}(2P)$) ×B($\chi_{b2}(2P) \to \gamma\,\Upsilon(1S)$) × 2 B($\Upsilon(1S) \to \ell^+\ell^-$) = (5.03 ± 0.94 ± 0.63) 10^{-4}.

[17] Recalculated by us. HEINTZ 92 quotes B($\Upsilon(3S) \to \gamma\chi_{b2}(2P)$) ×B($\chi_{b2}(2P) \to \gamma\,\Upsilon(1S)$) =(0.77 ± 0.11 ± 0.05)% using B($\Upsilon(1S) \to \mu^+\mu^-$) = (2.57 ± 0.05)%. Supersedes HEINTZ 91.

$\Gamma(\pi\pi\chi_{b2}(1P))/\Gamma_{total}$ Γ_4/Γ

VALUE (units 10^{-3})	EVTS	DOCUMENT ID		TECN	COMMENT
5.1±0.9 OUR AVERAGE					
4.9±0.7±0.6	17k	[18] LEES	11C	BABR	$e^+e^- \to \pi^+\pi^- X$
6.0±1.6±1.4		[19] CAWLFIELD	06	CLE3	$\Upsilon(3S) \to 2(\gamma\pi\ell)$

[18] $(0.64 \pm 0.05 \pm 0.08) \times 10^{-3}$. We derive the value assuming $B(\Upsilon(3S) \to \chi_{b2}(2P)X) = B(\Upsilon(3S) \to \chi_{b2}(2P)\gamma) = (13.1 \pm 1.6) \times 10^{-2}$.

[19] CAWLFIELD 06 quote $\Gamma(\chi_b(2P) \to \pi\pi\chi_b(1P)) = 0.83 \pm 0.22 \pm 0.08 \pm 0.19$ keV assuming I-spin conservation, no D-wave contribution, $\Gamma(\chi_{b1}(2P)) = 96 \pm 16$keV, and $\Gamma(\chi_{b2}(2P)) = 138 \pm 19$ keV.

$\Gamma(D^0X)/\Gamma_{total}$ Γ_5/Γ

VALUE	CL%	DOCUMENT ID		TECN	COMMENT
<2.4 × 10⁻²	90	[20,21] BRIERE	08	CLEO	$\Upsilon(3S) \to \gamma D^0 X$

[20] For $p_{D^0} > 2.5$ GeV/c.

[21] The authors also present their result as $(0.2 \pm 1.4 \pm 0.1) \times 10^{-2}$.

$\Gamma(\pi^+\pi^-K^+K^-\pi^0)/\Gamma_{total}$ Γ_6/Γ

VALUE (units 10^{-4})	CL%	DOCUMENT ID		TECN	COMMENT
<1.1	90	[22] ASNER	08A	CLEO	$\Upsilon(3S) \to \gamma\pi^+\pi^-K^+K^-\pi^0$

[22] ASNER 08A reports $[\Gamma(\chi_{b2}(2P) \to \pi^+\pi^-K^+K^-\pi^0)/\Gamma_{total}] \times [B(\Upsilon(3S) \to \gamma\chi_{b2}(2P))] < 14 \times 10^{-6}$ which we divide by our best value $B(\Upsilon(3S) \to \gamma\chi_{b2}(2P)) = 13.1 \times 10^{-2}$.

$\Gamma(2\pi^+\pi^-K^-K^0_S)/\Gamma_{total}$ Γ_7/Γ

VALUE (units 10^{-4})	CL%	DOCUMENT ID		TECN	COMMENT
<0.9	90	[23] ASNER	08A	CLEO	$\Upsilon(3S) \to \gamma 2\pi^+\pi^-K^-K^0_S$

[23] ASNER 08A reports $[\Gamma(\chi_{b2}(2P) \to 2\pi^+\pi^-K^-K^0_S)/\Gamma_{total}] \times [B(\Upsilon(3S) \to \gamma\chi_{b2}(2P))] < 12 \times 10^{-6}$ which we divide by our best value $B(\Upsilon(3S) \to \gamma\chi_{b2}(2P)) = 13.1 \times 10^{-2}$.

$\Gamma(2\pi^+\pi^-K^-K^0_S2\pi^0)/\Gamma_{total}$ Γ_8/Γ

VALUE (units 10^{-4})	CL%	DOCUMENT ID		TECN	COMMENT
<7	90	[24] ASNER	08A	CLEO	$\Upsilon(3S) \to \gamma 2\pi^+\pi^-K^-2\pi^0$

[24] ASNER 08A reports $[\Gamma(\chi_{b2}(2P) \to 2\pi^+\pi^-K^-K^0_S2\pi^0)/\Gamma_{total}] \times [B(\Upsilon(3S) \to \gamma\chi_{b2}(2P))] < 87 \times 10^{-6}$ which we divide by our best value $B(\Upsilon(3S) \to \gamma\chi_{b2}(2P)) = 13.1 \times 10^{-2}$.

$\Gamma(2\pi^+2\pi^-2\pi^0)/\Gamma_{total}$ Γ_9/Γ

VALUE (units 10^{-4})	EVTS	DOCUMENT ID		TECN	COMMENT
3.9±1.6±0.5	23	[25] ASNER	08A	CLEO	$\Upsilon(3S) \to \gamma 2\pi^+2\pi^-2\pi^0$

[25] ASNER 08A reports $[\Gamma(\chi_{b2}(2P) \to 2\pi^+2\pi^-2\pi^0)/\Gamma_{total}] \times [B(\Upsilon(3S) \to \gamma\chi_{b2}(2P))] = (51 \pm 16 \pm 13) \times 10^{-6}$ which we divide by our best value $B(\Upsilon(3S) \to \gamma\chi_{b2}(2P)) = (13.1 \pm 1.6) \times 10^{-2}$. Our first error is their experiment's error and our second error is the systematic error from using our best value.

$\Gamma(2\pi^+2\pi^-K^+K^-)/\Gamma_{total}$ Γ_{10}/Γ

VALUE (units 10^{-4})	EVTS	DOCUMENT ID		TECN	COMMENT
0.9±0.4±0.1	11	[26] ASNER	08A	CLEO	$\Upsilon(3S) \to \gamma 2\pi^+2\pi^-K^+K^-$

[26] ASNER 08A reports $[\Gamma(\chi_{b2}(2P) \to 2\pi^+2\pi^-K^+K^-)/\Gamma_{total}] \times [B(\Upsilon(3S) \to \gamma\chi_{b2}(2P))] = (12 \pm 4 \pm 3) \times 10^{-6}$ which we divide by our best value $B(\Upsilon(3S) \to \gamma\chi_{b2}(2P)) = (13.1 \pm 1.6) \times 10^{-2}$. Our first error is their experiment's error and our second error is the systematic error from using our best value.

$\Gamma(2\pi^+2\pi^-K^+K^-\pi^0)/\Gamma_{total}$ Γ_{11}/Γ

VALUE (units 10^{-4})	EVTS	DOCUMENT ID		TECN	COMMENT
2.4±1.0±0.3	16	[27] ASNER	08A	CLEO	$\Upsilon(3S) \to \gamma 2\pi^+2\pi^-K^+K^-\pi^0$

[27] ASNER 08A reports $[\Gamma(\chi_{b2}(2P) \to 2\pi^+2\pi^-K^+K^-\pi^0)/\Gamma_{total}] \times [B(\Upsilon(3S) \to \gamma\chi_{b2}(2P))] = (32 \pm 11 \pm 8) \times 10^{-6}$ which we divide by our best value $B(\Upsilon(3S) \to \gamma\chi_{b2}(2P)) = (13.1 \pm 1.6) \times 10^{-2}$. Our first error is their experiment's error and our second error is the systematic error from using our best value.

$\Gamma(2\pi^+2\pi^-K^+K^-2\pi^0)/\Gamma_{total}$ Γ_{12}/Γ

VALUE (units 10^{-4})	EVTS	DOCUMENT ID		TECN	COMMENT
4.7±2.2±0.6	14	[28] ASNER	08A	CLEO	$\Upsilon(3S) \to \gamma 2\pi^+2\pi^-K^+K^-2\pi^0$

[28] ASNER 08A reports $[\Gamma(\chi_{b2}(2P) \to 2\pi^+2\pi^-K^+K^-2\pi^0)/\Gamma_{total}] \times [B(\Upsilon(3S) \to \gamma\chi_{b2}(2P))] = (62 \pm 23 \pm 17) \times 10^{-6}$ which we divide by our best value $B(\Upsilon(3S) \to \gamma\chi_{b2}(2P)) = (13.1 \pm 1.6) \times 10^{-2}$. Our first error is their experiment's error and our second error is the systematic error from using our best value.

$\Gamma(3\pi^+2\pi^-K^-K^0_S\pi^0)/\Gamma_{total}$ Γ_{13}/Γ

VALUE (units 10^{-4})	CL%	DOCUMENT ID		TECN	COMMENT
<4	90	[29] ASNER	08A	CLEO	$\Upsilon(3S) \to \gamma 3\pi^+2\pi^-K^-K^0_S\pi^0$

[29] ASNER 08A reports $[\Gamma(\chi_{b2}(2P) \to 3\pi^+2\pi^-K^-K^0_S\pi^0)/\Gamma_{total}] \times [B(\Upsilon(3S) \to \gamma\chi_{b2}(2P))] < 58 \times 10^{-6}$ which we divide by our best value $B(\Upsilon(3S) \to \gamma\chi_{b2}(2P)) = 13.1 \times 10^{-2}$.

$\Gamma(3\pi^+3\pi^-)/\Gamma_{total}$ Γ_{14}/Γ

VALUE (units 10^{-4})	EVTS	DOCUMENT ID		TECN	COMMENT
0.9±0.4±0.1	14	[30] ASNER	08A	CLEO	$\Upsilon(3S) \to \gamma 3\pi^+3\pi^-$

[30] ASNER 08A reports $[\Gamma(\chi_{b2}(2P) \to 3\pi^+3\pi^-)/\Gamma_{total}] \times [B(\Upsilon(3S) \to \gamma\chi_{b2}(2P))] = (12 \pm 4 \pm 3) \times 10^{-6}$ which we divide by our best value $B(\Upsilon(3S) \to \gamma\chi_{b2}(2P)) = (13.1 \pm 1.6) \times 10^{-2}$. Our first error is their experiment's error and our second error is the systematic error from using our best value.

$\Gamma(3\pi^+3\pi^-2\pi^0)/\Gamma_{total}$ Γ_{15}/Γ

VALUE (units 10^{-4})	EVTS	DOCUMENT ID		TECN	COMMENT
12±4±1	45	[31] ASNER	08A	CLEO	$\Upsilon(3S) \to \gamma 3\pi^+3\pi^-2\pi^0$

[31] ASNER 08A reports $[\Gamma(\chi_{b2}(2P) \to 3\pi^+3\pi^-2\pi^0)/\Gamma_{total}] \times [B(\Upsilon(3S) \to \gamma\chi_{b2}(2P))] = (159 \pm 33 \pm 43) \times 10^{-6}$ which we divide by our best value $B(\Upsilon(3S) \to \gamma\chi_{b2}(2P)) = (13.1 \pm 1.6) \times 10^{-2}$. Our first error is their experiment's error and our second error is the systematic error from using our best value.

$\Gamma(3\pi^+3\pi^-K^+K^-)/\Gamma_{total}$ Γ_{16}/Γ

VALUE (units 10^{-4})	EVTS	DOCUMENT ID		TECN	COMMENT
1.4±0.7±0.2	12	[32] ASNER	08A	CLEO	$\Upsilon(3S) \to \gamma 3\pi^+3\pi^-K^+K^-$

[32] ASNER 08A reports $[\Gamma(\chi_{b2}(2P) \to 3\pi^+3\pi^-K^+K^-)/\Gamma_{total}] \times [B(\Upsilon(3S) \to \gamma\chi_{b2}(2P))] = (19 \pm 7 \pm 5) \times 10^{-6}$ which we divide by our best value $B(\Upsilon(3S) \to \gamma\chi_{b2}(2P)) = (13.1 \pm 1.6) \times 10^{-2}$. Our first error is their experiment's error and our second error is the systematic error from using our best value.

$\Gamma(3\pi^+3\pi^-K^+K^-\pi^0)/\Gamma_{total}$ Γ_{17}/Γ

VALUE (units 10^{-4})	EVTS	DOCUMENT ID		TECN	COMMENT
4.2±1.7±0.5	16	[33] ASNER	08A	CLEO	$\Upsilon(3S) \to \gamma 3\pi^+3\pi^-K^+K^-\pi^0$

[33] ASNER 08A reports $[\Gamma(\chi_{b2}(2P) \to 3\pi^+3\pi^-K^+K^-\pi^0)/\Gamma_{total}] \times [B(\Upsilon(3S) \to \gamma\chi_{b2}(2P))] = (55 \pm 16 \pm 15) \times 10^{-6}$ which we divide by our best value $B(\Upsilon(3S) \to \gamma\chi_{b2}(2P)) = (13.1 \pm 1.6) \times 10^{-2}$. Our first error is their experiment's error and our second error is the systematic error from using our best value.

$\Gamma(4\pi^+4\pi^-)/\Gamma_{total}$ Γ_{18}/Γ

VALUE (units 10^{-4})	EVTS	DOCUMENT ID		TECN	COMMENT
0.9±0.4±0.1	9	[34] ASNER	08A	CLEO	$\Upsilon(3S) \to \gamma 4\pi^+4\pi^-$

[34] ASNER 08A reports $[\Gamma(\chi_{b2}(2P) \to 4\pi^+4\pi^-)/\Gamma_{total}] \times [B(\Upsilon(3S) \to \gamma\chi_{b2}(2P))] = (12 \pm 5 \pm 3) \times 10^{-6}$ which we divide by our best value $B(\Upsilon(3S) \to \gamma\chi_{b2}(2P)) = (13.1 \pm 1.6) \times 10^{-2}$. Our first error is their experiment's error and our second error is the systematic error from using our best value.

$\Gamma(4\pi^+4\pi^-2\pi^0)/\Gamma_{total}$ Γ_{19}/Γ

VALUE (units 10^{-4})	EVTS	DOCUMENT ID		TECN	COMMENT
13±5±2	27	[35] ASNER	08A	CLEO	$\Upsilon(3S) \to \gamma 4\pi^+4\pi^-2\pi^0$

[35] ASNER 08A reports $[\Gamma(\chi_{b2}(2P) \to 4\pi^+4\pi^-2\pi^0)/\Gamma_{total}] \times [B(\Upsilon(3S) \to \gamma\chi_{b2}(2P))] = (165 \pm 46 \pm 50) \times 10^{-6}$ which we divide by our best value $B(\Upsilon(3S) \to \gamma\chi_{b2}(2P)) = (13.1 \pm 1.6) \times 10^{-2}$. Our first error is their experiment's error and our second error is the systematic error from using our best value.

$\chi_{b2}(2P)$ Cross-Particle Branching Ratios

$\Gamma(\chi_{b2}(2P) \to \gamma\Upsilon(1S))/\Gamma_{total} \times \Gamma(\Upsilon(3S) \to \gamma\chi_{b2}(2P))/\Gamma_{total}$ $\Gamma_3/\Gamma \times \Gamma_{20}^{\Upsilon(3S)}/\Gamma^{\Upsilon(3S)}$

VALUE (units 10^{-3})	EVTS	DOCUMENT ID		TECN	COMMENT
9.2±0.3±0.4	11k	LEES	11J	BABR	$\Upsilon(3S) \to X\gamma$

$\Gamma(\chi_{b2}(2P) \to \gamma\Upsilon(2S))/\Gamma_{total} \times \Gamma(\Upsilon(3S) \to \gamma\chi_{b2}(2P))/\Gamma_{total}$ $\Gamma_2/\Gamma \times \Gamma_{20}^{\Upsilon(3S)}/\Gamma^{\Upsilon(3S)}$

VALUE (units 10^{-2})	EVTS	DOCUMENT ID		TECN	COMMENT
1.1±0.1±0.1	2.5k	LEES	11J	BABR	$\Upsilon(3S) \to X\gamma$

$B(\chi_{b2}(2P) \to \chi_{b2}(1P)\pi^+\pi^-) \times B(\Upsilon(3S) \to \chi_{b2}(2P)X)$

VALUE (units 10^{-3})	EVTS	DOCUMENT ID		TECN	COMMENT
0.64±0.05±0.08	17k	LEES	11C	BABR	$e^+e^- \to \pi^+\pi^- X$

$B(\chi_{b2}(2P) \to \gamma\Upsilon(1S)) \times B(\Upsilon(3S) \to \gamma\chi_{b2}(2P)) \times B(\Upsilon(1S) \to \ell^+\ell^-)$

VALUE (units 10^{-4})	EVTS	DOCUMENT ID		TECN	COMMENT
2.02±0.18 OUR AVERAGE					
$1.95^{+0.22}_{-0.21}{}^{+0.10}_{-0.16}$		[36] LEES	14M	BABR	$\Upsilon(3S) \to \gamma\gamma\mu^+\mu^-$
2.52±0.47±0.32	48	[37] CRAWFORD	92B	CLE2	$\Upsilon(3S) \to \gamma\gamma\ell^+\ell^-$
1.98±0.28±0.12		[38] HEINTZ	92	CSB2	$\Upsilon(3S) \to \gamma\gamma\ell^+\ell^-$

[36] From a sample of $\Upsilon(3S) \to \gamma\gamma\mu^+\mu^-$ with converted photons.

[37] CRAWFORD 92B quotes $2 \times B(\Upsilon(3S) \to \gamma\chi_{b,J}(2P))\ B(\chi_{b,J}(2P) \to \gamma\Upsilon(nS))\ B(\Upsilon(nS) \to \ell^+\ell^-)$.

[38] Calculated by us. HEINTZ 92 quotes $B(\Upsilon(3S) \to \gamma\chi_{b2}(2P)) \times B(\chi_{b2}(2P) \to \gamma\Upsilon(1S)) = (0.77 \pm 0.11 \pm 0.05)\%$ using $B(\Upsilon(1S) \to \mu^+\mu^-) = (2.57 \pm 0.05)\%$.

$[B(\chi_{b2}(2P) \to \gamma\Upsilon(1S)) \times B(\Upsilon(3S) \to \gamma\chi_{b2}(2P))]\ /\ [B(\chi_{b1}(2P) \to \gamma\Upsilon(1S)) \times B(\Upsilon(3S) \to \gamma\chi_{b1}(2P))]$

VALUE (%)	DOCUMENT ID		TECN	COMMENT
66.6±3.0	[39] LEES	14M	BABR	$\Upsilon(3S) \to \gamma\gamma\mu^+\mu^-$

[39] From a sample of $\Upsilon(3S) \to \gamma\gamma\mu^+\mu^-$ events without converted photons.

$B(\chi_{b2}(2P) \to \gamma\Upsilon(2S)) \times B(\Upsilon(3S) \to \gamma\chi_{b2}(2P)) \times B(\Upsilon(2S) \to \ell^+\ell^-)$

VALUE (units 10^{-4})	EVTS	DOCUMENT ID		TECN	COMMENT
2.74±0.29 OUR AVERAGE					
$3.22^{+0.58}_{-0.53}{}^{+0.16}_{-0.71}$		[40] LEES	14M	BABR	$\Upsilon(3S) \to \gamma\gamma\mu^+\mu^-$
2.49±0.47±0.31	53	[41] CRAWFORD	92B	CLE2	$\Upsilon(3S) \to \gamma\gamma\ell^+\ell^-$
2.74±0.33±0.18		[42] HEINTZ	92	CSB2	$\Upsilon(3S) \to \gamma\gamma\ell^+\ell^-$

[40] From a sample of $\Upsilon(3S) \to \gamma\gamma\mu^+\mu^-$ with converted photons.

[41] CRAWFORD 92B quotes $2\times B(\Upsilon(3S) \to \gamma\chi_{bJ}(2P))\ B(\chi_{bJ}(2P) \to \gamma\Upsilon(nS))\ B(\Upsilon(nS) \to \ell^+\ell^-)$.

[42] Calculated by us. HEINTZ 92 quotes $B(\Upsilon(3S) \to \gamma\chi_{b2}(2P)) \times B(\chi_{b2}(2P) \to \gamma\Upsilon(2S)) = (1.90 \pm 0.23 \pm 0.18)$ % using $B(\Upsilon(2S) \to \mu^+\mu^-) = (1.44 \pm 0.10)$%.

$[B(\chi_{b2}(2P) \to \gamma\Upsilon(2S)) \times B(\Upsilon(3S) \to \gamma\chi_{b2}(2P))] / [B(\chi_{b1}(2P) \to \gamma\Upsilon(2S)) \times B(\Upsilon(3S) \to \gamma\chi_{b1}(2P))]$

VALUE (%)	DOCUMENT ID		TECN	COMMENT
46.9±2.0	[43] LEES	14M	BABR	$\Upsilon(3S) \to \gamma\gamma\mu^+\mu^-$

[43] From a sample of $\Upsilon(3S) \to \gamma\gamma\mu^+\mu^-$ without converted photons.

$\chi_{b2}(2P)$ REFERENCES

AAIJ	14BG	JHEP 1410 088	R. Aaij *et al.*	(LHCb Collab.)
LEES	14M	PR D90 112010	J.P. Lees *et al.*	(BABAR Collab.)
LEES	11C	PR D84 011104	J.P. Lees *et al.*	(BABAR Collab.)
LEES	11J	PR D84 072002	J.P. Lees *et al.*	(BABAR Collab.)
ASNER	08A	PR D78 091103	D.M. Asner *et al.*	(CLEO Collab.)
BRIERE	08	PR D78 092007	R.A. Briere *et al.*	(CLEO Collab.)
CAWLFIELD	06	PR D73 012003	C. Cawlfield *et al.*	(CLEO Collab.)
ARTUSO	05	PRL 94 032001	M. Artuso *et al.*	(CLEO Collab.)
CRONIN-HEN...	04	PRL 92 222002	D. Cronin-Hennessy *et al.*	(CLEO Collab.)
CRAWFORD	92B	PL B294 139	G. Crawford *et al.*	(CLEO Collab.)
HEINTZ	92	PR D46 1928	U. Heintz *et al.*	(CUSB II Collab.)
HEINTZ	91	PRL 66 1563	U. Heintz *et al.*	(CUSB Collab.)
MORRISON	91	PRL 67 1696	R.J. Morrison *et al.*	(CLEO Collab.)
NARAIN	91	PRL 66 3113	M. Narain *et al.*	(CUSB Collab.)

$\Upsilon(3S)$

$I^G(J^{PC}) = 0^-(1^{--})$

$\Upsilon(3S)$ MASS

VALUE (MeV)	DOCUMENT ID		TECN	COMMENT
10355.2±0.5	[1] ARTAMONOV 00		MD1	$e^+e^- \to$ hadrons
• • • We do not use the following data for averages, fits, limits, etc. • • •				
10355.3±0.5	[2,3] BARU	86B	REDE	$e^+e^- \to$ hadrons

[1] Reanalysis of BARU 86B using new electron mass (COHEN 87).
[2] Reanalysis of ARTAMONOV 84.
[3] Superseded by ARTAMONOV 00.

$m_{\Upsilon(3S)} - m_{\Upsilon(2S)}$

VALUE (MeV)	DOCUMENT ID		TECN	COMMENT
331.50±0.02±0.13	LEES	11C	BABR	$e^+e^- \to \pi^+\pi^- X$

$\Upsilon(3S)$ WIDTH

VALUE (keV)	DOCUMENT ID
20.32±1.85 OUR EVALUATION	See the Note on "Width Determinations of the Υ States"

$\Upsilon(3S)$ DECAY MODES

	Mode	Fraction (Γ_i/Γ)	Scale factor/ Confidence level
Γ_1	$\Upsilon(2S)$ anything	(10.6 ± 0.8) %	
Γ_2	$\Upsilon(2S)\pi^+\pi^-$	(2.82± 0.18) %	S=1.6
Γ_3	$\Upsilon(2S)\pi^0\pi^0$	(1.85± 0.14) %	
Γ_4	$\Upsilon(2S)\gamma\gamma$	(5.0 ± 0.7) %	
Γ_5	$\Upsilon(2S)\pi^0$	< 5.1 $\times 10^{-4}$	CL=90%
Γ_6	$\Upsilon(1S)\pi^+\pi^-$	(4.37± 0.08) %	
Γ_7	$\Upsilon(1S)\pi^0\pi^0$	(2.20± 0.13) %	
Γ_8	$\Upsilon(1S)\eta$	< 1 $\times 10^{-4}$	CL=90%
Γ_9	$\Upsilon(1S)\pi^0$	< 7 $\times 10^{-5}$	CL=90%
Γ_{10}	$h_b(1P)\pi^0$	< 1.2 $\times 10^{-3}$	CL=90%
Γ_{11}	$h_b(1P)\pi^0 \to \gamma\eta_b(1S)\pi^0$	(4.3 ± 1.4) $\times 10^{-4}$	
Γ_{12}	$h_b(1P)\pi^+\pi^-$	< 1.2 $\times 10^{-4}$	CL=90%
Γ_{13}	$\tau^+\tau^-$	(2.29± 0.30) %	
Γ_{14}	$\mu^+\mu^-$	(2.18± 0.21) %	S=2.1
Γ_{15}	e^+e^-	(2.18± 0.20) %	
Γ_{16}	hadrons	(93 ±12) %	
Γ_{17}	ggg	(35.7 ± 2.6) %	
Γ_{18}	γgg	(9.7 ± 1.8) $\times 10^{-3}$	
Γ_{19}	^2H anything	(2.33± 0.33) $\times 10^{-5}$	

Radiative decays

Γ_{20}	$\gamma\chi_{b2}(2P)$	(13.1 ± 1.6) %		S=3.4
Γ_{21}	$\gamma\chi_{b1}(2P)$	(12.6 ± 1.2) %		S=2.4
Γ_{22}	$\gamma\chi_{b0}(2P)$	(5.9 ± 0.6) %		S=1.4
Γ_{23}	$\gamma\chi_{b2}(1P)$	(9.9 ± 1.2) $\times 10^{-3}$		S=1.9
Γ_{24}	$\gamma\chi_{b1}(1P)$	(9 ± 5) $\times 10^{-4}$		S=1.8
Γ_{25}	$\gamma\chi_{b0}(1P)$	(2.7 ± 0.4) $\times 10^{-3}$		
Γ_{26}	$\gamma\eta_b(2S)$	< 6.2 $\times 10^{-4}$		CL=90%
Γ_{27}	$\gamma\eta_b(1S)$	(5.1 ± 0.7) $\times 10^{-4}$		
Γ_{28}	$\gamma A^0 \to \gamma$ hadrons	< 8 $\times 10^{-5}$		CL=90%
Γ_{29}	$\gamma X \to \gamma +$ ≥ 4 prongs	[a] < 2.2 $\times 10^{-4}$		CL=95%
Γ_{30}	$\gamma a_1^0 \to \gamma\mu^+\mu^-$	< 5.5 $\times 10^{-6}$		CL=90%
Γ_{31}	$\gamma a_1^0 \to \gamma\tau^+\tau^-$	[b] < 1.6 $\times 10^{-4}$		CL=90%

Lepton Family number (*LF*) violating modes

Γ_{32}	$e^\pm\tau^\mp$	*LF*	< 4.2 $\times 10^{-6}$		CL=90%
Γ_{33}	$\mu^\pm\tau^\mp$	*LF*	< 3.1 $\times 10^{-6}$		CL=90%

[a] 1.5 GeV < m_X < 5.0 GeV

[b] For $m_{\tau^+\tau^-}$ in the ranges 4.03–9.52 and 9.61–10.10 GeV.

$\Upsilon(3S)$ $\Gamma(i)\Gamma(e^+e^-)/\Gamma(\text{total})$

$\Gamma(\text{hadrons}) \times \Gamma(e^+e^-)/\Gamma_{\text{total}}$ $\Gamma_{16}\Gamma_{15}/\Gamma$

VALUE (keV)	DOCUMENT ID		TECN	COMMENT
0.414±0.007 OUR AVERAGE				
0.413±0.004±0.006	ROSNER	06	CLEO	10.4 $e^+e^- \to$ hadrons
0.45 ±0.03 ±0.03	[4] GILES	84B	CLEO	$e^+e^- \to$ hadrons

[4] Radiative corrections reevaluated by BUCHMUELLER 88 following KURAEV 85.

$\Gamma(\Upsilon(1S)\pi^+\pi^-) \times \Gamma(e^+e^-)/\Gamma_{\text{total}}$ $\Gamma_6\Gamma_{15}/\Gamma$

VALUE (eV)	EVTS	DOCUMENT ID		TECN	COMMENT
18.46±0.27±0.77	6.4K	[5] AUBERT	08BP	BABR	$e^+e^- \to \gamma\pi^+\pi^-\ell^+\ell^-$

[5] Using $B(\Upsilon(1S) \to e^+e^-) = (2.38 \pm 0.11)$% and $B(\Upsilon(1S) \to \mu^+\mu^-) = (2.48 \pm 0.05)$%.

$\Upsilon(3S)$ PARTIAL WIDTHS

$\Gamma(e^+e^-)$ Γ_{15}

VALUE (keV)	DOCUMENT ID
0.443±0.008 OUR EVALUATION	

$\Upsilon(3S)$ BRANCHING RATIOS

$\Gamma(\Upsilon(2S)\text{anything})/\Gamma_{\text{total}}$ Γ_1/Γ

VALUE	EVTS	DOCUMENT ID		TECN	COMMENT
0.106 ±0.008 OUR AVERAGE					
0.1023±0.0105	4625	[6,7,8] BUTLER	94B	CLE2	$e^+e^- \to \ell^+\ell^-$X
0.111 ±0.012	4891	[7,8,9] BROCK	91	CLEO	$e^+e^- \to \pi^+\pi^-$X, $\pi^+\pi^-\ell^+\ell^-$

[6] Using $B(\Upsilon(2S) \to \Upsilon(1S)\gamma\gamma) = (0.038 \pm 0.007)$%, and $B(\Upsilon(2S) \to \Upsilon(1S)\pi^0\pi^0) = (1/2)B(\Upsilon(2S) \to \Upsilon(1S)\pi^+\pi^-)$.

[7] Using $B(\Upsilon(1S) \to \mu^+\mu^-) = (2.48 \pm 0.06)$%. With the assumption of $e\mu$ universality.

[8] Using $B(\Upsilon(2S) \to \Upsilon(1S)\pi^+\pi^-) = (18.5 \pm 0.8)$%.

[9] Using $B(\Upsilon(2S) \to \mu^+\mu^-) = (1.31 \pm 0.21)$%, $B(\Upsilon(2S) \to \Upsilon(1S)\gamma\gamma) \times 2B(\Upsilon(1S) \to \mu^+\mu^-) = (0.188 \pm 0.035)$%, and $B(\Upsilon(2S) \to \Upsilon(1S)\pi^0\pi^0) \times 2B(\Upsilon(1S) \to \mu^+\mu^-) = (0.436 \pm 0.056)$%. With the assumption of $e\mu$ universality.

$\Gamma(\Upsilon(2S)\pi^+\pi^-)/\Gamma_{\text{total}}$ Γ_2/Γ

VALUE (units 10^{-2})	EVTS	DOCUMENT ID		TECN	COMMENT
2.82±0.18 OUR AVERAGE Error includes scale factor of 1.6. See the ideogram below.					
3.00±0.02±0.14	543k	LEES	11C	BABR	$e^+e^- \to \pi^+\pi^- X$
2.40±0.10±0.26	800	[10] AUBERT	08BP	BABR	$e^+e^- \to \gamma\pi^+\pi^- e^+e^-$
3.12±0.49	980	[11,12] BUTLER	94B	CLE2	$e^+e^- \to \pi^+\pi^-\ell^+\ell^-$
2.13±0.38	974	[13] BROCK	91	CLEO	$e^+e^- \to \pi^+\pi^-$X, $\pi^+\pi^-\ell^+\ell^-$
• • • We do not use the following data for averages, fits, limits, etc. • • •					
4.82±0.65±0.53	138	[13] WU	93	CUSB	$\Upsilon(3S) \to \pi^+\pi^-\ell^+\ell^-$
3.1 ±2.0	5	MAGERAS	82	CUSB	$\Upsilon(3S) \to \pi^+\pi^-\ell^+\ell^-$

[10] Using $B(\Upsilon(1S) \to e^+e^-) = (2.38 \pm 0.11)$%, $B(\Upsilon(1S) \to \mu^+\mu^-) = (2.48 \pm 0.05)$%, and $\Gamma_{ee}(\Upsilon(3S)) = 0.443 \pm 0.008$ keV.

[11] From the exclusive mode.

[12] Using $B(\Upsilon(2S) \to \Upsilon(1S)\gamma\gamma) = (0.038 \pm 0.007)$%, and $B(\Upsilon(2S) \to \Upsilon(1S)\pi^0\pi^0) = (1/2)B(\Upsilon(2S) \to \Upsilon(1S)\pi^+\pi^-)$.

[13] Using $B(\Upsilon(2S) \to \mu^+\mu^-) = (1.31 \pm 0.21)$%, $B(\Upsilon(2S) \to \Upsilon(1S)\gamma\gamma) \times 2B(\Upsilon(1S) \to \mu^+\mu^-) = (0.188 \pm 0.035)$%, and $B(\Upsilon(2S) \to \Upsilon(1S)\pi^0\pi^0) \times 2B(\Upsilon(1S) \to \mu^+\mu^-) = (0.436 \pm 0.056)$%. With the assumption of $e\mu$ universality.

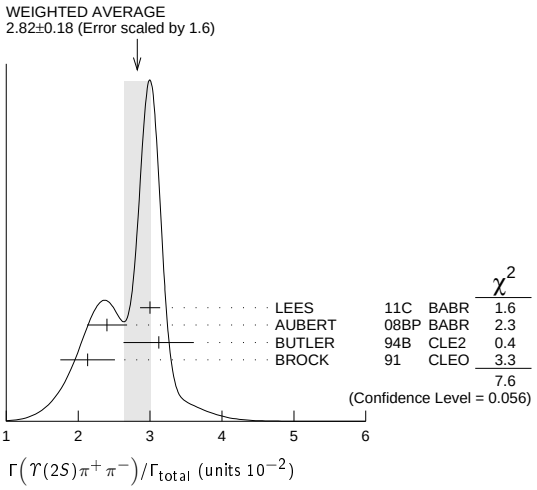

$\Gamma(\Upsilon(2S)\pi^0\pi^0)/\Gamma_{total}$ Γ_3/Γ

VALUE (units 10^{-2})	EVTS	DOCUMENT ID		TECN	COMMENT
1.85±0.14 OUR AVERAGE					
1.82±0.09±0.12	4391	[14] BHARI	09	CLEO	$e^+e^- \to \pi^0\pi^0\ell^+\ell^-$
2.16±0.39		[15,16] BUTLER	94B	CLE2	$e^+e^- \to \pi^0\pi^0\ell^+\ell^-$
1.7 ±0.5 ±0.2	10	[17] HEINTZ	92	CSB2	$e^+e^- \to \pi^0\pi^0\ell^+\ell^-$

[14] Authors assume B($\Upsilon(1S) \to e^+e^-$) + B($\Upsilon(1S) \to \mu^+\mu^-$) = 4.06%.
[15] B($\Upsilon(2S) \to \mu^+\mu^-$) = (1.31 ± 0.21)% and assuming $e\mu$ universality.
[16] From the exclusive mode.
[17] B($\Upsilon(2S) \to \mu^+\mu^-$) = (1.44 ± 0.10)% and assuming $e\mu$ universality. Supersedes HEINTZ 91.

$\Gamma(\Upsilon(2S)\gamma\gamma)/\Gamma_{total}$ Γ_4/Γ

VALUE	DOCUMENT ID		TECN	COMMENT
0.0502±0.0069	[18] BUTLER	94B	CLE2	$e^+e^- \to \ell^+\ell^- 2\gamma$

[18] From the exclusive mode.

$\Gamma(\Upsilon(2S)\pi^0)/\Gamma_{total}$ Γ_5/Γ

VALUE (units 10^{-3})	CL%	DOCUMENT ID		TECN	COMMENT
<0.51	90	[19] HE	08A	CLEO	$e^+e^- \to \ell^+\ell^-\gamma\gamma$

[19] Authors assume B($\Upsilon(2S) \to e^+e^-$) + B($\Upsilon(1S) \to \mu^+\mu^-$) = 4.06%.

$\Gamma(\Upsilon(1S)\pi^+\pi^-)/\Gamma_{total}$ Γ_6/Γ

Abbreviation MM in the *COMMENT* field below stands for missing mass.

VALUE (units 10^{-2})	EVTS	DOCUMENT ID		TECN	COMMENT
4.37±0.08 OUR AVERAGE					
4.32±0.07±0.13	90k	[20] LEES	11L	BABR	$\Upsilon(3S) \to \pi^+\pi^-\ell^+\ell^-$
4.46±0.01±0.13	190k	[21] BHARI	09	CLEO	$e^+e^- \to \pi^+\pi^-$ MM
4.17±0.06±0.19	6.4K	[22] AUBERT	08BP	BABR	10.58 $e^+e^- \to \gamma\pi^+\pi^-\ell^+\ell^-$
4.52±0.35	11830	[23] BUTLER	94B	CLE2	$e^+e^- \to \pi^+\pi^-$X, $\pi^+\pi^-\ell^+\ell^-$
4.46±0.34±0.50	451	[23] WU	93	CUSB	$\Upsilon(3S) \to \pi^+\pi^-\ell^+\ell^-$
4.46±0.30	11221	[23] BROCK	91	CLEO	$e^+e^- \to \pi^+\pi^-$X, $\pi^+\pi^-\ell^+\ell^-$
• • • We do not use the following data for averages, fits, limits, etc. • • •					
4.9 ±1.0	22	GREEN	82	CLEO	$\Upsilon(3S) \to \pi^+\pi^-\ell^+\ell^-$
3.9 ±1.3	26	MAGERAS	82	CUSB	$\Upsilon(3S) \to \pi^+\pi^-\ell^+\ell^-$

[20] Using B($\Upsilon(1S) \to e^+e^-$) = (2.38 ± 0.11)% and B($\Upsilon(1S) \to \mu^+\mu^-$) = (2.48 ± 0.05)%.
[21] A weighted average of the inclusive and exclusive results.
[22] Using B($\Upsilon(2S) \to e^+e^-$) = (1.91 ± 0.16)%, B($\Upsilon(2S) \to \mu^+\mu^-$) = (1.93 ± 0.17)%, and $\Gamma_{ee}(\Upsilon(3S))$ = 0.443 ± 0.008 keV.
[23] Using B($\Upsilon(1S) \to \mu^+\mu^-$) = (2.48 ± 0.06)%. With the assumption of $e\mu$ universality.

$\Gamma(\Upsilon(2S)\pi^+\pi^-)/\Gamma(\Upsilon(1S)\pi^+\pi^-)$ Γ_2/Γ_6

VALUE	EVTS	DOCUMENT ID		TECN	COMMENT
• • • We do not use the following data for averages, fits, limits, etc. • • •					
0.577±0.026±0.060	800	[24] AUBERT	08BP	BABR	$e^+e^- \to \gamma\pi^+\pi^-\ell^+\ell^-$

[24] Using B($\Upsilon(1S) \to e^+e^-$) = (2.38 ± 0.11)%, B($\Upsilon(1S) \to \mu^+\mu^-$) = (2.48 ± 0.05)%, B($\Upsilon(2S) \to e^+e^-$) = (1.91 ± 0.16)%, and B($\Upsilon(2S) \to \mu^+\mu^-$) = (1.93 ± 0.17)%. Not independent of other values reported by AUBERT 08BP.

$\Gamma(\Upsilon(1S)\pi^0\pi^0)/\Gamma_{total}$ Γ_7/Γ

VALUE (units 10^{-2})	EVTS	DOCUMENT ID		TECN	COMMENT
2.20±0.13 OUR AVERAGE					
2.24±0.09±0.11	6584	[25] BHARI	09	CLEO	$e^+e^- \to \pi^0\pi^0\ell^+\ell^-$
1.99±0.34	56	[26] BUTLER	94B	CLE2	$e^+e^- \to \pi^0\pi^0\ell^+\ell^-$
2.2 ±0.4 ±0.3	33	[27] HEINTZ	92	CSB2	$e^+e^- \to \pi^0\pi^0\ell^+\ell^-$

[25] Authors assume B($\Upsilon(1S) \to e^+e^-$) + B($\Upsilon(1S) \to \mu^+\mu^-$) = 4.96%.
[26] Using B($\Upsilon(1S) \to \mu^+\mu^-$) = (2.48 ± 0.06)% and assuming $e\mu$ universality.
[27] Using B($\Upsilon(1S) \to \mu^+\mu^-$) = (2.57 ± 0.07)% and assuming $e\mu$ universality. Supersedes HEINTZ 91.

$\Gamma(\Upsilon(1S)\pi^0\pi^0)/\Gamma(\Upsilon(1S)\pi^+\pi^-)$ Γ_7/Γ_6

VALUE	DOCUMENT ID		TECN	COMMENT
• • • We do not use the following data for averages, fits, limits, etc. • • •				
0.501±0.043	[28] BHARI	09	CLEO	$e^+e^- \to \Upsilon(3S)$

[28] Not independent of other values reported by BHARI 09.

$\Gamma(\Upsilon(1S)\eta)/\Gamma_{total}$ Γ_8/Γ

VALUE (units 10^{-3})	CL%	DOCUMENT ID		TECN	COMMENT
<0.1	90	[29] LEES	11L	BABR	$\Upsilon(3S) \to (\pi^+\pi^-)(\gamma\gamma)\ell^+\ell^-$
• • • We do not use the following data for averages, fits, limits, etc. • • •					
<0.8	90	[29,30] AUBERT	08BP	BABR	$e^+e^- \to \gamma\pi^+\pi^-\pi^0\ell^+\ell^-$
<0.18	90	[31] HE	08A	CLEO	$e^+e^- \to \ell^+\ell^-\eta$
<2.2	90	BROCK	91	CLEO	$e^+e^- \to \ell^+\ell^-\eta$

[29] Using B($\Upsilon(1S) \to e^+e^-$) = (2.38 ± 0.11)%, B($\Upsilon(1S) \to \mu^+\mu^-$) = (2.48 ± 0.05)%.
[30] Using $\Gamma_{ee}(\Upsilon(3S))$ = 0.443 ± 0.008 keV.
[31] Authors assume B($\Upsilon(1S) \to e^+e^-$) + B($\Upsilon(1S) \to \mu^+\mu^-$) = 4.96%.

$\Gamma(\Upsilon(1S)\eta)/\Gamma(\Upsilon(1S)\pi^+\pi^-)$ Γ_8/Γ_6

VALUE (units 10^{-2})	CL%	DOCUMENT ID		TECN	COMMENT
<0.23	90	[32] LEES	11L	BABR	$\Upsilon(3S) \to (\pi^+\pi^-)(\gamma\gamma)\ell^+\ell^-$
• • • We do not use the following data for averages, fits, limits, etc. • • •					
<1.9	90	[33] AUBERT	08BP	BABR	$e^+e^- \to \gamma\pi^+\pi^-(\pi^0)\ell^+\ell^-$

[32] Not independent of other values reported by LEES 11L.
[33] Not independent of other values reported by AUBERT 08BP.

$\Gamma(\Upsilon(1S)\pi^0)/\Gamma_{total}$ Γ_9/Γ

VALUE (units 10^{-3})	CL%	DOCUMENT ID		TECN	COMMENT
<0.07	90	[34] HE	08A	CLEO	$e^+e^- \to \ell^+\ell^-\gamma\gamma$

[34] Authors assume B($\Upsilon(1S) \to e^+e^-$) + B($\Upsilon(1S) \to \mu^+\mu^-$) = 4.96%.

$\Gamma(h_b(1P)\pi^0)/\Gamma_{total}$ Γ_{10}/Γ

VALUE	CL%	DOCUMENT ID		TECN	COMMENT
<1.2 × 10^{-3}	90	[35] GE	11	CLEO	$\Upsilon(3S) \to \pi^0$ anything

[35] Assuming $M(h_b(1P))$ = 9900 MeV and $\Gamma(h_b(1P))$ = 0 MeV, and allowing B($h_b(1P) \to \gamma\eta_b(1S)$) to vary from 0–100%.

$\Gamma(h_b(1P)\pi^0 \to \gamma\eta_b(1S)\pi^0)/\Gamma_{total}$ Γ_{11}/Γ

VALUE (units 10^{-4})	DOCUMENT ID		TECN	COMMENT
4.3±1.1±0.9	LEES	11K	BABR	$\Upsilon(3S) \to \eta_b\gamma\pi^0$

$\Gamma(h_b(1P)\pi^+\pi^-)/\Gamma_{total}$ Γ_{12}/Γ

VALUE (units 10^{-4})	CL%	DOCUMENT ID		TECN	COMMENT
< 1.2	90	[36] LEES	11C	BABR	$e^+e^- \to \pi^+\pi^-X$
• • • We do not use the following data for averages, fits, limits, etc. • • •					
<18		[36] BUTLER	94B	CLE2	$e^+e^- \to \pi^+\pi^-X$
<15		[36] BROCK	91	CLEO	$e^+e^- \to \pi^+\pi^-X$

[36] For $M(h_b(1P))$ = 9900 MeV.

$\Gamma(\tau^+\tau^-)/\Gamma_{total}$ Γ_{13}/Γ

VALUE (units 10^{-2})	EVTS	DOCUMENT ID		TECN	COMMENT
2.29±0.21±0.22	15k	[37] BESSON	07	CLEO	$e^+e^- \to \Upsilon(3S) \to \tau^+\tau^-$

[37] BESSON 07 reports [$\Gamma(\Upsilon(3S) \to \tau^+\tau^-)/\Gamma_{total}$] / [B($\Upsilon(3S) \to \mu^+\mu^-$)] = 1.05 ± 0.08 ± 0.05 which we multiply by our best value B($\Upsilon(3S) \to \mu^+\mu^-$) = (2.18 ± 0.21) × 10^{-2}. Our first error is their experiment's error and our second error is the systematic error from using our best value.

$\Gamma(\tau^+\tau^-)/\Gamma(\mu^+\mu^-)$ Γ_{13}/Γ_{14}

VALUE	EVTS	DOCUMENT ID		TECN	COMMENT
1.05±0.08±0.05	15k	BESSON	07	CLEO	$e^+e^- \to \Upsilon(3S)$

$\Gamma(\mu^+\mu^-)/\Gamma_{total}$ Γ_{14}/Γ

VALUE	EVTS	DOCUMENT ID		TECN	COMMENT
0.0218±0.0021 OUR AVERAGE Error includes scale factor of 2.1. See the ideogram below.					
0.0239±0.0007±0.0010	81k	ADAMS	05	CLEO	$e^+e^- \to \mu^+\mu^-$
0.0202±0.0019±0.0033		CHEN	89B	CLEO	$e^+e^- \to \mu^+\mu^-$
0.0173±0.0015±0.0011		KAARSBERG	89	CSB2	$e^+e^- \to \mu^+\mu^-$
0.033 ±0.013 ±0.007	1096	ANDREWS	83	CLEO	$e^+e^- \to \mu^+\mu^-$

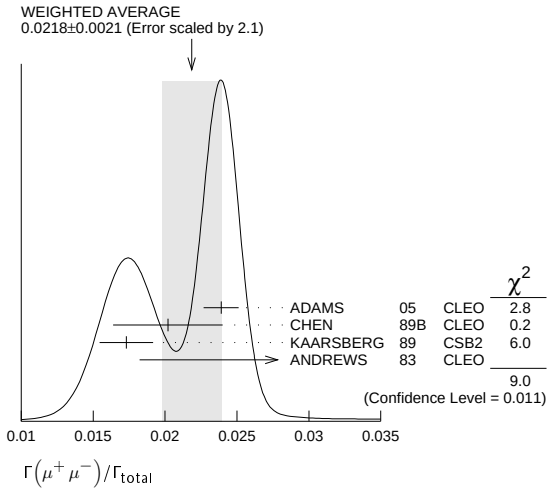

$\Gamma(ggg)/\Gamma_{total}$ Γ_{17}/Γ

VALUE (units 10^{-2})	EVTS	DOCUMENT ID		TECN	COMMENT
35.7±2.6	3M	[38] BESSON	06A	CLEO	$\Upsilon(3S) \to$ hadrons

[38] Calculated using BESSON 06A value of $\Gamma(\gamma gg)/\Gamma(ggg) = (2.72 \pm 0.06 \pm 0.32 \pm 0.37)\%$ and the PDG 08 values of $B(\Upsilon(2S) + \text{anything}) = (10.6 \pm 0.8)\%$, $B(\pi^+\pi^-\Upsilon(1S)) = (4.40 \pm 0.10)\%$, $B(\pi^0\pi^0\Upsilon(1S)) = (2.20 \pm 0.13)\%$, $B(\gamma\chi_{b2}(2P)) = (13.1 \pm 1.6)\%$, $B(\gamma\chi_{b1}(2P)) = (12.6 \pm 1.2)\%$, $B(\gamma\chi_{b0}(2P)) = (5.9 \pm 0.6)\%$, $B(\gamma\chi_{b0}(1P)) = (0.30 \pm 0.11)\%$,$B(\mu^+\mu^-) = (2.18 \pm 0.21)\%$, and $R_{hadrons} = 3.51$. The statistical error is negligible and the systematic error is partially correlated with $\Gamma(\gamma gg)/\Gamma_{total}$ BESSON 06A value.

$\Gamma(\gamma gg)/\Gamma_{total}$ Γ_{18}/Γ

VALUE (units 10^{-2})	EVTS	DOCUMENT ID		TECN	COMMENT
0.97±0.18	60k	[39] BESSON	06A	CLEO	$\Upsilon(3S) \to \gamma +$ hadrons

[39] Calculated using BESSON 06A values of $\Gamma(\gamma gg)/\Gamma(ggg) = (2.72 \pm 0.06 \pm 0.32 \pm 0.37)\%$ and $\Gamma(ggg)/\Gamma_{total}$. The statistical error is negligible and the systematic error is partially correlated with $\Gamma(ggg)/\Gamma_{total}$ BESSON 06A value.

$\Gamma(\gamma gg)/\Gamma(ggg)$ Γ_{18}/Γ_{17}

VALUE (units 10^{-2})	EVTS	DOCUMENT ID		TECN	COMMENT
2.72±0.06±0.49	3M	BESSON	06A	CLEO	$\Upsilon(3S) \to (\gamma +)$ hadrons

$\Gamma(\overline{^2H}\text{ anything})/\Gamma_{total}$ Γ_{19}/Γ

VALUE (units 10^{-5})	DOCUMENT ID		TECN	COMMENT
$2.33 \pm 0.15 \pm 0.31 \atop -0.28$	LEES	14G	BABR	$e^+e^- \to \overline{^2H}X$

$\Gamma(\gamma\chi_{b2}(2P))/\Gamma_{total}$ Γ_{20}/Γ

VALUE	EVTS	DOCUMENT ID		TECN	COMMENT
0.131 ±0.016 OUR AVERAGE Error includes scale factor of 3.4. See the ideogram below.					
0.1579±0.0017±0.0073	568k	ARTUSO	05	CLEO	$e^+e^- \to \gamma X$
0.111 ±0.005 ±0.004	10319	[40] HEINTZ	92	CSB2	$e^+e^- \to \gamma X$
0.135 ±0.003 ±0.017	30741	MORRISON	91	CLE2	$e^+e^- \to \gamma X$

[40] Supersedes NARAIN 91.

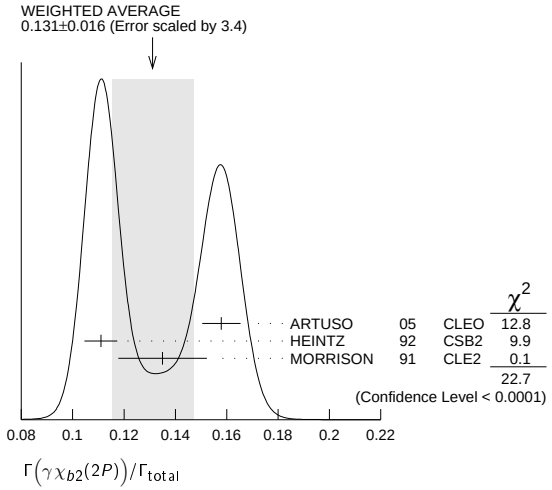

$\Gamma(\gamma\chi_{b1}(2P))/\Gamma_{total}$ Γ_{21}/Γ

VALUE	EVTS	DOCUMENT ID		TECN	COMMENT
0.126 ±0.012 OUR AVERAGE Error includes scale factor of 2.4. See the ideogram below.					
0.1454±0.0018±0.0073	537k	ARTUSO	05	CLEO	$e^+e^- \to \gamma X$
0.115 ±0.005 ±0.005	11147	[41] HEINTZ	92	CSB2	$e^+e^- \to \gamma X$
0.105 $^{+0.003}_{-0.002}$ ±0.013	25759	MORRISON	91	CLE2	$e^+e^- \to \gamma X$

[41] Supersedes NARAIN 91.

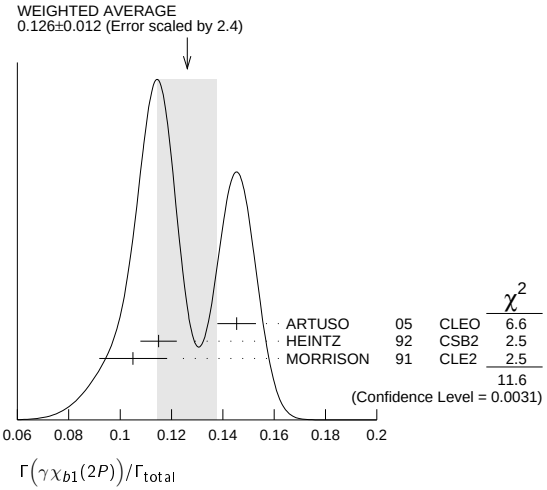

$\Gamma(\gamma\chi_{b0}(2P))/\Gamma_{total}$ Γ_{22}/Γ

VALUE	EVTS	DOCUMENT ID		TECN	COMMENT
0.059 ±0.006 OUR AVERAGE Error includes scale factor of 1.4. See the ideogram below.					
0.0677±0.0020±0.0065	225k	ARTUSO	05	CLEO	$e^+e^- \to \gamma X$
0.060 ±0.004 ±0.006	4959	[42] HEINTZ	92	CSB2	$e^+e^- \to \gamma X$
0.049 $^{+0.003}_{-0.004}$ ±0.006	9903	MORRISON	91	CLE2	$e^+e^- \to \gamma X$

[42] Supersedes NARAIN 91.

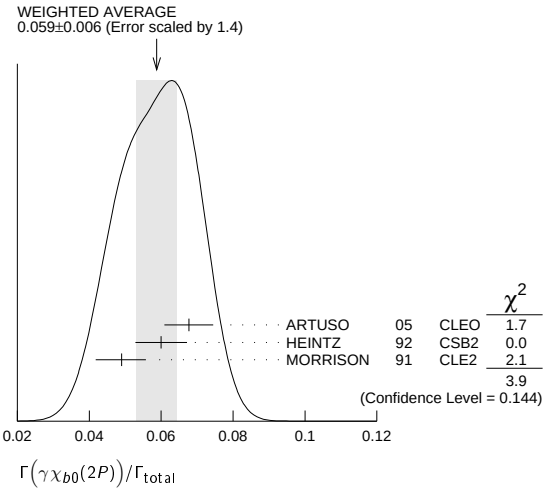

$\Gamma(\gamma\chi_{b2}(1P))/\Gamma_{total}$ Γ_{23}/Γ

VALUE (units 10^{-3})	CL%	EVTS	DOCUMENT ID		TECN	COMMENT
9.9±1.2 OUR AVERAGE Error includes scale factor of 1.9.						
7.6±1.2±0.4		126	[43,44] KORNICER	11	CLEO	$e^+e^- \to \gamma\gamma\ell^+\ell^-$
10.5±0.3 $^{+0.7}_{-0.6}$		9.7k	LEES	11J	BABR	$\Upsilon(3S) \to X\gamma$
• • • We do not use the following data for averages, fits, limits, etc. • • •						
<19	90		[45] ASNER	08A	CLEO	$\Upsilon(3S) \to \gamma +$ hadrons
seen			[46] HEINTZ	92	CSB2	$e^+e^- \to \gamma\gamma\ell^+\ell^-$

[43] Assuming $B(\Upsilon(1S) \to \ell^+\ell^-) = (2.48 \pm 0.05)\%$.

[44] KORNICER 11 reports $[\Gamma(\Upsilon(3S) \to \gamma\chi_{b2}(1P))/\Gamma_{total}] \times [B(\chi_{b2}(1P) \to \gamma\Upsilon(1S))] = (1.435 \pm 0.162 \pm 0.169) \times 10^{-3}$ which we divide by our best value $B(\chi_{b2}(1P) \to \gamma\Upsilon(1S)) = (18.8 \pm 1.1) \times 10^{-2}$. Our first error is their experiment's error and our second error is the systematic error from using our best value.

[45] ASNER 08A reports $[\Gamma(\Upsilon(3S) \to \gamma\chi_{b2}(1P))/\Gamma_{total}] / [B(\Upsilon(2S) \to \gamma\chi_{b2}(1P))] < 27.1 \times 10^{-2}$ which we multiply by our best value $B(\Upsilon(2S) \to \gamma\chi_{b2}(1P)) = 7.15 \times 10^{-2}$.

[46] HEINTZ 92, while unable to distinguish between different J states, measures $\sum_J B(\Upsilon(3S) \to \gamma\chi_{bJ}) \times B(\chi_{bJ} \to \gamma\Upsilon(1S)) = (1.7 \pm 0.4 \pm 0.6) \times 10^{-3}$ for J = 0,1,2 using inclusive $\Upsilon(1S)$ decays and $(1.2^{+0.4}_{-0.3} \pm 0.09) \times 10^{-3}$ for $J = 1,2$ using $\Upsilon(1S) \to \ell^+\ell^-$.

$\Gamma(\gamma\chi_{b1}(1P))/\Gamma_{total}$ Γ_{24}/Γ

VALUE (units 10^{-3})	CL%	EVTS	DOCUMENT ID		TECN	COMMENT
0.9±0.5 OUR AVERAGE Error includes scale factor of 1.8.						
$1.5 \pm 0.4 \pm 0.1$		50	[47,48] KORNICER	11	CLEO	$e^+e^- \to \gamma\gamma\ell^+\ell^-$
$0.5 \pm 0.3^{+0.2}_{-0.1}$			LEES	11J	BABR	$\Upsilon(3S) \to X\gamma$
• • • We do not use the following data for averages, fits, limits, etc. • • •						
<1.7	90		[49] ASNER	08A	CLEO	$\Upsilon(3S) \to \gamma +$ hadrons
seen			[50] HEINTZ	92	CSB2	$e^+e^- \to \gamma\gamma\ell^+\ell^-$

[47] Assuming $B(\Upsilon(1S) \to \ell^+\ell^-) = (2.48 \pm 0.05)\%$.

[48] KORNICER 11 reports $[\Gamma(\Upsilon(3S) \to \gamma\chi_{b1}(1P))/\Gamma_{total}] \times [B(\chi_{b1}(1P) \to \gamma\Upsilon(1S))] = (5.38 \pm 1.20 \pm 0.95) \times 10^{-4}$ which we divide by our best value $B(\chi_{b1}(1P) \to \gamma\Upsilon(1S)) = (35.0 \pm 2.1) \times 10^{-2}$. Our first error is their experiment's error and our second error is the systematic error from using our best value.

[49] ASNER 08A reports $[\Gamma(\Upsilon(3S) \to \gamma\chi_{b1}(1P))/\Gamma_{total}] / [B(\Upsilon(2S) \to \gamma\chi_{b1}(1P))] < 2.5 \times 10^{-2}$ which we multiply by our best value $B(\Upsilon(2S) \to \gamma\chi_{b1}(1P)) = 6.9 \times 10^{-2}$.

[50] HEINTZ 92, while unable to distinguish between different J states, measures $\sum_J B(\Upsilon(3S) \to \gamma\chi_{bJ}) \times B(\chi_{bJ} \to \gamma\Upsilon(1S)) = (1.7 \pm 0.4 \pm 0.6) \times 10^{-3}$ for J = 0,1,2 using inclusive $\Upsilon(1S)$ decays and $(1.2^{+0.4}_{-0.3} \pm 0.09) \times 10^{-3}$ for $J = 1,2$ using $\Upsilon(1S) \to \ell^+\ell^-$.

$\Gamma(\gamma\chi_{b0}(1P))/\Gamma_{total}$ Γ_{25}/Γ

VALUE (units 10^{-2})	CL%	EVTS	DOCUMENT ID		TECN	COMMENT
0.27±0.04 OUR AVERAGE						
$0.27 \pm 0.04 \pm 0.02$		2.3k	LEES	11J	BABR	$\Upsilon(3S) \to X\gamma$
$0.30 \pm 0.04 \pm 0.10$		8.7k	ARTUSO	05	CLEO	$e^+e^- \to \gamma X$
• • • We do not use the following data for averages, fits, limits, etc. • • •						
<0.8	90		[51] ASNER	08A	CLEO	$\Upsilon(3S) \to \gamma +$ hadrons

[51] ASNER 08A reports $[\Gamma(\Upsilon(3S) \to \gamma\chi_{b0}(1P))/\Gamma_{total}] / [B(\Upsilon(2S) \to \gamma\chi_{b0}(1P))] < 21.9 \times 10^{-2}$ which we multiply by our best value $B(\Upsilon(2S) \to \gamma\chi_{b0}(1P)) = 3.8 \times 10^{-2}$.

$\Gamma(\gamma\eta_b(2S))/\Gamma_{total}$ Γ_{26}/Γ

VALUE (units 10^{-4})	CL%	DOCUMENT ID		TECN	COMMENT
< 6.2	90	ARTUSO	05	CLEO	$e^+e^- \to \gamma X$
• • • We do not use the following data for averages, fits, limits, etc. • • •					
<19	90	LEES	11J	BABR	$\Upsilon(3S) \to X\gamma$

$\Gamma(\gamma\eta_b(1S))/\Gamma_{total}$ Γ_{27}/Γ

VALUE (units 10^{-4})	CL%	EVTS	DOCUMENT ID		TECN	COMMENT
5.1±0.7 OUR AVERAGE						
$7.1 \pm 1.8 \pm 1.3$		2.3 ± 0.5k	[52] BONVICINI	10	CLEO	$\Upsilon(3S) \to \gamma X$
$4.8 \pm 0.5 \pm 0.6$		19 ± 3k	[52] AUBERT	09AQ	BABR	$\Upsilon(3S) \to \gamma X$
• • • We do not use the following data for averages, fits, limits, etc. • • •						
<8.5	90		LEES	11J	BABR	$\Upsilon(3S) \to X\gamma$
$4.8 \pm 0.5 \pm 1.2$		19 ± 3k	[52,53] AUBERT	08V	BABR	$\Upsilon(3S) \to \gamma X$
<4.3	90		[54] ARTUSO	05	CLEO	$e^+e^- \to \gamma X$

[52] Assuming $\Gamma_{\eta_b(1S)} = 10$ MeV.

[53] Systematic error re-evaluated by AUBERT 09AQ.

[54] Superseded by BONVICINI 10.

$\Gamma(\gamma A^0 \to \gamma$ hadrons$)/\Gamma_{total}$ Γ_{28}/Γ

(0.3 GeV < m_{A^0} < 7 GeV)

VALUE	CL%	DOCUMENT ID		TECN	COMMENT
<8 × 10⁻⁵	90	[55] LEES	11H	BABR	$\Upsilon(3S) \to \gamma$ hadrons

[55] For a narrow scalar or pseudoscalar A^0, excluding known resonances, with mass in the range 0.3–7 GeV. Measured 90% CL limits as a function of m_{A^0} range from 1×10^{-6} to 8×10^{-5}.

$\Gamma(\gamma X \to \gamma + \geq 4$ prongs$)/\Gamma_{total}$ Γ_{29}/Γ

(1.5 GeV < m_X < 5.0 GeV)

VALUE (units 10^{-4})	CL%	DOCUMENT ID		TECN	COMMENT
<2.2	95	ROSNER	07A	CLEO	$e^+e^- \to \gamma X$

$\Gamma(\gamma a_1^0 \to \gamma\mu^+\mu^-)/\Gamma_{total}$ Γ_{30}/Γ

VALUE (units 10^{-6})	CL%	DOCUMENT ID		TECN	COMMENT
<5.5	90	[56] AUBERT	09Z	BABR	$e^+e^- \to \gamma a_1^0 \to \gamma\mu^+\mu^-$

[56] For a narrow scalar or pseudoscalar a_1^0 with mass in the range 212–9300 MeV, excluding J/ψ and $\psi(2S)$. Measured 90% CL limits as a function of $m_{a_1^0}$ range from 0.27–5.5 × 10^{-6}.

$\Gamma(\gamma a_1^0 \to \gamma\tau^+\tau^-)/\Gamma_{total}$ Γ_{31}/Γ

VALUE	CL%	DOCUMENT ID		TECN	COMMENT
<1.6 × 10⁻⁴	90	[57] AUBERT	09P	BABR	$e^+e^- \to \gamma a_1^0 \to \gamma\tau^+\tau^-$

[57] For a narrow scalar or pseudoscalar a_1^0 with $M(\tau^+\tau^-)$ in the ranges 4.03–9.52 and 9.61–10.10 GeV. Measured 90% CL limits as a function of $M(\tau^+\tau^-)$ range from 1.5–16 × 10^{-5}.

LEPTON FAMILY NUMBER (*LF*) VIOLATING MODES

$\Gamma(e^\pm\tau^\mp)/\Gamma_{total}$ Γ_{32}/Γ

VALUE (units 10^{-6})	CL%	DOCUMENT ID		TECN	COMMENT
<4.2	90	LEES	10B	BABR	$e^+e^- \to e^\pm\tau^\mp$

$\Gamma(\mu^\pm\tau^\mp)/\Gamma_{total}$ Γ_{33}/Γ

VALUE (units 10^{-6})	CL%	DOCUMENT ID		TECN	COMMENT
< 3.1	90	LEES	10B	BABR	$e^+e^- \to \mu^\pm\tau^\mp$
• • • We do not use the following data for averages, fits, limits, etc. • • •					
<20.3	95	LOVE	08A	CLEO	$e^+e^- \to \mu^\pm\tau^\mp$

$\Upsilon(3S)$ REFERENCES

LEES	14G	PR D89 111102	J.P. Lees *et al.*	(BABAR Collab.)
GE	11	PR D84 032008	J.Y. Ge *et al.*	(CLEO Collab.)
KORNICER	11	PR D83 054003	M. Kornicer *et al.*	(CLEO Collab.)
LEES	11C	PR D84 011104	J.P. Lees *et al.*	(BABAR Collab.)
LEES	11H	PRL 107 221803	J.P. Lees *et al.*	(BABAR Collab.)
LEES	11J	PR D84 072002	J.P. Lees *et al.*	(BABAR Collab.)
LEES	11K	PR D84 091101	J.P. Lees *et al.*	(BABAR Collab.)
LEES	11L	PR D84 092003	J.P. Lees *et al.*	(BABAR Collab.)
BONVICINI	10	PR D81 031104	G. Bonvicini *et al.*	(CLEO Collab.)
LEES	10B	PRL 104 151802	J.P. Lees *et al.*	(BABAR Collab.)
AUBERT	09AQ	PRL 103 161801	B. Aubert *et al.*	(BABAR Collab.)
AUBERT	09P	PRL 103 181801	B. Aubert *et al.*	(BABAR Collab.)
AUBERT	09Z	PRL 103 081803	B. Aubert *et al.*	(BABAR Collab.)
BHARI	09	PR D79 011103	S.R. Bhari *et al.*	(CLEO Collab.)
ASNER	08A	PR D78 091103	D.M. Asner *et al.*	(CLEO Collab.)
AUBERT	08BP	PR D78 112002	B. Aubert *et al.*	(BABAR Collab.)
AUBERT	08V	PRL 101 071801	B. Aubert *et al.*	(BABAR Collab.)
HE	08A	PRL 101 192001	Q. He *et al.*	(CLEO Collab.)
LOVE	08A	PRL 101 201601	W. Love *et al.*	(CLEO Collab.)
PDG	08	PL B667 1	C. Amsler *et al.*	(PDG Collab.)
BESSON	07	PRL 98 052002	D. Besson *et al.*	(CLEO Collab.)
ROSNER	07A	PR D76 117102	J.L. Rosner *et al.*	(CLEO Collab.)
BESSON	06A	PR D74 012003	D. Besson *et al.*	(CLEO Collab.)
ROSNER	06	PRL 96 092003	J.L. Rosner *et al.*	(CLEO Collab.)
ADAMS	05	PRL 94 012001	G.S. Adams *et al.*	(CLEO Collab.)
ARTUSO	05	PRL 94 032001	M. Artuso *et al.*	(CLEO Collab.)
ARTAMONOV	00	PL B474 427	A.S. Artamonov *et al.*	
BUTLER	94B	PR D49 40	F. Butler *et al.*	(CLEO Collab.)
WU	93	PL B301 307	Q.W. Wu *et al.*	(CUSB Collab.)
HEINTZ	92	PR D46 1928	U. Heintz *et al.*	(CUSB II Collab.)
BROCK	91	PR D43 1448	I.C. Brock *et al.*	(CLEO Collab.)
HEINTZ	91	PRL 66 1563	U. Heintz *et al.*	(CUSB Collab.)
MORRISON	91	PRL 67 1696	R.J. Morrison *et al.*	(CLEO Collab.)
NARAIN	91	PRL 66 3113	M. Narain *et al.*	(CUSB Collab.)
CHEN	89B	PR D39 3528	W.Y. Chen *et al.*	(CLEO Collab.)
KAARSBERG	89	PRL 62 2077	T.M. Kaarsberg *et al.*	(CUSB Collab.)
BUCHMUEL...	88	HE e^+e^- Physics 412 Editors: A. Ali and P. Soeding, World Scientific, Singapore	W. Buchmueller, S. Cooper	(HANN, DESY, MIT)
COHEN	87	RMP 59 1121	E.R. Cohen, B.N. Taylor	(RISC, NBS)
BARU	86B	ZPHY C32 622 (erratum)	S.E. Baru *et al.*	(NOVO)
KURAEV	85	SJNP 41 466 Translated from YAF 41 733.	E.A. Kuraev, V.S. Fadin	(NOVO)
ARTAMONOV	84	PL 137B 272	A.S. Artamonov *et al.*	(NOVO)
GILES	84B	PR D29 1285	R. Giles *et al.*	(CLEO Collab.)
ANDREWS	83	PRL 50 807	D.E. Andrews *et al.*	(CLEO Collab.)
GREEN	82	PRL 49 617	J. Green *et al.*	(CLEO Collab.)
MAGERAS	82	PL 118B 453	G. Mageras *et al.*	(COLU, CORN, LSU+)

$\chi_{b1}(3P)$

$I^G(J^{PC}) = 0^+(1^{++})$

Observed in the radiative decay to $\Upsilon(1S, 2S, 3S)$, therefore $C = +$.
J needs confirmation.

$\chi_{b1}(3P)$ MASS

VALUE (MeV)	EVTS	DOCUMENT ID		TECN	COMMENT
10512.1± 2.1± 0.9	351	[1] AAIJ	14BG	LHCB	$pp \to \gamma\mu^+\mu^- X$
• • • We do not use the following data for averages, fits, limits, etc. • • •					
$10515.7^{+\ 2.2\ +\ 1.5}_{-\ 3.9\ -\ 2.1}$	169	[2] AAIJ	14BG	LHCB	$pp \to \gamma\mu^+\mu^- X$
$10511.3 \pm 1.7 \pm 2.5$	182	[3] AAIJ	14BI	LHCB	$pp \to \gamma\mu^+\mu^- X$
10530 ± 5 ± 9		[4] AAD	12A	ATLS	$pp \to \gamma\mu^+\mu^- X$
10551 ±14 ±17		[4] ABAZOV	12Q	D0	$p\overline{p} \to \gamma\mu^+\mu^- X$

[1] The mass of the $\chi_{b1}(3P)$ state obtained by combining the results of AAIJ 14BG with that of AAIJ 14BI. The first uncertainty is experimental and the second attributable to the unknown mass splitting, assumed to be $m_{\chi_{b2}(3P)} - m_{\chi_{b1}(3P)} = 10.5 \pm 1.5$ MeV.

[2] From $\chi_{b1}(3P) \to \Upsilon(1S, 2S)\gamma$ transitions assuming $m_{\chi_{b2}(3P)} - m_{\chi_{b1}(3P)} = 10.5 \pm 1.5$ MeV and allowing for ±30% variation in the $\chi_{b2}(3P)$ production rate relative to that of $\chi_{b1}(3P)$.

[3] From $\chi_{b1}(3P) \to \Upsilon(3S)\gamma$ transition assuming $m_{\chi_{b2}(3P)} - m_{\chi_{b1}(3P)} = 10.5 \pm 1.5$ MeV.

[4] The mass barycenter of the merged lineshapes from the $J = 1$ and 2 states.

$\chi_{b1}(3P)$ DECAY MODES

	Mode	Fraction (Γ_i/Γ)
Γ_1	$\Upsilon(1S)\gamma$	seen
Γ_2	$\Upsilon(2S)\gamma$	seen
Γ_3	$\Upsilon(3S)\gamma$	seen

$\chi_{b1}(3P)$ BRANCHING RATIOS

$\Gamma(\Upsilon(1S)\gamma)/\Gamma_{total}$ Γ_1/Γ

VALUE	EVTS	DOCUMENT ID		TECN	COMMENT
seen	169	[5] AAIJ	14BG	LHCB	$pp \to \gamma\mu^+\mu^- X$
• • • We do not use the following data for averages, fits, limits, etc. • • •					
seen		AAD	12A	ATLS	$pp \to \gamma\mu^+\mu^- X$
seen		ABAZOV	12Q	D0	$p\overline{p} \to \gamma\mu^+\mu^- X$

[5] From $\chi_{b1}(3P) \to \Upsilon(1S,2S)\gamma$ transitions assuming $m_{\chi_{b2}(3P)} - m_{\chi_{b1}(3P)} = 10.5 \pm 1.5$ MeV and allowing for $\pm 30\%$ variation in the $\chi_{b2}(3P)$ production rate relative to that of $\chi_{b1}(3P)$.

$\Gamma(\Upsilon(2S)\gamma)/\Gamma_{total}$ Γ_2/Γ

VALUE	EVTS	DOCUMENT ID		TECN	COMMENT
seen	169	[6] AAIJ	14BG	LHCB	$pp \to \gamma\mu^+\mu^- X$
• • • We do not use the following data for averages, fits, limits, etc. • • •					
seen		AAD	12A	ATLS	$pp \to \gamma\mu^+\mu^- X$

[6] From $\chi_{b1}(3P) \to \Upsilon(1S,2S)\gamma$ transitions assuming $m_{\chi_{b2}(3P)} - m_{\chi_{b1}(3P)} = 10.5 \pm 1.5$ MeV and allowing for $\pm 30\%$ variation in the $\chi_{b2}(3P)$ production rate relative to that of $\chi_{b1}(3P)$.

$\Gamma(\Upsilon(3S)\gamma)/\Gamma_{total}$ Γ_3/Γ

VALUE	EVTS	DOCUMENT ID		TECN	COMMENT
seen	182	AAIJ	14BI	LHCB	$pp \to \gamma\mu^+\mu^- X$

$\chi_{b1}(3P)$ REFERENCES

AAIJ	14BG	JHEP 1410 088	R. Aaij *et al.*	(LHCb Collab.)
AAIJ	14BI	EPJ C74 3092	R. Aaij *et al.*	(LHCb Collab.)
AAD	12A	PRL 108 152001	G. Aad *et al.*	(ATLAS Collab.)
ABAZOV	12Q	PR D86 031103	V.M. Abazov *et al.*	(D0 Collab.)

$\Upsilon(4S)$

$I^G(J^{PC}) = 0^-(1^{--})$

also known as $\Upsilon(10580)$

$\Upsilon(4S)$ MASS

VALUE (MeV)	DOCUMENT ID		TECN	COMMENT
10579.4±1.2 OUR AVERAGE				
10579.3±0.4±1.2	AUBERT	05Q	BABR	$e^+e^- \to$ hadrons
10580.0±3.5	[1] BEBEK	87	CLEO	$e^+e^- \to$ hadrons
• • • We do not use the following data for averages, fits, limits, etc. • • •				
10577.4±1.0	[2] LOVELOCK	85	CUSB	$e^+e^- \to$ hadrons

[1] Reanalysis of BESSON 85.
[2] No systematic error given.

$\Upsilon(4S)$ WIDTH

VALUE (MeV)	DOCUMENT ID		TECN	COMMENT
20.5±2.5 OUR AVERAGE				
20.7±1.6±2.5	AUBERT	05Q	BABR	$e^+e^- \to$ hadrons
20 ±2 ±4	BESSON	85	CLEO	$e^+e^- \to$ hadrons
• • • We do not use the following data for averages, fits, limits, etc. • • •				
25 ±2.5	LOVELOCK	85	CUSB	$e^+e^- \to$ hadrons

$\Upsilon(4S)$ DECAY MODES

	Mode	Fraction (Γ_i/Γ)	Confidence level
Γ_1	$B\overline{B}$	> 96 %	95%
Γ_2	B^+B^-	(51.4 ±0.6) %	
Γ_3	D_s^+ anything + c.c.	(17.8 ±2.6) %	
Γ_4	$B^0\overline{B}^0$	(48.6 ±0.6) %	
Γ_5	$J/\psi K_S^0 + (J/\psi,\ \eta_c) K_S^0$	< 4 $\times 10^{-7}$	90%
Γ_6	non-$B\overline{B}$	< 4 %	95%
Γ_7	e^+e^-	(1.57±0.08) $\times 10^{-5}$	
Γ_8	$\rho^+\rho^-$	< 5.7 $\times 10^{-6}$	90%
Γ_9	$K^*(892)^0\overline{K}^0$	< 2.0 $\times 10^{-6}$	90%
Γ_{10}	$J/\psi(1S)$ anything	< 1.9 $\times 10^{-4}$	95%
Γ_{11}	D^{*+} anything + c.c.	< 7.4 %	90%
Γ_{12}	ϕ anything	(7.1 ±0.6) %	
Γ_{13}	$\phi\eta$	< 1.8 $\times 10^{-6}$	90%
Γ_{14}	$\phi\eta'$	< 4.3 $\times 10^{-6}$	90%
Γ_{15}	$\rho\eta$	< 1.3 $\times 10^{-6}$	90%
Γ_{16}	$\rho\eta'$	< 2.5 $\times 10^{-6}$	90%
Γ_{17}	$\Upsilon(1S)$ anything	< 4 $\times 10^{-3}$	90%
Γ_{18}	$\Upsilon(1S)\pi^+\pi^-$	(8.2 ±0.4) $\times 10^{-5}$	
Γ_{19}	$\Upsilon(1S)\eta$	(1.81±0.18) $\times 10^{-4}$	
Γ_{20}	$\Upsilon(2S)\pi^+\pi^-$	(8.2 ±0.8) $\times 10^{-5}$	
Γ_{21}	$h_b(1P)\pi^+\pi^-$	not seen	
Γ_{22}	$h_b(1P)\eta$	(2.18±0.21) $\times 10^{-3}$	
Γ_{23}	$\overline{2H}$ anything	< 1.3 $\times 10^{-5}$	90%

Double Radiative Decays

Γ_{24}	$\gamma\gamma\,\Upsilon(D) \to \gamma\gamma\eta\,\Upsilon(1S)$	< 2.3 $\times 10^{-5}$		90%

$\Upsilon(4S)$ PARTIAL WIDTHS

$\Gamma(e^+e^-)$ Γ_7

VALUE (keV)	DOCUMENT ID		TECN	COMMENT
0.272±0.029 OUR AVERAGE	Error includes scale factor of 1.5.			See the ideogram below.
0.321±0.017±0.029	AUBERT	05Q	BABR	$e^+e^- \to$ hadrons
0.28 ±0.05 ±0.01	[1] ALBRECHT	95E	ARG	$e^+e^- \to$ hadrons
0.192±0.007±0.038	BESSON	85	CLEO	$e^+e^- \to$ hadrons
0.283±0.037	LOVELOCK	85	CUSB	$e^+e^- \to$ hadrons

[1] Using LEYAOUANC 77 parametrization of $\Gamma(s)$.

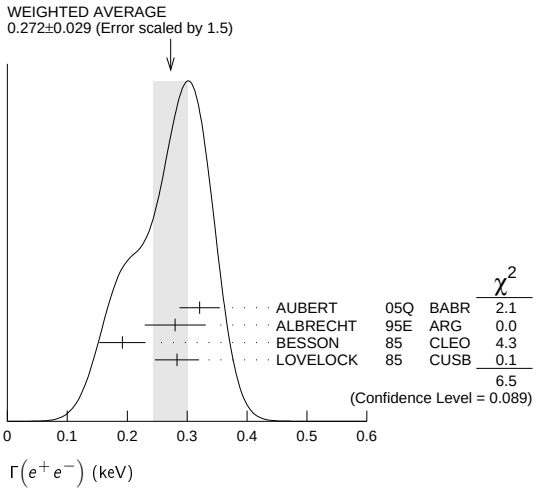

$\Upsilon(4S)$ BRANCHING RATIOS

$B\overline{B}$ DECAYS

The ratio of branching fraction to charged and neutral B mesons is often derived assuming isospin invariance in the decays, and relies on the knowledge of the B^+/B^0 lifetime ratio. "OUR EVALUATION" is obtained based on averages of rescaled data listed below. The average and rescaling were performed by the Heavy Flavor Averaging Group (HFLAV) and are described at http://www.slac.stanford.edu/xorg/hflav/. The averaging/rescaling procedure takes into account the common dependence of the measurement on the value of the lifetime ratio.

$\Gamma(B^+B^-)/\Gamma_{total}$ Γ_2/Γ

VALUE	DOCUMENT ID
0.514±0.006 OUR EVALUATION	Assuming B($\Upsilon(4S) \to B\overline{B}$) = 1

$\Gamma(D_s^+$ anything + c.c.$)/\Gamma_{total}$ Γ_3/Γ

VALUE	DOCUMENT ID		TECN	COMMENT
0.178±0.021±0.016	[1] ARTUSO	05B	CLE3	$e^+e^- \to D_s X$

[1] ARTUSO 05B reports $[\Gamma(\Upsilon(4S) \to D_s^+$ anything + c.c.$)/\Gamma_{total}] \times [B(D_s^+ \to \phi\pi^+)]$ = (8.0 ± 0.2 ± 0.9) × 10^{-3} which we divide by our best value $B(D_s^+ \to \phi\pi^+)$ = (4.5 ± 0.4) × 10^{-2}. Our first error is their experiment's error and our second error is the systematic error from using our best value.

$\Gamma(B^0\overline{B}^0)/\Gamma_{total}$ Γ_4/Γ

VALUE	DOCUMENT ID		TECN	COMMENT
0.486±0.006 OUR EVALUATION	Assuming B($\Upsilon(4S) \to B\overline{B}$) = 1			
• • • We do not use the following data for averages, fits, limits, etc. • • •				
0.487±0.010±0.008	[1] AUBERT,B	05H	BABR	$\Upsilon(4S) \to \overline{B}B \to D^*\ell\nu_\ell$

[1] Direct measurement. This value is averaged with the value extracted from the $\Gamma(B^+B^-)$ / $\Gamma(B^0\overline{B}^0)$ measurements.

Meson Particle Listings

$\Upsilon(4S)$

$\Gamma(B^+B^-)/\Gamma(B^0\overline{B}^0)$ Γ_2/Γ_4

VALUE	DOCUMENT ID		TECN	COMMENT
1.058±0.024 OUR EVALUATION				
1.006±0.036±0.031	[1] AUBERT	04F	BABR	$\Upsilon(4S) \to B\overline{B} \to J/\psi K$
1.01 ±0.03 ±0.09	[1] HASTINGS	03	BELL	$\Upsilon(4S) \to B\overline{B} \to$ dileptons
1.058±0.084±0.136	[2] ATHAR	02	CLEO	$\Upsilon(4S) \to B\overline{B} \to D^*\ell\nu$
1.10 ±0.06 ±0.05	[3] AUBERT	02	BABR	$\Upsilon(4S) \to B\overline{B} \to (c\overline{c})K^*$
1.04 ±0.07 ±0.04	[4] ALEXANDER	01	CLEO	$\Upsilon(4S) \to B\overline{B} \to J/\psi K^*$

[1] HASTINGS 03 and AUBERT 04F assume $\tau(B^+)\ /\ \tau(B^0) = 1.083 \pm 0.017$.
[2] ATHAR 02 assumes $\tau(B^+)\ /\ \tau(B^0) = 1.074 \pm 0.028$. Supersedes BARISH 95.
[3] AUBERT 02 assumes $\tau(B^+)\ /\ \tau(B^0) = 1.062 \pm 0.029$.
[4] ALEXANDER 01 assumes $\tau(B^+)\ /\ \tau(B^0) = 1.066 \pm 0.024$.

$[\Gamma(J/\psi K^0_S) + \Gamma((J/\psi, \eta_c)K^0_S)]/\Gamma_{\text{total}}$ Γ_5/Γ

Forbidden by CP invariance.

VALUE (units 10^{-7})	CL%	DOCUMENT ID		TECN	COMMENT
<4	90	[1] TAJIMA	07A	BELL	$\Upsilon(4S) \to B^0\overline{B}^0$

[1] $\Upsilon(4S)$ with $CP = +1$ decays to the final state with $CP = -1$.

non-$B\overline{B}$ DECAYS

$\Gamma(\text{non-}B\overline{B})/\Gamma_{\text{total}}$ Γ_6/Γ

VALUE	CL%	DOCUMENT ID		TECN	COMMENT
<0.04	95	BARISH	96B	CLEO	e^+e^-

$\Gamma(e^+e^-)/\Gamma_{\text{total}}$ Γ_7/Γ

VALUE (units 10^{-5})	DOCUMENT ID		TECN	COMMENT
1.57±0.08 OUR AVERAGE				
1.55±0.04±0.07	AUBERT	05Q	BABR	$e^+e^- \to$ hadrons
2.77±0.50±0.49	[1] ALBRECHT	95E	ARG	$e^+e^- \to$ hadrons

[1] Using LEYAOUANC 77 parametrization of $\Gamma(s)$.

$\Gamma(\rho^+\rho^-)/\Gamma_{\text{total}}$ Γ_8/Γ

VALUE	CL%	DOCUMENT ID		TECN	COMMENT
<5.7 × 10^{-6}	90	AUBERT	08BO	BABR	$e^+e^- \to \pi^+\pi^- 2\pi^0$

$\Gamma(K^*(892)^0\overline{K}^0)/\Gamma_{\text{total}}$ Γ_9/Γ

VALUE	CL%	DOCUMENT ID		TECN	COMMENT
<2.0 × 10^{-6}	90	SHEN	13A	BELL	$e^+e^- \to K^*(892)^0\overline{K}^0$

$\Gamma(J/\psi(1S)\text{ anything})/\Gamma_{\text{total}}$ Γ_{10}/Γ

VALUE (units 10^{-4})	CL%	DOCUMENT ID		TECN	COMMENT
<1.9	95	[1] ABE	02D	BELL	$e^+e^- \to J/\psi X \to \ell^+\ell^- X$
• • • We do not use the following data for averages, fits, limits, etc. • • •					
<4.7	90	[1] AUBERT	01C	BABR	$e^+e^- \to J/\psi X \to \ell^+\ell^- X$

[1] Uses $B(J/\psi \to e^+e^-) = 0.0593 \pm 0.0010$ and $B(J/\psi \to \mu^+\mu^-) = 0.0588 \pm 0.0010$.

$\Gamma(D^{*+}\text{ anything} + \text{c.c.})/\Gamma_{\text{total}}$ Γ_{11}/Γ

VALUE	CL%	DOCUMENT ID		TECN	COMMENT
<0.074	90	[1] ALEXANDER	90C	CLEO	e^+e^-

[1] For $x > 0.473$.

$\Gamma(\phi\text{ anything})/\Gamma_{\text{total}}$ Γ_{12}/Γ

VALUE (units 10^{-2})	CL%	DOCUMENT ID		TECN	COMMENT
7.1 ±0.1±0.6		HUANG	07	CLEO	$\Upsilon(4S) \to \phi X$
• • • We do not use the following data for averages, fits, limits, etc. • • •					
<0.23	90	[1] ALEXANDER	90C	CLEO	e^+e^-

[1] For $x > 0.52$.

$\Gamma(\phi\eta)/\Gamma_{\text{total}}$ Γ_{13}/Γ

VALUE (units 10^{-6})	CL%	DOCUMENT ID		TECN	COMMENT
<1.8	90	[1] BELOUS	09	BELL	$e^+e^- \to \phi\eta$
• • • We do not use the following data for averages, fits, limits, etc. • • •					
<2.5	90	AUBERT,BE	06F	BABR	$e^+e^- \to \phi\eta$

[1] Using all intermedite branching fraction values from PDG 08.

$\Gamma(\phi\eta')/\Gamma_{\text{total}}$ Γ_{14}/Γ

VALUE (units 10^{-6})	CL%	DOCUMENT ID		TECN	COMMENT
<4.3	90	[1] BELOUS	09	BELL	$e^+e^- \to \phi\eta'$

[1] Using all intermedite branching fraction values from PDG 08.

$\Gamma(\rho\eta)/\Gamma_{\text{total}}$ Γ_{15}/Γ

VALUE (units 10^{-6})	CL%	DOCUMENT ID		TECN	COMMENT
<1.3	90	[1] BELOUS	09	BELL	$e^+e^- \to \rho\eta$

[1] Using all intermedite branching fraction values from PDG 08.

$\Gamma(\rho\eta')/\Gamma_{\text{total}}$ Γ_{16}/Γ

VALUE (units 10^{-6})	CL%	DOCUMENT ID		TECN	COMMENT
<2.5	90	[1] BELOUS	09	BELL	$e^+e^- \to \rho\eta'$

[1] Using all intermedite branching fraction values from PDG 08.

$\Gamma(\Upsilon(1S)\text{ anything})/\Gamma_{\text{total}}$ Γ_{17}/Γ

VALUE	CL%	DOCUMENT ID		TECN	COMMENT
<0.004	90	ALEXANDER	90C	CLEO	e^+e^-

$\Gamma(\Upsilon(1S)\pi^+\pi^-)/\Gamma_{\text{total}}$ Γ_{18}/Γ

VALUE (units 10^{-5})	CL%	EVTS	DOCUMENT ID		TECN	COMMENT
8.2 ±0.4 OUR AVERAGE						
8.2 ±0.5 ±0.4		515	GUIDO	17	BELL	$\Upsilon(4S) \to \pi^+\pi^-\mu^+\mu^-$
8.5 ±1.3 ±0.2		113 ± 16	[1] SOKOLOV	09	BELL	$e^+e^- \to \pi^+\pi^-\mu^+\mu^-$
8.00±0.64±0.27		430	[2] AUBERT	08BP	BABR	$\Upsilon(4S) \to \pi^+\pi^-\ell^+\ell^-$
• • • We do not use the following data for averages, fits, limits, etc. • • •						
17.8 ±4.0 ±0.3			[3,4] SOKOLOV	07	BELL	$e^+e^- \to \pi^+\pi^-\mu^+\mu^-$
9.0 ±1.5 ±0.2		167 ± 19	[5] AUBERT	06R	BABR	$e^+e^- \to \pi^+\pi^-\mu^+\mu^-$
<12	90		GLENN	99	CLE2	e^+e^-

[1] SOKOLOV 09 reports $[\Gamma(\Upsilon(4S) \to \Upsilon(1S)\pi^+\pi^-)/\Gamma_{\text{total}}] \times [B(\Upsilon(1S) \to \mu^+\mu^-)] = (0.211 \pm 0.030 \pm 0.014) \times 10^{-5}$ which we divide by our best value $B(\Upsilon(1S) \to \mu^+\mu^-) = (2.48 \pm 0.05) \times 10^{-2}$. Our first error is their experiment's error and our second error is the systematic error from using our best value.
[2] Using $B(\Upsilon(1S) \to e^+e^-) = (2.38 \pm 0.11)\%$ and $B(\Upsilon(1S) \to \mu^+\mu^-) = (2.48 \pm 0.05)\%$.
[3] SOKOLOV 07 reports $[\Gamma(\Upsilon(4S) \to \Upsilon(1S)\pi^+\pi^-)/\Gamma_{\text{total}}] \times [B(\Upsilon(1S) \to \mu^+\mu^-)] = (4.42 \pm 0.81 \pm 0.56) \times 10^{-6}$ which we divide by our best value $B(\Upsilon(1S) \to \mu^+\mu^-) = (2.48 \pm 0.05) \times 10^{-2}$. Our first error is their experiment's error and our second error is the systematic error from using our best value.
[4] According to the authors, systematic errors were underestimated.
[5] Superseded by AUBERT 08BP. AUBERT 06R reports $[\Gamma(\Upsilon(4S) \to \Upsilon(1S)\pi^+\pi^-)/\Gamma_{\text{total}}] \times [B(\Upsilon(1S) \to \mu^+\mu^-)] = (2.23 \pm 0.25 \pm 0.27) \times 10^{-6}$ which we divide by our best value $B(\Upsilon(1S) \to \mu^+\mu^-) = (2.48 \pm 0.05) \times 10^{-2}$. Our first error is their experiment's error and our second error is the systematic error from using our best value.

$\Gamma(\Upsilon(1S)\eta)/\Gamma_{\text{total}}$ Γ_{19}/Γ

VALUE (units 10^{-4})	CL%	EVTS	DOCUMENT ID		TECN	COMMENT
1.81±0.18 OUR AVERAGE						
1.70±0.23±0.08		49	GUIDO	17	BELL	$\Upsilon(4S) \to \pi^+\pi^-\pi^0\mu^+\mu^-$
1.96±0.26±0.09		56	[1] AUBERT	08BP	BABR	$\Upsilon(4S) \to \pi^+\pi^-\pi^0\ell^+\ell^-$
• • • We do not use the following data for averages, fits, limits, etc. • • •						
<2.7	90		[2] TAMPONI	15	BELL	$e^+e^- \to \gamma\eta +$ hadrons

[1] Using $B(\Upsilon(1S) \to e^+e^-) = (2.38 \pm 0.11)\%$ and $B(\Upsilon(1S) \to \mu^+\mu^-) = (2.48 \pm 0.05)\%$.
[2] Using $B(\eta \to 2\gamma) = (39.41 \pm 0.20)\%$.

$\Gamma(\Upsilon(1S)\eta)/\Gamma(\Upsilon(1S)\pi^+\pi^-)$ Γ_{19}/Γ_{18}

VALUE	EVTS	DOCUMENT ID		TECN	COMMENT
• • • We do not use the following data for averages, fits, limits, etc. • • •					
2.41±0.40±0.12	56	[1] AUBERT	08BP	BABR	$\Upsilon(4S) \to \pi^+\pi^-(\pi^0)\ell^+\ell^-$

[1] Not independent of other values reported by AUBERT 08BP.

$\Gamma(\Upsilon(2S)\pi^+\pi^-)/\Gamma_{\text{total}}$ Γ_{20}/Γ

VALUE (units 10^{-5})	CL%	EVTS	DOCUMENT ID		TECN	COMMENT
8.2±0.8 OUR AVERAGE						
7.9±1.0±0.4		181	GUIDO	17	BELL	$\Upsilon(4S) \to \pi^+\pi^-\mu^+\mu^-$
8.6±1.1±0.7		220	[1] AUBERT	08BP	BABR	$\Upsilon(4S) \to \pi^+\pi^-\ell^+\ell^-$
• • • We do not use the following data for averages, fits, limits, etc. • • •						
8.8±1.7±0.8		97 ± 15	[2] AUBERT	06R	BABR	$e^+e^- \to \pi^+\pi^-\mu^+\mu^-$
<3.9	90		GLENN	99	CLE2	e^+e^-

[1] Using $B(\Upsilon(2S) \to e^+e^-) = (1.91 \pm 0.16)\%$ and $B(\Upsilon(2S) \to \mu^+\mu^-) = (1.93 \pm 0.17)\%$.
[2] Superseded by AUBERT 08BP. AUBERT 06R reports $[\Gamma(\Upsilon(4S) \to \Upsilon(2S)\pi^+\pi^-)/\Gamma_{\text{total}}] \times [B(\Upsilon(2S) \to \mu^+\mu^-)] = (1.69 \pm 0.26 \pm 0.20) \times 10^{-6}$ which we divide by our best value $B(\Upsilon(2S) \to \mu^+\mu^-) = (1.93 \pm 0.17) \times 10^{-2}$. Our first error is their experiment's error and our second error is the systematic error from using our best value.

$\Gamma(\Upsilon(2S)\pi^+\pi^-)/\Gamma(\Upsilon(1S)\pi^+\pi^-)$ Γ_{20}/Γ_{18}

VALUE	EVTS	DOCUMENT ID		TECN	COMMENT
• • • We do not use the following data for averages, fits, limits, etc. • • •					
1.16±0.16±0.14	220	[1] AUBERT	08BP	BABR	$\Upsilon(4S) \to \pi^+\pi^-\ell^+\ell^-$

[1] Using $B(\Upsilon(1S) \to e^+e^-) = (2.38 \pm 0.11)\%$, $B(\Upsilon(1S) \to \mu^+\mu^-) = (2.48 \pm 0.05)\%$, $B(\Upsilon(2S) \to e^+e^-) = (1.91 \pm 0.16)\%$, and $B(\Upsilon(2S) \to \mu^+\mu^-) = (1.93 \pm 0.17)\%$. Not independent of other values reported by AUBERT 08BP.

$\Gamma(h_b(1P)\pi^+\pi^-)/\Gamma_{\text{total}}$ Γ_{21}/Γ

VALUE	EVTS	DOCUMENT ID		TECN	COMMENT
not seen	(35^{+32}_{-26})k	[1] ADACHI	12	BELL	10.58 $e^+e^- \to h_b(1P)\pi^+\pi^-$

[1] From the upper limit on the ratio of $\sigma(e^+e^- \to h_b(1P)\pi^+\pi^-)$ at the $\Upsilon(4S)$ to that at the $\Upsilon(5S)$ of 0.27.

$\Gamma(h_b(1P)\eta)/\Gamma_{\text{total}}$ Γ_{22}/Γ

VALUE (units 10^{-3})	EVTS	DOCUMENT ID		TECN	COMMENT
2.18±0.11±0.18	112k	[1] TAMPONI	15	BELL	$e^+e^- \to h_b(1P)\eta$

[1] Using $B(\eta \to 2\gamma) = (39.41 \pm 0.20)\%$.

$\Gamma(\overline{^2H}\text{ anything})/\Gamma_{\text{total}}$ Γ_{23}/Γ

VALUE (units 10^{-5})	CL%	DOCUMENT ID		TECN	COMMENT
<1.3	90	ASNER	07	CLEO	$e^+e^- \to \overline{d}X$

Double Radiative Decays

$\Gamma(\gamma\gamma\Upsilon(D) \to \gamma\gamma\eta\Upsilon(1S))/\Gamma_{\text{total}}$ Γ_{24}/Γ

VALUE	CL%	DOCUMENT ID		TECN	COMMENT
$<2.3\times10^{-5}$	90	GUIDO	17	BELL	$\Upsilon(4S) \to \gamma\gamma\pi^+\pi^-\pi^0\mu^+\mu^-$

$\Upsilon(4S)$ REFERENCES

GUIDO	17	PR D96 052005	E. Guido *et al.*	(BELLE Collab.)
TAMPONI	15	PRL 115 142001	U. Tamponi *et al.*	(BELLE Collab.)
SHEN	13A	PR D88 052019	C.P. Shen *et al.*	(BELLE Collab.)
ADACHI	12	PRL 108 032001	I. Adachi *et al.*	(BELLE Collab.)
BELOUS	09	PL B681 400	K. Belous *et al.*	(BELLE Collab.)
SOKOLOV	09	PR D79 051103	A. Sokolov *et al.*	(BELLE Collab.)
AUBERT	08BO	PR D78 071103	B. Aubert *et al.*	(BABAR Collab.)
AUBERT	08BP	PR D78 112002	B. Aubert *et al.*	(BABAR Collab.)
PDG	08	PL B667 1	C. Amsler *et al.*	(PDG Collab.)
ASNER	07	PR D75 012009	D.M. Asner *et al.*	(CLEO Collab.)
HUANG	07	PR D75 012002	G.S. Huang *et al.*	(CLEO Collab.)
SOKOLOV	07	PR D75 071103	A. Sokolov *et al.*	(BELLE Collab.)
TAJIMA	07A	PRL 99 211601	O. Tajima *et al.*	(BELLE Collab.)
AUBERT	06R	PRL 96 232001	B. Aubert *et al.*	(BABAR Collab.)
AUBERT,BE	06F	PR D74 111103	B. Aubert *et al.*	(BABAR Collab.)
ARTUSO	05B	PRL 95 261801	M. Artuso *et al.*	(CLEO Collab.)
AUBERT	05Q	PR D72 032005	B. Aubert *et al.*	(BABAR Collab.)
AUBERT,B	05H	PRL 95 042001	B. Aubert *et al.*	(BABAR Collab.)
AUBERT	04F	PR D69 071101	B.Aubert *et al.*	
HASTINGS	03	PR D67 052004	N.C. Hastings *et al.*	(BELLE Collab.)
ABE	02D	PRL 88 052001	K. Abe *et al.*	(BELLE Collab.)
ATHAR	02	PR D66 052003	S.B. Athar *et al.*	(CLEO Collab.)
AUBERT	02	PR D65 032001	B. Aubert *et al.*	(BABAR Collab.)
ALEXANDER	01	PRL 86 2737	J.P. Alexander *et al.*	(CLEO Collab.)
AUBERT	01C	PRL 87 162002	B. Aubert *et al.*	(BABAR Collab.)
GLENN	99	PR D59 052003	S. Glenn *et al.*	
BARISH	96B	PRL 76 1570	B.C. Barish *et al.*	(CLEO Collab.)
ALBRECHT	95E	ZPHY C65 619	H. Albrecht *et al.*	(ARGUS Collab.)
BARISH	95	PR D51 1014	B.C. Barish *et al.*	(CLEO Collab.)
ALEXANDER	90C	PRL 64 2226	J. Alexander *et al.*	(CLEO Collab.)
BEBEK	87	PR D36 1289	C. Bebek *et al.*	(CLEO Collab.)
BESSON	85	PRL 54 381	D. Besson *et al.*	(CLEO Collab.)
LOVELOCK	85	PRL 54 377	D.M.J. Lovelock *et al.*	(CUSB Collab.)
LEYAOUANC	77	PL B71 397	A. Le Yaouanc *et al.*	(ORSAY)

$Z_b(10610)$

$I^G(J^{PC}) = 1^+(1^{+-})$

was $X(10610)$

Properties incompatible with a $q\overline{q}$ structure (exotic state). See the review on non-$q\overline{q}$ states.

Observed by BONDAR 12 in $\Upsilon(5S)$ decays to $\Upsilon(nS)\pi^+\pi^-$ (n = 1, 2, 3) and $h_b(mP)\pi^+\pi^-$ (m = 1, 2). $J^P = 1^+$ is favored from angular analyses. Isospin = 1 is favored due to observation by KROKOVNY 13 of a corresponding neutral state produced in $\Upsilon(10860) \to \Upsilon(2S)/\Upsilon(3S)\pi^0\pi^0$ decays at a consistent mass.

$Z_b(10610)^\pm$ MASS

VALUE (MeV)	DOCUMENT ID		TECN	COMMENT
10607.2±2.0	[1] BONDAR	12	BELL	$e^+e^- \to$ hadrons
• • • We do not use the following data for averages, fits, limits, etc. • • •				
$10608.5 \pm 3.4^{+3.7}_{-1.4}$	[2] GARMASH	15	BELL	$e^+e^- \to \Upsilon(1S)\pi^+\pi^-$
$10608.1 \pm 1.2^{+1.5}_{-0.2}$	[2] GARMASH	15	BELL	$e^+e^- \to \Upsilon(2S)\pi^+\pi^-$
$10607.4 \pm 1.5^{+0.8}_{-0.2}$	[2] GARMASH	15	BELL	$e^+e^- \to \Upsilon(3S)\pi^+\pi^-$
$10611 \pm 4 \pm 3$	[3] BONDAR	12	BELL	$e^+e^- \to \Upsilon(1S)\pi^+\pi^-$
$10609 \pm 2 \pm 3$	[3] BONDAR	12	BELL	$e^+e^- \to \Upsilon(2S)\pi^+\pi^-$
$10608 \pm 2 \pm 3$	[3] BONDAR	12	BELL	$e^+e^- \to \Upsilon(3S)\pi^+\pi^-$
$10605 \pm 2 \, {}^{+3}_{-1}$	[3] BONDAR	12	BELL	$e^+e^- \to h_b(1P)\pi^+\pi^-$
$10599 \, {}^{+6}_{-3} \, {}^{+5}_{-4}$	[3] BONDAR	12	BELL	$e^+e^- \to h_b(2P)\pi^+\pi^-$

[1] Average of the BONDAR 12 measurements in separate channels.
[2] Correlated with the corresponding result from BONDAR 12.
[3] Superseded by the average measurement of BONDAR 12.

$Z_b(10610)^0$ MASS

VALUE (MeV)	DOCUMENT ID		TECN	COMMENT
10609±4±4	[1] KROKOVNY	13	BELL	$e^+e^- \to \Upsilon(2S)/\Upsilon(3S)\pi^0\pi^0$

[1] From a simultaneous fit to the KROKOVNY 13 Dalitz analysis of $e^+e^- \to \Upsilon(2S)/\Upsilon(3S)\pi^0\pi^0$ decays with fixed width $\Gamma(Z_b(10610)^0) = 18.4$ MeV.

$Z_b(10610)^\pm$ WIDTH

VALUE (MeV)	DOCUMENT ID		TECN	COMMENT
18.4± 2.4	[1] BONDAR	12	BELL	$e^+e^- \to$ hadrons
• • • We do not use the following data for averages, fits, limits, etc. • • •				
$18.5 \pm 5.3^{+6.1}_{-2.3}$	[2] GARMASH	15	BELL	$e^+e^- \to \Upsilon(1S)\pi^+\pi^-$
$20.8 \pm 2.5^{+0.3}_{-2.1}$	[2] GARMASH	15	BELL	$e^+e^- \to \Upsilon(2S)\pi^+\pi^-$
$18.7 \pm 3.4^{+2.5}_{-1.3}$	[2] GARMASH	15	BELL	$e^+e^- \to \Upsilon(3S)\pi^+\pi^-$
$22.3 \pm 7.7^{+3.0}_{-4.0}$	[3] BONDAR	12	BELL	$e^+e^- \to \Upsilon(1S)\pi^+\pi^-$
$24.2 \pm 3.1^{+2.0}_{-3.0}$	[3] BONDAR	12	BELL	$e^+e^- \to \Upsilon(2S)\pi^+\pi^-$
$17.6 \pm 3.0 \pm 3.0$	[3] BONDAR	12	BELL	$e^+e^- \to \Upsilon(3S)\pi^+\pi^-$
$11.4 \, {}^{+}_{-} \, {}^{4.5}_{3.9} \, {}^{+2.1}_{-1.2}$	[3] BONDAR	12	BELL	$e^+e^- \to h_b(1P)\pi^+\pi^-$
$13 \, {}^{+10}_{-8} \, {}^{+9}_{-7}$	[3] BONDAR	12	BELL	$e^+e^- \to h_b(2P)\pi^+\pi^-$

[1] Average of the BONDAR 12 measurements in separate channels.
[2] Correlated with the corresponding result from BONDAR 12.
[3] Superseded by the average measurement of BONDAR 12.

$Z_b(10610)$ DECAY MODES

	Mode	Fraction (Γ_i/Γ)
Γ_1	$\Upsilon(1S)\pi^+$	$(5.4^{+1.9}_{-1.5}) \times 10^{-3}$
Γ_2	$\Upsilon(1S)\pi^0$	not seen
Γ_3	$\Upsilon(2S)\pi^+$	$(3.6^{+1.1}_{-0.8})$ %
Γ_4	$\Upsilon(2S)\pi^0$	seen
Γ_5	$\Upsilon(3S)\pi^+$	$(2.1^{+0.8}_{-0.6})$ %
Γ_6	$\Upsilon(3S)\pi^0$	seen
Γ_7	$h_b(1P)\pi^+$	$(3.5^{+1.2}_{-0.9})$ %
Γ_8	$h_b(2P)\pi^+$	$(4.7^{+1.7}_{-1.3})$ %
Γ_9	$B^+\overline{B}^0$	not seen
Γ_{10}	$B^+\overline{B}^{*0} + B^{*+}\overline{B}^0$	$(85.6^{+2.1}_{-2.9})$ %
Γ_{11}	$B^{*+}\overline{B}^{*0}$	not seen

$Z_b(10610)$ BRANCHING RATIOS

$\Gamma(\Upsilon(1S)\pi^+)/\Gamma_{\text{total}}$ Γ_1/Γ

VALUE (units 10^{-3})	DOCUMENT ID		TECN	COMMENT
$5.4^{+1.6}_{-1.3}{}^{+1.1}_{-0.8}$	[1] GARMASH	16	BELL	$e^+e^- \to \pi^-B^+\overline{B}^{*0}$, $\pi^-\overline{B}^0B^{*+}$
• • • We do not use the following data for averages, fits, limits, etc. • • •				
seen	GARMASH	15	BELL	$e^+e^- \to \Upsilon(1S)\pi^+\pi^-$
seen	BONDAR	12	BELL	$e^+e^- \to \Upsilon(1S)\pi^+\pi^-$

[1] Assuming the $Z_b(10610)$ decay width is saturated by the channels $\pi^+\Upsilon(1S, 2S, 3S)$, $\pi^+h_b(1P, 2P)$, and $B^+\overline{B}^{*0} + \overline{B}^0B^{*+}$, and using the results from BONDAR 12 and MIZUK 16.

$\Gamma(\Upsilon(1S)\pi^0)/\Gamma_{\text{total}}$ Γ_2/Γ

VALUE	DOCUMENT ID		TECN	COMMENT
not seen	KROKOVNY	13	BELL	$e^+e^- \to \Upsilon(1S)\pi^0\pi^0$

$\Gamma(\Upsilon(2S)\pi^+)/\Gamma_{\text{total}}$ Γ_3/Γ

VALUE (units 10^{-2})	DOCUMENT ID		TECN	COMMENT
$3.62^{+0.76}_{-0.59}{}^{+0.79}_{-0.53}$	[1] GARMASH	16	BELL	$e^+e^- \to \pi^-B^+\overline{B}^{*0}$, $\pi^-\overline{B}^0B^{*+}$
• • • We do not use the following data for averages, fits, limits, etc. • • •				
seen	GARMASH	15	BELL	$e^+e^- \to \Upsilon(2S)\pi^+\pi^-$
seen	BONDAR	12	BELL	$e^+e^- \to \Upsilon(2S)\pi^+\pi^-$

[1] Assuming the $Z_b(10610)$ decay width is saturated by the channels $\pi^+\Upsilon(1S, 2S, 3S)$, $\pi^+h_b(1P, 2P)$, and $B^+\overline{B}^{*0} + \overline{B}^0B^{*+}$, and using the results from BONDAR 12 and MIZUK 16.

$\Gamma(\Upsilon(2S)\pi^0)/\Gamma_{\text{total}}$ Γ_4/Γ

VALUE	DOCUMENT ID		TECN	COMMENT
seen	[1] KROKOVNY	13	BELL	$e^+e^- \to \Upsilon(2S)\pi^0\pi^0$

[1] Combined significance in $e^+e^- \to \Upsilon(2S)/\Upsilon(3S)\pi^0\pi^0$, including systematics, of 6.5σ.

$\Gamma(\Upsilon(3S)\pi^+)/\Gamma_{\text{total}}$ Γ_5/Γ

VALUE (units 10^{-2})	DOCUMENT ID		TECN	COMMENT
$2.15^{+0.55}_{-0.42}{}^{+0.60}_{-0.43}$	[1] GARMASH	16	BELL	$e^+e^- \to \pi^-B^+\overline{B}^{*0}$, $\pi^-\overline{B}^0B^{*+}$
• • • We do not use the following data for averages, fits, limits, etc. • • •				
seen	GARMASH	15	BELL	$e^+e^- \to \Upsilon(3S)\pi^+\pi^-$
seen	BONDAR	12	BELL	$e^+e^- \to \Upsilon(3S)\pi^+\pi^-$

[1] Assuming the $Z_b(10610)$ decay width is saturated by the channels $\pi^+\Upsilon(1S, 2S, 3S)$, $\pi^+h_b(1P, 2P)$, and $B^+\overline{B}^{*0} + \overline{B}^0B^{*+}$, and using the results from BONDAR 12 and MIZUK 16.

$\Gamma(\Upsilon(3S)\pi^0)/\Gamma_{total}$ Γ_6/Γ

VALUE	DOCUMENT ID		TECN	COMMENT
seen	[1] KROKOVNY	13	BELL	$e^+e^- \to \Upsilon(3S)\pi^0\pi^0$

[1] Combined significance in $e^+e^- \to \Upsilon(2S)/\Upsilon(3S)\pi^0\pi^0$, including systematics, of 6.5σ.

$\Gamma(h_b(1P)\pi^+)/\Gamma_{total}$ Γ_7/Γ

VALUE (units 10^{-2})	DOCUMENT ID		TECN	COMMENT
$\mathbf{3.45^{+0.87+0.86}_{-0.71-0.63}}$	[1] GARMASH	16	BELL	$e^+e^- \to \pi^- B^+ \overline{B}^{*0}$, $\pi^- \overline{B}^0 B^{*+}$
• • • We do not use the following data for averages, fits, limits, etc. • • •				
possibly seen	[2] MIZUK	16	BELL	$e^+e^- \to h_b(1P)\pi^+\pi^-$
seen	[3] BONDAR	12	BELL	$e^+e^- \to h_b(1P)\pi^+\pi^-$

[1] Assuming the $Z_b(10610)$ decay width is saturated by the channels $\pi^+\Upsilon(1S,2S,3S)$, $\pi^+ h_b(1P,2P)$, and $B^+\overline{B}^{*0} + \overline{B}^0 B^{*+}$, and using the results from BONDAR 12 and MIZUK 16.
[2] Using e^+e^- energies near the $\Upsilon(11020)$.
[3] Using e^+e^- energies near the $\Upsilon(10860)$.

$\Gamma(h_b(2P)\pi^+)/\Gamma_{total}$ Γ_8/Γ

VALUE (units 10^{-2})	DOCUMENT ID		TECN	COMMENT
$\mathbf{4.67^{+1.24+1.18}_{-1.00-0.89}}$	[1] GARMASH	16	BELL	$e^+e^- \to \pi^- B^+ \overline{B}^{*0}$, $\pi^- \overline{B}^0 B^{*+}$
• • • We do not use the following data for averages, fits, limits, etc. • • •				
possibly seen	[2] MIZUK	16	BELL	$e^+e^- \to h_b(2P)\pi^+\pi^-$
seen	[3] BONDAR	12	BELL	$e^+e^- \to h_b(2P)\pi^+\pi^-$

[1] Assuming the $Z_b(10610)$ decay width is saturated by the channels $\pi^+\Upsilon(1S,2S,3S)$, $\pi^+ h_b(1P,2P)$, and $B^+\overline{B}^{*0} + \overline{B}^0 B^{*+}$, and using the results from BONDAR 12 and MIZUK 16.
[2] Using e^+e^- energies near the $\Upsilon(11020)$.
[3] Using e^+e^- energies near the $\Upsilon(10860)$.

$\Gamma(B^+\overline{B}^0)/\Gamma_{total}$ Γ_9/Γ

VALUE	DOCUMENT ID		TECN	COMMENT
not seen	GARMASH	16	BELL	$e^+e^- \to \pi^- B^+ \overline{B}^0$

$[\Gamma(B^+\overline{B}^{*0}) + \Gamma(B^{*+}\overline{B}^0)]/\Gamma_{total}$ Γ_{10}/Γ

VALUE (units 10^{-2})	EVTS	DOCUMENT ID		TECN	COMMENT
$\mathbf{85.6^{+1.5+1.5}_{-2.0-2.1}}$	357	[1] GARMASH	16	BELL	$e^+e^- \to \pi^- B^+ \overline{B}^{*0}$, $\pi^- B^{*+} \overline{B}^0$

[1] Assuming the $Z_b(10610)$ decay width is saturated by the channels $\pi^+\Upsilon(1S,2S,3S)$, $\pi^+ h_b(1P,2P)$, and $B^+\overline{B}^{*0} + B^{*+}\overline{B}^0$, and using the results from BONDAR 12 and MIZUK 16. Using the mass and width of the $Z_b(10610)$ from BONDAR 12.

$\Gamma(B^{*+}\overline{B}^{*0})/\Gamma_{total}$ Γ_{11}/Γ

VALUE	DOCUMENT ID		TECN	COMMENT
not seen	GARMASH	16	BELL	$e^+e^- \to \pi^- B^{*+} \overline{B}^{*0}$

$[\Gamma(B^+\overline{B}^{*0}) + \Gamma(B^{*+}\overline{B}^0)]/[\Gamma(\Upsilon(1S)\pi^+) + \Gamma(\Upsilon(2S)\pi^+) + \Gamma(\Upsilon(3S)\pi^+) + \Gamma(h_b(1P)\pi^+) + \Gamma(h_b(2P)\pi^+)]$ $\Gamma_{10}/(\Gamma_1+\Gamma_3+\Gamma_5+\Gamma_7+\Gamma_8)$

VALUE (units 10^{-2})	EVTS	DOCUMENT ID		TECN	COMMENT
• • • We do not use the following data for averages, fits, limits, etc. • • •					
$5.93^{+0.99+1.01}_{-0.69-0.73}$	357	[1] GARMASH	16	BELL	$e^+e^- \to \pi^- B^+ \overline{B}^{*0}$, $\pi^- \overline{B}^0 B^{*+}$

[1] Combined with the results of BONDAR 12 and MIZUK 16. Not independent from $Z_b(10610)$ branching fractions to $\pi^+\Upsilon(1S,2S,3S)$, $\pi^+ h_b(1P,2P)$, and $B^+\overline{B}^{*0} + \overline{B}^0 B^{*+}$.

$Z_b(10610)$ REFERENCES

GARMASH	16	PRL 116 212001	A. Garmash *et al.*	(BELLE Collab.)
MIZUK	16	PRL 117 142001	R. Mizuk *et al.*	(BELLE Collab.)
GARMASH	15	PR D91 072003	A. Garmash *et al.*	(BELLE Collab.)
KROKOVNY	13	PR D88 052016	P. Krokovny *et al.*	(BELLE Collab.)
BONDAR	12	PRL 108 122001	A. Bondar *et al.*	(BELLE Collab.)

$Z_b(10650)$

$I^G(J^{PC}) = 1^+(1^{+-})$
I, *G*, *C* need confirmation.

OMITTED FROM SUMMARY TABLE
was $X(10650)^\pm$

Properties incompatible with a $q\overline{q}$ structure (exotic state). See the review on non-$q\overline{q}$ states.

Observed by BONDAR 12 in $\Upsilon(5S)$ decays to $\Upsilon(nS)\pi^+\pi^-$ (n = 1, 2, 3) and $h_b(mP)\pi^+\pi^-$ (m = 1, 2). $J^P = 1^+$ is favored from angular analyses.

$Z_b(10650)$ MASS

VALUE (MeV)	DOCUMENT ID		TECN	COMMENT
10652.2±1.5	[1] BONDAR	12	BELL	$e^+e^- \to$ hadrons
• • • We do not use the following data for averages, fits, limits, etc. • • •				
$10656.7 \pm 5.0^{+1.1}_{-3.1}$	[2] GARMASH	15	BELL	$e^+e^- \to \Upsilon(1S)\pi^+\pi^-$
$10650.7 \pm 1.5^{+0.5}_{-0.2}$	[2] GARMASH	15	BELL	$e^+e^- \to \Upsilon(2S)\pi^+\pi^-$
$10651.2 \pm 1.0^{+0.4}_{-0.3}$	[2] GARMASH	15	BELL	$e^+e^- \to \Upsilon(3S)\pi^+\pi^-$
10657 ±6 ±3	[3] BONDAR	12	BELL	$e^+e^- \to \Upsilon(1S)\pi^+\pi^-$
10651 ±2 ±3	[3] BONDAR	12	BELL	$e^+e^- \to \Upsilon(2S)\pi^+\pi^-$
10652 ±1 ±2	[3] BONDAR	12	BELL	$e^+e^- \to \Upsilon(3S)\pi^+\pi^-$
$10654 \pm 3^{+1}_{-2}$	[3] BONDAR	12	BELL	$e^+e^- \to h_b(1P)\pi^+\pi^-$
$10651^{+2}_{-3} \pm 2^{+3}_{-2}$	[3] BONDAR	12	BELL	$e^+e^- \to h_b(2P)\pi^+\pi^-$

[1] Average of the BONDAR 12 measurements in separate channels.
[2] Correlated with the corresponding result from BONDAR 12.
[3] Superseded by the average measurement of BONDAR 12.

$Z_b(10650)$ WIDTH

VALUE (MeV)	DOCUMENT ID		TECN	COMMENT
11.5± 2.2	[4] BONDAR	12	BELL	e^+e^- → hadrons
• • • We do not use the following data for averages, fits, limits, etc. • • •				
$12.1^{+11.3}_{-4.8} \pm 2.7 \pm 0.6$	[5] GARMASH	15	BELL	$e^+e^- \to \Upsilon(1S)\pi^+\pi^-$
$14.2 \pm 3.7^{+0.9}_{-0.4}$	[5] GARMASH	15	BELL	$e^+e^- \to \Upsilon(2S)\pi^+\pi^-$
$9.3 \pm 2.2^{+0.3}_{-0.5}$	[5] GARMASH	15	BELL	$e^+e^- \to \Upsilon(3S)\pi^+\pi^-$
16.3± 9.8$^{+6.0}_{-2.0}$	[6] BONDAR	12	BELL	$e^+e^- \to \Upsilon(1S)\pi^+\pi^-$
13.3± 3.3$^{+4.0}_{-3.0}$	[6] BONDAR	12	BELL	$e^+e^- \to \Upsilon(2S)\pi^+\pi^-$
8.4± 2.0± 2.0	[6] BONDAR	12	BELL	$e^+e^- \to \Upsilon(3S)\pi^+\pi^-$
$20.9^{+5.4}_{-4.7} \pm 2.1 \pm 5.7$	[6] BONDAR	12	BELL	$e^+e^- \to h_b(1P)\pi^+\pi^-$
19 ± 7 $^{+11}_{-7}$	[6] BONDAR	12	BELL	$e^+e^- \to h_b(2P)\pi^+\pi^-$

[4] Average of the BONDAR 12 measurements in separate channels.
[5] Correlated with the corresponding result from BONDAR 12.
[6] Superseded by the average measurement of BONDAR 12.

$Z_b(10650)^+$ DECAY MODES

$Z_b(10650)^-$ decay modes are charge conjugates of the modes below.

	Mode	Fraction (Γ_i/Γ)
Γ_1	$\Upsilon(1S)\pi^+$	$(1.7^{+0.8}_{-0.6}) \times 10^{-3}$
Γ_2	$\Upsilon(2S)\pi^+$	$(1.4^{+0.6}_{-0.4})$ %
Γ_3	$\Upsilon(3S)\pi^+$	$(1.6^{+0.7}_{-0.5})$ %
Γ_4	$h_b(1P)\pi^+$	$(8.4^{+2.9}_{-2.4})$ %
Γ_5	$h_b(2P)\pi^+$	(15 ±4) %
Γ_6	$B^+\overline{B}^0$	not seen
Γ_7	$B^+\overline{B}^{*0} + B^{*+}\overline{B}^0$	not seen
Γ_8	$B^{*+}\overline{B}^{*0}$	(74 $^{+4}_{-6}$) %

$Z_b(10650)$ BRANCHING RATIOS

$\Gamma(\Upsilon(1S)\pi^+)/\Gamma_{total}$ Γ_1/Γ

VALUE (units 10^{-3})	DOCUMENT ID		TECN	COMMENT
$\mathbf{1.7^{+0.7+0.3}_{-0.6-0.2}}$	[7] GARMASH	16	BELL	$e^+e^- \to \pi^- B^{*+} \overline{B}^{*0}$
• • • We do not use the following data for averages, fits, limits, etc. • • •				
seen	GARMASH	15	BELL	$e^+e^- \to \Upsilon(1S)\pi^+\pi^-$
seen	BONDAR	12	BELL	$e^+e^- \to \Upsilon(1S)\pi^+\pi^-$

[7] Assuming the $Z_b(10650)$ decay width is saturated by the channels $\pi^+\Upsilon(1S,2S,3S)$, $\pi^+ h_b(1P,2P)$, and $B^{*+}\overline{B}^{*0}$, and using the results from BONDAR 12 and MIZUK 16.

$\Gamma(\Upsilon(2S)\pi^+)/\Gamma_{total}$ Γ_2/Γ

VALUE (units 10^{-2})	DOCUMENT ID		TECN	COMMENT
$\mathbf{1.39^{+0.48+0.34}_{-0.38-0.23}}$	[8] GARMASH	16		$e^+e^- \to \pi^- B^{*+} \overline{B}^{*0}$
• • • We do not use the following data for averages, fits, limits, etc. • • •				
seen	GARMASH	15	BELL	$e^+e^- \to \Upsilon(2S)\pi^+\pi^-$
seen	BONDAR	12	BELL	$e^+e^- \to \Upsilon(2S)\pi^+\pi^-$

[8] Assuming the $Z_b(10650)$ decay width is saturated by the channels $\pi^+\Upsilon(1S,2S,3S)$, $\pi^+ h_b(1P,2P)$, and $B^{*+}\overline{B}^{*0}$, and using the results from BONDAR 12 and MIZUK 16.

$\Gamma(\Upsilon(3S)\pi^+)/\Gamma_{total}$ Γ_3/Γ

VALUE (units 10^{-2})	DOCUMENT ID		TECN	COMMENT
$1.63^{+0.53}_{-0.42}{}^{+0.39}_{-0.28}$	[9] GARMASH	16	BELL	$e^+e^- \to \pi^- B^{*+}\overline{B}^{*0}$
• • • We do not use the following data for averages, fits, limits, etc. • • •				
seen	GARMASH	15	BELL	$e^+e^- \to \Upsilon(3S)\pi^+\pi^-$
seen	BONDAR	12	BELL	$e^+e^- \to \Upsilon(3S)\pi^+\pi^-$

[9] Assuming the $Z_b(10650)$ decay width is saturated by the channels $\pi^+\Upsilon(1S,2S,3S)$, $\pi^+ h_b(1P,2P)$, and $B^{*+}\overline{B}^{*0}$, and using the results from BONDAR 12 and MIZUK 16.

$\Gamma(h_b(1P)\pi^+)/\Gamma_{total}$ Γ_4/Γ

VALUE (units 10^{-2})	DOCUMENT ID		TECN	COMMENT
$8.41^{+2.43}_{-2.12}{}^{+1.49}_{-1.06}$	[10] GARMASH	16	BELL	$e^+e^- \to \pi^- B^{*+}\overline{B}^{*0}$
• • • We do not use the following data for averages, fits, limits, etc. • • •				
seen	[11] MIZUK	16	BELL	$e^+e^- \to h_b(1P)\pi^+\pi^-$
seen	[12] BONDAR	12	BELL	$e^+e^- \to h_b(1P)\pi^+\pi^-$

[10] Assuming the $Z_b(10650)$ decay width is saturated by the channels $\pi^+\Upsilon(1S,2S,3S)$, $\pi^+ h_b(1P,2P)$, and $B^{*+}\overline{B}^{*0}$, and using the results from BONDAR 12 and MIZUK 16.
[11] Using e^+e^- energies near the $\Upsilon(11020)$.
[12] Using e^+e^- energies near the $\Upsilon(10860)$.

$\Gamma(h_b(2P)\pi^+)/\Gamma_{total}$ Γ_5/Γ

VALUE (units 10^{-2})	DOCUMENT ID		TECN	COMMENT
$14.7^{+3.2}_{-2.8}{}^{+2.8}_{-2.3}$	[13] GARMASH	16	BELL	$e^+e^- \to \pi^- B^{*+}\overline{B}^{*0}$
• • • We do not use the following data for averages, fits, limits, etc. • • •				
possibly seen	[14] MIZUK	16	BELL	$e^+e^- \to h_b(2P)\pi^+\pi^-$
seen	[15] BONDAR	12	BELL	$e^+e^- \to h_b(2P)\pi^+\pi^-$

[13] Assuming the $Z_b(10650)$ decay width is saturated by the channels $\pi^+\Upsilon(1S,2S,3S)$, $\pi^+ h_b(1P,2P)$, and $B^{*+}\overline{B}^{*0}$, and using the results from BONDAR 12 and MIZUK 16.
[14] Using e^+e^- energies near the $\Upsilon(11020)$.
[15] Using e^+e^- energies near the $\Upsilon(10860)$.

$\Gamma(B^+\overline{B}^0)/\Gamma_{total}$ Γ_6/Γ

VALUE	DOCUMENT ID		TECN	COMMENT
not seen	GARMASH	16	BELL	$e^+e^- \to \pi^- B^+\overline{B}^0$

$[\Gamma(B^+\overline{B}^{*0}) + \Gamma(B^{*+}\overline{B}^0)]/\Gamma_{total}$ Γ_7/Γ

VALUE	DOCUMENT ID		TECN	COMMENT
not seen	GARMASH	16	BELL	$e^+e^- \to \pi^- B^+\overline{B}^{*0}$, $\pi^-\overline{B}^0 B^{*+}$

$\Gamma(B^{*+}\overline{B}^{*0})/\Gamma_{total}$ Γ_8/Γ

VALUE (units 10^{-2})	EVTS	DOCUMENT ID		TECN	COMMENT
$73.7^{+3.4}_{-4.4}{}^{+2.7}_{-3.5}$	161	[16] GARMASH	16	BELL	$e^+e^- \to \pi^- B^{*+}\overline{B}^{*0}$

[16] Assuming the $Z_b(10650)$ decay width is saturated by the channels $\pi^+\Upsilon(1S,2S,3S)$, $\pi^+ h_b(1P,2P)$, and $B^{*+}\overline{B}^{*0}$, and using the results from BONDAR 12 and MIZUK 16. Using the mass and width of the $Z_b(10650)$ from BONDAR 12.

$\Gamma(B^{*+}\overline{B}^{*0})/[\Gamma(\Upsilon(1S)\pi^+) + \Gamma(\Upsilon(2S)\pi^+) + \Gamma(\Upsilon(3S)\pi^+) + \Gamma(h_b(1P)\pi^+) + \Gamma(h_b(2P)\pi^+)]$ $\Gamma_8/(\Gamma_1+\Gamma_2+\Gamma_3+\Gamma_4+\Gamma_5)$

VALUE (units 10^{-2})	EVTS	DOCUMENT ID		TECN	COMMENT
• • • We do not use the following data for averages, fits, limits, etc. • • •					
$2.80^{+0.69}_{-0.40}{}^{+0.54}_{-0.36}$	161	[17] GARMASH	16	BELL	$e^+e^- \to \pi^- B^{*+}\overline{B}^{*0}$

[17] Combined with the results of BONDAR 12 and MIZUK 16. Not independent from $Z_b(10650)$ branching fractions to $\pi^+\Upsilon(1S,2S,3S)$, $\pi^+ h_b(1P,2P)$, and $B^{*+}\overline{B}^{*0}$.

$Z_b(10650)$ REFERENCES

GARMASH	16	PRL 116 212001	A. Garmash *et al.*	(BELLE Collab.)
MIZUK	16	PRL 117 142001	R. Mizuk *et al.*	(BELLE Collab.)
GARMASH	15	PR D91 072003	A. Garmash *et al.*	(BELLE Collab.)
BONDAR	12	PRL 108 122001	A. Bondar *et al.*	(BELLE Collab.)

$\Upsilon(10860)$

$I^G(J^{PC}) = 0^-(1^{--})$

$\Upsilon(10860)$ MASS

VALUE (MeV)	DOCUMENT ID		TECN	COMMENT
$10889.9 \pm {}^{3.2}_{2.6}$ OUR AVERAGE				
$10884.7^{+3.6}_{-3.4}{}^{+8.9}_{-1.0}$	[1] MIZUK	16	BELL	$e^+e^- \to h_b(1P,2P)\pi^+\pi^-$
$10891.1 \pm 3.2^{+1.2}_{-2.0}$	[2] SANTEL	16	BELL	$e^+e^- \to \Upsilon(1S,2S,3S)\pi^+\pi^-$
• • • We do not use the following data for averages, fits, limits, etc. • • •				
$10881.8^{+1.0}_{-1.1} \pm 1.2$	[3,4] SANTEL	16	BELL	$e^+e^- \to$ hadrons
10879 ± 3	[5,6] CHEN	10	BELL	$e^+e^- \to$ hadrons
$10888.4^{+2.7}_{-2.6} \pm 1.2$	[7] CHEN	10	BELL	$e^+e^- \to \Upsilon(1S,2S,3S)\pi^+\pi^-$
10876 ± 2	[5] AUBERT	09E	BABR	$e^+e^- \to$ hadrons
10869 ± 2	[8] AUBERT	09E	BABR	$e^+e^- \to$ hadrons
$10868 \pm 6 \pm 5$	[9] BESSON	85	CLEO	$e^+e^- \to$ hadrons
10845 ± 20	[10] LOVELOCK	85	CUSB	$e^+e^- \to$ hadrons

[1] From a simultaneous fit to the $h_b(nP)\pi^+\pi^-$, $n = 1, 2$ cross sections at 22 energy points within $\sqrt{s} = 10.77$–11.02 GeV to a pair of interfering Breit-Wigner amplitudes modified by phase space factors, with eight resonance parameters (a mass and width for each of $\Upsilon(10860)$ and $\Upsilon(11020)$, a single relative phase, a single relative amplitude, and two overall normalization factors, one for each n). The systematic error estimate is dominated by possible interference with a small nonresonant continuum amplitude.
[2] From a simultaneous fit to the $\Upsilon(nS)\pi^+\pi^-$, $n = 1, 2, 3$ cross sections at 25 energy points within $\sqrt{s} = 10.6$–11.05 GeV to a pair of interfering Breit-Wigner amplitudes modified by phase space factors, with fourteen resonance parameters (a mass, width, and three amplitudes for each of $\Upsilon(10860)$ and $\Upsilon(11020)$, a single universal relative phase, and three decoherence coefficients, one for each n). Continuum contributions were measured (and therefore fixed) to be zero.
[3] From a fit to the total hadronic cross sections measured at 60 energy points within $\sqrt{s} = 10.82$–11.05 GeV to a pair of interfering Breit-Wigner amplitudes and two floating continuum amplitudes with $1/\sqrt{s}$ dependence, one coherent with the resonances and one incoherent, with six resonance parameters (a mass, width, and an amplitude for each of $\Upsilon(10860)$ and $\Upsilon(11020)$, one relative phase, and one decoherence coefficient).
[4] Not including uncertain and potentially large systematic errors due to assumed continuum amplitude $1/\sqrt{s}$ dependence and related interference contributions.
[5] In a model where a flat non-resonant $b\overline{b}$-continuum is incoherently added to a second flat component interfering with two Breit-Wigner resonances. Systematic uncertainties not estimated.
[6] The parameters of the $\Upsilon(11020)$ are fixed to those in AUBERT 09E.
[7] In a model where a flat nonresonant $\Upsilon(1S,2S,3S)\pi^+\pi^-$ continuum interferes with a single Breit-Wigner resonance.
[8] In a model where a non-resonant $b\overline{b}$-continuum represented by a threshold function at $\sqrt{s}=2m_B$ is incoherently added to a flat component interfering with two Breit-Wigner resonances. Not independent of other AUBERT 09E results. Systematic uncertainties not estimated.
[9] Assuming four Gaussians with radiative tails and a single step in R.
[10] In a coupled-channel model with three resonances and a smooth step in R.

$\Upsilon(10860)$ WIDTH

VALUE (MeV)	DOCUMENT ID		TECN	COMMENT
$51 \pm {}^{6}_{7}$ OUR AVERAGE				
$40.6^{+12.7}_{-8.0}{}^{+1.1}_{-19.1}$	[11] MIZUK	16	BELL	$e^+e^- \to h_b(1P,2P)\pi^+\pi^-$
$53.7^{+7.1}_{-5.6}{}^{+1.3}_{-5.4}$	[12] SANTEL	16	BELL	$e^+e^- \to \Upsilon(1S,2S,3S)\pi^+\pi^-$
• • • We do not use the following data for averages, fits, limits, etc. • • •				
$48.5^{+1.9}_{-1.8}{}^{+2.0}_{-2.8}$	[13,14] SANTEL	16	BELL	$e^+e^- \to$ hadrons
$46 {}^{+9}_{-7}$	[15,16] CHEN	10	BELL	$e^+e^- \to$ hadrons
$30.7^{+8.3}_{-7.0} \pm 3.1$	[17] CHEN	10	BELL	$e^+e^- \to \Upsilon(1S,2S,3S)\pi^+\pi^-$
43 ± 4	[15] AUBERT	09E	BABR	$e^+e^- \to$ hadrons
74 ± 4	[18] AUBERT	09E	BABR	$e^+e^- \to$ hadrons
$112 \pm 17 \pm 23$	[19] BESSON	85	CLEO	$e^+e^- \to$ hadrons
110 ± 15	[20] LOVELOCK	85	CUSB	$e^+e^- \to$ hadrons

[11] From a simultaneous fit to the $h_b(nP)\pi^+\pi^-$, $n = 1, 2$ cross sections at 22 energy points within $\sqrt{s} = 10.77$–11.02 GeV to a pair of interfering Breit-Wigner amplitudes modified by phase space factors, with eight resonance parameters (a mass and width for each of $\Upsilon(10860)$ and $\Upsilon(11020)$, a single relative phase, a single relative amplitude, and two overall normalization factors, one for each n). The systematic error estimate is dominated by possible interference with a small nonresonant continuum amplitude.
[12] From a simultaneous fit to the $\Upsilon(nS)\pi^+\pi^-$, $n = 1, 2, 3$ cross sections at 25 energy points within $\sqrt{s} = 10.6$–11.05 GeV to a pair of interfering Breit-Wigner amplitudes modified by phase space factors, with fourteen resonance parameters (a mass, width, and three amplitudes for each of $\Upsilon(10860)$ and $\Upsilon(11020)$, a single universal relative phase, and three decoherence coefficients, one for each n). Continuum contributions were measured (and therefore fixed) to be zero.
[13] From a fit to the total hadronic cross sections measured at 60 energy points within $\sqrt{s} = 10.82$–11.05 GeV to a pair of interfering Breit-Wigner amplitudes and two floating continuum amplitudes with $1/\sqrt{s}$ dependence, one coherent with the resonances and one incoherent, with six resonance parameters (a mass, width, and an amplitude for each of $\Upsilon(10860)$ and $\Upsilon(11020)$, one relative phase, and one decoherence coefficient).
[14] Not including uncertain and potentially large systematic errors due to assumed continuum amplitude $1/\sqrt{s}$ dependence and related interference contributions.
[15] In a model where a flat non-resonant $b\overline{b}$-continuum is incoherently added to a second flat component interfering with two Breit-Wigner resonances. Systematic uncertainties not estimated.
[16] The parameters of the $\Upsilon(11020)$ are fixed to those in AUBERT 09E.
[17] In a model where a flat nonresonant $\Upsilon(1S,2S,3S)\pi^+\pi^-$ continuum interferes with a single Breit-Wigner resonance.
[18] In a model where a non-resonant $b\overline{b}$-continuum represented by a threshold function at $\sqrt{s}=2m_B$ is incoherently added to a flat component interfering with two Breit-Wigner resonances. Not independent of other AUBERT 09E results. Systematic uncertainties not estimated.
[19] Assuming four Gaussians with radiative tails and a single step in R.
[20] In a coupled-channel model with three resonances and a smooth step in R.

Meson Particle Listings

$\Upsilon(10860)$

$\Upsilon(10860)$ DECAY MODES

	Mode	Fraction (Γ_i/Γ)	Confidence level
Γ_1	$B\overline{B}X$	$(76.2\ ^{+2.7}_{-4.0})$ %	
Γ_2	$B\overline{B}$	(5.5 ± 1.0) %	
Γ_3	$B\overline{B}^* +$ c.c.	(13.7 ± 1.6) %	
Γ_4	$B^*\overline{B}^*$	(38.1 ± 3.4) %	
Γ_5	$B\overline{B}^{(*)}\pi$	< 19.7 %	90%
Γ_6	$B\overline{B}\pi$	(0.0 ± 1.2) %	
Γ_7	$B^*\overline{B}\pi + B\overline{B}^*\pi$	(7.3 ± 2.3) %	
Γ_8	$B^*\overline{B}^*\pi$	(1.0 ± 1.4) %	
Γ_9	$B\overline{B}\pi\pi$	< 8.9 %	90%
Γ_{10}	$B_s^{(*)}\overline{B}_s^{(*)}$	(20.1 ± 3.1) %	
Γ_{11}	$B_s\overline{B}_s$	$(5 \pm 5) \times 10^{-3}$	
Γ_{12}	$B_s\overline{B}_s^* +$ c.c.	(1.35 ± 0.32) %	
Γ_{13}	$B_s^*\overline{B}_s^*$	(17.6 ± 2.7) %	
Γ_{14}	no open-bottom	$(3.8\ ^{+5.0}_{-0.5})$ %	
Γ_{15}	e^+e^-	$(6.1 \pm 1.6) \times 10^{-6}$	
Γ_{16}	$K^*(892)^0\overline{K}^0$	$< 1.0 \times 10^{-5}$	90%
Γ_{17}	$\Upsilon(1S)\pi^+\pi^-$	$(5.3 \pm 0.6) \times 10^{-3}$	
Γ_{18}	$\Upsilon(2S)\pi^+\pi^-$	$(7.8 \pm 1.3) \times 10^{-3}$	
Γ_{19}	$\Upsilon(3S)\pi^+\pi^-$	$(4.8\ ^{+1.9}_{-1.7}) \times 10^{-3}$	
Γ_{20}	$\Upsilon(1S)K^+K^-$	$(6.1 \pm 1.8) \times 10^{-4}$	
Γ_{21}	$h_b(1P)\pi^+\pi^-$	$(3.5\ ^{+1.0}_{-1.3}) \times 10^{-3}$	
Γ_{22}	$h_b(2P)\pi^+\pi^-$	$(5.7\ ^{+1.7}_{-2.1}) \times 10^{-3}$	
Γ_{23}	$\chi_{b0}(1P)\pi^+\pi^-\pi^0$	$< 6.3 \times 10^{-3}$	90%
Γ_{24}	$\chi_{b0}(1P)\omega$	$< 3.9 \times 10^{-3}$	90%
Γ_{25}	$\chi_{b0}(1P)(\pi^+\pi^-\pi^0)_{\text{non}-\omega}$	$< 4.8 \times 10^{-3}$	90%
Γ_{26}	$\chi_{b1}(1P)\pi^+\pi^-\pi^0$	$(1.85 \pm 0.33) \times 10^{-3}$	
Γ_{27}	$\chi_{b1}(1P)\omega$	$(1.57 \pm 0.30) \times 10^{-3}$	
Γ_{28}	$\chi_{b1}(1P)(\pi^+\pi^-\pi^0)_{\text{non}-\omega}$	$(5.2 \pm 1.9) \times 10^{-4}$	
Γ_{29}	$\chi_{b2}(1P)\pi^+\pi^-\pi^0$	$(1.17 \pm 0.30) \times 10^{-3}$	
Γ_{30}	$\chi_{b2}(1P)\omega$	$(6.0 \pm 2.7) \times 10^{-4}$	
Γ_{31}	$\chi_{b2}(1P)(\pi^+\pi^-\pi^0)_{\text{non}-\omega}$	$(6 \pm 4) \times 10^{-4}$	
Γ_{32}	$\gamma X_b \to \gamma\,\Upsilon(1S)\omega$	$< 3.8 \times 10^{-5}$	90%

Inclusive Decays.

These decay modes are submodes of one or more of the decay modes above.

Γ_{33}	ϕ anything	$(13.8\ ^{+2.4}_{-1.7})$ %	
Γ_{34}	D^0 anything + c.c.	(108 ± 8) %	
Γ_{35}	D_s anything + c.c.	(46 ± 6) %	
Γ_{36}	J/ψ anything	(2.06 ± 0.21) %	
Γ_{37}	B^0 anything + c.c.	(77 ± 8) %	
Γ_{38}	B^+ anything + c.c.	(72 ± 6) %	

$\Upsilon(10860)$ PARTIAL WIDTHS

$\Gamma(e^+e^-)$ Γ_{15}

VALUE (keV)	DOCUMENT ID		TECN	COMMENT
0.31 ±0.07 OUR AVERAGE	Error includes scale factor of 1.3.			
0.22 ±0.05 ±0.07	BESSON	85	CLEO	$e^+e^- \to$ hadrons
0.365±0.070	LOVELOCK	85	CUSB	$e^+e^- \to$ hadrons

$\Upsilon(10860)$ BRANCHING RATIOS

"OUR EVALUATION" is obtained based on averages of rescaled data listed below. The averages and rescaling were performed by the Heavy Flavor Averaging Group (HFLAV) and are described at http://www.slac.stanford.edu/xorg/hflav/.

$\Gamma(B\overline{B}X)/\Gamma_{\text{total}}$ Γ_1/Γ

VALUE	EVTS	DOCUMENT ID		TECN	COMMENT
$0.762^{+0.027}_{-0.043}$ OUR EVALUATION					
0.71 ±0.06 OUR AVERAGE					
0.737±0.032±0.051	1063	[21] DRUTSKOY	10	BELL	$\Upsilon(5S) \to B^+X,\ B^0X$
0.589±0.100±0.092		[22] HUANG	07	CLEO	$\Upsilon(5S) \to$ hadrons

$\Gamma(B\overline{B})/\Gamma_{\text{total}}$ Γ_2/Γ

VALUE (units 10^{-2})	CL%	DOCUMENT ID		TECN	COMMENT
$5.5^{+1.0}_{-0.9}$±0.4		[23] DRUTSKOY	10	BELL	$\Upsilon(5S) \to B^+X,\ B^0X$
• • • We do not use the following data for averages, fits, limits, etc. • • •					
<13.8	90	[22] HUANG	07	CLEO	$\Upsilon(5S) \to$ hadrons

$\Gamma(B\overline{B})/\Gamma(B\overline{B}X)$ Γ_2/Γ_1

VALUE	CL%	DOCUMENT ID		TECN	COMMENT
<0.22	90	AQUINES	06	CLE3	$\Upsilon(5S) \to$ hadrons

$\Gamma(B\overline{B}^* + \text{c.c.})/\Gamma_{\text{total}}$ Γ_3/Γ

VALUE	DOCUMENT ID		TECN	COMMENT
0.137±0.016 OUR AVERAGE				
0.137±0.013±0.011	[23] DRUTSKOY	10	BELL	$\Upsilon(5S) \to B^+X,\ B^0X$
0.143±0.053±0.027	[22] HUANG	07	CLEO	$\Upsilon(5S) \to$ hadrons

$\Gamma(B\overline{B}^* + \text{c.c.})/\Gamma(B\overline{B}X)$ Γ_3/Γ_1

VALUE	EVTS	DOCUMENT ID		TECN	COMMENT
0.24±0.09±0.03	10	AQUINES	06	CLE3	$\Upsilon(5S) \to$ hadrons

$\Gamma(B^*\overline{B}^*)/\Gamma_{\text{total}}$ Γ_4/Γ

VALUE	DOCUMENT ID		TECN	COMMENT
0.381±0.034 OUR AVERAGE				
$0.375\ ^{+0.021}_{-0.019}$±0.030	[23] DRUTSKOY	10	BELL	$\Upsilon(5S) \to B^+X,\ B^0X$
0.436±0.083±0.072	[22] HUANG	07	CLEO	$\Upsilon(5S) \to$ hadrons

$\Gamma(B^*\overline{B}^*)/\Gamma(B\overline{B}X)$ Γ_4/Γ_1

VALUE	EVTS	DOCUMENT ID		TECN	COMMENT
0.74±0.15±0.08	31	AQUINES	06	CLE3	$\Upsilon(5S) \to$ hadrons

$\Gamma(B\overline{B}^{(*)}\pi)/\Gamma_{\text{total}}$ Γ_5/Γ

VALUE	CL%	DOCUMENT ID		TECN	COMMENT
<0.197	90	[22] HUANG	07	CLEO	$\Upsilon(5S) \to$ hadrons

$\Gamma(B\overline{B}^{(*)}\pi)/\Gamma(B\overline{B}X)$ Γ_5/Γ_1

VALUE	CL%	DOCUMENT ID		TECN	COMMENT
<0.32	90	AQUINES	06	CLE3	$\Upsilon(5S) \to$ hadrons

$\Gamma(B\overline{B}\pi)/\Gamma_{\text{total}}$ Γ_6/Γ

VALUE (units 10^{-2})	EVTS	DOCUMENT ID		TECN	COMMENT
0.0±1.2±0.3	0	[23] DRUTSKOY	10	BELL	$\Upsilon(5S) \to B^{+,0}\pi^-X$

$[\Gamma(B^*\overline{B}\pi) + \Gamma(B\overline{B}^*\pi)]/\Gamma_{\text{total}}$ Γ_7/Γ

VALUE (units 10^{-2})	EVTS	DOCUMENT ID		TECN	COMMENT
$7.3^{+2.3}_{-2.1}$±0.8	38	[23] DRUTSKOY	10	BELL	$\Upsilon(5S) \to B^{+,0}\pi^-X$

$\Gamma(B^*\overline{B}^*\pi)/\Gamma_{\text{total}}$ Γ_8/Γ

VALUE (units 10^{-2})	EVTS	DOCUMENT ID		TECN	COMMENT
$1.0^{+1.4}_{-1.3}$±0.4	5	[23] DRUTSKOY	10	BELL	$\Upsilon(5S) \to B^{+,0}\pi^-X$

$\Gamma(B\overline{B}\pi\pi)/\Gamma_{\text{total}}$ Γ_9/Γ

VALUE	CL%	DOCUMENT ID		TECN	COMMENT
<0.089	90	[22] HUANG	07	CLEO	$\Upsilon(5S) \to$ hadrons

$\Gamma(B\overline{B}\pi\pi)/\Gamma(B\overline{B}X)$ Γ_9/Γ_1

VALUE	CL%	DOCUMENT ID		TECN	COMMENT
<0.14	90	AQUINES	06	CLE3	$\Upsilon(5S) \to$ hadrons

$\Gamma(B_s^{(*)}\overline{B}_s^{(*)})/\Gamma_{\text{total}}$ $\Gamma_{10}/\Gamma = (\Gamma_{11}+\Gamma_{12}+\Gamma_{13})/\Gamma$

VALUE	DOCUMENT ID		TECN	COMMENT
$0.201^{+0.030}_{-0.031}$ OUR EVALUATION				
$0.189^{+0.027}_{-0.021}$ OUR AVERAGE				
0.172±0.030	[24] ESEN	13	BELL	$\Upsilon(5S) \to D^0X,\ D_sX$
$0.21\ ^{+0.06}_{-0.03}$	[25] HUANG	07	CLEO	$\Upsilon(5S) \to D_sX$
• • • We do not use the following data for averages, fits, limits, etc. • • •				
0.180±0.013±0.032	[26] DRUTSKOY	07	BELL	$\Upsilon(5S) \to D^0X,\ D_sX$
0.160±0.026±0.058	[27] ARTUSO	05B	CLEO	$e^+e^- \to D_sX$

$\Gamma(B_s^{(*)}\overline{B}_s^{(*)})/\Gamma(B\overline{B}X)$ Γ_{10}/Γ_1

VALUE	DOCUMENT ID
$0.264^{+0.052}_{-0.045}$ OUR EVALUATION	

$\Gamma(B_s^*\overline{B}_s^*)/\Gamma(B_s^{(*)}\overline{B}_s^{(*)})$ $\Gamma_{13}/\Gamma_{10} = \Gamma_{13}/(\Gamma_{11}+\Gamma_{12}+\Gamma_{13})$

VALUE (units 10^{-2})	EVTS	DOCUMENT ID		TECN	COMMENT
87.8±1.5 OUR AVERAGE					
87.0±1.7		[28,29] ESEN	13	BELL	$B_s^0 \to D_s^-\pi^+$
90.5±3.2±0.1	227	[29,30] LI	12	BELL	$B_s^0 \to J/\psi\eta^{(\prime)}$
• • • We do not use the following data for averages, fits, limits, etc. • • •					
$90.1\ ^{+3.8}_{-4.0}$±0.2		[31] LOUVOT	09	BELL	10.86 $e^+e^- \to B_s^{(*)}\overline{B}_s^{(*)}$
$93\ ^{+7}_{-9}$ ±1		[31] DRUTSKOY	07A	BELL	Superseded by LOUVOT 09

$\Gamma(B_s\overline{B}_s)/\Gamma(B_s^{(*)}\overline{B}_s^{(*)})$ $\Gamma_{11}/\Gamma_{10}=\Gamma_{11}/(\Gamma_{11}+\Gamma_{12}+\Gamma_{13})$

VALUE	DOCUMENT ID		TECN	COMMENT
$2.6^{+2.6}_{-2.5}$	LOUVOT	09	BELL	10.86 $e^+e^- \to B_s^{(*)}\overline{B}_s^{(*)}$

$\Gamma(B_s\overline{B}_s)/\Gamma(B_s^*\overline{B}_s^*)$ Γ_{11}/Γ_{13}

VALUE	CL%	DOCUMENT ID		TECN	COMMENT
<0.16	90	BONVICINI	06	CLE3	e^+e^-

$\Gamma(B_s\overline{B}_s^* + \text{c.c.})/\Gamma(B_s^{(*)}\overline{B}_s^{(*)})$ $\Gamma_{12}/\Gamma_{10}=\Gamma_{12}/(\Gamma_{11}+\Gamma_{12}+\Gamma_{13})$

VALUE	EVTS	DOCUMENT ID		TECN	COMMENT
6.7±1.2 OUR AVERAGE					
7.3±1.4	28,29	ESEN	13	BELL	$B_s^0 \to D_s^-\pi^+$
4.9±2.5±0.0	227	29,30 LI	12	BELL	$B_s^0 \to J/\psi\eta^{(\prime)}$
• • • We do not use the following data for averages, fits, limits, etc. • • •					
$7.3^{+3.3}_{-3.0}$±0.1		LOUVOT	09	BELL	10.86 $e^+e^- \to B_s^{(*)}\overline{B}_s^{(*)}$

$\Gamma(B_s\overline{B}_s^* + \text{c.c.})/\Gamma(B_s^*\overline{B}_s^*)$ Γ_{12}/Γ_{13}

VALUE	CL%	DOCUMENT ID		TECN	COMMENT
<0.16	90	BONVICINI	06	CLE3	e^+e^-

$\Gamma(\text{no open-bottom})/\Gamma_{\text{total}}$ Γ_{14}/Γ

VALUE	DOCUMENT ID
$0.038^{+0.051}_{-0.005}$ **OUR EVALUATION**	

$\Gamma(K^*(892)^0\overline{K}^0)/\Gamma_{\text{total}}$ Γ_{16}/Γ

VALUE	CL%	DOCUMENT ID		TECN	COMMENT
$<1.0\times10^{-5}$	90	SHEN	13A	BELL	$e^+e^- \to K^*(892)^0\overline{K}^0$

$\Gamma(\Upsilon(1S)\pi^+\pi^-)/\Gamma_{\text{total}}$ Γ_{17}/Γ

VALUE (units 10^{-3})	EVTS	DOCUMENT ID		TECN	COMMENT
5.3±0.3±0.5	325	32 CHEN	08	BELL	10.87 $e^+e^- \to \Upsilon(1S)\pi^+\pi^-$

$\Gamma(\Upsilon(2S)\pi^+\pi^-)/\Gamma_{\text{total}}$ Γ_{18}/Γ

VALUE (units 10^{-3})	EVTS	DOCUMENT ID		TECN	COMMENT
7.8±0.6±1.1	186	32 CHEN	08	BELL	10.87 $e^+e^- \to \Upsilon(2S)\pi^+\pi^-$

$\Gamma(\Upsilon(3S)\pi^+\pi^-)/\Gamma_{\text{total}}$ Γ_{19}/Γ

VALUE (units 10^{-3})	EVTS	DOCUMENT ID		TECN	COMMENT
$4.8^{+1.8}_{-1.5}$±0.7	10	32 CHEN	08	BELL	10.87 $e^+e^- \to \Upsilon(3S)\pi^+\pi^-$

$\Gamma(\Upsilon(1S)K^+K^-)/\Gamma_{\text{total}}$ Γ_{20}/Γ

VALUE (units 10^{-4})	EVTS	DOCUMENT ID		TECN	COMMENT
$6.1^{+1.6}_{-1.4}$±1.0	20	32 CHEN	08	BELL	10.87 $e^+e^- \to \Upsilon(1S)K^+K^-$

$\Gamma(h_b(1P)\pi^+\pi^-)/\Gamma(\Upsilon(2S)\pi^+\pi^-)$ Γ_{21}/Γ_{18}

VALUE	DOCUMENT ID		TECN	COMMENT
$0.45\pm0.08^{+0.07}_{-0.12}$	ADACHI	12	BELL	10.86 e^+e^- → hadrons

$\Gamma(h_b(2P)\pi^+\pi^-)/\Gamma(\Upsilon(2S)\pi^+\pi^-)$ Γ_{22}/Γ_{18}

VALUE	DOCUMENT ID		TECN	COMMENT
$0.77\pm0.08^{+0.22}_{-0.17}$	ADACHI	12	BELL	10.86 e^+e^- → hadrons

$\Gamma(h_b(1P)\pi^+\pi^-)/\Gamma(h_b(2P)\pi^+\pi^-)$ Γ_{21}/Γ_{22}

VALUE	DOCUMENT ID		TECN	COMMENT
0.616±0.052±0.017	MIZUK	16	BELL	$e^+e^- \to h_b(1P,2P)\pi^+\pi^-$

$\Gamma(\chi_{b0}(1P)\pi^+\pi^-\pi^0)/\Gamma_{\text{total}}$ Γ_{23}/Γ

VALUE	CL%	DOCUMENT ID		TECN	COMMENT
$<6.3\times10^{-3}$	90	33 HE	14	BELL	$\Upsilon(5S) \to \pi^+\pi^-\pi^0\gamma\Upsilon(1S)$

$\Gamma(\chi_{b0}(1P)\omega)/\Gamma_{\text{total}}$ Γ_{24}/Γ

VALUE	CL%	DOCUMENT ID		TECN	COMMENT
$<3.9\times10^{-3}$	90	33 HE	14	BELL	$\Upsilon(5S) \to \pi^+\pi^-\pi^0\gamma\Upsilon(1S)$

$\Gamma(\chi_{b0}(1P)(\pi^+\pi^-\pi^0)_{\text{non}-\omega})/\Gamma_{\text{total}}$ Γ_{25}/Γ

VALUE	CL%	DOCUMENT ID		TECN	COMMENT
$<4.8\times10^{-3}$	90	33 HE	14	BELL	$\Upsilon(5S) \to \pi^+\pi^-\pi^0\gamma\Upsilon(1S)$

$\Gamma(\chi_{b1}(1P)\pi^+\pi^-\pi^0)/\Gamma_{\text{total}}$ Γ_{26}/Γ

VALUE (units 10^{-3})	EVTS	DOCUMENT ID		TECN	COMMENT
1.85±0.23±0.23	80	33 HE	14	BELL	$\Upsilon(5S) \to \pi^+\pi^-\pi^0\gamma\Upsilon(1S)$

$\Gamma(\chi_{b1}(1P)\omega)/\Gamma_{\text{total}}$ Γ_{27}/Γ

VALUE (units 10^{-3})	EVTS	DOCUMENT ID		TECN	COMMENT
1.57±0.22±0.21	60	33 HE	14	BELL	$\Upsilon(5S) \to \pi^+\pi^-\pi^0\gamma\Upsilon(1S)$

$\Gamma(\chi_{b1}(1P)(\pi^+\pi^-\pi^0)_{\text{non}-\omega})/\Gamma_{\text{total}}$ Γ_{28}/Γ

VALUE (units 10^{-3})	EVTS	DOCUMENT ID		TECN	COMMENT
0.52±0.15±0.11	24	33 HE	14	BELL	$\Upsilon(5S) \to \pi^+\pi^-\pi^0\gamma\Upsilon(1S)$

$\Gamma(\chi_{b2}(1P)\pi^+\pi^-\pi^0)/\Gamma_{\text{total}}$ Γ_{29}/Γ

VALUE (units 10^{-3})	EVTS	DOCUMENT ID		TECN	COMMENT
1.17±0.27±0.14	29	33 HE	14	BELL	$\Upsilon(5S) \to \pi^+\pi^-\pi^0\gamma\Upsilon(1S)$

$\Gamma(\chi_{b2}(1P)\omega)/\Gamma_{\text{total}}$ Γ_{30}/Γ

VALUE (units 10^{-3})	EVTS	DOCUMENT ID		TECN	COMMENT
0.60±0.23±0.15	13	33 HE	14	BELL	$\Upsilon(5S) \to \pi^+\pi^-\pi^0\gamma\Upsilon(1S)$

$\Gamma(\chi_{b2}(1P)\omega)/\Gamma(\chi_{b1}(1P)\omega)$ Γ_{30}/Γ_{27}

VALUE	DOCUMENT ID		TECN	COMMENT
• • • We do not use the following data for averages, fits, limits, etc. • • •				
0.38±0.16±0.09	34 HE	14	BELL	$\Upsilon(5S) \to \pi^+\pi^-\pi^0\gamma\Upsilon(1S)$

$\Gamma(\chi_{b2}(1P)(\pi^+\pi^-\pi^0)_{\text{non}-\omega})/\Gamma_{\text{total}}$ Γ_{31}/Γ

VALUE (units 10^{-3})	EVTS	DOCUMENT ID		TECN	COMMENT
0.61±0.22±0.28	16	33 HE	14	BELL	$\Upsilon(5S) \to \pi^+\pi^-\pi^0\gamma\Upsilon(1S)$

$\Gamma(\chi_{b2}(1P)(\pi^+\pi^-\pi^0)_{\text{non}-\omega})/\Gamma(\chi_{b1}(1P)(\pi^+\pi^-\pi^0)_{\text{non}-\omega})$ Γ_{31}/Γ_{28}

VALUE	DOCUMENT ID		TECN	COMMENT
• • • We do not use the following data for averages, fits, limits, etc. • • •				
1.20±0.55±0.65	34 HE	14	BELL	$\Upsilon(5S) \to \pi^+\pi^-\pi^0\gamma\Upsilon(1S)$

$\Gamma(\gamma X_b \to \gamma\Upsilon(1S)\omega)/\Gamma_{\text{total}}$ Γ_{32}/Γ

VALUE	CL%	DOCUMENT ID		TECN	COMMENT
$<3.8\times10^{-5}$	90	35 HE	14	BELL	$\Upsilon(5S) \to \pi^+\pi^-\pi^0\gamma\Upsilon(1S)$

$\Gamma(\phi \text{ anything})/\Gamma_{\text{total}}$ Γ_{33}/Γ

VALUE	DOCUMENT ID		TECN	COMMENT
$0.138\pm0.007^{+0.023}_{-0.015}$	HUANG	07	CLEO	$\Upsilon(5S) \to \phi X$

$\Gamma(D^0 \text{ anything} + \text{c.c.})/\Gamma_{\text{total}}$ Γ_{34}/Γ

VALUE	DOCUMENT ID		TECN	COMMENT
1.076±0.040±0.068	DRUTSKOY	07	BELL	$\Upsilon(5S) \to D^0X$

$\Gamma(D_s \text{ anything} + \text{c.c.})/\Gamma_{\text{total}}$ Γ_{35}/Γ

VALUE	DOCUMENT ID		TECN	COMMENT
0.46 ±0.06 OUR AVERAGE				
0.472±0.024±0.072	26 DRUTSKOY	07	BELL	$\Upsilon(5S) \to D_sX$
0.44 ±0.09 ±0.04	36 ARTUSO	05B	CLE3	$e^+e^- \to D_sX$

$\Gamma(J/\psi \text{ anything})/\Gamma_{\text{total}}$ Γ_{36}/Γ

VALUE (units 10^{-2})	DOCUMENT ID		TECN	COMMENT
2.060±0.160±0.134	DRUTSKOY	07	BELL	$\Upsilon(5S) \to J/\psi X$

$\Gamma(B^0 \text{ anything} + \text{c.c.})/\Gamma_{\text{total}}$ Γ_{37}/Γ

VALUE	EVTS	DOCUMENT ID		TECN	COMMENT
$0.770^{+0.058}_{-0.056}\pm0.061$	352	DRUTSKOY	10	BELL	$\Upsilon(5S) \to B^0X$

$\Gamma(B^+ \text{ anything} + \text{c.c.})/\Gamma_{\text{total}}$ Γ_{38}/Γ

VALUE	EVTS	DOCUMENT ID		TECN	COMMENT
$0.721^{+0.039}_{-0.038}\pm0.050$	711	DRUTSKOY	10	BELL	$\Upsilon(5S) \to B^+X$

[21] Not independent of DRUTSKOY 10 values for $\Upsilon(5S) \to B^{\pm,0}$ anything.
[22] Using measurements or limits from AQUINES 06.
[23] Assuming isospin conservation.
[24] Supersedes DRUTSKOY 07.
[25] Supersedes ARTUSO 05B. Combining inclusive ϕ, D_s, and B measurements. Using $B(D_s^+ \to \phi\pi^+) = 4.4 \pm 0.6\%$ from PDG 06.
[26] Using $B(D_s^+ \to \phi\pi^+) = (4.4 \pm 0.6)\%$ from PDG 06.
[27] Uses a model-dependent estimate $B(B_s \to D_sX) = (92 \pm 11)\%$.
[28] Supersedes LOUVOT 09.
[29] With $N(B_s^{(*)}\overline{B}_s^{(*)}) = (7.11 \pm 1.30) \times 10^6$.
[30] The ratios $N(B_s^*\overline{B}_s^*)$ / $N(B_s^{(*)}\overline{B}_s^{(*)})$ and $N(B_s^*\overline{B}_s^0)$ / $N(B_s^{(*)}\overline{B}_s^{(*)})$ are measured with a correlation coefficient of −0.72.
[31] From a measurement of $\sigma(e^+e^- \to B_s^*\overline{B}_s^*)$ / $\sigma(e^+e^- \to B_s^{(*)}\overline{B}_s^{(*)})$ at $\sqrt{s} = 10.86$ GeV.
[32] Assuming that the observed events are solely due to the $\Upsilon(5S)$ resonance.
[33] Assuming that all the $b\overline{b}$ events are from $\Upsilon(5S)$ resonance decays and using $\sigma(e^+e^- \to b\overline{b}) = 0.340 \pm 0.016$ nb from ESEN 13. Correlated with other results from HE 14.
[34] Accounting for correlated systematics.
[35] Assuming that all the $b\overline{b}$ events are from $\Upsilon(5S)$ resonance decays and using $\sigma(e^+e^- \to b\overline{b}) = 0.340 \pm 0.016$ nb from ESEN 13. Correlated with other results from HE 14. For a state X_b with mass between 10.55 GeV/c^2 and 10.65 GeV/c^2, the obtained 90% upper limit as a function of m_{X_b} varies from 2.6×10^{-5} to 3.8×10^{-5}.
[36] ARTUSO 05B reports $[\Gamma(\Upsilon(10860) \to D_s \text{ anything} + \text{c.c.})/\Gamma_{\text{total}}] \times [B(D_s^+ \to \phi\pi^+)] = 0.0198 \pm 0.0019 \pm 0.0038$ which we divide by our best value $B(D_s^+ \to \phi\pi^+) = (4.5 \pm 0.4) \times 10^{-2}$. Our first error is their experiment's error and our second error is the systematic error from using our best value.

Meson Particle Listings

$\Upsilon(10860)$, $\Upsilon(11020)$

$\Upsilon(10860)$ REFERENCES

MIZUK	16	PRL 117 142001	R. Mizuk *et al.*	(BELLE Collab.)
SANTEL	16	PR D93 011101	D. Santel *et al.*	(BELLE Collab.)
HE	14	PRL 113 142001	X.H. He *et al.*	(BELLE Collab.)
ESEN	13	PR D87 031101	S. Esen *et al.*	(BELLE Collab.)
SHEN	13A	PR D88 052019	C.P. Shen *et al.*	(BELLE Collab.)
ADACHI	12	PRL 108 032001	I. Adachi *et al.*	(BELLE Collab.)
LI	12	PRL 108 181808	J. Li *et al.*	(BELLE Collab.)
CHEN	10	PR D82 091106	K.-F. Chen *et al.*	(BELLE Collab.)
DRUTSKOY	10	PR D81 112003	A. Drutskoy *et al.*	(BELLE Collab.)
AUBERT	09E	PRL 102 012001	B. Aubert *et al.*	(BABAR Collab.)
LOUVOT	09	PRL 102 021801	R. Louvot *et al.*	(BELLE Collab.)
CHEN	08	PRL 100 112001	K.-F. Chen *et al.*	(BELLE Collab.)
DRUTSKOY	07	PRL 98 052001	A. Drutskoy *et al.*	(BELLE Collab.)
DRUTSKOY	07A	PR D76 012002	A. Drutskoy *et al.*	(BELLE Collab.)
HUANG	07	PR D75 012002	G.S. Huang *et al.*	(CLEO Collab.)
AQUINES	06	PRL 96 152001	O. Aquines *et al.*	(CLEO Collab.)
BONVICINI	06	PRL 96 022002	G. Bonvicini *et al.*	(CLEO Collab.)
PDG	06	JP G33 1	W.-M. Yao *et al.*	(PDG Collab.)
ARTUSO	05B	PRL 95 261801	M. Artuso *et al.*	(CLEO Collab.)
BESSON	85	PRL 54 381	D. Besson *et al.*	(CLEO Collab.)
LOVELOCK	85	PRL 54 377	D.M.J. Lovelock *et al.*	(CUSB Collab.)

$\Upsilon(11020)$

$I^G(J^{PC}) = 0^-(1^{--})$

$\Upsilon(11020)$ MASS

VALUE (MeV)	*DOCUMENT ID*		*TECN*	*COMMENT*
$10992.9^{+10.0}_{-3.1}$ OUR AVERAGE				
$10999.0^{+7.3}_{-7.8}{}^{+16.9}_{-1.0}$	[1] MIZUK	16	BELL	$e^+e^- \to h_b(1P,2P)\pi^+\pi^-$
$10987.5^{+6.4}_{-2.5}{}^{+9.1}_{-2.3}$	[2] SANTEL	16	BELL	$e^+e^- \to \Upsilon(1S,2S,3S)\pi^+\pi^-$
• • • We do not use the following data for averages, fits, limits, etc. • • •				
$11003.0 \pm 1.1^{+0.9}_{-1.0}$	[3,4] SANTEL	16	BELL	$e^+e^- \to$ hadrons
10996 ± 2	[5] AUBERT	09E	BABR	$e^+e^- \to$ hadrons
$11019 \pm 5 \pm 7$	BESSON	85	CLEO	$e^+e^- \to$ hadrons
11020 ± 30	LOVELOCK	85	CUSB	$e^+e^- \to$ hadrons

[1] From a simultaneous fit to the $h_b(nP)\pi^+\pi^-$, $n = 1$, 2 cross sections at 22 energy points within $\sqrt{s} = 10.77$–11.02 GeV to a pair of interfering Breit-Wigner amplitudes modified by phase space factors, with eight resonance parameters (a mass and width for each of $\Upsilon(10860)$ and $\Upsilon(11020)$, a single relative phase, a single relative amplitude, and two overall normalization factors, one for each n). The systematic error estimate is dominated by possible interference with a small nonresonant continuum amplitude.

[2] From a simultaneous fit to the $\Upsilon(nS)\pi^+\pi^-$, $n = 1$, 2, 3 cross sections at 25 energy points within $\sqrt{s} = 10.6$–11.05 GeV to a pair of interfering Breit-Wigner amplitudes modified by phase space factors, with fourteen resonance parameters (a mass, width, and three amplitudes for each of $\Upsilon(10860)$ and $\Upsilon(11020)$, a single universal relative phase, and three decoherence coefficients, one for each n). Continuum contributions were measured (and therefore fixed) to be zero.

[3] From a fit to the total hadronic cross sections measured at 60 energy points within $\sqrt{s} = 10.82$–11.05 GeV to a pair of interfering Breit-Wigner amplitudes and two floating continuum amplitudes with $1/\sqrt{s}$ dependence, one coherent with the resonances and one incoherent, with six resonance parameters (a mass, width, and an amplitude for each of $\Upsilon(10860)$ and $\Upsilon(11020)$, one relative phase, and one decoherence coefficient).

[4] Not including uncertain and potentially large systematic errors due to assumed continuum amplitude $1/\sqrt{s}$ dependence and related interference contributions.

[5] In a model where a flat non-resonant $b\overline{b}$-continuum is incoherently added to a second flat component interfering with two Breit-Wigner resonances. Systematic uncertainties not estimated.

$\Upsilon(11020)$ WIDTH

VALUE (MeV)	*DOCUMENT ID*		*TECN*	*COMMENT*
49^{+9}_{-15} OUR AVERAGE				
$27^{+27}_{-11}{}^{+5}_{-12}$	[6] MIZUK	16	BELL	$e^+e^- \to h_b(1P,2P)\pi^+\pi^-$
$61^{+9}_{-19}{}^{+2}_{-20}$	[7] SANTEL	16	BELL	$e^+e^- \to \Upsilon(1S,2S,3S)\pi^+\pi^-$
• • • We do not use the following data for averages, fits, limits, etc. • • •				
$39.3^{+1.7}_{-1.6}{}^{+1.3}_{-2.4}$	[8,9] SANTEL	16	BELL	$e^+e^- \to$ hadrons
37 ± 3	[10] AUBERT	09E	BABR	$e^+e^- \to$ hadrons
$61 \pm 13 \pm 22$	BESSON	85	CLEO	$e^+e^- \to$ hadrons
90 ± 20	LOVELOCK	85	CUSB	$e^+e^- \to$ hadrons

[6] From a simultaneous fit to the $h_b(nP)\pi^+\pi^-$, $n = 1$, 2 cross sections at 22 energy points within $\sqrt{s} = 10.77$–11.02 GeV to a pair of interfering Breit-Wigner amplitudes modified by phase space factors, with eight resonance parameters (a mass and width for each of $\Upsilon(10860)$ and $\Upsilon(11020)$, a single relative phase, a single relative amplitude, and two overall normalization factors, one for each n). The systematic error estimate is dominated by possible interference with a small nonresonant continuum amplitude.

[7] From a simultaneous fit to the $\Upsilon(nS)\pi^+\pi^-$, n=1, 2, 3 cross sections at 25 energy points within $\sqrt{s} = 10.6$–11.05 GeV to a pair of interfering Breit-Wigner amplitudes modified by phase space factors, with fourteen resonance parameters (a mass, width, and three amplitudes for each of $\Upsilon(10860)$ and $\Upsilon(11020)$, a single universal relative phase, and three decoherence coefficients, one for each n). Continuum contributions were measured (and therefore fixed) to be zero.

[8] From a fit to the total hadronic cross sections measured at 60 energy points within $\sqrt{s} = 10.82$–11.05 GeV to a pair of interfering Breit-Wigner amplitudes and two floating continuum amplitudes with $1/\sqrt{s}$ dependence, one coherent with the resonances and one incoherent, with six resonance parameters (a mass, width, and an amplitude for each of $\Upsilon(10860)$ and $\Upsilon(11020)$, one relative phase, and one decoherence coefficient).

[9] Not including uncertain and potentially large systematic errors due to assumed continuum amplitude $1/\sqrt{s}$ dependence and related interference contributions.

[10] In a model where a flat non-resonant $b\overline{b}$-continuum is incoherently added to a second flat component interfering with two Breit-Wigner resonances. Systematic uncertainties not estimated.

$\Upsilon(11020)$ DECAY MODES

	Mode	Fraction (Γ_i/Γ)
Γ_1	e^+e^-	$(2.7^{+1.0}_{-0.8}) \times 10^{-6}$

$\Upsilon(11020)$ PARTIAL WIDTHS

$\Gamma(e^+e^-)$ **Γ_1**

VALUE (keV)	*DOCUMENT ID*		*TECN*	*COMMENT*
0.130 ± 0.030 OUR AVERAGE				
$0.095 \pm 0.03 \pm 0.035$	BESSON	85	CLEO	$e^+e^- \to$ hadrons
0.156 ± 0.040	LOVELOCK	85	CUSB	$e^+e^- \to$ hadrons

$\Upsilon(11020)$ REFERENCES

MIZUK	16	PRL 117 142001	R. Mizuk *et al.*	(BELLE Collab.)
SANTEL	16	PR D93 011101	D. Santel *et al.*	(BELLE Collab.)
AUBERT	09E	PRL 102 012001	B. Aubert *et al.*	(BABAR Collab.)
BESSON	85	PRL 54 381	D. Besson *et al.*	(CLEO Collab.)
LOVELOCK	85	PRL 54 377	D.M.J. Lovelock *et al.*	(CUSB Collab.)

N BARYONS
(S = 0, I = 1/2)

p, $N^+ = uud$; n, $N^0 = udd$

p

$I(J^P) = \frac{1}{2}(\frac{1}{2}^+)$ Status: ****

p MASS (atomic mass units u)

The mass is known much more precisely in u (atomic mass units) than in MeV. See the next data block.

VALUE (u)	DOCUMENT ID		TECN	COMMENT
1.007276466879±0.000000000091	MOHR	16	RVUE	2014 CODATA value
• • • We do not use the following data for averages, fits, limits, etc. • • •				
1.007276466583±0.000000000032	[1] HEISSE	17	SPEC	Penning trap
1.007276466812±0.000000000090	MOHR	12	RVUE	2010 CODATA value
1.00727646677 ±0.00000000010	MOHR	08	RVUE	2006 CODATA value
1.00727646688 ±0.00000000013	MOHR	05	RVUE	2002 CODATA value
1.00727646688 ±0.00000000013	MOHR	99	RVUE	1998 CODATA value
1.007276470 ±0.000000012	COHEN	87	RVUE	1986 CODATA value

[1] The statistical and systematic errors are 15 and 29 in the last two places of the value. The value disagrees with the MOHR 16 value by over 3 standard deviations.

p MASS (MeV)

The mass is known much more precisely in u (atomic mass units) than in MeV. The conversion from u to MeV, 1 u = 931.494 0054(57) MeV/c^2 (MOHR 16, the 2014 CODATA value), involves the relatively poorly known electronic charge.

VALUE (MeV)	DOCUMENT ID		TECN	COMMENT
938.2720813±0.0000058	MOHR	16	RVUE	2014 CODATA value
• • • We do not use the following data for averages, fits, limits, etc. • • •				
938.272046 ±0.000021	MOHR	12	RVUE	2010 CODATA value
938.272013 ±0.000023	MOHR	08	RVUE	2006 CODATA value
938.272029 ±0.000080	MOHR	05	RVUE	2002 CODATA value
938.271998 ±0.000038	MOHR	99	RVUE	1998 CODATA value
938.27231 ±0.00028	COHEN	87	RVUE	1986 CODATA value
938.2796 ±0.0027	COHEN	73	RVUE	1973 CODATA value

$|m_p - m_{\overline{p}}|/m_p$

A test of *CPT* invariance. Note that the comparison of the $\overline{p}$ and p charge-to-mass ratio, given in the next data block, is much better determined.

VALUE	CL%	DOCUMENT ID		TECN	COMMENT
<7 × 10⁻¹⁰	90	[1] HORI	11	SPEC	$\overline{p}e^-$He atom
• • • We do not use the following data for averages, fits, limits, etc. • • •					
<2 × 10⁻⁹	90	[1] HORI	06	SPEC	$\overline{p}e^-$He atom
<1.0 × 10⁻⁸	90	[1] HORI	03	SPEC	$\overline{p}e^-$ ^{4}He, $\overline{p}e^-$ ^{3}He
<6 × 10⁻⁸	90	[1] HORI	01	SPEC	$\overline{p}e^-$He atom
<5 × 10⁻⁷		[2] TORII	99	SPEC	$\overline{p}e^-$He atom

[1] HORI 01, HORI 03, HORI 06, and HORI 11 use the more-precisely-known constraint on the $\overline{p}$ charge-to-mass ratio of GABRIELSE 99 (see below) to get their results. Their results are not independent of the HORI 01, HORI 03, HORI 06, and HORI 11 values for $|q_p+q_{\overline{p}}|/e$, below.

[2] TORII 99 uses the more-precisely-known constraint on the $\overline{p}$ charge-to-mass ratio of GABRIELSE 95 (see below) to get this result. This is not independent of the TORII 99 value for $|q_p+q_{\overline{p}}|/e$, below.

$\overline{p}/p$ CHARGE-TO-MASS RATIO, $|\frac{q_{\overline{p}}}{m_{\overline{p}}}|/(\frac{q_p}{m_p})$

A test of *CPT* invariance. Listed here are measurements involving the *inertial* masses. For a discussion of what may be inferred about the ratio of $\overline{p}$ and p *gravitational* masses, see ERICSON 90; they obtain an upper bound of 10^{-6}–10^{-7} for violation of the equivalence principle for $\overline{p}$'s.

VALUE	DOCUMENT ID		TECN	COMMENT
1.000000000001±0.000000000069	ULMER	15	TRAP	Penning trap
• • • We do not use the following data for averages, fits, limits, etc. • • •				
0.99999999991 ±0.00000000009	GABRIELSE	99	TRAP	Penning trap
1.0000000015 ±0.0000000011	[1] GABRIELSE	95	TRAP	Penning trap
1.000000023 ±0.000000042	[2] GABRIELSE	90	TRAP	Penning trap

[1] Equation (2) of GABRIELSE 95 should read $M(\overline{p})/M(p) = 0.999\,999\,998\underline{5}\,(11)$ (G. Gabrielse, private communication).

[2] GABRIELSE 90 also measures $m_{\overline{p}}/m_{e^-} = 1836.152660 \pm 0.000083$ and $m_p/m_{e^-} = 1836.152680 \pm 0.000088$. Both are completely consistent with the 1986 CODATA (COHEN 87) value for m_p/m_{e^-} of 1836.152701 ± 0.000037.

$(|\frac{q_{\overline{p}}}{m_{\overline{p}}}|-\frac{q_p}{m_p})/\frac{q_p}{m_p}$

A test of *CPT* invariance. Taken from the $\overline{p}/p$ charge-to-mass ratio, above.

VALUE	DOCUMENT ID
(−9±9) × 10⁻¹¹ OUR EVALUATION	

$|q_p + q_{\overline{p}}|/e$

A test of *CPT* invariance. Note that the comparison of the $\overline{p}$ and p charge-to-mass ratios given above is much better determined. See also a similar test involving the electron.

VALUE	CL%	DOCUMENT ID		TECN	COMMENT
<7 × 10⁻¹⁰	90	[1] HORI	11	SPEC	$\overline{p}e^-$He atom
• • • We do not use the following data for averages, fits, limits, etc. • • •					
<2 × 10⁻⁹	90	[1] HORI	06	SPEC	$\overline{p}e^-$He atom
<1.0 × 10⁻⁸	90	[1] HORI	03	SPEC	$\overline{p}e^-$ ^{4}He, $\overline{p}e^-$ ^{3}He
<6 × 10⁻⁸	90	[1] HORI	01	SPEC	$\overline{p}e^-$He atom
<5 × 10⁻⁷		[2] TORII	99	SPEC	$\overline{p}e^-$He atom
<2 × 10⁻⁵		[3] HUGHES	92	RVUE	

[1] HORI 01, HORI 03, HORI 06, and HORI 11 use the more-precisely-known constraint on the $\overline{p}$ charge-to-mass ratio of GABRIELSE 99 (see above) to get their results. Their results are not independent of the HORI 01, HORI 03, HORI 06, and HORI 11 values for $|m_p-m_{\overline{p}}|/m_p$, above.

[2] TORII 99 uses the more-precisely-known constraint on the $\overline{p}$ charge-to-mass ratio of GABRIELSE 95 (see above) to get this result. This is not independent of the TORII 99 value for $|m_p-m_{\overline{p}}|/m_p$, above.

[3] HUGHES 92 uses recent measurements of Rydberg-energy and cyclotron-frequency ratios.

$|q_p + q_e|/e$

See BRESSI 11 for a summary of experiments on the neutrality of matter.
See also "*n* CHARGE" in the neutron Listings.

VALUE	DOCUMENT ID		COMMENT
<1 × 10⁻²¹	[1] BRESSI	11	Neutrality of SF_6
• • • We do not use the following data for averages, fits, limits, etc. • • •			
<3.2 × 10⁻²⁰	[2] SENGUPTA	00	binary pulsar
<0.8 × 10⁻²¹	MARINELLI	84	Magnetic levitation
<1.0 × 10⁻²¹	[1] DYLLA	73	Neutrality of SF_6

[1] BRESSI 11 uses the method of DYLLA 73 but finds serious errors in that experiment that greatly reduce its accuracy. The BRESSI 11 limit assumes that $n \rightarrow p e^- \nu_e$ conserves charge. Thus the limit applies equally to the charge of the neutron.

[2] SENGUPTA 00 uses the difference between the observed rate of of rotational energy loss by the binary pulsar PSR B1913+16 and the rate predicted by general relativity to set this limit. See the paper for assumptions.

p MAGNETIC MOMENT

See the "Note on Baryon Magnetic Moments" in the Λ Listings.

VALUE (μ_N)	DOCUMENT ID		TECN	COMMENT
2.79284734462±0.00000000082	SCHNEIDER	17	TRAP	Double Penning trap
• • • We do not use the following data for averages, fits, limits, etc. • • •				
2.7928473508 ±0.0000000085	MOHR	16	RVUE	2014 CODATA value
2.792847356 ±0.000000023	MOHR	12	RVUE	2010 CODATA value
2.792847356 ±0.000000023	MOHR	08	RVUE	2006 CODATA value
2.792847351 ±0.000000028	MOHR	05	RVUE	2002 CODATA value
2.792847337 ±0.000000029	MOHR	99	RVUE	1998 CODATA value
2.792847386 ±0.000000063	COHEN	87	RVUE	1986 CODATA value

$\overline{p}$ MAGNETIC MOMENT

A few early results have been omitted.

VALUE (μ_N)	DOCUMENT ID		TECN	COMMENT
−2.7928473441±0.0000000042	SMORRA	17	TRAP	Hot/cold $\overline{p}$ frequencies, Penning traps
• • • We do not use the following data for averages, fits, limits, etc. • • •				
−2.7928465 ±0.0000023	NAGAHAMA	17	TRAP	Single $\overline{p}$, Penning trap
−2.792845 ±0.000012	DISCIACCA	13	TRAP	Single $\overline{p}$, Penning trap
−2.7862 ±0.0083	PASK	09	CNTR	$\overline{p}$ He^+ hyperfine structure
−2.8005 ±0.0090	KREISSL	88	CNTR	$\overline{p}$ ^{208}Pb 11→ 10 X-ray
−2.817 ±0.048	ROBERTS	78	CNTR	
−2.791 ±0.021	HU	75	CNTR	Exotic atoms

$(\mu_p + \mu_{\overline{p}}) / \mu_p$

A test of CPT invariance.

VALUE (units 10^{-6})	DOCUMENT ID		TECN	COMMENT
0.3±0.8 OUR AVERAGE				
0.3±0.8	NAGAHAMA	17	TRAP	Single $\overline{p}$, Penning trap
0 ±5	DISCIACCA	13	TRAP	Single $\overline{p}$, Penning trap

p ELECTRIC DIPOLE MOMENT

A nonzero value is forbidden by both T invariance and P invariance.

VALUE (10^{-23} e cm)	DOCUMENT ID		TECN	COMMENT
< 0.021	[1] SAHOO	17		Theory plus ^{199}Hg atom EDM
• • • We do not use the following data for averages, fits, limits, etc. • • •				
< 0.54	[1] DMITRIEV	03		Theory plus ^{199}Hg atom EDM
− 3.7 ± 6.3	CHO	89	NMR	Tl F molecules
< 400	DZUBA	85	THEO	Uses ^{129}Xe moment
130 ± 200	[2] WILKENING	84		
900 ±1400	[3] WILKENING	84		
700 ± 900	HARRISON	69	MBR	Molecular beam

[1] SAHOO 17 and DMITRIEV 03 are not direct measurements of the proton electric dipole moment. They use theory to calculate this limit from the limit on the electric dipole moment of the ^{199}Hg atom.
[2] This WILKENING 84 value includes a finite-size effect and a magnetic effect.
[3] This WILKENING 84 value is more cautious than the other and excludes the finite-size effect, which relies on uncertain nuclear integrals.

p ELECTRIC POLARIZABILITY α_p

For a very complete review of the "polarizability of the nucleon and Compton scattering," see SCHUMACHER 05. His recommended values for the proton are $\alpha_p = (12.0 \pm 0.6) \times 10^{-4}$ fm^3 and $\beta_p = (1.9 \mp 0.6) \times 10^{-4}$ fm^3, almost exactly our averages.

VALUE (10^{-4} fm^3)	DOCUMENT ID		TECN	COMMENT
11.2 ±0.4 OUR AVERAGE				
10.65±0.35±0.36	MCGOVERN	13	RVUE	χEFT + Compton scattering
12.1 ±1.1 ±0.5	[1] BEANE	03		EFT + γp
$11.82 \pm 0.98^{+0.52}_{-0.98}$	[2] BLANPIED	01	LEGS	$p(\vec{\gamma},\gamma)$, $p(\vec{\gamma},\pi^0)$, $p(\vec{\gamma},\pi^+)$
11.9 ±0.5 ±1.3	[3] OLMOSDEL...	01	CNTR	γp Compton scattering
12.1 ±0.8 ±0.5	[4] MACGIBBON	95	RVUE	global average
• • • We do not use the following data for averages, fits, limits, etc. • • •				
11.7 ±0.8 ±0.7	[5] BARANOV	01	RVUE	Global average
12.5 ±0.6 ±0.9	MACGIBBON	95	CNTR	γp Compton scattering
9.8 ±0.4 ±1.1	HALLIN	93	CNTR	γp Compton scattering
$10.62^{+1.25}_{-1.19} \pm 1.07 - 1.03$	ZIEGER	92	CNTR	γp Compton scattering
10.9 ±2.2 ±1.3	[6] FEDERSPIEL	91	CNTR	γp Compton scattering

[1] BEANE 03 uses effective field theory and low-energy γp and γd Compton-scattering data. It also gets for the isoscalar polarizabilities (see the erratum) $\alpha_N = (13.0 \pm 1.9^{+3.9}_{-1.5}) \times 10^{-4}$ fm^3 and $\beta_N = (-1.8 \pm 1.9^{+2.1}_{-0.9}) \times 10^{-4}$ fm^3.
[2] BLANPIED 01 gives $\alpha_p + \beta_p$ and $\alpha_p - \beta_p$. The separate α_p and β_p are provided to us by A. Sandorfi. The first error above is statistics plus systematics; the second is from the model.
[3] This OLMOSDELEON 01 result uses the TAPS data alone, and does not use the (re-evaluated) sum-rule constraint that $\alpha + \beta = (13.8 \pm 0.4) \times 10^{-4}$ fm^3. See the paper for a discussion.
[4] MACGIBBON 95 combine the results of ZIEGER 92, FEDERSPIEL 91, and their own experiment to get a "global average" in which model errors and systematic errors are treated in a consistent way. See MACGIBBON 95 for a discussion.
[5] BARANOV 01 combines the results of 10 experiments from 1958 through 1995 to get a global average that takes into account both systematic and model errors and does not use the theoretical constraint on the sum $\alpha_p + \beta_p$.
[6] FEDERSPIEL 91 obtains for the (static) electric polarizability α_p, defined in terms of the induced electric dipole moment by $\mathbf{D} = 4\pi\epsilon_0\alpha_p\mathbf{E}$, the value $(7.0 \pm 2.2 \pm 1.3) \times 10^{-4}$ fm^3.

p MAGNETIC POLARIZABILITY β_p

The electric and magnetic polarizabilities are subject to a dispersion sum-rule constraint $\overline{\alpha} + \overline{\beta} = (14.2 \pm 0.5) \times 10^{-4}$ fm^3. Errors here are anticorrelated with those on $\overline{\alpha}_p$ due to this constraint.

VALUE (10^{-4} fm^3)	DOCUMENT ID		TECN	COMMENT
2.5 ±0.4 OUR AVERAGE Error includes scale factor of 1.2.				
3.15±0.35±0.36	MCGOVERN	13	RVUE	χEFT + Compton scattering
3.4 ±1.1 ±0.1	[1] BEANE	03		EFT + γp
$1.43 \pm 0.98^{+0.52}_{-0.98}$	[2] BLANPIED	01	LEGS	$p(\vec{\gamma},\gamma)$, $p(\vec{\gamma},\pi^0)$, $p(\vec{\gamma},\pi^+)$
1.2 ±0.7 ±0.5	[3] OLMOSDEL...	01	CNTR	γp Compton scattering
2.1 ±0.8 ±0.5	[4] MACGIBBON	95	RVUE	global average
• • • We do not use the following data for averages, fits, limits, etc. • • •				
2.3 ±0.9 ±0.7	[5] BARANOV	01	RVUE	Global average
1.7 ±0.6 ±0.9	MACGIBBON	95	CNTR	γp Compton scattering
4.4 ±0.4 ±1.1	HALLIN	93	CNTR	γp Compton scattering
$3.58^{+1.19}_{-1.25} \pm 1.03 - 1.07$	ZIEGER	92	CNTR	γp Compton scattering
3.3 ±2.2 ±1.3	FEDERSPIEL	91	CNTR	γp Compton scattering

[1] BEANE 03 uses effective field theory and low-energy γp and γd Compton-scattering data. It also gets for the isoscalar polarizabilities (see the erratum) $\alpha_N = (13.0 \pm 1.9^{+3.9}_{-1.5}) \times 10^{-4}$ fm^3 and $\beta_N = (-1.8 \pm 1.9^{+2.1}_{-0.9}) \times 10^{-4}$ fm^3.
[2] BLANPIED 01 gives $\alpha_p + \beta_p$ and $\alpha_p - \beta_p$. The separate α_p and β_p are provided to us by A. Sandorfi. The first error above is statistics plus systematics; the second is from the model.
[3] This OLMOSDELEON 01 result uses the TAPS data alone, and does not use the (re-evaluated) sum-rule constraint that $\alpha + \beta = (13.8 \pm 0.4) \times 10^{-4}$ fm^3. See the paper for a discussion.
[4] MACGIBBON 95 combine the results of ZIEGER 92, FEDERSPIEL 91, and their own experiment to get a "global average" in which model errors and systematic errors are treated in a consistent way. See MACGIBBON 95 for a discussion.
[5] BARANOV 01 combines the results of 10 experiments from 1958 through 1995 to get a global average that takes into account both systematic and model errors and does not use the theoretical constraint on the sum $\alpha_p + \beta_p$.

p CHARGE RADIUS

This is the rms electric charge radius, $\sqrt{\langle r_E^2 \rangle}$.

There are in fact three kinds of measurements of the proton radius: with atomic hydrogen, with electron scattering off of hydrogen, and with muonic hydrogen. Most measurements of the radius of the proton involve electron-proton interactions, and most of those values, the most precise of which is $r_p = 0.879(8)$ fm (BERNAUER 10), agree with one another. The MOHR 16 value (2014 CODATA), obtained from the electronic results available at the time, is 0.8751(61) fm.

Compared to this MOHR 16 value, however, the best measurement using muonic hydrogen got $r_p = 0.84087(39)$ fm (ANTOGNINI 13), which is 16 times more precise but differs by 5.6 standard deviations.

The earlier face-off seemed to be between the two electronic methods and muonic hydrogen. But a purely statistical reanalysis of electron-scattering data by HIGINBOTHAM 16 found consistency with muonic hydrogen—so that (the paper claims) it "is the atomic hydrogen results that are the outliers." But still more recently there is a new atomic-hydrogen value, $r_p = 0.8335(95)$ fm (BEYER 17), that agrees with the muonic hydrogen value!

Since POHL 10 (the first μp result), there has been a lot of discussion about the disagreement, especially concerning the modeling of muonic hydrogen. Here is an incomplete list of papers: DERUJULA 10, CLOET 11, DISTLER 11, DERUJULA 11, ARRINGTON 11, BERNAUER 11, HILL 11, LORENZ 14, KARSHENBOIM 14A, PESET 15, SICK 17, and HORBATSCH 17.

Until the differences between the three methods are resolved, it does not make sense to average the values together. For the present, we give both the 2014 CODATA value and the best μp value. It is up to workers in the field to solve this puzzle.

See our 2014 edition (Chinese Physics **C38** 070001 (2014)) for values published before 2003.

VALUE (fm)	DOCUMENT ID		TECN	COMMENT
0.8751 ±0.0061	MOHR	16	RVUE	2014 CODATA value
0.84087±0.00026±0.00029	ANTOGNINI	13	LASR	μp-atom Lamb shift
• • • We do not use the following data for averages, fits, limits, etc. • • •				
0.8335 ±0.0095	[1] BEYER	17	LASR	2S-4P transition in H
0.895 ±0.014 ±0.014	[2] LEE	15	SPEC	Just 2010 Mainz data
0.916 ±0.024	LEE	15	SPEC	World data, no Mainz
0.8775 ±0.0051	MOHR	12	RVUE	2010 CODATA, ep data
0.875 ±0.008 ±0.006	ZHAN	11	SPEC	Recoil polarimetry
0.879 ±0.005 ±0.006	BERNAUER	10	SPEC	$ep \to ep$ form factor
0.912 ±0.009 ±0.007	BORISYUK	10		reanalyzes old ep data
0.871 ±0.009 ±0.003	HILL	10		z-expansion reanalysis
0.84184±0.00036±0.00056	POHL	10	LASR	See ANTOGNINI 13
0.8768 ±0.0069	MOHR	08	RVUE	2006 CODATA value
$0.844 \; {}^{+0.008}_{-0.004}$	BELUSHKIN	07		Dispersion analysis
0.897 ±0.018	BLUNDEN	05		SICK 03 + 2γ correction
0.8750 ±0.0068	MOHR	05	RVUE	2002 CODATA value
0.895 ±0.010 ±0.013	SICK	03		$ep \to ep$ reanalysis

[1] The BEYER 17 result is 3.3 combined standard deviations below the MOHR 16 (2014 CODATA) value. The experiment measures the 2S-4P transition in hydrogen and gets the proton radius and the Rydberg constant.
[2] Authors also provide values for combinations of all available data.

p MAGNETIC RADIUS

This is the rms magnetic radius, $\sqrt{\langle r_M^2 \rangle}$.

VALUE (fm)	DOCUMENT ID		TECN	COMMENT
0.776±0.034±0.017	[1] LEE	15	SPEC	Just 2010 Mainz data
• • • We do not use the following data for averages, fits, limits, etc. • • •				
0.914±0.035	LEE	15	SPEC	World data, no Mainz
0.87 ±0.02	EPSTEIN	14		Using ep, en, $\pi\pi$ data
0.867±0.009±0.018	ZHAN	11	SPEC	Recoil polarimetry
0.777±0.013±0.010	BERNAUER	10	SPEC	$ep \to ep$ form factor
0.876±0.010±0.016	BORISYUK	10		Reanalyzes old $ep \to ep$ data
0.854±0.005	BELUSHKIN	07		Dispersion analysis

[1] Authors also provide values for a combination of all available data.

p MEAN LIFE

A test of baryon conservation. See the "p Partial Mean Lives" section below for limits for identified final states. The limits here are to "anything" or are for "disappearance" modes of a bound proton (p) or (n). See also the 3ν modes in the "Partial Mean Lives" section. Table 1 of BACK 03 is a nice summary.

LIMIT (years)	PARTICLE	CL%	DOCUMENT ID		TECN	COMMENT
$>5.8 \times 10^{29}$	***n***	90	[1] ARAKI	06	KLND	$n \to$ invisible
$>2.1 \times 10^{29}$	***p***	90	[2] AHMED	04	SNO	$p \to$ invisible
• • • We do not use the following data for averages, fits, limits, etc. • • •						
$>1.9 \times 10^{29}$	n	90	[2] AHMED	04	SNO	$n \to$ invisible
$>1.8 \times 10^{25}$	n	90	[3] BACK	03	BORX	
$>1.1 \times 10^{26}$	p	90	[3] BACK	03	BORX	
$>3.5 \times 10^{28}$	p	90	[4] ZDESENKO	03		$p \to$ invisible
$>1 \times 10^{28}$	p	90	[5] AHMAD	02	SNO	$p \to$ invisible
$>4 \times 10^{23}$	p	95	TRETYAK	01		$d \to n +$?
$>1.9 \times 10^{24}$	p	90	[6] BERNABEI	00B	DAMA	
$>1.6 \times 10^{25}$	p, n		[7,8] EVANS	77		
$>3 \times 10^{23}$	p		[8] DIX	70	CNTR	
$>3 \times 10^{23}$	p, n		[8,9] FLEROV	58		

[1] ARAKI 06 looks for signs of de-excitation of the residual nucleus after disappearance of a neutron from the s shell of ^{12}C.

[2] AHMED 04 looks for γ rays from the de-excitation of a residual ^{15}O* or ^{15}N* following the disappearance of a neutron or proton in ^{16}O.

[3] BACK 03 looks for decays of unstable nuclides left after N decays of parent ^{12}C, ^{13}C, ^{16}O nuclei. These are "invisible channel" limits.

[4] ZDESENKO 03 gets this limit on proton disappearance in deuterium by analyzing SNO data in AHMAD 02.

[5] AHMAD 02 (see its footnote 7) looks for neutrons left behind after the disappearance of the proton in deuterons.

[6] BERNABEI 00B looks for the decay of a $^{128}_{53}$I nucleus following the disappearance of a proton in the otherwise-stable $^{129}_{54}$Xe nucleus.

[7] EVANS 77 looks for the daughter nuclide ^{129}Xe from possible ^{130}Te decays in ancient Te ore samples.

[8] This mean-life limit has been obtained from a half-life limit by dividing the latter by ln(2) = 0.693.

[9] FLEROV 58 looks for the spontaneous fission of a ^{232}Th nucleus after the disappearance of one of its nucleons.

$\overline{p}$ MEAN LIFE

Of the two astrophysical limits here, that of GEER 00D involves considerably more refinements in its modeling. The other limits come from direct observations of stored antiprotons. See also "$\overline{p}$ Partial Mean Lives" after "p Partial Mean Lives," below, for exclusive-mode limits. The best (lifetime/branching fraction) limit there is 7×10^5 years, for $\overline{p} \to e^-\gamma$. We advance only the exclusive-mode limits to our Summary Tables.

LIMIT (years)	CL%	EVTS	DOCUMENT ID		TECN	COMMENT
• • • We do not use the following data for averages, fits, limits, etc. • • •						
>5.0	90		SELLNER	17	TRAP	Penning trap
$>8 \times 10^5$	90		[1] GEER	00D		$\overline{p}/p$ ratio, cosmic rays
>0.28			GABRIELSE	90	TRAP	Penning trap
>0.08	90	1	BELL	79	CNTR	Storage ring
$>1 \times 10^7$			GOLDEN	79	SPEC	$\overline{p}/p$ ratio, cosmic rays
$>3.7 \times 10^{-3}$			BREGMAN	78	CNTR	Storage ring

[1] GEER 00D uses agreement between a model of galactic $\overline{p}$ production and propagation and the observed $\overline{p}/p$ cosmic-ray spectrum to set this limit.

p DECAY MODES

See the "Note on Nucleon Decay" in our 1994 edition (Phys. Rev. **D50**, 1173) for a short review.

The "partial mean life" limits tabulated here are the limits on τ/B_i, where τ is the total mean life and B_i is the branching fraction for the mode in question. For N decays, p and n indicate proton and neutron partial lifetimes.

	Mode	Partial mean life (10^{30} years)	Confidence level
	Antilepton + meson		
τ_1	$N \to e^+\pi$	>2000 (n), >8200 (p)	90%
τ_2	$N \to \mu^+\pi$	>1000 (n), >6600 (p)	90%
τ_3	$N \to \nu\pi$	>1100 (n), >390 (p)	90%
τ_4	$p \to e^+\eta$	>4200	90%
τ_5	$p \to \mu^+\eta$	>1300	90%
τ_6	$n \to \nu\eta$	>158	90%
τ_7	$N \to e^+\rho$	>217 (n), >710 (p)	90%
τ_8	$N \to \mu^+\rho$	>228 (n), >160 (p)	90%
τ_9	$N \to \nu\rho$	>19 (n), >162 (p)	90%
τ_{10}	$p \to e^+\omega$	>320	90%
τ_{11}	$p \to \mu^+\omega$	>780	90%
τ_{12}	$n \to \nu\omega$	>108	90%
τ_{13}	$N \to e^+K$	>17 (n), >1000 (p)	90%
τ_{14}	$p \to e^+K^0_S$		
τ_{15}	$p \to e^+K^0_L$		
τ_{16}	$N \to \mu^+K$	>26 (n), >1600 (p)	90%
τ_{17}	$p \to \mu^+K^0_S$		
τ_{18}	$p \to \mu^+K^0_L$		
τ_{19}	$N \to \nu K$	>86 (n), >5900 (p)	90%
τ_{20}	$n \to \nu K^0_S$	>260	90%
τ_{21}	$p \to e^+K^*(892)^0$	>84	90%
τ_{22}	$N \to \nu K^*(892)$	>78 (n), >51 (p)	90%
	Antilepton + mesons		
τ_{23}	$p \to e^+\pi^+\pi^-$	>82	90%
τ_{24}	$p \to e^+\pi^0\pi^0$	>147	90%
τ_{25}	$n \to e^+\pi^-\pi^0$	>52	90%
τ_{26}	$p \to \mu^+\pi^+\pi^-$	>133	90%
τ_{27}	$p \to \mu^+\pi^0\pi^0$	>101	90%
τ_{28}	$n \to \mu^+\pi^-\pi^0$	>74	90%
τ_{29}	$n \to e^+K^0\pi^-$	>18	90%
	Lepton + meson		
τ_{30}	$n \to e^-\pi^+$	>65	90%
τ_{31}	$n \to \mu^-\pi^+$	>49	90%
τ_{32}	$n \to e^-\rho^+$	>62	90%
τ_{33}	$n \to \mu^-\rho^+$	>7	90%
τ_{34}	$n \to e^-K^+$	>32	90%
τ_{35}	$n \to \mu^-K^+$	>57	90%
	Lepton + mesons		
τ_{36}	$p \to e^-\pi^+\pi^+$	>30	90%
τ_{37}	$n \to e^-\pi^+\pi^0$	>29	90%
τ_{38}	$p \to \mu^-\pi^+\pi^+$	>17	90%
τ_{39}	$n \to \mu^-\pi^+\pi^0$	>34	90%
τ_{40}	$p \to e^-\pi^+K^+$	>75	90%
τ_{41}	$p \to \mu^-\pi^+K^+$	>245	90%
	Antilepton + photon(s)		
τ_{42}	$p \to e^+\gamma$	>670	90%
τ_{43}	$p \to \mu^+\gamma$	>478	90%
τ_{44}	$n \to \nu\gamma$	>550	90%
τ_{45}	$p \to e^+\gamma\gamma$	>100	90%
τ_{46}	$n \to \nu\gamma\gamma$	>219	90%
	Antilepton + single massless		
τ_{47}	$p \to e^+X$	>790	90%
τ_{48}	$p \to \mu^+X$	>410	90%
	Three (or more) leptons		
τ_{49}	$p \to e^+e^+e^-$	>793	90%
τ_{50}	$p \to e^+\mu^+\mu^-$	>359	90%
τ_{51}	$p \to e^+\nu\nu$	>170	90%
τ_{52}	$n \to e^+e^-\nu$	>257	90%
τ_{53}	$n \to \mu^+e^-\nu$	>83	90%
τ_{54}	$n \to \mu^+\mu^-\nu$	>79	90%
τ_{55}	$p \to \mu^+e^+e^-$	>529	90%
τ_{56}	$p \to \mu^+\mu^+\mu^-$	>675	90%
τ_{57}	$p \to \mu^+\nu\nu$	>220	90%
τ_{58}	$p \to e^-\mu^+\mu^+$	>6	90%
τ_{59}	$n \to 3\nu$	$>5 \times 10^{-4}$	90%
τ_{60}	$n \to 5\nu$		

Baryon Particle Listings

p

Inclusive modes

τ_{61}	$N \rightarrow e^+$ anything	> 0.6 (n, p)	90%
τ_{62}	$N \rightarrow \mu^+$ anything	> 12 (n, p)	90%
τ_{63}	$N \rightarrow \nu$ anything		
τ_{64}	$N \rightarrow e^+ \pi^0$ anything	> 0.6 (n, p)	90%
τ_{65}	$N \rightarrow$ 2 bodies, ν-free		

$\Delta B = 2$ dinucleon modes

The following are lifetime limits per iron nucleus.

τ_{66}	$pp \rightarrow \pi^+\pi^+$	> 72.2	90%
τ_{67}	$pn \rightarrow \pi^+\pi^0$	> 170	90%
τ_{68}	$nn \rightarrow \pi^+\pi^-$	> 0.7	90%
τ_{69}	$nn \rightarrow \pi^0\pi^0$	> 404	90%
τ_{70}	$pp \rightarrow K^+K^+$	> 170	90%
τ_{71}	$pp \rightarrow e^+e^+$	> 5.8	90%
τ_{72}	$pp \rightarrow e^+\mu^+$	> 3.6	90%
τ_{73}	$pp \rightarrow \mu^+\mu^+$	> 1.7	90%
τ_{74}	$pn \rightarrow e^+\overline{\nu}$	> 260	90%
τ_{75}	$pn \rightarrow \mu^+\overline{\nu}$	> 200	90%
τ_{76}	$pn \rightarrow \tau^+\overline{\nu}_\tau$	> 29	90%
τ_{77}	$nn \rightarrow \nu_e\overline{\nu}_e$	> 1.4	90%
τ_{78}	$nn \rightarrow \nu_\mu\overline{\nu}_\mu$	> 1.4	90%
τ_{79}	$pn \rightarrow$ invisible	$> 2.1 \times 10^{-5}$	90%
τ_{80}	$pp \rightarrow$ invisible	$> 5 \times 10^{-5}$	90%

$\overline{p}$ DECAY MODES

	Mode	Partial mean life (years)	Confidence level
τ_{81}	$\overline{p} \rightarrow e^-\gamma$	$> 7 \times 10^5$	90%
τ_{82}	$\overline{p} \rightarrow \mu^-\gamma$	$> 5 \times 10^4$	90%
τ_{83}	$\overline{p} \rightarrow e^-\pi^0$	$> 4 \times 10^5$	90%
τ_{84}	$\overline{p} \rightarrow \mu^-\pi^0$	$> 5 \times 10^4$	90%
τ_{85}	$\overline{p} \rightarrow e^-\eta$	$> 2 \times 10^4$	90%
τ_{86}	$\overline{p} \rightarrow \mu^-\eta$	$> 8 \times 10^3$	90%
τ_{87}	$\overline{p} \rightarrow e^-K^0_S$	> 900	90%
τ_{88}	$\overline{p} \rightarrow \mu^-K^0_S$	$> 4 \times 10^3$	90%
τ_{89}	$\overline{p} \rightarrow e^-K^0_L$	$> 9 \times 10^3$	90%
τ_{90}	$\overline{p} \rightarrow \mu^-K^0_L$	$> 7 \times 10^3$	90%
τ_{91}	$\overline{p} \rightarrow e^-\gamma\gamma$	$> 2 \times 10^4$	90%
τ_{92}	$\overline{p} \rightarrow \mu^-\gamma\gamma$	$> 2 \times 10^4$	90%
τ_{93}	$\overline{p} \rightarrow e^-\omega$	> 200	90%

p PARTIAL MEAN LIVES

The "partial mean life" limits tabulated here are the limits on τ/B_i, where τ is the total mean life for the proton and B_i is the branching fraction for the mode in question.

Decaying particle: p = proton, n = bound neutron. The same event may appear under more than one partial decay mode. Background estimates may be accurate to a factor of two.

Antilepton + meson

$\tau(N \rightarrow e^+\pi)$ τ_1

LIMIT (10^{30} years)	PARTICLE	CL%	EVTS	BKGD EST	DOCUMENT ID		TECN
>16000	**p**	**90**	**0**	**0.61**	ABE	17	SKAM
> 5300	**n**	**90**	**0**	**0.41**	ABE	17D	SKAM
• • • We do not use the following data for averages, fits, limits, etc. • • •							
> 2000	n	90	0	0.27	NISHINO	12	SKAM
> 8200	p	90	0	0.3	NISHINO	09	SKAM
> 540	p	90	0	0.2	MCGREW	99	IMB3
> 158	n	90	3	5	MCGREW	99	IMB3
> 1600	p	90	0	0.1	SHIOZAWA	98	SKAM
> 70	p	90	0	0.5	BERGER	91	FREJ
> 70	n	90	0	≤ 0.1	BERGER	91	FREJ
> 550	p	90	0	0.7	[1] BECKER-SZ...	90	IMB3
> 260	p	90	0	<0.04	HIRATA	89C	KAMI
> 130	n	90	0	<0.2	HIRATA	89C	KAMI
> 310	p	90	0	0.6	SEIDEL	88	IMB
> 100	n	90	0	1.6	SEIDEL	88	IMB
> 1.3	n	90	0		BARTELT	87	SOUD
> 1.3	p	90	0		BARTELT	87	SOUD
> 250	p	90	0	0.3	HAINES	86	IMB
> 31	n	90	8	9	HAINES	86	IMB
> 64	p	90	0	<0.4	ARISAKA	85	KAMI
> 26	n	90	0	<0.7	ARISAKA	85	KAMI
> 82	p (free)	90	0	0.2	BLEWITT	85	IMB
> 250	p	90	0	0.2	BLEWITT	85	IMB
> 25	n	90	4	4	PARK	85	IMB
> 15	p, n	90	0		BATTISTONI	84	NUSX
> 0.5	p	90	1	0.3	[2] BARTELT	83	SOUD
> 0.5	n	90	1	0.3	[2] BARTELT	83	SOUD
> 5.8	p	90	2		[3] KRISHNA...	82	KOLR
> 5.8	n	90	2		[3] KRISHNA...	82	KOLR
> 0.1	n	90			[4] GURR	67	CNTR

[1] This BECKER-SZENDY 90 result includes data from SEIDEL 88.
[2] Limit based on zero events.
[3] We have calculated 90% CL limit from 1 confined event.
[4] We have converted half-life to 90% CL mean life.

$\tau(N \rightarrow \mu^+\pi)$ τ_2

LIMIT (10^{30} years)	PARTICLE	CL%	EVTS	BKGD EST	DOCUMENT ID		TECN
>7700	**p**	**90**	**2**	**0.87**	ABE	17	SKAM
>3500	**n**	**90**	**1**	**0.77**	ABE	17D	SKAM
• • • We do not use the following data for averages, fits, limits, etc. • • •							
>1000	n	90	1	0.43	NISHINO	12	SKAM
>6600	p	90	0	0.3	NISHINO	09	SKAM
> 473	p	90	0	0.6	MCGREW	99	IMB3
> 90	n	90	1	1.9	MCGREW	99	IMB3
> 81	p	90	0	0.2	BERGER	91	FREJ
> 35	n	90	1	1.0	BERGER	91	FREJ
> 230	p	90	0	<0.07	HIRATA	89C	KAMI
> 100	n	90	0	<0.2	HIRATA	89C	KAMI
> 270	p	90	0	0.5	SEIDEL	88	IMB
> 63	n	90	0	0.5	SEIDEL	88	IMB
> 76	p	90	2	1	HAINES	86	IMB
> 23	n	90	8	7	HAINES	86	IMB
> 46	p	90	0	<0.7	ARISAKA	85	KAMI
> 20	n	90	0	<0.4	ARISAKA	85	KAMI
> 59	p (free)	90	0	0.2	BLEWITT	85	IMB
> 100	p	90	1	0.4	BLEWITT	85	IMB
> 38	n	90	1	4	PARK	85	IMB
> 10	p, n	90	0		BATTISTONI	84	NUSX
> 1.3	p, n	90	0		ALEKSEEV	81	BAKS

$\tau(N \rightarrow \nu\pi)$ τ_3

LIMIT (10^{30} years)	PARTICLE	CL%	EVTS	BKGD EST	DOCUMENT ID		TECN
> 390	**p**	**90**	**52.8**		ABE	14E	SKAM
>1100	**n**	**90**	**19.1**		ABE	14E	SKAM
• • • We do not use the following data for averages, fits, limits, etc. • • •							
> 16	p	90	6	6.7	WALL	00B	SOU2
> 39	n	90	4	3.8	WALL	00B	SOU2
> 10	p	90	15	20.3	MCGREW	99	IMB3
> 112	n	90	6	6.6	MCGREW	99	IMB3
> 13	n	90	1	1.2	BERGER	89	FREJ
> 10	p	90	11	14	BERGER	89	FREJ
> 25	p	90	32	32.8	[1] HIRATA	89C	KAMI
> 100	n	90	1	3	HIRATA	89C	KAMI
> 6	n	90	73	60	HAINES	86	IMB
> 2	p	90	16	13	KAJITA	86	KAMI
> 40	n	90	0	1	KAJITA	86	KAMI
> 7	n	90	28	19	PARK	85	IMB
> 7	n	90	0		BATTISTONI	84	NUSX
> 2	p	90	≤ 3		BATTISTONI	84	NUSX
> 5.8	p	90	1		[2] KRISHNA...	82	KOLR
> 0.3	p	90	2		[3] CHERRY	81	HOME
> 0.1	p	90			[4] GURR	67	CNTR

[1] In estimating the background, this HIRATA 89C limit (as opposed to the later limits of WALL 00B and MCGREW 99) does not take into account present understanding that the flux of ν_μ originating in the upper atmosphere is depleted. Doing so would reduce the background and thus also would reduce the limit here.
[2] We have calculated 90% CL limit from 1 confined event.
[3] We have converted 2 possible events to 90% CL limit.
[4] We have converted half-life to 90% CL mean life.

$\tau(p \rightarrow e^+\eta)$ τ_4

LIMIT (10^{30} years)	PARTICLE	CL%	EVTS	BKGD EST	DOCUMENT ID		TECN
>10000	**p**	**90**	**0**	**0.78**	ABE	17D	SKAM
• • • We do not use the following data for averages, fits, limits, etc. • • •							
> 4200	p	90	0	0.44	NISHINO	12	SKAM
> 81	p	90	1	1.7	WALL	00B	SOU2
> 313	p	90	0	0.2	MCGREW	99	IMB3
> 44	p	90	0	0.1	BERGER	91	FREJ
> 140	p	90	0	<0.04	HIRATA	89C	KAMI
> 100	p	90	0	0.6	SEIDEL	88	IMB
> 200	p	90	5	3.3	HAINES	86	IMB
> 64	p	90	0	<0.8	ARISAKA	85	KAMI
> 64	p (free)	90	5	6.5	BLEWITT	85	IMB
> 200	p	90	5	4.7	BLEWITT	85	IMB
> 1.2	p	90	2		[1] CHERRY	81	HOME

[1] We have converted 2 possible events to 90% CL limit.

See key on page 885

$\tau(p \to \mu^+ \eta)$ τ_5

LIMIT (10^{30} years)	PARTICLE	CL%	EVTS	BKGD EST	DOCUMENT ID		TECN
>4700	***p***	**90**	**2**	**0.85**	ABE	17D	SKAM
• • • We do not use the following data for averages, fits, limits, etc. • • •							
>1300	*p*	90	2	0.49	NISHINO	12	SKAM
> 89	*p*	90	0	1.6	WALL	00B	SOU2
> 126	*p*	90	3	2.8	MCGREW	99	IMB3
> 26	*p*	90	1	0.8	BERGER	91	FREJ
> 69	*p*	90	1	<0.08	HIRATA	89C	KAMI
> 1.3	*p*	90	0	0.7	PHILLIPS	89	HPW
> 34	*p*	90	1	1.5	SEIDEL	88	IMB
> 46	*p*	90	7	6	HAINES	86	IMB
> 26	*p*	90	1	<0.8	ARISAKA	85	KAMI
> 17	*p* (free)	90	6	6	BLEWITT	85	IMB
> 46	*p*	90	7	8	BLEWITT	85	IMB

$\tau(n \to \nu \eta)$ τ_6

LIMIT (10^{30} years)	PARTICLE	CL%	EVTS	BKGD EST	DOCUMENT ID		TECN
>158	***n***	**90**	**0**	**1.2**	MCGREW	99	IMB3
• • • We do not use the following data for averages, fits, limits, etc. • • •							
> 71	*n*	90	2	3.7	WALL	00B	SOU2
> 29	*n*	90	0	0.9	BERGER	89	FREJ
> 54	*n*	90	2	0.9	HIRATA	89C	KAMI
> 16	*n*	90	3	2.1	SEIDEL	88	IMB
> 25	*n*	90	7	6	HAINES	86	IMB
> 30	*n*	90	0	0.4	KAJITA	86	KAMI
> 18	*n*	90	4	3	PARK	85	IMB
> 0.6	*n*	90	2		[1] CHERRY	81	HOME

[1] We have converted 2 possible events to 90% CL limit.

$\tau(N \to e^+ \rho)$ τ_7

LIMIT (10^{30} years)	PARTICLE	CL%	EVTS	BKGD EST	DOCUMENT ID		TECN
>720	***p***	**90**	**2**	**0.64**	ABE	17D	SKAM
>217	***n***	**90**	**4**	**4.8**	MCGREW	99	IMB3
• • • We do not use the following data for averages, fits, limits, etc. • • •							
> 30	*n*	90	4	0.87	ABE	17D	SKAM
>710	*p*	90	0	0.35	NISHINO	12	SKAM
> 70	*n*	90	1	0.38	NISHINO	12	SKAM
> 29	*p*	90	0	2.2	BERGER	91	FREJ
> 41	*n*	90	0	1.4	BERGER	91	FREJ
> 75	*p*	90	2	2.7	HIRATA	89C	KAMI
> 58	*n*	90	0	1.9	HIRATA	89C	KAMI
> 38	*n*	90	2	4.1	SEIDEL	88	IMB
> 1.2	*p*	90	0		BARTELT	87	SOUD
> 1.5	*n*	90	0		BARTELT	87	SOUD
> 17	*p*	90	7	7	HAINES	86	IMB
> 14	*n*	90	9	4	HAINES	86	IMB
> 12	*p*	90	0	<1.2	ARISAKA	85	KAMI
> 6	*n*	90	2	<1	ARISAKA	85	KAMI
> 6.7	*p* (free)	90	6	6	BLEWITT	85	IMB
> 17	*p*	90	7	7	BLEWITT	85	IMB
> 12	*n*	90	4	2	PARK	85	IMB
> 0.6	*n*	90	1	0.3	[1] BARTELT	83	SOUD
> 0.5	*p*	90	1	0.3	[1] BARTELT	83	SOUD
> 9.8	*p*	90	1		[2] KRISHNA...	82	KOLR
> 0.8	*p*	90	2		[3] CHERRY	81	HOME

[1] Limit based on zero events.
[2] We have calculated 90% CL limit from 0 confined events.
[3] We have converted 2 possible events to 90% CL limit.

$\tau(N \to \mu^+ \rho)$ τ_8

LIMIT (10^{30} years)	PARTICLE	CL%	EVTS	BKGD EST	DOCUMENT ID		TECN
>570	***p***	**90**	**1**	**1.30**	ABE	17D	SKAM
>228	***n***	**90**	**3**	**9.5**	MCGREW	99	IMB3
• • • We do not use the following data for averages, fits, limits, etc. • • •							
> 60	*n*	90	1	0.96	ABE	17D	SKAM
>160	*p*	90	1	0.42	NISHINO	12	SKAM
> 36	*n*	90	0	0.29	NISHINO	12	SKAM
> 12	*p*	90	0	0.5	BERGER	91	FREJ
> 22	*n*	90	0	1.1	BERGER	91	FREJ
>110	*p*	90	0	1.7	HIRATA	89C	KAMI
> 23	*n*	90	1	1.8	HIRATA	89C	KAMI
> 4.3	*p*	90	0	0.7	PHILLIPS	89	HPW
> 30	*p*	90	0	0.5	SEIDEL	88	IMB
> 11	*n*	90	1	1.1	SEIDEL	88	IMB
> 16	*p*	90	4	4.5	HAINES	86	IMB
> 7	*n*	90	6	5	HAINES	86	IMB
> 12	*p*	90	0	<0.7	ARISAKA	85	KAMI
> 5	*n*	90	1	<1.2	ARISAKA	85	KAMI
> 5.5	*p* (free)	90	4	5	BLEWITT	85	IMB
> 16	*p*	90	4	5	BLEWITT	85	IMB
> 9	*n*	90	1	2	PARK	85	IMB

$\tau(N \to \nu \rho)$ τ_9

LIMIT (10^{30} years)	PARTICLE	CL%	EVTS	BKGD EST	DOCUMENT ID		TECN
>162	***p***	**90**	**18**	**21.7**	MCGREW	99	IMB3
> 19	***n***	**90**	**0**	**0.5**	SEIDEL	88	IMB
• • • We do not use the following data for averages, fits, limits, etc. • • •							
> 9	*n*	90	4	2.4	BERGER	89	FREJ
> 24	*p*	90	0	0.9	BERGER	89	FREJ
> 27	*p*	90	5	1.5	HIRATA	89C	KAMI
> 13	*n*	90	4	3.6	HIRATA	89C	KAMI
> 13	*p*	90	1	1.1	SEIDEL	88	IMB
> 8	*p*	90	6	5	HAINES	86	IMB
> 2	*n*	90	15	10	HAINES	86	IMB
> 11	*p*	90	2	1	KAJITA	86	KAMI
> 4	*n*	90	2	2	KAJITA	86	KAMI
> 4.1	*p* (free)	90	6	7	BLEWITT	85	IMB
> 8.4	*p*	90	6	5	BLEWITT	85	IMB
> 2	*n*	90	7	3	PARK	85	IMB
> 0.9	*p*	90	2		[1] CHERRY	81	HOME
> 0.6	*n*	90	2		[1] CHERRY	81	HOME

[1] We have converted 2 possible events to 90% CL limit.

$\tau(p \to e^+ \omega)$ τ_{10}

LIMIT (10^{30} years)	PARTICLE	CL%	EVTS	BKGD EST	DOCUMENT ID		TECN
>1600	***p***	**90**	**1**	**1.35**	ABE	17D	SKAM
• • • We do not use the following data for averages, fits, limits, etc. • • •							
> 320	*p*	90	1	0.53	NISHINO	12	SKAM
> 107	*p*	90	7	10.8	MCGREW	99	IMB3
> 17	*p*	90	0	1.1	BERGER	91	FREJ
> 45	*p*	90	2	1.45	HIRATA	89C	KAMI
> 26	*p*	90	1	1.0	SEIDEL	88	IMB
> 1.5	*p*	90	0		BARTELT	87	SOUD
> 37	*p*	90	6	5.3	HAINES	86	IMB
> 25	*p*	90	1	<1.4	ARISAKA	85	KAMI
> 12	*p* (free)	90	6	7.5	BLEWITT	85	IMB
> 37	*p*	90	6	5.7	BLEWITT	85	IMB
> 0.6	*p*	90	1	0.3	[1] BARTELT	83	SOUD
> 9.8	*p*	90	1		[2] KRISHNA...	82	KOLR
> 2.8	*p*	90	2		[3] CHERRY	81	HOME

[1] Limit based on zero events.
[2] We have calculated 90% CL limit from 0 confined events.
[3] We have converted 2 possible events to 90% CL limit.

$\tau(p \to \mu^+ \omega)$ τ_{11}

LIMIT (10^{30} years)	PARTICLE	CL%	EVTS	BKGD EST	DOCUMENT ID		TECN
>2800	***p***	**90**	**0**	**1.09**	ABE	17D	SKAM
> 780	***p***	**90**	**0**	**0.48**	NISHINO	12	SKAM
• • • We do not use the following data for averages, fits, limits, etc. • • •							
> 117	*p*	90	11	12.1	MCGREW	99	IMB3
> 11	*p*	90	0	1.0	BERGER	91	FREJ
> 57	*p*	90	2	1.9	HIRATA	89C	KAMI
> 4.4	*p*	90	0	0.7	PHILLIPS	89	HPW
> 10	*p*	90	2	1.3	SEIDEL	88	IMB
> 23	*p*	90	2	1	HAINES	86	IMB
> 6.5	*p* (free)	90	9	8.7	BLEWITT	85	IMB
> 23	*p*	90	8	7	BLEWITT	85	IMB

$\tau(n \to \nu \omega)$ τ_{12}

LIMIT (10^{30} years)	PARTICLE	CL%	EVTS	BKGD EST	DOCUMENT ID		TECN
>108	***n***	**90**	**12**	**22.5**	MCGREW	99	IMB3
• • • We do not use the following data for averages, fits, limits, etc. • • •							
> 17	*n*	90	1	0.7	BERGER	89	FREJ
> 43	*n*	90	3	2.7	HIRATA	89C	KAMI
> 6	*n*	90	2	1.3	SEIDEL	88	IMB
> 12	*n*	90	6	6	HAINES	86	IMB
> 18	*n*	90	2	2	KAJITA	86	KAMI
> 16	*n*	90	1	2	PARK	85	IMB
> 2.0	*n*	90	2		[1] CHERRY	81	HOME

[1] We have converted 2 possible events to 90% CL limit.

$\tau(N \to e^+ K)$ τ_{13}

LIMIT (10^{30} years)	PARTICLE	CL%	EVTS	BKGD EST	DOCUMENT ID		TECN
>1000	**p**	**90**	**6**	**4.7**	KOBAYASHI	05	SKAM
> 17	***n***	**90**	**35**	**29.4**	MCGREW	99	IMB3
• • • We do not use the following data for averages, fits, limits, etc. • • •							
> 85	*p*	90	3	4.9	WALL	00	SOU2
> 31	*p*	90	23	25.2	MCGREW	99	IMB3
> 60	*p*	90	0		BERGER	91	FREJ
> 150	*p*	90	0	<0.27	HIRATA	89C	KAMI
> 70	*p*	90	0	1.8	SEIDEL	88	IMB
> 77	*p*	90	5	4.5	HAINES	86	IMB

> 38	p	90	0	<0.8	ARISAKA	85	KAMI
> 24	p (free)	90	7	8.5	BLEWITT	85	IMB
> 77	p	90	5	4	BLEWITT	85	IMB
> 1.3	p	90	0		ALEKSEEV	81	BAKS
> 1.3	n	90	0		ALEKSEEV	81	BAKS

$\tau(p \to e^+ K_S^0)$ τ_{14}

LIMIT (10^{30} years)	PARTICLE	CL%	EVTS	BKGD EST	DOCUMENT ID		TECN
• • • We do not use the following data for averages, fits, limits, etc. • • •							
>120	p	90	1	1.3	WALL	00	SOU2
> 76	p	90	0	0.5	BERGER	91	FREJ

$\tau(p \to e^+ K_L^0)$ τ_{15}

LIMIT (10^{30} years)	PARTICLE	CL%	EVTS	BKGD EST	DOCUMENT ID		TECN
• • • We do not use the following data for averages, fits, limits, etc. • • •							
>51	p	90	2	3.5	WALL	00	SOU2
>44	p	90	0	≤ 0.1	BERGER	91	FREJ

$\tau(N \to \mu^+ K)$ τ_{16}

LIMIT (10^{30} years)	PARTICLE	CL%	EVTS	BKGD EST	DOCUMENT ID		TECN
>1600	**p**	**90**	**13**	**13.2**	REGIS	12	SKAM
> 26	**n**	**90**	**20**	**28.4**	MCGREW	99	IMB3
• • • We do not use the following data for averages, fits, limits, etc. • • •							
>1300	p	90	3	3.9	KOBAYASHI	05	SKAM
> 120	p	90	0	<1.2	WALL	00	SOU2
> 120	p	90	4	7.2	MCGREW	99	IMB3
> 54	p	90	0		BERGER	91	FREJ
> 120	p	90	1	0.4	HIRATA	89C	KAMI
> 3.0	p	90	0	0.7	PHILLIPS	89	HPW
> 19	p	90	3	2.5	SEIDEL	88	IMB
> 1.5	p	90	0		[1] BARTELT	87	SOUD
> 1.1	n	90	0		BARTELT	87	SOUD
> 40	p	90	7	6	HAINES	86	IMB
> 19	p	90	1	<1.1	ARISAKA	85	KAMI
> 6.7	p (free)	90	11	13	BLEWITT	85	IMB
> 40	p	90	7	8	BLEWITT	85	IMB
> 6	p	90	1		BATTISTONI	84	NUSX
> 0.6	p	90	0		[2] BARTELT	83	SOUD
> 0.4	n	90	0		[2] BARTELT	83	SOUD
> 5.8	p	90	2		[3] KRISHNA...	82	KOLR
> 2.0	p	90	0		CHERRY	81	HOME
> 0.2	n	90			[4] GURR	67	CNTR

[1] BARTELT 87 limit applies to $p \to \mu^+ K_S^0$.
[2] Limit based on zero events.
[3] We have calculated 90% CL limit from 1 confined event.
[4] We have converted half-life to 90% CL mean life.

$\tau(p \to \mu^+ K_S^0)$ τ_{17}

LIMIT (10^{30} years)	PARTICLE	CL%	EVTS	BKGD EST	DOCUMENT ID		TECN
• • • We do not use the following data for averages, fits, limits, etc. • • •							
>150	p	90	0	<0.8	WALL	00	SOU2
> 64	p	90	0	1.2	BERGER	91	FREJ

$\tau(p \to \mu^+ K_L^0)$ τ_{18}

LIMIT (10^{30} years)	PARTICLE	CL%	EVTS	BKGD EST	DOCUMENT ID		TECN
• • • We do not use the following data for averages, fits, limits, etc. • • •							
>83	p	90	0	0.4	WALL	00	SOU2
>44	p	90	0	≤ 0.1	BERGER	91	FREJ

$\tau(N \to \nu K)$ τ_{19}

LIMIT (10^{30} years)	PARTICLE	CL%	EVTS	BKGD EST	DOCUMENT ID		TECN
>5900	**p**	**90**	**0**	**1.0**	ABE	14G	SKAM
> 86	**n**	**90**	**0**	**2.4**	HIRATA	89C	KAMI
• • • We do not use the following data for averages, fits, limits, etc. • • •							
> 540	p	90	0	0.9	ASAKURA	15	KLND
>2300	p	90	0	1.3	KOBAYASHI	05	SKAM
> 26	n	90	16	9.1	WALL	00	SOU2
> 670	p	90			HAYATO	99	SKAM
> 151	p	90	15	21.4	MCGREW	99	IMB3
> 30	n	90	34	34.1	MCGREW	99	IMB3
> 43	p	90	1	1.54	[1] ALLISON	98	SOU2
> 15	n	90	1	1.8	BERGER	89	FREJ
> 15	p	90	1	1.8	BERGER	89	FREJ
> 100	p	90	9	7.3	HIRATA	89C	KAMI
> 0.28	p	90	0	0.7	PHILLIPS	89	HPW
> 0.3	p	90	0		BARTELT	87	SOUD
> 0.75	n	90	0		[2] BARTELT	87	SOUD
> 10	p	90	6	5	HAINES	86	IMB
> 15	n	90	3	5	HAINES	86	IMB
> 28	p	90	3	3	KAJITA	86	KAMI
> 32	n	90	0	1.4	KAJITA	86	KAMI
> 1.8	p (free)	90	6	11	BLEWITT	85	IMB
> 9.6	p	90	6	5	BLEWITT	85	IMB
> 10	n	90	2	2	PARK	85	IMB
> 5	n	90	0		BATTISTONI	84	NUSX
> 2	p	90	0		BATTISTONI	84	NUSX
> 0.3	n	90	0		[3] BARTELT	83	SOUD
> 0.1	p	90	0		[3] BARTELT	83	SOUD
> 5.8	p	90	1		[4] KRISHNA...	82	KOLR
> 0.3	n	90	2		[5] CHERRY	81	HOME

[1] This ALLISON 98 limit is with no background subtraction; with subtraction the limit becomes $> 46 \times 10^{30}$ years.
[2] BARTELT 87 limit applies to $n \to \nu K_S^0$.
[3] Limit based on zero events.
[4] We have calculated 90% CL limit from 1 confined event.
[5] We have converted 2 possible events to 90% CL limit.

$\tau(n \to \nu K_S^0)$ τ_{20}

LIMIT (10^{30} years)	PARTICLE	CL%	EVTS	BKGD EST	DOCUMENT ID		TECN
>260	**n**	**90**	**34**	**30**	[1] KOBAYASHI	05	SKAM
• • • We do not use the following data for averages, fits, limits, etc. • • •							
> 51	n	90	16	9.1	WALL	00	SOU2

[1] We have doubled the $n \to \nu K^0$ limit given in KOBAYASHI 05 to obtain this $n \to \nu K_S^0$ limit.

$\tau(p \to e^+ K^*(892)^0)$ τ_{21}

LIMIT (10^{30} years)	PARTICLE	CL%	EVTS	BKGD EST	DOCUMENT ID		TECN
>84	**p**	**90**	**38**	**52.0**	MCGREW	99	IMB3
• • • We do not use the following data for averages, fits, limits, etc. • • •							
>10	p	90	0	0.8	BERGER	91	FREJ
>52	p	90	2	1.55	HIRATA	89C	KAMI
>10	p	90	1	<1	ARISAKA	85	KAMI

$\tau(N \to \nu K^*(892))$ τ_{22}

LIMIT (10^{30} years)	PARTICLE	CL%	EVTS	BKGD EST	DOCUMENT ID		TECN
>51	**p**	**90**	**7**	**9.1**	MCGREW	99	IMB3
>78	**n**	**90**	**40**	**50**	MCGREW	99	IMB3
• • • We do not use the following data for averages, fits, limits, etc. • • •							
>22	n	90	0	2.1	BERGER	89	FREJ
>17	p	90	0	2.4	BERGER	89	FREJ
>20	p	90	5	2.1	HIRATA	89C	KAMI
>21	n	90	4	2.4	HIRATA	89C	KAMI
>10	p	90	7	6	HAINES	86	IMB
> 5	n	90	8	7	HAINES	86	IMB
> 8	p	90	3	2	KAJITA	86	KAMI
> 6	n	90	2	1.6	KAJITA	86	KAMI
> 5.8	p (free)	90	10	16	BLEWITT	85	IMB
> 9.6	p	90	7	6	BLEWITT	85	IMB
> 7	n	90	1	4	PARK	85	IMB
> 2.1	p	90	1		[1] BATTISTONI	82	NUSX

[1] We have converted 1 possible event to 90% CL limit.

Antilepton + mesons

$\tau(p \to e^+ \pi^+ \pi^-)$ τ_{23}

LIMIT (10^{30} years)	PARTICLE	CL%	EVTS	BKGD EST	DOCUMENT ID		TECN
>82	**p**	**90**	**16**	**23.1**	MCGREW	99	IMB3
• • • We do not use the following data for averages, fits, limits, etc. • • •							
>21	p	90	0	2.2	BERGER	91	FREJ

$\tau(p \to e^+ \pi^0 \pi^0)$ τ_{24}

LIMIT (10^{30} years)	PARTICLE	CL%	EVTS	BKGD EST	DOCUMENT ID		TECN
>147	**p**	**90**	**2**	**0.8**	MCGREW	99	IMB3
• • • We do not use the following data for averages, fits, limits, etc. • • •							
> 38	p	90	1	0.5	BERGER	91	FREJ

$\tau(n \to e^+ \pi^- \pi^0)$ τ_{25}

LIMIT (10^{30} years)	PARTICLE	CL%	EVTS	BKGD EST	DOCUMENT ID		TECN
>52	**n**	**90**	**38**	**34.2**	MCGREW	99	IMB3
• • • We do not use the following data for averages, fits, limits, etc. • • •							
>32	n	90	1	0.8	BERGER	91	FREJ

$\tau(p \to \mu^+ \pi^+ \pi^-)$ τ_{26}

LIMIT (10^{30} years)	PARTICLE	CL%	EVTS	BKGD EST	DOCUMENT ID		TECN
>133	**p**	**90**	**25**	**38.0**	MCGREW	99	IMB3
• • • We do not use the following data for averages, fits, limits, etc. • • •							
> 17	p	90	1	2.6	BERGER	91	FREJ
> 3.3	p	90	0	0.7	PHILLIPS	89	HPW

See key on page 885

$\tau(p \to \mu^+ \pi^0 \pi^0)$ τ_{27}

LIMIT (10^{30} years)	PARTICLE	CL%	EVTS	BKGD EST	DOCUMENT ID		TECN
>101	**p**	**90**	**3**	**1.6**	MCGREW	99	IMB3
• • • We do not use the following data for averages, fits, limits, etc. • • •							
> 33	p	90	1	0.9	BERGER	91	FREJ

$\tau(n \to \mu^+ \pi^- \pi^0)$ τ_{28}

LIMIT (10^{30} years)	PARTICLE	CL%	EVTS	BKGD EST	DOCUMENT ID		TECN
>74	**n**	**90**	**17**	**20.8**	MCGREW	99	IMB3
• • • We do not use the following data for averages, fits, limits, etc. • • •							
>33	n	90	0	1.1	BERGER	91	FREJ

$\tau(n \to e^+ K^0 \pi^-)$ τ_{29}

LIMIT (10^{30} years)	PARTICLE	CL%	EVTS	BKGD EST	DOCUMENT ID		TECN
>18	**n**	**90**	**1**	**0.2**	BERGER	91	FREJ

Lepton + meson

$\tau(n \to e^- \pi^+)$ τ_{30}

LIMIT (10^{30} years)	PARTICLE	CL%	EVTS	BKGD EST	DOCUMENT ID		TECN
>65	**n**	**90**	**0**	**1.6**	SEIDEL	88	IMB
• • • We do not use the following data for averages, fits, limits, etc. • • •							
>55	n	90	0	1.09	BERGER	91B	FREJ
>16	n	90	9	7	HAINES	86	IMB
>25	n	90	2	4	PARK	85	IMB

$\tau(n \to \mu^- \pi^+)$ τ_{31}

LIMIT (10^{30} years)	PARTICLE	CL%	EVTS	BKGD EST	DOCUMENT ID		TECN
>49	**n**	**90**	**0**	**0.5**	SEIDEL	88	IMB
• • • We do not use the following data for averages, fits, limits, etc. • • •							
>33	n	90	0	1.40	BERGER	91B	FREJ
> 2.7	n	90	0	0.7	PHILLIPS	89	HPW
>25	n	90	7	6	HAINES	86	IMB
>27	n	90	2	3	PARK	85	IMB

$\tau(n \to e^- \rho^+)$ τ_{32}

LIMIT (10^{30} years)	PARTICLE	CL%	EVTS	BKGD EST	DOCUMENT ID		TECN
>62	**n**	**90**	**2**	**4.1**	SEIDEL	88	IMB
• • • We do not use the following data for averages, fits, limits, etc. • • •							
>12	n	90	13	6	HAINES	86	IMB
>12	n	90	5	3	PARK	85	IMB

$\tau(n \to \mu^- \rho^+)$ τ_{33}

LIMIT (10^{30} years)	PARTICLE	CL%	EVTS	BKGD EST	DOCUMENT ID		TECN
>7	**n**	**90**	**1**	**1.1**	SEIDEL	88	IMB
• • • We do not use the following data for averages, fits, limits, etc. • • •							
>2.6	n	90	0	0.7	PHILLIPS	89	HPW
>9	n	90	7	5	HAINES	86	IMB
>9	n	90	2	2	PARK	85	IMB

$\tau(n \to e^- K^+)$ τ_{34}

LIMIT (10^{30} years)	PARTICLE	CL%	EVTS	BKGD EST	DOCUMENT ID		TECN
>32	**n**	**90**	**3**	**2.96**	BERGER	91B	FREJ
• • • We do not use the following data for averages, fits, limits, etc. • • •							
> 0.23	n	90	0	0.7	PHILLIPS	89	HPW

$\tau(n \to \mu^- K^+)$ τ_{35}

LIMIT (10^{30} years)	PARTICLE	CL%	EVTS	BKGD EST	DOCUMENT ID		TECN
>57	**n**	**90**	**0**	**2.18**	BERGER	91B	FREJ
• • • We do not use the following data for averages, fits, limits, etc. • • •							
> 4.7	n	90	0	0.7	PHILLIPS	89	HPW

Lepton + mesons

$\tau(p \to e^- \pi^+ \pi^+)$ τ_{36}

LIMIT (10^{30} years)	PARTICLE	CL%	EVTS	BKGD EST	DOCUMENT ID		TECN
>30	**p**	**90**	**1**	**2.50**	BERGER	91B	FREJ
• • • We do not use the following data for averages, fits, limits, etc. • • •							
> 2.0	p	90	0	0.7	PHILLIPS	89	HPW

$\tau(n \to e^- \pi^+ \pi^0)$ τ_{37}

LIMIT (10^{30} years)	PARTICLE	CL%	EVTS	BKGD EST	DOCUMENT ID		TECN
>29	**n**	**90**	**1**	**0.78**	BERGER	91B	FREJ

$\tau(p \to \mu^- \pi^+ \pi^+)$ τ_{38}

LIMIT (10^{30} years)	PARTICLE	CL%	EVTS	BKGD EST	DOCUMENT ID		TECN
>17	**p**	**90**	**1**	**1.72**	BERGER	91B	FREJ
• • • We do not use the following data for averages, fits, limits, etc. • • •							
> 7.8	p	90	0	0.7	PHILLIPS	89	HPW

$\tau(n \to \mu^- \pi^+ \pi^0)$ τ_{39}

LIMIT (10^{30} years)	PARTICLE	CL%	EVTS	BKGD EST	DOCUMENT ID		TECN
>34	**n**	**90**	**0**	**0.78**	BERGER	91B	FREJ

$\tau(p \to e^- \pi^+ K^+)$ τ_{40}

LIMIT (10^{30} years)	PARTICLE	CL%	EVTS	BKGD EST	DOCUMENT ID		TECN
>75	**p**	**90**	**81**	**127.2**	MCGREW	99	IMB3
• • • We do not use the following data for averages, fits, limits, etc. • • •							
>20	p	90	3	2.50	BERGER	91B	FREJ

$\tau(p \to \mu^- \pi^+ K^+)$ τ_{41}

LIMIT (10^{30} years)	PARTICLE	CL%	EVTS	BKGD EST	DOCUMENT ID		TECN
>245	**p**	**90**	**3**	**4.0**	MCGREW	99	IMB3
• • • We do not use the following data for averages, fits, limits, etc. • • •							
> 5	p	90	2	0.78	BERGER	91B	FREJ

Antilepton + photon(s)

$\tau(p \to e^+ \gamma)$ τ_{42}

LIMIT (10^{30} years)	PARTICLE	CL%	EVTS	BKGD EST	DOCUMENT ID		TECN
>670	**p**	**90**	**0**	**0.1**	MCGREW	99	IMB3
• • • We do not use the following data for averages, fits, limits, etc. • • •							
>133	p	90	0	0.3	BERGER	91	FREJ
>460	p	90	0	0.6	SEIDEL	88	IMB
>360	p	90	0	0.3	HAINES	86	IMB
> 87	p (free)	90	0	0.2	BLEWITT	85	IMB
>360	p	90	0	0.2	BLEWITT	85	IMB
> 0.1	p	90			[1] GURR	67	CNTR

[1] We have converted half-life to 90% CL mean life.

$\tau(p \to \mu^+ \gamma)$ τ_{43}

LIMIT (10^{30} years)	PARTICLE	CL%	EVTS	BKGD EST	DOCUMENT ID		TECN
>478	**p**	**90**	**0**	**0.1**	MCGREW	99	IMB3
• • • We do not use the following data for averages, fits, limits, etc. • • •							
>155	p	90	0	0.1	BERGER	91	FREJ
>380	p	90	0	0.5	SEIDEL	88	IMB
> 97	p	90	3	2	HAINES	86	IMB
> 61	p (free)	90	0	0.2	BLEWITT	85	IMB
>280	p	90	0	0.6	BLEWITT	85	IMB
> 0.3	p	90			[1] GURR	67	CNTR

[1] We have converted half-life to 90% CL mean life.

$\tau(n \to \nu \gamma)$ τ_{44}

LIMIT (10^{30} years)	PARTICLE	CL%	EVTS	BKGD EST	DOCUMENT ID		TECN
>550		**90**			TAKHISTOV	15	SKAM
• • • We do not use the following data for averages, fits, limits, etc. • • •							
> 28	n	90	163	144.7	MCGREW	99	IMB3
> 24	n	90	10	6.86	BERGER	91B	FREJ
> 9	n	90	73	60	HAINES	86	IMB
> 11	n	90	28	19	PARK	85	IMB

$\tau(p \to e^+ \gamma\gamma)$ τ_{45}

LIMIT (10^{30} years)	PARTICLE	CL%	EVTS	BKGD EST	DOCUMENT ID		TECN
>100	**p**	**90**	**1**	**0.8**	BERGER	91	FREJ

$\tau(n \to \nu \gamma\gamma)$ τ_{46}

LIMIT (10^{30} years)	PARTICLE	CL%	EVTS	BKGD EST	DOCUMENT ID		TECN
>219	**n**	**90**	**5**	**7.5**	MCGREW	99	IMB3

Antilepton + single massless

$\tau(p \to e^+ X)$ τ_{47}

VALUE (10^{30} years)	CL%	DOCUMENT ID		TECN
>790	90	TAKHISTOV	15	SKAM

$\tau(p \to \mu^+ X)$ τ_{48}

VALUE (10^{30} years)	CL%	DOCUMENT ID		TECN
>410	90	TAKHISTOV	15	SKAM

Baryon Particle Listings

p

Three (or more) leptons

$\tau(p \to e^+ e^+ e^-)$ τ_{49}

LIMIT (10^{30} years)	PARTICLE	CL%	EVTS	BKGD EST	DOCUMENT ID		TECN
>793	**p**	**90**	**0**	**0.5**	MCGREW	99	IMB3
• • • We do not use the following data for averages, fits, limits, etc. • • •							
>147	p	90	0	0.1	BERGER	91	FREJ
>510	p	90	0	0.3	HAINES	86	IMB
> 89	p (free)	90	0	0.5	BLEWITT	85	IMB
>510	p	90	0	0.7	BLEWITT	85	IMB

$\tau(p \to e^+ \mu^+ \mu^-)$ τ_{50}

LIMIT (10^{30} years)	PARTICLE	CL%	EVTS	BKGD EST	DOCUMENT ID		TECN
>359	**p**	**90**	**1**	**0.9**	MCGREW	99	IMB3
• • • We do not use the following data for averages, fits, limits, etc. • • •							
> 81	p	90	0	0.16	BERGER	91	FREJ
> 5.0	p	90	0	0.7	PHILLIPS	89	HPW

$\tau(p \to e^+ \nu\nu)$ τ_{51}

LIMIT (10^{30} years)	PARTICLE	CL%	EVTS	BKGD EST	DOCUMENT ID		TECN
>170	**p**	**90**			[1] TAKHISTOV	14	SKAM
• • • We do not use the following data for averages, fits, limits, etc. • • •							
> 17	p	90	152	153.7	MCGREW	99	IMB3
> 11	p	90	11	6.08	BERGER	91B	FREJ

[1] Allowed events at 90% CL are 459.

$\tau(n \to e^+ e^- \nu)$ τ_{52}

LIMIT (10^{30} years)	PARTICLE	CL%	EVTS	BKGD EST	DOCUMENT ID		TECN
>257	**n**	**90**	**5**	**7.5**	MCGREW	99	IMB3
• • • We do not use the following data for averages, fits, limits, etc. • • •							
> 74	n	90	0	< 0.1	BERGER	91B	FREJ
> 45	n	90	5	5	HAINES	86	IMB
> 26	n	90	4	3	PARK	85	IMB

$\tau(n \to \mu^+ e^- \nu)$ τ_{53}

LIMIT (10^{30} years)	PARTICLE	CL%	EVTS	BKGD EST	DOCUMENT ID		TECN
>83	**n**	**90**	**25**	**29.4**	MCGREW	99	IMB3
• • • We do not use the following data for averages, fits, limits, etc. • • •							
>47	n	90	0	< 0.1	BERGER	91B	FREJ

$\tau(n \to \mu^+ \mu^- \nu)$ τ_{54}

LIMIT (10^{30} years)	PARTICLE	CL%	EVTS	BKGD EST	DOCUMENT ID		TECN
>79	**n**	**90**	**100**	**145**	MCGREW	99	IMB3
• • • We do not use the following data for averages, fits, limits, etc. • • •							
>42	n	90	0	1.4	BERGER	91B	FREJ
> 5.1	n	90	0	0.7	PHILLIPS	89	HPW
>16	n	90	14	7	HAINES	86	IMB
>19	n	90	4	7	PARK	85	IMB

$\tau(p \to \mu^+ e^+ e^-)$ τ_{55}

LIMIT (10^{30} years)	PARTICLE	CL%	EVTS	BKGD EST	DOCUMENT ID		TECN
>529	**p**	**90**	**0**	**1.0**	MCGREW	99	IMB3
• • • We do not use the following data for averages, fits, limits, etc. • • •							
> 91	p	90	0	$\leq$ 0.1	BERGER	91	FREJ

$\tau(p \to \mu^+ \mu^+ \mu^-)$ τ_{56}

LIMIT (10^{30} years)	PARTICLE	CL%	EVTS	BKGD EST	DOCUMENT ID		TECN
>675	**p**	**90**	**0**	**0.3**	MCGREW	99	IMB3
• • • We do not use the following data for averages, fits, limits, etc. • • •							
>119	p	90	0	0.2	BERGER	91	FREJ
> 10.5	p	90	0	0.7	PHILLIPS	89	HPW
>190	p	90	1	0.1	HAINES	86	IMB
> 44	p (free)	90	1	0.7	BLEWITT	85	IMB
>190	p	90	1	0.9	BLEWITT	85	IMB
> 2.1	p	90	1		[1] BATTISTONI	82	NUSX

[1] We have converted 1 possible event to 90% CL limit.

$\tau(p \to \mu^+ \nu\nu)$ τ_{57}

LIMIT (10^{30} years)	PARTICLE	CL%	EVTS	BKGD EST	DOCUMENT ID		TECN
>220	**p**	**90**			[1] TAKHISTOV	14	SKAM
• • • We do not use the following data for averages, fits, limits, etc. • • •							
> 21	p	90	7	11.23	BERGER	91B	FREJ

[1] Allowed events at 90% CL are 286.

$\tau(p \to e^- \mu^+ \mu^+)$ τ_{58}

LIMIT (10^{30} years)	PARTICLE	CL%	EVTS	BKGD EST	DOCUMENT ID		TECN
>6.0	**p**	**90**	**0**	**0.7**	PHILLIPS	89	HPW

$\tau(n \to 3\nu)$ τ_{59}

See also the "to anything" and "disappearance" limits for bound nucleons in the "p Mean Life" data block just in front of the list of possible p decay modes. Such modes could of course be to three (or five) neutrinos, and the limits are stronger, but we do not repeat them here.

LIMIT (10^{30} years)	PARTICLE	CL%	EVTS	BKGD EST	DOCUMENT ID		TECN
>0.00049	**n**	**90**	**2**	**2**	[1] SUZUKI	93B	KAMI
• • • We do not use the following data for averages, fits, limits, etc. • • •							
>0.0023	n	90			[2] GLICENSTEIN	97	KAMI
>0.00003	n	90	11	6.1	[3] BERGER	91B	FREJ
>0.00012	n	90	7	11.2	[3] BERGER	91B	FREJ
>0.0005	n	90	0		LEARNED	79	RVUE

[1] The SUZUKI 93B limit applies to any of $\nu_e\nu_e\overline{\nu}_e$, $\nu_\mu\nu_\mu\overline{\nu}_\mu$, or $\nu_\tau\nu_\tau\overline{\nu}_\tau$.

[2] GLICENSTEIN 97 uses Kamioka data and the idea that the disappearance of the neutron's magnetic moment should produce radiation.

[3] The first BERGER 91B limit is for $n \to \nu_e\nu_e\overline{\nu}_e$, the second is for $n \to \nu_\mu\nu_\mu\overline{\nu}_\mu$.

$\tau(n \to 5\nu)$ τ_{60}

See the note on $\tau(n \to 3\nu)$ on the previous data block.

LIMIT (10^{30} years)	PARTICLE	CL%	EVTS	BKGD EST	DOCUMENT ID		TECN
• • • We do not use the following data for averages, fits, limits, etc. • • •							
>0.0017	n	90			[1] GLICENSTEIN	97	KAMI

[1] GLICENSTEIN 97 uses Kamioka data and the idea that the disappearance of the neutron's magnetic moment should produce radiation.

Inclusive modes

$\tau(N \to e^+ \text{anything})$ τ_{61}

LIMIT (10^{30} years)	PARTICLE	CL%	EVTS	BKGD EST	DOCUMENT ID		TECN
>0.6	**p, n**	**90**			[1] LEARNED	79	RVUE

[1] The electron may be primary or secondary.

$\tau(N \to \mu^+ \text{anything})$ τ_{62}

LIMIT (10^{30} years)	PARTICLE	CL%	EVTS	BKGD EST	DOCUMENT ID		TECN
>12	**p, n**	**90**	**2**		[1,2] CHERRY	81	HOME
• • • We do not use the following data for averages, fits, limits, etc. • • •							
> 1.8	p, n	90			[2] COWSIK	80	CNTR
> 6	p, n	90			[2] LEARNED	79	RVUE

[1] We have converted 2 possible events to 90% CL limit.

[2] The muon may be primary or secondary.

$\tau(N \to \nu \text{anything})$ τ_{63}

Anything = π, ρ, K, etc.

LIMIT (10^{30} years)	PARTICLE	CL%	EVTS	BKGD EST	DOCUMENT ID		TECN
• • • We do not use the following data for averages, fits, limits, etc. • • •							
>0.0002	p, n	90	0		LEARNED	79	RVUE

$\tau(N \to e^+ \pi^0 \text{anything})$ τ_{64}

LIMIT (10^{30} years)	PARTICLE	CL%	EVTS	BKGD EST	DOCUMENT ID		TECN
>0.6	**p, n**	**90**	**0**		LEARNED	79	RVUE

$\tau(N \to 2 \text{bodies}, \nu\text{-free})$ τ_{65}

LIMIT (10^{30} years)	PARTICLE	CL%	EVTS	BKGD EST	DOCUMENT ID		TECN
• • • We do not use the following data for averages, fits, limits, etc. • • •							
>1.3	p, n	90	0		ALEKSEEV	81	BAKS

$\Delta B = 2$ dinucleon modes

$\tau(pp \to \pi^+\pi^+)$ τ_{66}

LIMIT (10^{30} years)	CL%	EVTS	BKGD EST	DOCUMENT ID		TECN	COMMENT
>72.2	**90**	**2**	**4.45**	GUSTAFSON	15	SKAM	per oxygen nucleus
• • • We do not use the following data for averages, fits, limits, etc. • • •							
> 0.7	90	4	2.34	BERGER	91B	FREJ	per iron nucleus

$\tau(pn \to \pi^+\pi^0)$ τ_{67}

LIMIT (10^{30} years)	CL%	EVTS	BKGD EST	DOCUMENT ID		TECN	COMMENT
>170	**90**			GUSTAFSON	15	SKAM	per oxygen nucleus
• • • We do not use the following data for averages, fits, limits, etc. • • •							
> 2.0	90	0	0.31	BERGER	91B	FREJ	per iron nucleus

See key on page 885

$\tau(nn \to \pi^+\pi^-)$ τ_{68}

LIMIT (10^{30} years)	CL%	EVTS	BKGD EST	DOCUMENT ID		TECN	COMMENT
>0.7	**90**	**4**	**2.18**	BERGER	91B	FREJ	τ per iron nucleus

$\tau(nn \to \pi^0\pi^0)$ τ_{69}

LIMIT (10^{30} years)	CL%	EVTS	BKGD EST	DOCUMENT ID		TECN	COMMENT
>404	**90**			GUSTAFSON	15	SKAM	per oxygen nucleus
• • • We do not use the following data for averages, fits, limits, etc. • • •							
> 3.4	90	0	0.78	BERGER	91B	FREJ	per iron nucleus

$\tau(pp \to K^+K^+)$ τ_{70}

LIMIT (10^{30} years)	CL%	EVTS	BKGD EST	DOCUMENT ID		TECN	COMMENT
>170	**90**	**0**	**0.28**	LITOS	14	SKAM	τ per oxygen nucleus

$\tau(pp \to e^+e^+)$ τ_{71}

LIMIT (10^{30} years)	CL%	EVTS	BKGD EST	DOCUMENT ID		TECN	COMMENT
>5.8	**90**	**0**	**<0.1**	BERGER	91B	FREJ	τ per iron nucleus

$\tau(pp \to e^+\mu^+)$ τ_{72}

LIMIT (10^{30} years)	CL%	EVTS	BKGD EST	DOCUMENT ID		TECN	COMMENT
>3.6	**90**	**0**	**<0.1**	BERGER	91B	FREJ	τ per iron nucleus

$\tau(pp \to \mu^+\mu^+)$ τ_{73}

LIMIT (10^{30} years)	CL%	EVTS	BKGD EST	DOCUMENT ID		TECN	COMMENT
>1.7	**90**	**0**	**0.62**	BERGER	91B	FREJ	τ per iron nucleus

$\tau(pn \to e^+\overline{\nu})$ τ_{74}

LIMIT (10^{30} years)	CL%	EVTS	BKGD EST	DOCUMENT ID		TECN	COMMENT
>260	**90**			TAKHISTOV	15	SKAM	
• • • We do not use the following data for averages, fits, limits, etc. • • •							
> 2.8	90	5	9.67	BERGER	91B	FREJ	τ per iron nucleus

$\tau(pn \to \mu^+\overline{\nu})$ τ_{75}

LIMIT (10^{30} years)	CL%	EVTS	BKGD EST	DOCUMENT ID		TECN	COMMENT
>200	**90**			TAKHISTOV	15	SKAM	
• • • We do not use the following data for averages, fits, limits, etc. • • •							
> 1.6	90	4	4.37	BERGER	91B	FREJ	τ per iron nucleus

$\tau(pn \to \tau^+\overline{\nu}_\tau)$ τ_{76}

LIMIT (10^{30} years)	CL%	EVTS	BKGD EST	DOCUMENT ID		TECN	COMMENT
>29	**90**			TAKHISTOV	15	SKAM	
• • • We do not use the following data for averages, fits, limits, etc. • • •							
> 1	90			[1] BRYMAN	14	CHER	

[1] BRYMAN 14 uses a MCGREW 99 limit on the $p \to e^+\nu\nu$ lifetime to extract this value.

$\tau(nn \to \nu_e\overline{\nu}_e)$ τ_{77}

We include "invisible" modes here.

LIMIT (10^{30} years)	CL%	EVTS	BKGD EST	DOCUMENT ID		TECN	COMMENT
>1.4	**90**			[1] ARAKI	06	KLND	$nn \to$ invisible
• • • We do not use the following data for averages, fits, limits, etc. • • •							
>0.000042	90			[2] TRETYAK	04	CNTR	$nn \to$ invisible
>0.000049	90			[3] BACK	03	BORX	$nn \to$ invisible
>0.000012	90			[4] BERNABEI	00B	DAMA	$nn \to$ invisible
>0.000012	90	5	9.7	BERGER	91B	FREJ	τ per iron nucleus

[1] ARAKI 06 looks for signs of de-excitation of the residual nucleus after disappearance of two neutrons from the s shell of ^{12}C.
[2] TRETYAK 04 uses data from an old Homestake-mine radiochemical experiment on limits for invisible decays of ^{39}K to ^{37}Ar.
[3] BACK 03 looks for decays of unstable nuclides left after NN decays of parent ^{12}C, ^{13}C, ^{16}O nuclei. These are "invisible channel" limits.
[4] BERNABEI 00B looks for the decay of a $^{127}_{52}$Te nucleus following the disappearance of an nn pair in the otherwise-stable $^{129}_{54}$Xe nucleus. The limit here applies as well to $nn \to \nu_\mu\overline{\nu}_\mu$, $nn \to \nu_\tau\overline{\nu}_\tau$, or any "disappearance" mode.

$\tau(nn \to \nu_\mu\overline{\nu}_\mu)$ τ_{78}

See the proceeding data block. "Invisible modes" would include any multi-neutrino mode.

LIMIT (10^{30} years)	CL%	EVTS	BKGD EST	CL%	DOCUMENT ID	TECN	COMMENT
>1.4	**(CL = 90%) OUR LIMIT**						
• • • We do not use the following data for averages, fits, limits, etc. • • •							
>0.000006	90	4	4.4		BERGER 91B	FREJ	τ per iron nucleus

$\tau(pn \to \text{invisible})$ τ_{79}

This violates charge conservation as well as baryon number conservation.

VALUE (10^{30} years)	CL%	DOCUMENT ID		TECN
>0.000021	90	[1] TRETYAK	04	CNTR

[1] TRETYAK 04 uses data from an old Homestake-mine radiochemical experiment on limits for invisible decays of ^{39}K to ^{37}Ar.

$\tau(pp \to \text{invisible})$ τ_{80}

This violates charge conservation as well as baryon number conservation.

LIMIT (10^{30} years)	CL%	EVTS	BKGD EST	CL%	DOCUMENT ID		TECN
>0.00005				90	[1] BACK	03	BORX
• • • We do not use the following data for averages, fits, limits, etc. • • •							
>0.00000055	90				[2] BERNABEI	00B	DAMA

[1] BACK 03 looks for decays of unstable nuclides left after NN decays of parent ^{12}C, ^{13}C, ^{16}O nuclei. These are "invisible channel" limits.
[2] BERNABEI 00B looks for the decay of a $^{127}_{52}$Te nucleus following the disappearance of a pp pair in the otherwise-stable $^{129}_{54}$Xe nucleus.

$\overline{p}$ PARTIAL MEAN LIVES

The "partial mean life" limits tabulated here are the limits on $\overline{\tau}/B_i$, where $\overline{\tau}$ is the total mean life for the antiproton and B_i is the branching fraction for the mode in question.

$\tau(\overline{p} \to e^-\gamma)$ τ_{81}

VALUE (years)	CL%	DOCUMENT ID		TECN	COMMENT
> 7×10^5	90	GEER	00	APEX	8.9 GeV/c $\overline{p}$ beam
• • • We do not use the following data for averages, fits, limits, etc. • • •					
>1848	95	GEER	94	CALO	8.9 GeV/c $\overline{p}$ beam

$\tau(\overline{p} \to \mu^-\gamma)$ τ_{82}

VALUE (years)	CL%	DOCUMENT ID		TECN	COMMENT
> $\times 10^4$	90	GEER	00	APEX	8.9 GeV/c $\overline{p}$ beam
• • • We do not use the following data for averages, fits, limits, etc. • • •					
>5.0×10^4	90	HU	98B	APEX	8.9 GeV/c $\overline{p}$ beam

$\tau(\overline{p} \to e^-\pi^0)$ τ_{83}

VALUE (years)	CL%	DOCUMENT ID		TECN	COMMENT
> 4×10^5	90	GEER	00	APEX	8.9 GeV/c $\overline{p}$ beam
• • • We do not use the following data for averages, fits, limits, etc. • • •					
>554	95	GEER	94	CALO	8.9 GeV/c $\overline{p}$ beam

$\tau(\overline{p} \to \mu^-\pi^0)$ τ_{84}

VALUE (years)	CL%	DOCUMENT ID		TECN	COMMENT
> $\times 10^4$	90	GEER	00	APEX	8.9 GeV/c $\overline{p}$ beam
• • • We do not use the following data for averages, fits, limits, etc. • • •					
>4.8×10^4	90	HU	98B	APEX	8.9 GeV/c $\overline{p}$ beam

$\tau(\overline{p} \to e^-\eta)$ τ_{85}

VALUE (years)	CL%	DOCUMENT ID		TECN	COMMENT
> 2×10^4	90	GEER	00	APEX	8.9 GeV/c $\overline{p}$ beam
• • • We do not use the following data for averages, fits, limits, etc. • • •					
>171	95	GEER	94	CALO	8.9 GeV/c $\overline{p}$ beam

$\tau(\overline{p} \to \mu^-\eta)$ τ_{86}

VALUE (years)	CL%	DOCUMENT ID		TECN	COMMENT
> $\times 10^3$	90	GEER	00	APEX	8.9 GeV/c $\overline{p}$ beam
• • • We do not use the following data for averages, fits, limits, etc. • • •					
>7.9×10^3	90	HU	98B	APEX	8.9 GeV/c $\overline{p}$ beam

$\tau(\overline{p} \to e^- K^0_S)$ τ_{87}

VALUE (years)	CL%	DOCUMENT ID		TECN	COMMENT
>900	90	GEER	00	APEX	8.9 GeV/c $\overline{p}$ beam
• • • We do not use the following data for averages, fits, limits, etc. • • •					
> 29	95	GEER	94	CALO	8.9 GeV/c $\overline{p}$ beam

$\tau(\overline{p} \to \mu^- K^0_S)$ τ_{88}

VALUE (years)	CL%	DOCUMENT ID		TECN	COMMENT
> $\times 10^3$	90	GEER	00	APEX	8.9 GeV/c $\overline{p}$ beam
• • • We do not use the following data for averages, fits, limits, etc. • • •					
>4.3×10^3	90	HU	98B	APEX	8.9 GeV/c $\overline{p}$ beam

$\tau(\overline{p} \to e^- K^0_L)$ τ_{89}

VALUE (years)	CL%	DOCUMENT ID		TECN	COMMENT
> 9×10^3	90	GEER	00	APEX	8.9 GeV/c $\overline{p}$ beam
• • • We do not use the following data for averages, fits, limits, etc. • • •					
>9	95	GEER	94	CALO	8.9 GeV/c $\overline{p}$ beam

$\tau(\overline{p} \to \mu^- K_L^0)$ τ_{90}

VALUE (years)	CL%	DOCUMENT ID		TECN	COMMENT
$>7 \times 10^3$	90	GEER	00	APEX	8.9 GeV/c $\overline{p}$ beam
• • • We do not use the following data for averages, fits, limits, etc. • • •					
$>6.5 \times 10^3$	90	HU	98B	APEX	8.9 GeV/c $\overline{p}$ beam

$\tau(\overline{p} \to e^- \gamma\gamma)$ τ_{91}

VALUE (years)	CL%	DOCUMENT ID		TECN	COMMENT
$>2 \times 10^4$	90	GEER	00	APEX	8.9 GeV/c $\overline{p}$ beam

$\tau(\overline{p} \to \mu^- \gamma\gamma)$ τ_{92}

VALUE (years)	CL%	DOCUMENT ID		TECN	COMMENT
$>2 \times 10^4$	90	GEER	00	APEX	8.9 GeV/c $\overline{p}$ beam
• • • We do not use the following data for averages, fits, limits, etc. • • •					
$>2.3 \times 10^4$	90	HU	98B	APEX	8.9 GeV/c $\overline{p}$ beam

$\tau(\overline{p} \to e^- \omega)$ τ_{93}

VALUE (years)	CL%	DOCUMENT ID		TECN	COMMENT
>200	90	GEER	00	APEX	8.9 GeV/c $\overline{p}$ beam

p REFERENCES

ABE 17 PR D95 012004 K. Abe *et al.* (Super-Kamiokande Collab.)
ABE 17D PR D96 012003 K. Abe *et al.* (Super-Kamiokande Collab.)
BEYER 17 SCI 358 79 A. Beyer *et al.* (MPQG Collab.)
HEISSE 17 PRL 119 033001 F. Heisse *et al.* (MPIH, GSI, MANZ, RIKEN)
HORBATSCH 17 PR C95 035203 M. Horbatsch, E.A. Hessels, A. Pineda (YORKC+)
NAGAHAMA 17 NATC 8 14084 H. Nagahama *et al.* (RIKEN, TOKY, CERN+)
SAHOO 17 PR D95 013002 B.K. Sahoo (AHMEB)
SCHNEIDER 17 SCI 358 1081 G. Schneider *et al.* (MANZ, RIKEN, +)
SELLNER 17 NJP 19 083023 S. Sellner *et al.* (RIKEN, MPIK, +)
SICK 17 PR C95 012501 I. Sick, D. Trautmann (BASL)
SMORRA 17 NAT 550 371 C. Smorra *et al.* (RIKEN, CERN, +)
HIGINBOTHAM 16 PR C93 055207 D.W. Higinbotham *et al.* (JLAB, KENT, +)
MOHR 16 RMP 88 035009 P.J. Mohr, D.B. Newell, B.N. Taylor (NIST)
ASAKURA 15 PR D92 052006 K. Asakura *et al.* (KamLAND Collab.)
GUSTAFSON 15 PR D91 072009 J. Gustafson *et al.* (Super-Kamiokande Collab.)
LEE 15 PR D92 013013 G. Lee, J.R. Arrington, R.J. Hill (ANL, EFI+)
PESET 15 EPJ A51 32 C. Peset, A. Pineda (BARC)
TAKHISTOV 15 PRL 115 121803 V. Takhistov *et al.* (Super-Kamiokande Collab.)
ULMER 15 NAT 524 196 S. Ulmer *et al.* (RIKEN, CERN, MPIH, +)
ABE 14E PRL 113 121802 K. Abe *et al.* (Super-Kamiokande Collab.)
ABE 14G PR D90 072005 K. Abe *et al.* (Super-Kamiokande Collab.)
BRYMAN 14 PL B733 190 D. Bryman (BRCO)
EPSTEIN 14 PR D90 074027 Z. Epstein, G. Paz, J. Roy (UMD, WAYN)
KARSHENBOI... 14A PR D90 053012 S.G. Karshenboim (MPIG)
LITOS 14 PRL 112 131803 M. Litos *et al.* (Super-Kamiokande Collab.)
LORENZ 14 PL B737 57 I.T. Lorentz, U.-G. Meissner (BONN, JULI)
PDG 14 CP C38 070001 K. Olive *et al.* (PDG Collab.)
TAKHISTOV 14 PRL 113 101801 V. Takhistov *et al.* (Super-Kamiokande Collab.)
ANTOGNINI 13 SCI 339 417 A. Antognini *et al.* (MPIM, ETH, UPMC+)
DISCIACCA 13 PRL 110 130801 J. DiSciacca *et al.* (ATRAP Collab.)
MCGOVERN 13 EPJ A49 12 J.A. McGovern, D.R. Phillips, H.W. Griesshammer
MOHR 12 RMP 84 1527 P.J. Mohr, B.N. Taylor, D.B. Newell (NIST)
NISHINO 12 PR D85 112001 H. Nishino *et al.* (Super-Kamiokande Collab.)
REGIS 12 PR D86 012006 C. Regis *et al.* (Super-Kamiokande Collab.)
ARRINGTON 11 PRL 107 119101 J. Arrington (ANL)
BERNAUER 11 PRL 107 119102 J.C. Bernauer *et al.* (MAMI A1 Collab.)
BRESSI 11 PR A83 052101 G. Bressi *et al.* (LEGN, PAVI, PADO, TRST+)
CLOET 11 PR C83 012201 I.C. Cloet, G.A. Miller (WASH)
DERUJULA 11 PL B697 26 A. de Rujula (MADE, BOST, CERN)
DISTLER 11 PL B696 343 M.O. Distler, J.C. Bernauer, T. Walcher (MANZ)
HILL 11 PRL 107 160402 R.J. Hill, G. Paz (EFI)
HORI 11 NAT 475 484 M. Hori *et al.* (MPIG, TOKY, BUDA, +)
ZHAN 11 PL B705 59 X. Zhan *et al.* (JLAB-Hall A Collab.)
BERNAUER 10 PRL 105 242001 J.C. Bernauer *et al.* (MAMI A1 Collab.)
Also PR C90 015206 J.C. Bernauer *et al.* (MAMI A1 Collab.)
BORISYUK 10 NP A843 59 D. Borisyuk (KIEV)
DERUJULA 10 PL B693 555 A. De Rujula (MADU, CERN)
HILL 10 PR D82 113005 R.J. Hill, G. Paz (CHIC)
POHL 10 NAT 466 213 R. Pohl *et al.* (MPIQ, ENSP, COIM, +)
NISHINO 09 PRL 102 141801 H. Nishino *et al.* (Super-Kamiokande Collab.)
PASK 09 PL B678 55 T. Pask *et al.* (Stefan Meyer Inst., Vienna, TOKY+)
MOHR 08 RMP 80 633 P.J. Mohr, B.N. Taylor, D.B. Newell (NIST)
BELUSHKIN 07 PR C75 035202 M.A. Belushkin, H.W. Hammer, U.-G. Meissner (BONN+)
ARAKI 06 PRL 96 101802 T. Araki *et al.* (KamLAND Collab.)
HORI 06 PRL 96 243401 M. Hori *et al.* (CERN, TOKYO+)
BLUNDEN 05 PR C72 057601 P.G. Blunden, I. Sick (MANI, BASL)
KOBAYASHI 05 PR D72 052007 K. Kobayashi *et al.* (Super-Kamiokande Collab.)
MOHR 05 RMP 77 1 P.J. Mohr, B.N. Taylor (NIST)
SCHUMACHER 05 PPNP 55 567 M. Schumacher (GOET)
AHMED 04 PRL 92 102004 S.N. Ahmed *et al.* (SNO Collab.)
TRETYAK 04 JETPL 79 106 V.I. Tretyak, V.Yu. Denisov, Yu.G. Zdesenko (KIEV)
Translated from ZETFP 79 136.
BACK 03 PL B563 23 H.O. Back *et al.* (BOREXINO Collab.)
BEANE 03 PL B567 200 S.R. Beane *et al.*
Also PL B607 320 (errat.) S.R. Beane *et al.*
DMITRIEV 03 PRL 91 212303 V.F. Dmitriev, R.A. Senkov (NOVO)
HORI 03 PRL 91 123401 M. Hori *et al.* (CERN ASACUSA Collab.)
SICK 03 PL B576 62 I. Sick (BASL)
ZDESENKO 03 PL B553 135 Yu.G. Zdesenko, V.I. Tretyak (KIEV)
AHMAD 02 PRL 89 011301 Q.R. Ahmad *et al.* (SNO Collab.)
BARANOV 01 PPN 32 376 P.S. Baranov *et al.*
Translated from FECAY 32 699.
BLANPIED 01 PR C64 025203 G. Blanpied *et al.* (BNL LEGS Collab.)
HORI 01 PRL 87 093401 M. Hori *et al.* (CERN ASACUSA Collab.)
OLMOSDEL... 01 EPJ A10 207 V. Olmos de Leon *et al.* (MAMI TAPS Collab.)
TRETYAK 01 PL B505 59 V.I. Tretyak, Yu.G. Zdesenko (KIEV)
BERNABEI 00B PL B493 12 R. Bernabei *et al.* (Gran Sasso DAMA Collab.)
GEER 00 PRL 84 590 S. Geer *et al.* (FNAL APEX Collab.)
Also PR D62 052004 S. Geer *et al.* (FNAL APEX Collab.)
Also PRL 85 3546 (errat.) S. Geer *et al.* (FNAL APEX Collab.)
GEER 00D APJ 532 648 S.H. Geer, D.C. Kennedy
SENGUPTA 00 PL B484 275 S. Sengupta
WALL 00 PR D61 072004 D. Wall *et al.* (Soudan-2 Collab.)
WALL 00B PR D62 092003 D. Wall *et al.* (Soudan-2 Collab.)
GABRIELSE 99 PRL 82 3198 G. Gabrielse *et al.*
HAYATO 99 PRL 83 1529 Y. Hayato *et al.* (Super-Kamiokande Collab.)
MCGREW 99 PR D59 052004 C. McGrew *et al.* (IMB-3 Collab.)
MOHR 99 JPCRD 28 1713 P.J. Mohr, B.N. Taylor (NIST)
Also RMP 72 351 P.J. Mohr, B.N. Taylor (NIST)
TORII 99 PR A59 223 H.A. Torii *et al.* (CERN PS-205 Collab.)
ALLISON 98 PL B427 217 W.W.M. Allison *et al.* (Soudan-2 Collab.)
HU 98B PR D58 111101 M. Hu *et al.* (FNAL APEX Collab.)
SHIOZAWA 98 PRL 81 3319 M. Shiozawa *et al.* (Super-Kamiokande Collab.)
GLICENSTEIN 97 PL B411 326 J.F. Glicenstein (SACL)
GABRIELSE 95 PRL 74 3544 G. Gabrielse *et al.* (HARV, MANZ, SEOUL)
MACGIBBON 95 PR C52 2097 B.E. MacGibbon *et al.* (ILL, SASK, INRM)
GEER 94 PRL 72 1596 S. Geer *et al.* (FNAL, UCLA, PSU)
HALLIN 93 PR C48 1497 E.L. Hallin *et al.* (SASK, BOST, ILL)
SUZUKI 93B PL B311 357 Y. Suzuki *et al.* (Kamiokande Collab.)
HUGHES 92 PRL 69 578 R.J. Hughes, B.I. Deutch (LANL, AARH)
ZIEGER 92 PL B278 34 A. Zieger *et al.* (MPCM)
Also PL B281 417 (erratum) A. Zieger *et al.* (MPCM)
BERGER 91 ZPHY C50 385 C. Berger *et al.* (FREJUS Collab.)
BERGER 91B PL B269 227 C. Berger *et al.* (FREJUS Collab.)
FEDERSPIEL 91 PRL 67 1511 F.J. Federspiel *et al.* (ILL)
BECKER-SZ... 90 PR D42 2974 R.A. Becker-Szendy *et al.* (IMB-3 Collab.)
ERICSON 90 EPL 11 295 T.E.O. Ericson, A. Richter (CERN, DARM)
GABRIELSE 90 PRL 65 1317 G. Gabrielse *et al.* (HARV, MANZ, WASH+)
BERGER 89 NP B313 509 C. Berger *et al.* (FREJUS Collab.)
CHO 89 PRL 63 2559 D. Cho, K. Sangster, E.A. Hinds (YALE)
HIRATA 89C PL B220 308 K.S. Hirata *et al.* (Kamiokande Collab.)
PHILLIPS 89 PL B224 348 T.J. Phillips *et al.* (HPW Collab.)
KREISSL 88 ZPHY C37 557 A. Kreissl *et al.* (CERN PS176 Collab.)
SEIDEL 88 PRL 61 2522 S. Seidel *et al.* (IMB Collab.)
BARTELT 87 PR D36 1990 J.E. Bartelt *et al.* (Soudan Collab.)
Also PR D40 1701 (erratum) J.E. Bartelt *et al.* (Soudan Collab.)
COHEN 87 RMP 59 1121 E.R. Cohen, B.N. Taylor (RISC, NBS)
HAINES 86 PRL 57 1986 T.J. Haines *et al.* (IMB Collab.)
KAJITA 86 JPSJ 55 711 T. Kajita *et al.* (Kamiokande Collab.)
ARISAKA 85 JPSJ 54 3213 K. Arisaka *et al.* (Kamiokande Collab.)
BLEWITT 85 PRL 55 2114 G.B. Blewitt *et al.* (IMB Collab.)
DZUBA 85 PL 154B 93 V.A. Dzuba, V.V. Flambaum, P.G. Silvestrov (NOVO)
PARK 85 PRL 54 22 H.S. Park *et al.* (IMB Collab.)
BATTISTONI 84 PL 133B 454 G. Battistoni *et al.* (NUSEX Collab.)
MARINELLI 84 PL 137B 439 M. Marinelli, G. Morpurgo (GENO)
WILKENING 84 PR A29 425 D.A. Wilkening, N.F. Ramsey, D.J. Larson (HARV+)
BARTELT 83 PRL 50 651 J.E. Bartelt *et al.* (MINN, ANL)
BATTISTONI 82 PL 118B 461 G. Battistoni *et al.* (NUSEX Collab.)
KRISHNA... 82 PL 115B 349 M.R. Krishnaswamy *et al.* (TATA, OSKC+)
ALEKSEEV 81 JETPL 33 651 E.N. Alekseev *et al.* (PNPI)
Translated from ZETFP 33 664.
CHERRY 81 PRL 47 1507 M.L. Cherry *et al.* (PENN, BNL)
COWSIK 80 PR D22 2204 R. Cowsik, V.S. Narasimham (TATA)
BELL 79 PL 86B 215 M. Bell *et al.* (CERN)
GOLDEN 79 PRL 43 1196 R.L. Golden *et al.* (NASA, PSLL)
LEARNED 79 PRL 43 907 J.G. Learned, F. Reines, A. Soni (UCI)
BREGMAN 78 PL 78B 174 M. Bregman *et al.* (CERN)
ROBERTS 78 PR D17 358 B.L. Roberts (WILL, RHEL)
EVANS 77 SCI 197 989 J.C. Evans Jr., R.I. Steinberg (BNL, PENN)
HU 75 NP A254 403 E. Hu *et al.* (COLU, YALE)
COHEN 73 JPCRD 2 664 E.R. Cohen, B.N. Taylor (RISC, NBS)
DYLLA 73 PR A7 1224 H.F. Dylla, J.G. King (MIT)
DIX 70 Thesis Case F.W. Dix (CASE)
HARRISON 69 PRL 22 1263 G.E. Harrison, P.G.H. Sandars, S.J. Wright (OXF)
GURR 67 PR 158 1321 H.S. Gurr *et al.* (CASE, WITW)
FLEROV 58 DOKL 3 79 G.N. Flerov *et al.* (ASCI)

n

$I(J^P) = \frac{1}{2}(\frac{1}{2}^+)$ Status: ****

We have omitted some results that have been superseded by later experiments. See our earlier editions.

Anyone interested in the neutron should look at these two review articles: D. Dubbers and M.G. Schmidt, "The neutron and its role in cosmology and particle physics," Reviews of Modern Physics **83** 1111 (2011); and F.E. Wietfeldt and G.L. Greene, "The neutron lifetime," Reviews of Modern Physics **83** 1173 (2011).

n MASS (atomic mass units u)

The mass is known much more precisely in u (atomic mass units) than in MeV. See the next data block.

VALUE (u)	DOCUMENT ID		TECN	COMMENT
1.00866491588±0.00000000049	MOHR	16	RVUE	2014 CODATA value
• • • We do not use the following data for averages, fits, limits, etc. • • •				
1.00866491600±0.00000000043	MOHR	12	RVUE	2010 CODATA value
1.00866491597±0.00000000043	MOHR	08	RVUE	2006 CODATA value
1.00866491560±0.00000000055	MOHR	05	RVUE	2002 CODATA value
1.00866491578±0.00000000055	MOHR	99	RVUE	1998 CODATA value
1.008665904 ±0.000000014	COHEN	87	RVUE	1986 CODATA value

n MASS (MeV)

The mass is known much more precisely in u (atomic mass units) than in MeV. The conversion from u to MeV, 1 u = 931.494 0054(57) MeV/c^2 (MOHR 16, the 2014 CODATA value), involves the relatively poorly known electronic charge.

VALUE (MeV)		DOCUMENT ID		TECN	COMMENT
939.5654133±0.0000058		MOHR	16	RVUE	2014 CODATA value
• • • We do not use the following data for averages, fits, limits, etc. • • •					
939.565379 ±0.000021		MOHR	12	RVUE	2010 CODATA value
939.565346 ±0.000023		MOHR	08	RVUE	2006 CODATA value
939.565360 ±0.000081		MOHR	05	RVUE	2002 CODATA value
939.565331 ±0.000037	[1]	KESSLER	99	SPEC	$np \to d\gamma$
939.565330 ±0.000038		MOHR	99	RVUE	1998 CODATA value
939.56565 ±0.00028	[2,3]	DIFILIPPO	94	TRAP	Penning trap
939.56563 ±0.00028		COHEN	87	RVUE	1986 CODATA value
939.56564 ±0.00028	[3,4]	GREENE	86	SPEC	$np \to d\gamma$
939.5731 ±0.0027	[3]	COHEN	73	RVUE	1973 CODATA value

[1] We use the 1998 CODATA u-to-MeV conversion factor (see the heading above) to get this mass in MeV from the much more precisely measured KESSLER 99 value of 1.00866491637 ± 0.00000000082 u.
[2] The mass is known much more precisely in u: m = 1.0086649235 ± 0.0000000023 u. We use the 1986 CODATA conversion factor to get the mass in MeV.
[3] These determinations are not independent of the $m_n - m_p$ measurements below.
[4] The mass is known much more precisely in u: m = 1.008664919 ± 0.000000014 u.

$\overline{n}$ MASS

VALUE (MeV)	EVTS	DOCUMENT ID		TECN	COMMENT
939.485 ± 0.051	59	[1] CRESTI	86	HBC	$\overline{p}p \to \overline{n}n$

[1] This is a corrected result (see the erratum). The error is statistical. The maximum systematic error is 0.029 MeV.

$(m_n - m_{\overline{n}})/\, m_n$

A test of CPT invariance. Calculated from the n and $\overline{n}$ masses, above.

VALUE	DOCUMENT ID
(9 ± 6) × 10^{-5} OUR EVALUATION	

$m_n - m_p$

VALUE (MeV)	DOCUMENT ID		TECN	COMMENT
1.29333205 ± 0.00000051	[1] MOHR	16	RVUE	2014 CODATA value
• • • We do not use the following data for averages, fits, limits, etc. • • •				
1.29333217 ± 0.00000042	[2] MOHR	12	RVUE	2010 CODATA value
1.29333214 ± 0.00000043	[3] MOHR	08	RVUE	2006 CODATA value
1.2933317 ± 0.0000005	[4] MOHR	05	RVUE	2002 CODATA value
1.2933318 ± 0.0000005	[5] MOHR	99	RVUE	1998 CODATA value
1.293318 ± 0.000009	[6] COHEN	87	RVUE	1986 CODATA value
1.2933328 ± 0.0000072	GREENE	86	SPEC	$np \to d\gamma$
1.293429 ± 0.000036	COHEN	73	RVUE	1973 CODATA value

[1] The 2014 CODATA mass difference in u is $m_n - m_p$ = 1.001 388 449 00(51) × 10^{-3} u.
[2] The 2010 CODATA mass difference in u is $m_n - m_p$ = 1.388 449 19(45) × 10^{-3} u.
[3] Calculated by us from the MOHR 08 ratio m_n/m_p = 1.00137841918(46). In u, $m_n - m_p$ = 1.38844920(46) × 10^{-3} u.
[4] Calculated by us from the MOHR 05 ratio m_n/m_p = 1.00137841870 ± 0.00000000058. In u, $m_n - m_p$ = (1.3884487 ± 0.0000006) × 10^{-3} u.
[5] Calculated by us from the MOHR 99 ratio m_n/m_p = 1.00137841887 ± 0.00000000058. In u, $m_n - m_p$ = (1.3884489 ± 0.0000006) × 10^{-3} u.
[6] Calculated by us from the COHEN 87 ratio m_n/m_p = 1.001378404 ± 0.000000009. In u, $m_n - m_p$ = 0.001388434 ± 0.000000009 u.

n MEAN LIFE

Limits on lifetimes for *bound* neutrons are given in the section "p PARTIAL MEAN LIVES."

We average the best seven measurements. The result, 880.2 ± 1.0 s (including a scale factor of 1.9), is 5.5 seconds lower than the value we gave in 2010—a drop of 6.9 old and 5.5 new standard deviations.

For a full review of all matters concerning the neutron lifetime, see F.E. Wietfeldt and G.L. Greene, "The neutron lifetime," Reviews of Modern Physics **83** 1173 (2011). In particular, there is a full discussion of the experimental methods and results; and an average lifetime is obtained making several different selections of the results then available.

VALUE (s)	DOCUMENT ID		TECN	COMMENT
880.2 ± 1.0 OUR AVERAGE	Error includes scale factor of 1.9. See the ideogram below.			
880.2 ± 1.2	[1] ARZUMANOV	15	CNTR	UCN double bottle
887.7 ± 1.2 ± 1.9	[2] YUE	13	CNTR	In-beam n, trapped p
882.5 ± 1.4 ± 1.5	[3] STEYERL	12	CNTR	UCN material bottle
880.7 ± 1.3 ± 1.2	PICHLMAIER	10	CNTR	UCN material bottle
878.5 ± 0.7 ± 0.3	SEREBROV	05	CNTR	UCN gravitational trap
889.2 ± 3.0 ± 3.8	BYRNE	96	CNTR	Penning trap
882.6 ± 2.7	[4] MAMPE	93	CNTR	UCN material bottle
• • • We do not use the following data for averages, fits, limits, etc. • • •				
881.6 ± 0.8 ± 1.9	[5] ARZUMANOV	12	CNTR	See ARZUMANOV 15
886.3 ± 1.2 ± 3.2	NICO	05	CNTR	See YUE 13
886.8 ± 1.2 ± 3.2	DEWEY	03	CNTR	See NICO 05
885.4 ± 0.9 ± 0.4	ARZUMANOV	00	CNTR	See ARZUMANOV 12
888.4 ± 3.1 ± 1.1	[6] NESVIZHEV...	92	CNTR	UCN material bottle
888.4 ± 2.9	ALFIMENKOV	90	CNTR	See NESVIZHEVSKII 92
893.6 ± 3.8 ± 3.7	BYRNE	90	CNTR	See BYRNE 96
878 ±27 ±14	KOSSAKOW...	89	TPC	Pulsed beam
887.6 ± 3.0	MAMPE	89	CNTR	See STEYERL 12
877 ±10	PAUL	89	CNTR	Magnetic storage ring
876 ±10 ±19	LAST	88	SPEC	Pulsed beam
891 ± 9	SPIVAK	88	CNTR	Beam
903 ±13	KOSVINTSEV	86	CNTR	UCN material bottle
937 ±18	[7] BYRNE	80	CNTR	
875 ±95	KOSVINTSEV	80	CNTR	
881 ± 8	BONDAREN...	78	CNTR	See SPIVAK 88
918 ±14	CHRISTENSEN	72	CNTR	

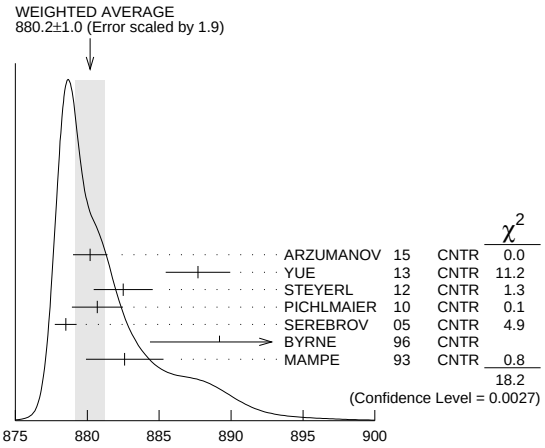

[1] ARZUMANOV 15 is a reanalysis of their 2008–2010 dataset, with improved systematic corrections of of ARZUMANOV 00 and ARZUMANOV 12.
[2] YUE 13 differs from NICO 05 in that a different and better method was used to measure the neutron density in the fiducial volume. This shifted the lifetime by +1.4 seconds and reduced the previously largest source of systematic uncertainty by a factor of five.
[3] STEYERL 12 is a detailed reanalysis of neutron storage loss corrections to the raw data of MAMPE 89, and it replaces that value.
[4] IGNATOVICH 95 calls into question some of the corrections and averaging procedures used by MAMPE 93. The response, BONDARENKO 96, denies the validity of the criticisms.
[5] ARZUMANOV 12 reanalyzes its systematic corrections in ARZUMANOV 00 and obtains this corrected value.
[6] The NESVIZHEVSKII 92 measurement has been withdrawn by A. Serebrov.
[7] The BYRNE 80 measurement has been withdrawn (J. Byrne, private communication, 1990).

n MAGNETIC MOMENT

See the "Note on Baryon Magnetic Moments" in the Λ Listings.

VALUE (μ_N)	DOCUMENT ID		TECN	COMMENT
−1.91304273 ± 0.00000045	MOHR	16	RVUE	2014 CODATA value
• • • We do not use the following data for averages, fits, limits, etc. • • •				
−1.91304272 ± 0.00000045	MOHR	12	RVUE	2010 CODATA value
−1.91304273 ± 0.00000045	MOHR	08	RVUE	2006 CODATA value
−1.91304273 ± 0.00000045	MOHR	05	RVUE	2002 CODATA value
−1.91304272 ± 0.00000045	MOHR	99	RVUE	1998 CODATA value
−1.91304275 ± 0.00000045	COHEN	87	RVUE	1986 CODATA value
−1.91304277 ± 0.00000048	[1] GREENE	82	MRS	

[1] GREENE 82 measures the moment to be (1.04187564 ± 0.00000026) × 10^{-3} Bohr magnetons. The value above is obtained by multiplying this by m_p/m_e = 1836.152701 ± 0.000037 (the 1986 CODATA value from COHEN 87).

n ELECTRIC DIPOLE MOMENT

A nonzero value is forbidden by both T invariance and P invariance. A number of early results have been omitted. See RAMSEY 90, GOLUB 94, and LAMOREAUX 09 for reviews.

The results are upper limits on $|d_n|$.

VALUE (10^{-25} ecm)	CL%	DOCUMENT ID		TECN	COMMENT
< 0.30	90	PENDLEBURY	15	MRS	$d = (-0.21 \pm 1.82) \times 10^{-26}$
• • • We do not use the following data for averages, fits, limits, etc. • • •					
< 0.22	95	[1] SAHOO	17		^{199}Hg atom EDM + theory
< 0.16	95	GRANER	16	MRS	^{199}Hg atom EDM + theory
< 0.55	90	SEREBROV	15	MRS	UCN's, $h\nu = 2\mu_n B \pm 2d_n E$
< 0.55	90	[2] SEREBROV	14	MRS	See SEREBROV 15
< 0.29	90	[3] BAKER	06	MRS	See PENDLEBURY 15
< 0.63	90	[4] HARRIS	99	MRS	$d = (-0.1 \pm 0.36) \times 10^{-25}$
< 0.97	90	ALTAREV	96	MRS	See SEREBROV 14
< 1.1	95	ALTAREV	92	MRS	See ALTAREV 96
< 1.2	95	SMITH	90	MRS	See HARRIS 99
< 2.6	95	ALTAREV	86	MRS	$d = (-1.4 \pm 0.6) \times 10^{-25}$
0.3 ±4.8		PENDLEBURY	84	MRS	Ultracold neutrons
< 6	90	ALTAREV	81	MRS	$d = (2.1 \pm 2.4) \times 10^{-25}$
<16	90	ALTAREV	79	MRS	$d = (4.0 \pm 7.5) \times 10^{-25}$

[1] SAHOO 17 develops theory to calculate this limit from the measured limit by GRANER 16 of the ^{199}Hg atom EDM.
[2] SEREBROV 14 includes the data of ALTAREV 96.
[3] LAMOREAUX 07 faults BAKER 06 for not including in the estimate of systematic error an effect due to the Earth's rotation. BAKER 07 replies (1) that the effect was included implicitly in the analysis and (2) that further analysis confirms that the BAKER 06 limit is correct as is. See also SILENKO 07.

[4] This HARRIS 99 result includes the result of SMITH 90. However, the averaging of the results of these two experiments has been criticized by LAMOREAUX 00.

n MEAN-SQUARE CHARGE RADIUS

The mean-square charge radius of the neutron, $\langle r_n^2 \rangle$, is related to the neutron-electron scattering length b_{ne} by $\langle r_n^2 \rangle = 3(m_e a_0/m_n) b_{ne}$, where m_e and m_n are the masses of the electron and neutron, and a_0 is the Bohr radius. Numerically, $\langle r_n^2 \rangle = 86.34\ b_{ne}$, if we use a_0 for a nucleus with infinite mass.

VALUE (fm^2)	DOCUMENT ID		COMMENT
−0.1161±0.0022 OUR AVERAGE	Error includes scale factor of 1.3. See the ideogram below.		
−0.115 ±0.002 ±0.003	KOPECKY	97	*ne* scattering (Pb)
−0.124 ±0.003 ±0.005	KOPECKY	97	*ne* scattering (Bi)
−0.114 ±0.003	KOESTER	95	*ne* scattering (Pb, Bi)
−0.134 ±0.009	ALEKSANDR...	86	*ne* scattering (Bi)
−0.115 ±0.003	[1] KROHN	73	*ne* scattering (Ne, Ar, Kr, Xe)
• • • We do not use the following data for averages, fits, limits, etc. • • •			
$-0.117\ ^{+0.007}_{-0.011}$	BELUSHKIN	07	Dispersion analysis
−0.113 ±0.003 ±0.004	KOPECKY	95	*ne* scattering (Pb)
−0.114 ±0.003	KOESTER	86	*ne* scattering (Pb, Bi)
−0.118 ±0.002	KOESTER	76	*ne* scattering (Pb)
−0.120 ±0.002	KOESTER	76	*ne* scattering (Bi)
−0.116 ±0.003	KROHN	66	*ne* scattering (Ne, Ar, Kr, Xe)

[1] This value is as corrected by KOESTER 76.

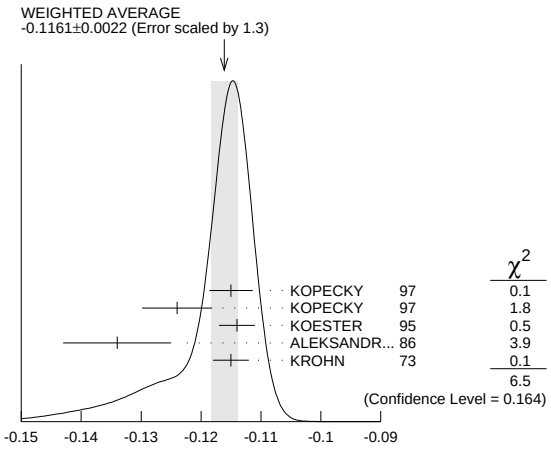

n mean-square charge radius

n MAGNETIC RADIUS

This is the rms magnetic radius, $\sqrt{\langle r_M^2 \rangle}$.

VALUE (fm)	DOCUMENT ID		COMMENT
$\mathbf{0.864\ ^{+0.009}_{-0.008}}$ **OUR AVERAGE**			
0.89 ±0.03	EPSTEIN	14	Using *ep*, *en*, $\pi\pi$ data
$0.862\ ^{+0.009}_{-0.008}$	BELUSHKIN	07	Dispersion analysis

n ELECTRIC POLARIZABILITY α_n

Following is the electric polarizability α_n defined in terms of the induced electric dipole moment by $\mathbf{D} = 4\pi\epsilon_0\alpha_n\mathbf{E}$. For a review, see SCHMIEDMAYER 89.

For very complete reviews of the polarizability of the nucleon and Compton scattering, see SCHUMACHER 05 and GRIESSHAMMER 12.

VALUE (10^{-4} fm^3)	DOCUMENT ID		TECN	COMMENT
11.8 ± 1.1 OUR AVERAGE				
11.55± 1.25±0.8	MYERS	14	CNTR	$\gamma d \to \gamma d$
$12.5 \pm 1.8\ ^{+1.6}_{-1.3}$	[1] KOSSERT	03	CNTR	$\gamma d \to \gamma p n$
12.0 ± 1.5 ±2.0	SCHMIEDM...	91	CNTR	*n* Pb transmission
$10.7\ ^{+3.3}_{-10.7}$	ROSE	90B	CNTR	$\gamma d \to \gamma n p$
• • • We do not use the following data for averages, fits, limits, etc. • • •				
8.8 ± 2.4 ±3.0	[2] LUNDIN	03	CNTR	$\gamma d \to \gamma d$
13.6	[3] KOLB	00	CNTR	$\gamma d \to \gamma n p$
0.0 ± 5.0	[4] KOESTER	95	CNTR	*n* Pb, *n* Bi transmission
$11.7\ ^{+4.3}_{-11.7}$	ROSE	90	CNTR	See ROSE 90B
8 ±10	KOESTER	88	CNTR	*n* Pb, *n* Bi transmission
12 ±10	SCHMIEDM...	88	CNTR	*n* Pb, *n* C transmission

[1] KOSSERT 03 gets $\alpha_n - \beta_n = (9.8 \pm 3.6\ ^{+2.1}_{-1.1} \pm 2.2) \times 10^{-4}$ fm^3, and uses $\alpha_n + \beta_n = (15.2 \pm 0.5) \times 10^{-4}$ fm^3 from LEVCHUK 00. Thus the errors on α_n and β_n are anti-correlated.

[2] LUNDIN 03 measures $\alpha_N - \beta_N = (6.4 \pm 2.4) \times 10^{-4}$ fm^3 and uses accurate values for α_p and α_p and a precise sum-rule result for $\alpha_n + \beta_n$. The second error is a model uncertainty, and errors on α_n and β_n are anticorrelated. The data from this paper aer included in the analysis of MYERS 14.

[3] KOLB 00 obtains this value with a lower limit of 7.6×10^{-4} fm^3 but no upper limit from this experiment alone. Combined with results of ROSE 90, the 1-σ range is (7.6–14.0) × 10^{-4} fm^3.

[4] KOESTER 95 uses natural Pb and the isotopes 208, 207, and 206. See this paper for a discussion of methods used by various groups to extract α_n from data.

n MAGNETIC POLARIZABILITY β_n

VALUE (10^{-4} fm^3)	DOCUMENT ID		TECN	COMMENT
3.7 ±1.2 OUR AVERAGE				
3.65±1.25±0.8	MYERS	14	CNTR	$\gamma d \to \gamma d$
$2.7 \pm 1.8\ ^{+1.3}_{-1.6}$	[1] KOSSERT	03	CNTR	$\gamma d \to \gamma p n$
6.5 ±2.4 ±3.0	[2] LUNDIN	03	CNTR	$\gamma d \to \gamma d$
• • • We do not use the following data for averages, fits, limits, etc. • • •				
1.6	[3] KOLB	00	CNTR	$\gamma d \to \gamma n p$

[1] KOSSERT 03 gets $\alpha_n - \beta_n = (9.8 \pm 3.6\ ^{+2.1}_{-1.1} \pm 2.2) \times 10^{-4}$ fm^3, and uses $\alpha_n + \beta_n = (15.2 \pm 0.5) \times 10^{-4}$ fm^3 from LEVCHUK 00. Thus the errors on α_n and β_n are anti-correlated.

[2] LUNDIN 03 measures $\alpha_N - \beta_N = (6.4 \pm 2.4) \times 10^{-4}$ fm^3 and uses accurate values for α_p and α_p and a precise sum-rule result for $\alpha_n + \beta_n$. The second error is a model uncertainty, and errors on α_n and β_n are anticorrelated.

[3] KOLB 00 obtains this value with an upper limit of 7.6×10^{-4} fm^3 but no lower limit from this experiment alone. Combined with results of ROSE 90, the 1-σ range is (1.2–7.6) × 10^{-4} fm^3.

n CHARGE

See also "$|q_p + q_e|/e$" in the proton Listings.

VALUE (10^{-21} *e*)	DOCUMENT ID		TECN	COMMENT
− 0.2± 0.8 OUR AVERAGE				
− 0.1± 1.1	[1] BRESSI	11		Neutrality of SF_6
− 0.4± 1.1	[2] BAUMANN	88		Cold *n* deflection
• • • We do not use the following data for averages, fits, limits, etc. • • •				
−15 ±22	[3] GAEHLER	82	CNTR	Cold *n* deflection

[1] As a limit, this BRESSI 11 value is $< 1 \times 10^{-21}$ *e*.

[2] The BAUMANN 88 error ±1.1 gives the 68% CL limits about the the value −0.4.

[3] The GAEHLER 82 error ±22 gives the 90% CL limits about the the value −15.

LIMIT ON $n\overline{n}$ OSCILLATIONS

Mean Time for $n\overline{n}$ Transition in Vacuum

A test of ΔB=2 baryon number nonconservation. MOHAPATRA 80 and MOHAPATRA 89 discuss the theoretical motivations for looking for $n\overline{n}$ oscillations. DOVER 83 and DOVER 85 give phenomenological analyses. The best limits come from looking for the decay of neutrons bound in nuclei. However, these analyses require model-dependent corrections for nuclear effects. See KABIR 83, DOVER 89, ALBERICO 91, and GAL 00 for discussions. Direct searches for $n \to \overline{n}$ transitions using reactor neutrons are cleaner but give somewhat poorer limits. We include limits for both free and bound neutrons in the Summary Table. See MOHAPATRA 09 and PHILLIPS 16 for recent reviews.

VALUE (s)	CL%	DOCUMENT ID		TECN	COMMENT
>2.7 × 10^8	90	ABE	15C	CNTR	*n* bound in oxygen
>8.6 × 10^7	90	BALDO-...	94	CNTR	Reactor (free) neutrons
• • • We do not use the following data for averages, fits, limits, etc. • • •					
>1.37 × 10^8	90	[1] AHARMIM	17	SNO	*n* bound in deuteron
>1.3 × 10^8	90	CHUNG	02B	SOU2	*n* bound in iron
>1 × 10^7	90	BALDO-...	90	CNTR	See BALDO-CEOLIN 94
>1.2 × 10^8	90	BERGER	90	FREJ	*n* bound in iron
>4.9 × 10^5	90	BRESSI	90	CNTR	Reactor neutrons
>4.7 × 10^5	90	BRESSI	89	CNTR	See BRESSI 90
>1.2 × 10^8	90	TAKITA	86	CNTR	*n* bound in oxygen
>1 × 10^6	90	FIDECARO	85	CNTR	Reactor neutrons
>8.8 × 10^7	90	PARK	85B	CNTR	
>3 × 10^7		BATTISTONI	84	NUSX	
> 0.27–1.1 × 10^8		JONES	84	CNTR	
>2 × 10^7		CHERRY	83	CNTR	

[1] The AHARMIM 17 value is an unbounded limit (it does not assume a positive lifetime). The bounded limit is 1.23×10^8 sec.

LIMIT ON nn' OSCILLATIONS

Lee and Yang (LEE 56) proposed the existence of mirror world in an attempt to restore global parity symmetry. See BEREZHIANI 06 for a recent discussion.

VALUE (s)	CL%	DOCUMENT ID		TECN	COMMENT
>414	90	SEREBROV	08	CNTR	UCN, B field on & off

• • • We do not use the following data for averages, fits, limits, etc. • • •

> 12	95	[1] ALTAREV	09A	CNTR	UCN, scan $0 \le B \le 12.5$ μT
>103	95	BAN	07	CNTR	UCN, B field on & off

[1] Losses of neutrons due to oscillations to mirror neutrons would be maximal when the magnetic fields B and B' in the two worlds were equal. Hence the scan over B by ALTAREV 09A: the limit applies for any B' over the given range. At $B' = 0$, the limit is 141 s (95% CL).

n DECAY MODES

	Mode	Fraction (Γ_i/Γ)	Confidence level
Γ_1	$p e^- \overline{\nu}_e$	100 %	
Γ_2	$p e^- \overline{\nu}_e \gamma$	[a] (9.2±0.7) × 10^{-3}	
Γ_3	hydrogen-atom $\overline{\nu}_e$		
	Charge conservation (Q) violating mode		
Γ_4	$p \nu_e \overline{\nu}_e$	Q < 8 × 10^{-27}	68%

[a] This limit is for γ energies between 0.4 and 782 keV.

n BRANCHING RATIOS

$\Gamma(p e^- \overline{\nu}_e \gamma)/\Gamma_{total}$ Γ_2/Γ

VALUE (units 10^{-3})	CL%	DOCUMENT ID		TECN	COMMENT
9.17±0.24±0.64		[1] BALES	16	RDK2	Two different set-ups
• • • We do not use the following data for averages, fits, limits, etc. • • •					
3.09±0.11±0.30		[2] COOPER	10	CNTR	See BALES 16
3.13±0.11±0.33		NICO	06	CNTR	See COOPER 10
<6.9	90	[3] BECK	02	CNTR	γ, p, e^- coincidence

[1] BALES 16 gets a branching fraction of $(5.82 \pm 0.23 \pm 0.62) \times 10^{-3}$ for a photon energy range 0.4 to 14.0 keV, and with a different detector array, $(3.35 \pm 0.05 \pm 0.15) \times 10^{-3}$ for 14.1 to 782 keV. Our result above is the sum; the error on the sum is completely dominated by the error on the lower range.
[2] This COOPER 10 result is for γ energies between 15 and 340 keV.
[3] This BECK 02 limit is for γ energies between 35 and 100 keV.

$\Gamma(\text{hydrogen-atom } \overline{\nu}_e)/\Gamma_{total}$ Γ_3/Γ

VALUE	CL%	DOCUMENT ID		TECN
• • • We do not use the following data for averages, fits, limits, etc. • • •				
<3 × 10^{-2}	95	[1] GREEN	90	RVUE

[1] GREEN 90 infers that τ(hydrogen-atom$\overline{\nu}_e$) > 3×10^4 s by comparing neutron lifetime measurements made in storage experiments with those made in β-decay experiments. However, the result depends sensitively on the lifetime measurements, and does not of course take into account more recent measurements of same.

$\Gamma(p \nu_e \overline{\nu}_e)/\Gamma_{total}$ Γ_4/Γ

Forbidden by charge conservation.

VALUE	CL%	DOCUMENT ID		TECN	COMMENT
<8 × 10^{-27}	68	[1] NORMAN	96	RVUE	^{71}Ga → ^{71}Ge neutrals
• • • We do not use the following data for averages, fits, limits, etc. • • •					
<9.7 × 10^{-18}	90	ROY	83	CNTR	^{113}Cd → ^{113m}Inneut.
<7.9 × 10^{-21}		VAIDYA	83	CNTR	^{87}Rb → ^{87m}Srneut.
<9 × 10^{-24}	90	BARABANOV	80	CNTR	^{71}Ga → ^{71}GeX
<3 × 10^{-19}		NORMAN	79	CNTR	^{87}Rb → ^{87m}Srneut.

[1] NORMAN 96 gets this limit by attributing SAGE and GALLEX counting rates to the charge-nonconserving transition ^{71}Ga → ^{71}Ge+neutrals rather than to solar-neutrino reactions.

See the related review(s):
Baryon Decay Parameters

n → $p e^- \overline{\nu}_e$ DECAY PARAMETERS

See the above "Note on Baryon Decay Parameters." For discussions of recent results, see the references cited at the beginning of the section on the neutron mean life. For discussions of the values of the weak coupling constants g_A and g_V obtained using the neutron lifetime and asymmetry parameter A, comparisons with other methods of obtaining these constants, and implications for particle physics and for astrophysics, see DUBBERS 91 and WOOLCOCK 91. For tests of the $V-A$ theory of neutron decay, see EROZOLIMSKII 91B, MOSTOVOI 96, NICO 05, SEVERIJNS 06, and ABELE 08.

$\lambda \equiv g_A / g_V$

VALUE			DOCUMENT ID		TECN	COMMENT
−1.2724 ±0.0023 OUR AVERAGE			Error includes scale factor of 2.2. See the ideogram below.			
−1.284	±0.014		[1] DARIUS	17	SPEC	Cold n, unpolarized
−1.2755	±0.0030		[2] MENDENHALL	13	UCNA	Ultracold n, polarized
−1.2748	±0.0008	$^{+0.0010}_{-0.0011}$	[3] MUND	13	SPEC	Cold n, polarized
−1.275	±0.006	±0.015	SCHUMANN	08	CNTR	Cold n, polarized
−1.2686	±0.0046	±0.0007	[4] MOSTOVOI	01	CNTR	A and B × polarizations
−1.266	±0.004		LIAUD	97	TPC	Cold n, polarized, A
−1.2594	±0.0038		[5] YEROZLIM...	97	CNTR	Cold n, polarized, A
−1.262	±0.005		BOPP	86	SPEC	Cold n, polarized, A
• • • We do not use the following data for averages, fits, limits, etc. • • •						
−1.27590	±0.00239	$^{+0.00331}_{-0.00377}$	[6] PLASTER	12	UCNA	See MENDENHALL 13
−1.27590		$^{+0.00409}_{-0.00445}$	LIU	10	UCNA	See PLASTER 12
−1.2739	±0.0019		[7] ABELE	02	SPEC	See MUND 13
−1.274	±0.003		ABELE	97D	SPEC	Cold n, polarized, A
−1.266	±0.004		SCHRECK...	95	TPC	See LIAUD 97
−1.2544	±0.0036		EROZOLIM...	91	CNTR	See YEROZOLIMSKY 97
−1.226	±0.042		MOSTOVOY	83	RVUE	
−1.261	±0.012		EROZOLIM...	79	CNTR	Cold n, polarized, A
−1.259	±0.017		[8] STRATOWA	78	CNTR	p recoil spectrum, a
−1.263	±0.015		EROZOLIM...	77	CNTR	See EROZOLIMSKII 79
−1.250	±0.036		[8] DOBROZE...	75	CNTR	See STRATOWA 78
−1.258	±0.015		[9] KROHN	75	CNTR	Cold n, polarized, A
−1.263	±0.016		[10] KROPF	74	RVUE	n decay alone
−1.250	±0.009		[10] KROPF	74	RVUE	n decay + nuclear ft

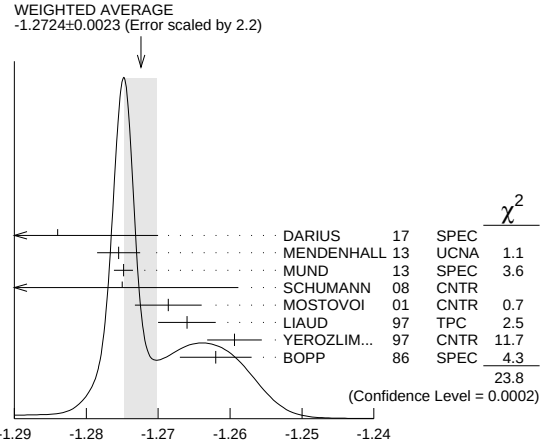

[1] DARIUS 17 calculates this value from the measurement of the a parameter (see below).
[2] MENDENHALL 13 gets $A = -0.11954 \pm 0.00055 \pm 0.00098$ and $\lambda = -1.2756 \pm 0.0030$. We quote the nearly identical values that include the earlier UCNA measurement (PLASTER 12), with a correction to that result.
[3] This MUND 13 value includes earlier PERKEO II measurements (ABELE 02 and ABELE 97D).
[4] MOSTOVOI 01 measures the two P-odd correlations A and B, or rather SA and SB, where S is the n polarization, in free neutron decay.
[5] YEROZOLIMSKY 97 makes a correction to the EROZOLIMSKII 91 value.
[6] This PLASTER 12 value is identical with that given in LIU 10, but the experiment is now described in detail.
[7] This is the combined result of ABELE 02 and ABELE 97D.
[8] These experiments measure the absolute value of g_A/g_V only.
[9] KROHN 75 includes events of CHRISTENSEN 70.
[10] KROPF 74 reviews all data through 1972.

e^- ASYMMETRY PARAMETER A

This is the neutron-spin electron-momentum correlation coefficient. Unless otherwise noted, the values are corrected for radiative effects and weak magnetism. In the Standard Model, A is related to $\lambda \equiv g_A/g_V$ by $A = -2\,\lambda\,(\lambda+1)\,/\,(1+3\lambda^2)$; this assumes that g_A and g_V are real.

VALUE			DOCUMENT ID		TECN	COMMENT
−0.1184 ±0.0010 OUR AVERAGE			Error includes scale factor of 2.4. See the ideogram below.			
−0.11952	±0.00110		[1] MENDENHALL	13	UCNA	Ultracold n, polarized
−0.11926	±0.00031	$^{+0.00036}_{-0.00042}$	[2] MUND	13	SPEC	Cold n, polarized
−0.1160	±0.0009	±0.0012	LIAUD	97	TPC	Cold n, polarized
−0.1135	±0.0014		[3] YEROZLIM...	97	CNTR	Cold n, polarized
−0.1146	±0.0019		BOPP	86	SPEC	Cold n, polarized
• • • We do not use the following data for averages, fits, limits, etc. • • •						
−0.11966	±0.00089	$^{+0.00123}_{-0.00140}$	[4] PLASTER	12	UCNA	See MENDENHALL 13
−0.11966	±0.00089	$^{+0.00123}_{-0.00140}$	LIU	10	UCNA	See PLASTER 12
−0.1138	±0.0046	±0.0021	PATTIE	09	SPEC	Ultracold n, polarized
−0.1189	±0.0007		[5] ABELE	02	SPEC	See MUND 13
−0.1168	±0.0017		[6] MOSTOVOI	01	CNTR	Inferred
−0.1189	±0.0012		ABELE	97D	SPEC	Cold n, polarized
−0.1160	±0.0009	±0.0011	SCHRECK...	95	TPC	See LIAUD 97
−0.1116	±0.0014		EROZOLIM...	91	CNTR	See YEROZOLIMSKY 97
−0.114	±0.005		[7] EROZOLIM...	79	CNTR	Cold n, polarized
−0.113	±0.006		[7] KROHN	75	CNTR	Cold n, polarized

[1] MENDENHALL 13 gets $A = -0.11954 \pm 0.00055 \pm 0.00098$ and $\lambda = -1.2756 \pm 0.0030$. We quote the nearly identical values that include the earlier UCNA measurement (PLASTER 12), with a correction to that result.

[2] This MUND 13 value includes earlier PERKEO II measurements (ABELE 02 and ABELE 97D), with a correction to those results.
[3] YEROZOLIMSKY 97 makes a correction to the EROZOLIMSKII 91 value.
[4] This PLASTER 12 value is identical with that given in LIU 10, but the experiment is now described in detail.
[5] This is the combined result of ABELE 02 and ABELE 97D.
[6] MOSTOVOI 01 calculates this from its measurement of $\lambda=g_A/g_V$ above.
[7] These results are not corrected for radiative effects and weak magnetism, but the corrections are small compared to the errors.

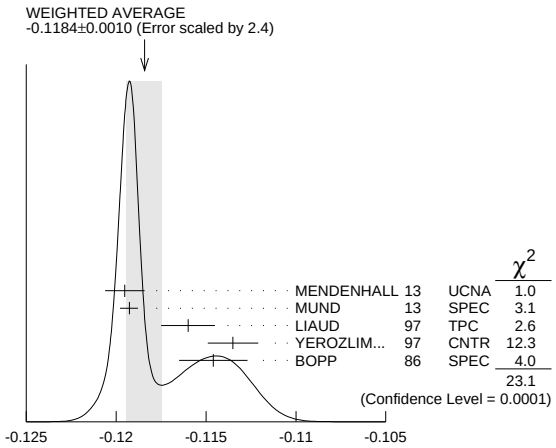

e^- asymmetry parameter A

$\bar{\nu}_e$ ASYMMETRY PARAMETER B

This is the neutron-spin antineutrino-momentum correlation coefficient. In the Standard Model, B is related to $\lambda \equiv g_A/g_V$ by $B = 2\lambda(\lambda-1)/(1+3\lambda^2)$; this assumes that g_A and g_V are real.

VALUE	DOCUMENT ID		TECN	COMMENT
0.9807±0.0030 OUR AVERAGE				
0.9802±0.0034±0.0036	SCHUMANN	07	CNTR	Cold *n*, polarized
0.967 ±0.006 ±0.010	KREUZ	05	CNTR	Cold *n*, polarized
0.9801±0.0046	SEREBROV	98	CNTR	Cold *n*, polarized
0.9894±0.0083	KUZNETSOV	95	CNTR	Cold *n*, polarized
1.00 ±0.05	CHRISTENSEN	70	CNTR	Cold *n*, polarized
0.995 ±0.034	EROZOLIM...	70C	CNTR	Cold *n*, polarized
• • • We do not use the following data for averages, fits, limits, etc. • • •				
0.9876±0.0004	[1] MOSTOVOI	01	CNTR	Inferred

[1] MOSTOVOI 01 calculates this from its measurement of $\lambda=g_A/g_V$ above.

PROTON ASYMMETRY PARAMETER C

Describes the correlation between the neutron spin and the proton momentum. In the Standard Model, C is related to $\lambda \equiv g_A/g_V$ by $C = -x_c\,(A+B) = x_c\,4\lambda/(1+3\lambda^2)$, where $x_c = 0.27484$ is a kinematic factor; this assumes that g_A and g_V are real.

VALUE	DOCUMENT ID		TECN	COMMENT
−0.2377±0.0010±0.0024	SCHUMANN	08	CNTR	Cold *n*, polarized

e-$\bar{\nu}_e$ ANGULAR CORRELATION COEFFICIENT a

For a review of past experiments and plans for future measurements of the a parameter, see WIETFELDT 05. In the Standard Model, a is related to $\lambda \equiv g_A/g_V$ by $a = (1-\lambda^2)/(1+3\lambda^2)$; this assumes that g_A and g_V are real.

VALUE	DOCUMENT ID		TECN	COMMENT
−0.1059±0.0028 OUR AVERAGE				
−0.1090±0.0030±0.0028	[1] DARIUS	17	SPEC	Cold *n*, unpolarized
−0.1054±0.0055	BYRNE	02	SPEC	Proton recoil spectrum
−0.1017±0.0051	STRATOWA	78	CNTR	Proton recoil spectrum
−0.091 ±0.039	GRIGOREV	68	SPEC	Proton recoil spectrum
• • • We do not use the following data for averages, fits, limits, etc. • • •				
−0.1045±0.0014	[2] MOSTOVOI	01	CNTR	Inferred

[1] DARIUS 17 exploits a "wishbone" correlation, where the p time of flight is correlated with the momentum of the electron in delayed coincidence.
[2] MOSTOVOI 01 calculates this from its measurement of $\lambda=g_A/g_V$ above.

ϕ_{AV}, PHASE OF g_A RELATIVE TO g_V

Time reversal invariance requires this to be 0 or 180°. This is related to D given in the next data block and $\lambda \equiv g_A/g_V$ by $\sin(\phi_{AV}) \equiv D(1+3\lambda^2)/2|\lambda|$; this assumes that g_A and g_V are real.

VALUE (°)	CL%	DOCUMENT ID		TECN	COMMENT
180.017±0.026 OUR AVERAGE					
180.012±0.028	68	CHUPP	12	CNTR	Cold *n*, polarized > 91%
180.04 ±0.09		SOLDNER	04	CNTR	Cold *n*, polarized
180.08 ±0.13		LISING	00	CNTR	Polarized > 93%
• • • We do not use the following data for averages, fits, limits, etc. • • •					
180.013±0.028		MUMM	11	CNTR	See CHUPP 12
179.71 ±0.39		EROZOLIM...	78	CNTR	Cold *n*, polarized
180.35 ±0.43		EROZOLIM...	74	CNTR	Cold *n*, polarized
181.1 ±1.3		[1] KROPF	74	RVUE	*n* decay
180.14 ±0.22		STEINBERG	74	CNTR	Cold *n*, polarized

[1] KROPF 74 reviews all data through 1972.

TRIPLE CORRELATION COEFFICIENT D

These are measurements of the component of n spin perpendicular to the decay plane in β decay. Should be zero if T invariance is not violated.

VALUE (units 10^{-4})	DOCUMENT ID		TECN	COMMENT
− 1.2 ± 2.0 OUR AVERAGE				
− 0.94± 1.89±0.97	CHUPP	12	CNTR	Cold *n*, polarized > 91%
− 2.8 ± 6.4 ±3.0	SOLDNER	04	CNTR	Cold *n*, polarized
− 6 ±12 ±5	LISING	00	CNTR	Polarized > 93%
• • • We do not use the following data for averages, fits, limits, etc. • • •				
− 0.96± 1.89±1.01	MUMM	11	CNTR	See CHUPP 12
+22 ±30	EROZOLIM...	78	CNTR	Cold *n*, polarized
−27 ±50	[1] EROZOLIM...	74	CNTR	Cold *n*, polarized
−11 ±17	STEINBERG	74	CNTR	Cold *n*, polarized

[1] EROZOLIMSKII 78 says asymmetric proton losses and nonuniform beam polarization may give a systematic error up to 30×10^{-4}, thus increasing the EROZOLIMSKII 74 error to 50×10^{-4}. STEINBERG 74 and STEINBERG 76 estimate these systematic errors to be insignificant in their experiment.

TRIPLE CORRELATION COEFFICIENT R

Another test of time-reversal invariance. R measures the polarization of the electron in the direction perpendicular to the plane defined by the neutron spin and the electron momentum. $R = 0$ for T invariance.

VALUE	DOCUMENT ID		TECN	COMMENT
+0.004±0.012±0.005	[1] KOZELA	12	CNTR	Mott polarimeter
• • • We do not use the following data for averages, fits, limits, etc. • • •				
+0.008±0.015±0.005	KOZELA	09	CNTR	See KOZELA 12

[1] KOZELA 12 also measures the polarization of the electron along the direction of the neutron spin. This is nonzero in the Standard Model; the correlation coefficient is $N = +0.067 \pm 0.011 \pm 0.004$.

n REFERENCES

We have omitted some papers that have been superseded by later experiments. See our earlier editions.

AHARMIM	17	PR D96 092005	B. Aharmin *et al.* (SNO Collab.)
DARIUS	17	PRL 119 042502	G. Darius *et al.* (aCORN at NIST)
SAHOO	17	PR D95 013002	B.K. Sahoo (AHMEB)
BALES	16	PRL 116 242501	M.J. Bales *et al.* (RDK II Collab.)
GRANER	16	PRL 116 161601	B. Graner *et al.* (WASH)
Also		PRL 119 119901 (errat.)	B. Graner *et al.* (WASH)
MOHR	16	RMP 88 035009	P.J. Mohr, D.B. Newell, B.N. Taylor (NIST)
PHILLIPS	16	PRPL 612 1	D.G. Phillips II *et al.*
ABE	15C	PR D91 072006	K. Abe *et al.* (Super-Kamiokande Collab.)
ARZUMANOV	15	PL B745 79	S. Arzumanov *et al.* (ILLG, KIAE)
PENDLEBURY	15	PR D92 092003	J.M. Pendlebury *et al.* (ETHZ, PSI, SUSS)
SEREBROV	15	PR C92 055501	A.P. Serebrov *et al.* (PNPI, ILLG, IOFF)
EPSTEIN	14	PR D90 074027	Z. Epstein, G. Paz, J. Roy (UMD, WAYN)
MYERS	14	PRL 113 262506	L.S. Myers *et al.* (COMPTON/MAX-lab Collab.)
SEREBROV	14	JETPL 99 4	A.P. Serebrov *et al.* (PNPI, ILL, IOFF)
MENDENHALL	13	PR C87 032501	M.P. Mendenhall *et al.* (UCNA Collab.)
MUND	13	PRL 110 172502	D. Mund *et al.* (HEID, ILLG)
YUE	13	PRL 111 222501	A.T. Yue *et al.* (UMD, NIST, TENN, ORNL+)
ARZUMANOV	12	JETPL 95 224	S.S. Arzumanov *et al.* (KIAE)
		Translated from ZETFP 95 248.	
CHUPP	12	PR C86 035505	T.E. Chupp *et al.* (MICH, UCB, WASH+)
GRIESSHAM...	12	PPNP 67 841	H.W. Griesshammer *et al.* (GWU, MCHS+)
KOZELA	12	PR C85 045501	A. Kozela *et al.* (nTRV Collab.)
MOHR	12	RMP 84 1527	P.J. Mohr, B.N. Taylor, D.B. Newell (NIST)
PLASTER	12	PR C86 055501	B. Plaster *et al.* (UCNA Collab.)
STEYERL	12	PR C85 065503	A. Steyerl *et al.* (URI, SUSS)
BRESSI	11	PR A83 052101	G. Bressi *et al.* (LEGN, PAVII, PADO, TRST+)
DUBBERS	11	RMP 83 1111	D. Dubbers, M.G. Schmidt (HEID)
MUMM	11	PRL 107 102301	H.P. Mumm *et al.* (NIST, WASH, MICH, LBL+)
WIETFELDT	11	RMP 83 1173	F.E. Wietfeldt, G.L. Greene (TULA, TENN)
COOPER	10	PR C81 035503	R.L. Cooper *et al.* (MICH, NIST, TULA+)
LIU	10	PRL 105 181803	J. Liu *et al.* (UCNA Collab.)
Also		PRL 105 219903 (errat.)	J. Liu *et al.* (UCNA Collab.)
PICHLMAIER	10	PL B693 221	A. Pichlmaier *et al.* (MUNT, PNPI, ILLG)
ALTAREV	09A	PR D80 032003	I. Altarev *et al.* (MUNT, RAL, CAEN+)
KOZELA	09	PRL 102 172301	A. Kozela *et al.* (JAGL, CRAC, PSI, CAEN+)
LAMOREAUX	09	JP G36 104002	S.K. Lamoreaux, R. Golub (YALE, NCSU)
MOHAPATRA	09	JP G36 104006	R.N. Mohapatra (UMD)
PATTIE	09	PRL 102 012301	R.W. Pattie Jr. *et al.* (Los Alamos UCNA Collab.)
ABELE	08	PPNP 60 1	H. Abele (HEID)
MOHR	08	RMP 80 633	P.J. Mohr, B.N. Taylor, D.B. Newell (NIST)
SCHUMANN	08	PRL 100 151801	M. Schumann *et al.* (HEID, ILLG, KARL+)
SEREBROV	08	PL B663 181	A.P. Serebrov *et al.* (PNPI, IOFF, ILLG+)
BAKER	07	PRL 98 149102	C.A. Baker *et al.* (RAL, SUSS, ILLG)
BAN	07	PRL 99 161603	G. Ban *et al.* (CAEN, JAGL, PSI, JINR+)
BELUSHKIN	07	PR C75 035202	M.A. Belushkin, H.W. Hammer, U.-G. Meissner (BONN+)
LAMOREAUX	07	PRL 98 149101	S.K. Lamoreaux, R. Golub (YALE, NCSU)
SCHUMANN	07	PRL 99 191803	M. Schumann *et al.* (HEID, ILLG, KARL+)
SILENKO	07	PPNL 4 468	A.Ya. Silenko (Belarussian U.)
		Translated from PFECAY 6 784.	
BAKER	06	PRL 97 131801	C.A. Baker *et al.* (RAL, SUSS, ILLG)
BEREZHIANI	06	PRL 96 081801	Z. Berezhiani, L. Bento (Aguila U., LISB)
NICO	06	NAT 444 1059	J.S. Nico *et al.* (NIST, TULN, MICH, UMD+)
SEVERIJNS	06	RMP 78 991	N. Severijns, M. Beck, O. Naviliat-Cuncic (LEUV+)
KREUZ	05	PL B619 263	M. Kreuz *et al.* (HEID, ILLG, MANZ, KARL+)
MOHR	05	RMP 77 1	P.J. Mohr, B.N. Taylor (NIST)
NICO	05	PR C71 055502	J.S. Nico *et al.* (NIST, TULN, IND, TENN+)
SCHUMACHER	05	PPNP 55 567	M. Schumacher (GOET)
SEREBROV	05	PL B605 72	A. Serebrov *et al.* (PNPI, JINR, ILLG)
Also		SPU 48 867	A.P. Serebrov *et al.* (PPNI, JINR, ILLG)
		Translated from UFN 175 905.	
WIETFELDT	05	MPLA20 1783	F.E. Wietfeldt (TULN)
SOLDNER	04	PL B581 49	T. Soldner *et al.* (ILLG, MUNT)
DEWEY	03	PRL 91 152302	M.S. Dewey *et al.* (NIST, TULN, IND+)
KOSSERT	03	EPJ A16 259	K. Kossert *et al.* (Mainz MAMI Collab.)
Also		PRL 88 162301	K. Kossert *et al.* (Mainz MAMI Collab.)
LUNDIN	03	PRL 90 192501	M. Lundin *et al.*
ABELE	02	PRL 88 211801	H. Abele *et al.* (PERKEO-II Collab.)
BECK	02	JETPL 76 332	M. Beck *et al.* (LEUV, SUSS, KIAE, PNPI)
		Translated from ZETFP 76 392.	
BYRNE	02	JP G28 1325	J. Byrne *et al.*
CHUNG	02B	PR D66 032004	J. Chung *et al.* (SOUDAN-2 Collab.)
MOSTOVOI	01	PAN 64 1955	Yu.A. Mostovoi *et al.*
		Translated from YAF 64 2040.	

ARZUMANOV 00 PL B483 15 S. Arzumanov *et al.*
GAL 00 PR C61 028201 A. Gal
KOLB 00 PRL 85 1388 N.R. Kolb *et al.*
LAMOREAUX 00 PR D61 051301 S.K. Lamoreaux, R. Golub
LEVCHUK 00 NP A674 449 M.I. Levchuk, A.I. L'vov (BELA, LEBD)
LISING 00 PR C62 055501 L.J. Lising *et al.* (NIST emiT Collab.)
HARRIS 99 PRL 82 904 P.G. Harris *et al.*
KESSLER 99 PL A255 221 E.G. Kessler Jr *et al.*
MOHR 99 JPCRD 28 1713 P.J. Mohr, B.N. Taylor (NIST)
Also RMP 72 351 P.J. Mohr, B.N. Taylor (NIST)
SEREBROV 98 JETP 86 1074 A.P. Serebrov *et al.*
Translated from ZETF 113 1963.
ABELE 97D PL B407 212 H. Abele *et al.* (HEIDP, ILLG)
KOPECKY 97 PR C56 2229 S. Kopecky *et al.*
LIAUD 97 NP A612 53 P. Liaud *et al.* (ILLG, LAPP)
YEROZLIM... 97 PL B412 240 B.G. Erozolimsky *et al.* (HARV, PNPI, KIAE)
ALTAREV 96 PAN 59 1152 I.S. Altarev *et al.* (PNPI)
Translated from YAF 59 1204.
BONDAREN... 96 JETPL 64 416 L.N. Bondarenko *et al.* (KIAE)
Translated from ZETFP 64 382.
BYRNE 96 EPL 33 187 J. Byrne *et al.* (SUSS, ILLG)
MOSTOVOI 96 PAN 59 968 Y.A. Mostovoy (KIAE)
Translated from YAF 59 1013.
NORMAN 96 PR D53 4086 E.B. Norman, J.N. Bahcall, M. Goldhaber (LBL+)
IGNATOVICH 95 JETPL 62 1 V.K. Ignatovich (JINR)
Translated from ZETFP 62 3.
KOESTER 95 PR C51 3363 L. Koester *et al.* (MUNT, JINR, LATV)
KOPECKY 95 PRL 74 2427 S. Kopecky *et al.*
KUZNETSOV 95 PRL 75 794 I.A. Kuznetsov *et al.* (PNPI, KIAE, HARV+)
SCHRECK... 95 PL B349 427 K. Schreckenbach *et al.* (MUNT, ILLG, LAPP)
BALDO-... 94 ZPHY C63 409 M. Baldo-Ceolin *et al.* (HEID, ILLG, PADO+)
DIFILIPPO 94 PRL 73 1481 F. DiFilippo *et al.* (MIT)
Also PRL 71 1998 V. Natarajan *et al.* (MIT)
GOLUB 94 PRPL 237C 1 R. Golub, K. Lamoreaux (HAHN, WASH)
MAMPE 93 JETPL 57 82 B. Mampe *et al.* (KIAE)
Translated from ZETFP 57 77.
ALTAREV 92 PL B276 242 I.S. Altarev *et al.* (PNPI)
NESVIZHEV... 92 JETP 75 405 V.V. Nesvizhevsky *et al.* (PNPI, JINR)
Translated from ZETF 102 740.
ALBERICO 91 NP A523 488 W.M. Alberico, A. de Pace, M. Pignone (TORI)
DUBBERS 91 NP A527 239c D. Dubbers (ILLG)
Also EPL 11 195 D. Dubbers, W. Mampe, J. Dohner (ILLG, HEID)
EROZOLIM... 91 PL B263 33 B.G. Erozolimsky *et al.* (PNPI, KIAE)
Also SJNP 52 999 B.G. Erozolimsky *et al.* (PNPI, KIAE)
Translated from YAF 52 1583.
EROZOLIM... 91B SJNP 53 260 B.G. Erozolimsky, Y.A. Mostovoy (KIAE)
Translated from YAF 53 418.
SCHMIEDM... 91 PRL 66 1015 J. Schmiedmayer *et al.* (TUW, ORNL)
WOOLCOCK 91 MPL A6 2579 W.S. Woolcock (CANB)
ALFIMENKOV 90 JETPL 52 373 V.P. Alfimenkov *et al.* (PNPI, JINR)
Translated from ZETFP 52 984.
BALDO-... 90 PL B236 95 M. Baldo-Ceolin *et al.* (PADO, PAVI, HEIDP+)
BERGER 90 PL B240 237 C. Berger *et al.* (FREJUS Collab.)
BRESSI 90 NC 103A 731 G. Bressi *et al.* (PAVI, ROMA, MILA)
BYRNE 90 PRL 65 289 J. Byrne *et al.* (SUSS, NBS, SCOT, CBNM)
GREEN 90 JP G16 L75 K. Green, D. Thompson (RAL)
RAMSEY 90 ARNPS 40 1 N.F. Ramsey (HARV)
ROSE 90 PL B234 460 K.W. Rose *et al.* (GOET, MPCM, MANZ)
ROSE 90B NP A514 621 K.W. Rose *et al.* (GOET, MPCM)
SMITH 90 PL B234 191 K.F. Smith *et al.* (SUSS, RAL, HARV+)
BRESSI 89 ZPHY C43 175 G. Bressi *et al.* (INFN, MILA, PAVI, ROMA)
DOVER 89 NIM A284 13 C.B. Dover, A. Gal, J.M. Richard (BNL, HEBR+)
KOSSAKOW... 89 NP A503 473 R. Kossakowski *et al.* (LAPP, SAVO, ISNG+)
MAMPE 89 PRL 63 593 W. Mampe *et al.* (ILLG, RISL, SUSS, URI)
MOHAPATRA 89 NIM A284 1 R.N. Mohapatra (UMD)
PAUL 89 ZPHY C45 25 W. Paul *et al.* (BONN, WUPP, MPIH, ILLG)
SCHMIEDM... 89 NIM A284 137 J. Schmiedmayer, H. Rauch, P. Riehs (WIEN)
BAUMANN 88 PR D37 3107 J. Baumann *et al.* (BAYR, MUNI, ILLG)
KOESTER 88 ZPHY A329 229 L. Koester, W. Waschkowski, J. Meier (MUNI, MUNT)
LAST 88 PRL 60 995 I. Last *et al.* (HEIDP, ILLG, ANL)
SCHMIEDM... 88 PRL 61 1065 J. Schmiedmayer, H. Rauch, P. Riehs (TUW)
Also PRL 61 2509 (erratum) J. Schmiedmayer, H. Rauch, P. Riehs (TUW)
SPIVAK 88 JETP 67 1735 P.E. Spivak (KIAE)
Translated from ZETF 94 1.
COHEN 87 RMP 59 1121 E.R. Cohen, B.N. Taylor (RISC, NBS)
ALEKSANDR... 86 SJNP 44 900 Yu.A. Aleksandrov *et al.*
Translated from YAF 44 1384.
ALTAREV 86 JETPL 44 460 I.S. Altarev *et al.* (PNPI)
Translated from ZETFP 44 360.
BOPP 86 PRL 56 919 P. Bopp *et al.* (HEIDP, ANL, ILLG)
Also ZPHY C37 179 E. Klempt *et al.* (HEIDP, ANL, ILLG)
CRESTI 86 PL B177 206 M. Cresti *et al.* (PADO)
Also PL B200 587 (erratum) M. Cresti *et al.* (PADO)
GREENE 86 PRL 56 819 G.L. Greene *et al.* (NBS, ILLG)
KOESTER 86 Physica B137 282 L. Koester *et al.*
KOSVINTSEV 86 JETPL 44 571 Y.Y. Kosvintsev, V.I. Morozov, G.I. Terekhov (KIAE)
Translated from ZETFP 44 444.
TAKITA 86 PR D34 902 M. Takita *et al.* (KEK, TOKY+)
DOVER 85 PR C31 1423 C.B. Dover, A. Gal, J.M. Richard (BNL)
FIDECARO 85 PL 156B 122 G. Fidecaro *et al.* (CERN, ILLG, PADO+)
PARK 85B NP B252 261 H.S. Park *et al.* (IMB Collab.)
BATTISTONI 84 PL 133B 454 G. Battistoni *et al.* (NUSEX Collab.)
JONES 84 PRL 52 720 T.W. Jones *et al.* (IMB Collab.)
PENDLEBURY 84 PL 136B 327 J.M. Pendlebury *et al.* (SUSS, HARV, RAL+)
CHERRY 83 PRL 50 1354 M.L. Cherry *et al.* (PENN, BNL)
DOVER 83 PR D27 1090 C.B. Dover, A. Gal, J.M. Richard (BNL)
KABIR 83 PRL 51 231 P.K. Kabir (HARV)
MOSTOVOY 83 JETPL 37 196 Y.A. Mostovoy (KIAE)
Translated from ZETFP 37 162.
ROY 83 PR D28 1770 A. Roy *et al.* (TATA)
VAIDYA 83 PR D27 486 S.C. Vaidya *et al.* (TATA)
GAEHLER 82 PR D25 2887 R. Gahler, J. Kalus, W. Mampe (BAYR, ILLG)
GREENE 82 Metrologia 18 93 G.L. Greene *et al.* (YALE, HARV, ILLG+)
ALTAREV 81 PL 102B 13 I.S. Altarev *et al.* (PNPI)
BARABANOV 80 JETPL 32 359 I.R. Barabanov *et al.* (PNPI)
Translated from ZETFP 32 384.
BYRNE 80 PL 92B 274 J. Byrne *et al.* (SUSS, RL)
KOSVINTSEV 80 JETPL 31 236 Y.Y. Kosvintsev *et al.* (JINR)
Translated from ZETFP 31 257.
MOHAPATRA 80 PRL 44 1316 R.N. Mohapatra, R.E. Marshak (CUNY, VPI)
ALTAREV 79 JETPL 29 730 I.S. Altarev *et al.* (PNPI)
Translated from ZETFP 29 794.
EROZOLIM... 79 SJNP 30 356 B.G. Erozolimsky *et al.* (KIAE)
Translated from YAF 30 692.
NORMAN 79 PRL 43 1226 E.B. Norman, A.G. Seamster (WASH)
BONDAREN... 78 JETPL 28 303 L.N. Bondarenko *et al.* (KIAE)
Translated from ZETFP 28 328.
Also Smolenice Conf. P.G. Bondarenko (KIAE)
EROZOLIM... 78 SJNP 28 48 B.G. Erozolimsky *et al.* (KIAE)
Translated from YAF 28 98.
STRATOWA 78 PR D18 3970 C. Stratowa, R. Dobrozemsky, P. Weinzierl (SEIB)
EROZOLIM... 77 JETPL 23 663 B.G. Erozolimsky *et al.* (KIAE)
Translated from ZETFP 23 720.
KOESTER 76 PRL 36 1021 L. Koester *et al.*
STEINBERG 76 PR D13 2469 R.I. Steinberg *et al.* (YALE, ISNG)
DOBROZE... 75 PR D11 510 R. Dobrozemsky *et al.* (SEIB)
KROHN 75 PL 55B 175 V.E. Krohn, G.R. Ringo (ANL)
EROZOLIM... 74 JETPL 20 345 B.G. Erozolimsky *et al.*
Translated from ZETFP 20 745.
KROPF 74 ZPHY 267 129 H. Kropf, E. Paul (LINZ)
Also NP A154 160 H. Paul (VIEN)
STEINBERG 74 PRL 33 41 R.I. Steinberg *et al.* (YALE, ISNG)
COHEN 73 JPCRD 2 664 E.R. Cohen, B.N. Taylor (RISC, NBS)
KROHN 73 PR D8 1305 V.E. Krohn, G.R. Ringo
CHRISTENSEN 72 PR D5 1628 C.J. Christensen *et al.* (RISO)
CHRISTENSEN 70 PR C1 1693 C.J. Christensen, V.E. Krohn, G.R. Ringo (ANL)
EROZOLIM... 70C PL 33B 351 B.G. Erozolimsky *et al.* (KIAE)
GRIGOREV 68 SJNP 6 239 V.K. Grigoriev *et al.* (ITEP)
Translated from YAF 6 329.
KROHN 66 PR 148 1303 V.E. Krohn, G.R. Ringo
LEE 56 PR 104 254 T.D. Lee, C.N. Yang (COLU, BNL)

See the related review(s):
N and Δ Resonances

N(1440) 1/2+

$I(J^P) = \frac{1}{2}(\frac{1}{2}^+)$ Status: ****

Older and obsolete values are listed and referenced in the 2014 edition, Chinese Physics **C38** 070001 (2014).

N(1440) POLE POSITION

REAL PART

VALUE (MeV)	*DOCUMENT ID*		*TECN*	*COMMENT*
1360 to 1380 (≈ 1370) OUR ESTIMATE				
1369± 3	SOKHOYAN	15A	DPWA	Multichannel
1363± 2±2	[1] SVARC	14	L+P	$\pi N \to \pi N$
1375±30	CUTKOSKY	80	IPWA	$\pi N \to \pi N$
• • • We do not use the following data for averages, fits, limits, etc. • • •				
1355	ROENCHEN	15A	DPWA	Multichannel
1386	SHKLYAR	13	DPWA	Multichannel
1370± 4	ANISOVICH	12A	DPWA	Multichannel
1370	SHRESTHA	12A	DPWA	Multichannel
1363±11	BATINIC	10	DPWA	$\pi N \to N\pi,\ N\eta$
1359	ARNDT	06	DPWA	$\pi N \to \pi N,\ \eta N$
1383	VRANA	00	DPWA	Multichannel
1385	HOEHLER	93	SPED	$\pi N \to \pi N$

[1] Fit to the amplitudes of HOEHLER 79.

−2×IMAGINARY PART

VALUE (MeV)	*DOCUMENT ID*		*TECN*	*COMMENT*
160 to 190 (≈ 175) OUR ESTIMATE				
189± 5	SOKHOYAN	15A	DPWA	Multichannel
180± 4±5	[1] SVARC	14	L+P	$\pi N \to \pi N$
180±40	CUTKOSKY	80	IPWA	$\pi N \to \pi N$
• • • We do not use the following data for averages, fits, limits, etc. • • •				
215	ROENCHEN	15A	DPWA	Multichannel
277	SHKLYAR	13	DPWA	Multichannel
190± 7	ANISOVICH	12A	DPWA	Multichannel
214	SHRESTHA	12A	DPWA	Multichannel
151±13	BATINIC	10	DPWA	$\pi N \to N\pi,\ N\eta$
162	ARNDT	06	DPWA	$\pi N \to \pi N,\ \eta N$
316	VRANA	00	DPWA	Multichannel
164	HOEHLER	93	SPED	$\pi N \to \pi N$

[1] Fit to the amplitudes of HOEHLER 79.

N(1440) ELASTIC POLE RESIDUE

MODULUS |*r*|

VALUE (MeV)	*DOCUMENT ID*		*TECN*	*COMMENT*
46 to 54 (≈ 50) OUR ESTIMATE				
49±3	SOKHOYAN	15A	DPWA	Multichannel
50±1±2	[1] SVARC	14	L+P	$\pi N \to \pi N$
52±5	CUTKOSKY	80	IPWA	$\pi N \to \pi N$
• • • We do not use the following data for averages, fits, limits, etc. • • •				
62	ROENCHEN	15A	DPWA	Multichannel
126	SHKLYAR	13	DPWA	Multichannel
48±3	ANISOVICH	12A	DPWA	Multichannel
44	BATINIC	10	DPWA	$\pi N \to N\pi,\ N\eta$
38	ARNDT	06	DPWA	$\pi N \to \pi N,\ \eta N$
40	HOEHLER	93	SPED	$\pi N \to \pi N$

[1] Fit to the amplitudes of HOEHLER 79.

PHASE θ

VALUE (°)	*DOCUMENT ID*		*TECN*	*COMMENT*
−100 to −80 (≈ −90) OUR ESTIMATE				
− 82± 5	SOKHOYAN	15A	DPWA	Multichannel
− 88± 1±2	[1] SVARC	14	L+P	$\pi N \to \pi N$
−100±35	CUTKOSKY	80	IPWA	$\pi N \to \pi N$

• • • We do not use the following data for averages, fits, limits, etc. • • •					
– 98	ROENCHEN	15A	DPWA	Multichannel	
– 60	SHKLYAR	13	DPWA	Multichannel	
– 78± 4	ANISOVICH	12A	DPWA	Multichannel	
– 88	BATINIC	10	DPWA	$\pi N \rightarrow N\pi, N\eta$	
– 98	ARNDT	06	DPWA	$\pi N \rightarrow \pi N, \eta N$	

[1] Fit to the amplitudes of HOEHLER 79.

N(1440) INELASTIC POLE RESIDUE

The "normalized residue" is the residue divided by $\Gamma_{pole}/2$.

Normalized residue in $N\pi \rightarrow N(1440) \rightarrow N\eta$

MODULUS	PHASE (°)	DOCUMENT ID	TECN	COMMENT
• • • We do not use the following data for averages, fits, limits, etc. • • •				
0.078	–27	ROENCHEN	15A	DPWA Multichannel

Normalized residue in $N\pi \rightarrow N(1440) \rightarrow \Delta\pi$, P-wave

MODULUS	PHASE (°)	DOCUMENT ID	TECN	COMMENT
0.27±0.02	38 ± 5	SOKHOYAN	15A	DPWA Multichannel
• • • We do not use the following data for averages, fits, limits, etc. • • •				
0.27±0.02	40 ± 5	ANISOVICH	12A	DPWA Multichannel

Normalized residue in $N\pi \rightarrow N(1440) \rightarrow \Lambda K$

MODULUS	PHASE (°)	DOCUMENT ID	TECN	COMMENT
• • • We do not use the following data for averages, fits, limits, etc. • • •				
0.016	145	ROENCHEN	15A	DPWA Multichannel

Normalized residue in $N\pi \rightarrow N(1440) \rightarrow \Sigma K$

MODULUS	PHASE (°)	DOCUMENT ID	TECN	COMMENT
• • • We do not use the following data for averages, fits, limits, etc. • • •				
0.027	113	ROENCHEN	15A	DPWA Multichannel

Normalized residue in $N\pi \rightarrow N(1440) \rightarrow N\,(\pi\pi)^{I=0}_{S-wave}$

MODULUS	PHASE (°)	DOCUMENT ID	TECN	COMMENT
0.21±0.04	–136 ± 4	SOKHOYAN	15A	DPWA Multichannel
• • • We do not use the following data for averages, fits, limits, etc. • • •				
0.21±0.05	–135 ± 7	ANISOVICH	12A	DPWA Multichannel

N(1440) BREIT-WIGNER MASS

VALUE (MeV)	DOCUMENT ID		TECN	COMMENT
1410 to 1470 (≈ 1440) OUR ESTIMATE				
1430 ±10	SOKHOYAN	15A	DPWA	Multichannel
1515 ±15	[1] SHKLYAR	13	DPWA	Multichannel
1412 ± 2	[1] SHRESTHA	12A	DPWA	Multichannel
1485.0± 1.2	[1] ARNDT	06	DPWA	$\pi N \rightarrow \pi N, \eta N$
1440 ±30	CUTKOSKY	80	IPWA	$\pi N \rightarrow \pi N$
1410 ±12	HOEHLER	79	IPWA	$\pi N \rightarrow \pi N$
• • • We do not use the following data for averages, fits, limits, etc. • • •				
1430 ± 8	ANISOVICH	12A	DPWA	Multichannel
1439 ±19	BATINIC	10	DPWA	$\pi N \rightarrow N\pi, N\eta$
1518 ± 5	PENNER	02C	DPWA	Multichannel
1479 ±80	VRANA	00	DPWA	Multichannel

[1] Statistical error only.

N(1440) BREIT-WIGNER WIDTH

VALUE (MeV)	DOCUMENT ID		TECN	COMMENT
250 to 450 (≈ 350) OUR ESTIMATE				
360± 30	SOKHOYAN	15A	DPWA	Multichannel
605± 90	[1] SHKLYAR	13	DPWA	Multichannel
248± 5	[1] SHRESTHA	12A	DPWA	Multichannel
284± 18	[1] ARNDT	06	DPWA	$\pi N \rightarrow \pi N, \eta N$
340± 70	CUTKOSKY	80	IPWA	$\pi N \rightarrow \pi N$
135± 10	HOEHLER	79	IPWA	$\pi N \rightarrow \pi N$
• • • We do not use the following data for averages, fits, limits, etc. • • •				
365± 35	ANISOVICH	12A	DPWA	Multichannel
437±141	BATINIC	10	DPWA	$\pi N \rightarrow N\pi, N\eta$
668± 41	PENNER	02C	DPWA	Multichannel
490±120	VRANA	00	DPWA	Multichannel

[1] Statistical error only.

N(1440) DECAY MODES

The following branching fractions are our estimates, not fits or averages.

	Mode	Fraction (Γ_i/Γ)
Γ_1	$N\pi$	55–75 %
Γ_2	$N\eta$	<1 %
Γ_3	$N\pi\pi$	17–50 %
Γ_4	$\Delta(1232)\pi$, P-wave	6–27 %
Γ_5	$N\sigma$	11–23 %
Γ_6	$p\gamma$, helicity=1/2	0.035–0.048 %
Γ_7	$n\gamma$, helicity=1/2	0.02–0.04 %

N(1440) BRANCHING RATIOS

$\Gamma(N\pi)/\Gamma_{total}$ Γ_1/Γ

VALUE (%)	DOCUMENT ID		TECN	COMMENT
55 to 75 (≈ 65) OUR ESTIMATE				
63 ±2	SOKHOYAN	15A	DPWA	Multichannel
56 ±2	[1] SHKLYAR	13	DPWA	Multichannel
64.8±0.9	[1] SHRESTHA	12A	DPWA	Multichannel
78.7±1.6	[1] ARNDT	06	DPWA	$\pi N \rightarrow \pi N, \eta N$
68 ±4	CUTKOSKY	80	IPWA	$\pi N \rightarrow \pi N$
51 ±5	HOEHLER	79	IPWA	$\pi N \rightarrow \pi N$
• • • We do not use the following data for averages, fits, limits, etc. • • •				
62 ±3	ANISOVICH	12A	DPWA	Multichannel
62 ±4	BATINIC	10	DPWA	$\pi N \rightarrow N\pi, N\eta$
57 ±1	PENNER	02C	DPWA	Multichannel
72 ±5	VRANA	00	DPWA	Multichannel

[1] Statistical error only.

$\Gamma(N\eta)/\Gamma_{total}$ Γ_2/Γ

VALUE (%)	DOCUMENT ID	TECN	COMMENT
• • • We do not use the following data for averages, fits, limits, etc. • • •			
0±1	VRANA	00	DPWA Multichannel

$\Gamma(\Delta(1232)\pi$, P-wave$)/\Gamma_{total}$ Γ_4/Γ

VALUE (%)	DOCUMENT ID		TECN	COMMENT
6 to 27 (≈ 15) OUR ESTIMATE				
$12\ ^{+5}_{-3}$	SHKLYAR	16	DPWA	Multichannel
20 ±7	SOKHOYAN	15A	DPWA	Multichannel
6.5±0.8	[1] SHRESTHA	12A	DPWA	Multichannel
• • • We do not use the following data for averages, fits, limits, etc. • • •				
21 ±8	ANISOVICH	12A	DPWA	Multichannel
16 ±1	VRANA	00	DPWA	Multichannel

[1] Statistical error only.

$\Gamma(N\sigma)/\Gamma_{total}$ Γ_5/Γ

VALUE (%)	DOCUMENT ID		TECN	COMMENT
$27\ ^{+4}_{-9}$	SHKLYAR	16	DPWA	Multichannel
17±6	SOKHOYAN	15A	DPWA	Multichannel
27±1	[1] SHRESTHA	12A	DPWA	Multichannel
• • • We do not use the following data for averages, fits, limits, etc. • • •				
17±7	ANISOVICH	12A	DPWA	Multichannel
12±1	VRANA	00	DPWA	Multichannel

[1] Statistical error only.

N(1440) PHOTON DECAY AMPLITUDES AT THE POLE

N(1440) → pγ, helicity-1/2 amplitude $A_{1/2}$

MODULUS ($GeV^{-1/2}$)	PHASE (°)	DOCUMENT ID	TECN	COMMENT
–0.044±0.005	–40 ± 8	SOKHOYAN	15A	DPWA Multichannel
$-0.054\ ^{+0.004}_{-0.003}$	$5\ ^{+2}_{-5}$	ROENCHEN	14	DPWA
• • • We do not use the following data for averages, fits, limits, etc. • • •				
–0.060	–23	ROENCHEN	15A	DPWA Multichannel

N(1440) BREIT-WIGNER PHOTON DECAY AMPLITUDES

N(1440) → pγ, helicity-1/2 amplitude $A_{1/2}$

VALUE ($GeV^{-1/2}$)	DOCUMENT ID		TECN	COMMENT
–0.080 to –0.050 (≈ – 0.065) OUR ESTIMATE				
–0.061±0.006	SOKHOYAN	15A	DPWA	Multichannel
–0.085±0.003	[1] SHKLYAR	13	DPWA	Multichannel
–0.056±0.001	[1] WORKMAN	12A	DPWA	$\gamma N \rightarrow N\pi$
–0.051±0.002	[1] DUGGER	07	DPWA	$\gamma N \rightarrow \pi N$
• • • We do not use the following data for averages, fits, limits, etc. • • •				
–0.061±0.008	ANISOVICH	12A	DPWA	Multichannel
–0.084±0.003	[1] SHRESTHA	12A	DPWA	Multichannel
–0.061	DRECHSEL	07	DPWA	$\gamma N \rightarrow \pi N$
–0.087	PENNER	02D	DPWA	Multichannel

[1] Statistical error only.

N(1440) → nγ, helicity-1/2 amplitude $A_{1/2}$

VALUE ($GeV^{-1/2}$)	DOCUMENT ID		TECN	COMMENT
0.035 to 0.055 (≈ 0.045) OUR ESTIMATE				
0.043±0.012	ANISOVICH	13B	DPWA	Multichannel
0.048±0.004	[1] CHEN	12A	DPWA	$\gamma N \rightarrow \pi N$
• • • We do not use the following data for averages, fits, limits, etc. • • •				
0.040±0.005	[1] SHRESTHA	12A	DPWA	Multichannel
0.054	DRECHSEL	07	DPWA	$\gamma N \rightarrow \pi N$
0.121	PENNER	02D	DPWA	Multichannel

[1] Statistical error only.

$N(1440)$ REFERENCES

For early references, see Physics Letters **111B** 1 (1982).

SHKLYAR	16	PR C93 045206	V. Shklyar, H. Lenske, U. Mosel	(GIES)
ROENCHEN	15A	EPJ A51 70	D. Roenchen *et al.*	
SOKHOYAN	15A	EPJ A51 95	V. Sokhoyan *et al.*	(CBELSA/TAPS Collab.)
PDG	14	CP C38 070001	K. Olive *et al.*	(PDG Collab.)
ROENCHEN	14	EPJ A50 101	D. Roenchen *et al.*	
Also		EPJ A51 63 (errat.)	D. Roenchen *et al.*	
SVARC	14	PR C89 045205	A. Svarc *et al.*	(RBI Zagreb, UNI Tuzla)
ANISOVICH	13B	EPJ A49 67	A.V. Anisovich *et al.*	
SHKLYAR	13	PR C87 015201	V. Shklyar, H. Lenske, U. Mosel	(GIES)
ANISOVICH	12A	EPJ A48 15	A.V. Anisovich *et al.*	(BONN, PNPI)
CHEN	12A	PR C86 015206	W. Chen *et al.*	(DUKE, GWU, MSST, ITEP+)
SHRESTHA	12A	PR C86 055203	M. Shrestha, D.M. Manley	(KSU)
WORKMAN	12A	PR C86 015202	R. Workman *et al.*	(GWU)
BATINIC	10	PR C82 038203	M. Batinic *et al.*	(ZAGR)
DRECHSEL	07	EPJ A34 69	D. Drechsel, S.S. Kamalov, L. Tiator	(MAINZ, JINR)
DUGGER	07	PR C76 025211	M. Dugger *et al.*	(JLab CLAS Collab.)
ARNDT	06	PR C74 045205	R.A. Arndt *et al.*	(GWU)
PENNER	02C	PR C66 055211	G. Penner, U. Mosel	(GIES)
PENNER	02D	PR C66 055212	G. Penner, U. Mosel	(GIES)
VRANA	00	PRPL 328 181	T.P. Vrana, S.A. Dytman, T.-S.H. Lee	(PITT, ANL)
HOEHLER	93	πN Newsletter 9 1	G. Hohler	(KARL)
CUTKOSKY	80	Toronto Conf. 19	R.E. Cutkosky *et al.*	(CMU, LBL) IJP
Also		PR D20 2839	R.E. Cutkosky *et al.*	(CMU, LBL) IJP
HOEHLER	79	PDAT 12-1	G. Hohler *et al.*	(KARLT) IJP
Also		Toronto Conf. 3	R. Koch	(KARLT) IJP

$N(1520)$ $3/2^-$

$I(J^P) = \frac{1}{2}(\frac{3}{2}^-)$ Status: ****

Older and obsolete values are listed and referenced in the 2014 edition, Chinese Physics **C38** 070001 (2014).

$N(1520)$ POLE POSITION

REAL PART

VALUE (MeV)	*DOCUMENT ID*		*TECN*	*COMMENT*
1505 to 1515 (≈ 1510) OUR ESTIMATE				
1507±2	SOKHOYAN	15A	DPWA	Multichannel
1506±1±1	[1] SVARC	14	L+P	$\pi N \to \pi N$
1510±5	CUTKOSKY	80	IPWA	$\pi N \to \pi N$
• • • We do not use the following data for averages, fits, limits, etc. • • •				
1512	ROENCHEN	15A	DPWA	Multichannel
1492	SHKLYAR	13	DPWA	Multichannel
1507±3	ANISOVICH	12A	DPWA	Multichannel
1501	SHRESTHA	12A	DPWA	Multichannel
1506±9	BATINIC	10	DPWA	$\pi N \to N\pi,\ N\eta$
1515	ARNDT	06	DPWA	$\pi N \to \pi N,\ \eta N$
1504	VRANA	00	DPWA	Multichannel
1510	HOEHLER	93	ARGD	$\pi N \to \pi N$

[1] Fit to the amplitudes of HOEHLER 79.

−2×IMAGINARY PART

VALUE (MeV)	*DOCUMENT ID*		*TECN*	*COMMENT*
105 to 120 (≈ 110) OUR ESTIMATE				
111± 3	SOKHOYAN	15A	DPWA	Multichannel
115± 2±1	[1] SVARC	14	L+P	$\pi N \to \pi N$
114±10	CUTKOSKY	80	IPWA	$\pi N \to \pi N$
• • • We do not use the following data for averages, fits, limits, etc. • • •				
89	ROENCHEN	15A	DPWA	Multichannel
94	SHKLYAR	13	DPWA	Multichannel
111± 5	ANISOVICH	12A	DPWA	Multichannel
112	SHRESTHA	12A	DPWA	Multichannel
122± 9	BATINIC	10	DPWA	$\pi N \to N\pi,\ N\eta$
113	ARNDT	06	DPWA	$\pi N \to \pi N,\ \eta N$
112	VRANA	00	DPWA	Multichannel
120	HOEHLER	93	ARGD	$\pi N \to \pi N$

[1] Fit to the amplitudes of HOEHLER 79.

$N(1520)$ ELASTIC POLE RESIDUE

MODULUS $|r|$

VALUE (MeV)	*DOCUMENT ID*		*TECN*	*COMMENT*
32 to 38 (≈ 35) OUR ESTIMATE				
36±2	SOKHOYAN	15A	DPWA	Multichannel
33±1±1	[1] SVARC	14	L+P	$\pi N \to \pi N$
35±2	CUTKOSKY	80	IPWA	$\pi N \to \pi N$
• • • We do not use the following data for averages, fits, limits, etc. • • •				
37	ROENCHEN	15A	DPWA	Multichannel
27	SHKLYAR	13	DPWA	Multichannel
36±3	ANISOVICH	12A	DPWA	Multichannel
35	BATINIC	10	DPWA	$\pi N \to N\pi,\ N\eta$
38	ARNDT	06	DPWA	$\pi N \to \pi N,\ \eta N$
32	HOEHLER	93	ARGD	$\pi N \to \pi N$

[1] Fit to the amplitudes of HOEHLER 79.

PHASE θ

VALUE (°)	*DOCUMENT ID*		*TECN*	*COMMENT*
−15 to −5 (≈ −10) OUR ESTIMATE				
−14±3	SOKHOYAN	15A	DPWA	Multichannel
−15±1±1	[1] SVARC	14	L+P	$\pi N \to \pi N$
−12±5	CUTKOSKY	80	IPWA	$\pi N \to \pi N$
• • • We do not use the following data for averages, fits, limits, etc. • • •				
− 6	ROENCHEN	15A	DPWA	Multichannel
−35	SHKLYAR	13	DPWA	Multichannel
−14±3	ANISOVICH	12A	DPWA	Multichannel
− 7	BATINIC	10	DPWA	$\pi N \to N\pi,\ N\eta$
− 5	ARNDT	06	DPWA	$\pi N \to \pi N,\ \eta N$
− 8	HOEHLER	93	ARGD	$\pi N \to \pi N$

[1] Fit to the amplitudes of HOEHLER 79.

$N(1520)$ INELASTIC POLE RESIDUE

The "normalized residue" is the residue divided by $\Gamma_{pole}/2$.

Normalized residue in $N\pi \to N(1520) \to \Delta\pi$, S-wave

MODULUS	*PHASE* (°)	*DOCUMENT ID*		*TECN*	*COMMENT*
0.33±0.04	155 ± 15	SOKHOYAN	15A	DPWA	Multichannel
• • • We do not use the following data for averages, fits, limits, etc. • • •					
0.33±0.05	150 ± 20	ANISOVICH	12A	DPWA	Multichannel

Normalized residue in $N\pi \to N(1520) \to \Delta\pi$, D-wave

MODULUS	*PHASE* (°)	*DOCUMENT ID*		*TECN*	*COMMENT*
0.25±0.03	105 ± 18	SOKHOYAN	15A	DPWA	Multichannel
• • • We do not use the following data for averages, fits, limits, etc. • • •					
0.25±0.03	100 ± 20	ANISOVICH	12A	DPWA	Multichannel

Normalized residue in $N\pi \to N(1520) \to N\eta$

MODULUS	*PHASE* (°)	*DOCUMENT ID*		*TECN*	*COMMENT*
• • • We do not use the following data for averages, fits, limits, etc. • • •					
0.026	95	ROENCHEN	15A	DPWA	Multichannel

Normalized residue in $N\pi \to N(1520) \to \Lambda K$

MODULUS	*PHASE* (°)	*DOCUMENT ID*		*TECN*	*COMMENT*
• • • We do not use the following data for averages, fits, limits, etc. • • •					
0.069	158	ROENCHEN	15A	DPWA	Multichannel

Normalized residue in $N\pi \to N(1520) \to \Sigma K$

MODULUS	*PHASE* (°)	*DOCUMENT ID*		*TECN*	*COMMENT*
• • • We do not use the following data for averages, fits, limits, etc. • • •					
0.049	−41	ROENCHEN	15A	DPWA	Multichannel

Normalized residue in $N\pi \to N(1520) \to N\sigma$

MODULUS	*PHASE* (°)	*DOCUMENT ID*		*TECN*	*COMMENT*
0.08±0.03	−45 ± 25	SOKHOYAN	15A	DPWA	Multichannel

$N(1520)$ BREIT-WIGNER MASS

VALUE (MeV)	*DOCUMENT ID*		*TECN*	*COMMENT*
1510 to 1520 (≈ 1515) OUR ESTIMATE				
1516 ± 2	SOKHOYAN	15A	DPWA	Multichannel
1505 ± 4	[1] SHKLYAR	13	DPWA	Multichannel
1512.6± 0.5	[1] SHRESTHA	12A	DPWA	Multichannel
1514.5± 0.2	[1] ARNDT	06	DPWA	$\pi N \to \pi N,\ \eta N$
1525 ±10	CUTKOSKY	80	IPWA	$\pi N \to \pi N$
1519 ± 4	HOEHLER	79	IPWA	$\pi N \to \pi N$
• • • We do not use the following data for averages, fits, limits, etc. • • •				
1517 ± 3	ANISOVICH	12A	DPWA	Multichannel
1522 ± 8	BATINIC	10	DPWA	$\pi N \to N\pi,\ N\eta$
1509 ± 1	PENNER	02C	DPWA	Multichannel
1518 ± 3	VRANA	00	DPWA	Multichannel

[1] Statistical error only.

$N(1520)$ BREIT-WIGNER WIDTH

VALUE (MeV)	*DOCUMENT ID*		*TECN*	*COMMENT*
100 to 120 (≈ 110) OUR ESTIMATE				
113 ± 4	SOKHOYAN	15A	DPWA	Multichannel
100 ± 2	[1] SHKLYAR	13	DPWA	Multichannel
117 ± 1	[1] SHRESTHA	12A	DPWA	Multichannel
103.6± 0.4	[1] ARNDT	06	DPWA	$\pi N \to \pi N,\ \eta N$
120 ±15	CUTKOSKY	80	IPWA	$\pi N \to \pi N$
114 ± 7	HOEHLER	79	IPWA	$\pi N \to \pi N$
• • • We do not use the following data for averages, fits, limits, etc. • • •				
114 ± 5	ANISOVICH	12A	DPWA	Multichannel
132 ±11	BATINIC	10	DPWA	$\pi N \to N\pi,\ N\eta$
100 ± 2	PENNER	02C	DPWA	Multichannel
124 ± 4	VRANA	00	DPWA	Multichannel

[1] Statistical error only.

$N(1520)$ DECAY MODES

The following branching fractions are our estimates, not fits or averages.

	Mode	Fraction (Γ_i/Γ)
Γ_1	$N\pi$	55–65 %
Γ_2	$N\eta$	0.07–0.09 %
Γ_3	$N\pi\pi$	25–35 %
Γ_4	$\Delta(1232)\pi$	22–34 %
Γ_5	$\Delta(1232)\pi$, S-wave	15–23 %
Γ_6	$\Delta(1232)\pi$, D-wave	7–11 %
Γ_7	$N\sigma$	< 2 %
Γ_8	$p\gamma$	0.31–0.52 %
Γ_9	$p\gamma$, helicity=1/2	0.01–0.02 %
Γ_{10}	$p\gamma$, helicity=3/2	0.30–0.50 %
Γ_{11}	$n\gamma$	0.30–0.53 %
Γ_{12}	$n\gamma$, helicity=1/2	0.04–0.10 %
Γ_{13}	$n\gamma$, helicity=3/2	0.25–0.45 %

$N(1520)$ BRANCHING RATIOS

$\Gamma(N\pi)/\Gamma_{total}$ Γ_1/Γ

VALUE (%)	DOCUMENT ID		TECN	COMMENT
55 to 65 (≈ 60) OUR ESTIMATE				
61 ±2	SOKHOYAN	15A	DPWA	Multichannel
57 ±2	[1] SHKLYAR	13	DPWA	Multichannel
62.7±0.5	[1] SHRESTHA	12A	DPWA	Multichannel
63.2±0.1	[1] ARNDT	06	DPWA	$\pi N \to \pi N$, ηN
58 ±3	CUTKOSKY	80	IPWA	$\pi N \to \pi N$
54 ±3	HOEHLER	79	IPWA	$\pi N \to \pi N$
• • • We do not use the following data for averages, fits, limits, etc. • • •				
62 ±3	ANISOVICH	12A	DPWA	Multichannel
55 ±5	BATINIC	10	DPWA	$\pi N \to N\pi$, $N\eta$
56 ±1	PENNER	02C	DPWA	Multichannel
63 ±2	VRANA	00	DPWA	Multichannel

[1] Statistical error only.

$\Gamma(N\eta)/\Gamma_{total}$ Γ_2/Γ

VALUE (%)	DOCUMENT ID		TECN	COMMENT
<1	SHKLYAR	13	DPWA	Multichannel
0.08±0.01	TIATOR	99	DPWA	$\gamma p \to p\eta$
• • • We do not use the following data for averages, fits, limits, etc. • • •				
0.1 ±0.1	BATINIC	10	DPWA	$\pi N \to N\pi$, $N\eta$
0.2 ±0.1	THOMA	08	DPWA	Multichannel
0.08 to 0.12	ARNDT	05	DPWA	Multichannel
0.23±0.04	PENNER	02C	DPWA	Multichannel
0 ±1	VRANA	00	DPWA	Multichannel

$\Gamma(\Delta(1232)\pi, S\text{-wave})/\Gamma_{total}$ Γ_5/Γ

VALUE (%)	DOCUMENT ID		TECN	COMMENT
19 ±4	SOKHOYAN	15A	DPWA	Multichannel
9.3±0.7	[1] SHRESTHA	12A	DPWA	Multichannel
• • • We do not use the following data for averages, fits, limits, etc. • • •				
19 ±4	ANISOVICH	12A	DPWA	Multichannel
15 ±2	VRANA	00	DPWA	Multichannel

[1] Statistical error only.

$\Gamma(\Delta(1232)\pi, D\text{-wave})/\Gamma_{total}$ Γ_6/Γ

VALUE (%)	DOCUMENT ID		TECN	COMMENT
9 ±2	SOKHOYAN	15A	DPWA	Multichannel
6.3±0.5	[1] SHRESTHA	12A	DPWA	Multichannel
• • • We do not use the following data for averages, fits, limits, etc. • • •				
9 ±2	ANISOVICH	12A	DPWA	Multichannel
11 ±2	VRANA	00	DPWA	Multichannel

[1] Statistical error only.

$\Gamma(N\sigma)/\Gamma_{total}$ Γ_7/Γ

VALUE (%)	DOCUMENT ID		TECN	COMMENT
<2	SOKHOYAN	15A	DPWA	Multichannel
<1	SHRESTHA	12A	DPWA	Multichannel
• • • We do not use the following data for averages, fits, limits, etc. • • •				
<4	THOMA	08	DPWA	Multichannel
1±1	VRANA	00	DPWA	Multichannel

$N(1520)$ PHOTON DECAY AMPLITUDES AT THE POLE

$N(1520) \to p\gamma$, helicity-1/2 amplitude $A_{1/2}$

MODULUS ($GeV^{-1/2}$)	PHASE (°)	DOCUMENT ID		TECN	COMMENT
−0.023±0.004	−6 ± 5	SOKHOYAN	15A	DPWA	Multichannel
$-0.024^{+0.008}_{-0.003}$	-17^{+16}_{-6}	ROENCHEN	14	DPWA	
• • • We do not use the following data for averages, fits, limits, etc. • • •					
−0.031	−17	ROENCHEN	15A	DPWA	Multichannel

$N(1520) \to p\gamma$, helicity-3/2 amplitude $A_{3/2}$

MODULUS ($GeV^{-1/2}$)	PHASE (°)	DOCUMENT ID	TECN	COMMENT
0.131±0.006	4 ± 4	SOKHOYAN	15A	DPWA Multichannel
$0.117^{+0.006}_{-0.010}$	26 ± 2	ROENCHEN	14	DPWA
• • • We do not use the following data for averages, fits, limits, etc. • • •				
0.075	1.7	ROENCHEN	15A	DPWA Multichannel

$N(1520)$ BREIT-WIGNER PHOTON DECAY AMPLITUDES

$N(1520) \to p\gamma$, helicity-1/2 amplitude $A_{1/2}$

VALUE ($GeV^{-1/2}$)	DOCUMENT ID		TECN	COMMENT
−0.030 to −0.015 (≈ −0.025) OUR ESTIMATE				
−0.024±0.004	SOKHOYAN	15A	DPWA	Multichannel
−0.015±0.001	[1] SHKLYAR	13	DPWA	Multichannel
−0.019±0.002	[1] WORKMAN	12A	DPWA	$\gamma N \to N\pi$
−0.028±0.002	[1] DUGGER	07	DPWA	$\gamma N \to \pi N$
−0.038±0.003	[1] AHRENS	02	DPWA	$\gamma N \to \pi N$
• • • We do not use the following data for averages, fits, limits, etc. • • •				
−0.022±0.004	ANISOVICH	12A	DPWA	Multichannel
−0.034±0.001	[1] SHRESTHA	12A	DPWA	Multichannel
−0.027	DRECHSEL	07	DPWA	$\gamma N \to \pi N$
−0.003	PENNER	02D	DPWA	Multichannel
−0.052±0.010±0.007	[1] MUKHOPAD...	98		$\gamma p \to \eta p$

[1] Statistical error only.

$N(1520) \to p\gamma$, helicity-3/2 amplitude $A_{3/2}$

VALUE ($GeV^{-1/2}$)	DOCUMENT ID		TECN	COMMENT
0.135 to 0.145 (≈ 0.140) OUR ESTIMATE				
0.130±0.006	SOKHOYAN	15A	DPWA	Multichannel
0.146±0.001	[1] SHKLYAR	13	DPWA	Multichannel
0.141±0.002	[1] WORKMAN	12A	DPWA	$\gamma N \to N\pi$
0.143±0.002	[1] DUGGER	07	DPWA	$\gamma N \to \pi N$
0.147±0.010	[1] AHRENS	02	DPWA	$\gamma N \to \pi N$
• • • We do not use the following data for averages, fits, limits, etc. • • •				
0.131±0.010	ANISOVICH	12A	DPWA	Multichannel
0.127±0.003	[1] SHRESTHA	12A	DPWA	Multichannel
0.161	DRECHSEL	07	DPWA	$\gamma N \to \pi N$
0.151	PENNER	02D	DPWA	Multichannel
0.130±0.020±0.015	[1] MUKHOPAD...	98		$\gamma p \to \eta p$

[1] Statistical error only.

$N(1520) \to n\gamma$, helicity-1/2 amplitude $A_{1/2}$

VALUE ($GeV^{-1/2}$)	DOCUMENT ID		TECN	COMMENT
−0.055 to −0.040 (≈ −0.050) OUR ESTIMATE				
−0.049±0.008	ANISOVICH	13B	DPWA	Multichannel
−0.046±0.006	[1] CHEN	12A	DPWA	$\gamma N \to \pi N$
• • • We do not use the following data for averages, fits, limits, etc. • • •				
−0.038±0.003	[1] SHRESTHA	12A	DPWA	Multichannel
−0.077	DRECHSEL	07	DPWA	$\gamma N \to \pi N$
−0.084	PENNER	02D	DPWA	Multichannel

[1] Statistical error only.

$N(1520) \to n\gamma$, helicity-3/2 amplitude $A_{3/2}$

VALUE ($GeV^{-1/2}$)	DOCUMENT ID		TECN	COMMENT
−0.120 to −0.100 (≈ −0.115) OUR ESTIMATE				
−0.113±0.012	ANISOVICH	13B	DPWA	Multichannel
−0.115±0.005	[1] CHEN	12A	DPWA	$\gamma N \to \pi N$
• • • We do not use the following data for averages, fits, limits, etc. • • •				
−0.101±0.004	[1] SHRESTHA	12A	DPWA	Multichannel
−0.154	DRECHSEL	07	DPWA	$\gamma N \to \pi N$
−0.159	PENNER	02D	DPWA	Multichannel

[1] Statistical error only.

$N(1520)$ REFERENCES

For early references, see Physics Letters **111B** 1 (1982). For very early references, see Reviews of Modern Physics **37** 633 (1965).

ROENCHEN	15A	EPJ A51 70	D. Roenchen *et al.*	
SOKHOYAN	15A	EPJ A51 95	V. Sokhoyan *et al.*	(CBELSA/TAPS Collab.)
PDG	14	CP C38 070001	K. Olive *et al.*	(PDG Collab.)
ROENCHEN	14	EPJ A50 101	D. Roenchen *et al.*	
Also		EPJ A51 63 (errat.)	D. Roenchen *et al.*	
SVARC	14	PR C89 045205	A. Svarc *et al.*	(RBI Zagreb, UNI Tuzla)
ANISOVICH	13B	EPJ A49 67	A.V. Anisovich *et al.*	
SHKLYAR	13	PR C87 015201	V. Shklyar, H. Lenske, U. Mosel	(GIES)
ANISOVICH	12A	EPJ A48 15	A.V. Anisovich *et al.*	(BONN, PNPI)
CHEN	12A	PR C86 015206	W. Chen *et al.*	(DUKE, GWU, MSST, ITEP+)
SHRESTHA	12A	PR C86 055203	M. Shrestha, D.M. Manley	(KSU)
WORKMAN	12A	PR C86 015202	R. Workman *et al.*	(GWU)
BATINIC	10	PR C82 038203	M. Batinic *et al.*	(ZAGR)
THOMA	08	PL B659 87	U. Thoma *et al.*	(CB-ELSA Collab.)

DRECHSEL	07	EPJ A34 69	D. Drechsel, S.S. Kamalov, L. Tiator	(MAINZ, JINR)
DUGGER	07	PR C76 025211	M. Dugger *et al.*	(JLab CLAS Collab.)
ARNDT	06	PR C74 045205	R.A. Arndt *et al.*	(GWU)
ARNDT	05	PR C72 045202	R.A. Arndt *et al.*	(GWU, PNPI)
AHRENS	02	PRL 88 232002	J. Ahrens *et al.*	(Mainz MAMI GDH/A2 Collab.)
PENNER	02C	PR C66 055211	G. Penner, U. Mosel	(GIES)
PENNER	02D	PR C66 055212	G. Penner, U. Mosel	(GIES)
VRANA	00	PRPL 328 181	T.P. Vrana, S.A. Dytman, T.-S.H. Lee	(PITT, ANL)
TIATOR	99	PR C60 035210	L. Tiator *et al.*	
MUKHOPAD...	98	PL B444 7	N.C. Mukhopadhyay, N. Mathur	
HOEHLER	93	πN Newsletter 9 1	G. Hohler	(KARL)
CUTKOSKY	80	Toronto Conf. 19	R.E. Cutkosky *et al.*	(CMU, LBL) IJP
Also		PR D20 2839	R.E. Cutkosky *et al.*	(CMU, LBL) IJP
HOEHLER	79	PDAT 12-1	G. Hohler *et al.*	(KARLT) IJP
Also		Toronto Conf. 3	R. Koch	(KARLT) IJP

$N(1535)$ $1/2^-$

$I(J^P) = \frac{1}{2}(\frac{1}{2}^-)$ Status: ****

Older and obsolete values are listed and referenced in the 2014 edition, Chinese Physics **C38** 070001 (2014).

$N(1535)$ POLE POSITION

REAL PART

VALUE (MeV)	DOCUMENT ID		TECN	COMMENT
1500 to 1520 (≈ 1510) OUR ESTIMATE				
1500± 4	SOKHOYAN	15A	DPWA	Multichannel
1509± 4±2	[1] SVARC	14	L+P	$\pi N \to \pi N$
1510±50	CUTKOSKY	80	IPWA	$\pi N \to \pi N$
• • • We do not use the following data for averages, fits, limits, etc. • • •				
1499	ROENCHEN	15A	DPWA	Multichannel
1490	SHKLYAR	13	DPWA	Multichannel
1501± 4	ANISOVICH	12A	DPWA	Multichannel
1515	SHRESTHA	12A	DPWA	Multichannel
1521±14	BATINIC	10	DPWA	$\pi N \to N\pi$, $N\eta$
1502	ARNDT	06	DPWA	$\pi N \to \pi N$, ηN
1525	VRANA	00	DPWA	Multichannel
1487	HOEHLER	93	SPED	$\pi N \to \pi N$

[1] Fit to the amplitudes of HOEHLER 79.

−2×IMAGINARY PART

VALUE (MeV)	DOCUMENT ID		TECN	COMMENT
110 to 150 (≈ 130) OUR ESTIMATE				
128± 9	SOKHOYAN	15A	DPWA	Multichannel
118± 9±2	[2] SVARC	14	L+P	$\pi N \to \pi N$
260±80	CUTKOSKY	80	IPWA	$\pi N \to \pi N$
• • • We do not use the following data for averages, fits, limits, etc. • • •				
104	ROENCHEN	15A	DPWA	Multichannel
100	SHKLYAR	13	DPWA	Multichannel
134±11	ANISOVICH	12A	DPWA	Multichannel
123	SHRESTHA	12A	DPWA	Multichannel
190±28	BATINIC	10	DPWA	$\pi N \to N\pi$, $N\eta$
95	ARNDT	06	DPWA	$\pi N \to \pi N$, ηN
102	VRANA	00	DPWA	Multichannel

[2] Fit to the amplitudes of HOEHLER 79.

$N(1535)$ ELASTIC POLE RESIDUE

MODULUS $|r|$

VALUE (MeV)	DOCUMENT ID		TECN	COMMENT
15 to 35 (≈ 25) OUR ESTIMATE				
29± 4	SOKHOYAN	15A	DPWA	Multichannel
22± 2±0.4	[3] SVARC	14	L+P	$\pi N \to \pi N$
120±40	CUTKOSKY	80	IPWA	$\pi N \to \pi N$
• • • We do not use the following data for averages, fits, limits, etc. • • •				
22	ROENCHEN	15A	DPWA	Multichannel
15	SHKLYAR	13	DPWA	Multichannel
31± 4	ANISOVICH	12A	DPWA	Multichannel
68	BATINIC	10	DPWA	$\pi N \to N\pi$, $N\eta$
16	ARNDT	06	DPWA	$\pi N \to \pi N$, ηN

[3] Fit to the amplitudes of HOEHLER 79.

PHASE θ

VALUE (°)	DOCUMENT ID		TECN	COMMENT
−30 to 0 (≈ −15) OUR ESTIMATE				
−20±10	SOKHOYAN	15A	DPWA	Multichannel
− 5± 5±3	[4] SVARC	14	L+P	$\pi N \to \pi N$
+15±45	CUTKOSKY	80	IPWA	$\pi N \to \pi N$
• • • We do not use the following data for averages, fits, limits, etc. • • •				
−46	ROENCHEN	15A	DPWA	Multichannel
−51	SHKLYAR	13	DPWA	Multichannel
−29± 5	ANISOVICH	12A	DPWA	Multichannel
12	BATINIC	10	DPWA	$\pi N \to N\pi$, $N\eta$
−16	ARNDT	06	DPWA	$\pi N \to \pi N$, ηN

[4] Fit to the amplitudes of HOEHLER 79.

$N(1535)$ INELASTIC POLE RESIDUE

The "normalized residue" is the residue divided by $\Gamma_{pole}/2$.

Normalized residue in $N\pi \to N(1535) \to N\eta$

MODULUS	PHASE (°)	DOCUMENT ID		TECN	COMMENT
0.43±0.03	−76 ± 5	ANISOVICH	12A	DPWA	Multichannel
• • • We do not use the following data for averages, fits, limits, etc. • • •					
0.51	112	ROENCHEN	15A	DPWA	Multichannel

Normalized residue in $N\pi \to N(1535) \to \Lambda K$

MODULUS	PHASE (°)	DOCUMENT ID		TECN	COMMENT
• • • We do not use the following data for averages, fits, limits, etc. • • •					
0.05	32	ROENCHEN	15A	DPWA	Multichannel

Normalized residue in $N\pi \to N(1535) \to \Sigma K$

MODULUS	PHASE (°)	DOCUMENT ID		TECN	COMMENT
• • • We do not use the following data for averages, fits, limits, etc. • • •					
0.05	−69	ROENCHEN	15A	DPWA	Multichannel

Normalized residue in $N\pi \to N(1535) \to \Delta\pi$, D-wave

MODULUS	PHASE (°)	DOCUMENT ID		TECN	COMMENT
0.11±0.02	160 ± 20	SOKHOYAN	15A	DPWA	Multichannel
• • • We do not use the following data for averages, fits, limits, etc. • • •					
0.12±0.03	145 ± 17	ANISOVICH	12A	DPWA	Multichannel

Normalized residue in $N\pi \to N(1535) \to N\sigma$

MODULUS	PHASE (°)	DOCUMENT ID		TECN	COMMENT
0.16±0.07	25 ± 40	SOKHOYAN	15A	DPWA	Multichannel

Normalized residue in $N\pi \to N(1535) \to N(1440)\pi$

MODULUS	PHASE (°)	DOCUMENT ID		TECN	COMMENT
0.21±0.14	−45 ± 50	SOKHOYAN	15A	DPWA	Multichannel

$N(1535)$ BREIT-WIGNER MASS

VALUE (MeV)	DOCUMENT ID		TECN	COMMENT
1515 to 1545 (≈ 1530) OUR ESTIMATE				
1528 ± 6	KASHEVAROV	17	DPWA	$\gamma p \to \eta p$, $\eta' p$
1517 ± 4	SOKHOYAN	15A	DPWA	Multichannel
1526 ± 2	[5] SHKLYAR	13	DPWA	Multichannel
1538 ± 1	[5] SHRESTHA	12A	DPWA	Multichannel
1547.0± 0.7	[5] ARNDT	06	DPWA	$\pi N \to \pi N$, ηN
1550 ±40	CUTKOSKY	80	IPWA	$\pi N \to \pi N$
1526 ± 7	HOEHLER	79	IPWA	$\pi N \to \pi N$
• • • We do not use the following data for averages, fits, limits, etc. • • •				
1519 ± 5	ANISOVICH	12A	DPWA	Multichannel
1553 ± 8	BATINIC	10	DPWA	$\pi N \to N\pi$, $N\eta$
1546.7± 2.2	ARNDT	04	DPWA	$\pi N \to \pi N$, ηN
1526 ± 2	PENNER	02C	DPWA	Multichannel
1530 ±10	BAI	01B	BES	$J/\psi \to p\bar{p}\eta$
1522 ±11	THOMPSON	01	CLAS	$\gamma^* p \to p\eta$
1542 ± 3	VRANA	00	DPWA	Multichannel
1532 ± 5	ARMSTRONG	99B	DPWA	$\gamma^* p \to p\eta$

[5] Statistical error only.

$N(1535)$ BREIT-WIGNER WIDTH

VALUE (MeV)	DOCUMENT ID		TECN	COMMENT
125 to 175 (≈ 150) OUR ESTIMATE				
163 ±25	KASHEVAROV	17	DPWA	$\gamma p \to \eta p$, $\eta' p$
120 ±10	SOKHOYAN	15A	DPWA	Multichannel
131 ±12	[6] SHKLYAR	13	DPWA	Multichannel
141 ± 4	[6] SHRESTHA	12A	DPWA	Multichannel
188.4± 3.8	[6] ARNDT	06	DPWA	$\pi N \to \pi N$, ηN
240 ±80	CUTKOSKY	80	IPWA	$\pi N \to \pi N$
120 ±20	HOEHLER	79	IPWA	$\pi N \to \pi N$
• • • We do not use the following data for averages, fits, limits, etc. • • •				
128 ±14	ANISOVICH	12A	DPWA	Multichannel
182 ±25	BATINIC	10	DPWA	$\pi N \to N\pi$, $N\eta$
129 ± 8	PENNER	02C	DPWA	Multichannel
95 ±25	BAI	01B	BES	$J/\psi \to p\bar{p}\eta$
143 ±18	THOMPSON	01	CLAS	$\gamma^* p \to p\eta$
112 ±19	VRANA	00	DPWA	Multichannel
154 ±20	ARMSTRONG	99B	DPWA	$\gamma^* p \to p\eta$

[6] Statistical error only.

$N(1535)$ DECAY MODES

The following branching fractions are our estimates, not fits or averages.

	Mode	Fraction (Γ_i/Γ)
Γ_1	$N\pi$	32–52 %
Γ_2	$N\eta$	30–55 %
Γ_3	$N\pi\pi$	3–14 %
Γ_4	$\Delta(1232)\pi$	
Γ_5	$\Delta(1232)\pi$, D-wave	1–4 %
Γ_6	$N\sigma$	2–10 %
Γ_7	$N(1440)\pi$	5–12 %
Γ_8	$p\gamma$, helicity=1/2	0.15–0.30 %
Γ_9	$n\gamma$, helicity=1/2	0.01–0.25 %

$N(1535)$ BRANCHING RATIOS

$\Gamma(N\pi)/\Gamma_{total}$ Γ_1/Γ

VALUE (%)	DOCUMENT ID		TECN	COMMENT
32 to 52 (≈ 42) OUR ESTIMATE				
52 ± 5	SOKHOYAN	15A	DPWA	Multichannel
35 ± 3	[7] SHKLYAR	13	DPWA	Multichannel
37 ± 1	[7] SHRESTHA	12A	DPWA	Multichannel
35.5 ± 0.2	[7] ARNDT	06	DPWA	$\pi N \to \pi N$, ηN
50 ±10	CUTKOSKY	80	IPWA	$\pi N \to \pi N$
38 ± 4	HOEHLER	79	IPWA	$\pi N \to \pi N$
• • • We do not use the following data for averages, fits, limits, etc. • • •				
54 ± 5	ANISOVICH	12A	DPWA	Multichannel
46 ± 7	BATINIC	10	DPWA	$\pi N \to N\pi$, $N\eta$
36 ± 1	PENNER	02C	DPWA	Multichannel
35 ± 8	VRANA	00	DPWA	Multichannel

[7] Statistical error only.

$\Gamma(N\eta)/\Gamma_{total}$ Γ_2/Γ

VALUE (%)	DOCUMENT ID		TECN	COMMENT
30 to 55 (≈ 42) OUR ESTIMATE				
41±4	[8] KASHEVAROV	17	DPWA	$\gamma p \to \eta p$, $\eta' p$
58±4	[9] SHKLYAR	13	DPWA	Multichannel
33±5	ANISOVICH	12A	DPWA	Multichannel
41±2	[9] SHRESTHA	12A	DPWA	Multichannel
53±1	PENNER	02C	DPWA	Multichannel
51±5	VRANA	00	DPWA	Multichannel
• • • We do not use the following data for averages, fits, limits, etc. • • •				
50±7	BATINIC	10	DPWA	$\pi N \to N\pi$, $N\eta$

[8] Assuming $A_{1/2} = 0.115$ GeV$^{-1/2}$.

[9] Statistical error only.

$\Gamma(N\eta)/\Gamma(N\pi)$ Γ_2/Γ_1

VALUE	DOCUMENT ID		TECN	COMMENT
• • • We do not use the following data for averages, fits, limits, etc. • • •				
0.95±0.03	AZNAURYAN	09	CLAS	π, η electroproduction

$\Gamma(\Delta(1232)\pi$, D-wave$)/\Gamma_{total}$ Γ_5/Γ

VALUE (%)	DOCUMENT ID		TECN	COMMENT
2.5±1.5	SOKHOYAN	15A	DPWA	Multichannel
1.8±0.8	[10] SHRESTHA	12A	DPWA	Multichannel
• • • We do not use the following data for averages, fits, limits, etc. • • •				
2.5±1.5	ANISOVICH	12A	DPWA	Multichannel
1 ±1	VRANA	00	DPWA	Multichannel

[10] Statistical error only.

$\Gamma(N\sigma)/\Gamma_{total}$ Γ_6/Γ

VALUE (%)	DOCUMENT ID		TECN	COMMENT
6 ±4	SOKHOYAN	15A	DPWA	Multichannel
1.5±0.5	[11] SHRESTHA	12A	DPWA	Multichannel
• • • We do not use the following data for averages, fits, limits, etc. • • •				
2 ±1	VRANA	00	DPWA	Multichannel

[11] Statistical error only.

$\Gamma(N(1440)\pi)/\Gamma_{total}$ Γ_7/Γ

VALUE (%)	DOCUMENT ID		TECN	COMMENT
12±8	SOKHOYAN	15A	DPWA	Multichannel
< 1	SHRESTHA	12A	DPWA	Multichannel
8±2	[12] STAROSTIN	03		$\pi^- p \to n3\pi^0$
• • • We do not use the following data for averages, fits, limits, etc. • • •				
10±9	VRANA	00	DPWA	Multichannel

[12] This STAROSTIN 03 value is an estimate made using simplest assumptions.

$N(1535)$ PHOTON DECAY AMPLITUDES AT THE POLE

$N(1535) \to p\gamma$, helicity-1/2 amplitude $A_{1/2}$

MODULUS (GeV$^{-1/2}$)	PHASE (°)	DOCUMENT ID		TECN	COMMENT
0.093±0.009	8 ± 4	ANISOVICH	17D	DPWA	Multichannel
0.050±0.004	-14^{+12}_{-10}	[13] ROENCHEN	14	DPWA	
• • • We do not use the following data for averages, fits, limits, etc. • • •					
0.114±0.008	10 ± 5	ANISOVICH	15A	DPWA	Multichannel
0.106	5.2	ROENCHEN	15A	DPWA	Multichannel
0.114±0.008	10 ± 5	SOKHOYAN	15A	DPWA	Multichannel

[13] T-Matrix amplitude

$N(1535) \to n\gamma$, helicity-1/2 amplitude $A_{1/2}$

MODULUS (GeV$^{-1/2}$)	PHASE (°)	DOCUMENT ID	TECN	COMMENT
−0.088±0.004	**5 ± 4**	ANISOVICH	17D	DPWA Multichannel
• • • We do not use the following data for averages, fits, limits, etc. • • •				
−0.095±0.006	8 ± 5	ANISOVICH	15A	DPWA Multichannel

$N(1535)$ BREIT-WIGNER PHOTON DECAY AMPLITUDES

$N(1535) \to p\gamma$, helicity-1/2 amplitude $A_{1/2}$

VALUE (GeV$^{-1/2}$)	DOCUMENT ID		TECN	COMMENT
0.090 to 0.120 (≈ 0.105) OUR ESTIMATE				
0.101±0.007	SOKHOYAN	15A	DPWA	Multichannel
0.091±0.004	[14] SHKLYAR	13	DPWA	Multichannel
0.128±0.004	[14] WORKMAN	12A	DPWA	$\gamma N \to N\pi$
0.091±0.002	[14] DUGGER	07	DPWA	$\gamma N \to \pi N$
• • • We do not use the following data for averages, fits, limits, etc. • • •				
0.105±0.010	ANISOVICH	12A	DPWA	Multichannel
0.059±0.003	[14] SHRESTHA	12A	DPWA	Multichannel
0.066	DRECHSEL	07	DPWA	$\gamma N \to \pi N$
0.090	PENNER	02D	DPWA	Multichannel

[14] Statistical error only.

$N(1535) \to n\gamma$, helicity-1/2 amplitude $A_{1/2}$

VALUE (GeV$^{-1/2}$)	DOCUMENT ID		TECN	COMMENT
−0.095 to −0.055 (≈ −0.075) OUR ESTIMATE				
−0.093±0.011	ANISOVICH	13B	DPWA	Multichannel
−0.058±0.006	[15] CHEN	12A	DPWA	$\gamma N \to \pi N$
• • • We do not use the following data for averages, fits, limits, etc. • • •				
−0.049±0.003	[15] SHRESTHA	12A	DPWA	Multichannel
−0.051	DRECHSEL	07	DPWA	$\gamma N \to \pi N$
−0.024	PENNER	02D	DPWA	Multichannel

[15] Statistical error only.

$N(1535) \to N\gamma$, ratio $A^n_{1/2}/A^p_{1/2}$

VALUE (GeV$^{-1/2}$)	DOCUMENT ID		TECN
• • • We do not use the following data for averages, fits, limits, etc. • • •			
−0.84±0.15	MUKHOPAD...	95B	IPWA

$N(1535)$ REFERENCES

For early references, see Physics Letters **111B** 1 (1982).

ANISOVICH	17D	PR C95 035211	A.V. Anisovich *et al.*	
KASHEVAROV	17	PRL 118 212001	V.L. Kashevarov *et al.*	(A2/MAMI Collab.)
ANISOVICH	15A	EPJ A51 72	A.V. Anisovich *et al.*	
ROENCHEN	15A	EPJ A51 70	D. Roenchen *et al.*	
SOKHOYAN	15A	EPJ A51 95	V. Sokhoyan *et al.*	(CBELSA/TAPS Collab.)
PDG	14	CP C38 070001	K. Olive *et al.*	(PDG Collab.)
ROENCHEN	14	EPJ A50 101	D. Roenchen *et al.*	
Also		EPJ A51 63 (errat.)	D. Roenchen *et al.*	
SVARC	14	PR C89 045205	A. Svarc *et al.*	(RBI Zagreb, UNI Tuzla)
ANISOVICH	13B	EPJ A49 67	A.V. Anisovich *et al.*	
SHKLYAR	13	PR C87 015201	V. Shklyar, H. Lenske, U. Mosel	(GIES)
ANISOVICH	12A	EPJ A48 15	A.V. Anisovich *et al.*	(BONN, PNPI)
CHEN	12A	PR C86 015206	W. Chen *et al.*	(DUKE, GWU, MSST, ITEP+)
SHRESTHA	12A	PR C86 055203	M. Shrestha, D.M. Manley	(KSU)
WORKMAN	12A	PR C86 015202	R. Workman *et al.*	(GWU)
BATINIC	10	PR C82 038203	M. Batinic *et al.*	(ZAGR)
AZNAURYAN	09	PR C80 055203	I.G. Aznauryan *et al.*	(JLab CLAS Collab.)
DRECHSEL	07	EPJ A34 69	D. Drechsel, S.S. Kamalov, L. Tiator	(MAINZ, JINR)
DUGGER	07	PR C76 025211	M. Dugger *et al.*	(JLab CLAS Collab.)
ARNDT	06	PR C74 045205	R.A. Arndt *et al.*	(GWU)
ARNDT	04	PR C69 035213	R.A. Arndt *et al.*	(GWU, TRIU)
STAROSTIN	03	PR C67 068201	A. Starostin *et al.*	(BNL Crystal Ball Collab.)
PENNER	02C	PR C66 055211	G. Penner, U. Mosel	(GIES)
PENNER	02D	PR C66 055212	G. Penner, U. Mosel	(GIES)
BAI	01B	PL B510 75	J.Z. Bai *et al.*	(BES Collab.)
THOMPSON	01	PRL 86 1702	R. Thompson *et al.*	(JLab CLAS Collab.)
VRANA	00	PRPL 328 181	T.P. Vrana, S.A. Dytman, T.-S.H. Lee	(PITT, ANL)
ARMSTRONG	99B	PR D60 052004	C.S. Armstrong *et al.*	
MUKHOPAD...	95B	PL B364 1	N.C. Mukhopadhyay, J.F. Zhang, M. Benmerrouche	
HOEHLER	93	πN Newsletter 9 1	G. Hohler	(KARL)
CUTKOSKY	80	Toronto Conf. 19	R.E. Cutkosky *et al.*	(CMU, LBL) IJP
Also		PR D20 2839	R.E. Cutkosky *et al.*	(CMU, LBL) IJP
HOEHLER	79	PDAT 12-1	G. Hohler *et al.*	(KARLT) IJP
Also		Toronto Conf. 3	R. Koch	(KARLT) IJP

$N(1650)\ 1/2^-$

$I(J^P) = \frac{1}{2}(\frac{1}{2}^-)$ Status: ****

Older and obsolete values are listed and referenced in the 2014 edition, Chinese Physics **C38** 070001 (2014).

$N(1650)$ POLE POSITION

REAL PART

VALUE (MeV)	DOCUMENT ID		TECN	COMMENT
1640 to 1670 (≈ 1655) OUR ESTIMATE				
1658±10	ANISOVICH	17A	DPWA	Multichannel
1660± 5	[1] ANISOVICH	17A	L+P	$\gamma p, \pi^- p \to K\Lambda$
1660± 3.5±1	[2] SVARC	14	L+P	$\pi N \to \pi N$
1640±20	CUTKOSKY	80	IPWA	$\pi N \to \pi N$
• • • We do not use the following data for averages, fits, limits, etc. • • •				
1672	ROENCHEN	15A	DPWA	Multichannel
1652± 7	SOKHOYAN	15A	DPWA	Multichannel
1650	SHKLYAR	13	DPWA	Multichannel
1647± 6	ANISOVICH	12A	DPWA	Multichannel
1655	SHRESTHA	12A	DPWA	Multichannel
1646± 8	BATINIC	10	DPWA	$\pi N \to N\pi, N\eta$
1648	ARNDT	06	DPWA	$\pi N \to \pi N, \eta N$
1663	VRANA	00	DPWA	Multichannel
1670	HOEHLER	93	ARGD	$\pi N \to \pi N$

[1] Statistical error only.
[2] Fit to the amplitudes of HOEHLER 79.

−2×IMAGINARY PART

VALUE (MeV)	DOCUMENT ID		TECN	COMMENT
100 to 170 (≈ 135) OUR ESTIMATE				
102± 8	ANISOVICH	17A	DPWA	Multichannel
59±16	[1] ANISOVICH	17A	L+P	$\gamma p, \pi^- p \to K\Lambda$
167± 8±2	[2] SVARC	14	L+P	$\pi N \to \pi N$
150±30	CUTKOSKY	80	IPWA	$\pi N \to \pi N$
• • • We do not use the following data for averages, fits, limits, etc. • • •				
137	ROENCHEN	15A	DPWA	Multichannel
102± 8	SOKHOYAN	15A	DPWA	Multichannel
89	SHKLYAR	13	DPWA	Multichannel
103± 8	ANISOVICH	12A	DPWA	Multichannel
123	SHRESTHA	12A	DPWA	Multichannel
204±17	BATINIC	10	DPWA	$\pi N \to N\pi, N\eta$
80	ARNDT	06	DPWA	$\pi N \to \pi N, \eta N$
240	VRANA	00	DPWA	Multichannel
163	HOEHLER	93	ARGD	$\pi N \to \pi N$

[1] Statistical error only.
[2] Fit to the amplitudes of HOEHLER 79.

$N(1650)$ ELASTIC POLE RESIDUE

MODULUS $|r|$

VALUE (MeV)	DOCUMENT ID		TECN	COMMENT
25 to 55 (≈ 45) OUR ESTIMATE				
27± 6	SOKHOYAN	15A	DPWA	Multichannel
47± 3±1	[1] SVARC	14	L+P	$\pi N \to \pi N$
60±10	CUTKOSKY	80	IPWA	$\pi N \to \pi N$
• • • We do not use the following data for averages, fits, limits, etc. • • •				
37	ROENCHEN	15A	DPWA	Multichannel
19	SHKLYAR	13	DPWA	Multichannel
24± 3	ANISOVICH	12A	DPWA	Multichannel
100	BATINIC	10	DPWA	$\pi N \to N\pi, N\eta$
14	ARNDT	06	DPWA	$\pi N \to \pi N, \eta N$
39	HOEHLER	93	ARGD	$\pi N \to \pi N$

[1] Fit to the amplitudes of HOEHLER 79.

PHASE θ

VALUE (°)	DOCUMENT ID		TECN	COMMENT
−80 to −50 (≈ − 70) OUR ESTIMATE				
−60±20	SOKHOYAN	15A	DPWA	Multichannel
−47± 3±1	[1] SVARC	14	L+P	$\pi N \to \pi N$
−75±25	CUTKOSKY	80	IPWA	$\pi N \to \pi N$
• • • We do not use the following data for averages, fits, limits, etc. • • •				
−59	ROENCHEN	15A	DPWA	Multichannel
−46	SHKLYAR	13	DPWA	Multichannel
−75±12	ANISOVICH	12A	DPWA	Multichannel
−65	BATINIC	10	DPWA	$\pi N \to N\pi, N\eta$
−69	ARNDT	06	DPWA	$\pi N \to \pi N, \eta N$
−37	HOEHLER	93	ARGD	$\pi N \to \pi N$

[1] Fit to the amplitudes of HOEHLER 79.

$N(1650)$ INELASTIC POLE RESIDUE

The "normalized residue" is the residue divided by $\Gamma_{pole}/2$.

Normalized residue in $N\pi \to N(1650) \to N\eta$

MODULUS	PHASE (°)	DOCUMENT ID		TECN	COMMENT
0.29±0.03	134 ± 10	ANISOVICH	12A	DPWA	Multichannel
• • • We do not use the following data for averages, fits, limits, etc. • • •					
0.21	48	ROENCHEN	15A	DPWA	Multichannel

Normalized residue in $N\pi \to N(1650) \to \Lambda K$

MODULUS	PHASE (°)	DOCUMENT ID		TECN	COMMENT
0.26±0.10	110 ± 20	ANISOVICH	17A	DPWA	Multichannel
0.10±0.10	95 ± 33	[1] ANISOVICH	17A	L+P	$\gamma p, \pi^- p \to K\Lambda$
• • • We do not use the following data for averages, fits, limits, etc. • • •					
0.20	−54	ROENCHEN	15A	DPWA	Multichannel
0.23±0.09	85 ± 9	ANISOVICH	12A	DPWA	Multichannel

[1] Statistical error only.

Normalized residue in $N\pi \to N(1650) \to \Sigma K$

MODULUS	PHASE (°)	DOCUMENT ID		TECN	COMMENT
• • • We do not use the following data for averages, fits, limits, etc. • • •					
0.026	−74	ROENCHEN	15A	DPWA	Multichannel

Normalized residue in $N\pi \to N(1650) \to \Delta\pi$, D-wave

MODULUS	PHASE (°)	DOCUMENT ID		TECN	COMMENT
0.19±0.06	−30 ± 20	SOKHOYAN	15A	DPWA	Multichannel
• • • We do not use the following data for averages, fits, limits, etc. • • •					
0.23±0.04	−30 ± 20	ANISOVICH	12A	DPWA	Multichannel

Normalized residue in $N\pi \to N(1650) \to N\sigma$

MODULUS	PHASE (°)	DOCUMENT ID		TECN	COMMENT
0.20±0.15	undefined	SOKHOYAN	15A	DPWA	Multichannel

Normalized residue in $N\pi \to N(1650) \to N(1440)\pi$

MODULUS	PHASE (°)	DOCUMENT ID		TECN	COMMENT
0.30±0.17	undefined	SOKHOYAN	15A	DPWA	Multichannel

$N(1650)$ BREIT-WIGNER MASS

VALUE (MeV)	DOCUMENT ID		TECN	COMMENT
1635 to 1665 (≈ 1650) OUR ESTIMATE				
1634 ± 5	KASHEVAROV	17	DPWA	$\gamma p \to \eta p, \eta' p$
1654 ± 6	SOKHOYAN	15A	DPWA	Multichannel
1665 ± 2	[1] SHKLYAR	13	DPWA	Multichannel
1664 ± 2	[1] SHRESTHA	12A	DPWA	Multichannel
1634.7± 1.1	[1] ARNDT	06	DPWA	$\pi N \to \pi N, \eta N$
1650 ±30	CUTKOSKY	80	IPWA	$\pi N \to \pi N$
1670 ± 8	HOEHLER	79	IPWA	$\pi N \to \pi N$
• • • We do not use the following data for averages, fits, limits, etc. • • •				
1651 ± 6	ANISOVICH	12A	DPWA	Multichannel
1652 ± 9	BATINIC	10	DPWA	$\pi N \to N\pi, N\eta$
1665 ± 2	PENNER	02C	DPWA	Multichannel
1647 ±20	BAI	01B	BES	$J/\psi \to p\overline{p}\eta$
1689 ±12	VRANA	00	DPWA	Multichannel

[1] Statistical error only.

$N(1650)$ BREIT-WIGNER WIDTH

VALUE (MeV)	DOCUMENT ID		TECN	COMMENT
100 to 150 (≈ 125) OUR ESTIMATE				
128 ±16	KASHEVAROV	17	DPWA	$\gamma p \to \eta p, \eta' p$
102 ± 8	SOKHOYAN	15A	DPWA	Multichannel
147 ±14	[1] SHKLYAR	13	DPWA	Multichannel
126 ± 3	[1] SHRESTHA	12A	DPWA	Multichannel
115.4± 2.8	[1] ARNDT	06	DPWA	$\pi N \to \pi N, \eta N$
150 ±40	CUTKOSKY	80	IPWA	$\pi N \to \pi N$
180 ±20	HOEHLER	79	IPWA	$\pi N \to \pi N$
• • • We do not use the following data for averages, fits, limits, etc. • • •				
104 ±10	ANISOVICH	12A	DPWA	Multichannel
202 ±16	BATINIC	10	DPWA	$\pi N \to N\pi, N\eta$
138 ± 7	PENNER	02C	DPWA	Multichannel
145 $^{+80}_{-45}$	BAI	01B	BES	$J/\psi \to p\overline{p}\eta$
202 ±40	VRANA	00	DPWA	Multichannel

[1] Statistical error only.

$N(1650)$ DECAY MODES

The following branching fractions are our estimates, not fits or averages.

	Mode	Fraction (Γ_i/Γ)
Γ_1	$N\pi$	50–70 %
Γ_2	$N\eta$	15–35 %
Γ_3	ΛK	5–15 %
Γ_4	$N\pi\pi$	8–36 %
Γ_5	$\Delta(1232)\pi$	
Γ_6	$\Delta(1232)\pi$, D-wave	6–18 %
Γ_7	$N\sigma$	2–18 %
Γ_8	$N(1440)\pi$	6–26 %
Γ_9	$p\gamma$, helicity=1/2	0.04–0.20 %
Γ_{10}	$n\gamma$, helicity=1/2	0.003–0.17 %

$N(1650)$ BRANCHING RATIOS

$\Gamma(N\pi)/\Gamma_{total}$ Γ_1/Γ

VALUE (%)	DOCUMENT ID		TECN	COMMENT
50 to 70 (≈ 60) OUR ESTIMATE				
51 ± 4	SOKHOYAN	15A	DPWA	Multichannel
74 ± 3	[1] SHKLYAR	13	DPWA	Multichannel
57 ± 2	[1] SHRESTHA	12A	DPWA	Multichannel
65 ± 10	CUTKOSKY	80	IPWA	$\pi N \to \pi N$
61 ± 4	HOEHLER	79	IPWA	$\pi N \to \pi N$
• • • We do not use the following data for averages, fits, limits, etc. • • •				
51 ± 4	ANISOVICH	12A	DPWA	Multichannel
79 ± 6	BATINIC	10	DPWA	$\pi N \to N\pi$, $N\eta$
100	ARNDT	06	DPWA	$\pi N \to \pi N$, ηN
65 ± 4	PENNER	02C	DPWA	Multichannel
74 ± 2	VRANA	00	DPWA	Multichannel

[1] Statistical error only.

$\Gamma(N\eta)/\Gamma_{total}$ Γ_2/Γ

VALUE (%)	DOCUMENT ID		TECN	COMMENT
15 to 35 (≈ 25) OUR ESTIMATE				
28 ±11	[1] KASHEVAROV	17	DPWA	$\gamma p \to \eta p$, $\eta' p$
< 3	SHKLYAR	13	DPWA	Multichannel
18 ± 4	ANISOVICH	12A	DPWA	Multichannel
21 ± 2	[2] SHRESTHA	12A	DPWA	Multichannel
• • • We do not use the following data for averages, fits, limits, etc. • • •				
13 ± 5	BATINIC	10	DPWA	$\pi N \to N\pi$, $N\eta$
1.0 ± 0.6	PENNER	02C	DPWA	Multichannel
6 ± 1	VRANA	00	DPWA	Multichannel

[1] Assuming $A_{1/2} = 0.045$ GeV$^{-1/2}$.

[2] Statistical error only.

$\Gamma(\Lambda K)/\Gamma_{total}$ Γ_3/Γ

VALUE (%)	DOCUMENT ID		TECN	COMMENT
5 to 15 (≈ 10) OUR ESTIMATE				
10 ±5	ANISOVICH	12A	DPWA	Multichannel
8 ±1	[1] SHRESTHA	12A	DPWA	Multichannel
4 ±1	[1] SHKLYAR	05	DPWA	Multichannel
• • • We do not use the following data for averages, fits, limits, etc. • • •				
2.7 ± 0.4	PENNER	02C	DPWA	Multichannel

[1] Statistical error only.

$\Gamma(\Delta(1232)\pi$, D-wave$)/\Gamma_{total}$ Γ_6/Γ

VALUE (%)	DOCUMENT ID		TECN	COMMENT
12 ± 6	SOKHOYAN	15A	DPWA	Multichannel
7 ± 2	[1] SHRESTHA	12A	DPWA	Multichannel
• • • We do not use the following data for averages, fits, limits, etc. • • •				
19 ± 9	ANISOVICH	12A	DPWA	Multichannel
2 ± 1	VRANA	00	DPWA	Multichannel

[1] Statistical error only.

$\Gamma(N\sigma)/\Gamma_{total}$ Γ_7/Γ

VALUE (%)	DOCUMENT ID		TECN	COMMENT
10 ± 8	SOKHOYAN	15A	DPWA	Multichannel
< 1	SHRESTHA	12A	DPWA	Multichannel
• • • We do not use the following data for averages, fits, limits, etc. • • •				
1 ± 1	VRANA	00	DPWA	Multichannel

$\Gamma(N(1440)\pi)/\Gamma_{total}$ Γ_8/Γ

VALUE (%)	DOCUMENT ID		TECN	COMMENT
16 ± 10	SOKHOYAN	15A	DPWA	Multichannel
< 1	SHRESTHA	12A	DPWA	Multichannel
• • • We do not use the following data for averages, fits, limits, etc. • • •				
3 ± 1	VRANA	00	DPWA	Multichannel

$N(1650)$ PHOTON DECAY AMPLITUDES AT THE POLE

$N(1650) \to p\gamma$, helicity-1/2 amplitude $A_{1/2}$

MODULUS (GeV$^{-1/2}$)	PHASE (°)	DOCUMENT ID		TECN	COMMENT
0.032 ± 0.006	7 ± 7	ANISOVICH	17D	DPWA	Multichannel
$0.023^{+0.003}_{-0.008}$	6^{+28}_{-15}	ROENCHEN	14	DPWA	
• • • We do not use the following data for averages, fits, limits, etc. • • •					
0.032 ± 0.007	−2 ± 11	ANISOVICH	15A	DPWA	Multichannel
0.059	−14	ROENCHEN	15A	DPWA	Multichannel
0.032 ± 0.006	−2 ± 11	SOKHOYAN	15A	DPWA	Multichannel

$N(1650) \to n\gamma$, helicity-1/2 amplitude $A_{1/2}$

MODULUS (GeV$^{-1/2}$)	PHASE (°)	DOCUMENT ID		TECN	COMMENT
0.016 ± 0.004	−28 ± 10	ANISOVICH	17D	DPWA	Multichannel
• • • We do not use the following data for averages, fits, limits, etc. • • •					
0.019 ± 0.006	0 ± 15	ANISOVICH	15A	DPWA	Multichannel

$N(1650)$ BREIT-WIGNER PHOTON DECAY AMPLITUDES

$N(1650) \to p\gamma$, helicity-1/2 amplitude $A_{1/2}$

VALUE (GeV$^{-1/2}$)	DOCUMENT ID		TECN	COMMENT
0.035 to 0.055 (≈ 0.045) OUR ESTIMATE				
0.032 ± 0.006	SOKHOYAN	15A	DPWA	Multichannel
0.063 ± 0.006	[1] SHKLYAR	13	DPWA	Multichannel
0.055 ± 0.030	[1] WORKMAN	12A	DPWA	$\gamma N \to N\pi$
0.022 ± 0.007	[1] DUGGER	07	DPWA	$\gamma N \to \pi N$
• • • We do not use the following data for averages, fits, limits, etc. • • •				
0.033 ± 0.007	ANISOVICH	12A	DPWA	Multichannel
0.030 ± 0.003	[1] SHRESTHA	12A	DPWA	Multichannel
0.033	DRECHSEL	07	DPWA	$\gamma N \to \pi N$
0.049	PENNER	02D	DPWA	Multichannel

[1] Statistical error only.

$N(1650) \to n\gamma$, helicity-1/2 amplitude $A_{1/2}$

VALUE (GeV$^{-1/2}$)	DOCUMENT ID		TECN	COMMENT
−0.040 to 0.030 (≈ −0.010) OUR ESTIMATE				
0.025 ± 0.020	ANISOVICH	13B	DPWA	Multichannel
−0.040 ± 0.010	[1] CHEN	12A	DPWA	$\gamma N \to \pi N$
• • • We do not use the following data for averages, fits, limits, etc. • • •				
0.011 ± 0.002	[1] SHRESTHA	12A	DPWA	Multichannel
0.009	DRECHSEL	07	DPWA	$\gamma N \to \pi N$
−0.011	PENNER	02D	DPWA	Multichannel

[1] Statistical error only.

$N(1650)$ REFERENCES

For early references, see Physics Letters **111B** 1 (1982).

ANISOVICH	17A	PRL 119 062004	A.V. Anisovich *et al.*
ANISOVICH	17D	PR C95 035211	A.V. Anisovich *et al.*
KASHEVAROV	17	PRL 118 212001	V.L. Kashevarov *et al.* (A2/MAMI Collab.)
ANISOVICH	15A	EPJ A51 72	A.V. Anisovich *et al.*
ROENCHEN	15A	EPJ A51 70	D. Roenchen *et al.*
SOKHOYAN	15A	EPJ A51 95	V. Sokhoyan *et al.* (CBELSA/TAPS Collab.)
PDG	14	CP C38 070001	K. Olive *et al.* (PDG Collab.)
ROENCHEN	14	EPJ A50 101	D. Roenchen *et al.*
Also		EPJ A51 63 (errat.)	D. Roenchen *et al.*
SVARC	14	PR C89 045205	A. Svarc *et al.* (RBI Zagreb, UNI Tuzla)
ANISOVICH	13B	EPJ A49 67	A.V. Anisovich *et al.*
SHKLYAR	13	PR C87 015201	V. Shklyar, H. Lenske, U. Mosel (GIES)
ANISOVICH	12A	EPJ A48 15	A.V. Anisovich *et al.* (BONN, PNPI)
CHEN	12A	PR C86 015206	W. Chen *et al.* (DUKE, GWU, MSST, ITEP+)
SHRESTHA	12A	PR C86 055203	M. Shrestha, D.M. Manley (KSU)
WORKMAN	12A	PR C86 015202	R. Workman *et al.* (GWU)
BATINIC	10	PR C82 038203	M. Batinic *et al.* (ZAGR)
DRECHSEL	07	EPJ A34 69	D. Drechsel, S.S. Kamalov, L. Tiator (MAINZ, JINR)
DUGGER	07	PR C76 025211	M. Dugger *et al.* (JLab CLAS Collab.)
ARNDT	06	PR C74 045205	R.A. Arndt *et al.* (GWU)
SHKLYAR	05	PR C72 015210	V. Shklyar, H. Lenske, U. Mosel (GIES)
PENNER	02C	PR C66 055211	G. Penner, U. Mosel (GIES)
PENNER	02D	PR C66 055212	G. Penner, U. Mosel (GIES)
BAI	01B	PL B510 75	J.Z. Bai *et al.* (BES Collab.)
VRANA	00	PRPL 328 181	T.P. Vrana, S.A. Dytman, T.-S.H. Lee (PITT, ANL)
HOEHLER	93	πN Newsletter 9 1	G. Hohler (KARL)
CUTKOSKY	80	Toronto Conf. 19	R.E. Cutkosky *et al.* (CMU, LBL) IJP
Also		PR D20 2839	R.E. Cutkosky *et al.* (CMU, LBL) IJP
HOEHLER	79	PDAT 12-1	G. Hohler *et al.* (KARLT) IJP
Also		Toronto Conf. 3	R. Koch (KARLT) IJP

$N(1675)$ $5/2^-$

$I(J^P) = \frac{1}{2}(\frac{5}{2}^-)$ Status: ****

Older and obsolete values are listed and referenced in the 2014 edition, Chinese Physics **C38** 070001 (2014).

$N(1675)$ POLE POSITION

REAL PART

VALUE (MeV)	DOCUMENT ID		TECN	COMMENT
1655 to 1665 (≈ 1660) OUR ESTIMATE				
1655 ± 4	SOKHOYAN	15A	DPWA	Multichannel
1654 ± 2	[1] SVARC	14	L+P	$\pi N \to \pi N$
1660 ± 10	CUTKOSKY	80	IPWA	$\pi N \to \pi N$
• • • We do not use the following data for averages, fits, limits, etc. • • •				
1646	ROENCHEN	15A	DPWA	Multichannel
1640	SHKLYAR	13	DPWA	Multichannel
1654 ± 4	ANISOVICH	12A	DPWA	Multichannel
1656	SHRESTHA	12A	DPWA	Multichannel
1658 ± 9	BATINIC	10	DPWA	$\pi N \to N\pi, N\eta$
1657	ARNDT	06	DPWA	$\pi N \to \pi N, \eta N$
1674	VRANA	00	DPWA	Multichannel
1656	HOEHLER	93	ARGD	$\pi N \to \pi N$

[1] Fit to the amplitudes of HOEHLER 79.

−2×IMAGINARY PART

VALUE (MeV)	DOCUMENT ID		TECN	COMMENT
125 to 150 (≈ 135) OUR ESTIMATE				
147 ± 5	SOKHOYAN	15A	DPWA	Multichannel
125 ± 3 ± 1	[1] SVARC	14	L+P	$\pi N \to \pi N$
140 ± 10	CUTKOSKY	80	IPWA	$\pi N \to \pi N$
• • • We do not use the following data for averages, fits, limits, etc. • • •				
125	ROENCHEN	15A	DPWA	Multichannel
108	SHKLYAR	13	DPWA	Multichannel
151 ± 5	ANISOVICH	12A	DPWA	Multichannel
128	SHRESTHA	12A	DPWA	Multichannel
137 ± 7	BATINIC	10	DPWA	$\pi N \to N\pi, N\eta$
139	ARNDT	06	DPWA	$\pi N \to \pi N, \eta N$
120	VRANA	00	DPWA	Multichannel
126	HOEHLER	93	ARGD	$\pi N \to \pi N$

[1] Fit to the amplitudes of HOEHLER 79.

$N(1675)$ ELASTIC POLE RESIDUE

MODULUS $|r|$

VALUE (MeV)	DOCUMENT ID		TECN	COMMENT
23 to 33 (≈ 28) OUR ESTIMATE				
28 ± 1	SOKHOYAN	15A	DPWA	Multichannel
23 ± 1	[1] SVARC	14	L+P	$\pi N \to \pi N$
31 ± 5	CUTKOSKY	80	IPWA	$\pi N \to \pi N$
• • • We do not use the following data for averages, fits, limits, etc. • • •				
24	ROENCHEN	15A	DPWA	Multichannel
20	SHKLYAR	13	DPWA	Multichannel
28 ± 1	ANISOVICH	12A	DPWA	Multichannel
25	BATINIC	10	DPWA	$\pi N \to N\pi, N\eta$
27	ARNDT	06	DPWA	$\pi N \to \pi N, \eta N$
23	HOEHLER	93	ARGD	$\pi N \to \pi N$

[1] Fit to the amplitudes of HOEHLER 79.

PHASE θ

VALUE (°)	DOCUMENT ID		TECN	COMMENT
−30 to −20 (≈ −25) OUR ESTIMATE				
−24 ± 4	SOKHOYAN	15A	DPWA	Multichannel
−25 ± 2	[1] SVARC	14	L+P	$\pi N \to \pi N$
−30 ± 10	CUTKOSKY	80	IPWA	$\pi N \to \pi N$
• • • We do not use the following data for averages, fits, limits, etc. • • •				
−22	ROENCHEN	15A	DPWA	Multichannel
−49	SHKLYAR	13	DPWA	Multichannel
−26 ± 4	ANISOVICH	12A	DPWA	Multichannel
−16	BATINIC	10	DPWA	$\pi N \to N\pi, N\eta$
−21	ARNDT	06	DPWA	$\pi N \to \pi N, \eta N$
−22	HOEHLER	93	ARGD	$\pi N \to \pi N$

[1] Fit to the amplitudes of HOEHLER 79.

$N(1675)$ INELASTIC POLE RESIDUE

The "normalized residue" is the residue divided by $\Gamma_{pole}/2$.

Normalized residue in $N\pi \to N(1675) \to \Delta\pi$, D-wave

MODULUS	PHASE (°)	DOCUMENT ID		TECN	COMMENT
0.33 ± 0.04	90 ± 15	SOKHOYAN	15A	DPWA	Multichannel
• • • We do not use the following data for averages, fits, limits, etc. • • •					
0.33 ± 0.05	82 ± 10	ANISOVICH	12A	DPWA	Multichannel

Normalized residue in $N\pi \to N(1675) \to N\eta$

MODULUS	PHASE (°)	DOCUMENT ID		TECN	COMMENT
• • • We do not use the following data for averages, fits, limits, etc. • • •					
0.044	−43	ROENCHEN	15A	DPWA	Multichannel

Normalized residue in $N\pi \to N(1675) \to \Lambda K$

MODULUS	PHASE (°)	DOCUMENT ID		TECN	COMMENT
• • • We do not use the following data for averages, fits, limits, etc. • • •					
0.001	100	ROENCHEN	15A	DPWA	Multichannel

Normalized residue in $N\pi \to N(1675) \to \Sigma K$

MODULUS	PHASE (°)	DOCUMENT ID		TECN	COMMENT
• • • We do not use the following data for averages, fits, limits, etc. • • •					
0.031	−175	ROENCHEN	15A	DPWA	Multichannel

Normalized residue in $N\pi \to N(1675) \to N\sigma$

MODULUS	PHASE (°)	DOCUMENT ID		TECN	COMMENT
0.13 ± 0.03	125 ± 20	SOKHOYAN	15A	DPWA	Multichannel
• • • We do not use the following data for averages, fits, limits, etc. • • •					
0.15 ± 0.04	132 ± 18	ANISOVICH	12A	DPWA	Multichannel

$N(1675)$ BREIT-WIGNER MASS

VALUE (MeV)	DOCUMENT ID		TECN	COMMENT
1665 to 1680 (≈ 1675) OUR ESTIMATE				
1663 ± 4	SOKHOYAN	15A	DPWA	Multichannel
1666 ± 2	[1] SHKLYAR	13	DPWA	Multichannel
1679 ± 1	[1] SHRESTHA	12A	DPWA	Multichannel
1674.1 ± 0.2	[1] ARNDT	06	DPWA	$\pi N \to \pi N, \eta N$
1675 ± 10	CUTKOSKY	80	IPWA	$\pi N \to \pi N$
1679 ± 8	HOEHLER	79	IPWA	$\pi N \to \pi N$
• • • We do not use the following data for averages, fits, limits, etc. • • •				
1664 ± 5	ANISOVICH	12A	DPWA	Multichannel
1679 ± 9	BATINIC	10	DPWA	$\pi N \to N\pi, N\eta$
1685 ± 4	VRANA	00	DPWA	Multichannel

[1] Statistical error only.

$N(1675)$ BREIT-WIGNER WIDTH

VALUE (MeV)	DOCUMENT ID		TECN	COMMENT
130 to 160 (≈ 145) OUR ESTIMATE				
146 ± 6	SOKHOYAN	15A	DPWA	Multichannel
148 ± 1	[1] SHKLYAR	13	DPWA	Multichannel
145 ± 4	[1] SHRESTHA	12A	DPWA	Multichannel
146.5 ± 1.0	[1] ARNDT	06	DPWA	$\pi N \to \pi N, \eta N$
160 ± 20	CUTKOSKY	80	IPWA	$\pi N \to \pi N$
120 ± 15	HOEHLER	79	IPWA	$\pi N \to \pi N$
• • • We do not use the following data for averages, fits, limits, etc. • • •				
152 ± 7	ANISOVICH	12A	DPWA	Multichannel
152 ± 8	BATINIC	10	DPWA	$\pi N \to N\pi, N\eta$
131 ± 10	VRANA	00	DPWA	Multichannel

[1] Statistical error only.

$N(1675)$ DECAY MODES

The following branching fractions are our estimates, not fits or averages.

	Mode	Fraction (Γ_i/Γ)
Γ_1	$N\pi$	38–42 %
Γ_2	$N\eta$	< 1 %
Γ_3	$N\pi\pi$	25–45 %
Γ_4	$\Delta(1232)\pi$	
Γ_5	$\Delta(1232)\pi$, D-wave	23–37 %
Γ_6	$N\sigma$	3–7 %
Γ_7	$p\gamma$	0–0.02 %
Γ_8	$p\gamma$, helicity=1/2	0–0.01 %
Γ_9	$p\gamma$, helicity=3/2	0–0.01 %
Γ_{10}	$n\gamma$	0–0.15 %
Γ_{11}	$n\gamma$, helicity=1/2	0–0.05 %
Γ_{12}	$n\gamma$, helicity=3/2	0–0.10 %

$N(1675)$ BRANCHING RATIOS

$\Gamma(N\pi)/\Gamma_{total}$ Γ_1/Γ

VALUE (%)	DOCUMENT ID		TECN	COMMENT
38 to 42 (≈ 40) OUR ESTIMATE				
41 ± 2	SOKHOYAN	15A	DPWA	Multichannel
41 ± 1	[1] SHKLYAR	13	DPWA	Multichannel
38.6 ± 0.6	[1] SHRESTHA	12A	DPWA	Multichannel
39.3 ± 0.1	[1] ARNDT	06	DPWA	$\pi N \to \pi N, \eta N$
38 ± 5	CUTKOSKY	80	IPWA	$\pi N \to \pi N$
38 ± 3	HOEHLER	79	IPWA	$\pi N \to \pi N$
• • • We do not use the following data for averages, fits, limits, etc. • • •				
40 ± 3	ANISOVICH	12A	DPWA	Multichannel
35 ± 4	BATINIC	10	DPWA	$\pi N \to N\pi, N\eta$
35 ± 1	VRANA	00	DPWA	Multichannel

[1] Statistical error only.

$\Gamma(N\eta)/\Gamma_{total}$ Γ_2/Γ

VALUE (%)	DOCUMENT ID		TECN	COMMENT
<1	SHKLYAR	13	DPWA	Multichannel
<1	SHRESTHA	12A	DPWA	Multichannel
• • • We do not use the following data for averages, fits, limits, etc. • • •				
0.1±0.1	BATINIC	10	DPWA	$\pi N \to N\pi$, $N\eta$
3 ±3	THOMA	08	DPWA	Multichannel
0 ±1	VRANA	00	DPWA	Multichannel

$\Gamma(\Delta(1232)\pi, D\text{-wave})/\Gamma_{total}$ Γ_5/Γ

VALUE (%)	DOCUMENT ID		TECN	COMMENT
30±7	SOKHOYAN	15A	DPWA	Multichannel
46±1	[1] SHRESTHA	12A	DPWA	Multichannel
• • • We do not use the following data for averages, fits, limits, etc. • • •				
33±8	ANISOVICH	12A	DPWA	Multichannel
63±2	VRANA	00	DPWA	Multichannel

[1] Statistical error only.

$\Gamma(N\sigma)/\Gamma_{total}$ Γ_6/Γ

VALUE (%)	DOCUMENT ID		TECN	COMMENT
5±2	SOKHOYAN	15A	DPWA	Multichannel
• • • We do not use the following data for averages, fits, limits, etc. • • •				
7±3	ANISOVICH	12A	DPWA	Multichannel

$N(1675)$ PHOTON DECAY AMPLITUDES AT THE POLE

$N(1675) \to p\gamma$, helicity-1/2 amplitude $A_{1/2}$

MODULUS ($GeV^{-1/2}$)	PHASE (°)	DOCUMENT ID		TECN	COMMENT
0.022±0.003	−12 ± 7	SOKHOYAN	15A	DPWA	Multichannel
$0.022^{+0.004}_{-0.007}$	49^{+5}_{-2}	ROENCHEN	14	DPWA	
• • • We do not use the following data for averages, fits, limits, etc. • • •					
0.032	36	ROENCHEN	15A	DPWA	Multichannel

$N(1675) \to p\gamma$, helicity-3/2 amplitude $A_{3/2}$

MODULUS ($GeV^{-1/2}$)	PHASE (°)	DOCUMENT ID		TECN	COMMENT
0.028±0.006	−17 ± 6	SOKHOYAN	15A	DPWA	Multichannel
$0.036^{+0.004}_{-0.005}$	−30 ± 4	ROENCHEN	14	DPWA	
• • • We do not use the following data for averages, fits, limits, etc. • • •					
0.051	−9.3	ROENCHEN	15A	DPWA	Multichannel

$N(1675)$ BREIT-WIGNER PHOTON DECAY AMPLITUDES

$N(1675) \to p\gamma$, helicity-1/2 amplitude $A_{1/2}$

VALUE ($GeV^{-1/2}$)	DOCUMENT ID		TECN	COMMENT
0.010 to 0.025 (≈ 0.018) OUR ESTIMATE				
0.022±0.003	SOKHOYAN	15A	DPWA	Multichannel
0.009±0.001	[1] SHKLYAR	13	DPWA	Multichannel
0.013±0.001	[1] WORKMAN	12A	DPWA	$\gamma N \to N\pi$
0.018±0.002	[1] DUGGER	07	DPWA	$\gamma N \to \pi N$
• • • We do not use the following data for averages, fits, limits, etc. • • •				
0.024±0.003	ANISOVICH	12A	DPWA	Multichannel
0.011±0.001	[1] SHRESTHA	12A	DPWA	Multichannel
0.015	DRECHSEL	07	DPWA	$\gamma N \to \pi N$

[1] Statistical error only.

$N(1675) \to p\gamma$, helicity-3/2 amplitude $A_{3/2}$

VALUE ($GeV^{-1/2}$)	DOCUMENT ID		TECN	COMMENT
0.015 to 0.030 (≈ 0.022) OUR ESTIMATE				
0.027±0.006	SOKHOYAN	15A	DPWA	Multichannel
0.021±0.001	[1] SHKLYAR	13	DPWA	Multichannel
0.016±0.001	[1] WORKMAN	12A	DPWA	$\gamma N \to N\pi$
0.021±0.001	[1] DUGGER	07	DPWA	$\gamma N \to \pi N$
• • • We do not use the following data for averages, fits, limits, etc. • • •				
0.025±0.007	ANISOVICH	12A	DPWA	Multichannel
0.020±0.001	[1] SHRESTHA	12A	DPWA	Multichannel
0.022	DRECHSEL	07	DPWA	$\gamma N \to \pi N$

[1] Statistical error only.

$N(1675) \to n\gamma$, helicity-1/2 amplitude $A_{1/2}$

VALUE ($GeV^{-1/2}$)	DOCUMENT ID		TECN	COMMENT
−0.065 to −0.055 (≈ −0.060) OUR ESTIMATE				
−0.060±0.007	ANISOVICH	13B	DPWA	Multichannel
−0.058±0.002	[1] CHEN	12A	DPWA	$\gamma N \to \pi N$
• • • We do not use the following data for averages, fits, limits, etc. • • •				
−0.040±0.004	[1] SHRESTHA	12A	DPWA	Multichannel
−0.062	DRECHSEL	07	DPWA	$\gamma N \to \pi N$

[1] Statistical error only.

$N(1675) \to n\gamma$, helicity-3/2 amplitude $A_{3/2}$

VALUE ($GeV^{-1/2}$)	DOCUMENT ID		TECN	COMMENT
−0.095 to −0.075 (≈ −0.085) OUR ESTIMATE				
−0.088±0.010	ANISOVICH	13B	DPWA	Multichannel
−0.080±0.005	[1] CHEN	12A	DPWA	$\gamma N \to \pi N$
• • • We do not use the following data for averages, fits, limits, etc. • • •				
−0.068±0.004	[1] SHRESTHA	12A	DPWA	Multichannel
−0.084	DRECHSEL	07	DPWA	$\gamma N \to \pi N$

[1] Statistical error only.

$N(1675)$ REFERENCES

For early references, see Physics Letters **111B** 1 (1982).

ROENCHEN	15A	EPJ A51 70	D. Roenchen *et al.*	
SOKHOYAN	15A	EPJ A51 95	V. Sokhoyan *et al.*	(CBELSA/TAPS Collab.)
PDG	14	CP C38 070001	K. Olive *et al.*	(PDG Collab.)
ROENCHEN	14	EPJ A50 101	D. Roenchen *et al.*	
Also		EPJ A51 63 (errat.)	D. Roenchen *et al.*	
SVARC	14	PR C89 045205	A. Svarc *et al.*	(RBI Zagreb, UNI Tuzla)
ANISOVICH	13B	EPJ A49 67	A.V. Anisovich *et al.*	
SHKLYAR	13	PR C87 015201	V. Shklyar, H. Lenske, U. Mosel	(GIES)
ANISOVICH	12A	EPJ A48 15	A.V. Anisovich *et al.*	(BONN, PNPI)
CHEN	12A	PR C86 015206	W. Chen *et al.*	(DUKE, GWU, MSST, ITEP+)
SHRESTHA	12A	PR C86 055203	M. Shrestha, D.M. Manley	(KSU)
WORKMAN	12A	PR C86 015202	R. Workman *et al.*	(GWU)
BATINIC	10	PR C82 038203	M. Batinic *et al.*	(ZAGR)
THOMA	08	PL B659 87	U. Thoma *et al.*	(CB-ELSA Collab.)
DRECHSEL	07	EPJ A34 69	D. Drechsel, S.S. Kamalov, L. Tiator	(MAINZ, JINR)
DUGGER	07	PR C76 025211	M. Dugger *et al.*	(JLab CLAS Collab.)
ARNDT	06	PR C74 045205	R.A. Arndt *et al.*	(GWU)
VRANA	00	PRPL 328 181	T.P. Vrana, S.A. Dytman, T.-S.H. Lee	(PITT, ANL)
HOEHLER	93	πN Newsletter 9 1	G. Hohler	(KARL)
CUTKOSKY	80	Toronto Conf. 19	R.E. Cutkosky *et al.*	(CMU, LBL) IJP
Also		PR D20 2839	R.E. Cutkosky *et al.*	(CMU, LBL) IJP
HOEHLER	79	PDAT 12-1	G. Hohler *et al.*	(KARLT) IJP
Also		Toronto Conf. 3	R. Koch	(KARLT) IJP

$N(1680)$ $5/2^+$

$I(J^P) = \frac{1}{2}(\frac{5}{2}^+)$ Status: ****

Older and obsolete values are listed and referenced in the 2014 edition, Chinese Physics **C38** 070001 (2014).

$N(1680)$ POLE POSITION

REAL PART

VALUE (MeV)	DOCUMENT ID		TECN	COMMENT
1665 to 1680 (≈ 1675) OUR ESTIMATE				
1678±5	SOKHOYAN	15A	DPWA	Multichannel
1674±2±1	[1] SVARC	14	L+P	$\pi N \to \pi N$
1667±5	CUTKOSKY	80	IPWA	$\pi N \to \pi N$
• • • We do not use the following data for averages, fits, limits, etc. • • •				
1669	ROENCHEN	15A	DPWA	Multichannel
1660	SHKLYAR	13	DPWA	Multichannel
1676±6	ANISOVICH	12A	DPWA	Multichannel
1669	SHRESTHA	12A	DPWA	Multichannel
1666±8	BATINIC	10	DPWA	$\pi N \to N\pi$, $N\eta$
1674	ARNDT	06	DPWA	$\pi N \to \pi N$, ηN
1667	VRANA	00	DPWA	Multichannel
1673	HOEHLER	93	ARGD	$\pi N \to \pi N$

[1] Fit to the amplitudes of HOEHLER 79.

−2×IMAGINARY PART

VALUE (MeV)	DOCUMENT ID		TECN	COMMENT
110 to 135 (≈ 120) OUR ESTIMATE				
113± 4	SOKHOYAN	15A	DPWA	Multichannel
129± 3±1	[1] SVARC	14	L+P	$\pi N \to \pi N$
110±10	CUTKOSKY	80	IPWA	$\pi N \to \pi N$
• • • We do not use the following data for averages, fits, limits, etc. • • •				
100	ROENCHEN	15A	DPWA	Multichannel
98	SHKLYAR	13	DPWA	Multichannel
113± 4	ANISOVICH	12A	DPWA	Multichannel
119	SHRESTHA	12A	DPWA	Multichannel
135± 6	BATINIC	10	DPWA	$\pi N \to N\pi$, $N\eta$
115	ARNDT	06	DPWA	$\pi N \to \pi N$, ηN
122	VRANA	00	DPWA	Multichannel
135	HOEHLER	93	ARGD	$\pi N \to \pi N$

[1] Fit to the amplitudes of HOEHLER 79.

$N(1680)$ ELASTIC POLE RESIDUE

MODULUS $|r|$

VALUE (MeV)	DOCUMENT ID		TECN	COMMENT
35 to 45 (≈ 40) OUR ESTIMATE				
45±4	SOKHOYAN	15A	DPWA	Multichannel
44±1±1	[1] SVARC	14	L+P	$\pi N \to \pi N$
34±2	CUTKOSKY	80	IPWA	$\pi N \to \pi N$

• • • We do not use the following data for averages, fits, limits, etc. • • •				
34	ROENCHEN	15A	DPWA	Multichannel
33	SHKLYAR	13	DPWA	Multichannel
43±4	ANISOVICH	12A	DPWA	Multichannel
44	BATINIC	10	DPWA	$\pi N \to N\pi$, $N\eta$
42	ARNDT	06	DPWA	$\pi N \to \pi N$, ηN
44	HOEHLER	93	ARGD	$\pi N \to \pi N$

[1] Fit to the amplitudes of HOEHLER 79.

PHASE θ

VALUE (°)	DOCUMENT ID		TECN	COMMENT
−20 to 10 (≈ −5) OUR ESTIMATE				
5±10	SOKHOYAN	15A	DPWA	Multichannel
−16± 1±1	[1] SVARC	14	L+P	$\pi N \to \pi N$
−25± 5	CUTKOSKY	80	IPWA	$\pi N \to \pi N$
• • • We do not use the following data for averages, fits, limits, etc. • • •				
−19	ROENCHEN	15A	DPWA	Multichannel
−32	SHKLYAR	13	DPWA	Multichannel
− 2±10	ANISOVICH	12A	DPWA	Multichannel
−19	BATINIC	10	DPWA	$\pi N \to N\pi$, $N\eta$
− 4	ARNDT	06	DPWA	$\pi N \to \pi N$, ηN
−17	HOEHLER	93	ARGD	$\pi N \to \pi N$

[1] Fit to the amplitudes of HOEHLER 79.

$N(1680)$ INELASTIC POLE RESIDUE

The "normalized residue" is the residue divided by $\Gamma_{pole}/2$.

Normalized residue in $N\pi \to N(1680) \to \Delta\pi$, P-wave

MODULUS	PHASE (°)	DOCUMENT ID		TECN	COMMENT
0.15±0.03	−60 ± 30	SOKHOYAN	15A	DPWA	Multichannel
• • • We do not use the following data for averages, fits, limits, etc. • • •					
0.15±0.03	−70 ± 45	ANISOVICH	12A	DPWA	Multichannel

Normalized residue in $N\pi \to N(1680) \to \Delta\pi$, F-wave

MODULUS	PHASE (°)	DOCUMENT ID		TECN	COMMENT
0.23±0.04	90 ± 12	SOKHOYAN	15A	DPWA	Multichannel
• • • We do not use the following data for averages, fits, limits, etc. • • •					
0.23±0.04	85 ± 15	ANISOVICH	12A	DPWA	Multichannel

Normalized residue in $N\pi \to N(1680) \to N\eta$

MODULUS	PHASE (°)	DOCUMENT ID		TECN	COMMENT
• • • We do not use the following data for averages, fits, limits, etc. • • •					
0.027	136	ROENCHEN	15A	DPWA	Multichannel

Normalized residue in $N\pi \to N(1680) \to \Lambda K$

MODULUS	PHASE (°)	DOCUMENT ID		TECN	COMMENT
• • • We do not use the following data for averages, fits, limits, etc. • • •					
0.001	90	ROENCHEN	15A	DPWA	Multichannel

Normalized residue in $N\pi \to N(1680) \to \Sigma K$

MODULUS	PHASE (°)	DOCUMENT ID		TECN	COMMENT
• • • We do not use the following data for averages, fits, limits, etc. • • •					
0.004	148	ROENCHEN	15A	DPWA	Multichannel

Normalized residue in $N\pi \to N(1680) \to N\,(\pi\pi)^{I=0}_{S-wave}$

MODULUS	PHASE (°)	DOCUMENT ID		TECN	COMMENT
0.29±0.06	−45 ± 15	SOKHOYAN	15A	DPWA	Multichannel
• • • We do not use the following data for averages, fits, limits, etc. • • •					
0.26±0.04	−56 ± 15	ANISOVICH	12A	DPWA	Multichannel

$N(1680)$ BREIT-WIGNER MASS

VALUE (MeV)	DOCUMENT ID		TECN	COMMENT
1680 to 1690 (≈ 1685) OUR ESTIMATE				
1690 ± 5	SOKHOYAN	15A	DPWA	Multichannel
1676 ± 2	[1] SHKLYAR	13	DPWA	Multichannel
1682.7± 0.5	[1] SHRESTHA	12A	DPWA	Multichannel
1680.1± 0.2	[1] ARNDT	06	DPWA	$\pi N \to \pi N$, ηN
1680 ±10	CUTKOSKY	80	IPWA	$\pi N \to \pi N$
1684 ± 3	HOEHLER	79	IPWA	$\pi N \to \pi N$
• • • We do not use the following data for averages, fits, limits, etc. • • •				
1689 ± 6	ANISOVICH	12A	DPWA	Multichannel
1680 ± 7	BATINIC	10	DPWA	$\pi N \to N\pi$, $N\eta$
1679 ± 3	VRANA	00	DPWA	Multichannel

[1] Statistical error only.

$N(1680)$ BREIT-WIGNER WIDTH

VALUE (MeV)	DOCUMENT ID		TECN	COMMENT
115 to 130 (≈ 120) OUR ESTIMATE				
119 ± 4	SOKHOYAN	15A	DPWA	Multichannel
115 ± 1	[1] SHKLYAR	13	DPWA	Multichannel
126 ± 1	[1] SHRESTHA	12A	DPWA	Multichannel
128.0± 1.1	[1] ARNDT	06	DPWA	$\pi N \to \pi N$, ηN
120 ±10	CUTKOSKY	80	IPWA	$\pi N \to \pi N$
128 ± 8	HOEHLER	79	IPWA	$\pi N \to \pi N$
• • • We do not use the following data for averages, fits, limits, etc. • • •				
118 ± 6	ANISOVICH	12A	DPWA	Multichannel
142 ± 7	BATINIC	10	DPWA	$\pi N \to N\pi$, $N\eta$
128 ± 9	VRANA	00	DPWA	Multichannel

[1] Statistical error only.

$N(1680)$ DECAY MODES

The following branching fractions are our estimates, not fits or averages.

	Mode	Fraction (Γ_i/Γ)
Γ_1	$N\pi$	60–70 %
Γ_2	$N\eta$	<1 %
Γ_3	$N\pi\pi$	20–40 %
Γ_4	$\Delta(1232)\pi$	11–23 %
Γ_5	$\Delta(1232)\pi$, P-wave	4–10 %
Γ_6	$\Delta(1232)\pi$, F-wave	1–13 %
Γ_7	$N\sigma$	9–19 %
Γ_8	$p\gamma$	0.21–0.32 %
Γ_9	$p\gamma$, helicity=1/2	0.001–0.011 %
Γ_{10}	$p\gamma$, helicity=3/2	0.20–0.32 %
Γ_{11}	$n\gamma$	0.021–0.046 %
Γ_{12}	$n\gamma$, helicity=1/2	0.004–0.029 %
Γ_{13}	$n\gamma$, helicity=3/2	0.01–0.024 %

$N(1680)$ BRANCHING RATIOS

$\Gamma(N\pi)/\Gamma_{total}$ Γ_1/Γ

VALUE (%)	DOCUMENT ID		TECN	COMMENT
60 to 70 (≈ 65) OUR ESTIMATE				
62 ±4	SOKHOYAN	15A	DPWA	Multichannel
68 ±1	[1] SHKLYAR	13	DPWA	Multichannel
68.0±0.5	[1] SHRESTHA	12A	DPWA	Multichannel
70.1±0.1	[1] ARNDT	06	DPWA	$\pi N \to \pi N$, ηN
62 ±5	CUTKOSKY	80	IPWA	$\pi N \to \pi N$
65 ±2	HOEHLER	79	IPWA	$\pi N \to \pi N$
• • • We do not use the following data for averages, fits, limits, etc. • • •				
64 ±5	ANISOVICH	12A	DPWA	Multichannel
67 ±3	BATINIC	10	DPWA	$\pi N \to N\pi$, $N\eta$
69 ±2	VRANA	00	DPWA	Multichannel

[1] Statistical error only.

$\Gamma(N\eta)/\Gamma_{total}$ Γ_2/Γ

VALUE (%)	DOCUMENT ID		TECN	COMMENT
<1	SHKLYAR	13	DPWA	Multichannel
1.0 ±0.3	[1] SHRESTHA	12A	DPWA	Multichannel
$0.15^{+0.35}_{-0.10}$	TIATOR	99	DPWA	$\gamma p \to p\eta$
• • • We do not use the following data for averages, fits, limits, etc. • • •				
0.4 ±0.2	BATINIC	10	DPWA	$\pi N \to N\pi$, $N\eta$
<1	THOMA	08	DPWA	Multichannel
0 ±1	VRANA	00	DPWA	Multichannel

[1] Statistical error only.

$\Gamma(\Delta(1232)\pi, P\text{-wave})/\Gamma_{total}$ Γ_5/Γ

VALUE (%)	DOCUMENT ID		TECN	COMMENT
7 ±3	SOKHOYAN	15A	DPWA	Multichannel
10.5±0.9	[1] SHRESTHA	12A	DPWA	Multichannel
• • • We do not use the following data for averages, fits, limits, etc. • • •				
5 ±3	ANISOVICH	12A	DPWA	Multichannel
14 ±3	VRANA	00	DPWA	Multichannel

[1] Statistical error only.

$\Gamma(\Delta(1232)\pi, F\text{-wave})/\Gamma_{total}$ Γ_6/Γ

VALUE (%)	DOCUMENT ID		TECN	COMMENT
10 ±3	SOKHOYAN	15A	DPWA	Multichannel
1.0±0.1	[1] SHRESTHA	12A	DPWA	Multichannel
• • • We do not use the following data for averages, fits, limits, etc. • • •				
10 ±3	ANISOVICH	12A	DPWA	Multichannel
1 ±1	VRANA	00	DPWA	Multichannel

[1] Statistical error only.

$\Gamma(N\sigma)/\Gamma_{total}$ Γ_7/Γ

VALUE (%)	DOCUMENT ID		TECN	COMMENT
14 ±5	SOKHOYAN	15A	DPWA	Multichannel
9.4±0.8	[1] SHRESTHA	12A	DPWA	Multichannel
• • • We do not use the following data for averages, fits, limits, etc. • • •				
14 ±7	ANISOVICH	12A	DPWA	Multichannel
9 ±1	VRANA	00	DPWA	Multichannel

[1] Statistical error only.

$N(1680)$ PHOTON DECAY AMPLITUDES AT THE POLE

$N(1680) \rightarrow p\gamma$, helicity-1/2 amplitude $A_{1/2}$

MODULUS ($GeV^{-1/2}$)	PHASE (°)	DOCUMENT ID		TECN	COMMENT
-0.013 ± 0.003	-20 ± 17	SOKHOYAN	15A	DPWA	Multichannel
$-0.013^{+0.002}_{-0.005}$	-42^{+9}_{-18}	ROENCHEN	14	DPWA	
• • • We do not use the following data for averages, fits, limits, etc. • • •					
-0.022	-28	ROENCHEN	15A	DPWA	Multichannel

$N(1680) \rightarrow p\gamma$, helicity-3/2 amplitude $A_{3/2}$

MODULUS ($GeV^{-1/2}$)	PHASE (°)	DOCUMENT ID		TECN	COMMENT
0.135 ± 0.005	1 ± 3	SOKHOYAN	15A	DPWA	Multichannel
$0.126^{+0.001}_{-0.002}$	-7^{+3}_{-2}	ROENCHEN	14	DPWA	
• • • We do not use the following data for averages, fits, limits, etc. • • •					
0.102	-11	ROENCHEN	15A	DPWA	Multichannel

$N(1680)$ BREIT-WIGNER PHOTON DECAY AMPLITUDES

$N(1680) \rightarrow p\gamma$, helicity-1/2 amplitude $A_{1/2}$

VALUE ($GeV^{-1/2}$)	DOCUMENT ID		TECN	COMMENT
-0.018 to -0.005 (≈ -0.010) OUR ESTIMATE				
-0.015 ± 0.002	SOKHOYAN	15A	DPWA	Multichannel
0.003 ± 0.001	[1] SHKLYAR	13	DPWA	Multichannel
-0.007 ± 0.002	[1] WORKMAN	12A	DPWA	$\gamma N \rightarrow N\pi$
-0.017 ± 0.001	[1] DUGGER	07	DPWA	$\gamma N \rightarrow \pi N$
• • • We do not use the following data for averages, fits, limits, etc. • • •				
-0.013 ± 0.003	ANISOVICH	12A	DPWA	Multichannel
-0.017 ± 0.001	[1] SHRESTHA	12A	DPWA	Multichannel
-0.025	DRECHSEL	07	DPWA	$\gamma N \rightarrow \pi N$

[1] Statistical error only.

$N(1680) \rightarrow p\gamma$, helicity-3/2 amplitude $A_{3/2}$

VALUE ($GeV^{-1/2}$)	DOCUMENT ID		TECN	COMMENT
0.130 to 0.140 (≈ 0.135) OUR ESTIMATE				
0.136 ± 0.005	SOKHOYAN	15A	DPWA	Multichannel
0.116 ± 0.001	[1] SHKLYAR	13	DPWA	Multichannel
0.140 ± 0.002	[1] WORKMAN	12A	DPWA	$\gamma N \rightarrow N\pi$
0.134 ± 0.002	[1] DUGGER	07	DPWA	$\gamma N \rightarrow \pi N$
• • • We do not use the following data for averages, fits, limits, etc. • • •				
0.135 ± 0.006	ANISOVICH	12A	DPWA	Multichannel
0.136 ± 0.001	[1] SHRESTHA	12A	DPWA	Multichannel
0.134	DRECHSEL	07	DPWA	$\gamma N \rightarrow \pi N$

[1] Statistical error only.

$N(1680) \rightarrow n\gamma$, helicity-1/2 amplitude $A_{1/2}$

VALUE ($GeV^{-1/2}$)	DOCUMENT ID		TECN	COMMENT
0.020 to 0.040 (≈ 0.030) OUR ESTIMATE				
0.034 ± 0.006	ANISOVICH	13B	DPWA	Multichannel
0.026 ± 0.004	[1] CHEN	12A	DPWA	$\gamma N \rightarrow \pi N$
• • • We do not use the following data for averages, fits, limits, etc. • • •				
0.029 ± 0.002	[1] SHRESTHA	12A	DPWA	Multichannel
0.028	DRECHSEL	07	DPWA	$\gamma N \rightarrow \pi N$

[1] Statistical error only.

$N(1680) \rightarrow n\gamma$, helicity-3/2 amplitude $A_{3/2}$

VALUE ($GeV^{-1/2}$)	DOCUMENT ID		TECN	COMMENT
-0.050 to -0.025 (≈ -0.035) OUR ESTIMATE				
-0.044 ± 0.009	ANISOVICH	13B	DPWA	Multichannel
-0.029 ± 0.002	[1] CHEN	12A	DPWA	$\gamma N \rightarrow \pi N$
• • • We do not use the following data for averages, fits, limits, etc. • • •				
-0.059 ± 0.002	[1] SHRESTHA	12A	DPWA	Multichannel
-0.038	DRECHSEL	07	DPWA	$\gamma N \rightarrow \pi N$

[1] Statistical error only.

$N(1680)$ REFERENCES

For early references, see Physics Letters **111B** 1 (1982). For very early references, see Reviews of Modern Physics **37** 633 (1965).

ROENCHEN	15A	EPJ A51 70	D. Roenchen *et al.*	
SOKHOYAN	15A	EPJ A51 95	V. Sokhoyan *et al.*	(CBELSA/TAPS Collab.)
PDG	14	CP C38 070001	K. Olive *et al.*	(PDG Collab.)
ROENCHEN	14	EPJ A50 101	D. Roenchen *et al.*	
Also		EPJ A51 63 (errat.)	D. Roenchen *et al.*	
SVARC	14	PR C89 045205	A. Svarc *et al.*	(RBI Zagreb, UNI Tuzla)
ANISOVICH	13B	EPJ A49 67	A.V. Anisovich *et al.*	
SHKLYAR	13	PR C87 015201	V. Shklyar, H. Lenske, U. Mosel	(GIES)
ANISOVICH	12A	EPJ A48 15	A.V. Anisovich *et al.*	(BONN, PNPI)
CHEN	12A	PR C86 015206	W. Chen *et al.*	(DUKE, GWU, MSST, ITEP+)
SHRESTHA	12A	PR C86 055203	M. Shrestha, D.M. Manley	(KSU)
WORKMAN	12A	PR C86 015202	R. Workman *et al.*	(GWU)
BATINIC	10	PR C82 038203	M. Batinic *et al.*	(ZAGR)
THOMA	08	PL B659 87	U. Thoma *et al.*	(CB-ELSA Collab.)
DRECHSEL	07	EPJ A34 69	D. Drechsel, S.S. Kamalov, L. Tiator	(MAINZ, JINR)
DUGGER	07	PR C76 025211	M. Dugger *et al.*	(JLab CLAS Collab.)
ARNDT	06	PR C74 045205	R.A. Arndt *et al.*	(GWU)
VRANA	00	PRPL 328 181	T.P. Vrana, S.A. Dytman, T.-S.H. Lee	(PITT, ANL)
TIATOR	99	PR C60 035210	L. Tiator *et al.*	
HOEHLER	93	πN Newsletter 9 1	G. Hohler	(KARL)
CUTKOSKY	80	Toronto Conf. 19	R.E. Cutkosky *et al.*	(CMU, LBL) IJP
Also		PR D20 2839	R.E. Cutkosky *et al.*	(CMU, LBL) IJP
HOEHLER	79	PDAT 12-1	G. Hohler *et al.*	(KARLT) IJP
Also		Toronto Conf. 3	R. Koch	(KARLT) IJP

$N(1700)\ 3/2^-$

$I(J^P) = \frac{1}{2}(\frac{3}{2}^-)$ Status: ***

Older and obsolete values are listed and referenced in the 2014 edition, Chinese Physics **C38** 070001 (2014).

$N(1700)$ POLE POSITION

REAL PART

VALUE (MeV)	DOCUMENT ID		TECN	COMMENT
1650 to 1750 (≈ 1700) OUR ESTIMATE				
1780 ± 35	SOKHOYAN	15A	DPWA	Multichannel
$1757 \pm 4 \pm 1$	[1] SVARC	14	L+P	$\pi N \rightarrow \pi N$
1660 ± 30	CUTKOSKY	80	IPWA	$\pi N \rightarrow \pi N$
• • • We do not use the following data for averages, fits, limits, etc. • • •				
1770 ± 40	ANISOVICH	12A	DPWA	Multichannel
1662	SHRESTHA	12A	DPWA	Multichannel
1806 ± 23	BATINIC	10	DPWA	$\pi N \rightarrow N\pi$, $N\eta$
1704	VRANA	00	DPWA	Multichannel
1700	HOEHLER	93	SPED	$\pi N \rightarrow \pi N$

[1] Fit to the amplitudes of HOEHLER 79.

$-2\times$IMAGINARY PART

VALUE (MeV)	DOCUMENT ID		TECN	COMMENT
100 to 300 (≈ 200) OUR ESTIMATE				
420 ± 140	SOKHOYAN	15A	DPWA	Multichannel
$136 \pm 7 \pm 4$	[1] SVARC	14	L+P	$\pi N \rightarrow \pi N$
90 ± 40	CUTKOSKY	80	IPWA	$\pi N \rightarrow \pi N$
• • • We do not use the following data for averages, fits, limits, etc. • • •				
420 ± 180	ANISOVICH	12A	DPWA	Multichannel
55	SHRESTHA	12A	DPWA	Multichannel
129 ± 33	BATINIC	10	DPWA	$\pi N \rightarrow N\pi$, $N\eta$
156	VRANA	00	DPWA	Multichannel
120	HOEHLER	93	SPED	$\pi N \rightarrow \pi N$

[1] Fit to the amplitudes of HOEHLER 79.

$N(1700)$ ELASTIC POLE RESIDUE

MODULUS $|r|$

VALUE (MeV)	DOCUMENT ID		TECN	COMMENT
5 to 50 (≈ 10) OUR ESTIMATE				
60 ± 30	SOKHOYAN	15A	DPWA	Multichannel
$7 \pm 1 \pm 1$	[1] SVARC	14	L+P	$\pi N \rightarrow \pi N$
6 ± 3	CUTKOSKY	80	IPWA	$\pi N \rightarrow \pi N$
• • • We do not use the following data for averages, fits, limits, etc. • • •				
50 ± 40	ANISOVICH	12A	DPWA	Multichannel
7	BATINIC	10	DPWA	$\pi N \rightarrow N\pi$, $N\eta$
5	HOEHLER	93	SPED	$\pi N \rightarrow \pi N$

[1] Fit to the amplitudes of HOEHLER 79.

PHASE θ

VALUE (°)	DOCUMENT ID		TECN	COMMENT
-120 to 0 (≈ -90) OUR ESTIMATE				
-115 ± 30	SOKHOYAN	15A	DPWA	Multichannel
$-113 \pm 4 \pm 2$	[1] SVARC	14	L+P	$\pi N \rightarrow \pi N$
0 ± 50	CUTKOSKY	80	IPWA	$\pi N \rightarrow \pi N$
• • • We do not use the following data for averages, fits, limits, etc. • • •				
-100 ± 40	ANISOVICH	12A	DPWA	Multichannel
-34	BATINIC	10	DPWA	$\pi N \rightarrow N\pi$, $N\eta$

[1] Fit to the amplitudes of HOEHLER 79.

$N(1700)$ INELASTIC POLE RESIDUE

The "normalized residue" is the residue divided by $\Gamma_{pole}/2$.

Normalized residue in $N\pi \rightarrow N(1700) \rightarrow \Delta\pi$, S-wave

MODULUS	PHASE (°)	DOCUMENT ID		TECN	COMMENT
0.33 ± 0.10	-70 ± 25	SOKHOYAN	15A	DPWA	Multichannel
• • • We do not use the following data for averages, fits, limits, etc. • • •					
0.34 ± 0.21	-60 ± 40	ANISOVICH	12A	DPWA	Multichannel

Normalized residue in $N\pi \rightarrow N(1700) \rightarrow \Delta\pi$, D-wave

MODULUS	PHASE (°)	DOCUMENT ID		TECN	COMMENT
0.10 ± 0.06	75 ± 30	SOKHOYAN	15A	DPWA	Multichannel
• • • We do not use the following data for averages, fits, limits, etc. • • •					
0.08 ± 0.06	90 ± 35	ANISOVICH	12A	DPWA	Multichannel

Normalized residue in $N\pi \to N(1700) \to N\sigma$

MODULUS	PHASE (°)	DOCUMENT ID		TECN	COMMENT
0.13±0.08	−100 ± 35	SOKHOYAN	15A	DPWA	Multichannel

Normalized residue in $N\pi \to N(1700) \to N(1440)\pi$

MODULUS	PHASE (°)	DOCUMENT ID		TECN	COMMENT
0.13±0.05	40 ± 35	SOKHOYAN	15A	DPWA	Multichannel

Normalized residue in $N\pi \to N(1700) \to N(1520)\pi$, P-wave

MODULUS	PHASE (°)	DOCUMENT ID		TECN	COMMENT
0.07±0.03	160 ± 45	SOKHOYAN	15A	DPWA	Multichannel

$N(1700)$ BREIT-WIGNER MASS

VALUE (MeV)	DOCUMENT ID		TECN	COMMENT
1650 to 1800 (≈ 1720) OUR ESTIMATE				
1800±35	SOKHOYAN	15A	DPWA	Multichannel
1665± 3	[1] SHRESTHA	12A	DPWA	Multichannel
1675±25	CUTKOSKY	80	IPWA	$\pi N \to \pi N$
1731±15	HOEHLER	79	IPWA	$\pi N \to \pi N$
• • • We do not use the following data for averages, fits, limits, etc. • • •				
1790±40	ANISOVICH	12A	DPWA	Multichannel
1817±22	BATINIC	10	DPWA	$\pi N \to N\pi, N\eta$
1736±33	VRANA	00	DPWA	Multichannel

[1] Statistical error only.

$N(1700)$ BREIT-WIGNER WIDTH

VALUE (MeV)	DOCUMENT ID		TECN	COMMENT
100 to 300 (≈ 200) OUR ESTIMATE				
400±100	SOKHOYAN	15A	DPWA	Multichannel
56± 8	[1] SHRESTHA	12A	DPWA	Multichannel
90± 40	CUTKOSKY	80	IPWA	$\pi N \to \pi N$
110± 30	HOEHLER	79	IPWA	$\pi N \to \pi N$
• • • We do not use the following data for averages, fits, limits, etc. • • •				
390±140	ANISOVICH	12A	DPWA	Multichannel
134± 37	BATINIC	10	DPWA	$\pi N \to N\pi, N\eta$
175±133	VRANA	00	DPWA	Multichannel

[1] Statistical error only.

$N(1700)$ DECAY MODES

The following branching fractions are our estimates, not fits or averages.

	Mode	Fraction (Γ_i/Γ)
Γ_1	$N\pi$	7–17 %
Γ_2	$N\eta$	seen
Γ_3	$N\omega$	10–34 %
Γ_4	$N\pi\pi$	60–90 %
Γ_5	$\Delta(1232)\pi$	55–85 %
Γ_6	$\Delta(1232)\pi$, S-wave	50–80 %
Γ_7	$\Delta(1232)\pi$, D-wave	4–14 %
Γ_8	$N(1440)\pi$	3–11 %
Γ_9	$N(1520)\pi$	<4 %
Γ_{10}	$N\rho$, S=3/2, S-wave	32–44 %
Γ_{11}	$N\sigma$	2–14 %
Γ_{12}	$p\gamma$	0.01–0.05 %
Γ_{13}	$p\gamma$, helicity=1/2	0.0–0.024 %
Γ_{14}	$p\gamma$, helicity=3/2	0.002–0.026 %
Γ_{15}	$n\gamma$	0.01–0.13 %
Γ_{16}	$n\gamma$, helicity=1/2	0.0–0.09 %
Γ_{17}	$n\gamma$, helicity=3/2	0.01–0.05 %

$N(1700)$ BRANCHING RATIOS

$\Gamma(N\pi)/\Gamma_{\text{total}}$ Γ_1/Γ

VALUE (%)	DOCUMENT ID		TECN	COMMENT
7 to 17 (≈ 12) OUR ESTIMATE				
15 ±6	SOKHOYAN	15A	DPWA	Multichannel
2.8±0.5	[1] SHRESTHA	12A	DPWA	Multichannel
11 ±5	CUTKOSKY	80	IPWA	$\pi N \to \pi N$
8 ±3	HOEHLER	79	IPWA	$\pi N \to \pi N$
• • • We do not use the following data for averages, fits, limits, etc. • • •				
12 ±5	ANISOVICH	12A	DPWA	Multichannel
9 ±6	BATINIC	10	DPWA	$\pi N \to N\pi, N\eta$
4 ±2	VRANA	00	DPWA	Multichannel

[1] Statistical error only.

$\Gamma(N\eta)/\Gamma_{\text{total}}$ Γ_2/Γ

VALUE (%)	DOCUMENT ID		TECN	COMMENT
• • • We do not use the following data for averages, fits, limits, etc. • • •				
14±5	BATINIC	10	DPWA	$\pi N \to N\pi, N\eta$
10±5	THOMA	08	DPWA	Multichannel
0±1	VRANA	00	DPWA	Multichannel

$\Gamma(N\omega)/\Gamma_{\text{total}}$ Γ_3/Γ

VALUE (%)	DOCUMENT ID		TECN	COMMENT
22±12	DENISENKO	16	DPWA	Multichannel

$\Gamma(\Delta(1232)\pi, S\text{-wave})/\Gamma_{\text{total}}$ Γ_6/Γ

VALUE (%)	DOCUMENT ID		TECN	COMMENT
65±15	SOKHOYAN	15A	DPWA	Multichannel
31± 9	[1] SHRESTHA	12A	DPWA	Multichannel
• • • We do not use the following data for averages, fits, limits, etc. • • •				
72±23	ANISOVICH	12A	DPWA	Multichannel
11± 1	VRANA	00	DPWA	Multichannel

[1] Statistical error only.

$\Gamma(\Delta(1232)\pi, D\text{-wave})/\Gamma_{\text{total}}$ Γ_7/Γ

VALUE (%)	DOCUMENT ID		TECN	COMMENT
9± 5	SOKHOYAN	15A	DPWA	Multichannel
3± 2	[1] SHRESTHA	12A	DPWA	Multichannel
• • • We do not use the following data for averages, fits, limits, etc. • • •				
<10	ANISOVICH	12A	DPWA	Multichannel
79±56	VRANA	00	DPWA	Multichannel

[1] Statistical error only.

$\Gamma(N(1440)\pi)/\Gamma_{\text{total}}$ Γ_8/Γ

VALUE (%)	DOCUMENT ID		TECN	COMMENT
7±4	SOKHOYAN	15A	DPWA	Multichannel

$\Gamma(N(1520)\pi)/\Gamma_{\text{total}}$ Γ_9/Γ

VALUE (%)	DOCUMENT ID		TECN	COMMENT
<4	SOKHOYAN	15A	DPWA	Multichannel

$\Gamma(N\rho, S\text{=}3/2, S\text{-wave})/\Gamma_{\text{total}}$ Γ_{10}/Γ

VALUE (%)	DOCUMENT ID		TECN	COMMENT
38±6	[1] SHRESTHA	12A	DPWA	Multichannel
• • • We do not use the following data for averages, fits, limits, etc. • • •				
7±1	VRANA	00	DPWA	Multichannel

[1] Statistical error only.

$\Gamma(N\sigma)/\Gamma_{\text{total}}$ Γ_{11}/Γ

VALUE (%)	DOCUMENT ID		TECN	COMMENT
8± 6	SOKHOYAN	15A	DPWA	Multichannel
24± 6	[1] SHRESTHA	12A	DPWA	Multichannel
• • • We do not use the following data for averages, fits, limits, etc. • • •				
18±12	THOMA	08	DPWA	Multichannel
0± 1	VRANA	00	DPWA	Multichannel

[1] Statistical error only.

$N(1700)$ PHOTON DECAY AMPLITUDES AT THE POLE

$N(1700) \to p\gamma$, helicity-1/2 amplitude $A_{1/2}$

MODULUS ($GeV^{-1/2}$)	PHASE (°)	DOCUMENT ID		TECN	COMMENT
0.047±0.016	75 ± 30	SOKHOYAN	15A	DPWA	Multichannel

$N(1700) \to p\gamma$, helicity-3/2 amplitude $A_{3/2}$

MODULUS ($GeV^{-1/2}$)	PHASE (°)	DOCUMENT ID		TECN	COMMENT
−0.041±0.014	0 ± 20	SOKHOYAN	15A	DPWA	Multichannel

$N(1700)$ BREIT-WIGNER PHOTON DECAY AMPLITUDES

$N(1700) \to p\gamma$, helicity-1/2 amplitude $A_{1/2}$

VALUE ($GeV^{-1/2}$)	DOCUMENT ID		TECN	COMMENT
0.041±0.017	ANISOVICH	12A	DPWA	Multichannel
• • • We do not use the following data for averages, fits, limits, etc. • • •				
0.021±0.005	[1] SHRESTHA	12A	DPWA	Multichannel

[1] Statistical error only.

$N(1700) \to p\gamma$, helicity-3/2 amplitude $A_{3/2}$

VALUE ($GeV^{-1/2}$)	DOCUMENT ID		TECN	COMMENT
−0.037±0.014	SOKHOYAN	15A	DPWA	Multichannel
• • • We do not use the following data for averages, fits, limits, etc. • • •				
−0.034±0.013	ANISOVICH	12A	DPWA	Multichannel
0.050±0.009	[1] SHRESTHA	12A	DPWA	Multichannel

[1] Statistical error only.

$N(1700) \rightarrow n\gamma$, helicity-1/2 amplitude $A_{1/2}$

VALUE ($GeV^{-1/2}$)	DOCUMENT ID		TECN	COMMENT
0.025 ± 0.010	ANISOVICH	13B	DPWA	Multichannel
• • • We do not use the following data for averages, fits, limits, etc. • • •				
-0.049 ± 0.008	[1] SHRESTHA	12A	DPWA	Multichannel

[1] Statistical error only.

$N(1700) \rightarrow n\gamma$, helicity-3/2 amplitude $A_{3/2}$

VALUE ($GeV^{-1/2}$)	DOCUMENT ID		TECN	COMMENT
-0.032 ± 0.018	ANISOVICH	13B	DPWA	Multichannel
• • • We do not use the following data for averages, fits, limits, etc. • • •				
-0.092 ± 0.014	[1] SHRESTHA	12A	DPWA	Multichannel

[1] Statistical error only.

$N(1700)$ REFERENCES

For early references, see Physics Letters **111B** 1 (1982).

DENISENKO	16	PL B755 97	I. Denisenko *et al.*	
SOKHOYAN	15A	EPJ A51 95	V. Sokhoyan *et al.*	(CBELSA/TAPS Collab.)
PDG	14	CP C38 070001	K. Olive *et al.*	(PDG Collab.)
SVARC	14	PR C89 045205	A. Svarc *et al.*	(RBI Zagreb, UNI Tuzla)
ANISOVICH	13B	EPJ A49 67	A.V. Anisovich *et al.*	
ANISOVICH	12A	EPJ A48 15	A.V. Anisovich *et al.*	(BONN, PNPI)
SHRESTHA	12A	PR C86 055203	M. Shrestha, D.M. Manley	(KSU)
BATINIC	10	PR C82 038203	M. Batinic *et al.*	(ZAGR)
THOMA	08	PL B659 87	U. Thoma *et al.*	(CB-ELSA Collab.)
VRANA	00	PRPL 328 181	T.P. Vrana, S.A. Dytman, T.-S.H. Lee	(PITT, ANL)
HOEHLER	93	πN Newsletter 9 1	G. Hohler	(KARL)
CUTKOSKY	80	Toronto Conf. 19	R.E. Cutkosky *et al.*	(CMU, LBL) IJP
Also		PR D20 2839	R.E. Cutkosky *et al.*	(CMU, LBL) IJP
HOEHLER	79	PDAT 12-1	G. Hohler *et al.*	(KARLT) IJP
Also		Toronto Conf. 3	R. Koch	(KARLT) IJP

$N(1710)\ 1/2^+$

$I(J^P) = \frac{1}{2}(\frac{1}{2}^+)$ Status: ****

Older and obsolete values are listed and referenced in the 2014 edition, Chinese Physics **C38** 070001 (2014).

$N(1710)$ POLE POSITION

REAL PART

VALUE (MeV)	DOCUMENT ID		TECN	COMMENT
1680 to 1720 (≈ 1700) OUR ESTIMATE				
1690 ± 15	ANISOVICH	17A	DPWA	Multichannel
1697 ± 23	[1] ANISOVICH	17A	L+P	$\gamma p,\ \pi^- p \rightarrow K\Lambda$
$1770 \pm 5 \pm 2$	[2] SVARC	14	L+P	$\pi N \rightarrow \pi N$
1690 ± 20	CUTKOSKY	80	IPWA	$\pi N \rightarrow \pi N$
• • • We do not use the following data for averages, fits, limits, etc. • • •				
1651	ROENCHEN	15A	DPWA	Multichannel
1690 ± 15	SOKHOYAN	15A	DPWA	Multichannel
1690 ± 15	GUTZ	14	DPWA	Multichannel
1670	SHKLYAR	13	DPWA	Multichannel
1687 ± 17	ANISOVICH	12A	DPWA	Multichannel
1644	SHRESTHA	12A	DPWA	Multichannel
1711 ± 15	[3] BATINIC	10	DPWA	$\pi N \rightarrow N\pi,\ N\eta$
1679	VRANA	00	DPWA	Multichannel
1690	HOEHLER	93	SPED	$\pi N \rightarrow \pi N$
1698	CUTKOSKY	90	IPWA	$\pi N \rightarrow \pi N$

[1] Statistical error only.
[2] Fit to the amplitudes of HOEHLER 79.
[3] BATINIC 10 finds evidence for a second P_{11} state with all parameters except for the phase of the pole residue very similar to the parameters we give here.

$-2\times$IMAGINARY PART

VALUE (MeV)	DOCUMENT ID		TECN	COMMENT
80 to 160 (≈ 120) OUR ESTIMATE				
155 ± 25	ANISOVICH	17A	DPWA	Multichannel
84 ± 34	[1] ANISOVICH	17A	L+P	$\gamma p,\ \pi^- p \rightarrow K\Lambda$
$98 \pm 8 \pm 5$	[2] SVARC	14	L+P	$\pi N \rightarrow \pi N$
80 ± 20	CUTKOSKY	80	IPWA	$\pi N \rightarrow \pi N$
• • • We do not use the following data for averages, fits, limits, etc. • • •				
121	ROENCHEN	15A	DPWA	Multichannel
170 ± 20	SOKHOYAN	15A	DPWA	Multichannel
170 ± 20	GUTZ	14	DPWA	Multichannel
159	SHKLYAR	13	DPWA	Multichannel
200 ± 25	ANISOVICH	12A	DPWA	Multichannel
104	SHRESTHA	12A	DPWA	Multichannel
174 ± 16	[3] BATINIC	10	DPWA	$\pi N \rightarrow N\pi,\ N\eta$
132	VRANA	00	DPWA	Multichannel
200	HOEHLER	93	SPED	$\pi N \rightarrow \pi N$
88	CUTKOSKY	90	IPWA	$\pi N \rightarrow \pi N$

[1] Statistical error only.
[2] Fit to the amplitudes of HOEHLER 79.
[3] BATINIC 10 finds evidence for a second P_{11} state with all parameters except for the phase of the pole residue very similar to the parameters we give here.

$N(1710)$ ELASTIC POLE RESIDUE

MODULUS $|r|$

VALUE (MeV)	DOCUMENT ID		TECN	COMMENT
4 to 10 (≈ 7) OUR ESTIMATE				
6 ± 3	SOKHOYAN	15A	DPWA	Multichannel
$5 \pm 1 \pm 1$	[1] SVARC	14	L+P	$\pi N \rightarrow \pi N$
8 ± 2	CUTKOSKY	80	IPWA	$\pi N \rightarrow \pi N$
• • • We do not use the following data for averages, fits, limits, etc. • • •				
3.2	ROENCHEN	15A	DPWA	Multichannel
6 ± 3	GUTZ	14	DPWA	Multichannel
11	SHKLYAR	13	DPWA	Multichannel
6 ± 4	ANISOVICH	12A	DPWA	Multichannel
24	[2] BATINIC	10	DPWA	$\pi N \rightarrow N\pi,\ N\eta$
15	HOEHLER	93	SPED	$\pi N \rightarrow \pi N$
9	CUTKOSKY	90	IPWA	$\pi N \rightarrow \pi N$

[1] Fit to the amplitudes of HOEHLER 79.
[2] BATINIC 10 finds evidence for a second P_{11} state with all parameters except for the phase of the pole residue very similar to the parameters we give here.

PHASE θ

VALUE (°)	DOCUMENT ID		TECN	COMMENT
120 to 260 (≈ 190) OUR ESTIMATE				
130 ± 35	SOKHOYAN	15A	DPWA	Multichannel
$-104 \pm 7 \pm 3$	[1] SVARC	14	L+P	$\pi N \rightarrow \pi N$
175 ± 35	CUTKOSKY	80	IPWA	$\pi N \rightarrow \pi N$
• • • We do not use the following data for averages, fits, limits, etc. • • •				
55	ROENCHEN	15A	DPWA	Multichannel
120 ± 45	GUTZ	14	DPWA	Multichannel
9	SHKLYAR	13	DPWA	Multichannel
120 ± 70	ANISOVICH	12A	DPWA	Multichannel
20	[2] BATINIC	10	DPWA	$\pi N \rightarrow N\pi,\ N\eta$
-167	CUTKOSKY	90	IPWA	$\pi N \rightarrow \pi N$

[1] Fit to the amplitudes of HOEHLER 79.
[2] BATINIC 10 finds evidence for a second P_{11} state with all parameters except for the phase of the pole residue very similar to the parameters we give here.

$N(1710)$ INELASTIC POLE RESIDUE

The "normalized residue" is the residue divided by $\Gamma_{pole}/2$.

Normalized residue in $N\pi \rightarrow N(1710) \rightarrow N\eta$

MODULUS	PHASE (°)	DOCUMENT ID		TECN	COMMENT
0.12 ± 0.04	0 ± 45	ANISOVICH	12A	DPWA	Multichannel
• • • We do not use the following data for averages, fits, limits, etc. • • •					
0.16	-180	ROENCHEN	15A	DPWA	Multichannel

Normalized residue in $N\pi \rightarrow N(1710) \rightarrow \Lambda K$

MODULUS	PHASE (°)	DOCUMENT ID		TECN	COMMENT
0.16 ± 0.05	-160 ± 25	ANISOVICH	17A	DPWA	Multichannel
$0.12^{+0.24}_{-0.12}$	-119 ± 83	[1] ANISOVICH	17A	L+P	$\gamma p,\ \pi^- p \rightarrow K\Lambda$
• • • We do not use the following data for averages, fits, limits, etc. • • •					
0.12	-32	ROENCHEN	15A	DPWA	Multichannel
0.17 ± 0.06	-110 ± 20	ANISOVICH	12A	DPWA	Multichannel

[1] Statistical error only.

Normalized residue in $N\pi \rightarrow N(1710) \rightarrow \Sigma K$

MODULUS	PHASE (°)	DOCUMENT ID		TECN	COMMENT
• • • We do not use the following data for averages, fits, limits, etc. • • •					
0.004	-43	ROENCHEN	15A	DPWA	Multichannel

Normalized residue in $N\pi \rightarrow N(1710) \rightarrow N(1535)\pi$

MODULUS	PHASE (°)	DOCUMENT ID		TECN	COMMENT
0.10 ± 0.04	140 ± 40	GUTZ	14	DPWA	Multichannel

$N(1710)$ BREIT-WIGNER MASS

VALUE (MeV)	DOCUMENT ID		TECN	COMMENT
1680 to 1740 (≈ 1710) OUR ESTIMATE				
1715 ± 20	SOKHOYAN	15A	DPWA	Multichannel
1737 ± 17	[1] SHKLYAR	13	DPWA	Multichannel
1662 ± 7	[1] SHRESTHA	12A	DPWA	Multichannel
1700 ± 50	CUTKOSKY	80	IPWA	$\pi N \rightarrow \pi N$
1723 ± 9	HOEHLER	79	IPWA	$\pi N \rightarrow \pi N$
• • • We do not use the following data for averages, fits, limits, etc. • • •				
1715 ± 20	GUTZ	14	DPWA	Multichannel
1710 ± 20	ANISOVICH	12A	DPWA	Multichannel
1729 ± 16	[2] BATINIC	10	DPWA	$\pi N \rightarrow N\pi,\ N\eta$
1752 ± 3	PENNER	02C	DPWA	Multichannel
1699 ± 65	VRANA	00	DPWA	Multichannel

[1] Statistical error only.
[2] BATINIC 10 finds evidence for a second P_{11} state with all parameters except for the phase of the pole residue very similar to the parameters we give here.

$N(1710)$ BREIT-WIGNER WIDTH

VALUE (MeV)	DOCUMENT ID		TECN	COMMENT
80 to 200 (≈ 140) OUR ESTIMATE				
175 ± 15	SOKHOYAN	15A	DPWA	Multichannel
368 ± 120	[1] SHKLYAR	13	DPWA	Multichannel
116 ± 17	[1] SHRESTHA	12A	DPWA	Multichannel
93 ± 30	CUTKOSKY	90	IPWA	$\pi N \to \pi N$
90 ± 30	CUTKOSKY	80	IPWA	$\pi N \to \pi N$
120 ± 15	HOEHLER	79	IPWA	$\pi N \to \pi N$
• • • We do not use the following data for averages, fits, limits, etc. • • •				
175 ± 15	GUTZ	14	DPWA	Multichannel
200 ± 18	ANISOVICH	12A	DPWA	Multichannel
180 ± 17	[2] BATINIC	10	DPWA	$\pi N \to N\pi$, $N\eta$
386 ± 59	PENNER	02C	DPWA	Multichannel
143 ± 100	VRANA	00	DPWA	Multichannel

[1] Statistical error only.
[2] BATINIC 10 finds evidence for a second P_{11} state with all parameters except for the phase of the pole residue very similar to the parameters we give here.

$N(1710)$ DECAY MODES

The following branching fractions are our estimates, not fits or averages.

	Mode	Fraction (Γ_i/Γ)
Γ_1	$N\pi$	5–20 %
Γ_2	$N\eta$	10–50 %
Γ_3	$N\omega$	1–5 %
Γ_4	ΛK	5–25 %
Γ_5	ΣK	seen
Γ_6	$N\pi\pi$	seen
Γ_7	$\Delta(1232)\pi$	
Γ_8	$\Delta(1232)\pi$, P-wave	3–9 %
Γ_9	$N(1535)\pi$	9–21 %
Γ_{10}	$N\rho$	
Γ_{11}	$N\rho$, S=1/2, P-wave	11–23 %
Γ_{12}	$p\gamma$, helicity=1/2	0.002–0.08 %
Γ_{13}	$n\gamma$, helicity=1/2	0.0–0.02%

$N(1710)$ BRANCHING RATIOS

$\Gamma(N\pi)/\Gamma_{\text{total}}$ Γ_1/Γ

VALUE (%)	DOCUMENT ID		TECN	COMMENT
5 to 20 (≈ 10) OUR ESTIMATE				
5 ± 3	SOKHOYAN	15A	DPWA	Multichannel
2 ± 2	[1] SHKLYAR	13	PWA	Multichannel
15 ± 4	[1] SHRESTHA	12A	DPWA	Multichannel
20 ± 4	CUTKOSKY	80	IPWA	$\pi N \to \pi N$
12 ± 4	HOEHLER	79	IPWA	$\pi N \to \pi N$
• • • We do not use the following data for averages, fits, limits, etc. • • •				
5 ± 3	GUTZ	14	DPWA	Multichannel
5 ± 4	ANISOVICH	12A	DPWA	Multichannel
22 ± 24	[2] BATINIC	10	DPWA	$\pi N \to N\pi$, $N\eta$
14 ± 8	PENNER	02C	DPWA	Multichannel
27 ± 13	VRANA	00	DPWA	Multichannel

[1] Statistical error only.
[2] BATINIC 10 finds evidence for a second P_{11} state with all parameters except for the phase of the pole residue very similar to the parameters we give here.

$\Gamma(N\eta)/\Gamma_{\text{total}}$ Γ_2/Γ

VALUE (%)	DOCUMENT ID		TECN	COMMENT
10 to 50 (≈ 30) OUR ESTIMATE				
45 ± 4	[1] SHKLYAR	13	DPWA	Multichannel
17 ± 10	ANISOVICH	12A	DPWA	Multichannel
11 ± 7	[1] SHRESTHA	12A	DPWA	Multichannel
• • • We do not use the following data for averages, fits, limits, etc. • • •				
6 ± 8	[2] BATINIC	10	DPWA	$\pi N \to N\pi$, $N\eta$
36 ± 11	PENNER	02C	DPWA	Multichannel
6 ± 1	VRANA	00	DPWA	Multichannel

[1] Statistical error only.
[2] BATINIC 10 finds evidence for a second P_{11} state with all parameters except for the phase of the pole residue very similar to the parameters we give here.

$\Gamma(N\omega)/\Gamma_{\text{total}}$ Γ_3/Γ

VALUE (%)	DOCUMENT ID		TECN	COMMENT
1 to 5 (≈ 3) OUR ESTIMATE				
2 ± 2	DENISENKO	16	DPWA	Multichannel
3 ± 2	[1] SHKLYAR	13	DPWA	Multichannel
• • • We do not use the following data for averages, fits, limits, etc. • • •				
13 ± 2	PENNER	02C	DPWA	Multichannel

[1] Statistical error only

$\Gamma(\Lambda K)/\Gamma_{\text{total}}$ Γ_4/Γ

VALUE (%)	DOCUMENT ID		TECN	COMMENT
5 to 25 (≈ 15) OUR ESTIMATE				
23 ± 7	ANISOVICH	12A	DPWA	Multichannel
8 ± 4	[1] SHRESTHA	12A	DPWA	Multichannel
5 ± 3	SHKLYAR	05	DPWA	Multichannel
• • • We do not use the following data for averages, fits, limits, etc. • • •				
5 ± 2	PENNER	02C	DPWA	Multichannel
10 ± 10	VRANA	00	DPWA	Multichannel

[1] Statistical error only.

$\Gamma(\Sigma K)/\Gamma_{\text{total}}$ Γ_5/Γ

VALUE (%)	DOCUMENT ID		TECN	COMMENT
• • • We do not use the following data for averages, fits, limits, etc. • • •				
7 ± 7	PENNER	02C	DPWA	Multichannel

$\Gamma(\Delta(1232)\pi, P\text{-wave})/\Gamma_{\text{total}}$ Γ_8/Γ

VALUE (%)	DOCUMENT ID		TECN	COMMENT
6 ± 3	[1] SHRESTHA	12A	DPWA	Multichannel
• • • We do not use the following data for averages, fits, limits, etc. • • •				
39 ± 8	VRANA	00	DPWA	Multichannel

[1] Statistical error only.

$\Gamma(N(1535)\pi)/\Gamma_{\text{total}}$ Γ_9/Γ

VALUE (%)	DOCUMENT ID		TECN	COMMENT
15 ± 6	GUTZ	14	DPWA	Multichannel

$\Gamma(N\rho, S{=}1/2, P\text{-wave})/\Gamma_{\text{total}}$ Γ_{11}/Γ

VALUE (%)	DOCUMENT ID		TECN	COMMENT
17 ± 6	[1] SHRESTHA	12A	DPWA	Multichannel
• • • We do not use the following data for averages, fits, limits, etc. • • •				
17 ± 1	VRANA	00	DPWA	Multichannel

[1] Statistical error only.

$N(1710)$ PHOTON DECAY AMPLITUDES AT THE POLE

$N(1710) \to p\gamma$, helicity-1/2 amplitude $A_{1/2}$

MODULUS ($\text{GeV}^{-1/2}$)	PHASE (°)	DOCUMENT ID		TECN	COMMENT
$0.028^{+0.009}_{-0.002}$	103^{+20}_{-6}	ROENCHEN	14	DPWA	
• • • We do not use the following data for averages, fits, limits, etc. • • •					
0.020	−83	ROENCHEN	15A	DPWA	Multichannel

$N(1710)$ BREIT-WIGNER PHOTON DECAY AMPLITUDES

$N(1710) \to p\gamma$, helicity-1/2 amplitude $A_{1/2}$

VALUE ($\text{GeV}^{-1/2}$)	DOCUMENT ID		TECN	COMMENT
0.050 ± 0.010	SOKHOYAN	15A	DPWA	Multichannel
−0.050 ± 0.001	[1] SHKLYAR	13	DPWA	Multichannel
• • • We do not use the following data for averages, fits, limits, etc. • • •				
0.05 ± 0.01	GUTZ	14	DPWA	Multichannel
0.052 ± 0.015	ANISOVICH	12A	DPWA	Multichannel
−0.008 ± 0.003	[2] SHRESTHA	12A	DPWA	Multichannel
0.044	PENNER	02D	DPWA	Multichannel

[1] Statistical error only
[2] Statistical error only.

$N(1710) \to n\gamma$, helicity-1/2 amplitude $A_{1/2}$

VALUE ($\text{GeV}^{-1/2}$)	DOCUMENT ID		TECN	COMMENT
−0.040 ± 0.020	ANISOVICH	13B	DPWA	Multichannel
• • • We do not use the following data for averages, fits, limits, etc. • • •				
0.017 ± 0.003	[1] SHRESTHA	12A	DPWA	Multichannel
−0.024	PENNER	02D	DPWA	Multichannel

[1] Statistical error only.

$N(1710)$ REFERENCES

For early references, see Physics Letters **111B** 1 (1982).

ANISOVICH	17A	PRL 119 062004	A.V. Anisovich *et al.*	
DENISENKO	16	PL B755 97	I. Denisenko *et al.*	
ROENCHEN	15A	EPJ A51 70	D. Roenchen *et al.*	
SOKHOYAN	15A	EPJ A51 95	V. Sokhoyan *et al.*	(CBELSA/TAPS Collab.)
GUTZ	14	EPJ A50 74	E. Gutz *et al.*	(CBELSA/TAPS Collab.)
PDG	14	CP C38 070001	K. Olive *et al.*	(PDG Collab.)
ROENCHEN	14	EPJ A50 101	D. Roenchen *et al.*	
Also		EPJ A51 63 (errat.)	D. Roenchen *et al.*	
SVARC	14	PR C89 045205	A. Svarc *et al.*	(RBI Zagreb, UNI Tuzla)
ANISOVICH	13B	EPJ A49 67	A.V. Anisovich *et al.*	
SHKLYAR	13	PR C87 015201	V. Shklyar, H. Lenske, U. Mosel	(GIES)
ANISOVICH	12A	EPJ A48 15	A.V. Anisovich *et al.*	(BONN, PNPI)

SHRESTHA	12A	PR C86 055203	M. Shrestha, D.M. Manley	(KSU)
BATINIC	10	PR C82 038203	M. Batinic *et al.*	(ZAGR)
SHKLYAR	05	PR C72 015210	V. Shklyar, H. Lenske, U. Mosel	(GIES)
PENNER	02C	PR C66 055211	G. Penner, U. Mosel	(GIES)
PENNER	02D	PR C66 055212	G. Penner, U. Mosel	(GIES)
VRANA	00	PRPL 328 181	T.P. Vrana, S.A. Dytman, T.-S.H. Lee	(PITT, ANL)
HOEHLER	93	πN Newsletter 9 1	G. Hohler	(KARL)
CUTKOSKY	90	PR D42 235	R.E. Cutkosky, S. Wang	(CMU)
CUTKOSKY	80	Toronto Conf. 19	R.E. Cutkosky *et al.*	(CMU, LBL) IJP
Also		PR D20 2839	R.E. Cutkosky *et al.*	(CMU, LBL) IJP
HOEHLER	79	PDAT 12-1	G. Hohler *et al.*	(KARL) IJP
Also		Toronto Conf. 3	R. Koch	(KARLT) IJP

$N(1720)\ 3/2^+$

$I(J^P) = \frac{1}{2}(\frac{3}{2}^+)$ Status: ****

Older and obsolete values are listed and referenced in the 2014 edition, Chinese Physics **C38** 070001 (2014).

$N(1720)$ POLE POSITION

REAL PART

VALUE (MeV)	DOCUMENT ID		TECN	COMMENT
1660 to 1690 (≈ 1675) OUR ESTIMATE				
1670±25	SOKHOYAN	15A	DPWA	Multichannel
1677± 4±1	[1] SVARC	14	L+P	$\pi N \to \pi N$
1680±30	CUTKOSKY	80	IPWA	$\pi N \to \pi N$
• • • We do not use the following data for averages, fits, limits, etc. • • •				
1710	ROENCHEN	15A	DPWA	Multichannel
1670	SHKLYAR	13	DPWA	Multichannel
1660±30	ANISOVICH	12A	DPWA	Multichannel
1687	SHRESTHA	12A	DPWA	Multichannel
1691±23	BATINIC	10	DPWA	$\pi N \to N\pi$, $N\eta$
1666	ARNDT	06	DPWA	$\pi N \to \pi N$, ηN
1692	VRANA	00	DPWA	Multichannel
1686	HOEHLER	93	SPED	$\pi N \to \pi N$

[1] Fit to the amplitudes of HOEHLER 79.

−2×IMAGINARY PART

VALUE (MeV)	DOCUMENT ID		TECN	COMMENT
150 to 400 (≈ 250) OUR ESTIMATE				
430±100	SOKHOYAN	15A	DPWA	Multichannel
184± 8±1	[1] SVARC	14	L+P	$\pi N \to \pi N$
120± 40	CUTKOSKY	80	IPWA	$\pi N \to \pi N$
• • • We do not use the following data for averages, fits, limits, etc. • • •				
219	ROENCHEN	15A	DPWA	Multichannel
118	SHKLYAR	13	DPWA	Multichannel
450±100	ANISOVICH	12A	DPWA	Multichannel
175	SHRESTHA	12A	DPWA	Multichannel
233± 23	BATINIC	10	DPWA	$\pi N \to N\pi$, $N\eta$
355	ARNDT	06	DPWA	$\pi N \to \pi N$, ηN
94	VRANA	00	DPWA	Multichannel
187	HOEHLER	93	SPED	$\pi N \to \pi N$

[1] Fit to the amplitudes of HOEHLER 79.

$N(1720)$ ELASTIC POLE RESIDUE

MODULUS $|r|$

VALUE (MeV)	DOCUMENT ID		TECN	COMMENT
10 to 25 (≈ 15) OUR ESTIMATE				
26 ±10	SOKHOYAN	15A	DPWA	Multichannel
13 ± 1	[1] SVARC	14	L+P	$\pi N \to \pi N$
8 ± 2	CUTKOSKY	80	IPWA	$\pi N \to \pi N$
• • • We do not use the following data for averages, fits, limits, etc. • • •				
4.2	ROENCHEN	15A	DPWA	Multichannel
12	SHKLYAR	13	DPWA	Multichannel
22 ± 8	ANISOVICH	12A	DPWA	Multichannel
20	BATINIC	10	DPWA	$\pi N \to N\pi$, $N\eta$
25	ARNDT	06	DPWA	$\pi N \to \pi N$, ηN
15	HOEHLER	93	SPED	$\pi N \to \pi N$

[1] Fit to the amplitudes of HOEHLER 79.

PHASE θ

VALUE (°)	DOCUMENT ID		TECN	COMMENT
−160 to −100 (≈ −130) OUR ESTIMATE				
−100±25	SOKHOYAN	15A	DPWA	Multichannel
−115± 3±2	[1] SVARC	14	L+P	$\pi N \to \pi N$
−160±30	CUTKOSKY	80	IPWA	$\pi N \to \pi N$
• • • We do not use the following data for averages, fits, limits, etc. • • •				
− 47	ROENCHEN	15A	DPWA	Multichannel
− 45	SHKLYAR	13	DPWA	Multichannel
−115±30	ANISOVICH	12A	DPWA	Multichannel
−109	BATINIC	10	DPWA	$\pi N \to N\pi$, $N\eta$
− 94	ARNDT	06	DPWA	$\pi N \to \pi N$, ηN

[1] Fit to the amplitudes of HOEHLER 79.

$N(1720)$ INELASTIC POLE RESIDUE

The "normalized residue" is the residue divided by $\Gamma_{pole}/2$.

Normalized residue in $N\pi \to N(1720) \to N\eta$

MODULUS	PHASE (°)	DOCUMENT ID		TECN	COMMENT
0.03 ±0.02		ANISOVICH	12A	DPWA	Multichannel
• • • We do not use the following data for averages, fits, limits, etc. • • •					
0.007	106	ROENCHEN	15A	DPWA	Multichannel

Normalized residue in $N\pi \to N(1720) \to \Lambda K$

MODULUS	PHASE (°)	DOCUMENT ID		TECN	COMMENT
0.06 ±0.04	−150 ± 45	ANISOVICH	12A	DPWA	Multichannel
• • • We do not use the following data for averages, fits, limits, etc. • • •					
0.011	−70	ROENCHEN	15A	DPWA	Multichannel

Normalized residue in $N\pi \to N(1720) \to \Sigma K$

MODULUS	PHASE (°)	DOCUMENT ID		TECN	COMMENT
• • • We do not use the following data for averages, fits, limits, etc. • • •					
0.002	79	ROENCHEN	15A	DPWA	Multichannel

Normalized residue in $N\pi \to N(1720) \to \Delta\pi$, P-wave

MODULUS	PHASE (°)	DOCUMENT ID		TECN	COMMENT
0.28±0.09	95 ± 30	SOKHOYAN	15A	DPWA	Multichannel
• • • We do not use the following data for averages, fits, limits, etc. • • •					
0.29±0.08	80 ± 40	ANISOVICH	12A	DPWA	Multichannel

Normalized residue in $N\pi \to N(1720) \to \Delta\pi$, F-wave

MODULUS	PHASE (°)	DOCUMENT ID		TECN	COMMENT
0.07±0.05		SOKHOYAN	15A	DPWA	Multichannel
• • • We do not use the following data for averages, fits, limits, etc. • • •					
0.03±0.03		ANISOVICH	12A	DPWA	Multichannel

Normalized residue in $N\pi \to N(1720) \to N\sigma$

MODULUS	PHASE (°)	DOCUMENT ID		TECN	COMMENT
0.08±0.04	−110 ± 35	SOKHOYAN	15A	DPWA	Multichannel

Normalized residue in $N\pi \to N(1720) \to N(1520)\pi$, S-wave

MODULUS	PHASE (°)	DOCUMENT ID		TECN	COMMENT
0.05±0.04	undefined	SOKHOYAN	15A	DPWA	Multichannel

$N(1720)$ BREIT-WIGNER MASS

VALUE (MeV)	DOCUMENT ID		TECN	COMMENT
1680 to 1750 (≈ 1720) OUR ESTIMATE				
1690 ± 30	SOKHOYAN	15A	DPWA	Multichannel
1700 ± 10	[1] SHKLYAR	13	DPWA	Multichannel
1720 ± 5	[1] SHRESTHA	12A	DPWA	Multichannel
1763.8± 4.6	ARNDT	06	DPWA	$\pi N \to \pi N$, ηN
1700 ± 50	CUTKOSKY	80	IPWA	$\pi N \to \pi N$
1710 ± 20	HOEHLER	79	IPWA	$\pi N \to \pi N$
• • • We do not use the following data for averages, fits, limits, etc. • • •				
1690 $^{+\ 70}_{-\ 35}$	ANISOVICH	12A	DPWA	Multichannel
1720 ± 18	BATINIC	10	DPWA	$\pi N \to N\pi$, $N\eta$
1705 ± 10	PENNER	02C	DPWA	Multichannel
1716 ±112	VRANA	00	DPWA	Multichannel

[1] Statistical error only.

$N(1720)$ BREIT-WIGNER WIDTH

VALUE (MeV)	DOCUMENT ID		TECN	COMMENT
150 to 400 (≈ 250) OUR ESTIMATE				
420± 80	SOKHOYAN	15A	DPWA	Multichannel
152± 2	[1] SHKLYAR	13	DPWA	Multichannel
200± 20	[1] SHRESTHA	12A	DPWA	Multichannel
210± 22	ARNDT	06	DPWA	$\pi N \to \pi N$, ηN
125± 70	CUTKOSKY	80	IPWA	$\pi N \to \pi N$
190± 30	HOEHLER	79	IPWA	$\pi N \to \pi N$
• • • We do not use the following data for averages, fits, limits, etc. • • •				
420±100	ANISOVICH	12A	DPWA	Multichannel
244± 28	BATINIC	10	DPWA	$\pi N \to N\pi$, $N\eta$
237± 73	PENNER	02C	DPWA	Multichannel
121± 39	VRANA	00	DPWA	Multichannel

[1] Statistical error only.

$N(1720)$ DECAY MODES

The following branching fractions are our estimates, not fits or averages.

	Mode	Fraction (Γ_i/Γ)
Γ_1	$N\pi$	8–14 %
Γ_2	$N\eta$	1–5 %
Γ_3	$N\omega$	12–40 %
Γ_4	ΛK	4–5 %
Γ_5	$N\pi\pi$	50–90 %
Γ_6	$\Delta(1232)\pi$	47–89 %
Γ_7	$\Delta(1232)\pi$, P-wave	47–77 %
Γ_8	$\Delta(1232)\pi$, F-wave	<12 %
Γ_9	$N\rho$	
Γ_{10}	$N\rho$, S=1/2, P-wave	1–2 %
Γ_{11}	$N\sigma$	2–14 %
Γ_{12}	$N(1440)\pi$	<2 %
Γ_{13}	$N(1520)\pi$, S-wave	1–5 %
Γ_{14}	$p\gamma$	0.05–0.25 %
Γ_{15}	$p\gamma$, helicity=1/2	0.05–0.15 %
Γ_{16}	$p\gamma$, helicity=3/2	0.002–0.16 %
Γ_{17}	$n\gamma$	0.0–0.016 %
Γ_{18}	$n\gamma$, helicity=1/2	0.0–0.01 %
Γ_{19}	$n\gamma$, helicity=3/2	0.0–0.015 %

$N(1720)$ BRANCHING RATIOS

$\Gamma(N\pi)/\Gamma_{total}$ Γ_1/Γ

VALUE (%)	DOCUMENT ID		TECN	COMMENT
8 to 14 (≈ 11) OUR ESTIMATE				
11 ±4	SOKHOYAN	15A	DPWA	Multichannel
17 ±2	[1] SHKLYAR	13	DPWA	Multichannel
13.6±0.6	[1] SHRESTHA	12A	DPWA	Multichannel
9.4±0.5	ARNDT	06	DPWA	$\pi N \to \pi N, \eta N$
10 ±4	CUTKOSKY	80	IPWA	$\pi N \to \pi N$
14 ±3	HOEHLER	79	IPWA	$\pi N \to \pi N$
• • • We do not use the following data for averages, fits, limits, etc. • • •				
10 ±5	ANISOVICH	12A	DPWA	Multichannel
18 ±3	BATINIC	10	DPWA	$\pi N \to N\pi, N\eta$
17 ±2	PENNER	02C	DPWA	Multichannel
5 ±5	VRANA	00	DPWA	Multichannel

[1] Statistical error only.

$\Gamma(N\eta)/\Gamma_{total}$ Γ_2/Γ

VALUE (%)	DOCUMENT ID		TECN	COMMENT
1 to 5 (≈ 3) OUR ESTIMATE				
< 1	SHKLYAR	13	DPWA	Multichannel
3 ±2	ANISOVICH	12A	DPWA	Multichannel
< 1	[1] SHRESTHA	12A	DPWA	Multichannel
• • • We do not use the following data for averages, fits, limits, etc. • • •				
0 ±1	BATINIC	10	DPWA	$\pi N \to N\pi, N\eta$
10 ±7	THOMA	08	DPWA	Multichannel
0.2±0.2	PENNER	02C	DPWA	Multichannel
4 ±1	VRANA	00	DPWA	Multichannel

[1] Statistical error only.

$\Gamma(N\omega)/\Gamma_{total}$ Γ_3/Γ

VALUE (%)	DOCUMENT ID		TECN	COMMENT
26±14	DENISENKO	16	DPWA	Multichannel

$\Gamma(\Lambda K)/\Gamma_{total}$ Γ_4/Γ

VALUE (%)	DOCUMENT ID		TECN	COMMENT
2.8±0.4	[1] SHRESTHA	12A	DPWA	Multichannel
4.3±0.4	SHKLYAR	05	DPWA	Multichannel
• • • We do not use the following data for averages, fits, limits, etc. • • •				
12 ±9	THOMA	08	DPWA	Multichannel
9 ±3	PENNER	02C	DPWA	Multichannel

[1] Statistical error only.

$\Gamma(\Delta(1232)\pi, P\text{-wave})/\Gamma_{total}$ Γ_7/Γ

VALUE (%)	DOCUMENT ID		TECN	COMMENT
62±15	SOKHOYAN	15A	DPWA	Multichannel
• • • We do not use the following data for averages, fits, limits, etc. • • •				
75±15	ANISOVICH	12A	DPWA	Multichannel

$\Gamma(\Delta(1232)\pi, F\text{-wave})/\Gamma_{total}$ Γ_8/Γ

VALUE (%)	DOCUMENT ID		TECN	COMMENT
6±6	SOKHOYAN	15A	DPWA	Multichannel

$\Gamma(N\rho, S{=}1/2, P\text{-wave})/\Gamma_{total}$ Γ_{10}/Γ

VALUE (%)	DOCUMENT ID		TECN	COMMENT
1.4±0.5	[1] SHRESTHA	12A	DPWA	Multichannel
• • • We do not use the following data for averages, fits, limits, etc. • • •				
91 ±1	VRANA	00	DPWA	Multichannel

[1] Statistical error only.

$\Gamma(N\sigma)/\Gamma_{total}$ Γ_{11}/Γ

VALUE (%)	DOCUMENT ID		TECN	COMMENT
8±6	SOKHOYAN	15A	DPWA	Multichannel

$\Gamma(N(1440)\pi)/\Gamma_{total}$ Γ_{12}/Γ

VALUE (%)	DOCUMENT ID		TECN	COMMENT
<2	SOKHOYAN	15A	DPWA	Multichannel

$\Gamma(N(1520)\pi, S\text{-wave})/\Gamma_{total}$ Γ_{13}/Γ

VALUE (%)	DOCUMENT ID		TECN	COMMENT
3±2	SOKHOYAN	15A	DPWA	Multichannel

$N(1720)$ PHOTON DECAY AMPLITUDES AT THE POLE

$N(1720) \to p\gamma$, helicity-1/2 amplitude $A_{1/2}$

MODULUS ($GeV^{-1/2}$)	PHASE (°)	DOCUMENT ID		TECN	COMMENT
0.115±0.045	0 ± 35	SOKHOYAN	15A	DPWA	Multichannel
$0.051^{+0.005}_{-0.004}$	57^{+9}_{-4}	ROENCHEN	14	DPWA	
• • • We do not use the following data for averages, fits, limits, etc. • • •					
0.039	5.3	ROENCHEN	15A	DPWA	Multichannel

$N(1720) \to p\gamma$, helicity-3/2 amplitude $A_{3/2}$

MODULUS ($GeV^{-1/2}$)	PHASE (°)	DOCUMENT ID		TECN	COMMENT
0.140±0.040	65 ± 35	SOKHOYAN	15A	DPWA	Multichannel
$0.014^{+0.009}_{-0.003}$	102^{+29}_{-59}	ROENCHEN	14	DPWA	
• • • We do not use the following data for averages, fits, limits, etc. • • •					
0.032	66	ROENCHEN	15A	DPWA	Multichannel

$N(1720)$ BREIT-WIGNER PHOTON DECAY AMPLITUDES

$N(1720) \to p\gamma$, helicity-1/2 amplitude $A_{1/2}$

VALUE ($GeV^{-1/2}$)	DOCUMENT ID		TECN	COMMENT
0.080 to 0.120 (≈ 0.100) OUR ESTIMATE				
0.115±0.045	SOKHOYAN	15A	DPWA	Multichannel
−0.065±0.002	[1] SHKLYAR	13	DPWA	Multichannel
0.095±0.002	WORKMAN	12A	DPWA	$\gamma N \to N\pi$
• • • We do not use the following data for averages, fits, limits, etc. • • •				
0.110±0.045	ANISOVICH	12A	DPWA	Multichannel
0.057±0.003	[1] SHRESTHA	12A	DPWA	Multichannel
0.073	DRECHSEL	07	DPWA	$\gamma N \to \pi N$
0.097±0.003	DUGGER	07	DPWA	$\gamma N \to \pi N$
−0.053	PENNER	02D	DPWA	Multichannel

[1] Statistical error only.

$N(1720) \to p\gamma$, helicity-3/2 amplitude $A_{3/2}$

VALUE ($GeV^{-1/2}$)	DOCUMENT ID		TECN	COMMENT
0.135±0.040	SOKHOYAN	15A	DPWA	Multichannel
0.035±0.002	[1] SHKLYAR	13	DPWA	Multichannel
−0.048±0.002	WORKMAN	12A	DPWA	$\gamma N \to N\pi$
• • • We do not use the following data for averages, fits, limits, etc. • • •				
0.150±0.030	ANISOVICH	12A	DPWA	Multichannel
−0.019±0.002	[1] SHRESTHA	12A	DPWA	Multichannel
−0.011	DRECHSEL	07	DPWA	$\gamma N \to \pi N$
−0.039±0.003	DUGGER	07	DPWA	$\gamma N \to \pi N$
0.027	PENNER	02D	DPWA	Multichannel

[1] Statistical error only.

$N(1720) \to n\gamma$, helicity-1/2 amplitude $A_{1/2}$

VALUE ($GeV^{-1/2}$)	DOCUMENT ID		TECN	COMMENT
−0.080±0.050	ANISOVICH	13B	DPWA	Multichannel
• • • We do not use the following data for averages, fits, limits, etc. • • •				
−0.002±0.001	[1] SHRESTHA	12A	DPWA	Multichannel
−0.003	DRECHSEL	07	DPWA	$\gamma N \to \pi N$
−0.004	PENNER	02D	DPWA	Multichannel

[1] Statistical error only.

$N(1720) \to n\gamma$, helicity-3/2 amplitude $A_{3/2}$

VALUE ($GeV^{-1/2}$)	DOCUMENT ID		TECN	COMMENT
−0.140±0.065	ANISOVICH	13B	DPWA	Multichannel

• • • We do not use the following data for averages, fits, limits, etc. • • •

−0.001 ± 0.002	[1]	SHRESTHA	12A	DPWA	Multichannel
−0.031		DRECHSEL	07	DPWA	$\gamma N \to \pi N$
0.003		PENNER	02D	DPWA	Multichannel

[1] Statistical error only.

$N(1720)$ REFERENCES

For early references, see Physics Letters **111B** 1 (1982).

DENISENKO	16	PL B755 97	I. Denisenko *et al.*	
ROENCHEN	15A	EPJ A51 70	D. Roenchen *et al.*	
SOKHOYAN	15A	EPJ A51 95	V. Sokhoyan *et al.*	(CBELSA/TAPS Collab.)
PDG	14	CP C38 070001	K. Olive *et al.*	(PDG Collab.)
ROENCHEN	14	EPJ A50 101	D. Roenchen *et al.*	
Also		EPJ A51 63 (errat.)	D. Roenchen *et al.*	
SVARC	14	PR C89 045205	A. Svarc *et al.*	(RBI Zagreb, UNI Tuzla)
ANISOVICH	13B	EPJ A49 67	A.V. Anisovich *et al.*	
SHKLYAR	13	PR C87 015201	V. Shklyar, H. Lenske, U. Mosel	(GIES)
ANISOVICH	12A	EPJ A48 15	A.V. Anisovich *et al.*	(BONN, PNPI)
SHRESTHA	12A	PR C86 055203	M. Shrestha, D.M. Manley	(KSU)
WORKMAN	12A	PR C86 015202	R. Workman *et al.*	(GWU)
BATINIC	10	PR C82 038203	M. Batinic *et al.*	(ZAGR)
THOMA	08	PL B659 87	U. Thoma *et al.*	(CB-ELSA Collab.)
DRECHSEL	07	EPJ A34 69	D. Drechsel, S.S. Kamalov, L. Tiator	(MAINZ, JINR)
DUGGER	07	PR C76 025211	M. Dugger *et al.*	(JLab CLAS Collab.)
ARNDT	06	PR C74 045205	R.A. Arndt *et al.*	(GWU)
SHKLYAR	05	PR C72 015210	V. Shklyar, H. Lenske, U. Mosel	(GIES)
PENNER	02C	PR C66 055211	G. Penner, U. Mosel	(GIES)
PENNER	02D	PR C66 055212	G. Penner, U. Mosel	(GIES)
VRANA	00	PRPL 328 181	T.P. Vrana, S.A. Dytman, T.-S.H. Lee	(PITT, ANL)
HOEHLER	93	πN Newsletter 9 1	G. Hohler	(KARL)
CUTKOSKY	80	Toronto Conf. 19	R.E. Cutkosky *et al.*	(CMU, LBL) IJP
Also		PR D20 2839	R.E. Cutkosky *et al.*	(CMU, LBL) IJP
HOEHLER	79	PDAT 12-1	G. Hohler *et al.*	(KARLT) IJP
Also		Toronto Conf. 3	R. Koch	(KARLT) IJP

$N(1860)$ $5/2^+$

$I(J^P) = \frac{1}{2}(\frac{5}{2}^+)$ Status: **

OMITTED FROM SUMMARY TABLE

Before the 2012 *Review*, all the evidence for a $J^P = 5/2^+$ state with a mass above 1800 MeV was filed under a two-star $N(2000)$. There is now some evidence from ANISOVICH 12A for two $5/2^+$ states in this region, so we have split the older data (according to mass) between two two-star $5/2^+$ states, an $N(1860)$ and an $N(2000)$.

$N(1860)$ POLE POSITION

REAL PART

VALUE (MeV)		DOCUMENT ID		TECN	COMMENT
1834 ± 19 ± 6	[1]	SVARC	14	L+P	$\pi N \to \pi N$
1830^{+120}_{-60}		ANISOVICH	12A	DPWA	Multichannel
• • • We do not use the following data for averages, fits, limits, etc. • • •					
1863		SHRESTHA	12A	DPWA	Multichannel
1807		ARNDT	06	DPWA	$\pi N \to \pi N, \eta N$

[1] Fit to the amplitudes of HOEHLER 79.

−2×IMAGINARY PART

VALUE (MeV)		DOCUMENT ID		TECN	COMMENT
122 ± 34 ± 7	[2]	SVARC	14	L+P	$\pi N \to \pi N$
250^{+150}_{-50}		ANISOVICH	12A	DPWA	Multichannel
• • • We do not use the following data for averages, fits, limits, etc. • • •					
189		SHRESTHA	12A	DPWA	Multichannel
109		ARNDT	06	DPWA	$\pi N \to \pi N, \eta N$

[2] Fit to the amplitudes of HOEHLER 79.

$N(1860)$ ELASTIC POLE RESIDUE

MODULUS $|r|$

VALUE (MeV)		DOCUMENT ID		TECN	COMMENT
4 ± 1 ± 1	[3]	SVARC	14	L+P	$\pi N \to \pi N$
50 ± 20		ANISOVICH	12A	DPWA	Multichannel
• • • We do not use the following data for averages, fits, limits, etc. • • •					
60		ARNDT	06	DPWA	$\pi N \to \pi N, \eta N$

[3] Fit to the amplitudes of HOEHLER 79.

PHASE θ

VALUE (°)		DOCUMENT ID		TECN	COMMENT
−39 ± 18 ± 9	[4]	SVARC	14	L+P	$\pi N \to \pi N$
−80 ± 40		ANISOVICH	12A	DPWA	Multichannel
• • • We do not use the following data for averages, fits, limits, etc. • • •					
−67		ARNDT	06	DPWA	$\pi N \to \pi N, \eta N$

[4] Fit to the amplitudes of HOEHLER 79.

$N(1860)$ BREIT-WIGNER MASS

VALUE (MeV)		DOCUMENT ID		TECN	COMMENT
$1860\ ^{+120}_{-60}$		ANISOVICH	12A	DPWA	Multichannel
1900 ± 7	[5]	SHRESTHA	12A	DPWA	Multichannel
1882 ± 10		HOEHLER	79	IPWA	$\pi N \to \pi N$
• • • We do not use the following data for averages, fits, limits, etc. • • •					
1817.7		ARNDT	06	DPWA	$\pi N \to \pi N, \eta N$

[5] Statistical error only.

$N(1860)$ BREIT-WIGNER WIDTH

VALUE (MeV)		DOCUMENT ID		TECN	COMMENT
$270\ ^{+140}_{-50}$		ANISOVICH	12A	DPWA	Multichannel
219 ± 23	[6]	SHRESTHA	12A	DPWA	Multichannel
95 ± 20		HOEHLER	79	IPWA	$\pi N \to \pi N$
• • • We do not use the following data for averages, fits, limits, etc. • • •					
117.6		ARNDT	06	DPWA	$\pi N \to \pi N, \eta N$

[6] Statistical error only.

$N(1860)$ DECAY MODES

	Mode	Fraction (Γ_i/Γ)
Γ_1	$N\pi$	4–20 %
Γ_2	$N\eta$	2–6 %
Γ_3	$N\pi\pi$	
Γ_4	$N\sigma$	35–47 %
Γ_5	$p\gamma$	
Γ_6	$p\gamma$, helicity=1/2	seen
Γ_7	$p\gamma$, helicity=3/2	seen
Γ_8	$n\gamma$	0.0017–0.062 %
Γ_9	$n\gamma$, helicity=1/2	0.0003–0.019 %
Γ_{10}	$n\gamma$, helicity=3/2	0.0014–0.043 %

$N(1860)$ BRANCHING RATIOS

$\Gamma(N\pi)/\Gamma_{total}$ Γ_1/Γ

VALUE (%)		DOCUMENT ID		TECN	COMMENT
20 ± 6		ANISOVICH	12A	DPWA	Multichannel
17 ± 1	[7]	SHRESTHA	12A	DPWA	Multichannel
4 ± 2		HOEHLER	79	IPWA	$\pi N \to \pi N$
• • • We do not use the following data for averages, fits, limits, etc. • • •					
12.7		ARNDT	06	DPWA	$\pi N \to \pi N, \eta N$

[7] Statistical error only.

$\Gamma(N\eta)/\Gamma_{total}$ Γ_2/Γ

VALUE (%)		DOCUMENT ID		TECN	COMMENT
4 ± 2	[8]	SHRESTHA	12A	DPWA	Multichannel

[8] Statistical error only.

$\Gamma(N\sigma)/\Gamma_{total}$ Γ_4/Γ

VALUE (%)		DOCUMENT ID		TECN	COMMENT
41 ± 6	[9]	SHRESTHA	12A	DPWA	Multichannel

[9] Statistical error only.

$N(1860)$ BREIT-WIGNER PHOTON DECAY AMPLITUDES

$N(1860) \to p\gamma$, helicity-1/2 amplitude $A_{1/2}$

VALUE ($GeV^{-1/2}$)		DOCUMENT ID		TECN	COMMENT
• • • We do not use the following data for averages, fits, limits, etc. • • •					
−0.017 ± 0.003	[10]	SHRESTHA	12A	DPWA	Multichannel

[10] Statistical error only.

$N(1860) \to p\gamma$, helicity-3/2 amplitude $A_{3/2}$

VALUE		DOCUMENT ID		TECN	COMMENT
• • • We do not use the following data for averages, fits, limits, etc. • • •					
0.029 ± 0.004	[11]	SHRESTHA	12A	DPWA	Multichannel

[11] Statistical error only.

$N(1860) \to n\gamma$, helicity-1/2 amplitude $A_{1/2}$

VALUE ($GeV^{-1/2}$)		DOCUMENT ID		TECN	COMMENT
0.021 ± 0.013		ANISOVICH	13B	DPWA	Multichannel
• • • We do not use the following data for averages, fits, limits, etc. • • •					
0.010 ± 0.005	[12]	SHRESTHA	12A	DPWA	Multichannel

[12] Statistical error only.

$N(1860) \rightarrow n\gamma$, helicity-3/2 amplitude $A_{3/2}$

VALUE ($GeV^{-1/2}$)	DOCUMENT ID		TECN	COMMENT
0.034 ± 0.017	ANISOVICH	13B	DPWA	Multichannel
• • • We do not use the following data for averages, fits, limits, etc. • • •				
-0.009 ± 0.005	[13] SHRESTHA	12A	DPWA	Multichannel

[13] Statistical error only.

$N(1860)$ REFERENCES

SVARC	14	PR C89 045205	A. Svarc *et al.*	(RBI Zagreb, UNI Tuzla)
ANISOVICH	13B	EPJ A49 67	A.V. Anisovich *et al.*	
ANISOVICH	12A	EPJ A48 15	A.V. Anisovich *et al.*	(BONN, PNPI)
SHRESTHA	12A	PR C86 055203	M. Shrestha, D.M. Manley	(KSU)
ARNDT	06	PR C74 045205	R.A. Arndt *et al.*	(GWU)
HOEHLER	79	PDAT 12-1	G. Hohler *et al.*	(KARLT)

$N(1875)\ 3/2^-$

$I(J^P) = \frac{1}{2}(\frac{3}{2}^-)$ Status: ***

Before the 2012 *Review*, all the evidence for a $J^P = 3/2^-$ state with a mass above 1800 MeV was filed under a two-star $N(2080)$. There is now evidence from ANISOVICH 12A for two $3/2^-$ states in this region, so we have split the older data (according to mass) between a three-star $N(1875)$ and a two-star $N(2120)$.

$N(1875)$ POLE POSITION

REAL PART

VALUE (MeV)	DOCUMENT ID		TECN	COMMENT
1850 to 1950 (≈ 1900) OUR ESTIMATE				
1870 ± 20	SOKHOYAN	15A	DPWA	Multichannel
1880 ± 100	CUTKOSKY	80	IPWA	$\pi N \rightarrow \pi N$ (lower m)
• • • We do not use the following data for averages, fits, limits, etc. • • •				
1810	SHKLYAR	13	DPWA	Multichannel
1860 ± 25	ANISOVICH	12A	DPWA	Multichannel
1975	SHRESTHA	12A	DPWA	Multichannel
1957 ± 49	BATINIC	10	DPWA	$\pi N \rightarrow N\pi, N\eta$
1824	VRANA	00	DPWA	Multichannel

$-2\times$IMAGINARY PART

VALUE (MeV)	DOCUMENT ID		TECN	COMMENT
100 to 220 (≈ 160) OUR ESTIMATE				
200 ± 15	SOKHOYAN	15A	DPWA	Multichannel
160 ± 80	CUTKOSKY	80	IPWA	$\pi N \rightarrow \pi N$ (lower m)
• • • We do not use the following data for averages, fits, limits, etc. • • •				
98	SHKLYAR	13	DPWA	Multichannel
200 ± 20	ANISOVICH	12A	DPWA	Multichannel
495	SHRESTHA	12A	DPWA	Multichannel
467 ± 106	BATINIC	10	DPWA	$\pi N \rightarrow N\pi, N\eta$
614	VRANA	00	DPWA	Multichannel

$N(1875)$ ELASTIC POLE RESIDUE

MODULUS $|r|$

VALUE (MeV)	DOCUMENT ID		TECN	COMMENT
3 to 12 (≈ 10) OUR ESTIMATE				
3 ± 1.5	SOKHOYAN	15A	DPWA	Multichannel
10 ± 5	CUTKOSKY	80	IPWA	$\pi N \rightarrow \pi N$ (lower m)
• • • We do not use the following data for averages, fits, limits, etc. • • •				
3	SHKLYAR	13	DPWA	Multichannel
2.5 ± 1.0	ANISOVICH	12A	DPWA	Multichannel
53	BATINIC	10	DPWA	$\pi N \rightarrow N\pi, N\eta$

PHASE θ

VALUE (°)	DOCUMENT ID		TECN	COMMENT
50 to 200 (≈ 100) OUR ESTIMATE				
160 ± 50	SOKHOYAN	15A	DPWA	Multichannel
100 ± 80	CUTKOSKY	80	IPWA	$\pi N \rightarrow \pi N$ (lower m)
• • • We do not use the following data for averages, fits, limits, etc. • • •				
− 76	SHKLYAR	13	DPWA	Multichannel
− 65	BATINIC	10	DPWA	$\pi N \rightarrow N\pi, N\eta$

$N(1875)$ INELASTIC POLE RESIDUE

The "normalized residue" is the residue divided by $\Gamma_{pole}/2$.

Normalized residue in $N\pi \rightarrow N(1875) \rightarrow \Lambda K$

MODULUS	PHASE (°)	DOCUMENT ID		TECN	COMMENT
0.015 ± 0.005		ANISOVICH	12A	DPWA	Multichannel

Normalized residue in $N\pi \rightarrow N(1875) \rightarrow \Sigma K$

MODULUS	PHASE (°)	DOCUMENT ID		TECN	COMMENT
0.04 ± 0.02		ANISOVICH	12A	DPWA	Multichannel

Normalized residue in $N\pi \rightarrow N(1875) \rightarrow N\sigma$

MODULUS	PHASE (°)	DOCUMENT ID		TECN	COMMENT
0.09 ± 0.03	-175 ± 45	SOKHOYAN	15A	DPWA	Multichannel
• • • We do not use the following data for averages, fits, limits, etc. • • •					
0.08 ± 0.03	-170 ± 65	ANISOVICH	12A	DPWA	Multichannel

Normalized residue in $N\pi \rightarrow N(1875) \rightarrow \Delta(1232)\pi$, S-wave

MODULUS	PHASE (°)	DOCUMENT ID		TECN	COMMENT
0.05 ± 0.03	undefined	SOKHOYAN	15A	DPWA	Multichannel

Normalized residue in $N\pi \rightarrow N(1875) \rightarrow \Delta(1232)\pi$, D-wave

MODULUS	PHASE (°)	DOCUMENT ID		TECN	COMMENT
0.04 ± 0.02	undefined	SOKHOYAN	15A	DPWA	Multichannel

Normalized residue in $N\pi \rightarrow N(1875) \rightarrow N(1440)\pi$

MODULUS	PHASE (°)	DOCUMENT ID		TECN	COMMENT
0.03 ± 0.02	undefined	SOKHOYAN	15A	DPWA	Multichannel

$N(1875)$ BREIT-WIGNER MASS

VALUE (MeV)	DOCUMENT ID		TECN	COMMENT
1850 to 1920 (≈ 1875) OUR ESTIMATE				
1875 ± 20	SOKHOYAN	15A	DPWA	Multichannel
1934 ± 10	[1] SHKLYAR	13	DPWA	Multichannel
1951 ± 27	[1] SHRESTHA	12A	DPWA	Multichannel
1880 ± 100	CUTKOSKY	80	IPWA	$\pi N \rightarrow \pi N$
• • • We do not use the following data for averages, fits, limits, etc. • • •				
1880 ± 20	ANISOVICH	12A	DPWA	Multichannel
2048 ± 65	BATINIC	10	DPWA	$\pi N \rightarrow N\pi, N\eta$
1946 ± 1	PENNER	02C	DPWA	Multichannel
1895	MART	00	DPWA	$\gamma p \rightarrow \Lambda K^+$
2003 ± 18	VRANA	00	DPWA	Multichannel

[1] Statistical error only.

$N(1875)$ BREIT-WIGNER WIDTH

VALUE (MeV)	DOCUMENT ID		TECN	COMMENT
120 to 250 (≈ 200) OUR ESTIMATE				
200 ± 25	SOKHOYAN	15A	DPWA	Multichannel
857 ± 100	[1] SHKLYAR	13	DPWA	Multichannel
500 ± 45	[1] SHRESTHA	12A	DPWA	Multichannel
180 ± 60	CUTKOSKY	80	IPWA	$\pi N \rightarrow \pi N$ (lower m)
• • • We do not use the following data for averages, fits, limits, etc. • • •				
200 ± 25	ANISOVICH	12A	DPWA	Multichannel
529 ± 128	BATINIC	10	DPWA	$\pi N \rightarrow N\pi, N\eta$
859 ± 7	PENNER	02C	DPWA	Multichannel
372	MART	00	DPWA	$\gamma p \rightarrow \Lambda K^+$
1070 ± 858	VRANA	00	DPWA	Multichannel

[1] Statistical error only.

$N(1875)$ DECAY MODES

	Mode	Fraction (Γ_i/Γ)
Γ_1	$N\pi$	3–11 %
Γ_2	$N\eta$	<1 %
Γ_3	$N\omega$	15–25 %
Γ_4	ΛK	seen
Γ_5	ΣK	seen
Γ_6	$N\pi\pi$	40–95 %
Γ_7	$\Delta(1232)\pi$	10–35 %
Γ_8	$\Delta(1232)\pi$, S-wave	7–21 %
Γ_9	$\Delta(1232)\pi$, D-wave	2–12 %
Γ_{10}	$N\rho$, $S=3/2$, S-wave	seen
Γ_{11}	$\Lambda K^*(892)$	
Γ_{12}	$N\sigma$	30–60 %
Γ_{13}	$N(1440)\pi$	2–8 %
Γ_{14}	$N(1520)\pi$	<2 %
Γ_{15}	$p\gamma$	0.001–0.025 %
Γ_{16}	$p\gamma$, helicity=1/2	0.001–0.021 %
Γ_{17}	$p\gamma$, helicity=3/2	<0.003 %
Γ_{18}	$n\gamma$	<0.040 %
Γ_{19}	$n\gamma$, helicity=1/2	<0.007 %
Γ_{20}	$n\gamma$, helicity=3/2	<0.033 %

$N(1875)$ BRANCHING RATIOS

$\Gamma(N\pi)/\Gamma_{total}$ Γ_1/Γ

VALUE (%)	DOCUMENT ID		TECN	COMMENT
3 to 11 (≈ 7) OUR ESTIMATE				
4±2	SOKHOYAN	15A	DPWA	Multichannel
11±1	[1] SHKLYAR	13	DPWA	Multichannel
7±2	[1] SHRESTHA	12A	DPWA	Multichannel
10±4	CUTKOSKY	80	IPWA	$\pi N \to \pi N$ (lower m)
• • • We do not use the following data for averages, fits, limits, etc. • • •				
3±2	ANISOVICH	12A	DPWA	Multichannel
17±7	BATINIC	10	DPWA	$\pi N \to N\pi$, $N\eta$
12±2	PENNER	02C	DPWA	Multichannel
13±3	VRANA	00	DPWA	Multichannel

[1] Statistical error only.

$\Gamma(N\eta)/\Gamma_{total}$ Γ_2/Γ

VALUE (%)	DOCUMENT ID		TECN	COMMENT
<1	SHKLYAR	13	DPWA	Multichannel
• • • We do not use the following data for averages, fits, limits, etc. • • •				
8±3	BATINIC	10	DPWA	$\pi N \to N\pi$, $N\eta$
7±2	PENNER	02C	DPWA	Multichannel
0±2	VRANA	00	DPWA	Multichannel

$\Gamma(N\omega)/\Gamma_{total}$ Γ_3/Γ

VALUE (%)	DOCUMENT ID		TECN	COMMENT
13±7	DENISENKO	16	DPWA	Multichannel
20±5	[1] SHKLYAR	13	DPWA	Multichannel
• • • We do not use the following data for averages, fits, limits, etc. • • •				
21±7	PENNER	02C	DPWA	Multichannel

[1] Statistical error only

$\Gamma(\Lambda K)/\Gamma_{total}$ Γ_4/Γ

VALUE (%)	DOCUMENT ID		TECN	COMMENT
• • • We do not use the following data for averages, fits, limits, etc. • • •				
0.2±0.2	PENNER	02C	DPWA	Multichannel

$\Gamma(\Sigma K)/\Gamma_{total}$ Γ_5/Γ

VALUE (%)	DOCUMENT ID		TECN	COMMENT
0.7±0.4	PENNER	02C	DPWA	Multichannel

$\Gamma(\Delta(1232)\pi$, S-wave$)/\Gamma_{total}$ Γ_8/Γ

VALUE (%)	DOCUMENT ID		TECN	COMMENT
14± 7	SOKHOYAN	15A	DPWA	Multichannel
87± 3	[1] SHRESTHA	12A	DPWA	Multichannel
• • • We do not use the following data for averages, fits, limits, etc. • • •				
40±10	VRANA	00	DPWA	Multichannel

[1] Statistical error only.

$\Gamma(\Delta(1232)\pi$, D-wave$)/\Gamma_{total}$ Γ_9/Γ

VALUE (%)	DOCUMENT ID		TECN	COMMENT
7± 5	SOKHOYAN	15A	DPWA	Multichannel
< 6	SHRESTHA	12A	DPWA	Multichannel
• • • We do not use the following data for averages, fits, limits, etc. • • •				
17±10	VRANA	00	DPWA	Multichannel

$\Gamma(N\rho$, S=3/2, S-wave$)/\Gamma_{total}$ Γ_{10}/Γ

VALUE (%)	DOCUMENT ID		TECN	COMMENT
<5	SHRESTHA	12A	DPWA	Multichannel
• • • We do not use the following data for averages, fits, limits, etc. • • •				
6±6	VRANA	00	DPWA	Multichannel

$\Gamma(\Lambda K^*(892))/\Gamma_{total}$ Γ_{11}/Γ

VALUE	DOCUMENT ID		TECN	COMMENT
<0.002	ANISOVICH	17B	DPWA	Multichannel

$\Gamma(N\sigma)/\Gamma_{total}$ Γ_{12}/Γ

VALUE (%)	DOCUMENT ID		TECN	COMMENT
45±15	SOKHOYAN	15A	DPWA	Multichannel
< 4	SHRESTHA	12A	DPWA	Multichannel
• • • We do not use the following data for averages, fits, limits, etc. • • •				
24±24	VRANA	00	DPWA	Multichannel

$\Gamma(N(1440)\pi)/\Gamma_{total}$ Γ_{13}/Γ

VALUE (%)	DOCUMENT ID		TECN	COMMENT
5±3	SOKHOYAN	15A	DPWA	Multichannel

$\Gamma(N(1520)\pi)/\Gamma_{total}$ Γ_{14}/Γ

VALUE (%)	DOCUMENT ID		TECN	COMMENT
<2	SOKHOYAN	15A	DPWA	Multichannel

$N(1875)$ PHOTON DECAY AMPLITUDES AT THE POLE

$N(1875) \to p\gamma$, helicity-1/2 amplitude $A_{1/2}$

MODULUS ($GeV^{-1/2}$)	PHASE (°)	DOCUMENT ID		TECN	COMMENT
0.017±0.009	−110 ± 40	SOKHOYAN	15A	DPWA	Multichannel

$N(1875) \to p\gamma$, helicity-3/2 amplitude $A_{3/2}$

MODULUS ($GeV^{-1/2}$)	PHASE (°)	DOCUMENT ID		TECN	COMMENT
0.008±0.004	180 ± 40	SOKHOYAN	15A	DPWA	Multichannel

$N(1875)$ BREIT-WIGNER PHOTON DECAY AMPLITUDES

$N(1875) \to p\gamma$, helicity-1/2 amplitude $A_{1/2}$

VALUE ($GeV^{-1/2}$)	DOCUMENT ID		TECN	COMMENT
0.010 to 0.025 (≈ 0.015) OUR ESTIMATE				
0.011±0.001	[1] SHKLYAR	13	DPWA	Multichannel
0.018±0.010	ANISOVICH	12A	DPWA	Multichannel
• • • We do not use the following data for averages, fits, limits, etc. • • •				
0.007±0.008	[1] SHRESTHA	12A	DPWA	Multichannel
0.012	PENNER	02D	DPWA	Multichannel

[1] Statistical error only.

$N(1875) \to p\gamma$, helicity-3/2 amplitude $A_{3/2}$

VALUE ($GeV^{-1/2}$)	DOCUMENT ID		TECN	COMMENT
−0.010 to 0.025 (≈ −0.005) OUR ESTIMATE				
−0.007±0.004	SOKHOYAN	15A	DPWA	Multichannel
0.026±0.001	[1] SHKLYAR	13	DPWA	Multichannel
• • • We do not use the following data for averages, fits, limits, etc. • • •				
−0.009±0.005	ANISOVICH	12A	DPWA	Multichannel
0.043±0.022	[1] SHRESTHA	12A	DPWA	Multichannel
−0.010	PENNER	02D	DPWA	Multichannel

[1] Statistical error only.

$N(1875) \to n\gamma$, helicity-1/2 amplitude $A_{1/2}$

VALUE ($GeV^{-1/2}$)	DOCUMENT ID		TECN	COMMENT
0.010±0.006	ANISOVICH	13B	DPWA	Multichannel
• • • We do not use the following data for averages, fits, limits, etc. • • •				
0.055±0.021	[1] SHRESTHA	12A	DPWA	Multichannel
0.023	PENNER	02D	DPWA	Multichannel

[1] Statistical error only.

$N(1875) \to n\gamma$, helicity-3/2 amplitude $A_{3/2}$

VALUE ($GeV^{-1/2}$)	DOCUMENT ID		TECN	COMMENT
−0.020±0.015	ANISOVICH	13B	DPWA	Multichannel
• • • We do not use the following data for averages, fits, limits, etc. • • •				
−0.085±0.031	[1] SHRESTHA	12A	DPWA	Multichannel
−0.009	PENNER	02D	DPWA	Multichannel

[1] Statistical error only.

$N(1875)$ REFERENCES

For early references, see Physics Letters **111B** 1 (1982).

ANISOVICH	17B	PL B771 142	A.V. Anisovich *et al.*	
DENISENKO	16	PL B755 97	I. Denisenko *et al.*	
SOKHOYAN	15A	EPJ A51 95	V. Sokhoyan *et al.*	(CBELSA/TAPS Collab.)
ANISOVICH	13B	EPJ A49 67	A.V. Anisovich *et al.*	
SHKLYAR	13	PR C87 015201	V. Shklyar, H. Lenske, U. Mosel	(GIES)
ANISOVICH	12A	EPJ A48 15	A.V. Anisovich *et al.*	(BONN, PNPI)
SHRESTHA	12A	PR C86 055203	M. Shrestha, D.M. Manley	(KSU)
BATINIC	10	PR C82 038203	M. Batinic *et al.*	(ZAGR)
PENNER	02C	PR C66 055211	G. Penner, U. Mosel	(GIES)
PENNER	02D	PR C66 055212	G. Penner, U. Mosel	(GIES)
MART	00	PR C61 012201	T. Mart, C. Bennhold	
VRANA	00	PRPL 328 181	T.P. Vrana, S.A. Dytman, T.-S.H. Lee	(PITT, ANL)
CUTKOSKY	80	Toronto Conf. 19	R.E. Cutkosky *et al.*	(CMU, LBL) IJP
Also		PR D20 2839	R.E. Cutkosky *et al.*	(CMU, LBL) IJP

$N(1880)$ $1/2^+$

$I(J^P) = \frac{1}{2}(\frac{1}{2}^+)$ Status: ***

$N(1880)$ POLE POSITION

REAL PART

VALUE (MeV)	DOCUMENT ID		TECN	COMMENT
1820 to 1900 (≈ 1860) OUR ESTIMATE				
1860±40	ANISOVICH	17A	DPWA	Multichannel
• • • We do not use the following data for averages, fits, limits, etc. • • •				
1875±11	[1] ANISOVICH	17A	L+P	γp, $\pi^- p \to K\Lambda$
1870±40	SOKHOYAN	15A	DPWA	Multichannel
1870±40	GUTZ	14	DPWA	Multichannel
1860±35	ANISOVICH	12A	DPWA	Multichannel
1801	SHRESTHA	12A	DPWA	Multichannel

[1] Statistical error only.

−2×IMAGINARY PART

VALUE (MeV)	DOCUMENT ID		TECN	COMMENT
180 to 280 (≈ 230) OUR ESTIMATE				
230±50	ANISOVICH	17A	DPWA	Multichannel
• • • We do not use the following data for averages, fits, limits, etc. • • •				
33± 9	[2] ANISOVICH	17A	L+P	$\gamma p,\ \pi^- p \rightarrow K\Lambda$
220±50	SOKHOYAN	15A	DPWA	Multichannel
220±50	GUTZ	14	DPWA	Multichannel
250±70	ANISOVICH	12A	DPWA	Multichannel
383	SHRESTHA	12A	DPWA	Multichannel

[2] Statistical error only.

$N(1880)$ ELASTIC POLE RESIDUE

MODULUS $|r|$

VALUE (MeV)	DOCUMENT ID		TECN	COMMENT
6±4	SOKHOYAN	15A	DPWA	Multichannel
• • • We do not use the following data for averages, fits, limits, etc. • • •				
6±4	GUTZ	14	DPWA	Multichannel
6±4	ANISOVICH	12A	DPWA	Multichannel

PHASE θ

VALUE (°)	DOCUMENT ID		TECN	COMMENT
70±60	SOKHOYAN	15A	DPWA	Multichannel
• • • We do not use the following data for averages, fits, limits, etc. • • •				
70±60	GUTZ	14	DPWA	Multichannel
80±65	ANISOVICH	12A	DPWA	Multichannel

$N(1880)$ INELASTIC POLE RESIDUE

The "normalized residue" is the residue divided by $\Gamma_{pole}/2$.

Normalized residue in $N\pi \rightarrow N(1880) \rightarrow N\eta$

MODULUS	PHASE (°)	DOCUMENT ID		TECN	COMMENT
0.11±0.07	−75 ± 55	ANISOVICH	12A	DPWA	Multichannel

Normalized residue in $N\pi \rightarrow N(1880) \rightarrow \Lambda K$

MODULUS	PHASE (°)	DOCUMENT ID		TECN	COMMENT
0.05±0.02	27 ± 30	ANISOVICH	17A	DPWA	$\gamma p, \pi^- p \rightarrow K\Lambda$
• • • We do not use the following data for averages, fits, limits, etc. • • •					
0.3 ±0.1	82 ± 9	[3] ANISOVICH	17A	L+P	$\gamma p,\ \pi^- p \rightarrow K\Lambda$
0.03±0.02	40 ± 40	ANISOVICH	12A	DPWA	Multichannel

[3] Statistical error only.

Normalized residue in $N\pi \rightarrow N(1880) \rightarrow \Sigma K$

MODULUS	PHASE (°)	DOCUMENT ID		TECN	COMMENT
• • • We do not use the following data for averages, fits, limits, etc. • • •					
0.11±0.06	95 ± 40	ANISOVICH	12A	DPWA	Multichannel

Normalized residue in $N\pi \rightarrow N(1880) \rightarrow \Delta\pi$, P-wave

MODULUS	PHASE (°)	DOCUMENT ID		TECN	COMMENT
0.14±0.08	−150 ± 55	SOKHOYAN	15A	DPWA	Multichannel
• • • We do not use the following data for averages, fits, limits, etc. • • •					
0.20±0.08	−150 ± 50	ANISOVICH	12A	DPWA	Multichannel

Normalized residue in $N\pi \rightarrow N(1880) \rightarrow N(1535)\pi$

MODULUS	PHASE (°)	DOCUMENT ID		TECN	COMMENT
0.09±0.05	130 ± 60	GUTZ	14	DPWA	Multichannel

Normalized residue in $N\pi \rightarrow N(1880) \rightarrow Na_0(980)$

MODULUS	PHASE (°)	DOCUMENT ID		TECN	COMMENT
0.04±0.03	40 ± 65	GUTZ	14	DPWA	Multichannel

Normalized residue in $N\pi \rightarrow N(1880) \rightarrow N\sigma$

MODULUS	PHASE (°)	DOCUMENT ID		TECN	COMMENT
0.10±0.05	−140 ± 55	SOKHOYAN	15A	DPWA	Multichannel

$N(1880)$ BREIT-WIGNER MASS

VALUE (MeV)	DOCUMENT ID		TECN	COMMENT
1830 to 1930 (≈ 1880) OUR ESTIMATE				
1875±40	SOKHOYAN	15A	DPWA	Multichannel
1900±36	[4] SHRESTHA	12A	DPWA	Multichannel
• • • We do not use the following data for averages, fits, limits, etc. • • •				
1875±40	GUTZ	14	DPWA	Multichannel
1870±35	ANISOVICH	12A	DPWA	Multichannel

[4] Statistical error only.

$N(1880)$ BREIT-WIGNER WIDTH

VALUE (MeV)	DOCUMENT ID		TECN	COMMENT
200 to 400 (≈ 300) OUR ESTIMATE				
230± 50	SOKHOYAN	15A	DPWA	Multichannel
485±142	[5] SHRESTHA	12A	DPWA	Multichannel
• • • We do not use the following data for averages, fits, limits, etc. • • •				
230± 50	GUTZ	14	DPWA	Multichannel
235± 65	ANISOVICH	12A	DPWA	Multichannel

[5] Statistical error only.

$N(1880)$ DECAY MODES

	Mode	Fraction (Γ_i/Γ)
Γ_1	$N\pi$	3–9 %
Γ_2	$N\eta$	5–55 %
Γ_3	$N\omega$	12–28 %
Γ_4	ΛK	12–28 %
Γ_5	ΣK	10–24 %
Γ_6	$N\pi\pi$	30–80 %
Γ_7	$\Delta(1232)\pi$	18–42 %
Γ_8	$N\sigma$	10–40 %
Γ_9	$N(1535)\pi$	4–12 %
Γ_{10}	$Na_0(980)$	1–5 %
Γ_{11}	$\Lambda K^*(892)$	0.5–1 %
Γ_{12}	$p\gamma$, helicity=1/2	seen
Γ_{13}	$n\gamma$, helicity=1/2	0.002–0.63 %

$N(1880)$ BRANCHING RATIOS

$\Gamma(N\pi)/\Gamma_{total}$ Γ_1/Γ

VALUE (%)	DOCUMENT ID		TECN	COMMENT
6±3	SOKHOYAN	15A	DPWA	Multichannel
15±5	[6] SHRESTHA	12A	DPWA	Multichannel
• • • We do not use the following data for averages, fits, limits, etc. • • •				
6±3	GUTZ	14	DPWA	Multichannel
5±3	ANISOVICH	12A	DPWA	Multichannel

[6] Statistical error only.

$\Gamma(N\eta)/\Gamma_{total}$ Γ_2/Γ

VALUE (%)	DOCUMENT ID		TECN	COMMENT
25^{+30}_{-20}	ANISOVICH	12A	DPWA	Multichannel
16± 7	[7] SHRESTHA	12A	DPWA	Multichannel

[7] Statistical error only.

$\Gamma(N\omega)/\Gamma_{total}$ Γ_3/Γ

VALUE (%)	DOCUMENT ID		TECN	COMMENT
20±8	DENISENKO	16	DPWA	Multichannel

$\Gamma(\Lambda K)/\Gamma_{total}$ Γ_4/Γ

VALUE (%)	DOCUMENT ID		TECN	COMMENT
2± 1	ANISOVICH	12A	DPWA	Multichannel
32±10	[8] SHRESTHA	12A	DPWA	Multichannel

[8] Statistical error only.

$\Gamma(\Sigma K)/\Gamma_{total}$ Γ_5/Γ

VALUE (%)	DOCUMENT ID		TECN	COMMENT
17±7	ANISOVICH	12A	DPWA	Multichannel

$\Gamma(\Delta(1232)\pi)/\Gamma_{total}$ Γ_7/Γ

VALUE (%)	DOCUMENT ID		TECN	COMMENT
30±12	SOKHOYAN	15A	DPWA	Multichannel
< 2	SHRESTHA	12A	DPWA	Multichannel
• • • We do not use the following data for averages, fits, limits, etc. • • •				
29±12	ANISOVICH	12A	DPWA	Multichannel

$\Gamma(N\sigma)/\Gamma_{total}$ Γ_8/Γ

VALUE (%)	DOCUMENT ID		TECN	COMMENT
25±15	SOKHOYAN	15A	DPWA	Multichannel
8± 5	[9] SHRESTHA	12A	DPWA	Multichannel

[9] Statistical error only.

$\Gamma(N(1535)\pi)/\Gamma_{total}$ Γ_9/Γ

VALUE (%)	DOCUMENT ID		TECN	COMMENT
8±4	GUTZ	14	DPWA	Multichannel

$\Gamma(Na_0(980))/\Gamma_{total}$ Γ_{10}/Γ

VALUE (%)	DOCUMENT ID		TECN	COMMENT
3±2	GUTZ	14	DPWA	Multichannel

$\Gamma(\Lambda K^*(892))/\Gamma_{total}$ Γ_{11}/Γ

VALUE	DOCUMENT ID		TECN	COMMENT
0.008±0.003	ANISOVICH	17B	DPWA	Multichannel

$N(1880)$ BREIT-WIGNER PHOTON DECAY AMPLITUDES

$N(1880) \to p\gamma$, helicity-1/2 amplitude $A_{1/2}$

VALUE (GeV$^{-1/2}$)	DOCUMENT ID		TECN	COMMENT
• • • We do not use the following data for averages, fits, limits, etc. • • •				
0.021±0.006	[10] SHRESTHA	12A	DPWA	Multichannel

[10] Statistical error only.

$N(1880) \to n\gamma$, helicity-1/2 amplitude $A_{1/2}$

VALUE (GeV$^{-1/2}$)	DOCUMENT ID		TECN	COMMENT
−0.060±0.050	ANISOVICH	13B	DPWA	Multichannel
• • • We do not use the following data for averages, fits, limits, etc. • • •				
0.014±0.007	[11] SHRESTHA	12A	DPWA	Multichannel

[11] Statistical error only.

$N(1880)$ REFERENCES

ANISOVICH	17A	PRL 119 062004	A.V. Anisovich *et al.*	
ANISOVICH	17B	PL B771 142	A.V. Anisovich *et al.*	
DENISENKO	16	PL B755 97	I. Denisenko *et al.*	
SOKHOYAN	15A	EPJ A51 95	V. Sokhoyan *et al.*	(CBELSA/TAPS Collab.)
GUTZ	14	EPJ A50 74	E. Gutz *et al.*	(CBELSA/TAPS Collab.)
ANISOVICH	13B	EPJ A49 67	A.V. Anisovich *et al.*	
ANISOVICH	12A	EPJ A48 15	A.V. Anisovich *et al.*	(BONN, PNPI)
SHRESTHA	12A	PR C86 055203	M. Shrestha, D.M. Manley	(KSU)

$N(1895)\ 1/2^-$

$I(J^P) = \frac{1}{2}(\frac{1}{2}^-)$ Status: ****

Before our 2012 *Review*, this state appeared in our Listings as the $N(2090)$. Any structure in the S_{11} wave above 1800 MeV is listed here. A few early results that are now obsolete have been omitted.

$N(1895)$ POLE POSITION

REAL PART

VALUE (MeV)	DOCUMENT ID		TECN	COMMENT
1890 to 1930 (≈ 1910) OUR ESTIMATE				
1895±15	ANISOVICH	17A	DPWA	Multichannel
1906±17	[1] ANISOVICH	17A	L+P	$\gamma p,\ \pi^- p \to K\Lambda$
1917±19±1	[2] SVARC	14	L+P	$\pi N \to \pi N$
• • • We do not use the following data for averages, fits, limits, etc. • • •				
1907±10	ANISOVICH	17C	DPWA	Multichannel
1907±10	SOKHOYAN	15A	DPWA	Multichannel
1900±15	ANISOVICH	12A	DPWA	Multichannel
1858	SHRESTHA	12A	DPWA	Multichannel
1797±26	BATINIC	10	DPWA	$\pi N \to N\pi,\ N\eta$
1795	VRANA	00	DPWA	Multichannel
2150±70	CUTKOSKY	80	IPWA	$\pi N \to \pi N$

[1] Statistical error only.
[2] Fit to the amplitudes of HOEHLER 79.

−2×IMAGINARY PART

VALUE (MeV)	DOCUMENT ID		TECN	COMMENT
80 to 140 (≈ 110) OUR ESTIMATE				
132± 30	ANISOVICH	17A	DPWA	Multichannel
100± 10	[1] ANISOVICH	17A	L+P	$\gamma p,\ \pi^- p \to K\Lambda$
101± 36±1	[1,2] SVARC	14	L+P	$\pi N \to \pi N$
• • • We do not use the following data for averages, fits, limits, etc. • • •				
$100^{+\ 40}_{-\ 10}$	ANISOVICH	17C	DPWA	Multichannel
$100^{+\ 40}_{-\ 15}$	SOKHOYAN	15A	DPWA	Multichannel
$90^{+\ 30}_{-\ 15}$	ANISOVICH	12A	DPWA	Multichannel
479	SHRESTHA	12A	DPWA	Multichannel
420± 45	BATINIC	10	DPWA	$\pi N \to N\pi,\ N\eta$
220	VRANA	00	DPWA	Multichannel
350±100	CUTKOSKY	80	IPWA	$\pi N \to \pi N$

[1] Statistical error only.
[2] Fit to the amplitudes of HOEHLER 79.

$N(1895)$ ELASTIC POLE RESIDUE

MODULUS $|r|$

VALUE (MeV)	DOCUMENT ID		TECN	COMMENT
1 to 5 (≈ 3) OUR ESTIMATE				
3 ± 2	SOKHOYAN	15A	DPWA	Multichannel
3.1± 1.4	[1] SVARC	14	L+P	$\pi N \to \pi N$
• • • We do not use the following data for averages, fits, limits, etc. • • •				
1 ± 1	ANISOVICH	12A	DPWA	Multichannel
60	BATINIC	10	DPWA	$\pi N \to N\pi,\ N\eta$
40 ±20	CUTKOSKY	80	IPWA	$\pi N \to \pi N$

[1] Fit to the amplitudes of HOEHLER 79.

PHASE θ

VALUE (°)	DOCUMENT ID		TECN	COMMENT
125±45	SOKHOYAN	15A	DPWA	Multichannel
−107±23±2	[1] SVARC	14	L+P	$\pi N \to \pi N$
0±90	CUTKOSKY	80	IPWA	$\pi N \to \pi N$
• • • We do not use the following data for averages, fits, limits, etc. • • •				
−164	BATINIC	10	DPWA	$\pi N \to N\pi,\ N\eta$

[1] Fit to the amplitudes of HOEHLER 79.

$N(1895)$ INELASTIC POLE RESIDUE

The "normalized residue" is the residue divided by $\Gamma_{pole}/2$.

Normalized residue in $N\pi \to N(1895) \to \Lambda K$

MODULUS	PHASE (°)	DOCUMENT ID		TECN	COMMENT
0.09±0.03	8 ± 30	ANISOVICH	17A	DPWA	Multichannel
0.06±0.02	87 ± 27	[1] ANISOVICH	17A	L+P	$\gamma p,\ \pi^- p \to K\Lambda$
• • • We do not use the following data for averages, fits, limits, etc. • • •					
0.05±0.02	−90 ± 30	ANISOVICH	12A	DPWA	Multichannel

[1] Statistical error only.

Normalized residue in $N\pi \to N(1895) \to \Sigma K$

MODULUS	PHASE (°)	DOCUMENT ID		TECN	COMMENT
0.06±0.02	40 ± 30	ANISOVICH	12A	DPWA	Multichannel

Normalized residue in $N\pi \to N(1895) \to \Delta(1232)\pi$

MODULUS	PHASE (°)	DOCUMENT ID		TECN	COMMENT
0.05±0.025	−100 ± 45	SOKHOYAN	15A	DPWA	Multichannel

Normalized residue in $N\pi \to N(1895) \to N(1440)\pi$

MODULUS	PHASE (°)	DOCUMENT ID		TECN	COMMENT
0.05±0.025	−100 ± 45	SOKHOYAN	15A	DPWA	Multichannel

$N(1895)$ BREIT-WIGNER MASS

VALUE (MeV)	DOCUMENT ID		TECN	COMMENT
1870 to 1920 (≈ 1895) OUR ESTIMATE				
$1890^{+\ 9}_{-\ 23}$	KASHEVAROV	17	DPWA	$\gamma p \to \eta p,\ \eta' p$
1905±12	SOKHOYAN	15A	DPWA	Multichannel
1910±15	[1] SHRESTHA	12A	DPWA	Multichannel
1880±20	HOEHLER	79	IPWA	$\pi N \to \pi N$
• • • We do not use the following data for averages, fits, limits, etc. • • •				
1895±15	ANISOVICH	12A	DPWA	Multichannel
1812±25	BATINIC	10	DPWA	$\pi N \to N\pi,\ N\eta$
1822±43	VRANA	00	DPWA	Multichannel
2180±80	CUTKOSKY	80	IPWA	$\pi N \to \pi N$

[1] Statistical error only.

$N(1895)$ BREIT-WIGNER WIDTH

VALUE (MeV)	DOCUMENT ID		TECN	COMMENT
80 to 200 (≈ 120) OUR ESTIMATE				
150± 57	KASHEVAROV	17	DPWA	$\gamma p \to \eta p,\ \eta' p$
$100^{+\ 30}_{-\ 10}$	SOKHOYAN	15A	DPWA	Multichannel
502± 47	[1] SHRESTHA	12A	DPWA	Multichannel
95± 30	HOEHLER	79	IPWA	$\pi N \to \pi N$
• • • We do not use the following data for averages, fits, limits, etc. • • •				
$90^{+\ 30}_{-\ 15}$	ANISOVICH	12A	DPWA	Multichannel
405± 40	BATINIC	10	DPWA	$\pi N \to N\pi,\ N\eta$
248±185	VRANA	00	DPWA	Multichannel
350±100	CUTKOSKY	80	IPWA	$\pi N \to \pi N$

[1] Statistical error only.

$N(1895)$ DECAY MODES

	Mode	Fraction (Γ_i/Γ)
Γ_1	$N\pi$	2–18 %
Γ_2	$N\eta$	15–40 %
Γ_3	$N\eta'$	10–40 %
Γ_4	$N\omega$	16–40 %
Γ_5	ΛK	13–23 %
Γ_6	ΣK	6–20 %
Γ_7	$N\pi\pi$	
Γ_8	$\Delta(1232)\pi$	
Γ_9	$\Delta(1232)\pi$, D-wave	3–11 %
Γ_{10}	$N\rho$	
Γ_{11}	$N\rho$, S=1/2, S-wave	seen

Γ_{12}	$N\rho$, S=3/2, D-wave	3–12 %
Γ_{13}	$\Lambda K^*(892)$	4–9 %
Γ_{14}	$N\sigma$	seen
Γ_{15}	$N(1440)\pi$	1–4 %
Γ_{16}	$p\gamma$, helicity=1/2	0.01–0.06 %
Γ_{17}	$n\gamma$, helicity=1/2	0.003–0.05 %

$N(1895)$ BRANCHING RATIOS

$\Gamma(N\pi)/\Gamma_{total}$ Γ_1/Γ

VALUE (%)	DOCUMENT ID		TECN	COMMENT
2 to 18 (≈ 10) OUR ESTIMATE				
2.5±1.5	SOKHOYAN	15A	DPWA	Multichannel
17 ±2	[1] SHRESTHA	12A	DPWA	Multichannel
9 ±5	HOEHLER	79	IPWA	$\pi N \to \pi N$
• • • We do not use the following data for averages, fits, limits, etc. • • •				
2 ±1	ANISOVICH	12A	DPWA	Multichannel
32 ±6	BATINIC	10	DPWA	$\pi N \to N\pi$, $N\eta$
17 ±3	VRANA	00	DPWA	Multichannel
18 ±8	CUTKOSKY	80	IPWA	$\pi N \to \pi N$

[1] Statistical error only.

$\Gamma(N\eta)/\Gamma_{total}$ Γ_2/Γ

VALUE (%)	DOCUMENT ID		TECN	COMMENT
15 to 40 (≈ 25) OUR ESTIMATE				
10± 5	ANISOVICH	17C	DPWA	Multichannel
20± 6	[1] KASHEVAROV	17	DPWA	$\gamma p \to \eta p$, $\eta' p$
40± 4	[2] SHRESTHA	12A	DPWA	Multichannel
• • • We do not use the following data for averages, fits, limits, etc. • • •				
21± 6	ANISOVICH	12A	DPWA	Multichannel
22±10	BATINIC	10	DPWA	$\pi N \to N\pi$, $N\eta$
41± 4	VRANA	00	DPWA	Multichannel

[1] Assuming $A_{1/2} = -0.030$ GeV$^{-1/2}$.

[2] Statistical error only.

$\Gamma(N\eta')/\Gamma_{total}$ Γ_3/Γ

VALUE	DOCUMENT ID		TECN	COMMENT
0.10 to 0.40 (≈ 0.20) OUR ESTIMATE				
0.13±0.05	ANISOVICH	17C	DPWA	Multichannel
0.38±0.20	[1] KASHEVAROV	17	DPWA	$\gamma p \to \eta p$, $\eta' p$

[1] Assuming $A_{1/2} = -0.030$ GeV$^{-1/2}$.

$\Gamma(N\omega)/\Gamma_{total}$ Γ_4/Γ

VALUE (%)	DOCUMENT ID		TECN	COMMENT
28±12	DENISENKO	16	DPWA	Multichannel

$\Gamma(\Lambda K)/\Gamma_{total}$ Γ_5/Γ

VALUE (%)	DOCUMENT ID		TECN	COMMENT
18 ±5	ANISOVICH	12A	DPWA	Multichannel
1.8±0.8	[1] SHRESTHA	12A	DPWA	Multichannel

[1] Statistical error only.

$\Gamma(\Sigma K)/\Gamma_{total}$ Γ_6/Γ

VALUE (%)	DOCUMENT ID		TECN	COMMENT
13±7	ANISOVICH	12A	DPWA	Multichannel

$\Gamma(\Delta(1232)\pi$, D-wave$)/\Gamma_{total}$ Γ_9/Γ

VALUE (%)	DOCUMENT ID		TECN	COMMENT
7±4	SOKHOYAN	15A	DPWA	Multichannel
7±3	[1] SHRESTHA	12A	DPWA	Multichannel
• • • We do not use the following data for averages, fits, limits, etc. • • •				
1±1	VRANA	00	DPWA	Multichannel

[1] Statistical error only.

$\Gamma(N\rho$, S=1/2, S-wave$)/\Gamma_{total}$ Γ_{11}/Γ

VALUE (%)	DOCUMENT ID		TECN	COMMENT
< 2	[1] SHRESTHA	12A	DPWA	Multichannel
• • • We do not use the following data for averages, fits, limits, etc. • • •				
36±1	VRANA	00	DPWA	Multichannel

[1] Statistical error only.

$\Gamma(N\rho$, S=3/2, D-wave$)/\Gamma_{total}$ Γ_{12}/Γ

VALUE (%)	DOCUMENT ID		TECN	COMMENT
9±3	[1] SHRESTHA	12A	DPWA	Multichannel
• • • We do not use the following data for averages, fits, limits, etc. • • •				
1±1	VRANA	00	DPWA	Multichannel

[1] Statistical error only.

$\Gamma(\Lambda K^*(892))/\Gamma_{total}$ Γ_{13}/Γ

VALUE	DOCUMENT ID		TECN	COMMENT
0.063±0.025	ANISOVICH	17B	DPWA	Multichannel

$\Gamma(N\sigma)/\Gamma_{total}$ Γ_{14}/Γ

VALUE (%)	DOCUMENT ID		TECN	COMMENT
<2	[1] SHRESTHA	12A	DPWA	Multichannel
• • • We do not use the following data for averages, fits, limits, etc. • • •				
2±1	VRANA	00	DPWA	Multichannel

[1] Statistical error only.

$\Gamma(N(1440)\pi)/\Gamma_{total}$ Γ_{15}/Γ

VALUE (%)	DOCUMENT ID		TECN	COMMENT
2.5±1.5	SOKHOYAN	15A	DPWA	Multichannel
24 ±4	[1] SHRESTHA	12A	DPWA	Multichannel
• • • We do not use the following data for averages, fits, limits, etc. • • •				
2 ±1	VRANA	00	DPWA	Multichannel

[1] Statistical error only.

$N(1895)$ PHOTON DECAY AMPLITUDES AT THE POLE

$N(1895) \to p\gamma$, helicity-1/2 amplitude $A_{1/2}$

MODULUS (GeV$^{-1/2}$)	PHASE (°)	DOCUMENT ID		TECN	COMMENT
−0.015±0.006	−35 ± 35	ANISOVICH	17C	DPWA	Multichannel
• • • We do not use the following data for averages, fits, limits, etc. • • •					
0.015±0.006	145 ± 35	SOKHOYAN	15A	DPWA	Multichannel

$N(1895)$ BREIT-WIGNER PHOTON DECAY AMPLITUDES

$N(1895) \to p\gamma$, helicity-1/2 amplitude $A_{1/2}$

VALUE (GeV$^{-1/2}$)	DOCUMENT ID		TECN	COMMENT
−0.016±0.006	SOKHOYAN	15A	DPWA	Multichannel
• • • We do not use the following data for averages, fits, limits, etc. • • •				
0.012±0.006	[1] SHRESTHA	12A	DPWA	Multichannel

[1] Statistical error only.

$N(1895) \to n\gamma$, helicity-1/2 amplitude $A_{1/2}$

VALUE (GeV$^{-1/2}$)	DOCUMENT ID		TECN	COMMENT
0.013±0.006	ANISOVICH	13B	DPWA	Multichannel
• • • We do not use the following data for averages, fits, limits, etc. • • •				
0.003±0.007	[1] SHRESTHA	12A	DPWA	Multichannel

[1] Statistical error only.

$N(1895)$ REFERENCES

ANISOVICH	17A	PRL 119 062004	A.V. Anisovich *et al.*	
ANISOVICH	17B	PL B771 142	A.V. Anisovich *et al.*	
ANISOVICH	17C	PL B772 247	A.V. Anisovich *et al.*	
KASHEVAROV	17	PRL 118 212001	V.L. Kashevarov *et al.*	(A2/MAMI Collab.)
DENISENKO	16	PL B755 97	I. Denisenko *et al.*	
SOKHOYAN	15A	EPJ A51 95	V. Sokhoyan *et al.*	(CBELSA/TAPS Collab.)
SVARC	14	PR C89 045205	A. Svarc *et al.*	(RBI Zagreb, UNI Tuzla)
ANISOVICH	13B	EPJ A49 67	A.V. Anisovich *et al.*	
ANISOVICH	12A	EPJ A48 15	A.V. Anisovich *et al.*	(BONN, PNPI)
SHRESTHA	12A	PR C86 055203	M. Shrestha, D.M. Manley	(KSU)
BATINIC	10	PR C82 038203	M. Batinic *et al.*	(ZAGR)
VRANA	00	PRPL 328 181	T.P. Vrana, S.A. Dytman, T.-S.H. Lee	(PITT, ANL)
CUTKOSKY	80	Toronto Conf. 19	R.E. Cutkosky *et al.*	(CMU, LBL) IJP
Also		PR D20 2839	R.E. Cutkosky *et al.*	(CMU, LBL)
HOEHLER	79	PDAT 12-1	G. Hohler *et al.*	(KARLT) IJP
Also		Toronto Conf. 3	R. Koch	(KARLT) IJP

$N(1900)$ $3/2^+$

$I(J^P) = \frac{1}{2}(\frac{3}{2}^+)$ Status: ****

$N(1900)$ POLE POSITION

REAL PART

VALUE (MeV)	DOCUMENT ID		TECN	COMMENT
1900 to 1940 (≈ 1920) OUR ESTIMATE				
1945±35	ANISOVICH	17A	DPWA	Multichannel
1928±18±2	[1] SVARC	14	L+P	$\pi N \to \pi N$
• • • We do not use the following data for averages, fits, limits, etc. • • •				
1912±30	[2] ANISOVICH	17A	L+P	γp, $\pi^- p \to K\Lambda$
1910±30	SOKHOYAN	15A	DPWA	Multichannel
1910±30	GUTZ	14	DPWA	Multichannel
1910	SHKLYAR	13	DPWA	Multichannel
1900±30	ANISOVICH	12A	DPWA	Multichannel
1895	SHRESTHA	12A	DPWA	Multichannel

[1] Fit to the amplitudes of HOEHLER 79.

[2] Statistical error only.

−2×IMAGINARY PART

VALUE (MeV)	DOCUMENT ID		TECN	COMMENT
100 to 200 (≈ 150) OUR ESTIMATE				
135^{+70}_{-30}	ANISOVICH	17A	DPWA	Multichannel
152 ± 40 ± 9	[1] SVARC	14	L+P	$\pi N \to \pi N$
• • • We do not use the following data for averages, fits, limits, etc. • • •				
166 ± 30	[2] ANISOVICH	17A	L+P	$\gamma p, \pi^- p \to K\Lambda$
280 ± 50	SOKHOYAN	15A	DPWA	Multichannel
280 ± 50	GUTZ	14	DPWA	Multichannel
173	SHKLYAR	13	DPWA	Multichannel
200^{+100}_{-60}	ANISOVICH	12A	DPWA	Multichannel
100	SHRESTHA	12A	DPWA	Multichannel

[1] Fit to the amplitudes of HOEHLER 79.
[2] Statistical error only.

N(1900) ELASTIC POLE RESIDUE

MODULUS |r|

VALUE (MeV)	DOCUMENT ID		TECN	COMMENT
2 to 6 (≈ 4) OUR ESTIMATE				
4 ± 2	SOKHOYAN	15A	DPWA	Multichannel
4 ± 1 ± 1	[1] SVARC	14	L+P	$\pi N \to \pi N$
• • • We do not use the following data for averages, fits, limits, etc. • • •				
4 ± 2	GUTZ	14	DPWA	Multichannel
10	SHKLYAR	13	DPWA	Multichannel
3 ± 2	ANISOVICH	12A	DPWA	Multichannel

[1] Fit to the amplitudes of HOEHLER 79.

PHASE θ

VALUE (°)	DOCUMENT ID		TECN	COMMENT
−50 to 10 (≈ − 20) OUR ESTIMATE				
−10 ± 40	SOKHOYAN	15A	DPWA	Multichannel
−29 ± 15 ± 2	[1] SVARC	14	L+P	$\pi N \to \pi N$
• • • We do not use the following data for averages, fits, limits, etc. • • •				
−10 ± 40	GUTZ	14	DPWA	Multichannel
−64	SHKLYAR	13	DPWA	Multichannel
10 ± 35	ANISOVICH	12A	DPWA	Multichannel

[1] Fit to the amplitudes of HOEHLER 79.

N(1900) INELASTIC POLE RESIDUE

The "normalized residue" is the residue divided by $\Gamma_{pole}/2$.

Normalized residue in $N\pi \to N(1900) \to N\eta$

MODULUS	PHASE (°)	DOCUMENT ID		TECN	COMMENT
0.05 ± 0.02	70 ± 60	ANISOVICH	12A	DPWA	Multichannel

Normalized residue in $N\pi \to N(1900) \to \Lambda K$

MODULUS	PHASE (°)	DOCUMENT ID		TECN	COMMENT
0.03 ± 0.02	90 ± 40	ANISOVICH	17A	DPWA	Multichannel
• • • We do not use the following data for averages, fits, limits, etc. • • •					
0.07 ± 0.03	135 ± 25	ANISOVICH	12A	DPWA	Multichannel

Normalized residue in $N\pi \to N(1900) \to \Sigma K$

MODULUS	PHASE (°)	DOCUMENT ID		TECN	COMMENT
0.04 ± 0.02	110 ± 30	ANISOVICH	12A	DPWA	Multichannel

Normalized residue in $N\pi \to N(1900) \to N(1535)\pi$

MODULUS	PHASE (°)	DOCUMENT ID		TECN	COMMENT
0.04 ± 0.01	170 ± 30	GUTZ	14	DPWA	Multichannel

Normalized residue in $N\pi \to N(1900) \to \Delta(1232)\pi$, P-wave

MODULUS	PHASE (°)	DOCUMENT ID		TECN	COMMENT
0.07 ± 0.04	−65 ± 30	SOKHOYAN	15A	DPWA	Multichannel

Normalized residue in $N\pi \to N(1900) \to \Delta(1232)\pi$, F-wave

MODULUS	PHASE (°)	DOCUMENT ID		TECN	COMMENT
0.10 ± 0.05	80 ± 30	SOKHOYAN	15A	DPWA	Multichannel

Normalized residue in $N\pi \to N(1900) \to N(1520)\pi$

MODULUS	PHASE (°)	DOCUMENT ID		TECN	COMMENT
0.07 ± 0.04	−105 ± 35	SOKHOYAN	15A	DPWA	Multichannel

Normalized residue in $N\pi \to N(1900) \to N\sigma$

MODULUS	PHASE (°)	DOCUMENT ID		TECN	COMMENT
0.03 ± 0.02	−110 ± 35	SOKHOYAN	15A	DPWA	Multichannel

N(1900) BREIT-WIGNER MASS

VALUE (MeV)	DOCUMENT ID		TECN	COMMENT
1890 to 1950 (≈ 1920) OUR ESTIMATE				
1910 ± 30	SOKHOYAN	15A	DPWA	Multichannel
1998 ± 3	[1] SHKLYAR	13	DPWA	Multichannel
1900 ± 8	[1] SHRESTHA	12A	DPWA	Multichannel
• • • We do not use the following data for averages, fits, limits, etc. • • •				
1910 ± 30	GUTZ	14	DPWA	Multichannel
1905 ± 30	ANISOVICH	12A	DPWA	Multichannel
1951 ± 53	PENNER	02C	DPWA	Multichannel

[1] Statistical error only.

N(1900) BREIT-WIGNER WIDTH

VALUE (MeV)	DOCUMENT ID		TECN	COMMENT
100 to 320 (≈ 200) OUR ESTIMATE				
270 ± 50	SOKHOYAN	15A	DPWA	Multichannel
359 ± 10	[1] SHKLYAR	13	DPWA	Multichannel
101 ± 15	[1] SHRESTHA	12A	DPWA	Multichannel
• • • We do not use the following data for averages, fits, limits, etc. • • •				
270 ± 50	GUTZ	14	DPWA	Multichannel
250^{+120}_{-50}	ANISOVICH	12A	DPWA	Multichannel
622 ± 42	PENNER	02C	DPWA	Multichannel

[1] Statistical error only.

N(1900) DECAY MODES

	Mode	Fraction (Γ_i/Γ)
Γ_1	$N\pi$	1–20 %
Γ_2	$N\eta$	2–14 %
Γ_3	$N\eta'$	4–8 %
Γ_4	$N\omega$	7–13 %
Γ_5	ΛK	2–20 %
Γ_6	ΣK	3–7 %
Γ_7	$N\pi\pi$	40–80 %
Γ_8	$\Delta(1232)\pi$	30–70 %
Γ_9	$\Delta(1232)\pi$, P-wave	9–25 %
Γ_{10}	$\Delta(1232)\pi$, F-wave	21–45 %
Γ_{11}	$\Lambda K^*(892)$	< 0.2 %
Γ_{12}	$N\sigma$	1–7 %
Γ_{13}	$N(1520)\pi$	7–23 %
Γ_{14}	$N(1535)\pi$	4–10 %
Γ_{15}	$p\gamma$	0.001–0.025 %
Γ_{16}	$p\gamma$, helicity=1/2	0.001–0.021 %
Γ_{17}	$p\gamma$, helicity=3/2	<0.003 %
Γ_{18}	$n\gamma$	<0.040 %
Γ_{19}	$n\gamma$, helicity=1/2	<0.007 %
Γ_{20}	$n\gamma$, helicity=3/2	<0.033 %

N(1900) BRANCHING RATIOS

$\Gamma(N\pi)/\Gamma_{total}$ Γ_1/Γ

VALUE (%)	DOCUMENT ID		TECN	COMMENT
2 to 20 (≈ 10) OUR ESTIMATE				
3 ± 2	SOKHOYAN	15A	DPWA	Multichannel
25 ± 1	[1] SHKLYAR	13	DPWA	Multichannel
7 ± 4	[1] SHRESTHA	12A	DPWA	Multichannel
• • • We do not use the following data for averages, fits, limits, etc. • • •				
3 ± 2	GUTZ	14	DPWA	Multichannel
3 ± 2	ANISOVICH	12A	DPWA	Multichannel
16 ± 2	PENNER	02C	DPWA	Multichannel

[1] Statistical error only.

$\Gamma(N\eta)/\Gamma_{total}$ Γ_2/Γ

VALUE (%)	DOCUMENT ID		TECN	COMMENT
2 ± 2	[1] SHKLYAR	13	DPWA	Multichannel
10 ± 4	ANISOVICH	12A	DPWA	Multichannel
< 1	SHRESTHA	12A	DPWA	Multichannel
• • • We do not use the following data for averages, fits, limits, etc. • • •				
14 ± 5	PENNER	02C	DPWA	Multichannel

[1] Statistical error only.

$\Gamma(N\eta')/\Gamma_{total}$ Γ_3/Γ

VALUE	DOCUMENT ID		TECN	COMMENT
0.06 ± 0.02	ANISOVICH	17C	DPWA	Multichannel

$\Gamma(N\omega)/\Gamma_{total}$ Γ_4/Γ

VALUE (%)	DOCUMENT ID		TECN	COMMENT
15±8	DENISENKO	16	DPWA	Multichannel
10±3	[1] SHKLYAR	13	DPWA	Multichannel
• • • We do not use the following data for averages, fits, limits, etc. • • •				
39±9	PENNER	02C	DPWA	Multichannel

[1] Statistical error only.

$\Gamma(\Lambda K)/\Gamma_{total}$ Γ_5/Γ

VALUE (%)	DOCUMENT ID		TECN	COMMENT
16 ±5	ANISOVICH	12A	DPWA	Multichannel
14 ±5	[1] SHRESTHA	12A	DPWA	Multichannel
2.4±0.3	[1] SHKLYAR	05	DPWA	Multichannel
• • • We do not use the following data for averages, fits, limits, etc. • • •				
5 to 15	NIKONOV	08	DPWA	Multichannel
0.1±0.1	PENNER	02C	DPWA	Multichannel

[1] Statistical error only.

$\Gamma(\Sigma K)/\Gamma_{total}$ Γ_6/Γ

VALUE (%)	DOCUMENT ID		TECN	COMMENT
5±2	ANISOVICH	12A	DPWA	Multichannel
• • • We do not use the following data for averages, fits, limits, etc. • • •				
1±1	PENNER	02C	DPWA	Multichannel

$\Gamma(\Lambda K^*(892))/\Gamma_{total}$ Γ_{11}/Γ

VALUE	DOCUMENT ID		TECN	COMMENT
<0.002	ANISOVICH	17B	DPWA	Multichannel

$\Gamma(N\sigma)/\Gamma_{total}$ Γ_{12}/Γ

VALUE (%)	DOCUMENT ID		TECN	COMMENT
4±3	SOKHOYAN	15A	DPWA	Multichannel

$\Gamma(N(1520)\pi)/\Gamma_{total}$ Γ_{13}/Γ

VALUE (%)	DOCUMENT ID		TECN	COMMENT
15±8	SOKHOYAN	15A	DPWA	Multichannel

$\Gamma(N(1535)\pi)/\Gamma_{total}$ Γ_{14}/Γ

VALUE (%)	DOCUMENT ID		TECN	COMMENT
7±3	GUTZ	14	DPWA	Multichannel

$\Gamma(\Delta(1232)\pi, P\text{-wave})/\Gamma_{total}$ Γ_9/Γ

VALUE (%)	DOCUMENT ID		TECN	COMMENT
17±8	SOKHOYAN	15A	DPWA	Multichannel

$\Gamma(\Delta(1232)\pi, F\text{-wave})/\Gamma_{total}$ Γ_{10}/Γ

VALUE (%)	DOCUMENT ID		TECN	COMMENT
33±12	SOKHOYAN	15A	DPWA	Multichannel

$N(1900)$ PHOTON DECAY AMPLITUDES AT THE POLE

$N(1900) \to p\gamma$, helicity-1/2 amplitude $A_{1/2}$

MODULUS ($GeV^{-1/2}$)	PHASE (°)	DOCUMENT ID		TECN	COMMENT
0.026±0.014	60 ± 35	SOKHOYAN	15A	DPWA	Multichannel

$N(1900) \to p\gamma$, helicity-3/2 amplitude $A_{3/2}$

MODULUS ($GeV^{-1/2}$)	PHASE (°)	DOCUMENT ID		TECN	COMMENT
−0.070±0.030	70 ± 50	SOKHOYAN	15A	DPWA	Multichannel

$N(1900)$ BREIT-WIGNER PHOTON DECAY AMPLITUDES

$N(1900) \to p\gamma$, helicity-1/2 amplitude $A_{1/2}$

VALUE ($GeV^{-1/2}$)	DOCUMENT ID		TECN	COMMENT
0.024±0.014	SOKHOYAN	15A	DPWA	Multichannel
−0.008±0.001	[1] SHKLYAR	13	DPWA	Multichannel
• • • We do not use the following data for averages, fits, limits, etc. • • •				
0.024±0.014	GUTZ	14	DPWA	Multichannel
0.026±0.015	ANISOVICH	12A	DPWA	Multichannel
0.041±0.008	[1] SHRESTHA	12A	DPWA	Multichannel
−0.017	PENNER	02D	DPWA	Multichannel

[1] Statistical error only.

$N(1900) \to p\gamma$, helicity-3/2 amplitude $A_{3/2}$

VALUE ($GeV^{-1/2}$)	DOCUMENT ID		TECN	COMMENT
−0.067±0.030	SOKHOYAN	15A	DPWA	Multichannel
< 0.001	SHKLYAR	13	DPWA	Multichannel
• • • We do not use the following data for averages, fits, limits, etc. • • •				
−0.067±0.030	GUTZ	14	DPWA	Multichannel
−0.065±0.030	ANISOVICH	12A	DPWA	Multichannel
−0.004±0.006	[1] SHRESTHA	12A	DPWA	Multichannel
0.031	PENNER	02D	DPWA	Multichannel

[1] Statistical error only.

$N(1900) \to n\gamma$, helicity-1/2 amplitude $A_{1/2}$

VALUE ($GeV^{-1/2}$)	DOCUMENT ID		TECN	COMMENT
0.000±0.030	ANISOVICH	13B	DPWA	Multichannel
• • • We do not use the following data for averages, fits, limits, etc. • • •				
−0.010±0.004	[1] SHRESTHA	12A	DPWA	Multichannel
−0.016	PENNER	02D	DPWA	Multichannel

[1] Statistical error only.

$N(1900) \to n\gamma$, helicity-3/2 amplitude $A_{3/2}$

VALUE ($GeV^{-1/2}$)	DOCUMENT ID		TECN	COMMENT
−0.060±0.045	ANISOVICH	13B	DPWA	Multichannel
• • • We do not use the following data for averages, fits, limits, etc. • • •				
−0.011±0.007	[1] SHRESTHA	12A	DPWA	Multichannel
−0.002	PENNER	02D	DPWA	Multichannel

[1] Statistical error only.

$N(1900)$ REFERENCES

ANISOVICH	17A	PRL 119 062004	A.V. Anisovich *et al.*	
ANISOVICH	17B	PL B771 142	A.V. Anisovich *et al.*	
ANISOVICH	17C	PL B772 247	A.V. Anisovich *et al.*	
DENISENKO	16	PL B755 97	I. Denisenko *et al.*	
SOKHOYAN	15A	EPJ A51 95	V. Sokhoyan *et al.*	(CBELSA/TAPS Collab.)
GUTZ	14	EPJ A50 74	E. Gutz *et al.*	(CBELSA/TAPS Collab.)
SVARC	14	PR C89 045205	A. Svarc *et al.*	(RBI Zagreb, UNI Tuzla)
ANISOVICH	13B	EPJ A49 67	A.V. Anisovich *et al.*	
SHKLYAR	13	PR C87 015201	V. Shklyar, H. Lenske, U. Mosel	(GIES)
ANISOVICH	12A	EPJ A48 15	A.V. Anisovich *et al.*	(BONN, PNPI)
SHRESTHA	12A	PR C86 055203	M. Shrestha, D.M. Manley	(KSU)
NIKONOV	08	PL B662 245	V.A. Nikonov *et al.*	(Bonn, Gatchina)
SHKLYAR	05	PR C72 015210	V. Shklyar, H. Lenske, U. Mosel	(GIES)
PENNER	02C	PR C66 055211	G. Penner, U. Mosel	(GIES)
PENNER	02D	PR C66 055212	G. Penner, U. Mosel	(GIES)
HOEHLER	79	PDAT 12-1	G. Hohler *et al.*	(KARLT)

$N(1990)\ 7/2^+$

$I(J^P) = \frac{1}{2}(\frac{7}{2}^+)$ Status: **

OMITTED FROM SUMMARY TABLE

Older and obsolete values are listed and referenced in the 2014 edition, Chinese Physics **C38** 070001 (2014).

$N(1990)$ POLE POSITION

REAL PART

VALUE (MeV)	DOCUMENT ID		TECN	COMMENT
2030±65	ANISOVICH	12A	DPWA	Multichannel
1900±30	CUTKOSKY	80	IPWA	$\pi N \to \pi N$
• • • We do not use the following data for averages, fits, limits, etc. • • •				
1738	ROENCHEN	15A	DPWA	Multichannel
1941	SHRESTHA	12A	DPWA	Multichannel
2301	VRANA	00	DPWA	Multichannel

−2×IMAGINARY PART

VALUE (MeV)	DOCUMENT ID		TECN	COMMENT
240±60	ANISOVICH	12A	DPWA	Multichannel
260±60	CUTKOSKY	80	IPWA	$\pi N \to \pi N$
• • • We do not use the following data for averages, fits, limits, etc. • • •				
188	ROENCHEN	15A	DPWA	Multichannel
130	SHRESTHA	12A	DPWA	Multichannel
202	VRANA	00	DPWA	Multichannel

$N(1990)$ ELASTIC POLE RESIDUE

MODULUS $|r|$

VALUE (MeV)	DOCUMENT ID		TECN	COMMENT
2 ±1	ANISOVICH	12A	DPWA	Multichannel
9 ±3	CUTKOSKY	80	IPWA	$\pi N \to \pi N$
• • • We do not use the following data for averages, fits, limits, etc. • • •				
4.3	ROENCHEN	15A	DPWA	Multichannel

PHASE θ

VALUE (°)	DOCUMENT ID		TECN	COMMENT
125±65	ANISOVICH	12A	DPWA	Multichannel
− 60±30	CUTKOSKY	80	IPWA	$\pi N \to \pi N$
• • • We do not use the following data for averages, fits, limits, etc. • • •				
− 70	ROENCHEN	15A	DPWA	Multichannel

$\Delta(1990)$ INELASTIC POLE RESIDUE

The "normalized residue" is the residue divided by $\Gamma_{pole}/2$.

Normalized residue in $N\pi \to N(1990) \to N\eta$

MODULUS	PHASE (°)	DOCUMENT ID		TECN	COMMENT
• • • We do not use the following data for averages, fits, limits, etc. • • •					
0.013	−82	ROENCHEN	15A	DPWA	Multichannel

Normalized residue in $N\pi \to N(1990) \to \Lambda K$

MODULUS	PHASE (°)	DOCUMENT ID		TECN	COMMENT
• • • We do not use the following data for averages, fits, limits, etc. • • •					
0.022	−111	ROENCHEN	15A	DPWA	Multichannel

Normalized residue in $N\pi \to N(1990) \to \Sigma K$

MODULUS	PHASE (°)	DOCUMENT ID		TECN	COMMENT
• • • We do not use the following data for averages, fits, limits, etc. • • •					
0.005	24	ROENCHEN	15A	DPWA	Multichannel

$N(1990)$ BREIT-WIGNER MASS

VALUE (MeV)	DOCUMENT ID		TECN	COMMENT
1950 to 2100 (≈ 2020) OUR ESTIMATE				
2060 ± 65	ANISOVICH	12A	DPWA	Multichannel
1990 ± 45	[1] SHRESTHA	12A	DPWA	Multichannel
1970 ± 50	CUTKOSKY	80	IPWA	$\pi N \to \pi N$
2005 ± 150	HOEHLER	79	IPWA	$\pi N \to \pi N$
• • • We do not use the following data for averages, fits, limits, etc. • • •				
2311 ± 16	VRANA	00	DPWA	Multichannel

[1] Statistical error only.

$N(1990)$ BREIT-WIGNER WIDTH

VALUE (MeV)	DOCUMENT ID		TECN	COMMENT
200 to 400 (≈ 300) OUR ESTIMATE				
240 ± 50	ANISOVICH	12A	DPWA	Multichannel
203 ± 161	[1] SHRESTHA	12A	DPWA	Multichannel
350 ± 120	CUTKOSKY	80	IPWA	$\pi N \to \pi N$
350 ± 100	HOEHLER	79	IPWA	$\pi N \to \pi N$
• • • We do not use the following data for averages, fits, limits, etc. • • •				
205 ± 72	VRANA	00	DPWA	Multichannel

[1] Statistical error only.

$N(1990)$ DECAY MODES

	Mode	Fraction (Γ_i/Γ)
Γ_1	$N\pi$	2–6 %
Γ_2	$p\gamma$	0.01–0.12 %
Γ_3	$p\gamma$, helicity=1/2	0.003–0.042 %
Γ_4	$p\gamma$, helicity=3/2	0.009–0.075 %
Γ_5	$n\gamma$	0.01–0.16 %
Γ_6	$n\gamma$, helicity=1/2	0.003–0.066 %
Γ_7	$n\gamma$, helicity=3/2	0.003–0.098 %

$N(1990)$ BRANCHING RATIOS

$\Gamma(N\pi)/\Gamma_{\text{total}}$ Γ_1/Γ

VALUE (%)	DOCUMENT ID		TECN	COMMENT
2 to 6 (≈ 4) OUR ESTIMATE				
2 ± 1	ANISOVICH	12A	DPWA	Multichannel
2 ± 1	[1] SHRESTHA	12A	DPWA	Multichannel
6 ± 2	CUTKOSKY	80	IPWA	$\pi N \to \pi N$
4 ± 2	HOEHLER	79	IPWA	$\pi N \to \pi N$
• • • We do not use the following data for averages, fits, limits, etc. • • •				
22 ± 11	VRANA	00	DPWA	Multichannel

[1] Statistical error only.

$N(1990)$ PHOTON DECAY AMPLITUDES AT THE POLE

$N(1990) \to p\gamma$, helicity-1/2 amplitude $A_{1/2}$

MODULUS ($GeV^{-1/2}$)	PHASE (°)	DOCUMENT ID		TECN	COMMENT
$0.010^{+0.011}_{-0.006}$	-103^{+108}_{-155}	ROENCHEN	14	DPWA	
• • • We do not use the following data for averages, fits, limits, etc. • • •					
0.029	67	ROENCHEN	15A	DPWA	Multichannel

$N(1990) \to p\gamma$, helicity-3/2 amplitude $A_{3/2}$

MODULUS ($GeV^{-1/2}$)	PHASE (°)	DOCUMENT ID		TECN	COMMENT
$0.053^{+0.023}_{-0.028}$	36^{+17}_{-4}	ROENCHEN	14	DPWA	
• • • We do not use the following data for averages, fits, limits, etc. • • •					
0.033	39	ROENCHEN	15A	DPWA	Multichannel

$N(1990)$ BREIT-WIGNER PHOTON DECAY AMPLITUDES

$N(1990) \to p\gamma$, helicity-1/2 amplitude $A_{1/2}$

VALUE ($GeV^{-1/2}$)	DOCUMENT ID		TECN	COMMENT
0.040 ± 0.012	ANISOVICH	12A	DPWA	Multichannel

$N(1990) \to p\gamma$, helicity-3/2 amplitude $A_{3/2}$

VALUE ($GeV^{-1/2}$)	DOCUMENT ID		TECN	COMMENT
0.057 ± 0.012	ANISOVICH	12A	DPWA	Multichannel

$N(1990) \to n\gamma$, helicity-1/2 amplitude $A_{1/2}$

VALUE ($GeV^{-1/2}$)	DOCUMENT ID		TECN	COMMENT
−0.045 ± 0.020	ANISOVICH	13B	DPWA	Multichannel

$N(1990) \to n\gamma$, helicity-3/2 amplitude $A_{3/2}$

VALUE ($GeV^{-1/2}$)	DOCUMENT ID		TECN	COMMENT
−0.052 ± 0.027	ANISOVICH	13B	DPWA	Multichannel

$N(1990)$ REFERENCES

For early references, see Physics Letters **111B** 1 (1982).

ROENCHEN	15A	EPJ A51 70	D. Roenchen *et al.*	
PDG	14	CP C38 070001	K. Olive *et al.*	(PDG Collab.)
ROENCHEN	14	EPJ A50 101	D. Roenchen *et al.*	
Also		EPJ A51 63 (errat.)	D. Roenchen *et al.*	
ANISOVICH	13B	EPJ A49 67	A.V. Anisovich *et al.*	
ANISOVICH	12A	EPJ A48 15	A.V. Anisovich *et al.*	(BONN, PNPI)
SHRESTHA	12A	PR C86 055203	M. Shrestha, D.M. Manley	(KSU)
VRANA	00	PRPL 328 181	T.P. Vrana, S.A. Dytman, T.-S.H. Lee	(PITT, ANL)
CUTKOSKY	80	Toronto Conf. 19	R.E. Cutkosky *et al.*	(CMU, LBL) IJP
Also		PR D20 2839	R.E. Cutkosky *et al.*	(CMU, LBL) IJP
HOEHLER	79	PDAT 12-1	G. Hohler *et al.*	(KARLT) IJP
Also		Toronto Conf. 3	R. Koch	(KARLT) IJP

$N(2000)\ 5/2^+$

$I(J^P) = \frac{1}{2}(\frac{5}{2}^+)$ Status: **

OMITTED FROM SUMMARY TABLE

Before the 2012 *Review*, all the evidence for a $J^P = 5/2^+$ state with a mass above 1800 MeV was filed under a two-star $N(2000)$. There is now some evidence from ANISOVICH 12A for two $5/2^+$ states in this region, so we have split the older data (according to mass) between two two-star $5/2^+$ states, an $N(1860)$ and an $N(2000)$.

$N(2000)$ POLE POSITION

REAL PART

VALUE (MeV)	DOCUMENT ID		TECN	COMMENT
2030 ± 40	SOKHOYAN	15A	DPWA	Multichannel
• • • We do not use the following data for averages, fits, limits, etc. • • •				
1900	SHKLYAR	13	DPWA	Multichannel
2030 ± 110	ANISOVICH	12A	DPWA	Multichannel

−2×IMAGINARY PART

VALUE (MeV)	DOCUMENT ID		TECN	COMMENT
380 ± 60	SOKHOYAN	15A	DPWA	Multichannel
• • • We do not use the following data for averages, fits, limits, etc. • • •				
123	SHKLYAR	13	DPWA	Multichannel
480 ± 100	ANISOVICH	12A	DPWA	Multichannel

$N(2000)$ ELASTIC POLE RESIDUE

MODULUS $|r|$

VALUE (MeV)	DOCUMENT ID		TECN	COMMENT
18 ± 8	SOKHOYAN	15A	DPWA	Multichannel
• • • We do not use the following data for averages, fits, limits, etc. • • •				
11	SHKLYAR	13	DPWA	Multichannel
35^{+80}_{-15}	ANISOVICH	12A	DPWA	Multichannel

PHASE θ

VALUE (°)	DOCUMENT ID		TECN	COMMENT
−150 ± 40	SOKHOYAN	15A	DPWA	Multichannel
• • • We do not use the following data for averages, fits, limits, etc. • • •				
− 6	SHKLYAR	13	DPWA	Multichannel
−100 ± 40	ANISOVICH	12A	DPWA	Multichannel

$N(2000)$ INELASTIC POLE RESIDUE

The "normalized residue" is the residue divided by $\Gamma_{pole}/2$.

Normalized residue in $N\pi \to N(2000) \to \Delta(1232)\pi$, P-wave

MODULUS	PHASE (°)	DOCUMENT ID		TECN	COMMENT
0.16 ± 0.06	100 ± 50	SOKHOYAN	15A	DPWA	Multichannel

Normalized residue in $N\pi \to N(2000) \to \Delta(1232)\pi$, F-wave

MODULUS	PHASE (°)	DOCUMENT ID		TECN	COMMENT
0.20 ± 0.10	−20 ± 45	SOKHOYAN	15A	DPWA	Multichannel

Normalized residue in $N\pi \to N(2000) \to N\sigma$

MODULUS	PHASE (°)	DOCUMENT ID		TECN	COMMENT
0.12 ± 0.06	80 ± 40	SOKHOYAN	15A	DPWA	Multichannel

Normalized residue in $N\pi \rightarrow N(2000) \rightarrow N(1520)\pi$, D-wave

MODULUS	PHASE (°)	DOCUMENT ID		TECN	COMMENT
0.17±0.09	−60 ± 35	SOKHOYAN	15A	DPWA	Multichannel

$N(2000)$ BREIT-WIGNER MASS

VALUE (MeV)	DOCUMENT ID		TECN	COMMENT
2060± 30	SOKHOYAN	15A	DPWA	Multichannel
1946± 4	[1] SHKLYAR	13	DPWA	Multichannel
• • • We do not use the following data for averages, fits, limits, etc. • • •				
2090±120	ANISOVICH	12A	DPWA	Multichannel

[1] Statistical error only.

$N(2000)$ BREIT-WIGNER WIDTH

VALUE (MeV)	DOCUMENT ID		TECN	COMMENT
390± 55	SOKHOYAN	15A	DPWA	Multichannel
198± 2	[2] SHKLYAR	13	DPWA	Multichannel
• • • We do not use the following data for averages, fits, limits, etc. • • •				
460±100	ANISOVICH	12A	DPWA	Multichannel

[2] Statistical error only.

$N(2000)$ DECAY MODES

	Mode	Fraction (Γ_i/Γ)
Γ_1	$N\pi$	6–10 %
Γ_2	$N\eta$	<4 %
Γ_3	$N\omega$	<2 %
Γ_4	$N\pi\pi$	35–90 %
Γ_5	$\Delta(1232)\pi$	30–80 %
Γ_6	$\Delta(1232)\pi$, P-wave	12–32 %
Γ_7	$\Delta(1232)\pi$, F-wave	19–49 %
Γ_8	$\Lambda K^*(892)$	(2.2±1.0) %
Γ_9	$N\sigma$	5–15 %
Γ_{10}	$N(1520)\pi$, D-wave	11–31 %
Γ_{11}	$N(1680)\pi$, P-wave	17–25 %
Γ_{12}	$p\gamma$	0.01–0.08 %
Γ_{13}	$p\gamma$, helicity=1/2	0.003–0.031 %
Γ_{14}	$p\gamma$, helicity=3/2	0.008–0.048 %
Γ_{15}	$n\gamma$	0.002–0.07 %
Γ_{16}	$n\gamma$, helicity=1/2	<0.017 %
Γ_{17}	$n\gamma$, helicity=3/2	0.001–0.056 %

$N(2000)$ BRANCHING RATIOS

$\Gamma(N\pi)/\Gamma_{total}$ Γ_1/Γ

VALUE (%)	DOCUMENT ID		TECN	COMMENT
6 to 10 (≈ 8) OUR ESTIMATE				
8±4	SOKHOYAN	15A	DPWA	Multichannel
10±1	[3] SHKLYAR	13	DPWA	Multichannel
• • • We do not use the following data for averages, fits, limits, etc. • • •				
9±4	ANISOVICH	12A	DPWA	Multichannel

[3] Statistical error only.

$\Gamma(N\eta)/\Gamma_{total}$ Γ_2/Γ

VALUE (%)	DOCUMENT ID		TECN	COMMENT
2±2	[4] SHKLYAR	13	DPWA	Multichannel

[4] Statistical error only.

$\Gamma(N\omega)/\Gamma_{total}$ Γ_3/Γ

VALUE (%)	DOCUMENT ID		TECN	COMMENT
18±8	DENISENKO	16	DPWA	Multichannel
1±1	[5] SHKLYAR	13	DPWA	Multichannel

[5] Statistical error only.

$\Gamma(\Delta(1232)\pi, P\text{-wave})/\Gamma_{total}$ Γ_6/Γ

VALUE (%)	DOCUMENT ID		TECN	COMMENT
22±10	SOKHOYAN	15A	DPWA	Multichannel

$\Gamma(\Delta(1232)\pi, F\text{-wave})/\Gamma_{total}$ Γ_7/Γ

VALUE (%)	DOCUMENT ID		TECN	COMMENT
34±15	SOKHOYAN	15A	DPWA	Multichannel

$\Gamma(\Lambda K^*(892))/\Gamma_{total}$ Γ_8/Γ

VALUE	DOCUMENT ID		TECN	COMMENT
0.022±0.010	ANISOVICH	17B	DPWA	Multichannel

$\Gamma(N\sigma)/\Gamma_{total}$ Γ_9/Γ

VALUE (%)	DOCUMENT ID		TECN	COMMENT
10±5	SOKHOYAN	15A	DPWA	Multichannel

$\Gamma(N(1520)\pi, D\text{-wave})/\Gamma_{total}$ Γ_{10}/Γ

VALUE (%)	DOCUMENT ID		TECN	COMMENT
21±10	SOKHOYAN	15A	DPWA	Multichannel

$\Gamma(N(1680)\pi, P\text{-wave})/\Gamma_{total}$ Γ_{11}/Γ

VALUE (%)	DOCUMENT ID		TECN	COMMENT
16±9	SOKHOYAN	15A	DPWA	Multichannel

$N(2000)$ PHOTON DECAY AMPLITUDES AT THE POLE

$N(2000) \rightarrow p\gamma$, helicity-1/2 amplitude $A_{1/2}$

MODULUS ($GeV^{-1/2}$)	PHASE (°)	DOCUMENT ID		TECN	COMMENT
0.033±0.010	15 ± 25	SOKHOYAN	15A	DPWA	Multichannel

$N(2000) \rightarrow p\gamma$, helicity-3/2 amplitude $A_{3/2}$

MODULUS ($GeV^{-1/2}$)	PHASE (°)	DOCUMENT ID		TECN	COMMENT
0.045±0.008	−140 ± 25	SOKHOYAN	15A	DPWA	Multichannel

$N(2000)$ BREIT-WIGNER PHOTON DECAY AMPLITUDES

$N(2000) \rightarrow p\gamma$, helicity-1/2 amplitude $A_{1/2}$

VALUE ($GeV^{-1/2}$)	DOCUMENT ID		TECN	COMMENT
0.031±0.010	SOKHOYAN	15A	DPWA	Multichannel
0.011±0.001	[6] SHKLYAR	13	DPWA	Multichannel

[6] Statistical error only.

$N(2000) \rightarrow p\gamma$, helicity-3/2 amplitude $A_{3/2}$

VALUE ($GeV^{-1/2}$)	DOCUMENT ID		TECN	COMMENT
−0.043±0.008	SOKHOYAN	15A	DPWA	Multichannel
0.025±0.001	[7] SHKLYAR	13	DPWA	Multichannel

[7] Statistical error only.

$N(2000) \rightarrow n\gamma$, helicity-1/2 amplitude $A_{1/2}$

VALUE ($GeV^{-1/2}$)	DOCUMENT ID		TECN	COMMENT
−0.018±0.012	ANISOVICH	13B	DPWA	Multichannel

$N(2000) \rightarrow n\gamma$, helicity-3/2 amplitude $A_{3/2}$

VALUE ($GeV^{-1/2}$)	DOCUMENT ID		TECN	COMMENT
−0.035±0.020	ANISOVICH	13B	DPWA	Multichannel

$N(2000)$ REFERENCES

ANISOVICH	17B	PL B771 142	A.V. Anisovich *et al.*	
DENISENKO	16	PL B755 97	I. Denisenko *et al.*	
SOKHOYAN	15A	EPJ A51 95	V. Sokhoyan *et al.*	(CBELSA/TAPS Collab.)
ANISOVICH	13B	EPJ A49 67	A.V. Anisovich *et al.*	
SHKLYAR	13	PR C87 015201	V. Shklyar, H. Lenske, U. Mosel	(GIES)
ANISOVICH	12A	EPJ A48 15	A.V. Anisovich *et al.*	(BONN, PNPI)

$N(2040)$ $3/2^+$

$J^P = \frac{3}{2}^+$ Status: *

OMITTED FROM SUMMARY TABLE

$N(2040)$ MASS

VALUE (MeV)	DOCUMENT ID		TECN	COMMENT
$2040^{+3}_{-4}\pm25$	ABLIKIM	09B	BES2	$J/\psi \rightarrow p\overline{p}\pi^0$
$2068\pm3^{+15}_{-40}$	ABLIKIM	06K	BES2	$J/\psi \rightarrow p\overline{n}\pi^-$, $n\overline{p}\pi^+$

$N(2040)$ WIDTH

VALUE (MeV)	DOCUMENT ID		TECN	COMMENT
230± 8±52	ABLIKIM	09B	BES2	$J/\psi \rightarrow p\overline{p}\pi^0$
165±14±40	ABLIKIM	06K	BES2	$J/\psi \rightarrow p\overline{n}\pi^-$, $n\overline{p}\pi^+$

$N(2040)$ REFERENCES

ABLIKIM	09B	PR D80 052004	M. Ablikim *et al.*	(BES II Collab.)
ABLIKIM	06K	PRL 97 062001	M. Ablikim *et al.*	(BES II Collab.)

N(2060) 5/2⁻

$I(J^P) = \frac{1}{2}(\frac{5}{2}^-)$ Status: ***

Before our 2012 *Review*, this state appeared in our Listings as the $N(2200)$.

N(2060) POLE POSITION

REAL PART

VALUE (MeV)	DOCUMENT ID		TECN	COMMENT
2020 to 2130 (≈ 2070) OUR ESTIMATE				
2030±15	SOKHOYAN	15A	DPWA	Multichannel
2119±11±1	[1] SVARC	14	L+P	$\pi N \to \pi N$
2100±60	CUTKOSKY	80	IPWA	$\pi N \to \pi N$
• • • We do not use the following data for averages, fits, limits, etc. • • •				
2040±15	ANISOVICH	12A	DPWA	Multichannel
2064	SHRESTHA	12A	DPWA	Multichannel
2144±31	BATINIC	10	DPWA	$\pi N \to N\pi, N\eta$

[1] Fit to the amplitudes of HOEHLER 79.

−2×IMAGINARY PART

VALUE (MeV)	DOCUMENT ID		TECN	COMMENT
350 to 430 (≈ 400) OUR ESTIMATE				
400±35	SOKHOYAN	15A	DPWA	Multichannel
370±20±5	[1] SVARC	14	L+P	$\pi N \to \pi N$
360±80	CUTKOSKY	80	IPWA	$\pi N \to \pi N$
• • • We do not use the following data for averages, fits, limits, etc. • • •				
390±25	ANISOVICH	12A	DPWA	Multichannel
267	[2] SHRESTHA	12A	DPWA	Multichannel
438±13	BATINIC	10	DPWA	$\pi N \to N\pi, N\eta$

[1] Fit to the amplitudes of HOEHLER 79.
[2] Statistical error only.

N(2060) ELASTIC POLE RESIDUE

MODULUS |r|

VALUE (MeV)	DOCUMENT ID		TECN	COMMENT
15 to 30 (≈ 20) OUR ESTIMATE				
25± 8	SOKHOYAN	15A	DPWA	Multichannel
19± 1±1	[1] SVARC	14	L+P	$\pi N \to \pi N$
20±10	CUTKOSKY	80	IPWA	$\pi N \to \pi N$
• • • We do not use the following data for averages, fits, limits, etc. • • •				
19± 5	ANISOVICH	12A	DPWA	Multichannel
26	BATINIC	10	DPWA	$\pi N \to N\pi, N\eta$

[1] Fit to the amplitudes of HOEHLER 79.

PHASE θ

VALUE (°)	DOCUMENT ID		TECN	COMMENT
−130 to −90 (≈ −110) OUR ESTIMATE				
−130±20	SOKHOYAN	15A	DPWA	Multichannel
− 94± 5±1	[1] SVARC	14	L+P	$\pi N \to \pi N$
− 90±50	CUTKOSKY	80	IPWA	$\pi N \to \pi N$
• • • We do not use the following data for averages, fits, limits, etc. • • •				
−125±20	ANISOVICH	12A	DPWA	Multichannel
− 71	BATINIC	10	DPWA	$\pi N \to N\pi, N\eta$

[1] Fit to the amplitudes of HOEHLER 79.

N(2060) INELASTIC POLE RESIDUE

The "normalized residue" is the residue divided by $\Gamma_{pole}/2$.

Normalized residue in $N\pi \to N(2060) \to N\eta$

MODULUS	PHASE (°)	DOCUMENT ID		TECN	COMMENT
0.05±0.03	40 ± 25	ANISOVICH	12A	DPWA	Multichannel

Normalized residue in $N\pi \to N(2060) \to \Lambda K$

MODULUS	DOCUMENT ID		TECN	COMMENT
0.01±0.005	ANISOVICH	12A	DPWA	Multichannel

Normalized residue in $N\pi \to N(2060) \to \Sigma K$

MODULUS	PHASE (°)	DOCUMENT ID		TECN	COMMENT
0.04±0.02	−70 ± 30	ANISOVICH	12A	DPWA	Multichannel

Normalized residue in $N\pi \to N(2060) \to \Delta(1232)\pi$, D-wave

MODULUS	PHASE (°)	DOCUMENT ID		TECN	COMMENT
0.06±0.03	−90 ± 40	SOKHOYAN	15A	DPWA	Multichannel

Normalized residue in $N\pi \to N(2060) \to N\sigma$

MODULUS	PHASE (°)	DOCUMENT ID		TECN	COMMENT
0.12±0.06	80 ± 40	SOKHOYAN	15A	DPWA	Multichannel

Normalized residue in $N\pi \to N(2060) \to N(1440)\pi$

MODULUS	PHASE (°)	DOCUMENT ID		TECN	COMMENT
0.17±0.09	−60 ± 35	SOKHOYAN	15A	DPWA	Multichannel

Normalized residue in $N\pi \to N(2060) \to N(1520)\pi$, P-wave

MODULUS	PHASE (°)	DOCUMENT ID		TECN	COMMENT
0.14±0.06	−45 ± 15	SOKHOYAN	15A	DPWA	Multichannel

N(2060) BREIT-WIGNER MASS

VALUE (MeV)	DOCUMENT ID		TECN	COMMENT
2030 to 2200 (≈ 2100) OUR ESTIMATE				
2045±15	SOKHOYAN	15A	DPWA	Multichannel
2116±21	[1] SHRESTHA	12A	DPWA	Multichannel
2180±80	CUTKOSKY	80	IPWA	$\pi N \to \pi N$
2228±30	HOEHLER	79	IPWA	$\pi N \to \pi N$
• • • We do not use the following data for averages, fits, limits, etc. • • •				
2060±15	ANISOVICH	12A	DPWA	Multichannel
2217±27	BATINIC	10	DPWA	$\pi N \to N\pi, N\eta$

[1] Statistical error only.

N(2060) BREIT-WIGNER WIDTH

VALUE (MeV)	DOCUMENT ID		TECN	COMMENT
300 to 450 (≈ 400) OUR ESTIMATE				
420± 30	SOKHOYAN	15A	DPWA	Multichannel
307±112	[1] SHRESTHA	12A	DPWA	Multichannel
400±100	CUTKOSKY	80	IPWA	$\pi N \to \pi N$
310± 50	HOEHLER	79	IPWA	$\pi N \to \pi N$
• • • We do not use the following data for averages, fits, limits, etc. • • •				
375± 25	ANISOVICH	12A	DPWA	Multichannel
481± 17	BATINIC	10	DPWA	$\pi N \to N\pi, N\eta$

[1] Statistical error only.

N(2060) DECAY MODES

	Mode	Fraction (Γ_i/Γ)
Γ_1	$N\pi$	7–12 %
Γ_2	$N\eta$	2–6 %
Γ_3	$N\omega$	1–7 %
Γ_4	ΛK	seen
Γ_5	ΣK	1–5 %
Γ_6	$N\pi\pi$	7–19 %
Γ_7	$\Delta(1232)\pi$	
Γ_8	$\Delta(1232)\pi$, D-wave	4–10 %
Γ_9	$N\rho$	
Γ_{10}	$N\rho$, S=1/2, P-wave	seen
Γ_{11}	$\Lambda K^*(892)$	0.3–1.3 %
Γ_{12}	$N\sigma$	3–9 %
Γ_{13}	$N(1440)\pi$	4–14 %
Γ_{14}	$N(1520)\pi$, P-wave	9–21 %
Γ_{15}	$N(1680)\pi$, S-wave	8–22 %
Γ_{16}	$p\gamma$	0.03–0.19 %
Γ_{17}	$p\gamma$, helicity=1/2	0.02–0.08 %
Γ_{18}	$p\gamma$, helicity=3/2	0.01–0.10 %
Γ_{19}	$n\gamma$	0.003–0.07 %
Γ_{20}	$n\gamma$, helicity=1/2	0.001–0.02 %
Γ_{21}	$n\gamma$, helicity=3/2	0.002–0.05 %

N(2060) BRANCHING RATIOS

$\Gamma(N\pi)/\Gamma_{total}$ Γ_1/Γ

VALUE (%)	DOCUMENT ID		TECN	COMMENT
7 to 12 (≈ 10) OUR ESTIMATE				
11±2	SOKHOYAN	15A	DPWA	Multichannel
9±2	[1] SHRESTHA	12A	DPWA	Multichannel
10±3	CUTKOSKY	80	IPWA	$\pi N \to \pi N$
7±2	HOEHLER	79	IPWA	$\pi N \to \pi N$
• • • We do not use the following data for averages, fits, limits, etc. • • •				
8±2	ANISOVICH	12A	DPWA	Multichannel
13±4	BATINIC	10	DPWA	$\pi N \to N\pi, N\eta$

[1] Statistical error only.

$\Gamma(N\eta)/\Gamma_{total}$ Γ_2/Γ

VALUE (%)	DOCUMENT ID		TECN	COMMENT
4 ±2	ANISOVICH	12A	DPWA	Multichannel
<1	[1] SHRESTHA	12A	DPWA	Multichannel
• • • We do not use the following data for averages, fits, limits, etc. • • •				
0.2±1.0	BATINIC	10	DPWA	$\pi N \to N\pi, N\eta$

[1] Statistical error only.

$\Gamma(N\omega)/\Gamma_{total}$ Γ_3/Γ

VALUE (%)	DOCUMENT ID		TECN	COMMENT
4±3	DENISENKO	16	DPWA	Multichannel

$\Gamma(\Sigma K)/\Gamma_{total}$ Γ_5/Γ

VALUE (%)	DOCUMENT ID		TECN	COMMENT
3±2	ANISOVICH	12A	DPWA	Multichannel

$\Gamma(\Delta(1232)\pi$, D-wave$)/\Gamma_{total}$ Γ_8/Γ

VALUE (%)	DOCUMENT ID		TECN	COMMENT
7± 3	SOKHOYAN	15A	DPWA	Multichannel
40±13	[1] SHRESTHA	12A	DPWA	Multichannel

[1] Statistical error only.

$\Gamma(N\rho$, S=1/2, P-wave$)/\Gamma_{total}$ Γ_{10}/Γ

VALUE (%)	DOCUMENT ID		TECN	COMMENT
21±15	[1] SHRESTHA	12A	DPWA	Multichannel

[1] Statistical error only.

$\Gamma(\Lambda K^*(892))/\Gamma_{total}$ Γ_{11}/Γ

VALUE	DOCUMENT ID		TECN	COMMENT
0.008±0.005	ANISOVICH	17B	DPWA	Multichannel

$\Gamma(N\sigma)/\Gamma_{total}$ Γ_{12}/Γ

VALUE (%)	DOCUMENT ID		TECN	COMMENT
6±3	SOKHOYAN	15A	DPWA	Multichannel

$\Gamma(N(1440)\pi)/\Gamma_{total}$ Γ_{13}/Γ

VALUE (%)	DOCUMENT ID		TECN	COMMENT
9±5	SOKHOYAN	15A	DPWA	Multichannel

$\Gamma(N(1520)\pi$, P-wave$)/\Gamma_{total}$ Γ_{14}/Γ

VALUE (%)	DOCUMENT ID		TECN	COMMENT
15±6	SOKHOYAN	15A	DPWA	Multichannel

$\Gamma(N(1680)\pi$, S-wave$)/\Gamma_{total}$ Γ_{15}/Γ

VALUE (%)	DOCUMENT ID		TECN	COMMENT
15±7	SOKHOYAN	15A	DPWA	Multichannel

$N(2060)$ PHOTON DECAY AMPLITUDES AT THE POLE

$N(2060) \to p\gamma$, helicity-1/2 amplitude $A_{1/2}$

MODULUS ($GeV^{-1/2}$)	PHASE (°)	DOCUMENT ID		TECN	COMMENT
0.064±0.010	12 ± 8	SOKHOYAN	15A	DPWA	Multichannel

$N(2060) \to p\gamma$, helicity-3/2 amplitude $A_{3/2}$

MODULUS ($GeV^{-1/2}$)	PHASE (°)	DOCUMENT ID		TECN	COMMENT
0.060±0.020	13 ± 10	SOKHOYAN	15A	DPWA	Multichannel

$N(2060)$ BREIT-WIGNER PHOTON DECAY AMPLITUDES

$N(2060) \to p\gamma$, helicity-1/2 amplitude $A_{1/2}$

VALUE ($GeV^{-1/2}$)	DOCUMENT ID		TECN	COMMENT
0.062±0.010	SOKHOYAN	15A	DPWA	Multichannel
• • • We do not use the following data for averages, fits, limits, etc. • • •				
0.018±0.004	[1] SHRESTHA	12A	DPWA	Multichannel

[1] Statistical error only.

$N(2060) \to p\gamma$, helicity-3/2 amplitude $A_{3/2}$

VALUE ($GeV^{-1/2}$)	DOCUMENT ID		TECN	COMMENT
0.062±0.020	SOKHOYAN	15A	DPWA	Multichannel
• • • We do not use the following data for averages, fits, limits, etc. • • •				
0.010±0.004	[1] SHRESTHA	12A	DPWA	Multichannel

[1] Statistical error only.

$N(2060) \to n\gamma$, helicity-1/2 amplitude $A_{1/2}$

VALUE ($GeV^{-1/2}$)	DOCUMENT ID		TECN	COMMENT
0.025±0.011	ANISOVICH	13B	DPWA	Multichannel
• • • We do not use the following data for averages, fits, limits, etc. • • •				
−0.012±0.017	[1] SHRESTHA	12A	DPWA	Multichannel

[1] Statistical error only.

$N(2060) \to n\gamma$, helicity-3/2 amplitude $A_{3/2}$

VALUE ($GeV^{-1/2}$)	DOCUMENT ID		TECN	COMMENT
−0.037±0.017	ANISOVICH	13B	DPWA	Multichannel
• • • We do not use the following data for averages, fits, limits, etc. • • •				
−0.023±0.023	[1] SHRESTHA	12A	DPWA	Multichannel

[1] Statistical error only.

$N(2060)$ REFERENCES

ANISOVICH	17B	PL B771 142	A.V. Anisovich *et al.*	
DENISENKO	16	PL B755 97	I. Denisenko *et al.*	
SOKHOYAN	15A	EPJ A51 95	V. Sokhoyan *et al.*	(CBELSA/TAPS Collab.)
SVARC	14	PR C89 045205	A. Svarc *et al.*	(RBI Zagreb, UNI Tuzla)
ANISOVICH	13B	EPJ A49 67	A.V. Anisovich *et al.*	
ANISOVICH	12A	EPJ A48 15	A.V. Anisovich *et al.*	(BONN, PNPI)
SHRESTHA	12A	PR C86 055203	M. Shrestha, D.M. Manley	(KSU)
BATINIC	10	PR C82 038203	M. Batinic *et al.*	(ZAGR)
CUTKOSKY	80	Toronto Conf. 19	R.E. Cutkosky *et al.*	(CMU, LBL) IJP
Also		PR D20 2839	R.E. Cutkosky *et al.*	(CMU, LBL)
HOEHLER	79	PDAT 12-1	G. Hohler *et al.*	(KARLT) IJP
Also		Toronto Conf. 3	R. Koch	(KARLT) IJP

$N(2100)$ $1/2^+$

$I(J^P) = \frac{1}{2}(\frac{1}{2}^+)$ Status: ***

$N(2100)$ POLE POSITION

REAL PART

VALUE (MeV)	DOCUMENT ID		TECN	COMMENT
2050 to 2150 (≈ 2100) OUR ESTIMATE				
2120±25	SOKHOYAN	15A	DPWA	Multichannel
2052± 6±3	[1] SVARC	14	L+P	$\pi N \to \pi N$
2120±40	CUTKOSKY	80	IPWA	$\pi N \to \pi N$
• • • We do not use the following data for averages, fits, limits, etc. • • •				
2120±47	BATINIC	10	DPWA	$\pi N \to N\pi$, $N\eta$
1810	VRANA	00	DPWA	Multichannel

[1] Fit to the amplitudes of HOEHLER 79.

−2×IMAGINARY PART

VALUE (MeV)	DOCUMENT ID		TECN	COMMENT
240 to 340 (≈ 300) OUR ESTIMATE				
290±30	SOKHOYAN	15A	DPWA	Multichannel
337±10±4	[1] SVARC	14	L+P	$\pi N \to \pi N$
240±80	CUTKOSKY	80	IPWA	$\pi N \to \pi N$
• • • We do not use the following data for averages, fits, limits, etc. • • •				
346±80	BATINIC	10	DPWA	$\pi N \to N\pi$, $N\eta$
622	VRANA	00	DPWA	Multichannel

[1] Fit to the amplitudes of HOEHLER 79.

$N(2100)$ ELASTIC POLE RESIDUE

MODULUS $|r|$

VALUE (MeV)	DOCUMENT ID		TECN	COMMENT
15 to 30 (≈ 20) OUR ESTIMATE				
23±5	SOKHOYAN	15A	DPWA	Multichannel
30±1±1	[1] SVARC	14	L+P	$\pi N \to \pi N$
14±7	CUTKOSKY	80	IPWA	$\pi N \to \pi N$
• • • We do not use the following data for averages, fits, limits, etc. • • •				
33	BATINIC	10	DPWA	$\pi N \to N\pi$, $N\eta$

[1] Fit to the amplitudes of HOEHLER 79.

PHASE θ

VALUE (°)	DOCUMENT ID		TECN	COMMENT
−100 to −60 (≈ − 80) OUR ESTIMATE				
− 70±25	SOKHOYAN	15A	DPWA	Multichannel
− 92± 3±2	[1] SVARC	14	L+P	$\pi N \to \pi N$
35±25	CUTKOSKY	80	IPWA	$\pi N \to \pi N$
• • • We do not use the following data for averages, fits, limits, etc. • • •				
− 59	BATINIC	10	DPWA	$\pi N \to N\pi$, $N\eta$

[1] Fit to the amplitudes of HOEHLER 79.

$N(2100)$ INELASTIC POLE RESIDUE

Normalized residue in $N\pi \to N(2100) \to \Delta(1232)\pi$

MODULUS	PHASE (°)	DOCUMENT ID		TECN	COMMENT
0.11±0.05	20 ± 60	SOKHOYAN	15A	DPWA	Multichannel

Normalized residue in $N\pi \to N(2100) \to N\sigma$

MODULUS	PHASE (°)	DOCUMENT ID		TECN	COMMENT
0.18±0.06	125 ± 25	SOKHOYAN	15A	DPWA	Multichannel

Normalized residue in $N\pi \to N(2100) \to N(1535)\pi$

MODULUS	PHASE (°)	DOCUMENT ID		TECN	COMMENT
0.22±0.06	−40 ± 25	SOKHOYAN	15A	DPWA	Multichannel

$N(2100)$ BREIT-WIGNER MASS

VALUE (MeV)	DOCUMENT ID		TECN	COMMENT
2050 to 2150 (≈ 2100) OUR ESTIMATE				
2115±20	SOKHOYAN	15A	DPWA	Multichannel
2125±75	CUTKOSKY	80	IPWA	$\pi N \to \pi N$
2050±20	HOEHLER	79	IPWA	$\pi N \to \pi N$

• • • We do not use the following data for averages, fits, limits, etc. • • •				
2157±42	BATINIC	10	DPWA	$\pi N \to N\pi$, $N\eta$
2068± 3^{+15}_{-40}	ABLIKIM	06K	BES2	$J/\psi \to (p\pi^-)\overline{n}$
2084±93	VRANA	00	DPWA	Multichannel

$N(2100)$ BREIT-WIGNER WIDTH

VALUE (MeV)	DOCUMENT ID		TECN	COMMENT
200 to 320 (≈ 260) OUR ESTIMATE				
290± 20	SOKHOYAN	15A	DPWA	Multichannel
260±100	CUTKOSKY	80	IPWA	$\pi N \to \pi N$
200± 30	HOEHLER	79	IPWA	$\pi N \to \pi N$
• • • We do not use the following data for averages, fits, limits, etc. • • •				
355± 88	BATINIC	10	DPWA	$\pi N \to N\pi$, $N\eta$
165± 14±40	ABLIKIM	06K	BES2	$J/\psi \to (p\pi^-)\overline{n}$
1077±643	VRANA	00	DPWA	Multichannel

$N(2100)$ DECAY MODES

	Mode	Fraction (Γ_i/Γ)
Γ_1	$N\pi$	8–18 %
Γ_2	$N\eta$	seen
Γ_3	$N\eta'$	5–11 %
Γ_4	$N\omega$	10–25 %
Γ_5	ΛK	seen
Γ_6	$N\pi\pi$	20–40 %
Γ_7	$\Delta(1232)\pi$	
Γ_8	$\Delta(1232)\pi$, P-wave	6–14 %
Γ_9	$N\rho$	
Γ_{10}	$N\rho$, S=1/2, P-wave	seen
Γ_{11}	$\Lambda K^*(892)$	3–11 %
Γ_{12}	$N\sigma$	14–26 %
Γ_{13}	$N(1535)\pi$	26–34 %
Γ_{14}	$N\gamma$, helicity=1/2	0.001–0.012 %

$N(2100)$ BRANCHING RATIOS

$\Gamma(N\pi)/\Gamma_{\text{total}}$ Γ_1/Γ

VALUE (%)	DOCUMENT ID		TECN	COMMENT
8 to 18 (≈ 12) OUR ESTIMATE				
16±5	SOKHOYAN	15A	DPWA	Multichannel
12±3	CUTKOSKY	80	IPWA	$\pi N \to \pi N$
10±4	HOEHLER	79	IPWA	$\pi N \to \pi N$
• • • We do not use the following data for averages, fits, limits, etc. • • •				
16±5	BATINIC	10	DPWA	$\pi N \to N\pi$, $N\eta$
2±5	VRANA	00	DPWA	Multichannel

$\Gamma(N\eta)/\Gamma_{\text{total}}$ Γ_2/Γ

VALUE (%)	DOCUMENT ID		TECN	COMMENT
• • • We do not use the following data for averages, fits, limits, etc. • • •				
83± 5	BATINIC	10	DPWA	$\pi N \to N\pi$, $N\eta$
61±61	VRANA	00	DPWA	Multichannel

$\Gamma(N\eta')/\Gamma_{\text{total}}$ Γ_3/Γ

VALUE	DOCUMENT ID		TECN	COMMENT
0.08±0.03	ANISOVICH	17C	DPWA	Multichannel

$\Gamma(N\omega)/\Gamma_{\text{total}}$ Γ_4/Γ

VALUE (%)	DOCUMENT ID		TECN	COMMENT
15±10	DENISENKO	16	DPWA	Multichannel

$\Gamma(\Lambda K)/\Gamma_{\text{total}}$ Γ_5/Γ

VALUE (%)	DOCUMENT ID		TECN	COMMENT
• • • We do not use the following data for averages, fits, limits, etc. • • •				
21±20	VRANA	00	DPWA	Multichannel

$\Gamma(\Delta(1232)\pi$, P-wave$)/\Gamma_{\text{total}}$ Γ_8/Γ

VALUE (%)	DOCUMENT ID		TECN	COMMENT
10±4	SOKHOYAN	15A	DPWA	Multichannel
• • • We do not use the following data for averages, fits, limits, etc. • • •				
2±1	VRANA	00	DPWA	Multichannel

$\Gamma(N\rho$, S=1/2, P-wave$)/\Gamma_{\text{total}}$ Γ_{10}/Γ

VALUE (%)	DOCUMENT ID		TECN	COMMENT
• • • We do not use the following data for averages, fits, limits, etc. • • •				
4±1	VRANA	00	DPWA	Multichannel

$\Gamma(\Lambda K^*(892))/\Gamma_{\text{total}}$ Γ_{11}/Γ

VALUE	DOCUMENT ID		TECN	COMMENT
0.07±0.04	ANISOVICH	17B	DPWA	Multichannel

$\Gamma(N\sigma)/\Gamma_{\text{total}}$ Γ_{12}/Γ

VALUE (%)	DOCUMENT ID		TECN	COMMENT
20±6	SOKHOYAN	15A	DPWA	Multichannel
• • • We do not use the following data for averages, fits, limits, etc. • • •				
10±1	VRANA	00	DPWA	Multichannel

$\Gamma(N(1535)\pi)/\Gamma_{\text{total}}$ Γ_{13}/Γ

VALUE (%)	DOCUMENT ID		TECN	COMMENT
30±4	SOKHOYAN	15A	DPWA	Multichannel

$N(2100)$ PHOTON DECAY AMPLITUDES AT THE POLE

$N(2100) \to p\gamma$, helicity-1/2 amplitude $A_{1/2}$

MODULUS ($GeV^{-1/2}$)	PHASE (°)	DOCUMENT ID		TECN	COMMENT
0.011±0.004	65 ± 30	SOKHOYAN	15A	DPWA	Multichannel

$N(2100)$ BREIT-WIGNER PHOTON DECAY AMPLITUDES

$N(2100) \to p\gamma$, helicity-1/2 amplitude $A_{1/2}$

VALUE ($GeV^{-1/2}$)	DOCUMENT ID		TECN	COMMENT
0.010±0.004	SOKHOYAN	15A	DPWA	Multichannel

$N(2100)$ REFERENCES

ANISOVICH	17B	PL B771 142	A.V. Anisovich *et al.*	
ANISOVICH	17C	PL B772 247	A.V. Anisovich *et al.*	
DENISENKO	16	PL B755 97	I. Denisenko *et al.*	
SOKHOYAN	15A	EPJ A51 95	V. Sokhoyan *et al.*	(CBELSA/TAPS Collab.)
SVARC	14	PR C89 045205	A. Svarc *et al.*	(RBI Zagreb, UNI Tuzla)
BATINIC	10	PR C82 038203	M. Batinic *et al.*	(ZAGR)
ABLIKIM	06K	PRL 97 062001	M. Ablikim *et al.*	(BES II Collab.)
VRANA	00	PRPL 328 181	T.P. Vrana, S.A. Dytman, T.-S.H. Lee	(PITT, ANL)
CUTKOSKY	80	Toronto Conf. 19	R.E. Cutkosky *et al.*	(CMU, LBL) IJP
Also		PR D20 2839	R.E. Cutkosky *et al.*	(CMU, LBL)
HOEHLER	79	PDAT 12-1	G. Hohler *et al.*	(KARLT) IJP
Also		Toronto Conf. 3	R. Koch	(KARLT) IJP

$N(2120)$ $3/2^-$

$I(J^P) = \frac{1}{2}(\frac{3}{2}^-)$ Status: ***

Before the 2012 *Review*, all the evidence for a $J^P = 3/2^-$ state with a mass above 1800 MeV was filed under a two-star $N(2080)$. There is now evidence from ANISOVICH 12A for two $3/2^-$ states in this region, so we have split the older data (according to mass) between a three-star $N(1875)$ and a two-star $N(2120)$.

$N(2120)$ POLE POSITION

REAL PART

VALUE (MeV)	DOCUMENT ID		TECN	COMMENT
2050 to 2150 (≈ 2100) OUR ESTIMATE				
2115±40	SOKHOYAN	15A	DPWA	Multichannel
2094± 7±11	SVARC	14	L+P	$\pi N \to \pi N$
2050±70	CUTKOSKY	80	IPWA	$\pi N \to \pi N$ (higher m)
• • • We do not use the following data for averages, fits, limits, etc. • • •				
2115±40	GUTZ	14	DPWA	Multichannel
2110±50	ANISOVICH	12A	DPWA	Multichannel

−2×IMAGINARY PART

VALUE (MeV)	DOCUMENT ID		TECN	COMMENT
200 to 360 (≈ 280) OUR ESTIMATE				
345±35	SOKHOYAN	15A	DPWA	Multichannel
296±15±4	SVARC	14	L+P	$\pi N \to \pi N$
200±80	CUTKOSKY	80	IPWA	$\pi N \to \pi N$ (higher m)
• • • We do not use the following data for averages, fits, limits, etc. • • •				
345±35	GUTZ	14	DPWA	Multichannel
340±45	ANISOVICH	12A	DPWA	Multichannel

$N(2120)$ ELASTIC POLE RESIDUE

MODULUS $|r|$

VALUE (MeV)	DOCUMENT ID		TECN	COMMENT
10 to 30 (≈ 20) OUR ESTIMATE				
11± 6	SOKHOYAN	15A	DPWA	Multichannel
13± 1±1	SVARC	14	L+P	$\pi N \to \pi N$
30±20	CUTKOSKY	80	IPWA	$\pi N \to \pi N$ (higher m)
• • • We do not use the following data for averages, fits, limits, etc. • • •				
11± 6	GUTZ	14	DPWA	Multichannel
13± 3	ANISOVICH	12A	DPWA	Multichannel

PHASE θ

VALUE (°)	DOCUMENT ID		TECN	COMMENT
−40 to 20 (≈ − 10) OUR ESTIMATE				
−30± 20	SOKHOYAN	15A	DPWA	Multichannel
− 2± 4±9	SVARC	14	L+P	$\pi N \to \pi N$
0±100	CUTKOSKY	80	IPWA	$\pi N \to \pi N$ (higher m)
• • • We do not use the following data for averages, fits, limits, etc. • • •				
−30± 20	GUTZ	14	DPWA	Multichannel
−20± 10	ANISOVICH	12A	DPWA	Multichannel

N(2120) INELASTIC POLE RESIDUE

The "normalized residue" is the residue divided by $\Gamma_{pole}/2$.

Normalized residue in $N\pi \to N(2120) \to \Lambda K$

MODULUS	PHASE (°)	DOCUMENT ID		TECN	COMMENT
0.03±0.01	100 ± 30	ANISOVICH	12A	DPWA	Multichannel

Normalized residue in $N\pi \to N(2120) \to \Sigma K$

MODULUS	PHASE (°)	DOCUMENT ID		TECN	COMMENT
0.02±0.015	−50 ± 40	ANISOVICH	12A	DPWA	Multichannel

Normalized residue in $N\pi \to N(2120) \to N(1535)\pi$

MODULUS	PHASE (°)	DOCUMENT ID		TECN	COMMENT
0.15±0.08	−90 ± 40	GUTZ	14	DPWA	Multichannel

Normalized residue in $N\pi \to N(2120) \to \Delta(1232)\pi$, S-wave

MODULUS	PHASE (°)	DOCUMENT ID		TECN	COMMENT
0.25±0.10	undefined	SOKHOYAN	15A	DPWA	Multichannel

Normalized residue in $N\pi \to N(2120) \to \Delta(1232)\pi$, D-wave

MODULUS	PHASE (°)	DOCUMENT ID		TECN	COMMENT
0.15±0.06	−35 ± 30	SOKHOYAN	15A	DPWA	Multichannel

Normalized residue in $N\pi \to N(2120) \to N\sigma$

MODULUS	PHASE (°)	DOCUMENT ID		TECN	COMMENT
0.09±0.05	−80 ± 50	SOKHOYAN	15A	DPWA	Multichannel

N(2120) BREIT-WIGNER MASS

VALUE (MeV)	DOCUMENT ID		TECN	COMMENT
2060 to 2160 (≈ 2120) OUR ESTIMATE				
2120±45	SOKHOYAN	15A	DPWA	Multichannel
2060±80	CUTKOSKY	80	IPWA	$\pi N \to \pi N$
2081±20	HOEHLER	79	IPWA	$\pi N \to \pi N$
• • • We do not use the following data for averages, fits, limits, etc. • • •				
2120±35	GUTZ	14	DPWA	Multichannel
2150±60	ANISOVICH	12A	DPWA	Multichannel

N(2120) BREIT-WIGNER WIDTH

VALUE (MeV)	DOCUMENT ID		TECN	COMMENT
260 to 360 (≈ 300) OUR ESTIMATE				
340± 35	SOKHOYAN	15A	DPWA	Multichannel
300±100	CUTKOSKY	80	IPWA	$\pi N \to \pi N$ (higher m)
265± 40	HOEHLER	79	IPWA	$\pi N \to \pi N$
• • • We do not use the following data for averages, fits, limits, etc. • • •				
340± 35	GUTZ	14	DPWA	Multichannel
330± 45	ANISOVICH	12A	DPWA	Multichannel

N(2120) DECAY MODES

	Mode	Fraction (Γ_i/Γ)
Γ_1	$N\pi$	5–15 %
Γ_2	$N\eta'$	2–6 %
Γ_3	$N\omega$	4–20 %
Γ_4	$N\pi\pi$	50–95 %
Γ_5	$\Delta(1232)\pi$	40–90 %
Γ_6	$\Delta(1232)\pi$, S-wave	30–70 %
Γ_7	$\Delta(1232)\pi$, D-wave	8–32 %
Γ_8	$\Lambda K^*(892)$	< 0.2 %
Γ_9	$N\sigma$	7–15 %
Γ_{10}	$N(1535)\pi$	7–23 %
Γ_{11}	$p\gamma$	0.16–2.1 %
Γ_{12}	$p\gamma$, helicity=1/2	0.07–0.80 %
Γ_{13}	$p\gamma$, helicity=3/2	0.09–1.3 %
Γ_{14}	$n\gamma$	0.04–0.72 %
Γ_{15}	$n\gamma$, helicity=1/2	0.04–0.60 %
Γ_{16}	$n\gamma$, helicity=3/2	0.001–0.12 %

N(2120) BRANCHING RATIOS

$\Gamma(N\pi)/\Gamma_{total}$ — Γ_1/Γ

VALUE (%)	DOCUMENT ID		TECN	COMMENT
5 to 15 (≈ 10) OUR ESTIMATE				
5±3	SOKHOYAN	15A	DPWA	Multichannel
14±7	CUTKOSKY	80	IPWA	$\pi N \to \pi N$ (higher m)
6±2	HOEHLER	79	IPWA	$\pi N \to \pi N$
• • • We do not use the following data for averages, fits, limits, etc. • • •				
5±3	GUTZ	14	DPWA	Multichannel
6±2	ANISOVICH	12A	DPWA	Multichannel

$\Gamma(N\eta')/\Gamma_{total}$ — Γ_2/Γ

VALUE	DOCUMENT ID		TECN	COMMENT
0.04±0.02	ANISOVICH	17C	DPWA	Multichannel

$\Gamma(N\omega)/\Gamma_{total}$ — Γ_3/Γ

VALUE (%)	DOCUMENT ID		TECN	COMMENT
12±8	DENISENKO	16	DPWA	Multichannel

$\Gamma(\Delta(1232)\pi, S\text{-wave})/\Gamma_{total}$ — Γ_6/Γ

VALUE (%)	DOCUMENT ID		TECN	COMMENT
50±20	SOKHOYAN	15A	DPWA	Multichannel

$\Gamma(\Delta(1232)\pi, D\text{-wave})/\Gamma_{total}$ — Γ_7/Γ

VALUE (%)	DOCUMENT ID		TECN	COMMENT
20±12	SOKHOYAN	15A	DPWA	Multichannel

$\Gamma(\Lambda K^*(892))/\Gamma_{total}$ — Γ_8/Γ

VALUE	DOCUMENT ID		TECN	COMMENT
<0.002	ANISOVICH	17B	DPWA	Multichannel

$\Gamma(N\sigma)/\Gamma_{total}$ — Γ_9/Γ

VALUE (%)	DOCUMENT ID		TECN	COMMENT
11±4	SOKHOYAN	15A	DPWA	Multichannel

$\Gamma(N(1535)\pi)/\Gamma_{total}$ — Γ_{10}/Γ

VALUE (%)	DOCUMENT ID		TECN	COMMENT
15±8	GUTZ	14	DPWA	Multichannel

N(2120) PHOTON DECAY AMPLITUDES AT THE POLE

$N(2120) \to p\gamma$, helicity-1/2 amplitude $A_{1/2}$

MODULUS ($GeV^{-1/2}$)	PHASE (°)	DOCUMENT ID		TECN	COMMENT
0.130±0.045	−40 ± 25	SOKHOYAN	15A	DPWA	Multichannel

$N(2120) \to p\gamma$, helicity-3/2 amplitude $A_{3/2}$

MODULUS ($GeV^{-1/2}$)	PHASE (°)	DOCUMENT ID		TECN	COMMENT
0.160±0.060	−30 ± 15	SOKHOYAN	15A	DPWA	Multichannel

N(2120) BREIT-WIGNER PHOTON DECAY AMPLITUDES

$N(2120) \to p\gamma$, helicity-1/2 amplitude $A_{1/2}$

VALUE ($GeV^{-1/2}$)	DOCUMENT ID		TECN	COMMENT
0.130±0.050	SOKHOYAN	15A	DPWA	Multichannel
• • • We do not use the following data for averages, fits, limits, etc. • • •				
0.130±0.050	GUTZ	14	DPWA	Multichannel

$N(2120) \to p\gamma$, helicity-3/2 amplitude $A_{3/2}$

VALUE ($GeV^{-1/2}$)	DOCUMENT ID		TECN	COMMENT
0.160±0.065	SOKHOYAN	15A	DPWA	Multichannel
• • • We do not use the following data for averages, fits, limits, etc. • • •				
0.160±0.065	GUTZ	14	DPWA	Multichannel

$N(2120) \to n\gamma$, helicity-1/2 amplitude $A_{1/2}$

VALUE ($GeV^{-1/2}$)	DOCUMENT ID		TECN	COMMENT
0.110±0.045	ANISOVICH	13B	DPWA	Multichannel

$N(2120) \to n\gamma$, helicity-3/2 amplitude $A_{3/2}$

VALUE ($GeV^{-1/2}$)	DOCUMENT ID		TECN	COMMENT
0.040±0.030	ANISOVICH	13B	DPWA	Multichannel

N(2120) REFERENCES

ANISOVICH	17B	PL B771 142	A.V. Anisovich *et al.*	
ANISOVICH	17C	PL B772 247	A.V. Anisovich *et al.*	
DENISENKO	16	PL B755 97	I. Denisenko *et al.*	
SOKHOYAN	15A	EPJ A51 95	V. Sokhoyan *et al.*	(CBELSA/TAPS Collab.)
GUTZ	14	EPJ A50 74	E. Gutz *et al.*	(CBELSA/TAPS Collab.)
SVARC	14	PR C89 045205	A. Svarc *et al.*	(RBI Zagreb, UNI Tuzla)
ANISOVICH	13B	EPJ A49 67	A.V. Anisovich *et al.*	
ANISOVICH	12A	EPJ A48 15	A.V. Anisovich *et al.*	(BONN, PNPI)
CUTKOSKY	80	Toronto Conf. 19	R.E. Cutkosky *et al.*	(CMU, LBL)
HOEHLER	79	PDAT 12-1	G. Hohler *et al.*	(KARLT)

Baryon Particle Listings

$N(2190)$

$N(2190)\ 7/2^-$

$I(J^P) = \frac{1}{2}(\frac{7}{2}^-)$ Status: ****

Older and obsolete values are listed and referenced in the 2014 edition, Chinese Physics **C38** 070001 (2014).

$N(2190)$ POLE POSITION

REAL PART

VALUE (MeV)	DOCUMENT ID		TECN	COMMENT
2050 to 2150 (≈ 2100) OUR ESTIMATE				
2150±25	SOKHOYAN	15A	DPWA	Multichannel
2079± 4±9	[1] SVARC	14	L+P	$\pi N \to \pi N$
2100±50	CUTKOSKY	80	IPWA	$\pi N \to \pi N$
• • • We do not use the following data for averages, fits, limits, etc. • • •				
2074	ROENCHEN	15A	DPWA	Multichannel
2150±25	ANISOVICH	12A	DPWA	Multichannel
2062	SHRESTHA	12A	DPWA	Multichannel
2063±32	BATINIC	10	DPWA	$\pi N \to N\pi, N\eta$
2070	ARNDT	06	DPWA	$\pi N \to \pi N, \eta N$
2107	VRANA	00	DPWA	Multichannel
2042	HOEHLER	93	SPED	$\pi N \to \pi N$

[1] Fit to the amplitudes of HOEHLER 79.

−2×IMAGINARY PART

VALUE (MeV)	DOCUMENT ID		TECN	COMMENT
300 to 500 (≈ 400) OUR ESTIMATE				
325± 25	SOKHOYAN	15A	DPWA	Multichannel
509± 7±16	[1] SVARC	14	L+P	$\pi N \to \pi N$
400±160	CUTKOSKY	80	IPWA	$\pi N \to \pi N$
• • • We do not use the following data for averages, fits, limits, etc. • • •				
327	ROENCHEN	15A	DPWA	Multichannel
330± 30	ANISOVICH	12A	DPWA	Multichannel
428	SHRESTHA	12A	DPWA	Multichannel
330±101	BATINIC	10	DPWA	$\pi N \to N\pi, N\eta$
520	ARNDT	06	DPWA	$\pi N \to \pi N, \eta N$
380	VRANA	00	DPWA	Multichannel
482	HOEHLER	93	SPED	$\pi N \to \pi N$

[1] Fit to the amplitudes of HOEHLER 79.

$N(2190)$ ELASTIC POLE RESIDUE

MODULUS $|r|$

VALUE (MeV)	DOCUMENT ID		TECN	COMMENT
25 to 70 (≈ 50) OUR ESTIMATE				
30± 4	SOKHOYAN	15A	DPWA	Multichannel
54± 1±3	[1] SVARC	14	L+P	$\pi N \to \pi N$
25±10	CUTKOSKY	80	IPWA	$\pi N \to \pi N$
• • • We do not use the following data for averages, fits, limits, etc. • • •				
35	ROENCHEN	15A	DPWA	Multichannel
30± 5	ANISOVICH	12A	DPWA	Multichannel
34	BATINIC	10	DPWA	$\pi N \to N\pi, N\eta$
72	ARNDT	06	DPWA	$\pi N \to \pi N, \eta N$
45	HOEHLER	93	SPED	$\pi N \to \pi N$

[1] Fit to the amplitudes of HOEHLER 79.

PHASE θ

VALUE (°)	DOCUMENT ID		TECN	COMMENT
−30 to 30 (≈ 0) OUR ESTIMATE				
28±10	SOKHOYAN	15A	DPWA	Multichannel
−18± 1±3	[1] SVARC	14	L+P	$\pi N \to \pi N$
−30±50	CUTKOSKY	80	IPWA	$\pi N \to \pi N$
• • • We do not use the following data for averages, fits, limits, etc. • • •				
−40	ROENCHEN	15A	DPWA	Multichannel
30±10	ANISOVICH	12A	DPWA	Multichannel
−19	BATINIC	10	DPWA	$\pi N \to N\pi, N\eta$
−32	ARNDT	06	DPWA	$\pi N \to \pi N, \eta N$

[1] Fit to the amplitudes of HOEHLER 79.

$N(2190)$ INELASTIC POLE RESIDUE

The "normalized residue" is the residue divided by $\Gamma_{pole}/2$.

Normalized residue in $N\pi \to N(2190) \to \Lambda K$

MODULUS	PHASE (°)	DOCUMENT ID		TECN	COMMENT
0.03 ±0.01	20 ± 15	ANISOVICH	12A	DPWA	Multichannel
• • • We do not use the following data for averages, fits, limits, etc. • • •					
0.005	−51	ROENCHEN	15A	DPWA	Multichannel

Normalized residue in $N\pi \to N(2190) \to \Sigma K$

MODULUS	PHASE (°)	DOCUMENT ID		TECN	COMMENT
• • • We do not use the following data for averages, fits, limits, etc. • • •					
0.013	−69	ROENCHEN	15A	DPWA	Multichannel

Normalized residue in $N\pi \to N(2190) \to N\eta$

MODULUS	PHASE (°)	DOCUMENT ID		TECN	COMMENT
• • • We do not use the following data for averages, fits, limits, etc. • • •					
0.016	129	ROENCHEN	15A	DPWA	Multichannel

Normalized residue in $N\pi \to N(2190) \to \Delta(1232)\pi$, D-wave

MODULUS	PHASE (°)	DOCUMENT ID		TECN	COMMENT
0.27±0.04	−165 ± 20	SOKHOYAN	15A	DPWA	Multichannel

Normalized residue in $N\pi \to N(2190) \to N\sigma$

MODULUS	PHASE (°)	DOCUMENT ID		TECN	COMMENT
0.13±0.05	50 ± 15	SOKHOYAN	15A	DPWA	Multichannel

$N(2190)$ BREIT-WIGNER MASS

VALUE (MeV)	DOCUMENT ID		TECN	COMMENT
2140 to 2220 (≈ 2180) OUR ESTIMATE				
2205 ±18	SOKHOYAN	15A	DPWA	Multichannel
2150 ±26	[1] SHRESTHA	12A	DPWA	Multichannel
2152.4± 1.4	[1] ARNDT	06	DPWA	$\pi N \to \pi N, \eta N$
2200 ±70	CUTKOSKY	80	IPWA	$\pi N \to \pi N$
2140 ±12	HOEHLER	79	IPWA	$\pi N \to \pi N$
• • • We do not use the following data for averages, fits, limits, etc. • • •				
2180 ±20	ANISOVICH	12A	DPWA	Multichannel
2125 ±61	BATINIC	10	DPWA	$\pi N \to N\pi, N\eta$
2168 ±18	VRANA	00	DPWA	Multichannel

[1] Statistical error only.

$N(2190)$ BREIT-WIGNER WIDTH

VALUE (MeV)	DOCUMENT ID		TECN	COMMENT
300 to 500 (≈ 400) OUR ESTIMATE				
355± 30	SOKHOYAN	15A	DPWA	Multichannel
500± 74	[1] SHRESTHA	12A	DPWA	Multichannel
484± 13	[1] ARNDT	06	DPWA	$\pi N \to \pi N, \eta N$
500±150	CUTKOSKY	80	IPWA	$\pi N \to \pi N$
390± 30	HOEHLER	79	IPWA	$\pi N \to \pi N$
• • • We do not use the following data for averages, fits, limits, etc. • • •				
335± 40	ANISOVICH	12A	DPWA	Multichannel
381±160	BATINIC	10	DPWA	$\pi N \to N\pi, N\eta$
453±101	VRANA	00	DPWA	Multichannel

[1] Statistical error only.

$N(2190)$ DECAY MODES

The following branching fractions are our estimates, not fits or averages.

	Mode	Fraction (Γ_i/Γ)
Γ_1	$N\pi$	10–20 %
Γ_2	$N\eta$	1–3 %
Γ_3	$N\omega$	8–20 %
Γ_4	ΛK	
Γ_5	$N\pi\pi$	
Γ_6	$\Delta(1232)\pi$	
Γ_7	$\Delta(1232)\pi$, D-wave	19–31 %
Γ_8	$N\rho$	
Γ_9	$N\rho$, $S=3/2$, D-wave	seen
Γ_{10}	$\Lambda K^*(892)$	0.2–0.8 %
Γ_{11}	$N\sigma$	3–9 %
Γ_{12}	$p\gamma$	0.014–0.077 %
Γ_{13}	$p\gamma$, helicity=1/2	
Γ_{14}	$p\gamma$, helicity=3/2	
Γ_{15}	$n\gamma$	<0.04 %
Γ_{16}	$n\gamma$, helicity=1/2	
Γ_{17}	$n\gamma$, helicity=3/2	<0.03 %

$N(2190)$ BRANCHING RATIOS

$\Gamma(N\pi)/\Gamma_{total}$ Γ_1/Γ

VALUE (%)	DOCUMENT ID		TECN	COMMENT
10 to 20 (≈ 15) OUR ESTIMATE				
16 ± 2	SOKHOYAN	15A	DPWA	Multichannel
20 ± 1	[1] SHRESTHA	12A	DPWA	Multichannel
23.8± 0.1	[1] ARNDT	06	DPWA	$\pi N \to \pi N, \eta N$
12 ± 6	CUTKOSKY	80	IPWA	$\pi N \to \pi N$
14 ± 2	HOEHLER	79	IPWA	$\pi N \to \pi N$
• • • We do not use the following data for averages, fits, limits, etc. • • •				
16 ± 2	ANISOVICH	12A	DPWA	Multichannel
18 ±12	BATINIC	10	DPWA	$\pi N \to N\pi, N\eta$
20 ± 4	VRANA	00	DPWA	Multichannel

[1] Statistical error only.

$\Gamma(N\eta)/\Gamma_{total}$ Γ_2/Γ

VALUE (%)	DOCUMENT ID		TECN	COMMENT
2 ±1	[1] SHRESTHA	12A	DPWA	Multichannel
• • • We do not use the following data for averages, fits, limits, etc. • • •				
0.1±0.3	BATINIC	10	DPWA	$\pi N \to \pi N, N\eta$
0 ±1	VRANA	00	DPWA	Multichannel

[1] Statistical error only.

$\Gamma(N\omega)/\Gamma_{total}$ Γ_3/Γ

VALUE (%)	DOCUMENT ID		TECN	COMMENT
14±6	DENISENKO	16	DPWA	Multichannel
• • • We do not use the following data for averages, fits, limits, etc. • • •				
seen	WILLIAMS	09	IPWA	$\gamma p \to p\omega$

$\Gamma(\Lambda K)/\Gamma_{total}$ Γ_4/Γ

VALUE (%)	DOCUMENT ID		TECN	COMMENT
0.5±0.3	ANISOVICH	12A	DPWA	Multichannel
<1	SHRESTHA	12A	DPWA	Multichannel

$\Gamma(\Delta(1232)\pi, D\text{-wave})/\Gamma_{total}$ Γ_7/Γ

VALUE (%)	DOCUMENT ID		TECN	COMMENT
25±6	SOKHOYAN	15A	DPWA	Multichannel

$\Gamma(N\rho, S=3/2, D\text{-wave})/\Gamma_{total}$ Γ_9/Γ

VALUE (%)	DOCUMENT ID		TECN	COMMENT
• • • We do not use the following data for averages, fits, limits, etc. • • •				
29±28	VRANA	00	DPWA	Multichannel

$\Gamma(\Lambda K^*(892))/\Gamma_{total}$ Γ_{10}/Γ

VALUE	DOCUMENT ID		TECN	COMMENT
0.005±0.003	ANISOVICH	17B	DPWA	Multichannel

$\Gamma(N\sigma)/\Gamma_{total}$ Γ_{11}/Γ

VALUE (%)	DOCUMENT ID		TECN	COMMENT
6±3	SOKHOYAN	15A	DPWA	Multichannel

$N(2190)$ PHOTON DECAY AMPLITUDES AT THE POLE

$N(2190) \to p\gamma$, helicity-1/2 amplitude $A_{1/2}$

MODULUS ($GeV^{-1/2}$)	PHASE (°)	DOCUMENT ID		TECN	COMMENT
0.068±0.005	−170 ± 12	SOKHOYAN	15A	DPWA	Multichannel
$-0.083^{+0.007}_{-0.003}$	-11^{+6}_{-2}	ROENCHEN	14	DPWA	
• • • We do not use the following data for averages, fits, limits, etc. • • •					
−0.041	−21	ROENCHEN	15A	DPWA	Multichannel

$N(2190) \to p\gamma$, helicity-3/2 amplitude $A_{3/2}$

MODULUS ($GeV^{-1/2}$)	PHASE (°)	DOCUMENT ID		TECN	COMMENT
0.025±0.010	22 ± 10	SOKHOYAN	15A	DPWA	Multichannel
$0.095^{+0.013}_{-0.010}$	-3^{+3}_{-5}	ROENCHEN	14	DPWA	
• • • We do not use the following data for averages, fits, limits, etc. • • •					
0.085	−22	ROENCHEN	15A	DPWA	Multichannel

$N(2190)$ BREIT-WIGNER PHOTON DECAY AMPLITUDES

$N(2190) \to p\gamma$, helicity-1/2 amplitude $A_{1/2}$

VALUE ($GeV^{-1/2}$)	DOCUMENT ID		TECN	COMMENT
−0.071±0.006	SOKHOYAN	15A	DPWA	Multichannel
• • • We do not use the following data for averages, fits, limits, etc. • • •				
−0.065±0.008	ANISOVICH	12A	DPWA	Multichannel

$N(2190) \to p\gamma$, helicity-3/2 amplitude $A_{3/2}$

VALUE ($GeV^{-1/2}$)	DOCUMENT ID		TECN	COMMENT
0.027±0.010	SOKHOYAN	15A	DPWA	Multichannel
• • • We do not use the following data for averages, fits, limits, etc. • • •				
0.035±0.017	ANISOVICH	12A	DPWA	Multichannel

$N(2190) \to p\gamma$, ratio of helicity amplitudes $A_{3/2}/A_{1/2}$

VALUE	DOCUMENT ID		TECN	COMMENT
• • • We do not use the following data for averages, fits, limits, etc. • • •				
−0.17±0.15	WILLIAMS	09	IPWA	$\gamma p \to p\omega$

$N(2190) \to n\gamma$, helicity-1/2 amplitude $A_{1/2}$

VALUE ($GeV^{-1/2}$)	DOCUMENT ID		TECN	COMMENT
−0.015±0.013	ANISOVICH	13B	DPWA	Multichannel

$N(2190) \to n\gamma$, helicity-3/2 amplitude $A_{3/2}$

VALUE ($GeV^{-1/2}$)	DOCUMENT ID		TECN	COMMENT
−0.034±0.022	ANISOVICH	13B	DPWA	Multichannel

$N(2190)$ REFERENCES

For early references, see Physics Letters **111B** 1 (1982).

ANISOVICH	17B	PL B771 142	A.V. Anisovich *et al.*	
DENISENKO	16	PL B755 97	I. Denisenko *et al.*	
ROENCHEN	15A	EPJ A51 70	D. Roenchen *et al.*	
SOKHOYAN	15A	EPJ A51 95	V. Sokhoyan *et al.*	(CBELSA/TAPS Collab.)
PDG	14	CP C38 070001	K. Olive *et al.*	(PDG Collab.)
ROENCHEN	14	EPJ A50 101	D. Roenchen *et al.*	
Also		EPJ A51 63 (errat.)	D. Roenchen *et al.*	
SVARC	14	PR C89 045205	A. Svarc *et al.*	(RBI Zagreb, UNI Tuzla)
ANISOVICH	13B	EPJ A49 67	A.V. Anisovich *et al.*	
ANISOVICH	12A	EPJ A48 15	A.V. Anisovich *et al.*	(BONN, PNPI)
SHRESTHA	12A	PR C86 055203	M. Shrestha, D.M. Manley	(KSU)
BATINIC	10	PR C82 038203	M. Batinic *et al.*	(ZAGR)
WILLIAMS	09	PR C80 065209	M. Williams *et al.*	(JLab CLAS Collab.)
ARNDT	06	PR C74 045205	R.A. Arndt *et al.*	(GWU)
VRANA	00	PRPL 328 181	T.P. Vrana, S.A. Dytman, T.-S.H. Lee	(PITT, ANL)
HOEHLER	93	πN Newsletter 9 1	G. Hohler	(KARL)
CUTKOSKY	80	Toronto Conf. 19	R.E. Cutkosky *et al.*	(CMU, LBL) IJP
Also		PR D20 2839	R.E. Cutkosky *et al.*	(CMU, LBL) IJP
HOEHLER	79	PDAT 12-1	G. Hohler *et al.*	(KARLT) IJP
Also		Toronto Conf. 3	R. Koch	(KARLT) IJP

$N(2220)$ $9/2^+$

$I(J^P) = \frac{1}{2}(\frac{9}{2}^+)$ Status: ****

Older and obsolete values are listed and referenced in the 2014 edition, Chinese Physics **C38** 070001 (2014).

$N(2220)$ POLE POSITION

REAL PART

VALUE (MeV)	DOCUMENT ID		TECN	COMMENT
2130 to 2200 (≈ 2170) OUR ESTIMATE				
2127± 3±24	[1] SVARC	14	L+P	$\pi N \to \pi N$
2150±35	ANISOVICH	12A	DPWA	Multichannel
2160±80	CUTKOSKY	80	IPWA	$\pi N \to \pi N$
• • • We do not use the following data for averages, fits, limits, etc. • • •				
2171	ROENCHEN	15A	DPWA	Multichannel
2199	ARNDT	06	DPWA	$\pi N \to \pi N, \eta N$
2135	HOEHLER	93	ARGD	$\pi N \to \pi N$

[1] Fit to the amplitudes of HOEHLER 79.

−2×IMAGINARY PART

VALUE (MeV)	DOCUMENT ID		TECN	COMMENT
360 to 480 (≈ 400) OUR ESTIMATE				
380± 7±22	[1] SVARC	14	L+P	$\pi N \to \pi N$
440± 40	ANISOVICH	12A	DPWA	Multichannel
480±100	CUTKOSKY	80	IPWA	$\pi N \to \pi N$
• • • We do not use the following data for averages, fits, limits, etc. • • •				
593	ROENCHEN	15A	DPWA	Multichannel
372	ARNDT	06	DPWA	$\pi N \to \pi N, \eta N$
400	HOEHLER	93	ARGD	$\pi N \to \pi N$

[1] Fit to the amplitudes of HOEHLER 79.

$N(2220)$ ELASTIC POLE RESIDUE

MODULUS $|r|$

VALUE (MeV)	DOCUMENT ID		TECN	COMMENT
35 to 60 (≈ 45) OUR ESTIMATE				
38± 1±5	[1] SVARC	14	L+P	$\pi N \to \pi N$
60±12	ANISOVICH	12A	DPWA	Multichannel
45±20	CUTKOSKY	80	IPWA	$\pi N \to \pi N$
• • • We do not use the following data for averages, fits, limits, etc. • • •				
62	ROENCHEN	15A	DPWA	Multichannel
33	ARNDT	06	DPWA	$\pi N \to \pi N, \eta N$
40	HOEHLER	93	ARGD	$\pi N \to \pi N$

[1] Fit to the amplitudes of HOEHLER 79.

PHASE θ

VALUE (°)	DOCUMENT ID		TECN	COMMENT
−60 to −30 (≈ −50) OUR ESTIMATE				
−52± 1±14	[1] SVARC	14	L+P	$\pi N \to \pi N$
−58±12	ANISOVICH	12A	DPWA	Multichannel
−45±25	CUTKOSKY	80	IPWA	$\pi N \to \pi N$
• • • We do not use the following data for averages, fits, limits, etc. • • •				
−59	ROENCHEN	15A	DPWA	Multichannel
−33	ARNDT	06	DPWA	$\pi N \to \pi N, \eta N$
−50	HOEHLER	93	ARGD	$\pi N \to \pi N$

[1] Fit to the amplitudes of HOEHLER 79.

$N(2220)$ INELASTIC POLE RESIDUE

The "normalized residue" is the residue divided by $\Gamma_{pole}/2$.

Normalized residue in $N\pi \to N(2220) \to N\eta$

MODULUS	PHASE (°)	DOCUMENT ID		TECN	COMMENT
• • • We do not use the following data for averages, fits, limits, etc. • • •					
0.004	−101	ROENCHEN	15A	DPWA	Multichannel

Normalized residue in $N\pi \to N(2220) \to \Lambda K$

MODULUS	PHASE (°)	DOCUMENT ID		TECN	COMMENT
• • • We do not use the following data for averages, fits, limits, etc. • • •					
0.007	62	ROENCHEN	15A	DPWA	Multichannel

Normalized residue in $N\pi \to N(2220) \to \Sigma K$

MODULUS	PHASE (°)	DOCUMENT ID		TECN	COMMENT
• • • We do not use the following data for averages, fits, limits, etc. • • •					
0.009	−128	ROENCHEN	15A	DPWA	Multichannel

N(2220) BREIT-WIGNER MASS

VALUE (MeV)	DOCUMENT ID		TECN	COMMENT
2200 to 2300 (≈ 2250) OUR ESTIMATE				
2316.3± 2.9	[1] ARNDT	06	DPWA	$\pi N \to \pi N, \eta N$
2230 ±80	CUTKOSKY	80	IPWA	$\pi N \to \pi N$
2205 ±10	HOEHLER	79	IPWA	$\pi N \to \pi N$

[1] Statistical error only.

N(2220) BREIT-WIGNER WIDTH

VALUE (MeV)	DOCUMENT ID		TECN	COMMENT
350 to 500 (≈ 400) OUR ESTIMATE				
633± 17	[1] ARNDT	06	DPWA	$\pi N \to \pi N, \eta N$
500±150	CUTKOSKY	80	IPWA	$\pi N \to \pi N$
365± 30	HOEHLER	79	IPWA	$\pi N \to \pi N$

[1] Statistical error only.

N(2220) DECAY MODES

The following branching fractions are our estimates, not fits or averages.

	Mode	Fraction (Γ_i/Γ)
Γ_1	$N\pi$	15–30 %

N(2220) BRANCHING RATIOS

$\Gamma(N\pi)/\Gamma_{total}$ Γ_1/Γ

VALUE (%)	DOCUMENT ID		TECN	COMMENT
15 to 30 (≈ 25) OUR ESTIMATE				
24 ±5	ANISOVICH	12A	DPWA	Multichannel
24.6±0.1	[1] ARNDT	06	DPWA	$\pi N \to \pi N, \eta N$
15 ±3	CUTKOSKY	80	IPWA	$\pi N \to \pi N$
18.0±1.5	HOEHLER	79	IPWA	$\pi N \to \pi N$

[1] Statistical error only.

N(2220) PHOTON DECAY AMPLITUDES AT THE POLE

N(2220) → pγ, helicity-1/2 amplitude $A_{1/2}$

MODULUS ($GeV^{-1/2}$)	PHASE (°)	DOCUMENT ID		TECN	COMMENT
$-0.233^{+0.084}_{-0.044}$	-47^{+10}_{-6}	ROENCHEN	14	DPWA	
• • • We do not use the following data for averages, fits, limits, etc. • • •					
0.135	114	ROENCHEN	15A	DPWA	Multichannel

N(2220) → pγ, helicity-3/2 amplitude $A_{3/2}$

MODULUS ($GeV^{-1/2}$)	PHASE (°)	DOCUMENT ID		TECN	COMMENT
$0.162^{+0.041}_{-0.038}$	-27^{+26}_{-13}	ROENCHEN	14	DPWA	
• • • We do not use the following data for averages, fits, limits, etc. • • •					
0.082	−41	ROENCHEN	15A	DPWA	Multichannel

N(2220) REFERENCES

For early references, see Physics Letters **111B** 1 (1982).

ROENCHEN	15A	EPJ A51 70	D. Roenchen *et al.*	
PDG	14	CP C38 070001	K. Olive *et al.*	(PDG Collab.)
ROENCHEN	14	EPJ A50 101	D. Roenchen *et al.*	
Also		EPJ A51 63 (errat.)	D. Roenchen *et al.*	
SVARC	14	PR C89 045205	A. Svarc *et al.*	(RBI Zagreb, UNI Tuzla)
ANISOVICH	12A	EPJ A48 15	A.V. Anisovich *et al.*	(BONN, PNPI)
ARNDT	06	PR C74 045205	R.A. Arndt *et al.*	(GWU)
HOEHLER	93	πN Newsletter 9 1	G. Hohler	(KARL)
CUTKOSKY	80	Toronto Conf. 19	R.E. Cutkosky *et al.*	(CMU, LBL) IJP
Also		PR D20 2839	R.E. Cutkosky *et al.*	(CMU, LBL) IJP
HOEHLER	79	PDAT 12-1	G. Hohler *et al.*	(KARLT) IJP
Also		Toronto Conf. 3	R. Koch	(KARLT) IJP

N(2250) 9/2⁻

$I(J^P) = \frac{1}{2}(\frac{9}{2}^-)$ Status: ****

Older and obsolete values are listed and referenced in the 2014 edition, Chinese Physics **C38** 070001 (2014).

N(2250) POLE POSITION

REAL PART

VALUE (MeV)	DOCUMENT ID		TECN	COMMENT
2150 to 2250 (≈ 2200) OUR ESTIMATE				
2157± 3±14	[1] SVARC	14	L+P	$\pi N \to \pi N$
2195±45	ANISOVICH	12A	DPWA	Multichannel
2150±50	CUTKOSKY	80	IPWA	$\pi N \to \pi N$
• • • We do not use the following data for averages, fits, limits, etc. • • •				
2062	ROENCHEN	15A	DPWA	Multichannel
2217	ARNDT	06	DPWA	$\pi N \to \pi N, \eta N$
2187	HOEHLER	93	SPED	$\pi N \to \pi N$

[1] Fit to the amplitudes of HOEHLER 79.

−2×IMAGINARY PART

VALUE (MeV)	DOCUMENT ID		TECN	COMMENT
350 to 500 (≈ 420) OUR ESTIMATE				
412± 7±44	[1] SVARC	14	L+P	$\pi N \to \pi N$
470± 50	ANISOVICH	12A	DPWA	Multichannel
360±100	CUTKOSKY	80	IPWA	$\pi N \to \pi N$
• • • We do not use the following data for averages, fits, limits, etc. • • •				
403	ROENCHEN	15A	DPWA	Multichannel
431	ARNDT	06	DPWA	$\pi N \to \pi N, \eta N$
388	HOEHLER	93	SPED	$\pi N \to \pi N$

[1] Fit to the amplitudes of HOEHLER 79.

N(2250) ELASTIC POLE RESIDUE

MODULUS |r|

VALUE (MeV)	DOCUMENT ID		TECN	COMMENT
20 to 30 (≈ 25) OUR ESTIMATE				
24 ±1±5	[1] SVARC	14	L+P	$\pi N \to \pi N$
26 ±5	ANISOVICH	12A	DPWA	Multichannel
20 ±6	CUTKOSKY	80	IPWA	$\pi N \to \pi N$
• • • We do not use the following data for averages, fits, limits, etc. • • •				
8.2	ROENCHEN	15A	DPWA	Multichannel
21	ARNDT	06	DPWA	$\pi N \to \pi N, \eta N$
21	HOEHLER	93	SPED	$\pi N \to \pi N$

[1] Fit to the amplitudes of HOEHLER 79.

PHASE θ

VALUE (°)	DOCUMENT ID		TECN	COMMENT
−60 to −20 (≈ −40) OUR ESTIMATE				
−62± 1±11	[1] SVARC	14	L+P	$\pi N \to \pi N$
−38±25	ANISOVICH	12A	DPWA	Multichannel
−50±20	CUTKOSKY	80	IPWA	$\pi N \to \pi N$
• • • We do not use the following data for averages, fits, limits, etc. • • •				
−64	ROENCHEN	15A	DPWA	Multichannel
−20	ARNDT	06	DPWA	$\pi N \to \pi N, \eta N$

[1] Fit to the amplitudes of HOEHLER 79.

N(2250) INELASTIC POLE RESIDUE

The "normalized residue" is the residue divided by $\Gamma_{pole}/2$.

Normalized residue in $N\pi \to N(2250) \to N\eta$

MODULUS	PHASE (°)	DOCUMENT ID		TECN	COMMENT
• • • We do not use the following data for averages, fits, limits, etc. • • •					
0.017	−89	ROENCHEN	15A	DPWA	Multichannel

Normalized residue in $N\pi \to N(2250) \to \Lambda K$

MODULUS	PHASE (°)	DOCUMENT ID		TECN	COMMENT
• • • We do not use the following data for averages, fits, limits, etc. • • •					
0.006	−101	ROENCHEN	15A	DPWA	Multichannel

Normalized residue in $N\pi \to N(2250) \to \Sigma K$

MODULUS	PHASE (°)	DOCUMENT ID		TECN	COMMENT
• • • We do not use the following data for averages, fits, limits, etc. • • •					
0.002	70	ROENCHEN	15A	DPWA	Multichannel

N(2250) BREIT-WIGNER MASS

VALUE (MeV)	DOCUMENT ID		TECN	COMMENT
2250 to 2320 (≈ 2280) OUR ESTIMATE				
2280±40	ANISOVICH	12A	DPWA	Multichannel
2302± 6	[1] ARNDT	06	DPWA	$\pi N \to \pi N, \eta N$
2250±80	CUTKOSKY	80	IPWA	$\pi N \to \pi N$
2268±15	HOEHLER	79	IPWA	$\pi N \to \pi N$

[1] Statistical error only.

N(2250) BREIT-WIGNER WIDTH

VALUE (MeV)	DOCUMENT ID		TECN	COMMENT
300 to 600 (≈ 500) OUR ESTIMATE				
520± 50	ANISOVICH	12A	DPWA	Multichannel
628± 28	[1] ARNDT	06	DPWA	$\pi N \to \pi N, \eta N$
480±120	CUTKOSKY	80	IPWA	$\pi N \to \pi N$
300± 40	HOEHLER	79	IPWA	$\pi N \to \pi N$

[1] Statistical error only.

$N(2250)$ DECAY MODES

The following branching fractions are our estimates, not fits or averages.

	Mode	Fraction (Γ_i/Γ)
Γ_1	$N\pi$	0.05 to 0.15 (≈ 0.10)

$N(2250)$ BRANCHING RATIOS

$\Gamma(N\pi)/\Gamma_{\text{total}}$ **Γ_1/Γ**

VALUE (%)	DOCUMENT ID		TECN	COMMENT
5 to 15 ($\approx$ 10) OUR ESTIMATE				
12 $\pm$4	ANISOVICH	12A	DPWA	Multichannel
8.9$\pm$0.1	[1] ARNDT	06	DPWA	$\pi N \to \pi N$, ηN
10 $\pm$2	CUTKOSKY	80	IPWA	$\pi N \to \pi N$
10 $\pm$2	HOEHLER	79	IPWA	$\pi N \to \pi N$

[1] Statistical error only.

$N(2250)$ PHOTON DECAY AMPLITUDES AT THE POLE

$N(2250) \to p\gamma$, helicity-1/2 amplitude $A_{1/2}$

MODULUS ($GeV^{-1/2}$)	PHASE (°)	DOCUMENT ID		TECN	COMMENT
$-0.090^{+0.025}_{-0.022}$	-49^{+17}_{-11}	ROENCHEN	14	DPWA	
• • • We do not use the following data for averages, fits, limits, etc. • • •					
0.026	-26	ROENCHEN	15A	DPWA	Multichannel

$N(2250) \to p\gamma$, helicity-3/2 amplitude $A_{3/2}$

MODULUS ($GeV^{-1/2}$)	PHASE (°)	DOCUMENT ID		TECN	COMMENT
$0.049^{+0.031}_{-0.019}$	171^{+36}_{-43}	ROENCHEN	14	DPWA	
• • • We do not use the following data for averages, fits, limits, etc. • • •					
0.119	-42	ROENCHEN	15A	DPWA	Multichannel

$N(2250)$ REFERENCES

ROENCHEN	15A	EPJ A51 70	D. Roenchen *et al.*	
PDG	14	CP C38 070001	K. Olive *et al.*	(PDG Collab.)
ROENCHEN	14	EPJ A50 101	D. Roenchen *et al.*	
Also		EPJ A51 63 (errat.)	D. Roenchen *et al.*	
SVARC	14	PR C89 045205	A. Svarc *et al.*	(RBI Zagreb, UNI Tuzla)
ANISOVICH	12A	EPJ A48 15	A.V. Anisovich *et al.*	(BONN, PNPI)
ARNDT	06	PR C74 045205	R.A. Arndt *et al.*	(GWU)
HOEHLER	93	πN Newsletter 9 1	G. Hohler	(KARL)
CUTKOSKY	80	Toronto Conf. 19	R.E. Cutkosky *et al.*	(CMU, LBL) IJP
Also		PR D20 2839	R.E. Cutkosky *et al.*	(CMU, LBL) IJP
HOEHLER	79	PDAT 12-1	G. Hohler *et al.*	(KARLT) IJP
Also		Toronto Conf. 3	R. Koch	(KARLT) IJP

$N(2300)\ 1/2^+$

$I(J^P) = \frac{1}{2}(\frac{1}{2}^+)$ Status: **

OMITTED FROM SUMMARY TABLE

$N(2300)$ MASS

VALUE (MeV)	DOCUMENT ID		TECN	COMMENT
$2300^{+40}_{-30}{}^{+109}_{-0}$	ABLIKIM	13A	BES3	$\psi(2S) \to p\overline{p}\pi^0$

$N(2300)$ WIDTH

VALUE (MeV)	DOCUMENT ID		TECN	COMMENT
$340\pm30^{+110}_{-58}$	ABLIKIM	13A	BES3	$\psi(2S) \to p\overline{p}\pi^0$

$N(2300)$ REFERENCES

ABLIKIM	13A	PRL 110 022001	M. Ablikim *et al.*	(BES III Collab.)

$N(2570)\ 5/2^-$

$I(J^P) = \frac{1}{2}(\frac{5}{2}^-)$ Status: **

OMITTED FROM SUMMARY TABLE

$N(2570)$ MASS

VALUE (MeV)	DOCUMENT ID		TECN	COMMENT
$2570^{+19}_{-10}{}^{+34}_{-10}$	ABLIKIM	13A	BES3	$\psi(2S) \to p\overline{p}\pi^0$

$N(2570)$ WIDTH

VALUE (MeV)	DOCUMENT ID		TECN	COMMENT
$250^{+14}_{-24}{}^{+69}_{-21}$	ABLIKIM	13A	BES3	$\psi(2S) \to p\overline{p}\pi^0$

$N(2570)$ REFERENCES

ABLIKIM	13A	PRL 110 022001	M. Ablikim *et al.*	(BES III Collab.)

$N(2600)\ 11/2^-$

$I(J^P) = \frac{1}{2}(\frac{11}{2}^-)$ Status: ***

$N(2600)$ BREIT-WIGNER MASS

VALUE (MeV)	DOCUMENT ID		TECN	COMMENT
2550 to 2750 ($\approx$ 2600) OUR ESTIMATE				
2623$\pm$197	ARNDT	06	DPWA	$\pi N \to \pi N$, ηN
2577$\pm$ 50	HOEHLER	79	IPWA	$\pi N \to \pi N$

$N(2600)$ BREIT-WIGNER WIDTH

VALUE (MeV)	DOCUMENT ID		TECN	COMMENT
500 to 800 ($\approx$ 650) OUR ESTIMATE				
1311$\pm$996	ARNDT	06	DPWA	$\pi N \to \pi N$, ηN
400$\pm$100	HOEHLER	79	IPWA	$\pi N \to \pi N$

$N(2600)$ DECAY MODES

	Mode	Fraction (Γ_i/Γ)
Γ_1	$N\pi$	3–8 %

$N(2600)$ BRANCHING RATIOS

$\Gamma(N\pi)/\Gamma_{\text{total}}$ **Γ_1/Γ**

VALUE (%)	DOCUMENT ID		TECN	COMMENT
3 to 8 ($\approx$ 5) OUR ESTIMATE				
5.0$\pm$1.8	ARNDT	06	DPWA	$\pi N \to \pi N$, ηN
5 $\pm$1	HOEHLER	79	IPWA	$\pi N \to \pi N$

$N(2600)$ REFERENCES

ARNDT	06	PR C74 045205	R.A. Arndt *et al.*	(GWU)
HOEHLER	79	PDAT 12-1	G. Hohler *et al.*	(KARLT) IJP
Also		Toronto Conf. 3	R. Koch	(KARLT) IJP

$N(2700)\ 13/2^+$

$I(J^P) = \frac{1}{2}(\frac{13}{2}^+)$ Status: **

OMITTED FROM SUMMARY TABLE

$N(2700)$ BREIT-WIGNER MASS

VALUE (MeV)	DOCUMENT ID		TECN	COMMENT
2612$\pm$45	HOEHLER	79	IPWA	$\pi N \to \pi N$

$N(2700)$ BREIT-WIGNER WIDTH

VALUE (MeV)	DOCUMENT ID		TECN	COMMENT
350$\pm$50	HOEHLER	79	IPWA	$\pi N \to \pi N$

$N(2700)$ DECAY MODES

	Mode	Fraction (Γ_i/Γ)
Γ_1	$N\pi$	3–5 %

$N(2700)$ BRANCHING RATIOS

$\Gamma(N\pi)/\Gamma_{\text{total}}$ **Γ_1/Γ**

VALUE (%)	DOCUMENT ID		TECN	COMMENT
4$\pm$1	HOEHLER	79	IPWA	$\pi N \to \pi N$

$N(2700)$ REFERENCES

HOEHLER	79	PDAT 12-1	G. Hohler *et al.*	(KARLT) IJP
Also		Toronto Conf. 3	R. Koch	(KARLT) IJP

$N(\sim 3000$ Region) Partial-Wave Analyses

OMITTED FROM SUMMARY TABLE

We list here miscellaneous high-mass candidates for isospin-1/2 resonances found in partial-wave analyses.

Our 1982 edition had an $N(3245)$, an $N(3690)$, and an $N(3755)$, each a narrow peak seen in a production experiment. Since nothing has been heard from them since the 1960's, we declare them to be dead. There was also an $N(3030)$, deduced from total cross-section and 180° elastic cross-section measurements; it is the KOCH 80 $L_{1,15}$ state below.

$N(\sim 3000)$ BREIT-WIGNER MASS

VALUE (MeV)	DOCUMENT ID		TECN	COMMENT
≈ 3000 OUR ESTIMATE				
2600	KOCH	80	IPWA	$\pi N \rightarrow \pi N\ D_{13}$
3100	KOCH	80	IPWA	$\pi N \rightarrow \pi N\ L_{1,15}$ wave
3500	KOCH	80	IPWA	$\pi N \rightarrow \pi N\ M_{1,17}$ wave
3500 to 4000	KOCH	80	IPWA	$\pi N \rightarrow \pi N\ N_{1,19}$ wave
3500±200	HENDRY	78	MPWA	$\pi N \rightarrow \pi N\ L_{1,15}$ wave
3800±200	HENDRY	78	MPWA	$\pi N \rightarrow \pi N\ M_{1,17}$ wave
4100±200	HENDRY	78	MPWA	$\pi N \rightarrow \pi N\ N_{1,19}$ wave

$N(\sim 3000)$ BREIT-WIGNER WIDTH

VALUE (MeV)	DOCUMENT ID		TECN	COMMENT
1300±200	HENDRY	78	MPWA	$\pi N \rightarrow \pi N\ L_{1,15}$ wave
1600±200	HENDRY	78	MPWA	$\pi N \rightarrow \pi N\ M_{1,17}$ wave
1900±300	HENDRY	78	MPWA	$\pi N \rightarrow \pi N\ N_{1,19}$ wave

$N(\sim 3000)$ DECAY MODES

	Mode
Γ_1	$N\pi$

$N(\sim 3000)$ BRANCHING RATIOS

$\Gamma(N\pi)/\Gamma_{total}$ Γ_1/Γ

VALUE (%)	DOCUMENT ID		TECN	COMMENT
6 ±2	HENDRY	78	MPWA	$\pi N \rightarrow \pi N\ L_{1,15}$ wave
4.0±1.5	HENDRY	78	MPWA	$\pi N \rightarrow \pi N\ M_{1,17}$ wave
3.0±1.5	HENDRY	78	MPWA	$\pi N \rightarrow \pi N\ N_{1,19}$ wave

$N(\sim 3000)$ REFERENCES

KOCH	80	Toronto Conf. 3	R. Koch	(KARLT) IJP
HENDRY	78	PRL 41 222	A.W. Hendry	(IND, LBL) IJP
Also		ANP 136 1	A.W. Hendry	(IND) IJP

Δ BARYONS
(S = 0, I = 3/2)

$\Delta^{++} = uuu$, $\Delta^{+} = uud$, $\Delta^{0} = udd$, $\Delta^{-} = ddd$

Δ(1232) 3/2+

$I(J^P) = \frac{3}{2}(\frac{3}{2}^+)$ Status: ****

Older and obsolete values are listed and referenced in the 2014 edition, Chinese Physics **C38** 070001 (2014).

Δ(1232) POLE POSITIONS

REAL PART, MIXED CHARGES

VALUE (MeV)	DOCUMENT ID		TECN	COMMENT
1209 to 1211 (≈ 1210) OUR ESTIMATE				
1211 ±1 ±1	[1] SVARC	14	L+P	$\pi N \to \pi N$
1210.5 ±1.0	ANISOVICH	12A	DPWA	Multichannel
1210 ±1	CUTKOSKY	80	IPWA	$\pi N \to \pi N$
• • • We do not use the following data for averages, fits, limits, etc. • • •				
1218	ROENCHEN	15A	DPWA	Multichannel
1212	SHRESTHA	12A	DPWA	Multichannel
1211 ±1	ANISOVICH	10	DPWA	Multichannel
1211	ARNDT	06	DPWA	$\pi N \to \pi N, \eta N$
1210	ARNDT	04	DPWA	$\pi N \to \pi N, \eta N$
1209	[2] HOEHLER	93	ARGD	$\pi N \to \pi N$

[1] Fit to the amplitudes of HOEHLER 79.
[2] See HOEHLER 93 for a detailed discussion of the evidence for and the pole parameters of N and Δ resonances as determined from Argand diagrams of πN elastic partial-wave amplitudes and from plots of the speeds with which the amplitudes traverse the diagrams.

−2×IMAGINARY PART, MIXED CHARGES

VALUE (MeV)	DOCUMENT ID		TECN	COMMENT
98 to 102 (≈ 100) OUR ESTIMATE				
98±2±1	[1] SVARC	14	L+P	$\pi N \to \pi N$
99±2	ANISOVICH	12A	DPWA	Multichannel
100±2	CUTKOSKY	80	IPWA	$\pi N \to \pi N$
• • • We do not use the following data for averages, fits, limits, etc. • • •				
92	ROENCHEN	15A	DPWA	Multichannel
98	SHRESTHA	12A	DPWA	Multichannel
100±2	ANISOVICH	10	DPWA	Multichannel
99	ARNDT	06	DPWA	$\pi N \to \pi N, \eta N$
100	ARNDT	04	DPWA	$\pi N \to \pi N, \eta N$
100	[2] HOEHLER	93	ARGD	$\pi N \to \pi N$

[1] Fit to the amplitudes of HOEHLER 79.
[2] See HOEHLER 93 for a detailed discussion of the evidence for and the pole parameters of N and Δ resonances as determined from Argand diagrams of πN elastic partial-wave amplitudes and from plots of the speeds with which the amplitudes traverse the diagrams.

REAL PART, Δ(1232)++

VALUE (MeV)	DOCUMENT ID		COMMENT
• • • We do not use the following data for averages, fits, limits, etc. • • •			
1212.50±0.24	BERNICHA	96	Fit to PEDRONI 78

−2×IMAGINARY PART, Δ(1232)++

VALUE (MeV)	DOCUMENT ID		COMMENT
• • • We do not use the following data for averages, fits, limits, etc. • • •			
97.37±0.42	BERNICHA	96	Fit to PEDRONI 78

REAL PART, Δ(1232)+

VALUE (MeV)	DOCUMENT ID		TECN	COMMENT
• • • We do not use the following data for averages, fits, limits, etc. • • •				
1211 ±1 to 1212 ± 1	HANSTEIN	96	DPWA	$\gamma N \to \pi N$
1206.9±0.9 to 1210.5 ± 1.8	MIROSHNIC...	79		Fit photoproduction

−2×IMAGINARY PART, Δ(1232)+

VALUE (MeV)	DOCUMENT ID		TECN	COMMENT
• • • We do not use the following data for averages, fits, limits, etc. • • •				
102 ±2 to 99 ± 2	[1] HANSTEIN	96	DPWA	$\gamma N \to \pi N$
111.2±2.0 to 116.6 ± 2.2	MIROSHNIC...	79		Fit photoproduction

[1] The second (lower) value of HANSTEIN 96 here goes with the second (higher) value of the real part in the preceding data block.

REAL PART, Δ(1232)0

VALUE (MeV)	DOCUMENT ID		COMMENT
• • • We do not use the following data for averages, fits, limits, etc. • • •			
1213.20±0.66	BERNICHA	96	Fit to PEDRONI 78

−2×IMAGINARY PART, Δ(1232)0

VALUE (MeV)	DOCUMENT ID		COMMENT
• • • We do not use the following data for averages, fits, limits, etc. • • •			
104.10±1.01	BERNICHA	96	Fit to PEDRONI 78

Δ(1232) ELASTIC POLE RESIDUES

ABSOLUTE VALUE, MIXED CHARGES

VALUE (MeV)	DOCUMENT ID		TECN	COMMENT
49 to 52 (≈ 50) OUR ESTIMATE				
50 ±1 ±1	[1] SVARC	14	L+P	$\pi N \to \pi N$
51.6±0.6	ANISOVICH	12A	DPWA	Multichannel
53 ±2	CUTKOSKY	80	IPWA	$\pi N \to \pi N$
• • • We do not use the following data for averages, fits, limits, etc. • • •				
46	ROENCHEN	15A	DPWA	Multichannel
52	ARNDT	06	DPWA	$\pi N \to \pi N, \eta N$
53	ARNDT	04	DPWA	$\pi N \to \pi N, \eta N$
50	HOEHLER	93	ARGD	$\pi N \to \pi N$

PHASE, MIXED CHARGES

VALUE (°)	DOCUMENT ID		TECN	COMMENT
−48 to −45 (≈ −46) OUR ESTIMATE				
−46±1±1	[1] SVARC	14	L+P	$\pi N \to \pi N$
−46±1	ANISOVICH	12A	DPWA	Multichannel
−47±1	CUTKOSKY	80	IPWA	$\pi N \to \pi N$
• • • We do not use the following data for averages, fits, limits, etc. • • •				
−36	ROENCHEN	15A	DPWA	Multichannel
−47	ARNDT	06	DPWA	$\pi N \to \pi N, \eta N$
−47	ARNDT	04	DPWA	$\pi N \to \pi N, \eta N$
−48	HOEHLER	93	ARGD	$\pi N \to \pi N$

[1] Fit to the amplitudes of HOEHLER 79.

Δ(1232) BREIT-WIGNER MASSES

MIXED CHARGES

VALUE (MeV)	DOCUMENT ID		TECN	COMMENT
1230 to 1234 (≈ 1232) OUR ESTIMATE				
1228 ±2	ANISOVICH	12A	DPWA	Multichannel
1231.1±0.2	[1] SHRESTHA	12A	DPWA	Multichannel
1233.4±0.4	[1] ARNDT	06	DPWA	$\pi N \to \pi N, \eta N$
1232 ±3	CUTKOSKY	80	IPWA	$\pi N \to \pi N$
1233 ±2	HOEHLER	79	IPWA	$\pi N \to \pi N$
• • • We do not use the following data for averages, fits, limits, etc. • • •				
1230 ±2	ANISOVICH	10	DPWA	Multichannel
1232.9±1.2	ARNDT	04	DPWA	$\pi N \to \pi N, \eta N$
1228 ±1	PENNER	02C	DPWA	Multichannel

[1] Statistical error only.

Δ(1232)++ MASS

VALUE (MeV)	DOCUMENT ID		TECN	COMMENT
• • • We do not use the following data for averages, fits, limits, etc. • • •				
1230.55±0.20	GRIDNEV	06	DPWA	$\pi N \to \pi N$
1231.88±0.29	BERNICHA	96		Fit to PEDRONI 78
1230.5 ±0.2	ABAEV	95	IPWA	$\pi N \to \pi N$
1230.9 ±0.3	KOCH	80B	IPWA	$\pi N \to \pi N$
1231.1 ±0.2	PEDRONI	78		$\pi N \to \pi N$ 70–370 MeV

Δ(1232)+ MASS

VALUE (MeV)	DOCUMENT ID		COMMENT
• • • We do not use the following data for averages, fits, limits, etc. • • •			
1234.9±1.4	MIROSHNIC...	79	Fit photoproduction

Δ(1232)0 MASS

VALUE (MeV)	DOCUMENT ID		TECN	COMMENT
• • • We do not use the following data for averages, fits, limits, etc. • • •				
1231.3 ±0.6	BREITSCHOP...	06	CNTR	Using new CHEX data
1233.40±0.22	GRIDNEV	06	DPWA	$\pi N \to \pi N$
1234.35±0.75	BERNICHA	96		Fit to PEDRONI 78
1233.1 ±0.3	ABAEV	95	IPWA	$\pi N \to \pi N$
1233.6 ±0.5	KOCH	80B	IPWA	$\pi N \to \pi N$
1233.8 ±0.2	PEDRONI	78		$\pi N \to \pi N$ 70–370 MeV

$m_{\Delta^0} - m_{\Delta^{++}}$

VALUE (MeV)	DOCUMENT ID		TECN	COMMENT
• • • We do not use the following data for averages, fits, limits, etc. • • •				
2.86±0.30	GRIDNEV	06	DPWA	$\pi N \to \pi N$
2.25±0.68	BERNICHA	96		Fit to PEDRONI 78
2.6 ±0.4	ABAEV	95	IPWA	$\pi N \to \pi N$
2.7 ±0.3	[1] PEDRONI	78		See the masses

[1] Using $\pi^{\pm} d$ as well, PEDRONI 78 determine $(M^- - M^{++}) + (M^0 - M^+)/3 = 4.6 \pm 0.2$ MeV.

Δ(1232) BREIT-WIGNER WIDTHS

MIXED CHARGES

VALUE (MeV)	DOCUMENT ID		TECN	COMMENT
114 to 120 (≈ 117) OUR ESTIMATE				
110 ±3	ANISOVICH	12A	DPWA	Multichannel
113.0±0.5	[1] SHRESTHA	12A	DPWA	Multichannel
118.7±0.6	[1] ARNDT	06	DPWA	$\pi N \to \pi N, \eta N$
120 ±5	CUTKOSKY	80	IPWA	$\pi N \to \pi N$
116 ±5	HOEHLER	79	IPWA	$\pi N \to \pi N$
• • • We do not use the following data for averages, fits, limits, etc. • • •				
112 ±4	ANISOVICH	10	DPWA	Multichannel
118.0±2.2	ARNDT	04	DPWA	$\pi N \to \pi N, \eta N$
106 ±1	PENNER	02C	DPWA	Multichannel

[1] Statistical error only.

Δ(1232)++ WIDTH

VALUE (MeV)	DOCUMENT ID		TECN	COMMENT
• • • We do not use the following data for averages, fits, limits, etc. • • •				
112.2 ±0.7	GRIDNEV	06	DPWA	$\pi N \to \pi N$
109.07±0.48	BERNICHA	96		Fit to PEDRONI 78
111.0 ±1.0	KOCH	80B	IPWA	$\pi N \to \pi N$
111.3 ±0.5	PEDRONI	78		$\pi N \to \pi N$ 70–370 MeV

Δ(1232)+ WIDTH

VALUE (MeV)	DOCUMENT ID		COMMENT
• • • We do not use the following data for averages, fits, limits, etc. • • •			
131.1±2.4	MIROSHNIC...	79	Fit photoproduction

Δ(1232)0 WIDTH

VALUE (MeV)	DOCUMENT ID		TECN	COMMENT
• • • We do not use the following data for averages, fits, limits, etc. • • •				
112.5 ±1.9	BREITSCHOP...06		CNTR	Using new CHEX data
116.9 ±0.7	GRIDNEV	06	DPWA	$\pi N \to \pi N$
117.58±1.16	BERNICHA	96		Fit to PEDRONI 78
113.0 ±1.5	KOCH	80B	IPWA	$\pi N \to \pi N$
117.9 ±0.9	PEDRONI	78		$\pi N \to \pi N$ 70–370 MeV

Δ0-Δ++ WIDTH DIFFERENCE

VALUE (MeV)	DOCUMENT ID		TECN	COMMENT
• • • We do not use the following data for averages, fits, limits, etc. • • •				
4.66±1.0	GRIDNEV	06	DPWA	$\pi N \to \pi N$
8.45±1.11	BERNICHA	96		Fit to PEDRONI 78
5.1 ±1.0	ABAEV	95	IPWA	$\pi N \to \pi N$
6.6 ±1.0	PEDRONI	78		See the widths

Δ(1232) DECAY MODES

The following branching fractions are our estimates, not fits or averages.

	Mode	Fraction (Γ_j/Γ)
Γ_1	$N\pi$	99.4 %
Γ_2	$N\gamma$	0.55–0.65 %
Γ_3	$N\gamma$, helicity=1/2	0.11–0.13 %
Γ_4	$N\gamma$, helicity=3/2	0.44–0.52 %
Γ_5	pe^+e^-	$(4.2\pm0.7)\times10^{-5}$

Δ(1232) BRANCHING RATIOS

$\Gamma(N\pi)/\Gamma_{total}$ Γ_1/Γ

VALUE	DOCUMENT ID		TECN	COMMENT
0.994 OUR ESTIMATE				
1.00	ARNDT	06	DPWA	$\pi N \to \pi N, \eta N$
1.0	CUTKOSKY	80	IPWA	$\pi N \to \pi N$
1.0	HOEHLER	79	IPWA	$\pi N \to \pi N$
• • • We do not use the following data for averages, fits, limits, etc. • • •				
0.994	SHRESTHA	12A	DPWA	Multichannel
1.0	ANISOVICH	10	DPWA	Multichannel
1.000	ARNDT	04	DPWA	$\pi N \to \pi N, \eta N$
1.00	PENNER	02C	DPWA	Multichannel

$\Gamma(pe^+e^-)/\Gamma_{total}$ Γ_5/Γ

VALUE (units 10^{-5})	DOCUMENT ID	
4.19±0.34±0.62	[1] ADAMCZEW...	17

[1] The systematic uncertainty includes the model dependence.

Δ(1232) PHOTON DECAY AMPLITUDES AT THE POLE

Δ(1232) → Nγ, helicity-1/2 amplitude $A_{1/2}$

MODULUS ($GeV^{-1/2}$)	PHASE (°)	DOCUMENT ID		TECN	COMMENT
$-0.114^{+0.010}_{-0.003}$	-9^{+4}_{-2}	ROENCHEN	14	DPWA	
• • • We do not use the following data for averages, fits, limits, etc. • • •					
−0.117	−6.6	ROENCHEN	15A	DPWA	Multichannel

Δ(1232) → Nγ, helicity-3/2 amplitude $A_{3/2}$

MODULUS ($GeV^{-1/2}$)	PHASE (°)	DOCUMENT ID		TECN	COMMENT
$-0.229^{+0.003}_{-0.004}$	$3^{+0.3}_{-0.4}$	ROENCHEN	14	DPWA	
• • • We do not use the following data for averages, fits, limits, etc. • • •					
−0.226	2.8	ROENCHEN	15A	DPWA	Multichannel

Δ(1232) BREIT-WIGNER PHOTON DECAY AMPLITUDES

Papers on γN amplitudes predating 1981 may be found in our 2006 edition, Journal of Physics **G33** 1 (2006).

Δ(1232) → Nγ, helicity-1/2 amplitude $A_{1/2}$

VALUE ($GeV^{-1/2}$)	DOCUMENT ID		TECN	COMMENT
−0.142 to −0.129 (≈ −0.135) OUR ESTIMATE				
−0.131 ±0.004	ANISOVICH	12A	DPWA	Multichannel
−0.139 ±0.002	[1] WORKMAN	12A	DPWA	$\gamma N \to N\pi$
−0.139 ±0.004	[1] DUGGER	07	DPWA	$\gamma N \to \pi N$
−0.137 ±0.005	AHRENS	04A	DPWA	$\vec{\gamma}\vec{p} \to N\pi$
−0.1357±0.0013±0.0037	BLANPIED	01	LEGS	$\gamma p \to p\gamma, p\pi^0, n\pi^+$
−0.131 ±0.001	[1] BECK	00	IPWA	$\vec{\gamma}p \to p\pi^0, n\pi^+$
−0.140 ±0.005	KAMALOV	99	DPWA	$\gamma N \to \pi N$
−0.1294±0.0013	HANSTEIN	98	IPWA	$\gamma N \to \pi N$
−0.1278±0.0012	DAVIDSON	97	DPWA	$\gamma N \to \pi N$
• • • We do not use the following data for averages, fits, limits, etc. • • •				
−0.137 ±0.001	[1] SHRESTHA	12A	DPWA	Multichannel
−0.136 ±0.005	ANISOVICH	10	DPWA	Multichannel
−0.140	DRECHSEL	07	DPWA	$\gamma N \to \pi N$
−0.129 ±0.001	ARNDT	02	DPWA	$\gamma p \to N\pi$
−0.128	PENNER	02D	DPWA	Multichannel
−0.1312	HANSTEIN	98	DPWA	$\gamma N \to \pi N$

[1] Statistical error only.

Δ(1232) → Nγ, helicity-3/2 amplitude $A_{3/2}$

VALUE ($GeV^{-1/2}$)	DOCUMENT ID		TECN	COMMENT
−0.262 to −0.248 (≈ −0.255) OUR ESTIMATE				
−0.254 ±0.005	ANISOVICH	12A	DPWA	Multichannel
−0.262 ±0.003	WORKMAN	12A	DPWA	$\gamma N \to N\pi$
−0.258 ±0.005	DUGGER	07	DPWA	$\gamma N \to \pi N$
−0.256 ±0.003	AHRENS	04A	DPWA	$\vec{\gamma}\vec{p} \to N\pi$
−0.2669±0.0016±0.0078	BLANPIED	01	LEGS	$\gamma p \to p\gamma, p\pi^0, n\pi^+$
−0.251 ±0.001	BECK	00	IPWA	$\vec{\gamma}p \to p\pi^0, n\pi^+$
−0.258 ±0.006	KAMALOV	99	DPWA	$\gamma N \to \pi N$
−0.2466±0.0013	HANSTEIN	98	IPWA	$\gamma N \to \pi N$
−0.2524±0.0013	DAVIDSON	97	DPWA	$\gamma N \to \pi N$
• • • We do not use the following data for averages, fits, limits, etc. • • •				
−0.251 ±0.001	[1] SHRESTHA	12A	DPWA	Multichannel
−0.267 ±0.008	ANISOVICH	10	DPWA	Multichannel
−0.265	DRECHSEL	07	DPWA	$\gamma N \to \pi N$
−0.243 ±0.001	ARNDT	02	DPWA	$\gamma p \to N\pi$
−0.247	PENNER	02D	DPWA	Multichannel
−0.2522	HANSTEIN	98	DPWA	$\gamma N \to \pi N$

[1] Statistical error only.

Δ(1232) → Nγ, E_2/M_1 ratio

VALUE	DOCUMENT ID		TECN	COMMENT
−0.030 to −0.020 (≈ −0.025) OUR ESTIMATE				
−0.0274±0.0003±0.0030	AHRENS	04A	DPWA	$\vec{\gamma}\vec{p} \to N\pi$
−0.020 ±0.002	ARNDT	02	DPWA	$\gamma p \to N\pi$
−0.0307±0.0026±0.0024	BLANPIED	01	LEGS	$\gamma p \to p\gamma, p\pi^0, n\pi^+$
−0.016 ±0.004 ±0.002	GALLER	01	DPWA	$\gamma p \to \gamma p$
−0.025 ±0.001 ±0.002	BECK	00	IPWA	$\vec{\gamma}p \to p\pi^0, n\pi^+$
−0.0233±0.0017	HANSTEIN	98	IPWA	$\gamma N \to \pi N$
−0.015 ±0.005	[1] ARNDT	97	IPWA	$\gamma N \to \pi N$
−0.0319±0.0024	DAVIDSON	97	DPWA	$\gamma N \to \pi N$
• • • We do not use the following data for averages, fits, limits, etc. • • •				
−0.022	DRECHSEL	07	DPWA	$\gamma N \to \pi N$
−0.026	PENNER	02D	DPWA	Multichannel
−0.0254±0.0010	HANSTEIN	98	DPWA	$\gamma N \to \pi N$
−0.025 ±0.002 ±0.002	BECK	97	IPWA	$\gamma N \to \pi N$
−0.030 ±0.003 ±0.002	BLANPIED	97	DPWA	$\gamma N \to \pi N, \gamma N$

[1] This ARNDT 97 value is very sensitive to the database being fitted. The result is from a fit to the full pion photoproduction database, apart from the BLANPIED 97 cross-section measurements.

Δ(1232) → Nγ, absolute value of E_2/M_1 ratio at pole

VALUE	DOCUMENT ID		TECN	COMMENT
• • • We do not use the following data for averages, fits, limits, etc. • • •				
0.065±0.007	ARNDT	97	DPWA	$\gamma N \to \pi N$
0.058	HANSTEIN	96	DPWA	$\gamma N \to \pi N$

$\Delta(1232) \rightarrow N\gamma$, phase of E_2/M_1 ratio at pole

VALUE	DOCUMENT ID		TECN	COMMENT
• • • We do not use the following data for averages, fits, limits, etc. • • •				
-122 ± 5	ARNDT	97	DPWA	$\gamma N \rightarrow \pi N$
-127.2	HANSTEIN	96	DPWA	$\gamma N \rightarrow \pi N$

$\Delta(1232)$ MAGNETIC MOMENTS

$\Delta(1232)^{++}$ MAGNETIC MOMENT

The values are extracted from UCLA and SIN data on $\pi^+ p$ bremsstrahlung using a variety of different theoretical approximations and methods. Our estimate is *only* a rough guess of the range we expect the moment to lie within.

VALUE (μ_N)	DOCUMENT ID		TECN	COMMENT
• • • We do not use the following data for averages, fits, limits, etc. • • •				
6.14 ± 0.51	LOPEZCAST...	01	DPWA	$\pi^+ p \rightarrow \pi^+ p\gamma$
$4.52 \pm 0.50 \pm 0.45$	BOSSHARD	91		$\pi^+ p \rightarrow \pi^+ p\gamma$ (SIN data)
3.7 to 4.2	LIN	91B		$\pi^+ p \rightarrow \pi^+ p\gamma$ (from UCLA data)
4.6 to 4.9	LIN	91B		$\pi^+ p \rightarrow \pi^+ p\gamma$ (from SIN data)
5.6 to 7.5	WITTMAN	88		$\pi^+ p \rightarrow \pi^+ p\gamma$ (from UCLA data)
6.9 to 9.8	HELLER	87		$\pi^+ p \rightarrow \pi^+ p\gamma$ (from UCLA data)
4.7 to 6.7	NEFKENS	78		$\pi^+ p \rightarrow \pi^+ p\gamma$ (UCLA data)

$\Delta(1232)^{+}$ MAGNETIC MOMENT

VALUE (μ_N)	DOCUMENT ID		COMMENT
• • • We do not use the following data for averages, fits, limits, etc. • • •			
$2.7^{+1.0}_{-1.3} \pm 1.5 \pm 3$	[1] KOTULLA	02	$\gamma p \rightarrow p\pi^0\gamma'$

[1] The second error is systematic, the third is an estimate of theoretical uncertainties.

$\Delta(1232)$ REFERENCES

For early references, see Physics Letters **111B** 1 (1982).

ADAMCZEW...	17	PR C95 065205	J. Adamczewski-Musch *et al.*	(HADES Collab.)
ROENCHEN	15A	EPJ A51 70	D. Roenchen *et al.*	
PDG	14	CP C38 070001	K. Olive *et al.*	(PDG Collab.)
ROENCHEN	14	EPJ A50 101	D. Roenchen *et al.*	
Also		EPJ A51 63 (errat.)	D. Roenchen *et al.*	
SVARC	14	PR C89 045205	A. Svarc *et al.*	(RBI Zagreb, UNI Tuzla)
ANISOVICH	12A	EPJ A48 15	A.V. Anisovich *et al.*	(BONN, PNPI)
SHRESTHA	12A	PR C86 055203	M. Shrestha, D.M. Manley	(KSU)
WORKMAN	12A	PR C86 015202	R. Workman *et al.*	(GWU)
ANISOVICH	10	EPJ A44 203	A.V. Anisovich *et al.*	(BONN, PNPI)
DRECHSEL	07	EPJ A34 69	D. Drechsel, S.S. Kamalov, L. Tiator	(MAINZ, JINR)
DUGGER	07	PR C76 025211	M. Dugger *et al.*	(JLab CLAS Collab.)
ARNDT	06	PR C74 045205	R.A. Arndt *et al.*	(GWU)
BREITSCHOP...	06	PL B639 424	J. Breitschopf *et al.*	(TUBIN, HEBR, CSUS)
GRIDNEV	06	PAN 69 1542	A.B. Gridnev *et al.*	(PNPI, BONN, GWU)
PDG	06	JP G33 1	W.-M. Yao *et al.*	(PDG Collab.)
AHRENS	04A	EPJ A21 323	J. Ahrens *et al.*	(Mainz GDH, A2 Collab.)
ARNDT	04	PR C69 035213	R.A. Arndt *et al.*	(GWU, TRIU)
ARNDT	02	PR C66 055213	R. A. Arndt *et al.*	(GWU)
KOTULLA	02	PRL 89 272001	M. Kotulla *et al.*	(MAMI TAPS Collab.)
PENNER	02C	PR C66 055211	G. Penner, U. Mosel	(GIES)
PENNER	02D	PR C66 055212	G. Penner, U. Mosel	(GIES)
BLANPIED	01	PR C64 025203	G. Blanpied *et al.*	(BNL LEGS Collab.)
GALLER	01	PL B503 245	G. Galler *et al.*	(Mainz LARA Collab.)
LOPEZCAST...	01	PL B517 339	G. Lopez Castro, A. Mariano	
Also		NP A697 440	G. Lopez Castro, A. Mariano	
BECK	00	PR C61 035204	R. Beck *et al.*	(Mainz Microtron DAPHNE Col.)
KAMALOV	99	PRL 83 4494	S.S. Kamalov, S.N. Yang	(Taiwan U.)
HANSTEIN	98	NP A632 561	O. Hanstein, D. Drechsel, L. Tiator	
ARNDT	97	PR C56 577	R.A. Arndt, I.I. Strakovsky, R.L. Workman	(VPI)
BECK	97	PRL 78 606	R. Beck *et al.*	(MANZ, SACL, PAVI, GLAS)
Also		PRL 79 4510	R.L. Beck, H.P. Krahn	(MANZ)
Also		PRL 79 4512	R.L. Beck, H.P. Krahn	(MANZ)
Also		PRL 79 4515 (erratum)	R.L. Beck *et al.*	(MANZ, SACL, PAVI, GLAS)
BLANPIED	97	PRL 79 4337	G.S. Blanpied *et al.*	(LEGS Collab.)
DAVIDSON	97	PRL 79 4509	R.M. Davidson, N.C.A. Mukhopadhyay	(RPI)
BERNICHA	96	NP A597 623	A. Bernicha, G. Lopez Castro, J. Pestieau	(LOUV+)
HANSTEIN	96	PL B385 45	O. Hanstein, D. Drechsel, L. Tiator	(MANZ)
ABAEV	95	ZPHY A352 85	V.V. Abaev, S.P. Kruglov	(PNPI)
HOEHLER	93	πN Newsletter 9 1	G. Hohler	(KARL)
BOSSHARD	91	PR D44 1962	A. Bosshard *et al.*	(ZURI, LBL, VILL+)
Also		PRL 64 2619	A. Bosshard *et al.*	(CATH, LAUS, LBL+)
LIN	91B	PR C44 1819	D.H. Lin, M.K. Liou, Z.M. Ding	(CUNY, CSOK)
Also		PR C43 R930	D. Lin, M.K. Liou	(CUNY)
WITTMAN	88	PR C37 2075	R. Wittman	(TRIU)
HELLER	87	PR C35 718	L. Heller *et al.*	(LANL, MIT, ILL)
CUTKOSKY	80	Toronto Conf. 19	R.E. Cutkosky *et al.*	(CMU, LBL) IJP
Also		PR D20 2839	R.E. Cutkosky *et al.*	(CMU, LBL)
KOCH	80B	NP A336 331	R. Koch, E. Pietarinen	(KARLT) IJP
HOEHLER	79	PDAT 12-1	G. Hohler *et al.*	(KARLT) IJP
Also		Toronto Conf. 3	R. Koch	(KARLT) IJP
MIROSHNIC...	79	SJNP 29 94 Translated from YAF 29 188.	I.I. Miroshnichenko *et al.*	(KFTI) IJP
NEFKENS	78	PR D18 3911	B.M.K. Nefkens *et al.*	(UCLA, CATH) IJP
PEDRONI	78	NP A300 321	E. Pedroni *et al.*	(SIN, ISNG, KARLE+) IJP

$\Delta(1600)$ $3/2^+$

$I(J^P) = \frac{3}{2}(\frac{3}{2}^+)$ Status: ****

Older and obsolete values are listed and referenced in the 2014 edition, Chinese Physics **C38** 070001 (2014).

$\Delta(1600)$ POLE POSITION

REAL PART

VALUE (MeV)	DOCUMENT ID		TECN	COMMENT
1460 to 1560 (≈ 1510) OUR ESTIMATE				
1515 ± 20	SOKHOYAN	15A	DPWA	Multichannel
$1469 \pm 10 \pm 5$	[1] SVARC	14	L+P	$\pi N \rightarrow \pi N$
1550 ± 40	CUTKOSKY	80	IPWA	$\pi N \rightarrow \pi N$
• • • We do not use the following data for averages, fits, limits, etc. • • •				
1552	ROENCHEN	15A	DPWA	Multichannel
1498 ± 25	ANISOVICH	12A	DPWA	Multichannel
1599	SHRESTHA	12A	DPWA	Multichannel
1457	ARNDT	06	DPWA	$\pi N \rightarrow \pi N, \eta N$
1599	VRANA	00	DPWA	Multichannel
1550	HOEHLER	93	SPED	$\pi N \rightarrow \pi N$

[1] Fit to the amplitudes of HOEHLER 79.

$-2\times$IMAGINARY PART

VALUE (MeV)	DOCUMENT ID		TECN	COMMENT
200 to 340 (≈ 270) OUR ESTIMATE				
250 ± 30	SOKHOYAN	15A	DPWA	Multichannel
$314 \pm 18 \pm 8$	[1] SVARC	14	L+P	$\pi N \rightarrow \pi N$
200 ± 60	CUTKOSKY	80	IPWA	$\pi N \rightarrow \pi N$
• • • We do not use the following data for averages, fits, limits, etc. • • •				
350	ROENCHEN	15A	DPWA	Multichannel
230 ± 50	ANISOVICH	12A	DPWA	Multichannel
211	SHRESTHA	12A	DPWA	Multichannel
400	ARNDT	06	DPWA	$\pi N \rightarrow \pi N, \eta N$
312	VRANA	00	DPWA	Multichannel

[1] Fit to the amplitudes of HOEHLER 79.

$\Delta(1600)$ ELASTIC POLE RESIDUE

MODULUS $|r|$

VALUE (MeV)	DOCUMENT ID		TECN	COMMENT
10 to 40 (≈ 25) OUR ESTIMATE				
13 ± 3	SOKHOYAN	15A	DPWA	Multichannel
$38 \pm 2 \pm 2$	[1] SVARC	14	L+P	$\pi N \rightarrow \pi N$
17 ± 4	CUTKOSKY	80	IPWA	$\pi N \rightarrow \pi N$
• • • We do not use the following data for averages, fits, limits, etc. • • •				
23	ROENCHEN	15A	DPWA	Multichannel
11 ± 6	ANISOVICH	12A	DPWA	Multichannel
44	ARNDT	06	DPWA	$\pi N \rightarrow \pi N, \eta N$

[1] Fit to the amplitudes of HOEHLER 79.

PHASE θ

VALUE (°)	DOCUMENT ID		TECN	COMMENT
150 to 210 (≈ 180) OUR ESTIMATE				
-155 ± 20	SOKHOYAN	15A	DPWA	Multichannel
$173 \pm 5 \pm 5$	[1] SVARC	14	L+P	$\pi N \rightarrow \pi N$
-150 ± 30	CUTKOSKY	80	IPWA	$\pi N \rightarrow \pi N$
• • • We do not use the following data for averages, fits, limits, etc. • • •				
-155	ROENCHEN	15A	DPWA	Multichannel
-160 ± 33	ANISOVICH	12A	DPWA	Multichannel
$+147$	ARNDT	06	DPWA	$\pi N \rightarrow \pi N, \eta N$

[1] Fit to the amplitudes of HOEHLER 79.

$\Delta(1600)$ INELASTIC POLE RESIDUE

The "normalized residue" is the residue divided by $\Gamma_{pole}/2$.

Normalized residue in $N\pi \rightarrow \Delta(1600) \rightarrow \Delta\pi$, P-wave

MODULUS	PHASE (°)	DOCUMENT ID		TECN	COMMENT
0.15 ± 0.04	30 ± 35	SOKHOYAN	15A	DPWA	Multichannel
• • • We do not use the following data for averages, fits, limits, etc. • • •					
0.31	31	ROENCHEN	15A	DPWA	Multichannel
0.14 ± 0.10	154 ± 40	ANISOVICH	12A	DPWA	Multichannel

Normalized residue in $N\pi \rightarrow \Delta(1600) \rightarrow \Delta\pi$, F-wave

MODULUS	PHASE (°)	DOCUMENT ID		TECN	COMMENT
0.010 ± 0.005		SOKHOYAN	15A	DPWA	Multichannel
• • • We do not use the following data for averages, fits, limits, etc. • • •					
0.013	29	ROENCHEN	15A	DPWA	Multichannel
0.010 ± 0.005		ANISOVICH	12A	DPWA	Multichannel

Normalized residue in $N\pi \rightarrow \Delta(1600) \rightarrow \Sigma K$

MODULUS	PHASE (°)	DOCUMENT ID		TECN	COMMENT
• • • We do not use the following data for averages, fits, limits, etc. • • •					
0.13	-5.6	ROENCHEN	15A	DPWA	Multichannel

$\Delta(1600)$ BREIT-WIGNER MASS

VALUE (MeV)	DOCUMENT ID		TECN	COMMENT
1500 to 1640 (≈ 1570) OUR ESTIMATE				
1520 ± 20	SOKHOYAN	15A	DPWA	Multichannel
1626 ± 8	[1] SHRESTHA	12A	DPWA	Multichannel
1600 ± 50	CUTKOSKY	80	IPWA	$\pi N \rightarrow \pi N$
1522 ± 13	HOEHLER	79	IPWA	$\pi N \rightarrow \pi N$

• • • We do not use the following data for averages, fits, limits, etc. • • •

1510±20	ANISOVICH	12A	DPWA	Multichannel
1667± 1	PENNER	02C	DPWA	Multichannel
1687±44	VRANA	00	DPWA	Multichannel

[1] Statistical error only.

Δ(1600) BREIT-WIGNER WIDTH

VALUE (MeV)	DOCUMENT ID		TECN	COMMENT
200 to 300 (≈ 250) OUR ESTIMATE				
235± 30	SOKHOYAN	15A	DPWA	Multichannel
225± 18	[1] SHRESTHA	12A	DPWA	Multichannel
300±100	CUTKOSKY	80	IPWA	$\pi N \to \pi N$
220± 40	HOEHLER	79	IPWA	$\pi N \to \pi N$
• • • We do not use the following data for averages, fits, limits, etc. • • •				
220± 45	ANISOVICH	12A	DPWA	Multichannel
397± 10	PENNER	02C	DPWA	Multichannel
493± 75	VRANA	00	DPWA	Multichannel

[1] Statistical error only.

Δ(1600) DECAY MODES

The following branching fractions are our estimates, not fits or averages.

	Mode	Fraction (Γ_i/Γ)
Γ_1	$N\pi$	8–24 %
Γ_2	$N\pi\pi$	75–90 %
Γ_3	$\Delta(1232)\pi$	73–83 %
Γ_4	$\Delta(1232)\pi$, P-wave	72–82 %
Γ_5	$\Delta(1232)\pi$, F-wave	<2 %
Γ_6	$N(1440)\pi$	
Γ_7	$N(1440)\pi$, P-wave	15–25 %
Γ_8	$N\gamma$	0.001–0.035 %
Γ_9	$N\gamma$, helicity=1/2	0.0–0.02 %
Γ_{10}	$N\gamma$, helicity=3/2	0.001–0.015 %

Δ(1600) BRANCHING RATIOS

$\Gamma(N\pi)/\Gamma_{total}$ Γ_1/Γ

VALUE (%)	DOCUMENT ID		TECN	COMMENT
8 to 24 (≈ 16) OUR ESTIMATE				
14±4	SOKHOYAN	15A	DPWA	Multichannel
8±2	[1] SHRESTHA	12A	DPWA	Multichannel
18±4	CUTKOSKY	80	IPWA	$\pi N \to \pi N$
21±6	HOEHLER	79	IPWA	$\pi N \to \pi N$
• • • We do not use the following data for averages, fits, limits, etc. • • •				
12±5	ANISOVICH	12A	DPWA	Multichannel
13±1	PENNER	02C	DPWA	Multichannel
28±5	VRANA	00	DPWA	Multichannel

[1] Statistical error only.

$\Gamma(\Delta(1232)\pi, P\text{-wave})/\Gamma_{total}$ Γ_4/Γ

VALUE (%)	DOCUMENT ID		TECN	COMMENT
77± 5	SOKHOYAN	15A	DPWA	Multichannel
70± 3	[1] SHRESTHA	12A	DPWA	Multichannel
• • • We do not use the following data for averages, fits, limits, etc. • • •				
78± 6	ANISOVICH	12A	DPWA	Multichannel
59±10	VRANA	00	DPWA	Multichannel

[1] Statistical error only.

$\Gamma(\Delta(1232)\pi, F\text{-wave})/\Gamma_{total}$ Γ_5/Γ

VALUE (%)	DOCUMENT ID	TECN	COMMENT
<2	SOKHOYAN 15A	DPWA	Multichannel

$\Gamma(N(1440)\pi)/\Gamma_{total}$ Γ_6/Γ

VALUE (%)	DOCUMENT ID		TECN	COMMENT
22±3	[1] SHRESTHA	12A	DPWA	Multichannel
• • • We do not use the following data for averages, fits, limits, etc. • • •				
13±4	VRANA	00	DPWA	Multichannel

[1] Statistical error only.

Δ(1600) PHOTON DECAY AMPLITUDES AT THE POLE

Δ(1600) → $N\gamma$, helicity-1/2 amplitude $A_{1/2}$

MODULUS ($GeV^{-1/2}$)	PHASE (°)	DOCUMENT ID		TECN	COMMENT
0.053±0.010	130 ± 15	SOKHOYAN	15A	DPWA	Multichannel
$0.193^{+0.023}_{-0.024}$	151^{+9}_{-15}	ROENCHEN	14	DPWA	
• • • We do not use the following data for averages, fits, limits, etc. • • •					
−0.230	−42	ROENCHEN	15A	DPWA	Multichannel

Δ(1600) → $N\gamma$, helicity-3/2 amplitude $A_{3/2}$

MODULUS ($GeV^{-1/2}$)	PHASE (°)	DOCUMENT ID	TECN	COMMENT
0.055±0.010	152 ± 15	SOKHOYAN 15A	DPWA	Multichannel
$-0.254^{+0.085}_{-0.086}$	110^{+10}_{-6}	ROENCHEN 14	DPWA	
• • • We do not use the following data for averages, fits, limits, etc. • • •				
0.332	−71	ROENCHEN 15A	DPWA	Multichannel

Δ(1600) BREIT-WIGNER PHOTON DECAY AMPLITUDES

Δ(1600) → $N\gamma$, helicity-1/2 amplitude $A_{1/2}$

VALUE ($GeV^{-1/2}$)	DOCUMENT ID		TECN	COMMENT
−0.060 to −0.030 (≈ −0.045) OUR ESTIMATE				
−0.051±0.010	SOKHOYAN	15A	DPWA	Multichannel
−0.018±0.015	[1] ARNDT	96	IPWA	$\gamma N \to \pi N$
• • • We do not use the following data for averages, fits, limits, etc. • • •				
−0.050±0.009	ANISOVICH	12A	DPWA	Multichannel
0.006±0.005	[1] SHRESTHA	12A	DPWA	Multichannel
0.0	PENNER	02D	DPWA	Multichannel

[1] Statistical error only.

Δ(1600) → $N\gamma$, helicity-3/2 amplitude $A_{3/2}$

VALUE ($GeV^{-1/2}$)	DOCUMENT ID		TECN	COMMENT
−0.050 to −0.020 (≈ −0.035) OUR ESTIMATE				
−0.055±0.010	SOKHOYAN	15A	DPWA	Multichannel
−0.025±0.015	[1] ARNDT	96	IPWA	$\gamma N \to \pi N$
• • • We do not use the following data for averages, fits, limits, etc. • • •				
−0.040±0.012	ANISOVICH	12A	DPWA	Multichannel
0.052±0.008	[1] SHRESTHA	12A	DPWA	Multichannel
−0.024	PENNER	02D	DPWA	Multichannel

[1] Statistical error only.

Δ(1600) REFERENCES

For early references, see Physics Letters **111B** 1 (1982).

ROENCHEN	15A	EPJ A51 70	D. Roenchen *et al.*	
SOKHOYAN	15A	EPJ A51 95	V. Sokhoyan *et al.*	(CBELSA/TAPS Collab.)
PDG	14	CP C38 070001	K. Olive *et al.*	(PDG Collab.)
ROENCHEN	14	EPJ A50 101	D. Roenchen *et al.*	
Also		EPJ A51 63 (errat.)	D. Roenchen *et al.*	
SVARC	14	PR C89 045205	A. Svarc *et al.*	(RBI Zagreb, UNI Tuzla)
ANISOVICH	12A	EPJ A48 15	A.V. Anisovich *et al.*	(BONN, PNPI)
SHRESTHA	12A	PR C86 055203	M. Shrestha, D.M. Manley	(KSU)
ARNDT	06	PR C74 045205	R.A. Arndt *et al.*	(GWU)
PENNER	02C	PR C66 055211	G. Penner, U. Mosel	(GIES)
PENNER	02D	PR C66 055212	G. Penner, U. Mosel	(GIES)
VRANA	00	PRPL 328 181	T.P. Vrana, S.A. Dytman, T.-S.H. Lee	(PITT, ANL)
ARNDT	96	PR C53 430	R.A. Arndt, I.I. Strakovsky, R.L. Workman	(VPI)
HOEHLER	93	πN Newsletter 9 1	G. Hohler	(KARL)
CUTKOSKY	80	Toronto Conf. 19	R.E. Cutkosky *et al.*	(CMU, LBL) IJP
Also		PR D20 2839	R.E. Cutkosky *et al.*	(CMU, LBL) IJP
HOEHLER	79	PDAT 12-1	G. Hohler *et al.*	(KARLT) IJP
Also		Toronto Conf. 3	R. Koch	(KARLT) IJP

Δ(1620) 1/2⁻

$I(J^P) = \frac{3}{2}(\frac{1}{2}^-)$ Status: ****

Older and obsolete values are listed and referenced in the 2014 edition, Chinese Physics **C38** 070001 (2014).

Δ(1620) POLE POSITION

REAL PART

VALUE (MeV)	DOCUMENT ID		TECN	COMMENT
1590 to 1610 (≈ 1600) OUR ESTIMATE				
1597± 5	SOKHOYAN	15A	DPWA	Multichannel
1603± 7±2	[1] SVARC	14	L+P	$\pi N \to \pi N$
1600±15	CUTKOSKY	80	IPWA	$\pi N \to \pi N$
• • • We do not use the following data for averages, fits, limits, etc. • • •				
1600	ROENCHEN	15A	DPWA	Multichannel
1597± 4	ANISOVICH	12A	DPWA	Multichannel
1587	SHRESTHA	12A	DPWA	Multichannel
1595	ARNDT	06	DPWA	$\pi N \to \pi N$, ηN
1607	VRANA	00	DPWA	Multichannel
1608	HOEHLER	93	SPED	$\pi N \to \pi N$

[1] Fit to the amplitudes of HOEHLER 79.

−2×IMAGINARY PART

VALUE (MeV)	DOCUMENT ID		TECN	COMMENT
100 to 140 (≈ 120) OUR ESTIMATE				
134± 8	SOKHOYAN	15A	DPWA	Multichannel
114±12±4	[1] SVARC	14	L+P	$\pi N \to \pi N$
120±20	CUTKOSKY	80	IPWA	$\pi N \to \pi N$

• • • We do not use the following data for averages, fits, limits, etc. • • •				
65	ROENCHEN	15A	DPWA	Multichannel
130± 9	ANISOVICH	12A	DPWA	Multichannel
107	SHRESTHA	12A	DPWA	Multichannel
135	ARNDT	06	DPWA	$\pi N \to \pi N, \eta N$
148	VRANA	00	DPWA	Multichannel
116	HOEHLER	93	SPED	$\pi N \to \pi N$

[1] Fit to the amplitudes of HOEHLER 79.

Δ(1620) ELASTIC POLE RESIDUE

MODULUS |r|

VALUE (MeV)	DOCUMENT ID		TECN	COMMENT
15 to 20 (≈ 17) OUR ESTIMATE				
20±3	SOKHOYAN	15A	DPWA	Multichannel
17±2±1	[1] SVARC	14	L+P	$\pi N \to \pi N$
15±2	CUTKOSKY	80	IPWA	$\pi N \to \pi N$
• • • We do not use the following data for averages, fits, limits, etc. • • •				
16	ROENCHEN	15A	DPWA	Multichannel
18±2	ANISOVICH	12A	DPWA	Multichannel
15	ARNDT	06	DPWA	$\pi N \to \pi N, \eta N$
19	HOEHLER	93	SPED	$\pi N \to \pi N$

[1] Fit to the amplitudes of HOEHLER 79.

PHASE θ

VALUE (°)	DOCUMENT ID		TECN	COMMENT
−120 to −80 (≈ −100) OUR ESTIMATE				
− 90±15	SOKHOYAN	15A	DPWA	Multichannel
−106±10±4	[1] SVARC	14	L+P	$\pi N \to \pi N$
−110±20	CUTKOSKY	80	IPWA	$\pi N \to \pi N$
• • • We do not use the following data for averages, fits, limits, etc. • • •				
−104	ROENCHEN	15A	DPWA	Multichannel
−100± 5	ANISOVICH	12A	DPWA	Multichannel
− 92	ARNDT	06	DPWA	$\pi N \to \pi N, \eta N$
− 95	HOEHLER	93	SPED	$\pi N \to \pi N$

[1] Fit to the amplitudes of HOEHLER 79.

Δ(1620) INELASTIC POLE RESIDUE

The "normalized residue" is the residue divided by $\Gamma_{pole}/2$.

Normalized residue in $N\pi \to \Delta(1620) \to \Delta\pi$, D-wave

MODULUS	PHASE (°)	DOCUMENT ID		TECN	COMMENT
0.42±0.06	−90 ± 20	SOKHOYAN	15A	DPWA	Multichannel
• • • We do not use the following data for averages, fits, limits, etc. • • •					
0.57	105	ROENCHEN	15A	DPWA	Multichannel
0.38±0.09	−85 ± 30	ANISOVICH	12A	DPWA	Multichannel

Normalized residue in $N\pi \to \Delta(1620) \to \Sigma K$

MODULUS	PHASE (°)	DOCUMENT ID		TECN	COMMENT
• • • We do not use the following data for averages, fits, limits, etc. • • •					
0.22	−105	ROENCHEN	15A	DPWA	Multichannel

Normalized residue in $N\pi \to \Delta(1620) \to N(1440)\pi$

MODULUS	PHASE (°)	DOCUMENT ID		TECN	COMMENT
0.10±0.06	−65 ± 30	SOKHOYAN	15A	DPWA	Multichannel

Δ(1620) BREIT-WIGNER MASS

VALUE (MeV)	DOCUMENT ID		TECN	COMMENT
1590 to 1630 (≈ 1610) OUR ESTIMATE				
1595 ± 8	SOKHOYAN	15A	DPWA	Multichannel
1600 ± 1	[1] SHRESTHA	12A	DPWA	Multichannel
1615.2± 0.4	[1] ARNDT	06	DPWA	$\pi N \to \pi N, \eta N$
1620 ±20	CUTKOSKY	80	IPWA	$\pi N \to \pi N$
1610 ± 7	HOEHLER	79	IPWA	$\pi N \to \pi N$
• • • We do not use the following data for averages, fits, limits, etc. • • •				
1600 ± 8	ANISOVICH	12A	DPWA	Multichannel
1612 ± 2	PENNER	02C	DPWA	Multichannel
1617 ±15	VRANA	00	DPWA	Multichannel

[1] Statistical error only.

Δ(1620) BREIT-WIGNER WIDTH

VALUE (MeV)	DOCUMENT ID		TECN	COMMENT
110 to 150 (≈ 130) OUR ESTIMATE				
135 ± 9	SOKHOYAN	15A	DPWA	Multichannel
112 ± 2	[1] SHRESTHA	12A	DPWA	Multichannel
146.9± 1.9	[1] ARNDT	06	DPWA	$\pi N \to \pi N, \eta N$
140 ±20	CUTKOSKY	80	IPWA	$\pi N \to \pi N$
139 ±18	HOEHLER	79	IPWA	$\pi N \to \pi N$
• • • We do not use the following data for averages, fits, limits, etc. • • •				
130 ±11	ANISOVICH	12A	DPWA	Multichannel
202 ± 7	PENNER	02C	DPWA	Multichannel
143 ±42	VRANA	00	DPWA	Multichannel

[1] Statistical error only.

Δ(1620) DECAY MODES

The following branching fractions are our estimates, not fits or averages.

	Mode	Fraction (Γ_i/Γ)
Γ_1	$N\pi$	25–35 %
Γ_2	$N\pi\pi$	55–80 %
Γ_3	$\Delta(1232)\pi$	
Γ_4	$\Delta(1232)\pi$, D-wave	52–72 %
Γ_5	$N\rho$	
Γ_6	$N\rho$, S=1/2, S-wave	seen
Γ_7	$N\rho$, S=3/2, D-wave	seen
Γ_8	$N(1440)\pi$	3–9 %
Γ_9	$N\gamma$, helicity=1/2	0.03–0.10 %

Δ(1620) BRANCHING RATIOS

$\Gamma(N\pi)/\Gamma_{total}$ Γ_1/Γ

VALUE (%)	DOCUMENT ID		TECN	COMMENT
25 to 35 (≈ 30) OUR ESTIMATE				
28 ±3	SOKHOYAN	15A	DPWA	Multichannel
33 ±2	[1] SHRESTHA	12A	DPWA	Multichannel
31.5±0.1	[1] ARNDT	06	DPWA	$\pi N \to \pi N, \eta N$
25 ±3	CUTKOSKY	80	IPWA	$\pi N \to \pi N$
35 ±6	HOEHLER	79	IPWA	$\pi N \to \pi N$
• • • We do not use the following data for averages, fits, limits, etc. • • •				
28 ±3	ANISOVICH	12A	DPWA	Multichannel
34 ±1	PENNER	02C	DPWA	Multichannel
45 ±5	VRANA	00	DPWA	Multichannel

[1] Statistical error only.

$\Gamma(\Delta(1232)\pi, D\text{-wave})/\Gamma_{total}$ Γ_4/Γ

VALUE (%)	DOCUMENT ID		TECN	COMMENT
62±10	SOKHOYAN	15A	DPWA	Multichannel
32± 2	[1] SHRESTHA	12A	DPWA	Multichannel
• • • We do not use the following data for averages, fits, limits, etc. • • •				
60±17	ANISOVICH	12A	DPWA	Multichannel
39± 2	VRANA	00	DPWA	Multichannel

[1] Statistical error only.

$\Gamma(N\rho, S=1/2, S\text{-wave})/\Gamma_{total}$ Γ_6/Γ

VALUE (%)	DOCUMENT ID		TECN	COMMENT
26±2	[1] SHRESTHA	12A	DPWA	Multichannel
• • • We do not use the following data for averages, fits, limits, etc. • • •				
14±3	VRANA	00	DPWA	Multichannel

[1] Statistical error only.

$\Gamma(N\rho, S=3/2, D\text{-wave})/\Gamma_{total}$ Γ_7/Γ

VALUE (%)	DOCUMENT ID		TECN	COMMENT
• • • We do not use the following data for averages, fits, limits, etc. • • •				
2±1	VRANA	00	DPWA	Multichannel

$\Gamma(N(1440)\pi)/\Gamma_{total}$ Γ_8/Γ

VALUE (%)	DOCUMENT ID		TECN	COMMENT
6±3	SOKHOYAN	15A	DPWA	Multichannel
9±1	[1] SHRESTHA	12A	DPWA	Multichannel
• • • We do not use the following data for averages, fits, limits, etc. • • •				
0±1	VRANA	00	DPWA	Multichannel

[1] Statistical error only.

Δ(1620) PHOTON DECAY AMPLITUDES AT THE POLE

$\Delta(1620) \to N\gamma$, helicity-1/2 amplitude $A_{1/2}$

MODULUS ($GeV^{-1/2}$)	PHASE (°)	DOCUMENT ID		TECN	COMMENT
0.054±0.007	−6 ± 7	SOKHOYAN	15A	DPWA	Multichannel
$-0.028^{+0.006}_{-0.002}$	-166^{+1}_{-4}	ROENCHEN	14	DPWA	
• • • We do not use the following data for averages, fits, limits, etc. • • •					
0.014	26	ROENCHEN	15A	DPWA	Multichannel

Δ(1620) BREIT-WIGNER PHOTON DECAY AMPLITUDES

Δ(1620) → Nγ, helicity-1/2 amplitude $A_{1/2}$

VALUE ($GeV^{-1/2}$)	DOCUMENT ID		TECN	COMMENT
0.030 to 0.060 (≈ 0.050) OUR ESTIMATE				
0.055±0.007	SOKHOYAN	15A	DPWA	Multichannel
0.029±0.003	[1] WORKMAN	12A	DPWA	$\gamma N \to N\pi$
0.050±0.002	[1] DUGGER	07	DPWA	$\gamma N \to \pi N$
• • • We do not use the following data for averages, fits, limits, etc. • • •				
0.052±0.005	ANISOVICH	12A	DPWA	Multichannel
−0.003±0.003	[1] SHRESTHA	12A	DPWA	Multichannel
0.066	DRECHSEL	07	DPWA	$\gamma N \to \pi N$
−0.050	PENNER	02D	DPWA	Multichannel

[1] Statistical error only.

Δ(1620) REFERENCES

For early references, see Physics Letters **111B** 1 (1982).

ROENCHEN	15A	EPJ A51 70	D. Roenchen *et al.*	
SOKHOYAN	15A	EPJ A51 95	V. Sokhoyan *et al.*	(CBELSA/TAPS Collab.)
PDG	14	CP C38 070001	K. Olive *et al.*	(PDG Collab.)
ROENCHEN	14	EPJ A50 101	D. Roenchen *et al.*	
Also		EPJ A51 63 (errat.)	D. Roenchen *et al.*	
SVARC	14	PR C89 045205	A. Svarc *et al.*	(RBI Zagreb, UNI Tuzla)
ANISOVICH	12A	EPJ A48 15	A.V. Anisovich *et al.*	(BONN, PNPI)
SHRESTHA	12A	PR C86 055203	M. Shrestha, D.M. Manley	(KSU)
WORKMAN	12A	PR C86 015202	R. Workman *et al.*	(GWU)
DRECHSEL	07	EPJ A34 69	D. Drechsel, S.S. Kamalov, L. Tiator	(MAINZ, JINR)
DUGGER	07	PR C76 025211	M. Dugger *et al.*	(JLab CLAS Collab.)
ARNDT	06	PR C74 045205	R.A. Arndt *et al.*	(GWU)
PENNER	02C	PR C66 055211	G. Penner, U. Mosel	(GIES)
PENNER	02D	PR C66 055212	G. Penner, U. Mosel	(GIES)
VRANA	00	PRPL 328 181	T.P. Vrana, S.A. Dytman, T.-S.H. Lee	(PITT, ANL)
HOEHLER	93	πN Newsletter 9 1	G. Hohler	(KARL)
CUTKOSKY	80	Toronto Conf. 19	R.E. Cutkosky *et al.*	(CMU, LBL) IJP
Also		PR D20 2839	R.E. Cutkosky *et al.*	(CMU, LBL) IJP
HOEHLER	79	PDAT 12-1	G. Hohler *et al.*	(KARLT) IJP
Also		Toronto Conf. 3	R. Koch	(KARLT) IJP

Δ(1700) 3/2⁻

$I(J^P) = \frac{3}{2}(\frac{3}{2}^-)$ Status: ****

Older and obsolete values are listed and referenced in the 2014 edition, Chinese Physics **C38** 070001 (2014).

Δ(1700) POLE POSITION

REAL PART

VALUE (MeV)	DOCUMENT ID		TECN	COMMENT
1640 to 1690 (≈ 1665) OUR ESTIMATE				
1685±10	SOKHOYAN	15A	DPWA	Multichannel
1643± 6±3	[1] SVARC	14	L+P	$\pi N \to \pi N$
1675±25	CUTKOSKY	80	IPWA	$\pi N \to \pi N$
• • • We do not use the following data for averages, fits, limits, etc. • • •				
1677	ROENCHEN	15A	DPWA	Multichannel
1685±10	GUTZ	14	DPWA	Multichannel
1680±10	ANISOVICH	12A	DPWA	Multichannel
1656	SHRESTHA	12A	DPWA	Multichannel
1632	ARNDT	06	DPWA	$\pi N \to \pi N, \eta N$
1726	VRANA	00	DPWA	Multichannel
1651	HOEHLER	93	SPED	$\pi N \to \pi N$

[1] Fit to the amplitudes of HOEHLER 79.

−2×IMAGINARY PART

VALUE (MeV)	DOCUMENT ID		TECN	COMMENT
200 to 300 (≈ 250) OUR ESTIMATE				
300±15	SOKHOYAN	15A	DPWA	Multichannel
217±10±8	[1] SVARC	14	L+P	$\pi N \to \pi N$
220±40	CUTKOSKY	80	IPWA	$\pi N \to \pi N$
• • • We do not use the following data for averages, fits, limits, etc. • • •				
305	ROENCHEN	15A	DPWA	Multichannel
300±15	GUTZ	14	DPWA	Multichannel
305±15	ANISOVICH	12A	DPWA	Multichannel
226	SHRESTHA	12A	DPWA	Multichannel
253	ARNDT	06	DPWA	$\pi N \to \pi N, \eta N$
118	VRANA	00	DPWA	Multichannel
159	HOEHLER	93	SPED	$\pi N \to \pi N$

[1] Fit to the amplitudes of HOEHLER 79.

Δ(1700) ELASTIC POLE RESIDUE

MODULUS |r|

VALUE (MeV)	DOCUMENT ID		TECN	COMMENT
10 to 40 (≈ 25) OUR ESTIMATE				
40±6	SOKHOYAN	15A	DPWA	Multichannel
13±1±1	[1] SVARC	14	L+P	$\pi N \to \pi N$
13±3	CUTKOSKY	80	IPWA	$\pi N \to \pi N$
• • • We do not use the following data for averages, fits, limits, etc. • • •				
24	ROENCHEN	15A	DPWA	Multichannel
40±6	GUTZ	14	DPWA	Multichannel
42±7	ANISOVICH	12A	DPWA	Multichannel
18	ARNDT	06	DPWA	$\pi N \to \pi N, \eta N$
10	HOEHLER	93	SPED	$\pi N \to \pi N$

[1] Fit to the amplitudes of HOEHLER 79.

PHASE θ

VALUE (°)	DOCUMENT ID		TECN	COMMENT
−40 to 0 (≈ −20) OUR ESTIMATE				
− 1 ±10	SOKHOYAN	15A	DPWA	Multichannel
−30 ± 4±3	[1] SVARC	14	L+P	$\pi N \to \pi N$
−40	ARNDT	06	DPWA	$\pi N \to \pi N, \eta N$
−20 ±25	CUTKOSKY	80	IPWA	$\pi N \to \pi N$
• • • We do not use the following data for averages, fits, limits, etc. • • •				
− 7.3	ROENCHEN	15A	DPWA	Multichannel
− 1 ±10	GUTZ	14	DPWA	Multichannel
− 3 ±15	ANISOVICH	12A	DPWA	Multichannel

[1] Fit to the amplitudes of HOEHLER 79.

Δ(1700) INELASTIC POLE RESIDUE

The "normalized residue" is the residue divided by $\Gamma_{pole}/2$.

Normalized residue in $N\pi \to \Delta(1700) \to \Delta\eta$

MODULUS	PHASE (°)	DOCUMENT ID		TECN	COMMENT
0.12±0.02	−60 ± 12	GUTZ	14	DPWA	Multichannel
• • • We do not use the following data for averages, fits, limits, etc. • • •					
0.12±0.03	−60 ± 15	ANISOVICH	12A	DPWA	Multichannel

Normalized residue in $N\pi \to \Delta(1700) \to \Sigma K$

MODULUS	PHASE (°)	DOCUMENT ID		TECN	COMMENT
• • • We do not use the following data for averages, fits, limits, etc. • • •					
0.011	−147	ROENCHEN	15A	DPWA	Multichannel

Normalized residue in $N\pi \to \Delta(1700) \to N(1535)\pi$

MODULUS	PHASE (°)	DOCUMENT ID		TECN	COMMENT
0.035±0.015	−75 ± 30	GUTZ	14	DPWA	Multichannel

Normalized residue in $N\pi \to \Delta(1700) \to \Delta(1232)\pi$, S-wave

MODULUS	PHASE (°)	DOCUMENT ID		TECN	COMMENT
0.25±0.12	135 ± 45	SOKHOYAN	15A	DPWA	Multichannel
• • • We do not use the following data for averages, fits, limits, etc. • • •					
0.39	151	ROENCHEN	15A	DPWA	Multichannel

Normalized residue in $N\pi \to \Delta(1700) \to \Delta(1232)\pi$, D-wave

MODULUS	PHASE (°)	DOCUMENT ID		TECN	COMMENT
0.12 ±0.06	−160 ± 30	SOKHOYAN	15A	DPWA	Multichannel
• • • We do not use the following data for averages, fits, limits, etc. • • •					
0.054	166	ROENCHEN	15A	DPWA	Multichannel

Normalized residue in $N\pi \to \Delta(1700) \to N(1520)\pi$, P-wave

MODULUS	PHASE (°)	DOCUMENT ID		TECN	COMMENT
0.10±0.03	−10 ± 20	SOKHOYAN	15A	DPWA	Multichannel

Δ(1700) BREIT-WIGNER MASS

VALUE (MeV)	DOCUMENT ID		TECN	COMMENT
1690 to 1730 (≈ 1710) OUR ESTIMATE				
1715 ±20	SOKHOYAN	15A	DPWA	Multichannel
1691 ± 4	[1] SHRESTHA	12A	DPWA	Multichannel
1695.0± 1.3	[1] ARNDT	06	DPWA	$\pi N \to \pi N, \eta N$
1710 ±30	CUTKOSKY	80	IPWA	$\pi N \to \pi N$
1680 ±70	HOEHLER	79	IPWA	$\pi N \to \pi N$
• • • We do not use the following data for averages, fits, limits, etc. • • •				
1715 ±20	GUTZ	14	DPWA	Multichannel
1715 $^{+30}_{-15}$	ANISOVICH	12A	DPWA	Multichannel
1678 ± 1	PENNER	02C	DPWA	Multichannel
1732 ±23	VRANA	00	DPWA	Multichannel

[1] Statistical error only.

Δ(1700) BREIT-WIGNER WIDTH

VALUE (MeV)	DOCUMENT ID		TECN	COMMENT
220 to 380 (≈ 300) OUR ESTIMATE				
300 ±25	SOKHOYAN	15A	DPWA	Multichannel
248 ± 9	[1] SHRESTHA	12A	DPWA	Multichannel
375.5± 7.0	[1] ARNDT	06	DPWA	$\pi N \to \pi N, \eta N$
280 ±80	CUTKOSKY	80	IPWA	$\pi N \to \pi N$
230 ±80	HOEHLER	79	IPWA	$\pi N \to \pi N$

• • • We do not use the following data for averages, fits, limits, etc. • • •

300	±25	GUTZ	14	DPWA	Multichannel
310	$^{+40}_{-15}$	ANISOVICH	12A	DPWA	Multichannel
606	±15	PENNER	02C	DPWA	Multichannel
119	±70	VRANA	00	DPWA	Multichannel

[1] Statistical error only.

$\Delta(1700)$ DECAY MODES

The following branching fractions are our estimates, not fits or averages.

	Mode	Fraction (Γ_i/Γ)
Γ_1	$N\pi$	10–20 %
Γ_2	$N\pi\pi$	10–55 %
Γ_3	$\Delta(1232)\pi$	10–50 %
Γ_4	$\Delta(1232)\pi$, S-wave	5–35 %
Γ_5	$\Delta(1232)\pi$, D-wave	4–16 %
Γ_6	$N\rho$	
Γ_7	$N\rho$, S=3/2, S-wave	seen
Γ_8	$N(1520)\pi$, P-wave	1–5 %
Γ_9	$N(1535)\pi$	0.5–1.5 %
Γ_{10}	$\Delta(1232)\eta$	3–7 %
Γ_{11}	$N\gamma$	0.22–0.60 %
Γ_{12}	$N\gamma$, helicity=1/2	0.12–0.30 %
Γ_{13}	$N\gamma$, helicity=3/2	0.10–0.30 %

$\Delta(1700)$ BRANCHING RATIOS

$\Gamma(N\pi)/\Gamma_{total}$ Γ_1/Γ

VALUE (%)	DOCUMENT ID		TECN	COMMENT
10 to 20 OUR ESTIMATE				
22 ±4	SOKHOYAN	15A	DPWA	Multichannel
14 ±1	[1] SHRESTHA	12A	DPWA	Multichannel
15.6±0.1	[1] ARNDT	06	DPWA	$\pi N \to \pi N$, ηN
12 ±3	CUTKOSKY	80	IPWA	$\pi N \to \pi N$
20 ±3	HOEHLER	79	IPWA	$\pi N \to \pi N$
• • • We do not use the following data for averages, fits, limits, etc. • • •				
22 ±4	GUTZ	14	DPWA	Multichannel
22 ±4	ANISOVICH	12A	DPWA	Multichannel
14 ±1	PENNER	02C	DPWA	Multichannel
5 ±1	VRANA	00	DPWA	Multichannel

[1] Statistical error only.

$\Gamma(\Delta(1232)\pi, S\text{-wave})/\Gamma_{total}$ Γ_4/Γ

VALUE (%)	DOCUMENT ID		TECN	COMMENT
20±15	SOKHOYAN	15A	DPWA	Multichannel
54± 3	[1] SHRESTHA	12A	DPWA	Multichannel
• • • We do not use the following data for averages, fits, limits, etc. • • •				
20^{+25}_{-13}	ANISOVICH	12A	DPWA	Multichannel
90± 2	VRANA	00	DPWA	Multichannel

[1] Statistical error only.

$\Gamma(\Delta(1232)\pi, D\text{-wave})/\Gamma_{total}$ Γ_5/Γ

VALUE (%)	DOCUMENT ID		TECN	COMMENT
10± 6	SOKHOYAN	15A	DPWA	Multichannel
1± 1	[1] SHRESTHA	12A	DPWA	Multichannel
• • • We do not use the following data for averages, fits, limits, etc. • • •				
12^{+14}_{-7}	ANISOVICH	12A	DPWA	Multichannel
4± 1	VRANA	00	DPWA	Multichannel

[1] Statistical error only.

$\Gamma(N\rho, S=3/2, S\text{-wave})/\Gamma_{total}$ Γ_7/Γ

VALUE (%)	DOCUMENT ID		TECN	COMMENT
30±3	[1] SHRESTHA	12A	DPWA	Multichannel
• • • We do not use the following data for averages, fits, limits, etc. • • •				
1±1	VRANA	00	DPWA	Multichannel

[1] Statistical error only.

$\Gamma(N(1520)\pi, P\text{-wave})/\Gamma_{total}$ Γ_8/Γ

VALUE (%)	DOCUMENT ID		TECN	COMMENT
3±2	SOKHOYAN	15A	DPWA	Multichannel

$\Gamma(N(1535)\pi)/\Gamma_{total}$ Γ_9/Γ

VALUE (%)	DOCUMENT ID		TECN	COMMENT
1.0±0.5	GUTZ	14	DPWA	Multichannel
• • • We do not use the following data for averages, fits, limits, etc. • • •				
4 ±2	HORN	08A	DPWA	Multichannel

$\Gamma(\Delta(1232)\eta)/\Gamma_{total}$ Γ_{10}/Γ

VALUE (%)	DOCUMENT ID		TECN	COMMENT
5±2	GUTZ	14	DPWA	Multichannel
• • • We do not use the following data for averages, fits, limits, etc. • • •				
5±2	ANISOVICH	12A	DPWA	Multichannel

$\Gamma(N(1535)\pi)/\Gamma(\Delta(1232)\eta)$ Γ_9/Γ_{10}

VALUE	DOCUMENT ID		TECN	COMMENT
• • • We do not use the following data for averages, fits, limits, etc. • • •				
0.67	KASHEVAROV	09	CBAL	$\gamma p \to p\pi^0\eta$

$\Delta(1700)$ PHOTON DECAY AMPLITUDES AT THE POLE

$\Delta(1700) \to N\gamma$, helicity-1/2 amplitude $A_{1/2}$

MODULUS ($GeV^{-1/2}$)	PHASE (°)	DOCUMENT ID		TECN	COMMENT
0.175±0.020	50 ± 10	SOKHOYAN	15A	DPWA	Multichannel
0.109±0.010	-21^{+12}_{-6}	ROENCHEN	14	DPWA	
• • • We do not use the following data for averages, fits, limits, etc. • • •					
0.123	1.1	ROENCHEN	15A	DPWA	Multichannel

$\Delta(1700) \to N\gamma$, helicity-3/2 amplitude $A_{3/2}$

MODULUS ($GeV^{-1/2}$)	PHASE (°)	DOCUMENT ID		TECN	COMMENT
0.180±0.020	45 ± 10	SOKHOYAN	15A	DPWA	Multichannel
$0.111^{+0.027}_{-0.006}$	12^{+9}_{-11}	ROENCHEN	14	DPWA	
• • • We do not use the following data for averages, fits, limits, etc. • • •					
0.124	22	ROENCHEN	15A	DPWA	Multichannel

$\Delta(1700)$ BREIT-WIGNER PHOTON DECAY AMPLITUDES

$\Delta(1700) \to N\gamma$, helicity-1/2 amplitude $A_{1/2}$

VALUE ($GeV^{-1/2}$)	DOCUMENT ID		TECN	COMMENT
0.100 to 0.160 (≈ 0.130) OUR ESTIMATE				
0.165±0.020	SOKHOYAN	15A	DPWA	Multichannel
0.132±0.005	[1] DUGGER	13	DPWA	$\gamma N \to \pi N$
0.105±0.005	[1] WORKMAN	12A	DPWA	$\gamma N \to \pi N$
• • • We do not use the following data for averages, fits, limits, etc. • • •				
0.165±0.020	GUTZ	14	DPWA	Multichannel
0.160±0.020	ANISOVICH	12A	DPWA	Multichannel
0.058±0.010	[1] SHRESTHA	12A	DPWA	Multichannel
0.226	DRECHSEL	07	DPWA	$\gamma N \to \pi N$
0.125±0.003	DUGGER	07	DPWA	$\gamma N \to \pi N$
0.096	PENNER	02D	DPWA	Multichannel

[1] Statistical error only.

$\Delta(1700) \to N\gamma$, helicity-3/2 amplitude $A_{3/2}$

VALUE ($GeV^{-1/2}$)	DOCUMENT ID		TECN	COMMENT
0.090 to 0.170 (≈ 0.130) OUR ESTIMATE				
0.170±0.025	SOKHOYAN	15A	DPWA	Multichannel
0.108±0.005	[1] DUGGER	13	DPWA	$\gamma N \to \pi N$
0.092±0.004	[1] WORKMAN	12A	DPWA	$\gamma N \to \pi N$
• • • We do not use the following data for averages, fits, limits, etc. • • •				
0.170±0.025	GUTZ	14	DPWA	Multichannel
0.165±0.025	ANISOVICH	12A	DPWA	Multichannel
0.097±0.008	[1] SHRESTHA	12A	DPWA	Multichannel
0.210	DRECHSEL	07	DPWA	$\gamma N \to \pi N$
0.105±0.003	DUGGER	07	DPWA	$\gamma N \to \pi N$
0.154	PENNER	02D	DPWA	Multichannel

[1] Statistical error only.

$\Delta(1700)$ REFERENCES

For early references, see Physics Letters **111B** 1 (1982).

ROENCHEN	15A	EPJ A51 70	D. Roenchen *et al.*	
SOKHOYAN	15A	EPJ A51 95	V. Sokhoyan *et al.*	(CBELSA/TAPS Collab.)
GUTZ	14	EPJ A50 74	E. Gutz *et al.*	(CBELSA/TAPS Collab.)
PDG	14	CP C38 070001	K. Olive *et al.*	(PDG Collab.)
ROENCHEN	14	EPJ A50 101	D. Roenchen *et al.*	
Also		EPJ A51 63 (errat.)	D. Roenchen *et al.*	
SVARC	14	PR C89 045205	A. Svarc *et al.*	(RBI Zagreb, UNI Tuzla)
DUGGER	13	PR C88 065203	M. Dugger *et al.*	(JLab CLAS Collab.)
ANISOVICH	12A	EPJ A48 15	A.V. Anisovich *et al.*	(BONN, PNPI)
SHRESTHA	12A	PR C86 055203	M. Shrestha, D.M. Manley	(KSU)
WORKMAN	12A	PR C86 015202	R. Workman *et al.*	(GWU)
KASHEVAROV	09	EPJ A42 141	V.L. Kashevarov *et al.*	(MAMI Crystal Ball/TAPS)
HORN	08A	EPJ A38 173	I. Horn *et al.*	(CB-ELSA Collab.)
Also		PRL 101 202002	I. Horn *et al.*	(CB-ELSA Collab.)
DRECHSEL	07	EPJ A34 69	D. Drechsel, S.S. Kamalov, L. Tiator	(MAINZ, JINR)
DUGGER	07	PR C76 025211	M. Dugger *et al.*	(JLab CLAS Collab.)
ARNDT	06	PR C74 045205	R.A. Arndt *et al.*	(GWU)
PENNER	02C	PR C66 055211	G. Penner, U. Mosel	(GIES)
PENNER	02D	PR C66 055212	G. Penner, U. Mosel	(GIES)
VRANA	00	PRPL 328 181	T.P. Vrana, S.A. Dytman, T.-S.H. Lee	(PITT, ANL)
HOEHLER	93	πN Newsletter 9 1	G. Hohler	(KARL)

Baryon Particle Listings

Δ(1700), Δ(1750), Δ(1900)

CUTKOSKY	80	Toronto Conf. 19	R.E. Cutkosky *et al.*	(CMU, LBL) IJP
Also		PR D20 2839	R.E. Cutkosky *et al.*	(CMU, LBL) IJP
HOEHLER	79	PDAT 12-1	G. Hohler *et al.*	(KARLT) IJP
Also		Toronto Conf. 3	R. Koch	(KARLT) IJP

Δ(1750) 1/2+

$I(J^P) = \frac{3}{2}(\frac{1}{2}^+)$ Status: *

OMITTED FROM SUMMARY TABLE

Δ(1750) POLE POSITION

REAL PART

VALUE (MeV)	DOCUMENT ID		TECN	COMMENT
• • • We do not use the following data for averages, fits, limits, etc. • • •				
1748	ARNDT	04	DPWA	$\pi N \to \pi N, \eta N$
1714	VRANA	00	DPWA	Multichannel

−2×IMAGINARY PART

VALUE (MeV)	DOCUMENT ID		TECN	COMMENT
• • • We do not use the following data for averages, fits, limits, etc. • • •				
524	ARNDT	04	DPWA	$\pi N \to \pi N, \eta N$
68	VRANA	00	DPWA	Multichannel

Δ(1750) ELASTIC POLE RESIDUE

MODULUS |r|

VALUE (MeV)	DOCUMENT ID		TECN	COMMENT
• • • We do not use the following data for averages, fits, limits, etc. • • •				
48	ARNDT	04	DPWA	$\pi N \to \pi N, \eta N$

PHASE θ

VALUE (°)	DOCUMENT ID		TECN	COMMENT
• • • We do not use the following data for averages, fits, limits, etc. • • •				
158	ARNDT	04	DPWA	$\pi N \to \pi N, \eta N$

Δ(1750) BREIT-WIGNER MASS

VALUE (MeV)	DOCUMENT ID		TECN	COMMENT
• • • We do not use the following data for averages, fits, limits, etc. • • •				
1712 ± 1	PENNER	02C	DPWA	Multichannel
1721 ± 61	VRANA	00	DPWA	Multichannel

Δ(1750) BREIT-WIGNER WIDTH

VALUE (MeV)	DOCUMENT ID		TECN	COMMENT
• • • We do not use the following data for averages, fits, limits, etc. • • •				
643 ± 17	PENNER	02C	DPWA	Multichannel
70 ± 50	VRANA	00	DPWA	Multichannel

Δ(1750) DECAY MODES

	Mode	Fraction (Γ_i/Γ)
Γ_1	$N\pi$	seen
Γ_2	$N\pi\pi$	
Γ_3	$N(1440)\pi$	seen
Γ_4	ΣK	seen

Δ(1750) BRANCHING RATIOS

Γ(Nπ)/Γtotal — Γ1/Γ

VALUE (%)	DOCUMENT ID		TECN	COMMENT
• • • We do not use the following data for averages, fits, limits, etc. • • •				
1 ± 1	PENNER	02C	DPWA	Multichannel
6 ± 9	VRANA	00	DPWA	Multichannel

Γ(N(1440)π)/Γtotal — Γ3/Γ

VALUE (%)	DOCUMENT ID		TECN	COMMENT
• • • We do not use the following data for averages, fits, limits, etc. • • •				
83 ± 1	VRANA	00	DPWA	Multichannel

Γ(ΣK)/Γtotal — Γ4/Γ

VALUE (%)	DOCUMENT ID		TECN	COMMENT
• • • We do not use the following data for averages, fits, limits, etc. • • •				
0.1 ± 0.1	PENNER	02C	DPWA	Multichannel

Δ(1750) BREIT-WIGNER PHOTON DECAY AMPLITUDES

Papers on γN amplitudes predating 1981 may be found in our 2006 edition, Journal of Physics **G33** 1 (2006).

Δ(1750) → Nγ, helicity-1/2 amplitude $A_{1/2}$

VALUE ($GeV^{-1/2}$)	DOCUMENT ID		TECN	COMMENT
• • • We do not use the following data for averages, fits, limits, etc. • • •				
0.053	PENNER	02D	DPWA	Multichannel

Δ(1750) REFERENCES

PDG	06	JP G33 1	W.-M. Yao *et al.*	(PDG Collab.)
ARNDT	04	PR C69 035213	R.A. Arndt *et al.*	(GWU, TRIU)
PENNER	02C	PR C66 055211	G. Penner, U. Mosel	(GIES)
PENNER	02D	PR C66 055212	G. Penner, U. Mosel	(GIES)
VRANA	00	PRPL 328 181	T.P. Vrana, S.A. Dytman, T.-S.H. Lee	(PITT, ANL)

Δ(1900) 1/2−

$I(J^P) = \frac{3}{2}(\frac{1}{2}^-)$ Status: ***

Older and obsolete values are listed and referenced in the 2014 edition, Chinese Physics **C38** 070001 (2014).

Δ(1900) POLE POSITION

REAL PART

VALUE (MeV)	DOCUMENT ID		TECN	COMMENT
1830 to 1900 (≈ 1865) OUR ESTIMATE				
1845 ± 20	SOKHOYAN	15A	DPWA	Multichannel
1865 ± 35 ± 19	[1] SVARC	14	L+P	$\pi N \to \pi N$
1870 ± 40	CUTKOSKY	80	IPWA	$\pi N \to \pi N$
• • • We do not use the following data for averages, fits, limits, etc. • • •				
1845 ± 20	GUTZ	14	DPWA	Multichannel
1845 ± 25	ANISOVICH	12A	DPWA	Multichannel
1844	SHRESTHA	12A	DPWA	Multichannel
1795	VRANA	00	DPWA	Multichannel
1780	HOEHLER	93	SPED	$\pi N \to \pi N$

[1] Fit to the amplitudes of HOEHLER 79.

−2×IMAGINARY PART

VALUE (MeV)	DOCUMENT ID		TECN	COMMENT
180 to 300 (≈ 240) OUR ESTIMATE				
295 ± 35	SOKHOYAN	15A	DPWA	Multichannel
187 ± 50 ± 19	[1] SVARC	14	L+P	$\pi N \to \pi N$
180 ± 50	CUTKOSKY	80	IPWA	$\pi N \to \pi N$
• • • We do not use the following data for averages, fits, limits, etc. • • •				
295 ± 35	GUTZ	14	DPWA	Multichannel
300 ± 45	ANISOVICH	12A	DPWA	Multichannel
223	SHRESTHA	12A	DPWA	Multichannel
58	VRANA	00	DPWA	Multichannel

[1] Fit to the amplitudes of HOEHLER 79.

Δ(1900) ELASTIC POLE RESIDUE

MODULUS |r|

VALUE (MeV)	DOCUMENT ID		TECN	COMMENT
8 to 14 (≈ 11) OUR ESTIMATE				
11 ± 2	SOKHOYAN	15A	DPWA	Multichannel
11 ± 4 ± 2	[1] SVARC	14	L+P	$\pi N \to \pi N$
10 ± 3	CUTKOSKY	80	IPWA	$\pi N \to \pi N$
• • • We do not use the following data for averages, fits, limits, etc. • • •				
11 ± 2	GUTZ	14	DPWA	Multichannel
10 ± 3	ANISOVICH	12A	DPWA	Multichannel

[1] Fit to the amplitudes of HOEHLER 79.

PHASE θ

VALUE (°)	DOCUMENT ID		TECN	COMMENT
−115 ± 20	SOKHOYAN	15A	DPWA	Multichannel
20 ± 27 ± 19	[1] SVARC	14	L+P	$\pi N \to \pi N$
+ 20 ± 40	CUTKOSKY	80	IPWA	$\pi N \to \pi N$
• • • We do not use the following data for averages, fits, limits, etc. • • •				
−115 ± 20	GUTZ	14	DPWA	Multichannel
−125 ± 20	ANISOVICH	12A	DPWA	Multichannel

[1] Fit to the amplitudes of HOEHLER 79.

Δ(1900) INELASTIC POLE RESIDUE

The "normalized residue" is the residue divided by $\Gamma_{pole}/2$.

Normalized residue in Nπ → Δ(1900) → ΣK

MODULUS	PHASE (°)	DOCUMENT ID		TECN	COMMENT
0.07 ± 0.02	−50 ± 30	ANISOVICH	12A	DPWA	Multichannel

Normalized residue in $N\pi \to \Delta(1900) \to \Delta\pi$, D-wave

MODULUS	PHASE (°)	DOCUMENT ID		TECN	COMMENT
0.18 ± 0.10	105 ± 25	SOKHOYAN	15A	DPWA	Multichannel
• • • We do not use the following data for averages, fits, limits, etc. • • •					
$0.12^{+0.08}_{-0.05}$	110 ± 20	ANISOVICH	12A	DPWA	Multichannel

Normalized residue in $N\pi \to \Delta(1900) \to \Delta(1232)\eta$

MODULUS	PHASE (°)	DOCUMENT ID		TECN	COMMENT
0.013 ± 0.006	undefined	GUTZ	14	DPWA	Multichannel

Normalized residue in $N\pi \to \Delta(1900) \to N(1440)\pi$

MODULUS	PHASE (°)	DOCUMENT ID		TECN	COMMENT
0.11 ± 0.06	115 ± 30	SOKHOYAN	15A	DPWA	Multichannel

Normalized residue in $N\pi \to \Delta(1900) \to N(1520)\pi$

MODULUS	PHASE (°)	DOCUMENT ID		TECN	COMMENT
0.06 ± 0.03	undefined	SOKHOYAN	15A	DPWA	Multichannel

$\Delta(1900)$ BREIT-WIGNER MASS

VALUE (MeV)	DOCUMENT ID		TECN	COMMENT
1840 to 1920 (≈ 1860) OUR ESTIMATE				
1840 ± 20	SOKHOYAN	15A	DPWA	Multichannel
1868 ± 12	[1] SHRESTHA	12A	DPWA	Multichannel
1890 ± 50	CUTKOSKY	80	IPWA	$\pi N \to \pi N$
1908 ± 30	HOEHLER	79	IPWA	$\pi N \to \pi N$
• • • We do not use the following data for averages, fits, limits, etc. • • •				
1840 ± 20	GUTZ	14	DPWA	Multichannel
1840 ± 30	ANISOVICH	12A	DPWA	Multichannel
1802 ± 87	VRANA	00	DPWA	Multichannel

[1] Statistical error only.

$\Delta(1900)$ BREIT-WIGNER WIDTH

VALUE (MeV)	DOCUMENT ID		TECN	COMMENT
180 to 320 (≈ 250) OUR ESTIMATE				
295 ± 30	SOKHOYAN	15A	DPWA	Multichannel
234 ± 27	[1] SHRESTHA	12A	DPWA	Multichannel
170 ± 50	CUTKOSKY	80	IPWA	$\pi N \to \pi N$
140 ± 40	HOEHLER	79	IPWA	$\pi N \to \pi N$
• • • We do not use the following data for averages, fits, limits, etc. • • •				
295 ± 30	GUTZ	14	DPWA	Multichannel
300 ± 45	ANISOVICH	12A	DPWA	Multichannel
48 ± 45	VRANA	00	DPWA	Multichannel

[1] Statistical error only.

$\Delta(1900)$ DECAY MODES

The following branching fractions are our estimates, not fits or averages.

	Mode	Fraction (Γ_i/Γ)
Γ_1	$N\pi$	4–12 %
Γ_2	ΣK	seen
Γ_3	$N\pi\pi$	45–85 %
Γ_4	$\Delta(1232)\pi$	
Γ_5	$\Delta(1232)\pi$, D-wave	30–70 %
Γ_6	$N\rho$	
Γ_7	$N\rho$, S=1/2, S-wave	8–16 %
Γ_8	$N\rho$, S=3/2, D-wave	18–28 %
Γ_9	$N(1440)\pi$	8–32 %
Γ_{10}	$N(1520)\pi$	2–10 %
Γ_{11}	$\Delta(1232)\eta$	0–2 %
Γ_{12}	$N\gamma$, helicity=1/2	0.06–0.43 %

$\Delta(1900)$ BRANCHING RATIOS

$\Gamma(N\pi)/\Gamma_{\text{total}}$ Γ_1/Γ

VALUE (%)	DOCUMENT ID		TECN	COMMENT
4 to 12 (≈ 8) OUR ESTIMATE				
7 ± 2	SOKHOYAN	15A	DPWA	Multichannel
8 ± 1	[1] SHRESTHA	12A	DPWA	Multichannel
10 ± 3	CUTKOSKY	80	IPWA	$\pi N \to \pi N$
8 ± 4	HOEHLER	79	IPWA	$\pi N \to \pi N$
• • • We do not use the following data for averages, fits, limits, etc. • • •				
7 ± 2	GUTZ	14	DPWA	Multichannel
7 ± 3	ANISOVICH	12A	DPWA	Multichannel
33 ± 10	VRANA	00	DPWA	Multichannel

[1] Statistical error only.

$\Gamma(\Delta(1232)\pi$, D-wave$)/\Gamma_{\text{total}}$ Γ_5/Γ

VALUE (%)	DOCUMENT ID		TECN	COMMENT
50 ± 20	SOKHOYAN	15A	DPWA	Multichannel
56 ± 6	[1] SHRESTHA	12A	DPWA	Multichannel
• • • We do not use the following data for averages, fits, limits, etc. • • •				
15^{+50}_{-10}	ANISOVICH	12A	DPWA	Multichannel
28 ± 1	VRANA	00	DPWA	Multichannel

[1] Statistical error only.

$\Gamma(N\rho, S$=1/2, S-wave$)/\Gamma_{\text{total}}$ Γ_7/Γ

VALUE (%)	DOCUMENT ID		TECN	COMMENT
12 ± 4	[1] SHRESTHA	12A	DPWA	Multichannel
• • • We do not use the following data for averages, fits, limits, etc. • • •				
30 ± 2	VRANA	00	DPWA	Multichannel

[1] Statistical error only.

$\Gamma(N\rho, S$=3/2, D-wave$)/\Gamma_{\text{total}}$ Γ_8/Γ

VALUE (%)	DOCUMENT ID		TECN	COMMENT
23 ± 5	[1] SHRESTHA	12A	DPWA	Multichannel
• • • We do not use the following data for averages, fits, limits, etc. • • •				
5 ± 1	VRANA	00	DPWA	Multichannel

[1] Statistical error only.

$\Gamma(N(1440)\pi)/\Gamma_{\text{total}}$ Γ_9/Γ

VALUE (%)	DOCUMENT ID		TECN	COMMENT
20 ± 12	SOKHOYAN	15A	DPWA	Multichannel
< 1	[1] SHRESTHA	12A	DPWA	Multichannel
• • • We do not use the following data for averages, fits, limits, etc. • • •				
4 ± 1	VRANA	00	DPWA	Multichannel

[1] Statistical error only.

$\Gamma(N(1520)\pi)/\Gamma_{\text{total}}$ Γ_{10}/Γ

VALUE (%)	DOCUMENT ID		TECN	COMMENT
6 ± 4	SOKHOYAN	15A	DPWA	Multichannel

$\Gamma(\Delta(1232)\eta)/\Gamma_{\text{total}}$ Γ_{11}/Γ

VALUE (%)	DOCUMENT ID		TECN	COMMENT
1 ± 1	GUTZ	14	DPWA	Multichannel

$\Delta(1900)$ PHOTON DECAY AMPLITUDES AT THE POLE

$\Delta(1900) \to N\gamma$, helicity-1/2 amplitude $A_{1/2}$

MODULUS (GeV$^{-1/2}$)	PHASE (°)	DOCUMENT ID		TECN	COMMENT
0.064 ± 0.015	60 ± 20	SOKHOYAN	15A	DPWA	Multichannel

$\Delta(1900)$ BREIT-WIGNER PHOTON DECAY AMPLITUDES

$\Delta(1900) \to N\gamma$, helicity-1/2 amplitude $A_{1/2}$

VALUE (GeV$^{-1/2}$)	DOCUMENT ID		TECN	COMMENT
0.065 ± 0.015	SOKHOYAN	15A	DPWA	Multichannel
• • • We do not use the following data for averages, fits, limits, etc. • • •				
0.057 ± 0.014	GUTZ	14	DPWA	Multichannel
-0.082 ± 0.009	[1] SHRESTHA	12A	DPWA	Multichannel

[1] Statistical error only.

$\Delta(1900)$ REFERENCES

For early references, see Physics Letters **111B** 1 (1982).

SOKHOYAN	15A	EPJ A51 95	V. Sokhoyan *et al.*	(CBELSA/TAPS Collab.)
GUTZ	14	EPJ A50 74	E. Gutz *et al.*	(CBELSA/TAPS Collab.)
PDG	14	CP C38 070001	K. Olive *et al.*	(PDG Collab.)
SVARC	14	PR C89 045205	A. Svarc *et al.*	(RBI Zagreb, UNI Tuzla)
ANISOVICH	12A	EPJ A48 15	A.V. Anisovich *et al.*	(BONN, PNPI)
SHRESTHA	12A	PR C86 055203	M. Shrestha, D.M. Manley	(KSU)
VRANA	00	PRPL 328 181	T.P. Vrana, S.A. Dytman, T.-S.H. Lee	(PITT, ANL)
HOEHLER	93	πN Newsletter 9 1	G. Hohler	(KARL)
CUTKOSKY	80	Toronto Conf. 19	R.E. Cutkosky *et al.*	(CMU, LBL) IJP
Also		PR D20 2839	R.E. Cutkosky *et al.*	(CMU, LBL) IJP
HOEHLER	79	PDAT 12-1	G. Hohler *et al.*	(KARLT) IJP
Also		Toronto Conf. 3	R. Koch	(KARLT) IJP

$\Delta(1905)\ 5/2^+$

$I(J^P) = \frac{3}{2}(\frac{5}{2}^+)$ Status: ****

Older and obsolete values are listed and referenced in the 2014 edition, Chinese Physics **C38** 070001 (2014).

$\Delta(1905)$ POLE POSITION

REAL PART

VALUE (MeV)	DOCUMENT ID		TECN	COMMENT
1770 to 1830 (≈ 1800) OUR ESTIMATE				
1800 ± 6	SOKHOYAN	15A	DPWA	Multichannel
$1752 \pm 3 \pm 2$	[1] SVARC	14	L+P	$\pi N \to \pi N$
1830 ± 40	CUTKOSKY	80	IPWA	$\pi N \to \pi N$

• • • We do not use the following data for averages, fits, limits, etc. • • •

1795	ROENCHEN	15A	DPWA	Multichannel
1800± 6	GUTZ	14	DPWA	Multichannel
1805±10	ANISOVICH	12A	DPWA	Multichannel
1769	SHRESTHA	12A	DPWA	Multichannel
1819	ARNDT	06	DPWA	$\pi N \to \pi N, \eta N$
1793	VRANA	00	DPWA	Multichannel
1829	HOEHLER	93	SPED	$\pi N \to \pi N$

[1] Fit to the amplitudes of HOEHLER 79.

−2×IMAGINARY PART

VALUE (MeV)	DOCUMENT ID		TECN	COMMENT
260 to 340 (≈ 300) OUR ESTIMATE				
290±15	SOKHOYAN	15A	DPWA	Multichannel
346± 6±2	[1] SVARC	14	L+P	$\pi N \to \pi N$
280±60	CUTKOSKY	80	IPWA	$\pi N \to \pi N$
• • • We do not use the following data for averages, fits, limits, etc. • • •				
247	ROENCHEN	15A	DPWA	Multichannel
290±15	GUTZ	14	DPWA	Multichannel
300±15	ANISOVICH	12A	DPWA	Multichannel
239	SHRESTHA	12A	DPWA	Multichannel
247	ARNDT	06	DPWA	$\pi N \to \pi N, \eta N$
302	VRANA	00	DPWA	Multichannel
303	HOEHLER	93	SPED	$\pi N \to \pi N$

[1] Fit to the amplitudes of HOEHLER 79.

Δ(1905) ELASTIC POLE RESIDUE

MODULUS |r|

VALUE (MeV)	DOCUMENT ID		TECN	COMMENT
15 to 25 (≈ 20) OUR ESTIMATE				
19 ±2	SOKHOYAN	15A	DPWA	Multichannel
24 ±1±1	[1] SVARC	14	L+P	$\pi N \to \pi N$
25 ±8	CUTKOSKY	80	IPWA	$\pi N \to \pi N$
• • • We do not use the following data for averages, fits, limits, etc. • • •				
5.3	ROENCHEN	15A	DPWA	Multichannel
19 ±2	GUTZ	14	DPWA	Multichannel
20 ±2	ANISOVICH	12A	DPWA	Multichannel
15	ARNDT	06	DPWA	$\pi N \to \pi N, \eta N$
25	HOEHLER	93	SPED	$\pi N \to \pi N$

[1] Fit to the amplitudes of HOEHLER 79.

PHASE θ

VALUE (°)	DOCUMENT ID		TECN	COMMENT
−120 to −30 (≈ −50) OUR ESTIMATE				
− 45± 4	SOKHOYAN	15A	DPWA	Multichannel
−114± 1±2	[1] SVARC	14	L+P	$\pi N \to \pi N$
− 50±20	CUTKOSKY	80	IPWA	$\pi N \to \pi N$
• • • We do not use the following data for averages, fits, limits, etc. • • •				
− 89	ROENCHEN	15A	DPWA	Multichannel
− 45± 4	GUTZ	14	DPWA	Multichannel
− 44± 5	ANISOVICH	12A	DPWA	Multichannel
− 30	ARNDT	06	DPWA	$\pi N \to \pi N, \eta N$

[1] Fit to the amplitudes of HOEHLER 79.

Δ(1905) INELASTIC POLE RESIDUE

The "normalized residue" is the residue divided by $\Gamma_{pole}/2$.

Normalized residue in $N\pi \to \Delta(1905) \to \Delta\pi$, P-wave

MODULUS	PHASE (°)	DOCUMENT ID		TECN	COMMENT
0.19 ±0.07	10 ± 30	SOKHOYAN	15A	DPWA	Multichannel
• • • We do not use the following data for averages, fits, limits, etc. • • •					
0.0870	72	ROENCHEN	15A	DPWA	Multichannel
0.25 ±0.06	0 ± 15	ANISOVICH	12A	DPWA	Multichannel

Normalized residue in $N\pi \to \Delta(1905) \to \Delta\pi$, F-wave

MODULUS	PHASE (°)	DOCUMENT ID		TECN	COMMENT
• • • We do not use the following data for averages, fits, limits, etc. • • •					
0.009	64	ROENCHEN	15A	DPWA	Multichannel

Normalized residue in $N\pi \to \Delta(1905) \to \Sigma K$

MODULUS	PHASE (°)	DOCUMENT ID		TECN	COMMENT
• • • We do not use the following data for averages, fits, limits, etc. • • •					
0.001	−155	ROENCHEN	15A	DPWA	Multichannel

Normalized residue in $N\pi \to \Delta(1905) \to N(1535)\pi$

MODULUS	PHASE (°)	DOCUMENT ID		TECN	COMMENT
0.025±0.010	130 ± 35	GUTZ	14	DPWA	Multichannel

Normalized residue in $N\pi \to \Delta(1905) \to \Delta(1232)\eta$

MODULUS	PHASE (°)	DOCUMENT ID		TECN	COMMENT
0.07±0.02	40 ± 20	GUTZ	14	DPWA	Multichannel

Δ(1905) BREIT-WIGNER MASS

VALUE (MeV)	DOCUMENT ID		TECN	COMMENT
1855 to 1910 (≈ 1880) OUR ESTIMATE				
1856 ± 6	SOKHOYAN	15A	DPWA	Multichannel
1818 ± 8	[1] SHRESTHA	12A	DPWA	Multichannel
1857.8± 1.6	[1] ARNDT	06	DPWA	$\pi N \to \pi N, \eta N$
1910 ±30	CUTKOSKY	80	IPWA	$\pi N \to \pi N$
1905 ±20	HOEHLER	79	IPWA	$\pi N \to \pi N$
• • • We do not use the following data for averages, fits, limits, etc. • • •				
1856 ± 6	GUTZ	14	DPWA	Multichannel
1861 ± 6	ANISOVICH	12A	DPWA	Multichannel
1873 ±77	VRANA	00	DPWA	Multichannel

[1] Statistical error only.

Δ(1905) BREIT-WIGNER WIDTH

VALUE (MeV)	DOCUMENT ID		TECN	COMMENT
270 to 400 (≈ 330) OUR ESTIMATE				
325 ± 15	SOKHOYAN	15A	DPWA	Multichannel
278 ± 18	[1] SHRESTHA	12A	DPWA	Multichannel
320.6± 8.6	[1] ARNDT	06	DPWA	$\pi N \to \pi N, \eta N$
400 ±100	CUTKOSKY	80	IPWA	$\pi N \to \pi N$
260 ± 20	HOEHLER	79	IPWA	$\pi N \to \pi N$
• • • We do not use the following data for averages, fits, limits, etc. • • •				
325 ± 15	GUTZ	14	DPWA	Multichannel
335 ± 18	ANISOVICH	12A	DPWA	Multichannel
461 ±111	VRANA	00	DPWA	Multichannel

[1] Statistical error only.

Δ(1905) DECAY MODES

The following branching fractions are our estimates, not fits or averages.

	Mode	Fraction (Γ_i/Γ)
Γ_1	$N\pi$	9–15 %
Γ_2	$N\pi\pi$	
Γ_3	$\Delta(1232)\pi$	80–100 %
Γ_4	$\Delta(1232)\pi$, P-wave	23–43 %
Γ_5	$\Delta(1232)\pi$, F-wave	56–72 %
Γ_6	$N\rho$	
Γ_7	$N\rho$, $S=3/2$, P-wave	seen
Γ_8	$N(1535)\pi$	< 1 %
Γ_9	$N(1680)\pi$, P-wave	5–15 %
Γ_{10}	$\Delta(1232)\eta$	2–6 %
Γ_{11}	$N\gamma$	0.012–0.036 %
Γ_{12}	$N\gamma$, helicity=1/2	0.002–0.006 %
Γ_{13}	$N\gamma$, helicity=3/2	0.01–0.03 %

Δ(1905) BRANCHING RATIOS

$\Gamma(N\pi)/\Gamma_{total}$ Γ_1/Γ

VALUE (%)	DOCUMENT ID		TECN	COMMENT
9 to 15 (≈ 12) OUR ESTIMATE				
13 ±2	SOKHOYAN	15A	DPWA	Multichannel
6 ±1	[1] SHRESTHA	12A	DPWA	Multichannel
12.2±0.1	[1] ARNDT	06	DPWA	$\pi N \to \pi N, \eta N$
8 ±3	CUTKOSKY	80	IPWA	$\pi N \to \pi N$
15 ±2	HOEHLER	79	IPWA	$\pi N \to \pi N$
• • • We do not use the following data for averages, fits, limits, etc. • • •				
13 ±2	GUTZ	14	DPWA	Multichannel
13 ±2	ANISOVICH	12A	DPWA	Multichannel
9 ±1	VRANA	00	DPWA	Multichannel

[1] Statistical error only.

$\Gamma(\Delta(1232)\pi$, P-wave$)/\Gamma_{total}$ Γ_4/Γ

VALUE (%)	DOCUMENT ID		TECN	COMMENT
33±10	SOKHOYAN	15A	DPWA	Multichannel
28± 7	[1] SHRESTHA	12A	DPWA	Multichannel
• • • We do not use the following data for averages, fits, limits, etc. • • •				
45±14	ANISOVICH	12A	DPWA	Multichannel
23± 1	VRANA	00	DPWA	Multichannel

[1] Statistical error only.

$\Gamma(\Delta(1232)\pi$, F-wave$)/\Gamma_{total}$ Γ_5/Γ

VALUE (%)	DOCUMENT ID		TECN	COMMENT
64±8	[1] SHRESTHA	12A	DPWA	Multichannel
• • • We do not use the following data for averages, fits, limits, etc. • • •				
44±1	VRANA	00	DPWA	Multichannel

[1] Statistical error only.

$\Gamma(N\rho, S{=}3/2, P\text{-wave})/\Gamma_{total}$ Γ_7/Γ

VALUE (%)	DOCUMENT ID		TECN	COMMENT
< 6	SHRESTHA	12A	DPWA	Multichannel
• • • We do not use the following data for averages, fits, limits, etc. • • •				
24 ± 1	VRANA	00	DPWA	Multichannel

$\Gamma(N(1535)\pi)/\Gamma_{total}$ Γ_8/Γ

VALUE (%)	DOCUMENT ID		TECN	COMMENT
<1	GUTZ	14	DPWA	Multichannel

$\Gamma(N(1680)\pi, P\text{-wave})/\Gamma_{total}$ Γ_9/Γ

VALUE (%)	DOCUMENT ID		TECN	COMMENT
10 ± 5	SOKHOYAN	15A	DPWA	Multichannel

$\Gamma(\Delta(1232)\eta)/\Gamma_{total}$ Γ_{10}/Γ

VALUE (%)	DOCUMENT ID		TECN	COMMENT
4 ± 2	GUTZ	14	DPWA	Multichannel

$\Delta(1905)$ PHOTON DECAY AMPLITUDES AT THE POLE

$\Delta(1905) \rightarrow N\gamma$, helicity-1/2 amplitude $A_{1/2}$

MODULUS ($GeV^{-1/2}$)	PHASE (°)	DOCUMENT ID		TECN	COMMENT
0.025 ± 0.005	-28 ± 12	SOKHOYAN	15A	DPWA	Multichannel
$0.013^{+0.013}_{-0.005}$	64^{+72}_{-36}	ROENCHEN	14	DPWA	
• • • We do not use the following data for averages, fits, limits, etc. • • •					
0.053	89	ROENCHEN	15A	DPWA	Multichannel

$\Delta(1905) \rightarrow N\gamma$, helicity-3/2 amplitude $A_{3/2}$

MODULUS ($GeV^{-1/2}$)	PHASE (°)	DOCUMENT ID		TECN	COMMENT
-0.050 ± 0.004	5 ± 10	SOKHOYAN	15A	DPWA	Multichannel
0.072 ± 0.016	113^{+13}_{-7}	ROENCHEN	14	DPWA	
• • • We do not use the following data for averages, fits, limits, etc. • • •					
-0.030	80	ROENCHEN	15A	DPWA	Multichannel

$\Delta(1905)$ BREIT-WIGNER PHOTON DECAY AMPLITUDES

$\Delta(1905) \rightarrow N\gamma$, helicity-1/2 amplitude $A_{1/2}$

VALUE ($GeV^{-1/2}$)	DOCUMENT ID		TECN	COMMENT
0.017 to 0.027 (≈ 0.022) OUR ESTIMATE				
0.025 ± 0.005	SOKHOYAN	15A	DPWA	Multichannel
0.020 ± 0.002	[1] DUGGER	13	DPWA	$\gamma N \rightarrow \pi N$
0.019 ± 0.002	[1] WORKMAN	12A	DPWA	$\gamma N \rightarrow \pi N$
• • • We do not use the following data for averages, fits, limits, etc. • • •				
0.025 ± 0.005	GUTZ	14	DPWA	Multichannel
0.025 ± 0.004	ANISOVICH	12A	DPWA	Multichannel
0.066 ± 0.018	[1] SHRESTHA	12A	DPWA	Multichannel
0.018	DRECHSEL	07	DPWA	$\gamma N \rightarrow \pi N$

[1] Statistical error only.

$\Delta(1905) \rightarrow N\gamma$, helicity-3/2 amplitude $A_{3/2}$

VALUE ($GeV^{-1/2}$)	DOCUMENT ID		TECN	COMMENT
-0.055 to -0.035 (≈ -0.045) OUR ESTIMATE				
-0.050 ± 0.005	SOKHOYAN	15A	DPWA	Multichannel
-0.049 ± 0.005	[1] DUGGER	13	DPWA	$\gamma N \rightarrow \pi N$
-0.038 ± 0.004	WORKMAN	12A	DPWA	$\gamma N \rightarrow \pi N$
• • • We do not use the following data for averages, fits, limits, etc. • • •				
-0.050 ± 0.005	GUTZ	14	DPWA	Multichannel
-0.049 ± 0.004	ANISOVICH	12A	DPWA	Multichannel
-0.223 ± 0.029	[1] SHRESTHA	12A	DPWA	Multichannel
-0.028	DRECHSEL	07	DPWA	$\gamma N \rightarrow \pi N$

[1] Statistical error only.

$\Delta(1905)$ REFERENCES

For early references, see Physics Letters **111B** 1 (1982).

ROENCHEN	15A	EPJ A51 70	D. Roenchen *et al.*	
SOKHOYAN	15A	EPJ A51 95	V. Sokhoyan *et al.*	(CBELSA/TAPS Collab.)
GUTZ	14	EPJ A50 74	E. Gutz *et al.*	(CBELSA/TAPS Collab.)
PDG	14	CP C38 070001	K. Olive *et al.*	(PDG Collab.)
ROENCHEN	14	EPJ A50 101	D. Roenchen *et al.*	
Also		EPJ A51 63 (errat.)	D. Roenchen *et al.*	
SVARC	14	PR C89 045205	A. Svarc *et al.*	(RBI Zagreb, UNI Tuzla)
DUGGER	13	PR C88 065203	M. Dugger *et al.*	(JLab CLAS Collab.)
ANISOVICH	12A	EPJ A48 15	A.V. Anisovich *et al.*	(BONN, PNPI)
SHRESTHA	12A	PR C86 055203	M. Shrestha, D.M. Manley	(KSU)
WORKMAN	12A	PR C86 015202	R. Workman *et al.*	(GWU)
DRECHSEL	07	EPJ A34 69	D. Drechsel, S.S. Kamalov, L. Tiator	(MAINZ, JINR)
ARNDT	06	PR C74 045205	R.A. Arndt *et al.*	(GWU)
VRANA	00	PRPL 328 181	T.P. Vrana, S.A. Dytman, T.-S.H. Lee	(PITT, ANL)
HOEHLER	93	πN Newsletter 9 1	G. Hohler	(KARL)
CUTKOSKY	80	Toronto Conf. 19	R.E. Cutkosky *et al.*	(CMU, LBL) IJP
Also		PR D20 2839	R.E. Cutkosky *et al.*	(CMU, LBL) IJP
HOEHLER	79	PDAT 12-1	G. Hohler *et al.*	(KARLT) IJP
Also		Toronto Conf. 3	R. Koch	(KARLT) IJP

$\Delta(1910)$ $1/2^+$

$I(J^P) = \frac{3}{2}(\frac{1}{2}^+)$ Status: ****

Older and obsolete values are listed and referenced in the 2014 edition, Chinese Physics **C38** 070001 (2014).

$\Delta(1910)$ POLE POSITION

REAL PART

VALUE (MeV)	DOCUMENT ID		TECN	COMMENT
1830 to 1890 (≈ 1860) OUR ESTIMATE				
1840 ± 40	SOKHOYAN	15A	DPWA	Multichannel
1896 ± 11	[1] SVARC	14	L+P	$\pi N \rightarrow \pi N$
1880 ± 30	CUTKOSKY	80	IPWA	$\pi N \rightarrow \pi N$
• • • We do not use the following data for averages, fits, limits, etc. • • •				
1799	ROENCHEN	15A	DPWA	Multichannel
1840 ± 40	GUTZ	14	DPWA	Multichannel
1850 ± 40	ANISOVICH	12A	DPWA	Multichannel
1910	SHRESTHA	12A	DPWA	Multichannel
1771	ARNDT	06	DPWA	$\pi N \rightarrow \pi N, \eta N$
1880	VRANA	00	DPWA	Multichannel
1874	HOEHLER	93	SPED	$\pi N \rightarrow \pi N$

[1] Fit to the amplitudes of HOEHLER 79.

$-2\times$IMAGINARY PART

VALUE (MeV)	DOCUMENT ID		TECN	COMMENT
200 to 400 (≈ 300) OUR ESTIMATE				
370 ± 60	SOKHOYAN	15A	DPWA	Multichannel
302 ± 22	[1] SVARC	14	L+P	$\pi N \rightarrow \pi N$
200 ± 40	CUTKOSKY	80	IPWA	$\pi N \rightarrow \pi N$
• • • We do not use the following data for averages, fits, limits, etc. • • •				
648	ROENCHEN	15A	DPWA	Multichannel
370 ± 60	GUTZ	14	DPWA	Multichannel
350 ± 45	ANISOVICH	12A	DPWA	Multichannel
199	SHRESTHA	12A	DPWA	Multichannel
479	ARNDT	06	DPWA	$\pi N \rightarrow \pi N, \eta N$
496	VRANA	00	DPWA	Multichannel
283	HOEHLER	93	SPED	$\pi N \rightarrow \pi N$

[1] Fit to the amplitudes of HOEHLER 79.

$\Delta(1910)$ ELASTIC POLE RESIDUE

MODULUS $|r|$

VALUE (MeV)	DOCUMENT ID		TECN	COMMENT
20 to 30 (≈ 25) OUR ESTIMATE				
25 ± 6	SOKHOYAN	15A	DPWA	Multichannel
29 ± 2	[1] SVARC	14	L+P	$\pi N \rightarrow \pi N$
20 ± 4	CUTKOSKY	80	IPWA	$\pi N \rightarrow \pi N$
• • • We do not use the following data for averages, fits, limits, etc. • • •				
90	ROENCHEN	15A	DPWA	Multichannel
25 ± 6	GUTZ	14	DPWA	Multichannel
24 ± 6	ANISOVICH	12A	DPWA	Multichannel
45	ARNDT	06	DPWA	$\pi N \rightarrow \pi N, \eta N$
38	HOEHLER	93	SPED	$\pi N \rightarrow \pi N$

[1] Fit to the amplitudes of HOEHLER 79.

PHASE θ

VALUE (°)	DOCUMENT ID		TECN	COMMENT
-180 to -80 (≈ -130) OUR ESTIMATE				
-155 ± 30	SOKHOYAN	15A	DPWA	Multichannel
$-83 \pm 4 \pm 1$	[1] SVARC	14	L+P	$\pi N \rightarrow \pi N$
-90 ± 30	CUTKOSKY	80	IPWA	$\pi N \rightarrow \pi N$
• • • We do not use the following data for averages, fits, limits, etc. • • •				
-83	ROENCHEN	15A	DPWA	Multichannel
-155 ± 30	GUTZ	14	DPWA	Multichannel
-145 ± 30	ANISOVICH	12A	DPWA	Multichannel
$+172$	ARNDT	06	DPWA	$\pi N \rightarrow \pi N, \eta N$

[1] Fit to the amplitudes of HOEHLER 79.

$\Delta(1910)$ INELASTIC POLE RESIDUE

The "normalized residue" is the residue divided by $\Gamma_{pole}/2$.

Normalized residue in $N\pi \rightarrow \Delta(1910) \rightarrow \Sigma K$

MODULUS	PHASE (°)	DOCUMENT ID		TECN	COMMENT
0.07 ± 0.02	-110 ± 30	ANISOVICH	12A	DPWA	Multichannel
• • • We do not use the following data for averages, fits, limits, etc. • • •					
0.019	-123	ROENCHEN	15A	DPWA	Multichannel

Baryon Particle Listings

$\Delta(1910)$, $\Delta(1920)$

Normalized residue in $N\pi \to \Delta(1910) \to \Delta\pi$, P-wave

MODULUS	PHASE (°)	DOCUMENT ID		TECN	COMMENT
0.24±0.10	85 ± 35	SOKHOYAN	15A	DPWA	Multichannel
• • • We do not use the following data for averages, fits, limits, etc. • • •					
0.58	131	ROENCHEN	15A	DPWA	Multichannel
0.16±0.09	95 ± 40	ANISOVICH	12A	DPWA	Multichannel

Normalized residue in $N\pi \to \Delta(1910) \to \Delta(1232)\eta$

MODULUS	PHASE (°)	DOCUMENT ID		TECN	COMMENT
0.11±0.04	−150 ± 50	GUTZ	14	DPWA	Multichannel

Normalized residue in $N\pi \to \Delta(1910) \to N(1440)\pi$

MODULUS	PHASE (°)	DOCUMENT ID		TECN	COMMENT
0.06±0.03	170 ± 45	SOKHOYAN	15A	DPWA	Multichannel

$\Delta(1910)$ BREIT-WIGNER MASS

VALUE (MeV)	DOCUMENT ID		TECN	COMMENT
1850 to 1950 (≈ 1900) OUR ESTIMATE				
1845 ±40	SOKHOYAN	15A	DPWA	Multichannel
1934 ± 5	[1] SHRESTHA	12A	DPWA	Multichannel
2067.9± 1.7	[1] ARNDT	06	DPWA	$\pi N \to \pi N$, ηN
1910 ±40	CUTKOSKY	80	IPWA	$\pi N \to \pi N$
1888 ±20	HOEHLER	79	IPWA	$\pi N \to \pi N$
• • • We do not use the following data for averages, fits, limits, etc. • • •				
1845 ±40	GUTZ	14	DPWA	Multichannel
1860 ±40	ANISOVICH	12A	DPWA	Multichannel
1995 ±12	VRANA	00	DPWA	Multichannel

[1] Statistical error only.

$\Delta(1910)$ BREIT-WIGNER WIDTH

VALUE (MeV)	DOCUMENT ID		TECN	COMMENT
200 to 400 (≈ 300) OUR ESTIMATE				
360± 60	SOKHOYAN	15A	DPWA	Multichannel
211± 11	[1] SHRESTHA	12A	DPWA	Multichannel
543± 10	[1] ARNDT	06	DPWA	$\pi N \to \pi N$, ηN
225± 50	CUTKOSKY	80	IPWA	$\pi N \to \pi N$
280± 50	HOEHLER	79	IPWA	$\pi N \to \pi N$
• • • We do not use the following data for averages, fits, limits, etc. • • •				
360± 60	GUTZ	14	DPWA	Multichannel
350± 55	ANISOVICH	12A	DPWA	Multichannel
713±465	VRANA	00	DPWA	Multichannel

[1] Statistical error only.

$\Delta(1910)$ DECAY MODES

The following branching fractions are our estimates, not fits or averages.

	Mode	Fraction (Γ_i/Γ)
Γ_1	$N\pi$	15–30 %
Γ_2	ΣK	4–14 %
Γ_3	$N\pi\pi$	
Γ_4	$\Delta(1232)\pi$	34–66 %
Γ_5	$N(1440)\pi$	3–9 %
Γ_6	$\Delta(1232)\eta$	5–13 %
Γ_7	$N\gamma$, helicity=1/2	0.0–0.02 %

$\Delta(1910)$ BRANCHING RATIOS

$\Gamma(N\pi)/\Gamma_{total}$ Γ_1/Γ

VALUE (%)	DOCUMENT ID		TECN	COMMENT
15 to 30 (≈ 20) OUR ESTIMATE				
12 ± 3	SOKHOYAN	15A	DPWA	Multichannel
17 ± 1	[1] SHRESTHA	12A	DPWA	Multichannel
23.9± 0.1	[1] ARNDT	06	DPWA	$\pi N \to \pi N$, ηN
19 ± 3	CUTKOSKY	80	IPWA	$\pi N \to \pi N$
24 ± 6	HOEHLER	79	IPWA	$\pi N \to \pi N$
• • • We do not use the following data for averages, fits, limits, etc. • • •				
12 ± 3	GUTZ	14	DPWA	Multichannel
12 ± 3	ANISOVICH	12A	DPWA	Multichannel
29 ±21	VRANA	00	DPWA	Multichannel

[1] Statistical error only.

$\Gamma(\Sigma K)/\Gamma_{total}$ Γ_2/Γ

VALUE (%)	DOCUMENT ID	TECN	COMMENT
9±5	ANISOVICH 12A	DPWA	Multichannel

$\Gamma(\Delta(1232)\pi)/\Gamma_{total}$ Γ_4/Γ

VALUE (%)	DOCUMENT ID		TECN	COMMENT
50±16	SOKHOYAN	15A	DPWA	Multichannel
• • • We do not use the following data for averages, fits, limits, etc. • • •				
60±28	ANISOVICH	12A	DPWA	Multichannel

$\Gamma(N(1440)\pi)/\Gamma_{total}$ Γ_5/Γ

VALUE (%)	DOCUMENT ID		TECN	COMMENT
6±3	SOKHOYAN	15A	DPWA	Multichannel
47±6	[1] SHRESTHA	12A	DPWA	Multichannel
• • • We do not use the following data for averages, fits, limits, etc. • • •				
56±7	VRANA	00	DPWA	Multichannel

[1] Statistical error only.

$\Gamma(\Delta(1232)\eta)/\Gamma_{total}$ Γ_6/Γ

VALUE (%)	DOCUMENT ID	TECN	COMMENT
9±4	GUTZ 14	DPWA	Multichannel

$\Delta(1910)$ PHOTON DECAY AMPLITUDES AT THE POLE

$\Delta(1910) \to N\gamma$, helicity-1/2 amplitude $A_{1/2}$

MODULUS ($GeV^{-1/2}$)	PHASE (°)	DOCUMENT ID		TECN	COMMENT
0.027±0.009	−30 ± 60	SOKHOYAN	15A	DPWA	Multichannel
$-0.246^{+0.024}_{-0.047}$	159^{+9}_{-4}	ROENCHEN	14	DPWA	
• • • We do not use the following data for averages, fits, limits, etc. • • •					
0.321	39	ROENCHEN	15A	DPWA	Multichannel

$\Delta(1910)$ BREIT-WIGNER PHOTON DECAY AMPLITUDES

$\Delta(1910) \to N\gamma$, helicity-1/2 amplitude $A_{1/2}$

VALUE ($GeV^{-1/2}$)	DOCUMENT ID		TECN	COMMENT
0.010 to 0.030 (≈ 0.020) OUR ESTIMATE				
0.026±0.008	SOKHOYAN	15A	DPWA	Multichannel
−0.002±0.008	[1] ARNDT	96	IPWA	$\gamma N \to \pi N$
• • • We do not use the following data for averages, fits, limits, etc. • • •				
0.026±0.008	GUTZ	14	DPWA	Multichannel
0.022±0.009	ANISOVICH	12A	DPWA	Multichannel
0.030±0.002	[1] SHRESTHA	12A	DPWA	Multichannel

[1] Statistical error only.

$\Delta(1910)$ REFERENCES

For early references, see Physics Letters **111B** 1 (1982).

ROENCHEN	15A	EPJ A51 70	D. Roenchen *et al.*	
SOKHOYAN	15A	EPJ A51 95	V. Sokhoyan *et al.*	(CBELSA/TAPS Collab.)
GUTZ	14	EPJ A50 74	E. Gutz *et al.*	(CBELSA/TAPS Collab.)
PDG	14	CP C38 070001	K. Olive *et al.*	(PDG Collab.)
ROENCHEN	14	EPJ A50 101	D. Roenchen *et al.*	
Also		EPJ A51 63 (errat.)	D. Roenchen *et al.*	
SVARC	14	PR C89 045205	A. Svarc *et al.*	(RBI Zagreb, UNI Tuzla)
ANISOVICH	12A	EPJ A48 15	A.V. Anisovich *et al.*	(BONN, PNPI)
SHRESTHA	12A	PR C86 055203	M. Shrestha, D.M. Manley	(KSU)
ARNDT	06	PR C74 045205	R.A. Arndt *et al.*	(GWU)
VRANA	00	PRPL 328 181	T.P. Vrana, S.A. Dytman, T.-S.H. Lee	(PITT, ANL)
ARNDT	96	PR C53 430	R.A. Arndt, I.I. Strakovsky, R.L. Workman	(VPI)
HOEHLER	93	πN Newsletter 9 1	G. Hohler	(KARL)
CUTKOSKY	80	Toronto Conf. 19	R.E. Cutkosky *et al.*	(CMU, LBL) IJP
Also		PR D20 2839	R.E. Cutkosky *et al.*	(CMU, LBL) IJP
HOEHLER	79	PDAT 12-1	G. Hohler *et al.*	(KARLT) IJP
Also		Toronto Conf. 3	R. Koch	(KARLT) IJP

$\Delta(1920)\ 3/2^+$

$I(J^P) = \frac{3}{2}(\frac{3}{2}^+)$ Status: ***

Older and obsolete values are listed and referenced in the 2014 edition, Chinese Physics **C38** 070001 (2014).

$\Delta(1920)$ POLE POSITION

REAL PART

VALUE (MeV)	DOCUMENT ID		TECN	COMMENT
1850 to 1950 (≈ 1900) OUR ESTIMATE				
1875±30	SOKHOYAN	15A	DPWA	Multichannel
1906±10±2	[1] SVARC	14	L+P	$\pi N \to \pi N$
1900±80	CUTKOSKY	80	IPWA	$\pi N \to \pi N$
• • • We do not use the following data for averages, fits, limits, etc. • • •				
1715	ROENCHEN	15A	DPWA	Multichannel
1875±30	GUTZ	14	DPWA	Multichannel
1890±30	ANISOVICH	12A	DPWA	Multichannel
2110	SHRESTHA	12A	DPWA	Multichannel
1880	VRANA	00	DPWA	Multichannel
1900	HOEHLER	93	SPED	$\pi N \to \pi N$

[1] Fit to the amplitudes of HOEHLER 79.

−2×IMAGINARY PART

VALUE (MeV)	DOCUMENT ID		TECN	COMMENT
200 to 400 (≈ 300) OUR ESTIMATE				
300± 40	SOKHOYAN	15A	DPWA	Multichannel
310± 20±11	[1] SVARC	14	L+P	$\pi N \to \pi N$
300±100	CUTKOSKY	80	IPWA	$\pi N \to \pi N$

• • • We do not use the following data for averages, fits, limits, etc. • • •				
882	ROENCHEN	15A	DPWA	Multichannel
300± 40	GUTZ	14	DPWA	Multichannel
300± 60	ANISOVICH	12A	DPWA	Multichannel
386	SHRESTHA	12A	DPWA	Multichannel
120	VRANA	00	DPWA	Multichannel

[1] Fit to the amplitudes of HOEHLER 79.

Δ(1920) ELASTIC POLE RESIDUE

MODULUS |r|

VALUE (MeV)	DOCUMENT ID		TECN	COMMENT
8 to 24 (≈ 16) OUR ESTIMATE				
16±6	SOKHOYAN	15A	DPWA	Multichannel
26±3±2	[1] SVARC	14	L+P	$\pi N \to \pi N$
24±4	CUTKOSKY	80	IPWA	$\pi N \to \pi N$
• • • We do not use the following data for averages, fits, limits, etc. • • •				
38	ROENCHEN	15A	DPWA	Multichannel
16±6	GUTZ	14	DPWA	Multichannel
17±8	ANISOVICH	12A	DPWA	Multichannel

[1] Fit to the amplitudes of HOEHLER 79.

PHASE θ

VALUE (°)	DOCUMENT ID		TECN	COMMENT
−150 to −50 (≈ −100) OUR ESTIMATE				
− 50±25	SOKHOYAN	15A	DPWA	Multichannel
−130± 5±3	[1] SVARC	14	L+P	$\pi N \to \pi N$
−150±30	CUTKOSKY	80	IPWA	$\pi N \to \pi N$
• • • We do not use the following data for averages, fits, limits, etc. • • •				
146	ROENCHEN	15A	DPWA	Multichannel
− 50±25	GUTZ	14	DPWA	Multichannel
− 40±20	ANISOVICH	12A	DPWA	Multichannel

[1] Fit to the amplitudes of HOEHLER 79.

Δ(1920) INELASTIC POLE RESIDUE

The "normalized residue" is the residue divided by $\Gamma_{pole}/2$.

Normalized residue in $N\pi \to \Delta(1920) \to \Delta\eta$

MODULUS	PHASE (°)	DOCUMENT ID		TECN	COMMENT
0.15±0.04	70 ± 20	GUTZ	14	DPWA	Multichannel
• • • We do not use the following data for averages, fits, limits, etc. • • •					
0.17±0.08	70 ± 20	ANISOVICH	12A	DPWA	Multichannel

Normalized residue in $N\pi \to \Delta(1920) \to \Sigma K$

MODULUS	PHASE (°)	DOCUMENT ID		TECN	COMMENT
0.09±0.03	80 ± 40	ANISOVICH	12A	DPWA	Multichannel
• • • We do not use the following data for averages, fits, limits, etc. • • •					
0.17	−35	ROENCHEN	15A	DPWA	Multichannel

Normalized residue in $N\pi \to \Delta(1920) \to \Delta\pi$, P-wave

MODULUS	PHASE (°)	DOCUMENT ID		TECN	COMMENT
0.20 ±0.08	−105 ± 25	SOKHOYAN	15A	DPWA	Multichannel
• • • We do not use the following data for averages, fits, limits, etc. • • •					
0.069	131	ROENCHEN	15A	DPWA	Multichannel
0.20 ±0.12	−120 ± 30	ANISOVICH	12A	DPWA	Multichannel

Normalized residue in $N\pi \to \Delta(1920) \to \Delta\pi$, F-wave

MODULUS	PHASE (°)	DOCUMENT ID		TECN	COMMENT
0.37 ±0.10	−90 ± 20	SOKHOYAN	15A	DPWA	Multichannel
• • • We do not use the following data for averages, fits, limits, etc. • • •					
0.013	−115	ROENCHEN	15A	DPWA	Multichannel
0.28 ±0.07	−95 ± 35	ANISOVICH	12A	DPWA	Multichannel

Normalized residue in $N\pi \to \Delta(1920) \to N(1535)\pi$

MODULUS	PHASE (°)	DOCUMENT ID		TECN	COMMENT
0.03±0.02	35 ± 45	GUTZ	14	DPWA	Multichannel

Normalized residue in $N\pi \to \Delta(1920) \to Na_0(980)$

MODULUS	PHASE (°)	DOCUMENT ID		TECN	COMMENT
0.03±0.02	−85 ± 45	GUTZ	14	DPWA	Multichannel

Normalized residue in $N\pi \to \Delta(1920) \to N(1440)\pi$

MODULUS	PHASE (°)	DOCUMENT ID		TECN	COMMENT
0.04±0.03	undefined	SOKHOYAN	15A	DPWA	Multichannel

Normalized residue in $N\pi \to \Delta(1920) \to N(1520)\pi$, S-wave

MODULUS	PHASE (°)	DOCUMENT ID		TECN	COMMENT
0.05±0.05	undefined	SOKHOYAN	15A	DPWA	Multichannel

Δ(1920) BREIT-WIGNER MASS

VALUE (MeV)	DOCUMENT ID		TECN	COMMENT
1870 to 1970 (≈ 1920) OUR ESTIMATE				
1880± 30	SOKHOYAN	15A	DPWA	Multichannel
2146± 32	[1] SHRESTHA	12A	DPWA	Multichannel
1920± 80	CUTKOSKY	80	IPWA	$\pi N \to \pi N$
1868± 10	HOEHLER	79	IPWA	$\pi N \to \pi N$
• • • We do not use the following data for averages, fits, limits, etc. • • •				
1880± 30	GUTZ	14	DPWA	Multichannel
1900± 30	ANISOVICH	12A	DPWA	Multichannel
2057± 1	PENNER	02C	DPWA	Multichannel
1889±100	VRANA	00	DPWA	Multichannel

[1] Statistical error only.

Δ(1920) BREIT-WIGNER WIDTH

VALUE (MeV)	DOCUMENT ID		TECN	COMMENT
240 to 360 (≈ 300) OUR ESTIMATE				
300± 40	SOKHOYAN	15A	DPWA	Multichannel
400± 80	[1] SHRESTHA	12A	DPWA	Multichannel
300±100	CUTKOSKY	80	IPWA	$\pi N \to \pi N$
220± 80	HOEHLER	79	IPWA	$\pi N \to \pi N$
• • • We do not use the following data for averages, fits, limits, etc. • • •				
300± 40	GUTZ	14	DPWA	Multichannel
310± 60	ANISOVICH	12A	DPWA	Multichannel
525± 32	PENNER	02C	DPWA	Multichannel
123± 53	VRANA	00	DPWA	Multichannel

[1] Statistical error only.

Δ(1920) DECAY MODES

The following branching fractions are our estimates, not fits or averages.

	Mode	Fraction (Γ_i/Γ)
Γ_1	$N\pi$	5–20 %
Γ_2	ΣK	2–6 %
Γ_3	$N\pi\pi$	
Γ_4	$\Delta(1232)\pi$	50–90 %
Γ_5	$\Delta(1232)\pi$, P-wave	8–28 %
Γ_6	$\Delta(1232)\pi$, F-wave	44–72 %
Γ_7	$N(1440)\pi$, P-wave	<4 %
Γ_8	$N(1520)\pi$, S-wave	<5 %
Γ_9	$N(1535)\pi$	<2 %
Γ_{10}	$Na_0(980)$	seen
Γ_{11}	$\Delta(1232)\eta$	5–17 %

Δ(1920) BRANCHING RATIOS

$\Gamma(N\pi)/\Gamma_{total}$ — Γ_1/Γ

VALUE (%)	DOCUMENT ID		TECN	COMMENT
5 to 20 (≈ 12) OUR ESTIMATE				
8±4	SOKHOYAN	15A	DPWA	Multichannel
16±4	[1] SHRESTHA	12A	DPWA	Multichannel
20±5	CUTKOSKY	80	IPWA	$\pi N \to \pi N$
14±4	HOEHLER	79	IPWA	$\pi N \to \pi N$
• • • We do not use the following data for averages, fits, limits, etc. • • •				
8±4	GUTZ	14	DPWA	Multichannel
8±4	ANISOVICH	12A	DPWA	Multichannel
15±1	PENNER	02C	DPWA	Multichannel
5±4	VRANA	00	DPWA	Multichannel

[1] Statistical error only.

$\Gamma(\Sigma K)/\Gamma_{total}$ — Γ_2/Γ

VALUE (%)	DOCUMENT ID		TECN	COMMENT
4 ±2	ANISOVICH	12A	DPWA	Multichannel
• • • We do not use the following data for averages, fits, limits, etc. • • •				
2.1±0.3	PENNER	02C	DPWA	Multichannel

$\Gamma(\Delta(1232)\pi$, P-wave$)/\Gamma_{total}$ — Γ_5/Γ

VALUE (%)	DOCUMENT ID		TECN	COMMENT
18±10	SOKHOYAN	15A	DPWA	Multichannel
7± 5	[1] SHRESTHA	12A	DPWA	Multichannel
• • • We do not use the following data for averages, fits, limits, etc. • • •				
22±12	ANISOVICH	12A	DPWA	Multichannel
41± 3	VRANA	00	DPWA	Multichannel

[1] Statistical error only.

$\Gamma(\Delta(1232)\pi$, F-wave$)/\Gamma_{total}$ — Γ_6/Γ

VALUE (%)	DOCUMENT ID		TECN	COMMENT
58±14	SOKHOYAN	15A	DPWA	Multichannel
• • • We do not use the following data for averages, fits, limits, etc. • • •				
45±20	ANISOVICH	12A	DPWA	Multichannel

$\Gamma(N(1440)\pi$, P-wave$)/\Gamma_{total}$ — Γ_7/Γ

VALUE (%)	DOCUMENT ID		TECN	COMMENT
< 4	SOKHOYAN	15A	DPWA	Multichannel
<20	SHRESTHA	12A	DPWA	Multichannel

• • • We do not use the following data for averages, fits, limits, etc. • • •

53±8	VRANA	00	DPWA	Multichannel

Γ(Nπ, S-wave)/Γ_total Γ8/Γ

VALUE (%)	DOCUMENT ID		TECN	COMMENT
<5	SOKHOYAN	15A	DPWA	Multichannel

Γ(Nπ)/Γ_total Γ9/Γ

VALUE (%)	DOCUMENT ID		TECN	COMMENT
<2	GUTZ	14	DPWA	Multichannel

Γ(Na0(980))/Γ_total Γ10/Γ

VALUE (%)	DOCUMENT ID		TECN	COMMENT
• • • We do not use the following data for averages, fits, limits, etc. • • •				
4±2	HORN	08A	DPWA	Multichannel

Γ(Δ(1232)η)/Γ_total Γ11/Γ

VALUE (%)	DOCUMENT ID		TECN	COMMENT
11±6	GUTZ	14	DPWA	Multichannel
• • • We do not use the following data for averages, fits, limits, etc. • • •				
15±8	ANISOVICH	12A	DPWA	Multichannel

Δ(1920) PHOTON DECAY AMPLITUDES AT THE POLE

Δ(1920) → Nγ, helicity-1/2 amplitude A_1/2

MODULUS (GeV^-1/2)	PHASE (°)	DOCUMENT ID		TECN	COMMENT
0.110±0.030	−50 ± 20	SOKHOYAN	15A	DPWA	Multichannel
$0.190^{+0.050}_{-0.022}$	-160^{+24}_{-11}	ROENCHEN	14	DPWA	
• • • We do not use the following data for averages, fits, limits, etc. • • •					
−0.192	46	ROENCHEN	15A	DPWA	Multichannel

Δ(1920) → Nγ, helicity-3/2 amplitude A_3/2

MODULUS (GeV^-1/2)	PHASE (°)	DOCUMENT ID		TECN	COMMENT
−0.100±0.040	0 ± 20	SOKHOYAN	15A	DPWA	Multichannel
$-0.398^{+0.070}_{-0.067}$	-110^{+4}_{-5}	ROENCHEN	14	DPWA	
• • • We do not use the following data for averages, fits, limits, etc. • • •					
0.522	67	ROENCHEN	15A	DPWA	Multichannel

Δ(1920) BREIT-WIGNER PHOTON DECAY AMPLITUDES

Δ(1920) → Nγ, helicity-1/2 amplitude A_1/2

VALUE (GeV^-1/2)	DOCUMENT ID		TECN	COMMENT
0.110±0.030	SOKHOYAN	15A	DPWA	Multichannel
• • • We do not use the following data for averages, fits, limits, etc. • • •				
0.110±0.030	GUTZ	14	DPWA	Multichannel
$0.130^{+0.030}_{-0.060}$	ANISOVICH	12A	DPWA	Multichannel
0.051±0.010	[1] SHRESTHA	12A	DPWA	Multichannel
−0.007	PENNER	02D	DPWA	Multichannel

[1] Statistical error only.

Δ(1920) → Nγ, helicity-3/2 amplitude A_3/2

VALUE (GeV^-1/2)	DOCUMENT ID		TECN	COMMENT
−0.105±0.035	SOKHOYAN	15A	DPWA	Multichannel
• • • We do not use the following data for averages, fits, limits, etc. • • •				
−0.105±0.035	GUTZ	14	DPWA	Multichannel
$-0.115^{+0.025}_{-0.050}$	ANISOVICH	12A	DPWA	Multichannel
0.017±0.015	[1] SHRESTHA	12A	DPWA	Multichannel
−0.001	PENNER	02D	DPWA	Multichannel

[1] Statistical error only.

Δ(1920) REFERENCES

For early references, see Physics Letters **111B** 1 (1982).

ROENCHEN	15A	EPJ A51 70	D. Roenchen *et al.*	
SOKHOYAN	15A	EPJ A51 95	V. Sokhoyan *et al.*	(CBELSA/TAPS Collab.)
GUTZ	14	EPJ A50 74	E. Gutz *et al.*	(CBELSA/TAPS Collab.)
PDG	14	CP C38 070001	K. Olive *et al.*	(PDG Collab.)
ROENCHEN	14	EPJ A50 101	D. Roenchen *et al.*	
Also		EPJ A51 63 (errat.)	D. Roenchen *et al.*	
SVARC	14	PR C89 045205	A. Svarc *et al.*	(RBI Zagreb, UNI Tuzla)
ANISOVICH	12A	EPJ A48 15	A.V. Anisovich *et al.*	(BONN, PNPI)
SHRESTHA	12A	PR C86 055203	M. Shrestha, D.M. Manley	(KSU)
HORN	08A	EPJ A38 173	I. Horn *et al.*	(CB-ELSA Collab.)
Also		PRL 101 202002	I. Horn *et al.*	(CB-ELSA Collab.)
PENNER	02C	PR C66 055211	G. Penner, U. Mosel	(GIES)
PENNER	02D	PR C66 055212	G. Penner, U. Mosel	(GIES)
VRANA	00	PRPL 328 181	T.P. Vrana, S.A. Dytman, T.-S.H. Lee	(PITT, ANL)
HOEHLER	93	πN Newsletter 9 1	G. Hohler	(KARL)
CUTKOSKY	80	Toronto Conf. 19	R.E. Cutkosky *et al.*	(CMU, LBL) IJP
Also		PR D20 2839	R.E. Cutkosky *et al.*	(CMU, LBL) IJP
HOEHLER	79	PDAT 12-1	G. Hohler *et al.*	(KARLT) IJP
Also		Toronto Conf. 3	R. Koch	(KARLT) IJP

Δ(1930) 5/2⁻

$I(J^P) = \frac{3}{2}(\frac{5}{2}^-)$ Status: ***

Older and obsolete values are listed and referenced in the 2014 edition, Chinese Physics **C38** 070001 (2014).

Δ(1930) POLE POSITION

REAL PART

VALUE (MeV)	DOCUMENT ID		TECN	COMMENT
1840 to 1920 (≈ 1880) OUR ESTIMATE				
1848± 9±19	[1] SVARC	14	L+P	$\pi N \to \pi N$
1890±50	CUTKOSKY	80	IPWA	$\pi N \to \pi N$
• • • We do not use the following data for averages, fits, limits, etc. • • •				
1836	ROENCHEN	15A	DPWA	Multichannel
1882	SHRESTHA	12A	DPWA	Multichannel
2001	ARNDT	06	DPWA	$\pi N \to \pi N, \eta N$
1883	VRANA	00	DPWA	Multichannel
1850	HOEHLER	93	SPED	$\pi N \to \pi N$

[1] Fit to the amplitudes of HOEHLER 79.

−2×IMAGINARY PART

VALUE (MeV)	DOCUMENT ID		TECN	COMMENT
230 to 330 (≈ 280) OUR ESTIMATE				
321±17±7	[1] SVARC	14	L+P	$\pi N \to \pi N$
260±60	CUTKOSKY	80	IPWA	$\pi N \to \pi N$
• • • We do not use the following data for averages, fits, limits, etc. • • •				
724	ROENCHEN	15A	DPWA	Multichannel
187	SHRESTHA	12A	DPWA	Multichannel
387	ARNDT	06	DPWA	$\pi N \to \pi N, \eta N$
250	VRANA	00	DPWA	Multichannel
180	HOEHLER	93	SPED	$\pi N \to \pi N$

[1] Fit to the amplitudes of HOEHLER 79.

Δ(1930) ELASTIC POLE RESIDUE

MODULUS |r|

VALUE (MeV)	DOCUMENT ID		TECN	COMMENT
8 to 20 (≈ 14) OUR ESTIMATE				
9±1±1	[1] SVARC	14	L+P	$\pi N \to \pi N$
18±6	CUTKOSKY	80	IPWA	$\pi N \to \pi N$
• • • We do not use the following data for averages, fits, limits, etc. • • •				
34	ROENCHEN	15A	DPWA	Multichannel
7	ARNDT	06	DPWA	$\pi N \to \pi N, \eta N$
20	HOEHLER	93	SPED	$\pi N \to \pi N$

[1] Fit to the amplitudes of HOEHLER 79.

PHASE θ

VALUE (°)	DOCUMENT ID		TECN	COMMENT
− 40 to −10 (≈ − 30) OUR ESTIMATE				
− 37± 3±7	[1] SVARC	14	L+P	$\pi N \to \pi N$
− 20±40	CUTKOSKY	80	IPWA	$\pi N \to \pi N$
• • • We do not use the following data for averages, fits, limits, etc. • • •				
−155	ROENCHEN	15A	DPWA	Multichannel
− 12	ARNDT	06	DPWA	$\pi N \to \pi N, \eta N$

[1] Fit to the amplitudes of HOEHLER 79.

Δ(1930) INELASTIC POLE RESIDUE

The "normalized residue" is the residue divided by $\Gamma_{pole}/2$.

Normalized residue in Nπ → Δ(1930) → ΣK

MODULUS	PHASE (°)	DOCUMENT ID		TECN	COMMENT
• • • We do not use the following data for averages, fits, limits, etc. • • •					
0.043	−0.5	ROENCHEN	15A	DPWA	Multichannel

Normalized residue in Nπ → Δ(1930) → Δπ, D-wave

MODULUS	PHASE (°)	DOCUMENT ID		TECN	COMMENT
• • • We do not use the following data for averages, fits, limits, etc. • • •					
0.15	30	ROENCHEN	15A	DPWA	Multichannel

Normalized residue in Nπ → Δ(1930) → Δπ, G-wave

MODULUS	PHASE (°)	DOCUMENT ID		TECN	COMMENT
• • • We do not use the following data for averages, fits, limits, etc. • • •					
0.009	121	ROENCHEN	15A	DPWA	Multichannel

$\Delta(1930)$ BREIT-WIGNER MASS

VALUE (MeV)	DOCUMENT ID		TECN	COMMENT
1900 to 2000 (≈ 1950) OUR ESTIMATE				
1930± 12	[1] SHRESTHA	12A	DPWA	Multichannel
2233± 53	[1] ARNDT	06	DPWA	$\pi N \to \pi N$, ηN
1940± 30	CUTKOSKY	80	IPWA	$\pi N \to \pi N$
1901± 15	HOEHLER	79	IPWA	$\pi N \to \pi N$
• • • We do not use the following data for averages, fits, limits, etc. • • •				
1932±100	VRANA	00	DPWA	Multichannel

[1] Statistical error only.

$\Delta(1930)$ BREIT-WIGNER WIDTH

VALUE (MeV)	DOCUMENT ID		TECN	COMMENT
200 to 400 (≈ 300) OUR ESTIMATE				
235± 39	[1] SHRESTHA	12A	DPWA	Multichannel
773±187	ARNDT	06	DPWA	$\pi N \to \pi N$, ηN
320± 60	CUTKOSKY	80	IPWA	$\pi N \to \pi N$
195± 60	HOEHLER	79	IPWA	$\pi N \to \pi N$
• • • We do not use the following data for averages, fits, limits, etc. • • •				
316±237	VRANA	00	DPWA	Multichannel

[1] Statistical error only.

$\Delta(1930)$ DECAY MODES

The following branching fractions are our estimates, not fits or averages.

	Mode	Fraction (Γ_i/Γ)
Γ_1	$N\pi$	5–15 %
Γ_2	$N\gamma$	0.0–0.01 %
Γ_3	$N\gamma$, helicity=1/2	0.0–0.005 %
Γ_4	$N\gamma$, helicity=3/2	0.0–0.004 %

$\Delta(1930)$ BRANCHING RATIOS

$\Gamma(N\pi)/\Gamma_{total}$ Γ_1/Γ

VALUE (%)	DOCUMENT ID		TECN	COMMENT
5 to 15 (≈ 10) OUR ESTIMATE				
7.9±0.4	[1] SHRESTHA	12A	DPWA	Multichannel
8.1±1.2	[1] ARNDT	06	DPWA	$\pi N \to \pi N$, ηN
14 ±4	CUTKOSKY	80	IPWA	$\pi N \to \pi N$
4 ±3	HOEHLER	79	IPWA	$\pi N \to \pi N$
• • • We do not use the following data for averages, fits, limits, etc. • • •				
9 ±8	VRANA	00	DPWA	Multichannel

[1] Statistical error only.

$\Delta(1930)$ PHOTON DECAY AMPLITUDES AT THE POLE

$\Delta(1930) \to N\gamma$, helicity-1/2 amplitude $A_{1/2}$

MODULUS ($GeV^{-1/2}$)	PHASE (°)	DOCUMENT ID		TECN	COMMENT
$0.130^{+0.073}_{-0.096}$	-50^{+77}_{-26}	ROENCHEN	14	DPWA	
• • • We do not use the following data for averages, fits, limits, etc. • • •					
−0.270	33	ROENCHEN	15A	DPWA	Multichannel

$\Delta(1930) \to N\gamma$, helicity-3/2 amplitude $A_{3/2}$

MODULUS ($GeV^{-1/2}$)	PHASE (°)	DOCUMENT ID		TECN	COMMENT
$-0.056^{+0.003}_{-0.151}$	168^{+72}_{-76}	ROENCHEN	14	DPWA	
• • • We do not use the following data for averages, fits, limits, etc. • • •					
0.153	81	ROENCHEN	15A	DPWA	Multichannel

$\Delta(1930)$ BREIT-WIGNER PHOTON DECAY AMPLITUDES

$\Delta(1930) \to N\gamma$, helicity-1/2 amplitude $A_{1/2}$

VALUE ($GeV^{-1/2}$)	DOCUMENT ID		TECN	COMMENT
−0.007±0.010	[1] ARNDT	96	IPWA	$\gamma N \to \pi N$
• • • We do not use the following data for averages, fits, limits, etc. • • •				
0.011±0.003	[1] SHRESTHA	12A	DPWA	Multichannel

[1] Statistical error only.

$\Delta(1930) \to N\gamma$, helicity-3/2 amplitude $A_{3/2}$

VALUE ($GeV^{-1/2}$)	DOCUMENT ID		TECN	COMMENT
0.005±0.010	[1] ARNDT	96	IPWA	$\gamma N \to \pi N$
• • • We do not use the following data for averages, fits, limits, etc. • • •				
0.002±0.002	[1] SHRESTHA	12A	DPWA	Multichannel

[1] Statistical error only.

$\Delta(1930)$ REFERENCES

For early references, see Physics Letters **111B** 1 (1982).

ROENCHEN	15A	EPJ A51 70	D. Roenchen *et al.*	
PDG	14	CP C38 070001	K. Olive *et al.*	(PDG Collab.)
ROENCHEN	14	EPJ A50 101	D. Roenchen *et al.*	
Also		EPJ A51 63 (errat.)	D. Roenchen *et al.*	
SVARC	14	PR C89 045205	A. Svarc *et al.*	(RBI Zagreb, UNI Tuzla)
SHRESTHA	12A	PR C86 055203	M. Shrestha, D.M. Manley	(KSU)
ARNDT	06	PR C74 045205	R.A. Arndt *et al.*	(GWU)
VRANA	00	PRPL 328 181	T.P. Vrana, S.A. Dytman, T.-S.H. Lee	(PITT, ANL)
ARNDT	96	PR C53 430	R.A. Arndt, I.I. Strakovsky, R.L. Workman	(VPI)
HOEHLER	93	πN Newsletter 9 1	G. Hohler	(KARL)
CUTKOSKY	80	Toronto Conf. 19	R.E. Cutkosky *et al.*	(CMU, LBL) IJP
Also		PR D20 2839	R.E. Cutkosky *et al.*	(CMU, LBL) IJP
HOEHLER	79	PDAT 12-1	G. Hohler *et al.*	(KARLT) IJP
Also		Toronto Conf. 3	R. Koch	(KARLT) IJP

$\Delta(1940)\ 3/2^-$

$I(J^P) = \frac{3}{2}(\frac{3}{2}^-)$ Status: **

OMITTED FROM SUMMARY TABLE

$\Delta(1940)$ POLE POSITION

REAL PART

VALUE (MeV)	DOCUMENT ID		TECN	COMMENT
1850 to 2050 (≈ 1950) OUR ESTIMATE				
2040± 50	SOKHOYAN	15A	DPWA	Multichannel
1878± 11±5.5	[1] SVARC	14	L+P	$\pi N \to \pi N$
1900±100	CUTKOSKY	80	IPWA	$\pi N \to \pi N$
• • • We do not use the following data for averages, fits, limits, etc. • • •				
2040± 50	GUTZ	14	DPWA	Multichannel
1990^{+100}_{-50}	ANISOVICH	12A	DPWA	Multichannel

[1] Fit to the amplitudes of HOEHLER 79.

−2×IMAGINARY PART

VALUE (MeV)	DOCUMENT ID		TECN	COMMENT
200 to 500 (≈ 350) OUR ESTIMATE				
450±90	SOKHOYAN	15A	DPWA	Multichannel
212±21±6	[1] SVARC	14	L+P	$\pi N \to \pi N$
200±60	CUTKOSKY	80	IPWA	$\pi N \to \pi N$
• • • We do not use the following data for averages, fits, limits, etc. • • •				
450±90	GUTZ	14	DPWA	Multichannel
450±90	ANISOVICH	12A	DPWA	Multichannel

[1] Fit to the amplitudes of HOEHLER 79.

$\Delta(1940)$ ELASTIC POLE RESIDUE

MODULUS $|r|$

VALUE (MeV)	DOCUMENT ID		TECN	COMMENT
4 to 10 (≈ 7) OUR ESTIMATE				
6±3	SOKHOYAN	15A	DPWA	Multichannel
9±1±1	[1] SVARC	14	L+P	$\pi N \to \pi N$
8±3	CUTKOSKY	80	IPWA	$\pi N \to \pi N$
• • • We do not use the following data for averages, fits, limits, etc. • • •				
4±3	GUTZ	14	DPWA	Multichannel
4±4	ANISOVICH	12A	DPWA	Multichannel

[1] Fit to the amplitudes of HOEHLER 79.

PHASE θ

VALUE (°)	DOCUMENT ID		TECN	COMMENT
150 to 250 (≈ 200) OUR ESTIMATE				
− 90±35	SOKHOYAN	15A	DPWA	Multichannel
140± 7±7	[1] SVARC	14	L+P	$\pi N \to \pi N$
135±45	CUTKOSKY	80	IPWA	$\pi N \to \pi N$
• • • We do not use the following data for averages, fits, limits, etc. • • •				
− 50±35	GUTZ	14	DPWA	Multichannel

[1] Fit to the amplitudes of HOEHLER 79.

$\Delta(1940)$ INELASTIC POLE RESIDUE

The "normalized residue" is the residue divided by $\Gamma_{pole}/2$.

Normalized residue in $N\pi \to \Delta(1940) \to \Delta(1232)\eta$

MODULUS	PHASE (°)	DOCUMENT ID		TECN	COMMENT
<0.01	undefined	GUTZ	14	DPWA	Multichannel

Normalized residue in $N\pi \to \Delta(1940) \to N(1535)\pi$

MODULUS	PHASE (°)	DOCUMENT ID		TECN	COMMENT
<0.03	undefined	GUTZ	14	DPWA	Multichannel

Normalized residue in $N\pi \to \Delta(1940) \to \Delta(1232)\pi$, S-wave

MODULUS	PHASE (°)	DOCUMENT ID		TECN	COMMENT
0.12±0.06	120 ± 45	SOKHOYAN	15A	DPWA	Multichannel

Normalized residue in $N\pi \to \Delta(1940) \to \Delta(1232)\pi$, D-wave

MODULUS	PHASE (°)	DOCUMENT ID		TECN	COMMENT
0.06±0.04	−80 ± 35	SOKHOYAN	15A	DPWA	Multichannel

$\Delta(1940)$ BREIT-WIGNER MASS

VALUE (MeV)	DOCUMENT ID		TECN	COMMENT
1940 to 2060 (≈ 2000) OUR ESTIMATE				
2050± 40	SOKHOYAN	15A	DPWA	Multichannel
1940±100	CUTKOSKY	80	IPWA	$\pi N \to \pi N$
• • • We do not use the following data for averages, fits, limits, etc. • • •				
2050± 40	GUTZ	14	DPWA	Multichannel
1995^{+105}_{-60}	ANISOVICH	12A	DPWA	Multichannel

$\Delta(1940)$ BREIT-WIGNER WIDTH

VALUE (MeV)	DOCUMENT ID		TECN	COMMENT
300 to 500 (≈ 400) OUR ESTIMATE				
450± 70	SOKHOYAN	15A	DPWA	Multichannel
200±100	CUTKOSKY	80	IPWA	$\pi N \to \pi N$
• • • We do not use the following data for averages, fits, limits, etc. • • •				
450± 70	GUTZ	14	DPWA	Multichannel
450±100	ANISOVICH	12A	DPWA	Multichannel

$\Delta(1940)$ DECAY MODES

	Mode	Fraction (Γ_i/Γ)
Γ_1	$N\pi$	1–7 %
Γ_2	$N\pi\pi$	
Γ_3	$\Delta(1232)\pi$	30–85 %
Γ_4	$\Delta(1232)\pi$, S-wave	25–65 %
Γ_5	$\Delta(1232)\pi$, D-wave	5–20 %
Γ_6	$N(1535)\pi$	2–14 %
Γ_7	$N a_0(980)$	seen
Γ_8	$\Delta(1232)\eta$	4–16 %
Γ_9	$N\gamma$, helicity=1/2	seen
Γ_{10}	$N\gamma$, helicity=3/2	seen

$\Delta(1940)$ BRANCHING RATIOS

$\Gamma(N\pi)/\Gamma_{\text{total}}$ Γ_1/Γ

VALUE (%)	DOCUMENT ID		TECN	COMMENT
1 to 7 (≈ 4) OUR ESTIMATE				
2±1	SOKHOYAN	15A	DPWA	Multichannel
5±2	CUTKOSKY	80	IPWA	$\pi N \to \pi N$
• • • We do not use the following data for averages, fits, limits, etc. • • •				
2±1	GUTZ	14	DPWA	Multichannel

$\Gamma(\Delta(1232)\pi, S\text{-wave})/\Gamma_{\text{total}}$ Γ_4/Γ

VALUE (%)	DOCUMENT ID		TECN	COMMENT
46±20	SOKHOYAN	15A	DPWA	Multichannel

$\Gamma(\Delta(1232)\pi, D\text{-wave})/\Gamma_{\text{total}}$ Γ_5/Γ

VALUE (%)	DOCUMENT ID		TECN	COMMENT
12±7	SOKHOYAN	15A	DPWA	Multichannel

$\Gamma(N(1535)\pi)/\Gamma_{\text{total}}$ Γ_6/Γ

VALUE (%)	DOCUMENT ID		TECN	COMMENT
8±6	GUTZ	14	DPWA	Multichannel
• • • We do not use the following data for averages, fits, limits, etc. • • •				
2±1	HORN	08A	DPWA	Multichannel

$\Gamma(N a_0(980))/\Gamma_{\text{total}}$ Γ_7/Γ

VALUE (%)	DOCUMENT ID		TECN	COMMENT
• • • We do not use the following data for averages, fits, limits, etc. • • •				
2±1	HORN	08A	DPWA	Multichannel

$\Gamma(\Delta(1232)\eta)/\Gamma_{\text{total}}$ Γ_8/Γ

VALUE (%)	DOCUMENT ID		TECN	COMMENT
10±6	GUTZ	14	DPWA	Multichannel
• • • We do not use the following data for averages, fits, limits, etc. • • •				
4±2	HORN	08A	DPWA	Multichannel

$\Delta(1940)$ PHOTON DECAY AMPLITUDES AT THE POLE

$\Delta(1940) \to N\gamma$, helicity-1/2 amplitude $A_{1/2}$

MODULUS (GeV$^{-1/2}$)	PHASE (°)	DOCUMENT ID		TECN	COMMENT
$0.170^{+0.120}_{-0.100}$	−10 ± 30	SOKHOYAN	15A	DPWA	Multichannel

$\Delta(1940) \to N\gamma$, helicity-3/2 amplitude $A_{3/2}$

MODULUS (GeV$^{-1/2}$)	PHASE (°)	DOCUMENT ID		TECN	COMMENT
0.150±0.080	−10 ± 30	SOKHOYAN	15A	DPWA	Multichannel

$\Delta(1940)$ BREIT-WIGNER PHOTON DECAY AMPLITUDES

$\Delta(1940) \to N\gamma$, helicity-1/2 amplitude $A_{1/2}$

VALUE (GeV$^{-1/2}$)	DOCUMENT ID		TECN	COMMENT
$0.170^{+0.110}_{-0.080}$	SOKHOYAN	15A	DPWA	Multichannel
• • • We do not use the following data for averages, fits, limits, etc. • • •				
$0.170^{+0.110}_{-0.080}$	GUTZ	14	DPWA	Multichannel

$\Delta(1940) \to N\gamma$, helicity-3/2 amplitude $A_{3/2}$

VALUE (GeV$^{-1/2}$)	DOCUMENT ID		TECN	COMMENT
0.150±0.080	SOKHOYAN	15A	DPWA	Multichannel
• • • We do not use the following data for averages, fits, limits, etc. • • •				
0.150±0.080	GUTZ	14	DPWA	Multichannel

$\Delta(1940)$ REFERENCES

SOKHOYAN	15A	EPJ A51 95	V. Sokhoyan *et al.*	(CBELSA/TAPS Collab.)
GUTZ	14	EPJ A50 74	E. Gutz *et al.*	(CBELSA/TAPS Collab.)
SVARC	14	PR C89 045205	A. Svarc *et al.*	(RBI Zagreb, UNI Tuzla)
ANISOVICH	12A	EPJ A48 15	A.V. Anisovich *et al.*	(BONN, PNPI)
HORN	08A	EPJ A38 173	I. Horn *et al.*	(CB-ELSA Collab.)
Also		PRL 101 202002	I. Horn *et al.*	(CB-ELSA Collab.)
CUTKOSKY	80	Toronto Conf. 19	R.E. Cutkosky *et al.*	(CMU, LBL) IJP
Also		PR D20 2839	R.E. Cutkosky *et al.*	(CMU, LBL)
HOEHLER	79	PDAT 12-1	G. Hohler *et al.*	(KARLT)

$\Delta(1950)\ 7/2^+$

$I(J^P) = \frac{3}{2}(\frac{7}{2}^+)$ Status: ****

Older and obsolete values are listed and referenced in the 2014 edition, Chinese Physics **C38** 070001 (2014).

$\Delta(1950)$ POLE POSITION

REAL PART

VALUE (MeV)	DOCUMENT ID		TECN	COMMENT
1870 to 1890 (≈ 1880) OUR ESTIMATE				
1888± 4	SOKHOYAN	15A	DPWA	Multichannel
1877± 2±1	[1] SVARC	14	L+P	$\pi N \to \pi N$
1890±15	CUTKOSKY	80	IPWA	$\pi N \to \pi N$
• • • We do not use the following data for averages, fits, limits, etc. • • •				
1874	ROENCHEN	15A	DPWA	Multichannel
1888± 4	GUTZ	14	DPWA	Multichannel
1890± 4	ANISOVICH	12A	DPWA	Multichannel
1871	SHRESTHA	12A	DPWA	Multichannel
1876	ARNDT	06	DPWA	$\pi N \to \pi N, \eta N$
1910	VRANA	00	DPWA	Multichannel
1878	HOEHLER	93	ARGD	$\pi N \to \pi N$

[1] Fit to the amplitudes of HOEHLER 79.

−2×IMAGINARY PART

VALUE (MeV)	DOCUMENT ID		TECN	COMMENT
220 to 260 (≈ 240) OUR ESTIMATE				
245± 8	SOKHOYAN	15A	DPWA	Multichannel
223± 4±1	[1] SVARC	14	L+P	$\pi N \to \pi N$
260±40	CUTKOSKY	80	IPWA	$\pi N \to \pi N$
• • • We do not use the following data for averages, fits, limits, etc. • • •				
239	ROENCHEN	15A	DPWA	Multichannel
245± 8	GUTZ	14	DPWA	Multichannel
243± 8	ANISOVICH	12A	DPWA	Multichannel
220	SHRESTHA	12A	DPWA	Multichannel
227	ARNDT	06	DPWA	$\pi N \to \pi N, \eta N$
230	VRANA	00	DPWA	Multichannel
230	HOEHLER	93	ARGD	$\pi N \to \pi N$

[1] Fit to the amplitudes of HOEHLER 79.

$\Delta(1950)$ ELASTIC POLE RESIDUE

MODULUS $|r|$

VALUE (MeV)	DOCUMENT ID		TECN	COMMENT
44 to 60 (≈ 52) OUR ESTIMATE				
58±2	SOKHOYAN	15A	DPWA	Multichannel
44±1	[1] SVARC	14	L+P	$\pi N \to \pi N$
50±7	CUTKOSKY	80	IPWA	$\pi N \to \pi N$
• • • We do not use the following data for averages, fits, limits, etc. • • •				
56	ROENCHEN	15A	DPWA	Multichannel
58±2	GUTZ	14	DPWA	Multichannel
58±2	ANISOVICH	12A	DPWA	Multichannel
53	ARNDT	06	DPWA	$\pi N \to \pi N, \eta N$

47	HOEHLER	93	ARGD	$\pi N \to \pi N$

[1] Fit to the amplitudes of HOEHLER 79.

PHASE θ

VALUE (°)	DOCUMENT ID		TECN	COMMENT
−40 to −24 (≈ −32) OUR ESTIMATE				
−24±3	SOKHOYAN	15A	DPWA	Multichannel
−39±1±1	[1] SVARC	14	L+P	$\pi N \to \pi N$
−33±8	CUTKOSKY	80	IPWA	$\pi N \to \pi N$
• • • We do not use the following data for averages, fits, limits, etc. • • •				
−33	ROENCHEN	15A	DPWA	Multichannel
−24±3	GUTZ	14	DPWA	Multichannel
−24±3	ANISOVICH	12A	DPWA	Multichannel
−31	ARNDT	06	DPWA	$\pi N \to \pi N, \eta N$
−32	HOEHLER	93	ARGD	$\pi N \to \pi N$

[1] Fit to the amplitudes of HOEHLER 79.

Δ(1950) INELASTIC POLE RESIDUE

The "normalized residue" is the residue divided by $\Gamma_{pole}/2$.

Normalized residue in $N\pi \to \Delta(1950) \to \Sigma K$

MODULUS	PHASE (°)	DOCUMENT ID		TECN	COMMENT
0.05 ±0.01	−65 ± 25	ANISOVICH	12A	DPWA	Multichannel
• • • We do not use the following data for averages, fits, limits, etc. • • •					
0.031	−87	ROENCHEN	15A	DPWA	Multichannel

Normalized residue in $N\pi \to \Delta(1950) \to \Delta\pi$, F-wave

MODULUS	PHASE (°)	DOCUMENT ID		TECN	COMMENT
0.12±0.04	undefined	SOKHOYAN	15A	DPWA	Multichannel
• • • We do not use the following data for averages, fits, limits, etc. • • •					
0.54	131	ROENCHEN	15A	DPWA	Multichannel
0.12±0.04	12 ± 10	ANISOVICH	12A	DPWA	Multichannel

Normalized residue in $N\pi \to \Delta(1950) \to \Delta\pi$, H-wave

MODULUS	PHASE (°)	DOCUMENT ID		TECN	COMMENT
• • • We do not use the following data for averages, fits, limits, etc. • • •					
0.033	−97	ROENCHEN	15A	DPWA	Multichannel

Normalized residue in $N\pi \to \Delta(1950) \to \Delta(1232)\eta$

MODULUS	PHASE (°)	DOCUMENT ID		TECN	COMMENT
0.035±0.005	90 ± 25	GUTZ	14	DPWA	Multichannel

Δ(1950) BREIT-WIGNER MASS

VALUE (MeV)	DOCUMENT ID		TECN	COMMENT
1915 to 1950 (≈ 1930) OUR ESTIMATE				
1917 ± 4	ANISOVICH	17	DPWA	Multichannel
1918 ± 1	[1] SHRESTHA	12A	DPWA	Multichannel
1921.3± 0.2	[1] ARNDT	06	DPWA	$\pi N \to \pi N, \eta N$
1950 ±15	CUTKOSKY	80	IPWA	$\pi N \to \pi N$
1913 ± 8	HOEHLER	79	IPWA	$\pi N \to \pi N$
• • • We do not use the following data for averages, fits, limits, etc. • • •				
1917 ± 4	SOKHOYAN	15A	DPWA	Multichannel
1917 ± 4	GUTZ	14	DPWA	Multichannel
1915 ± 6	ANISOVICH	12A	DPWA	Multichannel
1936 ± 5	VRANA	00	DPWA	Multichannel

[1] Statistical error only.

Δ(1950) BREIT-WIGNER WIDTH

VALUE (MeV)	DOCUMENT ID		TECN	COMMENT
235 to 335 (≈ 285) OUR ESTIMATE				
251 ± 8	ANISOVICH	17	DPWA	Multichannel
259 ± 4	[1] SHRESTHA	12A	DPWA	Multichannel
271.1± 1.1	[1] ARNDT	06	DPWA	$\pi N \to \pi N, \eta N$
340 ±50	CUTKOSKY	80	IPWA	$\pi N \to \pi N$
224 ±10	HOEHLER	79	IPWA	$\pi N \to \pi N$
• • • We do not use the following data for averages, fits, limits, etc. • • •				
251 ± 8	SOKHOYAN	15A	DPWA	Multichannel
251 ± 8	GUTZ	14	DPWA	Multichannel
246 ±10	ANISOVICH	12A	DPWA	Multichannel
245 ±12	VRANA	00	DPWA	Multichannel

[1] Statistical error only.

Δ(1950) DECAY MODES

The following branching fractions are our estimates, not fits or averages.

	Mode	Fraction (Γ_i/Γ)
Γ_1	$N\pi$	35–45 %
Γ_2	ΣK	0.3–0.5 %
Γ_3	$N\pi\pi$	
Γ_4	$\Delta(1232)\pi$, F-wave	1–9 %
Γ_5	$N(1680)\pi$, P-wave	3–9 %
Γ_6	$\Delta(1232)\eta$	< 0.6 %

Δ(1950) BRANCHING RATIOS

$\Gamma(N\pi)/\Gamma_{total}$ Γ_1/Γ

VALUE (%)	DOCUMENT ID		TECN	COMMENT
35 to 45 (≈ 40) OUR ESTIMATE				
46 ±2	ANISOVICH	17	DPWA	Multichannel
45.6 ±0.4	[1] SHRESTHA	12A	DPWA	Multichannel
47.1 ±0.1	[1] ARNDT	06	DPWA	$\pi N \to \pi N, \eta N$
39 ±4	CUTKOSKY	80	IPWA	$\pi N \to \pi N$
38 ±2	HOEHLER	79	IPWA	$\pi N \to \pi N$
• • • We do not use the following data for averages, fits, limits, etc. • • •				
0.046±0.002	SOKHOYAN	15A	DPWA	Multichannel
46 ±2	GUTZ	14	DPWA	Multichannel
45 ±2	ANISOVICH	12A	DPWA	Multichannel
44 ±1	VRANA	00	DPWA	Multichannel

[1] Statistical error only.

$\Gamma(\Sigma K)/\Gamma_{total}$ Γ_2/Γ

VALUE (%)	DOCUMENT ID		TECN	COMMENT
0.6±0.2	ANISOVICH	17	DPWA	Multichannel
• • • We do not use the following data for averages, fits, limits, etc. • • •				
0.4±0.1	ANISOVICH	12A	DPWA	Multichannel

$\Gamma(\Delta(1232)\pi$, F-wave$)/\Gamma_{total}$ Γ_4/Γ

VALUE (%)	DOCUMENT ID		TECN	COMMENT
5 ±3	ANISOVICH	17	DPWA	Multichannel
8 ±1	[1] SHRESTHA	12A	DPWA	Multichannel
• • • We do not use the following data for averages, fits, limits, etc. • • •				
5 ±4	SOKHOYAN	15A	DPWA	Multichannel
2.8±1.4	ANISOVICH	12A	DPWA	Multichannel
36 ±1	VRANA	00	DPWA	Multichannel

[1] Statistical error only.

$\Gamma(N(1680)\pi$, P-wave$)/\Gamma_{total}$ Γ_5/Γ

VALUE (%)	DOCUMENT ID		TECN	COMMENT
6±3	SOKHOYAN	15A	DPWA	Multichannel

$\Gamma(\Delta(1232)\eta)/\Gamma_{total}$ Γ_6/Γ

VALUE (%)	DOCUMENT ID		TECN	COMMENT
0.3±0.3	ANISOVICH	17	DPWA	Multichannel
• • • We do not use the following data for averages, fits, limits, etc. • • •				
<1	GUTZ	14	DPWA	Multichannel

Δ(1950) PHOTON DECAY AMPLITUDES AT THE POLE

Δ(1950) → Nγ, helicity-1/2 amplitude $A_{1/2}$

MODULUS ($GeV^{-1/2}$)	PHASE (°)	DOCUMENT ID		TECN	COMMENT
−0.067±0.004	−10 ± 5	SOKHOYAN	15A	DPWA	Multichannel
−0.071±0.004	-14^{+2}_{-4}	ROENCHEN	14	DPWA	
• • • We do not use the following data for averages, fits, limits, etc. • • •					
−0.068	−19	ROENCHEN	15A	DPWA	Multichannel

Δ(1950) → Nγ, helicity-3/2 amplitude $A_{3/2}$

MODULUS ($GeV^{-1/2}$)	PHASE (°)	DOCUMENT ID		TECN	COMMENT
−0.095±0.004	−10 ± 5	SOKHOYAN	15A	DPWA	Multichannel
$-0.089^{+0.008}_{-0.007}$	-10^{+3}_{-1}	ROENCHEN	14	DPWA	
• • • We do not use the following data for averages, fits, limits, etc. • • •					
−0.084	−19	ROENCHEN	15A	DPWA	Multichannel

Δ(1950) BREIT-WIGNER PHOTON DECAY AMPLITUDES

Δ(1950) → Nγ, helicity-1/2 amplitude $A_{1/2}$

VALUE ($GeV^{-1/2}$)	DOCUMENT ID		TECN	COMMENT
−0.075 to −0.065 (≈ −0.070) OUR ESTIMATE				
−0.067±0.005	ANISOVICH	17	DPWA	Multichannel
−0.083±0.004	WORKMAN	12A	DPWA	$\gamma N \to N\pi$
• • • We do not use the following data for averages, fits, limits, etc. • • •				
−0.067±0.005	SOKHOYAN	15A	DPWA	Multichannel
−0.067±0.005	GUTZ	14	DPWA	Multichannel
−0.071±0.004	ANISOVICH	12A	DPWA	Multichannel
−0.065±0.001	[1] SHRESTHA	12A	DPWA	Multichannel
−0.094	DRECHSEL	07	DPWA	$\gamma N \to \pi N$

[1] Statistical error only.

Δ(1950) → Nγ, helicity-3/2 amplitude $A_{3/2}$

VALUE ($GeV^{-1/2}$)	DOCUMENT ID		TECN	COMMENT
−0.100 to −0.080 (≈ −0.090) OUR ESTIMATE				
−0.094±0.004	ANISOVICH	17	DPWA	Multichannel
−0.096±0.004	WORKMAN	12A	DPWA	$\gamma N \rightarrow N\pi$
• • • We do not use the following data for averages, fits, limits, etc. • • •				
−0.094±0.004	SOKHOYAN	15A	DPWA	Multichannel
−0.094±0.004	GUTZ	14	DPWA	Multichannel
−0.094±0.005	ANISOVICH	12A	DPWA	Multichannel
−0.083±0.001	[1] SHRESTHA	12A	DPWA	Multichannel
−0.121	DRECHSEL	07	DPWA	$\gamma N \rightarrow \pi N$

[1] Statistical error only.

Δ(1950) REFERENCES

ANISOVICH	17	PL B766 357	A.V. Anisovich *et al.*	
ROENCHEN	15A	EPJ A51 70	D. Roenchen *et al.*	
SOKHOYAN	15A	EPJ A51 95	V. Sokhoyan *et al.*	(CBELSA/TAPS Collab.)
GUTZ	14	EPJ A50 74	E. Gutz *et al.*	(CBELSA/TAPS Collab.)
PDG	14	CP C38 070001	K. Olive *et al.*	(PDG Collab.)
ROENCHEN	14	EPJ A50 101	D. Roenchen *et al.*	
Also		EPJ A51 63 (errat.)	D. Roenchen *et al.*	
SVARC	14	PR C89 045205	A. Svarc *et al.*	(RBI Zagreb, UNI Tuzla)
ANISOVICH	12A	EPJ A48 15	A.V. Anisovich *et al.*	(BONN, PNPI)
SHRESTHA	12A	PR C86 055203	M. Shrestha, D.M. Manley	(KSU)
WORKMAN	12A	PR C86 015202	R. Workman *et al.*	(GWU)
DRECHSEL	07	EPJ A34 69	D. Drechsel, S.S. Kamalov, L. Tiator	(MAINZ, JINR)
ARNDT	06	PR C74 045205	R.A. Arndt *et al.*	(GWU)
VRANA	00	PRPL 328 181	T.P. Vrana, S.A. Dytman, T.-S.H. Lee	(PITT, ANL)
HOEHLER	93	πN Newsletter 9 1	G. Hohler	(KARL)
CUTKOSKY	80	Toronto Conf. 19	R.E. Cutkosky *et al.*	(CMU, LBL) IJP
Also		PR D20 2839	R.E. Cutkosky *et al.*	(CMU, LBL) IJP
HOEHLER	79	PDAT 12-1	G. Hohler *et al.*	(KARLT) IJP
Also		Toronto Conf. 3	R. Koch	(KARLT) IJP

Δ(2000) 5/2+

$I(J^P) = \frac{3}{2}(\frac{5}{2}^+)$ Status: **

OMITTED FROM SUMMARY TABLE

Δ(2000) POLE POSITION

REAL PART

VALUE (MeV)	DOCUMENT ID		TECN	COMMENT
1998± 4±4	[1] SVARC	14	L+P	$\pi N \rightarrow \pi N$
1976	SHRESTHA	12A	DPWA	Multichannel
2150±100	CUTKOSKY	80	IPWA	$\pi N \rightarrow \pi N$
• • • We do not use the following data for averages, fits, limits, etc. • • •				
1697	VRANA	00	DPWA	Multichannel

[1] Fit to the amplitudes of HOEHLER 79.

−2×IMAGINARY PART

VALUE (MeV)	DOCUMENT ID		TECN	COMMENT
404± 10±4	[1] SVARC	14	L+P	$\pi N \rightarrow \pi N$
350±100	CUTKOSKY	80	IPWA	$\pi N \rightarrow \pi N$
• • • We do not use the following data for averages, fits, limits, etc. • • •				
488	SHRESTHA	12A	DPWA	Multichannel
112	VRANA	00	DPWA	Multichannel

[1] Fit to the amplitudes of HOEHLER 79.

Δ(2000) ELASTIC POLE RESIDUE

MODULUS |r|

VALUE (MeV)	DOCUMENT ID		TECN	COMMENT
34±1±1	[1] SVARC	14	L+P	$\pi N \rightarrow \pi N$
16±5	CUTKOSKY	80	IPWA	$\pi N \rightarrow \pi N$

[1] Fit to the amplitudes of HOEHLER 79.

PHASE θ

VALUE (°)	DOCUMENT ID		TECN	COMMENT
110± 1±3	[1] SVARC	14	L+P	$\pi N \rightarrow \pi N$
150±90	CUTKOSKY	80	IPWA	$\pi N \rightarrow \pi N$

[1] Fit to the amplitudes of HOEHLER 79.

Δ(2000) BREIT-WIGNER MASS

VALUE (MeV)	DOCUMENT ID		TECN	COMMENT
2015± 24	[1] SHRESTHA	12A	DPWA	Multichannel
2200±125	CUTKOSKY	80	IPWA	$\pi N \rightarrow \pi N$
• • • We do not use the following data for averages, fits, limits, etc. • • •				
1724± 61	VRANA	00	DPWA	Multichannel
1752± 32	MANLEY	92	IPWA	$\pi N \rightarrow \pi N$ & $N\pi\pi$

[1] Statistical error only.

Δ(2000) BREIT-WIGNER WIDTH

VALUE (MeV)	DOCUMENT ID		TECN	COMMENT
500± 52	[1] SHRESTHA	12A	DPWA	Multichannel
400±125	CUTKOSKY	80	IPWA	$\pi N \rightarrow \pi N$
• • • We do not use the following data for averages, fits, limits, etc. • • •				
138± 68	VRANA	00	DPWA	Multichannel
251± 93	MANLEY	92	IPWA	$\pi N \rightarrow \pi N$ & $N\pi\pi$

[1] Statistical error only.

Δ(2000) DECAY MODES

	Mode	Fraction (Γ_i/Γ)
Γ_1	$N\pi$	3–11 %
Γ_2	$N\pi\pi$	
Γ_3	$\Delta(1232)\pi$, *P*-wave	seen
Γ_4	$\Delta(1232)\pi$, *F*-wave	seen
Γ_5	$N\rho$, *S*=3/2, *P*-wave	seen
Γ_6	$N\gamma$	
Γ_7	$N\gamma$, helicity=1/2	seen
Γ_8	$N\gamma$, helicity=3/2	seen

Δ(2000) BRANCHING RATIOS

$\Gamma(N\pi)/\Gamma_{total}$ Γ_1/Γ

VALUE (%)	DOCUMENT ID		TECN	COMMENT
7±1	[1] SHRESTHA	12A	DPWA	Multichannel
7±4	CUTKOSKY	80	IPWA	$\pi N \rightarrow \pi N$
• • • We do not use the following data for averages, fits, limits, etc. • • •				
0±1	VRANA	00	DPWA	Multichannel
2±1	MANLEY	92	IPWA	$\pi N \rightarrow \pi N$ & $N\pi\pi$

[1] Statistical error only.

$\Gamma(\Delta(1232)\pi, P\text{-wave})/\Gamma_{total}$ Γ_3/Γ

VALUE (%)	DOCUMENT ID		TECN	COMMENT
3±3	[1] SHRESTHA	12A	DPWA	Multichannel
• • • We do not use the following data for averages, fits, limits, etc. • • •				
0±1	VRANA	00	DPWA	Multichannel

[1] Statistical error only.

$\Gamma(\Delta(1232)\pi, F\text{-wave})/\Gamma_{total}$ Γ_4/Γ

VALUE (%)	DOCUMENT ID		TECN	COMMENT
< 3	SHRESTHA	12A	DPWA	Multichannel
• • • We do not use the following data for averages, fits, limits, etc. • • •				
40±1	VRANA	00	DPWA	Multichannel

$\Gamma(N\rho, S=3/2, P\text{-wave})/\Gamma_{total}$ Γ_5/Γ

VALUE (%)	DOCUMENT ID		TECN	COMMENT
90± 3	[1] SHRESTHA	12A	DPWA	Multichannel
• • • We do not use the following data for averages, fits, limits, etc. • • •				
60±60	VRANA	00	DPWA	Multichannel

[1] Statistical error only.

Δ(2000) BREIT-WIGNER PHOTON DECAY AMPLITUDES

Δ(2000) → pγ, helicity-1/2 amplitude $A_{1/2}$

VALUE ($GeV^{-1/2}$)	DOCUMENT ID		TECN	COMMENT
• • • We do not use the following data for averages, fits, limits, etc. • • •				
−0.061±0.018	[1] SHRESTHA	12A	DPWA	Multichannel

[1] Statistical error only.

Δ(2000) → pγ, helicity-3/2 amplitude $A_{3/2}$

VALUE ($GeV^{-1/2}$)	DOCUMENT ID		TECN	COMMENT
• • • We do not use the following data for averages, fits, limits, etc. • • •				
0.158±0.032	[1] SHRESTHA	12A	DPWA	Multichannel

[1] Statistical error only.

Δ(2000) REFERENCES

SVARC	14	PR C89 045205	A. Svarc *et al.*	(RBI Zagreb, UNI Tuzla)
SHRESTHA	12A	PR C86 055203	M. Shrestha, D.M. Manley	(KSU)
VRANA	00	PRPL 328 181	T.P. Vrana, S.A. Dytman, T.-S.H. Lee	(PITT, ANL)
MANLEY	92	PR D45 4002	D.M. Manley, E.M. Saleski	(KSA) IJP
Also		PR D30 904	D.M. Manley *et al.*	(VPI)
CUTKOSKY	80	Toronto Conf. 19	R.E. Cutkosky *et al.*	(CMU, LBL)
Also		PR D20 2839	R.E. Cutkosky *et al.*	(CMU, LBL)
HOEHLER	79	PDAT 12-1	G. Hohler *et al.*	(KARLT)

$\Delta(2150)\ 1/2^-$

$I(J^P) = \frac{3}{2}(\frac{1}{2}^-)$ Status: *

OMITTED FROM SUMMARY TABLE

$\Delta(2150)$ POLE POSITION

REAL PART

VALUE (MeV)	DOCUMENT ID		TECN	COMMENT
2140±80	CUTKOSKY	80	IPWA	$\pi N \to \pi N$

−2×IMAGINARY PART

VALUE (MeV)	DOCUMENT ID		TECN	COMMENT
200±80	CUTKOSKY	80	IPWA	$\pi N \to \pi N$

$\Delta(2150)$ ELASTIC POLE RESIDUE

MODULUS $|r|$

VALUE (MeV)	DOCUMENT ID		TECN	COMMENT
7±2	CUTKOSKY	80	IPWA	$\pi N \to \pi N$

PHASE θ

VALUE (°)	DOCUMENT ID		TECN	COMMENT
−60±90	CUTKOSKY	80	IPWA	$\pi N \to \pi N$

$\Delta(2150)$ BREIT-WIGNER MASS

VALUE (MeV)	DOCUMENT ID		TECN	COMMENT
2150±100	CUTKOSKY	80	IPWA	$\pi N \to \pi N$

$\Delta(2150)$ BREIT-WIGNER WIDTH

VALUE (MeV)	DOCUMENT ID		TECN	COMMENT
200±100	CUTKOSKY	80	IPWA	$\pi N \to \pi N$

$\Delta(2150)$ DECAY MODES

	Mode	Fraction (Γ_i/Γ)
Γ_1	$N\pi$	6–10 %

$\Delta(2150)$ BRANCHING RATIOS

$\Gamma(N\pi)/\Gamma_{total}$ **Γ_1/Γ**

VALUE (%)	DOCUMENT ID		TECN	COMMENT
8±2	CUTKOSKY	80	IPWA	$\pi N \to \pi N$

$\Delta(2150)$ REFERENCES

CUTKOSKY 80 Toronto Conf. 19 R.E. Cutkosky *et al.* (CMU, LBL) IJP
Also PR D20 2839 R.E. Cutkosky *et al.* (CMU, LBL)

$\Delta(2200)\ 7/2^-$

$I(J^P) = \frac{3}{2}(\frac{7}{2}^-)$ Status: ***

$\Delta(2200)$ POLE POSITION

REAL PART

VALUE (MeV)	DOCUMENT ID		TECN	COMMENT
2050 to 2150 (≈ 2100) OUR ESTIMATE				
2100±50	CUTKOSKY	80	IPWA	$\pi N \to \pi N$
• • • We do not use the following data for averages, fits, limits, etc. • • •				
2142	ROENCHEN	15A	DPWA	Multichannel

−2×IMAGINARY PART

VALUE (MeV)	DOCUMENT ID		TECN	COMMENT
260 to 420 (≈ 340) OUR ESTIMATE				
340±80	CUTKOSKY	80	IPWA	$\pi N \to \pi N$
• • • We do not use the following data for averages, fits, limits, etc. • • •				
486	ROENCHEN	15A	DPWA	Multichannel

$\Delta(2200)$ ELASTIC POLE RESIDUE

MODULUS $|r|$

VALUE (MeV)	DOCUMENT ID		TECN	COMMENT
8±3	CUTKOSKY	80	IPWA	$\pi N \to \pi N$
• • • We do not use the following data for averages, fits, limits, etc. • • •				
17	ROENCHEN	15A	DPWA	Multichannel

PHASE θ

VALUE (°)	DOCUMENT ID		TECN	COMMENT
−70±40	CUTKOSKY	80	IPWA	$\pi N \to \pi N$
• • • We do not use the following data for averages, fits, limits, etc. • • •				
−56	ROENCHEN	15A	DPWA	Multichannel

$\Delta(2200)$ INELASTIC POLE RESIDUE

The "normalized residue" is the residue divided by $\Gamma_{pole}/2$.

Normalized residue in $N\pi \to \Delta(2200) \to \Sigma K$

MODULUS	PHASE (°)	DOCUMENT ID		TECN	COMMENT
• • • We do not use the following data for averages, fits, limits, etc. • • •					
0.005	−103	ROENCHEN	15A	DPWA	Multichannel

Normalized residue in $N\pi \to \Delta(2200) \to \Delta\pi$, D-wave

MODULUS	PHASE (°)	DOCUMENT ID		TECN	COMMENT
• • • We do not use the following data for averages, fits, limits, etc. • • •					
0.23	107	ROENCHEN	15A	DPWA	Multichannel

Normalized residue in $N\pi \to \Delta(2200) \to \Delta\pi$, G-wave

MODULUS	PHASE (°)	DOCUMENT ID		TECN	COMMENT
• • • We do not use the following data for averages, fits, limits, etc. • • •					
0.022	−151	ROENCHEN	15A	DPWA	Multichannel

$\Delta(2200)$ BREIT-WIGNER MASS

VALUE (MeV)	DOCUMENT ID		TECN	COMMENT
2150 to 2250 (≈ 2200) OUR ESTIMATE				
2176±40	ANISOVICH	17	DPWA	Multichannel
2200±80	CUTKOSKY	80	IPWA	$\pi N \to \pi N$
2215±60	HOEHLER	79	IPWA	$\pi N \to \pi N$

$\Delta(2200)$ BREIT-WIGNER WIDTH

VALUE (MeV)	DOCUMENT ID		TECN	COMMENT
200 to 500 (≈ 350) OUR ESTIMATE				
210± 70	ANISOVICH	17	DPWA	Multichannel
450±100	CUTKOSKY	80	IPWA	$\pi N \to \pi N$
400±100	HOEHLER	79	IPWA	$\pi N \to \pi N$

$\Delta(2200)$ DECAY MODES

	Mode	Fraction (Γ_i/Γ)
Γ_1	$N\pi$	2–8 %
Γ_2	ΣK	1–7 %
Γ_3	$\Delta\pi$, D-wave	40–100 %
Γ_4	$\Delta\pi$, G-wave	5–25 %
Γ_5	$\Delta\eta$, D-wave	seen

$\Delta(2200)$ BRANCHING RATIOS

$\Gamma(N\pi)/\Gamma_{total}$ **Γ_1/Γ**

VALUE (%)	DOCUMENT ID		TECN	COMMENT
2 to 8 (≈ 5) OUR ESTIMATE				
3.5±1.5	ANISOVICH	17	DPWA	Multichannel
6 ±2	CUTKOSKY	80	IPWA	$\pi N \to \pi N$
5 ±2	HOEHLER	79	IPWA	$\pi N \to \pi N$

$\Gamma(\Sigma K)/\Gamma_{total}$ **Γ_2/Γ**

VALUE	DOCUMENT ID		TECN	COMMENT
0.04±0.03	ANISOVICH	17	DPWA	Multichannel

$\Gamma(\Delta\pi, D\text{-wave})/\Gamma_{total}$ **Γ_3/Γ**

VALUE	DOCUMENT ID		TECN	COMMENT
0.70±0.30	ANISOVICH	17	DPWA	Multichannel

$\Gamma(\Delta\pi, G\text{-wave})/\Gamma_{total}$ **Γ_4/Γ**

VALUE	DOCUMENT ID		TECN	COMMENT
0.15±0.10	ANISOVICH	17	DPWA	Multichannel

$\Gamma(\Delta\eta, D\text{-wave})/\Gamma_{total}$ **Γ_5/Γ**

VALUE	DOCUMENT ID		TECN	COMMENT
~ 0.01	ANISOVICH	17	DPWA	Multichannel

$\Delta(2200)$ PHOTON DECAY AMPLITUDES AT THE POLE

$\Delta(2200) \to N\gamma$, helicity-1/2 amplitude $A_{1/2}$

MODULUS ($GeV^{-1/2}$)	PHASE (°)	DOCUMENT ID		TECN	COMMENT
$0.107^{+0.011}_{-0.020}$	−36 ± 5	ROENCHEN	14	DPWA	
• • • We do not use the following data for averages, fits, limits, etc. • • •					
0.106	−23	ROENCHEN	15A	DPWA	Multichannel

$\Delta(2200) \rightarrow N\gamma$, helicity-3/2 amplitude $A_{3/2}$

MODULUS (GeV$^{-1/2}$)	PHASE (°)	DOCUMENT ID		TECN	COMMENT
$-0.131^{+0.024}_{-0.009}$	113^{+9}_{-5}	ROENCHEN	14	DPWA	
• • • We do not use the following data for averages, fits, limits, etc. • • •					
0.157	−60	ROENCHEN	15A	DPWA	Multichannel

$\Delta(2200)$ REFERENCES

ANISOVICH	17	PL B766 357	A.V. Anisovich *et al.*	
ROENCHEN	15A	EPJ A51 70	D. Roenchen *et al.*	
ROENCHEN	14	EPJ A50 101	D. Roenchen *et al.*	
Also		EPJ A51 63 (errat.)	D. Roenchen *et al.*	
CUTKOSKY	80	Toronto Conf. 19	R.E. Cutkosky *et al.*	(CMU, LBL) IJP
Also		PR D20 2839	R.E. Cutkosky *et al.*	(CMU, LBL) IJP
HOEHLER	79	PDAT 12-1	G. Hohler *et al.*	(KARLT) IJP
Also		Toronto Conf. 3	R. Koch	(KARLT) IJP

$\Delta(2300)\ 9/2^+$

$I(J^P) = \frac{3}{2}(\frac{9}{2}^+)$ Status: **

OMITTED FROM SUMMARY TABLE

$\Delta(2300)$ POLE POSITION

REAL PART

VALUE (MeV)	DOCUMENT ID		TECN	COMMENT
2370±80	CUTKOSKY	80	IPWA	$\pi N \rightarrow \pi N$

−2×IMAGINARY PART

VALUE (MeV)	DOCUMENT ID		TECN	COMMENT
420±160	CUTKOSKY	80	IPWA	$\pi N \rightarrow \pi N$

$\Delta(2300)$ ELASTIC POLE RESIDUE

MODULUS $|r|$

VALUE (MeV)	DOCUMENT ID		TECN	COMMENT
10±4	CUTKOSKY	80	IPWA	$\pi N \rightarrow \pi N$

PHASE θ

VALUE (°)	DOCUMENT ID		TECN	COMMENT
−20±30	CUTKOSKY	80	IPWA	$\pi N \rightarrow \pi N$

$\Delta(2300)$ BREIT-WIGNER MASS

VALUE (MeV)	DOCUMENT ID		TECN	COMMENT
2400±125	CUTKOSKY	80	IPWA	$\pi N \rightarrow \pi N$
2217± 80	HOEHLER	79	IPWA	$\pi N \rightarrow \pi N$

$\Delta(2300)$ BREIT-WIGNER WIDTH

VALUE (MeV)	DOCUMENT ID		TECN	COMMENT
425±150	CUTKOSKY	80	IPWA	$\pi N \rightarrow \pi N$
300±100	HOEHLER	79	IPWA	$\pi N \rightarrow \pi N$

$\Delta(2300)$ DECAY MODES

	Mode	Fraction (Γ_i/Γ)
Γ_1	$N\pi$	1–8 %

$\Delta(2300)$ BRANCHING RATIOS

$\Gamma(N\pi)/\Gamma_{total}$ **Γ_1/Γ**

VALUE (%)	DOCUMENT ID		TECN	COMMENT
6±2	CUTKOSKY	80	IPWA	$\pi N \rightarrow \pi N$
3±2	HOEHLER	79	IPWA	$\pi N \rightarrow \pi N$

$\Delta(2300)$ REFERENCES

CUTKOSKY	80	Toronto Conf. 19	R.E. Cutkosky *et al.*	(CMU, LBL) IJP
Also		PR D20 2839	R.E. Cutkosky *et al.*	(CMU, LBL)
HOEHLER	79	PDAT 12-1	G. Hohler *et al.*	(KARLT) IJP
Also		Toronto Conf. 3	R. Koch	(KARLT) IJP

$\Delta(2350)\ 5/2^-$

$I(J^P) = \frac{3}{2}(\frac{5}{2}^-)$ Status: *

OMITTED FROM SUMMARY TABLE

$\Delta(2350)$ POLE POSITION

REAL PART

VALUE (MeV)	DOCUMENT ID		TECN	COMMENT
2400±125	CUTKOSKY	80	IPWA	$\pi N \rightarrow \pi N$
• • • We do not use the following data for averages, fits, limits, etc. • • •				
2427	VRANA	00	DPWA	Multichannel

−2×IMAGINARY PART

VALUE (MeV)	DOCUMENT ID		TECN	COMMENT
400±150	CUTKOSKY	80	IPWA	$\pi N \rightarrow \pi N$
• • • We do not use the following data for averages, fits, limits, etc. • • •				
458	VRANA	00	DPWA	Multichannel

$\Delta(2350)$ ELASTIC POLE RESIDUE

MODULUS $|r|$

VALUE (MeV)	DOCUMENT ID		TECN	COMMENT
15±8	CUTKOSKY	80	IPWA	$\pi N \rightarrow \pi N$

PHASE θ

VALUE (°)	DOCUMENT ID		TECN	COMMENT
−70±70	CUTKOSKY	80	IPWA	$\pi N \rightarrow \pi N$

$\Delta(2350)$ BREIT-WIGNER MASS

VALUE (MeV)	DOCUMENT ID		TECN	COMMENT
2400±125	CUTKOSKY	80	IPWA	$\pi N \rightarrow \pi N$
2305± 26	HOEHLER	79	IPWA	$\pi N \rightarrow \pi N$
• • • We do not use the following data for averages, fits, limits, etc. • • •				
2459±100	VRANA	00	DPWA	Multichannel

$\Delta(2350)$ BREIT-WIGNER WIDTH

VALUE (MeV)	DOCUMENT ID		TECN	COMMENT
400±150	CUTKOSKY	80	IPWA	$\pi N \rightarrow \pi N$
300± 70	HOEHLER	79	IPWA	$\pi N \rightarrow \pi N$
• • • We do not use the following data for averages, fits, limits, etc. • • •				
480±360	VRANA	00	DPWA	Multichannel

$\Delta(2350)$ DECAY MODES

	Mode	Fraction (Γ_i/Γ)
Γ_1	$N\pi$	4–30 %

$\Delta(2350)$ BRANCHING RATIOS

$\Gamma(N\pi)/\Gamma_{total}$ **Γ_1/Γ**

VALUE (%)	DOCUMENT ID		TECN	COMMENT
20±10	CUTKOSKY	80	IPWA	$\pi N \rightarrow \pi N$
4± 2	HOEHLER	79	IPWA	$\pi N \rightarrow \pi N$
• • • We do not use the following data for averages, fits, limits, etc. • • •				
7±14	VRANA	00	DPWA	Multichannel

$\Delta(2350)$ REFERENCES

VRANA	00	PRPL 328 181	T.P. Vrana, S.A. Dytman, T.-S.H. Lee	(PITT, ANL)
CUTKOSKY	80	Toronto Conf. 19	R.E. Cutkosky *et al.*	(CMU, LBL) IJP
Also		PR D20 2839	R.E. Cutkosky *et al.*	(CMU, LBL)
HOEHLER	79	PDAT 12-1	G. Hohler *et al.*	(KARLT) IJP
Also		Toronto Conf. 3	R. Koch	(KARLT) IJP

$\Delta(2390)\ 7/2^+$

$I(J^P) = \frac{3}{2}(\frac{7}{2}^+)$ Status: *

OMITTED FROM SUMMARY TABLE

$\Delta(2390)$ POLE POSITION

REAL PART

VALUE (MeV)	DOCUMENT ID		TECN	COMMENT
2223± 15±19	[1] SVARC	14	L+P	$\pi N \rightarrow \pi N$
2350±100	CUTKOSKY	80	IPWA	$\pi N \rightarrow \pi N$

−2×IMAGINARY PART

VALUE (MeV)	DOCUMENT ID		TECN	COMMENT
431± 26±7	[1] SVARC	14	L+P	$\pi N \rightarrow \pi N$
260±100	CUTKOSKY	80	IPWA	$\pi N \rightarrow \pi N$

$\Delta(2390)$ ELASTIC POLE RESIDUE

MODULUS $|r|$

VALUE (MeV)	DOCUMENT ID		TECN	COMMENT
26±2±1	[1] SVARC	14	L+P	$\pi N \rightarrow \pi N$
12±6	CUTKOSKY	80	IPWA	$\pi N \rightarrow \pi N$

PHASE θ

VALUE (°)		DOCUMENT ID		TECN	COMMENT
−160 ± 5 ± 11	[1]	SVARC	14	L+P	$\pi N \rightarrow \pi N$
− 90 ± 60		CUTKOSKY	80	IPWA	$\pi N \rightarrow \pi N$

Δ(2390) BREIT-WIGNER MASS

VALUE (MeV)	DOCUMENT ID		TECN	COMMENT
2350 ± 100	CUTKOSKY	80	IPWA	$\pi N \rightarrow \pi N$
2425 ± 60	HOEHLER	79	IPWA	$\pi N \rightarrow \pi N$

Δ(2390) BREIT-WIGNER WIDTH

VALUE (MeV)	DOCUMENT ID		TECN	COMMENT
300 ± 100	CUTKOSKY	80	IPWA	$\pi N \rightarrow \pi N$
300 ± 80	HOEHLER	79	IPWA	$\pi N \rightarrow \pi N$

Δ(2390) DECAY MODES

	Mode	Fraction (Γ_i/Γ)
Γ_1	$N\pi$	3–12 %

Δ(2390) BRANCHING RATIOS

$\Gamma(N\pi)/\Gamma_{total}$ **Γ_1/Γ**

VALUE (%)	DOCUMENT ID		TECN	COMMENT
8 ± 4	CUTKOSKY	80	IPWA	$\pi N \rightarrow \pi N$
7 ± 4	HOEHLER	79	IPWA	$\pi N \rightarrow \pi N$

Δ(2390) FOOTNOTES

[1] Fit to the amplitudes of HOEHLER 79.

Δ(2390) REFERENCES

SVARC	14	PR C89 045205	A. Svarc *et al.*	(RBI Zagreb, UNI Tuzla)
CUTKOSKY	80	Toronto Conf. 19	R.E. Cutkosky *et al.*	(CMU, LBL) IJP
Also		PR D20 2839	R.E. Cutkosky *et al.*	(CMU, LBL)
HOEHLER	79	PDAT 12-1	G. Hohler *et al.*	(KARLT) IJP
Also		Toronto Conf. 3	R. Koch	(KARLT) IJP

Δ(2400) 9/2⁻

$I(J^P) = \frac{3}{2}(\frac{9}{2}^-)$ Status: **

OMITTED FROM SUMMARY TABLE

Δ(2400) POLE POSITION

REAL PART

VALUE (MeV)	DOCUMENT ID		TECN	COMMENT
2260 ± 60	CUTKOSKY	80	IPWA	$\pi N \rightarrow \pi N$
• • • We do not use the following data for averages, fits, limits, etc. • • •				
1931	ROENCHEN	15A	DPWA	Multichannel
1983	ARNDT	06	DPWA	$\pi N \rightarrow \pi N, \eta N$

−2×IMAGINARY PART

VALUE (MeV)	DOCUMENT ID		TECN	COMMENT
320 ± 160	CUTKOSKY	80	IPWA	$\pi N \rightarrow \pi N$
• • • We do not use the following data for averages, fits, limits, etc. • • •				
442	ROENCHEN	15A	DPWA	Multichannel
878	ARNDT	06	DPWA	$\pi N \rightarrow \pi N, \eta N$

Δ(2400) ELASTIC POLE RESIDUE

MODULUS |r|

VALUE (MeV)	DOCUMENT ID		TECN	COMMENT
8 ± 4	CUTKOSKY	80	IPWA	$\pi N \rightarrow \pi N$
• • • We do not use the following data for averages, fits, limits, etc. • • •				
13	ROENCHEN	15A	DPWA	Multichannel
24	ARNDT	06	DPWA	$\pi N \rightarrow \pi N, \eta N$

PHASE θ

VALUE (°)	DOCUMENT ID		TECN	COMMENT
− 25 ± 15	CUTKOSKY	80	IPWA	$\pi N \rightarrow \pi N$
• • • We do not use the following data for averages, fits, limits, etc. • • •				
− 96	ROENCHEN	15A	DPWA	Multichannel
−139	ARNDT	06	DPWA	$\pi N \rightarrow \pi N, \eta N$

Δ(2400) INELASTIC POLE RESIDUE

The "normalized residue" is the residue divided by $\Gamma_{pole}/2$.

Normalized residue in $N\pi \rightarrow \Delta(2400) \rightarrow \Sigma K$

MODULUS	PHASE (°)	DOCUMENT ID		TECN	COMMENT
• • • We do not use the following data for averages, fits, limits, etc. • • •					
0.009	25	ROENCHEN	15A	DPWA	Multichannel

Normalized residue in $N\pi \rightarrow \Delta(2400) \rightarrow \Delta\pi$, *G*-wave

MODULUS	PHASE (°)	DOCUMENT ID		TECN	COMMENT
• • • We do not use the following data for averages, fits, limits, etc. • • •					
0.18	−110	ROENCHEN	15A	DPWA	Multichannel

Normalized residue in $N\pi \rightarrow \Delta(2400) \rightarrow \Delta\pi$, *I*-wave

MODULUS	PHASE (°)	DOCUMENT ID		TECN	COMMENT
• • • We do not use the following data for averages, fits, limits, etc. • • •					
0.012	−1.0	ROENCHEN	15A	DPWA	Multichannel

Δ(2400) BREIT-WIGNER MASS

VALUE (MeV)	DOCUMENT ID		TECN	COMMENT
2643 ± 141	[1] ARNDT	06	DPWA	$\pi N \rightarrow \pi N, \eta N$
2300 ± 100	CUTKOSKY	80	IPWA	$\pi N \rightarrow \pi N$
2468 ± 50	HOEHLER	79	IPWA	$\pi N \rightarrow \pi N$

[1] Statistical error only.

Δ(2400) BREIT-WIGNER WIDTH

VALUE (MeV)	DOCUMENT ID		TECN	COMMENT
895 ± 432	[2] ARNDT	06	DPWA	$\pi N \rightarrow \pi N, \eta N$
330 ± 100	CUTKOSKY	80	IPWA	$\pi N \rightarrow \pi N$
480 ± 100	HOEHLER	79	IPWA	$\pi N \rightarrow \pi N$

[2] Statistical error only.

Δ(2400) DECAY MODES

	Mode	Fraction (Γ_i/Γ)
Γ_1	$N\pi$	3–9 %

Δ(2400) BRANCHING RATIOS

$\Gamma(N\pi)/\Gamma_{total}$ **Γ_1/Γ**

VALUE (%)	DOCUMENT ID		TECN	COMMENT
6.4 ± 2.2	[3] ARNDT	06	DPWA	$\pi N \rightarrow \pi N, \eta N$
5 ± 2	CUTKOSKY	80	IPWA	$\pi N \rightarrow \pi N$
6 ± 3	HOEHLER	79	IPWA	$\pi N \rightarrow \pi N$

[3] Statistical error only.

Δ(2400) PHOTON DECAY AMPLITUDES AT THE POLE

Δ(2400) → $N\gamma$, helicity-1/2 amplitude $A_{1/2}$

MODULUS ($GeV^{-1/2}$)	PHASE (°)	DOCUMENT ID		TECN	COMMENT
$-0.128^{+0.046}_{-0.012}$	118^{+24}_{-3}	ROENCHEN	14	DPWA	
• • • We do not use the following data for averages, fits, limits, etc. • • •					
−0.034	63	ROENCHEN	15A	DPWA	Multichannel

Δ(2400) → $N\gamma$, helicity-3/2 amplitude $A_{3/2}$

MODULUS ($GeV^{-1/2}$)	PHASE (°)	DOCUMENT ID		TECN	COMMENT
$-0.115^{+0.042}_{-0.024}$	140^{+17}_{-28}	ROENCHEN	14	DPWA	
• • • We do not use the following data for averages, fits, limits, etc. • • •					
0.054	−75	ROENCHEN	15A	DPWA	Multichannel

Δ(2400) REFERENCES

ROENCHEN	15A	EPJ A51 70	D. Roenchen *et al.*	
ROENCHEN	14	EPJ A50 101	D. Roenchen *et al.*	
Also		EPJ A51 63 (errat.)	D. Roenchen *et al.*	
ARNDT	06	PR C74 045205	R.A. Arndt *et al.*	(GWU)
CUTKOSKY	80	Toronto Conf. 19	R.E. Cutkosky *et al.*	(CMU, LBL) IJP
Also		PR D20 2839	R.E. Cutkosky *et al.*	(CMU, LBL)
HOEHLER	79	PDAT 12-1	G. Hohler *et al.*	(KARLT) IJP
Also		Toronto Conf. 3	R. Koch	(KARLT) IJP

Δ(2420) 11/2+

$I(J^P) = \frac{3}{2}(\frac{11}{2}^+)$ Status: ****

Older and obsolete values are listed and referenced in the 2014 edition, Chinese Physics **C38** 070001 (2014).

Δ(2420) POLE POSITION

REAL PART

VALUE (MeV)	DOCUMENT ID		TECN	COMMENT
2300 to 2500 (≈ 2400) OUR ESTIMATE				
2454± 4±11	[1] SVARC	14	L+P	$\pi N \to \pi N$
2360±100	CUTKOSKY	80	IPWA	$\pi N \to \pi N$
• • • We do not use the following data for averages, fits, limits, etc. • • •				
2529	ARNDT	06	DPWA	$\pi N \to \pi N, \eta N$
2300	HOEHLER	93	ARGD	$\pi N \to \pi N$

[1] Fit to the amplitudes of HOEHLER 79.

−2×IMAGINARY PART

VALUE (MeV)	DOCUMENT ID		TECN	COMMENT
350 to 550 (≈ 450) OUR ESTIMATE				
462± 8±50	[1] SVARC	14	L+P	$\pi N \to \pi N$
420±100	CUTKOSKY	80	IPWA	$\pi N \to \pi N$
• • • We do not use the following data for averages, fits, limits, etc. • • •				
621	ARNDT	06	DPWA	$\pi N \to \pi N, \eta N$
620	HOEHLER	93	ARGD	$\pi N \to \pi N$

[1] Fit to the amplitudes of HOEHLER 79.

Δ(2420) ELASTIC POLE RESIDUE

MODULUS |r|

VALUE (MeV)	DOCUMENT ID		TECN	COMMENT
20 to 40 (≈ 30) OUR ESTIMATE				
30±1±7	[1] SVARC	14	L+P	$\pi N \to \pi N$
18±6	CUTKOSKY	80	IPWA	$\pi N \to \pi N$
• • • We do not use the following data for averages, fits, limits, etc. • • •				
33	ARNDT	06	DPWA	$\pi N \to \pi N, \eta N$
39	HOEHLER	93	ARGD	$\pi N \to \pi N$

[1] Fit to the amplitudes of HOEHLER 79.

PHASE θ

VALUE (°)	DOCUMENT ID		TECN	COMMENT
−60 to 20 (≈ − 20) OUR ESTIMATE				
11± 1±8	[1] SVARC	14	L+P	$\pi N \to \pi N$
−30±40	CUTKOSKY	80	IPWA	$\pi N \to \pi N$
• • • We do not use the following data for averages, fits, limits, etc. • • •				
−45	ARNDT	06	DPWA	$\pi N \to \pi N, \eta N$
−60	HOEHLER	93	ARGD	$\pi N \to \pi N$

[1] Fit to the amplitudes of HOEHLER 79.

Δ(2420) BREIT-WIGNER MASS

VALUE (MeV)	DOCUMENT ID		TECN	COMMENT
2300 to 2600 (≈ 2450) OUR ESTIMATE				
2633± 29	[1] ARNDT	06	DPWA	$\pi N \to \pi N, \eta N$
2400±125	CUTKOSKY	80	IPWA	$\pi N \to \pi N$
2416± 17	HOEHLER	79	IPWA	$\pi N \to \pi N$

[1] Statistical error only.

Δ(2420) BREIT-WIGNER WIDTH

VALUE (MeV)	DOCUMENT ID		TECN	COMMENT
300 to 700 (≈ 500) OUR ESTIMATE				
692± 47	[1] ARNDT	06	DPWA	$\pi N \to \pi N, \eta N$
450±150	CUTKOSKY	80	IPWA	$\pi N \to \pi N$
340± 28	HOEHLER	79	IPWA	$\pi N \to \pi N$

[1] Statistical error only.

Δ(2420) DECAY MODES

The following branching fractions are our estimates, not fits or averages.

	Mode	Fraction (Γ_i/Γ)
Γ_1	$N\pi$	5–10 %

Δ(2420) BRANCHING RATIOS

$\Gamma(N\pi)/\Gamma_{total}$ Γ_1/Γ

VALUE (%)	DOCUMENT ID		TECN	COMMENT
5 to 10 (≈ 8) OUR ESTIMATE				
8.5±0.8	[1] ARNDT	06	DPWA	$\pi N \to \pi N, \eta N$
8 ±3	CUTKOSKY	80	IPWA	$\pi N \to \pi N$
8.0±1.5	HOEHLER	79	IPWA	$\pi N \to \pi N$

[1] Statistical error only.

Δ(2420) REFERENCES

PDG	14	CP C38 070001	K. Olive *et al.*	(PDG Collab.)
SVARC	14	PR C89 045205	A. Svarc *et al.*	(RBI Zagreb, UNI Tuzla)
ARNDT	06	PR C74 045205	R.A. Arndt *et al.*	(GWU)
HOEHLER	93	πN Newsletter 9 1	G. Hohler	(KARL)
CUTKOSKY	80	Toronto Conf. 19	R.E. Cutkosky *et al.*	(CMU, LBL) IJP
Also		PR D20 2839	R.E. Cutkosky *et al.*	(CMU, LBL)
HOEHLER	79	PDAT 12-1	G. Hohler *et al.*	(KARLT) IJP
Also		Toronto Conf. 3	R. Koch	(KARLT) IJP

Δ(2750) 13/2−

$I(J^P) = \frac{3}{2}(\frac{13}{2}^-)$ Status: **

OMITTED FROM SUMMARY TABLE

Δ(2750) BREIT-WIGNER MASS

VALUE (MeV)	DOCUMENT ID		TECN	COMMENT
2794±80	HOEHLER	79	IPWA	$\pi N \to \pi N$

Δ(2750) BREIT-WIGNER WIDTH

VALUE (MeV)	DOCUMENT ID		TECN	COMMENT
350±100	HOEHLER	79	IPWA	$\pi N \to \pi N$

Δ(2750) DECAY MODES

	Mode	Fraction (Γ_i/Γ)
Γ_1	$N\pi$	2–6 %

Δ(2750) BRANCHING RATIOS

$\Gamma(N\pi)/\Gamma_{total}$ Γ_1/Γ

VALUE (%)	DOCUMENT ID		TECN	COMMENT
4.0±1.5	HOEHLER	79	IPWA	$\pi N \to \pi N$

Δ(2750) REFERENCES

HOEHLER	79	PDAT 12-1	G. Hohler *et al.*	(KARLT) IJP
Also		Toronto Conf. 3	R. Koch	(KARLT) IJP

Δ(2950) 15/2+

$I(J^P) = \frac{3}{2}(\frac{15}{2}^+)$ Status: **

OMITTED FROM SUMMARY TABLE

Δ(2950) BREIT-WIGNER MASS

VALUE (MeV)	DOCUMENT ID		TECN	COMMENT
2990±100	HOEHLER	79	IPWA	$\pi N \to \pi N$

Δ(2950) BREIT-WIGNER WIDTH

VALUE (MeV)	DOCUMENT ID		TECN	COMMENT
330±100	HOEHLER	79	IPWA	$\pi N \to \pi N$

Δ(2950) DECAY MODES

	Mode	Fraction (Γ_i/Γ)
Γ_1	$N\pi$	2–6 %

Δ(2950) BRANCHING RATIOS

$\Gamma(N\pi)/\Gamma_{total}$ Γ_1/Γ

VALUE (%)	DOCUMENT ID		TECN	COMMENT
4±2	HOEHLER	79	IPWA	$\pi N \to \pi N$

Δ(2950) REFERENCES

HOEHLER	79	PDAT 12-1	G. Hohler *et al.*	(KARLT) IJP
Also		Toronto Conf. 3	R. Koch	(KARLT) IJP

See key on page 885

$\Delta(\sim 3000$ Region) Partial-Wave Analyses

OMITTED FROM SUMMARY TABLE

We list here miscellaneous high-mass candidates for isospin-3/2 resonances found in partial-wave analyses.

Our 1982 edition also had a $\Delta(2850)$ and a $\Delta(3230)$. The evidence for them was deduced from total cross-section and 180° elastic cross-section measurements. The $\Delta(2850)$ has been resolved into the $\Delta(2750)$ $I_{3,13}$ and $\Delta(2950)$ $K_{3,15}$. The $\Delta(3230)$ is perhaps related to the $K_{3,13}$ of HENDRY 78 and to the $L_{3,17}$ of KOCH 80.

$\Delta(\sim 3000)$ BREIT-WIGNER MASS

VALUE (MeV)	DOCUMENT ID		TECN	COMMENT
3300	[1] KOCH	80	IPWA	$\pi N \to \pi N$ $L_{3,17}$ wave
3500	[1] KOCH	80	IPWA	$\pi N \to \pi N$ $M_{3,19}$ wave
2850 ± 150	HENDRY	78	MPWA	$\pi N \to \pi N$ $I_{3,11}$ wave
3200 ± 200	HENDRY	78	MPWA	$\pi N \to \pi N$ $K_{3,13}$ wave
3300 ± 200	HENDRY	78	MPWA	$\pi N \to \pi N$ $L_{3,17}$ wave
3700 ± 200	HENDRY	78	MPWA	$\pi N \to \pi N$ $M_{3,19}$ wave
4100 ± 300	HENDRY	78	MPWA	$\pi N \to \pi N$ $N_{3,21}$ wave

$\Delta(\sim 3000)$ BREIT-WIGNER WIDTH

VALUE (MeV)	DOCUMENT ID		TECN	COMMENT
700 ± 200	HENDRY	78	MPWA	$\pi N \to \pi N$ $I_{3,11}$ wave
1000 ± 300	HENDRY	78	MPWA	$\pi N \to \pi N$ $K_{3,13}$ wave
1100 ± 300	HENDRY	78	MPWA	$\pi N \to \pi N$ $L_{3,17}$ wave
1300 ± 400	HENDRY	78	MPWA	$\pi N \to \pi N$ $M_{3,19}$ wave
1600 ± 500	HENDRY	78	MPWA	$\pi N \to \pi N$ $N_{3,21}$ wave

$\Delta(\sim 3000)$ DECAY MODES

	Mode	Fraction (Γ_i/Γ)
Γ_1	$N\pi$	seen

$\Delta(\sim 3000)$ BRANCHING RATIOS

$\Gamma(N\pi)/\Gamma_{total}$ Γ_1/Γ

VALUE (%)	DOCUMENT ID		TECN	COMMENT
6 ± 2	HENDRY	78	MPWA	$\pi N \to \pi N$ $I_{3,11}$ wave
5 ± 2	HENDRY	78	MPWA	$\pi N \to \pi N$ $K_{3,13}$ wave
3 ± 1	HENDRY	78	MPWA	$\pi N \to \pi N$ $L_{3,17}$ wave
3 ± 1	HENDRY	78	MPWA	$\pi N \to \pi N$ $M_{3,19}$ wave
2 ± 1	HENDRY	78	MPWA	$\pi N \to \pi N$ $N_{3,21}$ wave

$\Delta(\sim 3000)$ FOOTNOTES

[1] In addition, KOCH 80 reports some evidence for an S_{31} $\Delta(2700)$ and a P_{33} $\Delta(2800)$.

$\Delta(\sim 3000)$ REFERENCES

KOCH	80	Toronto Conf. 3	R. Koch	(KARLT) IJP
HENDRY	78	PRL 41 222	A.W. Hendry	(IND, LBL) IJP
Also		ANP 136 1	A.W. Hendry	(IND)

Λ BARYONS
($S = -1$, $I = 0$)

$\Lambda^0 = uds$

Λ $I(J^P) = 0(\frac{1}{2}^+)$ Status: ****

We have omitted some results that have been superseded by later experiments. See our earlier editions.

Λ MASS

The fit uses Λ, Σ^+, Σ^0, Σ^- mass and mass-difference measurements.

VALUE (MeV)	EVTS	DOCUMENT ID		TECN	COMMENT
1115.683±0.006 OUR FIT					
1115.683±0.006 OUR AVERAGE					
1115.678±0.006±0.006	20k	HARTOUNI	94	SPEC	pp 27.5 GeV/c
1115.690±0.008±0.006	18k	[1] HARTOUNI	94	SPEC	pp 27.5 GeV/c
• • • We do not use the following data for averages, fits, limits, etc. • • •					
1115.59 ±0.08	935	HYMAN	72	HEBC	
1115.39 ±0.12	195	MAYEUR	67	EMUL	
1115.6 ±0.4		LONDON	66	HBC	
1115.65 ±0.07	488	[2] SCHMIDT	65	HBC	
1115.44 ±0.12		[3] BHOWMIK	63	RVUE	

[1] We assume CPT invariance: this is the $\overline{\Lambda}$ mass as measured by HARTOUNI 94. See below for the fractional mass difference, testing CPT.
[2] The SCHMIDT 65 masses have been reevaluated using our April 1973 proton and $K^\pm$ and $\pi^\pm$ masses. P. Schmidt, private communication (1974).
[3] The mass has been raised 35 keV to take into account a 46 keV increase in the proton mass and an 11 keV decrease in the $\pi^\pm$ mass (note added Reviews of Modern Physics **39** 1 (1967)).

$(m_\Lambda - m_{\overline{\Lambda}}) / m_\Lambda$

A test of CPT invariance.

VALUE (units 10^{-5})	EVTS	DOCUMENT ID		TECN	COMMENT
− 0.1 ± 1.1 OUR AVERAGE		Error includes scale factor of 1.6.			
+ 1.3 ± 1.2	31k	[1] RYBICKI	96	NA32	π^- Cu, 230 GeV
− 1.08± 0.90		HARTOUNI	94	SPEC	pp 27.5 GeV/c
4.5 ± 5.4		CHIEN	66	HBC	6.9 GeV/c $\overline{p}p$
• • • We do not use the following data for averages, fits, limits, etc. • • •					
−26 ±13		BADIER	67	HBC	2.4 GeV/c $\overline{p}p$

[1] RYBICKI 96 is an analysis of old ACCMOR (NA32) data.

Λ MEAN LIFE

Measurements with an error $\geq 0.1 \times 10^{-10}$ s have been omitted altogether, and only the latest high-statistics measurements are used for the average.

VALUE (10^{-10} s)	EVTS	DOCUMENT ID		TECN	COMMENT
2.632±0.020 OUR AVERAGE		Error includes scale factor of 1.6.			See the ideogram below.
2.69 ±0.03	53k	ZECH	77	SPEC	Neutral hyperon beam
2.611±0.020	34k	CLAYTON	75	HBC	0.96–1.4 GeV/c K^-p
2.626±0.020	36k	POULARD	73	HBC	0.4–2.3 GeV/c K^-p
• • • We do not use the following data for averages, fits, limits, etc. • • •					
2.69 ±0.05	6582	ALTHOFF	73B	OSPK	$\pi^+ n \to \Lambda K^+$
2.54 ±0.04	4572	BALTAY	71B	HBC	K^-p at rest
2.535±0.035	8342	GRIMM	68	HBC	
2.47 ±0.08	2600	HEPP	68	HBC	
2.35 ±0.09	916	BURAN	66	HLBC	
$2.452^{+0.056}_{-0.054}$	2213	ENGELMANN	66	HBC	
2.59 ±0.09	794	HUBBARD	64	HBC	
2.59 ±0.07	1378	SCHWARTZ	64	HBC	
2.36 ±0.06	2239	BLOCK	63	HEBC	

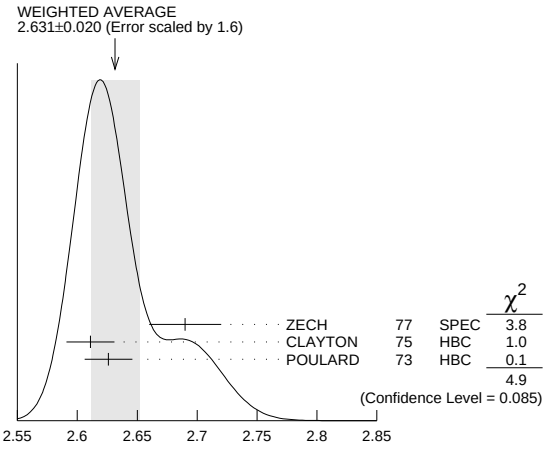

$(\tau_\Lambda - \tau_{\overline{\Lambda}}) / \tau_\Lambda$

A test of CPT invariance.

VALUE	DOCUMENT ID		TECN	COMMENT
−0.001 ±0.009 OUR AVERAGE				
−0.0018±0.0066±0.0056	BARNES	96	CNTR	LEAR $\overline{p}p \to \overline{\Lambda}\Lambda$
0.044 ±0.085	BADIER	67	HBC	2.4 GeV/c $\overline{p}p$

See the related review(s):
Baryon Magnetic Moments

Λ MAGNETIC MOMENT

See the "Note on Baryon Magnetic Moments" above. Measurements with an error $\geq 0.15\ \mu_N$ have been omitted.

VALUE (μ_N)	EVTS	DOCUMENT ID		TECN	COMMENT
−0.613 ±0.004 OUR AVERAGE					
−0.606 ±0.015	200k	COX	81	SPEC	
−0.6138±0.0047	3M	SCHACHIN...	78	SPEC	
−0.59 ±0.07	350k	HELLER	77	SPEC	
−0.57 ±0.05	1.2M	BUNCE	76	SPEC	
−0.66 ±0.07	1300	DAHL-JENSEN	71	EMUL	200 kG field

Λ ELECTRIC DIPOLE MOMENT

A nonzero value is forbidden by both T invariance and P invariance.

VALUE (10^{-16} ecm)	CL%	DOCUMENT ID		TECN
< 1.5	95	[1] PONDROM	81	SPEC
• • • We do not use the following data for averages, fits, limits, etc. • • •				
<100	95	[2] BARONI	71	EMUL
<500	95	GIBSON	66	EMUL

[1] PONDROM 81 measures $(-3.0 \pm 7.4) \times 10^{-17}$ e-cm.
[2] BARONI 71 measures $(-5.9 \pm 2.9) \times 10^{-15}$ e-cm.

Λ DECAY MODES

	Mode		Fraction (Γ_i/Γ)		Confidence level
Γ_1	$p\pi^-$		(63.9 ±0.5) %		
Γ_2	$n\pi^0$		(35.8 ±0.5) %		
Γ_3	$n\gamma$		(1.75±0.15)	$\times 10^{-3}$	
Γ_4	$p\pi^-\gamma$	[a]	(8.4 ±1.4)	$\times 10^{-4}$	
Γ_5	$pe^-\overline{\nu}_e$		(8.32±0.14)	$\times 10^{-4}$	
Γ_6	$p\mu^-\overline{\nu}_\mu$		(1.57±0.35)	$\times 10^{-4}$	
	Lepton (L) and/or Baryon (B) number violating decay modes				
Γ_7	$\pi^+ e^-$	L,B	< 6	$\times 10^{-7}$	90%
Γ_8	$\pi^+ \mu^-$	L,B	< 6	$\times 10^{-7}$	90%
Γ_9	$\pi^- e^+$	L,B	< 4	$\times 10^{-7}$	90%
Γ_{10}	$\pi^- \mu^+$	L,B	< 6	$\times 10^{-7}$	90%
Γ_{11}	$K^+ e^-$	L,B	< 2	$\times 10^{-6}$	90%
Γ_{12}	$K^+ \mu^-$	L,B	< 3	$\times 10^{-6}$	90%
Γ_{13}	$K^- e^+$	L,B	< 2	$\times 10^{-6}$	90%
Γ_{14}	$K^- \mu^+$	L,B	< 3	$\times 10^{-6}$	90%
Γ_{15}	$K^0_S \nu$	L,B	< 2	$\times 10^{-5}$	90%
Γ_{16}	$\overline{p}\pi^+$	B	< 9	$\times 10^{-7}$	90%

[a] See the Listings below for the pion momentum range used in this measurement.

CONSTRAINED FIT INFORMATION

An overall fit to 5 branching ratios uses 20 measurements and one constraint to determine 5 parameters. The overall fit has a $\chi^2 = 10.5$ for 16 degrees of freedom.

The following *off-diagonal* array elements are the correlation coefficients $\langle \delta x_i \delta x_j \rangle / (\delta x_i \cdot \delta x_j)$, in percent, from the fit to the branching fractions, $x_i \equiv \Gamma_i/\Gamma_{\text{total}}$. The fit constrains the x_i whose labels appear in this array to sum to one.

x_2	−100			
x_3	−2	−1		
x_5	46	−46	−1	
x_6	0	0	0	0
	x_1	x_2	x_3	x_5

Λ BRANCHING RATIOS

$\Gamma(p\pi^-)/\Gamma(N\pi)$ $\Gamma_1/(\Gamma_1+\Gamma_2)$

VALUE	EVTS	DOCUMENT ID		TECN	COMMENT
0.641±0.005 OUR FIT					
0.640±0.005 OUR AVERAGE					
0.646±0.008	4572	BALTAY	71B	HBC	K^-p at rest
0.635±0.007	6736	DOYLE	69	HBC	$\pi^-p \to \Lambda K^0$
0.643±0.016	903	HUMPHREY	62	HBC	
0.624±0.030		CRAWFORD	59B	HBC	$\pi^-p \to \Lambda K^0$

$\Gamma(n\pi^0)/\Gamma(N\pi)$ $\Gamma_2/(\Gamma_1+\Gamma_2)$

VALUE	EVTS	DOCUMENT ID		TECN
0.359±0.005 OUR FIT				
0.310±0.028 OUR AVERAGE				
0.35 ±0.05		BROWN	63	HLBC
0.291±0.034	75	CHRETIEN	63	HLBC

$\Gamma(n\gamma)/\Gamma_{\text{total}}$ Γ_3/Γ

VALUE (units 10^{-3})	EVTS	DOCUMENT ID		TECN	COMMENT
1.75±0.15 OUR FIT					
1.75±0.15	1816	LARSON	93	SPEC	K^-p at rest
• • • We do not use the following data for averages, fits, limits, etc. • • •					
$1.78 \pm 0.24 \,^{+0.14}_{-0.16}$	287	NOBLE	92	SPEC	See LARSON 93

$\Gamma(n\gamma)/\Gamma(n\pi^0)$ Γ_3/Γ_2

VALUE (units 10^{-3})	EVTS	DOCUMENT ID		TECN	COMMENT
• • • We do not use the following data for averages, fits, limits, etc. • • •					
2.86±0.74±0.57	24	BIAGI	86	SPEC	SPS hyperon beam

$\Gamma(p\pi^-\gamma)/\Gamma(p\pi^-)$ Γ_4/Γ_1

VALUE (units 10^{-3})	EVTS	DOCUMENT ID		TECN	COMMENT
1.32±0.22	72	BAGGETT	72C	HBC	π^- < 95 MeV/c

$\Gamma(pe^-\overline{\nu}_e)/\Gamma(p\pi^-)$ Γ_5/Γ_1

VALUE (units 10^{-3})	EVTS	DOCUMENT ID		TECN	COMMENT
1.301±0.019 OUR FIT					
1.301±0.019 OUR AVERAGE					
1.335±0.056	7111	BOURQUIN	83	SPEC	SPS hyperon beam
1.313±0.024	10k	WISE	80	SPEC	
1.23 ±0.11	544	LINDQUIST	77	SPEC	$\pi^-p \to K^0\Lambda$
1.27 ±0.07	1089	KATZ	73	HBC	
1.31 ±0.06	1078	ALTHOFF	71	OSPK	
1.17 ±0.13	86	[1] CANTER	71	HBC	K^-p at rest
1.20 ±0.12	143	[2] MALONEY	69	HBC	
1.17 ±0.18	120	[2] BAGLIN	64	FBC	K^- freon 1.45 GeV/c
1.23 ±0.20	150	[2] ELY	63	FBC	
• • • We do not use the following data for averages, fits, limits, etc. • • •					
1.32 ±0.15	218	[1] LINDQUIST	71	OSPK	See LINDQUIST 77

[1] Changed by us from $\Gamma(pe^-\overline{\nu}_e)/\Gamma(N\pi)$ assuming the authors used $\Gamma(p\pi^-)/\Gamma_{\text{total}} = 2/3$.

[2] Changed by us from $\Gamma(pe^-\overline{\nu}_e)/\Gamma(N\pi)$ because $\Gamma(pe^-\nu)/\Gamma(p\pi^-)$ is the directly measured quantity.

$\Gamma(p\mu^-\overline{\nu}_\mu)/\Gamma(N\pi)$ $\Gamma_6/(\Gamma_1+\Gamma_2)$

VALUE (units 10^{-4})	EVTS	DOCUMENT ID		TECN	COMMENT
1.57±0.35 OUR FIT					
1.57±0.35 OUR AVERAGE					
1.4 ±0.5	14	BAGGETT	72B	HBC	K^-p at rest
2.4 ±0.8	9	CANTER	71B	HBC	K^-p at rest
1.3 ±0.7	3	LIND	64	RVUE	
1.5 ±1.2	2	RONNE	64	FBC	

Lepton (L) and/or Baryon (B) number violating decay modes

$\Gamma(\pi^+e^-)/\Gamma_{\text{total}}$ Γ_7/Γ

VALUE	CL%	DOCUMENT ID		TECN	COMMENT
<6 × 10⁻⁷	90	[1] MCCRACKEN	15	CLAS	$\gamma p \to K^+\Lambda$

[1] Uses B($\Lambda \to p\pi^-$) = (63.9 ± 0.5)% for normalization mode.

$\Gamma(\pi^+\mu^-)/\Gamma_{\text{total}}$ Γ_8/Γ

VALUE	CL%	DOCUMENT ID		TECN	COMMENT
<6 × 10⁻⁷	90	[1] MCCRACKEN	15	CLAS	$\gamma p \to K^+\Lambda$

[1] Uses B($\Lambda \to p\pi^-$) = (63.9 ± 0.5)% for normalization mode.

$\Gamma(\pi^-e^+)/\Gamma_{\text{total}}$ Γ_9/Γ

VALUE	CL%	DOCUMENT ID		TECN	COMMENT
<4 × 10⁻⁷	90	[1] MCCRACKEN	15	CLAS	$\gamma p \to K^+\Lambda$

[1] Uses B($\Lambda \to p\pi^-$) = (63.9 ± 0.5)% for normalization mode.

$\Gamma(\pi^-\mu^+)/\Gamma_{\text{total}}$ Γ_{10}/Γ

VALUE	CL%	DOCUMENT ID		TECN	COMMENT
<6 × 10⁻⁷	90	[1] MCCRACKEN	15	CLAS	$\gamma p \to K^+\Lambda$

[1] Uses B($\Lambda \to p\pi^-$) = (63.9 ± 0.5)% for normalization mode.

$\Gamma(K^+e^-)/\Gamma_{\text{total}}$ Γ_{11}/Γ

VALUE	CL%	DOCUMENT ID		TECN	COMMENT
<2 × 10⁻⁶	90	[1] MCCRACKEN	15	CLAS	$\gamma p \to K^+\Lambda$

[1] Uses B($\Lambda \to p\pi^-$) = (63.9 ± 0.5)% for normalization mode.

$\Gamma(K^+\mu^-)/\Gamma_{\text{total}}$ Γ_{12}/Γ

VALUE	CL%	DOCUMENT ID		TECN	COMMENT
<3 × 10⁻⁶	90	[1] MCCRACKEN	15	CLAS	$\gamma p \to K^+\Lambda$

[1] Uses B($\Lambda \to p\pi^-$) = (63.9 ± 0.5)% for normalization mode.

$\Gamma(K^-e^+)/\Gamma_{\text{total}}$ Γ_{13}/Γ

VALUE	CL%	DOCUMENT ID		TECN	COMMENT
<2 × 10⁻⁶	90	[1] MCCRACKEN	15	CLAS	$\gamma p \to K^+\Lambda$

[1] Uses B($\Lambda \to p\pi^-$) = (63.9 ± 0.5)% for normalization mode.

$\Gamma(K^-\mu^+)/\Gamma_{\text{total}}$ Γ_{14}/Γ

VALUE	CL%	DOCUMENT ID		TECN	COMMENT
<3 × 10⁻⁶	90	[1] MCCRACKEN	15	CLAS	$\gamma p \to K^+\Lambda$

[1] Uses B($\Lambda \to p\pi^-$) = (63.9 ± 0.5)% for normalization mode.

$\Gamma(K^0_S\nu)/\Gamma_{\text{total}}$ Γ_{15}/Γ

VALUE	CL%	DOCUMENT ID		TECN	COMMENT
<2 × 10⁻⁵	90	[1] MCCRACKEN	15	CLAS	$\gamma p \to K^+\Lambda$

[1] Uses B($\Lambda \to p\pi^-$) = (63.9 ± 0.5)% for normalization mode.

$\Gamma(\overline{p}\pi^+)/\Gamma_{\text{total}}$ Γ_{16}/Γ

VALUE	CL%	DOCUMENT ID		TECN	COMMENT
<9 × 10⁻⁷	90	[1] MCCRACKEN	15	CLAS	$\gamma p \to K^+\Lambda$

[1] Uses B($\Lambda \to p\pi^-$) = (63.9 ± 0.5)% for normalization mode.

Λ DECAY PARAMETERS

See the "Note on Baryon Decay Parameters" in the neutron Listings. Some early results have been omitted.

α_- FOR $\Lambda \to p\pi^-$

VALUE	EVTS	DOCUMENT ID		TECN	COMMENT
0.642±0.013 OUR AVERAGE					
0.584±0.046	8500	ASTBURY	75	SPEC	
0.649±0.023	10325	CLELAND	72	OSPK	
0.67 ±0.06	3520	DAUBER	69	HBC	From Ξ decay
0.645±0.017	10130	OVERSETH	67	OSPK	Λ from π^-p
0.62 ±0.07	1156	CRONIN	63	CNTR	Λ from π^-p

α_+ FOR $\overline{\Lambda} \to \overline{p}\pi^+$

VALUE	EVTS	DOCUMENT ID		TECN	COMMENT
−0.71 ±0.08 OUR AVERAGE					
−0.755±0.083±0.063	≈ 8.7k	ABLIKIM	10	BES	$J/\psi \to \Lambda\overline{\Lambda}$
−0.63 ±0.13	770	TIXIER	88	DM2	$J/\psi \to \Lambda\overline{\Lambda}$

ϕ ANGLE FOR $\Lambda \to p\pi^-$ $(\tan\phi = \beta/\gamma)$

VALUE (°)	EVTS	DOCUMENT ID		TECN	COMMENT
− 6.5± 3.5 OUR AVERAGE					
− 7.0± 4.5	10325	CLELAND	72	OSPK	Λ from π^-p
− 8.0± 6.0	10130	OVERSETH	67	OSPK	Λ from π^-p
13.0±17.0	1156	CRONIN	63	OSPK	Λ from π^-p

Baryon Particle Listings

Λ, Λ's and Σ's, $\Lambda(1405)$

α_0 / α_- = $\alpha(\Lambda \to n\pi^0)$ / $\alpha(\Lambda \to p\pi^-)$

VALUE	EVTS	DOCUMENT ID		TECN	COMMENT
1.01 ±0.07 OUR AVERAGE					
1.000±0.068	4760	[1] OLSEN	70	OSPK	$\pi^+ n \to \Lambda K^+$
1.10 ±0.27		CORK	60	CNTR	

[1] OLSEN 70 compares proton and neutron distributions from Λ decay.

$(\alpha + \overline{\alpha})/(\alpha - \overline{\alpha})$ in $\Lambda \to p\pi^-$, $\overline{\Lambda} \to \overline{p}\pi^+$

Zero if CP is conserved; α_- and α_+ are the asymmetry parameters for $\Lambda \to p\pi^-$ and $\overline{\Lambda} \to \overline{p}\pi^+$ decay. See also the Ξ^- for a similar test involving the decay chain $\Xi^- \to \Lambda\pi^-$, $\Lambda \to p\pi^-$ and the corresponding antiparticle chain.

VALUE	EVTS	DOCUMENT ID		TECN	COMMENT
0.006±0.021 OUR AVERAGE					
−0.081±0.055±0.059	≈ 8.7k	ABLIKIM	10	BES	$J/\psi \to \Lambda\overline{\Lambda}$
+0.013±0.022	96k	BARNES	96	CNTR	LEAR $\overline{p}p \to \overline{\Lambda}\Lambda$
+0.01 ±0.10	770	TIXIER	88	DM2	$J/\psi \to \Lambda\overline{\Lambda}$
−0.02 ±0.14	10k	[1] CHAUVAT	85	CNTR	pp, $\overline{p}p$ ISR
• • • We do not use the following data for averages, fits, limits, etc. • • •					
−0.07 ±0.09	4063	BARNES	87	CNTR	See BARNES 96

[1] CHAUVAT 85 actually gives $\alpha_+(\overline{\Lambda})/\alpha_-(\Lambda) = -1.04 \pm 0.29$. Assumes polarization is same in $\overline{p}p \to \overline{\Lambda}X$ and $pp \to \Lambda X$. Tests of this assumption, based on C-invariance and fragmentation, are satisfied by the data.

g_A / g_V FOR $\Lambda \to pe^-\overline{\nu}_e$

Measurements with fewer than 500 events have been omitted. Where necessary, signs have been changed to agree with our conventions, which are given in the "Note on Baryon Decay Parameters" in the neutron Listings. The measurements all assume that the form factor $g_2 = 0$. See also the footnote on DWORKIN 90.

VALUE	EVTS	DOCUMENT ID		TECN	COMMENT
−0.718±0.015 OUR AVERAGE					
−0.719±0.016±0.012	37k	[1] DWORKIN	90	SPEC	$e\nu$ angular corr.
−0.70 ±0.03	7111	BOURQUIN	83	SPEC	$\Xi \to \Lambda\pi^-$
−0.734±0.031	10k	[2] WISE	81	SPEC	$e\nu$ angular correl.
• • • We do not use the following data for averages, fits, limits, etc. • • •					
−0.63 ±0.06	817	ALTHOFF	73	OSPK	Polarized Λ

[1] The tabulated result assumes the weak-magnetism coupling $w \equiv g_W(0)/g_V(0)$ to be 0.97, as given by the CVC hypothesis and as assumed by the other listed measurements. However, DWORKIN 90 *measures* w to be 0.15 ± 0.30, and then $g_A/g_V = -0.731 \pm 0.016$.

[2] This experiment measures only the absolute value of g_A/g_V.

Λ REFERENCES

We have omitted some papers that have been superseded by later experiments. See our earlier editions.

MCCRACKEN	15	PR D92 072002	M.E. McCracken *et al.*	(JLab CLAS Collab.)
ABLIKIM	10	PR D81 012003	M. Ablikim *et al.*	(BES Collab.)
BARNES	96	PR C54 1877	P.D. Barnes *et al.*	(CERN PS-185 Collab.)
RYBICKI	96	APP B27 2155	K. Rybicki	
HARTOUNI	94	PRL 72 1322	E.P. Hartouni *et al.*	(BNL E766 Collab.)
Also		PRL 72 2821 (erratum)	E.P. Hartouni *et al.*	(BNL E766 Collab.)
LARSON	93	PR D47 799	K.D. Larson *et al.*	(BNL-811 Collab.)
NOBLE	92	PRL 69 414	A.J. Noble *et al.*	(BIRM, BOST, BRCO+)
DWORKIN	90	PR D41 780	J. Dworkin *et al.*	(MICH, WISC, RUTG+)
TIXIER	88	PL B212 523	M.H. Tixier *et al.*	(DM2 Collab.)
BARNES	87	PL B199 147	P.D. Barnes *et al.*	(CMU, SACL, LANL+)
BIAGI	86	ZPHY C30 201	S.F. Biagi *et al.*	(BRIS, CERN, GEVA+)
CHAUVAT	85	PL 163B 273	P. Chauvat *et al.*	(CERN, CLER, UCLA+)
BOURQUIN	83	ZPHY C21 1	M.H. Bourquin *et al.*	(BRIS, GEVA, HEIDP+)
COX	81	PRL 46 877	P.T. Cox *et al.*	(MICH, WISC, RUTG, MINN+)
PONDROM	81	PR D23 814	L. Pondrom *et al.*	(WISC, MICH, RUTG+)
WISE	81	PL 98B 123	J.E. Wise *et al.*	(MASA, BNL)
WISE	80	PL 91B 165	J.E. Wise *et al.*	(MASA, BNL)
SCHACHIN...	78	PRL 41 1348	L. Schachinger *et al.*	(MICH, RUTG, WISC)
HELLER	77	PL 68B 480	K. Heller *et al.*	(MICH, WISC, HEIDH)
LINDQUIST	77	PR D16 2104	J. Lindquist *et al.*	(EFI, OSU, ANL)
Also		JP G2 L211	J. Lindquist *et al.*	(EFI, WUSL, OSU+)
ZECH	77	NP B124 413	G. Zech *et al.*	(SIEG, CERN, DORT, HEIDH)
BUNCE	76	PRL 36 1113	G.R.M. Bunce *et al.*	(WISC, MICH, RUTG)
ASTBURY	75	NP B99 30	P. Astbury *et al.*	(LOIC, CERN, ETH+)
CLAYTON	75	NP B95 130	E.F. Clayton *et al.*	(LOIC, RHEL)
ALTHOFF	73	PL 43B 237	K.H. Althoff *et al.*	(CERN, HEID)
ALTHOFF	73B	NP B66 29	K.H. Althoff *et al.*	(CERN, HEID)
KATZ	73	Thesis MDDP-TR-74-044	C.N. Katz	(UMD)
POULARD	73	PL 46B 135	G. Poulard, A. Givernaud, A.C. Borg	(SACL)
BAGGETT	72B	ZPHY 252 362	M.J. Baggett *et al.*	(HEID)
BAGGETT	72C	PL 42B 379	M.J. Baggett *et al.*	(HEID)
CLELAND	72	NP B40 221	W.E. Cleland *et al.*	(CERN, GEVA, LUND)
HYMAN	72	PR D5 1063	L.G. Hyman *et al.*	(ANL, CMU)
ALTHOFF	71	PL 37B 531	K.H. Althoff *et al.*	(CERN, HEID)
BALTAY	71B	PR D4 670	C. Baltay *et al.*	(COLU, BING)
BARONI	71	LNC 2 1256	G. Baroni, S. Petrera, G. Romano	(ROMA)
CANTER	71	PRL 26 868	J. Canter *et al.*	(STON, COLU)
CANTER	71B	PRL 27 59	J. Canter *et al.*	(STON, COLU)
DAHL-JENSEN	71	NC 3A 1	E. Dahl-Jensen *et al.*	(CERN, ANKA, LAUS+)
LINDQUIST	71	PRL 27 612	J. Lindquist *et al.*	(EFI, WUSL, OSU+)
OLSEN	70	PRL 24 843	S.L. Olsen *et al.*	(WISC, MICH)
DAUBER	69	PR 179 1262	P.M. Dauber *et al.*	(LRL)
DOYLE	69	Thesis UCRL 18139	J.C. Doyle	(LRL)
MALONEY	69	PRL 23 425	J.E. Maloney, B. Sechi-Zorn	(UMD)
GRIMM	68	NC 54A 187	H.J. Grimm	(HEID)
HEPP	68	ZPHY 214 71	V. Hepp, H. Schleich	(HEID)
BADIER	67	PL 25B 152	J. Badier *et al.*	(EPOL)
MAYEUR	67	U.Libr.Brux.Bul. 32	C. Mayeur, E. Tompa, J.H. Wickens	(BELG, LOUC)
OVERSETH	67	PRL 19 391	O.E. Overseth, R.F. Roth	(MICH, PRIN)
PDG	67	RMP 39 1	A.H. Rosenfeld *et al.*	(LRL, CERN, YALE)
BURAN	66	PL 20 318	T. Buran *et al.*	(OSLO)
CHIEN	66	PR 152 1171	C.Y. Chien *et al.*	(YALE, BNL)
ENGELMANN	66	NC 45A 1038	R. Engelmann *et al.*	(HEID, REHO)
GIBSON	66	NC 45A 882	W.M. Gibson, K. Green	(BRIS)
LONDON	66	PR 143 1034	G.W. London *et al.*	(BNL, SYRA)
SCHMIDT	65	PR 140 B1328	P. Schmidt	(COLU)
BAGLIN	64	NC 35 977	C. Baglin *et al.*	(EPOL, CERN, LOUC, RHEL+)
HUBBARD	64	PR 135 B183	J.R. Hubbard *et al.*	(LRL)
LIND	64	PR 135 B1483	V.G. Lind *et al.*	(WISC)
RONNE	64	PL 11 357	B.E. Ronne *et al.*	(CERN, EPOL, LOUC+)
SCHWARTZ	64	Thesis UCRL 11360	J.A. Schwartz	(LRL)
BHOWMIK	63	NC 28 1494	B. Bhowmik, D.P. Goyal	(DELH)
BLOCK	63	PR 130 766	M.M. Block *et al.*	(NWES, BGNA, SYRA+)
BROWN	63	PR 130 769	J.L. Brown *et al.*	(LRL, MICH)
CHRETIEN	63	PR 131 2208	M. Chretien *et al.*	(BRAN, BROW, HARV+)
CRONIN	63	PR 129 1795	J.W. Cronin, O.E. Overseth	(PRIN)
ELY	63	PR 131 868	R.P. Ely *et al.*	(LRL)
HUMPHREY	62	PR 127 1305	W.E. Humphrey, R.R. Ross	(LRL)
CORK	60	PR 120 1000	B. Cork *et al.*	(LRL, PRIN, BNL)
CRAWFORD	59B	PRL 2 266	F.S. Crawford *et al.*	(LRL)

See the related review(s):
Λ and Σ Resonances

$\Lambda(1405)$ $1/2^-$

$I(J^P) = 0(\frac{1}{2}^-)$ Status: ****

In the 1998 Note on the $\Lambda(1405)$ in PDG 98, R.H. Dalitz discussed the S-shaped cusp behavior of the intensity at the N-$\overline{K}$ threshold observed in THOMAS 73 and HEMINGWAY 85. He commented that this behavior "is characteristic of S-wave coupling; the other below threshold hyperon, the $\Sigma(1385)$, has no such threshold distortion because its N-$\overline{K}$ coupling is P-wave. For $\Lambda(1405)$ this asymmetry is the sole direct evidence that $J^P = 1/2^-$."

A recent measurement by the CLAS collaboration, MORIYA 14, definitively established the long-assumed $J^P = 1/2^-$ spin-parity assignment of the $\Lambda(1405)$. The experiment produced the $\Lambda(1405)$ spin-polarized in the photoproduction process $\gamma p \to K^+\Lambda(1405)$ and measured the decay of the $\Lambda(1405)$(polarized) $\to \Sigma^+$(polarized)π^-. The observed isotropic decay of $\Lambda(1405)$ is consistent with spin $J = 1/2$. The polarization transfer to the Σ^+(polarized) direction revealed negative parity, and thus established $J^P = 1/2^-$.

See the related review(s):
Pole Structure of the $\Lambda(1405)$ Region

$\Lambda(1405)$ REGION POLE POSITIONS

REAL PART

VALUE (MeV)		DOCUMENT ID		TECN	
• • • We do not use the following data for averages, fits, limits, etc. • • •					
1429^{+8}_{-7}	[1]	MAI	15	DPWA	
1325^{+15}_{-15}	[2]	MAI	15	DPWA	
1434^{+2}_{-2}	[3]	MAI	15	DPWA	
1330^{+4}_{-5}	[4]	MAI	15	DPWA	
1421^{+3}_{-2}	[5]	GUO	13	DPWA	
1388 ± 9	[6]	GUO	13	DPWA	
1424^{+7}_{-23}	[7]	IKEDA	12	DPWA	
1381^{+18}_{-6}	[8]	IKEDA	12	DPWA	

[1] High-mass pole, solution number 4.
[2] Low-mass pole, solution number 4.
[3] High-mass pole, solution number 2.
[4] Low-mass pole, solution number 2.
[5] High-mass pole, fit II
[6] Low-mass pole, fit II.
[7] High-mass pole
[8] Low-mass pole

−2×IMAGINARY PART

VALUE (MeV)		DOCUMENT ID		TECN	
• • • We do not use the following data for averages, fits, limits, etc. • • •					
24^{+4}_{-6}	[1]	MAI	15	DPWA	
180^{+24}_{-36}	[2]	MAI	15	DPWA	
20^{+4}_{-2}	[3]	MAI	15	DPWA	
112^{+34}_{-22}	[4]	MAI	15	DPWA	
38^{+16}_{-10}	[5]	GUO	13	DPWA	
228^{+48}_{-50}	[6]	GUO	13	DPWA	
52^{+6}_{-28}	[7]	IKEDA	12	DPWA	
162^{+38}_{-16}	[8]	IKEDA	12	DPWA	

[1] High-mass pole, solution number 4.
[2] Low-mass pole, solution number 4.
[3] High-mass pole, solution number 2.
[4] Low-mass pole, solution number 2.
[5] High-mass pole, fit II
[6] Low-mass pole, fit II.
[7] High-mass pole
[8] Low-mass pole

Λ(1405) MASS

PRODUCTION EXPERIMENTS

VALUE (MeV)	EVTS	DOCUMENT ID		TECN	COMMENT
1405.1 $^{+1.3}_{-1.0}$ OUR AVERAGE					
1405 $^{+11}_{-9}$		HASSANVAND	13	SPEC	$pp \to p\Lambda(1405)K^+$
1405 $^{+1.4}_{-1.0}$		ESMAILI	10	RVUE	^{4}He $K^- \to \Sigma^\pm\pi^\mp X$ at rest
1406.5 ± 4.0		[1] DALITZ	91		M-matrix fit
• • • We do not use the following data for averages, fits, limits, etc. • • •					
1391 ± 1	700	[1] HEMINGWAY	85	HBC	K^-p 4.2 GeV/c
~ 1405	400	[2] THOMAS	73	HBC	π^-p 1.69 GeV/c
1405	120	BARBARO-...	68B	DBC	K^-d 2.1–2.7 GeV/c
1400 ± 5	67	BIRMINGHAM	66	HBC	K^-p 3.5 GeV/c
1382 ± 8		ENGLER	65	HDBC	π^-p, π^+d 1.68 GeV/c
1400 ±24		MUSGRAVE	65	HBC	$\overline{p}p$ 3–4 GeV/c
1410		ALEXANDER	62	HBC	π^-p 2.1 GeV/c
1405		ALSTON	62	HBC	K^-p 1.2–0.5 GeV/c
1405		ALSTON	61B	HBC	K^-p 1.15 GeV/c

[1] DALITZ 91 fits the HEMINGWAY 85 data.
[2] THOMAS 73 data is fit by CHAO 73 (see next section).

EXTRAPOLATIONS BELOW $N\overline{K}$ THRESHOLD

VALUE (MeV)	DOCUMENT ID		TECN	COMMENT
• • • We do not use the following data for averages, fits, limits, etc. • • •				
1407.56 or 1407.50	[1] KIMURA	00		potential model
1411	[2] MARTIN	81		K-matrix fit
1406	[3] CHAO	73	DPWA	0–range fit (sol. B)
1421	MARTIN	70	RVUE	Constant K-matrix
1416 ±4	MARTIN	69	HBC	Constant K-matrix
1403 ±3	KIM	67	HBC	K-matrix fit
1407.5 ± 1.2	[4] KITTEL	66	HBC	0–effective-range fit
1410.7 ± 1.0	KIM	65	HBC	0–effective-range fit
1409.6 ± 1.7	[4] SAKITT	65	HBC	0–effective-range fit

[1] The KIMURA 00 values are from fits A and B from a coupled-channel potential model using low-energy $\overline{K}N$ and $\Sigma\pi$ data, kaonic-hydrogen x-ray measurements, and our Λ(1405) mass and width. The results bear mainly on the *nature* of the Λ(1405): three-quark state or $\overline{K}N$ bound state.
[2] The MARTIN 81 fit includes the $K^\pm p$ forward scattering amplitudes and the dispersion relations they must satisfy.
[3] See also the accompanying paper of THOMAS 73.
[4] Data of SAKITT 65 are used in the fit by KITTEL 66.

Λ(1405) WIDTH

PRODUCTION EXPERIMENTS

VALUE (MeV)	EVTS	DOCUMENT ID		TECN	COMMENT
50.5 ± 2.0 OUR AVERAGE					
62 ±10		HASSANVAND	13	SPEC	$pp \to p\Lambda(1405)K^+$
50 ± 2		[1] DALITZ	91		M-matrix fit
• • • We do not use the following data for averages, fits, limits, etc. • • •					
24 $^{+4}_{-3}$		ESMAILI	10	RVUE	^{4}He $K^- \to \Sigma^\pm\pi^\mp X$ at rest
32 ± 1	700	[1] HEMINGWAY	85	HBC	K^-p 4.2 GeV/c
45 to 55	400	[2] THOMAS	73	HBC	π^-p 1.69 GeV/c
35	120	BARBARO-...	68B	DBC	K^-d 2.1–2.7 GeV/c
50 ±10	67	BIRMINGHAM	66	HBC	K^-p 3.5 GeV/c
89 ±20		ENGLER	65	HDBC	
60 ±20		MUSGRAVE	65	HBC	
35 ± 5		ALEXANDER	62	HBC	
50		ALSTON	62	HBC	
20		ALSTON	61B	HBC	

[1] DALITZ 91 fits the HEMINGWAY 85 data.
[2] THOMAS 73 data is fit by CHAO 73 (see next section).

EXTRAPOLATIONS BELOW $N\overline{K}$ THRESHOLD

VALUE (MeV)	DOCUMENT ID		TECN	COMMENT
• • • We do not use the following data for averages, fits, limits, etc. • • •				
50.24 or 50.26	[1] KIMURA	00		potential model
30	[2] MARTIN	81		K-matrix fit
55	[3,4] CHAO	73	DPWA	0–range fit (sol. B)
20	MARTIN	70	RVUE	Constant K-matrix
29 ±6	MARTIN	69	HBC	Constant K-matrix
50 ±5	KIM	67	HBC	K-matrix fit
34.1 ± 4.1	[5] KITTEL	66	HBC	
37.0 ± 3.2	KIM	65	HBC	
28.2 ± 4.1	[5] SAKITT	65	HBC	

[1] The KIMURA 00 values are from fits A and B from a coupled-channel potential model using low-energy $\overline{K}N$ and $\Sigma\pi$ data, kaonic-hydrogen x-ray measurements, and our Λ(1405) mass and width. The results bear mainly on the *nature* of the Λ(1405): three-quark state or $\overline{K}N$ bound state.
[2] The MARTIN 81 fit includes the $K^\pm p$ forward scattering amplitudes and the dispersion relations they must satisfy.
[3] An asymmetric shape, with $\Gamma/2 = 41$ MeV below resonance, 14 MeV above.
[4] See also the accompanying paper of THOMAS 73.
[5] Data of SAKITT 65 are used in the fit by KITTEL 66.

Λ(1405) DECAY MODES

	Mode	Fraction (Γ_i/Γ)
Γ_1	$\Sigma\pi$	100 %
Γ_2	$\Lambda\gamma$	
Γ_3	$\Sigma^0\gamma$	
Γ_4	$N\overline{K}$	

Λ(1405) PARTIAL WIDTHS

Γ(Λγ) Γ2

VALUE (keV)	DOCUMENT ID	COMMENT
• • • We do not use the following data for averages, fits, limits, etc. • • •		
27 ± 8	BURKHARDT 91	Isobar model fit

Γ(Σ⁰γ) Γ3

VALUE (keV)	DOCUMENT ID	COMMENT
• • • We do not use the following data for averages, fits, limits, etc. • • •		
10 ± 4 or 23 ± 7	BURKHARDT 91	Isobar model fit

Λ(1405) BRANCHING RATIOS

Γ(N$\overline{K}$)/Γ(Σπ) Γ4/Γ1

VALUE	CL%	DOCUMENT ID		TECN	COMMENT
• • • We do not use the following data for averages, fits, limits, etc. • • •					
<3	95	HEMINGWAY	85	HBC	K^-p 4.2 GeV/c

Λ(1405) REFERENCES

MAI	15	EPJ A51 30	M. Mai, U.-G. Meissner	(BONN, JULI)
MORIYA	14	PRL 112 082004	K. Moriya *et al.*	(CLAS Collab.) JP
GUO	13	PR C87 035202	Z.-H. Guo, J. Oller	
HASSANVAND	13	PR C87 055202	M. Hassanvand *et al.*	
Also		PR C88 019905 (errat.)	M. Hassanvand *et al.*	
IKEDA	12	NP A881 98	Y. Ikeda, T. Hyodo, W. Weise	(MUNT, RIKEN, TINT)
ESMAILI	10	PL B686 23	J. Esmaili, Y. Akaishi, T. Yamazaki	(RIKEN, ISUT+)
KIMURA	00	PR C62 015206	M. Kimura *et al.*	
PDG	98	EPJ C3 1	C. Caso *et al.*	(PDG Collab.)
BURKHARDT	91	PR C44 607	H. Burkhardt, J. Lowe	(NOTT, UNM, BIRM)
DALITZ	91	JP G17 289	R.H. Dalitz, A. Deloff	(OXFTP, WINR)
HEMINGWAY	85	NP B253 742	R.J. Hemingway	(CERN) J
MARTIN	81	NP B179 33	A.D. Martin	(DURH)
CHAO	73	NP B56 46	Y.A. Chao *et al.*	(RHEL, CMU, LOUC)
THOMAS	73	NP B56 15	D.W. Thomas *et al.*	(CMU) J
MARTIN	70	NP B16 479	A.D. Martin, G.G. Ross	(DURH)
MARTIN	69	PR 183 1352	B.R. Martin, M. Sakitt	(LOUC, BNL)
Also		PR 183 1345	B.R. Martin, M. Sakitt	(LOUC, BNL)
BARBARO-...	68B	PRL 21 573	A. Barbaro-Galtieri *et al.*	(LRL, SLAC)
KIM	67	PRL 19 1074	J.K. Kim	(YALE)
BIRMINGHAM	66	PR 152 1148	M. Haque *et al.*	(BIRM, GLAS, LOIC, OXF+)
KITTEL	66	PL 21 349	W. Kittel, G. Otter, I. Wacek	(VIEN)
ENGLER	65	PRL 15 224	A. Engler *et al.*	(CMU, BNL) IJ
KIM	65	PRL 14 29	J.K. Kim	(COLU)
MUSGRAVE	65	NC 35 735	B. Musgrave *et al.*	(BIRM, CERN, EPOL+)
SAKITT	65	PR 139 B719	M. Sakitt *et al.*	(UMD, LRL)
ALEXANDER	62	PRL 8 447	G. Alexander *et al.*	(LRL) I
ALSTON	62	CERN Conf. 311	M.H. Alston *et al.*	(LRL) I
ALSTON	61B	PRL 6 698	M.H. Alston *et al.*	(LRL) I

OTHER RELATED PAPERS

IWASAKI	97	PRL 78 3067	M. Iwasaki *et al.*	(KEK 228 Collab.)
FINK	90	PR C41 2720	P.J.Jr. Fink *et al.*	(IBMY, ORST, ANSM)
LEINWEBER	90	ANP 198 203	D.B. Leinweber	(MCMS)
MUELLER-GR...	90	NP A513 557	A. Mueller-Groeling, K. Holinde, J. Speth	(JULI)
BARRETT	89	NC 102A 179	R.C. Barrett	(SURR)
BATTY	89	NC 102A 255	C.J. Batty, A. Gal	(RAL, HEBR)
CAPSTICK	89	Excited Baryons 88, p.32	S. Capstick	(GUEL)
LOWE	89	NC 102A 167	J. Lowe	(BIRM)
WHITEHOUSE	89	PRL 63 1352	D.A. Whitehouse *et al.*	(BIRM, BOST, BRCO+)
SIEGEL	88	PR C38 2221	P.B. Siegel, W. Weise	(REGE)
WORKMAN	88	PR D37 3117	R.L. Workman, H.W. Fearing	(TRIU)
SCHNICK	87	PRL 58 1719	J. Schnick, R.H. Landau	(ORST)
CAPSTICK	86	PR D34 2809	S. Capstick, N. Isgur	(TNTO)
JENNINGS	86	PL B176 229	B.K. Jennings	(TRIU)
MALTMAN	86	PR D34 1372	K. Maltman, N. Isgur	(LANL, TNTO)
ZHONG	86	PL B171 471	Y.S. Zhong *et al.*	(ADLD, TRIU, SURR)
BURKHARDT	85	NP A440 653	H. Burkhardt, J. Lowe, A.S. Rosenthal	(NOTT+)
DAREWYCH	85	PR D32 1765	J.W. Darewych, R. Koniuk, N. Isgur	(YORKC, TNTO)
VEIT	85	PR D31 1033	E.A. Veit *et al.*	(TRIU, ADLD, SURR)
KIANG	84	PR C30 1638	D. Kiang *et al.*	(DALH, MCMS)
MILLER	84	Conference paper	D.J. Miller	(LOUC)
		Conf. Intersections between Particle and Nuclear Physics, p. 783		
VANDIJK	84	PR D30 937	W. van Dijk	(MCMS)
VEIT	84	PL 137B 415	E.A. Veit *et al.*	(TRIU, SURR, CERN)
DALITZ	82	Heid. Conf.	R.H. Dalitz *et al.*	(OXFTP)
		Heidelberg Conf., p. 201		
DALITZ	81	Kaon Conf.	R.H. Dalitz, J.G. McGinley	(OXFTP)
		Low and Intermediate Energy Kaon-Nucleon Physics, p.381		

MARTIN	81B	Kaon Conf.	A.D. Martin	(DURH)
Low and Intermediate Energy Kaon-Nucelon Physics, p. 97				
OADES	77	NC 42A 462	G.C. Oades, G. Rasche	(AARH, ZURI)
SHAW	73	Purdue Conf. 417	G.L. Shaw	(UCI)
BARBARO-...	72	LBL-555	A. Barbaro-Galtieri	(LBL)
DOBSON	72	PR D6 3256	P.N. Dobson, R. McElhaney	(HAWA)
RAJASEKA...	72	PR D5 610	G. Rajasekaran	(TATA)
Earlier papers also cited in RAJASEKARAN 72.				
CLINE	71	PRL 26 1194	D. Cline, R. Laumann, J. Mapp	(WISC)
MARTIN	71	PL 35B 62	A.D. Martin, A.D. Martin, G.G. Ross	(DURH, LOUC+)
DALITZ	67	PR 153 1617	R.H. Dalitz, T.C. Wong, G. Rajasekaran	(OXFTP+)
DONALD	66	PL 22 711	R.A. Donald *et al.*	(LIVP)
KADYK	66	PRL 17 599	J.A. Kadyk *et al.*	(LRL)
ABRAMS	65	PR 139 B454	G.S. Abrams, B. Sechi-Zorn	(UMD)

Λ(1520) 3/2⁻

$I(J^P) = 0(\frac{3}{2}^-)$ Status: ****

Discovered by FERRO-LUZZI 62; the elaboration in WATSON 63 is the classic paper on the Breit-Wigner analysis of a multichannel resonance.

The measurements of the mass, width, and elasticity published before 1975 are now obsolete and have been omitted. They were last listed in our 1982 edition Physics Letters **111B** 1 (1982).

Production and formation experiments agree quite well, so they are listed together here.

Λ(1520) POLE POSITION

REAL PART

VALUE (MeV)	DOCUMENT ID		TECN	COMMENT
1517 $^{+4}_{-4}$	[1] KAMANO	15	DPWA	Multichannel
• • • We do not use the following data for averages, fits, limits, etc. • • •				
1518	ZHANG	13A	DPWA	Multichannel
1518.8	QIANG	10	SPEC	$ep \to e' K^+ X$ (fit to X)

[1] From the preferred solution A in KAMANO 15.

−2×IMAGINARY PART

VALUE (MeV)	DOCUMENT ID		TECN	COMMENT
15 $^{+10}_{-8}$	[1] KAMANO	15	DPWA	Multichannel
• • • We do not use the following data for averages, fits, limits, etc. • • •				
16	ZHANG	13A	DPWA	Multichannel
17.2	QIANG	10	SPEC	$ep \to e' K^+ X$ (fit to X)

[1] From the preferred solution A in KAMANO 15.

Λ(1520) POLE RESIDUES

The normalized residue is the residue divided by $\Gamma_{pole}/2$.

Normalized residue in $N\overline{K} \to \Lambda(1520) \to N\overline{K}$

MODULUS	PHASE (°)	DOCUMENT ID		TECN	COMMENT
• • • We do not use the following data for averages, fits, limits, etc. • • •					
0.431	−11	[1] KAMANO	15	DPWA	Multichannel

[1] From the preferred solution A in KAMANO 15.

Normalized residue in $N\overline{K} \to \Lambda(1520) \to \Sigma\pi$

MODULUS	PHASE (°)	DOCUMENT ID		TECN	COMMENT
• • • We do not use the following data for averages, fits, limits, etc. • • •					
0.435	−10	[1] KAMANO	15	DPWA	Multichannel

[1] From the preferred solution A in KAMANO 15.

Normalized residue in $N\overline{K} \to \Lambda(1520) \to \Sigma(1385)\pi$, *S*-wave

MODULUS	PHASE (°)	DOCUMENT ID		TECN	COMMENT
• • • We do not use the following data for averages, fits, limits, etc. • • •					
0.431	−123	[1] KAMANO	15	DPWA	Multichannel

[1] From the preferred solution A in KAMANO 15.

Normalized residue in $N\overline{K} \to \Lambda(1520) \to \Sigma(1385)\pi$, *D*-wave

MODULUS	PHASE (°)	DOCUMENT ID		TECN	COMMENT
• • • We do not use the following data for averages, fits, limits, etc. • • •					
0.0141	122	[1] KAMANO	15	DPWA	Multichannel

[1] From the preferred solution A in KAMANO 15.

Λ(1520) MASS

VALUE (MeV)	EVTS	DOCUMENT ID		TECN	COMMENT
1519.5 ±1.0 OUR ESTIMATE					
1519.54±0.17 OUR AVERAGE					
1519.6 ±0.5		ZHANG	13A	DPWA	Multichannel
1520.4 ±0.6 ±1.5		QIANG	10	SPEC	$ep \to e' K^+ X$ (fit to X)
1517.3 ±1.5	300	BARBER	80D	SPEC	$\gamma p \to \Lambda(1520) K^+$
1517.8 ±1.2	5k	BARLAG	79	HBC	$K^- p$ 4.2 GeV/c
1520.0 ±0.5		ALSTON-...	78	DPWA	$\overline{K}N \to \overline{K}N$
1519.7 ±0.3	4k	CAMERON	77	HBC	$K^- p$ 0.96–1.36 GeV/c
1519 ±1		GOPAL	77	DPWA	$\overline{K}N$ multichannel
1519.4 ±0.3	2000	CORDEN	75	DBC	$K^- d$ 1.4–1.8 GeV/c

Λ(1520) WIDTH

VALUE (MeV)	EVTS	DOCUMENT ID		TECN	COMMENT
15.6 ±1.0 OUR ESTIMATE					
15.73±0.29 OUR AVERAGE Error includes scale factor of 1.1.					
17 ±1		ZHANG	13A	DPWA	Multichannel
18.6 ±1.9 ±1.0		QIANG	10	SPEC	$ep \to e' K^+ X$ (fit to X)
16.3 ±3.3	300	BARBER	80D	SPEC	$\gamma p \to \Lambda(1520) K^+$
16 ±1		GOPAL	80	DPWA	$\overline{K}N \to \overline{K}N$
14 ±3	677	[1] BARLAG	79	HBC	$K^- p$ 4.2 GeV/c
15.4 ±0.5		ALSTON-...	78	DPWA	$\overline{K}N \to \overline{K}N$
16.3 ±0.5	4k	CAMERON	77	HBC	$K^- p$ 0.96–1.36 GeV/c
15.0 ±0.5		GOPAL	77	DPWA	$\overline{K}N$ multichannel
15.5 ±1.6	2000	CORDEN	75	DBC	$K^- d$ 1.4–1.8 GeV/c

[1] From the best-resolution sample of $\Lambda\pi\pi$ events only.

Λ(1520) DECAY MODES

	Mode	Fraction (Γ_j/Γ)
Γ_1	$N\overline{K}$	(45 ±1) %
Γ_2	$\Sigma\pi$	(42 ±1) %
Γ_3	$\Lambda\pi\pi$	(10 ±1) %
Γ_4	$\Sigma(1385)\pi$, *S*-wave	
Γ_5	$\Sigma(1385)\pi$, *D*-wave	
Γ_6	$\Sigma(1385)\pi$	
Γ_7	$\Sigma(1385)\pi(\to \Lambda\pi\pi)$	
Γ_8	$\Lambda(\pi\pi)_{S\text{-wave}}$	
Γ_9	$\Sigma\pi\pi$	(0.9 ±0.1) %
Γ_{10}	$\Lambda\gamma$	(0.85±0.15) %
Γ_{11}	$\Sigma^0\gamma$	

CONSTRAINED FIT INFORMATION

An overall fit to 9 branching ratios uses 28 measurements and one constraint to determine 6 parameters. The overall fit has a $\chi^2 = 18.9$ for 23 degrees of freedom.

The following *off-diagonal* array elements are the correlation coefficients $\langle \delta x_i \delta x_j \rangle / (\delta x_i \cdot \delta x_j)$, in percent, from the fit to the branching fractions, $x_i \equiv \Gamma_i/\Gamma_{\text{total}}$. The fit constrains the x_i whose labels appear in this array to sum to one.

	x_1	x_2	x_3	x_9	x_{10}
x_2	−63				
x_3	−32	−34			
x_9	−4	−3	−1		
x_{10}	−8	−7	−3	0	
x_{11}	−24	−21	−10	−1	−1

Λ(1520) BRANCHING RATIOS

See "Sign conventions for resonance couplings" in the Note on Λ and Σ Resonances.

$\Gamma(N\overline{K})/\Gamma_{\text{total}}$ Γ_1/Γ

VALUE	DOCUMENT ID		TECN	COMMENT
0.45 ±0.01 OUR ESTIMATE				
0.448±0.007 OUR FIT Error includes scale factor of 1.2.				
0.456±0.010 OUR AVERAGE				
0.47 ±0.04	ZHANG	13A	DPWA	Multichannel
0.47 ±0.02	GOPAL	80	DPWA	$\overline{K}N \to \overline{K}N$
0.45 ±0.03	ALSTON-...	78	DPWA	$\overline{K}N \to \overline{K}N$
0.448±0.014	CORDEN	75	DBC	$K^- d$ 1.4–1.8 GeV/c
• • • We do not use the following data for averages, fits, limits, etc. • • •				
0.43	[1] KAMANO	15	DPWA	Multichannel
0.47 ±0.01	GOPAL	77	DPWA	See GOPAL 80
0.42	MAST	76	HBC	$K^- p \to \overline{K}^0 n$

[1] From the preferred solution A in KAMANO 15.

$\Gamma(\Sigma\pi)/\Gamma_{\text{total}}$ Γ_2/Γ

VALUE	DOCUMENT ID		TECN	COMMENT
0.42 ±0.01 OUR ESTIMATE				
0.421±0.007 OUR FIT Error includes scale factor of 1.2.				
0.425±0.011 OUR AVERAGE				
0.47 ±0.05	ZHANG	13A	DPWA	Multichannel
0.426±0.014	CORDEN	75	DBC	$K^- d$ 1.4–1.8 GeV/c

0.418±0.017	BARBARO-...	69B	HBC	$K^- p$ 0.28–0.45 GeV/c

• • • We do not use the following data for averages, fits, limits, etc. • • •

0.446	[1] KAMANO	15	DPWA	Multichannel	
0.46	KIM	71	DPWA	K-matrix analysis	

[1] From the preferred solution A in KAMANO 15.

$\Gamma(\Sigma\pi)/\Gamma(N\overline{K})$ Γ_2/Γ_1

VALUE	DOCUMENT ID		TECN	COMMENT
0.940±0.026 OUR FIT	Error includes scale factor of 1.3.			
0.95 ±0.04 OUR AVERAGE	Error includes scale factor of 1.7. See the ideogram below.			
0.98 ±0.03	[1] GOPAL	77	DPWA	$\overline{K}N$ multichannel
0.82 ±0.08	BURKHARDT	69	HBC	$K^- p$ 0.8–1.2 GeV/c
1.06 ±0.14	SCHEUER	68	DBC	$K^- N$ 3 GeV/c
0.96 ±0.20	DAHL	67	HBC	$\pi^- p$ 1.6–4 GeV/c
0.73 ±0.11	DAUBER	67	HBC	$K^- p$ 2 GeV/c

• • • We do not use the following data for averages, fits, limits, etc. • • •

1.06 ±0.12	BERTHON	74	HBC	Quasi-2-body σ
1.72 ±0.78	MUSGRAVE	65	HBC	

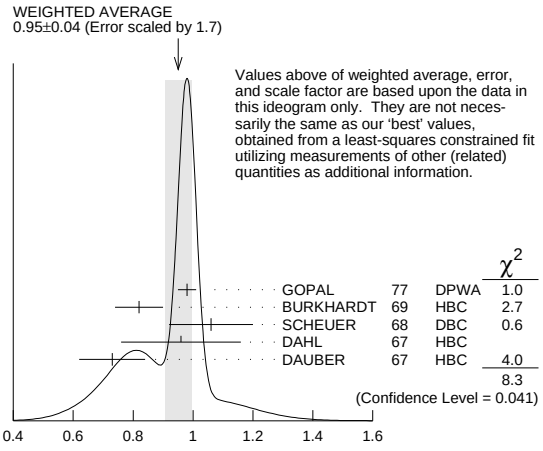

[1] The $\overline{K}N \to \Sigma\pi$ amplitude at resonance is $+0.46 \pm 0.01$.

$\Gamma(\Lambda\pi\pi)/\Gamma_{\text{total}}$ Γ_3/Γ

VALUE	DOCUMENT ID		TECN	COMMENT
0.10 ±0.01 OUR ESTIMATE				
0.095±0.005 OUR FIT	Error includes scale factor of 1.2.			
0.096±0.008 OUR AVERAGE	Error includes scale factor of 1.6.			
0.091±0.006	CORDEN	75	DBC	$K^- d$ 1.4–1.8 GeV/c
0.11 ±0.01	[1] MAST	73B	IPWA	$K^- p \to \Lambda\pi\pi$

[1] Assumes $\Gamma(N\overline{K})/\Gamma_{\text{total}} = 0.46 \pm 0.02$.

$\Gamma(\Lambda\pi\pi)/\Gamma(N\overline{K})$ Γ_3/Γ_1

VALUE	DOCUMENT ID		TECN	COMMENT
0.212±0.012 OUR FIT	Error includes scale factor of 1.2.			
0.202±0.021 OUR AVERAGE				
0.22 ±0.03	BURKHARDT	69	HBC	$K^- p$ 0.8–1.2 GeV/c
0.19 ±0.04	SCHEUER	68	DBC	$K^- N$ 3 GeV/c
0.17 ±0.05	DAHL	67	HBC	$\pi^- p$ 1.6–4 GeV/c
0.21 ±0.18	DAUBER	67	HBC	$K^- p$ 2 GeV/c

• • • We do not use the following data for averages, fits, limits, etc. • • •

0.27 ±0.13	BERTHON	74	HBC	Quasi-2-body σ
0.2	KIM	71	DPWA	K-matrix analysis

$\Gamma(\Sigma\pi)/\Gamma(\Lambda\pi\pi)$ Γ_2/Γ_3

VALUE	DOCUMENT ID		TECN	COMMENT
4.43±0.25 OUR FIT	Error includes scale factor of 1.2.			
3.9 ±0.6 OUR AVERAGE				
3.9 ±1.0	UHLIG	67	HBC	$K^- p$ 0.9–1.0 GeV/c
3.3 ±1.1	BIRMINGHAM	66	HBC	$K^- p$ 3.5 GeV/c
4.5 ±1.0	ARMENTEROS	65C	HBC	

$\Gamma(\Sigma(1385)\pi$, S-wave$)/\Gamma_{\text{total}}$ Γ_4/Γ

VALUE	DOCUMENT ID		TECN	COMMENT

• • • We do not use the following data for averages, fits, limits, etc. • • •

0.121	[1] KAMANO	15	DPWA	Multichannel

[1] From the preferred solution A in KAMANO 15.

$\Gamma(\Sigma(1385)\pi$, D-wave$)/\Gamma_{\text{total}}$ Γ_5/Γ

VALUE	DOCUMENT ID		TECN	COMMENT

• • • We do not use the following data for averages, fits, limits, etc. • • •

0.003	[1] KAMANO	15	DPWA	Multichannel

[1] From the preferred solution A in KAMANO 15.

$\Gamma(\Sigma(1385)\pi)/\Gamma_{\text{total}}$ Γ_6/Γ

VALUE	DOCUMENT ID		TECN	COMMENT
0.041±0.005	CHAN	72	HBC	$K^- p \to \Lambda\pi\pi$

$\Gamma(\Sigma(1385)\pi(\to \Lambda\pi\pi))/\Gamma(\Lambda\pi\pi)$ Γ_7/Γ_3

The $\Lambda\pi\pi$ mode is largely due to $\Sigma(1385)\pi$. Only the values of $(\Sigma(1385)\pi)\ /\ (\Lambda 2\pi)$ given by MAST 73B and CORDEN 75 are based on real 3-body partial-wave analyses. The discrepancy between the two results is essentially due to the different hypotheses made concerning the shape of the $(\pi\pi)_{S\text{-wave}}$ state.

VALUE	CL%	DOCUMENT ID		TECN	COMMENT
0.58±0.22		CORDEN	75	DBC	$K^- d$ 1.4–1.8 GeV/c
0.82±0.10		[1] MAST	73B	IPWA	$K^- p \to \Lambda\pi\pi$

• • • We do not use the following data for averages, fits, limits, etc. • • •

<0.44	90	WIELAND	11	SPHR	$\gamma p \to K^+\Lambda(1520)$
0.39±0.10		[2] BURKHARDT	71	HBC	$K^- p \to (\Lambda\pi\pi)\pi$

[1] Both $\Sigma(1385)\pi$ DS_{03} and $\Sigma(\pi\pi)$ DP_{03} contribute.

[2] The central bin (1514–1524 MeV) gives 0.74 ± 0.10; other bins are lower by 2-to-5 standard deviations.

$\Gamma(\Lambda(\pi\pi)_{S\text{-wave}})/\Gamma(\Lambda\pi\pi)$ Γ_8/Γ_3

VALUE	DOCUMENT ID		TECN	COMMENT
0.20±0.08	CORDEN	75	DBC	$K^- d$ 1.4–1.8 GeV/c

$\Gamma(\Sigma\pi\pi)/\Gamma_{\text{total}}$ Γ_9/Γ

VALUE	DOCUMENT ID		TECN	COMMENT
0.009 ±0.001 OUR ESTIMATE				
0.0086±0.0005 OUR FIT				
0.0086±0.0005 OUR AVERAGE				
0.007 ±0.002	[1] CORDEN	75	DBC	$K^- d$ 1.4–1.8 GeV/c
0.0085±0.0006	[2] MAST	73	MPWA	$K^- p \to \Sigma\pi\pi$
0.010 ±0.0015	BARBARO-...	69B	HBC	$K^- p$ 0.28–0.45 GeV/c

[1] Much of the $\Sigma\pi\pi$ decay proceeds via $\Sigma(1385)\pi$.

[2] Assumes $\Gamma(N\overline{K})/\Gamma_{\text{total}} = 0.46$.

$\Gamma(\Lambda\gamma)/\Gamma_{\text{total}}$ Γ_{10}/Γ

VALUE (units 10^{-3})	EVTS	DOCUMENT ID		TECN	COMMENT
8.5±1.5 OUR ESTIMATE					
8.8±1.1 OUR FIT					
8.8±1.1 OUR AVERAGE					
$10.7 \pm 2.9^{+1.5}_{-0.4}$	32	TAYLOR	05	CLAS	$\gamma p \to K^+\Lambda\gamma$
10.2±2.1±1.5	290	ANTIPOV	04A	SPNX	$p\,N(\text{C}) \to \Lambda(1520)\,K^+\,N(\text{C})$
8.0±1.4	238	MAST	68B	HBC	Using $\Gamma(N\overline{K})/\Gamma_{\text{total}} = 0.45$

$\Gamma(\Sigma^0\gamma)/\Gamma_{\text{total}}$ Γ_{11}/Γ

VALUE	DOCUMENT ID		TECN	COMMENT
0.0193±0.0034 OUR FIT				
0.02 ±0.0035	[1] MAST	68B	HBC	Not measured; see note

[1] Calculated from $\Gamma(\Lambda\gamma)/\Gamma_{\text{total}}$, assuming SU(3). Needed to constrain the sum of all the branching ratios to be unity.

$\Lambda(1520)$ REFERENCES

KAMANO	15	PR C92 025205	H. Kamano *et al.*	(ANL, OSAK)
ZHANG	13A	PR C88 035205	H. Zhang *et al.*	(KSU)
WIELAND	11	EPJ A47 47	F. Wieland *et al.*	(ELSA SAPHIR Collab.)
QIANG	10	PL B694 123	Y. Qiang *et al.*	(DUKE, JEFF, PNPI, GWU+)
TAYLOR	05	PR C71 054609	S. Taylor *et al.*	(JLab CLAS Collab.)
Also		PR C72 039902 (errat.)	S. Taylor *et al.*	(JLab CLAS Collab.)
ANTIPOV	04A	PL B604 22	Yu.M. Antipov *et al.*	(IHEP SPHINX Collab.)
PDG	82	PL 111B 1	M. Roos *et al.*	(HELS, CIT, CERN)
BARBER	80D	ZPHY C7 17	D.P. Barber *et al.*	(DARE, LANC, SHEF)
GOPAL	80	Toronto Conf. 159	G.P. Gopal	(RHEL) IJP
BARLAG	79	NP B149 220	S.J.M. Barlag *et al.*	(AMST, CERN, NIJM+)
ALSTON-...	78	PR D18 182	M. Alston-Garnjost *et al.*	(LBL, MTHO+) IJP
Also		PRL 38 1007	M. Alston-Garnjost *et al.*	(LBL, MTHO+) IJP
CAMERON	77	NP B131 399	W. Cameron *et al.*	(RHEL, LOIC) IJP
GOPAL	77	NP B119 362	G.P. Gopal *et al.*	(LOIC, RHEL) IJP
MAST	76	PR D14 13	T.S. Mast *et al.*	(LBL)
CORDEN	75	NP B84 306	M.J. Corden *et al.*	(BIRM)
BERTHON	74	NC 21A 146	A. Berthon *et al.*	(CDEF, RHEL, SACL+)
MAST	73	PR D7 3212	T.S. Mast *et al.*	(LBL) IJP
MAST	73B	PR D7 5	T.S. Mast *et al.*	(LBL) IJP
CHAN	72	PRL 28 256	S.B. Chan *et al.*	(MASA, YALE)
BURKHARDT	71	NP B27 64	E. Burkhardt *et al.*	(HEID, CERN, SACL)
KIM	71	PRL 27 356	J.K. Kim	(HARV) IJP
Also		Duke Conf. 161 Hyperon Resonances, 1970	J.K. Kim	(HARV) IJP
BARBARO-...	69B	Lund Conf. 352	A. Barbaro-Galtieri *et al.*	(LRL)
Also		Duke Conf. 95 Hyperon Resonances 1970	R.D. Tripp	(LRL)
BURKHARDT	69	NP B14 106	E. Burkhardt *et al.*	(HEID, EFI, CERN+)
MAST	68B	PRL 21 1715	T.S. Mast *et al.*	(LRL)
SCHEUER	68	NP B8 503	J.C. Scheuer *et al.*	(SABRE Collab.)
DAHL	67	PR 163 1377	O.I. Dahl *et al.*	(LRL)
DAUBER	67	PL 24B 525	P.M. Dauber *et al.*	(UCLA)
UHLIG	67	PR 155 1448	R.P. Uhlig *et al.*	(UMD, NRL)
BIRMINGHAM	66	PR 152 1148	M. Haque *et al.*	(BIRM, GLAS, LOIC, OXF+)
ARMENTEROS	65C	PL 19 338	R. Armenteros *et al.*	(CERN, HEID, SACL)
MUSGRAVE	65	NC 35 735	B. Musgrave *et al.*	(BIRM, CERN, EPOL+)
WATSON	63	PR 131 2248	M.B. Watson, M. Ferro-Luzzi, R.D. Tripp	(LRL) IJP
FERRO-LUZZI	62	PRL 8 28	M. Ferro-Luzzi, R.D. Tripp, M.B. Watson	(LRL) IJP

Λ(1600) 1/2+

$I(J^P) = 0(\frac{1}{2}^+)$ Status: ***

See also the Λ(1810) P_{01}. There are quite possibly two P_{01} states in this region.

Λ(1600) POLE POSITION

REAL PART

VALUE (MeV)	DOCUMENT ID		TECN	COMMENT
1544^{+3}_{-3}	[1] KAMANO	15	DPWA	Multichannel
• • • We do not use the following data for averages, fits, limits, etc. • • •				
1572	ZHANG	13A	DPWA	Multichannel

[1] From the preferred solution A in KAMANO 15.

−2×IMAGINARY PART

VALUE (MeV)	DOCUMENT ID		TECN	COMMENT
112^{+12}_{-2}	[1] KAMANO	15	DPWA	Multichannel
• • • We do not use the following data for averages, fits, limits, etc. • • •				
138	ZHANG	13A	DPWA	Multichannel

[1] From the preferred solution A in KAMANO 15.

Λ(1600) POLE RESIDUES

The normalized residue is the residue divided by $\Gamma_{pole}/2$.

Normalized residue in $N\overline{K} \rightarrow$ Λ(1600) $\rightarrow N\overline{K}$

MODULUS	PHASE (°)	DOCUMENT ID		TECN	COMMENT
• • • We do not use the following data for averages, fits, limits, etc. • • •					
0.105	−80	[1] KAMANO	15	DPWA	Multichannel

[1] From the preferred solution A in KAMANO 15.

Normalized residue in $N\overline{K} \rightarrow$ Λ(1600) $\rightarrow \Sigma\pi$

MODULUS	PHASE (°)	DOCUMENT ID		TECN	COMMENT
• • • We do not use the following data for averages, fits, limits, etc. • • •					
0.232	108	[1] KAMANO	15	DPWA	Multichannel

[1] From the preferred solution A in KAMANO 15.

Normalized residue in $N\overline{K} \rightarrow$ Λ(1600) $\rightarrow \Sigma(1385)\pi$

MODULUS	PHASE (°)	DOCUMENT ID		TECN	COMMENT
• • • We do not use the following data for averages, fits, limits, etc. • • •					
0.183	77	[1] KAMANO	15	DPWA	Multichannel

[1] From the preferred solution A in KAMANO 15.

Λ(1600) MASS

VALUE (MeV)	DOCUMENT ID		TECN	COMMENT
1560 to 1700 (≈ 1600) OUR ESTIMATE				
1592± 10	ZHANG	13A	DPWA	Multichannel
1568± 20	GOPAL	80	DPWA	$\overline{K}N \rightarrow \overline{K}N$
1703±100	ALSTON-...	78	DPWA	$\overline{K}N \rightarrow \overline{K}N$
1573± 25	GOPAL	77	DPWA	$\overline{K}N$ multichannel
1596± 6	KANE	74	DPWA	$K^-p \rightarrow \Sigma\pi$
1620± 10	LANGBEIN	72	IPWA	$\overline{K}N$ multichannel
• • • We do not use the following data for averages, fits, limits, etc. • • •				
1572 or 1617	[1] MARTIN	77	DPWA	$\overline{K}N$ multichannel
1646± 7	[2] CARROLL	76	DPWA	Isospin-0 total σ
1570	KIM	71	DPWA	K-matrix analysis

[1] The two MARTIN 77 values are from a T-matrix pole and from a Breit-Wigner fit.
[2] A total cross-section bump with (J+1/2) Γ_{el} / Γ_{total} = 0.04.

Λ(1600) WIDTH

VALUE (MeV)	DOCUMENT ID		TECN	COMMENT
50 to 250 (≈ 150) OUR ESTIMATE				
150± 28	ZHANG	13A	DPWA	Multichannel
116± 20	GOPAL	80	DPWA	$\overline{K}N \rightarrow \overline{K}N$
593±200	ALSTON-...	78	DPWA	$\overline{K}N \rightarrow \overline{K}N$
147± 50	GOPAL	77	DPWA	$\overline{K}N$ multichannel
175± 20	KANE	74	DPWA	$K^-p \rightarrow \Sigma\pi$
60± 10	LANGBEIN	72	IPWA	$\overline{K}N$ multichannel
• • • We do not use the following data for averages, fits, limits, etc. • • •				
247 or 271	[1] MARTIN	77	DPWA	$\overline{K}N$ multichannel
20	[2] CARROLL	76	DPWA	Isospin-0 total σ
50	KIM	71	DPWA	K-matrix analysis

[1] The two MARTIN 77 values are from a T-matrix pole and from a Breit-Wigner fit.
[2] A total cross-section bump with (J+1/2) Γ_{el} / Γ_{total} = 0.04.

Λ(1600) DECAY MODES

	Mode	Fraction (Γ_i/Γ)
Γ_1	$N\overline{K}$	15–30 %
Γ_2	$\Sigma\pi$	10–60 %
Γ_3	$\Sigma(1385)\pi$	

Λ(1600) BRANCHING RATIOS

See "Sign conventions for resonance couplings" in the Note on Λ and Σ Resonances.

$\Gamma(N\overline{K})/\Gamma_{total}$ Γ_1/Γ

VALUE	DOCUMENT ID		TECN	COMMENT
0.15 to 0.30 OUR ESTIMATE				
0.14 ±0.04	ZHANG	13A	DPWA	Multichannel
0.23 ±0.04	GOPAL	80	DPWA	$\overline{K}N \rightarrow \overline{K}N$
0.14 ±0.05	ALSTON-...	78	DPWA	$\overline{K}N \rightarrow \overline{K}N$
0.25 ±0.15	LANGBEIN	72	IPWA	$\overline{K}N$ multichannel
• • • We do not use the following data for averages, fits, limits, etc. • • •				
0.064	[1] KAMANO	15	DPWA	Multichannel
0.24 ±0.04	GOPAL	77	DPWA	See GOPAL 80
0.30 or 0.29	[2] MARTIN	77	DPWA	$\overline{K}N$ multichannel

[1] From the preferred solution A in KAMANO 15.
[2] The two MARTIN 77 values are from a T-matrix pole and from a Breit-Wigner fit.

$\Gamma(\Sigma\pi)/\Gamma_{total}$ Γ_2/Γ

VALUE	DOCUMENT ID		TECN	COMMENT
• • • We do not use the following data for averages, fits, limits, etc. • • •				
0.851	[1] KAMANO	15	DPWA	Multichannel

[1] From the preferred solution A in KAMANO 15.

$\Gamma(\Sigma(1385)\pi)/\Gamma_{total}$ Γ_3/Γ

VALUE	DOCUMENT ID		TECN	COMMENT
• • • We do not use the following data for averages, fits, limits, etc. • • •				
0.085	[1] KAMANO	15	DPWA	Multichannel

[1] From the preferred solution A in KAMANO 15.

$(\Gamma_i\Gamma_f)^{1/2}/\Gamma_{total}$ in $N\overline{K} \rightarrow$ Λ(1600) $\rightarrow \Sigma\pi$ $(\Gamma_1\Gamma_2)^{1/2}/\Gamma$

VALUE	DOCUMENT ID		TECN	COMMENT
−0.23±0.03	ZHANG	13A	DPWA	Multichannel
−0.16±0.04	GOPAL	77	DPWA	$\overline{K}N$ multichannel
−0.33±0.11	KANE	74	DPWA	$K^-p \rightarrow \Sigma\pi$
0.28±0.09	LANGBEIN	72	IPWA	$\overline{K}N$ multichannel
• • • We do not use the following data for averages, fits, limits, etc. • • •				
−0.39 or −0.39	[1] MARTIN	77	DPWA	$\overline{K}N$ multichannel
not seen	HEPP	76B	DPWA	$K^-N \rightarrow \Sigma\pi$

[1] The two MARTIN 77 values are from a T-matrix pole and from a Breit-Wigner fit.

Λ(1600) REFERENCES

KAMANO	15	PR C92 025205	H. Kamano *et al.*	(ANL, OSAK)
ZHANG	13A	PR C88 035205	H. Zhang *et al.*	(KSU)
GOPAL	80	Toronto Conf. 159	G.P. Gopal	(RHEL) IJP
ALSTON-...	78	PR D18 182	M. Alston-Garnjost *et al.*	(LBL, MTHO+) IJP
Also		PRL 38 1007	M. Alston-Garnjost *et al.*	(LBL, MTHO+) IJP
GOPAL	77	NP B119 362	G.P. Gopal *et al.*	(LOIC, RHEL) IJP
MARTIN	77	NP B127 349	B.R. Martin, M.K. Pidcock, R.G. Moorhouse	(LOUC+) IJP
Also		NP B126 266	B.R. Martin, M.K. Pidcock	(LOUC)
Also		NP B126 285	B.R. Martin, M.K. Pidcock	(LOUC) IJP
CARROLL	76	PRL 37 806	A.S. Carroll *et al.*	(BNL) I
HEPP	76B	PL 65B 487	V. Hepp *et al.*	(CERN, HEIDH, MPIM) IJP
KANE	74	LBL-2452	D.F. Kane	(LBL) IJP
LANGBEIN	72	NP B47 477	W. Langbein, F. Wagner	(MPIM) IJP
KIM	71	PRL 27 356	J.K. Kim	(HARV) IJP

Λ(1670) 1/2−

$I(J^P) = 0(\frac{1}{2}^-)$ Status: ****

The measurements of the mass, width, and elasticity published before 1974 are now obsolete and have been omitted. They were last listed in our 1982 edition Physics Letters **111B** 1 (1982).

Λ(1670) POLE POSITIONS

REAL PART

VALUE (MeV)	DOCUMENT ID		TECN	COMMENT
1669^{+3}_{-8}	[1] KAMANO	15	DPWA	Multichannel
• • • We do not use the following data for averages, fits, limits, etc. • • •				
1667	ZHANG	13A	DPWA	Multichannel

[1] From the preferred solution A in KAMANO 15.

−2×IMAGINARY PART

VALUE (MeV)	DOCUMENT ID		TECN	COMMENT
19^{+18}_{-2}	[1] KAMANO	15	DPWA	Multichannel
• • • We do not use the following data for averages, fits, limits, etc. • • •				
26	ZHANG	13A	DPWA	Multichannel

[1] From the preferred solution A in KAMANO 15.

Λ(1670) POLE RESIDUES

The normalized residue is the residue divided by $\Gamma_{pole}/2$.

Normalized residue in $\overline{K}N \rightarrow \Lambda(1670) \rightarrow \overline{K}N$

MODULUS	PHASE (°)	DOCUMENT ID		TECN	COMMENT
• • • We do not use the following data for averages, fits, limits, etc. • • •					
0.351	164	[1] KAMANO	15	DPWA	Multichannel

[1] From the preferred solution A in KAMANO 15.

Normalized residue in $N\overline{K} \rightarrow \Lambda(1670) \rightarrow \Sigma\pi$

MODULUS	PHASE (°)	DOCUMENT ID		TECN	COMMENT
• • • We do not use the following data for averages, fits, limits, etc. • • •					
0.327	125	[1] KAMANO	15	DPWA	Multichannel

[1] From the preferred solution A in KAMANO 15.

Normalized residue in $N\overline{K} \rightarrow \Lambda(1670) \rightarrow \Lambda\eta$

MODULUS	PHASE (°)	DOCUMENT ID		TECN	COMMENT
• • • We do not use the following data for averages, fits, limits, etc. • • •					
0.474	59	[1] KAMANO	15	DPWA	Multichannel

[1] From the preferred solution A in KAMANO 15.

Normalized residue in $N\overline{K} \rightarrow \Lambda(1670) \rightarrow \Sigma(1385)\pi$

MODULUS	PHASE (°)	DOCUMENT ID		TECN	COMMENT
• • • We do not use the following data for averages, fits, limits, etc. • • •					
0.0988	−104	[1] KAMANO	15	DPWA	Multichannel

[1] From the preferred solution A in KAMANO 15.

Λ(1670) MASS

VALUE (MeV)	DOCUMENT ID		TECN	COMMENT
1660 to 1680 (≈ 1670) OUR ESTIMATE				
1672 ±3	ZHANG	13A	DPWA	Multichannel
1677.5 ± 0.8	[1] GARCIA-REC...	03	DPWA	$\overline{K}N$ multichannel
1673 ±2	MANLEY	02	DPWA	$\overline{K}N$ multichannel
1670.8 ± 1.7	KOISO	85	DPWA	$K^-p \rightarrow \Sigma\pi$
1667 ±5	GOPAL	80	DPWA	$\overline{K}N \rightarrow \overline{K}N$
1671 ±3	ALSTON-...	78	DPWA	$\overline{K}N \rightarrow \overline{K}N$
1670 ±5	GOPAL	77	DPWA	$\overline{K}N$ multichannel
1675 ±2	HEPP	76B	DPWA	$K^-N \rightarrow \Sigma\pi$
1679 ±1	KANE	74	DPWA	$K^-p \rightarrow \Sigma\pi$
1665 ±5	PREVOST	74	DPWA	$K^-N \rightarrow \Sigma(1385)\pi$
• • • We do not use the following data for averages, fits, limits, etc. • • •				
1668.9 ± 2.0	ABAEV	96	DPWA	$K^-p \rightarrow \Lambda\eta$
1664	[2] MARTIN	77	DPWA	$\overline{K}N$ multichannel

[1] GARCIA-RECIO 03 gives pole, not Breit-Wigner, parameters, but the narrow width of the Λ(1670) means there will be little difference.

[2] MARTIN 77 obtains identical resonance parameters from a T-matrix pole and from a Breit-Wigner fit.

Λ(1670) WIDTH

VALUE (MeV)	DOCUMENT ID		TECN	COMMENT
25 to 50 (≈ 35) OUR ESTIMATE				
29 ± 5	ZHANG	13A	DPWA	Multichannel
29.2 ± 1.4	[1] GARCIA-REC...	03	DPWA	$\overline{K}N$ multichannel
23 ± 6	MANLEY	02	DPWA	$\overline{K}N$ multichannel
34.1 ± 3.7	KOISO	85	DPWA	$K^-p \rightarrow \Sigma\pi$
29 ± 5	GOPAL	80	DPWA	$\overline{K}N \rightarrow \overline{K}N$
29 ± 5	ALSTON-...	78	DPWA	$\overline{K}N \rightarrow \overline{K}N$
45 ±10	GOPAL	77	DPWA	$\overline{K}N$ multichannel
46 ± 5	HEPP	76B	DPWA	$K^-N \rightarrow \Sigma\pi$
40 ± 3	KANE	74	DPWA	$K^-p \rightarrow \Sigma\pi$
19 ± 5	PREVOST	74	DPWA	$K^-N \rightarrow \Sigma(1385)\pi$
• • • We do not use the following data for averages, fits, limits, etc. • • •				
21.1 ± 3.6	ABAEV	96	DPWA	$K^-p \rightarrow \Lambda\eta$
12	[2] MARTIN	77	DPWA	$\overline{K}N$ multichannel

[1] GARCIA-RECIO 03 gives pole, not Breit-Wigner, parameters, but the narrow width of the Λ(1670) means there will be little difference.

[2] MARTIN 77 obtains identical resonance parameters from a T-matrix pole and from a Breit-Wigner fit.

Λ(1670) DECAY MODES

	Mode	Fraction (Γ_i/Γ)
Γ_1	$N\overline{K}$	20–30 %
Γ_2	$\Sigma\pi$	25–55 %
Γ_3	$\Lambda\eta$	10–25 %
Γ_4	$\Sigma(1385)\pi$, D-wave	
Γ_5	$N\overline{K}^*(892)$, S=1/2, S-wave	
Γ_6	$N\overline{K}^*(892)$, S=3/2, D-wave	(5 ± 4) %

Λ(1670) BRANCHING RATIOS

See "Sign conventions for resonance couplings" in the Note on Λ and Σ Resonances.

$\Gamma(N\overline{K})/\Gamma_{total}$ Γ_1/Γ

VALUE	DOCUMENT ID		TECN	COMMENT
0.20 to 0.30 OUR ESTIMATE				
0.26 ±0.25	ZHANG	13A	DPWA	Multichannel
0.37 ±0.07	MANLEY	02	DPWA	$\overline{K}N$ multichannel
0.18 ±0.03	GOPAL	80	DPWA	$\overline{K}N \rightarrow \overline{K}N$
0.17 ±0.03	ALSTON-...	78	DPWA	$\overline{K}N \rightarrow \overline{K}N$
• • • We do not use the following data for averages, fits, limits, etc. • • •				
0.318	[1] KAMANO	15	DPWA	Multichannel
0.20 ±0.03	GOPAL	77	DPWA	See GOPAL 80
0.15	[2] MARTIN	77	DPWA	$\overline{K}N$ multichannel

[1] From the preferred solution A in KAMANO 15.

[2] MARTIN 77 obtains identical resonance parameters from a T-matrix pole and from a Breit-Wigner fit.

$\Gamma(\Sigma\pi)/\Gamma_{total}$ Γ_2/Γ

VALUE	DOCUMENT ID		TECN	COMMENT
• • • We do not use the following data for averages, fits, limits, etc. • • •				
0.289	[1] KAMANO	15	DPWA	Multichannel

[1] From the preferred solution A in KAMANO 15.

$\Gamma(\Lambda\eta)/\Gamma_{total}$ Γ_3/Γ

VALUE	DOCUMENT ID		TECN	COMMENT
• • • We do not use the following data for averages, fits, limits, etc. • • •				
0.373	KAMANO	15	DPWA	Multichannel
0.30 ±0.08	ABAEV	96	DPWA	$K^-p \rightarrow \Lambda\eta$

$\Gamma(\Sigma(1385)\pi, D\text{-wave})/\Gamma_{total}$ Γ_4/Γ

VALUE	DOCUMENT ID		TECN	COMMENT
• • • We do not use the following data for averages, fits, limits, etc. • • •				
0.019	KAMANO	15	DPWA	Multi-channel

$\Gamma(N\overline{K}^*(892), S{=}1/2, S\text{-wave})/\Gamma_{total}$ Γ_5/Γ

VALUE	DOCUMENT ID		TECN	COMMENT
• • • We do not use the following data for averages, fits, limits, etc. • • •				
not seen	[1] KAMANO	15	DPWA	Multichannel

[1] Not seen in the preferred solution A in KAMANO 15.

$\Gamma(N\overline{K}^*(892), S{=}3/2, D\text{-wave})/\Gamma_{total}$ Γ_6/Γ

VALUE	DOCUMENT ID		TECN	COMMENT
0.05 ± 0.04	ZHANG	13A	DPWA	Multichannel
• • • We do not use the following data for averages, fits, limits, etc. • • •				
not seen	[1] KAMANO	15	DPWA	Multichannel

[1] Not seen in the preferred solution A in KAMANO 15.

$(\Gamma_i\Gamma_f)^{1/2}/\Gamma_{total}$ in $N\overline{K} \rightarrow \Lambda(1670) \rightarrow \Sigma\pi$ $(\Gamma_1\Gamma_2)^{1/2}/\Gamma$

VALUE	DOCUMENT ID		TECN	COMMENT
−0.29 ± 0.06	ZHANG	13A	DPWA	Multichannel
−0.38 ± 0.03	MANLEY	02	DPWA	$\overline{K}N$ multichannel
−0.26 ± 0.02	KOISO	85	DPWA	$K^-p \rightarrow \Sigma\pi$
−0.31 ± 0.03	GOPAL	77	DPWA	$\overline{K}N$ multichannel
−0.29 ± 0.03	HEPP	76B	DPWA	$K^-N \rightarrow \Sigma\pi$
−0.23 ± 0.03	LONDON	75	HLBC	$K^-p \rightarrow \Sigma^0\pi^0$
−0.27 ± 0.02	KANE	74	DPWA	$K^-p \rightarrow \Sigma\pi$
• • • We do not use the following data for averages, fits, limits, etc. • • •				
−0.13	[1] MARTIN	77	DPWA	$\overline{K}N$ multichannel

[1] MARTIN 77 obtains identical resonance parameters from a T-matrix pole and from a Breit-Wigner fit.

$(\Gamma_i\Gamma_f)^{1/2}/\Gamma_{total}$ in $N\overline{K} \rightarrow \Lambda(1670) \rightarrow \Lambda\eta$ $(\Gamma_1\Gamma_3)^{1/2}/\Gamma$

VALUE	DOCUMENT ID		TECN	COMMENT
−0.30 ± 0.10	ZHANG	13A	DPWA	Multichannel
+0.24 ± 0.04	MANLEY	02	DPWA	$\overline{K}N$ multichannel
+0.20 ± 0.05	BAXTER	73	DPWA	$K^-p \rightarrow$ neutrals
• • • We do not use the following data for averages, fits, limits, etc. • • •				
0.24	KIM	71	DPWA	K-matrix analysis
0.26	ARMENTEROS	69C	HBC	
0.20 or 0.23	BERLEY	65	HBC	

$(\Gamma_i\Gamma_f)^{1/2}/\Gamma_{total}$ in $N\overline{K} \to \Lambda(1670) \to \Sigma(1385)\pi$, D-wave — $(\Gamma_1\Gamma_4)^{1/2}/\Gamma$

VALUE	DOCUMENT ID		TECN	COMMENT
-0.17 ± 0.06	MANLEY	02	DPWA	$\overline{K}N$ multichannel
-0.18 ± 0.05	PREVOST	74	DPWA	$K^-N \to \Sigma(1385)\pi$

Λ(1670) REFERENCES

KAMANO	15	PR C92 025205	H. Kamano *et al.*	(ANL, OSAK)
ZHANG	13A	PR C88 035205	H. Zhang *et al.*	(KSU)
GARCIA-REC...	03	PR D67 076009	C. Garcia-Recio *et al.*	(GRAN, VALE)
MANLEY	02	PRL 88 012002	D.M. Manley *et al.*	(BNL Crystal Ball Collab.)
ABAEV	96	PR C53 385	V.V. Abaev, B.M.K. Nefkens	(UCLA)
KOISO	85	NP A433 619	H. Koiso *et al.*	(TOKY, MASA)
PDG	82	PL 111B 1	M. Roos *et al.*	(HELS, CIT, CERN)
GOPAL	80	Toronto Conf. 159	G.P. Gopal	(RHEL) IJP
ALSTON-...	78	PR D18 182	M. Alston-Garnjost *et al.*	(LBL, MTHO+) IJP
Also		PRL 38 1007	M. Alston-Garnjost *et al.*	(LBL, MTHO+) IJP
GOPAL	77	NP B119 362	G.P. Gopal *et al.*	(LOIC, RHEL) IJP
MARTIN	77	NP B127 349	B.R. Martin, M.K. Pidcock, R.G. Moorhouse	(LOUC+) IJP
Also		NP B126 266	B.R. Martin, M.K. Pidcock	(LOUC)
Also		NP B126 285	B.R. Martin, M.K. Pidcock	(LOUC) IJP
HEPP	76B	PL 65B 487	V. Hepp *et al.*	(CERN, HEIDH, MPIM) IJP
LONDON	75	NP B85 289	G.W. London *et al.*	(BNL, CERN, EPOL+)
KANE	74	LBL-2452	D.F. Kane	(LBL) IJP
PREVOST	74	NP B69 246	J. Prevost *et al.*	(SACL, CERN, HEID)
BAXTER	73	NP B67 125	D.F. Baxter *et al.*	(OXF) IJP
KIM	71	PRL 27 356	J.K. Kim	(HARV) IJP
Also		Duke Conf. 161 Hyperon Resonances, 1970	J.K. Kim	(HARV) IJP
ARMENTEROS 69C		Lund Paper 229 Values are quoted in LEVI-SETTI 69.	R. Armenteros *et al.*	(CERN, HEID, SACL) IJP
BERLEY	65	PRL 15 641	D. Berley *et al.*	(BNL) IJP

Λ(1690) 3/2⁻

$I(J^P) = 0(\frac{3}{2}^-)$ Status: ****

The measurements of the mass, width, and elasticity published before 1974 are now obsolete and have been omitted. They were last listed in our 1982 edition Physics Letters **111B** 1 (1982).

Λ(1690) POLE POSITION

REAL PART

VALUE (MeV)	DOCUMENT ID		TECN	COMMENT
1697^{+6}_{-6}	[1] KAMANO	15	DPWA	Multichannel
• • • We do not use the following data for averages, fits, limits, etc. • • •				
1689	ZHANG	13A	DPWA	Multichannel

[1] From the preferred solution A in KAMANO 15.

$-2\times$IMAGINARY PART

VALUE (MeV)	DOCUMENT ID		TECN	COMMENT
65 ± 14	[1] KAMANO	15	DPWA	Multichannel
• • • We do not use the following data for averages, fits, limits, etc. • • •				
53	ZHANG	13A	DPWA	Multichannel

[1] From the preferred solution A in KAMANO 15.

Λ(1690) POLE RESIDUES

The normalized residue is the residue divided by $\Gamma_{pole}/2$.

Normalized residue in $N\overline{K} \to \Lambda(1690) \to N\overline{K}$

MODULUS	PHASE (°)	DOCUMENT ID		TECN	COMMENT
• • • We do not use the following data for averages, fits, limits, etc. • • •					
0.251	3	[1] KAMANO	15	DPWA	Multichannel

[1] From the preferred solution A in KAMANO 15.

Normalized residue in $N\overline{K} \to \Lambda(1690) \to \Sigma\pi$

MODULUS	PHASE (°)	DOCUMENT ID		TECN	COMMENT
• • • We do not use the following data for averages, fits, limits, etc. • • •					
0.315	-173	[1] KAMANO	15	DPWA	Multichannel

[1] From the preferred solution A in KAMANO 15.

Normalized residue in $N\overline{K} \to \Lambda(1690) \to \Lambda\eta$

MODULUS	PHASE (°)	DOCUMENT ID		TECN	COMMENT
• • • We do not use the following data for averages, fits, limits, etc. • • •					
0.00567	81	[1] KAMANO	15	DPWA	Multichannel

[1] From the preferred solution A in KAMANO 15.

Normalized residue in $N\overline{K} \to \Lambda(1690) \to \Sigma(1385)\pi$, S-wave

MODULUS	PHASE (°)	DOCUMENT ID		TECN	COMMENT
• • • We do not use the following data for averages, fits, limits, etc. • • •					
0.134	168	[1] KAMANO	15	DPWA	Multichannel

[1] From the preferred solution A in KAMANO 15.

Normalized residue in $N\overline{K} \to \Lambda(1690) \to \Sigma(1385)\pi$, D-wave

MODULUS	PHASE (°)	DOCUMENT ID		TECN	COMMENT
• • • We do not use the following data for averages, fits, limits, etc. • • •					
0.319	-22	[1] KAMANO	15	DPWA	Multichannel

[1] From the preferred solution A in KAMANO 15.

Λ(1690) MASS

VALUE (MeV)	DOCUMENT ID		TECN	COMMENT
1685 to 1695 (≈ 1690) OUR ESTIMATE				
1691 ±3	ZHANG	13A	DPWA	Multichannel
1695.7 ± 2.6	KOISO	85	DPWA	$K^-p \to \Sigma\pi$
1690 ±5	GOPAL	80	DPWA	$\overline{K}N \to \overline{K}N$
1692 ±5	ALSTON-...	78	DPWA	$\overline{K}N \to \overline{K}N$
1690 ±5	GOPAL	77	DPWA	$\overline{K}N$ multichannel
1690 ±3	HEPP	76B	DPWA	$K^-N \to \Sigma\pi$
1689 ±1	KANE	74	DPWA	$K^-p \to \Sigma\pi$
• • • We do not use the following data for averages, fits, limits, etc. • • •				
1687 or 1689	[1] MARTIN	77	DPWA	$\overline{K}N$ multichannel
1692 ±4	CARROLL	76	DPWA	Isospin-0 total σ

[1] The two MARTIN 77 values are from a T-matrix pole and from a Breit-Wigner fit. Another D_{03} Λ at 1966 MeV is also suggested by MARTIN 77, but is very uncertain.

Λ(1690) WIDTH

VALUE (MeV)	DOCUMENT ID		TECN	COMMENT
50 to 70 (≈ 60) OUR ESTIMATE				
54 ± 5	ZHANG	13A	DPWA	Multichannel
67.2 ± 5.6	KOISO	85	DPWA	$K^-p \to \Sigma\pi$
61 ± 5	GOPAL	80	DPWA	$\overline{K}N \to \overline{K}N$
64 ±10	ALSTON-...	78	DPWA	$\overline{K}N \to \overline{K}N$
60 ± 5	GOPAL	77	DPWA	$\overline{K}N$ multichannel
82 ± 8	HEPP	76B	DPWA	$K^-N \to \Sigma\pi$
60 ± 4	KANE	74	DPWA	$K^-p \to \Sigma\pi$
• • • We do not use the following data for averages, fits, limits, etc. • • •				
62 or 62	[1] MARTIN	77	DPWA	$\overline{K}N$ multichannel
38	CARROLL	76	DPWA	Isospin-0 total σ

[1] The two MARTIN 77 values are from a T-matrix pole and from a Breit-Wigner fit. Another D_{03} Λ at 1966 MeV is also suggested by MARTIN 77, but is very uncertain.

Λ(1690) DECAY MODES

	Mode	Fraction (Γ_i/Γ)
Γ_1	$N\overline{K}$	20–30 %
Γ_2	$\Sigma\pi$	20–40 %
Γ_3	$\Lambda\pi\pi$	∼ 25 %
Γ_4	$\Sigma\pi\pi$	∼ 20 %
Γ_5	$\Lambda\eta$	
Γ_6	$\Sigma(1385)\pi$, S-wave	
Γ_7	$\Sigma(1385)\pi$, D-wave	
Γ_8	$N\overline{K}^*(892)$, S=1/2, D-wave	
Γ_9	$N\overline{K}^*(892)$, S=3/2, S-wave	
Γ_{10}	$N\overline{K}^*(892)$, S=3/2, D-wave	

Λ(1690) BRANCHING RATIOS

The sum of all the quoted branching ratios is more than 1.0. The two-body ratios are from partial-wave analyses, and thus probably are more reliable than the three-body ratios, which are determined from bumps in cross sections. Of the latter, the $\Sigma\pi\pi$ bump looks more significant. (The error given for the $\Lambda\pi\pi$ ratio looks unreasonably small.) Hardly any of the $\Sigma\pi\pi$ decay can be via Σ(1385), for then seven times as much $\Lambda\pi\pi$ decay would be required. See "Sign conventions for resonance couplings" in the Note on Λ and Σ Resonances.

$\Gamma(N\overline{K})/\Gamma_{total}$ — Γ_1/Γ

VALUE	DOCUMENT ID		TECN	COMMENT
0.2 to 0.3 OUR ESTIMATE				
0.25 ± 0.04	ZHANG	13A	DPWA	Multichannel
0.23 ± 0.03	GOPAL	80	DPWA	$\overline{K}N \to \overline{K}N$
0.22 ± 0.03	ALSTON-...	78	DPWA	$\overline{K}N \to \overline{K}N$
• • • We do not use the following data for averages, fits, limits, etc. • • •				
0.239	[1] KAMANO	15	DPWA	Multichannel
0.24 ± 0.03	GOPAL	77	DPWA	See GOPAL 80
0.28 or 0.26	[2] MARTIN	77	DPWA	$\overline{K}N$ multichannel

[1] From the preferred solution A in KAMANO 15.

[2] The two MARTIN 77 values are from a T-matrix pole and from a Breit-Wigner fit. Another D_{03} Λ at 1966 MeV is also suggested by MARTIN 77, but is very uncertain.

$\Gamma(\Sigma\pi)/\Gamma_{total}$ Γ_2/Γ

VALUE	DOCUMENT ID		TECN	COMMENT
• • • We do not use the following data for averages, fits, limits, etc. • • •				
0.387	[1] KAMANO	15	DPWA	Multichannel

[1] From the preferred solution A in KAMANO 15.

$\Gamma(\Lambda\eta)/\Gamma_{total}$ Γ_5/Γ

VALUE	DOCUMENT ID		TECN	COMMENT
• • • We do not use the following data for averages, fits, limits, etc. • • •				
not seen	[1] KAMANO	15	DPWA	Multichannel

[1] From the preferred solution A in KAMANO 15.

$\Gamma(\Sigma(1385)\pi$, S-wave$)/\Gamma_{total}$ Γ_6/Γ

VALUE	DOCUMENT ID		TECN	COMMENT
• • • We do not use the following data for averages, fits, limits, etc. • • •				
0.062	[1] KAMANO	15	DPWA	Multichannel

[1] From the preferred solution A in KAMANO 15.

$\Gamma(\Sigma(1385)\pi$, D-wave$)/\Gamma_{total}$ Γ_7/Γ

VALUE	DOCUMENT ID		TECN	COMMENT
• • • We do not use the following data for averages, fits, limits, etc. • • •				
0.308	[1] KAMANO	15	DPWA	Multichannel

[1] From the preferred solution A in KAMANO 15.

$\Gamma(N\overline{K}^*(892)$, S=1/2, D-wave$)/\Gamma_{total}$ Γ_8/Γ

VALUE	DOCUMENT ID		TECN	COMMENT
• • • We do not use the following data for averages, fits, limits, etc. • • •				
not seen	[1] KAMANO	15	DPWA	Multichannel

[1] From the preferred solution A in KAMANO 15.

$\Gamma(N\overline{K}^*(892)$, S=3/2, S-wave$)/\Gamma_{total}$ Γ_9/Γ

VALUE	DOCUMENT ID		TECN	COMMENT
• • • We do not use the following data for averages, fits, limits, etc. • • •				
0.003	KAMANO	15	DPWA	Multichannel

$\Gamma(N\overline{K}^*(892)$, S=3/2, D-wave$)/\Gamma_{total}$ Γ_{10}/Γ

VALUE	DOCUMENT ID		TECN	COMMENT
• • • We do not use the following data for averages, fits, limits, etc. • • •				
not seen	[1] KAMANO	15	DPWA	Multichannel

[1] From the preferred solution A in KAMANO 15.

$(\Gamma_i\Gamma_f)^{1/2}/\Gamma_{total}$ in $N\overline{K} \to \Lambda(1690) \to \Sigma\pi$ $(\Gamma_1\Gamma_2)^{1/2}/\Gamma$

VALUE	DOCUMENT ID		TECN	COMMENT
-0.27 ± 0.03	ZHANG	13A	DPWA	Multichannel
-0.34 ± 0.02	KOISO	85	DPWA	$K^-p \to \Sigma\pi$
-0.25 ± 0.03	GOPAL	77	DPWA	$\overline{K}N$ multichannel
-0.29 ± 0.03	HEPP	76B	DPWA	$K^-N \to \Sigma\pi$
-0.28 ± 0.03	LONDON	75	HLBC	$K^-p \to \Sigma^0\pi^0$
-0.28 ± 0.02	KANE	74	DPWA	$K^-p \to \Sigma\pi$
• • • We do not use the following data for averages, fits, limits, etc. • • •				
-0.30 or -0.28	[1] MARTIN	77	DPWA	$\overline{K}N$ multichannel

[1] The two MARTIN 77 values are from a T-matrix pole and from a Breit-Wigner fit. Another D_{03} Λ at 1966 MeV is also suggested by MARTIN 77, but is very uncertain.

$(\Gamma_i\Gamma_f)^{1/2}/\Gamma_{total}$ in $N\overline{K} \to \Lambda(1690) \to \Lambda\pi\pi$ $(\Gamma_1\Gamma_3)^{1/2}/\Gamma$

VALUE	DOCUMENT ID		TECN	COMMENT
• • • We do not use the following data for averages, fits, limits, etc. • • •				
0.25 ± 0.02	[1] BARTLEY	68	HDBC	$K^-p \to \Lambda\pi\pi$

[1] BARTLEY 68 uses only cross-section data. The enhancement is not seen by PREVOST 71.

$(\Gamma_i\Gamma_f)^{1/2}/\Gamma_{total}$ in $N\overline{K} \to \Lambda(1690) \to \Sigma\pi\pi$ $(\Gamma_1\Gamma_4)^{1/2}/\Gamma$

VALUE	DOCUMENT ID		TECN	COMMENT
0.21	ARMENTEROS	68C	HDBC	$K^-N \to \Sigma\pi\pi$

$(\Gamma_i\Gamma_f)^{1/2}/\Gamma_{total}$ in $N\overline{K} \to \Lambda(1690) \to \Lambda\eta$ $(\Gamma_1\Gamma_5)^{1/2}/\Gamma$

VALUE	DOCUMENT ID		TECN	COMMENT
0.00 ± 0.03	BAXTER	73	DPWA	$K^-p \to$ neutrals

$(\Gamma_i\Gamma_f)^{1/2}/\Gamma_{total}$ in $N\overline{K} \to \Lambda(1690) \to \Sigma(1385)\pi$, S-wave $(\Gamma_1\Gamma_6)^{1/2}/\Gamma$

VALUE	DOCUMENT ID		TECN	COMMENT
-0.28 ± 0.06	ZHANG	13A	DPWA	Multichannel
$+0.27\pm0.04$	PREVOST	74	DPWA	$K^-N \to \Sigma(1385)\pi$

$\Lambda(1690)$ REFERENCES

KAMANO	15	PR C92 025205	H. Kamano *et al.*	(ANL, OSAK)
ZHANG	13A	PR C88 035205	H. Zhang *et al.*	(KSU)
KOISO	85	NP A433 619	H. Koiso *et al.*	(TOKY, MASA)
PDG	82	PL 111B 1	M. Roos *et al.*	(HELS, CIT, CERN)
GOPAL	80	Toronto Conf. 159	G.P. Gopal	(RHEL) IJP
ALSTON-...	78	PR D18 182	M. Alston-Garnjost *et al.*	(LBL, MTHO+) IJP
Also		PRL 38 1007	M. Alston-Garnjost *et al.*	(LBL, MTHO+) IJP
GOPAL	77	NP B119 362	G.P. Gopal *et al.*	(LOIC, RHEL) IJP
MARTIN	77	NP B127 349	B.R. Martin, M.K. Pidcock, R.G. Moorhouse	(LOUC+) IJP
Also		NP B126 266	B.R. Martin, M.K. Pidcock	(LOUC)
Also		NP B126 285	B.R. Martin, M.K. Pidcock	(LOUC) IJP
CARROLL	76	PRL 37 806	A.S. Carroll *et al.*	(BNL) I
HEPP	76B	PL 65B 487	V. Hepp *et al.*	(CERN, HEIDH, MPIM) IJP
LONDON	75	NP B85 289	G.W. London *et al.*	(BNL, CERN, EPOL+)
KANE	74	LBL-2452	D.F. Kane	(LBL) IJP
PREVOST	74	NP B69 246	J. Prevost *et al.*	(SACL, CERN, HEID)
BAXTER	73	NP B67 125	D.F. Baxter *et al.*	(OXF) IJP
PREVOST	71	Amsterdam Conf.	J. Prevost	(CERN, HEID, SACL)
ARMENTEROS	68C	NP B8 216	R. Armenteros *et al.*	(CERN, HEID, SACL) I
BARTLEY	68	PRL 21 1111	J.H. Bartley *et al.*	(TUFTS, FSU, BRAN) I

$\Lambda(1710)\ 1/2^+$

$I(J^P) = 0(\frac{1}{2}^+)$ Status: *

OMITTED FROM SUMMARY TABLE

$\Lambda(1710)$ MASS

VALUE (MeV)	DOCUMENT ID		TECN	COMMENT
1713±13	ZHANG	13A	DPWA	Multichannel

$\Lambda(1710)$ WIDTH

VALUE (MeV)	DOCUMENT ID		TECN	COMMENT
180±42	ZHANG	13A	DPWA	Multichannel

$\Lambda(1710)$ DECAY MODES

	Mode	Fraction (Γ_i/Γ)
Γ_1	$N\overline{K}$	(43±4) %
Γ_2	$\Sigma\pi$	(21±5) %
Γ_3	$\Sigma^*(1385)\pi$, P-wave	(20±8) %
Γ_4	$N\overline{K}^*(892)$	
Γ_5	$N\overline{K}^*(892)$, S=1/2	(5±4) %
Γ_6	$N\overline{K}^*(892)$, S=3/2, P-wave	(10±8) %

$\Lambda(1710)$ BRANCHING RATIOS

$\Gamma(N\overline{K})/\Gamma_{total}$ Γ_1/Γ

VALUE	DOCUMENT ID		TECN	COMMENT
0.43±0.04	ZHANG	13A	DPWA	Multichannel

$\Gamma(\Sigma\pi)/\Gamma_{total}$ Γ_2/Γ

VALUE	DOCUMENT ID		TECN	COMMENT
0.21±0.05	ZHANG	13A	DPWA	Multichannel

$\Gamma(\Sigma^*(1385)\pi$, P-wave$)/\Gamma_{total}$ Γ_3/Γ

VALUE	DOCUMENT ID		TECN	COMMENT
0.20±0.08	ZHANG	13A	DPWA	Multichannel

$\Gamma(N\overline{K}^*(892)$, S=1/2$)/\Gamma_{total}$ Γ_5/Γ

VALUE	DOCUMENT ID		TECN	COMMENT
0.05±0.04	ZHANG	13A	DPWA	Multichannel

$\Gamma(N\overline{K}^*(892)$, S=3/2, P-wave$)/\Gamma_{total}$ Γ_6/Γ

VALUE	DOCUMENT ID		TECN	COMMENT
0.10±0.08	ZHANG	13A	DPWA	Multichannel

$\Lambda(1710)$ REFERENCES

ZHANG	13A	PR C88 035205	H. Zhang *et al.*	(KSU)

$\Lambda(1800)\ 1/2^-$

$I(J^P) = 0(\frac{1}{2}^-)$ Status: ***

This is the second resonance in the S_{01} wave, the first being the $\Lambda(1670)$.

$\Lambda(1800)$ POLE POSITION

REAL PART

VALUE (MeV)	DOCUMENT ID		TECN	COMMENT
• • • We do not use the following data for averages, fits, limits, etc. • • •				
1729	ZHANG	13A	DPWA	Multichannel

Baryon Particle Listings

Λ(1800), Λ(1810)

−2×IMAGINARY PART

VALUE (MeV)	DOCUMENT ID		TECN	COMMENT
• • • We do not use the following data for averages, fits, limits, etc. • • •				
198	ZHANG	13A	DPWA	Multichannel

Λ(1800) MASS

VALUE (MeV)	DOCUMENT ID		TECN	COMMENT
1720 to 1850 (≈ 1800) OUR ESTIMATE				
1783±19	ZHANG	13A	DPWA	Multichannel
1845±10	MANLEY	02	DPWA	$\overline{K}N$ multichannel
1841±10	GOPAL	80	DPWA	$\overline{K}N \to \overline{K}N$
1725±20	ALSTON-...	78	DPWA	$\overline{K}N \to \overline{K}N$
1825±20	GOPAL	77	DPWA	$\overline{K}N$ multichannel
1830±20	LANGBEIN	72	IPWA	$\overline{K}N$ multichannel
• • • We do not use the following data for averages, fits, limits, etc. • • •				
1767 or 1842	[1] MARTIN	77	DPWA	$\overline{K}N$ multichannel
1780	KIM	71	DPWA	K-matrix analysis
1872±10	BRICMAN	70B	DPWA	$\overline{K}N \to \overline{K}N$

Λ(1800) WIDTH

VALUE (MeV)	DOCUMENT ID		TECN	COMMENT
200 to 400 (≈ 300) OUR ESTIMATE				
256±35	ZHANG	13A	DPWA	Multichannel
518±84	MANLEY	02	DPWA	$\overline{K}N$ multichannel
228±20	GOPAL	80	DPWA	$\overline{K}N \to \overline{K}N$
185±20	ALSTON-...	78	DPWA	$\overline{K}N \to \overline{K}N$
230±20	GOPAL	77	DPWA	$\overline{K}N$ multichannel
70±15	LANGBEIN	72	IPWA	$\overline{K}N$ multichannel
• • • We do not use the following data for averages, fits, limits, etc. • • •				
435 or 473	[1] MARTIN	77	DPWA	$\overline{K}N$ multichannel
40	KIM	71	DPWA	K-matrix analysis
100±20	BRICMAN	70B	DPWA	$\overline{K}N \to \overline{K}N$

Λ(1800) DECAY MODES

	Mode	Fraction (Γ_i/Γ)
Γ_1	$N\overline{K}$	25–40 %
Γ_2	$\Sigma\pi$	seen
Γ_3	$\Sigma(1385)\pi$	seen
Γ_4	$\Lambda\eta$	(6±5) %
Γ_5	$N\overline{K}^*(892)$	seen
Γ_6	$N\overline{K}^*(892)$, S=1/2, S-wave	
Γ_7	$N\overline{K}^*(892)$, S=3/2, D-wave	

Λ(1800) BRANCHING RATIOS

See "Sign conventions for resonance couplings" in the Note on Λ and Σ Resonances.

$\Gamma(N\overline{K})/\Gamma_{total}$ Γ_1/Γ

VALUE	DOCUMENT ID		TECN	COMMENT
0.25 to 0.40 OUR ESTIMATE				
0.13±0.06	ZHANG	13A	DPWA	Multichannel
0.24±0.10	MANLEY	02	DPWA	$\overline{K}N$ multichannel
0.36±0.04	GOPAL	80	DPWA	$\overline{K}N \to \overline{K}N$
0.28±0.05	ALSTON-...	78	DPWA	$\overline{K}N \to \overline{K}N$
0.35±0.15	LANGBEIN	72	IPWA	$\overline{K}N$ multichannel
• • • We do not use the following data for averages, fits, limits, etc. • • •				
0.37±0.05	GOPAL	77	DPWA	See GOPAL 80
1.21 or 0.70	[1] MARTIN	77	DPWA	$\overline{K}N$ multichannel
0.80	KIM	71	DPWA	K-matrix analysis
0.18±0.02	BRICMAN	70B	DPWA	$\overline{K}N \to \overline{K}N$

$(\Gamma_i\Gamma_f)^{1/2}/\Gamma_{total}$ in $N\overline{K} \to \Lambda(1800) \to \Sigma\pi$ $(\Gamma_1\Gamma_2)^{1/2}/\Gamma$

VALUE	DOCUMENT ID		TECN	COMMENT
−0.07±0.02	ZHANG	13A	DPWA	Multichannel
−0.08±0.05	GOPAL	77	DPWA	$\overline{K}N$ multichannel
• • • We do not use the following data for averages, fits, limits, etc. • • •				
−0.74 or −0.43	[1] MARTIN	77	DPWA	$\overline{K}N$ multichannel
0.24	KIM	71	DPWA	K-matrix analysis

$(\Gamma_i\Gamma_f)^{1/2}/\Gamma_{total}$ in $N\overline{K} \to \Lambda(1800) \to \Sigma(1385)\pi$ $(\Gamma_1\Gamma_3)^{1/2}/\Gamma$

VALUE	DOCUMENT ID		TECN	COMMENT
−0.09 ±0.05	ZHANG	13A	DPWA	Multichannel
+0.056±0.028	[2] CAMERON	78	DPWA	$K^-p \to \Sigma(1385)\pi$

$\Gamma(\Lambda\eta)/\Gamma_{total}$ Γ_4/Γ

VALUE	DOCUMENT ID		TECN	COMMENT
0.06±0.05	ZHANG	13A	DPWA	Multichannel

$(\Gamma_i\Gamma_f)^{1/2}/\Gamma_{total}$ in $N\overline{K} \to \Lambda(1800) \to N\overline{K}^*(892)$, S=1/2, S-wave $(\Gamma_1\Gamma_6)^{1/2}/\Gamma$

VALUE	DOCUMENT ID		TECN	COMMENT
−0.13±0.02	ZHANG	13A	DPWA	Multichannel
−0.17±0.03	[2] CAMERON	78B	DPWA	$K^-p \to N\overline{K}^*$

$(\Gamma_i\Gamma_f)^{1/2}/\Gamma_{total}$ in $N\overline{K} \to \Lambda(1800) \to N\overline{K}^*(892)$, S=3/2, D-wave $(\Gamma_1\Gamma_7)^{1/2}/\Gamma$

VALUE	DOCUMENT ID		TECN	COMMENT
−0.13±0.04	CAMERON	78B	DPWA	$K^-p \to N\overline{K}^*$

Λ(1800) FOOTNOTES

[1] The two MARTIN 77 values are from a T-matrix pole and from a Breit-Wigner fit.
[2] The published sign has been changed to be in accord with the baryon-first convention.

Λ(1800) REFERENCES

ZHANG	13A	PR C88 035205	H. Zhang *et al.*	(KSU)
MANLEY	02	PRL 88 012002	D.M. Manley *et al.*	(BNL Crystal Ball Collab.)
GOPAL	80	Toronto Conf. 159	G.P. Gopal	(RHEL) IJP
ALSTON-...	78	PR D18 182	M. Alston-Garnjost *et al.*	(LBL, MTHO+) IJP
Also		PRL 38 1007	M. Alston-Garnjost *et al.*	(LBL, MTHO+) IJP
CAMERON	78	NP B143 189	W. Cameron *et al.*	(RHEL, LOIC) IJP
CAMERON	78B	NP B146 327	W. Cameron *et al.*	(RHEL, LOIC) IJP
GOPAL	77	NP B119 362	G.P. Gopal *et al.*	(LOIC, RHEL) IJP
MARTIN	77	NP B127 349	B.R. Martin, M.K. Pidcock, R.G. Moorhouse	(LOUC+) IJP
Also		NP B126 266	B.R. Martin, M.K. Pidcock	(LOUC)
Also		NP B126 285	B.R. Martin, M.K. Pidcock	(LOUC) IJP
LANGBEIN	72	NP B47 477	W. Langbein, F. Wagner	(MPIM) IJP
KIM	71	PRL 27 356	J.K. Kim	(HARV) IJP
Also		Duke Conf. 161	J.K. Kim	(HARV) IJP
Hyperon Resonances, 1970				
BRICMAN	70B	PL 33B 511	C. Bricman, M. Ferro-Luzzi, J.P. Lagnaux	(CERN) IJP

Λ(1810) 1/2+

$I(J^P) = 0(\frac{1}{2}^+)$ Status: ***

Almost all the recent analyses contain a P_{01} state, and sometimes two of them, but the masses, widths, and branching ratios vary greatly. See also the Λ(1600) P_{01}.

Λ(1810) POLE POSITION

REAL PART

VALUE (MeV)	DOCUMENT ID		TECN	COMMENT
• • • We do not use the following data for averages, fits, limits, etc. • • •				
2097^{+40}_{-1}	[1] KAMANO	15	DPWA	Multichannel
1780	ZHANG	13A	DPWA	Multichannel

[1] From the preferred solution A in KAMANO 15. Solution B reports M = 1841^{+3}_{-4} MeV.

−2×IMAGINARY PART

VALUE (MeV)	DOCUMENT ID		TECN	COMMENT
• • • We do not use the following data for averages, fits, limits, etc. • • •				
166^{+64}_{-12}	[1] KAMANO	15	DPWA	Multichannel
64	ZHANG	13A	DPWA	Multichannel

[1] From the preferred solution A in KAMANO 15. Solution B Reports Γ = 62^{+6}_{-4} MeV.

Λ(1810) POLE RESIDUES

The normalized residue is the residue divided by $\Gamma_{pole}/2$.

Normalized residue in $N\overline{K} \to \Lambda(1810) \to N\overline{K}$

MODULUS	PHASE (°)	DOCUMENT ID		TECN	COMMENT
• • • We do not use the following data for averages, fits, limits, etc. • • •					
0.205	−63	[1] KAMANO	15	DPWA	Multichannel

[1] From the preferred solution A in KAMANO 15.

Normalized residue in $N\overline{K} \to \Lambda(1810) \to \Sigma\pi$

MODULUS	PHASE (°)	DOCUMENT ID		TECN	COMMENT
• • • We do not use the following data for averages, fits, limits, etc. • • •					
0.0325	29	[1] KAMANO	15	DPWA	Multichannel

[1] From the preferred solution A in KAMANO 15.

Normalized residue in $N\overline{K} \to \Lambda(1810) \to \Lambda\eta$

MODULUS	PHASE (°)	DOCUMENT ID		TECN	COMMENT
• • • We do not use the following data for averages, fits, limits, etc. • • •					
0.155	165	[1] KAMANO	15	DPWA	Multichannel

[1] From the preferred solution A in KAMANO 15.

Normalized residue in $N\overline{K} \to \Lambda(1810) \to \Xi K$

MODULUS	PHASE (°)	DOCUMENT ID		TECN	COMMENT
• • • We do not use the following data for averages, fits, limits, etc. • • •					
0.0937	−64	[1] KAMANO	15	DPWA	Multichannel

[1] From the preferred solution A in KAMANO 15.

Normalized residue in $N\overline{K} \to \Lambda(1810) \to \Sigma(1385)\pi$

MODULUS	PHASE (°)	DOCUMENT ID		TECN	COMMENT
• • • We do not use the following data for averages, fits, limits, etc. • • •					
0.244	−10	[1] KAMANO	15	DPWA	Multichannel

[1] From the preferred solution A in KAMANO 15.

Normalized residue in $N\overline{K} \to \Lambda(1810) \to N\overline{K}^*(892)$, S=1/2, P-wave

MODULUS	PHASE (°)	DOCUMENT ID		TECN	COMMENT
• • • We do not use the following data for averages, fits, limits, etc. • • •					
0.159	−97	[1] KAMANO	15	DPWA	Multichannel

[1] From the preferred solution A in KAMANO 15.

Normalized residue in $N\overline{K} \to \Lambda(1810) \to N\overline{K}^*(892)$, S=3/2, P-wave

MODULUS	PHASE (°)	DOCUMENT ID		TECN	COMMENT
• • • We do not use the following data for averages, fits, limits, etc. • • •					
0.0497	2	[1] KAMANO	15	DPWA	Multichannel

[1] From the preferred solution A in KAMANO 15.

Λ(1810) MASS

VALUE (MeV)	DOCUMENT ID		TECN	COMMENT
1750 to 1850 (≈ 1810) OUR ESTIMATE				
1821±10	ZHANG	13A	DPWA	Multichannel
1841±20	GOPAL	80	DPWA	$\overline{K}N \to \overline{K}N$
1853±20	GOPAL	77	DPWA	$\overline{K}N$ multichannel
1735± 5	CARROLL	76	DPWA	Isospin-0 total σ
1746±10	PREVOST	74	DPWA	$K^-N \to \Sigma(1385)\pi$
1780±20	LANGBEIN	72	IPWA	$\overline{K}N$ multichannel
• • • We do not use the following data for averages, fits, limits, etc. • • •				
1861 or 1953	[1] MARTIN	77	DPWA	$\overline{K}N$ multichannel
1755	KIM	71	DPWA	K-matrix analysis
1800	ARMENTEROS	70	HBC	$\overline{K}N \to \overline{K}N$
1750	ARMENTEROS	70	HBC	$\overline{K}N \to \Sigma\pi$
1690±10	BARBARO-...	70	HBC	$\overline{K}N \to \Sigma\pi$
1740	BAILEY	69	DPWA	$\overline{K}N \to \overline{K}N$
1745	ARMENTEROS	68B	HBC	$\overline{K}N \to \overline{K}N$

[1] The two MARTIN 77 values are from a T-matrix pole and from a Breit-Wigner fit.

Λ(1810) WIDTH

VALUE (MeV)	DOCUMENT ID		TECN	COMMENT
50 to 250 (≈ 150) OUR ESTIMATE				
174±50	ZHANG	13A	DPWA	Multichannel
164±20	GOPAL	80	DPWA	$\overline{K}N \to \overline{K}N$
90±20	CAMERON	78B	DPWA	$K^-p \to N\overline{K}^*$
166±20	GOPAL	77	DPWA	$\overline{K}N$ multichannel
46±20	PREVOST	74	DPWA	$K^-N \to \Sigma(1385)\pi$
120±10	LANGBEIN	72	IPWA	$\overline{K}N$ multichannel
• • • We do not use the following data for averages, fits, limits, etc. • • •				
535 or 585	[1] MARTIN	77	DPWA	$\overline{K}N$ multichannel
28	CARROLL	76	DPWA	Isospin-0 total σ
35	KIM	71	DPWA	K-matrix analysis
30	ARMENTEROS	70	HBC	$\overline{K}N \to \overline{K}N$
70	ARMENTEROS	70	HBC	$\overline{K}N \to \Sigma\pi$
22	BARBARO-...	70	HBC	$\overline{K}N \to \Sigma\pi$
300	BAILEY	69	DPWA	$\overline{K}N \to \overline{K}N$
147	ARMENTEROS	68B	HBC	

[1] The two MARTIN 77 values are from a T-matrix pole and from a Breit-Wigner fit.

Λ(1810) DECAY MODES

	Mode	Fraction (Γ_j/Γ)
Γ_1	$N\overline{K}$	20–50 %
Γ_2	$\Sigma\pi$	10–40 %
Γ_3	$\Lambda\eta$	
Γ_4	ΞK	
Γ_5	$\Sigma(1385)\pi$	seen
Γ_6	$N\overline{K}^*(892)$	30–60 %
Γ_7	$N\overline{K}^*(892)$, S=1/2, P-wave	
Γ_8	$N\overline{K}^*(892)$, S=3/2, P-wave	

Λ(1810) BRANCHING RATIOS

See "Sign conventions for resonance couplings" in the Note on Λ and Σ Resonances.

$\Gamma(N\overline{K})/\Gamma_{total}$ Γ_1/Γ

VALUE	DOCUMENT ID		TECN	COMMENT
0.2 to 0.5 OUR ESTIMATE				
0.19 ±0.08	ZHANG	13A	DPWA	Multichannel
0.24 ±0.04	GOPAL	80	DPWA	$\overline{K}N \to \overline{K}N$
0.36 ±0.05	LANGBEIN	72	IPWA	$\overline{K}N$ multichannel
• • • We do not use the following data for averages, fits, limits, etc. • • •				
0.225	[1] KAMANO	15	DPWA	Multichannel
0.21 ±0.04	GOPAL	77	DPWA	See GOPAL 80
0.52 or 0.49	[2] MARTIN	77	DPWA	$\overline{K}N$ multichannel
0.30	KIM	71	DPWA	K-matrix analysis
0.15	ARMENTEROS	70	DPWA	$\overline{K}N \to \overline{K}N$
0.55	BAILEY	69	DPWA	$\overline{K}N \to \overline{K}N$
0.4	ARMENTEROS	68B	DPWA	$\overline{K}N \to \overline{K}N$

[1] From the preferred solution A in KAMANO 15.
[2] The two MARTIN 77 values are from a T-matrix pole and from a Breit-Wigner fit.

$\Gamma(\Sigma\pi)/\Gamma_{total}$ Γ_2/Γ

VALUE	DOCUMENT ID		TECN	COMMENT
• • • We do not use the following data for averages, fits, limits, etc. • • •				
0.009	[1] KAMANO	15	DPWA	Multichannel

[1] From the preferred solution A in KAMANO 15.

$\Gamma(\Lambda\eta)/\Gamma_{total}$ Γ_3/Γ

VALUE	DOCUMENT ID		TECN	COMMENT
• • • We do not use the following data for averages, fits, limits, etc. • • •				
0.111	[1] KAMANO	15	DPWA	Multichannel

[1] From the preferred solution A in KAMANO 15.

$\Gamma(\Xi K)/\Gamma_{total}$ Γ_4/Γ

VALUE	DOCUMENT ID		TECN	COMMENT
• • • We do not use the following data for averages, fits, limits, etc. • • •				
0.051	[1] KAMANO	15	DPWA	Multichannel

[1] From the preferred solution A in KAMANO 15.

$\Gamma(\Sigma(1385)\pi)/\Gamma_{total}$ Γ_5/Γ

VALUE	DOCUMENT ID		TECN	COMMENT
• • • We do not use the following data for averages, fits, limits, etc. • • •				
0.600	[1] KAMANO	15	DPWA	Multichannel

[1] From the preferred solution A in KAMANO 15.

$\Gamma(N\overline{K}^*(892), S$=1/2, P-wave$)/\Gamma_{total}$ Γ_7/Γ

VALUE	DOCUMENT ID		TECN	COMMENT
• • • We do not use the following data for averages, fits, limits, etc. • • •				
0.003	[1] KAMANO	15	DPWA	Multichannel

[1] From the preferred solution A in KAMANO 15.

$(\Gamma_j\Gamma_f)^{1/2}/\Gamma_{total}$ in $N\overline{K} \to \Lambda(1810) \to \Sigma\pi$ $(\Gamma_1\Gamma_2)^{1/2}/\Gamma$

VALUE	DOCUMENT ID		TECN	COMMENT
−0.08±0.05	ZHANG	13A	DPWA	Multichannel
−0.24±0.04	GOPAL	77	DPWA	$\overline{K}N$ multichannel
• • • We do not use the following data for averages, fits, limits, etc. • • •				
+0.25 or +0.23	[1] MARTIN	77	DPWA	$\overline{K}N$ multichannel
< 0.01	LANGBEIN	72	IPWA	$\overline{K}N$ multichannel
0.17	KIM	71	DPWA	K-matrix analysis
+0.20	[2] ARMENTEROS	70	DPWA	$\overline{K}N \to \Sigma\pi$
−0.13±0.03	BARBARO-...	70	DPWA	$\overline{K}N \to \Sigma\pi$

[1] The two MARTIN 77 values are from a T-matrix pole and from a Breit-Wigner fit.
[2] The published sign has been changed to be in accord with the baryon-first convention.

$(\Gamma_j\Gamma_f)^{1/2}/\Gamma_{total}$ in $N\overline{K} \to \Lambda(1810) \to \Sigma(1385)\pi$ $(\Gamma_1\Gamma_5)^{1/2}/\Gamma$

VALUE	DOCUMENT ID		TECN	COMMENT
+0.18±0.10	PREVOST	74	DPWA	$K^-N \to \Sigma(1385)\pi$

$(\Gamma_j\Gamma_f)^{1/2}/\Gamma_{total}$ in $N\overline{K} \to \Lambda(1810) \to N\overline{K}^*(892), S$=1/2, P-wave $(\Gamma_1\Gamma_7)^{1/2}/\Gamma$

VALUE	DOCUMENT ID		TECN	COMMENT
−0.14±0.03	[1] CAMERON	78B	DPWA	$K^-p \to N\overline{K}^*$

[1] The published sign has been changed to be in accord with the baryon-first convention.

$(\Gamma_j\Gamma_f)^{1/2}/\Gamma_{total}$ in $N\overline{K} \to \Lambda(1810) \to N\overline{K}^*(892), S$=3/2, P-wave $(\Gamma_1\Gamma_8)^{1/2}/\Gamma$

VALUE	DOCUMENT ID		TECN	COMMENT
+0.38±0.06	ZHANG	13A	DPWA	Multichannel
+0.35±0.06	CAMERON	78B	DPWA	$K^-p \to N\overline{K}^*$

Λ(1810) REFERENCES

KAMANO	15	PR C92 025205	H. Kamano *et al.*	(ANL, OSAK)
ZHANG	13A	PR C88 035205	H. Zhang *et al.*	(KSU)
GOPAL	80	Toronto Conf. 159	G.P. Gopal	(RHEL) IJP
CAMERON	78B	NP B146 327	W. Cameron *et al.*	(RHEL, LOIC) IJP
GOPAL	77	NP B119 362	G.P. Gopal *et al.*	(LOIC, RHEL) IJP
MARTIN	77	NP B127 349	B.R. Martin, M.K. Pidcock, R.G. Moorhouse	(LOUC+) IJP
Also		NP B126 266	B.R. Martin, M.K. Pidcock	(LOUC)
Also		NP B126 285	B.R. Martin, M.K. Pidcock	(LOUC) IJP
CARROLL	76	PRL 37 806	A.S. Carroll *et al.*	(BNL) I
PREVOST	74	NP B69 246	J. Prevost *et al.*	(SACL, CERN, HEID)
LANGBEIN	72	NP B47 477	W. Langbein, F. Wagner	(MPIM) IJP
KIM	71	PRL 27 356	J.K. Kim	(HARV) IJP
Also		Duke Conf. 161 Hyperon Resonances, 1970	J.K. Kim	(HARV) IJP
ARMENTEROS	70	Duke Conf. 123 Hyperon Resonances, 1970	R. Armenteros *et al.*	(CERN, HEID, SACL) IJP
BARBARO-...	70	Duke Conf. 173 Hyperon Resonances, 1970	A. Barbaro-Galtieri	(LRL) IJP
BAILEY	69	Thesis UCRL 50617	J.M. Bailey	(LLL) IJP
ARMENTEROS	68B	NP B8 195	R. Armenteros *et al.*	(CERN, HEID, SACL) IJP

Baryon Particle Listings

Λ(1820)

Λ(1820) $5/2^+$

$I(J^P) = 0(\frac{5}{2}^+)$ Status: ****

This resonance is the cornerstone for all partial-wave analyses in this region. Most of the results published before 1973 are now obsolete and have been omitted. They may be found in our 1982 edition Physics Letters **111B** 1 (1982).

Most of the quoted errors are statistical only; the systematic errors due to the particular parametrizations used in the partial-wave analyses are not included. For this reason we do not calculate weighted averages for the mass and width.

Λ(1820) POLE POSITION

REAL PART

VALUE (MeV)	DOCUMENT ID		TECN	COMMENT
1824^{+2}_{-1}	[1] KAMANO	15	DPWA	Multichannel
• • • We do not use the following data for averages, fits, limits, etc. • • •				
1814	ZHANG	13A	DPWA	Multichannel

[1] From the preferred solution A in KAMANO 15.

−2×IMAGINARY PART

VALUE (MeV)	DOCUMENT ID		TECN	COMMENT
77±2	[1] KAMANO	15	DPWA	Multichannel
• • • We do not use the following data for averages, fits, limits, etc. • • •				
85	ZHANG	13A	DPWA	Multichannel

[1] From the preferred solution A in KAMANO 15.

Λ(1820) POLE RESIDUES

The normalized residue is the residue divided by $\Gamma_{pole}/2$.

Normalized residue in $N\overline{K} \to \Lambda(1820) \to N\overline{K}$

MODULUS	PHASE (°)	DOCUMENT ID		TECN	COMMENT
• • • We do not use the following data for averages, fits, limits, etc. • • •					
0.558	−13	[1] KAMANO	15	DPWA	Multichannel

[1] From the preferred solution A in KAMANO 15.

Normalized residue in $N\overline{K} \to \Lambda(1820) \to \Sigma\pi$

MODULUS	PHASE (°)	DOCUMENT ID		TECN	COMMENT
• • • We do not use the following data for averages, fits, limits, etc. • • •					
0.357	168	[1] KAMANO	15	DPWA	Multichannel

[1] From the preferred solution A in KAMANO 15.

Normalized residue in $N\overline{K} \to \Lambda(1820) \to \Lambda\eta$

MODULUS	PHASE (°)	DOCUMENT ID		TECN	COMMENT
• • • We do not use the following data for averages, fits, limits, etc. • • •					
0.0184	−3	[1] KAMANO	15	DPWA	Multichannel

[1] From the preferred solution A in KAMANO 15.

Normalized residue in $N\overline{K} \to \Lambda(1820) \to \Xi K$

MODULUS	PHASE (°)	DOCUMENT ID		TECN	COMMENT
• • • We do not use the following data for averages, fits, limits, etc. • • •					
0.00111	70	[1] KAMANO	15	DPWA	Multichannel

[1] From the preferred solution A in KAMANO 15.

Normalized residue in $N\overline{K} \to \Lambda(1820) \to \Sigma(1385)\pi$, *P*-wave

MODULUS	PHASE (°)	DOCUMENT ID		TECN	COMMENT
• • • We do not use the following data for averages, fits, limits, etc. • • •					
0.340	161	[1] KAMANO	15	DPWA	Multichannel

[1] From the preferred solution A in KAMANO 15.

Normalized residue in $N\overline{K} \to \Lambda(1820) \to \Sigma(1385)\pi$, *F*-wave

MODULUS	PHASE (°)	DOCUMENT ID		TECN	COMMENT
• • • We do not use the following data for averages, fits, limits, etc. • • •					
0.201	151	[1] KAMANO	15	DPWA	Multichannel

[1] From the preferred solution A in KAMANO 15.

Normalized residue in $N\overline{K} \to \Lambda(1820) \to N\overline{K}^*(892)$, S=1/2 , *F*-wave

MODULUS	PHASE (°)	DOCUMENT ID		TECN	COMMENT
• • • We do not use the following data for averages, fits, limits, etc. • • •					
0.00750	41	[1] KAMANO	15	DPWA	Multichannel

[1] From the preferred solution A in KAMANO 15.

Normalized residue in $N\overline{K} \to \Lambda(1820) \to N\overline{K}^*(892)$, S=3/2 , *P*-wave

MODULUS	PHASE (°)	DOCUMENT ID		TECN	COMMENT
• • • We do not use the following data for averages, fits, limits, etc. • • •					
0.171	−139	[1] KAMANO	15	DPWA	Multichannel

[1] From the preferred solution A in KAMANO 15.

Normalized residue in $N\overline{K} \to \Lambda(1820) \to N\overline{K}^*(892)$, S=3/2 , *F*-wave

MODULUS	PHASE (°)	DOCUMENT ID		TECN	COMMENT
• • • We do not use the following data for averages, fits, limits, etc. • • •					
0.000517	161	[1] KAMANO	15	DPWA	Multichannel

[1] From the preferred solution A in KAMANO 15.

Λ(1820) MASS

VALUE (MeV)	DOCUMENT ID		TECN	COMMENT
1815 to 1825 (≈ 1820) OUR ESTIMATE				
1823.5 ± 0.8	ZHANG	13A	DPWA	Multichannel
1823 ± 3	GOPAL	80	DPWA	$\overline{K}N \to \overline{K}N$
1819 ± 2	ALSTON-...	78	DPWA	$\overline{K}N \to \overline{K}N$
1822 ± 2	GOPAL	77	DPWA	$\overline{K}N$ multichannel
1821 ± 2	KANE	74	DPWA	$K^-p \to \Sigma\pi$
• • • We do not use the following data for averages, fits, limits, etc. • • •				
1830	DECLAIS	77	DPWA	$\overline{K}N \to \overline{K}N$
1817 or 1819	[1] MARTIN	77	DPWA	$\overline{K}N$ multichannel

[1] The two MARTIN 77 values are from a T-matrix pole and from a Breit-Wigner fit.

Λ(1820) WIDTH

VALUE (MeV)	DOCUMENT ID		TECN	COMMENT
70 to 90 (≈ 80) OUR ESTIMATE				
89 ± 2	ZHANG	13A	DPWA	Multichannel
77 ± 5	GOPAL	80	DPWA	$\overline{K}N \to \overline{K}N$
72 ± 5	ALSTON-...	78	DPWA	$\overline{K}N \to \overline{K}N$
81 ± 5	GOPAL	77	DPWA	$\overline{K}N$ multichannel
87 ± 3	KANE	74	DPWA	$K^-p \to \Sigma\pi$
• • • We do not use the following data for averages, fits, limits, etc. • • •				
82	DECLAIS	77	DPWA	$\overline{K}N \to \overline{K}N$
76 or 76	[1] MARTIN	77	DPWA	$\overline{K}N$ multichannel

[1] The two MARTIN 77 values are from a T-matrix pole and from a Breit-Wigner fit.

Λ(1820) DECAY MODES

	Mode	Fraction (Γ_i/Γ)
Γ_1	$N\overline{K}$	55–65 %
Γ_2	$\Sigma\pi$	8–14 %
Γ_3	$\Sigma(1385)\pi$	5–10 %
Γ_4	$\Sigma(1385)\pi$, *P*-wave	
Γ_5	$\Sigma(1385)\pi$, *F*-wave	
Γ_6	$\Lambda\eta$	
Γ_7	ΞK	
Γ_8	$\Sigma\pi\pi$	
Γ_9	$N\overline{K}^*(892)$, S=1/2, *F*-wave	
Γ_{10}	$N\overline{K}^*(892)$, S=3/2, *P*-wave	(3.0±1.0) %
Γ_{11}	$N\overline{K}^*(892)$, S=3/2, *F*-wave	

Λ(1820) BRANCHING RATIOS

Errors quoted do not include uncertainties in the parametrizations used in the partial-wave analyses and are thus too small. See also "Sign conventions for resonance couplings" in the Note on Λ and Σ Resonances.

$\Gamma(N\overline{K})/\Gamma_{total}$ Γ_1/Γ

VALUE	DOCUMENT ID		TECN	COMMENT
0.55 to 0.65 OUR ESTIMATE				
0.54 ±0.01	ZHANG	13A	DPWA	Multichannel
0.58 ±0.02	GOPAL	80	DPWA	$\overline{K}N \to \overline{K}N$
0.60 ±0.03	ALSTON-...	78	DPWA	$\overline{K}N \to \overline{K}N$
• • • We do not use the following data for averages, fits, limits, etc. • • •				
0.547	[1] KAMANO	15	DPWA	Multichannel
0.51	DECLAIS	77	DPWA	$\overline{K}N \to \overline{K}N$
0.57 ±0.02	GOPAL	77	DPWA	See GOPAL 80
0.59 or 0.58	[2] MARTIN	77	DPWA	$\overline{K}N$ multichannel

[1] From the preferred solution A in KAMANO 15.
[2] The two MARTIN 77 values are from a T-matrix pole and from a Breit-Wigner fit.

$\Gamma(\Sigma\pi)/\Gamma_{total}$ Γ_2/Γ

VALUE	DOCUMENT ID		TECN	COMMENT
• • • We do not use the following data for averages, fits, limits, etc. • • •				
0.218	[1] KAMANO	15	DPWA	Multichannel

[1] From the preferred solution A in KAMANO 15.

$\Gamma(\Sigma(1385)\pi$, *P*-wave$)/\Gamma_{total}$ Γ_4/Γ

VALUE	DOCUMENT ID		TECN	COMMENT
• • • We do not use the following data for averages, fits, limits, etc. • • •				
0.173	[1] KAMANO	15	DPWA	Multichannel

[1] From the preferred solution A in KAMANO 15.

$\Gamma(\Sigma(1385)\pi$, F-wave$)/\Gamma_{total}$ Γ_5/Γ

VALUE	DOCUMENT ID		TECN	COMMENT
• • • We do not use the following data for averages, fits, limits, etc. • • •				
0.055	[1] KAMANO	15	DPWA	Multichannel

[1] From the preferred solution A in KAMANO 15.

$\Gamma(\Lambda\eta)/\Gamma_{total}$ Γ_6/Γ

VALUE	DOCUMENT ID		TECN	COMMENT
• • • We do not use the following data for averages, fits, limits, etc. • • •				
0.001	[1] KAMANO	15	DPWA	Multichannel

[1] From the preferred solution A in KAMANO 15.

$\Gamma(\Xi K)/\Gamma_{total}$ Γ_7/Γ

VALUE	DOCUMENT ID		TECN	COMMENT
• • • We do not use the following data for averages, fits, limits, etc. • • •				
not seen	[1] KAMANO	15	DPWA	Multichannel

[1] From the preferred solution A in KAMANO 15.

$\Gamma(\Sigma\pi\pi)/\Gamma_{total}$ Γ_8/Γ

VALUE	DOCUMENT ID		TECN	COMMENT
no clear signal	[1] ARMENTEROS 68C		HDBC	$K^- N \to \Sigma\pi\pi$

[1] There is a suggestion of a bump, enough to be consistent with what is expected from $\Sigma(1385) \to \Sigma\pi$ decay.

$\Gamma(N\overline{K}^*(892)$, S=1/2, F-wave$)/\Gamma_{total}$ Γ_9/Γ

VALUE	DOCUMENT ID		TECN	COMMENT
• • • We do not use the following data for averages, fits, limits, etc. • • •				
not seen	[1] KAMANO	15	DPWA	Multichannel

[1] From the preferred solution A in KAMANO 15.

$\Gamma(N\overline{K}^*(892)$, S=3/2, P-wave$)/\Gamma_{total}$ Γ_{10}/Γ

VALUE	DOCUMENT ID		TECN	COMMENT
0.03 ±0.01	ZHANG	13A	DPWA	Multichannel
• • • We do not use the following data for averages, fits, limits, etc. • • •				
0.006	[1] KAMANO	15	DPWA	Multichannel

[1] From the preferred solution A in KAMANO 15.

$\Gamma(N\overline{K}^*(892)$, S=3/2, F-wave$)/\Gamma_{total}$ Γ_{11}/Γ

VALUE	DOCUMENT ID		TECN	COMMENT
• • • We do not use the following data for averages, fits, limits, etc. • • •				
not seen	[1] KAMANO	15	DPWA	Multichannel

[1] From the preferred solution A in KAMANO 15.

$(\Gamma_i\Gamma_f)^{1/2}/\Gamma_{total}$ in $N\overline{K} \to \Lambda(1820) \to \Sigma\pi$ $(\Gamma_1\Gamma_2)^{1/2}/\Gamma$

VALUE	DOCUMENT ID		TECN	COMMENT
-0.28 ± 0.01	ZHANG	13A	DPWA	Multichannel
-0.28 ± 0.03	GOPAL	77	DPWA	$\overline{K}N$ multichannel
-0.28 ± 0.01	KANE	74	DPWA	$K^- p \to \Sigma\pi$
• • • We do not use the following data for averages, fits, limits, etc. • • •				
-0.25 or -0.25	[1] MARTIN	77	DPWA	$\overline{K}N$ multichannel

[1] The two MARTIN 77 values are from a T-matrix pole and from a Breit-Wigner fit.

$(\Gamma_i\Gamma_f)^{1/2}/\Gamma_{total}$ in $N\overline{K} \to \Lambda(1820) \to \Sigma(1385)\pi$, P-wave $(\Gamma_1\Gamma_4)^{1/2}/\Gamma$

VALUE	DOCUMENT ID		TECN	COMMENT
-0.20 ±0.02	ZHANG	13A	DPWA	Multichannel
-0.167 ± 0.054	[1] CAMERON	78	DPWA	$K^- p \to \Sigma(1385)\pi$
$+0.27$ ±0.03	PREVOST	74	DPWA	$K^- N \to \Sigma(1385)\pi$

[1] The published sign has been changed to be in accord with the baryon-first convention.

$(\Gamma_i\Gamma_f)^{1/2}/\Gamma_{total}$ in $N\overline{K} \to \Lambda(1820) \to \Sigma(1385)\pi$, F-wave $(\Gamma_1\Gamma_5)^{1/2}/\Gamma$

VALUE	DOCUMENT ID		TECN	COMMENT
$+0.065\pm0.029$	[1] CAMERON	78	DPWA	$K^- p \to \Sigma(1385)\pi$

[1] The published sign has been changed to be in accord with the baryon-first convention.

$(\Gamma_i\Gamma_f)^{1/2}/\Gamma_{total}$ in $N\overline{K} \to \Lambda(1820) \to \Lambda\eta$ $(\Gamma_1\Gamma_6)^{1/2}/\Gamma$

VALUE	DOCUMENT ID		TECN
$-0.096^{+0.040}_{-0.020}$	RADER	73	MPWA

$\Lambda(1820)$ REFERENCES

KAMANO	15	PR C92 025205	H. Kamano *et al.*	(ANL, OSAK)
ZHANG	13A	PR C88 035205	H. Zhang *et al.*	(KSU)
PDG	82	PL 111B 1	M. Roos *et al.*	(HELS, CIT, CERN)
GOPAL	80	Toronto Conf. 159	G.P. Gopal	(RHEL) IJP
ALSTON-...	78	PR D18 182	M. Alston-Garnjost *et al.*	(LBL, MTHO+) IJP
Also		PRL 38 1007	M. Alston-Garnjost *et al.*	(LBL, MTHO+) IJP
CAMERON	78	NP B143 189	W. Cameron *et al.*	(RHEL, LOIC) IJP
DECLAIS	77	CERN 77-16	Y. Declais *et al.*	(CAEN, CERN) IJP
GOPAL	77	NP B119 362	G.P. Gopal *et al.*	(LOIC, RHEL) IJP
MARTIN	77	NP B127 349	B.R. Martin, M.K. Pidcock, R.G. Moorhouse	(LOUC+) IJP
Also		NP B126 266	B.R. Martin, M.K. Pidcock	(LOUC)
Also		NP B126 285	B.R. Martin, M.K. Pidcock	(LOUC) IJP
KANE	74	LBL-2452	D.F. Kane	(LBL) IJP
PREVOST	74	NP B69 246	J. Prevost *et al.*	(SACL, CERN, HEID)
RADER	73	NC 16A 178	R.K. Rader *et al.*	(SACL, HEID, CERN+)
ARMENTEROS	68C	NP B8 216	R. Armenteros *et al.*	(CERN, HEID, SACL) I

$\Lambda(1830)$ $5/2^-$

$I(J^P) = 0(\frac{5}{2}^-)$ Status: ****

For results published before 1973 (they are now obsolete), see our 1982 edition Physics Letters **111B** 1 (1982).

The best evidence for this resonance is in the $\Sigma\pi$ channel.

$\Lambda(1830)$ POLE POSITION

REAL PART

VALUE (MeV)	DOCUMENT ID		TECN	COMMENT
1899^{+35}_{-37}	[1] KAMANO	15	DPWA	Multichannel
• • • We do not use the following data for averages, fits, limits, etc. • • •				
1766^{+37}_{-34}	[2] KAMANO	15	DPWA	Multichannel
1809	ZHANG	13A	DPWA	Multichannel

[1] The preferred solution A in KAMANO 15 reports two poles. This entry is from the preferred solution A.
[2] From the preferred solution A in KAMANO 15. Not seen in solution B.

$-2\times$IMAGINARY PART

VALUE (MeV)	DOCUMENT ID		TECN	COMMENT
80^{+100}_{-34}	[1] KAMANO	15	DPWA	Multichannel
• • • We do not use the following data for averages, fits, limits, etc. • • •				
212^{+94}_{-62}	[2] KAMANO	15	DPWA	Multichannel
109	ZHANG	13A	DPWA	Multichannel

[1] The preferred solution A in KAMANO 15 reports two poles. This entry is from the preferred solution A.
[2] From the preferred solution A in KAMANO 15. Not seen in solution B.

$\Lambda(1830)$ POLE RESIDUES

The normalized residue is the residue divided by $\Gamma_{pole}/2$.

Normalized residue in $N\overline{K} \to \Lambda(1830) \to N\overline{K}$

MODULUS	PHASE (°)	DOCUMENT ID		TECN	COMMENT
• • • We do not use the following data for averages, fits, limits, etc. • • •					
0.00502	−80	[1] KAMANO	15	DPWA	Multichannel

[1] From the preferred solution A in KAMANO 15.

Normalized residue in $N\overline{K} \to \Lambda(1830) \to \Sigma\pi$

MODULUS	PHASE (°)	DOCUMENT ID		TECN	COMMENT
• • • We do not use the following data for averages, fits, limits, etc. • • •					
0.00581	179	[1] KAMANO	15	DPWA	Multichannel

[1] From the preferred solution A in KAMANO 15.

Normalized residue in $N\overline{K} \to \Lambda(1830) \to \Lambda\eta$

MODULUS	PHASE (°)	DOCUMENT ID		TECN	COMMENT
• • • We do not use the following data for averages, fits, limits, etc. • • •					
0.00941	−65	[1] KAMANO	15	DPWA	Multichannel

[1] From the preferred solution A in KAMANO 15.

Normalized residue in $N\overline{K} \to \Lambda(1830) \to \Xi K$

MODULUS	PHASE (°)	DOCUMENT ID		TECN	COMMENT
• • • We do not use the following data for averages, fits, limits, etc. • • •					
0.0477	94	[1] KAMANO	15	DPWA	Multichannel

[1] From the preferred solution A in KAMANO 15.

Normalized residue in $N\overline{K} \to \Lambda(1830) \to \Sigma(1385)\pi$, D-wave

MODULUS	PHASE (°)	DOCUMENT ID		TECN	COMMENT
• • • We do not use the following data for averages, fits, limits, etc. • • •					
0.0237	113	[1] KAMANO	15	DPWA	Multichannel

[1] From the preferred solution A in KAMANO 15.

Normalized residue in $N\overline{K} \to \Lambda(1830) \to \Sigma(1385)\pi$, G-wave

MODULUS	PHASE (°)	DOCUMENT ID		TECN	COMMENT
• • • We do not use the following data for averages, fits, limits, etc. • • •					
0.000726	127	[1] KAMANO	15	DPWA	Multichannel

[1] From the preferred solution A in KAMANO 15.

Normalized residue in $N\overline{K} \to \Lambda(1830) \to N\overline{K}^*(892)$, S=1/2 , D-wave

MODULUS	PHASE (°)	DOCUMENT ID		TECN	COMMENT
• • • We do not use the following data for averages, fits, limits, etc. • • •					
0.0278	−177	[1] KAMANO	15	DPWA	Multichannel

[1] From the preferred solution A in KAMANO 15.

Normalized residue in $N\overline{K} \to \Lambda(1830) \to N\overline{K}^*(892)$, S=3/2 , D-wave

MODULUS	PHASE (°)	DOCUMENT ID		TECN	COMMENT
• • • We do not use the following data for averages, fits, limits, etc. • • •					
0.0255	3	[1] KAMANO	15	DPWA	Multichannel

[1] From the preferred solution A in KAMANO 15.

Normalized residue in $N\overline{K} \to \Lambda(1830) \to N\overline{K}^*(892)$, S=3/2 , G-wave

MODULUS	PHASE (°)	DOCUMENT ID		TECN	COMMENT
• • • We do not use the following data for averages, fits, limits, etc. • • •					
0.00773	−17	[1] KAMANO	15	DPWA	Multichannel

[1] From the preferred solution A in KAMANO 15.

$\Lambda(1830)$ MASS

VALUE (MeV)	DOCUMENT ID		TECN	COMMENT
1810 to 1830 (≈ 1830) OUR ESTIMATE				
1820 ± 4	ZHANG	13A	DPWA	Multichannel
1831 ± 10	GOPAL	80	DPWA	$\overline{K}N \to \overline{K}N$
1825 ± 10	GOPAL	77	DPWA	$\overline{K}N$ multichannel
1825 ± 1	KANE	74	DPWA	$K^-p \to \Sigma\pi$
• • • We do not use the following data for averages, fits, limits, etc. • • •				
1817 or 1818	[1] MARTIN	77	DPWA	$\overline{K}N$ multichannel

[1] The two MARTIN 77 values are from a T-matrix pole and from a Breit-Wigner fit.

$\Lambda(1830)$ WIDTH

VALUE (MeV)	DOCUMENT ID		TECN	COMMENT
60 to 110 (≈ 95) OUR ESTIMATE				
114 ± 10	ZHANG	13A	DPWA	Multichannel
100 ± 10	GOPAL	80	DPWA	$\overline{K}N \to \overline{K}N$
94 ± 10	GOPAL	77	DPWA	$\overline{K}N$ multichannel
119 ± 3	KANE	74	DPWA	$K^-p \to \Sigma\pi$
• • • We do not use the following data for averages, fits, limits, etc. • • •				
56 or 56	[1] MARTIN	77	DPWA	$\overline{K}N$ multichannel

[1] The two MARTIN 77 values are from a T-matrix pole and from a Breit-Wigner fit.

$\Lambda(1830)$ DECAY MODES

	Mode	Fraction (Γ_i/Γ)
Γ_1	$N\overline{K}$	3–10 %
Γ_2	$\Sigma\pi$	35–75 %
Γ_3	ΞK	
Γ_4	$\Sigma(1385)\pi$	>15 %
Γ_5	$\Sigma(1385)\pi$, D-wave	(52 ± 6) %
Γ_6	$\Sigma(1385)\pi$, G-wave	
Γ_7	$\Lambda\eta$	
Γ_8	$N\overline{K}^*(892)$, S=1/2, D-wave	
Γ_9	$N\overline{K}^*(892)$, S=3/2, D-wave	
Γ_{10}	$N\overline{K}^*(892)$, S=3/2, G-wave	

$\Lambda(1830)$ BRANCHING RATIOS

See "Sign conventions for resonance couplings" in the Note on Λ and Σ Resonances.

$\Gamma(N\overline{K})/\Gamma_{total}$ Γ_1/Γ

VALUE	DOCUMENT ID		TECN	COMMENT
0.03 to 0.10 OUR ESTIMATE				
0.041 ± 0.005	ZHANG	13A	DPWA	Multichannel
0.08 ± 0.03	GOPAL	80	DPWA	$\overline{K}N \to \overline{K}N$
0.02 ± 0.02	ALSTON-...	78	DPWA	$\overline{K}N \to \overline{K}N$
• • • We do not use the following data for averages, fits, limits, etc. • • •				
0.006	[1] KAMANO	15	DPWA	Multichannel
0.04 ± 0.03	GOPAL	77	DPWA	See GOPAL 80
0.04 or 0.04	[2] MARTIN	77	DPWA	$\overline{K}N$ multichannel

[1] From the preferred solution A in KAMANO 15.
[2] The two MARTIN 77 values are from a T-matrix pole and from a Breit-Wigner fit.

$\Gamma(\Sigma\pi)/\Gamma_{total}$ Γ_2/Γ

VALUE	DOCUMENT ID		TECN	COMMENT
• • • We do not use the following data for averages, fits, limits, etc. • • •				
0.017	[1] KAMANO	15	DPWA	Multichannel

[1] From the preferred solution A in KAMANO 15.

$\Gamma(\Xi K)/\Gamma_{total}$ Γ_3/Γ

VALUE	DOCUMENT ID		TECN	COMMENT
• • • We do not use the following data for averages, fits, limits, etc. • • •				
0.562	[1] KAMANO	15	DPWA	Multichannel

[1] From the preferred solution A in KAMANO 15.

$\Gamma(\Sigma(1385)\pi, D\text{-wave})/\Gamma_{total}$ Γ_5/Γ

VALUE	DOCUMENT ID		TECN	COMMENT
0.52 ±0.06	ZHANG	13A	DPWA	Multichannel
• • • We do not use the following data for averages, fits, limits, etc. • • •				
0.134	[1] KAMANO	15	DPWA	Multichannel

[1] From the preferred solution A in KAMANO 15.

$\Gamma(\Lambda\eta)/\Gamma_{total}$ Γ_7/Γ

VALUE	DOCUMENT ID		TECN	COMMENT
• • • We do not use the following data for averages, fits, limits, etc. • • •				
0.024	[1] KAMANO	15	DPWA	Multichannel

[1] From the preferred solution A in KAMANO 15.

$\Gamma(N\overline{K}^*(892), S\text{=}1/2, D\text{-wave})/\Gamma_{total}$ Γ_8/Γ

VALUE	DOCUMENT ID		TECN	COMMENT
• • • We do not use the following data for averages, fits, limits, etc. • • •				
0.134	[1] KAMANO	15	DPWA	Multichannel

[1] From the preferred solution A in KAMANO 15.

$\Gamma(N\overline{K}^*(892), S\text{=}3/2, D\text{-wave})/\Gamma_{total}$ Γ_9/Γ

VALUE	DOCUMENT ID		TECN	COMMENT
• • • We do not use the following data for averages, fits, limits, etc. • • •				
0.115	[1] KAMANO	15	DPWA	Multichannel

[1] From the preferred solution A in KAMANO 15.

$\Gamma(N\overline{K}^*(892), S\text{=}3/2, G\text{-wave})/\Gamma_{total}$ Γ_{10}/Γ

VALUE	DOCUMENT ID		TECN	COMMENT
• • • We do not use the following data for averages, fits, limits, etc. • • •				
0.009	[1] KAMANO	15	DPWA	Multichannel

[1] From the preferred solution A in KAMANO 15.

$(\Gamma_i\Gamma_f)^{1/2}/\Gamma_{total}$ in $N\overline{K} \to \Lambda(1830) \to \Sigma\pi$ $(\Gamma_1\Gamma_2)^{1/2}/\Gamma$

VALUE	DOCUMENT ID		TECN	COMMENT
−0.13 ± 0.01	ZHANG	13A	DPWA	Multichannel
−0.17 ± 0.03	GOPAL	77	DPWA	$\overline{K}N$ multichannel
−0.15 ± 0.01	KANE	74	DPWA	$K^-p \to \Sigma\pi$
• • • We do not use the following data for averages, fits, limits, etc. • • •				
−0.17 or −0.17	[1] MARTIN	77	DPWA	$\overline{K}N$ multichannel

[1] The two MARTIN 77 values are from a T-matrix pole and from a Breit-Wigner fit.

$(\Gamma_i\Gamma_f)^{1/2}/\Gamma_{total}$ in $N\overline{K} \to \Lambda(1830) \to \Sigma(1385)\pi$ $(\Gamma_1\Gamma_4)^{1/2}/\Gamma$

VALUE	DOCUMENT ID		TECN	COMMENT
+0.141 ± 0.014	[1] CAMERON	78	DPWA	$K^-p \to \Sigma(1385)\pi$
+0.13 ±0.03	PREVOST	74	DPWA	$K^-N \to \Sigma(1385)\pi$

[1] The CAMERON 78 upper limit on G-wave decay is 0.03. The published sign has been changed to be in accord with the baryon-first convention.

$(\Gamma_i\Gamma_f)^{1/2}/\Gamma_{total}$ in $N\overline{K} \to \Lambda(1830) \to \Lambda\eta$ $(\Gamma_1\Gamma_7)^{1/2}/\Gamma$

VALUE	DOCUMENT ID		TECN
−0.044 ± 0.020	RADER	73	MPWA

$\Lambda(1830)$ REFERENCES

KAMANO	15	PR C92 025205	H. Kamano *et al.*	(ANL, OSAK)
ZHANG	13A	PR C88 035205	H. Zhang *et al.*	(KSU)
PDG	82	PL 111B 1	M. Roos *et al.*	(HELS, CIT, CERN)
GOPAL	80	Toronto Conf. 159	G.P. Gopal	(RHEL) IJP
ALSTON-...	78	PR D18 182	M. Alston-Garnjost *et al.*	(LBL, MTHO+) IJP
Also		PRL 38 1007	M. Alston-Garnjost *et al.*	(LBL, MTHO+) IJP
CAMERON	78	NP B143 189	W. Cameron *et al.*	(RHEL, LOIC) IJP
GOPAL	77	NP B119 362	G.P. Gopal *et al.*	(LOIC, RHEL) IJP
MARTIN	77	NP B127 349	B.R. Martin, M.K. Pidcock, R.G. Moorhouse	(LOUC+) IJP
Also		NP B126 266	B.R. Martin, M.K. Pidcock	(LOUC)
Also		NP B126 285	B.R. Martin, M.K. Pidcock	(LOUC) IJP
KANE	74	LBL-2452	D.F. Kane	(LBL) IJP
PREVOST	74	NP B69 246	J. Prevost *et al.*	(SACL, CERN, HEID)
RADER	73	NC 16A 178	R.K. Rader *et al.*	(SACL, HEID, CERN+)

$\Lambda(1890)$ $3/2^+$

$I(J^P) = 0(\frac{3}{2}^+)$ Status: ****

For results published before 1974 (they are now obsolete), see our 1982 edition Physics Letters **111B** 1 (1982).

The $J^P = 3/2^+$ assignment is consistent with all available data (including polarization) and recent partial-wave analyses. The dominant inelastic modes remain unknown.

Λ(1890) POLE POSITION

REAL PART

VALUE (MeV)	DOCUMENT ID		TECN	COMMENT
• • • We do not use the following data for averages, fits, limits, etc. • • •				
1859^{+5}_{-7}	[1] KAMANO	15	DPWA	Multichannel
1876	ZHANG	13A	DPWA	Multichannel

[1] From the preferred solution A in KAMANO 15, incompatible with solution B.

−2×IMAGINARY PART

VALUE (MeV)	DOCUMENT ID		TECN	COMMENT
• • • We do not use the following data for averages, fits, limits, etc. • • •				
113^{+20}_{-4}	[1] KAMANO	15	DPWA	Multichannel
145	ZHANG	13A	DPWA	Multichannel

[1] From the preferred solution A in KAMANO 15, incompatible with solution B.

Λ(1890) INELASTIC POLE RESIDUE

The "normalized residue" is the residue divided by $\Gamma_{pole}/2$.

Normalized residue in $N\overline{K} \to \Lambda(1890) \to N\overline{K}$

MODULUS	PHASE (°)	DOCUMENT ID		TECN	COMMENT
• • • We do not use the following data for averages, fits, limits, etc. • • •					
0.241	−23	[1] KAMANO	15	DPWA	Multichannel

[1] From the preferred solution A in KAMANO 15.

Normalized residue in $N\overline{K} \to \Lambda(1890) \to \Sigma\pi$

MODULUS	PHASE (°)	DOCUMENT ID		TECN	COMMENT
• • • We do not use the following data for averages, fits, limits, etc. • • •					
0.101	104	[1] KAMANO	15	DPWA	Multichannel

[1] From the preferred solution A in KAMANO 15.

Normalized residue in $N\overline{K} \to \Lambda(1890) \to \Lambda\eta$

MODULUS	PHASE (°)	DOCUMENT ID		TECN	COMMENT
• • • We do not use the following data for averages, fits, limits, etc. • • •					
0.0485	−54	[1] KAMANO	15	DPWA	Multichannel

[1] From the preferred solution A in KAMANO 15.

Normalized residue in $N\overline{K} \to \Lambda(1890) \to \Xi K$

MODULUS	PHASE (°)	DOCUMENT ID		TECN	COMMENT
• • • We do not use the following data for averages, fits, limits, etc. • • •					
0.0562	−85	[1] KAMANO	15	DPWA	Multichannel

[1] From the preferred solution A in KAMANO 15.

Normalized residue in $N\overline{K} \to \Lambda(1890) \to \Sigma(1385)\pi$, P-wave

MODULUS	PHASE (°)	DOCUMENT ID		TECN	COMMENT
• • • We do not use the following data for averages, fits, limits, etc. • • •					
0.295	−40	[1] KAMANO	15	DPWA	Multichannel

[1] From the preferred solution A in KAMANO 15.

Normalized residue in $N\overline{K} \to \Lambda(1890) \to \Sigma(1385)\pi$, F-wave

MODULUS	PHASE (°)	DOCUMENT ID		TECN	COMMENT
• • • We do not use the following data for averages, fits, limits, etc. • • •					
0.064	127	[1] KAMANO	15	DPWA	Multichannel

[1] From the preferred solution A in KAMANO 15.

Normalized residue in $N\overline{K} \to \Lambda(1890) \to N\overline{K}^*(892)$, S=1/2 , P-wave

MODULUS	PHASE (°)	DOCUMENT ID		TECN	COMMENT
• • • We do not use the following data for averages, fits, limits, etc. • • •					
0.188	−160	[1] KAMANO	15	DPWA	Multichannel

[1] From the preferred solution A in KAMANO 15.

Normalized residue in $N\overline{K} \to \Lambda(1890) \to N\overline{K}^*(892)$, S=3/2 , P-wave

MODULUS	PHASE (°)	DOCUMENT ID		TECN	COMMENT
• • • We do not use the following data for averages, fits, limits, etc. • • •					
0.209	15	[1] KAMANO	15	DPWA	Multichannel

[1] From the preferred solution A in KAMANO 15.

Normalized residue in $N\overline{K} \to \Lambda(1890) \to N\overline{K}^*(892)$, S=3/2, F-wave

MODULUS	PHASE (°)	DOCUMENT ID		TECN	COMMENT
• • • We do not use the following data for averages, fits, limits, etc. • • •					
0.0141	129	[1] KAMANO	15	DPWA	Multichannel

[1] From the preferred solution A in KAMANO 15.

Λ(1890) MASS

VALUE (MeV)	DOCUMENT ID		TECN	COMMENT
1850 to 1910 (≈ 1890) OUR ESTIMATE				
1900 ± 5	ZHANG	13A	DPWA	Multichannel
1897 ± 5	GOPAL	80	DPWA	$\overline{K}N \to \overline{K}N$
1908 ± 10	ALSTON-...	78	DPWA	$\overline{K}N \to \overline{K}N$
1900 ± 5	GOPAL	77	DPWA	$\overline{K}N$ multichannel
1894 ± 10	HEMINGWAY	75	DPWA	$K^-p \to \overline{K}N$
• • • We do not use the following data for averages, fits, limits, etc. • • •				
1856 or 1868	[1] MARTIN	77	DPWA	$\overline{K}N$ multichannel
1900	[2] NAKKASYAN	75	DPWA	$K^-p \to \Lambda\omega$

[1] The two MARTIN 77 values are from a T-matrix pole and from a Breit-Wigner fit.
[2] Found in one of two best solutions.

Λ(1890) WIDTH

VALUE (MeV)	DOCUMENT ID		TECN	COMMENT
60 to 200 (≈ 100) OUR ESTIMATE				
161 ± 15	ZHANG	13A	DPWA	Multichannel
74 ± 10	GOPAL	80	DPWA	$\overline{K}N \to \overline{K}N$
119 ± 20	ALSTON-...	78	DPWA	$\overline{K}N \to \overline{K}N$
72 ± 10	GOPAL	77	DPWA	$\overline{K}N$ multichannel
107 ± 10	HEMINGWAY	75	DPWA	$K^-p \to \overline{K}N$
• • • We do not use the following data for averages, fits, limits, etc. • • •				
191 or 193	[1] MARTIN	77	DPWA	$\overline{K}N$ multichannel
100	[2] NAKKASYAN	75	DPWA	$K^-p \to \Lambda\omega$

[1] The two MARTIN 77 values are from a T-matrix pole and from a Breit-Wigner fit.
[2] Found in one of two best solutions.

Λ(1890) DECAY MODES

	Mode	Fraction (Γ_i/Γ)
Γ_1	$N\overline{K}$	20–35 %
Γ_2	$\Sigma\pi$	3–10 %
Γ_3	$\Lambda\eta$	
Γ_4	ΞK	
Γ_5	$\Sigma(1385)\pi$	seen
Γ_6	$\Sigma(1385)\pi$, P-wave	
Γ_7	$\Sigma(1385)\pi$, F-wave	
Γ_8	$N\overline{K}^*(892)$	seen
Γ_9	$N\overline{K}^*(892)$, S=1/2	
Γ_{10}	$N\overline{K}^*(892)$, S=1/2, P-wave	
Γ_{11}	$N\overline{K}^*(892)$, S=3/2, P-wave	
Γ_{12}	$N\overline{K}^*(892)$, S=3/2, F-wave	
Γ_{13}	$\Lambda\omega$	

Λ(1890) BRANCHING RATIOS

See "Sign conventions for resonance couplings" in the Note on Λ and Σ Resonances.

$\Gamma(N\overline{K})/\Gamma_{total}$ Γ_1/Γ

VALUE	DOCUMENT ID		TECN	COMMENT
0.20 to 0.35 OUR ESTIMATE				
0.37 ±0.03	ZHANG	13A	DPWA	Multichannel
0.20 ±0.02	GOPAL	80	DPWA	$\overline{K}N \to \overline{K}N$
0.34 ±0.05	ALSTON-...	78	DPWA	$\overline{K}N \to \overline{K}N$
0.24 ±0.04	HEMINGWAY	75	DPWA	$K^-p \to \overline{K}N$
• • • We do not use the following data for averages, fits, limits, etc. • • •				
0.305	[1] KAMANO	15	DPWA	Multichannel
0.18 ±0.02	GOPAL	77	DPWA	See GOPAL 80
0.36 or 0.34	[2] MARTIN	77	DPWA	$\overline{K}N$ multichannel

[1] From the preferred solution A in KAMANO 15.
[2] The two MARTIN 77 values are from a T-matrix pole and from a Breit-Wigner fit.

$\Gamma(\Sigma\pi)/\Gamma_{total}$ Γ_2/Γ

VALUE	DOCUMENT ID		TECN	COMMENT
<0.03	LANGBEIN	72	IPWA	$\overline{K}N$ multichannel
• • • We do not use the following data for averages, fits, limits, etc. • • •				
0.04	[1] KAMANO	15	DPWA	Multichannel

[1] From the preferred solution A in KAMANO 15.

$\Gamma(\Lambda\eta)/\Gamma_{total}$ Γ_3/Γ

VALUE	DOCUMENT ID		TECN	COMMENT
• • • We do not use the following data for averages, fits, limits, etc. • • •				
0.012	[1] KAMANO	15	DPWA	Multichannel

[1] From the preferred solution A in KAMANO 15.

Γ(ΞK)/Γtotal Γ4/Γ

VALUE	DOCUMENT ID		TECN	COMMENT
• • • We do not use the following data for averages, fits, limits, etc. • • •				
0.009	[1] KAMANO	15	DPWA	Multichannel

[1] From the preferred solution A in KAMANO 15.

Γ(Σ(1385)π, P-wave)/Γtotal Γ6/Γ

VALUE	DOCUMENT ID		TECN	COMMENT
• • • We do not use the following data for averages, fits, limits, etc. • • •				
0.453	[1] KAMANO	15	DPWA	Multichannel

[1] From the preferred solution A in KAMANO 15.

Γ(Σ(1385)π, F-wave)/Γtotal Γ7/Γ

VALUE	DOCUMENT ID		TECN	COMMENT
• • • We do not use the following data for averages, fits, limits, etc. • • •				
0.019	[1] KAMANO	15	DPWA	Multichannel

[1] From the preferred solution A in KAMANO 15.

Γ(NK̄*(892), S=1/2, P-wave)/Γtotal Γ10/Γ

VALUE	DOCUMENT ID		TECN	COMMENT
• • • We do not use the following data for averages, fits, limits, etc. • • •				
0.073	[1] KAMANO	15	DPWA	Multichannel

[1] From the preferred solution A in KAMANO 15.

Γ(NK̄*(892), S=3/2, P-wave)/Γtotal Γ11/Γ

VALUE	DOCUMENT ID		TECN	COMMENT
• • • We do not use the following data for averages, fits, limits, etc. • • •				
0.088	[1] KAMANO	15	DPWA	Multichannel

[1] From the preferred solution A in KAMANO 15.

Γ(NK̄*(892), S=3/2, F-wave)/Γtotal Γ12/Γ

VALUE	DOCUMENT ID		TECN	COMMENT
• • • We do not use the following data for averages, fits, limits, etc. • • •				
0.001	[1] KAMANO	15	DPWA	Multichannel

[1] From the preferred solution A in KAMANO 15.

(ΓiΓf)^½/Γtotal in NK̄ → Λ(1890) → Σπ (Γ1Γ2)^½/Γ

VALUE	DOCUMENT ID		TECN	COMMENT
−0.09±0.02	ZHANG	13A	DPWA	Multichannel
−0.09±0.03	GOPAL	77	DPWA	K̄N multichannel
• • • We do not use the following data for averages, fits, limits, etc. • • •				
+0.15 or +0.14	[1] MARTIN	77	DPWA	K̄N multichannel

[1] The two MARTIN 77 values are from a T-matrix pole and from a Breit-Wigner fit.

(ΓiΓf)^½/Γtotal in NK̄ → Λ(1890) → Σ(1385)π, P-wave (Γ1Γ6)^½/Γ

VALUE	DOCUMENT ID		TECN	COMMENT
<0.03	CAMERON	78	DPWA	$K^- p \to \Sigma(1385)\pi$

(ΓiΓf)^½/Γtotal in NK̄ → Λ(1890) → Σ(1385)π, F-wave (Γ1Γ7)^½/Γ

VALUE	DOCUMENT ID		TECN	COMMENT
−0.31 ±0.04	ZHANG	13A	DPWA	Multichannel
−0.126±0.055	[1] CAMERON	78	DPWA	$K^- p \to \Sigma(1385)\pi$

[1] The published sign has been changed to be in accord with the baryon-first convention.

(ΓiΓf)^½/Γtotal in NK̄ → Λ(1890) → NK̄*(892), S=1/2 (Γ1Γ9)^½/Γ

VALUE	DOCUMENT ID		TECN	COMMENT
−0.17±0.05	ZHANG	13A	DPWA	Multichannel
−0.07±0.03	[1,2] CAMERON	78B	DPWA	$K^- p \to N\overline{K}^*$

[1] Upper limits on the P_3 and F_3 waves are each 0.03.

[2] The published sign has been changed to be in accord with the baryon-first convention.

(ΓiΓf)^½/Γtotal in NK̄ → Λ(1890) → NK̄*(892), S=3/2, F-wave (Γ1Γ12)^½/Γ

VALUE	DOCUMENT ID		TECN	COMMENT
−0.11±0.03	ZHANG	13A	DPWA	Multichannel

(ΓiΓf)^½/Γtotal in NK̄ → Λ(1890) → Λω (Γ1Γ13)^½/Γ

VALUE	DOCUMENT ID		TECN	COMMENT
seen	BACCARI	77	IPWA	$K^- p \to \Lambda\omega$
0.032	[1] NAKKASYAN	75	DPWA	$K^- p \to \Lambda\omega$

[1] Found in one of two best solutions.

Λ(1890) REFERENCES

KAMANO	15	PR C92 025205	H. Kamano *et al.*	(ANL, OSAK)
ZHANG	13A	PR C88 035205	H. Zhang *et al.*	(KSU)
PDG	82	PL 111B 1	M. Roos *et al.*	(HELS, CIT, CERN)
GOPAL	80	Toronto Conf. 159	G.P. Gopal	(RHEL) IJP
ALSTON-...	78	PR D18 182	M. Alston-Garnjost *et al.*	(LBL, MTHO+) IJP
Also		PRL 38 1007	M. Alston-Garnjost *et al.*	(LBL, MTHO+) IJP
CAMERON	78	NP B143 189	W. Cameron *et al.*	(RHEL, LOIC) IJP
CAMERON	78B	NP B146 327	W. Cameron *et al.*	(RHEL, LOIC) IJP
BACCARI	77	NC 41A 96	B. Baccari *et al.*	(SACL, CDEF) IJP
GOPAL	77	NP B119 362	G.P. Gopal *et al.*	(LOIC, RHEL) IJP
MARTIN	77	NP B127 349	B.R. Martin, M.K. Pidcock, R.G. Moorhouse	(LOUC+) IJP
Also		NP B126 266	B.R. Martin, M.K. Pidcock	(LOUC)
Also		NP B126 285	B.R. Martin, M.K. Pidcock	(LOUC) IJP
HEMINGWAY	75	NP B91 12	R.J. Hemingway *et al.*	(CERN, HEIDH, MPIM) IJP
NAKKASYAN	75	NP B93 85	A. Nakkasyan	(CERN) IJP
LANGBEIN	72	NP B47 477	W. Langbein, F. Wagner	(MPIM) IJP

Λ(2000) $I(J^P) = 0(?^?)$ Status: *

OMITTED FROM SUMMARY TABLE

ZHANG 13A claims a $J^P = 1/2^-$ state.

We list here all the ambiguous resonance possibilities with a mass around 2 GeV. The proposed quantum numbers are D_3 (BARBAROGALTIERI 70 in $\Sigma\pi$), D_3+F_5, P_3+D_5, or P_1+D_3 (BRANDSTETTER 72 in $\Lambda\omega$), and S_1 (CAMERON 78B in $N\overline{K}^*$). The first two of the above analyses should now be considered obsolete. See also NAKKASYAN 75.

Λ(2000) MASS

VALUE (MeV)	DOCUMENT ID		TECN	COMMENT
≈ 2000 OUR ESTIMATE				
2020±16	ZHANG	13A	DPWA	Multichannel
2030±30	CAMERON	78B	DPWA	$K^- p \to N\overline{K}^*$
1935 to 1971	[1] BRANDSTET...	72	DPWA	$K^- p \to \Lambda\omega$
1951 to 2034	[1] BRANDSTET...	72	DPWA	$K^- p \to \Lambda\omega$
2010±30	BARBARO-...	70	DPWA	$K^- p \to \Sigma\pi$

Λ(2000) WIDTH

VALUE (MeV)	DOCUMENT ID		TECN	COMMENT
255±63	ZHANG	13A	DPWA	Multichannel
125±25	CAMERON	78B	DPWA	$K^- p \to N\overline{K}^*$
180 to 240	[1] BRANDSTET...	72	DPWA	(lower mass)
73 to 154	[1] BRANDSTET...	72	DPWA	(higher mass)
130±50	BARBARO-...	70	DPWA	$K^- p \to \Sigma\pi$

Λ(2000) DECAY MODES

	Mode	Fraction (Γi/Γ)
Γ1	NK̄	(27±6) %
Γ2	Σπ	
Γ3	Λη	(16±7) %
Γ4	Λω	
Γ5	NK̄*(892), S=1/2, S-wave	
Γ6	NK̄*(892), S=3/2, D-wave	

Λ(2000) BRANCHING RATIOS

See "Sign conventions for resonance couplings" in the Note on Λ and Σ Resonances.

Γ(NK̄)/Γtotal Γ1/Γ

VALUE	DOCUMENT ID		TECN	COMMENT
0.27±0.06	ZHANG	13A	DPWA	Multichannel

(ΓiΓf)^½/Γtotal in NK̄ → Λ(2000) → Σπ (Γ1Γ2)^½/Γ

VALUE	DOCUMENT ID		TECN	COMMENT
−0.07±0.03	ZHANG	13A	DPWA	Multichannel
−0.20±0.04	BARBARO-...	70	DPWA	$K^- p \to \Sigma\pi$

Γ(Λη)/Γtotal Γ3/Γ

VALUE	DOCUMENT ID		TECN	COMMENT
0.16±0.07	ZHANG	13A	DPWA	Multichannel

(ΓiΓf)^½/Γtotal in NK̄ → Λ(2000) → Λω (Γ1Γ4)^½/Γ

VALUE	DOCUMENT ID		TECN	COMMENT
0.17 to 0.25	[1] BRANDSTET...	72	DPWA	(lower mass)
0.04 to 0.15	[1] BRANDSTET...	72	DPWA	(higher mass)

(ΓiΓf)^½/Γtotal in NK̄ → Λ(2000) → NK̄*(892), S=1/2, S-wave (Γ1Γ5)^½/Γ

VALUE	DOCUMENT ID		TECN	COMMENT
−0.12±0.03	[2] CAMERON	78B	DPWA	$K^- p \to N\overline{K}^*$

$(\Gamma_i\Gamma_f)^{1/2}/\Gamma_{total}$ in $N\overline{K} \to \Lambda(2000) \to N\overline{K}^*(892)$, S=3/2, D-wave $(\Gamma_1\Gamma_6)^{1/2}/\Gamma$

VALUE	DOCUMENT ID		TECN	COMMENT
$+0.34\pm0.05$	ZHANG	13A	DPWA	Multichannel
$+0.09\pm0.03$	CAMERON	78B	DPWA	$K^-p \to N\overline{K}^*$

Λ(2000) FOOTNOTES

[1] The parameters quoted here are ranges from the three best fits; the lower state probably has $J \leq 3/2$, and the higher one probably has $J \leq 5/2$.

[2] The published sign has been changed to be in accord with the baryon-first convention.

Λ(2000) REFERENCES

ZHANG	13A	PR C88 035205	H. Zhang *et al.*	(KSU)
CAMERON	78B	NP B146 327	W. Cameron *et al.*	(RHEL, LOIC) IJP
NAKKASYAN	75	NP B93 85	A. Nakkasyan	(CERN) IJP
BRANDSTET...	72	NP B39 13	A.A. Brandstetter *et al.*	(RHEL, CDEF+)
BARBARO-...	70	Duke Conf. 173 Hyperon Resonances, 1970	A. Barbaro-Galtieri	(LRL) IJP

Λ(2020) 7/2+

$I(J^P) = 0(\frac{7}{2}^+)$ Status: *

OMITTED FROM SUMMARY TABLE

In LITCHFIELD 71, need for the state rests solely on a possibly inconsistent polarization measurement at 1.784 GeV/c. HEMINGWAY 75 does not require this state. GOPAL 77 does not need it in either $N\overline{K}$ or $\Sigma\pi$. With new K^-n angular distributions included, DECLAIS 77 sees it. However, this and other new data are included in GOPAL 80 and the state is not required. BACCARI 77 weakly supports it.

Λ(2020) POLE POSITION

REAL PART

VALUE	DOCUMENT ID		TECN	COMMENT
• • • We do not use the following data for averages, fits, limits, etc. • • •				
1757	[1] KAMANO	15	DPWA	Multichannel

[1] From the preferred solution A in KAMANO 15. Solution B reports $M = 2041^{+80}_{-82}$ MeV.

−2×IMAGINARY PART

VALUE	DOCUMENT ID		TECN	COMMENT
• • • We do not use the following data for averages, fits, limits, etc. • • •				
146	[1] KAMANO	15	DPWA	Multichannel

[1] From the preferred solution A in KAMANO 15. Solution B reports $M = 238^{+114}_{-34}$ MeV.

Λ(2020) POLE RESIDUES

The normalized residue is the residue divided by $\Gamma_{pole}/2$.

Normalized residue in $N\overline{K} \to \Lambda(2020) \to N\overline{K}$

MODULUS	PHASE (°)	DOCUMENT ID		TECN	COMMENT
• • • We do not use the following data for averages, fits, limits, etc. • • •					
0.000145	−77	[1] KAMANO	15	DPWA	Multichannel

[1] From the preferred solution A in KAMANO 15.

Normalized residue in $N\overline{K} \to \Lambda(2020) \to \Sigma\pi$

MODULUS	PHASE (°)	DOCUMENT ID		TECN	COMMENT
• • • We do not use the following data for averages, fits, limits, etc. • • •					
0.0112	120	[1] KAMANO	15	DPWA	Multichannel

[1] From the preferred solution A in KAMANO 15.

Normalized residue in $N\overline{K} \to \Lambda(2020) \to \Lambda\eta$

MODULUS	PHASE (°)	DOCUMENT ID		TECN	COMMENT
• • • We do not use the following data for averages, fits, limits, etc. • • •					
0.000786	−100	[1] KAMANO	15	DPWA	Multichannel

[1] From the preferred solution A in KAMANO 15.

Normalized residue in $N\overline{K} \to \Lambda(2020) \to \Sigma(1385)\pi$, F-wave

MODULUS	PHASE (°)	DOCUMENT ID		TECN	COMMENT
• • • We do not use the following data for averages, fits, limits, etc. • • •					
0.00451	−82	[1] KAMANO	15	DPWA	Multichannel

[1] From the preferred solution A in KAMANO 15.

Normalized residue in $N\overline{K} \to \Lambda(2020) \to \Sigma(1385)\pi$, H-wave

MODULUS	PHASE (°)	DOCUMENT ID		TECN	COMMENT
• • • We do not use the following data for averages, fits, limits, etc. • • •					
0.0000298	−128	[1] KAMANO	15	DPWA	Multichannel

[1] From the preferred solution A in KAMANO 15.

Λ(2020) MASS

VALUE (MeV)	DOCUMENT ID		TECN	COMMENT
≈ 2020 OUR ESTIMATE				
2043 ± 22	ZHANG	13A	DPWA	Multichannel
2140	BACCARI	77	DPWA	$K^-p \to \Lambda\omega$
2117	DECLAIS	77	DPWA	$\overline{K}N \to \overline{K}N$
2100 ± 30	LITCHFIELD	71	DPWA	$K^-p \to \overline{K}N$
2020 ± 20	BARBARO-...	70	DPWA	$K^-p \to \Sigma\pi$

Λ(2020) WIDTH

VALUE (MeV)	DOCUMENT ID		TECN	COMMENT
200 ± 75	ZHANG	13A	DPWA	Multichannel
128	BACCARI	77	DPWA	$K^-p \to \Lambda\omega$
167	DECLAIS	77	DPWA	$\overline{K}N \to \overline{K}N$
120 ± 30	LITCHFIELD	71	DPWA	$K^-p \to \overline{K}N$
160 ± 30	BARBARO-...	70	DPWA	$K^-p \to \Sigma\pi$

Λ(2020) DECAY MODES

	Mode	Fraction (Γ_i/Γ)
Γ_1	$N\overline{K}$	
Γ_2	$\Sigma\pi$	
Γ_3	$\Lambda\eta$	
Γ_4	$\Sigma(1385)\pi$, F-wave	
Γ_5	$\Sigma(1385)\pi$, H-wave	
Γ_6	$N\overline{K}^*(892)$, S=1/2, F-wave	
Γ_7	$N\overline{K}^*(892)$, S=3/2, F-wave	
Γ_8	$N\overline{K}^*(892)$, S=3/2, H-wave	
Γ_9	$\Lambda\omega$	
Γ_{10}	$N\overline{K}^*(892)$, S=1/2	(30±9) %

Λ(2020) BRANCHING RATIOS

See "Sign conventions for resonance couplings" in the Note on Λ and Σ Resonances.

$\Gamma(N\overline{K})/\Gamma_{total}$ Γ_1/Γ

VALUE	DOCUMENT ID		TECN	COMMENT
0.028 ± 0.005	ZHANG	13A	DPWA	Multichannel
0.05	DECLAIS	77	DPWA	$\overline{K}N \to \overline{K}N$
$0.05\ \pm0.02$	LITCHFIELD	71	DPWA	$K^-p \to \overline{K}N$
• • • We do not use the following data for averages, fits, limits, etc. • • •				
not seen	[1] KAMANO	15	DPWA	Multichannel

[1] From the preferred solution A in KAMANO 15.

$\Gamma(\Sigma\pi)/\Gamma_{total}$ Γ_2/Γ

VALUE	DOCUMENT ID		TECN	COMMENT
• • • We do not use the following data for averages, fits, limits, etc. • • •				
0.891	[1] KAMANO	15	DPWA	Multichannel

[1] From the preferred solution A in KAMANO 15.

$\Gamma(\Lambda\eta)/\Gamma_{total}$ Γ_3/Γ

VALUE	DOCUMENT ID		TECN	COMMENT
• • • We do not use the following data for averages, fits, limits, etc. • • •				
0.002	[1] KAMANO	15	DPWA	Multichannel

[1] From the preferred solution A in KAMANO 15.

$\Gamma(\Sigma(1385)\pi, F\text{-wave})/\Gamma_{total}$ Γ_4/Γ

VALUE	DOCUMENT ID		TECN	COMMENT
• • • We do not use the following data for averages, fits, limits, etc. • • •				
0.105	[1] KAMANO	15	DPWA	Multichannel

[1] From the preferred solution A in KAMANO 15.

$\Gamma(\Sigma(1385)\pi, H\text{-wave})/\Gamma_{total}$ Γ_5/Γ

VALUE	DOCUMENT ID		TECN	COMMENT
• • • We do not use the following data for averages, fits, limits, etc. • • •				
not seen	[1] KAMANO	15	DPWA	Multichannel

[1] From the preferred solution A in KAMANO 15.

$\Gamma(N\overline{K}^*(892), S\text{=}1/2, F\text{-wave})/\Gamma_{total}$ Γ_6/Γ

VALUE	DOCUMENT ID		TECN	COMMENT
• • • We do not use the following data for averages, fits, limits, etc. • • •				
not seen	[1] KAMANO	15	DPWA	Multichannel

[1] From the preferred solution A in KAMANO 15.

Γ(NK̄*(892), S=3/2, F-wave)/Γ_total — Γ7/Γ

VALUE	DOCUMENT ID	TECN	COMMENT
• • • We do not use the following data for averages, fits, limits, etc. • • •			
0.001	[1] KAMANO 15	DPWA	Multichannel

[1] From the preferred solution A in KAMANO 15.

Γ(NK̄*(892), S=3/2, H-wave)/Γ_total — Γ8/Γ

VALUE	DOCUMENT ID	TECN	COMMENT
• • • We do not use the following data for averages, fits, limits, etc. • • •			
not seen	[1] KAMANO 15	DPWA	Multichannel

[1] From the preferred solution A in KAMANO 15.

Γ(NK̄*(892), S=1/2)/Γ_total — Γ10/Γ

VALUE	DOCUMENT ID	TECN	COMMENT
0.30±0.09	ZHANG 13A	DPWA	Multichannel

(Γ_i Γ_f)^½/Γ_total in NK̄ → Λ(2020) → Σπ — (Γ1Γ2)^½/Γ

VALUE	DOCUMENT ID	TECN	COMMENT
+0.02±0.01	ZHANG 13A	DPWA	Multichannel
−0.15±0.02	BARBARO-... 70	DPWA	$K^- p \to \Sigma\pi$

(Γ_i Γ_f)^½/Γ_total in NK̄ → Λ(2020) → Λω — (Γ1Γ9)^½/Γ

VALUE	DOCUMENT ID	TECN	COMMENT
<0.05	BACCARI 77	DPWA	$K^- p \to \Lambda\omega$

Λ(2020) REFERENCES

KAMANO	15	PR C92 025205	H. Kamano *et al.*	(ANL, OSAK)
ZHANG	13A	PR C88 035205	H. Zhang *et al.*	(KSU)
GOPAL	80	Toronto Conf. 159	G.P. Gopal	(RHEL)
BACCARI	77	NC 41A 96	B. Baccari *et al.*	(SACL, CDEF) IJP
DECLAIS	77	CERN 77-16	Y. Declais *et al.*	(CAEN, CERN) IJP
GOPAL	77	NP B119 362	G.P. Gopal *et al.*	(LOIC, RHEL)
HEMINGWAY	75	NP B91 12	R.J. Hemingway *et al.*	(CERN, HEIDH, MPIM) IJP
LITCHFIELD	71	NP B30 125	P.J. Litchfield *et al.*	(RHEL, CDEF, SACL) IJP
BARBARO-...	70	Duke Conf. 173 Hyperon Resonances, 1970	A. Barbaro-Galtieri	(LRL) IJP

Λ(2050) 3/2⁻

$I(J^P) = 0(\frac{3}{2}^-)$ Status: *

OMITTED FROM SUMMARY TABLE

Λ(2050) MASS

VALUE (MeV)	DOCUMENT ID	TECN	COMMENT
2056±22	ZHANG 13A	DPWA	Multichannel

Λ(2050) WIDTH

VALUE (MeV)	DOCUMENT ID	TECN	COMMENT
493±61	ZHANG 13A	DPWA	Multichannel

Λ(2050) DECAY MODES

	Mode	Fraction (Γ_i/Γ)
Γ1	NK̄	(19 ±4) %
Γ2	Σπ	(6.0±3.0) %
Γ3	Σ*(1385)π, S-wave	(8 ±6) %
Γ4	Σ*(1385)π, D-wave	(4.0±3.0) %
Γ5	NK̄*(892), S=1/2	(23 ±7) %

Λ(2050) BRANCHING RATIOS

Γ(NK̄)/Γ_total — Γ1/Γ

VALUE	DOCUMENT ID	TECN	COMMENT
0.19±0.04	ZHANG 13A	DPWA	Multichannel

Γ(Σπ)/Γ_total — Γ2/Γ

VALUE	DOCUMENT ID	TECN	COMMENT
0.06±0.03	ZHANG 13A	DPWA	Multichannel

Γ(Σ*(1385)π, S-wave)/Γ_total — Γ3/Γ

VALUE	DOCUMENT ID	TECN	COMMENT
0.08±0.06	ZHANG 13A	DPWA	Multichannel

Γ(Σ*(1385)π, D-wave)/Γ_total — Γ4/Γ

VALUE	DOCUMENT ID	TECN	COMMENT
0.04±0.03	ZHANG 13A	DPWA	Multichannel

Γ(NK̄*(892), S=1/2)/Γ_total — Γ5/Γ

VALUE	DOCUMENT ID	TECN	COMMENT
0.23±0.07	ZHANG 13A	DPWA	Multichannel

Λ(2050) REFERENCES

ZHANG	13A	PR C88 035205	H. Zhang *et al.*	(KSU)

Λ(2100) 7/2⁻

$I(J^P) = 0(\frac{7}{2}^-)$ Status: ****

Most of the results published before 1973 are now obsolete and have been omitted. They may be found in our 1982 edition Physics Letters **111B** 1 (1982).

This entry only includes results from partial-wave analyses. Parameters of peaks seen in cross sections and in invariant-mass distributions around 2100 MeV used to be listed in a separate entry immediately following. It may be found in our 1986 edition Physics Letters **170B** 1 (1986).

Λ(2100) POLE POSITION

REAL PART

VALUE (MeV)	DOCUMENT ID	TECN	COMMENT
• • • We do not use the following data for averages, fits, limits, etc. • • •			
2023	ZHANG 13A	DPWA	Multichannel

−2×IMAGINARY PART

VALUE (MeV)	DOCUMENT ID	TECN	COMMENT
• • • We do not use the following data for averages, fits, limits, etc. • • •			
239	ZHANG 13A	DPWA	Multichannel

Λ(2100) MASS

VALUE (MeV)	DOCUMENT ID	TECN	COMMENT
2090 to 2110 (≈ 2100) OUR ESTIMATE			
2086± 6	ZHANG 13A	DPWA	Multichannel
2104±10	GOPAL 80	DPWA	$\overline{K}N \to \overline{K}N$
2106±30	DEBELLEFON 78	DPWA	$\overline{K}N \to \overline{K}N$
2110±10	GOPAL 77	DPWA	$\overline{K}N$ multichannel
2105±10	HEMINGWAY 75	DPWA	$K^- p \to \overline{K}N$
2115±10	KANE 74	DPWA	$K^- p \to \Sigma\pi$
• • • We do not use the following data for averages, fits, limits, etc. • • •			
2094	BACCARI 77	DPWA	$K^- p \to \Lambda\omega$
2094	DECLAIS 77	DPWA	$\overline{K}N \to \overline{K}N$
2110 or 2089	[1] NAKKASYAN 75	DPWA	$K^- p \to \Lambda\omega$

Λ(2100) WIDTH

VALUE (MeV)	DOCUMENT ID	TECN	COMMENT
100 to 250 (≈ 200) OUR ESTIMATE			
305±16	ZHANG 13A	DPWA	Multichannel
157±40	DEBELLEFON 78	DPWA	$\overline{K}N \to \overline{K}N$
250±30	GOPAL 77	DPWA	$\overline{K}N$ multichannel
241±30	HEMINGWAY 75	DPWA	$K^- p \to \overline{K}N$
152±15	KANE 74	DPWA	$K^- p \to \Sigma\pi$
• • • We do not use the following data for averages, fits, limits, etc. • • •			
98	BACCARI 77	DPWA	$K^- p \to \Lambda\omega$
250	DECLAIS 77	DPWA	$\overline{K}N \to \overline{K}N$
244 or 302	[1] NAKKASYAN 75	DPWA	$K^- p \to \Lambda\omega$

Λ(2100) DECAY MODES

	Mode	Fraction (Γ_i/Γ)
Γ1	NK̄	25–35 %
Γ2	Σπ	∼ 5 %
Γ3	Λη	<3 %
Γ4	ΞK	<3 %
Γ5	Λω	<8 %
Γ6	NK̄*(892)	10–20 %
Γ7	NK̄*(892), S=3/2, D-wave	
Γ8	NK̄*(892), S=1/2, G-wave	
Γ9	NK̄*(892), S=3/2, G-wave	

Λ(2100) BRANCHING RATIOS

See "Sign conventions for resonance couplings" in the Note on Λ and Σ Resonances.

Γ(NK̄)/Γ_total — Γ1/Γ

VALUE	DOCUMENT ID	TECN	COMMENT
0.25 to 0.35 OUR ESTIMATE			
0.23±0.01	ZHANG 13A	DPWA	Multichannel
0.34±0.03	GOPAL 80	DPWA	$\overline{K}N \to \overline{K}N$
0.24±0.06	DEBELLEFON 78	DPWA	$\overline{K}N \to \overline{K}N$
0.31±0.03	HEMINGWAY 75	DPWA	$K^- p \to \overline{K}N$
• • • We do not use the following data for averages, fits, limits, etc. • • •			
0.29	DECLAIS 77	DPWA	$\overline{K}N \to \overline{K}N$
0.30±0.03	GOPAL 77	DPWA	See GOPAL 80

$(\Gamma_i\Gamma_f)^{1/2}/\Gamma_{total}$ in $N\overline{K} \to \Lambda(2100) \to \Sigma\pi$ $(\Gamma_1\Gamma_2)^{1/2}/\Gamma$

VALUE	DOCUMENT ID		TECN	COMMENT
$+0.03\pm0.01$	ZHANG	13A	DPWA	Multichannel
$+0.12\pm0.04$	GOPAL	77	DPWA	$\overline{K}N$ multichannel
$+0.11\pm0.01$	KANE	74	DPWA	$K^-p \to \Sigma\pi$

$(\Gamma_i\Gamma_f)^{1/2}/\Gamma_{total}$ in $N\overline{K} \to \Lambda(2100) \to \Lambda\eta$ $(\Gamma_1\Gamma_3)^{1/2}/\Gamma$

VALUE	DOCUMENT ID		TECN	COMMENT
-0.050 ± 0.020	RADER	73	MPWA	$K^-p \to \Lambda\eta$

$(\Gamma_i\Gamma_f)^{1/2}/\Gamma_{total}$ in $N\overline{K} \to \Lambda(2100) \to \Xi K$ $(\Gamma_1\Gamma_4)^{1/2}/\Gamma$

VALUE	DOCUMENT ID		TECN	COMMENT
0.035 ± 0.018	LITCHFIELD	71	DPWA	$K^-p \to \Xi K$
• • • We do not use the following data for averages, fits, limits, etc. • • •				
0.003	MULLER	69B	DPWA	$K^-p \to \Xi K$
0.05	TRIPP	67	RVUE	$K^-p \to \Xi K$

$(\Gamma_i\Gamma_f)^{1/2}/\Gamma_{total}$ in $N\overline{K} \to \Lambda(2100) \to \Lambda\omega$ $(\Gamma_1\Gamma_5)^{1/2}/\Gamma$

VALUE	DOCUMENT ID		TECN	COMMENT
-0.070	[2] BACCARI	77	DPWA	GD_{37} wave
$+0.011$	[2] BACCARI	77	DPWA	GG_{17} wave
$+0.008$	[2] BACCARI	77	DPWA	GG_{37} wave
0.122 or 0.154	[1] NAKKASYAN	75	DPWA	$K^-p \to \Lambda\omega$

$(\Gamma_i\Gamma_f)^{1/2}/\Gamma_{total}$ in $N\overline{K} \to \Lambda(2100) \to N\overline{K}^*(892)$, S=3/2, D-wave $(\Gamma_1\Gamma_7)^{1/2}/\Gamma$

VALUE	DOCUMENT ID		TECN	COMMENT
$+0.16\pm0.02$	ZHANG	13A	DPWA	Multichannel
$+0.21\pm0.04$	CAMERON	78B	DPWA	$K^-p \to N\overline{K}^*$

$(\Gamma_i\Gamma_f)^{1/2}/\Gamma_{total}$ in $N\overline{K} \to \Lambda(2100) \to N\overline{K}^*(892)$, S=1/2, G-wave $(\Gamma_1\Gamma_8)^{1/2}/\Gamma$

VALUE	DOCUMENT ID		TECN	COMMENT
-0.03 ± 0.02	ZHANG	13A	DPWA	Multichannel
-0.04 ± 0.03	[3] CAMERON	78B	DPWA	$K^-p \to N\overline{K}^*$

$(\Gamma_i\Gamma_f)^{1/2}/\Gamma_{total}$ in $N\overline{K} \to \Lambda(2100) \to N\overline{K}^*(892)$, S=3/2, G-wave $(\Gamma_1\Gamma_9)^{1/2}/\Gamma$

VALUE	DOCUMENT ID		TECN	COMMENT
$+0.08\pm0.02$	ZHANG	13A	DPWA	Multichannel

$\Lambda(2100)$ FOOTNOTES

[1] The NAKKASYAN 75 values are from the two best solutions found. Each has the $\Lambda(2100)$ and one additional resonance (P_3 or F_5).

[2] Note that the three for BACCARI 77 entries are for three different waves.

[3] The published sign has been changed to be in accord with the baryon-first convention. The upper limit on the G_3 wave is 0.03.

$\Lambda(2100)$ REFERENCES

ZHANG	13A	PR C88 035205	H. Zhang *et al.*	(KSU)
PDG	86	PL 170B 1	M. Aguilar-Benitez *et al.*	(CERN, CIT+)
PDG	82	PL 111B 1	M. Roos *et al.*	(HELS, CIT, CERN)
GOPAL	80	Toronto Conf. 159	G.P. Gopal	(RHEL) IJP
CAMERON	78B	NP B146 327	W. Cameron *et al.*	(RHEL, LOIC) IJP
DEBELLEFON	78	NC 42A 403	A. de Bellefon *et al.*	(CDEF, SACL) IJP
BACCARI	77	NC 41A 96	B. Baccari *et al.*	(SACL, CDEF) IJP
DECLAIS	77	CERN 77-16	Y. Declais *et al.*	(CAEN, CERN) IJP
GOPAL	77	NP B119 362	G.P. Gopal *et al.*	(LOIC, RHEL) IJP
HEMINGWAY	75	NP B91 12	R.J. Hemingway *et al.*	(CERN, HEIDH, MPIM) IJP
NAKKASYAN	75	NP B93 85	A. Nakkasyan	(CERN) IJP
KANE	74	LBL-2452	D.F. Kane	(LBL) IJP
RADER	73	NC 16A 178	R.K. Rader *et al.*	(SACL, HEID, CERN+)
LITCHFIELD	71	NP B30 125	P.J. Litchfield *et al.*	(RHEL, CDEF, SACL) IJP
MULLER	69B	Thesis UCRL 19372	R.A. Muller	(LRL)
TRIPP	67	NP B3 10	R.D. Tripp *et al.*	(LRL, SLAC, CERN+)

$\Lambda(2110)$ $5/2^+$

$I(J^P) = 0(\frac{5}{2}^+)$ Status: ***

For results published before 1974 (they are now obsolete), see our 1982 edition Physics Letters **111B** 1 (1982). All the references have been retained.

This resonance is in the Baryon Summary Table, but the evidence for it could be better.

$\Lambda(2110)$ POLE POSITION

REAL PART

VALUE (MeV)	DOCUMENT ID		TECN	COMMENT
• • • We do not use the following data for averages, fits, limits, etc. • • •				
1970	ZHANG	13A	DPWA	Multichannel

$-2\times$IMAGINARY PART

VALUE (MeV)	DOCUMENT ID		TECN	COMMENT
• • • We do not use the following data for averages, fits, limits, etc. • • •				
350	ZHANG	13A	DPWA	Multichannel

$\Lambda(2110)$ MASS

VALUE (MeV)	DOCUMENT ID		TECN	COMMENT
2090 to 2140 (≈ 2110) OUR ESTIMATE				
2036 ± 13	ZHANG	13A	DPWA	Multichannel
2092 ± 25	GOPAL	80	DPWA	$\overline{K}N \to \overline{K}N$
2125 ± 25	CAMERON	78B	DPWA	$K^-p \to N\overline{K}^*$
2106 ± 50	DEBELLEFON	78	DPWA	$\overline{K}N \to \overline{K}N$
2140 ± 20	DEBELLEFON	77	DPWA	$K^-p \to \Sigma\pi$
2100 ± 50	GOPAL	77	DPWA	$\overline{K}N$ multichannel
$2112\pm\ 7$	KANE	74	DPWA	$K^-p \to \Sigma\pi$
• • • We do not use the following data for averages, fits, limits, etc. • • •				
2137	BACCARI	77	DPWA	$K^-p \to \Lambda\omega$
2103	[1] NAKKASYAN	75	DPWA	$K^-p \to \Lambda\omega$

$\Lambda(2110)$ WIDTH

VALUE (MeV)	DOCUMENT ID		TECN	COMMENT
150 to 250 (≈ 200) OUR ESTIMATE				
400 ± 38	ZHANG	13A	DPWA	Multichannel
245 ± 25	GOPAL	80	DPWA	$\overline{K}N \to \overline{K}N$
160 ± 30	CAMERON	78B	DPWA	$K^-p \to N\overline{K}^*$
251 ± 50	DEBELLEFON	78	DPWA	$\overline{K}N \to \overline{K}N$
140 ± 20	DEBELLEFON	77	DPWA	$K^-p \to \Sigma\pi$
200 ± 50	GOPAL	77	DPWA	$\overline{K}N$ multichannel
190 ± 30	KANE	74	DPWA	$K^-p \to \Sigma\pi$
• • • We do not use the following data for averages, fits, limits, etc. • • •				
132	BACCARI	77	DPWA	$K^-p \to \Lambda\omega$
391	[1] NAKKASYAN	75	DPWA	$K^-p \to \Lambda\omega$

$\Lambda(2110)$ DECAY MODES

	Mode	Fraction (Γ_j/Γ)
Γ_1	$N\overline{K}$	5–25 %
Γ_2	$\Sigma\pi$	10–40 %
Γ_3	$\Lambda\omega$	seen
Γ_4	$\Sigma(1385)\pi$	seen
Γ_5	$\Sigma(1385)\pi$, P-wave	
Γ_6	$N\overline{K}^*(892)$	10–60 %
Γ_7	$N\overline{K}^*(892)$, S=1/2	
Γ_8	$N\overline{K}^*(892)$, S=3/2, P-wave	

$\Lambda(2110)$ BRANCHING RATIOS

See "Sign conventions for resonance couplings" in the Note on Λ and Σ Resonances.

$\Gamma(N\overline{K})/\Gamma_{total}$ Γ_1/Γ

VALUE	DOCUMENT ID		TECN	COMMENT
0.05 to 0.25 OUR ESTIMATE				
0.083 ± 0.005	ZHANG	13A	DPWA	Multichannel
$0.07\ \pm0.03$	GOPAL	80	DPWA	$\overline{K}N \to \overline{K}N$
$0.27\ \pm0.06$	[2] DEBELLEFON	78	DPWA	$\overline{K}N \to \overline{K}N$
• • • We do not use the following data for averages, fits, limits, etc. • • •				
$0.07\ \pm0.03$	GOPAL	77	DPWA	See GOPAL 80

$(\Gamma_i\Gamma_f)^{1/2}/\Gamma_{total}$ in $N\overline{K} \to \Lambda(2110) \to \Sigma\pi$ $(\Gamma_1\Gamma_2)^{1/2}/\Gamma$

VALUE	DOCUMENT ID		TECN	COMMENT
$+0.04\pm0.01$	ZHANG	13A	DPWA	Multichannel
$+0.14\pm0.01$	DEBELLEFON	77	DPWA	$K^-p \to \Sigma\pi$
$+0.20\pm0.03$	KANE	74	DPWA	$K^-p \to \Sigma\pi$
• • • We do not use the following data for averages, fits, limits, etc. • • •				
$+0.10\pm0.03$	GOPAL	77	DPWA	$\overline{K}N$ multichannel

$(\Gamma_i\Gamma_f)^{1/2}/\Gamma_{total}$ in $N\overline{K} \to \Lambda(2110) \to \Lambda\omega$ $(\Gamma_1\Gamma_3)^{1/2}/\Gamma$

VALUE	DOCUMENT ID		TECN	COMMENT
<0.05	BACCARI	77	DPWA	$K^-p \to \Lambda\omega$
0.112	[1] NAKKASYAN	75	DPWA	$K^-p \to \Lambda\omega$

$(\Gamma_i\Gamma_f)^{1/2}/\Gamma_{total}$ in $N\overline{K} \to \Lambda(2110) \to \Sigma(1385)\pi$, P-wave $(\Gamma_1\Gamma_5)^{1/2}/\Gamma$

VALUE	DOCUMENT ID		TECN	COMMENT
$+0.04\ \pm0.01$	ZHANG	13A	DPWA	Multichannel
$+0.071\pm0.025$	[3] CAMERON	78	DPWA	$K^-p \to \Sigma(1385)\pi$

$(\Gamma_i\Gamma_f)^{1/2}/\Gamma_{total}$ in $N\overline{K} \to \Lambda(2110) \to N\overline{K}^*(892)$, S=1/2 **$(\Gamma_1\Gamma_7)^{1/2}/\Gamma$**

VALUE	DOCUMENT ID		TECN	COMMENT
−0.09±0.01	ZHANG	13A	DPWA	Multichannel
−0.17±0.04	[4] CAMERON	78B	DPWA	$K^-p \to N\overline{K}^*$

$(\Gamma_i\Gamma_f)^{1/2}/\Gamma_{total}$ in $N\overline{K} \to \Lambda(2110) \to N\overline{K}^*(892)$, S=3/2, P-wave **$(\Gamma_1\Gamma_8)^{1/2}/\Gamma$**

VALUE	DOCUMENT ID		TECN	COMMENT
0.24±0.01	ZHANG	13A	DPWA	Multichannel

Λ(2110) FOOTNOTES

[1] Found in one of two best solutions.
[2] The published error of 0.6 was a misprint.
[3] The CAMERON 78 upper limit on *F*-wave decay is 0.03. The sign here has been changed to be in accord with the baryon-first convention.
[4] The published sign has been changed to be in accord with the baryon-first convention. The CAMERON 78B upper limits on the P_3 and F_3 waves are each 0.03.

Λ(2110) REFERENCES

ZHANG	13A	PR C88 035205	H. Zhang *et al.*	(KSU)
PDG	82	PL 111B 1	M. Roos *et al.*	(HELS, CIT, CERN)
GOPAL	80	Toronto Conf. 159	G.P. Gopal	(RHEL) IJP
CAMERON	78	NP B143 189	W. Cameron *et al.*	(RHEL, LOIC) IJP
CAMERON	78B	NP B146 327	W. Cameron *et al.*	(RHEL, LOIC) IJP
DEBELLEFON	78	NC 42A 403	A. de Bellefon *et al.*	(CDEF, SACL) IJP
BACCARI	77	NC 41A 96	B. Baccari *et al.*	(SACL, CDEF) IJP
DEBELLEFON	77	NC 37A 175	A. de Bellefon *et al.*	(CDEF, SACL) IJP
GOPAL	77	NP B119 362	G.P. Gopal *et al.*	(LOIC, RHEL) IJP
NAKKASYAN	75	NP B93 85	A. Nakkasyan	(CERN) IJP
KANE	74	LBL-2452	D.F. Kane	(LBL) IJP

Λ(2325) 3/2⁻

$I(J^P) = 0(\frac{3}{2}^-)$ Status: *

OMITTED FROM SUMMARY TABLE

BACCARI 77 finds this state with either $J^P = 3/2^-$ or $3/2^+$ in a energy-dependent partial-wave analyses of $K^-p \to \Lambda\omega$ from 2070 to 2436 MeV. A subsequent semi-energy-independent analysis from threshold to 2436 MeV selects $3/2^-$. DEBELLEFON 78 (same group) also sees this state in an energy-dependent partial-wave analysis of $K^-p \to \overline{K}N$ data, and finds $J^P = 3/2^-$ or $3/2^+$. They again prefer $J^P = 3/2^-$, but only on the basis of model-dependent considerations.

Λ(2325) MASS

VALUE (MeV)	DOCUMENT ID		TECN	COMMENT
≈ 2325 OUR ESTIMATE				
2342±30	DEBELLEFON	78	DPWA	$\overline{K}N \to \overline{K}N$
2327±20	BACCARI	77	DPWA	$K^-p \to \Lambda\omega$

Λ(2325) WIDTH

VALUE (MeV)	DOCUMENT ID		TECN	COMMENT
177±40	DEBELLEFON	78	DPWA	$\overline{K}N \to \overline{K}N$
160±40	BACCARI	77	IPWA	$K^-p \to \Lambda\omega$

Λ(2325) DECAY MODES

	Mode
Γ_1	$N\overline{K}$
Γ_2	$\Lambda\omega$

Λ(2325) BRANCHING RATIOS

$\Gamma(N\overline{K})/\Gamma_{total}$ **Γ_1/Γ**

VALUE	DOCUMENT ID		TECN	COMMENT
0.19±0.06	DEBELLEFON	78	DPWA	$\overline{K}N \to \overline{K}N$

$(\Gamma_i\Gamma_f)^{1/2}/\Gamma_{total}$ in $N\overline{K} \to \Lambda(2325) \to \Lambda\omega$ **$(\Gamma_1\Gamma_2)^{1/2}/\Gamma$**

VALUE	DOCUMENT ID		TECN	COMMENT
0.06±0.02	[1] BACCARI	77	IPWA	DS_{33} wave
0.05±0.02	[1] BACCARI	77	DPWA	DD_{13} wave
0.08±0.03	[1] BACCARI	77	DPWA	DD_{33} wave

Λ(2325) FOOTNOTES

[1] Note that the three BACCARI 77 entries are for three different waves.

Λ(2325) REFERENCES

DEBELLEFON	78	NC 42A 403	A. de Bellefon *et al.*	(CDEF, SACL) IJP
BACCARI	77	NC 41A 96	B. Baccari *et al.*	(SACL, CDEF) IJP

Λ(2350) 9/2⁺

$I(J^P) = 0(\frac{9}{2}^+)$ Status: ***

DAUM 68 favors $J^P = 7/2^-$ or $9/2^+$. BRICMAN 70 favors $9/2^+$. LASINSKI 71 suggests three states in this region using a Pomeron + resonances model. There are now also three formation experiments from the College de France-Saclay group, DEBELLEFON 77, BACCARI 77, and DEBELLEFON 78, which find $9/2^+$ in energy-dependent partial-wave analyses of $\overline{K}N \to \Sigma\pi$, $\Lambda\omega$, and $N\overline{K}$.

Λ(2350) MASS

VALUE (MeV)	DOCUMENT ID		TECN	COMMENT
2340 to 2370 (≈ 2350) OUR ESTIMATE				
2370±50	DEBELLEFON	78	DPWA	$\overline{K}N \to \overline{K}N$
2365±20	DEBELLEFON	77	DPWA	$K^-p \to \Sigma\pi$
2358± 6	BRICMAN	70	CNTR	Total, charge exchange
• • • We do not use the following data for averages, fits, limits, etc. • • •				
2372	BACCARI	77	DPWA	$K^-p \to \Lambda\omega$
2344±15	COOL	70	CNTR	K^-p, K^-d total
2360±20	LU	70	CNTR	$\gamma p \to K^+Y^*$
2340± 7	BUGG	68	CNTR	K^-p, K^-d total

Λ(2350) WIDTH

VALUE (MeV)	DOCUMENT ID		TECN	COMMENT
100 to 250 (≈ 150) OUR ESTIMATE				
204±50	DEBELLEFON	78	DPWA	$\overline{K}N \to \overline{K}N$
110±20	DEBELLEFON	77	DPWA	$K^-p \to \Sigma\pi$
324±30	BRICMAN	70	CNTR	Total, charge exchange
• • • We do not use the following data for averages, fits, limits, etc. • • •				
257	BACCARI	77	DPWA	$K^-p \to \Lambda\omega$
190	COOL	70	CNTR	K^-p, K^-d total
55	LU	70	CNTR	$\gamma p \to K^+Y^*$
140±20	BUGG	68	CNTR	K^-p, K^-d total

Λ(2350) DECAY MODES

	Mode	Fraction (Γ_i/Γ)
Γ_1	$N\overline{K}$	∼ 12 %
Γ_2	$\Sigma\pi$	∼ 10 %
Γ_3	$\Lambda\omega$	

Λ(2350) BRANCHING RATIOS

See "Sign conventions for resonance couplings" in the Note on Λ and Σ Resonances.

$\Gamma(N\overline{K})/\Gamma_{total}$ **Γ_1/Γ**

VALUE	DOCUMENT ID		TECN	COMMENT
∼ 0.12 OUR ESTIMATE				
0.12±0.04	DEBELLEFON	78	DPWA	$\overline{K}N \to \overline{K}N$

$(\Gamma_i\Gamma_f)^{1/2}/\Gamma_{total}$ in $N\overline{K} \to \Lambda(2350) \to \Sigma\pi$ **$(\Gamma_1\Gamma_2)^{1/2}/\Gamma$**

VALUE	DOCUMENT ID		TECN	COMMENT
−0.11±0.02	DEBELLEFON	77	DPWA	$K^-p \to \Sigma\pi$

$(\Gamma_i\Gamma_f)^{1/2}/\Gamma_{total}$ in $N\overline{K} \to \Lambda(2350) \to \Lambda\omega$ **$(\Gamma_1\Gamma_3)^{1/2}/\Gamma$**

VALUE	DOCUMENT ID		TECN	COMMENT
<0.05	BACCARI	77	DPWA	$K^-p \to \Lambda\omega$

Λ(2350) REFERENCES

DEBELLEFON	78	NC 42A 403	A. de Bellefon *et al.*	(CDEF, SACL) IJP
BACCARI	77	NC 41A 96	B. Baccari *et al.*	(SACL, CDEF) IJP
DEBELLEFON	77	NC 37A 175	A. de Bellefon *et al.*	(CDEF, SACL) IJP
LASINSKI	71	NP B29 125	T.A. Lasinski	(EFI) IJP
BRICMAN	70	PL 31B 152	C. Bricman *et al.*	(CERN, CAEN, SACL)
COOL	70	PR D1 1887	R.L. Cool *et al.*	(BNL) I
Also		PRL 16 1228	R.L. Cool *et al.*	(BNL) I
LU	70	PR D2 1846	D.C. Lu *et al.*	(YALE)
BUGG	68	PR 168 1466	D.V. Bugg *et al.*	(RHEL, BIRM, CAVE) I
DAUM	68	NP B7 19	C. Daum *et al.*	(CERN) JP

Λ(2585) Bumps

$I(J^P) = 0(?^?)$ Status: **

OMITTED FROM SUMMARY TABLE

Λ(2585) MASS (BUMPS)

VALUE (MeV)	DOCUMENT ID		TECN	COMMENT
≈ 2585 OUR ESTIMATE				
2585 ± 45	ABRAMS	70	CNTR	K^-p, K^-d total
2530 ± 25	LU	70	CNTR	$\gamma p \rightarrow K^+ Y^*$

Λ(2585) WIDTH (BUMPS)

VALUE (MeV)	DOCUMENT ID		TECN	COMMENT
300	ABRAMS	70	CNTR	K^-p, K^-d total
150	LU	70	CNTR	$\gamma p \rightarrow K^+ Y^*$

Λ(2585) DECAY MODES (BUMPS)

	Mode
Γ_1	$N\overline{K}$

Λ(2585) BRANCHING RATIOS (BUMPS)

$(J+\frac{1}{2})\times\Gamma(N\overline{K})/\Gamma_{total}$ **Γ_1/Γ**

J is not known, so only $(J+\frac{1}{2}) \times \Gamma(N\overline{K})/\Gamma_{total}$ can be given.

VALUE	DOCUMENT ID		TECN	COMMENT
1	ABRAMS	70	CNTR	K^-p, K^-d total
0.12 ± 0.12	[1] BRICMAN	70	CNTR	Total, charge exchange

Λ(2585) FOOTNOTES (BUMPS)

[1] The resonance is at the end of the region analyzed — no clear signal.

Λ(2585) REFERENCES (BUMPS)

ABRAMS	70	PR D1 1917	R.J. Abrams *et al.*	(BNL) I
Also		PRL 16 1228	R.L. Cool *et al.*	(BNL) I
BRICMAN	70	PL 31B 152	C. Bricman *et al.*	(CERN, CAEN, SACL)
LU	70	PR D2 1846	D.C. Lu *et al.*	(YALE)

Σ BARYONS
($S = -1$, $I = 1$)

$\Sigma^+ = uus$, $\Sigma^0 = uds$, $\Sigma^- = dds$

Σ^+

$I(J^P) = 1(\frac{1}{2}^+)$ Status: ****

We have omitted some results that have been superseded by later experiments. See our earlier editions.

Σ^+ MASS

The fit uses Σ^+, Σ^0, Σ^-, and Λ mass and mass-difference measurements.

VALUE (MeV)	EVTS	DOCUMENT ID		TECN	COMMENT
1189.37±0.07 OUR FIT Error includes scale factor of 2.2.					
1189.37±0.06 OUR AVERAGE Error includes scale factor of 1.8. See the ideogram below.					
1189.33±0.04	607	[1] BOHM	72	EMUL	
1189.16±0.12		HYMAN	67	HEBC	
1189.61±0.08	4205	SCHMIDT	65	HBC	See note with Λ mass
1189.48±0.22	58	[2] BHOWMIK	64	EMUL	
1189.38±0.15	144	[2] BARKAS	63	EMUL	

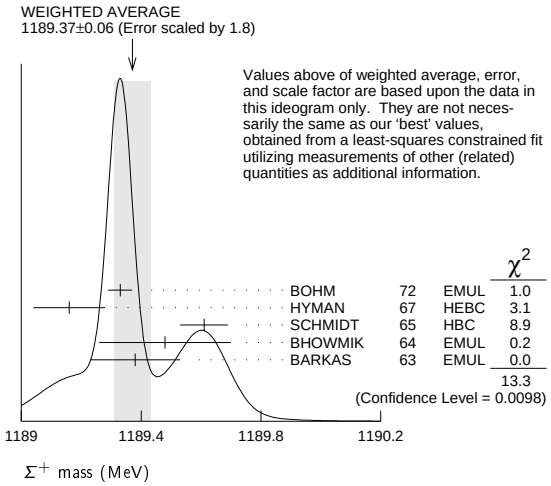

[1] BOHM 72 is updated with our 1973 K^-, π^-, and π^0 masses (Reviews of Modern Physics **45** S1 (1973)).

[2] These masses have been raised 30 keV to take into account a 46 keV increase in the proton mass and a 21 keV decrease in the π^0 mass (note added 1967 edition, Reviews of Modern Physics **39** 1 (1967)).

Σ^+ MEAN LIFE

Measurements with fewer than 1000 events have been omitted.

VALUE (10^{-10} s)	EVTS	DOCUMENT ID		TECN	COMMENT
0.8018±0.0026 OUR AVERAGE					
0.8038±0.0040±0.0014		BARBOSA	00	E761	hyperons, 375 GeV
0.8043±0.0080±0.0014		[3] BARBOSA	00	E761	hyperons, 375 GeV
0.798 ±0.005	30k	MARRAFFINO	80	HBC	K^-p 0.42–0.5 GeV/c
0.807 ±0.013	5719	CONFORTO	76	HBC	K^-p 1–1.4 GeV/c
0.795 ±0.010	20k	EISELE	70	HBC	K^-p at rest
0.803 ±0.008	10664	BARLOUTAUD	69	HBC	K^-p 0.4–1.2 GeV/c
0.83 ±0.032	1300	[4] CHANG	66	HBC	

[3] This is a measurement of the $\overline{\Sigma}^-$ lifetime. Here we assume CPT invariance; see below for the fractional Σ^+-$\overline{\Sigma}^-$ lifetime difference obtained by BARBOSA 00.

[4] We have increased the CHANG 66 error of 0.018; see our 1970 edition, Reviews of Modern Physics **42** 87 (1970).

$(\tau_{\Sigma^+} - \tau_{\overline{\Sigma}^-}) / \tau_{\Sigma^+}$

A test of CPT invariance.

VALUE	DOCUMENT ID		TECN	COMMENT
$(-6\pm12)\times10^{-4}$	BARBOSA	00	E761	hyperons, 375 GeV

Σ^+ MAGNETIC MOMENT

See the "Note on Baryon Magnetic Moments" in the Λ Listings. Measurements with an error $\geq 0.1\ \mu_N$ have been omitted.

VALUE (μ_N)	EVTS	DOCUMENT ID		TECN	COMMENT
2.458 ±0.010 OUR AVERAGE Error includes scale factor of 2.1. See the ideogram below.					
2.4613±0.0034±0.0040	250k	MORELOS	93	SPEC	pCu 800 GeV
2.428 ±0.036 ±0.007	12k	[5] MORELOS	93	SPEC	pCu 800 GeV
2.479 ±0.012 ±0.022	137k	WILKINSON	87	SPEC	pBe 400 GeV
2.4040±0.0198	44k	[6] ANKENBRA...	83	CNTR	pCu 400 GeV

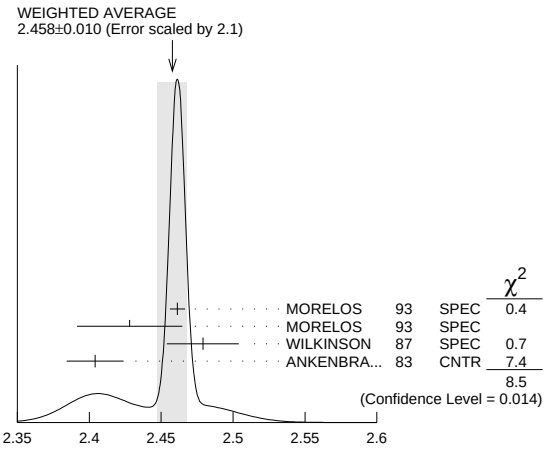

[5] We assume CPT invariance: this is (minus) the $\overline{\Sigma}^-$ magnetic moment as measured by MORELOS 93. See below for the moment difference testing CPT.

[6] ANKENBRANDT 83 gives the value $2.38 \pm 0.02\mu_N$. MORELOS 93 uses the same hyperon magnet and channel and claims to determine the field integral better, leading to the revised value given here.

$(\mu_{\Sigma^+} + \mu_{\overline{\Sigma}^-}) / \mu_{\Sigma^+}$

A test of CPT invariance.

VALUE	DOCUMENT ID		TECN	COMMENT
0.014±0.015	[7] MORELOS	93	SPEC	pCu 800 GeV

[7] This is our calculation from the MORELOS 93 measurements of the Σ^+ and $\overline{\Sigma}^-$ magnetic moments given above. The statistical error on $\mu_{\overline{\Sigma}^-}$ dominates the error here.

Σ^+ DECAY MODES

	Mode		Fraction (Γ_i/Γ)		Confidence level
Γ_1	$p\pi^0$		(51.57±0.30) %		
Γ_2	$n\pi^+$		(48.31±0.30) %		
Γ_3	$p\gamma$		(1.23±0.05)	$\times10^{-3}$	
Γ_4	$n\pi^+\gamma$	[a]	(4.5 ±0.5)	$\times10^{-4}$	
Γ_5	$\Lambda e^+\nu_e$		(2.0 ±0.5)	$\times10^{-5}$	
	$\Delta S = \Delta Q$ (SQ) violating modes or $\Delta S = 1$ weak neutral current ($S1$) modes				
Γ_6	$n e^+\nu_e$	SQ	< 5	$\times10^{-6}$	90%
Γ_7	$n\mu^+\nu_\mu$	SQ	< 3.0	$\times10^{-5}$	90%
Γ_8	$p e^+ e^-$	$S1$	< 7	$\times10^{-6}$	
Γ_9	$p\mu^+\mu^-$	$S1$	(9 $^{+9}_{-8}$)	$\times10^{-8}$	

[a] See the Listings below for the pion momentum range used in this measurement.

CONSTRAINED FIT INFORMATION

An overall fit to 2 branching ratios uses 14 measurements and one constraint to determine 3 parameters. The overall fit has a $\chi^2 = 7.7$ for 12 degrees of freedom.

The following *off-diagonal* array elements are the correlation coefficients $\langle \delta x_i \delta x_j \rangle / (\delta x_i \cdot \delta x_j)$, in percent, from the fit to the branching fractions, $x_i \equiv \Gamma_i/\Gamma_{\text{total}}$. The fit constrains the x_i whose labels appear in this array to sum to one.

x_2	−100		
x_3	12	−14	
	x_1	x_2	

Σ^+ BRANCHING RATIOS

$\Gamma(n\pi^+)/\Gamma(N\pi)$ — $\Gamma_2/(\Gamma_1+\Gamma_2)$

VALUE	EVTS	DOCUMENT ID		TECN	COMMENT
0.4836±0.0030 OUR FIT					
0.4836±0.0030 OUR AVERAGE					
0.4828±0.0036	10k	[8] MARRAFFINO	80	HBC	K^-p 0.42–0.5 GeV/c
0.488 ±0.008	1861	NOWAK	78	HBC	
0.484 ±0.015	537	TOVEE	71	EMUL	
0.488 ±0.010	1331	BARLOUTAUD	69	HBC	K^-p 0.4–1.2 GeV/c
0.46 ±0.02	534	CHANG	66	HBC	
0.490 ±0.024	308	HUMPHREY	62	HBC	

[8] MARRAFFINO 80 actually gives $\Gamma(p\pi^0)/\Gamma(\text{total}) = 0.5172 \pm 0.0036$.

$\Gamma(p\gamma)/\Gamma(p\pi^0)$ — Γ_3/Γ_1

VALUE (units 10^{-3})	EVTS	DOCUMENT ID		TECN	COMMENT
2.38±0.10 OUR FIT					
2.38±0.10 OUR AVERAGE					
2.32±0.11±0.10	32k	TIMM	95	E761	Σ^+ 375 GeV
$2.81 \pm 0.39^{+0.21}_{-0.43}$	408	HESSEY	89	CNTR	$K^-p \to \Sigma^+\pi^-$ at rest
2.52±0.28	190	[9] KOBAYASHI	87	CNTR	$\pi^+p \to \Sigma^+K^+$
$2.46^{+0.30}_{-0.35}$	155	BIAGI	85	CNTR	CERN hyperon beam
2.11±0.38	46	MANZ	80	HBC	$K^-p \to \Sigma^+\pi^-$
2.1 ±0.3	45	ANG	69B	HBC	K^-p at rest
2.76±0.51	31	GERSHWIN	69B	HBC	$K^-p \to \Sigma^+\pi^-$
3.7 ±0.8	24	BAZIN	65	HBC	K^-p at rest

[9] KOBAYASHI 87 actually gives $\Gamma(p\gamma)/\Gamma(\text{total}) = (1.30 \pm 0.15) \times 10^{-3}$.

$\Gamma(n\pi^+\gamma)/\Gamma(n\pi^+)$ — Γ_4/Γ_2

The π^+ momentum cuts differ, so we do not average the results but simply use the latest value in the Summary Table.

VALUE (units 10^{-3})	EVTS	DOCUMENT ID		TECN	COMMENT
0.93±0.10	180	EBENHOH	73	HBC	$\pi^+ < 150$ MeV/c
• • • We do not use the following data for averages, fits, limits, etc. • • •					
0.27±0.05	29	ANG	69B	HBC	$\pi^+ < 110$ MeV/c
~ 1.8		BAZIN	65B	HBC	$\pi^+ < 116$ MeV/c

$\Gamma(\Lambda e^+\nu_e)/\Gamma_{\text{total}}$ — Γ_5/Γ

VALUE (units 10^{-5})	EVTS	DOCUMENT ID		TECN	COMMENT
2.0±0.5 OUR AVERAGE					
1.6±0.7	5	BALTAY	69	HBC	K^-p at rest
2.9±1.0	10	EISELE	69	HBC	K^-p at rest
2.0±0.8	6	BARASH	67	HBC	K^-p at rest

$\Gamma(ne^+\nu_e)/\Gamma(n\pi^+)$ — Γ_6/Γ_2

Test of $\Delta S = \Delta Q$ rule. Experiments with an effective denominator less than 100,000 have been omitted.

EFFECTIVE DENOM.	EVTS	DOCUMENT ID		TECN	COMMENT
< 1.1 × 10⁻⁵ OUR LIMIT Our 90% CL limit = (2.3 events)/(effective denominator sum). [Number of events increased to 2.3 for a 90% confidence level.]					
111000	0	[10] EBENHOH	74	HBC	K^-p at rest
105000	0	[10] SECHI-ZORN	73	HBC	K^-p at rest

[10] Effective denominator calculated by us.

$\Gamma(n\mu^+\nu_\mu)/\Gamma(n\pi^+)$ — Γ_7/Γ_2

Test of $\Delta S = \Delta Q$ rule.

EFFECTIVE DENOM.	EVTS	DOCUMENT ID		TECN
< 6.2 × 10⁻⁵ OUR LIMIT Our 90% CL limit = (6.7 events)/(effective denominator sum). [Number of events increased to 6.7 for a 90% confidence level.]				
33800	0	BAGGETT	69B	HBC
62000	2	[11] EISELE	69B	HBC
10150	0	[12] COURANT	64	HBC
1710	0	[12] NAUENBERG	64	HBC
120	1	GALTIERI	62	EMUL

[11] Effective denominator calculated by us.
[12] Effective denominator taken from EISELE 67.

$\Gamma(pe^+e^-)/\Gamma_{\text{total}}$ — Γ_8/Γ

VALUE (units 10^{-6})	DOCUMENT ID		TECN	COMMENT
<7	[13] ANG	69B	HBC	K^-p at rest

[13] ANG 69B found three pe^+e^- events in agreement with $\gamma \to e^+e^-$ conversion from $\Sigma^+ \to p\gamma$. The limit given here is for neutral currents.

$\Gamma(p\mu^+\mu^-)/\Gamma_{\text{total}}$ — Γ_9/Γ

A test for a $\Delta S = 1$ weak neutral current, but also allowed by higher-order electroweak interactions.

VALUE (units 10^{-8})	EVTS	DOCUMENT ID		TECN	COMMENT
$8.6^{+6.6}_{-5.4} \pm 5.5$	3	[14] PARK	05	HYCP	p Cu, 800 GeV

[14] The masses of the three dimuons of PARK 05 are within 1 MeV of one another, perhaps indicating the existence of a new state P^0 with mass 214.3 ± 0.5 MeV. In that case, the decay is $\Sigma^+ \to pP^0$, $P^0 \to \mu^+\mu^-$, with a branching fraction of $(3.1^{+2.4}_{-1.9} \pm 1.5) \times 10^{-8}$.

$\Gamma(\Sigma^+ \to ne^+\nu_e)/\Gamma(\Sigma^- \to ne^-\overline{\nu}_e)$ — $\Gamma_6/\Gamma_3^{\Sigma^-}$

VALUE	CL%	EVTS	DOCUMENT ID		TECN	COMMENT
<0.009 OUR LIMIT Our 90% CL limit, using $\Gamma(ne^+\nu_e)/\Gamma(n\pi^+)$ above.						
• • • We do not use the following data for averages, fits, limits, etc. • • •						
<0.019	90	0	EBENHOH	74	HBC	K^-p at rest
<0.018	90	0	SECHI-ZORN	73	HBC	K^-p at rest
<0.12	95	0	COLE	71	HBC	K^-p at rest
<0.03	90	0	EISELE	69B	HBC	See EBENHOH 74

$\Gamma(\Sigma^+ \to n\mu^+\nu_\mu)/\Gamma(\Sigma^- \to n\mu^-\overline{\nu}_\mu)$ — $\Gamma_7/\Gamma_4^{\Sigma^-}$

VALUE	EVTS	DOCUMENT ID		TECN	COMMENT
<0.12 OUR LIMIT Our 90% CL limit, using $\Gamma(n\mu^+\nu_\mu)/\Gamma(n\pi^+)$ above.					
• • • We do not use the following data for averages, fits, limits, etc. • • •					
$0.06^{+0.045}_{-0.03}$	2	EISELE	69B	HBC	K^-p at rest

$\Gamma(\Sigma^+ \to n\ell^+\nu)/\Gamma(\Sigma^- \to n\ell^-\overline{\nu})$ — $(\Gamma_6+\Gamma_7)/(\Gamma_3^{\Sigma^-}+\Gamma_4^{\Sigma^-})$

Test of $\Delta S = \Delta Q$ rule.

VALUE	EVTS	DOCUMENT ID		TECN
<0.043 OUR LIMIT Our 90% CL limit, using $\left[\Gamma(ne^+\nu_e) + \Gamma(n\mu^+\nu_\mu)\right]/\Gamma(n\pi^+)$.				
• • • We do not use the following data for averages, fits, limits, etc. • • •				
<0.08	1	NORTON	69	HBC
<0.034	0	BAGGETT	67	HBC

Σ^+ DECAY PARAMETERS

See the "Note on Baryon Decay Parameters" in the neutron Listings. A few early results have been omitted.

α_0 FOR $\Sigma^+ \to p\pi^0$

VALUE	EVTS	DOCUMENT ID		TECN	COMMENT
$\mathbf{-0.980^{+0.017}_{-0.015}}$ **OUR FIT**					
$\mathbf{-0.980^{+0.017}_{-0.013}}$ **OUR AVERAGE**					
$-0.945^{+0.055}_{-0.042}$	1259	[15] LIPMAN	73	OSPK	$\pi^+p \to \Sigma^+$
−0.940±0.045	16k	BELLAMY	72	ASPK	$\pi^+p \to \Sigma^+K^+$
$-0.98^{+0.05}_{-0.02}$	1335	[16] HARRIS	70	OSPK	$\pi^+p \to \Sigma^+K^+$
−0.999±0.022	32k	BANGERTER	69	HBC	K^-p 0.4 GeV/c

[15] Decay protons scattered off aluminum.
[16] Decay protons scattered off carbon.

ϕ_0 ANGLE FOR $\Sigma^+ \to p\pi^0$ — $(\tan\phi_0 = \beta/\gamma)$

VALUE (°)	EVTS	DOCUMENT ID		TECN	COMMENT
36 ±34 OUR AVERAGE					
$38.1^{+35.7}_{-37.1}$	1259	[17] LIPMAN	73	OSPK	$\pi^+p \to \Sigma^+K^+$
22 ±90		[18] HARRIS	70	OSPK	$\pi^+p \to \Sigma^+K^+$

[17] Decay proton scattered off aluminum.
[18] Decay protons scattered off carbon.

α_+ / α_0

Older results have been omitted.

VALUE	EVTS	DOCUMENT ID		TECN	COMMENT
−0.069±0.013 OUR FIT					
−0.073±0.021	23k	MARRAFFINO	80	HBC	K^-p 0.42–0.5 GeV/c

α_+ FOR $\Sigma^+ \to n\pi^+$

VALUE	EVTS	DOCUMENT ID		TECN	COMMENT
0.068±0.013 OUR FIT					
0.066±0.016 OUR AVERAGE					
0.037±0.049	4101	BERLEY	70B	HBC	
0.069±0.017	35k	BANGERTER	69	HBC	K^-p 0.4 GeV/c

ϕ_+ ANGLE FOR $\Sigma^+ \to n\pi^+$ — $(\tan\phi_+ = \beta/\gamma)$

VALUE (°)	EVTS	DOCUMENT ID		TECN	COMMENT
167±20 OUR AVERAGE Error includes scale factor of 1.1.					
184±24	1054	[19] BERLEY	70B	HBC	
143±29	560	BANGERTER	69B	HBC	K^-p 0.4 GeV/c

[19] Changed from 176 to 184° to agree with our sign convention.

Baryon Particle Listings

Σ^+, Σ^0

α_γ FOR $\Sigma^+ \to p\gamma$

VALUE	EVTS	DOCUMENT ID		TECN	COMMENT
−0.76 ±0.08 OUR AVERAGE					
−0.720±0.086±0.045	35k	[20] FOUCHER	92	SPEC	Σ^+ 375 GeV
−0.86 ±0.13 ±0.04	190	KOBAYASHI	87	CNTR	$\pi^+ p \to \Sigma^+ K^+$
$-0.53\ ^{+0.38}_{-0.36}$	46	MANZ	80	HBC	$K^- p \to \Sigma^+ \pi^-$
$-1.03\ ^{+0.52}_{-0.42}$	61	GERSHWIN	69B	HBC	$K^- p \to \Sigma^+ \pi^-$

[20] See TIMM 95 for a detailed description of the analysis.

Σ^+ REFERENCES

We have omitted some papers that have been superseded by later experiments. See our earlier editions.

PARK	05	PRL 94 021801	H.K. Park *et al.*	(FNAL HyperCP Collab.)
BARBOSA	00	PR D61 031101	R.F. Barbosa *et al.*	(FNAL E761 Collab.)
TIMM	95	PR D51 4638	S. Timm *et al.*	(FNAL E761 Collab.)
MORELOS	93	PRL 71 3417	A. Morelos *et al.*	(FNAL E761 Collab.)
FOUCHER	92	PRL 68 3004	M. Foucher *et al.*	(FNAL E761 Collab.)
HESSEY	89	ZPHY C42 175	N.P. Hessey *et al.*	(BNL-811 Collab.)
KOBAYASHI	87	PRL 59 868	M. Kobayashi *et al.*	(KYOT)
WILKINSON	87	PRL 58 855	C.A. Wilkinson *et al.*	(WISC, MICH, RUTG+)
BIAGI	85	ZPHY C28 495	S.F. Biagi *et al.*	(CERN WA62 Collab.)
ANKENBRA...	83	PRL 51 863	C.M. Ankenbrandt *et al.*	(FNAL, IOWA, ISU+)
MANZ	80	PL 96B 217	A. Manz *et al.*	(MPIM, VAND)
MARRAFFINO	80	PR D21 2501	J. Marraffino *et al.*	(VAND, MPIM)
NOWAK	78	NP B139 61	R.J. Nowak *et al.*	(LOUC, BELG, DURH+)
CONFORTO	76	NP B105 189	B. Conforto *et al.*	(RHEL, LOIC)
EBENHOH	74	ZPHY 266 367	H. Ebenhoh *et al.*	(HEIDT)
EBENHOH	73	ZPHY 264 413	W. Ebenhoh *et al.*	(HEIDT)
LIPMAN	73	PL 43B 89	N.H. Lipman *et al.*	(RHEL, SUSS, LOWC)
PDG	73	RMP 45 S1	T.A. Lasinski *et al.*	(LBL, BRAN, CERN+)
SECHI-ZORN	73	PR D8 12	B. Sechi-Zorn, G.A. Snow	(UMD)
BELLAMY	72	PL 39B 299	E.H. Bellamy *et al.*	(LOWC, RHEL, SUSS)
BOHM	72	NP B48 1	G. Bohm *et al.*	(BERL, KIDR, BRUX, IASD+)
Also		IIHE-73.2 Nov	G. Bohm	(BERL, KIDR, BRUX, IASD, DUUC+)
COLE	71	PR D4 631	J. Cole *et al.*	(STON, COLU)
TOVEE	71	NP B33 493	D.N. Tovee *et al.*	(LOUC, KIDR, BERL+)
BERLEY	70B	PR D1 2015	D. Berley *et al.*	(BNL, MASA, YALE)
EISELE	70	ZPHY 238 372	F. Eisele *et al.*	(HEID)
HARRIS	70	PRL 24 165	F. Harris *et al.*	(MICH, WISC)
PDG	70	RMP 42 87	A. Barbaro-Galtieri *et al.*	(LRL, BRAN+)
ANG	69B	ZPHY 228 151	G. Ang *et al.*	(HEID)
BAGGETT	69B	Thesis MDDP-TR-973	N.V. Baggett	(UMD)
BALTAY	69	PRL 22 615	C. Baltay *et al.*	(COLU, STON)
BANGERTER	69	Thesis UCRL 19244	R.O. Bangerter	(LRL)
BANGERTER	69B	PR 187 1821	R.O. Bangerter *et al.*	(LRL)
BARLOUTAUD	69	NP B14 153	R. Barloutaud *et al.*	(SACL, CERN, HEID)
EISELE	69	ZPHY 221 1	F. Eisele *et al.*	(HEID)
Also		PRL 13 291	W. Willis *et al.*	(BNL, CERN, HEID, UMD)
EISELE	69B	ZPHY 221 401	F. Eisele *et al.*	(HEID)
GERSHWIN	69B	PR 188 2077	L.K. Gershwin *et al.*	(LRL)
Also		Thesis UCRL 19246	L.K. Gershwin	(LRL)
NORTON	69	Thesis Nevis 175	H. Norton	(COLU)
BAGGETT	67	PRL 19 1458	N. Baggett *et al.*	(UMD)
Also		Vienna Abs. 374	N.V. Baggett, B. Kehoe	(UMD)
Also		Private Comm.	N.V. Baggett	(UMD)
BARASH	67	PRL 19 181	N. Barash *et al.*	(UMD)
EISELE	67	ZPHY 205 409	F. Eisele *et al.*	(HEID)
HYMAN	67	PL 25B 376	L.G. Hyman *et al.*	(ANL, CMU, NWES)
PDG	67	RMP 39 1	A.H. Rosenfeld *et al.*	(LRL, CERN, YALE)
CHANG	66	PR 151 1081	C.Y. Chang	(COLU)
Also		Thesis Nevis 145	C.Y. Chang	(COLU)
BAZIN	65	PRL 14 154	M. Bazin *et al.*	(PRIN, COLU)
BAZIN	65B	PR 140 B1358	M. Bazin *et al.*	(PRIN, RUTG, COLU)
SCHMIDT	65	PR 140 B1328	P. Schmidt	(COLU)
BHOWMIK	64	NP 53 22	B. Bhowmik *et al.*	(DELH)
COURANT	64	PR 136 B1791	H. Courant *et al.*	(CERN, HEID, UMD+)
NAUENBERG	64	PRL 12 679	U. Nauenberg *et al.*	(COLU, RUTG, PRIN)
BARKAS	63	PRL 11 26	W.H. Barkas, J.N. Dyer, H.H. Heckman	(LRL)
Also		Thesis UCRL 9450	J.N. Dyer	(LRL)
GALTIERI	62	PRL 9 26	A. Barbaro-Galtieri *et al.*	(LRL)
HUMPHREY	62	PRL 127 1305	W.E. Humphrey, R.R. Ross	(LRL)

Σ^0

$I(J^P) = 1(\frac{1}{2}^+)$ Status: ****

COURANT 63 and ALFF 65, using $\Sigma^0 \to \Lambda e^+ e^-$ decays (Dalitz decays), determined the Σ^0 parity to be positive, given that $J = 1/2$ and that certain very reasonable assumptions about form factors are true. The results of experiments involving the Primakoff effect, from which the Σ^0 mean life and $\Sigma^0 \to \Lambda$ transition magnetic moment come (see below), strongly support $J = 1/2$.

Σ^0 MASS

The fit uses Σ^+, Σ^0, Σ^-, and Λ mass and mass-difference measurements.

VALUE (MeV)	EVTS	DOCUMENT ID		TECN	COMMENT
1192.642±0.024 OUR FIT					
• • • We do not use the following data for averages, fits, limits, etc. • • •					
1192.65 ±0.020±0.014	3327	[1] WANG	97	SPEC	$\Sigma^0 \to \Lambda\gamma \to (p\pi^-)(e^+e^-)$

[1] This WANG 97 result is redundant with the Σ^0-Λ mass-difference measurement below.

$m_{\Sigma^-} - m_{\Sigma^0}$

VALUE (MeV)	EVTS	DOCUMENT ID		TECN	COMMENT
4.807±0.035 OUR FIT	Error includes scale factor of 1.1.				
4.86 ±0.08 OUR AVERAGE	Error includes scale factor of 1.2.				
4.87 ±0.12	37	DOSCH	65	HBC	
5.01 ±0.12	12	SCHMIDT	65	HBC	See note with Λ mass
4.75 ±0.1	18	BURNSTEIN	64	HBC	

$m_{\Sigma^0} - m_\Lambda$

VALUE (MeV)	EVTS	DOCUMENT ID		TECN	COMMENT
76.959±0.023 OUR FIT					
76.966±0.020±0.013	3327	WANG	97	SPEC	$\Sigma^0 \to \Lambda\gamma \to (p\pi^-)(e^+e^-)$
• • • We do not use the following data for averages, fits, limits, etc. • • •					
76.23 ±0.55	109	COLAS	75	HLBC	$\Sigma^0 \to \Lambda\gamma$
76.63 ±0.28	208	SCHMIDT	65	HBC	See note with Λ mass

Σ^0 MEAN LIFE

These lifetimes are deduced from measurements of the cross sections for the Primakoff process $\Lambda \to \Sigma^0$ in nuclear Coulomb fields. An alternative expression of the same information is the Σ^0-Λ transition magnetic moment given in the following section. The relation is $(\mu_{\Sigma\Lambda}/\mu_N)^2\,\tau = 1.92951 \times 10^{-19}$ s (see DEVLIN 86).

VALUE (10^{-20} s)	DOCUMENT ID		TECN	COMMENT
7.4±0.7 OUR EVALUATION	Using $\mu_{\Sigma\Lambda}$ (see the above note).			
$6.5\ ^{+1.7}_{-1.1}$	[2] DEVLIN	86	SPEC	Primakoff effect
7.6±0.5±0.7	[3] PETERSEN	86	SPEC	Primakoff effect
• • • We do not use the following data for averages, fits, limits, etc. • • •				
5.8±1.3	[2] DYDAK	77	SPEC	See DEVLIN 86

[2] DEVLIN 86 is a recalculation of the results of DYDAK 77 removing a numerical approximation made in that work.
[3] An additional uncertainty of the Primakoff formalism is estimated to be $< 5\%$.

$|\mu(\Sigma^0 \to \Lambda)|$ TRANSITION MAGNETIC MOMENT

See the note in the Σ^0 mean-life section above. Also, see the "Note on Baryon Magnetic Moments" in the Λ Listings.

VALUE (μ_N)	DOCUMENT ID		TECN	COMMENT
1.61±0.08 OUR AVERAGE				
$1.72\ ^{+0.17}_{-0.19}$	[4] DEVLIN	86	SPEC	Primakoff effect
1.59±0.05±0.07	[5] PETERSEN	86	SPEC	Primakoff effect
• • • We do not use the following data for averages, fits, limits, etc. • • •				
$1.82\ ^{+0.25}_{-0.18}$	[4] DYDAK	77	SPEC	See DEVLIN 86

[4] DEVLIN 86 is a recalculation of the results of DYDAK 77 removing a numerical approximation made in that work.
[5] An additional uncertainty of the Primakoff formalism is estimated to be $< 2.5\%$.

Σ^0 DECAY MODES

	Mode	Fraction (Γ_i/Γ)	Confidence level
Γ_1	$\Lambda\gamma$	100 %	
Γ_2	$\Lambda\gamma\gamma$	$< 3\ \%$	90%
Γ_3	$\Lambda e^+ e^-$	[a] 5×10^{-3}	

[a] A theoretical value using QED.

Σ^0 BRANCHING RATIOS

$\Gamma(\Lambda\gamma\gamma)/\Gamma_{total}$ Γ_2/Γ

VALUE	CL%	DOCUMENT ID		TECN
<0.03	90	COLAS	75	HLBC

$\Gamma(\Lambda e^+ e^-)/\Gamma_{total}$ Γ_3/Γ

See COURANT 63 and ALFF 65 for measurements of the invariant-mass spectrum of the Dalitz pairs.

VALUE	DOCUMENT ID		COMMENT
0.00545	FEINBERG	58	Theoretical QED calculation

Σ^0 REFERENCES

WANG	97	PR D56 2544	M.H.L.S. Wang *et al.*	(BNL-E766 Collab.)
DEVLIN	86	PR D34 1626	T. Devlin, P.C. Petersen, A. Beretvas	(RUTG)
PETERSEN	86	PRL 57 949	P.C. Petersen *et al.*	(RUTG, WISC, MICH+)
DYDAK	77	NP B118 1	F. Dydak *et al.*	(CERN, DORT, HEIDH)
COLAS	75	NP B91 253	J. Colas *et al.*	(ORSAY)
ALFF	65	PR 137 B1105	C. Alff *et al.*	(COLU, RUTG, BNL) P

DOSCH	65	PL 14 239	H.C. Dosch *et al.*	(HEID)
SCHMIDT	65	PR 140 B1328	P. Schmidt	(COLU)
BURNSTEIN	64	PRL 13 66	R.A. Burnstein *et al.*	(UMD)
COURANT	63	PRL 10 409	H. Courant *et al.*	(CERN, UMD) P
FEINBERG	58	PR 109 1019	G. Feinberg	(BNL)

Σ^-

$I(J^P) = 1(\frac{1}{2}^+)$ Status: ****

We have omitted some results that have been superseded by later experiments. See our earlier editions.

Σ^- MASS

The fit uses Σ^+, Σ^0, Σ^-, and Λ mass and mass-difference measurements.

VALUE (MeV)	EVTS	DOCUMENT ID		TECN	COMMENT
1197.449±0.030 OUR FIT		Error includes scale factor of 1.2.			
1197.45 ±0.04 OUR AVERAGE		Error includes scale factor of 1.2.			
1197.417±0.040		GUREV	93	SPEC	Σ^- C atom, crystal diff.
1197.532±0.057		GALL	88	CNTR	Σ^- Pb, Σ^- W atoms
1197.43 ±0.08	3000	SCHMIDT	65	HBC	See note with Λ mass
• • • We do not use the following data for averages, fits, limits, etc. • • •					
1197.24 ±0.15		[1] DUGAN	75	CNTR	Exotic atoms

[1] GALL 88 concludes that the DUGAN 75 mass needs to be reevaluated.

$m_{\Sigma^-} - m_{\Sigma^+}$

VALUE (MeV)	EVTS	DOCUMENT ID		TECN
8.08±0.08 OUR FIT	Error includes scale factor of 1.9.			
8.09±0.16 OUR AVERAGE				
7.91±0.23	86	BOHM	72	EMUL
8.25±0.25	2500	DOSCH	65	HBC
8.25±0.40	87	BARKAS	63	EMUL

$m_{\Sigma^-} - m_{\Lambda}$

VALUE (MeV)	EVTS	DOCUMENT ID		TECN	COMMENT
81.766±0.030 OUR FIT	Error includes scale factor of 1.2.				
81.69 ±0.07 OUR AVERAGE					
81.64 ±0.09	2279	HEPP	68	HBC	
81.80 ±0.13	85	SCHMIDT	65	HBC	See note with Λ mass
81.70 ±0.19		BURNSTEIN	64	HBC	

Σ^- MEAN LIFE

Measurements with an error $\geq 0.2 \times 10^{-10}$ s have been omitted.

VALUE (10^{-10} s)	EVTS	DOCUMENT ID		TECN	COMMENT
1.479±0.011 OUR AVERAGE	Error includes scale factor of 1.3.				See the ideogram below.
1.480±0.014	16k	MARRAFFINO	80	HBC	K^-p 0.42–0.5 GeV/c
1.49 ±0.03	8437	CONFORTO	76	HBC	K^-p 1–1.4 GeV/c
1.463±0.039	2400	ROBERTSON	72	HBC	K^-p 0.25 GeV/c
1.42 ±0.05	1383	BAKKER	71	DBC	$K^-N \to \Sigma^-\pi\pi$
1.41 $^{+0.09}_{-0.08}$		TOVEE	71	EMUL	
1.485±0.022	100k	EISELE	70	HBC	K^-p at rest
1.472±0.016	10k	BARLOUTAUD	69	HBC	K^-p 0.4–1.2 GeV/c
1.38 ±0.07	506	WHITESIDE	68	HBC	K^-p at rest
1.666±0.075	3267	[2] CHANG	66	HBC	K^-p at rest
1.58 ±0.06	1208	HUMPHREY	62	HBC	K^-p at rest

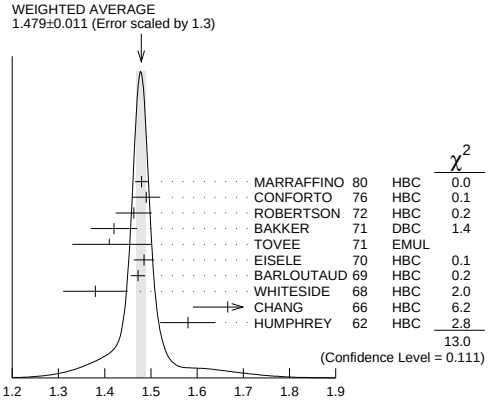

Σ^- mean life (10^{-10} s)

[2] We have increased the CHANG 66 error of 0.026; see our 1970 edition, Reviews of Modern Physics **42** 87 (1970).

Σ^- MAGNETIC MOMENT

See the "Note on Baryon Magnetic Moments" in the Λ Listings. Measurements with an error $\geq 0.3\ \mu_N$ have been omitted.

VALUE (μ_N)	EVTS	DOCUMENT ID		TECN	COMMENT
−1.160±0.025 OUR AVERAGE	Error includes scale factor of 1.7. See the ideogram below.				
−1.105±0.029±0.010		HERTZOG	88	CNTR	Σ^- Pb, Σ^- W atoms
−1.166±0.014±0.010	671k	ZAPALAC	86	SPEC	$ne^-\nu$, $n\pi^-$ decays
−1.23 ±0.03 ±0.03		WAH	85	CNTR	p Cu $\to \Sigma^-$ X
• • • We do not use the following data for averages, fits, limits, etc. • • •					
−0.89 ±0.14	516k	DECK	83	SPEC	pBe $\to \Sigma^-$ X

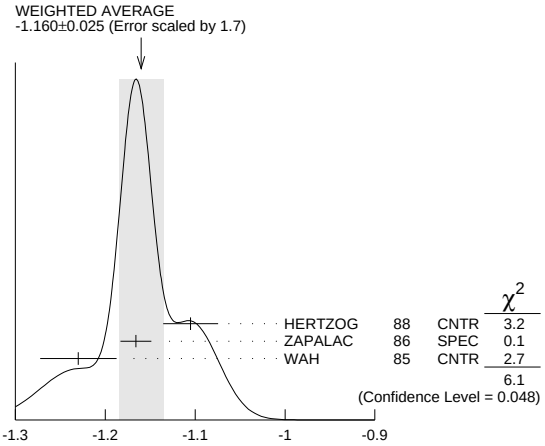

Σ^- magnetic moment (μ_N)

Σ^- CHARGE RADIUS

VALUE (fm)	DOCUMENT ID		TECN	COMMENT
0.780±0.080±0.060	[3] ESCHRICH	01	SELX	$\Sigma^- e \to \Sigma^- e$

[3] ESCHRICH 01 actually gives $\langle r^2 \rangle = (0.61 \pm 0.12 \pm 0.09)$ fm^2.

Σ^- DECAY MODES

	Mode	Fraction (Γ_i/Γ)
Γ_1	$n\pi^-$	(99.848±0.005) %
Γ_2	$n\pi^-\gamma$	[a] (4.6 ±0.6) × 10^{-4}
Γ_3	$ne^-\overline{\nu}_e$	(1.017±0.034) × 10^{-3}
Γ_4	$n\mu^-\overline{\nu}_\mu$	(4.5 ±0.4) × 10^{-4}
Γ_5	$\Lambda e^-\overline{\nu}_e$	(5.73 ±0.27) × 10^{-5}

[a] See the Listings below for the pion momentum range used in this measurement.

CONSTRAINED FIT INFORMATION

An overall fit to 3 branching ratios uses 16 measurements and one constraint to determine 4 parameters. The overall fit has a $\chi^2 = 8.7$ for 13 degrees of freedom.

The following *off-diagonal* array elements are the correlation coefficients $\langle \delta x_i \delta x_j \rangle / (\delta x_i \cdot \delta x_j)$, in percent, from the fit to the branching fractions, $x_i \equiv \Gamma_i/\Gamma_{\text{total}}$. The fit constrains the x_i whose labels appear in this array to sum to one.

x_3	−64		
x_4	−77	0	
x_5	−5	0	0
	x_1	x_3	x_4

Baryon Particle Listings

Σ^-

Σ^- BRANCHING RATIOS

$\Gamma(n\pi^-\gamma)/\Gamma(n\pi^-)$ Γ_2/Γ_1

The π^+ momentum cuts differ, so we do not average the results but simply use the latest value for the Summary Table.

VALUE (units 10^{-3})	EVTS	DOCUMENT ID		TECN	COMMENT
0.46±0.06	292	EBENHOH	73	HBC	$\pi^+ < 150$ MeV/c
• • • We do not use the following data for averages, fits, limits, etc. • • •					
0.10±0.02	23	ANG	69B	HBC	$\pi^- < 110$ MeV/c
~ 1.1		BAZIN	65B	HBC	$\pi^- < 166$ MeV/c

$\Gamma(ne^-\overline{\nu}_e)/\Gamma(n\pi^-)$ Γ_3/Γ_1

Measurements with an error $\geq 0.2\times10^{-3}$ have been omitted.

VALUE (units 10^{-3})	EVTS	DOCUMENT ID		TECN	COMMENT
1.019±0.035 OUR FIT					
$1.019^{+0.031}_{-0.040}$ OUR AVERAGE					
0.96 ±0.05	2847	BOURQUIN	83C	SPEC	SPS hyperon beam
$1.09\ ^{+0.06}_{-0.08}$	601	[4] EBENHOH	74	HBC	K^-p at rest
$1.05\ ^{+0.07}_{-0.13}$	455	[4] SECHI-ZORN	73	HBC	K^-p at rest
0.97 ±0.15	57	COLE	71	HBC	K^-p at rest
1.11 ±0.09	180	BIERMAN	68	HBC	

[4] An additional negative systematic error is included for internal radiative corrections and latest form factors; see BOURQUIN 83C.

$\Gamma(n\mu^-\overline{\nu}_\mu)/\Gamma(n\pi^-)$ Γ_4/Γ_1

VALUE (units 10^{-3})	EVTS	DOCUMENT ID		TECN	COMMENT
0.45±0.04 OUR FIT					
0.45±0.04 OUR AVERAGE					
0.38±0.11	13	COLE	71	HBC	K^-p at rest
0.43±0.06	72	ANG	69	HBC	K^-p at rest
0.43±0.09	56	BAGGETT	69	HBC	K^-p at rest
0.56±0.20	11	BAZIN	65B	HBC	K^-p at rest
0.66±0.15	22	COURANT	64	HBC	

$\Gamma(\Lambda e^-\overline{\nu}_e)/\Gamma(n\pi^-)$ Γ_5/Γ_1

VALUE (units 10^{-4})	EVTS	DOCUMENT ID		TECN	COMMENT
0.574±0.027 OUR FIT					
0.574±0.027 OUR AVERAGE					
0.561±0.031	1620	[5] BOURQUIN	82	SPEC	SPS hyperon beam
0.63 ±0.11	114	THOMPSON	80	ASPK	Hyperon beam
0.52 ±0.09	31	BALTAY	69	HBC	K^-p at rest
0.69 ±0.12	31	EISELE	69	HBC	K^-p at rest
0.64 ±0.12	35	BARASH	67	HBC	K^-p at rest
0.75 ±0.28	11	COURANT	64	HBC	K^-p at rest

[5] The value is from BOURQUIN 83B, and includes radiation corrections and new acceptance.

Σ^- DECAY PARAMETERS

See the "Note on Baryon Decay Parameters" in the neutron Listings. Older, outdated results have been omitted.

α_- FOR $\Sigma^- \to n\pi^-$

VALUE	EVTS	DOCUMENT ID		TECN	COMMENT
−0.068±0.008 OUR AVERAGE					
−0.062±0.024	28k	HANSL	78	HBC	$K^-p \to \Sigma^-\pi^+$
−0.067±0.011	60k	BOGERT	70	HBC	K^-p 0.4 GeV/c
−0.071±0.012	51k	BANGERTER	69	HBC	K^-p 0.4 GeV/c

ϕ ANGLE FOR $\Sigma^- \to n\pi^-$ $(\tan\phi = \beta/\gamma)$

VALUE (°)	EVTS	DOCUMENT ID		TECN	COMMENT
10±15 OUR AVERAGE					
+ 5±23	1092	[6] BERLEY	70B	HBC	n rescattering
14±19	1385	BANGERTER	69B	HBC	K^-p 0.4 GeV/c

[6] BERLEY 70B changed from −5 to +5° to agree with our sign convention.

g_A/g_V FOR $\Sigma^- \to ne^-\overline{\nu}_e$

Measurements with fewer than 500 events have been omitted. Where necessary, signs have been changed to agree with our conventions, which are given in the "Note on Baryon Decay Parameters" in the neutron Listings. What is actually listed is $|g_1/f_1 - 0.237 g_2/f_1|$. This reduces to $g_A/g_V \equiv g_1(0)/f_1(0)$ on making the usual assumption that $g_2 = 0$. See also the note on HSUEH 88.

VALUE	EVTS	DOCUMENT ID		TECN	COMMENT
0.340±0.017 OUR AVERAGE					
+0.327±0.007±0.019	50k	[7] HSUEH	88	SPEC	Σ^- 250 GeV
+0.34 ±0.05	4456	[8] BOURQUIN	83C	SPEC	SPS hyperon beam
0.385±0.037	3507	[9] TANENBAUM	74	ASPK	
• • • We do not use the following data for averages, fits, limits, etc. • • •					
0.29 ±0.07	25k	HSUEH	85	SPEC	See HSUEH 88
$0.17\ ^{+0.07}_{-0.09}$	519	DECAMP	77	ELEC	Hyperon beam

[7] The sign is, *with our conventions*, unambiguously positive. The value assumes, as usual, that $g_2 = 0$. If g_2 is included in the fit, than (with our sign convention) $g_2 = -0.56 \pm 0.37$, with a corresponding reduction of g_A/g_V to $+0.20 \pm 0.08$.

[8] BOURQUIN 83C favors the positive sign by at least 2.6 standard deviations.

[9] TANENBAUM 74 gives 0.435 ± 0.035, assuming no q^2 dependence in g_A and g_V. The listed result allows q^2 dependence, and is taken from HSUEH 88.

$f_2(0)/f_1(0)$ FOR $\Sigma^- \to ne^-\overline{\nu}_e$

The signs have been changed to be in accord with our conventions, given in the "Note on Baryon Decay Parameters" in the neutron Listings.

VALUE	EVTS	DOCUMENT ID		TECN	COMMENT
0.97±0.14 OUR AVERAGE					
+0.96±0.07±0.13	50k	HSUEH	88	SPEC	Σ^- 250 GeV
+1.02±0.34	4456	BOURQUIN	83C	SPEC	SPS hyperon beam

TRIPLE CORRELATION COEFFICIENT D for $\Sigma^- \to ne^-\overline{\nu}_e$

The coefficient D of the term $D\ \mathbf{P}\cdot(\hat{\mathbf{p}}_e\times\hat{\mathbf{p}}_\nu)$ in the $\Sigma^- \to ne^-\overline{\nu}$ decay angular distribution. A nonzero value would indicate a violation of time-reversal invariance.

VALUE	EVTS	DOCUMENT ID		TECN	COMMENT
0.11±0.10	50k	HSUEH	88	SPEC	Σ^- 250 GeV

g_V/g_A FOR $\Sigma^- \to \Lambda e^-\overline{\nu}_e$

For the sign convention, see the "Note on Baryon Decay Parameters" in the neutron Listings. The value is predicted to be zero by conserved vector current theory. The values averaged assume CVC-SU(3) weak magnetism term.

VALUE	EVTS	DOCUMENT ID		TECN	COMMENT
0.01 ±0.10 OUR AVERAGE Error includes scale factor of 1.5. See the ideogram below.					
−0.034±0.080	1620	[10] BOURQUIN	82	SPEC	SPS hyperon beam
−0.29 ±0.29	114	THOMPSON	80	ASPK	BNL hyperon beam
−0.17 ±0.35	55	TANENBAUM	75B	SPEC	BNL hyperon beam
+0.45 ±0.20	186	[10,11] FRANZINI	72	HBC	

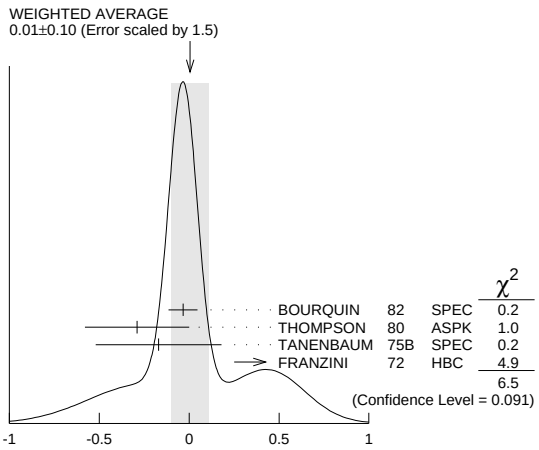

g_V/g_A for $\Sigma^- \to \Lambda e^-\overline{\nu}_e$

[10] The sign has been changed to agree with our convention.

[11] The FRANZINI 72 value includes the events of earlier papers.

g_{WM}/g_A FOR $\Sigma^- \to \Lambda e^-\overline{\nu}_e$

The values quoted assume the CVC prediction $g_V = 0$.

VALUE	EVTS	DOCUMENT ID		TECN	COMMENT
2.4 ±1.7 OUR AVERAGE					
1.75±3.5	114	THOMPSON	80	ASPK	BNL hyperon beam
3.5 ±4.5	55	TANENBAUM	75B	SPEC	BNL hyperon beam
2.4 ±2.1	186	FRANZINI	72	HBC	

Σ^- REFERENCES

We have omitted some papers that have been superseded by later experiments. See our earlier editions.

ESCHRICH	01	PL B522 233	I. Eschrich *et al.* (FNAL SELEX Collab.)
GUREV	93	JETPL 57 400 Translated from ZETFP 57 389.	M.P. Gurev *et al.* (PNPI)
GALL	88	PRL 60 186	K.P. Gall *et al.* (BOST, MIT, WILL, CIT+)
HERTZOG	88	PR D37 1142	D.W. Hertzog *et al.* (WILL, BOST, MIT+)
HSUEH	88	PR D38 2056	S.Y. Hsueh *et al.* (CHIC, ELMT, FNAL+)
ZAPALAC	86	PRL 57 1526	G. Zapalac *et al.* (EFI, ELMT, FNAL+)
HSUEH	85	PRL 54 2399	S.Y. Hsueh *et al.* (CHIC, ELMT, FNAL+)
WAH	85	PRL 55 2551	Y.W. Wah *et al.* (FNAL, IOWA, ISU)
BOURQUIN	83B	ZPHY C21 27	M.H. Bourquin *et al.* (BRIS, GEVA, HEIDP+)
BOURQUIN	83C	ZPHY C21 17	M.H. Bourquin *et al.* (BRIS, GEVA, HEIDP+)
DECK	83	PR D28 1	L. Deck *et al.* (RUTG, WISC, MICH, MINN)
BOURQUIN	82	ZPHY C12 307	M.H. Bourquin *et al.* (BRIS, GEVA, HEIDP+)
MARRAFFINO	80	PR D21 2501	J. Marraffino *et al.* (VAND, MPIM)
THOMPSON	80	PR D21 25	J.A. Thompson *et al.* (PITT, BNL)
HANSL	78	NP B132 45	T. Hansl *et al.* (MPIM, VAND)
DECAMP	77	PL 66B 295	D. Decamp *et al.* (LALO, EPOL)
CONFORTO	76	NP B105 189	B. Conforto *et al.* (RHEL, LOIC)
DUGAN	75	NP A254 396	G. Dugan *et al.* (COLU, YALE)
TANENBAUM	75B	PR D12 1871	W. Tanenbaum *et al.* (YALE, FNAL, BNL)
EBENHOH	74	ZPHY 266 367	H. Ebenhoh *et al.* (HEIDT)
TANENBAUM	74	PRL 33 175	W. Tanenbaum *et al.* (YALE, FNAL, BNL)
EBENHOH	73	ZPHY 264 413	W. Ebenhoh *et al.* (HEIDT)
SECHI-ZORN	73	PR D8 12	B. Sechi-Zorn, G.A. Snow (UMD)
BOHM	72	NP B48 1	G. Bohm *et al.* (BERL, KIDR, BRUX, IASD+)
FRANZINI	72	PR D6 2417	P. Franzini *et al.* (COLU, HEID, UMD+)

ROBERTSON	72	Thesis UMI 78-00877	R.M. Robertson	(IIT)
BAKKER	71	LNC 1 37	A.M. Bakker *et al.*	(SABRE Collab.)
COLE	71	PR D4 631	J. Cole *et al.*	(STON, COLU)
Also		Thesis Nevis 175	H. Norton	(COLU)
TOVEE	71	NP B33 493	D.N. Tovee *et al.*	(LOUC, KIDR, BERL+)
BERLEY	70B	PR D1 2015	D. Berley *et al.*	(BNL, MASA, YALE)
BOGERT	70	PR D2 6	D.V. Bogert *et al.*	(BNL, MASA, YALE)
EISELE	70	ZPHY 238 372	F. Eisele *et al.*	(HEID)
PDG	70	RMP 42 87	A. Barbaro-Galtieri *et al.*	(LRL, BRAN+)
ANG	69	ZPHY 223 103	G. Ang *et al.*	(HEID)
ANG	69B	ZPHY 228 151	G. Ang *et al.*	(HEID)
BAGGETT	69	PRL 23 249	N.V. Baggett, B. Kehoe, G.A. Snow	(UMD)
BALTAY	69	PRL 22 615	C. Baltay *et al.*	(COLU, STON)
BANGERTER	69	Thesis UCRL 19244	R.O. Bangerter	(LRL)
BANGERTER	69B	PR 187 1821	R.O. Bangerter *et al.*	(LRL)
BARLOUTAUD	69	NP B14 153	R. Barloutaud *et al.*	(SACL, CERN, HEID)
EISELE	69	ZPHY 221 1	F. Eisele *et al.*	(HEID)
BIERMAN	68	PRL 20 1459	E. Bierman *et al.*	(PRIN)
HEPP	68	ZPHY 214 71	V. Hepp, H. Schleich	(HEID)
WHITESIDE	68	NC 54A 537	H. Whiteside, J. Gollub	(OBER)
BARASH	67	PRL 19 181	N. Barash *et al.*	(UMD)
CHANG	66	PR 151 1081	C.Y. Chang	(COLU)
BAZIN	65B	PR 140 B1358	M. Bazin *et al.*	(PRIN, RUTG, COLU)
DOSCH	65	PL 14 239	H.C. Dosch *et al.*	(HEID)
Also		PR 151 1081	C.Y. Chang	(COLU)
SCHMIDT	65	PR 140 B1328	P. Schmidt	(COLU)
BURNSTEIN	64	PRL 13 66	R.A. Burnstein *et al.*	(UMD)
COURANT	64	PR 136 B1791	H. Courant *et al.*	(CERN, HEID, UMD+)
BARKAS	63	PRL 11 26	W.H. Barkas, J.N. Dyer, H.H. Heckman	(LRL)
HUMPHREY	62	PR 127 1305	W.E. Humphrey, R.R. Ross	(LRL)

$\Sigma(1385)\ 3/2^+$

$I(J^P) = 1(\frac{3}{2}^+)$ Status: ****

Discovered by ALSTON 60. Early measurements of the mass and width for combined charge states have been omitted. They may be found in our 1984 edition Reviews of Modern Physics **56** S1 (1984).

We average only the most significant determinations. We do not average results from inclusive experiments with large backgrounds or results which are not accompanied by some discussion of experimental resolution. Nevertheless systematic differences between experiments remain. (See the ideograms in the Listings below.) These differences could arise from interference effects that change with production mechanism and/or beam momentum. They can also be accounted for in part by differences in the parametrizations employed. (See BORENSTEIN 74 for a discussion on this point.) Thus BORENSTEIN 74 uses a Breit-Wigner with energy-independent width, since a P-wave was found to give unsatisfactory fits. CAMERON 78 uses the same form. On the other hand HOLMGREN 77 obtains a good fit to their $\Lambda\pi$ spectrum with a P-wave Breit-Wigner, but includes the partial width for the $\Sigma\pi$ decay mode in the parametrization. AGUILAR-BENITEZ 81D gives masses and widths for five different Breit-Wigner shapes. The results vary considerably. Only the best-fit S-wave results are given here.

$\Sigma(1385)$ POLE POSITIONS

$\Sigma(1385)^+$ REAL PART

VALUE	DOCUMENT ID	COMMENT
1379±1	LICHTENBERG74	Extrapolates HABIBI 73

$\Sigma(1385)^+$ −IMAGINARY PART

VALUE	DOCUMENT ID	COMMENT
17.5±1.5	LICHTENBERG74	Extrapolates HABIBI 73

$\Sigma(1385)^-$ REAL PART

VALUE	DOCUMENT ID	COMMENT
1383±1	LICHTENBERG74	Extrapolates HABIBI 73

$\Sigma(1385)^-$ −IMAGINARY PART

VALUE	DOCUMENT ID	COMMENT
22.5±1.5	LICHTENBERG74	Extrapolates HABIBI 73

$\Sigma(1385)$ MASSES

$\Sigma(1385)^+$ MASS

VALUE (MeV)	EVTS	DOCUMENT ID		TECN	COMMENT
1382.80±0.35 OUR AVERAGE		Error includes scale factor of 1.9. See the ideogram below.			
1383.2 ±0.9 $^{+0.1}_{-1.5}$		AGAKISHIEV	12	SPEC	$pp \to \Sigma(1385)^+ K^+ n$, 3.5 GeV
1384.1 ±0.7	1897	BAUBILLIER	84	HBC	$K^- p$ 8.25 GeV/c
1384.5 ±0.5	5256	AGUILAR-...	81D	HBC	$K^- p \to \Lambda\pi\pi$ 4.2 GeV/c
1383.0 ±0.4	9361	AGUILAR-...	81D	HBC	$K^- p \to \Lambda 3\pi$ 4.2 GeV/c
1381.9 ±0.3	6900	CAMERON	78	HBC	$K^- p$ 0.96–1.36 GeV/c
1381 ±1	6846	BORENSTEIN	74	HBC	$K^- p$ 2.18 GeV/c
1383.5 ±0.85	2300	HABIBI	73	HBC	$K^- p \to \Lambda\pi\pi$
1382 ±2	400	AGUILAR-...	72B	HBC	$K^- p \to \Lambda\pi$'s
1384.4 ±1.0	1260	SIEGEL	67	HBC	$K^- p$ 2.1 GeV/c
1382 ±1	750	ARMENTEROS	65B	HBC	$K^- p$ 0.9–1.2 GeV/c
1381.0 ±1.6	859	HUWE	64	HBC	$K^- p$ 1.22 GeV/c

• • • We do not use the following data for averages, fits, limits, etc. • • •

1385.1 ±1.2	600	BAKER	80	HYBR	$\pi^+ p$ 7 GeV/c
1383.2 ±1.0	750	BAKER	80	HYBR	$K^- p$ 7 GeV/c
1381 ±2	7k	[1] BAUBILLIER	79B	HBC	$K^- p$ 8.25 GeV/c
1391 ±2	2k	CAUTIS	79	HYBR	$\pi^+ p/K^- p$ 11.5 GeV
1390 ±2	100	[1] SUGAHARA	79B	HBC	$\pi^- p$ 6 GeV/c
1385 ±3	22k	[1,2] BARREIRO	77B	HBC	$K^- p$ 4.2 GeV/c
1385 ±1	2594	HOLMGREN	77	HBC	See AGUILAR-BENITEZ 81D
1380 ±2		[1] BARDADIN-...	75	HBC	$K^- p$ 14.3 GeV/c
1382 ±1	3740	[3] BERTHON	74	HBC	$K^- p$ 1263–1843 MeV/c
1390 ±6	46	AGUILAR-...	70B	HBC	$K^- p \to \Sigma\pi$'s 4 GeV/c
1383 ±8	62	[4] BIRMINGHAM	66	HBC	$K^- p$ 3.5 GeV/c
1378 ±5	135	LONDON	66	HBC	$K^- p$ 2.24 GeV/c
1384.3 ±1.9	250	[4] SMITH	65	HBC	$K^- p$ 1.8 GeV/c
1382.6 ±2.1	250	[4] SMITH	65	HBC	$K^- p$ 1.95 GeV/c
1375.0 ±3.9	170	COOPER	64	HBC	$K^- p$ 1.45 GeV/c
1376.0 ±3.9	154	[4] ELY	61	HLBC	$K^- p$ 1.11 GeV/c

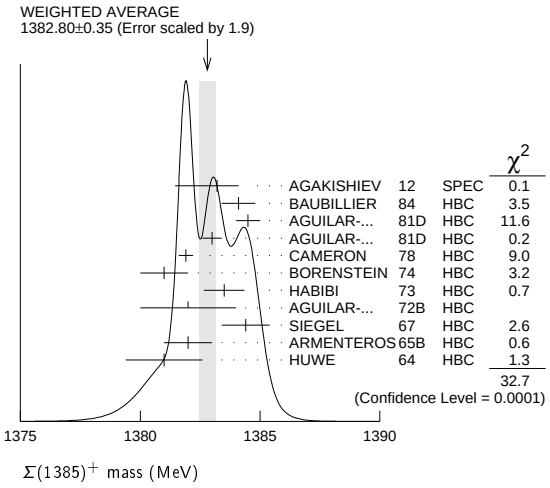

$\Sigma(1385)^0$ MASS

VALUE (MeV)	EVTS	DOCUMENT ID		TECN	COMMENT
1383.7±1.0 OUR AVERAGE		Error includes scale factor of 1.4. See the ideogram below.			
1384.1±0.8	5722	AGUILAR-...	81D	HBC	$K^- p \to \Lambda 3\pi$ 4.2 GeV/c
1380 ±2	3100	[5] BORENSTEIN	74	HBC	$K^- p \to \Lambda 3\pi$ 2.18 GeV/c
1385.1±2.5	240	[4] THOMAS	73	HBC	$\pi^- p \to \Lambda\pi^0 K^0$

• • • We do not use the following data for averages, fits, limits, etc. • • •

1389 ±3	500	[6] BAUBILLIER	79B	HBC	$K^- p$ 8.25 GeV/c

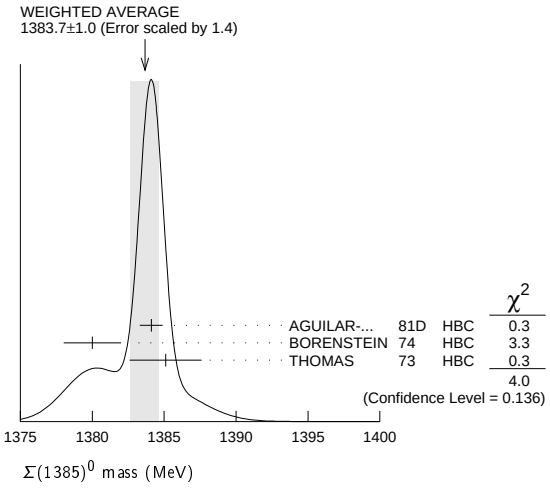

$\Sigma(1385)^-$ MASS

VALUE (MeV)	EVTS	DOCUMENT ID		TECN	COMMENT
1387.2±0.5 OUR AVERAGE		Error includes scale factor of 2.2. See the ideogram below.			
1388.3±1.7	620	AGUILAR-...	81D	HBC	$K^- p \to \Lambda\pi\pi$ 4.2 GeV/c
1384.9±0.8	3346	AGUILAR-...	81D	HBC	$K^- p \to \Lambda 3\pi$ 4.2 GeV/c
1387.6±0.3	9720	CAMERON	78	HBC	$K^- p$ 0.96–1.36 GeV/c
1383 ±2	2303	BORENSTEIN	74	HBC	$K^- p$ 2.18 GeV/c
1390.7±1.2	1900	HABIBI	73	HBC	$K^- p \to \Lambda\pi\pi$

1387.1±1.9	630	[4] THOMAS	73	HBC	$\pi^- p \to \Lambda\pi^- K^+$
1390.7±2.0	370	SIEGEL	67	HBC	$K^- p$ 2.1 GeV/c
1384 ±1	1380	ARMENTEROS	65B	HBC	$K^- p$ 0.9–1.2 GeV/c
1385.3±1.9	1086	[4] HUWE	64	HBC	$K^- p$ 1.15–1.30 GeV/c
• • • We do not use the following data for averages, fits, limits, etc. • • •					
1383 ±1	4.5k	[1] BAUBILLIER	79B	HBC	$K^- p$ 8.25 GeV/c
1380 ±6	150	[1] SUGAHARA	79B	HBC	$\pi^- p$ 6 GeV/c
1387 ±3	12k	[1,2] BARREIRO	77B	HBC	$K^- p$ 4.2 GeV/c
1391 ±3	193	HOLMGREN	77	HBC	See AGUILAR-BENITEZ 81D
1383 ±2		[1] BARDADIN-...	75	HBC	$K^- p$ 14.3 GeV/c
1389 ±1	3060	[3] BERTHON	74	HBC	$K^- p$ 1263–1843 MeV/c
1389 ±9	15	LONDON	66	HBC	$K^- p$ 2.24 GeV/c
1391.5±2.6	120	[4] SMITH	65	HBC	$K^- p$ 1.8 GeV/c
1399.8±2.2	58	[4] SMITH	65	HBC	$K^- p$ 1.95 GeV/c
1392.0±6.2	200	COOPER	64	HBC	$K^- p$ 1.45 GeV/c
1382 ±3	93	DAHL	61	DBC	$K^- d$ 0.45 GeV/c
1376.0±4.4	224	[4] ELY	61	HLBC	$K^- p$ 1.11 GeV/c

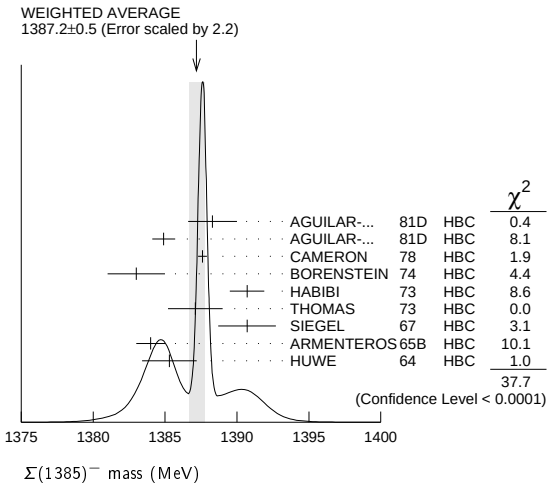

$m_{\Sigma(1385)^-} - m_{\Sigma(1385)^+}$

VALUE (MeV)	CL%	DOCUMENT ID		TECN	COMMENT
• • • We do not use the following data for averages, fits, limits, etc. • • •					
− 2 to +6	95	[7] BORENSTEIN	74	HBC	$K^- p$ 2.18 GeV/c
7.2±1.4		[7] HABIBI	73	HBC	$K^- p \to \Lambda\pi\pi$
6.3±2.0		[7] SIEGEL	67	HBC	$K^- p$ 2.1 GeV/c
11 ±9		[7] LONDON	66	HBC	$K^- p$ 2.24 GeV/c
9 ±6		LONDON	66	HBC	$\Lambda 3\pi$ events
2.0±1.5		[7] ARMENTEROS	65B	HBC	$K^- p$ 0.9–1.2 GeV/c
7.2±2.1		[7] SMITH	65	HBC	$K^- p$ 1.8 GeV/c
17.2±2.0		[7] SMITH	65	HBC	$K^- p$ 1.95 GeV/c
17 ±7		[7] COOPER	64	HBC	$K^- p$ 1.45 GeV/c
4.3±2.2		[7] HUWE	64	HBC	$K^- p$ 1.22 GeV/c
0.0±4.2		[7] ELY	61	HLBC	$K^- p$ 1.11 GeV/c

$m_{\Sigma(1385)^0} - m_{\Sigma(1385)^+}$

VALUE (MeV)	CL%	DOCUMENT ID		TECN	COMMENT
• • • We do not use the following data for averages, fits, limits, etc. • • •					
−4 to +4	95	[7] BORENSTEIN	74	HBC	$K^- p$ 2.18 GeV/c

$m_{\Sigma(1385)^-} - m_{\Sigma(1385)^0}$

VALUE (MeV)	DOCUMENT ID		TECN	COMMENT
• • • We do not use the following data for averages, fits, limits, etc. • • •				
2.0±2.4	[7] THOMAS	73	HBC	$\pi^- p \to \Lambda\pi^- K^+$

$\Sigma(1385)$ WIDTHS

$\Sigma(1385)^+$ WIDTH

VALUE (MeV)	EVTS	DOCUMENT ID		TECN	COMMENT
36.0± 0.7 OUR AVERAGE					
40.2± 2.1 $^{+1.2}_{-2.8}$		AGAKISHIEV	12	SPEC	$pp \to \Sigma(1385)^+ K^+ n$, 3.5 GeV
37.2± 2.0	1897	BAUBILLIER	84	HBC	$K^- p$ 8.25 GeV/c
35.1± 1.7	5256	AGUILAR-...	81D	HBC	$K^- p \to \Lambda\pi\pi$ 4.2 GeV/c
37.5± 2.0	9361	AGUILAR-...	81D	HBC	$K^- p \to \Lambda 3\pi$ 4.2 GeV/c
35.5± 1.9	6900	CAMERON	78	HBC	$K^- p$ 0.96–1.36 GeV/c
34.0± 1.6	6846	[8] BORENSTEIN	74	HBC	$K^- p$ 2.18 GeV/c
38.3± 3.2	2300	[9] HABIBI	73	HBC	$K^- p \to \Lambda\pi\pi$
32.5± 6.0	400	AGUILAR-...	72B	HBC	$K^- p \to \Lambda\pi$'s
36 ± 4	1260	[9] SIEGEL	67	HBC	$K^- p$ 2.1 GeV/c
32.0± 4.7	750	[9] ARMENTEROS	65B	HBC	$K^- p$ 0.95–1.20 GeV/c
46.5± 6.4	859	[9] HUWE	64	HBC	$K^- p$ 1.15–1.30 GeV/c
• • • We do not use the following data for averages, fits, limits, etc. • • •					
40 ± 3	600	BAKER	80	HYBR	$\pi^+ p$ 7 GeV/c
37 ± 2	750	BAKER	80	HYBR	$K^- p$ 7 GeV/c
37 ± 2	7k	[1] BAUBILLIER	79B	HBC	$K^- p$ 8.25 GeV/c
30 ± 4	2k	CAUTIS	79	HYBR	$\pi^+ p/K^- p$ 11.5 GeV
30 ± 6	100	[1] SUGAHARA	79B	HBC	$\pi^- p$ 6 GeV/c
43 ± 5	22k	[1,2] BARREIRO	77B	HBC	$K^- p$ 4.2 GeV/c
34 ± 2	2594	HOLMGREN	77	HBC	See AGUILAR-BENITEZ 81D
40.0± 3.2		[1] BARDADIN-...	75	HBC	$K^- p$ 14.3 GeV/c
48 ± 3	3740	[3] BERTHON	74	HBC	$K^- p$ 1263–1843 MeV/c
33 ±20	46	[9] AGUILAR-...	70B	HBC	$K^- p \to \Sigma\pi$'s 4 GeV/c
25 ±32	62	[9] BIRMINGHAM	66	HBC	$K^- p$ 3.5 GeV/c
30.3± 7.5	250	[9] SMITH	65	HBC	$K^- p$ 1.8 GeV/c
33.1± 8.3	250	[9] SMITH	65	HBC	$K^- p$ 1.95 GeV/c
51 ±16	170	[9] COOPER	64	HBC	$K^- p$ 1.45 GeV/c
48 ±16	154	[9] ELY	61	HLBC	$K^- p$ 1.11 GeV/c

$\Sigma(1385)^0$ WIDTH

VALUE (MeV)	EVTS	DOCUMENT ID		TECN	COMMENT
36 ± 5 OUR AVERAGE					
34.8± 5.6	5722	AGUILAR-...	81D	HBC	$K^- p \to \Lambda 3\pi$ 4.2 GeV/c
39.3±10.2	240	[9] THOMAS	73	HBC	$\pi^- p \to \Lambda\pi^0 K^0$
• • • We do not use the following data for averages, fits, limits, etc. • • •					
53 ± 8	3100	[10] BORENSTEIN	74	HBC	$K^- p \to \Lambda 3\pi$ 2.18 GeV/c
30 ± 9	106	CURTIS	63	OSPK	$\pi^- p$ 1.5 GeV/c

$\Sigma(1385)^-$ WIDTH

VALUE (MeV)	EVTS	DOCUMENT ID		TECN	COMMENT
39.4± 2.1 OUR AVERAGE		Error includes scale factor of 1.7. See the ideogram below.			
38.4±10.7	620	AGUILAR-...	81D	HBC	$K^- p \to \Lambda\pi\pi$ 4.2 GeV/c
34.6± 4.2	3346	AGUILAR-...	81D	HBC	$K^- p \to \Lambda 3\pi$ 4.2 GeV/c
39.2± 1.7	9720	CAMERON	78	HBC	$K^- p$ 0.96–1.36 GeV/c
35 ± 3	2303	[8] BORENSTEIN	74	HBC	$K^- p$ 2.18 GeV/c
51.9± 4.8	1900	[9] HABIBI	73	HBC	$K^- p \to \Lambda\pi\pi$
48.2± 7.7	630	[9] THOMAS	73	HBC	$\pi^- p \to \Lambda\pi^- K^0$
31.0± 6.5	370	[9] SIEGEL	67	HBC	$K^- p$ 2.1 GeV/c
38.0± 4.1	1382	[9] ARMENTEROS	65B	HBC	$K^- p$ 0.95–1.20 GeV/c
62 ± 7	1086	HUWE	64	HBC	$K^- p$ 1.15–1.30 GeV/c
• • • We do not use the following data for averages, fits, limits, etc. • • •					
44 ± 4	4.5k	[1] BAUBILLIER	79B	HBC	$K^- p$ 8.25 GeV/c
58 ± 4	150	[1] SUGAHARA	79B	HBC	$\pi^- p$ 6 GeV/c
45 ± 5	12k	[1,2] BARREIRO	77B	HBC	$K^- p$ 4.2 GeV/c
35 ±10	193	HOLMGREN	77	HBC	See AGUILAR-BENITEZ 81D
47 ± 6		[1] BARDADIN-...	75	HBC	$K^- p$ 14.3 GeV/c
40 ± 3	3060	[3] BERTHON	74	HBC	$K^- p$ 1263–1843 MeV/c
29.2±10.6	120	[9] SMITH	65	HBC	$K^- p$ 1.80 GeV/c
17.1± 8.9	58	[9] SMITH	65	HBC	$K^- p$ 1.95 GeV/c
88 ±24	200	[9] COOPER	64	HBC	$K^- p$ 1.45 GeV/c
40		DAHL	61	DBC	$K^- d$ 0.45 GeV/c
66 ±18	224	[9] ELY	61	HLBC	$K^- p$ 1.11 GeV/c

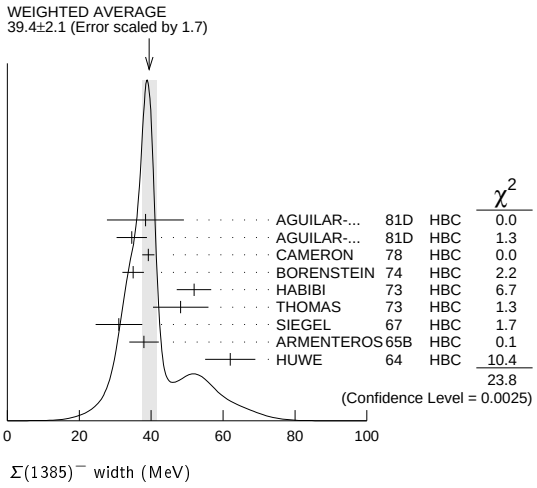

$\Sigma(1385)$ DECAY MODES

	Mode	Fraction (Γ_i/Γ)	Confidence level
Γ_1	$\Lambda\pi$	(87.0 ±1.5) %	
Γ_2	$\Sigma\pi$	(11.7 ±1.5) %	
Γ_3	$\Lambda\gamma$	($1.25^{+0.13}_{-0.12}$) %	
Γ_4	$\Sigma^+\gamma$	(7.0 ±1.7) $\times 10^{-3}$	
Γ_5	$\Sigma^-\gamma$	< 2.4 $\times 10^{-4}$	90%
Γ_6	$N\overline{K}$		

$\Sigma(1385)$ BRANCHING RATIOS

$\Gamma(\Sigma\pi)/\Gamma(\Lambda\pi)$ Γ_2/Γ_1

VALUE	DOCUMENT ID		TECN	CHG	COMMENT
0.135±0.011 OUR AVERAGE					
0.20 ±0.06	DIONISI	78B	HBC	±	$K^-p \to Y^*K\overline{K}$
0.16 ±0.03	BERTHON	74	HBC	+	K^-p 1.26–1.84 GeV/c
0.11 ±0.02	BERTHON	74	HBC	−	K^-p 1.26–1.84 GeV/c
0.21 ±0.05	BORENSTEIN	74	HBC	+	$K^-p \to \Lambda\pi^+\pi^-$, $\Sigma^0\pi^+\pi^-$
0.18 ±0.04	MAST	73	MPWA	±	$K^-p \to \Lambda\pi^+\pi^-$, $\Sigma^0\pi^+\pi^-$
0.10 ±0.05	THOMAS	73	HBC	−	$\pi^-p \to \Lambda K\pi$, $\Sigma K\pi$
0.16 ±0.07	AGUILAR-...	72B	HBC	+	K^-p 3.9, 4.6 GeV/c
0.13 ±0.04	COLLEY	71B	DBC	−0	K^-N 1.5 GeV/c
0.13 ±0.04	PAN	69	HBC	+	$\pi^+p \to \Lambda K\pi$, $\Sigma K\pi$
0.08 ±0.06	LONDON	66	HBC	+	K^-p 2.24 GeV/c
0.163±0.041	ARMENTEROS	65B	HBC	±	K^-p 0.95–1.20 GeV/c
0.09 ±0.04	HUWE	64	HBC	±	K^-p 1.2–1.7 GeV
• • • We do not use the following data for averages, fits, limits, etc. • • •					
<0.04	ALSTON	62	HBC	±0	K^-p 1.15 GeV/c
0.04 ±0.04	BASTIEN	61	HBC	±	

$\Gamma(\Lambda\gamma)/\Gamma(\Lambda\pi)$ Γ_3/Γ_1

This ratio is of course for $\Sigma(1385)^0 \to \Lambda\gamma$ and $\Lambda\pi^0$.

VALUE (units 10^{-2})	EVTS	DOCUMENT ID		TECN	COMMENT
$1.43^{+0.15}_{-0.13}$ OUR AVERAGE					
$1.42\pm0.12^{+0.11}_{-0.07}$	624 ± 25	KELLER	11	CLAS	$\gamma p \to K^+\Lambda\gamma$, E_γ 1.6–3.8 GeV
$1.53\pm0.39^{+0.15}_{-0.24}$	61	TAYLOR	05	CLAS	$\gamma p \to K^+\Lambda\gamma$

$\Gamma(\Sigma^+\gamma)/\Gamma(\Sigma\pi)$ Γ_4/Γ_2

This ratio is for $\Sigma(1385)^+ \to \Sigma^+\gamma$ over $\Sigma(1385)^+ \to \Sigma\pi$.

VALUE (%)	DOCUMENT ID		TECN	COMMENT
$5.98\pm1.11^{+0.27}_{-0.61}$	[11] KELLER	12	CLAS	$\gamma p \to K^0\Sigma(1385)^+$

$\Gamma(\Sigma^-\gamma)/\Gamma_{total}$ Γ_5/Γ

VALUE	CL%	DOCUMENT ID		TECN	CHG	COMMENT
$<2.4\times10^{-4}$	90	[12] MOLCHANOV	04	SELX	−	Σ^- Pb → $\Sigma(1385)^-$ Pb, 600 GeV
• • • We do not use the following data for averages, fits, limits, etc. • • •						
$<6.1\times10^{-4}$	90	[13] ARIK	77	SPEC	−	Σ^- Pb → $\Sigma(1385)^-$ Pb, 23 GeV

$(\Gamma_i\Gamma_f)^{1/2}/\Gamma_{total}$ in $N\overline{K} \to \Sigma(1385) \to \Lambda\pi$ $(\Gamma_6\Gamma_1)^{1/2}/\Gamma$

VALUE	DOCUMENT ID		CHG	COMMENT
+0.586±0.319	[14] DEVENISH	74B	0	Fixed-t dispersion rel.

$\Sigma(1385)$ FOOTNOTES

[1] From fit to inclusive $\Lambda\pi$ spectrum.
[2] Includes data of HOLMGREN 77.
[3] The errors are statistical only. The resolution is not unfolded.
[4] The error is enlarged to $\Gamma/\sqrt{N}$. See the note on the $K^*(892)$ mass in the 1984 edition.
[5] From a fit to $\Lambda\pi^0$ with the width fixed at 34 MeV.
[6] From fit to inclusive $\Lambda\pi^0$ spectrum with the width fixed at 40 MeV.
[7] Redundant with data in the mass Listings.
[8] Results from $\Lambda\pi^+\pi^-$ and $\Lambda\pi^+\pi^-\pi^0$ combined by us.
[9] The error is enlarged to $4\Gamma/\sqrt{N}$. See the note on the $K^*(892)$ mass in the 1984 edition.
[10] Consistent with +, 0, and − widths equal.
[11] KELLER 12 gives $\Gamma(\Sigma^+\gamma)/\Gamma(\Sigma^+\pi^0) = (11.95 \pm 2.21^{+0.53}_{-1.21})\%$, using 1/2 our total $\Sigma(1385) \to \Sigma\pi$ fraction for $\Sigma^+\pi^0$. We divide the KELLER 12 value by two.
[12] We calculate this from the MOLCHANOV 04 upper limit of 9.5 keV on the $\Sigma^-\gamma$ width.
[13] We calculate this from the ARIK 77 upper limit of 24 keV on the $\Sigma^-\gamma$ width.
[14] An extrapolation of the parametrized amplitude below threshold.

$\Sigma(1385)$ REFERENCES

AGAKISHIEV	12	PR C85 035203	G. Agakishiev *et al.* (HADES Collab.)
KELLER	12	PR D85 052004	D. Keller *et al.* (JLab CLAS Collab.)
KELLER	11	PR D83 072004	D. Keller *et al.* (JLab CLAS Collab.)
TAYLOR	05	PR C71 054609	S. Taylor *et al.* (JLab CLAS Collab.)
Also		PR C72 039902 (errat.)	S. Taylor *et al.* (JLab CLAS Collab.)
MOLCHANOV	04	PL B590 161	V.V. Molchanov *et al.* (FNAL SELEX Collab.)
BAUBILLIER	84	ZPHY C23 213	M. Baubillier *et al.* (BIRM, CERN, GLAS+)
PDG	84	RMP 56 S1	C.G. Wohl *et al.* (LBL, CIT, CERN)
AGUILAR-...	81D	AFIS A77 144	M. Aguilar-Benitez, J. Salicio (MADR)
BAKER	80	NP B166 207	P.A. Baker *et al.* (LOIC)
BAUBILLIER	79B	NP B148 18	M. Baubillier *et al.* (BIRM, CERN, GLAS+)
CAUTIS	79	NP B156 507	C.V. Cautis *et al.* (SLAC)
SUGAHARA	79B	NP B156 237	R. Sugahara *et al.* (KEK, OSKC, KINK)
CAMERON	78	NP B143 189	W. Cameron *et al.* (RHEL, LOIC)
DIONISI	78B	PL 78B 154	C. Dionisi, R. Armenteros, J. Diaz (CERN, AMST+)
ARIK	77	PRL 38 1000	E. Arik *et al.* (PITT, BNL, MASA)
BARREIRO	77B	NP B126 319	F. Barreiro *et al.* (CERN, AMST, NIJM)
HOLMGREN	77	NP B119 261	S.O. Holmgren *et al.* (CERN, AMST, NIJM)
BARDADIN-...	75	NP B98 418	M. Bardadin-Otwinowska *et al.* (SACL, EPOL+)
BERTHON	74	NC 21A 146	A. Berthon *et al.* (CDEF, RHEL, SACL+)
BORENSTEIN	74	PR D9 3006	S.R. Borenstein *et al.* (BNL, MICH)
DEVENISH	74B	NP B81 330	R.C.E. Devenish, C.D. Froggatt, B.R. Martin (DESY+)
LICHTENBERG	74	PR D10 3865	D.B. Lichtenberg (IND)
Also		Private Comm.	D.B. Lichtenberg (IND)
HABIBI	73	Thesis Nevis 199	M. Habibi (COLU)
Also		Purdue Conf. 387	C. Baltay *et al.* (COLU, BING)
MAST	73	PR D7 3212	T.S. Mast *et al.* (LBL) IJP
Also		PR D7 5	T.S. Mast *et al.* (LBL) IJP
THOMAS	73	NP B56 15	D.W. Thomas *et al.* (CMU) JP
AGUILAR-...	72B	PR D6 29	M. Aguilar-Benitez *et al.* (BNL)
COLLEY	71B	NP B31 61	D.C. Colley *et al.* (BIRM, EDIN, GLAS+)
AGUILAR-...	70B	PRL 25 58	M. Aguilar-Benitez *et al.* (BNL, SYRA)
PAN	69	PRL 23 808	Y.L. Pan, F.L. Forman (PENN) I
SIEGEL	67	Thesis UCRL 18041	D.M. Siegel (LRL)
BIRMINGHAM	66	PR 152 1148	M. Haque *et al.* (BIRM, GLAS, LOIC, OXF+)
LONDON	66	PR 143 1034	G.W. London *et al.* (BNL, SYRA) J
ARMENTEROS	65B	PL 19 75	R. Armenteros *et al.* (CERN, HEID, SACL)
SMITH	65	Thesis UCLA	L.T. Smith (UCLA)
COOPER	64	PL 8 365	W.A. Cooper *et al.* (CERN, AMST)
HUWE	64	Thesis UCRL 11291	D.O. Huwe (LRL) JP
Also		PR 181 1824	D.O. Huwe (LRL)
CURTIS	63	PR 132 1771	L.J. Curtis *et al.* (MICH) J
ALSTON	62	CERN Conf. 311	M.H. Alston *et al.* (LRL)
BASTIEN	61	PRL 6 702	P.L. Bastien, M. Ferro-Luzzi, A.H. Rosenfeld (LRL)
DAHL	61	PRL 6 142	O.I. Dahl *et al.* (LRL)
ELY	61	PRL 7 461	R.P. Ely *et al.* (LRL) J
ALSTON	60	PRL 5 520	M.H. Alston *et al.* (LRL) I

$\Sigma(1480)$ Bumps

$I(J^P) = 1(?^?)$ Status: *

OMITTED FROM SUMMARY TABLE

These are peaks seen in $\Lambda\pi$ and $\Sigma\pi$ spectra in the reaction $\pi^+p \to (Y\pi)K^+$ at 1.7 GeV/c. Also, the Y polarization oscillates in the same region.

MILLER 70 suggests a possible alternate explanation in terms of a reflection of $N(1675) \to \Lambda K$ decay. However, such an explanation for the $(\Sigma^+\pi^0)K^+$ channel in terms of $\Delta(1650) \to \Sigma K$ decay seems unlikely (see PAN 70). In addition such reflections would also have to account for the oscillation of the Y polarization in the 1480 MeV region.

HANSON 71, with less data than PAN 70, can neither confirm nor deny the existence of this state. MAST 75 sees no structure in this region in $K^-p \to \Lambda\pi^0$.

ENGELEN 80 performs a multichannel analysis of $K^-p \to p\overline{K}^0\pi^-$ at 4.2 GeV/c. They observe a 3.5 standard-deviation signal at 1480 MeV in $p\overline{K}^0$ which cannot be explained as a reflection of any competing channel.

PRAKHOV 04 sees no evidence for this or other light Σ resonances, aside from the $\Sigma(1385)$, in $K^-p \to \Lambda\pi^0\pi^0$.

ZYCHOR 06 finds peaks in $pp \to pK^+(\pi^\pm X^\mp)$ at p_{beam} = 3.65 GeV/c.

$\Sigma(1480)$ MASS (PRODUCTION EXPERIMENTS)

VALUE (MeV)	EVTS	DOCUMENT ID		TECN	COMMENT
≈ 1480 OUR ESTIMATE					
1480±15	365 ± 60	ZYCHOR	06	SPEC	$pp \to pK^+(\pi^\pm X^\mp)$
1480	120	ENGELEN	80	HBC	$K^-p \to (p\overline{K}^0)\pi^-$
1485±10		CLINE	73	MPWA	$K^-d \to (\Lambda\pi^-)p$
1479±10		PAN	70	HBC	$\pi^+p \to (\Lambda\pi^+)K^+$
1465±15		PAN	70	HBC	$\pi^+p \to (\Sigma\pi)K^+$

$\Sigma(1480)$ WIDTH (PRODUCTION EXPERIMENTS)

VALUE (MeV)	EVTS	DOCUMENT ID		TECN	COMMENT
60±15	365 ± 60	ZYCHOR	06	SPEC	$pp \to pK^+(\pi^\pm X^\mp)$
80±20	120	ENGELEN	80	HBC	$K^-p \to (p\overline{K}^0)\pi^-$
40±20		CLINE	73	MPWA	$K^-d \to (\Lambda\pi^-)p$

31±15	PAN	70	HBC	$\pi^+ p \rightarrow (\Lambda\pi^+) K^+$	
30±20	PAN	70	HBC	$\pi^+ p \rightarrow (\Sigma\pi) K^+$	

$\Sigma(1480)$ DECAY MODES (PRODUCTION EXPERIMENTS)

	Mode
Γ_1	$N\overline{K}$
Γ_2	$\Lambda\pi$
Γ_3	$\Sigma\pi$

$\Sigma(1480)$ BRANCHING RATIOS (PRODUCTION EXPERIMENTS)

$\Gamma(\Sigma\pi)/\Gamma(\Lambda\pi)$ — Γ_3/Γ_2

VALUE	DOCUMENT ID		TECN	CHG
0.82±0.51	PAN	70	HBC	+

$\Gamma(N\overline{K})/\Gamma(\Lambda\pi)$ — Γ_1/Γ_2

VALUE	DOCUMENT ID		TECN	CHG
0.72±0.50	PAN	70	HBC	+

$\Gamma(N\overline{K})/\Gamma_{total}$ — Γ_1/Γ

VALUE	DOCUMENT ID		TECN	COMMENT
small	CLINE	73	MPWA	$K^- d \rightarrow (\Lambda\pi^-) p$

$\Sigma(1480)$ REFERENCES (PRODUCTION EXPERIMENTS)

ZYCHOR	06	PRL 96 012002	I. Zychor *et al.*	(ANKE Collab.)
PRAKHOV	04	PR C69 042202	S. Prakhov *et al.*	(BNL Crystal Ball Collab.)
ENGELEN	80	NP B167 61	J.J. Engelen *et al.*	(NIJM, AMST, CERN+)
MAST	75	PR D11 3078	T.S. Mast *et al.*	(LBL)
CLINE	73	LNC 6 205	D. Cline, R. Laumann, J. Mapp	(WISC) IJP
HANSON	71	PR D4 1296	P. Hanson, G.E. Kalmus, J. Louie	(LBL) I
MILLER	70	Duke Conf. 229 Hyperon Resonances, 1970	D.H. Miller	(PURD)
PAN	70	PR D2 449	Y.L. Pan *et al.*	(PENN)
Also		PRL 23 808	Y.L. Pan, F.L. Forman	(PENN) I
Also		PRL 23 806	Y.L. Pan, F.L. Forman	(PENN) I

$\Sigma(1560)$ Bumps

$I(J^P) = 1(?^?)$ Status: **

OMITTED FROM SUMMARY TABLE

This entry lists peaks reported in mass spectra around 1560 MeV without implying that they are necessarily related.

DIONISI 78B observes a 6 standard-deviation enhancement at 1553 MeV in the charged $\Lambda/\Sigma\pi$ mass spectra from $K^- p \rightarrow (\Lambda/\Sigma)\pi K\overline{K}$ at 4.2 GeV/c. In a CERN ISR experiment, LOCKMAN 78 reports a narrow 6 standard-deviation enhancement at 1572 MeV in $\Lambda\pi^{\pm}$ from the reaction $pp \rightarrow \Lambda\pi^+\pi^- X$. These enhancements are unlikely to be associated with the $\Sigma(1580)$ (which has not been confirmed by several recent experiments – see the next entry in the Listings).

CARROLL 76 observes a bump at 1550 MeV (as well as one at 1580 MeV) in the isospin-1 $\overline{K}N$ total cross section, but uncertainties in cross section measurements outside the mass range of the experiment preclude estimating its significance.

See also MEADOWS 80 for a review of this state.

$\Sigma(1560)$ MASS (PRODUCTION EXPERIMENTS)

VALUE (MeV)	EVTS	DOCUMENT ID		TECN	CHG	COMMENT
≈ 1560 OUR ESTIMATE						
1553±7	121	DIONISI	78B	HBC	±	$K^- p \rightarrow (Y\pi) K\overline{K}$
1572±4	40	LOCKMAN	78	SPEC	±	$pp \rightarrow \Lambda\pi^+\pi^- X$

$\Sigma(1560)$ WIDTH (PRODUCTION EXPERIMENTS)

VALUE (MeV)	EVTS	DOCUMENT ID		TECN	CHG	COMMENT
79±30	121	DIONISI	78B	HBC	±	$K^- p \rightarrow (Y\pi) K\overline{K}$
15± 6	40	[1] LOCKMAN	78	SPEC	±	$pp \rightarrow \Lambda\pi^+\pi^- X$

$\Sigma(1560)$ DECAY MODES (PRODUCTION EXPERIMENTS)

	Mode	Fraction (Γ_i/Γ)
Γ_1	$\Lambda\pi$	seen
Γ_2	$\Sigma\pi$	

$\Sigma(1560)$ BRANCHING RATIOS (PRODUCTION EXPERIMENTS)

$\Gamma(\Sigma\pi)/[\Gamma(\Lambda\pi)+\Gamma(\Sigma\pi)]$ — $\Gamma_2/(\Gamma_1+\Gamma_2)$

VALUE	DOCUMENT ID		TECN	CHG	COMMENT
0.35±0.12	DIONISI	78B	HBC	±	$K^- p \rightarrow (Y\pi) K\overline{K}$

$\Gamma(\Lambda\pi)/\Gamma_{total}$ — Γ_1/Γ

VALUE	DOCUMENT ID		TECN	CHG	COMMENT
seen	LOCKMAN	78	SPEC	±	$pp \rightarrow \Lambda\pi^+\pi^- X$

$\Sigma(1560)$ FOOTNOTES (PRODUCTION EXPERIMENTS)

[1] The width observed by LOCKMAN 78 is consistent with experimental resolution.

$\Sigma(1560)$ REFERENCES (PRODUCTION EXPERIMENTS)

MEADOWS	80	Toronto Conf. 283	B.T. Meadows	(CINC)
DIONISI	78B	PL 78B 154	C. Dionisi, R. Armenteros, J. Diaz	(CERN, AMST+) I
LOCKMAN	78	Saclay DPHPE 78-01	W. Lockman *et al.*	(UCLA, SACL)
CARROLL	76	PRL 37 806	A.S. Carroll *et al.*	(BNL) I

$\Sigma(1580)$ $3/2^-$

$I(J^P) = 1(\frac{3}{2}^-)$ Status: *

OMITTED FROM SUMMARY TABLE

Seen in the isospin-1 $\overline{K}N$ cross section at BNL (LI 73, CARROLL 76) and in a partial-wave analysis of $K^- p \rightarrow \Lambda\pi^0$ for c.m. energies 1560–1600 MeV by LITCHFIELD 74. LITCHFIELD 74 finds $J^P = 3/2^-$. Not seen by ENGLER 78 or by CAMERON 78C (with larger statistics in $K^0_L p \rightarrow \Lambda\pi^+$ and $\Sigma^0\pi^+$).

Neither OLMSTED 04 (in $K^- p \rightarrow \Lambda\pi^0$) nor PRAKHOV 04 (in $K^- p \rightarrow \Lambda\pi^0\pi^0$) see any evidence for this state.

$\Sigma(1580)$ POLE POSITION

REAL PART

VALUE (MeV)	DOCUMENT ID		TECN	COMMENT
• • • We do not use the following data for averages, fits, limits, etc. • • •				
1607^{+13}_{-11}	[1] KAMANO	15	DPWA	Multichannel

[1] From the preferred solution A in KAMANO 15. Solution B reports M = 1492^{+4}_{-7} MeV.

−2×IMAGINARY PART

VALUE (MeV)	DOCUMENT ID		TECN	COMMENT
• • • We do not use the following data for averages, fits, limits, etc. • • •				
253^{+30}_{-18}	[2] KAMANO	15	DPWA	Multichannel

[2] From the preferred solution A in KAMANO 15. Solution B reports M = 138^{+8}_{-14} MeV.

$\Sigma(1580)$ POLE RESIDUES

The normalized residue is the residue divided by $\Gamma_{pole}/2$.

Normalized residue in $N\overline{K} \rightarrow \Sigma(1580) \rightarrow N\overline{K}$

MODULUS	PHASE (°)	DOCUMENT ID		TECN	COMMENT
• • • We do not use the following data for averages, fits, limits, etc. • • •					
0.00778	51	[3] KAMANO	15	DPWA	Multichannel

[3] From the preferred solution A in KAMANO 15.

Normalized residue in $N\overline{K} \rightarrow \Sigma(1580) \rightarrow \Sigma\pi$

MODULUS	PHASE (°)	DOCUMENT ID		TECN	COMMENT
• • • We do not use the following data for averages, fits, limits, etc. • • •					
0.0625	−6	[4] KAMANO	15	DPWA	Multichannel

[4] From the preferred solution A in KAMANO 15.

Normalized residue in $N\overline{K} \rightarrow \Sigma(1580) \rightarrow \Lambda\pi$

MODULUS	PHASE (°)	DOCUMENT ID		TECN	COMMENT
• • • We do not use the following data for averages, fits, limits, etc. • • •					
0.059	156	[5] KAMANO	15	DPWA	Multichannel

[5] From the preferred solution A in KAMANO 15.

Normalized residue in $N\overline{K} \rightarrow \Sigma(1580) \rightarrow \Sigma(1385)\pi$, S-wave

MODULUS	PHASE (°)	DOCUMENT ID		TECN	COMMENT
• • • We do not use the following data for averages, fits, limits, etc. • • •					
0.0368	−18	[6] KAMANO	15	DPWA	Multichannel

[6] From the preferred solution A in KAMANO 15.

Normalized residue in $N\overline{K} \rightarrow \Sigma(1580) \rightarrow \Sigma(1385)\pi$, D-wave

MODULUS	PHASE (°)	DOCUMENT ID		TECN	COMMENT
• • • We do not use the following data for averages, fits, limits, etc. • • •					
0.0103	123	[7] KAMANO	15	DPWA	Multichannel

[7] From the preferred solution A in KAMANO 15.

$\Sigma(1580)$ MASS

VALUE (MeV)	DOCUMENT ID		TECN	COMMENT
≈ 1580 OUR ESTIMATE				
1583±4	[8] CARROLL	76	DPWA	Isospin-1 total σ
1582±4	[9] LITCHFIELD	74	DPWA	$K^-p \rightarrow \Lambda\pi^0$

[8] CARROLL 76 sees a total-cross-section bump with $(J+1/2)\ \Gamma_{el}\ /\ \Gamma_{total} = 0.06$.

[9] The main effect observed by LITCHFIELD 74 is in the $\Lambda\pi$ final state; the $\overline{K}N$ and $\Sigma\pi$ couplings are estimated from a multichannel fit including total-cross-section data of LI 73.

$\Sigma(1580)$ WIDTH

VALUE (MeV)	DOCUMENT ID		TECN	COMMENT
15	[10] CARROLL	76	DPWA	Isospin-1 total σ
11±4	[11] LITCHFIELD	74	DPWA	$K^-p \rightarrow \Lambda\pi^0$

[10] CARROLL 76 sees a total-cross-section bump with $(J+1/2)\ \Gamma_{el}\ /\ \Gamma_{total} = 0.06$.

[11] The main effect observed by LITCHFIELD 74 is in the $\Lambda\pi$ final state; the $\overline{K}N$ and $\Sigma\pi$ couplings are estimated from a multichannel fit including total-cross-section data of LI 73.

$\Sigma(1580)$ DECAY MODES

	Mode
Γ_1	$N\overline{K}$
Γ_2	$\Lambda\pi$
Γ_3	$\Sigma\pi$
Γ_4	$\Sigma(1385)\pi$, S-wave
Γ_5	$\Sigma(1385)\pi$, D-wave
Γ_6	$N\overline{K}^*(892)$, S=1/2, D-wave
Γ_7	$N\overline{K}^*(892)$, S=3/2, S-wave
Γ_8	$N\overline{K}^*(892)$, S=3/2, D-wave

$\Sigma(1580)$ BRANCHING RATIOS

See "Sign conventions for resonance couplings" in the Note on Λ and Σ Resonances.

$\Gamma(N\overline{K})/\Gamma_{total}$ Γ_1/Γ

VALUE	DOCUMENT ID		TECN	COMMENT
+0.03 ±0.01	[12] LITCHFIELD	74	DPWA	$\overline{K}N$ multichannel
• • • We do not use the following data for averages, fits, limits, etc. • • •				
0.003	[13] KAMANO	15	DPWA	Multichannel

[12] The main effect observed by LITCHFIELD 74 is in the $\Lambda\pi$ final state; the $\overline{K}N$ and $\Sigma\pi$ couplings are estimated from a multichannel fit including total-cross-section data of LI 73.

[13] From the preferred solution A in KAMANO 15.

$\Gamma(\Lambda\pi)/\Gamma_{total}$ Γ_2/Γ

VALUE	DOCUMENT ID		TECN	COMMENT
• • • We do not use the following data for averages, fits, limits, etc. • • •				
0.490	[14] KAMANO	15	DPWA	Multichannel

[14] From the preferred solution A in KAMANO 15.

$\Gamma(\Sigma\pi)/\Gamma_{total}$ Γ_3/Γ

VALUE	DOCUMENT ID		TECN	COMMENT
• • • We do not use the following data for averages, fits, limits, etc. • • •				
0.387	[15] KAMANO	15	DPWA	Multichannel

[15] From the preferred solution A in KAMANO 15.

$\Gamma(\Sigma(1385)\pi$, S-wave$)/\Gamma_{total}$ Γ_4/Γ

VALUE	DOCUMENT ID		TECN	COMMENT
• • • We do not use the following data for averages, fits, limits, etc. • • •				
0.12	[16] KAMANO	15	DPWA	Multichannel

[16] From the preferred solution A in KAMANO 15.

$\Gamma(\Sigma(1385)\pi$, D-wave$)/\Gamma_{total}$ Γ_5/Γ

VALUE	DOCUMENT ID		TECN	COMMENT
• • • We do not use the following data for averages, fits, limits, etc. • • •				
0.001	[17] KAMANO	15	DPWA	Multichannel

[17] From the preferred solution A in KAMANO 15.

$\Gamma(N\overline{K}^*(892)$, S=1/2, D-wave$)/\Gamma_{total}$ Γ_6/Γ

VALUE	DOCUMENT ID		TECN	COMMENT
• • • We do not use the following data for averages, fits, limits, etc. • • •				
not seen	[18] KAMANO	15	DPWA	Multichannel

[18] From the preferred solution A in KAMANO 15.

$\Gamma(N\overline{K}^*(892)$, S=3/2, S-wave$)/\Gamma_{total}$ Γ_7/Γ

VALUE	DOCUMENT ID		TECN	COMMENT
• • • We do not use the following data for averages, fits, limits, etc. • • •				
not seen	[19] KAMANO	15	DPWA	Multichannel

[19] From the preferred solution A in KAMANO 15.

$\Gamma(N\overline{K}^*(892)$, S=3/2, D-wave$)/\Gamma_{total}$ Γ_8/Γ

VALUE	DOCUMENT ID		TECN	COMMENT
• • • We do not use the following data for averages, fits, limits, etc. • • •				
not seen	[20] KAMANO	15	DPWA	Multichannel

[20] From the preferred solution A in KAMANO 15.

$(\Gamma_i\Gamma_f)^{1/2}/\Gamma_{total}$ in $N\overline{K} \rightarrow \Sigma(1580) \rightarrow \Lambda\pi$ $(\Gamma_1\Gamma_2)^{1/2}/\Gamma$

VALUE	DOCUMENT ID		TECN	COMMENT
not seen	CAMERON	78C	HBC	$K_L^0 p \rightarrow \Lambda\pi^+$
not seen	ENGLER	78	HBC	$K_L^0 p \rightarrow \Lambda\pi^+$
+0.10±0.02	[21] LITCHFIELD	74	DPWA	$K^-p \rightarrow \Lambda\pi^0$

[21] The main effect observed by LITCHFIELD 74 is in the $\Lambda\pi$ final state; the $\overline{K}N$ and $\Sigma\pi$ couplings are estimated from a multichannel fit including total-cross-section data of LI 73.

$(\Gamma_i\Gamma_f)^{1/2}/\Gamma_{total}$ in $N\overline{K} \rightarrow \Sigma(1580) \rightarrow \Sigma\pi$ $(\Gamma_1\Gamma_3)^{1/2}/\Gamma$

VALUE	DOCUMENT ID		TECN	COMMENT
not seen	CAMERON	78C	HBC	$K_L^0 p \rightarrow \Sigma^0\pi^+$
not seen	ENGLER	78	HBC	$K_L^0 p \rightarrow \Sigma^0\pi^+$
+0.03±0.04	[22] LITCHFIELD	74	DPWA	$\overline{K}N$ multichannel

[22] The main effect observed by LITCHFIELD 74 is in the $\Lambda\pi$ final state; the $\overline{K}N$ and $\Sigma\pi$ couplings are estimated from a multichannel fit including total-cross-section data of LI 73.

$\Sigma(1580)$ REFERENCES

KAMANO	15	PR C92 025205	H. Kamano *et al.*	(ANL, OSAK)
OLMSTED	04	PL B588 29	J. Olmsted *et al.*	(BNL Crystal Ball Collab.)
PRAKHOV	04	PR C69 042202	S. Prakhov *et al.*	(BNL Crystal Ball Collab.)
CAMERON	78C	NP B132 189	W. Cameron *et al.*	(BGNA, EDIN, GLAS+) I
ENGLER	78	PR D18 3061	A. Engler *et al.*	(CMU, ANL)
CARROLL	76	PRL 37 806	A.S. Carroll *et al.*	(BNL) I
LITCHFIELD	74	PL 51B 509	P.J. Litchfield	(CERN) IJP
LI	73	Purdue Conf. 283	K.K. Li	(BNL) I

$\Sigma(1620)\ 1/2^-$

$I(J^P) = 1(\frac{1}{2}^-)$ Status: *

OMITTED FROM SUMMARY TABLE

The S_{11} state at 1697 MeV reported by VANHORN 75 is tentatively listed under the $\Sigma(1750)$. CARROLL 76 sees two bumps in the isospin-1 total cross section near this mass. GAO 12 sees no evidence for this resonance.

Production experiments are listed separately in the next entry.

$\Sigma(1620)$ POLE POSITION

REAL PART

VALUE (MeV)	DOCUMENT ID		TECN	COMMENT
• • • We do not use the following data for averages, fits, limits, etc. • • •				
1501	ZHANG	13A	DPWA	Multichannel

−2×IMAGINARY PART

VALUE (MeV)	DOCUMENT ID		TECN	COMMENT
• • • We do not use the following data for averages, fits, limits, etc. • • •				
171	ZHANG	13A	DPWA	Multichannel

Baryon Particle Listings

$\Sigma(1620)$, $\Sigma(1620)$ Production Experiments, $\Sigma(1660)$

$\Sigma(1620)$ MASS

VALUE (MeV)		DOCUMENT ID		TECN	COMMENT
≈ 1620 OUR ESTIMATE					
1600±15		ZHANG	13A	DPWA	Multichannel
1600± 6	[1]	MORRIS	78	DPWA	$K^- n \to \Lambda\pi^-$
1608± 5	[2]	CARROLL	76	DPWA	Isospin-1 total σ
1633±10	[3]	CARROLL	76	DPWA	Isospin-1 total σ
1630±10		LANGBEIN	72	IPWA	$\overline{K}N$ multichannel
1620		KIM	71	DPWA	K-matrix analysis

$\Sigma(1620)$ WIDTH

VALUE (MeV)		DOCUMENT ID		TECN	COMMENT
400±152		ZHANG	13A	DPWA	Multichannel
87± 19	[1]	MORRIS	78	DPWA	$K^- n \to \Lambda\pi^-$
15	[2]	CARROLL	76	DPWA	Isospin-1 total σ
10	[3]	CARROLL	76	DPWA	Isospin-1 total σ
65± 20		LANGBEIN	72	IPWA	$\overline{K}N$ multichannel
40		KIM	71	DPWA	K-matrix analysis

$\Sigma(1620)$ DECAY MODES

	Mode
Γ_1	$N\overline{K}$
Γ_2	$\Lambda\pi$
Γ_3	$\Sigma\pi$

$\Sigma(1620)$ BRANCHING RATIOS

$\Gamma(N\overline{K})/\Gamma_{total}$ — **Γ_1/Γ**

VALUE	DOCUMENT ID		TECN	COMMENT
0.59±0.10	ZHANG	13A	DPWA	Multichannel
0.22±0.02	LANGBEIN	72	IPWA	$\overline{K}N$ multichannel
0.05	KIM	71	DPWA	K-matrix analysis

$(\Gamma_i\Gamma_f)^{1/2}/\Gamma_{total}$ in $N\overline{K} \to \Sigma(1620) \to \Lambda\pi$ — **$(\Gamma_1\Gamma_2)^{1/2}/\Gamma$**

VALUE	DOCUMENT ID		TECN	COMMENT
0.12±0.02	[1] MORRIS	78	DPWA	$K^- n \to \Lambda\pi^-$
not seen	BAILLON	75	IPWA	$\overline{K}N \to \Lambda\pi$
0.15	KIM	71	DPWA	K-matrix analysis

$(\Gamma_i\Gamma_f)^{1/2}/\Gamma_{total}$ in $N\overline{K} \to \Sigma(1620) \to \Sigma\pi$ — **$(\Gamma_1\Gamma_3)^{1/2}/\Gamma$**

VALUE	DOCUMENT ID		TECN	COMMENT
+0.32±0.03	ZHANG	13A	DPWA	Multichannel
not seen	HEPP	76B	DPWA	$K^- N \to \Sigma\pi$
+0.40±0.06	LANGBEIN	72	IPWA	$\overline{K}N$ multichannel
+0.08	KIM	71	DPWA	K-matrix analysis

$\Sigma(1620)$ FOOTNOTES

[1] MORRIS 78 obtains an equally good fit without including this resonance.
[2] Total cross-section bump with $(J+1/2)$ Γ_{el} / Γ_{total} is 0.06 seen by CARROLL 76.
[3] Total cross-section bump with $(J+1/2)$ Γ_{el} / Γ_{total} is 0.04 seen by CARROLL 76.

$\Sigma(1620)$ REFERENCES

ZHANG	13A	PR C88 035205	H. Zhang *et al.*	(KSU)
GAO	12	PR C86 025201	P. Gao, J. Shi, B.S. Zou	(BHEP, BEIJT)
Also		NP A867 41	P. Gao, B.S. Zou, A. Sibirtsev	(BHEP, BEIJT+)
MORRIS	78	PR D17 55	W.A. Morris *et al.*	(FSU) IJP
CARROLL	76	PRL 37 806	A.S. Carroll *et al.*	(BNL) I
HEPP	76B	PL 65B 487	V. Hepp *et al.*	(CERN, HEIDH, MPIM) IJP
BAILLON	75	NP B94 39	P.H. Baillon, P.J. Litchfield	(CERN, RHEL) IJP
VANHORN	75	NP B87 145	A.J. van Horn	(LBL) IJP
Also		NP B87 157	A.J. van Horn	(LBL) IJP
LANGBEIN	72	NP B47 477	W. Langbein, F. Wagner	(MPIM) IJP
KIM	71	PRL 27 356	J.K. Kim	(HARV) IJP
Also		Duke Conf. 161 Hyperon Resonances, 1970	J.K. Kim	(HARV) IJP

$\Sigma(1620)$ Production Experiments

$I(J^P) = 1(?^?)$

OMITTED FROM SUMMARY TABLE

Formation experiments are listed separately in the previous entry.

The results of CRENNELL 69B at 3.9 GeV/c are not confirmed by SABRE 70 at 3.0 GeV/c. However, at 4.5 GeV/c, AMMANN 70 sees a peak at 1642 MeV which on the basis of branching ratios they do not associate with the $\Sigma(1670)$. See MILLER 70 for a review of these conflicts.

$\Sigma(1620)$ MASS (PRODUCTION EXPERIMENTS)

VALUE (MeV)	EVTS	DOCUMENT ID		TECN	CHG	COMMENT
≈ 1620 OUR ESTIMATE						
1642±12		AMMANN	70	DBC		$K^- N$ 4.5 GeV/c
1618± 3	20	BLUMENFELD	69	HBC	+	$K^0_L p$
1619± 8		CRENNELL	69B	DBC	±	$K^- N \to \Lambda\pi\pi\pi$
• • • We do not use the following data for averages, fits, limits, etc. • • •						
1616± 8		CRENNELL	68	DBC	±	See CRENNELL 69B

$\Sigma(1620)$ WIDTH (PRODUCTION EXPERIMENTS)

VALUE (MeV)	EVTS	DOCUMENT ID		TECN	CHG	COMMENT
55±24		AMMANN	70	DBC		$K^- N$ 4.5 GeV/c
30±10	20	BLUMENFELD	69	HBC	+	
72^{+22}_{-15}		CRENNELL	69B	DBC	±	
• • • We do not use the following data for averages, fits, limits, etc. • • •						
66±16		CRENNELL	68	DBC	±	See CRENNELL 69B

$\Sigma(1620)$ DECAY MODES (PRODUCTION EXPERIMENTS)

	Mode
Γ_1	$N\overline{K}$
Γ_2	$\Lambda\pi$
Γ_3	$\Sigma\pi$
Γ_4	$\Lambda\pi\pi$
Γ_5	$\Sigma(1385)\pi$
Γ_6	$\Lambda(1405)\pi$

$\Sigma(1620)$ BRANCHING RATIOS (PRODUCTION EXPERIMENTS)

$\Gamma(\Lambda\pi\pi)/\Gamma(\Lambda\pi)$ — **Γ_4/Γ_2**

VALUE	EVTS	DOCUMENT ID		TECN	CHG
~ 2.5	14	BLUMENFELD	69	HBC	+

$\Gamma(N\overline{K})/\Gamma(\Lambda\pi)$ — **Γ_1/Γ_2**

VALUE	DOCUMENT ID		TECN	CHG	COMMENT
0.4±0.4	AMMANN	70	DBC		$K^- p$ 4.5 GeV/c
0.0±0.1	CRENNELL	68	DBC	+	See CRENNELL 69B

$\Gamma(\Lambda\pi)/\Gamma_{total}$ — **Γ_2/Γ**

VALUE	DOCUMENT ID		TECN	CHG
large	CRENNELL	68	DBC	±

$\Gamma(\Sigma(1385)\pi)/\Gamma(\Lambda\pi)$ — **Γ_5/Γ_2**

VALUE	CL%	DOCUMENT ID		TECN	CHG	COMMENT
<0.3	95	AMMANN	70	DBC		$K^- p$ 4.5 GeV/c
0.2±0.1		CRENNELL	68	DBC	±	

$\Gamma(\Sigma\pi)/\Gamma(\Lambda\pi)$ — **Γ_3/Γ_2**

VALUE	CL%	DOCUMENT ID		TECN	COMMENT
<1.1	95	AMMANN	70	DBC	$K^- N$ 4.5 GeV/c

$\Gamma(\Lambda(1405)\pi)/\Gamma(\Lambda\pi)$ — **Γ_6/Γ_2**

VALUE	DOCUMENT ID		TECN	COMMENT
0.7±0.4	AMMANN	70	DBC	$K^- p$ 4.5 GeV/c

$\Sigma(1620)$ REFERENCES (PRODUCTION EXPERIMENTS)

AMMANN	70	PRL 24 327	A.C. Ammann *et al.*	(PURD, IND)
Also		PR D7 1345	A.C. Ammann *et al.*	(PURD, IUPU)
MILLER	70	Duke Conf. 229 Hyperon Resonances, 1970	D.H. Miller	(PURD)
SABRE	70	NP B16 201	R. Barloutaud *et al.*	(SABRE Collab.)
BLUMENFELD	69	PL 29B 58	B.J. Blumenfeld, G.R. Kalbfleisch	(BNL) I
CRENNELL	69B	Lund Paper 183 Results are quoted in LEVI-SETTI 69C.	D.J. Crennell *et al.*	(BNL, CUNY) I
Also		Lund Conf.	R. Levi-Setti	(EFI)
CRENNELL	68	PRL 21 648	D.J. Crennell *et al.*	(BNL, CUNY) I

$\Sigma(1660)$ $1/2^+$

$I(J^P) = 1(\frac{1}{2}^+)$ Status: ***

For results published before 1974 (they are now obsolete), see our 1982 edition Physics Letters **111B** 1 (1982).

$\Sigma(1660)$ POLE POSITION

REAL PART

VALUE (MeV)	DOCUMENT ID		TECN	COMMENT
• • • We do not use the following data for averages, fits, limits, etc. • • •				
1547^{+111}_{-59}	[1] KAMANO	15	DPWA	Multichannel

[1] From the preferred solution A in KAMANO 15. Solution B reports $M = 1457^{+5}_{-1}$ MeV.

$-2\times$IMAGINARY PART

VALUE (MeV)	DOCUMENT ID		TECN	COMMENT
• • • We do not use the following data for averages, fits, limits, etc. • • •				
183^{+86}_{-78}	[1] KAMANO	15	DPWA	Multichannel

[1] From the preferred solution A in KAMANO 15. Solution B reports $\Gamma = 78^{+2}_{-8}$ MeV.

$\Sigma(1660)$ POLE RESIDUES

The normalized residue is the residue divided by $\Gamma_{pole}/2$.

Normalized residue in $N\overline{K} \rightarrow \Sigma(1660) \rightarrow N\overline{K}$

MODULUS	PHASE (°)	DOCUMENT ID		TECN	COMMENT
• • • We do not use the following data for averages, fits, limits, etc. • • •					
0.0247	168	[1] KAMANO	15	DPWA	Multichannel

[1] From the preferred solution A in KAMANO 15.

Normalized residue in $N\overline{K} \rightarrow \Sigma(1660) \rightarrow \Sigma\pi$

MODULUS	PHASE (°)	DOCUMENT ID		TECN	COMMENT
• • • We do not use the following data for averages, fits, limits, etc. • • •					
0.16	78	[1] KAMANO	15	DPWA	Multichannel

[1] From the preferred solution A in KAMANO 15.

Normalized residue in $N\overline{K} \rightarrow \Sigma(1660) \rightarrow \Lambda\pi$

MODULUS	PHASE (°)	DOCUMENT ID		TECN	COMMENT
• • • We do not use the following data for averages, fits, limits, etc. • • •					
0.0614	−84	[1] KAMANO	15	DPWA	Multichannel

[1] From the preferred solution A in KAMANO 15.

Normalized residue in $N\overline{K} \rightarrow \Sigma(1660) \rightarrow \Sigma(1385)\pi$

MODULUS	PHASE (°)	DOCUMENT ID		TECN	COMMENT
• • • We do not use the following data for averages, fits, limits, etc. • • •					
0.0513	−44	[1] KAMANO	15	DPWA	Multichannel

[1] From the preferred solution A in KAMANO 15.

$\Sigma(1660)$ MASS

VALUE (MeV)	DOCUMENT ID		TECN	COMMENT
1630 to 1690 (≈ 1660) OUR ESTIMATE				
1633 ± 3	GAO	12	DPWA	$\overline{K}N \rightarrow \Lambda\pi$
1665.1 ± 11.2	[1] KOISO	85	DPWA	$K^-p \rightarrow \Sigma\pi$
1670 ±10	GOPAL	80	DPWA	$\overline{K}N \rightarrow \overline{K}N$
1679 ±10	ALSTON-...	78	DPWA	$\overline{K}N \rightarrow \overline{K}N$
1676 ±15	GOPAL	77	DPWA	$\overline{K}N$ multichannel
1668 ±25	VANHORN	75	DPWA	$K^-p \rightarrow \Lambda\pi^0$
1670 ±20	KANE	74	DPWA	$K^-p \rightarrow \Sigma\pi$
• • • We do not use the following data for averages, fits, limits, etc. • • •				
1565 or 1597	[2] MARTIN	77	DPWA	$\overline{K}N$ multichannel
1660 ±30	[3] BAILLON	75	IPWA	$\overline{K}N \rightarrow \Lambda\pi$
1671 ± 2	[4] PONTE	75	DPWA	$K^-p \rightarrow \Lambda\pi^0$

[1] The evidence of KOISO 85 is weak.
[2] The two MARTIN 77 values are from a T-matrix pole and from a Breit-Wigner fit.
[3] From solution 1 of BAILLON 75; not present in solution 2.
[4] From solution 2 of PONTE 75; not present in solution 1.

$\Sigma(1660)$ WIDTH

VALUE (MeV)	DOCUMENT ID		TECN	COMMENT
40 to 200 (≈ 100) OUR ESTIMATE				
121^{+4}_{-7}	GAO	12	DPWA	$\overline{K}N \rightarrow \Lambda\pi$
81.5 ± 22.2	[1] KOISO	85	DPWA	$K^-p \rightarrow \Sigma\pi$
152 ± 20	GOPAL	80	DPWA	$\overline{K}N \rightarrow \overline{K}N$
38 ± 10	ALSTON-...	78	DPWA	$\overline{K}N \rightarrow \overline{K}N$
120 ± 20	GOPAL	77	DPWA	$\overline{K}N$ multichannel
230^{+165}_{-60}	VANHORN	75	DPWA	$K^-p \rightarrow \Lambda\pi^0$
250 ±110	KANE	74	DPWA	$K^-p \rightarrow \Sigma\pi$
• • • We do not use the following data for averages, fits, limits, etc. • • •				
202 or 217	[2] MARTIN	77	DPWA	$\overline{K}N$ multichannel
80 ± 40	[3] BAILLON	75	IPWA	$\overline{K}N \rightarrow \Lambda\pi$
81 ± 10	[4] PONTE	75	DPWA	$K^-p \rightarrow \Lambda\pi^0$

[1] The evidence of KOISO 85 is weak.
[2] The two MARTIN 77 values are from a T-matrix pole and from a Breit-Wigner fit.
[3] From solution 1 of BAILLON 75; not present in solution 2.
[4] From solution 2 of PONTE 75; not present in solution 1.

$\Sigma(1660)$ DECAY MODES

	Mode	Fraction (Γ_j/Γ)
Γ_1	$N\overline{K}$	10–30 %
Γ_2	$\Lambda\pi$	seen
Γ_3	$\Sigma\pi$	seen
Γ_4	$\Sigma(1385)\pi$	

$\Sigma(1660)$ BRANCHING RATIOS

See "Sign conventions for resonance couplings" in the Note on Λ and Σ Resonances.

$\Gamma(N\overline{K})/\Gamma_{total}$ Γ_1/Γ

VALUE	DOCUMENT ID		TECN	COMMENT
0.1 to 0.3 OUR ESTIMATE				
0.12 ±0.03	GOPAL	80	DPWA	$\overline{K}N \rightarrow \overline{K}N$
0.10 ±0.05	ALSTON-...	78	DPWA	$\overline{K}N \rightarrow \overline{K}N$
penalty-50				
• • • We do not use the following data for averages, fits, limits, etc. • • •				
0.005	[1] KAMANO	15	DPWA	Multichannel
<0.04	GOPAL	77	DPWA	See GOPAL 80
0.27 or 0.29	[2] MARTIN	77	DPWA	$\overline{K}N$ multichannel

[1] From the preferred solution A in KAMANO 15.
[2] The two MARTIN 77 values are from a T-matrix pole and from a Breit-Wigner fit.

$\Gamma(\Lambda\pi)/\Gamma_{total}$ Γ_2/Γ

VALUE	DOCUMENT ID		TECN	COMMENT
• • • We do not use the following data for averages, fits, limits, etc. • • •				
0.128	[1] KAMANO	15	DPWA	Multichannel

[1] From the preferred solution A in KAMANO 15.

$\Gamma(\Sigma\pi)/\Gamma_{total}$ Γ_3/Γ

VALUE	DOCUMENT ID		TECN	COMMENT
• • • We do not use the following data for averages, fits, limits, etc. • • •				
0.865	[1] KAMANO	15	DPWA	Multichannel

[1] From the preferred solution A in KAMANO 15.

$\Gamma(\Sigma(1385)\pi)/\Gamma_{total}$ Γ_4/Γ

VALUE	DOCUMENT ID		TECN	COMMENT
• • • We do not use the following data for averages, fits, limits, etc. • • •				
0.001	[1] KAMANO	15	DPWA	Multichannel

[1] From the preferred solution A in KAMANO 15.

$(\Gamma_i\Gamma_f)^{1/2}/\Gamma_{total}$ in $N\overline{K} \rightarrow \Sigma(1660) \rightarrow \Lambda\pi$ $(\Gamma_1\Gamma_2)^{1/2}/\Gamma$

VALUE	DOCUMENT ID		TECN	COMMENT
$-0.064^{+0.005}_{-0.003}$	GAO	12	DPWA	$\overline{K}N \rightarrow \Lambda\pi$
< 0.04	GOPAL	77	DPWA	$\overline{K}N$ multichannel
$0.12^{+0.12}_{-0.04}$	VANHORN	75	DPWA	$K^-p \rightarrow \Lambda\pi^0$
penalty-50				
• • • We do not use the following data for averages, fits, limits, etc. • • •				
−0.10 or −0.11	[1] MARTIN	77	DPWA	$\overline{K}N$ multichannel
−0.04 ±0.02	[2] BAILLON	75	IPWA	$\overline{K}N \rightarrow \Lambda\pi$
+0.16 ±0.01	[3] PONTE	75	DPWA	$K^-p \rightarrow \Lambda\pi^0$

[1] The two MARTIN 77 values are from a T-matrix pole and from a Breit-Wigner fit.
[2] From solution 1 of BAILLON 75; not present in solution 2.
[3] From solution 2 of PONTE 75; not present in solution 1.

$(\Gamma_i\Gamma_f)^{1/2}/\Gamma_{total}$ in $N\overline{K} \rightarrow \Sigma(1660) \rightarrow \Sigma\pi$ $(\Gamma_1\Gamma_3)^{1/2}/\Gamma$

VALUE	DOCUMENT ID		TECN	COMMENT
−0.13 ± 0.04	[1] KOISO	85	DPWA	$K^-p \rightarrow \Sigma\pi$
−0.16 ± 0.03	GOPAL	77	DPWA	$\overline{K}N$ multichannel
−0.11 ± 0.01	KANE	74	DPWA	$K^-p \rightarrow \Sigma\pi$
• • • We do not use the following data for averages, fits, limits, etc. • • •				
−0.34 or −0.37	[2] MARTIN	77	DPWA	$\overline{K}N$ multichannel
not seen	HEPP	76B	DPWA	$K^-N \rightarrow \Sigma\pi$

[1] The evidence of KOISO 85 is weak.
[2] The two MARTIN 77 values are from a T-matrix pole and from a Breit-Wigner fit.

Baryon Particle Listings

$\Sigma(1660)$, $\Sigma(1670)$

$\Sigma(1660)$ REFERENCES

KAMANO	15	PR C92 025205	H. Kamano *et al.*	(ANL, OSAK)
GAO	12	PR C86 025201	P. Gao, J. Shi, B.S. Zou	(BHEP, BEIJT)
Also		NP A867 41	P. Gao, B.S. Zou, A. Sibirtsev	(BHEP, BEIJT+)
KOISO	85	NP A433 619	H. Koiso *et al.*	(TOKY, MASA)
PDG	82	PL 111B 1	M. Roos *et al.*	(HELS, CIT, CERN)
GOPAL	80	Toronto Conf. 159	G.P. Gopal	(RHEL) IJP
ALSTON-...	78	PR D18 182	M. Alston-Garnjost *et al.*	(LBL, MTHO+) IJP
Also		PRL 38 1007	M. Alston-Garnjost *et al.*	(LBL, MTHO+) IJP
GOPAL	77	NP B119 362	G.P. Gopal *et al.*	(LOIC, RHEL) IJP
MARTIN	77	NP B127 349	B.R. Martin, M.K. Pidcock, R.G. Moorhouse	(LOUC+) IJP
Also		NP B126 266	B.R. Martin, M.K. Pidcock	(LOUC)
Also		NP B126 285	B.R. Martin, M.K. Pidcock	(LOUC) IJP
HEPP	76B	PL 65B 487	V. Hepp *et al.*	(CERN, HEIDH, MPIM) IJP
BAILLON	75	NP B94 39	P.H. Baillon, P.J. Litchfield	(CERN, RHEL) IJP
PONTE	75	PR D12 2597	R.A. Ponte *et al.*	(MASA, TENN, UCR) IJP
VANHORN	75	NP B87 145	A.J. van Horn	(LBL) IJP
Also		NP B87 157	A.J. van Horn	(LBL) IJP
KANE	74	LBL-2452	D.F. Kane	(LBL) IJP

See the related review(s):

$\Sigma(1670)$ Region

$\Sigma(1670)\ 3/2^-$

$I(J^P) = 1(\frac{3}{2}^-)$ Status: ****

For most results published before 1974 (they are now obsolete), see our 1982 edition Physics Letters **111B** 1 (1982).

Results from production experiments are listed separately in the next entry.

$\Sigma(1670)$ POLE POSITION

REAL PART

VALUE (MeV)		DOCUMENT ID		TECN	COMMENT
$\mathbf{1669^{+7}_{-7}}$	[1]	KAMANO	15	DPWA	Multichannel
• • • We do not use the following data for averages, fits, limits, etc. • • •					
1674		ZHANG	13A	DPWA	Multichannel

[1] From the preferred solution A in KAMANO 15.

$-2\times$IMAGINARY PART

VALUE (MeV)		DOCUMENT ID		TECN	COMMENT
$\mathbf{64^{+10}_{-14}}$	[1]	KAMANO	15	DPWA	Multichannel
• • • We do not use the following data for averages, fits, limits, etc. • • •					
54		ZHANG	13A	DPWA	Multichannel

[1] From the preferred solution A in KAMANO 15.

$\Sigma(1670)$ POLE RESIDUES

The normalized residue is the residue divided by $\Gamma_{pole}/2$.

Normalized residue in $N\overline{K} \to \Sigma(1670) \to N\overline{K}$

MODULUS	PHASE (°)	DOCUMENT ID		TECN	COMMENT
• • • We do not use the following data for averages, fits, limits, etc. • • •					
0.129	−20	[1] KAMANO	15	DPWA	Multichannel

[1] From the preferred solution A in KAMANO 15.

Normalized residue in $N\overline{K} \to \Sigma(1670) \to \Sigma\pi$

MODULUS	PHASE (°)	DOCUMENT ID		TECN	COMMENT
• • • We do not use the following data for averages, fits, limits, etc. • • •					
0.249	−21	[1] KAMANO	15	DPWA	Multichannel

[1] From the preferred solution A in KAMANO 15.

Normalized residue in $N\overline{K} \to \Sigma(1670) \to \Lambda\pi$

MODULUS	PHASE (°)	DOCUMENT ID		TECN	COMMENT
• • • We do not use the following data for averages, fits, limits, etc. • • •					
0.0818	−7	[1] KAMANO	15	DPWA	Multichannel

[1] From the preferred solution A in KAMANO 15.

Normalized residue in $N\overline{K} \to \Sigma(1670) \to \Sigma(1385)\pi$, *S*-wave

MODULUS	PHASE (°)	DOCUMENT ID		TECN	COMMENT
• • • We do not use the following data for averages, fits, limits, etc. • • •					
0.228	167	[1] KAMANO	15	DPWA	Multichannel

[1] From the preferred solution A in KAMANO 15.

Normalized residue in $N\overline{K} \to \Sigma(1670) \to \Sigma(1385)\pi$, *D*-wave

MODULUS	PHASE (°)	DOCUMENT ID		TECN	COMMENT
• • • We do not use the following data for averages, fits, limits, etc. • • •					
0.0915	141	KAMANO	15	DPWA	Multichannel

$\Sigma(1670)$ MASS

VALUE (MeV)		DOCUMENT ID		TECN	COMMENT
1665 to 1685 (≈ 1670) OUR ESTIMATE					
1678 ± 2		ZHANG	13A	DPWA	Multichannel
1673 ± 1		GAO	12	DPWA	$\overline{K}N \to \Lambda\pi$
1665.1 ± 4.1		KOISO	85	DPWA	$K^-p \to \Sigma\pi$
1682 ± 5		GOPAL	80	DPWA	$\overline{K}N \to \overline{K}N$
1679 ±10		ALSTON-...	78	DPWA	$\overline{K}N \to \overline{K}N$
1670 ± 5		GOPAL	77	DPWA	$\overline{K}N$ multichannel
1670 ± 6		HEPP	76B	DPWA	$K^-N \to \Sigma\pi$
1685 ±20		BAILLON	75	IPWA	$\overline{K}N \to \Lambda\pi$
1659 $^{+12}_{-5}$		VANHORN	75	DPWA	$K^-p \to \Lambda\pi^0$
1670 ± 2 penalty-50		KANE	74	DPWA	$K^-p \to \Sigma\pi$
• • • We do not use the following data for averages, fits, limits, etc. • • •					
1667 or 1668	[1]	MARTIN	77	DPWA	$\overline{K}N$ multichannel
1650		DEBELLEFON	76	IPWA	$K^-p \to \Lambda\pi^0$
1671 ± 3		PONTE	75	DPWA	$K^-p \to \Lambda\pi^0$ (sol. 1)
1655 ± 2		PONTE	75	DPWA	$K^-p \to \Lambda\pi^0$ (sol. 2)

[1] The two MARTIN 77 values are from a T-matrix pole and from a Breit-Wigner fit.

$\Sigma(1670)$ WIDTH

VALUE (MeV)		DOCUMENT ID		TECN	COMMENT
40 to 80 (≈ 60) OUR ESTIMATE					
55 ± 4		ZHANG	13A	DPWA	Multichannel
52 $^{+5}_{-2}$		GAO	12	DPWA	$\overline{K}N \to \Lambda\pi$
65.0 ± 7.3		KOISO	85	DPWA	$K^-p \to \Sigma\pi$
79 ±10		GOPAL	80	DPWA	$\overline{K}N \to \overline{K}N$
56 ±20		ALSTON-...	78	DPWA	$\overline{K}N \to \overline{K}N$
50 ± 5		GOPAL	77	DPWA	$\overline{K}N$ multichannel
56 ± 3		HEPP	76B	DPWA	$K^-N \to \Sigma\pi$
85 ±25		BAILLON	75	IPWA	$\overline{K}N \to \Lambda\pi$
32 ±11		VANHORN	75	DPWA	$K^-p \to \Lambda\pi^0$
79 ± 6 penalty-50		KANE	74	DPWA	$K^-p \to \Sigma\pi$
• • • We do not use the following data for averages, fits, limits, etc. • • •					
46 or 46	[1]	MARTIN	77	DPWA	$\overline{K}N$ multichannel
80		DEBELLEFON	76	IPWA	$K^-p \to \Lambda\pi^0$
44 ±11		PONTE	75	DPWA	$K^-p \to \Lambda\pi^0$ (sol. 1)
76 ± 5		PONTE	75	DPWA	$K^-p \to \Lambda\pi^0$ (sol. 2)

[1] The two MARTIN 77 values are from a T-matrix pole and from a Breit-Wigner fit.

$\Sigma(1670)$ DECAY MODES

	Mode	Fraction (Γ_i/Γ)
Γ_1	$N\overline{K}$	7–13 %
Γ_2	$\Lambda\pi$	5–15 %
Γ_3	$\Sigma\pi$	30–60 %
Γ_4	$\Lambda\pi\pi$	
Γ_5	$\Sigma\pi\pi$	
Γ_6	$\Sigma(1385)\pi$	
Γ_7	$\Sigma(1385)\pi$, *S*-wave	
Γ_8	$\Sigma(1385)\pi$, *S*-wave	
Γ_9	$\Sigma(1385)\pi$, *D*-wave	
Γ_{10}	$N\overline{K}^*(892)$, S=1/2, *D*-wave	
Γ_{11}	$N\overline{K}^*(892)$, S=3/2, *S*-wave	
Γ_{12}	$N\overline{K}^*(892)$, S=3/2, *D*-wave	
Γ_{13}	$\Lambda(1405)\pi$	
Γ_{14}	$\Lambda(1520)\pi$	

$\Sigma(1670)$ BRANCHING RATIOS

See "Sign conventions for resonance couplings" in the Note on Λ and Σ Resonances.

$\Gamma(N\overline{K})/\Gamma_{total}$ Γ_1/Γ

VALUE	DOCUMENT ID		TECN	COMMENT
0.07 to 0.13 OUR ESTIMATE				
0.062±0.007	ZHANG	13A	DPWA	Multichannel
0.10 ±0.03	GOPAL	80	DPWA	$\overline{K}N \to \overline{K}N$
0.11 ±0.03	ALSTON-...	78	DPWA	$\overline{K}N \to \overline{K}N$
• • • We do not use the following data for averages, fits, limits, etc. • • •				
0.121	[1] KAMANO	15	DPWA	Multichannel
0.08 ±0.03	GOPAL	77	DPWA	See GOPAL 80
0.07 or 0.07	[2] MARTIN	77	DPWA	$\overline{K}N$ multichannel

[1] From the preferred solution A in KAMANO 15.
[2] The two MARTIN 77 values are from a T-matrix pole and from a Breit-Wigner fit.

$\Gamma(\Lambda\pi)/\Gamma_{total}$ Γ_2/Γ

VALUE	DOCUMENT ID		TECN	COMMENT
• • • We do not use the following data for averages, fits, limits, etc. • • •				
0.058	[1] KAMANO	15	DPWA	Multichannel

[1] From the preferred solution A in KAMANO 15.

$\Gamma(\Sigma\pi)/\Gamma_{total}$ Γ_3/Γ

VALUE	DOCUMENT ID		TECN	COMMENT
• • • We do not use the following data for averages, fits, limits, etc. • • •				
0.465	[1] KAMANO	15	DPWA	Multichannel

[1] From the preferred solution A in KAMANO 15.

$\Gamma(\Lambda\pi\pi)/\Gamma_{total}$ Γ_4/Γ

VALUE	DOCUMENT ID		TECN	COMMENT
• • • We do not use the following data for averages, fits, limits, etc. • • •				
<0.11	ARMENTEROS	68E	HBC	$K^- p$ (Γ_1=0.09)

$\Gamma(\Sigma\pi\pi)/\Gamma_{total}$ Γ_5/Γ

VALUE	DOCUMENT ID		TECN	COMMENT
• • • We do not use the following data for averages, fits, limits, etc. • • •				
<0.14	[1] ARMENTEROS	68E	HBC	$K^- p$, $K^- d$ (Γ_1=0.09)

[1] Ratio only for $\Sigma 2\pi$ system in $I = 1$, which cannot be $\Sigma(1385)$.

$\Gamma(\Sigma(1385)\pi$, S-wave$)/\Gamma_{total}$ Γ_8/Γ

VALUE	DOCUMENT ID		TECN	COMMENT
• • • We do not use the following data for averages, fits, limits, etc. • • •				
0.309	[1] KAMANO	15	DPWA	Multichannel

[1] From the preferred solution A in KAMANO 15.

$\Gamma(\Sigma(1385)\pi$, D-wave$)/\Gamma_{total}$ Γ_9/Γ

VALUE	DOCUMENT ID		TECN	COMMENT
• • • We do not use the following data for averages, fits, limits, etc. • • •				
0.044	[1] KAMANO	15	DPWA	Multichannel

[1] From the preferred solution A in KAMANO 15.

$\Gamma(N\overline{K}^*(892)$, S=1/2, D-wave$)/\Gamma_{total}$ Γ_{10}/Γ

VALUE	DOCUMENT ID		TECN	COMMENT
• • • We do not use the following data for averages, fits, limits, etc. • • •				
0.001	[1] KAMANO	15	DPWA	Multichannel

[1] From the preferred solution A in KAMANO 15.

$\Gamma(N\overline{K}^*(892)$, S=3/2, S-wave$)/\Gamma_{total}$ Γ_{11}/Γ

VALUE	DOCUMENT ID		TECN	COMMENT
• • • We do not use the following data for averages, fits, limits, etc. • • •				
0.002	[1] KAMANO	15	DPWA	Multichannel

[1] From the preferred solution A in KAMANO 15.

$\Gamma(N\overline{K}^*(892)$, S=3/2, D-wave$)/\Gamma_{total}$ Γ_{12}/Γ

VALUE	DOCUMENT ID		TECN	COMMENT
• • • We do not use the following data for averages, fits, limits, etc. • • •				
0.001	[1] KAMANO	15	DPWA	Multichannel

[1] From the preferred solution A in KAMANO 15.

$\Gamma(\Lambda(1405)\pi)/\Gamma_{total}$ Γ_{13}/Γ

VALUE	DOCUMENT ID		TECN	COMMENT
• • • We do not use the following data for averages, fits, limits, etc. • • •				
<0.06	ARMENTEROS	68E	HBC	$K^- p$, $K^- d$ (Γ_1=0.09)

$\Gamma(\Lambda(1405)\pi)/\Gamma(\Sigma(1385)\pi)$ Γ_{13}/Γ_6

VALUE	DOCUMENT ID		TECN	COMMENT
0.23±0.08	BRUCKER	70	DBC	$K^- N \to \Sigma\pi\pi$

$(\Gamma_i\Gamma_f)^{1/2}/\Gamma_{total}$ in $N\overline{K} \to \Sigma(1670) \to \Lambda\pi$ $(\Gamma_1\Gamma_2)^{1/2}/\Gamma$

VALUE	DOCUMENT ID		TECN	COMMENT
+0.08 ±0.01	ZHANG	13A	DPWA	Multichannel
$+0.081^{+0.002}_{-0.004}$	GAO	12	DPWA	$\overline{K}N \to \Lambda\pi$
+0.17 ±0.03	[1] MORRIS	78	DPWA	$K^- n \to \Lambda\pi^-$
+0.13 ±0.02	[1] MORRIS	78	DPWA	$K^- n \to \Lambda\pi^-$
+0.10 ±0.02	GOPAL	77	DPWA	$\overline{K}N$ multichannel
+0.06 ±0.02	BAILLON	75	IPWA	$\overline{K}N \to \Lambda\pi$
+0.09 ±0.02	VANHORN	75	DPWA	$K^- p \to \Lambda\pi^0$
+0.018±0.060	DEVENISH	74B		Fixed-t dispersion rel.
• • • We do not use the following data for averages, fits, limits, etc. • • •				
+0.08 or +0.08	[2] MARTIN	77	DPWA	$\overline{K}N$ multichannel
+0.05	DEBELLEFON	76	IPWA	$K^- p \to \Lambda\pi^0$
+0.08 ±0.01	PONTE	75	DPWA	$K^- p \to \Lambda\pi^0$ (sol. 1)
+0.17 ±0.01	PONTE	75	DPWA	$K^- p \to \Lambda\pi^0$ (sol. 2)

[1] Results are with and without an S_{11} $\Sigma(1620)$ in the fit.

[2] The two MARTIN 77 values are from a T-matrix pole and from a Breit-Wigner fit.

$(\Gamma_i\Gamma_f)^{1/2}/\Gamma_{total}$ in $N\overline{K} \to \Sigma(1670) \to \Sigma\pi$ $(\Gamma_1\Gamma_3)^{1/2}/\Gamma$

VALUE	DOCUMENT ID		TECN	COMMENT
+0.20±0.01	ZHANG	13A	DPWA	Multichannel
+0.20±0.02	KOISO	85	DPWA	$K^- p \to \Sigma\pi$
+0.21±0.02	GOPAL	77	DPWA	$\overline{K}N$ multichannel
+0.20±0.01	HEPP	76B	DPWA	$K^- N \to \Sigma\pi$
+0.21±0.03	KANE	74	DPWA	$K^- p \to \Sigma\pi$
• • • We do not use the following data for averages, fits, limits, etc. • • •				
+0.18 or +0.17	[1] MARTIN	77	DPWA	$\overline{K}N$ multichannel

[1] The two MARTIN 77 values are from a T-matrix pole and from a Breit-Wigner fit.

$(\Gamma_i\Gamma_f)^{1/2}/\Gamma_{total}$ in $N\overline{K} \to \Sigma(1670) \to \Sigma(1385)\pi$, S-wave $(\Gamma_1\Gamma_7)^{1/2}/\Gamma$

VALUE	DOCUMENT ID		TECN	COMMENT
+0.11±0.03	PREVOST	74	DPWA	$K^- N \to \Sigma(1385)\pi$
• • • We do not use the following data for averages, fits, limits, etc. • • •				
0.17±0.02	[1] SIMS	68	DBC	$K^- N \to \Lambda\pi\pi$

[1] SIMS 68 uses only cross-section data. Result used as upper limit only.

$\Gamma_i\Gamma_f/\Gamma^2_{total}$ in $N\overline{K} \to \Sigma(1670) \to \Lambda(1405)\pi$ $\Gamma_1\Gamma_{13}/\Gamma^2$

VALUE	DOCUMENT ID		TECN	COMMENT
0.007±0.002	[1] BRUCKER	70	DBC	$K^- N \to \Sigma\pi\pi$
• • • We do not use the following data for averages, fits, limits, etc. • • •				
<0.03	BERLEY	69	HBC	$K^- p$ 0.6–0.82 GeV/c

[1] Assuming the $\Lambda(1405)\pi$ cross-section bump is due only to $3/2^-$ resonance.

$(\Gamma_i\Gamma_f)^{1/2}/\Gamma_{total}$ in $N\overline{K} \to \Sigma(1670) \to \Lambda(1520)\pi$ $(\Gamma_1\Gamma_{14})^{1/2}/\Gamma$

VALUE	DOCUMENT ID		TECN	COMMENT
0.081±0.016	[1] CAMERON	77	DPWA	P-wave decay

[1] The CAMERON 77 upper limit on F-wave decay is 0.03.

$\Sigma(1670)$ REFERENCES

KAMANO	15	PR C92 025205	H. Kamano *et al.*	(ANL, OSAK)
ZHANG	13A	PR C88 035205	H. Zhang *et al.*	(KSU)
GAO	12	PR C86 025201	P. Gao, J. Shi, B.S. Zou	(BHEP, BEIJT)
Also		NP A867 41	P. Gao, B.S. Zou, A. Sibirtsev	(BHEP, BEIJT+)
KOISO	85	NP A433 619	H. Koiso *et al.*	(TOKY, MASA)
PDG	82	PL 111B 1	M. Roos *et al.*	(HELS, CIT, CERN)
GOPAL	80	Toronto Conf. 159	G.P. Gopal	(RHEL) IJP
ALSTON-...	78	PR D18 182	M. Alston-Garnjost *et al.*	(LBL, MTHO+) IJP
Also		PRL 38 1007	M. Alston-Garnjost *et al.*	(LBL, MTHO+) IJP
MORRIS	78	PR D17 55	W.A. Morris *et al.*	(FSU) IJP
CAMERON	77	NP B131 399	W. Cameron *et al.*	(RHEL, LOIC) IJP
GOPAL	77	NP B119 362	G.P. Gopal *et al.*	(LOIC, RHEL) IJP
MARTIN	77	NP B127 349	B.R. Martin, M.K. Pidcock, R.G. Moorhouse	(LOUC+) IJP
Also		NP B126 266	B.R. Martin, M.K. Pidcock	(LOUC)
Also		NP B126 285	B.R. Martin, M.K. Pidcock	(LOUC) IJP
DEBELLEFON	76	NP B109 129	A. de Bellefon, A. Berthon	(CDEF) IJP
HEPP	76B	PL 65B 487	V. Hepp *et al.*	(CERN, HEIDH, MPIM) IJP
BAILLON	75	NP B94 39	P.H. Baillon, P.J. Litchfield	(CERN, RHEL) IJP
PONTE	75	PR D12 2597	R.A. Ponte *et al.*	(MASA, TENN, UCR) IJP
VANHORN	75	NP B87 145	A.J. van Horn	(LBL) IJP
Also		NP B87 157	A.J. van Horn	(LBL) IJP
DEVENISH	74B	NP B81 330	R.C.E. Devenish, C.D. Froggatt, B.R. Martin	(DESY+)
KANE	74	LBL-2452	D.F. Kane	(LBL) IJP
PREVOST	74	NP B69 246	J. Prevost *et al.*	(SACL, CERN, HEID)
BRUCKER	70	Duke Conf. 155 Hyperon Resonances, 1970	E.B. Brucker *et al.*	(FSU) I
BERLEY	69	PL 30B 430	D. Berley *et al.*	(BNL)
ARMENTEROS	68E	PL 28B 521	R. Armenteros *et al.*	(CERN, HEID, SACL) I
SIMS	68	PRL 21 1413	W.H. Sims *et al.*	(FSU, TUFTS, BRAN)

$\Sigma(1670)$ Bumps

$I(J^P) = 1(?^?)$

OMITTED FROM SUMMARY TABLE

Formation experiments are listed separately in the preceding entry.

Probably there are two states at the same mass with the same quantum numbers, one decaying to $\Sigma\pi$ and $\Lambda\pi$, the other to $\Lambda(1405)\pi$. See the note in front of the preceding entry.

$\Sigma(1670)$ MASS (PRODUCTION EXPERIMENTS)

VALUE (MeV)	EVTS	DOCUMENT ID		TECN	CHG	COMMENT
≈ 1670 OUR ESTIMATE						
1670± 4		[1] CARROLL	76	DPWA		Isospin-1 total σ
1675±10		[2] HEPP	76	DBC	−	$K^- N$ 1.6–1.75 GeV/c
1665± 1		APSELL	74	HBC		$K^- p$ 2.87 GeV/c
1688± 2 or 1683 ± 5	1.2k	BERTHON	74	HBC	0	Quasi-2-body σ
1670± 6		AGUILAR-...	70B	HBC		$K^- p \to \Sigma\pi\pi$ 4 GeV
1668±10		AGUILAR-...	70B	HBC		$K^- p \to \Sigma 3\pi$ 4 GeV
1660±10		ALVAREZ	63	HBC	+	$K^- p$ 1.51 GeV/c

• • • We do not use the following data for averages, fits, limits, etc. • • •						
1668±10	150	[3] FERRERSORIA	81	OMEG	−	$\pi^- p$ 9,12 GeV/c
1655 to 1677		TIMMERMANS	76	HBC	+	$K^- p$ 4.2 GeV/c
1665± 5		BUGG	68	CNTR		$K^- p$, d total σ
1661± 9	70	PRIMER	68	HBC	+	See BARNES 69E
1685		ALEXANDER	62C	HBC	−0	$\pi^- p$ 2–2.2 GeV/c

$\Sigma(1670)$ WIDTH (PRODUCTION EXPERIMENTS)

VALUE (MeV)	EVTS	DOCUMENT ID		TECN	CHG	COMMENT
67.0± 2.4		APSELL	74	HBC		$K^- p$ 2.87 GeV/c
110 ±12		AGUILAR-...	70B	HBC		$K^- p \to \Sigma\pi\pi$ 4 GeV
135 $^{+40}_{-30}$		AGUILAR-...	70B	HBC		$K^- p \to \Sigma 3\pi$ 4 GeV
40 ±10		ALVAREZ	63	HBC	+	
• • • We do not use the following data for averages, fits, limits, etc. • • •						
90 ±20	150	[3] FERRERSORIA	81	OMEG	−	$\pi^- p$ 9,12 GeV/c
52		[1] CARROLL	76	DPWA		Isospin-1 total σ
48 to 63		TIMMERMANS	76	HBC	+	$K^- p$ 4.2 GeV/c
30 ±15		BUGG	68	CNTR		
60 ±20	70	PRIMER	68	HBC	+	See BARNES 69E
45		ALEXANDER	62C	HBC	−0	

$\Sigma(1670)$ DECAY MODES (PRODUCTION EXPERIMENTS)

	Mode
Γ_1	$N\overline{K}$
Γ_2	$\Lambda\pi$
Γ_3	$\Sigma\pi$
Γ_4	$\Lambda\pi\pi$
Γ_5	$\Sigma\pi\pi$
Γ_6	$\Sigma(1385)\pi$
Γ_7	$\Lambda(1405)\pi$

$\Sigma(1670)$ BRANCHING RATIOS (PRODUCTION EXPERIMENTS)

$\Gamma(N\overline{K})/\Gamma(\Sigma\pi)$ Γ_1/Γ_3

VALUE	EVTS	DOCUMENT ID		TECN	CHG	COMMENT
<0.03		TIMMERMANS	76	HBC	+	$K^- p$ 4.2 GeV/c
<0.10		BERTHON	74	HBC	0	Quasi-2-body σ
<0.2		AGUILAR-...	70B	HBC		
<0.26		BARNES	69E	HBC	+	$K^- p$ 3.9–5 GeV/c
0.025		BUGG	68	CNTR	0	Assuming $J = 3/2$
<0.24	0	PRIMER	68	HBC	+	$K^- p$ 4.6–5 GeV/c
<0.6		LONDON	66	HBC	+	$K^- p$ 2.25 GeV/c
<0.19	0	ALVAREZ	63	HBC	+	$K^- p$ 1.15 GeV/c
≥ 0.5 ±0.25		SMITH	63	HBC	−0	

$\Gamma(\Lambda\pi)/\Gamma(\Sigma\pi)$ Γ_2/Γ_3

VALUE	EVTS	DOCUMENT ID		TECN	CHG	COMMENT
0.76±0.09		ESTES	74	HBC	0	$K^- p$ 2.1,2.6 GeV/c
0.45±0.15		BARNES	69E	HBC	+	$K^- p$ 3.9–5 GeV/c
0.15±0.07		HUWE	69	HBC	+	
0.11±0.06	33	BUTTON-...	68	HBC	+	$K^- p$ 1.7 GeV/c
• • • We do not use the following data for averages, fits, limits, etc. • • •						
≤ 0.45±0.07		TIMMERMANS	76	HBC	+	$K^- p$ 4.2 GeV/c
0.55±0.11		BERTHON	74	HBC	0	Quasi-2-body σ
0	0	PRIMER	68	HBC	+	See BARNES 69E
<0.6		LONDON	66	HBC	+	$K^- p$ 2.25 GeV/c
1.2	130	ALVAREZ	63	HBC	+	$K^- p$ 1.15 GeV/c
1.2		SMITH	63	HBC	−0	

$\Gamma(\Lambda\pi\pi)/\Gamma(\Sigma\pi)$ Γ_4/Γ_3

VALUE	EVTS	DOCUMENT ID		TECN	CHG	COMMENT
<0.6		LONDON	66	HBC	+	$K^- p$ 2.25 GeV/c
0.56	90	ALVAREZ	63	HBC	+	$K^- p$ 1.15 GeV/c
0.17		SMITH	63	HBC	−0	

$\Gamma(\Sigma\pi\pi)/\Gamma(\Sigma\pi)$ Γ_5/Γ_3

VALUE	EVTS	DOCUMENT ID		TECN	CHG	COMMENT
largest at small angles		ESTES	74	HBC	0	$K^- p$ 2.1,2.6 GeV/c
• • • We do not use the following data for averages, fits, limits, etc. • • •						
<0.2		[2] HEPP	76	DBC	−	$K^- N$ 1.6–1.75 GeV/c
0.56	180	ALVAREZ	63	HBC	+	$K^- p$ 1.15 GeV/c

$\Gamma(\Lambda(1405)\pi)/\Gamma(\Sigma\pi)$ Γ_7/Γ_3

VALUE	EVTS	DOCUMENT ID		TECN	CHG	COMMENT
1.8 ±0.3 to 0.02 ± 0.07		[3,4] TIMMERMANS	76	HBC	+	$K^- p$ 4.2 GeV/c
largest at small angles		ESTES	74	HBC	±	$K^- p$ 2.1,2.6 GeV/c
3.0 ±1.6	50	LONDON	66	HBC	+	$K^- p$ 2.25 GeV/c
• • • We do not use the following data for averages, fits, limits, etc. • • •						
0.58±0.20	17	PRIMER	68	HBC	+	See BARNES 69E

$\Gamma(\Sigma\pi)/\Gamma(\Sigma\pi\pi)$ Γ_3/Γ_5

VALUE	DOCUMENT ID		TECN	CHG	COMMENT
varies with prod. angle	[5] APSELL	74	HBC	+	$K^- p$ 2.87 GeV/c
1.39±0.16	BERTHON	74	HBC	0	Quasi-2-body σ
2.5 to 0.24	[4] EBERHARD	69	HBC		$K^- p$ 2.6 GeV/c
<0.4	BIRMINGHAM	66	HBC	+	$K^- p$ 3.5 GeV/c
0.30±0.15	LONDON	66	HBC	+	$K^- p$ 2.25 GeV/c

$\Gamma(\Lambda(1405)\pi)/\Gamma(\Sigma\pi\pi)$ Γ_7/Γ_5

VALUE	DOCUMENT ID		TECN	CHG	COMMENT
0.97±0.08	TIMMERMANS	76	HBC		$K^- p$ 4.2 GeV/c
1.00±0.02	APSELL	74	HBC		$K^- p$ 2.87 GeV/c
0.90 $^{+0.10}_{-0.16}$	EBERHARD	65	HBC	+	$K^- p$ 2.45 GeV/c

$\Gamma(\Lambda(1405)\pi)/\Gamma(\Sigma(1385)\pi)$ Γ_7/Γ_6

VALUE	DOCUMENT ID		TECN	CHG	COMMENT
<0.8	EBERHARD	65	HBC	+	$K^- p$ 2.45 GeV/c

$\Gamma(\Lambda\pi\pi)/\Gamma(\Sigma\pi\pi)$ Γ_4/Γ_5

VALUE	DOCUMENT ID		TECN	CHG	COMMENT
0.35±0.2	BIRMINGHAM	66	HBC	+	$K^- p$ 3.5 GeV/c

$\Gamma(\Lambda\pi)/\Gamma(\Sigma\pi\pi)$ Γ_2/Γ_5

VALUE	DOCUMENT ID		TECN	CHG	COMMENT
<0.2	BIRMINGHAM	66	HBC	+	$K^- p$ 3.5 GeV/c

$\Gamma(\Lambda\pi)/[\Gamma(\Lambda\pi)+\Gamma(\Sigma\pi)]$ $\Gamma_2/(\Gamma_2+\Gamma_3)$

VALUE	DOCUMENT ID		TECN
<0.6	AGUILAR-...	70B	HBC

$\Gamma(\Sigma(1385)\pi)/\Gamma(\Sigma\pi)$ Γ_6/Γ_3

VALUE	DOCUMENT ID		TECN	COMMENT
≤ 0.21±0.05	TIMMERMANS	76	HBC	$K^- p$ 4.2 GeV/c

$\Sigma(1670)$ QUANTUM NUMBERS (PRODUCTION EXPERIMENTS)

VALUE	EVTS	DOCUMENT ID		TECN	CHG	COMMENT
$J^P = 3/2^-$	400	BUTTON-...	68	HBC	±	$\Sigma^0\pi$
$J^P = 3/2^-$		EBERHARD	67	HBC	+	$\Lambda(1405)\pi$
$J^P = 3/2^+$		LEVEQUE	65	HBC		$\Lambda(1405)\pi$

$\Sigma(1670)$ FOOTNOTES

[1] Total cross-section bump with $(J+1/2)\ \Gamma_{el}\ /\ \Gamma_{total} = 0.23$.
[2] Enhancements in $\Sigma\pi$ and $\Sigma\pi\pi$ cross sections.
[3] Backward production in the $\Lambda\pi^- K^+$ final state.
[4] Depending on production angle.
[5] APSELL 74, ESTES 74, and TIMMERMANS 76 find strong branching ratio dependence on production angle, as in earlier production experiments.

$\Sigma(1670)$ REFERENCES (PRODUCTION EXPERIMENTS)

FERRERSORIA	81	NP B178 373	A. Ferrer Soria *et al.*	(CERN, CDEF, EPOL+)
CARROLL	76	PRL 37 806	A.S. Carroll *et al.*	(BNL) I
HEPP	76	NP B115 82	V. Hepp *et al.*	(CERN, HEID, MPIM) I
TIMMERMANS	76	NP B112 77	J.J.M. Timmermans *et al.*	(NIJM, CERN+) JP
APSELL	74	PR D10 1419	S.P. Apsell *et al.*	(BRAN, UMD, SYRA+) I
BERTHON	74	NC 21A 146	A. Berthon *et al.*	(CDEF, RHEL, SACL+)
ESTES	74	Thesis LBL-3827	R.D. Estes	(LBL)
AGUILAR-...	70B	PRL 25 58	M. Aguilar-Benitez *et al.*	(BNL, SYRA)
BARNES	69E	BNL 13823	V.E. Barnes *et al.*	(BNL, SYRA)
EBERHARD	69	PRL 22 200	P.H. Eberhard *et al.*	(LRL)
HUWE	69	PR 181 1824	D.O. Huwe	(LRL)
BUGG	68	PR 168 1466	D.V. Bugg *et al.*	(RHEL, BIRM, CAVE) I
BUTTON-...	68	PRL 21 1123	J. Button-Shafer	(MASA, LRL) JP
PRIMER	68	PRL 20 610	M. Primer *et al.*	(SYRA, BNL)
EBERHARD	67	PR 163 1446	P. Eberhard *et al.*	(LRL, ILL) IJP
BIRMINGHAM	66	PR 152 1148	M. Haque *et al.*	(BIRM, GLAS, LOIC, OXF+)
LONDON	66	PR 143 1034	G.W. London *et al.*	(BNL, SYRA) IJ
EBERHARD	65	PRL 14 466	P.H. Eberhard *et al.*	(LRL, ILL) I
LEVEQUE	65	PL 18 69	A. Leveque *et al.*	(SACL, EPOL, GLAS+) JP
ALVAREZ	63	PRL 10 184	L.W. Alvarez *et al.*	(LRL) I
SMITH	63	Athens Conf. 67	G.A. Smith	(LRL)
ALEXANDER	62C	CERN Conf. 320	G. Alexander *et al.*	(LRL) I

$\Sigma(1690)$ Bumps

$I(J^P) = 1(?^?)$ Status: **

OMITTED FROM SUMMARY TABLE

See the note preceding the $\Sigma(1670)$ Listings. Seen in production experiments only, mainly in $\Lambda\pi$.

$\Sigma(1690)$ MASS (PRODUCTION EXPERIMENTS)

VALUE (MeV)	EVTS	DOCUMENT ID		TECN	CHG	COMMENT
≈ 1690 OUR ESTIMATE						
1698±20	70	[1] GODDARD	79	HBC	+	$\pi^+ p$ 10.3 GeV/c
1707±20	40	[2] GODDARD	79	HBC	+	$\pi^+ p$ 10.3 GeV/c
1698±20	15	ADERHOLZ	69	HBC	+	$\pi^+ p$ 8 GeV/c
1682± 2	46	BLUMENFELD	69	HBC	+	$K^0_L p$
1700±20		MOTT	69	HBC	+	$K^- p$ 5.5 GeV/c
1694±24	60	[3] PRIMER	68	HBC	+	$K^- p$ 4.6–5 GeV/c
1700± 6		[4] SIMS	68	HBC	−	$K^- N \to \Lambda\pi\pi$
1715±12	30	COLLEY	67	HBC	+	$K^- p$ 6 GeV/c

$\Sigma(1690)$ WIDTH (PRODUCTION EXPERIMENTS)

VALUE (MeV)	EVTS	DOCUMENT ID		TECN	CHG	COMMENT
240± 60	70	[1] GODDARD	79	HBC	+	$\pi^+ p$ 10.3 GeV/c
$130^{+100}_{-\ 60}$	40	[2] GODDARD	79	HBC	+	$\pi^+ p$ 10.3 GeV/c
142± 40	15	ADERHOLZ	69	HBC	+	$\pi^+ p$ 8 GeV/c
25± 10	46	BLUMENFELD	69	HBC	+	$K^0_L p$
130± 25		MOTT	69	HBC	+	$K^- p$ 5.5 GeV/c
105± 35	60	[3] PRIMER	68	HBC	+	$K^- p$ 4.6–5 GeV/c
62± 14		[4] SIMS	68	HBC	−	$K^- N \to \Lambda\pi\pi$
100± 35	30	COLLEY	67	HBC	+	$K^- p$ 6 GeV/c

$\Sigma(1690)$ DECAY MODES (PRODUCTION EXPERIMENTS)

	Mode
Γ_1	$N\overline{K}$
Γ_2	$\Lambda\pi$
Γ_3	$\Sigma\pi$
Γ_4	$\Sigma(1385)\pi$
Γ_5	$\Lambda\pi\pi$ (including $\Sigma(1385)\pi$)

$\Sigma(1690)$ BRANCHING RATIOS (PRODUCTION EXPERIMENTS)

$\Gamma(N\overline{K})/\Gamma(\Lambda\pi)$ Γ_1/Γ_2

VALUE	EVTS	DOCUMENT ID		TECN	CHG	COMMENT
small		GODDARD	79	HBC	+	$\pi^+ p$ 10.2 GeV/c
<0.2		MOTT	69	HBC	+	$K^- p$ 5.5 GeV/c
0.4±0.25	18	COLLEY	67	HBC	+	6/30 events

$\Gamma(\Sigma\pi)/\Gamma(\Lambda\pi)$ Γ_3/Γ_2

VALUE	CL%	DOCUMENT ID		TECN	CHG	COMMENT
small		GODDARD	79	HBC	+	$\pi^+ p$ 10.2 GeV/c
<0.4	90	MOTT	69	HBC	+	$K^- p$ 5.5 GeV/c
0.3±0.3		COLLEY	67	HBC	+	4/30 events

$\Gamma(\Sigma(1385)\pi)/\Gamma(\Lambda\pi)$ Γ_4/Γ_2

VALUE	DOCUMENT ID		TECN	CHG	COMMENT
<0.5	MOTT	69	HBC	+	$K^- p$ 5.5 GeV/c

$\Gamma(\Lambda\pi\pi$ (including $\Sigma(1385)\pi))/\Gamma(\Lambda\pi)$ Γ_5/Γ_2

VALUE	DOCUMENT ID		TECN	CHG	COMMENT
2.0±0.6	BLUMENFELD	69	HBC	+	31/15 events
0.5±0.25	COLLEY	67	HBC	+	15/30 events

$\Gamma(\Sigma(1385)\pi)/\Gamma(\Lambda\pi\pi$ (including $\Sigma(1385)\pi))$ Γ_4/Γ_5

VALUE	DOCUMENT ID		TECN	CHG	COMMENT
large	SIMS	68	HBC	−	$K^- N \to \Lambda\pi\pi$
small	COLLEY	67	HBC	+	$K^- p$ 6 GeV/c

$\Sigma(1690)$ FOOTNOTES (PRODUCTION EXPERIMENTS)

[1] From $\pi^+ p \to (\Lambda\pi^+) K^+$. $J > 1/2$ is not required by the data.

[2] From $\pi^+ p \to (\Lambda\pi^+)(K\pi)^+$. $J > 1/2$ is indicated, but large background precludes a definite conclusion.

[3] See the $\Sigma(1670)$ Listings. AGUILAR-BENITEZ 70B with three times the data of PRIMER 68 find no evidence for the $\Sigma(1690)$.

[4] This analysis, which is difficult and requires several assumptions and shows no unambiguous $\Sigma(1690)$ signal, suggests $J^P = 5/2^+$. Such a state would lead all previously known Y^* trajectories.

$\Sigma(1690)$ REFERENCES (PRODUCTION EXPERIMENTS)

GODDARD	79	PR D19 1350	M.C. Goddard *et al.*	(TNTO, BNL) IJ
AGUILAR-...	70B	PRL 25 58	M. Aguilar-Benitez *et al.*	(BNL, SYRA)
ADERHOLZ	69	NP B11 259	M. Aderholz *et al.*	(AACH3, BERL, CERN+) I
BLUMENFELD	69	PL 29B 58	B.J. Blumenfeld, G.R. Kalbfleisch	(BNL) I
MOTT	69	PR 177 1966	J. Mott *et al.*	(NWES, ANL) I
Also		PRL 18 266	M. Derrick *et al.*	(ANL, NWES) I
PRIMER	68	PRL 20 610	M. Primer *et al.*	(SYRA, BNL) I
SIMS	68	PRL 21 1413	W.H. Sims *et al.*	(FSU, TUFTS, BRAN) I
COLLEY	67	PL 24B 489	D.C. Colley	(BIRM, GLAS, LOIC, MUNI, OXF+) I

$\Sigma(1730)$ $3/2^+$

$I(J^P) = 1(\frac{3}{2}^+)$ Status: *

OMITTED FROM SUMMARY TABLE

$\Sigma(1730)$ MASS

VALUE (MeV)	DOCUMENT ID		TECN	COMMENT
1727±27	ZHANG	13A	DPWA	Multichannel

$\Lambda(1730)$ WIDTH

VALUE (MeV)	DOCUMENT ID		TECN	COMMENT
276±87	ZHANG	13A	DPWA	Multichannel

$\Sigma(1730)$ DECAY MODES

	Mode	Fraction (Γ_i/Γ)
Γ_1	$N\overline{K}$	(2.0± 1.0) %
Γ_2	$\Lambda\pi$	(70 ±17) %
Γ_3	$\Sigma\pi$	(12 ± 6) %

$\Sigma(1730)$ BRANCHING RATIOS

$\Gamma(N\overline{K})/\Gamma_{total}$ Γ_1/Γ

VALUE	DOCUMENT ID		TECN	COMMENT
0.02±0.01	ZHANG	13A	DPWA	Multichannel

$\Gamma(\Lambda\pi)/\Gamma_{total}$ Γ_2/Γ

VALUE	DOCUMENT ID		TECN	COMMENT
0.70±0.17	ZHANG	13A	DPWA	Multichannel

$\Gamma(\Sigma\pi)/\Gamma_{total}$ Γ_3/Γ

VALUE	DOCUMENT ID		TECN	COMMENT
0.12±0.06	ZHANG	13A	DPWA	Multichannel

$\Sigma(1730)$ REFERENCES

ZHANG	13A	PR C88 035205	H. Zhang *et al.*	(KSU)

$\Sigma(1750)$ $1/2^-$

$I(J^P) = 1(\frac{1}{2}^-)$ Status: ***

For most results published before 1974 (they are now obsolete), see our 1982 edition Physics Letters **111B** 1 (1982).

There is evidence for this state in many partial-wave analyses, but with wide variations in the mass, width, and couplings. The latest analyses indicated significant couplings to $N\overline{K}$ and $\Lambda\pi$, as well as to $\Sigma\eta$ whose threshold is at 1746 MeV (JONES 74).

$\Sigma(1750)$ POLE POSITION

REAL PART

VALUE (MeV)	DOCUMENT ID		TECN	COMMENT
• • • We do not use the following data for averages, fits, limits, etc. • • •				
1704^{+3}_{-6}	[1] KAMANO	15	DPWA	Multichannel
1708	ZHANG	13A	DPWA	Multichannel

[1] From the preferred solution A in KAMANO 15. Solution B reports two poles at M = 1551^{+2}_{-9} MeV and 1940^{+2}_{-2} MeV.

Baryon Particle Listings

$\Sigma(1750)$

−2×IMAGINARY PART

VALUE (MeV)	DOCUMENT ID		TECN	COMMENT
• • • We do not use the following data for averages, fits, limits, etc. • • •				
86^{+14}_{-4}	[1] KAMANO	15	DPWA	Multichannel
158	ZHANG	13A	DPWA	Multichannel

[1] From the preferred solution A in KAMANO 15. Solution B Reports two poles with $\Gamma = 376^{+12}_{-2}$ and 172^{+4}_{-4} MeV.

$\Sigma(1750)$ POLE RESIDUES

The normalized residue is the residue divided by $\Gamma_{pole}/2$.

Normalized residue in $N\overline{K} \to \Sigma(1750) \to N\overline{K}$

MODULUS	PHASE (°)	DOCUMENT ID		TECN	COMMENT
• • • We do not use the following data for averages, fits, limits, etc. • • •					
0.0982	178	[1] KAMANO	15	DPWA	Multichannel

[1] From the preferred solution A in KAMANO 15.

Normalized residue in $N\overline{K} \to \Sigma(1750) \to \Sigma\pi$

MODULUS	PHASE (°)	DOCUMENT ID		TECN	COMMENT
• • • We do not use the following data for averages, fits, limits, etc. • • •					
0.192	137	[1] KAMANO	15	DPWA	Multichannel

[1] From the preferred solution A in KAMANO 15.

Normalized residue in $N\overline{K} \to \Sigma(1750) \to \Lambda\pi$

MODULUS	PHASE (°)	DOCUMENT ID		TECN	COMMENT
• • • We do not use the following data for averages, fits, limits, etc. • • •					
0.207	169	[1] KAMANO	15	DPWA	Multichannel

[1] From the preferred solution A in KAMANO 15.

Normalized residue in $N\overline{K} \to \Sigma(1750) \to \Sigma(1385)\pi$, D-wave

MODULUS	PHASE (°)	DOCUMENT ID		TECN	COMMENT
• • • We do not use the following data for averages, fits, limits, etc. • • •					
0.0536	73	[1] KAMANO	15	DPWA	Multichannel

[1] From the preferred solution A in KAMANO 15.

$\Sigma(1750)$ MASS

VALUE (MeV)	DOCUMENT ID		TECN	COMMENT
1730 to 1800 (≈ 1750) OUR ESTIMATE				
1739 ± 8	ZHANG	13A	DPWA	Multichannel
1756 ± 10	GOPAL	80	DPWA	$\overline{K}N \to \overline{K}N$
1770 ± 10	ALSTON-...	78	DPWA	$\overline{K}N \to \overline{K}N$
1770 ± 15	GOPAL	77	DPWA	$\overline{K}N$ multichannel
• • • We do not use the following data for averages, fits, limits, etc. • • •				
1800 or 1813	[1] MARTIN	77	DPWA	$\overline{K}N$ multichannel
1715 ± 10	[2] CARROLL	76	DPWA	Isospin-1 total σ
1730	DEBELLEFON	76	IPWA	$K^-p \to \Lambda\pi^0$
1780 ± 30	BAILLON	75	IPWA	$\overline{K}N \to \Lambda\pi$ (sol. 1)
1700 ± 30	BAILLON	75	IPWA	$\overline{K}N \to \Lambda\pi$ (sol. 2)
1697^{+20}_{-10}	VANHORN	75	DPWA	$K^-p \to \Lambda\pi^0$
1785 ± 12	CHU	74	DBC	Fits $\sigma(K^-n \to \Sigma^-\eta)$
1760 ± 5	[3] JONES	74	HBC	Fits $\sigma(K^-p \to \Sigma^0\eta)$
1739 ± 10	PREVOST	74	DPWA	$K^-N \to \Sigma(1385)\pi$

[1] The two MARTIN 77 values are from a T-matrix pole and from a Breit-Wigner fit.
[2] A total cross-section bump with $(J+1/2)\ \Gamma_{el}\ /\ \Gamma_{total} = 0.30$.
[3] An S-wave Breit-Wigner fit to the threshold cross section with no background and errors statistical only.

$\Sigma(1750)$ WIDTH

VALUE (MeV)	DOCUMENT ID		TECN	COMMENT
60 to 160 (≈ 90) OUR ESTIMATE				
182 ± 60	ZHANG	13A	DPWA	Multichannel
64 ± 10	GOPAL	80	DPWA	$\overline{K}N \to \overline{K}N$
161 ± 20	ALSTON-...	78	DPWA	$\overline{K}N \to \overline{K}N$
60 ± 10	GOPAL	77	DPWA	$\overline{K}N$ multichannel
• • • We do not use the following data for averages, fits, limits, etc. • • •				
117 or 119	[1] MARTIN	77	DPWA	$\overline{K}N$ multichannel
10	[2] CARROLL	76	DPWA	Isospin-1 total σ
110	DEBELLEFON	76	IPWA	$K^-p \to \Lambda\pi^0$
140 ± 30	BAILLON	75	IPWA	$\overline{K}N \to \Lambda\pi$ (sol. 1)
160 ± 50	BAILLON	75	IPWA	$\overline{K}N \to \Lambda\pi$ (sol. 2)
66^{+14}_{-12}	VANHORN	75	DPWA	$K^-p \to \Lambda\pi^0$
89 ± 33	CHU	74	DBC	Fits $\sigma(K^-n \to \Sigma^-\eta)$
92 ± 7	[3] JONES	74	HBC	Fits $\sigma(K^-p \to \Sigma^0\eta)$
108 ± 20	PREVOST	74	DPWA	$K^-N \to \Sigma(1385)\pi$

[1] The two MARTIN 77 values are from a T-matrix pole and from a Breit-Wigner fit.
[2] A total cross-section bump with $(J+1/2)\ \Gamma_{el}\ /\ \Gamma_{total} = 0.30$.
[3] An S-wave Breit-Wigner fit to the threshold cross section with no background and errors statistical only.

$\Sigma(1750)$ DECAY MODES

	Mode	Fraction (Γ_i/Γ)
Γ_1	$N\overline{K}$	10–40 %
Γ_2	$\Lambda\pi$	seen
Γ_3	$\Sigma\pi$	<8 %
Γ_4	$\Sigma\eta$	15–55 %
Γ_5	$\Sigma(1385)\pi$, D-wave	
Γ_6	$\Lambda(1520)\pi$	
Γ_7	$N\overline{K}^*(892)$, S=1/2	(8±4) %
Γ_8	$N\overline{K}^*(892)$, S=3/2, D-wave	

$\Sigma(1750)$ BRANCHING RATIOS

See "Sign conventions for resonance couplings" in the Note on Λ and Σ Resonances.

$\Gamma(N\overline{K})/\Gamma_{total}$ Γ_1/Γ

VALUE	DOCUMENT ID		TECN	COMMENT
0.1 to 0.4 OUR ESTIMATE				
0.09 ±0.07	ZHANG	13A	DPWA	Multichannel
0.14 ±0.03	GOPAL	80	DPWA	$\overline{K}N \to \overline{K}N$
0.33 ±0.05	ALSTON-...	78	DPWA	$\overline{K}N \to \overline{K}N$
• • • We do not use the following data for averages, fits, limits, etc. • • •				
0.154	[1] KAMANO	15	DPWA	Multichannel
0.15 ±0.03	GOPAL	77	DPWA	See GOPAL 80
0.06 or 0.05	[2] MARTIN	77	DPWA	$\overline{K}N$ multichannel

[1] From the preferred solution A in KAMANO 15.
[2] The two MARTIN 77 values are from a T-matrix pole and from a Breit-Wigner fit.

$\Gamma(\Lambda\pi)/\Gamma_{total}$ Γ_2/Γ

VALUE	DOCUMENT ID		TECN	COMMENT
• • • We do not use the following data for averages, fits, limits, etc. • • •				
0.435	[1] KAMANO	15	DPWA	Multichannel

[1] From the preferred solution A in KAMANO 15.

$\Gamma(\Sigma\pi)/\Gamma_{total}$ Γ_3/Γ

VALUE	DOCUMENT ID		TECN	COMMENT
• • • We do not use the following data for averages, fits, limits, etc. • • •				
0.373	[1] KAMANO	15	DPWA	Multichannel

[1] From the preferred solution A in KAMANO 15.

$\Gamma(\Sigma(1385)\pi, D\text{-wave})/\Gamma_{total}$ Γ_5/Γ

VALUE	DOCUMENT ID		TECN	COMMENT
• • • We do not use the following data for averages, fits, limits, etc. • • •				
0.024	[1] KAMANO	15	DPWA	Multichannel

[1] From the preferred solution A in KAMANO 15.

$\Gamma(N\overline{K}^*(892), S{=}1/2)/\Gamma_{total}$ Γ_7/Γ

VALUE	DOCUMENT ID		TECN	COMMENT
0.08 ±0.04	ZHANG	13A	DPWA	Multichannel
• • • We do not use the following data for averages, fits, limits, etc. • • •				
0.004	[1] KAMANO	15	DPWA	Multichannel

[1] From the preferred solution A in KAMANO 15.

$\Gamma(N\overline{K}^*(892), S{=}3/2, D\text{-wave})/\Gamma_{total}$ Γ_8/Γ

VALUE	DOCUMENT ID		TECN	COMMENT
• • • We do not use the following data for averages, fits, limits, etc. • • •				
0.01	[1] KAMANO	15	DPWA	Multichannel

[1] From the preferred solution A in KAMANO 15.

$(\Gamma_i\Gamma_f)^{1/2}/\Gamma_{total}$ in $N\overline{K} \to \Sigma(1750) \to \Lambda\pi$ $(\Gamma_1\Gamma_2)^{1/2}/\Gamma$

VALUE	DOCUMENT ID		TECN	COMMENT
+0.10 ±0.04	ZHANG	13A	DPWA	Multichannel
0.04 ±0.03	GOPAL	77	DPWA	$\overline{K}N$ multichannel
• • • We do not use the following data for averages, fits, limits, etc. • • •				
−0.10 or −0.09	[1] MARTIN	77	DPWA	$\overline{K}N$ multichannel
−0.12	DEBELLEFON	76	IPWA	$K^-p \to \Lambda\pi^0$
−0.12 ±0.02	BAILLON	75	IPWA	$\overline{K}N \to \Lambda\pi$ (sol. 1)
−0.13 ±0.03	BAILLON	75	IPWA	$\overline{K}N \to \Lambda\pi$ (sol. 2)
−0.13 ±0.04	VANHORN	75	DPWA	$K^-p \to \Lambda\pi^0$
−0.120±0.077	DEVENISH	74B		Fixed-t dispersion rel.

[1] The two MARTIN 77 values are from a T-matrix pole and from a Breit-Wigner fit.

$(\Gamma_i\Gamma_f)^{1/2}/\Gamma_{total}$ in $N\overline{K} \to \Sigma(1750) \to \Sigma\pi$ $(\Gamma_1\Gamma_3)^{1/2}/\Gamma$

VALUE	DOCUMENT ID		TECN	COMMENT
$+0.17\pm0.07$	ZHANG	13A	DPWA	Multichannel
-0.09 ± 0.05	GOPAL	77	DPWA	$\overline{K}N$ multichannel
• • • We do not use the following data for averages, fits, limits, etc. • • •				
$+0.06$ or $+0.06$	[1] MARTIN	77	DPWA	$\overline{K}N$ multichannel
0.13 ± 0.02	LANGBEIN	72	IPWA	$\overline{K}N$ multichannel

[1] The two MARTIN 77 values are from a T-matrix pole and from a Breit-Wigner fit.

$(\Gamma_i\Gamma_f)^{1/2}/\Gamma_{total}$ in $N\overline{K} \to \Sigma(1750) \to \Sigma\eta$ $(\Gamma_1\Gamma_4)^{1/2}/\Gamma$

VALUE	DOCUMENT ID		TECN	COMMENT
0.23 ± 0.01	[1] JONES	74	HBC	Fits $\sigma(K^-p \to \Sigma^0\eta)$
• • • We do not use the following data for averages, fits, limits, etc. • • •				
seen	CLINE	69	DBC	Threshold bump

[1] An S-wave Breit-Wigner fit to the threshold cross section with no background and errors statistical only.

$(\Gamma_i\Gamma_f)^{1/2}/\Gamma_{total}$ in $N\overline{K} \to \Sigma(1750) \to \Sigma(1385)\pi$, D-wave $(\Gamma_1\Gamma_5)^{1/2}/\Gamma$

VALUE	DOCUMENT ID		TECN	COMMENT
$+0.17\pm0.07$	ZHANG	13A	DPWA	Multichannel
$+0.18\pm0.15$	PREVOST	74	DPWA	$K^-N \to \Sigma(1385)\pi$

$(\Gamma_i\Gamma_f)^{1/2}/\Gamma_{total}$ in $N\overline{K} \to \Sigma(1750) \to \Lambda(1520)\pi$ $(\Gamma_1\Gamma_6)^{1/2}/\Gamma$

VALUE	DOCUMENT ID		TECN	COMMENT
• • • We do not use the following data for averages, fits, limits, etc. • • •				
0.032 ± 0.021	CAMERON	77	DPWA	P-wave decay

$\Sigma(1750)$ REFERENCES

KAMANO	15	PR C92 025205	H. Kamano *et al.*	(ANL, OSAK)
ZHANG	13A	PR C88 035205	H. Zhang *et al.*	(KSU)
PDG	82	PL 111B 1	M. Roos *et al.*	(HELS, CIT, CERN)
GOPAL	80	Toronto Conf. 159	G.P. Gopal	(RHEL) IJP
ALSTON-...	78	PR D18 182	M. Alston-Garnjost *et al.*	(LBL, MTHO+) IJP
Also		PRL 38 1007	M. Alston-Garnjost *et al.*	(LBL, MTHO+) IJP
CAMERON	77	NP B131 399	W. Cameron *et al.*	(RHEL, LOIC) IJP
GOPAL	77	NP B119 362	G.P. Gopal *et al.*	(LOIC, RHEL) IJP
MARTIN	77	NP B127 349	B.R. Martin, M.K. Pidcock, R.G. Moorhouse	(LOUC+) IJP
Also		NP B126 266	B.R. Martin, M.K. Pidcock	(LOUC)
Also		NP B126 285	B.R. Martin, M.K. Pidcock	(LOUC) IJP
CARROLL	76	PRL 37 806	A.S. Carroll *et al.*	(BNL) I
DEBELLEFON	76	NP B109 129	A. de Bellefon, A. Berthon	(CDEF) IJP
BAILLON	75	NP B94 39	P.H. Baillon, P.J. Litchfield	(CERN, RHEL) IJP
VANHORN	75	NP B87 145	A.J. van Horn	(LBL) IJP
Also		NP B87 157	A.J. van Horn	(LBL) IJP
CHU	74	NC 20A 35	R.Y.L. Chu *et al.*	(PLAT, TUFTS, BRAN) IJP
DEVENISH	74B	NP B81 330	R.C.E. Devenish, C.D. Froggatt, B.R. Martin	(DESY+)
JONES	74	NP B73 141	M.D. Jones	(CHIC) IJP
PREVOST	74	NP B69 246	J. Prevost *et al.*	(SACL, CERN, HEID)
LANGBEIN	72	NP B47 477	W. Langbein, F. Wagner	(MPIM) IJP
CLINE	69	LNC 2 407	D. Cline, R. Laumann, J. Mapp	(WISC)

$\Sigma(1770)$ $1/2^+$

$I(J^P) = 1(\frac{1}{2}^+)$ Status: *

OMITTED FROM SUMMARY TABLE

Evidence for this state now rests solely on solution 1 of BAILLON 75, (see the footnotes) but the $\Lambda\pi$ partial-wave amplitudes of this solution are in disagreement with amplitudes from most other $\Lambda\pi$ analyses. ZHANG 13A finds no evidence for this state.

$\Sigma(1770)$ POLE POSITION

REAL PART

VALUE (MeV)	DOCUMENT ID		TECN	COMMENT
• • • We do not use the following data for averages, fits, limits, etc. • • •				
1706^{+67}_{-60}	[1] KAMANO	15	DPWA	Multichannel

[1] From the preferred solution A in KAMANO 15. Solution B Reports two poles at 1605^{+2}_{-4} and $2014^{+\ 6}_{-13}$ MeV.

$-2\times$IMAGINARY PART

VALUE (MeV)	DOCUMENT ID		TECN	COMMENT
• • • We do not use the following data for averages, fits, limits, etc. • • •				
$101^{+158}_{-\ 84}$	[1] KAMANO	15	DPWA	Multichannel

[1] From the preferred solution A in KAMANO 15. Solution B reports two poles with $192^{+\ 2}_{-10}$ and $140^{+28}_{-\ 2}$ MeV width.

$\Sigma(1770)$ POLE RESIDUES

The normalized residue is the residue divided by $\Gamma_{pole}/2$.

Normalized residue in $N\overline{K} \to \Sigma(1770) \to N\overline{K}$

MODULUS	PHASE (°)	DOCUMENT ID		TECN	COMMENT
• • • We do not use the following data for averages, fits, limits, etc. • • •					
0.0268	91	[1] KAMANO	15	DPWA	Multichannel

[1] From the preferred solution A in KAMANO 15.

Normalized residue in $N\overline{K} \to \Sigma(1770) \to \Sigma\pi$

MODULUS	PHASE (°)	DOCUMENT ID		TECN	COMMENT
• • • We do not use the following data for averages, fits, limits, etc. • • •					
0.145	-171	[1] KAMANO	15	DPWA	Multichannel

[1] From the preferred solution A in KAMANO 15.

Normalized residue in $N\overline{K} \to \Sigma(1770) \to \Lambda\pi$

MODULUS	PHASE (°)	DOCUMENT ID		TECN	COMMENT
• • • We do not use the following data for averages, fits, limits, etc. • • •					
0.117	-76	[1] KAMANO	15	DPWA	Multichannel

[1] From the preferred solution A in KAMANO 15.

Normalized residue in $N\overline{K} \to \Sigma(1770) \to \Sigma(1385)\pi$

MODULUS	PHASE (°)	DOCUMENT ID		TECN	COMMENT
• • • We do not use the following data for averages, fits, limits, etc. • • •					
0.0722	-128	[1] KAMANO	15	DPWA	Multichannel

[1] From the preferred solution A in KAMANO 15.

$\Sigma(1770)$ MASS

VALUE (MeV)	DOCUMENT ID		TECN	COMMENT
≈ 1770 OUR ESTIMATE				
1738 ± 10	[1] GOPAL	77	DPWA	$\overline{K}N$ multichannel
1770 ± 20	[2] BAILLON	75	IPWA	$\overline{K}N \to \Lambda\pi$
1772	[3] KANE	72	DPWA	$K^-p \to \Sigma\pi$

[1] Required to fit the isospin-1 total cross section of CARROLL 76 in the $\overline{K}N$ channel. The addition of new K^-p polarization and K^-n differential cross-section data in GOPAL 80 find it to be more consistent with the $\Sigma(1660)$ P_{11}.
[2] From solution 1 of BAILLON 75; not present in solution 2.
[3] Not required in KANE 74, which supersedes KANE 72.

$\Sigma(1770)$ WIDTH

VALUE (MeV)	DOCUMENT ID		TECN	COMMENT
72 ± 10	[1] GOPAL	77	DPWA	$\overline{K}N$ multichannel
80 ± 30	[2] BAILLON	75	IPWA	$\overline{K}N \to \Lambda\pi$
80	[3] KANE	72	DPWA	$K^-p \to \Sigma\pi$

[1] Required to fit the isospin-1 total cross section of CARROLL 76 in the $\overline{K}N$ channel. The addition of new K^-p polarization and K^-n differential cross-section data in GOPAL 80 find it to be more consistent with the $\Sigma(1660)$ P_{11}.
[2] From solution 1 of BAILLON 75; not present in solution 2.
[3] Not required in KANE 74, which supersedes KANE 72.

$\Sigma(1770)$ DECAY MODES

	Mode
Γ_1	$N\overline{K}$
Γ_2	$\Lambda\pi$
Γ_3	$\Sigma\pi$
Γ_4	$\Sigma(1385)\pi$
Γ_5	$N\overline{K}^*(892)$, S=1/2, P-wave
Γ_6	$N\overline{K}^*(892)$, S=3/2, P-wave

$\Sigma(1770)$ BRANCHING RATIOS

See "Sign conventions for resonance couplings" in the Note on Λ and Σ Resonances.

$\Gamma(N\overline{K})/\Gamma_{total}$ Γ_1/Γ

VALUE	DOCUMENT ID		TECN	COMMENT
$0.14\ \pm0.04$	[1] GOPAL	77	DPWA	$\overline{K}N$ multichannel
• • • We do not use the following data for averages, fits, limits, etc. • • •				
0.016	[2] KAMANO	15	DPWA	Multichannel

[1] Required to fit the isospin-1 total cross section of CARROLL 76 in the $\overline{K}N$ channel. The addition of new K^-p polarization and K^-n differential cross-section data in GOPAL 80 find it to be more consistent with the $\Sigma(1660)$ P_{11}.
[2] From the preferred solution A in KAMANO 15.

$\Gamma(\Lambda\pi)/\Gamma_{total}$ Γ_2/Γ

VALUE	DOCUMENT ID		TECN	COMMENT
• • • We do not use the following data for averages, fits, limits, etc. • • •				
0.283	[1] KAMANO	15	DPWA	Multichannel

[1] From the preferred solution A in KAMANO 15.

$\Gamma(\Sigma\pi)/\Gamma_{total}$ Γ_3/Γ

VALUE	DOCUMENT ID		TECN	COMMENT
• • • We do not use the following data for averages, fits, limits, etc. • • •				
0.595	[1] KAMANO	15	DPWA	Multichannel

[1] From the preferred solution A in KAMANO 15.

$\Gamma(\Sigma(1385)\pi)/\Gamma_{total}$ Γ_4/Γ

VALUE	DOCUMENT ID		TECN	COMMENT
• • • We do not use the following data for averages, fits, limits, etc. • • •				
0.103	[1] KAMANO	15	DPWA	Multichannel

[1] From the preferred solution A in KAMANO 15.

$\Gamma(N\overline{K}^*(892), S=1/2, P\text{-wave})/\Gamma_{total}$ Γ_5/Γ

VALUE	DOCUMENT ID		TECN	COMMENT
• • • We do not use the following data for averages, fits, limits, etc. • • •				
0.004	[1] KAMANO	15	DPWA	Multichannel

[1] From the preferred solution A in KAMANO 15.

$\Gamma(N\overline{K}^*(892), S=3/2, P\text{-wave})/\Gamma_{total}$ Γ_6/Γ

VALUE	DOCUMENT ID		TECN	COMMENT
• • • We do not use the following data for averages, fits, limits, etc. • • •				
not seen	[1] KAMANO	15	DPWA	Multichannel

[1] From the preferred solution A in KAMANO 15.

$(\Gamma_i\Gamma_f)^{1/2}/\Gamma_{total}$ in $N\overline{K} \to \Sigma(1770) \to \Lambda\pi$ $(\Gamma_1\Gamma_2)^{1/2}/\Gamma$

VALUE	DOCUMENT ID		TECN	COMMENT
< 0.04	GOPAL	77	DPWA	$\overline{K}N$ multichannel
-0.08 ± 0.02	[1] BAILLON	75	IPWA	$\overline{K}N \to \Lambda\pi$

[1] From solution 1 of BAILLON 75; not present in solution 2.

$(\Gamma_i\Gamma_f)^{1/2}/\Gamma_{total}$ in $N\overline{K} \to \Sigma(1770) \to \Sigma\pi$ $(\Gamma_1\Gamma_3)^{1/2}/\Gamma$

VALUE	DOCUMENT ID		TECN	COMMENT
< 0.04	GOPAL	77	DPWA	$\overline{K}N$ multichannel
-0.108	[1] KANE	72	DPWA	$K^-p \to \Sigma\pi$

[1] Not required in KANE 74, which supersedes KANE 72.

$\Sigma(1770)$ REFERENCES

KAMANO	15	PR C92 025205	H. Kamano *et al.*	(ANL, OSAK)
ZHANG	13A	PR C88 035205	H. Zhang *et al.*	(KSU)
GOPAL	80	Toronto Conf. 159	G.P. Gopal	(RHEL)
GOPAL	77	NP B119 362	G.P. Gopal *et al.*	(LOIC, RHEL) IJP
CARROLL	76	PRL 37 806	A.S. Carroll *et al.*	(BNL) I
BAILLON	75	NP B94 39	P.H. Baillon, P.J. Litchfield	(CERN, RHEL) IJP
KANE	74	LBL-2452	D.F. Kane	(LBL) IJP
KANE	72	PR D5 1583	D.F.J. Kane	(LBL)

$\Sigma(1775)\ 5/2^-$

$I(J^P) = 1(\frac{5}{2}^-)$ Status: ****

Discovered by GALTIERI 63, this resonance plays the same role as cornerstone for isospin-1 analyses in this region as the $\Lambda(1820)F_{05}$ does in the isospin-0 channel.

For most results published before 1974 (they are now obsolete), see our 1982 edition Physics Letters **111B** 1 (1982).

$\Sigma(1775)$ POLE POSITION

REAL PART

VALUE (MeV)	DOCUMENT ID		TECN	COMMENT
$\mathbf{1767^{+2}_{-2}}$	[1] KAMANO	15	DPWA	Multichannel
• • • We do not use the following data for averages, fits, limits, etc. • • •				
1759	ZHANG	13A	DPWA	Multichannel

[1] From the preferred solution A in KAMANO 15.

$-2\times$IMAGINARY PART

VALUE (MeV)	DOCUMENT ID		TECN	COMMENT
$\mathbf{128^{+4}_{-2}}$	[1] KAMANO	15	DPWA	Multichannel
• • • We do not use the following data for averages, fits, limits, etc. • • •				
118	ZHANG	13A	DPWA	Multichannel

[1] From the preferred solution A in KAMANO 15.

$\Sigma(1775)$ POLE RESIDUES

The normalized residue is the residue divided by $\Gamma_{pole}/2$.

Normalized residue in $N\overline{K} \to \Sigma(1775) \to N\overline{K}$

MODULUS	PHASE (°)	DOCUMENT ID		TECN	COMMENT
• • • We do not use the following data for averages, fits, limits, etc. • • •					
0.371	-32	[1] KAMANO	15	DPWA	Multichannel

[1] From the preferred solution A in KAMANO 15.

Normalized residue in $N\overline{K} \to \Sigma(1775) \to \Sigma\pi$

MODULUS	PHASE (°)	DOCUMENT ID		TECN	COMMENT
• • • We do not use the following data for averages, fits, limits, etc. • • •					
0.115	-24	[1] KAMANO	15	DPWA	Multichannel

[1] From the preferred solution A in KAMANO 15.

Normalized residue in $N\overline{K} \to \Sigma(1775) \to \Lambda\pi$

MODULUS	PHASE (°)	DOCUMENT ID		TECN	COMMENT
• • • We do not use the following data for averages, fits, limits, etc. • • •					
0.325	157	[1] KAMANO	15	DPWA	Multichannel

[1] From the preferred solution A in KAMANO 15.

Normalized residue in $N\overline{K} \to \Sigma(1775) \to \Sigma(1385)\pi$, D-wave

MODULUS	PHASE (°)	DOCUMENT ID		TECN	COMMENT
• • • We do not use the following data for averages, fits, limits, etc. • • •					
0.391	137	[1] KAMANO	15	DPWA	Multichannel

[1] From the preferred solution A in KAMANO 15.

Normalized residue in $N\overline{K} \to \Sigma(1775) \to \Sigma(1385)\pi$, G-wave

MODULUS	PHASE (°)	DOCUMENT ID		TECN	COMMENT
• • • We do not use the following data for averages, fits, limits, etc. • • •					
0.0129	-58	[1] KAMANO	15	DPWA	Multichannel

[1] From the preferred solution A in KAMANO 15.

$\Sigma(1775)$ MASS

VALUE (MeV)	DOCUMENT ID		TECN	COMMENT
1770 to 1780 ($\approx$ 1775) OUR ESTIMATE				
1778 ± 1	ZHANG	13A	DPWA	Multichannel
1778 ± 5	GOPAL	80	DPWA	$\overline{K}N \to \overline{K}N$
1777 ± 5	ALSTON-...	78	DPWA	$\overline{K}N \to \overline{K}N$
1774 ± 5	GOPAL	77	DPWA	$\overline{K}N$ multichannel
1775 ± 10	BAILLON	75	IPWA	$\overline{K}N \to \Lambda\pi$
1774 ± 10	VANHORN	75	DPWA	$K^-p \to \Lambda\pi^0$
1772 ± 6	KANE	74	DPWA	$K^-p \to \Sigma\pi$
• • • We do not use the following data for averages, fits, limits, etc. • • •				
1772 or 1777	[1] MARTIN	77	DPWA	$\overline{K}N$ multichannel
1765	DEBELLEFON	76	IPWA	$K^-p \to \Lambda\pi^0$

[1] The two MARTIN 77 values are from a T-matrix pole and from a Breit-Wigner fit.

$\Sigma(1775)$ WIDTH

VALUE (MeV)	DOCUMENT ID		TECN	COMMENT
105 to 135 ($\approx$ 120) OUR ESTIMATE				
131 ± 3	ZHANG	13A	DPWA	Multichannel
137 ± 10	GOPAL	80	DPWA	$\overline{K}N \to \overline{K}N$
116 ± 10	ALSTON-...	78	DPWA	$\overline{K}N \to \overline{K}N$
130 ± 10	GOPAL	77	DPWA	$\overline{K}N$ multichannel
125 ± 15	BAILLON	75	IPWA	$\overline{K}N \to \Lambda\pi$
146 ± 18	VANHORN	75	DPWA	$K^-p \to \Lambda\pi^0$
154 ± 10	KANE	74	DPWA	$K^-p \to \Sigma\pi$
• • • We do not use the following data for averages, fits, limits, etc. • • •				
102 or 103	[1] MARTIN	77	DPWA	$\overline{K}N$ multichannel
120	DEBELLEFON	76	IPWA	$K^-p \to \Lambda\pi^0$

[1] The two MARTIN 77 values are from a T-matrix pole and from a Breit-Wigner fit.

$\Sigma(1775)$ DECAY MODES

	Mode	Fraction (Γ_i/Γ)
Γ_1	$N\overline{K}$	37–43%
Γ_2	$\Lambda\pi$	14–20%
Γ_3	$\Sigma\pi$	2–5%
Γ_4	$\Sigma(1385)\pi$	8–12%
Γ_5	$\Sigma(1385)\pi$, D-wave	
Γ_6	$\Sigma(1385)\pi$, D-wave	
Γ_7	$\Sigma(1385)\pi$, G-wave	
Γ_8	$\Lambda(1520)\pi$, P-wave	17–23%
Γ_9	$\Sigma\pi\pi$	
Γ_{10}	$\Delta(1232)\overline{K}$, D-wave	
Γ_{11}	$N\overline{K}^*(892)$, $S=1/2$	
Γ_{12}	$N\overline{K}^*(892)$, $S=1/2$, D-wave	
Γ_{13}	$N\overline{K}^*(892)$, $S=3/2$, D-wave	
Γ_{14}	$N\overline{K}^*(892)$, $S=3/2$, G-wave	

CONSTRAINED FIT INFORMATION

An overall fit to 7 branching ratios uses 18 measurements and one constraint to determine 5 parameters. The overall fit has a $\chi^2 = 363.4$ for 14 degrees of freedom.

The following *off-diagonal* array elements are the correlation coefficients $\langle \delta x_i \delta x_j \rangle / (\delta x_i \cdot \delta x_j)$, in percent, from the fit to the branching fractions, $x_i \equiv \Gamma_i/\Gamma_{\text{total}}$. The fit constrains the x_i whose labels appear in this array to sum to one.

x_2	−44			
x_3	−23	10		
x_4	−23	−32	−4	
x_8	−3	1	1	−84
	x_1	x_2	x_3	x_4

$\Sigma(1775)$ BRANCHING RATIOS

See "Sign conventions for resonance couplings" in the Note on Λ and Σ Resonances. Also, the errors quoted do not include uncertainties due to the parametrization used in the partial-wave analyses and are thus too small.

$\Gamma(N\overline{K})/\Gamma_{\text{total}}$ Γ_1/Γ

VALUE	DOCUMENT ID		TECN	COMMENT
0.37 to 0.43 OUR ESTIMATE				
0.421±0.020 OUR FIT Error includes scale factor of 2.5.				
0.398±0.009 OUR AVERAGE				
0.40 ±0.01	ZHANG	13A	DPWA	Multichannel
0.40 ±0.02	GOPAL	80	DPWA	$\overline{K}N \to \overline{K}N$
0.37 ±0.03	ALSTON-...	78	DPWA	$\overline{K}N \to \overline{K}N$
• • • We do not use the following data for averages, fits, limits, etc. • • •				
0.402	[1] KAMANO	15	DPWA	Multichannel
0.41 ±0.03	GOPAL	77	DPWA	See GOPAL 80
0.37 or 0.36	[2] MARTIN	77	DPWA	$\overline{K}N$ multichannel

[1] From the preferred solution A in KAMANO 15.
[2] The two MARTIN 77 values are from a T-matrix pole and from a Breit-Wigner fit.

$\Gamma(\Lambda\pi)/\Gamma_{\text{total}}$ Γ_2/Γ

VALUE	DOCUMENT ID		TECN	COMMENT
• • • We do not use the following data for averages, fits, limits, etc. • • •				
0.244	[1] KAMANO	15	DPWA	Multichannel

[1] From the preferred solution A in KAMANO 15.

$\Gamma(\Lambda\pi)/\Gamma(N\overline{K})$ Γ_2/Γ_1

VALUE	DOCUMENT ID		TECN	COMMENT
0.48±0.06 OUR FIT Error includes scale factor of 2.3.				
0.33±0.05	UHLIG	67	HBC	$K^- p$ 0.9 GeV/c

$\Gamma(\Sigma\pi)/\Gamma_{\text{total}}$ Γ_3/Γ

VALUE	DOCUMENT ID		TECN	COMMENT
• • • We do not use the following data for averages, fits, limits, etc. • • •				
0.042	[1] KAMANO	15	DPWA	Multichannel

[1] From the preferred solution A in KAMANO 15.

$\Gamma(\Sigma(1385)\pi)/\Gamma(N\overline{K})$ Γ_4/Γ_1

VALUE	DOCUMENT ID		TECN	COMMENT
0.79±0.11 OUR FIT Error includes scale factor of 3.2.				
0.25±0.09	UHLIG	67	HBC	$K^- p$ 0.9 GeV/c

$\Gamma(\Sigma(1385)\pi$, D-wave$)/\Gamma_{\text{total}}$ Γ_6/Γ

VALUE	DOCUMENT ID		TECN	COMMENT
• • • We do not use the following data for averages, fits, limits, etc. • • •				
0.309	[1] KAMANO	15	DPWA	Multichannel

[1] From the preferred solution A in KAMANO 15.

$\Gamma(\Sigma(1385)\pi$, G-wave$)/\Gamma_{\text{total}}$ Γ_7/Γ

VALUE	DOCUMENT ID		TECN	COMMENT
• • • We do not use the following data for averages, fits, limits, etc. • • •				
not seen	[1] KAMANO	15	DPWA	Multichannel

[1] From the preferred solution A in KAMANO 15.

$\Gamma(\Lambda(1520)\pi$, P-wave$)/\Gamma(N\overline{K})$ Γ_8/Γ_1

VALUE	DOCUMENT ID		TECN	COMMENT
$0.053^{+0.080}_{-0.035}$ OUR FIT Error includes scale factor of 11.8.				
0.28 ±0.05	UHLIG	67	HBC	$K^- p$ 0.9 GeV/c

$\Gamma(\Sigma\pi\pi)/\Gamma_{\text{total}}$ Γ_9/Γ

VALUE	DOCUMENT ID		TECN	COMMENT
• • • We do not use the following data for averages, fits, limits, etc. • • •				
0.12	[1] ARMENTEROS68C		HDBC	$K^- N \to \Sigma\pi\pi$

[1] For about 3/4 of this, the $\Sigma\pi$ system has $I = 0$ and is almost entirely $\Lambda(1520)$. For the rest, the $\Sigma\pi$ has $I = 1$, which is about what is expected from the known $\Sigma(1775) \to \Sigma(1385)\pi$ rate, as seen in $\Lambda\pi\pi$.

$\Gamma(N\overline{K}^*(892)$, S=1/2, D-wave$)/\Gamma_{\text{total}}$ Γ_{12}/Γ

VALUE	DOCUMENT ID		TECN	COMMENT
• • • We do not use the following data for averages, fits, limits, etc. • • •				
not seen	[1] KAMANO	15	DPWA	Multichannel

[1] From the preferred solution A in KAMANO 15.

$\Gamma(N\overline{K}^*(892)$, S=3/2, D-wave$)/\Gamma_{\text{total}}$ Γ_{13}/Γ

VALUE	DOCUMENT ID		TECN	COMMENT
• • • We do not use the following data for averages, fits, limits, etc. • • •				
0.003	[1] KAMANO	15	DPWA	Multichannel

[1] From the preferred solution A in KAMANO 15.

$\Gamma(N\overline{K}^*(892)$, S=3/2, G-wave$)/\Gamma_{\text{total}}$ Γ_{14}/Γ

VALUE	DOCUMENT ID		TECN	COMMENT
• • • We do not use the following data for averages, fits, limits, etc. • • •				
not seen	[1] KAMANO	15	DPWA	Multichannel

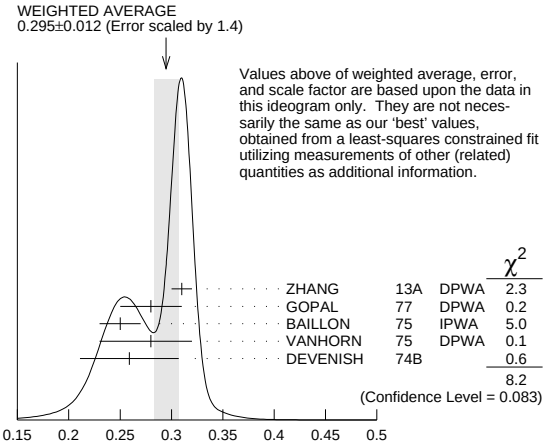

[1] From the preferred solution A in KAMANO 15.

$(\Gamma_i\Gamma_f)^{1/2}/\Gamma_{\text{total}}$ in $N\overline{K} \to \Sigma(1775) \to \Lambda\pi$ $(\Gamma_1\Gamma_2)^{1/2}/\Gamma$

VALUE	DOCUMENT ID		TECN	COMMENT
0.293±0.013 OUR FIT Error includes scale factor of 1.8.				
0.295±0.012 OUR AVERAGE Signs on measurements were ignored. Error includes scale factor of 1.4. See the ideogram below.				
−0.31 ±0.01	ZHANG	13A	DPWA	Multichannel
−0.28 ±0.03	GOPAL	77	DPWA	$\overline{K}N$ multichannel
−0.25 ±0.02	BAILLON	75	IPWA	$\overline{K}N \to \Lambda\pi$
$-0.28\ ^{+0.04}_{-0.05}$	VANHORN	75	DPWA	$K^- p \to \Lambda\pi^0$
−0.259±0.048	DEVENISH	74B		Fixed-t dispersion rel.
• • • We do not use the following data for averages, fits, limits, etc. • • •				
−0.29 or −0.28	[1] MARTIN	77	DPWA	$\overline{K}N$ multichannel
−0.30	DEBELLEFON	76	IPWA	$K^- p \to \Lambda\pi^0$

[1] The two MARTIN 77 values are from a T-matrix pole and from a Breit-Wigner fit.

$(\Gamma_i\Gamma_f)^{1/2}/\Gamma_{\text{total}}$ in $N\overline{K} \to \Sigma(1775) \to \Lambda\pi$

$(\Gamma_i\Gamma_f)^{1/2}/\Gamma_{\text{total}}$ in $N\overline{K} \to \Sigma(1775) \to \Sigma\pi$ $(\Gamma_1\Gamma_3)^{1/2}/\Gamma$

VALUE	DOCUMENT ID		TECN	COMMENT
0.090±0.009 OUR FIT Error includes scale factor of 1.4.				
0.090±0.011 OUR AVERAGE Signs on measurements were ignored. Error includes scale factor of 1.6. See the ideogram below.				
+0.08 ±0.01	ZHANG	13A	DPWA	Multichannel
+0.13 ±0.02	GOPAL	77	DPWA	$\overline{K}N$ multichannel
0.09 ±0.01	KANE	74	DPWA	$K^- p \to \Sigma\pi$
• • • We do not use the following data for averages, fits, limits, etc. • • •				
+0.08 or +0.08	[1] MARTIN	77	DPWA	$\overline{K}N$ multichannel

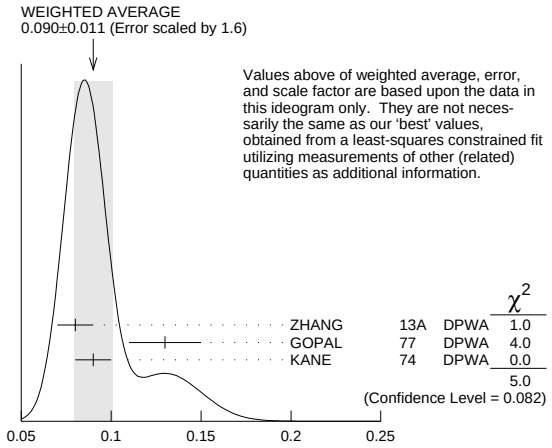

$(\Gamma_i\Gamma_f)^{1/2}/\Gamma_{total}$ in $N\overline{K} \rightarrow \Sigma(1775) \rightarrow \Sigma\pi$

[1] The two MARTIN 77 values are from a T-matrix pole and from a Breit-Wigner fit.

$(\Gamma_i\Gamma_f)^{1/2}/\Gamma_{total}$ in $N\overline{K} \rightarrow \Sigma(1775) \rightarrow \Sigma(1385)\pi$, D-wave — $(\Gamma_1\Gamma_5)^{1/2}/\Gamma$

VALUE	DOCUMENT ID		TECN	COMMENT
0.155 ± 0.024 OUR AVERAGE	Signs on measurements were ignored. Error includes scale factor of 3.5. See the ideogram below.			
−0.12 ± 0.01	ZHANG	13A	DPWA	Multichannel
−0.184 ± 0.011	[1] CAMERON	78	DPWA	$K^-p \rightarrow \Sigma(1385)\pi$
+0.20 ± 0.02	PREVOST	74	DPWA	$K^-N \rightarrow \Sigma(1385)\pi$
• • • We do not use the following data for averages, fits, limits, etc. • • •				
0.32 ± 0.06	SIMS	68	DBC	$K^-N \rightarrow \Lambda\pi\pi$
0.24 ± 0.03	ARMENTEROS	67C	HBC	$K^-p \rightarrow \Lambda\pi\pi$

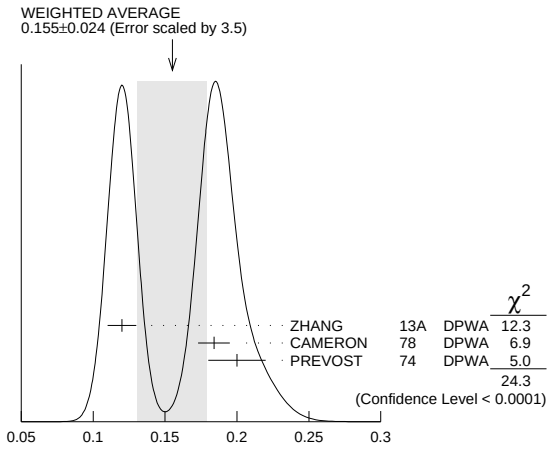

$(\Gamma_i\Gamma_f)^{1/2}/\Gamma_{total}$ in $N\overline{K} \rightarrow \Sigma(1775) \rightarrow \Sigma(1385)\pi$, D-wave

[1] The CAMERON 78 upper limit on G-wave decay is 0.03.

$(\Gamma_i\Gamma_f)^{1/2}/\Gamma_{total}$ in $N\overline{K} \rightarrow \Sigma(1775) \rightarrow \Lambda(1520)\pi$, P-wave — $(\Gamma_1\Gamma_8)^{1/2}/\Gamma$

VALUE	DOCUMENT ID		TECN	COMMENT
0.10 ± 0.06 OUR FIT	Error includes scale factor of 11.5.			
0.20 ± 0.07 OUR AVERAGE	Signs on measurements were ignored. Error includes scale factor of 10.7. See the ideogram below.			
−0.06 ± 0.01	ZHANG	13A	DPWA	Multichannel
−0.305 ± 0.010	[1] CAMERON	77	DPWA	$K^-p \rightarrow \Lambda(1520)\pi^0$
0.31 ± 0.02	BARLETTA	72	DPWA	$K^-p \rightarrow \Lambda(1520)\pi^0$
0.27 ± 0.03	ARMENTEROS	65C	HBC	$K^-p \rightarrow \Lambda(1520)\pi^0$

[1] This rate combines P-wave- and F-wave decays. The CAMERON 77 results for the separate P-wave- and F-wave decays are -0.303 ± 0.010 and -0.037 ± 0.014. The published signs have been changed here to be in accord with the baryon-first convention.

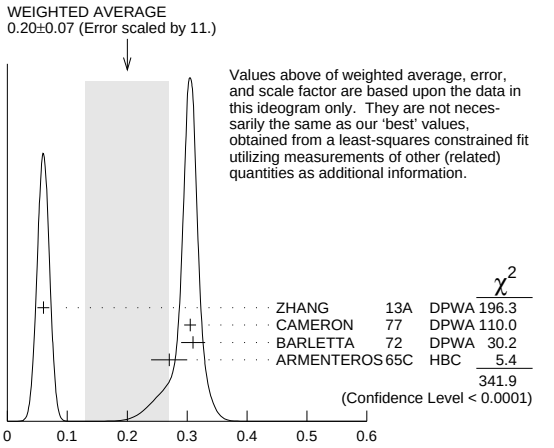

$(\Gamma_i\Gamma_f)^{1/2}/\Gamma_{total}$ in $N\overline{K} \rightarrow \Sigma(1775) \rightarrow \Lambda(1520)\pi$, P-wave

$(\Gamma_i\Gamma_f)^{1/2}/\Gamma_{total}$ in $N\overline{K} \rightarrow \Sigma(1775) \rightarrow \Delta(1232)\overline{K}$, D-wave — $(\Gamma_1\Gamma_{10})^{1/2}/\Gamma$

VALUE	DOCUMENT ID		TECN	COMMENT
+0.06 ± 0.03	ZHANG	13A	DPWA	Multichannel

$(\Gamma_i\Gamma_f)^{1/2}/\Gamma_{total}$ in $N\overline{K} \rightarrow \Sigma(1775) \rightarrow N\overline{K}^*(892)$, S=1/2 — $(\Gamma_1\Gamma_{11})^{1/2}/\Gamma$

VALUE	DOCUMENT ID		TECN	COMMENT
+0.04 ± 0.01	ZHANG	13A	DPWA	Multichannel

$(\Gamma_i\Gamma_f)^{1/2}/\Gamma_{total}$ in $N\overline{K} \rightarrow \Sigma(1775) \rightarrow N\overline{K}^*(892)$, S=3/2, D-wave — $(\Gamma_1\Gamma_{13})^{1/2}/\Gamma$

VALUE	DOCUMENT ID		TECN	COMMENT
+0.04 ± 0.01	ZHANG	13A	DPWA	Multichannel

$\Sigma(1775)$ REFERENCES

KAMANO	15	PR C92 025205	H. Kamano *et al.*	(ANL, OSAK)
ZHANG	13A	PR C88 035205	H. Zhang *et al.*	(KSU)
PDG	82	PL 111B 1	M. Roos *et al.*	(HELS, CIT, CERN)
GOPAL	80	Toronto Conf. 159	G.P. Gopal	(RHEL) IJP
ALSTON-...	78	PR D18 182	M. Alston-Garnjost *et al.*	(LBL, MTHO+) IJP
Also		PRL 38 1007	M. Alston-Garnjost *et al.*	(LBL, MTHO+) IJP
CAMERON	78	NP B143 189	W. Cameron *et al.*	(RHEL, LOIC) IJP
CAMERON	77	NP B131 399	W. Cameron *et al.*	(RHEL, LOIC) IJP
GOPAL	77	NP B119 362	G.P. Gopal *et al.*	(LOIC, RHEL) IJP
MARTIN	77	NP B127 349	B.R. Martin, M.K. Pidcock, R.G. Moorhouse	(LOUC+) IJP
Also		NP B126 266	B.R. Martin, M.K. Pidcock	(LOUC)
Also		NP B126 285	B.R. Martin, M.K. Pidcock	(LOUC) IJP
DEBELLEFON	76	NP B109 129	A. de Bellefon, A. Berthon	(CDEF) IJP
BAILLON	75	NP B94 39	P.H. Baillon, P.J. Litchfield	(CERN, RHEL) IJP
VANHORN	75	NP B87 145	A.J. van Horn	(LBL) IJP
Also		NP B87 157	A.J. van Horn	(LBL) IJP
DEVENISH	74B	NP B81 330	R.C.E. Devenish, C.D. Froggatt, B.R. Martin	(DESY+)
KANE	74	LBL-2452	D.F. Kane	(LBL) IJP
PREVOST	74	NP B69 246	J. Prevost *et al.*	(SACL, CERN, HEID)
BARLETTA	72	NP B40 45	W.A. Barletta	(EFI) IJP
Also		PRL 17 841	S. Fenster *et al.*	(CHIC, ANL, CERN) IJP
ARMENTEROS	68C	NP B8 216	R. Armenteros *et al.*	(CERN, HEID, SACL) I
SIMS	68	PRL 21 1413	W.H. Sims *et al.*	(FSU, TUFTS, BRAN)
ARMENTEROS	67C	ZPHY 202 486	R. Armenteros *et al.*	(CERN, HEID, SACL)
UHLIG	67	PR 155 1448	R.P. Uhlig *et al.*	(UMD, NRL)
ARMENTEROS	65C	PL 19 338	R. Armenteros *et al.*	(CERN, HEID, SACL) IJP
GALTIERI	63	PL 6 296	A. Galtieri, A. Hussain, R. Tripp	(LRL) IJ

$\Sigma(1840)\ 3/2^+$

$I(J^P) = 1(\frac{3}{2}^+)$ Status: *

OMITTED FROM SUMMARY TABLE

For the time being, we list together here all resonance claims in the P_{13} wave between 1700 and 1900 MeV.

$\Sigma(1840)$ MASS

VALUE (MeV)	DOCUMENT ID		TECN	COMMENT
≈ 1840 OUR ESTIMATE				
1798 or 1802	[1] MARTIN	77	DPWA	$\overline{K}N$ multichannel
1720 ± 30	[2] BAILLON	75	IPWA	$\overline{K}N \rightarrow \Lambda\pi$
1925 ± 200	VANHORN	75	DPWA	$K^-p \rightarrow \Lambda\pi^0$
1840 ± 10	LANGBEIN	72	IPWA	$\overline{K}N$ multichannel

$\Sigma(1840)$ WIDTH

VALUE (MeV)	DOCUMENT ID		TECN	COMMENT
93 or 93	[1] MARTIN	77	DPWA	$\overline{K}N$ multichannel
120 ± 30	[2] BAILLON	75	IPWA	$\overline{K}N \rightarrow \Lambda\pi$
65^{+50}_{-20}	VANHORN	75	DPWA	$K^-p \rightarrow \Lambda\pi^0$
120 ± 10	LANGBEIN	72	IPWA	$\overline{K}N$ multichannel

$\Sigma(1840)$ DECAY MODES

	Mode
Γ_1	$N\overline{K}$
Γ_2	$\Lambda\pi$
Γ_3	$\Sigma\pi$

$\Sigma(1840)$ BRANCHING RATIOS

See "Sign conventions for resonance couplings" in the Note on Λ and Σ Resonances.

$\Gamma(N\overline{K})/\Gamma_{total}$ Γ_1/Γ

VALUE	DOCUMENT ID		TECN	COMMENT
0 or 0	[1] MARTIN	77	DPWA	$\overline{K}N$ multichannel
0.37±0.13	LANGBEIN	72	IPWA	$\overline{K}N$ multichannel

$(\Gamma_i\Gamma_f)^{1/2}/\Gamma_{total}$ in $N\overline{K}\to\Sigma(1840)\to\Lambda\pi$ $(\Gamma_1\Gamma_2)^{1/2}/\Gamma$

VALUE	DOCUMENT ID		TECN	COMMENT
+0.03 or +0.03	[1] MARTIN	77	DPWA	$\overline{K}N$ multichannel
+0.11 ±0.02	[2] BAILLON	75	IPWA	$\overline{K}N\to\Lambda\pi$
+0.06 ±0.04	VANHORN	75	DPWA	$K^-p\to\Lambda\pi^0$
+0.122±0.078	DEVENISH	74B		Fixed-t dispersion rel.
0.20 ±0.04	LANGBEIN	72	IPWA	$\overline{K}N$ multichannel

$(\Gamma_i\Gamma_f)^{1/2}/\Gamma_{total}$ in $N\overline{K}\to\Sigma(1840)\to\Sigma\pi$ $(\Gamma_1\Gamma_3)^{1/2}/\Gamma$

VALUE	DOCUMENT ID		TECN	COMMENT
−0.04 or −0.04	[1] MARTIN	77	DPWA	$\overline{K}N$ multichannel
0.15±0.04	LANGBEIN	72	IPWA	$\overline{K}N$ multichannel

$\Sigma(1840)$ FOOTNOTES

[1] The two MARTIN 77 values are from a T-matrix pole and from a Breit-Wigner fit.
[2] From solution 1 of BAILLON 75; not present in solution 2.

$\Sigma(1840)$ REFERENCES

MARTIN	77	NP B127 349	B.R. Martin, M.K. Pidcock, R.G. Moorhouse	(LOUC+) IJP
Also		NP B126 266	B.R. Martin, M.K. Pidcock	(LOUC)
Also		NP B126 285	B.R. Martin, M.K. Pidcock	(LOUC) IJP
BAILLON	75	NP B94 39	P.H. Baillon, P.J. Litchfield	(CERN, RHEL) IJP
VANHORN	75	NP B87 145	A.J. van Horn	(LBL) IJP
Also		NP B87 157	A.J. van Horn	(LBL) IJP
DEVENISH	74B	NP B81 330	R.C.E. Devenish, C.D. Froggatt, B.R. Martin	(DESY+)
LANGBEIN	72	NP B47 477	W. Langbein, F. Wagner	(MPIM) IJP

$\Sigma(1880)$ $1/2^+$

$I(J^P) = 1(\frac{1}{2}^+)$ Status: **

OMITTED FROM SUMMARY TABLE

A P_{11} resonance is suggested by several partial-wave analyses, but with wide variations in the mass and other parameters. We list here all claims which lie well above the P_{11} $\Sigma(1770)$.

$\Sigma(1880)$ POLE POSITION

REAL PART

VALUE (MeV)	DOCUMENT ID		TECN	COMMENT
• • • We do not use the following data for averages, fits, limits, etc. • • •				
1776	ZHANG	13A	DPWA	Multichannel

−2×IMAGINARY PART

VALUE (MeV)	DOCUMENT ID		TECN	COMMENT
• • • We do not use the following data for averages, fits, limits, etc. • • •				
270	ZHANG	13A	DPWA	Multichannel

$\Sigma(1880)$ MASS

VALUE (MeV)	DOCUMENT ID		TECN	COMMENT
≈ 1880 OUR ESTIMATE				
1821±17	ZHANG	13A	DPWA	Multichannel
1826±20	GOPAL	80	DPWA	$\overline{K}N\to\overline{K}N$
1870±10	CAMERON	78B	DPWA	$K^-p\to N\overline{K}^*$
1847 or 1863	[1] MARTIN	77	DPWA	$\overline{K}N$ multichannel
1960±30	[2] BAILLON	75	IPWA	$\overline{K}N\to\Lambda\pi$
1985±50	VANHORN	75	DPWA	$K^-p\to\Lambda\pi^0$
1898	[3] LEA	73	DPWA	Multichannel K-matrix
∼ 1850	ARMENTEROS	70	IPWA	$\overline{K}N\to\overline{K}N$
1950±50	BARBARO-...	70	DPWA	$K^-N\to\Lambda\pi$
1920±30	LITCHFIELD	70	DPWA	$K^-N\to\Lambda\pi$
1850	BAILEY	69	DPWA	$\overline{K}N\to\overline{K}N$
1882±40	SMART	68	DPWA	$K^-N\to\Lambda\pi$

$\Sigma(1880)$ WIDTH

VALUE (MeV)	DOCUMENT ID		TECN	COMMENT
300± 59	ZHANG	13A	DPWA	Multichannel
86± 15	GOPAL	80	DPWA	$\overline{K}N\to\overline{K}N$
80± 10	CAMERON	78B	DPWA	$K^-p\to N\overline{K}^*$
216 or 220	[1] MARTIN	77	DPWA	$\overline{K}N$ multichannel
260± 40	[2] BAILLON	75	IPWA	$\overline{K}N\to\Lambda\pi$
220±140	VANHORN	75	DPWA	$K^-p\to\Lambda\pi^0$
222	[3] LEA	73	DPWA	Multichannel K-matrix
∼ 30	ARMENTEROS	70	IPWA	$\overline{K}N\to\overline{K}N$
200± 50	BARBARO-...	70	DPWA	$K^-N\to\Lambda\pi$
170± 40	LITCHFIELD	70	DPWA	$K^-N\to\Lambda\pi$
200	BAILEY	69	DPWA	$\overline{K}N\to\overline{K}N$
222±150	SMART	68	DPWA	$K^-N\to\Lambda\pi$

$\Sigma(1880)$ DECAY MODES

	Mode	Fraction (Γ_j/Γ)
Γ_1	$N\overline{K}$	
Γ_2	$\Lambda\pi$	
Γ_3	$\Sigma\pi$	
Γ_4	$\Lambda(1520)\pi$, D-wave	(2.0±1.0) %
Γ_5	$N\overline{K}^*(892)$, S=1/2, P-wave	
Γ_6	$N\overline{K}^*(892)$, S=3/2, P-wave	
Γ_7	$\Delta(1232)\overline{K}$, P-wave	(39 ±8) %

$\Sigma(1880)$ BRANCHING RATIOS

See "Sign conventions for resonance couplings" in the Note on Λ and Σ Resonances.

$\Gamma(N\overline{K})/\Gamma_{total}$ Γ_1/Γ

VALUE	DOCUMENT ID		TECN	COMMENT
0.10±0.03	ZHANG	13A	DPWA	Multichannel
0.06±0.02	GOPAL	80	DPWA	$\overline{K}N\to\overline{K}N$
0.27 or 0.27	[1] MARTIN	77	DPWA	$\overline{K}N$ multichannel
0.31	[3] LEA	73	DPWA	Multichannel K-matrix
0.20	ARMENTEROS	70	IPWA	$\overline{K}N\to\overline{K}N$
0.22	BAILEY	69	DPWA	$\overline{K}N\to\overline{K}N$

$(\Gamma_i\Gamma_f)^{1/2}/\Gamma_{total}$ in $N\overline{K}\to\Sigma(1880)\to\Lambda\pi$ $(\Gamma_1\Gamma_2)^{1/2}/\Gamma$

VALUE	DOCUMENT ID		TECN	COMMENT
−0.24 or −0.24	[1] MARTIN	77	DPWA	$\overline{K}N$ multichannel
−0.12 ±0.02	[2] BAILLON	75	IPWA	$\overline{K}N\to\Lambda\pi$
$+0.05\ {}^{+0.07}_{-0.02}$	VANHORN	75	DPWA	$K^-p\to\Lambda\pi^0$
−0.169±0.119	DEVENISH	74B		Fixed-t dispersion rel.
−0.30	[3] LEA	73	DPWA	Multichannel K-matrix
−0.09 ±0.04	BARBARO-...	70	DPWA	$K^-N\to\Lambda\pi$
−0.14 ±0.03	LITCHFIELD	70	DPWA	$K^-N\to\Lambda\pi$
−0.11 ±0.03	SMART	68	DPWA	$K^-N\to\Lambda\pi$

$(\Gamma_i\Gamma_f)^{1/2}/\Gamma_{total}$ in $N\overline{K}\to\Sigma(1880)\to\Sigma\pi$ $(\Gamma_1\Gamma_3)^{1/2}/\Gamma$

VALUE	DOCUMENT ID		TECN	COMMENT
+0.30 or +0.29	[1] MARTIN	77	DPWA	$\overline{K}N$ multichannel
not seen	[3] LEA	73	DPWA	Multichannel K-matrix

$\Gamma(\Lambda(1520)\pi, D\text{-wave})/\Gamma_{total}$ Γ_4/Γ

VALUE	DOCUMENT ID		TECN	COMMENT
0.02±0.01	ZHANG	13A	DPWA	Multichannel

$(\Gamma_i\Gamma_f)^{1/2}/\Gamma_{total}$ in $N\overline{K}\to\Sigma(1880)\to N\overline{K}^*(892)$, S=1/2, P-wave $(\Gamma_1\Gamma_5)^{1/2}/\Gamma$

VALUE	DOCUMENT ID		TECN	COMMENT
−0.05±0.03	[4] CAMERON	78B	DPWA	$K^-p\to N\overline{K}^*$

$(\Gamma_i\Gamma_f)^{1/2}/\Gamma_{total}$ in $N\overline{K}\to\Sigma(1880)\to N\overline{K}^*(892)$, S=3/2, P-wave $(\Gamma_1\Gamma_6)^{1/2}/\Gamma$

VALUE	DOCUMENT ID		TECN	COMMENT
+0.11±0.03	CAMERON	78B	DPWA	$K^-p\to N\overline{K}^*$

$\Gamma(\Delta(1232)\overline{K}, P\text{-wave})/\Gamma_{total}$ Γ_7/Γ

VALUE	DOCUMENT ID		TECN	COMMENT
0.39±0.08	ZHANG	13A	DPWA	Multichannel

$\Sigma(1880)$ FOOTNOTES

[1] The two MARTIN 77 values are from a T-matrix pole and from a Breit-Wigner fit.
[2] From solution 1 of BAILLON 75; not present in solution 2.
[3] Only unconstrained states from table 1 of LEA 73 are listed.
[4] The published sign has been changed to be in accord with the baryon-first convention.

Baryon Particle Listings

$\Sigma(1880)$, $\Sigma(1900)$, $\Sigma(1915)$

$\Sigma(1880)$ REFERENCES

ZHANG	13A	PR C88 035205	H. Zhang *et al.*	(KSU)
GOPAL	80	Toronto Conf. 159	G.P. Gopal	(RHEL) IJP
CAMERON	78B	NP B146 327	W. Cameron *et al.*	(RHEL, LOIC) IJP
MARTIN	77	NP B127 349	B.R. Martin, M.K. Pidcock, R.G. Moorhouse	(LOUC+) IJP
Also		NP B126 266	B.R. Martin, M.K. Pidcock	(LOUC)
Also		NP B126 285	B.R. Martin, M.K. Pidcock	(LOUC) IJP
BAILLON	75	NP B94 39	P.H. Baillon, P.J. Litchfield	(CERN, RHEL) IJP
VANHORN	75	NP B87 145	A.J. van Horn	(LBL) IJP
Also		NP B87 157	A.J. van Horn	(LBL) IJP
DEVENISH	74B	NP B81 330	R.C.E. Devenish, C.D. Froggatt, B.R. Martin	(DESY+)
LEA	73	NP B56 77	A.T. Lea *et al.*	(RHEL, LOUC, GLAS, AARH) IJP
ARMENTEROS	70	Duke Conf. 123 Hyperon Resonances, 1970	R. Armenteros *et al.*	(CERN, HEID, SACL) IJP
BARBARO-...	70	Duke Conf. 173 Hyperon Resonances, 1970	A. Barbaro-Galtieri	(LRL) IJP
LITCHFIELD	70	NP B22 269	P.J. Litchfield	(RHEL) IJP
BAILEY	69	Thesis UCRL 50617	J.M. Bailey	(LLL) IJP
SMART	68	PR 169 1330	W.M. Smart	(LRL) IJP

$\Sigma(1900)\ 1/2^-$

$I(J^P) = 1(\frac{1}{2}^-)$ Status: *

OMITTED FROM SUMMARY TABLE

$\Sigma(1900)$ MASS

VALUE (MeV)	DOCUMENT ID		TECN	COMMENT
1900±21	ZHANG	13A	DPWA	Multichannel

$\Lambda(1900)$ WIDTH

VALUE (MeV)	DOCUMENT ID		TECN	COMMENT
191±47	ZHANG	13A	DPWA	Multichannel

$\Sigma(1900)$ DECAY MODES

	Mode	Fraction (Γ_i/Γ)
Γ_1	$N\overline{K}$	(67±17) %
Γ_2	$\Sigma\pi$	(10± 5) %

$\Sigma(1900)$ BRANCHING RATIOS

$\Gamma(N\overline{K})/\Gamma_{total}$ **Γ_1/Γ**

VALUE	DOCUMENT ID		TECN	COMMENT
0.67±0.17	ZHANG	13A	DPWA	Multichannel

$\Gamma(\Sigma\pi)/\Gamma_{total}$ **Γ_2/Γ**

VALUE	DOCUMENT ID		TECN	COMMENT
0.10±0.05	ZHANG	13A	DPWA	Multichannel

$\Sigma(1900)$ REFERENCES

ZHANG	13A	PR C88 035205	H. Zhang *et al.*	(KSU)

$\Sigma(1915)\ 5/2^+$

$I(J^P) = 1(\frac{5}{2}^+)$ Status: ****

Discovered by COOL 66. For results published before 1974 (they are now obsolete), see our 1982 edition Physics Letters **111B** 1 (1982).

This entry only includes results from partial-wave analyses. Parameters of peaks seen in cross sections and invariant-mass distributions in this region used to be listed in in a separate entry immediately following. They may be found in our 1986 edition Physics Letters **170B** 1 (1986).

$\Sigma(1915)$ POLE POSITION

REAL PART

VALUE (MeV)	DOCUMENT ID		TECN	COMMENT
1890^{+3}_{-2}	[1] KAMANO	15	DPWA	Multichannel
• • • We do not use the following data for averages, fits, limits, etc. • • •				
1897	ZHANG	13A	DPWA	Multichannel

[1] From the preferred solution A in KAMANO 15.

$-2\times$IMAGINARY PART

VALUE (MeV)	DOCUMENT ID		TECN	COMMENT
97^{+4}_{-6}	[1] KAMANO	15	DPWA	Multichannel
• • • We do not use the following data for averages, fits, limits, etc. • • •				
133	ZHANG	13A	DPWA	Multichannel

[1] From the preferred solution A in KAMANO 15.

$\Sigma(1915)$ POLE RESIDUES

The normalized residue is the residue divided by $\Gamma_{pole}/2$.

Normalized residue in $N\overline{K} \to \Sigma(1915) \to N\overline{K}$

MODULUS	PHASE (°)	DOCUMENT ID		TECN	COMMENT
• • • We do not use the following data for averages, fits, limits, etc. • • •					
0.0391	−15	[1] KAMANO	15	DPWA	Multichannel

[1] From the preferred solution A in KAMANO 15.

Normalized residue in $N\overline{K} \to \Sigma(1915) \to \Sigma\pi$

MODULUS	PHASE (°)	DOCUMENT ID		TECN	COMMENT
• • • We do not use the following data for averages, fits, limits, etc. • • •					
0.157	157	[1] KAMANO	15	DPWA	Multichannel

[1] From the preferred solution A in KAMANO 15.

Normalized residue in $N\overline{K} \to \Sigma(1915) \to \Lambda\pi$

MODULUS	PHASE (°)	DOCUMENT ID		TECN	COMMENT
• • • We do not use the following data for averages, fits, limits, etc. • • •					
0.0757	166	[1] KAMANO	15	DPWA	Multichannel

[1] From the preferred solution A in KAMANO 15.

Normalized residue in $N\overline{K} \to \Sigma(1915) \to \Xi K$

MODULUS	PHASE (°)	DOCUMENT ID		TECN	COMMENT
• • • We do not use the following data for averages, fits, limits, etc. • • •					
0.002	−88	[1] KAMANO	15	DPWA	Multichannel

[1] From the preferred solution A in KAMANO 15.

Normalized residue in $N\overline{K} \to \Lambda(1915) \to \Sigma(1385)\pi$, P-wave

MODULUS	PHASE (°)	DOCUMENT ID		TECN	COMMENT
• • • We do not use the following data for averages, fits, limits, etc. • • •					
0.0724	161	[1] KAMANO	15	DPWA	Multichannel

[1] From the preferred solution A in KAMANO 15.

Normalized residue in $N\overline{K} \to \Lambda(1915) \to \Sigma(1385)\pi$, F-wave

MODULUS	PHASE (°)	DOCUMENT ID		TECN	COMMENT
• • • We do not use the following data for averages, fits, limits, etc. • • •					
0.0162	−163	[1] KAMANO	15	DPWA	Multichannel

[1] From the preferred solution A in KAMANO 15.

Normalized residue in $N\overline{K} \to \Sigma(1915) \to N\overline{K}^*(892)$, S=1/2 , F-wave

MODULUS	PHASE (°)	DOCUMENT ID		TECN	COMMENT
• • • We do not use the following data for averages, fits, limits, etc. • • •					
0.00476	4	[1] KAMANO	15	DPWA	Multichannel

[1] From the preferred solution A in KAMANO 15.

Normalized residue in $N\overline{K} \to \Sigma(1915) \to N\overline{K}^*(892)$, S=3/2 , P-wave

MODULUS	PHASE (°)	DOCUMENT ID		TECN	COMMENT
• • • We do not use the following data for averages, fits, limits, etc. • • •					
0.0494	51	[1] KAMANO	15	DPWA	Multichannel

[1] From the preferred solution A in KAMANO 15.

Normalized residue in $N\overline{K} \to \Sigma(1915) \to N\overline{K}^*(892)$, S=3/2 , F-wave

MODULUS	PHASE (°)	DOCUMENT ID		TECN	COMMENT
• • • We do not use the following data for averages, fits, limits, etc. • • •					
0.000314	16	[1] KAMANO	15	DPWA	Multichannel

[1] From the preferred solution A in KAMANO 15.

$\Sigma(1915)$ MASS

VALUE (MeV)	DOCUMENT ID		TECN	COMMENT
1900 to 1935 (≈ 1915) OUR ESTIMATE				
1920± 7	ZHANG	13A	DPWA	Multichannel
1937±20	ALSTON-...	78	DPWA	$\overline{K}N \to \overline{K}N$
1894± 5	[1] CORDEN	77C		$K^-n \to \Sigma\pi$
1909± 5	[1] CORDEN	77C		$K^-n \to \Sigma\pi$
1920±10	GOPAL	77	DPWA	$\overline{K}N$ multichannel
1900± 4	[2] CORDEN	76	DPWA	$K^-n \to \Lambda\pi^-$
1920±30	BAILLON	75	IPWA	$\overline{K}N \to \Lambda\pi$
1914±10	HEMINGWAY	75	DPWA	$K^-p \to \overline{K}N$
1920^{+15}_{-20}	VANHORN	75	DPWA	$K^-p \to \Lambda\pi^0$
1920± 5	KANE	74	DPWA	$K^-p \to \Sigma\pi$
• • • We do not use the following data for averages, fits, limits, etc. • • •				
not seen	DECLAIS	77	DPWA	$\overline{K}N \to \overline{K}N$
1925 or 1933	[3] MARTIN	77	DPWA	$\overline{K}N$ multichannel
1915	DEBELLEFON	76	IPWA	$K^-p \to \Lambda\pi^0$

[1] The two entries for CORDEN 77C are from two different acceptable solutions.
[2] Preferred solution 3; see CORDEN 76 for other possibilities.

[3] The two MARTIN 77 values are from a T-matrix pole and from a Breit-Wigner fit.

$\Sigma(1915)$ WIDTH

VALUE (MeV)	DOCUMENT ID		TECN	COMMENT
80 to 160 (≈ 120) OUR ESTIMATE				
149±17	ZHANG	13A	DPWA	Multichannel
161±20	ALSTON-...	78	DPWA	$\overline{K}N \rightarrow \overline{K}N$
107±14	[1] CORDEN	77C		$K^-n \rightarrow \Sigma\pi$
85±13	[1] CORDEN	77C		$K^-n \rightarrow \Sigma\pi$
130±10	GOPAL	77	DPWA	$\overline{K}N$ multichannel
75±14	[2] CORDEN	76	DPWA	$K^-n \rightarrow \Lambda\pi^-$
70±20	BAILLON	75	IPWA	$\overline{K}N \rightarrow \Lambda\pi$
85±15	HEMINGWAY	75	DPWA	$K^-p \rightarrow \overline{K}N$
102±18	VANHORN	75	DPWA	$K^-p \rightarrow \Lambda\pi^0$
162±25	KANE	74	DPWA	$K^-p \rightarrow \Sigma\pi$
• • • We do not use the following data for averages, fits, limits, etc. • • •				
171 or 173	[3] MARTIN	77	DPWA	$\overline{K}N$ multichannel
60	DEBELLEFON	76	IPWA	$K^-p \rightarrow \Lambda\pi^0$

[1] The two entries for CORDEN 77C are from two different acceptable solutions.
[2] Preferred solution 3; see CORDEN 76 for other possibilities.
[3] The two MARTIN 77 values are from a T-matrix pole and from a Breit-Wigner fit.

$\Sigma(1915)$ DECAY MODES

	Mode	Fraction (Γ_i/Γ)
Γ_1	$N\overline{K}$	5–15 %
Γ_2	$\Lambda\pi$	seen
Γ_3	$\Sigma\pi$	seen
Γ_4	ΞK	
Γ_5	$\Sigma(1385)\pi$, P-wave	
Γ_6	$\Sigma(1385)\pi$, F-wave	
Γ_7	$\Sigma(1385)\pi$	<5 %
Γ_8	$\Sigma(1385)\pi$, P-wave	
Γ_9	$\Sigma(1385)\pi$, F-wave	
Γ_{10}	$N\overline{K}^*(892)$, S=1/2, F-wave	
Γ_{11}	$N\overline{K}^*(892)$, S=3/2, P-wave	
Γ_{12}	$N\overline{K}^*(892)$, S=3/2, F-wave	

$\Sigma(1915)$ BRANCHING RATIOS

See "Sign conventions for resonance couplings" in the Note on Λ and Σ Resonances.

$\Gamma(N\overline{K})/\Gamma_{total}$ Γ_1/Γ

VALUE	DOCUMENT ID		TECN	COMMENT
0.05 to 0.15 OUR ESTIMATE				
0.026±0.004	ZHANG	13A	DPWA	Multichannel
0.03 ±0.02	[1] GOPAL	80	DPWA	$\overline{K}N \rightarrow \overline{K}N$
0.14 ±0.05	ALSTON-...	78	DPWA	$\overline{K}N \rightarrow \overline{K}N$
0.11 ±0.04	HEMINGWAY	75	DPWA	$K^-p \rightarrow \overline{K}N$
• • • We do not use the following data for averages, fits, limits, etc. • • •				
0.036	[2] KAMANO	15	DPWA	Multichannel
0.05 ±0.03	GOPAL	77	DPWA	See GOPAL 80
0.08 or 0.08	[3] MARTIN	77	DPWA	$\overline{K}N$ multichannel

[1] The mass and width are fixed to the GOPAL 77 values due to the low elasticity.
[2] From the preferred solution A in KAMANO 15.
[3] The two MARTIN 77 values are from a T-matrix pole and from a Breit-Wigner fit.

$\Gamma(\Lambda\pi)/\Gamma_{total}$ Γ_2/Γ

VALUE	DOCUMENT ID		TECN	COMMENT
• • • We do not use the following data for averages, fits, limits, etc. • • •				
0.127	[1] KAMANO	15	DPWA	Multichannel

[1] From the preferred solution A in KAMANO 15.

$\Gamma(\Sigma\pi)/\Gamma_{total}$ Γ_3/Γ

VALUE	DOCUMENT ID		TECN	COMMENT
• • • We do not use the following data for averages, fits, limits, etc. • • •				
0.678	[1] KAMANO	15	DPWA	Multichannel

[1] From the preferred solution A in KAMANO 15.

$\Gamma(\Xi K)/\Gamma_{total}$ Γ_4/Γ

VALUE	DOCUMENT ID		TECN	COMMENT
• • • We do not use the following data for averages, fits, limits, etc. • • •				
not seen	[1] KAMANO	15	DPWA	Multichannel

[1] From the preferred solution A in KAMANO 15.

$\Gamma(\Sigma(1385)\pi$, P-wave$)/\Gamma_{total}$ Γ_5/Γ

VALUE	DOCUMENT ID		TECN	COMMENT
• • • We do not use the following data for averages, fits, limits, etc. • • •				
0.112	[1] KAMANO	15	DPWA	Multichannel

[1] From the preferred solution A in KAMANO 15.

$\Gamma(\Sigma(1385)\pi$, F-wave$)/\Gamma_{total}$ Γ_6/Γ

VALUE	DOCUMENT ID		TECN	COMMENT
• • • We do not use the following data for averages, fits, limits, etc. • • •				
0.004	[1] KAMANO	15	DPWA	Multichannel

[1] From the preferred solution A in KAMANO 15.

$\Gamma(N\overline{K}^*(892)$, S=1/2, F-wave$)/\Gamma_{total}$ Γ_{10}/Γ

VALUE	DOCUMENT ID		TECN	COMMENT
• • • We do not use the following data for averages, fits, limits, etc. • • •				
0.001	[1] KAMANO	15	DPWA	Multichannel

[1] From the preferred solution A in KAMANO 15.

$\Gamma(N\overline{K}^*(892)$, S=3/2, P-wave$)/\Gamma_{total}$ Γ_{11}/Γ

VALUE	DOCUMENT ID		TECN	COMMENT
• • • We do not use the following data for averages, fits, limits, etc. • • •				
0.042	[1] KAMANO	15	DPWA	Multichannel

[1] From the preferred solution A in KAMANO 15.

$\Gamma(N\overline{K}^*(892)$, S=3/2, F-wave$)/\Gamma_{total}$ Γ_{12}/Γ

VALUE	DOCUMENT ID		TECN	COMMENT
• • • We do not use the following data for averages, fits, limits, etc. • • •				
not seen	[1] KAMANO	15	DPWA	Multichannel

[1] From the preferred solution A in KAMANO 15.

$(\Gamma_i\Gamma_f)^{1/2}/\Gamma_{total}$ in $N\overline{K} \rightarrow \Sigma(1915) \rightarrow \Lambda\pi$ $(\Gamma_1\Gamma_2)^{1/2}/\Gamma$

VALUE	DOCUMENT ID		TECN	COMMENT
−0.09 ±0.03	GOPAL	77	DPWA	$\overline{K}N$ multichannel
−0.10 ±0.01	[1] CORDEN	76	DPWA	$K^-n \rightarrow \Lambda\pi^-$
−0.06 ±0.02	BAILLON	75	IPWA	$\overline{K}N \rightarrow \Lambda\pi$
−0.09 ±0.02	VANHORN	75	DPWA	$K^-p \rightarrow \Lambda\pi^0$
−0.087±0.056	DEVENISH	74B		Fixed-t dispersion rel.
• • • We do not use the following data for averages, fits, limits, etc. • • •				
−0.09 or −0.09	[2] MARTIN	77	DPWA	$\overline{K}N$ multichannel
−0.10	DEBELLEFON	76	IPWA	$K^-p \rightarrow \Lambda\pi^0$

[1] Preferred solution 3; see CORDEN 76 for other possibilities.
[2] The two MARTIN 77 values are from a T-matrix pole and from a Breit-Wigner fit.

$(\Gamma_i\Gamma_f)^{1/2}/\Gamma_{total}$ in $N\overline{K} \rightarrow \Sigma(1915) \rightarrow \Sigma\pi$ $(\Gamma_1\Gamma_3)^{1/2}/\Gamma$

VALUE	DOCUMENT ID		TECN	COMMENT
−0.14±0.01	ZHANG	13A	DPWA	Multichannel
−0.17±0.01	[1] CORDEN	77C		$K^-n \rightarrow \Sigma\pi$
−0.15±0.02	[1] CORDEN	77C		$K^-n \rightarrow \Sigma\pi$
−0.19±0.03	GOPAL	77	DPWA	$\overline{K}N$ multichannel
−0.16±0.03	KANE	74	DPWA	$K^-p \rightarrow \Sigma\pi$
• • • We do not use the following data for averages, fits, limits, etc. • • •				
−0.05 or −0.05	[2] MARTIN	77	DPWA	$\overline{K}N$ multichannel

[1] The two entries for CORDEN 77C are from two different acceptable solutions.
[2] The two MARTIN 77 values are from a T-matrix pole and from a Breit-Wigner fit.

$(\Gamma_i\Gamma_f)^{1/2}/\Gamma_{total}$ in $N\overline{K} \rightarrow \Sigma(1915) \rightarrow \Sigma(1385)\pi$, P-wave $(\Gamma_1\Gamma_8)^{1/2}/\Gamma$

VALUE	DOCUMENT ID		TECN	COMMENT
<0.01	CAMERON	78	DPWA	$K^-p \rightarrow \Sigma(1385)\pi$

$(\Gamma_i\Gamma_f)^{1/2}/\Gamma_{total}$ in $N\overline{K} \rightarrow \Sigma(1915) \rightarrow \Sigma(1385)\pi$, F-wave $(\Gamma_1\Gamma_9)^{1/2}/\Gamma$

VALUE	DOCUMENT ID		TECN	COMMENT
+0.06 ±0.02	ZHANG	13A	DPWA	Multichannel
+0.039±0.009	[1] CAMERON	78	DPWA	$K^-p \rightarrow \Sigma(1385)\pi$

[1] The published sign has been changed to be in accord with the baryon-first convention.

$\Sigma(1915)$ REFERENCES

KAMANO	15	PR C92 025205	H. Kamano *et al.*	(ANL, OSAK)
ZHANG	13A	PR C88 035205	H. Zhang *et al.*	(KSU)
PDG	86	PL 170B 1	M. Aguilar-Benitez *et al.*	(CERN, CIT+)
PDG	82	PL 111B 1	M. Roos *et al.*	(HELS, CIT, CERN)
GOPAL	80	Toronto Conf. 159	G.P. Gopal	(RHEL) IJP
ALSTON-...	78	PR D18 182	M. Alston-Garnjost *et al.*	(LBL, MTHO+) IJP
Also		PRL 38 1007	M. Alston-Garnjost *et al.*	(LBL, MTHO+) IJP
CAMERON	78	NP B143 189	W. Cameron *et al.*	(RHEL, LOIC) IJP
CORDEN	77C	NP B125 61	M.J. Corden *et al.*	(BIRM) IJP
DECLAIS	77	CERN 77-16	Y. Declais *et al.*	(CAEN, CERN) IJP
GOPAL	77	NP B119 362	G.P. Gopal *et al.*	(LOIC, RHEL) IJP
MARTIN	77	NP B127 349	B.R. Martin, M.K. Pidcock, R.G. Moorhouse	(LOUC+) IJP
Also		NP B126 266	B.R. Martin, M.K. Pidcock	(LOUC)
Also		NP B126 285	B.R. Martin, M.K. Pidcock	(LOUC) IJP
CORDEN	76	NP B104 382	M.J. Corden *et al.*	(BIRM) IJP
DEBELLEFON	76	NP B109 129	A. de Bellefon, A. Berthon	(CDEF) IJP
BAILLON	75	NP B94 39	P.H. Baillon, P.J. Litchfield	(CERN, RHEL) IJP
HEMINGWAY	75	NP B91 12	R.J. Hemingway *et al.*	(CERN, HEIDH, MPIM) IJP
VANHORN	75	NP B87 145	A.J. van Horn	(LBL) IJP
Also		NP B87 157	A.J. van Horn	(LBL) IJP
DEVENISH	74B	NP B81 330	R.C.E. Devenish, C.D. Froggatt, B.R. Martin	(DESY+)
KANE	74	LBL-2452	D.F. Kane	(LBL) IJP
COOL	66	PRL 16 1228	R.L. Cool *et al.*	(BNL)

Baryon Particle Listings

$\Sigma(1915)$, $\Sigma(1940)$, $\Sigma(1940)$

$\Sigma(1940)\ 3/2^+$

$I(J^P) = 1(\frac{3}{2}^+)$ Status: *

OMITTED FROM SUMMARY TABLE

$\Sigma(1940)$ MASS

VALUE (MeV)	DOCUMENT ID		TECN	COMMENT
1941±18	ZHANG	13A	DPWA	Multichannel

$\Lambda(1945)$ WIDTH

VALUE (MeV)	DOCUMENT ID		TECN	COMMENT
400±49	ZHANG	13A	DPWA	Multichannel

$\Sigma(1940)$ DECAY MODES

	Mode	Fraction (Γ_i/Γ)
Γ_1	$N\overline{K}$	(13.0±2.0) %
Γ_2	$\Sigma\pi$	(4.0±2.0) %
Γ_3	$\Sigma(1385)\pi$, P-wave	(22 ±7) %
Γ_4	$\Lambda(1520)\pi$, S-wave	(5.0±2.0) %

$\Sigma(1940)$ BRANCHING RATIOS

$\Gamma(N\overline{K})/\Gamma_{total}$ Γ_1/Γ

VALUE	DOCUMENT ID		TECN	COMMENT
0.13±0.02	ZHANG	13A	DPWA	Multichannel

$\Gamma(\Sigma\pi)/\Gamma_{total}$ Γ_2/Γ

VALUE	DOCUMENT ID		TECN	COMMENT
0.04±0.02	ZHANG	13A	DPWA	Multichannel

$\Gamma(\Sigma(1385)\pi$, P-wave$)/\Gamma_{total}$ Γ_3/Γ

VALUE	DOCUMENT ID		TECN	COMMENT
0.22±0.07	ZHANG	13A	DPWA	Multichannel

$\Gamma(\Lambda(1520)\pi$, S-wave$)/\Gamma_{total}$ Γ_4/Γ

VALUE	DOCUMENT ID		TECN	COMMENT
0.05±0.02	ZHANG	13A	DPWA	Multichannel

$\Sigma(1940)$ REFERENCES

ZHANG 13A PR C88 035205 H. Zhang *et al.* (KSU)

$\Sigma(1940)\ 3/2^-$

$I(J^P) = 1(\frac{3}{2}^-)$ Status: ***

For results published before 1974 (they are now obsolete), see our 1982 edition Physics Letters **111B** 1 (1982).

Not all analyses require this state. It is not required by the GOYAL 77 analysis of $K^-n \to (\Sigma\pi)^-$ nor by the GOPAL 80 analysis of $K^-n \to K^-n$. See also HEMINGWAY 75.

$\Sigma(1940)$ MASS

VALUE (MeV)	DOCUMENT ID		TECN	COMMENT
1900 to 1950 (≈ 1940) OUR ESTIMATE				
1920±50	GOPAL	77	DPWA	$\overline{K}N$ multichannel
1950±30	BAILLON	75	IPWA	$\overline{K}N \to \Lambda\pi$
1949^{+40}_{-60}	VANHORN	75	DPWA	$K^-p \to \Lambda\pi^0$
1935±80	KANE	74	DPWA	$K^-p \to \Sigma\pi$
1940±20	LITCHFIELD	74B	DPWA	$K^-p \to \Lambda(1520)\pi^0$
1950±20	LITCHFIELD	74C	DPWA	$K^-p \to \Delta(1232)\overline{K}$
• • • We do not use the following data for averages, fits, limits, etc. • • •				
1886 or 1893	[1] MARTIN	77	DPWA	$\overline{K}N$ multichannel
1940	DEBELLEFON	76	IPWA	$K^-p \to \Lambda\pi^0$, F_{17} wave

$\Sigma(1940)$ WIDTH

VALUE (MeV)	DOCUMENT ID		TECN	COMMENT
150 to 300 (≈ 220) OUR ESTIMATE				
170±25	CAMERON	78B	DPWA	$K^-p \to N\overline{K}^*$
300±80	GOPAL	77	DPWA	$\overline{K}N$ multichannel
150±75	BAILLON	75	IPWA	$\overline{K}N \to \Lambda\pi$
160^{+70}_{-40}	VANHORN	75	DPWA	$K^-p \to \Lambda\pi^0$
330±80	KANE	74	DPWA	$K^-p \to \Sigma\pi$
60±20	LITCHFIELD	74B	DPWA	$K^-p \to \Lambda(1520)\pi^0$
70^{+30}_{-20}	LITCHFIELD	74C	DPWA	$K^-p \to \Delta(1232)\overline{K}$
• • • We do not use the following data for averages, fits, limits, etc. • • •				
157 or 159	[1] MARTIN	77	DPWA	$\overline{K}N$ multichannel

$\Sigma(1940)$ DECAY MODES

	Mode	Fraction (Γ_i/Γ)
Γ_1	$N\overline{K}$	<20 %
Γ_2	$\Lambda\pi$	seen
Γ_3	$\Sigma\pi$	seen
Γ_4	$\Sigma(1385)\pi$	seen
Γ_5	$\Sigma(1385)\pi$, S-wave	
Γ_6	$\Lambda(1520)\pi$	seen
Γ_7	$\Lambda(1520)\pi$, P-wave	
Γ_8	$\Lambda(1520)\pi$, F-wave	
Γ_9	$\Delta(1232)\overline{K}$	seen
Γ_{10}	$\Delta(1232)\overline{K}$, S-wave	
Γ_{11}	$\Delta(1232)\overline{K}$, D-wave	
Γ_{12}	$N\overline{K}^*(892)$	seen
Γ_{13}	$N\overline{K}^*(892)$, S=3/2, S-wave	

$\Sigma(1940)$ BRANCHING RATIOS

See "Sign conventions for resonance couplings" in the Note on Λ and Σ Resonances.

$\Gamma(N\overline{K})/\Gamma_{total}$ Γ_1/Γ

VALUE	DOCUMENT ID		TECN	COMMENT
<0.2 OUR ESTIMATE				
<0.04	GOPAL	77	DPWA	$\overline{K}N$ multichannel
0.14 or 0.13	[1] MARTIN	77	DPWA	$\overline{K}N$ multichannel

$(\Gamma_i\Gamma_f)^{1/2}/\Gamma_{total}$ in $N\overline{K} \to \Sigma(1940) \to \Lambda\pi$ $(\Gamma_1\Gamma_2)^{1/2}/\Gamma$

VALUE	DOCUMENT ID		TECN	COMMENT
−0.06 ±0.03	GOPAL	77	DPWA	$\overline{K}N$ multichannel
−0.04 ±0.02	BAILLON	75	IPWA	$\overline{K}N \to \Lambda\pi$
$-0.05\ ^{+0.03}_{-0.02}$	VANHORN	75	DPWA	$K^-p \to \Lambda\pi^0$
−0.153±0.070	DEVENISH	74B		Fixed-t dispersion rel.
• • • We do not use the following data for averages, fits, limits, etc. • • •				
−0.15 or −0.14	[1] MARTIN	77	DPWA	$\overline{K}N$ multichannel

$(\Gamma_i\Gamma_f)^{1/2}/\Gamma_{total}$ in $N\overline{K} \to \Sigma(1940) \to \Sigma\pi$ $(\Gamma_1\Gamma_3)^{1/2}/\Gamma$

VALUE	DOCUMENT ID		TECN	COMMENT
−0.08±0.04	GOPAL	77	DPWA	$\overline{K}N$ multichannel
−0.14±0.04	KANE	74	DPWA	$K^-p \to \Sigma\pi$
• • • We do not use the following data for averages, fits, limits, etc. • • •				
+0.16 or +0.16	[1] MARTIN	77	DPWA	$\overline{K}N$ multichannel

$(\Gamma_i\Gamma_f)^{1/2}/\Gamma_{total}$ in $N\overline{K} \to \Sigma(1940) \to \Lambda(1520)\pi$, P-wave $(\Gamma_1\Gamma_7)^{1/2}/\Gamma$

VALUE	DOCUMENT ID		TECN	COMMENT
< 0.03	CAMERON	77	DPWA	$K^-p \to \Lambda(1520)\pi^0$
−0.11±0.04	LITCHFIELD	74B	DPWA	$K^-p \to \Lambda(1520)\pi^0$

$(\Gamma_i\Gamma_f)^{1/2}/\Gamma_{total}$ in $N\overline{K} \to \Sigma(1940) \to \Lambda(1520)\pi$, F-wave $(\Gamma_1\Gamma_8)^{1/2}/\Gamma$

VALUE	DOCUMENT ID		TECN	COMMENT
0.062±0.021	CAMERON	77	DPWA	$K^-p \to \Lambda(1520)\pi^0$
−0.08 ±0.04	LITCHFIELD	74B	DPWA	$K^-p \to \Lambda(1520)\pi^0$

$(\Gamma_i\Gamma_f)^{1/2}/\Gamma_{total}$ in $N\overline{K} \to \Sigma(1940) \to \Delta(1232)\overline{K}$, S-wave $(\Gamma_1\Gamma_{10})^{1/2}/\Gamma$

VALUE	DOCUMENT ID		TECN	COMMENT
−0.16±0.05	LITCHFIELD	74C	DPWA	$K^-p \to \Delta(1232)\overline{K}$

$(\Gamma_i\Gamma_f)^{1/2}/\Gamma_{total}$ in $N\overline{K} \to \Sigma(1940) \to \Delta(1232)\overline{K}$, D-wave $(\Gamma_1\Gamma_{11})^{1/2}/\Gamma$

VALUE	DOCUMENT ID		TECN	COMMENT
−0.14±0.05	LITCHFIELD	74C	DPWA	$K^-p \to \Delta(1232)\overline{K}$

$(\Gamma_i\Gamma_f)^{1/2}/\Gamma_{total}$ in $N\overline{K} \to \Sigma(1940) \to \Sigma(1385)\pi$ $(\Gamma_1\Gamma_4)^{1/2}/\Gamma$

VALUE	DOCUMENT ID		TECN	COMMENT
+0.066±0.025	[2] CAMERON	78	DPWA	$K^-p \to \Sigma(1385)\pi$

$(\Gamma_i\Gamma_f)^{1/2}/\Gamma_{total}$ in $N\overline{K} \to \Sigma(1940) \to N\overline{K}^*(892)$ $(\Gamma_1\Gamma_{12})^{1/2}/\Gamma$

VALUE	DOCUMENT ID		TECN	COMMENT
−0.09±0.02	[3] CAMERON	78B	DPWA	$K^-p \to N\overline{K}^*$

$\Sigma(1940)$ FOOTNOTES

[1] The two MARTIN 77 values are from a T-matrix pole and from a Breit-Wigner fit.
[2] The published sign has been changed to be in accord with the baryon-first convention.
[3] Upper limits on the D_1 and D_3 waves are each 0.03.

$\Sigma(1940)$ REFERENCES

PDG	82	PL 111B 1	M. Roos *et al.*	(HELS, CIT, CERN)
GOPAL	80	Toronto Conf. 159	G.P. Gopal	(RHEL)
CAMERON	78	NP B143 189	W. Cameron *et al.*	(RHEL, LOIC) IJP
CAMERON	78B	NP B146 327	W. Cameron *et al.*	(RHEL, LOIC) IJP
CAMERON	77	NP B131 399	W. Cameron *et al.*	(RHEL, LOIC) IJP
GOPAL	77	NP B119 362	G.P. Gopal *et al.*	(LOIC, RHEL) IJP
GOYAL	77	PR D16 2746	D.P. Goyal, A.V. Sodhi	(DELH)
MARTIN	77	NP B127 349	B.R. Martin, M.K. Pidcock, R.G. Moorhouse	(LOUC+) IJP
Also		NP B126 266	B.R. Martin, M.K. Pidcock	(LOUC) IJP
Also		NP B126 285	B.R. Martin, M.K. Pidcock	(LOUC) IJP
DEBELLEFON	76	NP B109 129	A. de Bellefon, A. Berthon	(CDEF) IJP
BAILLON	75	NP B94 39	P.H. Baillon, P.J. Litchfield	(CERN, RHEL) IJP
HEMINGWAY	75	NP B91 12	R.J. Hemingway *et al.*	(CERN, HEIDH, MPIM) IJP
VANHORN	75	NP B87 145	A.J. van Horn	(LBL) IJP
Also		NP B87 157	A.J. van Horn	(LBL) IJP
DEVENISH	74B	NP B81 330	R.C.E. Devenish, C.D. Froggatt, B.R. Martin	(DESY+)
KANE	74	LBL-2452	D.F. Kane	(LBL) IJP
LITCHFIELD	74B	NP B74 19	P.J. Litchfield *et al.*	(CERN, HEIDH) IJP
LITCHFIELD	74C	NP B74 39	P.J. Litchfield *et al.*	(CERN, HEIDH) IJP

$\Sigma(2000)\ 1/2^-$

$I(J^P) = 1(\frac{1}{2}^-)$ Status: *

OMITTED FROM SUMMARY TABLE

We list here all reported S_{11} states lying above the $\Sigma(1750)$ S_{11}. ZHANG 13A finds no evidence for those states.

$\Sigma(2000)$ MASS

VALUE (MeV)	DOCUMENT ID		TECN	COMMENT
≈ 2000 OUR ESTIMATE				
1944±15	GOPAL	80	DPWA	$\overline{K}N \to \overline{K}N$
1955±15	GOPAL	77	DPWA	$\overline{K}N$ multichannel
1755 or 1834	[1] MARTIN	77	DPWA	$\overline{K}N$ multichannel
2004±40	VANHORN	75	DPWA	$K^-p \to \Lambda\pi^0$

$\Sigma(2000)$ WIDTH

VALUE (MeV)	DOCUMENT ID		TECN	COMMENT
215±25	GOPAL	80	DPWA	$\overline{K}N \to \overline{K}N$
170±40	GOPAL	77	DPWA	$\overline{K}N$ multichannel
413 or 450	[1] MARTIN	77	DPWA	$\overline{K}N$ multichannel
116±40	VANHORN	75	DPWA	$K^-p \to \Lambda\pi^0$

$\Sigma(2000)$ DECAY MODES

	Mode
Γ_1	$N\overline{K}$
Γ_2	$\Lambda\pi$
Γ_3	$\Sigma\pi$
Γ_4	$\Lambda(1520)\pi$
Γ_5	$N\overline{K}^*(892)$, S=1/2, S-wave
Γ_6	$N\overline{K}^*(892)$, S=3/2, D-wave

$\Sigma(2000)$ BRANCHING RATIOS

See "Sign conventions for resonance couplings" in the Note on Λ and Σ Resonances.

$\Gamma(N\overline{K})/\Gamma_{total}$ Γ_1/Γ

VALUE	DOCUMENT ID		TECN	COMMENT
0.51±0.05	GOPAL	80	DPWA	$\overline{K}N \to \overline{K}N$
0.44±0.05	GOPAL	77	DPWA	See GOPAL 80
0.62 or 0.57	[1] MARTIN	77	DPWA	$\overline{K}N$ multichannel

$(\Gamma_i\Gamma_f)^{1/2}/\Gamma_{total}$ in $N\overline{K} \to \Sigma(2000) \to \Lambda\pi$ $(\Gamma_1\Gamma_2)^{1/2}/\Gamma$

VALUE	DOCUMENT ID		TECN	COMMENT
0.08±0.03	GOPAL	77	DPWA	$\overline{K}N$ multichannel
−0.19 or −0.18	[1] MARTIN	77	DPWA	$\overline{K}N$ multichannel
not seen	BAILLON	75	IPWA	$\overline{K}N \to \Lambda\pi$
$+0.07^{+0.02}_{-0.01}$	VANHORN	75	DPWA	$K^-p \to \Lambda\pi^0$

$(\Gamma_i\Gamma_f)^{1/2}/\Gamma_{total}$ in $N\overline{K} \to \Sigma(2000) \to \Sigma\pi$ $(\Gamma_1\Gamma_3)^{1/2}/\Gamma$

VALUE	DOCUMENT ID		TECN	COMMENT
+0.20±0.04	GOPAL	77	DPWA	$\overline{K}N$ multichannel
+0.26 or +0.24	[1] MARTIN	77	DPWA	$\overline{K}N$ multichannel

$(\Gamma_i\Gamma_f)^{1/2}/\Gamma_{total}$ in $N\overline{K} \to \Sigma(2000) \to \Lambda(1520)\pi$ $(\Gamma_1\Gamma_4)^{1/2}/\Gamma$

VALUE	DOCUMENT ID		TECN	COMMENT
+0.081±0.021	[2] CAMERON	77	DPWA	P-wave decay

$(\Gamma_i\Gamma_f)^{1/2}/\Gamma_{total}$ in $N\overline{K} \to \Sigma(2000) \to N\overline{K}^*(892)$, S=1/2, S-wave $(\Gamma_1\Gamma_5)^{1/2}/\Gamma$

VALUE	DOCUMENT ID		TECN	COMMENT
+0.10±0.02	[2] CAMERON	78B	DPWA	$K^-p \to N\overline{K}^*$

$(\Gamma_i\Gamma_f)^{1/2}/\Gamma_{total}$ in $N\overline{K} \to \Sigma(2000) \to N\overline{K}^*(892)$, S=3/2, D-wave $(\Gamma_1\Gamma_6)^{1/2}/\Gamma$

VALUE	DOCUMENT ID		TECN	COMMENT
−0.07±0.03	CAMERON	78B	DPWA	$K^-p \to N\overline{K}^*$

$\Sigma(2000)$ FOOTNOTES

[1] The two MARTIN 77 values are from a T-matrix pole and from a Breit-Wigner fit.
[2] The published sign has been changed to be in accord with the baryon-first convention.

$\Sigma(2000)$ REFERENCES

ZHANG	13A	PR C88 035205	H. Zhang *et al.*	(KSU)
GOPAL	80	Toronto Conf. 159	G.P. Gopal	(RHEL) IJP
CAMERON	78B	NP B146 327	W. Cameron *et al.*	(RHEL, LOIC) IJP
CAMERON	77	NP B131 399	W. Cameron *et al.*	(RHEL, LOIC) IJP
GOPAL	77	NP B119 362	G.P. Gopal *et al.*	(LOIC, RHEL) IJP
MARTIN	77	NP B127 349	B.R. Martin, M.K. Pidcock, R.G. Moorhouse	(LOUC+) IJP
Also		NP B126 266	B.R. Martin, M.K. Pidcock	(LOUC) IJP
Also		NP B126 285	B.R. Martin, M.K. Pidcock	(LOUC) IJP
BAILLON	75	NP B94 39	P.H. Baillon, P.J. Litchfield	(CERN, RHEL) IJP
VANHORN	75	NP B87 145	A.J. van Horn	(LBL) IJP
Also		NP B87 157	A.J. van Horn	(LBL) IJP

$\Sigma(2030)\ 7/2^+$

$I(J^P) = 1(\frac{7}{2}^+)$ Status: ****

Discovered by COOL 66 and by WOHL 66. For most results published before 1974 (they are now obsolete), see our 1982 edition Physics Letters **111B** 1 (1982).

This entry only includes results from partial-wave analyses. Parameters of peaks seen in cross sections and invariant-mass distributions around 2030 MeV may be found in our 1984 edition, Reviews of Modern Physics **56** S1 (1984).

$\Sigma(2030)$ POLE POSITION

REAL PART

VALUE (MeV)	DOCUMENT ID		TECN	COMMENT
$\mathbf{2025^{+10}_{-5}}$	[1] KAMANO	15	DPWA	Multichannel
• • • We do not use the following data for averages, fits, limits, etc. • • •				
1993	ZHANG	13A	DPWA	Multichannel

[1] From the preferred solution A in KAMANO 15.

−2×IMAGINARY PART

VALUE (MeV)	DOCUMENT ID		TECN	COMMENT
$\mathbf{130^{+6}_{-24}}$	[1] KAMANO	15	DPWA	Multichannel
• • • We do not use the following data for averages, fits, limits, etc. • • •				
176	ZHANG	13A	DPWA	Multichannel

[1] From the preferred solution A in KAMANO 15.

$\Sigma(2030)$ POLE RESIDUES

The normalized residue is the residue divided by $\Gamma_{pole}/2$.

Normalized residue in $N\overline{K} \to \Sigma(2030) \to N\overline{K}$

MODULUS	PHASE (°)	DOCUMENT ID		TECN	COMMENT
• • • We do not use the following data for averages, fits, limits, etc. • • •					
0.220	−38	[1] KAMANO	15	DPWA	Multichannel

[1] From the preferred solution A in KAMANO 15.

Normalized residue in $N\overline{K} \to \Sigma(2030) \to \Sigma\pi$

MODULUS	PHASE (°)	DOCUMENT ID		TECN	COMMENT
• • • We do not use the following data for averages, fits, limits, etc. • • •					
0.0807	135	[1] KAMANO	15	DPWA	Multichannel

[1] From the preferred solution A in KAMANO 15.

Normalized residue in $N\overline{K} \to \Sigma(2030) \to \Lambda\pi$

MODULUS	PHASE (°)	DOCUMENT ID		TECN	COMMENT
• • • We do not use the following data for averages, fits, limits, etc. • • •					
0.138	−24	[1] KAMANO	15	DPWA	Multichannel

[1] From the preferred solution A in KAMANO 15.

Normalized residue in $N\overline{K} \to \Sigma(2030) \to \Xi K$

MODULUS	PHASE (°)	DOCUMENT ID		TECN	COMMENT
• • • We do not use the following data for averages, fits, limits, etc. • • •					
0.0348	129	[1] KAMANO	15	DPWA	Multichannel

[1] From the preferred solution A in KAMANO 15.

Baryon Particle Listings

$\Sigma(2030)$

Normalized residue in $N\overline{K} \rightarrow \Sigma(2030) \rightarrow \Sigma(1385)\pi$, F-wave

MODULUS	PHASE (°)	DOCUMENT ID		TECN	COMMENT
• • • We do not use the following data for averages, fits, limits, etc. • • •					
0.089	−23	[1] KAMANO	15	DPWA	Multichannel

[1] From the preferred solution A in KAMANO 15.

Normalized residue in $N\overline{K} \rightarrow \Sigma(2030) \rightarrow \Sigma(1385)\pi$, H-wave

MODULUS	PHASE (°)	DOCUMENT ID		TECN	COMMENT
• • • We do not use the following data for averages, fits, limits, etc. • • •					
0.0245	132	[1] KAMANO	15	DPWA	Multichannel

[1] From the preferred solution A in KAMANO 15.

Normalized residue in $N\overline{K} \rightarrow \Sigma(2030) \rightarrow N\overline{K}^*(892)$, S=1/2 , F-wave

MODULUS	PHASE (°)	DOCUMENT ID		TECN	COMMENT
• • • We do not use the following data for averages, fits, limits, etc. • • •					
0.193	38	[1] KAMANO	15	DPWA	Multichannel

[1] From the preferred solution A in KAMANO 15.

Normalized residue in $N\overline{K} \rightarrow \Sigma(2030) \rightarrow N\overline{K}^*(892)$, S=3/2 , F-wave

MODULUS	PHASE (°)	DOCUMENT ID		TECN	COMMENT
• • • We do not use the following data for averages, fits, limits, etc. • • •					
0.320	37	[1] KAMANO	15	DPWA	Multichannel

[1] From the preferred solution A in KAMANO 15.

Normalized residue in $N\overline{K} \rightarrow \Sigma(2030) \rightarrow N\overline{K}^*(892)$, S=3/2 , H-wave

MODULUS	PHASE (°)	DOCUMENT ID		TECN	COMMENT
• • • We do not use the following data for averages, fits, limits, etc. • • •					
0.00358	22	[1] KAMANO	15	DPWA	Multichannel

[1] From the preferred solution A in KAMANO 15.

$\Sigma(2030)$ MASS

VALUE (MeV)	DOCUMENT ID		TECN	COMMENT
2025 to 2040 (≈ 2030) OUR ESTIMATE				
2030 ± 5	ZHANG	13A	DPWA	Multichannel
2036 ± 5	GOPAL	80	DPWA	$\overline{K}N \rightarrow \overline{K}N$
2038 ± 10	CORDEN	77B		$K^-N \rightarrow N\overline{K}^*$
2040 ± 5	GOPAL	77	DPWA	$\overline{K}N$ multichannel
2030 ± 3	[1] CORDEN	76	DPWA	$K^-n \rightarrow \Lambda\pi^-$
2035 ± 15	BAILLON	75	IPWA	$\overline{K}N \rightarrow \Lambda\pi$
2038 ± 10	HEMINGWAY	75	DPWA	$K^-p \rightarrow \overline{K}N$
2042 ± 11	VANHORN	75	DPWA	$K^-p \rightarrow \Lambda\pi^0$
2020 ± 6	KANE	74	DPWA	$K^-p \rightarrow \Sigma\pi$
2035 ± 10	LITCHFIELD	74B	DPWA	$K^-p \rightarrow \Lambda(1520)\pi^0$
2020 ± 30	LITCHFIELD	74C	DPWA	$K^-p \rightarrow \Delta(1232)\overline{K}$
2025 ± 10	LITCHFIELD	74D	DPWA	$K^-p \rightarrow \Lambda(1820)\pi^0$
• • • We do not use the following data for averages, fits, limits, etc. • • •				
2027 to 2057	GOYAL	77	DPWA	$K^-N \rightarrow \Sigma\pi$
2030	DEBELLEFON	76	IPWA	$K^-p \rightarrow \Lambda\pi^0$

[1] Preferred solution 3; see CORDEN 76 for other possibilities.

$\Sigma(2030)$ WIDTH

VALUE (MeV)	DOCUMENT ID		TECN	COMMENT
150 to 200 (≈ 180) OUR ESTIMATE				
207 ± 17	ZHANG	13A	DPWA	Multichannel
172 ± 10	GOPAL	80	DPWA	$\overline{K}N \rightarrow \overline{K}N$
137 ± 40	CORDEN	77B		$K^-N \rightarrow N\overline{K}^*$
190 ± 10	GOPAL	77	DPWA	$\overline{K}N$ multichannel
201 ± 9	[1] CORDEN	76	DPWA	$K^-n \rightarrow \Lambda\pi^-$
180 ± 20	BAILLON	75	IPWA	$\overline{K}N \rightarrow \Lambda\pi$
172 ± 15	HEMINGWAY	75	DPWA	$K^-p \rightarrow \overline{K}N$
178 ± 13	VANHORN	75	DPWA	$K^-p \rightarrow \Lambda\pi^0$
111 ± 5	KANE	74	DPWA	$K^-p \rightarrow \Sigma\pi$
160 ± 20	LITCHFIELD	74B	DPWA	$K^-p \rightarrow \Lambda(1520)\pi^0$
200 ± 30	LITCHFIELD	74C	DPWA	$K^-p \rightarrow \Delta(1232)\overline{K}$
• • • We do not use the following data for averages, fits, limits, etc. • • •				
260	DECLAIS	77	DPWA	$\overline{K}N \rightarrow \overline{K}N$
126 to 195	GOYAL	77	DPWA	$K^-N \rightarrow \Sigma\pi$
160	DEBELLEFON	76	IPWA	$K^-p \rightarrow \Lambda\pi^0$
70 to 125	LITCHFIELD	74D	DPWA	$K^-p \rightarrow \Lambda(1820)\pi^0$

[1] Preferred solution 3; see CORDEN 76 for other possibilities.

$\Sigma(2030)$ DECAY MODES

	Mode	Fraction (Γ_i/Γ)
Γ_1	$N\overline{K}$	17–23 %
Γ_2	$\Lambda\pi$	17–23 %
Γ_3	$\Sigma\pi$	5–10 %
Γ_4	ΞK	<2 %
Γ_5	$\Sigma(1385)\pi$	5–15 %
Γ_6	$\Sigma(1385)\pi$, F-wave	
Γ_7	$\Sigma(1385)\pi$, F-wave	
Γ_8	$\Sigma(1385)\pi$, H-wave	
Γ_9	$\Lambda(1520)\pi$	10–20 %
Γ_{10}	$\Lambda(1520)\pi$, D-wave	
Γ_{11}	$\Lambda(1520)\pi$, G-wave	
Γ_{12}	$\Delta(1232)\overline{K}$	10–20 %
Γ_{13}	$\Delta(1232)\overline{K}$, F-wave	
Γ_{14}	$\Delta(1232)\overline{K}$, H-wave	
Γ_{15}	$N\overline{K}^*(892)$	<5 %
Γ_{16}	$N\overline{K}^*(892)$, S=1/2, F-wave	
Γ_{17}	$N\overline{K}^*(892)$, S=3/2, F-wave	
Γ_{18}	$N\overline{K}^*(892)$, S=3/2, H-wave	
Γ_{19}	$\Lambda(1820)\pi$, P-wave	

$\Sigma(2030)$ BRANCHING RATIOS

See "Sign conventions for resonance couplings" in the Note on Λ and Σ Resonances.

$\Gamma(N\overline{K})/\Gamma_{\text{total}}$ Γ_1/Γ

VALUE	DOCUMENT ID		TECN	COMMENT
0.17 to 0.23 OUR ESTIMATE				
0.13 ±0.01	ZHANG	13A	DPWA	Multichannel
0.19 ±0.03	GOPAL	80	DPWA	$\overline{K}N \rightarrow \overline{K}N$
0.18 ±0.03	HEMINGWAY	75	DPWA	$K^-p \rightarrow \overline{K}N$
• • • We do not use the following data for averages, fits, limits, etc. • • •				
0.269	[1] KAMANO	15	DPWA	Multichannel
0.15	DECLAIS	77	DPWA	$\overline{K}N \rightarrow \overline{K}N$
0.24 ±0.02	GOPAL	77	DPWA	See GOPAL 80

[1] From the preferred solution A in KAMANO 15.

$\Gamma(\Lambda\pi)/\Gamma_{\text{total}}$ Γ_2/Γ

VALUE	DOCUMENT ID		TECN	COMMENT
• • • We do not use the following data for averages, fits, limits, etc. • • •				
0.080	[1] KAMANO	15	DPWA	Multichannel

[1] From the preferred solution A in KAMANO 15.

$\Gamma(\Sigma\pi)/\Gamma_{\text{total}}$ Γ_3/Γ

VALUE	DOCUMENT ID		TECN	COMMENT
• • • We do not use the following data for averages, fits, limits, etc. • • •				
0.037	[1] KAMANO	15	DPWA	Multichannel

[1] From the preferred solution A in KAMANO 15.

$\Gamma(\Xi K)/\Gamma_{\text{total}}$ Γ_4/Γ

VALUE	DOCUMENT ID		TECN	COMMENT
• • • We do not use the following data for averages, fits, limits, etc. • • •				
0.006	[1] KAMANO	15	DPWA	Multichannel

[1] From the preferred solution A in KAMANO 15.

$\Gamma(\Sigma(1385)\pi, F\text{-wave})/\Gamma_{\text{total}}$ Γ_7/Γ

VALUE	DOCUMENT ID		TECN	COMMENT
• • • We do not use the following data for averages, fits, limits, etc. • • •				
0.030	[1] KAMANO	15	DPWA	Multichannel

[1] From the preferred solution A in KAMANO 15.

$\Gamma(\Sigma(1385)\pi, H\text{-wave})/\Gamma_{\text{total}}$ Γ_8/Γ

VALUE	DOCUMENT ID		TECN	COMMENT
• • • We do not use the following data for averages, fits, limits, etc. • • •				
0.003	[1] KAMANO	15	DPWA	Multichannel

[1] From the preferred solution A in KAMANO 15.

$\Gamma(N\overline{K}^*(892), S$=1/2, $F\text{-wave})/\Gamma_{\text{total}}$ Γ_{16}/Γ

VALUE	DOCUMENT ID		TECN	COMMENT
• • • We do not use the following data for averages, fits, limits, etc. • • •				
0.154	[1] KAMANO	15	DPWA	Multichannel

[1] From the preferred solution A in KAMANO 15.

$\Gamma(N\overline{K}^*(892), S$=3/2, $F\text{-wave})/\Gamma_{\text{total}}$ Γ_{17}/Γ

VALUE	DOCUMENT ID		TECN	COMMENT
• • • We do not use the following data for averages, fits, limits, etc. • • •				
0.422	[1] KAMANO	15	DPWA	Multichannel

[1] From the preferred solution A in KAMANO 15.

$\Gamma(N\overline{K}^*(892), S=3/2, H\text{-wave})/\Gamma_{total}$ Γ_{18}/Γ

VALUE	DOCUMENT ID		TECN	COMMENT
• • • We do not use the following data for averages, fits, limits, etc. • • •				
not seen	[1] KAMANO	15	DPWA	Multichannel

[1] From the preferred solution A in KAMANO 15.

$(\Gamma_i\Gamma_f)^{1/2}/\Gamma_{total}$ in $N\overline{K} \to \Sigma(2030) \to \Lambda\pi$ $(\Gamma_1\Gamma_2)^{1/2}/\Gamma$

VALUE	DOCUMENT ID		TECN	COMMENT
$+0.15 \pm 0.01$	ZHANG	13A	DPWA	Multichannel
$+0.18 \pm 0.02$	GOPAL	77	DPWA	$\overline{K}N$ multichannel
$+0.20 \pm 0.01$	[1] CORDEN	76	DPWA	$K^- n \to \Lambda\pi^-$
$+0.18 \pm 0.02$	BAILLON	75	IPWA	$\overline{K}N \to \Lambda\pi$
$+0.20 \pm 0.01$	VANHORN	75	DPWA	$K^- p \to \Lambda\pi^0$
$+0.195 \pm 0.053$	DEVENISH	74B		Fixed-t dispersion rel.
• • • We do not use the following data for averages, fits, limits, etc. • • •				
0.20	DEBELLEFON	76	IPWA	$K^- p \to \Lambda\pi^0$

[1] Preferred solution 3; see CORDEN 76 for other possibilities.

$(\Gamma_i\Gamma_f)^{1/2}/\Gamma_{total}$ in $N\overline{K} \to \Sigma(2030) \to \Sigma\pi$ $(\Gamma_1\Gamma_3)^{1/2}/\Gamma$

VALUE	DOCUMENT ID		TECN	COMMENT
-0.08 ± 0.01	ZHANG	13A	DPWA	Multichannel
-0.09 ± 0.01	[1] CORDEN	77C		$K^- n \to \Sigma\pi$
-0.06 ± 0.01	[1] CORDEN	77C		$K^- n \to \Sigma\pi$
-0.15 ± 0.03	GOPAL	77	DPWA	$\overline{K}N$ multichannel
-0.10 ± 0.01	KANE	74	DPWA	$K^- p \to \Sigma\pi$
• • • We do not use the following data for averages, fits, limits, etc. • • •				
-0.085 ± 0.02	[2] GOYAL	77	DPWA	$K^- N \to \Sigma\pi$

[1] The two entries for CORDEN 77C are from two different acceptable solutions.
[2] This coupling is extracted from unnormalized data.

$(\Gamma_i\Gamma_f)^{1/2}/\Gamma_{total}$ in $N\overline{K} \to \Sigma(2030) \to \Xi K$ $(\Gamma_1\Gamma_4)^{1/2}/\Gamma$

VALUE	DOCUMENT ID		TECN	COMMENT
0.023	MULLER	69B	DPWA	$K^- p \to \Xi K$
<0.05	BURGUN	68	DPWA	$K^- p \to \Xi K$
<0.05	TRIPP	67	RVUE	$K^- p \to \Xi K$

$(\Gamma_i\Gamma_f)^{1/2}/\Gamma_{total}$ in $N\overline{K} \to \Sigma(2030) \to \Sigma(1385)\pi$, F-wave $(\Gamma_1\Gamma_6)^{1/2}/\Gamma$

VALUE	DOCUMENT ID		TECN	COMMENT
$+0.16 \pm 0.01$	ZHANG	13A	DPWA	Multichannel
$+0.153 \pm 0.026$	[1] CAMERON	78	DPWA	$K^- p \to \Sigma(1385)\pi$

[1] The published sign has been changed to be in accord with the baryon-first convention.

$(\Gamma_i\Gamma_f)^{1/2}/\Gamma_{total}$ in $N\overline{K} \to \Sigma(2030) \to \Lambda(1520)\pi$, D-wave $(\Gamma_1\Gamma_{10})^{1/2}/\Gamma$

VALUE	DOCUMENT ID		TECN	COMMENT
$+0.114 \pm 0.010$	[1] CAMERON	77	DPWA	$K^- p \to \Lambda(1520)\pi^0$
0.14 ± 0.03	LITCHFIELD	74B	DPWA	$K^- p \to \Lambda(1520)\pi^0$
• • • We do not use the following data for averages, fits, limits, etc. • • •				
0.10 ± 0.03	[2] CORDEN	75B	DBC	$K^- n \to N\overline{K}\pi^-$

[1] The published sign has been changed to be in accord with the baryon-first convention.
[2] An upper limit.

$(\Gamma_i\Gamma_f)^{1/2}/\Gamma_{total}$ in $N\overline{K} \to \Sigma(2030) \to \Lambda(1520)\pi$, G-wave $(\Gamma_1\Gamma_{11})^{1/2}/\Gamma$

VALUE	DOCUMENT ID		TECN	COMMENT
$+0.146 \pm 0.010$	[1] CAMERON	77	DPWA	$K^- p \to \Lambda(1520)\pi^0$
0.02 ± 0.02	LITCHFIELD	74B	DPWA	$K^- p \to \Lambda(1520)\pi^0$

[1] The published sign has been changed to be in accord with the baryon-first convention.

$(\Gamma_i\Gamma_f)^{1/2}/\Gamma_{total}$ in $N\overline{K} \to \Sigma(2030) \to \Delta(1232)\overline{K}$, F-wave $(\Gamma_1\Gamma_{13})^{1/2}/\Gamma$

VALUE	DOCUMENT ID		TECN	COMMENT
$+0.12 \pm 0.02$	ZHANG	13A	DPWA	Multichannel
0.16 ± 0.03	LITCHFIELD	74C	DPWA	$K^- p \to \Delta(1232)\overline{K}$
• • • We do not use the following data for averages, fits, limits, etc. • • •				
0.17 ± 0.03	[1] CORDEN	75B	DBC	$K^- n \to N\overline{K}\pi^-$

[1] An upper limit.

$(\Gamma_i\Gamma_f)^{1/2}/\Gamma_{total}$ in $N\overline{K} \to \Sigma(2030) \to \Delta(1232)\overline{K}$, H-wave $(\Gamma_1\Gamma_{14})^{1/2}/\Gamma$

VALUE	DOCUMENT ID		TECN	COMMENT
0.00 ± 0.02	LITCHFIELD	74C	DPWA	$K^- p \to \Delta(1232)\overline{K}$

$(\Gamma_i\Gamma_f)^{1/2}/\Gamma_{total}$ in $N\overline{K} \to \Sigma(2030) \to N\overline{K}^*(892)$, $S=1/2$, F-wave $(\Gamma_1\Gamma_{16})^{1/2}/\Gamma$

VALUE	DOCUMENT ID		TECN	COMMENT
$+0.06 \pm 0.02$	ZHANG	13A	DPWA	Multichannel
$+0.06 \pm 0.03$	[1] CAMERON	78B	DPWA	$K^- p \to N\overline{K}^*$
-0.02 ± 0.01	CORDEN	77B		$K^- d \to NN\overline{K}^*$

[1] The published sign has been changed to be in accord with the baryon-first convention.

$(\Gamma_i\Gamma_f)^{1/2}/\Gamma_{total}$ in $N\overline{K} \to \Sigma(2030) \to N\overline{K}^*(892)$, $S=3/2$, F-wave $(\Gamma_1\Gamma_{17})^{1/2}/\Gamma$

VALUE	DOCUMENT ID		TECN	COMMENT
$+0.05 \pm 0.01$	ZHANG	13A	DPWA	Multichannel
$+0.04 \pm 0.03$	[1] CAMERON	78B	DPWA	$K^- p \to N\overline{K}^*$
-0.12 ± 0.02	CORDEN	77B		$K^- d \to NN\overline{K}^*$

[1] The upper limit on the G_3 wave is 0.03.

$(\Gamma_i\Gamma_f)^{1/2}/\Gamma_{total}$ in $N\overline{K} \to \Sigma(2030) \to \Lambda(1820)\pi$, P-wave $(\Gamma_1\Gamma_{19})^{1/2}/\Gamma$

VALUE	DOCUMENT ID		TECN	COMMENT
0.14 ± 0.02	CORDEN	75B	DBC	$K^- n \to N\overline{K}\pi^-$
0.18 ± 0.04	LITCHFIELD	74D	DPWA	$K^- p \to \Lambda(1820)\pi^0$

$\Sigma(2030)$ REFERENCES

KAMANO	15	PR C92 025205	H. Kamano *et al.*	(ANL, OSAK)
ZHANG	13A	PR C88 035205	H. Zhang *et al.*	(KSU)
PDG	84	RMP 56 S1	C.G. Wohl *et al.*	(LBL, CIT, CERN)
PDG	82	PL 111B 1	M. Roos *et al.*	(HELS, CIT, CERN)
GOPAL	80	Toronto Conf. 159	G.P. Gopal	(RHEL) IJP
CAMERON	78	NP B143 189	W. Cameron *et al.*	(RHEL, LOIC) IJP
CAMERON	78B	NP B146 327	W. Cameron *et al.*	(RHEL, LOIC) IJP
CAMERON	77	NP B131 399	W. Cameron *et al.*	(RHEL, LOIC) IJP
CORDEN	77B	NP B121 365	M.J. Corden *et al.*	(BIRM) IJP
CORDEN	77C	NP B125 61	M.J. Corden *et al.*	(BIRM) IJP
DECLAIS	77	CERN 77-16	Y. Declais *et al.*	(CAEN, CERN) IJP
GOPAL	77	NP B119 362	G.P. Gopal *et al.*	(LOIC, RHEL) IJP
GOYAL	77	PR D16 2746	D.P. Goyal, A.V. Sodhi	(DELH) IJP
CORDEN	76	NP B104 382	M.J. Corden *et al.*	(BIRM) IJP
DEBELLEFON	76	NP B109 129	A. de Bellefon, A. Berthon	(CDEF) IJP
BAILLON	75	NP B94 39	P.H. Baillon, P.J. Litchfield	(CERN, RHEL) IJP
CORDEN	75B	NP B92 365	M.J. Corden *et al.*	(BIRM) IJP
HEMINGWAY	75	NP B91 12	R.J. Hemingway *et al.*	(CERN, HEIDH, MPIM) IJP
VANHORN	75	NP B87 145	A.J. van Horn	(LBL) IJP
Also		NP B87 157	A.J. van Horn	(LBL) IJP
DEVENISH	74B	NP B81 330	R.C.E. Devenish, C.D. Froggatt, B.R. Martin	(DESY+)
KANE	74	LBL-2452	D.F. Kane	(LBL) IJP
LITCHFIELD	74B	NP B74 19	P.J. Litchfield *et al.*	(CERN, HEIDH) IJP
LITCHFIELD	74C	NP B74 39	P.J. Litchfield *et al.*	(CERN, HEIDH) IJP
LITCHFIELD	74D	NP B74 12	P.J. Litchfield *et al.*	(CERN, HEIDH) IJP
MULLER	69B	Thesis UCRL 19372	R.A. Muller	(LRL)
BURGUN	68	NP B8 447	G. Burgun *et al.*	(SACL, CDEF, RHEL)
TRIPP	67	NP B3 10	R.D. Tripp *et al.*	(LRL, SLAC, CERN+)
COOL	66	PRL 16 1228	R.L. Cool *et al.*	(BNL)
WOHL	66	PRL 17 107	C.G. Wohl, F.T. Solmitz, M.L. Stevenson	(LRL) IJP

$\Sigma(2070)$ $5/2^+$

$I(J^P) = 1(\frac{5}{2}^+)$ Status: *

OMITTED FROM SUMMARY TABLE

This state suggested by BERTHON 70B finds support in GOPAL 80 with new $K^- p$ polarization and $K^- n$ angular distributions. The very broad state seen in KANE 72 is not required in the later (KANE 74) analysis of $\overline{K}N \to \Sigma\pi$.

$\Sigma(2070)$ MASS

VALUE (MeV)	DOCUMENT ID		TECN	COMMENT
≈ 2070 OUR ESTIMATE				
2051 ± 25	GOPAL	80	DPWA	$\overline{K}N \to \overline{K}N$
2057	KANE	72	DPWA	$K^- p \to \Sigma\pi$
2070 ± 10	BERTHON	70B	DPWA	$K^- p \to \Sigma\pi$

$\Sigma(2070)$ WIDTH

VALUE (MeV)	DOCUMENT ID		TECN	COMMENT
300 ± 30	GOPAL	80	DPWA	$\overline{K}N \to \overline{K}N$
906	KANE	72	DPWA	$K^- p \to \Sigma\pi$
140 ± 20	BERTHON	70B	DPWA	$K^- p \to \Sigma\pi$

$\Sigma(2070)$ DECAY MODES

	Mode
Γ_1	$N\overline{K}$
Γ_2	$\Sigma\pi$

$\Sigma(2070)$ BRANCHING RATIOS

See "Sign conventions for resonance couplings" in the Note on Λ and Σ Resonances.

$\Gamma(N\overline{K})/\Gamma_{total}$ Γ_1/Γ

VALUE	DOCUMENT ID		TECN	COMMENT
0.08 ± 0.03	GOPAL	80	DPWA	$\overline{K}N \to \overline{K}N$

$(\Gamma_i\Gamma_f)^{1/2}/\Gamma_{total}$ in $N\overline{K} \to \Sigma(2070) \to \Sigma\pi$ $(\Gamma_1\Gamma_2)^{1/2}/\Gamma$

VALUE	DOCUMENT ID		TECN	COMMENT
$+0.104$	KANE	72	DPWA	$K^- p \to \Sigma\pi$
$+0.12 \pm 0.02$	BERTHON	70B	DPWA	$K^- p \to \Sigma\pi$

Baryon Particle Listings

$\Sigma(2070)$, $\Sigma(2080)$, $\Sigma(2100)$, $\Sigma(2250)$

$\Sigma(2070)$ REFERENCES

GOPAL	80	Toronto Conf. 159	G.P. Gopal	(RHEL) IJP
KANE	74	LBL-2452	D.F. Kane	(LBL)
KANE	72	PR D5 1583	D.F.J. Kane	(LBL)
BERTHON	70B	NP B24 417	A. Berthon *et al.*	(CDEF, RHEL, SACL) IJP

$\Sigma(2080)\ 3/2^+$

$I(J^P) = 1(\frac{3}{2}^+)$ Status: **

OMITTED FROM SUMMARY TABLE

Suggested by some but not all partial-wave analyses across this region.

$\Sigma(2080)$ MASS

VALUE (MeV)	DOCUMENT ID		TECN	COMMENT
≈ 2080 OUR ESTIMATE				
2091 ± 7	[1] CORDEN	76	DPWA	$K^- n \to \Lambda\pi^-$
2070 to 2120	DEBELLEFON	76	IPWA	$K^- p \to \Lambda\pi^0$
2120 ± 40	BAILLON	75	IPWA	$\overline{K}N \to \Lambda\pi$ (sol. 1)
2140 ± 40	BAILLON	75	IPWA	$\overline{K}N \to \Lambda\pi$ (sol. 2)
2082 ± 4	COX	70	DPWA	See CORDEN 76
2070 ± 30	LITCHFIELD	70	DPWA	$K^- N \to \Lambda\pi$

$\Sigma(2080)$ WIDTH

VALUE (MeV)	DOCUMENT ID		TECN	COMMENT
186 ± 48	[1] CORDEN	76	DPWA	$K^- n \to \Lambda\pi^-$
100	DEBELLEFON	76	IPWA	$K^- p \to \Lambda\pi^0$
240 ± 50	BAILLON	75	IPWA	$\overline{K}N \to \Lambda\pi$ (sol. 1)
200 ± 50	BAILLON	75	IPWA	$\overline{K}N \to \Lambda\pi$ (sol. 2)
87 ± 20	COX	70	DPWA	See CORDEN 76
250 ± 40	LITCHFIELD	70	DPWA	$K^- N \to \Lambda\pi$

$\Sigma(2080)$ DECAY MODES

	Mode
Γ_1	$N\overline{K}$
Γ_2	$\Lambda\pi$

$\Sigma(2080)$ BRANCHING RATIOS

See "Sign conventions for resonance couplings" in the Note on Λ and Σ Resonances.

$(\Gamma_i\Gamma_f)^{1/2}/\Gamma_{total}$ in $N\overline{K} \to \Sigma(2080) \to \Lambda\pi$ **$(\Gamma_1\Gamma_2)^{1/2}/\Gamma$**

VALUE	DOCUMENT ID		TECN	COMMENT
−0.10 ± 0.03	[1] CORDEN	76	DPWA	$K^- n \to \Lambda\pi^-$
−0.10	DEBELLEFON	76	IPWA	$K^- p \to \Lambda\pi^0$
−0.13 ± 0.04	BAILLON	75	IPWA	$\overline{K}N \to \Lambda\pi$ (sol. 1 and 2)
−0.16 ± 0.03	COX	70	DPWA	See CORDEN 76
−0.09 ± 0.03	LITCHFIELD	70	DPWA	$K^- N \to \Lambda\pi$

$\Sigma(2080)$ FOOTNOTES

[1] Preferred solution 3; see CORDEN 76 for other possibilities, including a D_{15} at this mass.

$\Sigma(2080)$ REFERENCES

CORDEN	76	NP B104 382	M.J. Corden *et al.*	(BIRM) IJP
DEBELLEFON	76	NP B109 129	A. de Bellefon, A. Berthon	(CDEF) IJP
Also		NP B90 1	A. de Bellefon *et al.*	(CDEF, SACL) IJP
BAILLON	75	NP B94 39	P.H. Baillon, P.J. Litchfield	(CERN, RHEL) IJP
COX	70	NP B19 61	G.F. Cox *et al.*	(BIRM, EDIN, GLAS, LOIC) IJP
LITCHFIELD	70	NP B22 269	P.J. Litchfield	(RHEL) IJP

$\Sigma(2100)\ 7/2^-$

$I(J^P) = 1(\frac{7}{2}^-)$ Status: *

OMITTED FROM SUMMARY TABLE

$\Sigma(2100)$ MASS

VALUE (MeV)	DOCUMENT ID		TECN	COMMENT
≈ 2100 OUR ESTIMATE				
2060 ± 20	BARBARO-...	70	DPWA	$K^- p \to \Lambda\pi^0$
2120 ± 30	BARBARO-...	70	DPWA	$K^- p \to \Sigma\pi$

$\Sigma(2100)$ WIDTH

VALUE (MeV)	DOCUMENT ID		TECN	COMMENT
70 ± 30	BARBARO-...	70	DPWA	$K^- p \to \Lambda\pi^0$
135 ± 30	BARBARO-...	70	DPWA	$K^- p \to \Sigma\pi$

$\Sigma(2100)$ DECAY MODES

	Mode
Γ_1	$N\overline{K}$
Γ_2	$\Lambda\pi$
Γ_3	$\Sigma\pi$

$\Sigma(2100)$ BRANCHING RATIOS

See "Sign conventions for resonance couplings" in the Note on Λ and Σ Resonances.

$(\Gamma_i\Gamma_f)^{1/2}/\Gamma_{total}$ in $N\overline{K} \to \Sigma(2100) \to \Lambda\pi$ **$(\Gamma_1\Gamma_2)^{1/2}/\Gamma$**

VALUE	DOCUMENT ID		TECN	COMMENT
−0.07 ± 0.02	BARBARO-...	70	DPWA	$K^- p \to \Lambda\pi^0$

$(\Gamma_i\Gamma_f)^{1/2}/\Gamma_{total}$ in $N\overline{K} \to \Sigma(2100) \to \Sigma\pi$ **$(\Gamma_1\Gamma_3)^{1/2}/\Gamma$**

VALUE	DOCUMENT ID		TECN	COMMENT
+0.13 ± 0.02	BARBARO-...	70	DPWA	$K^- p \to \Sigma\pi$

$\Sigma(2100)$ REFERENCES

BARBARO-...	70	Duke Conf. 173 Hyperon Resonances, 1970	A. Barbaro-Galtieri	(LRL) IJP

$\Sigma(2250)$

$I(J^P) = 1(?^?)$ Status: ***

Results from partial-wave analyses are too weak to warrant separating them from the production and cross-section experiments. LASINSKI 71 in $\overline{K}N$ using a Pomeron + resonances model, and DEBELLEFON 76, DEBELLEFON 77, and DEBELLEFON 78 in energy-dependent partial-wave analyses of $\overline{K}N \to \Lambda\pi$, $\Sigma\pi$, and $N\overline{K}$, respectively, suggest two resonances around this mass.

$\Sigma(2250)$ MASS

VALUE (MeV)	DOCUMENT ID		TECN	COMMENT
2210 to 2280 (≈ 2250) OUR ESTIMATE				
2270 ± 50	DEBELLEFON	78	DPWA	D_5 wave
2210 ± 30	DEBELLEFON	78	DPWA	G_9 wave
2275 ± 20	DEBELLEFON	77	DPWA	D_5 wave
2215 ± 20	DEBELLEFON	77	DPWA	G_9 wave
2300 ± 30	[1] DEBELLEFON	75B	HBC	$K^- p \to \Xi^{*0} K^0$
2251^{+30}_{-20}	VANHORN	75	DPWA	$K^- p \to \Lambda\pi^0$, F_5 wave
2280 ± 14	AGUILAR-...	70B	HBC	$K^- p$ 3.9, 4.6 GeV/c
2237 ± 11	BRICMAN	70	CNTR	Total, charge exchange
2255 ± 10	COOL	70	CNTR	$K^- p$, $K^- d$ total
2250 ± 7	BUGG	68	CNTR	$K^- p$, $K^- d$ total
• • • We do not use the following data for averages, fits, limits, etc. • • •				
2260	DEBELLEFON	76	IPWA	D_5 wave
2215	DEBELLEFON	76	IPWA	G_9 wave
2250 ± 20	LU	70	CNTR	$\gamma p \to K^+ Y^*$
2245	BLANPIED	65	CNTR	$\gamma p \to K^+ Y^*$
2299 ± 6	BOCK	65	HBC	$\overline{p}p$ 5.7 GeV/c

$\Sigma(2250)$ WIDTH

VALUE (MeV)	DOCUMENT ID		TECN	COMMENT
60 to 150 (≈ 100) OUR ESTIMATE				
120 ± 40	DEBELLEFON	78	DPWA	D_5 wave
80 ± 20	DEBELLEFON	78	DPWA	G_9 wave
70 ± 20	DEBELLEFON	77	DPWA	D_5 wave
60 ± 20	DEBELLEFON	77	DPWA	G_9 wave
130 ± 20	[1] DEBELLEFON	75B	HBC	$K^- p \to \Xi^{*0} K^0$
192 ± 30	VANHORN	75	DPWA	$K^- p \to \Lambda\pi^0$, F_5 wave
100 ± 20	AGUILAR-...	70B	HBC	$K^- p$ 3.9, 4.6 GeV/c
164 ± 50	BRICMAN	70	CNTR	Total, charge exchange
230 ± 20	BUGG	68	CNTR	$K^- p$, $K^- d$ total
• • • We do not use the following data for averages, fits, limits, etc. • • •				
100	DEBELLEFON	76	IPWA	D_5 wave
140	DEBELLEFON	76	IPWA	G_9 wave
170	COOL	70	CNTR	$K^- p$, $K^- d$ total
125	LU	70	CNTR	$\gamma p \to K^+ Y^*$
150	BLANPIED	65	CNTR	$\gamma p \to K^+ Y^*$
21^{+17}_{-21}	BOCK	65	HBC	$\overline{p}p$ 5.7 GeV/c

$\Sigma(2250)$ DECAY MODES

	Mode	Fraction (Γ_i/Γ)
Γ_1	$N\overline{K}$	<10 %
Γ_2	$\Lambda\pi$	seen
Γ_3	$\Sigma\pi$	seen
Γ_4	$N\overline{K}\pi$	
Γ_5	$\Xi(1530)K$	

$\Sigma(2250)$ BRANCHING RATIOS

See "Sign conventions for resonance couplings" in the Note on Λ and Σ Resonances.

$\Gamma(N\overline{K})/\Gamma_{total}$ — Γ_1/Γ

VALUE	DOCUMENT ID		TECN	COMMENT
<0.1 OUR ESTIMATE				
0.08±0.02	DEBELLEFON	78	DPWA	D_5 wave
0.02±0.01	DEBELLEFON	78	DPWA	G_9 wave

$(J+\frac{1}{2})\times\Gamma(N\overline{K})/\Gamma_{total}$ — Γ_1/Γ

VALUE	DOCUMENT ID		TECN	COMMENT
• • • We do not use the following data for averages, fits, limits, etc. • • •				
0.16±0.12	BRICMAN	70	CNTR	Total, charge exchange
0.42	COOL	70	CNTR	K^-p, K^-d total
0.47	BUGG	68	CNTR	

$(\Gamma_i\Gamma_f)^{1/2}/\Gamma_{total}$ in $N\overline{K}\to\Sigma(2250)\to\Lambda\pi$ — $(\Gamma_1\Gamma_2)^{1/2}/\Gamma$

VALUE	DOCUMENT ID		TECN	COMMENT
−0.16±0.03	VANHORN	75	DPWA	$K^-p\to\Lambda\pi^0$, F_5 wave
• • • We do not use the following data for averages, fits, limits, etc. • • •				
+0.11	DEBELLEFON	76	IPWA	D_5 wave
−0.10	DEBELLEFON	76	IPWA	G_9 wave
−0.18	BARBARO-...	70	DPWA	$K^-p\to\Lambda\pi^0$, G_9 wave

$(\Gamma_i\Gamma_f)^{1/2}/\Gamma_{total}$ in $N\overline{K}\to\Sigma(2250)\to\Sigma\pi$ — $(\Gamma_1\Gamma_3)^{1/2}/\Gamma$

VALUE	DOCUMENT ID		TECN	COMMENT
+0.06±0.02	DEBELLEFON	77	DPWA	D_5 wave
−0.03±0.02	DEBELLEFON	77	DPWA	G_9 wave
+0.07	BARBARO-...	70	DPWA	$K^-p\to\Sigma\pi$, G_9 wave

$\Gamma(N\overline{K})/\Gamma(\Sigma\pi)$ — Γ_1/Γ_3

VALUE	DOCUMENT ID		TECN	COMMENT
• • • We do not use the following data for averages, fits, limits, etc. • • •				
<0.18	BARNES	69	HBC	1 standard dev. limit

$\Gamma(\Lambda\pi)/\Gamma(\Sigma\pi)$ — Γ_2/Γ_3

VALUE	DOCUMENT ID		TECN	COMMENT
• • • We do not use the following data for averages, fits, limits, etc. • • •				
<0.18	BARNES	69	HBC	1 standard dev. limit

$(\Gamma_i\Gamma_f)^{1/2}/\Gamma_{total}$ in $N\overline{K}\to\Sigma(2250)\to\Xi(1530)K$ — $(\Gamma_1\Gamma_5)^{1/2}/\Gamma$

VALUE	DOCUMENT ID		TECN	COMMENT
0.18±0.04	[1] DEBELLEFON	75B	HBC	$K^-p\to\Xi^{*0}K^0$

$\Sigma(2250)$ FOOTNOTES

[1] Seen in the (initial and final state) D_5 wave. Isospin not determined.

$\Sigma(2250)$ REFERENCES

DEBELLEFON	78	NC 42A 403	A. de Bellefon *et al.*	(CDEF, SACL) IJP
DEBELLEFON	77	NC 37A 175	A. de Bellefon *et al.*	(CDEF, SACL) IJP
DEBELLEFON	76	NP B109 129	A. de Bellefon, A. Berthon	(CDEF) IJP
Also		NP B90 1	A. de Bellefon *et al.*	(CDEF, SACL) IJP
DEBELLEFON	75B	NC 28A 289	A. de Bellefon *et al.*	(CDEF, SACL)
VANHORN	75	NP B87 145	A.J. van Horn	(LBL) IJP
Also		NP B87 157	A.J. van Horn	(LBL) IJP
LASINSKI	71	NP B29 125	T.A. Lasinski	(EFI) IJP
AGUILAR-...	70B	PRL 25 58	M. Aguilar-Benitez *et al.*	(BNL, SYRA)
BARBARO-...	70	Duke Conf. 173 Hyperon Resonances, 1970	A. Barbaro-Galtieri	(LRL) IJP
BRICMAN	70	PL 31B 152	C. Bricman *et al.*	(CERN, CAEN, SACL)
COOL	70	PR D1 1887	R.L. Cool *et al.*	(BNL) I
Also		PRL 16 1228	R.L. Cool *et al.*	(BNL) I
LU	70	PR D2 1846	D.C. Lu *et al.*	(YALE)
BARNES	69	PRL 22 479	V.E. Barnes *et al.*	(BNL, SYRA)
BUGG	68	PR 168 1466	D.V. Bugg *et al.*	(RHEL, BIRM, CAVE) I
BLANPIED	65	PRL 14 741	W.A. Blanpied *et al.*	(YALE, CEA)
BOCK	65	PL 17 166	R.K. Bock *et al.*	(CERN, SACL)

$\Sigma(2455)$ Bumps

$I(J^P) = 1(?^?)$ Status: **

OMITTED FROM SUMMARY TABLE

There is also some slight evidence for Y^* states in this mass region from the reaction $\gamma p\to K^+X$ — see GREENBERG 68.

$\Sigma(2455)$ MASS

VALUE (MeV)	DOCUMENT ID		TECN	COMMENT
≈ 2455 OUR ESTIMATE				
2455±10	ABRAMS	70	CNTR	K^-p, K^-d total
2455± 7	BUGG	68	CNTR	K^-p, K^-d total

$\Sigma(2455)$ WIDTH

VALUE (MeV)	DOCUMENT ID		TECN	COMMENT
140	ABRAMS	70	CNTR	K^-p, K^-d total
100±20	BUGG	68	CNTR	

$\Sigma(2455)$ DECAY MODES

	Mode
Γ_1	$N\overline{K}$

$\Sigma(2455)$ BRANCHING RATIOS

$(J+\frac{1}{2})\times\Gamma(N\overline{K})/\Gamma_{total}$ — Γ_1/Γ

VALUE	DOCUMENT ID		TECN	COMMENT
0.39	ABRAMS	70	CNTR	K^-p, K^-d total
0.05±0.05	[1] BRICMAN	70	CNTR	Total, charge exchange
0.3	BUGG	68	CNTR	

$\Sigma(2455)$ FOOTNOTES

[1] Fit of total cross section given by BRICMAN 70 is poor in this region.

$\Sigma(2455)$ REFERENCES

ABRAMS	70	PR D1 1917	R.J. Abrams *et al.*	(BNL) I
Also		PRL 19 678	R.J. Abrams *et al.*	(BNL)
BRICMAN	70	PL 31B 152	C. Bricman *et al.*	(CERN, CAEN, SACL)
BUGG	68	PR 168 1466	D.V. Bugg *et al.*	(RHEL, BIRM, CAVE) I
GREENBERG	68	PRL 20 221	J.S. Greenberg *et al.*	(YALE)

$\Sigma(2620)$ Bumps

$I(J^P) = 1(?^?)$ Status: **

OMITTED FROM SUMMARY TABLE

$\Sigma(2620)$ MASS

VALUE (MeV)	DOCUMENT ID		TECN	COMMENT
≈ 2620 OUR ESTIMATE				
2542±22	DIBIANCA	75	DBC	$K^-N\to\Xi K\pi$
2620±15	ABRAMS	70	CNTR	K^-p, K^-d total

$\Sigma(2620)$ WIDTH

VALUE (MeV)	DOCUMENT ID		TECN	COMMENT
221±81	DIBIANCA	75	DBC	$K^-N\to\Xi K\pi$
175	ABRAMS	70	CNTR	K^-p, K^-d total

$\Sigma(2620)$ DECAY MODES

	Mode
Γ_1	$N\overline{K}$

$\Sigma(2620)$ BRANCHING RATIOS

$(J+\frac{1}{2})\times\Gamma(N\overline{K})/\Gamma_{total}$ — Γ_1/Γ

VALUE	DOCUMENT ID		TECN	COMMENT
0.32	ABRAMS	70	CNTR	K^-p, K^-d total
0.36±0.12	BRICMAN	70	CNTR	Total, charge exchange

$\Sigma(2620)$ REFERENCES

DIBIANCA	75	NP B98 137	F.A. Dibianca, R.J. Endorf	(CMU)
ABRAMS	70	PR D1 1917	R.J. Abrams *et al.*	(BNL) I
Also		PRL 19 678	R.J. Abrams *et al.*	(BNL)
BRICMAN	70	PL 31B 152	C. Bricman *et al.*	(CERN, CAEN, SACL)

$\Sigma(3000)$ Bumps

$I(J^P) = 1(?^?)$ Status: *

OMITTED FROM SUMMARY TABLE

Seen as an enhancement in $\Lambda\pi$ and $\overline{K}N$ invariant mass spectra and in the missing mass of neutrals recoiling against a K^0.

Baryon Particle Listings

$\Sigma(3000)$ Bumps, $\Sigma(3170)$ Bumps

$\Sigma(3000)$ MASS

VALUE (MeV)	DOCUMENT ID		TECN	CHG	COMMENT
≈ 3000 OUR ESTIMATE					
3000	EHRLICH	66	HBC	0	$\pi^- p$ 7.91 GeV/c

$\Sigma(3000)$ DECAY MODES

	Mode
Γ_1	$N\overline{K}$
Γ_2	$\Lambda\pi$

$\Sigma(3000)$ REFERENCES

EHRLICH 66 PR 152 1194 R. Ehrlich, W. Selove, H. Yuta (PENN)I

$\Sigma(3170)$ Bumps

$I(J^P) = 1(?^?)$ Status: *

OMITTED FROM SUMMARY TABLE

Seen by AMIRZADEH 79 as a narrow 6.5-standard-deviation enhancement in the reaction $K^- p \rightarrow Y^{*+}\pi^-$ using data from independent high statistics bubble chamber experiments at 8.25 and 6.5 GeV/c. The dominant decay modes are multibody, multistrange final states and the production is via isospin-3/2 baryon exchange. Isospin 1 is favored.

Not seen in a $K^- p$ experiment in LASS at 11 GeV/c (ASTON 85B).

$\Sigma(3170)$ MASS (PRODUCTION EXPERIMENTS)

VALUE (MeV)	EVTS	DOCUMENT ID		TECN	COMMENT
≈ 3170 OUR ESTIMATE					
3170±5	35	AMIRZADEH	79	HBC	$K^- p \rightarrow Y^{*+}\pi^-$

$\Sigma(3170)$ WIDTH (PRODUCTION EXPERIMENTS)

VALUE (MeV)	EVTS	DOCUMENT ID		TECN	COMMENT
<20	35	[1] AMIRZADEH	79	HBC	$K^- p \rightarrow Y^{*+}\pi^-$

$\Sigma(3170)$ DECAY MODES (PRODUCTION EXPERIMENTS)

	Mode	Fraction (Γ_i/Γ)
Γ_1	$\Lambda K\overline{K}\pi$'s	seen
Γ_2	$\Sigma K\overline{K}\pi$'s	seen
Γ_3	$\Xi K\pi$'s	seen

$\Sigma(3170)$ BRANCHING RATIOS (PRODUCTION EXPERIMENTS)

$\Gamma(\Lambda K\overline{K}\pi\text{'s})/\Gamma_{total}$ **Γ_1/Γ**

VALUE	DOCUMENT ID		TECN	COMMENT
seen	AMIRZADEH	79	HBC	$K^- p \rightarrow Y^{*+}\pi^-$

$\Gamma(\Sigma K\overline{K}\pi\text{'s})/\Gamma_{total}$ **Γ_2/Γ**

VALUE	DOCUMENT ID		TECN	COMMENT
seen	AMIRZADEH	79	HBC	$K^- p \rightarrow Y^{*+}\pi^-$

$\Gamma(\Xi K\pi\text{'s})/\Gamma_{total}$ **Γ_3/Γ**

VALUE	DOCUMENT ID		TECN	COMMENT
seen	AMIRZADEH	79	HBC	$K^- p \rightarrow Y^{*+}\pi^-$

$\Sigma(3170)$ FOOTNOTES (PRODUCTION EXPERIMENTS)

[1] Observed width consistent with experimental resolution.

$\Sigma(3170)$ REFERENCES (PRODUCTION EXPERIMENTS)

ASTON 85B PR D32 2270 D. Aston *et al.* (SLAC, CARL, CNRC, CINC)
AMIRZADEH 79 PL 89B 125 J. Amirzadeh *et al.* (BIRM, CERN, GLAS+)I
Also Toronto Conf. 263 J.B. Kinson *et al.* (BIRM, CERN, GLAS+)I

Ξ BARYONS
($S = -2$, $I = 1/2$)

$\Xi^0 = uss$, $\Xi^- = dss$

Ξ^0 $I(J^P) = \frac{1}{2}(\frac{1}{2}^+)$ Status: ****

The parity has not actually been measured, but + is of course expected.

Ξ^0 MASS

The fit uses the Ξ^0, Ξ^-, and $\overline{\Xi}^+$ masses and the $\Xi^- - \Xi^0$ mass difference. It assumes that the Ξ^- and $\overline{\Xi}^+$ masses are the same.

VALUE (MeV)	EVTS	DOCUMENT ID		TECN	COMMENT
1314.86±0.20 OUR FIT					
1314.82±0.06±0.20	3120	FANTI	00	NA48	p Be, 450 GeV
• • • We do not use the following data for averages, fits, limits, etc. • • •					
1315.2 ±0.92	49	WILQUET	72	HLBC	
1313.4 ±1.8	1	PALMER	68	HBC	

$m_{\Xi^-} - m_{\Xi^0}$

The fit uses the Ξ^0, Ξ^-, and $\overline{\Xi}^+$ masses and the $\Xi^- - \Xi^0$ mass difference. It assumes that the Ξ^- and $\overline{\Xi}^+$ masses are the same.

VALUE (MeV)	EVTS	DOCUMENT ID		TECN	COMMENT
6.85±0.21 OUR FIT					
6.3 ±0.7 OUR AVERAGE					
6.9 ±2.2	29	LONDON	66	HBC	
6.1 ±0.9	88	PJERROU	65B	HBC	
6.8 ±1.6	23	JAUNEAU	63	FBC	
• • • We do not use the following data for averages, fits, limits, etc. • • •					
6.1 ±1.6	45	CARMONY	64B	HBC	See PJERROU 65B

Ξ^0 MEAN LIFE

VALUE (10^{-10} s)	EVTS	DOCUMENT ID		TECN	COMMENT
2.90±0.09 OUR AVERAGE					
2.83±0.16	6300	[1] ZECH	77	SPEC	Neutral hyperon beam
$2.88^{+0.21}_{-0.19}$	652	BALTAY	74	HBC	1.75 GeV/c K^-p
$2.90^{+0.32}_{-0.27}$	157	[2] MAYEUR	72	HLBC	2.1 GeV/c K^-
$3.07^{+0.22}_{-0.20}$	340	DAUBER	69	HBC	
3.0 ±0.5	80	PJERROU	65B	HBC	
$2.5\ ^{+0.4}_{-0.3}$	101	HUBBARD	64	HBC	
$3.9\ ^{+1.4}_{-0.8}$	24	JAUNEAU	63	FBC	
• • • We do not use the following data for averages, fits, limits, etc. • • •					
$3.5\ ^{+1.0}_{-0.8}$	45	CARMONY	64B	HBC	See PJERROU 65B

[1] The ZECH 77 result is $\tau_{\Xi^0} = [2.77-(\tau_\Lambda - 2.69)] \times 10^{-10}$ s, in which we use $\tau_\Lambda = 2.63 \times 10^{-10}$ s.
[2] The MAYEUR 72 value is modified for the erratum.

Ξ^0 MAGNETIC MOMENT

See the "Note on Baryon Magnetic Moments" in the Λ Listings.

VALUE (μ_N)	EVTS	DOCUMENT ID		TECN
−1.250±0.014 OUR AVERAGE				
−1.253±0.014	270k	COX	81	SPEC
−1.20 ±0.06	42k	BUNCE	79	SPEC

Ξ^0 DECAY MODES

	Mode	Fraction (Γ_i/Γ)	Confidence level
Γ_1	$\Lambda\pi^0$	(99.524±0.012) %	
Γ_2	$\Lambda\gamma$	(1.17 ±0.07) × 10^{-3}	
Γ_3	$\Lambda e^+ e^-$	(7.6 ±0.6) × 10^{-6}	
Γ_4	$\Sigma^0\gamma$	(3.33 ±0.10) × 10^{-3}	
Γ_5	$\Sigma^+ e^- \overline{\nu}_e$	(2.52 ±0.08) × 10^{-4}	
Γ_6	$\Sigma^+ \mu^- \overline{\nu}_\mu$	(2.33 ±0.35) × 10^{-6}	

$\Delta S = \Delta Q$ (SQ) violating modes or $\Delta S = 2$ forbidden ($S2$) modes

Γ_7	$\Sigma^- e^+ \nu_e$	SQ	<	9	× 10^{-4}	90%
Γ_8	$\Sigma^- \mu^+ \nu_\mu$	SQ	<	9	× 10^{-4}	90%
Γ_9	$p\pi^-$	$S2$	<	8	× 10^{-6}	90%
Γ_{10}	$p e^- \overline{\nu}_e$	$S2$	<	1.3	× 10^{-3}	
Γ_{11}	$p \mu^- \overline{\nu}_\mu$	$S2$	<	1.3	× 10^{-3}	

CONSTRAINED FIT INFORMATION

An overall fit to 5 branching ratios uses 11 measurements and one constraint to determine 5 parameters. The overall fit has a $\chi^2 = 7.5$ for 7 degrees of freedom.

The following *off-diagonal* array elements are the correlation coefficients $\langle \delta x_i \delta x_j \rangle / (\delta x_i \cdot \delta x_j)$, in percent, from the fit to the branching fractions, $x_i \equiv \Gamma_i/\Gamma_{\rm total}$. The fit constrains the x_i whose labels appear in this array to sum to one.

	x_1	x_2	x_4	x_5
x_2	−57			
x_4	−82	0		
x_5	−7	0	0	
x_6	0	0	0	1

Ξ^0 BRANCHING RATIOS

$\Gamma(\Lambda\gamma)/\Gamma(\Lambda\pi^0)$ Γ_2/Γ_1

VALUE (units 10^{-3})	EVTS	DOCUMENT ID		TECN	COMMENT
1.17±0.07 OUR FIT					
1.17±0.07 OUR AVERAGE					
1.17±0.05±0.06	672	[3] LAI	04A	NA48	p Be, 450 GeV
1.91±0.34±0.19	31	[4] FANTI	00	NA48	p Be, 450 GeV
1.06±0.12±0.11	116	JAMES	90	SPEC	FNAL hyperons

[3] LAI 04A used our 2002 value of 99.5% for the $\Xi^0 \to \Lambda\pi^0$ branching fraction to get $\Gamma(\Xi^0 \to \Lambda\gamma)/\Gamma_{\rm total} = (1.16 \pm 0.05 \pm 0.06) \times 10^{-3}$. We adjust slightly to go back to what was directly measured.
[4] FANTI 00 used our 1998 value of 99.5% for the $\Xi^0 \to \Lambda\pi^0$ branching fraction to get $\Gamma(\Xi^0 \to \Lambda\gamma)/\Gamma_{\rm total} = (1.90 \pm 0.34 \pm 0.19) \times 10^{-3}$. We adjust slightly to go back to what was directly measured.

$\Gamma(\Lambda e^+ e^-)/\Gamma_{\rm total}$ Γ_3/Γ

VALUE (units 10^{-6})	EVTS	DOCUMENT ID		TECN	COMMENT
7.6±0.4±0.5	397 ± 21	[5] BATLEY	07C	NA48	p Be, 400 GeV

[5] This BATLEY 07C result is consistent with internal bremsstrahlung.

$\Gamma(\Sigma^0\gamma)/\Gamma(\Lambda\pi^0)$ Γ_4/Γ_1

VALUE (units 10^{-3})	EVTS	DOCUMENT ID		TECN	COMMENT
3.35±0.10 OUR FIT					
3.35±0.10 OUR AVERAGE					
3.34±0.05±0.09	4045	ALAVI-HARATI	01C	KTEV	p nucleus, 800 GeV
3.16±0.76±0.32	17	[6] FANTI	00	NA48	p Be, 450 GeV
3.56±0.42±0.10	85	TEIGE	89	SPEC	FNAL hyperons

[6] FANTI 00 used our 1998 value of 99.5% for the $\Xi^0 \to \Lambda\pi^0$ branching fraction to get $\Gamma(\Xi^0 \to \Sigma^0\gamma)/\Gamma_{\rm total} = (3.14 \pm 0.76 \pm 0.32) \times 10^{-3}$. We adjust slightly to go back to what was directly measured.

$\Gamma(\Sigma^+ e^- \overline{\nu}_e)/\Gamma_{\rm total}$ Γ_5/Γ

VALUE (units 10^{-4})	EVTS	DOCUMENT ID		TECN	COMMENT
2.52±0.08 OUR FIT					
2.53±0.08 OUR AVERAGE					
2.51±0.03±0.09	6101	BATLEY	07	NA48	p Be, 400 GeV
2.55±0.14±0.10	419	[7] BATLEY	07	NA48	p Be, 400 GeV
2.71±0.22±0.31	176	AFFOLDER	99	KTEV	p nucleus, 800 GeV

[7] This BATLEY 07 result is for $\overline{\Xi}^0 \to \overline{\Sigma}^- e^+ \nu_e$ events.

$\Gamma(\Sigma^+ \mu^- \overline{\nu}_\mu)/\Gamma_{\rm total}$ Γ_6/Γ

VALUE (units 10^{-6})	EVTS	DOCUMENT ID		TECN	COMMENT
2.3 ±0.4 OUR FIT					
2.17±0.32±0.17	66	[8] BATLEY	13	NA48	p Be, 400 GeV

[8] BATLEY 13 used $\Xi^0 \to \Sigma^+ e^- \overline{\nu}_e$ decay as a normalization mode and its branching fraction value of (2.51 ± 0.03 ± 0.09) × 10^{-4} from BATLEY 07.

$\Gamma(\Sigma^+ \mu^- \overline{\nu}_\mu)/\Gamma(\Sigma^+ e^- \overline{\nu}_e)$ Γ_6/Γ_5

VALUE	EVTS	DOCUMENT ID		TECN	COMMENT
0.0092±0.0015 OUR FIT					
0.018 $^{+0.007}_{-0.005}$ ±0.002	9	ABOUZAID	05	KTEV	p nucleus 800 GeV

Baryon Particle Listings

Ξ^0, Ξ^-

$\Gamma(\Sigma^- e^+ \nu_e)/\Gamma(\Lambda\pi^0)$ Γ_7/Γ_1

Test of $\Delta S = \Delta Q$ rule.

VALUE (units 10^{-3})	CL%	EVTS	DOCUMENT ID		TECN	COMMENT
<0.9	90	0	YEH	74	HBC	Effective denom.=2500
• • • We do not use the following data for averages, fits, limits, etc. • • •						
<1.5			DAUBER	69	HBC	
<6			HUBBARD	66	HBC	

$\Gamma(\Sigma^- \mu^+ \nu_\mu)/\Gamma(\Lambda\pi^0)$ Γ_8/Γ_1

Test of $\Delta S = \Delta Q$ rule.

VALUE (units 10^{-3})	CL%	EVTS	DOCUMENT ID		TECN	COMMENT
<0.9	90	0	YEH	74	HBC	Effective denom.=2500
• • • We do not use the following data for averages, fits, limits, etc. • • •						
<1.5			DAUBER	69	HBC	
<6			HUBBARD	66	HBC	

$\Gamma(p\pi^-)/\Gamma(\Lambda\pi^0)$ Γ_9/Γ_1

ΔS=2. Forbidden in first-order weak interaction.

VALUE (units 10^{-6})	CL%	EVTS	DOCUMENT ID		TECN	COMMENT
< 8.2	90		WHITE	05	HYCP	p Cu, 800 GeV
• • • We do not use the following data for averages, fits, limits, etc. • • •						
< 36	90		GEWENIGER	75	SPEC	
<1800	90	0	YEH	74	HBC	Effective denom.=1300
< 900			DAUBER	69	HBC	
<5000			HUBBARD	66	HBC	

$\Gamma(pe^-\overline{\nu}_e)/\Gamma(\Lambda\pi^0)$ Γ_{10}/Γ_1

ΔS=2. Forbidden in first-order weak interaction.

VALUE (units 10^{-3})	CL%	EVTS	DOCUMENT ID		TECN	COMMENT
<1.3			DAUBER	69	HBC	
• • • We do not use the following data for averages, fits, limits, etc. • • •						
<3.4	90	0	YEH	74	HBC	Effective denom.=670
<6			HUBBARD	66	HBC	

$\Gamma(p\mu^-\overline{\nu}_\mu)/\Gamma(\Lambda\pi^0)$ Γ_{11}/Γ_1

ΔS=2. Forbidden in first-order weak interaction.

VALUE (units 10^{-3})	CL%	EVTS	DOCUMENT ID		TECN	COMMENT
<1.3			DAUBER	69	HBC	
• • • We do not use the following data for averages, fits, limits, etc. • • •						
<3.5	90	0	YEH	74	HBC	Effective denom.=664
<6			HUBBARD	66	HBC	

Ξ^0 DECAY PARAMETERS

See the "Note on Baryon Decay Parameters" in the neutron Listings.

$\alpha(\Xi^0)\ \alpha_-(\Lambda)$

This is a product of the $\Xi^0 \to \Lambda\pi^0$ and $\Lambda \to p\pi^-$ asymmetries.

VALUE	EVTS	DOCUMENT ID		TECN	COMMENT
-0.261 ± 0.006 OUR AVERAGE					
$-0.276\pm0.001\pm0.035$	4M	BATLEY	10B	NA48	p Be, 400 GeV
$-0.260\pm0.004\pm0.005$	300k	HANDLER	82	SPEC	FNAL hyperons
• • • We do not use the following data for averages, fits, limits, etc. • • •					
-0.317 ± 0.027	6075	BUNCE	78	SPEC	FNAL hyperons
$-0.35\ \pm0.06$	505	BALTAY	74	HBC	K^-p 1.75 GeV/c
$-0.28\ \pm0.06$	739	DAUBER	69	HBC	K^-p 1.7–2.6 GeV/c

α FOR $\Xi^0 \to \Lambda\pi^0$

The above average, $\alpha(\Xi^0)\alpha_-(\Lambda) = -0.261 \pm 0.006$, divided by our current average $\alpha_-(\Lambda) = 0.642 \pm 0.013$, gives the following value for $\alpha(\Xi^0)$.

VALUE	DOCUMENT ID
-0.406 ± 0.013 OUR EVALUATION	

ϕ ANGLE FOR $\Xi^0 \to \Lambda\pi^0$ $(\tan\phi = \beta/\gamma)$

VALUE (°)	EVTS	DOCUMENT ID		TECN	COMMENT
21 ± 12 OUR AVERAGE					
16 ± 17	652	BALTAY	74	HBC	1.75 GeV/c K^-p
38 ± 19	739	[9] DAUBER	69	HBC	
$-\ 8\pm30$	146	[10] BERGE	66	HBC	

[9] DAUBER 69 uses $\alpha_\Lambda = 0.647 \pm 0.020$.

[10] The errors have been multiplied by 1.2 due to approximations used for the Ξ polarization; see DAUBER 69 for a discussion.

See the related review(s):
Radiative Hyperon Decays

α FOR $\Xi^0 \to \Lambda\gamma$

See the note above on "Radiative Hyperon Decays."

VALUE	EVTS	DOCUMENT ID		TECN	COMMENT
$-0.704\pm0.019\pm0.064$	52k	[11] BATLEY	10B	NA48	p Be, 400 GeV
• • • We do not use the following data for averages, fits, limits, etc. • • •					
$-0.78\ \pm0.18\ \pm0.06$	672	LAI	04A	NA48	See BATLEY 10B
$-0.43\ \pm0.44$	87	[12] JAMES	90	SPEC	FNAL hyperons

[11] BATLEY 10B also measured the $\overline{\Xi}^0 \to \overline{\Lambda}\gamma$ asymmetry to be -0.798 ± 0.064 (no systematic error given) with 4769 events.

[12] The sign has been changed; see the erratum, JAMES 02.

α FOR $\Xi^0 \to \Lambda e^+ e^-$

VALUE	EVTS	DOCUMENT ID		TECN	COMMENT
-0.8 ± 0.2	397 ± 21	[13] BATLEY	07C	NA48	p Be, 400 GeV

[13] This BATLEY 07C result is consistent with the asymmetry α for $\Xi^0 \to \Lambda\gamma$, as expected if the mechanism is internal bremsstrahlung.

α FOR $\Xi^0 \to \Sigma^0\gamma$

See the note above on "Radiative Hyperon Decays."

VALUE	EVTS	DOCUMENT ID		TECN	COMMENT
$-0.69\ \pm0.06$ OUR AVERAGE					
$-0.729\pm0.030\pm0.076$	15k	[14] BATLEY	10B	NA48	p Be, 400 GeV
$-0.63\ \pm0.08\ \pm0.05$	4045	ALAVI-HARATI	01C	KTEV	p nucleus, 800 GeV
• • • We do not use the following data for averages, fits, limits, etc. • • •					
$+0.20\ \pm0.32\ \pm0.05$	85	[15] TEIGE	89	SPEC	FNAL hyperons

[14] BATLEY 10B also measured the $\overline{\Xi}^0 \to \overline{\Sigma}^0\gamma$ asymmetry to be -0.786 ± 0.104 (no systematic error given) with 1404 events.

[15] This result has been withdrawn, due to an error. See the erratum, TEIGE 02.

$g_1(0)/f_1(0)$ FOR $\Xi^0 \to \Sigma^+ e^- \overline{\nu}_e$

VALUE	EVTS	DOCUMENT ID		TECN	COMMENT
1.22 ± 0.05 OUR AVERAGE					
1.21 ± 0.05		BATLEY	13	NA48	p Be, 400 GeV
$1.32^{+0.21}_{-0.17}\pm0.05$	487	[16] ALAVI-HARATI	01I	KTEV	p nucleus, 800 GeV
• • • We do not use the following data for averages, fits, limits, etc. • • •					
$1.20\pm0.04\pm0.03$	6520	[17] BATLEY	07	NA48	See BATLEY 13

[16] ALAVI-HARATI 01I assumes here that the second-class current is zero and that the weak-magnetism term takes its exact SU(3) value.

[17] This BATLEY 07 result uses our 2006 value of V_{us} from semileptonic kaon decays as input.

$g_2(0)/f_1(0)$) FOR $\Xi^0 \to \Sigma^+ e^- \overline{\nu}_e$

VALUE	EVTS	DOCUMENT ID		TECN	COMMENT
$\mathbf{-1.7^{+2.1}_{-2.0}\pm0.5}$	487	[18] ALAVI-HARATI	01I	KTEV	p nucleus, 800 GeV

[18] ALAVI-HARATI 01I thus assumes that $g_2 = 0$ in calculating g_1/f_1, above.

$f_2(0)/f_1(0)$ FOR $\Xi^0 \to \Sigma^+ e^- \overline{\nu}_e$

VALUE	EVTS	DOCUMENT ID		TECN	COMMENT
2.0 ± 0.9 OUR AVERAGE					
2.0 ± 1.3		BATLEY	13	NA48	p Be, 400 GeV
$2.0\pm1.2\pm0.5$	487	ALAVI-HARATI	01I	KTEV	p nucleus, 800 GeV

Ξ^0 REFERENCES

BATLEY	13	PL B720 105	J.R. Batley *et al.*	(CERN NA48/1 Collab.)
BATLEY	10B	PL B693 241	J.R. Batley *et al.*	(CERN NA48/1 Collab.)
BATLEY	07	PL B645 36	J.R. Batley *et al.*	(CERN NA48/1 Collab.)
BATLEY	07C	PL B650 1	J.R. Batley *et al.*	(CERN NA48 Collab.)
ABOUZAID	05	PRL 95 081801	E. Abouzaid *et al.*	(FNAL KTeV Collab.)
WHITE	05	PRL 94 101804	C.G. White *et al.*	(FNAL HyperCP Collab.)
LAI	04A	PL B584 251	A. Lai *et al.*	(CERN NA48 Collab.)
JAMES	02	PRL 89 169901 (errat.)	C. James *et al.*	(MINN, MICH, WISC, RUTG)
TEIGE	02	PRL 89 169902 (errat.)	S. Teige *et al.*	(RUTG, MICH, MINN)
ALAVI-HARATI	01C	PRL 86 3239	A. Alavi-Harati *et al.*	(FNAL KTeV Collab.)
ALAVI-HARATI	01I	PRL 87 132001	A. Alavi-Harati *et al.*	(FNAL KTeV Collab.)
FANTI	00	EPJ C12 69	V. Fanti *et al.*	(CERN NA48 Collab.)
AFFOLDER	99	PRL 82 3751	A. Affolder *et al.*	(FNAL KTeV Collab.)
JAMES	90	PRL 64 843	C. James *et al.*	(MINN, MICH, WISC, RUTG)
TEIGE	89	PRL 63 2717	S. Teige *et al.*	(RUTG, MICH, MINN)
HANDLER	82	PR D25 639	R. Handler *et al.*	(WISC, MICH, MINN+)
COX	81	PRL 46 877	P.T. Cox *et al.*	(MICH, WISC, RUTG, MINN+)
BUNCE	79	PL B6B 386	G.R.M. Bunce *et al.*	(BNL, MICH, RUTG+)
BUNCE	78	PR D18 633	G.R.M. Bunce *et al.*	(WISC, MICH, RUTG)
ZECH	77	NP B124 413	G. Zech *et al.*	(SIEG, CERN, DORT, HEIDH)
GEWENIGER	75	PL 57B 193	C. Geweniger *et al.*	(CERN, HEIDH)
BALTAY	74	PR D9 49	C. Baltay *et al.*	(COLU, BING) J
YEH	74	PR D10 3545	N. Yeh *et al.*	(BING, COLU)
MAYEUR	72	NP B47 333	C. Mayeur *et al.*	(BRUX, CERN, TUFTS, LOUC)
Also		NP B53 268 (erratum)	C. Mayeur	
WILQUET	72	PL 42B 372	G. Wilquet *et al.*	(BRUX, CERN, TUFTS+)
DAUBER	69	PR 179 1262	P.M. Dauber *et al.*	(LRL)
PALMER	68	PL 26B 323	R.B. Palmer *et al.*	(BNL, SYRA)
BERGE	66	PR 147 945	J.P. Berge *et al.*	(LRL)
HUBBARD	66	Thesis UCRL 11510	J.R. Hubbard	(LRL)
LONDON	66	PR 143 1034	G.W. London *et al.*	(BNL, SYRA)
PJERROU	65B	PRL 14 275	G.M. Pjerrou *et al.*	(UCLA)
Also		Thesis	G.M. Pjerrou	(UCLA)
CARMONY	64B	PRL 12 482	D.D. Carmony *et al.*	(UCLA)
HUBBARD	64	PR 135 B183	J.R. Hubbard *et al.*	(LRL)
JAUNEAU	63	PL 4 49	L. Jauneau *et al.*	(EPOL, CERN, LOUC+)
Also		Siena Conf. 1 1	L. Jauneau *et al.*	(EPOL, CERN, LOUC+)

Ξ^-

$I(J^P) = \frac{1}{2}(\frac{1}{2}^+)$ Status: ****

The parity has not actually been measured, but + is of course expected.

We have omitted some results that have been superseded by later experiments. See our earlier editions.

Ξ^- MASS

The fit uses the Ξ^-, $\overline{\Xi}^+$, and Ξ^0 masses and the $\Xi^- - \overline{\Xi}^+$ mass difference. It assumes that the Ξ^- and $\overline{\Xi}^+$ masses are the same.

VALUE (MeV)	EVTS	DOCUMENT ID		TECN	COMMENT
1321.71±0.07 OUR FIT					
1321.70±0.08±0.05	2478 ± 68	ABDALLAH	06E	DLPH	from Z decays

See key on page 885

• • • We do not use the following data for averages, fits, limits, etc. • • •

1321.46±0.34	632	DIBIANCA	75	DBC	4.9 GeV/c K^-d
1321.12±0.41	268	WILQUET	72	HLBC	
1321.87±0.51	195	[1] GOLDWASSER	70	HBC	5.5 GeV/c K^-p
1321.67±0.52	6	CHIEN	66	HBC	6.9 GeV/c $\overline{p}p$
1321.4 ±1.1	299	LONDON	66	HBC	
1321.3 ±0.4	149	PJERROU	65B	HBC	
1321.1 ±0.3	241	[2] BADIER	64	HBC	
1321.4 ±0.4	517	[2] JAUNEAU	63D	FBC	
1321.1 ±0.65	62	[2] SCHNEIDER	63	HBC	

[1] GOLDWASSER 70 uses $m_\Lambda = 1115.58$ MeV.
[2] These masses have been increased 0.09 MeV because the Λ mass increased.

$\overline{\Xi}^+$ MASS

The fit uses the Ξ^-, $\overline{\Xi}^+$, and Ξ^0 masses and the $\Xi^- - \overline{\Xi}^+$ mass difference. It assumes that the Ξ^- and $\overline{\Xi}^+$ masses are the same.

VALUE (MeV)	EVTS	DOCUMENT ID		TECN	COMMENT
1321.71±0.07 OUR FIT					
1321.73±0.08±0.05	2256 ± 63	ABDALLAH	06E	DLPH	from Z decays

• • • We do not use the following data for averages, fits, limits, etc. • • •

1321.6 ±0.8	35	VOTRUBA	72	HBC	10 GeV/c K^+p
1321.2 ±0.4	34	STONE	70	HBC	
1320.69±0.93	5	CHIEN	66	HBC	6.9 GeV/c $\overline{p}p$

$(m_{\Xi^-} - m_{\overline{\Xi}^+}) / m_{\Xi^-}$

A test of CPT invariance.

VALUE	DOCUMENT ID		TECN	COMMENT
$(-2.5\pm8.7)\times10^{-5}$	ABDALLAH	06E	DLPH	from Z decays

Ξ^- MEAN LIFE

Measurements with an error $> 0.2\times10^{-10}$ s or with systematic errors not included have been omitted.

VALUE (10^{-10} s)	EVTS	DOCUMENT ID		TECN	COMMENT
1.639±0.015 OUR AVERAGE					
1.65 ±0.07 ±0.12	2478 ± 68	ABDALLAH	06E	DLPH	from Z decays
1.652±0.051	32k	BOURQUIN	84	SPEC	Hyperon beam
1.665±0.065	41k	BOURQUIN	79	SPEC	Hyperon beam
1.609±0.028	4286	HEMINGWAY	78	HBC	4.2 GeV/c K^-p
1.67 ±0.08		DIBIANCA	75	DBC	4.9 GeV/c K^-d
1.63 ±0.03	4303	BALTAY	74	HBC	1.75 GeV/c K^-p
$1.73\ ^{+0.08}_{-0.07}$	680	MAYEUR	72	HLBC	2.1 GeV/c K^-
1.61 ±0.04	2610	DAUBER	69	HBC	
1.80 ±0.16	299	LONDON	66	HBC	
1.70 ±0.12	246	PJERROU	65B	HBC	
1.69 ±0.07	794	HUBBARD	64	HBC	
$1.86\ ^{+0.15}_{-0.14}$	517	JAUNEAU	63D	FBC	

$\overline{\Xi}^+$ MEAN LIFE

VALUE (10^{-10} s)	EVTS	DOCUMENT ID		TECN	COMMENT
1.70±0.08±0.12	2256 ± 63	ABDALLAH	06E	DLPH	from Z decays

• • • We do not use the following data for averages, fits, limits, etc. • • •

$1.55\ ^{+0.35}_{-0.20}$	35	[3] VOTRUBA	72	HBC	10 GeV/c K^+p
1.6 ±0.3	34	STONE	70	HBC	
$1.9\ ^{+0.7}_{-0.5}$	12	[3] SHEN	67	HBC	
1.51±0.55	5	[3] CHIEN	66	HBC	6.9 GeV/c $\overline{p}p$

[3] The error is statistical only.

$(\tau_{\Xi^-} - \tau_{\overline{\Xi}^+}) / \tau_{\Xi^-}$

A test of CPT invariance.

VALUE	DOCUMENT ID		TECN	COMMENT
−0.01±0.07	ABDALLAH	06E	DLPH	from Z decays

Ξ^- MAGNETIC MOMENT

See the "Note on Baryon Magnetic Moments" in the Λ Listings.

VALUE (μ_N)	EVTS	DOCUMENT ID		TECN	COMMENT
−0.6507±0.0025 OUR AVERAGE					
−0.6505±0.0025	4.36M	DURYEA	92	SPEC	800 GeV p Be
−0.661 ±0.036 ±0.036	44k	TROST	89	SPEC	Ξ^- ∼ 250 GeV
−0.69 ±0.04	218k	RAMEIKA	84	SPEC	400 GeV pBe

• • • We do not use the following data for averages, fits, limits, etc. • • •

−0.674 ±0.021 ±0.020	122k	HO	90	SPEC	See DURYEA 92
−2.1 ±0.8	2436	COOL	74	OSPK	1.8 GeV/c K^-p
−0.1 ±2.1	2724	BINGHAM	70B	OSPK	1.8 GeV/c K^-p

$\overline{\Xi}^+$ MAGNETIC MOMENT

See the "Note on Baryon Magnetic Moments" in the Λ Listings.

VALUE (μ_N)	EVTS	DOCUMENT ID		TECN	COMMENT
+0.657±0.028±0.020	70k	HO	90	SPEC	800 GeV pBe

$(\mu_{\Xi^-} + \mu_{\overline{\Xi}^+}) / |\mu_{\Xi^-}|$

A test of CPT invariance. We calculate this from the Ξ^- and $\overline{\Xi}^+$ magnetic moments above.

VALUE	DOCUMENT ID
+0.01±0.05 OUR EVALUATION	

Ξ^- DECAY MODES

	Mode	Fraction (Γ_j/Γ)	Confidence level
Γ_1	$\Lambda\pi^-$	(99.887±0.035) %	
Γ_2	$\Sigma^-\gamma$	(1.27 ±0.23) × 10^{-4}	
Γ_3	$\Lambda e^-\overline{\nu}_e$	(5.63 ±0.31) × 10^{-4}	
Γ_4	$\Lambda\mu^-\overline{\nu}_\mu$	$(\ 3.5\ ^{+3.5}_{-2.2}\ )\times10^{-4}$	
Γ_5	$\Sigma^0 e^-\overline{\nu}_e$	(8.7 ±1.7) × 10^{-5}	
Γ_6	$\Sigma^0\mu^-\overline{\nu}_\mu$	< 8 × 10^{-4}	90%
Γ_7	$\Xi^0 e^-\overline{\nu}_e$	< 2.3 × 10^{-3}	90%
	$\Delta S = 2$ forbidden ($S2$) modes		
Γ_8	$n\pi^-$	$S2$ < 1.9 × 10^{-5}	90%
Γ_9	$n e^-\overline{\nu}_e$	$S2$ < 3.2 × 10^{-3}	90%
Γ_{10}	$n\mu^-\overline{\nu}_\mu$	$S2$ < 1.5 %	90%
Γ_{11}	$p\pi^-\pi^-$	$S2$ < 4 × 10^{-4}	90%
Γ_{12}	$p\pi^- e^-\overline{\nu}_e$	$S2$ < 4 × 10^{-4}	90%
Γ_{13}	$p\pi^-\mu^-\overline{\nu}_\mu$	$S2$ < 4 × 10^{-4}	90%
Γ_{14}	$p\mu^-\mu^-$	L < 4 × 10^{-8}	90%

CONSTRAINED FIT INFORMATION

An overall fit to 4 branching ratios uses 5 measurements and one constraint to determine 5 parameters. The overall fit has a $\chi^2 = 1.0$ for 1 degrees of freedom.

The following *off-diagonal* array elements are the correlation coefficients $\langle \delta x_i \delta x_j \rangle / (\delta x_i \cdot \delta x_j)$, in percent, from the fit to the branching fractions, $x_i \equiv \Gamma_i/\Gamma_{\rm total}$. The fit constrains the x_i whose labels appear in this array to sum to one.

	x_1	x_2	x_3	x_4
x_2	−6			
x_3	−8	0		
x_4	−99	0	−1	
x_5	−5	0	0	0

Ξ^- BRANCHING RATIOS

A number of early results have been omitted.

$\Gamma(\Sigma^-\gamma)/\Gamma(\Lambda\pi^-)$ Γ_2/Γ_1

VALUE (units 10^{-4})	EVTS	DOCUMENT ID		TECN	COMMENT
1.27±0.24 OUR FIT					
1.27±0.23 OUR AVERAGE					
1.22±0.23±0.06	211	[4] DUBBS	94	E761	Ξ^- 375 GeV
2.27±1.02	9	BIAGI	87B	SPEC	SPS hyperon beam

[4] DUBBS 94 also finds weak evidence that the asymmetry parameter α_γ is positive ($\alpha_\gamma = 1.0 \pm 1.3$).

$\Gamma(\Lambda e^-\overline{\nu}_e)/\Gamma(\Lambda\pi^-)$ Γ_3/Γ_1

VALUE (units 10^{-3})	EVTS	DOCUMENT ID		TECN	COMMENT
0.564±0.031 OUR FIT					
0.564±0.031	2857	BOURQUIN	83	SPEC	SPS hyperon beam

• • • We do not use the following data for averages, fits, limits, etc. • • •

0.30 ±0.13	11	THOMPSON	80	ASPK	Hyperon beam

$\Gamma(\Lambda\mu^-\overline{\nu}_\mu)/\Gamma(\Lambda\pi^-)$ Γ_4/Γ_1

VALUE (units 10^{-3})	CL%	EVTS	DOCUMENT ID		TECN	COMMENT
$0.35^{+0.35}_{-0.22}$ **OUR FIT**						
0.35±0.35		1	YEH	74	HBC	Effective denom.=2859
• • • We do not use the following data for averages, fits, limits, etc. • • •						
< 2.3	90	0	THOMPSON	80	ASPK	Effective denom.=1017
< 1.3			DAUBER	69	HBC	
<12			BERGE	66	HBC	

$\Gamma(\Sigma^0 e^-\overline{\nu}_e)/\Gamma(\Lambda\pi^-)$ Γ_5/Γ_1

VALUE (units 10^{-3})	EVTS	DOCUMENT ID		TECN	COMMENT
0.087±0.017 OUR FIT					
0.087±0.017	154	BOURQUIN	83	SPEC	SPS hyperon beam

$[\Gamma(\Lambda e^-\overline{\nu}_e)+\Gamma(\Sigma^0 e^-\overline{\nu}_e)]/\Gamma(\Lambda\pi^-)$ $(\Gamma_3+\Gamma_5)/\Gamma_1$

VALUE (units 10^{-3})	EVTS	DOCUMENT ID		TECN	COMMENT
• • • We do not use the following data for averages, fits, limits, etc. • • •					
0.651±0.031	3011	[5] BOURQUIN	83	SPEC	SPS hyperon beam
0.68 ±0.22	17	[6] DUCLOS	71	OSPK	

[5] See the separate BOURQUIN 83 values for $\Gamma(\Lambda e^-\overline{\nu}_e)/\Gamma(\Lambda\pi^-)$ and $\Gamma(\Sigma^0 e^-\overline{\nu}_e)/\Gamma(\Lambda\pi^-)$ above.

[6] DUCLOS 71 cannot distinguish Σ^0's from Λ's. The Cabibbo theory predicts the Σ^0 rate is about a factor 6 smaller than the Λ rate.

$\Gamma(\Sigma^0\mu^-\overline{\nu}_\mu)/\Gamma(\Lambda\pi^-)$ Γ_6/Γ_1

VALUE (units 10^{-3})	CL%	EVTS	DOCUMENT ID		TECN	COMMENT
<0.76	90	0	YEH	74	HBC	Effective denom.=3026
• • • We do not use the following data for averages, fits, limits, etc. • • •						
<5			BERGE	66	HBC	

$\Gamma(\Xi^0 e^-\overline{\nu}_e)/\Gamma(\Lambda\pi^-)$ Γ_7/Γ_1

VALUE (units 10^{-3})	CL%	EVTS	DOCUMENT ID		TECN	COMMENT
<2.3	90	0	YEH	74	HBC	Effective denom.=1000

$\Gamma(n\pi^-)/\Gamma(\Lambda\pi^-)$ Γ_8/Γ_1

ΔS=2. Forbidden in first-order weak interaction.

VALUE (units 10^{-3})	CL%	EVTS	DOCUMENT ID		TECN	COMMENT
<0.019	90		BIAGI	82B	SPEC	SPS hyperon beam
• • • We do not use the following data for averages, fits, limits, etc. • • •						
<3.0	90	0	YEH	74	HBC	Effective denom.=760
<1.1			DAUBER	69	HBC	
<5.0			FERRO-LUZZI	63	HBC	

$\Gamma(ne^-\overline{\nu}_e)/\Gamma(\Lambda\pi^-)$ Γ_9/Γ_1

ΔS=2. Forbidden in first-order weak interaction.

VALUE (units 10^{-3})	CL%	EVTS	DOCUMENT ID		TECN	COMMENT
< 3.2	90	0	YEH	74	HBC	Effective denom.=715
• • • We do not use the following data for averages, fits, limits, etc. • • •						
<10	90		BINGHAM	65	RVUE	

$\Gamma(n\mu^-\overline{\nu}_\mu)/\Gamma(\Lambda\pi^-)$ Γ_{10}/Γ_1

ΔS=2. Forbidden in first-order weak interaction.

VALUE (units 10^{-3})	CL%	EVTS	DOCUMENT ID		TECN	COMMENT
<15.3	90	0	YEH	74	HBC	Effective denom.=150

$\Gamma(p\pi^-\pi^-)/\Gamma(\Lambda\pi^-)$ Γ_{11}/Γ_1

ΔS=2. Forbidden in first-order weak interaction.

VALUE (units 10^{-4})	CL%	EVTS	DOCUMENT ID		TECN	COMMENT
<3.7	90	0	YEH	74	HBC	Effective denom.=6200

$\Gamma(p\pi^- e^-\overline{\nu}_e)/\Gamma(\Lambda\pi^-)$ Γ_{12}/Γ_1

ΔS=2. Forbidden in first-order weak interaction.

VALUE (units 10^{-4})	CL%	EVTS	DOCUMENT ID		TECN	COMMENT
<3.7	90	0	YEH	74	HBC	Effective denom.=6200

$\Gamma(p\pi^-\mu^-\overline{\nu}_\mu)/\Gamma(\Lambda\pi^-)$ Γ_{13}/Γ_1

ΔS=2. Forbidden in first-order weak interaction.

VALUE (units 10^{-4})	CL%	EVTS	DOCUMENT ID		TECN	COMMENT
<3.7	90	0	YEH	74	HBC	Effective denom.=6200

$\Gamma(p\mu^-\mu^-)/\Gamma(\Lambda\pi^-)$ Γ_{14}/Γ_1

A ΔL=2 decay, forbidden by total lepton number conservation.

VALUE (units 10^{-8})	CL%	DOCUMENT ID		TECN	COMMENT
<4.0	90	RAJARAM	05	HYCP	p Cu, 800 GeV
• • • We do not use the following data for averages, fits, limits, etc. • • •					
$<3.7\times10^4$	90	[7] LITTENBERG	92B	HBC	Uses YEH 74 data

[7] This LITTENBERG 92B limit and the identical YEH 74 limits for the preceding three modes all result from nonobservance of any 3-prong decays of the Ξ^-. One could as well apply the limit to the *sum* of the four modes.

Ξ^- DECAY PARAMETERS

See the "Note on Baryon Decay Parameters" in the neutron Listings.

$\alpha(\Xi^-)\alpha_-(\Lambda)$

VALUE	EVTS	DOCUMENT ID		TECN	COMMENT
−0.294 ±0.005 OUR AVERAGE		Error includes scale factor of 1.7. See the ideogram below.			
−0.2963±0.0042	189k	LUK	00	E756	p Be, 800 GeV
−0.2894±0.0073	63k	[8] LUK	00	E756	p Be, 800 GeV
−0.303 ±0.004 ±0.004	192k	RAMEIKA	86	SPEC	400 GeV pBe
−0.257 ±0.020	11k	ASTON	85B	LASS	11 GeV/c K^-p
−0.260 ±0.017	21k	BENSINGER	85	MPS	5 GeV/c K^-p
−0.299 ±0.007	150k	BIAGI	82	SPEC	SPS hyperon beam
−0.315 ±0.026	9046	CLELAND	80C	ASPK	BNL hyperon beam
−0.239 ±0.021	6599	HEMINGWAY	78	HBC	4.2 GeV/c K^-p
−0.243 ±0.025	4303	BALTAY	74	HBC	1.75 GeV/c K^-p
−0.252 ±0.032	2436	COOL	74	OSPK	1.8 GeV/c K^- p
−0.253 ±0.028	2781	DAUBER	69	HBC	

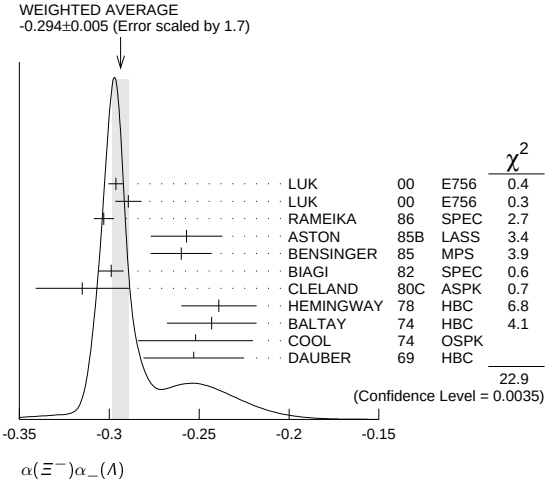

[8] This LUK 00 value is for $\alpha(\overline{\Xi}^+)\ \alpha_+(\overline{\Lambda})$. We assume CP conservation here by including it in the average for $\alpha(\Xi^-)\ \alpha_-(\Lambda)$. But see the second data block below for the CP test.

α FOR $\Xi^- \to \Lambda\pi^-$

The above average, $\alpha(\Xi^-)\ \alpha_-(\Lambda) = -0.294 \pm 0.005$, where the error includes a scale factor of 1.7, divided by our current average $\alpha_-(\Lambda) = 0.642 \pm 0.013$, gives the following value for $\alpha(\Xi^-)$.

VALUE	DOCUMENT ID
−0.458±0.012 OUR EVALUATION	Error includes scale factor of 1.8.

$\frac{[\alpha(\Xi^-)\alpha_-(\Lambda)-\alpha(\overline{\Xi}^+)\alpha_+(\overline{\Lambda})]}{[\alpha(\Xi^-)\alpha_-(\Lambda)+\alpha(\overline{\Xi}^+)\alpha_+(\overline{\Lambda})]}$

This is zero if CP is conserved. The α's are the decay-asymmetry parameters for $\Xi^- \to \Lambda\pi^-$ and $\Lambda \to p\pi^-$ and for $\overline{\Xi}^+ \to \overline{\Lambda}\pi^+$ and $\overline{\Lambda} \to \overline{p}\pi^+$.

VALUE (units 10^{-4})	EVTS	DOCUMENT ID		TECN	COMMENT
0.0± 5.1±4.4	158M	HOLMSTROM	04	HYCP	p Cu, 800 GeV
• • • We do not use the following data for averages, fits, limits, etc. • • •					
+120 ±140	252k	LUK	00	E756	p Be, 800 GeV

ϕ ANGLE FOR $\Xi^- \to \Lambda\pi^-$ $(\tan\phi = \beta/\gamma)$

VALUE (°)	EVTS	DOCUMENT ID		TECN	COMMENT
− 2.1 ± 0.8 OUR AVERAGE					
− 2.39± 0.64±0.64	144M	[9] HUANG	04	HYCP	p Cu, 800 GeV
− 1.61± 2.66±0.37	1.35M	[10] CHAKRAVO...	03	E756	p Be, 800 GeV
5 ±10	11k	ASTON	85B	LASS	K^-p
14.7 ±16.0	21k	[11] BENSINGER	85	MPS	5 GeV/c K^-p
11 ± 9	4303	BALTAY	74	HBC	1.75 GeV/c K^-p
5 ±16	2436	COOL	74	OSPK	1.8 GeV/c K^- p
−14 ±11	2781	DAUBER	69	HBC	Uses $\alpha_\Lambda = 0.647\pm0.020$
0 ±12	1004	[12] BERGE	66	HBC	
• • • We do not use the following data for averages, fits, limits, etc. • • •					
−26 ±30	2724	BINGHAM	70B	OSPK	
0 ±20.4	364	[12] LONDON	66	HBC	Using α_Λ=0.62
54 ±30	356	[12] CARMONY	64B	HBC	

[9] From this result and α_Ξ, HUANG 04 gets $\beta_\Xi = -0.037 \pm 0.011 \pm 0.010$ and $\gamma_\Xi = 0.888 \pm 0.0004 \pm 0.006$. And the strong p–s phase difference for $\Lambda\pi^-$ scattering is $(4.6 \pm 1.4 \pm 1.2)^\circ$.

[10] From this result and α_Ξ, CHAKRAVORTY 03 obtains $\beta_\Xi = -0.025 \pm 0.042 \pm 0.006$ and $\gamma_\Xi = 0.889\pm0.001\pm0.007$. And the strong p–s phase difference for $\Lambda\pi^-$ scattering is $(3.17 \pm 5.28 \pm 0.73)^\circ$.

[11] BENSINGER 85 used $\alpha_\Lambda = 0.642 \pm 0.013$.

[12] The errors have been multiplied by 1.2 due to approximations used for the Ξ polarization; see DAUBER 69 for a discussion.

g_A / g_V FOR $\Xi^- \to \Lambda e^- \overline{\nu}_e$

VALUE	EVTS	DOCUMENT ID		TECN	COMMENT
-0.25 ± 0.05	1992	[13] BOURQUIN	83	SPEC	SPS hyperon beam

[13] BOURQUIN 83 assumes that $g_2 = 0$. Also, the sign has been changed to agree with our conventions, given in the "Note on Baryon Decay Parameters" in the neutron Listings.

Ξ^- REFERENCES

We have omitted some papers that have been superseded by later experiments. See our earlier editions.

ABDALLAH	06E	PL B639 179	J. Abdallah *et al.*	(DELPHI Collab.)
RAJARAM	05	PRL 94 181801	D. Rajaram *et al.*	(FNAL HyperCP Collab.)
HOLMSTROM	04	PRL 93 262001	T. Holmstrom *et al.*	(FNAL HyperCP Collab.)
HUANG	04	PRL 93 011802	M. Huang *et al.*	(FNAL HyperCP Collab.)
CHAKRAVO...	03	PRL 91 031601	A. Chakravorty *et al.*	(FNAL E756 Collab.)
LUK	00	PRL 85 4860	K.B. Luk *et al.*	(FNAL E756 Collab.)
DUBBS	94	PRL 72 808	T. Dubbs *et al.*	(FNAL E761 Collab.)
DURYEA	92	PRL 68 768	J. Duryea *et al.*	(MINN, FNAL, MICH, RUTG)
LITTENBERG	92B	PR D46 892	L.S. Littenberg, R.E. Shrock	(BNL, STON)
HO	90	PRL 65 1713	P.M. Ho *et al.*	(MICH, FNAL, MINN, RUTG)
Also		PR D44 3402	P.M. Ho *et al.*	(MICH, FNAL, MINN, RUTG)
TROST	89	PR D40 1703	L.H. Trost *et al.*	(FNAL-715 Collab.)
BIAGI	87B	ZPHY C35 143	S.F. Biagi *et al.*	(BRIS, CERN, GEVA+)
RAMEIKA	86	PR D33 3172	R. Rameika *et al.*	(RUTG, MICH, WISC+)
ASTON	85B	PR D32 2270	D. Aston *et al.*	(SLAC, CARL, CNRC, CINC)
BENSINGER	85	NP B252 561	J.R. Bensinger *et al.*	(CHIC, ELMT, FNAL+)
BOURQUIN	84	NP B241 1	M.H. Bourquin *et al.*	(BRIS, GEVA, HEIDP+)
RAMEIKA	84	PRL 52 581	R. Rameika *et al.*	(RUTG, MICH, WISC+)
BOURQUIN	83	ZPHY C21 1	M.H. Bourquin *et al.*	(BRIS, GEVA, HEIDP+)
BIAGI	82	PL 112B 265	S.F. Biagi *et al.*	(BRIS, CAVE, GEVA+)
BIAGI	82B	PL 112B 277	S.F. Biagi *et al.*	(LOQM, GEVA, RL+)
CLELAND	80C	PR D21 12	W.E. Cleland *et al.*	(PITT, BNL)
THOMPSON	80	PR D21 25	J.A. Thompson *et al.*	(PITT, BNL)
BOURQUIN	79	PL 87B 297	M.H. Bourquin *et al.*	(BRIS, GEVA, HEIDP+)
HEMINGWAY	78	NP B142 205	R.J. Hemingway *et al.*	(CERN, ZEEM, NIJM+)
DIBIANCA	75	NP B98 137	F.A. Dibianca, R.J. Endorf	(CMU)
BALTAY	74	PR D9 49	C. Baltay *et al.*	(COLU, BING) J
COOL	74	PR D10 792	R.L. Cool *et al.*	(BNL)
Also		PRL 29 1630	R.L. Cool *et al.*	(BNL)
YEH	74	PR D10 3545	N. Yeh *et al.*	(BING, COLU)
MAYEUR	72	NP B47 333	C. Mayeur *et al.*	(BRUX, CERN, TUFTS, LOUC)
VOTRUBA	72	NP B45 77	M.F. Votruba, A. Safder, T.M. Ratcliffe	(BIRM+)
WILQUET	72	PL 42B 372	G. Wilquet *et al.*	(BRUX, CERN, TUFTS+)
DUCLOS	71	NP B32 493	J. Duclos *et al.*	(CERN)
BINGHAM	70B	PR D1 3010	G.M. Bingham *et al.*	(UCSD, WASH)
GOLDWASSER	70	PR D1 1960	E.L. Goldwasser, P.F. Schultz	(ILL)
STONE	70	PL 32B 515	S.L. Stone *et al.*	(ROCH)
DAUBER	69	PR 179 1262	P.M. Dauber *et al.*	(LRL) J
SHEN	67	PL 25B 443	B.C. Shen, A. Firestone, G. Goldhaber	(UCB+)
BERGE	66	PR 147 945	J.P. Berge *et al.*	(LRL)
CHIEN	66	PR 152 1171	C.Y. Chien *et al.*	(YALE, BNL)
LONDON	66	PR 143 1034	G.W. London *et al.*	(BNL, SYRA)
BINGHAM	65	PRSL 285 202	H.H. Bingham	(CERN)
PJERROU	65B	PRL 14 275	G.M. Pjerrou *et al.*	(UCLA)
Also		Thesis	G.M. Pjerrou	(UCLA)
BADIER	64	Dubna Conf. 1 593	J. Badier *et al.*	(EPOL, SACL, ZEEM)
CARMONY	64B	PRL 12 482	D.D. Carmony *et al.*	(UCLA) J
HUBBARD	64	PR 135 B183	J.R. Hubbard *et al.*	(LRL)
FERRO-LUZZI	63	PR 130 1568	M. Ferro-Luzzi *et al.*	(LRL)
JAUNEAU	63D	Siena Conf. 4	L. Jauneau *et al.*	(EPOL, CERN, LOUC+)
Also		PL 5 261	L. Jauneau *et al.*	(EPOL, CERN, LOUC+)
SCHNEIDER	63	PL 4 360	J. Schneider	(CERN)

See the related review(s):

Ξ Resonances

$\Xi(1530)\ 3/2^+$

$I(J^P) = \frac{1}{2}(\frac{3}{2}^+)$ Status: ****

This is the only Ξ resonance whose properties are all reasonably well known. Assuming that the Λ_c^+ has $J^P = 1/2^+$, AUBERT 08AK, in a study of $\Lambda_c^+ \to \Xi^-\pi^+K^+$, finds conclusively that the spin of the $\Xi(1530)^0$ is 3/2. In conjunction with SCHLEIN 63B and BUTTON-SHAFER 66, this proves also that the parity is +.

We use only those determinations of the mass and width that are accompanied by some discussion of systematics and resolution.

$\Xi(1530)$ POLE POSITIONS

$\Xi(1530)^0$ REAL PART

VALUE	DOCUMENT ID	COMMENT
1531.6 ± 0.4	LICHTENBERG74	Using HABIBI 73

$\Xi(1530)^0$ IMAGINARY PART

VALUE	DOCUMENT ID	COMMENT
4.45 ± 0.35	LICHTENBERG74	Using HABIBI 73

$\Xi(1530)^-$ REAL PART

VALUE	DOCUMENT ID	COMMENT
1534.4 ± 1.1	LICHTENBERG74	Using HABIBI 73

$\Xi(1530)^-$ IMAGINARY PART

VALUE	DOCUMENT ID	COMMENT
$3.9^{+1.75}_{-3.9}$	LICHTENBERG74	Using HABIBI 73

$\Xi(1530)$ MASSES

$\Xi(1530)^0$ MASS

VALUE (MeV)	EVTS	DOCUMENT ID		TECN	COMMENT
1531.80±0.32 OUR FIT Error includes scale factor of 1.3.					
1531.78±0.34 OUR AVERAGE Error includes scale factor of 1.4. See the ideogram below.					
1532.2 ±0.7		DEBELLEFON	75B	HBC	$K^-p \to \Xi^-\overline{K}\pi$
1533 ±1		ROSS	73B	HBC	$K^-p \to \Xi\overline{K}\pi(\pi)$
1531.4 ±0.8	59	BADIER	72	HBC	K^-p 3.95 GeV/c
1532.0 ±0.4	1262	BALTAY	72	HBC	K^-p 1.75 GeV/c
1531.3 ±0.6	324	BORENSTEIN	72	HBC	K^-p 2.2 GeV/c
1532.3 ±0.7	286	KIRSCH	72	HBC	K^-p 2.87 GeV/c
1528.7 ±1.1	76	LONDON	66	HBC	K^-p 2.24 GeV/c
• • • We do not use the following data for averages, fits, limits, etc. • • •					
1532.1 ±0.4	1244	ASTON	85B	LASS	K^-p 11 GeV/c
1532.1 ±0.6	2700	[1] BAUBILLIER	81B	HBC	K^-p 8.25 GeV/c
1530 ±1	450	BIAGI	81	SPEC	SPS hyperon beam
1527 ±6	80	SIXEL	79	HBC	K^-p 10 GeV/c
1535 ±4	100	SIXEL	79	HBC	K^-p 16 GeV/c
1533.6 ±1.4	97	BERTHON	74	HBC	Quasi-2-body σ

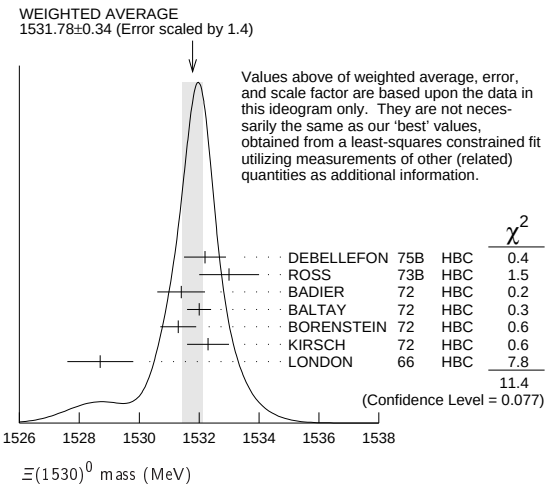

$\Xi(1530)^-$ MASS

VALUE (MeV)	EVTS	DOCUMENT ID		TECN	COMMENT
1535.0±0.6 OUR FIT					
1535.2±0.8 OUR AVERAGE					
1534.5 ±1.2		DEBELLEFON	75B	HBC	$K^-p \to \Xi^-\overline{K}\pi$
1535.3 ±2.0		ROSS	73B	HBC	$K^-p \to \Xi\overline{K}\pi(\pi)$
1536.2 ±1.6	185	KIRSCH	72	HBC	K^-p 2.87 GeV/c
1535.7 ±3.2	38	LONDON	66	HBC	K^-p 2.24 GeV/c
• • • We do not use the following data for averages, fits, limits, etc. • • •					
1540 ±3	48	BERTHON	74	HBC	Quasi-2-body σ
1534.7 ±1.1	334	BALTAY	72	HBC	K^-p 1.75 GeV/c

$m_{\Xi(1530)^-} - m_{\Xi(1530)}$

VALUE (MeV)	DOCUMENT ID		TECN	COMMENT
3.2±0.6 OUR FIT				
2.9±0.9 OUR AVERAGE				
2.7 ±1.0	BALTAY	72	HBC	K^-p 1.75 GeV/c
2.0 ±3.2	MERRILL	66	HBC	K^-p 1.7–2.7 GeV/c
5.7 ±3.0	PJERROU	65B	HBC	K^-p 1.8–1.95 GeV/c
• • • We do not use the following data for averages, fits, limits, etc. • • •				
3.9 ±1.8	[2] KIRSCH	72	HBC	K^-p 2.87 GeV/c
7 ±4	[2] LONDON	66	HBC	K^-p 2.24 GeV/c

$\Xi(1530)$ WIDTHS

$\Xi(1530)^0$ WIDTH

VALUE (MeV)	EVTS	DOCUMENT ID		TECN	COMMENT
9.1±0.5 OUR AVERAGE					
9.5 ±1.2		DEBELLEFON	75B	HBC	$K^-p \to \Xi^-\overline{K}\pi$
9.1 ±2.4		ROSS	73B	HBC	$K^-p \to \Xi\overline{K}\pi(\pi)$
11 ±2		BADIER	72	HBC	K^-p 3.95 GeV/c
9.0 ±0.7		BALTAY	72	HBC	K^-p 1.75 GeV/c
8.4 ±1.4		BORENSTEIN	72	HBC	$\Xi^-\pi^+$
11.0 ±1.8		KIRSCH	72	HBC	$\Xi^-\pi^+$
7 ±7		BERGE	66	HBC	K^-p 1.5–1.7 GeV/c
8.5 ±3.5		LONDON	66	HBC	K^-p 2.24 GeV/c
7 ±2		SCHLEIN	63B	HBC	K^-p 1.8, 1.95 GeV/c

Baryon Particle Listings

$\Xi(1530)$, $\Xi(1620)$, $\Xi(1690)$

• • • We do not use the following data for averages, fits, limits, etc. • • •

12.8±1.0	2700	[1] BAUBILLIER	81B	HBC	$K^- p$ 8.25 GeV/c
19 ±6	80	[3] SIXEL	79	HBC	$K^- p$ 10 GeV/c
14 ±5	100	[3] SIXEL	79	HBC	$K^- p$ 16 GeV/c

$\Xi(1530)^-$ WIDTH

VALUE (MeV)	DOCUMENT ID		TECN	COMMENT
$9.9^{+1.7}_{-1.9}$ OUR AVERAGE				
9.6±2.8	DEBELLEFON	75B	HBC	$K^- p \to \Xi^- \overline{K} \pi$
8.3±3.6	ROSS	73B	HBC	$K^- p \to \Xi \overline{K} \pi(\pi)$
$7.8^{+3.5}_{-7.8}$	BALTAY	72	HBC	$K^- p$ 1.75 GeV/c
16.2±4.6	KIRSCH	72	HBC	$\Xi^- \pi^0$, $\Xi^0 \pi^-$

$\Xi(1530)$ DECAY MODES

	Mode	Fraction (Γ_i/Γ)	Confidence level
Γ_1	$\Xi\pi$	100 %	
Γ_2	$\Xi\gamma$	<4 %	90%

$\Xi(1530)$ BRANCHING RATIOS

$\Gamma(\Xi\gamma)/\Gamma_{total}$ **Γ_2/Γ**

VALUE	CL%	DOCUMENT ID		TECN	COMMENT
<0.04	90	KALBFLEISCH	75	HBC	$K^- p$ 2.18 GeV/c

$\Xi(1530)$ FOOTNOTES

[1] BAUBILLIER 81B is a fit to the inclusive spectrum. The resolution (5 MeV) is not unfolded.
[2] Redundant with data in the mass Listings.
[3] SIXEL 79 doesn't unfold the experimental resolution of 15 MeV.

$\Xi(1530)$ REFERENCES

AUBERT	08AK	PR D78 034008	B. Aubert *et al.*	(BABAR Collab.)
ASTON	85B	PR D32 2270	D. Aston *et al.*	(SLAC, CARL, CNRC, CINC)
BAUBILLIER	81B	NP B192 1	M. Baubillier *et al.*	(BIRM, CERN, GLAS+)
BIAGI	81	ZPHY C9 305	S.F. Biagi *et al.*	(BRIS, CAVE, GEVA+)
SIXEL	79	NP B159 125	P. Sixel *et al.*	(AACH3, BERL, CERN, LOIC+)
DEBELLEFON	75B	NC 28A 289	A. de Bellefon *et al.*	(CDEF, SACL)
KALBFLEISCH	75	PR D11 987	G.R. Kalbfleisch, R.C. Strand, J.W. Chapman	(BNL+)
BERTHON	74	NC 21A 146	A. Berthon *et al.*	(CDEF, RHEL, SACL+)
LICHTENBERG	74	PR D10 3865	D.B. Lichtenberg	(IND)
Also		Private Comm.	D.B. Lichtenberg	(IND)
HABIBI	73	Thesis Nevis 199	M. Habibi	(COLU)
ROSS	73B	Purdue Conf. 355	R.T. Ross, J.L. Lloyd, D. Radojicic	(OXF)
BADIER	72	NP B37 429	J. Badier *et al.*	(EPOL)
BALTAY	72	PL 42B 129	C. Baltay *et al.*	(COLU, BING)
BORENSTEIN	72	PR D5 1559	S.R. Borenstein *et al.*	(BNL, MICH) I
KIRSCH	72	NP B40 349	L.E. Kirsch *et al.*	(BRAN, UMD, SYRA+) I
BERGE	66	PR 147 945	J.P. Berge *et al.*	(LRL) I
BUTTON-...	66	PR 142 883	J. Button-Shafer *et al.*	(LRL) JP
LONDON	66	PR 143 1034	G.W. London *et al.*	(BNL, SYRA) IJ
MERRILL	66	Thesis UCRL 16455	D.W. Merrill	(LRL) JP
PJERROU	65B	PRL 14 275	G.M. Pjerrou *et al.*	(UCLA)
SCHLEIN	63B	PRL 11 167	P.E. Schlein *et al.*	(UCLA) IJP

OTHER RELATED PAPERS

MAZZUCATO	81	NP B178 1	M. Mazzucato *et al.*	(AMST, CERN, NIJM+)
BRIEFEL	77	PR D16 2706	E. Briefel *et al.*	(BRAN, UMD, SYRA+)
BRIEFEL	75	PR D12 1859	E. Briefel *et al.*	(BRAN, UMD, SYRA+)
HUNGERBU...	74	PR D10 2051	V. Hungerbuhler *et al.*	(YALE, FNAL, BNL+)
BUTTON-...	66	PR 142 883	J. Button-Shafer *et al.*	(LRL) JP

$\Xi(1620)$

$I(J^P) = \frac{1}{2}(?^?)$ Status: *

J, P need confirmation.

OMITTED FROM SUMMARY TABLE

What little evidence there is consists of weak signals in the $\Xi\pi$ channel. A number of other experiments (e.g., BORENSTEIN 72 and HASSALL 81) have looked for but not seen any effect.

$\Xi(1620)$ MASS

VALUE (MeV)	EVTS	DOCUMENT ID		TECN	COMMENT
≈ 1620 OUR ESTIMATE					
1624± 3	31	BRIEFEL	77	HBC	$K^- p$ 2.87 GeV/c
1633±12	34	DEBELLEFON	75B	HBC	$K^- p \to \Xi^- \overline{K} \pi$
1606± 6	29	ROSS	72	HBC	$K^- p$ 3.1–3.7 GeV/c

$\Xi(1620)$ WIDTH

VALUE (MeV)	EVTS	DOCUMENT ID		TECN	COMMENT
22.5	31	[1] BRIEFEL	77	HBC	$K^- p$ 2.87 GeV/c
40 ±15	34	DEBELLEFON	75B	HBC	$K^- p \to \Xi^- \overline{K} \pi$
21 ± 7	29	ROSS	72	HBC	$K^- p \to \Xi^- \pi^+ K^{*0}(892)$

$\Xi(1620)$ DECAY MODES

	Mode
Γ_1	$\Xi\pi$

$\Xi(1620)$ FOOTNOTES

[1] The fit is insensitive to values between 15 and 30 MeV.

$\Xi(1620)$ REFERENCES

HASSALL	81	NP B189 397	J.K. Hassall *et al.*	(CAVE, MSU)
BRIEFEL	77	PR D16 2706	E. Briefel *et al.*	(BRAN, UMD, SYRA+)
Also		Duke Conf. 317	E. Briefel *et al.*	(BRAN, UMD, SYRA+)
Hyperon Resonances, 1970				
Also		PR D12 1859	E. Briefel *et al.*	(BRAN, UMD, SYRA+)
DEBELLEFON	75B	NC 28A 289	A. de Bellefon *et al.*	(CDEF, SACL)
BORENSTEIN	72	PR D5 1559	S.R. Borenstein *et al.*	(BNL, MICH) I
ROSS	72	PL 38B 177	R.T. Ross *et al.*	(OXF) I

OTHER RELATED PAPERS

HUNGERBU...	74	PR D10 2051	V. Hungerbuhler *et al.*	(YALE, FNAL, BNL+)
SCHMIDT	73	Purdue Conf. 363	P.E. Schmidt	(BRAN)
KALBFLEISCH	70	Duke Conf. 331	G.R. Kalbfleisch	(BNL) I
Hyperon Resonances 1970				
APSELL	69	PRL 23 884	S.P. Apsell *et al.*	(BRAN, UMD, SYRA+)
BARTSCH	69	PL 28B 439	J. Bartsch *et al.*	(AACH, BERL, CERN+)

$\Xi(1690)$

$I(J^P) = \frac{1}{2}(?^?)$ Status: ***

AUBERT 08AK, in a study of $\Lambda_c^+ \to \Xi^- \pi^+ K^+$, finds some evidence that the $\Xi(1690)$ has $J^P = 1/2^-$.

DIONISI 78 sees a threshold enhancement in both the neutral and negatively charged $\Sigma\overline{K}$ mass spectra in $K^- p \to (\Sigma\overline{K}) K \pi$ at 4.2 GeV/c. The data from the $\Sigma\overline{K}$ channels alone cannot distinguish between a resonance and a large scattering length. Weaker evidence at the same mass is seen in the corresponding $\Lambda\overline{K}$ channels, and a coupled-channel analysis yields results consistent with a new Ξ.

BIAGI 81 sees an enhancement at 1700 MeV in the diffractively produced ΛK^- system. A peak is also observed in the $\Lambda\overline{K}^0$ mass spectrum at 1660 MeV that is consistent with a 1720 MeV resonance decaying to $\Sigma^0\overline{K}^0$, with the γ from the Σ^0 decay not detected.

BIAGI 87 provides further confirmation of this state in diffractive dissociation of Ξ^- into ΛK^-. The significance claimed is 6.7 standard deviations.

ADAMOVICH 98 sees a peak of 1400 ± 300 events in the $\Xi^-\pi^+$ spectrum produced by 345 GeV/c Σ^--nucleus interactions.

$\Xi(1690)$ MASSES

MIXED CHARGES

VALUE (MeV)	DOCUMENT ID
1690±10 OUR ESTIMATE This is only an educated guess; the error given is larger than the error on the average of the published values.	

$\Xi(1690)^0$ MASS

VALUE (MeV)	EVTS	DOCUMENT ID		TECN	COMMENT
1686±4	1400	ADAMOVICH	98	WA89	Σ^- nucleus, 345 GeV/c
1699±5	175	[1] DIONISI	78	HBC	$K^- p$ 4.2 GeV/c
1684±5	183	[2] DIONISI	78	HBC	$K^- p$ 4.2 GeV/c

$\Xi(1690)^-$ MASS

VALUE (MeV)	EVTS	DOCUMENT ID		TECN	COMMENT
1691.1± 1.9±2.0	104	BIAGI	87	SPEC	Ξ^- Be 116 GeV
1700 ±10	150	[3] BIAGI	81	SPEC	Ξ^- H 100, 135 GeV
1694 ± 6	45	[4] DIONISI	78	HBC	$K^- p$ 4.2 GeV/c

$\Xi(1690)$ WIDTHS

MIXED CHARGES

VALUE (MeV)	DOCUMENT ID
<30 OUR ESTIMATE	

$\Xi(1690)^0$ WIDTH

VALUE (MeV)	EVTS	DOCUMENT ID		TECN	COMMENT
10± 6	1400	ADAMOVICH	98	WA89	Σ^- nucleus, 345 GeV/c
44±23	175	[1] DIONISI	78	HBC	$K^- p$ 4.2 GeV/c
20± 4	183	[2] DIONISI	78	HBC	$K^- p$ 4.2 GeV/c

Ξ(1690)⁻ WIDTH

VALUE (MeV)	CL%	EVTS	DOCUMENT ID		TECN	COMMENT
< 8	90	104	BIAGI	87	SPEC	Ξ^- Be 116 GeV
47±14		150	[3] BIAGI	81	SPEC	Ξ^- H 100, 135 GeV
26± 6		45	[4] DIONISI	78	HBC	K^-p 4.2 GeV/c

Ξ(1690) DECAY MODES

	Mode	Fraction (Γ_i/Γ)
Γ_1	$\Lambda\overline{K}$	seen
Γ_2	$\Sigma\overline{K}$	seen
Γ_3	$\Xi\pi$	seen
Γ_4	$\Xi^-\pi^+\pi^0$	
Γ_5	$\Xi^-\pi^+\pi^-$	possibly seen
Γ_6	$\Xi(1530)\pi$	

Ξ(1690) BRANCHING RATIOS

$\Gamma(\Lambda\overline{K})/\Gamma_{total}$ — Γ_1/Γ

VALUE	EVTS	DOCUMENT ID		TECN	CHG	COMMENT
seen	104	BIAGI	87	SPEC	–	Ξ^- Be 116 GeV

$\Gamma(\Sigma\overline{K})/\Gamma(\Lambda\overline{K})$ — Γ_2/Γ_1

VALUE	EVTS	DOCUMENT ID		TECN	CHG	COMMENT
0.75±0.39	75	ABE	02C	BELL		$e^+e^- \approx \Upsilon(4S)$
2.7 ±0.9		DIONISI	78	HBC	0	K^-p 4.2 GeV/c
3.1 ±1.4		DIONISI	78	HBC	–	K^-p 4.2 GeV/c

$\Gamma(\Xi\pi)/\Gamma(\Sigma\overline{K})$ — Γ_3/Γ_2

VALUE	DOCUMENT ID		TECN	CHG	COMMENT
<0.09	DIONISI	78	HBC	0	K^-p 4.2 GeV/c

$\Gamma(\Xi\pi)/\Gamma_{total}$ — Γ_3/Γ

VALUE	DOCUMENT ID		TECN	COMMENT
seen	ADAMOVICH	98	WA89	Σ^- nucleus, 345 GeV/c

$\Gamma(\Xi^-\pi^+\pi^0)/\Gamma(\Sigma\overline{K})$ — Γ_4/Γ_2

VALUE	DOCUMENT ID		TECN	CHG	COMMENT
<0.04	DIONISI	78	HBC	0	K^-p 4.2 GeV/c

$\Gamma(\Xi^-\pi^+\pi^-)/\Gamma_{total}$ — Γ_5/Γ

VALUE	EVTS	DOCUMENT ID		TECN	CHG	COMMENT
possibly seen	4	BIAGI	87	SPEC	–	Ξ^- Be 116 GeV

$\Gamma(\Xi^-\pi^+\pi^-)/\Gamma(\Sigma\overline{K})$ — Γ_5/Γ_2

VALUE	DOCUMENT ID		TECN	CHG	COMMENT
<0.03	DIONISI	78	HBC	–	K^-p 4.2 GeV/c

$\Gamma(\Xi(1530)\pi)/\Gamma(\Sigma\overline{K})$ — Γ_6/Γ_2

VALUE	DOCUMENT ID		TECN	CHG	COMMENT
<0.06	DIONISI	78	HBC	–	K^-p 4.2 GeV/c

Ξ(1690) FOOTNOTES

[1] From a fit to the Σ^+K^- spectrum.
[2] From a coupled-channel analysis of the Σ^+K^- and $\Lambda\overline{K}^0$ spectra.
[3] A fit to the inclusive spectrum from $\Xi^-N \to \Lambda K^-X$.
[4] From a coupled-channel analysis of the Σ^0K^- and ΛK^- spectra.

Ξ(1690) REFERENCES

AUBERT	08AK	PR D78 034008	B. Aubert *et al.*	(BABAR Collab.)
ABE	02C	PL B524 33	K. Abe *et al.*	(KEK BELLE Collab.)
ADAMOVICH	98	EPJ C5 621	M.I. Adamovich *et al.*	(CERN WA89 Collab.)
BIAGI	87	ZPHY C34 15	S.F. Biagi *et al.*	(BRIS, CERN, GEVA+) I
BIAGI	81	ZPHY C9 305	S.F. Biagi *et al.*	(BRIS, CAVE, GEVA+)
DIONISI	78	PL 80B 145	C. Dionisi *et al.*	(CERN, AMST, NIJM+) I

Ξ(1820) 3/2⁻

$I(J^P) = \frac{1}{2}(\frac{3}{2}^-)$ Status: ***

The clearest evidence is an 8-standard-deviation peak in ΛK^- seen by GAY 76C. TEODORO 78 favors $J = 3/2$, but cannot make a parity discrimination. BIAGI 87C is consistent with $J = 3/2$ and favors negative parity for this J value.

Ξ(1820) MASS

We only average the measurements that appear to us to be most significant and best determined.

VALUE (MeV)	EVTS	DOCUMENT ID		TECN	CHG	COMMENT
1823 ± 5 OUR ESTIMATE						
1823.4± 1.4 OUR AVERAGE						
1819.4± 3.1±2.0	280	[1] BIAGI	87	SPEC	0	Ξ^- Be → (ΛK^-) X
1826 ± 3 ±1	54	BIAGI	87C	SPEC	0	Ξ^- Be → $(\Lambda\overline{K}^0)$ X
1822 ± 6		JENKINS	83	MPS	–	$K^-p \to K^+$ (MM)
1830 ± 6	300	BIAGI	81	SPEC	–	SPS hyperon beam
1823 ± 2	130	GAY	76C	HBC	–	K^-p 4.2 GeV/c
• • • We do not use the following data for averages, fits, limits, etc. • • •						
1817 ± 3		ADAMOVICH	99B	WA89		Σ^- nucleus, 345 GeV
1797 ±19	74	BRIEFEL	77	HBC	0	K^-p 2.87 GeV/c
1829 ± 9	68	BRIEFEL	77	HBC	−0	$\Xi(1530)\pi$
1860 ±14	39	BRIEFEL	77	HBC	–	$\Sigma^-\overline{K}^0$
1870 ± 9	44	BRIEFEL	77	HBC	0	$\Lambda\overline{K}^0$
1813 ± 4	57	BRIEFEL	77	HBC	–	ΛK^-
1807 ±27		DIBIANCA	75	DBC	−0	$\Xi\pi\pi$, $\Xi^*\pi$
1762 ± 8	28	[2] BADIER	72	HBC	−0	$\Xi\pi$, $\Xi\pi\pi$, YK
1838 ± 5	38	[2] BADIER	72	HBC	−0	$\Xi\pi$, $\Xi\pi\pi$, YK
1830 ±10	25	[3] CRENNELL	70B	DBC	−0	3.6, 3.9 GeV/c
1826 ±12		[4] CRENNELL	70B	DBC	−0	3.6, 3.9 GeV/c
1830 ±10	40	ALITTI	69	HBC	–	Λ, $\Sigma\overline{K}$
1814 ± 4	30	BADIER	65	HBC	0	$\Lambda\overline{K}^0$
1817 ± 7	29	SMITH	65C	HBC	−0	$\Lambda\overline{K}^0$, ΛK^-
1770		HALSTEINSLID	63C	FBC	−0	K^- freon 3.5 GeV/c

Ξ(1820) WIDTH

VALUE (MeV)	EVTS	DOCUMENT ID		TECN	CHG	COMMENT
24^{+15}_{-10} OUR ESTIMATE						
24 ± 6 OUR AVERAGE Error includes scale factor of 1.5. See the ideogram below.						
24.6± 5.3	280	[1] BIAGI	87	SPEC	0	Ξ^- Be → (ΛK^-) X
12 ±14 ±1.7	54	BIAGI	87C	SPEC	0	Ξ^- Be → $(\Lambda\overline{K}^0)$ X
72 ±20	300	BIAGI	81	SPEC	–	SPS hyperon beam
21 ± 7	130	GAY	76C	HBC	–	K^-p 4.2 GeV/c
• • • We do not use the following data for averages, fits, limits, etc. • • •						
23 ±13		ADAMOVICH	99B	WA89		Σ^- nucleus, 345 GeV
99 ±57	74	BRIEFEL	77	HBC	0	K^-p 2.87 GeV/c
52 ±34	68	BRIEFEL	77	HBC	−0	$\Xi(1530)\pi$
72 ±17	39	BRIEFEL	77	HBC	–	$\Sigma^-\overline{K}^0$
44 ±11	44	BRIEFEL	77	HBC	0	$\Lambda\overline{K}^0$
26 ±11	57	BRIEFEL	77	HBC	–	ΛK^-
85 ±58		DIBIANCA	75	DBC	−0	$\Xi\pi\pi$, $\Xi^*\pi$
51 ±13		[2] BADIER	72	HBC	−0	Lower mass
58 ±13		[2] BADIER	72	HBC	−0	Higher mass
103^{+38}_{-24}		[3] CRENNELL	70B	DBC	−0	3.6, 3.9 GeV/c
48^{+36}_{-19}		[4] CRENNELL	70B	DBC	−0	3.6, 3.9 GeV/c
55^{+40}_{-20}		ALITTI	69	HBC	–	Λ, $\Sigma\overline{K}$
12 ± 4		BADIER	65	HBC	0	$\Lambda\overline{K}^0$
30 ± 7		SMITH	65B	HBC	−0	$\Lambda\overline{K}$
<80		HALSTEINSLID	63C	FBC	−0	K^- freon 3.5 GeV/c

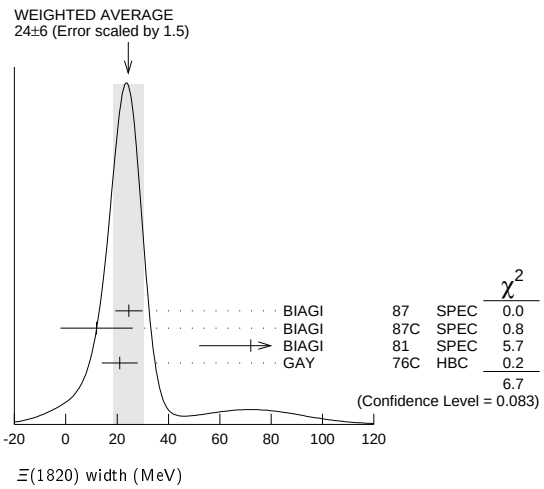

$\Xi(1820)$ DECAY MODES

	Mode	Fraction (Γ_i/Γ)
Γ_1	$\Lambda\overline{K}$	large
Γ_2	$\Sigma\overline{K}$	small
Γ_3	$\Xi\pi$	small
Γ_4	$\Xi(1530)\pi$	small
Γ_5	$\Xi\pi\pi$ (not $\Xi(1530)\pi$)	

$\Xi(1820)$ BRANCHING RATIOS

The dominant modes seem to be $\Lambda\overline{K}$ and (perhaps) $\Xi(1530)\pi$, but the branching fractions are very poorly determined.

$\Gamma(\Lambda\overline{K})/\Gamma_{total}$ Γ_1/Γ

VALUE	DOCUMENT ID		TECN	CHG	COMMENT
0.25±0.05 OUR AVERAGE					
0.24±0.05	ANISOVICH	12A	DPWA		Multichannel
0.30±0.15	ALITTI	69	HBC	−	K^-p 3.9–5 GeV/c

$\Gamma(\Xi\pi)/\Gamma_{total}$ Γ_3/Γ

VALUE	DOCUMENT ID		TECN	CHG	COMMENT
0.10±0.10	ALITTI	69	HBC	−	K^-p 3.9–5 GeV/c

$\Gamma(\Xi\pi)/\Gamma(\Lambda\overline{K})$ Γ_3/Γ_1

VALUE	CL%	DOCUMENT ID		TECN	CHG	COMMENT
<0.36	95	GAY	76C	HBC	−	K^-p 4.2 GeV/c
0.20±0.20		BADIER	65	HBC	0	K^-p 3 GeV/c

$\Gamma(\Xi\pi)/\Gamma(\Xi(1530)\pi)$ Γ_3/Γ_4

VALUE	DOCUMENT ID		TECN	CHG	COMMENT
$1.5^{+0.6}_{-0.4}$	APSELL	70	HBC	0	K^-p 2.87 GeV/c

$\Gamma(\Sigma\overline{K})/\Gamma_{total}$ Γ_2/Γ

VALUE	DOCUMENT ID		TECN	CHG	COMMENT
0.30±0.15	ALITTI	69	HBC	−	K^-p 3.9–5 GeV/c
• • • We do not use the following data for averages, fits, limits, etc. • • •					
<0.02	TRIPP	67	RVUE		Use SMITH 65C

$\Gamma(\Sigma\overline{K})/\Gamma(\Lambda\overline{K})$ Γ_2/Γ_1

VALUE	DOCUMENT ID		TECN	CHG	COMMENT
0.24±0.10	GAY	76C	HBC	−	K^-p 4.2 GeV/c

$\Gamma(\Xi(1530)\pi)/\Gamma_{total}$ Γ_4/Γ

VALUE	DOCUMENT ID		TECN	CHG	COMMENT
0.30±0.15	ALITTI	69	HBC	−	K^-p 3.9–5 GeV/c
• • • We do not use the following data for averages, fits, limits, etc. • • •					
seen	ASTON	85B	LASS		K^-p 11 GeV/c
not seen	[5] HASSALL	81	HBC		K^-p 6.5 GeV/c
<0.25	[6] DAUBER	69	HBC		K^-p 2.7 GeV/c

$\Gamma(\Xi(1530)\pi)/\Gamma(\Lambda\overline{K})$ Γ_4/Γ_1

VALUE	DOCUMENT ID		TECN	CHG	COMMENT
0.38±0.27 OUR AVERAGE	Error includes scale factor of 2.3.				
1.0 ±0.3	GAY	76C	HBC	−	K^-p 4.2 GeV/c
0.26±0.13	SMITH	65C	HBC	−0	K^-p 2.45–2.7 GeV/c

$\Gamma(\Xi\pi\pi(\text{not }\Xi(1530)\pi))/\Gamma(\Lambda\overline{K})$ Γ_5/Γ_1

VALUE	DOCUMENT ID		TECN	CHG	COMMENT
0.30±0.20	BIAGI	87	SPEC	−	Ξ^- Be 116 GeV
• • • We do not use the following data for averages, fits, limits, etc. • • •					
<0.14	[7] BADIER	65	HBC	0	1 st. dev. limit
>0.1	SMITH	65C	HBC	−0	K^-p 2.45–2.7 GeV/c

$\Gamma(\Xi\pi\pi(\text{not }\Xi(1530)\pi))/\Gamma(\Xi(1530)\pi)$ Γ_5/Γ_4

VALUE	DOCUMENT ID		TECN	CHG	COMMENT
consistent with zero	GAY	76C	HBC	−	K^-p 4.2 GeV/c
• • • We do not use the following data for averages, fits, limits, etc. • • •					
0.3±0.5	[8] APSELL	70	HBC	0	K^-p 2.87 GeV/c

$\Xi(1820)$ FOOTNOTES

[1] BIAGI 87 also sees weak signals in the in the $\Xi^-\pi^+\pi^-$ channel at 1782.6 ± 1.4 MeV (Γ = 6.0 ± 1.5 MeV) and 1831.9 ± 2.8 MeV (Γ = 9.6 ± 9.9 MeV).
[2] BADIER 72 adds all channels and divides the peak into lower and higher mass regions. The data can also be fitted with a single Breit-Wigner of mass 1800 MeV and width 150 MeV.
[3] From a fit to inclusive $\Xi\pi$, $\Xi\pi\pi$, and ΛK^- spectra.
[4] From a fit to inclusive $\Xi\pi$ and $\Xi\pi\pi$ spectra only.
[5] Including $\Xi\pi\pi$.
[6] DAUBER 69 uses in part the same data as SMITH 65C.
[7] For the decay mode $\Xi^-\pi^+\pi^0$ only. This limit includes $\Xi(1530)\pi$.
[8] Or less. Upper limit for the 3-body decay.

$\Xi(1820)$ REFERENCES

ANISOVICH	12A	EPJ A48 15	A.V. Anisovich *et al.* (BONN, PNPI)
ADAMOVICH	99B	EPJ C11 271	M.I. Adamovich *et al.* (CERN WA89 Collab.)
BIAGI	87	ZPHY C34 15	S.F. Biagi *et al.* (BRIS, CERN, GEVA+)
BIAGI	87C	ZPHY C34 175	S.F. Biagi *et al.* (BRIS, CERN, GEVA+) JP
ASTON	85B	PR D32 2270	D. Aston *et al.* (SLAC, CARL, CNRC, CINC)
JENKINS	83	PRL 51 951	C.M. Jenkins *et al.* (FSU, BRAN, LBL+)
BIAGI	81	ZPHY C9 305	S.F. Biagi *et al.* (BRIS, CAVE, GEVA+)
HASSALL	81	NP B189 397	J.K. Hassall *et al.* (CAVE, MSU)
TEODORO	78	PL 77B 451	D. Teodoro *et al.* (AMST, CERN, NIJM+) JP
BRIEFEL	77	PR D16 2706	E. Briefel *et al.* (BRAN, UMD, SYRA+)
Also		PRL 23 884	S.P. Apsell *et al.* (BRAN, UMD, SYRA+)
GAY	76C	PL 62B 477	J.B. Gay *et al.* (AMST, CERN, NIJM) IJ
DIBIANCA	75	NP B98 137	F.A. Dibianca, R.J. Endorf (CMU)
BADIER	72	NP B37 429	J. Badier *et al.* (EPOL)
APSELL	70	PRL 24 777	S.P. Apsell *et al.* (BRAN, UMD, SYRA+) I
CRENNELL	70B	PR D1 847	D.J. Crennell *et al.* (BNL)
ALITTI	69	PRL 22 79	J. Alitti *et al.* (BNL, SYRA) I
DAUBER	69	PR 179 1262	P.M. Dauber *et al.* (LRL)
TRIPP	67	NP B3 10	R.D. Tripp *et al.* (LRL, SLAC, CERN+)
BADIER	65	PL 16 171	J. Badier *et al.* (EPOL, SACL, AMST) I
SMITH	65B	Athens Conf. 251	G.A. Smith, J.S. Lindsey (LRL)
SMITH	65C	PRL 14 25	G.A. Smith *et al.* (LRL) IJP
HALSTEINSLID	63	Siena Conf. 1 73	A. Halsteinslid *et al.* (BERG, CERN, EPOL+) I

OTHER RELATED PAPERS

TEODORO	78	PL 77B 451	D. Teodoro *et al.* (AMST, CERN, NIJM+) JP
BRIEFEL	75	PR D12 1859	E. Briefel *et al.* (BRAN, UMD, SYRA+)
SCHMIDT	73	Purdue Conf. 363	P.E. Schmidt (BRAN)
MERRILL	68	PR 167 1202	D.W. Merrill, J. Button-Shafer (LRL)
SMITH	64	PRL 13 61	G.A. Smith *et al.* (LRL) IJP

$\Xi(1950)$

$I(J^P) = \frac{1}{2}(?^?)$ Status: ***

We list here everything reported between 1875 and 2000 MeV. The accumulated evidence for a Ξ near 1950 MeV seems strong enough to include a $\Xi(1950)$ in the main Baryon Table, but not much can be said about its properties. In fact, there may be more than one Ξ near this mass.

$\Xi(1950)$ MASS

VALUE (MeV)	EVTS	DOCUMENT ID		TECN	COMMENT
1950±15 OUR ESTIMATE					
1955± 6		ADAMOVICH	99B	WA89	Σ^- nucleus, 345 GeV
1944± 9	129	BIAGI	87	SPEC	Ξ^- Be → $(\Xi^-\pi^+)\pi^-$ X
1963± 5±2	63	BIAGI	87C	SPEC	Ξ^- Be → $(\Lambda\overline{K}^0)$ X
1937± 7	150	BIAGI	81	SPEC	SPS hyperon beam
1961±18	139	BRIEFEL	77	HBC	2.87 K^-p → $\Xi^-\pi^+$X
1936±22	44	BRIEFEL	77	HBC	2.87 K^-p → $\Xi^0\pi^-$X
1964±10	56	BRIEFEL	77	HBC	$\Xi(1530)\pi$
1900±12		DIBIANCA	75	DBC	$\Xi\pi$
1952±11	25	ROSS	73C		$(\Xi\pi)^-$
1956± 6	29	BADIER	72	HBC	$\Xi\pi$, $\Xi\pi\pi$, YK
1955±14	21	GOLDWASSER	70	HBC	$\Xi\pi$
1894±18	66	DAUBER	69	HBC	$\Xi\pi$
1930±20	27	ALITTI	68	HBC	$\Xi^-\pi^+$
1933±16	35	BADIER	65	HBC	$\Xi^-\pi^+$

$\Xi(1950)$ WIDTH

VALUE (MeV)	EVTS	DOCUMENT ID		TECN	COMMENT
60±20 OUR ESTIMATE					
68±22		ADAMOVICH	99B	WA89	Σ^- nucleus, 345 GeV
100±31	129	BIAGI	87	SPEC	Ξ^- Be → $(\Xi^-\pi^+)\pi^-$ X
25±15±1.2	63	BIAGI	87C	SPEC	Ξ^- Be → $(\Lambda\overline{K}^0)$ X
60± 8	150	BIAGI	81	SPEC	SPS hyperon beam
159±57	139	BRIEFEL	77	HBC	2.87 K^-p → $\Xi^-\pi^+$X
87±26	44	BRIEFEL	77	HBC	2.87 K^-p → $\Xi^0\pi^-$X
60±39	56	BRIEFEL	77	HBC	$\Xi(1530)\pi$
63±78		DIBIANCA	75	DBC	$\Xi\pi$
38±10		ROSS	73C		$(\Xi\pi)^-$
35±11	29	BADIER	72	HBC	$\Xi\pi$, $\Xi\pi\pi$, YK
56±26	21	GOLDWASSER	70	HBC	$\Xi\pi$
98±23	66	DAUBER	69	HBC	$\Xi\pi$
80±40	27	ALITTI	68	HBC	$\Xi^-\pi^+$
140±35	35	BADIER	65	HBC	$\Xi^-\pi^+$

$\Xi(1950)$ DECAY MODES

	Mode	Fraction (Γ_i/Γ)
Γ_1	$\Lambda\overline{K}$	seen
Γ_2	$\Sigma\overline{K}$	possibly seen
Γ_3	$\Xi\pi$	seen
Γ_4	$\Xi(1530)\pi$	
Γ_5	$\Xi\pi\pi$ (not $\Xi(1530)\pi$)	

$\Xi(1950)$ BRANCHING RATIOS

$\Gamma(\Sigma\overline{K})/\Gamma(\Lambda\overline{K})$ Γ_2/Γ_1

VALUE	CL%	EVTS	DOCUMENT ID		TECN	COMMENT
<2.3	90	0	BIAGI	87C	SPEC	Ξ^- Be 116 GeV

$\Gamma(\Sigma\overline{K})/\Gamma_{total}$ Γ_2/Γ

VALUE	EVTS	DOCUMENT ID		TECN	COMMENT
possibly seen	17	HASSALL	81	HBC	K^-p 6.5 GeV/c

$\Gamma(\Xi\pi)/\Gamma(\Xi(1530)\pi)$ Γ_3/Γ_4

VALUE	DOCUMENT ID		TECN
$2.8^{+0.7}_{-0.6}$	APSELL	70	HBC

$\Gamma(\Xi\pi\pi(\text{not }\Xi(1530)\pi))/\Gamma(\Xi(1530)\pi)$ Γ_5/Γ_4

VALUE	DOCUMENT ID		TECN
0.0 ± 0.3	APSELL	70	HBC

$\Xi(1950)$ REFERENCES

ADAMOVICH	99B	EPJ C11 271	M.I. Adamovich *et al.*	(CERN WA89 Collab.)
BIAGI	87	ZPHY C34 15	S.F. Biagi *et al.*	(BRIS, CERN, GEVA+)
BIAGI	87C	ZPHY C34 175	S.F. Biagi *et al.*	(BRIS, CERN, GEVA+)
BIAGI	81	ZPHY C9 305	S.F. Biagi *et al.*	(BRIS, CAVE, GEVA+)
HASSALL	81	NP B189 397	J.K. Hassall *et al.*	(CAVE, MSU)
BRIEFEL	77	PR D16 2706	E. Briefel *et al.*	(BRAN, UMD, SYRA+)
Also		Duke Conf. 317	E. Briefel *et al.*	(BRAN, UMD, SYRA+)
Hyperon Resonances, 1970				
DIBIANCA	75	NP B98 137	F.A. Dibianca, R.J. Endorf	(CMU)
ROSS	73C	Purdue Conf. 345	R.T. Ross, J.L. Lloyd, D. Radojicic	(OXF)
BADIER	72	NP B37 429	J. Badier *et al.*	(EPOL)
APSELL	70	PRL 24 777	S.P. Apsell *et al.*	(BRAN, UMD, SYRA+) I
GOLDWASSER	70	PR D1 1960	E.L. Goldwasser, P.F. Schultz	(ILL)
DAUBER	69	PR 179 1262	P.M. Dauber *et al.*	(LRL) I
ALITTI	68	PRL 21 1119	J. Alitti *et al.*	(BNL, SYRA) I
BADIER	65	PL 16 171	J. Badier *et al.*	(EPOL, SACL, AMST) I

$\Xi(2030)$

$I(J^P) = \frac{1}{2}(\geq\frac{5}{2}^?)$ Status: ***

The evidence for this state has been much improved by HEMINGWAY 77, who see an eight standard deviation enhancement in $\Sigma\overline{K}$ and a weaker coupling to $\Lambda\overline{K}$. ALITTI 68 and HEMINGWAY 77 observe no signals in the $\Xi\pi\pi$ (or $\Xi(1530)\pi$) channel, in contrast to DIBIANCA 75. The decay $(\Lambda/\Sigma)\overline{K}\pi$ reported by BARTSCH 69 is also not confirmed by HEMINGWAY 77.

A moments analysis of the HEMINGWAY 77 data indicates at a level of three standard deviations that $J \geq 5/2$.

$\Xi(2030)$ MASS

VALUE (MeV)	EVTS	DOCUMENT ID		TECN	CHG	COMMENT
2025 ± 5 OUR ESTIMATE						
2025.1± 2.4 OUR AVERAGE		Error includes scale factor of 1.3. See the ideogram below.				
2022 ± 7		JENKINS	83	MPS	–	$K^-p \rightarrow K^+$ MM
2024 ± 2	200	HEMINGWAY	77	HBC	–	K^-p 4.2 GeV/c
2044 ± 8		DIBIANCA	75	DBC	−0	$\Xi\pi\pi$, $\Xi^*\pi$
2019 ± 7	15	ROSS	73C	HBC	−0	$\Sigma\overline{K}$
2030 ±10	42	ALITTI	69	HBC	–	K^-p 3.9–5 GeV/c
2058 ±17	40	BARTSCH	69	HBC	−0	K^-p 10 GeV/c

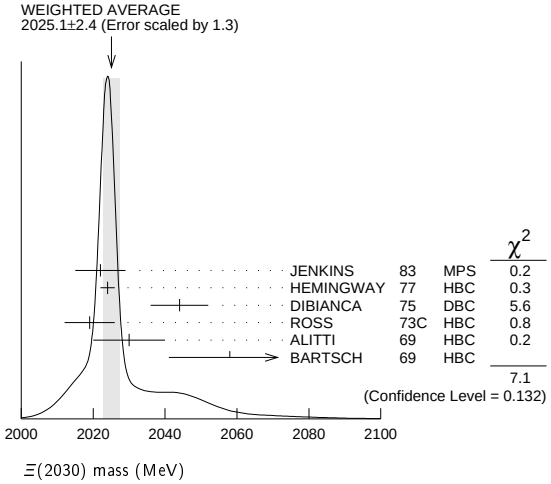

$\Xi(2030)$ WIDTH

VALUE (MeV)	EVTS	DOCUMENT ID		TECN	CHG	COMMENT
20^{+15}_{-5} OUR ESTIMATE						
21± 6 OUR AVERAGE		Error includes scale factor of 1.3. See the ideogram below.				
16± 5	200	HEMINGWAY	77	HBC	–	K^-p 4.2 GeV/c
60±24		DIBIANCA	75	DBC	−0	$\Xi\pi\pi$, $\Xi^*\pi$
33±17	15	ROSS	73C	HBC	−0	$\Sigma\overline{K}$
45^{+40}_{-20}		ALITTI	69	HBC	–	K^-p 3.9–5 GeV/c
57±30		BARTSCH	69	HBC	−0	K^-p 10 GeV/c

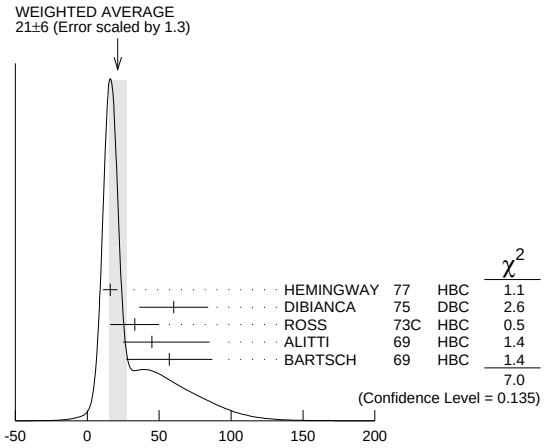

$\Xi(2030)$ DECAY MODES

	Mode	Fraction (Γ_i/Γ)
Γ_1	$\Lambda\overline{K}$	~ 20 %
Γ_2	$\Sigma\overline{K}$	~ 80 %
Γ_3	$\Xi\pi$	small
Γ_4	$\Xi(1530)\pi$	small
Γ_5	$\Xi\pi\pi$(not $\Xi(1530)\pi$)	small
Γ_6	$\Lambda\overline{K}\pi$	small
Γ_7	$\Sigma\overline{K}\pi$	small

$\Xi(2030)$ BRANCHING RATIOS

$\Gamma(\Xi\pi)/[\Gamma(\Lambda\overline{K})+\Gamma(\Sigma\overline{K})+\Gamma(\Xi\pi)+\Gamma(\Xi(1530)\pi)]$ $\Gamma_3/(\Gamma_1+\Gamma_2+\Gamma_3+\Gamma_4)$

VALUE	DOCUMENT ID		TECN	CHG	COMMENT
• • • We do not use the following data for averages, fits, limits, etc. • • •					
<0.30	ALITTI	69	HBC	–	1 standard dev. limit

$\Gamma(\Xi\pi)/\Gamma(\Sigma\overline{K})$ Γ_3/Γ_2

VALUE	CL%	DOCUMENT ID		TECN	CHG	COMMENT
<0.19	95	HEMINGWAY	77	HBC	–	K^-p 4.2 GeV/c

$\Gamma(\Lambda\overline{K})/[\Gamma(\Lambda\overline{K})+\Gamma(\Sigma\overline{K})+\Gamma(\Xi\pi)+\Gamma(\Xi(1530)\pi)]$ $\Gamma_1/(\Gamma_1+\Gamma_2+\Gamma_3+\Gamma_4)$

VALUE	DOCUMENT ID		TECN	CHG	COMMENT
0.25 ± 0.15	ALITTI	69	HBC	–	K^-p 3.9–5 GeV/c

$\Gamma(\Lambda\overline{K})/\Gamma(\Sigma\overline{K})$ Γ_1/Γ_2

VALUE	DOCUMENT ID		TECN	CHG	COMMENT
0.22 ± 0.09	HEMINGWAY	77	HBC	–	K^-p 4.2 GeV/c

$\Gamma(\Sigma\overline{K})/[\Gamma(\Lambda\overline{K})+\Gamma(\Sigma\overline{K})+\Gamma(\Xi\pi)+\Gamma(\Xi(1530)\pi)]$ $\Gamma_2/(\Gamma_1+\Gamma_2+\Gamma_3+\Gamma_4)$

VALUE	DOCUMENT ID		TECN	CHG	COMMENT
0.75 ± 0.20	ALITTI	69	HBC	–	K^-p 3.9–5 GeV/c

$\Gamma(\Xi(1530)\pi)/[\Gamma(\Lambda\overline{K})+\Gamma(\Sigma\overline{K})+\Gamma(\Xi\pi)+\Gamma(\Xi(1530)\pi)]$ $\Gamma_4/(\Gamma_1+\Gamma_2+\Gamma_3+\Gamma_4)$

VALUE	DOCUMENT ID		TECN	CHG	COMMENT
• • • We do not use the following data for averages, fits, limits, etc. • • •					
<0.15	ALITTI	69	HBC	–	1 standard dev. limit

$[\Gamma(\Xi(1530)\pi)+\Gamma(\Xi\pi\pi(\text{not }\Xi(1530)\pi))]/\Gamma(\Sigma\overline{K})$ $(\Gamma_4+\Gamma_5)/\Gamma_2$

VALUE	CL%	DOCUMENT ID		TECN	CHG	COMMENT
<0.11	95	[1] HEMINGWAY	77	HBC	–	K^-p 4.2 GeV/c

$\Gamma(\Lambda\overline{K}\pi)/\Gamma_{total}$ **Γ_6/Γ**

VALUE	DOCUMENT ID		TECN	COMMENT
• • • We do not use the following data for averages, fits, limits, etc. • • •				
seen	BARTSCH	69	HBC	K^-p 10 GeV

$\Gamma(\Lambda\overline{K}\pi)/\Gamma(\Sigma\overline{K})$ **Γ_6/Γ_2**

VALUE	CL%	DOCUMENT ID		TECN	CHG	COMMENT
<0.32	95	HEMINGWAY	77	HBC	–	K^-p 4.2 GeV/c

$\Gamma(\Sigma\overline{K}\pi)/\Gamma_{total}$ **Γ_7/Γ**

VALUE	DOCUMENT ID		TECN	COMMENT
• • • We do not use the following data for averages, fits, limits, etc. • • •				
seen	BARTSCH	69	HBC	K^-p 10 GeV

$\Gamma(\Sigma\overline{K}\pi)/\Gamma(\Sigma\overline{K})$ **Γ_7/Γ_2**

VALUE	CL%	DOCUMENT ID		TECN	CHG	COMMENT
<0.04	95	[2] HEMINGWAY	77	HBC	–	K^-p 4.2 GeV/c

$\Xi(2030)$ FOOTNOTES

[1] For the decay mode $\Xi^-\pi^+\pi^-$ only.
[2] For the decay mode $\Sigma^\pm K^-\pi^\mp$ only.

$\Xi(2030)$ REFERENCES

JENKINS	83	PRL 51 951	C.M. Jenkins *et al.*	(FSU, BRAN, LBL+)
HEMINGWAY	77	PL 68B 197	R.J. Hemingway *et al.*	(AMST, CERN, NIJM+) IJ
Also		PL 62B 477	J.B. Gay *et al.*	(AMST, CERN, NIJM)
DIBIANCA	75	NP B98 137	F.A. Dibianca, R.J. Endorf	(CMU)
ROSS	73C	Purdue Conf. 345	R.T. Ross, J.L. Lloyd, D. Radojicic	(OXF)
ALITTI	69	PRL 22 79	J. Alitti *et al.*	(BNL, SYRA) I
BARTSCH	69	PL 28B 439	J. Bartsch *et al.*	(AACH, BERL, CERN+)
ALITTI	68	PRL 21 1119	J. Alitti *et al.*	(BNL, SYRA)

$\Xi(2120)$

$I(J^P) = \frac{1}{2}(?^?)$ Status: * J, P need confirmation.

OMITTED FROM SUMMARY TABLE

$\Xi(2120)$ MASS

VALUE (MeV)	EVTS	DOCUMENT ID		TECN	COMMENT
≈ 2120 OUR ESTIMATE					
2137±4	18	[1] CHLIAPNIK...	79	HBC	K^+p 32 GeV/c
2123±7		[2] GAY	76C	HBC	K^-p 4.2 GeV/c

$\Xi(2120)$ WIDTH

VALUE (MeV)	EVTS	DOCUMENT ID		TECN	COMMENT
<20	18	[1] CHLIAPNIK...	79	HBC	K^+p 32 GeV/c
25±12		[2] GAY	76C	HBC	K^-p 4.2 GeV/c

$\Xi(2120)$ DECAY MODES

	Mode	Fraction (Γ_i/Γ)
Γ_1	$\Lambda\overline{K}$	seen

$\Xi(2120)$ BRANCHING RATIOS

$\Gamma(\Lambda\overline{K})/\Gamma_{total}$ **Γ_1/Γ**

VALUE	DOCUMENT ID		TECN	COMMENT
seen	[1] CHLIAPNIK...	79	HBC	$K^+p \to (\overline{\Lambda}K^+)$ X
seen	[2] GAY	76C	HBC	K^-p 4.2 GeV/c

$\Xi(2120)$ FOOTNOTES

[1] CHLIAPNIKOV 79 does not uniquely identify the K^+ in the $(\overline{\Lambda}K^+)$ X final state. It also reports bumps with fewer events at 2240, 2540, and 2830 MeV.
[2] GAY 76C sees a 4-standard deviation signal. However, HEMINGWAY 77, with more events from the same experiment points out that the signal is greatly reduced if a cut is made on the 4-momentum u. This suggests an anomalous production mechanism if the $\Xi(2120)$ is real.

$\Xi(2120)$ REFERENCES

CHLIAPNIK...	79	NP B158 253	P.V. Chliapnikov *et al.*	(CERN, BELG, MONS)
HEMINGWAY	77	PL 68B 197	R.J. Hemingway *et al.*	(AMST, CERN, NIJM+)
GAY	76C	PL 62B 477	J.B. Gay *et al.*	(AMST, CERN, NIJM)

$\Xi(2250)$

$I(J^P) = \frac{1}{2}(?^?)$ Status: ** J, P need confirmation.

OMITTED FROM SUMMARY TABLE

The evidence for this state is mixed. BARTSCH 69 sees a bump of not much statistical significance in $\Lambda\overline{K}\pi$, $\Sigma\overline{K}\pi$, and $\Xi\pi\pi$ mass spectra. GOLDWASSER 70 sees a narrower bump in $\Xi\pi\pi$ at a higher mass. Not seen by HASSALL 81 with 45 events/μb at 6.5 GeV/c. Seen by JENKINS 83. Perhaps seen by BIAGI 87.

$\Xi(2250)$ MASS

VALUE (MeV)	EVTS	DOCUMENT ID		TECN	CHG	COMMENT
≈ 2250 OUR ESTIMATE						
2189± 7	66	BIAGI	87	SPEC	–	Ξ^-Be → ($\Xi^-\pi^+\pi^-$) X
2214± 5		JENKINS	83	MPS	–	$K^-p \to K^+$ MM
2295±15	18	GOLDWASSER	70	HBC	–	K^-p 5.5 GeV/c
2244±52	35	BARTSCH	69	HBC		K^-p 10 GeV/c

$\Xi(2250)$ WIDTH

VALUE (MeV)	EVTS	DOCUMENT ID		TECN	CHG	COMMENT
46±27	66	BIAGI	87	SPEC	–	Ξ^-Be → ($\Xi^-\pi^+\pi^-$) X
< 30		GOLDWASSER	70	HBC	–	K^-p 5.5 GeV/c
130±80		BARTSCH	69	HBC		

$\Xi(2250)$ DECAY MODES

	Mode
Γ_1	$\Xi\pi\pi$
Γ_2	$\Lambda\overline{K}\pi$
Γ_3	$\Sigma\overline{K}\pi$

$\Xi(2250)$ REFERENCES

BIAGI	87	ZPHY C34 15	S.F. Biagi *et al.*	(BRIS, CERN, GEVA+)
JENKINS	83	PRL 51 951	C.M. Jenkins *et al.*	(FSU, BRAN, LBL+)
HASSALL	81	NP B189 397	J.K. Hassall *et al.*	(CAVE, MSU)
GOLDWASSER	70	PR D1 1960	E.L. Goldwasser, P.F. Schultz	(ILL)
BARTSCH	69	PL 28B 439	J. Bartsch *et al.*	(AACH, BERL, CERN+)

$\Xi(2370)$

$I(J^P) = \frac{1}{2}(?^?)$ Status: ** J, P need confirmation.

OMITTED FROM SUMMARY TABLE

$\Xi(2370)$ MASS

VALUE (MeV)	EVTS	DOCUMENT ID		TECN	CHG	COMMENT
≈ 2370 OUR ESTIMATE						
2356±10		JENKINS	83	MPS	–	$K^-p \to K^+$ MM
2370	50	HASSALL	81	HBC	–0	K^-p 6.5 GeV/c
2373± 8	94	AMIRZADEH	80	HBC	–0	K^-p 8.25 GeV/c
2392±27		DIBIANCA	75	DBC		$\Xi 2\pi$

$\Xi(2370)$ WIDTH

VALUE (MeV)	EVTS	DOCUMENT ID		TECN	CHG	COMMENT
80	50	HASSALL	81	HBC	–0	K^-p 6.5 GeV/c
80±25	94	AMIRZADEH	80	HBC	–0	K^-p 8.25 GeV/c
75±69		DIBIANCA	75	DBC		$\Xi 2\pi$

$\Xi(2370)$ DECAY MODES

	Mode	Fraction (Γ_i/Γ)
Γ_1	$\Lambda\overline{K}\pi$ Includes $\Gamma_4 + \Gamma_6$.	seen
Γ_2	$\Sigma\overline{K}\pi$ Includes $\Gamma_5 + \Gamma_6$.	seen
Γ_3	Ω^-K	
Γ_4	$\Lambda\overline{K}^*(892)$	
Γ_5	$\Sigma\overline{K}^*(892)$	
Γ_6	$\Sigma(1385)\overline{K}$	

$\Xi(2370)$ BRANCHING RATIOS

$\Gamma(\Lambda\overline{K}\pi)/\Gamma_{total}$ **Γ_1/Γ**

VALUE	DOCUMENT ID		TECN	CHG	COMMENT
seen	AMIRZADEH	80	HBC	–0	K^-p 8.25 GeV/c

$\Gamma(\Sigma\overline{K}\pi)/\Gamma_{total}$ **Γ_2/Γ**

VALUE	DOCUMENT ID		TECN	CHG	COMMENT
seen	AMIRZADEH	80	HBC	–0	K^-p 8.25 GeV/c

$[\Gamma(\Lambda\overline{K}\pi)+\Gamma(\Sigma\overline{K}\pi)]/\Gamma_{total}$ **$(\Gamma_1+\Gamma_2)/\Gamma$**

VALUE	EVTS	DOCUMENT ID		TECN	CHG	COMMENT
seen	50	HASSALL	81	HBC	−0	K^-p 6.5 GeV/c

$\Gamma(\Omega^-K)/\Gamma_{total}$ **Γ_3/Γ**

VALUE	DOCUMENT ID		TECN	CHG	COMMENT
0.09±0.04	[1] KINSON	80	HBC	–	K^-p 8.25 GeV/c

$[\Gamma(\Lambda\overline{K}^*(892))+\Gamma(\Sigma\overline{K}^*(892))]/\Gamma_{total}$ **$(\Gamma_4+\Gamma_5)/\Gamma$**

VALUE	DOCUMENT ID		TECN	CHG	COMMENT
0.22±0.13	[1] KINSON	80	HBC	–	K^-p 8.25 GeV/c

$\Gamma(\Sigma(1385)\overline{K})/\Gamma_{total}$ **Γ_6/Γ**

VALUE	DOCUMENT ID		TECN	CHG	COMMENT
0.12±0.08	[1] KINSON	80	HBC	–	K^-p 8.25 GeV/c

$\Xi(2370)$ FOOTNOTES

[1] KINSON 80 is a reanalysis of AMIRZADEH 80 with 50% more events.

$\Xi(2370)$ REFERENCES

JENKINS	83	PRL 51 951	C.M. Jenkins *et al.*	(FSU, BRAN, LBL+)
HASSALL	81	NP B189 397	J.K. Hassall *et al.*	(CAVE, MSU)
AMIRZADEH	80	PL 90B 324	J. Amirzadeh *et al.*	(BIRM, CERN, GLAS+) I
KINSON	80	Toronto Conf. 263	J.B. Kinson *et al.*	(BIRM, CERN, GLAS+) I
DIBIANCA	75	NP B98 137	F.A. Dibianca, R.J. Endorf	(CMU)

$\Xi(2500)$

$I(J^P) = \frac{1}{2}(?^?)$ Status: * J, P need confirmation.

OMITTED FROM SUMMARY TABLE

The ALITTI 69 peak might be instead the $\Xi(2370)$ or might be neither the $\Xi(2370)$ nor the $\Xi(2500)$.

$\Xi(2500)$ MASS

VALUE (MeV)	EVTS	DOCUMENT ID		TECN	CHG	COMMENT
≈ 2500 OUR ESTIMATE						
2505±10		JENKINS	83	MPS	–	$K^-p \to K^+$ MM
2430±20	30	ALITTI	69	HBC	–	K^-p 4.6–5 GeV/c
2500±10	45	BARTSCH	69	HBC	−0	K^-p 10 GeV/c

$\Xi(2500)$ WIDTH

VALUE (MeV)	DOCUMENT ID		TECN	CHG
150^{+60}_{-40}	ALITTI	69	HBC	–
59±27	BARTSCH	69	HBC	−0

$\Xi(2500)$ DECAY MODES

	Mode	Fraction (Γ_i/Γ)
Γ_1	$\Xi\pi$	
Γ_2	$\Lambda\overline{K}$	
Γ_3	$\Sigma\overline{K}$	
Γ_4	$\Xi\pi\pi$	seen
Γ_5	$\Xi(1530)\pi$	
Γ_6	$\Lambda\overline{K}\pi + \Sigma\overline{K}\pi$	seen

$\Xi(2500)$ BRANCHING RATIOS

$\Gamma(\Xi\pi)/[\Gamma(\Xi\pi)+\Gamma(\Lambda\overline{K})+\Gamma(\Sigma\overline{K})+\Gamma(\Xi(1530)\pi)]$ **$\Gamma_1/(\Gamma_1+\Gamma_2+\Gamma_3+\Gamma_5)$**

VALUE	DOCUMENT ID		TECN	COMMENT
<0.5	ALITTI	69	HBC	1 standard dev. limit

$\Gamma(\Lambda\overline{K})/[\Gamma(\Xi\pi)+\Gamma(\Lambda\overline{K})+\Gamma(\Sigma\overline{K})+\Gamma(\Xi(1530)\pi)]$ **$\Gamma_2/(\Gamma_1+\Gamma_2+\Gamma_3+\Gamma_5)$**

VALUE	DOCUMENT ID		TECN	CHG
0.5±0.2	ALITTI	69	HBC	–

$\Gamma(\Sigma\overline{K})/[\Gamma(\Xi\pi)+\Gamma(\Lambda\overline{K})+\Gamma(\Sigma\overline{K})+\Gamma(\Xi(1530)\pi)]$ **$\Gamma_3/(\Gamma_1+\Gamma_2+\Gamma_3+\Gamma_5)$**

VALUE	DOCUMENT ID		TECN	CHG
0.5±0.2	ALITTI	69	HBC	–

$\Gamma(\Xi(1530)\pi)/[\Gamma(\Xi\pi)+\Gamma(\Lambda\overline{K})+\Gamma(\Sigma\overline{K})+\Gamma(\Xi(1530)\pi)]$ **$\Gamma_5/(\Gamma_1+\Gamma_2+\Gamma_3+\Gamma_5)$**

VALUE	DOCUMENT ID		TECN	COMMENT
<0.2	ALITTI	69	HBC	1 standard dev. limit

$\Gamma(\Xi\pi\pi)/\Gamma_{total}$ **Γ_4/Γ**

VALUE	DOCUMENT ID		TECN	CHG
seen	BARTSCH	69	HBC	−0

$[\Gamma(\Lambda\overline{K}\pi)+\Gamma(\Sigma\overline{K}\pi)]/\Gamma_{total}$ **Γ_6/Γ**

VALUE	DOCUMENT ID		TECN	CHG
seen	BARTSCH	69	HBC	−0

$\Xi(2500)$ REFERENCES

JENKINS	83	PRL 51 951	C.M. Jenkins *et al.*	(FSU, BRAN, LBL+)
ALITTI	69	PRL 22 79	J. Alitti *et al.*	(BNL, SYRA) I
BARTSCH	69	PL 28B 439	J. Bartsch *et al.*	(AACH, BERL, CERN+)

Ω BARYONS
($S = -3$, $I = 0$)

$\Omega^- = sss$

Ω^-

$I(J^P) = 0(\frac{3}{2}^+)$ Status: ****

The unambiguous discovery in both production and decay was by BARNES 64. The quantum numbers follow from the assignment of the particle to the baryon decuplet. DEUTSCHMANN 78 and BAUBILLIER 78 rule out $J = 1/2$ and find consistency with $J = 3/2$. AUBERT,BE 06 finds from the decay angular distributions of $\Xi_c^0 \to \Omega^- K^+$ and $\Omega_c^0 \to \Omega^- K^+$ that $J = 3/2$; this depends on the spins of the Ξ_c^0 and Ω_c^0 being $J = 1/2$, their supposed values.

We have omitted some results that have been superseded by later experiments. See our earlier editions.

Ω^- MASS

The fit assumes the Ω^- and $\overline{\Omega}^+$ masses are the same, and averages them together.

VALUE (MeV)	EVTS	DOCUMENT ID		TECN	COMMENT
1672.45±0.29 OUR FIT					
1672.43±0.32 OUR AVERAGE					
1673 ±1	100	HARTOUNI	85	SPEC	80–280 GeV K_L^0C
1673.0 ±0.8	41	BAUBILLIER	78	HBC	8.25 GeV/c K^-p
1671.7 ±0.6	27	HEMINGWAY	78	HBC	4.2 GeV/c K^-p
1673.4 ±1.7	4	[1] DIBIANCA	75	DBC	4.9 GeV/c K^-d
1673.3 ±1.0	3	PALMER	68	HBC	K^-p 4.6, 5 GeV/c
1671.8 ±0.8	3	SCHULTZ	68	HBC	K^-p 5.5 GeV/c
1674.2 ±1.6	5	SCOTTER	68	HBC	K^-p 6 GeV/c
1672.1 ±1.0	1	[2] FRY	55	EMUL	
• • • We do not use the following data for averages, fits, limits, etc. • • •					
1671.43±0.78	13	[3] DEUTSCH...	73	HBC	K^-p 10 GeV/c
1671.9 ±1.2	6	[3] SPETH	69	HBC	See DEUTSCHMANN 73
1673.0 ±8.0	1	ABRAMS	64	HBC	$\to \Xi^-\pi^0$
1670.6 ±1.0	1	[2] FRY	55B	EMUL	
1615	1	[4] EISENBERG	54	EMUL	

[1] DIBIANCA 75 gives a mass for each event. We quote the average.
[2] The FRY 55 and FRY 55B events were identified as Ω^- by ALVAREZ 73. The masses assume decay to ΛK^- at rest. For FRY 55B, decay from an atomic orbit could Doppler shift the K^- energy and the resulting Ω^- mass by several MeV. This shift is negligible for FRY 55 because the Ω decay is approximately perpendicular to its orbital velocity, as is known because the Λ strikes the nucleus (L.Alvarez, private communication 1973). We have calculated the error assuming that the orbital n is 4 or larger.
[3] Excluded from the average; the Ω^- lifetimes measured by the experiments differ significantly from other measurements.
[4] The EISENBERG 54 mass was calculated for decay in flight. ALVAREZ 73 has shown that the Ω interacted with an Ag nucleus to give $K^-\Xi$Ag.

$\overline{\Omega}^+$ MASS

The fit assumes the Ω^- and $\overline{\Omega}^+$ masses are the same, and averages them together.

VALUE (MeV)	EVTS	DOCUMENT ID		TECN	COMMENT
1672.45±0.29 OUR FIT					
1672.5 ±0.7 OUR AVERAGE					
1672 ±1	72	HARTOUNI	85	SPEC	80–280 GeV K_L^0C
1673.1 ±1.0	1	FIRESTONE	71B	HBC	12 GeV/c K^+d

$(m_{\Omega^-} - m_{\overline{\Omega}^+}) / m_{\Omega^-}$

A test of CPT invariance.

VALUE	DOCUMENT ID		TECN	COMMENT
$(-1.44\pm7.98)\times10^{-5}$	CHAN	98	E756	p Be, 800 GeV

Ω^- MEAN LIFE

Measurements with an error $> 0.1\times10^{-10}$ s have been omitted. The fit assumes the Ω^- and $\overline{\Omega}^+$ mean lives are the same, and averages them together.

VALUE (10^{-10} s)	EVTS	DOCUMENT ID		TECN	COMMENT
0.821±0.011 OUR FIT					
0.821±0.011 OUR AVERAGE					
0.817±0.013±0.018	6934	CHAN	98	E756	p Be, 800 GeV
0.811±0.037	1096	LUK	88	SPEC	pBe 400 GeV
0.823±0.013	12k	BOURQUIN	84	SPEC	SPS hyperon beam
• • • We do not use the following data for averages, fits, limits, etc. • • •					
0.822±0.028	2437	BOURQUIN	79B	SPEC	See BOURQUIN 84

$\overline{\Omega}^+$ MEAN LIFE

The fit assumes the Ω^- and $\overline{\Omega}^+$ mean lives are the same, and averages them together.

VALUE (10^{-10} s)	EVTS	DOCUMENT ID		TECN	COMMENT
0.821±0.011 OUR FIT					
0.823±0.031±0.022	1801	CHAN	98	E756	p Be, 800 GeV

$(\tau_{\Omega^-} - \tau_{\overline{\Omega}^+}) / \tau_{\Omega^-}$

A test of CPT invariance. Our calculation, from the averages in the preceding two data blocks.

VALUE	DOCUMENT ID
0.00±0.05 OUR ESTIMATE	

Ω^- MAGNETIC MOMENT

VALUE (μ_N)	EVTS	DOCUMENT ID		TECN	COMMENT
−2.02 ±0.05 OUR AVERAGE					
−2.024±0.056	235k	WALLACE	95	SPEC	Ω^- 300–550 GeV
−1.94 ±0.17 ±0.14	25k	DIEHL	91	SPEC	Spin-transfer production

Ω^- DECAY MODES

	Mode	Fraction (Γ_i/Γ)		Confidence level
Γ_1	ΛK^-	(67.8±0.7) %		
Γ_2	$\Xi^0\pi^-$	(23.6±0.7) %		
Γ_3	$\Xi^-\pi^0$	(8.6±0.4) %		
Γ_4	$\Xi^-\pi^+\pi^-$	$(3.7^{+0.7}_{-0.6})\times10^{-4}$		
Γ_5	$\Xi(1530)^0\pi^-$	< 7	$\times10^{-5}$	90%
Γ_6	$\Xi^0 e^-\overline{\nu}_e$	$(5.6\pm2.8)\times10^{-3}$		
Γ_7	$\Xi^-\gamma$	< 4.6	$\times10^{-4}$	90%
	$\Delta S = 2$ forbidden ($S2$) modes			
Γ_8	$\Lambda\pi^-$ $S2$	< 2.9	$\times10^{-6}$	90%

Ω^- BRANCHING RATIOS

The BOURQUIN 84 values (which include results of BOURQUIN 79B, a separate experiment) are much more accurate than any other results, and so the other results have been omitted.

$\Gamma(\Lambda K^-)/\Gamma_{total}$ Γ_1/Γ

VALUE	EVTS	DOCUMENT ID		TECN	COMMENT
0.678±0.007	14k	BOURQUIN	84	SPEC	SPS hyperon beam
• • • We do not use the following data for averages, fits, limits, etc. • • •					
0.686±0.013	1920	BOURQUIN	79B	SPEC	See BOURQUIN 84

$\Gamma(\Xi^0\pi^-)/\Gamma_{total}$ Γ_2/Γ

VALUE	EVTS	DOCUMENT ID		TECN	COMMENT
0.236±0.007	1947	BOURQUIN	84	SPEC	SPS hyperon beam
• • • We do not use the following data for averages, fits, limits, etc. • • •					
0.234±0.013	317	BOURQUIN	79B	SPEC	See BOURQUIN 84

$\Gamma(\Xi^-\pi^0)/\Gamma_{total}$ Γ_3/Γ

VALUE	EVTS	DOCUMENT ID		TECN	COMMENT
0.086±0.004	759	BOURQUIN	84	SPEC	SPS hyperon beam
• • • We do not use the following data for averages, fits, limits, etc. • • •					
0.080±0.008	145	BOURQUIN	79B	SPEC	See BOURQUIN 84

$\Gamma(\Xi^-\pi^+\pi^-)/\Gamma_{total}$ Γ_4/Γ

VALUE (units 10^{-4})	EVTS	DOCUMENT ID		TECN	COMMENT
$3.74^{+0.67}_{-0.56}$	100	[5] KAMAEV	10	HYCP	p Cu, 800 GeV
• • • We do not use the following data for averages, fits, limits, etc. • • •					
$4.3\ ^{+3.4}_{-1.3}$	4	BOURQUIN	84	SPEC	SPS hyperon beam

[5] This KAMAEV 10 value uses 76 $\Omega^- \to \Xi^-\pi^+\pi^-$ and 24 $\overline{\Omega}^+ \to \overline{\Xi}^+\pi^-\pi^+$ decays. The Ω^- and $\overline{\Omega}^+$ branching fractions measurements are statistically equal. The errors given combine statistical and systematic contributions. The CP branching-fraction asymmetry, $(\Omega^- - \overline{\Omega}^+)$/sum, is $+0.12 \pm 0.20$.

$\Gamma(\Xi(1530)^0\pi^-)/\Gamma_{total}$ Γ_5/Γ

VALUE (units 10^{-4})	CL%	EVTS	DOCUMENT ID		TECN	COMMENT
<0.7	90		KAMAEV	10	HYCP	p Cu, 800 GeV
• • • We do not use the following data for averages, fits, limits, etc. • • •						
$6.4^{+5.1}_{-2.0}$		4	[6] BOURQUIN	84	SPEC	SPS hyperon beam

[6] The same 4 events as in the previous mode, with the isospin factor to take into account $\Xi(1530)^0 \to \Xi^0\pi^0$ decays included. BOURQUIN 84 adopted a theoretical assumption that $\Xi(1530)^0\pi^-$ would dominate $\Xi^-\pi^+\pi^-$ decay.

$\Gamma(\Xi^0 e^-\overline{\nu}_e)/\Gamma_{total}$ Γ_6/Γ

VALUE (units 10^{-3})	EVTS	DOCUMENT ID		TECN	COMMENT
5.6±2.8	14	BOURQUIN	84	SPEC	SPS hyperon beam
• • • We do not use the following data for averages, fits, limits, etc. • • •					
~ 10	3	BOURQUIN	79B	SPEC	See BOURQUIN 84

$\Gamma(\Xi^-\gamma)/\Gamma_{total}$ Γ_7/Γ

VALUE (units 10^{-4})	CL%	EVTS	DOCUMENT ID		TECN	COMMENT
< 4.6	90	0	ALBUQUERQ...94		E761	Ω^- 375 GeV
• • • We do not use the following data for averages, fits, limits, etc. • • •						
<22	90	9	BOURQUIN	84	SPEC	SPS hyperon beam
<31	90	0	BOURQUIN	79B	SPEC	See BOURQUIN 84

$\Gamma(\Lambda\pi^-)/\Gamma_{total}$ Γ_8/Γ

ΔS=2. Forbidden in first-order weak interaction.

VALUE (units 10^{-6})	CL%	DOCUMENT ID		TECN	COMMENT
< 2.9	90	WHITE	05	HYCP	p Cu, 800 GeV
• • • We do not use the following data for averages, fits, limits, etc. • • •					
< 190	90	BOURQUIN	84	SPEC	SPS hyperon beam
<1300	90	BOURQUIN	79B	SPEC	See BOURQUIN 84

Ω^- DECAY PARAMETERS

α FOR $\Omega^- \to \Lambda K^-$

Some early results have been omitted.

VALUE	EVTS	DOCUMENT ID		TECN	COMMENT
0.0180±0.0024 OUR AVERAGE					
$+0.0207\pm0.0051\pm0.0081$	960k	[7] CHEN	05	HYCP	p Cu, 800 GeV
$+0.0178\pm0.0019\pm0.0016$	4.5M	[7] LU	05A	HYCP	p Cu, 800 GeV
• • • We do not use the following data for averages, fits, limits, etc. • • •					
$-0.028\ \pm0.047$	6953	CHAN	98	E756	p Be, 800 GeV
$-0.034\ \pm0.079$	1743	LUK	88	SPEC	p Be 400 GeV
$-0.025\ \pm0.028$	12k	BOURQUIN	84	SPEC	SPS hyperon beam

[7] The results of CHEN 05 and LU 05A are from different experimental runs.

$\overline{\alpha}$ FOR $\overline{\Omega}^+ \to \overline{\Lambda}K^+$

VALUE	EVTS	DOCUMENT ID		TECN	COMMENT
$-0.0181\pm0.0028\pm0.0026$	1.89M	LU	06	HYCP	p Cu, 800 GeV
• • • We do not use the following data for averages, fits, limits, etc. • • •					
$+0.017\ \pm0.077$	1823	CHAN	98	E756	p Be, 800 GeV

$(\alpha+\overline{\alpha})/(\alpha-\overline{\alpha})$ in $\Omega^- \to \Lambda K^-, \overline{\Omega}^+ \to \overline{\Lambda}K^+$

Zero if CP is conserved.

VALUE	DOCUMENT ID		TECN	COMMENT
$-0.016\pm0.092\pm0.089$	[8] LU	06	HYCP	p Cu, 800 GeV

[8] This value uses the results of CHEN 05, LU 05A, and LU 06.

α FOR $\Omega^- \to \Xi^0\pi^-$

VALUE	EVTS	DOCUMENT ID		TECN	COMMENT
+0.09±0.14	1630	BOURQUIN	84	SPEC	SPS hyperon beam

α FOR $\Omega^- \to \Xi^-\pi^0$

VALUE	EVTS	DOCUMENT ID		TECN	COMMENT
+0.05±0.21	614	BOURQUIN	84	SPEC	SPS hyperon beam

Ω^- REFERENCES

We have omitted some papers that have been superseded by later experiments. See our earlier editions.

KAMAEV	10	PL B693 236	O. Kamaev *et al.*	(FNAL HyperCP Collab.)
AUBERT,BE	06	PRL 97 112001	B. Aubert *et al.*	(BABAR Collab.)
LU	06	PRL 96 242001	L.C. Lu *et al.*	(FNAL HyperCP Collab.)
CHEN	05	PR D71 051102	Y.C. Chen *et al.*	(FNAL HyperCP Collab.)
LU	05A	PL B617 11	L.C. Lu *et al.*	(FNAL HyperCP Collab.)
WHITE	05	PRL 94 101804	C.G. White *et al.*	(FNAL HyperCP Collab.)
CHAN	98	PR D58 072002	A.W. Chan *et al.*	(FNAL E756 Collab.)
WALLACE	95	PRL 74 3732	N.B. Wallace *et al.*	(MINN, ARIZ, MICH+)
ALBUQUERQ...	94	PR D50 18	I.F. Albuquerque *et al.*	(FNAL E761 Collab.)
DIEHL	91	PRL 67 804	H.T. Diehl *et al.*	(RUTG, FNAL, MICH+)
LUK	88	PR D38 19	K.B. Luk *et al.*	(RUTG, WISC, MICH, MINN)
HARTOUNI	85	PRL 54 628	E.P. Hartouni *et al.*	(COLU, ILL, FNAL)
BOURQUIN	84	NP B241 1	M.H. Bourquin *et al.*	(BRIS, GEVA, HEIDP+)
Also		PL 87B 297	M.H. Bourquin *et al.*	(BRIS, GEVA, HEIDP+)
BOURQUIN	79B	PL 88B 192	M.H. Bourquin *et al.*	(BRIS, GEVA, HEIDP+)
BAUBILLIER	78	PL 78B 342	M. Baubillier *et al.*	(BIRM, CERN, GLAS+) J
DEUTSCH...	78	PL 73B 96	M. Deutschmann *et al.*	(AACH3, BERL, CERN+) J
HEMINGWAY	78	NP B142 205	R.J. Hemingway *et al.*	(CERN, ZEEM, NIJM+)
DIBIANCA	75	NP B98 137	F.A. Dibianca, R.J. Endorf	(CMU)
ALVAREZ	73	PR D8 702	L.W. Alvarez	(LBL)
DEUTSCH...	73	NP B61 102	M. Deutschmann *et al.*	(ABCLV Collab.)
FIRESTONE	71B	PRL 26 410	I. Firestone *et al.*	(LRL)
SPETH	69	PL 29B 252	R. Speth *et al.*	(AACH, BERL, CERN, LOIC+)
PALMER	68	PL 26B 323	R.B. Palmer *et al.*	(BNL, SYRA)
SCHULTZ	68	PR 168 1509	P.F. Schultz *et al.*	(ILL, ANL, NWES+)
SCOTTER	68	PL 26B 474	D. Scotter *et al.*	(BIRM, GLAS, LOIC+)
ABRAMS	64	PRL 13 670	G.S. Abrams *et al.*	(UMD, NRL)
BARNES	64	PRL 12 204	V.E. Barnes *et al.*	(BNL)
FRY	55	PR 97 1189	W.F. Fry, J. Schneps, M.S. Swami	(WISC)
FRY	55B	NC 2 346	W.F. Fry, J. Schneps, M.S. Swami	(WISC)
EISENBERG	54	PR 96 541	Y. Eisenberg	(CORN)

$\Omega(2250)^-$ $I(J^P) = 0(?^?)$ Status: ***

$\Omega(2250)^-$ MASS

VALUE (MeV)	EVTS	DOCUMENT ID		TECN	COMMENT
2252± 9 OUR AVERAGE					
2253±13	44	ASTON	87B	LASS	K^-p 11 GeV/c
2251± 9±8	78	BIAGI	86B	SPEC	SPS Ξ^- beam

$\Omega(2250)^-$ WIDTH

VALUE (MeV)	EVTS	DOCUMENT ID		TECN	COMMENT
55±18 OUR AVERAGE					
81±38	44	ASTON	87B	LASS	K^-p 11 GeV/c
48±20	78	BIAGI	86B	SPEC	SPS Ξ^- beam

$\Omega(2250)^-$ DECAY MODES

	Mode	Fraction (Γ_i/Γ)
Γ_1	$\Xi^-\pi^+K^-$	seen
Γ_2	$\Xi(1530)^0K^-$	seen

$\Omega(2250)^-$ BRANCHING RATIOS

$\Gamma(\Xi(1530)^0K^-)/\Gamma(\Xi^-\pi^+K^-)$ Γ_2/Γ_1

VALUE	EVTS	DOCUMENT ID		TECN	COMMENT
~ 1.0	44	ASTON	87B	LASS	K^-p 11 GeV/c
0.70±0.20	49	BIAGI	86B	SPEC	Ξ^- Be 116 GeV/c

$\Omega(2250)^-$ REFERENCES

ASTON	87B	PL B194 579	D. Aston *et al.*	(SLAC, NAGO, CINC, INUS)
BIAGI	86B	ZPHY C31 33	S.F. Biagi *et al.*	(LOQM, GEVA, RAL+)

$\Omega(2380)^-$ Status: **

OMITTED FROM SUMMARY TABLE

$\Omega(2380)^-$ MASS

VALUE (MeV)	EVTS	DOCUMENT ID		TECN	COMMENT
≈ 2380 OUR ESTIMATE					
2384±9±8	45	BIAGI	86B	SPEC	SPS Ξ^- beam

$\Omega(2380)^-$ WIDTH

VALUE (MeV)	EVTS	DOCUMENT ID		TECN	COMMENT
26±23	45	BIAGI	86B	SPEC	SPS Ξ^- beam

$\Omega(2380)^-$ DECAY MODES

	Mode	Fraction (Γ_i/Γ)
Γ_1	$\Xi^-\pi^+K^-$	
Γ_2	$\Xi(1530)^0K^-$	seen
Γ_3	$\Xi^-\overline{K}^*(892)^0$	

$\Omega(2380)^-$ BRANCHING RATIOS

$\Gamma(\Xi(1530)^0K^-)/\Gamma(\Xi^-\pi^+K^-)$ Γ_2/Γ_1

VALUE	CL%	EVTS	DOCUMENT ID		TECN	COMMENT
<0.44	90	9	BIAGI	86B	SPEC	Ξ^- Be 116 GeV/c

Baryon Particle Listings

$\Omega(2380)^-$, $\Omega(2470)^-$

$\Gamma(\Xi^-\overline{K}^*(892)^0)/\Gamma(\Xi^-\pi^+K^-)$ Γ_3/Γ_1

VALUE	EVTS	DOCUMENT ID		TECN	COMMENT
0.5 ± 0.3	21	BIAGI	86B	SPEC	Ξ^- Be 116 GeV/c

$\Omega(2380)^-$ REFERENCES

BIAGI 86B ZPHY C31 33 S.F. Biagi *et al.* (LOQM, GEVA, RAL+)

$\Omega(2470)^-$

Status: **

OMITTED FROM SUMMARY TABLE

A peak in the $\Omega^-\pi^+\pi^-$ mass spectrum with a signal significance claimed to be at least 5.5 standard deviations. There is no reason to seriously doubt the existence of this state, but unless the evidence is overwhelming we usually wait for confirmation from a second experiment before elevating peaks to the Summary Table.

$\Omega(2470)^-$ MASS

VALUE (MeV)	EVTS	DOCUMENT ID		TECN	COMMENT
2474±12	59	ASTON	88G	LASS	K^-p 11 GeV/c

$\Omega(2470)^-$ WIDTH

VALUE (MeV)	EVTS	DOCUMENT ID		TECN	COMMENT
72±33	59	ASTON	88G	LASS	K^-p 11 GeV/c

$\Omega(2470)^-$ DECAY MODES

	Mode
Γ_1	$\Omega^-\pi^+\pi^-$

$\Omega(2470)^-$ REFERENCES

ASTON 88G PL B215 799 D. Aston *et al.* (SLAC, NAGO, CINC, INUS)

CHARMED BARYONS ($C = +1$)

$\Lambda_c^+ = udc$, $\Sigma_c^{++} = uuc$, $\Sigma_c^+ = udc$, $\Sigma_c^0 = ddc$,
$\Xi_c^+ = usc$, $\Xi_c^0 = dsc$, $\Omega_c^0 = ssc$

See the related review(s):
Charmed Baryons

Λ_c^+

$I(J^P) = 0(\frac{1}{2}^+)$ Status: ****

The parity of the Λ_c^+ is defined to be positive (as are the parities of the proton, neutron, and Λ). The quark content is udc. Results of an analysis of $pK^-\pi^+$ decays (JEZABEK 92) are consistent with $J = 1/2$. Nobody doubts that the spin is indeed 1/2.

We have omitted some results that have been superseded by later experiments. The omitted results may be found in earlier editions.

Λ_c^+ MASS

Our value in 2004, 2284.9 ± 0.6 MeV, was the average of the measurements now filed below as "not used." The BABAR measurement is so much better that we use it alone. Note that it is about 2.6 (old) standard deviations above the 2004 value.

The fit also includes Σ_c–Λ_c^+ and Λ_c^{*+}–Λ_c^+ mass-difference measurements, but this doesn't affect the Λ_c^+ mass. The new (in 2006) Λ_c^+ mass simply pushes all those other masses higher.

VALUE (MeV)	EVTS	DOCUMENT ID		TECN	COMMENT
2286.46±0.14 OUR FIT					
2286.46±0.14	4891	[1] AUBERT,B	05S	BABR	$\Lambda K_S^0 K^+$ and $\Sigma^0 K_S^0 K^+$
• • • We do not use the following data for averages, fits, limits, etc. • • •					
2284.7 ±0.6 ±0.7	1134	AVERY	91	CLEO	Six modes
2281.7 ±2.7 ±2.6	29	ALVAREZ	90B	NA14	$pK^-\pi^+$
2285.8 ±0.6 ±1.2	101	BARLAG	89	NA32	$pK^-\pi^+$
2284.7 ±2.3 ±0.5	5	AGUILAR-...	88B	LEBC	$pK^-\pi^+$
2283.1 ±1.7 ±2.0	628	ALBRECHT	88C	ARG	$pK^-\pi^+$, $p\overline{K}^0$, $\Lambda 3\pi$
2286.2 ±1.7 ±0.7	97	ANJOS	88B	E691	$pK^-\pi^+$
2281 ±3	2	JONES	87	HBC	$pK^-\pi^+$
2283 ±3	3	BOSETTI	82	HBC	$pK^-\pi^+$
2290 ±3	1	CALICCHIO	80	HYBR	$pK^-\pi^+$

[1] AUBERT,B 05S uses low-Q $\Lambda K_S^0 K^+$ and $\Sigma^0 K_S^0 K^+$ decays to minimize systematic errors. The error above includes systematic as well as statistical errors. Many cross checks and adjustments to properties of the BABAR detector, as well as the large number of clean events, make this by far the best measurement of the Λ_c^+ mass.

Λ_c^+ MEAN LIFE

Measurements with an error $\geq 100 \times 10^{-15}$ s or with fewer than 20 events have been omitted from the Listings.

VALUE (10^{-15} s)	EVTS	DOCUMENT ID		TECN	COMMENT
200 ± 6 OUR AVERAGE		Error includes scale factor of 1.6. See the ideogram below.			
204.6± 3.4± 2.5	8034	LINK	02C	FOCS	$pK^-\pi^+$
198.1± 7.0± 5.6	1630	KUSHNIR...	01	SELX	$\Lambda_c^+ \to pK^-\pi^+$
179.6± 6.9± 4.4	4749	MAHMOOD	01	CLE2	$e^+e^- \approx \Upsilon(4S)$
215 ±16 ± 8	1340	FRABETTI	93D	E687	γBe, $\Lambda_c^+ \to pK^-\pi^+$
• • • We do not use the following data for averages, fits, limits, etc. • • •					
180 ±30 ±30	29	ALVAREZ	90	NA14	γ, $\Lambda_c^+ \to pK^-\pi^+$
200 ±30 ±30	90	FRABETTI	90	E687	γBe, $\Lambda_c^+ \to pK^-\pi^+$
196 $^{+23}_{-20}$	101	BARLAG	89	NA32	$pK^-\pi^+$ + c.c.
220 ±30 ±20	97	ANJOS	88B	E691	$pK^-\pi^+$ + c.c.

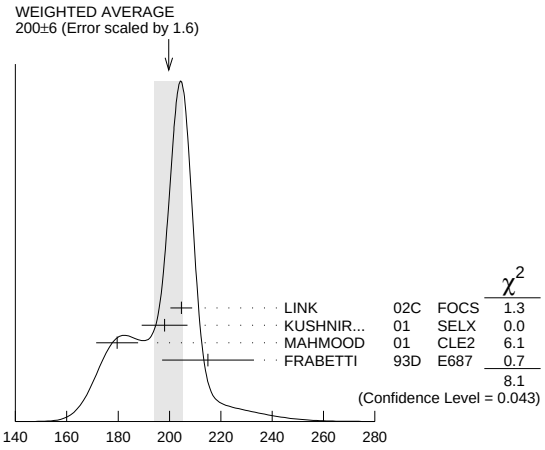

Λ_c^+ DECAY MODES

Branching fractions marked with a footnote, e.g. [a], have been corrected for decay modes not observed in the experiments. For example, the sub-mode fraction $\Lambda_c^+ \to p\overline{K}^*(892)^0$ seen in $\Lambda_c^+ \to pK^-\pi^+$ has been multiplied up to include $\overline{K}^*(892)^0 \to \overline{K}^0\pi^0$ decays.

	Mode		Fraction (Γ_i/Γ)	Scale factor / Confidence level
	Hadronic modes with a p or n: $S = -1$ final states			
Γ_1	pK_S^0		(1.58± 0.08) %	S=1.1
Γ_2	$pK^-\pi^+$		(6.23± 0.33) %	S=1.4
Γ_3	$p\overline{K}^*(892)^0$	[a]	(1.94± 0.27) %	
Γ_4	$\Delta(1232)^{++}K^-$		(1.07± 0.25) %	
Γ_5	$\Lambda(1520)\pi^+$	[a]	(2.2 ± 0.5) %	
Γ_6	$pK^-\pi^+$ nonresonant		(3.4 ± 0.4) %	
Γ_7	$pK_S^0\pi^0$		(1.96± 0.13) %	S=1.1
Γ_8	$nK_S^0\pi^+$		(1.82± 0.25) %	
Γ_9	$p\overline{K}^0\eta$		(1.6 ± 0.4) %	
Γ_{10}	$pK_S^0\pi^+\pi^-$		(1.59± 0.12) %	S=1.2
Γ_{11}	$pK^-\pi^+\pi^0$		(4.42± 0.31) %	S=1.5
Γ_{12}	$pK^*(892)^-\pi^+$	[a]	(1.4 ± 0.5) %	
Γ_{13}	$p(K^-\pi^+)_{\text{nonresonant}}\pi^0$		(4.5 ± 0.8) %	
Γ_{14}	$\Delta(1232)\overline{K}^*(892)$		seen	
Γ_{15}	$pK^-2\pi^+\pi^-$		(1.4 ± 0.9) $\times 10^{-3}$	
Γ_{16}	$pK^-\pi^+2\pi^0$		(10 ± 5) $\times 10^{-3}$	
Γ_{17}	$pK^-\pi^+3\pi^0$			
	Hadronic modes with a p: $S = 0$ final states			
Γ_{18}	$p\pi^0$		< 2.7 $\times 10^{-4}$	CL=90%
Γ_{19}	$p\eta$		(1.24± 0.30) $\times 10^{-3}$	
Γ_{20}	$p\pi^+\pi^-$		(4.2 ± 0.4) $\times 10^{-3}$	
Γ_{21}	$pf_0(980)$	[a]	(3.4 ± 2.3) $\times 10^{-3}$	
Γ_{22}	$p2\pi^+2\pi^-$		(2.2 ± 1.4) $\times 10^{-3}$	
Γ_{23}	pK^+K^-		(10 ± 4) $\times 10^{-4}$	
Γ_{24}	$p\phi$	[a]	(1.06± 0.14) $\times 10^{-3}$	
Γ_{25}	pK^+K^- non-ϕ		(5.2 ± 1.2) $\times 10^{-4}$	
Γ_{26}	$p\phi\pi^0$		(10 ± 4) $\times 10^{-5}$	
Γ_{27}	$pK^+K^-\pi^0$ nonresonant		< 6.3 $\times 10^{-5}$	CL=90%
	Hadronic modes with a hyperon: $S = -1$ final states			
Γ_{28}	$\Lambda\pi^+$		(1.29± 0.07) %	S=1.2
Γ_{29}	$\Lambda\pi^+\pi^0$		(7.0 ± 0.4) %	S=1.1
Γ_{30}	$\Lambda\rho^+$		< 6 %	CL=95%
Γ_{31}	$\Lambda\pi^-2\pi^+$		(3.61± 0.29) %	S=1.5
Γ_{32}	$\Sigma(1385)^+\pi^+\pi^-$, $\Sigma^{*+} \to \Lambda\pi^+$		(1.0 ± 0.5) %	
Γ_{33}	$\Sigma(1385)^-2\pi^+$, $\Sigma^{*-} \to \Lambda\pi^-$		(7.6 ± 1.4) $\times 10^{-3}$	
Γ_{34}	$\Lambda\pi^+\rho^0$		(1.4 ± 0.6) %	
Γ_{35}	$\Sigma(1385)^+\rho^0$, $\Sigma^{*+} \to \Lambda\pi^+$		(5 ± 4) $\times 10^{-3}$	
Γ_{36}	$\Lambda\pi^-2\pi^+$ nonresonant		< 1.1 %	CL=90%
Γ_{37}	$\Lambda\pi^-\pi^02\pi^+$ total		(2.2 ± 0.8) %	
Γ_{38}	$\Lambda\pi^+\eta$	[a]	(2.2 ± 0.5) %	
Γ_{39}	$\Sigma(1385)^+\eta$	[a]	(1.06± 0.32) %	
Γ_{40}	$\Lambda\pi^+\omega$	[a]	(1.5 ± 0.5) %	
Γ_{41}	$\Lambda\pi^-\pi^02\pi^+$, no η or ω		< 8 $\times 10^{-3}$	CL=90%

Baryon Particle Listings

Λ_c^+

Γ_{42}	$\Lambda K^+ \overline{K}^0$		$(5.6 \pm 1.1) \times 10^{-3}$		S=1.9
Γ_{43}	$\Xi(1690)^0 K^+$, $\Xi^{*0} \to \Lambda \overline{K}^0$		$(1.6 \pm 0.5) \times 10^{-3}$		
Γ_{44}	$\Sigma^0 \pi^+$		(1.28± 0.07) %		S=1.1
Γ_{45}	$\Sigma^+ \pi^0$		(1.24± 0.10) %		
Γ_{46}	$\Sigma^+ \eta$		$(6.9 \pm 2.3) \times 10^{-3}$		
Γ_{47}	$\Sigma^+ \pi^+ \pi^-$		(4.42± 0.28) %		S=1.2
Γ_{48}	$\Sigma^+ \rho^0$	<	1.7 %		CL=95%
Γ_{49}	$\Sigma^- 2\pi^+$		(1.86± 0.18) %		
Γ_{50}	$\Sigma^0 \pi^+ \pi^0$		(2.2 ± 0.8) %		
Γ_{51}	$\Sigma^0 \pi^- 2\pi^+$		(1.10± 0.30) %		
Γ_{52}	$\Sigma^+ \pi^+ \pi^- \pi^0$		—		
Γ_{53}	$\Sigma^+ \omega$	[a]	(1.69± 0.21) %		
Γ_{54}	$\Sigma^- \pi^0 2\pi^+$		(2.1 ± 0.4) %		
Γ_{55}	$\Sigma^+ K^+ K^-$		$(3.4 \pm 0.4) \times 10^{-3}$		S=1.1
Γ_{56}	$\Sigma^+ \phi$	[a]	$(3.8 \pm 0.6) \times 10^{-3}$		S=1.1
Γ_{57}	$\Xi(1690)^0 K^+$, $\Xi^{*0} \to \Sigma^+ K^-$		$(10.0 \pm 2.5) \times 10^{-4}$		
Γ_{58}	$\Sigma^+ K^+ K^-$ nonresonant	<	8 $\times 10^{-4}$		CL=90%
Γ_{59}	$\Xi^0 K^+$		$(4.9 \pm 1.2) \times 10^{-3}$		
Γ_{60}	$\Xi^- K^+ \pi^+$		$(6.2 \pm 0.6) \times 10^{-3}$		S=1.1
Γ_{61}	$\Xi(1530)^0 K^+$, $\Xi^0 \to \Xi^- \pi^+$		$(3.3 \pm 1.2) \times 10^{-3}$		

Hadronic modes with a hyperon: $S = 0$ final states

Γ_{62}	ΛK^+		$(6.0 \pm 1.2) \times 10^{-4}$		
Γ_{63}	$\Lambda K^+ \pi^+ \pi^-$	<	5 $\times 10^{-4}$		CL=90%
Γ_{64}	$\Sigma^0 K^+$		$(5.1 \pm 0.8) \times 10^{-4}$		
Γ_{65}	$\Sigma^0 K^+ \pi^+ \pi^-$	<	2.6 $\times 10^{-4}$		CL=90%
Γ_{66}	$\Sigma^+ K^+ \pi^-$		$(2.1 \pm 0.6) \times 10^{-3}$		
Γ_{67}	$\Sigma^+ K^*(892)^0$	[a]	$(3.4 \pm 1.0) \times 10^{-3}$		
Γ_{68}	$\Sigma^- K^+ \pi^+$	<	1.2 $\times 10^{-3}$		CL=90%

Doubly Cabibbo-suppressed modes

Γ_{69}	$p K^+ \pi^-$		$(1.46 \pm 0.23) \times 10^{-4}$		

Semileptonic modes

Γ_{70}	$\Lambda e^+ \nu_e$		(3.6 ± 0.4) %		
Γ_{71}	$\Lambda \mu^+ \nu_\mu$		(3.5 ± 0.5) %		

Inclusive modes

Γ_{72}	e^+ anything		(4.5 ± 1.7) %		
Γ_{73}	$p e^+$ anything		(1.8 ± 0.9) %		
Γ_{74}	Λe^+ anything				
Γ_{75}	p anything		(50 ±16) %		
Γ_{76}	p anything (no Λ)		(12 ±19) %		
Γ_{77}	p hadrons				
Γ_{78}	n anything		(50 ±16) %		
Γ_{79}	n anything (no Λ)		(29 ±17) %		
Γ_{80}	Λ anything		(35 ±11) %		S=1.4
Γ_{81}	$\Sigma^\pm$ anything	[b]	(10 ± 5) %		
Γ_{82}	3prongs		(24 ± 8) %		

$\Delta C = 1$ weak neutral current ($C1$) modes, or Lepton Family number (LF), or Lepton number (L), or Baryon number (B) violating modes

Γ_{83}	$p e^+ e^-$	$C1$	<	5.5 $\times 10^{-6}$		CL=90%
Γ_{84}	$p \mu^+ \mu^-$	$C1$	<	4.4 $\times 10^{-5}$		CL=90%
Γ_{85}	$p e^+ \mu^-$	LF	<	9.9 $\times 10^{-6}$		CL=90%
Γ_{86}	$p e^- \mu^+$	LF	<	1.9 $\times 10^{-5}$		CL=90%
Γ_{87}	$\overline{p} 2e^+$	L,B	<	2.7 $\times 10^{-6}$		CL=90%
Γ_{88}	$\overline{p} 2\mu^+$	L,B	<	9.4 $\times 10^{-6}$		CL=90%
Γ_{89}	$\overline{p} e^+ \mu^+$	L,B	<	1.6 $\times 10^{-5}$		CL=90%
Γ_{90}	$\Sigma^- \mu^+ \mu^+$	L	<	7.0 $\times 10^{-4}$		CL=90%

[a] This branching fraction includes all the decay modes of the final-state resonance.

[b] The value is for the sum of the charge states or particle/antiparticle states indicated.

CONSTRAINED FIT INFORMATION

An overall fit to 37 branching ratios uses 59 measurements and one constraint to determine 19 parameters. The overall fit has a $\chi^2 = 46.6$ for 41 degrees of freedom.

The following *off-diagonal* array elements are the correlation coefficients $\langle \delta x_i \delta x_j \rangle / (\delta x_i \cdot \delta x_j)$, in percent, from the fit to the branching fractions, $x_i \equiv \Gamma_i / \Gamma_{\text{total}}$. The fit constrains the x_i whose labels appear in this array to sum to one.

x_2	55									
x_7	47	57								
x_{10}	46	65	41							
x_{11}	53	61	41	61						
x_{28}	55	69	46	44	44					
x_{29}	47	63	43	40	37	66				
x_{31}	52	37	28	42	61	44	37			
x_{42}	17	24	15	15	15	27	20	13		
x_{44}	52	58	40	39	41	75	60	44	21	
x_{45}	39	41	32	27	30	35	35	23	11	31
x_{47}	47	78	47	57	59	53	51	38	18	46
x_{49}	5	10	6	6	6	7	6	4	2	6
x_{51}	14	15	10	13	16	14	12	21	4	13
x_{53}	20	31	19	24	27	20	19	18	7	18
x_{55}	24	41	24	29	30	28	26	19	10	24
x_{56}	20	32	20	24	24	22	21	16	8	19
x_{60}	31	41	26	27	26	53	37	24	15	40
	x_1	x_2	x_7	x_{10}	x_{11}	x_{28}	x_{29}	x_{31}	x_{42}	x_{44}

x_{47}	34						
x_{49}	4	8					
x_{51}	8	13	2				
x_{53}	15	28	3	6			
x_{55}	18	49	4	7	14		
x_{56}	14	42	3	6	12	20	
x_{60}	20	32	4	8	12	17	13
	x_{45}	x_{47}	x_{49}	x_{51}	x_{53}	x_{55}	x_{56}

Λ_c^+ BRANCHING RATIOS

A few really obsolete results have been omitted.

Hadronic modes with a p: $S = -1$ final states

$\Gamma(pK_S^0)/\Gamma_{\text{total}}$ Γ_1/Γ

VALUE (%)	EVTS	DOCUMENT ID		TECN	COMMENT
1.58±0.08 OUR FIT Error includes scale factor of 1.1.					
1.52±0.08±0.03	1243	ABLIKIM	16	BES3	$e^+e^- \to \Lambda_c \overline{\Lambda}_c$, 4.599 GeV

$\Gamma(pK_S^0)/\Gamma(pK^-\pi^+)$ Γ_1/Γ_2

Measurements given as a $\overline{K}^0$ ratio have been divided by 2 to convert to a K_S^0 ratio.

VALUE	EVTS	DOCUMENT ID		TECN	COMMENT
0.254±0.012 OUR FIT Error includes scale factor of 1.4.					
0.234±0.020 OUR AVERAGE					
0.23 ±0.01 ±0.02	1025	ALAM	98	CLE2	$e^+e^- \approx \Upsilon(4S)$
0.22 ±0.04 ±0.03	133	AVERY	91	CLEO	e^+e^- 10.5 GeV
0.28 ±0.09 ±0.07	45	ANJOS	90	E691	γBe 70–260 GeV
0.31 ±0.08 ±0.02	73	ALBRECHT	88C	ARG	e^+e^- 10 GeV

$\Gamma(pK^-\pi^+)/\Gamma_{\text{total}}$ Γ_2/Γ

VALUE (%)	EVTS	DOCUMENT ID		TECN	COMMENT
6.23±0.33 OUR FIT Error includes scale factor of 1.4.					
6.3 ±0.5 OUR AVERAGE Error includes scale factor of 2.0.					
5.84±0.27±0.23	6.3k	ABLIKIM	16	BES3	$e^+e^- \to \Lambda_c \overline{\Lambda}_c$, 4.599 GeV
$6.84 \pm 0.24 ^{+0.21}_{-0.27}$	1.4k	[1] ZUPANC	14	BELL	$e^+e^- \to D^{(*)-} \overline{p} \pi^+$ recoil
• • • We do not use the following data for averages, fits, limits, etc. • • •					
5.0 ±1.3		[2] PDG	02		See footnote

[1] This ZUPANC 14 value is the FIRST-EVER model-independent measurement of a Λ_c^+ branching fraction.

[2] See the note by P. Burchat, "Λ_c^+ Branching Fractions," in any edition of the Review from 2002 through 2014 for how this value was obtained. It is now obsolete.

$\Gamma(p\overline{K}^*(892)^0)/\Gamma(pK^-\pi^+)$ Γ_3/Γ_2

Unseen decay modes of the $\overline{K}^*(892)^0$ are included.

VALUE	EVTS	DOCUMENT ID		TECN	COMMENT
0.31±0.04 OUR AVERAGE					
0.29±0.04±0.03		[1] AITALA	00	E791	π^- N, 500 GeV
$0.35 ^{+0.06}_{-0.07} \pm 0.03$	39	BOZEK	93	NA32	π^- Cu 230 GeV
0.42±0.24	12	BASILE	81B	CNTR	$pp \to \Lambda_c^+ e^- X$
• • • We do not use the following data for averages, fits, limits, etc. • • •					
0.35±0.11		BARLAG	90D	NA32	See BOZEK 93

[1] AITALA 00 makes a coherent 5-dimensional amplitude analysis of 946 ± 38 $\Lambda_c^+ \to p K^- \pi^+$ decays.

See key on page 885

$\Gamma(\Delta(1232)^{++}K^-)/\Gamma(pK^-\pi^+)$ Γ_4/Γ_2

VALUE	EVTS	DOCUMENT ID		TECN	COMMENT
0.17±0.04 OUR AVERAGE Error includes scale factor of 1.1.					
0.18±0.03±0.03		[1] AITALA	00	E791	π^- N, 500 GeV
$0.12^{+0.04}_{-0.05}$±0.05	14	BOZEK	93	NA32	π^- Cu 230 GeV
0.40±0.17	17	BASILE	81B	CNTR	$pp \to \Lambda_c^+ e^- X$

[1] AITALA 00 makes a coherent 5-dimensional amplitude analysis of 946 ± 38 $\Lambda_c^+ \to pK^-\pi^+$ decays.

$\Gamma(\Lambda(1520)\pi^+)/\Gamma(pK^-\pi^+)$ Γ_5/Γ_2

Unseen decay modes of the $\Lambda(1520)$ are included.

VALUE	EVTS	DOCUMENT ID		TECN	COMMENT
0.35±0.08 OUR AVERAGE					
0.34±0.08±0.05		[1] AITALA	00	E791	π^- N, 500 GeV
$0.40^{+0.18}_{-0.13}$±0.09	12	BOZEK	93	NA32	π^- Cu 230 GeV

[1] AITALA 00 makes a coherent 5-dimensional amplitude analysis of 946 ± 38 $\Lambda_c^+ \to pK^-\pi^+$ decays.

$\Gamma(pK^-\pi^+ \text{nonresonant})/\Gamma(pK^-\pi^+)$ Γ_6/Γ_2

VALUE	EVTS	DOCUMENT ID		TECN	COMMENT
0.55±0.06 OUR AVERAGE					
0.55±0.06±0.04		[1] AITALA	00	E791	π^- N, 500 GeV
$0.56^{+0.07}_{-0.09}$±0.05	71	BOZEK	93	NA32	π^- Cu 230 GeV

[1] AITALA 00 makes a coherent 5-dimensional amplitude analysis of 946 ± 38 $\Lambda_c^+ \to pK^-\pi^+$ decays.

$\Gamma(pK_S^0\pi^0)/\Gamma_{\text{total}}$ Γ_7/Γ

VALUE (%)	EVTS	DOCUMENT ID		TECN	COMMENT
1.96±0.13 OUR FIT Error includes scale factor of 1.1.					
1.87±0.13±0.05	558	ABLIKIM	16	BES3	$e^+e^- \to \Lambda_c\overline{\Lambda}_c$, 4.599 GeV

$\Gamma(pK_S^0\pi^0)/\Gamma(pK^-\pi^+)$ Γ_7/Γ_2

Measurements given as a $\overline{K}^0$ ratio have been divided by 2 to convert to a K_S^0 ratio.

VALUE	EVTS	DOCUMENT ID		TECN	COMMENT
0.314±0.018 OUR FIT					
0.33 ±0.03 ±0.04	774	ALAM	98	CLE2	$e^+e^- \approx \Upsilon(4S)$

$\Gamma(nK_S^0\pi^+)/\Gamma_{\text{total}}$ Γ_8/Γ

VALUE (%)	EVTS	DOCUMENT ID		TECN	COMMENT
1.82±0.23±0.11	83	ABLIKIM	17H	BES3	e^+e^- at 4.6 GeV

$\Gamma(p\overline{K}^0\eta)/\Gamma(pK^-\pi^+)$ Γ_9/Γ_2

Unseen decay modes of the η are included.

VALUE	EVTS	DOCUMENT ID		TECN	COMMENT
0.25±0.04±0.04	57	AMMAR	95	CLE2	$e^+e^- \approx \Upsilon(4S)$

$\Gamma(pK_S^0\pi^+\pi^-)/\Gamma_{\text{total}}$ Γ_{10}/Γ

VALUE (%)	EVTS	DOCUMENT ID		TECN	COMMENT
1.59±0.12 OUR FIT Error includes scale factor of 1.2.					
1.53±0.11±0.09	485	ABLIKIM	16	BES3	$e^+e^- \to \Lambda_c\overline{\Lambda}_c$, 4.599 GeV

$\Gamma(pK_S^0\pi^+\pi^-)/\Gamma(pK^-\pi^+)$ Γ_{10}/Γ_2

Measurements given as a $\overline{K}^0$ ratio have been divided by 2 to convert to a K_S^0 ratio.

VALUE	EVTS	DOCUMENT ID		TECN	COMMENT
0.255±0.015 OUR FIT Error includes scale factor of 1.1.					
0.257±0.031 OUR AVERAGE					
0.26 ±0.02 ±0.03	985	ALAM	98	CLE2	$e^+e^- \approx \Upsilon(4S)$
0.22 ±0.06 ±0.02	83	AVERY	91	CLEO	e^+e^- 10.5 GeV
0.49 ±0.18 ±0.04	12	BARLAG	90D	NA32	π^- 230 GeV

$\Gamma(pK^-\pi^+\pi^0)/\Gamma_{\text{total}}$ Γ_{11}/Γ

VALUE (%)	EVTS	DOCUMENT ID		TECN	COMMENT
4.42±0.31 OUR FIT Error includes scale factor of 1.5.					
4.53±0.23±0.30	1849	ABLIKIM	16	BES3	$e^+e^- \to \Lambda_c\overline{\Lambda}_c$, 4.599 GeV

$\Gamma(pK^-\pi^+\pi^0)/\Gamma(pK^-\pi^+)$ Γ_{11}/Γ_2

VALUE	EVTS	DOCUMENT ID		TECN	COMMENT
0.71 ±0.04 OUR FIT Error includes scale factor of 2.4.					
0.685±0.019 OUR AVERAGE					
0.685±0.007±0.018	242k	PAL	17	BELL	$e^+e^- \approx \Upsilon(4S), \Upsilon(5S)$
0.67 ±0.04 ±0.11	2.6k	ALAM	98	CLE2	$e^+e^- \approx \Upsilon(4S)$

$\Gamma(pK^*(892)^-\pi^+)/\Gamma(pK_S^0\pi^+\pi^-)$ Γ_{12}/Γ_{10}

Unseen decay modes of the $K^*(892)^-$ are included.

VALUE	EVTS	DOCUMENT ID		TECN	COMMENT
0.88±0.28	17	ALEEV	94	BIS2	nN 20–70 GeV

$\Gamma(p(K^-\pi^+)_{\text{nonresonant}}\pi^0)/\Gamma(pK^-\pi^+)$ Γ_{13}/Γ_2

VALUE	EVTS	DOCUMENT ID		TECN	COMMENT
0.73±0.12±0.05	67	BOZEK	93	NA32	π^- Cu 230 GeV

$\Gamma(\Delta(1232)\overline{K}^*(892))/\Gamma_{\text{total}}$ Γ_{14}/Γ

VALUE	EVTS	DOCUMENT ID		TECN	COMMENT
seen	35	AMENDOLIA	87	SPEC	γGe-Si

$\Gamma(pK^-2\pi^+\pi^-)/\Gamma(pK^-\pi^+)$ Γ_{15}/Γ_2

VALUE	DOCUMENT ID		TECN	COMMENT
0.022±0.015	BARLAG	90D	NA32	π^- 230 GeV

$\Gamma(pK^-\pi^+2\pi^0)/\Gamma(pK^-\pi^+)$ Γ_{16}/Γ_2

VALUE	EVTS	DOCUMENT ID		TECN	COMMENT
0.16±0.07±0.03	15	BOZEK	93	NA32	π^- Cu 230 GeV

$\Gamma(pK^-\pi^+3\pi^0)/\Gamma(pK^-\pi^+)$ Γ_{17}/Γ_2

VALUE	EVTS	DOCUMENT ID		TECN	COMMENT
• • • We do not use the following data for averages, fits, limits, etc. • • •					
0.10±0.06±0.02	8	BOZEK	93	NA32	π^- Cu 230 GeV

Hadronic modes with a p: $S = 0$ final states

$\Gamma(p\pi^0)/\Gamma_{\text{total}}$ Γ_{18}/Γ

VALUE	CL%	DOCUMENT ID		TECN	COMMENT
$<2.7 \times 10^{-4}$	90	ABLIKIM	17Q	BES3	e^+e^- at 4.6 GeV

$\Gamma(p\eta)/\Gamma_{\text{total}}$ Γ_{19}/Γ

Unseen decay modes of the η are included.

VALUE (units 10^{-3})	EVTS	DOCUMENT ID		TECN	COMMENT
1.24±0.28±0.10	52	ABLIKIM	17Q	BES3	$\eta \to 2\gamma$, $\pi^+\pi^0\pi^-$

$\Gamma(p\pi^+\pi^-)/\Gamma(pK^-\pi^+)$ Γ_{20}/Γ_2

VALUE (units 10^{-2})	EVTS	DOCUMENT ID		TECN	COMMENT
6.7 ±0.5 OUR AVERAGE					
6.70±0.48±0.25	495	ABLIKIM	16U	BES3	e^+e^- at 4.599 GeV
6.9 ±3.6	5	BARLAG	90D	NA32	π^- 230 GeV

$\Gamma(pf_0(980))/\Gamma(pK^-\pi^+)$ Γ_{21}/Γ_2

Unseen decay modes of the $f_0(980)$ are included.

VALUE	DOCUMENT ID		TECN	COMMENT
0.055±0.036	BARLAG	90D	NA32	π^- 230 GeV

$\Gamma(p2\pi^+2\pi^-)/\Gamma(pK^-\pi^+)$ Γ_{22}/Γ_2

VALUE	DOCUMENT ID		TECN	COMMENT
0.036±0.023	BARLAG	90D	NA32	π^- 230 GeV

$\Gamma(pK^+K^-)/\Gamma(pK^-\pi^+)$ Γ_{23}/Γ_2

VALUE	EVTS	DOCUMENT ID		TECN	COMMENT
0.015±0.006 OUR AVERAGE Error includes scale factor of 2.1.					
0.014±0.002±0.002	676	ABE	02C	BELL	$e^+e^- \approx \Upsilon(4S)$
0.039±0.009±0.007	214	ALEXANDER	96C	CLE2	$e^+e^- \approx \Upsilon(4S)$
• • • We do not use the following data for averages, fits, limits, etc. • • •					
0.096±0.029±0.010	30	FRABETTI	93H	E687	γBe, $\overline{E}_\gamma$ 220 GeV
0.048±0.027		BARLAG	90D	NA32	π^- 230 GeV

$\Gamma(p\phi)/\Gamma(pK^-\pi^+)$ Γ_{24}/Γ_2

Unseen decay modes of the ϕ are included.

VALUE (units 10^{-2})	EVTS	DOCUMENT ID		TECN	COMMENT
1.70±0.21 OUR AVERAGE					
1.81±0.33±0.13	44	ABLIKIM	16U	BES3	e^+e^- at 4.599 GeV
1.5 ±0.2 ±0.2	345	ABE	02C	BELL	$e^+e^- \approx \Upsilon(4S)$
2.4 ±0.6 ±0.3	54	ALEXANDER	96C	CLE2	$e^+e^- \approx \Upsilon(4S)$
• • • We do not use the following data for averages, fits, limits, etc. • • •					
4.0 ±2.7		BARLAG	90D	NA32	π^- 230 GeV

$\Gamma(pK^+K^-\text{non-}\phi)/\Gamma(pK^-\pi^+)$ Γ_{25}/Γ_2

VALUE (units 10^{-3})	EVTS	DOCUMENT ID		TECN	COMMENT
8.4 ±1.8 OUR AVERAGE					
9.36±2.22±0.71	38	ABLIKIM	16U	BES3	e^+e^- at 4.599 GeV
7 ±2 ±2	344	ABE	02C	BELL	$e^+e^- \approx \Upsilon(4S)$

$\Gamma(p\phi\pi^0)/\Gamma(pK^-\pi^+)$ Γ_{26}/Γ_2

VALUE (units 10^{-3})	DOCUMENT ID		TECN	COMMENT
$1.538 \pm 0.641^{+0.077}_{-0.100}$	PAL	17	BELL	$e^+e^- \approx \Upsilon(4S), \Upsilon(5S)$

$\Gamma(pK^+K^-\pi^0 \text{nonresonant})/\Gamma_{\text{total}}$ Γ_{27}/Γ

VALUE	CL%	DOCUMENT ID		TECN	COMMENT
$<6.3 \times 10^{-5}$	90	PAL	17	BELL	$e^+e^- \approx \Upsilon(4S), \Upsilon(5S)$

Hadronic modes with a hyperon: $S = -1$ final states

$\Gamma(\Lambda\pi^+)/\Gamma_{\text{total}}$ Γ_{28}/Γ

VALUE (%)	EVTS	DOCUMENT ID		TECN	COMMENT
1.29±0.07 OUR FIT Error includes scale factor of 1.2.					
1.24±0.07±0.03	706	ABLIKIM	16	BES3	$e^+e^- \to \Lambda_c\overline{\Lambda}_c$, 4.599 GeV

Λ_c^+

$\Gamma(\Lambda\pi^+)/\Gamma(pK^-\pi^+)$ Γ_{28}/Γ_2

VALUE	CL%	EVTS	DOCUMENT ID		TECN	COMMENT
0.208±0.009 OUR FIT Error includes scale factor of 1.2.						
0.204±0.019 OUR AVERAGE						
0.217±0.013±0.020		750	LINK	05F	FOCS	γ nucleus, $\overline{E}_\gamma \approx 180$ GeV
0.18 ±0.03 ±0.04			ALBRECHT	92	ARG	$e^+e^- \approx 10.4$ GeV
0.18 ±0.03 ±0.03		87	AVERY	91	CLEO	e^+e^- 10.5 GeV
• • • We do not use the following data for averages, fits, limits, etc. • • •						
<0.33	90		ANJOS	90	E691	γBe 70–260 GeV
<0.16	90		ALBRECHT	88C	ARG	e^+e^- 10 GeV

$\Gamma(\Lambda\pi^+\pi^0)/\Gamma_{\text{total}}$ Γ_{29}/Γ

VALUE (%)	EVTS	DOCUMENT ID		TECN	COMMENT
7.0 ±0.4 OUR FIT Error includes scale factor of 1.1.					
7.01±0.37±0.19	1497	ABLIKIM	16	BES3	$e^+e^- \to \Lambda_c\overline{\Lambda}_c$, 4.599 GeV

$\Gamma(\Lambda\pi^+\pi^0)/\Gamma(pK^-\pi^+)$ Γ_{29}/Γ_2

VALUE	EVTS	DOCUMENT ID		TECN	COMMENT
1.13±0.06 OUR FIT Error includes scale factor of 1.1.					
0.73±0.09±0.16	464	AVERY	94	CLE2	$e^+e^- \approx \Upsilon(3S), \Upsilon(4S)$

$\Gamma(\Lambda\rho^+)/\Gamma(pK^-\pi^+)$ Γ_{30}/Γ_2

VALUE	CL%	DOCUMENT ID		TECN	COMMENT
<0.95	95	AVERY	94	CLE2	$e^+e^- \approx \Upsilon(3S), \Upsilon(4S)$

$\Gamma(\Lambda\pi^-2\pi^+)/\Gamma_{\text{total}}$ Γ_{31}/Γ

VALUE (%)	EVTS	DOCUMENT ID		TECN	COMMENT
3.61±0.29 OUR FIT Error includes scale factor of 1.5.					
3.81±0.24±0.18	609	ABLIKIM	16	BES3	$e^+e^- \to \Lambda_c\overline{\Lambda}_c$, 4.599 GeV

$\Gamma(\Lambda\pi^-2\pi^+)/\Gamma(pK^-\pi^+)$ Γ_{31}/Γ_2

VALUE	EVTS	DOCUMENT ID		TECN	COMMENT
0.58 ±0.05 OUR FIT Error includes scale factor of 2.0.					
0.522±0.032 OUR AVERAGE					
0.508±0.024±0.024	1356	LINK	05F	FOCS	γ nucleus, $\overline{E}_\gamma \approx 180$ GeV
0.65 ±0.11 ±0.12	289	AVERY	91	CLEO	e^+e^- 10.5 GeV
0.82 ±0.29 ±0.27	44	ANJOS	90	E691	γBe 70–260 GeV
0.94 ±0.41 ±0.13	10	BARLAG	90D	NA32	π^- 230 GeV
0.61 ±0.16 ±0.04	105	ALBRECHT	88C	ARG	e^+e^- 10 GeV

$\Gamma(\Sigma(1385)^+\pi^+\pi^-, \Sigma^{*+} \to \Lambda\pi^+)/\Gamma(\Lambda\pi^-2\pi^+)$ Γ_{32}/Γ_{31}

VALUE	DOCUMENT ID		TECN	COMMENT
0.28±0.10±0.08	LINK	05F	FOCS	γ nucleus, $\overline{E}_\gamma \approx 180$ GeV

$\Gamma(\Sigma(1385)^-2\pi^+, \Sigma^{*-} \to \Lambda\pi^-)/\Gamma(\Lambda\pi^-2\pi^+)$ Γ_{33}/Γ_{31}

VALUE	DOCUMENT ID		TECN	COMMENT
0.21±0.03±0.02	LINK	05F	FOCS	γ nucleus, $\overline{E}_\gamma \approx 180$ GeV

$\Gamma(\Lambda\pi^+\rho^0)/\Gamma(\Lambda\pi^-2\pi^+)$ Γ_{34}/Γ_{31}

VALUE	DOCUMENT ID		TECN	COMMENT
0.40±0.12±0.12	LINK	05F	FOCS	γ nucleus, $\overline{E}_\gamma \approx 180$ GeV

$\Gamma(\Sigma(1385)^+\rho^0, \Sigma^{*+} \to \Lambda\pi^+)/\Gamma(\Lambda\pi^-2\pi^+)$ Γ_{35}/Γ_{31}

VALUE	DOCUMENT ID		TECN	COMMENT
0.14±0.09±0.07	LINK	05F	FOCS	γ nucleus, $\overline{E}_\gamma \approx 180$ GeV

$\Gamma(\Lambda\pi^-2\pi^+ \text{nonresonant})/\Gamma(\Lambda\pi^-2\pi^+)$ Γ_{36}/Γ_{31}

VALUE	CL%	DOCUMENT ID		TECN	COMMENT
<0.3	90	LINK	05F	FOCS	γ nucleus, $\overline{E}_\gamma \approx 180$ GeV

$\Gamma(\Lambda\pi^-\pi^0 2\pi^+ \text{total})/\Gamma(pK^-\pi^+)$ Γ_{37}/Γ_2

VALUE	EVTS	DOCUMENT ID		TECN	COMMENT
0.36±0.09±0.09	50	[1] CRONIN-HEN...03		CLE3	$e^+e^- \approx \Upsilon(4S)$

[1] CRONIN-HENNESSY 03 finds this channel to be dominantly $\Lambda\eta\pi^+$ and $\Lambda\omega\pi^+$; see below.

$\Gamma(\Lambda\pi^+\eta)/\Gamma(pK^-\pi^+)$ Γ_{38}/Γ_2

Unseen decay modes of the η are included.

VALUE	EVTS	DOCUMENT ID		TECN	COMMENT
0.36±0.07 OUR AVERAGE					
0.41±0.17±0.10	11	CRONIN-HEN...03		CLE3	$e^+e^- \approx \Upsilon(4S)$
0.35±0.05±0.06	116	AMMAR	95	CLE2	$e^+e^- \approx \Upsilon(4S)$

$\Gamma(\Sigma(1385)^+\eta)/\Gamma(pK^-\pi^+)$ Γ_{39}/Γ_2

Unseen decay modes of the $\Sigma(1385)^+$ and η are included.

VALUE	EVTS	DOCUMENT ID		TECN	COMMENT
0.17±0.04±0.03	54	AMMAR	95	CLE2	$e^+e^- \approx \Upsilon(4S)$

$\Gamma(\Lambda\pi^+\omega)/\Gamma(pK^-\pi^+)$ Γ_{40}/Γ_2

Unseen decay modes of the ω are included.

VALUE	EVTS	DOCUMENT ID		TECN	COMMENT
0.24±0.06±0.06	32	CRONIN-HEN...03		CLE3	$e^+e^- \approx \Upsilon(4S)$

$\Gamma(\Lambda\pi^-\pi^0 2\pi^+, \text{no } \eta \text{ or } \omega)/\Gamma(pK^-\pi^+)$ Γ_{41}/Γ_2

VALUE	CL%	DOCUMENT ID		TECN	COMMENT
<0.13	90	CRONIN-HEN...03		CLE3	$e^+e^- \approx \Upsilon(4S)$

$\Gamma(\Lambda K^+\overline{K}^0)/\Gamma(pK^-\pi^+)$ Γ_{42}/Γ_2

VALUE	EVTS	DOCUMENT ID		TECN	COMMENT
0.091±0.017 OUR FIT Error includes scale factor of 1.9.					
0.131±0.020 OUR AVERAGE					
0.142±0.018±0.022	251	LINK	05F	FOCS	γ nucleus, $\overline{E}_\gamma \approx 180$ GeV
0.12 ±0.02 ±0.02	59	AMMAR	95	CLE2	$e^+e^- \approx \Upsilon(4S)$

$\Gamma(\Xi(1690)^0K^+, \Xi^{*0} \to \Lambda\overline{K}^0)/\Gamma(\Lambda K^+\overline{K}^0)$ Γ_{43}/Γ_{42}

VALUE	EVTS	DOCUMENT ID		TECN	COMMENT
0.28±0.07 OUR AVERAGE					
0.32±0.10±0.04	84±24	LINK	05F	FOCS	γ nucleus, $\overline{E}_\gamma \approx 180$ GeV
0.26±0.08±0.03	93	ABE	02C	BELL	$e^+e^- \approx \Upsilon(4S)$

$\Gamma(\Lambda K^+\overline{K}^0)/\Gamma(\Lambda\pi^+)$ Γ_{42}/Γ_{28}

VALUE	EVTS	DOCUMENT ID		TECN	COMMENT
0.44 ±0.08 OUR FIT Error includes scale factor of 2.0.					
0.395±0.026±0.036	460 ± 30	AUBERT	07U	BABR	$e^+e^- \approx \Upsilon(4S)$

$\Gamma(\Sigma^0\pi^+)/\Gamma_{\text{total}}$ Γ_{44}/Γ

VALUE (%)	EVTS	DOCUMENT ID		TECN	COMMENT
1.28±0.07 OUR FIT Error includes scale factor of 1.1.					
1.27±0.08±0.03	522	ABLIKIM	16	BES3	$e^+e^- \to \Lambda_c\overline{\Lambda}_c$, 4.599 GeV

$\Gamma(\Sigma^0\pi^+)/\Gamma(pK^-\pi^+)$ Γ_{44}/Γ_2

VALUE	EVTS	DOCUMENT ID		TECN	COMMENT
0.206±0.011 OUR FIT Error includes scale factor of 1.2.					
0.20 ±0.04 OUR AVERAGE					
0.21 ±0.02 ±0.04	196	AVERY	94	CLE2	$e^+e^- \approx \Upsilon(3S), \Upsilon(4S)$
0.17 ±0.06 ±0.04		ALBRECHT	92	ARG	$e^+e^- \approx 10.4$ GeV

$\Gamma(\Sigma^0\pi^+)/\Gamma(\Lambda\pi^+)$ Γ_{44}/Γ_{28}

VALUE	EVTS	DOCUMENT ID		TECN	COMMENT
0.99 ±0.04 OUR FIT					
0.98 ±0.05 OUR AVERAGE					
0.977±0.015±0.051	33k	AUBERT	07U	BABR	$e^+e^- \approx \Upsilon(4S)$
1.09 ±0.11 ±0.19	750	LINK	05F	FOCS	γ nucleus, $\overline{E}_\gamma \approx 180$ GeV

$\Gamma(\Sigma^+\pi^0)/\Gamma_{\text{total}}$ Γ_{45}/Γ

VALUE (%)	EVTS	DOCUMENT ID		TECN	COMMENT
1.24±0.10 OUR FIT					
1.18±0.10±0.03	309	ABLIKIM	16	BES3	$e^+e^- \to \Lambda_c\overline{\Lambda}_c$, 4.599 GeV

$\Gamma(\Sigma^+\pi^0)/\Gamma(pK^-\pi^+)$ Γ_{45}/Γ_2

VALUE	EVTS	DOCUMENT ID		TECN	COMMENT
0.199±0.015 OUR FIT					
0.20 ±0.03 ±0.03	93	KUBOTA	93	CLE2	$e^+e^- \approx \Upsilon(4S)$

$\Gamma(\Sigma^+\eta)/\Gamma(pK^-\pi^+)$ Γ_{46}/Γ_2

Unseen decay modes of the η are included.

VALUE	EVTS	DOCUMENT ID		TECN	COMMENT
0.11±0.03±0.02	26	AMMAR	95	CLE2	$e^+e^- \approx \Upsilon(4S)$

$\Gamma(\Sigma^+\pi^+\pi^-)/\Gamma_{\text{total}}$ Γ_{47}/Γ

VALUE (%)	EVTS	DOCUMENT ID		TECN	COMMENT
4.42±0.28 OUR FIT Error includes scale factor of 1.2.					
4.25±0.24±0.20	1156	ABLIKIM	16	BES3	$e^+e^- \to \Lambda_c\overline{\Lambda}_c$, 4.599 GeV

$\Gamma(\Sigma^+\pi^+\pi^-)/\Gamma(pK^-\pi^+)$ Γ_{47}/Γ_2

VALUE	EVTS	DOCUMENT ID		TECN	COMMENT
0.709±0.029 OUR FIT Error includes scale factor of 1.1.					
0.69 ±0.08 OUR AVERAGE					
0.72 ±0.14	47 ± 9	VAZQUEZ-JA...08		SELX	Σ^- nucleus, 600 GeV
0.74 ±0.07 ±0.09	487	KUBOTA	93	CLE2	$e^+e^- \approx \Upsilon(4S)$
$0.54\ ^{+0.18}_{-0.15}$	11	BARLAG	92	NA32	π^-Cu 230 GeV

$\Gamma(\Sigma^+\rho^0)/\Gamma(pK^-\pi^+)$ Γ_{48}/Γ_2

VALUE	CL%	DOCUMENT ID		TECN	COMMENT
<0.27	95	KUBOTA	93	CLE2	$e^+e^- \approx \Upsilon(4S)$

$\Gamma(\Sigma^-2\pi^+)/\Gamma_{\text{total}}$ Γ_{49}/Γ

VALUE (%)	EVTS	DOCUMENT ID		TECN	COMMENT
1.86±0.18 OUR FIT					
1.81±0.17±0.09	161	ABLIKIM	17Y	BES3	e^+e^- at 4.6 GeV

$\Gamma(\Sigma^-2\pi^+)/\Gamma(pK^-\pi^+)$ Γ_{49}/Γ_2

VALUE	EVTS	DOCUMENT ID		TECN	COMMENT
0.299±0.031 OUR FIT Error includes scale factor of 1.1.					
0.314±0.067	30 ± 6	VAZQUEZ-JA...08		SELX	Σ^- nucleus, 600 GeV

See key on page 885

$\Gamma(\Sigma^- 2\pi^+)/\Gamma(\Sigma^+\pi^+\pi^-)$ Γ_{49}/Γ_{47}

VALUE	EVTS	DOCUMENT ID		TECN	COMMENT
0.42±0.05 OUR FIT	Error includes scale factor of 1.1.				
0.53±0.15±0.07	56	FRABETTI	94E	E687	γBe, $\overline{E}_\gamma$ 220 GeV

$\Gamma(\Sigma^0\pi^+\pi^0)/\Gamma(pK^-\pi^+)$ Γ_{50}/Γ_2

VALUE	EVTS	DOCUMENT ID		TECN	COMMENT
0.36±0.09±0.10	117	AVERY	94	CLE2	$e^+e^- \approx \Upsilon(3S), \Upsilon(4S)$

$\Gamma(\Sigma^0\pi^-2\pi^+)/\Gamma(pK^-\pi^+)$ Γ_{51}/Γ_2

VALUE	EVTS	DOCUMENT ID		TECN	COMMENT
0.18±0.05 OUR FIT					
0.21±0.05±0.05	90	AVERY	94	CLE2	$e^+e^- \approx \Upsilon(3S), \Upsilon(4S)$

$\Gamma(\Sigma^0\pi^-2\pi^+)/\Gamma(\Lambda\pi^-2\pi^+)$ Γ_{51}/Γ_{31}

VALUE	EVTS	DOCUMENT ID		TECN	COMMENT
0.31±0.08 OUR FIT					
0.26±0.06±0.09	480	LINK	05F	FOCS	γ nucleus, $\overline{E}_\gamma \approx 180$ GeV

$\Gamma(\Sigma^+\omega)/\Gamma_{\text{total}}$ Γ_{53}/Γ

VALUE (%)	EVTS	DOCUMENT ID		TECN	COMMENT
1.69±0.21 OUR FIT					
1.56±0.20±0.07	157	ABLIKIM	16	BES3	$e^+e^- \to \Lambda_c\overline{\Lambda}_c$, 4.599 GeV

$\Gamma(\Sigma^+\omega)/\Gamma(pK^-\pi^+)$ Γ_{53}/Γ_2

Unseen decay modes of the ω are included.

VALUE	EVTS	DOCUMENT ID		TECN	COMMENT
0.271±0.032 OUR FIT					
0.54 ±0.13 ±0.06	107	KUBOTA	93	CLE2	$e^+e^- \approx \Upsilon(4S)$

$\Gamma(\Sigma^-\pi^0 2\pi^+)/\Gamma_{\text{total}}$ Γ_{54}/Γ

VALUE (%)	EVTS	DOCUMENT ID		TECN	COMMENT
2.11±0.33±0.14	88	ABLIKIM	17Y	BES3	e^+e^- at 4.6 GeV

$\Gamma(\Sigma^+K^+K^-)/\Gamma(pK^-\pi^+)$ Γ_{55}/Γ_2

VALUE	EVTS	DOCUMENT ID		TECN	COMMENT
0.055±0.006 OUR FIT					
0.070±0.011±0.011	59	AVERY	93	CLE2	$e^+e^- \approx 10.5$ GeV

$\Gamma(\Sigma^+K^+K^-)/\Gamma(\Sigma^+\pi^+\pi^-)$ Γ_{55}/Γ_{47}

VALUE	EVTS	DOCUMENT ID		TECN	COMMENT
0.078±0.009 OUR FIT					
0.074±0.009 OUR AVERAGE					
0.076±0.007±0.009	246	ABE	02C	BELL	$e^+e^- \approx \Upsilon(4S)$
0.071±0.011±0.011	103	LINK	02G	FOCS	γ nucleus, ≈ 180 GeV

$\Gamma(\Sigma^+\phi)/\Gamma(pK^-\pi^+)$ Γ_{56}/Γ_2

Unseen decay modes of the ϕ are included.

VALUE	EVTS	DOCUMENT ID		TECN	COMMENT
0.062±0.009 OUR FIT	Error includes scale factor of 1.1.				
0.069±0.023±0.016	26	AVERY	93	CLE2	$e^+e^- \approx 10.5$ GeV

$\Gamma(\Sigma^+\phi)/\Gamma(\Sigma^+\pi^+\pi^-)$ Γ_{56}/Γ_{47}

Unseen decay modes of the ϕ are included.

VALUE	EVTS	DOCUMENT ID		TECN	COMMENT
0.087±0.012 OUR FIT					
0.086±0.012 OUR AVERAGE					
0.085±0.012±0.012	129	ABE	02C	BELL	$e^+e^- \approx \Upsilon(4S)$
0.087±0.016±0.006	57	LINK	02G	FOCS	γ nucleus, ≈ 180 GeV

$\Gamma(\Xi(1690)^0K^+, \Xi^{*0}\to\Sigma^+K^-)/\Gamma(\Sigma^+\pi^+\pi^-)$ Γ_{57}/Γ_{47}

VALUE	EVTS	DOCUMENT ID		TECN	COMMENT
0.023±0.005 OUR AVERAGE					
0.023±0.005±0.005	75	ABE	02C	BELL	$e^+e^- \approx \Upsilon(4S)$
0.022±0.006±0.006	34	LINK	02G	FOCS	γ nucleus, ≈ 180 GeV

$\Gamma(\Sigma^+K^+K^-$ nonresonant$)/\Gamma(\Sigma^+\pi^+\pi^-)$ Γ_{58}/Γ_{47}

VALUE	CL%	DOCUMENT ID		TECN	COMMENT
<0.018	90	ABE	02C	BELL	$e^+e^- \approx \Upsilon(4S)$
• • • We do not use the following data for averages, fits, limits, etc. • • •					
<0.028	90	LINK	02G	FOCS	γ nucleus, ≈ 180 GeV

$\Gamma(\Xi^0K^+)/\Gamma(pK^-\pi^+)$ Γ_{59}/Γ_2

VALUE	EVTS	DOCUMENT ID		TECN	COMMENT
0.078±0.013±0.013	56	AVERY	93	CLE2	$e^+e^- \approx 10.5$ GeV

$\Gamma(\Xi^-K^+\pi^+)/\Gamma(pK^-\pi^+)$ Γ_{60}/Γ_2

VALUE	EVTS	DOCUMENT ID		TECN	COMMENT
0.099±0.009 OUR FIT	Error includes scale factor of 1.1.				
0.098±0.021 OUR AVERAGE	Error includes scale factor of 1.3. See the ideogram below.				
0.14 ±0.03 ±0.02	34	ALBRECHT	95B	ARG	$e^+e^- \approx 10.4$ GeV
0.079±0.013±0.014	60	AVERY	93	CLE2	$e^+e^- \approx 10.5$ GeV
0.15 ±0.04 ±0.03	30	AVERY	91	CLEO	e^+e^- 10.5 GeV

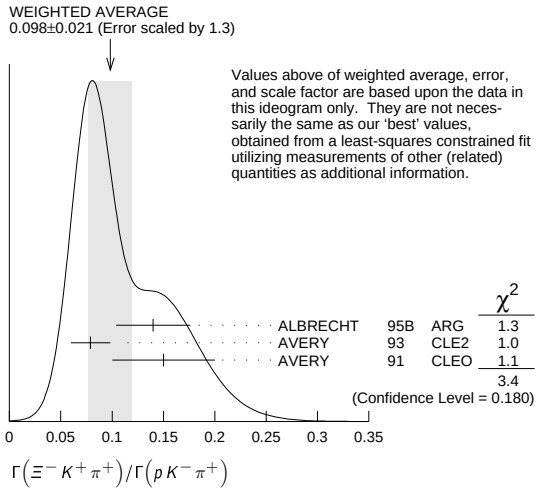

$\Gamma(\Xi^-K^+\pi^+)/\Gamma(\Lambda\pi^+)$ Γ_{60}/Γ_{28}

VALUE	EVTS	DOCUMENT ID		TECN	COMMENT
0.48 ±0.04 OUR FIT					
0.480±0.016±0.039	2665 ± 84	AUBERT	07U	BABR	$e^+e^- \approx \Upsilon(4S)$

$\Gamma(\Xi(1530)^0K^+, \Xi^0\to\Xi^-\pi^+)/\Gamma(pK^-\pi^+)$ Γ_{61}/Γ_2

VALUE	EVTS	DOCUMENT ID		TECN	COMMENT
0.053±0.016±0.010	24	AVERY	93	CLE2	$e^+e^- \approx 10.5$ GeV
• • • We do not use the following data for averages, fits, limits, etc. • • •					
0.05 ±0.02 ±0.01	11	ALBRECHT	95B	ARG	$e^+e^- \approx 10.4$ GeV

Hadronic modes with a hyperon: $S = 0$ final states

$\Gamma(\Lambda K^+)/\Gamma(\Lambda\pi^+)$ Γ_{62}/Γ_{28}

VALUE	EVTS	DOCUMENT ID		TECN	COMMENT
0.047±0.009 OUR AVERAGE	Error includes scale factor of 1.8.				
0.044±0.004±0.003	1162±101	AUBERT	07U	BABR	$e^+e^- \approx \Upsilon(4S)$
0.074±0.010±0.012	265	ABE	02C	BELL	$e^+e^- \approx \Upsilon(4S)$

$\Gamma(\Lambda K^+\pi^+\pi^-)/\Gamma(\Lambda\pi^+)$ Γ_{63}/Γ_{28}

VALUE	CL%	DOCUMENT ID		TECN	COMMENT
<4.1 × 10⁻²	90	AUBERT	07U	BABR	$e^+e^- \approx \Upsilon(4S)$

$\Gamma(\Sigma^0K^+)/\Gamma(\Sigma^0\pi^+)$ Γ_{64}/Γ_{44}

VALUE	EVTS	DOCUMENT ID		TECN	COMMENT
0.040±0.006 OUR AVERAGE					
0.038±0.005±0.003	366 ± 52	AUBERT	07U	BABR	$e^+e^- \approx \Upsilon(4S)$
0.056±0.014±0.008	75	ABE	02C	BELL	$e^+e^- \approx \Upsilon(4S)$

$\Gamma(\Sigma^0K^+\pi^+\pi^-)/\Gamma(\Sigma^0\pi^+)$ Γ_{65}/Γ_{44}

VALUE	CL%	DOCUMENT ID		TECN	COMMENT
<2.0 × 10⁻²	90	AUBERT	07U	BABR	$e^+e^- \approx \Upsilon(4S)$

$\Gamma(\Sigma^+K^+\pi^-)/\Gamma(\Sigma^+\pi^+\pi^-)$ Γ_{66}/Γ_{47}

VALUE	EVTS	DOCUMENT ID		TECN	COMMENT
0.047±0.011±0.008	105	ABE	02C	BELL	$e^+e^- \approx \Upsilon(4S)$

$\Gamma(\Sigma^+K^*(892)^0)/\Gamma(\Sigma^+\pi^+\pi^-)$ Γ_{67}/Γ_{47}

Unseen decay modes of the $K^*(892)^0$ are included.

VALUE	EVTS	DOCUMENT ID		TECN	COMMENT
0.078±0.018±0.013	49	LINK	02G	FOCS	γ nucleus, ≈ 180 GeV

$\Gamma(\Sigma^-K^+\pi^+)/\Gamma(\Sigma^+K^*(892)^0)$ Γ_{68}/Γ_{67}

VALUE	CL%	DOCUMENT ID		TECN	COMMENT
<0.35	90	LINK	02G	FOCS	γ nucleus, ≈ 180 GeV

Doubly Cabibbo-suppressed modes

$\Gamma(pK^+\pi^-)/\Gamma(pK^-\pi^+)$ Γ_{69}/Γ_2

VALUE (units 10^{-3})	CL%	EVTS	DOCUMENT ID		TECN	COMMENT
2.35±0.27±0.21		3379	YANG	16	BELL	At or near Υs
• • • We do not use the following data for averages, fits, limits, etc. • • •						
<4.6	90		[1] LINK		05K FOCS	180 GeV γ on BeO

[1] LINK 05K limit is equivalent to (0.05 ± 0.26 ± 0.02)% measurement.

Semileptonic modes

$\Gamma(\Lambda e^+\nu_e)/\Gamma_{\text{total}}$ Γ_{70}/Γ

VALUE (%)	EVTS	DOCUMENT ID		TECN	COMMENT
3.63±0.38±0.20	104	ABLIKIM	15Y	BES3	567 pb^{-1}, 4.599 GeV

$\Gamma(\Lambda e^+\nu_e)/\Gamma(pK^-\pi^+)$ Γ_{70}/Γ_2

VALUE	DOCUMENT ID		TECN	COMMENT
• • • We do not use the following data for averages, fits, limits, etc. • • •				
0.43±0.08	[1,2] BERGFELD	94	CLE2	$e^+e^- \approx \Upsilon(4S)$
0.38±0.14	[2,3] ALBRECHT	91G	ARG	$e^+e^- \approx 10.4$ GeV

[1] BERGFELD 94 measures $\sigma(e^+e^- \to \Lambda_c^+ X)\cdot B(\Lambda_c^+ \to \Lambda e^+\nu_e) = (4.87 \pm 0.28 \pm 0.69)$ pb.
[2] To extract $\Gamma(\Lambda_c^+ \to \Lambda e^+\nu_e)/\Gamma(\Lambda_c^+ \to pK^-\pi^+)$, we use $\sigma(e^+e^- \to \Lambda_c^+ X)\cdot B(\Lambda_c \to pK^-\pi^+) = (11.2 \pm 1.3)$ pb, which is the weighted average of measurements from ARGUS (ALBRECHT 96E) and CLEO (AVERY 91).
[3] ALBRECHT 91G measures $\sigma(e^+e^- \to \Lambda_c^+ X)\cdot B(\Lambda_c^+ \to \Lambda e^+\nu_e) = (4.20 \pm 1.28 \pm 0.71)$ pb.

$\Gamma(\Lambda\mu^+\nu_\mu)/\Gamma_{\text{total}}$ Γ_{71}/Γ

VALUE (%)	EVTS	DOCUMENT ID		TECN	COMMENT
3.49±0.46±0.27	79	ABLIKIM	17D	BES3	e^+e^- at 4.6 GeV

$\Gamma(\Lambda\mu^+\nu_\mu)/\Gamma(pK^-\pi^+)$ Γ_{71}/Γ_2

VALUE	DOCUMENT ID		TECN	COMMENT
• • • We do not use the following data for averages, fits, limits, etc. • • •				
0.40±0.09	[1,2] BERGFELD	94	CLE2	$e^+e^- \approx \Upsilon(4S)$
0.35±0.20	[2,3] ALBRECHT	91G	ARG	$e^+e^- \approx 10.4$ GeV

[1] BERGFELD 94 measures $\sigma(e^+e^- \to \Lambda_c^+ X)\cdot B(\Lambda_c^+ \to \Lambda\mu^+\nu_\mu) = (4.43 \pm 0.51 \pm 0.64)$ pb.
[2] To extract $\Gamma(\Lambda_c^+ \to \Lambda\mu^+\nu_\mu)/\Gamma(\Lambda_c^+ \to pK^-\pi^+)$, we use $\sigma(e^+e^- \to \Lambda_c^+ X)\cdot B(\Lambda_c \to pK^-\pi^+) = (11.2 \pm 1.3)$ pb, which is the weighted average of measurements from ARGUS (ALBRECHT 96E) and CLEO (AVERY 91).
[3] ALBRECHT 91G measures $\sigma(e^+e^- \to \Lambda_c^+ X)\cdot B(\Lambda_c^+ \to \Lambda\mu^+\nu_\mu) = (3.91 \pm 2.02 \pm 0.90)$ pb.

$\Gamma(\Lambda\mu^+\nu_\mu)/\Gamma(\Lambda e^+\nu_e)$ Γ_{71}/Γ_{70}

VALUE	DOCUMENT ID		TECN	COMMENT
• • • We do not use the following data for averages, fits, limits, etc. • • •				
0.96±0.16±0.04	[1] ABLIKIM	17D	BES3	e^+e^- at 4.6 GeV

[1] This is the ratio of the ABLIKIM 17D $\Lambda\mu^+\nu_e$ branching fraction and the ABLIKIM 15Y $\Lambda e^+\nu_e$ branching fraction (see above), and so is not an independent measurement.

Inclusive modes

$\Gamma(e^+ \text{anything})/\Gamma_{\text{total}}$ Γ_{72}/Γ

VALUE	DOCUMENT ID		TECN	COMMENT
0.045±0.017	VELLA	82	MRK2	e^+e^- 4.5–6.8 GeV

$\Gamma(pe^+ \text{anything})/\Gamma_{\text{total}}$ Γ_{73}/Γ

VALUE	DOCUMENT ID		TECN	COMMENT
0.018±0.009	[1] VELLA	82	MRK2	e^+e^- 4.5–6.8 GeV

[1] VELLA 82 includes protons from Λ decay.

$\Gamma(\Lambda e^+ \text{anything})/\Gamma_{\text{total}}$ Γ_{74}/Γ

VALUE	DOCUMENT ID		TECN	COMMENT
• • • We do not use the following data for averages, fits, limits, etc. • • •				
0.011±0.008	[1] VELLA	82	MRK2	e^+e^- 4.5–6.8 GeV

[1] VELLA 82 includes Λ's from Σ^0 decay.

$\Gamma(p \text{ anything})/\Gamma_{\text{total}}$ Γ_{75}/Γ

VALUE	DOCUMENT ID		TECN	COMMENT
0.50±0.08±0.14	[1] CRAWFORD	92	CLEO	e^+e^- 10.5 GeV

[1] This CRAWFORD 92 value includes protons from Λ decay. The value is model dependent, but account is taken of this in the systematic error.

$\Gamma(p \text{ anything (no } \Lambda))/\Gamma_{\text{total}}$ Γ_{76}/Γ

VALUE	DOCUMENT ID		TECN	COMMENT
0.12±0.10±0.16	CRAWFORD	92	CLEO	e^+e^- 10.5 GeV

$\Gamma(n \text{ anything})/\Gamma_{\text{total}}$ Γ_{78}/Γ

VALUE	DOCUMENT ID		TECN	COMMENT
0.50±0.08±0.14	[1] CRAWFORD	92	CLEO	e^+e^- 10.5 GeV

[1] This CRAWFORD 92 value includes neutrons from Λ decay. The value is model dependent, but account is taken of this in the systematic error.

$\Gamma(n \text{ anything (no } \Lambda))/\Gamma_{\text{total}}$ Γ_{79}/Γ

VALUE	DOCUMENT ID		TECN	COMMENT
0.29±0.09±0.15	CRAWFORD	92	CLEO	e^+e^- 10.5 GeV

$\Gamma(p \text{ hadrons})/\Gamma_{\text{total}}$ Γ_{77}/Γ

VALUE	DOCUMENT ID		TECN	COMMENT
• • • We do not use the following data for averages, fits, limits, etc. • • •				
0.41±0.24	ADAMOVICH	87	EMUL	γA 20–70 GeV/c

$\Gamma(\Lambda \text{ anything})/\Gamma_{\text{total}}$ Γ_{80}/Γ

VALUE	EVTS	DOCUMENT ID		TECN	COMMENT
0.35±0.11 OUR AVERAGE Error includes scale factor of 1.4. See the ideogram below.					
0.59±0.10±0.12		CRAWFORD	92	CLEO	e^+e^- 10.5 GeV
0.49±0.24		ADAMOVICH	87	EMUL	γA 20–70 GeV/c
0.23±0.10	8	[1] ABE	86	HYBR	20 GeV γp

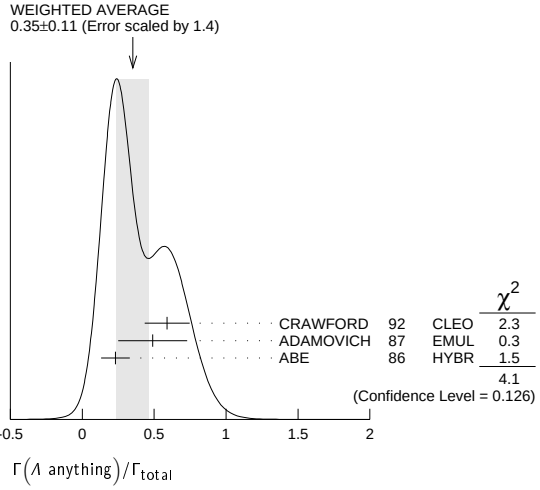

[1] ABE 86 includes Λ's from Σ^0 decay.

$\Gamma(\Sigma^\pm \text{anything})/\Gamma_{\text{total}}$ Γ_{81}/Γ

VALUE	EVTS	DOCUMENT ID		TECN	COMMENT
0.1±0.05	5	ABE	86	HYBR	20 GeV γp

$\Gamma(3\text{prongs})/\Gamma_{\text{total}}$ Γ_{82}/Γ

VALUE	DOCUMENT ID		TECN	COMMENT
0.24±0.07±0.04	KAYIS-TOPAK.03		CHRS	ν_μ emulsion, $\overline{E}$=27 GeV

Rare or forbidden modes

$\Gamma(pe^+e^-)/\Gamma_{\text{total}}$ Γ_{83}/Γ

A test for the ΔC=1 weak neutral current. Allowed by higher-order electroweak interactions.

VALUE	CL%	EVTS	DOCUMENT ID		TECN	COMMENT
<5.5 × 10⁻⁶	90	4.0 ± 7.1	LEES	11G	BABR	$e^+e^- \approx \Upsilon(4S)$

$\Gamma(p\mu^+\mu^-)/\Gamma_{\text{total}}$ Γ_{84}/Γ

A test for the ΔC=1 weak neutral current. Allowed by higher-order electroweak interactions.

VALUE	CL%	EVTS	DOCUMENT ID		TECN	COMMENT
<44 × 10⁻⁶	90	11.1 ± 5.6	LEES	11G	BABR	$e^+e^- \approx \Upsilon(4S)$
• • • We do not use the following data for averages, fits, limits, etc. • • •						
< 3.4 × 10⁻⁴	90	0	KODAMA	95	E653	π^- emulsion 600 GeV

$\Gamma(pe^+\mu^-)/\Gamma_{\text{total}}$ Γ_{85}/Γ

A test of lepton family-number conservation.

VALUE	CL%	EVTS	DOCUMENT ID		TECN	COMMENT
<9.9 × 10⁻⁶	90	−0.7 ± 3.0	LEES	11G	BABR	$e^+e^- \approx \Upsilon(4S)$

$\Gamma(pe^-\mu^+)/\Gamma_{\text{total}}$ Γ_{86}/Γ

A test of lepton family-number conservation.

VALUE	CL%	EVTS	DOCUMENT ID		TECN	COMMENT
<19 × 10⁻⁶	90	6.2 ± 4.9	LEES	11G	BABR	$e^+e^- \approx \Upsilon(4S)$

$\Gamma(\overline{p}2e^+)/\Gamma_{\text{total}}$ Γ_{87}/Γ

A test of lepton- and baryon-number conservation.

VALUE	CL%	EVTS	DOCUMENT ID		TECN	COMMENT
<2.7 × 10⁻⁶	90	−1.5 ± 4.5	LEES	11G	BABR	$e^+e^- \approx \Upsilon(4S)$

$\Gamma(\overline{p}2\mu^+)/\Gamma_{\text{total}}$ Γ_{88}/Γ

A test of lepton- and baryon-number conservation and of lepton family-number conservation.

VALUE	CL%	EVTS	DOCUMENT ID		TECN	COMMENT
<9.4 × 10⁻⁶	90	0.0 ± 2.2	LEES	11G	BABR	$e^+e^- \approx \Upsilon(4S)$

$\Gamma(\overline{p}e^+\mu^+)/\Gamma_{\text{total}}$ Γ_{89}/Γ

A test of lepton- and baryon-number conservation and of lepton family-number conservation.

VALUE	CL%	EVTS	DOCUMENT ID		TECN	COMMENT
<16 × 10⁻⁶	90	10.1 ± 6.8	LEES	11G	BABR	$e^+e^- \approx \Upsilon(4S)$

$\Gamma(\Sigma^-\mu^+\mu^+)/\Gamma_{\text{total}}$ Γ_{90}/Γ

A test of lepton-number conservation.

VALUE	CL%	EVTS	DOCUMENT ID		TECN	COMMENT
<7.0 × 10⁻⁴	90	0	KODAMA	95	E653	π^- emulsion 600 GeV

Λ_c^+ DECAY PARAMETERS

See the note on "Baryon Decay Parameters" in the neutron Listings.

α FOR $\Lambda_c^+ \to \Lambda\pi^+$

VALUE	EVTS	DOCUMENT ID		TECN	COMMENT
−0.91±0.15 OUR AVERAGE					
−0.78±0.16±0.19		LINK	06A	FOCS	γ A, $\overline{E}_\gamma \approx$ 180 GeV
−0.94±0.21±0.12	414	[1] BISHAI	95	CLE2	$e^+e^- \approx \Upsilon(4S)$
−0.96±0.42		ALBRECHT	92	ARG	$e^+e^- \approx$ 10.4 GeV
−1.1 ±0.4	86	AVERY	90B	CLEO	$e^+e^- \approx$ 10.6 GeV

[1] BISHAI 95 actually gives $\alpha = -0.94 \begin{smallmatrix}+0.21+0.12\\-0.06-0.06\end{smallmatrix}$, chopping the errors at the physical limit −1.0. However, for $\alpha \approx -1.0$, some experiments should *get* unphysical values ($\alpha < -1.0$), and for averaging with other measurements such values (or errors that extend below −1.0) should *not* be chopped.

α FOR $\Lambda_c^+ \to \Sigma^+\pi^0$

VALUE	EVTS	DOCUMENT ID		TECN	COMMENT
−0.45±0.31±0.06	89	BISHAI	95	CLE2	$e^+e^- \approx \Upsilon(4S)$

α FOR $\Lambda_c^+ \to \Lambda\ell^+\nu_\ell$

The experiments don't cover the complete (or same incomplete) $M(\Lambda\ell^+)$ range, but we average them together anyway.

VALUE	EVTS	DOCUMENT ID		TECN	COMMENT
−0.86±0.04 OUR AVERAGE					
−0.86±0.03±0.02	3201	[1] HINSON	05	CLEO	$e^+e^- \approx \Upsilon(4S)$
−0.91±0.42±0.25		[2] ALBRECHT	94B	ARG	$e^+e^- \approx$ 10 GeV
• • • We do not use the following data for averages, fits, limits, etc. • • •					
$-0.82 \begin{smallmatrix}+0.09+0.06\\-0.06-0.03\end{smallmatrix}$	700	[3] CRAWFORD	95	CLE2	See HINSON 05
$-0.89 \begin{smallmatrix}+0.17+0.09\\-0.11-0.05\end{smallmatrix}$	350	[4] BERGFELD	94	CLE2	See CRAWFORD 95

[1] HINSON 05 measures the form-factor ratio $R \equiv f_2/f_1$ for $\Lambda_c^+ \to \Lambda e^+\nu_e$ events to be $-0.31 \pm 0.05 \pm 0.04$ and the pole mass to be $2.21 \pm 0.08 \pm 0.14$ GeV/c^2, and from these calculates α, averaged over q^2, where $\langle q^2 \rangle = 0.67\,(\text{GeV/c})^2$.

[2] ALBRECHT 94B uses Λe^+ and $\Lambda\mu^+$ events in the mass range $1.85 < M(\Lambda\ell^+) < 2.20$ GeV.

[3] CRAWFORD 95 measures the form-factor ratio $R \equiv f_2/f_1$ for $\Lambda_c^+ \to \Lambda e^+\nu_e$ events to be $-0.25 \pm 0.14 \pm 0.08$ and from this calculates α, averaged over q^2, to be the above.

[4] BERGFELD 94 uses Λe^+ events.

Λ_c^+, $\overline{\Lambda}_c^-$ *CP*-VIOLATING DECAY ASYMMETRIES

$(\alpha + \overline{\alpha})/(\alpha - \overline{\alpha})$ in $\Lambda_c^+ \to \Lambda\pi^+$, $\overline{\Lambda}_c^- \to \overline{\Lambda}\pi^-$

This is zero if *CP* is conserved.

VALUE	DOCUMENT ID		TECN	COMMENT
−0.07±0.19±0.24	LINK	06A	FOCS	γ A, $\overline{E}_\gamma \approx$ 180 GeV

$(\alpha + \overline{\alpha})/(\alpha - \overline{\alpha})$ in $\Lambda_c^+ \to \Lambda e^+\nu_e$, $\overline{\Lambda}_c^- \to \overline{\Lambda} e^-\overline{\nu}_e$

This is zero if *CP* is conserved.

VALUE	DOCUMENT ID		TECN	COMMENT
0.00±0.03±0.02	HINSON	05	CLEO	$e^+e^- \approx \Upsilon(4S)$

Λ_c^+ REFERENCES

We have omitted some papers that have been superseded by later experiments. The omitted papers may be found in our 1992 edition (Physical Review **D45**, 1 June, Part II) or in earlier editions.

ABLIKIM	17D	PL B767 42	M. Ablikim *et al.*	(BES III Collab.)
ABLIKIM	17H	PRL 118 112001	M. Ablikim *et al.*	(BES III Collab.)
ABLIKIM	17Q	PR D95 111102	M. Ablikim *et al.*	(BES III Collab.)
ABLIKIM	17Y	PL B772 388	M. Ablikim *et al.*	(BES III Collab.)
PAL	17	PR D96 051102	B. Pal *et al.*	(BELLE Collab.)
ABLIKIM	16	PRL 116 052001	M. Ablikim *et al.*	(BES III Collab.)
ABLIKIM	16U	PRL 117 232002	M. Ablikim *et al.*	(BES III Collab.)
YANG	16	PRL 117 011801	S.B. Yang *et al.*	(BELLE Collab.)
ABLIKIM	15Y	PRL 115 221805	M. Ablikim *et al.*	(BES III Collab.)
ZUPANC	14	PRL 113 042002	A. Zupanc *et al.*	(BELLE Collab.)
LEES	11G	PR D84 072006	J.P. Lees *et al.*	(BABAR Collab.)
VAZQUEZ-JA...	08	PL B666 299	E. Vazquez-Jauregui *et al.*	(SELEX Collab.)
AUBERT	07U	PR D75 052002	B. Aubert *et al.*	(BABAR Collab.)
LINK	06A	PL B634 165	J.M. Link *et al.*	(FNAL FOCUS Collab.)
AUBERT,B	05S	PR D72 052006	B. Aubert *et al.*	(BABAR Collab.)
HINSON	05	PRL 94 191801	J.W. Hinson *et al.*	(CLEO Collab.)
LINK	05F	PL B624 22	J.M. Link *et al.*	(FNAL FOCUS Collab.)
LINK	05K	PL B624 166	J.M. Link *et al.*	(FNAL FOCUS Collab.)
CRONIN-HEN...	03	PR D67 012001	D. Cronin-Hennessy *et al.*	(CLEO Collab.)
KAYIS-TOPAK...	03	PL B555 156	A. Kayis-Topaksu *et al.*	(CERN CHORUS Collab.)
ABE	02C	PL B524 33	K. Abe *et al.*	(KEK BELLE Collab.)
LINK	02C	PRL 88 161801	J.M. Link *et al.*	(FNAL FOCUS Collab.)
LINK	02G	PL B540 25	J.M. Link *et al.*	(FNAL FOCUS Collab.)
PDG	02	PR D66 010001	K. Hagiwara *et al.*	(PDG Collab.)
KUSHNIR...	01	PRL 86 5243	A. Kushnirenko *et al.*	(FNAL SELEX Collab.)
MAHMOOD	01	PRL 86 2232	A.H. Mahmood *et al.*	(CLEO Collab.)
AITALA	00	PL B471 449	E.M. Aitala *et al.*	(FNAL E791 Collab.)
ALAM	98	PR D57 4467	M.S. Alam *et al.*	(CLEO Collab.)
ALBRECHT	96E	PRPL 276 223	H. Albrecht *et al.*	(ARGUS Collab.)
ALEXANDER	96C	PR D53 1013	J.P. Alexander *et al.*	(CLEO Collab.)
ALBRECHT	95B	PL B342 397	H. Albrecht *et al.*	(ARGUS Collab.)
AMMAR	95	PRL 74 3534	R. Ammar *et al.*	(CLEO Collab.)
BISHAI	95	PL B350 256	M. Bishai *et al.*	(CLEO Collab.)
CRAWFORD	95	PRL 75 624	G. Crawford *et al.*	(CLEO Collab.)
KODAMA	95	PL B345 85	K. Kodama *et al.*	(FNAL E653 Collab.)
ALBRECHT	94B	PL B326 320	H. Albrecht *et al.*	(ARGUS Collab.)
ALEEV	94	PAN 57 1370	A.N. Aleev *et al.*	(Serpukhov BIS-2 Collab.)
		Translated from YF 57 1443.		
AVERY	94	PL B325 257	P. Avery *et al.*	(CLEO Collab.)
BERGFELD	94	PL B323 219	T. Bergfeld *et al.*	(CLEO Collab.)
FRABETTI	94E	PL B328 193	P.L. Frabetti *et al.*	(FNAL E687 Collab.)
AVERY	93	PRL 71 2391	P. Avery *et al.*	(CLEO Collab.)
BOZEK	93	PL B312 247	A. Bozek *et al.*	(CERN NA32 Collab.)
FRABETTI	93D	PRL 70 1755	P.L. Frabetti *et al.*	(FNAL E687 Collab.)
FRABETTI	93H	PL B314 477	P.L. Frabetti *et al.*	(FNAL E687 Collab.)
KUBOTA	93	PRL 71 3255	Y. Kubota *et al.*	(CLEO Collab.)
ALBRECHT	92	PL B274 239	H. Albrecht *et al.*	(ARGUS Collab.)
BARLAG	92	PL B283 465	S. Barlag *et al.*	(ACCMOR Collab.)
CRAWFORD	92	PR D45 752	G. Crawford *et al.*	(CLEO Collab.)
JEZABEK	92	PL B286 175	M. Jezabek, K. Rybicki, R. Rylko	(CRAC)
ALBRECHT	91G	PL B269 234	H. Albrecht *et al.*	(ARGUS Collab.)
AVERY	91	PR D43 3599	P. Avery *et al.*	(CLEO Collab.)
ALVAREZ	90	ZPHY C47 539	M.P. Alvarez *et al.*	(CERN NA14/2 Collab.)
ALVAREZ	90B	PL B246 256	M.P. Alvarez *et al.*	(CERN NA14/2 Collab.)
ANJOS	90	PR D41 801	J.C. Anjos *et al.*	(FNAL E691 Collab.)
AVERY	90B	PRL 65 2842	P. Avery *et al.*	(CLEO Collab.)
BARLAG	90D	ZPHY C48 29	S. Barlag *et al.*	(ACCMOR Collab.)
FRABETTI	90	PL B251 639	P.L. Frabetti *et al.*	(FNAL E687 Collab.)
BARLAG	89	PL B218 374	S. Barlag *et al.*	(ACCMOR Collab.)
AGUILAR-...	88B	ZPHY C40 321	M. Aguilar-Benitez *et al.*	(LEBC-EHS Collab.)
Also		PL B189 254	M. Aguilar-Benitez *et al.*	(LEBC-EHS Collab.)
Also		PL B199 462	M. Aguilar-Benitez *et al.*	(LEBC-EHS Collab.)
Also		SJNP 48 833	M. Begalli *et al.*	(LEBC-EHS Collab.)
		Translated from YAF 48 1310.		
ALBRECHT	88C	PL B207 109	H. Albrecht *et al.*	(ARGUS Collab.)
ANJOS	88B	PRL 60 1379	J.C. Anjos *et al.*	(FNAL E691 Collab.)
ADAMOVICH	87	EPL 4 887	M.I. Adamovich *et al.*	(Photon Emulsion Collab.)
Also		SJNP 46 447	F. Viaggi *et al.*	(Photon Emulsion Collab.)
		Translated from YAF 46 799.		
AMENDOLIA	87	ZPHY C36 513	S.R. Amendolia *et al.*	(CERN NA1 Collab.)
JONES	87	ZPHY C36 593	G.T. Jones *et al.*	(CERN WA21 Collab.)
ABE	86	PR D33 1	K. Abe *et al.*	(SLAC HF Photon Collab.)
BOSETTI	82	PL 109B 234	P.C. Bosetti *et al.*	(AACH3, BONN, CERN+)
VELLA	82	PRL 48 1515	E. Vella *et al.*	(SLAC, LBL, UCB)
BASILE	81B	NC 62A 14	M. Basile *et al.*	(CERN, BGNA, PGIA, FRAS)
CALICCHIO	80	PL 93B 521	M. Calicchio *et al.*	(BARI, BIRM, BRUX+)

OTHER RELATED PAPERS

MIGLIOZZI	99	PL B462 217	P. Migliozzi *et al.*	
DUNIETZ	98	PR D58 094010	I. Dunietz	

$\Lambda_c(2595)^+$

$I(J^P) = 0(\frac{1}{2}^-)$ Status: ***

The $\Lambda_c^+\pi^+\pi^-$ mode is largely, and perhaps entirely, $\Sigma_c\pi$, which is just at threshold; since the Σ_c has $J^P = 1/2^+$, the J^P here is almost certainly $1/2^-$. This result is in accord with the theoretical expectation that this is the charm counterpart of the strange $\Lambda(1405)$.

$\Lambda_c(2595)^+$ MASS

The mass is obtained from the $\Lambda_c(2595)^+ - \Lambda_c^+$ mass-difference measurements below.

VALUE (MeV)	DOCUMENT ID
2592.25±0.28 OUR FIT	

$\Lambda_c(2595)^+ - \Lambda_c^+$ MASS DIFFERENCE

VALUE (MeV)	EVTS	DOCUMENT ID		TECN	COMMENT
305.79±0.24 OUR FIT					
305.79±0.14±0.20	3.5k	AALTONEN	11H	CDF	$p\overline{p}$ at 1.96 TeV
• • • We do not use the following data for averages, fits, limits, etc. • • •					
305.6 ±0.3		[1] BLECHMAN	03		Threshold shift
309.7 ±0.9 ±0.4	19	ALBRECHT	97	ARG	$e^+e^- \approx$ 10 GeV
309.2 ±0.7 ±0.3	14 ± 4.5	FRABETTI	96	E687	γBe, $\overline{E}_\gamma \approx$ 220 GeV
307.5 ±0.4 ±1.0	112 ± 17	EDWARDS	95	CLE2	$e^+e^- \approx$ 10.5 GeV

[1] BLECHMAN 03 finds that a more sophisticated treatment than a simple Breit-Wigner for the proximity of the threshold of the dominant decay, $\Sigma_c(2455)\pi$, lowers the $\Lambda_c(2595)^+ - \Lambda_c^+$ mass difference by 2 or 3 MeV. The analysis of AALTONEN 11H bears this out.

$\Lambda_c(2595)^+$ WIDTH

VALUE (MeV)	EVTS	DOCUMENT ID		TECN	COMMENT
2.59±0.30±0.47	3.5k	[2] AALTONEN	11H	CDF	$p\overline{p}$ at 1.96 TeV
• • • We do not use the following data for averages, fits, limits, etc. • • •					
$2.9 \begin{smallmatrix}+2.9+1.8\\-2.1-1.4\end{smallmatrix}$	19	ALBRECHT	97	ARG	$e^+e^- \approx$ 10 GeV
$3.9 \begin{smallmatrix}+1.4+2.0\\-1.2-1.0\end{smallmatrix}$	112 ± 17	EDWARDS	95	CLE2	$e^+e^- \approx$ 10.5 GeV

[2] AALTONEN 11H treats the three charged modes $\Lambda_c(2595)^+ \to \Sigma_c(2455)^{++}\pi^-$, $\Sigma_c(2455)^+\pi^0$, $\Sigma_c(2455)^0\pi^+$ separately in terms of a common coupling constant h_2 and obtains $h_2^2 = 0.36 \pm 0.08$. From this the width is determined.

Baryon Particle Listings

$\Lambda_c(2595)^+$, $\Lambda_c(2625)^+$

$\Lambda_c(2595)^+$ DECAY MODES

$\Lambda_c^+\pi\pi$ and its submode $\Sigma_c(2455)\pi$ — the latter just barely — are the only strong decays allowed to an excited Λ_c^+ having this mass; and the submode seems to dominate.

	Mode	Fraction (Γ_i/Γ)
Γ_1	$\Lambda_c^+\pi^+\pi^-$	[a] —
Γ_2	$\Sigma_c(2455)^{++}\pi^-$	24 ± 7 %
Γ_3	$\Sigma_c(2455)^0\pi^+$	24 ± 7 %
Γ_4	$\Lambda_c^+\pi^+\pi^-$ 3-body	18 ± 10 %
Γ_5	$\Lambda_c^+\pi^0$	[b] not seen
Γ_6	$\Lambda_c^+\gamma$	not seen

[a] See AALTONEN 11H, Fig. 8, for the calculated ratio of $\Lambda_c^+\pi^0\pi^0$ and $\Lambda_c^+\pi^+\pi^-$ partial widths as a function of the $\Lambda_c(2595)^+ - \Lambda_c^+$ mass difference. At our value of the mass difference, the ratio is about 4.

[b] A test that the isospin is indeed 0, so that the particle is indeed a Λ_c^+.

$\Lambda_c(2595)^+$ BRANCHING RATIOS

$\Gamma(\Sigma_c(2455)^{++}\pi^-)/\Gamma(\Lambda_c^+\pi^+\pi^-)$ Γ_2/Γ_1

VALUE	DOCUMENT ID		TECN	COMMENT
0.36±0.10 OUR AVERAGE				
0.37±0.12±0.13	ALBRECHT	97	ARG	$e^+e^-\approx$ 10 GeV
0.36±0.09±0.09	EDWARDS	95	CLE2	$e^+e^-\approx$ 10.5 GeV

$\Gamma(\Sigma_c(2455)^0\pi^+)/\Gamma(\Lambda_c^+\pi^+\pi^-)$ Γ_3/Γ_1

VALUE	DOCUMENT ID		TECN	COMMENT
0.37±0.10 OUR AVERAGE				
0.29±0.10±0.11	ALBRECHT	97	ARG	$e^+e^-\approx$ 10 GeV
0.42±0.09±0.09	EDWARDS	95	CLE2	$e^+e^-\approx$ 10.5 GeV

$[\Gamma(\Sigma_c(2455)^{++}\pi^-)+\Gamma(\Sigma_c(2455)^0\pi^+)]/\Gamma(\Lambda_c^+\pi^+\pi^-)$ $(\Gamma_2+\Gamma_3)/\Gamma_1$

VALUE	CL%	DOCUMENT ID		TECN	COMMENT
• • • We do not use the following data for averages, fits, limits, etc. • • •					
$0.66^{+0.13}_{-0.16}\pm0.07$		ALBRECHT	97	ARG	$e^+e^-\approx$ 10 GeV
>0.51	90	[3] FRABETTI	96	E687	γBe, $\overline{E}_\gamma\approx$ 220 GeV

[3] The results of FRABETTI 96 are consistent with this ratio being 100%.

$\Gamma(\Lambda_c^+\pi^0)/\Gamma(\Lambda_c^+\pi^+\pi^-)$ Γ_5/Γ_1

$\Lambda_c^+\pi^0$ decay is forbidden by isospin conservation if this state is in fact a Λ_c.

VALUE	CL%	DOCUMENT ID		TECN	COMMENT
<3.53	90	EDWARDS	95	CLE2	$e^+e^-\approx$ 10.5 GeV

$\Gamma(\Lambda_c^+\gamma)/\Gamma(\Lambda_c^+\pi^+\pi^-)$ Γ_6/Γ_1

VALUE	CL%	DOCUMENT ID		TECN	COMMENT
<0.98	90	EDWARDS	95	CLE2	$e^+e^-\approx$ 10.5 GeV

$\Lambda_c(2595)^+$ REFERENCES

AALTONEN	11H	PR D84 012003	T. Aaltonen *et al.*	(CDF Collab.)
BLECHMAN	03	PR D67 074033	A.E. Blechman *et al.*	(JHU, FLOR)
ALBRECHT	97	PL B402 207	H. Albrecht *et al.*	(ARGUS Collab.)
FRABETTI	96	PL B365 461	P.L. Frabetti *et al.*	(FNAL E687 Collab.)
EDWARDS	95	PRL 74 3331	K.W. Edwards *et al.*	(CLEO Collab.)

$\Lambda_c(2625)^+$

$I(J^P) = 0(\frac{3}{2}^-)$ Status: ***

The spin-parity has not been measured but is expected to be $3/2^-$: this is presumably the charm counterpart of the strange $\Lambda(1520)$.

$\Lambda_c(2625)^+$ MASS

The mass is obtained from the $\Lambda_c(2625)^+$–Λ_c^+ mass-difference measurements below.

VALUE (MeV)	EVTS	DOCUMENT ID		TECN	COMMENT
2628.11±0.19 OUR FIT Error includes scale factor of 1.1.					
• • • We do not use the following data for averages, fits, limits, etc. • • •					
2626.6 ±0.5 ±1.5	42 ± 9	ALBRECHT	93F	ARG	See ALBRECHT 97

$\Lambda_c(2625)^+ - \Lambda_c^+$ MASS DIFFERENCE

VALUE (MeV)	EVTS	DOCUMENT ID		TECN	COMMENT
341.65±0.13 OUR FIT Error includes scale factor of 1.1.					
341.65±0.15 OUR AVERAGE Error includes scale factor of 1.3. See the ideogram below.					
341.65±0.04±0.12	6.2k	AALTONEN	11H	CDF	$p\overline{p}$ at 1.96 TeV
342.1 ±0.5 ±0.5	51	ALBRECHT	97	ARG	$e^+e^-\approx$ 10 GeV
342.2 ±0.2 ±0.5	245 ± 19	EDWARDS	95	CLE2	$e^+e^-\approx$ 10.5 GeV
340.4 ±0.6 ±0.3	40 ± 9	FRABETTI	94	E687	γBe, $\overline{E}_\gamma$ = 220 GeV

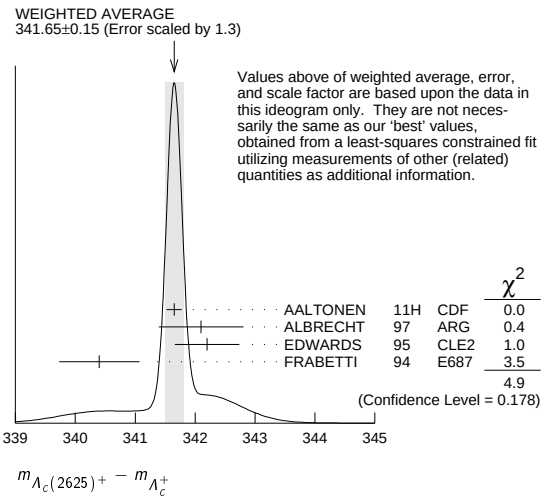

$\Lambda_c(2625)^+$ WIDTH

VALUE (MeV)	CL%	EVTS	DOCUMENT ID		TECN	COMMENT
<0.97	90	6.2k	AALTONEN	11H	CDF	$p\overline{p}$ at 1.96 TeV
• • • We do not use the following data for averages, fits, limits, etc. • • •						
<1.9	90	245 ± 19	EDWARDS	95	CLE2	$e^+e^-\approx$ 10.5 GeV
<3.2	90		ALBRECHT	93F	ARG	$e^+e^-\approx\Upsilon(4S)$

$\Lambda_c(2625)^+$ DECAY MODES

$\Lambda_c^+\pi\pi$ and its submode $\Sigma(2455)\pi$ are the only strong decays allowed to an excited Λ_c^+ having this mass.

	Mode		Fraction (Γ_i/Γ)	Confidence level
Γ_1	$\Lambda_c^+\pi^+\pi^-$		≈ 67%	
Γ_2	$\Sigma_c(2455)^{++}\pi^-$		<5	90%
Γ_3	$\Sigma_c(2455)^0\pi^+$		<5	90%
Γ_4	$\Lambda_c^+\pi^+\pi^-$ 3-body		large	
Γ_5	$\Lambda_c^+\pi^0$	[a]	not seen	
Γ_6	$\Lambda_c^+\gamma$		not seen	

[a] A test that the isospin is indeed 0, so that the particle is indeed a Λ_c^+.

$\Lambda_c(2625)^+$ BRANCHING RATIOS

$\Gamma(\Sigma_c(2455)^{++}\pi^-)/\Gamma(\Lambda_c^+\pi^+\pi^-)$ Γ_2/Γ_1

VALUE	CL%	DOCUMENT ID		TECN	COMMENT
<0.08	90	EDWARDS	95	CLE2	$e^+e^-\approx$ 10.5 GeV

$\Gamma(\Sigma_c(2455)^0\pi^+)/\Gamma(\Lambda_c^+\pi^+\pi^-)$ Γ_3/Γ_1

VALUE	CL%	DOCUMENT ID		TECN	COMMENT
<0.07	90	EDWARDS	95	CLE2	$e^+e^-\approx$ 10.5 GeV

$[\Gamma(\Sigma_c(2455)^{++}\pi^-)+\Gamma(\Sigma_c(2455)^0\pi^+)]/\Gamma(\Lambda_c^+\pi^+\pi^-)$ $(\Gamma_2+\Gamma_3)/\Gamma_1$

VALUE	CL%	EVTS	DOCUMENT ID		TECN	COMMENT
• • • We do not use the following data for averages, fits, limits, etc. • • •						
<0.36	90		FRABETTI	94	E687	γBe, $\overline{E}_\gamma$ = 220 GeV
0.46±0.14		21	ALBRECHT	93F	ARG	$e^+e^-\approx\Upsilon(4S)$

$\Gamma(\Lambda_c^+\pi^+\pi^-$ 3-body$)/\Gamma(\Lambda_c^+\pi^+\pi^-)$ Γ_4/Γ_1

VALUE	EVTS	DOCUMENT ID		TECN	COMMENT
• • • We do not use the following data for averages, fits, limits, etc. • • •					
0.54±0.14	16	ALBRECHT	93F	ARG	$e^+e^-\approx\Upsilon(4S)$

$\Gamma(\Lambda_c^+\pi^0)/\Gamma(\Lambda_c^+\pi^+\pi^-)$ Γ_5/Γ_1

$\Lambda_c^+\pi^0$ decay is forbidden by isospin conservation if this state is in fact a Λ_c.

VALUE	CL%	DOCUMENT ID		TECN	COMMENT
<0.91	90	EDWARDS	95	CLE2	$e^+e^-\approx$ 10.5 GeV

$\Gamma(\Lambda_c^+\gamma)/\Gamma(\Lambda_c^+\pi^+\pi^-)$ Γ_6/Γ_1

VALUE	CL%	DOCUMENT ID		TECN	COMMENT
<0.52	90	EDWARDS	95	CLE2	$e^+e^-\approx$ 10.5 GeV

$\Lambda_c(2625)^+$ REFERENCES

AALTONEN	11H	PR D84 012003	T. Aaltonen *et al.*	(CDF Collab.)
ALBRECHT	97	PL B402 207	H. Albrecht *et al.*	(ARGUS Collab.)
EDWARDS	95	PRL 74 3331	K.W. Edwards *et al.*	(CLEO Collab.)
FRABETTI	94	PRL 72 961	P.L. Frabetti *et al.*	(FNAL E687 Collab.)
ALBRECHT	93F	PL B317 227	H. Albrecht *et al.*	(ARGUS Collab.)

$\Lambda_c(2765)^+$ or $\Sigma_c(2765)$

$I(J^P) = ?(?^?)$ Status: *

OMITTED FROM SUMMARY TABLE

A broad, statistically significant peak (997^{+141}_{-129} events) seen in $\Lambda_c^+\pi^+\pi^-$. However, nothing at all is known about its quantum numbers, including whether it is a Λ_c^+ or a Σ_c, or whether the width might be due to overlapping states.

$\Lambda_c(2765)^+$ MASS

The mass is obtained from the $\Lambda_c(2765)^+ - \Lambda_c^+$ mass-difference measurement below.

VALUE (MeV)	DOCUMENT ID
2766.6±2.4 OUR FIT	

$\Lambda_c(2765)^+ - \Lambda_c^+$ MASS DIFFERENCE

VALUE (MeV)	EVTS	DOCUMENT ID		TECN	COMMENT
480.1±2.4 OUR FIT					
480.1±2.4	997^{+141}_{-129}	ARTUSO	01	CLE2	$e^+e^-\approx \Upsilon(4S)$

$\Lambda_c(2765)^+$ WIDTH

VALUE (MeV)	DOCUMENT ID		TECN	COMMENT
50	ARTUSO	01	CLE2	$e^+e^-\approx \Upsilon(4S)$

$\Lambda_c(2765)^+$ DECAY MODES

	Mode	Fraction (Γ_i/Γ)
Γ_1	$\Lambda_c^+\pi^+\pi^-$	seen

$\Lambda_c(2765)^+$ REFERENCES

ARTUSO	01	PRL 86 4479	M. Artuso *et al.*	(CLEO Collab.)

$\Lambda_c(2860)^+$

$I(J^P) = 0(\frac{3}{2}^+)$ Status: ***

$\Lambda_c(2860)^+$ MASS

VALUE (MeV)	DOCUMENT ID		TECN	COMMENT
$2856.1^{+2.0}_{-1.7}\pm0.5^{+1.1}_{-5.6}$	[1] AAIJ	17S	LHCB	in $\Lambda_b^0\to D^0p\pi^-$

[1] The third AAIJ 17S uncertainty comes from modeling the resonant shape of the nearby $\Lambda_c(2880)^+$ and the background (non-resonant) amplitudes.

$\Lambda_c(2860)^+$ WIDTH

VALUE (MeV)	DOCUMENT ID		TECN	COMMENT
$67.6^{+10.1}_{-8.1}\pm1.4^{+5.9}_{-20.0}$	[1] AAIJ	17S	LHCB	in $\Lambda_b^0\to D^0p\pi^-$

[1] The third AAIJ 17S uncertainty comes from modeling the resonant shape of the nearby $\Lambda_c(2880)^+$ and the background (non-resonant) amplitudes.

$\Lambda_c(2860)^+$ DECAY MODES

	Mode	Fraction (Γ_i/Γ)
Γ_1	D^0p	seen

$\Lambda_c(2860)^+$ BRANCHING RATIOS

$\Gamma(D^0p)/\Gamma_{total}$ Γ_1/Γ

VALUE	DOCUMENT ID		TECN	COMMENT
seen	AAIJ	17S	LHCB	in $\Lambda_b^0\to D^0p\pi^-$

$\Lambda_c(2860)^+$ REFERENCES

AAIJ	17S	JHEP 1705 030	R. Aaij *et al.*	(LHCb Collab.) JP

$\Lambda_c(2880)^+$

$I(J^P) = 0(\frac{5}{2}^+)$ Status: ***

A narrow peak seen in $\Lambda_c^+\pi^+\pi^-$ and in pD^0. It is not seen in pD^+, and therefore it is a Λ_c^+ and not a Σ_c.

$\Lambda_c(2880)^+$ MASS

VALUE (MeV)	EVTS	DOCUMENT ID		TECN	COMMENT
2881.63±0.24 OUR FIT					
2881.62±0.24 OUR AVERAGE					
$2881.75\pm0.29\pm0.07^{+0.14}_{-0.20}$		[1] AAIJ	17S	LHCB	in $\Lambda_b^0\to D^0p\pi^-$
2881.9 ±0.1 ±0.5	2.8k	AUBERT	07	BABR	in pD^0
2881.2 ±0.2 ±0.4	690	MIZUK	07	BELL	in $\Sigma_c(2455)^{0,++}\pi^\pm$

[1] The third AAIJ 17S uncertainty comes from modeling the resonant shape of the $\Lambda_c(2880)^+$ and the background (non-resonant) amplitudes.

$\Lambda_c(2880)^+ - \Lambda_c^+$ MASS DIFFERENCE

VALUE (MeV)	EVTS	DOCUMENT ID		TECN	COMMENT
595.17±0.28 OUR FIT					
596 ±1 ±2	350	ARTUSO	01	CLE2	in $\Lambda_c^+\pi^+\pi^-$

$\Lambda_c(2880)^+$ WIDTH

VALUE (MeV)	CL%	EVTS	DOCUMENT ID		TECN	COMMENT
$\mathbf{5.6\ ^{+0.8}_{-0.6}}$ **OUR AVERAGE**						
$5.43^{+0.77}_{-0.71}\pm0.81\ -0.29$			[2] AAIJ	17S	LHCB	in $\Lambda_b^0\to D^0p\pi^-$
5.8 ±1.5 ±1.1		2.8k	AUBERT	07	BABR	in pD^0
5.8 ±0.7 ±1.1		690	MIZUK	07	BELL	in $\Sigma_c(2455)^{0,++}\pi^\pm$
• • • We do not use the following data for averages, fits, limits, etc. • • •						
<8	90		ARTUSO	01	CLEO	in $\Lambda_c^+\pi^+\pi^-$

[2] AAIJ 17S reports $5.43^{+0.77}_{-0.71}\pm0.29^{+0.75}_{-0.00}$ MeV value where the third uncertainty comes from modeling the resonant shape of the $\Lambda_c(2880)^+$ and the background (non-resonant) amplitudes. We have combined in quadrature the systematic uncertainties.

$\Lambda_c(2880)^+$ DECAY MODES

	Mode	Fraction (Γ_i/Γ)
Γ_1	$\Lambda_c^+\pi^+\pi^-$	seen
Γ_2	$\Sigma_c(2455)^{0,++}\pi^\pm$	seen
Γ_3	$\Sigma_c(2520)^{0,++}\pi^\pm$	seen
Γ_4	pD^0	seen

$\Lambda_c(2880)^+$ BRANCHING RATIOS

$\Gamma(\Sigma_c(2455)^{0,++}\pi^\pm)/\Gamma(\Lambda_c^+\pi^+\pi^-)$ Γ_2/Γ_1

VALUE	EVTS	DOCUMENT ID		TECN	COMMENT
0.392±0.031 OUR AVERAGE		Error includes scale factor of 1.3.			
0.404±0.021±0.014		MIZUK	07	BELL	in $\Sigma_c(2455)^{0,++}\pi^\pm$
0.31 ±0.06 ±0.03	96	ARTUSO	01	CLE2	$e^+e^-\approx \Upsilon(4S)$

$\Gamma(\Sigma_c(2520)^{0,++}\pi^\pm)/\Gamma(\Lambda_c^+\pi^+\pi^-)$ Γ_3/Γ_1

VALUE	CL%	DOCUMENT ID		TECN	COMMENT
0.091±0.025±0.010		MIZUK	07	BELL	in $\Sigma_c(2455)^{0,++}\pi^\pm$
• • • We do not use the following data for averages, fits, limits, etc. • • •					
<0.11	90	ARTUSO	01	CLE2	$e^+e^-\approx \Upsilon(4S)$

$\Gamma(\Sigma_c(2520)^{0,++}\pi^{\pm})/\Gamma(\Sigma_c(2455)^{0,++}\pi^{\pm})$ Γ_3/Γ_2

VALUE	DOCUMENT ID		TECN	COMMENT
• • • We do not use the following data for averages, fits, limits, etc. • • •				
$0.225 \pm 0.062 \pm 0.025$	[3] MIZUK	07	BELL	in $\Sigma_c(2455)^{0,++}\pi^{\pm}$

[3] This MIZUK 07 ratio is redundant with MIZUK 07 ratios given above.

$\Lambda_c(2880)^+$ REFERENCES

AAIJ	17S	JHEP 1705 030	R. Aaij *et al.*	(LHCb Collab.) JP
AUBERT	07	PRL 98 012001	B. Aubert *et al.*	(BABAR Collab.)
MIZUK	07	PRL 98 262001	R. Mizuk *et al.*	(BELLE Collab.)
ARTUSO	01	PRL 86 4479	M. Artuso *et al.*	(CLEO Collab.)

$\Lambda_c(2940)^+$

$I(J^P) = 0(\frac{3}{2}^-)$ Status: ***

A narrow peak seen in pD^0 and in $\Lambda_c^+\pi^+\pi^-$. It is not seen in pD^+, and therefore it is a Λ_c^+ and not a Σ_c. $J^P = 3/2^-$ is favored, but not certain.

$\Lambda_c(2940)^+$ MASS

VALUE (MeV)	EVTS	DOCUMENT ID		TECN	COMMENT
$2939.6^{+1.3}_{-1.5}$ OUR AVERAGE					
$2944.8^{+3.5}_{-2.5} \pm 0.4^{+0.1}_{-4.6}$		[1] AAIJ	17S	LHCB	in $\Lambda_b^0 \to D^0 p\pi^-$
$2939.8 \pm 1.3 \pm 1.0$	2.2k	AUBERT	07	BABR	in pD^0
$2938.0 \pm 1.3^{+2.0}_{-4.0}$	220	MIZUK	07	BELL	in $\Sigma_c(2455)^{0,++}\pi^{\pm}$

[1] The third AAIJ 17S uncertainty comes from modeling the resonant shape of the nearby $\Lambda_c(2880)^+$ and the background (non-resonant) amplitudes.

$\Lambda_c(2940)^+$ WIDTH

VALUE (MeV)	EVTS	DOCUMENT ID		TECN	COMMENT
20^{+6}_{-5} OUR AVERAGE					
$27.7^{+8.2}_{-6.0} \pm 0.9^{+5.2}_{-10.4}$		[2] AAIJ	17S	LHCB	in $\Lambda_b^0 \to D^0 p\pi^-$
$17.5 \pm 5.2 \pm 5.9$	2.2k	AUBERT	07	BABR	in pD^0
$13^{+8}_{-5}{}^{+27}_{-7}$	220	MIZUK	07	BELL	in $\Sigma_c(2455)^{0,++}\pi^{\pm}$

[2] The third AAIJ 17S uncertainty comes from modeling the resonant shape of the nearby $\Lambda_c(2880)^+$ and the background (non-resonant) amplitudes.

$\Lambda_c(2940)^+$ DECAY MODES

	Mode	Fraction (Γ_i/Γ)
Γ_1	pD^0	seen
Γ_2	$\Sigma_c(2455)^{0,++}\pi^{\pm}$	seen

$\Lambda_c(2940)^+$ REFERENCES

AAIJ	17S	JHEP 1705 030	R. Aaij *et al.*	(LHCb Collab.) JP
AUBERT	07	PRL 98 012001	B. Aubert *et al.*	(BABAR Collab.)
MIZUK	07	PRL 98 262001	R. Mizuk *et al.*	(BELLE Collab.)

$\Sigma_c(2455)$

$I(J^P) = 1(\frac{1}{2}^+)$ Status: ****

The angular distribution of $B^- \to \Sigma_c(2455)^0\overline{p}$ favors $J = 1/2$ (as the quark model predicts). $J = 3/2$ is excluded by more than four σ see AUBERT 08BN.

$\Sigma_c(2455)$ MASSES

The masses are obtained from the mass-difference measurements that follow.

$\Sigma_c(2455)^{++}$ MASS

VALUE (MeV)	DOCUMENT ID
2453.97 ± 0.14 OUR FIT	

$\Sigma_c(2455)^+$ MASS

VALUE (MeV)	DOCUMENT ID
2452.9 ± 0.4 OUR FIT	

$\Sigma_c(2455)^0$ MASS

VALUE (MeV)	DOCUMENT ID
2453.75 ± 0.14 OUR FIT	

$\Sigma_c(2455) - \Lambda_c^+$ MASS DIFFERENCES

$m_{\Sigma_c^{++}} - m_{\Lambda_c^+}$

VALUE (MeV)	EVTS	DOCUMENT ID		TECN	COMMENT
167.510 ± 0.017 OUR FIT					
167.510 ± 0.022 OUR AVERAGE					
$167.51 \pm 0.01 \pm 0.02$	36k	LEE	14	BELL	e^+e^- at $\Upsilon(4S)$
$167.44 \pm 0.04 \pm 0.12$	13.8k	AALTONEN	11H	CDF	$p\overline{p}$ at 1.96 TeV
$167.4 \pm 0.1 \pm 0.2$	2k	ARTUSO	02	CLE2	$e^+e^- \approx \Upsilon(4S)$
$167.35 \pm 0.19 \pm 0.12$	461	LINK	00C	FOCS	γ A, $\overline{E}_\gamma$ 180 GeV
$167.76 \pm 0.29 \pm 0.15$	122	AITALA	96B	E791	π^- N, 500 GeV
$167.6 \pm 0.6 \pm 0.6$	56	FRABETTI	96	E687	γBe, $\overline{E}_\gamma \approx$ 220 GeV
$168.2 \pm 0.3 \pm 0.2$	126	CRAWFORD	93	CLE2	$e^+e^- \approx \Upsilon(4S)$
$167.8 \pm 0.4 \pm 0.3$	54	BOWCOCK	89	CLEO	e^+e^- 10 GeV
$168.2 \pm 0.5 \pm 1.6$	92	ALBRECHT	88D	ARG	e^+e^- 10 GeV
$167.4 \pm 0.5 \pm 2.0$	46	DIESBURG	87	SPEC	nA $\sim$ 600 GeV
• • • We do not use the following data for averages, fits, limits, etc. • • •					
167 ± 1	2	JONES	87	HBC	νp in BEBC
166 ± 1	1	BOSETTI	82	HBC	See JONES 87
168 ± 3	6	BALTAY	79	HLBC	ν Ne-H in 15-ft
166 ± 15	1	CAZZOLI	75	HBC	νp in BNL 7-ft

$m_{\Sigma_c^+} - m_{\Lambda_c^+}$

VALUE (MeV)	EVTS	DOCUMENT ID		TECN	COMMENT
166.4 ± 0.4 OUR FIT					
166.4 ± 0.2 ± 0.3	661	AMMAR	01	CLE2	$e^+e^- \approx \Upsilon(4S)$
• • • We do not use the following data for averages, fits, limits, etc. • • •					
$168.5 \pm 0.4 \pm 0.2$	111	CRAWFORD	93	CLE2	See AMMAR 01
168 ± 3	1	CALICCHIO	80	HBC	νp in BEBC-TST

$m_{\Sigma_c^0} - m_{\Lambda_c^+}$

VALUE (MeV)	EVTS	DOCUMENT ID		TECN	COMMENT
167.290 ± 0.017 OUR FIT					
167.290 ± 0.022 OUR AVERAGE					
$167.29 \pm 0.01 \pm 0.02$	32k	LEE	14	BELL	e^+e^- at $\Upsilon(4S)$
$167.28 \pm 0.03 \pm 0.12$	15.9k	AALTONEN	11H	CDF	$p\overline{p}$ at 1.96 TeV
$167.2 \pm 0.1 \pm 0.2$	2k	ARTUSO	02	CLE2	$e^+e^- \approx \Upsilon(4S)$
$167.38 \pm 0.21 \pm 0.13$	362	LINK	00C	FOCS	γ A, $\overline{E}_\gamma$ 180 GeV
$167.38 \pm 0.29 \pm 0.15$	143	AITALA	96B	E791	π^- N, 500 GeV
$167.8 \pm 0.6 \pm 0.2$		ALEEV	96	SPEC	n nucleus, 50 GeV/c
$166.6 \pm 0.5 \pm 0.6$	69	FRABETTI	96	E687	γBe, $\overline{E}_\gamma \approx$ 220 GeV
$167.1 \pm 0.3 \pm 0.2$	124	CRAWFORD	93	CLE2	$e^+e^- \approx \Upsilon(4S)$
$168.4 \pm 1.0 \pm 0.3$	14	ANJOS	89D	E691	γBe 90–260 GeV
• • • We do not use the following data for averages, fits, limits, etc. • • •					
$167.9 \pm 0.5 \pm 0.3$	48	[1] BOWCOCK	89	CLEO	e^+e^- 10 GeV
$167.0 \pm 0.5 \pm 1.6$	70	[1] ALBRECHT	88D	ARG	e^+e^- 10 GeV
$178.2 \pm 0.4 \pm 2.0$	85	[2] DIESBURG	87	SPEC	nA $\sim$ 600 GeV
163 ± 2	1	AMMAR	86	EMUL	νA

[1] This result enters the fit through $m_{\Sigma_c^{++}} - m_{\Sigma_c^0}$ given below.

[2] See the note on DIESBURG 87 in the $m_{\Sigma_c^{++}} - m_{\Sigma_c^0}$ section below.

$\Sigma_c(2455)$ MASS DIFFERENCES

$m_{\Sigma_c^{++}} - m_{\Sigma_c^0}$

VALUE (MeV)	DOCUMENT ID		TECN	COMMENT
0.220 ± 0.013 OUR FIT				
0.221 ± 0.014 OUR AVERAGE				
$0.22 \pm 0.01 \pm 0.01$	LEE	14	BELL	e^+e^- at $\Upsilon(4S)$
$0.2 \pm 0.1 \pm 0.1$	ARTUSO	02	CLE2	$e^+e^- \approx \Upsilon(4S)$
$-0.03 \pm 0.28 \pm 0.11$	LINK	00C	FOCS	γ A, $\overline{E}_\gamma$ 180 GeV
$0.38 \pm 0.40 \pm 0.15$	AITALA	96B	E791	π^- N, 500 GeV
$1.1 \pm 0.4 \pm 0.1$	CRAWFORD	93	CLE2	$e^+e^- \approx \Upsilon(4S)$
$-0.1 \pm 0.6 \pm 0.1$	BOWCOCK	89	CLEO	e^+e^- 10 GeV
$1.2 \pm 0.7 \pm 0.3$	ALBRECHT	88D	ARG	e^+e^- $\sim$ 10 GeV
• • • We do not use the following data for averages, fits, limits, etc. • • •				
-10.8 ± 2.9	[3] DIESBURG	87	SPEC	nA $\sim$ 600 GeV

[3] DIESBURG 87 is completely incompatible with the other experiments, which is surprising since it agrees with them about $m_{\Sigma_c(2455)^{++}} - m_{\Lambda_c^+}$. We go with the majority here.

$m_{\Sigma_c^+} - m_{\Sigma_c^0}$

VALUE (MeV)	DOCUMENT ID		TECN	COMMENT
−0.9 ± 0.4 OUR FIT				
• • • We do not use the following data for averages, fits, limits, etc. • • •				
$1.4 \pm 0.5 \pm 0.3$	CRAWFORD	93	CLE2	See AMMAR 01

$\Sigma_c(2455)$ WIDTHS

$\Sigma_c(2455)^{++}$ WIDTH

VALUE (MeV)	EVTS	DOCUMENT ID		TECN	COMMENT
$1.89^{+0.09}_{-0.18}$ OUR AVERAGE		Error includes scale factor of 1.1.			
$1.84 \pm 0.04^{+0.07}_{-0.20}$	36k	LEE	14	BELL	e^+e^- at $\Upsilon(4S)$
$2.34 \pm 0.13 \pm 0.45$	13.8k	AALTONEN	11H	CDF	$p\overline{p}$ at 1.96 TeV
$2.3 \pm 0.2 \pm 0.3$	2k	ARTUSO	02	CLE2	$e^+e^- \approx \Upsilon(4S)$
$2.05^{+0.41}_{-0.38} \pm 0.38$	1110	LINK	02	FOCS	γ A, $\overline{E}_\gamma \approx 180$ GeV

$\Sigma_c(2455)^{+}$ WIDTH

VALUE (MeV)	CL%	EVTS	DOCUMENT ID		TECN	COMMENT
<4.6	90	661	AMMAR	01	CLE2	$e^+e^- \approx \Upsilon(4S)$

$\Sigma_c(2455)^{0}$ WIDTH

VALUE (MeV)	EVTS	DOCUMENT ID		TECN	COMMENT
$1.83^{+0.11}_{-0.19}$ OUR AVERAGE		Error includes scale factor of 1.2.			
$1.76 \pm 0.04^{+0.09}_{-0.21}$	32k	LEE	14	BELL	e^+e^- at $\Upsilon(4S)$
$1.65 \pm 0.11 \pm 0.49$	15.9k	AALTONEN	11H	CDF	$p\overline{p}$ at 1.96 TeV
$2.6 \pm 0.5 \pm 0.3$		AUBERT	08BN	BABR	$B^- \to \overline{p}\Lambda_c^+\pi^-$
$2.5 \pm 0.2 \pm 0.3$	2k	ARTUSO	02	CLE2	$e^+e^- \approx \Upsilon(4S)$
$1.55^{+0.41}_{-0.37} \pm 0.38$	913	LINK	02	FOCS	γ A, $\overline{E}_\gamma \approx 180$ GeV

$\Sigma_c(2455)$ DECAY MODES

$\Lambda_c^+\pi$ is the only strong decay allowed to a Σ_c having this mass.

	Mode	Fraction (Γ_i/Γ)
Γ_1	$\Lambda_c^+\pi$	≈ 100 %

$\Sigma_c(2455)$ REFERENCES

LEE	14	PR D89 091102	S.-H. Lee *et al.*	(BELLE Collab.)
AALTONEN	11H	PR D84 012003	T. Aaltonen *et al.*	(CDF Collab.)
AUBERT	08BN	PR D78 112003	B. Aubert *et al.*	(BABAR Collab.)
ARTUSO	02	PR D65 071101	M. Artuso *et al.*	(CLEO Collab.)
LINK	02	PL B525 205	J.M. Link *et al.*	(FNAL FOCUS Collab.)
AMMAR	01	PRL 86 1167	R. Ammar *et al.*	(CLEO Collab.)
LINK	00C	PL B488 218	J.M. Link *et al.*	(FNAL FOCUS Collab.)
AITALA	96B	PL B379 292	E.M. Aitala *et al.*	(FNAL E791 Collab.)
ALEEV	96	JINRRC 3-77 31	A.N. Aleev *et al.*	(Serpukhov EXCHARM Collab.)
FRABETTI	96	PL B365 461	P.L. Frabetti *et al.*	(FNAL E687 Collab.)
CRAWFORD	93	PRL 71 3259	G. Crawford *et al.*	(CLEO Collab.)
ANJOS	89D	PRL 62 1721	J.C. Anjos *et al.*	(FNAL E691 Collab.)
BOWCOCK	89	PRL 62 1240	T.J.V. Bowcock *et al.*	(CLEO Collab.)
ALBRECHT	88D	PL B211 489	H. Albrecht *et al.*	(ARGUS Collab.)
DIESBURG	87	PRL 59 2711	M. Diesburg *et al.*	(FNAL E400 Collab.)
JONES	87	ZPHY C36 593	G.T. Jones *et al.*	(CERN WA21 Collab.)
AMMAR	86	JETPL 43 515	R. Ammar *et al.*	(ITEP)
		Translated from ZETFP 43 401.		
BOSETTI	82	PL 109B 234	P.C. Bosetti *et al.*	(AACH3, BONN, CERN+)
CALICCHIO	80	PL 93B 521	M. Calicchio *et al.*	(BARI, BIRM, BRUX+)
BALTAY	79	PRL 42 1721	C. Baltay *et al.*	(COLU, BNL) I
CAZZOLI	75	PRL 34 1125	E.G. Cazzoli *et al.*	(BNL)

$\Sigma_c(2520)$

$I(J^P) = 1(\frac{3}{2}^+)$ Status: ***

Seen in the $\Lambda_c^+\pi^\pm$ mass spectrum. The natural assignment is that this is the $J^P = 3/2^+$ excitation of the $\Sigma_c(2455)$, the charm counterpart of the $\Sigma(1385)$, but neither J nor P has been measured.

$\Sigma_c(2520)$ MASSES

The masses are obtained from the mass-difference measurements that follow.

$\Sigma_c(2520)^{++}$ MASS

VALUE (MeV)	EVTS	DOCUMENT ID		TECN	COMMENT
$2518.41^{+0.21}_{-0.19}$ OUR FIT		Error includes scale factor of 1.1.			
• • • We do not use the following data for averages, fits, limits, etc. • • •					
2530 ± 5 ± 5	6	[1] AMMOSOV	93	HLBC	$\nu p \to \mu^- \Sigma_c(2530)^{++}$

[1] AMMOSOV 93 sees a cluster of 6 events and estimates the background to be 1 event.

$\Sigma_c(2520)^{+}$ MASS

VALUE (MeV)	DOCUMENT ID
2517.5 $\pm$ 2.3 OUR FIT	

$\Sigma_c(2520)^{0}$ MASS

VALUE (MeV)	DOCUMENT ID
2518.48 $\pm$ 0.20 OUR FIT Error includes scale factor of 1.1.	

$\Sigma_c(2520)$ MASS DIFFERENCES

$m_{\Sigma_c(2520)^{++}} - m_{\Lambda_c^+}$

VALUE (MeV)	EVTS	DOCUMENT ID		TECN	COMMENT
$231.95^{+0.17}_{-0.12}$ OUR FIT		Error includes scale factor of 1.3.			
231.95 $\pm$ 0.16 OUR AVERAGE		Error includes scale factor of 1.6. See the ideogram below.			
$231.99 \pm 0.10 \pm 0.02$	44k	LEE	14	BELL	e^+e^- at $\Upsilon(4S)$
$230.73 \pm 0.56 \pm 0.16$	8.8k	AALTONEN	11H	CDF	$p\overline{p}$ at 1.96 TeV
$231.5 \pm 0.4 \pm 0.3$	1.3k	ATHAR	05	CLEO	e^+e^-, 9.4–11.5 GeV
$234.5 \pm 1.1 \pm 0.8$	677	BRANDENB...	97	CLE2	$e^+e^- \approx \Upsilon(4S)$

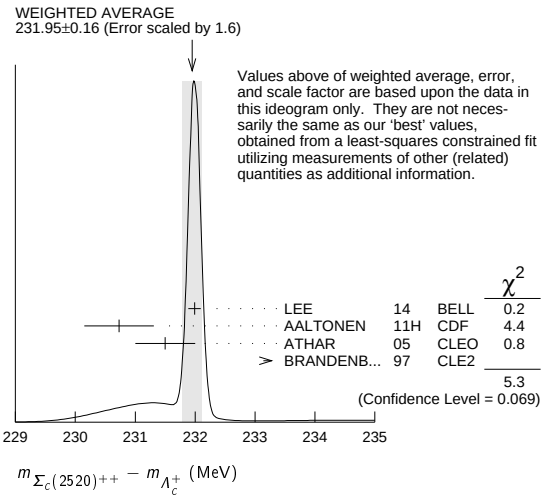

$m_{\Sigma_c(2520)^{+}} - m_{\Lambda_c^+}$

VALUE (MeV)	EVTS	DOCUMENT ID		TECN	COMMENT
231.0 $\pm$ 2.3 OUR FIT					
231.0 $\pm$ 1.1 $\pm$ 2.0	327	AMMAR	01	CLE2	$e^+e^- \approx \Upsilon(4S)$

$m_{\Sigma_c(2520)^{0}} - m_{\Lambda_c^+}$

VALUE (MeV)	EVTS	DOCUMENT ID		TECN	COMMENT
$232.02^{+0.15}_{-0.14}$ OUR FIT		Error includes scale factor of 1.3.			
232.02 $\pm$ 0.17 OUR AVERAGE		Error includes scale factor of 1.5. See the ideogram below.			
$231.98 \pm 0.11 \pm 0.04$	41k	LEE	14	BELL	e^+e^- at $\Upsilon(4S)$
$232.88 \pm 0.43 \pm 0.16$	9.0k	AALTONEN	11H	CDF	$p\overline{p}$ at 1.96 TeV
$231.4 \pm 0.5 \pm 0.3$	1.3k	ATHAR	05	CLEO	e^+e^-, 9.4–11.5 GeV
$232.6 \pm 1.0 \pm 0.8$	504	BRANDENB...	97	CLE2	$e^+e^- \approx \Upsilon(4S)$

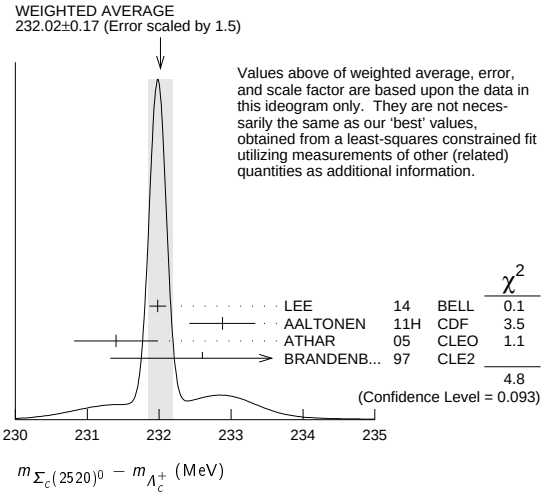

$m_{\Sigma_c(2520)^{++}} - m_{\Sigma_c(2520)^{0}}$

VALUE (MeV)	EVTS	DOCUMENT ID		TECN	COMMENT
0.01 $\pm$ 0.15 $\pm$ 0.03	44/41k	LEE	14	BELL	e^+e^- at $\Upsilon(4S)$
• • • We do not use the following data for averages, fits, limits, etc. • • •					
0.1 ± 0.8 ± 0.3		[2] ATHAR	05	CLEO	e^+e^-, 9.4–11.5 GeV
1.9 ± 1.4 ± 1.0		[3] BRANDENB...	97	CLE2	$e^+e^- \approx \Upsilon(4S)$

[2] This ATHAR 05 result is redundant with measurements in earlier entries.
[3] This BRANDENBURG 97 result is redundant with measurements in earlier entries.

Baryon Particle Listings

$\Sigma_c(2520)$, $\Sigma_c(2800)$, Ξ_c^+

$\Sigma_c(2520)$ WIDTHS

$\Sigma_c(2520)^{++}$ WIDTH

VALUE (MeV)	EVTS	DOCUMENT ID		TECN	COMMENT
$14.78^{+0.30}_{-0.40}$ OUR AVERAGE					
$14.77 \pm 0.25^{+0.18}_{-0.30}$	44k	LEE	14	BELL	e^+e^- at $\Upsilon(4S)$
$15.03 \pm 2.12 \pm 1.36$	8.8k	AALTONEN	11H	CDF	$p\overline{p}$ at 1.96 TeV
$14.4\ ^{+1.6}_{-1.5} \pm 1.4$	1.3k	ATHAR	05	CLEO	e^+e^-, 9.4–11.5 GeV
$17.9\ ^{+3.8}_{-3.2} \pm 4.0$	677	BRANDENB...	97	CLE2	$e^+e^- \approx \Upsilon(4S)$

$\Sigma_c(2520)^+$ WIDTH

VALUE (MeV)	CL%	EVTS	DOCUMENT ID		TECN	COMMENT
<17	90	327	AMMAR	01	CLE2	$e^+e^- \approx \Upsilon(4S)$

$\Sigma_c(2520)^0$ WIDTH

VALUE (MeV)	EVTS	DOCUMENT ID		TECN	COMMENT
$15.3\ ^{+0.4}_{-0.5}$ OUR AVERAGE					
$15.41 \pm 0.41^{+0.20}_{-0.32}$	41k	LEE	14	BELL	e^+e^- at $\Upsilon(4S)$
$12.51 \pm 1.82 \pm 1.37$	9.0k	AALTONEN	11H	CDF	$p\overline{p}$ at 1.96 TeV
$16.6\ ^{+1.9}_{-1.7} \pm 1.4$	1.3k	ATHAR	05	CLEO	e^+e^-, 9.4–11.5 GeV
$13.0\ ^{+3.7}_{-3.0} \pm 4.0$	504	BRANDENB...	97	CLE2	$e^+e^- \approx \Upsilon(4S)$

$\Sigma_c(2520)$ DECAY MODES

$\Lambda_c^+\pi$ is the only strong decay allowed to a Σ_c having this mass.

	Mode	Fraction (Γ_i/Γ)
Γ_1	$\Lambda_c^+\pi$	≈ 100 %

$\Sigma_c(2520)$ REFERENCES

LEE	14	PR D89 091102	S.-H. Lee *et al.*	(BELLE Collab.)
AALTONEN	11H	PR D84 012003	T. Aaltonen *et al.*	(CDF Collab.)
ATHAR	05	PR D71 051101	S.B. Athar *et al.*	(CLEO Collab.)
AMMAR	01	PRL 86 1167	R. Ammar *et al.*	(CLEO Collab.)
BRANDENB...	97	PRL 78 2304	G. Brandenburg *et al.*	(CLEO Collab.)
AMMOSOV	93	JETPL 58 247	V.V. Ammosov *et al.*	(SERP)

Translated from ZETFP 58 241.

$\Sigma_c(2800)$

$I(J^P) = 1(?^?)$ Status: ***

Seen in the $\Lambda_c^+\pi^+$, $\Lambda_c^+\pi^0$, and $\Lambda_c^+\pi^-$ mass spectra.

$\Sigma_c(2800)$ MASSES

The charged ++ and + masses are obtained from the mass-difference measurements that follow. The neutral mass is dominated by the mass-difference measurement, but is pulled up somewhat by the less well-determined but considerably higher direct-mass measurement. It is possible, in fact, that AUBERT 08BN is seeing a different Σ_c.

$\Sigma_c(2800)^{++}$ MASS

VALUE (MeV)	DOCUMENT ID
2801^{+4}_{-6} OUR FIT	

$\Sigma_c(2800)^+$ MASS

VALUE (MeV)	DOCUMENT ID
2792^{+14}_{-5} OUR FIT	

$\Sigma_c(2800)^0$ MASS

VALUE (MeV)	DOCUMENT ID	TECN	COMMENT
2806^{+5}_{-7} OUR FIT Error includes scale factor of 1.3.			
$2846 \pm 8 \pm 10$	AUBERT	08BN BABR	$B^- \to \overline{p}\Lambda_c^+\pi^-$

$\Sigma_c(2800)$ MASS DIFFERENCES

$m_{\Sigma_c(2800)^{++}} - m_{\Lambda_c^+}$

VALUE (MeV)	EVTS	DOCUMENT ID	TECN	COMMENT
$514\ ^{+4}_{-6}$ OUR FIT				
$514.5^{+3.4}_{-3.1}{}^{+2.8}_{-4.9}$	2810^{+1090}_{-775}	MIZUK 05	BELL	$e^+e^- \approx \Upsilon(4S)$

$m_{\Sigma_c(2800)^+} - m_{\Lambda_c^+}$

VALUE (MeV)	EVTS	DOCUMENT ID	TECN	COMMENT
$505\ ^{+14}_{-5}$ OUR FIT				
$505.4^{+5.8}_{-4.6}{}^{+12.4}_{-2.0}$	1540^{+1750}_{-1050}	MIZUK 05	BELL	$e^+e^- \approx \Upsilon(4S)$

$m_{\Sigma_c(2800)^0} - m_{\Lambda_c^+}$

VALUE (MeV)	EVTS	DOCUMENT ID	TECN	COMMENT
$519\ ^{+5}_{-7}$ OUR FIT Error includes scale factor of 1.3.				
$515.4^{+3.2}_{-3.1}{}^{+2.1}_{-6.0}$	2240^{+1300}_{-740}	MIZUK 05	BELL	$e^+e^- \approx \Upsilon(4S)$

$\Sigma_c(2800)$ WIDTHS

$\Sigma_c(2800)^{++}$ WIDTH

VALUE (MeV)	EVTS	DOCUMENT ID	TECN	COMMENT
$75^{+18}_{-13}{}^{+12}_{-11}$	2810^{+1090}_{-775}	MIZUK 05	BELL	$e^+e^- \approx \Upsilon(4S)$

$\Sigma_c(2800)^+$ WIDTH

VALUE (MeV)	EVTS	DOCUMENT ID	TECN	COMMENT
$62^{+37}_{-23}{}^{+52}_{-38}$	1540^{+1750}_{-1050}	MIZUK 05	BELL	$e^+e^- \approx \Upsilon(4S)$

$\Sigma_c(2800)^0$ WIDTH

VALUE (MeV)	EVTS	DOCUMENT ID	TECN	COMMENT
72^{+22}_{-15} OUR AVERAGE				
$86^{+33}_{-22} \pm 12$		AUBERT	08BN BABR	$B^- \to \overline{p}\Lambda_c^+\pi^-$
$61^{+18}_{-13}{}^{+22}_{-13}$	2240^{+1300}_{-740}	MIZUK 05	BELL	$e^+e^- \approx \Upsilon(4S)$

$\Sigma_c(2800)$ DECAY MODES

	Mode	Fraction (Γ_i/Γ)
Γ_1	$\Lambda_c^+\pi$	seen

$\Sigma_c(2800)$ REFERENCES

AUBERT	08BN	PR D78 112003	B. Aubert *et al.*	(BABAR Collab.)
MIZUK	05	PRL 94 122002	R. Mizuk *et al.*	(BELLE Collab.)

Ξ_c^+

$I(J^P) = \frac{1}{2}(\frac{1}{2}^+)$ Status: ***

According to the quark model, the Ξ_c^+ (quark content usc) and Ξ_c^0 form an isospin doublet, and the spin-parity ought to be $J^P = 1/2^+$. None of I, J, or P has actually been measured.

Ξ_c^+ MASS

The fit uses the Ξ_c^+ and Ξ_c^0 mass and mass-difference measurements.

VALUE (MeV)	EVTS	DOCUMENT ID		TECN	COMMENT
$2467.87 \pm$ 0.30 OUR FIT Error includes scale factor of 1.1.					
$2467.89\ ^{+0.34}_{-0.50}$ OUR AVERAGE					
$2468.00 \pm 0.18 \pm 0.51$	5.1k	AALTONEN	14B	CDF	$p\overline{p}$ at 1.96 TeV
$2468.1 \pm 0.4\ ^{+0.2}_{-1.4}$	4.9k	[1] LESIAK	05	BELL	e^+e^-, $\Upsilon(4S)$
$2465.8 \pm 1.9 \pm 2.5$	90	FRABETTI	98	E687	γ Be, $\overline{E}_\gamma = 220$ GeV
$2467.0 \pm 1.6 \pm 2.0$	147	EDWARDS	96	CLE2	$e^+e^- \approx \Upsilon(4S)$
$2465.1 \pm 3.6 \pm 1.9$	30	ALBRECHT	90F	ARG	e^+e^- at $\Upsilon(4S)$
$2467 \pm 3 \pm 4$	23	ALAM	89	CLEO	e^+e^- 10.6 GeV
$2466.5 \pm 2.7 \pm 1.2$	5	BARLAG	89C	ACCM	π^- Cu 230 GeV
• • • We do not use the following data for averages, fits, limits, etc. • • •					
$2464.4 \pm 2.0 \pm 1.4$	30	FRABETTI	93B	E687	See FRABETTI 98
$2459 \pm 5 \pm 30$	56	[2] COTEUS	87	SPEC	nA $\simeq$ 600 GeV
2460 ± 25	82	BIAGI	83	SPEC	Σ^- Be 135 GeV

[1] The systematic error was (wrongly) given the other way round in LESIAK 05; see the erratum.

[2] Although COTEUS 87 claims to agree well with BIAGI 83 on the mass and width, there appears to be a discrepancy between the two experiments. BIAGI 83 sees a single peak (stated significance about 6 standard deviations) in the $\Lambda K^-\pi^+\pi^+$ mass spectrum. COTEUS 87 sees *two* peaks in the same spectrum, one at the Ξ_c^+ mass, the other 75 MeV lower. The latter is attributed to $\Xi_c^+ \to \Sigma^0 K^-\pi^+\pi^+ \to (\Lambda\gamma)K^-\pi^+\pi^+$, with the γ unseen. The *combined* significance of the double peak is stated to be 5.5 standard deviations. But the absence of any trace of a lower peak in BIAGI 83 seems to us to throw into question the interpretation of the lower peak of COTEUS 87.

Ξ_c^+ MEAN LIFE

VALUE (10^{-15} s)	EVTS	DOCUMENT ID		TECN	COMMENT
442± 26 OUR AVERAGE		Error includes scale factor of 1.3.			See the ideogram below.
503± 47± 18	250	MAHMOOD	02	CLE2	$e^+e^- \approx \Upsilon(4S)$
439± 22± 9	532	LINK	01D	FOCS	γ nucleus, $\overline{E}_\gamma \approx 180$ GeV
$340^{+\ 70}_{-\ 50} \pm 20$	56	FRABETTI	98	E687	γ Be, $\overline{E}_\gamma = 220$ GeV
$400^{+180}_{-120} \pm 100$	102	COTEUS	87	SPEC	nA $\simeq$ 600 GeV
$480^{+210}_{-150} \pm 200$	53	BIAGI	85C	SPEC	Σ^- Be 135 GeV
• • • We do not use the following data for averages, fits, limits, etc. • • •					
$410^{+110}_{-\ 80} \pm 20$	30	FRABETTI	93B	E687	See FRABETTI 98
$200^{+110}_{-\ 60}$	6	BARLAG	89C	ACCM	π^- (K^-) Cu 230 GeV

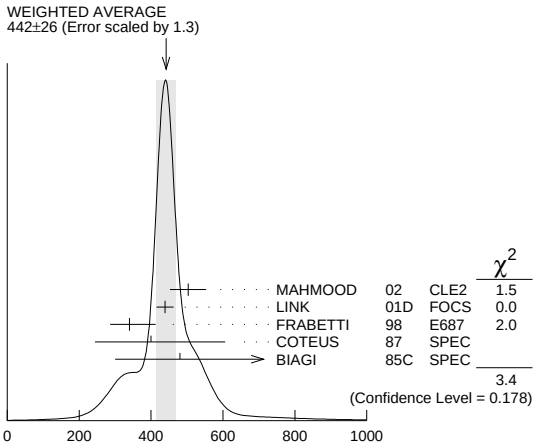

Ξ_c^+ DECAY MODES

Branching fractions marked with a footnote, e.g. [a], have been corrected for decay modes not observed in the experiments. For example, the submode fraction $\Xi_c^+ \to \Sigma^+ \overline{K}^*(892)^0$ seen in $\Xi_c^+ \to \Sigma^+ K^- \pi^+$ has been multiplied up to include $\overline{K}^*(892)^0 \to \overline{K}^0 \pi^0$ decays.

Mode	Fraction (Γ_i/Γ)	Confidence level

No absolute branching fractions have been measured.
The following are branching *ratios* relative to $\Xi^- 2\pi^+$.

Cabibbo-favored ($S = -2$) decays — relative to $\Xi^- 2\pi^+$

Γ_1	$p 2K_S^0$		0.087 ± 0.021	
Γ_2	$\Lambda \overline{K}^0 \pi^+$		—	
Γ_3	$\Sigma(1385)^+ \overline{K}^0$	[a]	1.0 ± 0.5	
Γ_4	$\Lambda K^- 2\pi^+$		0.323 ± 0.033	
Γ_5	$\Lambda \overline{K}^*(892)^0 \pi^+$	[a]	<0.16	90%
Γ_6	$\Sigma(1385)^+ K^- \pi^+$	[a]	<0.23	90%
Γ_7	$\Sigma^+ K^- \pi^+$		0.94 ± 0.10	
Γ_8	$\Sigma^+ \overline{K}^*(892)^0$	[a]	0.81 ± 0.15	
Γ_9	$\Sigma^0 K^- 2\pi^+$		0.27 ± 0.12	
Γ_{10}	$\Xi^0 \pi^+$		0.55 ± 0.16	
Γ_{11}	$\Xi^- 2\pi^+$		**DEFINED AS 1**	
Γ_{12}	$\Xi(1530)^0 \pi^+$	[a]	<0.10	90%
Γ_{13}	$\Xi^0 \pi^+ \pi^0$		2.3 ± 0.7	
Γ_{14}	$\Xi^0 \pi^- 2\pi^+$		1.7 ± 0.5	
Γ_{15}	$\Xi^0 e^+ \nu_e$		$2.3\ ^{+0.7}_{-0.8}$	
Γ_{16}	$\Omega^- K^+ \pi^+$		0.07 ± 0.04	

Cabibbo-suppressed decays — relative to $\Xi^- 2\pi^+$

Γ_{17}	$p K^- \pi^+$		0.21 ± 0.04	
Γ_{18}	$p \overline{K}^*(892)^0$	[a]	0.116 ± 0.030	
Γ_{19}	$\Sigma^+ \pi^+ \pi^-$		0.48 ± 0.20	
Γ_{20}	$\Sigma^- 2\pi^+$		0.18 ± 0.09	
Γ_{21}	$\Sigma^+ K^+ K^-$		0.15 ± 0.06	
Γ_{22}	$\Sigma^+ \phi$	[a]	<0.11	90%
Γ_{23}	$\Xi(1690)^0 K^+$, $\Xi^0 \to \Sigma^+ K^-$		<0.05	90%

[a] This branching fraction includes all the decay modes of the final-state resonance.

Ξ_c^+ BRANCHING RATIOS

Cabibbo-favored ($S = -2$) decays

$\Gamma(p 2K_S^0)/\Gamma(\Xi^- 2\pi^+)$ Γ_1/Γ_{11}

VALUE	EVTS	DOCUMENT ID		TECN	COMMENT
0.087±0.016±0.014	168 ± 27	LESIAK	05	BELL	e^+e^-, $\Upsilon(4S)$

$\Gamma(\Sigma(1385)^+ \overline{K}^0)/\Gamma(\Xi^- 2\pi^+)$ Γ_3/Γ_{11}

Unseen decay modes of the $\Sigma(1385)^+$ are included.

VALUE	EVTS	DOCUMENT ID		TECN	COMMENT
1.00±0.49±0.24	20	LINK	03E	FOCS	<1.72, 90% CL

$\Gamma(\Lambda K^- 2\pi^+)/\Gamma(\Xi^- 2\pi^+)$ Γ_4/Γ_{11}

VALUE	EVTS	DOCUMENT ID		TECN	COMMENT
0.323±0.033 OUR AVERAGE					
0.32 ±0.03 ±0.02	1177 ± 55	LESIAK	05	BELL	e^+e^-, $\Upsilon(4S)$
0.28 ±0.06 ±0.06	58	LINK	03E	FOCS	γ nucleus, $\overline{E}_\gamma \approx 180$ GeV
0.58 ±0.16 ±0.07	61	BERGFELD	96	CLE2	$e^+e^- \approx \Upsilon(4S)$

$\Gamma(\Lambda \overline{K}^*(892)^0 \pi^+)/\Gamma(\Lambda K^- 2\pi^+)$ Γ_5/Γ_4

Unseen decay modes of the $\overline{K}^*(892)^0$ are included.

VALUE	CL%	DOCUMENT ID		TECN	COMMENT
<0.5	90	BERGFELD	96	CLE2	$e^+e^- \approx \Upsilon(4S)$

$\Gamma(\Sigma(1385)^+ K^- \pi^+)/\Gamma(\Lambda K^- 2\pi^+)$ Γ_6/Γ_4

Unseen decay modes of the $\Sigma(1385)^+$ are included.

VALUE	CL%	DOCUMENT ID		TECN	COMMENT
<0.7	90	BERGFELD	96	CLE2	$e^+e^- \approx \Upsilon(4S)$

$\Gamma(\Sigma^+ K^- \pi^+)/\Gamma(\Xi^- 2\pi^+)$ Γ_7/Γ_{11}

VALUE	EVTS	DOCUMENT ID		TECN	COMMENT
0.94±0.10 OUR AVERAGE					
0.91±0.11±0.04	251	LINK	03E	FOCS	γ nucleus, $\overline{E}_\gamma \approx 180$ GeV
0.92±0.20±0.07		[3] JUN	00	SELX	Σ^- nucleus, 600 GeV
1.18±0.26±0.17	119	BERGFELD	96	CLE2	$e^+e^- \approx \Upsilon(4S)$

[3] This JUN 00 result is redundant with other results given below.

$\Gamma(\Sigma^+ \overline{K}^*(892)^0)/\Gamma(\Xi^- 2\pi^+)$ Γ_8/Γ_{11}

Unseen decay modes of the $\overline{K}^*(892)^0$ are included.

VALUE	EVTS	DOCUMENT ID		TECN	COMMENT
0.81±0.15 OUR AVERAGE					
0.78±0.16±0.06	119	LINK	03E	FOCS	γ nucleus, $\overline{E}_\gamma \approx 180$ GeV
0.92±0.27±0.14	61	BERGFELD	96	CLE2	$e^+e^- \approx \Upsilon(4S)$

$\Gamma(\Sigma^0 K^- 2\pi^+)/\Gamma(\Lambda K^- 2\pi^+)$ Γ_9/Γ_4

VALUE	EVTS	DOCUMENT ID		TECN	COMMENT
0.84±0.36	47	[4] COTEUS	87	SPEC	nA $\simeq$ 600 GeV

[4] See, however, the note on the COTEUS 87 Ξ_c^+ mass measurement.

$\Gamma(\Xi^0 \pi^+)/\Gamma(\Xi^- 2\pi^+)$ Γ_{10}/Γ_{11}

VALUE	EVTS	DOCUMENT ID		TECN	COMMENT
0.55±0.13±0.09	39	EDWARDS	96	CLE2	$e^+e^- \approx \Upsilon(4S)$

$\Gamma(\Xi^- 2\pi^+)/\Gamma_{\text{total}}$ Γ_{11}/Γ

VALUE	EVTS	DOCUMENT ID		TECN	COMMENT
• • • We do not use the following data for averages, fits, limits, etc. • • •					
seen	131	BERGFELD	96	CLE2	$e^+e^- \approx \Upsilon(4S)$
seen	160	AVERY	95	CLE2	$e^+e^- \approx \Upsilon(4S)$
seen	30	FRABETTI	93B	E687	γBe, $\overline{E}_\gamma = 220$ GeV
seen	30	ALBRECHT	90F	ARG	e^+e^- at $\Upsilon(4S)$
seen	23	ALAM	89	CLEO	e^+e^- 10.6 GeV

$\Gamma(\Xi(1530)^0 \pi^+)/\Gamma(\Xi^- 2\pi^+)$ Γ_{12}/Γ_{11}

Unseen decay modes of the $\Xi(1530)^0$ are included.

VALUE	CL%	DOCUMENT ID		TECN	COMMENT
<0.1	90	LINK	03E	FOCS	γ nucleus, $\overline{E}_\gamma \approx 180$ GeV
• • • We do not use the following data for averages, fits, limits, etc. • • •					
<0.2	90	BERGFELD	96	CLE2	$e^+e^- \approx \Upsilon(4S)$

$\Gamma(\Xi^0 \pi^+ \pi^0)/\Gamma(\Xi^- 2\pi^+)$ Γ_{13}/Γ_{11}

VALUE	EVTS	DOCUMENT ID		TECN	COMMENT
2.34±0.57±0.37	81	EDWARDS	96	CLE2	$e^+e^- \approx \Upsilon(4S)$

$\Gamma(\Xi(1530)^0 \pi^+)/\Gamma(\Xi^0 \pi^+ \pi^0)$ Γ_{12}/Γ_{13}

VALUE	CL%	DOCUMENT ID		TECN	COMMENT
• • • We do not use the following data for averages, fits, limits, etc. • • •					
<0.3	90	EDWARDS	96	CLE2	$e^+e^- \approx \Upsilon(4S)$

$\Gamma(\Xi^0\pi^-2\pi^+)/\Gamma(\Xi^-2\pi^+)$ Γ_{14}/Γ_{11}

VALUE	EVTS	DOCUMENT ID		TECN	COMMENT
1.74±0.42±0.27	57	EDWARDS	96	CLE2	$e^+e^-\approx\ \Upsilon(4S)$

$\Gamma(\Xi^0 e^+\nu_e)/\Gamma(\Xi^-2\pi^+)$ Γ_{15}/Γ_{11}

VALUE	EVTS	DOCUMENT ID		TECN	COMMENT
$2.3\pm0.6^{+0.3}_{-0.6}$	41	ALEXANDER	95B	CLE2	$e^+e^-\approx\ \Upsilon(4S)$

$\Gamma(\Omega^-K^+\pi^+)/\Gamma(\Xi^-2\pi^+)$ Γ_{16}/Γ_{11}

VALUE	EVTS	DOCUMENT ID		TECN	COMMENT
0.07±0.03±0.03	14	LINK	03E	FOCS	<0.12, 90% CL

Cabibbo-suppressed decays

$\Gamma(pK^-\pi^+)/\Gamma(\Xi^-2\pi^+)$ Γ_{17}/Γ_{11}

VALUE	EVTS	DOCUMENT ID		TECN	COMMENT
0.21 ±0.04 OUR AVERAGE					
0.194±0.054	47 ± 11	VAZQUEZ-JA...08		SELX	Σ^- nucleus, 600 GeV
0.234±0.047±0.022	202	LINK	01B	FOCS	γ nucleus
• • • We do not use the following data for averages, fits, limits, etc. • • •					
0.20 ±0.04 ±0.02	76	JUN	00	SELX	See VAZQUEZ-JAUREGUI 08

$\Gamma(p\overline{K}^*(892)^0)/\Gamma(pK^-\pi^+)$ Γ_{18}/Γ_{17}

Unseen decay modes of the $\overline{K}^*(892)^0$ are included.

VALUE	DOCUMENT ID		TECN	COMMENT
0.54±0.09±0.05	LINK	01B	FOCS	γ nucleus

$\Gamma(\Sigma^+\pi^+\pi^-)/\Gamma(\Xi^-2\pi^+)$ Γ_{19}/Γ_{11}

VALUE	EVTS	DOCUMENT ID		TECN	COMMENT
0.48±0.20	21 ± 8	VAZQUEZ-JA...08		SELX	Σ^- nucleus, 600 GeV

$\Gamma(\Sigma^-2\pi^+)/\Gamma(\Xi^-2\pi^+)$ Γ_{20}/Γ_{11}

VALUE	EVTS	DOCUMENT ID		TECN	COMMENT
0.18±0.09	10 ± 4	VAZQUEZ-JA...08		SELX	Σ^- nucleus, 600 GeV

$\Gamma(\Sigma^+K^+K^-)/\Gamma(\Sigma^+K^-\pi^+)$ Γ_{21}/Γ_7

VALUE	EVTS	DOCUMENT ID		TECN	COMMENT
0.16±0.06±0.01	17	LINK	03E	FOCS	γ nucleus, $\overline{E}_\gamma\approx180$ GeV

$\Gamma(\Sigma^+\phi)/\Gamma(\Sigma^+K^-\pi^+)$ Γ_{22}/Γ_7

Unseen decay modes of the ϕ are included.

VALUE	CL%	DOCUMENT ID		TECN	COMMENT
<0.12	90	LINK	03E	FOCS	γ nucleus, $\overline{E}_\gamma\approx180$ GeV

$\Gamma(\Xi(1690)^0K^+\times B(\Xi(1690)^0\to\ \Sigma^+K^-))/\Gamma(\Sigma^+K^-\pi^+)$ Γ_{23}/Γ_7

VALUE	CL%	DOCUMENT ID		TECN	COMMENT
<0.05	90	LINK	03E	FOCS	γ nucleus, $\overline{E}_\gamma\approx180$ GeV

Ξ_c^+ REFERENCES

AALTONEN	14B	PR D89 072014	T. Aaltonen *et al.*	(CDF Collab.)
VAZQUEZ-JA...	08	PL B666 299	E. Vazquez-Jauregui *et al.*	(SELEX Collab.)
LESIAK	05	PL B605 237	T. Lesiak *et al.*	(BELLE Collab.)
Also		PL B617 198 (errat.)	T. Lesiak *et al.*	(BELLE Collab.)
LINK	03E	PL B571 139	J.M. Link *et al.*	(FNAL FOCUS Collab.)
MAHMOOD	02	PR D65 031102	A.H. Mahmood *et al.*	(CLEO Collab.)
LINK	01B	PL B512 277	J.M. Link *et al.*	(FNAL FOCUS Collab.)
LINK	01D	PL B523 53	J.M. Link *et al.*	(FNAL FOCUS Collab.)
JUN	00	PRL 84 1857	S.Y. Jun *et al.*	(FNAL SELEX Collab.)
FRABETTI	98	PL B427 211	P.L. Frabetti *et al.*	(FNAL E687 Collab.)
BERGFELD	96	PL B365 431	T. Bergfeld *et al.*	(CLEO Collab.)
EDWARDS	96	PL B373 261	K.W. Edwards *et al.*	(CLEO Collab.)
ALEXANDER	95B	PRL 74 3113	J. Alexander *et al.*	(CLEO Collab.)
Also		PRL 75 4155 (erratum)	J. Alexander *et al.*	(CLEO Collab.)
AVERY	95	PRL 75 4364	P. Avery *et al.*	(CLEO Collab.)
FRABETTI	93B	PRL 70 1381	P.L. Frabetti *et al.*	(FNAL E687 Collab.)
ALBRECHT	90F	PL B247 121	H. Albrecht *et al.*	(ARGUS Collab.)
ALAM	89	PL B226 401	M.S. Alam *et al.*	(CLEO Collab.)
BARLAG	89C	PL B233 522	S. Barlag *et al.*	(ACCMOR Collab.)
COTEUS	87	PRL 59 1530	P. Coteus *et al.*	(FNAL E400 Collab.)
BIAGI	85C	PL 150B 230	S.F. Biagi *et al.*	(CERN WA62 Collab.)
BIAGI	83	PL 122B 455	S.F. Biagi *et al.*	(CERN WA62 Collab.)

Ξ_c^0

$I(J^P) = \frac{1}{2}(\frac{1}{2}^+)$ Status: ***

According to the quark model, the Ξ_c^0 (quark content dsc) and Ξ_c^+ form an isospin doublet, and the spin-parity ought to be $J^P = 1/2^+$. None of I, J, or P has actually been measured.

Ξ_c^0 MASS

The fit uses the Ξ_c^0 and Ξ_c^+ mass and mass-difference measurements.

VALUE (MeV)	EVTS	DOCUMENT ID		TECN	COMMENT
$2470.87^{+0.28}_{-0.31}$ OUR FIT					
$2470.99^{+0.30}_{-0.50}$ OUR AVERAGE					
$2470.85\pm0.24\pm0.55$	3.4k	AALTONEN	14B	CDF	$p\overline{p}$ at 1.96 TeV
$2471.0\ \pm0.3\ ^{+0.2}_{-1.4}$	8.6k	[1] LESIAK	05	BELL	e^+e^-, $\Upsilon(4S)$
2470.0 ±2.8 ±2.6	85	FRABETTI	98B	E687	γ Be, $\overline{E}_\gamma = 220$ GeV
2469 ±2 ±3	9	HENDERSON	92B	CLEO	Ω^-K^+
2472.1 ±2.7 ±1.6	54	ALBRECHT	90F	ARG	e^+e^- at $\Upsilon(4S)$
2473.3 ±1.9 ±1.2	4	BARLAG	90	ACCM	π^- (K^-) Cu 230 GeV
2472 ±3 ±4	19	ALAM	89	CLEO	e^+e^- 10.6 GeV
• • • We do not use the following data for averages, fits, limits, etc. • • •					
2462.1 ±3.1 ±1.4	42	[2] FRABETTI	93C	E687	See FRABETTI 98B
2471 ±3 ±4	14	AVERY	89	CLEO	See ALAM 89

[1] The systematic error was (wrongly) given the other way round in LESIAK 05.
[2] The FRABETTI 93C mass is well below the other measurements.

$\Xi_c^0 - \Xi_c^+$ MASS DIFFERENCE

VALUE (MeV)	EVTS	DOCUMENT ID		TECN	COMMENT
3.00±0.24 OUR FIT					
2.91±0.26 OUR AVERAGE					
$2.85\pm0.30\pm0.04$	5.1/3.4k	AALTONEN	14B	CDF	$p\overline{p}$ at 1.96 TeV
2.9 ±0.5		LESIAK	05	BELL	e^+e^-, $\Upsilon(4S)$
7.0 ±4.5 ±2.2		ALBRECHT	90F	ARG	e^+e^- at $\Upsilon(4S)$
6.8 ±3.3 ±0.5		BARLAG	90	ACCM	π^- (K^-) Cu 230 GeV
5 ±4 ±1		ALAM	89	CLEO	$\Xi_c^0\to\ \Xi^-\pi^+$, $\Xi_c^+\to\ \Xi^-\pi^+\pi^+$

Ξ_c^0 MEAN LIFE

VALUE (10^{-15} s)	EVTS	DOCUMENT ID		TECN	COMMENT
112^{+13}_{-10} OUR AVERAGE					
$118^{+14}_{-12}\pm5$	110	LINK	02H	FOCS	γ nucleus, ≈180 GeV
$101^{+25}_{-17}\pm5$	42	FRABETTI	93C	E687	γBe, $\overline{E}_\gamma = 220$ GeV
82^{+59}_{-30}	4	BARLAG	90	ACCM	π^- (K^-) Cu 230 GeV

Ξ_c^0 DECAY MODES

Branching fractions marked with a footnote, e.g. [*a*], have been corrected for decay modes not observed in the experiments. For example, the submode fraction $\Xi_c^0\to\ pK^-\overline{K}^*(892)^0$ seen in $\Xi_c^0\to\ pK^-K^-\pi^+$ has been multiplied up to include $\overline{K}^*(892)^0\to\ \overline{K}^0\pi^0$ decays.

Mode	Fraction (Γ_i/Γ)

No absolute branching fractions have been measured. The following are branching *ratios* relative to $\Xi^-\pi^+$.

Cabibbo-favored (S = −2) decays — relative to $\Xi^-\pi^+$

Γ_1	$pK^-K^-\pi^+$	0.34 ±0.04
Γ_2	$pK^-\overline{K}^*(892)^0$	[*a*] 0.21 ±0.05
Γ_3	$pK^-K^-\pi^+$ (no $\overline{K}^{*0}$)	0.21 ±0.04
Γ_4	ΛK_S^0	0.210±0.028
Γ_5	$\Lambda K^-\pi^+$	1.07 ±0.14
Γ_6	$\Lambda\overline{K}^0\pi^+\pi^-$	seen
Γ_7	$\Lambda K^-\pi^+\pi^+\pi^-$	seen
Γ_8	$\Xi^-\pi^+$	**DEFINED AS 1**
Γ_9	$\Xi^-\pi^+\pi^+\pi^-$	3.3 ±1.4
Γ_{10}	Ω^-K^+	0.297±0.024
Γ_{11}	$\Xi^-e^+\nu_e$	3.1 ±1.1
Γ_{12}	$\Xi^-\ell^+$ anything	1.0 ±0.5

Cabibbo-suppressed decays — relative to $\Xi^-\pi^+$

Γ_{13}	Ξ^-K^+	0.028±0.006
Γ_{14}	ΛK^+K^- (no ϕ)	0.029±0.007
Γ_{15}	$\Lambda\phi$	[*a*] 0.034±0.007

[*a*] This branching fraction includes all the decay modes of the final-state resonance.

Ξ_c^0 BRANCHING RATIOS

Cabibbo-favored (S = −2) decays

$\Gamma(pK^-K^-\pi^+)/\Gamma(\Xi^-\pi^+)$ Γ_1/Γ_8

VALUE	EVTS	DOCUMENT ID		TECN	COMMENT
0.34±0.04 OUR AVERAGE					
0.33±0.03±0.03	1908 ± 62	LESIAK	05	BELL	e^+e^-, $\Upsilon(4S)$
0.35±0.06±0.03	148 ± 18	DANKO	04	CLEO	e^+e^-

$\Gamma(pK^-\overline{K}^*(892)^0)/\Gamma(\Xi^-\pi^+)$ Γ_2/Γ_8

Unseen decay modes of the $\overline{K}^*(892)^0$ are included.

VALUE	DOCUMENT ID		TECN	COMMENT
0.210±0.045±0.015	DANKO	04	CLEO	e^+e^-
• • • We do not use the following data for averages, fits, limits, etc. • • •				
seen	BARLAG	90	ACCM	π^- (K^-) Cu 230 GeV

$\Gamma(pK^-K^-\pi^+(\text{no }\overline{K}^{*0}))/\Gamma(\Xi^-\pi^+)$ Γ_3/Γ_8

VALUE	DOCUMENT ID		TECN	COMMENT
0.21±0.04±0.02	DANKO	04	CLEO	e^+e^-

$\Gamma(\Lambda K_S^0)/\Gamma(\Xi^-\pi^+)$ Γ_4/Γ_8

VALUE	EVTS	DOCUMENT ID		TECN	COMMENT
0.21±0.02±0.02	465 ± 37	LESIAK	05	BELL	e^+e^-, $\Upsilon(4S)$
• • • We do not use the following data for averages, fits, limits, etc. • • •					
seen	7	ALBRECHT	95B	ARG	$e^+e^-\approx 10.4$ GeV

$\Gamma(\Lambda K^-\pi^+)/\Gamma(\Xi^-\pi^+)$ Γ_5/Γ_8

VALUE	EVTS	DOCUMENT ID		TECN	COMMENT
1.07±0.12±0.07	2979 ± 211	LESIAK	05	BELL	e^+e^-, $\Upsilon(4S)$

$\Gamma(\Lambda\overline{K}^0\pi^+\pi^-)/\Gamma_{\text{total}}$ Γ_6/Γ

VALUE	DOCUMENT ID		TECN	COMMENT
seen	FRABETTI	98B	E687	γ Be, $\overline{E}_\gamma$ = 220 GeV

$\Gamma(\Lambda K^-\pi^+\pi^+\pi^-)/\Gamma_{\text{total}}$ Γ_7/Γ

VALUE	DOCUMENT ID		TECN	COMMENT
seen	FRABETTI	98B	E687	γ Be, $\overline{E}_\gamma$ = 220 GeV

$\Gamma(\Xi^-\pi^+)/\Gamma(\Xi^-\pi^+\pi^+\pi^-)$ Γ_8/Γ_9

VALUE	DOCUMENT ID		TECN	COMMENT
0.30±0.12±0.05	ALBRECHT	90F	ARG	e^+e^- at $\Upsilon(4S)$

$\Gamma(\Omega^-K^+)/\Gamma(\Xi^-\pi^+)$ Γ_{10}/Γ_8

VALUE	EVTS	DOCUMENT ID		TECN	COMMENT
0.297±0.024 OUR AVERAGE					
0.294±0.018±0.016	650	AUBERT,B	05M	BABR	$e^+e^-\approx\ \Upsilon(4S)$
0.50 ±0.21 ±0.05	9	HENDERSON	92B	CLEO	$e^+e^-\approx 10.6$ GeV

$\Gamma(\Xi^-e^+\nu_e)/\Gamma(\Xi^-\pi^+)$ Γ_{11}/Γ_8

VALUE	EVTS	DOCUMENT ID		TECN	COMMENT
$3.1\pm1.0^{+0.3}_{-0.5}$	54	ALEXANDER	95B	CLE2	$e^+e^-\approx\ \Upsilon(4S)$

$\Gamma(\Xi^-\ell^+\text{anything})/\Gamma(\Xi^-\pi^+)$ Γ_{12}/Γ_8

The ratio is for the *average* (not the sum) of the Ξ^-e^+ anything and $\Xi^-\mu^+$ anything modes.

VALUE	EVTS	DOCUMENT ID		TECN	COMMENT
0.96±0.43±0.18	18	ALBRECHT	93B	ARG	$e^+e^-\approx 10.4$ GeV

$\Gamma(\Xi^-\ell^+\text{anything})/\Gamma(\Xi^-\pi^+\pi^+\pi^-)$ Γ_{12}/Γ_9

The ratio is for the *average* (not the sum) of the Ξ^-e^+ anything and $\Xi^-\mu^+$ anything modes.

VALUE	EVTS	DOCUMENT ID		TECN	COMMENT
0.29±0.12±0.04	18	ALBRECHT	93B	ARG	$e^+e^-\approx 10.4$ GeV

Cabibbo-suppressed decays

$\Gamma(\Xi^-K^+)/\Gamma(\Xi^-\pi^+)$ Γ_{13}/Γ_8

VALUE (units 10^{-2})	EVTS	DOCUMENT ID		TECN	COMMENT
2.75±0.51±0.25	314 ± 58	CHISTOV	13	BELL	$e^+e^-\approx\ \Upsilon(4S)$

$\Gamma(\Lambda K^+K^-(\text{no }\phi))/\Gamma(\Xi^-\pi^+)$ Γ_{14}/Γ_8

VALUE (units 10^{-2})	EVTS	DOCUMENT ID		TECN	COMMENT
2.86±0.61±0.37	510±110	CHISTOV	13	BELL	$e^+e^-\approx\ \Upsilon(4S)$

$\Gamma(\Lambda\phi)/\Gamma(\Xi^-\pi^+)$ Γ_{15}/Γ_8

Unseen decay modes of the ϕ are included.

VALUE (units 10^{-2})	EVTS	DOCUMENT ID		TECN	COMMENT
3.43±0.58±0.32	316 ± 54	CHISTOV	13	BELL	$e^+e^-\approx\ \Upsilon(4S)$

Ξ_c^0 DECAY PARAMETERS

See the note on "Baryon Decay Parameters" in the neutron Listings.

α FOR $\Xi_c^0\to\ \Xi^-\pi^+$

VALUE	EVTS	DOCUMENT ID		TECN	COMMENT
$-0.56\pm0.39^{+0.10}_{-0.09}$	138	CHAN	01	CLE2	$e^+e^-\approx\ \Upsilon(4S)$

Ξ_c^0 REFERENCES

AALTONEN	14B	PR D89 072014	T. Aaltonen *et al.*	(CDF Collab.)
CHISTOV	13	PR D88 071103	R. Chistov *et al.*	(BELLE Collab.)
AUBERT,B	05M	PRL 95 142003	B. Aubert *et al.*	(BABAR Collab.)
LESIAK	05	PL B605 237	T. Lesiak *et al.*	(BELLE Collab.)
Also		PL B617 198 (errat.)	T. Lesiak *et al.*	(BELLE Collab.)
DANKO	04	PR D69 052004	I. Danko *et al.*	(CLEO Collab.)
LINK	02H	PL B541 211	J.M. Link *et al.*	(FNAL FOCUS Collab.)
CHAN	01	PR D63 111102	S. Chan *et al.*	(CLEO Collab.)
FRABETTI	98B	PL B426 403	P.L. Frabetti *et al.*	(FNAL E687 Collab.)
ALBRECHT	95B	PL B342 397	H. Albrecht *et al.*	(ARGUS Collab.)
ALEXANDER	95B	PRL 74 3113	J. Alexander *et al.*	(CLEO Collab.)
Also		PRL 75 4155 (erratum)	J. Alexander *et al.*	(CLEO Collab.)
ALBRECHT	93B	PL B303 368	H. Albrecht *et al.*	(ARGUS Collab.)
FRABETTI	93C	PRL 70 2058	P.L. Frabetti *et al.*	(FNAL E687 Collab.)
HENDERSON	92B	PL B283 161	S. Henderson *et al.*	(CLEO Collab.)
ALBRECHT	90F	PL B247 121	H. Albrecht *et al.*	(ARGUS Collab.)
BARLAG	90	PL B236 495	S. Barlag *et al.*	(ACCMOR Collab.)
ALAM	89	PL B226 401	M.S. Alam *et al.*	(CLEO Collab.)
AVERY	89	PRL 62 863	P. Avery *et al.*	(CLEO Collab.)

$\Xi_c^{\prime+}$

$I(J^P) = \frac{1}{2}(\frac{1}{2}^+)$ Status: ***

The $\Xi_c^{\prime+}$ and $\Xi_c^{\prime 0}$ presumably complete the SU(3) sextet whose other members are the Σ_c^{++}, Σ_c^+, Σ_c^0, and Ω_c^0: see Fig. 3 in the note on Charmed Baryons. The quantum numbers given above come from this presumption but have not been measured.

$\Xi_c^{\prime+}$ MASS

The mass is obtained from the mass-difference measurement that follows.

VALUE (MeV)	DOCUMENT ID
2577.4±1.2 OUR FIT Error includes scale factor of 2.9.	

$\Xi_c^{\prime+} - \Xi_c^+$ MASS DIFFERENCE

VALUE (MeV)	EVTS	DOCUMENT ID		TECN	COMMENT
109.5±1.2 OUR FIT Error includes scale factor of 3.7.					
110.5±0.1±0.4	7055	YELTON	16	BELL	e^+e^-, Υ regions
• • • We do not use the following data for averages, fits, limits, etc. • • •					
107.8±1.7±2.5	25	JESSOP	99	CLE2	$e^+e^-\approx\ \Upsilon(4S)$

$\Xi_c^{\prime+} - \Xi_c^{\prime 0}$ MASS DIFFERENCE

VALUE (MeV)	DOCUMENT ID		TECN	COMMENT
−1.4±1.3 OUR FIT Error includes scale factor of 2.5.				
• • • We do not use the following data for averages, fits, limits, etc. • • •				
−0.8±0.1±0.5	YELTON	16	BELL	7055 and 11,560 evts

$\Xi_c^{\prime+}$ DECAY MODES

The $\Xi_c^{\prime+}$–Ξ_c^+ mass difference is too small for any strong decay to occur.

	Mode	Fraction (Γ_i/Γ)
Γ_1	$\Xi_c^+\gamma$	seen

$\Xi_c^{\prime+}$ REFERENCES

YELTON	16	PR D94 052011	J. Yelton *et al.*	(BELLE Collab.)
JESSOP	99	PRL 82 492	C.P. Jessop *et al.*	(CLEO Collab.)

$\Xi_c^{\prime 0}$

$I(J^P) = \frac{1}{2}(\frac{1}{2}^+)$ Status: ***

The $\Xi_c^{\prime 0}$ and $\Xi_c^{\prime+}$ presumably complete the SU(3) sextet whose other members are the Σ_c^{++}, Σ_c^+, Σ_c^0, and Ω_c^0: see Fig. 3 in the note on Charmed Baryons. The quantum numbers given above come from this presumption but have not been measured.

Baryon Particle Listings

$\Xi_c'^0$, $\Xi_c(2645)$, $\Xi_c(2790)$

$\Xi_c'^0$ MASS

The mass is obtained from the mass-difference measurement that follows.

VALUE (MeV)	DOCUMENT ID
2578.8±0.5 OUR FIT Error includes scale factor of 1.2.	

$\Xi_c'^0 - \Xi_c^0$ MASS DIFFERENCE

VALUE (MeV)	EVTS	DOCUMENT ID		TECN	COMMENT
108.0±0.4 OUR FIT Error includes scale factor of 1.2.					
108.3±0.1±0.4	11.5k	YELTON	16	BELL	e^+e^-, Υ regions
• • • We do not use the following data for averages, fits, limits, etc. • • •					
107.0±1.4±2.5	28	JESSOP	99	CLE2	$e^+e^- \approx \Upsilon(4S)$

$\Xi_c'^0$ DECAY MODES

The $\Xi_c'^0 - \Xi_c^0$ mass difference is too small for any strong decay to occur.

	Mode	Fraction (Γ_i/Γ)
Γ_1	$\Xi_c^0\gamma$	seen

$\Xi_c'^0$ REFERENCES

YELTON	16	PR D94 052011	J. Yelton *et al.*	(BELLE Collab.)
JESSOP	99	PRL 82 492	C.P. Jessop *et al.*	(CLEO Collab.)

$\Xi_c(2645)$

$I(J^P) = \frac{1}{2}(\frac{3}{2}^+)$ Status: ***

The natural assignment is that this is the $J^P = 3/2^+$ excitation of the Ξ_c in the same SU(4) multiplet as the $\Delta(1232)$, but the quantum numbers have not been measured.

$\Xi_c(2645)$ MASSES

$\Xi_c(2645)^+$ MASS

VALUE (MeV)	EVTS	DOCUMENT ID		TECN	COMMENT
2645.53±0.31 OUR FIT					
2645.6 ±0.2 $^{+0.6}_{-0.8}$	578 ± 32	LESIAK	08	BELL	$e^+e^- \approx \Upsilon(4S)$

$\Xi_c(2645)^0$ MASS

VALUE (MeV)	EVTS	DOCUMENT ID		TECN	COMMENT
2646.32±0.31 OUR FIT Error includes scale factor of 1.1.					
2645.7 ±0.2 $^{+0.6}_{-0.7}$	611 ± 32	LESIAK	08	BELL	$e^+e^- \approx \Upsilon(4S)$

$\Xi_c(2645) - \Xi_c$ MASS DIFFERENCES

$m_{\Xi_c(2645)^+} - m_{\Xi_c^0}$

VALUE (MeV)	EVTS	DOCUMENT ID		TECN	COMMENT
174.66±0.09 OUR FIT					
174.66±0.06±0.07	1260	YELTON	16	BELL	e^+e^- in Υ regions
• • • We do not use the following data for averages, fits, limits, etc. • • •					
177.1 ±0.5 ±1.1	47	FRABETTI	98B	E687	γ Be, $\overline{E}_\gamma = 220$ GeV
174.3 ±0.5 ±1.0	34	GIBBONS	96	CLE2	$e^+e^- \approx \Upsilon(4S)$

$m_{\Xi_c(2645)^0} - m_{\Xi_c^+}$

VALUE (MeV)	EVTS	DOCUMENT ID		TECN	COMMENT
178.44±0.11 OUR FIT Error includes scale factor of 1.1.					
178.46±0.07±0.07	975	YELTON	16	BELL	e^+e^- in Υ regions
• • • We do not use the following data for averages, fits, limits, etc. • • •					
178.2 ±0.5 ±1.0	55	AVERY	95	CLE2	$e^+e^- \approx \Upsilon(4S)$

$\Xi_c(2645)^+ - \Xi_c(2645)^0$ MASS DIFFERENCE

VALUE (MeV)	DOCUMENT ID		TECN	COMMENT
−0.79±0.27 OUR FIT				
• • • We do not use the following data for averages, fits, limits, etc. • • •				
−0.85±0.09±0.49	YELTON	16	BELL	1260 and 975 evts
−0.1 ±0.3 ±0.6	LESIAK	08	BELL	≈600 evts each

$\Xi_c(2645)$ WIDTHS

$\Xi_c(2645)^+$ WIDTH

VALUE (MeV)	CL%	EVTS	DOCUMENT ID		TECN	COMMENT
2.14±0.19 OUR AVERAGE Error includes scale factor of 1.1.						
2.06±0.13±0.13		1260	YELTON	16	BELL	e^+e^- in Υ regions
2.6 ±0.2 ±0.4		3.7k	KATO	14	BELL	e^+e^- $\Upsilon(1S)$-$\Upsilon(5S)$
• • • We do not use the following data for averages, fits, limits, etc. • • •						
<3.1	90		GIBBONS	96	CLE2	$e^+e^- \approx \Upsilon(4S)$

$\Xi_c(2645)^0$ WIDTH

VALUE (MeV)	CL%	EVTS	DOCUMENT ID		TECN	COMMENT
2.35±0.18±0.13		975	YELTON	16	BELL	e^+e^- in Υ regions
• • • We do not use the following data for averages, fits, limits, etc. • • •						
<5.5	90	55	AVERY	95	CLE2	$e^+e^- \approx \Upsilon(4S)$

$\Xi_c(2645)$ DECAY MODES

$\Xi_c\pi$ is the only strong decay allowed to a Ξ_c resonance having this mass.

	Mode	Fraction (Γ_i/Γ)
Γ_1	$\Xi_c^0\pi^+$	seen
Γ_2	$\Xi_c^+\pi^-$	seen

$\Xi_c(2645)$ REFERENCES

YELTON	16	PR D94 052011	J. Yelton *et al.*	(BELLE Collab.)
KATO	14	PR D89 052003	Y. Kato *et al.*	(BELLE Collab.)
LESIAK	08	PL B665 9	T. Lesiak *et al.*	(BELLE Collab.)
FRABETTI	98B	PL B426 403	P.L. Frabetti *et al.*	(FNAL E687 Collab.)
GIBBONS	96	PRL 77 810	L.K. Gibbons *et al.*	(CLEO Collab.)
AVERY	95	PRL 75 4364	P. Avery *et al.*	(CLEO Collab.)

$\Xi_c(2790)$

$I(J^P) = \frac{1}{2}(\frac{1}{2}^-)$ Status: ***

Seen in both $\Xi_c\pi$ and $\Xi_c'\pi$ decays. The simplest assignment, based on the mass, width, and decay mode, is that this belongs in the same SU(4) multiplet as the $\Lambda(1405)$ and the $\Lambda_c(2595)^+$, but the spin and parity have not been measured.

$\Xi_c(2790)$ MASSES

The masses are obtained from the mass-difference measurements that follow.

$\Xi_c(2790)^+$ MASS

VALUE (MeV)	DOCUMENT ID
2792.0±0.5 OUR FIT Error includes scale factor of 1.2.	

$\Xi_c(2790)^0$ MASS

VALUE (MeV)	DOCUMENT ID
2792.8±1.2 OUR FIT Error includes scale factor of 2.9.	

$\Xi_c(2790) - \Xi_c$ MASS DIFFERENCES

$m_{\Xi_c(2790)^+} - m_{\Xi_c^0}$

VALUE (MeV)	EVTS	DOCUMENT ID		TECN	COMMENT
321.1±0.4 OUR FIT Error includes scale factor of 1.2.					
320.7±0.2±0.4	2231	YELTON	16	BELL	e^+e^-, Υ regions
• • • We do not use the following data for averages, fits, limits, etc. • • •					
318.2±1.3±2.9	18	CSORNA	01	CLEO	$e^+e^- \approx \Upsilon(4S)$

$m_{\Xi_c(2790)^0} - m_{\Xi_c^+}$

VALUE (MeV)	EVTS	DOCUMENT ID		TECN	COMMENT
324.9±1.2 OUR FIT Error includes scale factor of 3.7.					
323.8±0.2±0.4	1241	YELTON	16	BELL	e^+e^-, Υ regions
• • • We do not use the following data for averages, fits, limits, etc. • • •					
324.0±1.3±3.0	14	CSORNA	01	CLEO	$e^+e^- \approx \Upsilon(4S)$

$\Xi_c(2790) - \Xi_c'$ MASS DIFFERENCES

$m_{\Xi_c(2790)^+} - m_{\Xi_c'^0}$

VALUE (MeV)	DOCUMENT ID		TECN	COMMENT
213.10±0.26 OUR FIT Error includes scale factor of 1.2.				
213.2 ±0.2 ±0.1	YELTON	16	BELL	2231 and 11,560 evts

$m_{\Xi_c(2790)^0} - m_{\Xi_c'^+}$

VALUE (MeV)	DOCUMENT ID		TECN	COMMENT
215.4±0.8 OUR FIT Error includes scale factor of 3.7.				
215.7±0.2±0.1	YELTON	16	BELL	1241 and 7055 evts

$\Xi_c(2790)^+ - \Xi_c(2790)^0$ MASS DIFFERENCE

VALUE (MeV)	DOCUMENT ID		TECN	COMMENT
−0.9±1.3 OUR FIT Error includes scale factor of 2.5.				
• • • We do not use the following data for averages, fits, limits, etc. • • •				
−3.3±0.4±0.5	YELTON	16	BELL	2231 and 1241 evts

$\Xi_c(2790)$ WIDTHS

$\Xi_c(2790)^+$ WIDTH

VALUE (MeV)	CL%	EVTS	DOCUMENT ID		TECN	COMMENT
8.9±0.6±0.8		2231	YELTON	16	BELL	e^+e^-, Υ regions
• • • We do not use the following data for averages, fits, limits, etc. • • •						
<15	90		CSORNA	01	CLEO	$e^+e^- \approx \Upsilon(4S)$

$\Xi_c(2790)^0$ WIDTH

VALUE (MeV)	CL%	EVTS	DOCUMENT ID		TECN	COMMENT
10.0±0.7±0.8		1241	YELTON	16	BELL	e^+e^-, Υ regions
• • • We do not use the following data for averages, fits, limits, etc. • • •						
<12	90		CSORNA	01	CLEO	$e^+e^- \approx \Upsilon(4S)$

$\Xi_c(2790)$ DECAY MODES

	Mode	Fraction (Γ_i/Γ)
Γ_1	$\Xi_c\pi$	seen
Γ_2	$\Xi_c'\pi$	seen

$\Xi_c(2790)$ REFERENCES

YELTON	16	PR D94 052011	J. Yelton *et al.*	(BELLE Collab.)
CSORNA	01	PRL 86 4243	S.E. Csorna *et al.*	(CLEO Collab.)

$\Xi_c(2815)$

$I(J^P) = \frac{1}{2}(\frac{3}{2}^-)$ Status: ***

Seen in both $\Xi_c\pi$ and $\Xi_c\pi\pi$ decays. The simplest assignment is that this belongs to the same SU(4) multiplet as the $\Lambda(1520)$ and the $\Lambda_c(2625)$, but the spin and parity have not been measured.

$\Xi_c(2815)$ MASSES

The masses are obtained from the mass-difference measurements that follow.

$\Xi_c(2815)^+$ MASS

VALUE (MeV)	EVTS	DOCUMENT ID		TECN	COMMENT
2816.67±0.31 OUR FIT	Error includes scale factor of 1.1.				
• • • We do not use the following data for averages, fits, limits, etc. • • •					
2817.0 ±1.2 $^{+0.7}_{-0.8}$	73 ± 10	LESIAK	08	BELL	$e^+e^- \approx \Upsilon(4S)$

$\Xi_c(2815)^0$ MASS

VALUE (MeV)	EVTS	DOCUMENT ID		TECN	COMMENT
2820.22±0.32 OUR FIT					
• • • We do not use the following data for averages, fits, limits, etc. • • •					
2820.4 ±1.4 $^{+0.9}_{-1.0}$	48 ± 8	LESIAK	08	BELL	$e^+e^- \approx \Upsilon(4S)$

$\Xi_c(2815) - \Xi_c$ MASS DIFFERENCES

$m_{\Xi_c(2815)^+} - m_{\Xi_c^+}$

VALUE (MeV)	EVTS	DOCUMENT ID		TECN	COMMENT
348.80±0.10 OUR FIT					
348.80±0.08±0.06	941	YELTON	16	BELL	e^+e^-, Υ regions
• • • We do not use the following data for averages, fits, limits, etc. • • •					
348.6 ±0.6 ±1.0	20	ALEXANDER	99B	CLE2	$e^+e^- \approx \Upsilon(4S)$

$m_{\Xi_c(2815)^0} - m_{\Xi_c^0}$

VALUE (MeV)	EVTS	DOCUMENT ID		TECN	COMMENT
349.35±0.11 OUR FIT					
349.35±0.08±0.07	1258	YELTON	16	BELL	e^+e^-, Υ regions
• • • We do not use the following data for averages, fits, limits, etc. • • •					
347.2 ±0.7 ±2.0	9	ALEXANDER	99B	CLE2	$e^+e^- \approx \Upsilon(4S)$

$\Xi_c(2815)^+ - \Xi_c(2815)^0$ MASS DIFFERENCE

$m_{\Xi_c(2815)^+} - m_{\Xi_c(2815)^0}$

VALUE (MeV)	DOCUMENT ID		TECN	COMMENT
−3.55±0.28 OUR FIT				
• • • We do not use the following data for averages, fits, limits, etc. • • •				
−3.47±0.12±0.48	YELTON	16	BELL	941 and 1258 evts
−3.4 ±1.9 ±0.9	LESIAK	08	BELL	73 & 48 events

$\Xi_c(2815)$ WIDTHS

$\Xi_c(2815)^+$ WIDTH

VALUE (MeV)	CL%	EVTS	DOCUMENT ID		TECN	COMMENT
2.43±0.20±0.17		941	YELTON	16	BELL	e^+e^-, Υ regions
• • • We do not use the following data for averages, fits, limits, etc. • • •						
<3.5	90		ALEXANDER	99B	CLE2	$e^+e^- \approx \Upsilon(4S)$

$\Xi_c(2815)^0$ WIDTH

VALUE (MeV)	CL%	EVTS	DOCUMENT ID		TECN	COMMENT
2.54±0.18±0.17		1258	YELTON	16	BELL	e^+e^-, Υ regions
• • • We do not use the following data for averages, fits, limits, etc. • • •						
<6.5	90		ALEXANDER	99B	CLE2	$e^+e^- \approx \Upsilon(4S)$

$\Xi_c(2815)$ DECAY MODES

The $\Xi_c\pi\pi$ modes are consistent with being entirely via $\Xi_c(2645)\pi$.

	Mode	Fraction (Γ_i/Γ)
Γ_1	$\Xi_c\pi$	seen
Γ_2	$\Xi_c^+\pi^+\pi^-$	seen
Γ_3	$\Xi_c^0\pi^+\pi^-$	seen

$\Xi_c(2815)$ REFERENCES

YELTON	16	PR D94 052011	J. Yelton *et al.*	(BELLE Collab.)
LESIAK	08	PL B665 9	T. Lesiak *et al.*	(BELLE Collab.)
ALEXANDER	99B	PRL 83 3390	J.P. Alexander *et al.*	(CLEO Collab.)

$\Xi_c(2930)$

$I(J^P) = ?(?^?)$ Status: *

OMITTED FROM SUMMARY TABLE

A peak seen in the $\Lambda_c^+ K^-$ mass projection of $B^- \to \Lambda_c^+ \overline{\Lambda}_c^- K^-$ events.

$\Xi_c(2930)$ MASS

VALUE (MeV)	EVTS	DOCUMENT ID		TECN	COMMENT
2931±3±5	≈ 34	AUBERT	08H	BABR	$\Upsilon(4S) \to B\overline{B}$

$\Xi_c(2930)$ WIDTH

VALUE (MeV)	EVTS	DOCUMENT ID		TECN	COMMENT
36±7±11	≈ 34	AUBERT	08H	BABR	$\Upsilon(4S) \to B\overline{B}$

$\Xi_c(2930)$ REFERENCES

AUBERT	08H	PR D77 031101	B. Aubert *et al.*	(BABAR Collab.)

$\Xi_c(2970)$

$I(J^P) = \frac{1}{2}(?^?)$ Status: ***

was $\Xi_c(2980)$

$\Xi_c(2970)$ MASSES

$\Xi_c(2970)^+$ MASS

VALUE (MeV)	EVTS	DOCUMENT ID		TECN	COMMENT
2969.4±0.8 OUR FIT	Error includes scale factor of 1.1.				
2970.7±2.2 OUR AVERAGE	Error includes scale factor of 1.5. See the ideogram below.				
2974.9±1.5±2.1	244 ± 39	KATO	14	BELL	e^+e^- $\Upsilon(1S)$ to $\Upsilon(5S)$
2969.3±2.2±1.7	756 ± 206	AUBERT	08J	BABR	$e^+e^- \approx$ 10.58 GeV
2967.7±2.3$^{+1.1}_{-1.2}$	78 ± 13	LESIAK	08	BELL	$e^+e^- \approx \Upsilon(4S)$
• • • We do not use the following data for averages, fits, limits, etc. • • •					
2978.5±2.1±2.0	405 ± 51	CHISTOV	06	BELL	See KATO 14

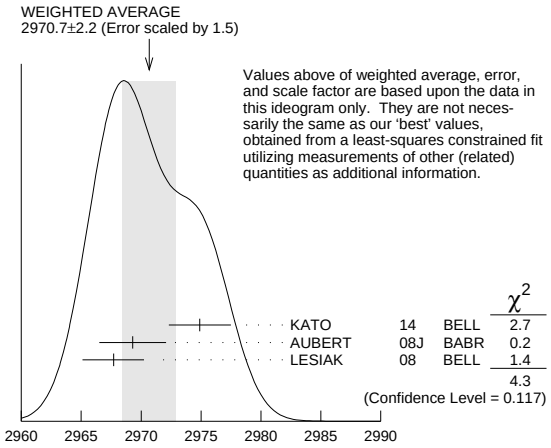

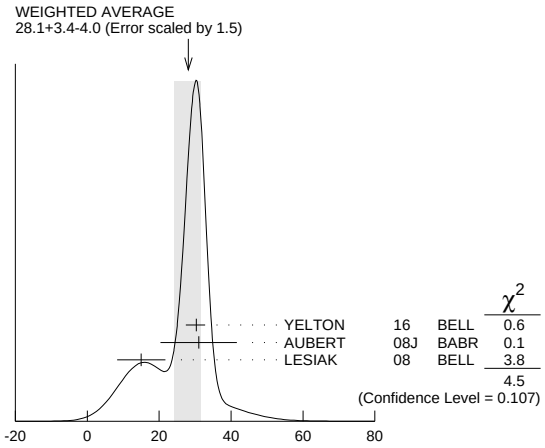

$\Xi_c(2970)^0$ MASS

The evidence is statistically weaker for this charge state.

VALUE (MeV)	EVTS	DOCUMENT ID		TECN	COMMENT
2967.8±0.8 OUR FIT	Error includes scale factor of 1.1.				
2968.0±2.6 OUR AVERAGE	Error includes scale factor of 1.2.				
2972.9±4.4±1.6	67 ± 44	AUBERT	08J	BABR	$e^+e^- \approx$ 10.58 GeV
$2965.7\pm2.4^{+1.1}_{-1.2}$	57 ± 13	LESIAK	08	BELL	$e^+e^- \approx \Upsilon(4S)$
2977.1±8.8±3.5	42 ± 24	CHISTOV	06	BELL	$e^+e^- \approx \Upsilon(4S)$

$\Xi_c(2970) - \Xi_c$ MASS DIFFERENCES

$m_{\Xi_c(2970)^+} - m_{\Xi_c^0}$

VALUE (MeV)	EVTS	DOCUMENT ID		TECN	COMMENT
498.5±0.8 OUR FIT	Error includes scale factor of 1.1.				
498.1±0.8±0.2	916	YELTON	16	BELL	e^+e^-, Υ regions

$m_{\Xi_c(2970)^0} - m_{\Xi_c^+}$

VALUE (MeV)	EVTS	DOCUMENT ID		TECN	COMMENT
$\mathbf{499.9^{+0.8}_{-0.7}}$ **OUR FIT**	Error includes scale factor of 1.1.				
499.9±0.7±0.2	1443	YELTON	16	BELL	e^+e^-, Υ regions

$\Xi_c(2970)^+ - \Xi_c(2970)^0$ MASS DIFFERENCE

VALUE (MeV)	DOCUMENT ID		TECN	COMMENT
1.6±1.1 OUR FIT	Error includes scale factor of 1.1.			
• • • We do not use the following data for averages, fits, limits, etc. • • •				
−4.8±0.1±0.5	YELTON	16	BELL	916 and 1443 evts

$\Xi_c(2970)$ WIDTHS

$\Xi_c(2970)^+$ WIDTH

VALUE (MeV)	EVTS	DOCUMENT ID		TECN	COMMENT
$\mathbf{20.9^{+2.4}_{-3.5}}$ **OUR AVERAGE**	Error includes scale factor of 1.2.				
$28.1\pm2.4^{+1.0}_{-5.0}$	916	YELTON	16	BELL	e^+e^-, Υ regions
14.8±2.5±4.1	244 ± 39	KATO	14	BELL	e^+e^- $\Upsilon(1S)$ to $\Upsilon(5S)$
27 ±8 ±2	756±206	AUBERT	08J	BABR	$e^+e^- \approx$ 10.58 GeV
18 ±6 ±3	78 ± 13	LESIAK	08	BELL	$e^+e^- \approx \Upsilon(4S)$
• • • We do not use the following data for averages, fits, limits, etc. • • •					
43.5±7.5±7.0	405 ± 51	CHISTOV	06	BELL	See KATO 14

$\Xi_c(2970)^0$ WIDTH

VALUE (MeV)	EVTS	DOCUMENT ID		TECN	COMMENT
$\mathbf{28.1^{+3.4}_{-4.0}}$ **OUR AVERAGE**	Error includes scale factor of 1.5. See the ideogram below.				
$30.3\pm2.3^{+1.0}_{-1.8}$	1443	YELTON	16	BELL	e^+e^-, Υ regions
31 ±7 ±8	67 ± 44	AUBERT	08J	BABR	$e^+e^- \approx$ 10.58 GeV
15 ±6 ±3	57 ± 13	LESIAK	08	BELL	$e^+e^- \approx \Upsilon(4S)$

$\Xi_c(2970)$ DECAY MODES

	Mode	Fraction (Γ_i/Γ)
Γ_1	$\Lambda_c^+ \overline{K}\pi$	seen
Γ_2	$\Sigma_c(2455)\overline{K}$	seen
Γ_3	$\Lambda_c^+ \overline{K}$	not seen
Γ_4	$\Xi_c 2\pi$	seen
Γ_5	$\Xi_c(2645)\pi$	seen

$\Xi_c(2970)$ BRANCHING RATIOS

$\Gamma(\Lambda_c^+\overline{K}\pi)/\Gamma_{\text{total}}$ Γ_1/Γ

VALUE	DOCUMENT ID		TECN	COMMENT
seen	AUBERT	08J	BABR	$e^+e^- \approx \Upsilon(4S)$
seen	CHISTOV	06	BELL	$e^+e^- \approx \Upsilon(4S)$

$\Gamma(\Sigma_c(2455)\overline{K})/\Gamma(\Lambda_c^+\overline{K}\pi)$ Γ_2/Γ_1

VALUE	DOCUMENT ID		TECN	COMMENT
0.55±0.07±0.13	AUBERT	08J	BABR	$e^+e^- \approx \Upsilon(4S)$

$\Gamma(\Xi_c(2645)\pi)/\Gamma_{\text{total}}$ Γ_5/Γ

VALUE	DOCUMENT ID		TECN	COMMENT
seen	LESIAK	08	BELL	$e^+e^- \approx \Upsilon(4S)$

$\Xi_c(2970)$ REFERENCES

YELTON	16	PR D94 052011	J. Yelton *et al.*	(BELLE Collab.)
KATO	14	PR D89 052003	Y. Kato *et al.*	(BELLE Collab.)
AUBERT	08J	PR D77 012002	B. Aubert *et al.*	(BABAR Collab.)
LESIAK	08	PL B665 9	T. Lesiak *et al.*	(BELLE Collab.)
CHISTOV	06	PRL 97 162001	R. Chistov *et al.*	(BELLE Collab.)

$\Xi_c(3055)$

$I(J^P) = ?(?^?)$ Status: ***

$\Xi_c(3055)$ MASSES

$\Xi_c(3055)^+$ MASS

VALUE (MeV)	EVTS	DOCUMENT ID		TECN	COMMENT
3055.9±0.4	894	KATO	16	BELL	e^+e^- Υ region
• • • We do not use the following data for averages, fits, limits, etc. • • •					
3058.1±1.0±2.1	199 ± 46	KATO	14	BELL	See KATO 16
3054.2±1.2±0.5	218 ± 95	AUBERT	08J	BABR	$e^+e^- \approx$ 10.58 GeV

$\Xi_c(3055)$ WIDTHS

$\Xi_c(3055)^+$ WIDTH

VALUE (MeV)	EVTS	DOCUMENT ID		TECN	COMMENT
7.8±1.2± 1.5		KATO	16	BELL	e^+e^- Υ region
• • • We do not use the following data for averages, fits, limits, etc. • • •					
9.7±3.4± 3.3	199 ± 46	KATO	14	BELL	e^+e^- $\Upsilon(1S)$ to $\Upsilon(5S)$
17 ±6 ±11	218 ± 95	AUBERT	08J	BABR	$e^+e^- \approx$ 10.58 GeV

$\Xi_c(3055)$ DECAY MODES

	Mode	Fraction (Γ_i/Γ)
Γ_1	$\Sigma^{++}K^-$	seen
Γ_2	ΛD^+	seen

$\Xi_c(3055)$ BRANCHING RATIOS

$\Gamma(\Lambda D^+)/\Gamma(\Sigma^{++}K^-)$ Γ_2/Γ_1

VALUE	DOCUMENT ID		TECN	COMMENT
5.09±1.01±0.76	KATO	16	BELL	721 and 103 evts

$\Xi_c(3055)$ REFERENCES

KATO	16	PR D94 032002	Y. Kato *et al.*	(BELLE Collab.)
KATO	14	PR D89 052003	Y. Kato *et al.*	(BELLE Collab.)
AUBERT	08J	PR D77 012002	B. Aubert *et al.*	(BABAR Collab.)

$\Xi_c(3080)$

$I(J^P) = \frac{1}{2}(?^?)$ Status: ***

$\Xi_c(3080)$ MASSES

$\Xi_c(3080)^+$ MASS

VALUE (MeV)	EVTS	DOCUMENT ID		TECN	COMMENT
3077.2±0.4 OUR AVERAGE					
3077.9±0.9	596	KATO	16	BELL	e^+e^- Υ region
3077.0±0.4±0.2	403 ± 60	AUBERT	08J	BABR	$e^+e^- \approx 10.58$ GeV
• • • We do not use the following data for averages, fits, limits, etc. • • •					
3076.9±0.3±0.2	210 ± 30	KATO	14	BELL	See KATO 16
3076.7±0.9±0.5	326 ± 40	CHISTOV	06	BELL	See KATO 14

$\Xi_c(3080)^0$ MASS

VALUE (MeV)	EVTS	DOCUMENT ID		TECN	COMMENT
3079.9±1.4 OUR AVERAGE Error includes scale factor of 1.3.					
3079.3±1.1±0.2	90 ± 27	AUBERT	08J	BABR	$e^+e^- \approx 10.58$ GeV
3082.8±1.8±1.5	67 ± 20	CHISTOV	06	BELL	$e^+e^- \approx \Upsilon(4S)$

$\Xi_c(3080)$ WIDTHS

$\Xi_c(3080)^+$ WIDTH

VALUE (MeV)	EVTS	DOCUMENT ID		TECN	COMMENT
3.6±1.1 OUR AVERAGE Error includes scale factor of 1.5.					
3.0±0.7±0.4	596	KATO	16	BELL	e^+e^- Υ region
5.5±1.3±0.6	403 ± 60	AUBERT	08J	BABR	$e^+e^- \approx 10.58$ GeV
• • • We do not use the following data for averages, fits, limits, etc. • • •					
2.4±0.9±1.6	210 ± 30	KATO	14	BELL	See KATO 16
6.2±1.2±0.8	326 ± 40	CHISTOV	06	BELL	See KATO 14

$\Xi_c(3080)^0$ WIDTH

VALUE (MeV)	EVTS	DOCUMENT ID		TECN	COMMENT
5.6±2.2 OUR AVERAGE					
5.9±2.3±1.5	90 ± 27	AUBERT	08J	BABR	$e^+e^- \approx 10.58$ GeV
5.2±3.1±1.8	67 ± 20	CHISTOV	06	BELL	$e^+e^- \approx \Upsilon(4S)$

$\Xi_c(3080)$ DECAY MODES

	Mode	Fraction (Γ_i/Γ)
Γ_1	$\Lambda_c^+\overline{K}\pi$	seen
Γ_2	$\Sigma_c(2455)\overline{K}$	seen
Γ_3	$\Sigma_c(2455)^{++}K^-$	seen
Γ_4	$\Sigma_c(2520)^{++}K^-$	seen
Γ_5	$\Sigma_c(2455)\overline{K} + \Sigma_c(2520)\overline{K}$	seen
Γ_6	$\Lambda_c^+\overline{K}$	not seen
Γ_7	$\Lambda_c^+\overline{K}\pi^+\pi^-$	not seen
Γ_8	ΛD^+	seen

$\Xi_c(3080)$ BRANCHING RATIOS

$\Gamma(\Sigma_c(2455)\overline{K})/\Gamma(\Lambda_c^+\overline{K}\pi)$ Γ_2/Γ_1

VALUE	DOCUMENT ID		TECN	COMMENT
0.45±0.06 OUR AVERAGE				
0.45±0.05±0.05	AUBERT	08J	BABR	in $\Lambda_c^+ K^-\pi^+$
0.44±0.12±0.07	AUBERT	08J	BABR	in $\Lambda_c^+ K_S^0\pi^-$

$\Gamma(\Sigma_c(2520)^{++}K^-)/\Gamma(\Sigma_c(2455)^{++}K^-)$ Γ_4/Γ_3

VALUE	DOCUMENT ID		TECN	COMMENT
1.07±0.27±0.04	KATO	16	BELL	234 and 176 evts

$[\Gamma(\Sigma_c(2455)\overline{K}) + \Gamma(\Sigma_c(2520)\overline{K})]/\Gamma(\Lambda_c^+\overline{K}\pi)$ Γ_5/Γ_1

VALUE	DOCUMENT ID		TECN	COMMENT
0.89±0.12 OUR AVERAGE				
0.95±0.14±0.06	AUBERT	08J	BABR	in $\Lambda_c^+ K^-\pi^+$
0.78±0.21±0.05	AUBERT	08J	BABR	in $\Lambda_c^+ K_S^0\pi^-$

$\Gamma(\Lambda D^+)/\Gamma(\Sigma_c(2455)^{++}K^-)$ Γ_8/Γ_3

VALUE	DOCUMENT ID		TECN	COMMENT
1.29±0.30±0.15	KATO	16	BELL	186 and 176 evts

$\Xi_c(3080)$ REFERENCES

KATO	16	PR D94 032002	Y. Kato *et al.*	(BELLE Collab.)
KATO	14	PR D89 052003	Y. Kato *et al.*	(BELLE Collab.)
AUBERT	08J	PR D77 012002	B. Aubert *et al.*	(BABAR Collab.)
CHISTOV	06	PRL 97 162001	R. Chistov *et al.*	(BELLE Collab.)

$\Xi_c(3123)$

$I(J^P) = ?(?^?)$ Status: *

OMITTED FROM SUMMARY TABLE

A peak in the $\Sigma_c(2520)^{++}K^- \to \Lambda_c^+ K^-\pi^+$ mass spectrum with a significance of 3.6 standard deviations. KATO 14 finds no evidence for this state.

$\Xi_c(3123)$ MASSES

$\Xi_c(3123)^+$ MASS

VALUE (MeV)	EVTS	DOCUMENT ID		TECN	COMMENT
3122.9±1.3±0.3	101 ± 35	AUBERT	08J	BABR	$e^+e^- \approx 10.58$ GeV

$\Xi_c(3123)$ WIDTHS

$\Xi_c(3123)^+$ WIDTH

VALUE (MeV)	EVTS	DOCUMENT ID		TECN	COMMENT
4.4±3.4±1.7	101 ± 35	AUBERT	08J	BABR	$e^+e^- \approx 10.58$ GeV

$\Xi_c(3123)$ REFERENCES

KATO	14	PR D89 052003	Y. Kato *et al.*	(BELLE Collab.)
AUBERT	08J	PR D77 012002	B. Aubert *et al.*	(BABAR Collab.)

Ω_c^0

$I(J^P) = 0(\frac{1}{2}^+)$ Status: ***

The quantum numbers have not been measured, but are simply assigned in accord with the quark model, in which the Ω_c^0 is the *ssc* ground state.

Ω_c^0 MASS

VALUE (MeV)	EVTS	DOCUMENT ID		TECN	COMMENT
2695.2± 1.7 OUR FIT Error includes scale factor of 1.3.					
2695.2$^{+\ 1.8}_{-\ 1.6}$ OUR AVERAGE Error includes scale factor of 1.3. See the ideogram below.					
2693.6± 0.3$^{+1.8}_{-1.5}$	725	SOLOVIEVA	09	BELL	$\Omega^-\pi^+$ in $e^+e^- \to \Upsilon(4S)$
2694.6± 2.6±1.9	40	[1] CRONIN-HEN..01		CLE2	$e^+e^- \approx 10.6$ GeV
2699.9± 1.5±2.5	42	[2] FRABETTI	94H	E687	γBe, $\overline{E}_\gamma = 221$ GeV
• • • We do not use the following data for averages, fits, limits, etc. • • •					
2705.9± 3.3±2.0	10	[3] FRABETTI	93	E687	γBe, $\overline{E}_\gamma = 221$ GeV
2719.0± 7.0±2.5	11	[4] ALBRECHT	92H	ARG	$e^+e^- \approx 10.6$ GeV
2740 ±20	3	BIAGI	85B	SPEC	Σ^-Be 135 GeV/c

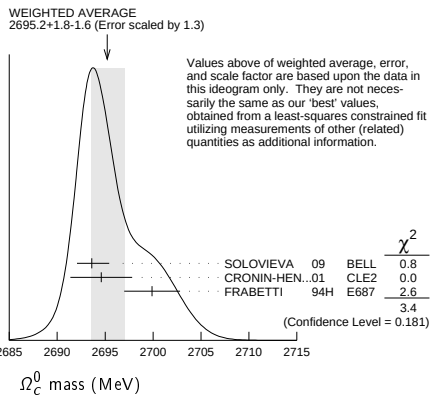

[1] CRONIN-HENNESSY 01 sees 40.4 ± 9.0 events in a sum over five channels.

[2] FRABETTI 94H claims a signal of 42.5 ± 8.8 $\Sigma^+ K^- K^- \pi^+$ events. The background is about 24 events.
[3] FRABETTI 93 claims a signal of 10.3 ± 3.9 $\Omega^- \pi^+$ events above a background of 5.8 events.
[4] ALBRECHT 92H claims a signal of 11.5 ± 4.3 $\Xi^- K^- \pi^+ \pi^+$ events. The background is about 5 events.

Ω_c^0 MEAN LIFE

VALUE (10^{-15} s)	EVTS	DOCUMENT ID		TECN	COMMENT
69±12 OUR AVERAGE					
72±11±11	64	LINK	03C	FOCS	$\Omega^- \pi^+$, $\Xi^- K^- \pi^+ \pi^+$
55^{+13+18}_{-11-23}	86	ADAMOVICH	95B	WA89	$\Omega^- \pi^- \pi^+ \pi^+$, $\Xi^- K^- \pi^+ \pi^+$
86^{+27}_{-20}±28	25	FRABETTI	95D	E687	$\Sigma^+ K^- K^- \pi^+$

Ω_c^0 DECAY MODES

Mode	Fraction (Γ_i/Γ)	Confidence level

No absolute branching fractions have been measured.
The following are branching *ratios* relative to $\Omega^- \pi^+$.

Cabibbo-favored ($S = -3$) decays — relative to $\Omega^- \pi^+$

Γ_1	$\Omega^- \pi^+$	**DEFINED AS 1**	
Γ_2	$\Omega^- \pi^+ \pi^0$	1.80±0.33	
Γ_3	$\Omega^- \rho^+$	>1.3	90%
Γ_4	$\Omega^- \pi^- 2\pi^+$	0.31±0.05	
Γ_5	$\Omega^- e^+ \nu_e$	2.4 ±1.2	
Γ_6	$\Xi^0 \overline{K}^0$	1.64±0.29	
Γ_7	$\Xi^0 K^- \pi^+$	1.20±0.18	
Γ_8	$\Xi^0 \overline{K}^{*0}$, $\overline{K}^{*0} \to K^- \pi^+$	0.68±0.16	
Γ_9	$\Xi^- \overline{K}^0 \pi^+$	2.12±0.28	
Γ_{10}	$\Xi^- K^- 2\pi^+$	0.63±0.09	
Γ_{11}	$\Xi(1530)^0 K^- \pi^+$, $\Xi^{*0} \to \Xi^- \pi^+$	0.21±0.06	
Γ_{12}	$\Xi^- \overline{K}^{*0} \pi^+$	0.34±0.11	
Γ_{13}	$\Sigma^+ K^- K^- \pi^+$	<0.32	90%
Γ_{14}	$\Lambda \overline{K}^0 \overline{K}^0$	1.72±0.35	

Ω_c^0 BRANCHING RATIOS

A few early but now obsolete measurements have been omitted. See K.A. Olive, et al. (Particle Data Group), Chinese Physics **C38** 070001 (2014).

$\Gamma(\Omega^- \pi^+ \pi^0)/\Gamma(\Omega^- \pi^+)$ Γ_2/Γ_1

VALUE	EVTS	DOCUMENT ID		TECN	COMMENT
1.80±0.33 OUR AVERAGE		Error includes scale factor of 1.9.			
2.00±0.17±0.11	403	YELTON	18	BELL	$e^+ e^- \to \Upsilon(4S)$, +higher
1.27±0.31±0.11	64	AUBERT	07AH	BABR	$e^+ e^- \approx \Upsilon(4S)$

$\Gamma(\Omega^- \rho^+)/\Gamma(\Omega^- \pi^+ \pi^0)$ Γ_3/Γ_2

VALUE	CL%	DOCUMENT ID		TECN	COMMENT
>0.71	90	[1] YELTON	18	BELL	$e^+ e^- \to \Upsilon(4S)$, +higher

[1] This submode fraction is evaluated from a background-subtracted signal in a mass plot. Result ignores interference effects and systematic uncertainties, which YELTON 18 claim are both small.

$\Gamma(\Omega^- \pi^- 2\pi^+)/\Gamma(\Omega^- \pi^+)$ Γ_4/Γ_1

VALUE	EVTS	DOCUMENT ID		TECN	COMMENT
0.31±0.05 OUR AVERAGE					
0.32±0.05±0.02	108	YELTON	18	BELL	$e^+ e^- \to \Upsilon(4S)$, +higher
0.28±0.09±0.01	25	AUBERT	07AH	BABR	$e^+ e^- \approx \Upsilon(4S)$

$\Gamma(\Omega^- \pi^+)/\Gamma(\Omega^- e^+ \nu_e)$ Γ_1/Γ_5

VALUE	EVTS	DOCUMENT ID		TECN	COMMENT
0.41±0.19±0.04	11	AMMAR	02	CLE2	$e^+ e^- \approx \Upsilon(4S)$

$\Gamma(\Xi^0 \overline{K}^0)/\Gamma(\Omega^- \pi^+)$ Γ_6/Γ_1

VALUE	EVTS	DOCUMENT ID		TECN	COMMENT
1.64±0.26±0.12	98	YELTON	18	BELL	$e^+ e^- \to \Upsilon(4S)$, +higher

$\Gamma(\Xi^0 K^- \pi^+)/\Gamma(\Omega^- \pi^+)$ Γ_7/Γ_1

VALUE	EVTS	DOCUMENT ID		TECN	COMMENT
1.20±0.16±0.08	168	YELTON	18	BELL	$e^+ e^- \to \Upsilon(4S)$, +higher

$\Gamma(\Xi^0 \overline{K}^{*0}, \overline{K}^{*0} \to K^- \pi^+)/\Gamma(\Xi^0 K^- \pi^+)$ Γ_8/Γ_7

VALUE	EVTS	DOCUMENT ID		TECN	COMMENT
0.57±0.10	95	[1] YELTON	18	BELL	$e^+ e^- \to \Upsilon(4S)$, +higher

[1] This submode fraction is evaluated from a background-subtracted signal in a mass plot. Result ignores interference effects and systematic uncertainties, which YELTON 18 claim are both small.

$\Gamma(\Xi^- \overline{K}^0 \pi^+)/\Gamma(\Omega^- \pi^+)$ Γ_9/Γ_1

VALUE	EVTS	DOCUMENT ID		TECN	COMMENT
2.12±0.24±0.14	349	YELTON	18	BELL	$e^+ e^- \to \Upsilon(4S)$, +higher

$\Gamma(\Xi^- K^- 2\pi^+)/\Gamma(\Omega^- \pi^+)$ Γ_{10}/Γ_1

VALUE	EVTS	DOCUMENT ID		TECN	COMMENT
0.63±0.09 OUR AVERAGE		Error includes scale factor of 1.4.			
0.68±0.07±0.03	278	YELTON	18	BELL	$e^+ e^- \to \Upsilon(4S)$, +higher
0.46±0.13±0.03	45	AUBERT	07AH	BABR	$e^+ e^- \approx \Upsilon(4S)$

$\Gamma(\Xi(1530)^0 K^- \pi^+, \Xi^{*0} \to \Xi^- \pi^+)/\Gamma(\Xi^- K^- 2\pi^+)$ Γ_{11}/Γ_{10}

VALUE	EVTS	DOCUMENT ID		TECN	COMMENT
0.33±0.09	74	[1] YELTON	18	BELL	$e^+ e^- \to \Upsilon(4S)$, +higher

[1] This submode fraction is evaluated from a background-subtracted signal in a mass plot. Result ignores interference effects and systematic uncertainties, which YELTON 18 claim are both small.

$\Gamma(\Xi^- \overline{K}^{*0} \pi^+)/\Gamma(\Xi^- K^- 2\pi^+)$ Γ_{12}/Γ_{10}

VALUE	EVTS	DOCUMENT ID		TECN	COMMENT
0.55±0.16	136	[1] YELTON	18	BELL	$e^+ e^- \to \Upsilon(4S)$, +higher

[1] This submode fraction is evaluated from a background-subtracted signal in a mass plot. Result ignores interference effects and systematic uncertainties, which YELTON 18 claim are both small.

$\Gamma(\Sigma^+ K^- K^- \pi^+)/\Gamma(\Omega^- \pi^+)$ Γ_{13}/Γ_1

VALUE	CL%	EVTS	DOCUMENT ID		TECN	COMMENT
<0.32	90	17	YELTON	18	BELL	$e^+ e^- \to \Upsilon(4S)$, +higher

$\Gamma(\Lambda \overline{K}^0 \overline{K}^0)/\Gamma(\Omega^- \pi^+)$ Γ_{14}/Γ_1

VALUE	EVTS	DOCUMENT ID		TECN	COMMENT
1.72±0.32±0.14	95	YELTON	18	BELL	$e^+ e^- \to \Upsilon(4S)$, +higher

Ω_c^0 REFERENCES

YELTON	18	PR D97 032001	J. Yelton *et al.*	(BELLE Collab.)
PDG	14	CP C38 070001	K. Olive *et al.*	(PDG Collab.)
SOLOVIEVA	09	PL B672 1	E. Solovieva *et al.*	(BELLE Collab.)
AUBERT	07AH	PRL 99 062001	B. Aubert *et al.*	(BABAR Collab.)
LINK	03C	PL B561 41	J.M. Link *et al.*	(FNAL FOCUS Collab.)
AMMAR	02	PRL 89 171803	R. Ammar *et al.*	(CLEO Collab.)
CRONIN-HEN...	01	PRL 86 3730	D. Cronin-Hennessy *et al.*	(CLEO Collab.)
ADAMOVICH	95B	PL B358 151	M.I. Adamovich *et al.*	(CERN WA89 Collab.)
FRABETTI	95D	PL B357 678	P.L. Frabetti *et al.*	(FNAL E687 Collab.)
FRABETTI	94H	PL B338 106	P.L. Frabetti *et al.*	(FNAL E687 Collab.)
FRABETTI	93	PL B300 190	P.L. Frabetti *et al.*	(FNAL E687 Collab.)
ALBRECHT	92H	PL B288 367	H. Albrecht *et al.*	(ARGUS Collab.)
BIAGI	85B	ZPHY C28 175	S.F. Biagi *et al.*	(CERN WA62 Collab.)

$\Omega_c(2770)^0$

$I(J^P) = 0(\frac{3}{2}^+)$ Status: ***

The natural assignment is that this goes with the $\Sigma_c(2520)$ and $\Xi_c(2645)$ to complete the lowest mass $J^P = \frac{3}{2}^+$ SU(3) sextet, part of the SU(4) 20-plet that includes the $\Delta(1232)$. But J and P have not been measured.

$\Omega_c(2770)^0$ MASS

The mass is obtained from the mass-difference measurement that follows.

VALUE (MeV)	DOCUMENT ID
2765.9±2.0 OUR FIT	Error includes scale factor of 1.2.

$\Omega_c(2770)^0 - \Omega_c^0$ MASS DIFFERENCE

VALUE (MeV)	EVTS	DOCUMENT ID		TECN	COMMENT
$70.7^{+0.8}_{-0.9}$ OUR FIT					
$70.7^{+0.8}_{-1.0}$ OUR AVERAGE					
$70.7 \pm 0.9^{+0.1}_{-0.9}$	54 ± 9	SOLOVIEVA	09	BELL	$\Omega_c^0 \gamma$ in $e^+ e^- \to \Upsilon(4S)$
70.8±1.0±1.1	105 ± 22	AUBERT,BE	06I	BABR	$e^+ e^- \approx \Upsilon(4S)$

$\Omega_c(2770)^0$ DECAY MODES

The $\Omega_c(2770)^0 - \Omega_c^0$ mass difference is too small for any strong decay to occur.

	Mode	Fraction (Γ_i/Γ)
Γ_1	$\Omega_c^0 \gamma$	presumably 100%

$\Omega_c(2770)^0$ REFERENCES

SOLOVIEVA	09	PL B672 1	E. Solovieva *et al.*	(BELLE Collab.)
AUBERT,BE	06I	PRL 97 232001	B. Aubert *et al.*	(BABAR Collab.)

$\Omega_c(3000)^0$

$I(J^P) = ?(?^?)$ Status: ***

$\Omega_c(3000)^0$ MASS

VALUE (MeV)	EVTS	DOCUMENT ID		TECN	COMMENT
3000.4±0.2±0.1±0.3	1.3k	[1] AAIJ	17AH	LHCB	*pp* at 7, 8, 13 TeV

[1] The third error is the uncertainty on the Ξ_c^+ mass. (AAIJ 17AH gave $^{+0.3}_{-0.5}$ MeV here, but as of 2018 it is ±0.3.)

$\Omega_c(3000)^0$ WIDTH

VALUE (MeV)	EVTS	DOCUMENT ID		TECN	COMMENT
4.5±0.6±0.3	1.3k	AAIJ	17AH	LHCB	*pp* at 7, 8, 13 TeV

$\Omega_c(3000)^0$ DECAY MODES

	Mode	Fraction (Γ_i/Γ)
Γ_1	$\Xi_c^+ K^-$	seen

$\Omega_c(3000)^0$ BRANCHING RATIOS

$\Gamma(\Xi_c^+ K^-)/\Gamma_{total}$ Γ_1/Γ

VALUE	DOCUMENT ID		TECN	COMMENT
seen	AAIJ	17AH	LHCB	*pp* at 7, 8, 13 TeV

$\Omega_c(3000)^0$ REFERENCES

AAIJ	17AH	PRL 118 182001	R. Aaij *et al.*	(LHCb Collab.)

$\Omega_c(3050)^0$

$I(J^P) = ?(?^?)$ Status: ***

$\Omega_c(3050)^0$ MASS

VALUE (MeV)	EVTS	DOCUMENT ID		TECN	COMMENT
3050.2±0.1±0.1±0.3	970	[1] AAIJ	17AH	LHCB	*pp* at 7, 8, 13 TeV

[1] The third error is the uncertainty on the Ξ_c^+ mass. (AAIJ 17AH gave $^{+0.3}_{-0.5}$ MeV here, but as of 2018 it is ±0.3.)

$\Omega_c(3050)^0$ WIDTH

VALUE (MeV)	CL%	DOCUMENT ID		TECN	COMMENT
<1.2	95	AAIJ	17AH	LHCB	*pp* at 7, 8, 13 TeV

$\Omega_c(3050)^0$ DECAY MODES

	Mode	Fraction (Γ_i/Γ)
Γ_1	$\Xi_c^+ K^-$	seen

$\Omega_c(3050)^0$ BRANCHING RATIOS

$\Gamma(\Xi_c^+ K^-)/\Gamma_{total}$ Γ_1/Γ

VALUE	DOCUMENT ID		TECN	COMMENT
seen	AAIJ	17AH	LHCB	*pp* at 7, 8, 13 TeV

$\Omega_c(3050)^0$ REFERENCES

AAIJ	17AH	PRL 118 182001	R. Aaij *et al.*	(LHCb Collab.)

$\Omega_c(3065)^0$

$I(J^P) = ?(?^?)$ Status: ***

$\Omega_c(3065)^0$ MASS

VALUE (MeV)	EVTS	DOCUMENT ID		TECN	COMMENT
3065.6±0.1±0.3±0.3	1.74k	[1] AAIJ	17AH	LHCB	*pp* at 7, 8, 13 TeV

[1] The third error is the uncertainty on the Ξ_c^+ mass. (AAIJ 17AH gave $^{+0.3}_{-0.5}$ MeV here, but as of 2018 it is ±0.3.)

$\Omega_c(3065)^0$ WIDTH

VALUE (MeV)	EVTS	DOCUMENT ID		TECN	COMMENT
3.5±0.4±0.2	1.74k	AAIJ	17AH	LHCB	*pp* at 7, 8, 13 TeV

$\Omega_c(3065)^0$ DECAY MODES

	Mode	Fraction (Γ_i/Γ)
Γ_1	$\Xi_c^+ K^-$	seen

$\Omega_c(3065)^0$ BRANCHING RATIOS

$\Gamma(\Xi_c^+ K^-)/\Gamma_{total}$ Γ_1/Γ

VALUE	DOCUMENT ID		TECN	COMMENT
seen	AAIJ	17AH	LHCB	*pp* at 7, 8, 13 TeV

$\Omega_c(3065)^0$ REFERENCES

AAIJ	17AH	PRL 118 182001	R. Aaij *et al.*	(LHCb Collab.)

$\Omega_c(3090)^0$

$I(J^P) = ?(?^?)$ Status: ***

$\Omega_c(3090)^0$ MASS

VALUE (MeV)	EVTS	DOCUMENT ID		TECN	COMMENT
3090.2±0.3±0.5±0.3	2.0k	[1] AAIJ	17AH	LHCB	*pp* at 7, 8, 13 TeV

[1] The third error is the uncertainty on the Ξ_c^+ mass. (AAIJ 17AH gave $^{+0.3}_{-0.5}$ MeV here, but as of 2018 it is ±0.3.)

$\Omega_c(3090)^0$ WIDTH

VALUE (MeV)	EVTS	DOCUMENT ID		TECN	COMMENT
8.7±1.0±0.8	2.0k	AAIJ	17AH	LHCB	*pp* at 7, 8, 13 TeV

$\Omega_c(3090)^0$ DECAY MODES

	Mode	Fraction (Γ_i/Γ)
Γ_1	$\Xi_c^+ K^-$	seen

$\Omega_c(3090)^0$ BRANCHING RATIOS

$\Gamma(\Xi_c^+ K^-)/\Gamma_{total}$ Γ_1/Γ

VALUE	DOCUMENT ID		TECN	COMMENT
seen	AAIJ	17AH	LHCB	*pp* at 7, 8, 13 TeV

$\Omega_c(3090)^0$ REFERENCES

AAIJ	17AH	PRL 118 182001	R. Aaij *et al.*	(LHCb Collab.)

$\Omega_c(3120)^0$

$I(J^P) = ?(?^?)$ Status: ***

$\Omega_c(3120)^0$ MASS

VALUE (MeV)	EVTS	DOCUMENT ID		TECN	COMMENT
3119.1±0.3±0.9±0.3	480	[1] AAIJ	17AH	LHCB	*pp* at 7, 8, 13 TeV

[1] The third error is the uncertainty on the Ξ_c^+ mass. (AAIJ 17AH gave $^{+0.3}_{-0.5}$ MeV here, but as of 2018 it is ±0.3.)

$\Omega_c(3120)^0$ WIDTH

VALUE (MeV)	CL%	DOCUMENT ID		TECN	COMMENT
<2.6	95	AAIJ	17AH	LHCB	*pp* at 7, 8, 13 TeV

$\Omega_c(3120)^0$ DECAY MODES

	Mode	Fraction (Γ_i/Γ)
Γ_1	$\Xi_c^+ K^-$	seen

$\Omega_c(3120)^0$ BRANCHING RATIOS

$\Gamma(\Xi_c^+ K^-)/\Gamma_{\text{total}}$ Γ_1/Γ

VALUE	DOCUMENT ID		TECN	COMMENT
seen	AAIJ	17AH	LHCB	pp at 7, 8, 13 TeV

$\Omega_c(3120)^0$ REFERENCES

AAIJ 17AH PRL 118 182001 R. Aaij *et al.* (LHCb Collab.)

DOUBLY CHARMED BARYONS ($C = +2$)

$\Xi_{cc}^{++} = ucc$, $\Xi_{cc}^{+} = dcc$, $\Omega_{cc}^{+} = scc$

Ξ_{cc}^{+}

$I(J^P) = ?(?^?)$ Status: *

OMITTED FROM SUMMARY TABLE

This would presumably be an isospin-1/2 particle, a ccu Ξ_{cc}^{++} and a ccd Ξ_{cc}^{+}. However, opposed to the evidence cited below, the BABAR experiment has found no evidence for a Ξ_{cc}^{+} in a search in $\Lambda_c^+ K^- \pi^+$ and $\Xi_c^0 \pi^+$ modes, and no evidence of a Ξ_{cc}^{++} in $\Lambda_c^+ K^- \pi^+ \pi^+$ and $\Xi_c^0 \pi^+ \pi^+$ modes (AUBERT,B 06D). Nor have the BELLE (CHISTOV 06, KATO 14) or LHCb (AAIJ 13CD) experiments found any evidence for this state.

Ξ_{cc}^{+} MASS

VALUE (MeV)	EVTS	DOCUMENT ID		TECN	COMMENT
3518.9±0.9 OUR AVERAGE					
3518 ±3	6	[1] OCHERASHVI..05		SELX	Σ^- nucleus ≈ 600 GeV
3519 ±1	16	[2] MATTSON	02	SELX	Σ^- nucleus ≈ 600 GeV

[1] OCHERASHVILI 05 claims "an excess of 5.62 events over ... 1.38 ± 0.13 events" for a significance of 4.8 σ in pD^+K^- events.

[2] MATTSON 02 claims "an excess of 15.9 events over an expected background of 6.1 ± 0.5 events, a statistical significance of 6.3 σ" in the $\Lambda_c^+ K^- \pi^+$ invariant-mass spectrum. The probability that the peak is a fluctuation increases from 1.0×10^{-6} to 1.1×10^{-4} when the number of bins searched is considered.

Ξ_{cc}^{+} MEAN LIFE

VALUE (10^{-15} s)	CL%	DOCUMENT ID		TECN	COMMENT
<33	90	MATTSON	02	SELX	Σ^- nucleus, ≈ 600 GeV

Ξ_{cc}^{+} DECAY MODES

	Mode
Γ_1	$\Lambda_c^+ K^- \pi^+$
Γ_2	pD^+K^-

$\Gamma(pD^+K^-)/\Gamma(\Lambda_c^+ K^- \pi^+)$ Γ_2/Γ_1

VALUE	EVTS	DOCUMENT ID	TECN	COMMENT
0.36±0.21	6	OCHERASHVI..05	SELX	Σ^- ≈ 600 GeV

Ξ_{cc}^{+} REFERENCES

KATO	14	PR D89 052003	Y. Kato *et al.*	(BELLE Collab.)
AAIJ	13CD	JHEP 1312 090	R. Aaij *et al.*	(LHCb Collab.)
AUBERT,B	06D	PR D74 011103	B. Aubert *et al.*	(BABAR Collab.)
CHISTOV	06	PRL 97 162001	R. Chistov *et al.*	(BELLE Collab.)
OCHERASHVI...05		PL B628 18	A. Ocherashvili *et al.*	(FNAL SELEX Collab.)
MATTSON	02	PRL 89 112001	M. Mattson *et al.*	(FNAL SELEX Collab.)

Ξ_{cc}^{++}

$I(J^P) = ?(?^?)$ Status: ***

A nerrow peak seen in 13 TeV pp collisions in $\Lambda_c^+ K^- 2\pi^+$ with a significance of 12 standard deviations. Supported by measurements at 8 TeV by the same collaboration.

Ξ_{cc}^{++} MASS

VALUE (MeV)	EVTS	DOCUMENT ID		TECN	COMMENT
3621.40±0.72±0.27±0.14	313	[1] AAIJ	17BC	LHCB	pp at 13 TeV

[1] The third error in AAIJ 17BC value is from the uncertainty of the Λ_c^+ mass. The width of the signal is 6.6 ± 0.8 MeV, consistent with the experimental resolution.

Ξ_{cc}^{++} DECAY MODES

	Mode	Fraction (Γ_i/Γ)
Γ_1	$\Lambda_c^+ K^- \pi^+ \pi^+$	seen

$\Gamma(\Lambda_c^+ K^- \pi^+ \pi^+)/\Gamma_{total}$ Γ_1/Γ

VALUE	DOCUMENT ID	TECN	COMMENT
seen	AAIJ	17BC LHCB	pp at 13 TeV

Ξ_{cc}^{++} REFERENCES

AAIJ	17BC	PRL 119 112001	R. Aaij *et al.*	(LHCb Collab.)

BOTTOM BARYONS
($B = -1$)

$\Lambda_b^0 = udb$, $\Xi_b^0 = usb$, $\Xi_b^- = dsb$, $\Omega_b^- = ssb$

Λ_b^0

$I(J^P) = 0(\frac{1}{2}^+)$ Status: ***

In the quark model, a Λ_b^0 is an isospin-0 udb state. The lowest Λ_b^0 ought to have $J^P = 1/2^+$. None of I, J, or P have actually been measured.

Λ_b^0 MASS

$m_{\Lambda_b^0}$

VALUE (MeV)	EVTS	DOCUMENT ID		TECN	COMMENT
5619.60± 0.17 OUR AVERAGE					
5619.62± 0.16± 0.13		[1] AAIJ	17AM	LHCB	pp at 7, 8 TeV
5619.30± 0.34		[2] AAIJ	14AA	LHCB	pp at 7 TeV
5620.15± 0.31± 0.47		[3] AALTONEN	14B	CDF	$p\overline{p}$ at 1.96 TeV
5619.7 ± 0.7 ± 1.1		[3] AAD	13U	ATLS	pp at 7 TeV
5621 ± 4 ± 3		[4] ABE	97B	CDF	$p\overline{p}$ at 1.8 TeV
5668 ± 16 ± 8	4	[5] ABREU	96N	DLPH	$e^+e^- \to Z$
5614 ± 21 ± 4	4	[5] BUSKULIC	96L	ALEP	$e^+e^- \to Z$
• • • We do not use the following data for averages, fits, limits, etc. • • •					
5619.65± 0.17± 0.17		[6] AAIJ	16Y	LHCB	Repl. by AAIJ 17AM
5619.44± 0.13± 0.38		[3] AAIJ	13AV	LHCB	Repl. by AAIJ 17AM
5619.19± 0.70± 0.30		[3] AAIJ	12E	LHCB	Repl. by AAIJ 13AV
5619.7 ± 1.2 ± 1.2		[7] ACOSTA	06	CDF	Repl. by AALTONEN 14B
not seen		[8] ABE	93B	CDF	Repl. by ABE 97B
5640 ± 50 ±30	16	[9] ALBAJAR	91E	UA1	$p\overline{p}$ 630 GeV
5640 $^{+100}_{-210}$	52	BARI	91	SFM	$\Lambda_b^0 \to pD^0\pi^-$
5650 $^{+150}_{-200}$	90	BARI	91	SFM	$\Lambda_b^0 \to \Lambda_c^+\pi^+\pi^-\pi^-$

[1] Uses $\Lambda_b^0 \to \chi_{c1} p K^-$, $\Lambda_b^0 \to \chi_{c2} p K^-$, $\Lambda_b^0 \to J/\psi\Lambda$, $\Lambda_b^0 \to p\psi(2S) K^-$, $\Lambda_b^0 \to p J/\psi\pi^+\pi^- K^-$, and $\Lambda_b^0 \to p J/\psi K^-$ decays.

[2] Uses exclusively reconstructed final states $\Lambda_b^0 \to \Lambda_c^+ D_s^-$, $\Lambda_c^+ D^-$ and $\overline{B}^0 \to D^+ D_s^-$ decays. The uncertainty includes both statistical and systematic contributions.

[3] Uses $\Lambda_b^0 \to J/\psi\Lambda$ fully reconstructed decays.

[4] ABE 97B observed 38 events with a background of 18 ± 1.6 events in the mass range 5.60–5.65 GeV/c^2, a significance of > 3.4 standard deviations.

[5] Uses 4 fully reconstructed Λ_b events.

[6] Uses $\Lambda_b^0 \to p\psi(2S) K^-$, $\Lambda_b^0 \to p J/\psi\pi^+\pi^- K^-$, and $\Lambda_b^0 \to p J/\psi K^-$ decays.

[7] Uses exclusively reconstructed final states containing a $J/\psi \to \mu^+\mu^-$ decays.

[8] ABE 93B states that, based on the signal claimed by ALBAJAR 91E, CDF should have found 30 ± 23 $\Lambda_b^0 \to J/\psi(1S)\Lambda$ events. Instead, CDF found not more than 2 events.

[9] ALBAJAR 91E claims 16 ± 5 events above a background of 9 ± 1 events, a significance of about 5 standard deviations.

$m_{\Lambda_b^0} - m_{B^0}$

VALUE (MeV)	DOCUMENT ID		TECN	COMMENT
339.2±1.4±0.1	[1] ACOSTA	06	CDF	$p\overline{p}$ at 1.96 TeV

[1] Uses exclusively reconstructed final states containing $J/\psi \to \mu^+\mu^-$ decays.

$m_{\Lambda_b^0} - m_{B^+}$

VALUE (MeV)	DOCUMENT ID		TECN	COMMENT
339.72±0.28 OUR AVERAGE				
339.72±0.24±0.18	[1] AAIJ	14AA	LHCB	pp at 7 TeV
339.71±0.71±0.09	[2] AAIJ	12E	LHCB	pp at 7 TeV

[1] Uses exclusively reconstructed final states $\Lambda_b^0 \to \Lambda_c^+ D_s^-$, $\Lambda_c^+ D^-$ and $\overline{B}^0 \to D^+ D_s^-$ decays.

[2] Uses exclusively reconstructed final states containing $J/\psi \to \mu^+\mu^-$ decays.

Λ_b^0 MEAN LIFE

See b-baryon Admixture section for data on b-baryon mean life average over species of b-baryon particles.

"OUR EVALUATION" is an average using rescaled values of the data listed below. The average and rescaling were performed by the Heavy Flavor Averaging Group (HFLAV) and are described at http://www.slac.stanford.edu/xorg/hflav/. The averaging/rescaling procedure takes into account correlations between the measurements and asymmetric lifetime errors.

VALUE (10^{-12} s)	EVTS	DOCUMENT ID		TECN	COMMENT
1.470±0.010 OUR EVALUATION					
1.415±0.027±0.006		[1] AAIJ	14E	LHCB	pp at 7 TeV
1.479±0.009±0.010		[2] AAIJ	14U	LHCB	pp at 7, 8 TeV
1.565±0.035±0.020		[1] AALTONEN	14B	CDF	$p\overline{p}$ at 1.96 TeV
1.449±0.036±0.017		[1] AAD	13U	ATLS	pp at 7 TeV
1.503±0.052±0.031		[1] CHATRCHYAN	13AC	CMS	pp at 7 TeV
1.303±0.075±0.035		[1] ABAZOV	12U	D0	$p\overline{p}$ at 1.96 TeV
1.401±0.046±0.035		[3] AALTONEN	10B	CDF	$p\overline{p}$ at 1.96 TeV
• • • We do not use the following data for averages, fits, limits, etc. • • •					
1.482±0.018±0.012		[4] AAIJ	13BB	LHCB	Repl. by AAIJ 14U
1.537±0.045±0.014		[1] AALTONEN	11	CDF	Repl. by AALTONEN 14B
1.218 $^{+0.130}_{-0.115}$ ±0.042		[1] ABAZOV	07S	D0	Repl. by ABAZOV 12U
1.290 $^{+0.119}_{-0.110}$ $^{+0.087}_{-0.091}$		[5] ABAZOV	07U	D0	$p\overline{p}$ at 1.96 TeV
1.593 $^{+0.083}_{-0.078}$ ±0.033		[1] ABULENCIA	07A	CDF	Repl. by AALTONEN 11
1.22 $^{+0.22}_{-0.18}$ ±0.04		[1] ABAZOV	05C	D0	Repl. by ABAZOV 07S
1.11 $^{+0.19}_{-0.18}$ ±0.05		[6] ABREU	99W	DLPH	$e^+e^- \to Z$
1.29 $^{+0.24}_{-0.22}$ ±0.06		[6] ACKERSTAFF	98G	OPAL	$e^+e^- \to Z$
1.21 ±0.11		[6] BARATE	98D	ALEP	$e^+e^- \to Z$
1.32 ±0.15 ±0.07		[7] ABE	96M	CDF	$p\overline{p}$ at 1.8 TeV
1.19 $^{+0.21}_{-0.18}$ $^{+0.07}_{-0.08}$		ABREU	96D	DLPH	Repl. by ABREU 99W
1.14 $^{+0.22}_{-0.19}$ ±0.07	69	AKERS	95K	OPAL	Repl. by ACKERSTAFF 98G
1.02 $^{+0.23}_{-0.18}$ ±0.06	44	BUSKULIC	95L	ALEP	Repl. by BARATE 98D

[1] Measured mean life using fully reconstructed $\Lambda_b^0 \to J/\psi\Lambda$ decays.

[2] Used $\Lambda_b^0 \to J/\psi p K^-$ decays.

[3] Measured mean life using fully reconstructed $\Lambda_b^0 \to \Lambda_c^+\pi^-$ decays.

[4] Measured the lifetime ratio of decays $\Lambda_b^0 \to J/\psi p K^-$ to $B^0 \to J/\psi\pi^+ K^-$ to be 0.976 ± 0.012 ± 0.006 with $\tau_{B^0} = 1.519 \pm 0.007$ ps.

[5] Measured using semileptonic decays $\Lambda_b^0 \to \Lambda_c^+ \mu\nu X$ and $\Lambda_c^+ \to K_S^0 p$.

[6] Measured using $\Lambda_c \ell^-$ and $\Lambda \ell^+ \ell^-$.

[7] Excess $\Lambda_c \ell^-$, decay lengths.

$\tau_{\Lambda_b^0}/\tau_{\overline{\Lambda}_b^0}$

VALUE	DOCUMENT ID		TECN	COMMENT
0.940±0.035±0.006	[1] AAIJ	14E	LHCB	pp at 7 TeV

[1] Measured using $\Lambda_b^0 \to J/\psi\Lambda$ decays.

$\tau_{\Lambda_b^0}/\tau_{B^0}$ MEAN LIFE RATIO

$\tau_{\Lambda_b^0}/\tau_{B^0}$ (direct measurements)

"OUR EVALUATION" has been obtained by the Heavy Flavor Averaging Group (HFLAV) by including both B^0 and B^+ decays.

VALUE	DOCUMENT ID		TECN	COMMENT
0.964±0.007 OUR EVALUATION				
0.969±0.010 OUR AVERAGE Error includes scale factor of 1.6. See the ideogram below.				
0.929±0.018±0.004	[1] AAIJ	14E	LHCB	pp at 7 TeV
0.974±0.006±0.004	[2] AAIJ	14U	LHCB	pp at 7, 8 TeV
0.960±0.025±0.016	[3] AAD	13U	ATLS	pp at 7 TeV
0.864±0.052±0.033	[4,5] ABAZOV	12U	D0	$p\overline{p}$ at 1.96 TeV
1.020±0.030±0.008	[4] AALTONEN	11	CDF	$p\overline{p}$ at 1.96 TeV
• • • We do not use the following data for averages, fits, limits, etc. • • •				
0.976±0.012±0.006	[6] AAIJ	13BB	LHCB	Repl. by AAIJ 14U
0.811 $^{+0.096}_{-0.087}$ ±0.034	[4,5] ABAZOV	07S	D0	Repl. by ABAZOV 12U
1.041±0.057	[7] ABULENCIA	07A	CDF	Repl. by AALTONEN 11
0.87 $^{+0.17}_{-0.14}$ ±0.03	[7] ABAZOV	05C	D0	Repl. by ABAZOV 07S

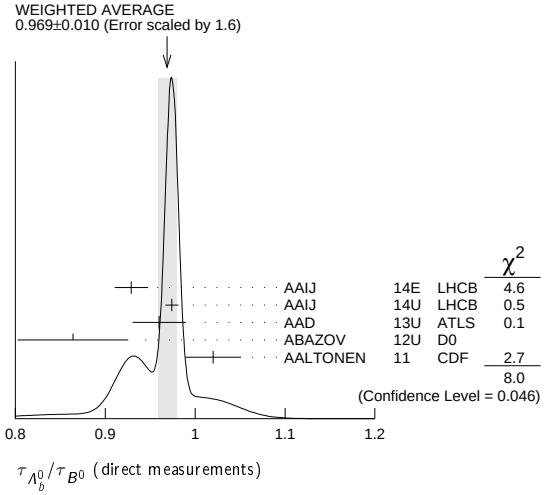

[1] Measured using $\Lambda_b^0 \to J/\psi\Lambda$ and $B^0 \to J/\psi K^{*0}$ decays.
[2] Used $\Lambda_b^0 \to J/\psi p K^-$ and $B^0 \to J/\psi K^*(892)^0$ decays.
[3] Measured with $\Lambda_b^0 \to J/\psi(\mu^+\mu^-)\,\Lambda^0(p\pi^-)$ decays.
[4] Uses fully reconstructed $\Lambda_b \to J/\psi\Lambda$ decays.
[5] Uses $B^0 \to J/\psi K_S^0$ decays for denominator.
[6] Measures $1/\tau_{\Lambda_b^0} - 1/\tau_{B^0}$ and uses $\tau_{B^0} = 1.519 \pm 0.007$ ps to extract lifetime ratio.
[7] Measured mean life ratio using fully reconstructed decays.

Λ_b^0 DECAY MODES

The branching fractions B(b-baryon $\to \Lambda\ell^-\overline{\nu}_\ell$anything) and B($\Lambda_b^0 \to \Lambda_c^+\ell^-\overline{\nu}_\ell$anything) are not pure measurements because the underlying measured products of these with B($b \to b$-baryon) were used to determine B($b \to b$-baryon), as described in the note "Production and Decay of b-Flavored Hadrons."

For inclusive branching fractions, *e.g.*, $\Lambda_b \to \overline{\Lambda}_c$anything, the values usually are multiplicities, not branching fractions. They can be greater than one.

	Mode		Fraction (Γ_i/Γ)	Scale factor/ Confidence level
Γ_1	$J/\psi(1S)\Lambda \times$ B($b \to \Lambda_b^0$)		$(5.8 \pm 0.8) \times 10^{-5}$	
Γ_2	$J/\psi(1S)\Lambda$			
Γ_3	$\psi(2S)\Lambda$			
Γ_4	$pD^0\pi^-$		$(6.3 \pm 0.7) \times 10^{-4}$	
Γ_5	$\Lambda_c(2860)^+\pi^-$, $\Lambda_c^+ \to D^0 p$			
Γ_6	$\Lambda_c(2880)^+\pi^-$, $\Lambda_c^+ \to D^0 p$			
Γ_7	$\Lambda_c(2940)^+\pi^-$, $\Lambda_c^+ \to D^0 p$			
Γ_8	pD^0K^-		$(4.6 \pm 0.8) \times 10^{-5}$	
Γ_9	$pJ/\psi\pi^-$		$(2.6\ ^{+0.5}_{-0.4}) \times 10^{-5}$	
Γ_{10}	$p\pi^- J/\psi$, $J/\psi \to \mu^+\mu^-$		$(1.6 \pm 0.8) \times 10^{-6}$	
Γ_{11}	$pJ/\psi K^-$		$(3.2\ ^{+0.6}_{-0.5}) \times 10^{-4}$	
Γ_{12}	$P_c(4380)^+K^-$, $P_c \to pJ/\psi$	[a]	$(2.7 \pm 1.4) \times 10^{-5}$	
Γ_{13}	$P_c(4450)^+K^-$, $P_c \to pJ/\psi$	[a]	$(1.3 \pm 0.4) \times 10^{-5}$	
Γ_{14}	$\chi_{c1}(1P)pK^-$		$(7.6\ ^{+1.5}_{-1.3}) \times 10^{-5}$	
Γ_{15}	$\chi_{c2}(1P)pK^-$		$(7.9\ ^{+1.6}_{-1.4}) \times 10^{-5}$	
Γ_{16}	$pJ/\psi(1S)\pi^+\pi^-K^-$		$(6.6\ ^{+1.3}_{-1.1}) \times 10^{-5}$	
Γ_{17}	$p\psi(2S)K^-$		$(6.6\ ^{+1.2}_{-1.0}) \times 10^{-5}$	
Γ_{18}	$p\overline{K}^0\pi^-$		$(1.3 \pm 0.4) \times 10^{-5}$	
Γ_{19}	pK^-K^-		$< 3.5 \times 10^{-6}$	CL=90%
Γ_{20}	$\Lambda_c^+\pi^-$		$(4.9 \pm 0.4) \times 10^{-3}$	S=1.2
Γ_{21}	$\Lambda_c^+K^-$		$(3.59 \pm 0.30) \times 10^{-4}$	S=1.2
Γ_{22}	$\Lambda_c^+ a_1(1260)^-$		seen	
Γ_{23}	$\Lambda_c^+ D^-$		$(4.6 \pm 0.6) \times 10^{-4}$	
Γ_{24}	$\Lambda_c^+ D_s^-$		(1.10 ± 0.10) %	
Γ_{25}	$\Lambda_c^+\pi^+\pi^-\pi^-$		$(7.7 \pm 1.1) \times 10^{-3}$	S=1.1
Γ_{26}	$\Lambda_c(2595)^+\pi^-$, $\Lambda_c(2595)^+ \to \Lambda_c^+\pi^+\pi^-$		$(3.4 \pm 1.5) \times 10^{-4}$	
Γ_{27}	$\Lambda_c(2625)^+\pi^-$, $\Lambda_c(2625)^+ \to \Lambda_c^+\pi^+\pi^-$		$(3.3 \pm 1.3) \times 10^{-4}$	
Γ_{28}	$\Sigma_c(2455)^0\pi^+\pi^-$, $\Sigma_c^0 \to \Lambda_c^+\pi^-$		$(5.7 \pm 2.2) \times 10^{-4}$	
Γ_{29}	$\Sigma_c(2455)^{++}\pi^-\pi^-$, $\Sigma_c^{++} \to \Lambda_c^+\pi^+$		$(3.2 \pm 1.6) \times 10^{-4}$	
Γ_{30}	$\Lambda K^0 2\pi^+ 2\pi^-$			
Γ_{31}	$\Lambda_c^+\ell^-\overline{\nu}_\ell$anything	[b]	(10.3 ± 2.1) %	
Γ_{32}	$\Lambda_c^+\ell^-\overline{\nu}_\ell$		$(6.2\ ^{+1.4}_{-1.3})$ %	
Γ_{33}	$\Lambda_c^+\pi^+\pi^-\ell^-\overline{\nu}_\ell$		(5.6 ± 3.1) %	
Γ_{34}	$\Lambda_c(2595)^+\ell^-\overline{\nu}_\ell$		$(7.9\ ^{+4.0}_{-3.5}) \times 10^{-3}$	
Γ_{35}	$\Lambda_c(2625)^+\ell^-\overline{\nu}_\ell$		$(1.3\ ^{+0.6}_{-0.5})$ %	
Γ_{36}	$\Sigma_c(2455)^0\pi^+\ell^-\overline{\nu}_\ell$			
Γ_{37}	$\Sigma_c(2455)^{++}\pi^-\ell^-\overline{\nu}_\ell$			
Γ_{38}	ph^-	[c]	$< 2.3 \times 10^{-5}$	CL=90%
Γ_{39}	$p\pi^-$		$(4.2 \pm 0.8) \times 10^{-6}$	
Γ_{40}	pK^-		$(5.1 \pm 0.9) \times 10^{-6}$	
Γ_{41}	pD_s^-		$< 4.8 \times 10^{-4}$	CL=90%
Γ_{42}	$p\mu^-\overline{\nu}_\mu$		$(4.1 \pm 1.0) \times 10^{-4}$	
Γ_{43}	$\Lambda\mu^+\mu^-$		$(1.08 \pm 0.28) \times 10^{-6}$	
Γ_{44}	$p\pi^-\mu^+\mu^-$		$(6.9 \pm 2.5) \times 10^{-8}$	
Γ_{45}	$\Lambda\gamma$		$< 1.3 \times 10^{-3}$	CL=90%
Γ_{46}	$\Lambda^0\eta$		$(9\ ^{+7}_{-5}) \times 10^{-6}$	
Γ_{47}	$\Lambda^0\eta'(958)$		$< 3.1 \times 10^{-6}$	CL=90%
Γ_{48}	$\Lambda\pi^+\pi^-$		$(4.6 \pm 1.9) \times 10^{-6}$	
Γ_{49}	$\Lambda K^+\pi^-$		$(5.7 \pm 1.2) \times 10^{-6}$	
Γ_{50}	ΛK^+K^-		$(1.61 \pm 0.23) \times 10^{-5}$	
Γ_{51}	$\Lambda^0\phi$		$(9.2 \pm 2.5) \times 10^{-6}$	
Γ_{52}	$p\pi^-\pi^+\pi^-$			
Γ_{53}	$pK^-K^+\pi^-$			

[a] P_c^+ is a pentaquark-charmonium state.
[b] Not a pure measurement. See note at head of Λ_b^0 Decay Modes.
[c] Here h^- means π^- or K^-.

CONSTRAINED FIT INFORMATION

An overall fit to 10 branching ratios uses 12 measurements and one constraint to determine 7 parameters. The overall fit has a $\chi^2 = 10.7$ for 6 degrees of freedom.

The following *off-diagonal* array elements are the correlation coefficients $\langle \delta x_i \delta x_j \rangle / (\delta x_i \cdot \delta x_j)$, in percent, from the fit to the branching fractions, $x_i \equiv \Gamma_i/\Gamma_{\text{total}}$. The fit constrains the x_i whose labels appear in this array to sum to one.

x_{21}	94				
x_{25}	50	47			
x_{32}	14	14	7		
x_{39}	0	0	0	0	
x_{40}	0	0	0	0	83
	x_{20}	x_{21}	x_{25}	x_{32}	x_{39}

Λ_b^0 BRANCHING RATIOS

$\Gamma(J/\psi(1S)\Lambda \times$ B($b \to \Lambda_b^0$)$)/\Gamma_{\text{total}}$ Γ_1/Γ

VALUE (units 10^{-5})	EVTS	DOCUMENT ID		TECN	COMMENT
5.8 ± 0.8 OUR AVERAGE					
$6.01 \pm 0.60 \pm 0.58 \pm 0.28$		[1] ABAZOV	11O	D0	$p\overline{p}$ at 1.96 TeV
$4.7 \pm 2.3 \pm 0.2$		[2] ABE	97B	CDF	$p\overline{p}$ at 1.8 TeV
• • • We do not use the following data for averages, fits, limits, etc. • • •					
$180 \pm 60 \pm 90$	16	ALBAJAR	91E	UA1	$p\overline{p}$ at 630 GeV

[1] ABAZOV 11O uses B($B^0 \to J/\psi K_S^0$) × B($b \to B^0$) $= (1.74 \pm 0.08) \times 10^{-4}$ to obtain the result. The $(\pm 0.08) \times 10^{-4}$ uncertainty of this product is listed as the last uncertainty of the measurement, $(\pm 0.28) \times 10^{-5}$.
[2] ABE 97B reports [B($\Lambda_b^0 \to J/\psi\Lambda$) × B($b \to \Lambda_b^0$)] / [B($B^0 \to J/\psi K_S^0$) × B($b \to B^0$)] $= 0.27 \pm 0.12 \pm 0.05$. We multiply by our best value B($B^0 \to J/\psi K_S^0$) × B($b \to B^0$) $= (1.74 \pm 0.08) \times 10^{-4}$. Our first error is their experiment error and our second error is the systematic error from using our best value.

$\Gamma(\psi(2S)\Lambda)/\Gamma(J/\psi(1S)\Lambda)$ Γ_3/Γ_2

VALUE	DOCUMENT ID		TECN	COMMENT
0.50 ± 0.03 ± 0.02	[1] AAD	15CH	ATLS	pp at 8 TeV

[1] AAD 15CH uses B($J/\psi \to \mu^+\mu^-$) $= (5.961 \pm 0.033) \times 10^{-2}$ (PDG 14). And B($\psi(2S) \to \mu^+\mu^-$) $= (7.89 \pm 0.17) \times 10^{-3}$ (PDG 14) is used assuming lepton universality.

$\Gamma(pD^0\pi^-)/\Gamma_{\text{total}}$ Γ_4/Γ

VALUE	EVTS	DOCUMENT ID		TECN	COMMENT
• • • We do not use the following data for averages, fits, limits, etc. • • •					
seen	52	BARI	91	SFM	$D^0 \to K^-\pi^+$
seen		BASILE	81	SFM	$D^0 \to K^-\pi^+$

$\Gamma(\Lambda_c(2860)^+\pi^-, \Lambda_c^+ \to D^0 p)/\Gamma(\Lambda_c(2880)^+\pi^-, \Lambda_c^+ \to D^0 p)$ Γ_5/Γ_6

VALUE	DOCUMENT ID		TECN	COMMENT
$4.54\ ^{+0.51}_{-0.39}\ ^{+0.21}_{-0.59}$	AAIJ	17S	LHCB	pp at 7, 8 TeV

$\Gamma(\Lambda_c(2940)^+\pi^-, \Lambda_c^+ \to D^0 p)/\Gamma(\Lambda_c(2880)^+\pi^-, \Lambda_c^+ \to D^0 p)$ Γ_7/Γ_6

VALUE	DOCUMENT ID		TECN	COMMENT
$0.83\ ^{+0.31}_{-0.10}\ ^{+0.18}_{-0.43}$	AAIJ	17S	LHCB	pp at 7, 8 TeV

$\Gamma(pD^0K^-)/\Gamma(pD^0\pi^-)$ Γ_8/Γ_4

VALUE (units 10^{-2})	DOCUMENT ID		TECN	COMMENT
$7.3 \pm 0.8\ ^{+0.5}_{-0.6}$	AAIJ	14H	LHCB	pp at 7 TeV

Λ_b^0

$\Gamma(\chi_{c1}(1P)pK^-)/\Gamma(pJ/\psi K^-)$ Γ_{14}/Γ_{11}

VALUE	DOCUMENT ID		TECN	COMMENT
0.239±0.019±0.007	[1] AAIJ	17AM	LHCB	pp at 7, 8 TeV

[1] AAIJ 17AM reports 0.242 ± 0.014 ± 0.016 from a measurement of $[\Gamma(\Lambda_b^0 \to \chi_{c1}(1P)pK^-)/\Gamma(\Lambda_b^0 \to pJ/\psi K^-)] \times [B(\chi_{c1}(1P) \to \gamma J/\psi(1S))]$ assuming $B(\chi_{c1}(1P) \to \gamma J/\psi(1S)) = (33.9 \pm 1.2) \times 10^{-2}$, which we rescale to our best value $B(\chi_{c1}(1P) \to \gamma J/\psi(1S)) = (34.3 \pm 1.0) \times 10^{-2}$. Our first error is their experiment's error and our second error is the systematic error from using our best value.

$\Gamma(\chi_{c2}(1P)pK^-)/\Gamma(pJ/\psi K^-)$ Γ_{15}/Γ_{11}

VALUE	DOCUMENT ID		TECN	COMMENT
0.250±0.025±0.007	[1] AAIJ	17AM	LHCB	pp at 7, 8 TeV

[1] AAIJ 17AM reports 0.248 ± 0.02 ± 0.017 from a measurement of $[\Gamma(\Lambda_b^0 \to \chi_{c2}(1P)pK^-)/\Gamma(\Lambda_b^0 \to pJ/\psi K^-)] \times [B(\chi_{c2}(1P) \to \gamma J/\psi(1S))]$ assuming $B(\chi_{c2}(1P) \to \gamma J/\psi(1S)) = (19.2 \pm 0.7) \times 10^{-2}$, which we rescale to our best value $B(\chi_{c2}(1P) \to \gamma J/\psi(1S)) = (19.0 \pm 0.5) \times 10^{-2}$. Our first error is their experiment's error and our second error is the systematic error from using our best value.

$\Gamma(pJ/\psi\pi^-)/\Gamma(pJ/\psi K^-)$ Γ_9/Γ_{11}

VALUE (units 10^{-2})	DOCUMENT ID		TECN	COMMENT
8.24±0.25±0.42	AAIJ	14K	LHCB	pp at 7, 8 TeV

$\Gamma(pJ/\psi K^-)/\Gamma_{total}$ Γ_{11}/Γ

VALUE (units 10^{-4})	DOCUMENT ID		TECN	COMMENT
$3.17 \pm 0.04 ^{+0.57}_{-0.45}$	[1] AAIJ	16A	LHCB	pp at 7, 8 TeV

[1] AAIJ 16A reported the measurement of $(3.17 \pm 0.04 \pm 0.07 \pm 0.34 ^{+0.45}_{-0.28}) \times 10^{-4}$ where the first uncertainty is statistical, the second is systematic, the third is due to the branching fraction of $B^0 \to J/\psi K^*(892)^0$, and the fourth is due to the knowledge of f_{Λ_b}/f_d. We combined in quadrature second to fourth uncertainties to a total systematic uncertainty.

$\Gamma(P_c(4380)^+K^-,\ P_c \to pJ/\psi)/\Gamma_{total}$ Γ_{12}/Γ

P_c^+ is a pentaquark-charmonium state.

VALUE (units 10^{-5})	DOCUMENT ID		TECN	COMMENT
$2.66 \pm 0.22 ^{+1.41}_{-1.38}$	[1] AAIJ	16A	LHCB	pp at 7, 8 TeV

[1] AAIJ 16 total systematic includes the uncertainties on $f(P_c^+)$ and $B(\Lambda_b \to pJ/\psi K^-)$.

$\Gamma(P_c(4450)^+K^-,\ P_c \to pJ/\psi)/\Gamma_{total}$ Γ_{13}/Γ

P_c^+ is a pentaquark-charmonium state.

VALUE (units 10^{-5})	DOCUMENT ID		TECN	COMMENT
$1.30 \pm 0.16 ^{+0.42}_{-0.39}$	[1] AAIJ	16A	LHCB	pp at 7, 8 TeV

[1] AAIJ 16 total systematic includes the uncertainties on $f(P_c^+)$ and $B(\Lambda_b \to pJ/\psi K^-)$.

$\Gamma(pJ/\psi(1S)\pi^+\pi^-K^-)/\Gamma(pJ/\psi K^-)$ Γ_{16}/Γ_{11}

VALUE	DOCUMENT ID		TECN	COMMENT
0.2086±0.0096±0.0134	[1] AAIJ	16Y	LHCB	pp at 7, 8 TeV

[1] Excludes $\psi(2S) \to J/\psi\pi^+\pi^-$.

$\Gamma(p\psi(2S)K^-)/\Gamma(pJ/\psi K^-)$ Γ_{17}/Γ_{11}

VALUE	DOCUMENT ID		TECN	COMMENT
0.2070±0.0076±0.0059	[1] AAIJ	16Y	LHCB	pp at 7, 8 TeV

[1] AAIJ 16Y reports a measurement of 0.2070 ± 0.0076 ± 0.0046 ± 0.0037 where the third uncertainty is due to the knowledge of J/ψ and $\psi(2S)$ branching fractions. We have combined both systematic uncertainties in quadrature.

$\Gamma(p\overline{K}^0\pi^-)/\Gamma_{total}$ Γ_{18}/Γ

VALUE (units 10^{-5})	DOCUMENT ID		TECN	COMMENT
1.26±0.19±0.36	[1] AAIJ	14Q	LHCB	pp at 7 TeV

[1] Used the normalizing mode branching fraction value of $B(B^0 \to K^0\pi^+\pi^-) = (4.96 \pm 0.20) \times 10^{-5}$.

$\Gamma(pK^0K^-)/\Gamma_{total}$ Γ_{19}/Γ

VALUE	CL%	DOCUMENT ID	TECN	COMMENT
$<3.5 \times 10^{-6}$	90	AAIJ	14Q LHCB	pp at 7 TeV

$\Gamma(\Lambda_c^+\pi^-)/\Gamma_{total}$ Γ_{20}/Γ

VALUE (units 10^{-3})	EVTS	DOCUMENT ID		TECN	COMMENT
4.9 ±0.4 OUR FIT		Error includes scale factor of 1.2.			
4.9 ±0.5 OUR AVERAGE		Error includes scale factor of 1.5.			
$4.57 ^{+0.31}_{-0.30} \pm 0.23$		[1] AAIJ	14I	LHCB	pp at 7 TeV
$5.97 \pm 0.28 \pm 0.81$		[2] AAIJ	14Q	LHCB	pp at 7 TeV
8.8 ±2.8 ±1.5		[3] ABULENCIA	07B	CDF	$p\overline{p}$ at 1.96 TeV
• • • We do not use the following data for averages, fits, limits, etc. • • •					
seen	3	ABREU	96N	DLPH	$\Lambda_c^+ \to pK^-\pi^+$
seen	4	BUSKULIC	96L	ALEP	$\Lambda_c^+ \to pK^-\pi^+$, $p\overline{K}^0$, $\Lambda\pi^+\pi^+\pi^-$

[1] AAIJ 14I reports $(4.30 \pm 0.03 ^{+0.12}_{-0.11} \pm 0.26 \pm 0.21) \times 10^{-3}$ from a measurement of $[\Gamma(\Lambda_b^0 \to \Lambda_c^+\pi^-)/\Gamma_{total}] \times [B(B^0 \to D^-\pi^+)]$ assuming $B(B^0 \to D^-\pi^+) = (2.68 \pm 0.13) \times 10^{-3}$, which we rescale to our best value $B(B^0 \to D^-\pi^+) = (2.52 \pm 0.13) \times 10^{-3}$. Our first error is their experiment's error and our second error is the systematic error from using our best value. Uses information on f_{baryon}/f_d from measurement in semileptonic decays by the same authors.

[2] Obtained using the branching fraction of $\Lambda_c^+ \to pK^-\pi^+$ decay.

[3] The result is obtained from $(f_{baryon}/f_d)\ (B(\Lambda_b^0 \to \Lambda_c^+\pi^-)/B(\overline{B}^0 \to D^+\pi^-)) = 0.82 \pm 0.08 \pm 0.11 \pm 0.22$, assuming $f_{baryon}/f_d = 0.25 \pm 0.04$ and $B(\overline{B}^0 \to D^+\pi^-) = (2.68 \pm 0.13) \times 10^{-3}$.

$\Gamma(pD^0\pi^-)/\Gamma(\Lambda_c^+\pi^-)$ Γ_4/Γ_{20}

VALUE	DOCUMENT ID		TECN	COMMENT
0.129±0.007±0.007	[1] AAIJ	14H	LHCB	pp at 7 TeV

[1] AAIJ 14H reports $[\Gamma(\Lambda_b^0 \to pD^0\pi^-)/\Gamma(\Lambda_b^0 \to \Lambda_c^+\pi^-)] \times [B(D^0 \to K^-\pi^+)] / [B(\Lambda_c^+ \to pK^-\pi^+)] = (8.06 \pm 0.23 \pm 0.35) \times 10^{-2}$ which we multiply or divide by our best values $B(D^0 \to K^-\pi^+) = (3.89 \pm 0.04) \times 10^{-2}$, $B(\Lambda_c^+ \to pK^-\pi^+) = (6.23 \pm 0.33) \times 10^{-2}$. Our first error is their experiment's error and our second error is the systematic error from using our best values.

$\Gamma(\Lambda_c^+K^-)/\Gamma_{total}$ Γ_{21}/Γ

VALUE (units 10^{-4})	DOCUMENT ID		TECN	COMMENT
3.59±0.30 OUR FIT	Error includes scale factor of 1.2.			
3.55±0.44±0.50	[1] AAIJ	14Q	LHCB	pp at 7 TeV

[1] Obtained using the branching fraction of $\Lambda_c^+ \to pK^-\pi^+$ decay.

$\Gamma(\Lambda_c^+K^-)/\Gamma(\Lambda_c^+\pi^-)$ Γ_{21}/Γ_{20}

VALUE (units 10^{-2})	DOCUMENT ID		TECN	COMMENT
7.31±0.22 OUR FIT				
7.31±0.16±0.16	AAIJ	14H	LHCB	pp at 7 TeV

$\Gamma(\Lambda_c^+a_1(1260)^-)/\Gamma_{total}$ Γ_{22}/Γ

VALUE	EVTS	DOCUMENT ID		TECN	COMMENT
seen	1	ABREU	96N	DLPH	$\Lambda_c^+ \to pK^-\pi^+$, $a_1^- \to \rho^0\pi^- \to \pi^+\pi^-\pi^-$

$\Gamma(\Lambda_c^+D_s^-)/\Gamma_{total}$ Γ_{24}/Γ

VALUE (units 10^{-2})	DOCUMENT ID		TECN	COMMENT
1.1±0.1	[1] AAIJ	14AA	LHCB	pp at 7 TeV

[1] Uses $B(\overline{B}^0 \to D^+D_s^-) = (7.2 \pm 0.8) \times 10^{-3}$ and their measured $B(\Lambda_b^0 \to \Lambda_c^+\pi^-))/B(\overline{B}^0 \to D^+\pi^-)$ values.

$\Gamma(\Lambda_c^+D^-)/\Gamma(\Lambda_c^+D_s^-)$ Γ_{23}/Γ_{24}

VALUE	DOCUMENT ID		TECN	COMMENT
0.042±0.003±0.003	AAIJ	14AA	LHCB	pp at 7 TeV

$\Gamma(\Lambda_c^+\pi^+\pi^-\pi^-)/\Gamma_{total}$ Γ_{25}/Γ

VALUE (units 10^{-3})	EVTS	DOCUMENT ID		TECN	COMMENT
7.7±1.1 OUR FIT		Error includes scale factor of 1.1.			
$14.9 ^{+3.8}_{-3.2} \pm 1.2$		[1] AALTONEN	12A	CDF	$p\overline{p}$ at 1.96 TeV
• • • We do not use the following data for averages, fits, limits, etc. • • •					
seen	90	BARI	91	SFM	$\Lambda_c^+ \to pK^-\pi^+$

[1] AALTONEN 12A reports $[\Gamma(\Lambda_b^0 \to \Lambda_c^+\pi^+\pi^-\pi^-)/\Gamma_{total}] / [B(\Lambda_b^0 \to \Lambda_c^+\pi^-)] = 3.04 \pm 0.33 ^{+0.70}_{-0.55}$ which we multiply by our best value $B(\Lambda_b^0 \to \Lambda_c^+\pi^-) = (4.9 \pm 0.4) \times 10^{-3}$. Our first error is their experiment's error and our second error is the systematic error from using our best value.

$\Gamma(\Lambda_c^+\pi^+\pi^-\pi^-)/\Gamma(\Lambda_c^+\pi^-)$ Γ_{25}/Γ_{20}

VALUE	DOCUMENT ID		TECN	COMMENT
1.56±0.21 OUR FIT				
1.43±0.16±0.13	AAIJ	11E	LHCB	pp at 7 TeV

$\Gamma(\Lambda_c(2595)^+\pi^-, \Lambda_c(2595)^+ \to \Lambda_c^+\pi^+\pi^-)/\Gamma(\Lambda_c^+\pi^+\pi^-\pi^-)$ Γ_{26}/Γ_{25}

VALUE (units 10^{-2})	DOCUMENT ID		TECN	COMMENT
$4.4 \pm 1.7 ^{+0.6}_{-0.4}$	AAIJ	11E	LHCB	pp at 7 TeV

$\Gamma(\Lambda_c(2625)^+\pi^-, \Lambda_c(2625)^+ \to \Lambda_c^+\pi^+\pi^-)/\Gamma(\Lambda_c^+\pi^+\pi^-\pi^-)$ Γ_{27}/Γ_{25}

VALUE (units 10^{-2})	DOCUMENT ID		TECN	COMMENT
4.3±1.5±0.4	AAIJ	11E	LHCB	pp at 7 TeV

$\Gamma(\Sigma_c(2455)^0\pi^+\pi^-, \Sigma_c^0 \to \Lambda_c^+\pi^-)/\Gamma(\Lambda_c^+\pi^+\pi^-\pi^-)$ Γ_{28}/Γ_{25}

VALUE (units 10^{-2})	DOCUMENT ID		TECN	COMMENT
7.4±2.4±1.2	AAIJ	11E	LHCB	pp at 7 TeV

$\Gamma(\Sigma_c(2455)^{++}\pi^-\pi^-, \Sigma_c^{++} \to \Lambda_c^+\pi^+)/\Gamma(\Lambda_c^+\pi^+\pi^-\pi^-)$ Γ_{29}/Γ_{25}

VALUE (units 10^{-2})	DOCUMENT ID		TECN	COMMENT
4.2±1.8±0.7	AAIJ	11E	LHCB	pp at 7 TeV

$\Gamma(\Lambda K^0 2\pi^+ 2\pi^-)/\Gamma_{total}$ Γ_{30}/Γ

VALUE	EVTS	DOCUMENT ID		TECN	COMMENT
• • • We do not use the following data for averages, fits, limits, etc. • • •					
seen	4	[1] ARENTON	86	FMPS	$\Lambda K_S^0 2\pi^+ 2\pi^-$

[1] See the footnote to the ARENTON 86 mass value.

$\Gamma(\Lambda_c^+ \ell^- \overline{\nu}_\ell \text{anything})/\Gamma_{total}$ Γ_{31}/Γ

The values and averages in this section serve only to show what values result if one assumes our B($b \to$ b-baryon). They cannot be thought of as measurements since the underlying product branching fractions were also used to determine B($b \to$ b-baryon) as described in the note on "Production and Decay of b-Flavored Hadrons."

VALUE	EVTS	DOCUMENT ID		TECN	COMMENT
0.103±0.021 OUR AVERAGE					
0.097±0.018±0.013		[1] BARATE	98D	ALEP	$e^+e^- \to Z$
0.13 $^{+0.05}_{-0.04}$ ±0.02	29	[2] ABREU	95S	DLPH	$e^+e^- \to Z$
• • • We do not use the following data for averages, fits, limits, etc. • • •					
0.085±0.021±0.011	55	[3] BUSKULIC	95L	ALEP	Repl. by BARATE 98D
0.17 ±0.06 ±0.02	21	[4] BUSKULIC	92E	ALEP	$\Lambda_c^+ \to pK^-\pi^+$

[1] BARATE 98D reports $[\Gamma(\Lambda_b^0 \to \Lambda_c^+ \ell^- \overline{\nu}_\ell \text{anything})/\Gamma_{total}] \times [B(\overline{b} \to b\text{-baryon})] = 0.0086 \pm 0.0007 \pm 0.0014$ which we divide by our best value $B(\overline{b} \to b\text{-baryon}) = (8.9 \pm 1.2) \times 10^{-2}$. Our first error is their experiment's error and our second error is the systematic error from using our best value. Measured using $\Lambda_c \ell^-$ and $\Lambda \ell^+ \ell^-$.

[2] ABREU 95S reports $[\Gamma(\Lambda_b^0 \to \Lambda_c^+ \ell^- \overline{\nu}_\ell \text{anything})/\Gamma_{total}] \times [B(\overline{b} \to b\text{-baryon})] = 0.0118 \pm 0.0026 ^{+0.0031}_{-0.0021}$ which we divide by our best value $B(\overline{b} \to b\text{-baryon}) = (8.9 \pm 1.2) \times 10^{-2}$. Our first error is their experiment's error and our second error is the systematic error from using our best value.

[3] BUSKULIC 95L reports $[\Gamma(\Lambda_b^0 \to \Lambda_c^+ \ell^- \overline{\nu}_\ell \text{anything})/\Gamma_{total}] \times [B(\overline{b} \to b\text{-baryon})] = 0.00755 \pm 0.0014 \pm 0.0012$ which we divide by our best value $B(\overline{b} \to b\text{-baryon}) = (8.9 \pm 1.2) \times 10^{-2}$. Our first error is their experiment's error and our second error is the systematic error from using our best value.

[4] BUSKULIC 92E reports $[\Gamma(\Lambda_b^0 \to \Lambda_c^+ \ell^- \overline{\nu}_\ell \text{anything})/\Gamma_{total}] \times [B(\overline{b} \to b\text{-baryon})] = 0.015 \pm 0.0035 \pm 0.0045$ which we divide by our best value $B(\overline{b} \to b\text{-baryon}) = (8.9 \pm 1.2) \times 10^{-2}$. Our first error is their experiment's error and our second error is the systematic error from using our best value. Superseded by BUSKULIC 95L.

$\Gamma(\Lambda_c^+ \ell^- \overline{\nu}_\ell)/\Gamma_{total}$ Γ_{32}/Γ

VALUE	DOCUMENT ID		TECN	COMMENT
0.062 $^{+0.014}_{-0.013}$ OUR FIT				
0.050 $^{+0.011}_{-0.008}$ ±0.016	[1] ABDALLAH	04A	DLPH	$e^+e^- \to Z^0$

[1] Derived from a combined likelihood and event rate fit to the distribution of the Isgur-Wise variable and using HQET. The slope of the form factor is measured to be $\rho^2 = 2.03 \pm 0.46 ^{+0.72}_{-1.00}$.

$\Gamma(\Lambda_c^+ \ell^- \overline{\nu}_\ell)/\Gamma(\Lambda_c^+ \pi^-)$ Γ_{32}/Γ_{20}

VALUE	DOCUMENT ID		TECN	COMMENT
12.7 $^{+3.1}_{-2.7}$ OUR FIT				
16.6±3.0 $^{+2.8}_{-3.6}$	AALTONEN	09E	CDF	$p\overline{p}$ at 1.96 TeV

$\Gamma(\Lambda_c^+ \pi^+ \pi^- \ell^- \overline{\nu}_\ell)/\Gamma_{total}$ Γ_{33}/Γ

VALUE	DOCUMENT ID		TECN	COMMENT
0.056 $^{+0.031}_{-0.030}$	[1] ABDALLAH	04A	DLPH	$e^+e^- \to Z^0$

[1] Derived from the fraction of $\Gamma(\Lambda_b^0 \to \Lambda_c^+ \ell^- \overline{\nu}_\ell)$ / ($\Gamma(\Lambda_b^0 \to \Lambda_c^+ \ell^- \overline{\nu}_\ell) + \Gamma(\Lambda_b^0 \to \Lambda_c^+ \pi^+ \pi^- \ell^- \overline{\nu}_\ell)$) $= 0.47 ^{+0.10}_{-0.08} \pm 0.07 \pm 0.06$.

$\Gamma(\Lambda_c^+ \ell^- \overline{\nu}_\ell)/[\Gamma(\Lambda_c^+ \ell^- \overline{\nu}_\ell) + \Gamma(\Lambda_c^+ \pi^+ \pi^- \ell^- \overline{\nu}_\ell)]$ $\Gamma_{32}/(\Gamma_{32}+\Gamma_{33})$

VALUE	DOCUMENT ID		TECN	COMMENT
0.47 $^{+0.10}_{-0.08}$ ±0.07 ±0.06	ABDALLAH	04A	DLPH	$e^+e^- \to Z^0$

$\Gamma(\Lambda_c(2595)^+ \ell^- \overline{\nu}_\ell)/\Gamma(\Lambda_c^+ \ell^- \overline{\nu}_\ell)$ Γ_{34}/Γ_{32}

VALUE	DOCUMENT ID		TECN	COMMENT
0.126±0.033 $^{+0.047}_{-0.038}$	AALTONEN	09E	CDF	$p\overline{p}$ at 1.96 TeV

$\Gamma(\Lambda_c(2625)^+ \ell^- \overline{\nu}_\ell)/\Gamma(\Lambda_c^+ \ell^- \overline{\nu}_\ell)$ Γ_{35}/Γ_{32}

VALUE	DOCUMENT ID		TECN	COMMENT
0.210±0.042 $^{+0.071}_{-0.050}$	AALTONEN	09E	CDF	$p\overline{p}$ at 1.96 TeV

$[\frac{1}{2}\Gamma(\Sigma_c(2455)^0 \pi^+ \ell^- \overline{\nu}_\ell) + \frac{1}{2}\Gamma(\Sigma_c(2455)^{++} \pi^- \ell^- \overline{\nu}_\ell)]/\Gamma(\Lambda_c^+ \ell^- \overline{\nu}_\ell)$ $(\frac{1}{2}\Gamma_{36}+\frac{1}{2}\Gamma_{37})/\Gamma_{32}$

VALUE	DOCUMENT ID		TECN	COMMENT
0.054±0.022 $^{+0.021}_{-0.018}$	AALTONEN	09E	CDF	$p\overline{p}$ at 1.96 TeV

$\Gamma(ph^-)/\Gamma_{total}$ Γ_{38}/Γ

VALUE	CL%	DOCUMENT ID		TECN	COMMENT
<2.3 × 10^{-5}	90	[1] ACOSTA	05O	CDF	$p\overline{p}$ at 1.96 TeV

[1] Assumes f_Λ / $f_d = 0.25$, and equal momentum distribution for Λ_b and B mesons.

$\Gamma(p\pi^-)/\Gamma_{total}$ Γ_{39}/Γ

VALUE (units 10^{-6})	CL%	DOCUMENT ID		TECN	COMMENT
4.2±0.8 OUR FIT					
3.7±0.8±0.5		[1] AALTONEN	09C	CDF	$p\overline{p}$ at 1.96 TeV
• • • We do not use the following data for averages, fits, limits, etc. • • •					
<5.0	90	[2] BUSKULIC	96V	ALEP	$e^+e^- \to Z$

[1] AALTONEN 09C reports $[\Gamma(\Lambda_b^0 \to p\pi^-)/\Gamma_{total}]$ / $[B(B^0 \to K^+\pi^-)] \times [B(\overline{b} \to b\text{-baryon})]$ / $[B(\overline{b} \to B^0)] = 0.042 \pm 0.007 \pm 0.006$ which we multiply or divide by our best values $B(B^0 \to K^+\pi^-) = (1.96 \pm 0.05) \times 10^{-5}$, $B(\overline{b} \to b\text{-baryon}) = (8.9 \pm 1.2) \times 10^{-2}$, $B(\overline{b} \to B^0) = (40.5 \pm 0.6) \times 10^{-2}$. Our first error is their experiment's error and our second error is the systematic error from using our best values.

[2] BUSKULIC 96V assumes PDG 96 production fractions for B^0, B^+, B_s, b baryons.

$\Gamma(pK^-)/\Gamma_{total}$ Γ_{40}/Γ

VALUE (units 10^{-6})	CL%	DOCUMENT ID		TECN	COMMENT
5.1±0.9 OUR FIT					
5.9±1.1±0.8		[1] AALTONEN	09C	CDF	$p\overline{p}$ at 1.96 TeV
• • • We do not use the following data for averages, fits, limits, etc. • • •					
<360	90	[2] ADAM	96D	DLPH	$e^+e^- \to Z$
< 50	90	[3] BUSKULIC	96V	ALEP	$e^+e^- \to Z$

[1] AALTONEN 09C reports $[\Gamma(\Lambda_b^0 \to pK^-)/\Gamma_{total}]$ / $[B(B^0 \to K^+\pi^-)] \times [B(\overline{b} \to b\text{-baryon})]$ / $[B(\overline{b} \to B^0)] = 0.066 \pm 0.009 \pm 0.008$ which we multiply or divide by our best values $B(B^0 \to K^+\pi^-) = (1.96 \pm 0.05) \times 10^{-5}$, $B(\overline{b} \to b\text{-baryon}) = (8.9 \pm 1.2) \times 10^{-2}$, $B(\overline{b} \to B^0) = (40.5 \pm 0.6) \times 10^{-2}$. Our first error is their experiment's error and our second error is the systematic error from using our best values.

[2] ADAM 96D assumes $f_{B^0} = f_{B^-} = 0.39$ and $f_{B_s} = 0.12$.

[3] BUSKULIC 96V assumes PDG 96 production fractions for B^0, B^+, B_s, b baryons.

$\Gamma(p\pi^-)/\Gamma(pK^-)$ Γ_{39}/Γ_{40}

VALUE	DOCUMENT ID		TECN	COMMENT
0.84±0.09 OUR FIT				
0.86±0.08±0.05	AAIJ	12AR	LHCB	pp at 7 TeV

$\Gamma(pD_s^-)/\Gamma_{total}$ Γ_{41}/Γ

VALUE	CL%	DOCUMENT ID		TECN	COMMENT
<4.8 × 10^{-4}	90	AAIJ	14Q	LHCB	pp at 7 TeV

$\Gamma(p\mu^-\overline{\nu}_\mu)/\Gamma_{total}$ Γ_{42}/Γ

VALUE (units 10^{-4})	DOCUMENT ID		TECN	COMMENT
4.1±1.0	[1] AAIJ	15BG	LHCB	pp at 8 TeV

[1] The ratio of $B(\Lambda_b^0 \to p\mu^-\overline{\nu}_\mu)$ to $B(\Lambda_b^0 \to \Lambda_c^+ \mu^-\overline{\nu}_\mu)$ is measured within a restricted q^2 region. Combined with theoretical calculations of the form factors and the previously measured value of $|V_{cb}|$, the first $|V_{ub}| = (3.27 \pm 0.15 \pm 0.16 \pm 0.06) \times 10^{-3}$ measurement from the Λ_b decay is obtained, consistent with the exclusively measured world averages.

$\Gamma(p\mu^-\overline{\nu}_\mu)/\Gamma(\Lambda_c^+ \ell^- \overline{\nu}_\ell)$ Γ_{42}/Γ_{32}

VALUE (units 10^{-2})	DOCUMENT ID		TECN	COMMENT
• • • We do not use the following data for averages, fits, limits, etc. • • •				
1.0±0.04±0.08	[1] AAIJ	15BG	LHCB	pp at 8 TeV

[1] This measurement is a ratio of $\Gamma(\Lambda_b^0 \to p\mu^-\overline{\nu}_\mu)[q^2 > 15$ GeV/c$^2]$ to $\Gamma(\Lambda_b^0 \to \Lambda_c^+ \mu^-\overline{\nu}_\mu)[q^2 > 7$ GeV/c$^2]$ within a restricted q^2 region. Combined with theoretical calculations of the form factors and the previously measured value of $|V_{cb}|$, the first $|V_{ub}| = (3.27 \pm 0.15 \pm 0.16 \pm 0.06) \times 10^{-3}$ measurement from the Λ_b decay is obtained, consistent with the exclusively measured world averages.

$\Gamma(\Lambda\mu^+\mu^-)/\Gamma_{total}$ Γ_{43}/Γ

VALUE (units 10^{-7})	DOCUMENT ID		TECN	COMMENT
10.8±2.8 OUR AVERAGE				
9.6±1.6±2.5	[1] AAIJ	13AJ	LHCB	pp at 7 TeV
17.3±4.2±5.5	AALTONEN	11AI	CDF	$p\overline{p}$ at 1.96 TeV

[1] Uses $B(\Lambda_b^0 \to J/\psi\Lambda) = (6.2 \pm 1.4) \times 10^{-4}$. This measurement comes from the sum of the differential rates in q^2 regions excluding those corresponding to J/ψ and $\psi(2S)$ ([8.68,10.09] and [12.86, 14.18] GeV^2/c^4).

$\Gamma(p\pi^-\mu^+\mu^-)/\Gamma_{total}$ Γ_{44}/Γ

VALUE (units 10^{-8})	DOCUMENT ID		TECN	COMMENT
6.9±1.9 $^{+1.7}_{-1.5}$	[1] AAIJ	17P	LHCB	pp at 7, 8 TeV

[1] Excludes J/ψ and $\psi(2S)$ decays to $\mu^+\mu^-$.

$\Gamma(p\pi^-\mu^+\mu^-)/\Gamma(p\pi^- J/\psi, J/\psi \to \mu^+\mu^-)$ Γ_{44}/Γ_{10}

VALUE (units 10^{-2})	DOCUMENT ID		TECN	COMMENT
4.4±1.2±0.7	[1] AAIJ	17P	LHCB	pp at 7, 8 TeV

[1] The $p\pi^-\mu^+\mu^-$ mode excludes J/ψ and $\psi(2S)$ decays to $\mu^+\mu^-$.

Baryon Particle Listings

Λ_b^0

$\Gamma(\Lambda\gamma)/\Gamma_{\text{total}}$ Γ_{45}/Γ

VALUE	CL%	DOCUMENT ID		TECN	COMMENT
$<1.3\times10^{-3}$	90	ACOSTA	02G	CDF	$p\overline{p}$ at 1.8 TeV

$\Gamma(\Lambda^0\eta)/\Gamma_{\text{total}}$ Γ_{46}/Γ

VALUE (units 10^{-6})	DOCUMENT ID		TECN	COMMENT
$9^{+7}_{-5}\pm1$	[1] AAIJ	15AH	LHCB	pp at 7, 8 TeV

[1] AAIJ 15AH reports $[\Gamma(\Lambda_b^0\to\Lambda^0\eta)/\Gamma_{\text{total}}]$ / $[B(B^0\to\eta' K^0)] = 0.142^{+0.11}_{-0.08}$ which we multiply by our best value $B(B^0\to\eta' K^0) = (6.6\pm0.4)\times10^{-5}$. Our first error is their experiment's error and our second error is the systematic error from using our best value. The single uncertainty quoted with the original measurement combines in quadrature statistical and systematic uncertainties.

$\Gamma(\Lambda^0\eta'(958))/\Gamma_{\text{total}}$ Γ_{47}/Γ

VALUE	CL%	DOCUMENT ID		TECN	COMMENT
$<3.1\times10^{-6}$	90	[1] AAIJ	15AH	LHCB	pp at 7, 8 TeV

[1] AAIJ 15AH reports $[\Gamma(\Lambda_b^0\to\Lambda^0\eta'(958))/\Gamma_{\text{total}}]$ / $[B(B^0\to\eta' K^0)] <$ 0.047 which we multiply by our best value $B(B^0\to\eta' K^0) = 6.6\times10^{-5}$.

$\Gamma(\Lambda\pi^+\pi^-)/\Gamma(\Lambda_c^+\pi^-)$ Γ_{48}/Γ_{20}

VALUE (units 10^{-4})	DOCUMENT ID		TECN	COMMENT
$9.4\pm3.8\pm0.5$	[1] AAIJ	16W	LHCB	pp at 7, 8 TeV

[1] AAIJ 16W reports $[\Gamma(\Lambda_b^0\to\Lambda\pi^+\pi^-)/\Gamma(\Lambda_b^0\to\Lambda_c^+\pi^-)]$ / $[B(\Lambda_c^+\to\Lambda\pi^+)] = (7.3\pm1.9\pm2.2)\times10^{-2}$ which we multiply by our best value $B(\Lambda_c^+\to\Lambda\pi^+) = (1.29\pm0.07)\times10^{-2}$. Our first error is their experiment's error and our second error is the systematic error from using our best value.

$\Gamma(\Lambda K^+\pi^-)/\Gamma(\Lambda_c^+\pi^-)$ Γ_{49}/Γ_{20}

VALUE (units 10^{-4})	DOCUMENT ID		TECN	COMMENT
$11.5\pm2.3\pm0.6$	[1] AAIJ	16W	LHCB	pp at 7, 8 TeV

[1] AAIJ 16W reports $[\Gamma(\Lambda_b^0\to\Lambda K^+\pi^-)/\Gamma(\Lambda_b^0\to\Lambda_c^+\pi^-)]$ / $[B(\Lambda_c^+\to\Lambda\pi^+)] = (8.9\pm1.2\pm1.3)\times10^{-2}$ which we multiply by our best value $B(\Lambda_c^+\to\Lambda\pi^+) = (1.29\pm0.07)\times10^{-2}$. Our first error is their experiment's error and our second error is the systematic error from using our best value.

$\Gamma(\Lambda K^+K^-)/\Gamma(\Lambda_c^+\pi^-)$ Γ_{50}/Γ_{20}

VALUE (units 10^{-3})	DOCUMENT ID		TECN	COMMENT
$3.27\pm0.35^{+0.17}_{-0.18}$	[1] AAIJ	16W	LHCB	pp at 7, 8 TeV

[1] AAIJ 16W reports $[\Gamma(\Lambda_b^0\to\Lambda K^+K^-)/\Gamma(\Lambda_b^0\to\Lambda_c^+\pi^-)]$ / $[B(\Lambda_c^+\to\Lambda\pi^+)] = (25.3\pm1.9\pm1.9)\times10^{-2}$ which we multiply by our best value $B(\Lambda_c^+\to\Lambda\pi^+) = (1.29\pm0.07)\times10^{-2}$. Our first error is their experiment's error and our second error is the systematic error from using our best value.

$\Gamma(\Lambda^0\phi)/\Gamma_{\text{total}}$ Γ_{51}/Γ

VALUE (units 10^{-6})	DOCUMENT ID		TECN	COMMENT
$9.2\pm1.9\pm1.5$	[1] AAIJ	16J	LHCB	pp at 7, 8 TeV

[1] AAIJ 16J reports $[\Gamma(\Lambda_b^0\to\Lambda^0\phi)/\Gamma_{\text{total}}]$ / $[B(B^0\to K^0\phi)]\times[B(\overline{b}\to b\text{-baryon})]$ / $[B(\overline{b}\to B^0)] = 0.275\pm0.055\pm0.020$ which we multiply or divide by our best values $B(B^0\to K^0\phi) = (7.3\pm0.7)\times10^{-6}$, $B(\overline{b}\to b\text{-baryon}) = (8.9\pm1.2)\times10^{-2}$, $B(\overline{b}\to B^0) = (40.5\pm0.6)\times10^{-2}$. Our first error is their experiment's error and our second error is the systematic error from using our best values.

PARTIAL BRANCHING FRACTIONS IN $\Lambda_b\to\Lambda\mu^+\mu^-$

$B(\Lambda_b\to\Lambda\mu^+\mu^-)$ $(q^2<2.0\ \text{GeV}^2/c^4)$

VALUE (units 10^{-7})	DOCUMENT ID		TECN	COMMENT
0.71 ± 0.27 OUR AVERAGE				
$0.72^{+0.24}_{-0.22}\pm0.14$	[1] AAIJ	15AE	LHCB	pp at 7, 8 TeV
$0.15\pm2.01\pm0.05$	AALTONEN	11AI	CDF	$p\overline{p}$ at 1.96 TeV
• • • We do not use the following data for averages, fits, limits, etc. • • •				
$0.56\pm0.76\pm0.80$	[2] AAIJ	13AJ	LHCB	Repl. by AAIJ 15AE

[1] AAIJ 15AE measurement covers $0.1 < q^2 < 2.0\ \text{GeV}^2/c^4$.
[2] Uses $B(\Lambda_b^0\to J/\psi\Lambda) = (6.2\pm1.4)\times10^{-4}$.

$B(\Lambda_b\to\Lambda\mu^+\mu^-)$ $(2.0<q^2<4.3\ \text{GeV}^2/c^4)$

VALUE (units 10^{-7})	DOCUMENT ID		TECN	COMMENT
$0.28\ ^{+0.28}_{-0.21}$ OUR AVERAGE				
$0.253^{+0.276}_{-0.207}\pm0.046$	[1] AAIJ	15AE	LHCB	pp at 7, 8 TeV
$1.8\ \pm1.7\ \pm0.6$	AALTONEN	11AI	CDF	$p\overline{p}$ at 1.96 TeV
• • • We do not use the following data for averages, fits, limits, etc. • • •				
$0.71\ \pm0.60\ \pm0.23$	[2] AAIJ	13AJ	LHCB	Repl. by AAIJ 15AE

[1] AAIJ 15AE measurement covers $2.0 < q^2 < 4.0\ \text{GeV}^2/c^4$.
[2] Uses $B(\Lambda_b^0\to J/\psi\Lambda) = (6.2\pm1.4)\times10^{-4}$.

$B(\Lambda_b\to\Lambda\mu^+\mu^-)$ $(q^2<4.3\ \text{GeV}^2/c^4)$

VALUE (units 10^{-7})	DOCUMENT ID		TECN	COMMENT
$2.7\pm2.5\pm0.9$	AALTONEN	11AI	CDF	$p\overline{p}$ at 1.96 TeV

$B(\Lambda_b\to\Lambda\mu^+\mu^-)$ $(4.0<q^2<6.0\ \text{GeV}^2/c^4)$

VALUE (units 10^{-7})	DOCUMENT ID		TECN	COMMENT
$0.04^{+0.18}_{-0.00}\pm0.02$	AAIJ	15AE	LHCB	pp at 7, 8 TeV

$B(\Lambda_b\to\Lambda\mu^+\mu^-)$ $(1.0<q^2<6.0\ \text{GeV}^2/c^4)$

VALUE (units 10^{-7})	DOCUMENT ID		TECN	COMMENT
$0.47^{+0.31}_{-0.27}$ OUR AVERAGE				
$0.45^{+0.30}_{-0.25}\pm0.10$	[1] AAIJ	15AE	LHCB	pp at 7 and 8 TeV
$1.3\ \pm2.1\ \pm0.4$	AALTONEN	11AI	CDF	$p\overline{p}$ at 1.96 TeV

[1] AAIJ 15AE measurement covers $1.1 < q^2 < 6.0\ \text{GeV}^2/c^4$.

$B(\Lambda_b\to\Lambda\mu^+\mu^-)$ $(6.0<q^2<8.0\ \text{GeV}^2/c^4)$

VALUE (units 10^{-7})	DOCUMENT ID		TECN	COMMENT
$0.50^{+0.24}_{-0.22}\pm0.10$	AAIJ	15AE	LHCB	pp at 7, 8 TeV

$B(\Lambda_b\to\Lambda\mu^+\mu^-)$ $(4.3<q^2<8.68\ \text{GeV}^2/c^4)$

VALUE (units 10^{-7})	DOCUMENT ID		TECN	COMMENT
$0.5\ \pm0.7$ OUR AVERAGE				
$0.66\pm0.74\pm0.18$	[1] AAIJ	13AJ	LHCB	pp at 7 TeV
$-0.2\ \pm1.6\ \pm0.1$	AALTONEN	11AI	CDF	$p\overline{p}$ at 1.96 TeV

[1] Uses $B(\Lambda_b^0\to J/\psi\Lambda) = (6.2\pm1.4)\times10^{-4}$.

$B(\Lambda_b\to\Lambda\mu^+\mu^-)$ $(10.09<q^2<12.86\ \text{GeV}^2/c^4)$

VALUE (units 10^{-7})	DOCUMENT ID		TECN	COMMENT
$2.2\ \pm0.6$ OUR AVERAGE				
$2.08^{+0.42}_{-0.39}\pm0.42$	[1] AAIJ	15AE	LHCB	pp at 7, 8 TeV
$3.0\ \pm1.5\ \pm1.0$	AALTONEN	11AI	CDF	$p\overline{p}$ at 1.96 TeV
• • • We do not use the following data for averages, fits, limits, etc. • • •				
$1.55\pm0.58\pm0.55$	[2] AAIJ	13AJ	LHCB	Repl. by AAIJ 15AE

[1] AAIJ 15AE measurement covers $11.0 < q^2 < 12.5\ \text{GeV}^2/c^4$.
[2] Uses $B(\Lambda_b^0\to J/\psi\Lambda) = (6.2\pm1.4)\times10^{-4}$.

$B(\Lambda_b\to\Lambda\mu^+\mu^-)$ $(14.18<q^2<16.0\ \text{GeV}^2/c^4)$

VALUE (units 10^{-7})	DOCUMENT ID		TECN	COMMENT
$1.7\ \pm0.5$ OUR AVERAGE Error includes scale factor of 1.1.				
$2.04^{+0.35}_{-0.33}\pm0.42$	[1] AAIJ	15AE	LHCB	pp at 7, 8 TeV
$1.0\ \pm0.7\ \pm0.3$	AALTONEN	11AI	CDF	$p\overline{p}$ at 1.96 TeV
• • • We do not use the following data for averages, fits, limits, etc. • • •				
$1.44\pm0.44\pm0.42$	[2] AAIJ	13AJ	LHCB	Repl. by AAIJ 15AE

[1] AAIJ 15AE measurement covers $15.0 < q^2 < 16.0\ \text{GeV}^2/c^4$.
[2] Uses $B(\Lambda_b^0\to J/\psi\Lambda) = (6.2\pm1.4)\times10^{-4}$.

$B(\Lambda_b\to\Lambda\mu^+\mu^-)$ $(16.0<q^2\ \text{GeV}^2/c^4)$

VALUE (units 10^{-7})	DOCUMENT ID		TECN	COMMENT
$7.0\ \pm1.9\ \pm2.2$	AALTONEN	11AI	CDF	$p\overline{p}$ at 1.96 TeV
• • • We do not use the following data for averages, fits, limits, etc. • • •				
$4.73\pm0.77\pm1.25$	[1,2] AAIJ	13AJ	LHCB	Repl. by AAIJ 15AE

[1] Uses $B(\Lambda_b^0\to J/\psi\Lambda) = (6.2\pm1.4)\times10^{-4}$.
[2] Requires $16.00 < q^2 < 20.30\ \text{GeV}^2/c^4$.

$B(\Lambda_b\to\Lambda\mu^+\mu^-)$ $(18.0<q^2<20.0\ \text{GeV}^2/c^4)$

VALUE (units 10^{-7})	DOCUMENT ID		TECN	COMMENT
$2.44\pm0.28\pm0.50$	AAIJ	15AE	LHCB	pp at 7, 8 TeV

$B(\Lambda_b\to\Lambda\mu^+\mu^-)$ $(15.0<q^2<20.0\ \text{GeV}^2/c^4)$

VALUE (units 10^{-7})	DOCUMENT ID		TECN	COMMENT
$6.00\pm0.45\pm1.25$	AAIJ	15AE	LHCB	pp at 7, 8 TeV

CP VIOLATION

A_{CP} is defined as

$$A_{CP} = \frac{B(\Lambda_b^0\to f) - B(\overline{\Lambda}_b^0\to\overline{f})}{B(\Lambda_b^0\to f) + B(\overline{\Lambda}_b^0\to\overline{f})},$$

the *CP*-violation asymmetry of exclusive Λ_b^0 and $\overline{\Lambda}_b^0$ decay.

$A_{CP}(\Lambda_b\to p\pi^-)$

VALUE	DOCUMENT ID		TECN	COMMENT
$0.06\pm0.07\pm0.03$	AALTONEN	14P	CDF	$p\overline{p}$ at 1.96 TeV
• • • We do not use the following data for averages, fits, limits, etc. • • •				
$0.03\pm0.17\pm0.05$	AALTONEN	11N	CDF	Repl. by AALTONEN 14P

$A_{CP}(\Lambda_b \to pK^-)$

VALUE	DOCUMENT ID		TECN	COMMENT
$-0.10\pm0.08\pm0.04$	AALTONEN	14P	CDF	$p\overline{p}$ at 1.96 TeV

• • • We do not use the following data for averages, fits, limits, etc. • • •

$0.37\pm0.17\pm0.03$	AALTONEN	11N	CDF	Repl. by AALTONEN 14P

$A_{CP}(\Lambda_b \to p\overline{K}^0\pi^-)$

VALUE	DOCUMENT ID		TECN	COMMENT
$0.22\pm0.13\pm0.03$	AAIJ	14Q	LHCB	pp at 7 TeV

$\Delta A_{CP}(J/\psi p\pi^-/K^-) \equiv A_{CP}(J/\psi p\pi^-) - A_{CP}(J/\psi pK^-)$

VALUE (units 10^{-2})	DOCUMENT ID		TECN	COMMENT
$5.7\pm2.4\pm1.2$	AAIJ	14K	LHCB	pp at 7, 8 TeV

$A_{CP}(\Lambda_b \to \Lambda K^+\pi^-)$

VALUE	DOCUMENT ID		TECN	COMMENT
$-0.53\pm0.23\pm0.11$	[1] AAIJ	16W	LHCB	pp at 7, 8 TeV

[1] Measured relative to $\Lambda_b^0 \to \Lambda_c^+\pi^-$ decay.

$A_{CP}(\Lambda_b \to \Lambda K^+K^-)$

VALUE	DOCUMENT ID		TECN	COMMENT
$-0.28\pm0.10\pm0.07$	[1] AAIJ	16W	LHCB	pp at 7, 8 TeV

[1] Measured relative to $\Lambda_b^0 \to \Lambda_c^+\pi^-$ decay.

$\Delta A_{CP}(\Lambda_b^0 \to pK^-\mu^+\mu^-) \equiv A_{CP}(pK^-\mu^+\mu^-) - A_{CP}(pK^-J/\psi)$

VALUE (units 10^{-2})	DOCUMENT ID		TECN	COMMENT
$-3.5\pm5.0\pm0.2$	AAIJ	17T	LHCB	pp at 7, 8 TeV

CP AND *T* VIOLATION PARAMETERS

Measured values of the triple-product asymmetry parameters, odd under time-reversal, are defined as $A_{c(s)}(\Lambda/\phi) = (N^+_{c(s)} - N^-_{c(s)})$ / (sum) where $N^+_{c(s)}$, $N^-_{c(s)}$ are the number of Λ or ϕ candidates for which the cos(Φ) and sin(Φ) observables are positive and negative, respectively. Angles cos(Φ) and sin(Φ) are defined as in LEITNER 07.

$A_c(\Lambda)$

VALUE	DOCUMENT ID		TECN	COMMENT
$-0.22\pm0.12\pm0.06$	AAIJ	16J	LHCB	pp at 7, 8 TeV

$A_s(\Lambda)$

VALUE	DOCUMENT ID		TECN	COMMENT
$0.13\pm0.12\pm0.05$	AAIJ	16J	LHCB	pp at 7, 8 TeV

$A_c(\phi)$

VALUE	DOCUMENT ID		TECN	COMMENT
$-0.01\pm0.12\pm0.03$	AAIJ	16J	LHCB	pp at 7, 8 TeV

$A_s(\phi)$

VALUE	DOCUMENT ID		TECN	COMMENT
$-0.07\pm0.12\pm0.01$	AAIJ	16J	LHCB	pp at 7, 8 TeV

$a_P(\Lambda_b^0 \to p\pi^-\pi^+\pi^-)$

Observable calculated as average of the triple products for Λ_b^0 and $\overline{\Lambda}_b^0$, which is sensitive to parity violation.

VALUE (%)	DOCUMENT ID		TECN	COMMENT
$-3.71\pm1.45\pm0.32$	[1] AAIJ	17H	LHCB	pp at 7, 8 TeV

[1] Measured over full phase space of the decay.

$a_P(\Lambda_b^0 \to pK^-K^+\pi^-)$

Observable calculated as average of the triple products for Λ_b^0 and $\overline{\Lambda}_b^0$, which is sensitive to parity violation.

VALUE (%)	DOCUMENT ID		TECN	COMMENT
$3.62\pm4.54\pm0.42$	[1] AAIJ	17H	LHCB	pp at 7, 8 TeV

[1] Measured over full phase space of the decay.

$a_{CP}(\Lambda_b^0 \to p\pi^-\pi^+\pi^-)$

Observable calculated as half of the difference between triple products for Λ_b^0 and $\overline{\Lambda}_b^0$, which is sensitive to *CP* violation.

VALUE (%)	DOCUMENT ID		TECN	COMMENT
$1.15\pm1.45\pm0.32$	[1] AAIJ	17H	LHCB	pp at 7, 8 TeV

[1] Measured over full phase space of the decay.

$a_{CP}(\Lambda_b^0 \to pK^-K^+\pi^-)$

Observable calculated as half of the difference between triple products for Λ_b^0 and $\overline{\Lambda}_b^0$, which is sensitive to *CP* violation.

VALUE (%)	DOCUMENT ID		TECN	COMMENT
$-0.93\pm4.54\pm0.42$	[1] AAIJ	17H	LHCB	pp at 7, 8 TeV

[1] Measured over full phase space of the decay.

$a_P(\Lambda_b^0 \to pK^-\mu^+\mu^-)$

VALUE (%)	DOCUMENT ID		TECN	COMMENT
$-4.8\pm5.0\pm0.7$	AAIJ	17T	LHCB	pp at 7, 8 TeV

$a_{CP}(\Lambda_b^0 \to pK^-\mu^+\mu^-)$

VALUE (%)	DOCUMENT ID		TECN	COMMENT
$1.2\pm5.0\pm0.7$	AAIJ	17T	LHCB	pp at 7, 8 TeV

Λ_b^0 DECAY PARAMETERS

See the note on "Baryon Decay Parameters" in the neutron Listings.

α decay parameter for $\Lambda_b \to J/\psi\Lambda$

VALUE	DOCUMENT ID		TECN	COMMENT
0.18 ± 0.13 OUR AVERAGE				
$0.30\pm0.16\pm0.06$	[1] AAD	14L	ATLS	pp at 7 TeV
$0.05\pm0.17\pm0.07$	[2] AAIJ	13AG	LHCB	pp at 7 TeV

[1] An angular analysis of $\Lambda_b \to J/\psi\Lambda$ decay is performed and magnitudes of all helicity amplitudes are also reported.

[2] An angular analysis of $\Lambda_b \to J/\psi\Lambda$ decay is performed and a Λ_b transverse production polarization of $0.06 \pm 0.07 \pm 0.02$ is also reported.

$A^{\ell}_{FB}(\mu\mu)$ in $\Lambda_b \to \Lambda\mu^+\mu^-$

VALUE	DOCUMENT ID		TECN	COMMENT
$-0.05\pm0.09\pm0.03$	[1] AAIJ	15AE	LHCB	pp at 7, 8 TeV

[1] AAIJ 15AE measurement covers $15.0 < q^2 < 20.0$ GeV$^2/c^4$.

$A^{h}_{FB}(p\pi)$ in $\Lambda_b \to \Lambda(p\pi)\mu^+\mu^-$

VALUE	DOCUMENT ID		TECN	COMMENT
$-0.29\pm0.07\pm0.03$	[1] AAIJ	15AE	LHCB	pp at 7, 8 TeV

[1] AAIJ 15AE measurement covers $15.0 < q^2 < 20.0$ GeV$^2/c^4$.

$f_L(\mu\mu)$ longitudinal polarization fraction in $\Lambda_b \to \Lambda\mu^+\mu^-$

VALUE	DOCUMENT ID		TECN	COMMENT
$0.61^{+0.11}_{-0.14}\pm0.03$	[1] AAIJ	15AE	LHCB	pp at 7, 8 TeV

[1] AAIJ 15AE measurement covers $15.0 < q^2 < 20.0$ GeV$^2/c^4$.

FORWARD-BACKWARD ASYMMETRIES

The forward-backward assymmetry is defined as $A_{FB}(\Lambda_b^0)$ = [N(F) − N(B)] / [N(F) + N(B)], where the forward (F) direction corresponds to a particle (Λ_b^0 or Λ_b^-) sharing valence quark flavors with a beam particle with the same sign of rapidity.

$A_{FB}(\Lambda_b^0 \to J/\psi\Lambda)$

VALUE	DOCUMENT ID		TECN	COMMENT
$0.04\pm0.07\pm0.02$	[1] ABAZOV	15I	D0	pp at 1.96 TeV

[1] The measured asymmetry integrated over rapidity y in the range of $0.1 < |y| < 2.0$.

$A_P(\Lambda_b^0)$

$A_P(\Lambda_b^0) = [\sigma(\Lambda_b^0) - \sigma(\overline{\Lambda}_b^0)] / [\sigma(\Lambda_b^0) + \sigma(\overline{\Lambda}_b^0)]$

VALUE (units 10^{-2})	DOCUMENT ID		TECN	COMMENT
$2.4\ \pm1.6$ OUR AVERAGE	Error includes scale factor of 1.1.			
$-0.11\pm2.53\pm1.08$	[1] AAIJ	17BF	LHCB	pp at 7 TeV
$3.44\pm1.61\pm0.76$	[1] AAIJ	17BF	LHCB	pp at 8 TeV

[1] Indirect determination in kinematic range $2 < p_T < 30$ GeV/c and $2.1 < \eta < 4.5$ from production asymmetries of B^+, B^0 and B_s^0.

Λ_b^0 REFERENCES

AAIJ	17AM	PRL 119 062001	R. Aaij *et al.*	(LHCb Collab.)
AAIJ	17BF	PL B774 139	R. Aaij *et al.*	(LHCb Collab.)
AAIJ	17H	NATP 13 391	R. Aaij *et al.*	(LHCb Collab.)
AAIJ	17P	JHEP 1704 029	R. Aaij *et al.*	(LHCb Collab.)
AAIJ	17S	JHEP 1705 030	R. Aaij *et al.*	(LHCb Collab.)
AAIJ	17T	JHEP 1706 108	R. Aaij *et al.*	(LHCb Collab.)
AAIJ	16	JHEP 1601 012	R. Aaij *et al.*	(LHCb Collab.)
AAIJ	16A	CP C40 011001	R. Aaij *et al.*	(LHCb Collab.)
AAIJ	16J	PL B759 282	R. Aaij *et al.*	(LHCb Collab.)
AAIJ	16W	JHEP 1605 081	R. Aaij *et al.*	(LHCb Collab.)
AAIJ	16Y	JHEP 1605 132	R. Aaij *et al.*	(LHCb Collab.)
AAD	15CH	PL B751 63	G. Aad *et al.*	(ATLAS Collab.)
AAIJ	15AE	JHEP 1506 115	R. Aaij *et al.*	(LHCb Collab.)
AAIJ	15AH	JHEP 1509 006	R. Aaij *et al.*	(LHCb Collab.)
AAIJ	15BG	NATP 11 743	R. Aaij *et al.*	(LHCb Collab.)
ABAZOV	15I	PR D91 072008	V.M. Abazov *et al.*	(D0 Collab.)
AAD	14L	PR D89 092009	G. Aad *et al.*	(ATLAS Collab.)
AAIJ	14AA	PRL 112 202001	R. Aaij *et al.*	(LHCb Collab.)
AAIJ	14E	JHEP 1404 114	R. Aaij *et al.*	(LHCb Collab.)
AAIJ	14H	PR D89 032001	R. Aaij *et al.*	(LHCb Collab.)
AAIJ	14I	JHEP 1408 143	R. Aaij *et al.*	(LHCb Collab.)
AAIJ	14K	JHEP 1407 103	R. Aaij *et al.*	(LHCb Collab.)
AAIJ	14Q	JHEP 1404 087	R. Aaij *et al.*	(LHCb Collab.)
AAIJ	14U	PL B734 122	R. Aaij *et al.*	(LHCb Collab.)
AALTONEN	14B	PR D89 072014	T. Aaltonen *et al.*	(CDF Collab.)
AALTONEN	14P	PRL 113 242001	T. Aaltonen *et al.*	(CDF Collab.)
PDG	14	CP C38 070001	K. Olive *et al.*	(PDG Collab.)
AAD	13U	PR D87 032002	G. Aad *et al.*	(ATLAS Collab.)
AAIJ	13AG	PL B724 27	R. Aaij *et al.*	(LHCb Collab.)
AAIJ	13AJ	PL B725 25	R. Aaij *et al.*	(LHCb Collab.)
AAIJ	13AV	PRL 110 182001	R. Aaij *et al.*	(LHCb Collab.)
AAIJ	13BB	PRL 111 102003	R. Aaij *et al.*	(LHCb Collab.)
CHATRCHYAN	13AC	JHEP 1307 163	S. Chatrchyan *et al.*	(CMS Collab.)
AAIJ	12AR	JHEP 1210 037	R. Aaij *et al.*	(LHCb Collab.)
AAIJ	12E	PL B708 241	R. Aaij *et al.*	(LHCb Collab.)
AALTONEN	12A	PR D85 032003	T. Aaltonen *et al.*	(CDF Collab.)
ABAZOV	12U	PR D85 112003	V.M. Abazov *et al.*	(D0 Collab.)

AAIJ	11E	PR D84 092001	R. Aaij *et al.*	(LHCb Collab.)
Also		PR D85 039904 (errat.)	R. Aaij *et al.*	(LHCb Collab.)
AALTONEN	11	PRL 106 121804	T. Aaltonen *et al.*	(CDF Collab.)
AALTONEN	11AI	PRL 107 201802	T. Aaltonen *et al.*	(CDF Collab.)
AALTONEN	11N	PRL 106 181802	T. Aaltonen *et al.*	(CDF Collab.)
ABAZOV	11O	PR D84 031102	V.M. Abazov *et al.*	(D0 Collab.)
AALTONEN	10B	PRL 104 102002	T. Aaltonen *et al.*	(CDF Collab.)
AALTONEN	09C	PRL 103 031801	T. Aaltonen *et al.*	(CDF Collab.)
AALTONEN	09E	PR D79 032001	T. Aaltonen *et al.*	(CDF Collab.)
ABAZOV	07S	PRL 99 142001	V.M. Abazov *et al.*	(D0 Collab.)
ABAZOV	07U	PRL 99 182001	V.M. Abazov *et al.*	(D0 Collab.)
ABULENCIA	07A	PRL 98 122001	A. Abulencia *et al.*	(FNAL CDF Collab.)
ABULENCIA	07B	PRL 98 122002	A. Abulencia *et al.*	(FNAL CDF Collab.)
LEITNER	07	NPBPS 174 169	O. Leitner, Z.J. Ajaltouni	
ACOSTA	06	PRL 96 202001	D. Acosta *et al.*	(CDF Collab.)
ABAZOV	05C	PRL 94 102001	V.M. Abazov *et al.*	(D0 Collab.)
ACOSTA	05O	PR D72 051104	D. Acosta *et al.*	(CDF Collab.)
ABDALLAH	04A	PL B585 63	J. Abdallah *et al.*	(DELPHI Collab.)
ACOSTA	02G	PR D66 112002	D. Acosta *et al.*	(CDF Collab.)
ABREU	99W	EPJ C10 185	P. Abreu *et al.*	(DELPHI Collab.)
ACKERSTAFF	98G	PL B426 161	K. Ackerstaff *et al.*	(OPAL Collab.)
BARATE	98D	EPJ C2 197	R. Barate *et al.*	(ALEPH Collab.)
ABE	97B	PR D55 1142	F. Abe *et al.*	(CDF Collab.)
ABE	96M	PRL 77 1439	F. Abe *et al.*	(CDF Collab.)
ABREU	96D	ZPHY C71 199	P. Abreu *et al.*	(DELPHI Collab.)
ABREU	96N	PL B374 351	P. Abreu *et al.*	(DELPHI Collab.)
ADAM	96D	ZPHY C72 207	W. Adam *et al.*	(DELPHI Collab.)
BUSKULIC	96L	PL B380 442	D. Buskulic *et al.*	(ALEPH Collab.)
BUSKULIC	96V	PL B384 471	D. Buskulic *et al.*	(ALEPH Collab.)
PDG	96	PR D54 1	R. M. Barnett *et al.*	(PDG Collab.)
ABREU	95S	ZPHY C68 375	P. Abreu *et al.*	(DELPHI Collab.)
AKERS	95K	PL B353 402	R. Akers *et al.*	(OPAL Collab.)
BUSKULIC	95L	PL B357 685	D. Buskulic *et al.*	(ALEPH Collab.)
ABE	93B	PR D47 2639	F. Abe *et al.*	(CDF Collab.)
BUSKULIC	92E	PL B294 145	D. Buskulic *et al.*	(ALEPH Collab.)
ALBAJAR	91E	PL B273 540	C. Albajar *et al.*	(UA1 Collab.)
BARI	91	NC 104A 1787	G. Bari *et al.*	(CERN R422 Collab.)
ARENTON	86	NP B274 707	M.W. Arenton *et al.*	(ARIZ, NDAM, VAND)
BASILE	81	LNC 31 97	M. Basile *et al.*	(CERN R415 Collab.)

$\Lambda_b(5912)^0$

$J^P = \frac{1}{2}^-$ Status: ***

Quantum numbers are based on quark model expectations.

$\Lambda_b(5912)^0$ MASS

VALUE (MeV)	DOCUMENT ID		TECN	COMMENT
5912.20±0.13±0.17	[1,2] AAIJ	12AL	LHCB	pp at 7 TeV

[1] Observed in $\Lambda_b(5912)^0 \to \Lambda_b^0\pi^+\pi^-$ decays with 17.6 ± 4.8 candidates with a significance of 5.2 sigma.

[2] AAIJ 12AL measures $m(\Lambda_b(5912)^0) - m(\Lambda_b^0) = 292.60 \pm 0.12 \pm 0.04$ MeV. We have adjusted the measurement to our best value of $m(\Lambda_b^0) = 5619.60 \pm 0.17$ MeV. Our first error is their experiment's error and our second error is the systematic error from using our best values.

$\Lambda_b(5912)^0$ WIDTH

VALUE (MeV)	CL%	DOCUMENT ID		TECN	COMMENT
<0.66	90	AAIJ	12AL	LHCB	pp at 7 TeV

$\Lambda_b(5912)^0$ DECAY MODES

	Mode	Fraction (Γ_i/Γ)
Γ_1	$\Lambda_b^0\pi^+\pi^-$	seen

$\Lambda_b(5912)^0$ BRANCHING RATIOS

$\Gamma(\Lambda_b^0\pi^+\pi^-)/\Gamma_{total}$ Γ_1/Γ

VALUE	DOCUMENT ID		TECN	COMMENT
seen	AAIJ	12AL	LHCB	pp at 7 TeV

$\Lambda_b(5912)^0$ REFERENCES

AAIJ	12AL	PRL 109 172003	R. Aaij *et al.*	(LHCb Collab.)

$\Lambda_b(5920)^0$

$J^P = \frac{3}{2}^-$ Status: ***

Quantum numbers are based on quark model expectations.

$\Lambda_b(5920)^0$ MASS

VALUE (MeV)	DOCUMENT ID		TECN	COMMENT
5919.92±0.19 OUR AVERAGE	Error includes scale factor of 1.1.			
5919.4 ±0.5 ±0.2	[1,2] AALTONEN	13V	CDF	$p\overline{p}$ at 1.96 TeV
5920.00±0.09±0.17	[3,4] AAIJ	12AL	LHCB	pp at 7 TeV

[1] Measured in $\Lambda_b(5920)^0 \to \Lambda_b^0\pi^+\pi^-$ decays with $17.3^{+5.3}_{-4.6}$ events, with a significance of 3.5 sigma.

[2] AALTONEN 13V measures $m(\Lambda_b(5920)^0) - m(\Lambda_b^0) - 2m(\pi) = 20.68 \pm 0.35 \pm 0.30$ MeV. We have adjusted the measurement to our best values of $m(\Lambda_b^0) = 5619.60 \pm 0.17$ MeV and $m(\pi) = 139.57061 \pm 0.00024$ MeV. Our first error is their experiment's error and our second error is the systematic error from using our best values.

[3] Observed in $\Lambda_b(5920)^0 \to \Lambda_b^0\pi^+\pi^-$ decays with 52.5 ± 8.1 candidates with a significance of 10.2 sigma.

[4] AAIJ 12AL measures $m(\Lambda_b(5920)^0) - m(\Lambda_b^0) = 300.40 \pm 0.08 \pm 0.04$ MeV. We have adjusted the measurement to our best value of $m(\Lambda_b^0) = 5619.60 \pm 0.17$ MeV. Our first error is their experiment's error and our second error is the systematic error from using our best values.

$\Lambda_b(5920)^0$ WIDTH

VALUE (MeV)	CL%	DOCUMENT ID		TECN	COMMENT
<0.63	90	AAIJ	12AL	LHCB	pp at 7 TeV

$\Lambda_b(5920)^0$ DECAY MODES

	Mode	Fraction (Γ_i/Γ)
Γ_1	$\Lambda_b^0\pi^+\pi^-$	seen

$\Lambda_b(5920)^0$ BRANCHING RATIOS

$\Gamma(\Lambda_b^0\pi^+\pi^-)/\Gamma_{total}$ Γ_1/Γ

VALUE	DOCUMENT ID		TECN	COMMENT
seen	AAIJ	12AL	LHCB	pp at 7 TeV

$\Lambda_b(5920)^0$ REFERENCES

AALTONEN	13V	PR D88 071101	T. Aaltonen *et al.*	(CDF Collab.)
AAIJ	12AL	PRL 109 172003	R. Aaij *et al.*	(LHCb Collab.)

Σ_b

$I(J^P) = 1(\frac{1}{2}^+)$ Status: ***

I, *J*, *P* need confirmation.

In the quark model Σ_b^+, Σ_b^0, Σ_b^- are an isotriplet (*uub*, *udb*, *ddb*) state. The lowest Σ_b ought to have $J^P = 1/2^+$. None of *I*, *J*, or *P* have actually been measured.

Σ_b MASS

Σ_b^+ MASS

VALUE (MeV)	DOCUMENT ID		TECN	COMMENT
$5811.3^{+0.9}_{-0.8}\pm1.7$	[1] AALTONEN	12F	CDF	$p\overline{p}$ at 1.96 TeV
• • • We do not use the following data for averages, fits, limits, etc. • • •				
$5807.8^{+2.0}_{-2.2}\pm1.7$	[2] AALTONEN	07K	CDF	Repl. by AALTONEN 12F

Σ_b^- MASS

VALUE (MeV)	DOCUMENT ID		TECN	COMMENT
$5815.5^{+0.6}_{-0.5}\pm1.7$	[1] AALTONEN	12F	CDF	$p\overline{p}$ at 1.96 TeV
• • • We do not use the following data for averages, fits, limits, etc. • • •				
5815.2±1.0±1.7	[2] AALTONEN	07K	CDF	Repl. by AALTONEN 12F

$m_{\Sigma_b^+} - m_{\Sigma_b^-}$

VALUE (MeV)	DOCUMENT ID		TECN	COMMENT
$-4.2^{+1.1}_{-1.0}\pm0.1$	[1] AALTONEN	12F	CDF	$p\overline{p}$ at 1.96 TeV

[1] Measured using the fully reconstructed $\Lambda_b^0 \to \Lambda_c^+\pi^-$ and $\Lambda_c^+ \to K^-\pi^+$ decays.

[2] Observed four $\Lambda_b^0\pi^\pm$ resonances in the fully reconstructed decay mode $\Lambda_b^0 \to \Lambda_c^+\pi^-$, where $\Lambda_c^+ \to pK^-\pi^+$.

Σ_b WIDTH

Σ_b^+ WIDTH

VALUE (MeV)	DOCUMENT ID		TECN	COMMENT
$9.7^{+3.8}_{-2.8}{}^{+1.2}_{-1.1}$	[3] AALTONEN	12F	CDF	$p\overline{p}$ at 1.96 TeV

Σ_b^- WIDTH

VALUE (MeV)	DOCUMENT ID		TECN	COMMENT
$4.9^{+3.1}_{-2.1}\pm1.1$	[3] AALTONEN	12F	CDF	$p\overline{p}$ at 1.96 TeV

[3] Measured using the fully reconstructed $\Lambda_b^0 \to \Lambda_c^+\pi^-$ and $\Lambda_c^+ \to K^-\pi^+$ decays.

Σ_b DECAY MODES

	Mode	Fraction (Γ_i/Γ)
Γ_1	$\Lambda_b^0\pi$	dominant

Σ_b BRANCHING RATIOS

$\Gamma(\Lambda_b^0\pi)/\Gamma_{\text{total}}$ Γ_1/Γ

VALUE	DOCUMENT ID		TECN	COMMENT
dominant	AALTONEN	07K	CDF	$p\overline{p}$ at 1.96 TeV

Σ_b REFERENCES

AALTONEN	12F	PR D85 092011	T. Aaltonen *et al.*	(CDF Collab.)
AALTONEN	07K	PRL 99 202001	T. Aaltonen *et al.*	(CDF Collab.)

Σ_b^*

$I(J^P) = 1(\frac{3}{2}^+)$ Status: ***

I, *J*, *P* need confirmation.

I, *J*, *P* need confirmation. Quantum numbers shown are quark-model predictions.

Σ_b^* MASS

Σ_b^{*+} MASS

VALUE (MeV)	DOCUMENT ID		TECN	COMMENT
$\mathbf{5832.1 \pm 0.7^{+1.7}_{-1.8}}$	[1] AALTONEN	12F	CDF	$p\overline{p}$ at 1.96 TeV

Σ_b^{*-} MASS

VALUE (MeV)	DOCUMENT ID		TECN	COMMENT
$\mathbf{5835.1 \pm 0.6^{+1.7}_{-1.8}}$	[1] AALTONEN	12F	CDF	$p\overline{p}$ at 1.96 TeV

$m_{\Sigma_b^{*+}} - m_{\Sigma_b^{*-}}$

VALUE (MeV)	DOCUMENT ID		TECN	COMMENT
$\mathbf{-3.0^{+1.0}_{-0.9} \pm 0.1}$	[1] AALTONEN	12F	CDF	$p\overline{p}$ at 1.96 TeV

[1] Measured using the fully reconstructed $\Lambda_b^0 \to \Lambda_c^+\pi^-$ and $\Lambda_c^+ \to K^-\pi^+$ decays.

Σ_b^* WIDTH

Σ_b^{*+} WIDTH

VALUE (MeV)	DOCUMENT ID		TECN	COMMENT
$\mathbf{11.5^{+2.7+1.0}_{-2.2-1.5}}$	[2] AALTONEN	12F	CDF	$p\overline{p}$ at 1.96 TeV

Σ_b^{*-} WIDTH

VALUE (MeV)	DOCUMENT ID		TECN	COMMENT
$\mathbf{7.5^{+2.2+0.9}_{-1.8-1.4}}$	[2] AALTONEN	12F	CDF	$p\overline{p}$ at 1.96 TeV

[2] Measured using the fully reconstructed $\Lambda_b^0 \to \Lambda_c^+\pi^-$ and $\Lambda_c^+ \to K^-\pi^+$ decays.

$m_{\Sigma_b^*} - m_{\Sigma_b}$

VALUE (MeV)	DOCUMENT ID		TECN	COMMENT
$\mathbf{21.2^{+2.0+0.4}_{-1.9-0.3}}$	[3] AALTONEN	07K	CDF	$p\overline{p}$ at 1.96 TeV

[3] Observed four $\Lambda_b^0\pi^\pm$ resonances in the fully reconstructed decay mode $\Lambda_b^0 \to \Lambda_c^+\pi^-$, where $\Lambda_c^+ \to pK^-\pi^+$. Assumes $m_{\Sigma_b^{*+}} - m_{\Sigma_b^+} = m_{\Sigma_b^{*-}} - m_{\Sigma_b^-}$

Σ_b^* DECAY MODES

	Mode	Fraction (Γ_i/Γ)
Γ_1	$\Lambda_b^0\pi$	dominant

Σ_b^* BRANCHING RATIOS

$\Gamma(\Lambda_b^0\pi)/\Gamma_{\text{total}}$ Γ_1/Γ

VALUE	DOCUMENT ID		TECN	COMMENT
dominant	AALTONEN	07K	CDF	$p\overline{p}$ at 1.96 TeV

Σ_b^* REFERENCES

AALTONEN	12F	PR D85 092011	T. Aaltonen *et al.*	(CDF Collab.)
AALTONEN	07K	PRL 99 202001	T. Aaltonen *et al.*	(CDF Collab.)

Ξ_b^0, Ξ_b^-

$I(J^P) = \frac{1}{2}(\frac{1}{2}^+)$ Status: ***

I, *J*, *P* need confirmation.

In the quark model, Ξ_b^0 and Ξ_b^- are an isodoublet (*usb*, *dsb*) state; the lowest Ξ_b^0 and Ξ_b^- ought to have $J^P = 1/2^+$. None of *I*, *J*, or *P* have actually been measured.

Ξ_b MASSES

Ξ_b^- MASS

VALUE (MeV)	DOCUMENT ID		TECN	COMMENT
5797.0 ± 0.9 OUR AVERAGE	Error includes scale factor of 1.8. See the ideogram below.			
5797.72 ± 0.46 ± 0.31	[1] AAIJ	14BJ	LHCB	pp at 7, 8 TeV
5793.4 ± 1.8 ± 0.7	[2] AALTONEN	14B	CDF	$p\overline{p}$ at 1.96 TeV
5795.8 ± 0.9 ± 0.4	[3] AAIJ	13AV	LHCB	pp at 7 TeV
5774 ±11 ±15	[4] ABAZOV	07K	D0	$p\overline{p}$ at 1.96 TeV
• • • We do not use the following data for averages, fits, limits, etc. • • •				
5796.7 ± 5.1 ± 1.4	[5] AALTONEN	11X	CDF	Repl. by AALTONEN 14B
5790.9 ± 2.6 ± 0.8	[6] AALTONEN	09AP	CDF	Repl. by AALTONEN 14B
5792.9 ± 2.5 ± 1.7	[7] AALTONEN	07A	CDF	Repl. by AALTONEN 09AP

[1] Reconstructed in $\Xi_b^- \to \Xi_c^0\pi^-$, $\Xi_c^0 \to pK^-K^-\pi^+$ decays. Reference Λ_b^0 mass 5619.30 ± 0.34 MeV from AAIJ 14AA.

[2] Uses $\Xi_b^- \to J/\psi\Xi^-$ and $\Xi_c^0\pi^-$ decays.

[3] Measured in $\Xi_b^- \to J/\psi\Xi^-$ decays.

[4] Observed in $\Xi_b^- \to J/\psi\Xi^-$ decays with $15.2 \pm 4.4^{+1.9}_{-0.4}$ candidates, a significance of 5.5 sigma.

[5] Measured in $\Xi_b^- \to \Xi_c^0\pi^-$ with $25.8^{+5.5}_{-5.2}$ candidates.

[6] Measured in $\Xi_b^- \to J/\psi\Xi^-$ decays with 66^{+14}_{-9} candidates.

[7] Observed in $\Xi_b^- \to J/\psi\Xi^-$ decays with 17.5 ± 4.3 candidates, a significance of 7.7 sigma.

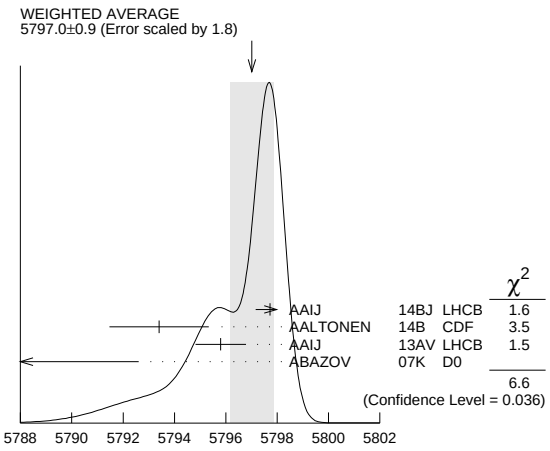

Ξ_b^0 MASS

VALUE (MeV)	DOCUMENT ID		TECN	COMMENT
5791.9 ±0.5 OUR AVERAGE				
5794.3 ±2.4 ±0.7	AAIJ	14H	LHCB	pp at 7 TeV
5791.80 ± 0.39 ± 0.31	[1] AAIJ	14Z	LHCB	pp at 7, 8 TeV
5788.7 ±4.3 ±1.4	[2] AALTONEN	14B	CDF	$p\overline{p}$ at 1.96 TeV
• • • We do not use the following data for averages, fits, limits, etc. • • •				
5787.8 ±5.0 ±1.3	[3] AALTONEN	11X	CDF	Repl. by AALTONEN 14B

[1] Uses $\Xi_b^0 \to \Xi_c^+\pi^-$ and $\Xi_c^+ \to pK^-\pi^+$ decays. The measurement comes from the mass difference of Ξ_b^0 and Λ_b^0.

[2] Uses $\Xi_b^0 \to \Xi_c^+\pi^-$ decays.

[3] Measured in $\Xi_b^0 \to \Xi_c^+\pi^-$ with $25.3^{+5.6}_{-5.4}$ candidates.

$m_{\Xi_b^-} - m_{\Lambda_b^0}$

VALUE (MeV)	DOCUMENT ID		TECN	COMMENT
177.5 ±0.5 OUR AVERAGE	Error includes scale factor of 1.6.			
177.73 ± 0.33 ± 0.14	[1] AAIJ	17BE	LHCB	pp at 7, 8 TeV
176.2 ±0.9 ±0.1	[2] AAIJ	13AV	LHCB	pp at 7 TeV
• • • We do not use the following data for averages, fits, limits, etc. • • •				
177.08 ± 0.47 ± 0.16	[3] AAIJ	17BE	LHCB	pp at 7, 8 TeV
178.36 ± 0.46 ± 0.16	[4,5] AAIJ	14BJ	LHCB	pp at 7, 8 TeV

[1] Combination of the original statistically independent measurements of AAIJ 14BE and AAIJ 17BJ taking into account correlation between systematic uncertainties.

[2] Reconstructed in $\Xi_b^- \to J/\psi\Xi^-$ decays.

[3] Reconstructed in $\Xi_b^- \to J/\psi\Lambda K^-$ decays. Reference decays $\Lambda_b^0 \to J/\psi\Lambda$ were used.

[4] Reconstructed in $\Xi_b^- \to \Xi_c^0\pi^-$, $\Xi_c^0 \to pK^-K^-\pi^+$ decays. Reference $\Lambda_b^0 \to \Lambda_c^+\pi^-$.

[5] Combined with AAIJ 17BE.

Baryon Particle Listings

Ξ_b^0, Ξ_b^-

$m_{\Xi_b^0} - m_{\Lambda_b^0}$

VALUE (MeV)	DOCUMENT ID		TECN	COMMENT
172.5 ±0.4 OUR AVERAGE				
174.8 ±2.4 ±0.5	AAIJ	14H	LHCB	pp at 7 TeV
172.44±0.39±0.17	[1] AAIJ	14Z	LHCB	pp at 7, 8 TeV

[1] Uses $\Xi_b^0 \to \Xi_c^+\pi^-$ and $\Xi_c^+ \to pK^-\pi^+$ decays.

$m_{\Xi_b^-} - m_{\Xi_b^0}$

VALUE (MeV)	DOCUMENT ID		TECN	COMMENT
5.9 ±0.6 OUR AVERAGE				
5.92±0.60±0.23	[1] AAIJ	14BJ	LHCB	pp at 7, 8 TeV
3.1 ±5.6 ±1.3	[2] AALTONEN	11X	CDF	$p\overline{p}$ at 1.96 TeV

[1] Reconstructed in $\Xi_b^- \to \Xi_c^0\pi^-$, $\Xi_c^0 \to pK^-K^-\pi^+$ decays. Uses $m(\Xi_b^0) - m(\Lambda_b^0) = 172.44 \pm 0.39 \pm 0.17$ MeV from AAIJ 14Z.
[2] Derived from measurements in $\Xi_b^0 \to \Xi_c^+\pi^-$ and $\Xi_b^- \to J/\psi\Xi^-$ from AALTONEN 09AP taking correlated systematic uncertainties into account.

Ξ_b MEAN LIFE

"OUR EVALUATION" is an average using rescaled values of the data listed below. The average and rescaling were performed by the Heavy Flavor Averaging Group (HFLAV) and are described at http://www.slac.stanford.edu/xorg/hflav/. The averaging/rescaling procedure takes into account correlations between the measurements and asymmetric lifetime errors.

Ξ_b^- MEAN LIFE

VALUE (10^{-12} s)	DOCUMENT ID		TECN	COMMENT
1.571±0.040 OUR EVALUATION				
1.57 ±0.04 OUR AVERAGE Error includes scale factor of 1.1.				
1.599±0.041±0.022	[1] AAIJ	14BJ	LHCB	pp at 7, 8 TeV
1.55 $^{+0.10}_{-0.09}$ ±0.03	[2] AAIJ	14T	LHCB	pp at 7, 8 TeV
1.36 ±0.15 ±0.02	AALTONEN	14B	CDF	$p\overline{p}$ at 1.96 TeV
• • • We do not use the following data for averages, fits, limits, etc. • • •				
1.56 $^{+0.27}_{-0.25}$ ±0.02	[3] AALTONEN	09AP	CDF	Repl. by AALTONEN 14B

[1] Reconstructed in $\Xi_b^- \to \Xi_c^0\pi^-$, $\Xi_c^0 \to pK^-K^-\pi^+$ decays. Reference Λ_b^0 lifetime $1.479 \pm 0.009 \pm 0.010$ ps from AAIJ 14U.
[2] Measured in $\Xi_b^- \to J/\psi\Xi^-$ decays.
[3] Measured in $\Xi_b^- \to J/\psi\Xi^-$ decays with 66^{+14}_{-9} candidates.

Ξ_b^0 MEAN LIFE

VALUE (10^{-12} s)	DOCUMENT ID		TECN	COMMENT
1.479±0.031 OUR EVALUATION				
1.477±0.026±0.019	[1] AAIJ	14Z	LHCB	pp at 7, 8 TeV

[1] Uses $\Xi_b^0 \to \Xi_c^+\pi^-$ and $\Xi_c^+ \to pK^-\pi^+$ decays. The measurement comes from the value of relative lifetime of Ξ_b^0 to Λ_b^0.

Ξ_b MEAN LIFE

VALUE (10^{-12} s)	DOCUMENT ID		TECN	COMMENT
• • • We do not use the following data for averages, fits, limits, etc. • • •				
1.48 $^{+0.40}_{-0.31}$ ±0.12	[1] ABDALLAH	05C	DLPH	$e^+e^- \to Z^0$
1.35 $^{+0.37}_{-0.28}$ $^{+0.15}_{-0.17}$	[2] BUSKULIC	96T	ALEP	$e^+e^- \to Z$
1.5 $^{+0.7}_{-0.4}$ ±0.3	[3] ABREU	95V	DLPH	Repl. by ABDALLAH 05C

[1] Used the decay length of Ξ^- accompanied by a lepton of the same sign.
[2] Excess $\Xi^-\ell^-$, impact parameters.
[3] Excess $\Xi^-\ell^-$, decay lengths.

τ_{mix} (1/2π) times the oscillation period

VALUE (s)	DOCUMENT ID		TECN	COMMENT
$>13 \times 10^{-12}$	[1] AAIJ	17BH	LHCB	pp at 7, 8 TeV

[1] Uses Ξ_b^{*-} and $\Xi_b^{\prime-}$ decays to $\Xi_b^0\pi^-$, where $\Xi_b^0 \to \Xi_c^+\pi^-$, $\Xi_c^+ \to pK^-\pi^+$.

MEAN LIFE RATIOS

$\tau_{\Xi_b^-}$ / $\tau_{\Lambda_b^0}$ mean life ratio

VALUE	DOCUMENT ID		TECN	COMMENT
1.089±0.026±0.011	[1] AAIJ	14BJ	LHCB	pp at 7, 8 TeV

[1] Reconstructed in $\Xi_b^- \to \Xi_c^0\pi^-$, $\Xi_c^0 \to pK^-K^-\pi^+$ decays. Reference $\Lambda_b^0 \to \Lambda_c^+\pi^-$.

$\tau_{\Xi_b^-}$ / $\tau_{\Xi_b^0}$ mean life ratio

VALUE	DOCUMENT ID		TECN	COMMENT
1.083±0.032±0.016	[1] AAIJ	14BJ	LHCB	pp at 7, 8 TeV

[1] Reconstructed in $\Xi_b^- \to \Xi_c^0\pi^-$, $\Xi_c^0 \to pK^-K^-\pi^+$ decays. Uses Ξ_b^0 measurements from AAIJ 14Z.

Ξ_b DECAY MODES

	Mode	Fraction (Γ_i/Γ)	Scale factor/ Confidence level
Γ_1	$\Xi^-\ell^-\overline{\nu}_\ell X \times B(\overline{b} \to \Xi_b)$	$(3.9 \pm 1.2) \times 10^{-4}$	S=1.4
Γ_2	$J/\psi\Xi^- \times B(b \to \Xi_b^-)$	$(1.02^{+0.26}_{-0.21}) \times 10^{-5}$	
Γ_3	$J/\psi\Lambda K^- \times B(b \to \Xi_b^-)$	$(2.5 \pm 0.4) \times 10^{-6}$	
Γ_4	$pD^0K^- \times B(\overline{b} \to \Xi_b)$	$(1.8 \pm 0.6) \times 10^{-6}$	
Γ_5	$p\overline{K}^0\pi^- \times B(\overline{b} \to \Xi_b)/B(\overline{b} \to B^0)$	$< 1.6 \times 10^{-6}$	CL=90%
Γ_6	$pK^0K^- \times B(\overline{b} \to \Xi_b)/B(\overline{b} \to B^0)$	$< 1.1 \times 10^{-6}$	CL=90%
Γ_7	$pK^-K^- \times B(\overline{b} \to \Xi_b)$	$(3.6 \pm 0.8) \times 10^{-8}$	
Γ_8	pK^-K^-		
Γ_9	$p\pi^-\pi^-$		
Γ_{10}	$pK^-\pi^-$		
Γ_{11}	$\Lambda\pi^+\pi^- \times B(b \to \Xi_b^0)/B(b \to \Lambda_b^0)$	$< 1.7 \times 10^{-6}$	CL=90%
Γ_{12}	$\Lambda K^-\pi^+ \times B(b \to \Xi_b^0)/B(b \to \Lambda_b^0)$	$< 8 \times 10^{-7}$	CL=90%
Γ_{13}	$\Lambda K^+K^- \times B(b \to \Xi_b^0)/B(b \to \Lambda_b^0)$	$< 3 \times 10^{-7}$	CL=90%
Γ_{14}	$\Lambda_c^+K^- \times B(\overline{b} \to \Xi_b)$	$(6 \pm 4) \times 10^{-7}$	
Γ_{15}	$\Lambda_b^0\pi^- \times B(b \to \Xi_b^-)/B(b \to \Lambda_b^0)$	$(5.7 \pm 2.0) \times 10^{-4}$	

Ξ_b BRANCHING RATIOS

$\Gamma(\Xi^-\ell^-\overline{\nu}_\ell X \times B(\overline{b} \to \Xi_b))/\Gamma_{total}$ Γ_1/Γ

VALUE (units 10^{-4})	DOCUMENT ID		TECN	COMMENT
3.9±1.2 OUR AVERAGE Error includes scale factor of 1.4.				
3.0±1.0±0.3	ABDALLAH	05C	DLPH	$e^+e^- \to Z^0$
5.4±1.1±0.8	BUSKULIC	96T	ALEP	Excess $\Xi^-\ell^-$ over $\Xi^-\ell^+$
• • • We do not use the following data for averages, fits, limits, etc. • • •				
5.9±2.1±1.0	ABREU	95V	DLPH	Repl. by ABDALLAH 05C

$\Gamma(J/\psi\Xi^- \times B(b \to \Xi_b^-))/\Gamma_{total}$ Γ_2/Γ

VALUE (units 10^{-4})	DOCUMENT ID		TECN	COMMENT
0.102$^{+0.026}_{-0.021}$ OUR AVERAGE				
0.098$^{+0.023}_{-0.016}$±0.014	[1] AALTONEN	09AP	CDF	$p\overline{p}$ at 1.96 TeV
0.16 ±0.07 ±0.02	[2] ABAZOV	07K	D0	$p\overline{p}$ at 1.96 TeV

[1] AALTONEN 09AP reports $[\Gamma(\Xi_b \to J/\psi\Xi^- \times B(b \to \Xi_b^-))/\Gamma_{total}] / [B(\Lambda_b^0 \to J/\psi(1S)\Lambda \times B(b \to \Lambda_b^0))] = 0.167^{+0.037}_{-0.025} \pm 0.012$ which we multiply by our best value $B(\Lambda_b^0 \to J/\psi(1S)\Lambda \times B(b \to \Lambda_b^0)) = (5.8 \pm 0.8) \times 10^{-5}$. Our first error is their experiment's error and our second error is the systematic error from using our best value.
[2] ABAZOV 07K reports $[\Gamma(\Xi_b \to J/\psi\Xi^- \times B(b \to \Xi_b^-))/\Gamma_{total}] / [B(\Lambda_b^0 \to J/\psi(1S)\Lambda \times B(b \to \Lambda_b^0))] = 0.28 \pm 0.09^{+0.09}_{-0.08}$ which we multiply by our best value $B(\Lambda_b^0 \to J/\psi(1S)\Lambda \times B(b \to \Lambda_b^0)) = (5.8 \pm 0.8) \times 10^{-5}$. Our first error is their experiment's error and our second error is the systematic error from using our best value.

$\Gamma(J/\psi\Lambda K^- \times B(b \to \Xi_b^-))/\Gamma_{total}$ Γ_3/Γ

VALUE (10^{-6})	DOCUMENT ID		TECN	COMMENT
2.45±0.19±0.35	[1,2] AAIJ	17BE	LHCB	pp at 7 and 8 TeV

[1] AAIJ 17BE reports $[\Gamma(\Xi_b \to J/\psi\Lambda K^- \times B(b \to \Xi_b^-))/\Gamma_{total}] / [B(\Lambda_b^0 \to J/\psi(1S)\Lambda \times B(b \to \Lambda_b^0))] = (4.19 \pm 0.29 \pm 0.15) \times 10^{-2}$ which we multiply by our best value $B(\Lambda_b^0 \to J/\psi(1S)\Lambda \times B(b \to \Lambda_b^0)) = (5.8 \pm 0.8) \times 10^{-5}$. Our first error is their experiment's error and our second error is the systematic error from using our best value.
[2] Integrated over the b-baryon transverse momentum $p_T < 25$ GeV and rapidity $2.0 < y < 4.5$.

$\Gamma(pD^0K^- \times B(\overline{b} \to \Xi_b))/\Gamma_{total}$ Γ_4/Γ

VALUE	DOCUMENT ID		TECN	COMMENT
(1.8±0.4±0.4) × 10^{-6}	[1] AAIJ	14H	LHCB	pp at 7 TeV

[1] AAIJ 14H reports $[\Gamma(\Xi_b \to pD^0K^- \times B(\overline{b} \to \Xi_b))/\Gamma_{total}] / [B(\Lambda_b^0 \to pD^0K^-)] = 0.44 \pm 0.09 \pm 0.06$ which we multiply by our best values $B(\overline{b} \to b\text{-baryon}) = (8.9 \pm 1.2) \times 10^{-2}$, $B(\Lambda_b^0 \to pD^0K^-) = (4.6 \pm 0.8) \times 10^{-5}$. Our first error is their experiment's error and our second error is the systematic error from using our best values.

$\Gamma(p\overline{K}^0\pi^- \times B(\overline{b} \to \Xi_b)/B(\overline{b} \to B^0))/\Gamma_{total}$ Γ_5/Γ

VALUE	CL%	DOCUMENT ID		TECN	COMMENT
< 1.6 × 10^{-6}	90	AAIJ	14Q	LHCB	pp at 7 TeV

$\Gamma(pK^0K^- \times B(\overline{b} \to \Xi_b)/B(\overline{b} \to B^0))/\Gamma_{total}$ Γ_6/Γ

VALUE	CL%	DOCUMENT ID		TECN	COMMENT
< 1.1 × 10^{-6}	90	AAIJ	14Q	LHCB	pp at 7 TeV

$\Gamma(p K^- K^-\times B(\overline{b}\to \Xi_b))/\Gamma_{total}$ Γ_7/Γ

VALUE (units 10^{-8})	DOCUMENT ID		TECN	COMMENT
3.6±0.8±0.2	[1] AAIJ	17F	LHCB	pp at 7, 8 TeV

[1] AAIJ 17F reports $[\Gamma(\Xi_b \to p K^- K^-\times B(\overline{b}\to \Xi_b))/\Gamma_{total}] / [B(B^+ \to K^+ K^- K^+)] / [B(\overline{b}\to B^+)] = (2.65 \pm 0.35 \pm 0.47)\times 10^{-3}$ which we multiply by our best values $B(B^+ \to K^+ K^- K^+) = (3.40 \pm 0.14)\times 10^{-5}$, $B(\overline{b}\to B^+) = (40.5 \pm 0.6)\times 10^{-2}$. Our first error is their experiment's error and our second error is the systematic error from using our best values.

$\Gamma(p\pi^-\pi^-)/\Gamma(p K^- K^-)$ Γ_9/Γ_8

VALUE	CL%	DOCUMENT ID		TECN	COMMENT
<0.56	90	[1] AAIJ	17F	LHCB	pp at 7, 8 TeV

[1] Measures the ratio as $0.28 \pm 0.16 \pm 0.13$.

$\Gamma(p K^-\pi^-)/\Gamma(p K^- K^-)$ Γ_{10}/Γ_8

VALUE	DOCUMENT ID		TECN	COMMENT
0.98±0.27±0.09	AAIJ	17F	LHCB	pp at 7, 8 TeV

$\Gamma(\Lambda\pi^+\pi^-\times B(b\to \Xi_b^0)/B(b\to \Lambda_b^0))/\Gamma_{total}$ Γ_{11}/Γ

VALUE	CL%	DOCUMENT ID		TECN	COMMENT
$<1.7\times 10^{-6}$	90	AAIJ	16W	LHCB	pp at 7, 8 TeV

$\Gamma(\Lambda K^-\pi^+\times B(b\to \Xi_b^0)/B(b\to \Lambda_b^0))/\Gamma_{total}$ Γ_{12}/Γ

VALUE	CL%	DOCUMENT ID		TECN	COMMENT
$<0.8\times 10^{-6}$	90	AAIJ	16W	LHCB	pp at 7, 8 TeV

$\Gamma(\Lambda K^+ K^-\times B(b\to \Xi_b^0)/B(b\to \Lambda_b^0))/\Gamma_{total}$ Γ_{13}/Γ

VALUE	CL%	DOCUMENT ID		TECN	COMMENT
$<0.3\times 10^{-6}$	90	AAIJ	16W	LHCB	pp at 7, 8 TeV

$\Gamma(\Lambda_c^+ K^-\times B(\overline{b}\to \Xi_b))/\Gamma(p D^0 K^-\times B(\overline{b}\to \Xi_b))$ Γ_{14}/Γ_4

VALUE	DOCUMENT ID		TECN	COMMENT
0.36±0.19±0.02	[1] AAIJ	14H	LHCB	pp at 7 TeV

[1] AAIJ 14H reports $[\Gamma(\Xi_b \to \Lambda_c^+ K^-\times B(\overline{b}\to \Xi_b))/\Gamma(\Xi_b \to p D^0 K^-\times B(\overline{b}\to \Xi_b))] \times [B(\Lambda_c^+ \to p K^-\pi^+)] / [B(D^0 \to K^-\pi^+)] = 0.57 \pm 0.22 \pm 0.21$ which we multiply or divide by our best values $B(\Lambda_c^+ \to p K^-\pi^+) = (6.23 \pm 0.33)\times 10^{-2}$, $B(D^0 \to K^-\pi^+) = (3.89 \pm 0.04)\times 10^{-2}$. Our first error is their experiment's error and our second error is the systematic error from using our best values.

$\Gamma(\Lambda_b^0\pi^-\times B(b\to \Xi_b^-)/B(b\to \Lambda_b^0))/\Gamma_{total}$ Γ_{15}/Γ

VALUE (units 10^{-4})	DOCUMENT ID		TECN	COMMENT
$5.7\pm1.8^{+0.8}_{-0.9}$	[1] AAIJ	15BA	LHCB	pp at 7, 8 TeV

[1] A signal is reported with a significance of 3.2 standard deviations in the decay chain of $\Xi_b^- \to \Lambda_b^0\pi^-$, $\Lambda_b^0 \to \Lambda_c^+\pi^-$, and $\Lambda_c^+ \to p K^-\pi^+$.

Ξ_b REFERENCES

AAIJ	17BE	PL B772 265	R. Aaij *et al.*	(LHCb Collab.)
AAIJ	17BH	PRL 119 181807	R. Aaij *et al.*	(LHCb Collab.)
AAIJ	17BJ	PRL 119 232001	R. Aaij *et al.*	(LHCb Collab.)
AAIJ	17F	PRL 118 071801	R. Aaij *et al.*	(LHCb Collab.)
AAIJ	16W	JHEP 1605 081	R. Aaij *et al.*	(LHCb Collab.)
AAIJ	15BA	PRL 115 241801	R. Aaij *et al.*	(LHCb Collab.)
AAIJ	14AA	PRL 112 202001	R. Aaij *et al.*	(LHCb Collab.)
AAIJ	14BE	NP B888 169	R. Aaij *et al.*	(LHCb Collab.)
AAIJ	14BJ	PRL 113 242002	R. Aaij *et al.*	(LHCb Collab.)
AAIJ	14H	PR D89 032001	R. Aaij *et al.*	(LHCb Collab.)
AAIJ	14Q	JHEP 1404 087	R. Aaij *et al.*	(LHCb Collab.)
AAIJ	14T	PL B736 154	R. Aaij *et al.*	(LHCb Collab.)
AAIJ	14U	PL B734 122	R. Aaij *et al.*	(LHCb Collab.)
AAIJ	14Z	PRL 113 032001	R. Aaij *et al.*	(LHCb Collab.)
AALTONEN	14B	PR D89 072014	T. Aaltonen *et al.*	(CDF Collab.)
AAIJ	13AV	PRL 110 182001	R. Aaij *et al.*	(LHCb Collab.)
AALTONEN	11X	PRL 107 102001	T. Aaltonen *et al.*	(CDF Collab.)
AALTONEN	09AP	PR D80 072003	T. Aaltonen *et al.*	(CDF Collab.)
AALTONEN	07A	PRL 99 052002	T. Aaltonen *et al.*	(CDF Collab.)
ABAZOV	07K	PRL 99 052001	V.M. Abazov *et al.*	(D0 Collab.)
ABDALLAH	05C	EPJ C44 299	J. Abdallah *et al.*	(DELPHI Collab.)
BUSKULIC	96T	PL B384 449	D. Buskulic *et al.*	(ALEPH Collab.)
ABREU	95V	ZPHY C68 541	P. Abreu *et al.*	(DELPHI Collab.)

$\Xi_b'(5935)^-$ $J^P = \frac{1}{2}^+$ Status: ***

$\Xi_b'(5935)^-$ MASS

VALUE (MeV)	DOCUMENT ID		TECN	COMMENT
5935.02±0.02±0.05	[1] AAIJ	15H	LHCB	pp at 7, 8 TeV

[1] Not independent of the mass difference measurement below. Observed in $\Xi_b^0\pi^-$ channel with $\Xi_b^0 \to \Xi_c^+\pi^-$ and $\Xi_c^+ \to p K^-\pi^+$.

$m_{\Xi_b'(5935)^-} - m_{\Xi_b^0} - m_{\pi^-}$

VALUE (MeV)	DOCUMENT ID		TECN	COMMENT
3.653±0.018±0.006	[2] AAIJ	15H	LHCB	pp at 7, 8 TeV

[2] Observed in $\Xi_b^0\pi^-$ channel with $\Xi_b^0 \to \Xi_c^+\pi^-$ and $\Xi_c^+ \to p K^-\pi^+$.

$\Xi_b'(5935)^-$ WIDTH

VALUE (MeV)	CL%	DOCUMENT ID		TECN	COMMENT
<0.08	95	[3] AAIJ	15H	LHCB	pp at 7, 8 TeV

[3] Observed in $\Xi_b^0\pi^-$ channel with $\Xi_b^0 \to \Xi_c^+\pi^-$ and $\Xi_c^+ \to p K^-\pi^+$.

$\Xi_b'(5935)^-$ DECAY MODES

	Mode	Fraction (Γ_i/Γ)
Γ_1	$\Xi_b^0\pi^-\times B(\overline{b}\to \Xi_b'(5935)^-)/B(\overline{b}\to \Xi_b^0)$	(11.8±1.8) %

$\Xi_b'(5935)^-$ BRANCHING RATIOS

$\Gamma(\Xi_b^0\pi^-\times B(\overline{b}\to \Xi_b'(5935)^-)/B(\overline{b}\to \Xi_b^0))/\Gamma_{total}$ Γ_1/Γ

VALUE	DOCUMENT ID		TECN	COMMENT
0.118±0.017±0.007	[4] AAIJ	15H	LHCB	pp at 7, 8 TeV

[4] Observed in $\Xi_b^0\pi^-$ channel with $\Xi_b^0 \to \Xi_c^+\pi^-$ and $\Xi_c^+ \to p K^-\pi^+$.

$\Xi_b'(5935)^-$ REFERENCES

AAIJ	15H	PRL 114 062004	R. Aaij *et al.*	(LHCb Collab.)

$\Xi_b(5945)^0$ $J^P = \frac{3}{2}^+$ Status: ***

Quantum numbers are based on quark model expectations.

$\Xi_b(5945)^0$ MASS

VALUE (MeV)	DOCUMENT ID		TECN	COMMENT
5949.8±1.4 OUR AVERAGE				
5952.3±0.1±0.9	[1] AAIJ	16AE	LHCB	pp at 7, 8 TeV
5951.4±0.8±0.9	[2] CHATRCHYAN	12S	CMS	pp at 7 TeV, 5.3 fb^{-1}

[1] AAIJ 16AE measures $m(\Xi_b(5945)^0) - m(\Xi_b^-) - m(\pi^+) = 15.727 \pm 0.068 \pm 0.023$ MeV. We have adjusted the measurement to our best values of $m(\Xi_b^-) = 5797.0 \pm 0.9$ MeV, $m(\pi^+) = 139.57061 \pm 0.00024$ MeV. Our first error is their experiment's error and our second error is the systematic error from using our best values.

[2] CHATRCHYAN 12S measures $m(\Xi_b(5945)^0) - m(\Xi_b^-) - m(\pi^+) = 14.84 \pm 0.74 \pm 0.28$ MeV. We have adjusted the measurement to our best values of $m(\Xi_b^-) = 5797.0 \pm 0.9$ MeV, $m(\pi^+) = 139.57061 \pm 0.00024$ MeV. Our first error is their experiment's error and our second error is the systematic error from using our best values.

$\Xi_b(5945)^0$ WIDTH

VALUE (MeV)	DOCUMENT ID		TECN	COMMENT
0.90±0.16±0.08	[3] AAIJ	16AE	LHCB	pp at 7, 8 TeV
• • • We do not use the following data for averages, fits, limits, etc. • • •				
2.1 ±1.7	[4] CHATRCHYAN	12S	CMS	pp at 7 TeV, 5.3 fb^{-1}

[3] Measured using $\Xi_b(5945)^0 \to \Xi_b^-\pi^+$, $\Xi_b^- \to \Xi_c^0\pi^-$, $\Xi_c^0 \to p K^- K^-\pi^+$ decays.

[4] Systematic uncertainty not evaluated.

$\Xi_b(5945)^0$ DECAY MODES

	Mode	Fraction (Γ_i/Γ)
Γ_1	$\Xi_b^-\pi^+$	seen

$\Xi_b(5945)^0$ BRANCHING RATIOS

$\Gamma(\Xi_b^-\pi^+)/\Gamma_{total}$ Γ_1/Γ

VALUE	DOCUMENT ID		TECN	COMMENT
seen	AAIJ	16AE	ATLS	pp at 7, 8 TeV
seen	CHATRCHYAN	12S	CMS	pp at 7 TeV, 5.3 fb^{-1}

$\Xi_b(5945)^0$ REFERENCES

AAIJ	16AE	JHEP 1605 161	R. Aaij *et al.*	(LHCb Collab.)
CHATRCHYAN	12S	PRL 108 252002	S. Chatrchyan *et al.*	(CMS Collab.)

Baryon Particle Listings

$\Xi_b(5945)^0$, $\Xi_b(5955)^-$, Ω_b^-

$\Xi_b(5955)^-$

$J^P = \frac{3}{2}^+$ Status: ***

$\Xi_b(5955)^-$ MASS

VALUE (MeV)	DOCUMENT ID		TECN	COMMENT
5955.33±0.12±0.05	[1] AAIJ	15H	LHCB	pp at 7, 8 TeV

[1] Not independent of the mass difference measurement below. Observed in $\Xi_b^0\pi^-$ channel with $\Xi_b^0 \to \Xi_c^+\pi^-$ and $\Xi_c^+ \to pK^-\pi^+$.

$m_{\Xi_b(5955)^-} - m_{\Xi_b^0} - m_{\pi^-}$

VALUE (MeV)	DOCUMENT ID		TECN	COMMENT
23.96±0.12±0.06	[1] AAIJ	15H	LHCB	pp at 7, 8 TeV

[1] Observed in $\Xi_b^0\pi^-$ channel with $\Xi_b^0 \to \Xi_c^+\pi^-$ and $\Xi_c^+ \to pK^-\pi^+$.

$\Xi_b(5955)^-$ WIDTH

VALUE (MeV)	DOCUMENT ID		TECN	COMMENT
1.65±0.31±0.10	[1] AAIJ	15H	LHCB	pp at 7, 8 TeV

[1] Observed in $\Xi_b^0\pi^-$ channel with $\Xi_b^0 \to \Xi_c^+\pi^-$ and $\Xi_c^+ \to pK^-\pi^+$.

$\Xi_b(5955)^-$ DECAY MODES

	Mode	Fraction (Γ_i/Γ)
Γ_1	$\Xi_b^0\pi^- \times$ B($\overline{b} \to \Xi_b^*(5955)^-$)/B($\overline{b} \to \Xi_b^0$)	(20.7±3.5) %

$\Xi_b(5955)^-$ BRANCHING RATIOS

$\Gamma(\Xi_b^0\pi^- \times$ B($\overline{b} \to \Xi_b^*(5955)^-$)/B($\overline{b} \to \Xi_b^0$))/$\Gamma_{\text{total}}$ Γ_1/Γ

VALUE	DOCUMENT ID		TECN	COMMENT
0.207±0.032±0.015	[1] AAIJ	15H	LHCB	pp at 7, 8 TeV

[1] Observed in $\Xi_b^0\pi^-$ channel with $\Xi_b^0 \to \Xi_c^+\pi^-$ and $\Xi_c^+ \to pK^-\pi^+$.

$\Xi_b(5955)^-$ REFERENCES

AAIJ 15H PRL 114 062004 R. Aaij *et al.* (LHCb Collab.)

Ω_b^-

$I(J^P) = 0(\frac{1}{2}^+)$ Status: ***
I, J, P need confirmation.

In the quark model Ω_b^- is ssb ground state. None of its quantum numbers has been measured.

Ω_b^- MASS

VALUE (MeV)	DOCUMENT ID		TECN	COMMENT
6046.1± 1.7 OUR AVERAGE				
6045.1± 3.2± 0.8	[1] AAIJ	16O	LHCB	pp at 7, 8 TeV
6047.5± 3.8± 0.6	[2] AALTONEN	14B	CDF	$p\overline{p}$ at 1.96 TeV
6046.0± 2.2± 0.5	[3] AAIJ	13AV	LHCB	pp at 7 TeV
• • • We do not use the following data for averages, fits, limits, etc. • • •				
6054.4± 6.8± 0.9	[4] AALTONEN	09AP	CDF	Repl. by AALTONEN 14B
6165 ±10 ±13	[5] ABAZOV	08AL	D0	$p\overline{p}$ at 1.96 TeV

[1] Reconstructed in $\Omega_b^- \to \Omega_c^0\pi^-$, $\Omega_c^0 \to pK^-K^-\pi^+$ decays. Reference Ξ_b^- mass 5797.72 ± 0.6 MeV from AAIJ 14B.

[2] Uses $\Omega_b^- \to J/\psi\Omega^-$ and $\Omega_c^0\pi^-$ decays, with the first evidence for $\Omega_b^- \to \Omega_c^0\pi^-$ at 3.3 σ significance.

[3] Measured in $\Omega_b^- \to J/\psi\Omega^-$ with 19 ± 5 events.

[4] Observed in $\Omega_b^- \to J/\psi\Omega^-$ decays with 16^{+6}_{-4} candidates, a significance of 5.5 sigma from a combined mass-lifetime fit.

[5] Observed in $\Omega_b^- \to J/\psi\Omega^-$ decays with 17.8 ± 4.9 ± 0.8 candidates, a significance of 5.4 sigma.

$m_{\Omega_b^-} - m_{\Lambda_b^0}$

VALUE (MeV)	DOCUMENT ID		TECN	COMMENT
426.4±2.2±0.4	AAIJ	13AV	LHCB	pp at 7 TeV

$m_{\Omega_b^-} - m_{\Xi_b^-}$

VALUE (MeV)	DOCUMENT ID		TECN	COMMENT
247.3±3.2±0.5	[1] AAIJ	16O	LHCB	pp at 7, 8 TeV

[1] Uses $\Omega_b^- \to \Omega_c^0\pi^-$, $\Omega_c^0 \to pK^-K^-\pi^+$ and $\Xi_b^- \to \Xi_c^0\pi^-$, $\Xi_c^0 \to pK^-K^-\pi^+$ decays.

Ω_b MEAN LIFE

VALUE (10^{-12} s)	DOCUMENT ID		TECN	COMMENT
$1.64^{+0.18}_{-0.17}$ OUR EVALUATION				
$1.65^{+0.18}_{-0.16}$ OUR AVERAGE				
1.78±0.26±0.05±0.06	[1] AAIJ	16O	LHCB	pp at 7, 8 TeV
$1.54^{+0.26}_{-0.21}$±0.05	[2] AAIJ	14T	LHCB	pp at 7, 8 TeV
$1.66^{+0.53}_{-0.40}$±0.02	[2] AALTONEN	14B	CDF	$p\overline{p}$ at 1.96 TeV
• • • We do not use the following data for averages, fits, limits, etc. • • •				
$1.13^{+0.53}_{-0.40}$±0.02	[3] AALTONEN	09AP	CDF	Repl. by AALTONEN 14B

[1] Measured in $\Omega_b^- \to \Omega_c^0\pi^-$, $\Omega_c^0 \to pK^-K^-\pi^+$ decays relative to $\Xi_b^- \to \Xi_c^0\pi^-$, $\Xi_c^0 \to pK^-K^-\pi^+$ decays with reference Ξ_b^- mean life 1.599 ± 0.06 ps from AAIJ 14B.

[2] Measured in $\Omega_b^- \to J/\psi\Omega^-$ decays.

[3] Observed in $\Omega_b^- \to J/\psi\Omega^-$ decays with 16^{+6}_{-4} candidates, a significance of 5.5 sigma from a combined mass-lifetime fit.

$\tau(\Omega_b^-)/\tau(\Xi_b^-)$ mean life ratio

VALUE	DOCUMENT ID		TECN	COMMENT
1.11±0.16±0.03	[1] AAIJ	16O	LHCB	pp at 7, 8 TeV

[1] Uses $\Omega_b^- \to \Omega_c^0\pi^-$, $\Omega_c^0 \to pK^-K^-\pi^+$ and $\Xi_b^- \to \Xi_c^0\pi^-$, $\Xi_c^0 \to pK^-K^-\pi^+$ decays.

Ω_b^- DECAY MODES

	Mode	Fraction (Γ_i/Γ)	Confidence level
Γ_1	$J/\psi\Omega^- \times$B($b \to \Omega_b$)	$(2.9^{+1.1}_{-0.8}) \times 10^{-6}$	
Γ_2	$pK^-K^- \times$B($\overline{b} \to \Omega_b$)	$< 2.5 \times 10^{-9}$	90%
Γ_3	$p\pi^-\pi^- \times$B($\overline{b} \to \Omega_b$)	$< 1.5 \times 10^{-8}$	90%
Γ_4	$pK^-\pi^- \times$B($\overline{b} \to \Omega_b$)	$< 7 \times 10^{-9}$	90%

Ω_b^- BRANCHING RATIOS

$\Gamma(J/\psi\Omega^- \times$B($b \to \Omega_b$))/$\Gamma_{\text{total}}$ Γ_1/Γ

VALUE (units 10^{-4})	DOCUMENT ID		TECN	COMMENT
$0.029^{+0.011}_{-0.008}$ OUR AVERAGE				
$0.026^{+0.010}_{-0.007}$±0.004	[1] AALTONEN	09AP	CDF	$p\overline{p}$ at 1.96 TeV
0.08 ±0.04 ±0.02	[2] ABAZOV	08AL	D0	$p\overline{p}$ at 1.96 TeV

[1] AALTONEN 09AP reports [$\Gamma(\Omega_b^- \to J/\psi\Omega^- \times$B($b \to \Omega_b$))/$\Gamma_{\text{total}}$] / [B($\Lambda_b^0 \to J/\psi(1S)\Lambda \times$ B($b \to \Lambda_b^0$))] = $0.045^{+0.017}_{-0.012}$ ± 0.004 which we multiply by our best value B($\Lambda_b^0 \to J/\psi(1S)\Lambda \times$ B($b \to \Lambda_b^0$)) = (5.8 ± 0.8) × 10^{-5}. Our first error is their experiment's error and our second error is the systematic error from using our best value.

[2] ABAZOV 08AL reports [$\Gamma(\Omega_b^- \to J/\psi\Omega^- \times$B($b \to \Omega_b$))/$\Gamma_{\text{total}}$] / [B($\Xi_b \to J/\psi\Xi^- \times$ B($b \to \Xi_b^-$))] = 0.80 ± $0.32^{+0.14}_{-0.22}$ which we multiply by our best value B($\Xi_b \to J/\psi\Xi^- \times$ B($b \to \Xi_b^-$)) = ($1.02^{+0.26}_{-0.21}$) × 10^{-5}. Our first error is their experiment's error and our second error is the systematic error from using our best value.

$\Gamma(pK^-K^- \times$B($\overline{b} \to \Omega_b$))/$\Gamma_{\text{total}}$ Γ_2/Γ

VALUE (units 10^{-5})	CL%	DOCUMENT ID		TECN	COMMENT
$< 2.5 \times 10^{-4}$	90	[1] AAIJ	17F	LHCB	pp at 7, 8 TeV

[1] AAIJ 17F reports [$\Gamma(\Omega_b^- \to pK^-K^- \times$B($\overline{b} \to \Omega_b$))/$\Gamma_{\text{total}}$] / [B($B^+ \to K^+K^-K^+$)] / [B($\overline{b} \to B^+$)] < 18×10^{-5} which we multiply by our best values B($B^+ \to K^+K^-K^+$) = 3.40×10^{-5}, B($\overline{b} \to B^+$) = 40.5×10^{-2}.

$\Gamma(p\pi^-\pi^- \times$B($\overline{b} \to \Omega_b$))/$\Gamma_{\text{total}}$ Γ_3/Γ

VALUE (units 10^{-5})	CL%	DOCUMENT ID		TECN	COMMENT
$< 1.5 \times 10^{-3}$	90	[1] AAIJ	17F	LHCB	pp at 7, 8 TeV

[1] AAIJ 17F reports [$\Gamma(\Omega_b^- \to p\pi^-\pi^- \times$B($\overline{b} \to \Omega_b$))/$\Gamma_{\text{total}}$] / [B($B^+ \to K^+K^-K^+$)] / [B($\overline{b} \to B^+$)] < 109×10^{-5} which we multiply by our best values B($B^+ \to K^+K^-K^+$) = 3.40×10^{-5}, B($\overline{b} \to B^+$) = 40.5×10^{-2}.

$\Gamma(pK^-\pi^- \times$B($\overline{b} \to \Omega_b$))/$\Gamma_{\text{total}}$ Γ_4/Γ

VALUE (units 10^{-5})	CL%	DOCUMENT ID		TECN	COMMENT
$< 7 \times 10^{-4}$	90	[1] AAIJ	17F	LHCB	pp at 7, 8 TeV

[1] AAIJ 17F reports [$\Gamma(\Omega_b^- \to pK^-\pi^- \times$B($\overline{b} \to \Omega_b$))/$\Gamma_{\text{total}}$] / [B($B^+ \to K^+K^-K^+$)] / [B($\overline{b} \to B^+$)] < 51×10^{-5} which we multiply by our best values B($B^+ \to K^+K^-K^+$) = 3.40×10^{-5}, B($\overline{b} \to B^+$) = 40.5×10^{-2}.

Ω_b^- REFERENCES

AAIJ	17F	PRL 118 071801	R. Aaij *et al.*	(LHCb Collab.)
AAIJ	16O	PR D93 092007	R. Aaij *et al.*	(LHCb Collab.)
AAIJ	14B	PL B728 234	R. Aaij *et al.*	(LHCb Collab.)
AAIJ	14T	PL B736 154	R. Aaij *et al.*	(LHCb Collab.)
AALTONEN	14B	PR D89 072014	T. Aaltonen *et al.*	(CDF Collab.)
AAIJ	13AV	PRL 110 182001	R. Aaij *et al.*	(LHCb Collab.)
AALTONEN	09AP	PR D80 072003	T. Aaltonen *et al.*	(CDF Collab.)
ABAZOV	08AL	PRL 101 232002	V.M. Abazov *et al.*	(D0 Collab.)

b-baryon ADMIXTURE (Λ_b, Ξ_b, Σ_b, Ω_b)

b-baryon ADMIXTURE MEAN LIFE

Each measurement of the b-baryon mean life is an average over an admixture of various b baryons which decay weakly. Different techniques emphasize different admixtures of produced particles, which could result in a different b-baryon mean life. More b-baryon flavor specific channels are not included in the measurement.

VALUE (10^{-12} s)	EVTS	DOCUMENT ID		TECN	COMMENT
• • • We do not use the following data for averages, fits, limits, etc. • • •					
$1.218^{+0.130}_{-0.115}\pm0.042$		[1] ABAZOV	07S	D0	Repl. by ABAZOV 12U
$1.22\ ^{+0.22}_{-0.18}\pm0.04$		[1] ABAZOV	05C	D0	Repl. by ABAZOV 07S
$1.16\ \pm0.20\ \pm0.08$		[2] ABREU	99W	DLPH	$e^+e^-\to Z$
$1.19\ \pm0.14\ \pm0.07$		[3] ABREU	99W	DLPH	$e^+e^-\to Z$
$1.14\ \pm0.08\ \pm0.04$		[4] ABREU	99W	DLPH	$e^+e^-\to Z$
$1.11\ ^{+0.19}_{-0.18}\ \pm0.05$		[5] ABREU	99W	DLPH	$e^+e^-\to Z$
$1.29\ ^{+0.24}_{-0.22}\ \pm0.06$		[5] ACKERSTAFF	98G	OPAL	$e^+e^-\to Z$
$1.20\ \pm0.08\ \pm0.06$		[6] BARATE	98D	ALEP	$e^+e^-\to Z$
$1.21\ \pm0.11$		[5] BARATE	98D	ALEP	$e^+e^-\to Z$
$1.32\ \pm0.15\ \pm0.07$		[7] ABE	96M	CDF	$p\overline{p}$ at 1.8 TeV
$1.46\ ^{+0.22}_{-0.21}\ ^{+0.07}_{-0.09}$		ABREU	96D	DLPH	Repl. by ABREU 99W
$1.10\ ^{+0.19}_{-0.17}\ \pm0.09$		[5] ABREU	96D	DLPH	$e^+e^-\to Z$
$1.16\ \pm0.11\ \pm0.06$		[5] AKERS	96	OPAL	$e^+e^-\to Z$
$1.27\ ^{+0.35}_{-0.29}\ \pm0.09$		ABREU	95S	DLPH	Repl. by ABREU 99W
$1.05\ ^{+0.12}_{-0.11}\ \pm0.09$	290	BUSKULIC	95L	ALEP	Repl. by BARATE 98D
$1.04\ ^{+0.48}_{-0.38}\ \pm0.10$	11	[8] ABREU	93F	DLPH	Excess $\Lambda\mu^-$, decay lengths
$1.05\ ^{+0.23}_{-0.20}\ \pm0.08$	157	[9] AKERS	93	OPAL	Excess $\Lambda\ell^-$, decay lengths
$1.12\ ^{+0.32}_{-0.29}\ \pm0.16$	101	[10] BUSKULIC	92I	ALEP	Excess $\Lambda\ell^-$, impact parameters

[1] Measured mean life using fully reconstructed $\Lambda_b^0\to J/\psi\Lambda$ decays.
[2] Measured using $\Lambda\ell^-$ decay length.
[3] Measured using $p\ell^-$ decay length.
[4] This ABREU 99W result is the combined result of the $\Lambda\ell^-$, $p\ell^-$, and excess $\Lambda\mu^-$ impact parameter measurements.
[5] Measured using $\Lambda_c\ell^-$ and $\Lambda\ell^+\ell^-$.
[6] Measured using the excess of $\Lambda\ell^-$, lepton impact parameter.
[7] Measured using $\Lambda_c\ell^-$.
[8] ABREU 93F superseded by ABREU 96D.
[9] AKERS 93 superseded by AKERS 96.
[10] BUSKULIC 92I superseded by BUSKULIC 95L.

b-baryon ADMIXTURE DECAY MODES (Λ_b, Ξ_b, Σ_b, Ω_b)

These branching fractions are actually an average over weakly decaying b-baryons weighted by their production rates at the LHC, LEP, and Tevatron, branching ratios, and detection efficiencies. They scale with the b-baryon production fraction B($b\to$ b-baryon).

The branching fractions B(b-baryon $\to \Lambda\ell^-\overline{\nu}_\ell$anything) and B($\Lambda_b^0\to\Lambda_c^+\ell^-\overline{\nu}_\ell$anything) are not pure measurements because the underlying measured products of these with B($b\to$ b-baryon) were used to determine B($b\to$ b-baryon), as described in the note "Production and Decay of b-Flavored Hadrons."

For inclusive branching fractions, *e.g.*, $B\to D^\pm$anything, the values usually are multiplicities, not branching fractions. They can be greater than one.

	Mode	Fraction (Γ_i/Γ)
Γ_1	$p\mu^-\overline{\nu}$anything	($5.5^{+\ 2.2}_{-\ 1.9}$) %
Γ_2	$p\ell\overline{\nu}_\ell$anything	(5.3± 1.1) %
Γ_3	$p$anything	(66 ±21) %
Γ_4	$\Lambda\ell^-\overline{\nu}_\ell$anything	(3.6± 0.6) %
Γ_5	$\Lambda\ell^+\nu_\ell$anything	(3.0± 0.8) %
Γ_6	Λanything	(37 ± 7) %
Γ_7	$\Xi^-\ell^-\overline{\nu}_\ell$anything	(6.2± 1.6) $\times10^{-3}$

b-baryon ADMIXTURE (Λ_b, Ξ_b, Σ_b, Ω_b) BRANCHING RATIOS

$\Gamma(p\mu^-\overline{\nu}$anything$)/\Gamma_{\rm total}$ Γ_1/Γ

VALUE (%)	EVTS	DOCUMENT ID		TECN	COMMENT
$\mathbf{5.5^{+2.1}_{-1.7}\pm0.7}$	125	[11] ABREU	95S	DLPH	$e^+e^-\to Z$

[11] ABREU 95S reports [$\Gamma(b$-baryon $\to p\mu^-\overline{\nu}$anything$)/\Gamma_{\rm total}$] × [B($\overline{b}\to$ b-baryon)] = 0.0049 ± 0.0011 $^{+0.0015}_{-0.0011}$ which we divide by our best value B($\overline{b}\to$ b-baryon) = (8.9 ± 1.2) × 10^{-2}. Our first error is their experiment's error and our second error is the systematic error from using our best value.

$\Gamma(p\ell\overline{\nu}_\ell$anything$)/\Gamma_{\rm total}$ Γ_2/Γ

VALUE (%)	DOCUMENT ID		TECN	COMMENT
5.3±0.9±0.7	[12] BARATE	98V	ALEP	$e^+e^-\to Z$

[12] BARATE 98V reports [$\Gamma(b$-baryon $\to p\ell\overline{\nu}_\ell$anything$)/\Gamma_{\rm total}$] × [B($\overline{b}\to$ b-baryon)] = (4.72 ± 0.66 ± 0.44) × 10^{-3} which we divide by our best value B($\overline{b}\to$ b-baryon) = (8.9 ± 1.2) × 10^{-2}. Our first error is their experiment's error and our second error is the systematic error from using our best value.

$\Gamma(p\ell\overline{\nu}_\ell$anything$)/\Gamma(p$anything$)$ Γ_2/Γ_3

VALUE (%)	DOCUMENT ID		TECN	COMMENT
8.0±1.2±1.4	BARATE	98V	ALEP	$e^+e^-\to Z$

$\Gamma(\Lambda\ell^-\overline{\nu}_\ell$anything$)/\Gamma_{\rm total}$ Γ_4/Γ

The values and averages in this section serve only to show what values result if one assumes our B($b\to$ b-baryon). They cannot be thought of as measurements since the underlying product branching fractions were also used to determine B($b\to$ b-baryon) as described in the note on "Production and Decay of b-Flavored Hadrons."

VALUE (%)	EVTS	DOCUMENT ID		TECN	COMMENT
3.6±0.6 OUR AVERAGE					
3.7±0.5±0.5		[13] BARATE	98D	ALEP	$e^+e^-\to Z$
3.3±0.4±0.4		[14] AKERS	96	OPAL	Excess of $\Lambda\ell^-$ over $\Lambda\ell^+$
3.4±0.8±0.5	262	[15] ABREU	95S	DLPH	Excess of $\Lambda\ell^-$ over $\Lambda\ell^+$
6.9±1.3±0.9	290	[16] BUSKULIC	95L	ALEP	Excess of $\Lambda\ell^-$ over $\Lambda\ell^+$
• • • We do not use the following data for averages, fits, limits, etc. • • •					
seen	157	[17] AKERS	93	OPAL	Excess of $\Lambda\ell^-$ over $\Lambda\ell^+$
7.9±2.3±1.1	101	[18] BUSKULIC	92I	ALEP	Excess of $\Lambda\ell^-$ over $\Lambda\ell^+$

[13] BARATE 98D reports [$\Gamma(b$-baryon $\to \Lambda\ell^-\overline{\nu}_\ell$anything$)/\Gamma_{\rm total}$] × [B($\overline{b}\to$ b-baryon)] = 0.00326 ± 0.00016 ± 0.00039 which we divide by our best value B($\overline{b}\to$ b-baryon) = (8.9 ± 1.2) × 10^{-2}. Our first error is their experiment's error and our second error is the systematic error from using our best value. Measured using the excess of $\Lambda\ell^-$, lepton impact parameter.
[14] AKERS 96 reports [$\Gamma(b$-baryon $\to \Lambda\ell^-\overline{\nu}_\ell$anything$)/\Gamma_{\rm total}$] × [B($\overline{b}\to$ b-baryon)] = 0.00291 ± 0.00023 ± 0.00025 which we divide by our best value B($\overline{b}\to$ b-baryon) = (8.9 ± 1.2) × 10^{-2}. Our first error is their experiment's error and our second error is the systematic error from using our best value.
[15] ABREU 95S reports [$\Gamma(b$-baryon $\to \Lambda\ell^-\overline{\nu}_\ell$anything$)/\Gamma_{\rm total}$] × [B($\overline{b}\to$ b-baryon)] = 0.0030 ± 0.0006 ± 0.0004 which we divide by our best value B($\overline{b}\to$ b-baryon) = (8.9 ± 1.2) × 10^{-2}. Our first error is their experiment's error and our second error is the systematic error from using our best value.
[16] BUSKULIC 95L reports [$\Gamma(b$-baryon $\to \Lambda\ell^-\overline{\nu}_\ell$anything$)/\Gamma_{\rm total}$] × [B($\overline{b}\to$ b-baryon)] = 0.0061 ± 0.0006 ± 0.0010 which we divide by our best value B($\overline{b}\to$ b-baryon) = (8.9 ± 1.2) × 10^{-2}. Our first error is their experiment's error and our second error is the systematic error from using our best value.
[17] AKERS 93 superseded by AKERS 96.
[18] BUSKULIC 92I reports [$\Gamma(b$-baryon $\to \Lambda\ell^-\overline{\nu}_\ell$anything$)/\Gamma_{\rm total}$] × [B($\overline{b}\to$ b-baryon)] = 0.0070 ± 0.0010 ± 0.0018 which we divide by our best value B($\overline{b}\to$ b-baryon) = (8.9 ± 1.2) × 10^{-2}. Our first error is their experiment's error and our second error is the systematic error from using our best value. Superseded by BUSKULIC 95L.

$\Gamma(\Lambda\ell^+\nu_\ell$anything$)/\Gamma(\Lambda$anything$)$ Γ_5/Γ_6

VALUE (units 10^{-2})	DOCUMENT ID		TECN	COMMENT
8.0±1.2±0.8	ABBIENDI	99L	OPAL	$e^+e^-\to Z$
• • • We do not use the following data for averages, fits, limits, etc. • • •				
7.0±1.2±0.7	ACKERSTAFF	97N	OPAL	Repl. by ABBIENDI 99L

$\Gamma(\Lambda$anything$)/\Gamma_{\rm total}$ Γ_6/Γ

VALUE (%)	DOCUMENT ID		TECN	COMMENT
37± 7 OUR AVERAGE				
39± 5±5	[19] ABBIENDI	99L	OPAL	$e^+e^-\to Z$
$25^{+14}_{-9}\pm3$	[20] ABREU	95C	DLPH	$e^+e^-\to Z$
• • • We do not use the following data for averages, fits, limits, etc. • • •				
44± 7±6	[21] ACKERSTAFF	97N	OPAL	Repl. by ABBIENDI 99L

[19] ABBIENDI 99L reports [$\Gamma(b$-baryon $\to \Lambda$anything$)/\Gamma_{\rm total}$] × [B($\overline{b}\to$ b-baryon)] = 0.035 ± 0.0032 ± 0.0035 which we divide by our best value B($\overline{b}\to$ b-baryon) = (8.9 ± 1.2) × 10^{-2}. Our first error is their experiment's error and our second error is the systematic error from using our best value.

[20] ABREU 95C reports $0.28^{+0.17}_{-0.12}$ from a measurement of $[\Gamma(b\text{-baryon} \to \Lambda\text{anything})/\Gamma_{total}] \times [B(\overline{b} \to b\text{-baryon})]$ assuming $B(\overline{b} \to b\text{-baryon}) = 0.08 \pm 0.02$, which we rescale to our best value $B(\overline{b} \to b\text{-baryon}) = (8.9 \pm 1.2) \times 10^{-2}$. Our first error is their experiment's error and our second error is the systematic error from using our best value.

[21] ACKERSTAFF 97N reports $[\Gamma(b\text{-baryon} \to \Lambda\text{anything})/\Gamma_{total}] \times [B(\overline{b} \to b\text{-baryon})] = 0.0393 \pm 0.0046 \pm 0.0037$ which we divide by our best value $B(\overline{b} \to b\text{-baryon}) = (8.9 \pm 1.2) \times 10^{-2}$. Our first error is their experiment's error and our second error is the systematic error from using our best value.

$\Gamma(\Xi^- \ell^- \overline{\nu}_\ell \text{anything})/\Gamma_{total}$ Γ_7/Γ

VALUE (units 10^{-3})	DOCUMENT ID		TECN	COMMENT
6.2±1.6 OUR AVERAGE				
6.1±1.5±0.8	[22] BUSKULIC	96T	ALEP	Excess $\Xi^- \ell^-$ over $\Xi^- \ell^+$
6.6±2.6±0.9	[23] ABREU	95V	DLPH	Excess $\Xi^- \ell^-$ over $\Xi^- \ell^+$

[22] BUSKULIC 96T reports $[\Gamma(b\text{-baryon} \to \Xi^- \ell^- \overline{\nu}_\ell \text{anything})/\Gamma_{total}] \times [B(\overline{b} \to b\text{-baryon})] = 0.00054 \pm 0.00011 \pm 0.00008$ which we divide by our best value $B(\overline{b} \to b\text{-baryon}) = (8.9 \pm 1.2) \times 10^{-2}$. Our first error is their experiment's error and our second error is the systematic error from using our best value.

[23] ABREU 95V reports $[\Gamma(b\text{-baryon} \to \Xi^- \ell^- \overline{\nu}_\ell \text{anything})/\Gamma_{total}] \times [B(\overline{b} \to b\text{-baryon})] = 0.00059 \pm 0.00021 \pm 0.0001$ which we divide by our best value $B(\overline{b} \to b\text{-baryon}) = (8.9 \pm 1.2) \times 10^{-2}$. Our first error is their experiment's error and our second error is the systematic error from using our best value.

b-baryon ADMIXTURE (Λ_b, Ξ_b, Σ_b, Ω_b) REFERENCES

ABAZOV	12U	PR D85 112003	V.M. Abazov *et al.*	(D0 Collab.)
ABAZOV	07S	PRL 99 142001	V.M. Abazov *et al.*	(D0 Collab.)
ABAZOV	05C	PRL 94 102001	V.M. Abazov *et al.*	(D0 Collab.)
ABBIENDI	99L	EPJ C9 1	G. Abbiendi *et al.*	(OPAL Collab.)
ABREU	99W	EPJ C10 185	P. Abreu *et al.*	(DELPHI Collab.)
ACKERSTAFF	98G	PL B426 161	K. Ackerstaff *et al.*	(OPAL Collab.)
BARATE	98D	EPJ C2 197	R. Barate *et al.*	(ALEPH Collab.)
BARATE	98V	EPJ C5 205	R. Barate *et al.*	(ALEPH Collab.)
ACKERSTAFF	97N	ZPHY C74 423	K. Ackerstaff *et al.*	(OPAL Collab.)
ABE	96M	PRL 77 1439	F. Abe *et al.*	(CDF Collab.)
ABREU	96D	ZPHY C71 199	P. Abreu *et al.*	(DELPHI Collab.)
AKERS	96	ZPHY C69 195	R. Akers *et al.*	(OPAL Collab.)
BUSKULIC	96T	PL B384 449	D. Buskulic *et al.*	(ALEPH Collab.)
ABREU	95C	PL B347 447	P. Abreu *et al.*	(DELPHI Collab.)
ABREU	95S	ZPHY C68 375	P. Abreu *et al.*	(DELPHI Collab.)
ABREU	95V	ZPHY C68 541	P. Abreu *et al.*	(DELPHI Collab.)
BUSKULIC	95L	PL B357 685	D. Buskulic *et al.*	(ALEPH Collab.)
ABREU	93F	PL B311 379	P. Abreu *et al.*	(DELPHI Collab.)
AKERS	93	PL B316 435	R. Akers *et al.*	(OPAL Collab.)
BUSKULIC	92I	PL B297 449	D. Buskulic *et al.*	(ALEPH Collab.)

EXOTIC BARYONS

See the related review(s):

Pentaquarks

$P_c(4380)^+$

Status: *

A resonance seen in $\Lambda_b^0 \to P_c^+ K^-$, then $P_c \to J/\psi p$, with a significance of 9 standard deviations. The $J/\psi p$ quark content is $uudc\overline{c}$, a pentaquark. See also the $P_c(4450)^+$. In the best amplitude fit, the two states have opposite parity, one having $J = 3/2$, the other $J = 5/2$.

Extraction of the pentaquark signals requires some understanding of the dominant $K^- p$ background. AAIJ 15P used a model-dependent approach. AAIJ 16AG reanalyzed the data making minimal assumptions about the $K^- p$ background, and thus confirmed the strong significance of the pentaquark signals.

$P_c(4380)^+$ MASS

VALUE (MeV)	DOCUMENT ID		TECN	COMMENT
4380±8±29	AAIJ	15P	LHCB	pp at 7, 8 TeV

$P_c(4380)^+$ WIDTH

VALUE (MeV)	DOCUMENT ID		TECN	COMMENT
205±18±86	AAIJ	15P	LHCB	pp at 7, 8 TeV

$P_c(4380)^+$ DECAY MODES

	Mode	Fraction (Γ_i/Γ)
Γ_1	$J/\psi p$	seen

$P_c(4380)^+$ BRANCHING RATIOS

$\Gamma(J/\psi p)/\Gamma_{total}$ Γ_1/Γ

VALUE	DOCUMENT ID		TECN	COMMENT
seen	AAIJ	15P	LHCB	pp at 7, 8 TeV

$P_c(4380)^+$ REFERENCES

AAIJ 16AG PRL 117 082002 R. Aaij *et al.* (LHCb Collab.)
AAIJ 15P PRL 115 072001 R. Aaij *et al.* (LHCb Collab.)

$P_c(4450)^+$

Status: *

A resonance seen in $\Lambda_b^0 \to P_c^+ K^-$, then $P_c \to J/\psi p$, with a significance of 12 standard deviations. The $J/\psi p$ quark content is $uudc\overline{c}$, a pentaquark. See also the $P_c(4380)^+$. In the best amplitude fit, the two states have opposite parity, one having $J = 3/2$, the other $J = 5/2$.

Extraction of the pentaquark signals requires some understanding of the dominant $K^- p$ background. AAIJ 15P used a model-dependent approach. AAIJ 16AG reanalyzed the data making minimal assumptions about the $K^- p$ background, and thus confirmed the strong significance of the pentaquark signals.

$P_c(4450)^+$ MASS

VALUE (MeV)	DOCUMENT ID		TECN	COMMENT
4449.8±1.7±2.5	AAIJ	15P	LHCB	pp at 7, 8 TeV

$P_c(4450)^+$ WIDTH

VALUE (MeV)	DOCUMENT ID		TECN	COMMENT
39±5±19	AAIJ	15P	LHCB	pp at 7, 8 TeV

$P_c(4450)^+$ DECAY MODES

	Mode	Fraction (Γ_i/Γ)
Γ_1	$J/\psi p$	seen

$P_c(4450)^+$ BRANCHING RATIOS

$\Gamma(J/\psi p)/\Gamma_{total}$ Γ_1/Γ

VALUE	DOCUMENT ID		TECN	COMMENT
seen	AAIJ	15P	LHCB	pp at 7, 8 TeV

$P_c(4450)^+$ REFERENCES

AAIJ 16AG PRL 117 082002 R. Aaij *et al.* (LHCb Collab.)
AAIJ 15P PRL 115 072001 R. Aaij *et al.* (LHCb Collab.)

MISCELLANEOUS SEARCHES

SEARCHES IN OTHER SECTIONS

Related Reviews in Volume 1

SEARCHES NOT IN OTHER SECTIONS

Magnetic Monopole Searches

See the related review(s):
Magnetic Monopoles

Monopole Production Cross Section — Accelerator Searches

X-SECT (cm^2)	MASS (GeV)	CHG (g)	ENERGY (GeV)	BEAM	DOCUMENT ID		TECN
<2.5E−37	200–6000	1	13000	pp	[1] ACHARYA	17	INDU
<2E−37	200–6000	2	13000	pp	[1] ACHARYA	17	INDU
<4E−37	200–5000	3	13000	pp	[1] ACHARYA	17	INDU
<1.5E−36	400–4000	4	13000	pp	[1] ACHARYA	17	INDU
<7E−36	1000–3000	5	13000	pp	[1] ACHARYA	17	INDU
<5E−40	200–2500	0.5–2.0	8000	pp	[2] AAD	16AB	ATLS
<2E−37	100–3500	1	8000	pp	[3] ACHARYA	16	INDU
<2E−37	100–3500	2	8000	pp	[3] ACHARYA	16	INDU
<6E−37	500–3000	3	8000	pp	[3] ACHARYA	16	INDU
<7E−36	1000–2000	4	8000	pp	[3] ACHARYA	16	INDU
<1.6E−38	200–1200	1	7000	pp	[4] AAD	12CS	ATLS
<5E−38	45–102	1	206	e^+e^-	[5] ABBIENDI	08	OPAL
<0.2E−36	200–700	1	1960	$p\overline{p}$	[6] ABULENCIA	06K	CNTR
< 2.E−36		1	300	e^+p	[7,8] AKTAS	05A	INDU
< 0.2 E−36		2	300	e^+p	[7,8] AKTAS	05A	INDU
< 0.09E−36		3	300	e^+p	[7,8] AKTAS	05A	INDU
< 0.05E−36		≥ 6	300	e^+p	[7,8] AKTAS	05A	INDU
< 2.E−36		1	300	e^+p	[7,9] AKTAS	05A	INDU
< 0.2E−36		2	300	e^+p	[7,9] AKTAS	05A	INDU
< 0.07E−36		3	300	e^+p	[7,9] AKTAS	05A	INDU
< 0.06E−36		≥ 6	300	e^+p	[7,9] AKTAS	05A	INDU
< 0.6E−36	>265	1	1800	$p\overline{p}$	[10] KALBFLEISCH	04	INDU
< 0.2E−36	>355	2	1800	$p\overline{p}$	[10] KALBFLEISCH	04	INDU
< 0.07E−36	>410	3	1800	$p\overline{p}$	[10] KALBFLEISCH	04	INDU
< 0.2E−36	>375	6	1800	$p\overline{p}$	[10] KALBFLEISCH	04	INDU
< 0.7E−36	>295	1	1800	$p\overline{p}$	[11,12] KALBFLEISCH	00	INDU
< 7.8E−36	>260	2	1800	$p\overline{p}$	[11,12] KALBFLEISCH	00	INDU
< 2.3E−36	>325	3	1800	$p\overline{p}$	[11,13] KALBFLEISCH	00	INDU
< 0.11E−36	>420	6	1800	$p\overline{p}$	[11,13] KALBFLEISCH	00	INDU
<0.65E−33	<3.3	≥ 2	11A	^{197}Au	[14,15] HE	97	
<1.90E−33	<8.1	≥ 2	160A	^{208}Pb	[14,15] HE	97	
<3.E−37	<45.0	1.0	88–94	e^+e^-	PINFOLD	93	PLAS
<3.E−37	<41.6	2.0	88–94	e^+e^-	PINFOLD	93	PLAS
<7.E−35	<44.9	0.2–1.0	89–93	e^+e^-	KINOSHITA	92	PLAS
<2.E−34	<850	≥ 0.5	1800	$p\overline{p}$	BERTANI	90	PLAS
<1.2E−33	<800	≥ 1	1800	$p\overline{p}$	PRICE	90	PLAS
<1.E−37	<29	1	50–61	e^+e^-	KINOSHITA	89	PLAS
<1.E−37	<18	2	50–61	e^+e^-	KINOSHITA	89	PLAS
<1.E−38	<17	<1	35	e^+e^-	BRAUNSCH...	88B	CNTR
<8.E−37	<24	1	50–52	e^+e^-	KINOSHITA	88	PLAS
<1.3E−35	<22	2	50–52	e^+e^-	KINOSHITA	88	PLAS
<9.E−37	<4	<0.15	10.6	e^+e^-	GENTILE	87	CLEO
<3.E−32	<800	≥ 1	1800	$p\overline{p}$	PRICE	87	PLAS
<3.E−38		<3	29	e^+e^-	FRYBERGER	84	PLAS
<1.E−31		1,3	540	$p\overline{p}$	AUBERT	83B	PLAS
<4.E−38	<10	<6	34	e^+e^-	MUSSET	83	PLAS
<8.E−36	<20		52	pp	[16] DELL	82	CNTR
<9.E−37	<30	<3	29	e^+e^-	KINOSHITA	82	PLAS
<1.E−37	<20	<24	63	pp	CARRIGAN	78	CNTR
<1.E−37	<30	<3	56	pp	HOFFMANN	78	PLAS
			62	pp	[16] DELL	76	SPRK
<4.E−33			300	p	[16] STEVENS	76B	SPRK
<1.E−40	<5	<2	70	p	[17] ZRELOV	76	CNTR
<2.E−30			300	n	[16] BURKE	75	OSPK
<1.E−38			8	ν	[18] CARRIGAN	75	HLBC
<5.E−43	<12	<10	400	p	EBERHARD	75B	INDU
<2.E−36	<30	<3	60	pp	GIACOMELLI	75	PLAS
<5.E−42	<13	<24	400	p	CARRIGAN	74	CNTR
<6.E−42	<12	<24	300	p	CARRIGAN	73	CNTR
<2.E−36		1	0.001	γ	[17] BARTLETT	72	CNTR
<1.E−41	<5		70	p	GUREVICH	72	EMUL
<1.E−40	<3	<2	28	p	AMALDI	63	EMUL
<2.E−40	<3	<2	30	p	PURCELL	63	CNTR
<1.E−35	<3	<4	28	p	FIDECARO	61	CNTR
<2.E−35	<1	1	6	p	BRADNER	59	EMUL

[1] The search was sensitive to monopoles which had stopped in aluminium trapping volumes. Monopoles with spins 0 and 1/2 were considered; mass-dependent spin 1/2 monopole limits are quoted here.
[2] AAD 16AB model-independent 95% CL limits estimated using a fiducial region of approximately constant acceptance. Limits are mass-dependent.
[3] ACHARYA 16 limits at 95% CL estimated using a Drell-Yan-like production mechanism for scalar monopoles.
[4] AAD 12CS searched for monopoles as highly ionising objects. The cross section limits are based on an assumed Drell Yan-like production process for spin 1/2 monopoles. The limits are mass- and scenario-dependent.
[5] ABBIENDI 08 assume production of spin 1/2 monopoles with effective charge $g\beta$ (n=1), via $e^+e^- \rightarrow \gamma^* \rightarrow M\overline{M}$, so that the cross section is proportional to $(1 + \cos^2\theta)$. There is no z information for such highly saturated tracks, so a parabolic track in the jet chamber is projected onto the xy plane. Charge per hit in the chamber produces a clean separation of signal and background.
[6] ABULENCIA 06K searches for high-ionizing signals in CDF central outer tracker and time-of-flight detector. For Drell-Yan $M\overline{M}$ production, the cross section limit implies $M > 360$ GeV at 95% CL.
[7] AKTAS 05A model-dependent limits as a function of monopole mass shown for arbitrary mass of 60 GeV. Based on search for stopped monopoles in the H1 Al beam pipe.
[8] AKTAS 05A limits with assumed elastic spin 0 monopole pair production.
[9] AKTAS 05A limits with assumed inelastic spin 1/2 monopole pair production.
[10] KALBFLEISCH 04 reports searches for stopped magnetic monopoles in Be, Al, and Pb samples obtained from discarded material from the upgrading of DØ and CDF. A large-aperture warm-bore cryogenic detector was used. The approach was an extension of the methods of KALBFLEISCH 00. Cross section results moderately model dependent; interpretation as a mass lower limit depends on possibly invalid perturbation expansion.
[11] KALBFLEISCH 00 used an induction method to search for stopped monopoles in pieces of the DØ (FNAL) beryllium beam pipe and in extensions to the drift chamber aluminum support cylinder. Results are model dependent.
[12] KALBFLEISCH 00 result is for aluminum.
[13] KALBFLEISCH 00 result is for beryllium.
[14] HE 97 used a lead target and barium phosphate glass detectors. Cross-section limits are well below those predicted via the Drell-Yan mechanism.
[15] This work has also been reinterpreted in the framework of monopole production via the thermal Schwinger process (GOULD 17); this gives rise to lower mass limits.
[16] Multiphoton events.
[17] Cherenkov radiation polarization.
[18] Re-examines CERN neutrino experiments.

Monopole Production — Other Accelerator Searches

MASS (GeV)	CHG (g)	SPIN	ENERGY (GeV)	BEAM	DOCUMENT ID		TECN
> 610	≥ 1	0	1800	$p\overline{p}$	[1] ABBOTT	98K	D0
> 870	≥ 1	1/2	1800	$p\overline{p}$	[1] ABBOTT	98K	D0
>1580	≥ 1	1	1800	$p\overline{p}$	[1] ABBOTT	98K	D0
> 510			88–94	e^+e^-	[2] ACCIARRI	95C	L3

[1] ABBOTT 98K search for heavy pointlike Dirac monopoles via central production of a pair of photons with high transverse energies.
[2] ACCIARRI 95C finds a limit $B(Z \rightarrow \gamma\gamma\gamma) < 0.8 \times 10^{-5}$ (which is possible via a monopole loop) at 95% CL and sets the mass limit via a cross section model.

Monopole Flux — Cosmic Ray Searches

"Caty" in the charge column indicates a search for monopole-catalyzed nucleon decay.

FLUX ($cm^{-2}sr^{-1}s^{-1}$)	MASS (GeV)	CHG (g)	COMMENTS ($\beta = v/c$)	EVTS	DOCUMENT ID		TECN
<1.5E−18		1	$\beta > 0.6$	0	[1] ALBERT	17	ANTR
<2.5E−21		1	1E8< γ <1E13	0	[2] AAB	16	AUGE
<1.55E-18			$\beta > 0.51$	0	[3] AARTSEN	16B	ICCB
<1E-17		Caty	1E-3< β <1E-2	0	[4] AARTSEN	14	ICCB
<3E-18		1	$\beta > 0.8$	0	[5] ABBASI	13	ICCB
<1.3E-17		1	$\beta > 0.625$	0	[6] ADRIAN-MAR...	12A	ANTR
<6E-28	<1E17	Caty	1E-5< β <0.04	0	[7] UENO	12	SKAM
<1E-19		**1**	**γ >1E10**	0	[8] DETRIXHE	11	ANIT
<3.8E-17		1	$\beta > 0.76$	0	[5] ABBASI	10A	ICCB
<1.3E−15	1E4<M<5E13	1	$\beta > 0.05$	0	[9] BALESTRA	08	PLAS
<0.65E−15	>5E13	1	$\beta > 0.05$	0	[9] BALESTRA	08	PLAS
<1E−18		**1**	**γ >1 E8**	0	[8] HOGAN	08	RICE
<1.4E−16		**1**	**1.1E−4 < β <1**	0	[10] AMBROSIO	02B	MCRO
<3E−16		Caty	1.1E−4 < β <5E−3	0	[11] AMBROSIO	02C	MCRO
<1.5E−15		1	5E−3 < β < 0.99	0	[12] AMBROSIO	02D	MCRO
<1E−15		1	1.1×10^{-4}–0.1	0	[13] AMBROSIO	97	MCRO
<5.6E−15		1	(0.18–3.0)E−3	0	[14] AHLEN	94	MCRO
<2.7E−15		Caty	$\beta \sim 1 \times 10^{-3}$	0	[15] BECKER-SZ...	94	IMB
<8.7E−15		1	>2.E−3	0	THRON	92	SOUD
<4.4E−12		1	all β	0	GARDNER	91	INDU
<7.2E−13		1	all β	0	HUBER	91	INDU
<3.7E−15	>E12	1	β=1.E−4	0	[16] ORITO	91	PLAS
<3.2E−16	>E10	1	$\beta > 0.05$	0	[16] ORITO	91	PLAS
<3.2E−16	>E10–E12	2, 3		0	[16] ORITO	91	PLAS
<3.8E−13		1	all β	0	BERMON	90	INDU
<5.E−16		Caty	β <1.E−3	0	[15] BEZRUKOV	90	CHER
<1.8E−14		1	β >1.1E−4	0	[17] BUCKLAND	90	HEPT
<1E−18			3.E−4 < β <1.5E−3	0	[18] GHOSH	90	MICA
<7.2E−13		1	all β	0	HUBER	90	INDU
<5.E−12	>E7	1	3.E−4 < β <5.E−3	0	BARISH	87	CNTR
<1.E−13		Caty	1.E−5 < β <1	0	[15] BARTELT	87	SOUD
<1.E−10		1	all β	0	EBISU	87	INDU
<2.E−13			1.E−4 < β <6.E−4	0	MASEK	87	HEPT
<2.E−14			4.E−5 < β <2.E−4	0	NAKAMURA	87	PLAS
<2.E−14			1.E−3 < β <1	0	NAKAMURA	87	PLAS
<5.E−14			9.E−4 < β <1.E−2	0	SHEPKO	87	CNTR
<2.E−13			4.E−4 < β <1	0	TSUKAMOTO	87	CNTR
<5.E−14		1	all β	1	[19] CAPLIN	86	INDU
<5.E−12		1		0	CROMAR	86	INDU
<1.E−13		1	7.E−4 < β	0	HARA	86	CNTR

Searches Particle Listings

Magnetic Monopole Searches

<7.E−11		1	all β	0	INCANDELA	86	INDU
<1.E−18			4.E−4 < β <1.E−3	0	[18] PRICE	86	MICA
<5.E−12		1		0	BERMON	85	INDU
<6.E−12		1		0	CAPLIN	85	INDU
<6.E−10		1		0	EBISU	85	INDU
<3.E−15		Caty	5.E−5 ≤ β ≤ 1.E−3	0	[15] KAJITA	85	KAMI
<2.E−21		Caty	β <1.E−3	0	[15,20] KAJITA	85	KAMI
<3.E−15		Caty	1.E−3 < β <1.E−1	0	[15] PARK	85B	CNTR
<5.E−12		1	1.E−4 < β <1	0	BATTISTONI	84	NUSX
<7.E−12		1		0	INCANDELA	84	INDU
<7.E−13		1	3.E−4 < β	0	[17] KAJINO	84	CNTR
<2.E−12		1	3.E−4 < β <1.E−1	0	KAJINO	84B	CNTR
<6.E−13		1	5.E−4 < β <1	0	KAWAGOE	84	CNTR
<2.E−14			1.E−3 < β	0	[15] KRISHNA...	84	CNTR
<4.E−13		1	6.E−4 < β <2.E−3	0	LISS	84	CNTR
<1.E−16			3.E−4 < β <1.E−3	0	[18] PRICE	84	MICA
<1.E−13		1	1.E−4 < β	0	PRICE	84B	PLAS
<4.E−13		1	6.E−4 < β <2.E−3	0	TARLE	84	CNTR
				7	[21] ANDERSON	83	EMUL
<4.E−13		1	1.E−2 < β <1.E−3	0	BARTELT	83B	CNTR
<1.E−12		1	7.E−3 < β <1	0	BARWICK	83	PLAS
<3.E−13		1	1.E−3 < β <4.E−1	0	BONARELLI	83	CNTR
<3.E−12		Caty	5.E−4 < β <5.E−2	0	[15] BOSETTI	83	CNTR
<4.E−11		1		0	CABRERA	83	INDU
<5.E−15		1	1.E−2 < β <1	0	DOKE	83	PLAS
<8.E−15		Caty	1.E−4 < β <1.E−1	0	[15] ERREDE	83	IMB
<5.E−12		1	1.E−4 < β <3.E−2	0	GROOM	83	CNTR
<2.E−12			6.E−4 < β <1	0	MASHIMO	83	CNTR
<1.E−13		1	β=3.E−3	0	ALEXEYEV	82	CNTR
<2.E−12		1	7.E−3 < β <6.E−1	0	BONARELLI	82	CNTR
6.E−10		1	all β	1	[22] CABRERA	82	INDU
<2.E−11			1.E−2 < β <1.E−1	0	MASHIMO	82	CNTR
<2.E−15			concentrator	0	BARTLETT	81	PLAS
<1.E−13	>1		1.E−3 < β	0	KINOSHITA	81B	PLAS
<5.E−11	<E17		3.E−4 < β <1.E−3	0	ULLMAN	81	CNTR
<2.E−11			concentrator	0	BARTLETT	78	PLAS
1.E−1	>200	2		1	[23] PRICE	75	PLAS
<2.E−13		>2		0	FLEISCHER	71	PLAS
<1.E−19		>2	obsidian, mica	0	FLEISCHER	69C	PLAS
<5.E−15	<15	<3	concentrator	0	CARITHERS	66	ELEC
<2.E−11		<1–3	concentrator	0	MALKUS	51	EMUL

[1] ALBERT 17 limits were estimated using a Cherenkov light in an array of optical modules under the Mediterranean Sea. The limits are for MM masses between 10^{10} and 10^{14} GeV. The limits are speed-dependent.

[2] AAB 16 search was made with a set of telescopes sampling the longitudinal profile of fluorescence light emitted by extensive air showers. Limits are speed dependent.

[3] AARTSEN 16B was based on a Cherenkov signature in an array of optical modules which were sunk in the Antarctic ice cap. Limits are speed-dependent.

[4] Beyond the monopole speed, the limits of AARTSEN 14 depend on the catalysis cross section (σ) which corresponds to the monopole radiating $\hat{l}$ times the light per track length compared to the Cherenkov light from a single electrically charged, relativistic particle. The values quoted here correspond to $\sigma = 1$ barn or $\hat{l} = 30$.

[5] ABBASI 13 and ABBASI 10A were based on a Cherenkov signature in an array of optical modules which were sunk in the Antarctic ice cap. Limits are speed-dependent.

[6] ADRIAN-MARTINEZ 12A measurements were based on a Cherenkov signature in an underwater telescope in the Western Mediterranean Sea. Limits are speed-dependent.

[7] The limits from UENO 12 depend on the monopole speed and are also sensitive to assumed values of monopole mass and the catalysis cross section.

[8] HOGAN 08 and DETRIXHE 11 limits on relativistic monopoles are based on nonobservation of radio Cherenkov signals at the South Pole. Limits are speed-dependent.

[9] BALESTRA 08 exposed of nuclear track detector modules totaling 400 m^2 for 4 years at the Chacaltaya Laboratory (5230 m) in search for intermediate-mass monopoles with $\beta > 0.05$. The analysis is mainly based on three CR39 modules. For $M > 5 \times 10^{13}$ GeV there can be upward-going monopoles as well, hence the flux limit is half that obtained for less massive monopoles. Previous experiments (e.g. MACRO and OHYA (ORITO 91)) had set limits only for $M > 1 \times 10^{9}$ GeV.

[10] AMBROSIO 02B direct search final result for $m \geq 10^{17}$ GeV, based upon 4.2 to 9.5 years of running, depending upon the subsystem. Limit with CR39 track-etch detector extends the limit from β=4 × 10^{-5} (3.1×10^{-16} cm^{-2} sr^{-1} s^{-1}) to $\beta = 1 \times 10^{-4}$ (2.1×10^{-16} cm^{-2} sr^{-1} s^{-1}). Limit curve in paper is piecewise continuous due to different detection techniques for different β ranges.

[11] AMBROSIO 02C limit for catalysis of nucleon decay with catalysis cross section of ≈ 1 mb. The flux limit increases by ∼ 3 at the higher β limit, and increases to 1×10^{-14} cm^{-2} sr^{-1} s^{-1} if the catalysis cross section is 0.01 mb. Based upon 71193 hr of data with the streamer detector, with an acceptance of 4250 m^2 sr.

[12] AMBROSIO 02D result for "more than two years of data." Ionization search using several subsystems. Limit curve as a function of β not given. Included in AMBROSIO 02B.

[13] AMBROSIO 97 global MACRO 90%CL is 0.78×10^{-15} at $\beta = 1.1 \times 10^{-4}$, goes through a minimum at 0.61×10^{-15} near $\beta = (1.1–2.7) \times 10^{-3}$, then rises to 0.84×10^{-15} at β=0.1. The global limit in this region is below the Parker bound at 10^{-15}. Less stringent limits are established for $4 \times 10^{-5} < \beta < 1 \times 10^{-4}$. Limits set by various triggers and different subdetectors are given in the paper. All limits assume a catalysis cross section smaller than a few mb.

[14] AHLEN 94 limit for dyons extends down to β=0.9E−4 and a limit of 1.3E−14 extends to β = 0.8E−4. Also see comment by PRICE 94 and reply of BARISH 94. One loophole in the AHLEN 94 result is that in the case of monopoles catalyzing nucleon decay, relativistic particles could veto the events. See AMBROSIO 97 for additional results.

[15] Catalysis of nucleon decay; sensitive to assumed catalysis cross section.

[16] ORITO 91 limits are functions of velocity. Lowest limits are given here.

[17] Used DKMPR mechanism and Penning effect.

[18] Assumes monopole attaches fermion nucleus.

[19] Limit from combining data of CAPLIN 86, BERMON 85, INCANDELA 84, and CABRERA 83. For a discussion of controversy about CAPLIN 86 observed event, see GUY 87. Also see SCHOUTEN 87.

[20] Based on lack of high- energy solar neutrinos from catalysis in the sun.

[21] Anomalous long-range α (^{4}He) tracks.

[22] CABRERA 82 candidate event has single Dirac charge within ±5%.

[23] ALVAREZ 75, FLEISCHER 75, and FRIEDLANDER 75 explain as fragmenting nucleus. EBERHARD 75 and ROSS 76 discuss conflict with other experiments. HAGSTROM 77 reinterprets as antinucleus. PRICE 78 reassesses.

Monopole Flux — Astrophysics

FLUX ($cm^{-2}sr^{-1}s^{-1}$)	MASS (GeV)	CHG (g)	COMMENTS ($\beta = v/c$)	DOCUMENT ID		TECN
<1.3E−20			faint white dwarf	[1] FREESE	99	ASTR
<1.E−16	E17	1	galactic field	[2] ADAMS	93	COSM
<1.E−23			Jovian planets	[1] ARAFUNE	85	ASTR
<1.E−16	E15		solar trapping	BRACCI	85B	ASTR
<1.E−18		1		[1] HARVEY	84	COSM
<3.E−23			neutron stars	KOLB	84	ASTR
<7.E−22			pulsars	[1] FREESE	83B	ASTR
<1.E−18	<E18	1	intergalactic field	[1] REPHAELI	83	COSM
<1.E−23			neutron stars	[1] DIMOPOUL...	82	COSM
<5.E−22			neutron stars	[1] KOLB	82	COSM
<5.E−15	>E21		galactic halo	SALPETER	82	COSM
<1.E−12	E19	1	β=3.E−3	[3] TURNER	82	COSM
<1.E−16		1	galactic field	PARKER	70	COSM

[1] Catalysis of nucleon decay.

[2] ADAMS 93 limit based on "survival and growth of a small galactic seed field" is 10^{-16} ($m/10^{17}$ GeV) cm^{-2} s^{-1} sr^{-1}. Above 10^{17} GeV, limit 10^{-16} (10^{17} GeV/m) cm^{-2} s^{-1} sr^{-1} (from requirement that monopole density does not overclose the universe) is more stringent.

[3] Re-evaluates PARKER 70 limit for GUT monopoles.

Monopole Density — Matter Searches

DENSITY	CHG (g)	MATERIAL	DOCUMENT ID		TECN
<9.8E−5/gram	≥ 1	Polar rock	BENDTZ	13	INDU
<6.9E−6/gram	>1/3	Meteorites and other	JEON	95	INDU
<2.E−7/gram	>0.6	Fe ore	[1] EBISU	87	INDU
<4.6E−6/gram	> 0.5	deep schist	KOVALIK	86	INDU
<1.6E−6/gram	> 0.5	manganese nodules	[2] KOVALIK	86	INDU
<1.3E−6/gram	> 0.5	seawater	KOVALIK	86	INDU
>1.E+14/gram	>1/3	iron aerosols	MIKHAILOV	83	SPEC
<6.E−4/gram		air, seawater	CARRIGAN	76	CNTR
<5.E−1/gram	>0.04	11 materials	CABRERA	75	INDU
<2.E−4/gram	>0.05	moon rock	ROSS	73	INDU
<6.E−7/gram	<140	seawater	KOLM	71	CNTR
<1.E−2/gram	<120	manganese nodules	FLEISCHER	69	PLAS
<1.E−4/gram	>0	manganese	FLEISCHER	69B	PLAS
<2.E−3/gram	<1–3	magnetite, meteor	GOTO	63	EMUL
<2.E−2/gram		meteorite	PETUKHOV	63	CNTR

[1] Mass 1×10^{14}–1×10^{17} GeV.

[2] KOVALIK 86 examined 498 kg of schist from two sites which exhibited clear mineralogical evidence of having been buried at least 20 km deep and held below the Curie temperature.

Monopole Density — Astrophysics

DENSITY	CHG (g)	MATERIAL	DOCUMENT ID		TECN
<1.E−9/gram	1	sun, catalysis	[1] ARAFUNE	83	COSM
<6.E−33/nucl	1	moon wake	SCHATTEN	83	ELEC
<2.E−28/nucl		earth heat	CARRIGAN	80	COSM
<2.E−4/prot		42cm absorption	BRODERICK	79	COSM
<2.E−13/m^3		moon wake	SCHATTEN	70	ELEC

[1] Catalysis of nucleon decay.

REFERENCES FOR Magnetic Monopole Searches

ACHARYA	17	PRL 118 061801	B. Acharya *et al.*	(MoEDAL Collab.)
ALBERT	17	JHEP 1707 054	A. Albert *et al.*	(ANTARES Collab.)
GOULD	17	PRL 119 241601	O. Gould, A. Rajantie	
AAB	16	PR D94 082002	A. Aab *et al.*	(Pierre Auger Collab.)
AAD	16AB	PR D93 052009	G. Aad *et al.*	(ATLAS Collab.)
AARTSEN	16B	EPJ C76 133	M.G. Aartsen *et al.*	(IceCube Collab.)
ACHARYA	16	JHEP 1608 067	B. Acharya *et al.*	(MoEDAL Collab.)
AARTSEN	14	EPJ C74 2938	M.G. Aartsen *et al.*	(IceCube Collab.)
ABBASI	13	PR D87 022001	R. Abbasi *et al.*	(IceCube Collab.)
BENDTZ	13	PRL 110 121803	K. Bendtz *et al.*	
AAD	12CS	PRL 109 261803	G. Aad *et al.*	(ATLAS Collab.)
ADRIAN-MAR...	12A	ASP 35 634	S. Adrian-Martinez *et al.*	(ANTARES Collab.)
UENO	12	ASP 36 131	K. Ueno *et al.*	(Super-Kamiokande Collab.)
DETRIXHE	11	PR D83 023513	M. Detrixhe *et al.*	(ANITA Collab.)
ABBASI	10A	EPJ C69 361	R. Abbasi *et al.*	(IceCube Collab.)
ABBIENDI	08	PL B663 37	G. Abbiendi *et al.*	(OPAL Collab.)
BALESTRA	08	EPJ C55 57	S. Balestra *et al.*	(SLIM Collab.)
HOGAN	08	PR D78 075031	D.P. Hogan *et al.*	(KANS, NEBR, DELA)
ABULENCIA	06K	PRL 96 201801	A. Abulencia *et al.*	(CDF Collab.)
AKTAS	05A	EPJ C41 133	A. Aktas *et al.*	(H1 Collab.)
KALBFLEISCH	04	PR D69 052002	G.R. Kalbfleisch *et al.*	(OKLA)
AMBROSIO	02B	EPJ C25 511	M. Ambrosio *et al.*	(MACRO Collab.)
AMBROSIO	02C	EPJ C26 163	M. Ambrosio *et al.*	(MACRO Collab.)
AMBROSIO	02D	ASP 18 27	M. Ambrosio *et al.*	(MACRO Collab.)
KALBFLEISCH	00	PRL 85 5292	G.R. Kalbfleisch *et al.*	

FREESE	99	PR D59 063007	K. Freese, E. Krasteva	
ABBOTT	98K	PRL 81 524	B. Abbott *et al.*	(D0 Collab.)
AMBROSIO	97	PL B406 249	M. Ambrosio *et al.*	(MACRO Collab.)
HE	97	PRL 79 3134	Y.D. He	(UCB)
ACCIARRI	95C	PL B345 609	M. Acciarri *et al.*	(L3 Collab.)
JEON	95	PRL 75 1443	H. Jeon, M.J. Longo	(MICH)
Also		PRL 76 159 (erratum)	H. Jeon, M.J. Longo	
AHLEN	94	PRL 72 608	S.P. Ahlen *et al.*	(MACRO Collab.)
BARISH	94	PRL 73 1306	B.C. Barish, G. Giacomelli, J.T. Hong	(CIT+)
BECKER-SZ...	94	PR D49 2169	R.A. Becker-Szendy *et al.*	(IMB Collab.)
PRICE	94	PRL 73 1305	P.B. Price	(UCB)
ADAMS	93	PRL 70 2511	F.C. Adams *et al.*	(MICH, FNAL)
PINFOLD	93	PL B316 407	J.L. Pinfold *et al.*	(ALBE, HARV, MONT+)
KINOSHITA	92	PR D46 881	K. Kinoshita *et al.*	(HARV, BGNA, REHO)
THRON	92	PR D46 4846	J.L. Thron *et al.*	(SOUDAN-2 Collab.)
GARDNER	91	PR D44 622	R.D. Gardner *et al.*	(STAN)
HUBER	91	PR D44 636	M.E. Huber *et al.*	(STAN)
ORITO	91	PRL 66 1951	S. Orito *et al.*	(ICEPP, WASCR, NIHO, ICRR)
BERMON	90	PRL 64 839	S. Bermon *et al.*	(IBM, BNL)
BERTANI	90	EPL 12 613	M. Bertani *et al.*	(BGNA, INFN)
BEZRUKOV	90	SJNP 52 54	L.B. Bezrukov *et al.*	(INRM)
		Translated from YAF 52 86.		
BUCKLAND	90	PR D41 2726	K.N. Buckland *et al.*	(UCSD)
GHOSH	90	EPL 12 25	D.C. Ghosh, S. Chatterjea	(JADA)
HUBER	90	PRL 64 835	M.E. Huber *et al.*	(STAN)
PRICE	90	PRL 65 149	P.B. Price, J. Guiru, K. Kinoshita	(UCB, HARV)
KINOSHITA	89	PL B228 543	K. Kinoshita *et al.*	(HARV, TISA, KEK+)
BRAUNSCH...	88B	ZPHY C38 543	R. Braunschweig *et al.*	(TASSO Collab.)
KINOSHITA	88	PRL 60 1610	K. Kinoshita *et al.*	(HARV, TISA, KEK+)
BARISH	87	PR D36 2641	B.C. Barish, G. Liu, C. Lane	(CIT)
BARTELT	87	PR D36 1990	J.E. Bartelt *et al.*	(Soudan Collab.)
Also		PR D40 1701 (erratum)	J.E. Bartelt *et al.*	(Soudan Collab.)
EBISU	87	PR D36 3359	T. Ebisu, T. Watanabe	(KOBE)
Also		JP G11 883	T. Ebisu, T. Watanabe	(KOBE)
GENTILE	87	PR D35 1081	T. Gentile *et al.*	(CLEO Collab.)
GUY	87	NAT 325 463	J. Guy	(LOIC)
MASEK	87	PR D35 2758	G.E. Masek *et al.*	(UCSD)
NAKAMURA	87	PL B183 395	S. Nakamura *et al.*	(INUS, WASCR, NIHO)
PRICE	87	PRL 59 2523	P.B. Price, R. Guoxiao, K. Kinoshita	(UCB, HARV)
SCHOUTEN	87	JP E20 850	J.C. Schouten *et al.*	(LOIC)
SHEPKO	87	PR D35 2917	M.J. Shepko *et al.*	(TAMU)
TSUKAMOTO	87	EPL 3 39	T. Tsukamoto *et al.*	(ICRR)
CAPLIN	86	NAT 321 402	A.D. Caplin *et al.*	(LOIC)
Also		JP E20 850	J.C. Schouten *et al.*	(LOIC)
Also		NAT 325 463	J. Guy	(LOIC)
CROMAR	86	PRL 56 2561	M.W. Cromar, A.F. Clark, F.R. Fickett	(NBSB)
HARA	86	PRL 56 553	T. Hara *et al.*	(ICRR, KYOT, KEK, KOBE+)
INCANDELA	86	PR D34 2637	J. Incandela *et al.*	(CHIC, FNAL, MICH)
KOVALIK	86	PR A33 1183	J.M. Kovalik, J.L. Kirschvink	(CIT)
PRICE	86	PRL 56 1226	P.B. Price, M.H. Salamon	(UCB)
ARAFUNE	85	PR D32 2586	J. Arafune, M. Fukugita, S. Yanagita	(ICRR, KYOTU+)
BERMON	85	PRL 55 1850	S. Bermon *et al.*	(IBM)
BRACCI	85B	NP B258 726	L. Bracci, G. Fiorentini, G. Mezzorani	(PISA+)
Also		LNC 42 123	L. Bracci, G. Fiorentini	(PISA)
CAPLIN	85	NAT 317 234	A.D. Caplin *et al.*	(LOIC)
EBISU	85	JP G11 883	T. Ebisu, T. Watanabe	(KOBE)
KAJITA	85	JPSJ 54 4065	T. Kajita *et al.*	(ICRR, KEK, NIIG)
PARK	85B	NP B252 261	H.S. Park *et al.*	(IMB Collab.)
BATTISTONI	84	PL 133B 454	G. Battistoni *et al.*	(NUSEX Collab.)
FRYBERGER	84	PR D29 1524	D. Fryberger *et al.*	(SLAC, UCB)
HARVEY	84	NP B236 255	J.A. Harvey	(PRIN)
INCANDELA	84	PRL 53 2067	J. Incandela *et al.*	(CHIC, FNAL, MICH)
KAJINO	84	PRL 52 1373	F. Kajino *et al.*	(ICRR)
KAJINO	84B	JP G10 447	F. Kajino *et al.*	(ICRR)
KAWAGOE	84	LNC 41 315	K. Kawagoe *et al.*	(TOKY)
KOLB	84	APJ 286 702	E.W. Kolb, M.S. Turner	(FNAL, CHIC)
KRISHNA...	84	PL 142B 99	M.R. Krishnaswamy *et al.*	(TATA, OSKC+)
LISS	84	PR D30 884	T.M. Liss, S.P. Ahlen, G. Tarle	(UCB, IND+)
PRICE	84	PRL 52 1265	P.B. Price *et al.*	(ROMA, UCB, IND+)
PRICE	84B	PL 140B 112	P.B. Price	(CERN)
TARLE	84	PRL 52 90	G. Tarle, S.P. Ahlen, T.M. Liss	(UCB, MICH+)
ANDERSON	83	PR D28 2308	S.N. Anderson *et al.*	(WASH)
ARAFUNE	83	PL 133B 380	J. Arafune, M. Fukugita	(ICRR, KYOTU)
AUBERT	83B	PL 120B 465	B. Aubert *et al.*	(CERN, LAPP)
BARTELT	83B	PRL 50 655	J.E. Bartelt *et al.*	(MINN, ANL)
BARWICK	83	PR D28 2338	S.W. Barwick, K. Kinoshita, P.B. Price	(UCB)
BONARELLI	83	PL 126B 137	R. Bonarelli, P. Capiluppi, I. d'Antone	(BGNA)
BOSETTI	83	PL 133B 265	P.C. Bosetti *et al.*	(AACH3, HAWA, TOKY)
CABRERA	83	PRL 51 1933	B. Cabrera *et al.*	(STAN)
DOKE	83	PL 129B 370	T. Doke *et al.*	(WASU, RIKK, TTAM, RIKEN)
ERREDE	83	PRL 51 245	S.M. Errede *et al.*	(IMB Collab.)
FREESE	83B	PRL 51 1625	K. Freese, M.S. Turner, D.N. Schramm	(CHIC)
GROOM	83	PRL 50 573	D.E. Groom *et al.*	(UTAH, STAN)
MASHIMO	83	PL 128B 327	T. Mashimo *et al.*	(ICEPP)
MIKHAILOV	83	PL 130B 331	V.F. Mikhailov	(KAZA)
MUSSET	83	PL 128B 333	P. Musset, M. Price, E. Lohrmann	(CERN, HAMB)
REPHAELI	83	PL 121B 115	Y. Rephaeli, M.S. Turner	(CHIC)
SCHATTEN	83	PR D27 1525	K.H. Schatten	(NASA)
ALEXEYEV	82	LNC 35 413	E.N. Alekseev *et al.*	(INRM)
BONARELLI	82	PL 112B 100	R. Bonarelli *et al.*	(BGNA)
CABRERA	82	PRL 48 1378	B. Cabrera	(STAN)
DELL	82	NP B209 45	G.F. Dell *et al.*	(BNL, ADEL, ROMA)
DIMOPOUL...	82	PL 119B 320	S. Dimopoulos, J. Preskill, F. Wilczek	(HARV+)
KINOSHITA	82	PRL 48 77	K. Kinoshita, P.B. Price, D. Fryberger	(UCB+)
KOLB	82	PRL 49 1373	E.W. Kolb, S.A. Colgate, J.A. Harvey	(LASL, PRIN)
MASHIMO	82	JPSJ 51 3067	T. Mashimo, K. Kawagoe, M. Koshiba	(INUS)
SALPETER	82	PRL 49 1114	E.E. Salpeter, S.L. Shapiro, I. Wasserman	(CORN)
TURNER	82	PR D26 1296	M.S. Turner, E.N. Parker, T.J. Bogdan	(CHIC)
BARTLETT	81	PR D24 612	D.F. Bartlett *et al.*	(COLO, GESC)
KINOSHITA	81B	PR D24 1707	K. Kinoshita, P.B. Price	(UCB)
ULLMAN	81	PRL 47 289	J.D. Ullman	(LEHM, BNL)
CARRIGAN	80	NAT 288 348	R.A. Carrigan	(FNAL)
BRODERICK	79	PR D19 1046	J.J. Broderick *et al.*	(VPI)
BARTLETT	78	PR D18 2253	D.F. Bartlett, D. Soo, M.G. White	(COLO, PRIN)
CARRIGAN	78	PR D17 1754	R.A. Carrigan, B.P. Strauss, G. Giacomelli	(FNAL+)
HOFFMANN	78	LNC 23 357	H. Hoffmann *et al.*	(CERN, ROMA)
PRICE	78	PR D18 1382	P.B. Price *et al.*	(UCB, HOUS)
HAGSTROM	77	PRL 38 729	R. Hagstrom	(LBL)
CARRIGAN	76	PR D13 1823	R.A. Carrigan, F.A. Nezrick, B.P. Strauss	(FNAL)
DELL	76	LNC 15 269	G.F. Dell *et al.*	(CERN, BNL, ROMA, ADEL)
ROSS	76	LBL-4665	R.R. Ross	(LBL)
STEVENS	76B	PR D14 2207	D.M. Stevens *et al.*	(VPI, BNL)
ZRELOV	76	CZJP B26 1306	V.P. Zrelov *et al.*	(JINR)
ALVAREZ	75	LBL-4260	L.W. Alvarez	(LBL)
BURKE	75	PL 60B 113	D.L. Burke *et al.*	(MICH)
CABRERA	75	Thesis	B. Cabrera	(STAN)
CARRIGAN	75	NP B91 279	R.A. Carrigan, F.A. Nezrick	(FNAL)
Also		PR D3 56	R.A. Carrigan, F.A. Nezrick	(FNAL)
EBERHARD	75	PR D11 3099	P.H. Eberhard *et al.*	(LBL, MPIM)
EBERHARD	75B	LBL-4289	P.H. Eberhard	(LBL)
FLEISCHER	75	PRL 35 1412	R.L. Fleischer, R.N.F. Walker	(GESC, WUSL)
FRIEDLANDER	75	PRL 35 1167	M.W. Friedlander	(WUSL)
GIACOMELLI	75	NC 28A 21	G. Giacomelli *et al.*	(BGNA, CERN, SACL+)
PRICE	75	PRL 35 487	P.B. Price *et al.*	(UCB, HOUS)
CARRIGAN	74	PR D10 3867	R.A. Carrigan, F.A. Nezrick, B.P. Strauss	(FNAL)
CARRIGAN	73	PR D8 3717	R.A. Carrigan, F.A. Nezrick, B.P. Strauss	(FNAL)
ROSS	73	PR D8 698	R.R. Ross *et al.*	(LBL, SLAC)
Also		PR D4 3260	P.H. Eberhard *et al.*	(LBL, SLAC)
Also		SCI 167 701	L.W. Alvarez *et al.*	(LBL, SLAC)
BARTLETT	72	PR D6 1817	D.F. Bartlett, M.D. Lahana	(COLO)
GUREVICH	72	PL 38B 549	I.I. Gurevich *et al.*	(KIAE, NOVO, SERP)
Also		JETP 34 917	L.M. Barkov, I.I. Gurevich, M.S. Zolotorev	(KIAE+)
		Translated from ZETF 61 1721.		
Also		PL 31B 394	I.I. Gurevich *et al.*	(KIAE, NOVO, SERP)
FLEISCHER	71	PR D4 24	R.L. Fleischer *et al.*	(GESC)
KOLM	71	PR D4 1285	H.H. Kolm, F. Villa, A. Odian	(MIT, SLAC)
PARKER	70	APJ 160 383	E.N. Parker	(CHIC)
SCHATTEN	70	PR D1 2245	K.H. Schatten	(NASA)
FLEISCHER	69	PR 177 2029	R.L. Fleischer *et al.*	(GESC, FSU)
FLEISCHER	69B	PR 184 1393	R.L. Fleischer *et al.*	(GESC, UNCS, GSCO)
FLEISCHER	69C	PR 184 1398	R.L. Fleischer, P.B. Price, R.T. Woods	(GESC)
Also		JAP 41 958	R.L. Fleischer *et al.*	(GESC)
CARITHERS	66	PR 149 1070	W.C.J. Carithers, R.J. Stefanski, R.K. Adair	
AMALDI	63	NC 28 773	E. Amaldi *et al.*	(ROMA, UCSD, CERN)
GOTO	63	PR 132 387	E. Goto, H.H. Kolm, K.W. Ford	(TOKY, MIT, BRAN)
PETUKHOV	63	NP 49 87	V.A. Petukhov, M.N. Yakimenko	(LEBD)
PURCELL	63	PR 129 2326	E.M. Purcell *et al.*	(HARV, BNL)
FIDECARO	61	NC 22 657	M. Fidecaro, G. Finocchiaro, G. Giacomelli	(CERN)
BRADNER	59	PR 114 603	H. Bradner, W.M. Isbell	(LBL)
MALKUS	51	PR 83 899	W.V.R. Malkus	(CHIC)

OTHER RELATED PAPERS

GROOM	86	PRPL 140 323	D.E. Groom	(UTAH)
Review				

Supersymmetric Particle Searches

The exclusion of particle masses within a mass range (m_1, m_2) will be denoted with the notation "none m_1–m_2" in the VALUE column of the following Listings. The latest unpublished results are described in the "Supersymmetry: Experiment" review.

See the related review(s):

Supersymmetry, Part I (Theory)

Supersymmetry, Part II (Experiment)

CONTENTS:

Most of the results shown below, unless stated otherwise, are based on the Minimal Supersymmetric Standard Model (MSSM), as described in the Note on Supersymmetry. Unless otherwise indicated, this includes the assumption of common gaugino and scalar masses at the scale of Grand Unification (GUT), and use of the resulting relations in the spectrum and

decay branching ratios. Unless otherwise indicated, it is also assumed that R-parity (R) is conserved and that:

1) The $\widetilde{\chi}_1^0$ is the lighest supersymmetric particle (LSP)
2) $m_{\widetilde{f}_L} = m_{\widetilde{f}_R}$, where $\widetilde{f}_{L,R}$ refer to the scalar partners of left- and right-handed fermions.

Limits involving different assumptions are identified in the Comments or in the Footnotes. We summarize here the notations used in this Chapter to characterize some of the most common deviations from the MSSM (for further details, see the Note on Supersymmetry).

Theories with R-parity violation ($\not{R}$) are characterized by a superpotential of the form: $\lambda_{ijk} L_i L_j e_k^c + \lambda'_{ijk} L_i Q_j d_k^c + \lambda''_{ijk} u_i^c d_j^c d_k^c$, where i, j, k are generation indices. The presence of any of these couplings is often identified in the following by the symbols $LL\overline{E}$, $LQ\overline{D}$, and $\overline{UDD}$. Mass limits in the presence of $\not{R}$ will often refer to "direct" and "indirect" decays. Direct refers to $\not{R}$ decays of the particle in consideration. Indirect refers to cases where $\not{R}$ appears in the decays of the LSP. The LSP need not be the $\widetilde{\chi}_1^0$.

In several models, most notably in theories with so-called Gauge Mediated Supersymmetry Breaking (GMSB), the gravitino ($\widetilde{G}$) is the LSP. It is usually much lighter than any other massive particle in the spectrum, and $m_{\widetilde{G}}$ is then neglected in all decay processes involving gravitinos. In these scenarios, particles other than the neutralino are sometimes considered as the next-to-lighest supersymmetric particle (NLSP), and are assumed to decay to their even-R partner plus $\widetilde{G}$. If the lifetime is short enough for the decay to take place within the detector, $\widetilde{G}$ is assumed to be undetected and to give rise to missing energy ($\not{E}$) or missing transverse energy ($\not{E}_T$) signatures.

When needed, specific assumptions on the eigenstate content of $\widetilde{\chi}^0$ and $\widetilde{\chi}^\pm$ states are indicated, using the notation $\widetilde{\gamma}$ (photino), $\widetilde{H}$ (higgsino), $\widetilde{W}$ (wino), and $\widetilde{Z}$ (zino) to signal that the limit of pure states was used. The terms gaugino is also used, to generically indicate wino-like charginos and zino-like neutralinos.

In the listings we have made use of the following abbreviations for simplified models employed by the experimental collaborations in supersymmetry searches published in the past year.

Simplified Models Table

Tglu1A: gluino pair production with $\tilde{g} \to q\bar{q}\tilde{\chi}_1^0$.

Tglu1B: gluino pair production with $\tilde{g} \to qq'\tilde{\chi}_1^\pm$, $\tilde{\chi}_1^\pm \to W^\pm\tilde{\chi}_1^0$.

Tglu1C: gluino pair production with a 2/3 probability of having a $\tilde{g} \to qq'\tilde{\chi}_1^\pm$, $\tilde{\chi}_1^\pm \to W^\pm\tilde{\chi}_1^0$ decay and a 1/3 probability of having a $\tilde{g} \to qq\tilde{\chi}_2^0$, $\tilde{\chi}_2^0 \to Z^\pm\tilde{\chi}_1^0$ decay.

Tglu1D: gluino pair production with one gluino decaying to $q\bar{q}'\tilde{\chi}_1^\pm$ with $\tilde{\chi}_1^\pm \to W^\pm + \tilde{G}$, and the other gluino decaying to $q\bar{q}\tilde{\chi}_1^0$ with $\tilde{\chi}_1^0 \to \gamma + \tilde{G}$.

Tglu1E: gluino pair production with $\tilde{g} \to qq'\tilde{\chi}_1^\pm$, $\tilde{\chi}_1^\pm \to W^\pm\tilde{\chi}_2^0$ and $\tilde{\chi}_2^0 \to Z^\pm\tilde{\chi}_1^0$ where $m_{\tilde{\chi}_1^\pm} = (m_{\tilde{g}} + m_{\tilde{\chi}_1^0})/2$, $m_{\tilde{\chi}_2^0} = (m_{\tilde{\chi}_1^\pm} + m_{\tilde{\chi}_1^0})/2$.

Tglu1F: gluino pair production with $\tilde{g} \to qq'\tilde{\chi}_1^\pm$ or $\tilde{g} \to qq\tilde{\chi}_2^0$ with equal branching ratios, where $\tilde{\chi}_1^\pm$ decays through an intermediate scalar tau lepton or sneutrino to $\tau\nu\tilde{\chi}_1^0$ and where $\tilde{\chi}_2^0$ decays through an intermediate scalar tau lepton or sneutrino to $\tau^+\tau^-\tilde{\chi}_1^0$ or $\nu\bar{\nu}\tilde{\chi}_1^0$; the mass hierarchy is such that $m_{\chi_1^\pm} \sim m_{\tilde{\chi}_2^0} = (m_{\tilde{g}} + m_{\chi_1^0})/2$ and $m_{\tilde{\tau},\tilde{\nu}} = (m_{\tilde{\chi}_1^\pm} + m_{\tilde{\chi}_1^0})/2$.

Tglu1G: gluino pair production with $\tilde{g} \to q\bar{q}\tilde{\chi}_2^0$, and $\tilde{\chi}_2^0$ decaying through an intermediate slepton or sneutrino to $l^+l^-\tilde{\chi}_1^0$ or $\nu\bar{\nu}\tilde{\chi}_1^0$ where $m_{\tilde{\chi}_2^0} = (m_{\tilde{g}} + m_{\tilde{\chi}_1^0})/2$ and $m_{\tilde{\ell},\tilde{\nu}} = (m_{\tilde{\chi}_2^0} + m_{\tilde{\chi}_1^0})/2$.

Tglu1H: gluino pair production with $\tilde{g} \to q\bar{q}\tilde{\chi}_2^0$, and $\tilde{\chi}_2^0 \to \tilde{\chi}_1^0 Z^{0(*)}$.

Tglu2A: gluino pair production with $\tilde{g} \to b\bar{b}\tilde{\chi}_1^0$.

Tglu3A: gluino pair production with $\tilde{g} \to t\bar{t}\tilde{\chi}_1^0$.

Tglu3B: gluino pair production with $\tilde{g} \to t\bar{\tilde{t}}$ where $\tilde{t}$ decays exclusively to $t\tilde{\chi}_1^0$.

Tglu3C: gluino pair production with $\tilde{g} \to t\bar{\tilde{t}}$ where $\tilde{t}$ decays exclusively to $c\tilde{\chi}_1^0$.

Tglu3D: gluino pair production with $\tilde{g} \to t\bar{b}\tilde{\chi}_1^\pm$ with $\tilde{\chi}_1^\pm \to W^\pm\tilde{\chi}_1^0$.

Tglu3E: gluino pair production where the gluino decays 25% of the time through $\tilde{g} \to t\bar{t}\tilde{\chi}_1^0$, 25% of the time through $\tilde{g} \to b\bar{b}\tilde{\chi}_1^0$ and 50% of the time through $\tilde{g} \to t\bar{b}\tilde{\chi}_1^\pm$ with $\tilde{\chi}_1^\pm \to W^\pm\tilde{\chi}_1^0$

Tglu4A: gluino pair production with one gluino decaying to $q\bar{q}'\tilde{\chi}_1^\pm$ with $\tilde{\chi}_1^\pm \to W^\pm + \tilde{G}$, and the other gluino decaying to $q\bar{q}\tilde{\chi}_1^0$ with $\tilde{\chi}_1^0 \to \gamma + \tilde{G}$.

Tglu4B: gluino pair production with gluinos decaying to $q\bar{q}\tilde{\chi}_1^0$ and $\tilde{\chi}_1^0 \to \gamma + \tilde{G}$.

Tglu4C: gluino pair production with gluinos decaying to $\tilde{g} \to q\bar{q}\tilde{\chi}_1^0$ and $\tilde{\chi}_1^0 \to Z + \tilde{G}$.

Tsqk1: squark pair production with $\tilde{q} \to q\tilde{\chi}_1^0$.

Tsqk2: squark pair production with $\tilde{q} \to q\tilde{\chi}_2^0$ and $\tilde{\chi}_2^0 \to Z + \tilde{\chi}_1^0$.

Tsqk3: squark pair production with $\tilde{q} \to q'\tilde{\chi}_1^\pm$, $\tilde{\chi}_1^\pm \to W^\pm\tilde{\chi}_1^0$ (like Tglu1B but for squarks)

Tsqk4: squark pair production with squarks decaying to $q\tilde{\chi}_1^0$ and $\tilde{\chi}_1^0 \to \gamma + \tilde{G}$.

Tsqk4A: squark pair production with one squark decaying to $q\tilde{\chi}_1^\pm$ with $\tilde{\chi}_1^\pm \to W^\pm + \tilde{G}$, and the other squark decaying to $q\tilde{\chi}_1^0$ with $\tilde{\chi}_1^0 \to \gamma + \tilde{G}$.

Tsqk4B: squark pair production with squarks decaying to $q\tilde{\chi}_1^0$ and $\tilde{\chi}_1^0 \to \gamma + \tilde{G}$.

Tstop1: stop pair production with $\tilde{t} \to t\tilde{\chi}_1^0$.

Tstop2: stop pair production with $\tilde{t} \to b\tilde{\chi}_1^\pm$ with $\tilde{\chi}_1^\pm \to W^\pm\tilde{\chi}_1^0$.

Tstop3: stop pair production with the subsequent four-body decay $\tilde{t} \to bff'\tilde{\chi}_1^0$ where f represents a lepton or a quark.

Tstop4: stop pair production with $\tilde{t} \to c\tilde{\chi}_1^0$.

Tstop5: stop pair production with $\tilde{t} \to b\bar{\nu}\tilde{\tau}$ with $\tilde{\tau} \to \tau\tilde{G}$.

Tstop6: stop pair production with $\tilde{t} \to t + \tilde{\chi}_2^0$, where $\tilde{\chi}_2^0 \to Z + \tilde{\chi}_1^0$ or $H + \tilde{\chi}_1^0$ each with Br=50%.

Tstop7: stop pair production with $\tilde{t}_2 \to \tilde{t}_1 + H/Z$, where $\tilde{t}_1 \to t + \tilde{\chi}_1^0$.

Tstop8: stop pair production with equal probability of the stop decaying via $\tilde{t} \to t\tilde{\chi}_1^0$ or via $\tilde{t} \to b\tilde{\chi}_1^\pm$ with $\tilde{\chi}_1^\pm \to W^\pm\tilde{\chi}_1^0$.

Tstop9: stop pair production with equal probability of the stop decaying via $\tilde{t} \to c\tilde{\chi}_1^0$ or via the four-body decay $\tilde{t} \to bff'\tilde{\chi}_1^0$ where f represents a lepton or a quark.

Tstop10: stop pair production with $\tilde{t} \to b\tilde{\chi}_1^\pm$ and $\tilde{\chi}_1^\pm \to W^{\pm *}\tilde{\chi}_1^0 \to (f\bar{f}') + \tilde{\chi}_1^0$ with a virtual W-boson.

Tstop11: stop pair production with $\tilde{t} \to b\tilde{\chi}_1^\pm$ with $\tilde{\chi}_1^\pm$ decaying through an intermediate slepton to $l\nu\tilde{\chi}_1^0$

Tstop1RPV: stop pair production with $\tilde{t} \to \bar{b}\bar{s}$ via RPV coupling λ''_{323}.

Tsbot1: sbottom pair production with $\tilde{b} \to b\tilde{\chi}_1^0$.

Tsbot2: sbottom pair production with $\tilde{b} \to t\chi_1^-$, $\chi_1^- \to W^-\tilde{\chi}_1^0$.

Tsbot3: sbottom pair production with $\tilde{b} \to b\tilde{\chi}_2^0$, where one of the $\tilde{\chi}_2^0 \to Z^{(*)}\tilde{\chi}_1^0 \to f\bar{f}\tilde{\chi}_1^0$ and the other $\tilde{\chi}_2^0 \to \tilde{\ell}\ell^+ \to \ell^+\ell^-\tilde{\chi}_1^0$.

Tchi1chi1A: electroweak pair and associated production of nearly mass-degenerate charginos $\tilde{\chi}_1^\pm$ and neutralinos $\tilde{\chi}_1^0$, where $\tilde{\chi}_1^\pm$ decays to $\tilde{\chi}_1^0$ plus soft radiation, and where one of the $\tilde{\chi}_1^0$ decays to $\gamma + \tilde{G}$ while the other one decays to $Z/H + \tilde{G}$ (with equal probability).

Tchi1chi1B: electroweak pair production of charginos $\tilde{\chi}_1^\pm$, where $\tilde{\chi}_1^\pm$ decays through an intermediate slepton or sneutrino to $l\nu\tilde{\chi}_1^0$ and where the slepton or sneutrino mass is 5%, 25%, 50%, 75% and 95% of the $\tilde{\chi}_1^\pm$ mass.

Tchi1chi1C: electroweak pair production of charginos $\tilde{\chi}_1^\pm$, where $\tilde{\chi}_1^\pm$ decays through an intermediate slepton or sneutrino to $l\nu\tilde{\chi}_1^0$ and where $m_{\tilde{\ell},\tilde{\nu}} = (m_{\tilde{\chi}_1^\pm} + m_{\tilde{\chi}_1^0})/2$.

Tchi1n1A: electroweak associated production of mass-degenerate charginos $\tilde{\chi}_1^\pm$ and neutralinos $\tilde{\chi}_1^0$, where $\tilde{\chi}_1^\pm$ decays exclusively to $W^\pm + \tilde{G}$ and $\tilde{\chi}_1^0$ decays exclusively to $\gamma + \tilde{G}$.

Tchi1n2A: electroweak associated production of mass-degenerate charginos $\tilde{\chi}_1^\pm$ and neutralinos $\tilde{\chi}_2^0$, where $\tilde{\chi}_1^\pm$ decays through an intermediate slepton or sneutrino to $l\nu\tilde{\chi}_1^0$ and where $\tilde{\chi}_2^0$ decays through an intermediate slepton or sneutrino to $l^+l^-\tilde{\chi}_1^0$ or $\nu\bar{\nu}\tilde{\chi}_1^0$.

Tchi1n2B: electroweak associated production of mass-degenerate charginos $\tilde{\chi}_1^\pm$ and neutralinos $\tilde{\chi}_2^0$, where $\tilde{\chi}_1^\pm$ decays through an intermediate slepton or sneutrino to $l\nu\tilde{\chi}_1^0$ and where $chiz_2$ decays through an intermediate slepton or sneutrino to $l^+l^-\tilde{\chi}_1^0$ or $\nu\bar{\nu}\tilde{\chi}_1^0$ and where the slepton or sneutrino mass is 5%, 25%, 50%, 75% and 95% of the $\tilde{\chi}_1^\pm$ mass.

Tchi1n2C: electroweak associated production of mass-degenerate charginos $\tilde{\chi}_1^\pm$ and neutralinos $\tilde{\chi}_2^0$, where $\tilde{\chi}_1^\pm$ decays through an intermediate slepton or sneutrino to $l\nu\tilde{\chi}_1^0$ and where $chiz_2$ decays through an intermediate slepton or sneutrino to $l^+l^-\tilde{\chi}_1^0$ or $\nu\bar{\nu}\tilde{\chi}_1^0$ and where $m_{\tilde{\ell},\tilde{\nu}} = (m_{\tilde{\chi}_1^\pm} + m_{\tilde{\chi}_1^0})/2$.

Tchi1n2D: electroweak associated production of mass-degenerate charginos $\tilde{\chi}_1^\pm$ and neutralinos $\tilde{\chi}_2^0$, where $\tilde{\chi}_1^\pm$ decays through an intermediate scalar tau lepton or sneutrino to $\tau\nu\tilde{\chi}_1^0$ and where $chiz_2$ decays through an intermediate scalar tau lepton or sneutrino to $\tau^+\tau^-\tilde{\chi}_1^0$ or $\nu\bar{\nu}\tilde{\chi}_1^0$ and where $m_{\tilde{\tau},\tilde{\nu}} = (m_{\tilde{\chi}_1^\pm} + m_{\tilde{\chi}_1^0})/2$.

Tchi1n2E: electroweak associated production of mass-degenerate charginos $\tilde{\chi}_1^\pm$ and neutralinos $\tilde{\chi}_2^0$, where $\tilde{\chi}_1^\pm \to W^\pm + \tilde{\chi}_1^0$ and $\tilde{\chi}_2^0 \to H + \tilde{\chi}_1^0$.

Tn2n3A: electroweak associated production of mass-degenerate neutralinos $\tilde{\chi}_2^0$ and $\tilde{\chi}_3^0$, where $\tilde{\chi}_2^0$ and $\tilde{\chi}_3^0$ decay through intermediate sleptons to $l^+l^-\tilde{\chi}_1^0$ and where the slepton mass is 5%, 25%, 50%, 75% and 95% of the $\tilde{\chi}_2^0$ mass.

Tn2n3B: electroweak associated production of mass-degenerate neutralinos $\tilde{\chi}_2^0$ and $\tilde{\chi}_3^0$, where $\tilde{\chi}_2^0$ and $\tilde{\chi}_3^0$ decay through intermediate sleptons to $l^+l^-\tilde{\chi}_1^0$ and where $m_{\tilde{\ell}} = (m_{\tilde{\chi}_2^0} + m_{\tilde{\chi}_1^0})/2$.

$\tilde{\chi}_1^0$ (Lightest Neutralino) mass limit

$\tilde{\chi}_1^0$ is often assumed to be the lightest supersymmetric particle (LSP). See also the $\tilde{\chi}_2^0$, $\tilde{\chi}_3^0$, $\tilde{\chi}_4^0$ section below.

We have divided the $\tilde{\chi}_1^0$ listings below into five sections:

1) Accelerator limits for stable $\tilde{\chi}_1^0$,

2) Bounds on $\tilde{\chi}_1^0$ from dark matter searches,

3) $\tilde{\chi}_1^0 - p$ elastic cross section (spin-dependent, spin-independent interactions),

4) Other bounds on $\tilde{\chi}_1^0$ from astrophysics and cosmology, and

5) Unstable $\tilde{\chi}_1^0$ (Lightest Neutralino) mass limit.

Accelerator limits for stable $\tilde{\chi}_1^0$

Unless otherwise stated, results in this section assume spectra, production rates, decay modes, and branching ratios as evaluated in the MSSM, with gaugino and sfermion mass unification at the GUT scale. These papers generally study production of $\tilde{\chi}_i^0\tilde{\chi}_j^0$ ($i \geq 1$, $j \geq 2$), $\tilde{\chi}_1^+\tilde{\chi}_1^-$, and (in the case of hadronic collisions) $\tilde{\chi}_1^+\tilde{\chi}_2^0$ pairs. The mass limits on $\tilde{\chi}_1^0$ are either direct, or follow indirectly from the constraints set by the non-observation of $\tilde{\chi}_1^\pm$ and $\tilde{\chi}_2^0$ states on the gaugino and higgsino MSSM parameters M_2 and μ. In some cases, information is used from the nonobservation of slepton decays.

Obsolete limits obtained from e^+e^- collisions up to $\sqrt{s}$=184 GeV have been removed from this compilation and can be found in the 2000 Edition (The European Physical Journal **C15** 1 (2000)) of this Review. $\Delta m = m_{\tilde{\chi}_2^0} - m_{\tilde{\chi}_1^0}$.

VALUE (GeV)	CL%	DOCUMENT ID		TECN	COMMENT
		[1] DREINER	09	THEO	
>40	95	[2] ABBIENDI	04H	OPAL	all tanβ, Δm >5 GeV, m_0 >500 GeV, $A_0 = 0$
>42.4	95	[3] HEISTER	04	ALEP	all tanβ, all Δm, all m_0
>39.2	95	[4] ABDALLAH	03M	DLPH	all tanβ, $m_{\tilde{\nu}}$ >500 GeV
>46	95	[5] ABDALLAH	03M	DLPH	all tanβ, all Δm, all m_0
>32.5	95	[6] ACCIARRI	00D	L3	tan$\beta > 0.7$, $\Delta m > 3$ GeV, all m_0
• • • We do not use the following data for averages, fits, limits, etc. • • •					
		[7] AAD	14K	ATLS	

[1] DREINER 09 show that in the general MSSM with non-universal gaugino masses there exists no model-independent laboratory bound on the mass of the lightest neutralino. An essentially massless χ_1^0 is allowed by the experimental and observational data, imposing some constraints on other MSSM parameters, including M_2, μ and the slepton and squark masses.

[2] ABBIENDI 04H search for charginos and neutralinos in events with acoplanar leptons+jets and multi-jet final states in the 192–209 GeV data, combined with the results on leptonic final states from ABBIENDI 04. The results hold for a scan over the parameter space covering the region $0 < M_2 < 5000$ GeV, $-1000 < \mu < 1000$ GeV and tanβ from 1 to 40. This limit supersedes ABBIENDI 00H.

[3] HEISTER 04 data collected up to 209 GeV. Updates earlier analysis of selectrons from HEISTER 02E, includes a new analysis of charginos and neutralinos decaying into stau and uses results on charginos with initial state radiation from HEISTER 02J. The limit is based on the direct search for charginos and neutralinos, the constraints from the slepton search and the Higgs mass limits from HEISTER 02 using a top mass of 175 GeV, interpreted in a framework with universal gaugino and sfermion masses. Assuming the mixing in the stau sector to be negligible, the limit improves to 43.1 GeV. Under the assumption of MSUGRA with unification of the Higgs and sfermion masses, the limit improves to 50 GeV, and reaches 53 GeV for $A_0 = 0$. These limits include and update the results of BARATE 01.

[4] ABDALLAH 03M uses data from $\sqrt{s} = 192$–208 GeV. A limit on the mass of $\tilde{\chi}_1^0$ is derived from direct searches for neutralinos combined with the chargino search. Neutralinos are searched in the production of $\tilde{\chi}_1^0\tilde{\chi}_2^0$, $\tilde{\chi}_1^0\tilde{\chi}_3^0$, as well as $\tilde{\chi}_2^0\tilde{\chi}_3^0$ and $\tilde{\chi}_2^0\tilde{\chi}_4^0$ giving rise to cascade decays, and $\tilde{\chi}_1^0\tilde{\chi}_2^0$ and $\tilde{\chi}_1^0\tilde{\chi}_2^0$, followed by the decay $\tilde{\chi}_2^0 \to \tilde{\tau}\tau$. The results hold for the parameter space defined by values of $M_2 < 1$ TeV, $|\mu| \leq 2$ TeV with the $\tilde{\chi}_1^0$ as LSP. The limit is obtained for tan$\beta = 1$ and large m_0, where $\tilde{\chi}_2^0\tilde{\chi}_4^0$ and chargino pair production are important. If the constraint from Higgs searches is also imposed, the limit improves to 49.0 GeV in the $m_h^{\max}$ scenario with m_t=174.3 GeV. These limits update the results of ABREU 00J.

[5] ABDALLAH 03M uses data from $\sqrt{s}$ = 192–208 GeV. An indirect limit on the mass of $\tilde{\chi}_1^0$ is derived by constraining the MSSM parameter space by the results from direct searches for neutralinos (including cascade decays and $\tilde{\tau}\tau$ final states), for charginos (for all Δm_+) and for sleptons, stop and sbottom. The results hold for the full parameter space defined by values of $M_2 < 1$ TeV, $|\mu| \leq 2$ TeV with the $\tilde{\chi}_1^0$ as LSP. Constraints from the Higgs search in the $m_h^{\max}$ scenario assuming m_t=174.3 GeV are included. The limit is obtained for tan$\beta \geq 5$ when stau mixing leads to mass degeneracy between $\tilde{\tau}_1$ and $\tilde{\chi}_1^0$ and the limit is based on $\tilde{\chi}_2^0$ production followed by its decay to $\tilde{\tau}_1\tau$. In the pathological scenario where m_0 and $|\mu|$ are large, so that the $\tilde{\chi}_2^0$ production cross section is negligible, and where there is mixing in the stau sector but not in stop nor sbottom, the limit is based on charginos with soft decay products and an ISR photon. The limit then degrades to 39 GeV. See Figs. 40–42 for the dependence of the limit on tanβ and $m_{\tilde{\nu}}$. These limits update the results of ABREU 00W.

[6] ACCIARRI 00D data collected at $\sqrt{s}$=189 GeV. The results hold over the full parameter space defined by $0.7 \leq$ tan$\beta \leq 60$, $0 \leq M_2 \leq 2$ TeV, $m_0 \leq 500$ GeV, $|\mu| \leq 2$ TeV The minimum mass limit is reached for tanβ=1 and large m_0. The results of slepton searches from ACCIARRI 99W are used to help set constraints in the region of small m_0. The limit improves to 48 GeV for $m_0 \gtrsim 200$ GeV and tan$\beta \gtrsim 10$. See their Figs. 6–8 for the tanβ and m_0 dependence of the limits. Updates ACCIARRI 98F.

[7] AAD 14K sets limits on the χ-nucleon spin-dependent and spin-independent cross sections out to $m_\chi = 10$ TeV.

Bounds on $\tilde{\chi}_1^0$ from dark matter searches

These papers generally exclude regions in the $M_2 - \mu$ parameter plane assuming that $\tilde{\chi}_1^0$ is the dominant form of dark matter in the galactic halo. These limits are based on the lack of detection in laboratory experiments, telescopes, or by the absence of a signal in underground neutrino detectors. The latter signal is expected if $\tilde{\chi}_1^0$ accumulates in the Sun or the Earth and annihilates into high-energy ν's.

VALUE	DOCUMENT ID		TECN
• • • We do not use the following data for averages, fits, limits, etc. • • •			
	[1] AARTSEN	17	ICCB
	[2] AARTSEN	17A	ICCB
	[3] AARTSEN	17C	ICCB
	[4] ALBERT	17A	ANTR
	[5] ARCHAMBAU..	17	VRTS
	[6] AARTSEN	16D	ICCB
	[7] ABDALLAH	16	HESS
	[8] ABDALLAH	16A	HESS
	[9] ADRIAN-MAR..	16	ANTR
	[10] AHNEN	16	MGFL
	[11] AVRORIN	16	BAIK
	[12] CIRELLI	16	THEO
	[12] LEITE	16	THEO
	[13] ABRAMOWSKI	15	HESS
	[14] ACKERMANN	15	FLAT
	[15] ACKERMANN	15A	FLAT
	[16] ACKERMANN	15B	FLAT
	[17] BUCKLEY	15	THEO
	[18] CHOI	15	SKAM
	[19] ALEKSIC	14	MGIC
	[20] AVRORIN	14	BAIK
	[21] AARTSEN	13C	ICCB
	[22] ABRAMOWSKI	13	HESS
	[23] BERGSTROM	13	COSM
	[24] BOLIEV	13	BAKS

[23] JIN	13	ASTR	
[23] KOPP	13	COSM	
[25] ABBASI	12	ICCB	
[26] ABRAMOWSKI	11	HESS	
[27] ABDO	10	FLAT	
[28] ACKERMANN	10	FLAT	
[29] ACHTERBERG	06	AMND	
[30] ACKERMANN	06	AMND	
[31] DEBOER	06	RVUE	
[32] DESAI	04	SKAM	
[32] AMBROSIO	99	MCRO	
[33] LOSECCO	95	RVUE	
[34] MORI	93	KAMI	
[35] BOTTINO	92	COSM	
[36] BOTTINO	91	RVUE	
[37] GELMINI	91	COSM	
[38] KAMIONKOW...	91	RVUE	
[39] MORI	91B	KAMI	
[40] OLIVE	88	COSM	

none 4–15 GeV

[1] AARTSEN 17 is based on data collected during 327 days of detector livetime with IceCube. They looked for interactions of ν's resulting from neutralino annihilations in the Earth over a background of atmospheric neutrinos and set 90% CL limits on the spin independent neutralino-proton cross section for neutralino masses in the range 10–10000 GeV.

[2] AARTSEN 17A is based on data collected during 532 days of livetime with the IceCube 86-string detector including the DeepCore sub-array. They looked for interactions of ν's from neutralino annihilations in the Sun over a background of atmospheric neutrinos and set 90% CL limits on the spin dependent neutralino-proton cross section for neutralino masses in the range 10–10000 GeV. This updates AARTSEN 16C.

[3] AARTSEN 17C is based on 1005 days of running with the IceCube detector. They set a limit on the annihilation cross section for dark matter with masses between 10–1000 GeV annihilating in the Galactic center assuming an NFW profile. The limit is of 1.2×10^{23} cm^{3}s^{-1} in the $\tau^+\tau^-$ channel. Supercedes AARTSEN 15E.

[4] ALBERT 17A is based on data from the ANTARES neutrino telescope. They looked for interactions of ν's from neutralino annihilations in the Milky Way galaxy over a background of atmospheric neutrinos and set 90% CL limits on the muon neutrino flux. They also obtain limits on the thermally averaged cross section for neutralino masses in the range 50 to 100,000 GeV. This updates ADRIAN-MARTINEZ 15.

[5] ARCHAMBAULT 17 performs a joint statistical analysis of four dwarf galaxies with VERITAS looking for gamma-ray emission from neutralino annihilation. They set limits on the neutralino annihilation cross section.

[6] AARTSEN 16D is based on 329 live days of running with the DeepCore subdetector of the IceCube detector. They set a limit of 10^{-23} cm^{3}s^{-1} on the annihilation cross section to $\nu\overline{\nu}$. This updates AARTSEN 15C.

[7] ABDALLAH 16 places constraints on the dark matter annihilation cross section for annihilations in the Galactic center for masses between 200 GeV to 70 TeV. This updates ABRAMOWSKI 15.

[8] ABDALLAH 16A place upper limits on the annihilation cross section with final states in the energy range of 0.1 to 2 TeV. This complements ABRAMOWSKI 13.

[9] ADRIAN-MARTINEZ 16 is based on data from the ANTARES neutrino telescope. They looked for interactions of ν's from neutralino annihilations in the Sun over a background of atmospheric neutrinos and set 90% CL limits on the muon neutrino flux. They also obtain limits on the spin dependent and spin independent neutralino-proton cross section for neutralino masses in the range 50 to 5,000 GeV. This updates ADRIAN-MARTINEZ 13.

[10] AHNEN 16 combines 158 hours of Segue 1 observations with MAGIC with 6 year observations of 15 dwarf satellite galaxies by Fermi-LAT to set limits on annihilation cross sections for dark matter masses between 10 GeV and 100 TeV.

[11] AVRORIN 16 is based on 2.76 years with Lake Baikal neutrino telescope. They derive 90% upper limits on the annihilation cross section from dark matter annihilations in the Galactic center.

[12] CIRELLI 16 and LEITE 16 derive bounds on the annihilation cross section from radio observations.

[13] ABRAMOWSKI 15 places constraints on the dark matter annihilation cross section for annihilations in the Galactic center for masses between 300 GeV to 10 TeV.

[14] ACKERMANN 15 is based on 5.8 years of data with Fermi-LAT and search for monochromatic gamma-rays in the energy range of 0.2–500 GeV from dark matter annihilations. This updates ACKERMANN 13A.

[15] ACKERMANN 15A is based on 50 months of data with Fermi-LAT and search for dark matter annihilation signals in the isotropic gamma-ray background as well as galactic subhalos in the energy range of a few GeV to a few tens of TeV.

[16] ACKERMANN 15B is based on 6 years of data with Fermi-LAT observations of Milky Way dwarf spheroidal galaxies. Set limits on the annihilation cross section from $m_\chi =$ 2 GeV to 10 TeV. This updates ACKERMANN 14.

[17] BUCKLEY 15 is based on 5 years of Fermi-LAT data searching for dark matter annihilation signals from Large Magellanic Cloud.

[18] CHOI 15 is based on 3903 days of SuperKamiokande data searching for neutrinos produced from dark matter annihilations in the sun. They place constraints on the dark matter-nucleon scattering cross section for dark matter masses between 4–200 GeV.

[19] ALEKSIC 14 is based on almost 160 hours of observations of Segue 1 satellite dwarf galaxy using the MAGIC telescopes between 2011 and 2013. Sets limits on the annihilation cross section out to $m_\chi = 10$ TeV.

[20] AVRORIN 14 is based on almost 2.76 years with Lake Baikal neutrino telescope. They derive 90% upper limits on the fluxes of muons and muon neutrinos from dark matter annihilations in the Sun.

[21] AARTSEN 13C is based on data collected during 339.8 effective days with the IceCube 59-string detector. They looked for interactions of ν_μ's from neutralino annihilations in nearby galaxies and galaxy clusters. They obtain limits on the neutralino annihilation cross section for neutralino masses in the range 30–100, 000 GeV.

[22] ABRAMOWSKI 13 place upper limits on the annihilation cross section with $\gamma\gamma$ final states in the energy range of 0.5–25 TeV.

[23] BERGSTROM 13, JIN 13, and KOPP 13 derive limits on the mass and annihilation cross section using AMS-02 data. JIN 13 also sets a limit on the lifetime of the dark matter particle.

[24] BOLIEV 13 is based on data collected during 24.12 years of live time with the Bakson Underground Scintillator Telescope. They looked for interactions of ν_μ's from neutralino annihilations in the Sun over a background of atmospheric neutrinos and set 90% CL limits on the muon flux. They also obtain limits on the spin dependent and spin independent neutralino-proton cross section for neutralino masses in the range 10–1000 GeV.

[25] ABBASI 12 is based on data collected during 812 effective days with AMANDA II and 149 days of the IceCube 40-string detector combined with the data of ABBASI 09B. They looked for interactions of ν_μ's from neutralino annihilations in the Sun over a background of atmospheric neutrinos and set 90% CL limits on the muon flux. No excess is observed. They also obtain limits on the spin dependent neutralino-proton cross section for neutralino masses in the range 50–5000 GeV.

[26] ABRAMOWSKI 11 place upper limits on the annihilation cross section with $\gamma\gamma$ final states.

[27] ABDO 10 place upper limits on the annihilation cross section with $\gamma\gamma$ or $\mu^+\mu^-$ final states.

[28] ACKERMANN 10 place upper limits on the annihilation cross section with $b\overline{b}$ or $\mu^+\mu^-$ final states.

[29] ACHTERBERG 06 is based on data collected during 421.9 effective days with the AMANDA detector. They looked for interactions of ν_μs from the centre of the Earth over a background of atmospheric neutrinos and set 90 % CL limits on the muon flux. Their limit is compared with the muon flux expected from neutralino annihilations into W^+W^- and $b\overline{b}$ at the centre of the Earth for MSSM parameters compatible with the relic dark matter density, see their Fig. 7.

[30] ACKERMANN 06 is based on data collected during 143.7 days with the AMANDA-II detector. They looked for interactions of ν_μs from the Sun over a background of atmospheric neutrinos and set 90 % CL limits on the muon flux. Their limit is compared with the muon flux expected from neutralino annihilations into W^+W^- in the Sun for SUSY model parameters compatible with the relic dark matter density, see their Fig. 3.

[31] DEBOER 06 interpret an excess of diffuse Galactic gamma rays observed with the EGRET satellite as originating from π^0 decays from the annihilation of neutralinos into quark jets. They analyze the corresponding parameter space in a supergravity inspired MSSM model with radiative electroweak symmetry breaking, see their Fig. 3 for the preferred region in the $(m_0, m_{1/2})$ plane of a scenario with large tanβ.

[32] AMBROSIO 99 and DESAI 04 set new neutrino flux limits which can be used to limit the parameter space in supersymmetric models based on neutralino annihilation in the Sun and the Earth.

[33] LOSECCO 95 reanalyzed the IMB data and places lower limit on $m_{\widetilde{\chi}^0_1}$ of 18 GeV if the LSP is a photino and 10 GeV if the LSP is a higgsino based on LSP annihilation in the sun producing high-energy neutrinos and the limits on neutrino fluxes from the IMB detector.

[34] MORI 93 excludes some region in M_2-μ parameter space depending on tanβ and lightest scalar Higgs mass for neutralino dark matter $m_{\widetilde{\chi}^0} > m_W$, using limits on upgoing muons produced by energetic neutrinos from neutralino annihilation in the Sun and the Earth.

[35] BOTTINO 92 excludes some region M_2-μ parameter space assuming that the lightest neutralino is the dark matter, using upgoing muons at Kamiokande, direct searches by Ge detectors, and by LEP experiments. The analysis includes top radiative corrections on Higgs parameters and employs two different hypotheses for nucleon-Higgs coupling. Effects of rescaling in the local neutralino density according to the neutralino relic abundance are taken into account.

[36] BOTTINO 91 excluded a region in $M_2 - \mu$ plane using upgoing muon data from Kamioka experiment, assuming that the dark matter surrounding us is composed of neutralinos and that the Higgs boson is not too heavy.

[37] GELMINI 91 exclude a region in $M_2 - \mu$ plane using dark matter searches.

[38] KAMIONKOWSKI 91 excludes a region in the M_2-μ plane using IMB limit on upgoing muons originated by energetic neutrinos from neutralino annihilation in the sun, assuming that the dark matter is composed of neutralinos and that $m_{H^0_1} \lesssim 50$ GeV. See Fig. 8 in the paper.

[39] MORI 91B exclude a part of the region in the M_2-μ plane with $m_{\widetilde{\chi}^0_1} \lesssim 80$ GeV using a limit on upgoing muons originated by energetic neutrinos from neutralino annihilation in the earth, assuming that the dark matter surrounding us is composed of neutralinos and that $m_{H^0_1} \lesssim 80$ GeV.

[40] OLIVE 88 result assumes that photinos make up the dark matter in the galactic halo. Limit is based on annihilations in the sun and is due to an absence of high energy neutrinos detected in underground experiments. The limit is model dependent.

$\widetilde{\chi}^0_1$-p elastic cross section

Experimental results on the $\widetilde{\chi}^0_1$-p elastic cross section are evaluated at $m_{\widetilde{\chi}^0_1}$=100 GeV. The experimental results on the cross section are often mass dependent. Therefore, the mass and cross section results are also given where the limit is strongest, when appropriate. Results are quoted separately for spin-dependent interactions (based on an effective 4-Fermi Lagrangian of the form $\overline{\chi}\gamma^\mu\gamma^5\chi\overline{q}\gamma_\mu\gamma^5 q$) and spin-independent interactions ($\overline{\chi}\chi\overline{q}q$). For calculational details see GRIEST 88B, ELLIS 88D, BARBIERI 89C, DREES 93B, ARNOWITT 96, BERGSTROM 96, and BAER 97 in addition to the theory papers listed in the Tables. For a description of the theoretical assumptions and experimental techniques underlying most of the listed papers, see the review on "Dark matter" in this "Review of Particle Physics," and references therein. Most of the following papers use galactic halo and nuclear interaction assumptions from (LEWIN 96).

Spin-dependent interactions

VALUE (pb)	CL%	DOCUMENT ID		TECN	COMMENT
• • • We do not use the following data for averages, fits, limits, etc. • • •					
$< 8 \times 10^{-4}$	90	[1] AKERIB	17A	LUX	Xe
$< 5 \times 10^{-5}$	90	[2] AMOLE	17	PICO	C_3F_8
< 0.28	90	[3] BATTAT	17	DRFT	CS_2; CF_4
< 0.027	90	[4] BEHNKE	17	PICA	C_4F_{10}
$< 2 \times 10^{-3}$	90	[5] FU	17	PNDX	Xe
$< 5 \times 10^{-4}$	90	[6] AMOLE	16	PICO	CF_3I

$<$ 6.8	$\times 10^{-3}$	90	[7] APRILE	16B	X100 Xe
$<$ 6.3	$\times 10^{-3}$	90	[8] FELIZARDO	14	SMPL C_2ClF_5
$<$ 0.01		90	[9] AKIMOV	12	ZEP3 Xe
$<$ 7	$\times 10^{-3}$		[10] BEHNKE	12	COUP CF_3I
$<$ 8.5	$\times 10^{-3}$		[11] FELIZARDO	12	SMPL C_2ClF_5
$<$ 0.016		90	[12] KIM	12	KIMS CsI
5×10^{-10} to 10^{-5}		95	[13] BUCHMUEL...	11B	THEO
$<$ 1		90	[14] ANGLE	08A	XE10 Xe
$<$ 0.055			[15] BEDNYAKOV	08	HDMS Ge
$<$ 0.33		90	[16] BEHNKE	08	COUP CF_3I
$<$ 5			[17] AKERIB	06	CDMS Ge
$<$ 2			[18] SHIMIZU	06A	CNTR CaF_2
$<$ 0.4			[19] ALNER	05	NAIA NaI Spin Dep.
$<$ 2			[20] BARNABE-HE...	05	PICA C
2×10^{-11} to 1×10^{-4}			[21] ELLIS	04	THEO $\mu > 0$
$<$ 0.8			[22] AHMED	03	NAIA NaI Spin Dep.
$<$ 40			[23] TAKEDA	03	BOLO NaF Spin Dep.
$<$ 10			[24] ANGLOHER	02	CRES Saphire
8×10^{-7} to 2×10^{-5}			[25] ELLIS	01C	THEO $\tan\beta \leq 10$
$<$ 3.8			[26] BERNABEI	00D	DAMA Xe
$<$ 0.8			SPOONER	00	UKDM NaI
$<$ 4.8			[27] BELLI	99C	DAMA F
$<$100			[28] OOTANI	99	BOLO LiF
$<$ 0.6			BERNABEI	98C	DAMA Xe
$<$ 5			[27] BERNABEI	97	DAMA F

[1] The strongest limit is 5×10^{-4} pb at $m_\chi = 35$ GeV. The limit for scattering on neutrons is 3×10^{-5} pb at 100 GeV and is 1.6×10^{-5} pb at 35 GeV. This updates AKERIB 16A.

[2] The strongest limit is 3.4×10^{-5} pb at $m_\chi = 30$ GeV. This updates AMOLE 16A.

[3] Directional recoil detector. This updates DAW 12.

[4] This result updates ARCHAMBAULT 12. The strongest limit is 0.013 pb at $m_\chi = 20$ GeV.

[5] The strongest limit is 1.2×10^{-3} pb at 40 GeV. The limit for scattering on neutrons is 5×10^{-5} pb at 100 GeV and the strongest limit is 4.1×10^{-5} pb at 40 GeV.

[6] The strongest limit is 5×10^{-4} pb at $m_\chi = 80$ GeV.

[7] The strongest limit is 5.2×10^{-3} pb at 50 GeV. The limit for scattering on neutrons is 2.8×10^{-4} pb at 100 GeV and the strongest limit is 2.0×10^{-4} pb at 50 GeV. This updates APRILE 13.

[8] The strongest limit is 0.0043 pb and occurs at $m_\chi = 35$ GeV. FELIZARDO 14 also presents limits for the scattering on neutrons. At $m_\chi = 100$ GeV, the upper limit is 0.13 pb and the strongest limit is 0.066 pb at $m_\chi = 35$ GeV.

[9] This result updates LEBEDENKO 09A. The strongest limit is 8×10^{-3} pb at $m_\chi = 50$ GeV. Limit applies to the neutralino neutron elastic cross section.

[10] The strongest limit is 6×10^{-3} at $m_\chi = 60$ GeV.

[11] The strongest limit is 5.7×10^{-3} at $m_\chi = 35$ GeV.

[12] This result updates LEE 07A. The strongest limit is at $m_\chi = 80$ GeV.

[13] Predictions for the spin-dependent elastic cross section based on a frequentist approach to electroweak observables in the framework of $N = 1$ supergravity models with radiative breaking of the electroweak gauge symmetry.

[14] The strongest limit is 0.6 pb and occurs at m_χ= 30 GeV. The limit for scattering on neutrons is 0.01 pb at m_χ= 100 GeV, and the strongest limit is 0.0045 pb at m_χ= 30 GeV.

[15] Limit applies to neutron elastic cross section.

[16] The strongest upper limit is 0.25 pb and occurs at $m_\chi \simeq 40$ GeV.

[17] The strongest upper limit is 4 pb and occurs at $m_\chi \simeq 60$ GeV. The limit on the neutron spin-dependent elastic cross section is 0.07 pb. This latter limit is improved in AHMED 09, where a limit of 0.02 pb is obtained at $m_\chi = 100$ GeV. The strongest limit in AHMED 09 is 0.018 pb and occurs at $m_\chi = 60$ GeV.

[18] The strongest upper limit is 1.2 pb and occurs at $m_\chi \simeq 40$ GeV. The limit on the neutron spin-dependent cross section is 35 pb.

[19] The strongest upper limit is 0.35 pb and occurs at $m_\chi \simeq 60$ GeV.

[20] The strongest upper limit is 1.2 pb and occurs $m_\chi \simeq 30$ GeV.

[21] ELLIS 04 calculates the χp elastic scattering cross section in the framework of N=1 supergravity models with radiative breaking of the electroweak gauge symmetry, but without universal scalar masses. In the case of universal squark and slepton masses, but non-universal Higgs masses, the limit becomes 2×10^{-4}, see ELLIS 03E.

[22] The strongest upper limit is 0.75 pb and occurs at $m_\chi \approx 70$ GeV.

[23] The strongest upper limit is 30 pb and occurs at $m_\chi \approx 20$ GeV.

[24] The strongest upper limit is 8 pb and occurs at $m_\chi \simeq 30$ GeV.

[25] ELLIS 01C calculates the χ-p elastic scattering cross section in the framework of N=1 supergravity models with radiative breaking of the electroweak gauge symmetry. In models with nonuniversal Higgs masses, the upper limit to the cross section is 6×10^{-4}.

[26] The strongest upper limit is 3 pb and occurs at $m_\chi \simeq 60$ GeV. The limits are for inelastic scattering $X^0 + {}^{129}Xe \rightarrow X^0 + {}^{129}Xe^*$ (39.58 keV).

[27] The strongest upper limit is 4.4 pb and occurs at $m_\chi \simeq 60$ GeV.

[28] The strongest upper limit is about 35 pb and occurs at $m_\chi \simeq 15$ GeV.

Spin-independent interactions

VALUE (pb)	CL%	DOCUMENT ID		TECN	COMMENT
• • • We do not use the following data for averages, fits, limits, etc. • • •					
$<1.8\times10^{-10}$	90	[1] AKERIB	17	LUX	Xe
$<1.5\times10^{-10}$	90	[2] APRILE	17G	XE1T	Xe
$<1.4\times10^{-10}$	90	[3] CUI	17A	PNDX	Xe
$<3\times10^{-8}$	90	AMOLE	16	PICO	CF_3I
$<1.5\times10^{-9}$	90	[4] APRILE	16B	X100	Xe
$<6.1\times10^{-8}$	90	AGNES	15	DS50	Ar
$<2.2\times10^{-8}$	90	[5] AGNESE	15B	CDMS	Ge
$<1.5\times10^{-9}$	90	[6] AKERIB	14	LUX	Xe
10^{-11}–10^{-7}	95	[7] BUCHMUEL...	14A	THEO	
$<4.6\times10^{-6}$	90	[8] FELIZARDO	14	SMPL	C_2ClF_5
10^{-11}–10^{-8}	95	[9] ROSZKOWSKI	14	THEO	
$<2.2\times10^{-6}$	90	[10] AGNESE	13	CDMS	Si
$<5\times10^{-8}$	90	[11] AKIMOV	12	ZEP3	Xe
1.6×10^{-6}; 3.7×10^{-5}		[12] ANGLOHER	12	CRES	$CaWO_4$
3×10^{-12} to 3×10^{-9}	95	[13] BECHTLE	12	THEO	
$<1.6\times10^{-7}$		[14] BEHNKE	12	COUP	CF_3I
$<6.5\times10^{-6}$		[15] FELIZARDO	12	SMPL	C_2ClF_5
$<2.3\times10^{-7}$	90	[16] KIM	12	KIMS	CsI
$<3.3\times10^{-8}$	90	[17] AHMED	11A		Ge
$<4.4\times10^{-8}$	90	[18] ARMENGAUD	11	EDE2	Ge
$<7\times10^{-7}$	90	[19] ANGLOHER	09	CRES	$CaWO_4$
$<1\times10^{-7}$	90	[20] ANGLE	08	XE10	Xe
$<1\times10^{-6}$	90	BENETTI	08	WARP	Ar
$<7.5\times10^{-7}$	90	[21] ALNER	07A	ZEP2	Xe
$<2\times10^{-7}$		[22] AKERIB	06A	CDMS	Ge
$<90\times10^{-7}$		ALNER	05	NAIA	NaI Spin Indep.
$<12\times10^{-7}$		[23] ALNER	05A	ZEPL	
$<20\times10^{-7}$		[24] ANGLOHER	05	CRES	$CaWO_4$
$<14\times10^{-7}$		SANGLARD	05	EDEL	Ge
$<4\times10^{-7}$		[25] AKERIB	04	CDMS	Ge
2×10^{-11} to 1.5×10^{-7}	95	[26] BALTZ	04	THEO	
2×10^{-11} to 8×10^{-6}		[27,28] ELLIS	04	THEO	$\mu > 0$
$<5\times10^{-8}$		[29] PIERCE	04A	THEO	
$<2\times10^{-5}$		[30] AHMED	03	NAIA	NaI Spin Indep.
$<3\times10^{-6}$		[31] AKERIB	03	CDMS	Ge
2×10^{-13} to 2×10^{-7}		[32] BAER	03A	THEO	
$<1.4\times10^{-5}$		[33] KLAPDOR-K...	03	HDMS	Ge
$<6\times10^{-6}$		[34] ABRAMS	02	CDMS	Ge
$<1.4\times10^{-6}$		[35] BENOIT	02	EDEL	Ge
1×10^{-12} to 7×10^{-6}		[27] KIM	02B	THEO	
$<3\times10^{-5}$		[36] MORALES	02B	CSME	Ge
$<1\times10^{-5}$		[37] MORALES	02C	IGEX	Ge
$<1\times10^{-6}$		BALTZ	01	THEO	
$<3\times10^{-5}$		[38] BAUDIS	01	HDMS	Ge
$<4.5\times10^{-6}$		BENOIT	01	EDEL	Ge
$<7\times10^{-6}$		[39] BOTTINO	01	THEO	
$<1\times10^{-8}$		[40] CORSETTI	01	THEO	$\tan\beta \leq 25$
5×10^{-10} to 1.5×10^{-8}		[41] ELLIS	01C	THEO	$\tan\beta \leq 10$
$<4\times10^{-6}$		[40] GOMEZ	01	THEO	
2×10^{-10} to 1×10^{-7}		[40] LAHANAS	01	THEO	
$<3\times10^{-6}$		ABUSAIDI	00	CDMS	Ge, Si
$<6\times10^{-7}$		[42] ACCOMANDO	00	THEO	
		[43] BERNABEI	00	DAMA	NaI
2.5×10^{-9} to 3.5×10^{-8}		[44] FENG	00	THEO	$\tan\beta$=10
$<1.5\times10^{-5}$		MORALES	00	IGEX	Ge
$<4\times10^{-5}$		SPOONER	00	UKDM	NaI
$<7\times10^{-6}$		BAUDIS	99	HDMO	^{76}Ge
$<7\times10^{-6}$		BERNABEI	98C	DAMA	Xe

[1] The strongest limit is 1.1×10^{-10} at 50 GeV. This updates AKERIB 16.

[2] The strongest limit is 7.7×10^{-11} pb at $m_\chi = 35$ GeV.

[3] The strongest limit is 8.6×10^{-11} pb at 40 GeV. This updates TAN 16B.

[4] The strongest limit is 1.1×10^{-9} pb at 50 GeV. This updates APRILE 12.

[5] AGNESE 15B result updates AHMED 10 and AHMED 09. The strongest limit is 1.8×10^{-8} pb and occurs at $m_\chi = 60$ GeV.

[6] The strongest upper limit is 7.6×10^{-10} at $m_\chi = 33$ GeV.

[7] Predictions for the spin-independent elastic cross section based on a frequentist approach to electroweak observables in the framework of $N = 1$ supergravity models with radiative breaking of the electroweak gauge symmetry using the 20 fb^{-1} 8 TeV and the 5 fb^{-1} 7 TeV LHC data and the LUX data.

[8] The strongest limit is 3.6×10^{-6} pb and occurs at $m_\chi = 35$ GeV.

[9] Predictions for the spin-independent elastic cross section based on a Bayesian approach to electroweak observables in the framework of $N = 1$ supergravity models with radiative breaking of the electroweak gauge symmetry using the 20 fb^{-1} LHC data and LUX.

[10] AGNESE 13 presents 90% CL limits on the elastic cross section for masses in the range 7–100 GeV using the Si based detector. The strongest upper limit is 1.8×10^{-6} pb at $m_\chi = 50$ GeV. This limit is improved to 7×10^{-7} pb in AGNESE 13A.

[11] This result updates LEBEDENKO 09. The strongest limit is 3.9×10^{-8} pb at m_χ = 52 GeV.

[12] ANGLOHER 12 presents results of 730 kg days from the CRESST-II dark matter detector. They find two maxima in the likelihood function corresponding to best fit WIMP masses of 25.3 and 11.6 GeV with elastic cross sections of 1.6×10^{-6} and 3.7×10^{-5} pb respectively, see their Table 4. The statistical significance is more than 4σ.

[13] Predictions for the spin-independent elastic cross section based on a frequentist approach to electroweak observables in the framework of $N = 1$ supergravity models with radiative breaking of the electroweak gauge symmetry using the 5 fb^{-1} LHC data and XENON100.

[14] The strongest limit is 1.4×10^{-7} at $m_\chi = 60$ GeV.

[15] The strongest limit is 4.7×10^{-6} at $m_\chi = 35$ GeV.

[16] This result updates LEE 07A. The strongest limit is 2.1×10^{-7} at $m_\chi = 70$ GeV.

[17] AHMED 11A gives combined results from CDMS and EDELWEISS. The strongest limit is at $m_\chi = 90$ GeV.

[18] ARMENGAUD 11 updates result of ARMENGAUD 10. Strongest limit at $m_\chi = 85$ GeV.

[19] The strongest upper limit is 4.8×10^{-7} pb and occurs at $m_\chi = 50$ GeV.

[20] The strongest upper limit is 5.1×10^{-8} pb and occurs at $m_\chi \simeq 30$ GeV. The values quoted here are based on the analysis performed in ANGLE 08 with the update from SORENSEN 09.

[21] The strongest upper limit is 6.6×10^{-7} pb and occurs at $m_\chi \simeq 65$ GeV.

[22] AKERIB 06A updates the results of AKERIB 05. The strongest upper limit is 1.6×10^{-7} pb and occurs at $m_\chi \approx 60$ GeV.

[23] The strongest upper limit is also close to 1.0×10^{-6} pb and occurs at $m_\chi \simeq 70$ GeV. BENOIT 06 claim that the discrimination power of ZEPLIN-I measurement (ALNER 05A) is not reliable enough to obtain a limit better than 1×10^{-3} pb. However, SMITH 06 do not agree with the criticisms of BENOIT 06.

[24] The strongest upper limit is also close to 1.4×10^{-6} pb and occurs at $m_\chi \simeq 70$ GeV.

[25] AKERIB 04 is incompatible with BERNABEI 00 most likely value, under the assumption of standard WIMP-halo interactions. The strongest upper limit is 4×10^{-7} pb and occurs at $m_\chi \simeq 60$ GeV.

[26] Predictions for the spin-independent elastic cross section in the framework of $N = 1$ supergravity models with radiative breaking of the electroweak gauge symmetry.

[27] KIM 02 and ELLIS 04 calculate the χp elastic scattering cross section in the framework of N=1 supergravity models with radiative breaking of the electroweak gauge symmetry, but without universal scalar masses.

[28] In the case of universal squark and slepton masses, but non-universal Higgs masses, the limit becomes 2×10^{-6} (2×10^{-11} when constraint from the BNL $g-2$ experiment are included), see ELLIS 03E. ELLIS 05 display the sensitivity of the elastic scattering cross section to the π-Nucleon Σ term.

[29] PIERCE 04A calculates the χp elastic scattering cross section in the framework of models with very heavy scalar masses. See Fig. 2 of the paper.

[30] The strongest upper limit is 1.8×10^{-5} pb and occurs at $m_\chi \approx 80$ GeV.

[31] Under the assumption of standard WIMP-halo interactions, Akerib 03 is incompatible with BERNABEI 00 most likely value at the 99.98% CL. See Fig. 4.

[32] BAER 03A calculates the χp elastic scattering cross section in several models including the framework of N=1 supergravity models with radiative breaking of the electroweak gauge symmetry.

[33] The strongest upper limit is 7×10^{-6} pb and occurs at $m_\chi \simeq 30$ GeV.

[34] ABRAMS 02 is incompatible with the DAMA most likely value at the 99.9% CL. The strongest upper limit is 3×10^{-6} pb and occurs at $m_\chi \simeq 30$ GeV.

[35] BENOIT 02 excludes the central result of DAMA at the 99.8%CL.

[36] The strongest upper limit is 2×10^{-5} pb and occurs at $m_\chi \simeq 40$ GeV.

[37] The strongest upper limit is 7×10^{-6} pb and occurs at $m_\chi \simeq 46$ GeV.

[38] The strongest upper limit is 1.8×10^{-5} pb and occurs at $m_\chi \simeq 32$ GeV

[39] BOTTINO 01 calculates the χ-p elastic scattering cross section in the framework of the following supersymmetric models: N=1 supergravity with the radiative breaking of the electroweak gauge symmetry, N=1 supergravity with nonuniversal scalar masses and an effective MSSM model at the electroweak scale.

[40] Calculates the χ-p elastic scattering cross section in the framework of N=1 supergravity models with radiative breaking of the electroweak gauge symmetry.

[41] ELLIS 01C calculates the χ-p elastic scattering cross section in the framework of N=1 supergravity models with radiative breaking of the electroweak gauge symmetry. ELLIS 02B find a range 2×10^{-8}–1.5×10^{-7} at $\tan\beta$=50. In models with nonuniversal Higgs masses, the upper limit to the cross section is 4×10^{-7}.

[42] ACCOMANDO 00 calculate the χ-p elastic scattering cross section in the framework of minimal N=1 supergravity models with radiative breaking of the electroweak gauge symmetry. The limit is relaxed by at least an order of magnitude when models with nonuniversal scalar masses are considered. A subset of the authors in ARNOWITT 02 updated the limit to $< 9 \times 10^{-8}$ ($\tan\beta < 55$).

[43] BERNABEI 00 search for annual modulation of the WIMP signal. The data favor the hypothesis of annual modulation at 4σ and are consistent, for a particular model framework quoted there, with m_{χ^0}=44 $^{+12}_{-9}$ GeV and a spin-independent χ^0-proton cross section of $(5.4 \pm 1.0) \times 10^{-6}$ pb. See also BERNABEI 01 and BERNABEI 00C.

[44] FENG 00 calculate the χ-p elastic scattering cross section in the framework of N=1 supergravity models with radiative breaking of the electroweak gauge symmetry with a particular emphasis on focus point models. At $\tan\beta$=50, the range is 8×10^{-8}–4×10^{-7}.

Other bounds on $\tilde{\chi}_1^0$ from astrophysics and cosmology

Most of these papers generally exclude regions in the $M_2 - \mu$ parameter plane by requiring that the $\tilde{\chi}_1^0$ contribution to the overall cosmological density is less than some maximal value to avoid overclosure of the Universe. Those not based on the cosmological density are indicated. Many of these papers also include LEP and /or other bounds.

VALUE	DOCUMENT ID		TECN	COMMENT
>46 GeV	[1] ELLIS	00	RVUE	
• • • We do not use the following data for averages, fits, limits, etc. • • •				
	[2] BUCHMUEL...	14	COSM	
	[3] BUCHMUEL...	14A	COSM	
	[4] ROSZKOWSKI	14	COSM	
	[5] CABRERA	13	COSM	
	[6] ELLIS	13B	COSM	
	[5] STREGE	13	COSM	
	[2] AKULA	12	COSM	
	[2] ARBEY	12A	COSM	
	[2] BAER	12	COSM	
	[7] BALAZS	12	COSM	
	[8] BECHTLE	12	COSM	
	[9] BESKIDT	12	COSM	
> 18 GeV	[10] BOTTINO	12	COSM	
	[2] BUCHMUEL...	12	COSM	
	[2] CAO	12A	COSM	
	[2] ELLIS	12B	COSM	
	[11] FENG	12B	COSM	
	[2] KADASTIK	12	COSM	
	[7] STREGE	12	COSM	
	[12] BUCHMUEL...	11	COSM	
	[13] ROSZKOWSKI	11	COSM	
	[14] ELLIS	10	COSM	
	[15] BUCHMUEL...	09	COSM	
	[16] DREINER	09	THEO	
	[17] BUCHMUEL...	08	COSM	
	[13] ELLIS	08	COSM	
	[18] CALIBBI	07	COSM	
	[19] ELLIS	07	COSM	
	[20] ALLANACH	06	COSM	
	[21] DE-AUSTRI	06	COSM	
	[13] BAER	05	COSM	
	[22] BALTZ	04	COSM	
> 6 GeV	[10,23] BELANGER	04	THEO	
	[24] ELLIS	04B	COSM	
	[25] PIERCE	04A	COSM	
	[26] BAER	03	COSM	
> 6 GeV	[10] BOTTINO	03	COSM	
	[26] CHATTOPAD...	03	COSM	
	[27] ELLIS	03	COSM	
	[13] ELLIS	03B	COSM	
	[26] ELLIS	03C	COSM	
	[26] LAHANAS	03	COSM	
	[28] LAHANAS	02	COSM	
	[29] BARGER	01C	COSM	
	[30] ELLIS	01B	COSM	
	[27] BOEHM	00B	COSM	
	[31] FENG	00	COSM	
< 600 GeV	[32] ELLIS	98B	COSM	
	[33] EDSJO	97	COSM	Co-annihilation
	[34] BAER	96	COSM	
	[13] BEREZINSKY	95	COSM	
	[35] FALK	95	COSM	*CP*-violating phases
	[36] DREES	93	COSM	Minimal supergravity
	[37] FALK	93	COSM	Sfermion mixing
	[36] KELLEY	93	COSM	Minimal supergravity
	[38] MIZUTA	93	COSM	Co-annihilation
	[39] LOPEZ	92	COSM	Minimal supergravity, m_0=A=0
	[40] MCDONALD	92	COSM	
	[41] GRIEST	91	COSM	
	[42] NOJIRI	91	COSM	Minimal supergravity
	[43] OLIVE	91	COSM	
	[44] ROSZKOWSKI	91	COSM	
	[45] GRIEST	90	COSM	
	[43] OLIVE	89	COSM	
none 100 eV – 15 GeV	SREDNICKI	88	COSM	$\tilde{\gamma}$; $m_{\tilde{f}}$=100 GeV
none 100 eV–5 GeV	ELLIS	84	COSM	$\tilde{\gamma}$; for $m_{\tilde{f}}$=100 GeV
	GOLDBERG	83	COSM	$\tilde{\gamma}$
	[46] KRAUSS	83	COSM	$\tilde{\gamma}$
	VYSOTSKII	83	COSM	$\tilde{\gamma}$

[1] ELLIS 00 updates ELLIS 98. Uses LEP e^+e^- data at $\sqrt{s}$=202 and 204 GeV to improve bound on neutralino mass to 51 GeV when scalar mass universality is assumed and 46 GeV when Higgs mass universality is relaxed. Limits on $\tan\beta$ improve to > 2.7 ($\mu > 0$), > 2.2 ($\mu < 0$) when scalar mass universality is assumed and > 1.9 (both signs of μ) when Higgs mass universality is relaxed.

[2] Implications of the LHC result on the Higgs mass and on the SUSY parameter space in the framework of $N = 1$ supergravity models with radiative breaking of the electroweak gauge symmetry.

[3] BUCHMUELLER 14A places constraints on the SUSY parameter space in the framework of $N = 1$ supergravity models with radiative breaking of the electroweak gauge symmetry using indirect experimental searches using the 20 fb^{-1} 8 TeV and the 5 fb^{-1} 7 TeV LHC and the LUX data.

[4] ROSZKOWSKI 14 places constraints on the SUSY parameter space in the framework of $N = 1$ supergravity models with radiative breaking of the electroweak gauge symmetry using Bayesian statistics and indirect experimental searches using the 20 fb^{-1} LHC and the LUX data.

[5] CABRERA 13 and STREGE 13 place constraints on the SUSY parameter space in the framework of $N = 1$ supergravity models with radiative breaking of the electroweak gauge symmetry with and without non-universal Higgs masses using the 5.8 fb^{-1}, $\sqrt{s} = 7$ TeV ATLAS supersymmetry searches and XENON100 results.

[6] ELLIS 13B place constraints on the SUSY parameter space in the framework of $N = 1$ supergravity models with radiative breaking of the electroweak gauge symmetry with and without Higgs mass universality. Models with universality below the GUT scale are also considered.

[7] BALAZS 12 and STREGE 12 place constraints on the SUSY parameter space in the framework of $N = 1$ supergravity models with radiative breaking of the electroweak gauge symmetry using the 1 fb^{-1} LHC supersymmetry searches, the 5 fb^{-1} Higgs mass constraints, both with $\sqrt{s} = 7$ TeV, and XENON100 results.

[8] BECHTLE 12 places constraints on the SUSY parameter space in the framework of $N = 1$ supergravity models with radiative breaking of the electroweak gauge symmetry using indirect experimental searches, using the 5 fb^{-1} LHC and XENON100 data.

[9] BESKIDT 12 places constraints on the SUSY parameter space in the framework of $N = 1$ supergravity models with radiative breaking of the electroweak gauge symmetry using indirect experimental searches, the 5 fb^{-1} LHC and the XENON100 data.

[10] BELANGER 04 and BOTTINO 12 (see also BOTTINO 03, BOTTINO 03A and BOTTINO 04) do not assume gaugino or scalar mass unification.

[11] FENG 12B places constraints on the SUSY parameter space in the framework of $N = 1$ supergravity models with radiative breaking of the electroweak gauge symmetry and large sfermion masses using the 1 fb^{-1} LHC supersymmetry searches, the 5 fb^{-1} LHC Higgs mass constraints both with $\sqrt{s} = 7$ TeV, and XENON100 results.

[12] BUCHMUELLER 11 places constraints on the SUSY parameter space in the framework of $N = 1$ supergravity models with radiative breaking of the electroweak gauge symmetry using indirect experimental searches and including supersymmetry breaking relations between A and B parameters.

[13] Places constraints on the SUSY parameter space in the framework of N=1 supergravity models with radiative breaking of the electroweak gauge symmetry but non-Universal Higgs masses.

[14] ELLIS 10 places constraints on the SUSY parameter space in the framework of $N = 1$ supergravity models with radiative breaking of the electroweak gauge symmetry with universality above the GUT scale.

[15] BUCHMUELLER 09 places constraints on the SUSY parameter space in the framework of $N = 1$ supergravity models with radiative breaking of the electroweak gauge symmetry using indirect experimental searches.

[16] DREINER 09 show that in the general MSSM with non-universal gaugino masses there exists no model-independent laboratory bound on the mass of the lightest neutralino. An essentially massless χ_1^0 is allowed by the experimental and observational data, imposing some constraints on other MSSM parameters, including M_2, μ and the slepton and squark masses.

[17] BUCHMUELLER 08 places constraints on the SUSY parameter space in the framework of $N = 1$ supergravity models with radiative breaking of the electroweak gauge symmetry using indirect experimental searches.

[18] CALIBBI 07 places constraints on the SUSY parameter space in the framework of $N = 1$ supergravity models with radiative breaking of the electroweak gauge symmetry with universality above the GUT scale including the effects of right-handed neutrinos.

[19] ELLIS 07 places constraints on the SUSY parameter space in the framework of $N = 1$ supergravity models with radiative breaking of the electroweak gauge symmetry with universality below the GUT scale.

[20] ALLANACH 06 places constraints on the SUSY parameter space in the framework of $N = 1$ supergravity models with radiative breaking of the electroweak gauge symmetry.

[21] DE-AUSTRI 06 places constraints on the SUSY parameter space in the framework of $N = 1$ supergravity models with radiative breaking of the electroweak gauge symmetry.

[22] BALTZ 04 places constraints on the SUSY parameter space in the framework of $N = 1$ supergravity models with radiative breaking of the electroweak gauge symmetry.

[23] Limit assumes a pseudo scalar mass < 200 GeV. For larger pseudo scalar masses, $m_\chi > 18(29)$ GeV for $\tan\beta = 50(10)$. Bounds from WMAP, $(g-2)_\mu$, $b \to s\gamma$, LEP.

[24] ELLIS 04B places constraints on the SUSY parameter space in the framework of N=1 supergravity models with radiative breaking of the electroweak gauge symmetry including supersymmetry breaking relations between A and B parameters. See also ELLIS 03D.

[25] PIERCE 04A places constraints on the SUSY parameter space in the framework of models with very heavy scalar masses.

[26] BAER 03, CHATTOPADHYAY 03, ELLIS 03C and LAHANAS 03 place constraints on the SUSY parameter space in the framework of N=1 supergravity models with radiative breaking of the electroweak gauge symmetry based on WMAP results for the cold dark matter density.

[27] BOEHM 00B and ELLIS 03 place constraints on the SUSY parameter space in the framework of minimal N=1 supergravity models with radiative breaking of the electroweak gauge symmetry. Includes the effect of χ-$\tilde{t}$ co-annihilations.

[28] LAHANAS 02 places constraints on the SUSY parameter space in the framework of minimal N=1 supergravity models with radiative breaking of the electroweak gauge symmetry. Focuses on the role of pseudo-scalar Higgs exchange.

[29] BARGER 01C use the cosmic relic density inferred from recent CMB measurements to constrain the parameter space in the framework of minimal N=1 supergravity models with radiative breaking of the electroweak gauge symmetry.

[30] ELLIS 01B places constraints on the SUSY parameter space in the framework of minimal N=1 supergravity models with radiative breaking of the electroweak gauge symmetry. Focuses on models with large $\tan\beta$.

[31] FENG 00 explores cosmologically allowed regions of MSSM parameter space with multi-TeV masses.

[32] ELLIS 98B assumes a universal scalar mass and radiative supersymmetry breaking with universal gaugino masses. The upper limit to the LSP mass is increased due to the inclusion of $\chi - \tilde{\tau}_R$ coannihilations.

[33] EDSJO 97 included all coannihilation processes between neutralinos and charginos for any neutralino mass and composition.

[34] Notes the location of the neutralino Z resonance and h resonance annihilation corridors in minimal supergravity models with radiative electroweak breaking.

[35] Mass of the bino (=LSP) is limited to $m_{\widetilde{B}} \lesssim 350$ GeV for $m_t = 174$ GeV.

[36] DREES 93, KELLEY 93 compute the cosmic relic density of the LSP in the framework of minimal N=1 supergravity models with radiative breaking of the electroweak gauge symmetry.

[37] FALK 93 relax the upper limit to the LSP mass by considering sfermion mixing in the MSSM.

[38] MIZUTA 93 include coannihilations to compute the relic density of Higgsino dark matter.

[39] LOPEZ 92 calculate the relic LSP density in a minimal SUSY GUT model.

[40] MCDONALD 92 calculate the relic LSP density in the MSSM including exact tree-level annihilation cross sections for all two-body final states.

[41] GRIEST 91 improve relic density calculations to account for coannihilations, pole effects, and threshold effects.

[42] NOJIRI 91 uses minimal supergravity mass relations between squarks and sleptons to narrow cosmologically allowed parameter space.

[43] Mass of the bino (=LSP) is limited to $m_{\widetilde{B}} \lesssim 350$ GeV for $m_t \leq 200$ GeV. Mass of the higgsino (=LSP) is limited to $m_{\widetilde{H}} \lesssim 1$ TeV for $m_t \leq 200$ GeV.

[44] ROSZKOWSKI 91 calculates LSP relic density in mixed gaugino/higgsino region.

[45] Mass of the bino (=LSP) is limited to $m_{\widetilde{B}} \lesssim 550$ GeV. Mass of the higgsino (=LSP) is limited to $m_{\widetilde{H}} \lesssim 3.2$ TeV.

[46] KRAUSS 83 finds $m_{\widetilde{\gamma}}$ not 30 eV to 2.5 GeV. KRAUSS 83 takes into account the gravitino decay. Find that limits depend strongly on reheated temperature. For example a new allowed region $m_{\widetilde{\gamma}} = 4$–20 MeV exists if $m_{\text{gravitino}} < 40$ TeV. See figure 2.

Unstable $\widetilde{\chi}_1^0$ (Lightest Neutralino) mass limit

Unless otherwise stated, results in this section assume spectra and production rates as evaluated in the MSSM. Unless otherwise stated, the goldstino or gravitino mass $m_{\widetilde{G}}$ is assumed to be negligible relative to all other masses. In the following, $\widetilde{G}$ is assumed to be undetected and to give rise to a missing energy ($\not{E}$) signature.

Some earlier papers are now obsolete and have been omitted. They were last listed in our PDG 14 edition: K. Olive, *et al.* (Particle Data Group), Chinese Physics **C38** 070001 (2014) (http://pdg.lbl.gov).

VALUE (GeV)	CL%	DOCUMENT ID		TECN	COMMENT
>380	95	[1] KHACHATRY...14L		CMS	$\widetilde{\chi}_1^0 \to Z\widetilde{G}$ simplified models,GMSB
• • • We do not use the following data for averages, fits, limits, etc. • • •					
		[2] AAIJ	17Z		displaced vertex with associated μ
		[3] KHACHATRY...16BX			$\geq 3\ell^\pm$, RPV, λ or λ' couplings, wino- or higgsino-like neutralinos
		[4] AAD	14BH	ATLS	$2\gamma + \not{E}_T$, GMSB, SPS8
		[5] AAD	13AP	ATLS	$2\gamma + \not{E}_T$, GMSB, SPS8
none 220–380	95	[6] AAD	13Q	ATLS	$\gamma + b + \not{E}_T$, higgsino-like neutralino, GMSB
		[7] AAD	13R	ATLS	$\widetilde{\chi}_1^0 \to \mu jj$, RPV, $\lambda'_{211} \neq 0$
		[8] AALTONEN	13I	CDF	$\widetilde{\chi}_1^0 \to \gamma\widetilde{G}$, $\not{E}_T$, GMSB
>220	95	[9] CHATRCHYAN	13AH	CMS	$\widetilde{\chi}_1^0 \to \gamma\widetilde{G}$, GMSB, SPS8, $c\tau <$ 500 mm
		[10] AAD	12CP	ATLS	$2\gamma + \not{E}_T$, GMSB
		[11] AAD	12CT	ATLS	$\geq 4\ell^\pm$, RPV
		[12] AAD	12R	ATLS	$\widetilde{\chi}_1^0 \to \mu jj$, RPV, $\lambda'_{211} \neq 0$
		[13] ABAZOV	12AD	D0	$\widetilde{\chi}_1^0\widetilde{\chi}_1^0 \to \gamma Z\widetilde{G}\widetilde{G}$, GMSB
		[14] CHATRCHYAN	12BK	CMS	$2\gamma + \not{E}_T$, GMSB
		[15] CHATRCHYAN	11B	CMS	$\widetilde{W}^0 \to \gamma\widetilde{G}$, $\widetilde{W}^\pm \to \ell^\pm\widetilde{G}$, GMSB
>149	95	[16] AALTONEN	10	CDF	$p\overline{p} \to \widetilde{\chi}\widetilde{\chi}$, $\widetilde{\chi}$=$\widetilde{\chi}_2^0$, $\widetilde{\chi}_1^\pm$, $\widetilde{\chi}_1^0 \to \gamma\widetilde{G}$, GMSB
>175	95	[17] ABAZOV	10P	D0	$\widetilde{\chi}_1^0 \to \gamma\widetilde{G}$, GMSB
>125	95	[18] ABAZOV	08F	D0	$p\overline{p} \to \widetilde{\chi}\widetilde{\chi}$, $\widetilde{\chi}$=$\widetilde{\chi}_2^0$, $\widetilde{\chi}_1^\pm$, $\widetilde{\chi}_1^0 \to \gamma\widetilde{G}$, GMSB
		[19] ABULENCIA	07H	CDF	RPV, $LL\overline{E}$
> 96.8	95	[20] ABBIENDI	06B	OPAL	$e^+e^- \to \widetilde{B}\widetilde{B}$, ($\widetilde{B} \to \widetilde{G}\gamma$)
		[21] ABDALLAH	05B	DLPH	$e^+e^- \to \widetilde{G}\widetilde{\chi}_1^0$, ($\widetilde{\chi}_1^0 \to \widetilde{G}\gamma$)
> 96	95	[22] ABDALLAH	05B	DLPH	$e^+e^- \to \widetilde{B}\widetilde{B}$, ($\widetilde{B} \to \widetilde{G}\gamma$)

[1] KHACHATRYAN 14L searched in 19.5 fb^{-1} of pp collisions at $\sqrt{s} = 8$ TeV for evidence of direct pair production of neutralinos with Higgs or Z-bosons in the decay chain, leading to HH, HZ and ZZ final states with missing transverse energy. The decays of 16–20. a Higgs boson to a b-quark pair, to a photon pair, and to final states with leptons are considered in conjunction with hadronic and leptonic decay modes of the Z and W bosons. No significant excesses over the expected SM backgrounds are observed. The results are interpreted in the context of GMSB simplified models where the decays $\widetilde{\chi}_1^0 \to H\widetilde{G}$ or $\widetilde{\chi}_1^0 \to Z\widetilde{G}$ take place either 100% or 50% of the time, see Figs. 16–20.

[2] AAIJ 17Z searched in 1 fb^{-1} of pp collisions at $\sqrt{s} = 7$ TeV and in 2 fb^{-1} of pp collisions at $\sqrt{s} = 8$ TeV for events containing a displaced vertex with one associated high transverse momentum μ. No excess is observed above the background expected from Standard Model processes. The results are used to set 95% C.L. upper limits on the cross section times branching fractions of pair-produced neutralinos decaying non-promptly into a muon and two quarks. Long-lived particles in a mass range 23–198 GeV are considered, see their Fig. 5 and Fig. 6.

[3] KHACHATRYAN 16BX searched in 19.5 fb^{-1} of pp collisions at $\sqrt{s} = 8$ TeV for events containing 3 or more leptons coming from the electroweak production of wino- or higgsino-like neutralinos, assuming non-zero R-parity-violating leptonic couplings λ_{122}, λ_{123}, and λ_{233} or semileptonic couplings λ'_{131}, λ'_{233}, λ'_{331}, and λ'_{333}. No excess over the expected background is observed and limits are derived on the neutralino mass, see Figs. 24 and 25.

[4] AAD 14BH searched in 20.3 fb^{-1} of pp collisions at $\sqrt{s} = 8$ TeV for events containing non-pointing photons in a diphoton plus missing transverse energy final state. No excess is observed above the background expected from Standard Model processes. The results are used to set 95% C.L. exclusion limits in the contact of gauge-mediated supersymmetric breaking models, with the lightest neutralino being the next-to-lightest supersymmetric particle and decaying with a lifetime in the range from 0.25 ns to about 100 ns into a photon and a gravitino. For limits on the NLSP lifetime versus Λ plane, for the SPS8 model, see their Fig. 7.

[5] AAD 13AP searched in 4.8 fb^{-1} of pp collisions at $\sqrt{s} = 7$ TeV for events containing non-pointing photons in a diphoton plus missing transverse energy final state. No excess is observed above the background expected from Standard Model processes. The results are used to set 95% C.L. exclusion limits in the context of gauge-mediated supersymmetric breaking models, with the lightest neutralino being the next-to-lightest supersymmetric particle and decaying with a lifetime in excess of 0.25 ns into a photon and a gravitino. For limits in the NLSP lifetime versus Λ plane, for the SPS8 model, see their Fig. 8.

[6] AAD 13Q searched in 4.7 fb^{-1} of pp collisions at $\sqrt{s} = 7$ TeV for events containing a high-p_T isolated photon, at least one jet identified as originating from a bottom quark, and high missing transverse momentum. Such signatures may originate from supersymmetric models with gauge-mediated supersymmetry breaking in events in which one of a pair of higgsino-like neutralinos decays into a photon and a gravitino while the other decays into a Higgs boson and a gravitino. No significant excess above the expected background was found and limits were set on the neutralino mass in a generalized GMSB model (GGM) with a higgsino-like neutralino NLSP, see their Fig. 4. Intermediate

neutralino masses between 220 and 380 GeV are excluded at 95% C.L, regardless of the squark and gluino masses, purely on the basis of the expected weak production.

[7] AAD 13R looked in 4.4 fb^{-1} of pp collisions at $\sqrt{s}$ = 7 TeV for events containing new, heavy particles that decay at a significant distance from their production point into a final state containing a high-momentum muon and charged hadrons. No excess over the expected background is observed and limits are placed on the production cross-section of neutralinos via squarks for various $m_{\widetilde{q}}$, $m_{\widetilde{\chi}^0_1}$ in an R-parity violating scenario with $\lambda'_{211} \neq 0$, as a function of the neutralino lifetime, see their Fig. 6.

[8] AALTONEN 13I searched in 6.3 fb^{-1} of $p\overline{p}$ collisions at $\sqrt{s}$ = 1.96 TeV for events containing $\not\!\!E_T$ and a delayed photon that arrives late in the detector relative to the time expected from prompt production. No evidence of delayed photon production is observed.

[9] CHATRCHYAN 13AH searched in 4.9 fb^{-1} of pp collisions at $\sqrt{s}$ = 7 TeV for events containing $\not\!\!E_T$ and a delayed photon that arrives late in the detector relative to the time expected from prompt production. No significant excess above the expected background was found and limits were set on the pair production of $\widetilde{\chi}^0_1$ depending on the neutralino proper decay length, see Fig. 8. Supersedes CHATRCHYAN 12BK.

[10] AAD 12CP searched in 4.8 fb^{-1} of pp collisions at $\sqrt{s}$ = 7 TeV for events with two photons and large $\not\!\!E_T$ due to $\widetilde{\chi}^0_1 \rightarrow \gamma\widetilde{G}$ decays in a GMSB framework. No significant excess above the expected background was found and limits were set on the neutralino mass in a generalized GMSB model (GGM) with a bino-like neutralino NLSP, see Figs. 6 and 7. The other sparticle masses were decoupled, tanβ = 2 and $c\tau_{NLSP} < 0.1$ mm. Also, in the framework of the SPS8 model, limits are presented in Fig. 8.

[11] AAD 12CT searched in 4.7 fb^{-1} of pp collisions at $\sqrt{s}$ = 7 TeV for events containing four or more leptons (electrons or muons) and either moderate values of missing transverse momentum or large effective mass. No significant excess is found in the data. Limits are presented in a simplified model of R-parity violating supersymmetry in which charginos are pair-produced and then decay into a W-boson and a $\widetilde{\chi}^0_1$, which in turn decays through an RPV coupling into two charged leptons ($e^{\pm}e^{\mp}$ or $\mu^{\pm}\mu^{\mp}$) and a neutrino. In this model, limits are set on the neutralino mass as a function of the chargino mass, see Fig. 3a. Limits are also set in an R-parity violating mSUGRA model, see Fig. 3b.

[12] AAD 12R looked in 33 pb^{-1} of pp collisions at $\sqrt{s}$ = 7 TeV for events containing new, heavy particles that decay at a significant distance from their production point into a final state containing a high-momentum muon and charged hadrons. No excess over the expected background is observed and limits are placed on the production cross-section of neutralinos via squarks for various ($m_{\widetilde{q}}$, $m_{\widetilde{\chi}^0_1}$) in an R-parity violating scenario with $\lambda'_{211} \neq 0$, as a function of the neutralino lifetime, see their Fig. 8. Superseded by AAD 13R.

[13] ABAZOV 12AD looked in 6.2 fb^{-1} of pp collisions at $\sqrt{s}$ = 1.96 TeV for events with a photon, a Z-boson, and large $\not\!\!E_T$ in the final state. This topology corresponds to a GMSB model where pairs of neutralino NLSPs are either pair produced promptly or from decays of other supersymmetric particles and then decay to either $Z\widetilde{G}$ or $\gamma\widetilde{G}$. No significant excess over the SM expectation is observed and a limit at 95% C.L. on the cross section is derived as a function of the effective SUSY breaking scale Λ, see Fig. 3. Assuming N_{mes} = 2, M_{mes} = 3 Λ, tanβ = 3, μ = 0.75 M_1, and C_{grav} = 1, the model is excluded at 95% C.L. for values of $\Lambda < 87$ TeV.

[14] CHATRCHYAN 12BK searched in 2.23 fb^{-1} of pp collisions at $\sqrt{s}$ = 7 TeV for events with two photons and large $\not\!\!E_T$ due to $\widetilde{\chi}^0_1 \rightarrow \gamma\widetilde{G}$ decays in a GMSB framework. No significant excess above the expected background was found and limits were set on the pair production of $\widetilde{\chi}^0_1$ depending on the neutralino lifetime, see Fig. 6.

[15] CHATRCHYAN 11B looked in 35 pb^{-1} of pp collisions at $\sqrt{s}$=7 TeV for events with an isolated lepton (e or μ), a photon and $\not\!\!E_T$ which may arise in a generalized gauge mediated model from the decay of Wino-like NLSPs. No evidence for an excess over the expected background is observed. Limits are derived in the plane of squark/gluino mass versus Wino mass (see Fig. 4). Mass degeneracy of the produced squarks and gluinos is assumed.

[16] AALTONEN 10 searched in 2.6 fb^{-1} of $p\overline{p}$ collisions at $\sqrt{s}$ = 1.96 TeV for diphoton events with large $\not\!\!E_T$. They may originate from the production of $\widetilde{\chi}^{\pm}$ in pairs or associated to a $\widetilde{\chi}^0_2$, decaying into $\widetilde{\chi}^0_1$ which itself decays in GMSB to $\gamma\widetilde{G}$. There is no excess of events beyond expectation. An upper limit on the cross section is calculated in the GMSB model as a function of the $\widetilde{\chi}^0_1$ mass and lifetime, see their Fig. 2. A limit is derived on the $\widetilde{\chi}^0_1$ mass of 149 GeV for $\tau_{\widetilde{\chi}^0_1} \ll 1$ ns, which improves the results of previous searches.

[17] ABAZOV 10P looked in 6.3 fb^{-1} of $p\overline{p}$ collisions at $\sqrt{s}$ = 1.96 TeV for events with at least two isolated γs and large $\not\!\!E_T$. These could be the signature of $\widetilde{\chi}^0_2$ and $\widetilde{\chi}^{\pm}_1$ production, decaying to $\widetilde{\chi}^0_1$ and finally $\widetilde{\chi}^0_1 \rightarrow \gamma\widetilde{G}$ in a GMSB framework. No significant excess over the SM expectation is observed, and a limit at 95% C.L. on the cross section is derived for N_{mes} = 1, tanβ = 15 and $\mu > 0$, see their Fig. 2. This allows them to set a limit on the effective SUSY breaking scale $\Lambda > 124$ TeV, from which the excluded $\widetilde{\chi}^0_1$ mass range is obtained.

[18] ABAZOV 08F looked in 1.1 fb^{-1} of $p\overline{p}$ collisions at $\sqrt{s}$ = 1.96 TeV for diphoton events with large $\not\!\!E_T$. They may originate from the production of $\widetilde{\chi}^{\pm}$ in pairs or associated to a $\widetilde{\chi}^0_2$, decaying to a $\widetilde{\chi}^0_1$ which itself decays promptly in GMSB to $\widetilde{\chi}^0_1 \rightarrow \gamma\widetilde{G}$. No significant excess was found compared to the background expectation. A limit is derived on the masses of SUSY particles in the GMSB framework for $M = 2\Lambda$, N = 1, tanβ = 15 and $\mu > 0$, see Figure 2. It also excludes $\Lambda < 91.5$ TeV. Supersedes the results of ABAZOV 05A. Superseded by ABAZOV 10P.

[19] ABULENCIA 07H searched in 346 pb^{-1} of $p\overline{p}$ collisions at $\sqrt{s}$ = 1.96 TeV for events with at least three leptons (e or μ) from the decay of $\widetilde{\chi}^0_1$ via $LL\overline{E}$ couplings. The results are consistent with the hypothesis of no signal. Upper limits on the cross-section are extracted and a limit is derived in the framework of mSUGRA on the masses of $\widetilde{\chi}^0_1$ and $\widetilde{\chi}^{\pm}_1$, see e.g. their Fig. 3 and Tab. II.

[20] ABBIENDI 06B use 600 pb^{-1} of data from $\sqrt{s}$ = 189–209 GeV. They look for events with diphotons + $\not\!\!E$ final states originating from prompt decays of pair-produced neutralinos in a GMSB scenario with $\widetilde{\chi}^0_1$ NLSP. Limits on the cross-section are computed as a function of m($\widetilde{\chi}^0_1$), see their Fig. 14. The limit on the $\widetilde{\chi}^0_1$ mass is for a pure Bino state assuming a prompt decay, with lifetimes up to 10^{-9}s. Supersedes the results of ABBIENDI 04N.

[21] ABDALLAH 05B use data from $\sqrt{s}$ = 180–209 GeV. They look for events with single photons + $\not\!\!E$ final states. Limits are computed in the plane (m($\widetilde{G}$) , m($\widetilde{\chi}^0_1$)), shown in their Fig. 9b for a pure Bino state in the GMSB framework and in Fig. 9c for a no-scale supergravity model. Supersedes the results of ABREU 00Z.

[22] ABDALLAH 05B use data from $\sqrt{s}$ = 130–209 GeV. They look for events with diphotons + $\not\!\!E$ final states and single photons not pointing to the vertex, expected in GMSB when the $\widetilde{\chi}^0_1$ is the NLSP. Limits are computed in the plane (m($\widetilde{G}$), m($\widetilde{\chi}^0_1$)), see their Fig. 10. The lower limit is derived on the $\widetilde{\chi}^0_1$ mass for a pure Bino state assuming a prompt decay and $m_{\widetilde{e}_R} = m_{\widetilde{e}_L} = 2\ m_{\widetilde{\chi}^0_1}$. It improves to 100 GeV for $m_{\widetilde{e}_R} = m_{\widetilde{e}_L} = 1.1\ m_{\widetilde{\chi}^0_1}$ and the limit in the plane (m($\widetilde{\chi}^0_1$), m($\widetilde{e}_R$)) is shown in Fig. 10b. For long-lived neutralinos, cross-section limits are displayed in their Fig 11. Supersedes the results of ABREU 00Z.

$\widetilde{\chi}^0_2$, $\widetilde{\chi}^0_3$, $\widetilde{\chi}^0_4$ (Neutralinos) mass limits

Neutralinos are unknown mixtures of photinos, z-inos, and neutral higgsinos (the supersymmetric partners of photons and of Z and Higgs bosons). The limits here apply only to $\widetilde{\chi}^0_2$, $\widetilde{\chi}^0_3$, and $\widetilde{\chi}^0_4$. $\widetilde{\chi}^0_1$ is the lightest supersymmetric particle (LSP); see $\widetilde{\chi}^0_1$ Mass Limits. It is not possible to quote rigorous mass limits because they are extremely model dependent; i.e. they depend on branching ratios of various $\widetilde{\chi}^0$ decay modes, on the masses of decay products ($\widetilde{e}$, $\widetilde{\gamma}$, $\widetilde{q}$, $\widetilde{g}$), and on the $\widetilde{e}$ mass exchanged in $e^+e^- \rightarrow \widetilde{\chi}^0_i\widetilde{\chi}^0_j$. Limits arise either from direct searches, or from the MSSM constraints set on the gaugino and higgsino mass parameters M_2 and μ through searches for lighter charginos and neutralinos. Often limits are given as contour plots in the $m_{\widetilde{\chi}^0} - m_{\widetilde{e}}$ plane vs other parameters. When specific assumptions are made, e.g, the neutralino is a pure photino ($\widetilde{\gamma}$), pure z-ino ($\widetilde{Z}$), or pure neutral higgsino ($\widetilde{H}^0$), the neutralinos will be labelled as such.

Limits obtained from e^+e^- collisions at energies up to 136 GeV, as well as other limits from different techniques, are now superseded and have not been included in this compilation. They can be found in the 1998 Edition (The European Physical Journal **C3** 1 (1998)) of this Review. Some later papers are now obsolete and have been omitted. They were last listed in our PDG 14 edition: K. Olive, *et al.* (Particle Data Group), Chinese Physics **C38** 070001 (2014) (http://pdg.lbl.gov).

VALUE (GeV)	CL%	DOCUMENT ID		TECN	COMMENT
none 220–490	95	[1] SIRUNYAN	17AW	CMS	1ℓ+ 2 b-jets + $\not\!\!E_T$, Tchi1n2E, $m_{\widetilde{\chi}^0_1}$ = 0 GeV
>600	95	[2] AAD	16AA	ATLS	3/4ℓ + $\not\!\!E_T$, Tn2n3A, $m_{\widetilde{\chi}^0_1}$=0GeV
>670	95	[2] AAD	16AA	ATLS	3/4ℓ+$\not\!\!E_T$,Tn2n3B,$m_{\widetilde{\chi}^0_1}$ < 200GeV
>250	95	[3] AAD	15BA	ATLS	$m_{\widetilde{\chi}^{\pm}_1} = m_{\widetilde{\chi}^0_2}$, $m_{\widetilde{\chi}^0_1}$ = 0 GeV
>380	95	[4] AAD	14H	ATLS	$\widetilde{\chi}^{\pm}_1\widetilde{\chi}^0_2 \rightarrow \tau^{\pm}\nu\widetilde{\chi}^0_1\tau^{\mp}\tau\widetilde{\chi}^0_1$, simplified model, $m_{\widetilde{\chi}^{\pm}_1} = m_{\widetilde{\chi}^0_2}$, $m_{\widetilde{\chi}^0_1}$ = 0 GeV
>700	95	[4] AAD	14H	ATLS	$\widetilde{\chi}^{\pm}_1\widetilde{\chi}^0_2 \rightarrow \ell^{\pm}\nu\widetilde{\chi}^0_1\ell^{\pm}\ell^{\mp}\widetilde{\chi}^0_1$, simplified model, $m_{\widetilde{\chi}^{\pm}_1} = m_{\widetilde{\chi}^0_2}$, $m_{\widetilde{\chi}^0_1}$ = 0 GeV
>345	95	[4] AAD	14H	ATLS	$\widetilde{\chi}^{\pm}_1\widetilde{\chi}^0_2 \rightarrow W\widetilde{\chi}^0_1 Z\widetilde{\chi}^0_1$, simplified model, $m_{\widetilde{\chi}^{\pm}_1} = m_{\widetilde{\chi}^0_2}$, $m_{\widetilde{\chi}^0_1}$ = 0 GeV
>148	95	[4] AAD	14H	ATLS	$\widetilde{\chi}^{\pm}_1\widetilde{\chi}^0_2 \rightarrow W\widetilde{\chi}^0_1 H\widetilde{\chi}^0_1$, simplified model, $m_{\widetilde{\chi}^{\pm}_1} = m_{\widetilde{\chi}^0_2}$, $m_{\widetilde{\chi}^0_1}$ = 0 GeV
>620	95	[5] AAD	14X	ATLS	$\geq 4\ell^{\pm}$, $\widetilde{\chi}^0_{2,3} \rightarrow \ell^{\pm}\ell^{\mp}\widetilde{\chi}^0_1$, $m_{\widetilde{\chi}^0_1}$ = 0 GeV
		[6] AAD	13	ATLS	$3\ell^{\pm} + \not\!\!E_T$, pMSSM, SMS
		[7] CHATRCHYAN	12BJ	CMS	$\geq 2\ \ell$, jets + $\not\!\!E_T$, $pp \rightarrow \widetilde{\chi}^{\pm}_1\widetilde{\chi}^0_2$
>116.0	95	[8] ABREU	00W	DLPH	$\widetilde{\chi}^0_4$, $1 \leq$ tan$\beta \leq$ 40, all Δm, all m_0
• • • We do not use the following data for averages, fits, limits, etc. • • •					
none 180–355	95	[9] AAD	14G	ATLS	$\widetilde{\chi}^{\pm}_1\widetilde{\chi}^0_2 \rightarrow W\widetilde{\chi}^0_1 Z\widetilde{\chi}^0_1$, simplified model, $m_{\widetilde{\chi}^{\pm}_1} = m_{\widetilde{\chi}^0_2}$, $m_{\widetilde{\chi}^0_1}$ = 0 GeV
		[10] KHACHATRY...14I		CMS	$\widetilde{\chi}^0_2 \rightarrow (Z,\ H)\widetilde{\chi}^0_1\ \widetilde{\ell}\ell$, simplified model
		[11] AAD	12AS	ATLS	$3\ell^{\pm} + \not\!\!E_T$, pMSSM
		[12] AAD	12T	ATLS	$\ell^{\pm}\ell^{\pm} + \not\!\!E_T$, $pp \rightarrow \widetilde{\chi}^{\pm}_1\widetilde{\chi}^0_2$

[1] SIRUNYAN 17AW searched in 35.9 fb^{-1} of pp collisions at $\sqrt{s}$ = 13 TeV for events with a charged lepton (electron or muon), two jets identified as originating from a b-quark, and large $\not\!\!E_T$. No significant excess above the Standard Model expectations is observed. Limits are set on the mass of the chargino and the next-to-lightest neutralino in the Tchi1n2E simplified model, see their Figure 6.

[2] AAD 16AA summarized and extended ATLAS searches for electroweak supersymmetry in final states containing several charged leptons, $\not\!\!E_T$, with or without hadronic jets, in 20 fb^{-1} of pp collisions at $\sqrt{s}$ = 8 TeV. The paper reports the results of new interpretations and statistical combinations of previously published analyses, as well as new analyses. Exclusion limits at 95% C.L. are set on mass-degenerate $\widetilde{\chi}^0_2$ and $\widetilde{\chi}^0_3$ masses in the Tn2n3A and Tn2n3B simplified models. See their Fig. 15.

[3] AAD 15BA searched in 20.3 fb^{-1} of pp collisions at $\sqrt{s}$ = 8 TeV for electroweak production of charginos and neutralinos decaying to a final state containing a W boson and a 125 GeV Higgs boson, plus missing transverse momentum. No excess beyond the Standard Model expectation is observed. Exclusion limits are derived in simplified models of direct chargino and next-to-lightest neutralino production, with the decays

$\tilde{\chi}_1^\pm \to W^\pm \tilde{\chi}_1^0$ and $\tilde{\chi}_2^0 \to H\tilde{\chi}_1^0$ having 100% branching fraction, see Fig. 8. A combination of the multiple final states for the Higgs decay yields the best limits (Fig. 8d).

[4] AAD 14H searched in 20.3 fb^{-1} of pp collisions at $\sqrt{s} = 8$ TeV for electroweak production of charginos and neutralinos decaying to a final sate with three leptons and missing transverse momentum. No excess beyond the Standard Model expectation is observed. Exclusion limits are derived in simplified models of direct chargino and next-to-lightest neutralino production, with decays to the lightest neutralino via either all three generations of leptons, staus only, gauge bosons, or Higgs bosons, see Fig. 7. An interpretation in the pMSSM is also given, see Fig. 8.

[5] AAD 14X searched in 20.3 fb^{-1} of pp collisions at $\sqrt{s} = 8$ TeV for events with at least four leptons (electrons, muons, taus) in the final state. No significant excess above the Standard Model expectations is observed. Limits are set on the neutralino mass in an R-parity conserving simplified model where the decay $\tilde{\chi}_{2,3}^0 \to \ell^\pm \ell^\mp \tilde{\chi}_1^0$ takes place with a branching ratio of 100%, see Fig. 10.

[6] AAD 13 searched in 4.7 fb^{-1} of pp collisions at $\sqrt{s} = 7$ TeV for charginos and neutralinos decaying to a final state with three leptons (e and μ) and missing transverse energy. No excess beyond the Standard Model expectation is observed. Exclusion limits are derived in the phenomenological MSSM, see Fig. 2 and 3, and in simplified models, see Fig. 4. For the simplified models with intermediate slepton decays, degenerate $\tilde{\chi}_1^\pm$ and $\tilde{\chi}_2^0$ masses up to 500 GeV are excluded at 95% C.L. for very large mass differences with the $\tilde{\chi}_1^0$. Supersedes AAD 12AS.

[7] CHATRCHYAN 12BJ searched in 4.98 fb^{-1} of pp collisions at $\sqrt{s} = 7$ TeV for direct electroweak production of charginos and neutralinos in events with at least two leptons, jets and missing transverse momentum. No significant excesses over the expected SM backgrounds are observed and 95% C.L. limits on the production cross section of $\tilde{\chi}_1^\pm \tilde{\chi}_2^0$ pair production were set in a number of simplified models, see Figs. 7 to 12. Most limits are for exactly 3 jets.

[8] ABREU 00W combines data collected at $\sqrt{s}$=189 GeV with results from lower energies. The mass limit is obtained by constraining the MSSM parameter space with gaugino and sfermion mass universality at the GUT scale, using the results of negative direct searches for neutralinos (including cascade decays and $\tilde{\tau}\tilde{\tau}$ final states) from ABREU 01, for charginos from ABREU 00J and ABREU 00T (for all Δm_+), and for charged sleptons from ABREU 01B. The results hold for the full parameter space defined by all values of M_2 and $|\mu| \leq 2$ TeV with the $\tilde{\chi}_1^0$ as LSP.

[9] AAD 14G searched in 20.3 fb^{-1} of pp collisions at $\sqrt{s} = 8$ TeV for electroweak production of chargino-neutralino pairs, decaying to a final sate with two leptons (e and μ) and missing transverse momentum. No excess beyond the Standard Model expectation is observed. Exclusion limits are derived in simplified models of chargino and next-to-lightest neutralino production, with decays to the lightest neutralino via gauge bosons, see Fig. 7. An interpretation in the pMSSM is also given, see Fig. 10.

[10] KHACHATRYAN 14I searched in 19.5 fb^{-1} of pp collisions at $\sqrt{s} = 8$ TeV for electroweak production of charginos and neutralinos decaying to a final state with three leptons (e or μ) and missing transverse momentum, or with a Z-boson, dijets and missing transverse momentum. No excess beyond the Standard Model expectation is observed. Exclusion limits are derived in simplified models, see Figs. 12–16.

[11] AAD 12AS searched in 2.06 fb^{-1} of pp collisions at $\sqrt{s} = 7$ TeV for charginos and neutralinos decaying to a final state with three leptons (e and μ) and missing transverse energy. No excess beyond the Standard Model expectation is observed. Exclusion limits are derived in the phenomenological MSSM, see Fig. 2 (top), and in simplified models, see Fig. 2 (bottom).

[12] AAD 12T looked in 1 fb^{-1} of pp collisions at $\sqrt{s} = 7$ TeV for the production of supersymmetric particles decaying into final states with missing transverse momentum and exactly two isolated leptons (e or μ). Same-sign dilepton events were separately studied. Additionally, in opposite-sign events, a search was made for an excess of same-flavor over different-flavor lepton pairs. No excess over the expected background is observed and limits are placed on the effective production cross section of opposite-sign dilepton events with $\not{E}_T > 250$ GeV and on same-sign dilepton events with $\not{E}_T > 100$ GeV. The latter limit is interpreted in a simplified electroweak gaugino production model.

$\tilde{\chi}_1^\pm$, $\tilde{\chi}_2^\pm$ (Charginos) mass limits

Charginos are unknown mixtures of w-inos and charged higgsinos (the supersymmetric partners of W and Higgs bosons). A lower mass limit for the lightest chargino ($\tilde{\chi}_1^\pm$) of approximately 45 GeV, independent of the field composition and of the decay mode, has been obtained by the LEP experiments from the analysis of the Z width and decays. These results, as well as other now superseded limits from e^+e^- collisions at energies below 136 GeV, and from hadronic collisions, can be found in the 1998 Edition (The European Physical Journal **C3** 1 (1998)) of this Review.

Unless otherwise stated, results in this section assume spectra, production rates, decay modes and branching ratios as evaluated in the MSSM, with gaugino and sfermion mass unification at the GUT scale. These papers generally study production of $\tilde{\chi}_1^0 \tilde{\chi}_2^0$, $\tilde{\chi}_1^+ \tilde{\chi}_1^-$ and (in the case of hadronic collisions) $\tilde{\chi}_1^+ \tilde{\chi}_2^0$ pairs, including the effects of cascade decays. The mass limits on $\tilde{\chi}_1^\pm$ are either direct, or follow indirectly from the constraints set by the non-observation of $\tilde{\chi}_2^0$ states on the gaugino and higgsino MSSM parameters M_2 and μ. For generic values of the MSSM parameters, limits from high-energy e^+e^- collisions coincide with the highest value of the mass allowed by phase-space, namely $m_{\tilde{\chi}_1^\pm} \lesssim \sqrt{s}/2$. The still unpublished combination of the results of the four LEP collaborations from the 2000 run of LEP2 at $\sqrt{s}$ up to $\simeq 209$ GeV yields a lower mass limit of 103.5 GeV valid for general MSSM models. The limits become however weaker in certain regions of the MSSM parameter space where the detection efficiencies or production cross sections are suppressed. For example, this may happen when: (i) the mass differences $\Delta m_+ = m_{\tilde{\chi}_1^\pm} - m_{\tilde{\chi}_1^0}$ or $\Delta m_\nu = m_{\tilde{\chi}_1^\pm} - m_{\tilde{\nu}}$ are very small, and the detection efficiency is reduced; (ii) the electron sneutrino mass is small, and the $\tilde{\chi}_1^\pm$ production rate is suppressed due to a destructive interference between s and t channel exchange diagrams. The regions of MSSM parameter space where the following limits are valid are indicated in the comment lines or in the footnotes.

Some earlier papers are now obsolete and have been omitted. They were last listed in our PDG 14 edition: K. Olive, *et al.* (Particle Data Group), Chinese Physics **C38** 070001 (2014) (http://pdg.lbl.gov).

VALUE (GeV)	CL%	DOCUMENT ID		TECN	COMMENT
> 420	95	[1] KHACHATRY...17L		CMS	2 τ+$\not{E}_T$, Tchi1chi1C and $\tilde{\tau}$-only, $m_{\tilde{\chi}_1^0}$=0 GeV
none 220–490	95	[2] SIRUNYAN	17AW		1ℓ + 2b-jets + $\not{E}_T$, Tchi1n2E, $m_{\tilde{\chi}_1^0} = 0$ GeV
> 500	95	[3] AAD	16AA	ATLS	2$\ell^\pm$+$\not{E}_T$,Tchi1chi1B,$m_{\tilde{\chi}_1^0}$=0 GeV
> 220	95	[3] AAD	16AA	ATLS	2$\ell^\pm$+$\not{E}_T$, Tchi1chi1C, low Δm for $\tilde{\chi}_1^\pm$, $\tilde{\chi}_1^0$
> 700	95	[4] AAD	16AA	ATLS	3/4ℓ+$\not{E}_T$,Tchi1n2B, $m_{\tilde{\chi}_1^0}$=0 GeV
> 700	95	[4] AAD	16AA	ATLS	3/4ℓ+$\not{E}_T$, Tchi1n2C, $m_{\tilde{\ell}} = m_{\tilde{\chi}_1^0}$ + 0.5 (or 0.95) ($m_{\tilde{\chi}_1^\pm} - m_{\tilde{\chi}_1^0}$)
> 400	95	[4] AAD	16AA	ATLS	2 hadronic τ+$\not{E}_T$ & 3ℓ+$\not{E}_T$ combination,Tchi1n2D,$m_{\tilde{\chi}_1^0}$=0 GeV
> 540	95	[5] KHACHATRY...16R		CMS	$\geq 1\gamma + 1$ e or μ + $\not{E}_T$, Tchi1n1A
> 250	95	[6] AAD	15BA	ATLS	$m_{\tilde{\chi}_1^\pm} = m_{\tilde{\chi}_2^0}$, $m_{\tilde{\chi}_1^0} = 0$ GeV
> 590	95	[7] AAD	15CA	ATLS	$\geq 2\ \gamma + \not{E}_T$, GGM, bino-like NLSP, any NLSP mass
none 124–361	95	[7] AAD	15CA	ATLS	$\geq 1\ \gamma + e,\mu + \not{E}_T$, GGM, wino-like NLSP
> 700	95	[8] AAD	14H	ATLS	$\tilde{\chi}_1^\pm \tilde{\chi}_2^0 \to \ell^\pm \nu \tilde{\chi}_1^0 \ell^\pm \ell^\mp \tilde{\chi}_1^0$, simplified model, $m_{\tilde{\chi}_1^\pm} = m_{\tilde{\chi}_2^0}$, $m_{\tilde{\chi}_1^0} = 0$ GeV
> 345	95	[8] AAD	14H	ATLS	$\tilde{\chi}_1^\pm \tilde{\chi}_2^0 \to W\tilde{\chi}_1^0 Z\tilde{\chi}_1^0$, simplified model, $m_{\tilde{\chi}_1^\pm} = m_{\tilde{\chi}_2^0}$, $m_{\tilde{\chi}_1^0} = 0$ GeV
> 148	95	[8] AAD	14H	ATLS	$\tilde{\chi}_1^\pm \tilde{\chi}_2^0 \to W\tilde{\chi}_1^0 H\tilde{\chi}_1^0$, simplified model, $m_{\tilde{\chi}_1^\pm} = m_{\tilde{\chi}_2^0}$, $m_{\tilde{\chi}_1^0} = 0$ GeV
> 380	95	[8] AAD	14H	ATLS	$\tilde{\chi}_1^\pm \tilde{\chi}_2^0 \to \tau^\pm \nu \tilde{\chi}_1^0 \tau^\pm \tau^\mp \tilde{\chi}_1^0$, simplified model, $m_{\tilde{\chi}_1^\pm} = m_{\tilde{\chi}_2^0}$, $m_{\tilde{\chi}_1^0} = 0$ GeV
> 750	95	[9] AAD	14X	ATLS	RPV, $\geq 4\ell^\pm$, $\tilde{\chi}_1^\pm \to W^{(*)\pm}\tilde{\chi}_1^0$, $\tilde{\chi}_1^0 \to \ell^\pm \ell^\mp \nu$
> 210	95	[10] KHACHATRY...14L		CMS	$\tilde{\chi}_2^0 \to H\tilde{\chi}_1^0$ and $\tilde{\chi}_1^\pm \to W^\pm \tilde{\chi}_1^0$ simplified models, $m_{\tilde{\chi}_2^0} = m_{\tilde{\chi}_1^\pm}$, $m_{\tilde{\chi}_1^0} = 0$ GeV
		[11] AAD	13	ATLS	3$\ell^\pm$ + $\not{E}_T$, pMSSM, SMS
		[12] AAD	13B	ATLS	2$\ell^\pm$ + $\not{E}_T$, pMSSM, SMS
> 540	95	[13] AAD	12CT	ATLS	$\geq 4\ell^\pm$, RPV, $m_{\tilde{\chi}_1^0} > 300$ GeV
		[14] CHATRCHYAN	12BJ	CMS	$\geq 2\ \ell$, jets + $\not{E}_T$, $pp \to \tilde{\chi}_1^\pm \tilde{\chi}_2^0$
> 94	95	[15] ABDALLAH	03M	DLPH	$\tilde{\chi}_1^\pm$, $\tan\beta \leq 40$, $\Delta m_+ > 3$ GeV,all m_0
• • • We do not use the following data for averages, fits, limits, etc. • • •					
> 570	95	[16] KHACHATRY...16AA		CMS	$\geq 1\gamma$ + jets + $\not{E}_T$, Tchi1chi1A
> 680	95	[16] KHACHATRY...16AA		CMS	$\geq 1\gamma$ + jets + $\not{E}_T$, Tchi1n1A
> 710	95	[16] KHACHATRY...16AA		CMS	$\geq 1\gamma$ + jets + $\not{E}_T$, GGM, $\tilde{\chi}_2^0 \tilde{\chi}_1^\pm$ pair production, wino-like NLSP
>1000	95	[17] KHACHATRY...16R		CMS	$\geq 1\gamma + 1$ e or μ + $\not{E}_T$, Tglu1F, $m_{\tilde{\chi}_1^\pm} = m_{\tilde{\chi}_2^0} > 200$ GeV
> 307	95	[18] KHACHATRY...16Y		CMS	1 or 2 soft $\ell^\pm$+jets+$\not{E}_T$, Tchi1n2A, $m_{\tilde{\chi}_1^\pm} - m_{\tilde{\chi}_1^0}$=20 GeV
> 410	95	[19] AAD	14AV	ATLS	$\geq 2\ \tau + \not{E}_T$, direct $\tilde{\chi}_1^\pm \tilde{\chi}_2^0$, $\tilde{\chi}_1^\pm \tilde{\chi}_1^\mp$ production, $m_{\tilde{\chi}_2^0} = m_{\tilde{\chi}_1^\pm}$, $m_{\tilde{\chi}_1^0} = 0$ GeV
> 345	95	[20] AAD	14AV	ATLS	$\geq 2\ \tau + \not{E}_T$, direct $\tilde{\chi}_1^\pm \tilde{\chi}_1^\mp$ production, $m_{\tilde{\chi}_1^0} = 0$ GeV
none 100–105, 120–135, 145–160	95	[21] AAD	14G	ATLS	$\tilde{\chi}_1^\pm \tilde{\chi}_1^\mp \to W^+ \tilde{\chi}_1^0 W^- \tilde{\chi}_1^0$, simplified model, $m_{\tilde{\chi}_1^0} = 0$ GeV
none 140–465	95	[21] AAD	14G	ATLS	$\tilde{\chi}_1^\pm \tilde{\chi}_1^\mp \to \ell^+ \nu \tilde{\chi}_1^0 \ell^- \overline{\nu} \tilde{\chi}_1^0$, simplified model, $m_{\tilde{\chi}_1^0} = 0$ GeV
none 180–355	95	[21] AAD	14G	ATLS	$\tilde{\chi}_1^\pm \tilde{\chi}_2^0 \to W\tilde{\chi}_1^0 Z\tilde{\chi}_1^0$, simplified model, $m_{\tilde{\chi}_1^\pm} = m_{\tilde{\chi}_2^0}$, $m_{\tilde{\chi}_1^0} = 0$ GeV
> 168	95	[22] AALTONEN	14	CDF	3$\ell^\pm$+ $\not{E}_T$, $\tilde{\chi}_1^\pm \to \ell\nu\tilde{\chi}_1^0$, mSUGRA with m_0=60 GeV
		[23] KHACHATRY...14I		CMS	$\tilde{\chi}_1^\pm \to W\tilde{\chi}_1^0$, $\ell\tilde{\nu}$, $\tilde{\ell}\nu$, simplified model

		[24] AALTONEN	13Q	CDF	$\tilde{\chi}_1^\pm \to \tau X$, simplified gravity- and gauge-mediated models
		[25] AAD	12AS	ATLS	$3\ell^\pm + \not{E}_T$, pMSSM
		[26] AAD	12T	ATLS	$\ell^\pm\ell^\mp + \not{E}_T$, $\ell^\pm\ell^\pm + \not{E}_T$, $pp \to \tilde{\chi}_1^\pm \tilde{\chi}_2^0$
		[27] CHATRCHYAN	11B	CMS	$\widetilde{W}^0 \to \gamma\widetilde{G}$,$\widetilde{W}^\pm \to \ell^\pm\widetilde{G}$,GMSB
> 163	95	[28] CHATRCHYAN	11V	CMS	$\tan\beta$=3, m_0=60 GeV, A_0=0, μ >0

[1] KHACHATRYAN 17L searched in about 19 fb^{-1} of pp collisions at $\sqrt{s}$ = 8 TeV for events with two τ (at least one decaying hadronically) and $\not{E}_T$. In the Tchi1chi1C model, assuming decays via intermediate $\tilde{\tau}$ or $\tilde{\nu}_\tau$ with equivalent mass, the observed limits rule out $\tilde{\chi}_1^\pm$ masses up to 420 GeV for a massless $\tilde{\chi}_1^0$. See their Fig.5.

[2] SIRUNYAN 17AW searched in 35.9 fb^{-1} of pp collisions at $\sqrt{s}$ = 13 TeV for events with a charged lepton (electron or muon), two jets identified as originating from a b-quark, and large $\not{E}_T$. No significant excess above the Standard Model expectations is observed. Limits are set on the mass of the chargino and the next-to-lightest neutralino in the Tchi1n2E simplified model, see their Figure 6.

[3] AAD 16AA summarized and extended ATLAS searches for electroweak supersymmetry in final states containing several charged leptons, $\not{E}_T$, with or without hadronic jets, in 20 fb^{-1} of pp collisions at $\sqrt{s}$ = 8 TeV. The paper reports the results of new interpretations and statistical combinations of previously published analyses, as well as new analyses. Exclusion limits at 95% C.L. are set on the $\tilde{\chi}_1^\pm$ mass in the Tchi1chi1B and Tchi1chi1C simplified models. See their Fig. 13.

[4] AAD 16AA summarized and extended ATLAS searches for electroweak supersymmetry in final states containing several charged leptons, $\not{E}_T$, with or without hadronic jets, in 20 fb^{-1} of pp collisions at $\sqrt{s}$ = 8 TeV. The paper reports the results of new interpretations and statistical combinations of previously published analyses, as well as new analyses. Exclusion limits at 95% C.L. are set on mass-degenerate $\tilde{\chi}_1^\pm$ and $\tilde{\chi}_2^0$ masses in the Tchi1n2B, Tchi1n2C, and Tchi1n2D simplified models. See their Figs. 16, 17, and 18. Interpretations in phenomenological-MSSM, two-parameter Non Universal Higgs Masses (NUHM2), and gauge-mediated symmetry breaking (GMSB) models are also given in their Figs. 20, 21 and 22.

[5] KHACHATRYAN 16R searched in 19.7 fb^{-1} of pp collisions at $\sqrt{s}$ = 8 TeV for events with one or more photons, one electron or muon, and $\not{E}_T$. No significant excess above the Standard Model expectations is observed. Limits are set on wino masses in a general gauge-mediated SUSY breaking model (GGM), for a wino-like neutralino NLSP scenario, see Fig. 5. Limits are also set in the Tglu1D and Tchi1n1A simplified models, see Fig. 6. The Tchi1n1A limit is reduced to 340 GeV for a branching ratio reduced by the weak mixing angle.

[6] AAD 15BA searched in 20.3 fb^{-1} of pp collisions at $\sqrt{s}$ = 8 TeV for electroweak production of charginos and neutralinos decaying to a final state containing a W boson and a 125 GeV Higgs boson, plus missing transverse momentum. No excess beyond the Standard Model expectation is observed. Exclusion limits are derived in simplified models of direct chargino and next-to-lightest neutralino production, with the decays $\tilde{\chi}_1^\pm \to W^\pm\tilde{\chi}_1^0$ and $\tilde{\chi}_2^0 \to H\tilde{\chi}_1^0$ having 100% branching fraction, see Fig. 8. A combination of the multiple final states for the Higgs decay yields the best limits (Fig. 8d).

[7] AAD 15CA searched in 20.3 fb^{-1} of pp collisions at $\sqrt{s}$ = 8 TeV for events with one or more photons and $\not{E}_T$, with or without leptons (e, μ). No significant excess above the Standard Model expectations is observed. Limits are set on wino masses in the general gauge-mediated SUSY breaking model (GGM), for wino-like NLSP, see Fig. 9, 12

[8] AAD 14H searched in 20.3 fb^{-1} of pp collisions at $\sqrt{s}$ = 8 TeV for electroweak production of charginos and neutralinos decaying to a final sate with three leptons and missing transverse momentum. No excess beyond the Standard Model expectation is observed. Exclusion limits are derived in simplified models of direct chargino and next-to-lightest neutralino production, with decays to the lightest neutralino via either all three generations of leptons, staus only, gauge bosons, or Higgs bosons, see Fig. 7. An interpretation in the pMSSM is also given, see Fig. 8.

[9] AAD 14X searched in 20.3 fb^{-1} of pp collisions at $\sqrt{s}$ = 8 TeV for events with at least four leptons (electrons, muons, taus) in the final state. No significant excess above the Standard Model expectations is observed. Limits are set on the wino-like chargino mass in an R-parity violating simplified model where the decay $\tilde{\chi}_1^\pm \to W^{(*)}\pm\tilde{\chi}_1^0$, with $\tilde{\chi}_1^0 \to \ell^\pm\ell^\mp\nu$, takes place with a branching ratio of 100%, see Fig. 8.

[10] KHACHATRYAN 14L searched in 19.5 fb^{-1} of pp collisions at $\sqrt{s}$ = 8 TeV for evidence of chargino-neutralino $\tilde{\chi}_1^\pm\tilde{\chi}_2^0$ pair production with Higgs or W-bosons in the decay chain, leading to HW final states with missing transverse energy. The decays of a Higgs boson to a photon pair are considered in conjunction with hadronic and leptonic decay modes of the W bosons. No significant excesses over the expected SM backgrounds are observed. The results are interpreted in the context of simplified models where the decays $\tilde{\chi}_2^0 \to H\tilde{\chi}_1^0$ and $\tilde{\chi}_1^\pm \to W^\pm\tilde{\chi}_1^0$ take place 100% of the time, see Figs. 22–23.

[11] AAD 13 searched in 4.7 fb^{-1} of pp collisions at $\sqrt{s}$ = 7 TeV for charginos and neutralinos decaying to a final state with three leptons (e and μ) and missing transverse energy. No excess beyond the Standard Model expectation is observed. Exclusion limits are derived in the phenomenological MSSM, see Fig. 2 and 3, and in simplified models, see Fig. 4. For the simplified models with intermediate slepton decays, degenerate $\tilde{\chi}_1^\pm$ and $\tilde{\chi}_2^0$ masses up to 500 GeV are excluded at 95% C.L. for very large mass differences with the $\tilde{\chi}_1^0$. Supersedes AAD 12AS.

[12] AAD 13B searched in 4.7 fb^{-1} of pp collisions at $\sqrt{s}$ = 7 TeV for gauginos decaying to a final state with two leptons (e and μ) and missing transverse energy. No excess beyond the Standard Model expectation is observed. Limits are derived in a simplified model of wino-like chargino pair production, where the chargino always decays to the lightest neutralino via an intermediate on-shell charged slepton, see Fig. 2(b). Chargino masses between 110 and 340 GeV are excluded at 95% C.L. for $m_{\tilde{\chi}_1^0}$ = 10 GeV. Exclusion limits are also derived in the phenomenological MSSM, see Fig. 3.

[13] AAD 12CT searched in 4.7 fb^{-1} of pp collisions at $\sqrt{s}$ = 7 TeV for events containing four or more leptons (electrons or muons) and either moderate values of missing transverse momentum or large effective mass. No significant excess is found in the data. Limits are presented in a simplified model of R-parity violating supersymmetry in which charginos are pair-produced and then decay into a W-boson and a $\tilde{\chi}_1^0$, which in turn decays through an RPV coupling into two charged leptons ($e^\pm e^\mp$ or $e^\pm\mu^\mp$) and a neutrino. In this model, chargino masses up to 540 GeV are excluded at 95% C.L. for $m_{\tilde{\chi}_1^0}$ above 300 GeV, see Fig. 3a. The limit deteriorates for lighter $\tilde{\chi}_1^0$. Limits are also set in an R-parity violating mSUGRA model, see Fig. 3b.

[14] CHATRCHYAN 12BJ searched in 4.98 fb^{-1} of pp collisions at $\sqrt{s}$ = 7 TeV for direct electroweak production of charginos and neutralinos in events with at least two leptons, jets and missing transverse momentum. No significant excesses over the expected SM backgrounds are observed and 95% C.L. limits on the production cross section of $\tilde{\chi}_1^\pm\tilde{\chi}_2^0$ pair production were set in a number of simplified models, see Figs. 7 to 12.

[15] ABDALLAH 03M uses data from $\sqrt{s}$ = 192–208 GeV to obtain limits in the framework of the MSSM with gaugino and sfermion mass universality at the GUT scale. An indirect limit on the mass of charginos is derived by constraining the MSSM parameter space by the results from direct searches for neutralinos (including cascade decays), for charginos and for sleptons. These limits are valid for values of $M_2 < 1$ TeV, $|\mu| \leq 2$ TeV with the $\tilde{\chi}_1^0$ as LSP. Constraints from the Higgs search in the $m_h^{\max}$ scenario assuming m_t= 174.3 GeV are included. The quoted limit applies if there is no mixing in the third family or when $m_{\tilde{\tau}_1} - m_{\tilde{\chi}_1^0} > 6$ GeV. If mixing is included the limit degrades to 90 GeV. See Fig. 43 for the mass limits as a function of $\tan\beta$. These limits update the results of ABREU 00W.

[16] KHACHATRYAN 16AA searched in 7.4 fb^{-1} of pp collisions at $\sqrt{s}$ = 8 TeV for events with one or more photons, hadronic jets and $\not{E}_T$. No significant excess above the Standard Model expectations is observed. Limits are set on wino masses in the general gauge-mediated SUSY breaking model (GGM), for a wino-like neutralino NLSP scenario and with the wino mass fixed at 10 GeV above the bino mass, see Fig. 4. Limits are also set in the Tchi1chi1A and Tchi1n1A simplified models, see Fig. 3.

[17] KHACHATRYAN 16R searched in 19.7 fb^{-1} of pp collisions at $\sqrt{s}$ = 8 TeV for events with one or more photons, one electron or muon, and $\not{E}_T$. No significant excess above the Standard Model expectations is observed. Limits are also set in the Tglu1F simplified model, see Fig. 6.

[18] KHACHATRYAN 16Y searched in 19.7 fb^{-1} of pp collisions at $\sqrt{s}$ = 8 TeV for events with one or two soft isolated leptons, hadronic jets, and $\not{E}_T$. No significant excess above the Standard Model expectations is observed. Limits are set on the $\tilde{\chi}_1^\pm$ mass (which is degenerate with the $\tilde{\chi}_2^0$) in the Tchi1n2A simplified model, see Fig. 4.

[19] AAD 14AV searched in 20.3 fb^{-1} of pp collisions at $\sqrt{s}$ = 8 TeV for the direct production of charginos, neutralinos and staus in events containing at last two hadronically decaying τ-leptons, large missing transverse momentum and low jet activity. The quoted limit was derived for direct $\tilde{\chi}_1^\pm\tilde{\chi}_2^0$ and $\tilde{\chi}_1^\pm\tilde{\chi}_1^\mp$ production with $\tilde{\chi}_2^0 \to \tilde{\tau}\tau \to \tau\tau\tilde{\chi}_1^0$ and $\tilde{\chi}_1^\pm \to \tilde{\tau}\nu(\tilde{\nu}_\tau\tau) \to \tau\nu\tilde{\chi}_1^0$, $m_{\tilde{\chi}_2^0} = m_{\tilde{\chi}_1^\pm}$, $m_{\tilde{\tau}} = 0.5\,(m_{\tilde{\chi}_1^\pm} + m_{\tilde{\chi}_1^0})$, $m_{\tilde{\chi}_1^0} = 0$ GeV. No excess over the expected SM background is observed. Exclusion limits are set in simplified models of $\tilde{\chi}_1^\pm\tilde{\chi}_1^\mp$ and $\tilde{\chi}_1^\pm\tilde{\chi}_2^0$ pair production, see their Figure 7. Upper limits on the cross section and signal strength for direct di-stau production are derived, see Figures 8 and 9. Also, limits are derived in a pMSSM model where the only light slepton is the $\tilde{\tau}_R$, see Figure 10.

[20] AAD 14AV searched in 20.3 fb^{-1} of pp collisions at $\sqrt{s}$ = 8 TeV for the direct production of charginos, neutralinos and staus in events containing at last two hadronically decaying τ-leptons, large missing transverse momentum and low jet activity. The quoted limit was derived for direct $\tilde{\chi}_1^\pm\tilde{\chi}_1^\mp$ production with $\tilde{\chi}_1^\pm \to \tilde{\tau}\nu(\tilde{\nu}_\tau\tau) \to \tau\nu\tilde{\chi}_1^0$, $m_{\tilde{\tau}} = 0.5\,(m_{\tilde{\chi}_1^\pm} + m_{\tilde{\chi}_1^0})$, $m_{\tilde{\chi}_1^0} = 0$ GeV. No excess over the expected SM background is observed.

Exclusion limits are set in simplified models of $\tilde{\chi}_1^\pm\tilde{\chi}_1^\mp$ and $\tilde{\chi}_1^\pm\tilde{\chi}_2^0$ pair production, see their Figure 7. Upper limits on the cross section and signal strength for direct di-stau production are derived, see Figures 8 and 9. Also, limits are derived in a pMSSM model where the only light slepton is the $\tilde{\tau}_R$, see Figure 10.

[21] AAD 14G searched in 20.3 fb^{-1} of pp collisions at $\sqrt{s}$ = 8 TeV for electroweak production of chargino pairs, or chargino-neutralino pairs, decaying to a final sate with two leptons (e and μ) and missing transverse momentum. No excess beyond the Standard Model expectation is observed. Exclusion limits are derived in simplified models of chargino pair production, with chargino decays to the lightest neutralino via either sleptons or gauge bosons, see Fig 5.; or in simplified models of chargino and next-to-lightest neutralino production, with decays to the lightest neutralino via gauge bosons, see Fig. 7. An interpretation in the pMSSM is also given, see Fig. 10.

[22] AALTONEN 14 searched in 5.8 fb^{-1} of $p\overline{p}$ collisions at $\sqrt{s}$ = 1.96 TeV for evidence of chargino and next-to-lightest neutralino associated production in final states consisting of three leptons (electrons, muons or taus) and large missing transverse momentum. The results are consistent with the Standard Model predictions within 1.85 σ. Limits on the chargino mass are derived in an mSUGRA model with m_0 = 60 GeV, $\tan\beta$ = 3, A_0 = 0 and μ >0, see their Fig. 2.

[23] KHACHATRYAN 14I searched in 19.5 fb^{-1} of pp collisions at $\sqrt{s}$ = 8 TeV for electroweak production of chargino pairs decaying to a final state with opposite-sign lepton pairs (e or μ) and missing transverse momentum. No excess beyond the Standard Model expectation is observed. Exclusion limits are derived in simplified models, see Fig. 18.

[24] AALTONEN 13Q searched in 6.0 fb^{-1} of $p\overline{p}$ collisions at $\sqrt{s}$ = 1.96 TeV for evidence of chargino-neutralino associated production in like-sign dilepton final states. One lepton is identified as the hadronic decay of a tau lepton, while the other is an electron or muon. Good agreement with the Standard Model predictions is observed and limits are set on the chargino-neutralino cross section for simplified gravity- and gauge-mediated models, see their Figs. 2 and 3.

[25] AAD 12AS searched in 2.06 fb^{-1} of pp collisions at $\sqrt{s}$ = 7 TeV for charginos and neutralinos decaying to a final state with three leptons (e and μ) and missing transverse energy. No excess beyond the Standard Model expectation is observed. Exclusion limits are derived in the phenomenological MSSM, see Fig. 2 (top), and in simplified models, see Fig. 2 (bottom).

[26] AAD 12T looked in 1 fb^{-1} of pp collisions at $\sqrt{s}$ = 7 TeV for the production of supersymmetric particles decaying into final states with missing transverse momentum and exactly two isolated leptons (e or μ). Opposite-sign and same-sign dilepton events were separately studied. Additionally, in opposite-sign events, a search was made for an excess of same-flavor over different-flavor lepton pairs. No excess over the expected background is observed and limits are placed on the effective production cross section of opposite-sign dilepton events with $\not{E}_T$ > 250 GeV and on same-sign dilepton events with $\not{E}_T$ > 100 GeV. The latter limit is interpreted in a simplified electroweak gaugino production model as a lower chargino mass limit.

[27] CHATRCHYAN 11B looked in 35 pb^{-1} of pp collisions at $\sqrt{s}$=7 TeV for events with an isolated lepton (e or μ), a photon and $\not{E}_T$ which may arise in a generalized gauge

mediated model from the decay of Wino-like NLSPs. No evidence for an excess over the expected background is observed. Limits are derived in the plane of squark/gluino mass versus Wino mass (see Fig. 4). Mass degeneracy of the produced squarks and gluinos is assumed.

[28] CHATRCHYAN 11V looked in 35 pb^{-1} of pp collisions at $\sqrt{s} = 7$ TeV for events with ≥ 3 isolated leptons (e, μ or τ), with or without jets and $\not{E}_T$. No evidence for an excess over the expected background is observed. Limits are derived in the CMSSM (m_0, $m_{1/2}$) plane for $\tan\beta = 3$ (see Fig. 5).

Long-lived $\widetilde{\chi}^{\pm}$ (Chargino) mass limit

Limits on charginos which leave the detector before decaying.

VALUE (GeV)	CL%	DOCUMENT ID		TECN	COMMENT
>620	95	[1] AAD	15AE	ATLS	stable $\widetilde{\chi}^{\pm}$
>534	95	[2] AAD	15BM	ATLS	stable $\widetilde{\chi}^{\pm}$
>239	95	[2] AAD	15BM	ATLS	$\widetilde{\chi}^{\pm} \to \widetilde{\chi}^0_1 \pi^{\pm}$, lifetime 1 ns, $m_{\widetilde{\chi}^{\pm}} - m_{\widetilde{\chi}^0_1} = 0.14$ GeV
>482	95	[2] AAD	15BM	ATLS	$\widetilde{\chi}^{\pm} \to \widetilde{\chi}^0_1 \pi^{\pm}$, lifetime 15 ns, $m_{\widetilde{\chi}^{\pm}} - m_{\widetilde{\chi}^0_1} = 0.14$ GeV
>103	95	[3] AAD	13H	ATLS	long-lived $\widetilde{\chi}^{\pm} \to \widetilde{\chi}^0_1 \pi^{\pm}$, mAMSB, $\Delta m_{\widetilde{\chi}^0_1} = 160$ MeV
> 92	95	[4] AAD	12BJ	ATLS	long-lived $\widetilde{\chi}^{\pm} \to \pi^{\pm} \widetilde{\chi}^0_1$, mAMSB
>171	95	[5] ABAZOV	09M	D0	$\widetilde{H}$
>102	95	[6] ABBIENDI	03L	OPAL	$m_{\widetilde{\nu}}$ >500 GeV
none 2–93.0	95	[7] ABREU	00T	DLPH	$\widetilde{H}^{\pm}$ or $m_{\widetilde{\nu}} > m_{\widetilde{\chi}^{\pm}}$
• • • We do not use the following data for averages, fits, limits, etc. • • •					
>260	95	[8] KHACHATRY...15AB		CMS	$\widetilde{\chi}^{\pm}_1 \to \widetilde{\chi}^0_1 \pi^{\pm}$, $\tau_{\widetilde{\chi}^{\pm}_1}$=0.2ns, AMSB
>800	95	[9] KHACHATRY...15AO		CMS	long-lived $\widetilde{\chi}^{\pm}_1$, mAMSB, τ >100ns
>100	95	[9] KHACHATRY...15AO		CMS	long-lived $\widetilde{\chi}^{\pm}_1$, mAMSB, $\tau > 3$ ns
	95	[10] KHACHATRY...15W		CMS	long-lived $\widetilde{\chi}^0$, $\widetilde{q} \to q\widetilde{\chi}^0$, $\widetilde{\chi}^0 \to \ell^+\ell^-\nu$, RPV
>270	95	[11] AAD	13BD	ATLS	disappearing-track signature, AMSB
>278	95	[12] ABAZOV	13B	D0	long-lived $\widetilde{\chi}^{\pm}$, gaugino-like
>244	95	[12] ABAZOV	13B	D0	long-lived $\widetilde{\chi}^{\pm}$, higgsino-like

[1] AAD 15AE searched in 19.1 fb^{-1} of pp collisions at $\sqrt{s} = 8$ TeV for heavy long-lived charged particles, measured through their specific ionization energy loss in the ATLAS pixel detector or their time-of-flight in the ALTAS muon system. In the absence of an excess of events above the expected backgrounds, limits are set on stable charginos, see Fig. 10.

[2] AAD 15BM searched in 18.4 fb^{-1} of pp collisions at $\sqrt{s} = 8$ TeV for stable and metastable non-relativistic charged particles through their anomalous specific ionization energy loss in the ATLAS pixel detector. In absence of an excess of events above the expected backgrounds, limits are set on stable charginos (see Table 5) and on metastable charginos decaying to $\widetilde{\chi}^0_1 \pi^{\pm}$, see Fig. 11.

[3] AAD 13H searched in 4.7 fb^{-1} of pp collisions at $\sqrt{s} = 7$ TeV for direct electroweak production of long-lived charginos in the context of AMSB scenarios. The search is based on the signature of a high-momentum isolated track with few associated hits in the outer part of the tracking system, arising from a chargino decay into a neutralino and a low-momentum pion. The p_T spectrum of the tracks was found to be consistent with the SM expectations. Constraints on the lifetime and the production cross section were obtained, see Fig. 6. In the minimal AMSB framework with $\tan\beta = 5$, and $\mu > 0$, a chargino having a mass below 103 (85) GeV for a chargino-neutralino mass splitting $\Delta m_{\widetilde{\chi}^0_1}$ of 160 (170) MeV is excluded at the 95% C.L. See Fig. 7 for more precise bounds.

[4] AAD 12BJ looked in 1.02 fb^{-1} of pp collisions at $\sqrt{s} = 7$ TeV for signatures of decaying charginos resulting in isolated tracks with few associated hits in the outer region of the tracking system. The p_T spectrum of the tracks was found to be consistent with the SM expectations. Constraints on the lifetime and the production cross section were obtained. In the minimal AMSB framework with $m_{3/2} < 32$ TeV, $m_0 < 1.5$ TeV, $\tan\beta = 5$, and $\mu > 0$, a chargino having a mass below 92 GeV and a lifetime between 0.5 ns and 2 ns is excluded at the 95% C.L. See their Fig. 8 for more precise bounds.

[5] ABAZOV 09M searched in 1.1 fb^{-1} of $p\overline{p}$ collisions at $\sqrt{s} = 1.96$ TeV for events with direct production of a pair of charged massive stable particles identified by their TOF. The number of the observed events is consistent with the predicted background. The data are used to constrain the production cross section as a function of the $\widetilde{\chi}^{\pm}_1$ mass, see their Fig. 2. The quoted limit improves to 206 GeV for gaugino-like charginos.

[6] ABBIENDI 03L used e^+e^- data at $\sqrt{s} = 130$–209 GeV to select events with two high momentum tracks with anomalous dE/dx. The excluded cross section is compared to the theoretical expectation as a function of the heavy particle mass in their Fig. 3. The bounds are valid for colorless fermions with lifetime longer than 10^{-6} s. Supersedes the results from ACKERSTAFF 98P.

[7] ABREU 00T searches for the production of heavy stable charged particles, identified by their ionization or Cherenkov radiation, using data from $\sqrt{s}$= 130 to 189 GeV. These limits include and update the results of ABREU 98P.

[8] KHACHATRYAN 15AB searched in 19.5 fb^{-1} of pp collisions at $\sqrt{s} = 8$ TeV for events containing tracks with little or no associated calorimeter energy deposits and with missing hits in the outer layers of the tracking system (disappearing-track signature). Such disappearing tracks can result from the decay of charginos that are nearly mass degenerate with the lightest neutralino. The number of observed events is in agreement with the background expectation. Limits are set on the cross section of electroweak chargino production in terms of the chargino mass and mean proper lifetime, see Fig. 4. In the minimal AMSB model, a chargino mass below 260 GeV is excluded at 95% C.L., see their Fig. 5.

[9] KHACHATRYAN 15O searched in 18.8 fb^{-1} of pp collisions at $\sqrt{s} = 8$ TeV for evidence of long-lived charginos in the context of AMSB and pMSSM scenarios. The results are based on a previously published search for heavy stable charged particles at 7 and 8 TeV. In the minimal AMSB framework with $\tan\beta = 5$ and $\mu \geq 0$, constraints on the chargino mass and lifetime were placed, see Fig. 5. Charginos with a mass below 800 (100) GeV are excluded at the 95% C.L. for lifetimes above 100 ns (3 ns). Constraints are also placed on the pMSSM parameter space, see Fig. 3.

[10] KHACHATRYAN 15W searched in up to 20.5 fb^{-1} of pp collisions at $\sqrt{s} = 8$ TeV for evidence of long-lived neutralinos produced through $\widetilde{q}$-pair production, with $\widetilde{q} \to q\widetilde{\chi}^0$ and $\widetilde{\chi}^0 \to \ell^+\ell^-\nu$ (RPV: $\lambda_{121}, \lambda_{122} \neq 0$). 95% C.L. exclusion limits on cross section times branching ratio are set as a function of mean proper decay length of the neutralino, see Figs. 6 and 9.

[11] AAD 13BD searched in 20.3 fb^{-1} of pp collisions at $\sqrt{s} = 8$ TeV for events containing tracks with no associated hits in the outer region of the tracking system resulting from the decay of charginos that are nearly mass degenerate with the lightest neutralino, as is often the case in AMSB scenarios. No significant excess above the background expectation is observed for candidate tracks with large transverse momentum. Constraints on chargino properties are obtained and in the minimal AMSB model, a chargino mass below 270 GeV is excluded at 95% C.L., see their Fig. 7.

[12] ABAZOV 13B looked in 6.3 fb^{-1} of $p\overline{p}$ collisions at $\sqrt{s} = 1.96$ TeV for charged massive long-lived particles in events with muon-like particles that have both speed and ionization energy loss inconsistent with muons produced in beam collisions. In the absence of an excess, limits are set at 95% C.L. on gaugino- and higgsino-like charginos, see their Table 20 and Fig. 23.

$\widetilde{\nu}$ (Sneutrino) mass limit

The limits may depend on the number, $N(\widetilde{\nu})$, of sneutrinos assumed to be degenerate in mass. Only $\widetilde{\nu}_L$ (not $\widetilde{\nu}_R$) is assumed to exist. It is possible that $\widetilde{\nu}$ could be the lightest supersymmetric particle (LSP).

We report here, but do not include in the Listings, the limits obtained from the fit of the final results obtained by the LEP Collaborations on the invisible width of the Z boson ($\Delta\Gamma_{\text{inv.}} < 2.0$ MeV, LEP-SLC 06): $m_{\widetilde{\nu}} > 43.7$ GeV ($N(\widetilde{\nu})$=1) and $m_{\widetilde{\nu}} > 44.7$ GeV ($N(\widetilde{\nu})$=3) .

Some earlier papers are now obsolete and have been omitted. They were last listed in our PDG 14 edition: K. Olive, *et al.* (Particle Data Group), Chinese Physics **C38** 070001 (2014) (http://pdg.lbl.gov).

VALUE (GeV)	CL%	DOCUMENT ID		TECN	COMMENT
>2300	95	[1] AABOUD	16P	ATLS	RPV, $\widetilde{\nu}_\tau \to e\mu$, $\lambda'_{311} = 0.11$
>2200	95	[1] AABOUD	16P	ATLS	RPV, $\widetilde{\nu}_\tau \to e\tau$, $\lambda'_{311} = 0.11$
>1900	95	[1] AABOUD	16P	ATLS	RPV, $\widetilde{\nu}_\tau \to \mu\tau$, $\lambda'_{311} = 0.11$
> 400	95	[2] AAD	14X	ATLS	RPV, $\geq 4\ell^{\pm}$, $\widetilde{\nu} \to \nu\widetilde{\chi}^0_1$, $\widetilde{\chi}^0_1 \to \ell^{\pm}\ell^{\mp}\nu$
		[3] AAD	11Z	ATLS	RPV, $\widetilde{\nu}_\tau \to e\mu$
> 94	95	[4] ABDALLAH	03M	DLPH	$1 \leq \tan\beta \leq 40$, $m_{\widetilde{e}_R} - m_{\widetilde{\chi}^0_1}$ >10 GeV
> 84	95	[5] HEISTER	02N	ALEP	$\widetilde{\nu}_e$, any Δm
> 41	95	[6] DECAMP	92	ALEP	$\Gamma(Z \to$ invisible); $N(\widetilde{\nu})$=3, model independent
• • • We do not use the following data for averages, fits, limits, etc. • • •					
>1280	95	[7] KHACHATRY...16BE		CMS	RPV, $\widetilde{\nu}_\tau \to e\mu$, $\lambda_{132} = \lambda_{231} = \lambda'_{311} = 0.01$
>2300	95	[7] KHACHATRY...16BE		CMS	RPV, $\widetilde{\nu}_\tau \to e\mu$, $\lambda_{132} = \lambda_{231} =$ 0.07, $\lambda'_{311} = 0.11$
>2000	95	[8] AAD	15O	ATLS	RPV ($e\mu$), $\widetilde{\nu}_\tau$, $\lambda'_{311} = 0.11$, $\lambda_{i3k} = 0.07$
>1700	95	[8] AAD	15O	ATLS	RPV ($\tau\mu$, $e\tau$), $\widetilde{\nu}_\tau$, $\lambda'_{311} = 0.11$, $\lambda_{i3k} = 0.07$
		[9] AAD	13AI	ATLS	RPV, $\widetilde{\nu}_\tau \to e\mu$, $e\tau$, $\mu\tau$
		[10] AAD	11H	ATLS	RPV, $\widetilde{\nu}_\tau \to e\mu$
		[11] AALTONEN	10Z	CDF	RPV, $\widetilde{\nu}_\tau \to e\mu$, $e\tau$, $\mu\tau$
		[12] ABAZOV	10M	D0	RPV, $\widetilde{\nu}_\tau \to e\mu$
> 95	95	[13] ABDALLAH	04H	DLPH	AMSB, $\mu > 0$
> 37.1	95	[14] ADRIANI	93M	L3	$\Gamma(Z \to$ invisible); $N(\widetilde{\nu})$=1
> 36	95	ABREU	91F	DLPH	$\Gamma(Z \to$ invisible); $N(\widetilde{\nu})$=1
> 31.2	95	[15] ALEXANDER	91F	OPAL	$\Gamma(Z \to$ invisible); $N(\widetilde{\nu})$=1

[1] AABOUD 16P searched in 3.2 fb^{-1} of pp collisions at $\sqrt{s} = 13$ TeV for events with different flavour dilepton pairs ($e\mu$, $e\tau$, $\mu\tau$) from the production of $\widetilde{\nu}_\tau$ via an RPV λ'_{311} coupling and followed by a decay via $\lambda_{312} = \lambda_{321} = 0.07$ for $e + \mu$, via $\lambda_{313} = \lambda_{331} = 0.07$ for $e + \tau$ and via $\lambda_{323} = \lambda_{332} = 0.07$ for $\mu + \tau$. No evidence for a dilepton resonance over the SM expectation is observed, and limits are derived on $m_{\widetilde{\nu}}$ at 95% CL, see their Figs. 2(b), 3(b), 4(b), and Table 3.

[2] AAD 14X searched in 20.3 fb^{-1} of pp collisions at $\sqrt{s} = 8$ TeV for events with at least four leptons (electrons, muons, taus) in the final state. No significant excess above the Standard Model expectations is observed. Limits are set on the sneutrino mass in an R-parity violating simplified model where the decay $\widetilde{\nu} \to \nu\widetilde{\chi}^0_1$, with $\widetilde{\chi}^0_1 \to \ell^{\pm}\ell^{\mp}\nu$, takes place with a branching ratio of 100%, see Fig. 9.

[3] AAD 11Z looked in 1.07 fb^{-1} of pp collisions at $\sqrt{s} = 7$ TeV for events with one electron and one muon of opposite charge from the production of $\widetilde{\nu}_\tau$ via an RPV λ'_{311} coupling and followed by a decay via λ_{312} into $e + \mu$. No evidence for an (e, μ) resonance over the SM expectation is observed, and a limit is derived in the plane of λ'_{311} versus $m_{\widetilde{\nu}}$ for three values of λ_{312}, see their Fig. 2. Masses $m_{\widetilde{\nu}} < 1.32$ (1.45) TeV are excluded for $\lambda'_{311} = 0.10$ and $\lambda_{312} = 0.05$ ($\lambda'_{311} = 0.11$ and $\lambda_{312} = 0.07$).

[4] ABDALLAH 03M uses data from $\sqrt{s} = 192$–208 GeV to obtain limits in the framework of the MSSM with gaugino and sfermion mass universality at the GUT scale. An indirect limit on the mass is derived by constraining the MSSM parameter space by the results from direct searches for neutralinos (including cascade decays) and for sleptons. These limits are valid for values of $M_2 < 1$ TeV, $|\mu| \leq 1$ TeV with the $\widetilde{\chi}^0_1$ as LSP. The quoted limit is obtained when there is no mixing in the third family. See Fig. 43 for the mass limits as a function of $\tan\beta$. These limits update the results of ABREU 00W.

[5] HEISTER 02N derives a bound on $m_{\tilde{\nu}_e}$ by exploiting the mass relation between the $\tilde{\nu}_e$ and $\tilde{e}$, based on the assumption of universal GUT scale gaugino and scalar masses $m_{1/2}$ and m_0 and the search described in the $\tilde{e}$ section. In the MSUGRA framework with radiative electroweak symmetry breaking, the limit improves to $m_{\tilde{\nu}_e}$ >130 GeV, assuming a trilinear coupling A_0=0 at the GUT scale. See Figs. 5 and 7 for the dependence of the limits on tanβ.

[6] DECAMP 92 limit is from $\Gamma(\text{invisible})/\Gamma(\ell\ell) = 5.91 \pm 0.15$ ($N_\nu = 2.97 \pm 0.07$).

[7] KHACHATRYAN 16BE searched in 19.7 fb^{-1} of pp collisions at $\sqrt{s} = 8$ TeV for evidence of narrow resonances decaying into $e\mu$ final states. No significant excess above the Standard Model expectation is observed and 95% C.L. exclusions are placed on the cross section times branching ratio for the production of an R-parity-violating supersymmetric tau sneutrino, see their Fig. 3.

[8] AAD 15O searched in 20.3 fb^{-1} of pp collisions at $\sqrt{s} = 8$ TeV for evidence of heavy particles decaying into $e\mu$, $e\tau$ or $\mu\tau$ final states. No significant excess above the Standard Model expectation is observed, and 95% C.L. exclusions are placed on the cross section times branching ratio for the production of an R-parity-violating supersymmetric tau sneutrino, applicable to any sneutrino flavour, see their Fig. 2.

[9] AAD 13AI searched in 4.6 fb^{-1} of pp collisions at $\sqrt{s} = 7$ TeV for evidence of heavy particles decaying into $e\mu$, $e\tau$ or $\mu\tau$ final states. No significant excess above the Standard Model expectation is observed, and 95% C.L. exclusions are placed on the cross section times branching ratio for the production of an R-parity-violating supersymmetric tau sneutrino, see their Fig. 2. For couplings $\lambda'_{311} = 0.10$ and $\lambda_{i3k} = 0.05$, the lower limits on the $\tilde{\nu}_\tau$ mass are 1610, 1110, 1100 GeV in the $e\mu$, $e\tau$, and $\mu\tau$ channels, respectively.

[10] AAD 11H looked in 35 pb^{-1} of pp collisions at $\sqrt{s} = 7$ TeV for events with one electron and one muon of opposite charge from the production of $\tilde{\nu}_\tau$ via an RPV λ'_{311} coupling and followed by a decay via λ_{312} into $e + \mu$. No evidence for an excess over the SM expectation is observed, and a limit is derived in the plane of λ'_{311} versus $m_{\tilde{\nu}}$ for several values of λ_{312}, see their Fig. 2. Superseded by AAD 11Z.

[11] AALTONEN 10Z searched in 1 fb^{-1} of $p\overline{p}$ collisions at $\sqrt{s} = 1.96$ TeV for events from the production $d\overline{d} \to \tilde{\nu}_\tau$ with the subsequent decays $\tilde{\nu}_\tau \to e\mu$, $\mu\tau$, $e\tau$ in the MSSM framework with RPV. Two isolated leptons of different flavor and opposite charges are required, with τs identified by their hadronic decay. No statistically significant excesses are observed over the SM background. Upper limits on λ'^2_{311} times the branching ratio are listed in their Table III for various $\tilde{\nu}_\tau$ masses. Limits on the cross section times branching ratio for $\lambda'_{311} = 0.10$ and $\lambda_{i3k} = 0.05$, displayed in Fig. 2, are used to set limits on the $\tilde{\nu}_\tau$ mass of 558 GeV for the $e\mu$, 441 GeV for the $\mu\tau$ and 442 GeV for the $e\tau$ channels.

[12] ABAZOV 10M looked in 5.3 fb^{-1} of $p\overline{p}$ collisions at $\sqrt{s} = 1.96$ TeV for events with exactly one pair of high p_T isolated $e\mu$ and a veto against hard jets. No evidence for an excess over the SM expectation is observed, and a limit at 95% C.L. on the cross section times branching ratio is derived, see their Fig. 3. These limits are translated into limits on couplings as a function of $m_{\tilde{\nu}_\tau}$ as shown on their Fig. 4. As an example, for $m_{\tilde{\nu}_\tau}$ = 100 GeV and $\lambda_{312} \leq 0.07$, couplings $\lambda'_{311} > 7.7 \times 10^{-4}$ are excluded.

[13] ABDALLAH 04H use data from LEP 1 and $\sqrt{s}$ = 192–208 GeV. They re-use results or re-analyze the data from ABDALLAH 03M to put limits on the parameter space of anomaly-mediated supersymmetry breaking (AMSB), which is scanned in the region 1< $m_{3/2}$ <50 TeV, 0< m_0 <1000 GeV, 1.5<tanβ <35, both signs of μ. The constraints are obtained from the searches for mass degenerate chargino and neutralino, for SM-like and invisible Higgs, for leptonically decaying charginos and from the limit on non-SM Z width of 3.2 MeV. The limit is for m_t = 174.3 GeV (see Table 2 for other m_t values). The limit improves to 114 GeV for $\mu < 0$.

[14] ADRIANI 93M limit from $\Delta\Gamma(Z)$(invisible)< 16.2 MeV.

[15] ALEXANDER 91F limit is for one species of $\tilde{\nu}$ and is derived from Γ(invisible, new)/$\Gamma(\ell\ell)$ < 0.38.

Charged sleptons

This section contains limits on charged scalar leptons ($\tilde{\ell}$, with ℓ=e,μ,τ). Studies of width and decays of the Z boson (use is made here of $\Delta\Gamma_{\text{inv}} < 2.0$ MeV, LEP 00) conclusively rule out $m_{\tilde{\ell}_R} < 40$ GeV (41 GeV for $\tilde{\ell}_L$) , independently of decay modes, for each individual slepton. The limits improve to 43 GeV (43.5 GeV for $\tilde{\ell}_L$) assuming all 3 flavors to be degenerate. Limits on higher mass sleptons depend on model assumptions and on the mass splitting $\Delta m = m_{\tilde{\ell}} - m_{\tilde{\chi}^0_1}$. The mass and composition of $\tilde{\chi}^0_1$ may affect the selectron production rate in e^+e^- collisions through t-channel exchange diagrams. Production rates are also affected by the potentially large mixing angle of the lightest mass eigenstate $\tilde{\ell}_1 = \tilde{\ell}_R \sin\theta_\ell + \tilde{\ell}_L \cos\theta_\ell$. It is generally assumed that only $\tilde{\tau}$ may have significant mixing. The coupling to the Z vanishes for θ_ℓ=0.82. In the high-energy limit of e^+e^- collisions the interference between γ and Z exchange leads to a minimal cross section for θ_ℓ=0.91, a value which is sometimes used in the following entries relative to data taken at LEP 2. When limits on $m_{\tilde{\ell}_R}$ are quoted, it is understood that limits on $m_{\tilde{\ell}_L}$ are usually at least as strong.

Possibly open decays involving gauginos other than $\tilde{\chi}^0_1$ will affect the detection efficiencies. Unless otherwise stated, the limits presented here result from the study of $\tilde{\ell}^+\tilde{\ell}^-$ production, with production rates and decay properties derived from the MSSM. Limits made obsolete by the recent analyses of e^+e^- collisions at high energies can be found in previous Editions of this Review.

For decays with final state gravitinos ($\tilde{G}$), $m_{\tilde{G}}$ is assumed to be negligible relative to all other masses.

R-parity conserving $\tilde{e}$ (Selectron) mass limit

Some earlier papers are now obsolete and have been omitted. They were last listed in our PDG 14 edition: K. Olive, *et al.* (Particle Data Group), Chinese Physics **C38** 070001 (2014) (http://pdg.lbl.gov).

VALUE (GeV)	CL%	DOCUMENT ID		TECN	COMMENT
		[1] CHATRCHYAN	14R	CMS	$\geq 3\ell^\pm$, $\tilde{\ell} \to \ell^\pm\tau^\mp\tau^\mp\tilde{G}$ simplified model, GMSB, stau (N)NLSP scenario
		[2] AAD	13B	ATLS	$2\ell^\pm + \not{E}_T$, SMS, pMSSM
> 97.5		[3] ABBIENDI	04	OPAL	$\tilde{e}_R$,$\Delta m > 11$ GeV, $\lvert\mu\rvert$ >100 GeV, tanβ=1.5
> 94.4		[4] ACHARD	04	L3	$\tilde{e}_R$,$\Delta m > 10$ GeV, $\lvert\mu\rvert$ >200 GeV, tan$\beta \geq 2$
> 71.3		[4] ACHARD	04	L3	$\tilde{e}_R$, all Δm
none 30–94	95	[5] ABDALLAH	03M	DLPH	Δm >15 GeV, $\tilde{e}^+_R\tilde{e}^-_R$
> 94	95	[6] ABDALLAH	03M	DLPH	$\tilde{e}_R$,$1 \leq \tan\beta \leq 40$, Δm >10 GeV
> 95	95	[7] HEISTER	02E	ALEP	$\Delta m > 15$ GeV, $\tilde{e}^+_R\tilde{e}^-_R$
> 73	95	[8] HEISTER	02N	ALEP	$\tilde{e}_R$, any Δm
>107	95	[8] HEISTER	02N	ALEP	$\tilde{e}_L$, any Δm
• • • We do not use the following data for averages, fits, limits, etc. • • •					
none 90–325	95	[9] AAD	14G	ATLS	$\tilde{\ell}\tilde{\ell} \to \ell^+\tilde{\chi}^0_1\ell^-\tilde{\chi}^0_1$, simplified model, $m_{\tilde{\ell}_L} = m_{\tilde{\ell}_R}$, $m_{\tilde{\chi}^0_1}$ = 0 GeV
		[10] KHACHATRY...14I		CMS	$\tilde{\ell} \to \ell\tilde{\chi}^0_1$, simplified model

[1] CHATRCHYAN 14R searched in 19.5 fb^{-1} of pp collisions at $\sqrt{s} = 8$ TeV for events with at least three leptons (electrons, muons, taus) in the final state. No significant excess above the Standard Model expectations is observed. Limits are set on the slepton mass in a stau (N)NLSP simplified model (GMSB) where the decay $\tilde{\ell} \to \ell^\pm\tau^\pm\tau^\mp\tilde{G}$ takes place with a branching ratio of 100%, see Fig. 8.

[2] AAD 13B searched in 4.7 fb^{-1} of pp collisions at $\sqrt{s} = 7$ TeV for sleptons decaying to a final state with two leptons (e and μ) and missing transverse energy. No excess beyond the Standard Model expectation is observed. Limits are derived in a simplified model of direct left-handed slepton pair production, where left-handed slepton masses between 85 and 195 GeV are excluded at 95% C.L. for $m_{\tilde{\chi}^0_1} = 20$ GeV. See also Fig. 2(a). Exclusion limits are also derived in the phenomenological MSSM, see Fig. 3.

[3] ABBIENDI 04 search for $\tilde{e}_R\tilde{e}_R$ production in acoplanar di-electron final states in the 183–208 GeV data. See Fig. 13 for the dependence of the limits on $m_{\tilde{\chi}^0_1}$ and for the limit at tanβ=35 This limit supersedes ABBIENDI 00G.

[4] ACHARD 04 search for $\tilde{e}_R\tilde{e}_L$ and $\tilde{e}_R\tilde{e}_R$ production in single- and acoplanar di-electron final states in the 192–209 GeV data. Absolute limits on $m_{\tilde{e}_R}$ are derived from a scan over the MSSM parameter space with universal GUT scale gaugino and scalar masses $m_{1/2}$ and m_0, $1 \leq \tan\beta \leq 60$ and $-2 \leq \mu \leq 2$ TeV. See Fig. 4 for the dependence of the limits on $m_{\tilde{\chi}^0_1}$. This limit supersedes ACCIARRI 99W.

[5] ABDALLAH 03M looked for acoplanar dielectron $+\not{E}$ final states at $\sqrt{s}$ = 189–208 GeV. The limit assumes μ=$-$200 GeV and tanβ=1.5 in the calculation of the production cross section and B($\tilde{e} \to e\tilde{\chi}^0_1$). See Fig. 15 for limits in the ($m_{\tilde{e}_R}$, $m_{\tilde{\chi}^0_1}$) plane. These limits include and update the results of ABREU 01

[6] ABDALLAH 03M uses data from $\sqrt{s}$ = 192–208 GeV to obtain limits in the framework of the MSSM with gaugino and sfermion mass universality at the GUT scale. An indirect limit on the mass is derived by constraining the MSSM parameter space by the results from direct searches for neutralinos (including cascade decays) and for sleptons. These limits are valid for values of M_2 <1 TeV, $\lvert\mu\rvert \leq 1$ TeV with the $\tilde{\chi}^0_1$ as LSP. The quoted limit is obtained when there is no mixing in the third family. See Fig. 43 for the mass limits as a function of tanβ. These limits update the results of ABREU 00W.

[7] HEISTER 02E looked for acoplanar dielectron $+\not{E}_T$ final states from e^+e^- interactions between 183 and 209 GeV. The mass limit assumes $\mu < -200$ GeV and tanβ=2 for the production cross section and B($\tilde{e} \to e\tilde{\chi}^0_1$)=1. See their Fig. 4 for the dependence of the limit on Δm. These limits include and update the results of BARATE 01.

[8] HEISTER 02N search for $\tilde{e}_R\tilde{e}_L$ and $\tilde{e}_R\tilde{e}_R$ production in single- and acoplanar di-electron final states in the 183–208 GeV data. Absolute limits on $m_{\tilde{e}_R}$ are derived from a scan over the MSSM parameter space with universal GUT scale gaugino and scalar masses $m_{1/2}$ and m_0, $1 \leq \tan\beta \leq 50$ and $-10 \leq \mu \leq 10$ TeV. The region of small $\lvert\mu\rvert$, where cascade decays are important, is covered by a search for $\tilde{\chi}^0_1\tilde{\chi}^0_3$ in final states with leptons and possibly photons. Limits on $m_{\tilde{e}_L}$ are derived by exploiting the mass relation between the $\tilde{e}_L$ and $\tilde{e}_R$, based on universal m_0 and $m_{1/2}$. When the constraint from the mass limit of the lightest Higgs from HEISTER 02 is included, the bounds improve to $m_{\tilde{e}_R}$ >77(75) GeV and $m_{\tilde{e}_L}$ >115(115) GeV for a top mass of 175(180) GeV. In the MSUGRA framework with radiative electroweak symmetry breaking, the limits improve further to $m_{\tilde{e}_R}$ >95 GeV and $m_{\tilde{e}_L}$ >152 GeV, assuming a trilinear coupling A_0=0 at the GUT scale. See Figs. 4, 5, 7 for the dependence of the limits on tanβ.

[9] AAD 14G searched in 20.3 fb^{-1} of pp collisions at $\sqrt{s} = 8$ TeV for electroweak production of slepton pairs, decaying to a final sate with two leptons (e and μ) and missing transverse momentum. No excess beyond the Standard Model expectation is observed. Exclusion limits are derived in simplified models of slepton pair production, see Fig. 8. An interpretation in the pMSSM is also given, see Fig. 10.

[10] KHACHATRYAN 14I searched in 19.5 fb^{-1} of pp collisions at $\sqrt{s} = 8$ TeV for electroweak production of slepton pairs decaying to a final state with opposite-sign lepton pairs (e or μ) and missing transverse momentum. No excess beyond the Standard Model expectation is observed. Exclusion limits are derived in simplified models, see Fig. 18.

R-partiy violating $\tilde{e}$ (Selectron) mass limit

Some earlier papers are now obsolete and have been omitted. They were last listed in our PDG 14 edition: K. Olive, *et al.* (Particle Data Group), Chinese Physics **C38** 070001 (2014) (http://pdg.lbl.gov).

VALUE (GeV)	CL%	DOCUMENT ID		TECN	COMMENT
>410	95	[1] AAD	14X	ATLS	RPV, $\geq 4\ell^\pm$, $\tilde{\ell} \to l\tilde{\chi}^0_1$, $\tilde{\chi}^0_1 \to \ell^\pm\ell^\mp\nu$

• • • We do not use the following data for averages, fits, limits, etc. • • •

> 89	95	[2] ABBIENDI	04F	OPAL	RPV, $\tilde{e}_L$	
> 92	95	[3] ABDALLAH	04M	DLPH	RPV, $\tilde{e}_R$, indirect, Δm >5 GeV	

[1] AAD 14X searched in 20.3 fb^{-1} of pp collisions at $\sqrt{s}$ = 8 TeV for events with at least four leptons (electrons, muons, taus) in the final state. No significant excess above the Standard Model expectations is observed. Limits are set on the slepton mass in an R-parity violating simplified model where the decay $\tilde{\ell} \rightarrow \ell\tilde{\chi}_1^0$, with $\tilde{\chi}_1^0 \rightarrow \ell^{\pm}\ell^{\mp}\nu$, takes place with a branching ratio of 100%, see Fig. 9.

[2] ABBIENDI 04F use data from $\sqrt{s}$ = 189–209 GeV. They derive limits on sparticle masses under the assumption of RPV with $LL\overline{E}$ or $LQ\overline{D}$ couplings. The results are valid for tanβ = 1.5, $\mu = -200$ GeV, with, in addition, $\Delta m \geq 5$ GeV for indirect decays via $LQ\overline{D}$. The limit quoted applies to direct decays via $LL\overline{E}$ or $LQ\overline{D}$ couplings. For indirect decays, the limits on the $\tilde{e}_R$ mass are respectively 99 and 92 GeV for $LL\overline{E}$ and $LQ\overline{D}$ couplings and $m_{\tilde{\chi}_1^0}$ = 10 GeV and degrade slightly for larger $\tilde{\chi}_1^0$ mass. Supersedes the results of ABBIENDI 00.

[3] ABDALLAH 04M use data from $\sqrt{s}$ = 192–208 GeV to derive limits on sparticle masses under the assumption of RPV with $LL\overline{E}$ or $\overline{UDD}$ couplings. The results are valid for $\mu = -200$ GeV, tanβ = 1.5, $\Delta m \geq 5$ GeV and assuming a BR of 1 for the given decay. The limit quoted is for indirect $\overline{UDD}$ decays using the neutralino constraint of 39.5 GeV for $LL\overline{E}$ and of 38.0 GeV for $\overline{UDD}$ couplings, also derived in ABDALLAH 04M. For indirect decays via $LL\overline{E}$ the limit improves to 95 GeV if the constraint from the neutralino is used and to 94 GeV if it is not used. For indirect decays via $\overline{UDD}$ couplings it remains unchanged when the neutralino constraint is not used. Supersedes the result of ABREU 00U.

R-parity conserving $\tilde{\mu}$ (Smuon) mass limit

VALUE (GeV)	CL%	DOCUMENT ID		TECN	COMMENT
		[1] CHATRCHYAN	14R	CMS	$\geq 3\ell^{\pm}$, $\tilde{\ell} \rightarrow \ell^{\pm}\tau^{\mp}\tau^{\mp}\tilde{G}$ simplified model, GMSB, stau (N)NLSP scenario
		[2] AAD	13B	ATLS	$2\ell^{\pm} + \not{E}_T$, SMS, pMSSM
>91.0		[3] ABBIENDI	04	OPAL	Δm >3 GeV, $\tilde{\mu}_R^+\tilde{\mu}_R^-$, $\lvert\mu\rvert$ >100 GeV, tanβ=1.5
>86.7		[4] ACHARD	04	L3	Δm >10 GeV, $\tilde{\mu}_R^+\tilde{\mu}_R^-$, $\lvert\mu\rvert$ >200 GeV, tan$\beta \geq 2$
none 30–88	95	[5] ABDALLAH	03M	DLPH	Δm >5 GeV, $\tilde{\mu}_R^+\tilde{\mu}_R^-$
>94	95	[6] ABDALLAH	03M	DLPH	$\tilde{\mu}_R$, $1 \leq$ tan$\beta \leq$ 40, Δm >10 GeV
>88	95	[7] HEISTER	02E	ALEP	$\Delta m >$ 15 GeV, $\tilde{\mu}_R^+\tilde{\mu}_R^-$

• • • We do not use the following data for averages, fits, limits, etc. • • •

none 90–325	95	[8] AAD	14G	ATLS	$\tilde{\ell}\tilde{\ell} \rightarrow \ell^+\tilde{\chi}_1^0\ell^-\tilde{\chi}_1^0$, simplified model, $m_{\tilde{\ell}_L} = m_{\tilde{\ell}_R}$, $m_{\tilde{\chi}_1^0}$ = 0 GeV
		[9] KHACHATRY...14I		CMS	$\tilde{\ell} \rightarrow \ell\tilde{\chi}_1^0$, simplified model
>80	95	[10] ABREU	00V	DLPH	$\tilde{\mu}_R\tilde{\mu}_R$ ($\tilde{\mu}_R \rightarrow \mu\tilde{G}$), $m_{\tilde{G}}$ >8 eV

[1] CHATRCHYAN 14R searched in 19.5 fb^{-1} of pp collisions at $\sqrt{s}$ = 8 TeV for events with at least three leptons (electrons, muons, taus) in the final state. No significant excess above the Standard Model expectations is observed. Limits are set on the slepton mass in a stau (N)NLSP simplified model (GMSB) where the decay $\tilde{\ell} \rightarrow \ell^{\pm}\tau^{\pm}\tau^{\mp}\tilde{G}$ takes place with a branching ratio of 100%, see Fig. 8.

[2] AAD 13B searched in 4.7 fb^{-1} of pp collisions at $\sqrt{s}$ = 7 TeV for sleptons decaying to a final state with two leptons (e and μ) and missing transverse energy. No excess beyond the Standard Model expectation is observed. Limits are derived in a simplified model of direct left-handed slepton pair production, where left-handed slepton masses between 85 and 195 GeV are excluded at 95% C.L. for $m_{\tilde{\chi}_1^0}$ = 20 GeV. See also Fig. 2(a). Exclusion limits are also derived in the phenomenological MSSM, see Fig. 3.

[3] ABBIENDI 04 search for $\tilde{\mu}_R\tilde{\mu}_R$ production in acoplanar di-muon final states in the 183–208 GeV data. See Fig. 14 for the dependence of the limits on $m_{\tilde{\chi}_1^0}$ and for the limit at tanβ=35. Under the assumption of 100% branching ratio for $\tilde{\mu}_R \rightarrow \mu\tilde{\chi}_1^0$, the limit improves to 94.0 GeV for $\Delta m > 4$ GeV. See Fig. 11 for the dependence of the limits on $m_{\tilde{\chi}_1^0}$ at several values of the branching ratio. This limit supersedes ABBIENDI 00G.

[4] ACHARD 04 search for $\tilde{\mu}_R\tilde{\mu}_R$ production in acoplanar di-muon final states in the 192–209 GeV data. Limits on $m_{\tilde{\mu}_R}$ are derived from a scan over the MSSM parameter space with universal GUT scale gaugino and scalar masses $m_{1/2}$ and m_0, $1 \leq$ tan$\beta \leq 60$ and $-2 \leq \mu \leq 2$ TeV. See Fig. 4 for the dependence of the limits on $m_{\tilde{\chi}_1^0}$. This limit supersedes ACCIARRI 99W.

[5] ABDALLAH 03M looked for acoplanar dimuon $+\not{E}$ final states at $\sqrt{s}$ = 189–208 GeV. The limit assumes B($\tilde{\mu} \rightarrow \mu\tilde{\chi}_1^0$) = 100%. See Fig. 16 for limits on the ($m_{\tilde{\mu}_R}$, $m_{\tilde{\chi}_1^0}$) plane. These limits include and update the results of ABREU 01.

[6] ABDALLAH 03M uses data from $\sqrt{s}$ = 192–208 GeV to obtain limits in the framework of the MSSM with gaugino and sfermion mass universality at the GUT scale. An indirect limit on the mass is derived by constraining the MSSM parameter space by the results from direct searches for neutralinos (including cascade decays) and for sleptons. These limits are valid for values of $M_2 < 1$ TeV, $\lvert\mu\rvert \leq 1$ TeV with the $\tilde{\chi}_1^0$ as LSP. The quoted limit is obtained when there is no mixing in the third family. See Fig. 43 for the mass limits as a function of tanβ. These limits update the results of ABREU 00W.

[7] HEISTER 02E looked for acoplanar dimuon + $\not{E}_T$ final states from e^+e^- interactions between 183 and 209 GeV. The mass limit assumes B($\tilde{\mu} \rightarrow \mu\tilde{\chi}_1^0$)=1. See their Fig. 4 for the dependence of the limit on Δm. These limits include and update the results of BARATE 01.

[8] AAD 14G searched in 20.3 fb^{-1} of pp collisions at $\sqrt{s}$ = 8 TeV for electroweak production of slepton pairs, decaying to a final sate with two leptons (e and μ) and missing transverse momentum. No excess beyond the Standard Model expectation is observed. Exclusion limits are derived in simplified models of slepton pair production, see Fig. 8. An interpretation in the pMSSM is also given, see Fig. 10.

[9] KHACHATRYAN 14I searched in 19.5 fb^{-1} of pp collisions at $\sqrt{s}$ = 8 TeV for electroweak production of slepton pairs decaying to a final state with opposite-sign lepton pairs (e or μ) and missing transverse momentum. No excess beyond the Standard Model expectation is observed. Exclusion limits are derived in simplified models, see Fig. 18.

[10] ABREU 00V use data from $\sqrt{s}$= 130–189 GeV to search for tracks with large impact parameter or visible decay vertices. Limits are obtained as function of $m_{\tilde{G}}$, after combining these results with the search for slepton pair production in the SUGRA framework from ABREU 01 to cover prompt decays and on stable particle searches from ABREU 00Q. For limits at different $m_{\tilde{G}}$, see their Fig. 12.

R-parity violating $\tilde{\mu}$ (Smuon) mass limit

VALUE (GeV)	CL%	DOCUMENT ID		TECN	COMMENT
>410	95	[1] AAD	14X	ATLS	RPV, $\geq 4\ell^{\pm}$, $\tilde{\ell} \rightarrow \ell\tilde{\chi}_1^0$, $\tilde{\chi}_1^0 \rightarrow \ell^{\pm}\ell^{\mp}\nu$

• • • We do not use the following data for averages, fits, limits, etc. • • •

> 87	95	[2] ABDALLAH	04M	DLPH	RPV, $\tilde{\mu}_R$, indirect, Δm >5 GeV
> 81	95	[3] HEISTER	03G	ALEP	RPV, $\tilde{\mu}_L$

[1] AAD 14X searched in 20.3 fb^{-1} of pp collisions at $\sqrt{s}$ = 8 TeV for events with at least four leptons (electrons, muons, taus) in the final state. No significant excess above the Standard Model expectations is observed. Limits are set on the slepton mass in an R-parity violating simplified model where the decay $\tilde{\ell} \rightarrow \ell\tilde{\chi}_1^0$, with $\tilde{\chi}_1^0 \rightarrow \ell^{\pm}\ell^{\mp}\nu$, takes place with a branching ratio of 100%, see Fig. 9.

[2] ABDALLAH 04M use data from $\sqrt{s}$ = 192–208 GeV to derive limits on sparticle masses under the assumption of RPV with $LL\overline{E}$ or $\overline{UDD}$ couplings. The results are valid for $\mu = -200$ GeV, tanβ = 1.5, $\Delta m \geq 5$ GeV and assuming a BR of 1 for the given decay. The limit quoted is for indirect $\overline{UDD}$ decays using the neutralino constraint of 39.5 GeV for $LL\overline{E}$ and of 38.0 GeV for $\overline{UDD}$ couplings, also derived in ABDALLAH 04M. For indirect decays via $LL\overline{E}$ the limit improves to 90 GeV if the constraint from the neutralino is used and remains at 87 GeV if it is not used. For indirect decays via $\overline{UDD}$ couplings it degrades to 85 GeV when the neutralino constraint is not used. Supersedes the result of ABREU 00U.

[3] HEISTER 03G searches for the production of smuons in the case of RPV prompt decays with $LL\overline{E}$, $LQ\overline{D}$ or $\overline{UDD}$ couplings at $\sqrt{s}$ = 189–209 GeV. The search is performed for direct and indirect decays, assuming one coupling at a time to be non-zero. The limit holds for direct decays mediated by RPV $LQ\overline{D}$ couplings and improves to 90 GeV for indirect decays (for $\Delta m > 10$ GeV). Limits are also given for $LL\overline{E}$ direct ($m_{\tilde{\mu}R}$ > 87 GeV) and indirect decays ($m_{\tilde{\mu}R}$ > 96 GeV for $m(\tilde{\chi}_1^0) > 23$ GeV from BARATE 98S) and for $\overline{UDD}$ indirect decays ($m_{\tilde{\mu}R}$ > 85 GeV for $\Delta m > 10$ GeV). Supersedes the results from BARATE 01B.

R-parity conserving $\tilde{\tau}$ (Stau) mass limit

Some earlier papers are now obsolete and have been omitted. They were last listed in our PDG 14 edition: K. Olive, *et al.* (Particle Data Group), Chinese Physics **C38** 070001 (2014) (http://pdg.lbl.gov).

VALUE (GeV)	CL%	DOCUMENT ID		TECN	COMMENT
>85.2		[1] ABBIENDI	04	OPAL	$\Delta m > 6$ GeV, θ_τ=π/2, $\lvert\mu\rvert$ > 100 GeV, tanβ=1.5
>78.3		[2] ACHARD	04	L3	$\Delta m > 15$ GeV, θ_τ=π/2, $\lvert\mu\rvert$ >200 GeV,tan$\beta \geq 2$
>81.9	95	[3] ABDALLAH	03M	DLPH	Δm >15 GeV, all θ_τ
>79	95	[4] HEISTER	02E	ALEP	$\Delta m > 15$ GeV, θ_τ=π/2
>76	95	[4] HEISTER	02E	ALEP	$\Delta m > 15$ GeV, θ_τ=0.91

• • • We do not use the following data for averages, fits, limits, etc. • • •

	95	[5] KHACHATRY...17L		CMS	2 τ+$\not{E}_T$, $\tilde{\tau}_L \rightarrow \tau\tilde{\chi}_1^0$, $m_{\tilde{\chi}_1^0}$ = 0 GeV
none 109	95	[6] AAD	16AA	ATLS	2 hadronic $\tau + \not{E}_T$, $\tilde{\tau}_{R/L} \rightarrow \tau\tilde{\chi}_1^0$, $m_{\tilde{\chi}_1^0}$ = 0 GeV
		[7] AAD	12AF	ATLS	2τ + jets + $\not{E}_T$, GMSB
		[8] AAD	12AG	ATLS	$\geq 1\tau_h$ + jets + $\not{E}_T$, GMSB
		[9] AAD	12CM	ATLS	$\geq 1\tau$ + jets + $\not{E}_T$, GMSB
>87.4	95	[10] ABBIENDI	06B	OPAL	$\tilde{\tau}_R \rightarrow \tau\tilde{G}$, all $\tau(\tilde{\tau}_R)$
>68	95	[11] ABDALLAH	04H	DLPH	AMSB, $\mu > 0$
none m_τ– 26.3	95	[3] ABDALLAH	03M	DLPH	$\Delta m > m_\tau$, all θ_τ

[1] ABBIENDI 04 search for $\tilde{\tau}\tilde{\tau}$ production in acoplanar di-tau final states in the 183–208 GeV data. See Fig. 15 for the dependence of the limits on $m_{\tilde{\chi}_1^0}$ and for the limit at tanβ=35. Under the assumption of 100% branching ratio for $\tilde{\tau}_R \rightarrow \tau\tilde{\chi}_1^0$, the limit improves to 89.8 GeV for $\Delta m > 8$ GeV. See Fig. 12 for the dependence of the limits on $m_{\tilde{\chi}_1^0}$ at several values of the branching ratio and for their dependence on θ_τ. This limit supersedes ABBIENDI 00G.

[2] ACHARD 04 search for $\tilde{\tau}\tilde{\tau}$ production in acoplanar di-tau final states in the 192–209 GeV data. Limits on $m_{\tilde{\tau}_R}$ are derived from a scan over the MSSM parameter space with universal GUT scale gaugino and scalar masses $m_{1/2}$ and m_0, $1 \leq$ tan$\beta \leq 60$ and $-2 \leq \mu \leq 2$ TeV. See Fig. 4 for the dependence of the limits on $m_{\tilde{\chi}_1^0}$.

[3] ABDALLAH 03M looked for acoplanar ditaus $+\not{E}$ final states at $\sqrt{s}$ = 130–208 GeV. A dedicated search was made for low mass $\tilde{\tau}$s decoupling from the Z^0. The limit assumes B($\tilde{\tau} \rightarrow \tau\tilde{\chi}_1^0$) = 100%. See Fig. 20 for limits on the ($m_{\tilde{\tau}}$,$m_{\tilde{\chi}_1^0}$) plane and as function of the $\tilde{\chi}_1^0$ mass and of the branching ratio. The limit in the low-mass region improves to 29.6 and 31.1 GeV for $\tilde{\tau}_R$ and $\tilde{\tau}_L$, respectively, at $\Delta m > m_\tau$. The limit in the high-mass region improves to 84.7 GeV for $\tilde{\tau}_R$ and $\Delta m > 15$ GeV. These limits include and update the results of ABREU 01.

[4] HEISTER 02E looked for acoplanar ditau + $\not{E}_T$ final states from e^+e^- interactions between 183 and 209 GeV. The mass limit assumes B($\tilde{\tau} \rightarrow \tau\tilde{\chi}_1^0$)=1. See their Fig. 4 for the dependence of the limit on Δm. These limits include and update the results of BARATE 01.

[5] KHACHATRYAN 17L searched in about 19 fb^{-1} of pp collisions at $\sqrt{s}$ = 8 TeV for events with two τ (at least one decaying hadronically) and $\not{E}_T$. Results were interpreted to set constraints on the cross section for production of $\tilde{\tau}_L$ pairs for $m_{\tilde{\chi}^0_1}$=1 GeV. No mass constraints are set, see their Fig. 7.

[6] AAD 16AA summarized and extended ATLAS searches for electroweak supersymmetry in final states containing several charged leptons, $\not{E}_T$, with or without hadronic jets, in 20 fb^{-1} of pp collisions at $\sqrt{s}$ = 8 TeV. The paper reports 95% C.L. exclusion limits on the cross-section for production of $\tilde{\tau}_R$ and $\tilde{\tau}_L$ pairs for various $m_{\tilde{\chi}^0_1}$, using the 2 hadronic $\tau + \not{E}_T$ analysis. The $m_{\tilde{\tau}_{R/L}}$ = 109 GeV is excluded for $m_{\tilde{\chi}^0_1}$ = 0 GeV, with the constraints being stronger for $\tilde{\tau}_R$. See their Fig. 12.

[7] AAD 12AF searched in 2 fb^{-1} of pp collisions at $\sqrt{s}$ = 7 TeV for events with two tau leptons, jets and large $\not{E}_T$ in a GMSB framework. No significant excess above the expected background was found and an upper limit on the visible cross section for new phenomena is set. A 95% C.L. lower limit of 32 TeV on the mGMSB breaking scale Λ is set for M_{mess} = 250 TeV, N_S = 3, μ > 0 and C_{grav} = 1, independent of tanβ.

[8] AAD 12AG searched in 2.05 fb^{-1} of pp collisions at $\sqrt{s}$ = 7 TeV for events with at least one hadronically decaying tau lepton, jets, and large $\not{E}_T$ in a GMSB framework. No significant excess above the expected background was found and an upper limit on the visible cross section for new phenomena is set. A 95% C.L. lower limit of 30 TeV on the mGMSB breaking scale Λ is set for M_{mess} = 250 TeV, N_S = 3, μ > 0 and C_{grav} = 1, independent of tanβ. For large values of tanβ, the limit on Λ increases to 43 TeV.

[9] AAD 12CM searched in 4.7 fb^{-1} of pp collisions at $\sqrt{s}$=7 TeV for events with at least one tau lepton, zero or one additional light lepton (e/μ) jets, and large $\not{E}_T$ in a GMSB framework. No significant excess above the expected background was found and an upper limit on the visible cross section for new phenomena is set. A 95% C. L. lower limit of 54 TeV on the mGMSB breaking scale Λ is set for M_{mess} = 250 TeV, N_S = 3, μ > 0 and C_{grav} = 1, for tanβ > 20. Here the $\tilde{\tau}_1$ is the NLSP.

[10] ABBIENDI 06B use 600 pb^{-1} of data from $\sqrt{s}$ = 189–209 GeV. They look for events from pair-produced staus in a GMSB scenario with $\tilde{\tau}$ NLSP including prompt $\tilde{\tau}$ decays to ditaus + $\not{E}$ final states, large impact parameters, kinked tracks and heavy stable charged particles. Limits on the cross-section are computed as a function of m($\tilde{\tau}$) and the lifetime, see their Fig. 7. The limit is compared to the $\sigma \cdot BR^2$ from a scan over the GMSB parameter space.

[11] ABDALLAH 04H use data from LEP 1 and $\sqrt{s}$ = 192–208 GeV. They re-use results or re-analyze the data from ABDALLAH 03M to put limits on the parameter space of anomaly-mediated supersymmetry breaking (AMSB), which is scanned in the region 1< $m_{3/2}$ <50 TeV, 0< m_0 <1000 GeV, 1.5<tanβ <35, both signs of μ. The constraints are obtained from the searches for mass degenerate chargino and neutralino, for SM-like and invisible Higgs, for leptonically decaying charginos and from the limit on non-SM Z width of 3.2 MeV. The limit is for m_t = 174.3 GeV (see Table 2 for other m_t values). The limit improves to 75 GeV for μ < 0.

R-parity violating $\tilde{\tau}$ (Stau) mass limit

Some earlier papers are now obsolete and have been omitted. They were last listed in our PDG 14 edition: K. Olive, *et al.* (Particle Data Group), Chinese Physics **C38** 070001 (2014) (http://pdg.lbl.gov).

VALUE (GeV)	CL%	DOCUMENT ID		TECN	COMMENT
• • • We do not use the following data for averages, fits, limits, etc. • • •					
>74	95	[1] ABBIENDI	04F	OPAL	RPV, $\tilde{\tau}_L$
>90	95	[2] ABDALLAH	04M	DLPH	RPV, $\tilde{\tau}_R$, indirect, Δm >5 GeV

[1] ABBIENDI 04F use data from $\sqrt{s}$ = 189–209 GeV. They derive limits on sparticle masses under the assumption of RPV with $LL\overline{E}$ or $LQ\overline{D}$ couplings. The results are valid for tanβ = 1.5, μ = −200 GeV, with, in addition, Δm > 5 GeV for indirect decays via $LQ\overline{D}$. The limit quoted applies to direct decays with $LL\overline{E}$ couplings and improves to 75 GeV for $LQ\overline{D}$ couplings. The limit on the $\tilde{\tau}_R$ mass for indirect decays is 92 GeV for $LL\overline{E}$ couplings at $m_{\tilde{\chi}^0}$ = 10 GeV and no exclusion is obtained for $LQ\overline{D}$ couplings. Supersedes the results of ABBIENDI 00.

[2] ABDALLAH 04M use data from $\sqrt{s}$ = 192–208 GeV to derive limits on sparticle masses under the assumption of RPV with $LL\overline{E}$ couplings. The results are valid for μ = −200 GeV, tanβ = 1.5, Δm > 5 GeV and assuming a BR of 1 for the given decay. The limit quoted is for indirect decays using the neutralino constraint of 39.5 GeV, also derived in ABDALLAH 04M. For indirect decays via $LL\overline{E}$ the limit decreases to 86 GeV if the constraint from the neutralino is not used. Supersedes the result of ABREU 00U.

Long-lived $\tilde{\ell}$ (Slepton) mass limit

Limits on scalar leptons which leave detector before decaying. Limits from Z decays are independent of lepton flavor. Limits from continuum e^+e^- annihilation are also independent of flavor for smuons and staus. Selectron limits from e^+e^- collisions in the continuum depend on MSSM parameters because of the additional neutralino exchange contribution.

VALUE (GeV)	CL%	DOCUMENT ID		TECN	COMMENT
>490	95	[1] KHACHATRY...16BW		CMS	long-lived $\tilde{\tau}$ from inclusive production, mGMSB SPS line 7 scenario
>240	95	[1] KHACHATRY...16BW		CMS	long-lived $\tilde{\tau}$ from direct pair production, mGMSB SPS line 7 scenario
>440	95	[2] AAD	15AE	ATLS	mGMSB, M_{mess}= 250 TeV, N_5 = 3, μ > 0, C_{grav} = 5000, tanβ = 10
>385	95	[2] AAD	15AE	ATLS	mGMSB, M_{mess}= 250 TeV, N_5 = 3, μ > 0, C_{grav} = 5000, tanβ = 50
>286	95	[2] AAD	15AE	ATLS	direct $\tilde{\tau}$ production
none 124–309	95	[3] AAIJ	15BD	LHCB	long-lived $\tilde{\tau}$, mGMSB, SPS7
> 98	95	[4] ABBIENDI	03L	OPAL	$\tilde{\mu}_R$, $\tilde{\tau}_R$
none 2–87.5	95	[5] ABREU	00Q	DLPH	$\tilde{\mu}_R$, $\tilde{\tau}_R$
> 81.2	95	[6] ACCIARRI	99H	L3	$\tilde{\mu}_R$, $\tilde{\tau}_R$
> 81	95	[7] BARATE	98K	ALEP	$\tilde{\mu}_R$, $\tilde{\tau}_R$
• • • We do not use the following data for averages, fits, limits, etc. • • •					
>300	95	[8] AAD	13AA	ATLS	long-lived $\tilde{\tau}$, GMSB, tanβ = 5–20
		[9] ABAZOV	13B	D0	long-lived $\tilde{\tau}$, 100 <$m_{\tilde{\tau}}$ <300 GeV
>339	95	[10,11] CHATRCHYAN	13AB	CMS	long-lived $\tilde{\tau}$, direct $\tilde{\tau}_1$ pair prod., minimal GMSB, SPS line 7
>500	95	[10,12] CHATRCHYAN	13AB	CMS	long-lived $\tilde{\tau}$, $\tilde{\tau}_1$ from direct pair prod. and from decay of heavier SUSY particles, minimal GMSB, SPS line 7
>314	95	[13] CHATRCHYAN	12L	CMS	long-lived $\tilde{\tau}$, $\tilde{\tau}_1$ from decay of heavier SUSY particles, minimal GMSB, SPS line 7
>136	95	[14] AAD	11P	ATLS	stable $\tilde{\tau}$, GMSB scenario, tanβ=5

[1] KHACHATRYAN 16BW searched in 2.5 fb^{-1} of pp collisions at $\sqrt{s}$ = 13 TeV for events with heavy stable charged particles, identified by their anomalously high energy deposits in the silicon tracker and/or long time-of-flight measurements by the muon system. No evidence for an excess over the expected background is observed. Limits are derived for pair production of tau sleptons as a function of mass, depending on their direct or inclusive production in a minimal GMSB scenario along the Snowmass Points and Slopes (SPS) line 7, see Fig. 4 and Table 7.

[2] AAD 15AE searched in 19.1 fb^{-1} of pp collisions at $\sqrt{s}$ = 8 TeV for heavy long-lived charged particles, measured through their specific ionization energy loss in the ATLAS pixel detector or their time-of-flight in the ALTAS muon system. In the absence of an excess of events above the expected backgrounds, limits are set on stable $\tilde{\tau}$ sleptons in various scenarios, see Figs. 5-7.

[3] AAIJ 15BD searched in 3.0 fb^{-1} of pp collisions at $\sqrt{s}$ = 7 and 8 TeV for evidence of Drell-Yan pair production of long-lived $\tilde{\tau}$ particles. No evidence for such particles is observed and 95% C.L. upper limits on the cross section of $\tilde{\tau}$ pair production are derived, see Fig. 7. In the mGMSB, assuming the SPS7 benchmark scenario $\tilde{\tau}$ masses between 124 and 309 GeV are excluded at 95% C.L.

[4] ABBIENDI 03L used e^+e^- data at $\sqrt{s}$ = 130–209 GeV to select events with two high momentum tracks with anomalous dE/dx. The excluded cross section is compared to the theoretical expectation as a function of the heavy particle mass in their Fig. 3. The limit improves to 98.5 GeV for $\tilde{\mu}_L$ and $\tilde{\tau}_L$. The bounds are valid for colorless spin 0 particles with lifetimes longer than 10^{-6} s. Supersedes the results from ACKERSTAFF 98P.

[5] ABREU 00Q searches for the production of pairs of heavy, charged stable particles in e^+e^- annihilation at $\sqrt{s}$= 130–189 GeV. The upper bound improves to 88 GeV for $\tilde{\mu}_L$, $\tilde{\tau}_L$. These limits include and update the results of ABREU 98P.

[6] ACCIARRI 99H searched for production of pairs of back-to-back heavy charged particles at $\sqrt{s}$=130–183 GeV. The upper bound improves to 82.2 GeV for $\tilde{\mu}_L$, $\tilde{\tau}_L$.

[7] The BARATE 98K mass limit improves to 82 GeV for $\tilde{\mu}_L$,$\tilde{\tau}_L$. Data collected at $\sqrt{s}$=161–184 GeV.

[8] AAD 13AA searched in 4.7 fb^{-1} of pp collisions at $\sqrt{s}$ = 7 TeV for events containing long-lived massive particles in a GMSB framework. No significant excess above the expected background was found. A 95% C.L. lower limit of 300 GeV is placed on long-lived $\tilde{\tau}$'s in the GMSB model with M_{mess} = 250 TeV, N_S = 3, μ > 0, for tanβ = 5–20. The lower limit on the GMSB breaking scale Λ was found to be 99–110 TeV, for tanβ values between 5 and 40, see Fig. 4 (top). Also, directly produced long-lived sleptons, or sleptons decaying to long-lived ones, are excluded at 95% C.L. up to a $\tilde{\tau}$ mass of 278 GeV for models with slepton splittings smaller than 50 GeV.

[9] ABAZOV 13B looked in 6.3 fb^{-1} of $p\overline{p}$ collisions at $\sqrt{s}$ = 1.96 TeV for charged massive long-lived particles in events with muon-like particles that have both speed and ionization energy loss inconsistent with muons produced in beam collisions. In the absence of an excess, limits are set at 95% C.L. on the production cross section of stau leptons in the mass range 100–300 GeV, see their Table 20 and Fig. 23.

[10] CHATRCHYAN 13AB looked in 5.0 fb^{-1} of pp collisions at $\sqrt{s}$ = 7 TeV and in 18.8 fb^{-1} of pp collisions at $\sqrt{s}$ = 8 TeV for events with heavy stable particles, identified by their anomalous dE/dx in the tracker or additionally requiring that it be identified as muon in the muon chambers, from pair production of $\tilde{\tau}_1$'s. No evidence for an excess over the expected background is observed. Supersedes CHATRCHYAN 12L.

[11] CHATRCHYAN 13AB limits are derived for pair production of $\tilde{\tau}_1$ as a function of mass in minimal GMSB scenarios along the Snowmass Points and Slopes (SPS) line 7 (see Fig. 8 and Table 7). The limit given here is valid for direct pair $\tilde{\tau}_1$ production.

[12] CHATRCHYAN 13AB limits are derived for the production of $\tilde{\tau}_1$ as a function of mass in minimal GMSB scenarios along the Snowmass Points and Slopes (SPS) line 7 (see Fig. 8 and Table 7). The limit given here is valid for the production of $\tilde{\tau}_1$ from both direct pair production and from the decay of heavier supersymmetric particles.

[13] CHATRCHYAN 12L looked in 5.0 fb^{-1} of pp collisions at $\sqrt{s}$ = 7 TeV for events with heavy stable particles, identified by their anomalous dE/dx in the tracker or additionally requiring that it be identified as muon in the muon chambers, from pair production of $\tilde{\tau}_1$'s. No evidence for an excess over the expected background is observed. Limits are derived for the production of $\tilde{\tau}_1$ as a function of mass in minimal GMSB scenarios along the Snowmass Points and Slopes (SPS) line 7 (see Fig. 3). The limit given here is valid for the production of $\tilde{\tau}_1$ in the decay of heavier supersymmetric particles.

[14] AAD 11P looked in 37 pb^{-1} of pp collisions at $\sqrt{s}$ = 7 TeV for events with two heavy stable particles, reconstructed in the Inner tracker and the Muon System and identified by their time of flight in the Muon System. No evidence for an excess over the SM expectation is observed. Limits on the mass are derived, see Fig. 3, for $\tilde{\tau}$ in a GMSB scenario and for sleptons produced by electroweak processes only, in which case the limit degrades to 110 GeV.

$\tilde{q}$ (Squark) mass limit

For $m_{\tilde{q}}$ > 60–70 GeV, it is expected that squarks would undergo a cascade decay via a number of neutralinos and/or charginos rather than undergo a direct decay to photinos as assumed by some papers. Limits obtained when direct decay is assumed are usually higher than limits when cascade decays are included.

Limits from e^+e^- collisions depend on the mixing angle of the lightest mass eigenstate $\tilde{q}_1$=$\tilde{q}_R$sinθ_q+$\tilde{q}_L$cosθ_q. It is usually assumed that only the sbottom and stop squarks have non-trivial mixing angles (see the stop and sbottom sections). Here, unless otherwise noted, squarks are always taken to be either left/right degenerate, or purely of left or right type. Data from Z decays have set squark mass limits above 40 GeV, in the

case of $\tilde{q} \to q\tilde{\chi}_1$ decays if $\Delta m = m_{\tilde{q}} - m_{\tilde{\chi}_1^0} \gtrsim 5$ GeV. For smaller values of Δm, current constraints on the invisible width of the Z ($\Delta\Gamma_{\rm inv} < 2.0$ MeV, LEP 00) exclude $m_{\tilde{u}_{L,R}} < 44$ GeV, $m_{\tilde{d}_R} < 33$ GeV, $m_{\tilde{d}_L} < 44$ GeV and, assuming all squarks degenerate, $m_{\tilde{q}} < 45$ GeV.

Some earlier papers are now obsolete and have been omitted. They were last listed in our PDG 14 edition: K. Olive, *et al.* (Particle Data Group), Chinese Physics **C38** 070001 (2014) (http://pdg.lbl.gov).

R-parity conserving $\tilde{q}$ (Squark) mass limit

VALUE (GeV)	CL%	DOCUMENT ID		TECN	COMMENT
>1450 (CL = 95%) OUR EVALUATION					CMSSM, tanβ=30, μ >0
>1550 (CL = 95%) OUR EVALUATION					Mass degenerate squarks
>1050 (CL = 95%) OUR EVALUATION					Single light squark bounds
>1220	95	[1] AABOUD	17AR	ATLS	1ℓ+jets+$\not{E}_T$, Tsqk3, $m_{\tilde{\chi}_1^0} = 0$ GeV
>1000	95	[2] AABOUD	17N	ATLS	2 same-flavour, opposite-sign ℓ + jets + $\not{E}_T$, Tsqk2, $m_{\tilde{\chi}_1^0} = 0$ GeV
>1150	95	[3] KHACHATRY...	17P	CMS	1 or more jets+$\not{E}_T$, Tsqk1, 4(flavor) x 2(isospin) = 8 mass degenerate states, $m_{\tilde{\chi}_1^0} = 0$ GeV
> 575	95	[3] KHACHATRY...	17P	CMS	1 or more jets+$\not{E}_T$, Tsqk1, one light flavor state, $m_{\tilde{\chi}_1^0} = 0$ GeV
>1370	95	[4] KHACHATRY...	17V	CMS	2 γ + $\not{E}_T$, GGM, Tsqk4, any NLSP mass
>1600	95	[5] SIRUNYAN	17AY	CMS	γ + jets+$\not{E}_T$, Tsqk4B, $m_{\tilde{\chi}_1^0} = 0$ GeV
>1370	95	[5] SIRUNYAN	17AY	CMS	γ + jets+$\not{E}_T$, Tsqk4A, $m_{\tilde{\chi}_1^0} = 0$ GeV
>1050	95	[6] SIRUNYAN	17AZ	CMS	$\geq$ 1 jets+$\not{E}_T$, Tsqk1, single light flavor state, $m_{\tilde{\chi}_1^0} = 0$ GeV
>1550	95	[6] SIRUNYAN	17AZ	CMS	$\geq$ 1 jets+$\not{E}_T$, Tsqk1, 4(flavor) x 2(isospin) = 8 degenerate mass states, $m_{\tilde{\chi}_1^0} = 0$ GeV
>1390	95	[7] SIRUNYAN	17P	CMS	jets+$\not{E}_T$, Tsqk1, 4(flavor) x 2(isospin) = 8 degenerate mass states, $m_{\tilde{\chi}_1^0} = 0$ GeV
> 950	95	[7] SIRUNYAN	17P	CMS	jets+$\not{E}_T$, Tsqk1, one light flavor state, $m_{\tilde{\chi}_1^0} = 0$ GeV
> 608	95	[8] AABOUD	16D	ATLS	$\geq$ 1 jet + $\not{E}_T$, Tsqk1, $m_{\tilde{q}} - m_{\tilde{\chi}_1^0} = 5$ GeV
>1030	95	[9] AABOUD	16N	ATLS	$\geq$ 2 jets + $\not{E}_T$, Tsqk1, $m_{\tilde{\chi}_1^0} = 0$ GeV
> 600	95	[10] KHACHATRY...	16BS	CMS	jets + $\not{E}_T$, Tsqk1, single light squark, $m_{\tilde{\chi}_1^0} = 0$ GeV
>1260	95	[10] KHACHATRY...	16BS	CMS	jets + $\not{E}_T$, Tsqk1, 8 degenerate light squarks, $m_{\tilde{\chi}_1^0} = 0$ GeV
> 850	95	[11] AAD	15BV	ATLS	jets + $\not{E}_T$, $\tilde{q} \to q\tilde{\chi}_1^0$, $m_{\tilde{\chi}_1^0} =$ 100 GeV
> 250	95	[12] AAD	15CS	ATLS	photon + $\not{E}_T$, $pp \to \tilde{q}\tilde{q}^*\gamma$, $\tilde{q} \to q\tilde{\chi}_1^0$, $m_{\tilde{q}} - m_{\tilde{\chi}_1^0} = m_c$
> 490	95	[13] AAD	15K	ATLS	$\tilde{c} \to c\tilde{\chi}_1^0$, $m_{\tilde{\chi}_1^0} < 200$ GeV
> 875	95	[14] KHACHATRY...	15AF	CMS	$\tilde{q} \to q\tilde{\chi}_1^0$, simplified model, 8 degenerate light $\tilde{q}$, $m_{\tilde{\chi}_1^0} = 0$
> 520	95	[14] KHACHATRY...	15AF	CMS	$\tilde{q} \to q\tilde{\chi}_1^0$, simplified model, single light squark, $m_{\tilde{\chi}_1^0} = 0$
>1450	95	[14] KHACHATRY...	15AF	CMS	CMSSM, tanβ = 30, $A_0 = -2\max(m_0, m_{1/2})$, $\mu > 0$
> 850	95	[15] AAD	14AE	ATLS	jets + $\not{E}_T$, $\tilde{q} \to q\tilde{\chi}_1^0$ simplified model, mass degenerate first and second generation squarks, $m_{\tilde{\chi}_1^0} = 0$ GeV
> 440	95	[15] AAD	14AE	ATLS	jets + $\not{E}_T$, $\tilde{q} \to q\tilde{\chi}_1^0$ simplified model, single light-flavour squark, $m_{\tilde{\chi}_1^0} = 0$ GeV
>1700	95	[15] AAD	14AE	ATLS	jets + $\not{E}_T$, mSUGRA/CMSSM, $m_{\tilde{q}} = m_{\tilde{g}}$
> 800	95	[16] CHATRCHYAN	14AH	CMS	jets + $\not{E}_T$, $\tilde{q} \to q\tilde{\chi}_1^0$ simplified model, $m_{\tilde{\chi}_1^0} = 50$ GeV
> 780	95	[17] CHATRCHYAN	14I	CMS	multijets + $\not{E}_T$, $\tilde{q} \to q\tilde{\chi}_1^0$ simplified model, $m_{\tilde{\chi}_1^0} < 200$ GeV
>1360	95	[18] AAD	13L	ATLS	jets + $\not{E}_T$, CMSSM, $m_{\tilde{g}} = m_{\tilde{q}}$
>1200	95	[19] AAD	13Q	ATLS	γ+b+$\not{E}_T$,higgsino-like neutralino, $m_{\tilde{\chi}_1^0} > 220$ GeV, GMSB
		[20] CHATRCHYAN	13	CMS	$\ell^\pm\ell^\mp$ + jets + $\not{E}_T$, CMSSM
>1250	95	[21] CHATRCHYAN	13G	CMS	0,1,2, $\geq$ 3 b-jets + $\not{E}_T$, CMSSM, $m_{\tilde{q}} = m_{\tilde{g}}$
>1430	95	[22] CHATRCHYAN	13H	CMS	2γ + $\geq$ 4 jets + low $\not{E}_T$, stealth SUSY model
> 750	95	[23] CHATRCHYAN	13T	CMS	jets + $\not{E}_T$, $\tilde{q} \to q\tilde{\chi}_1^0$ simplified model, $m_{\tilde{\chi}_1^0} = 0$ GeV
> 820	95	[24] AAD	12AX	ATLS	ℓ +jets +$\not{E}_T$, CMSSM, $m_{\tilde{q}} = m_{\tilde{g}}$
>1200	95	[25] AAD	12CJ	ATLS	$\ell^\pm$+jets+$\not{E}_T$, CMSSM, $m_{\tilde{q}} = m_{\tilde{g}}$
> 870	95	[26] AAD	12CP	ATLS	2γ +$\not{E}_T$, GMSB, bino NLSP, $m_{\tilde{\chi}_1^0} > 50$ GeV
> 950	95	[27] AAD	12W	ATLS	jets + $\not{E}_T$, CMSSM, $m_{\tilde{q}} = m_{\tilde{g}}$
		[28] CHATRCHYAN	12	CMS	e, μ, jets, razor, CMSSM
> 760	95	[29] CHATRCHYAN	12AE	CMS	jets + $\not{E}_T$, $\tilde{q} \to q\tilde{\chi}_1^0$, $m_{\tilde{\chi}_1^0} <$ 200 GeV
>1110	95	[30] CHATRCHYAN	12AT	CMS	jets + $\not{E}_T$, CMSSM
>1180	95	[30] CHATRCHYAN	12AT	CMS	jets + $\not{E}_T$, CMSSM, $m_{\tilde{q}} = m_{\tilde{g}}$
• • • We do not use the following data for averages, fits, limits, etc. • • •					
> 300	95	[31] KHACHATRY...	16BT	CMS	19-parameter pMSSM model, global Bayesian analysis, flat prior
	95	[32] AAD	15AI	ATLS	$\ell^\pm$ + jets + $\not{E}_T$
>1650	95	[11] AAD	15BV	ATLS	jets + $\not{E}_T$, $m_{\tilde{g}} = m_{\tilde{q}}$, $m_{\tilde{\chi}_1^0} = 1$ GeV
> 790	95	[11] AAD	15BV	ATLS	jets + $\not{E}_T$, $\tilde{q} \to qW\tilde{\chi}_1^0$, $m_{\tilde{\chi}_1^0} =$ 100 GeV
> 820	95	[11] AAD	15BV	ATLS	2 or 3 leptons + jets, $\tilde{q}$ decays via sleptons, $m_{\tilde{\chi}_1^0} = 100$ GeV
> 850	95	[11] AAD	15BV	ATLS	τ, $\tilde{q}$ decays via staus, $m_{\tilde{\chi}_1^0} = 50$ GeV
> 700	95	[33] KHACHATRY...	15AR	CMS	$\tilde{q} \to q\tilde{\chi}_1^0$, $\tilde{\chi}_1^0 \to \tilde{S}g$, $\tilde{S} \to S\tilde{G}$, $S \to gg$, $m_{\tilde{S}} = 100$ GeV, $m_S = 90$ GeV
> 550	95	[33] KHACHATRY...	15AR	CMS	$\ell^\pm$, $\tilde{q} \to q\tilde{\chi}_1^\pm$, $\tilde{\chi}_1^\pm \to \tilde{S}W^\pm$, $\tilde{S} \to S\tilde{G}$, $S \to gg$, $m_{\tilde{S}} =$ 100 GeV, $m_S = 90$ GeV
>1500	95	[34] KHACHATRY...	15AZ	CMS	$\geq$ 2 γ, $\geq$ 1 jet, (Razor), bino-like NLSP, $m_{\tilde{\chi}_1^0} = 375$ GeV
>1000	95	[34] KHACHATRY...	15AZ	CMS	$\geq$ 1 γ, $\geq$ 2 jet, wino-like NLSP, $m_{\tilde{\chi}_1^0} = 375$ GeV
> 670	95	[35] AAD	14E	ATLS	$\ell^\pm\ell^\pm(\ell^\mp)$ + jets, $\tilde{q} \to q'\tilde{\chi}_1^\pm$, $\tilde{\chi}_1^\pm \to W^{(*)\pm}\tilde{\chi}_2^0$, $\tilde{\chi}_2^0 \to Z^{(*)}\tilde{\chi}_1^0$ simplified model, $m_{\tilde{\chi}_1^0} < 300$ GeV
> 780	95	[35] AAD	14E	ATLS	$\ell^\pm\ell^\pm(\ell^\mp)$ + jets, $\tilde{q} \to q'\tilde{\chi}_1^\pm/\tilde{\chi}_2^0$, $\tilde{\chi}_1^\pm \to \ell^\pm\nu\tilde{\chi}_1^0$, $\tilde{\chi}_2^0 \to \ell^\pm\ell^\mp(\nu\nu)\tilde{\chi}_1^0$ simplified model
> 700	95	[36] CHATRCHYAN	13AO	CMS	$\ell^\pm\ell^\mp$ + jets + $\not{E}_T$, CMSSM, $m_0 < 700$ GeV
>1350	95	[37] CHATRCHYAN	13AV	CMS	jets (+ leptons) + $\not{E}_T$, CMSSM, $m_{\tilde{g}} = m_{\tilde{q}}$
> 800	95	[38] CHATRCHYAN	13W	CMS	$\geq$ 1 photons + jets + $\not{E}_T$, GGM, wino-like NLSP, $m_{\tilde{\chi}_1^0} =$ 375 GeV
>1000	95	[38] CHATRCHYAN	13W	CMS	$\geq$ 2 photons + jets + $\not{E}_T$, GGM, bino-like NLSP, $m_{\tilde{\chi}_1^0} =$ 375 GeV
> 340	95	[39] DREINER	12A	THEO	$m_{\tilde{q}} \sim m_{\tilde{\chi}_1^0}$
> 650	95	[40] DREINER	12A	THEO	$m_{\tilde{q}} = m_{\tilde{g}} \sim m_{\tilde{\chi}_1^0}$

[1] AABOUD 17AR searched in 36.1 fb^{-1} of pp collisions at $\sqrt{s} = 13$ TeV for events with one isolated lepton, at least two jets and large missing transverse momentum. No significant excess above the Standard Model expectations is observed. Limits up to 1.25 TeV are set on the 1st and 2nd generation squark masses in Tsqk3 simplified models, with $x = (m_{\tilde{\chi}_1^\pm} - m_{\tilde{\chi}_1^0}) / (m_{\tilde{q}} - m_{\tilde{\chi}_1^0}) = 1/2$. Similar limits are obtained for variable x and fixed neutralino mass, $m_{\tilde{\chi}_1^0} = 60$ GeV. See their Figure 13.

[2] AABOUD 17N searched in 14.7 fb^{-1} of pp collisions at $\sqrt{s} = 13$ TeV for events with 2 same-flavour, opposite-sign leptons (electrons or muons), jets and large missing transverse momentum. The results are interpreted as 95% C.L. limits in Tsqk2 models, assuming $m_{\tilde{\chi}_1^0} = 0$ GeV and $m_{\tilde{\chi}_2^0} = 600$ GeV. See their Fig. 12 for exclusion limits as a function of $m_{\tilde{\chi}_2^0}$.

[3] KHACHATRYAN 17P searched in 2.3 fb^{-1} of pp collisions at $\sqrt{s} = 13$ TeV for events with one or more jets and large $\not{E}_T$. No significant excess above the Standard Model expectations is observed. Limits are set on the gluino mass in the Tglu1A, Tglu2A, Tglu3A, Tglu3B, Tglu3C and Tglu3D simplified models, see their Figures 7 and 8. Limits are also set on the squark mass in the Tsqk1 simplified model, see their Fig. 7, and on the sbottom mass in the Tsbot1 simplified model, see Fig. 8. Finally, limits are set on the stop mass in the Tstop1, Tstop3, Tstop4, Tstop6 and Tstop7 simplified models, see Fig. 8.

[4] KHACHATRYAN 17V searched in 2.3 fb^{-1} of pp collisions at $\sqrt{s} = 13$ TeV for events with two photons and large $\not{E}_T$. No significant excess above the Standard Model expectations is observed. Limits are set on the gluino and squark mass in the context of general gauge mediation models Tglu4B and Tsqk4, see their Fig. 4.

[5] SIRUNYAN 17AY searched in 35.9 fb^{-1} of pp collisions at $\sqrt{s} = 13$ TeV for events with at least one photon, jets and large $\not{E}_T$. No significant excess above the Standard Model expectations is observed. Limits are set on the gluino mass in the Tglu4A and Tglu4B simplified models, and on the squark mass in the Tskq4A and Tsqk4B simplified models, see their Figure 6.

[6] SIRUNYAN 17AZ searched in 35.9 fb^{-1} of pp collisions at $\sqrt{s} = 13$ TeV for events with one or more jets and large $\not{E}_T$. No significant excess above the Standard Model expectations is observed. Limits are set on the gluino mass in the Tglu1A, Tglu2A, Tglu3A simplified models, see their Figures 6. Limits are also set on the squark mass in the Tsqk1 simplified model (for single light squark and for 8 degenerate light squarks), on the sbottom mass in the Tsbot1 simplified model and on the stop mass in the Tstop1 simplified model, see their Fig. 7. Finally, limits are set on the stop mass in the Tstop2, Tstop4 and Tstop8 simplified models, see Fig. 8.

[7] SIRUNYAN 17P searched in 35.9 fb^{-1} of pp collisions at $\sqrt{s} = 13$ TeV for events with multiple jets and large $\not{E}_T$. No significant excess above the Standard Model expectations is observed. Limits are set on the gluino mass in the Tglu1A, Tglu1C, Tglu2A, Tglu3A and Tglu3D simplified models, see their Fig. 12. Limits are also set on the squark mass in the Tsqk1 simplified model, on the stop mass in the Tstop1 simplified model, and on the sbottom mass in the Tsbot1 simplified model, see Fig. 13.

[8] AABOUD 16D searched in 3.2 fb^{-1} of pp collisions at $\sqrt{s} = 13$ TeV for events with an energetic jet and large missing transverse momentum. The results are interpreted as 95% C.L. limits on masses of first and second generation squarks decaying into a quark and the lightest neutralino in scenarios with $m_{\tilde{q}} - m_{\tilde{\chi}_1^0} < 25$ GeV. See their Fig. 6.

[9] AABOUD 16N searched in 3.2 fb^{-1} of pp collisions at $\sqrt{s} = 13$ TeV for events containing hadronic jets, large $\not{E}_T$, and no electrons or muons. No significant excess above the Standard Model expectations is observed. First- and second-generation squark masses below 1030 GeV are excluded at the 95% C.L. decaying to quarks and a massless lightest neutralino. See their Fig. 7a.

[10] KHACHATRYAN 16BS searched in 2.3 fb^{-1} of pp collisions at $\sqrt{s} = 13$ TeV for events with at least one energetic jet , no isolated leptons, and significant $\not{E}_T$, using the transverse mass variable M_{T2} to discriminate between signal and background processes. No significant excess above the Standard Model expectations is observed. Limits are set on the squark mass in the Tskq1 simplified model, both in the assumption of a single light squark and of 8 degenerate squarks, see Fig. 11 and Table 3.

[11] AAD 15BV summarized and extended ATLAS searches for gluinos and first- and second-generation squarks in final states containing jets and missing transverse momentum, with or without leptons or b-jets in the $\sqrt{s} = 8$ TeV data set collected in 2012. The paper reports the results of new interpretations and statistical combinations of previously published analyses, as well as new analyses. Exclusion limits at 95% C.L. are set on the squark mass in several R-parity conserving models. See their Figs. 9, 11, 18, 22, 24, 27, 28.

[12] AAD 15CS searched in 20.3 fb^{-1} of pp collisions at $\sqrt{s} = 8$ TeV for evidence of pair production of squarks, decaying into a quark and a neutralino, where a photon was radiated either from an initial-state quark, from an intermediate squark, or from a final-state quark. No evidence was found for an excess above the expected level of Standard Model background and a 95% C.L. exclusion limit was set on the squark mass as a function of the squark-neutralino mass difference, see Fig. 19.

[13] AAD 15K searched in 20.3 fb^{-1} of pp collisions at $\sqrt{s} = 8$ TeV for events containing at least two jets, where the two leading jets are each identified as originating from c-quarks, and large missing transverse momentum. No excess of events above the expected level of Standard Model background was found. Exclusion limits at 95% C.L. are set on the mass of superpartners of charm quarks ($\tilde{c}$). Assuming that the decay $\tilde{c} \rightarrow c\tilde{\chi}_1^0$ takes place 100% of the time, a scalar charm mass below 490 GeV is excluded for $m_{\tilde{\chi}_1^0} < 200$ GeV. For more details, see their Fig. 2.

[14] KHACHATRYAN 15AF searched in 19.5 fb^{-1} of pp collisions at $\sqrt{s} = 8$ TeV for events with at least two energetic jets and significant $\not{E}_T$, using the transverse mass variable M_{T2} to discriminate between signal and background processes. No significant excess above the Standard Model expectations is observed. Limits are set on the squark mass in simplified models where the decay $\tilde{q} \rightarrow q\tilde{\chi}_1^0$ takes place with a branching ratio of 100%, both for the case of a single light squark or 8 degenerate squarks, see Fig. 12. See also Table 5. Exclusions in the CMSSM, assuming $\tan\beta = 30$, $A_0 = -2$ max(m_0, $m_{1/2}$) and $\mu > 0$, are also presented, see Fig. 15.

[15] AAD 14AE searched in 20.3 fb^{-1} of pp collisions at $\sqrt{s} = 8$ TeV for strongly produced supersymmetric particles in events containing jets and large missing transverse momentum, and no electrons or muons. No excess over the expected SM background is observed. Exclusion limits are derived in simplified models containing squarks that decay via $\tilde{q} \rightarrow q\tilde{\chi}_1^0$, where either a single light state or two degenerate generations of squarks are assumed, see Fig. 10.

[16] CHATRCHYAN 14AH searched in 4.7 fb^{-1} of pp collisions at $\sqrt{s} = 7$ TeV for events with at least two energetic jets and significant $\not{E}_T$, using the razor variables (M_R and R^2) to discriminate between signal and background processes. No significant excess above the Standard Model expectations is observed. Limits are set on squark masses in simplified models where the decay $\tilde{q} \rightarrow q\tilde{\chi}_1^0$ takes place with a branching ratio of 100%, see Fig. 28. Exclusions in the CMSSM, assuming $\tan\beta = 10$, $A_0 = 0$ and $\mu > 0$, are also presented, see Fig. 26.

[17] CHATRCHYAN 14I searched in 19.5 fb^{-1} of pp collisions at $\sqrt{s} = 8$ TeV for events containing multijets and large $\not{E}_T$. No excess over the expected SM background is observed. Exclusion limits are derived in simplified models containing squarks that decay via $\tilde{q} \rightarrow q\tilde{\chi}_1^0$, where either a single light state or two degenerate generations of squarks are assumed, see Fig. 7a.

[18] AAD 13L searched in 4.7 fb^{-1} of pp collisions at $\sqrt{s} = 7$ TeV for the production of squarks and gluinos in events containing jets, missing transverse momentum and no high-p_T electrons or muons. No excess over the expected SM background is observed. In mSUGRA/CMSSM models with $\tan\beta = 10$, $A_0 = 0$ and $\mu > 0$, squarks and gluinos of equal mass are excluded for masses below 1360 GeV at 95% C.L. In a simplified model containing only squarks of the first two generations, a gluino octet and a massless neutralino, squark masses below 1320 GeV are excluded at 95% C.L. for gluino masses below 2 TeV. See Figures 10–15 for more precise bounds.

[19] AAD 13Q searched in 4.7 fb^{-1} of pp collisions at $\sqrt{s} = 7$ TeV for events containing a high-p_T isolated photon, at least one jet identified as originating from a bottom quark, and high missing transverse momentum. Such signatures may originate from supersymmetric models with gauge-mediated supersymmetry breaking in events in which one of a pair of higgsino-like neutralinos decays into a photon and a gravitino while the other decays into a Higgs boson and a gravitino. No significant excess above the expected background was found and limits were set on the squark mass as a function of the neutralino mass in a generalized GMSB model (GGM) with a higgsino-like neutralino NLSP, see their Fig. 4. For neutralino masses greater than 220 GeV, squark masses below 1020 GeV are excluded at 95% C.L.

[20] CHATRCHYAN 13 looked in 4.98 fb^{-1} of pp collisions at $\sqrt{s} = 7$ TeV for events with two opposite-sign leptons (e, μ, τ), jets and missing transverse energy. No excess beyond the Standard Model expectation is observed. Exclusion limits are derived in the mSUGRA/CMSSM model with $\tan\beta = 10$, $A_0 = 0$ and $\mu > 0$, see Fig. 6.

[21] CHATRCHYAN 13G searched in 4.98 fb^{-1} of pp collisions at $\sqrt{s} = 7$ TeV for the production of squarks and gluinos in events containing 0,1,2, ≥ 3 b-jets, missing transverse momentum and no electrons or muons. No excess over the expected SM background is observed. In mSUGRA/CMSSM models with $\tan\beta = 10$, $A_0 = 0$, and $\mu > 0$, squarks and gluinos of equal mass are excluded for masses below 1250 GeV at 95% C.L. Exclusions are also derived in various simplified models, see Fig. 7.

[22] CHATRCHYAN 13H searched in 4.96 fb^{-1} of pp collisions at $\sqrt{s} = 7$ TeV for events with two photons, ≥ 4 jets and low $\not{E}_T$ due to $\tilde{q} \rightarrow \gamma\tilde{\chi}_1^0$ decays in a stealth SUSY framework, where the $\tilde{\chi}_1^0$ decays through a singlino ($\tilde{S}$) intermediate state to $\gamma S\,\tilde{G}$, with the singlet state S decaying to two jets. No significant excess above the expected background was found and limits were set in a particular R-parity conserving stealth SUSY model. The model assumes $m_{\tilde{\chi}_1^0} = 0.5\ m_{\tilde{q}}$, $m_{\tilde{S}} = 100$ GeV and $m_S = 90$ GeV. Under these assumptions, squark masses less than 1430 GeV were excluded at the 95% C.L.

[23] CHATRCHYAN 13T searched in 11.7 fb^{-1} of pp collisions at $\sqrt{s} = 8$ TeV for events with at least two energetic jets and significant $\not{E}_T$, using the α_T variable to discriminate between processes with genuine and misreconstructed $\not{E}_T$. No significant excess above the Standard Model expectations is observed. Limits are set on squark masses in simplified models where the decay $\tilde{q} \rightarrow q\tilde{\chi}_1^0$ takes place with a branching ratio of 100%, assuming an eightfold degeneracy of the masses of the first two generation squarks, see Fig. 8 and Table 9. Also limits in the case of a single light squark are given.

[24] AAD 12AX searched in 1.04 fb^{-1} of pp collisions at $\sqrt{s} = 7$ TeV for supersymmetry in events containing jets, missing transverse momentum and one isolated electron or muon. No excess over the expected SM background is observed and model-independent limits are set on the cross section of new physics contributions to the signal regions. In mSUGRA/CMSSM models with $\tan\beta = 10$, $A_0 = 0$ and $\mu > 0$, squarks and gluinos of equal mass are excluded for masses below 820 GeV at 95% C.L. Limits are also set on simplified models for squark production and decay via an intermediate chargino and on supersymmetric models with bilinear R-parity violation. Supersedes AAD 11G.

[25] AAD 12CJ searched in 4.7 fb^{-1} of pp collisions at $\sqrt{s} = 7$ TeV for events containing one or more isolated leptons (electrons or muons), jets and $\not{E}_T$. The observations are in good agreement with the SM expectations and exclusion limits have been set in number of SUSY models. In the mSUGRA/CMSSM model with $\tan\beta = 10$, $A_0 = 0$, and $\mu > 0$, 95% C.L. exclusion limits have been derived for $m_{\tilde{q}} < 1200$ GeV, assuming equal squark and gluino masses. In minimal GMSB, values of the effective SUSY breaking scale $\Lambda <$ 50 TeV are excluded at 95% C.L. for $\tan\beta < 45$. Also exclusion limits in a number of simplified models have been presented, see Figs. 10 and 12.

[26] AAD 12CP searched in 4.8 fb^{-1} of pp collisions at $\sqrt{s} = 7$ TeV for events with two photons and large $\not{E}_T$ due to $\tilde{\chi}_1^0 \rightarrow \gamma\tilde{G}$ decays in a GMSB framework. No significant excess above the expected background was found and limits were set on the squark mass as a function of the neutralino mass in a generalized GMSB model (GGM) with a bino-like neutralino NLSP. The other sparticle masses were decoupled, $\tan\beta = 2$ and $c\tau_{NLSP} < 0.1$ mm. Also, in the framework of the SPS8 model, a 95% C.L. lower limit was set on the breaking scale Λ of 196 TeV.

[27] AAD 12W searched in 1.04 fb^{-1} of pp collisions at $\sqrt{s} = 7$ TeV for the production of squarks and gluinos in events containing jets, missing transverse momentum and no electrons or muons. No excess over the expected SM background is observed. In mSUGRA/CMSSM models with $\tan\beta = 10$, $A_0 = 0$ and $\mu > 0$, squarks and gluinos of equal mass are excluded for masses below 950 GeV at 95% C.L. In a simplified model containing only squarks of the first two generations, a gluino octet and a massless neutralino, squark masses below 875 GeV are excluded at 95% C.L.

[28] CHATRCHYAN 12 looked in 35 pb^{-1} of pp collisions at $\sqrt{s} = 7$ TeV for events with e and/or μ and/or jets, a large total transverse energy, and $\not{E}_T$. The event selection is based on the dimensionless razor variable R, related to the $\not{E}_T$ and M_R, an indicator of the heavy particle mass scale. No evidence for an excess over the expected background is observed. Limits are derived in the CMSSM (m_0, $m_{1/2}$) plane for $\tan\beta = 3$, 10 and 50 (see Fig. 7 and 8). Limits are also obtained for Simplified Model Spectra.

[29] CHATRCHYAN 12AE searched in 4.98 fb^{-1} of pp collisions at $\sqrt{s} = 7$ TeV for events with at least three jets and large missing transverse momentum. No significant excesses over the expected SM backgrounds are observed and 95% C.L. limits on the production cross section of squarks in a scenario where $\tilde{q} \rightarrow q\tilde{\chi}_1^0$ with a 100% branching ratio, see Fig. 3. For $m_{\tilde{\chi}_1^0} < 200$ GeV, values of $m_{\tilde{q}}$ below 760 GeV are excluded at 95% C.L. Also limits in the CMSSM are presented, see Fig. 2.

[30] CHATRCHYAN 12AT searched in 4.73 fb^{-1} of pp collisions at $\sqrt{s} = 7$ TeV for the production of squarks and gluinos in events containing jets, missing transverse momentum and no electrons or muons. No excess over the expected SM background is observed. In mSUGRA/CMSSM models with $\tan\beta = 10$, $A_0 = 0$ and $\mu > 0$, squarks with masses below 1110 GeV are excluded at 95% C.L. Squarks and gluinos of equal mass are excluded for masses below 1180 GeV at 95% C.L. Exclusions are also derived in various simplified models, see Fig. 6.

[31] KHACHATRYAN 16BT performed a global Bayesian analysis of a wide range of CMS results obtained with data samples corresponding to 5.0 fb^{-1} of pp collisions at $\sqrt{s} =$ 7 TeV and in 19.5 fb^{-1} of pp collisions at $\sqrt{s} = 8$ TeV. The set of searches considered, both individually and in combination, includes those with all-hadronic final states, same-sign and opposite-sign dileptons, and multi-lepton final states. An interpretation was given in a scan of the 19-parameter pMSSM. No scan points with a gluino mass less than 500 GeV survived and 98% of models with a squark mass less than 300 GeV were excluded.

[32] AAD 15AI searched in 20 fb^{-1} of pp collisions at $\sqrt{s} = 8$ TeV for events containing at least one isolated lepton (electron or muon), jets, and large missing transverse momentum. No excess of events above the expected level of Standard Model background was found. Exclusion limits at 95% C.L. are set on the squark masses in the CMSSM/mSUGRA, see Fig. 15, in the NUHMG, see Fig. 16, and in various simplified models, see Figs. 19–21.

[33] KHACHATRYAN 15AR searched in 19.7 fb^{-1} of pp collisions at $\sqrt{s}$ = 8 TeV for events containing jets, either a charged lepton or a photon, and low missing transverse momentum. No significant excess above the Standard Model expectations is observed. Limits are set on the squark mass in a stealth SUSY model where the decays $\tilde{q} \to q\tilde{\chi}_1^{\pm}$, $\tilde{\chi}_1^{\pm} \to \tilde{S}\,W^{\pm}$, $\tilde{S} \to S\,\tilde{G}$ and $S \to gg$, with $m_{\tilde{S}}$ = 100 GeV and m_S = 90 GeV, take place with a branching ratio of 100%. See Fig. 6 for γ or Fig. 7 for $\ell^{\pm}$ analyses.

[34] KHACHATRYAN 15AZ searched in 19.7 fb^{-1} of pp collisions at $\sqrt{s}$ = 8 TeV for events with either at least one photon, hadronic jets and $\not{E}_T$ (single photon channel) or with at least two photons and at least one jet and using the razor variables. No significant excess above the Standard Model expectations is observed. Limits are set on gluino masses in the general gauge-mediated SUSY breaking model (GGM), for both a bino-like and wino-like neutralino NLSP scenario, see Fig. 8 and 9.

[35] AAD 14E searched in 20.3 fb^{-1} of pp collisions at $\sqrt{s}$ = 8 TeV for strongly produced supersymmetric particles in events containing jets and two same-sign leptons or three leptons. The search also utilises jets originating from b-quarks, missing transverse momentum and other variables. No excess over the expected SM background is observed. Exclusion limits are derived in simplified models containing gluinos and squarks, see Figures 5 and 6. In the $\tilde{q} \to q'\tilde{\chi}_1^{\pm}$, $\tilde{\chi}_1^{\pm} \to W^{(*)\pm}\tilde{\chi}_2^0$, $\tilde{\chi}_2^0 \to Z^{(*)}\tilde{\chi}_1^0$ simplified model, the following assumptions have been made: $m_{\tilde{\chi}_1^{\pm}} = 0.5\ m_{\tilde{\chi}_1^0} + m_{\tilde{g}}$, $m_{\tilde{\chi}_2^0} = 0.5\ (\ m_{\tilde{\chi}_1^0} + m_{\tilde{\chi}_1^{\pm}}\ )$. In the $\tilde{q} \to q'\tilde{\chi}_1^{\pm}$ or $\tilde{q} \to q'\tilde{\chi}_2^0$, $\tilde{\chi}_1^{\pm} \to \ell^{\pm}\nu\tilde{\chi}_1^0$ or $\tilde{\chi}_2^0 \to \ell^{\pm}\ell^{\mp}(\nu\nu)\tilde{\chi}_1^0$ simplified model, the following assumptions have been made: $m_{\tilde{\chi}_1^{\pm}} = m_{\tilde{\chi}_2^0} = 0.5\ (\ m_{\tilde{\chi}_1^0} + m_{\tilde{q}}\ )$, $m_{\tilde{\chi}_1^0} < 460$ GeV. Limits are also derived in the mSUGRA/CMSSM, bRPV and GMSB models, see their Fig. 8.

[36] CHATRCHYAN 13AO searched in 4.98 fb^{-1} of pp collisions at $\sqrt{s}$ = 7 TeV for events with two opposite-sign isolated leptons accompanied by hadronic jets and $\not{E}_T$. No significant excesses over the expected SM backgrounds are observed and 95% C.L. exclusion limits are derived in the mSUGRA/CMSSM model with tanβ = 10, A_0 = 0 and $\mu > 0$, see Fig. 8.

[37] CHATRCHYAN 13AV searched in 4.7 fb^{-1} of pp collisions at $\sqrt{s}$ = 7 TeV for new heavy particle pairs decaying into jets (possibly b-tagged), leptons and $\not{E}_T$ using the Razor variables. No significant excesses over the expected SM backgrounds are observed and 95% C.L. exclusion limits are derived in the mSUGRA/CMSSM model with tanβ = 10, A_0 = 0 and $\mu > 0$, see Fig. 3. The results are also interpreted in various simplified models, see Fig. 4.

[38] CHATRCHYAN 13W searched in 4.93 fb^{-1} of pp collisions at $\sqrt{s}$ = 7 TeV for events with one or more photons, hadronic jets and $\not{E}_T$. No significant excess above the Standard Model expectations is observed. Limits are set on squark masses in the general gauge-mediated SUSY breaking model (GGM), for both a wino-like and bino-like neutralino NLSP scenario, see Fig. 5.

[39] DREINER 12A reassesses constraints from CMS (at 7 TeV, $\sim$ 4.4 fb^{-1}) under the assumption that the fist and second generation squarks and the lightest SUSY particle are quasi-degenerate in mass (compressed spectrum).

[40] DREINER 12A reassesses constraints from CMS (at 7 TeV, $\sim$ 4.4 fb^{-1}) under the assumption that the first and second generation squarks, the gluino, and the lightest SUSY particle are quasi-degenerate in mass (compressed spectrum).

R-parity violating $\tilde{q}$ (Squark) mass limit

VALUE (GeV)	CL%	DOCUMENT ID		TECN	COMMENT
>1600	95	[1] KHACHATRY...16BX		CMS	RPV, $\tilde{q} \to q\tilde{\chi}_1^0$, $\tilde{\chi}_1^0 \to \ell\ell\nu$, λ_{121} or $\lambda_{122} \neq 0$, $m_{\tilde{g}}$ = 2400 GeV
>1000	95	[2] AAD	15CB	ATLS	RPV, jets, $\tilde{q} \to q\tilde{\chi}_1^0$, $\tilde{\chi}_1^0 \to \ell qq$, $m_{\tilde{\chi}_1^0}$ = 108 GeV and $2.5 < c\tau_{\tilde{\chi}_1^0} < 200$ mm
		[3] AAD	12AX	ATLS	ℓ +jets +$\not{E}_T$, CMSSM, $m_{\tilde{q}}$=$m_{\tilde{g}}$
		[4] CHATRCHYAN	12AL	CMS	RPV, $\geq 3\ell^{\pm}$

[1] KHACHATRYAN 16BX searched in 19.5 fb^{-1} of pp collisions at $\sqrt{s}$ = 8 TeV for events containing 4 leptons coming from R-parity-violating decays of $\tilde{\chi}_1^0 \to \ell\ell\nu$ with $\lambda_{121} \neq 0$ or $\lambda_{122} \neq 0$. No excess over the expected background is observed. Limits are derived on the gluino, squark and stop masses, see Fig. 23.

[2] AAD 15CB searched for events containing at least one long-lived particle that decays at a significant distance from its production point (displaced vertex, DV) into two leptons or into five or more charged particles in 20.3 fb^{-1} of pp collisions at $\sqrt{s}$ = 8 TeV. The dilepton signature is characterised by DV formed from at least two lepton candidates. Four different final states were considered for the multitrack signature, in which the DV must be accompanied by a high-transverse momentum muon or electron candidate that originates from the DV, jets or missing transverse momentum. No events were observed in any of the signal regions. Results were interpreted in SUSY scenarios involving R-parity violation, split supersymmetry, and gauge mediation. See their Fig. 14–20.

[3] AAD 12AX searched in 1.04 fb^{-1} of pp collisions at $\sqrt{s}$ = 7 TeV for supersymmetry in events containing jets, missing transverse momentum and one isolated electron or muon. No excess over the expected SM background is observed and model-independent limits are set on the cross section of new physics contributions to the signal regions. In mSUGRA/CMSSM models with tanβ = 10, A_0 = 0 and $\mu > 0$, squarks and gluinos of equal mass are excluded for masses below 820 GeV at 95% C.L. Limits are also set on simplified models for squark production and decay via an intermediate chargino and on supersymmetric models with bilinear R-parity violation. Supersedes AAD 11G.

[4] CHATRCHYAN 12AL looked in 4.98 fb^{-1} of pp collisions at $\sqrt{s}$ = 7 TeV for anomalous production of events with three or more isolated leptons. Limits on squark and gluino masses are set in RPV SUSY models with leptonic $LL\bar{E}$couplings, $\lambda_{123} > 0.05$, and hadronic $\overline{UDD}$ couplings, $\lambda''_{112} > 0.05$, see their Fig. 5. In the $\overline{UDD}$ case the leptons arise from supersymmetric cascade decays. A very specific supersymmetric spectrum is assumed. All decays are prompt.

Long-lived $\tilde{q}$ (Squark) mass limit

The following are bounds on long-lived scalar quarks, assumed to hadronise into hadrons with lifetime long enough to escape the detector prior to a possible decay. Limits may depend on the mixing angle of mass eigenstates: $\tilde{q}_1$=$\tilde{q}_L\cos\theta_q + \tilde{q}_R\sin\theta_q$.

The coupling to the Z^0 boson vanishes for up-type squarks when θ_u=0.98, and for down type squarks when θ_d=1.17.

VALUE (GeV)	CL%	DOCUMENT ID		TECN	COMMENT
> 805	95	[1] AABOUD	16B	ATLS	$\tilde{b}$ R-hadrons
> 890	95	[2] AABOUD	16B	ATLS	$\tilde{t}$ R-hadrons
>1040	95	[3] KHACHATRY...16BW		CMS	$\tilde{t}$ R-hadrons, cloud interaction model
>1000	95	[3] KHACHATRY...16BW		CMS	$\tilde{t}$ R-hadrons, charge-suppressed interaction model
> 845	95	[4] AAD	15AE	ATLS	$\tilde{b}$ R-hadron, stable, Regge model
> 900	95	[4] AAD	15AE	ATLS	$\tilde{t}$ R-hadron, stable, Regge model
>1500	95	[4] AAD	15AE	ATLS	$\tilde{g}$ decaying to 300 GeV stable sleptons, LeptoSUSY model
> 751	95	[5] AAD	15BM	ATLS	$\tilde{b}$ R-hadron, stable, Regge model
> 766	95	[5] AAD	15BM	ATLS	$\tilde{t}$ R-hadron, stable, Regge model
> 525	95	[6] KHACHATRY...15AK		CMS	$\tilde{t}$ R-hadrons, 10 μs< τ <1000 s
> 470	95	[6] KHACHATRY...15AK		CMS	$\tilde{t}$ R-hadrons, 1 μs< τ <1000 s
• • • We do not use the following data for averages, fits, limits, etc. • • •					
> 683	95	[7] AAD	13AA	ATLS	$\tilde{t}$, R-hadrons, generic interaction model
> 612	95	[8] AAD	13AA	ATLS	$\tilde{b}$, R-hadrons, generic interaction model
> 344	95	[9] AAD	13BC	ATLS	R-hadrons, $\tilde{t} \to b\tilde{\chi}_1^0$, Regge model, lifetime between 10^{-5} and 10^3 s, $m_{\tilde{\chi}_1^0}$ = 100 GeV
> 379	95	[10] AAD	13BC	ATLS	R-hadrons, $\tilde{t} \to t\tilde{\chi}_1^0$, Regge model, lifetime between 10^{-5} and 10^3 s, $m_{\tilde{\chi}_1^0}$ = 100 GeV
> 935	95	[11] CHATRCHYAN	13AB	CMS	long-lived $\tilde{t}$ forming R-hadrons, cloud interaction model

[1] AABOUD 16B searched in 3.2 fb^{-1} of pp collisions at $\sqrt{s}$ = 13 TeV for long-lived R-hadrons using observables related to large ionization losses and slow propagation velocities, which are signatures of heavy charged particles traveling significantly slower than the speed of light. Exclusion limits at 95% C.L. are set on the long-lived sbottom masses exceeding 805 GeV. See their Fig. 5.

[2] AABOUD 16B searched in 3.2 fb^{-1} of pp collisions at $\sqrt{s}$ = 13 TeV for long-lived R-hadrons using observables related to large ionization losses and slow propagation velocities, which are signatures of heavy charged particles traveling significantly slower than the speed of light. Exclusion limits at 95% C.L. are set on the long-lived stop masses exceeding 890 GeV. See their Fig. 5.

[3] KHACHATRYAN 16BW searched in 2.5 fb^{-1} of pp collisions at $\sqrt{s}$ = 13 TeV for events with heavy stable charged particles, identified by their anomalously high energy deposits in the silicon tracker and/or long time-of-flight measurements by the muon system. No evidence for an excess over the expected background is observed. Limits are derived for pair production of top squarks as a function of mass, depending on the interaction model, see Fig. 4 and Table 7.

[4] AAD 15AE searched in 19.1 fb^{-1} of pp collisions at $\sqrt{s}$ = 8 TeV for heavy long-lived charged particles, measured through their specific ionization energy loss in the ATLAS pixel detector or their time-of-flight in the ALTAS muon system. In the absence of an excess of events above the expected backgrounds, limits are set R-hadrons in various scenarios, see Fig. 11. Limits are also set in LeptoSUSY models where the gluino decays to stable 300 GeV leptons, see Fig. 9.

[5] AAD 15BM searched in 18.4 fb^{-1} of pp collisions at $\sqrt{s}$ = 8 TeV for stable and metastable non-relativistic charged particles through their anomalous specific ionization energy loss in the ATLAS pixel detector. In absence of an excess of events above the expected backgrounds, limits are set on stable bottom and top squark R-hadrons, see Table 5.

[6] KHACHATRYAN 15AK looked in a data set corresponding to fb^{-1} of pp collisions at $\sqrt{s}$ = 8 TeV, and a search interval corresponding to 281 h of trigger lifetime, for long-lived particles that have stopped in the CMS detector. No evidence for an excess over the expected background in a cloud interaction model is observed. Assuming the decay $\tilde{t} \to t\tilde{\chi}_1^0$ and lifetimes between 1 μs and 1000 s, limits are derived on $\tilde{t}$ production as a function of $m_{\tilde{\chi}_1^0}$, see Figs. 4 and 7. The exclusions require that $m_{\tilde{\chi}_1^0}$ is kinematically consistent with the minimum values of the jet energy thresholds used.

[7] AAD 13AA searched in 4.7 fb^{-1} of pp collisions at $\sqrt{s}$ = 7 TeV for events containing colored long-lived particles that hadronize forming R-hadrons. No significant excess above the expected background was found. Long-lived R-hadrons containing a $\tilde{t}$ are excluded for masses up to 683 GeV at 95% C.L in a general interaction model. Also, limits independent of the fraction of R-hadrons that arrive charged in the muon system were derived, see Fig. 6.

[8] AAD 13AA searched in 4.7 fb^{-1} of pp collisions at $\sqrt{s}$ = 7 TeV for events containing colored long-lived particles that hadronize forming R-hadrons. No significant excess above the expected background was found. Long-lived R-hadrons containing a $\tilde{b}$ are excluded for masses up to 612 GeV at 95% C.L in a general interaction model. Also, limits independent of the fraction of R-hadrons that arrive charged in the muon system were derived, see Fig. 6.

[9] AAD 13BC searched in 5.0 fb^{-1} of pp collisions at $\sqrt{s}$ = 7 TeV and in 22.9 fb^{-1} of pp collisions at $\sqrt{s}$ = 8 TeV for bottom squark R-hadrons that have come to rest within the ATLAS calorimeter and decay at some later time to hadronic jets and a neutralino. In absence of an excess of events above the expected backgrounds, limits are set on sbottom masses for the decay $\tilde{b} \to b\tilde{\chi}_1^0$, for different lifetimes, and for a neutralino mass of 100 GeV, see their Table 6 and Fig 10.

[10] AAD 13BC searched in 5.0 fb^{-1} of pp collisions at $\sqrt{s}$ = 7 TeV and in 22.9 fb^{-1} of pp collisions at $\sqrt{s}$ = 8 TeV for bottom squark R-hadrons that have come to rest within the ATLAS calorimeter and decay at some later time to hadronic jets and a neutralino. In absence of an excess of events above the expected backgrounds, limits are set on stop masses for the decay $\tilde{t} \to t\tilde{\chi}_1^0$, for different lifetimes, and for a neutralino mass of 100 GeV, see their Table 6 and Fig 10.

[11] CHATRCHYAN 13AB looked in 5.0 fb^{-1} of pp collisions at $\sqrt{s}$ = 7 TeV and in 18.8 fb^{-1} of pp collisions at $\sqrt{s}$ = 8 TeV for events with heavy stable particles, identified by their anomalous dE/dx in the tracker or additionally requiring that it be identified as muon in the muon chambers, from pair production of $\tilde{t}_1$'s. No evidence for an excess over the expected background is observed. Limits are derived for pair production of stops as a function of mass in the cloud interaction model (see Fig. 8 and Table 6). In the charge-suppressed model, the limit decreases to 818 GeV.

$\tilde{b}$ (Sbottom) mass limit

Limits in e^+e^- depend on the mixing angle of the mass eigenstate $\tilde{b}_1 = \tilde{b}_L \cos\theta_b + \tilde{b}_R \sin\theta_b$. Coupling to the Z vanishes for $\theta_b \sim 1.17$. As a consequence, no absolute constraint in the mass region $\lesssim$40 GeV is available in the literature at this time from e^+e^- collisions. In the Listings below, we use $\Delta m = m_{\tilde{b}_1} - m_{\tilde{\chi}^0_1}$.

Some earlier papers are now obsolete and have been omitted. They were last listed in our PDG 14 edition: K. Olive, *et al.* (Particle Data Group), Chinese Physics **C38** 070001 (2014) (http://pdg.lbl.gov).

R-parity conserving $\tilde{b}$ (Sbottom) mass limit

VALUE (GeV)	CL%	DOCUMENT ID		TECN	COMMENT
>1230	95	[1] SIRUNYAN	18B	CMS	jets+$\not{E}_T$, Tsbot1, $m_{\tilde{\chi}^0_1}$ = 0 GeV
> 700	95	[2] AABOUD	17AJ	ATLS	same-sign $\ell^\pm\ell^\pm$ / 3 ℓ + jets + $\not{E}_T$, Tsbot2, $m_{\tilde{\chi}^0_1}$ = 0 GeV
> 950	95	[3] AABOUD	17AX	ATLS	2 b-jets+$\not{E}_T$, Tsbot1, $m_{\tilde{\chi}^0_1}$ = 0 GeV
> 880	95	[4] AABOUD	17AX	ATLS	2 b-jets + $\not{E}_T$, mixture Tsbot1 and Tsbot2 BR=50%, $m_{\tilde{\chi}^0_1}$ = 0 GeV, $m_{\tilde{\chi}^\pm_1} - m_{\tilde{\chi}^0_1}$ = 1 GeV
> 315	95	[5] KHACHATRY...17A		CMS	2 VBF jets + $\not{E}_T$, Tsbot1, $m_{\tilde{b}} - m_{\tilde{\chi}^0_1}$ = 5 GeV
> 450	95	[6] KHACHATRY...17AW		CMS	$\geq 3\ell^\pm$, 2 jets, Tsbot2, $m_{\tilde{\chi}^0_1}$ = 50 GeV, $m_{\tilde{\chi}^\pm_1}$ = 200 GeV
> 800	95	[7] KHACHATRY...17P		CMS	1 or more jets+$\not{E}_T$, Tsbot1, $m_{\tilde{\chi}^0_1}$ = 0 GeV
>1175	95	[8] SIRUNYAN	17AZ	CMS	$\geq$ 1 jets+$\not{E}_T$, Tsbot1, $m_{\tilde{\chi}^0_1}$ = 0 GeV
> 890	95	[9] SIRUNYAN	17K	CMS	jets+$\not{E}_T$, Tsbot1, $m_{\tilde{\chi}^0_1}$ = 0 GeV
> 810	95	[10] SIRUNYAN	17S	CMS	same-sign $\ell^\pm\ell^\pm$ + jets + $\not{E}_T$, Tsbot2, $m_{\tilde{\chi}^0_1}$ = 50 GeV, $m_{\tilde{\chi}^\pm_1}$ = 100 GeV
> 323	95	[11] AABOUD	16D	ATLS	$\geq$1 jet + $\not{E}_T$, Tsbot1, $m_{\tilde{b}_1} - m_{\tilde{\chi}^0_1}$ = 5 GeV
> 840	95	[12] AABOUD	16Q	ATLS	2 b-jets + $\not{E}_T$, Tsbot1, $m_{\tilde{\chi}^0_1}$ = 100 GeV
> 540	95	[13] AAD	16BB	ATLS	2 same-sign/3ℓ + jets + $\not{E}_T$, Tsbot2, $m_{\tilde{\chi}^0_1}$ < 55 GeV
> 680	95	[14] KHACHATRY...16BJ		CMS	same-sign $\ell^\pm\ell^\pm$, Tsbot2, $m_{\tilde{\chi}^\pm_1}$ < 550 GeV, $m_{\tilde{\chi}^0_1}$ = 50 GeV
> 500	95	[14] KHACHATRY...16BJ		CMS	same-sign $\ell^\pm\ell^\pm$, Tsbot2, $m_{\tilde{b}} - m_{\tilde{\chi}^\pm_1}$ <100 GeV, $m_{\tilde{\chi}^0_1}$=50 GeV
> 880	95	[15] KHACHATRY...16BS		CMS	jets + $\not{E}_T$, Tsbot1, $m_{\tilde{\chi}^0_1}$ = 0 GeV
> 550	95	[16] KHACHATRY...16BY		CMS	opposite-sign $\ell^\pm\ell^\pm$, Tsbot3, $m_{\tilde{\chi}^0_1}$ = 100 GeV
> 600	95	[17] AAD	15CJ	ATLS	$\tilde{b} \to b\tilde{\chi}^0_1$, $m_{\tilde{\chi}^0_1}$ < 250 GeV
> 440	95	[17] AAD	15CJ	ATLS	$\tilde{b} \to t\tilde{\chi}^\pm_1$, $\tilde{\chi}^\pm_1 \to W^{(*)}\tilde{\chi}^0_1$, $m_{\tilde{\chi}^0_1}$ = 60 GeV, $m_{\tilde{b}} - m_{\tilde{\chi}^\pm_1} < m_t$
none 300–650	95	[17] AAD	15CJ	ATLS	$\tilde{b} \to \tilde{b}b\tilde{\chi}^0_2$, $\tilde{\chi}^0_2 \to h\tilde{\chi}^0_1$, $m_{\tilde{\chi}^0_1}$ = 60 GeV, $m_{\tilde{\chi}^0_2}$ > 250 GeV
> 640	95	[18] KHACHATRY...15AF		CMS	$\tilde{b} \to b\tilde{\chi}^0_1$, $m_{\tilde{\chi}^0_1}$ = 0
> 650	95	[19] KHACHATRY...15AH		CMS	$\tilde{b} \to b\tilde{\chi}^0_1$, $m_{\tilde{\chi}^0_1}$ = 0
> 250	95	[19] KHACHATRY...15AH		CMS	$\tilde{b} \to b\tilde{\chi}^0_1$, $m_{\tilde{b}} - m_{\tilde{\chi}^0_1}$ < 10 GeV
> 570	95	[20] KHACHATRY...15I		CMS	$\tilde{b} \to t\tilde{\chi}^\pm_1$, $\tilde{\chi}^\pm_1 \to W^\pm\tilde{\chi}^0_1$, $m_{\tilde{\chi}^0_1}$ =50 GeV, 150<$m_{\tilde{\chi}^\pm_1}$ <300 GeV
> 255	95	[21] AAD	14T	ATLS	$\tilde{b}_1 \to b\tilde{\chi}^0_1$, $m_{\tilde{b}_1} - m_{\tilde{\chi}^0_1} \approx m_b$
> 400	95	[22] CHATRCHYAN	14AH	CMS	jets + $\not{E}_T$, $\tilde{b} \to b\tilde{\chi}^0_1$ simplified model, $m_{\tilde{\chi}^0_1}$ = 50 GeV
		[23] CHATRCHYAN	14R	CMS	$\geq 3\ell^\pm$, $\tilde{b} \to t\tilde{\chi}^\pm_1$, $\tilde{\chi}^\pm_1 \to W^\pm\tilde{\chi}^0_1$ simplified model, $m_{\tilde{\chi}^0_1}$ = 50 GeV

• • • We do not use the following data for averages, fits, limits, etc. • • •

		[24] KHACHATRY...15AD		CMS	$\ell^\pm\ell^\mp$ + jets + $\not{E}_T$, $\tilde{b} \to b\ell^\pm\ell^\mp\tilde{\chi}^0_1$
none 340–600	95	[25] AAD	14AX	ATLS	$\geq$ 3 b-jets + $\not{E}_T$, $\tilde{b} \to b\tilde{\chi}^0_2$ simplified model with $\tilde{\chi}^0_2 \to h\tilde{\chi}^0_1$, $m_{\tilde{\chi}^0_1}$=60 GeV, $m_{\tilde{\chi}^0_2}$=300 GeV
> 440	95	[26] AAD	14E	ATLS	$\ell^\pm\ell^\pm(\ell^\mp)$ + jets, $\tilde{b}_1 \to t\tilde{\chi}^\pm_1$ with $\tilde{\chi}^\pm_1 \to W^{(*)\pm}\tilde{\chi}^0_1$ simplified model, $m_{\tilde{\chi}^\pm_1} = 2\, m_{\tilde{\chi}^0_1}$
> 500	95	[27] CHATRCHYAN	14H	CMS	same-sign $\ell^\pm\ell^\pm$, $\tilde{b} \to t\tilde{\chi}^\pm_1$, $\tilde{\chi}^\pm_1 \to W^\pm\tilde{\chi}^0_1$ simplified model, $m_{\tilde{\chi}^\pm_1}$ = 2 GeV, $m_{\tilde{\chi}^0_1}$ = 100 GeV
> 620	95	[28] AAD	13AU	ATLS	2 b-jets + $\not{E}_T$, $\tilde{b}_1 \to b\tilde{\chi}^0_1$, $m_{\tilde{\chi}^0_1}$ < 120 GeV
> 550	95	[29] CHATRCHYAN	13AT	CMS	jets + $\not{E}_T$, $\tilde{b} \to b\tilde{\chi}^0_1$ simplified model, $m_{\tilde{\chi}^0_1}$= 50 GeV
> 600	95	[30] CHATRCHYAN	13T	CMS	jets + $\not{E}_T$, $\tilde{b} \to b\tilde{\chi}^0_1$ simplified model, $m_{\tilde{\chi}^0_1}$= 0 GeV
> 450	95	[31] CHATRCHYAN	13V	CMS	same-sign $\ell^\pm\ell^\pm$ + $\geq$ 2 b-jets, $\tilde{b} \to t\tilde{\chi}^\pm_1$, $\tilde{\chi}^\pm_1 \to W^\pm\tilde{\chi}^0_1$ simplified model, $m_{\tilde{\chi}^0_1}$ = 50 GeV
> 390		[32] AAD	12AN	ATLS	$\tilde{b}_1 \to b\tilde{\chi}^0_1$, simplified model, $m_{\tilde{\chi}^0_1}$ < 60 GeV
		[33] CHATRCHYAN	12AI	CMS	$\ell^\pm\ell^\pm$ + b-jets + $\not{E}_T$
> 410	95	[34] CHATRCHYAN	12BO	CMS	$\tilde{b}_1 \to b\tilde{\chi}^0_1$, simplified model, $m_{\tilde{\chi}^0_1}$ = 50 GeV
> 294	95	[35] AAD	11K	ATLS	stable b
		[36] AAD	11O	ATLS	$\tilde{g} \to \tilde{b}_1 b$, $\tilde{b}_1 \to b\tilde{\chi}^0_1$, $m_{\tilde{\chi}^0_1}$=60 GeV
		[37] CHATRCHYAN	11D	CMS	$\tilde{b}, \tilde{t} \to b$
> 230	95	[38] AALTONEN	10R	CDF	$\tilde{b}_1 \to b\tilde{\chi}^0_1$, $m_{\tilde{\chi}^0_1}$ < 70 GeV
> 247	95	[39] ABAZOV	10L	D0	$\tilde{b}_1 \to b\tilde{\chi}^0_1$, $m_{\tilde{\chi}^0_1}$ = 0 GeV

[1] SIRUNYAN 18B searched in 35.9 fb^{-1} of pp collisions at $\sqrt{s}$ = 13 TeV for the pair production of third-generation squarks in events with jets and large $\not{E}_T$. No significant excess above the Standard Model expectations is observed. Limits are set on the sbottom mass in the Tsbot1 simplified model, see their Figure 5, and on the stop mass in the Tstop4 simplified model, see their Figure 6.

[2] AABOUD 17AJ searched in 36.1 fb^{-1} of pp collisions at $\sqrt{s}$ = 13 TeV for events with two same-sign or three leptons, jets and large missing transverse momentum. No significant excess above the Standard Model expectations is observed. Limits up to 700 GeV are set on the bottom squark mass in Tsbot2 simplified models assuming $m_{\tilde{\chi}^0_1}$ = 0 GeV. See their Figure 4(d).

[3] AABOUD 17AX searched in 36 fb^{-1} of pp collisions at $\sqrt{s}$ = 13 TeV for events containing two jets identified as originating from b-quarks and large missing transverse momentum. No excess of events above the expected level of Standard Model background was found. Exclusion limits at 95% C.L. are set on the masses of bottom squarks. In the Tsbot1 simplified model, a $\tilde{b}_1$ mass below 950 GeV is excluded for $m_{\tilde{\chi}^0_1}$ = 0 (<420) GeV. See their Fig. 7(a).

[4] AABOUD 17AX searched in 36 fb^{-1} of pp collisions at $\sqrt{s}$ = 13 TeV for events containing two jets identified as originating from b-quarks and large missing transverse momentum, with or without leptons. No excess of events above the expected level of Standard Model background was found. Exclusion limits at 95% C.L. are set on the masses of bottom squarks. Assuming 50% BR for Tsbot1 and Tsbot2 simplified models, a $\tilde{b}_1$ mass below 880 (860) GeV is excluded for $m_{\tilde{\chi}^0_1}$ = 0 (<250) GeV. See their Fig. 7(b).

[5] KHACHATRYAN 17A searched in 18.5 fb^{-1} of pp collisions at $\sqrt{s}$ = 8 TeV for events with two forward jets, produced through vector boson fusion, and missing transverse momentum. No significant excess above the Standard Model expectations is observed. A limit is set on sbottom masses in the Tsbot1 simplified model, see Fig. 3.

[6] KHACHATRYAN 17AW searched in 2.3 fb^{-1} of pp collisions at $\sqrt{s}$ = 13 TeV for events with at least three charged leptons, in any combination of electrons and muons, and significant $\not{E}_T$. No significant excess above the Standard Model expectations is observed. Limits are set on the gluino mass in the Tglu3A and Tglu1C simplified models, and on the sbottom mass in the Tsbot2 simplified model, see their Figure 4.

[7] KHACHATRYAN 17P searched in 2.3 fb^{-1} of pp collisions at $\sqrt{s}$ = 13 TeV for events with one or more jets and large $\not{E}_T$. No significant excess above the Standard Model expectations is observed. Limits are set on the gluino mass in the Tglu1A, Tglu2A, Tglu3A, Tglu3B, Tglu3C and Tglu3D simplified models, see their Figures 7 and 8. Limits are also set on the squark mass in the Tsqk1 simplified model, see their Fig. 7, and on the sbottom mass in the Tsbot1 simplified model, see Fig. 8. Finally, limits are set on the stop mass in the Tstop1, Tstop3, Tstop4, Tstop6 and Tstop7 simplified models, see Fig. 8.

[8] SIRUNYAN 17AZ searched in 35.9 fb^{-1} of pp collisions at $\sqrt{s}$ = 13 TeV for events with one or more jets and large $\not{E}_T$. No significant excess above the Standard Model expectations is observed. Limits are set on the gluino mass in the Tglu1A, Tglu2A, Tglu3A simplified models, see their Figures 6. Limits are also set on the squark mass in the Tsqk1 simplified model (for single light squark and for 8 degenerate light squarks), on the sbottom mass in the Tsbot1 simplified model and on the stop mass in the Tstop1 simplified model, see their Fig. 7. Finally, limits are set on the stop mass in the Tstop2, Tstop4 and Tstop8 simplified models, see Fig. 8.

[9] SIRUNYAN 17K searched in 2.3 fb^{-1} of pp collisions at $\sqrt{s}$ = 13 TeV for direct production of stop or sbottom pairs in events with multiple jets and significant $\not{E}_T$. A second search also requires an isolated lepton and is combined with the all-hadronic search. No significant excess above the Standard Model expectations is observed. Limits are set on the stop mass in the Tstop1, Tstop8 and Tstop4 simplified models, see their Figures 7, 8 and 9 (for the Tstop4 limits, only the results of the all-hadronic search are used). Limits are also set on the sbottom mass in the Tsbot1 simplified model, see Fig. 10 (also here, only the results of the all-hadronic search are used).

[10] SIRUNYAN 17S searched in 35.9 fb^{-1} of pp collisions at $\sqrt{s}$ = 13 TeV for events with two isolated same-sign leptons, jets, and large $\not{E}_T$. No significant excess above the Standard Model expectations is observed. Limits are set on the mass of the gluino mass in the Tglu3A, Tglu3B, Tglu3C, Tglu3D and Tglu1B simplified models, see their Figures 5 and 6, and on the sbottom mass in the Tsbot2 simplified model, see their Figure 6.

[11] AABOUD 16D searched in 3.2 fb^{-1} of pp collisions at $\sqrt{s}$ = 13 TeV for events with an energetic jet and large missing transverse momentum. The results are interpreted as 95%C.L. limits on mass of sbottom decaying into a b-quark and the lightest neutralino in scenarios with $m_{\tilde{b}_1} - m_{\tilde{\chi}_1^0}$ between 5 and 20 GeV. See their Fig. 6.

[12] AABOUD 16Q searched in 3.2 fb^{-1} of pp collisions at $\sqrt{s}$ = 13 TeV for events containing two jets identified as originating from b-quarks and large missing transverse momentum. No excess of events above the expected level of Standard Model background was found. Exclusion limits at 95% C.L. are set on the masses of third-generation squarks. Assuming that the decay $\tilde{b}_1 \rightarrow b\tilde{\chi}_1^0$ (Tsbot1) takes place 100% of the time, a $\tilde{b}_1$ mass below 840 (800) GeV is excluded for $m_{\tilde{\chi}_1^0} < 100$ (360) GeV. Differences in mass above 100 GeV between the $\tilde{b}_1$ and the $\tilde{\chi}_1^0$ are excluded up to a $\tilde{b}_1$ mass of 500 GeV. For more details, see their Fig. 4.

[13] AAD 16BB searched in 3.2 fb^{-1} of pp collisions at $\sqrt{s}$ = 13 TeV for events with exactly two same-sign leptons or at least three leptons, multiple hadronic jets, b-jets, and $\not{E}_T$. No significant excess over the Standard Model expectation is found. Exclusion limits at 95% C.L. are set on the sbottom mass for the Tsbot2 model, assuming $m_{\tilde{\chi}_1^\pm} = m_{\tilde{\chi}_1^0}$ + 100 GeV. See their Fig. 4c.

[14] KHACHATRYAN 16BJ searched in 2.3 fb^{-1} of pp collisions at $\sqrt{s}$ = 13 TeV for events with two isolated same-sign dileptons and jets in the final state. No significant excess above the Standard Model expectations is observed. Limits are set on the sbottom mass in the Tsbot2 simplified model, see Fig. 6.

[15] KHACHATRYAN 16BS searched in 2.3 fb^{-1} of pp collisions at $\sqrt{s}$ = 13 TeV for events with at least one energetic jet , no isolated leptons, and significant $\not{E}_T$, using the transverse mass variable M_{T2} to discriminate between signal and background processes. No significant excess above the Standard Model expectations is observed. Limits are set on the sbottom mass in the Tsbot1 simplified model, see Fig. 11 and Table 3.

[16] KHACHATRYAN 16BY searched in 2.3 fb^{-1} of pp collisions at $\sqrt{s}$ = 13 TeV for events with two opposite-sign, same-flavour leptons, jets, and missing transverse momentum. No significant excess above the Standard Model expectations is observed. Limits are set on the gluino mass in the Tglu4C simplified model, see Fig. 4, and on sbottom masses in the Tsbot3 simplified model, see Fig. 5.

[17] AAD 15CJ searched in 20 fb^{-1} of pp collisions at $\sqrt{s}$ = 8 TeV for evidence of third generation squarks by combining a large number of searches covering various final states. Limits on the sbottom mass are shown, either assuming the $\tilde{b} \rightarrow b\tilde{\chi}_1^0$ decay, see Fig. 11, or assuming the $\tilde{b} \rightarrow t\tilde{\chi}_1^\pm$ decay, with $\tilde{\chi}_1^\pm \rightarrow W^{(*)}\tilde{\chi}_1^0$, see Fig. 12a, or assuming the $\tilde{b} \rightarrow b\tilde{\chi}_2^0$ decay, with $\tilde{\chi}_2^0 \rightarrow h\tilde{\chi}_1^0$, see Fig. 12b. Interpretations in the pMSSM are also discussed, see Figures 13–15.

[18] KHACHATRYAN 15AF searched in 19.5 fb^{-1} of pp collisions at $\sqrt{s}$ = 8 TeV for events with at least two energetic jets and significant $\not{E}_T$, using the transverse mass variable M_{T2} to discriminate between signal and background processes. No significant excess above the Standard Model expectations is observed. Limits are set on the sbottom mass in simplified models where the decay $\tilde{b} \rightarrow b\tilde{\chi}_1^0$ takes place with a branching ratio of 100%, see Fig. 12. See also Table 5. Exclusions in the CMSSM, assuming tanβ = 30, $A_0 = -2$ max(m_0, $m_{1/2}$) and $\mu > 0$, are also presented, see Fig. 15.

[19] KHACHATRYAN 15AH searched in 19.4 or 19.7 fb^{-1} of pp collisions at $\sqrt{s}$ = 8 TeV for events containing either a fully reconstructed top quark, or events containing dijets requiring one or both jets to originate from b-quarks, or events containing a mono-jet. No significant excess above the Standard Model expectations is observed. Limits are set on the sbottom mass in simplified models where the decay $\tilde{b} \rightarrow b\tilde{\chi}_1^0$ takes place with a branching ratio of 100%, see Fig. 12. Limits are also set in a simplified model where the decay $\tilde{b} \rightarrow c\tilde{\chi}_1^0$ takes place with a branching ratio of 100%, see Fig. 12.

[20] KHACHATRYAN 15I searched in 19.5 fb^{-1} of pp collisions at $\sqrt{s}$ = 8 TeV for events in which b-jets and four W-bosons are produced. Five individual search channels are combined (fully hadronic, single lepton, same-sign dilepton, opposite-sign dilepton, multilepton). No significant excess above the Standard Model expectations is observed. Limits are set on the sbottom mass in a simplified model where the decay $\tilde{b} \rightarrow t\tilde{\chi}_1^\pm$, with $\tilde{\chi}_1^\pm \rightarrow W^\pm\tilde{\chi}_1^0$, takes place with a branching ratio of 100%, see Fig. 7.

[21] AAD 14T searched in 20.3 fb^{-1} of pp collisions at $\sqrt{s}$ = 8 TeV for monojet-like events. No excess of events above the expected level of Standard Model background was found. Exclusion limits at 95% C.L. are set on the masses of third-generation squarks in simplified models which assume that the decay $\tilde{b}_1 \rightarrow b\tilde{\chi}_1^0$ takes place 100% of the time, see Fig. 12.

[22] CHATRCHYAN 14AH searched in 4.7 fb^{-1} of pp collisions at $\sqrt{s}$ = 7 TeV for events with at least two energetic jets and significant $\not{E}_T$, using the razor variables (M_R and R^2) to discriminate between signal and background processes. A second analysis requires at least one of the jets to be originating from a b-quark. No significant excess above the Standard Model expectations is observed. Limits are set on sbottom masses in simplified models where the decay $\tilde{b} \rightarrow b\tilde{\chi}_1^0$ takes place with a branching ratio of 100%, see Figs. 28 and 29. Exclusions in the CMSSM, assuming tanβ = 10, A_0 = 0 and μ >0, are also presented, see Fig. 26.

[23] CHATRCHYAN 14R searched in 19.5 fb^{-1} of pp collisions at $\sqrt{s}$ = 8 TeV for events with at least three leptons (electrons, muons, taus) in the final state. No significant excess above the Standard Model expectations is observed. Limits are set on the gluino mass in a simplified model where the decay $\tilde{b} \rightarrow t\tilde{\chi}_1^\pm$, with $\tilde{\chi}_1^\pm \rightarrow W^\pm\tilde{\chi}_1^0$, takes place with a branching ratio of 100%, see Fig. 11.

[24] KHACHATRYAN 15AD searched in 19.4 fb^{-1} of pp collisions at $\sqrt{s}$ = 8 TeV for events with two opposite-sign same flavor isolated leptons featuring either a kinematic edge, or a peak at the Z-boson mass, in the invariant mass spectrum. No evidence for a statistically significant excess over the expected SM backgrounds is observed and 95% C.L. exclusion limits are derived in a simplified model of sbottom pair production where the sbottom decays into a b-quark, two opposite-sign dileptons and a neutralino LSP, through an intermediate state containing either an off-shell Z-boson or a slepton, see Fig. 8.

[25] AAD 14AX searched in 20.1 fb^{-1} of pp collisions at $\sqrt{s}$ = 8 TeV for the strong production of supersymmetric particles in events containing either zero or at last one high high-p_T lepton, large missing transverse momentum, high jet multiplicity and at least three jets identified as originating from b-quarks. No excess over the expected SM background is observed. Limits are derived in mSUGRA/CMSSM models with tanβ = 30, $A_0 = -2\ m_0$ and $\mu > 0$, see their Fig. 14. Also, exclusion limits are set in simplified models containing scalar bottom quarks, where the decay $\tilde{b} \rightarrow b\tilde{\chi}_2^0$ and $\tilde{\chi}_2^0 \rightarrow h\tilde{\chi}_1^0$ takes place with a branching ratio of 100%, see their Figures 11.

[26] AAD 14E searched in 20.3 fb^{-1} of pp collisions at $\sqrt{s}$ = 8 TeV for strongly produced supersymmetric particles in events containing jets and two same-sign leptons or three leptons. The search also utilises jets originating from b-quarks, missing transverse momentum and other variables. No excess over the expected SM background is observed. Exclusion limits are derived in simplified models containing bottom, see Fig. 7. Limits are also derived in the mSUGRA/CMSSM, bRPV and GMSB models, see their Fig. 8.

[27] CHATRCHYAN 14H searched in 19.5 fb^{-1} of pp collisions at $\sqrt{s}$ = 8 TeV for events with two isolated same-sign dileptons and jets in the final state. No significant excess above the Standard Model expectations is observed. Limits are set on the sbottom mass in a simplified models where the decay $\tilde{b} \rightarrow t\tilde{\chi}_1^\pm$, $\tilde{\chi}_1^\pm \rightarrow W^\pm\tilde{\chi}_1^0$ takes place with a branching ratio of 100%, with varying mass of the $\tilde{\chi}_1^\pm$, for $m_{\tilde{\chi}_1^0}$ = 50 GeV, see Fig. 6.

[28] AAD 13AU searched in 20.1 fb^{-1} of pp collisions at $\sqrt{s}$ = 8 TeV for events containing two jets identified as originating from b-quarks and large missing transverse momentum. No excess of events above the expected level of Standard Model background was found. Exclusion limits at 95% C.L. are set on the masses of third-generation squarks. Assuming that the decay $\tilde{b}_1 \rightarrow b\tilde{\chi}_1^0$ takes place 100% of the time, a $\tilde{b}_1$ mass below 620 GeV is excluded for $m_{\tilde{\chi}_1^0} < 120$ GeV. For more details, see their Fig. 5.

[29] CHATRCHYAN 13AT provides interpretations of various searches for supersymmetry by the CMS experiment based on 4.73–4.98 fb^{-1} of pp collisions at $\sqrt{s}$ = 7 TeV in the framework of simplified models. Limits are set on the sbottom mass in a simplified models where sbottom quarks are pair-produced and the decay $\tilde{b} \rightarrow b\tilde{\chi}_1^0$ takes place with a branching ratio of 100%, see Fig. 4.

[30] CHATRCHYAN 13T searched in 11.7 fb^{-1} of pp collisions at $\sqrt{s}$ = 8 TeV for events with at least two energetic jets and significant $\not{E}_T$, using the α_T variable to discriminate between processes with genuine and misreconstructed $\not{E}_T$. No significant excess above the Standard Model expectations is observed. Limits are set on sbottom masses in simplified models where the decay $\tilde{b} \rightarrow b\tilde{\chi}_1^0$ takes place with a branching ratio of 100%, see Fig. 8 and Table 9.

[31] CHATRCHYAN 13V searched in 10.5 fb^{-1} of pp collisions at $\sqrt{s}$ = 8 TeV for events with two isolated same-sign dileptons and at least two b-jets in the final state. No significant excess above the Standard Model expectations is observed. Limits are set on the bottom mass in a simplified models where the decay $\tilde{b} \rightarrow t\tilde{\chi}_1^\pm$, $\tilde{\chi}_1^\pm \rightarrow W^\pm\tilde{\chi}_1^0$ takes place with a branching ratio of 100%, with varying mass of the $\tilde{\chi}_1^\pm$, for $m_{\tilde{\chi}_1^0}$ = 50 GeV, see Fig. 4.

[32] AAD 12AN searched in 2.05 fb^{-1} of pp collisions at $\sqrt{s}$ = 7 TeV for scalar bottom quarks in events with large missing transverse momentum and two b-jets in the final state. The data are found to be consistent with the Standard Model expectations. Limits are set in an R-parity conserving minimal supersymmetric scenario, assuming B($\tilde{b}_1 \rightarrow b\tilde{\chi}_1^0$) = 100%, see their Fig. 2.

[33] CHATRCHYAN 12AI looked in 4.98 fb^{-1} of pp collisions at $\sqrt{s}$ = 7 TeV for events with two same-sign leptons (e, μ), but not necessarily same flavor, at least 2 b-jets and missing transverse energy. No excess beyond the Standard Model expectation is observed. Exclusion limits are derived in a simplified model for sbottom pair production, where the sbottom decays through $\tilde{b}_1 \rightarrow t\tilde{\chi}_1 W$, see Fig. 8.

[34] CHATRCHYAN 12BO searched in 4.7 fb^{-1} of pp collisions at $\sqrt{s}$ = 7 TeV for scalar bottom quarks in events with large missing transverse momentum and two b-jets in the final state. The data are found to be consistent with the Standard Model expectations. Limits are set in an R-parity conserving minimal supersymmetric scenario, assuming B($\tilde{b}_1 \rightarrow b\tilde{\chi}_1^0$) = 100%, see their Fig. 2.

[35] AAD 11K looked in 34 pb^{-1} of pp collisions at $\sqrt{s}$ = 7 TeV for events with heavy stable particles, identified by their anomalous dE/dx in the tracker or time of flight in the tile calorimeter, from pair production of $\tilde{b}$. No evidence for an excess over the SM expectation is observed and limits on the mass are derived for pair production of sbottom, see Fig. 4.

[36] AAD 11O looked in 35 pb^{-1} of pp collisions at $\sqrt{s}$ = 7 TeV for events with jets, of which at least one is a b-jet, and $\not{E}_T$. No excess above the Standard Model was found. Limits are derived in the ($m_{\tilde{g}}$, $m_{\tilde{b}_1}$) plane (see Fig. 2) under the assumption of 100% branching ratios and $\tilde{b}_1$ being the lightest squark. The quoted limit is valid for $m_{\tilde{b}_1} <$ 500 GeV. A similar approach for $\tilde{t}_1$ as the lightest squark with $\tilde{g} \rightarrow \tilde{t}_1 t$ and $\tilde{t}_1 \rightarrow b\tilde{\chi}_1^\pm$ with 100% branching ratios leads to a gluino mass limit of 520 GeV for 130 < $m_{\tilde{t}_1} <$ 300 GeV. Limits are also derived in the CMSSM (m_0, $m_{1/2}$) plane for tanβ = 40, see Fig. 4, and in scenarios based on the gauge group SO(10).

[37] CHATRCHYAN 11D looked in 35 pb^{-1} of pp collisions at $\sqrt{s}$ = 7 TeV for events with $\geq$ 2 jets, at least one of which is b-tagged, and $\not{E}_T$, where the b-jets are decay products of $\tilde{t}$ or $\tilde{b}$. No evidence for an excess over the expected background is observed. Limits are derived in the CMSSM (m_0, $m_{1/2}$) plane for tanβ = 50 (see Fig. 2).

[38] AALTONEN 10R searched in 2.65 fb^{-1} of $p\overline{p}$ collisions at $\sqrt{s}$ = 1.96 TeV for events with $\not{E}_T$ and exactly two jets, at least one of which is b-tagged. The results are in agreement with the SM prediction, and a limit on the cross section of 0.1 pb is obtained for the range of masses 80 < $m_{\tilde{b}_1}$ < 280 GeV assuming that the sbottom decays exclusively to $b\tilde{\chi}_1^0$. The excluded mass region in the framework of conserved R_p is shown in a plane of ($m_{\tilde{b}_1}$, $m_{\tilde{\chi}_1^0}$), see their Fig.2.

[39] ABAZOV 10L looked in 5.2 fb^{-1} of $p\overline{p}$ collisions at $\sqrt{s}$ = 1.96 TeV for events with at least 2 b-jets and $\not{E}_T$ from the production of $\tilde{b}_1\,\tilde{b}_1$. No evidence for an excess over the SM expectation is observed, and a limit on the cross section is derived under the assumption of 100% branching ratio. The excluded mass region in the framework of conserved R_p is shown in a plane of ($m_{\tilde{b}_1}$,$m_{\tilde{\chi}^0_1}$), see their Fig. 3b. The exclusion also extends to $m_{\tilde{\chi}^0_1}$ = 110 GeV for 160< $m_{\tilde{b}_1}$ < 200 GeV.

R-parity violating $\tilde{b}$ (Sbottom) mass limit

VALUE (GeV)	CL%	DOCUMENT ID		TECN	COMMENT
>307	95	[1] KHACHATRY...16BX		CMS	RPV, $\tilde{b} \to t\,d$ or $t\,s$, λ''_{332} or λ''_{331} coupling
• • • We do not use the following data for averages, fits, limits, etc. • • •					
		[2] AAD	14E	ATLS	$\ell^\pm\ell^\pm(\ell^\mp)$ + jets, $\tilde{b}_1 \to t\,\tilde{\chi}^\pm_1$ with $\tilde{\chi}^\pm_1 \to W^{(*)\pm}\tilde{\chi}^0_1$ simplified model, $m_{\tilde{\chi}^\pm_1} = 2\,m_{\tilde{\chi}^0_1}$

[1] KHACHATRYAN 16BX searched in 19.5 fb^{-1} of pp collisions at $\sqrt{s}$ = 8 TeV for events containing 2 leptons coming from R-parity-violating decays of supersymmetric particles. No excess over the expected background is observed. Limits are derived on the sbottom mass, assuming the RPV $\tilde{b} \to t\,d$ or $\tilde{b} \to t\,s$ decay, see Fig. 15.

[2] AAD 14E searched in 20.3 fb^{-1} of pp collisions at $\sqrt{s}$ = 8 TeV for strongly produced supersymmetric particles in events containing jets and two same-sign leptons or three leptons. The search also utilises jets originating from b-quarks, missing transverse momentum and other variables. No excess over the expected SM background is observed. Exclusion limits are derived in simplified models containing bottom, see Fig. 7. Limits are also derived in the mSUGRA/CMSSM, bRPV and GMSB models, see their Fig. 8.

$\tilde{t}$ (Stop) mass limit

Limits depend on the decay mode. In e^+e^- collisions they also depend on the mixing angle of the mass eigenstate $\tilde{t}_1 = \tilde{t}_L\cos\theta_t + \tilde{t}_R\sin\theta_t$. The coupling to the Z vanishes when θ_t = 0.98. In the Listings below, we use $\Delta m \equiv m_{\tilde{t}_1} - m_{\tilde{\chi}^0_1}$ or $\Delta m \equiv m_{\tilde{t}_1} - m_{\tilde{\nu}}$, depending on relevant decay mode. See also bounds in "$\tilde{q}$ (Squark) MASS LIMIT."

Some earlier papers are now obsolete and have been omitted. They were last listed in our PDG 14 edition: K. Olive, *et al.* (Particle Data Group), Chinese Physics **C38** 070001 (2014) (http://pdg.lbl.gov).

R-parity conserving $\tilde{t}$ (Stop) mass limit

VALUE (GeV)	CL%	DOCUMENT ID		TECN	COMMENT
> 510	95	[1] SIRUNYAN	18B	CMS	jets+$\not{E}_T$, Tstop4, $m_{\tilde{t}} - m_{\tilde{\chi}^0_1}$ = 10 GeV
> 800	95	[2] SIRUNYAN	18C	CMS	$\ell^\pm\ell^\mp$ + b-jets + $\not{E}_T$, Tstop1, $m_{\tilde{\chi}^0_1}$ = 0
> 750	95	[2] SIRUNYAN	18C	CMS	$\ell^\pm\ell^\mp$ + b-jets + $\not{E}_T$, Tstop2, $m_{\tilde{\chi}^\pm_1} = (m_{\tilde{t}} + m_{\tilde{\chi}^0_1})/2$, $m_{\tilde{\chi}^0_1}$ = 0
>1050	95	[2] SIRUNYAN	18C	CMS	Combination of all-hadronic, 1 $\ell^\pm$ and $\ell^\pm\ell^\mp$ searches, Tstop1, $m_{\tilde{\chi}^0_1}$ = 0
>1000	95	[2] SIRUNYAN	18C	CMS	Combination of all-hadronic, 1 $\ell^\pm$ and $\ell^\pm\ell^\mp$ searches, Tstop2, $m_{\tilde{\chi}^\pm_1} = (m_{\tilde{t}} + m_{\tilde{\chi}^0_1})/2$, $m_{\tilde{\chi}^0_1}$ = 0
>1200	95	[2] SIRUNYAN	18C	CMS	$\ell^\pm\ell^\mp$ + b-jets + $\not{E}_T$, Tstop11, $m_{\tilde{\chi}^\pm_1}$ = 0.5 ($m_{\tilde{t}} + m_{\tilde{\chi}^0_1}$), $m_{\tilde{l}}$ = 0.5 $m_{\tilde{\chi}^\pm_1}$, $m_{\tilde{\chi}^0_1}$ = 0
>1300	95	[2] SIRUNYAN	18C	CMS	$\ell^\pm\ell^\mp$ + b-jets + $\not{E}_T$, Tstop11, $m_{\tilde{\chi}^\pm_1}$ = 0.5 ($m_{\tilde{t}} + m_{\tilde{\chi}^0_1}$), $m_{\tilde{l}}$ = 0.95 $m_{\tilde{\chi}^\pm_1}$, $m_{\tilde{\chi}^0_1}$ = 0
none 460–1060	95	[2] SIRUNYAN	18C	CMS	$\ell^\pm\ell^\mp$ + b-jets + $\not{E}_T$, Tstop11, $m_{\tilde{\chi}^\pm_1}$ = 0.5 ($m_{\tilde{t}} + m_{\tilde{\chi}^0_1}$), $m_{\tilde{l}}$ = 0.05 $m_{\tilde{\chi}^\pm_1}$, $m_{\tilde{\chi}^0_1}$ = 0
>1020	95	[3] SIRUNYAN	18D	CMS	top quark (hadronically decaying) + jets + $\not{E}_T$, Tstop1, $m_{\tilde{\chi}^0_1}$ = 0 GeV
> 700	95	[4] AABOUD	17AJ	ATLS	same-sign $\ell^\pm\ell^\pm$ / 3 ℓ + jets + $\not{E}_T$, Tstop11, $m_{\tilde{\chi}^0_2} = m_{\tilde{\chi}^0_1}$ + 100 GeV
> 880	95	[5] AABOUD	17AX	ATLS	b-jets+$\not{E}_T$, mixture Tstop1 and Tstop2 with BR=50%, $m_{\tilde{\chi}^0_1}$ = 0 GeV, $m_{\tilde{\chi}^\pm_1}$ - $m_{\tilde{\chi}^0_1}$ = 1 GeV
none 250–1000	95	[6] AABOUD	17AY	ATLS	jets+$\not{E}_T$, Tstop1, $m_{\tilde{\chi}^0_1}$ = 0 GeV
none 450–850	95	[7] AABOUD	17AY	ATLS	jets+$\not{E}_T$, mixture of Tstop1 and Tstop2 with BR=50%, $m_{\tilde{\chi}^\pm_1} - m_{\tilde{\chi}^0_1}$ = 1 GeV
> 720	95	[8] AABOUD	17BE	ATLS	$\ell^\pm\ell^\mp$ + $\not{E}_T$, Tstop1, $m_{\tilde{\chi}^0_1}$ = 0 GeV
> 400	95	[9] AABOUD	17BE	ATLS	$\ell^\pm\ell^\mp$ + $\not{E}_T$, Tstop3, $m_{\tilde{t}_1} - m_{\tilde{\chi}^0_1}$ = 40 GeV
> 430	95	[10] AABOUD	17BE	ATLS	$\ell^\pm\ell^\mp$ + $\not{E}_T$, Tstop1 (offshell t), $m_{\tilde{t}_1} - m_{\tilde{\chi}^0_1} \sim m_W$
> 700	95	[11] AABOUD	17BE	ATLS	$\ell^\pm\ell^\mp$ + $\not{E}_T$, Tstop2, $m_{\tilde{t}_1} - m_{\tilde{\chi}^\pm_1}$ = 10 GeV, $m_{\tilde{\chi}^0_1}$ = 0 GeV
> 750	95	[12] KHACHATRY...17		CMS	jets+$\not{E}_T$,Tstop1,$m_{\tilde{\chi}^0_1}$=100GeV
none 250–740	95	[13] KHACHATRY...17AD		CMS	jets+b-jets+$\not{E}_T$, Tstop1, $m_{\tilde{\chi}^0_1}$ = 0 GeV
> 610	95	[14] KHACHATRY...17AD		CMS	jets+b-jets+$\not{E}_T$, mixture Tstop1 and Tstop2 with BR=50%, $m_{\tilde{\chi}^0_1}$ = 60 GeV
> 590	95	[15] KHACHATRY...17P		CMS	1 or more jets+$\not{E}_T$, Tstop8, $m_{\tilde{\chi}^\pm_1} - m_{\tilde{\chi}^0_1}$ = 5 GeV, $m_{\tilde{\chi}^0_1}$ = 100 GeV
none 280–640	95	[15] KHACHATRY...17P		CMS	1 or more jets+$\not{E}_T$, Tstop1, $m_{\tilde{\chi}^0_1}$ = 0 GeV
> 350	95	[15] KHACHATRY...17P		CMS	1 or more jets+$\not{E}_T$, Tstop4, 10 GeV < $m_{\tilde{t}_1} - m_{\tilde{\chi}^0_1}$ < 80 GeV
> 280	95	[15] KHACHATRY...17P		CMS	1 or more jets+$\not{E}_T$, Tstop3, 10 GeV < $m_{\tilde{t}_1} - m_{\tilde{\chi}^0_1}$ < 80 GeV
> 320	95	[15] KHACHATRY...17P		CMS	1 or more jets+$\not{E}_T$, Tstop9, 10 GeV < $m_{\tilde{t}_1} - m_{\tilde{\chi}^0_1}$ < 80 GeV
> 240	95	[16] KHACHATRY...17S		CMS	jets+$\not{E}_T$, Tstop4, $m_{\tilde{t}} - m_{\tilde{\chi}^0_1}$ = 10 GeV
> 225	95	[17] KHACHATRY...17S		CMS	jets+$\not{E}_T$, Tstop3, $m_{\tilde{t}} - m_{\tilde{\chi}^0_1}$ = 10 GeV
> 325	95	[18] KHACHATRY...17S		CMS	jets+$\not{E}_T$, Tstop2, $m_{\tilde{\chi}^\pm_1}$ = 0.25 $m_{\tilde{t}}$ + 0.75 $m_{\tilde{\chi}^0_1}$, $m_{\tilde{\chi}^0_1}$ = 225 GeV
> 400	95	[19] KHACHATRY...17S		CMS	jets+$\not{E}_T$, Tstop2, $m_{\tilde{\chi}^\pm_1}$ = 0.75 $m_{\tilde{t}}$ + 0.25 $m_{\tilde{\chi}^0_1}$, $m_{\tilde{\chi}^0_1}$ = 0 GeV
> 500	95	[20] KHACHATRY...17S		CMS	jets+$\not{E}_T$, Tstop1, $m_{\tilde{\chi}^0_1}$ = 0 GeV
>1120	95	[21] SIRUNYAN	17AS	CMS	1ℓ+jets+$\not{E}_T$, Tstop1, $m_{\tilde{\chi}^0_1}$ = 0 GeV
>1000	95	[21] SIRUNYAN	17AS	CMS	1ℓ+jets+$\not{E}_T$, Tstop2, $m_{\tilde{\chi}^\pm_1} = (m_{\tilde{t}} + m_{\tilde{\chi}^0_1})/2$, $m_{\tilde{\chi}^0_1}$ = 0 GeV
> 980	95	[21] SIRUNYAN	17AS	CMS	1ℓ+jets+$\not{E}_T$, Tstop8, $m_{\tilde{\chi}^\pm_1} - m_{\tilde{\chi}^0_1}$ = 5 GeV, $m_{\tilde{\chi}^0_1}$ = 0 GeV
>1040	95	[22] SIRUNYAN	17AT	CMS	jets+$\not{E}_T$, Tstop1, $m_{\tilde{\chi}^0_1}$ = 0 GeV
> 750	95	[22] SIRUNYAN	17AT	CMS	jets+$\not{E}_T$, Tstop2, $m_{\tilde{\chi}^\pm_1} = (m_{\tilde{t}} + m_{\tilde{\chi}^0_1})/2$, $m_{\tilde{\chi}^0_1}$ = 0 GeV
> 940	95	[22] SIRUNYAN	17AT	CMS	jets+$\not{E}_T$, Tstop8, $m_{\tilde{\chi}^\pm_1} - m_{\tilde{\chi}^0_1}$ = 5 GeV, $m_{\tilde{\chi}^0_1}$ = 100 GeV
> 540	95	[22] SIRUNYAN	17AT	CMS	jets+$\not{E}_T$, Tstop3, 10 GeV < $m_{\tilde{t}_1} - m_{\tilde{\chi}^0_1}$ < 80 GeV
> 480	95	[22] SIRUNYAN	17AT	CMS	jets+$\not{E}_T$, Tstop4, 10 GeV < $m_{\tilde{t}_1} - m_{\tilde{\chi}^0_1}$ < 80 GeV
> 530	95	[22] SIRUNYAN	17AT	CMS	jets+$\not{E}_T$, Tstop10, $m_{\tilde{\chi}^\pm_1} = (m_{\tilde{t}} + m_{\tilde{\chi}^0_1})/2$, 10 GeV < $m_{\tilde{t}_1} - m_{\tilde{\chi}^0_1}$ < 80 GeV
>1070	95	[23] SIRUNYAN	17AZ	CMS	$\geq$ 1 jets+$\not{E}_T$, Tstop1, $m_{\tilde{\chi}^0_1}$ = 0 GeV
> 900	95	[23] SIRUNYAN	17AZ	CMS	$\geq$ 1 jets+$\not{E}_T$, Tstop2, $m_{\tilde{\chi}^\pm_1} = (m_{\tilde{t}} + m_{\tilde{\chi}^0_1})/2$, $m_{\tilde{\chi}^0_1}$ = 0 GeV
>1020	95	[23] SIRUNYAN	17AZ	CMS	$\geq$ 1jets+$\not{E}_T$, Tstop8, $m_{\tilde{\chi}^\pm_1} - m_{\tilde{\chi}^0_1}$ = 5 GeV, $m_{\tilde{\chi}^0_1}$ = 100 GeV
> 540	95	[23] SIRUNYAN	17AZ	CMS	$\geq$ 1 jets+$\not{E}_T$, Tstop4, 10 GeV < $m_{\tilde{t}_1} - m_{\tilde{\chi}^0_1}$ < 80 GeV
none 280–830	95	[24] SIRUNYAN	17K	CMS	0, 1 $\ell^\pm$+jets+$\not{E}_T$ (combination), Tstop1, $m_{\tilde{\chi}^0_1}$ = 0 GeV

> 700	95	[24] SIRUNYAN	17K	CMS	0, 1 $\ell^{\pm}$+jets+$\not{E}_T$ (combination), Tstop8, $m_{\widetilde{\chi}_1^{\pm}} - m_{\widetilde{\chi}_1^0}$ = 5 GeV, $m_{\widetilde{\chi}_1^0}$ = 100 GeV	
> 160	95	[24] SIRUNYAN	17K	CMS	jets+$\not{E}_T$, Tstop4, 10 < $m_{\widetilde{t}} - m_{\widetilde{\chi}_1^0}$ < 80 GeV	
none 230–960	95	[25] SIRUNYAN	17P	CMS	jets+$\not{E}_T$, Tstop1, $m_{\widetilde{\chi}_1^0}$ = 0 GeV	
> 990	95	[25] SIRUNYAN	17P	CMS	jets+$\not{E}_T$, Tsbot1, $m_{\widetilde{\chi}_1^0}$ = 0 GeV	
> 323	95	[26] AABOUD	16D	ATLS	$\geq$ 1 jet + $\not{E}_T$, Tstop4, $m_{\widetilde{t}_1} - m_{\widetilde{\chi}_1^0}$ = 5 GeV	
none, 745–780	95	[27] AABOUD	16J	ATLS	1 $\ell^{\pm}$ + $\geq$ 4 jets + $\not{E}_T$, Tstop1, $m_{\widetilde{\chi}_1^0}$ = 0 GeV	
> 490–650	95	[28] AAD	16AY	ATLS	2ℓ (including hadronic τ) + $\not{E}_T$, Tstop5, 87 GeV< $m_{\widetilde{\tau}} < m_{\widetilde{t}_1}$	
> 700	95	[29] KHACHATRY...	16AV	CMS	1 or 2 $\ell^{\pm}$+jets+b-jets+$\not{E}_T$, Tstop1, $m_{\widetilde{\chi}_1^0}$ < 250 GeV	
> 700	95	[29] KHACHATRY...	16AV	CMS	1 or 2 $\ell^{\pm}$+jets+b-jets $\not{E}_T$, Tstop2, $m_{\widetilde{\chi}_1^0}$ = 0 GeV, $m_{\widetilde{\chi}_1^{\pm}}$ = 0.75 $m_{\widetilde{t}_1}$ + 0.25 $m_{\widetilde{\chi}_1^0}$	
> 775	95	[30] KHACHATRY...	16BK	CMS	jets+$\not{E}_T$,Tstop1,$m_{\widetilde{\chi}_1^0}$ <200GeV	
> 620	95	[30] KHACHATRY...	16BK	CMS	jets+$\not{E}_T$, Tstop2, $m_{\widetilde{\chi}_1^0}$=0 GeV	
> 800	95	[31] KHACHATRY...	16BS	CMS	jets+$\not{E}_T$, Tstop1, $m_{\widetilde{\chi}_1^0}$=0 GeV	
> 316	95	[32] KHACHATRY...	16Y	CMS	1 or 2 soft $\ell^{\pm}$ + jets + $\not{E}_T$, Tstop3,$m_{\widetilde{t}} - m_{\widetilde{\chi}_1^0}$=25 GeV	
> 250	95	[33] AAD	15CJ	ATLS	B($\widetilde{t} \to c\widetilde{\chi}_1^0$)+B($\widetilde{t} \to bf f'\widetilde{\chi}_1^0$) = 1, $m_{\widetilde{t}} - m_{\widetilde{\chi}_1^0}$ = 10 GeV	
> 270	95	[33] AAD	15CJ	ATLS	$\widetilde{t} \to c\widetilde{\chi}_1^0$, $m_{\widetilde{t}} - m_{\widetilde{\chi}_1^0}$=80 GeV	
none, 200–700	95	[33] AAD	15CJ	ATLS	$\widetilde{t} \to t\widetilde{\chi}_1^0$, $m_{\widetilde{\chi}_1^0}$ = 0	
> 500	95	[33] AAD	15CJ	ATLS	B($\widetilde{t} \to t\widetilde{\chi}_1^0$) + B($\widetilde{t} \to b\widetilde{\chi}_1^{\pm}$) = 1, $\widetilde{\chi}_1^{\pm} \to W^{(*)}\widetilde{\chi}_1^0$, $m_{\widetilde{\chi}_1^{\pm}}$ = 2$m_{\widetilde{\chi}_1^0}$, $m_{\widetilde{\chi}_1^0}$ < 160 GeV	
> 600	95	[33] AAD	15CJ	ATLS	$\widetilde{t}_2 \to Z\widetilde{t}_1$, $m_{\widetilde{t}_1} - m_{\widetilde{\chi}_1^0}$ = 180 GeV, $m_{\widetilde{\chi}_1^0}$ = 0	
> 600	95	[33] AAD	15CJ	ATLS	$\widetilde{t}_2 \to h\widetilde{t}_1$, $m_{\widetilde{t}_1} - m_{\widetilde{\chi}_1^0}$ = 180 GeV, $m_{\widetilde{\chi}_1^0}$ = 0	
none, 172.5–191	95	[34] AAD	15J	ATLS	$\widetilde{t} \to t\widetilde{\chi}_1^0$, $m_{\widetilde{\chi}_1^0}$ = 1 GeV	
> 450	95	[35] KHACHATRY...	15AF	CMS	$\widetilde{t} \to t\widetilde{\chi}_1^0$, $m_{\widetilde{\chi}_1^0}$ = 0, $m_{\widetilde{t}} > m_t + m_{\widetilde{\chi}_1^0}$	
> 560	95	[36] KHACHATRY...	15AH	CMS	$\widetilde{t} \to t\widetilde{\chi}_1^0$, $m_{\widetilde{\chi}_1^0}$ = 0, $m_{\widetilde{t}} > m_t + m_{\widetilde{\chi}_1^0}$	
> 250	95	[37] KHACHATRY...	15AH	CMS	$\widetilde{t} \to c\widetilde{\chi}_1^0$, $m_{\widetilde{t}} - m_{\widetilde{\chi}_1^0}$ <10 GeV	
none, 200–350	95	[38] KHACHATRY...	15L	CMS	$\widetilde{t} \to qq$, RPV, $\lambda''_{312} \neq 0$	
none, 200–385	95	[38] KHACHATRY...	15L	CMS	$\widetilde{t} \to qb$, RPV, $\lambda''_{323} \neq 0$	
> 730	95	[39] KHACHATRY...	15X	CMS	$\widetilde{t} \to t\widetilde{\chi}_1^0$, $m_{\widetilde{\chi}_1^0}$ = 100 GeV, $m_{\widetilde{t}} > m_t + m_{\widetilde{\chi}_1^0}$	
none 400–645	95	[39] KHACHATRY...	15X	CMS	$\widetilde{t} \to t\widetilde{\chi}_1^0$ or $\widetilde{t} \to b\widetilde{\chi}_1^{\pm}$, $m_{\widetilde{\chi}_1^0}$ = 100 GeV, $m_{\widetilde{\chi}_1^{\pm}} - m_{\widetilde{\chi}_1^0}$ = 5 GeV	
none 270–645	95	[40] AAD	14AJ	ATLS	$\geq$ 4 jets + $\not{E}_T$, $\widetilde{t}_1 \to t\widetilde{\chi}_1^0$, $m_{\widetilde{\chi}_1^0}$ < 30 GeV	
none 250–550	95	[40] AAD	14AJ	ATLS	$\geq$ 4 jets + $\not{E}_T$, B($\widetilde{t}_1 \to b\widetilde{\chi}_1^{\pm}$) = 50 %, $m_{\widetilde{\chi}_1^{\pm}} = 2\, m_{\widetilde{\chi}_1^0}$, $m_{\widetilde{\chi}_1^0}$ < 60 GeV	
none 210–640	95	[41] AAD	14BD	ATLS	$\ell^{\pm}$ + jets + $\not{E}_T$, $\widetilde{t}_1 \to t\widetilde{\chi}_1^0$, $m_{\widetilde{\chi}_1^0}$ = 0 GeV	
> 500	95	[41] AAD	14BD	ATLS	$\ell^{\pm}$ + jets + $\not{E}_T$, $\widetilde{t}_1 \to b\widetilde{\chi}_1^{\pm}$, $m_{\widetilde{\chi}_1^{\pm}} = 2\, m_{\widetilde{\chi}_1^0}$, 100 GeV< $m_{\widetilde{\chi}_1^0}$ < 150 GeV	
none 150–445	95	[42] AAD	14F	ATLS	$\ell^{\pm}\ell^{\mp}$ final state, $\widetilde{t}_1 \to b\widetilde{\chi}_1^{\pm}$, $m_{\widetilde{t}_1} - m_{\widetilde{\chi}_1^{\pm}}$ = 10 GeV, $m_{\widetilde{\chi}_1^0}$ = 1 GeV	
none 215–530	95	[42] AAD	14F	ATLS	$\ell^{\pm}\ell^{\mp}$ final state, $\widetilde{t}_1 \to t\widetilde{\chi}_1^0$, $m_{\widetilde{\chi}_1^0}$ = 1 GeV	
> 270	95	[43] AAD	14T	ATLS	$\widetilde{t}_1 \to c\widetilde{\chi}_1^0$, $m_{\widetilde{\chi}_1^0}$ = 200 GeV	
> 240	95	[43] AAD	14T	ATLS	$\widetilde{t}_1 \to c\widetilde{\chi}_1^0$,$m_{\widetilde{t}_1} - m_{\widetilde{\chi}_1^0}$ <85 GeV	
> 255	95	[43] AAD	14T	ATLS	$\widetilde{t}_1 \to bf f'\widetilde{\chi}_1^0$, $m_{\widetilde{t}_1} - m_{\widetilde{\chi}_1^0} \approx m_b$	
> 400	95	[44] CHATRCHYAN	14AH	CMS	jets + $\not{E}_T$, $\widetilde{t} \to t\widetilde{\chi}_1^0$ simplified model, $m_{\widetilde{\chi}_1^0}$ = 50 GeV	
		[45] CHATRCHYAN	14R	CMS	$\geq 3\ell^{\pm}$, $\widetilde{t} \to (b\widetilde{\chi}_1^{\pm}/t\widetilde{\chi}_1^0)$, $\widetilde{\chi}_1^{\pm} \to (qq'/\ell\nu)\widetilde{\chi}_1^0$, $\widetilde{\chi}_1^0 \to (H/Z)\widetilde{G}$, GMSB, natural higgsino NLSP scenario	
> 740	95	[46] KHACHATRY...	14T	CMS	τ + b-jets, RPV, $LQ\overline{D}$, $\lambda'_{333} \neq 0$, $\widetilde{t} \to \tau b$ simplified model	
> 580	95	[46] KHACHATRY...	14T	CMS	τ + b-jets, RPV, $LQ\overline{D}$, $\lambda'_{3jk} \neq 0$ ($j \neq 3$), $\widetilde{t} \to \widetilde{\chi}^{\pm} b$, $\widetilde{\chi}^{\pm} \to qq\tau^{\pm}$ simplified model	
• • • We do not use the following data for averages, fits, limits, etc. • • •						
> 850	95	[47] AABOUD	17AF	ATLS	2ℓ+jets+b-jets+$\not{E}_T$, Tstop6, $m_{\widetilde{\chi}_1^0}$ = 0	
> 800	95	[48] AABOUD	17AF	ATLS	2ℓ+jets+b-jets+$\not{E}_T$, Tstop7 with 100% decays via Z, $m_{\widetilde{\chi}_1^0}$ = 50 GeV	
> 880	95	[49] AABOUD	17AF	ATLS	2ℓ+jets+b-jets+$\not{E}_T$, Tstop7 with 100% decays via higgs, $m_{\widetilde{\chi}_1^0}$ = 50 GeV	
		[50] AABOUD	17AY	ATLS	jets+$\not{E}_T$, pMSSM-inspired	
> 230		ROLBIECKI	15	THEO	WW xsection, $\widetilde{t}_1 \to bW\widetilde{\chi}_1^0$, $m_{\widetilde{t}_1} \simeq m_b + m_W + m_{\widetilde{\chi}_1^0}$	
> 600	95	[51] AAD	14B	ATLS	Z+b $\not{E}_T$, $\widetilde{t}_2 \to Z\widetilde{t}_1$, $\widetilde{t}_1 \to t\widetilde{\chi}_1^0$, $m_{\widetilde{\chi}_1^0}$ < 200 GeV	
> 540	95	[51] AAD	14B	ATLS	Z+b $\not{E}_T$, $\widetilde{t}_1 \to t\widetilde{\chi}_1^0$, $\widetilde{\chi}_1^0 \to Z\widetilde{G}$, natural GMSB, 100 GeV < $m_{\widetilde{\chi}_1^0}$ < $m_{\widetilde{t}_1}$−10 GeV	
> 360	95	[52] CHATRCHYAN	14U	CMS	$\widetilde{t}_1 \to b\widetilde{\chi}_1^{\pm}$r, $\widetilde{\chi}_1^{\pm} \to f f'\widetilde{\chi}_1^0$, $\widetilde{\chi}_1^0 \to H\widetilde{G}$ simplified model, $m_{\widetilde{\chi}_1^{\pm}} - m_{\widetilde{\chi}_1^0}$ = 5 GeV,GMSB	
> 215	95	CZAKON	14		$\widetilde{t} \to t\chi_1^0$, $m_{\chi_1^0}$ < 10 GeV	
		[53] KHACHATRY...	14C	CMS	$\widetilde{t}_2 \to H\widetilde{t}_1$ or $\widetilde{t}_2 \to Z\widetilde{t}_1$ simplified model	

[1] SIRUNYAN 18B searched in 35.9 fb^{-1} of pp collisions at $\sqrt{s}$ = 13 TeV for the pair production of third-generation squarks in events with jets and large $\not{E}_T$. No significant excess above the Standard Model expectations is observed. Limits are set on the sbottom mass in the Tsbot1 simplified model, see their Figure 5, and on the stop mass in the Tstop4 simplified model, see their Figure 6.

[2] SIRUNYAN 18C searched in 35.9 fb^{-1} of pp collisions at $\sqrt{s}$ = 13 TeV for the pair production of top squarks in events with two oppositely charged leptons (electrons or muons), jets identified as originating from a b-quark and large $\not{E}_T$. No significant excess above the Standard Model expectations is observed. Limits are set on the stop mass in the Tstop1, Tstop2 and Tstop11 simplified models, see their Figures 11 and 12. The Tstop1 and Tstop2 results are combined with complementary searches in the all-hadronic and single lepton channels, see their Figures 13 and 14.

[3] SIRUNYAN 18D searched in 35.9 fb^{-1} of pp collisions at $\sqrt{s}$ = 13 TeV for events containing identified hadronically decaying top quarks, no leptons, and $\not{E}_T$. No significant excess above the Standard Model expectations is observed. Limits are set on the stop mass in the Tstop1 simplified model, see their Figure 8, and on the gluino mass in the Tglu3A, Tglu3B, Tglu3C and Tglu3E simplified models, see their Figure 9.

[4] AABOUD 17AJ searched in 36.1 fb^{-1} of pp collisions at $\sqrt{s}$ = 13 TeV for events with two same-sign or three leptons, jets and large missing transverse momentum. No significant excess above the Standard Model expectations is observed. Limits up to 700 GeV are set on the top squark mass in Tstop11 simplified models, assuming $m_{\widetilde{\chi}_1^0} = m_{\widetilde{t}} - 275$ GeV and $m_{\widetilde{\chi}_2^0} = m_{\widetilde{\chi}_1^0} + 100$ GeV. See their Figure 4(e).

[5] AABOUD 17AX searched in 36 fb^{-1} of pp collisions at $\sqrt{s}$ = 13 TeV for events containing two jets identified as originating from b-quarks and large missing transverse momentum, with or without leptons. No excess of events above the expected level of Standard Model background was found. Exclusion limits at 95% C.L. are set on the masses of top squarks. Assuming 50% BR for Tstop1 and Tstop2 simplified models, a $\widetilde{t}_1$ mass below 880 (860) GeV is excluded for $m_{\widetilde{\chi}_1^0}$ = 0 (<250) GeV. See their Fig. 7(b).

[6] AABOUD 17AY searched in 36.1 fb^{-1} of pp collisions at $\sqrt{s}$ = 13 TeV for events with at least four jets and large missing transverse momentum. No significant excess above the Standard Model expectations is observed. Limits in the range 250–1000 GeV are set on the top squark mass in Tstop1 simplified models. For the first time, additional constraints are set for the region $m_{\widetilde{t}_1} \sim m_t + m_{\widetilde{\chi}_1^0}$, with exclusion of the $\widetilde{t}_1$ mass range 235–590 GeV. See their Figure 8.

[7] AABOUD 17AY searched in 36.1 fb^{-1} of pp collisions at $\sqrt{s}$ = 13 TeV for events with at least four jets and large missing transverse momentum. No significant excess above the Standard Model expectations is observed. Limits in the range 450-850 GeV are set on the top squark mass in a mixture of Tstop1 and Tstop2 simplified models with BR=50% and assuming $m_{\widetilde{\chi}_1^{\pm}} - m_{\widetilde{\chi}_1^0} = 1$ GeV and $m_{\chi_1^0} < 240$ GeV. Constraints are given for various values of the BR. See their Figure 9.

[8] AABOUD 17BE searched in 36.1 fb^{-1} of pp collisions at $\sqrt{s}$ = 13 TeV for events with two opposite-charge leptons (electrons and muons) and large missing transverse momentum. No significant excess above the Standard Model expectations is observed. Limits up to 720 GeV are set on the top squark mass in Tstop1 simplified models, assuming massless neutralinos. See their Figure 9 (2-body area).

[9] AABOUD 17BE searched in 36.1 fb^{-1} of pp collisions at $\sqrt{s}$ = 13 TeV for events with two opposite-charge leptons (electrons and muons) and large missing transverse momentum. No significant excess above the Standard Model expectations is observed. Limits up to 400 GeV are set on the top squark mass in Tstop3 simplified models, assuming $m_{\tilde{t}_1} - m_{\tilde{\chi}_1^0}$ = 40 GeV. See their Figure 9 (4-body area).

[10] AABOUD 17BE searched in 36.1 fb^{-1} of pp collisions at $\sqrt{s}$ = 13 TeV for events with two opposite-charge leptons (electrons and muons) and large missing transverse momentum. No significant excess above the Standard Model expectations is observed. Limits up to 430 GeV are set on the top squark mass in Tstop1 simplified models where top quarks are offshell, assuming $m_{\tilde{t}_1} - m_{\tilde{\chi}_1^0}$ close to the W mass. See their Figure 9 (3-body area).

[11] AABOUD 17BE searched in 36.1 fb^{-1} of pp collisions at $\sqrt{s}$ = 13 TeV for events with two opposite-charge leptons (electrons and muons) and large missing transverse momentum. No significant excess above the Standard Model expectations is observed. Limits up to 700 GeV are set on the top squark mass in Tstop2 simplified models, assuming $m_{\tilde{t}_1} - m_{\tilde{\chi}_1^\pm}$ = 10 GeV and massless neutralinos. See their Figure 10.

[12] KHACHATRYAN 17 searched in 2.3 fb^{-1} of pp collisions at $\sqrt{s}$ = 13 TeV for events containing four or more jets, no more than one lepton, and missing transverse momentum, using the razor variables (M_R and R^2) to discriminate between signal and background processes. No evidence for an excess over the expected background is observed. Limits are derived on the stop mass in the Tstop1 simplified model, see Fig. 17.

[13] KHACHATRYAN 17AD searched in 2.3 fb^{-1} of pp collisions at $\sqrt{s}$ = 13 TeV for events containing at least four jets (including b-jets), missing transverse momentum and tagged top quarks. No evidence for an excess over the expected background is observed. Top squark masses in the range 250–740 GeV and neutralino masses up to 240 GeV are excluded at 95% C.L. See Fig. 12.

[14] KHACHATRYAN 17AD searched in 2.3 fb^{-1} of pp collisions at $\sqrt{s}$ = 13 TeV for events containing at least four jets (including b-jets), missing transverse momentum and tagged top quarks. No evidence for an excess over the expected background is observed. Limits are derived on the $\tilde{t}$ mass in simplified models that are a mixture of Tstop1 and Tstop2 with branching fractions 50% for each of the two decay modes: top squark masses of up to 610 GeV and neutralino masses up to 190 GeV are excluded at 95% C.L. The $\tilde{\chi}_1^\pm$ and the $\tilde{\chi}_1^0$ are assumed to be nearly degenerate in mass, with a 5 GeV difference between their masses. See Fig. 12.

[15] KHACHATRYAN 17P searched in 2.3 fb^{-1} of pp collisions at $\sqrt{s}$ = 13 TeV for events with one or more jets and large $\not{E}_T$. No significant excess above the Standard Model expectations is observed. Limits are set on the gluino mass in the Tglu1A, Tglu2A, Tglu3A, Tglu3B, Tglu3C and Tglu3D simplified models, see their Figures 7 and 8. Limits are also set on the squark mass in the Tsqk1 simplified model, see their Fig. 7, and on the sbottom mass in the Tsbot1 simplified model, see Fig. 8. Finally, limits are set on the stop mass in the Tstop1, Tstop3, Tstop4, Tstop6 and Tstop7 simplified models, see Fig. 8.

[16] KHACHATRYAN 17S searched in 18.5 fb^{-1} of pp collisions at $\sqrt{s}$ = 8 TeV for events containing multiple jets and missing transverse momentum, using the α_T variable to discriminate between signal and background processes. No evidence for an excess over the expected background is observed. Limits are derived on the stop mass in the Tstop4 model: for $\Delta m = m_{\tilde{t}} - m_{\tilde{\chi}_1^0}$ equal to 10 and 80 GeV, masses of stop below 240 and 260 GeV are excluded, respectively. See their Fig.3.

[17] KHACHATRYAN 17S searched in 18.5 fb^{-1} of pp collisions at $\sqrt{s}$ = 8 TeV for events containing multiple jets and missing transverse momentum, using the α_T variable to discriminate between signal and background processes. No evidence for an excess over the expected background is observed. Limits are derived on the stop mass in the Tstop3 model: for $\Delta m = m_{\tilde{t}} - m_{\tilde{\chi}_1^0}$ equal to 10 and 80 GeV, masses of stop below 225 and 130 GeV are excluded, respectively. See their Fig.3.

[18] KHACHATRYAN 17S searched in 18.5 fb^{-1} of pp collisions at $\sqrt{s}$ = 8 TeV for events containing multiple jets and missing transverse momentum, using the α_T variable to discriminate between signal and background processes. No evidence for an excess over the expected background is observed. Limits are derived on the stop mass in the Tstop2 model: assuming $m_{\tilde{\chi}_1^\pm} = 0.25\ m_{\tilde{t}} + 0.75\ m_{\tilde{\chi}_1^0}$, masses of stop up to 325 GeV and masses of the neutralino up to 225 GeV are excluded. See their Fig.3.

[19] KHACHATRYAN 17S searched in 18.5 fb^{-1} of pp collisions at $\sqrt{s}$ = 8 TeV for events containing multiple jets and missing transverse momentum, using the α_T variable to discriminate between signal and background processes. No evidence for an excess over the expected background is observed. Limits are derived on the stop mass in the Tstop2 model: assuming $m_{\tilde{\chi}_1^\pm} = 0.75\ m_{\tilde{t}} + 0.25\ m_{\tilde{\chi}_1^0}$, masses of stop up to 400 GeV are excluded for low neutralino masses. See their Fig.3.

[20] KHACHATRYAN 17S searched in 18.5 fb^{-1} of pp collisions at $\sqrt{s}$ = 8 TeV for events containing multiple jets and missing transverse momentum, using the α_T variable to discriminate between signal and background processes. No evidence for an excess over the expected background is observed. Limits are derived on the stop mass in the Tstop1 model: assuming masses of stop up to 500 GeV and masses of the neutralino up to 105 GeV are excluded. See their Fig.3.

[21] SIRUNYAN 17AS searched in 35.9 fb^{-1} of pp collisions at $\sqrt{s}$ = 13 TeV for events with a single lepton (electron or muon), jets, and large $\not{E}_T$. No significant excess above the Standard Model expectations is observed. Limits are set on the stop mass in the Tstop1, Tstop2 and Tstop8 simplified models, see their Figures 5, 6 and 7.

[22] SIRUNYAN 17AT searched in 35.9 fb^{-1} of pp collisions at $\sqrt{s}$ = 13 TeV for direct production of top squarks in events with jets and large $\not{E}_T$. No significant excess above the Standard Model expectations is observed. Limits are set on the stop mass in the Tstop1, Tstop2 , Tstop3, Tstop4, Tstop8 and Tstop10 simplified models, see their Figures 9 to 14.

[23] SIRUNYAN 17AZ searched in 35.9 fb^{-1} of pp collisions at $\sqrt{s}$ = 13 TeV for events with one or more jets and large $\not{E}_T$. No significant excess above the Standard Model expectations is observed. Limits are set on the gluino mass in the Tglu1A, Tglu2A, Tglu3A simplified models, see their Figures 6. Limits are also set on the squark mass in the Tsqk1 simplified model (for single light squark and for 8 degenerate light squarks), on the sbottom mass in the Tsbot1 simplified model and on the stop mass in the Tstop1 simplified model, see their Fig. 7. Finally, limits are set on the stop mass in the Tstop2, Tstop4 and Tstop8 simplified models, see Fig. 8.

[24] SIRUNYAN 17K searched in 2.3 fb^{-1} of pp collisions at $\sqrt{s}$ = 13 TeV for direct production of stop or sbottom pairs in events with multiple jets and significant $\not{E}_T$. A second search also requires an isolated lepton and is combined with the all-hadronic search. No significant excess above the Standard Model expectations is observed. Limits are set on the stop mass in the Tstop1, Tstop8 and Tstop4 simplified models, see their Figures 7, 8 and 9 (for the Tstop4 limits, only the results of the all-hadronic search are used). Limits are also set on the sbottom mass in the Tsbot1 simplified model, see Fig. 10 (also here, only the results of the all-hadronic search are used).

[25] SIRUNYAN 17P searched in 35.9 fb^{-1} of pp collisions at $\sqrt{s}$ = 13 TeV for events with multiple jets and large $\not{E}_T$. No significant excess above the Standard Model expectations is observed. Limits are set on the gluino mass in the Tglu1A, Tglu1C, Tglu2A, Tglu3A and Tglu3D simplified models, see their Fig. 12. Limits are also set on the squark mass in the Tsqk1 simplified model, on the stop mass in the Tstop1 simplified model, and on the sbottom mass in the Tsbot1 simplified model, see Fig. 13.

[26] AABOUD 16D searched in 3.2 fb^{-1} of pp collisions at $\sqrt{s}$ = 13 TeV in events with an energetic jet and large missing transverse momentum. The results are interpreted as 95% C.L. limits on mass of stop decaying into a charm-quark and the lightest neutralino in scenarios with $m_{\tilde{t}_1} - m_{\tilde{\chi}_1^0}$ between 5 and 20 GeV. See their Fig. 5.

[27] AABOUD 16J searched in 3.2 fb^{-1} of pp collisions at $\sqrt{s}$ = 13 TeV in final states with one isolated electron or muon, jets, and missing transverse momentum. For the direct stop pair production model where the stop decays via top and lightest neutralino, the results exclude at 95% C.L. stop masses between 745 GeV and 780 GeV for a massless $\tilde{\chi}_1^0$. See their Fig. 8.

[28] AAD 16AY searched in 20 fb^{-1} of pp collisions at $\sqrt{s}$ = 8 TeV for events with either two hadronically decaying tau leptons, one hadronically decaying tau and one light lepton, or two light leptons. No significant excess over the Standard Model expectation is found. Exclusion limits at 95% C.L. on the mass of top squarks decaying via $\tilde{\tau}$ to a nearly massless gravitino are placed depending on $m_{\tilde{\tau}}$ which is ranging from the 87 GeV LEP limit to $m_{\tilde{t}_1}$. See their Figs. 9 and 10.

[29] KHACHATRYAN 16AV searched in 19.7 fb^{-1} of pp collisions at $\sqrt{s}$ = 8 TeV for events with one or two isolated leptons, hadronic jets, b-jets and $\not{E}_T$. No significant excess above the Standard Model expectations is observed. Limits are set on the stop mass in the Tstop1 and Tstop2 simplified models, see Fig. 11.

[30] KHACHATRYAN 16BK searched in 18.9 fb^{-1} of pp collisions at $\sqrt{s}$ = 8 TeV for events with hadronic jets and $\not{E}_T$. No significant excess above the Standard Model expectations is observed. Limits are set on the stop mass in the Tstop1 and Tstop2 simplified models, see Fig. 16.

[31] KHACHATRYAN 16BS searched in 2.3 fb^{-1} of pp collisions at $\sqrt{s}$ = 13 TeV for events with at least one energetic jet , no isolated leptons, and significant $\not{E}_T$, using the transverse mass variable M_{T2} to discriminate between signal and background processes. No significant excess above the Standard Model expectations is observed. Limits are set on the stop mass in the Tstop1 simplified model, see Fig. 11 and Table 3.

[32] KHACHATRYAN 16Y searched in 19.7 fb^{-1} of pp collisions at $\sqrt{s}$ = 8 TeV for events with one or two soft isolated leptons, hadronic jets, and $\not{E}_T$. No significant excess above the Standard Model expectations is observed. Limits are set on the stop mass in the Tstop3 simplified model, see Fig. 3.

[33] AAD 15CJ searched in 20 fb^{-1} of pp collisions at $\sqrt{s}$ = 8 TeV for evidence of third generation squarks by combining a large number of searches covering various final states. Stop decays with and without charginos in the decay chain are considered and summaries of all ATLAS Run 1 searches for direct stop production can be found in Fig. 4 (no intermediate charginos) and Fig. 7 (intermediate charginos). Limits are set on stop masses in compressed mass regions regions, with $B(\tilde{t} \to c\tilde{\chi}_1^0) + B(\tilde{t} \to bff'\tilde{\chi}_1^0)$ = 1, see Fig. 5. Limits are also set on stop masses assuming that both the decay $\tilde{t} \to t\tilde{\chi}_1^0$ and $\tilde{t} \to b\tilde{\chi}_1^\pm$ are possible, with both their branching rations summing up to 1, assuming $\tilde{\chi}_1^\pm \to W^{(*)}\tilde{\chi}_1^0$ and $m_{\tilde{\chi}_1^\pm} = 2\ m_{\tilde{\chi}_1^0}$, see Fig. 6. Limits on the mass of the next-to-lightest stop $\tilde{t}_2$, decaying either to $Z\tilde{t}_1$, $h\tilde{t}_1$ or $t\tilde{\chi}_1^0$, are also presented, see Figs. 9 and 10.Interpretations in the pMSSM are also discussed, see Figs 13–15.

[34] AAD 15J interpreted the measurement of spin correlations in $t\bar{t}$ production using 20.3 fb^{-1} of pp collisions at $\sqrt{s}$ = 8 TeV in exclusion limits on the pair production of light $\tilde{t}_1$ squarks with masses similar to the top quark mass. The $\tilde{t}_1$ is assumed to decay through $\tilde{t}_1 \to t\tilde{\chi}_1^0$ with predominantly right-handed top and a 100% branching ratio. The data are found to be consistent with the Standard Model expectations and masses between the top quark mass and 191 GeV are excluded, see their Fig. 2

[35] KHACHATRYAN 15AF searched in 19.5 fb^{-1} of pp collisions at $\sqrt{s}$ = 8 TeV for events with at least two energetic jets and significant $\not{E}_T$, using the transverse mass variable M_{T2} to discriminate between signal and background processes. No significant excess above the Standard Model expectations is observed. Limits are set on the stop mass in simplified models where the decay $\tilde{t} \to t\tilde{\chi}_1^0$ takes place with a branching ratio of 100%, see Fig. 12. See also Table 5. Exclusions in the CMSSM, assuming tanβ = 30, A_0 = -2 max(m_0, $m_{1/2}$) and $\mu > 0$, are also presented, see Fig. 15.

[36] KHACHATRYAN 15AH searched in 19.4 or 19.7 fb^{-1} of pp collisions at $\sqrt{s}$ = 8 TeV for events containing either a fully reconstructed top quark, or events containing dijets requiring one or both jets to originate from b-quarks, or events containing a mono-jet. No significant excess above the Standard Model expectations is observed. Limits are set on the stop mass in simplified models where the decay $\tilde{t} \to t\tilde{\chi}_1^0$ takes place with a branching ratio of 100%, see Fig. 9. Limits are also set in simplified models where the decays $\tilde{t} \to t\tilde{\chi}_1^0$ and $\tilde{t} \to b\tilde{\chi}_1^\pm$, with $m_{\tilde{\chi}_1^\pm}$ - $m_{\tilde{\chi}_1^0}$ = 5 GeV, each take place with a branching ratio of 50%, see Fig. 10, or with other fractions, see Fig. 11. Finally, limits are set in a simplified model where the decay $\tilde{t} \to c\tilde{\chi}_1^0$ takes place with a branching ratio of 100%, see Figs. 9, 10 and 11.

[37] KHACHATRYAN 15AH searched in 19.4 or 19.7 fb^{-1} of pp collisions at $\sqrt{s}$ = 8 TeV for events containing either a fully reconstructed top quark, or events containing dijets requiring one or both jets to originate from b-quarks, or events containing a mono-jet. No significant excess above the Standard Model expectations is observed. Limits are set on the stop mass in simplified models where the decay $\tilde{t} \to t\tilde{\chi}_1^0$ takes place with a branching ratio of 100%, see Fig. 9. Limits are also set in simplified models where the decays $\tilde{t} \to t\tilde{\chi}_1^0$ and $\tilde{t} \to b\tilde{\chi}_1^\pm$, with $m_{\tilde{\chi}_1^\pm} - m_{\tilde{\chi}_1^0}$ = 5 GeV, each take place with a branching ratio of 50%, see Fig. 10, or with other fractions, see Fig. 11. Finally, limits

are set in a simplified model where the decay $\tilde{t} \rightarrow c\tilde{\chi}_1^0$ takes place with a branching ratio of 100%, see Figs. 9, 10, and 11.

[38] KHACHATRYAN 15L searched in 19.4 fb^{-1} of pp collisions at $\sqrt{s} = 8$ TeV for pair production of heavy resonances decaying to pairs of jets in four jet events. No significant excess above the Standard Model expectations is observed. Limits are set on the stop mass in R-parity-violating supersymmetry models where $\tilde{t} \rightarrow qq$ ($\lambda''_{312} \neq 0$), see Fig. 6 (top) and $\tilde{t} \rightarrow qb$ ($\lambda''_{323} \neq 0$), see Fig. 6 (bottom).

[39] KHACHATRYAN 15X searched in 19.3 fb^{-1} of pp collisions at $\sqrt{s} = 8$ TeV for events with at least two energetic jets, at least one of which is required to originate from a b quark, possibly a lepton, and significant $\not{E}_T$, using the razor variables (M_R and R^2) to discriminate between signal and background processes. No significant excess above the Standard Model expectations is observed. Limits are set on the stop mass in simplified models where the decay $\tilde{t} \rightarrow t\tilde{\chi}_1^0$ and the decay $\tilde{t} \rightarrow b\tilde{\chi}_1^{\pm}$, with $m_{\tilde{\chi}_1^{\pm}} - m_{\tilde{\chi}_1^0} = 5$ GeV, take place with branching ratios varying between 0 and 100%, see Figs. 15, 16 and 17.

[40] AAD 14AJ searched in 20.1 fb^{-1} of pp collisions at $\sqrt{s} = 8$ TeV for events containing four or more jets and large missing transverse momentum. No excess of events above the expected level of Standard Model background was found. Exclusion limits at 95% C.L. are set on the masses of third-generation squarks in simplified models which either assume that the decay $\tilde{t}_1 \rightarrow t\tilde{\chi}_1^0$ takes place 100% of the time, see Fig. 8, or that this decay takes place 50% of the time, while the decay $\tilde{t}_1 \rightarrow b\tilde{\chi}_1^{\pm}$ takes place the other 50% of the time, see Fig. 9.

[41] AAD 14BD searched in 20 fb^{-1} of pp collisions at $\sqrt{s} = 8$ TeV for events containing one isolated lepton, jets and large missing transverse momentum. No excess of events above the expected level of Standard Model background was found. Exclusion limits at 95% C.L. are set on the masses of third-generation squarks in simplified models which either assume that the decay $\tilde{t}_1 \rightarrow t\tilde{\chi}_1^0$ takes place 100% of the time, see Fig. 15, or the decay $\tilde{t}_1 \rightarrow b\tilde{\chi}_1^{\pm}$ takes place 100% of the time, see Fig. 16–22. For the mixed decay scenario, see Fig. 23.

[42] AAD 14F searched in 20.3 fb^{-1} of pp collisions at $\sqrt{s} = 8$ TeV for events containing two leptons (e or μ), and possibly jets and missing transverse momentum. No excess of events above the expected level of Standard Model background was found. Exclusion limits at 95% C.L. are set on the masses of third-generation squarks in simplified models which either assume that the decay $\tilde{t}_1 \rightarrow b\tilde{\chi}_1^{\pm}$ takes place 100% of the time, see Figs. 14–17 and 20, or that the decay $\tilde{t}_1 \rightarrow t\tilde{\chi}_1^0$ takes place 100% of the time, see Figs. 18 and 19.

[43] AAD 14T searched in 20.3 fb^{-1} of pp collisions at $\sqrt{s} = 8$ TeV for monojet-like and c-tagged events. No excess of events above the expected level of Standard Model background was found. Exclusion limits at 95% C.L. are set on the masses of third-generation squarks in simplified models which assume that the decay $\tilde{t}_1 \rightarrow c\tilde{\chi}_1^0$ takes place 100% of the time, see Fig. 9 and 10. The results of the monojet-like analysis are also interpreted in terms of stop pair production in the four-body decay $\tilde{t}_1 \rightarrow bff'\tilde{\chi}_1^0$, see Fig. 11.

[44] CHATRCHYAN 14AH searched in 4.7 fb^{-1} of pp collisions at $\sqrt{s} = 7$ TeV for events with at least two energetic jets and significant $\not{E}_T$, using the razor variables (M_R and R^2) to discriminate between signal and background processes. A second analysis requires at least one of the jets to be originating from a b-quark. No significant excess above the Standard Model expectations is observed. Limits are set on sbottom masses in simplified models where the decay $\tilde{t} \rightarrow t\tilde{\chi}_1^0$ takes place with a branching ratio of 100%, see Figs. 28 and 29. Exclusions in the CMSSM, assuming $\tan\beta = 10$, $A_0 = 0$ and $\mu > 0$, are also presented, see Fig. 26.

[45] CHATRCHYAN 14R searched in 19.5 fb^{-1} of pp collisions at $\sqrt{s} = 8$ TeV for events with at least three leptons (electrons, muons, taus) in the final state. No significant excess above the Standard Model expectations is observed. Limits are set on the stop mass in a natural higgsino NLSP simplified model (GMSB) where the decay $\tilde{t} \rightarrow b\tilde{\chi}_1^{\pm}$, with $\tilde{\chi}_1^{\pm} \rightarrow (qq'/\ell\nu)H$, $Z\tilde{G}$, takes place with a branching ratio of 100% (the particles between brackets have a soft p_T spectrum), see Figs. 4–6.

[46] KHACHATRYAN 14T searched in 19.7 fb^{-1} of pp collisions at $\sqrt{s} = 8$ TeV for events with τ-leptons and b-quark jets, possibly with extra light-flavour jets. No excess above the Standard Model expectations is observed. Limits are set on stop masses in RPV SUSY models with $LQ\overline{D}$ couplings, in two simplified models. In the first model, the decay $\tilde{t} \rightarrow \tau b$ is considered, with $\lambda'_{333} \neq 0$, see Fig. 3. In the second model, the decay $\tilde{t} \rightarrow \tilde{\chi}^{\pm} b$, with the subsequent decay $\tilde{\chi}^{\pm} \rightarrow qq\tau^{\pm}$ is considered, with $\lambda'_{3jk} \neq 0$ and the mass splitting between the top squark and the charging chosen to be 100 GeV, see Fig. 4.

[47] AABOUD 17AF searched in 36 fb^{-1} of pp collisions at $\sqrt{s} = 13$ TeV for evidence of top squarks in events containing 2 leptons, jets, b-jets and $\not{E}_T$. In Tstop6 model, assuming $m_{\tilde{\chi}_1^0} = 0$ GeV, $\tilde{t}_1$ masses up to 850 GeV are excluded for $m_{\tilde{\chi}_2^0} > 200$ GeV.

[48] AABOUD 17AF searched in 36 fb^{-1} of pp collisions at $\sqrt{s} = 13$ TeV for evidence of $\tilde{t}_2$ in events containing 2 leptons, jets, b-jets and $\not{E}_T$. In Tstop7 model, assuming $m_{\tilde{\chi}_1^0} = 50$ GeV and 100% decays via Z boson, $\tilde{t}_2$ masses up to 800 GeV are excluded. Exclusion limits are also shown as a function of the $\tilde{t}_2$ branching ratios in their Figure 7.

[49] AABOUD 17AF searched in 36 fb^{-1} of pp collisions at $\sqrt{s} = 13$ TeV for evidence of $\tilde{t}_2$ in events containing 2 leptons, jets, b-jets and $\not{E}_T$. In Tstop7 model, assuming $m_{\tilde{\chi}_1^0} = 50$ GeV and 100% decays via higgs boson, $\tilde{t}_2$ masses up to 880 GeV are excluded. Exclusion limits are also shown as a function of the $\tilde{t}_2$ branching ratios in their Figure 7.

[50] AABOUD 17AY searched in 36.1 fb^{-1} of pp collisions at $\sqrt{s} = 13$ TeV for events with at least four jets and large missing transverse momentum. No significant excess above the Standard Model expectations is observed. Limits are set on the top squark mass assuming three pMSSM-inspired models. The first one, referred to as Higgsino LSP model, assumes $m_{\tilde{\chi}_1^{\pm}} - m_{\tilde{\chi}_1^0} = 5$ GeV and $m_{\tilde{\chi}_2^0} - m_{\tilde{\chi}_1^0} = 10$ GeV, with a mixture of decay modes as in Tstop1, Tstop2 and Tstop6. See their Figure 10. The second and third models are referred to as Wino NLSP and well-tempered pMSSM models, respectively. See their Figure 11 and Figure 12, and text for details on assumptions.

[51] AAD 14B searched in 20.3 fb^{-1} of pp collisions at $\sqrt{s} = 8$ TeV for events containing a Z boson, with or without additional leptons, plus jets originating from b-quarks and significant missing transverse momentum. No excess over the expected SM background is observed. Limits are derived in simplified models featuring $\tilde{t}_2$ production, with $\tilde{t}_2 \rightarrow Z\tilde{t}_1$, $\tilde{t}_1 \rightarrow t\tilde{\chi}_1^0$ with a 100% branching ratio, see Fig. 4, and in the framework of natural GMSB, see Fig. 6.

[52] CHATRCHYAN 14U searched in 19.7 fb^{-1} of pp collisions at $\sqrt{s} = 8$ TeV for evidence of direct pair production of top squarks, with Higgs bosons in the decay chain. The search is performed using a selection of events containing two Higgs bosons, each decaying to a photon pair, missing transverse energy and possibly b-quark jets. No significant excesses over the expected SM backgrounds are observed. The results are interpreted in the context of a "natural SUSY" simplified model where the decays $\tilde{t}_1 \rightarrow b\tilde{\chi}_1^{\pm}$, with $\tilde{\chi}_1^{\pm} \rightarrow ff'\tilde{\chi}_1^0$, and $\tilde{\chi}_1^0 \rightarrow H\tilde{G}$, all happen with 100% branching ratio, see Fig. 4.

[53] KHACHATRYAN 14C searched in 19.5 fb^{-1} of pp collisions at $\sqrt{s} = 8$ TeV for evidence of direct pair production of top squarks, with Higgs or Z-bosons in the decay chain. The search is performed using a selection of events containing leptons and b-quark jets. No significant excesses over the expected SM backgrounds are observed. The results are interpreted in the context of a simplified model with pair production of a heavier top-squark mass eigenstate $\tilde{t}_2$ decaying to a lighter top-squark eigenstate $\tilde{t}_1$ via either $\tilde{t}_2 \rightarrow H\tilde{t}_1$ or $\tilde{t}_2 \rightarrow Z\tilde{t}_1$, followed in both cases by $\tilde{t}_1 \rightarrow t\tilde{\chi}_1^0$. The interpretation is performed in the region where the mass difference between the $\tilde{t}_1$ and $\tilde{\chi}_1^0$ is approximately equal to the top-quark mass, which is not probed by searches for direct $\tilde{t}_1$ pair production, see Figs. 5 and 6. The analysis excludes top squarks with masses $m_{\tilde{t}_2} < 575$ GeV and $m_{\tilde{t}_1} < 400$ GeV at 95% C.L.

R-parity violating $\tilde{t}$ (Stop) mass limit

VALUE (GeV)	CL%	DOCUMENT ID		TECN	COMMENT
>1200	95	[1] AABOUD	17AI	ATLS	RPV, $\geq 1\ell + \geq 8$ jets, Tstop1 with $\tilde{\chi}_1^0 \rightarrow tbs$, λ''_{323} coupling, $m_{\tilde{\chi}_1^0}$=500 GeV
none, 100–315	95	[2] AAD	16AM	ATLS	2 large-radius jets, Tstop1RPV
• • • We do not use the following data for averages, fits, limits, etc. • • •					
> 890	95	[3] KHACHATRY...16AC		CMS	$e^+e^- + \geq 5$ jets; $\tilde{t} \rightarrow b\tilde{\chi}_1^{\pm}$; $\tilde{\chi}_1^{\pm} \rightarrow \ell^{\pm}jj$, RPV, λ'_{ijk}
>1000	95	[3] KHACHATRY...16AC		CMS	$\mu^+\mu^- + \geq 5$ jets; $\tilde{t} \rightarrow b\tilde{\chi}_1^{\pm}$; $\tilde{\chi}_1^{\pm} \rightarrow \ell^{\pm}jj$, RPV, λ'_{ijk}
> 950	95	[4] KHACHATRY...16BX		CMS	$\tilde{t} \rightarrow t\tilde{\chi}_1^0$, $\tilde{\chi}_1^0 \rightarrow \ell\ell\nu$, RPV, λ_{121} or $\lambda_{122} \neq 0$
> 790	95	[5] KHACHATRY...15E		CMS	$\tilde{t}_1 \rightarrow b\ell$, RPV, $c\tau = 2$ cm

[1] AABOUD 17AI searched in 36.1 fb^{-1} of pp collisions at $\sqrt{s} = 13$ TeV for events with one or more isolated lepton, at least eight jets, either zero or many b-jets, for evidence of R-parity violating decays of the top squark. No significant excess above the Standard Model expectations is observed. Limits up to 1.25 (1.10) TeV are set on the top squark mass in R-parity-violating supersymmetry models where $\tilde{t}_1$ decays for a bino LSP as: $\tilde{t} \rightarrow t\tilde{\chi}_1^0$ and for a higgsino LSP as $\tilde{t} \rightarrow t\tilde{\chi}_{1,2}^0/b\tilde{\chi}_1^+$. These is followed by the decays through the non-zero λ''_{323} coupling $\tilde{\chi}_{1,2}^0 \rightarrow tbs$, $\tilde{\chi}_1^{\pm} \rightarrow bbs$. See their Figure 10 and text for details on model assumptions.

[2] AAD 16AM searched in 17.4 fb^{-1} of pp collisions at $\sqrt{s} = 8$ TeV for events containing two large-radius hadronic jets. No deviation from the background prediction is observed. Top squarks with masses between 100 and 315 GeV are excluded at 95% C.L. in the hypothesis that they both decay via R-parity violating coupling λ''_{323} to b- and s-quarks. See their Fig. 10.

[3] KHACHATRYAN 16AC searched in 19.7 fb^{-1} of pp collisions at $\sqrt{s} = 8$ TeV for events with low missing transverse momentum, two oppositely charged electrons or muons, and at least five jets, at least one of which is a b-jet, for evidence of R-parity violating, charging-mediated decays of the top squark. No significant excess above the Standard Model expectations is observed. Limits are set on the stop mass in R-parity-violating supersymmetry models where $\tilde{t} \rightarrow b\tilde{\chi}_1^{\pm}$ with $\tilde{\chi}_1^{\pm} \rightarrow \ell^{\pm}jj$, $\lambda'_{ijk} \neq 0$ ($i,j,k \leq 2$), and with $m_{\tilde{t}} - m_{\tilde{\chi}_1^{\pm}} = 100$ GeV, see Fig. 3.

[4] KHACHATRYAN 16BX searched in 19.5 fb^{-1} of pp collisions at $\sqrt{s} = 8$ TeV for events containing 4 leptons coming from R-parity-violating decays of $\tilde{\chi}_1^0 \rightarrow \ell\ell\nu$ with $\lambda_{121} \neq 0$ or $\lambda_{122} \neq 0$. No excess over the expected background is observed. Limits are derived on the gluino, squark and stop masses, see Fig. 23.

[5] KHACHATRYAN 15E searched for long-lived particles decaying to leptons in 19.7 fb^{-1} of pp collisions at $\sqrt{s} = 8$ TeV. Events were selected with an electron and muon with opposite charges and each with transverse impact parameter values between 0.02 and 2 cm. Limits are set on SUSY benchmark models with pair production of top squarks decaying into an $e\mu$ final state via RPV interactions. See their Fig. 2

Heavy $\tilde{g}$ (Gluino) mass limit

For $m_{\tilde{g}} > 60$–70 GeV, it is expected that gluinos would undergo a cascade decay via a number of neutralinos and/or charginos rather than undergo a direct decay to photinos as assumed by some papers. Limits obtained when direct decay is assumed are usually higher than limits when cascade decays are included.

Some earlier papers are now obsolete and have been omitted. They were last listed in our PDG 14 edition: K. Olive, *et al.* (Particle Data Group), Chinese Physics **C38** 070001 (2014) (http://pdg.lbl.gov).

VALUE (GeV)	CL%	DOCUMENT ID		TECN	COMMENT
>2040	95	[1] SIRUNYAN	18D	CMS	top quark (hadronically decaying) + jets + $\not{E}_T$, Tglu3A, $m_{\tilde{\chi}_1^0}$ = 0 GeV
>1930	95	[1] SIRUNYAN	18D	CMS	top quark (hadronically decaying) + jets + $\not{E}_T$, Tglu3B, $m_{\tilde{t}_1} - m_{\tilde{\chi}_1^0} = 175$ GeV, $m_{\tilde{\chi}_1^0}$ = 200 GeV

>1690	95	[1] SIRUNYAN	18D	CMS	top quark (hadronically decaying) + jets + $\not{E}_T$, Tglu3C, $m_{\widetilde{t}_1} - m_{\widetilde{\chi}^0_1} = 20$ GeV, $m_{\widetilde{\chi}^0_1} = 0$ GeV	
>1990	95	[1] SIRUNYAN	18D	CMS	top quark (hadronically decaying) + jets + $\not{E}_T$, Tglu3E, $m_{\widetilde{\chi}^\pm_1} = m_{\widetilde{\chi}^0_1} + 5$ GeV, $m_{\widetilde{\chi}^0_1} = 100$ GeV	
>2100	95	[2] AABOUD	17AI	ATLS	RPV, $\geq 1\ell +$ ≥ 8 jets, Tglu3A and $\widetilde{\chi}^0_1 \to uds$, λ''_{112} coupling, $m_{\widetilde{\chi}^0_1}$=1000 GeV	
>1650	95	[3] AABOUD	17AI	ATLS	RPV, $\geq 1\ell +$ ≥ 8 jets, $\widetilde{g} \to t\widetilde{t}$, $\widetilde{t} \to bs$, λ''_{323} coupling, $m_{\widetilde{t}}$=1000 GeV	
>1800	95	[4] AABOUD	17AI	ATLS	RPV, $\geq 1\ell +$ ≥ 8 jets, Tglu1A and $\widetilde{\chi}^0_1 \to qql$, λ' coupling, $m_{\widetilde{\chi}^0_1}$=1000 GeV	
>1750	95	[5] AABOUD	17AJ	ATLS	same-sign $\ell^\pm\ell^\pm$ / 3 ℓ + jets + $\not{E}_T$, Tglu3A, $m_{\widetilde{\chi}^0_1} = 100$ GeV	
>1570	95	[6] AABOUD	17AJ	ATLS	same-sign $\ell^\pm\ell^\pm$ / 3 ℓ + jets + $\not{E}_T$, Tglu1E, $m_{\widetilde{\chi}^0_1} = 100$ GeV	
>1860	95	[7] AABOUD	17AJ	ATLS	same-sign $\ell^\pm\ell^\pm$ / 3 ℓ + jets + $\not{E}_T$, Tglu1G, $m_{\widetilde{\chi}^0_1} = 200$ GeV	
>1800	95	[8] AABOUD	17AJ	ATLS	RPV, same-sign $\ell^\pm\ell^\pm$ / 3 ℓ + jets + $\not{E}_T$, Tglu3A, λ''_{112} coupling, $m_{\widetilde{\chi}^0_1} = 50$ GeV	
>1750	95	[9] AABOUD	17AJ	ATLS	RPV, same-sign $\ell^\pm\ell^\pm$ / 3 ℓ + jets + $\not{E}_T$, Tglu1A and $\widetilde{\chi}^0_1 \to qq\ell$, λ' coupling	
>1450	95	[10] AABOUD	17AJ	ATLS	RPV, same-sign $\ell^\pm\ell^\pm$ / 3 ℓ + jets + $\not{E}_T$, $\widetilde{g} \to t\widetilde{t}_1$ and $\widetilde{t}_1 \to sd$, λ''_{321} coupling	
>1450	95	[11] AABOUD	17AJ	ATLS	RPV, same-sign $\ell^\pm\ell^\pm$ / 3 ℓ + jets + $\not{E}_T$, $\widetilde{g} \to t\widetilde{t}_1$ and $\widetilde{t}_1 \to bd$, λ''_{313} coupling	
> 400	95	[12] AABOUD	17AJ	ATLS	RPV, same-sign $\ell^\pm\ell^\pm$ / 3 ℓ + jets + $\not{E}_T$, $\widetilde{d}_R \to tb(ts)$, λ''_{313} (λ''_{321}) coupling	
>2100	95	[13] AABOUD	17AR	ATLS	1ℓ+jets+$\not{E}_T$, Tglu1B, $m_{\widetilde{\chi}^0_1} = 0$ GeV	
>1740	95	[14] AABOUD	17AR	ATLS	1ℓ+jets+$\not{E}_T$, Tglu1E, $m_{\widetilde{\chi}^0_1} = 0$ GeV	
>1800	95	[15] AABOUD	17AY	ATLS	jets+$\not{E}_T$, Tglu3A, $m_{\widetilde{t}_1} - m_{\widetilde{\chi}^0_1} = 5$ GeV	
>1800	95	[16] AABOUD	17AZ	ATLS	≥ 7 jets+$\not{E}_T$, large R-jets and/or b-jets, Tglu1E, $m_{\widetilde{\chi}^0_1} = 100$ GeV	
>1540	95	[17] AABOUD	17AZ	ATLS	≥ 7 jets+$\not{E}_T$, large R-jets and/or b-jets, Tglu3A, $m_{\widetilde{\chi}^0_1} = 0$ GeV	
none 625–1375	95	[18] AABOUD	17AZ	ATLS	RPV, ≥ 7 jets+$\not{E}_T$, large R-jets and/or b-jets, $\widetilde{g} \to t\widetilde{t}_1$ and $\widetilde{t}_1 \to bs$, λ''_{323} coupling	
>1340	95	[19] AABOUD	17N	ATLS	2 same-flavor, opposite-sign ℓ + jets + $\not{E}_T$, Tglu1H, $m_{\widetilde{\chi}^0_1} = 0$ GeV	
>1310	95	[20] AABOUD	17N	ATLS	2 same-flavor, opposite-sign ℓ + jets + $\not{E}_T$, Tglu1H, $m_{\widetilde{\chi}^0_2} = (m_{\widetilde{g}}+m_{\widetilde{\chi}^0_1})/2$, $m_{\widetilde{\chi}^0_1} < 400$ GeV	
>1700	95	[21] AABOUD	17N	ATLS	2 same-flavor, opposite-sign ℓ + jets + $\not{E}_T$, Tglu1G, $m_{\widetilde{\chi}^0_1} \sim 1$ GeV	
>1400	95	[22] KHACHATRY...17		CMS	jets+$\not{E}_T$,Tglu1A,$m_{\widetilde{\chi}^0_1}$=200GeV	
>1650	95	[22] KHACHATRY...17		CMS	jets+$\not{E}_T$,Tglu2A,$m_{\widetilde{\chi}^0_1}$=200 GeV	
>1600	95	[22] KHACHATRY...17		CMS	jets+$\not{E}_T$,Tglu3A,$m_{\widetilde{\chi}^0_1}$=200GeV	
>1550	95	[23] KHACHATRY...17AD		CMS	jets+b-jets+$\not{E}_T$, Tglu3A, $m_{\widetilde{\chi}^0_1} = 0$ GeV	
>1450	95	[24] KHACHATRY...17AD		CMS	jets+b-jets+$\not{E}_T$, Tglu3C, 200 < $m_{\widetilde{\chi}^0_1}$ < 400 GeV	
>1570	95	[25] KHACHATRY...17AS		CMS	1ℓ, Tglu3A, $m_{\widetilde{\chi}^0_1} < 600$ GeV	
>1500	95	[25] KHACHATRY...17AS		CMS	1ℓ, Tglu3A, $m_{\widetilde{\chi}^0_1} < 775$ GeV	
>1400	95	[25] KHACHATRY...17AS		CMS	1ℓ, Tglu1B, $m_{\widetilde{\chi}^\pm_1} = (m_{\widetilde{g}} + m_{\widetilde{\chi}^0_1})/2$, $m_{\widetilde{\chi}^0_1} < 725$ GeV	
none 1050–1350	95	[25] KHACHATRY...17AS		CMS	1ℓ, Tglu1B, $m_{\widetilde{\chi}^\pm_1} = (m_{\widetilde{g}} + m_{\widetilde{\chi}^0_1})/2$, $m_{\widetilde{\chi}^0_1} < 850$ GeV	
>1175	95	[26] KHACHATRY...17AW		CMS	$\geq 3\ell^\pm$, 2 jets, Tglu3A, $m_{\widetilde{\chi}^0_1} = 0$ GeV	
> 825	95	[26] KHACHATRY...17AW		CMS	$\geq 3\ell^\pm$, 2 jets, Tglu1C, $m_{\widetilde{\chi}^\pm_1} = (m_{\widetilde{g}} + m_{\widetilde{\chi}^0_1})/2$, $m_{\widetilde{\chi}^0_1} = 0$ GeV	
>1350	95	[27] KHACHATRY...17P		CMS	1 or more jets+$\not{E}_T$, Tglu1A, $m_{\widetilde{\chi}^0_1} = 0$ GeV	
>1545	95	[27] KHACHATRY...17P		CMS	1 or more jets+$\not{E}_T$, Tglu2A, $m_{\widetilde{\chi}^0_1} = 0$ GeV	
>1120	95	[27] KHACHATRY...17P		CMS	1 or more jets+$\not{E}_T$, Tglu3A, $m_{\widetilde{\chi}^0_1} = 0$ GeV	
>1300	95	[27] KHACHATRY...17P		CMS	1 or more jets+$\not{E}_T$, Tglu3D, $m_{\widetilde{\chi}^\pm_1} = m_{\widetilde{\chi}^0_1} + 5$ GeV, $m_{\widetilde{\chi}^0_1} = 100$ GeV	
> 780	95	[27] KHACHATRY...17P		CMS	1 or more jets+$\not{E}_T$, Tglu3B, $m_{\widetilde{t}_1} - m_{\widetilde{\chi}^0_1} = 175$ GeV, $m_{\widetilde{\chi}^0_1} = 50$ GeV	
> 790	95	[27] KHACHATRY...17P		CMS	1 or more jets+$\not{E}_T$, Tglu3C, $m_{\widetilde{t}_1} - m_{\widetilde{\chi}^0_1} = 20$ GeV, $m_{\widetilde{\chi}^0_1} = 0$ GeV	
>1650	95	[28] KHACHATRY...17V		CMS	2 $\gamma + \not{E}_T$, GGM, Tglu4B, any NLSP mass	
none 600–650	95	[29] KHACHATRY...17Y		CMS	$\widetilde{g} \to qqqqq$, RPV, λ''_{212} coupling, $m_{\widetilde{q}} = 100$ GeV	
none 600–1030	95	[29] KHACHATRY...17Y		CMS	$\widetilde{g} \to qqqqq$, RPV, λ''_{212} coupling, $m_{\widetilde{q}} = 900$ GeV	
none 600–650	95	[29] KHACHATRY...17Y		CMS	$\widetilde{g} \to qqqqb$, RPV, λ''_{213} coupling, $m_{\widetilde{q}} = 100$ GeV	
none 600–1080	95	[29] KHACHATRY...17Y		CMS	$\widetilde{g} \to qqqqb$, RPV, λ''_{213} coupling, $m_{\widetilde{q}} = 900$ GeV	
none 600–680	95	[29] KHACHATRY...17Y		CMS	$\widetilde{g} \to qqqbb$, RPV, λ''_{212} coupling, $m_{\widetilde{q}} = 100$ GeV	
none 600–1080	95	[29] KHACHATRY...17Y		CMS	$\widetilde{g} \to qqqbb$, RPV, λ''_{212} coupling, $m_{\widetilde{q}} = 900$ GeV	
none 600–650	95	[29] KHACHATRY...17Y		CMS	$\widetilde{g} \to qqbbb$, RPV, λ''_{213} coupling, $m_{\widetilde{q}} = 100$ GeV	
none 600–1100	95	[29] KHACHATRY...17Y		CMS	$\widetilde{g} \to qqbbb$, RPV, λ''_{213} coupling, $m_{\widetilde{q}} = 900$ GeV	
>1900	95	[30] SIRUNYAN	17AF	CMS	1ℓ+jets+b-jets+$\not{E}_T$, Tglu3A, $m_{\widetilde{\chi}^0_1} = 0$ GeV	
>1600	95	[30] SIRUNYAN	17AF	CMS	1ℓ+jets+b-jets+$\not{E}_T$, Tglu3B, $m_{\widetilde{t}_1} - m_{\widetilde{\chi}^0_1} = 175$ GeV, $m_{\widetilde{\chi}^0_1} = 50$ GeV	
>1800	95	[31] SIRUNYAN	17AY	CMS	γ + jets+$\not{E}_T$, Tglu4B, $m_{\widetilde{\chi}^0_1} = 0$ GeV	
>1600	95	[31] SIRUNYAN	17AY	CMS	γ + jets+$\not{E}_T$, Tglu4A, $m_{\widetilde{\chi}^0_1} = 0$ GeV	
>1860	95	[32] SIRUNYAN	17AZ	CMS	≥ 1 jets + $\not{E}_T$, Tglu1A, $m_{\widetilde{\chi}^0_1} = 0$ GeV	
>2025	95	[32] SIRUNYAN	17AZ	CMS	≥ 1 jets+$\not{E}_T$, Tglu2A, $m_{\widetilde{\chi}^0_1} = 0$ GeV	
>1900	95	[32] SIRUNYAN	17AZ	CMS	≥ 1 jets+$\not{E}_T$, Tglu3A, $m_{\widetilde{\chi}^0_1} = 0$ GeV	
>1825	95	[33] SIRUNYAN	17P	CMS	jets+$\not{E}_T$, Tglu1A, $m_{\widetilde{\chi}^0_1} = 0$ GeV	
>1950	95	[33] SIRUNYAN	17P	CMS	jets+$\not{E}_T$, Tglu2A, $m_{\widetilde{\chi}^0_1} = 0$ GeV	
>1960	95	[33] SIRUNYAN	17P	CMS	jets+$\not{E}_T$, Tglu3A, $m_{\widetilde{\chi}^0_1} = 0$ GeV	
>1800	95	[33] SIRUNYAN	17P	CMS	jets+$\not{E}_T$, Tglu1C, $m_{\widetilde{\chi}^\pm_1} = m_{\widetilde{\chi}^0_2} = (m_{\widetilde{g}}+m_{\widetilde{\chi}^0_1})/2$, $m_{\widetilde{\chi}^0_1} = 0$ GeV	
>1870	95	[33] SIRUNYAN	17P	CMS	jets+$\not{E}_T$, Tglu3D, $m_{\widetilde{\chi}^\pm_1} = m_{\widetilde{\chi}^0_1} + 5$ GeV, $m_{\widetilde{\chi}^0_1} = 1000$ GeV	
>1520	95	[34] SIRUNYAN	17S	CMS	same-sign $\ell^\pm\ell^\pm$ + jets + $\not{E}_T$, Tglu3A, $m_{\widetilde{\chi}^0_1} = 0$ GeV	
>1200	95	[34] SIRUNYAN	17S	CMS	same-sign $\ell^\pm\ell^\pm$ + jets + $\not{E}_T$, Tglu3D, $m_{\widetilde{\chi}^\pm_1} = m_{\widetilde{\chi}^0_1} + 5$ GeV, $m_{\widetilde{\chi}^0_1} = 100$ GeV	
>1370	95	[34] SIRUNYAN	17S	CMS	same-sign $\ell^\pm\ell^\pm$ + jets + $\not{E}_T$, Tglu3B, $m_{\widetilde{t}_1} - m_{\widetilde{\chi}^0_1} = 175$ GeV, $m_{\widetilde{\chi}^0_1} = 50$ GeV	
>1180	95	[34] SIRUNYAN	17S	CMS	same-sign $\ell^\pm\ell^\pm$ + jets + $\not{E}_T$, Tglu3C, $m_{\widetilde{t}_1} - m_{\widetilde{\chi}^0_1} = 20$ GeV, $m_{\widetilde{\chi}^0_1} = 0$ GeV	
>1280	95	[34] SIRUNYAN	17S	CMS	same-sign $\ell^\pm\ell^\pm$ + jets + $\not{E}_T$, Tglu1B, $m_{\widetilde{\chi}^\pm_1} = (m_{\widetilde{g}} + m_{\widetilde{\chi}^0_1})/2$, $m_{\widetilde{\chi}^0_1} = 0$ GeV	

>1300	95	[34] SIRUNYAN	17S	CMS	same-sign $\ell^\pm\ell^\pm$ + jets + $\not{E}_T$, Tglu1B, $m_{\widetilde{t}_1}-m_{\widetilde{\chi}^0_1}$ = 20 GeV, $m_{\widetilde{\chi}^0_1}$ = 100 GeV	
>1570	95	[35] AABOUD	16AC	ATLS	$\geq$ 2 jets + 1 or 2 τ + $\not{E}_T$, Tglu1F, $m_{\widetilde{\chi}^0_1}$ = 100 GeV	
>1460	95	[36] AABOUD	16J	ATLS	1 $\ell^\pm$ + $\geq$ 4 jets + $\not{E}_T$, Tglu3C, $m_{\widetilde{t}_1}-m_{\widetilde{\chi}^0_1}$ = 5 GeV	
>1650	95	[37] AABOUD	16M	ATLS	2 γ + $\not{E}_T$, Tglu1D, any NLSP mass	
>1510	95	[38] AABOUD	16N	ATLS	$\geq$ 4 jets + $\not{E}_T$, Tglu1A, $m_{\widetilde{\chi}^0_1}$ = 0 GeV	
>1500	95	[39] AABOUD	16N	ATLS	$\geq$ 4 jets + $\not{E}_T$, Tglu1B, $m_{\widetilde{\chi}^\pm_1}$ = $(m_{\widetilde{g}}+m_{\widetilde{\chi}^0_1})/2$, $m_{\widetilde{\chi}^0_1}$=200GeV	
>1780	95	[40] AAD	16AD	ATLS	0ℓ, $\geq$ 3 b-jets + $\not{E}_T$, Tglu2A, $m_{\widetilde{\chi}^0_1}$ < 800 GeV	
>1760	95	[41] AAD	16AD	ATLS	1ℓ, $\geq$ 3 b-jets + $\not{E}_T$, Tglu3A, $m_{\widetilde{\chi}^0_1}$ < 700 GeV	
>1300	95	[42] AAD	16BB	ATLS	2 same-sign/3ℓ + jets + $\not{E}_T$, Tglu1D, $m_{\widetilde{\chi}^0_1}$ < 600 GeV	
>1100	95	[42] AAD	16BB	ATLS	2 same-sign/3ℓ + jets + $\not{E}_T$, Tglu1E, $m_{\widetilde{\chi}^0_1}$ < 300 GeV	
>1200	95	[42] AAD	16BB	ATLS	2 same-sign /3ℓ + jets + $\not{E}_T$, Tglu3A, $m_{\widetilde{\chi}^0_1}$ < 600 GeV	
>1600		[43] AAD	16BG	ATLS	1ℓ, $\geq$ 4 jets, $\not{E}_T$, Tglu1B, $m_{\widetilde{\chi}^\pm_1}=(m_{\widetilde{g}}+m_{\widetilde{\chi}^0_1})/2$, $m_{\widetilde{\chi}^0_1}$= 100 GeV	
>1400	95	[44] AAD	16V	ATLS	$\geq$ 7 to $\geq$ 10 jets + $\not{E}_T$, Tglu1E, $m_{\widetilde{\chi}^0_1}$ < 200 GeV	
>1400	95	[44] AAD	16V	ATLS	$\geq$ 7 to $\geq$ 10 jets + $\not{E}_T$, pMSSM M_1 = 60 GeV, M_2 = 3 TeV, tanβ=10, μ < 0	
>1100	95	[45] KHACHATRY...16AM		CMS	boosted W+b, Tglu3C, $m_{\widetilde{t}_1}-m_{\widetilde{\chi}^0_1}$ <80GeV,$m_{\widetilde{\chi}^0_1}$ <400GeV	
> 700	95	[45] KHACHATRY...16AM		CMS	boosted W+b, Tglu3B, $m_{\widetilde{t}_1}-m_{\widetilde{\chi}^0_1}$=175 GeV, $m_{\widetilde{\chi}^0_1}$=0 GeV	
>1050	95	[46] KHACHATRY...16BJ		CMS	same-sign $\ell^\pm\ell^\pm$, Tglu3A, $m_{\widetilde{\chi}^0_1}$ < 800 GeV	
>1300	95	[46] KHACHATRY...16BJ		CMS	same-sign $\ell^\pm\ell^\pm$,Tglu3A,$m_{\widetilde{\chi}^0_1}$=0	
>1140	95	[46] KHACHATRY...16BJ		CMS	same-sign $\ell^\pm\ell^\pm$, Tglu3B, $m_{\widetilde{t}}-m_{\widetilde{\chi}^0_1}$ = 20 GeV, $m_{\widetilde{\chi}^0_1}$ = 0	
> 850	95	[46] KHACHATRY...16BJ		CMS	same-sign $\ell^\pm\ell^\pm$, Tglu3B, $m_{\widetilde{t}}-m_{\widetilde{\chi}^0_1}$=20 GeV,$m_{\widetilde{\chi}^0_1}$ <700 GeV	
> 950	95	[46] KHACHATRY...16BJ		CMS	same-sign $\ell^\pm\ell^\pm$, Tglu3D, $m_{\widetilde{\chi}^\pm_1}$ = $m_{\widetilde{\chi}^0_1}$ + 5 GeV	
>1100	95	[46] KHACHATRY...16BJ		CMS	same-sign $\ell^\pm\ell^\pm$,Tglu1B,$m_{\widetilde{\chi}^\pm_1}$= 0.5($m_{\widetilde{g}}$+$m_{\widetilde{\chi}^0_1}$),$m_{\widetilde{\chi}^0_1}$ <400GeV	
> 830	95	[46] KHACHATRY...16BJ		CMS	same-sign $\ell^\pm\ell^\pm$,Tglu1B,$m_{\widetilde{\chi}^\pm_1}$= 0.5($m_{\widetilde{g}}$+$m_{\widetilde{\chi}^0_1}$),$m_{\widetilde{\chi}^0_1}$ <700GeV	
>1300	95	[46] KHACHATRY...16BJ		CMS	same-sign $\ell^\pm\ell^\pm$, Tglu3B, $m_{\widetilde{t}}-m_{\widetilde{\chi}^0_1}=m_t$, $m_{\widetilde{\chi}^0_1}$ = 0	
>1050	95	[46] KHACHATRY...16BJ		CMS	same-sign $\ell^\pm\ell^\pm$, Tglu3B, $m_{\widetilde{t}}-m_{\widetilde{\chi}^0_1}=m_t$, $m_{\widetilde{\chi}^0_1}$ < 800 GeV	
>1725	95	[47] KHACHATRY...16BS		CMS	jets + $\not{E}_T$, Tglu1A, $m_{\widetilde{\chi}^0_1}$ = 0	
>1750	95	[47] KHACHATRY...16BS		CMS	jets + $\not{E}_T$, Tglu2A, $m_{\widetilde{\chi}^0_1}$ = 0	
>1550	95	[47] KHACHATRY...16BS		CMS	jets + $\not{E}_T$, Tglu3A, $m_{\widetilde{\chi}^0_1}$ = 0	
>1030	95	[48] KHACHATRY...16BX		CMS	$\widetilde{g}\rightarrow tbs$, RPV, λ''_{332} coupling	
>1280	95	[49] KHACHATRY...16BY		CMS	opposite-sign $\ell^\pm\ell^\pm$, Tglu4C, $m_{\widetilde{\chi}^0_1}$ = 1000 GeV	
>1030	95	[49] KHACHATRY...16BY		CMS	opposite-sign $\ell^\pm\ell^\pm$, Tglu4C, $m_{\widetilde{\chi}^0_1}$ = 0 GeV	
>1440	95	[50] KHACHATRY...16V		CMS	jets + $\not{E}_T$, Tglu1A, $m_{\widetilde{\chi}^0_1}$ = 0	
>1600	95	[50] KHACHATRY...16V		CMS	jets + $\not{E}_T$, Tglu2A, $m_{\widetilde{\chi}^0_1}$ = 0	
>1550	95	[50] KHACHATRY...16V		CMS	jets + $\not{E}_T$, Tglu3A, $m_{\widetilde{\chi}^0_1}$ = 0	
>1450	95	[50] KHACHATRY...16V		CMS	jets + $\not{E}_T$, Tglu1C, $m_{\widetilde{\chi}^0_1}$ = 0	
> 820	95	[51] AAD	15BG	ATLS	GGM, $\widetilde{g}\rightarrow q\bar{q}Z\widetilde{G}$, tan$\beta$ = 30, μ > 600 GeV	
> 850	95	[51] AAD	15BG	ATLS	GGM, $\widetilde{g}\rightarrow q\bar{q}Z\widetilde{G}$, tan$\beta$ = 1.5, μ > 450 GeV	
>1150	95	[52] AAD	15BV	ATLS	general RPC $\widetilde{g}$ decays, $m_{\widetilde{\chi}^0_1}$ < 100 GeV	
> 700	95	[53] AAD	15BX	ATLS	$\widetilde{g}\rightarrow X\widetilde{\chi}^0_1$, independent of $m_{\widetilde{\chi}^0_1}$	
>1290	95	[54] AAD	15CA	ATLS	$\geq$ 2 γ + $\not{E}_T$, GGM, bino-like NLSP, any NLSP mass	
>1260	95	[54] AAD	15CA	ATLS	$\geq$ 1 γ + b-jets + $\not{E}_T$, GGM, higgsino-bino admix. NLSP and μ <0, m(NLSP)>450 GeV	
>1140	95	[54] AAD	15CA	ATLS	$\geq$ 1 γ + jets + $\not{E}_T$, GGM, higgsino-bino admixture NLSP, all μ >0	
>1225	95	[55] KHACHATRY...15AF		CMS	$\widetilde{g}\rightarrow q\bar{q}\widetilde{\chi}^0_1$, $m_{\widetilde{\chi}^0_1}$ = 0	
>1300	95	[55] KHACHATRY...15AF		CMS	$\widetilde{g}\rightarrow b\bar{b}\widetilde{\chi}^0_1$, $m_{\widetilde{\chi}^0_1}$ = 0	
>1225	95	[55] KHACHATRY...15AF		CMS	$\widetilde{g}\rightarrow t\bar{t}\widetilde{\chi}^0_1$, $m_{\widetilde{\chi}^0_1}$ = 0	
>1550	95	[55] KHACHATRY...15AF		CMS	CMSSM, tanβ=30, $m_{\widetilde{g}}$=$m_{\widetilde{q}}$, A_0=$-2\max(m_0,m_{1/2})$, μ >0	
>1150	95	[55] KHACHATRY...15AF		CMS	CMSSM, tanβ=30, A_0=$-2\max(m_0,m_{1/2})$, μ >0	
>1280	95	[56] KHACHATRY...15I		CMS	$\widetilde{g}\rightarrow t\bar{t}\widetilde{\chi}^0_1$, $m_{\widetilde{\chi}^0_1}$ = 0	
>1310	95	[57] KHACHATRY...15X		CMS	$\widetilde{g}\rightarrow b\bar{b}\widetilde{\chi}^0_1$, $m_{\widetilde{\chi}^0_1}$ = 100 GeV	
>1175	95	[57] KHACHATRY...15X		CMS	$\widetilde{g}\rightarrow t\bar{t}\widetilde{\chi}^0_1$, $m_{\widetilde{\chi}^0_1}$ = 100 GeV	
>1330	95	[58] AAD	14AE	ATLS	jets + $\not{E}_T$, $\widetilde{g}\rightarrow q\bar{q}\widetilde{\chi}^0_1$ simplified model, $m_{\widetilde{\chi}^0_1}$ = 0 GeV	
>1700	95	[58] AAD	14AE	ATLS	jets + $\not{E}_T$, mSUGRA/CMSSM, $m_{\widetilde{q}}=m_{\widetilde{g}}$	
>1090	95	[59] AAD	14AG	ATLS	τ + jets + $\not{E}_T$, natural Gauge Mediation	
>1600	95	[59] AAD	14AG	ATLS	τ + jets + $\not{E}_T$, mGMSB, M_{mess} = 250 GeV, N_5 = 3, μ > 0, C_{grav} = 1	
>1350	95	[60] AAD	14X	ATLS	$\geq 4\ell^\pm$, $\widetilde{g}\rightarrow q\bar{q}\widetilde{\chi}^0_1$, $\widetilde{\chi}^0_1\rightarrow \ell^\pm\ell^\mp\nu$, RPV	
> 640	95	[61] AAD	14X	ATLS	$\geq 4\ell^\pm$, $\widetilde{g}\rightarrow q\bar{q}\widetilde{\chi}^0_1$, $\widetilde{\chi}^0_1\rightarrow \ell^\pm\ell^\mp\widetilde{G}$, tan$\beta$ = 30, GGM	
>1000	95	[62] CHATRCHYAN14AH		CMS	jets + $\not{E}_T$, $\widetilde{g}\rightarrow q\bar{q}\widetilde{\chi}^0_1$ simplified model, $m_{\widetilde{\chi}^0_1}$ = 50 GeV	
>1350	95	[62] CHATRCHYAN14AH		CMS	jets + $\not{E}_T$, CMSSM, $m_{\widetilde{g}}=m_{\widetilde{q}}$	
>1000	95	[63] CHATRCHYAN14AH		CMS	jets + $\not{E}_T$, $\widetilde{g}\rightarrow b\bar{b}\widetilde{\chi}^0_1$ simplified model, $m_{\widetilde{\chi}^0_1}$ = 50 GeV	
>1000	95	[64] CHATRCHYAN14AH		CMS	jets + $\not{E}_T$, $\widetilde{g}\rightarrow t\bar{t}\widetilde{\chi}^0_1$ simplified model, $m_{\widetilde{\chi}^0_1}$ = 50 GeV	
>1160	95	[65] CHATRCHYAN14I		CMS	jets + $\not{E}_T$, $\widetilde{g}\rightarrow q\bar{q}\widetilde{\chi}^0_1$ simplified model, $m_{\widetilde{\chi}^0_1}$ < 100 GeV	
>1130	95	[65] CHATRCHYAN14I		CMS	multijets + $\not{E}_T$, $\widetilde{g}\rightarrow t\bar{t}\widetilde{\chi}^0_1$ simplified model, $m_{\widetilde{\chi}^0_1}$ < 100 GeV	
>1210	95	[65] CHATRCHYAN14I		CMS	multijets + $\not{E}_T$, $\widetilde{g}\rightarrow q\bar{q}W/Z\widetilde{\chi}^0_1$ simplified model, $m_{\widetilde{\chi}^0_1}$ < 100 GeV	
>1260	95	[66] CHATRCHYAN14N		CMS	1$\ell^\pm$+ jets + $\geq$ 2b-jets, $\widetilde{g}\rightarrow t\bar{t}\chi^0_1$ simplified model, $m_{\chi^0_1}$=0 GeV, $m_{\widetilde{t}}>m_{\widetilde{g}}$	
> 650	95	[67] CHATRCHYAN14P		CMS	$\widetilde{g}\rightarrow jjj$, RPV	
none 200–835	95	[67] CHATRCHYAN14P		CMS	$\widetilde{g}\rightarrow bjj$, RPV	
		[68] CHATRCHYAN14R		CMS	$\geq 3\ell^\pm$, $(\widetilde{g}/\widetilde{q})\rightarrow q\ell^\pm\ell^\mp\widetilde{G}$ simplified model, GMSB, slepton co-NLSP scenario	
		[69] CHATRCHYAN14R		CMS	$\geq 3\ell^\pm$, $\widetilde{g}\rightarrow t\bar{t}\widetilde{\chi}^0_1$ simplified model	

• • • We do not use the following data for averages, fits, limits, etc. • • •

>1600	95	[70] AABOUD	17AZ	ATLS	$\geq$ 7 jets+$\not{E}_T$, large R-jets and/or b-jets, pMSSM, $m_{\widetilde{\chi}^\pm_1}$ = 200 GeV	
>1600	95	[71] KHACHATRY...16AY		CMS	1$\ell^\pm$ + jets + b-jets + $\not{E}_T$, Tglu3A, $m_{\widetilde{\chi}^0_1}$ = 0 GeV	
> 500	95	[72] KHACHATRY...16BT		CMS	19-parameter pMSSM model, global Bayesian analysis, flat prior	
>1400	95	[73] KHACHATRY...16BX		CMS	$\widetilde{g}\rightarrow qq\widetilde{\chi}^0_1$, $\widetilde{\chi}^0_1\rightarrow \ell\ell\nu$, RPV, λ_{121} or $\lambda_{122}\neq 0$, $m_{\widetilde{\chi}^0_1}$ > 400 GeV	
	95	[74] AAD	15AB	ATLS	$\widetilde{g}\rightarrow Sg$, $c\tau$ = 1 m, $\widetilde{S}\rightarrow S\widetilde{G}$ and $S\rightarrow gg$, BR = 100%	
	95	[75] AAD	15AI	ATLS	$\ell^\pm$ + jets + $\not{E}_T$	
>1600	95	[52] AAD	15BV	ATLS	pMSSM, M_1 = 60 GeV, $m_{\widetilde{q}}$ < 1500 GeV	
>1280	95	[52] AAD	15BV	ATLS	mSUGRA, m_0 > 2 TeV	
>1100	95	[52] AAD	15BV	ATLS	via $\tilde{\tau}$, natural GMSB, all $m_{\widetilde{\tau}}$	
>1330	95	[52] AAD	15BV	ATLS	jets + $\not{E}_T$, $\widetilde{g}\rightarrow q\bar{q}\widetilde{\chi}^0_1$, $m_{\widetilde{\chi}^0_1}$ = 1 GeV	
>1500	95	[52] AAD	15BV	ATLS	jets + $\not{E}_T$, $\widetilde{g}\rightarrow \widetilde{q}q$, $\widetilde{q}\rightarrow q\widetilde{\chi}^0_1$, $m_{\widetilde{\chi}^0_1}$ = 1 GeV	

>1650	95	[52] AAD	15BV	ATLS	jets + $\not{E}_T$, $m_{\tilde{g}} = m_{\tilde{q}}$, $m_{\tilde{\chi}_1^0} = 1$ GeV
> 850	95	[52] AAD	15BV	ATLS	jets + $\not{E}_T$, $\tilde{g} \to g\tilde{\chi}_1^0$, $m_{\tilde{\chi}_1^0} <$ 550 GeV
>1270	95	[52] AAD	15BV	ATLS	jets + $\not{E}_T$, $\tilde{g} \to q\overline{q}W\tilde{\chi}_1^0$, $m_{\tilde{\chi}_1^0}$ = 100 GeV
>1150	95	[52] AAD	15BV	ATLS	jets + $\ell^{\pm}\ell^{\pm}$, $\tilde{g} \to q\overline{q}WZ\tilde{\chi}_1^0$, $m_{\tilde{\chi}_1^0} = 100$ GeV
>1320	95	[52] AAD	15BV	ATLS	jets + $\ell^{\pm}\ell^{\pm}$, $\tilde{g}$ decays via sleptons, $m_{\tilde{\chi}_1^0} = 100$ GeV
>1220	95	[52] AAD	15BV	ATLS	τ, $\tilde{q}$ decays via staus, $m_{\tilde{\chi}_1^0} = 100$ GeV
>1310	95	[52] AAD	15BV	ATLS	b-jets, $\tilde{g} \to t\overline{t}\tilde{\chi}_1^0$, $m_{\tilde{\chi}_1^0} < 400$ GeV
>1220	95	[52] AAD	15BV	ATLS	b-jets, $\tilde{g} \to \tilde{t}_1 t$ and $\tilde{t}_1 \to t\tilde{\chi}_1^0$, $m_{\tilde{T}_1} < 1000$ GeV
>1180	95	[52] AAD	15BV	ATLS	b-jets, $\tilde{g} \to \tilde{t}_1 t$ and $\tilde{t}_1 \to b\tilde{\chi}_1^{\pm}$, $m_{\tilde{T}_1} < 1000$ GeV, $m_{\tilde{\chi}_1^0} = 60$ GeV
>1260	95	[52] AAD	15BV	ATLS	b-jets, $\tilde{g} \to \tilde{t}_1 t$ and $\tilde{g} \to c\tilde{\chi}_1^0$
> 880	95	[52] AAD	15BV	ATLS	jets, $\tilde{g} \to \tilde{t}_1 t$ and $\tilde{t}_1 \to sb$, RPV, $400 < m_{\tilde{t}_1} < 1000$ GeV
>1200	95	[52] AAD	15BV	ATLS	b-jets, $\tilde{g} \to \tilde{b}_1 b$ and $\tilde{b}_1 \to b\tilde{\chi}_1^0$, $m_{\tilde{b}_1} < 1000$ GeV
>1250	95	[52] AAD	15BV	ATLS	b-jets, $\tilde{g} \to b\overline{b}\tilde{\chi}_1^0$, $m_{\tilde{\chi}_1^0} < 400$ GeV
none, 750–1250	95	[52] AAD	15BV	ATLS	b-jets, $\tilde{g}$ decay via offshell $\tilde{t}_1$ and $\tilde{b}_1$, $m_{\tilde{\chi}_1^0} < 500$ GeV
		[76] AAD	15CB	ATLS	ℓ, $\tilde{g} \to (e/\mu)qq$, RPV, benchmark gluino, neutralino masses
> 600	95	[76] AAD	15CB	ATLS	$\ell\ell/Z$, $\tilde{g} \to (ee/\mu\mu/e\mu)qq$, RPV, $m_{\tilde{\chi}_1^0} = 400$ GeV and $0.7 < c\tau_{\tilde{\chi}_1^0} < 3 \times 10^5$ mm
>1100	95	[76] AAD	15CB	ATLS	jets, $\tilde{g} \to qq\tilde{\chi}_1^0$, $\tilde{\chi}_1^0 \to Z\tilde{G}$, GGM, $m_{\tilde{\chi}_1^0} = 400$ GeV and $3 < c\tau_{\tilde{\chi}_1^0} < 500$ mm
>1400	95	[76] AAD	15CB	ATLS	jets or $\not{E}_T$, $\tilde{g} \to qq\tilde{\chi}_1^0$, Split SUSY, $m_{\tilde{\chi}_1^0} = 100$ GeV and $15 < c\tau < 300$ mm
>1500	95	[76] AAD	15CB	ATLS	$\not{E}_T$, $\tilde{g} \to qq\tilde{\chi}_1^0$, Split SUSY, $m_{\tilde{\chi}_1^0} = 100$ GeV and $20 < c\tau < 250$ mm
>1000	95	[77] AAD	15X	ATLS	≥ 10 jets, $\tilde{g} \to q\overline{q}\tilde{\chi}_1^0$, $\tilde{\chi}_1^0 \to qqq$ (RPV), $m_{\tilde{\chi}_1^0}$=500 GeV
> 917	95	[77] AAD	15X	ATLS	$\geq$ 6,7 jets, $\tilde{g} \to qqq$, (light-quark, λ'' couplings, RPV)
> 929	95	[77] AAD	15X	ATLS	$\geq$ 6,7 jets, $\tilde{g} \to qqq$, (b-quark, λ'' couplings, RPV)
		[78] KHACHATRY...	15AD	CMS	$\ell^{\pm}\ell^{\mp}$ + jets + $\not{E}_T$, GMSB, $\tilde{g} \to q\overline{q}Z\tilde{G}$
>1300	95	[79] KHACHATRY...	15AZ	CMS	$\geq 2\ \gamma$, ≥ 1 jet, (Razor), bino-like NLSP, $m_{\tilde{\chi}_1^0} = 375$ GeV
> 800	95	[79] KHACHATRY...	15AZ	CMS	$\geq 1\ \gamma$, ≥ 2 jet, wino-like NLSP, $m_{\tilde{\chi}_1^0} = 375$ GeV
>1280	95	[80] AAD	14AX	ATLS	≥ 3 b-jets + $\not{E}_T$, CMSSM
>1250	95	[80] AAD	14AX	ATLS	≥ 3 b-jets + $\not{E}_T$, $\tilde{g} \to \tilde{b}_1 b\tilde{\chi}_1^0$ simplified model, $\tilde{b}_1 \to b\tilde{\chi}_1^0$, $m_{\tilde{\chi}_1^0} = 60$ GeV, $m_{\tilde{b}_1} < 900$ GeV
>1190	95	[80] AAD	14AX	ATLS	≥ 3 b-jets + $\not{E}_T$, $\tilde{g} \to \tilde{t}_1 t\tilde{\chi}_1^0$ simplified model, $\tilde{t}_1 \to t\tilde{\chi}_1^0$, $m_{\tilde{\chi}_1^0} = 60$ GeV, $m_{\tilde{T}_1} < 1000$ GeV
>1180	95	[80] AAD	14AX	ATLS	≥ 3 b-jets + $\not{E}_T$, $\tilde{g} \to \tilde{t}_1 t\tilde{\chi}_1^0$ simplified model, $\tilde{t}_1 \to b\tilde{\chi}_1^{\pm}$, $m_{\tilde{\chi}_1^{\pm}}$=2$m_{\tilde{\chi}_1^0}$, $m_{\tilde{\chi}_1^0}$=60 GeV, $m_{\tilde{T}_1}$ <1000 GeV
>1250	95	[80] AAD	14AX	ATLS	≥ 3 b-jets + $\not{E}_T$, $\tilde{g} \to b\overline{b}\tilde{\chi}_1^0$ simplified model, $m_{\tilde{\chi}_1^0} < 400$ GeV
>1340	95	[80] AAD	14AX	ATLS	≥ 3 b-jets + $\not{E}_T$, $\tilde{g} \to t\overline{t}\tilde{\chi}_1^0$ simplified model, $m_{\tilde{\chi}_1^0} < 400$ GeV
>1300	95	[80] AAD	14AX	ATLS	≥ 3 b-jets + $\not{E}_T$, $\tilde{g} \to t\overline{b}\tilde{\chi}_1^{\pm}$ simplified model, $\tilde{\chi}_1^{\pm} \to f f'\tilde{\chi}_1^0$, $m_{\tilde{\chi}_1^{\pm}} - m_{\tilde{\chi}_1^0} = 2$ GeV, $m_{\tilde{\chi}_1^0} < 300$ GeV
> 950	95	[81] AAD	14E	ATLS	$\ell^{\pm}\ell^{\pm}(\ell^{\mp})$ + jets, $\tilde{g} \to t\overline{t}\tilde{\chi}_1^0$ simplified model
>1000	95	[81] AAD	14E	ATLS	$\ell^{\pm}\ell^{\pm}(\ell^{\mp})$ + jets, $\tilde{g} \to t\tilde{t}_1$ with $\tilde{t}_1 \to b\tilde{\chi}_1^{\pm}$ simplified model, $m_{\tilde{t}_1} < 200$ GeV, $m_{\tilde{\chi}_1^{\pm}}$ = 118 GeV, $m_{\tilde{\chi}_1^0} = 60$ GeV
> 640	95	[81] AAD	14E	ATLS	$\ell^{\pm}\ell^{\pm}(\ell^{\mp})$ + jets, $\tilde{g} \to t\tilde{t}_1$ with $\tilde{t}_1 \to c\tilde{\chi}_1^0$ simplified model, $m_{\tilde{t}_1} = m_{\tilde{\chi}_1^0} + 20$ GeV
> 850	95	[81] AAD	14E	ATLS	$\ell^{\pm}\ell^{\pm}(\ell^{\mp})$ + jets, $\tilde{g} \to t\tilde{t}_1$ with $\tilde{t}_1 \to bs$ simplified model, RPV
> 860	95	[81] AAD	14E	ATLS	$\ell^{\pm}\ell^{\pm}(\ell^{\mp})$ + jets, $\tilde{g} \to qq'\tilde{\chi}_1^{\pm}$, $\tilde{\chi}_1^{\pm} \to W^{(*)\pm}\tilde{\chi}_1^0$ simplified model, $m_{\tilde{\chi}_1^{\pm}} = 2\ m_{\tilde{\chi}_1^0}$, $m_{\tilde{\chi}_1^0} < 400$ GeV
>1040	95	[81] AAD	14E	ATLS	$\ell^{\pm}\ell^{\pm}(\ell^{\mp})$ + jets, $\tilde{g} \to qq'\tilde{\chi}_1^{\pm}$, $\tilde{\chi}_1^{\pm} \to W^{(*)\pm}\tilde{\chi}_2^0$, $\tilde{\chi}_2^0 \to Z^{(*)}\tilde{\chi}_1^0$ simplified model, $m_{\tilde{\chi}_1^0} < 520$ GeV
>1200	95	[81] AAD	14E	ATLS	$\ell^{\pm}\ell^{\pm}(\ell^{\mp})$ + jets, $\tilde{g} \to qq'\tilde{\chi}_1^{\pm}/\tilde{\chi}_2^0$, $\tilde{\chi}_1^{\pm} \to \ell^{\pm}\nu\tilde{\chi}_1^0$, $\tilde{\chi}_2^0 \to \ell^{\pm}\ell^{\mp}(\nu\nu)\tilde{\chi}_1^0$ simplified model
>1050	95	[82] CHATRCHYAN	14H	CMS	same-sign $\ell^{\pm}\ell^{\pm}$, $\tilde{g} \to t\overline{t}\tilde{\chi}_1^0$ simplified model, massless $\tilde{\chi}_1^0$
> 900	95	[83] CHATRCHYAN	14H	CMS	same-sign $\ell^{\pm}\ell^{\pm}$, $\tilde{g} \to qq'\tilde{\chi}_1^{\pm}$, $\tilde{\chi}_1^{\pm} \to W^{\pm}\tilde{\chi}_1^0$ simplified model, $m_{\tilde{\chi}_1^{\pm}} = 0.5\ m_{\tilde{g}}$, massless $\tilde{\chi}_1^0$
>1050	95	[84] CHATRCHYAN	14H	CMS	same-sign $\ell^{\pm}\ell^{\pm}$, $\tilde{g} \to b\overline{t}\tilde{\chi}_1^{\pm}$, $\tilde{\chi}_1^{\pm} \to W^{\pm}\tilde{\chi}_1^0$ simplified model, $m_{\tilde{\chi}_1^{\pm}} = 300$ GeV, $m_{\tilde{\chi}_1^0}$ = 50 GeV
> 900	95	[85] CHATRCHYAN	14H		same-sign $\ell^{\pm}\ell^{\pm}$, $\tilde{g} \to tbs$ simplified model, RPV

[1] SIRUNYAN 18D searched in 35.9 fb^{-1} of pp collisions at $\sqrt{s} = 13$ TeV for events containing identified hadronically decaying top quarks, no leptons, and $\not{E}_T$. No significant excess above the Standard Model expectations is observed. Limits are set on the stop mass in the Tstop1 simplified model, see their Figure 8, and on the gluino mass in the Tglu3A, Tglu3B, Tglu3C and Tglu3E simplified models, see their Figure 9.

[2] AABOUD 17AI searched in 36.1 fb^{-1} of pp collisions at $\sqrt{s} = 13$ TeV for events with one or more isolated lepton, at least eight jets, either zero or many b-jets, for evidence of R-parity violating decays of the gluino. No significant excess above the Standard Model expectations is observed. Limits up to 2.1 TeV are set on the gluino mass in R-parity-violating supersymmetry models as Tglu3A with LSP decay through the non-zero λ''_{112} coupling as $\tilde{\chi}_1^0 \to uds$. See their Figure 9.

[3] AABOUD 17AI searched in 36.1 fb^{-1} of pp collisions at $\sqrt{s} = 13$ TeV for events with one or more isolated lepton, at least eight jets, either zero or many b-jets, for evidence of R-parity violating decays of the gluino. No significant excess above the Standard Model expectations is observed. Limits up to 1.65 TeV are set on the gluino mass in R-parity-violating supersymmetry models with $\tilde{g} \to t\tilde{t}$, $\tilde{t} \to bs$ through the non-zero λ''_{323} coupling. See their Figure 9.

[4] AABOUD 17AI searched in 36.1 fb^{-1} of pp collisions at $\sqrt{s} = 13$ TeV for events with one or more isolated lepton, at least eight jets, either zero or many b-jets, for evidence of R-parity violating decays of the gluino. No significant excess above the Standard Model expectations is observed. Limits up to 1.8 TeV are set on the gluino mass in R-parity-violating supersymmetry models as Tglu1A with the LSP decay through the non-zero λ' coupling as $\tilde{\chi}_1^0 \to qq\ell$. See their Figure 9.

[5] AABOUD 17AJ searched in 36.1 fb^{-1} of pp collisions at $\sqrt{s} = 13$ TeV for events with two same-sign or three leptons, jets and large missing transverse momentum. No significant excess above the Standard Model expectations is observed. Limits up to 1.75 TeV are set on the gluino mass in Tglu3A simplified models in case of off-shell top squarks and for $m_{\tilde{\chi}_1^0} = 100$ GeV. See their Figure 4(a).

[6] AABOUD 17AJ searched in 36.1 fb^{-1} of pp collisions at $\sqrt{s} = 13$ TeV for events with two same-sign or three leptons, jets and large missing transverse momentum. No significant excess above the Standard Model expectations is observed. Limits up to 1.57 TeV are set on the gluino mass in Tglu1E simplified models (2-step models) for $m_{\tilde{\chi}_1^0} = 100$ GeV. See their Figure 4(b).

[7] AABOUD 17AJ searched in 36.1 fb^{-1} of pp collisions at $\sqrt{s} = 13$ TeV for events with two same-sign or three leptons, jets and large missing transverse momentum. No significant excess above the Standard Model expectations is observed. Limits up to 1.86 TeV are set on the gluino mass in Tglu1G simplified models for $m_{\tilde{\chi}_1^0} = 200$ GeV. See their Figure 4(c).

[8] AABOUD 17AJ searched in 36.1 fb^{-1} of pp collisions at $\sqrt{s} = 13$ TeV for events with two same-sign or three leptons, jets and large missing transverse momentum. No significant excess above the Standard Model expectations is observed. Limits up to 1.8 TeV are set on the gluino mass in R-parity-violating supersymmetry models as Tglu3A with LSP decaying through the non-zero λ''_{112} coupling as $\widetilde{\chi}^0_1 \rightarrow u\,d\,s$. See their Figure 5(d).

[9] AABOUD 17AJ searched in 36.1 fb^{-1} of pp collisions at $\sqrt{s} = 13$ TeV for events with two same-sign or three leptons, jets and large missing transverse momentum. No significant excess above the Standard Model expectations is observed. Limits up to 1.75 TeV are set on the gluino mass in R-parity-violating supersymmetry models as Tglu1A with LSP decaying through the non-zero λ' coupling as $\widetilde{\chi}^0_1 \rightarrow q\,q\,\ell$. See their Figure 5(c).

[10] AABOUD 17AJ searched in 36.1 fb^{-1} of pp collisions at $\sqrt{s} = 13$ TeV for events with two same-sign or three leptons, jets and large missing transverse momentum. No significant excess above the Standard Model expectations is observed. Limits up to 1.45 TeV are set on the gluino mass in R-parity-violating supersymmetry models where $\widetilde{g} \rightarrow t\,\widetilde{t}_1$ and $\widetilde{t}_1 \rightarrow s\,d$ through the non-zero λ''_{321} coupling. See their Figure 5(b).

[11] AABOUD 17AJ searched in 36.1 fb^{-1} of pp collisions at $\sqrt{s} = 13$ TeV for events with two same-sign or three leptons, jets and large missing transverse momentum. No significant excess above the Standard Model expectations is observed. Limits up to 1.45 TeV are set on the gluino mass in R-parity-violating supersymmetry models where $\widetilde{g} \rightarrow t\,\widetilde{t}_1$ and $\widetilde{t}_1 \rightarrow b\,d$ through the non-zero λ''_{313} coupling. See their Figure 5(a).

[12] AABOUD 17AJ searched in 36.1 fb^{-1} of pp collisions at $\sqrt{s} = 13$ TeV for events with two same-sign or three leptons, jets and large missing transverse momentum. No significant excess above the Standard Model expectations is observed. Limits up to 400 GeV are set on the down type squark ($\widetilde{d}_R$ mass in R-parity-violating supersymmetry models where $\widetilde{d}_R \rightarrow t\,b$ through the non-zero λ''_{313} coupling or $\widetilde{d}_R \rightarrow t\,s$ through the non-zero λ''_{321}. See their Figure 5(e) and 5(f).

[13] AABOUD 17AR searched in 36.1 fb^{-1} of pp collisions at $\sqrt{s} = 13$ TeV for events with one isolated lepton, at least two jets and large missing transverse momentum. No significant excess above the Standard Model expectations is observed. Limits up to 2.1 TeV are set on the gluino mass in Tglu1B simplified models, with $x = (m_{\widetilde{\chi}^\pm_1} - m_{\widetilde{\chi}^0_1}) / (m_{\widetilde{g}} - m_{\widetilde{\chi}^0_1}) = 1/2$.Similar limits are obtained for variable x and fixed neutralino mass, $m_{\widetilde{\chi}^0_1} = 60$ GeV. See their Figure 13.

[14] AABOUD 17AR searched in 36.1 fb^{-1} of pp collisions at $\sqrt{s} = 13$ TeV for events with one isolated lepton, at least two jets and large missing transverse momentum. No significant excess above the Standard Model expectations is observed. Limits up to 1.74 TeV are set on the gluino mass in Tglu1E simplified model. Limits up to 1.7 TeV are also set on pMSSM models leading to similar signal event topologies. See their Figure 13.

[15] AABOUD 17AY searched in 36.1 fb^{-1} of pp collisions at $\sqrt{s} = 13$ TeV for events with at least four jets and large missing transverse momentum. No significant excess above the Standard Model expectations is observed. Limits up to 1.8 TeV are set on the gluino mass in Tglu3A simplified models assuming $m_{\widetilde{t}_1} - m_{\widetilde{\chi}^0_1} = 5$ GeV. See their Figure 13.

[16] AABOUD 17AZ searched in 36.1 fb^{-1} of pp collisions at $\sqrt{s} = 13$ TeV for events with at least seven jets and large missing transverse momentum. Selected events are further classified based on the presence of large R-jets or b-jets and no leptons. No significant excess above the Standard Model expectations is observed. Limits up to 1.8 TeV are set on the gluino mass in Tglu1E simplified models. See their Figure 6b.

[17] AABOUD 17AZ searched in 36.1 fb^{-1} of pp collisions at $\sqrt{s} = 13$ TeV for events with at least seven jets and large missing transverse momentum. Selected events are further classified based on the presence of large R-jets or b-jets and no leptons. No significant excess above the Standard Model expectations is observed. Limits up to 1.54 TeV are set on the gluino mass in Tglu3A simplified models. See their Figure 7a.

[18] AABOUD 17AZ searched in 36.1 fb^{-1} of pp collisions at $\sqrt{s} = 13$ TeV for events with at least seven jets and large missing transverse momentum. Selected events are further classified based on the presence of large R-jets or b-jets and no leptons. No significant excess above the Standard Model expectations is observed. Limits are set for R-parity violating decays of the gluino assuming $\widetilde{g} \rightarrow t\,\widetilde{t}_1$ and $\widetilde{t}_1 \rightarrow b\,s$ through the non-zero λ''_{323} couplings. The range 625–1375 GeV is excluded for $m_{\widetilde{t}_1} = 400$ GeV. See their Figure 7b.

[19] AABOUD 17N searched in 14.7 fb^{-1} of pp collisions at $\sqrt{s} = 13$ TeV in final states with 2 same-flavor, opposite-sign leptons (electrons or muons), jets and large missing transverse momentum. In Tglu1J models, gluino masses are excluded at 95% C.L. up to 1300 GeV for $m_{\widetilde{\chi}^0_1} = 0$ GeV and $m_{\widetilde{\chi}^0_2} = 1100$ GeV. See their Fig. 12 for exclusion limits as a function of $m_{\widetilde{\chi}^0_2}$. Limits are also presented assuming $m_{\widetilde{\chi}^0_2} = m_{\widetilde{\chi}^0_1} + 100$ GeV, see their Fig. 13.

[20] AABOUD 17N searched in 14.7 fb^{-1} of pp collisions at $\sqrt{s} = 13$ TeV in final states with 2 same-flavor, opposite-sign leptons (electrons or muons), jets and large missing transverse momentum. In Tglu1H models, gluino masses are excluded at 95% C.L. up to 1310 GeV for $m_{\widetilde{\chi}^0_1} < 400$ GeV and assuming $m_{\widetilde{\chi}^0_2} = (m_{\widetilde{g}} + m_{\widetilde{\chi}^0_1})/2$. See their Fig. 15.

[21] AABOUD 17N searched in 14.7 fb^{-1} of pp collisions at $\sqrt{s} = 13$ TeV in final states with 2 same-flavor, opposite-sign leptons (electrons or muons), jets and large missing transverse momentum. In Tglu1G models, gluino masses are excluded at 95% C.L. up to 1700 GeV for small $m_{\widetilde{\chi}^0_1}$. The results probe kinematic endpoints as small as $m_{\widetilde{\chi}^0_2} - m_{\widetilde{\chi}^0_1} = (m_{\widetilde{g}} - m_{\widetilde{\chi}^0_1})/2 = 50$ GeV. See their Fig. 14.

[22] KHACHATRYAN 17 searched in 2.3 fb^{-1} of pp collisions at $\sqrt{s} = 13$ TeV for events containing four or more jets, no more than one lepton, and missing transverse momentum, using the razor variables (M_R and R^2) to discriminate between signal and background processes. No evidence for an excess over the expected background is observed. Limits are derived on the gluino mass in the Tglu1A, Tglu2A and Tglu3A simplified models, see Figs. 16 and 17. Also, assuming gluinos decay only via three-body processes involving third-generation quarks plus a neutralino/chargino, and assuming $m_{\widetilde{\chi}^\pm_1} = m_{\widetilde{\chi}^0_1} + 5$ GeV, a branching ratio-independent limit on the gluino mass is given, see Fig. 16.

[23] KHACHATRYAN 17AD searched in 2.3 fb^{-1} of pp collisions at $\sqrt{s} = 13$ TeV for events containing at least four jets (including b-jets), missing transverse momentum and tagged top quarks. No evidence for an excess over the expected background is observed. Gluino masses up to 1550 GeV and neutralino masses up to 900 GeV are excluded at 95% C.L. See Fig. 13.

[24] KHACHATRYAN 17AD searched in 2.3 fb^{-1} of pp collisions at $\sqrt{s} = 13$ TeV for events containing at least four jets (including b-jets), missing transverse momentum and tagged top quarks. No evidence for an excess over the expected background is observed. Gluino masses up to 1450 GeV and neutralino masses up to 820 GeV are excluded at 95% C.L. See Fig. 13.

[25] KHACHATRYAN 17AS searched in 2.3 fb^{-1} of pp collisions at $\sqrt{s} = 13$ TeV for events with a single electron or muon and multiple jets. No significant excess above the Standard Model expectations is observed. Limits are set on the gluino mass in the Tglu3A and Tglu1B simplified models, see their Fig. 7.

[26] KHACHATRYAN 17AW searched in 2.3 fb^{-1} of pp collisions at $\sqrt{s} = 13$ TeV for events with at least three charged leptons, in any combination of electrons and muons, and significant $\not{E}_T$. No significant excess above the Standard Model expectations is observed. Limits are set on the gluino mass in the Tglu3A and Tglu1C simplified models, and on the sbottom mass in the Tsbot2 simplified model, see their Figure 4.

[27] KHACHATRYAN 17P searched in 2.3 fb^{-1} of pp collisions at $\sqrt{s} = 13$ TeV for events with one or more jets and large $\not{E}_T$. No significant excess above the Standard Model expectations is observed. Limits are set on the gluino mass in the Tglu1A, Tglu2A, Tglu3A, Tglu3B, Tglu3C and Tglu3D simplified models, see their Figures 7 and 8. Limits are also set on the squark mass in the Tsqk1 simplified model, see their Fig. 7, and on the sbottom mass in the Tsbot1 simplified model, see Fig. 8. Finally, limits are set on the stop mass in the Tstop1, Tstop3, Tstop4, Tstop6 and Tstop7 simplified models, see Fig. 8.

[28] KHACHATRYAN 17V searched in 2.3 fb^{-1} of pp collisions at $\sqrt{s} = 13$ TeV for events with two photons and large $\not{E}_T$. No significant excess above the Standard Model expectations is observed. Limits are set on the gluino and squark mass in the context of general gauge mediation models Tglu4B and Tsqk4, see their Fig. 4.

[29] KHACHATRYAN 17Y searched in 19.7 fb^{-1} of pp collisions at $\sqrt{s} = 8$ TeV for events containing at least 8 or 10 jets, possibly b-tagged, coming from R-parity-violating decays of supersymmetric particles. No excess over the expected background is observed. Limits are derived on the gluino mass, assuming various RPV decay modes, see Fig. 7.

[30] SIRUNYAN 17AF searched in 35.9 fb^{-1} of pp collisions at $\sqrt{s} = 13$ TeV for events with a single lepton (electron or muon), jets, including at least one jet originating from a b-quark, and large $\not{E}_T$. No significant excess above the Standard Model expectations is observed. Limits are set on the gluino mass in the Tglu3A and Tglu3B simplified models, see their Figure 2.

[31] SIRUNYAN 17AY searched in 35.9 fb^{-1} of pp collisions at $\sqrt{s} = 13$ TeV for events with at least one photon, jets and large $\not{E}_T$. No significant excess above the Standard Model expectations is observed. Limits are set on the gluino mass in the Tglu4A and Tglu4B simplified models, and on the squark mass in the Tskq4A and Tsqk4B simplified models, see their Figure 6.

[32] SIRUNYAN 17AZ searched in 35.9 fb^{-1} of pp collisions at $\sqrt{s} = 13$ TeV for events with one or more jets and large $\not{E}_T$. No significant excess above the Standard Model expectations is observed. Limits are set on the gluino mass in the Tglu1A, Tglu2A, Tglu3A simplified models, see their Figures 6. Limits are also set on the squark mass in the Tsqk1 simplified model (for single light squark and for 8 degenerate light squarks), on the sbottom mass in the Tsbot1 simplified model and on the stop mass in the Tstop1 simplified model, see their Fig. 7. Finally, limits are set on the stop mass in the Tstop2, Tstop4 and Tstop8 simplified models, see Fig. 8.

[33] SIRUNYAN 17P searched in 35.9 fb^{-1} of pp collisions at $\sqrt{s} = 13$ TeV for events with multiple jets and large $\not{E}_T$. No significant excess above the Standard Model expectations is observed. Limits are set on the gluino mass in the Tglu1A, Tglu1C, Tglu2A, Tglu3A and Tglu3D simplified models, see their Fig. 12. Limits are also set on the squark mass in the Tsqk1 simplified model, on the stop mass in the Tstop1 simplified model, and on the sbottom mass in the Tsbot1 simplified model, see Fig. 13.

[34] SIRUNYAN 17S searched in 35.9 fb^{-1} of pp collisions at $\sqrt{s} = 13$ TeV for events with two isolated same-sign leptons, jets, and large $\not{E}_T$. No significant excess above the Standard Model expectations is observed. Limits are set on the mass of the gluino mass in the Tglu3A, Tglu3B, Tglu3C, Tglu3D and Tglu1B simplified models, see their Figures 5 and 6, and on the sbottom mass in the Tsbot2 simplified model, see their Figure 6.

[35] AABOUD 16AC searched in 3.2 fb^{-1} of pp collisions at $\sqrt{s} = 13$ TeV in final states with hadronic jets, 1 or two hadronically decaying τ and $\not{E}_T$. In Tglu1F, gluino masses are excluded at 95% C.L. up to 1570 GeV for neutralino masses of 100 GeV or below. Neutralino masses up to 700 GeV are excluded for all gluino masses between 800 GeV and 1500 GeV, while the strongest neutralino-mass exclusion of 750 GeV is achieved for gluino masses around 1400 GeV. See their Fig. 8. Limits are also presented in the context of Gauge-Mediated Symmetry Breaking models: in this case, values of Λ below 92 TeV are excluded at the 95% CL, corresponding to gluino masses below 2000 GeV. See their Fig. 9.

[36] AABOUD 16J searched in 3.2 fb^{-1} of pp collisions at $\sqrt{s} = 13$ TeV in final states with one isolated electron or muon, hadronic jets, and $\not{E}_T$. Gluino-mediated pair production of stops with a nearly mass-degenerate stop and neutralino are targeted and gluino masses are excluded at 95% C.L. up to 1460 GeV. A 100% of stops decaying via charm + neutralino is assumed. The results are also valid in case of 4-body decays $\widetilde{t}_1 \rightarrow f\,f'\,b\,\widetilde{\chi}^0_1$. See their Fig. 8.

[37] AABOUD 16M searched in 3.2 fb^{-1} of pp collisions at $\sqrt{s} = 13$ TeV for events with two photons, hadronic jets and $\not{E}_T$. No significant excess above the Standard Model expectations is observed. Exclusion limits at 95% C.L. are set on gluino masses in the general gauge-mediated SUSY breaking model (GGM), for bino-like NLSP. See their Fig. 3.

[38] AABOUD 16N searched in 3.2 fb^{-1} of pp collisions at $\sqrt{s} = 13$ TeV for events containing hadronic jets, large $\not{E}_T$, and no electrons or muons. No significant excess above the Standard Model expectations is observed. Gluino masses below 1510 GeV are excluded at the 95% C.L. in a simplified model with only gluinos and the lightest neutralino. See their Fig. 7b.

[39] AABOUD 16N searched in 3.2 fb^{-1} of pp collisions at $\sqrt{s} = 13$ TeV for events containing hadronic jets, large $\not{E}_T$, and no electrons or muons. No significant excess above the Standard Model expectations is observed. Gluino masses below 1500 GeV are excluded at the 95% C.L. in a simplified model with gluinos decaying via an intermediate $\widetilde{\chi}^\pm_1$ to two quarks, a W boson and a $\widetilde{\chi}^0_1$, for $m_{\widetilde{\chi}^0_1} = 200$ GeV. See their Fig 8.

[40] AAD 16AD searched in 3.2 fb^{-1} of pp collisions at $\sqrt{s} = 13$ TeV for events containing several energetic jets, of which at least three must be identified as b-jets, large $\not{E}_T$ and no electrons or muons. No significant excess above the Standard Model expectations is observed. For $\widetilde{\chi}^0_1$ below 800 GeV, gluino masses below 1780 GeV are excluded at 95% C.L. for gluinos decaying via bottom squarks. See their Fig. 7a.

[41] AAD 16AD searched in 3.2 fb^{-1} of pp collisions at $\sqrt{s}$ = 13 TeV for events containing several energetic jets, of which at least three must be identified as b-jets, large $\not{E}_T$ and one electron or muon. Large-radius jets with a high mass are also used to identify highly boosted top quarks. No significant excess above the Standard Model expectations is observed. For $\tilde{\chi}_1^0$ below 700 GeV, gluino masses below 1760 GeV are excluded at 95% C.L. for gluinos decaying via top squarks. See their Fig. 7b.

[42] AAD 16BB searched in 3.2 fb^{-1} of pp collisions at $\sqrt{s}$ = 13 TeV for events with exactly two same-sign leptons or at least three leptons, multiple hadronic jets, b-jets, and $\not{E}_T$. No significant excess over the Standard Model expectation is found. Exclusion limits at 95% C.L. are set on the gluino mass in various simplified models (Tglu1D, Tglu1E, Tglu3A). See their Figs. 4.a, 4.b, and 4.d.

[43] AAD 16BG searched in 3.2 fb^{-1} of pp collisions at $\sqrt{s}$ = 13 TeV in final states with one isolated electron or muon, hadronic jets, and $\not{E}_T$. The data agree with the SM background expectation in the six signal selections defined in the search, and the largest deviation is a 2.1 standard deviation excess. Gluinos are excluded at 95% C.L. up to 1600 GeV assuming they decay via the lightest chargino to the lightest neutralino as in the model Tglu1B for $m_{\tilde{\chi}_1^0}$=100 GeV, assuming $m_{\tilde{\chi}_1^\pm}$=($m_{\tilde{g}}$ + $m_{\tilde{\chi}_1^0}$)/2. See their Fig. 6.

[44] AAD 16V searched in 3.2 fb^{-1} of pp collisions at $\sqrt{s}$ = 13 TeV for events with $\not{E}_T$ various hadronic jet multiplicities from $\geq$ 7 to $\geq$ 10 and with various b-jet multiplicity requirements. No significant excess over the Standard Model expectation is found. Exclusion limits at 95% C.L. are set on the gluino mass in one simplified model (Tglu1E) and a pMSSM-inspired model. See their Fig. 5.

[45] KHACHATRYAN 16AM searched in 19.7 fb^{-1} of pp collisions at $\sqrt{s}$ = 8 TeV for events with highly boosted W-bosons and b-jets, using the razor variables (M_R and R^2) to discriminate between signal and background processes. No significant excess above the Standard Model expectations is observed. Limits are set on the gluino mass in the Tglu3C and Tglu3B simplified models, see Fig. 12.

[46] KHACHATRYAN 16BJ searched in 2.3 fb^{-1} of pp collisions at $\sqrt{s}$ = 13 TeV for events with two isolated same-sign dileptons and jets in the final state. No significant excess above the Standard Model expectations is observed. Limits are set on the gluino mass in the following simplified models: Tglu3A and Tglu3D, see Fig. 4, Tglu3B and Tglu3C, see Fig. 5, and Tglu1B, see Fig. 7.

[47] KHACHATRYAN 16BS searched in 2.3 fb^{-1} of pp collisions at $\sqrt{s}$ = 13 TeV for events with at least one energetic jet , no isolated leptons, and significant $\not{E}_T$, using the transverse mass variable M_{T2} to discriminate between signal and background processes. No significant excess above the Standard Model expectations is observed. Limits are set on the gluino mass in the Tglu1A, Tglu2A and Tglu3A simplified models, see Fig. 10 and Table 3.

[48] KHACHATRYAN 16BX searched in 19.5 fb^{-1} of pp collisions at $\sqrt{s}$ = 8 TeV for events containing 0 or 1 leptons and b-tagged jets, coming from R-parity-violating decays of supersymmetric particles. No excess over the expected background is observed. Limits are derived on the gluino mass, assuming the RPV $\tilde{g} \rightarrow t\,b\,s$ decay, see Fig. 7 and 10.

[49] KHACHATRYAN 16BY searched in 2.3 fb^{-1} of pp collisions at $\sqrt{s}$ = 13 TeV for events with two opposite-sign, same-flavour leptons, jets, and missing transverse momentum. No significant excess above the Standard Model expectations is observed. Limits are set on the gluino mass in the Tglu4C simplified model, see Fig. 4, and on sbottom masses in the Tsbot3 simplified model, see Fig. 5.

[50] KHACHATRYAN 16V searched in 2.3 fb^{-1} of pp collisions at $\sqrt{s}$ = 13 TeV for events with at least four energetic jets and significant $\not{E}_T$, no identified isolated electron or muon or charged track. No significant excess above the Standard Model expectations is observed. Limits are set on the gluino mass in the Tglu1A, Tglu1C, Tglu2A, and Tglu3A simplified models, see Fig. 8.

[51] AAD 15BG searched in 20.3 fb^{-1} of pp collisions at $\sqrt{s}$ = 8 TeV for events with jets, missing E_T, and two opposite-sign same flavor isolated leptons featuring either a kinematic edge, or a peak at the Z-boson mass, in the invariant mass spectrum. No evidence for a statistically significant excess over the expected SM backgrounds are observed and 95% C.L. exclusion limits are derived in a GGM simplified model of gluino pair production where the gluino decays into quarks, a Z-boson, and a massless gravitino LSP, see Fig. 12. Also, limits are set in simplified models with slepton /sneutrino intermediate states, see Fig. 13.

[52] AAD 15BV summarized and extended ATLAS searches for gluinos and first- and second-generation squarks in final states containing jets and missing transverse momentum, with or without leptons or b-jets in the $\sqrt{s}$ =8 TeV data set collected in 2012. The paper reports the results of new interpretations and statistical combinations of previously published analyses, as well as new analyses. Exclusion limits at 95% C.L. are set on the gluino mass in several R-parity conserving models, leading to a generalized constraint on gluino masses exceeding 1150 GeV for lightest supersymmetric particle masses below 100 GeV. See their Figs. 10, 19, 20, 21, 23, 25, 26, 29-37.

[53] AAD 15BX interpreted the results of a wide range of ATLAS direct searches for supersymmetry, during the first run of the LHC using the $\sqrt{s}$ =7 TeV and $\sqrt{s}$ = 8 TeV data set collected in 2012, within the wider framework of the phenomenological MSSM (pMSSM). The integrated luminosity was up to 20.3 fb^{-1}. From an initial random sampling of 500 million pMSSM points, generated from the 19-parameter pMSSM, a total of 310,327 model points with $\tilde{\chi}_1^0$ LSP were selected each of which satisfies constraints from previous collider searches, precision measurements, cold dark matter energy density measurements and direct dark matter searches. The impact of the ATLAS Run 1 searches on this space was presented, considering the fraction of model points surviving, after projection into two-dimensional spaces of sparticle masses. Good complementarity is observed between different ATLAS analyses, with almost all showing regions of unique sensitivity. ATLAS searches have good sensitivity at LSP mass below 800 GeV.

[54] AAD 15CA searched in 20.3 fb^{-1} of pp collisions at $\sqrt{s}$ = 8 TeV for events with one or more photons, hadronic jets or b-jets and $\not{E}_T$. No significant excess above the Standard Model expectations is observed. Limits are set on gluino masses in the general gauge-mediated SUSY breaking model (GGM), for bino-like or higgsino-bino admixtures NLSP, see Fig. 8, 10, 11

[55] KHACHATRYAN 15AF searched in 19.5 fb^{-1} of pp collisions at $\sqrt{s}$ = 8 TeV for events with at least two energetic jets and significant $\not{E}_T$, using the transverse mass variable M_{T2} to discriminate between signal and background processes. No significant excess above the Standard Model expectations is observed. Limits are set on the gluino mass in simplified models where the decay $\tilde{g} \rightarrow q\overline{q}\tilde{\chi}_1^0$ takes place with a branching ratio of 100%, see Fig. 13(a), or where the decay $\tilde{g} \rightarrow b\overline{b}\tilde{\chi}_1^0$ takes place with a branching ratio of 100%, see Fig. 13(b), or where the decay $\tilde{g} \rightarrow t\overline{t}\tilde{\chi}_1^0$ takes place with a branching ratio of 100%, see Fig. 13(c). See also Table 5. Exclusions in the CMSSM, assuming tanβ = 30, $A_0 = -2$ max(m_0, $m_{1/2}$) and $\mu > 0$, are also presented, see Fig. 15.

[56] KHACHATRYAN 15I searched in 19.5 fb^{-1} of pp collisions at $\sqrt{s}$ = 8 TeV for events in which b-jets and four W-bosons are produced. Five individual search channels are combined (fully hadronic, single lepton, same-sign dilepton, opposite-sign dilepton, multilepton). No significant excess above the Standard Model expectations is observed. Limits are set on the gluino mass in a simplified model where the decay $\tilde{g} \rightarrow t\overline{t}\tilde{\chi}_1^0$ takes place with a branching ratio of 100%, see Fig. 5. Also a simplified model with gluinos decaying into on-shell top squarks is considered, see Fig. 6.

[57] KHACHATRYAN 15X searched in 19.3fb^{-1} of pp collisions at $\sqrt{s}$ = 8 TeV for events with at least two energetic jets, at least one of which is required to originate from a b quark, and significant $\not{E}_T$, using the razor variables (M_R) and R^2) to discriminate between signal and background processes. No significant excess above the Standard Model expectations is observed. Limits are set on the gluino mass in simplified models where the decay $\tilde{g} \rightarrow b\overline{b}\tilde{\chi}_1^0$ and the decay $\tilde{g} \rightarrow t\overline{t}\tilde{\chi}_1^0$ take place with branching ratios varying between 0, 50 and 100%, see Figs. 13 and 14.

[58] AAD 14AE searched in 20.3 fb^{-1} of pp collisions at $\sqrt{s}$ = 8 TeV for strongly produced supersymmetric particles in events containing jets and large missing transverse momentum, and no electrons or muons. No excess over the expected SM background is observed. Exclusion limits are derived in simplified models containing gluinos and squarks, see Figures 5, 6 and 7. Limits are also derived in the mSUGRA/CMSSM with parameters tanβ = 30, $A_0 = -2\ m_0$ and $\mu > 0$, see their Fig. 8.

[59] AAD 14AG searched in 20.3 fb^{-1} of pp collisions at $\sqrt{s}$ = 8 TeV for events containing one hadronically decaying τ-lepton, zero or one additional light leptons (electrons or muons), jets and large missing transverse momentum. No excess of events above the expected level of Standard Model background was found. Exclusion limits at 95% C.L. are set in several SUSY scenarios. For an interpretation in the minimal GMSB model, see their Fig. 8. For an interpretation in the mSUGRA/CMSSM with parameters tanβ = 30, $A_0 = -2\ m_0$ and $\mu > 0$, see their Fig. 9. For an interpretation in the framework of natural Gauge Mediation, see Fig. 10. For an interpretation in the bRPV scenario, see their Fig. 11.

[60] AAD 14X searched in 20.3 fb^{-1} of pp collisions at $\sqrt{s}$ = 8 TeV for events with at least four leptons (electrons, muons, taus) in the final state. No significant excess above the Standard Model expectations is observed. Limits are set on the gluino mass in an R-parity violating simplified model where the decay $\tilde{g} \rightarrow q\overline{q}\tilde{\chi}_1^0$, with $\tilde{\chi}_1^0 \rightarrow \ell^\pm\ell^\mp\nu$, takes place with a branching ratio of 100%, see Fig. 8.

[61] AAD 14X searched in 20.3 fb^{-1} of pp collisions at $\sqrt{s}$ = 8 TeV for events with at least four leptons (electrons, muons, taus) in the final state. No significant excess above the Standard Model expectations is observed. Limits are set on the gluino mass in a general gauge-mediation model (GGM) where the decay $\tilde{g} \rightarrow q\overline{q}\tilde{\chi}_1^0$, with $\tilde{\chi}_1^0 \rightarrow \ell^\pm\ell^\mp\tilde{G}$, takes place with a branching ratio of 100%, for two choices of tanβ = 1.5 and 30, see Fig. 11. Also some constraints on the higgsino mass parameter μ are discussed.

[62] CHATRCHYAN 14AH searched in 4.7 fb^{-1} of pp collisions at $\sqrt{s}$ = 7 TeV for events with at least two energetic jets and significant $\not{E}_T$, using the razor variables (M_R and R^2) to discriminate between signal and background processes. No significant excess above the Standard Model expectations is observed. Limits are set on sbottom masses in simplified models where the decay $\tilde{g} \rightarrow q\overline{q}\tilde{\chi}_1^0$ takes place with a branching ratio of 100%, see Fig. 28. Exclusions in the CMSSM, assuming tanβ = 10, A_0 = 0 and $\mu > 0$, are also presented, see Fig. 26.

[63] CHATRCHYAN 14AH searched in 4.7 fb^{-1} of pp collisions at $\sqrt{s}$ = 7 TeV for events with at least two energetic jets and significant $\not{E}_T$, using the razor variables (M_R and R^2) to discriminate between signal and background processes. A second analysis requires at least one of the jets to be originating from a b-quark. No significant excess above the Standard Model expectations is observed. Limits are set on sbottom masses in simplified models where the decay $\tilde{g} \rightarrow b\overline{b}\tilde{\chi}_1^0$ takes place with a branching ratio of 100%, see Figs. 28 and 29. Exclusions in the CMSSM, assuming tanβ = 10, A_0 = 0 and $\mu > 0$, are also presented, see Fig. 26.

[64] CHATRCHYAN 14AH searched in 4.7 fb^{-1} of pp collisions at $\sqrt{s}$ = 7 TeV for events with at least two energetic jets and significant $\not{E}_T$, using the razor variables (M_R and R^2) to discriminate between signal and background processes. A second analysis requires at least one of the jets to be originating from a b-quark. No significant excess above the Standard Model expectations is observed. Limits are set on sbottom masses in simplified models where the decay $\tilde{g} \rightarrow t\overline{t}\tilde{\chi}_1^0$ takes place with a branching ratio of 100%, see Figs. 28 and 29. Exclusions in the CMSSM, assuming tanβ = 10, A_0 = 0 and μ >0, are also presented, see Fig. 26.

[65] CHATRCHYAN 14I searched in 19.5 fb^{-1} of pp collisions at $\sqrt{s}$ = 8 TeV for events containing multijets and large $\not{E}_T$. No excess over the expected SM background is observed. Exclusion limits are derived in simplified models containing gluinos that decay via $\tilde{g} \rightarrow q\overline{q}\tilde{\chi}_1^0$ with a 100% branching ratio, see Fig. 7b, or via $\tilde{g} \rightarrow t\overline{t}\tilde{\chi}_1^0$ with a 100% branching ratio, see Fig. 7c, or via $\tilde{g} \rightarrow q\overline{q}W/Z\tilde{\chi}_1^0$, see Fig. 7d.

[66] CHATRCHYAN 14N searched in 19.3 fb^{-1} of pp collisions at $\sqrt{s}$ = 8 TeV for events containing a single isolated electron or muon and multiple jets, at least two of which are identified as originating from a b-quark. No significant excesses over the expected SM backgrounds are observed. The results are interpreted in three simplified models of gluino pair production with subsequent decay into virtual or on-shell top squarks, where each of the top squarks decays in turn into a top quark and a $\tilde{\chi}_1^0$, see Fig. 4. The models differ in which masses are allowed to vary.

[67] CHATRCHYAN 14P searched in 19.4 fb^{-1} of pp collisions at $\sqrt{s}$ = 8 TeV for three-jet resonances produced in the decay of a gluino in R-parity violating supersymmetric models. No excess over the expected SM background is observed. Assuming a 100% branching ratio for the gluino decay into three light-flavour jets, limits are set on the cross section of gluino pair production, see Fig. 7, and gluino masses below 650 GeV are excluded at 95% C.L. Assuming a 100% branching ratio for the gluino decaying to one b-quark jet and two light-flavour jets, gluino masses between 200 GeV and 835 GeV are excluded at 95% C L.

[68] CHATRCHYAN 14R searched in 19.5 fb^{-1} of pp collisions at $\sqrt{s}$ = 8 TeV for events with at least three leptons (electrons, muons, taus) in the final state. No significant excess above the Standard Model expectations is observed. Limits are set on the gluino mass in a slepton co-NLSP simplified model (GMSB) where the decay $\tilde{g} \rightarrow q\ell^\pm\ell^\mp\tilde{G}$ takes place with a branching ratio of 100%, see Fig. 8.

[69] CHATRCHYAN 14R searched in 19.5 fb^{-1} of pp collisions at $\sqrt{s}$ = 8 TeV for events with at least three leptons (electrons, muons, taus) in the final state. No significant excess above the Standard Model expectations is observed. Limits are set on the gluino mass in a simplified model where the decay $\tilde{g} \rightarrow t\overline{t}\tilde{\chi}_1^0$ takes place with a branching ratio of 100%, see Fig. 11.

[70] AABOUD 17AZ searched in 36.1 fb^{-1} of pp collisions at $\sqrt{s}$ = 13 TeV for events with at least seven jets and large missing transverse momentum. Selected events are further classified based on the presence of large R-jets or b-jets and no leptons. No significant excess above the Standard Model expectations is observed. Limits are set for pMSSM models with M_1 = 60 GeV, tan(β) = 10, μ < 0 varying the soft-breaking parameters M_3 and μ. Gluino masses up to 1600 GeV are excluded for $m_{\widetilde{\chi}_1^\pm}$ = 200 GeV. See their Figure 6a and text for details on the model.

[71] KHACHATRYAN 16AY searched in 2.3 fb^{-1} of pp collisions at $\sqrt{s}$ = 13 TeV for events with one isolated high transverse momentum lepton (e or μ), hadronic jets of which at least one is identified as coming from a b-quark, and large $\not{E}_T$. No significant excess above the Standard Model expectations is observed. Limits are set on the gluino mass in the Tglu3A simplified model, see Fig. 10, and in the Tglu3B model, see Fig. 11.

[72] KHACHATRYAN 16BT performed a global Bayesian analysis of a wide range of CMS results obtained with data samples corresponding to 5.0 fb^{-1} of pp collisions at $\sqrt{s}$ = 7 TeV and in 19.5 fb^{-1} of pp collisions at $\sqrt{s}$ = 8 TeV. The set of searches considered, both individually and in combination, includes those with all-hadronic final states, same-sign and opposite-sign dileptons, and multi-lepton final states. An interpretation was given in a scan of the 19-parameter pMSSM. No scan points with a gluino mass less than 500 GeV survived and 98% of models with a squark mass less than 300 GeV were excluded.

[73] KHACHATRYAN 16BX searched in 19.5 fb^{-1} of pp collisions at $\sqrt{s}$ = 8 TeV for events containing 4 leptons coming from R-parity-violating decays of $\widetilde{\chi}_1^0 \to \ell\ell\nu$ with $\lambda_{121} \neq 0$ or $\lambda_{122} \neq 0$. No excess over the expected background is observed. Limits are derived on the gluino, squark and stop masses, see Fig. 23.

[74] AAD 15AB searched for the decay of neutral, weakly interacting, long-lived particles in 20.3 fb^{-1} of pp collisions at $\sqrt{s}$ = 8 TeV. Signal events require at least two reconstructed vertices possibly originating from long-lived particles decaying to jets in the inner tracking detector and muon spectrometer. No significant excess of events over the expected background was found. Results were interpreted in Stealth SUSY benchmark models where a pair of gluinos decay to long-lived singlinos, $\widetilde{S}$, which in turn each decay to a low-mass gravitino and a pair of jets. The 95% confidence-level limits are set on the cross section × branching ratio for the decay $\widetilde{g} \to \widetilde{S}g$, as a function of the singlino proper lifetime ($c\tau$). See their Fig. 10(f)

[75] AAD 15AI searched in 20 fb^{-1} of pp collisions at $\sqrt{s}$ = 8 TeV for events containing at least one isolated lepton (electron or muon), jets, and large missing transverse momentum. No excess of events above the expected level of Standard Model background was found. Exclusion limits at 95% C.L. are set on the gluino mass in the CMSSM/mSUGRA, see Fig. 15, in the NUHMG, see Fig. 16, and in various simplified models, see Figs. 18–22.

[76] AAD 15CB searched for events containing at least one long-lived particle that decays at a significant distance from its production point (displaced vertex, DV) into two leptons or into five or more charged particles in 20.3 fb^{-1} of pp collisions at $\sqrt{s}$ = 8 TeV. The dilepton signature is characterised by DV formed from at least two lepton candidates. Four different final states were considered for the multitrak signature, in which the DV must be accompanied by a high-transverse momentum muon or electron candidate that originates from the DV, jets or missing transverse momentum. No events were observed in any of the signal regions. Results were interpreted in SUSY scenarios involving R-parity violation, split supersymmetry, and gauge mediation. See their Fig. 12–20.

[77] AAD 15X searched in 20.3 fb^{-1} of pp collisions at $\sqrt{s}$ = 8 TeV for events containing large number of jets, no requirements on missing transverse momentum and no isolated electrons or muons. The sensitivity of the search is enhanced by considering the number of b-tagged jets and the scalar sum of masses of large-radius jets in an event. No evidence was found for excesses above the expected level of Standard Model background. Exclusion limits at 95% C.L. are set on the gluino mass assuming the gluino decays to various quark flavors, and for various neutralino masses. See their Fig. 11–16.

[78] KHACHATRYAN 15AD searched in 19.4 fb^{-1} of pp collisions at $\sqrt{s}$ = 8 TeV for events with two opposite-sign same flavor isolated leptons featuring either a kinematic edge, or a peak at the Z-boson mass, in the invariant mass spectrum. No evidence for a statistically significant excess over the expected SM backgrounds is observed and 95% C.L. exclusion limits are derived in a simplified model of gluino pair production where the gluino decays into quarks, a Z-boson, and a massless gravitino LSP, see Fig. 9.

[79] KHACHATRYAN 15AZ searched in 19.7 fb^{-1} of pp collisions at $\sqrt{s}$ = 8 TeV for events with either at least one photon, hadronic jets and $\not{E}_T$ (single photon channel) or with at least two photons and at least one jet and using the razor variables. No significant excess above the Standard Model expectations is observed. Limits are set on gluino masses in the general gauge-mediated SUSY breaking model (GGM), for both a bino-like and wino-like neutralino NLSP scenario, see Fig. 8 and 9.

[80] AAD 14AX searched in 20.1 fb^{-1} of pp collisions at $\sqrt{s}$ = 8 TeV for the strong production of supersymmetric particles in events containing either zero or at last one high high-p_T lepton, large missing transverse momentum, high jet multiplicity and at least three jets identified as originating from b-quarks. No excess over the expected SM background is observed. Limits are derived in mSUGRA/CMSSM models with tanβ = 30, $A_0 = -2m_0$ and $\mu > 0$, see their Fig. 14. Also, exclusion limits in simplified models containing gluinos and scalar top and bottom quarks are set, see their Figures 12, 13.

[81] AAD 14E searched in 20.3 fb^{-1} of pp collisions at $\sqrt{s}$ = 8 TeV for strongly produced supersymmetric particles in events containing jets and two same-sign leptons or three leptons. The search also utilises jets originating from b-quarks, missing transverse momentum and other variables. No excess over the expected SM background is observed. Exclusion limits are derived in simplified models containing gluinos and squarks, see Figures 5 and 6. In the $\widetilde{g} \to qq'\widetilde{\chi}_1^\pm$, $\widetilde{\chi}_1^\pm \to W^{(*)\pm}\widetilde{\chi}_2^0$, $\widetilde{\chi}_2^0 \to Z^{(*)}\widetilde{\chi}_1^0$ simplified model, the following assumptions have been made: $m_{\widetilde{\chi}_1^\pm} = 0.5\ m_{\widetilde{\chi}_1^0} + m_{\widetilde{g}}$, $m_{\widetilde{\chi}_2^0} = 0.5\ (m_{\widetilde{\chi}_1^0} + m_{\widetilde{\chi}_1^\pm})$, $m_{\widetilde{\chi}_1^0} < 520$ GeV. In the $\widetilde{g} \to qq'\widetilde{\chi}_1^\pm$, $\widetilde{\chi}_1^\pm \to \ell^\pm\nu\widetilde{\chi}_1^0$ or $\widetilde{g} \to qq'\widetilde{\chi}_2^0$, $\widetilde{\chi}_2^0 \to \ell^\pm\ell^\mp(\nu\nu)\widetilde{\chi}_1^0$ simplified model, the following assumptions have been made: $m_{\widetilde{\chi}_1^\pm} = m_{\widetilde{\chi}_2^0} = 0.5\ (m_{\widetilde{\chi}_1^0} + m_{\widetilde{g}})$, $m_{\widetilde{\chi}_1^0} < 660$ GeV. Limits are also derived in the mSUGRA/CMSSM, bRPV and GMSB models, see their Fig. 8.

[82] CHATRCHYAN 14H searched in 19.5 fb^{-1} of pp collisions at $\sqrt{s}$ = 8 TeV for events with two isolated same-sign dileptons and jets in the final state. No significant excess above the Standard Model expectations is observed. Limits are set on the gluino mass in simplified models where the decay $\widetilde{g} \to t\overline{t}\widetilde{\chi}_1^0$ takes place with a branching ratio of 100%, or where the decay $\widetilde{g} \to \widetilde{t}t$, $\widetilde{t} \to t\widetilde{\chi}_1^0$ takes place with a branching ratio of 100%, with varying mass of the $\widetilde{\chi}_1^0$, or where the decay $\widetilde{g} \to \widetilde{b}b$, $\widetilde{b} \to t\widetilde{\chi}_1^\pm$, $\widetilde{\chi}_1^\pm \to W^\pm\widetilde{\chi}_1^0$ takes place with a branching ratio of 100%, with varying mass of the $\widetilde{\chi}_1^\pm$, see Fig. 5.

[83] CHATRCHYAN 14H searched in 19.5 fb^{-1} of pp collisions at $\sqrt{s}$ = 8 TeV for events with two isolated same-sign dileptons and jets in the final state. No significant excess above the Standard Model expectations is observed. Limits are set on the gluino mass in simplified models where the decay $\widetilde{g} \to qq'\widetilde{\chi}_1^\pm$, $\widetilde{\chi}_1^\pm \to W^\pm\widetilde{\chi}_1^0$ takes place with a branching ratio of 100%, with varying mass of the $\widetilde{\chi}_1^\pm$ and $\widetilde{\chi}_1^0$, see Fig. 7.

[84] CHATRCHYAN 14H searched in 19.5 fb^{-1} of pp collisions at $\sqrt{s}$ = 8 TeV for events with two isolated same-sign dileptons and jets in the final state. No significant excess above the Standard Model expectations is observed. Limits are set on the gluino mass in simplified models where the decay $\widetilde{g} \to b\overline{t}\widetilde{\chi}_1^\pm$, $\widetilde{\chi}_1^\pm \to W^\pm\widetilde{\chi}_1^0$ takes place with a branching ratio of 100%, for two choices of $m_{\widetilde{\chi}_1^\pm}$ and fixed $m_{\widetilde{\chi}_1^0}$, see Fig. 6.

[85] CHATRCHYAN 14H searched in 19.5 fb^{-1} of pp collisions at $\sqrt{s}$ = 8 TeV for events with two isolated same-sign dileptons and jets in the final state. No significant excess above the Standard Model expectations is observed. Limits are set on the gluino mass in simplified models where the R-parity violating decay $\widetilde{g} \to tbs$ takes place with a branching ratio of 100%, see Fig. 8.

Long-lived $\widetilde{g}$ (Gluino) mass limit

Limits on light gluinos ($m_{\widetilde{g}}$ < 5 GeV) were last listed in our PDG 14 edition: K. Olive, *et al.* (Particle Data Group), Chinese Physics **C38** 070001 (2014) (http://pdg.lbl.gov).

VALUE (GeV)	CL%	DOCUMENT ID		TECN	COMMENT
>1000	95	[1] KHACHATRY...17AR		CMS	long-lived $\widetilde{g}$, RPV, $\widetilde{g} \to t\overline{b}s$, $c\tau$ = 0.3 mm
>1300	95	[1] KHACHATRY...17AR		CMS	long-lived $\widetilde{g}$, RPV, $\widetilde{g} \to t\overline{b}s$, $c\tau$ = 1.0 mm
>1400	95	[1] KHACHATRY...17AR		CMS	long-lived $\widetilde{g}$, RPV, $\widetilde{g} \to t\overline{b}s$, 2 mm < $c\tau$ < 30 mm
>1580	95	[2] AABOUD	16B	ATLS	long-lived R-hadrons
> 740–1590	95	[3] AABOUD	16C	ATLS	R-hadrons, Tglu1A, $\tau \geq 0.4$ ns, $m_{\widetilde{\chi}_1^0}$ = 100 GeV
>1570	95	[3] AABOUD	16C	ATLS	R-hadrons, Tglu1A, stable
>1610	95	[4] KHACHATRY...16BW		CMS	long-lived $\widetilde{g}$ forming R-hadrons, f = 0.1, cloud interaction model
>1580	95	[4] KHACHATRY...16BW		CMS	long-lived $\widetilde{g}$ forming R-hadrons, f = 0.1, charge-suppressed interaction model
>1520	95	[4] KHACHATRY...16BW		CMS	long-lived $\widetilde{g}$ forming R-hadrons, f = 0.5, cloud interaction model
>1540	95	[4] KHACHATRY...16BW		CMS	long-lived $\widetilde{g}$ forming R-hadrons, f = 0.5, charge-suppressed interaction model
>1270	95	[5] AAD	15AE	ATLS	$\widetilde{g}$ R-hadron, generic R-hadron model
>1360	95	[5] AAD	15AE	ATLS	$\widetilde{g}$ decaying to 300 GeV stable sleptons, LeptoSUSY model
>1115	95	[6] AAD	15BM	ATLS	$\widetilde{g}$ R-hadron, stable
>1185	95	[6] AAD	15BM	ATLS	$\widetilde{g} \to (g/q\overline{q})\widetilde{\chi}_1^0$, lifetime 10 ns, $m_{\widetilde{\chi}_1^0}$ = 100 GeV
>1099	95	[6] AAD	15BM	ATLS	$\widetilde{g} \to (g/q\overline{q})\widetilde{\chi}_1^0$, lifetime 10 ns, $m_{\widetilde{g}} - m_{\widetilde{\chi}_1^0}$ = 100 GeV
>1182	95	[6] AAD	15BM	ATLS	$\widetilde{g} \to t\overline{t}\widetilde{\chi}_1^0$, lifetime 10 ns, $m_{\widetilde{\chi}_1^0}$ = 100 GeV
>1157	95	[6] AAD	15BM	ATLS	$\widetilde{g} \to t\overline{t}\widetilde{\chi}_1^0$, lifetime 10 ns, $m_{\widetilde{g}} - m_{\widetilde{\chi}_1^0}$ = 480 GeV
> 869	95	[6] AAD	15BM	ATLS	$\widetilde{g} \to (g/q\overline{q})\widetilde{\chi}_1^0$, lifetime 1 ns, $m_{\widetilde{\chi}_1^0}$ = 100 GeV
> 821	95	[6] AAD	15BM	ATLS	$\widetilde{g} \to (g/q\overline{q})\widetilde{\chi}_1^0$, lifetime 1 ns, $m_{\widetilde{g}} - m_{\widetilde{\chi}_1^0}$ = 100 GeV
> 836	95	[6] AAD	15BM	ATLS	$\widetilde{g} \to t\overline{t}\widetilde{\chi}_1^0$, lifetime 1 ns, $m_{\widetilde{\chi}_1^0}$ = 100 GeV
> 836	95	[6] AAD	15BM	ATLS	$\widetilde{g} \to t\overline{t}\widetilde{\chi}_1^0$, lifetime 10 ns, $m_{\widetilde{g}} - m_{\widetilde{\chi}_1^0}$ = 480 GeV
>1000	95	[7] KHACHATRY...15AK		CMS	$\widetilde{g}$ R-hadrons, 10 μs< τ <1000 s
> 880	95	[7] KHACHATRY...15AK		CMS	$\widetilde{g}$ R-hadrons, 1 μs< τ <1000 s
• • • We do not use the following data for averages, fits, limits, etc. • • •					
> 985	95	[8] AAD	13AA	ATLS	$\widetilde{g}$, R-hadrons, generic interaction model
> 832	95	[9] AAD	13BC	ATLS	R-hadrons, $\widetilde{g} \to g/q\overline{q}\widetilde{\chi}_1^0$, generic R-hadron model, lifetime between 10^{-5} and 10^3 s, $m_{\widetilde{\chi}_1^0}$ = 100 GeV
>1322	95	[10] CHATRCHYAN	13AB	CMS	long-lived $\widetilde{g}$ forming R-hadrons, f = 0.1, cloud interaction model
none 200–341	95	[11] AAD	12P	ATLS	long-lived $\widetilde{g} \to g\widetilde{\chi}_1^0$, $m_{\widetilde{\chi}_1^0}$ = 100 GeV
> 640	95	[12] CHATRCHYAN	12AN	CMS	long-lived $\widetilde{g} \to g\widetilde{\chi}_1^0$
>1098	95	[13] CHATRCHYAN	12L	CMS	long-lived $\widetilde{g}$ forming R-hadrons, f = 0.1

> 586	95	[14] AAD	11K	ATLS	stable $\tilde{g}$	
> 544	95	[15] AAD	11P	ATLS	stable $\tilde{g}$, GMSB scenario, $\tan\beta$=5	
> 370	95	[16] KHACHATRY...11		CMS	long lived $\tilde{g}$	
> 398	95	[17] KHACHATRY...11C		CMS	stable $\tilde{g}$	

[1] KHACHATRYAN 17AR searched in 17.6 fb^{-1} of pp collisions at $\sqrt{s}$ = 8 TeV for R-parity-violating SUSY in which long-lived neutralinos or gluinos decay into multijet final states. No significant excess above the Standard Model expectations is observed. Limits are set on the gluino mass for a range of mean proper decay lengths ($c\tau$), see their Fig. 7. The upper limits on the production cross section times branching ratio squared (Fig. 7) are also applicable to long-lived neutralinos.

[2] AABOUD 16B searched in 3.2 fb^{-1} of pp collisions at $\sqrt{s}$ = 13 TeV for long-lived R-hadrons using observables related to large ionization losses and slow propagation velocities, which are signatures of heavy charged particles traveling significantly slower than the speed of light. Exclusion limits at 95% C.L. are set on the long-lived gluino masses exceeding 1580 GeV. See their Fig. 5.

[3] AABOUD 16C searched in 3.2 fb^{-1} of pp collisions at $\sqrt{s}$ = 13 TeV for long-lived and stable R-hadrons identified by anomalous specific ionization energy loss in the ATLAS Pixel detector. Gluino R-hadrons with lifetimes above 0.4 ns are excluded at 95% C.L. with lower mass limit range between 740 GeV and 1590 GeV. In the case of stable R-hadrons, the lower mass limit is 1570 GeV. See their Figs. 5 and 6.

[4] KHACHATRYAN 16BW searched in 2.5 fb^{-1} of pp collisions at $\sqrt{s}$ = 13 TeV for events with heavy stable charged particles, identified by their anomalously high energy deposits in the silicon tracker and/or long time-of-flight measurements by the muon system. No evidence for an excess over the expected background is observed. Limits are derived for pair production of gluinos as a function of mass, depending on the interaction model and on the fraction f, of produced gluinos hadronizing into a $\tilde{g}$ - gluon state, see Fig. 4 and Table 7.

[5] AAD 15AE searched in 19.1 fb^{-1} of pp collisions at $\sqrt{s}$ = 8 TeV for heavy long-lived charged particles, measured through their specific ionization energy loss in the ATLAS pixel detector or their time-of-flight in the ALTAS muon system. In the absence of an excess of events above the expected backgrounds, limits are set R-hadrons in various scenarios, see Fig. 11. Limits are also set in LeptoSUSY models where the gluino decays to stable 300 GeV leptons, see Fig. 9.

[6] AAD 15BM searched in 18.4 fb^{-1} of pp collisions at $\sqrt{s}$ = 8 TeV for stable and metastable non-relativistic charged particles through their anomalous specific ionization energy loss in the ATLAS pixel detector. In absence of an excess of events above the expected backgrounds, limits are set within a generic R-hadron model, on stable gluino R-hadrons (see Table 5) and on metastable gluino R-hadrons decaying to (g / $q\overline{q}$) plus a light $\tilde{\chi}_1^0$ (see Fig. 7) and decaying to $t\overline{t}$ plus a light $\tilde{\chi}_1^0$ (see Fig. 9).

[7] KHACHATRYAN 15AK looked in a data set corresponding to 18.6 fb^{-1} of pp collisions at $\sqrt{s}$ = 8 TeV, and a search interval corresponding to 281 h of trigger lifetime, for long-lived particles that have stopped in the CMS detector. No evidence for an excess over the expected background in a cloud interaction model is observed. Assuming the decay $\tilde{g} \rightarrow g\tilde{\chi}_1^0$ and lifetimes between 1 μs and 1000 s, limits are derived on $\tilde{g}$ production as a function of $m_{\tilde{\chi}_1^0}$, see Figs. 4 and 6. The exclusions require that $m_{\tilde{\chi}_1^0}$ is kinematically consistent with the minimum values of the jet energy thresholds used.

[8] AAD 13AA searched in 4.7 fb^{-1} of pp collisions at $\sqrt{s}$ = 7 TeV for events containing colored long-lived particles that hadronize forming R-hadrons. No significant excess above the expected background was found. Long-lived R-hadrons containing a $\tilde{g}$ are excluded for masses up to 985 GeV at 95% C.L in a general interaction model. Also, limits independent of the fraction of R-hadrons that arrive charged in the muon system were derived, see Fig. 6.

[9] AAD 13BC searched in 5.0 fb^{-1} of pp collisions at $\sqrt{s}$ = 7 TeV and in 22.9 fb^{-1} of pp collisions at $\sqrt{s}$ = 8 TeV for bottom squark R-hadrons that have come to rest within the ATLAS calorimeter and decay at some later time to hadronic jets and a neutralino. In absence of an excess of events above the expected backgrounds, limits are set on gluino masses for different decays, lifetimes, and neutralino masses, see their Table 6 and Fig. 10.

[10] CHATRCHYAN 13AB looked in 5.0 fb^{-1} of pp collisions at $\sqrt{s}$ = 7 TeV and in 18.8 fb^{-1} of pp collisions at $\sqrt{s}$ = 8 TeV for events with heavy stable particles, identified by their anomalous dE/dx in the tracker or additionally requiring that it be identified as muon in the muon chambers, from pair production of $\tilde{g}$'s. No evidence for an excess over the expected background is observed. Limits are derived for pair production of gluinos as a function of mass (see Fig. 8 and Table 5), depending on the fraction, f, of formation of $\tilde{g}$–g (R-gluonball) states. The quoted limit is for f = 0.1, while for f = 0.5 it degrades to 1276 GeV. In the conservative scenario where every hadronic interaction causes it to become neutral, the limit decreases to 928 GeV for f = 0.1.

[11] AAD 12P looked in 31 pb^{-1} of pp collisions at $\sqrt{s}$ = 7 TeV for events with pair production of long-lived gluinos. The hadronization of the gluinos leads to R-hadrons which may stop inside the detector and later decay via $\tilde{g} \rightarrow g\tilde{\chi}_1^0$ during gaps between the proton bunches. No significant excess over the expected background is observed. From a counting experiment, a limit at 95% C.L. on the cross section as a function of $m_{\tilde{g}}$ is derived for $m_{\tilde{\chi}_1^0}$ = 100 GeV, see Fig. 4. The limit is valid for lifetimes between 10^{-5} and 10^3 seconds and assumes the *Generic* matter interaction model for the production cross section.

[12] CHATRCHYAN 12AN looked in 4.0 fb^{-1} of pp collisions at $\sqrt{s}$ = 7 TeV for events with pair production of long-lived gluinos. The hadronization of the gluinos leads to R-hadrons which may stop inside the detector and later decay via $\tilde{g} \rightarrow g\tilde{\chi}_1^0$ during gaps between the proton bunches. No significant excess over the expected background is observed. From a counting experiment, a limit at 95% C.L. on the cross section as a function of $m_{\tilde{g}}$ is derived, see Fig. 3. The mass limit is valid for lifetimes between 10^{-5} and 10^3 seconds, for what they call "the daughter gluon energy E_g >" 100 GeV and assuming the *cloud* interaction model for R-hadrons. Supersedes KHACHATRYAN 11.

[13] CHATRCHYAN 12L looked in 5.0 fb^{-1} of pp collisions at $\sqrt{s}$ = 7 TeV for events with heavy stable particles, identified by their anomalous dE/dx in the tracker or additionally requiring that it be identified as muon in the muon chambers, from pair production of $\tilde{g}$'s. No evidence for an excess over the expected background is observed. Limits are derived for pair production of gluinos as a function of mass (see Fig. 3), depending on the fraction, f, of formation of $\tilde{g}$–g (R-glueball) states. The quoted limit is for f = 0.1, while for f = 0.5 it degrades to 1046 GeV. In the conservative scenario where every hadronic interaction causes it to become neutral, the limit decreases to 928 GeV for f=0.1. Supersedes KHACHATRYAN 11C.

[14] AAD 11K looked in 34 pb^{-1} of pp collisions at $\sqrt{s}$ = 7 TeV for events with heavy stable particles, identified by their anomalous dE/dx in the tracker or time of flight in the tile calorimeter, from pair production of $\tilde{g}$. No evidence for an excess over the SM expectation is observed. Limits are derived for pair production of gluinos as a function of mass (see Fig. 4), for a fraction, f = 10%, of formation of $\tilde{g} - g$ (R-gluonball). If instead of a phase space driven approach for the hadronic scattering of the R-hadrons, a triple-Regge model or a bag-model is used, the limit degrades to 566 and 562 GeV, respectively.

[15] AAD 11P looked in 37 pb^{-1} of pp collisions at $\sqrt{s}$ = 7 TeV for events with heavy stable particles, reconstructed and identified by their time of flight in the Muon System. There is no requirement on their observation in the tracker to increase the sensitivity to cases where gluinos have a large fraction, f, of formation of neutral $\tilde{g} - g$ (R-gluonball). No evidence for an excess over the SM expectation is observed. Limits are derived as a function of mass (see Fig. 4), for f=0.1. For fractions f = 0.5 and 1.0 the limit degrades to 537 and 530 GeV, respectively.

[16] KHACHATRYAN 11 looked in 10 pb^{-1} of pp collisions at $\sqrt{s}$ = 7 TeV for events with pair production of long-lived gluinos. The hadronization of the gluinos leads to R-hadrons which may stop inside the detector and later decay via $\tilde{g} \rightarrow g\tilde{\chi}_1^0$ during gaps between the proton bunches. No significant excess over the expected background is observed. From a counting experiment, a limit at 95% C.L. on the cross section times branching ratio is derived for $m_{\tilde{g}} - m_{\tilde{\chi}_1^0} > 100$ GeV, see their Fig. 2. Assuming 100% branching ratio, lifetimes between 75 ns and 3×10^5 s are excluded for $m_{\tilde{g}}$ = 300 GeV. The $\tilde{g}$ mass exclusion is obtained with the same assumptions for lifetimes between 10 μs and 1000 s, but shows some dependence on the model for R-hadron interactions with matter, illustrated in Fig. 3. From a time-profile analysis, the mass exclusion is 382 GeV for a lifetime of 10 μs under the same assumptions as above.

[17] KHACHATRYAN 11C looked in 3.1 pb^{-1} of pp collisions at $\sqrt{s}$ = 7 TeV for events with heavy stable particles, identified by their anomalous dE/dx in the tracker or additionally requiring that it be identified as muon in the muon chambers, from pair production of $\tilde{g}$. No evidence for an excess over the expected background is observed. Limits are derived for pair production of gluinos as a function of mass (see Fig. 3), depending on the fraction, f, of formation of $\tilde{g} - g$ (R-gluonball). The quoted limit is for f=0.1, while for f=0.5 it degrades to 357 GeV. In the conservative scenario where every hadronic interaction causes it to become neutral, the limit decreases to 311 GeV for f=0.1.

Light $\tilde{G}$ (Gravitino) mass limits from collider experiments

The following are bounds on light ($\ll$ 1 eV) gravitino indirectly inferred from its coupling to matter suppressed by the gravitino decay constant.

Unless otherwise stated, all limits assume that other supersymmetric particles besides the gravitino are too heavy to be produced. The gravitino is assumed to be undetected and to give rise to a missing energy ($\not{E}$) signature.

Some earlier papers are now obsolete and have been omitted. They were last listed in our PDG 14 edition: K. Olive, *et al.* (Particle Data Group), Chinese Physics **C38** 070001 (2014) (http://pdg.lbl.gov).

VALUE (eV)	CL%	DOCUMENT ID		TECN	COMMENT
• • • We do not use the following data for averages, fits, limits, etc. • • •					
> 3.5 $\times 10^{-4}$	95	[1] AAD	15BH	ATLS	jet + $\not{E}_T$, $pp \rightarrow (\tilde{q}/\tilde{g})\tilde{G}$, $m_{\tilde{q}} = m_{\tilde{g}}$ = 500 GeV
> 3 $\times 10^{-4}$	95	[1] AAD	15BH	ATLS	jet + $\not{E}_T$, $pp \rightarrow (\tilde{q}/\tilde{g})\tilde{G}$, $m_{\tilde{q}} = m_{\tilde{g}}$ = 1000 GeV
> 2 $\times 10^{-4}$	95	[1] AAD	15BH	ATLS	jet + $\not{E}_T$, $pp \rightarrow (\tilde{q}/\tilde{g})\tilde{G}$, $m_{\tilde{q}} = m_{\tilde{g}}$ = 1500 GeV
> 1.09 $\times 10^{-5}$	95	[2] ABDALLAH	05B	DLPH	$e^+e^- \rightarrow \tilde{G}\tilde{G}\gamma$
> 1.35 $\times 10^{-5}$	95	[3] ACHARD	04E	L3	$e^+e^- \rightarrow \tilde{G}\tilde{G}\gamma$
> 1.3 $\times 10^{-5}$		[4] HEISTER	03C	ALEP	$e^+e^- \rightarrow \tilde{G}\tilde{G}\gamma$
>11.7 $\times 10^{-6}$	95	[5] ACOSTA	02H	CDF	$p\overline{p} \rightarrow \tilde{G}\tilde{G}\gamma$
> 8.7 $\times 10^{-6}$	95	[6] ABBIENDI,G	00D	OPAL	$e^+e^- \rightarrow \tilde{G}\tilde{G}\gamma$

[1] AAD 15BH searched in 20.3 fb^{-1} of pp collisions at $\sqrt{s}$ = 8 TeV for associated production of a light gravitino and a squark or gluino. The squark (gluino) is assumed to decay exclusively to a quark (gluon) and a gravitino. No evidence was found for an excess above the expected level of Standard Model background and 95% C.L. lower limits were set on the gravitino mass as a function of the squark/gluino mass, both in the case of degenerate and non-degenerate squark/gluino masses, see Figs. 14 and 15.

[2] ABDALLAH 05B use data from $\sqrt{s}$ = 180–208 GeV. They look for events with a single photon + $\not{E}$ final states from which a cross section limit of $\sigma < 0.18$ pb at 208 GeV is obtained, allowing a limit on the mass to be set. Supersedes the results of ABREU 00Z.

[3] ACHARD 04E use data from $\sqrt{s}$ = 189–209 GeV. They look for events with a single photon + $\not{E}$ final states from which a limit on the Gravitino mass is set corresponding to $\sqrt{F} > 238$ GeV. Supersedes the results of ACCIARRI 99R.

[4] HEISTER 03C use the data from $\sqrt{s}$ = 189–209 GeV to search for $\gamma\not{E}_T$ final states.

[5] ACOSTA 02H looked in 87 pb^{-1} of $p\overline{p}$ collisions at $\sqrt{s}$=1.8 TeV for events with a high-E_T photon and $\not{E}_T$. They compared the data with a GMSB model where the final state could arise from $q\overline{q} \rightarrow \tilde{G}\tilde{G}\gamma$. Since the cross section for this process scales as $1/|F|^4$, a limit at 95% CL is derived on $|F|^{1/2} > 221$ GeV. A model independent limit for the above topology is also given in the paper.

[6] ABBIENDI,G 00D searches for $\gamma\not{E}$ final states from $\sqrt{s}$=189 GeV.

Supersymmetry miscellaneous results

Results that do not appear under other headings or that make nonminimal assumptions.

Some earlier papers are now obsolete and have been omitted. They were last listed in our PDG 14 edition: K. Olive, *et al.* (Particle Data Group), Chinese Physics **C38** 070001 (2014) (http://pdg.lbl.gov).

VALUE	CL%	DOCUMENT ID		TECN	COMMENT
• • • We do not use the following data for averages, fits, limits, etc. • • •					
>65	95	[1] AABOUD	16AF	ATLS	selected ATLAS searches on EWK sector

none 0–2	95	[2] AAD	16AG	ATLS	dark photon, γ_d, in SUSY- and Higgs-portal models
		[3] AAD	13P	ATLS	dark γ, hidden valley
		[4] AALTONEN	12AB	CDF	hidden-valley Higgs
none 100–185	95	[5] AAD	11AA	ATLS	scalar gluons
		[6] CHATRCHYAN	11E	CMS	$\mu\mu$ resonances
		[7] ABAZOV	10N	D0	γ_D, hidden valley

[1] AABOUD 16AF uses a selection of searches by ATLAS for the electroweak production of SUSY particles studying resulting constraints on dark matter candidates. They use 20 fb^{-1} of pp collisions at $\sqrt{s} = 8$ TeV. A likelihood-driven scan of an effective model focusing on the gaugino-higgsino and Higgs sector of the pMSSM is performed. The ATLAS searches impact models where $m_{\widetilde{\chi}_1^0} < 65$ GeV, excluding 86% of them. See their Figs. 2, 4, and 6.

[2] AAD 16AG searches for prompt lepton-jets using 20 fb^{-1} of pp collisions at $\sqrt{s} = 8$ TeV collected with the ATLAS detector. Lepton-jets are expected from decays of low-mass dark photons in SUSY-portal and Higgs-portal models. No significant excess of events is observed and 95% CL upper limits are computed on the production cross section times branching ratio for two prompt lepton-jets in models predicting 2 or 4 γ_d via SUSY-portal topologies, for γ_d mass values between 0 and 2 GeV. See their Figs 9 and 10. The results are also interpreted in terms of a 90% CL exclusion region in kinetic mixing and dark-photon mass parameter space. See their Fig. 13.

[3] AAD 13P searched in 5 fb^{-1} of pp collisions at $\sqrt{s} = 7$ TeV for single lepton-jets with at least four muons; pairs of lepton-jets, each with two or more muons; and pairs of lepton-jets with two or more electrons. All of these could be signatures of Hidden Valley supersymmetric models. No statistically significant deviations from the Standard Model expectations are found. 95% C.L. limits are placed on the production cross section times branching ratio of dark photons for several parameter sets of a Hidden Valley model.

[4] AALTONEN 12AB looked in 5.1 fb^{-1} of $p\overline{p}$ collisions at $\sqrt{s} = 1.96$ TeV for anomalous production of multiple low-energy leptons in association with a W or Z boson. Such events may occur in hidden valley models in which a supersymmetric Higgs boson is produced in association with a W or Z boson, with $H \rightarrow \widetilde{\chi}_1^0\widetilde{\chi}_1^0$ pair and with the $\widetilde{\chi}_1^0$ further decaying into a dark photon (γ_D) and the unobservable lightest SUSY particle of the hidden sector. As the γ_D is expected to be light, it may decay into a lepton pair. No significant excess over the SM expectation is observed and a limit at 95% C.L. is set on the cross section for a benchmark model of supersymmetric hidden-valley Higgs production.

[5] AAD 11AA looked in 34 pb^{-1} of pp collisions at $\sqrt{s} = 7$ TeV for events with ≥ 4 jets originating from pair production of scalar gluons, each decaying to two gluons. No two-jet resonances are observed over the SM background. Limits are derived on the cross section times branching ratio (see Fig. 3). Assuming 100% branching ratio for the decay to two gluons, the quoted exclusion range is obtained, except for a 5 GeV mass window around 140 GeV.

[6] CHATRCHYAN 11E looked in 35 pb^{-1} of pp collisions at $\sqrt{s} = 7$ TeV for events with collimated μ pairs (leptonic jets) from the decay of hidden sector states. No evidence for new resonance production is found. Limits are derived and compared to various SUSY models (see Fig. 4) where the LSP, either the $\widetilde{\chi}_1^0$ or a $\widetilde{q}$, decays to dark sector particles.

[7] ABAZOV 10N looked in 5.8 fb^{-1} of $p\overline{p}$ collisions at $\sqrt{s} = 1.96$ TeV for events from hidden valley models in which a $\widetilde{\chi}_1^0$ decays into a dark photon, γ_D, and the unobservable lightest SUSY particle of the hidden sector. As the γ_D is expected to be light, it may decay into a tightly collimated lepton pair, called lepton jet. They searched for events with $\not{E}_T$ and two isolated lepton jets observable by an opposite charged lepton pair ee, $e\mu$ or $\mu\mu$. No significant excess over the SM expectation is observed, and a limit at 95% C.L. on the cross section times branching ratio is derived, see their Table I. They also examined the invariant mass of the lepton jets for a narrow resonance, see their Fig. 4, but found no evidence for a signal.

REFERENCES FOR Supersymmetric Particle Searches

SIRUNYAN	18B	PL B778 263	A.M. Sirunyan *et al.*	(CMS Collab.)
SIRUNYAN	18C	PR D97 032009	A.M. Sirunyan *et al.*	(CMS Collab.)
SIRUNYAN	18D	PR D97 012007	A.M. Sirunyan *et al.*	(CMS Collab.)
AABOUD	17AF	JHEP 1708 006	M. Aaboud *et al.*	(ATLAS Collab.)
AABOUD	17AI	JHEP 1709 088	M. Aaboud *et al.*	(ATLAS Collab.)
AABOUD	17AJ	JHEP 1709 084	M. Aaboud *et al.*	(ATLAS Collab.)
AABOUD	17AR	PR D96 112010	M. Aaboud *et al.*	(ATLAS Collab.)
AABOUD	17AX	JHEP 1711 195	M. Aaboud *et al.*	(ATLAS Collab.)
AABOUD	17AY	JHEP 1712 085	M. Aaboud *et al.*	(ATLAS Collab.)
AABOUD	17AZ	JHEP 1712 034	M. Aaboud *et al.*	(ATLAS Collab.)
AABOUD	17BE	EPJ C77 898	M. Aaboud *et al.*	(ATLAS Collab.)
AABOUD	17N	EPJ C77 144	M. Aaboud *et al.*	(ATLAS Collab.)
AAIJ	17Z	EPJ C77 224	R. Aaij *et al.*	(LHCb Collab.)
AARTSEN	17	EPJ C77 82	M.G. Aartsen *et al.*	(IceCube Collab.)
AARTSEN	17A	EPJ C77 146	M.G. Aartsen *et al.*	(IceCube Collab.)
AARTSEN	17C	EPJ C77 627	M.G. Aartsen *et al.*	(IceCube Collab.)
AKERIB	17	PRL 118 021303	D.S. Akerib *et al.*	(LUX Collab.)
AKERIB	17A	PRL 118 251302	D.S. Akerib *et al.*	(LUX Collab.)
ALBERT	17A	PL B769 249	A. Albert *et al.*	(ANTARES Collab.)
AMOLE	17	PRL 118 251301	C. Amole *et al.*	(PICO Collab.)
APRILE	17G	PRL 119 181301	E. Aprile *et al.*	(XENON Collab.)
ARCHAMBAU...	17	PR D95 082001	S. Archambault *et al.*	(VERITAS Collab.)
BATTAT	17	ASP 91 65	J.B.R. Battat *et al.*	(DRIFT-IId Collab.)
BEHNKE	17	ASP 90 85	E. Behnke *et al.*	(PICASSO Collab.)
CUI	17A	PRL 119 181302	X. Cui *et al.*	(PandaX-II Collab.)
FU	17	PRL 118 071301	C. Fu *et al.*	(PandaX Collab.)
KHACHATRY...	17	PR D95 012003	V. Khachatryan *et al.*	(CMS Collab.)
KHACHATRY...	17A	PRL 118 021802	V. Khachatryan *et al.*	(CMS Collab.)
KHACHATRY...	17AD	PR D96 012004	V. Khachatryan *et al.*	(CMS Collab.)
KHACHATRY...	17AR	PR D95 012009	V. Khachatryan *et al.*	(CMS Collab.)
KHACHATRY...	17AS	PR D95 012011	V. Khachatryan *et al.*	(CMS Collab.)
KHACHATRY...	17AW	EPJ C77 635	V. Khachatryan *et al.*	(CMS Collab.)
KHACHATRY...	17L	JHEP 1704 018	V. Khachatryan *et al.*	(CMS Collab.)
KHACHATRY...	17P	EPJ C77 294	V. Khachatryan *et al.*	(CMS Collab.)
KHACHATRY...	17S	PL B767 403	V. Khachatryan *et al.*	(CMS Collab.)
KHACHATRY...	17V	PL B769 391	V. Khachatryan *et al.*	(CMS Collab.)
KHACHATRY...	17Y	PL B770 257	V. Khachatryan *et al.*	(CMS Collab.)
SIRUNYAN	17AF	PRL 119 151802	A.M. Sirunyan *et al.*	(CMS Collab.)
SIRUNYAN	17AS	JHEP 1710 019	A.M. Sirunyan *et al.*	(CMS Collab.)
SIRUNYAN	17AT	JHEP 1710 005	A.M. Sirunyan *et al.*	(CMS Collab.)
SIRUNYAN	17AW	JHEP 1711 029	A.M. Sirunyan *et al.*	(CMS Collab.)
SIRUNYAN	17AY	JHEP 1712 142	A.M. Sirunyan *et al.*	(CMS Collab.)
SIRUNYAN	17AZ	EPJ C77 710	A.M. Sirunyan *et al.*	(CMS Collab.)
SIRUNYAN	17K	EPJ C77 327	A.M. Sirunyan *et al.*	(CMS Collab.)
SIRUNYAN	17P	PR D96 032003	A.M. Sirunyan *et al.*	(CMS Collab.)
SIRUNYAN	17S	EPJ C77 578	A.M. Sirunyan *et al.*	(CMS Collab.)
AABOUD	16AC	EPJ C76 683	M. Aaboud *et al.*	(ATLAS Collab.)
AABOUD	16AF	JHEP 1609 175	M. Aaboud et al	(ATLAS Collab.)
AABOUD	16B	PL B760 647	M. Aaboud *et al.*	(ATLAS Collab.)
AABOUD	16C	PR D93 112015	M. Aaboud *et al.*	(ATLAS Collab.)
AABOUD	16D	PR D94 032005	M. Aaboud *et al.*	(ATLAS Collab.)
AABOUD	16J	PR D94 052009	M. Aaboud *et al.*	(ATLAS Collab.)
AABOUD	16M	EPJ C76 517	M. Aaboud *et al.*	(ATLAS Collab.)
AABOUD	16N	EPJ C76 392	M. Aaboud *et al.*	(ATLAS Collab.)
AABOUD	16P	EPJ C76 541	M. Aaboud *et al.*	(ATLAS Collab.)
AABOUD	16Q	EPJ C76 547	M. Aaboud *et al.*	(ATLAS Collab.)
AAD	16AA	PR D93 052002	G. Aad *et al.*	(ATLAS Collab.)
AAD	16AD	PR D94 032003	G. Aad *et al.*	(ATLAS Collab.)
AAD	16AG	JHEP 1602 062	G. Aad *et al.*	(ATLAS Collab.)
AAD	16AM	JHEP 1606 067	G. Aad *et al.*	(ATLAS Collab.)
AAD	16AY	EPJ C76 81	G. Aad *et al.*	(ATLAS Collab.)
AAD	16BB	EPJ C76 259	G. Aad *et al.*	(ATLAS Collab.)
AAD	16BG	EPJ C76 565	G. Aad *et al.*	(ATLAS Collab.)
AAD	16V	PL B757 334	G. Aad *et al.*	(ATLAS Collab.)
AARTSEN	16C	JCAP 1604 022	M.G. Aartsen *et al.*	(IceCube Collab.)
AARTSEN	16D	EPJ C76 531	M.G. Aartsen *et al.*	(IceCube Collab.)
ABDALLAH	16	PRL 117 111301	H. Abdallah *et al.*	(H.E.S.S. Collab.)
ABDALLAH	16A	PRL 117 151302	H. Abdallah *et al.*	(H.E.S.S. Collab.)
ADRIAN-MAR...	16	PL B759 69	S. Adrian-Martinez *et al.*	(ANTARES Collab.)
AHNEN	16	JCAP 1602 039	M.L. Ahnen *et al.*	(MAGIC and Fermi-LAT Collab.)
AKERIB	16	PRL 116 161301	D.S. Akerib *et al.*	(LUX Collab.)
AKERIB	16A	PRL 116 161302	D.S. Akerib *et al.*	(LUX Collab.)
AMOLE	16	PR D93 052014	C. Amole *et al.*	(PICO Collab.)
AMOLE	16A	PR D93 061101	C. Amole *et al.*	(PICO Collab.)
APRILE	16B	PR D94 122001	E. Aprile *et al.*	(XENON100 Collab.)
AVRORIN	16	ASP 81 12	A.D. Avrorin *et al.*	(BAIKAL Collab.)
CIRELLI	16	JCAP 1607 041	M. Cirelli, M. Taoso	(LPNHE, MADE)
KHACHATRY...	16AA	PL B759 479	V. Khachatryan *et al.*	(CMS Collab.)
KHACHATRY...	16AC	PL B760 178	V. Khachatryan *et al.*	(CMS Collab.)
KHACHATRY...	16AM	PR D93 092009	V. Khachatryan *et al.*	(CMS Collab.)
KHACHATRY...	16AV	JHEP 1607 027	V. Khachatryan *et al.*	(CMS Collab.)
KHACHATRY...	16AY	JHEP 1608 122	V. Khachatryan *et al.*	(CMS Collab.)
KHACHATRY...	16BE	EPJ C76 317	V. Khachatryan *et al.*	(CMS Collab.)
KHACHATRY...	16BJ	EPJ C76 439	V. Khachatryan *et al.*	(CMS Collab.)
KHACHATRY...	16BK	EPJ C76 460	V. Khachatryan *et al.*	(CMS Collab.)
KHACHATRY...	16BS	JHEP 1610 006	V. Khachatryan *et al.*	(CMS Collab.)
KHACHATRY...	16BT	JHEP 1610 129	V. Khachatryan *et al.*	(CMS Collab.)
KHACHATRY...	16BW	PR D94 112004	V. Khachatryan *et al.*	(CMS Collab.)
KHACHATRY...	16BX	PR D94 112009	V. Khachatryan *et al.*	(CMS Collab.)
KHACHATRY...	16BY	JHEP 1612 013	V. Khachatryan *et al.*	(CMS Collab.)
KHACHATRY...	16R	PL B757 6	V. Khachatryan *et al.*	(CMS Collab.)
KHACHATRY...	16V	PL B758 152	V. Khachatryan *et al.*	(CMS Collab.)
KHACHATRY...	16Y	PL B759 9	V. Khachatryan *et al.*	(CMS Collab.)
LEITE	16	JCAP 1611 021	N. Leite *et al.*	
TAN	16B	PRL 117 121303	A. Tan *et al.*	(PandaX Collab.)
AAD	15AB	PR D92 012010	G. Aad *et al.*	(ATLAS Collab.)
AAD	15AE	JHEP 1501 068	G. Aad *et al.*	(ATLAS Collab.)
AAD	15AI	JHEP 1504 116	G. Aad *et al.*	(ATLAS Collab.)
AAD	15BA	EPJ C75 208	G. Aad *et al.*	(ATLAS Collab.)
AAD	15BG	EPJ C75 318	G. Aad *et al.*	(ATLAS Collab.)
Also		EPJ C75 463	G. Aad *et al.*	(ATLAS Collab.)
AAD	15BH	EPJ C75 299	G. Aad *et al.*	(ATLAS Collab.)
Also		EPJ C75 408 (errat.)	G. Aad *et al.*	(ATLAS Collab.)
AAD	15BM	EPJ C75 407	G. Aad *et al.*	(ATLAS Collab.)
AAD	15BV	JHEP 1510 054	G. Aad *et al.*	(ATLAS Collab.)
AAD	15BX	JHEP 1510 134	G. Aad *et al.*	(ATLAS Collab.)
AAD	15CA	PR D92 072001	G. Aad *et al.*	(ATLAS Collab.)
AAD	15CB	PR D92 072004	G. Aad *et al.*	(ATLAS Collab.)
AAD	15CJ	EPJ C75 510	G. Aad	(ATLAS Collab.)
AAD	15CS	PR D91 012008	G. Aad *et al.*	(ATLAS Collab.)
Also		PR D92 059903 (errat.)	G. Aad *et al.*	(ATLAS Collab.)
AAD	15J	PRL 114 142001	G. Aad *et al.*	(ATLAS Collab.)
AAD	15K	PRL 114 161801	G. Aad *et al.*	(ATLAS Collab.)
AAD	15O	PRL 115 031801	G. Aad *et al.*	(ATLAS Collab.)
AAD	15X	PR D91 112016	G. Aad *et al.*	(ATLAS Collab.)
AAIJ	15BD	EPJ C75 595	R. Aaij *et al.*	(LHCb Collab.)
AARTSEN	15C	EPJ C75 20	M.G. Aartsen *et al.*	(IceCube Collab.)
AARTSEN	15E	EPJ C75 492	M.G. Aartsen *et al.*	(IceCube Collab.)
ABRAMOWSKI	15	PRL 114 081301	A. Abramowski *et al.*	(H.E.S.S. Collab.)
ACKERMANN	15	PR D91 122002	M. Ackermann *et al.*	(Fermi-LAT Collab.)
ACKERMANN	15A	JCAP 1509 008	M. Ackermann *et al.*	(Fermi-LAT Collab.)
ACKERMANN	15B	PRL 115 231301	M. Ackermann *et al.*	(Fermi-LAT Collab.)
ADRIAN-MAR...	15	JCAP 1510 068	S. Adrian-Martinez *et al.*	(ANTARES Collab.)
AGNES	15	PL B743 456	P. Agnes *et al.*	(DarkSide-50 Collab.)
AGNESE	15B	PR D92 072003	R. Agnese *et al.*	(SuperCDMS Collab.)
BUCKLEY	15	PR D91 102001	M.R. Buckley *et al.*	
CHOI	15	PRL 114 141301	K. Choi *et al.*	(Super-Kamiokande Collab.)
KHACHATRY...	15AB	JHEP 1501 096	V. Khachatryan *et al.*	(CMS Collab.)
KHACHATRY...	15AD	JHEP 1504 124	V. Khachatryan *et al.*	(CMS Collab.)
KHACHATRY...	15AF	JHEP 1505 078	V. Khachatryan *et al.*	(CMS Collab.)
KHACHATRY...	15AH	JHEP 1506 116	V. Khachatryan *et al.*	(CMS Collab.)
KHACHATRY...	15AK	EPJ C75 151	V. Khachatryan *et al.*	(CMS Collab.)
KHACHATRY...	15AO	EPJ C75 325	V. Khachatryan *et al.*	(CMS Collab.)
KHACHATRY...	15AR	PL B743 503	V. Khachatryan *et al.*	(CMS Collab.)
KHACHATRY...	15AZ	PR D92 072006	V. Khachatryan *et al.*	(CMS Collab.)
KHACHATRY...	15E	PRL 114 061801	V. Khachatryan *et al.*	(CMS Collab.)
KHACHATRY...	15I	PL B745 5	V. Khachatryan *et al.*	(CMS Collab.)
KHACHATRY...	15L	PL B747 98	V. Khachatryan *et al.*	(CMS Collab.)
KHACHATRY...	15O	PL B748 255	V. Khachatryan *et al.*	(CMS Collab.)
KHACHATRY...	15W	PR D91 052012	V. Khachatryan *et al.*	(CMS Collab.)
KHACHATRY...	15X	PR D91 052018	V. Khachatryan *et al.*	(CMS Collab.)
ROLBIECKI	15	PL B750 247	K. Rolbiecki, J. Tattersall	(MADE, HEID)
AAD	14AE	JHEP 1409 176	G. Aad *et al.*	(ATLAS Collab.)
AAD	14AG	JHEP 1409 103	G. Aad *et al.*	(ATLAS Collab.)
AAD	14AJ	JHEP 1409 015	G. Aad *et al.*	(ATLAS Collab.)
AAD	14AV	JHEP 1410 096	G. Aad *et al.*	(ATLAS Collab.)
AAD	14AX	JHEP 1410 024	G. Aad *et al.*	(ATLAS Collab.)
AAD	14B	EPJ C74 2883	G. Aad *et al.*	(ATLAS Collab.)
AAD	14BD	JHEP 1411 118	G. Aad *et al.*	(ATLAS Collab.)
AAD	14BH	PR D90 112005	G. Aad *et al.*	(ATLAS Collab.)
AAD	14E	JHEP 1406 035	G. Aad *et al.*	(ATLAS Collab.)
AAD	14F	JHEP 1406 124	G. Aad *et al.*	(ATLAS Collab.)
AAD	14G	JHEP 1405 071	G. Aad *et al.*	(ATLAS Collab.)
AAD	14H	JHEP 1404 169	G. Aad *et al.*	(ATLAS Collab.)
AAD	14K	PR D90 012004	G. Aad *et al.*	(ATLAS Collab.)
AAD	14T	PR D90 052008	G. Aad *et al.*	(ATLAS Collab.)
AAD	14X	PR D90 052001	G. Aad *et al.*	(ATLAS Collab.)
AALTONEN	14	PR D90 012011	T. Aaltonen *et al.*	(CDF Collab.)
ACKERMANN	14	PR D89 042001	M. Ackermann *et al.*	(Fermi-LAT Collab.)
AKERIB	14	PRL 112 091303	D.S. Akerib *et al.*	(LUX Collab.)
ALEKSIC	14	JCAP 1402 008	J. Aleksic *et al.*	(MAGIC Collab.)
AVRORIN	14	ASP 62 12	A.D. Avrorin *et al.*	(BAIKAL Collab.)
BUCHMUEL...	14	EPJ C74 2809	O. Buchmueller *et al.*	
BUCHMUEL...	14A	EPJ C74 2922	O. Buchmueller *et al.*	
CHATRCHYAN	14AH	PR D90 112001	S. Chatrchyan *et al.*	(CMS Collab.)
CHATRCHYAN	14H	JHEP 1401 163	S. Chatrchyan *et al.*	(CMS Collab.)
CHATRCHYAN	14I	JHEP 1406 055	S. Chatrchyan *et al.*	(CMS Collab.)

Searches Particle Listings

Supersymmetric Particle Searches

CHATRCHYAN 14N PL B733 328 S. Chatrchyan *et al.* (CMS Collab.)
CHATRCHYAN 14P PL B730 193 S. Chatrchyan *et al.* (CMS Collab.)
CHATRCHYAN 14R PR D90 032006 S. Chatrchyan *et al.* (CMS Collab.)
CHATRCHYAN 14U PRL 112 161802 S. Chatrchyan *et al.* (CMS Collab.)
CZAKON 14 PRL 113 201803 M. Czakon *et al.* (AACH, CAMB, UCB, LBL+)
FELIZARDO 14 PR D89 072013 M. Felizardo *et al.* (SIMPLE Collab.)
KHACHATRY... 14C PL B736 371 V. Khachatryan *et al.* (CMS Collab.)
KHACHATRY... 14I EPJ C74 3036 V. Khachatryan *et al.* (CMS Collab.)
KHACHATRY... 14L PR D90 092007 V. Khachatryan *et al.* (CMS Collab.)
KHACHATRY... 14T PL B739 229 V. Khachatryan *et al.* (CMS Collab.)
PDG 14 CP C38 070001 K. Olive *et al.* (PDG Collab.)
ROSZKOWSKI 14 JHEP 1408 067 L. Roszkowski, E.M. Sessolo, A.J. Williams (WINR)
AAD 13 PL B718 841 G. Aad *et al.* (ATLAS Collab.)
AAD 13AA PL B720 277 G. Aad *et al.* (ATLAS Collab.)
AAD 13AI PL B723 15 G. Aad *et al.* (ATLAS Collab.)
AAD 13AP PR D88 012001 G. Aad *et al.* (ATLAS Collab.)
AAD 13AU JHEP 1310 189 G. Aad *et al.* (ATLAS Collab.)
AAD 13B PL B718 879 G. Aad *et al.* (ATLAS Collab.)
AAD 13BC PR D88 112003 G. Aad *et al.* (ATLAS Collab.)
AAD 13BD PR D88 112006 G. Aad *et al.* (ATLAS Collab.)
AAD 13H JHEP 1301 131 G. Aad *et al.* (ATLAS Collab.)
AAD 13L PR D87 012008 G. Aad *et al.* (ATLAS Collab.)
AAD 13P PL B719 299 G. Aad *et al.* (ATLAS Collab.)
AAD 13Q PL B719 261 G. Aad *et al.* (ATLAS Collab.)
AAD 13R PL B719 280 G. Aad *et al.* (ATLAS Collab.)
AALTONEN 13I PR D88 031103 T. Aaltonen *et al.* (CDF Collab.)
AALTONEN 13Q PRL 110 201802 T. Aaltonen *et al.* (CDF Collab.)
AARTSEN 13C PR D88 122001 M.G. Aartsen *et al.* (IceCube Collab.)
ABAZOV 13B PR D87 052011 V.M. Abazov *et al.* (D0 Collab.)
ABRAMOWSKI 13 PRL 110 041301 A. Abramowski *et al.* (H.E.S.S. Collab.)
ACKERMANN 13A PR D88 082002 M. Ackermann *et al.* (Fermi-LAT Collab.)
ADRIAN-MAR... 13 JCAP 1311 032 S. Adrian-Martinez *et al.* (ANTARES Collab.)
AGNESE 13 PR D88 031104 R. Agnese *et al.* (CDMS Collab.)
AGNESE 13A PRL 111 251301 R. Agnese *et al.* (CDMS Collab.)
APRILE 13 PRL 111 021301 E. Aprile *et al.* (XENON100 Collab.)
BERGSTROM 13 PRL 111 171101 L. Bergstrom *et al.*
BOLIEV 13 JCAP 1309 019 M. Boliev *et al.*
CABRERA 13 JHEP 1307 182 M. Cabrera, J. Casas, R. de Austri
CHATRCHYAN 13 PL B718 815 S. Chatrchyan *et al.* (CMS Collab.)
CHATRCHYAN 13AB JHEP 1307 122 S. Chatrchyan *et al.* (CMS Collab.)
CHATRCHYAN 13AH PL B722 273 S. Chatrchyan *et al.* (CMS Collab.)
CHATRCHYAN 13AO PR D87 072001 S. Chatrchyan *et al.* (CMS Collab.)
CHATRCHYAN 13AT PR D88 052017 S. Chatrchyan *et al.* (CMS Collab.)
CHATRCHYAN 13AV PRL 111 081802 S. Chatrchyan *et al.* (CMS Collab.)
CHATRCHYAN 13G JHEP 1301 077 S. Chatrchyan *et al.* (CMS Collab.)
CHATRCHYAN 13H PL B719 42 S. Chatrchyan *et al.* (CMS Collab.)
CHATRCHYAN 13T EPJ C73 2568 S. Chatrchyan *et al.* (CMS Collab.)
CHATRCHYAN 13V JHEP 1303 037 S. Chatrchyan *et al.* (CMS Collab.)
Also JHEP 1307 041 (errat.) S. Chatrchyan *et al.* (CMS Collab.)
CHATRCHYAN 13W JHEP 1303 111 S. Chatrchyan *et al.* (CMS Collab.)
ELLIS 13B EPJ C73 2403 J. Ellis *et al.*
JIN 13 JCAP 1311 026 H.-B. Jin, Y.-L. Wu, Y.-F. Zhou
KOPP 13 PR D88 076013 J. Kopp
STREGE 13 JCAP 1304 013 C. Strege *et al.*
AAD 12AF PL B714 180 G. Aad *et al.* (ATLAS Collab.)
AAD 12AG PL B714 197 G. Aad *et al.* (ATLAS Collab.)
AAD 12AN PRL 108 181802 G. Aad *et al.* (ATLAS Collab.)
AAD 12AS PRL 108 261804 G. Aad *et al.* (ATLAS Collab.)
AAD 12AX PR D85 012006 G. Aad *et al.* (ATLAS Collab.)
Also PR D87 099903 (errat.) G. Aad *et al.* (ATLAS Collab.)
AAD 12BJ EPJ C72 1993 G. Aad *et al.* (ATLAS Collab.)
AAD 12CJ PR D86 092002 G. Aad *et al.* (ATLAS Collab.)
AAD 12CM EPJ C72 2215 G. Aad *et al.* (ATLAS Collab.)
AAD 12CP PL B718 411 G. Aad *et al.* (ATLAS Collab.)
AAD 12CT JHEP 1212 124 G. Aad *et al.* (ATLAS Collab.)
AAD 12P EPJ C72 1965 G. Aad *et al.* (ATLAS Collab.)
AAD 12R PL B707 478 G. Aad *et al.* (ATLAS Collab.)
AAD 12T PL B709 137 G. Aad *et al.* (ATLAS Collab.)
AAD 12W PL B710 67 G. Aad *et al.* (ATLAS Collab.)
AALTONEN 12AB PR D85 092001 T. Aaltonen *et al.* (CDF Collab.)
ABAZOV 12AD PR D86 071701 V.M. Abazov *et al.* (D0 Collab.)
ABBASI 12 PR D85 042002 R. Abbasi *et al.* (IceCube Collab.)
AKIMOV 12 PL B709 14 D.Yu. Akimov *et al.* (ZEPLIN-III Collab.)
AKULA 12 PR D85 075001 S. Akula *et al.* (NEAS, MICH)
ANGLOHER 12 EPJ C72 1971 G. Angloher *et al.* (CRESST-II Collab.)
APRILE 12 PRL 109 181301 E. Aprile *et al.* (XENON100 Collab.)
ARBEY 12A PL B708 162 A. Arbey *et al.*
ARCHAMBAU... 12 PL B711 153 S. Archambault *et al.* (PICASSO Collab.)
BAER 12 JHEP 1205 091 H. Baer, V. Barger, A. Mustafayev (OKLA, WISC+)
BALAZS 12 EPJ C73 2563 C. Balazs *et al.*
BECHTLE 12 JHEP 1206 098 P. Bechtle *et al.*
BEHNKE 12 PR D86 052001 E. Behnke *et al.* (COUPP Collab.)
Also PR D90 079902 (errat.) E. Behnke *et al.* (COUPP Collab.)
BESKIDT 12 EPJ C72 2166 C. Beskidt *et al.* (KARLE, JINR, ITEP)
BOTTINO 12 PR D85 095013 A. Bottino, N. Fornengo, S. Scopel (TORI, SOGA)
BUCHMUEL... 12 EPJ C72 2020 O. Buchmueller *et al.*
CAO 12A PL B710 665 J. Cao *et al.*
CHATRCHYAN 12 PR D85 012004 S. Chatrchyan *et al.* (CMS Collab.)
CHATRCHYAN 12AE PRL 109 171803 S. Chatrchyan *et al.* (CMS Collab.)
CHATRCHYAN 12AI JHEP 1208 110 S. Chatrchyan *et al.* (CMS Collab.)
CHATRCHYAN 12AL JHEP 1206 169 S. Chatrchyan *et al.* (CMS Collab.)
CHATRCHYAN 12AN JHEP 1208 026 S. Chatrchyan *et al.* (CMS Collab.)
CHATRCHYAN 12AT JHEP 1210 018 S. Chatrchyan *et al.* (CMS Collab.)
CHATRCHYAN 12BJ JHEP 1211 147 S. Chatrchyan *et al.* (CMS Collab.)
CHATRCHYAN 12BK JHEP 1211 172 S. Chatrchyan *et al.* (CMS Collab.)
CHATRCHYAN 12BO JHEP 1212 055 S. Chatrchyan *et al.* (CMS Collab.)
CHATRCHYAN 12L PL B713 408 S. Chatrchyan *et al.* (CMS Collab.)
DAW 12 ASP 35 397 E. Daw *et al.* (DRIFT-IId Collab.)
DREINER 12A EPL 99 61001 H.K. Dreiner, M. Kramer, J. Tattersall (BONN+)
ELLIS 12B EPJ C72 2005 J. Ellis, K. Olive
FELIZARDO 12 PRL 108 201302 M. Felizardo *et al.* (SIMPLE Collab.)
FENG 12B PR D85 075007 J. Feng, K. Matchev, D. Sanford
KADASTIK 12 JHEP 1205 061 M. Kadastik *et al.*
KIM 12 PRL 108 181301 S.C. Kim *et al.* (KIMS Collab.)
STREGE 12 JCAP 1203 030 C. Strege *et al.* (LOIC, AMST, MADU, GRAN+)
AAD 11AA EPJ C71 1828 G. Aad *et al.* (ATLAS Collab.)
AAD 11G PRL 106 131802 G. Aad *et al.* (ATLAS Collab.)
AAD 11H PRL 106 251801 G. Aad *et al.* (ATLAS Collab.)
AAD 11K PL B701 1 G. Aad *et al.* (ATLAS Collab.)
AAD 11O PL B701 398 G. Aad *et al.* (ATLAS Collab.)
AAD 11P PL B703 428 G. Aad *et al.* (ATLAS Collab.)
AAD 11Z EPJ C71 1809 G. Aad *et al.* (ATLAS Collab.)
ABRAMOWSKI 11 PRL 106 161301 A. Abramowski *et al.* (H.E.S.S. Collab.)
AHMED 11A PR D84 011102 Z. Ahmed *et al.* (CDMS and EDELWEISS Collabs.)
ARMENGAUD 11 PL B702 329 E. Armengaud *et al.* (EDELWEISS II Collab.)
BUCHMUEL... 11 EPJ C71 1583 O. Buchmueller *et al.*
BUCHMUEL... 11B EPJ C71 1722 O. Buchmueller *et al.*
CHATRCHYAN 11B JHEP 1106 093 S. Chatrchyan *et al.* (CMS Collab.)
CHATRCHYAN 11D JHEP 1107 113 S. Chatrchyan *et al.* (CMS Collab.)
CHATRCHYAN 11E JHEP 1107 098 S. Chatrchyan *et al.* (CMS Collab.)
CHATRCHYAN 11V PL B704 411 S. Chatrchyan *et al.* (CMS Collab.)
KHACHATRY... 11 PRL 106 011801 V. Khachatryan *et al.* (CMS Collab.)
KHACHATRY... 11C JHEP 1103 024 V. Khachatryan *et al.* (CMS Collab.)
ROSZKOWSKI 11 PR D83 015014 L. Roszkowski *et al.*
AALTONEN 10 PRL 104 011801 T. Aaltonen *et al.* (CDF Collab.)
AALTONEN 10R PRL 105 081802 T. Aaltonen *et al.* (CDF Collab.)
AALTONEN 10Z PRL 105 191801 T. Aaltonen *et al.* (CDF Collab.)
ABAZOV 10L PL B693 95 V.M. Abazov *et al.* (D0 Collab.)
ABAZOV 10M PRL 105 191802 V.M. Abazov *et al.* (D0 Collab.)
ABAZOV 10N PRL 105 211802 V.M. Abazov *et al.* (D0 Collab.)
ABAZOV 10P PRL 105 221802 V.M. Abazov *et al.* (D0 Collab.)
ABDO 10 JCAP 1004 014 A.A. Abdo *et al.* (Fermi-LAT Collab.)
ACKERMANN 10 JCAP 1005 025 M. Ackermann (Fermi-LAT Collab.)
AHMED 10 SCI 327 1619 Z. Ahmed *et al.* (CDMS II Collab.)
ARMENGAUD 10 PL B687 294 E. Armengaud *et al.* (EDELWEISS II Collab.)
ELLIS 10 EPJ C69 201 J. Ellis, A. Mustafayev, K. Olive
ABAZOV 09M PRL 102 161802 V.M. Abazov *et al.* (D0 Collab.)
ABBASI 09B PRL 102 201302 R. Abbasi *et al.* (IceCube Collab.)
AHMED 09 PRL 102 011301 Z. Ahmed *et al.* (CDMS Collab.)
ANGLOHER 09 ASP 31 270 G. Angloher *et al.* (CRESST Collab.)
BUCHMUEL... 09 EPJ C64 391 O. Buchmueller *et al.* (LOIC, FNAL, CERN+)
DREINER 09 EPJ C62 547 H. Dreiner *et al.*
LEBEDENKO 09 PR D80 052010 V.N. Lebedenko *et al.* (ZEPLIN-III Collab.)
LEBEDENKO 09A PRL 103 151302 V.N. Lebedenko *et al.* (ZEPLIN-III Collab.)
SORENSEN 09 NIM A601 339 P. Sorensen *et al.* (XENON10 Collab.)
ABAZOV 08F PL B659 856 V.M. Abazov *et al.* (D0 Collab.)
ANGLE 08 PRL 100 021303 J. Angle *et al.* (XENON10 Collab.)
ANGLE 08A PRL 101 091301 J. Angle *et al.* (XENON10 Collab.)
BEDNYAKOV 08 PAN 71 111 V.A. Bednyakov, H.P. Klapdor-Kleingrothaus, I.V. Krivosheina
Translated from YAF 71 112.
BEHNKE 08 SCI 319 933 E. Behnke (COUPP Collab.)
BENETTI 08 ASP 28 495 P. Benetti *et al.* (WARP Collab.)
BUCHMUEL... 08 JHEP 0809 117 O. Buchmueller *et al.*
ELLIS 08 PR D78 075012 J. Ellis, K. Olive, P. Sandick (CERN, MINN)
ABULENCIA 07H PR 98 131804 A. Abulencia *et al.* (CDF Collab.)
ALNER 07A ASP 28 287 G.J. Alner *et al.* (ZEPLIN-II Collab.)
CALIBBI 07 JHEP 0709 081 L. Calibbi *et al.*
ELLIS 07 JHEP 0706 079 J. Ellis, K. Olive, P. Sandick (CERN, MINN)
LEE 07A PRL 99 091301 H.S. Lee *et al.* (KIMS Collab.)
ABBIENDI 06B EPJ C46 307 G. Abbiendi *et al.* (OPAL Collab.)
ACHTERBERG 06 ASP 26 129 A. Achterberg *et al.* (AMANDA Collab.)
ACKERMANN 06 ASP 24 459 M. Ackermann *et al.* (AMANDA Collab.)
AKERIB 06 PR D73 011102 D.S. Akerib *et al.* (CDMS Collab.)
AKERIB 06A PRL 96 011302 D.S. Akerib *et al.* (CDMS Collab.)
ALLANACH 06 PR D73 015013 B.C. Allanach *et al.*
BENOIT 06 PL B637 156 A. Benoit *et al.*
DE-AUSTRI 06 JHEP 0605 002 R.R. de Austri, R. Trotta, L. Roszkowski
DEBOER 06 PL B636 13 W. de Boer *et al.*
LEP-SLC 06 PRPL 427 257 ALEPH, DELPHI, L3, OPAL, SLD and working groups
SHIMIZU 06A PL B633 195 Y. Shimizu *et al.*
SMITH 06 PL B642 567 N.J.T. Smith, A.S. Murphy, T.J. Summer
ABAZOV 05A PRL 94 041801 V.M. Abazov *et al.* (D0 Collab.)
ABDALLAH 05B EPJ C38 395 J. Abdallah *et al.* (DELPHI Collab.)
AKERIB 05 PR D72 052009 D.S. Akerib *et al.* (CDMS Collab.)
ALNER 05 PL B616 17 G.J. Alner *et al.* (UK Dark Matter Collab.)
ALNER 05A ASP 23 444 G.J. Alner *et al.* (UK Dark Matter Collab.)
ANGLOHER 05 ASP 23 325 G. Angloher *et al.* (CRESST-II Collab.)
BAER 05 JHEP 0507 065 H. Baer *et al.* (FSU, MSU, HAWA)
BARNABE-HE... 05 PL B624 186 M. Barnabe-Heider *et al.* (PICASSO Collab.)
ELLIS 05 PR D71 095007 J. Ellis *et al.*
SANGLARD 05 PR D71 122002 V. Sanglard *et al.* (EDELWEISS Collab.)
ABBIENDI 04 EPJ C32 453 G. Abbiendi *et al.* (OPAL Collab.)
ABBIENDI 04F EPJ C33 149 G. Abbiendi *et al.* (OPAL Collab.)
ABBIENDI 04H EPJ C35 1 G. Abbiendi *et al.* (OPAL Collab.)
ABBIENDI 04N PL B602 167 G. Abbiendi *et al.* (OPAL Collab.)
ABDALLAH 04H EPJ C34 145 J. Abdallah *et al.* (DELPHI Collab.)
ABDALLAH 04M EPJ C36 1 J. Abdallah *et al.* (DELPHI Collab.)
Also EPJ C37 129 (errat.) J. Abdallah *et al.* (DELPHI Collab.)
ACHARD 04 PL B580 37 P. Achard *et al.* (L3 Collab.)
ACHARD 04E PL B587 16 P. Achard *et al.* (L3 Collab.)
AKERIB 04 PRL 93 211301 D.S. Akerib *et al.* (CDMSII Collab.)
BALTZ 04 JHEP 0410 052 E. Baltz, P. Gondolo
BELANGER 04 JHEP 0403 012 G. Belanger *et al.*
BOTTINO 04 PR D69 037302 A. Bottino *et al.*
DESAI 04 PR D70 083523 S. Desai *et al.* (Super-Kamiokande Collab.)
ELLIS 04 PR D69 015005 J. Ellis *et al.*
ELLIS 04B PR D70 055005 J. Ellis *et al.*
HEISTER 04 PL B583 247 A. Heister *et al.* (ALEPH Collab.)
PIERCE 04A PR D70 075006 A. Pierce
ABBIENDI 03L PL B572 8 G. Abbiendi *et al.* (OPAL Collab.)
ABDALLAH 03M EPJ C31 421 J. Abdallah *et al.* (DELPHI Collab.)
AHMED 03 ASP 19 691 B. Ahmed *et al.* (UK Dark Matter Collab.)
AKERIB 03 PR D68 082002 D.S. Akerib *et al.* (CDMS Collab.)
BAER 03 JCAP 0305 006 H. Baer, C. Balazs
BAER 03A JCAP 0309 007 H. Baer *et al.*
BOTTINO 03 PR D68 043506 A. Bottino *et al.*
BOTTINO 03A PR D67 063519 A. Bottino, N. Fornengo, S. Scopel
CHATTOPAD... 03 PR D68 035005 U. Chattopadhyay, A. Corsetti, P. Nath
ELLIS 03 ASP 18 395 J. Ellis, K.A. Olive, Y. Santoso
ELLIS 03B NP B652 259 J. Ellis *et al.*
ELLIS 03C PL B565 176 J. Ellis *et al.*
ELLIS 03D PL B573 162 J. Ellis *et al.*
ELLIS 03E PR D67 123502 J. Ellis *et al.*
HEISTER 03C EPJ C28 1 A. Heister *et al.* (ALEPH Collab.)
HEISTER 03G EPJ C31 1 A. Heister *et al.* (ALEPH Collab.)
KLAPDOR-K... 03 ASP 18 525 H.V. Klapdor-Kleingrothaus *et al.*
LAHANAS 03 PL B568 55 A. Lahanas, D. Nanopoulos
TAKEDA 03 PL B572 145 A. Takeda *et al.*
ABRAMS 02 PR D66 122003 D. Abrams *et al.* (CDMS Collab.)
ACOSTA 02H PRL 89 281801 D. Acosta *et al.* (CDF Collab.)
ANGLOHER 02 ASP 18 43 G. Angloher *et al.* (CRESST Collab.)
ARNOWITT 02 hep-ph/0211417 R. Arnowitt, B. Dutta
BENOIT 02 PL B545 43 A. Benoit *et al.* (EDELWEISS Collab.)
ELLIS 02B PL B532 318 J. Ellis, A. Ferstl, K.A. Olive
HEISTER 02 PL B526 191 A. Heister *et al.* (ALEPH Collab.)
HEISTER 02E PL B526 206 A. Heister *et al.* (ALEPH Collab.)
HEISTER 02J PL B533 223 A. Heister *et al.* (ALEPH Collab.)
HEISTER 02N PL B544 73 A. Heister *et al.* (ALEPH Collab.)
KIM 02 PL B527 18 H.B. Kim *et al.*
KIM 02B JHEP 0212 034 Y.G. Kim *et al.*
LAHANAS 02 EPJ C23 185 A. Lahanas, V.C. Spanos
MORALES 02B ASP 16 325 A. Morales *et al.* (COSME Collab.)
MORALES 02C PL B532 8 A. Morales *et al.* (IGEX Collab.)
ABREU 01 EPJ C19 29 P. Abreu *et al.* (DELPHI Collab.)
ABREU 01B EPJ C19 201 P. Abreu *et al.* (DELPHI Collab.)
BALTZ 01 PR 86 5004 E. Baltz, P. Gondolo
BARATE 01 PL B499 67 R. Barate *et al.* (ALEPH Collab.)
BARATE 01B EPJ C19 415 R. Barate *et al.* (ALEPH Collab.)
BARGER 01C PL B518 117 V. Barger, C. Kao
BAUDIS 01 PR D63 022001 L. Baudis *et al.* (Heidelberg-Moscow Collab.)
BENOIT 01 PL B513 15 A. Benoit *et al.* (EDELWEISS Collab.)
BERNABEI 01 PL B509 197 R. Bernabei *et al.* (DAMA Collab.)
BOTTINO 01 PR D63 125003 A. Bottino *et al.*
CORSETTI 01 PR D64 125010 A. Corsetti, P. Nath

ELLIS 01B PL B510 236 J. Ellis *et al.*
ELLIS 01C PR D63 065016 J. Ellis, A. Ferstl, K.A. Olive
GOMEZ 01 PL B512 252 M.E. Gomez, J.D. Vergados
LAHANAS 01 PL B518 94 A. Lahanas, D.V. Nanopoulos, V. Spanos
ABBIENDI 00 EPJ C12 1 G. Abbiendi *et al.* (OPAL Collab.)
ABBIENDI 00G EPJ C14 51 G. Abbiendi *et al.* (OPAL Collab.)
ABBIENDI 00H EPJ C14 187 G. Abbiendi *et al.* (OPAL Collab.)
Also EPJ C16 707 (errat.) G. Abbiendi *et al.* (OPAL Collab.)
ABBIENDI,G 00D EPJ C18 253 G. Abbiendi *et al.* (OPAL Collab.)
ABREU 00J PL B479 129 P. Abreu *et al.* (DELPHI Collab.)
ABREU 00Q PL B478 65 P. Abreu *et al.* (DELPHI Collab.)
ABREU 00T PL B485 95 P. Abreu *et al.* (DELPHI Collab.)
ABREU 00U PL B487 36 P. Abreu *et al.* (DELPHI Collab.)
ABREU 00V EPJ C16 211 P. Abreu *et al.* (DELPHI Collab.)
ABREU 00W PL B489 38 P. Abreu *et al.* (DELPHI Collab.)
ABREU 00Z EPJ C17 53 P. Abreu *et al.* (DELPHI Collab.)
ABUSAIDI 00 PRL 84 5699 R. Abusaidi *et al.* (CDMS Collab.)
ACCIARRI 00D PL B472 420 M. Acciarri *et al.* (L3 Collab.)
ACCOMANDO 00 NP B585 124 E. Accomando *et al.*
BERNABEI 00 PL B480 23 R. Bernabei *et al.* (DAMA Collab.)
BERNABEI 00C EPJ C18 283 R. Bernabei *et al.* (DAMA Collab.)
BERNABEI 00D NJP 2 15 R. Bernabei *et al.* (DAMA Collab.)
BOEHM 00B PR D62 035012 C. Boehm, A. Djouadi, M. Drees
ELLIS 00 PR D62 075010 J. Ellis *et al.*
FENG 00 PL B482 388 J.L. Feng, K.T. Matchev, F. Wilczek
LEP 00 CERN-EP-2000-016 LEP Collabs. (ALEPH, DELPHI, L3, OPAL, SLD+)
MORALES 00 PL B489 268 A. Morales *et al.* (IGEX Collab.)
PDG 00 EPJ C15 1 D.E. Groom *et al.* (PDG Collab.)
SPOONER 00 PL B473 330 N.J.C. Spooner *et al.* (UK Dark Matter Col.)
ACCIARRI 99H PL B456 283 M. Acciarri *et al.* (L3 Collab.)
ACCIARRI 99R PL B470 268 M. Acciarri *et al.* (L3 Collab.)
ACCIARRI 99W PL B471 280 M. Acciarri *et al.* (L3 Collab.)
AMBROSIO 99 PR D60 082002 M. Ambrosio *et al.* (Macro Collab.)
BAUDIS 99 PR D59 022001 L. Baudis *et al.* (Heidelberg-Moscow Collab.)
BELLI 99C NP B563 97 P. Belli *et al.* (DAMA Collab.)
OOTANI 99 PL B461 371 W. Ootani *et al.*
ABREU 98P PL B444 491 P. Abreu *et al.* (DELPHI Collab.)
ACCIARRI 98F EPJ C4 207 M. Acciarri *et al.* (L3 Collab.)
ACKERSTAFF 98P PL B433 195 K. Ackerstaff *et al.* (OPAL Collab.)
BARATE 98K PL B433 176 R. Barate *et al.* (ALEPH Collab.)
BARATE 98S EPJ C4 433 R. Barate *et al.* (ALEPH Collab.)
BERNABEI 98C PL B436 379 R. Bernabei *et al.* (DAMA Collab.)
ELLIS 98 PR D58 095002 J. Ellis *et al.*
ELLIS 98B PL B444 367 J. Ellis, T. Falk, K. Olive
PDG 98 EPJ C3 1 C. Caso *et al.* (PDG Collab.)
BAER 97 PR D57 567 H. Baer, M. Brhlik
BERNABEI 97 ASP 7 73 R. Bernabei *et al.* (DAMA Collab.)
EDSJO 97 PR D56 1879 J. Edsjo, P. Gondolo
ARNOWITT 96 PR D54 2374 R. Arnowitt, P. Nath
BAER 96 PR D53 597 H. Baer, M. Brhlik
BERGSTROM 96 ASP 5 263 L. Bergstrom, P. Gondolo
LEWIN 96 ASP 6 87 J.D. Lewin, P.F. Smith
BEREZINSKY 95 ASP 5 1 V. Berezinsky *et al.*
FALK 95 PL B354 99 T. Falk, K.A. Olive, M. Srednicki (MINN, UCSB)
LOSECCO 95 PL B342 392 J.M. LoSecco (NDAM)
ADRIANI 93M PRPL 236 1 O. Adriani *et al.* (L3 Collab.)
DREES 93 PR D47 376 M. Drees, M.M. Nojiri (DESY, SLAC)
DREES 93B PR D48 3483 M. Drees, M.M. Nojiri
FALK 93 PL B318 354 T. Falk *et al.* (UCB, UCSB, MINN)
KELLEY 93 PR D47 2461 S. Kelley *et al.* (TAMU, ALAH)
MIZUTA 93 PL B298 120 S. Mizuta, M. Yamaguchi (TOHO)
MORI 93 PR D48 5505 M. Mori *et al.* (KEK, NIIG, TOKY, TOKA+)
BOTTINO 92 MPL A7 733 A. Bottino *et al.* (TORI, ZARA)
Also PL B265 57 A. Bottino *et al.* (TORI, INFN)
DECAMP 92 PRPL 216 253 D. Decamp *et al.* (ALEPH Collab.)
LOPEZ 92 NP B370 445 J.L. Lopez, D.V. Nanopoulos, K.J. Yuan (TAMU)
MCDONALD 92 PL B283 80 J. McDonald, K.A. Olive, M. Srednicki (LISB+)
ABREU 91F NP B367 511 P. Abreu *et al.* (DELPHI Collab.)
ALEXANDER 91F ZPHY C52 175 G. Alexander *et al.* (OPAL Collab.)
BOTTINO 91 PL B265 57 A. Bottino *et al.* (TORI, INFN)
GELMINI 91 NP B351 623 G.B. Gelmini, P. Gondolo, E. Roulet (UCLA, TRST)
GRIEST 91 PR D43 3191 K. Griest, D. Seckel
KAMIONKOW...91 PR D44 3021 M. Kamionkowski (CHIC, FNAL)
MORI 91B PL B270 89 M. Mori *et al.* (Kamiokande Collab.)
NOJIRI 91 PL B261 76 M.M. Nojiri (KEK)
OLIVE 91 NP B355 208 K.A. Olive, M. Srednicki (MINN, UCSB)
ROSZKOWSKI 91 PR D41 3565 L. Roszkowski (CERN)
GRIEST 90 PR D41 3565 K. Griest, M. Kamionkowski, M.S. Turner (UCB+)
BARBIERI 89C NP B313 725 R. Barbieri, M. Frigeni, G. Giudice
OLIVE 89 PL B230 78 K.A. Olive, M. Srednicki (MINN, UCSB)
ELLIS 88D NP B307 883 J. Ellis, R. Flores
GRIEST 88B PR D38 2357 K. Griest
OLIVE 88 PL B205 553 K.A. Olive, M. Srednicki (MINN, UCSB)
SREDNICKI 88 NP B310 693 M. Srednicki, R. Watkins, K.A. Olive (MINN, UCSB)
ELLIS 84 NP B238 453 J. Ellis *et al.* (CERN)
GOLDBERG 83 PRL 50 1419 H. Goldberg (NEAS)
KRAUSS 83 NP B227 556 L.M. Krauss (HARV)
VYSOTSKII 83 SJNP 37 948 M.I. Vysotsky (ITEP)
Translated from YAF 37 1597.

Technicolor

See the related review(s):

Dynamical Electroweak Symmetry Breaking: Implications of the H^0

The latest unpublished results are described in "Dynamical Electroweak Symmetry Breaking" review.

MASS LIMITS for Resonances in Models of Dynamical Electroweak Symmetry Breaking

VALUE (GeV)	CL%	DOCUMENT ID		TECN	COMMENT
• • • We do not use the following data for averages, fits, limits, etc. • • •					
		[1] AAD	16W	ATLS	color octet vector resonance
>2400	95	[2] KHACHATRY...	16E	CMS	top-color Z'
		[3] AAD	15AB	ATLS	$h \to \pi_V \pi_V$
>1800	95	[4] AAD	15AO	ATLS	top-color Z'
		[5] AAD	15BB	ATLS	$pp \to \rho_T/a_{1T} \to Wh$ or Zh
		[6] AAD	15Q	ATLS	$h \to \pi_V \pi_V$
		[7] AAIJ	15AN	LHCB	$h \to \pi_V \pi_V$
>1140	95	[8] KHACHATRY...	15C	CMS	$\rho_T \to WZ$
		[9] KHACHATRY...	15W	CMS	$H \to \pi_V \pi_V$
none 200–700, 750–890	95	[10] AAD	14AT	ATLS	$pp \to \omega_T \to Z\gamma$
none 275–960	95	[10] AAD	14AT	ATLS	$pp \to a_T \to W\gamma$
		[11] AAD	14V	ATLS	color singlet techni-vector
> 703		[12] AAD	13AN	ATLS	$pp \to a_T \to W\gamma$
> 494		[13] AAD	13AN	ATLS	$pp \to \omega_T \to Z\gamma$
none 500–1740	95	[14] AAD	13AQ	ATLS	top-color Z'
>1300	95	[15] CHATRCHYAN	13AP	CMS	top-color Z'
>2100	95	[14] CHATRCHYAN	13BM	CMS	top-color Z'
		[16] BAAK	12	RVUE	QCD-like technicolor
none 167–687	95	[17] CHATRCHYAN	12AF	CMS	$\rho_T \to WZ$
> 805	95	[14] AALTONEN	11AD	CDF	top-color Z'
> 805	95	[14] AALTONEN	11AE	CDF	top-color Z'
		[18] CHIVUKULA	11	RVUE	top-Higgs
		[19] CHIVUKULA	11A	RVUE	techini-π
		[20] AALTONEN	10I	CDF	$p\overline{p} \to \rho_T/\omega_T \to W\pi_T$
none 208–408	95	[21] ABAZOV	10A	D0	$\rho_T \to WZ$
		[22] ABAZOV	07I	D0	$p\overline{p} \to \rho_T/\omega_T \to W\pi_T$
> 280	95	[23] ABULENCIA	05A	CDF	$\rho_T \to e^+e^-, \mu^+\mu^-$
		[24] CHEKANOV	02B	ZEUS	color octet techni-π
> 207	95	[25] ABAZOV	01B	D0	$\rho_T \to e^+e^-$
none 90–206.7	95	[26] ABDALLAH	01	DLPH	$e^+e^- \to \rho_T$
		[27] AFFOLDER	00F	CDF	color-singlet techni-ρ, $\rho_T \to W\pi_T, 2\pi_T$
> 600	95	[28] AFFOLDER	00K	CDF	color-octet techni-ρ, $\rho_{T8} \to 2\pi_{LQ}$
none 350–440	95	[29] ABE	99F	CDF	color-octet techni-ρ, $\rho_{T8} \to \overline{b}b$
		[30] ABE	99N	CDF	techni-ω, $\omega_T \to \gamma\overline{b}b$
none 260–480	95	[31] ABE	97G	CDF	color-octet techni-ρ, $\rho_{T8} \to$ 2jets

[1] AAD 16W search for color octet vector resonance decaying to bB in pp collisions at $\sqrt{s}$ = 8 TeV. The vector like quark B is assumed to decay to bH. See their Fig.3 and Fig.4 for limits on $\sigma \cdot B$.

[2] KHACHATRYAN 16E search for top-color Z' decaying to $t\overline{t}$. The quoted limit is for $\Gamma_{Z'}/m_{Z'} = 0.012$. Also exclude $m_{Z'} < 2.9$ TeV for wider topcolor Z' with $\Gamma_{Z'}/m_{Z'} = 0.1$.

[3] AAD 15AB search for long-lived hidden valley π_V particles which are produced in pairs by the decay of a scalar boson. π_V is assumed to decay into dijets. See their Fig. 10 for the limit on σB.

[4] AAD 15AO search for top-color Z' decaying to $t\overline{t}$. The quoted limit is for $\Gamma_{Z'}/m_{Z'} = 0.012$.

[5] AAD 15BB search for minimal walking technicolor (MWT) isotriplet vector and axial-vector resonances decaying to Wh or Zh. See their Fig. 3 for the exclusion limit in the MWT parameter space.

[6] AAD 15Q search for long-lived hidden valley π_V particles which are produced in pairs by the decay of scalar boson. π_V is assumed to decay into dijets. See their Fig. 5 and Fig. 6 for the limit on σB.

[7] AAIJ 15AN search for long-lived hidden valley π_V particles which are produced in pairs by the decay of scalar boson with a mass of 120GeV. π_V is assumed to decay into dijets. See their Fig. 4 for the limit on σB.

[8] KHACHATRYAN 15C search for a vector techni-resonance decaying to WZ. The limit assumes $M_{\pi_T} = (3/4)\ M_{\rho_T} - 25$ GeV. See their Fig.3 for the limit in $M_{\pi_T} - M_{\rho_T}$ plane of the low scale technicolor model.

[9] KHACHATRYAN 15W search for long-lived hidden valley π_V particles which are produced in pairs in the decay of heavy higgs boson H. π_V is assumed to decay into $\ell^+\ell^-$. See their Fig. 7 and Fig. 8 for the limits on σB.

[10] AAD 14AT search for techni-ω and techni-a resonances decaying to $V\gamma$ with $V = W(\to \ell\nu)$ or $Z(\to \ell^+\ell^-)$.

[11] AAD 14V search for vector techni-resonances decaying into electron or muon pairs in pp collisions at $\sqrt{s} = 8$ TeV. See their table IX for exclusion limits with various assumptions.

[12] AAD 13AN search for vector techni-resonance a_T decaying into $W\gamma$.

[13] AAD 13AN search for vector techni-resonance ω_T decaying into $Z\gamma$.

[14] Search for top-color Z' decaying to $t\overline{t}$. The quoted limit is for $\Gamma_{Z'}/m_{Z'} = 0.012$.

[15] CHATRCHYAN 13AP search for top-color leptophobic Z' decaying to $t\overline{t}$. The quoted limit is for $\Gamma_{Z'}/m_{Z'} = 0.012$.

[16] BAAK 12 give electroweak oblique parameter constraints on the QCD-like technicolor models. See their Fig. 28.

[17] CHATRCHYAN 12AF search for a vector techni-resonance decaying to WZ. The limit assumes $M_{\pi_T} = (3/4)\ M_{\rho_T} - 25$ GeV. See their Fig. 3 for the limit in $M_{\pi_T} - M_{\rho_T}$ plane of the low scale technicolor model.

[18] Using the LHC limit on the Higgs boson production cross section, CHIVUKULA 11 obtain a limit on the top-Higgs mass > 300 GeV at 95% CL assuming 150 GeV top-pion mass.

[19] Using the LHC limit on the Higgs boson production cross section, CHIVUKULA 11A obtain a limit on the techinipion mass ruling out the region 110 GeV $< m_P < 2m_t$. Existence of color techni-fermions, top-color mechanism, and $N_{TC} \geq 3$ are assumed.

[20] AALTONEN 10I search for the vector techni-resonances (ρ_T, ω_T) decaying into $W\pi_T$ with $W \to \ell\nu$ and $\pi_T \to b\overline{b}$, $b\overline{c}$, or $b\overline{u}$. See their Fig. 3 for the exclusion plot in $M_{\pi_T} - M_{\rho_T}$ plane.

[21] ABAZOV 10A search for a vector techni-resonance decaying into WZ. The limit assumes $M_{\rho_T} < M_{\pi_T} + M_W$.

[22] ABAZOV 07I search for the vector techni-resonances (ρ_T, ω_T) decaying into $W\pi_T$ with $W \to e\nu$ and $\pi_T \to b\overline{b}$ or $b\overline{c}$. See their Fig. 2 for the exclusion plot in $M_{\pi_T} - M_{\rho_T}$ plane.

[23] ABULENCIA 05A search for resonances decaying to electron or muon pairs in $p\overline{p}$ collisions. at $\sqrt{s} = 1.96$ TeV. The limit assumes Technicolor-scale mass parameters $M_V = M_A = 500$ GeV.

[24] CHEKANOV 02B search for color octet techni-π P decaying into dijets in ep collisions. See their Fig. 5 for the limit on $\sigma(ep \to eP X)\cdot B(P \to 2j)$.

[25] ABAZOV 01B searches for vector techni-resonances (ρ_T, ω_T) decaying to e^+e^-. The limit assumes $M_{\rho_T} = M_{\omega_T} < M_{\pi_T} + M_W$.

[26] The limit is independent of the π_T mass. See their Fig. 9 and Fig. 10 for the exclusion plot in the $M_{\rho_T} - M_{\pi_T}$ plane. ABDALLAH 01 limit on the techni-pion mass is $M_{\pi_T} > 79.8$ GeV for $N_D = 2$, assuming its point-like coupling to gauge bosons.

[27] AFFOLDER 00F search for ρ_T decaying into $W\pi_T$ or $\pi_T\pi_T$ with $W \to \ell\nu$ and $\pi_T \to \overline{b}b, \overline{b}c$. See Fig. 1 in the above Note on "Dynamical Electroweak Symmetry Breaking" for the exclusion plot in the $M_{\rho_T} - M_{\pi_T}$ plane.

[28] AFFOLDER 00K search for the ρ_{T8} decaying into $\pi_{LQ}\pi_{LQ}$ with $\pi_{LQ} \to b\nu$. For $\pi_{LQ} \to c\nu$, the limit is $M_{\rho_{T8}} > 510$ GeV. See their Fig. 2 and Fig. 3 for the exclusion plot in the $M_{\rho_{T8}} - M_{\pi_{LQ}}$ plane.

[29] ABE 99F search for a new particle X decaying into $b\overline{b}$ in $p\overline{p}$ collisions at $E_{cm} = 1.8$ TeV. See Fig. 7 in the above Note on "Dynamical Electroweak Symmetry Breaking" for the upper limit on $\sigma(p\overline{p} \to X)\times B(X \to b\overline{b})$. ABE 99F also exclude top gluons of width $\Gamma = 0.3M$ in the mass interval $280 < M < 670$ GeV, of width $\Gamma = 0.5M$ in the mass interval $340 < M < 640$ GeV, and of width $\Gamma = 0.7M$ in the mass interval $375 < M < 560$ GeV.

[30] ABE 99N search for the techni-ω decaying into $\gamma\pi_T$. The technipion is assumed to decay $\pi_T \to b\overline{b}$. See Fig. 2 in the above Note on "Dynamical Electroweak Symmetry Breaking" for the exclusion plot in the $M_{\omega_T} - M_{\pi_T}$ plane.

[31] ABE 97G search for a new particle X decaying into dijets in $p\overline{p}$ collisions at $E_{cm} = 1.8$ TeV. See Fig. 5 in the above Note on "Dynamical Electroweak Symmetry Breaking" for the upper limit on $\sigma(p\overline{p} \to X)\times B(X \to 2j)$.

REFERENCES FOR Technicolor

AAD	16W	PL B758 249	G. Aad *et al.*	(ATLAS Collab.)
KHACHATRY...	16E	PR D93 012001	V. Khachatryan *et al.*	(CMS Collab.)
AAD	15AB	PR D92 012010	G. Aad *et al.*	(ATLAS Collab.)
AAD	15AO	JHEP 1508 148	G. Aad *et al.*	(ATLAS Collab.)
AAD	15BB	EPJ C75 263	G. Aad *et al.*	(ATLAS Collab.)
AAD	15Q	PL B743 15	G. Aad *et al.*	(ATLAS Collab.)
AAIJ	15AN	EPJ C75 152	R. Aaij *et al.*	(LHCb Collab.)
KHACHATRY...	15C	PL B740 83	V. Khachatryan *et al.*	(CMS Collab.)
KHACHATRY...	15W	PR D91 052012	V. Khachatryan *et al.*	(CMS Collab.)
AAD	14AT	PL B738 428	G. Aad *et al.*	(ATLAS Collab.)
AAD	14V	PR D90 052005	G. Aad *et al.*	(ATLAS Collab.)
AAD	13AN	PR D87 112003	G. Aad *et al.*	(ATLAS Collab.)
Also		PR D91 119901 (errat.)	G. Aad *et al.*	(ATLAS Collab.)
AAD	13AQ	PR D88 012004	G. Aad *et al.*	(ATLAS Collab.)
CHATRCHYAN	13AP	PR D87 072002	S. Chatrchyan *et al.*	(CMS Collab.)
CHATRCHYAN	13BM	PRL 111 211804	S. Chatrchyan *et al.*	(CMS Collab.)
Also		PRL 112 119903 (errat.)	S. Chatrchyan *et al.*	(CMS Collab.)
BAAK	12	EPJ C72 2003	M. Baak *et al.*	(Gfitter Group)
CHATRCHYAN	12AF	PRL 109 141801	S. Chatrchyan *et al.*	(CMS Collab.)
AALTONEN	11AD	PR D84 072003	T. Aaltonen *et al.*	(CDF Collab.)
AALTONEN	11AE	PR D84 072004	T. Aaltonen *et al.*	(CDF Collab.)
CHIVUKULA	11	PR D84 095022	R.S. Chivukula *et al.*	
CHIVUKULA	11A	PR D84 115025	R. S. Chivukula *et al.*	
AALTONEN	10I	PRL 104 111802	T. Aaltonen *et al.*	(CDF Collab.)
ABAZOV	10A	PRL 104 061801	V.M. Abazov *et al.*	(D0 Collab.)
ABAZOV	07I	PRL 98 221801	V.M. Abazov *et al.*	(D0 Collab.)
ABULENCIA	05A	PRL 95 252001	A. Abulencia *et al.*	(CDF Collab.)
CHEKANOV	02B	PL B531 9	S. Chekanov *et al.*	(ZEUS Collab.)
ABAZOV	01B	PRL 87 061802	V.M. Abazov *et al.*	(D0 Collab.)
ABDALLAH	01	EPJ C22 17	J. Abdallah *et al.*	(DELPHI Collab.)
AFFOLDER	00F	PRL 84 1110	T. Affolder *et al.*	(CDF Collab.)
AFFOLDER	00K	PRL 85 2056	T. Affolder *et al.*	(CDF Collab.)
ABE	99F	PRL 82 2038	F. Abe *et al.*	(CDF Collab.)
ABE	99N	PRL 83 3124	F. Abe *et al.*	(CDF Collab.)
ABE	97G	PR D55 5263	F. Abe *et al.*	(CDF Collab.)

Quark and Lepton Compositeness, Searches for

The latest unpublished results are described in the "Quark and Lepton Compositeness" review.

See the related review(s):

Searches for Quark and Lepton Compositeness

CONTENTS:

SCALE LIMITS for Contact Interactions: $\Lambda(eeee)$

Limits are for $\Lambda^{\pm}_{LL}$ only. For other cases, see each reference.

Λ^+_{LL}(TeV)	Λ^-_{LL}(TeV)	CL%	DOCUMENT ID		TECN	COMMENT
>8.3	**>10.3**	95	[1] BOURILKOV	01	RVUE	E_{cm}= 192–208 GeV
• • • We do not use the following data for averages, fits, limits, etc. • • •						
>4.5	>7.0	95	[2] SCHAEL	07A	ALEP	E_{cm}= 189–209 GeV
>5.3	>6.8	95	ABDALLAH	06C	DLPH	E_{cm}= 130–207 GeV
>4.7	>6.1	95	[3] ABBIENDI	04G	OPAL	E_{cm}= 130–207 GeV
>4.3	>4.9	95	ACCIARRI	00P	L3	E_{cm}= 130–189 GeV

[1] A combined analysis of the data from ALEPH, DELPHI, L3, and OPAL.
[2] SCHAEL 07A limits are from R_c, Q^{depl}_{FB}, and hadronic cross section measurements.
[3] ABBIENDI 04G limits are from $e^+e^- \to e^+e^-$ cross section at $\sqrt{s}$ = 130–207 GeV.

SCALE LIMITS for Contact Interactions: $\Lambda(ee\mu\mu)$

Limits are for $\Lambda^{\pm}_{LL}$ only. For other cases, see each reference.

Λ^+_{LL}(TeV)	Λ^-_{LL}(TeV)	CL%	DOCUMENT ID		TECN	COMMENT
>6.6	**>9.5**	95	[1] SCHAEL	07A	ALEP	E_{cm}= 189–209 GeV
> 8.5	>3.8	95	ACCIARRI	00P	L3	E_{cm}= 130–189 GeV
• • • We do not use the following data for averages, fits, limits, etc. • • •						
>7.3	>7.6	95	ABDALLAH	06C	DLPH	E_{cm}= 130–207 GeV
>8.1	>7.3	95	[2] ABBIENDI	04G	OPAL	E_{cm}= 130–207 GeV

[1] SCHAEL 07A limits are from R_c, Q^{depl}_{FB}, and hadronic cross section measurements.
[2] ABBIENDI 04G limits are from $e^+e^- \to \mu\mu$ cross section at $\sqrt{s}$ = 130–207 GeV.

SCALE LIMITS for Contact Interactions: $\Lambda(ee\tau\tau)$

Limits are for $\Lambda^{\pm}_{LL}$ only. For other cases, see each reference.

Λ^+_{LL}(TeV)	Λ^-_{LL}(TeV)	CL%	DOCUMENT ID		TECN	COMMENT
>7.9	>5.8	95	[1] SCHAEL	07A	ALEP	E_{cm}= 189–209 GeV
>7.9	>4.6	95	ABDALLAH	06C	DLPH	E_{cm}= 130–207 GeV
>4.9	**>7.2**	95	[2] ABBIENDI	04G	OPAL	E_{cm}= 130–207 GeV
• • • We do not use the following data for averages, fits, limits, etc. • • •						
>5.4	>4.7	95	ACCIARRI	00P	L3	E_{cm}= 130–189 GeV

[1] SCHAEL 07A limits are from R_c, Q^{depl}_{FB}, and hadronic cross section measurements.
[2] ABBIENDI 04G limits are from $e^+e^- \to \tau\tau$ cross section at $\sqrt{s}$ = 130–207 GeV.

SCALE LIMITS for Contact Interactions: $\Lambda(\ell\ell\ell\ell)$

Lepton universality assumed. Limits are for $\Lambda^{\pm}_{LL}$ only. For other cases, see each reference.

Λ^+_{LL}(TeV)	Λ^-_{LL}(TeV)	CL%	DOCUMENT ID		TECN	COMMENT
>7.9	**> 10.3**	95	[1] SCHAEL	07A	ALEP	E_{cm}= 189–209 GeV
>9.1	>8.2	95	ABDALLAH	06C	DLPH	E_{cm}= 130–207 GeV
• • • We do not use the following data for averages, fits, limits, etc. • • •						
>7.7	>9.5	95	[2] ABBIENDI	04G	OPAL	E_{cm}= 130–207 GeV
			[3] BABICH	03	RVUE	
>9.0	>5.2	95	ACCIARRI	00P	L3	E_{cm}= 130–189 GeV

[1] SCHAEL 07A limits are from R_c, Q^{depl}_{FB}, and hadronic cross section measurements.
[2] ABBIENDI 04G limits are from $e^+e^- \to \ell^+\ell^-$ cross section at $\sqrt{s}$ = 130–207 GeV.
[3] BABICH 03 obtain a bound -0.175 TeV$^{-2} < 1/\Lambda^2_{LL} < 0.095$ TeV^{-2} (95%CL) in a model independent analysis allowing all of Λ_{LL}, Λ_{LR}, Λ_{RL}, Λ_{RR} to coexist.

SCALE LIMITS for Contact Interactions: $\Lambda(eeqq)$

Limits are for $\Lambda^{\pm}_{LL}$ only. For other cases, see each reference.

Λ^+_{LL}(TeV)	Λ^-_{LL}(TeV)	CL%	DOCUMENT ID		TECN	COMMENT
>24	**>37**	95	[1] AABOUD	17AT	ATLS	$(eeqq)$
> 8.4	**>10.2**	95	[2] ABDALLAH	09	DLPH	$(eebb)$
> 9.4	**>5.6**	95	[3] SCHAEL	07A	ALEP	$(eecc)$
> 9.4	>4.9	95	[2] SCHAEL	07A	ALEP	$(eebb)$
>23.3	**>12.5**	95	[4] CHEUNG	01B	RVUE	$(eeuu)$
>11.1	**>26.4**	95	[4] CHEUNG	01B	RVUE	$(eedd)$

• • • We do not use the following data for averages, fits, limits, etc. • • •

>15.5	>19.5	95	[5] AABOUD	16U	ATLS	$(eeqq)$
>13.5	>18.3	95	[6] KHACHATRY...	15AE	CMS	$(eeqq)$
>16.4	>20.7	95	[7] AAD	14BE	ATLS	$(eeqq)$
> 9.5	>12.1	95	[8] AAD	13E	ATLS	$(eeqq)$
>10.1	>9.4	95	[9] AAD	12AB	ATLS	$(eeqq)$
> 4.2	>4.0	95	[10] AARON	11C	H1	$(eeqq)$
> 3.8	>3.8	95	[11] ABDALLAH	11	DLPH	$(eetc)$
>12.9	>7.2	95	[12] SCHAEL	07A	ALEP	$(eeqq)$
> 3.7	>5.9	95	[13] ABULENCIA	06L	CDF	$(eeqq)$

[1] AABOUD 17AT limits are from pp collisions at $\sqrt{s} = 13$ TeV. The quoted limit uses a uniform positive prior in $1/\Lambda^2$.

[2] ABDALLAH 09 and SCHAEL 07A limits are from R_b, A^b_{FB}.

[3] SCHAEL 07A limits are from R_c, Q^{depl}_{FB}, and hadronic cross section measurements.

[4] CHEUNG 01B is an update of BARGER 98E.

[5] AABOUD 16U limits are from pp collisions at $\sqrt{s} = 13$ TeV. The quoted limit uses a uniform positive prior in $1/\Lambda^2$.

[6] KHACHATRYAN 15AE limit is from e^+e^- mass distribution in pp collisions at $E_{cm} = 8$ TeV.

[7] AAD 14BE limits are from pp collisions at $\sqrt{s} = 8$ TeV. The quoted limit uses a uniform positive prior in $1/\Lambda^2$.

[8] AAD 13E limis are from e^+e^- mass distribution in pp collisions at $E_{cm} = 7$ TeV.

[9] AAD 12AB limis are from e^+e^- mass distribution in pp collisions at $E_{cm} = 7$ TeV.

[10] AARON 11C limits are from Q^2 spectrum measurements of $e^\pm p \to e^\pm X$.

[11] ABDALLAH 11 limit is from $e^+e^- \to t\overline{c}$ cross section. $\Lambda_{LL} = \Lambda_{LR} = \Lambda_{RL} = \Lambda_{RR}$ is assumed.

[12] SCHAEL 07A limit assumes quark flavor universality of the contact interactions.

[13] ABULENCIA 06L limits are from $p\overline{p}$ collisions at $\sqrt{s} = 1.96$ TeV.

SCALE LIMITS for Contact Interactions: $\Lambda(\mu\mu qq)$

Λ^+_{LL}(TeV)	Λ^-_{LL}(TeV)	CL%	DOCUMENT ID		TECN	COMMENT
>20	**>30**	95	[1] AABOUD	17AT	ATLS	$(\mu\mu qq)$

• • • We do not use the following data for averages, fits, limits, etc. • • •

>15.8	>21.8	95	[2] AABOUD	16U	ATLS	$(\mu\mu qq)$	
>12.0	>15.2	95	[3] KHACHATRY...	15AE	CMS	$(\mu\mu qq)$	
>12.5	>16.7	95	[4] AAD	14BE	ATLS	$(\mu\mu qq)$	
> 9.6	>12.9	95	[5] AAD	13E	ATLS	$(\mu\mu qq)$	(isosinglet)
> 9.5	>13.1	95	[6] CHATRCHYAN	13K	CMS	$(\mu\mu qq)$	(isosinglet)
> 8.0	>7.0	95	[7] AAD	12AB	ATLS	$(\mu\mu qq)$	(isosinglet)

[1] AABOUD 17AT limits are from pp collisions at $\sqrt{s} = 13$ TeV. The quoted limit uses a uniform positive prior in $1/\Lambda^2$.

[2] AABOUD 16U limits are from pp collisions at $\sqrt{s} = 13$ TeV. The quoted limit uses a uniform positive prior in $1/\Lambda^2$.

[3] KHACHATRYAN 15AE limit is from $\mu^+\mu^-$ mass distribution in pp collisions at $E_{cm} = 8$ TeV.

[4] AAD 14BE limits are from pp collisions at $\sqrt{s} = 8$ TeV. The quoted limit uses a uniform positive prior in $1/\Lambda^2$.

[5] AAD 13E limis are from $\mu^+\mu^-$ mass distribution in pp collisions at $E_{cm} = 7$ TeV.

[6] CHATRCHYAN 13K limis are from $\mu^+\mu^-$ mass distribution in pp collisions at $E_{cm} = 7$ TeV.

[7] AAD 12AB limis are from $\mu^+\mu^-$ mass distribution in pp collisions at $E_{cm} = 7$ TeV.

SCALE LIMITS for Contact Interactions: $\Lambda(\ell\nu\ell\nu)$

VALUE (TeV)	CL%	DOCUMENT ID		TECN	COMMENT
>3.10	90	[1] JODIDIO	86	SPEC	$\Lambda^\pm_{LR}(\nu_\mu\nu_e\mu e)$

• • • We do not use the following data for averages, fits, limits, etc. • • •

>3.8	[2] DIAZCRUZ	94	RVUE	$\Lambda^+_{LL}(\tau\nu_\tau e\nu_e)$	
>8.1	[2] DIAZCRUZ	94	RVUE	$\Lambda^-_{LL}(\tau\nu_\tau e\nu_e)$	
>4.1	[3] DIAZCRUZ	94	RVUE	$\Lambda^+_{LL}(\tau\nu_\tau\mu\nu_\mu)$	
>6.5	[3] DIAZCRUZ	94	RVUE	$\Lambda^-_{LL}(\tau\nu_\tau\mu\nu_\mu)$	

[1] JODIDIO 86 limit is from $\mu^+ \to \overline{\nu}_\mu e^+\nu_e$. Chirality invariant interactions $L = (g^2/\Lambda^2)$ $[\eta_{LL}\ (\overline{\nu}_{\mu L}\gamma^\alpha\mu_L)\ (\overline{e}_L\gamma_\alpha\nu_{eL}) + \eta_{LR}\ (\overline{\nu}_{\mu L}\gamma^\alpha\nu_{eL}\ (\overline{e}_R\gamma_\alpha\mu_R)]$ with $g^2/4\pi = 1$ and $(\eta_{LL},\eta_{LR}) = (0,\pm1)$ are taken. No limits are given for $\Lambda^\pm_{LL}$ with $(\eta_{LL},\eta_{LR}) = (\pm1,0)$. For more general constraints with right-handed neutrinos and chirality nonconserving contact interactions, see their text.

[2] DIAZCRUZ 94 limits are from $\Gamma(\tau \to e\nu\nu)$ and assume flavor-dependent contact interactions with $\Lambda(\tau\nu_\tau e\nu_e) \ll \Lambda(\mu\nu_\mu e\nu_e)$.

[3] DIAZCRUZ 94 limits are from $\Gamma(\tau \to \mu\nu\nu)$ and assume flavor-dependent contact interactions with $\Lambda(\tau\nu_\tau\mu\nu_\mu) \ll \Lambda(\mu\nu_\mu e\nu_e)$.

SCALE LIMITS for Contact Interactions: $\Lambda(e\nu qq)$

VALUE (TeV)	CL%	DOCUMENT ID		TECN
>2.81	95	[1] AFFOLDER	01I	CDF

[1] AFFOLDER 00I bound is for a scalar interaction $\overline{q}_R\, q_L\, \overline{\nu}e_L$.

SCALE LIMITS for Contact Interactions: $\Lambda(qqqq)$

Λ^+_{LL}(TeV)	Λ^-_{LL}(TeV)	CL%	DOCUMENT ID		TECN	COMMENT
>13.1 none 17.4–29.5	**>21.8**	95	[1] AABOUD	17AK	ATLS	pp dijet angl.

• • • We do not use the following data for averages, fits, limits, etc. • • •

>11.5	>14.7	95	[2] SIRUNYAN	17F	CMS	pp dijet angl.
>12.0	>17.5	95	[3] AAD	16S	ATLS	pp dijet angl.
			[4] AAD	15AR	ATLS	$pp \to t\overline{t}t\overline{t}$
			[5] AAD	15BY	ATLS	$pp \to t\overline{t}t\overline{t}$
> 8.1	>12.0	95	[6] AAD	15L	ATLS	pp dijet angl.
> 9.0	>11.7	95	[7] KHACHATRY...	15J	CMS	pp dijet angl.
> 5		95	[8] FABBRICHESI	14	RVUE	$q\overline{q}\,t\overline{t}$

[1] AABOUD 17AK limit is from dijet angular distribution in pp collisions at $\sqrt{s} = 13$ TeV. u, d, and s quarks are assumed to be composite.

[2] SIRUNYAN 17F limit is from dijet angular cross sections in pp collisions at $E_{cm} = 13$ TeV. All quarks are assumed to be composite.

[3] AAD 16S limit is from dijet angular selections in pp collisions at $E_{cm} = 13$ TeV. u, d, and s quarks are assumed to be composite.

[4] AAD 15AR obtain limit on the t_R compositeness $2\pi/\Lambda^2_{RR} < 6.6$ TeV^{-2} at 95% CL from the $t\overline{t}t\overline{t}$ production in the pp collisions at $E_{cm} = 8$ TeV.

[5] AAD 15BY obtain limit on the t_R compositeness $2\pi/\Lambda^2_{RR} < 15.1$ TeV^{-2} at 95% CL from the $t\overline{t}t\overline{t}$ production in the pp collisions at $E_{cm} = 8$ TeV.

[6] AAD 15L limit is from dijet angular distribution in pp collisions at $E_{cm} = 8$ TeV. u, d, and s quarks are assumed to be composite.

[7] KHACHATRYAN 15J limit is from dijet angular distribution in pp collisions at $E_{cm} = 8$ TeV. u, d, s, c, and b quarks are assumed to be composite.

[8] FABBRICHESI 14 obtain bounds on chromoelectric and chromomagnetic form factors of the top-quark using $pp \to t\overline{t}$ and $p\overline{p} \to t\overline{t}$ cross sections. The quoted limit on the $q\overline{q}\,t\overline{t}$ contact interaction is derived from their bound on the chromoelectric form factor.

SCALE LIMITS for Contact Interactions: $\Lambda(\nu\nu qq)$

Limits are for $\Lambda^\pm_{LL}$ only. For other cases, see each reference.

Λ^+_{LL}(TeV)	Λ^-_{LL}(TeV)	CL%	DOCUMENT ID		TECN	COMMENT
>5.0	**>5.4**	95	[1] MCFARLAND	98	CCFR	νN scattering

[1] MCFARLAND 98 assumed a flavor universal interaction. Neutrinos were mostly of muon type.

MASS LIMITS for Excited e (e^*)

Most e^+e^- experiments assume one-photon or Z exchange. The limits from some e^+e^- experiments which depend on λ have assumed transition couplings which are chirality violating ($\eta_L = \eta_R$). However they can be interpreted as limits for chirality-conserving interactions after multiplying the coupling value λ by $\sqrt{2}$; see Note.

Excited leptons have the same quantum numbers as other ortholeptons. See also the searches for ortholeptons in the "Searches for Heavy Leptons" section.

Limits for Excited e (e^*) from Pair Production

These limits are obtained from $e^+e^- \to e^{*+}e^{*-}$ and thus rely only on the (electroweak) charge of e^*. Form factor effects are ignored unless noted. For the case of limits from Z decay, the e^* coupling is assumed to be of sequential type. Possible t channel contribution from transition magnetic coupling is neglected. All limits assume a dominant $e^* \to e\gamma$ decay except the limits from $\Gamma(Z)$.

For limits prior to 1987, see our 1992 edition (Physical Review **D45** S1 (1992)).

VALUE (GeV)	CL%	DOCUMENT ID		TECN	COMMENT
>103.2	95	[1] ABBIENDI	02G	OPAL	$e^+e^- \to e^*e^*$ Homodoublet type

• • • We do not use the following data for averages, fits, limits, etc. • • •

>102.8	95	[2] ACHARD	03B	L3	$e^+e^- \to e^*e^*$ Homodoublet type

[1] From e^+e^- collisions at $\sqrt{s} = 183$–209 GeV. $f = f'$ is assumed.

[2] From e^+e^- collisions at $\sqrt{s} = 189$–209 GeV. $f = f'$ is assumed. ACHARD 03B also obtain limit for $f = -f'$: $m_{e^*} > 96.6$ GeV.

Limits for Excited e (e^*) from Single Production

These limits are from $e^+e^- \to e^*e$, $W \to e^*\nu$, or $ep \to e^*X$ and depend on transition magnetic coupling between e and e^*. All limits assume $e^* \to e\gamma$ decay except as noted. Limits from LEP, UA2, and H1 are for chiral coupling, whereas all other limits are for nonchiral coupling, $\eta_L = \eta_R = 1$. In most papers, the limit is expressed in the form of an excluded region in the λ–m_{e^*} plane. See the original papers.

For limits prior to 1987, see our 1992 edition (Physical Review **D45** S1 (1992)).

VALUE (GeV)	CL%	DOCUMENT ID		TECN	COMMENT
>3000	95	[1] AAD	15AP	ATLS	$pp \to e^{(*)}e^*X$

• • • We do not use the following data for averages, fits, limits, etc. • • •

>2450	95	[2] KHACHATRY...	16AQ	CMS	$pp \to ee^*X$
>2200	95	[3] AAD	13BB	ATLS	$pp \to ee^*X$
>1900	95	[4] CHATRCHYAN	13AE	CMS	$pp \to ee^*X$
>1870	95	[5] AAD	12AZ	ATLS	$pp \to e^{(*)}e^*X$

[1] AAD 15AP search for e^* production in evens with three or more charged leptons in pp collisions at $\sqrt{s} = 8$ TeV. The quoted limit assumes $\Lambda = m_{e^*}$, $f = f' = 1$. The contact interaction is included in the e^* production and decay amplitudes.

[2] KHACHATRYAN 16AQ search for single e^* production in pp collisions at $\sqrt{s} = 8$ TeV. The limit above is from the $e^* \to e\gamma$ search channel assuming $f = f' = 1$, $m_{e^*} = \Lambda$. See their Table 7 for limits in other search channels or with different assumptions.

[3] AAD 13BB search for single e^* production in pp collisions with $e^* \to e\gamma$ decay. $f = f' = 1$, and e^* production via contact interaction with $\Lambda = m_{e^*}$ are assumed.

[4] CHATRCHYAN 13AE search for single e^* production in pp collisions with $e^* \to e\gamma$ decay. $f = f' = 1$, and e^* production via contact interaction with $\Lambda = m_{e^*}$ are assumed.

[5] AAD 12AZ search for e^* production via four-fermion contact interaction in pp collisions with $e^* \to e\gamma$ decay. The quoted limit assumes $\Lambda = m_{e^*}$. See their Fig. 8 for the exclusion plot in the mass-coupling plane.

Limits for Excited e (e^*) from $e^+e^- \to \gamma\gamma$

These limits are derived from indirect effects due to e^* exchange in the t channel and depend on transition magnetic coupling between e and e^*. All limits are for $\lambda_\gamma = 1$. All limits except ABE 89J and ACHARD 02D are for nonchiral coupling with $\eta_L = \eta_R = 1$. We choose the chiral coupling limit as the best limit and list it in the Summary Table.

For limits prior to 1987, see our 1992 edition (Physical Review **D45** S1 (1992)).

VALUE (GeV)	CL%	DOCUMENT ID		TECN	COMMENT
>356	95	[1] ABDALLAH	04N	DLPH	$\sqrt{s}$= 161–208 GeV
• • • We do not use the following data for averages, fits, limits, etc. • • •					
>310	95	ACHARD	02D	L3	$\sqrt{s}$= 192–209 GeV

[1] ABDALLAH 04N also obtain a limit on the excited electron mass with ee^* chiral coupling, $m_{e^*} > 295$ GeV at 95% CL.

Indirect Limits for Excited e (e^*)

These limits make use of loop effects involving e^* and are therefore subject to theoretical uncertainty.

VALUE (GeV)	DOCUMENT ID		TECN	COMMENT
• • • We do not use the following data for averages, fits, limits, etc. • • •				
	[1] DORENBOS...	89	CHRM	$\overline{\nu}_\mu e \to \overline{\nu}_\mu e$, $\nu_\mu e \to \nu_\mu e$
	[2] GRIFOLS	86	THEO	$\nu_\mu e \to \nu_\mu e$
	[3] RENARD	82	THEO	$g-2$ of electron

[1] DORENBOSCH 89 obtain the limit $\lambda_\gamma^2 \Lambda_{\rm cut}^2 / m_{e^*}^2 < 2.6$ (95% CL), where $\Lambda_{\rm cut}$ is the cutoff scale, based on the one-loop calculation by GRIFOLS 86. If one assumes that $\Lambda_{\rm cut} = 1$ TeV and $\lambda_\gamma = 1$, one obtains $m_{e^*} > 620$ GeV. However, one generally expects $\lambda_\gamma \approx m_{e^*}/\Lambda_{\rm cut}$ in composite models.

[2] GRIFOLS 86 uses $\nu_\mu e \to \nu_\mu e$ and $\overline{\nu}_\mu e \to \overline{\nu}_\mu e$ data from CHARM Collaboration to derive mass limits which depend on the scale of compositeness.

[3] RENARD 82 derived from $g-2$ data limits on mass and couplings of e^* and μ^*. See figures 2 and 3 of the paper.

MASS LIMITS for Excited μ (μ^*)

Limits for Excited μ (μ^*) from Pair Production

These limits are obtained from $e^+e^- \to \mu^{*+}\mu^{*-}$ and thus rely only on the (electroweak) charge of μ^*. Form factor effects are ignored unless noted. For the case of limits from Z decay, the μ^* coupling is assumed to be of sequential type. All limits assume a dominant $\mu^* \to \mu\gamma$ decay except the limits from $\Gamma(Z)$.

For limits prior to 1987, see our 1992 edition (Physical Review **D45** S1 (1992)).

VALUE (GeV)	CL%	DOCUMENT ID		TECN	COMMENT
>103.2	95	[1] ABBIENDI	02G	OPAL	$e^+e^- \to \mu^*\mu^*$ Homodoublet type
• • • We do not use the following data for averages, fits, limits, etc. • • •					
>102.8	95	[2] ACHARD	03B	L3	$e^+e^- \to \mu^*\mu^*$ Homodoublet type

[1] From e^+e^- collisions at $\sqrt{s} = 183$–209 GeV. $f = f'$ is assumed.

[2] From e^+e^- collisions at $\sqrt{s} = 189$–209 GeV. $f = f'$ is assumed. ACHARD 03B also obtain limit for $f = -f'$: $m_{\mu^*} > 96.6$ GeV.

Limits for Excited μ (μ^*) from Single Production

These limits are from $e^+e^- \to \mu^*\mu$ and depend on transition magnetic coupling between μ and μ^*. All limits assume $\mu^* \to \mu\gamma$ decay. Limits from LEP are for chiral coupling, whereas all other limits are for nonchiral coupling, $\eta_L = \eta_R = 1$. In most papers, the limit is expressed in the form of an excluded region in the λ–m_{μ^*} plane. See the original papers.

For limits prior to 1987, see our 1992 edition (Physical Review **D45** S1 (1992)).

VALUE (GeV)	CL%	DOCUMENT ID		TECN	COMMENT
>3000	95	[1] AAD	15AP	ATLS	$pp \to \mu^{(*)}\mu^* X$
• • • We do not use the following data for averages, fits, limits, etc. • • •					
>2800	95	[2] AAD	16BM	ATLS	$pp \to \mu\mu^* X$
>2470	95	[3] KHACHATRY...16AQ		CMS	$pp \to \mu\mu^* X$
>2200	95	[4] AAD	13BB	ATLS	$pp \to \mu\mu^* X$
>1900	95	[5] CHATRCHYAN	13AE	CMS	$pp \to \mu\mu^* X$
>1750	95	[6] AAD	12AZ	ATLS	$pp \to \mu^{(*)}\mu^* X$

[1] AAD 15AP search for μ^* production in evens with three or more charged leptons in pp collisions at $\sqrt{s} = 8$ TeV. The quoted limit assumes $\Lambda = m_{\mu^*}$, $f = f' = 1$. The contact interaction is included in the μ^* production and decay amplitudes.

[2] AAD 16BM search for μ^* production in $\mu\mu jj$ events in pp collisions at $\sqrt{s} = 8$ TeV. Both the production and decay are assumed to occur via a contact interaction with $\Lambda = m_{\mu^*}$.

[3] KHACHATRYAN 16AQ search for single μ^* production in pp collisions at $\sqrt{s} = 8$ TeV. The limit above is from the $\mu^* \to \mu\gamma$ search channel assuming $f = f' = 1$, $m_{\mu^*} = \Lambda$. See their Table 7 for limits in other search channels or with different assumptions.

[4] AAD 13BB search for single μ^* production in pp collisions with $\mu^* \to \mu\gamma$ decay. $f = f' = 1$, and μ^* production via contact interaction with $\Lambda = m_{\mu^*}$ are assumed.

[5] CHATRCHYAN 13AE search for single μ^* production in pp collisions with $\mu^* \to \mu\gamma$ decay. $f = f' = 1$, and μ^* production via contact interaction with $\Lambda = m_{\mu^*}$ are assumed.

[6] AAD 12AZ search for μ^* production via four-fermion contact interaction in pp collisions with $\mu^* \to \mu\gamma$ decay. The quoted limit assumes $\Lambda = m_{\mu^*}$. See their Fig. 8 for the exclusion plot in the mass-coupling plane.

Indirect Limits for Excited μ (μ^*)

These limits make use of loop effects involving μ^* and are therefore subject to theoretical uncertainty.

VALUE (GeV)	DOCUMENT ID		TECN	COMMENT
• • • We do not use the following data for averages, fits, limits, etc. • • •				
	[1] RENARD	82	THEO	$g-2$ of muon

[1] RENARD 82 derived from $g-2$ data limits on mass and couplings of e^* and μ^*. See figures 2 and 3 of the paper.

MASS LIMITS for Excited τ (τ^*)

Limits for Excited τ (τ^*) from Pair Production

These limits are obtained from $e^+e^- \to \tau^{*+}\tau^{*-}$ and thus rely only on the (electroweak) charge of τ^*. Form factor effects are ignored unless noted. For the case of limits from Z decay, the τ^* coupling is assumed to be of sequential type. All limits assume a dominant $\tau^* \to \tau\gamma$ decay except the limits from $\Gamma(Z)$.

For limits prior to 1987, see our 1992 edition (Physical Review **D45** S1 (1992)).

VALUE (GeV)	CL%	DOCUMENT ID		TECN	COMMENT
>103.2	95	[1] ABBIENDI	02G	OPAL	$e^+e^- \to \tau^*\tau^*$ Homodoublet type
• • • We do not use the following data for averages, fits, limits, etc. • • •					
>102.8	95	[2] ACHARD	03B	L3	$e^+e^- \to \tau^*\tau^*$ Homodoublet type

[1] From e^+e^- collisions at $\sqrt{s} = 183$–209 GeV. $f = f'$ is assumed.

[2] From e^+e^- collisions at $\sqrt{s} = 189$–209 GeV. $f = f'$ is assumed. ACHARD 03B also obtain limit for $f = -f'$: $m_{\tau^*} > 96.6$ GeV.

Limits for Excited τ (τ^*) from Single Production

These limits are from $e^+e^- \to \tau^*\tau$ and depend on transition magnetic coupling between τ and τ^*. All limits assume $\tau^* \to \tau\gamma$ decay. Limits from LEP are for chiral coupling, whereas all other limits are for nonchiral coupling, $\eta_L = \eta_R = 1$. In most papers, the limit is expressed in the form of an excluded region in the λ–m_{τ^*} plane. See the original papers.

VALUE (GeV)	CL%	DOCUMENT ID		TECN	COMMENT
>2500	95	[1] AAD	15AP	ATLS	$pp \to \tau^{(*)}\tau^* X$
• • • We do not use the following data for averages, fits, limits, etc. • • •					
> 180	95	[2] ACHARD	03B	L3	$e^+e^- \to \tau\tau^*$
> 185	95	[3] ABBIENDI	02G	OPAL	$e^+e^- \to \tau\tau^*$

[1] AAD 15AP search for τ^* production in events with three or more charged leptons in pp collisions at $\sqrt{s} = 8$ TeV. The quoted limit assumes $\Lambda = m_{\tau^*}$, $f = f' = 1$. The contact interaction is included in the τ^* production and decay amplitudes.

[2] ACHARD 03B result is from e^+e^- collisions at $\sqrt{s} = 189$–209 GeV. $f = f' = \Lambda/m_{\tau^*}$ is assumed. See their Fig. 4 for the exclusion plot in the mass-coupling plane.

[3] ABBIENDI 02G result is from e^+e^- collisions at $\sqrt{s} = 183$–209 GeV. $f = f' = \Lambda/m_{\tau^*}$ is assumed for τ^* coupling. See their Fig. 4c for the exclusion limit in the mass-coupling plane.

MASS LIMITS for Excited Neutrino (ν^*)

Limits for Excited ν (ν^*) from Pair Production

These limits are obtained from $e^+e^- \to \nu^*\nu^*$ and thus rely only on the (electroweak) charge of ν^*. Form factor effects are ignored unless noted. The ν^* coupling is assumed to be of sequential type unless otherwise noted. All limits assume a dominant $\nu^* \to \nu\gamma$ decay except the limits from $\Gamma(Z)$.

VALUE (GeV)	CL%	DOCUMENT ID		TECN	COMMENT
>1600	95	[1] AAD	15AP	ATLS	$pp \to \nu^*\nu^* X$
• • • We do not use the following data for averages, fits, limits, etc. • • •					
		[2] ABBIENDI	04N	OPAL	
> 102.6	95	[3] ACHARD	03B	L3	$e^+e^- \to \nu^*\nu^*$ Homodoublet type

[1] AAD 15AP search for ν^* pair production in evens with three or more charged leptons in pp collisions at $\sqrt{s} = 8$ TeV. The quoted limit assumes $\Lambda = m_{\nu^*}$, $f = f' = 1$. The contact interaction is included in the ν^* production and decay amplitudes.

[2] From e^+e^- collisions at $\sqrt{s} = 192$–209 GeV, ABBIENDI 04N obtain limit on $\sigma(e^+e^- \to \nu^*\nu^*)\,B^2(\nu^* \to \nu\gamma)$. See their Fig.2. The limit ranges from 20 to 45 fb for $m_{\nu^*} > 45$ GeV.

[3] From e^+e^- collisions at $\sqrt{s} = 189$–209 GeV. $f = -f'$ is assumed. ACHARD 03B also obtain limit for $f = f'$: $m_{\nu_e^*} > 101.7$ GeV, $m_{\nu_\mu^*} > 101.8$ GeV, and $m_{\nu_\tau^*} > 92.9$ GeV. See their Fig. 4 for the exclusion plot in the mass-coupling plane.

Limits for Excited ν (ν^*) from Single Production

These limits are from $e^+e^- \to \nu\nu^*$, $Z \to \nu\nu^*$, or $ep \to \nu^* X$ and depend on transition magnetic coupling between ν/e and ν^*. Assumptions about ν^* decay mode are given in footnotes.

VALUE (GeV)	CL%	DOCUMENT ID		TECN	COMMENT
>213	95	[1] AARON	08	H1	$ep \to \nu^* X$
• • • We do not use the following data for averages, fits, limits, etc. • • •					
>190	95	[2] ACHARD	03B	L3	$e^+e^- \to \nu\nu^*$
none 50–150	95	[3] ADLOFF	02	H1	$ep \to \nu^* X$
>158	95	[4] CHEKANOV	02D	ZEUS	$ep \to \nu^* X$

[1] AARON 08 search for single ν^* production in ep collisions with the decays $\nu^* \to \nu\gamma$, νZ, eW. The quoted limit assumes $f = -f' = \Lambda/m_{\nu^*}$. See their Fig. 3 and Fig. 4 for the exclusion plots in the mass-coupling plane.

[2] ACHARD 03B result is from e^+e^- collisions at $\sqrt{s}$ = 189–209 GeV. The quoted limit is for ν_e^*. $f = -f' = \Lambda/m_{\nu^*}$ is assumed. See their Fig. 4 for the exclusion plot in the mass-coupling plane.

[3] ADLOFF 02 search for single ν^* production in ep collisions with the decays $\nu^* \to \nu\gamma$, νZ, eW. The quoted limit assumes $f = -f' = \Lambda/m_{\nu^*}$. See their Fig. 1 for the exclusion plots in the mass-coupling plane.

[4] CHEKANOV 02D search for single ν^* production in ep collisions with the decays $\nu^* \to \nu\gamma$, νZ, eW. $f = -f' = \Lambda/m_{\nu^*}$ is assumed for the e^* coupling. CHEKANOV 02D also obtain limit for $f = f' = \Lambda/m_{\nu^*}$: m_{ν^*} >135 GeV. See their Fig. 5c and Fig. 5d for the exclusion plot in the mass-coupling plane.

MASS LIMITS for Excited q (q^*)

Limits for Excited q (q^*) from Pair Production

These limits are mostly obtained from $e^+e^- \to q^*\overline{q}^*$ and thus rely only on the (electroweak) charge of the q^*. Form factor effects are ignored unless noted. Assumptions about the q^* decay are given in the comments and footnotes.

VALUE (GeV)	CL%	DOCUMENT ID		TECN	COMMENT
>338	95	[1] AALTONEN	10H	CDF	$q^* \to tW^-$
• • • We do not use the following data for averages, fits, limits, etc. • • •					
		[2] BARATE	98U	ALEP	$Z \to q^*q^*$
> 45.6	95	[3] ADRIANI	93M	L3	u or d type, $Z \to q^*q^*$
> 41.7	95	[4] BARDADIN-...	92	RVUE	u-type, $\Gamma(Z)$
> 44.7	95	[4] BARDADIN-...	92	RVUE	d-type, $\Gamma(Z)$
> 40.6	95	[5] DECAMP	92	ALEP	u-type, $\Gamma(Z)$
> 44.2	95	[5] DECAMP	92	ALEP	d-type, $\Gamma(Z)$
> 45	95	[6] DECAMP	92	ALEP	u or d type, $Z \to q^*q^*$
> 45	95	[5] ABREU	91F	DLPH	u-type, $\Gamma(Z)$
> 45	95	[5] ABREU	91F	DLPH	d-type, $\Gamma(Z)$

[1] AALTONEN 10H obtain limits on the q^*q^* production cross section in $p\overline{p}$ collisions. See their Fig. 3.

[2] BARATE 98U obtain limits on the form factor. See their Fig. 16 for limits in mass-form factor plane.

[3] ADRIANI 93M limit is valid for B($q^* \to qg$)> 0.25 (0.17) for up (down) type.

[4] BARDADIN-OTWINOWSKA 92 limit based on $\Delta\Gamma(Z)$<36 MeV.

[5] These limits are independent of decay modes.

[6] Limit is for B($q^* \to qg$)+B($q^* \to q\gamma$)=1.

Limits for Excited q (q^*) from Single Production

These limits are from $e^+e^- \to q^*\overline{q}$, $p\overline{p} \to q^*X$, or $pp \to q^*X$ and depend on transition magnetic couplings between q and q^*. Assumptions about q^* decay mode are given in the footnotes and comments.

VALUE (GeV)	CL%	DOCUMENT ID		TECN	COMMENT
>6000	95	[1] AABOUD	17AK	ATLS	$pp \to q^*X,\ q^* \to qg$
• • • We do not use the following data for averages, fits, limits, etc. • • •					
none 600–5400	95	[2] KHACHATRY...	17W	CMS	$pp \to q^*X,\ q^* \to qg$
none 1100–2100	95	[3] AABOUD	16	ATLS	$pp \to b^*X,\ b^* \to bg$
>1500	95	[4] AAD	16AH	ATLS	$pp \to b^*X,\ b^* \to tW$
>4400	95	[5] AAD	16AI	ATLS	$pp \to q^*X,\ q^* \to q\gamma$
		[6] AAD	16AV	ATLS	$pp \to q^*X,\ q^* \to Wb$
>5200	95	[7] AAD	16S	ATLS	$pp \to q^*X,\ q^* \to qg$
>1390	95	[8] KHACHATRY...	16I	CMS	$pp \to b^*X,\ b^* \to tW$
>5000	95	[9] KHACHATRY...	16K	CMS	$pp \to q^*X,\ q^* \to qg$
none 500–1600	95	[10] KHACHATRY...	16L	CMS	$pp \to q^*X,\ q^* \to qg$
>4060	95	[11] AAD	15V	ATLS	$pp \to q^*X,\ q^* \to qg$
>3500	95	[12] KHACHATRY...	15V	CMS	$pp \to q^*X,\ q^* \to qg$
>3500	95	[13] AAD	14A	ATLS	$pp \to q^*X,\ q^* \to q\gamma$
>3200	95	[14] KHACHATRY...	14	CMS	$pp \to q^*X,\ q^* \to qW$
>2900	95	[15] KHACHATRY...	14	CMS	$pp \to q^*X,\ q^* \to qZ$
none 700–3500	95	[16] KHACHATRY...	14J	CMS	$pp \to q^*X,\ q^* \to q\gamma$
>2380	95	[17] CHATRCHYAN	13AJ	CMS	$pp \to q^*X,\ q^* \to qW$
>2150	95	[18] CHATRCHYAN	13AJ	CMS	$pp \to q^*X,\ q^* \to qZ$

[1] AABOUD 17AK assume $\Lambda = m_{q^*}$, $f_s = f = f' = 1$. The contact interactions are not included in q^* production and decay amplitudes. Only the decay of $q^* \to gu$ and $q^* \to gd$ is simulated as the benchmark signals in the analysis.

[2] KHACHATRYAN 17W assume $\Lambda = m_{q^*}$, $f_s = f = f' = 1$. The contact interactions are not included in q^* production and decay amplitudes.

[3] AABOUD 16 assume $\Lambda = m_{b^*}$, $f_s = f = f' = 1$. The contact interactions are not included in the b^* production and decay amplitudes.

[4] AAD 16AH search for b^* decaying to tW in pp collisions at $\sqrt{s}$ = 8 TeV. $f_g = f_L = f_R = 1$ are assumed. See their Fig. 12b for limits on $\sigma \cdot B$.

[5] AAD 16AI assume $\Lambda = m_{q^*}$, $f_s = f = f' = 1$.

[6] AAD 16AV search for single production of vector-like quarks decaying to Wb in pp collisions. See their Fig. 8 for the limits on couplings and mixings.

[7] AAD 16S assume $\Lambda = m_{q^*}$, $f_s = f = f' = 1$. The contact interactions are not included in q^* production and decay amplitudes.

[8] KHACHATRYAN 16I search for b^* decaying to tW in pp collisions at $\sqrt{s}$ = 8 TeV. $\kappa_L^b = g_L = 1$, $\kappa_R^b = g_R = 0$ are assumed. See their Fig. 8 for limits on $\sigma \cdot B$.

[9] KHACHATRYAN 16K assume $\Lambda = m_{q^*}$, $f_s = f = f' = 1$. The contact interactions are not included in q^* production and decay amplitudes.

[10] KHACHATRYAN 16L search for resonances decaying to dijets in pp collisions at $\sqrt{s}$ = 8 TeV using the data scouting technique which increases the sensitivity to the low mass resonances.

[11] AAD 15V assume $\Lambda = m_{q^*}$, $f_s = f = f' = 1$. The contact interactions are not included in q^* production and decay amplitudes.

[12] KHACHATRYAN 15V assume $\Lambda = m_{q^*}$, $f_s = f = f' = 1$. The contact interactions are not included in q^* production and decay amplitudes.

[13] AAD 14A assume $\Lambda = m_{q^*}$, $f_s = f = f' = 1$.

[14] KHACHATRYAN 14 use the hadronic decay of W, assuming $\Lambda = m_{q^*}$, f_s=f=f' = 1.

[15] KHACHATRYAN 14 use the hadronic decay of Z, assuming $\Lambda = m_{q^*}$, f_s=f=f' = 1.

[16] KHACHATRYAN 14J assume $f_s = f = f' = \Lambda$ / m_{q^*}.

[17] CHATRCHYAN 13AJ use the hadronic decay of W.

[18] CHATRCHYAN 13AJ use the hadronic decay of Z.

MASS LIMITS for Color Sextet Quarks (q_6)

VALUE (GeV)	CL%	DOCUMENT ID		TECN	COMMENT
>84	95	[1] ABE	89D	CDF	$p\overline{p} \to q_6\overline{q}_6$

[1] ABE 89D look for pair production of unit-charged particles which leave the detector before decaying. In the above limit the color sextet quark is assumed to fragment into a unit-charged or neutral hadron with equal probability and to have long enough lifetime not to decay within the detector. A limit of 121 GeV is obtained for a color decuplet.

MASS LIMITS for Color Octet Charged Leptons (ℓ_8)

$\lambda \equiv m_{\ell_8}/\Lambda$

VALUE (GeV)	CL%	DOCUMENT ID		TECN	COMMENT
>86	95	[1] ABE	89D	CDF	Stable ℓ_8: $p\overline{p} \to \ell_8\overline{\ell}_8$
• • • We do not use the following data for averages, fits, limits, etc. • • •					
		[2] ABT	93	H1	e_8: $ep \to e_8 X$

[1] ABE 89D look for pair production of unit-charged particles which leave the detector before decaying. In the above limit the color octet lepton is assumed to fragment into a unit-charged or neutral hadron with equal probability and to have long enough lifetime not to decay within the detector. The limit improves to 99 GeV if it always fragments into a unit-charged hadron.

[2] ABT 93 search for e_8 production via e-gluon fusion in ep collisions with $e_8 \to eg$. See their Fig. 3 for exclusion plot in the m_{e_8}–Λ plane for m_{e_8} = 35–220 GeV.

MASS LIMITS for Color Octet Neutrinos (ν_8)

$\lambda \equiv m_{\ell_8}/\Lambda$

VALUE (GeV)	CL%	DOCUMENT ID		TECN	COMMENT
>110	90	[1] BARGER	89	RVUE	ν_8: $p\overline{p} \to \nu_8\overline{\nu}_8$
• • • We do not use the following data for averages, fits, limits, etc. • • •					
none 3.8–29.8	95	[2] KIM	90	AMY	ν_8: $e^+e^- \to$ acoplanar jets
none 9–21.9	95	[3] BARTEL	87B	JADE	ν_8: $e^+e^- \to$ acoplanar jets

[1] BARGER 89 used ABE 89B limit for events with large missing transverse momentum. Two-body decay $\nu_8 \to \nu g$ is assumed.

[2] KIM 90 is at E_{cm} = 50–60.8 GeV. The same assumptions as in BARTEL 87B are used.

[3] BARTEL 87B is at E_{cm} = 46.3–46.78 GeV. The limit assumes the ν_8 pair production cross section to be eight times larger than that of the corresponding heavy neutrino pair production. This assumption is not valid in general for the weak couplings, and the limit can be sensitive to its $SU(2)_L \times U(1)_Y$ quantum numbers.

MASS LIMITS for W_8 (Color Octet W Boson)

VALUE (GeV)	DOCUMENT ID		TECN	COMMENT
• • • We do not use the following data for averages, fits, limits, etc. • • •				
	[1] ALBAJAR	89	UA1	$p\overline{p} \to W_8 X,\ W_8 \to Wg$

[1] ALBAJAR 89 give $\sigma(W_8 \to W + \text{jet})/\sigma(W) < 0.019$ (90% CL) for $m_{W_8} > 220$ GeV.

REFERENCES FOR Searches for Quark and Lepton Compositeness

AABOUD	17AK	PR D96 052004	M. Aaboud *et al.*	(ATLAS Collab.)
AABOUD	17AT	JHEP 1710 182	M. Aaboud *et al.*	(ATLAS Collab.)
KHACHATRY...	17W	PL B769 520	V. Khachatryan *et al.*	(CMS Collab.)
SIRUNYAN	17F	JHEP 1707 013	A.M. Sirunyan *et al.*	(CMS Collab.)
AABOUD	16	PL B759 229	M. Aaboud *et al.*	(ATLAS Collab.)
AABOUD	16U	PL B761 372	M. Aaboud *et al.*	(ATLAS Collab.)
AAD	16AH	JHEP 1602 110	G. Aad *et al.*	(ATLAS Collab.)
AAD	16AI	JHEP 1603 041	G. Aad *et al.*	(ATLAS Collab.)

Searches Particle Listings

Quark and Lepton Compositeness, Extra Dimensions

AAD	16AV	EPJ C76 442	G. Aad *et al.*	(ATLAS Collab.)
AAD	16BM	NJP 18 073021	G. Aad *et al.*	(ATLAS Collab.)
AAD	16S	PL B754 302	G. Aad *et al.*	(ATLAS Collab.)
KHACHATRY...	16AQ	JHEP 1603 125	V. Khachatryan *et al.*	(CMS Collab.)
KHACHATRY...	16I	JHEP 1601 166	V. Khachatryan *et al.*	(CMS Collab.)
KHACHATRY...	16K	PRL 116 071801	V. Khachatryan *et al.*	(CMS Collab.)
KHACHATRY...	16L	PRL 117 031802	V. Khachatryan *et al.*	(CMS Collab.)
AAD	15AP	JHEP 1508 138	G. Aad *et al.*	(ATLAS Collab.)
AAD	15AR	JHEP 1508 105	G. Aad *et al.*	(ATLAS Collab.)
AAD	15BY	JHEP 1510 150	G. Aad *et al.*	(ATLAS Collab.)
AAD	15L	PRL 114 221802	G. Aad *et al.*	(ATLAS Collab.)
AAD	15V	PR D91 052007	G. Aad *et al.*	(ATLAS Collab.)
KHACHATRY...	15AE	JHEP 1504 025	V. Khachatryan *et al.*	(CMS Collab.)
KHACHATRY...	15J	PL B746 79	V. Khachatryan *et al.*	(CMS Collab.)
KHACHATRY...	15V	PR D91 052009	V. Khachatryan *et al.*	(CMS Collab.)
AAD	14A	PL B728 562	G. Aad *et al.*	(ATLAS Collab.)
AAD	14BE	EPJ C74 3134	G. Aad *et al.*	(ATLAS Collab.)
FABBRICHESI	14	PR D89 074028	M. Fabbrichesi, M. Pinamonti, A. Tonero	
KHACHATRY...	14	JHEP 1408 173	V. Khachatryan *et al.*	(CMS Collab.)
KHACHATRY...	14J	PL B738 274	V. Khachatryan *et al.*	(CMS Collab.)
AAD	13BB	NJP 15 093011	G. Aad *et al.*	(ATLAS Collab.)
AAD	13E	PR D87 015010	G. Aad *et al.*	(ATLAS Collab.)
CHATRCHYAN	13AE	PL B720 309	S. Chatrchyan *et al.*	(CMS Collab.)
CHATRCHYAN	13AJ	PL B723 280	S. Chatrchyan *et al.*	(CMS Collab.)
CHATRCHYAN	13K	PR D87 032001	S. Chatrchyan *et al.*	(CMS Collab.)
AAD	12AB	PL B712 40	G. Aad *et al.*	(ATLAS Collab.)
AAD	12AZ	PR D85 072003	G. Aad *et al.*	(ATLAS Collab.)
AARON	11C	PL B705 52	F. D. Aaron *et al.*	(H1 Collab.)
ABDALLAH	11	EPJ C71 1555	J. Abdallah *et al.*	(DELPHI Collab.)
AALTONEN	10H	PRL 104 091801	T. Aaltonen *et al.*	(CDF Collab.)
ABDALLAH	09	EPJ C60 1	J. Abdallah *et al.*	(DELPHI Collab.)
AARON	08	PL B663 382	F.D. Aaron *et al.*	(H1 Collab.)
SCHAEL	07A	EPJ C49 411	S. Schael *et al.*	(ALEPH Collab.)
ABDALLAH	06C	EPJ C45 589	J. Abdallah *et al.*	(DELPHI Collab.)
ABULENCIA	06L	PRL 96 211801	A. Abulencia *et al.*	(CDF Collab.)
ABBIENDI	04G	EPJ C33 173	G. Abbiendi *et al.*	(OPAL Collab.)
ABBIENDI	04N	PL B602 167	G. Abbiendi *et al.*	(OPAL Collab.)
ABDALLAH	04N	EPJ C37 405	J. Abdallah *et al.*	(DELPHI Collab.)
ACHARD	03B	PL B568 23	P. Achard *et al.*	(L3 Collab.)
BABICH	03	EPJ C29 103	A.A. Babich *et al.*	
ABBIENDI	02G	PL B544 57	G. Abbiendi *et al.*	(OPAL Collab.)
ACHARD	02D	PL B531 28	P. Achard *et al.*	(L3 Collab.)
ADLOFF	02	PL B525 9	C. Adloff *et al.*	(H1 Collab.)
CHEKANOV	02D	PL B549 32	S. Chekanov *et al.*	(ZEUS Collab.)
AFFOLDER	01I	PRL 87 231803	T. Affolder *et al.*	(CDF Collab.)
BOURILKOV	01	PR D64 071701	D. Bourilkov	
CHEUNG	01B	PL B517 167	K. Cheung	
ACCIARRI	00P	PL B489 81	M. Acciarri *et al.*	(L3 Collab.)
AFFOLDER	00I	PR D62 012004	T. Affolder *et al.*	(CDF Collab.)
BARATE	98U	EPJ C4 571	R. Barate *et al.*	(ALEPH Collab.)
BARGER	98E	PR D57 391	V. Barger *et al.*	
MCFARLAND	98	EPJ C1 509	K.S. McFarland *et al.*	(CCFR/NuTeV Collab.)
DIAZCRUZ	94	PR D49 2149	J.L. Diaz Cruz, O.A. Sampayo	(CINV)
ABT	93	NP B396 3	I. Abt *et al.*	(H1 Collab.)
ADRIANI	93M	PRPL 236 1	O. Adriani *et al.*	(L3 Collab.)
BARDADIN-...	92	ZPHY C55 163	M. Bardadin-Otwinowska	(CLER)
DECAMP	92	PRPL 216 253	D. Decamp *et al.*	(ALEPH Collab.)
PDG	92	PR D45 S1	K. Hikasa *et al.*	(KEK, LBL, BOST+)
ABREU	91F	NP B367 511	P. Abreu *et al.*	(DELPHI Collab.)
KIM	90	PL B240 243	G.N. Kim *et al.*	(AMY Collab.)
ABE	89B	PRL 62 1825	F. Abe *et al.*	(CDF Collab.)
ABE	89D	PRL 63 1447	F. Abe *et al.*	(CDF Collab.)
ABE	89J	ZPHY C45 175	K. Abe *et al.*	(VENUS Collab.)
ALBAJAR	89	ZPHY C44 15	C. Albajar *et al.*	(UA1 Collab.)
BARGER	89	PL B220 464	V. Barger *et al.*	(WISC, KEK)
DORENBOS...	89	ZPHY C41 567	J. Dorenbosch *et al.*	(CHARM Collab.)
BARTEL	87B	ZPHY C36 15	W. Bartel *et al.*	(JADE Collab.)
GRIFOLS	86	PL 168B 264	J.A. Grifols, S. Peris	(BARC)
JODIDIO	86	PR D34 1967	A. Jodidio *et al.*	(LBL, NWES, TRIU)
Also		PR D37 237 (erratum)	A. Jodidio *et al.*	(LBL, NWES, TRIU)
RENARD	82	PL 116B 264	F.M. Renard	(CERN)

Extra Dimensions

For explanation of terms used and discussion of significant model dependence of following limits, see the "Extra Dimensions" review. Footnotes describe originally quoted limit. δ indicates the number of extra dimensions.

Limits not encoded here are summarized in the "Extra Dimensions" review, where the latest unpublished results are also described.

See the related review(s):

Extra Dimensions Searches

CONTENTS:

Limits on R from Deviations in Gravitational Force Law

This section includes limits on the size of extra dimensions from deviations in the Newtonian ($1/r^2$) gravitational force law at short distances. Deviations are parametrized by a gravitational potential of the form $V = -(G\ m\ m'/r)\ [1 + \alpha\ \exp(-r/R)]$. For δ toroidal extra dimensions of equal size, $\alpha = 8\delta/3$. Quoted bounds are for $\delta = 2$ unless otherwise noted.

VALUE (μm)	CL%	DOCUMENT ID		COMMENT
< 30	95	[1] KAPNER	07	Torsion pendulum
• • • We do not use the following data for averages, fits, limits, etc. • • •				
		[2] KLIMCHITSK...	17A	Torsion oscillator
		[3] XU	13	Nuclei properties
		[4] BEZERRA	11	Torsion oscillator
		[5] SUSHKOV	11	Torsion pendulum
		[6] BEZERRA	10	Microcantilever
		[7] MASUDA	09	Torsion pendulum
		[8] GERACI	08	Microcantilever
		[9] TRENKEL	08	Newton's constant
		[10] DECCA	07A	Torsion oscillator
< 47	95	[11] TU	07	Torsion pendulum
		[12] SMULLIN	05	Microcantilever
<130	95	[13] HOYLE	04	Torsion pendulum
		[14] CHIAVERINI	03	Microcantilever
$\lesssim$200	95	[15] LONG	03	Microcantilever
<190	95	[16] HOYLE	01	Torsion pendulum
		[17] HOSKINS	85	Torsion pendulum

[1] KAPNER 07 search for new forces, probing a range of $\alpha \simeq 10^{-3}$–10^5 and length scales $R \simeq$ 10–1000 μm. For $\delta = 1$ the bound on R is 44 μm. For $\delta = 2$, the bound is expressed in terms of M_*, here translated to a bound on the radius. See their Fig. 6 for details on the bound.

[2] KLIMCHITSKAYA 17A uses an experiment that measures the difference of Casimir forces to obtain bounds on non-Newtonian forces with strengths $|\alpha| \simeq 10^5$–10^{17} and length scales $R = 0.03$–10 μm. See their Fig. 3. These constraints do not place limits on the size of extra flat dimensions.

[3] XU 13 obtain constraints on non-Newtonian forces with strengths $|\alpha| \simeq 10^{34}$–10^{36} and length scales $R \simeq$ 1–10 fm. See their Fig. 4 for more details. These constraints do not place limits on the size of extra flat dimensions.

[4] BEZERRA 11 obtain constraints on non-Newtonian forces with strengths $10^{11} \lesssim |\alpha| \lesssim 10^{18}$ and length scales $R =$ 30–1260 nm. See their Fig. 2 for more details. These constraints do not place limits on the size of extra flat dimensions.

[5] SUSHKOV 11 obtain improved limits on non-Newtonian forces with strengths $10^7 \lesssim |\alpha| \lesssim 10^{11}$ and length scales 0.4 μm $< R <$ 4 μm (95% CL). See their Fig. 2. These bounds do not place limits on the size of extra flat dimensions. However, a model dependent bound of $M_* > 70$ TeV is obtained assuming gauge bosons that couple to baryon number also propagate in $(4 + \delta)$ dimensions.

[6] BEZERRA 10 obtain improved constraints on non-Newtonian forces with strengths $10^{19} \lesssim |\alpha| \lesssim 10^{29}$ and length scales $R =$ 1.6–14 nm (95% CL). See their Fig. 1. This bound does not place limits on the size of extra flat dimensions.

[7] MASUDA 09 obtain improved constraints on non-Newtonian forces with strengths $10^9 \lesssim |\alpha| \lesssim 10^{11}$ and length scales $R =$ 1.0–2.9 μm (95% CL). See their Fig. 3. This bound does not place limits on the size of extra flat dimensions.

[8] GERACI 08 obtain improved constraints on non-Newtonian forces with strengths $|\alpha| >$ 14,000 and length scales $R =$ 5–15 μm. See their Fig. 9. This bound does not place limits on the size of extra flat dimensions.

[9] TRENKEL 08 uses two independent measurements of Newton's constant G to constrain new forces with strength $|\alpha| \simeq 10^{-4}$ and length scales $R =$ 0.02–1 m. See their Fig. 1. This bound does not place limits on the size of extra flat dimensions.

[10] DECCA 07A search for new forces and obtain bounds in the region with strengths $|\alpha| \simeq 10^{13}$–10^{18} and length scales $R =$ 20–86 nm. See their Fig. 6. This bound does not place limits on the size of extra flat dimensions.

[11] TU 07 search for new forces probing a range of $|\alpha| \simeq 10^{-1}$–10^5 and length scales $R \simeq$ 20–1000 μm. For $\delta = 1$ the bound on R is 53 μm. See their Fig. 3 for details on the bound.

[12] SMULLIN 05 search for new forces, and obtain bounds in the region with strengths $\alpha \simeq 10^3$–10^8 and length scales $R =$ 6–20 μm. See their Figs. 1 and 16 for details on the bound. This work does not place limits on the size of extra flat dimensions.

[13] HOYLE 04 search for new forces, probing α down to 10^{-2} and distances down to 10μm. Quoted bound on R is for $\delta = 2$. For $\delta = 1$, bound goes to 160 μm. See their Fig. 34 for details on the bound.

[14] CHIAVERINI 03 search for new forces, probing α above 10^4 and λ down to 3μm, finding no signal. See their Fig. 4 for details on the bound. This bound does not place limits on the size of extra flat dimensions.

[15] LONG 03 search for new forces, probing α down to 3, and distances down to about 10μm. See their Fig. 4 for details on the bound.

[16] HOYLE 01 search for new forces, probing α down to 10^{-2} and distances down to 20μm. See their Fig. 4 for details on the bound. The quoted bound is for $\alpha \geq 3$.

[17] HOSKINS 85 search for new forces, probing distances down to 4 mm. See their Fig. 13 for details on the bound. This bound does not place limits on the size of extra flat dimensions.

Limits on R from On-Shell Production of Gravitons: $\delta = 2$

This section includes limits on on-shell production of gravitons in collider and astrophysical processes. Bounds quoted are on R, the assumed common radius of the flat extra dimensions, for $\delta = 2$ extra dimensions. Studies often quote bounds in terms of derived parameter; experiments are actually sensitive to the masses of the KK gravitons: $m_{\vec{n}} = |\vec{n}|/R$. See the Review on "Extra Dimensions" for details. Bounds are given in μm for $\delta = 2$.

VALUE (μm)	CL%	DOCUMENT ID		TECN	COMMENT
< 10.9	95	[1] AABOUD	16D	ATLS	$pp \to jG$
< 0.00016	95	[2] HANNESTAD	03		Neutron star heating
• • • We do not use the following data for averages, fits, limits, etc. • • •					
		[3] SIRUNYAN	17AQ	CMS	$pp \to \gamma G$
< 90	95	[4] AABOUD	16F	ATLS	$pp \to \gamma G$
		[5] KHACHATRY...	16N	CMS	$pp \to \gamma G$
< 17.2	95	[6] AAD	15BH	ATLS	$pp \to jG$
		[7] AAD	15CS	ATLS	$pp \to \gamma G$
< 15	95	[8] KHACHATRY...	15AL	CMS	$pp \to jG$
< 25	95	[9] AAD	13AD	ATLS	$pp \to jG$
< 127	95	[10] AAD	13C	ATLS	$pp \to \gamma G$
< 34.4	95	[11] AAD	13D	ATLS	$pp \to jj$
< 0.0087	95	[12] AJELLO	12	FLAT	Neutron star γ sources
< 23	95	[13] CHATRCHYAN	12AP	CMS	$pp \to jG$

< 92	95	[14] AAD	11S	ATLS	$pp \to jG$
< 72	95	[15] CHATRCHYAN	11U	CMS	$pp \to jG$
< 245	95	[16] AALTONEN	08AC	CDF	$p\overline{p} \to \gamma G, jG$
< 615	95	[17] ABAZOV	08S	D0	$p\overline{p} \to \gamma G$
< 0.916	95	[18] DAS	08		Supernova cooling
< 350	95	[19] ABULENCIA,A	06	CDF	$p\overline{p} \to jG$
< 270	95	[20] ABDALLAH	05B	DLPH	$e^+e^- \to \gamma G$
< 210	95	[21] ACHARD	04E	L3	$e^+e^- \to \gamma G$
< 480	95	[22] ACOSTA	04C	CDF	$\overline{p}p \to jG$
< 0.00038	95	[23] CASSE	04		Neutron star γ sources
< 610	95	[24] ABAZOV	03	D0	$\overline{p}p \to jG$
< 0.96	95	[25] HANNESTAD	03		Supernova cooling
< 0.096	95	[26] HANNESTAD	03		Diffuse γ background
< 0.051	95	[27] HANNESTAD	03		Neutron star γ sources
< 300	95	[28] HEISTER	03C	ALEP	$e^+e^- \to \gamma G$
		[29] FAIRBAIRN	01		Cosmology
< 0.66	95	[30] HANHART	01		Supernova cooling
		[31] CASSISI	00		Red giants
<1300	95	[32] ACCIARRI	99S	L3	$e^+e^- \to ZG$

[1] AABOUD 16D search for $pp \to jG$, using 3.2 fb^{-1} of data at $\sqrt{s} = 13$ TeV to place lower limits on M_D for two to six extra dimensions (see their Table X), from which this bound on R is derived.

[2] HANNESTAD 03 obtain a limit on R from the heating of old neutron stars by the surrounding cloud of trapped KK gravitons. Limits for all $\delta \leq 7$ are given in their Tables V and VI. These limits supersede those in HANNESTAD 02.

[3] SIRUNYAN 17AQ search for $pp \to \gamma G$, using 12.9 fb^{-1} of data at $\sqrt{s} = 13$ TeV to place limits on M_D for three to six extra dimensions (see their Table 3).

[4] AABOUD 16F search for $pp \to \gamma G$, using 3.2 fb^{-1} of data at $\sqrt{s} = 13$ TeV to place limits on M_D for two to six extra dimensions (see their Figure 9), from which this bound on R is derived.

[5] KHACHATRYAN 16N search for $pp \to \gamma G$, using 19.6 fb^{-1} of data at $\sqrt{s} = 8$ TeV to place limits on M_D for three to six extra dimensions (see their Table 5).

[6] AAD 15BH search for $pp \to jG$, using 20.3 fb^{-1} of data at $\sqrt{s} = 8$ TeV to place bounds on M_D for two to six extra dimensions, from which this bound on R is derived. See their Figure 9 for bounds on all $\delta \leq 6$.

[7] AAD 15CS search for $pp \to \gamma G$, using 20.3 fb^{-1} of data at $\sqrt{s} = 8$ TeV to place lower limits on M_D for two to six extra dimensions (see their Fig. 18).

[8] KHACHATRYAN 15AL search for $pp \to jG$, using 19.7 fb^{-1} of data at $\sqrt{s} = 8$ TeV to place bounds on M_D for two to six extra dimensions (see their Table 7), from which this bound on R is derived.

[9] AAD 13AD search for $pp \to jG$, using 4.7 fb^{-1} of data at $\sqrt{s} = 7$ TeV to place bounds on M_D for two to six extra dimensions, from which this bound on R is derived. See their Table 8 for bounds on all $\delta \leq 6$.

[10] AAD 13C search for $pp \to \gamma G$, using 4.6 fb^{-1} of data at $\sqrt{s} = 7$ TeV to place bounds on M_D for two to six extra dimensions, from which this bound on R is derived.

[11] AAD 13D search for the dijet decay of quantum black holes in 4.8 fb^{-1} of data produced in pp collisions at $\sqrt{s} = 7$ TeV to place bounds on M_D for two to seven extra dimensions, from which these bounds on R are derived. Limits on M_D for all $\delta \leq 7$ are given in their Table 3.

[12] AJELLO 12 obtain a limit on R from the gamma-ray emission of point γ sources that arise from the photon decay of KK gravitons which are gravitationally bound around neutron stars. Limits for all $\delta \leq 7$ are given in their Table 7.

[13] CHATRCHYAN 12AP search for $pp \to jG$, using 5.0 fb^{-1} of data at $\sqrt{s} = 7$ TeV to place bounds on M_D for two to six extra dimensions, from which this bound on R is derived. See their Table 7 for bounds on all $\delta \leq 6$.

[14] AAD 11S search for $pp \to jG$, using 33 pb^{-1} of data at $\sqrt{s} = 7$ TeV, to place bounds on M_D for two to four extra dimensions, from which these bounds on R are derived. See their Table 3 for bounds on all $\delta \leq 4$.

[15] CHATRCHYAN 11U search for $pp \to jG$, using 36 pb^{-1} of data at $\sqrt{s} = 7$ TeV, to place bounds on M_D for two to six extra dimensions, from which these bounds on R are derived. See their Table 3 for bounds on all $\delta \leq 6$.

[16] AALTONEN 08AC search for $p\overline{p} \to \gamma G$ and $p\overline{p} \to jG$ at $\sqrt{s} = 1.96$ TeV with 2.0 fb^{-1} and 1.1 fb^{-1} respectively, in order to place bounds on the fundamental scale and size of the extra dimensions. See their Table III for limits on all $\delta \leq 6$.

[17] ABAZOV 08S search for $p\overline{p} \to \gamma G$, using 1 fb^{-1} of data at $\sqrt{s} = 1.96$ TeV to place bounds on M_D for two to eight extra dimensions, from which these bounds on R are derived. See their paper for intermediate values of δ.

[18] DAS 08 obtain a limit on R from Kaluza-Klein graviton cooling of SN1987A due to plasmon-plasmon annihilation.

[19] ABULENCIA,A 06 search for $p\overline{p} \to jG$ using 368 pb^{-1} of data at $\sqrt{s} = 1.96$ TeV. See their Table II for bounds for all $\delta \leq 6$.

[20] ABDALLAH 05B search for $e^+e^- \to \gamma G$ at $\sqrt{s} = 180$–209 GeV to place bounds on the size of extra dimensions and the fundamental scale. Limits for all $\delta \leq 6$ are given in their Table 6. These limits supersede those in ABREU 00Z.

[21] ACHARD 04E search for $e^+e^- \to \gamma G$ at $\sqrt{s} = 189$–209 GeV to place bounds on the size of extra dimensions and the fundamental scale. See their Table 8 for limits with $\delta \leq 8$. These limits supersede those in ACCIARRI 99R.

[22] ACOSTA 04C search for $\overline{p}p \to jG$ at $\sqrt{s} = 1.8$ TeV to place bounds on the size of extra dimensions and the fundamental scale. See their paper for bounds on $\delta = 4, 6$.

[23] CASSE 04 obtain a limit on R from the gamma-ray emission of point γ sources that arises from the photon decay of gravitons around newly born neutron stars, applying the technique of HANNESTAD 03 to neutron stars in the galactic bulge. Limits for all $\delta \leq 7$ are given in their Table I.

[24] ABAZOV 03 search for $p\overline{p} \to jG$ at $\sqrt{s}$=1.8 TeV to place bounds on M_D for 2 to 7 extra dimensions, from which these bounds on R are derived. See their paper for bounds on intermediate values of δ. We quote results without the approximate NLO scaling introduced in the paper.

[25] HANNESTAD 03 obtain a limit on R from graviton cooling of supernova SN1987a. Limits for all $\delta \leq 7$ are given in their Tables V and VI.

[26] HANNESTAD 03 obtain a limit on R from gravitons emitted in supernovae and which subsequently decay, contaminating the diffuse cosmic γ background. Limits for all $\delta \leq 7$ are given in their Tables V and VI. These limits supersede those in HANNESTAD 02.

[27] HANNESTAD 03 obtain a limit on R from gravitons emitted in two recent supernovae and which subsequently decay, creating point γ sources. Limits for all $\delta \leq 7$ are given in their Tables V and VI. These limits are corrected in the published erratum.

[28] HEISTER 03C use the process $e^+e^- \to \gamma G$ at $\sqrt{s} = 189$–209 GeV to place bounds on the size of extra dimensions and the scale of gravity. See their Table 4 for limits with $\delta \leq 6$ for derived limits on M_D.

[29] FAIRBAIRN 01 obtains bounds on R from over production of KK gravitons in the early universe. Bounds are quoted in paper in terms of fundamental scale of gravity. Bounds depend strongly on temperature of QCD phase transition and range from $R <$ 0.13 μm to 0.001 μm for δ=2; bounds for δ=3,4 can be derived from Table 1 in the paper.

[30] HANHART 01 obtain bounds on R from limits on graviton cooling of supernova SN 1987a using numerical simulations of proto-neutron star neutrino emission.

[31] CASSISI 00 obtain rough bounds on M_D (and thus R) from red giant cooling for δ=2,3. See their paper for details.

[32] ACCIARRI 99S search for $e^+e^- \to ZG$ at $\sqrt{s}$=189 GeV. Limits on the gravity scale are found in their Table 2, for $\delta \leq 4$.

Mass Limits on M_{TT}

This section includes limits on the cut-off mass scale, M_{TT}, of dimension-8 operators from KK graviton exchange in models of large extra dimensions. Ambiguities in the UV-divergent summation are absorbed into the parameter λ, which is taken to be $\lambda = \pm 1$ in the following analyses. Bounds for $\lambda = -1$ are shown in parenthesis after the bound for $\lambda = +1$, if appropriate. Different papers use slightly different definitions of the mass scale. The definition used here is related to another popular convention by $M_{TT}^4 = (2/\pi)\,\Lambda_T^4$, as discussed in the above Review on "Extra Dimensions."

VALUE (TeV)		CL%	DOCUMENT ID		TECN	COMMENT
> 8.4		95	[1] SIRUNYAN	17F	CMS	$pp \to$ dijet, ang. distrib.
>20.6	**(> 15.7)**	95	[2] GIUDICE	03	RVUE	Dim-6 operators
• • • We do not use the following data for averages, fits, limits, etc. • • •						
> 7.2		95	[3] AABOUD	17AP	ATLS	$pp \to \gamma\gamma$
> 3.7		95	[4] KHACHATRY...	15AE	CMS	$pp \to e^+e^-,\ \mu^+\mu^-$
> 6.3		95	[5] KHACHATRY...	15J	CMS	$pp \to$ dijet, ang. distrib.
> 3.8		95	[6] AAD	14BE	ATLS	$pp \to e^+e^-,\ \mu^+\mu^-$
> 2.94	(>2.52)	95	[7] AAD	13AS	ATLS	$pp \to \gamma\gamma$
> 3.2		95	[8] AAD	13E	ATLS	$pp \to e^+e^-,\mu^+\mu^-,\gamma\gamma$
> 2.66	(>2.27)	95	[9] AAD	12Y	ATLS	$pp \to \gamma\gamma$
			[10] BAAK	12	RVUE	Electroweak
> 2.86		95	[11] CHATRCHYAN	12J	CMS	$pp \to e^+e^-, \mu^+\mu^-$
> 2.84	(>2.41)	95	[12] CHATRCHYAN	12R	CMS	$pp \to \gamma\gamma$
> 0.90	(>0.92)	95	[13] AARON	11C	H1	$e^\pm p \to e^\pm X$
> 1.74	(>1.71)	95	[14] CHATRCHYAN	11A	CMS	$pp \to \gamma\gamma$
> 1.48		95	[15] ABAZOV	09AE	D0	$p\overline{p} \to$ dijet, ang. distrib.
> 1.45		95	[16] ABAZOV	09D	D0	$p\overline{p} \to e^+e^-, \gamma\gamma$
> 1.1	(> 1.0)	95	[17] SCHAEL	07A	ALEP	$e^+e^- \to e^+e^-$
> 0.898	(> 0.998)	95	[18] ABDALLAH	06C	DLPH	$e^+e^- \to \ell^+\ell^-$
> 0.853	(> 0.939)	95	[19] GERDES	06		$p\overline{p} \to e^+e^-, \gamma\gamma$
> 0.96	(> 0.93)	95	[20] ABAZOV	05V	D0	$p\overline{p} \to \mu^+\mu^-$
> 0.78	(> 0.79)	95	[21] CHEKANOV	04B	ZEUS	$e^\pm p \to e^\pm X$
> 0.805	(> 0.956)	95	[22] ABBIENDI	03D	OPAL	$e^+e^- \to \gamma\gamma$
> 0.7	(> 0.7)	95	[23] ACHARD	03D	L3	$e^+e^- \to ZZ$
> 0.82	(> 0.78)	95	[24] ADLOFF	03	H1	$e^\pm p \to e^\pm X$
> 1.28	(> 1.25)	95	[25] GIUDICE	03	RVUE	
> 0.80	(> 0.85)	95	[26] HEISTER	03C	ALEP	$e^+e^- \to \gamma\gamma$
> 0.84	(> 0.99)	95	[27] ACHARD	02D	L3	$e^+e^- \to \gamma\gamma$
> 1.2	(> 1.1)	95	[28] ABBOTT	01	D0	$p\overline{p} \to e^+e^-, \gamma\gamma$
> 0.60	(> 0.63)	95	[29] ABBIENDI	00R	OPAL	$e^+e^- \to \mu^+\mu^-$
> 0.63	(> 0.50)	95	[29] ABBIENDI	00R	OPAL	$e^+e^- \to \tau^+\tau^-$
> 0.68	(> 0.61)	95	[29] ABBIENDI	00R	OPAL	$e^+e^- \to \mu^+\mu^-,\tau^+\tau^-$
			[30] ABREU	00A	DLPH	$e^+e^- \to \gamma\gamma$
> 0.680	(> 0.542)	95	[31] ABREU	00S	DLPH	$e^+e^- \to \mu^+\mu^-,\tau^+\tau^-$
> 15–28		99.7	[32] CHANG	00B	RVUE	Electroweak
> 0.98		95	[33] CHEUNG	00	RVUE	$e^+e^- \to \gamma\gamma$
> 0.29–0.38		95	[34] GRAESSER	00	RVUE	$(g-2)_\mu$
> 0.50–1.1		95	[35] HAN	00	RVUE	Electroweak
> 2.0	(> 2.0)	95	[36] MATHEWS	00	RVUE	$\overline{p}p \to jj$
> 1.0	(> 1.1)	95	[37] MELE	00	RVUE	$e^+e^- \to VV$
			[38] ABBIENDI	99P	OPAL	
			[39] ACCIARRI	99M	L3	
			[40] ACCIARRI	99S	L3	
> 1.412	(> 1.077)	95	[41] BOURILKOV	99		$e^+e^- \to e^+e^-$

[1] SIRUNYAN 17F use dijet angular distributions in 2.6 fb^{-1} of data from pp collisions at $\sqrt{s} = 13$ TeV to place a lower bound on Λ_T, here converted to M_{TT}.

[2] GIUDICE 03 place bounds on Λ_6, the coefficient of the gravitationally-induced dimension-6 operator $(2\pi\lambda/\Lambda_6^2)(\sum \overline{f}\gamma_\mu\gamma^5 f)(\sum \overline{f}\gamma^\mu\gamma^5 f)$, using data from a variety of experiments. Results are quoted for $\lambda = \pm 1$ and are independent of δ.

[3] AABOUD 17AP use 36.7 fb^{-1} of data from pp collisions at $\sqrt{s} = 13$ TeV to place lower limits on M_{TT} (equivalent to their M_S).

[4] KHACHATRYAN 15AE use 20.6 (19.7) fb^{-1} of data from pp collisions at $\sqrt{s} = 8$ TeV in the dimuon (dielectron) channel to place a lower limit on Λ_T, here converted to M_{TT}.

[5] KHACHATRYAN 15J use dijet angular distributions in 19.7 fb^{-1} of data from pp collisions at $\sqrt{s} = 8$ TeV to place a lower bound on Λ_T, here converted to M_{TT}.

[6] AAD 14BE use 20 fb^{-1} of data from pp collisions at $\sqrt{s} = 8$ TeV in the dilepton channel to place lower limits on M_{TT} (equivalent to their M_S).

[7] AAD 13AS use 4.9 fb^{-1} of data from pp collisions at $\sqrt{s} = 7$ TeV to place lower limits on M_{TT} (equivalent to their M_S).

[8] AAD 13E use 4.9 and 5.0 fb^{-1} of data from pp collisions at $\sqrt{s}$ = 7 TeV in the dielectron and dimuon channels, respectively, to place lower limits on M_{TT} (equivalent to their M_S). The dielectron and dimuon channels are combined with previous results in the diphoton channel to set the best limit. Bounds on individual channels and different priors can be found in their Table VIII.

[9] AAD 12Y use 2.12 fb^{-1} of data from pp collisions at $\sqrt{s}$ = 7 TeV to place lower limits on M_{TT} (equivalent to their M_S).

[10] BAAK 12 use electroweak precision observables to place bounds on the ratio Λ_T/M_D as a function of M_D. See their Fig. 22 for constraints with a Higgs mass of 120 GeV.

[11] CHATRCHYAN 12J use approximately 2 fb^{-1} of data from pp collisions at $\sqrt{s}$ = 7 TeV in the dielectron and dimuon channels to place lower limits on Λ_T, here converted to M_{TT}.

[12] CHATRCHYAN 12R use 2.2 fb^{-1} of data from pp collisions at $\sqrt{s}$ = 7 TeV to place lower limits on M_{TT} (equivalent to their M_S).

[13] AARON 11C search for deviations in the differential cross section of $e^{\pm}p \rightarrow e^{\pm}X$ in 446 pb^{-1} of data taken at $\sqrt{s}$ = 301 and 319 GeV to place a bound on M_{TT}.

[14] CHATRCHYAN 11A use 36 pb^{-1} of data from pp collisions at $\sqrt{s}$ = 7 TeV to place lower limits on Λ_T, here converted to M_{TT}.

[15] ABAZOV 09AE use dijet angular distributions in 0.7 fb^{-1} of data from $p\overline{p}$ collisions at $\sqrt{s}$ = 1.96 TeV to place lower bounds on Λ_T (equivalent to their M_S), here converted to M_{TT}.

[16] ABAZOV 09D use 1.05 fb^{-1} of data from $p\overline{p}$ collisions at $\sqrt{s}$ = 1.96 TeV to place lower bounds on Λ_T (equivalent to their M_s), here converted to M_{TT}.

[17] SCHAEL 07A use e^+e^- collisions at $\sqrt{s}$ = 189–209 GeV to place lower limits on Λ_T, here converted to limits on M_{TT}.

[18] ABDALLAH 06C use e^+e^- collisions at $\sqrt{s} \sim$ 130–207 GeV to place lower limits on M_{TT}, which is equivalent to their definition of M_s. Bound shown includes all possible final state leptons, $\ell = e, \mu, \tau$. Bounds on individual leptonic final states can be found in their Table 31.

[19] GERDES 06 use 100 to 110 pb^{-1} of data from $p\overline{p}$ collisions at $\sqrt{s}$ = 1.8 TeV, as recorded by the CDF Collaboration during Run I of the Tevatron. Bound shown includes a K-factor of 1.3. Bounds on individual e^+e^- and $\gamma\gamma$ final states are found in their Table I.

[20] ABAZOV 05V use 246 pb^{-1} of data from $p\overline{p}$ collisions at $\sqrt{s}$ = 1.96 TeV to search for deviations in the differential cross section to $\mu^+\mu^-$ from graviton exchange.

[21] CHEKANOV 04B search for deviations in the differential cross section of $e^{\pm}p \rightarrow e^{\pm}X$ with 130 pb^{-1} of combined data and Q^2 values up to 40,000 GeV^2 to place a bound on M_{TT}.

[22] ABBIENDI 03D use e^+e^- collisions at $\sqrt{s}$=181–209 GeV to place bounds on the ultraviolet scale M_{TT}, which is equivalent to their definition of M_S.

[23] ACHARD 03D look for deviations in the cross section for $e^+e^- \rightarrow ZZ$ from $\sqrt{s}$ = 200–209 GeV to place a bound on M_{TT}.

[24] ADLOFF 03 search for deviations in the differential cross section of $e^{\pm}p \rightarrow e^{\pm}X$ at $\sqrt{s}$=301 and 319 GeV to place bounds on M_{TT}.

[25] GIUDICE 03 review existing experimental bounds on M_{TT} and derive a combined limit.

[26] HEISTER 03C use e^+e^- collisions at $\sqrt{s}$= 189–209 GeV to place bounds on the scale of dim-8 gravitational interactions. Their $M_s^{\pm}$ is equivalent to our M_{TT} with λ=$\pm$1.

[27] ACHARD 02 search for s-channel graviton exchange effects in $e^+e^- \rightarrow \gamma\gamma$ at $E_{\rm cm}$ = 192–209 GeV.

[28] ABBOTT 01 search for variations in differential cross sections to e^+e^- and $\gamma\gamma$ final states at the Tevatron.

[29] ABBIENDI 00R uses e^+e^- collisions at $\sqrt{s}$= 189 GeV.

[30] ABREU 00A search for s-channel graviton exchange effects in $e^+e^- \rightarrow \gamma\gamma$ at $E_{\rm cm}$= 189–202 GeV.

[31] ABREU 00S uses e^+e^- collisions at $\sqrt{s}$=183 and 189 GeV. Bounds on μ and τ individual final states given in paper.

[32] CHANG 00B derive 3σ limit on M_{TT} of (28,19,15) TeV for δ=(2,4,6) respectively assuming the presence of a torsional coupling in the gravitational action. Highly model dependent.

[33] CHEUNG 00 obtains limits from anomalous diphoton production at OPAL due to graviton exchange. Original limit for δ=4. However, unknown UV theory renders δ dependence unreliable. Original paper works in HLZ convention.

[34] GRAESSER 00 obtains a bound from graviton contributions to $g-2$ of the muon through loops of 0.29 TeV for δ=2 and 0.38 TeV for δ=4,6. Limits scale as $\lambda^{1/2}$. However calculational scheme not well-defined without specification of high-scale theory. See the "Extra Dimensions Review."

[35] HAN 00 calculates corrections to gauge boson self-energies from KK graviton loops and constrain them using S and T. Bounds on M_{TT} range from 0.5 TeV (δ=6) to 1.1 TeV (δ=2); see text. Limits have strong dependence, $\lambda^{\delta+2}$, on unknown λ coefficient.

[36] MATHEWS 00 search for evidence of graviton exchange in CDF and DØ dijet production data. See their Table 2 for slightly stronger δ-dependent bounds. Limits expressed in terms of $\widetilde{M}_S^4 = M_{TT}^4/8$.

[37] MELE 00 obtains bound from KK graviton contributions to $e^+e^- \rightarrow VV$ (V=γ,W,Z) at LEP. Authors use Hewett conventions.

[38] ABBIENDI 99P search for s-channel graviton exchange effects in $e^+e^- \rightarrow \gamma\gamma$ at $E_{\rm cm}$=189 GeV. The limits $G_+ > 660$ GeV and $G_- > 634$ GeV are obtained from combined $E_{\rm cm}$=183 and 189 GeV data, where $G_{\pm}$ is a scale related to the fundamental gravity scale.

[39] ACCIARRI 99M search for the reaction $e^+e^- \rightarrow \gamma G$ and s-channel graviton exchange effects in $e^+e^- \rightarrow \gamma\gamma$, W^+W^-, ZZ, e^+e^-, $\mu^+\mu^-$, $\tau^+\tau^-$, $q\overline{q}$ at $E_{\rm cm}$=183 GeV. Limits on the gravity scale are listed in their Tables 1 and 2.

[40] ACCIARRI 99S search for the reaction $e^+e^- \rightarrow ZG$ and s-channel graviton exchange effects in $e^+e^- \rightarrow \gamma\gamma$, W^+W^-, ZZ, e^+e^-, $\mu^+\mu^-$, $\tau^+\tau^-$, $q\overline{q}$ at $E_{\rm cm}$=189 GeV. Limits on the gravity scale are listed in their Tables 1 and 2.

[41] BOURILKOV 99 performs global analysis of LEP data on e^+e^- collisions at $\sqrt{s}$=183 and 189 GeV. Bound is on Λ_T.

Limits on $1/R = M_C$

This section includes limits on $1/R = M_C$, the compactification scale in models with one TeV-sized extra dimension, due to exchange of Standard Model KK excitations. Bounds assume fermions are not in the bulk, unless stated otherwise. See the "Extra Dimensions" review for discussion of model dependence.

VALUE (TeV)	CL%	DOCUMENT ID		TECN	COMMENT
>4.16	95	[1] AAD	12CC	ATLS	$pp \rightarrow \ell\overline{\ell}$
>6.1		[2] BARBIERI	04	RVUE	Electroweak
• • • We do not use the following data for averages, fits, limits, etc. • • •					
>3.8	95	[3] ACCOMANDO	15	RVUE	Electroweak
>3.40	95	[4] KHACHATRY...15T		CMS	$pp \rightarrow \ell X$
		[5] CHATRCHYAN	13AQ	CMS	$pp \rightarrow \ell X$
>1.38	95	[6] CHATRCHYAN	13W	CMS	$pp \rightarrow \gamma\gamma$, δ=6, M_D=5 TeV
>0.715	95	[7] EDELHAUSER	13	RVUE	$pp \rightarrow \ell\overline{\ell} + X$
>1.40	95	[8] AAD	12CP	ATLS	$pp \rightarrow \gamma\gamma$, δ=6, M_D=5 TeV
>1.23	95	[9] AAD	12X	ATLS	$pp \rightarrow \gamma\gamma$, δ=6, M_D=5 TeV
>0.26	95	[10] ABAZOV	12M	D0	$p\overline{p} \rightarrow \mu\mu$
>0.75	95	[11] BAAK	12	RVUE	Electroweak
		[12] FLACKE	12	RVUE	Electroweak
>0.43	95	[13] NISHIWAKI	12	RVUE	$H \rightarrow WW, \gamma\gamma$
>0.729	95	[14] AAD	11F	ATLS	$pp \rightarrow \gamma\gamma$, δ=6, M_D=5 TeV
>0.961	95	[15] AAD	11X	ATLS	$pp \rightarrow \gamma\gamma$, δ=6, M_D=5 TeV
>0.477	95	[16] ABAZOV	10P	D0	$p\overline{p} \rightarrow \gamma\gamma$, δ=6, M_D=5 TeV
>1.59	95	[17] ABAZOV	09AE	D0	$p\overline{p} \rightarrow$ dijet, angular dist.
>0.6	95	[18] HAISCH	07	RVUE	$\overline{B} \rightarrow X_s\gamma$
>0.6	90	[19] GOGOLADZE	06	RVUE	Electroweak
>3.3	95	[20] CORNET	00	RVUE	Electroweak
> 3.3–3.8	95	[21] RIZZO	00	RVUE	Electroweak

[1] AAD 12CC use 4.9 and 5.0 fb^{-1} of data from pp collisions at $\sqrt{s}$ = 7 TeV in the dielectron and dimuon channels, respectively, to place a lower bound on the mass of the lightest KK Z/γ boson (equivalent to $1/R = M_C$). The limit quoted here assumes a flat prior corresponding to when the pure Z/γ KK cross section term dominates. See their Section 15 for more details.

[2] BARBIERI 04 use electroweak precision observables to place a lower bound on the compactification scale $1/R$. Both the gauge bosons and the Higgs boson are assumed to propagate in the bulk.

[3] ACCOMANDO 15 use electroweak precision observables to place a lower bound on the compactification scale $1/R$. See their Fig. 2 for the bound as a function of sinβ, which parametrizes the VEV contribution from brane and bulk Higgs fields. The quoted value is for the minimum bound which occurs at sinβ = 0.45.

[4] KHACHATRYAN 15T use 19.7 fb^{-1} of data from pp collisions at $\sqrt{s}$ = 8 TeV to place a lower bound on the compactification scale $1/R$.

[5] CHATRCHYAN 13AQ use 5.0 fb^{-1} of data from pp collisions at $\sqrt{s}$ = 7 TeV and a further 3.7 fb^{-1} of data at $\sqrt{s}$ = 8 TeV to place a lower bound on the compactification scale $1/R$, in models with universal extra dimensions and Standard Model fields propagating in the bulk. See their Fig. 5 for the bound as a function of the universal bulk fermion mass parameter μ.

[6] CHATRCHYAN 13W use diphoton events with large missing transverse momentum in 4.93 fb^{-1} of data produced from pp collisions at $\sqrt{s}$ = 7 TeV to place a lower bound on the compactification scale in a universal extra dimension model with gravitational decays. The bound assumes that the cutoff scale Λ, for the radiative corrections to the Kaluza-Klein masses, satisfies $\Lambda/M_C = 20$. The model parameters are chosen such that the decay $\gamma^* \rightarrow G\gamma$ occurs with an appreciable branching fraction.

[7] EDELHAUSER 13 use 19.6 and 20.6 fb^{-1} of data from pp collisions at $\sqrt{s}$ = 8 TeV analyzed by the CMS Collaboration in the dielectron and dimuon channels, respectively, to place a lower bound on the mass of the second lightest Kaluza-Klein Z/γ boson (converted to a limit on $1/R = M_C$). The bound assumes Standard Model fields propagating in the bulk and that the cutoff scale Λ, for the radiative corrections to the Kaluza-Klein masses, satisfies $\Lambda/M_C = 20$.

[8] AAD 12CP use diphoton events with large missing transverse momentum in 4.8 fb^{-1} of data produced from pp collisions at $\sqrt{s}$ = 7 TeV to place a lower bound on the compactification scale in a universal extra dimension model with gravitational decays. The bound assumes that the cutoff scale Λ, for the radiative corrections to the Kaluza-Klein masses, satisfies $\Lambda/M_C = 20$. The model parameters are chosen such that the decay $\gamma^* \rightarrow G\gamma$ occurs with an appreciable branching fraction.

[9] AAD 12X use diphoton events with large missing transverse momentum in 1.07 fb^{-1} of data produced from pp collisions at $\sqrt{s}$ = 7 TeV to place a lower bound on the compactification scale in a universal extra dimension model with gravitational decays. The bound assumes that the cutoff scale Λ, for the radiative corrections to the Kaluza-Klein masses, satisfies $\Lambda/M_C = 20$. The model parameters are chosen such that the decay $\gamma^* \rightarrow G\gamma$ occurs with an appreciable branching fraction.

[10] ABAZOV 12M use same-sign dimuon events in 7.3 fb^{-1} of data from $p\overline{p}$ collisions at $\sqrt{s}$ = 1.96 TeV to place a lower bound on the compactification scale $1/R$, in models with universal extra dimensions where all Standard Model fields propagate in the bulk.

[11] BAAK 12 use electroweak precision observables to place a lower bound on the compactification scale $1/R$, in models with universal extra dimensions and Standard Model fields propagating in the bulk. Bound assumes a 125 GeV Higgs mass. See their Fig. 25 for the bound as a function of the Higgs mass.

[12] FLACKE 12 use electroweak precision observables to place a lower bound on the compactification scale $1/R$, in models with universal extra dimensions and Standard Model fields propagating in the bulk. See their Fig. 1 for the bound as a function of the universal bulk fermion mass parameter μ.

[13] NISHIWAKI 12 use up to 2 fb^{-1} of data from the ATLAS and CMS experiments that constrains the production cross section of a Higgs-like particle to place a lower bound on the compactification scale $1/R$ in universal extra dimension models. The quoted bound assumes Standard Model fields propagating in the bulk and a 125 GeV Higgs mass. See their Fig. 1 for the bound as a function of the Higgs mass.

[14] AAD 11F use diphoton events with large missing transverse energy in 3.1 pb^{-1} of data produced from pp collisions at $\sqrt{s}$ = 7 TeV to place a lower bound on the compactification scale in a universal extra dimension model with gravitational decays. The bound assumes that the cutoff scale Λ, for the radiative corrections to the Kaluza-Klein masses,

satisfies $\Lambda/M_c = 20$. The model parameters are chosen such that the decay $\gamma^* \rightarrow G\gamma$ occurs with an appreciable branching fraction.

[15] AAD 11X use diphoton events with large missing transverse energy in 36 pb^{-1} of data produced from pp collisions at $\sqrt{s} = 7$ TeV to place a lower bound on the compactification scale in a universal extra dimension model with gravitational decays. The bound assumes that the cutoff scale Λ, for the radiative corrections to the Kaluza-Klein masses, satisfies $\Lambda/M_c = 20$. The model parameters are chosen such that the decay $\gamma^* \rightarrow G\gamma$ occurs with an appreciable branching fraction.

[16] ABAZOV 10P use diphoton events with large missing transverse energy in 6.3 fb^{-1} of data produced from $p\overline{p}$ collisions at $\sqrt{s} = 1.96$ TeV to place a lower bound on the compactification scale in a universal extra dimension model with gravitational decays. The bound assumes that the cutoff scale Λ, for the radiative corrections to the Kaluza-Klein masses, satisfies Λ/M_c=20. The model parameters are chosen such that the decay $\gamma^* \rightarrow G\gamma$ occurs with an appreciable branching fraction.

[17] ABAZOV 09AE use dijet angular distributions in 0.7 fb^{-1} of data from $p\overline{p}$ collisions at $\sqrt{s} = 1.96$ TeV to place a lower bound on the compactification scale.

[18] HAISCH 07 use inclusive $\overline{B}$-meson decays to place a Higgs mass independent bound on the compactification scale $1/R$ in the minimal universal extra dimension model.

[19] GOGOLADZE 06 use electroweak precision observables to place a lower bound on the compactification scale in models with universal extra dimensions. Bound assumes a 115 GeV Higgs mass. See their Fig. 3 for the bound as a function of the Higgs mass.

[20] CORNET 00 translates a bound on the coefficient of the 4-fermion operator $(\overline{\ell}\gamma_\mu\tau^a\ell)(\overline{\ell}\gamma^\mu\tau^a\ell)$ derived by Hagiwara and Matsumoto into a limit on the mass scale of KK W bosons.

[21] RIZZO 00 obtains limits from global electroweak fits in models with a Higgs in the bulk (3.8 TeV) or on the standard brane (3.3 TeV).

Limits on Kaluza-Klein Gravitons in Warped Extra Dimensions

This section places limits on the mass of the first Kaluza-Klein (KK) excitation of the graviton in the warped extra dimension model of Randall and Sundrum. Bounds in parenthesis assume Standard Model fields propagate in the bulk. Experimental bounds depend strongly on the warp parameter, k. See the "Extra Dimensions" review for a full discussion.

Here we list limits for the value of the warp parameter $k/\overline{M}_P = 0.1$.

VALUE (TeV)	CL%	DOCUMENT ID		TECN	COMMENT
>4.1	95	[1] AABOUD	17AP	ATLS	$pp \rightarrow G \rightarrow \gamma\gamma$
• • • We do not use the following data for averages, fits, limits, etc. • • •					
		[2] SIRUNYAN	18F	CMS	$pp \rightarrow G \rightarrow hh$
>3.11	95	[3] KHACHATRY...	17T	CMS	$pp \rightarrow G \rightarrow e^+e^-, \mu^+\mu^-$
>1.9	95	[4] KHACHATRY...	17W	CMS	$pp \rightarrow G \rightarrow jj$
		[5] SIRUNYAN	17AK	CMS	$pp \rightarrow G \rightarrow WW,\ ZZ$
		[6] AABOUD	16AE	ATLS	$pp \rightarrow G \rightarrow WW,ZZ$
		[7] AABOUD	16H	ATLS	$pp \rightarrow G \rightarrow \gamma\gamma$
		[8] AABOUD	16I	ATLS	$pp \rightarrow G \rightarrow hh$
		[9] AAD	16R	ATLS	$pp \rightarrow G \rightarrow WW,ZZ$
		[10] KHACHATRY...	16BQ	CMS	$pp \rightarrow G \rightarrow hh$
>3.3	95	[11] KHACHATRY...	16M	CMS	$pp \rightarrow G \rightarrow \gamma\gamma$
>2.66	95	[12] AAD	15AD	ATLS	$pp \rightarrow G \rightarrow \gamma\gamma$
		[13] AAD	15AU	ATLS	$pp \rightarrow G \rightarrow ZZ$
		[14] AAD	15AZ	ATLS	$pp \rightarrow G \rightarrow WW$
		[15] AAD	15BK	ATLS	$pp \rightarrow G \rightarrow hh$
		[16] AAD	15CT	ATLS	$pp \rightarrow G \rightarrow WW,ZZ$
>2.73	95	[17] KHACHATRY...	15AE	CMS	$pp \rightarrow e^+e^-,\ \mu^+\mu^-$
		[18] KHACHATRY...	15R	CMS	$pp \rightarrow G \rightarrow hh$
>2.68	95	[19] AAD	14V	ATLS	$pp \rightarrow G \rightarrow e^+e^-, \mu^+\mu^-$
		[20] KHACHATRY...	14A	CMS	$pp \rightarrow G \rightarrow WW,ZZ,WZ$
>1.23 (>0.84)	95	[21] AAD	13A	ATLS	$pp \rightarrow G \rightarrow WW$
>0.94 (>0.71)	95	[22] AAD	13AO	ATLS	$pp \rightarrow G \rightarrow WW$
>2.23	95	[23] AAD	13AS	ATLS	$pp \rightarrow \gamma\gamma, e^+e^-, \mu^+\mu^-$
>2.39	95	[24] CHATRCHYAN	13AF	CMS	$pp \rightarrow e^+e^-, \mu^+\mu^-$
		[25] CHATRCHYAN	13U	CMS	$pp \rightarrow G \rightarrow ZZ$
>0.845	95	[26] AAD	12AD	ATLS	$pp \rightarrow G \rightarrow ZZ$
>2.16	95	[27] AAD	12CC	ATLS	$pp \rightarrow G \rightarrow \ell\overline{\ell}$
>1.95	95	[28] AAD	12Y	ATLS	$pp \rightarrow \gamma\gamma, e^+e^-, \mu^+\mu^-$
		[29] AALTONEN	12V	CDF	$p\overline{p} \rightarrow G \rightarrow ZZ$
		[30] BAAK	12	RVUE	Electroweak
>1.84	95	[31] CHATRCHYAN	12R	CMS	$pp \rightarrow G \rightarrow \gamma\gamma$
>1.63	95	[32] AAD	11AD	ATLS	$pp \rightarrow G \rightarrow \ell\overline{\ell}$
		[33] AALTONEN	11G	CDF	$p\overline{p} \rightarrow G \rightarrow ZZ$
>1.058	95	[34] AALTONEN	11R	CDF	$p\overline{p} \rightarrow G \rightarrow e^+e^-, \gamma\gamma$
>0.754	95	[35] ABAZOV	11H	D0	$p\overline{p} \rightarrow G \rightarrow WW$
>1.079	95	[36] CHATRCHYAN	11	CMS	$pp \rightarrow G \rightarrow \ell\overline{\ell}$
>0.607		[37] AALTONEN	10N	CDF	$p\overline{p} \rightarrow G \rightarrow WW$
>1.05		[38] ABAZOV	10F	D0	$p\overline{p} \rightarrow G \rightarrow e^+e^-,\ \gamma\gamma$
		[39] AALTONEN	08S	CDF	$p\overline{p} \rightarrow G \rightarrow ZZ$
>0.90		[40] ABAZOV	08J	D0	$p\overline{p} \rightarrow G \rightarrow e^+e^-, \gamma\gamma$
		[41] AALTONEN	07G	CDF	$p\overline{p} \rightarrow G \rightarrow \gamma\gamma$
>0.889		[42] AALTONEN	07H	CDF	$p\overline{p} \rightarrow G \rightarrow e\overline{e}$
>0.785		[43] ABAZOV	05N	D0	$p\overline{p} \rightarrow G \rightarrow \ell\ell, \gamma\gamma$
>0.71		[44] ABULENCIA	05A	CDF	$p\overline{p} \rightarrow G \rightarrow \ell\overline{\ell}$

[1] AABOUD 17AP use 36.7 fb^{-1} of data from pp collisions at $\sqrt{s} = 13$ TeV in the diphoton channel to place a lower limit on the mass of the lightest KK graviton.

[2] SIRUNYAN 18F use 35.9 fb^{-1} of data from pp collisions at $\sqrt{s} = 13$ TeV to search for Higgs boson pair production in the $b\overline{b}\ell\nu\ell\nu$ final state. See their Figure 7 for limits on the cross section times branching fraction as a function of the KK graviton mass with a warp parameter value $k/\overline{M}_P = 0.1$.

[3] KHACHATRYAN 17T use 2.7 (2.9) fb^{-1} of data from pp collisions at $\sqrt{s} = 13$ TeV in the dielectron (dimuon) channel. This 13 TeV data is combined with 20 fb^{-1} of a previously analyzed set of 8 TeV data to place a lower bound on the mass of the lightest KK graviton. See their paper for the limit with warp parameter value $k/\overline{M}_P = 0.01$.

[4] KHACHATRYAN 17W use 12.9 fb^{-1} of data from pp collisions at $\sqrt{s} = 13$ TeV to place a lower bound on the mass of the lightest KK graviton. (The quoted bound is for a warp parameter value of $k/\overline{M}_P = 0.1$, although it was not disclosed in the publication.)

[5] SIRUNYAN 17AK use 19.7 fb^{-1} and up to 2.7 fb^{-1} of data from pp collisions at $\sqrt{s}$ = 8 TeV and 13 TeV, respectively, to place limits on the production cross section of a KK graviton resonance. See their Figure 3 for exclusion limits on the signal strength for $k/\overline{M}_P = 0.5$ and a mass range of 0.6 to 4.0 TeV .

[6] AABOUD 16AE use 3.2 fb^{-1} of data from pp collisions at $\sqrt{s} = 13$ TeV to place a lower bound on the mass of the lightest KK graviton. See their Figure 8 for the limit on the KK graviton mass as a function of the cross section times branching fraction for $k/\overline{M}_P = 1$.

[7] AABOUD 16H use 3.2 fb^{-1} of data from pp collisions at $\sqrt{s} = 13$ TeV in the diphoton channel to place a lower limit on the mass of the lightest KK graviton. See their Figure 11 for limits on the cross section times branching fraction as a function of the graviton mass with warp parameter values $k/\overline{M}_P$ between 0.01 and 0.3.

[8] AABOUD 16I use 3.2 fb^{-1} of data from pp collisions at $\sqrt{s} = 13$ TeV to search for Higgs boson pair production in the $b\overline{b}b\overline{b}$ final state. See their Figure 10 for limits on the cross section times branching fraction as a function of the KK graviton mass with warp parameter values $k/\overline{M}_P = 1.0$ and 2.0.

[9] AAD 16R use 20.3 fb^{-1} of data from pp collisions at $\sqrt{s} = 8$ TeV to place a lower bound on the mass of the lightest KK graviton. See their Figure 4 for the limit on the KK graviton mass as a function of the cross section times branching fraction.

[10] KHACHATRYAN 16BQ use 19.7 fb^{-1} of data from pp collisions at $\sqrt{s} = 8$ TeV to search for Higgs boson pair production in the $\gamma\gamma b\overline{b}$ final state. See their Figure 9 for limits on the cross section times branching fraction as a function of the KK graviton mass with a warp parameter value $k/\overline{M}_P = 0.2$.

[11] KHACHATRYAN 16M use 19.7 fb^{-1} and 3.3 fb^{-1} of data from pp collisions at $\sqrt{s}$ = 8 TeV and 13 TeV, respectively, in the diphoton channel to place a lower limit on the mass of the lightest KK graviton. See their paper for limits with other warp parameter values $k/\overline{M}_P = 0.01$ and 0.2.

[12] AAD 15AD use 20.3 fb^{-1} of data from pp collisions at $\sqrt{s} = 8$ TeV in the diphoton channel to place a lower limit on the mass of the lightest KK graviton. See their Table IV for limits with warp parameter values $k/\overline{M}_P$ between 0.01 and 0.1.

[13] AAD 15AU use 20 fb^{-1} of data from pp collisions at $\sqrt{s} = 8$ TeV to search for KK gravitons in a warped extra dimension decaying to ZZ dibosons. See their Figure 2 for limits on the KK graviton mass as a function of the cross section times branching fraction.

[14] AAD 15AZ use 20.3 fb^{-1} of data from pp collisions at $\sqrt{s} = 8$ TeV to place a lower bound on the mass of the lightest KK graviton. See their Figure 2 for limits on the KK graviton mass as a function of the cross section times branching ratio.

[15] AAD 15BK use 19.5 fb^{-1} of data from pp collisions at $\sqrt{s} = 8$ TeV to search for Higgs boson pair production in the $b\overline{b}b\overline{b}$ final state, and exclude masses of the lightest KK graviton. See their Table 9 for the excluded mass ranges with warp parameter values $k/\overline{M}_P = 1.0$, 1.5, and 2.0.

[16] AAD 15CT use 20.3 fb^{-1} of data from pp collisions at $\sqrt{s} = 8$ TeV to place a lower bound on the mass of the lightest KK graviton. See their Figures 6b and 6c for the limit on the KK graviton mass as a function of the cross section times branching fraction.

[17] KHACHATRYAN 15AE use 20.6 (19.7) fb^{-1} of data from pp collisions at $\sqrt{s} = 8$ TeV in the dimuon (dielectron) channel to place a lower bound on the mass of the lightest KK graviton.

[18] KHACHATRYAN 15R use 17.9 fb^{-1} of data from pp collisions at $\sqrt{s} = 8$ TeV to search for Higgs boson pair production in the $b\overline{b}b\overline{b}$ final state, and exclude a KK graviton with mass from 380 to 830 GeV.

[19] AAD 14V use 20 fb^{-1} of data from pp collisions at $\sqrt{s} = 8$ TeV in the dielectron and dimuon channels to place a lower bound on the mass of the lightest KK graviton.

[20] KHACHATRYAN 14A use 19.7 fb^{-1} of data from pp collisions at $\sqrt{s} = 8$ TeV to search for KK gravitons in a warped extra dimension decaying to dibosons. See their Figure 9 for limits on the cross section times branching fraction as a function of the KK graviton mass.

[21] AAD 13A use 4.7 fb^{-1} of data from pp collisions at $\sqrt{s} = 7$ TeV in the $\ell\nu\ell\nu$ channel, to place a lower bound on the mass of the lightest KK graviton.

[22] AAD 13AO use 4.7 fb^{-1} of data from pp collisions at $\sqrt{s} = 7$ TeV in the $\ell\nu jj$ channel, to place a lower bound on the mass of the lightest KK graviton.

[23] AAD 13AS use 4.9 fb^{-1} of data from pp collisions at $\sqrt{s} = 7$ TeV in the diphoton channel to place lower limits on the mass of the lightest KK graviton. The diphoton channel is combined with previous results in the dielectron and dimuon channels to set the best limit. See their Table 2 for warp parameter values $k/\overline{M}_P$ between 0.01 and 0.1.

[24] CHATRCHYAN 13AF use 5.3 and 4.1 fb^{-1} of data from pp collisions at $\sqrt{s} = 7$ TeV and 8 TeV, respectively, in the dielectron and dimuon channels, to place a lower bound on the mass of the lightest KK graviton.

[25] CHATRCHYAN 13U use 5 fb^{-1} of data from pp collisions at $\sqrt{s} = 7$ TeV to search for KK gravitons in a warped extra dimension decaying to ZZ dibosons. See their Figure 5 for limits on the lightest KK graviton mass as a function of $k/\overline{M}_P$.

[26] AAD 12AD use 1.02 fb^{-1} of data from pp collisions at $\sqrt{s} = 7$ TeV to search for KK gravitons in a warped extra dimension decaying to ZZ dibosons in the $lljj$ and $llll$ channels (ℓ=e, μ). The limit is quoted for the combined $lljj + llll$ channels. See their Figure 5 for limits on the cross section $\sigma(G \rightarrow ZZ)$ as a function of the graviton mass.

[27] AAD 12CC use 4.9 and 5.0 fb^{-1} of data from pp collisions at $\sqrt{s} = 7$ TeV in the dielectron and dimuon channels, respectively, to place a lower bound on the mass of the lightest KK graviton. See their Figure 5 for limits on the lightest KK graviton mass as a function of $k/\overline{M}_P$.

[28] AAD 12Y use 2.12 fb^{-1} of data from pp collisions at $\sqrt{s} = 7$ TeV in the diphoton channel to place lower limits on the mass of the lightest KK graviton. The diphoton channel is combined with previous results in the dielectron and dimuon channels to set the best limit. See their Table 3 for warp parameter values $k/\overline{M}_P$ between 0.01 and 0.1.

[29] AALTONEN 12V use 6 fb^{-1} of data from $p\overline{p}$ collisions at $\sqrt{s} = 1.96$ TeV to search for KK gravitons in a warped extra dimension decaying to ZZ dibosons in the $lljj$ and $llll$ channels (ℓ=e, μ). It provides improved limits over the previous analysis in AALTONEN 11G. See their Figure 16 for limits from all channels combined on the cross section times branching ratio $\sigma(p\overline{p} \rightarrow G^* \rightarrow ZZ)$ as a function of the graviton mass.

[30] BAAK 12 use electroweak precision observables to place a lower bound on the compactification scale $k\,e^{-\pi k R}$, assuming Standard Model fields propagate in the bulk and the Higgs is confined to the IR brane. See their Fig. 27 for more details.

[31] CHATRCHYAN 12R use 2.2 fb^{-1} of data from pp collisions at $\sqrt{s} = 7$ TeV in the diphoton channel to place lower limits on the mass of the lightest KK graviton. See their Table III for warp parameter values $k/\overline{M}_P$ between 0.01 and 0.1.

[32] AAD 11AD use 1.08 and 1.21 fb^{-1} of data from pp collisions at $\sqrt{s} = 7$ TeV in the dielectron and dimuon channels, respectively, to place a lower bound on the mass of the lightest graviton. For warp parameter values $k/\overline{M}_P$ between 0.01 to 0.1 the lower limit on the mass of the lightest graviton is between 0.71 and 1.63 TeV. See their Table IV for more details.

[33] AALTONEN 11G use 2.5–2.9 fb^{-1} of data from $p\overline{p}$ collisions at $\sqrt{s} = 1.96$ TeV to search for KK gravitons in a warped extra dimension decaying to ZZ dibosons via the $eeee$, $ee\mu\mu$, $\mu\mu\mu\mu$, $eejj$, and $\mu\mu jj$ channels. See their Fig. 20 for limits on the cross section $\sigma(G \rightarrow ZZ)$ as a function of the graviton mass.

[34] AALTONEN 11R uses 5.7 fb^{-1} of data from $p\overline{p}$ collisions at $\sqrt{s} = 1.96$ TeV in the dielectron channel to place a lower bound on the mass of the lightest graviton. It provides combined limits with the diphoton channel analysis of AALTONEN 11U. For warp parameter values $k/\overline{M}_P$ between 0.01 to 0.1 the lower limit on the mass of the lightest graviton is between 612 and 1058 GeV. See their Table I for more details.

[35] ABAZOV 11H use 5.4 fb^{-1} of data from $p\overline{p}$ collisions at $\sqrt{s} = 1.96$ TeV to place a lower bound on the mass of the lightest graviton. Their 95% C.L. exclusion limit does not include masses less than 300 GeV.

[36] CHATRCHYAN 11 use 35 and 40 pb^{-1} of data from pp collisions at $\sqrt{s} = 7$ TeV in the dielectron and dimuon channels, respectively, to place a lower bound on the mass of the lightest graviton. For a warp parameter value $k/\overline{M}_P = 0.05$, the lower limit on the mass of the lightest graviton is 0.855 TeV.

[37] AALTONEN 10N use 2.9 fb^{-1} of data from $p\overline{p}$ collisions at $\sqrt{s} = 1.96$ TeV to place a lower bound on the mass of the lightest graviton.

[38] ABAZOV 10F use 5.4 fb^{-1} of data from $p\overline{p}$ collisions at $\sqrt{s} = 1.96$ TeV to place a lower bound on the mass of the lightest graviton. For warp parameter values of $k/\overline{M}_P$ between 0.01 and 0.1 the lower limit on the mass of the lightest graviton is between 560 and 1050 GeV. See their Fig. 3 for more details.

[39] AALTONEN 08S use $p\overline{p}$ collisions at $\sqrt{s} = 1.96$ TeV to search for KK gravitons in warped extra dimensions. They search for graviton resonances decaying to four electrons via two Z bosons using 1.1 fb^{-1} of data. See their Fig. 8 for limits on $\sigma \cdot \mathrm{B}(G \rightarrow ZZ)$ versus the graviton mass.

[40] ABAZOV 08J use $p\overline{p}$ collisions at $\sqrt{s} = 1.96$ TeV to search for KK gravitons in warped extra dimensions. They search for graviton resonances decaying to electrons and photons using 1 fb^{-1} of data. For warp parameter values of $k/\overline{M}_P$ between 0.01 and 0.1 the lower limit on the mass of the lightest excitation is between 300 and 900 GeV. See their Fig. 4 for more details.

[41] AALTONEN 07G use $p\overline{p}$ collisions at $\sqrt{s} = 1.96$ TeV to search for KK gravitons in warped extra dimensions. They search for graviton resonances decaying to photons using 1.2 fb^{-1} of data. For warp parameter values of $k/\overline{M}_P = 0.1$, 0.05, and 0.01 the bounds on the graviton mass are 850, 694, and 230 GeV, respectively. See their Fig. 3 for more details. See also AALTONEN 07H.

[42] AALTONEN 07H use $p\overline{p}$ collisions at $\sqrt{s} = 1.96$ TeV to search for KK gravitons in warped extra dimensions. They search for graviton resonances decaying to electrons using 1.3 fb^{-1} of data. For a warp parameter value of $k/\overline{M}_P = 0.1$ the bound on the graviton mass is 807 GeV. See their Fig. 4 for more details. A combined analysis with the diphoton data of AALTONEN 07G yields for $k/\overline{M}_P = 0.1$ a graviton mass lower bound of 889 GeV.

[43] ABAZOV 05N use $p\overline{p}$ collisions at $\sqrt{s} = 1.96$ TeV to search for KK gravitons in warped extra dimensions. They search for graviton resonances decaying to muons, electrons or photons, using 260 pb^{-1} of data. For warp parameter values of $k/\overline{M}_P = 0.1$, 0.05, and 0.01, the bounds on the graviton mass are 785, 650 and 250 GeV respectively. See their Fig. 3 for more details.

[44] ABULENCIA 05A use $p\overline{p}$ collisions at $\sqrt{s} = 1.96$ TeV to search for KK gravitons in warped extra dimensions. They search for graviton resonances decaying to muons or electrons, using 200 pb^{-1} of data. For warp parameter values of $k/\overline{M}_P = 0.1$, 0.05, and 0.01, the bounds on the graviton mass are 710, 510 and 170 GeV respectively.

Limits on Kaluza-Klein Gluons in Warped Extra Dimensions

This section places limits on the mass of the first Kaluza-Klein (KK) excitation of the gluon in warped extra dimension models with Standard Model fields propagating in the bulk. Bounds are given for a specific benchmark model with $\Gamma/m = 15.3\%$ where Γ is the width and m the mass of the KK gluon. See the "Extra Dimensions" review for more discussion.

VALUE (TeV)	CL%	DOCUMENT ID		TECN	COMMENT
>2.5	95	[1] CHATRCHYAN	13BM	CMS	$g_{KK} \rightarrow t\bar{t}$
• • • We do not use the following data for averages, fits, limits, etc. • • •					
>2.07	95	[2] AAD	13AQ	ATLS	$g_{KK} \rightarrow t\bar{t} \rightarrow \ell j$
		[3] CHEN	13A		$\overline{B} \rightarrow X_s\gamma$
>1.5	95	[4] AAD	12BV	ATLS	$g_{KK} \rightarrow t\bar{t} \rightarrow \ell j$

[1] CHATRCHYAN 13BM use 19.7 fb^{-1} of data from pp collisions at $\sqrt{s} = 8$ TeV. Bound is for a width of approximately 15–20% of the KK gluon mass.

[2] AAD 13AQ use 4.7 fb^{-1} of data from pp collisions at $\sqrt{s} = 7$ TeV.

[3] CHEN 13A place limits on the KK mass scale for a specific warped model with custodial symmetry and bulk fermions. See their Figures 4 and 5.

[4] AAD 12BV use 2.05 fb^{-1} of data from pp collisions at $\sqrt{s} = 7$ TeV.

REFERENCES FOR Extra Dimensions

SIRUNYAN	18F	JHEP 1801 054	A.M. Sirunyan *et al.*	(CMS Collab.)
AABOUD	17AP	PL B775 105	M. Aaboud *et al.*	(ATLAS Collab.)
KHACHATRY...	17T	PL B768 57	V. Khachatryan *et al.*	(CMS Collab.)
KHACHATRY...	17W	PL B769 520	V. Khachatryan *et al.*	(CMS Collab.)
KLIMCHITSK...	17A	PR D95 123013	G.L. Klimchitskaya, V.M. Mostepanenko	
SIRUNYAN	17AK	PL B774 533	A.M. Sirunyan *et al.*	(CMS Collab.)
SIRUNYAN	17AQ	JHEP 1710 073	A.M. Sirunyan *et al.*	(CMS Collab.)
SIRUNYAN	17F	JHEP 1707 013	A.M. Sirunyan *et al.*	(CMS Collab.)
AABOUD	16AE	JHEP 1609 173	M. Aaboud *et al.*	(ATLAS Collab.)
AABOUD	16D	PR D94 032005	M. Aaboud *et al.*	(ATLAS Collab.)
AABOUD	16F	JHEP 1606 059	M. Aaboud *et al.*	(ATLAS Collab.)
AABOUD	16H	JHEP 1609 001	M. Aaboud *et al.*	(ATLAS Collab.)
AABOUD	16I	PR D94 052002	M. Aaboud *et al.*	(ATLAS Collab.)
AAD	16R	PL B755 285	G. Aad *et al.*	(ATLAS Collab.)
KHACHATRY...	16BQ	PR D94 052012	V. Khachatryan *et al.*	(CMS Collab.)
KHACHATRY...	16M	PRL 117 051802	V. Khachatryan *et al.*	(CMS Collab.)
KHACHATRY...	16N	PL B755 102	V. Khachatryan *et al.*	(CMS Collab.)
AAD	15AD	PR D92 032004	G. Aad *et al.*	(ATLAS Collab.)
AAD	15AU	EPJ C75 69	G. Aad *et al.*	(ATLAS Collab.)
AAD	15AZ	EPJ C75 209	G. Aad *et al.*	(ATLAS Collab.)
Also		EPJ C75 370 (errat.)	G. Aad *et al.*	(ATLAS Collab.)
AAD	15BH	EPJ C75 299	G. Aad *et al.*	(ATLAS Collab.)
Also		EPJ C75 408 (errat.)	G. Aad *et al.*	(ATLAS Collab.)
AAD	15BK	EPJ C75 412	G. Aad *et al.*	(ATLAS Collab.)
AAD	15CS	PR D91 012008	G. Aad *et al.*	(ATLAS Collab.)
Also		PR D92 059903 (errat.)	G. Aad *et al.*	(ATLAS Collab.)
AAD	15CT	JHEP 1512 055	G. Aad *et al.*	(ATLAS Collab.)
ACCOMANDO	15	MPL A30 1540010	E. Accomando	(SHMP)
KHACHATRY...	15AE	JHEP 1504 025	V. Khachatryan *et al.*	(CMS Collab.)
KHACHATRY...	15AL	EPJ C75 235	V. Khachatryan *et al.*	(CMS Collab.)
KHACHATRY...	15J	PL B746 79	V. Khachatryan *et al.*	(CMS Collab.)
KHACHATRY...	15R	PL B749 560	V. Khachatryan *et al.*	(CMS Collab.)
KHACHATRY...	15T	PR D91 092005	V. Khachatryan *et al.*	(CMS Collab.)
AAD	14BE	EPJ C74 3134	G. Aad *et al.*	(ATLAS Collab.)
AAD	14V	PR D90 052005	G. Aad *et al.*	(ATLAS Collab.)
KHACHATRY...	14A	JHEP 1408 174	V. Khachatryan *et al.*	(CMS Collab.)
AAD	13A	PL B718 860	G. Aad *et al.*	(ATLAS Collab.)
AAD	13AD	JHEP 1304 075	G. Aad *et al.*	(ATLAS Collab.)
AAD	13AO	PR D87 112006	G. Aad *et al.*	(ATLAS Collab.)
AAD	13AQ	PR D88 012004	G. Aad *et al.*	(ATLAS Collab.)
AAD	13AS	NJP 15 043007	G. Aad *et al.*	(ATLAS Collab.)
AAD	13C	PRL 110 011802	G. Aad *et al.*	(ATLAS Collab.)
AAD	13D	JHEP 1301 029	G. Aad *et al.*	(ATLAS Collab.)
AAD	13E	PR D87 015010	G. Aad *et al.*	(ATLAS Collab.)
CHATRCHYAN	13AF	PL B720 63	S. Chatrchyan *et al.*	(CMS Collab.)
CHATRCHYAN	13AQ	PR D87 072005	S. Chatrchyan *et al.*	(CMS Collab.)
CHATRCHYAN	13BM	PRL 111 211804	S. Chatrchyan *et al.*	(CMS Collab.)
Also		PRL 112 119903 (errat.)	S. Chatrchyan *et al.*	(CMS Collab.)
CHATRCHYAN	13U	JHEP 1302 036	S. Chatrchyan *et al.*	(CMS Collab.)
CHATRCHYAN	13W	JHEP 1303 111	S. Chatrchyan *et al.*	(CMS Collab.)
CHEN	13A	CP C37 063102	J-B. Chen *et al.*	(DALI)
EDELHAUSER	13	JHEP 1308 091	L. Edelhauser, T. Flacke, M. Kramer	(AACH, KAIST)
XU	13	JP G40 035107	J. Xu *et al.*	
AAD	12AD	PL B712 331	G. Aad *et al.*	(ATLAS Collab.)
AAD	12BV	JHEP 1209 041	G. Aad *et al.*	(ATLAS Collab.)
AAD	12CC	JHEP 1211 138	G. Aad *et al.*	(ATLAS Collab.)
AAD	12CP	PL B718 411	G. Aad *et al.*	(ATLAS Collab.)
AAD	12X	PL B710 519	G. Aad *et al.*	(ATLAS Collab.)
AAD	12Y	PL B710 538	G. Aad *et al.*	(ATLAS Collab.)
AALTONEN	12V	PR D85 012008	T. Aaltonen *et al.*	(CDF Collab.)
ABAZOV	12M	PRL 108 131802	V.M. Abazov *et al.*	(D0 Collab.)
AJELLO	12	JCAP 1202 012	M. Ajello *et al.*	(Fermi-LAT Collab.)
BAAK	12	EPJ C72 2003	M. Baak *et al.*	(Gfitter Group)
CHATRCHYAN	12AP	JHEP 1209 094	S. Chatrchyan *et al.*	(CMS Collab.)
CHATRCHYAN	12J	PL B711 15	S. Chatrchyan *et al.*	(CMS Collab.)
CHATRCHYAN	12R	PRL 108 111801	S. Chatrchyan *et al.*	(CMS Collab.)
FLACKE	12	PR D85 126007	T. Flacke, C. Pasold	(WURZ)
NISHIWAKI	12	PL B707 506	K. Nishiwaki *et al.*	(KOBE, OSAK)
AAD	11AD	PRL 107 272002	G. Aad *et al.*	(ATLAS Collab.)
AAD	11F	PRL 106 121803	G. Aad *et al.*	(ATLAS Collab.)
AAD	11S	PL B705 294	G. Aad *et al.*	(ATLAS Collab.)
AAD	11X	EPJ C71 1744	G. Aad *et al.*	(ATLAS Collab.)
AALTONEN	11G	PR D83 112008	T. Aaltonen *et al.*	(CDF Collab.)
AALTONEN	11R	PRL 107 051801	T. Aaltonen *et al.*	(CDF Collab.)
AALTONEN	11U	PR D83 011102	T. Aaltonen *et al.*	(CDF Collab.)
AARON	11C	PL B705 52	F. D. Aaron *et al.*	(H1 Collab.)
ABAZOV	11H	PRL 107 011801	V.M. Abazov *et al.*	(D0 Collab.)
BEZERRA	11	PR D83 075004	V.B. Bezerra *et al.*	
CHATRCHYAN	11	JHEP 1105 093	S. Chatrchyan *et al.*	(CMS Collab.)
CHATRCHYAN	11A	JHEP 1105 085	S. Chatrchyan *et al.*	(CMS Collab.)
CHATRCHYAN	11U	PRL 107 201804	S. Chatychyan *et al.*	(CMS Collab.)
SUSHKOV	11	PRL 107 171101	A.O. Sushkov *et al.*	
AALTONEN	10N	PRL 104 241801	T. Aaltonen *et al.*	(CDF Collab.)
ABAZOV	10F	PRL 104 241802	V.M. Abazov *et al.*	(D0 Collab.)
ABAZOV	10P	PRL 105 221802	V.M. Abazov *et al.*	(D0 Collab.)
BEZERRA	10	PR D81 055003	V.B. Bezerra *et al.*	
ABAZOV	09AE	PRL 103 191803	V.M. Abazov *et al.*	(D0 Collab.)
ABAZOV	09D	PRL 102 051601	V.M. Abazov *et al.*	(D0 Collab.)
MASUDA	09	PRL 102 171101	M. Masuda, M. Sasaki	(ICRR)
AALTONEN	08AC	PRL 101 181602	T. Aaltonen *et al.*	(CDF Collab.)
AALTONEN	08S	PR D78 012008	T. Aaltonen *et al.*	(CDF Collab.)
ABAZOV	08J	PRL 100 091802	V.M. Abazov *et al.*	(D0 Collab.)
ABAZOV	08S	PRL 101 011601	V.M. Abazov *et al.*	(D0 Collab.)
DAS	08	PR D78 063011	P.K. Das, V.H.S. Kumar, P.K. Suresh	
GERACI	08	PR D78 022002	A.A. Geraci *et al.*	(STAN)
TRENKEL	08	PR D77 122001	C. Trenkel	
AALTONEN	07G	PRL 99 171801	T. Aaltonen *et al.*	(CDF Collab.)
AALTONEN	07H	PRL 99 171802	T. Aaltonen *et al.*	(CDF Collab.)
DECCA	07A	EPJ C51 963	R.S. Decca *et al.*	
HAISCH	07	PR D76 034014	U. Haisch, A. Weiler	
KAPNER	07	PRL 98 021101	D.J. Kapner *et al.*	
SCHAEL	07A	EPJ C49 411	S. Schael *et al.*	(ALEPH Collab.)
TU	07	PRL 98 201101	L.-C. Tu *et al.*	
ABDALLAH	06C	EPJ C45 589	J. Abdallah *et al.*	(DELPHI Collab.)
ABULENCIA,A	06	PRL 97 171802	A. Abulencia *et al.*	(CDF Collab.)
GERDES	06	PR D73 112008	D. Gerdes *et al.*	
GOGOLADZE	06	PR D74 093012	I. Gogoladze, C. Macesanu	
ABAZOV	05N	PRL 95 091801	V.M. Abazov *et al.*	(D0 Collab.)
ABAZOV	05V	PRL 95 161602	V.M. Abazov *et al.*	(D0 Collab.)
ABDALLAH	05B	EPJ C38 395	J. Abdallah *et al.*	(DELPHI Collab.)
ABULENCIA	05A	PRL 95 252001	A. Abulencia *et al.*	(CDF Collab.)
SMULLIN	05	PR D72 122001	S.J. Smullin *et al.*	
ACHARD	04E	PL B587 16	P. Achard *et al.*	(L3 Collab.)
ACOSTA	04C	PRL 92 121802	D. Acosta *et al.*	(CDF Collab.)
BARBIERI	04	NP B703 127	R. Barbieri *et al.*	
CASSE	04	PRL 92 111102	M. Casse *et al.*	
CHEKANOV	04B	PL B591 23	S. Chekanov *et al.*	(ZEUS Collab.)
HOYLE	04	PR D70 042004	C.D. Hoyle *et al.*	(WASH)
ABAZOV	03	PRL 90 251802	V.M. Abazov *et al.*	(D0 Collab.)
ABBIENDI	03D	EPJ C26 331	G. Abbiendi *et al.*	(OPAL Collab.)
ACHARD	03D	PL B572 133	P. Achard *et al.*	(L3 Collab.)
ADLOFF	03	PL B568 35	C. Adloff *et al.*	(H1 Collab.)
CHIAVERINI	03	PRL 90 151101	J. Chiaverini *et al.*	
GIUDICE	03	NP B663 377	G.F. Giudice, A. Strumia	
HANNESTAD	03	PR D67 125008	S. Hannestad, G.G. Raffelt	
Also		PR D69 029901(errat.)	S. Hannestad, G.G. Raffelt	
HEISTER	03C	EPJ C28 1	A. Heister *et al.*	(ALEPH Collab.)
LONG	03	Nature 421 922	J.C. Long *et al.*	
ACHARD	02	PL B524 65	P. Achard *et al.*	(L3 Collab.)
ACHARD	02D	PL B531 28	P. Achard *et al.*	(L3 Collab.)
HANNESTAD	02	PRL 88 071301	S. Hannestad, G. Raffelt	
ABBOTT	01	PRL 86 1156	B. Abbott *et al.*	(D0 Collab.)
FAIRBAIRN	01	PL B508 335	M. Fairbairn	

HANHART	01	PL B509 1	C. Hanhart *et al.*	
HOYLE	01	PRL 86 1418	C.D. Hoyle *et al.*	
ABBIENDI	00R	EPJ C13 553	G. Abbiendi *et al.*	(OPAL Collab.)
ABREU	00A	PL B491 67	P. Abreu *et al.*	(DELPHI Collab.)
ABREU	00S	PL B485 45	P. Abreu *et al.*	(DELPHI Collab.)
ABREU	00Z	EPJ C17 53	P. Abreu *et al.*	(DELPHI Collab.)
CASSISI	00	PL B481 323	S. Cassisi *et al.*	
CHANG	00B	PRL 85 3765	L.N. Chang *et al.*	
CHEUNG	00	PR D61 015005	K. Cheung	
CORNET	00	PR D61 037701	F. Cornet, M. Relano, J. Rico	
GRAESSER	00	PR D61 074019	M.L. Graesser	
HAN	00	PR D62 125018	T. Han, D. Marfatia, R.-J. Zhang	
MATHEWS	00	JHEP 0007 008	P. Mathews, S. Raychaudhuri, K. Sridhar	
MELE	00	PR D61 117901	S. Mele, E. Sanchez	
RIZZO	00	PR D61 016007	T.G. Rizzo, J.D. Wells	
ABBIENDI	99P	PL B465 303	G. Abbiendi *et al.*	(OPAL Collab.)
ACCIARRI	99M	PL B464 135	M. Acciarri *et al.*	(L3 Collab.)
ACCIARRI	99R	PL B470 268	M. Acciarri *et al.*	(L3 Collab.)
ACCIARRI	99S	PL B470 281	M. Acciarri *et al.*	(L3 Collab.)
BOURILKOV	99	JHEP 9908 006	D. Bourilkov	
HOSKINS	85	PR D32 3084	J.K. Hoskins *et al.*	

WIMP and Dark Matter Searches

OMITTED FROM SUMMARY TABLE

We omit papers on CHAMP's, millicharged particles, and other exotic particles.

GALACTIC WIMP SEARCHES

These limits are for weakly-interacting stable particles that may constitute the invisible mass in the galaxy. Unless otherwise noted, a local mass density of 0.3 GeV/cm^3 is assumed; see each paper for velocity distribution assumptions. In the papers the limit is given as a function of the X^0 mass. Here we list limits only for typical mass values of 20 GeV, 100 GeV, and 1 TeV. Specific limits on supersymmetric dark matter particles may be found in the Supersymmetry section.

Limits for Spin-Independent Cross Section of Dark Matter Particle (X^0) on Nucleon

Isoscalar coupling is assumed to extract the limits from those on X^0–nuclei cross section.

For m_{X^0} = 20 GeV

For limits from X^0 annihilation in the Sun, the assumed annihilation final state is shown in parenthesis in the comment.

VALUE (pb)	CL%	DOCUMENT ID		TECN	COMMENT
• • • We do not use the following data for averages, fits, limits, etc. • • •					
$<5 \times 10^{-6}$	95	[1] AGNESE	18	CDMS	Ge
$<2 \times 10^{-6}$	90	[2] AARTSEN	17	ICCB	ν, earth
$<1 \times 10^{4}$	90	[3] ANGLOHER	17A	CRES	χp
$<1 \times 10^{-3}$	90	[4] BARBOSA-D...	17	ICCB	NaI
$<7.3 \times 10^{-7}$	90	AGNES	16	DS50	Ar
$<1 \times 10^{-5}$	90	[5] AGNESE	16	CDMS	Ge
$<2 \times 10^{-4}$	90	[6] AGUILAR-AR...	16	DMIC	Si CCDs
$<4 \times 10^{-5}$	90	[7] ANGLOHER	16	CRES	$CaWO_4$
$<2 \times 10^{-6}$	90	[8] APRILE	16	X100	Xe
$<9.4 \times 10^{-8}$	90	[9] ARMENGAUD	16	EDE3	Ge
$<1.0 \times 10^{-7}$	90	[10] HEHN	16	EDE3	Ge
$<4 \times 10^{-6}$	90	[11] ZHAO	16	CDEX	Ge
$<1 \times 10^{-5}$	90	AGNES	15	DS50	Ar
$<1.5 \times 10^{-6}$	90	[12] AGNESE	15A	CDM2	Ge
$<1.5 \times 10^{-7}$	90	[13] AGNESE	15B	CDM2	Ge
$<2 \times 10^{-6}$	90	[14] AMOLE	15	PICO	C_3F_8
$<1.2 \times 10^{-5}$	90	CHOI	15	SKAM	H, solar ν ($b\overline{b}$)
$<1.19 \times 10^{-6}$	90	CHOI	15	SKAM	H, solar ν ($\tau^+\tau^-$)
$<2 \times 10^{-8}$	90	[15] XIAO	15	PNDX	Xe
$<2.0 \times 10^{-7}$	90	[16] AGNESE	14	SCDM	Ge
$<3.7 \times 10^{-5}$	90	[17] AGNESE	14A	SCDM	Ge
$<1 \times 10^{-9}$	90	[18] AKERIB	14	LUX	Xe
$<2 \times 10^{-6}$	90	[19] ANGLOHER	14	CRES	$CaWO_4$
$<5 \times 10^{-6}$	90	FELIZARDO	14	SMPL	C_2ClF_5
$<8 \times 10^{-6}$	90	[20] LEE	14A	KIMS	CsI
$<2 \times 10^{-4}$	90	[21] LIU	14A	CDEX	Ge
$<1 \times 10^{-5}$	90	[22] YUE	14	CDEX	Ge
$<1.08 \times 10^{-4}$	90	[23] AARTSEN	13	ICCB	H, solar ν ($\tau^+\tau^-$)
$<1.5 \times 10^{-5}$	90	[24] ABE	13B	XMAS	Xe
$<3.1 \times 10^{-6}$	90	[25] AGNESE	13	CDM2	Si
$<3.4 \times 10^{-6}$	90	[26] AGNESE	13A	CDM2	Si
$<2.2 \times 10^{-6}$	90	[27] AGNESE	13A	CDM2	Si
		[28] BERNABEI	13A	DAMA	NaI modulation
$<5 \times 10^{-5}$	90	[29] LI	13B	TEXO	Ge
		[30] ZHAO	13	CDEX	Ge
$<1.2 \times 10^{-7}$	90	AKIMOV	12	ZEP3	Xe
		[31] ANGLOHER	12	CRES	$CaWO_4$
$<8 \times 10^{-6}$	90	[32] ANGLOHER	12	CRES	$CaWO_4$
$<7 \times 10^{-9}$	90	[33] APRILE	12	X100	Xe
		[34] ARCHAMBAU...	12	PICA	F (C_4F_{10})
$<7 \times 10^{-7}$	90	[35] ARMENGAUD	12	EDE2	Ge
		[36] BARRETO	12	DMIC	CCD
$<2 \times 10^{-6}$	90	BEHNKE	12	COUP	CF_3I
$<7 \times 10^{-6}$		[37] FELIZARDO	12	SMPL	C_2ClF_5
$<1.5 \times 10^{-6}$	90	KIM	12	KIMS	CsI
$<5 \times 10^{-5}$	90	[38] AALSETH	11	CGNT	Ge
		[39] AALSETH	11A	CGNT	Ge
$<5 \times 10^{-7}$	90	[40] AHMED	11	CDM2	Ge, inelastic
$<2.7 \times 10^{-7}$	90	[41] AHMED	11A	RVUE	Ge
		[42] AHMED	11B	CDM2	Ge, low threshold
$<3 \times 10^{-6}$	90	[43] ANGLE	11	XE10	Xe
$<7 \times 10^{-8}$	90	[44] APRILE	11	X100	Xe
		[45] APRILE	11A	X100	Xe, inelastic
$<2 \times 10^{-8}$	90	[33] APRILE	11B	X100	Xe
		[46] HORN	11	ZEP3	Xe
$<2 \times 10^{-7}$	90	AHMED	10	CDM2	Ge
$<1 \times 10^{-5}$	90	[47] AKERIB	10	CDM2	Si, Ge, low threshold
$<1 \times 10^{-7}$	90	APRILE	10	X100	Xe
$<2 \times 10^{-6}$	90	ARMENGAUD	10	EDE2	Ge
$<4 \times 10^{-5}$	90	FELIZARDO	10	SMPL	C_2ClF_3
$<1.5 \times 10^{-7}$	90	[48] AHMED	09	CDM2	Ge
$<2 \times 10^{-4}$	90	[49] LIN	09	TEXO	Ge
		[50] AALSETH	08	CGNT	Ge

[1] AGNESE 18 give limits for $\sigma^{SI}(p_\chi)$ for m(WIMP) between 1.5 and 20 GeV using CDMSlite mode data.

[2] AARTSEN 17 obtain $\sigma(\mathrm{SI}) < 6 \times 10^{-6}$ pb for m(wimp) = 20 GeV from ν from earth.

[3] ANGLOHER 17A find $\sigma^{SI}(\chi p) < 10^4$ pb for m(WIMP) = 0.2 GeV.

[4] BARBOSA-DE-SOUZA 17 search for annual modulation of WIMP scatter on NaI using an exposure of 61 kg yr of DM-Ice17 for recoil energy in the 4–20 keV range (DAMA found modulation for recoil energy < 5 keV). No modulation seen. Sensitivity insufficient to distinguish DAMA signal from null.

[5] AGNESE 16 CDMSlite excludes low mass WIMPs 1.6–5.5 GeV and SI scattering cross section depending on m(WIMP); see Fig. 4.

[6] AGUILAR-AREVALO 16 search low mass 1–10 GeV WIMP scatter on Si CCDs; set limits Fig. 11.

[7] ANGLOHER 16 requires SI WIMP-nucleon cross section $< 9 \times 10^{-3}$ pb for m(WIMP) = 1 GeV on $CaWO_4$ target.

[8] APRILE 16 search low mass WIMP SI scatter on Xe; exclude $\sigma > 1.4 \times 10^{-5}$ pb for m(WIMP) = 6 GeV.

[9] ARMENGAUD 16 require SI WIMP-p cross section $< 4.3 \times 10^{-4}$ pb for m(WIMP) = 5 GeV on Ge target.

[10] HEHN 16 search for low mass WIMPs via SI scatter on Ge target; $\sigma(\mathrm{SI}) < 5.8 \times 10^{-4}$ pb for m(WIMP) = 5 GeV, Fig. 6.

[11] ZHAO 16 require SI scatter $< 4 \times 10^{-6}$ pb for m(WIMP) = 20 GeV using Ge target; limits also on SD scatter, see Fig. 19.

[12] AGNESE 15A reanalyse AHMED 11B low threshold data. See their Fig. 12 (left) for improved limits extending down to 5 GeV.

[13] AGNESE 15B reanalyse AHMED 10 data.

[14] See their Fig. 7 for limits extending down to 4 GeV.

[15] See their Fig. 13 for limits extending down to 5 GeV.

[16] This limit value is provided by the authors. See their Fig. 4 for limits extending down to $m_{X^0} = 3.5$ GeV.

[17] This limit value is provided by the authors. AGNESE 14A result is from CDMSlite mode operation with enhanced sensitivity to low mass m_{X^0}. See their Fig. 3 for limits extending down to $m_{X^0} = 3.5$ GeV (see also Fig. 4 in AGNESE 14).

[18] See their Fig. 5 for limits extending down to $m_{X^0} = 5.5$ GeV.

[19] See their Fig. 5 for limits extending down to $m_{X^0} = 1$ GeV.

[20] See their Fig. 5 for limits extending down to $m_{X^0} = 5$ GeV.

[21] LIU 14A result is based on prototype CDEX-0 detector. See their Fig. 13 for limits extending down to $m_{X^0} = 2$ GeV.

[22] See their Fig. 4 for limits extending down to $m_{X^0} = 4.5$ GeV.

[23] AARTSEN 13 search for neutrinos from the Sun arising from the pair annihilation of X^0 trapped by the sun in data taken between June 2010 and May 2011.

[24] See their Fig. 8 for limits extending down to $m_{X^0} = 7$ GeV.

[25] This limit value is provided by the authors. AGNESE 13 use data taken between Oct. 2006 and July 2007. See their Fig. 4 for limits extending down to $m_{X^0} = 7$ GeV.

[26] This limit value is provided by the authors. AGNESE 13A use data taken between July 2007 and Sep. 2008. Three candidate events are seen. Assuming these events are real, the best fit parameters are $m_{X^0} = 8.6$ GeV and $\sigma = 1.9 \times 10^{-5}$ pb.

[27] This limit value is provided by the authors. Limit from combined data of AGNESE 13 and AGNESE 13A. See their Fig. 4 for limits extending down to $m_{X^0} = 5.5$ GeV.

[28] BERNABEI 13A search for annual modulation of counting rate in the 2–6 keV recoil energy interval, in a 14 yr live time exposure of 1.33 t yr. Find a modulation of 0.0112 ± 0.0012 counts/(day kg keV) with 9.3 sigma C.L. Find period and phase in agreement with expectations from DM particles.

[29] See their Fig. 4 for limits extending down to $m_{X^0} = 4$ GeV.

[30] See their Fig. 5 for limits for $m_{X^0} = 4$–12 GeV.

[31] ANGLOHER 12 observe excess events above the expected background which are consistent with X^0 with mass $\sim$ 25 GeV (or 12 GeV) and spin-independent X^0-nucleon cross section of 2×10^{-6} pb (or 4×10^{-5} pb).

[32] Reanalysis of ANGLOHER 09 data with all three nuclides. See also BROWN 12.

[33] See also APRILE 14A.

[34] See their Fig. 7 for cross section limits for m_{X^0} between 4 and 12 GeV.

[35] See their Fig. 4 for limits extending down to $m_{X^0} = 7$ GeV.

[36] See their Fig. 13 for cross section limits for m_{X^0} between 1.2 and 10 GeV.

[37] See also DAHL 12 for a criticism.

[38] See their Fig. 4 for limits extending to $m_{X^0} = 3.5$ GeV.

[39] AALSETH 11A find indications of annual modulation of the data, the energy spectrum being compatible with X^0 mass around 8 GeV. See also AALSETH 13.
[40] AHMED 11 search for X^0 inelastic scattering. See their Fig. 8–10 for limits. The inelastic cross section reduces to the elastic cross section at the limit of zero mass splitting (Fig. 8, left).
[41] AHMED 11A combine CDMS II and EDELWEISS data.
[42] AHMED 11B give limits on spin-independent X^0-nucleon cross section for m_{X^0} = 4–12 GeV in the range 10^{-3}–10^{-5} pb. See their Fig. 3.
[43] See their Fig. 3 for limits down to m_{X^0} = 4 GeV.
[44] APRILE 11 reanalyze APRILE 10 data.
[45] APRILE 11A search for X^0 inelastic scattering. See their Fig. 2 and 3 for limits. See also APRILE 14A.
[46] HORN 11 perform detector calibration by neutrons. Earlier results are only marginally affected.
[47] See their Fig. 10 and 12 for limits extending to X^0 mass of 1 GeV.
[48] Superseded by AHMED 10.
[49] See their Fig. 6(a) for cross section limits for m_{X^0} extending down to 2 GeV.
[50] See their Fig. 2 for cross section limits for m_{X^0} between 4 and 10 GeV.

For m_{X^0} = 100 GeV

For limits from X^0 annihilation in the Sun, the assumed annihilation final state is shown in parenthesis in the comment.

VALUE (pb)	CL%	DOCUMENT ID		TECN	COMMENT
• • • We do not use the following data for averages, fits, limits, etc. • • •					
$<1 \times 10^{-8}$	90	[1] AGNESE	18A	CDMS	$\sigma^{SI}(\chi p)$
$<1.7 \times 10^{-10}$	90	[2] AKERIB	17	LUX	Xe
$<1.2 \times 10^{-10}$	90	[3] APRILE	17G	XE1T	Xe
$<1.2 \times 10^{-10}$	90	[4] CUI	17A	PNDX	Xe
$<2.0 \times 10^{-8}$	90	AGNES	16	DS50	Ar
$<1 \times 10^{-9}$	90	[5] AKERIB	16	LUX	Xe
$<1 \times 10^{-9}$	90	[6] APRILE	16B	X100	Xe
$<2 \times 10^{-8}$	90	[7] TAN	16	PNDX	Xe
$<4 \times 10^{-10}$	90	[8] TAN	16B	PNDX	Xe
$<6 \times 10^{-8}$	90	AGNES	15	DS50	Ar
$<4 \times 10^{-8}$	90	[9] AGNESE	15B	CDM2	Ge
$<7.13 \times 10^{-6}$	90	CHOI	15	SKAM	H, solar ν ($b\overline{b}$)
$<6.26 \times 10^{-7}$	90	CHOI	15	SKAM	H, solar ν (W^+W^-)
$<2.76 \times 10^{-7}$	90	CHOI	15	SKAM	H, solar ν ($\tau^+\tau^-$)
$<1.5 \times 10^{-8}$	90	XIAO	15	PNDX	Xe
$<1 \times 10^{-9}$	90	AKERIB	14	LUX	Xe
$<4.0 \times 10^{-6}$	90	[10] AVRORIN	14	BAIK	H, solar ν (W^+W^-)
$<1.0 \times 10^{-4}$	90	[10] AVRORIN	14	BAIK	H, solar ν ($b\overline{b}$)
$<1.6 \times 10^{-6}$	90	[10] AVRORIN	14	BAIK	H, solar ν ($\tau^+\tau^-$)
$<5 \times 10^{-6}$	90	FELIZARDO	14	SMPL	C_2ClF_5
$<6.01 \times 10^{-7}$	90	[11] AARTSEN	13	ICCB	H, solar ν (W^+W^-)
$<3.30 \times 10^{-5}$	90	[11] AARTSEN	13	ICCB	H, solar ν ($b\overline{b}$)
$<1.9 \times 10^{-6}$	90	[12] ADRIAN-MAR..13		ANTR	H, solar ν (W^+W^-)
$<1.2 \times 10^{-4}$	90	[12] ADRIAN-MAR..13		ANTR	H, solar ν ($b\overline{b}$)
$<7.6 \times 10^{-7}$	90	[12] ADRIAN-MAR..13		ANTR	H, solar ν ($\tau^+\tau^-$)
$<2 \times 10^{-6}$	90	[13] AGNESE	13	CDM2	Si
$<1.6 \times 10^{-6}$	90	[14] BOLIEV	13	BAKS	H, solar ν (W^+W^-)
$<1.9 \times 10^{-5}$	90	[14] BOLIEV	13	BAKS	H, solar ν ($b\overline{b}$)
$<7.1 \times 10^{-7}$	90	[14] BOLIEV	13	BAKS	H, solar ν ($\tau^+\tau^-$)
$<1.67 \times 10^{-6}$	90	[15] ABBASI	12	ICCB	H, solar ν (W^+W^-)
$<1.07 \times 10^{-4}$	90	[15] ABBASI	12	ICCB	H, solar ν ($b\overline{b}$)
$<4 \times 10^{-8}$	90	AKIMOV	12	ZEP3	Xe
$<1.4 \times 10^{-6}$	90	[16] ANGLOHER	12	CRES	$CaWO_4$
$<3 \times 10^{-9}$	90	[17] APRILE	12	X100	Xe
$<3 \times 10^{-7}$	90	BEHNKE	12	COUP	CF_3I
$<7 \times 10^{-6}$		FELIZARDO	12	SMPL	C_2ClF_5
$<2.5 \times 10^{-7}$	90	[18] KIM	12	KIMS	CsI
$<2 \times 10^{-4}$	90	AALSETH	11	CGNT	Ge
		[19] AHMED	11	CDM2	Ge, inelastic
$<3.3 \times 10^{-8}$	90	[20] AHMED	11A	RVUE	Ge
		[21] AJELLO	11	FLAT	
$<3 \times 10^{-8}$	90	[22] APRILE	11	X100	Xe
		[23] APRILE	11A	X100	Xe, inelastic
$<1 \times 10^{-8}$	90	[17] APRILE	11B	X100	Xe
$<5 \times 10^{-8}$	90	[24] ARMENGAUD	11	EDE2	Ge
		[25] HORN	11	ZEP3	Xe
$<4 \times 10^{-8}$	90	AHMED	10	CDM2	Ge
$<9 \times 10^{-6}$	90	AKERIB	10	CDM2	Si, Ge, low threshold
		[26] AKIMOV	10	ZEP3	Xe, inelastic
$<5 \times 10^{-8}$	90	APRILE	10	X100	Xe
$<1 \times 10^{-7}$	90	ARMENGAUD	10	EDE2	Ge
$<3 \times 10^{-5}$	90	FELIZARDO	10	SMPL	C_2ClF_3
$<5 \times 10^{-8}$	90	[27] AHMED	09	CDM2	Ge
		[28] ANGLE	09	XE10	Xe, inelastic
$<3 \times 10^{-4}$	90	LIN	09	TEXO	Ge
		[29] GIULIANI	05	RVUE	

[1] AGNESE 18A set limit $\sigma^{SI}(\chi p) < 10^{-8}$ pb for m(WIMP) = 100 GeV.
[2] AKERIB 17 exclude SI cross section $> 1.7\times10^{-10}$ pb for m(WIMP) = 100 GeV. Uses complete LUX data set.
[3] APRILE 17G set limit $\sigma^{SI}(\chi p) < 1.2\ 10^{-10}$ pb for m(WIMP) = 100 GeV using 1 ton fiducial mass Xe TPC. Exposure is 34.2 live days.
[4] CUI 17A require $\sigma^{SI}(\chi p) < 1.2\times10^{-10}$ pb for m(WIMP) = 100 GeV using 54 ton-day exposure of Xe.
[5] AKERIB 16 re-analysis of 2013 data exclude SI cross section $> 1\times10^{-9}$ pb for m(WIMP) = 100 GeV on Xe target.
[6] APRILE 16B combined 447 live days using Xe target exclude σ(SI) $> 1.1\times10^{-9}$ pb for m(WIMP) = 50 GeV.
[7] TAN 16 search for WIMP scatter off Xe target; see SI exclusion plot Fig. 6.
[8] TAN 16B search for WIMP-p scatter off Xe target; see Fig. 5 for SI exclusion.
[9] AGNESE 15B reanalyse AHMED 10 data.
[10] AVRORIN 14 search for neutrinos from the Sun arising from the pair annihilation of X^0 trapped by the Sun in data taken between 1998 and 2003. See their Table 1 for limits assuming annihilation into neutrino pairs.
[11] AARTSEN 13 search for neutrinos from the Sun arising from the pair annihilation of X^0 trapped by the sun in data taken between June 2010 and May 2011.
[12] ADRIAN-MARTINEZ 13 search for neutrinos from the Sun arising from the pair annihilation of X^0 trapped by the sun in data taken between Jan. 2007 and Dec. 2008.
[13] AGNESE 13 use data taken between Oct. 2006 and July 2007.
[14] BOLIEV 13 search for neutrinos from the Sun arising from the pair annihilation of X^0 trapped by the sun in data taken from 1978 to 2009. See also SUVOROVA 13 for an older analysis of the same data.
[15] ABBASI 12 search for neutrinos from the Sun arising from the pair annihilation of X^0 trapped by the Sun. The amount of X^0 depends on the X^0-proton cross section.
[16] Reanalysis of ANGLOHER 09 data with all three nuclides. See also BROWN 12.
[17] See also APRILE 14A.
[18] See their Fig. 6 for a limit on inelastically scattering X^0 for m_{X^0} = 70 GeV.
[19] AHMED 11 search for X^0 inelastic scattering. See their Fig. 8–10 for limits.
[20] AHMED 11A combine CDMS and EDELWEISS data.
[21] AJELLO 11 search for $e^{\pm}$ flux from X^0 annihilations in the Sun. Models in which X^0 annihilates into an intermediate long-lived weakly interacting particles or X^0 scatters inelastically are constrained. See their Fig. 6–8 for limits.
[22] APRILE 11 reanalyze APRILE 10 data.
[23] APRILE 11A search for X^0 inelastic scattering. See their Fig. 2 and 3 for limits. See also APRILE 14A.
[24] Supersedes ARMENGAUD 10. A limit on inelastic cross section is also given.
[25] HORN 11 perform detector calibration by neutrons. Earlier results are only marginally affected.
[26] AKIMOV 10 give cross section limits for inelastically scattering dark matter. See their Fig. 4.
[27] Superseded by AHMED 10.
[28] ANGLE 09 search for X^0 inelastic scattering. See their Fig. 4 for limits.
[29] GIULIANI 05 analyzes the spin-independent X^0-nucleon cross section limits with both isoscalar and isovector couplings. See their Fig. 3 and 4 for limits on the couplings.

For m_{X^0} = 1 TeV

For limits from X^0 annihilation in the Sun, the assumed annihilation final state is shown in parenthesis in the comment.

VALUE (pb)	CL%	DOCUMENT ID		TECN	COMMENT
• • • We do not use the following data for averages, fits, limits, etc. • • •					
<0.3	90	[1] CHEN	17E	PNDX	$\chi N \to \chi^* \to \chi\gamma$
$<8.6 \times 10^{-8}$	90	AGNES	16	DS50	Ar
$<2 \times 10^{-7}$	90	AGNES	15	DS50	Ar
$<2 \times 10^{-7}$	90	[2] AGNESE	15B	CDM2	Ge
$<1 \times 10^{-8}$	90	AKERIB	14	LUX	Xe
$<2.2 \times 10^{-6}$	90	[3] AVRORIN	14	BAIK	H, solar ν (W^+W^-)
$<5.5 \times 10^{-5}$	90	[3] AVRORIN	14	BAIK	H, solar ν ($b\overline{b}$)
$<6.8 \times 10^{-7}$	90	[3] AVRORIN	14	BAIK	H, solar ν ($\tau^+\tau^-$)
$<3.46 \times 10^{-7}$	90	[4] AARTSEN	13	ICCB	H, solar ν (W^+W^-)
$<7.75 \times 10^{-6}$	90	[4] AARTSEN	13	ICCB	H, solar ν ($b\overline{b}$)
$<6.9 \times 10^{-7}$	90	[5] ADRIAN-MAR..13		ANTR	H, solar ν (W^+W^-)
$<1.5 \times 10^{-5}$	90	[5] ADRIAN-MAR..13		ANTR	H, solar ν ($b\overline{b}$)
$<1.8 \times 10^{-7}$	90	[5] ADRIAN-MAR..13		ANTR	H, solar ν ($\tau^+\tau^-$)
$<4.3 \times 10^{-6}$	90	[6] BOLIEV	13	BAKS	H, solar ν (W^+W^-)
$<3.4 \times 10^{-5}$	90	[6] BOLIEV	13	BAKS	H, solar ν ($b\overline{b}$)
$<1.2 \times 10^{-6}$	90	[6] BOLIEV	13	BAKS	H, solar ν ($\tau^+\tau^-$)
$<2.12 \times 10^{-7}$	90	[7] ABBASI	12	ICCB	H, solar ν (W^+W^-)
$<6.56 \times 10^{-6}$	90	[7] ABBASI	12	ICCB	H, solar ν ($b\overline{b}$)
$<4 \times 10^{-7}$	90	AKIMOV	12	ZEP3	Xe
$<1.1 \times 10^{-5}$	90	[8] ANGLOHER	12	CRES	$CaWO_4$
$<2 \times 10^{-8}$	90	[9] APRILE	12	X100	Xe
$<2 \times 10^{-6}$	90	BEHNKE	12	COUP	CF_3I
$<4 \times 10^{-6}$		FELIZARDO	12	SMPL	C_2ClF_5
$<1.5 \times 10^{-6}$	90	KIM	12	KIMS	CsI
		[10] AHMED	11	CDM2	Ge, inelastic
$<1.5 \times 10^{-7}$	90	[11] AHMED	11A	RVUE	Ge
$<2 \times 10^{-7}$	90	[12] APRILE	11	X100	Xe
$<8 \times 10^{-8}$	90	[9] APRILE	11B	X100	Xe
$<2 \times 10^{-7}$	90	[13] ARMENGAUD	11	EDE2	Ge
		[14] HORN	11	ZEP3	Xe
$<2 \times 10^{-7}$	90	AHMED	10	CDM2	Ge
$<4 \times 10^{-7}$	90	APRILE	10	X100	Xe
$<6 \times 10^{-7}$	90	ARMENGAUD	10	EDE2	Ge
$<3.5 \times 10^{-7}$	90	[15] AHMED	09	CDM2	Ge

[1] CHEN 17E search for inelastic WIMP scatter on Xe; require $\sigma^{SI}(\chi N) < 0.3$ pb for m(χ) = 1 TeV and (mass difference) = 300 keV.
[2] AGNESE 15B reanalyse AHMED 10 data.
[3] AVRORIN 14 search for neutrinos from the Sun arising from the pair annihilation of X^0 trapped by the Sun in data taken between 1998 and 2003. See their Table 1 for limits assuming annihilation into neutrino pairs.

[4] AARTSEN 13 search for neutrinos from the Sun arising from the pair annihilation of X^0 trapped by the sun in data taken between June 2010 and May 2011.
[5] ADRIAN-MARTINEZ 13 search for neutrinos from the Sun arising from the pair annihilation of X^0 trapped by the sun in data taken between Jan. 2007 and Dec. 2008.
[6] BOLIEV 13 search for neutrinos from the Sun arising from the pair annihilation of X^0 trapped by the sun in data taken from 1978 to 2009. See also SUVOROVA 13 for an older analysis of the same data.
[7] ABBASI 12 search for neutrinos from the Sun arising from the pair annihilation of X^0 trapped by the Sun. The amount of X^0 depends on the X^0-proton cross section.
[8] Reanalysis of ANGLOHER 09 data with all three nuclides. See also BROWN 12.
[9] See also APRILE 14A.
[10] AHMED 11 search for X^0 inelastic scattering. See their Fig. 8–10 for limits.
[11] AHMED 11A combine CDMS and EDELWEISS data.
[12] APRILE 11 reanalyze APRILE 10 data.
[13] Supersedes ARMENGAUD 10. A limit on inelastic cross section is also given.
[14] HORN 11 perform detector calibration by neutrons. Earlier results are only marginally affected.
[15] Superseded by AHMED 10.

Limits for Spin-Dependent Cross Section of Dark Matter Particle (X^0) on Proton

For m_{X^0} = 20 GeV

For limits from X^0 annihilation in the Sun, the assumed annihilation final state is shown in parenthesis in the comment.

VALUE (pb)	CL%	DOCUMENT ID		TECN	COMMENT
• • • We do not use the following data for averages, fits, limits, etc. • • •					
< 30	95	[1] AGNESE	18	CDMS	Ge
$< 1.32 \times 10^{-2}$	90	[2] BEHNKE	17	PICA	C_4F_{10}
$< 5 \times 10^{-4}$	90	[3] AMOLE	16A	PICO	C_3F_8
$< 2 \times 10^{-6}$	90	[4] KHACHATRY...	16AJ	CMS	8 TeV $pp \to Z+\not{E}_T$; $Z \to \ell\overline{\ell}$
$< 1.2 \times 10^{-3}$	90	AMOLE	15	PICO	C_3F_8
$< 1.43 \times 10^{-3}$	90	CHOI	15	SKAM	H, solar ν ($b\overline{b}$)
$< 1.42 \times 10^{-4}$	90	CHOI	15	SKAM	H, solar ν ($\tau^+\tau^-$)
$< 5 \times 10^{-3}$	90	FELIZARDO	14	SMPL	C_2ClF_5
$< 1.29 \times 10^{-2}$	90	[5] AARTSEN	13	ICCB	H, solar ν ($\tau^+\tau^-$)
$< 3.17 \times 10^{-2}$	90	[6] APRILE	13	X100	Xe
$< 3 \times 10^{-2}$	90	ARCHAMBAU...	12	PICA	F (C_4F_{10})
$< 6 \times 10^{-2}$	90	BEHNKE	12	COUP	CF_3I
< 20	90	DAW	12	DRFT	F (CF_4)
$< 7 \times 10^{-3}$		FELIZARDO	12	SMPL	C_2ClF_5
< 0.15	90	KIM	12	KIMS	CsI
$< 1 \times 10^5$	90	[7] AHLEN	11	DMTP	F (CF_4)
< 0.1	90	[7] BEHNKE	11	COUP	CF_3I
$< 1.5 \times 10^{-2}$	90	[8] TANAKA	11	SKAM	H, solar ν ($b\overline{b}$)
< 0.2	90	ARCHAMBAU...	09	PICA	F
< 4	90	LEBEDENKO	09A	ZEP3	Xe
< 0.6	90	ANGLE	08A	XE10	Xe
<100	90	ALNER	07	ZEP2	Xe
< 1	90	LEE	07A	KIMS	CsI
< 20	90	[9] AKERIB	06	CDMS	^{73}Ge, ^{29}Si
< 2	90	SHIMIZU	06A	CNTR	F (CaF_2)
< 0.5	90	ALNER	05	NAIA	NaI
< 1.5	90	BARNABE-HE...	05	PICA	F (C_4F_{10})
< 1.5	90	GIRARD	05	SMPL	F (C_2ClF_5)
< 35	90	MIUCHI	03	BOLO	LiF
< 30	90	TAKEDA	03	BOLO	NaF

[1] AGNESE 18 give limits for $\sigma^{SD}(p\chi)$ for m(WIMP) between 1.5 and 20 GeV using CDMSlite mode data.
[2] BEHNKE 17 show final Picasso results based on 231.4 kg d exposure at SNOLab for WIMP scatter on C_4F_{10} search via superheated droplet; require $\sigma(\text{SD}) < 1.32 \times 10^{-2}$ pb for m(WIMP) = 20 GeV.
[3] AMOLE 16A require SD WIMP-p scattering $< 5 \times 10^{-4}$ pb for m(WIMP) = 20 GeV; bubbles from C_3F_8 target.
[4] KHACHATRYAN 16AJ require SD WIMP-p $< 2 \times 10^{-6}$ pb for m(WIMP) = 20 GeV from $pp \to Z + \not{E}_T$; $Z \to \ell\overline{\ell}$ signal.
[5] AARTSEN 13 search for neutrinos from the Sun arising from the pair annihilation of X^0 trapped by the sun in data taken between June 2010 and May 2011.
[6] The value has been provided by the authors. APRILE 13 note that the proton limits on Xe are highly sensitive to the theoretical model used. See also APRILE 14A.
[7] Use a direction-sensitive detector.
[8] TANAKA 11 search for neutrinos from the Sun arising from the pair annihilation of X^0 trapped by the Sun. The amount of X^0 depends on the X^0-proton cross section.
[9] See also AKERIB 05.

For m_{X^0} = 100 GeV

For limits from X^0 annihilation in the Sun, the assumed annihilation final state is shown in parenthesis in the comment.

VALUE (pb)	CL%	DOCUMENT ID		TECN	COMMENT
• • • We do not use the following data for averages, fits, limits, etc. • • •					
$< 5 \times 10^{-5}$	90	[1] AMOLE	17	PICO	C_3F_8
$< 3.3 \times 10^{-2}$	90	[2] APRILE	17A	X100	Xe inelastic
$< 2.8 \times 10^{-1}$	90	[3] BATTAT	17	DRFT	CS_2
$< 2 \times 10^{-3}$	90	[4] FU	17	PNDX	Xe
< 0.553–0.019	95	[5] AABOUD	16D	ATLS	$pp \to j + \not{E}_T$
$< 1 \times 10^{-5}$	90	[6] AABOUD	16F	ATLS	$pp \to \gamma + \not{E}_T$
$< 1 \times 10^{-4}$	90	[7] AARTSEN	16C	ICCB	solar ν (W^+W^-)
$< 2 \times 10^{-4}$	90	[8] ADRIAN-MAR...	16	ANTR	solar ν (WW, $b\overline{b}$, $\tau\overline{\tau}$)
$< 3 \times 10^{-3}$	90	[9] AKERIB	16A	LUX	Xe
$< 5 \times 10^{-4}$	90	[10] AMOLE	16	PICO	CF_3I
$< 1.5 \times 10^{-3}$	90	AMOLE	15	PICO	C_3F_8
$< 3.19 \times 10^{-3}$	90	CHOI	15	SKAM	H, solar ν ($b\overline{b}$)
$< 2.80 \times 10^{-4}$	90	CHOI	15	SKAM	H, solar ν (W^+W^-)
$< 1.24 \times 10^{-4}$	90	CHOI	15	SKAM	H, solar ν ($\tau^+\tau^-$)
$< 8 \times 10^2$	90	[11] NAKAMURA	15	NAGE	CF_4
$< 1.7 \times 10^{-3}$	90	[12] AVRORIN	14	BAIK	H, solar ν (W^+W^-)
$< 4.5 \times 10^{-2}$	90	[12] AVRORIN	14	BAIK	H, solar ν ($b\overline{b}$)
$< 7.1 \times 10^{-4}$	90	[12] AVRORIN	14	BAIK	H, solar ν ($\tau^+\tau^-$)
$< 6 \times 10^{-3}$	90	FELIZARDO	14	SMPL	C_2ClF_5
$< 2.68 \times 10^{-4}$	90	[13] AARTSEN	13	ICCB	H, solar ν (W^+W^-)
$< 1.47 \times 10^{-2}$	90	[13] AARTSEN	13	ICCB	H, solar ν ($b\overline{b}$)
$< 8.5 \times 10^{-4}$	90	[14] ADRIAN-MAR...	13	ANTR	H, solar ν (W^+W^-)
$< 5.5 \times 10^{-2}$	90	[14] ADRIAN-MAR...	13	ANTR	H, solar ν ($b\overline{b}$)
$< 3.4 \times 10^{-4}$	90	[14] ADRIAN-MAR...	13	ANTR	H, solar ν ($\tau^+\tau^-$)
$< 1.00 \times 10^{-2}$	90	[15] APRILE	13	X100	Xe
$< 7.1 \times 10^{-4}$	90	[16] BOLIEV	13	BAKS	H, solar ν (W^+W^-)
$< 8.4 \times 10^{-3}$	90	[16] BOLIEV	13	BAKS	H, solar ν ($b\overline{b}$)
$< 3.1 \times 10^{-4}$	90	[16] BOLIEV	13	BAKS	H, solar ν ($\tau^+\tau^-$)
$< 7.07 \times 10^{-4}$	90	[17] ABBASI	12	ICCB	H, solar ν (W^+W^-)
$< 4.53 \times 10^{-2}$	90	[17] ABBASI	12	ICCB	H, solar ν ($b\overline{b}$)
$< 7 \times 10^{-2}$	90	ARCHAMBAU...	12	PICA	F (C_4F_{10})
$< 1 \times 10^{-2}$	90	BEHNKE	12	COUP	CF_3I
< 1.8	90	DAW	12	DRFT	F (CF_4)
$< 9 \times 10^{-3}$		FELIZARDO	12	SMPL	C_2ClF_5
$< 2 \times 10^{-2}$	90	KIM	12	KIMS	CsI
$< 2 \times 10^3$	90	[11] AHLEN	11	DMTP	F (CF_4)
$< 7 \times 10^{-2}$	90	BEHNKE	11	COUP	CF_3I
$< 2.7 \times 10^{-4}$	90	[18] TANAKA	11	SKAM	H, solar ν (W^+W^-)
$< 4.5 \times 10^{-3}$	90	[18] TANAKA	11	SKAM	H, solar ν ($b\overline{b}$)
		[19] FELIZARDO	10	SMPL	C_2ClF_3
$< 6 \times 10^3$	90	[11] MIUCHI	10	NAGE	CF_4
< 0.4	90	ARCHAMBAU...	09	PICA	F
< 0.8	90	LEBEDENKO	09A	ZEP3	Xe
< 1.0	90	ANGLE	08A	XE10	Xe
< 15	90	ALNER	07	ZEP2	Xe
< 0.2	90	LEE	07A	KIMS	CsI
$< 1 \times 10^4$	90	[11] MIUCHI	07	NAGE	F (CF_4)
< 5	90	[20] AKERIB	06	CDMS	^{73}Ge, ^{29}Si
< 2	90	SHIMIZU	06A	CNTR	F (CaF_2)
< 0.3	90	ALNER	05	NAIA	NaI
< 2	90	BARNABE-HE...	05	PICA	F (C_4F_{10})
<100	90	BENOIT	05	EDEL	^{73}Ge
< 1.5	90	GIRARD	05	SMPL	F (C_2ClF_5)
< 0.7		[21] GIULIANI	05A	RVUE	
		[22] GIULIANI	04	RVUE	
		[23] GIULIANI	04A	RVUE	
< 35	90	MIUCHI	03	BOLO	LiF
< 40	90	TAKEDA	03	BOLO	NaF

[1] AMOLE 17 require $\sigma(\text{WIMP-}p)^{SD} < 5 \times 10^{-5}$ pb for m(WIMP) = 100 GeV using PICO-60 1167 kg-days exposure at SNOLab.
[2] APRILE 17A require require $\sigma(\text{WIMP-}p)(\text{inelastic})^{SD} < 3.3 \times 10^{-2}$ pb for m(WIMP) = 100 GeV, based on 7640 kg day exposure at LNGS.
[3] BATTAT 17 use directional detection of CS_2 ions to require $\sigma(\text{SD}) < 2.8 \times 10^{-1}$ pb for 100 GeV WIMP with a 55 days exposure at the Boulby Underground Science Facility.
[4] FU 17 from a 33000 kg d exposure at CJPL, PANDAX II derive for m(DM) = 100 GeV, $\sigma(\text{WIMP-p})^{SD} < 2 \times 10^{-3}$ pb and $\sigma(\text{WIMP-n})^{SD} < 6 \times 10^{-5}$ pb.
[5] AABOUD 16D use ATLAS 13 TeV 3.2 fb^{-1} of data to search for monojet plus missing E_T; agree with SM rates; present limits on large extra dimensions, compressed SUSY spectra and wimp pair production.
[6] AABOUD 16F search for monophoton plus missing E_T events at ATLAS with 13 Tev and 3.2 fb^{-1}; signal agrees with SM background; place limits on SD WIMP-proton scattering vs. mediator mass and large extra dimension models.
[7] AARTSEN 16C search for high energy νs from WIMP annihilation in solar core; limits set on SD WIMP-p scattering (Fig. 8).
[8] ADRIAN-MARTINEZ 16 search for WIMP annihilation into νs from solar core; exclude SD cross section $<$ few 10^{-4} depending on m(WIMP).
[9] AKERIB 16A using 2013 data exclude SD WIMP-proton scattering $> 3 \times 10^{-3}$ pb for m(WIMP) = 100 GeV.
[10] AMOLE 16 use bubble technique on CF_3I target to exclude SD WIMP-p scattering $> 5 \times 10^{-4}$ pb for m(WIMP) = 100 GeV.
[11] Use a direction-sensitive detector.
[12] AVRORIN 14 search for neutrinos from the Sun arising from the pair annihilation of X^0 trapped by the Sun in data taken between 1998 and 2003. See their Table 1 for limits assuming annihilation into neutrino pairs.
[13] AARTSEN 13 search for neutrinos from the Sun arising from the pair annihilation of X^0 trapped by the sun in data taken between June 2010 and May 2011.
[14] ADRIAN-MARTINEZ 13 search for neutrinos from the Sun arising from the pair annihilation of X^0 trapped by the sun in data taken between Jan. 2007 and Dec. 2008.
[15] The value has been provided by the authors. APRILE 13 note that the proton limits on Xe are highly sensitive to the theoretical model used. See also APRILE 14A.
[16] BOLIEV 13 search for neutrinos from the Sun arising from the pair annihilation of X^0 trapped by the sun in data taken from 1978 to 2009. See also SUVOROVA 13 for an older analysis of the same data.

[17] ABBASI 12 search for neutrinos from the Sun arising from the pair annihilation of X^0 trapped by the Sun. The amount of X^0 depends on the X^0-proton cross section.
[18] TANAKA 11 search for neutrinos from the Sun arising from the pair annihilation of X^0 trapped by the Sun. The amount of X^0 depends on the X^0-proton cross section.
[19] See their Fig. 3 for limits on spin-dependent proton couplings for X^0 mass of 50 GeV.
[20] See also AKERIB 05.
[21] GIULIANI 05A analyze available data and give combined limits.
[22] GIULIANI 04 reanalyze COLLAR 00 data and give limits for spin-dependent X^0-proton coupling.
[23] GIULIANI 04A give limits for spin-dependent X^0-proton couplings from existing data.

For m_{X^0} = 1 TeV

For limits from X^0 annihilation in the Sun, the assumed annihilation final state is shown in parenthesis in the comment.

VALUE (pb)	CL%	DOCUMENT ID		TECN	COMMENT
• • • We do not use the following data for averages, fits, limits, etc. • • •					
$< 2.05 \times 10^{-5}$	90	[1] AARTSEN	17A	ICCB	ν, sun
		[2] ADRIAN-MAR..	16B	ANTR	solar μ from WIMP annih.
$< 1 \times 10^{-2}$	90	AMOLE	15	PICO	C_3F_8
$< 1.5 \times 10^{3}$	90	NAKAMURA	15	NAGE	CF_4
$< 2.7 \times 10^{-3}$	90	[3] AVRORIN	14	BAIK	H, solar ν (W^+W^-)
$< 6.9 \times 10^{-2}$	90	[3] AVRORIN	14	BAIK	H, solar ν ($b\overline{b}$)
$< 8.4 \times 10^{-4}$	90	[3] AVRORIN	14	BAIK	H, solar ν ($\tau^+\tau^-$)
$< 4.48 \times 10^{-4}$	90	[4] AARTSEN	13	ICCB	H, solar ν (W^+W^-)
$< 1.00 \times 10^{-2}$	90	[4] AARTSEN	13	ICCB	H, solar ν ($b\overline{b}$)
$< 8.9 \times 10^{-4}$	90	[5] ADRIAN-MAR..	13	ANTR	H, solar ν (W^+W^-)
$< 2.0 \times 10^{-2}$	90	[5] ADRIAN-MAR..	13	ANTR	H, solar ν ($b\overline{b}$)
$< 2.3 \times 10^{-4}$	90	[5] ADRIAN-MAR..	13	ANTR	H, solar ν ($\tau^+\tau^-$)
$< 7.57 \times 10^{-2}$	90	[6] APRILE	13	X100	Xe
$< 5.4 \times 10^{-3}$	90	[7] BOLIEV	13	BAKS	H, solar ν (W^+W^-)
$< 4.2 \times 10^{-2}$	90	[7] BOLIEV	13	BAKS	H, solar ν ($b\overline{b}$)
$< 1.5 \times 10^{-3}$	90	[7] BOLIEV	13	BAKS	H, solar ν ($\tau^+\tau^-$)
$< 2.50 \times 10^{-4}$	90	[8] ABBASI	12	ICCB	H, solar ν (W^+W^-)
$< 7.86 \times 10^{-3}$	90	[8] ABBASI	12	ICCB	H, solar ν ($b\overline{b}$)
$< 8 \times 10^{-2}$	90	BEHNKE	12	COUP	CF_3I
< 8	90	DAW	12	DRFT	F (CF_4)
$< 6 \times 10^{-2}$		FELIZARDO	12	SMPL	C_2ClF_5
$< 8 \times 10^{-2}$	90	KIM	12	KIMS	CsI
$< 8 \times 10^{3}$	90	[9] AHLEN	11	DMTP	F (CF_4)
< 0.4	90	BEHNKE	11	COUP	CF_3I
$< 2 \times 10^{-3}$	90	[10] TANAKA	11	SKAM	H, solar ν ($b\overline{b}$)
$< 2 \times 10^{-2}$	90	[10] TANAKA	11	SKAM	H, solar ν (W^+W^-)
$< 1 \times 10^{-3}$	90	[11] ABBASI	10	ICCB	KK dark matter
$< 2 \times 10^{4}$	90	[9] MIUCHI	10	NAGE	CF_4
$< 8.7 \times 10^{-4}$	90	ABBASI	09B	ICCB	H, solar ν (W^+W^-)
$< 2.2 \times 10^{-2}$	90	ABBASI	09B	ICCB	H, solar ν ($b\overline{b}$)
< 3	90	ARCHAMBAU..	09	PICA	F
< 6	90	LEBEDENKO	09A	ZEP3	Xe
< 9	90	ANGLE	08A	XE10	Xe
<100	90	ALNER	07	ZEP2	Xe
< 0.8	90	LEE	07A	KIMS	CsI
$< 4 \times 10^{4}$	90	[9] MIUCHI	07	NAGE	F (CF_4)
< 30	90	[12] AKERIB	06	CDMS	^{73}Ge, ^{29}Si
< 1.5	90	ALNER	05	NAIA	NaI
< 15	90	BARNABE-HE..	05	PICA	F (C_4F_{10})
<600	90	BENOIT	05	EDEL	^{73}Ge
< 10	90	GIRARD	05	SMPL	F (C_2ClF_5)
<260	90	MIUCHI	03	BOLO	LiF
<150	90	TAKEDA	03	BOLO	NaF

[1] AARTSEN 17A search for neutrinos from solar WIMP annihilation into $\tau^+\tau^-$ in 532 days of live time.
[2] ADRIAN-MARTINEZ 16B search for secluded DM via WIMP annihilation in solar core into light mediator which later decays to μ or νs; limits presented in Figures 3 and 4.
[3] AVRORIN 14 search for neutrinos from the Sun arising from the pair annihilation of X^0 trapped by the Sun in data taken between 1998 and 2003. See their Table 1 for limits assuming annihilation into neutrino pairs.
[4] AARTSEN 13 search for neutrinos from the Sun arising from the pair annihilation of X^0 trapped by the sun in data taken between June 2010 and May 2011.
[5] ADRIAN-MARTINEZ 13 search for neutrinos from the Sun arising from the pair annihilation of X^0 trapped by the sun in data taken between Jan. 2007 and Dec. 2008.
[6] The value has been provided by the authors. APRILE 13 note that the proton limits on Xe are highly sensitive to the theoretical model used. See also APRILE 14A.
[7] BOLIEV 13 search for neutrinos from the Sun arising from the pair annihilation of X^0 trapped by the sun in data taken from 1978 to 2009. See also SUVOROVA 13 for an older analysis of the same data.
[8] ABBASI 12 search for neutrinos from the Sun arising from the pair annihilation of X^0 trapped by the Sun. The amount of X^0 depends on the X^0-proton cross section.
[9] Use a direction-sensitive detector.
[10] TANAKA 11 search for neutrinos from the Sun arising from the pair annihilation of X^0 trapped by the Sun. The amount of X^0 depends on the X^0-proton cross section.
[11] ABBASI 10 search for ν_μ from annihilations of Kaluza-Klein photon dark matter in the Sun.
[12] See also AKERIB 05.

Limits for Spin-Dependent Cross Section of Dark Matter Particle (X^0) on Neutron

For m_{X^0} = 20 GeV

VALUE (pb)	CL%	DOCUMENT ID		TECN	COMMENT
• • • We do not use the following data for averages, fits, limits, etc. • • •					
< 1.5	95	[1] AGNESE	18	CDMS	Ge
< 0.09	90	FELIZARDO	14	SMPL	C_2ClF_5
< 8	90	[2] UCHIDA	14	XMAS	^{129}Xe, inelastic
$< 1.13 \times 10^{-3}$	90	[3] APRILE	13	X100	Xe
< 0.02	90	AKIMOV	12	ZEP3	Xe
		[4] AHMED	11B	CDM2	Ge, low threshold
< 0.06	90	AHMED	09	CDM2	Ge
< 0.04	90	LEBEDENKO	09A	ZEP3	Xe
< 50		[5] LIN	09	TEXO	Ge
$< 6 \times 10^{-3}$	90	ANGLE	08A	XE10	Xe
< 0.5	90	ALNER	07	ZEP2	Xe
< 25	90	LEE	07A	KIMS	CsI
< 0.3	90	[6] AKERIB	06	CDMS	^{73}Ge, ^{29}Si
< 30	90	SHIMIZU	06A	CNTR	F (CaF_2)
< 60	90	ALNER	05	NAIA	NaI
< 20	90	BARNABE-HE..	05	PICA	F (C_4F_{10})
< 10	90	BENOIT	05	EDEL	^{73}Ge
< 4	90	KLAPDOR-K...	05	HDMS	^{73}Ge (enriched)
<600	90	TAKEDA	03	BOLO	NaF

[1] AGNESE 18 give limits for $\sigma^{SD}(n\chi)$ for m(WIMP) between 1.5 and 20 GeV using CDMSlite mode data.
[2] Derived limit from search for inelastic scattering $X^0 + {}^{129}\text{Xe} \rightarrow X^0 + {}^{129}\text{Xe}^*(39.58$ keV).
[3] The value has been provided by the authors. See also APRILE 14A.
[4] AHMED 11B give limits on spin-dependent X^0-neutron cross section for m_{X^0} = 4–12 GeV in the range 10^{-3}–10 pb. See their Fig. 3.
[5] See their Fig. 6(b) for cross section limits for m_{X^0} extending down to 2 GeV.
[6] See also AKERIB 05.

For m_{X^0} = 100 GeV

VALUE (pb)	CL%	DOCUMENT ID		TECN	COMMENT
• • • We do not use the following data for averages, fits, limits, etc. • • •					
$< 2.5 \times 10^{-5}$	90	[1] AKERIB	17A	LUX	Xe
< 0.1	90	FELIZARDO	14	SMPL	C_2ClF_5
< 0.05	90	[2] UCHIDA	14	XMAS	^{129}Xe, inelastic
$< 4.68 \times 10^{-4}$	90	[3] APRILE	13	X100	Xe
< 0.01	90	AKIMOV	12	ZEP3	Xe
		[4] FELIZARDO	10	SMPL	C_2ClF_3
< 0.02	90	AHMED	09	CDM2	Ge
< 0.01	90	LEBEDENKO	09A	ZEP3	Xe
<100	90	LIN	09	TEXO	Ge
< 0.01	90	ANGLE	08A	XE10	Xe
< 0.05	90	[5] BEDNYAKOV	08	RVUE	Ge
< 0.08	90	ALNER	07	ZEP2	Xe
< 6	90	LEE	07A	KIMS	CsI
< 0.07	90	[6] AKERIB	06	CDMS	^{73}Ge, ^{29}Si
< 30	90	SHIMIZU	06A	CNTR	F (CaF_2)
< 10	90	ALNER	05	NAIA	NaI
< 30	90	BARNABE-HE..	05	PICA	F (C_4F_{10})
< 0.7	90	BENOIT	05	EDEL	^{73}Ge
< 0.2		[7] GIULIANI	05A	RVUE	
< 1.5	90	KLAPDOR-K...	05	HDMS	^{73}Ge (enriched)
		[8] GIULIANI	04	RVUE	
		[9] GIULIANI	04A	RVUE	
		[10] MIUCHI	03	BOLO	LiF
<800	90	TAKEDA	03	BOLO	NaF

[1] AKERIB 17A require $\sigma(\chi p)_{SD} < 7 \times 10^{-4}$ pb for m(χ) = 100 GeV using 129.5 kg yr exposure.
[2] Derived limit from search for inelastic scattering $X^0 + {}^{129}\text{Xe}^* \rightarrow X^0 + {}^{129}\text{Xe}^*(39.58$ keV).
[3] The value has been provided by the authors. See also APRILE 14A.
[4] See their Fig. 3 for limits on spin-dependent neutron couplings for X^0 mass of 50 GeV.
[5] BEDNYAKOV 08 reanalyze KLAPDOR-KLEINGROTHAUS 05 and BAUDIS 01 data.
[6] See also AKERIB 05.
[7] GIULIANI 05A analyze available data and give combined limits.
[8] GIULIANI 04 reanalyze COLLAR 00 data and give limits for spin-dependent X^0-neutron coupling.
[9] GIULIANI 04A give limits for spin-dependent X^0-neutron couplings from existing data.
[10] MIUCHI 03 give model-independent limit for spin-dependent X^0-proton and neutron cross sections. See their Fig. 5.

For m_{X^0} = 1 TeV

VALUE (pb)	CL%	DOCUMENT ID		TECN	COMMENT
• • • We do not use the following data for averages, fits, limits, etc. • • •					
< 0.07	90	FELIZARDO	14	SMPL	C_2ClF_5
< 0.2	90	[1] UCHIDA	14	XMAS	^{129}Xe, inelastic
$< 3.64 \times 10^{-3}$	90	[2] APRILE	13	X100	Xe
< 0.08	90	AKIMOV	12	ZEP3	Xe
< 0.2	90	AHMED	09	CDM2	Ge
< 0.1	90	LEBEDENKO	09A	ZEP3	Xe

< 0.1		90		ANGLE	08A	XE10 Xe
< 0.25		90	[3]	BEDNYAKOV	08	RVUE Ge
< 0.6		90		ALNER	07	ZEP2 Xe
< 30		90		LEE	07A	KIMS CsI
< 0.5		90	[4]	AKERIB	06	CDMS ^{73}Ge, ^{29}Si
< 40		90		ALNER	05	NAIA NaI
<200		90		BARNABE-HE...	05	PICA $F(C_4F_{10})$
< 4		90		BENOIT	05	EDEL ^{73}Ge
< 10		90		KLAPDOR-K...	05	HDMS ^{73}Ge (enriched)
< 4	$\times 10^3$	90		TAKEDA	03	BOLO NaF

[1] Derived limit from search for inelastic scattering $X^0 + {}^{129}Xe^* \rightarrow X^0 + {}^{129}Xe^*$(39.58 keV).
[2] The value has been provided by the authors. See also APRILE 14A.
[3] BEDNYAKOV 08 reanalyze KLAPDOR-KLEINGROTHAUS 05 and BAUDIS 01 data.
[4] See also AKERIB 05.

Cross-Section Limits for Dark Matter Particles (X^0) on Nuclei

For m_{X^0} = 20 GeV

VALUE (nb)		CL%		DOCUMENT ID		TECN	COMMENT
• • • We do not use the following data for averages, fits, limits, etc. • • •							
< 0.03		90	[1]	UCHIDA	14	XMAS	^{129}Xe, inelastic
< 0.08		90	[2]	ANGLOHER	02	CRES	Al
			[3]	BENOIT	00	EDEL	Ge
< 0.04		95	[4]	KLIMENKO	98	CNTR	^{73}Ge, inel.
< 0.8				ALESSAND...	96	CNTR	O
< 6				ALESSAND...	96	CNTR	Te
< 0.02		90	[5]	BELLI	96	CNTR	^{129}Xe, inel.
			[6]	BELLI	96C	CNTR	^{129}Xe
< 4	$\times 10^{-3}$	90	[7]	BERNABEI	96	CNTR	Na
< 0.3		90	[7]	BERNABEI	96	CNTR	I
< 0.2		95	[8]	SARSA	96	CNTR	Na
< 0.015		90	[9]	SMITH	96	CNTR	Na
< 0.05		95	[10]	GARCIA	95	CNTR	Natural Ge
< 0.1		95		QUENBY	95	CNTR	Na
<90		90	[11]	SNOWDEN-...	95	MICA	^{16}O
< 4	$\times 10^3$	90	[11]	SNOWDEN-...	95	MICA	^{39}K
< 0.7		90		BACCI	92	CNTR	Na
< 0.12		90	[12]	REUSSER	91	CNTR	Natural Ge
< 0.06		95		CALDWELL	88	CNTR	Natural Ge

[1] UCHIDA 14 limit is for inelastic scattering $X^0 + {}^{129}Xe^* \rightarrow X^0 + {}^{129}Xe^*$ (39.58 keV).
[2] ANGLOHER 02 limit is for spin-dependent WIMP-Aluminum cross section.
[3] BENOIT 00 find four event categories in Ge detectors and suggest that low-energy surface nuclear recoils can explain anomalous events reported by UKDMC and Saclay NaI experiments.
[4] KLIMENKO 98 limit is for inelastic scattering $X^0\,{}^{73}Ge \rightarrow X^0\,{}^{73}Ge^*$ (13.26 keV).
[5] BELLI 96 limit for inelastic scattering $X^0\,{}^{129}Xe \rightarrow X^0\,{}^{129}Xe^*$(39.58 keV).
[6] BELLI 96C use background subtraction and obtain $\sigma < 150$ pb (< 1.5 fb) (90% CL) for spin-dependent (independent) X^0-proton cross section. The confidence level is from R. Bernabei, private communication, May 20, 1999.
[7] BERNABEI 96 use pulse shape discrimination to enhance the possible signal. The limit here is from R. Bernabei, private communication, September 19, 1997.
[8] SARSA 96 search for annual modulation of WIMP signal. See SARSA 97 for details of the analysis. The limit here is from M.L. Sarsa, private communication, May 26, 1997.
[9] SMITH 96 use pulse shape discrimination to enhance the possible signal. A dark matter density of 0.4 GeV cm^{-3} is assumed.
[10] GARCIA 95 limit is from the event rate. A weaker limit is obtained from searches for diurnal and annual modulation.
[11] SNOWDEN-IFFT 95 look for recoil tracks in an ancient mica crystal. Similar limits are also given for ^{27}Al and ^{28}Si. See COLLAR 96 and SNOWDEN-IFFT 96 for discussion on potential backgrounds.
[12] REUSSER 91 limit here is changed from published (0.04) after reanalysis by authors. J.L. Vuilleumier, private communication, March 29, 1996.

For m_{X^0} = 100 GeV

VALUE (nb)		CL%		DOCUMENT ID		TECN	COMMENT
• • • We do not use the following data for averages, fits, limits, etc. • • •							
< 3	$\times 10^{-3}$	90	[1]	UCHIDA	14	XMAS	^{129}Xe, inelastic
< 0.3		90	[2]	ANGLOHER	02	CRES	Al
			[3]	BELLI	02	RVUE	
			[4]	BERNABEI	02C	DAMA	
			[5]	GREEN	02	RVUE	
			[6]	ULLIO	01	RVUE	
			[7]	BENOIT	00	EDEL	Ge
< 4	$\times 10^{-3}$	90	[8]	BERNABEI	00D		^{129}Xe, inel.
			[9]	AMBROSIO	99	MCRO	
			[10]	BRHLIK	99	RVUE	
< 8	$\times 10^{-3}$	95	[11]	KLIMENKO	98	CNTR	^{73}Ge, inel.
< 0.08		95	[12]	KLIMENKO	98	CNTR	^{73}Ge, inel.
< 4				ALESSAND...	96	CNTR	O
<25				ALESSAND...	96	CNTR	Te
< 6	$\times 10^{-3}$	90	[13]	BELLI	96	CNTR	^{129}Xe, inel.
			[14]	BELLI	96C	CNTR	^{129}Xe
< 1	$\times 10^{-3}$	90	[15]	BERNABEI	96	CNTR	Na
< 0.3		90	[15]	BERNABEI	96	CNTR	I
< 0.7		95	[16]	SARSA	96	CNTR	Na
< 0.03		90	[17]	SMITH	96	CNTR	Na
< 0.8		90	[17]	SMITH	96	CNTR	I
< 0.35		95	[18]	GARCIA	95	CNTR	Natural Ge
< 0.6		95		QUENBY	95	CNTR	Na
< 3		95		QUENBY	95	CNTR	I
< 1.5	$\times 10^2$	90	[19]	SNOWDEN-...	95	MICA	^{16}O
< 4	$\times 10^2$	90	[19]	SNOWDEN-...	95	MICA	^{39}K
< 0.08		90	[20]	BECK	94	CNTR	^{76}Ge
< 2.5		90		BACCI	92	CNTR	Na
< 3		90		BACCI	92	CNTR	I
< 0.9		90	[21]	REUSSER	91	CNTR	Natural Ge
< 0.7		95		CALDWELL	88	CNTR	Natural Ge

[1] UCHIDA 14 limit is for inelastic scattering $X^0 + {}^{129}Xe^* \rightarrow X^0 + {}^{129}Xe^*$(39.58 keV).
[2] ANGLOHER 02 limit is for spin-dependent WIMP-Aluminum cross section.
[3] BELLI 02 discuss dependence of the extracted WIMP cross section on the assumptions of the galactic halo structure.
[4] BERNABEI 02C analyze the DAMA data in the scenario in which X^0 scatters into a slightly heavier state as discussed by SMITH 01.
[5] GREEN 02 discusses dependence of extracted WIMP cross section limits on the assumptions of the galactic halo structure.
[6] ULLIO 01 disfavor the possibility that the BERNABEI 99 signal is due to spin-dependent WIMP coupling.
[7] BENOIT 00 find four event categories in Ge detectors and suggest that low-energy surface nuclear recoils can explain anomalous events reported by UKDMC and Saclay NaI experiments.
[8] BERNABEI 00D limit is for inelastic scattering $X^0{}^{129}Xe \rightarrow X^0{}^{129}Xe$ (39.58 keV).
[9] AMBROSIO 99 search for upgoing muon events induced by neutrinos originating from WIMP annihilations in the Sun and Earth.
[10] BRHLIK 99 discuss the effect of astrophysical uncertainties on the WIMP interpretation of the BERNABEI 99 signal.
[11] KLIMENKO 98 limit is for inelastic scattering $X^0\,{}^{73}Ge \rightarrow X^0\,{}^{73}Ge^*$ (13.26 keV).
[12] KLIMENKO 98 limit is for inelastic scattering $X^0\,{}^{73}Ge \rightarrow X^0\,{}^{73}Ge^*$ (66.73 keV).
[13] BELLI 96 limit for inelastic scattering $X^0\,{}^{129}Xe \rightarrow X^0\,{}^{129}Xe^*$(39.58 keV).
[14] BELLI 96C use background subtraction and obtain $\sigma < 0.35$ pb (< 0.15 fb) (90% CL) for spin-dependent (independent) X^0-proton cross section. The confidence level is from R. Bernabei, private communication, May 20, 1999.
[15] BERNABEI 96 use pulse shape discrimination to enhance the possible signal. The limit here is from R. Bernabei, private communication, September 19, 1997.
[16] SARSA 96 search for annual modulation of WIMP signal. See SARSA 97 for details of the analysis. The limit here is from M.L. Sarsa, private communication, May 26, 1997.
[17] SMITH 96 use pulse shape discrimination to enhance the possible signal. A dark matter density of 0.4 GeV cm^{-3} is assumed.
[18] GARCIA 95 limit is from the event rate. A weaker limit is obtained from searches for diurnal and annual modulation.
[19] SNOWDEN-IFFT 95 look for recoil tracks in an ancient mica crystal. Similar limits are also given for ^{27}Al and ^{28}Si. See COLLAR 96 and SNOWDEN-IFFT 96 for discussion on potential backgrounds.
[20] BECK 94 uses enriched ^{76}Ge (86% purity).
[21] REUSSER 91 limit here is changed from published (0.3) after reanalysis by authors. J.L. Vuilleumier, private communication, March 29, 1996.

For m_{X^0} = 1 TeV

VALUE (nb)		CL%		DOCUMENT ID		TECN	COMMENT
• • • We do not use the following data for averages, fits, limits, etc. • • •							
< 0.03		90	[1]	UCHIDA	14	XMAS	^{129}Xe, inelastic
< 3		90	[2]	ANGLOHER	02	CRES	Al
			[3]	BENOIT	00	EDEL	Ge
			[4]	BERNABEI	99D	CNTR	SIMP
			[5]	DERBIN	99	CNTR	SIMP
< 0.06		95	[6]	KLIMENKO	98	CNTR	^{73}Ge, inel.
< 0.4		95	[7]	KLIMENKO	98	CNTR	^{73}Ge, inel.
< 40				ALESSAND...	96	CNTR	O
<700				ALESSAND...	96	CNTR	Te
< 0.05		90	[8]	BELLI	96	CNTR	^{129}Xe, inel.
< 1.5		90	[9]	BELLI	96	CNTR	^{129}Xe, inel.
			[10]	BELLI	96C	CNTR	^{129}Xe
< 0.01		90	[11]	BERNABEI	96	CNTR	Na
< 9		90	[11]	BERNABEI	96	CNTR	I
< 7		95	[12]	SARSA	96	CNTR	Na
< 0.3		90	[13]	SMITH	96	CNTR	Na
< 6		90	[13]	SMITH	96	CNTR	I
< 6		95	[14]	GARCIA	95	CNTR	Natural Ge
< 8		95		QUENBY	95	CNTR	Na
< 50		95		QUENBY	95	CNTR	I
<700		90	[15]	SNOWDEN-...	95	MICA	^{16}O
< 1	$\times 10^3$	90	[15]	SNOWDEN-...	95	MICA	^{39}K
< 0.8		90	[16]	BECK	94	CNTR	^{76}Ge
< 30		90		BACCI	92	CNTR	Na
< 30		90		BACCI	92	CNTR	I
< 15		90	[17]	REUSSER	91	CNTR	Natural Ge
< 6		95		CALDWELL	88	CNTR	Natural Ge

[1] UCHIDA 14 limit is for inelastic scattering $X^0 + {}^{129}Xe^* \rightarrow X^0 + {}^{129}Xe^*$ (39.58 keV).
[2] ANGLOHER 02 limit is for spin-dependent WIMP-Aluminum cross section.
[3] BENOIT 00 find four event categories in Ge detectors and suggest that low-energy surface nuclear recoils can explain anomalous events reported by UKDMC and Saclay NaI experiments.

[4] BERNABEI 99D search for SIMPs (Strongly Interacting Massive Particles) in the mass range 10^3–10^{16} GeV. See their Fig. 3 for cross-section limits.
[5] DERBIN 99 search for SIMPs (Strongly Interacting Massive Particles) in the mass range 10^2–10^{14} GeV. See their Fig. 3 for cross-section limits.
[6] KLIMENKO 98 limit is for inelastic scattering $X^0\,{}^{73}\mathrm{Ge} \rightarrow X^0\,{}^{73}\mathrm{Ge}^*$ (13.26 keV).
[7] KLIMENKO 98 limit is for inelastic scattering $X^0\,{}^{73}\mathrm{Ge} \rightarrow X^0\,{}^{73}\mathrm{Ge}^*$ (66.73 keV).
[8] BELLI 96 limit for inelastic scattering $X^0\,{}^{129}\mathrm{Xe} \rightarrow X^0\,{}^{129}\mathrm{Xe}^*$(39.58 keV).
[9] BELLI 96 limit for inelastic scattering $X^0\,{}^{129}\mathrm{Xe} \rightarrow X^0\,{}^{129}\mathrm{Xe}^*$(236.14 keV).
[10] BELLI 96C use background subtraction and obtain $\sigma < 0.7$ pb (< 0.7 fb) (90% CL) for spin-dependent (independent) X^0-proton cross section. The confidence level is from R. Bernabei, private communication, May 20, 1999.
[11] BERNABEI 96 use pulse shape discrimination to enhance the possible signal. The limit here is from R. Bernabei, private communication, September 19, 1997.
[12] SARSA 96 search for annual modulation of WIMP signal. See SARSA 97 for details of the analysis. The limit here is from M.L. Sarsa, private communication, May 26, 1997.
[13] SMITH 96 use pulse shape discrimination to enhance the possible signal. A dark matter density of 0.4 GeV cm^{-3} is assumed.
[14] GARCIA 95 limit is from the event rate. A weaker limit is obtained from searches for diurnal and annual modulation.
[15] SNOWDEN-IFFT 95 look for recoil tracks in an ancient mica crystal. Similar limits are also given for ^{27}Al and ^{28}Si. See COLLAR 96 and SNOWDEN-IFFT 96 for discussion on potential backgrounds.
[16] BECK 94 uses enriched ^{76}Ge (86% purity).
[17] REUSSER 91 limit here is changed from published (5) after reanalysis by authors. J.L. Vuilleumier, private communication, March 29, 1996.

Miscellaneous Results from Underground Dark Matter Searches

VALUE	CL%	DOCUMENT ID		TECN	COMMENT
• • • We do not use the following data for averages, fits, limits, etc. • • •					
$<1\times10^{-12}$	90	[1] AGUILAR-AR...17		DMIC	γ' on Si
		[2] APRILE	17	X100	Xe
		[3] APRILE	17D	X100	Xe
		[4] APRILE	17H	X100	keV bosonic DM search
		[5] APRILE	17K	X100	$\chi N \rightarrow \chi^* \rightarrow \chi\gamma$
$<4\times10^{-3}$	90	[6] ANGLOHER	16A	CRES	$CaWO_4$
		[7] APRILE	15	X100	Event rate modulation
		[8] APRILE	15A	X100	Electron scattering

[1] AGUILAR-AREVALO 17 search for hidden photon DM scatter on Si target CCD; limit kinetic mixing $\kappa < 1\times10^{-12}$ for m = 10 eV.
[2] APRILE 17 search for WIMP-e annual modulation signal for recoil energy in the 2.0–5.8 keV interval using 4 years data with Xe. No significant effect seen.
[3] APRILE 17D set limits on 14 WIMP-nucleon different interaction operators. No deviations found using 225 live days in the 6.6–240 keV recoil energy range.
[4] APRILE 17H search for keV bosonic DM via $e\chi \rightarrow e$, looking for electronic recoils with 224.6 live days of data and 34 kg of LXe. Limits set on $\chi e\,e$ coupling for m(χ) = 8–125 keV.
[5] APRILE 17K search for magnetic inelastic DM via $\chi N \rightarrow \chi^* \rightarrow \chi\gamma$. Limits set in DM magnetic moment vs. mass splitting plane for two DM masses corresponding to the DAMA/LIBRA best fit values.
[6] ANGLOHER 16A require q^2 dependent scattering $< 8\times10^{-3}$ pb for asymmetric DM m(WIMP) = 3 GeV on $CaWO_4$ target. It uses a local dark matter density of 0.38 GeV/cm^3.
[7] APRILE 15 search for periodic variation of electronic recoil event rate in the data between Feb. 2011 and Mar. 2012. No significant modulation is found for periods up to 500 days.
[8] APRILE 15A search for X^0 scattering off electrons. See their Fig. 4 for limits on cross section through axial-vector coupling for m_{X^0} between 0.6 GeV and 1 TeV. For m_{X^0} = 2 GeV, $\sigma < 60$ pb (90%CL) is obtained.

X^0 Annihilation Cross Section

Limits are on σv for X^0 pair annihilation at threshold.

VALUE ($\mathrm{cm}^3\mathrm{s}^{-1}$)	CL%	DOCUMENT ID		TECN	COMMENT
• • • We do not use the following data for averages, fits, limits, etc. • • •					
$<1.2\times10^{-23}$	95	[1] AARTSEN	17C	ICCB	$\chi\chi \rightarrow$ neutrinos
$<5\times10^{-25}$	90	[2] ALBERT	17A	ANTR	ν, Milky Way
$<1.32\times10^{-25}$	95	[3] ARCHAMBAU..17		VRTS	γ dwarf galaxies
$<7\times10^{-21}$	90	[4] AVRORIN	17	BAIK	cosmic ν
$<1\times10^{-28}$		[5] BOUDAUD	17		MeV DM to e^+e^-
		[6] AARTSEN	16D	ICCB	ν, galactic center
$<6\times10^{-26}$	95	[7] ABDALLAH	16	HESS	Central Galactic Halo
$<1\times10^{-27}$	95	[8] ABDALLAH	16A	HESS	WIMP+WIMP $\rightarrow \gamma\gamma$; galactic center
$<3\times10^{-26}$	95	[9] AHNEN	16	MGFL	Satellite galaxy, m(WIMP)=100 GeV
$<1.9\times10^{-21}$	90	[10] AVRORIN	16	BAIK	νs from galactic center
$<3\times10^{-26}$	95	[11] CAPUTO	16	FLAT	small Magellanic cloud
$<1\times10^{-25}$	95	[12] FORNASA	16	FLAT	Fermi-LAT γ-ray anisotropy
$<5\times10^{-27}$		[13] LEITE	16		WIMP, radio
$<2\times10^{-26}$	95	[14] LI	16	FLAT	dwarf galaxies
$<1\times10^{-25}$	95	[15] LI	16A	FLAT	Fermi-LAT; M31
$<1\times10^{-26}$		[16] LIANG	16	FLAT	Fermi-LAT, gamma line
$<1\times10^{-25}$	95	[17] LU	16	FLAT	Fermi-LAT and AMS-02
$<1\times10^{-23}$	95	[18] SHIRASAKI	16	FLAT	extra galactic
		[19] AARTSEN	15C	ICCB	ν, Galactic halo
		[20] AARTSEN	15E	ICCB	ν, Galactic center
		[21] ABRAMOWSKI	15	HESS	Galactic center
		[22] ACKERMANN	15	FLAT	monochromatic γ
		[23] ACKERMANN	15A	FLAT	isotropic γ background
		[24] ACKERMANN	15B	FLAT	Satellite galaxy
		[25] ADRIAN-MAR..15		ANTR	ν, Galactic center
$<2.90\times10^{-26}$	95	[26,27] ACKERMANN	14	FLAT	Satellite galaxy, m = 10 GeV
$<1.84\times10^{-25}$	95	[26,28] ACKERMANN	14	FLAT	Satellite galaxy, m = 100 GeV
$<1.75\times10^{-24}$	95	[26,28] ACKERMANN	14	FLAT	Satellite galaxy, m = 1 TeV
$<4.52\times10^{-24}$	95	[29] ALEKSIC	14	MGIC	Segue 1, m = 1.35 TeV
		[30] AARTSEN	13C	ICCB	Galaxies
		[31] ABRAMOWSKI	13	HESS	Central Galactic Halo
		[32] ACKERMANN	13A	FLAT	Galaxy
		[33] ABRAMOWSKI	12	HESS	Fornax Cluster
		[34] ACKERMANN	12	FLAT	Galaxy
		[35] ACKERMANN	12	FLAT	Galaxy
		[36] ALIU	12	VRTS	Segue 1
$<1\times10^{-22}$	90	[37] ABBASI	11C	ICCB	Galactic halo, m=1 TeV
$<3\times10^{-25}$	95	[38] ABRAMOWSKI	11	HESS	Near Galactic center, m=1 TeV
$<1\times10^{-26}$	95	[39] ACKERMANN	11	FLAT	Satellite galaxy, m=10 GeV
$<1\times10^{-25}$	95	[39] ACKERMANN	11	FLAT	Satellite galaxy, m=100 GeV
$<1\times10^{-24}$	95	[39] ACKERMANN	11	FLAT	Satellite galaxy, m=1 TeV

[1] AARTSEN 17C use 1005 days of IceCube data to search for $\chi\chi \rightarrow$ neutrinos via various annihilation channels. Limits set.
[2] ALBERT 17A maximum sensitivity to thermally averaged annihilation cross-section is for m(WIMP) = 10^5 GeV, where they require via $\tau\tau$ channel, $\langle\sigma\cdot v\rangle < 5\times10^{-25}$ cm^3/s assuming NFW halo profile, $\langle\sigma\cdot v\rangle < 2\times10^{-24}$ cm^3/s assuming McMillan profile, $\langle\sigma\cdot v\rangle < 1.2\times10^{-23}$ cm^3/s assuming Burkert profile.
[3] ARCHAMBAULT 17 set limits for WIMP mass between 100 GeV and 1 TeV on $\langle\sigma\cdot v\rangle$ for W^+W^-, ZZ, $b\overline{b}$, $s\overline{s}$, $u\overline{u}$, $d\overline{d}$, $t\overline{t}$, e^+e^-, gg, $c\overline{c}$, hh, $\gamma\gamma$, $\mu^+\mu^-$,$\tau^+\tau^-$ annihilation channels.
[4] AVRORIN 17 find upper limits for the annhilation cross section in various channels for DM particle mass between 30 GeV and 10 TeV. Strongest upper limits coming from the two neutrino channel require $\langle\sigma\cdot v\rangle < 6\times10^{-20}$ cm^3/s in dwarf galaxies and $\langle\sigma\cdot v\rangle < 7\times10^{-21}$ cm^3/s in LMC for 5 TeV WIMP mass.
[5] BOUDAUD 17 use data from the spacecraft Voyager 1, beyond the heliopause, and from AMS02 on $\chi\chi \rightarrow e^+e^-$ to require $\langle\sigma\cdot v\rangle < 1.\times10^{-28}$ cm^3/s for m(χ) = 10 MeV.
[6] AARTSEN 16D search for GeV νs from WIMP annihilation in galaxy; limits set on $\langle\sigma\cdot v\rangle$ in Fig. 6, 7.
[7] ABDALLAH 16 require $\langle\sigma\cdot v\rangle < 6\times10^{-26}$ cm^3/s for m(WIMP) = 1.5 TeV from 254 hours observation (WW channel) and $< 2\times10^{-26}$ cm^3/s for m(WIMP) = 1.0 TeV in $\tau^+\tau^-$ channel.
[8] ABDALLAH 16A search for line spectra from WIMP + WIMP $\rightarrow \gamma\gamma$ in 18 hr HESS data; rule out previous 130 GeV WIMP hint from Fermi-LAT data.
[9] AHNEN 16 require $\langle\sigma\cdot v\rangle < 3\times10^{-26}$ cm^3/s for m(WIMP) = 100 GeV (WW channel).
[10] AVRORIN 16 require $\langle$s.v$\rangle < 1.91\times10^{-21}$ cm^3/s from WIMP annihilation to νs via WW channel for m(WIMP) = 1 TeV.
[11] CAPUTO 16 place limits on WIMPs from annihilation to gamma rays in Small Magellanic Cloud using Fermi-LaT data: $\langle\sigma\cdot v\rangle < 3\times10^{-26}\mathrm{cm}^3$/s for m(WIMP) = 10 GeV.
[12] FORNASA 16 use anisotropies in the γ-ray diffuse emission detected by Fermi-LAT to bound $\langle\sigma\cdot v\rangle < 10^{-25}\mathrm{cm}^3$/s for m(WIMP) = 100 GeV in $b\overline{b}$ channel: see Fig. 28. The limit is driven by dark-matter subhalos in the Milky Way and it refers to their Most Constraining Scenario.
[13] LEITE 16 constrain WIMP annihilation via search for radio emissions from Smith cloud; $\langle\sigma\cdot v\rangle < 5\times10^{-27}\mathrm{cm}^3$/s in $e\,e$ channel for m(WIMP) = 5 GeV.
[14] LI 16 re-analyze Fermi-LAT data on 8 dwarf spheroidals; set limit $\langle\sigma\cdot v\rangle < 2\times10^{-26}$ cm^3/s for m(WIMP) = 100 GeV in $b\overline{b}$ mode with substructures included.
[15] LI 16A constrain $\langle\sigma\cdot v\rangle < 10^{-25}\mathrm{cm}^3$/s in $b\overline{b}$ channel for m(WIMP) = 100 GeV using Fermi-LAT data from M31; see Fig. 6.
[16] LIANG 16 search dwarf spheroidal galaxies, Large Magellanic Cloud, and Small Magellanic Cloud for γ-line in Fermi-LAT data.
[17] LU 16 re-analyze Fermi-LAT and AMS-02 data; require $\langle\sigma\cdot v\rangle < 10^{-25}\mathrm{cm}^3$/s for m_m(WIMP) = 1 TeV in $b\overline{b}$ channel .
[18] SHIRASAKI 16 re-anayze Fermi-LAT extra-galactic data; require $\langle\sigma\cdot v\rangle < 10^{-23}\mathrm{cm}^3$/s for m(WIMP) = 1 TeV in $b\overline{b}$ channel; see Fig. 8.
[19] AARTSEN 15C search for neutrinos from X^0 annihilation in the Galactic halo. See their Figs. 16 and 17, and Table 5 for limits on $\sigma\cdot$v for X^0 mass between 100 GeV and 100 TeV.
[20] AARTSEN 15E search for neutrinos from X^0 annihilation in the Galactic center. See their Figs. 7 and 9, and Table 3 for limits on $\sigma\cdot$v for X^0 mass between 30 GeV and 10 TeV.
[21] ABRAMOWSKI 15 search for γ from X^0 annihilation in the Galactic center. See their Fig. 4 for limits on $\sigma\cdot$v for X^0 mass between 250 GeV and 10 TeV.
[22] ACKERMANN 15 search for monochromatic γ from X^0 annihilation in the Galactic halo. See their Fig. 8 and Tables 2–4 for limits on $\sigma\cdot$v for X^0 mass between 0.2 GeV and 500 GeV.
[23] ACKERMANN 15A search for γ from X^0 annihilation (both Galactic and extragalactic) in the isotropic γ background. See their Fig. 7 for limits on $\sigma\cdot$v for X^0 mass between 10 GeV and 30 TeV.
[24] ACKERMANN 15B search for γ from X^0 annihilation in 15 dwarf spheroidal satellite galaxies of the Milky Way. See their Figs. 1 and 2 for limits on $\sigma\cdot$v for X^0 mass between 2 GeV and 10 TeV.
[25] ADRIAN-MARTINEZ 15 search for neutrinos from X^0 annihilation in the Galactic center. See their Figs. 10 and 11 and Tables 1 and 2 for limits on $\sigma\cdot$v for X^0 mass between 25 GeV and 10 TeV.
[26] ACKERMANN 14 search for γ from X^0 annihilation in 25 dwarf spheroidal satellite galaxies of the Milky Way. See their Tables II–VII for limits assuming annihilation into e^+e^-, $\mu^+\mu^-$, $\tau^+\tau^-$, $u\overline{u}$, $b\overline{b}$, and W^+W^-, for X^0 mass ranging from 2 GeV to 10 TeV.
[27] Limit assuming X^0 pair annihilation into $b\overline{b}$.
[28] Limit assuming X^0 pair annihilation into W^+W^-.
[29] ALEKSIC 14 search for γ from X^0 annihilation in the dwarf spheroidal galaxy Segue 1. The listed limit assumes annihilation into W^+W^-. See their Figs. 6, 7, and 16 for

limits on $\sigma \cdot v$ for annihilation channels $\mu^+\mu^-$, $\tau^+\tau^-$, $b\overline{b}$, $t\overline{t}$, $\gamma\gamma$, γZ, W^+W^-, ZZ for X^0 mass between 10^2 and 10^4 GeV.

[30] AARTSEN 13C search for neutrinos from X^0 annihilation in nearby galaxies and galaxy clusters. See their Figs. 5–7 for limits on $\sigma \cdot v$ for $X^0X^0 \to \nu\overline{\nu}$, $\mu^+\mu^-$, $\tau^+\tau^-$, and W^+W^- for X^0 mass between 300 GeV and 100 TeV.

[31] ABRAMOWSKI 13 search for monochromatic γ from X^0 annihilation in the Milky Way halo in the central region. Limit on $\sigma \cdot v$ between 10^{-28} and 10^{-25} cm^3 s^{-1} (95% CL) is obtained for X^0 mass between 500 GeV and 20 TeV for $X^0X^0 \to \gamma\gamma$. X^0 density distribution in the Galaxy by Einasto is assumed. See their Fig. 4.

[32] ACKERMANN 13A search for monochromatic γ from X^0 annihilation in the Milky Way. Limit on $\sigma \cdot v$ for the process $X^0X^0 \to \gamma\gamma$ in the range 10^{-29}–10^{-27} cm^3 s^{-1} (95% CL) is obtained for X^0 mass between 5 and 300 GeV. The limit depends slightly on the assumed density profile of X^0 in the Galaxy. See their Tables VII–X and Fig.10. Supersedes ACKERMANN 12.

[33] ABRAMOWSKI 12 search for γ's from X^0 annihilation in the Fornax galaxy cluster. See their Fig. 7 for limits on $\sigma \cdot v$ for X^0 mass between 0.1 and 100 TeV for the annihilation channels $\tau^+\tau^-$, $b\overline{b}$, and W^+W^-.

[34] ACKERMANN 12 search for monochromatic γ from X^0 annihilation in the Milky Way. Limit on $\sigma \cdot v$ in the range 10^{-28}–10^{-26} cm^{3}s^{-1} (95% CL) is obtained for X^0 mass between 7 and 200 GeV if X^0 annihilates into $\gamma\gamma$. The limit depends slightly on the assumed density profile of X^0 in the Galaxy. See their Table III and Fig. 15.

[35] ACKERMANN 12 search for γ from X^0 annihilation in the Milky Way in the diffuse γ background. Limit on $\sigma \cdot v$ of 10^{-24} cm^{3}s^{-1} or larger is obtained for X^0 mass between 5 GeV and 10 TeV for various annihilation channels including W^+W^-, $b\overline{b}$, gg, e^+e^-, $\mu^+\mu^-$, $\tau^+\tau^-$. The limit depends slightly on the assumed density profile of X^0 in the Galaxy. See their Figs. 17–20.

[36] ALIU 12 search for γ's from X^0 annihilation in the dwarf spheroidal galaxy Segue 1. Limit on $\sigma \cdot v$ in the range 10^{-24}–10^{-20} cm^{3}s^{-1} (95% CL) is obtained for X^0 mass between 10 GeV and 2 TeV for annihilation channels e^+e^-, $\mu^+\mu^-$, $\tau^+\tau^-$, $b\overline{b}$, and W^+W^-. See their Fig. 3.

[37] ABBASI 11C search for ν_μ from X^0 annihilation in the outer halo of the Milky Way. The limit assumes annihilation into $\nu\nu$. See their Fig. 9 for limits with other annihilation channels.

[38] ABRAMOWSKI 11 search for γ from X^0 annihilation near the Galactic center. The limit assumes Einasto DM density profile.

[39] ACKERMANN 11 search for γ from X^0 annihilation in ten dwarf spheroidal satellite galaxies of the Milky Way. The limit for $m = 10$ GeV assumes annihilation into $b\overline{b}$, the others W^+W^-. See their Fig. 2 for limits with other final states. See also GERINGER-SAMETH 11 for a different analysis of the same data.

Dark Matter Particle (X^0) Production in Hadron Collisions

Searches for X^0 production in association with observable particles (γ, jets, ...) in high energy hadron collisions. If a specific form of effective interaction Lagrangian is assumed, the limits may be translated into limits on X^0-nucleon scattering cross section.

VALUE	DOCUMENT ID		TECN	COMMENT
• • • We do not use the following data for averages, fits, limits, etc. • • •				
	[1] AABOUD	18	ATLS	$pp \to Z\chi\chi$; $Z \to \ell\ell$
	[2] AABOUD	18A	ATLS	$pp \to t\overline{t}\,\not{E}_T$; $pp \to b\overline{b}\,\not{E}_T$
	[3] AABOUD	18I	ATLS	jet(s) + $\not{E}_T$
	[4] SIRUNYAN	18C	CMS	$pp \to t\overline{t}\,\not{E}_T$
	[5] AABOUD	17A	ATLS	pp ($H \to b\overline{b}$ + WIMP pair)
	[6] AABOUD	17AM	ATLS	$pp \to Z' \to Ah \to h(b\overline{b}) + \not{E}_T$
	[7] AABOUD	17AQ	ATLS	$pp \to h(\gamma\gamma) + \not{E}_T$
	[8] AABOUD	17BD	ATLS	$pp \to$ jet(s) + $\not{E}_T$
	[9] AABOUD	17R	ATLS	$pp \to \gamma\not{E}_T$
	[10] AGUILAR-AR...	17A	MBNE	$pN \to \chi\chi X$; $\chi N \to \chi N$
	[11] BANERJEE	17	NA64	$eN \to eN\gamma'$
	[12] KHACHATRY...	17A	CMS	forward jets + $\not{E}_T$
	[13] KHACHATRY...	17F	CMS	$H \to$ invisibles
	[14] SIRUNYAN	17	CMS	$Z + \not{E}_T$
	[15] SIRUNYAN	17AP	CMS	$pp \to Z' \to Ah \to h$+MET
	[16] SIRUNYAN	17AQ	CMS	$pp \to \gamma$+MET
	[17] SIRUNYAN	17BB	CMS	$pp \to t\overline{t}$+$\not{E}_T$; $pp \to b\overline{b}$+$\not{E}_T$
	[18] SIRUNYAN	17G	CMS	$pp \to j + \not{E}_T$
	[19] SIRUNYAN	17U	CMS	$pp \to Z\chi\chi$; $Z \to \ell\overline{\ell}$
	[20] AABOUD	16AD	ATLS	(W or $Z \to$ jets) + $\not{E}_T$
	[21] AAD	16AF	ATLS	$VV \to$ forward jets +$\not{E}_T$
	[22] AAD	16AG	ATLS	ℓ + jets
	[23] AAD	16M	ATLS	$pp \to H + \not{E}_T$, $H \to b\overline{b}$
	[24] KHACHATRY...	16BZ	CMS	jet(s) + $\not{E}_T$
	[25] KHACHATRY...	16CA	CMS	jets + $\not{E}_T$
	[26] KHACHATRY...	16N	CMS	$pp \to \gamma + \not{E}_T$
	[27] AAD	15AS	ATLS	b ($\overline{b}$) + $\not{E}_T$, $t\overline{t}$ + $\not{E}_T$
	[28] AAD	15BH	ATLS	jet + $\not{E}_T$
	[29] AAD	15CF	ATLS	$H^0 + \not{E}_T$
	[30] AAD	15CS	ATLS	$\gamma + \not{E}_T$
	[31] KHACHATRY...	15AG	CMS	$t\overline{t} + \not{E}_T$
	[32] KHACHATRY...	15AL	CMS	jet + $\not{E}_T$
	[33] KHACHATRY...	15T	CMS	$\ell + \not{E}_T$
	[34] AAD	14AI	ATLS	$W + \not{E}_T$
	[35] AAD	14BK	ATLS	W, $Z + \not{E}_T$
	[36] AAD	14K	ATLS	$Z + \not{E}_T$
	[37] AAD	14O	ATLS	$Z + \not{E}_T$
	[38] AAD	13AD	ATLS	jet + $\not{E}_T$
	[39] AAD	13C	ATLS	$\gamma + \not{E}_T$
	[40] AALTONEN	12K	CDF	$t + \not{E}_T$
	[41] AALTONEN	12M	CDF	jet + $\not{E}_T$
	[42] CHATRCHYAN	12AP	CMS	jet + $\not{E}_T$
	[43] CHATRCHYAN	12T	CMS	$\gamma + \not{E}_T$

[1] AABOUD 18 search for $pp \to Z + \not{E}_T$ with $Z \to \ell\ell$ at 13 TeV with 36.1 fb^{-1} of data. Limits set for simplified models.

[2] AABOUD 18A search for $pp \to t\overline{t}\,\not{E}_T$ or $pp \to b\overline{b}\,\not{E}_T$ at 13 TeV, 36.1 fb^{-1} of data. Limits set for simplified models.

[3] AABOUD 18I search for $pp \to j + \not{E}_T$ at 13 TeV with 36.1 fb^{-1} of data. Limits set for simplified models with pair-produced weakly interacting dark-matter candidates.

[4] SIRUNYAN 18C search for new physics in $pp \to$ final states with two oppositely charged leptons at 13 TeV with 35.9 fb^{-1}. Limits placed on m(mediator) and top squark for various simplified models.

[5] AABOUD 17A search for $H \to b\overline{b} + \not{E}_T$. See Fig. 4b for limits set on VB mediator vs WIMP mass.

[6] AABOUD 17AM search for $pp \to Z' \to Ah \to h(b\overline{b}) + \not{E}_T$ at 13 TeV. Limits set in m(Z') vs. m(A) plane and on the visible cross section of $h(b\overline{b}) + \not{E}_T$ events in bins of $\not{E}_T$.

[7] AABOUD 17AQ search for WIMP in $pp \to h(\gamma\gamma) + \not{E}_T$ in 36.1 fb^{-1} of data. Limits on the visible cross section are also provided. Model dependent limits on spin independent DM - Nucleon cross-section are also presented, which are more stringent than those from direct searches for DM mass smaller than 2.5 GeV .

[8] AABOUD 17BD search for $pp \to$ jet(s) + $\not{E}_T$ at 13 TeV with 3.2 fb^{-1} of data. Limits set for simplified models. Observables corrected for detector effects can be used to constrain other models.

[9] AABOUD 17R, for an axial vector mediator in the s-channel, excludes m(mediator) < 750–1200 GeV for m(DM) < 230–480 GeV, depending on the couplings.

[10] AGUILAR-AREVALO 17A search for DM produced in 8 GeV proton collisions with steel beam dump followed by DM-nucleon scattering in MiniBooNE detector. Limit placed on DM cross section parameter $Y < 2 \times 10^{-8}$ for $\alpha_D = 0.5$ and for $0.01 < m(\text{DM}) < 0.3$ GeV.

[11] BANERJEE 17 search for dark photon invisible decay via eN scattering; exclude m(γ') < 100 MeV as an explanation of (g_μ−2) muon anomaly.

[12] KHACHATRYAN 17A search for WIMPs in forward jets + $\not{E}_T$ channel with 18.5 fb^{-1} at 8 TeV; limits set in effective theory model, Fig. 3.

[13] KHACHATRYAN 17F search for $H \to$ invisibles in pp collisions at 7, 8, and 13 TeV; place limits on Higgs portal DM.

[14] SIRUNYAN 17 search for $pp \to Z + \not{E}_T$ with 2.3 fb^{-1} at 13 TeV; no signal seen; limits placed on WIMPs and unparticles.

[15] SIRUNYAN 17AP search for $pp \to Z' \to Ah \to h$+MET with $h \to b\overline{b}$ or $\gamma\gamma$ and $A \to \chi\chi$ with 2.3 fb^{-1} at 13 TeV. Limits set in m(Z') vs. m(A) plane.

[16] SIRUNYAN 17AQ search for $pp \to \gamma$+MET at 13 TeV with 12.9 fb^{-1}. Limits derived for simplified DM models, effective electroweak-DM interaction and Extra Dimensions models.

[17] SIRUNYAN 17BB search for WIMPs via $pp \to t\overline{t}$+$\not{E}_T$, $pp \to b\overline{b}$+$\not{E}_T$ at 13 TeV with 2.2 fb^{-1}. Limits derived for various simplified models.

[18] SIRUNYAN 17G search for $pp \to j + \not{E}_T$ with 12.9 fb^{-1} at 13 TeV; limits placed on WIMP mass/mediators in DM simplified models.

[19] SIRUNYAN 17U search for WIMPs/unparticles via $pp \to Z\chi\chi$, $Z \to \ell\overline{\ell}$ at 13 TeV with 2.3 fb^{-1}. Limits derived for various simplified models.

[20] AABOUD 16AD place limits on $VVXX$ effective theory via search for hadronic W or Z plus WIMP pair production. See Fig. 5.

[21] AAD 16AF search for $VV \to (H \to$ WIMP pair) + forward jets with 20.3 fb^{-1} at 8 TeV; set limits in Higgs portal model, Fig. 8 .

[22] AAD 16AG search for lepton jets with 20.3 fb^{-1} of data at 8 TeV; Fig. 13 excludes dark photons around 0.1–1 GeV for kinetic mixing 10^{-6}–10^{-2}.

[23] AAD 16M search with 20.3 fb^{-1} of data at 8 TeV pp collisions; limits placed on EFT model (Fig. 7) and simplified Z' model (Fig. 6).

[24] KHACHATRYAN 16BZ search for jet(s) + $\not{E}_T$ in 19.7 fb^{-1} at 8 TeV; limits set for variety of simplified models.

[25] KHACHATRYAN 16CA search for WIMPs via jet(s) + $\not{E}_T$ using razor variable; require mediator scale > 1 TeV for various effective theories.

[26] KHACHATRYAN 16N search for γ + WIMPs in 19.6 fb^{-1} at 8 TeV; limits set on SI and SD WIMP-p scattering in Fig. 3.

[27] AAD 15AS search for events with one or more bottom quark and missing E_T, and also events with a top quark pair and missing E_T in pp collisions at E_{cm} = 8 TeV with L = 20.3 fb^{-1}. See their Figs. 5 and 6 for translated limits on X^0-nucleon cross section for m = 1–700 GeV.

[28] AAD 15BH search for events with a jet and missing E_T in pp collisions at E_{cm} = 8 TeV with L = 20.3 fb^{-1}. See their Fig. 12 for translated limits on X^0-nucleon cross section for m = 1–1200 GeV.

[29] AAD 15CF search for events with a H^0 ($\to \gamma\gamma$) and missing E_T in pp collisions at E_{cm} = 8 TeV with L = 20.3 fb^{-1}. See paper for limits on the strength of some contact interactions containing X^0 and the Higgs fields.

[30] AAD 15CS search for events with a photon and missing E_T in pp collisions at E_{cm} = 8 TeV with L = 20.3 fb^{-1}. See their Fig. 13 (see also erratum) for translated limits on X^0-nucleon cross section for m = 1–1000 GeV.

[31] KHACHATRYAN 15AG search for events with a top quark pair and missing E_T in pp collisions at E_{cm} = 8 TeV with L = 19.7 fb^{-1}. See their Fig. 8 for translated limits on X^0-nucleon cross section for m = 1–200 GeV.

[32] KHACHATRYAN 15AL search for events with a jet and missing E_T in pp collisions at E_{cm} = 8 TeV with L = 19.7 fb^{-1}. See their Fig. 5 and Tables 4–6 for translated limits on X^0-nucleon cross section for m = 1–1000 GeV.

[33] KHACHATRYAN 15T search for events with a lepton and missing E_T in pp collisions at E_{cm} = 8 TeV with L = 19.7 fb^{-1}. See their Fig. 17 for translated limits on X^0-proton cross section for m = 1–1000 GeV.

[34] AAD 14AI search for events with a W and missing E_T in pp collisions at E_{cm} = 8 TeV with L = 20.3 fb^{-1}. See their Fig. 4 for translated limits on X^0–nucleon cross section for m = 1–1500 GeV.

[35] AAD 14BK search for hadronically decaying W, Z in association with $\not{E}_T$ in 20.3 fb^{-1} at 8 TeV pp collisions. Fig. 5 presents exclusion results for SI and SD scattering cross section. In addition, cross section limits on the anomalous production of W or Z bosons with large missing transverse momentum are also set in two fiducial regions.

[36] AAD 14K search for events with a Z and missing E_T in pp collisions at E_{cm} = 8 TeV with L = 20.3 fb^{-1}. See their Fig. 5 and 6 for translated limits on X^0–nucleon cross section for m = 1–10^3 GeV.

[37] AAD 14O search for ZH^0 production with H^0 decaying to invisible final states. See their Fig. 4 for translated limits on X^0–nucleon cross section for m = 1–60 GeV in Higgs-portal X^0 scenario.

[38] AAD 13AD search for events with a jet and missing E_T in pp collisions at E_{cm} = 7 TeV with L = 4.7 fb^{-1}. See their Figs. 5 and 6 for translated limits on X^0–nucleon cross section for m = 1–1300 GeV.

[39] AAD 13C search for events with a photon and missing E_T in pp collisions at E_{cm} = 7 TeV with L = 4.6 fb^{-1}. See their Fig. 3 for translated limits on X^0–nucleon cross section for m = 1–1000 GeV.

[40] AALTONEN 12K search for events with a top quark and missing E_T in $p\overline{p}$ collisions at E_{cm} = 1.96 TeV with L = 7.7 fb^{-1}. Upper limits on $\sigma(tX^0)$ in the range 0.4–2 pb (95% CL) is given for m_{X^0} = 0–150 GeV.

[41] AALTONEN 12M search for events with a jet and missing E_T in $p\overline{p}$ collisions at E_{cm} = 1.96 TeV with L = 6.7 fb^{-1}. Upper limits on the cross section in the range 2–10 pb (90% CL) is given for m_{X^0} = 1–300 GeV. See their Fig. 2 for translated limits on X^0–nucleon cross section.

[42] CHATRCHYAN 12AP search for events with a jet and missing E_T in pp collisions at E_{cm} = 7 TeV with L = 5.0 fb^{-1}. See their Fig. 4 for translated limits on X^0–nucleon cross section for m_{X^0} = 0.1–1000 GeV.

[43] CHATRCHYAN 12T search for events with a photon and missing E_T in pp collisions at E_{cm} = 7 TeV with L = 5.0 fb^{-1}. Upper limits on the cross section in the range 13–15 fb (90% CL) is given for m_{X^0} = 1–1000 GeV. See their Fig. 2 for translated limits on X^0–nucleon cross section.

REFERENCES FOR WIMP and Dark Matter Searches

AABOUD	18	PL B776 318	M. Aaboud *et al.*	(ATLAS Collab.)
AABOUD	18A	EPJ C78 18	M. Aaboud *et al.*	(ATLAS Collab.)
AABOUD	18I	JHEP 1801 126	M. Aaboud *et al.*	(ATLAS Collab.)
AGNESE	18	PR D97 022002	R. Agnese *et al.*	(SuperCDMS Collab.)
AGNESE	18A	PRL 120 061802	R. Agnese *et al.*	(SuperCDMS Collab.)
SIRUNYAN	18C	PR D97 032009	A.M. Sirunyan *et al.*	(CMS Collab.)
AABOUD	17A	PL B765 11	M. Aaboud *et al.*	(ATLAS Collab.)
AABOUD	17AM	PRL 119 181804	M. Aaboud *et al.*	(ATLAS Collab.)
AABOUD	17AQ	PR D96 112004	M. Aaboud *et al.*	(ATLAS Collab.)
AABOUD	17BD	EPJ C77 765	M. Aaboud *et al.*	(ATLAS Collab.)
AABOUD	17R	EPJ C77 393	M. Aaboud *et al.*	(ATLAS Collab.)
AARTSEN	17	EPJ C77 82	M.G. Aartsen *et al.*	(IceCube Collab.)
AARTSEN	17A	EPJ C77 146	M.G. Aartsen *et al.*	(IceCube Collab.)
AARTSEN	17C	EPJ C77 627	M.G. Aartsen *et al.*	(IceCube Collab.)
AGUILAR-AR...	17	PRL 118 141803	A.A. Aguilar-Arevalo *et al.*	(DAMIC Collab.)
AGUILAR-AR...	17A	PRL 118 221803	A.A. Aguilar-Arevalo *et al.*	(MiniBooNE Collab.)
AKERIB	17	PRL 118 021303	D.S. Akerib *et al.*	(LUX Collab.)
AKERIB	17A	PRL 118 251302	D.S. Akerib *et al.*	(LUX Collab.)
ALBERT	17A	PL B769 249	A. Albert *et al.*	(ANTARES Collab.)
AMOLE	17	PRL 118 251301	C. Amole *et al.*	(PICO Collab.)
ANGLOHER	17A	EPJ C77 637	G. Angloher *et al.*	(CRESST Collab.)
APRILE	17	PRL 118 101101	E. Aprile *et al.*	(XENON100 Collab.)
APRILE	17A	PR D96 022008	E. Aprile *et al.*	(XENON100 Collab.)
APRILE	17D	PR D96 042004	E. Aprile *et al.*	(XENON100 Collab.)
APRILE	17G	PRL 119 181301	E. Aprile *et al.*	(XENON Collab.)
APRILE	17H	PR D96 122002	E. Aprile *et al.*	(XENON100 Collab.)
APRILE	17K	JCAP 1710 039	E. Aprile *et al.*	(XENON100 Collab.)
ARCHAMBAU...	17	PR D95 082001	S. Archambault *et al.*	(VERITAS Collab.)
AVRORIN	17	JETP 125 80	A.D. Avrorin *et al.*	(BAIKAL Collab.)
BANERJEE	17	PRL 118 011802	D. Banerjee *et al.*	(NA64 Collab.)
BARBOSA-D...	17	PR D95 032006	E. Barbosa de Souza *et al.*	(DM17 Collab.)
BATTAT	17	ASP 91 65	J.B.R. Battat *et al.*	(DRIFT-IId Collab.)
BEHNKE	17	ASP 90 85	E. Behnke *et al.*	(PICASSO Collab.)
BOUDAUD	17	PRL 119 021103	M. Boudaud, J. Lavalle, P. Salati	
CHEN	17E	PR D96 102007	X. Chen *et al.*	(PandaX-II Collab.)
CUI	17A	PRL 119 181302	X. Cui *et al.*	(PandaX-II Collab.)
FU	17	PRL 118 071301	C. Fu *et al.*	(PandaX Collab.)
KHACHATRY...	17A	PRL 118 021802	V. Khachatryan *et al.*	(CMS Collab.)
KHACHATRY...	17F	JHEP 1702 135	V. Khachatryan *et al.*	(CMS Collab.)
SIRUNYAN	17	JHEP 1703 061	A.M. Sirunyan *et al.*	(CMS Collab.)
SIRUNYAN	17AP	JHEP 1710 180	A.M. Sirunyan *et al.*	(CMS Collab.)
SIRUNYAN	17AQ	JHEP 1710 073	A.M. Sirunyan *et al.*	(CMS Collab.)
SIRUNYAN	17BB	EPJ C77 845	A.M. Sirunyan *et al.*	(CMS Collab.)
SIRUNYAN	17G	JHEP 1707 014	A.M. Sirunyan *et al.*	(CMS Collab.)
SIRUNYAN	17U	JHEP 1709 106	A.M. Sirunyan *et al.*	(CMS Collab.)
AABOUD	16AD	PL B763 251	M. Aaboud *et al.*	(ATLAS Collab.)
AABOUD	16D	PR D94 032005	M. Aaboud *et al.*	(ATLAS Collab.)
AABOUD	16F	JHEP 1606 059	M. Aaboud *et al.*	(ATLAS Collab.)
AAD	16AF	JHEP 1601 172	G. Aad *et al.*	(ATLAS Collab.)
AAD	16AG	JHEP 1602 062	G. Aad *et al.*	(ATLAS Collab.)
AAD	16M	PR D93 072007	G. Aad *et al.*	(ATLAS Collab.)
AARTSEN	16C	JCAP 1604 022	M.G. Aartsen *et al.*	(IceCube Collab.)
AARTSEN	16D	EPJ C76 531	M.G. Aartsen *et al.*	(IceCube Collab.)
ABDALLAH	16	PRL 117 111301	H. Abdallah *et al.*	(H.E.S.S. Collab.)
ABDALLAH	16A	PRL 117 151302	H. Abdallah *et al.*	(H.E.S.S. Collab.)
ADRIAN-MAR...	16	PL B759 69	S. Adrian-Martinez *et al.*	(ANTARES Collab.)
ADRIAN-MAR...	16B	JCAP 1605 016	S. Adrian-Martinez *et al.*	(ANTARES Collab.)
AGNES	16	PR D93 081101	P. Agnes *et al.*	(DarkSide-50 Collab.)
AGNESE	16	PRL 116 071301	R. Agnese *et al.*	(SuperCDMS Collab.)
AGUILAR-AR...	16	PR D94 082006	A.A. Aguilar-Arevalo *et al.*	(DAMIC Collab.)
AHNEN	16	JCAP 1602 039	M.L. Ahnen *et al.*	(MAGIC and Fermi-LAT Collab.)
AKERIB	16	PRL 116 161301	D.S. Akerib *et al.*	(LUX Collab.)
AKERIB	16A	PRL 116 161302	D.S. Akerib *et al.*	(LUX Collab.)
AMOLE	16	PR D93 052014	C. Amole *et al.*	(PICO Collab.)
AMOLE	16A	PR D93 061101	C. Amole *et al.*	(PICO Collab.)
ANGLOHER	16	EPJ C76 25	G. Angloher *et al.*	(CRESST-II Collab.)
ANGLOHER	16A	PRL 117 021303	G. Angloher *et al.*	(CRESST-II Collab.)
APRILE	16	PR D94 092001	E. Aprile *et al.*	(XENON100 Collab.)
APRILE	16B	PR D94 122001	E. Aprile *et al.*	(XENON100 Collab.)
ARMENGAUD	16	JCAP 1605 019	E. Armengaud *et al.*	(EDELWEISS-III Collab.)
AVRORIN	16	ASP 81 12	A.D. Avrorin *et al.*	(BAIKAL Collab.)
CAPUTO	16	PR D93 062004	R. Caputo *et al.*	
FORNASA	16	PR D94 123005	M. Fornasa *et al.*	(Fermi-LAT Collab.)
HEHN	16	EPJ C76 548	L. Hehn *et al.*	(EDELWEISS-III Collab.)
KHACHATRY...	16AJ	PR D93 052011	V. Khachatryan *et al.*	(CMS Collab.)
KHACHATRY...	16BZ	JHEP 1612 083	V. Khachatryan *et al.*	(CMS Collab.)
Also		JHEP 1708 035 (errat.)	V. Khachatryan *et al.*	(CMS Collab.)
KHACHATRY...	16CA	JHEP 1612 088	V. Khachatryan *et al.*	(CMS Collab.)
KHACHATRY...	16N	PL B755 102	V. Khachatryan *et al.*	(CMS Collab.)
LEITE	16	JCAP 1611 021	N. Leite *et al.*	
LI	16	PR D93 043518	S. Li *et al.*	
LI	16A	JCAP 1612 028	Z. Li *et al.*	
LIANG	16	PR D94 103502	Y.-F. Liang *et al.*	
LU	16	PR D93 103517	B-Q. Lu, H-S. Zong	
SHIRASAKI	16	PR D94 063522	M. Shirasaki *et al.*	
TAN	16	PR D93 122009	T.H. Tan *et al.*	(PandaX Collab.)
TAN	16B	PRL 117 121303	A. Tan *et al.*	(PandaX Collab.)
ZHAO	16	PR D93 092003	W. Zhao *et al.*	(CDEX Collab.)
AAD	15AS	EPJ C75 92	G. Aad *et al.*	(ATLAS Collab.)
AAD	15BH	EPJ C75 299	G. Aad *et al.*	(ATLAS Collab.)
Also		EPJ C75 408 (errat.)	G. Aad *et al.*	(ATLAS Collab.)
AAD	15CF	PRL 115 131801	G. Aad *et al.*	(ATLAS Collab.)
AAD	15CS	PR D91 012008	G. Aad *et al.*	(ATLAS Collab.)
Also		PR D92 059903 (errat.)	G. Aad *et al.*	(ATLAS Collab.)
AARTSEN	15C	EPJ C75 20	M.G. Aartsen *et al.*	(IceCube Collab.)
AARTSEN	15E	EPJ C75 492	M.G. Aartsen *et al.*	(IceCube Collab.)
ABRAMOWSKI	15	PRL 114 081301	A. Abramowski *et al.*	(H.E.S.S. Collab.)
ACKERMANN	15	PR D91 122002	M. Ackermann *et al.*	(Fermi-LAT Collab.)
ACKERMANN	15A	JCAP 1509 008	M. Ackermann *et al.*	(Fermi-LAT Collab.)
ACKERMANN	15B	PRL 115 231301	M. Ackermann *et al.*	(Fermi-LAT Collab.)
ADRIAN-MAR...	15	JCAP 1510 068	S. Adrian-Martinez *et al.*	(ANTARES Collab.)
AGNES	15	PL B743 456	P. Agnes *et al.*	(DarkSide-50 Collab.)
AGNESE	15A	PR D91 052021	R. Agnese *et al.*	(SuperCDMS Collab.)
AGNESE	15B	PR D92 072003	R. Agnese *et al.*	(SuperCDMS Collab.)
AMOLE	15	PRL 114 231302	C. Amole *et al.*	(PICO Collab.)
APRILE	15	PRL 115 091302	E. Aprile *et al.*	(XENON Collab.)
APRILE	15A	SCI 349 851	E. Aprile *et al.*	(XENON Collab.)
CHOI	15	PRL 114 141301	K. Choi *et al.*	(Super-Kamiokande Collab.)
KHACHATRY...	15AG	JHEP 1506 121	V. Khachatryan *et al.*	(CMS Collab.)
KHACHATRY...	15AL	EPJ C75 235	V. Khachatryan *et al.*	(CMS Collab.)
KHACHATRY...	15T	PR D91 092005	V. Khachatryan *et al.*	(CMS Collab.)
NAKAMURA	15	PTEP 2015 4 043F01	K. Nakamura *et al.*	(NEWAGE Collab.)
XIAO	15	PR D92 052004	X. Xiao *et al.*	(PandaX Collab.)
AAD	14AI	JHEP 1409 037	G. Aad *et al.*	(ATLAS Collab.)
AAD	14BK	PRL 112 041802	G. Aad *et al.*	(ATLAS Collab.)
AAD	14K	PR D90 012004	G. Aad *et al.*	(ATLAS Collab.)
AAD	14O	PRL 112 201802	G. Aad *et al.*	(ATLAS Collab.)
ACKERMANN	14	PR D89 042001	M. Ackermann *et al.*	(Fermi-LAT Collab.)
AGNESE	14	PRL 112 241302	R. Agnese *et al.*	(SuperCDMS Collab.)
AGNESE	14A	PRL 112 041302	R. Agnese *et al.*	(SuperCDMS Collab.)
AKERIB	14	PRL 112 091303	D.S. Akerib *et al.*	(LUX Collab.)
ALEKSIC	14	JCAP 1402 008	J. Aleksic *et al.*	(MAGIC Collab.)
ANGLOHER	14	EPJ C74 3184	G. Angloher *et al.*	(CRESST-II Collab.)
APRILE	14A	ASP 54 11	E. Aprile *et al.*	(XENON100 Collab.)
AVRORIN	14	ASP 62 12	A.D. Avrorin *et al.*	(BAIKAL Collab.)
FELIZARDO	14	PR D89 072013	M. Felizardo *et al.*	(SIMPLE Collab.)
LEE	14A	PR D90 052006	H.S. Lee *et al.*	(KIMS Collab.)
LIU	14A	PR D90 032003	S.K. Liu *et al.*	(CDEX Collab.)
UCHIDA	14	PTEP 2014 063C01	H. Uchida *et al.*	(XMASS Collab.)
YUE	14	PR D90 091701	Q. Yue *et al.*	(CDEX Collab.)
AAD	13AD	JHEP 1304 075	G. Aad *et al.*	(ATLAS Collab.)
AAD	13C	PRL 110 011802	G. Aad *et al.*	(ATLAS Collab.)
AALSETH	13	PR D88 012002	C.E. Aalseth *et al.*	(CoGeNT Collab.)
AARTSEN	13	PRL 110 131302	M.G. Aartsen *et al.*	(IceCube Collab.)
AARTSEN	13C	PR D88 122001	M.G. Aartsen *et al.*	(IceCube Collab.)
ABE	13B	PL B719 78	K. Abe *et al.*	(XMASS Collab.)
ABRAMOWSKI	13	PRL 110 041301	A. Abramowski *et al.*	(H.E.S.S. Collab.)
ACKERMANN	13A	PR D88 082002	M. Ackermann *et al.*	(Fermi-LAT Collab.)
ADRIAN-MAR...	13	JCAP 1311 032	S. Adrian-Martinez *et al.*	(ANTARES Collab.)
AGNESE	13	PR D88 031104	R. Agnese *et al.*	(CDMS Collab.)
AGNESE	13A	PRL 111 251301	R. Agnese *et al.*	(CDMS Collab.)
APRILE	13	PRL 111 021301	E. Aprile *et al.*	(XENON100 Collab.)
BERNABEI	13A	EPJ C73 2648	R. Bernabei *et al.*	(DAMA Collab.)
BOLIEV	13	JCAP 1309 019	M. Boliev *et al.*	
LI	13B	PRL 110 261301	H.B. Li *et al.*	(TEXONO Collab.)
SUVOROVA	13	PAN 76 1367 Translated from YAF 76 1433.	O.V. Suvorova *et al.*	(INRM)
ZHAO	13	PR D88 052004	W. Zhao *et al.*	(CDEX Collab.)
AALTONEN	12K	PRL 108 201802	T. Aaltonen *et al.*	(CDF Collab.)
AALTONEN	12M	PRL 108 211804	T. Aaltonen *et al.*	(CDF Collab.)
ABBASI	12	PR D85 042002	R. Abbasi *et al.*	(IceCube Collab.)
ABRAMOWSKI	12	APJ 750 123	A. Abramowski *et al.*	(H.E.S.S. Collab.)
ACKERMANN	12	PR D86 022002	M. Ackermann *et al.*	(Fermi-LAT Collab.)
AKIMOV	12	PL B709 14	D.Yu. Akimov *et al.*	(ZEPLIN-III Collab.)
ALIU	12	PR D85 062001	E. Aliu *et al.*	(VERITAS Collab.)
ANGLOHER	12	EPJ C72 1971	G. Angloher *et al.*	(CRESST-II Collab.)
APRILE	12	PRL 109 181301	E. Aprile *et al.*	(XENON100 Collab.)
ARCHAMBAU...	12	PL B711 153	S. Archambault *et al.*	(PICASSO Collab.)
ARMENGAUD	12	PR D86 051701	E. Armengaud *et al.*	(EDELWEISS Collab.)
BARRETO	12	PL B711 264	J. Barreto *et al.*	(DAMIC Collab.)
BEHNKE	12	PR D86 052001	E. Behnke *et al.*	(COUPP Collab.)
Also		PR D90 079902 (errat.)	E. Behnke *et al.*	(COUPP Collab.)
BROWN	12	PR D85 021301	A. Brown *et al.*	(OXF)
CHATRCHYAN	12AP	JHEP 1209 094	S. Chatrchyan *et al.*	(CMS Collab.)
CHATRCHYAN	12T	PRL 108 261803	S. Chatrchyan *et al.*	(CMS Collab.)
DAHL	12	PRL 108 259001	C.E. Dahl, J. Hall, W.H. Lippincott	(CHIC, FNAL)
DAW	12	ASP 35 397	E. Daw *et al.*	(DRIFT-IId Collab.)
FELIZARDO	12	PRL 108 201302	M. Felizardo *et al.*	(SIMPLE Collab.)
KIM	12	PRL 108 181301	S.C. Kim *et al.*	(KIMS Collab.)
AALSETH	11	PRL 106 131301	C.E. Aalseth *et al.*	(CoGeNT Collab.)
AALSETH	11A	PRL 107 141301	C.E. Aalseth *et al.*	(CoGeNT Collab.)
ABBASI	11C	PR D84 022004	R. Abbasi *et al.*	(IceCube Collab.)
ABRAMOWSKI	11	PRL 106 161301	A. Abramowski *et al.*	(H.E.S.S. Collab.)
ACKERMANN	11	PRL 107 241302	M. Ackermann *et al.*	(Fermi-LAT Collab.)
AHLEN	11	PL B695 124	S. Ahlen *et al.*	(DMTPC Collab.)
AHMED	11	PR D83 112002	Z. Ahmed *et al.*	(CDMS Collab.)
AHMED	11A	PR D84 011102	Z. Ahmed *et al.*	(CDMS and EDELWEISS Collabs.)
AHMED	11B	PRL 106 131302	Z. Ahmed *et al.*	(CDMS Collab.)
AJELLO	11	PR D84 032007	M. Ajello *et al.*	(Fermi-LAT Collab.)
ANGLE	11	PRL 107 051301	J. Angle *et al.*	(XENON10 Collab.)
Also		PRL 110 249901 (errat.)	J. Angle *et al.*	(XENON10 Collab.)
APRILE	11	PR D84 052003	E. Aprile *et al.*	(XENON100 Collab.)
APRILE	11A	PR D84 061101	E. Aprile *et al.*	(XENON100 Collab.)
APRILE	11B	PRL 107 131302	E. Aprile *et al.*	(XENON100 Collab.)
ARMENGAUD	11	PL B702 329	E. Armengaud *et al.*	(EDELWEISS II Collab.)
BEHNKE	11	PRL 106 021303	E. Behnke *et al.*	(COUPP Collab.)
GERINGER-SA...	11	PRL 107 241303	A. Geringer-Sameth, S.M. Koushiappas	
HORN	11	PL B705 471	M. Horn *et al.*	(ZEPLIN-III Collab.)
TANAKA	11	APJ 742 78	T. Tanaka *et al.*	(Super-Kamiokande Collab.)
ABBASI	10	PR D81 057101	R. Abbasi *et al.*	(IceCube Collab.)
AHMED	10	SCI 327 1619	Z. Ahmed *et al.*	(CDMS II Collab.)
AKERIB	10	PR D82 122004	D.S. Akerib *et al.*	(CDMS-II Collab.)
AKIMOV	10	PL B692 180	D.Yu. Akimov *et al.*	(ZEPLIN-III Collab.)
APRILE	10	PRL 105 131302	E. Aprile *et al.*	(XENON100 Collab.)
ARMENGAUD	10	PL B687 294	E. Armengaud *et al.*	(EDELWEISS II Collab.)
FELIZARDO	10	PRL 105 211301	M. Felizardo *et al.*	(The SIMPLE Collab.)
MIUCHI	10	PL B686 11	K. Miuchi *et al.*	(NEWAGE Collab.)

ABBASI	09B	PRL 102 201302	R. Abbasi *et al.*	(IceCube Collab.)
AHMED	09	PRL 102 011301	Z. Ahmed *et al.*	(CDMS Collab.)
ANGLE	09	PR D80 115005	J. Angle *et al.*	(XENON10 Collab.)
ANGLOHER	09	ASP 31 270	G. Angloher *et al.*	(CRESST Collab.)
ARCHAMBAU...	09	PL B682 185	S. Archambault *et al.*	(PICASSO Collab.)
LEBEDENKO	09A	PRL 103 151302	V.N. Lebedenko *et al.*	(ZEPLIN-III Collab.)
LIN	09	PR D79 061101	S.T. Lin *et al.*	(TEXONO Collab.)
AALSETH	08	PRL 101 251301	C.E. Aalseth *et al.*	(CoGeNT Collab.)
Also		PRL 102 109903 (errat.)	C.E. Aalseth *et al.*	(CoGeNT Collab.)
ANGLE	08A	PRL 101 091301	J. Angle *et al.*	(XENON10 Collab.)
BEDNYAKOV	08	PAN 71 111	V.A. Bednyakov, H.P. Klapdor-Kleingrothaus, I.V. Krivosheina	
		Translated from YAF 71 112.		
ALNER	07	PL B653 161	G.J. Alner *et al.*	(ZEPLIN-II Collab.)
LEE	07A	PRL 99 091301	H.S. Lee *et al.*	(KIMS Collab.)
MIUCHI	07	PL B654 58	K. Miuchi *et al.*	
AKERIB	06	PR D73 011102	D.S. Akerib *et al.*	(CDMS Collab.)
SHIMIZU	06A	PL B633 195	Y. Shimizu *et al.*	
AKERIB	05	PR D72 052009	D.S. Akerib *et al.*	(CDMS Collab.)
ALNER	05	PL B616 17	G.J. Alner *et al.*	(UK Dark Matter Collab.)
BARNABE-HE...	05	PL B624 186	M. Barnabe-Heider *et al.*	(PICASSO Collab.)
BENOIT	05	PL B616 25	A. Benoit *et al.*	(EDELWEISS Collab.)
GIRARD	05	PL B621 233	T.A. Girard *et al.*	(SIMPLE Collab.)
GIULIANI	05	PRL 95 101301	F. Giuliani	
GIULIANI	05A	PR D71 123503	F. Giuliani, T.A. Girard	
KLAPDOR-K...	05	PL B609 226	H.V. Klapdor-Kleingrothaus, I.V. Krivosheina, C. Tomei	
GIULIANI	04	PL B588 151	F. Giuliani, T.A. Girard	
GIULIANI	04A	PRL 93 161301	F. Giuliani	
MIUCHI	03	ASP 19 135	K. Miuchi *et al.*	
TAKEDA	03	PL B572 145	A. Takeda *et al.*	
ANGLOHER	02	ASP 18 43	G. Angloher *et al.*	(CRESST Collab.)
BELLI	02	PR D66 043503	P. Belli *et al.*	
BERNABEI	02C	EPJ C23 61	R. Bernabei *et al.*	(DAMA Collab.)
GREEN	02	PR D66 083003	A.M. Green	
BAUDIS	01	PR D63 022001	L. Baudis *et al.*	(Heidelberg-Moscow Collab.)
SMITH	01	PR D64 043502	D. Smith, N. Weiner	
ULLIO	01	JHEP 0107 044	P. Ullio, M. Kamionkowski, P. Vogel	
BENOIT	00	PL B479 8	A. Benoit *et al.*	(EDELWEISS Collab.)
BERNABEI	00D	NJP 2 15	R. Bernabei *et al.*	(DAMA Collab.)
COLLAR	00	PRL 85 3083	J.I. Collar *et al.*	(SIMPLE Collab.)
AMBROSIO	99	PR D60 082002	M. Ambrosio *et al.*	(Macro Collab.)
BERNABEI	99	PL B450 448	R. Bernabei *et al.*	(DAMA Collab.)
BERNABEI	99D	PRL 83 4918	R. Bernabei *et al.*	(DAMA Collab.)
BRHLIK	99	PL B464 303	M. Brhlik, L. Roszkowski	
DERBIN	99	PAN 62 1886	A.V. Derbin *et al.*	
		Translated from YAF 62 2034.		
KLIMENKO	98	JETPL 67 875	A.A. Klimenko *et al.*	
		Translated from ZETFP 67 835.		
SARSA	97	PR D56 1856	M.L. Sarsa *et al.*	(ZARA)
ALESSAND...	96	PL B384 316	A. Alessandrello *et al.*	(MILA, MILAI, SASSO)
BELLI	96	PL B387 222	P. Belli *et al.*	(DAMA Collab.)
Also		PL B389 783 (erratum)	P. Belli *et al.*	(DAMA Collab.)
BELLI	96C	NC C19 537	P. Belli *et al.*	(DAMA Collab.)
BERNABEI	96	PL B389 757	R. Bernabei *et al.*	(DAMA Collab.)
COLLAR	96	PRL 76 331	J.I. Collar	(SCUC)
SARSA	96	PL B386 458	M.L. Sarsa *et al.*	(ZARA)
Also		PR D56 1856	M.L. Sarsa *et al.*	(ZARA)
SMITH	96	PL B379 299	P.F. Smith *et al.*	(RAL, SHEF, LOIC+)
SNOWDEN-...	96	PRL 76 332	D.P. Snowden-Ifft, E.S. Freeman, P.B. Price	(UCB)
GARCIA	95	PR D51 1458	E. Garcia *et al.*	(ZARA, SCUC, PNL)
QUENBY	95	PL B351 70	J.J. Quenby *et al.*	(LOIC, RAL, SHEF+)
SNOWDEN-...	95	PRL 74 4133	D.P. Snowden-Ifft, E.S. Freeman, P.B. Price	(UCB)
Also		PRL 76 331	J.I. Collar	(SCUC)
Also		PRL 76 332	D.P. Snowden-Ifft, E.S. Freeman, P.B. Price	(UCB)
BECK	94	PL B336 141	M. Beck *et al.*	(MPIH, KIAE, SASSO)
BACCI	92	PL B293 460	C. Bacci *et al.*	(Beijing-Roma-Saclay Collab.)
REUSSER	91	PL B255 143	D. Reusser *et al.*	(NEUC, CIT, PSI)
CALDWELL	88	PRL 61 510	D.O. Caldwell *et al.*	(UCSB, UCB, LBL)

Other Particle Searches

OMITTED FROM SUMMARY TABLE

OTHER PARTICLE SEARCHES

Revised February 2018 by K. Hikasa (Tohoku University).

We collect here those searches which do not appear in any other search categories. These are listed in the following order:

- Concentration of stable particles in matter
- General new physics searches
- Limits on jet-jet resonance in hadron collisions
- Limits on neutral particle production at accelerators
- Limits on charged particles in e^+e^- collisions
- Limits on charged particles in hadron reactions
- Limits on charged particles in cosmic rays
- Searches for quantum black hole production

Note that searches appear in separate sections elsewhere for Higgs bosons (and technipions), other heavy bosons (including W_R, W', Z', leptoquarks, axigluons), axions (including pseudo-Goldstone bosons, Majorons, familons), WIMPs, heavy leptons, heavy neutrinos, free quarks, monopoles, supersymmetric particles, and compositeness.

We no longer list for limits on tachyons and centauros. See our 1994 edition for these limits.

CONCENTRATION OF STABLE PARTICLES IN MATTER

Concentration of Heavy (Charge +1) Stable Particles in Matter

VALUE	CL%	DOCUMENT ID		TECN	COMMENT
• • • We do not use the following data for averages, fits, limits, etc. • • •					
$<4\times10^{-17}$	95	[1] YAMAGATA	93	SPEC	Deep sea water, M=5–1600m_p
$<6\times10^{-15}$	95	[2] VERKERK	92	SPEC	Water, M= 10^5 to 3×10^7 GeV
$<7\times10^{-15}$	95	[2] VERKERK	92	SPEC	Water, M= 10^4, 6×10^7 GeV
$<9\times10^{-15}$	95	[2] VERKERK	92	SPEC	Water, M= 10^8 GeV
$<3\times10^{-23}$	90	[3] HEMMICK	90	SPEC	Water, $M=1000m_p$
$<2\times10^{-21}$	90	[3] HEMMICK	90	SPEC	Water, $M=5000m_p$
$<3\times10^{-20}$	90	[3] HEMMICK	90	SPEC	Water, $M=10000m_p$
$<1.\times10^{-29}$		SMITH	82B	SPEC	Water, M=30–400m_p
$<2.\times10^{-28}$		SMITH	82B	SPEC	Water, M=12–1000m_p
$<1.\times10^{-14}$		SMITH	82B	SPEC	Water, $M>1000\ m_p$
$<(0.2\text{–}1.)\times10^{-21}$		SMITH	79	SPEC	Water, M=6–350 m_p

[1] YAMAGATA 93 used deep sea water at 4000 m since the concentration is enhanced in deep sea due to gravity.

[2] VERKERK 92 looked for heavy isotopes in sea water and put a bound on concentration of stable charged massive particle in sea water. The above bound can be translated into into a bound on charged dark matter particle (5×10^6 GeV), assuming the local density, ρ=0.3 GeV/cm^3, and the mean velocity $\langle v\rangle$=300 km/s.

[3] See HEMMICK 90 Fig. 7 for other masses 100–10000 m_p.

Concentration of Heavy Stable Particles Bound to Nuclei

VALUE	CL%	DOCUMENT ID		TECN	COMMENT
• • • We do not use the following data for averages, fits, limits, etc. • • •					
$<1.2\times10^{-11}$	95	[1] JAVORSEK	01	SPEC	Au, M= 3 GeV
$<6.9\times10^{-10}$	95	[1] JAVORSEK	01	SPEC	Au, M= 144 GeV
$<1\ \times10^{-11}$	95	[2] JAVORSEK	01B	SPEC	Au, M= 188 GeV
$<1\ \times10^{-8}$	95	[2] JAVORSEK	01B	SPEC	Au, M= 1669 GeV
$<6\ \times10^{-9}$	95	[2] JAVORSEK	01B	SPEC	Fe, M= 188 GeV
$<1\ \times10^{-8}$	95	[2] JAVORSEK	01B	SPEC	Fe, M= 647 GeV
$<4\ \times10^{-20}$	90	[3] HEMMICK	90	SPEC	C, $M=100m_p$
$<8\ \times10^{-20}$	90	[3] HEMMICK	90	SPEC	C, $M=1000m_p$
$<2\ \times10^{-16}$	90	[3] HEMMICK	90	SPEC	C, $M=10000m_p$
$<6\ \times10^{-13}$	90	[3] HEMMICK	90	SPEC	Li, $M=1000m_p$
$<1\ \times10^{-11}$	90	[3] HEMMICK	90	SPEC	Be, $M=1000m_p$
$<6\ \times10^{-14}$	90	[3] HEMMICK	90	SPEC	B, $M=1000m_p$
$<4\ \times10^{-17}$	90	[3] HEMMICK	90	SPEC	O, $M=1000m_p$
$<4\ \times10^{-15}$	90	[3] HEMMICK	90	SPEC	F, $M=1000m_p$
$<1.5\times10^{-13}$/nucleon	68	[4] NORMAN	89	SPEC	^{206}PbX^-
$<1.2\times10^{-12}$/nucleon	68	[4] NORMAN	87	SPEC	^{56,58}FeX^-

[1] JAVORSEK 01 search for (neutral) SIMPs (strongly interacting massive particles) bound to Au nuclei. Here M is the effective SIMP mass.

[2] JAVORSEK 01B search for (neutral) SIMPs (strongly interacting massive particles) bound to Au and Fe nuclei from various origins with exposures on the earth's surface, in a satellite, heavy ion collisions, etc. Here M is the mass of the anomalous nucleus. See also JAVORSEK 02.

[3] See HEMMICK 90 Fig. 7 for other masses 100–10000 m_p.

[4] Bound valid up to $m_{X^-}\sim100$ TeV.

GENERAL NEW PHYSICS SEARCHES

This subsection lists some of the search experiments which look for general signatures characteristic of new physics, independent of the framework of a specific model.

The observed events are compatible with Standard Model expectation, unless noted otherwise.

VALUE	DOCUMENT ID		TECN	COMMENT
• • • We do not use the following data for averages, fits, limits, etc. • • •				
	[1] AAD	15AT	ATLS	$t+\not{E}_T$
	[2] KHACHATRY...	15F	CMS	$t+\not{E}_T$
	[3] AALTONEN	14J	CDF	W + 2 jets
	[4] AAD	13A	ATLS	$WW\to\ell\nu\ell'\nu$
	[5] AAD	13C	ATLS	$\gamma+\not{E}_T$
	[6] AALTONEN	13I	CDF	Delayed $\gamma+\not{E}_T$
	[7] CHATRCHYAN	13	CMS	$\ell^+\ell^-$ + jets + $\not{E}_T$
	[8] AAD	12C	ATLS	$t\bar{t}+\not{E}_T$
	[9] AALTONEN	12M	CDF	jet + $\not{E}_T$
	[10] CHATRCHYAN	12AP	CMS	jet + $\not{E}_T$
	[11] CHATRCHYAN	12Q	CMS	Z + jets + $\not{E}_T$
	[12] CHATRCHYAN	12T	CMS	$\gamma+\not{E}_T$
	[13] AAD	11S	ATLS	jet + $\not{E}_T$
	[14] AALTONEN	11AF	CDF	$\ell^\pm\ell^\pm$
	[15] CHATRCHYAN	11C	CMS	$\ell^+\ell^-$ + jets + $\not{E}_T$
	[16] CHATRCHYAN	11U	CMS	jet + $\not{E}_T$
	[17] AALTONEN	10AF	CDF	$\gamma\gamma+\ \ell,\not{E}_T$

[18] AALTONEN 09AF CDF $\ell\gamma b\,\not{E}_T$
[19] AALTONEN 09G CDF $\ell\ell\ell\,\not{E}_T$

[1] AAD 15AT search for events with a top quark and mssing E_T in pp collisions at E_{cm} = 8 TeV with L = 20.3 fb^{-1}.
[2] KHACHATRYAN 15F search for events with a top quark and mssing E_T in pp collisions at E_{cm} = 8 TeV with L = 19.7 fb^{-1}.
[3] AALTONEN 14J examine events with a W and two jets in $p\overline{p}$ collisions at E_{cm} = 1.96 TeV with L = 8.9 fb^{-1}. Invariant mass distributions of the two jets are consistent with the Standard Model expectation.
[4] AAD 13A search for resonant WW production in pp collisions at E_{cm} = 7 TeV with L = 4.7 fb^{-1}.
[5] AAD 13C search for events with a photon and missing $\not{E}_T$ in pp collisions at E_{cm} = 7 TeV with L = 4.6 fb^{-1}.
[6] AALTONEN 13I search for events with a photon and missing E_T, where the photon is detected after the expected timing, in $p\overline{p}$ collisions at E_{cm} = 1.96 TeV with L = 6.3 fb^{-1}. The data are consistent with the Standard Model expectation.
[7] CHATRCHYAN 13 search for events with an opposite-sign lepton pair, jets, and missing E_T in pp collisions at E_{cm} = 7 TeV with L = 4.98 fb^{-1}.
[8] AAD 12C search for events with a $t\overline{t}$ pair and missing $\not{E}_T$ in pp collisions at E_{cm} = 7 TeV with L = 1.04 fb^{-1}.
[9] AALTONEN 12M search for events with a jet and missing E_T in $p\overline{p}$ collisions at E_{cm} = 1.96 TeV with L = 6.7 fb^{-1}.
[10] CHATRCHYAN 12AP search for events with a jet and missing E_T in pp collisions at E_{cm} = 7 TeV with L = 5.0 fb^{-1}.
[11] CHATRCHYAN 12Q search for events with a Z, jets, and missing $\not{E}_T$ in pp collisions at E_{cm} = 7 TeV with L = 4.98 fb^{-1}.
[12] CHATRCHYAN 12T search for events with a photon and missing $\not{E}_T$ in pp collisions at E_{cm} = 7 TeV with L = 5.0 fb^{-1}.
[13] AAD 11S search for events with one jet and missing E_T in pp collisions at E_{cm} = 7 TeV with L = 33 pb^{-1}.
[14] AALTONEN 11AF search for high-p_T like-sign dileptons in $p\overline{p}$ collisions at E_{cm} = 1.96 TeV with L = 6.1 fb^{-1}.
[15] CHATRCHYAN 11C search for events with an opposite-sign lepton pair, jets, and missing E_T in pp collisions at E_{cm} = 7 TeV with L = 34 pb^{-1}.
[16] CHATRCHYAN 11U search for events with one jet and missing E_T in pp collisions at E_{cm} = 7 TeV with L = 36 pb^{-1}.
[17] AALTONEN 10AF search for $\gamma\gamma$ events with e, μ, τ, or missing E_T in $p\overline{p}$ collisions at E_{cm} = 1.96 TeV with L = 1.1–2.0 fb^{-1}.
[18] AALTONEN 09AF search for $\ell\gamma b$ events with missing E_T in $p\overline{p}$ collisions at E_{cm} = 1.96 TeV with L = 1.9 fb^{-1}. The observed events are compatible with Standard Model expectation including $t\overline{t}\gamma$ production.
[19] AALTONEN 09G search for $\mu\mu\mu$ and $\mu\mu e$ events with missing E_T in $p\overline{p}$ collisions at E_{cm} = 1.96 TeV with L = 976 pb^{-1}.

LIMITS ON JET-JET RESONANCES

Heavy Particle Production Cross Section

Limits are for a particle decaying to two hadronic jets.

Units(pb)	CL%	Mass(GeV)	DOCUMENT ID		TECN	COMMENT
• • • We do not use the following data for averages, fits, limits, etc. • • •						
			[1] KHACHATRY...17W	CMS		$pp \to jj$ resonance
			[2] KHACHATRY...17Y	CMS		$pp \to$ (8–10) $j+\not{E}_T$
			[3] SIRUNYAN	17F CMS		$pp \to jj$ angular distribution
			[4] AABOUD	16 ATLS		$pp \to b$ + jet
			[5] AAD	16N ATLS		$pp \to$ 3 high E_T jets
			[6] AAD	16S ATLS		$pp \to jj$ resonance
			[7] KHACHATRY...16K	CMS		$pp \to jj$ resonance
			[8] KHACHATRY...16L	CMS		$pp \to jj$ resonance
			[9] AAD	13D ATLS		7 TeV $pp \to 2$ jets
			[10] AALTONEN	13R CDF		1.96 TeV $p\overline{p} \to 4$ jets
			[11] CHATRCHYAN	13A CMS		7 TeV $pp \to 2$ jets
			[12] CHATRCHYAN	13A CMS		7 TeV $pp \to b\overline{b}X$
			[13] AAD	12S ATLS		7 TeV $pp \to 2$ jets
			[14] CHATRCHYAN	12BL CMS		7 TeV $pp \to t\overline{t}X$
			[15] AAD	11AG ATLS		7 TeV $pp \to 2$ jets
			[16] AALTONEN	11M CDF		1.96 TeV $p\overline{p} \to W+2$ jets
			[17] ABAZOV	11I D0		1.96 TeV $p\overline{p} \to W+2$ jets
			[18] AAD	10 ATLS		7 TeV $pp \to 2$ jets
			[19] KHACHATRY...10	CMS		7 TeV $pp \to 2$ jets
			[20] ABE	99F CDF		1.8 TeV $p\overline{p} \to b\overline{b}+$ anything
			[21] ABE	97G CDF		1.8 TeV $p\overline{p} \to 2$ jets
<2603	95	200	[22] ABE	93G CDF		1.8 TeV $p\overline{p} \to 2$ jets
< 44	95	400	[22] ABE	93G CDF		1.8 TeV $p\overline{p} \to 2$ jets
< 7	95	600	[22] ABE	93G CDF		1.8 TeV $p\overline{p} \to 2$ jets

[1] KHACHATRYAN 17W search for dijet resonance in 12.9 fb^{-1} data at 13 TeV; see Fig. 2 for limits on axigluons, diquarks, dark matter mediators etc.
[2] KHACHATRYAN 17Y search for $pp \to$ (8–10) j in 19.7 fb^{-1} at 8 TeV. No signal seen. Limits set on colorons, axigluons, RPV, and SUSY.
[3] SIRUNYAN 17F measure $pp \to jj$ angular distribution in 2.6 fb^{-1} at 13 TeV; limits set on LEDs and quantum black holes.
[4] AABOUD 16 search for resonant dijets including one or two b-jets with 3.2 fb^{-1} at 13 TeV; exclude excited b^* quark from 1.1–2.1 TeV; exclude leptophilic Z' with SM couplings from 1.1–1.5 TeV.
[5] AAD 16N search for ≥ 3 jets with 3.6 fb^{-1} at 13 TeV; limits placed on micro black holes (Fig. 10) and string balls (Fig. 11).
[6] AAD 16S search for high mass jet-jet resonance with 3.6 fb^{-1} at 13 TeV; exclude portions of excited quarks, W', Z' and contact interaction parameter space.
[7] KHACHATRYAN 16K search for dijet resonance in 2.4 fb^{-1} data at 13 TeV; see Fig. 3 for limits on axigluons, diquarks etc.
[8] KHACHATRYAN 16L use data scouting technique to search for jj resonance on 18.8 fb^{-1} of data at 8 TeV. Limits on the coupling of a leptophobic Z' to quarks are set, improving on the results by other experiments in the mass range between 500–800 GeV.
[9] AAD 13D search for dijet resonances in pp collisions at E_{cm} = 7 TeV with L = 4.8 fb^{-1}. The observed events are compatible with Standard Model expectation. See their Fig. 6 and Table 2 for limits on resonance cross section in the range m = 1.0–4.0 TeV.
[10] AALTONEN 13R search for production of a pair of jet-jet resonances in $p\overline{p}$ collisions at E_{cm} = 1.96 TeV with L = 6.6 fb^{-1}. See their Fig. 5 and Tables I, II for cross section limits.
[11] CHATRCHYAN 13A search for qq, qg, and gg resonances in pp collisions at E_{cm} = 7 TeV with L = 4.8 fb^{-1}. See their Fig. 3 and Table 1 for limits on resonance cross section in the range m = 1.0–4.3 TeV.
[12] CHATRCHYAN 13A search for $b\overline{b}$ resonances in pp collisions at E_{cm} = 7 TeV with L = 4.8 fb^{-1}. See their Fig. 8 and Table 4 for limits on resonance cross section in the range m = 1.0–4.0 TeV.
[13] AAD 12S search for dijet resonances in pp collisions at E_{cm} = 7 TeV with L = 1.0 fb^{-1}. See their Fig. 3 and Table 2 for limits on resonance cross section in the range m = 0.9–4.0 TeV.
[14] CHATRCHYAN 12BL search for $t\overline{t}$ resonances in pp collisions at E_{cm} = 7 TeV with L = 4.4 fb^{-1}. See their Fig. 4 for limits on resonance cross section in the range m = 0.5–3.0 TeV.
[15] AAD 11AG search for dijet resonances in pp collisions at E_{cm} = 7 TeV with L = 36 pb^{-1}. Limits on number of events for m = 0.6–4 TeV are given in their Table 3.
[16] AALTONEN 11M find a peak in two jet invariant mass distribution around 140 GeV in W + 2 jet events in $p\overline{p}$ collisions at E_{cm} = 1.96 TeV with L = 4.3 fb^{-1}.
[17] ABAZOV 11I search for two-jet resonances in W + 2 jet events in $p\overline{p}$ collisions at E_{cm} = 1.96 TeV with L = 4.3 fb^{-1} and give limits $\sigma <$ (2.6–1.3) pb (95% CL) for m = 110–170 GeV. The result is incompatible with AALTONEN 11M.
[18] AAD 10 search for narrow dijet resonances in pp collisions at E_{cm} = 7 TeV with L = 315 nb^{-1}. Limits on the cross section in the range 10–10^3 pb is given for m = 0.3–1.7 TeV.
[19] KHACHATRYAN 10 search for narrow dijet resonances in pp collisions at E_{cm} = 7 TeV with L = 2.9 pb^{-1}. Limits on the cross section in the range 1–300 pb is given for m = 0.5–2.6 TeV separately in the final states qq, qg, and gg.
[20] ABE 99F search for narrow $b\overline{b}$ resonances in $p\overline{p}$ collisions at E_{cm}=1.8 TeV. Limits on $\sigma(p\overline{p} \to X+$ anything$)\times$B($X \to b\overline{b}$) in the range 3–10^3 pb (95%CL) are given for m_X=200–750 GeV. See their Table I.
[21] ABE 97G search for narrow dijet resonances in $p\overline{p}$ collisions with 106 pb^{-1} of data at E_{cm} = 1.8 TeV. Limits on $\sigma(p\overline{p} \to X +$ anything$)\cdot$B($X \to jj$) in the range 10^4–10^{-1} pb (95%CL) are given for dijet mass m=200–1150 GeV with both jets having $|\eta| < 2.0$ and the dijet system having $|\cos\theta^*| < 0.67$. See their Table I for the list of limits. Supersedes ABE 93G.
[22] ABE 93G give cross section times branching ratio into light (d, u, s, c, b) quarks for Γ = 0.02 M. Their Table II gives limits for M = 200–900 GeV and Γ = (0.02–0.2) M.

LIMITS ON NEUTRAL PARTICLE PRODUCTION

Production Cross Section of Radiatively-Decaying Neutral Particle

VALUE (pb)	CL%	DOCUMENT ID		TECN	COMMENT
• • • We do not use the following data for averages, fits, limits, etc. • • •					
		[1] KHACHATRY...17D	CMS		$Z\gamma$ resonance
<0.0008	95	[2] AAD	16AI ATLS		$pp \to \gamma$ + jet
		[3] KHACHATRY...16M	CMS		$pp \to \gamma\gamma$ resonance
<(0.043–0.17)	95	[4] ABBIENDI	00D OPAL		$e^+e^- \to X^0Y^0$, $X^0 \to Y^0\gamma$
<(0.05–0.8)	95	[5] ABBIENDI	00D OPAL		$e^+e^- \to X^0X^0$, $X^0 \to Y^0\gamma$
<(2.5–0.5)	95	[6] ACKERSTAFF	97B OPAL		$e^+e^- \to X^0Y^0$, $X^0 \to Y^0\gamma$
<(1.6–0.9)	95	[7] ACKERSTAFF	97B OPAL		$e^+e^- \to X^0X^0$, $X^0 \to Y^0\gamma$

[1] KHACHATRYAN 17D search for new scalar resonance decaying to $Z\gamma$ with $Z \to e^+e^-$, $\mu^+\mu^-$ in pp collisions at 8 and 13 TeV; no signal seen.
[2] AAD 16AI search for excited quarks (EQ) and quantum black holes (QBH) in 3.2 fb^{-1} at 13 TeV of data; exclude EQ below 4.4 TeV and QBH below 3.8 (6.2) TeV for RS1 (ADD) models. The visible cross section limit was obtained for 5 TeV resonance with σ_G/M_G = 2%.
[3] KHACHATRYAN 16M search for $\gamma\gamma$ resonance using 19.7 fb^{-1} at 8 TeV and 3.3 fb^{-1} at 13 Tev; slight excess at 750 GeV noted; limit set on RS graviton.
[4] ABBIENDI 00D associated production limit is for m_{X^0}= 90–188 GeV, m_{Y^0}=0 at E_{cm}=189 GeV. See also their Fig. 9.
[5] ABBIENDI 00D pair production limit is for m_{X^0} = 45–94 GeV, m_{Y^0}=0 at E_{cm}=189 GeV. See also their Fig. 12.
[6] ACKERSTAFF 97B associated production limit is for m_{X^0} = 80–160 GeV, m_{Y^0}=0 from 10.0 pb^{-1} at E_{cm} = 161 GeV. See their Fig. 3(a).
[7] ACKERSTAFF 97B pair production limit is for m_{X^0} = 40–80 GeV, m_{Y^0}=0 from 10.0 pb^{-1} at E_{cm} = 161 GeV. See their Fig. 3(b).

Heavy Particle Production Cross Section

VALUE (cm^2/N)	CL%	DOCUMENT ID		TECN	COMMENT
• • • We do not use the following data for averages, fits, limits, etc. • • •					
		[1] AABOUD	17B ATLS		WH, ZH resonance
		[2] AAIJ	17BR LHCB		$pp \to \pi_V\pi_V$, $\pi_V \to jj$

		[3] AAD	16O	ATLS	ℓ + (ℓs or jets)
		[4] AAD	16R	ATLS	WW, WZ, ZZ resonance
		[5] LEES	15E	BABR	e^+e^- collisions
		[6] ADAMS	97B	KTEV	m= 1.2–5 GeV
$<10^{-36}$–10^{-33}	90	[7] GALLAS	95	TOF	m= 0.5–20 GeV
$<(4$–$0.3)\times10^{-31}$	95	[8] AKESSON	91	CNTR	m = 0–5 GeV
$<2\ \times10^{-36}$	90	[9] BADIER	86	BDMP	$\tau=(0.05$–$1.)\times10^{-8}$ s
$<2.5\times10^{-35}$		[10] GUSTAFSON	76	CNTR	$\tau>10^{-7}$ s

[1] AABOUD 17B exclude m(W', Z') < 1.49–2.31 TeV depending on the couplings and W'/Z' degeneracy assumptions via WH, ZH search in pp collisions at 13 TeV with 3.2 fb^{-1} of data.

[2] AAIJ 17BR search for long-lived hidden valley pions from Higgs decay. Limits are set on the signal strength as a function of the mass and lifetime of the long-lived particle in their Fig. 4 and Tab. 4.

[3] AAD 16O search for high E_T ℓ + (ℓs or jets) with 3.2 fb^{-1} at 13 TeV; exclude micro black holes mass < 8 TeV (Fig. 3) for models with two extra dimensions.

[4] AAD 16R search for WW, WZ, ZZ resonance in 20.3 fb^{-1} at 8 TeV data; limits placed on massive RS graviton (Fig. 4).

[5] LEES 15E search for long-lived neutral particles produced in e^+e^- collisions in the Upsilon region, which decays into e^+e^-, $\mu^+\mu^-$, $e^\pm\mu^\mp$, $\pi^+\pi^-$, K^+K^-, or $\pi^\pm K^\mp$. See their Fig. 2 for cross section limits.

[6] ADAMS 97B search for a hadron-like neutral particle produced in pN interactions, which decays into a ρ^0 and a weakly interacting massive particle. Upper limits are given for the ratio to K_L production for the mass range 1.2–5 GeV and lifetime 10^{-9}–10^{-4} s. See also our Light Gluino Section.

[7] GALLAS 95 limit is for a weakly interacting neutral particle produced in 800 GeV/c pN interactions decaying with a lifetime of 10^{-4}–10^{-8} s. See their Figs. 8 and 9. Similar limits are obtained for a stable particle with interaction cross section 10^{-29}–10^{-33} cm^2. See Fig. 10.

[8] AKESSON 91 limit is from weakly interacting neutral long-lived particles produced in pN reaction at 450 GeV/c performed at CERN SPS. Bourquin-Gaillard formula is used as the production model. The above limit is for $\tau > 10^{-7}$ s. For $\tau > 10^{-9}$ s, $\sigma < 10^{-30}$ cm^{-2}/nucleon is obtained.

[9] BADIER 86 looked for long-lived particles at 300 GeV π^- beam dump. The limit applies for nonstrongly interacting neutral or charged particles with mass >2 GeV. The limit applies for particle modes, $\mu^+\pi^-$, $\mu^+\mu^-$, $\pi^+\pi^-$X, $\pi^+\pi^-\pi^\pm$ etc. See their figure 5 for the contours of limits in the mass-τ plane for each mode.

[10] GUSTAFSON 76 is a 300 GeV FNAL experiment looking for heavy (m >2 GeV) long-lived neutral hadrons in the M4 neutral beam. The above typical value is for m = 3 GeV and assumes an interaction cross section of 1 mb. Values as a function of mass and interaction cross section are given in figure 2.

Production of New Penetrating Non-ν Like States in Beam Dump

VALUE	DOCUMENT ID		TECN	COMMENT
• • • We do not use the following data for averages, fits, limits, etc. • • •				
	[1] LOSECCO	81	CALO	28 GeV protons

[1] No excess neutral-current events leads to σ(production) × σ(interaction)×acceptance $< 2.26\times10^{-71}$ cm^4/nucleon^2 (CL = 90%) for light neutrals. Acceptance depends on models (0.1 to 4. × 10^{-4}).

LIMITS ON CHARGED PARTICLES IN e^+e^-

Heavy Particle Production Cross Section in e^+e^-

Ratio to $\sigma(e^+e^-\to\mu^+\mu^-)$ unless noted. See also entries in Free Quark Search and Magnetic Monopole Searches.

VALUE	CL%	DOCUMENT ID		TECN	COMMENT
• • • We do not use the following data for averages, fits, limits, etc. • • •					
$<1\ \times10^{-3}$	90	[1] ABLIKIM	17AA	BES3	$e^+e^-\to\ell\bar{\ell}\gamma$
		[2] ACKERSTAFF	98P	OPAL	Q=1,2/3, m=45–89.5 GeV
		[3] ABREU	97D	DLPH	Q=1,2/3, m=45–84 GeV
		[4] BARATE	97K	ALEP	Q=1, m=45–85 GeV
$<2\ \times10^{-5}$	95	[5] AKERS	95R	OPAL	Q=1, m= 5–45 GeV
$<1\ \times10^{-5}$	95	[5] AKERS	95R	OPAL	Q=2, m= 5–45 GeV
$<2\ \times10^{-3}$	90	[6] BUSKULIC	93C	ALEP	Q=1, m=32–72 GeV
$<(10^{-2}$–1)	95	[7] ADACHI	90C	TOPZ	Q=1, m=1–16, 18–27 GeV
$<7\ \times10^{-2}$	90	[8] ADACHI	90E	TOPZ	Q = 1, m = 5–25 GeV
$<1.6\times10^{-2}$	95	[9] KINOSHITA	82	PLAS	Q=3–180, m <14.5 GeV
$<5.0\times10^{-2}$	90	[10] BARTEL	80	JADE	Q=(3,4,5)/3 2–12 GeV

[1] ABLIKIM 17AA search for dark photon $A\to\ell\bar{\ell}$ at 3.773 GeV with 2.93 fb^{-1}. Limits are set in ϵ vs m(A) plane.

[2] ACKERSTAFF 98P search for pair production of long-lived charged particles at E_{cm} between 130 and 183 GeV and give limits $\sigma<(0.05$–$0.2)$ pb (95%CL) for spin-0 and spin-1/2 particles with m=45–89.5 GeV, charge 1 and 2/3. The limit is translated to the cross section at E_{cm}=183 GeV with the s dependence described in the paper. See their Figs. 2–4.

[3] ABREU 97D search for pair production of long-lived particles and give limits $\sigma<(0.4$–$2.3)$ pb (95%CL) for various center-of-mass energies E_{cm}=130–136, 161, and 172 GeV, assuming an almost flat production distribution in cosθ.

[4] BARATE 97K search for pair production of long-lived charged particles at E_{cm} = 130, 136, 161, and 172 GeV and give limits $\sigma<(0.2$–$0.4)$ pb (95%CL) for spin-0 and spin-1/2 particles with m=45–85 GeV. The limit is translated to the cross section at E_{cm}=172 GeV with the E_{cm} dependence described in the paper. See their Figs. 2 and 3 for limits on J = 1/2 and J = 0 cases.

[5] AKERS 95R is a CERN-LEP experiment with $W_{cm}\sim m_Z$. The limit is for the production of a stable particle in multihadron events normalized to $\sigma(e^+e^-\to$ hadrons). Constant phase space distribution is assumed. See their Fig. 3 for bounds for $Q=\pm2/3$, $\pm4/3$.

[6] BUSKULIC 93C is a CERN-LEP experiment with $W_{cm}=m_Z$. The limit is for a pair or single production of heavy particles with unusual ionization loss in TPC. See their Fig. 5 and Table 1.

[7] ADACHI 90C is a KEK-TRISTAN experiment with W_{cm} = 52–60 GeV. The limit is for pair production of a scalar or spin-1/2 particle. See Figs. 3 and 4.

[8] ADACHI 90E is KEK-TRISTAN experiment with W_{cm} = 52–61.4 GeV. The above limit is for inclusive production cross section normalized to $\sigma(e^+e^-\to\mu^+\mu^-)\cdot\beta(3-\beta^2)/2$, where $\beta=(1-4m^2/W_{cm}^2)^{1/2}$. See the paper for the assumption about the production mechanism.

[9] KINOSHITA 82 is SLAC PEP experiment at W_{cm} = 29 GeV using lexan and ^{39}Cr plastic sheets sensitive to highly ionizing particles.

[10] BARTEL 80 is DESY-PETRA experiment with W_{cm} = 27–35 GeV. Above limit is for inclusive pair production and ranges between 1. × 10^{-1} and 1. × 10^{-2} depending on mass and production momentum distributions. (See their figures 9, 10, 11).

Branching Fraction of Z^0 to a Pair of Stable Charged Heavy Fermions

VALUE	CL%	DOCUMENT ID		TECN	COMMENT
• • • We do not use the following data for averages, fits, limits, etc. • • •					
$<5\times10^{-6}$	95	[1] AKERS	95R	OPAL	m= 40.4–45.6 GeV
$<1\times10^{-3}$	95	AKRAWY	90O	OPAL	m = 29–40 GeV

[1] AKERS 95R give the 95% CL limit $\sigma(X\overline{X})/\sigma(\mu\mu)<1.8\times10^{-4}$ for the pair production of singly- or doubly-charged stable particles. The limit applies for the mass range 40.4–45.6 GeV for $X^\pm$ and < 45.6 GeV for $X^{\pm\pm}$. See the paper for bounds for $Q=\pm2/3$, $\pm4/3$.

LIMITS ON CHARGED PARTICLES IN HADRONIC REACTIONS

MASS LIMITS for Long-Lived Charged Heavy Fermions

Limits are for spin 1/2 particles with no color and SU(2)$_L$ charge. The electric charge Q of the particle (in the unit of e) is therefore equal to its weak hypercharge. Pair production by Drell-Yan like γ and Z exchange is assumed to derive the limits.

VALUE (GeV)	CL%	DOCUMENT ID		TECN	COMMENT
• • • We do not use the following data for averages, fits, limits, etc. • • •					
>660	95	[1] AAD	15BJ	ATLS	$\|Q\|$ = 2
>200	95	[2] CHATRCHYAN	13AB	CMS	$\|Q\|$ = 1/3
>480	95	[2] CHATRCHYAN	13AB	CMS	$\|Q\|$ = 2/3
>574	95	[2] CHATRCHYAN	13AB	CMS	$\|Q\|$ = 1
>685	95	[2] CHATRCHYAN	13AB	CMS	$\|Q\|$ = 2
>140	95	[3] CHATRCHYAN	13AR	CMS	$\|Q\|$ = 1/3
>310	95	[3] CHATRCHYAN	13AR	CMS	$\|Q\|$ = 2/3

[1] AAD 15BJ use 20.3 fb^{-1} of pp collisions at E_{cm} = 8 TeV. See paper for limits for $|Q|$ = 3, 4, 5, 6.

[2] CHATRCHYAN 13AB use 5.0 fb^{-1} of pp collisions at E_{cm} = 7 TeV and 18.8 fb^{-1} at E_{cm} = 8 TeV. See paper for limits for $|Q|$ = 3, 4,..., 8.

[3] CHATRCHYAN 13AR use 5.0 fb^{-1} of pp collisions at E_{cm} = 7 TeV.

Heavy Particle Production Cross Section

VALUE (nb)	CL%	DOCUMENT ID		TECN	COMMENT
• • • We do not use the following data for averages, fits, limits, etc. • • •					
		[1] AABOUD	17D	ATLS	anomalous $WWjj$, $WZjj$
		[2] AABOUD	17L	ATLS	m>870 GeV, $Z(\to\nu\nu)tX$
		[3] SIRUNYAN	17B	CMS	tH
		[4] SIRUNYAN	17C	CMS	$Z+(t$ or $b)$
		[5] SIRUNYAN	17J	CMS	$X_{5/3}\to tW$
		[6] AAIJ	15BD	LHCB	m=124–309 GeV
		[7] AAD	13AH	ATLS	$\|q\|$=(2–6)e, m=50–600 GeV
$<1.2\ \times10^{-3}$	95	[8] AAD	11I	ATLS	$\|q\|$=10e, m=0.2–1 TeV
$<1.0\ \times10^{-5}$	95	[9,10] AALTONEN	09Z	CDF	m>100 GeV, noncolored
$<4.8\ \times10^{-5}$	95	[9,11] AALTONEN	09Z	CDF	m>100 GeV, colored
<0.31–0.04×10^{-3}	95	[12] ABAZOV	09M	D0	pair production
<0.19	95	[13] AKTAS	04C	H1	m=3–10 GeV
<0.05	95	[14] ABE	92J	CDF	m=50–200 GeV
<30–130		[15] CARROLL	78	SPEC	m=2–2.5 GeV
<100		[16] LEIPUNER	73	CNTR	m=3–11 GeV

[1] AABOUD 17D search for $WWjj$, $WZjj$ in pp collisions at 8 TeV with 3.2 fb^{-1}; set limits on anomalous couplings.

[2] AABOUD 17L search for the pair production of heavy vector-like T quarks in the $Z(\to\nu\nu)tX$ final state.

[3] SIRUNYAN 17B search for vector-like quark $pp\to TX\to tHX$ in 2.3 fb^{-1} at 13 TeV; no signal seen; limits placed.

[4] SIRUNYAN 17C search for vector-like quark $pp\to TX\to Z+(t$ or $b)$ in 2.3 fb^{-1} at 13 TeV; no signal seen; limits placed.

[5] SIRUNYAN 17J search for $pp\to X_{5/3}X_{5/3}\to tWtW$ with 2.3 fb^{-1} at 13 TeV. No signal seen: m(X) > 1020 (990) GeV for RH (LH) new charge 5/3 quark.

[6] AAIJ 15BD search for production of long-lived particles in pp collisions at E_{cm} = 7 and 8 TeV. See their Table 6 for cross section limits.

[7] AAD 13AH search for production of long-lived particles with $|q|$=(2–6)e in pp collisions at E_{cm} = 7 TeV with 4.4 fb^{-1}. See their Fig. 8 for cross section limits.

[8] AAD 11I search for production of highly ionizing massive particles in pp collisions at E_{cm} = 7 TeV with L = 3.1 pb^{-1}. See their Table 5 for similar limits for $|q|=6e$ and 17e, Table 6 for limits on pair production cross section.

[9] AALTONEN 09Z search for long-lived charged particles in $p\overline{p}$ collisions at E_{cm} = 1.96 TeV with L = 1.0 fb^{-1}. The limits are on production cross section for a particle of mass above 100 GeV in the region $|\eta|\lesssim0.7$, $p_T>40$ GeV, and $0.4<\beta<1.0$.

[10] Limit for weakly interacting charge-1 particle.

[11] Limit for up-quark like particle.

[12] ABAZOV 09M search for pair production of long-lived charged particles in $p\overline{p}$ collisions at E_{cm} = 1.96 TeV with L = 1.1 fb^{-1}. Limit on the cross section of (0.31–0.04) pb (95% CL) is given for the mass range of 60–300 GeV, assuming the kinematics of stau pair production.
[13] AKTAS 04C look for charged particle photoproduction at HERA with mean c.m. energy of 200 GeV.
[14] ABE 92J look for pair production of unit-charged particles which leave detector before decaying. Limit shown here is for m=50 GeV. See their Fig. 5 for different charges and stronger limits for higher mass.
[15] CARROLL 78 look for neutral, $S = -2$ dihyperon resonance in $pp \rightarrow 2K^+X$. Cross section varies within above limits over mass range and p_{lab} = 5.1–5.9 GeV/c.
[16] LEIPUNER 73 is an NAL 300 GeV p experiment. Would have detected particles with lifetime greater than 200 ns.

Heavy Particle Production Differential Cross Section

VALUE (cm^{2}sr^{-1}GeV^{-1})	CL%	DOCUMENT ID		TECN	CHG	COMMENT
• • • We do not use the following data for averages, fits, limits, etc. • • •						
$<2.6\times10^{-36}$	90	[1] BALDIN	76	CNTR	−	Q= 1, m=2.1–9.4 GeV
$<2.2\times10^{-33}$	90	[2] ALBROW	75	SPEC	±	Q= ±1, m=4–15 GeV
$<1.1\times10^{-33}$	90	[2] ALBROW	75	SPEC	±	Q= ±2, m=6–27 GeV
$<8.\times10^{-35}$	90	[3] JOVANOV...	75	CNTR	±	m=15–26 GeV
$<1.5\times10^{-34}$	90	[3] JOVANOV...	75	CNTR	±	Q= ±2, m=3–10 GeV
$<6.\times10^{-35}$	90	[3] JOVANOV...	75	CNTR	±	Q= ±2, m=10–26 GeV
$<1.\times10^{-31}$	90	[4] APPEL	74	CNTR	±	m=3.2–7.2 GeV
$<5.8\times10^{-34}$	90	[5] ALPER	73	SPEC	±	m=1.5–24 GeV
$<1.2\times10^{-35}$	90	[6] ANTIPOV	71B	CNTR	−	Q=−, m=2.2–2.8
$<2.4\times10^{-35}$	90	[7] ANTIPOV	71C	CNTR	−	Q=−, m=1.2–1.7, 2.1–4
$<2.4\times10^{-35}$	90	BINON	69	CNTR	−	Q=−, m=1–1.8 GeV
$<1.5\times10^{-36}$		[8] DORFAN	65	CNTR		Be target m=3–7 GeV
$<3.0\times10^{-36}$		[8] DORFAN	65	CNTR		Fe target m=3–7 GeV

[1] BALDIN 76 is a 70 GeV Serpukhov experiment. Value is per Al nucleus at $\theta = 0$. For other charges in range −0.5 to −3.0, CL = 90% limit is $(2.6\times10^{-36})/|(\text{charge})|$ for mass range (2.1–9.4 GeV) × $|(\text{charge})|$. Assumes stable particle interacting with matter as do antiprotons.
[2] ALBROW 75 is a CERN ISR experiment with E_{cm} = 53 GeV. θ = 40 mr. See figure 5 for mass ranges up to 35 GeV.
[3] JOVANOVICH 75 is a CERN ISR 26+26 and 15+15 GeV pp experiment. Figure 4 covers ranges Q = 1/3 to 2 and m = 3 to 26 GeV. Value is per GeV momentum.
[4] APPEL 74 is NAL 300 GeV pW experiment. Studies forward production of heavy (up to 24 GeV) charged particles with momenta 24–200 GeV (−charge) and 40–150 GeV (+charge). Above typical value is for 75 GeV and is per GeV momentum per nucleon.
[5] ALPER 73 is CERN ISR 26+26 GeV pp experiment. p >0.9 GeV, 0.2 < β <0.65.
[6] ANTIPOV 71B is from same 70 GeV p experiment as ANTIPOV 71C and BINON 69.
[7] ANTIPOV 71C limit inferred from flux ratio. 70 GeV p experiment.
[8] DORFAN 65 is a 30 GeV/c p experiment at BNL. Units are per GeV momentum per nucleus.

Long-Lived Heavy Particle Invariant Cross Section

VALUE (cm^2/GeV^2/N)	CL%	DOCUMENT ID		TECN	CHG	COMMENT
• • • We do not use the following data for averages, fits, limits, etc. • • •						
<5–700×10^{-35}	90	[1] BERNSTEIN	88	CNTR		
<5–700×10^{-37}	90	[1] BERNSTEIN	88	CNTR		
$<2.5\times10^{-36}$	90	[2] THRON	85	CNTR	−	Q= 1, m=4–12 GeV
$<1.\times10^{-35}$	90	[2] THRON	85	CNTR	+	Q= 1, m=4–12 GeV
$<6.\times10^{-33}$	90	[3] ARMITAGE	79	SPEC		m=1.87 GeV
$<1.5\times10^{-33}$	90	[3] ARMITAGE	79	SPEC		m=1.5–3.0 GeV
		[4] BOZZOLI	79	CNTR	±	Q = (2/3, 1, 4/3, 2)
$<1.1\times10^{-37}$	90	[5] CUTTS	78	CNTR		m=4–10 GeV
$<3.0\times10^{-37}$	90	[6] VIDAL	78	CNTR		m=4.5–6 GeV

[1] BERNSTEIN 88 limits apply at x = 0.2 and p_T = 0. Mass and lifetime dependence of limits are shown in the regions: m = 1.5–7.5 GeV and $\tau = 10^{-8}$–2×10^{-6} s. First number is for hadrons; second is for weakly interacting particles.
[2] THRON 85 is FNAL 400 GeV proton experiment. Mass determined from measured velocity and momentum. Limits are for $\tau > 3\times10^{-9}$ s.
[3] ARMITAGE 79 is CERN-ISR experiment at E_{cm} = 53 GeV. Value is for x = 0.1 and p_T = 0.15. Observed particles at m = 1.87 GeV are found all consistent with being antideuterons.
[4] BOZZOLI 79 is CERN-SPS 200 GeV pN experiment. Looks for particle with τ larger than 10^{-8} s. See their figure 11–18 for production cross-section upper limits vs mass.
[5] CUTTS 78 is pBe experiment at FNAL sensitive to particles of $\tau > 5\times10^{-8}$ s. Value is for −0.3 <x <0 and p_T = 0.175.
[6] VIDAL 78 is FNAL 400 GeV proton experiment. Value is for x = 0 and p_T = 0. Puts lifetime limit of $< 5\times10^{-8}$ s on particle in this mass range.

Long-Lived Heavy Particle Production (σ(Heavy Particle) / $\sigma(\pi)$)

VALUE	EVTS	DOCUMENT ID		TECN	CHG	COMMENT
• • • We do not use the following data for averages, fits, limits, etc. • • •						
$<10^{-8}$		[1] NAKAMURA	89	SPEC	±	Q= (−5/3,±2)
	0	[2] BUSSIERE	80	CNTR	±	Q= (2/3,1,4/3,2)

[1] NAKAMURA 89 is KEK experiment with 12 GeV protons on Pt target. The limit applies for mass $\lesssim$ 1.6 GeV and lifetime $\gtrsim 10^{-7}$ s.
[2] BUSSIERE 80 is CERN-SPS experiment with 200–240 GeV protons on Be and Al target. See their figures 6 and 7 for cross-section ratio vs mass.

Production and Capture of Long-Lived Massive Particles

VALUE (10^{-36} cm^2)	DOCUMENT ID		TECN	COMMENT
• • • We do not use the following data for averages, fits, limits, etc. • • •				
<20 to 800	[1] ALEKSEEV	76	ELEC	τ=5 ms to 1 day
<200 to 2000	[1] ALEKSEEV	76B	ELEC	τ=100 ms to 1 day
<1.4 to 9	[2] FRANKEL	75	CNTR	τ=50 ms to 10 hours
<0.1 to 9	[3] FRANKEL	74	CNTR	τ=1 to 1000 hours

[1] ALEKSEEV 76 and ALEKSEEV 76B are 61–70 GeV p Serpukhov experiment. Cross section is per Pb nucleus.
[2] FRANKEL 75 is extension of FRANKEL 74.
[3] FRANKEL 74 looks for particles produced in thick Al targets by 300–400 GeV/c protons.

Long-Lived Particle Search at Hadron Collisions

Limits are for cross section times branching ratio.

VALUE (pb/nucleon)	CL%	DOCUMENT ID		TECN	COMMENT
• • • We do not use the following data for averages, fits, limits, etc. • • •					
		[1] AAIJ	16AR	LHCB	$H \rightarrow XX$ long-lived particles
		[2] KHACHATRY...	16BW	CMS	direct production: HSCPs
<2	90	[3] BADIER	86	BDMP	τ = (0.05–1.) × 10^{-8}s

[1] AAIJ 16AR search for long lived particles from $H \rightarrow XX$ with displaced X decay vertex using 0.62 fb^{-1} at 7 TeV; limits set in Fig. 7.
[2] KHACHATRYAN 16BW search for heavy stable charged particles via ToF with 2.5 fb^{-1} at 13 TeV; require stable m(gluinoball) > 1610 GeV.
[3] BADIER 86 looked for long-lived particles at 300 GeV π^- beam dump. The limit applies for nonstrongly interacting neutral or charged particles with mass >2 GeV. The limit applies for particle modes, $\mu^+\pi^-$, $\mu^+\mu^-$, $\pi^+\pi^-$X, $\pi^+\pi^-\pi^\pm$ etc. See their figure 5 for the contours of limits in the mass-τ plane for each mode.

Long-Lived Heavy Particle Cross Section

VALUE (pb/sr)	CL%	DOCUMENT ID		TECN	COMMENT
• • • We do not use the following data for averages, fits, limits, etc. • • •					
<34	95	[1] RAM	94	SPEC	1015<$m_{X^{++}}$ <1085 MeV
<75	95	[1] RAM	94	SPEC	920<$m_{X^{++}}$ <1025 MeV

[1] RAM 94 search for a long-lived doubly-charged fermion X^{++} with mass between m_N and m_N+m_π and baryon number +1 in the reaction $pp \rightarrow X^{++}n$. No candidate is found. The limit is for the cross section at 15° scattering angle at 460 MeV incident energy and applies for $\tau(X^{++}) \gg 0.1$ μs.

LIMITS ON CHARGED PARTICLES IN COSMIC RAYS

Heavy Particle Flux in Cosmic Rays

VALUE (cm^{-2}sr^{-1}s^{-1})		CL%	EVTS	DOCUMENT ID		TECN	CHG	COMMENT
• • • We do not use the following data for averages, fits, limits, etc. • • •								
< 1	$\times10^{-8}$	90	0	[1] AGNESE	15	CDM2		Q = 1/6
~ 6	$\times10^{-9}$		2	[2] SAITO	90			$Q \simeq$ 14, $m \simeq 370m_p$
< 1.4	$\times10^{-12}$	90	0	[3] MINCER	85	CALO		$m \geq$ 1 TeV
				[4] SAKUYAMA	83B	PLAS		$m \sim$ 1 TeV
< 1.7	$\times10^{-11}$	99	0	[5] BHAT	82	CC		
< 1.	$\times10^{-9}$	90	0	[6] MARINI	82	CNTR	±	Q= 1, $m \sim 4.5m_p$
2.	$\times10^{-9}$		3	[7] YOCK	81	SPRK	±	Q= 1, $m \sim 4.5m_p$
			3	[7] YOCK	81	SPRK		Fractionally charged
3.0	$\times10^{-9}$		3	[8] YOCK	80	SPRK		$m \sim 4.5$ m_p
(4 ±1)	$\times10^{-11}$		3	GOODMAN	79	ELEC		$m \geq$ 5 GeV
< 1.3	$\times10^{-9}$	90		[9] BHAT	78	CNTR	±	m >1 GeV
< 1.0	$\times10^{-9}$		0	BRIATORE	76	ELEC		
< 7.	$\times10^{-10}$	90	0	YOCK	75	ELEC	±	Q >7e or < −7e
> 6.	$\times10^{-9}$		5	[10] YOCK	74	CNTR		m >6 GeV
< 3.0	$\times10^{-8}$		0	DARDO	72	CNTR		
< 1.5	$\times10^{-9}$		0	TONWAR	72	CNTR		m >10 GeV
< 3.0	$\times10^{-10}$		0	BJORNBOE	68	CNTR		m >5 GeV
< 5.0	$\times10^{-11}$	90	0	JONES	67	ELEC		m=5–15 GeV

[1] See AGNESE 15 Fig. 6 for limits extending down to Q = 1/200.
[2] SAITO 90 candidates carry about 450 MeV/nucleon. Cannot be accounted for by conventional backgrounds. Consistent with strange quark matter hypothesis.
[3] MINCER 85 is high statistics study of calorimeter signals delayed by 20–200 ns. Calibration with AGS beam shows they can be accounted for by rare fluctuations in signals from low-energy hadrons in the shower. Claim that previous delayed signals including BJORNBOE 68, DARDO 72, BHAT 82, SAKUYAMA 83B below may be due to this fake effect.
[4] SAKUYAMA 83B analyzed 6000 extended air shower events. Increase of delayed particles and change of lateral distribution above 10^{17} eV may indicate production of very heavy parent at top of atmosphere.
[5] BHAT 82 observed 12 events with delay > 2.×10^{-8} s and with more than 40 particles. 1 eV has good hadron shower. However all events are delayed in only one of two detectors in cloud chamber, and could not be due to strongly interacting massive particle.
[6] MARINI 82 applied PEP-counter for TOF. Above limit is for velocity = 0.54 of light. Limit is inconsistent with YOCK 80 YOCK 81 events if isotropic dependence on zenith angle is assumed.
[7] YOCK 81 saw another 3 events with Q = ±1 and m about 4.5m_p as well as 2 events with m >5.3m_p, Q = ±0.75 ± 0.05 and m >2.8m_p, Q = ±0.70 ± 0.05 and 1 event with m = (9.3 ± 3.)m_p, Q = ±0.89 ± 0.06 as possible heavy candidates.

[8] YOCK 80 events are with charge exactly or approximately equal to unity.
[9] BHAT 78 is at Kolar gold fields. Limit is for $\tau > 10^{-6}$ s.
[10] YOCK 74 events could be tritons.

Superheavy Particle (Quark Matter) Flux in Cosmic Rays

VALUE ($cm^{-2}sr^{-1}s^{-1}$)	CL%	DOCUMENT ID		TECN	COMMENT
• • • We do not use the following data for averages, fits, limits, etc. • • •					
		[1] ADRIANI	15	PMLA	$4 < m < 1.2 \times 10^5$ m_p
$<5 \times 10^{-16}$	90	[2] AMBROSIO	00B	MCRO	$m > 5 \times 10^{14}$ GeV
$<1.8 \times 10^{-12}$	90	[3] ASTONE	93	CNTR	$m \geq 1.5 \times 10^{-13}$gram
$<1.1 \times 10^{-14}$	90	[4] AHLEN	92	MCRO	$10^{-10} < m < 0.1$ gram
$<2.2 \times 10^{-14}$	90	[5] NAKAMURA	91	PLAS	$m > 10^{11}$ GeV
$<6.4 \times 10^{-16}$	90	[6] ORITO	91	PLAS	$m > 10^{12}$ GeV
$<2.0 \times 10^{-11}$	90	[7] LIU	88	BOLO	$m > 1.5 \times 10^{-13}$ gram
$<4.7 \times 10^{-12}$	90	[8] BARISH	87	CNTR	$1.4 \times 10^8 < m < 10^{12}$ GeV
$<3.2 \times 10^{-11}$	90	[9] NAKAMURA	85	CNTR	$m > 1.5 \times 10^{-13}$gram
$<3.5 \times 10^{-11}$	90	[10] ULLMAN	81	CNTR	Planck-mass 10^{19}GeV
$<7. \times 10^{-11}$	90	[10] ULLMAN	81	CNTR	$m \leq 10^{16}$ GeV

[1] ADRIANI 15 search for relatively light quark matter with charge $Z = 1$–8. See their Figs. 2 and 3 for flux upper limits.
[2] AMBROSIO 00B searched for quark matter ("nuclearites") in the velocity range $(10^{-5}$–1$)\,c$. The listed limit is for $2 \times 10^{-3}\,c$.
[3] ASTONE 93 searched for quark matter ("nuclearites") in the velocity range $(10^{-3}$–1$)\,c$. Their Table 1 gives a compilation of searches for nuclearites.
[4] AHLEN 92 searched for quark matter ("nuclearites"). The bound applies to velocity $< 2.5 \times 10^{-3}\,c$. See their Fig. 3 for other velocity/c and heavier mass range.
[5] NAKAMURA 91 searched for quark matter in the velocity range $(4 \times 10^{-5}$–1$)\,c$.
[6] ORITO 91 searched for quark matter. The limit is for the velocity range $(10^{-4}$–$10^{-3})\,c$.
[7] LIU 88 searched for quark matter ("nuclearites") in the velocity range $(2.5 \times 10^{-3}$–1$)c$. A less stringent limit of 5.8×10^{-11} applies for (1–2.5) $\times 10^{-3}c$.
[8] BARISH 87 searched for quark matter ("nuclearites") in the velocity range $(2.7 \times 10^{-4}$–$5 \times 10^{-3})c$.
[9] NAKAMURA 85 at KEK searched for quark-matter. These might be lumps of strange quark matter with roughly equal numbers of u, d, s quarks. These lumps or nuclearites were assumed to have velocity of $(10^{-4}$–$10^{-3})\,c$.
[10] ULLMAN 81 is sensitive for heavy slow singly charge particle reaching earth with vertical velocity 100–350 km/s.

Highly Ionizing Particle Flux

VALUE ($m^{-2}yr^{-1}$)	CL%	EVTS	DOCUMENT ID	TECN	COMMENT
• • • We do not use the following data for averages, fits, limits, etc. • • •					
<0.4	95	0	KINOSHITA 81B	PLAS	Z/β 30–100

SEARCHES FOR BLACK HOLE PRODUCTION

VALUE	DOCUMENT ID		TECN	COMMENT
• • • We do not use the following data for averages, fits, limits, etc. • • •				
not seen	[1] AABOUD	16P	ATLS	13 TeV $pp \to e\mu,\ e\tau,\ \mu\tau$
	[2] AAD	15AN	ATLS	8 TeV $pp \to$ multijets
	[3] AAD	14A	ATLS	8 TeV $pp \to \gamma +$ jet
	[4] AAD	14AL	ATLS	8 TeV $pp \to \ell +$ jet
	[5] AAD	14C	ATLS	8 TeV $pp \to \ell +$ (ℓ or jets)
	[6] AAD	13D	ATLS	7 TeV $pp \to 2$ jets
	[7] CHATRCHYAN	13A	CMS	7 TeV $pp \to 2$ jets
	[8] CHATRCHYAN	13AD	CMS	8 TeV $pp \to$ multijets
	[9] AAD	12AK	ATLS	7 TeV $pp \to \ell +$ (ℓ or jets)
	[10] CHATRCHYAN	12W	CMS	7 TeV $pp \to$ multijets
	[11] AAD	11AG	ATLS	7 TeV $pp \to 2$ jets

[1] AABOUD 16P set limits on quantum BH production in n = 6 ADD or n = 1 RS models.
[2] AAD 15AN search for black hole or string ball formation followed by its decay to multijet final states, in pp collisions at $E_{cm} = 8$ TeV with $L = 20.3$ fb^{-1}. See their Figs. 6–8 for limits.
[3] AAD 14A search for quantum black hole formation followed by its decay to a γ and a jet, in pp collisions at $E_{cm} = 8$ TeV with $L = 20$ fb^{-1}. See their Fig. 3 for limits.
[4] AAD 14AL search for quantum black hole formation followed by its decay to a lepton and a jet, in pp collisions at $E_{cm} = 8$ TeV with $L = 20.3$ fb^{-1}. See their Fig. 2 for limits.
[5] AAD 14C search for microscopic (semiclassical) black hole formation followed by its decay to final states with a lepton and ≥ 2 (leptons or jets), in pp collisions at $E_{cm} = 8$ TeV with $L = 20.3$ fb^{-1}. See their Figures 8–11, Tables 7, 8 for limits.
[6] AAD 13D search for quantum black hole formation followed by its decay to two jets, in pp collisions at $E_{cm} = 7$ TeV with $L = 4.8$ fb^{-1}. See their Fig. 8 and Table 3 for limits.
[7] CHATRCHYAN 13A search for quantum black hole formation followed by its decay to two jets, in pp collisions at $E_{cm} = 7$ TeV with $L = 5$ fb^{-1}. See their Figs. 5 and 6 for limits.
[8] CHATRCHYAN 13AD search for microscopic (semiclassical) black hole formation followed by its evapolation to multiparticle final states, in multijet (including γ, ℓ) events in pp collisions at $E_{cm} = 8$ TeV with $L = 12$ fb^{-1}. See their Figs. 5–7 for limits.
[9] AAD 12AK search for microscopic (semiclassical) black hole formation followed by its decay to final states with a lepton and ≥ 2 (leptons or jets), in pp collisions at $E_{cm} = 7$ TeV with $L = 1.04$ fb^{-1}. See their Fig. 4 and 5 for limits.
[10] CHATRCHYAN 12W search for microscopic (semiclassical) black hole formation followed by its evapolation to multiparticle final states, in multijet (including γ, ℓ) events in pp collisions at $E_{cm} = 7$ TeV with $L = 4.7$ fb^{-1}. See their Figs. 5–8 for limits.
[11] AAD 11AG search for quantum black hole formation followed by its decay to two jets, in pp collisions at $E_{cm} = 7$ TeV with L = 36 pb^{-1}. See their Fig. 11 and Table 4 for limits.

REFERENCES FOR Other Particle Searches

AABOUD	17B	PL B765 32	M. Aaboud *et al.* (ATLAS Collab.)
AABOUD	17D	PR D95 032001	M. Aaboud *et al.* (ATLAS Collab.)
AABOUD	17L	JHEP 1708 052	M. Aaboud *et al.* (ATLAS Collab.)
AAIJ	17BR	EPJ C77 812	R. Aaij *et al.* (LHCb Collab.)
ABLIKIM	17AA	PL B774 252	M. Ablikim *et al.* (BES III Collab.)
KHACHATRY...	17D	JHEP 1701 076	V. Khachatryan *et al.* (CMS Collab.)
KHACHATRY...	17W	PL B769 520	V. Khachatryan *et al.* (CMS Collab.)
KHACHATRY...	17Y	PL B770 257	V. Khachatryan *et al.* (CMS Collab.)
SIRUNYAN	17B	JHEP 1704 136	A.M. Sirunyan *et al.* (CMS Collab.)
SIRUNYAN	17C	JHEP 1705 029	A.M. Sirunyan *et al.* (CMS Collab.)
SIRUNYAN	17F	JHEP 1707 013	A.M. Sirunyan *et al.* (CMS Collab.)
SIRUNYAN	17J	JHEP 1708 073	A.M. Sirunyan *et al.* (CMS Collab.)
AABOUD	16	PL B759 229	M. Aaboud *et al.* (ATLAS Collab.)
AABOUD	16P	EPJ C76 541	M. Aaboud *et al.* (ATLAS Collab.)
AAD	16AI	JHEP 1603 041	G. Aad *et al.* (ATLAS Collab.)
AAD	16N	JHEP 1603 026	G. Aad *et al.* (ATLAS Collab.)
AAD	16O	PL B760 520	G. Aad *et al.* (ATLAS Collab.)
AAD	16R	PL B755 285	G. Aad *et al.* (ATLAS Collab.)
AAD	16S	PL B754 302	G. Aad *et al.* (ATLAS Collab.)
AAIJ	16AR	EPJ C76 664	R. Aaij *et al.* (LHCb Collab.)
KHACHATRY...	16BW	PR D94 112004	V. Khachatryan *et al.* (CMS Collab.)
KHACHATRY...	16K	PRL 116 071801	V. Khachatryan *et al.* (CMS Collab.)
KHACHATRY...	16L	PRL 117 031802	V. Khachatryan *et al.* (CMS Collab.)
KHACHATRY...	16M	PRL 117 051802	V. Khachatryan *et al.* (CMS Collab.)
AAD	15AN	JHEP 1507 032	G. Aad *et al.* (ATLAS Collab.)
AAD	15AT	EPJ C75 79	G. Aad *et al.* (ATLAS Collab.)
AAD	15BJ	EPJ C75 362	G. Aad *et al.* (ATLAS Collab.)
AAIJ	15BD	EPJ C75 595	R. Aaij *et al.* (LHCb Collab.)
ADRIANI	15	PRL 115 111101	O. Adriani *et al.* (PAMELA Collab.)
AGNESE	15	PRL 114 111302	R. Agnese *et al.* (CDMS Collab.)
KHACHATRY...	15F	PRL 114 101801	V. Khachatryan *et al.* (CMS Collab.)
LEES	15E	PRL 114 171801	J.P. Lees *et al.* (BABAR Collab.)
AAD	14A	PL B728 562	G. Aad *et al.* (ATLAS Collab.)
AAD	14AL	PRL 112 091804	G. Aad *et al.* (ATLAS Collab.)
AAD	14C	JHEP 1408 103	G. Aad *et al.* (ATLAS Collab.)
AALTONEN	14J	PR D89 092001	T. Aaltonen *et al.* (CDF Collab.)
AAD	13A	PL B718 860	G. Aad *et al.* (ATLAS Collab.)
AAD	13AH	PL B722 305	G. Aad *et al.* (ATLAS Collab.)
AAD	13C	PRL 110 011802	G. Aad *et al.* (ATLAS Collab.)
AAD	13D	JHEP 1301 029	G. Aad *et al.* (ATLAS Collab.)
AALTONEN	13I	PR D88 031103	T. Aaltonen *et al.* (CDF Collab.)
AALTONEN	13R	PRL 111 031802	T. Aaltonen *et al.* (CDF Collab.)
CHATRCHYAN	13	PL B718 815	S. Chatrchyan *et al.* (CMS Collab.)
CHATRCHYAN	13A	JHEP 1301 013	S. Chatrchyan *et al.* (CMS Collab.)
CHATRCHYAN	13AB	JHEP 1307 122	S. Chatrchyan *et al.* (CMS Collab.)
CHATRCHYAN	13AD	JHEP 1307 178	S. Chatrchyan *et al.* (CMS Collab.)
CHATRCHYAN	13AR	PR D87 092008	S. Chatrchyan *et al.* (CMS Collab.)
AAD	12AK	PL B716 122	G. Aad *et al.* (ATLAS Collab.)
AAD	12C	PRL 108 041805	G. Aad *et al.* (ATLAS Collab.)
AAD	12S	PL B708 37	G. Aad *et al.* (ATLAS Collab.)
AALTONEN	12M	PRL 108 211804	T. Aaltonen *et al.* (CDF Collab.)
CHATRCHYAN	12AP	JHEP 1209 094	S. Chatrchyan *et al.* (CMS Collab.)
CHATRCHYAN	12BL	JHEP 1212 015	S. Chatrchyan *et al.* (CMS Collab.)
CHATRCHYAN	12Q	PL B716 260	S. Chatrchyan *et al.* (CMS Collab.)
CHATRCHYAN	12T	PRL 108 261803	S. Chatrchyan *et al.* (CMS Collab.)
CHATRCHYAN	12W	JHEP 1204 061	S. Chatrchyan *et al.* (CMS Collab.)
AAD	11AG	NJP 13 053044	G. Aad *et al.* (ATLAS Collab.)
AAD	11I	PL B698 353	G. Aad *et al.* (ATLAS Collab.)
AAD	11S	PL B705 294	G. Aad *et al.* (ATLAS Collab.)
AALTONEN	11AF	PRL 107 181801	T. Aaltonen *et al.* (CDF Collab.)
AALTONEN	11M	PRL 106 171801	T. Aaltonen *et al.* (CDF Collab.)
ABAZOV	11I	PRL 107 011804	V.M. Abazov *et al.* (D0 Collab.)
CHATRCHYAN	11C	JHEP 1106 026	S. Chatychyan *et al.* (CMS Collab.)
CHATRCHYAN	11U	PRL 107 201804	S. Chatychyan *et al.* (CMS Collab.)
AAD	10	PRL 105 161801	G. Aad *et al.* (ATLAS Collab.)
AALTONEN	10AF	PR D82 052005	T. Aaltonen *et al.* (CDF Collab.)
KHACHATRY...	10	PRL 105 211801	V. Khachatryan *et al.* (CMS Collab.)
Also		PRL 106 029902	V. Khachatryan *et al.* (CMS Collab.)
AALTONEN	09AF	PR D80 011102	T. Aaltonen *et al.* (CDF Collab.)
AALTONEN	09G	PR D79 052004	T. Aaltonen *et al.* (CDF Collab.)
AALTONEN	09Z	PRL 103 021802	T. Aaltonen *et al.* (CDF Collab.)
ABAZOV	09M	PRL 102 161802	V.M. Abazov *et al.* (D0 Collab.)
AKTAS	04C	EPJ C36 413	A. Atkas *et al.* (H1 Collab.)
JAVORSEK	02	PR D65 072003	D. Javorsek II *et al.*
JAVORSEK	01	PR D64 012005	D. Javorsek II *et al.*
JAVORSEK	01B	PRL 87 231804	D. Javorsek II *et al.*
ABBIENDI	00D	EPJ C13 197	G. Abbiendi *et al.* (OPAL Collab.)
AMBROSIO	00B	EPJ C13 453	M. Ambrosio *et al.* (MACRO Collab.)
ABE	99F	PRL 82 2038	F. Abe *et al.* (CDF Collab.)
ACKERSTAFF	98P	PL B433 195	K. Ackerstaff *et al.* (OPAL Collab.)
ABE	97G	PR D55 5263	F. Abe *et al.* (CDF Collab.)
ABREU	97D	PL B396 315	P. Abreu *et al.* (DELPHI Collab.)
ACKERSTAFF	97B	PL B391 210	K. Ackerstaff *et al.* (OPAL Collab.)
ADAMS	97B	PRL 79 4083	J. Adams *et al.* (FNAL KTeV Collab.)
BARATE	97K	PL B405 379	R. Barate *et al.* (ALEPH Collab.)
AKERS	95R	ZPHY C67 203	R. Akers *et al.* (OPAL Collab.)
GALLAS	95	PR D52 6	E. Gallas *et al.* (MSU, FNAL, MIT, FLOR)
RAM	94	PR D49 3120	S. Ram *et al.* (TELA, TRIU)
ABE	93G	PRL 71 2542	F. Abe *et al.* (CDF Collab.)
ASTONE	93	PR D47 4770	P. Astone *et al.* (ROMA, ROMAI, CATA, FRAS)
BUSKULIC	93C	PL B303 198	D. Buskulic *et al.* (ALEPH Collab.)
YAMAGATA	93	PR D47 1231	T. Yamagata, Y. Takamori, H. Utsunomiya (KONAN)
ABE	92J	PR D46 1889	F. Abe *et al.* (CDF Collab.)
AHLEN	92	PRL 69 1860	S.P. Ahlen *et al.* (MACRO Collab.)
VERKERK	92	PRL 68 1116	P. Verkerk *et al.* (ENSP, SACL, PAST)
AKESSON	91	ZPHY C52 219	T. Akesson *et al.* (HELIOS Collab.)
NAKAMURA	91	PL B263 529	S. Nakamura *et al.*
ORITO	91	PRL 66 1951	S. Orito *et al.* (ICEPP, WASCR, NIHO, ICRR)
ADACHI	90C	PL B244 352	I. Adachi *et al.* (TOPAZ Collab.)
ADACHI	90E	PL B249 336	I. Adachi *et al.* (TOPAZ Collab.)
AKRAWY	90O	PL B252 290	M.Z. Akrawy *et al.* (OPAL Collab.)
HEMMICK	90	PR D41 2074	T.K. Hemmick *et al.* (ROCH, MICH, OHIO+)
SAITO	90	PRL 65 2094	T. Saito *et al.* (ICRR, KOBE)
NAKAMURA	89	PR D39 1261	T.T. Nakamura *et al.* (KYOT, TMTC)
NORMAN	89	PR D39 2499	E.B. Norman *et al.* (LBL)
BERNSTEIN	88	PR D37 3103	R.M. Bernstein *et al.* (STAN, WISC)
LIU	88	PRL 61 271	G. Liu, B. Barish
BARISH	87	PR D36 2641	B.C. Barish, G. Liu, C. Lane (CIT)
NORMAN	87	PRL 58 1403	E.B. Norman, S.B. Gazes, D.A. Bennett (LBL)
BADIER	86	ZPHY C31 21	J. Badier *et al.* (NA3 Collab.)
MINCER	85	PR D32 541	A. Mincer *et al.* (UMD, GMAS, NSF)
NAKAMURA	85	PL 161B 417	K. Nakamura *et al.* (KEK, INUS)
THRON	85	PR D31 451	J.L. Thron *et al.* (YALE, FNAL, IOWA)

Searches Particle Listings

Other Particle Searches

SAKUYAMA	83B	LNC 37 17	H. Sakuyama, N. Suzuki	(MEIS)
Also		LNC 36 389	H. Sakuyama, K. Watanabe	(MEIS)
Also		NC 78A 147	H. Sakuyama, K. Watanabe	(MEIS)
Also		NC 6C 371	H. Sakuyama, K. Watanabe	(MEIS)
BHAT	82	PR D25 2820	P.N. Bhat *et al.*	(TATA)
KINOSHITA	82	PRL 48 77	K. Kinoshita, P.B. Price, D. Fryberger	(UCB+)
MARINI	82	PR D26 1777	A. Marini *et al.*	(FRAS, LBL, NWES, STAN+)
SMITH	82B	NP B206 333	P.F. Smith *et al.*	(RAL)
KINOSHITA	81B	PR D24 1707	K. Kinoshita, P.B. Price	(UCB)
LOSECCO	81	PL 102B 209	J.M. LoSecco *et al.*	(MICH, PENN, BNL)
ULLMAN	81	PRL 47 289	J.D. Ullman	(LEHM, BNL)
YOCK	81	PR D23 1207	P.C.M. Yock	(AUCK)
BARTEL	80	ZPHY C6 295	W. Bartel *et al.*	(JADE Collab.)
BUSSIERE	80	NP B174 1	A. Bussiere *et al.*	(BGNA, SACL, LAPP)
YOCK	80	PR D22 61	P.C.M. Yock	(AUCK)
ARMITAGE	79	NP B150 87	J.C.M. Armitage *et al.*	(CERN, DARE, FOM+)
BOZZOLI	79	NP B159 363	W. Bozzoli *et al.*	(BGNA, LAPP, SACL+)
GOODMAN	79	PR D19 2572	J.A. Goodman *et al.*	(UMD)
SMITH	79	NP B149 525	P.F. Smith, J.R.J. Bennett	(RHEL)
BHAT	78	PRAM 10 115	P.N. Bhat, P.V. Ramana Murthy	(TATA)
CARROLL	78	PRL 41 777	A.S. Carroll *et al.*	(BNL, PRIN)
CUTTS	78	PRL 41 363	D. Cutts *et al.*	(BROW, FNAL, ILL, BARI+)
VIDAL	78	PL 77B 344	R.A. Vidal *et al.*	(COLU, FNAL, STON+)
ALEKSEEV	76	SJNP 22 531 Translated from YAF 22 1021.	G.D. Alekseev *et al.*	(JINR)
ALEKSEEV	76B	SJNP 23 633 Translated from YAF 23 1190.	G.D. Alekseev *et al.*	(JINR)
BALDIN	76	SJNP 22 264 Translated from YAF 22 512.	B.Y. Baldin *et al.*	(JINR)
BRIATORE	76	NC 31A 553	L. Briatore *et al.*	(LCGT, FRAS, FREIB)
GUSTAFSON	76	PRL 37 474	H.R. Gustafson *et al.*	(MICH)
ALBROW	75	NP B97 189	M.G. Albrow *et al.*	(CERN, DARE, FOM+)
FRANKEL	75	PR D12 2561	S. Frankel *et al.*	(PENN, FNAL)
JOVANOV...	75	PL 56B 105	J.V. Jovanovich *et al.*	(MANI, AACH, CERN+)
YOCK	75	NP B86 216	P.C.M. Yock	(AUCK, SLAC)
APPEL	74	PRL 32 428	J.A. Appel *et al.*	(COLU, FNAL)
FRANKEL	74	PR D9 1932	S. Frankel *et al.*	(PENN, FNAL)
YOCK	74	NP B76 175	P.C.M. Yock	(AUCK)
ALPER	73	PL 46B 265	B. Alper *et al.*	(CERN, LIVP, LUND, BOHR+)
LEIPUNER	73	PRL 31 1226	L.B. Leipuner *et al.*	(BNL, YALE)
DARDO	72	NC 9A 319	M. Dardo *et al.*	(TORI)
TONWAR	72	JP A5 569	S.C. Tonwar, S. Naranan, B.V. Sreekantan	(TATA)
ANTIPOV	71B	NP B31 235	Y.M. Antipov *et al.*	(SERP)
ANTIPOV	71C	PL 34B 164	Y.M. Antipov *et al.*	(SERP)
BINON	69	PL 30B 510	F.G. Binon *et al.*	(SERP)
BJORNBOE	68	NC B53 241	J. Bjornboe *et al.*	(BOHR, TATA, BERN+)
JONES	67	PR 164 1584	L.W. Jones	(MICH, WISC, LBL, UCLA, MINN+)
DORFAN	65	PRL 14 999	D.E. Dorfan *et al.*	(COLU)

INDEX

Greek letters are alphabetized by their English-language spelling. Bold page numbers signify entries in the Particle Properties Summary Tables.

Greek letters are alphabetized by their English-language spelling. Bold page numbers signify entries in the Particle Properties Summary Tables.

Greek letters are alphabetized by their English-language spelling. Bold page numbers signify entries in the Particle Properties Summary Tables.

Greek letters are alphabetized by their English-language spelling. Bold page numbers signify entries in the Particle Properties Summary Tables.

Greek letters are alphabetized by their English-language spelling. Bold page numbers signify entries in the Particle Properties Summary Tables.

Greek letters are alphabetized by their English-language spelling. Bold page numbers signify entries in the Particle Properties Summary Tables.

Greek letters are alphabetized by their English-language spelling. Bold page numbers signify entries in the Particle Properties Summary Tables.

Greek letters are alphabetized by their English-language spelling. Bold page numbers signify entries in the Particle Properties Summary Tables.

Greek letters are alphabetized by their English-language spelling. Bold page numbers signify entries in the Particle Properties Summary Tables.

Greek letters are alphabetized by their English-language spelling. Bold page numbers signify entries in the Particle Properties Summary Tables.

Greek letters are alphabetized by their English-language spelling. Bold page numbers signify entries in the Particle Properties Summary Tables.

Greek letters are alphabetized by their English-language spelling. Bold page numbers signify entries in the Particle Properties Summary Tables.

Greek letters are alphabetized by their English-language spelling. Bold page numbers signify entries in the Particle Properties Summary Tables.

Greek letters are alphabetized by their English-language spelling. Bold page numbers signify entries in the Particle Properties Summary Tables.

Greek letters are alphabetized by their English-language spelling. Bold page numbers signify entries in the Particle Properties Summary Tables.